ENCYCLOPEDIA OF MOLECULAR BIOLOGY

VOLUMES 1 - 4

Thomas E. Creighton

European Molecular Biology Laboratory
London, England

A Wiley-Interscience Publication

John Wiley & Sons, Inc.

New York / Chichester / Weinheim / Brisbane / Singapore / Toronto

This book is printed on acid-free paper. ♾

For ordering and customer service, call 1-800-CALL-WILEY.

Library of Congress Cataloging-in-Publication Data:

Creighton, Thomas E., 1940–
The encyclopedia of molecular biology / Thomas E. Creighton.
p. cm.
Includes index.
ISBN 0-471-15302-8 (alk. paper)
1. Molecular biology–Encyclopedias. I. Title.
QH506.C74 1999 99-11575
572.8′03—dc21 CIP

Printed in the United States of America.

10 9 8 7 6 5 4 3 2 1

PREFACE

The Wiley Biotechnology Encyclopedias, composed of the *Encyclopedia of Molecular Biology*, the *Encyclopedia of Bioprocess Technology: Fermentation, Biocatalysis, and Bioseparation*, the *Encyclopedia of Cell Technology*, and the *Encyclopedia of Ethical, Legal, and Policy Issues in Biotechnology*, cover very broadly four major contemporary themes in biotechnology. The series comes at a fascinating time in that as we move into the twenty-first century, the discipline of biotechnology is undergoing striking paradigm changes.

Biotechnology is now beginning to be viewed as an informational science. In a simplistic sense, there are three types of biological information. First, there is the digital or linear information of our chromosomes and genes, with the four-letter alphabet composed of G, C, A, and T (the bases Guanine, Cytosine, Adenine, and Thymine). Variation in the order of these letters in the digital strings of our chromosomes or our expressed genes (or mRNAs) generates information of several distinct types: genes, regulatory machinery, and information that enables chromosomes to carry out their tasks as informational organelles (eg, centromeric and telomeric sequences).

Second, there is the three-dimensional information of proteins, the molecular machines of life. Proteins are strings of amino acids employing a 20-letter alphabet. Proteins pose four technical challenges: (i) Proteins are synthesized as linear strings and fold into precise three-dimensional structures as dictated by the order of amino acid residues in the string. Can we formulate the rules for protein folding to predict three-dimensional structure from primary amino acid sequence? The identification and comparative analysis of all human and model organism (bacteria, yeast, nematode, fly, mouse, etc.) genes and proteins will eventually lead to a lexicon of motifs that are the building block components of genes and proteins. These motifs will greatly constrain the shape space computational algorithms must search to successfully correlate primary amino acid sequence with the correct three-dimensional shapes. The protein-folding problem will probably be solved within the next 10 to 15 years. (ii) Can we predict protein function from knowledge of the three-dimensional structure? Once again the lexicon of motifs with their functional as well as structural correlations will play a critical role in solving this problem. (iii) How do the myriad of chemical modifications of proteins (eg, phosphorylation, acetylation) alter their structures and modify their functions? The mass spectrometer will play a key role in identifying secondary modifications. (iv) How do proteins interact with one another and/or with other macromolecules to form complex molecular machines (eg, the ribosomal subunits)? If these functional complexes can be isolated, the mass spectrometer, coupled with a knowledge of all protein sequences that can be derived from the complete genomic sequence of the organism, will serve as a powerful tool for identifying all the components of complex molecular machines.

The third type of biological information arises from complex biological systems and networks. Systems information is four-dimensional because it varies with time. For example, the human brain has 1012 neurons making approximately 1015 connections. From this network arises systems properties such a memory, consciousness, and the ability to learn. The important point is that systems properties cannot be understood from studying the network elements (eg, neurons) one at a time; rather, the collective behavior of the elements needs to be studied together. To study most biological systems, three issues need to be stressed. First, most biological systems are too complex to study directly; therefore they must be divided into tractable subsystems whose properties in part reflect those of the system. These subsystems must be sufficiently small to analyze all their elements and connections. Second, high-throughput analytic or global tools are required for studying many systems elements at one time (see below). Finally, the systems information needs to be modeled mathematically before systems properties can be predicted and ultimately understood. This will require recruiting computer scientists and applied mathematics into biology—just as the attempts to decipher the information of complete genomes and the protein folding and structure/function problems have required the recruitment of computational scientists.

I would be remiss not to point out that there are many other molecules that generate biological information—amino acids, carbohydrates, lipids, etc. These too must be studied in the context of their specific structures and specific functions.

The deciphering and manipulation of these various types of biological information represent an enormous technical challenge for biotechnology. Yet major new and powerful tools for doing so are emerging.

One class of tools for deciphering biological information is termed high-throughput analytic or global tools. These tools can study many genes or chromosome features (genomics), many proteins (proteomics), or many cells rapidly: large-scale DNA sequencing; genome-wide genetic mapping; cDNA or oligonucleotide arrays; two-dimensional gel electrophoresis and other global protein separation technologies; mass spectrometric analysis of proteins and protein fragments; multiparameter, high-throughput cell and chromosome sorting; and high-throughput phenotypic assays.

A second approach to the deciphering and manipulation of biological information centers around combinatorial strategies. The basic idea is to synthesize an informational string (DNA fragments, RNA fragments, protein fragments, antibody combining sites, etc.) using all combinations of the basic letters of the corresponding alphabet—thus creating many different shapes that can be used to activate, inhibit, or complement the biological functions of designated three-dimensional shapes (eg, a molecule in a signal transduction pathway). The power of combinational chemistry is just beginning to be appreciated.

A critical approach to deciphering biological information will ultimately be the ability to visualize the functioning of genes, proteins, cells, and other informational elements within living organisms (*in vivo* informational imaging).

Finally, there are the computational tools required to collect, store, analyze, model, and ultimately distribute the various types of biological information. The creation presents a challenge comparable to that of developing of new instrumentation and new chemistries. Once again, this means recruiting computer scientists and applied mathematicians to biology. The biggest challenge in this regard is the language barriers that separate different scientific disciplines. Teaching biology as an informational science has been a very effective means for breeching these language barriers.

The challenge is, of course, to decipher these various types of biological information and then be able to use this information to manipulate genes, proteins, cells, and informational pathways in living organisms to eliminate or prevent disease, produce higher yield crops, or increase the productivity of animal products and meat.

Biotechnology and its applications raise a host of social, ethical, and legal questions; for example, genetic privacy, germline genetic engineering, cloning animals, genes that influence behavior, cost of therapeutic drugs generated by biotechnology, animal rights, and the nature and control of intellectual property.

The challenge clearly is to educate society so that each citizen can thoughtfully and rationally deal with these issues, for ultimately society dictates the resources and regulations that circumscribe the development and practice of biotechnology. Ultimately, I feel enormous responsibility rests with scientists to inform and educate society about the challenges as well as the opportunities arising from biotechnology. These are critical issues for biotechnology that are developed in detail in the *Encyclopedia of Ethical, Legal, and Policy Issues in Biotechnology*.

The view that biotechnology is an informational science pervades virtually every aspect of this science—including discovery, reduction to practice, and societal concerns. These Encyclopedias of Biotechnology reinforce the emerging informational paradigm change that is powerfully positioning science as we move into the twenty-first century to more effectively decipher and manipulate for humankind's benefit the biological information of relevant living organisms.

LEROY HOOD
University of Washington

CONTRIBUTORS

Hanna E. Abboud, *University of Texas, Health Science Center, San Antonio, TX*
Sankar Adhya, *National Cancer Institute, National Institutes of Health, Bethesda, MD*
Hiroji Aiba, *Nagoya University, Chikusa, Nagoya, Japan*
Philip Aisen, *Albert Einstein College of Medicine, Bronx, NY*
Rudolf K. Allemann, *University of Birmingham, Birmingham, United Kingdom*
Nicholas Allen, *The Babraham Institute, Cambridge, United Kingdom*
Suresh Ambudkar, *National Cancer Institute, National Institutes of Health, Bethesda, MD*
Vernon E. Anderson, *Case Western Reserve University, Cleveland, OH*
Bertil Andersson, *Stockholm University, Stockholm, Sweden*
Ruth Hogue Angeletti, *Albert Einstein College of Medicine, Bronx, NY*
Rodolfo Aramayo, *Schering-Plough Research Institute, Kenilworth, NJ*
Yari Argon, *University of Chicago, Chicago, IL*
K. Arora, *University of California, Irvine, CA*
Leonie K. Ashman, *Hanson Center for Cancer Research, Adeleide, Australia*
John F. Atkins, *University of Utah, Salt Lake City, UT*
William M. Atkins, *University of Washington, Seattle, WA*
Daniel Atkinson, *UCLA, Los Angeles, CA*
David Auld, *Harvard Medical School, Boston, MA*
Paul Babitzke, *Pennsylvania State University, University Park, PA*
Andrew Baird, *Prizm Pharmaceuticals, San Diego, CA*
Stacey J. Baker, *Temple University School of Medicine, Philadelphia, PA*
Tom Baldwin, *Texas A&M University, College Station, TX*
Michael Bamshad, *University of Utah Health Sciences Center, Salt Lake City, UT*
Probal Banerjee, *College of Staten Island, New York, NY*
Ruma Banerjee, *University of Nebraska, Lincoln, NE*
William R. Bauer, *University of California, San Francisco, CA*
Christopher Baum, *Heinrich-Pette Institut, Hamburg, Germany*
Edward A. Bayer, *Weizmann Institute of Science, Rehovot, Israel*
Miguel Beato, *Philipps–Universitaet Marburg, Institut fuer Molekularbiologie, Marburg, Germany*
Dorothy Beckett, *University of Maryland, Baltimore, MD*
Samuel Benchimol, *University of Toronto, Toronto, Ontario, Canada*
Steven J. Benkovic, *Pennsylvania State University, University Park, PA*
Tomas Bergman, *Karolinska Institutet, Stockholm, Sweden*
Gerald Bergtrom, *University of Wisconsin, Milwaukee, WI*
Alan Bernstein, *Mount Sinai Hospital, Toronto, Ontario, Canada*
Harris D. Bernstein, *NIDDKD, National Institutes of Health, Bethesda, MD*
Sophie Bertrand, *Universiteit Gent, Gent, Belgium*
D. M. Bethea, *Thomas Jefferson University, Philadelphia, PA*
Dieter Beyer, *Rhone Poulenc Rorer Recherche Developpement, Vitry-sur-Seine, France*
Timothy R. Billiar, *University of Pittsburgh Medical Center, Pittsburgh, PA*
Asgeir Bjornsson, *University of Aarhus, Aarhus, Denmark*
Colin C. F. Blake, *Norfolk, United Kingdom*
F. Bonomi, *Universita Degli Studi Di Milano, Milano, Italy*
Ralph A. Bradshaw, *University of California, Irvine, CA*
Bertram Brenig, *Georg-August University, Göttingen, Germany*
Kenneth J. Breslauer, *Rutgers University, Piscataway, NJ*
Roy J. Britten, *California Institute of Technology, Corona del Mar, CA*
Maurizio Brunori, *University of Rome, "La Sapienza," Rome, Italy*
Bernd Bukau, *Albert-Ludwigs Universitat Freiburg, Freiburg, Germany*
Jens R. Bundgaard, *University of Copenhagen, Copenhagen, Denmark*
Arsene Burny, *Universite Libre de Bruxelles, Rhode Saint Genese, Belgium*
Kenneth Burtis, *University of California, Davis, CA*
Ana Busturia, *Universidad Aut noma de Madrid, Madrid, Spain*
Giulio L. Cantoni, *NIMH, National Institutes of Health, Bethesda, MD*
M. Stella Carlomango, *Università Degli Studi Di Napoli Federico II, Napoli, Italy*
Gerald M. Carlson, *University of Missouri, Kansas City, MO*
Graham Carpenter, *Vanderbilt University, Nashville, TN*
Robin W. Carrell, *University of Cambridge, Cambridge, United Kingdom*
James Castelli-Gair, *University of Cambridge, Cambridge, United Kingdom*
Enrique Cerda-Olmedo, *Universidad de Sevilla, Sevilla, Spain*
Jonathan Chaires, *University of Mississippi Medical Center, Jackson, MS*
Kung-Yao Chang, *MRC Laboratory of Molecular Biology, Cambridge, United Kingdom*
Lee Chao, *Medical University of South Carolina, Charleston, SC*
Ansuman Chattopadhyay, *Vanderbilt University School of Medicine, Nashville, TN*
Walter Chazin, *Scripps Research Institute, La Jolla, CA*
Elizabeth H. Chen, *University of Texas, Southwestern Medical Center, Dallas, TX*
Donald P. Cheney, *Northeastern University, Boston, MA*
Andreas Chrambach, *National Institutes of Health, Bethesda, MD*
Jason Christiansen, *Virginia Polytechnic Institute, Blacksburg, VA*
Jon A. Christopher, *Texas A&M University, College Station, TX*
Brian F. C. Clark, *Aarhus University, Aarhus, Denmark*
Dennis Clegg, *University of California, Santa Barbara, CA*
F. Cliften, *University of Colorado Health Sciences Center, Denver, CO*
Georges N. Cohen, *Institut Pasteur, Paris, France*
Roberta Colman, *University of Delaware, Newark, DE*
Orla M. Conneely, *Baylor College of Medicine, Houston, TX*
Barry S. Cooperman, *University of Pennsylvania, Philadelphia, PA*
Pamela Correll, *The Pennsylvania State University, University Park, PA*
Pascale Cossart, *Institut Pasteur, Paris, France*
Nancy Craig, *Johns Hopkins University, Baltimore, MD*
Elliott Crooke, *Georgetown University, Washington, DC*
Stanley T. Crooke, *ISIS Pharmaceuticals, Inc., Carlsbad, CA*
Richard D. Cummings, *University of Oklahoma, Oklahoma City, OK*
James Curran, *Wake Forest University, Winston-Salem, NC*
Michael A. Cusanovich, *University of Arizona, Tucson, AZ*
Giuseppe D'Alessio, *Universita di Napoli Federico II, Napoli, Italy*
Antoine Danchin, *Institut Pasteur, Paris, France*

P. L. Davies, *Queen's University, Kingston, Ontario, Canada*
Dennis R. Dean, *Virginia Polytechnic Institute & State University, Blacksburg, VA*
Pieter DeHaseth, *Case Western Reserve University, Cleveland, OH*
Andrew J. DeMello, *Imperial College, London, United Kingdom*
David T. Denhardt, *Rutgers University, Piscataway, NJ*
W. A. Denny, *University of Auckland, Auckland, New Zealand*
Zygmunt Derewenda, *University of Virginia, Charlottesville, VA*
Claude Desplan, *Rockefeller University, New York, NY*
Raymond Devoret, *Centre Universitaire, Orsay, France*
Beth Didomenico, *Schering-Plough Research Institute, Kenilworth, NJ*
Patrick DiMario, *Louisiana State University, Baton Rouge, LA*
Hal B. F. Dixon, *Cambridge University, Cambridge, United Kingdom*
Mark Dodson, *University of Arizona, Tucson, AZ*
Jan Drenth, *Laboratory of Biophysical Chemistry, Groningen, The Netherlands*
Gerhart Drews, *Institut fur Biologie, Freiburg, Germany*
Bernard Dujon, *Institut Pasteur, Paris, France*
Edward Egelman, *University of Minnesota, Minneapolis, MN*
Jean Marc Egly, *Parc d'Innovation, Illkirch, France*
John Ellis, *University of Warwick, Coventry, United Kingdom*
Vincent Ellis, *Thrombosis Research Institute, London, United Kingdom*
Walther Ellis, *Utah State University, Logan, UT*
Volker Erdmann, *Freie Universitat Berlin, Berlin, Germany*
Gerard Evan, *ICRF, London, United Kingdom*
Kenneth Ewan, *Max-Planck Institute of Biophysical Chemistry, Göttingen, Germany*
Hong Fang, *Vanderbilt University, Nashville, TN*
Lynette R. Ferguson, *University of Auckland Medical School, Auckland, New Zealand*
Carol A. Fierke, *Duke University, Durham, NC*
J. R. S. Fincham, *University of Edinburgh, Edinburgh, Scotland*
Anthony L. Fink, *University of California, Santa Cruz, CA*
Gunter Fischer, *MPG Arbeitsgruppe, Halle, Germany*
Darrell R. Fisher, *Pacific Northwest Laboratory, Richland, WA*
Catherine Florentz, *Institut de Biologic Moleculaire et Cellulaire, Strasbourg, France*
Ricardo Flores, *Instituto de Biologia Molecular y Cellularde Plantas, Valencia, Spain*
P. J. Foley, *Thomas Jefferson University, Philadelphia, PA*
Josiane Fontaine-Perus, *CNRS, Nantes Cedex, France*
Jefferson Foote, *Fred Hutchinson Cancer Research Center, Seattle, WA*
Patricia Foster, *Boston University, Boston, MA*
Michel Fougereau, *Centre d'Immunologie Marseille Luminy, Marseille, France*
Francois Franceschi, *Max-Planck Institute for Molecular Genetics, Berlin, Germany*
Murray J. Fraser, *Sydney Children's Hospital, Randwick, Australia*
Ian Freshney, *University of Glasgow, Glasgow, United Kingdom*
Terrence G. Frey, *San Diego State University, San Diego, CA*
Laura Frontali, *University of Rome, "La Sapienza," Rome, Italy*
Yasuo Fukami, *Kobe University, Nada, Kobe, Japan*
Carl W. Fuller, *Amersham Pharmacia Biotech, Cleveland, OH*
Betty Gaffney, *Florida State University, Tallahassee, FL*
Fernando Garcia-Arenal, *Ciudad Universitaria, Madrid, Spain*
Jean-Renaud Garel, *Laboratoire de Biologie Structurale, CNRS, Gif-sur-Yvette, France*
D. R. Garrod, *University of Manchester, Manchester, United Kingdom*
Frank R. Gasparro, *Jefferson University, Philadelphia, PA*
C. Gaspin, *Centre National de la Researche Scientifique, Strasbourg, France*
Anthony A. Gatenby, *E. I. duPont de Nemours & Co., Wilmington, DE*
Kunihiko Gekko, *Hiroshima University, Higashi-Hiroshima, Japan*
Herbert Geller, *UMDNJ—Robert Wood Johnson Medical School, Piscataway, NJ*
John Gerig, *University of California, Santa Barbara, CA*
Norman L. Gershfeld, *National Institutes of Health, Bethesda, MD*
Michael Gershon, *Columbia University, New York, NY*
Jonathan M. Gershoni, *Tel Aviv University, Tel Aviv, Israel*
Jean-Marie Ghuysen, *Universite de Liege, Liege, Belgium*
Toby Gibson, *European Molecular Biology Laboratory, Heidelberg, Germany*
J. A. Girault, *Chaire de Neuropharmacologie, College de France, Paris, France*
Adam Godzik, *Scripps Research Institute, La Jolla, CA*
Jefferey Godzik, *Scripps Research Institute, La Jolla, CA*
J. Peter Gogarten, *University of Connecticut, Storrs Mansfield, CT*
Takashi Gojobori, *National Institute of Genetics, Shizuoka, Japan*
Alfred L. Goldberg, *Harvard Medical School, Boston, MA*
Paul Gollnick, *State University of New York at Buffalo, Buffalo, NY*
Pierre Goldstein, *Centre d'Immunologie INSERM-CNRS de Marseille, Marseille, France*
H. Maurice Goodman, *University of Massachusetts Medical School, Worcester, MA*
Horace B. Gray, *University of Houston, Houston, TX*
Neil Green, *Vanderbilt University School of Medicine, Nashville, TN*
William Griffiths, *Karolinska Institutet, Stockholm, Sweden*
Frank Grosse, *Institut fur Molekulare Biotechnologie, Jena, Germany*
Marianne Grunberg-Manago, *Institut de Biologie Physico-Chemique, Paris, France*
Peter Gruss, *Max-Planck Institute for Biophysical Chemistry, Göttingen, Germany*
Richard Gumport, *University of Illinois, Urbana, IL*
Andras Guttman, *Genetich Biosystems, San Diego, CA*
William Hagan, *College of St. Rose, Albany, NY*
Klaus Hahlbrock, *Max-Planck Institut fur Biochemie, Martinsried, Germany*
Joshua W. Hamilton, *Dartmouth Medical School, Hanover, NH*
Susan Hamilton, *Baylor College of Medicine, Houston, TX*
Xianlin Han, *Washington University School of Medicine, St. Louis, MO*
Ryo Hanai, *Rikkyo University, Toshima, Tokyo, Japan*
Yusuf Hannun, *Duke University Medical Center, Durham, NC*
Stephen E. Harding, *University of Nottingham, Sutton Bonington, United Kingdom*
Peter Harland, *University of California, Berkeley, CA*
Ulrich Hartl, *Max-Planck Institut fur Biochemie, Martinsried, Germany*
R. W. Hartley, *National Institutes of Health, Bethesda, MD*
Enno Hartmann, *Georg-August Universitaet, Göttingen, Germany*
David L. Haviland, *The University of Texas, Houston Health Science Center, Houston, TX*
Toshihiko Hayashi, *University of Tokyo, Tokyo, Japan*
J. K. Heath, *University of Birmingham, Birmingham, United Kingdom*
Robert Helling, *University of Michigan, Ann Arbor, MI*
Ali Hemmati-Brivanlou, *Rockefeller University, New York, NY*
M. A. Hemminga, *Agricultural University of Wageningen, Daagenlaa, Wageningen, The Netherlands*
Beric Henderson, *University of Sydney, Westmead, Australia*
Roger W. Hendrix, *University of Pittsburgh, Pittsburgh, PA*
Leonard Herzenberg, *Stanford University, Stanford, CA*
George P. Hess, *Cornell University, Ithaca, NY*
Christa Heyting, *Agricultural University, Wageningen, The Netherlands*
D. J. Hill, *St. Joseph's Health Center, London, Ontario, Canada*
James A. Hoch, *Scripps Research Institute, La Jolla, CA*
Denis Hochstrasser, *Geneva University Hospital, Geneva, Switzerland*
Nicholas A. Hoenich, *The University of Newcastle upon Tyne, Newcastle, United Kingdom*
Wayne L. Hoffman, *University of Texas, Southwestern Medical Center, Dallas, TX*

J. John Holbrook, *University of Bristol, Bristol, United Kingdom*
Arne Holmgren, *Karolinska Institute, Stockholm, Sweden*
Thomas F. Holzman, *Abbot Laboratories, Abbot Park, IL*
H. Homareda, *Kyorin University, Tokyo, Japan*
Roger Hull, *John Innes Centre, Colney, Norwich, United Kingdom*
Martin Hum, *University of Texas, Southwestern Medical Center, Dallas, TX*
Jennifer A. Hunt, *Duke University Medical Center, Durham, NC*
Atsushi Ikai, *Tokyo Institute of Technology, Yokohama, Japan*
Kiyohiro Imai, *Osaka University, Osaka, Japan*
Taiji Imoto, *Kyushu University, Fukuoka, Japan*
Antonio Incardona, *University of Tennessee, Memphis, TN*
Edward E. Ishiguro, *University of Victoria, Victoria, B.C., Canada*
Akira Ishihama, *National Institute of Genetics, Shizuoka-ken, Japan*
Judith A. Jaehning, *University of Colorado, Denver, CO*
Yuh-Nung Jan, *University of California, San Francisco, CA*
Joel Janin, *Laboratoire de Biologie Structurale, Paris, France*
S. Jansen, *Georg-August University Göttingen, Göttingen, Germany*
Patricia A. Jennings, *University of California, San Diego, La Jolla, CA*
Randy L. Jirtle, *Duke University, Durham, NC*
Jonathan Jones, *John Innes Institute, Norwich, United Kingdom*
Rick Jones, *Southern Methodist University, Dallas, TX*
Hans Jornvall, *Karolinska Institutet, Stockholm, Sweden*
Akia Kaji, *University of Pennsylvania, Philadelphia, PA*
Barton A. Kamen, *University of Texas, Southwestern Medical Center, Dallas, TX*
Heather Kaminski, *Schering-Plough Research Institute, Kenilworth, NJ*
Minoru Kanehisa, *Kyoto University, Kyoto, Japan*
Jack Kaplan, *Oregon Health Sciences University, Portland, OR*
Francois Karch, *University of Geneva, Geneva, Switzerland*
Thom Kaufmann, *Indiana University, Bloomington, IN*
Jack D. Keene, *Duke University, Durham, NC*
Regis B. Kelly, *University of California, San Francisco, CA*
Zvi Kelman, *Memorial Sloan-Kettering Cancer Center, New York, NY*
Byron Kemper, *University of Illinois, Urbana, IL*
James Kennison, *National Institute of Child Health and Human Development, National Institutes of Health, Bethesda, MD*
Kathleen M. Kerr, *National Institutes of Health, Bethesda, MD*
John R. Kirby, *University of California, Berkeley, CA*
Jennifer Kitchen, *Georgetown University, Washington, DC*
Horst Kleinkauf, *Technische Universitat, Berlin, Germany*
Jorg Klug, *Phillips–Universitat Marburg, Marburg, Germany*
Peter Knight, *University of Leeds, Leeds, United Kingdom*
Charlotte Knudsen, *University of Aarhus, Aarhus, Denmark*
Yuji Kobayashi, *Osaka University, Osaka, Japan*
Ralf Koebnik, *Biozentrum Basel, Basel, Switzerland*
Andrzej Kolinski, *Scripps Research Institute, La Jolla, CA*
Gerald B. Koudelka, *State University of New York at Buffalo, Buffalo, NY*
Joseph Kraut, *University of California, San Diego, La Jolla, CA*
Toshio Kuroki, *Showa University, Tokyo, Japan*
Sidney R. Kushner, *University of Georgia, Athens, GA*
Kunihiro Kuwajima, *University of Tokyo, Tokyo, Japan*
Harold Lahm, *Institute of Molecular Animal Breeding, Munich, Germany*
Ratnesh Lal, *University of California, Santa Barbara, CA*
Marc Lalande, *Children's Hospital, Boston, MA*
David Lane, *Centre National de la Researche Scientifique, Strasbourg, France*
Janos Lanyi, *University of California, Irvine, CA*
Paul Lasko, *McGill University, Montreal, Quebec, Canada*
Michael Laskowski Jr., *Purdue University, West Lafayette, IN*
David S. Latchman, *University College London Medical School, London, United Kingdom*
Peter Lawrence, *Medical Research Council, Cambridge, United Kingdom*
Judith E. Layton, *Ludwig Institute for Cancer Research, Victoria, Australia*
Claude J. Lazdunski, *Laboratoire d'Ingeniere des Systèmes Macromoléculaires, Marseille, France*
Robin Leake, *University of Glasgow, Glasgow, United Kingdom*
Stewart H. Lecker, *Harvard Medical School, Boston, MA*
Stuart LeGrice, *Case Western Reserve School of Medicine, Cleveland, OH*
Ruth Lehmann, *New York University, New York, NY*
Arthur M. Lesk, *University of Cambridge, Cambridge, United Kingdom*
Michael Levine, *University of California, Berkeley, Berkeley, CA*
Joe D. Lewis, *Institute of Cell & Molecular Biology, Edinburgh, United Kingdom*
Uno Lindberg, *Stockholm University, Stockholm, Sweden*
Halina Lis, *Weizmann Institute of Science, Rehovot, Israel*
Uriel Littauer, *Weizmann Institute of Science, Rehovot, Israel*
John Little, *University of Arizona, Tucson, AZ*
Lawrence A. Loeb, *University of Washington, Seattle, WA*
Peter C. Loewen, *University of Manitoba, Winnipeg, Manitoba, Canada*
Douglas J. Loftus, *National Cancer Institute, National Institutes of Health, Bethesda, MD*
Kenton Longenecker, *University of Virginia Health Sciences Center, Charlottesville, VA*
J. Michael Lord, *University of Warwick, Conventry, United Kingdom*
Martin G. Low, *Columbia University, New York, NY*
Reinhard Luhrmann, *Institut fur Molekularbiologie und Tumorforschung, Marburg, Germany*
Paul MacDonald, *Stanford University, Stanford, CA*
Robert M. Macnab, *Yale University, New Haven, CT*
Neil B. Madsen, *University of Alberta, Edmonton, Alberta, Canada*
Hasaji Maki, *Ikoma City, Japan*
Gregory S. Makowski, *University of Connecticut, Farmington, CT*
Jack Maniloff, *University of Rochester, Rochester, NY*
Jeffrey R. Mann, *Beckman Research Institute of the City of Hope, Duarte, CA*
Bengt Mannervik, *Uppsala University, Uppsala, Sweden*
Armen Manoukian, *Ontario Cancer Institute, Toronto, Ontario, Canada*
Ahmed Mansouri, *Max-Planck Institute for Biophysical Chemistry, Göttingen, Germany*
Mohamed A. Marahiel, *Philipps–Universitat Marburg, Marburg, Germany*
Guglielmo Marin, *Universita Degli Studi di Padova, Padova, Italy*
Susan Marqusee, *University of California, Berkeley, CA*
Mike Marsh, *University College London, London, United Kingdom*
Garland Marshall, *Washington University, St. Louis, MO*
Jennifer Martin, *University of Queensland, Brisbane, Australia*
Nancy C. Martin, *University of Louisville, Louisville, KY*
Florence Maschat, *Institut de Genetique Humaine, Montpellier, France*
Christopher Mathews, *Oregon State University, Corvallis, OR*
Abdul Matin, *Stanford University, Stanford, CA*
Mark P. Mattson, *University of Kentucky, Lexington, KY*
Russell A. Maurer, *Case Western Reserve University, Cleveland, OH*
Nicola McCarthy, *Imperial Cancer Research Fund, London, United Kingdom*
Richard McCarty, *Johns Hopkins University, Baltimore, MD*
David R. McClay, *Duke University, Durham, NC*
John R. Menninger, *University of Iowa, Iowa City, IA*
Carl R. Merril, *National Institute of Mental Health, National Institutes of Health, Bethesda, MD*
David Metzler, *Iowa State University, Ames, IA*
Robert H. Michell, *The University of Birmingham, Birmingham, United Kingdom*
Marek Mlodzik, *European Molecular Biology Laboratory, Heidelberg, Germany*
Evita Mohr, *Universitat Hamburg, Hamburg, Germany*
Ian J. Molineux, *University of Texas, Austin, TX*

Cesare Montecucco, *Università degli Studi di Padova, Padova, Italy*
Carol Moore, *City University of New York Medical School, NY*
Henning D. Mootz, *Phillips–Universitat Marburg, Marburg, Germany*
Gines Morata, *University Autonoma De Madrid, Madrid, Spain*
Richard I. Morimoto, *Northwestern University, Evanston, IL*
John F. Morrison, *The Australian National University, Canberra, Australia*
Gisela Mosig, *Vanderbilt University, Nashville, TN*
Jan Mous, *F. Hoffmann-LaRoche Ltd., Basel, Switzerland*
Benno Müller-Hill, *Institut fur Genetik / Universitat Koln, Koln, Germany*
J. K. Myers, *Texas A&M University, College Station, TX*
Kyoshi Nagai, *MRC Laboratory of Molecular Biology, Cambridge, United Kingdom*
Haruki Nakamura, *Biomolecular Engineering Research Institute, Osaka, Japan*
Yoshikazu Nakamura, *University of Tokyo, Tokyo, Japan*
Aiguo Ni, *Medical University of South Carolina, Charleston, SC*
Allen W. Nicholson, *Wayne State University, Detroit, MI*
Christof Niehrs, *Deutsches Krebsforschungszentrum, Heidelberg, Germany*
Koich Nishigaki, *Saitama University, Urawa, Japan*
Ken Nishikawa, *National Institute of Genetics, Shizuoka, Japan*
Ralph A. Nixon, *Harvard Medical School, Belmont, MA*
Akio Nomoto, *University of Tokyo, Tokyo, Japan*
Bengt Norden, *Chalmers University of Technology, Gothenburg, Switzerland*
Shiao Li Oei, *Institute für Biochemie, Berlin, Germany*
Naotake Ogasawara, *Ikoma City, Japan*
Yoshio Okada, *Osaka University, Osaka, Japan*
Charles Ordahl, *University of California, San Francisco, CA*
George Ordal, *University of Illinois, Urbana, IL*
George Oster, *University of California, Berkeley, CA*
Malcolm G. P. Page, *F. Hoffmann-LaRoche Ltd., Basel, Switzerland*
Renato Paro, *University of Heidelberg, Heidelberg, Germany*
D. A. Parry, *Massey University, Palmerston North, New Zealand*
Premal H. Patel, *University of Washington School of Medicine, Seattle, WA*
Barbara Pearse, *MRC Laboratory of Molecular Biology, Cambridge, United Kingdom*
Israel Pecht, *Weizmann Institute of Science, Rehovot, Israel*
Iain K. Pemberton, *Institut Pasteur, Paris, France*
Bernard Perbal, *Centre Universitaire, Orsay, France*
Richard N. Perham, *University of Cambridge, Cambridge, United Kingdom*
Francine Perler, *New England Biolabs, Beverly, MA*
Charles L. Perrin, *University of California, San Diego, La Jolla, CA*
Steven Perrin, *ARIAD Pharmaceuticals, Cambridge, MA*
Bengt Persson, *Karolinska Institute, Stockholm, Sweden*
Donald W. Pettigrew, *Texas A&M University, College Station, TX*
Larry Pfeffer, *University of Tennessee, Memphis, TN*
K. Kevin Pfister, *University of Virginia, Charlottesville, VA*
Margaret A. Phillips, *University of Texas, Dallas, TX*
Don Phillips, *LaTrobe University, Victoria, Australia*
Thomas L. Poulos, *University of California, Irvine, CA*
Linda S. Powers, *Utah State University, Logan, UT*
Peter E. Prevelige, *University of Alabama, Birmingham, AL*
Peter L. Privalov, *Johns Hopkins University, Baltimore, MD*
Gudrun Rappold, *Institut fur Humangenetik Universitatsklinikum, Heidelberg, Germany*
Stephen W. Raso, *Texas A&M University, College Station, TX*
P. D. Rathjen, *University of Adelaide, Adelaide, Australia*
E. Prekumar Reddy, *The Fels Institute for Cancer Research and Molecular Biology, Philadelphia, PA*
Colin Reese, *King's College London, University of London, United Kingdom*
Peter Reichard, *Medical Nobel Institute, Karolinska Institutet, Stockholm, Sweden*
Steffen Reinbothe, *Universite Joseph Fourier, Grenoble, France*
Dietmar Richter, *Institut fur Zellbiochemie und klinische Neurobiologie, Hamburg, Germany*
P. G. Righetti, *University of Milan, Milan, Italy*
Richard J. Riopelle, *Queen's University, Kingston, Ontario, Canada*
James Riordan, *Harvard University, Boston, MA*
Anthony J. Robertson, *National Institutes of Health, Research Triangle Park, NC*
Jean-David Rochaix, *University of Geneva, Geneva, Switzerland*
Mario Roederer, *Stanford University, Stanford, CA*
William A. Rosche, *Boston University School of Medicine, Boston, MA*
Elliott M. Ross, *University of Texas, Southwestern Medical Center, Dallas, TX*
Gregory M. Ross, *Queen's University, Kingston, Ontario, Canada*
Lawrence Rothfield, *University of Connecticut, Farmington, CT*
Harry Rubin, *University of California, Berkeley, CA*
Thomas S. Rush, *Princeton University, Princeton, NJ*
M. S. Saedi, *Hybritech Co., San Diego, CA*
Alan Saltiel, *Parke-Davis Pharmaceutical Research, Ann Arbor, MI*
Aziz Sancar, *University of North Carolina, Chapel Hill, NC*
Matti Saraste, *European Molecular Biology Laboratory, Heidelberg, Germany*
Zuben E. Sauna, *National Institutes of Health, Bethesda, MD*
Lindsay Sawyer, *University of Edinburgh, Edinburgh, United Kingdom*
Walter Schaffner, *Universitat Zurich, Zurich, Switzerland*
Paul Schimmel, *Scripps Research Institute, La Jolla, CA*
Franz Schmid, *Universitat Bayreuth, Bayreuth, Germany*
Manfred Schnarr, *Institut de Biologie Moleculaire et Cellulaire, CNRS, Strasbourg, France*
J. Martin Scholtz, *Texas A&M University, College Station, TX*
Trudi Schupbach, *Princeton University, Princeton, NJ*
James Scott, *Royal Postgraduate Medical School, London, United Kingdom*
Barbara A. Seaton, *Boston University, Boston, MA*
Constantin E. Sekeris, *University of Wurzburg, Wurzburg, Germany*
Igor L. Shamovsky, *Queen's University, Kingston, Ontario, Canada*
Shmuel Shaltiel, *Weizmann Institute of Science, Rehovot, Israel*
Nathan Sharon, *Weizmann Institute of Science, Rehovot, Israel*
G. Shaw, *University of Florida, Gainesville, FL*
William V. Shaw, *Leicester University, Leicester, United Kingdom*
David Sherman, *University of Minnesota, St. Paul, MN*
Ben-Zion Shilo, *Weizmann Institute of Science, Rehovot, Israel*
Makoto Shimoyama, *Shimane Medical University, Izumo, Japan*
Israel Silman, *Weizmann Institute of Science, Rehovot, Israel*
Richard J. Simpson, *Ludwig Institute for Cancer Research, Victoria, Australia*
Gary Siuzdak, *Scripps Research Institute, La Jolla, CA*
James Skeath, *Washington University, St. Louis, MO*
Stephen J. Small, *New York University, New York, NY*
Colleen M. Smith, *Mercer University, Macon, GA*
Gerald R. Smith, *Fred Hutchinson Cancer Research Center, Seattle, WA*
Sarah M. Smolik, *Oregon Health Sciences University, Portland, OR*
Suzanne G. Sobel, *Yale University, New Haven, CT*
Kunitsugu Soda, *Nagaoka University of Technology, Niigata, Japan*
Lila Solnica-Krezel, *Vanderbilt University, Nashville, TN*
Mark Solomon, *Yale University, New Haven, CT*
Joseph Sperling, *The Hebrew University of Jerusalem, Jerusalem, Israel*
Ruth Sperling, *The Hebrew University of Jerusalem, Jerusalem, Israel*
Martin Spiess, *Biozentrum, Basel, Switzerland*
Tom Spiro, *Princeton University, Princeton, NJ*
Mathias Sprinzl, *Universitaet Bayreuth, Bayreuth, Germany*
R. B. Spruijt, *Wageningen Agricultural University, Wageningen, The Netherlands*
F. W. Stahl, *University of Oregon, Eugene, OR*
Martin F. Steiger, *F. Hoffmann-LaRoche Ltd., Basel, Switzerland*

Scott Strobel, *Yale University, New Haven, CT*
Shintaro Sugai, *Soka University, Tokyo, Japan*
Roy Sundick, *Wayne State University, Detroit, MI*
H. Eldon Sutton, *University of Texas, Austin, TX*
Sandra S. Szegedi, *University of Illinois at Urbana-Champaign, Urbana, IL*
Sevec Szmelcman, *Institut Pasteur, Paris, France*
Hatsumi Taniguchi, *University of Occupational and Environmental Health, Fukuota, Japan*
Joyce Taylor-Papadimitriou, *Imperial Cancer Research Fund Laboratories, London, United Kingdom*
Mariella Tegoni, *CNRS, Marseille, France*
Jean Thomas, *Cambridge University, Cambridge, United Kingdom*
Carl Thummel, *University of Utah, Salt Lake City, UT*
Serge Timasheff, *Brandeis University, Waltham, MA*
Thea D. Tlsty, *University of California, San Francisco, CA*
Andrew Travers, *MRC Laboratory of Molecular Biology, Cambridge, United Kingdom*
Jill Trewhella, *Los Alamos National Laboratory, Los Alamos, NM*
Edward Trifonov, *National Institute of Genetics, Shizuoka-ken, Japan*
Toshiki Tsurimoto, *Osaka, Japan*
Agnes Ullmann, *Institut Pasteur, Paris, France*
Dominiqe van der Straeten, *Universiteit Gent, Gent, Belgium*
M. van Lijsebettens, *Universiteit Gent, Gent, Belgium*
Marc Van Montagu, *Universiteit Gent, Gent, Belgium*
Klaas van Wijk, *Stöckholm University, Stockholm, Sweden*
G. Varani, *MRC Laboratory of Molecular Biology, Cambridge, United Kingdom*
Serge N. Vinogradov, *Wayne State University, Detroit, MI*
Hans von Dohren, *Technische Universitat Berlin, Berlin, Germany*
Edward Voss, *University of Illinois, Urbana, IL*
Richard Walden, *Horticulture Research International, Kent, United Kingdom*
Melinda Wales, *Texas A&M University, College Station, TX*
Valeria A. Wallace, *University College London, London, United Kingdom*
Frederick G. Walz, *Kent State University, Kent, OH*
Andrew H. J. Wang, *University of Illinois, Urbana, IL*
Hongyun Wang, *University of California, Berkeley, CA*
James C. Wang, *Harvard University, Cambridge, MA*
Michael J. Waring, *Cambridge University, Cambridge, United Kingdom*
Amy Warren, *Dartmouth College, Hanover, NH*
Graham Warren, *Imperial College Research Fund, London, United Kingdom*
Hans Warrick, *Stanford University, Stanford, CA*
Arieh Warshel, *University of Southern California, Los Angeles, CA*
Steven A. Wasserman, *University of Texas, Southwestern Medical Center, Dallas, TX*
Hans Weber, *Institut fur Molekularbiologie, Zurich, Switzerland*
Patricia C. Weber, *Schering-Plough Research Institute, Kenilworth, NJ*
Eric Westhof, *Institut de Biologie Moleculaire et Cellulaire, du CNRS, Strasbourg, France*
Richard A. Wetsel, *University of Texas, Houston, TX*
Paul Whiting, *Merck Sharp and Dohme Research Laboratories, Essex, United Kingdom*
Peter A. Whittaker, *Saint Patrick's College, Maynooth, Kildare, Ireland*
Pernilla Whittung-Stapshede, *California Institute of Technology, Pasadena, CA*
Meir Wilchek, *Weizmann Institute of Science, Rehovot, Israel*
Jim R. Wild, *Texas A&M University, College Station, TX*
Allison K. Wilson, *University of Wisconsin, Madison, WI*
David B. Wilson, *Cornell University, Ithaca, NY*
Leslie Wilson, *University of California, Santa Barbara, CA*
Sam H. Wilson, *NIEHS, National Institutes of Health, Research Triangle Park, NC*
R. Wolfenden, *University of North Carolina, Chapel Hill, NC*
Alan Paul Wolffe, *NICDH, National Institutes of Health, Bethesda, MD*
C. J. A. M. Wolfs, *Wageningen Agricultural University, Wageningen, The Netherlands*
William B. Wood, *University of Colorado, Boulder, CO*
Robert Woody, *Colorado State University, Fort Collins, CO*
Kenneth Yamada, *NIDR, National Institutes of Health, Bethesda, MD*
Charles Yanofsky, *Stanford University, Stanford, CA*
Ada Yonath, *Weizmann Institute of Science, Rehovot, Israel*
Hiroshi Yoshikawa, *Nara Institute of Science & Technology, Ikoma, Japan*
Jennifer Zamanian, *University of California, San Francisco, CA*
Guiliana Zanetti, *University of Milan, Milan, Italy*
Amanda Zeffman, *MRC Laboratory of Molecular Biology, Cambridge, United Kingdom*
Suisheng Zhang, *Institute of Molecular Biotechnology, Jena, Germany*
Mark Zoller, *Ariad Pharmaceuticals, Cambridge, MA*

COMMONLY USED ACRONYMS AND ABBREVIATIONS

Å	angstrom (10^{-10} m)
Ab	antibody
Ac	acetyl group
ADP	adenosine diphosphate
Ala	alanine residue (also A)
AMP	adenosine monophosphate
Arg	arginine residue (also R)
Asn	asparagine residue (also N)
Asp	aspartic acid residue (also D)
ATP	adenosine triphosphate
ATPase	adenosine triphosphatase
Bq	becquerel
bp	base-pair
BSA	bovine serum albumin
C	cytosine base
cal	calorie (4.18 J)
cAMP	3′,5′-cyclic AMP
CD	circular dichroism
CoA	coenzyme A
cDNA	complementary DNA
cGMP	3′,5′-cyclic GMP
Cmc	critical micelle concentration
Cys	cysteine residue (also C)
Da	dalton
DMSO	dimethyl sulfoxide
DNA	deoxyribonucleic acid
DNase	deoxyribonuclease
DTT	dithiothreitol
EDTA	ethylenediamine tetraacetic acid
EG	[ethylenebis(oxonitrilo)] tetraacetic acid
EGF	epidermal growth factor
ELISA	enzyme-linked immunosorbent assay
EM	electron microscopy
EPR, ESR	electron paramagnetic (or sign) resonance
ER	endoplasmic reticulum
EXAFS	extended X-ray absorption fine structure
FAD	flavin-adenine dinucleotide
fMet	*N*-formyl methionine
FMN	flavin mononucleotide
FPLC	fast protein liquid chromatography
G	Gibbs free energy of a system
G	guanine base
G-protein	guanine-nucleotide binding regulatory protein
GABA	g-aminobutyric acid
GalNAc	*N*-acetylgalactosamine residue
GdmCl	guanidinium chloride (guanidine hydrochloride)
GDP	guanosine diphosphate
Glc	glucose residue
GlcNAc	*N*-acetylglucosamine residue
Gln	glutamine residue (also Q)
Glu	glutamic acid residue (also E)
Gly	glycine residue (also G)
GMP	guanoine monophosphate
GSH	glutathione, thiol form
GSSG	glutathione, disulfide form
GTP	guanosine triphosphate
GTPase	guanosine triphosphatase
H	enthalpy of a system
h	hour
His	histidine residue (also H)
HLA	histocompatibility locus antigen
HPLC	high pressure liquid chromatography
Hz	hertz, frequency
IEF	isoelectric focusing IgG, IgA, IgM, etc. immunoglobuin G, A, M. etc.
Ile	isoleucine residue (also I)
Ins	inositol residue
IR	infrared
J	joule
K	degrees Kelvin, absolute temperature
k	rate constant for a specified reaction
K_a	association constant
K_d	dissociation constant
K_{eq}	equilibrium constant for a specified reaction
K_m	Michaelis constant
kb	kilobases
kcal	kilocalorie (4.18 kJ)
kDa	kilodalton
LDL	low density lipoprotein
Leu	leucine residue (also L)
Lys	lysine residue (also K)

m	meter
mAb	monoclonal antibody
Met	methionine residue (also M)
MHC	major histocompability locus
min	minute
mol	mole
M_r	relative molecular mass
mRNA	messenger RNA
MS	mass spectroscopy
mtDNA	mitochondrial DNA
Mur	muramic acid residue
MurNAc	*N*-acetylmuramic acid residue
NAD^+	nicotinamide adenine dinucleotide (oxidized)
NADH	nicotinamide adenine dinucleotide (reduced)
$NADP^+$	nicotinamide adenine dinucleotide phosphate (oxidized)
NADPH	nicotinamide adenine dinucleotide phosphate (reduced)
NMR	nuclear magnetic resonance
PAGE	polyacrylamide gel electrophoresis
PBS	phosphate-buffered saline
PCR	polymerase chain reaction
PEG	polyethylene glycol
pH	negative logarithm of hydrogen ion concentration
Phe	phenylalanine residue (also F)
P_i	inorganic phosphate
PP_i	inorganic pyrophosphate
p.p.m.	parts per million
Pro	proline residue (also P)
R	gas constant (8.21451 J/(K^1 mol^{-1}))
RIA	radioimmunoassay
RNA	ribonucleic acid
RNase	ribonuclease
RNP	ribonucleoprotein
rRNA	ribosomal RNA
S	entropy of a system
S	Svedberg sedimentation unit (10^{-13} s)
s	second
s	sedimentation coefficient
SDS	sodium dodecyl sulfate
snRNA	small nuclear RNA
SRP	signal recognition particle
T	temperature
T	thymine residue
TF	transcription factor
Thr	threonine residue (also T)
T_m	midpoint of temperature induced transition
Tri	tris(hydroxymethyl) aminomethane
tRNA	transfer RNA
Trp	tryptophan residue (also W)
TTP	thymidine triphosphate
Tyr	tyrosine residue (also Y)
U	uracil residue
UDP	uridine diphosphate
UMP	uridine monophosphate
UTP	uridine triphosphate
UV	ultraviolet
V	volume
V_{max}	maximum enzyme catalyzed velocity
Val	valine residue (also V)
WT	wild-type
Xyl	xylose residue

CONVERSION FACTORS

SI Units (Adopted 1960)

The International System of Units (abbreviated SI), is being implemented throughout the world. This measurement system is a modernized version of the MKSA (meter, kilogram, second, ampere) system, and its details are published and controlled by an international treaty organization (The International Bureau of Weights and Measures) (1).

SI units are divided into three classes:

BASE UNITS

length	meter[†] (m)
mass	kilogram (kg)
time	second (s)
electric current	ampere (A)
thermodynamic temperature[‡]	kelvin (K)
amount of substance	mole (mol)
luminous intensity	candela (cd)

SUPPLEMENTARY UNITS

plane angle	radian (rad)
solid angle	steradian (sr)

DERIVED UNITS AND OTHER ACCEPTABLE UNITS

These units are formed by combining base units, supplementary units, and other derived units (2–4). Those derived units having special names and symbols are marked with an asterisk in the list below.

Quantity	Unit	Symbol	Acceptable equivalent
*absorbed dose	gray	Gy	J/kg
acceleration	meter per second squared	m/s^2	
*activity (of a radionuclide)	becquerel	Bq	1/s
area	square kilometer	km^2	
	square hectometer	hm^2	ha (hectare)
	square meter	m^2	
concentration (of amount of substance)	mole per cubic meter	mol/m^3	
current density	ampere per square meter	A/m^2	
density, mass density	kilogram per cubic meter	kg/m^3	g/L; mg/cm^3
dipole moment (quantity)	coulomb meter	C·m	

[†]The spellings "metre" and "litre" are preferred by ASTM; however, "-er" is used in the *Encyclopedia*.

[‡]Wide use is made of Celsius temperature (t) defined by

$$t = T - T_0$$

where T is the thermodynamic temperature, expressed in kelvin, and $T_0 = 273.15$ K by definition. A temperature interval may be expressed in degrees Celsius as well as in kelvin.

Quantity	Unit	Symbol	Acceptable equivalent
*dose equivalent	sievert	Sv	J/kg
*electric capacitance	farad	F	C/V
*electric charge, quantity of electricity	coulomb	C	A·s
electric charge density	coulomb per cubic meter	C/m^3	
*electric conductance	siemens	S	A/V
electric field strength	volt per meter	V/m	
electric flux density	coulomb per square meter	C/m^2	
*electric potential, potential difference, electromotive force	volt	V	W/A
*electric resistance	ohm	Ω	V/A
*energy, work, quantity of heat	megajoule	MJ	
	kilojoule	kJ	
	joule	J	N·m
	electronvolt†	eV†	
	kilowatt-hour†	kW·h†	
energy density	joule per cubic meter	J/m^3	
*force	kilonewton	kN	
	newton	N	$kg{\cdot}m/s^2$
*frequency	megahertz	MHz	
	hertz	Hz	1/s
heat capacity, entropy	joule per kelvin	J/K	
heat capacity (specific), specific entropy	joule per kilogram kelvin	J/(kg·K)	
heat-transfer coefficient	watt per square meter kelvin	$W/(m^2{\cdot}K)$	
*illuminance	lux	lx	lm/m^2
*inductance	henry	H	Wb/A
linear density	kilogram per meter	kg/m	
luminance	candela per square meter	cd/m^2	
*luminous flux	lumen	lm	cd·sr
magnetic field strength	ampere per meter	A/m	
*magnetic flux	weber	Wb	V·s
*magnetic flux density	tesla	T	Wb/m^2
molar energy	joule per mole	J/mol	
molar entropy, molar heat capacity	joule per mole kelvin	J/(mol·K)	
moment of force, torque	newton meter	N·m	
momentum	kilogram meter per second	kg·m/s	
permeability	henry per meter	H/m	
permittivity	farad per meter	F/m	
*power, heat flow rate, radiant flux	kilowatt	kW	
	watt	W	J/s
power density, heat flux density, irradiance	watt per square meter	W/m^2	
*pressure, stress	megapascal	MPa	
	kilopascal	kPa	
	pascal	Pa	N/m^2
sound level	decibel	dB	
specific energy	joule per kilogram	J/kg	
specific volume	cubic meter per kilogram	m^3/kg	
surface tension	newton per meter	N/m	
thermal conductivity	watt per meter kelvin	W/(m·K)	
velocity	meter per second	m/s	
	kilometer per hour	km/h	
viscosity, dynamic	pascal second	Pa·s	
	millipascal second	mPa·s	
viscosity, kinematic	square meter per second	m^2/s	
	square millimeter per second	mm^2/s	
volume	cubic meter	m^3	
	cubic diameter	dm^3	L (liter) (5)
	cubic centimeter	cm^3	mL
wave number	1 per meter	m^{-1}	
	1 per centimeter	cm^{-1}	

†This non-SI unit is recognized by the CIPM as having to be retained because of practical importance or use in specialized fields (1).

In addition, there are 16 prefixes used to indicate order of magnitude, as follows:

Multiplication factor	Prefix	Symbol	Note
10^{18}	exa	E	
10^{15}	peta	P	
10^{12}	tera	T	
10^{9}	giga	G	
10^{6}	mega	M	
10^{3}	kilo	k	
10^{2}	hecto	h[a]	[a]Although hecto, deka, deci, and centi are SI prefixes, their use should be avoided except for SI unit-multiples for area and volume and nontechnical use of centimeter, as for body and clothing measurement.
10	deka	da[a]	
10^{-1}	deci	d[a]	
10^{-2}	centi	c[a]	
10^{-3}	milli	m	
10^{-6}	micro	μ	
10^{-9}	nano	n	
10^{-12}	pico	p	
10^{-15}	femto	f	
10^{-18}	atto	a	

For a complete description of SI and its use the reader is referred to ASTM E380 (4).

A representative list of conversion factors from non-SI to SI units is presented herewith. Factors are given to four significant figures. Exact relationships are followed by a dagger. A more complete list is given in the latest editions of ASTM E380 (4) and ANSI Z210.1 (6).

Conversion Factors to SI Units

To convert from	To	Multiply by
acre	square meter (m^2)	4.047×10^{3}
angstrom	meter (m)	$1.0 \times 10^{-10\dagger}$
are	square meter (m^2)	$1.0 \times 10^{2\dagger}$
astronomical unit	meter (m)	1.496×10^{11}
atmosphere, standard	pascal (Pa)	1.013×10^{5}
bar	pascal (Pa)	$1.0 \times 10^{5\dagger}$
barn	square meter (m^2)	$1.0 \times 10^{-28\dagger}$
barrel (42 U.S. liquid gallons)	cubic meter (m^3)	0.1590
Bohr magneton (μ_B)	J/T	9.274×10^{-24}
Btu (International Table)	joule (J)	1.055×10^{3}
Btu (mean)	joule (J)	1.056×10^{3}
Btu (thermochemical)	joule (J)	1.054×10^{3}
bushel	cubic meter (m^3)	3.524×10^{-2}
calorie (International Table)	joule (J)	4.187
calorie (mean)	joule (J)	4.190
calorie (thermochemical)	joule (J)	$4.184^{\dagger}$
centipoise	pascal second (Pa·s)	$1.0 \times 10^{-3\dagger}$
centistokes	square millimeter per second (mm^2/s)	$1.0^{\dagger}$
cfm (cubic foot per minute)	cubic meter per second (m^3/s)	4.72×10^{-4}
cubic inch	cubic meter (m^3)	1.639×10^{-5}
cubic foot	cubic meter (m^3)	2.832×10^{-2}
cubic yard	cubic meter (m^3)	0.7646
curie	becquerel (Bq)	$3.70 \times 10^{10\dagger}$
debye	coulomb meter (C·m)	3.336×10^{-30}
degree (angle)	radian (rad)	1.745×10^{-2}
denier (international)	kilogram per meter (kg/m)	1.111×10^{-7}
	tex[‡]	0.1111
dram (apothecaries')	kilogram (kg)	3.888×10^{-3}
dram (avoirdupois)	kilogram (kg)	1.772×10^{-3}
dram (U.S. fluid)	cubic meter (m^3)	3.697×10^{-6}
dyne	newton (N)	$1.0 \times 10^{-5\dagger}$
dyne/cm	newton per meter (N/m)	$1.0 \times 10^{-3\dagger}$
electronvolt	joule (J)	1.602×10^{-19}
erg	joule (J)	$1.0 \times 10^{-7\dagger}$

†Exact.

‡See footnote on p. xvi.

To convert from	To	Multiply by
fathom	meter (m)	1.829
fluid ounce (U.S.)	cubic meter (m^3)	2.957×10^{-5}
foot	meter (m)	0.3048†
footcandle	lux (lx)	10.76
furlong	meter (m)	2.012×10^{-2}
gal	meter per second squared (m/s^2)	1.0×10^{-2}†
gallon (U.S. dry)	cubic meter (m^3)	4.405×10^{-3}
gallon (U.S. liquid)	cubic meter (m^3)	3.785×10^{-3}
gallon per minute (gpm)	cubic meter per second (m^3/s)	6.309×10^{-5}
	cubic meter per hour (m^3/h)	0.2271
gauss	tesla (T)	1.0×10^{-4}
gilbert	ampere (A)	0.7958
gill (U.S.)	cubic meter (m^3)	1.183×10^{-4}
grade	radian	1.571×10^{-2}
grain	kilogram (kg)	6.480×10^{-5}
gram force per denier	newton per tex (N/tex)	8.826×10^{-2}
hectare	square meter (m^2)	1.0×10^{4}†
horsepower (550 ft·lbf/s)	watt (W)	7.457×10^{2}
horsepower (boiler)	watt (W)	9.810×10^{3}
horsepower (electric)	watt (W)	7.46×10^{2}†
hundredweight (long)	kilogram (kg)	50.80
hundredweight (short)	kilogram (kg)	45.36
inch	meter (m)	2.54×10^{-2}†
inch of mercury (32°F)	pascal (Pa)	3.386×10^{3}
inch of water (39.2°F)	pascal (Pa)	2.491×10^{2}
kilogram-force	newton (N)	9.807
kilowatt hour	megajoule (MJ)	3.6†
kip	newton (N)	4.448×10^{3}
knot (international)	meter per second (m/S)	0.5144
lambert	candela per square meter (cd/m^3)	3.183×10^{3}
league (British nautical)	meter (m)	5.559×10^{3}
league (statute)	meter (m)	4.828×10^{3}
light year	meter (m)	9.461×10^{15}
liter (for fluids only)	cubic meter (m^3)	1.0×10^{-3}†
maxwell	weber (Wb)	1.0×10^{-8}†
micron	meter (m)	1.0×10^{-6}†
mil	meter (m)	2.54×10^{-5}†
mile (statute)	meter (m)	1.609×10^{3}
mile (U.S. nautical)	meter (m)	1.852×10^{3}†
mile per hour	meter per second (m/s)	0.4470
millibar	pascal (Pa)	1.0×10^{2}
millimeter of mercury (0°C)	pascal (Pa)	1.333×10^{2}†
minute (angular)	radian	2.909×10^{-4}
myriagram	kilogram (kg)	10
myriameter	kilometer (km)	10
oersted	ampere per meter (A/m)	79.58
ounce (avoirdupois)	kilogram (kg)	2.835×10^{-2}
ounce (troy)	kilogram (kg)	3.110×10^{-2}
ounce (U.S. fluid)	cubic meter (m^3)	2.957×10^{-5}
ounce-force	newton (N)	0.2780
peck (U.S.)	cubic meter (m^3)	8.810×10^{-3}
pennyweight	kilogram (kg)	1.555×10^{-3}
pint (U.S. dry)	cubic meter (m^3)	5.506×10^{-4}
pint (U.S. liquid)	cubic meter (m^3)	4.732×10^{-4}
poise (absolute viscosity)	pascal second (Pa·s)	0.10†
pound (avoirdupois)	kilogram (kg)	0.4536
pound (troy)	kilogram (kg)	0.3732
poundal	newton (N)	0.1383
pound-force	newton (N)	4.448
pound force per square inch (psi)	pascal (Pa)	6.895×10^{3}
quart (U.S. dry)	cubic meter (m^3)	1.101×10^{-3}
quart (U.S. liquid)	cubic meter (m^3)	9.464×10^{-4}

To convert from	To	Multiply by
quintal	kilogram (kg)	$1.0 \times 10^{2\dagger}$
rad	gray (Gy)	$1.0 \times 10^{-2\dagger}$
rod	meter (m)	5.029
roentgen	coulomb per kilogram (C/kg)	2.58×10^{-4}
second (angle)	radian (rad)	$4.848 \times 10^{-6\dagger}$
section	square meter (m^2)	2.590×10^{6}
slug	kilogram (kg)	14.59
spherical candle power	lumen (lm)	12.57
square inch	square meter (m^2)	6.452×10^{-4}
square foot	square meter (m^2)	9.290×10^{-2}
square mile	square meter (m^2)	2.590×10^{6}
square yard	square meter (m^2)	0.8361
stere	cubic meter (m^3)	$1.0^{\dagger}$
stokes (kinematic viscosity)	square meter per second (m^2/s)	$1.0 \times 10^{-4\dagger}$
tex	kilogram per meter (kg/m)	$1.0 \times 10^{-6\dagger}$
ton (long, 2240 pounds)	kilogram (kg)	1.016×10^{3}
ton (metric) (tonne)	kilogram (kg)	$1.0 \times 10^{3\dagger}$
ton (short, 2000 pounds)	kilogram (kg)	9.072×10^{2}
torr	pascal (Pa)	1.333×10^{2}
unit pole	weber (Wb)	1.257×10^{-7}
yard	meter (m)	$0.9144^{\dagger}$

†Exact.

BIBLIOGRAPHY

1. The International Bureau of Weights and Measures, BIPM (Parc de Saint-Cloud, France) is described in Appendix X2 of Ref. 4. This bureau operates under the exclusive supervision of the International Committee for Weights and Measures (CIPM).
2. *Metric Editorial Guide* (*ANMC-78-1*), latest ed., American National Metric Council, 5410 Grosvenor Lane, Bethesda, Md. 20814, 1981.
3. *SI Units and Recommendations for the Use of Their Multiples and of Certain Other Units* (*ISO 1000-1981*), American National Standards Institute, 1430 Broadway, New York, 10018, 1981.
4. Based on *ASTM E380-89a* (*Standard Practice for Use of the International System of Units* (*SI*)), American Society for Testing and Materials, 1916 Race Street, Philadelphia, Pa. 19103, 1989.
5. *Fed. Reg.*, Dec. 10, 1976 (41 FR 36414).
6. For ANSI address, see Ref. 3.

R. P. LUKENS
ASTM Committee E-43 on SI Practice

A-DNA

A-DNA was first recognized as a DNA structure using fiber X-ray diffraction analysis. B-DNA can be converted to A-DNA under conditions of low hydration, and the process is reversible. The A-DNA double helix is short and fat, with the base pairs and backbone wrapped farther away from the helix axis (see Fig. 2 of DNA Structure). The base pairs are significantly tilted (~19°) with respect to the helix axis. The major groove has a very narrow width of ~3 Å and a depth of ~13 Å, whereas the minor groove has a broad width of 11 Å and a shallow depth of 3 Å. The base pairs also display a minor propeller twist.

There is increasing evidence that A-DNA may play an important role in biological processes such as protein recognition and transcription regulation, as in the TATA-box sequence bound with the TATA-box binding proteins (1, 2). There is a sequence-dependent propensity to form A-DNA. Guanine-rich regions readily form A-DNA, whereas stretches of adenine resist it. The crystal structures of DNA oligonucleotides having guanine-rich sequences showed a characteristic intrastrand guanine–guanine stacking interaction in the A-DNA double helix, which may explain the propensity of these sequences to adopt the A-DNA conformation. Moreover, the packing of the helices in the crystal lattice revealed a characteristic pattern of the terminal base pairs from one helix abutting the minor groove surface of the neighboring helix, thus minimizing the accessibility of solvent to the wide minor groove. Since a low humidity environment favors formation of A-type helix, the displacement of surface solvent molecules by **hydrophobic** base pairs provides a driving force in stabilizing short oligonucleotides in the A-DNA conformation. Recently, it has been demonstrated that complex ions such as spermine, cobalt(III)hexamine, and neomycin can facilitate the B-DNA to A-DNA transition for DNA containing stretches of $(dG)_n \cdot (dC)_n$ sequences.

Finally, the crystal structures of a number of DNA:RNA hybrids, such as the self-complementary r(GCG)d(TATACGC), showed that DNA–RNA hybrid helices are of the A-DNA type. All the ribose and 2′-deoxyribose sugars are in the C3′-*endo* conformation. The 2′-hydroxyl groups of the ribose are involved in different types of hydrogen bonding to the adjacent nucleotides in the chain.

Bibliography

1. J. L. Kim, D. B. Nikolov, and S. K. Burley (1993) Nature **365**, 520–527.
2. Y. Kim, J. H. Geiger, S. Hahn, and P. B. Sigler (1993) Nature **365**, 512–520.

abl Oncogenes

The *abl* gene was first identified as the transforming element of Abelson murine leukemia virus (A-MuLV), a replication-defective retrovirus that was isolated after inoculating Moloney murine leukemia virus (M-MuLV) into prednisolone-treated BALB/c mice (1). A-MuLV induces **B-cell** lymphomas *in vivo* and transforms both lymphoid and fibroblastic cells *in vitro*. The proviral genome of A-MuLV encodes a single polypeptide chain that is a fusion product of the virally-derived gag and cell-derived *abl* sequences (2). Sequence analysis of c-*abl* sequences revealed that, like the ***src* gene**, the *abl* gene codes for a **tyrosine kinase** that also contains the unique, SH3, SH2, and tyrosine kinase domains (3). Unlike the *src* gene, however, the *abl* gene product contains an additional C-terminal domain whose function is not entirely clear. In addition, the gene product of c-

abl does not contain the negative-regulatory **tyrosine** residue at its C-terminus. The tyrosine kinase activity of the c-Abl protein is negatively regulated by its SH3 domain, which is deleted from the v-*abl* gene product. Interestingly, it was also found that the v-*abl* gene product contains a point mutation in its C-terminal sequence, which enhances its tyrosine kinase and transforming activities (4). Thus, both the v-*src* and v-*abl* genes have alterations in their regulatory sequences that result in the constitutive activation of their tyrosine kinase activities, which correlates with their transforming function.

Gene mapping studies have established that the c-*abl* oncogene is located on human chromosome 9q34, the location where the break point occurs in the Philadelphia chromosome. The Philadelphia chromosome is generated when a portion of the c-*abl* gene is **translocated** to chromosome 22 and is fused to a portion of the gene called *bcr*, which itself is disrupted during the translocation process (Fig. 1). This process results in generating a new gene, called *bcr-abl*, that has enhanced oncogenic activity and whose expression leads to the development of leukemia (5, 6). It is interesting to note that the BCR-ABL gene is structurally similar to the *gag-abl* gene encoded by the Abelson murine leukemia virus. Both the *gag-abl* and *bcr-abl* genes exhibit high levels of tyrosine kinase activity, which is essential for their transforming activity.

Figure 1. Generation of the bcr-abl oncoprotein by chromosomal translocation. The abl gene in a normal cell, is located on chromosome 9 and encodes a tyrosine kinase. During malignant transformation of myeloid cells, a portion of chromosome 9 that contains the abl locus translocates to chromosome 22 at the breakpoint cluster region (bcr) locus and generates the chimeric bcr-abl oncoprotein. Because the translocation results in deleting the sequences that negatively regulate abl tryosine kinase activity, the fusion protein has constitutive and increased levels of enzymatic activity.

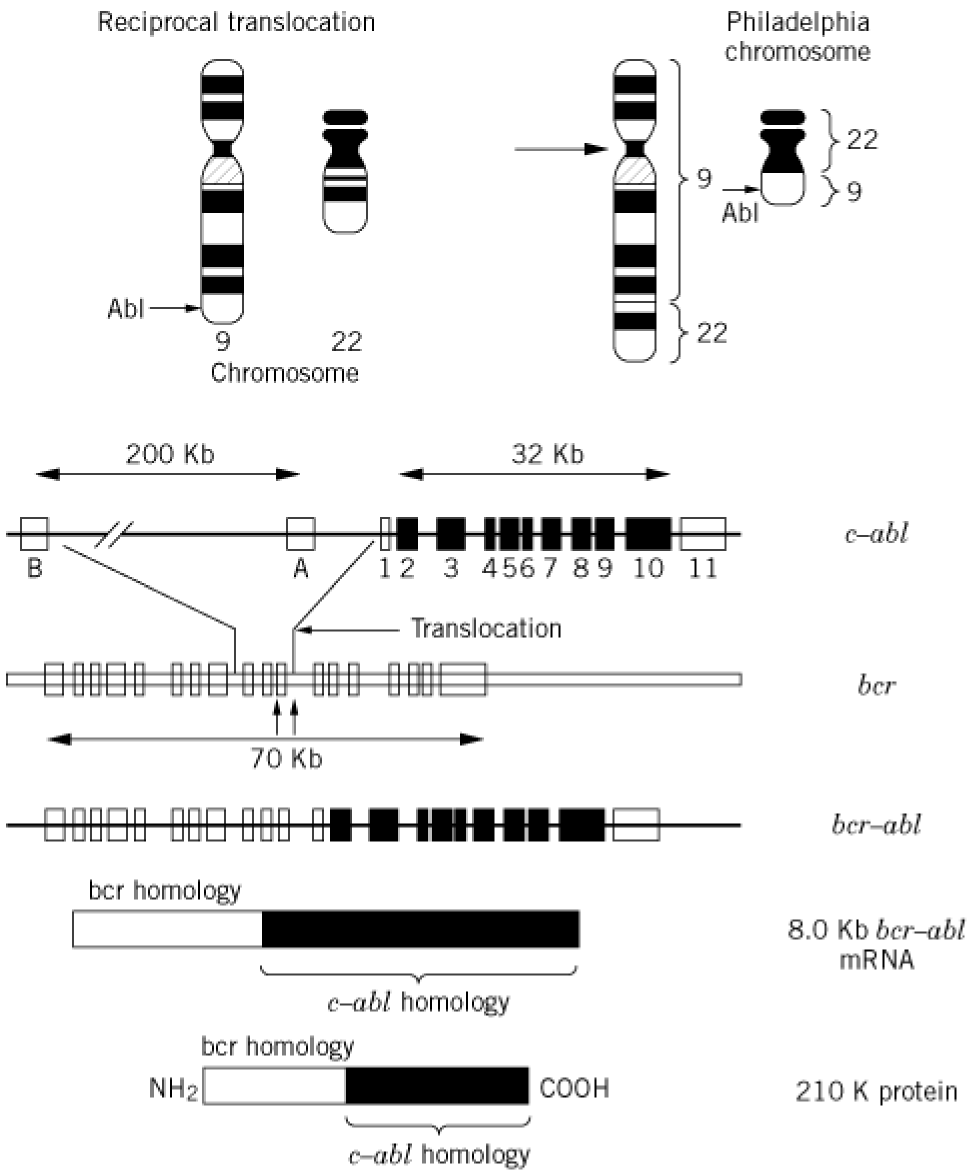

The function of c-abl in normal cell growth is not fully established. The c-abl gene codes for two 145-kDa proteins as a result of alternative splicing of the two first exons (see RNA Splicing and Introns, Exons). This results in synthesizing two proteins that differ in their amino-terminal sequences. Both forms of c-Abl are found in the cytoplasm and in the nucleus. The c-Abl protein can bind to DNA and to cell-cycle regulators like the **retinoblastoma** protein. Recent studies show that c-abl gene expression is induced during cellular stress caused by agents, such as ionizing radiation and certain other genotoxic agents. These agents induce the formation of a complex involving c-Abl, DNA-dependent protein kinase, and Ku antigen (7). The DNA-dependent protein kinase in this complex is activated by **DNA damage** and in turn phosphorylates and activates c-Abl. Recent studies have also shown that c-Abl associates with the product of the ATM gene, which in turn activates c-Abl in response to ionizing radiation. DNA damage also induces binding of c-Abl to p53 and contributes to cell-cycle arrest at the G1-phase, which is mediated by p53. Recent studies also show that the c-Abl protein binds to **protein kinase C**-δ and phosphorylates the latter, resulting in its activation and translocation to the nucleus, where it participates in inducing apoptosis (8). Thus, a substantial amount of evidence gathered in the past few years indicates that c-Abl protein has a pivotal role in mediating cellular growth arrest and the apoptotic effects that occur during exposure to ionizing radiation and genotoxic stress.

Bibliography

1. H. T. Abelson and L. S. Rabson (1970) Cancer Res. **30**, 2213–2222.
2. E. P. Reddy, M. J. Smith, and A. Srinivasan (1983) Proc. Natl. Acad. Sci. USA **80**, 3623–3627.
3. C. Oppi, S. K. Shore, and E. P. Reddy (1987) Proc. Natl. Acad. Sci. USA **84**, 8200–8204.
4. S. K. Shore, S. L. Bogart, and E. P. Reddy (1990) Proc. Natl. Acad. Sci. USA **87**, 6502–6506.
5. J. Groffen, J. R. Stephenson, N. Heisterkamp, A. De Klein, C. B. Bartam, and G. Grosveld (1984) Cell **36**, 93–99.
6. E. Shtivelman, R. P. Lifshitz, R. P. Gale, and E. Canaani (1985) Nature **315**, 550–553.
7. R. Baskaran, L. D. Wood, L. L. Whittaker, Y. Xu, C. Barlow, C. E. Canman, S. E. Morgan, D. Baltimore, A. Wynshaw-Boris, M. B. Kastan, and J. Y. J. Wang (1997) Nature **387**, 516–519.
8. Z-M. Yuan, T. Utsugisawa, T. Ishiko, S. Nakada, Y. Huang, S. Kharbanda, R. Weichselbaum, and D. Kufe (1998) Oncogene **16**, 1643–1648.

Abscisic Acid

1. History

The first evidence for the existence of an acidic inhibitor of coleoptile growth that promoted abscission and seed maturation dates back to the early 1950s, but it was not until 1963 that abscisic acid (ABA) was identified by Frederick Addicott and coworkers (1, 2). Addicott's team was studying compounds that stimulated abscission in cotton fruits and had named the active substances *abscisin I* and *abscisin II*; the latter proved to be ABA. Two other independent efforts also culminated in the discovery of ABA. A British group headed by Wareing (3) was investigating bud dormancy of woody plants and called the most active molecule *dormin*. In New Zealand, van Stevenick (4) studied compounds that accelerated abscission of flowers and fruits of *Lupinus luteus*. In 1964, it became evident that the three groups had discovered the same plant hormone, which was renamed *abscisic acid* 3 years later.

2. Biosynthesis and Metabolism

ABA is a universal compound in vascular plants; it is not found in bacteria, but has been reported in green algae, certain fungi, and mosses (5). ABA is a sesquiterpenoid, with mevalonic acid as a precursor. In certain fungi, ABA is produced by a direct, C15 pathway from farnesyl pyrophosphate. In higher plants, ABA is derived from xanthophylls, via an indirect C40 pathway (Fig. 1). Substantial progress in understanding the ABA biosynthetic pathway has been achieved by a combination of molecular and genetic techniques, primarily on mutants in *Arabidopsis thaliana, Zea mays, Nicotiana plumbaginifolia*, and tomato. Arabidopsis mutants impaired in ABA biosynthesis were isolated on the basis of their lack of seed dormancy due to ABA deficiency and their ability to overcome a gibberellin requirement for germination, which allowed them to germinate in the presence of inhibitors of gibberellin biosynthesis or in a gibberellin-deficient background (6, 7). ABA-deficient mutants show a wilty **phenotype** when subjected to water stress.

Figure 1. ABA biosynthesis in higher plants. Steps mediated by ABA1, ABA2, and ABA3 in *Arabidopsis* and by VP14 in *Zea mays* are indicated. (Adapted from Ref. 19.)

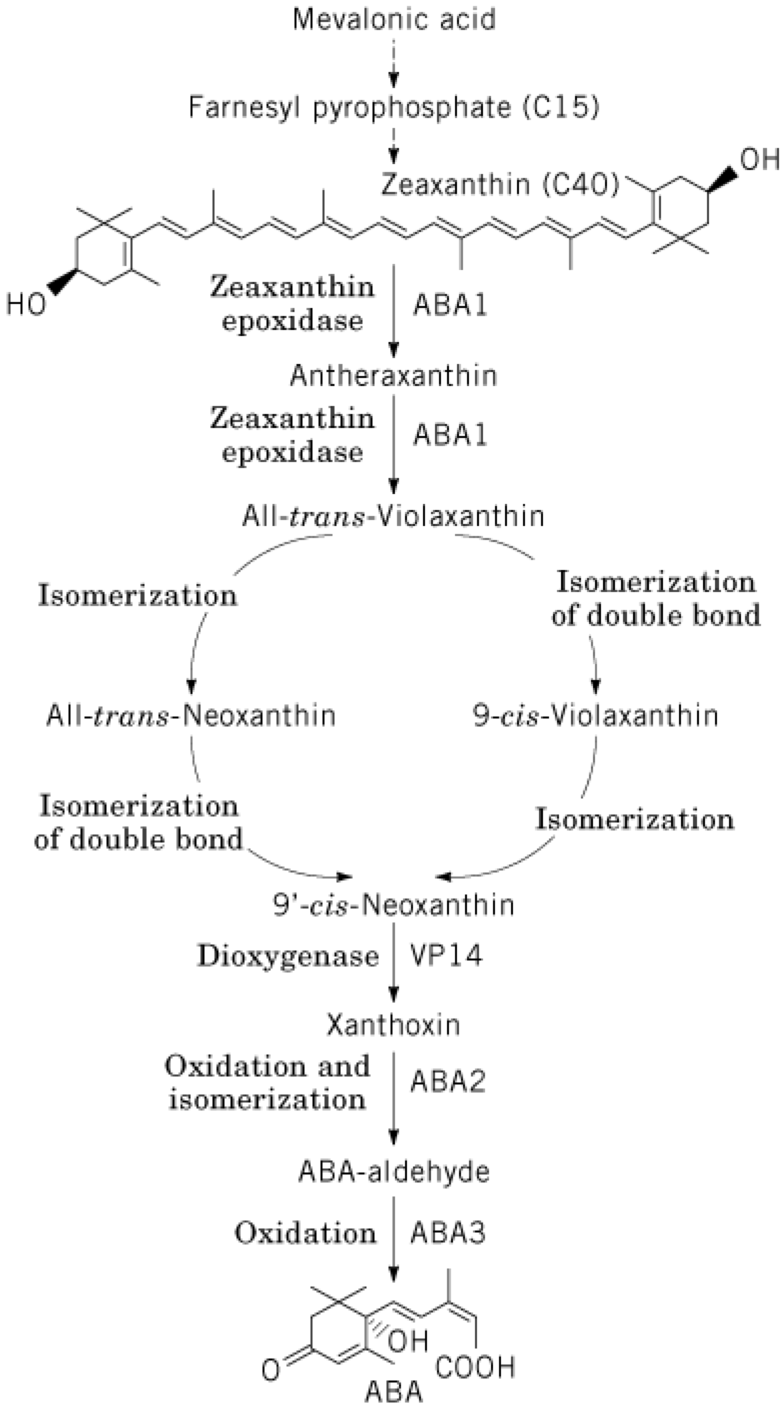

Mevalonic acid is converted to farnesyl pyrophosphate, a C15 compound, via several intermediates (Fig. 1). The subsequent conversion of farnesyl pyrophosphate to zeaxanthin, a C40 carotenoid, again involves multiple steps (8). A number of *viviparous* (*vp*) mutants of maize identify loci corresponding to these early conversions. The transformation of zeaxanthin to all-*trans*-violaxanthin consists of two epoxidations at the double bonds in both cyclohexenyl rings, with antheraxanthin as an intermediate. The *aba1* mutant impaired in zeaxanthin epoxidase activity has been characterized biochemically in *Arabidopsis* (6, 9, 10). The *N. plumbaginifolia ABA2* **gene** encoding zeaxanthin epoxidase was recently cloned by transposon tagging (11). The gene encodes a **chloroplast**-imported polypeptide chain with similarity to bacterial monooxygenases and oxidases. When the Nicotiana *ABA2* gene was expressed in *Escherichia coli* heterologously, the protein was shown to catalyze both epoxidations *in vitro*. Moreover, the complementary DNA (cDNA) complemented both the *N.*

plumbaginifolia aba2 mutant and the *Arabidopsis aba1* mutant. The ortholog in *Arabidopsis* (*ABA1*) was cloned by homology with *Nicotiana ABA2* (11). Although presumably a null **allele**, the *Nicotiana aba2* mutant retains up to half the ABA content of wild type in the absence of water stress. This characteristic might indicate the existence of a secondary biosynthetic pathway for ABA. Downstream of all-*trans*-violaxanthin, two isomerizations yield 9′-*cis*-neoxanthin.

The subsequent oxidative cleavage with xanthoxin as a product is thought to be the rate-limiting step in ABA biosynthesis (12, 13). A gene that most probably encodes the enzyme performing this reaction was cloned from maize, and by homology also from *Arabidopsis* (*VP14*) (13). Its overproduction in *E. coli* indicated that VP14 is probably a member of a novel class of dioxygenases.

Xanthoxin is subsequently converted to ABA-aldehyde by oxidation and isomerization. Biochemical analysis indicates that the *Arabidopsis aba2* mutant is blocked at this step in the pathway (7, 14). A final oxidation, catalyzed by ABA-aldehyde oxidase, produces ABA. Mutants in this step have been identified in several species (8). The *Arabidopsis aba3* mutant lacks several aldehyde oxidase activities that require a molybdenum cofactor (14). Yet the mutation blocks modification of the mobybdenum cofactor, rather than impairing the activity of the apoprotein. Cloning of the *ABA2* and *ABA3* genes should provide further clues as to the regulation of ABA biosynthesis in these final steps.

Metabolism of ABA is mainly to phaseic acid, dihydrophaseic acid, and their respective conjugates (15, 16). Direct conjugation of ABA to an ABA glucose ester, or an ABA-b-glucopyranoside, can also occur. Conjugation of ABA does not lead to its storage, probably because it is irreversible and yields unstable compounds. With the exception of phaseic acid, none of the metabolites carries biological activity (16).

3. Signal Perception and Transduction

Insight into the molecular basis of ABA responses was gathered by a combination of molecular-genetic, biochemical, and electrophysiological studies (12, 17-20). Currently, little is known about the perception of ABA, despite numerous efforts to isolate ABA receptors using different approaches (20). Two groups of mutants, ABA-insensitive and ABA-hypersensitive, have largely contributed to the understanding of ABA signal transduction. Whereas the five *abscisic acid-insensitive* (*abi*) mutants of *Arabidopsis* were identified by their ability to germinate on inhibiting concentrations of ABA (21, 22), the three *enhanced response to ABA* (*era*) mutants showed an increased dormancy in the presence of low ABA concentrations, compared to wild type (23). Besides their effects on seed development and dormancy, these mutants show altered responses to drought adaptation. The *abi* mutants differ from the above-mentioned *aba* mutants, because they do not have reduced endogenous ABA content and their phenotype cannot be reverted by exogenously supplied ABA. The characterization of *abi* mutants revealed that at least two ABA-response pathways exist: one primarily active in vegetative tissues, involving ABI1 and ABI2, and a second one operating predominantly during seed development and involving ABI3, ABI4, and ABI5 (19). Genes corresponding to four loci have been **cloned**. *ABI1* and *ABI2* encode highly homologous serine/threonine kinases and phosphatases 2C (24-26). These phosphatases might act in a phosphorylation/dephosphorylation cascade, as the protein phosphatase activity of recombinant ABI1 has been demonstrated *in vitro* (27). The functions of ABI1 and ABI2 are partially redundant (25). *ABI3* encodes a putative transcription factor that acts mainly during seed development and is the ortholog of *VP1* in maize (28-30). The suggested function of ABI3 consists of either activating the maturation program or preventing germination (30, 31). Finally, the predicted amino acid sequence of ERA1 shares similarity with the b-subunit of farnesyl transferases. In yeast and mammalian systems, this enzyme is known to modify signal transduction proteins for membrane anchoring (23). In wild-type *Arabidopsis*, ERA1 is proposed to modify a negative regulator of ABA signaling.

The current model of ABA signal transduction integrates ABI1/ABI2-dependent cascades in both seeds and vegetative tissues (Fig. 2). These cascades interact with the ABI3 protein in seeds only, because ABI3 is expressed exclusively in seeds (32). The role of ABI3 is not confined to ABA signaling (19); it is also thought to mediate developmental signals. This role is supported by the seed phenotype of *abi3*, which is more complex than that of *abi1, abi2*, or *aba1* mutants (19). The evidence that VP1 can also regulate transcription independently of ABA further supports the possibility of a less strict limitation of ABI3 to ABA signaling (33, 34). The same holds true for ABI4 and ABI5 (2).

Figure 2. A model for ABA signal transduction.

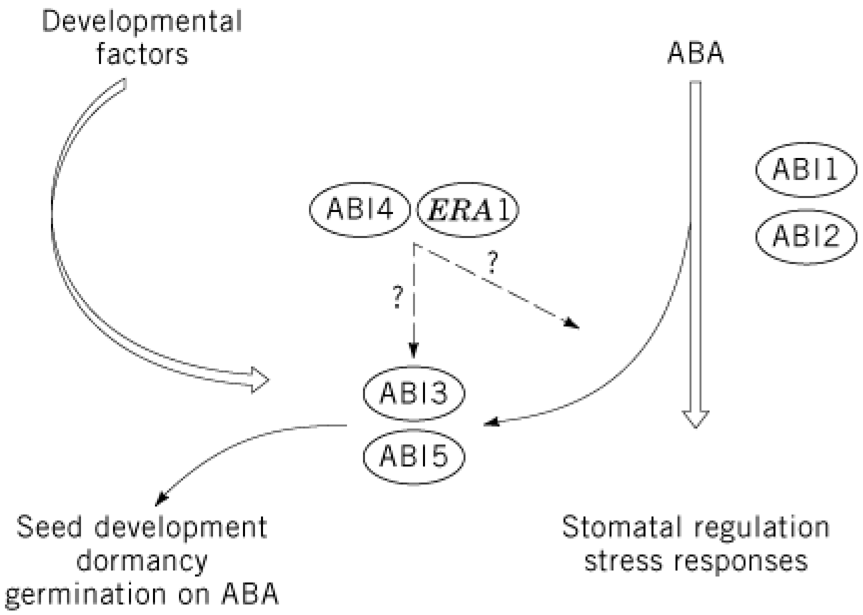

Intermediates in the ABA transduction chain were revealed by microinjection of putative second messengers into hypocotyl cells of the *aurea* mutant of tomato (35). Following injection of ABA-inducible *KIN2* and *RD29A* **promoters** linked to b-glucuronidase, coinjection of either Ca^{2+}, cyclic ADP-ribose (cADP), ADP-ribosyl cyclase, or inositol (1,4,5)-triphosphate (IP_3) (see Calcium Signaling) resulted in expression of the ABA-inducible genes in the absence of ABA, implying that cADP ribose, a Ca^{2+}-mobilizing second messenger, is involved in ABA responses. At present, it is difficult to integrate these data into the current model for the ABA signal transduction pathway (19). Electrophysiological studies (voltage clamp or patch clamp) on the ABA-insensitive mutants *abi1* and *abi2* have clearly shown an altered **ion channel** behavior in their stomatal guard cells and provided further evidence that phosphorylation/dephosphorylation cascades are involved in ABA signaling (36, 37).

Given the power of mutational approaches to identify signal transduction components, several groups are currently aiming at the identification of additional ABA signal transduction factors, exploiting novel screening procedures in *Arabidopsis* (12). At least eight *growth control via ABA* (*gca*) loci have been identified on the basis of their insensitivity to ABA inhibition of root growth (38). Furthermore, a *freezing sensitive* (*frs1*) mutant with a wilty phenotype appeared to be nonallelic to other ABA-deficient or -insensitive mutants of *Arabidopsis* (39). Other screens employ **transgenic** lines carrying chimeric promoter-**luciferase** constructs with promoters derived from ABA-responsive genes. Putative mutants are identified by aberrant expression of these genes in the mutagenized progeny (40). The identification of intragenic or extragenic enhancers and **suppressors** of known signaling components is yet another alternative.

Whereas part of the ABA signaling pathway is well established in seeds and stomatal guard cells, the implications of ABA signaling in the function of the vegetative meristem remain to be clarified. Furthermore, it will be most interesting to characterize the regulatory influence of light on ABA signaling, as well as the crosstalk with gibberellins, which are known to counteract ABA in many physiological processes (5).

4. Downstream Targets

Of all the plant hormones, ABA is probably best known from the point of view of responsiveness at the target gene level. ABA-responsive genes encode proteins with diverse functions and are often induced under water stress (drought, salinity, low temperature). It is important to mention, however, that certain water stress-related genes are independent of ABA (17, 18). ABA-responsive genes can be classified into two groups. Primary ABA response genes are rapidly induced and are independent of **protein biosynthesis**, implying that *trans*-acting factors controlling these genes are under post-translational control. A second class of ABA response genes consists of those that require the expression of other genes.

Cis-acting and trans-acting elements involved in ABA induction of **gene expression** have been studied extensively, often in relation to water stress (17, 18). A bipartite model for regulation of transcription of the primary response genes is proposed, as for the barley *HVA1* and *HVA22* genes (41, 42). The specificity of ABA responsiveness relies on the combination of an ABA response element (ABRE) and a coupling element. The ABRE has a **consensus sequence** (PyACGTGGC) that contains a G-box core sequence and has been shown to interact with bZIP factors (eg, wheat *Em* gene-binding protein EmBP-1) (43). A set of unique coupling elements would provide specificity in ABA response at the level of individual genes. In addition, in the case of *Em* induction, it has been demonstrated that a conserved domain of 18 amino acid residues of the VP1 protein enhances DNA-binding activity of the EmBP-1 bZIP factor, thereby acting as a DNA chaperone (44). A yeast two-hybrid system screen was used to identify proteins that interact specifically with VP1 on the promoter of the *Em* gene. One such protein was related to 14–3–3 proteins (45) and thus may help to stabilize and/or activate the regulatory complex at the *Em* promoter (20).

ABREs are not the only *cis* elements that confer ABA responsiveness. Both in the case of seed desiccation and in water stress conditions, other promoter elements can be involved. For example, ABA responses can be mediated in conjunction with the Sph box in germination-specific promoters. A direct interaction between the Sph box and a 140-residue conserved domain in the *C*-terminal region of VP1 has been demonstrated (46).

The second pathway for ABA-dependent gene expression requires protein biosynthesis, exemplified by the *Arabidopsis* ABA-inducible *RD22* gene. A 67-bp region in the promoter of this gene contains conserved motifs for MYC and MYB factor binding (47) (see Oncogenes, Oncoproteins). Factors binding to these promoter elements (RD22BP-1 and ATMYB2) were shown to activate transcription of *RD22* in transient transactivation assays (48). Cooperative binding of these factors has been proposed to control ABA-dependent expression of *RD22*.

One of the challenges for the future consists in making the link between the ABA-induced proteins and the tissue- and development-specific physiological responses, summarized below.

5. Effects

Although abscission was originally considered to be a process regulated by ABA, and the hormone was named accordingly, it is now clear that ethylene is the primary factor controlling abscission. Nevertheless, ABA also plays a key role in such diverse plant growth and developmental processes as seed maturation, germination, root growth, and stomatal closure (5). Stomatal movements involve changes in ion fluxes that occur very rapidly in response to ABA and do not require gene expression.

Furthermore, ABA is a major stress signal orchestrating responses to dehydration stress, including water stress induced by drought and high-salt concentration as well as by low-temperature conditions.

Bibliography

1. T. A. Bennet-Clark and N. P. Kefford (1953) Nature **171**, 645–647.
2. K. Ohkuma, O. E. Smith, J. L. Lyon, and F. T. Addicott (1963) Science **142**, 1592–1593.
3. P. F. Wareing (1956) Annu. Rev. Plant Physiol. **7**, 191–214.
4. R. F. M. van Stevenick (1957) J. Exp. Bot. **8**, 373–381.
5. P. J. Davies (1995) *Plant Hormones: Physiology, Biochemistry and Molecular Biology*, Kluwer, Dordrecht, The Netherlands.
6. M. Koornneef, M. L. Jorna, D. L. C. Brinkhorst-van der Swan, and C. M. Karssen (1982) Theor. Appl. Genet. **61**, 385–393.
7. K. M. Léon-Kloosterziel, M. Alvarez Gil, G. J. Ruijs, S. E. Jacobsen, N. E. Olszewski, S. H. Schwartz, J. A. D. Zeevaart, and M. Koornneef (1996) Plant J. **10**, 655–661.
8. I. B. Taylor (1991) In *Abscisic Acid, Physiology and Biochemistry* (W. J. Davies and H. G. Jones, eds.), Bios Scientific, Oxford, UK, pp. 23–37.
9. S. C. Duckham, R. S. T. Linforth, and I. B. Taylor (1991) Plant Cell Environ. **14**, 631–636.
10. C. D. Rock and J. A. D. Zeevaart (1991) Proc. Natl. Acad. Sci. USA **88**, 7496–7499.
11. E. Marin, L. Nussaume, A. Quesada, M. Gonneau, B. Sotta, P. Hugueney, A. Frey, and A. Marion-Poll (1996) EMBO J. **15**, 2331–2342.
12. M. Koornneef, K. M. Léon-Kloosterziel, S. H. Schwartz, and J. A. D. Zeevaart (1998) Plant Physiol. Biochem. **36**, 83–89.
13. S. H. Schwartz, K. M. Léon-Kloosterziel, M. Koornneef, and J. A. D. Zeevaart (1997) Plant Physiol. **114**, 161–166.
14. S. H. Schwartz, B. C. Cai, D. A. Gage, J. A. D. Zeevaart, and D. R. McCarty (1997) Science **276**, 1872–1874.
15. J. A. D. Zeevaart and R. A. Creelman (1988) Annu. Rev. Plant Physiol. Plant Mol. Biol. **39**, 439–473.
16. G. Sembdner, R. Atzorn, and G. Schneider (1994) Plant Mol. Biol. **26**, 1459–1481.
17. J. Ingram and D. Bartels (1996) Annu. Rev. Plant Physiol. Plant Mol. Biol. **47**, 377–403.
18. K. Shinozaki and K. Yamaguchi-Shinozaki (1996) Curr. Opin. Biotechnol. **7**, 161–167.
19. S. Merlot and J. Giraudat (1997) Plant Physiol. **114**, 751–757.
20. R. S. Quatrano, D. Bartels, T. H. D. Ho, and M. Pagés (1997) Plant Cell **9**, 470–475.
21. M. Koornneef, G. Reuling, and C. M. Karssen (1984) Physiol. Plant. **61**, 377–383.
22. R. R. Finkelstein (1994) Plant J. **5**, 765–771.
23. S. Cutler, M. Ghassemian, D. Bonetta, S. Cooney, and P. McCourt (1996) Science **273**, 1239–1241.
24. J. Leung, M. Bouvier-Durand, P.-C. Morris, D. Guerrier, F. Chefdor, and J. Giraudat (1994) Science **264**, 1448–1452.
25. J. Leung, S. Merlot, and J. Giraudat (1997) Plant Cell **9**, 759–771.
26. K. Meyer, M. P. Leube, and E. Grill (1994) Science **264**, 1452–1455.
27. N. Bertauche, J. Leung, and J. Giraudat (1996) Eur. J. Biochem. **241**, 193–200.
28. D. R. McCarty, T. Hattori, C. B. Carson, V. Vasil, M. Lazar, and I. K. Vasil (1991) Cell **66**, 895–905.
29. J. Giraudat, B. M. Hauge, C. Valon, J. Smalle, F. Parcy, and H. M. Goodman (1992) Plant Cell **4**, 1251–1261.
30. F. Parcy, C. Valon, M. Raynal, P. Gaubier-Comella, M. Delseny, and J. Giraudat (1994) Plant

Cell **6**, 1567–1582.
31. E. Nambara, K. Keith, P. McCourt, and S. Naito (1995) Development **121**, 629–636.
32. F. Parcy and J. Giraudat (1997) Plant J. **11**, 693–702.
33. V. Vasil, W. R. Marcotte Jr., L. Rosenkrans, S. M. Cocciolone, I. K. Vasil, R. S. Quatrano, and D. R. McCarty (1995) Plant Cell **7**, 1511–1518.
34. C.-Y. Kao, S. M. Cocciolone, I. K. Vasil, and D. R. McCarty (1996) Plant Cell **8**, 1171–1179.
35. Y. Wu, J. Kuzma, E. Maréchal, R. Graeff, H. C. Lee, R. Foster, and C.-H. Hua (1997) Science **278**, 2126–2130.
36. F. Armstrong, J. Leung, A. Grabov, J. Brearley, J. Giraudat, and M. R. Blatt (1995) Proc. Natl. Acad. Sci. USA **92**, 9520–9524.
37. Z.-M. Pei, K. Kuchitsu, J. M. Ward, M. Schwarz, and J. I. Schroeder (1997) Plant Cell **9**, 409–423.
38. G. Benning, T. Ehrler, K. Meyer, M. Leube, P. Rodriguez, and E. Grill (1996) In *Abscisic Acid Signal Transduction in Plants*. Centro de Reuniones Internacionales sobre Biología Workshop 60 (R. S. Quatrano and M. Pagès, eds.), Instituto Juan March de Estudios e Investigaciones, Madrid, p. 34.
39. J. Salinas, F. Llorente, and J. M. Martinez-Zapater (1996) In *Abscisic Acid Signal Transduction in Plants*. Centro de Reuniones Internacionales sobre Biología Workshop 60 (R. S. Quatrano and M. Pagès, eds.), Instituto Juan March de Estudios e Investigaciones, Madrid, p. 35.
40. N.-H. Chua, Y. Wu, and R. Foster (1996) In *Abscisic Acid Signal Transduction in Plants*. Centro de Reuniones Internacionales sobre Biología Workshop 60 (R. S. Quatrano and M. Pagès, eds.), Instituto Juan March de Estudios e Investigaciones, Madrid, p. 55.
41. Q. Shen and T.-H. D. Ho (1995) Plant Cell **7**, 295–307.
42. Q. Shen, P. Zhang, and T.-H. D. Ho (1996) Plant Cell **8**, 1107–1119.
43. M. J. Guiltinan, W. R. Marcotte Jr., and R. S. Quatrano (1990) Science **250**, 267–271.
44. A. Hill, A. Nantel, C. D. Rock, and R. S. Quatrano (1996) J. Biol. Chem. **271**, 3366–3374.
45. T. F. Schultz, J. Medina, A. Hill, and R. S. Quatrano (1998) Plant Cell **10**, 837–847.
46. M. Suzuki, C. Y. Kao, and D. R. McCarty (1997) Plant Cell **9**, 799–807.
47. T. Iwasaki, K. Yamaguchi-Shinozaki, and K. Shinozaki (1995) Mol. Gen. Genet. **247**, 391–398.
48. H. Abe, K. Yamaguchi-Shinozaki, T. Urao, T. Iwasaki, D. Hosokawa, and K. Shinozaki (1997) Plant Cell **9**, 1859–1868.

Absorption Spectroscopy

Light in the ultraviolet (UV) and visible (vis) range of the electromagnetic spectrum shows an energy that is equivalent to about 150 to 400 kJ/mol. Light with the appropriate energy is used to promote electrons from the ground state to an excited state. The absorption of energy from the incident light as a function of its wavelength is measured in absorption spectroscopy. Molecules with electrons that participate in delocalized aromatic systems often absorb light in the near-UV or visible region.

Absorption spectroscopy is usually performed on solutions of molecules in a transparent solvent. The absorbance of a solute depends linearly on its concentration, and therefore absorption spectroscopy is ideally suited for quantitative measurements. The spectral properties of a molecule depend on the molecular environment and the mobility of its chromophores. Absorption spectroscopy and difference spectroscopy (see Difference Spectroscopy) are therefore well-suited to follow **enzyme**-catalyzed reactions, **ligand binding**, and conformational transitions in proteins and nucleic acids. Spectroscopic measurements are very sensitive, nondestructive, and require only small amounts of material for analysis. Spectrophotometers are standard laboratory equipment, and the measurement of absorbance is technically simple.

1. Absorbance of Proteins

In proteins, the peptide bond absorbs light in the range of 180 to 230 nm (which is called the "far-UV" range). The aromatic residues, **tyrosine** (Tyr), **tryptophan** (Trp), and **phenylalanine** (Phe), also absorb light in this region and, in addition, show bands near 260 to 280 nm (in the "near-UV"). Disulfide bonds absorb weakly near 260 nm. Some protein cofactors, such as the heme group, show absorbance in the visible range. When the peptide groups and aromatic residues are part of an asymmetric structure, or when they are immobilized within an asymmetric environment (as in folded proteins), left- and right-handed circularly polarized light is absorbed to different extents. This phenomenon is called circular dichroism (CD).

Spectra of the aromatic amino acids and model proteins are found in (1). In the near-UV, the molar absorbance of a phenylalanine residue is much smaller than that of a tyrosine or a tryptophan, and the spectrum of a protein between 240 and 300 nm is therefore dominated by the contributions from the Tyr and Trp side-chains. Phe residues contribute fine structure ("wiggles") to the spectrum between 250 and 260 nm. The aromatic amino acids do not absorb above 310 nm, and therefore protein absorbance should be zero at wavelengths greater than 310 nm. Proteins without Trp residues do not absorb above 300 nm (see Fig. 1**c**).

Figure 1. Ultraviolet absorption spectra of (**a**) the wild-type form and (**c**) the Trp59Tyr variant of RNase T_1. The spectra of the native proteins (in 0.1 *M* sodium acetate, pH 5.0) are shown by the continuous lines. The spectra of the unfolded proteins (in 6.0 *M* GdmCl in the same buffer) are shown by broken lines. The difference spectra between the native and unfolded forms are shown in (**b**) and (**d**). Spectra of 15 μM protein were measured at 25°C in 1-cm cuvettes in a double-beam instrument with a band width of 1 nm at 25°C. The spectra of the native and unfolded proteins were recorded successively, stored, and subtracted. From Ref. 1.

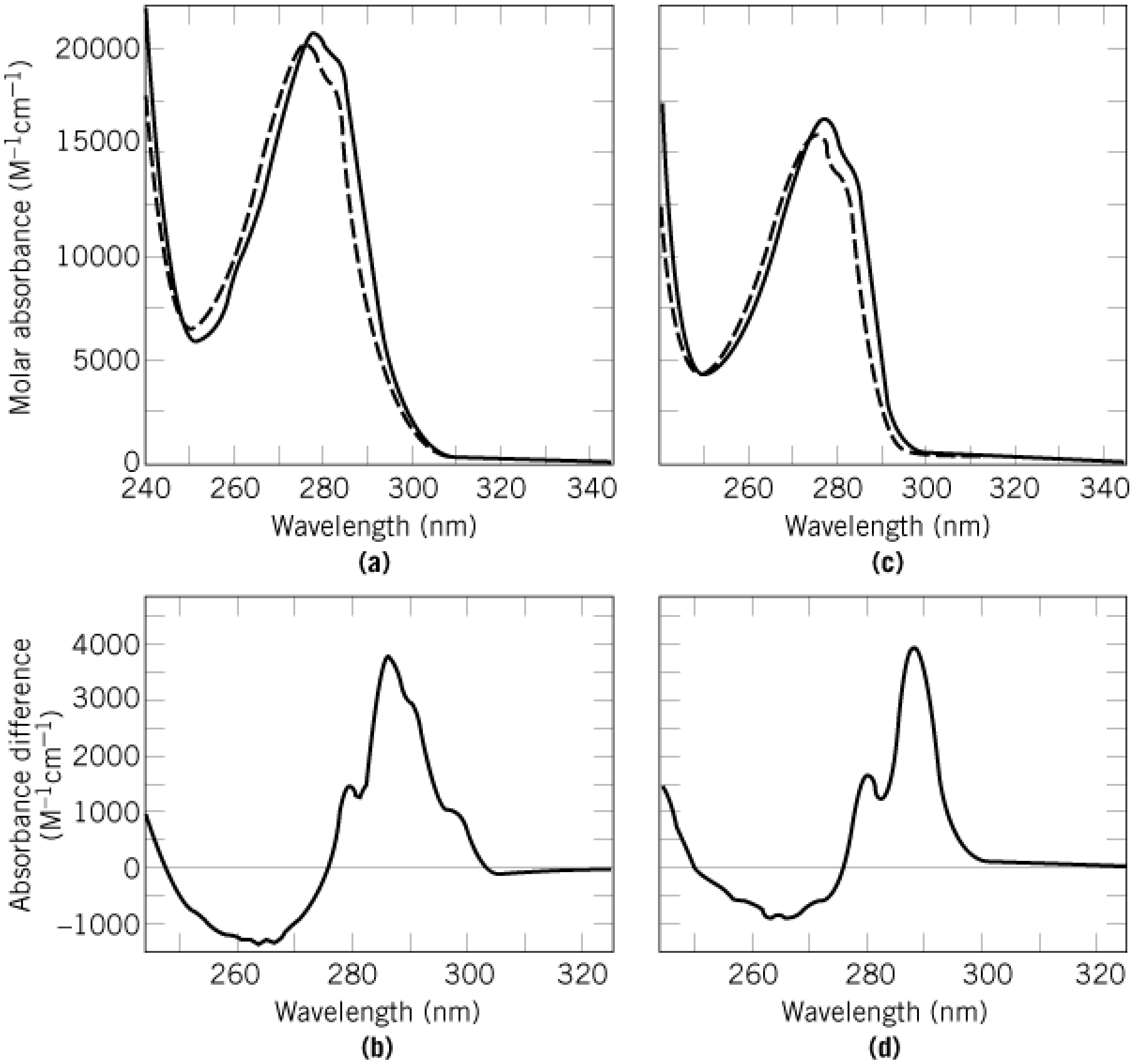

A fraction of the aromatic residues are buried in the **hydrophobic** core of a native, folded protein molecule (see Protein Structure). When these residues become exposed to the aqueous solvent upon unfolding, their absorption is shifted slightly to shorter wavelengths. This is clearly seen for two forms of **ribonuclease T$_1$** (Figs. 1**a** and 1**c**). The difference spectra in Figures 1**b** and **d** show that the maximal differences in absorbance occur in the 285 to 295 nm region. The **difference spectrum** for the form without a Trp residue (Fig. 1**d**) shows a prominent maximum at 287 nm. It is typical for proteins that contain Tyr residues only. The form with a single Trp residue (Fig. 1**b**) shows additional shoulders between 290 and 300 nm in the difference spectrum. They originate from the single Trp residue of this protein. The differences in the absorption spectra between the native and unfolded state of a protein are generally small, but they can be determined with good accuracy and are extremely useful for monitoring conformational changes of a protein.

Spectroscopic methods are, in general, the methods of choice (i) to investigate changes in the behavior of a protein under different solvent conditions, and (ii) to compare the properties of related molecules, such as homologous or mutated forms of a protein. In addition, they are widely used to measure protein stability and to follow structural transitions such as unfolding and refolding under a variety of conditions. Absorbance changes during fast reactions that occur in the milliseconds range can be followed by using rapid mixing techniques, such as in stopped-flow spectrometry (see Kinetics).

2. Absorbance of Nucleic Acids

Nucleic acids show a strong absorbance in the region of 240 to 275 nm. It originates from the $\pi \rightarrow \pi^*$ transitions of the **pyrimidine** and **purine** ring systems of the nucleobases. The bases can be protonated, and therefore the spectra of DNA and RNA are sensitive to pH. At neutral pH, the absorption maxima range from 253 nm (for guanosine) to 271 nm (for cytidine), and therefore polymeric DNA and RNA show a broad and strong absorbance near 260 nm.

In native DNA, the bases are stacked in the hydrophobic core of the double helix, and therefore their absorbance is considerably decreased relative to the absorbance of single-stranded DNA, and even more so relative to oligonucleotides. This phenomenon is called hypochromism. It is widely used to follow the melting of DNA double helices.

3. Absorbance to Determine Concentrations

Absorbance measurements are the methods of choice to determine the concentration of proteins or nucleic acids in solution. Spectrophotometers are standard laboratory equipment, and absorbance can be measured quickly and accurately. The absorbance A is related with the intensity of the light before I_0 and after I passage through the protein solution by Equation 1, and the absorbance depends linearly on concentration, according to the Lambert–Beer relationship (Eq. 2):

$$A = -\log_{10}(I/I_0) \qquad (1)$$

$$A = \varepsilon \times c \times l \qquad (2)$$

where c is the molar concentration, l the pathlength in cm, and ε the molar absorption coefficient. The concentration of a substance in solution can be determined very rapidly and accurately from its absorbance by using Equation 2. The measurement of absorbance values greater than 2 should be avoided, because only 1% of the incident light is transmitted through a solution with an absorbance of 2 (and is quantified by the photomultiplier). The value of e can be determined by a number of experimental techniques (2) or can be calculated for proteins by adding up the contributions of the constituent aromatic amino acids of a protein (2, 3).

The absorbance of nucleic acids does not vary much. The concentrations of nucleic acids in solution are routinely determined from the absorbance at 260 nm. In fact, amounts of nucleic acid are often given as "A_{260} units." For double-stranded DNA, one A_{260} unit is equivalent to 50 µg DNA; for single-stranded DNA, it is equivalent to 33 µg DNA; for single-stranded RNA, it is equivalent to 40 µg RNA. All these amounts would produce an A_{260} of 1 when dissolved in 1 mL and measured in a 1-cm cuvette. Proteins absorb much more weakly than nucleic acids. In a 1:1 mixture of nucleic acids and proteins, the proteins contribute only about 2% to the total absorbance at 260 nm. Consequently, these quantities of contaminating protein hardly affect the concentrations of nucleic acids measured by A_{260}.

4. Absorbance Spectrophotometers

Absorbance is measured by a spectrophotometer. Spectrophotometers consist usually of two light sources: a deuterium lamp, which emits light in the UV region, and a tungsten/halogen lamp for the visible region. After passing through a monochromator (or through optical filters), the light is focused into the cuvette, and the amount of light that passed through the sample is detected by a photomultiplier or photodiode. In diode array spectrophotometers, the sample is illuminated by the full lamp light; after passage through the cuvette, the transmitted light is spectrally decomposed by a prism into the individual components and quantified by an array of diodes, often in intervals of 2 nm. In diode array spectrometers, the entire spectrum is recorded at the same time and not by a time-dependent scan as in conventional instruments. This is of advantage for measuring time-dependent changes at several wavelengths simultaneously (see Kinetics).

5. Buffers for Absorbance Spectroscopy

Good buffers for measuring difference spectra ideally should not absorb light in the wavelength range of the experiment. For work in the near-UV, buffer absorbance should be small above 230 nm, and indeed most of the solvents commonly used in biochemical experiments do not absorb in this spectral region (1). Buffer absorbance is a major problem, however, in the far-UV region below 220 nm, because buffers that contain carboxyl and/or amino groups absorb light in this wavelength range. Buffers with negligible absorbance in the far-UV include phosphate, cacodylate, and borate. Detailed procedures for the measurement of difference spectra are found in Ref. 1.

Bibliography

1. F. X. Schmid (1997) "Optical spectroscopy to characterize protein conformation and conformational changes". In *Protein Structure: A Practical Approach*, 2nd ed. (T. E. Creighton, ed.), IRL Press, Oxford, UK, pp. 261–297.
2. S. C. Gill and P. H. von Hippel (1989) Anal. Biochem. **182**, 319–326.
3. C. N. Pace and F. X. Schmid (1997) "How to determine the molar absorption coefficient of a protein". In *Protein Structure: A Practical Approach*, 2nd ed. (T. E. Creighton, ed.), IRL Press, Oxford, UK, pp. 253–259.

Suggestions for Further Reading

4. S. B. Brown (1980) "Ultraviolet and visible spectroscopy". In *An Introduction to Spectroscopy for Biochemists* (S. B. Brown, ed.), Academic Press, London, pp. 14–69.
5. D. B. Gordon (1994) "Spectroscopic techniques". In *Principles and Techniques of Practical Biochemistry* (K. Wilson and J. Walker, eds.), Cambridge University Press, Cambridge, UK, Chap. "7", pp. 324–380.
6. D. A. Harris and C. L. Bashford (1987) *Spectrophotometry and Spectrofluorimetry: A Practical Approach*, IRL Press, Oxford, UK

Acceptor Stem

The acceptor stem is the site of attachment of amino acids to transfer RNA (tRNA). It is formed by 7 base pairs and has 4 single-stranded nucleotides. Nucleotides 1 to 7 from the 5′ end of the tRNA base pair with nucleotides 72–66, respectively, from the 3′ end of the molecule. Whereas the 5′ end of the RNA has a monophosphate group, the 3′ end contains a 3′-hydroxyl group, which is the site of esterification to the amino acid. The four 3′-end single-stranded nucleotides include residue 73, the discriminator base and the well-conserved nucleotides C74, C75, A76, the 3′-CCA sequence. In the three-dimensional structures of tRNA, the acceptor stem is stacked on the T arm, forming the acceptor "branch" of the L-shaped RNA fold (see Fig. 1 of Transfer RNA). The acceptor branch usually forms a regular A-type double helix, with the four single-stranded nucleotides extending in a regular helical continuity. In tRNA-like domains of some **viruses**, the acceptor stem is formed by a single RNA chain that folds into a helix due to the presence of a **pseudoknot** (1).

Specific aminoacylation of tRNA by their cognate aminoacyl-tRNA synthetases is dependent on the presence of a series of identity elements. Limited in number, these elements are preferentially located in the anticodon loop and in the acceptor stem (2-4). Residue 73, next to the CCA end, is called the “discriminator” base. The hypothesis that it contributes to discrimination of tRNA by cognate aminoacyl tRNA synthetases (5) has been largely confirmed. Residue 73 contributes strongly to specific aminoacylation of 17 different *Escherichia coli* tRNAs (6). It is the element making the major thermodynamic contribution toward aminoacylation of *E. coli* $tRNA^{Cys}$, *E. coli* $tRNA^{His}$, yeast $tRNA^{His}$ and *E. coli* $tRNA^{Leu}$. Replacement of A73 to G73 in human $tRNA^{Ser}$ converts it to a tRNA for isoleucine (7). The crystallographic structures of two tRNA-cognate synthetase complexes suggests two possible mechanisms by which the discriminator base contributes to aminoacylation specificity. One is a direct mechanism, involving direct hydrogen interactions with the synthetase. The other is an indirect mechanism that confers a conformational change to the acceptor end of the tRNA to facilitate aminoacylation. In the complex of yeast $tRNA^{Asp}$/aspartyl-tRNA synthetase, nucleotide G73 fits into the active site, forming hydrogen bond interactions with side chains of the synthetase. It does not cause a conformational change in the acceptor stem (8). Alternatively, the 2-amino group of G73 of *E. coli* $tRNA^{Gln}$ hydrogen bonds with the phosphate oxygen of the previous nucleotide, folding the backbone of G73 back toward the 3′ end of the tRNA. The formation of this fold-back hairpin enables the synthetase to open the first base pair of the acceptor stem and reach the second and third base pairs for specific interactions (9). In both complexes, additional contacts exist between the enzyme and the acceptor stems of the tRNA. The aspartyl-tRNA synthetase interacts with the $tRNA^{Asp}$ acceptor stem via the major groove of the RNA helix, whereas glutaminyl-tRNA synthetase interacts via the minor groove.

Acceptor stem identity-element nucleotides, as well as additional structural features, are important for synthetase recognition. Alanyl-tRNA synthetase is sensitive to both the exocyclic NH_2 group of G3 and local conformation of the helix due to structural characteristics of the G-U **wobble** pair (10-13). Alanine acceptance by alanyl-tRNA is modulated by additional signals within the acceptor stem, namely, A73, G1-C72, G2-C71 and G4-C69. The 5′ end of histidine-specific tRNA has an additional nucleotide, residue number –1, which is a guanosine. This nucleotide, opposite the discriminator base, does form a base pair with the discriminator in many, but not all, histidyl-tRNA. This –1 guanosine is the major histidine identity element. Its influence is complemented by base pairs U2-A71 and G3-C70. Base pairs 1–72, 2–71, 3–70, and/or 4–69 contribute to aminoacylation in several cases. Glutamine identity requires a weak 1–72 base pair, G2-C71, G3-C70, in addition to signals elsewhere in the tRNA. Glycine identity is dependent on C2-G71, G3-C70 sequences, and serine identity involves G2-C71, among other signals. Methionine identity is based on the presence of A73, G2-C71, C3-G70, in addition to the CAU anticodon.

At the three-dimensional level, tRNA molecules fold into a two-domain L-shaped structure with the amino acid acceptor terminus and the anticodon at opposite ends. Minihelices (small RNA molecules containing only part of a tRNA) that mimic the amino acid acceptor domain, specifically, the acceptor stem stacked on top of the TY stem, have been shown to be useful tools for determining the contribution of the acceptor stem to tRNA function (14, 15). Minihelices containing the identity elements from a tRNA are efficient substrates for its cognate aminoacyl-tRNA synthetases. Thus, alanyl-tRNA synthetase, glycyl-tRNA synthetase, and histidyl-tRNA synthetase aminoacylate minihelices efficiently. Minihelices containing partial identity sets of six additional tRNAs are specific substrates for their cognate synthetases. Since identity elements are located very close to the CCA end, minihelices may be reduced in size to microhelices, consisting only of the amino acceptor stem closed by a loop and remain active. The smallest substrate for an aminoacyl-tRNA synthetase is derived from yeast $tRNA^{Asp}$ and consists of only 14 nucleotides. There are three base pairs closed by a tetraloop, plus the discriminator base and the CCA sequence (16). Double-stranded RNA duplexes and RNA/DNA heteroduplexes may also be aminoacylated (15).

The aminoacylation efficiency of minihelices is generally reduced significantly compared to that of the corresponding full-length tRNA. The amino acid charging is, however, very specific and depends on just a few nucleotides. These minimal RNA substrates are devoid of the anticodons that read the genetic code and provide the link between amino acid and **codon**. Since the relationship between the sequences and structures of the minisubstrates and the specific amino acids is maintained, there appears to be an *operational RNA code* for primitive aminoacylation. This operational code may be the primitive code from which the contemporary genetic code evolved (17-20)

Acceptor stem properties are important for tRNA recognition by proteins other than synthetases. Aminoacylated initiator tRNA in **prokaryotes** is a substrate for a methionyl-tRNA transformylase that converts methionyl-$tRNA^{Met}$ to formylmethionine $tRNA^{Met}$. Recognition of initiator tRNA by the formylase depends on the presence of methionine. Sequence and/or structural elements in the tRNA that are important for formylation by methionyl-tRNA transformylase are clustered at the end of the acceptor stem (21). The key determinants appear to be a mismatch or a weak base pair between nucleotides 1 and 72, a G-C base pair between nucleotides 2 and 71, and a C-G or, less preferably, a G-C base-pair between nucleotides 3 and 70. Mutations at G4-C69 also affect formylation kinetics slightly. In addition to the positive elements A73, G2-C71, C3-G70, and G4-C69, the occurrence of a G-C or a C-G base pair between positions 1 and 72 acts as a major negative determinant for the formylase. Formylation is a prerequisite for interaction with initiation factor IF2, which delivers the initiator tRNA to the P site of the ribosome. Special structural features within the acceptor stem of eubacterial initiator tRNA contribute to their discrimination from elongator tRNA. They lack a Watson–Crick base pair between nucleotides 1 and 72 at the end of the acceptor stem. Eukaryotic initiator tRNA almost always has an A1-U72 pair, a feature not found in eukaryotic elongator tRNA.

A high-resolution X-ray crystallography structure of the ternary complex, formed by aminoacylated yeast $tRNA^{Phe}$, **elongation factor** Tu from *Thermus aquaticus*, and an analog of GTP, revealed numerous contacts between the protein and the acceptor stem of the tRNA (22). These contacts include specific interactions with residue A76, with phosphates 74, 75, 67, 64, 3, and with riboses 2, 3, 63, 64, 65 along the acceptor stem and the T stem.

The stability of the 1–72 base pair also governs the degree of sensitivity of a peptidyl-tRNA to peptidyl-tRNA hydrolase. This enzyme converts the peptidyl-tRNA of *N*-acetylaminoacyl-tRNA into free tRNA plus peptides or *N*-acetyl amino acids. It is believed to play a role in the translational apparatus through the recycling of free tRNA from immature peptidyl-tRNA created by abortive protein synthesis (23).

The acceptor stem also contains specific information required during synthesis of the tRNA. Ribonuclease P, an enzyme that removes extra nucleotides from the 5′ end of tRNA during tRNA biosynthesis, recognizes the -74CCA76- sequence in addition to nucleotides within the TY loop. Moreover, this enzyme locates its cleavage site by “measuring” the length of the helix formed by the amino acid acceptor stem fused to the TY stem. Processing at the 3′ end of the tRNA, as well as the addition and repair of the conserved CCA sequence by ATP(CTP)-tRNA nucleotidyltransferase, requires information within the acceptor stem. This enzyme interacts with tRNA at the corner of the structure, where the T and D loops interact, and extends that interaction across the aminoacyl stem to the 3′ end (24, 25).

Bibliography

1. K. Rietveld, C. W. A. Pleij, and L. Bosch (1983) EMBO J. **2**, 1079–1085.
2. R. Giegé, J. D. Puglisi, and C. Florentz (1993) Prog. Nucleic Acid Res. Mol. Biol. **45**, 129–206.
3. W. H. McClain (1993) J. Mol. Biol. **234**, 257–280.
4. M. E. Saks and J. R. Sampson (1995) J. Mol. Evol. **40**, 509–518.
5. D. M. Crothers, T. Seno, and D. G. Söll (1972) Proc. Natl. Acad. Sci. USA **69**, 3063–3067.

6. Y. M. Hou (1997) Chem. Biol. **4**, 93–96.
7. K. Breitshopf and H. J. Gross (1994) EMBO J. **13**, 3166–3169.
8. J. Cavarelli, B. Rees, M. Ruff, J.-C. Thierry, and D. Moras (1993) Nature **362**, 181–184.
9. M. A. Rould, J. J. Perona, D. Sâll, and T. A. Steitz (1989) Science **246**, 1135–1142.
10. Y. M. Hou and P. Schimmel (1988) Nature **333**, 140–145.
11. Y. M. Hou and P. Schimmel (1989) Biochemistry **28**(17), 6800–6804.
12. W. H. McClain and K. Foss (1988) Science **240**, 793–796.
13. K. Musier-Forsyth and P. Schimmel (1992) Nature **357**, 513–515.
14. C. Francklyn, K. Musier-Forsyth, and P. Schimmel (1992) Eur. J. Biochem. **206**, 315–321.
15. S. A. Martinis, and P. Schimmel (1995) In *tRNA: Structure, Biosynthesis, and Function* (D. Söll, and U. L. RajBhandary, eds.), American Society for Microbiology Press, Washington, DC, pp. 349–370.
16. M. Frugier, C. Florentz, and R. Giegé (1994) EMBO J. **13**, 2218–2226.
17. P. Schimmel, R. Giegé, D. Moras, and S. Yokoyama (1993) Proc. Natl. Acad. Sci. USA **90**, 8763–8768.
18. P. Schimmeland and L. Ribas de Pouplana (1995) Cell **81**, 983–986.
19. P. Schimmel (1995) J. Mol. Evol. **40**, 531–536.
20. P. Schimmel (1996) Proc. Natl. Acad. Sci. USA **93**, 4521–4522.
21. J. M. Guillon, T. Meinel, Y. Mechulam, C. Lazennec, S. Blanquet, and G. Fayat (1992) J. Mol. Biol. **224**, 359–367.
22. P. Nissen, M. Kjeldgaard, S. Thirup, G. Polekhina, L. Reshetnikova, B. F. C. Clark, and J. Nyborg (1995) Science **270**, 1464–1472.
23. S. Dutka, T. Meinnel, C. Lazennec, Y. Mechulam, and S. Blanquet (1993) Nucleic Acids Res. **21**, 4025–4030.
24. P. Spacciapoli, L. Doviken, J. J. Mulero, and D. L. Thurlow (1989) J. Biol. Chem. **264**, 3799–3805.
25. L. A. Hegg, and D. L. Thurlow (1990) Nucleic Acids Res. **18**, 5975–5979.

Accessible Surface

The surfaces of folded macromolecules, especially proteins, and the internal packing of their atoms have generally been analyzed using the procedure of Lee and Richards (1). The cross section of part of the surface of a native protein is depicted in Figure 1, which demonstrates a number of different surfaces and volumes (see Protein Structure). The **van der Waals surface** is defined by the spherical atoms that comprise the structure, but it is not very relevant to a folded macromolecule like a protein, where internal atoms and cavities are normally inaccessible to the solvent.

Figure 1. Schematic representation of possible molecular surface definitions. (**a**) A two-dimensional section through

part of the van der Waals envelope of a hypothetical protein including 12 atoms with the centers numbered 1–12. R_1 and R_2 show the radius of the probes. (**b**) Superposition of sections through the van der Waals and accessible surfaces of ribonucrease S. In places, the accessible surface is controlled by atoms above or below the section shown. The solid outline is the surface of carbon and sulfur atoms; the dashed outline nitrogen and oxygen. The arrow indicates a cavity inside the molecule large enough to accommodate a solvent molecule with a radius of 1.4 Å.[Taken from F. M. Richards (1977) *Ann. Rev. Biophys. Bioeng.* **6**, 151–176; B. Lee and F. M. Richards (1971) *J. Mol. Biol.* **55**, 279–400.]

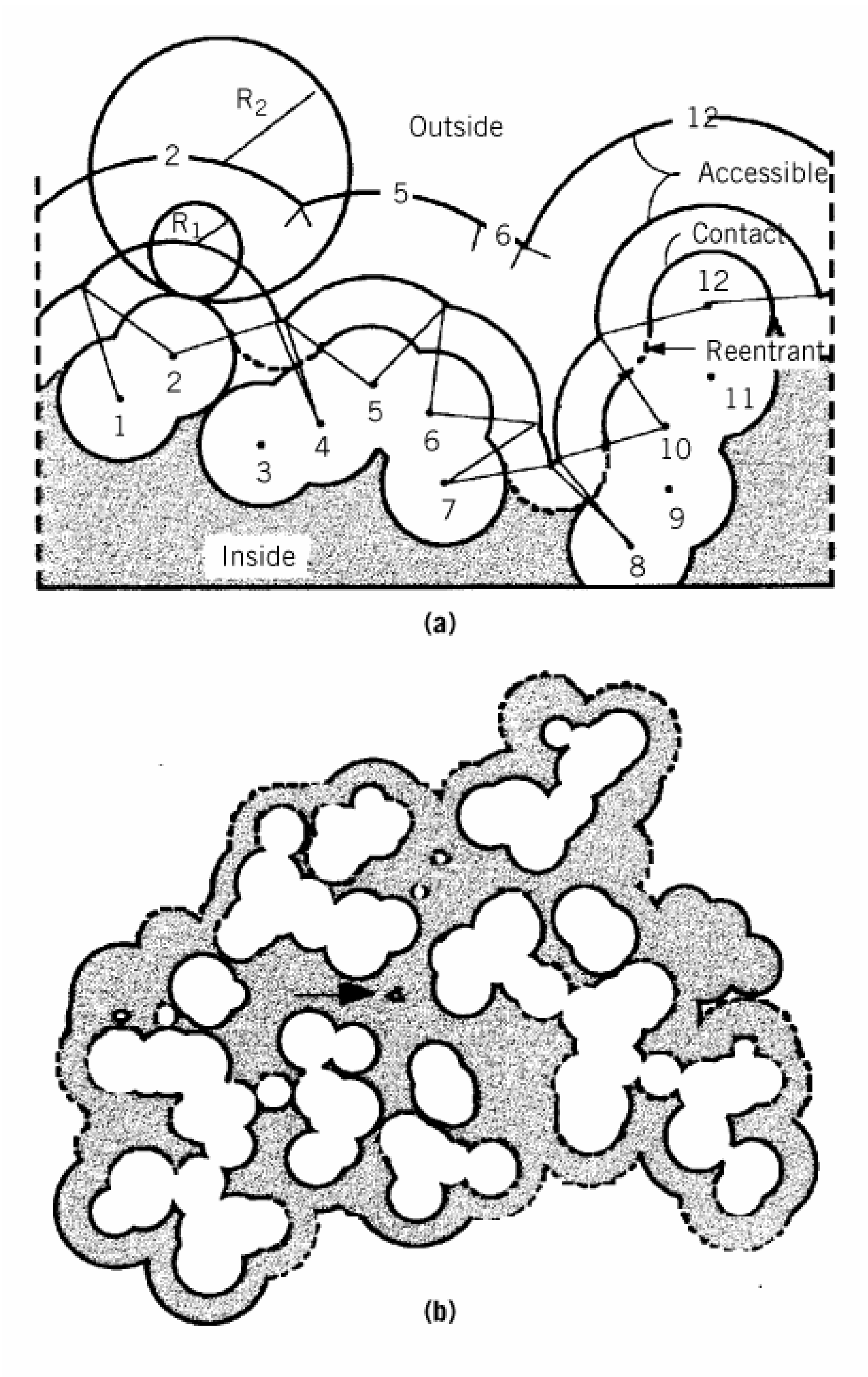

The most relevant surface is the accessible surface, which is defined by its contact with molecules of the solvent. This surface is defined by rolling a spherical probe of appropriate radius R_1 on the outside of the molecule, while maintaining contact with the van der Waals surface. For most purposes, the appropriate probe is a water molecule. The accessible surface is that depicted by the center of the probe as it moves over the surface of the protein. In Figure 1 the probe does not contact atoms 3, 9, or 11, and they have no accessible surface area. Such atoms are considered to be interior atoms, not part of the surface of the molecule. Those parts of the van der Waals surface in contact with the surface of the probe are designated the contact surface; they comprise a series of disconnected patches. When the probe is simultaneously in contact with more than one protein atom, its interior surface defines the reentrant surface. The contact surface and reentrant surface together make a continuous surface, which is defined as the **molecular surface**.

The accessible surface area depends on the size of the probe. When the radius of the probe increases from R_1 to R_2, the number of noncontact or interior atoms in Figure 1 increases from three to eight, and the accessible surface is much smoother. Thus, the smaller the probe, the larger the number of features that will be revealed. The probe is frequently taken to be a water molecule and approximated as a sphere with a radius of 1.4 Å. The accessible surface areas of individual amino acid residues are given in Table 1.

Table 1. Accessible Surface Areas of Amino Acid Residues

Residue	Accessible surface area[a] ($Å^2$)
Ala	113
Arg	241
Asn	158
Asp	151
Cys	140
Gln	189
Glu	183
Gly	85
His	194
Ile	182
Leu	180
Lys	211
Met	204
Phe	218
Pro	143
Ser	122
Thr	146
Trp	259
Tyr	229
Val	160

[a] Values estimated for a Gly-X-Gly tripeptide in an extended conformation (3).

The structures of protein determined by X-ray crystallography indicate that the total accessible surface area A_s of a protein is approximately proportional to the two-third power of its molecular weight. The A_s (in Å^2) of a typical small monomeric protein is usually related to its molecular weight M_w by the approximate relationship (2)

$$A_s = 6.3 M_w^{0.73} \tag{1}$$

For oligomeric proteins

$$A_s = 5.3 M_w^{0.76} \tag{2}$$

These equations are usually accurate to within ±4% on average for monomers and 5% for oligomers. Equations 1 and 2 imply that an oligomeric protein has a larger accessible surface area (by 7 to 13%) than a monomeric protein of the same molecular weight in the molecular weight range up to 35,000.

For an unfolded polypeptide chain, the total accessible surface area A_t in an extended conformation is directly proportional to its molecular weight, within ±3%

$$A_t = 1.45 M_w \tag{3}$$

Thus, for those proteins whose accessible surface area is given by Equation 1, the potential surface area buried by the protein's folding A_b will be approximately given by

$$A_b = 1.45 M_w - 6.3 M_w^{0.73} \tag{4}$$

This indicates that 55 to 75% of the surface area of the unfolded polypeptide chains is buried in the folding process.

The methodology of Lee and Richards (1) is also applicable to the calculation of the accessible surface area of **nucleic acids** (4). Two-thirds of the water-accessible surface area become buried on **double-helix** formation of **DNA** and **RNA**. When a probe corresponding to a single water molecule is used, the total accessible surface area is similar for A-DNA and B-DNA, although marked differences appear in the major and minor groove exposures. For the larger probes, there exist considerable differences in accessible surface area between the two conformations.

Bibliography

1. B. Lee and F. M. Richards (1971) J. Mol. Biol. **55**, 379–400.
2. J. Janin, S. Miller, and C. Chothia (1988) J. Mol. Biol. **204**, 155–164.
3. S. Miller et al. (1987) J. Mol. Biol. **196**, 641–656.
4. C. J. Alden and S. Kim (1979) J. Mol. Biol. **132**, 411–434.

Acentric Fragment

Fragments of chromosomes that lack centromeres are described as acentric fragments (Fig. 1). They are formed as a result of chromosomal damage. Lacking a centromere, there is no means of attachment to the mitotic spindle, which leads to a failure to segregate replicated chromatids in the acentric fragments to the daughter cells during cell division. Therefore, the acentric fragments are normally lost from most cells with progressive cell cycles. The breakage of the chromosome that separates the acentric fragment from the remainder of the chromosome containing the centromere can be a result of either inherent chromosomal fragility, radiation damage, or defective DNA repair mechanisms.

Figure 1. (**a**) A mitotic chromosome is shown with a fragile site, indicated. (**b**) Mitosis can create forces that break the chromosome at the fragile site, creating a residual chromosome that contains the centromere and an acentric fragment as indicated.

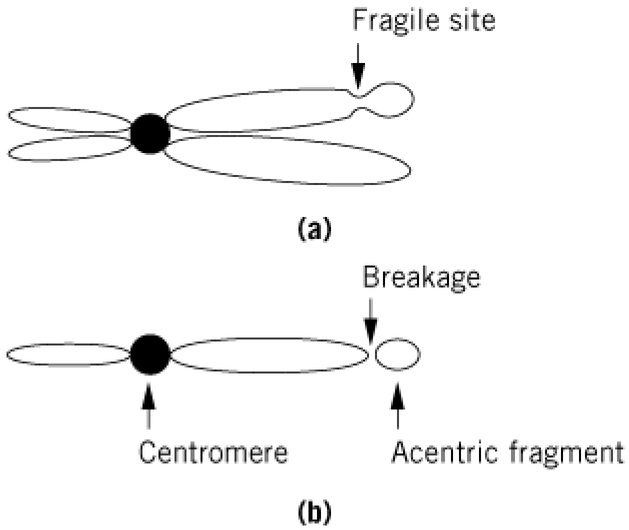

Chromosome fragile sites lead to acentric fragments in humans. The majority of recurrent cancer chromosome breakpoints are found at fragile sites (1). These breakpoints may promote oncogenic rearrangements and translocations. Chromosomal fragile sites can be induced by growing cells under abnormal conditions, by the addition of drugs or chemicals, and by infection with viruses. Fragility seems to be a consequence of incomplete compaction of the chromatin. A more open and accessible chromatin structure might explain the tendency of these sites to break, to recombine with other chromosomal regions, and to be sites of viral integration (2). A fragile site associated with a form of inherited mental retardation known as fragile X mental retardation has been characterized in some detail (5). A gene called FMR-1 (fragile X mental retardation gene 1) is present in the fragile site. This gene contains within it a trinucleotide repeat of CGG. A normal individual has between 6 and 50 of these trinucleotide repeats. Individuals with fragile X syndrome contain expansions of these repeat sequences such that they have several hundred CGG triplets. This expansion leads to chromosome fragility, to inactivation of FMR-1 gene expression, and to methylation of regulatory DNA within the gene. The expansion of the CGG trinucleotide sequences is associated with the assembly of an aberrant chromatin structure (3).

Defective chromosomal repair mechanisms lead to a much higher number of chromosomal breaks and translocations than found in normal cells. This high degree of chromosomal damage can eventually lead to malignancy. For example, in Bloom's syndrome there is a very high rate of sister chromatid exchange, and in Fanconi's anemia and ataxia telangiectasia there is a high incidence of chromosomal breakage and rejoining, leading to multicentric chromosomes and acentric fragments. Individuals with these syndromes are especially sensitive to environmental insults, such as chemical mutagens and ionizing radiation, which further increase chromosomal damage (4). Detection of acentric fragments is diagnostic of serious abnormalities in chromosomal metabolism.

Bibliography

1. J.J. Yunis and A.L. Soreng, Science **226**, 1199–1204 (1984).
2. A.D. Bailey, Z. Li, T. Pavelitz, and A.M. Weiner, Mol. Cell. Biol. **15**, 6246–6255 (1995).
3. R.S. Hansen et al., Cell **73**, 1403–1409 (1993).
4. C.J. Vessey, C.J. Norbury, I.D. Hickson, Prog Nucleic Acid Res Mol Biol **63**, 189–221 (1999).
5. P. Jin and S.T. Warren, Hum. Mol. Genet. **9**, 901–908 (2000).

Additional Reading

6. Clark M.S., and Wall W.J., *Chromosomes. The Complex Code*, Chapman and Hall, London, U.K., 1996.

Acetyl Coenzyme A

Acetyl coenzyme A (acetylCoA) consists of a two-carbon activated acetyl unit attached to coenzyme A in thioester linkage. AcetylCoA is central to energy generation from the degradative pathways of oxidative fuel metabolism and to a number of biosynthetic pathways that utilize the activated two-carbon acetyl unit. In aerobic cells, it is the product of all the major catabolic pathways of fuel metabolism, including b- oxidation of fatty acids, ketone body degradation, glycolysis and pyruvate oxidation, ethanol oxidation, and the oxidative degradation of many amino acids. The two-carbon acetyl unit of acetylCoA formed from these pathways can be completely oxidized to CO_2 in the tricarboxylic acid cycle (TCA cycle), thus providing aerobic cells with energy from the complete oxidation of fuels. The acetyl unit of acetylCoA is also the basic building block of fatty acids, cholesterol, and other compounds, and it can be transferred to other molecules in acetylation reactions (eg, synthesis of N-acetylated sugars).

1. Structure

The ability of acetylCoA to participate in these diverse metabolic pathways is derived from the thioester bond formed between the acyl carbon of the acetyl unit and the sulfhydryl group of coenzyme A (CoASH) (Fig. 1). Because sulfur does not share its electrons, the carbonyl carbon of the thioester bond carries a more positive partial charge than that of an oxygen ester, and electrons are pulled away from the C-H bonds of the terminal methyl group. This distribution of charge facilitates nucleophilic attack at the carbonyl carbon and enhances the ability of the terminal methyl carbon to act as an electrophilic agent in condensation reactions. The acetylCoA thioester bond is a high energy bond, with a $DG^{O'}$ for hydrolysis of –32.2 kJ/mol. Transfer of the acetyl unit to other molecules, therefore, usually occurs with the release of energy.

Figure 1. Structure of acetyl coenzyme A (acetyl CoA).

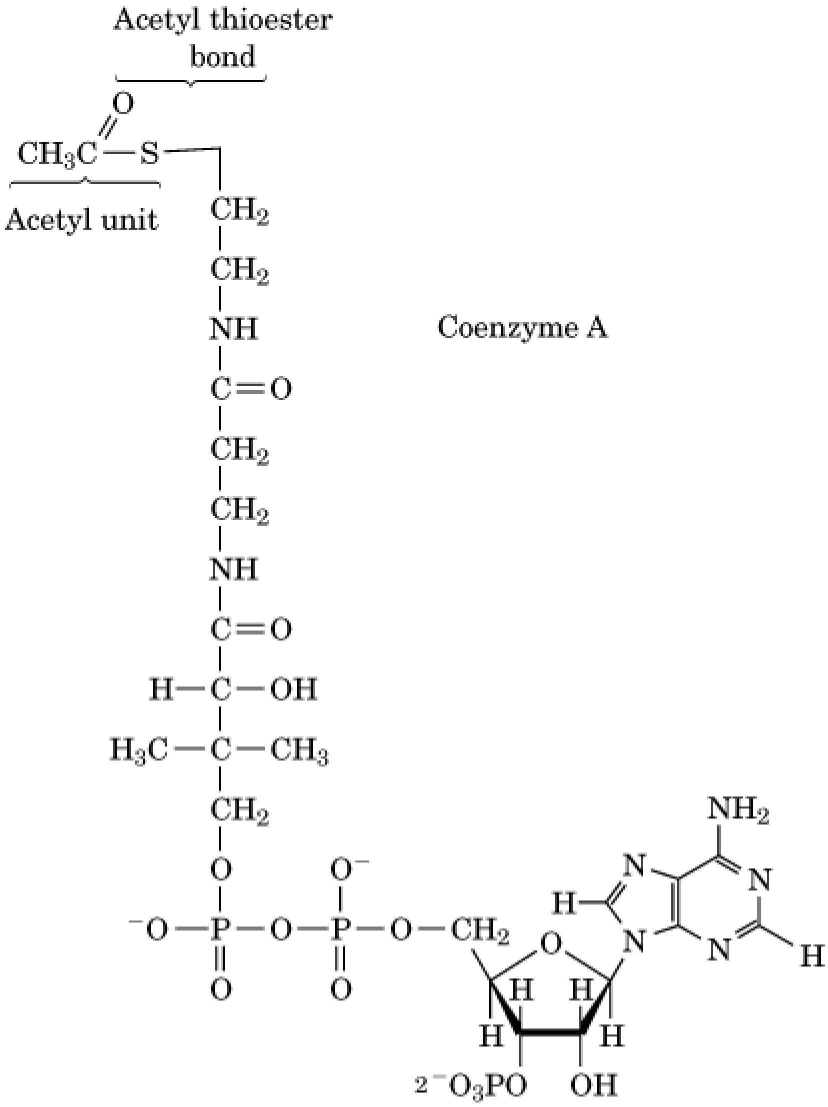

2. Formation of AcetylCoA in Oxidative Pathways

Three basic types of reactions exist in the oxidative pathways of fuel metabolism that generate acetylCoA: the activation of acetate, the thiolytic cleavage of b-ketoacyl CoAs and b-hydroxy acids, and the oxidative decarboxylation of pyruvate (Figure 2). In mammalian cells, acetate is the end product of ethanol metabolism and of threonine degradation. It is activated to acetylCoA in a single ATP- requiring step by the enzyme acetylCoA synthetase (Table 1). In an alternate route, bacterial cells can synthesize acetyl phosphate from acetate and then transfer the activated acetyl group to CoASH. Thiolytic cleavage of b-ketoacyl or b-hydroxy acylCoA derivatives to acetylCoA occurs in the pathways for oxidation of fatty acids, synthesis of the ketone bodies acetoacetate and b-hydroxybutyrate, and oxidative degradation of the amino acids isoleucine, leucine, lysine, tryptophan, phenylalanine, and tyrosine. (Most biochemistry textbooks contain general outlines of these pathways.) This type of reaction is illustrated by the b-oxidation spiral for fatty acids, in which one molecule of the C_{16}-fatty acid palmitate is converted to eight molecules of acetylCoA by enzymes that sequentially oxidize the molecule to a b-ketoacyl compound and then cleave acetylCoA from the carboxylic acid end (Table 1). The third type of reaction, the oxidative decarboxylation of pyruvate by the pyruvate dehydrogenase complex, provides the connecting link between pathways that produce pyruvate and the TCA cycle. The inhibition of the pyruvate dehydrogenase complex by acetylCoA has a regulatory role in controlling the flow of carbon into the various pathways of intermediary metabolism.

Figure 2. The role of acetyl CoA in oxidative fuel metabolism.

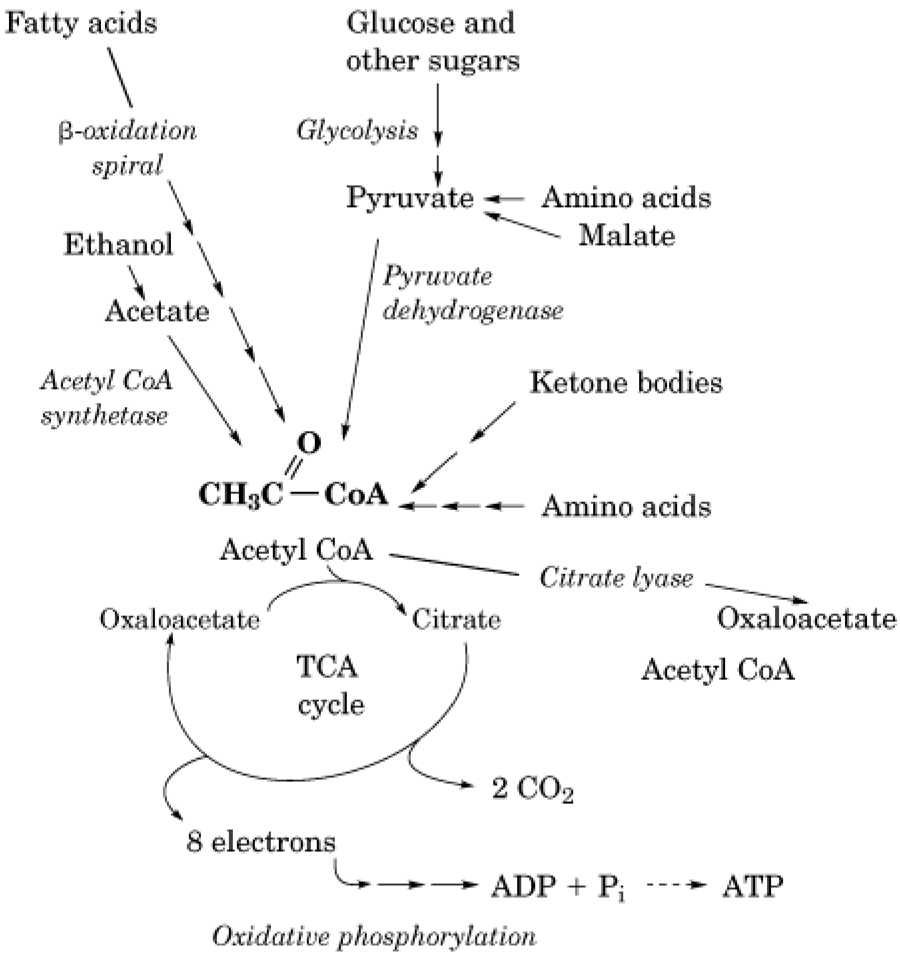

Table 1. Enzymes that Form Acetyl CoA

(1) $\text{acetate} + \text{ATP} + \text{CoASH} \xrightarrow{\textit{AcetylCoA synthetase}} \text{acetyl CoA} + \text{AMP} + \text{PP}_i$

(2) $CH_3(CH_2)_nCH_2\overset{\overset{\displaystyle O}{\|}}{C}-CH_2\overset{\overset{\displaystyle O}{\|}}{C}-SCoA \xrightarrow{\beta\textit{-Ketothiolase}} CH_3(CH_2)_nCH_2\overset{\overset{\displaystyle O}{\|}}{C}-SCoA + CH_3\overset{\overset{\displaystyle O}{\|}}{C}-SCoA$

Pyruvate dehydrogenase complex (thiamine-PP, lipoate, FAD)

(3) $\text{pyruvate} + \text{CoASH} + \text{NAD}^+ \longrightarrow \text{Acetyl CoA} + \text{NADH} + \text{H}^+ + \text{CO}_2$

(4) $\text{citrate} + \text{CoASH} + \text{ATP} \xrightarrow{\textit{Citrate lyase}} \text{acetyl CoA} + \text{oxaloacetate} + \text{ADP} + \text{P}_i$

3. Oxidation of the Acetyl Unit of AcetylCoA in the TCA Cycle

It is estimated that about two thirds of the energy requirements of aerobic cells is met by the complete oxidation of the acetyl group of acetylCoA to CO_2 in the TCA cycle (also called the citric acid cycle or the Krebs cycle.) In this cyclical sequence of reactions, acetylCoA condenses with oxaloacetate to form citrate in a reaction catalyzed by the enzyme citrate synthase. Subsequent reactions of the cycle donate electrons to the **coenzymes NAD$^+$** and **FAD** for ATP generation from oxidative phosphorylation, regenerate oxaloacetate, and release two carbons as CO_2. The net reaction of the TCA cycle is:

$$
\begin{aligned}
&\text{acetylCoA} + 3\ \text{NAD}^+ + \text{FAD} + \text{GDP} + \text{P}_i \\
&\qquad + 2\ \text{H}_2\text{O} \rightarrow \text{CoASH} + 2\ \text{CO}_2 \\
&\qquad + 3\ \text{NADH} + \text{FAD(2 H)} + 3\ \text{H}^+ + \text{GTP}
\end{aligned}
$$

Most of the pathways that produce acetylCoA in aerobic cells of **eukaryotic** organisms are located in the **mitochondrial** matrix, and most of the biosynthetic pathways that utilize acetylCoA are outside of the mitochondrion. AcetylCoA is not directly transported through the inner mitochondrial membrane but is “transferred” from the mitochondrial matrix to the **cytosol** as citrate. It is then regenerated in the cytosol by the enzyme citrate lyase.

4. AcetylCoA as a Precursor in Biosynthetic Reactions

The two-carbon acetyl unit of acetylCoA is the precursor of a number of compounds synthesized in cells. It is the basic building block of fatty acids, cholesterol, and other compounds derived from the five-carbon isoprenoid unit (Figure 3). In the synthesis of fatty acids, acetylCoA is carboxylated to malonylCoA by the **biotin**-requiring enzyme, **acetylCoA carboxylase** (Table 2). Subsequent reactions build the C_{16} fatty acid palmitate and other fatty acids from successive additions of the portion of malonyl CoA derived from acetylCoA, thereby providing the cell with the diverse fatty acids required for membrane lipids. In the synthesis of cholesterol, acetyl units from three acetylCoA molecules condense to form 3-hydroxy 3-methylglutaryl CoA (HMG CoA), which is subsequently decarboxylated and converted to the five-carbon isoprenoid unit isopentenyl pyrophosphate. This isoprenoid unit is one of the most common structural units of a number of compounds in mammalian cells, bacteria, and plants. AcetylCoA also contributes one carbon to compounds synthesized from the five-carbon intermediate a- ketoglutarate in the TCA cycle. The acetyl unit of acetylCoA can also be transferred either to hydroxyl groups of compounds to form an acetyl oxygen ester (eg, the neurotransmitter acetylcholine; see Acetylcholine Receptor) or to an amino group to form an amide in an N-acetylation reaction (eg, acetylated amino sugars such as N-acetylglucosamine).

Figure 3. The central role of acetyl CoA in biosynthetic pathways.

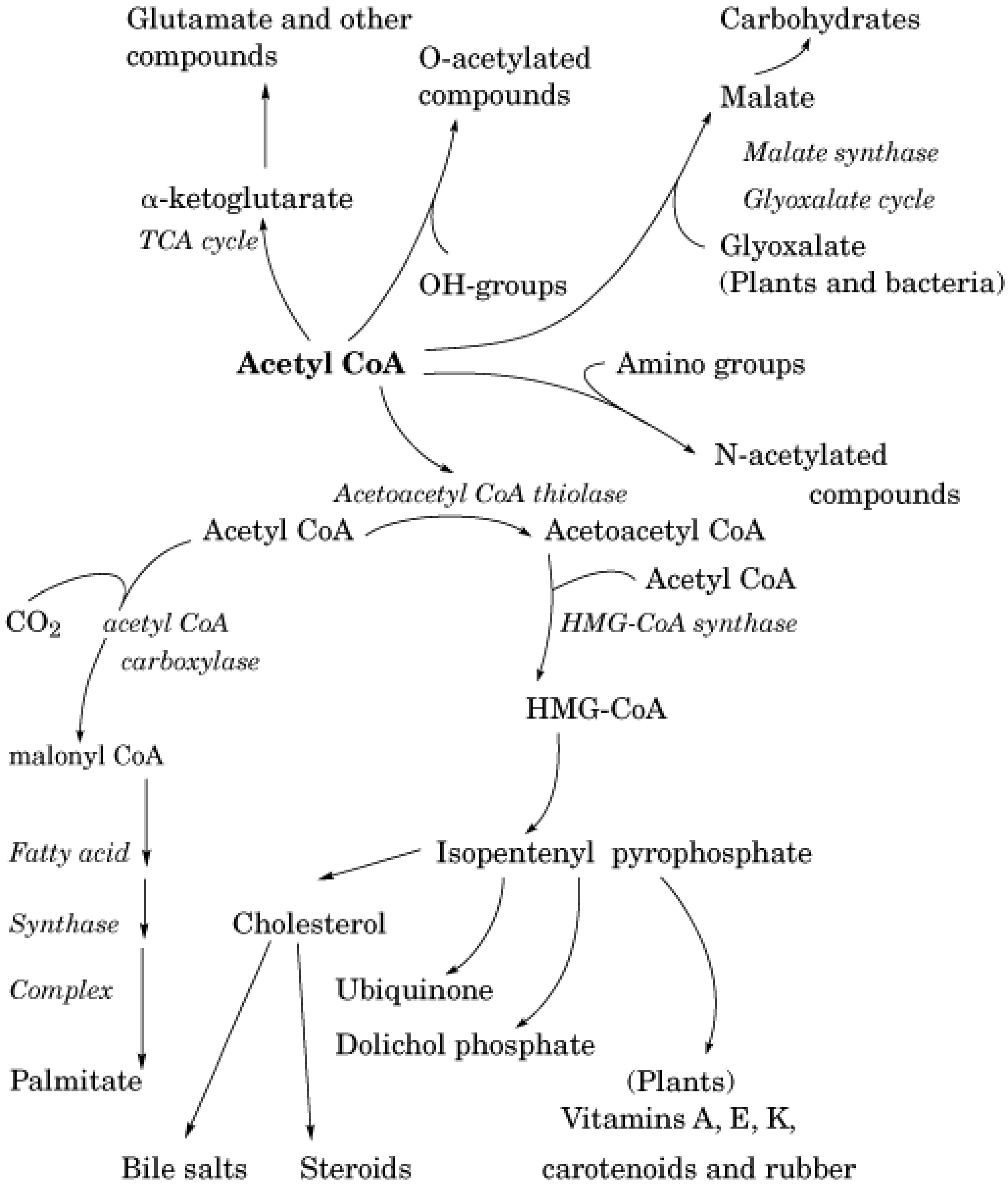

Table 2. Enzymes That Utilize AcetylCoA

$$\text{(5) acetyl CoA + oxaloacetate} \xrightarrow{\textit{Citrate synthase}} \text{citrate + CoASH}$$

$$\text{(6) acetyl CoA} + CO_2 + \text{ATP} \xrightarrow{\textit{AcetylCoA carboxylase (biotin)}} \text{malonyl CoA + ADP} + P_i$$

$$\text{(7) 2 acetyl CoA} \xleftrightarrow{\textit{AcetoacetylCoA thiolase}} \text{acetoacetyl CoA + CoASH}$$

$$\text{(8) acetyl CoA + acetoacetyl CoA} \xrightarrow{\textit{HMGCoA synthase}} \text{HMG CoA + CoASH}$$

$$\text{(9) acetyl CoA + choline} \xrightarrow{\textit{Choline acetyltransferase}} \text{acetylcholine + CoASH}$$

$$\text{(10) acetyl CoA + glyoxalate} \xrightarrow{\textit{Malate synthase}} \text{malate + CoASH}$$

In mammalian cells, acetylCoA cannot provide a net source of carbon for the synthesis of glucose or other sugars. However, plants, yeast, and bacteria contain the glyoxylate cycle, which serves as a bypass of the TCA cycle. The net result of the glyoxylate cycle is the conversion of two molecules of acetylCoA to succinate, utilizing TCA cycle enzymes plus isocitrate lyase and malate synthase. As a result, *Escherichia coli* and many other bacteria are able to convert acetate to carbohydrates and amino acids and can thus utilize and grow on acetate as their sole carbon source.

Suggestions for Further Reading

A. L. Lehninger, D. L. Nelson, and M. M. Cox (1990) *Principles of Biochemistry*, 2nd ed., Worth Publishers, New York. Although the pathways mentioned above can be found in more detail in most textbooks, this book is particularly good for outlines of major pathways found in mammals, bacteria, and plants.

D. B. Marks, A. D. Marks, and C. M. Smith (1996) *Basic Medical Biochemistry: A Clinical Approach*, Williams & Wilkins, Baltimore, MD. Provides a general outline of pathways found in humans and their relationship to human physiologic and pathologic conditions.

R. H. Bethal, D. B. Buxtion, J. G. Robertson, and M. S. Olson (1993) Regulation of the pyruvate dehydrogenase multienzyme complex. Ann. Rev. Nutr. **13**, 497–520. This article and the following one provide further information about the pyruvate dehydrogenase complex and acetylCoA carboxylase, two of the key enzymes in acetylCoA metabolism, which are highly regulated and the subject of current research.

G. M. Mabrouk, I. M. Helmy, K. G. Thampy, and S. J. Wakil (1990) Acute hormonal control of acetylCoA carboxylase: the roles of insulin, glucagon, and epinephrine. J. Biol. Chem. **265**, 6330–6338.

J. L. Goldstein, H. H. Hobbs, and M. S. Brown (1995) "Familial hypercholesterolemia". In *The Metabolic and Molecular Bases of Inherited Disease*, 7th ed. (C. R. Scriver, A. L. Beaudet, W. S. Sly, and D. Valle, eds.), McGraw Hill, New York: pp. 1981–2030. Covers certain aspects of pathway regulation for the synthesis of cholesterol from acetylCoA, which is of great interest for protection from heart disease.

Acetylcholine Receptor

Acetylcholine (ACh) is a widely distributed neurotransmitter in both the peripheral and central nervous systems (1). It is synthesized by the enzyme choline acetyltransferase within the cholinergic nerve terminal, where it is packaged into cholinergic vesicles. Arrival of an action potential at a cholinergic nerve terminal triggers quantal release of ACh by fusion of these vesicles with the presynaptic membrane and concomitant exocytosis of their contents into the synaptic cleft. The ACh released **diffuses** across the synapse to the postsynaptic membrane, where it activates its target, the acetylcholine receptor (AChR). Termination of transmission at cholinergic synapses involves rapid hydrolysis of ACh, by the enzyme acetylcholinesterase (AChE), which hydrolyzes it to choline and acetic acid (2).

The early observations of Dale (3) showed in various pharmacological preparations that ACh evoked responses similar to those evoked by either nicotine or muscarine. This provided the basis for the grouping of all AChRs into two families, nicotinic (nAChRs) and muscarinic (mAChRs). Dale's pioneering classification, based on the action of these two plant alkaloids, is still valid and used, although subtypes have been recognized and defined within each of the two families, both on the basis of specificity with respect to binding of agonists and antagonists and, in recent years, on the basis of gene cloning. Two additional plant alkaloids, *d*-tubocurarine and atropine, also provide useful tools by serving as specific antagonists of nAChRs and mAChRs, respectively (4).

nAChRs are ligand-gated **ion channels**, and their activation, by ACh or other agonists, causes a rapid change in ion permeability of the membrane in which they are embedded. mAChRs are members of the family of G-protein-coupled receptors and produce much slower responses, either excitatory or inhibitory, via their corresponding second messengers (5). Initial molecular cloning studies provided the primary structures of both nAChRs (6) and mAChRs (7), revealing that they belong to distinct families of proteins that share neither sequence identity nor a similar fold. As will be discussed in detail below, nAChRs are composed of pentamers of one or more subunits that display substantial sequence homology and, most likely, similar overall folds and transmembrane topologies. Muscarinic receptors are glycoproteins of molecular weight ~80,000 which, as already mentioned, belong to the family of G-protein-coupled receptors (8). Just as for other members of this family, hydrophobicity plots predict seven **transmembrane** sequences (8). The nAChR belongs to a larger family of ligand-gated ion channels, with which it too appears to share an overall fold, a common pattern of transmembrane sequences and other structural similarities (9, 10; see text below).

The recognition that the large electric organs of electric fish such as the electric eel, *Electrophorus electricus*, and the electric ray, *Torpedo* sp., provide a highly enriched and homogeneous preparation of cholinergic synapses (11) led to their use as an experimental model and also as the source of choice for purification and characterization of the nAChR, of AChE, and of homogeneous cholinergic synaptosomes and synaptic vesicles (2). The fact that the cholinergic synapse at the neuromuscular junction was the parallel system of choice for studying the electrophysiological characteristics of synaptic transmission (12), as well as many ultrastructural and developmental parameters (for recent reviews see Refs. 13-15), meant that many of the structural data garnered by use of the electric organ model system could be directly correlated with the functional data obtained with the neuromuscular preparation (2). Thus, the nAChR of electric organ closely resembles that of muscle (16), and the molecular forms of AChE present in electric organ tissue are homologous to those found at muscle endplates (17, 18).

The finding that injection into rabbits of purified nAChR elicited an **autoimmune** condition closely resembling the human muscle disease myasthenia gravis (19) was followed by detection of circulating antibodies to the nAChR in patients suffering from the disease. This opened up a fertile area of research in which clinical aspects were closely coupled to advances in basic research on the nAChR (20).

The cholinergic synapse has thus served as the prototypic synapse for understanding many fundamental aspects of synaptic transmission at chemical synapses. Even now, when improved electrophysiological techniques, and approaches such as Ca^{2+} imaging, allow better access to the CNS, and when genetic engineering allows expression of the receptor of choice in a system like the *Xenopus* oocyte that is amenable to user-friendly patch-clamp techniques, as well as in sufficient amounts to carry out structural characterization, the neuromuscular junction and electric organ tissue still occupy a position at the center of the stage.

1. The Nicotinic Acetylcholine Receptor

1.1. Identification and Characterization

As early as 1955, it was suggested by Nachmansohn (21) that the nAChR might be a protein in which a conformational change elicited by the neurotransmitter ACh could induce a change in permeability that would trigger the postsynaptic response, and it was in his laboratory, in the 1960s, that the first evidence was presented that the nAChR is indeed a protein. Thus, Karlin and Bartels (22), using the electric eel electroplaque preparation, showed that the response of the nAChR to carbamylcholine could be modified reversibly by reagents that either modified thiol groups or reduced disulfide bonds. Subsequently, Karlin and co-workers (23, 24) and Changeux et al. (25), also in the Nachmansohn laboratory, demonstrated *in situ* affinity labeling of the nAChR in the intact electroplaque. O'Brien and co-workers (26, 27), using specific binding of the reversible ligand muscarone and homogenates of electric organ tissue of *Torpedo*, were able to obtain a good estimate (~2 nmol/g tissue) of the number of nicotinic binding sites.

A major breakthrough in the identification of the nAChR, its localization, and its molecular characterization came about by use of (a) the neurotoxin a**-bungarotoxin** (aBgt), a 74-residue polypeptide chain purified by Lee and co-workers from the venom of the banded krait, *Bungarus multicinctus* (28), and (b) the homologous a-**neurotoxins** purified from cobra venom (29). Lee's group presented electrophysiological and pharmacological evidence that these neurotoxins acted as very high-affinity (dissociation constant in the pico-to-femtomolar range) antagonists of the nAChR (30). ^{125}I-aBgt was developed as a powerful tool for localization and quantification of the nAChR by high-resolution autoradiography (31). It was shown to be present as a dense quasi-crystalline array at the top of the folds of the postsynaptic membrane of skeletal muscle, opposite the putative ACh-release sites on the presynaptic membrane, with a density very similar to that in purified preparations of postsynaptic membranes obtained from *Torpedo* electroplax. A further step forward was taken when it was shown that binding of ^{125}I-aBgt was retained after solubilization in nonionic detergents, such as Triton X-100 and cholate, and that a single toxin-binding component, migrating at ~9 S, could be identified on sucrose gradient sedimentation velocity centrifugation (32, 33). Furthermore, the receptor so solubilized could be purified by affinity chromatography using resins to which either the a-neurotoxin (34) or a quaternary nitrogen ligand (35) had been attached. This permitted characterization of the nAChR as a multisubunit protein. Thus it was shown that it was a pentamer, of molecular weight ~250,000 (36), that contains four polypeptide subunits, a, b, g, and d, with apparent molecular weights of 39,000, 48,000, 58,000, and 64,000 and a stoichiometry of a$_2$bgd. In the electron microscope, such purified preparations displayed a rosette-like appearance (37), closely resembling similar, highly organized arrays of rosettes observed in purified postsynaptic membrane preparations (38). This led to the working hypothesis, still currently accepted, that the five subunits lie in the plane of the plasma membrane, surrounding the ion channel running through the center. A fifth polypeptide, the 43-kDa polypeptide (now known as rapsyn), which was found to be weakly associated with the pentamer (39), is believed to be involved in nAChR-clustering and anchoring to the cytoskeleton at the synapse (13). In skeletal muscle the g subunit is present in the nAChR of embryonic muscle, but is replaced by the ε subunit in adult muscle (40).

Studies on model systems were important in establishing the role of the nAChR in signal transduction at the cholinergic synapse. Thus the microsac preparation (41) was used to show that ACh could induce a permeability change in such nAChR-enriched vesicles. Furthermore, prolonged exposure to high concentrations of ACh was shown to produce a closed state, with high affinity for ACh (42), equivalent to the desensitized state first described in skeletal muscle by Katz and Thesleff

(43). The availability of purified native receptor permitted reconstitution studies into liposomes and into lipid bilayers, permitting recording of single channels induced in the presence of ACh (44, 45). The purified pentamer thus contained not only the ACh-binding site, but also the ion channel and the transducing elements involved in activation and desensitization (16).

Affinity labeling studies by Karlin and co-workers (46), using a radioactive reagent, established that the disulfide bond that was susceptible to reducing reagents, as originally demonstrated by Karlin and Bartels (22), was located on the a subunit, in proximity to the binding site for ACh and various quaternary ligands.

An important step forward was the finding of Raftery et al. (47) that the NH_2-terminal sequences of all four subunits display substantial **sequence homology**. When, not long after, the subunits were cloned (6), it was found that such homology extends throughout the whole polypeptide chain, and the receptor pentamer can be viewed as displaying pseudo-fivefold symmetry. One issue that still remains open is the arrangement of the subunits around the lumen. This has been approached primarily by electron microscopy using subunit-specific antibodies, with supplementary information coming from use of affinity labels directed toward the ACh-binding site, which label both the a subunit and an adjacent subunit (see text below). As many as 12 permutations are possible, but it is generally accepted that the two a-subunits are not adjacent to each other (48), and discussion focused on which of the b-, g-, and d-subunits is flanked on both sides by the a-subunit. Karlin et al. (49) proposed that it is the g-subunit that lies between the two a-subunits. Although Kubalek et al. (50) proposed that the b-subunit might occupy this position, the assignment of Karlin and co-workers is generally favored (for detailed discussions see Refs. 10 and 51).

Advances in cloning and expression, taken together with development of the patch-clamp technique, had a dramatic influence on research on the nAChR, just as they did on research on other receptors and on ion channels. In the case of the nAChR, however, the availability of large amounts of highly purified receptor from *Torpedo* electric organ resulted in fruitful synergy between these new techniques and the techniques of protein chemistry and structural biology.

In general, research has proceeded on two fronts, one concerned with the structure of the ACh-binding site and the other with that of the ion channel, with the eventual objective of understanding the physical mechanism by which ligand-binding causes channel opening. In the following, the overall topology of the receptor and of the individual subunits will first be reviewed briefly. The current status of our knowledge of the ACh-binding site, and then of the ion channel, will be summarized, followed by a discussion of the recent structural work from the laboratory of Unwin, which is beginning to give us a first glimpse of how the receptor may be functioning. For a number of recent reviews that cover these issues in more detail than is possible here, see Refs. 9, 10, 16, and 52, as well as the recent paper of Unwin (53), which summarizes the current status of the structural work.

1.2. Conformation and Topology

Analysis of the sequences of the four subunits, obtained on the basis of their complementary DNA sequences, showed that they shared a very similar topology: A long extracellular NH_2-terminal domain is followed by three putative transmembrane a-helices, identified on the basis of hydrophobicity, M1–M3, by a cytoplasmic loop containing ~100–150 residues, and finally, by a fourth transmembrane helix, M4, so that the COOH-terminus is believed to be on the extracellular side of the postsynaptic membrane (54). Other ligand-gated ion channels that belong to the same superfamily, including receptors for g-aminobutyric acid, glycine, and serotonin, display a similar topology (9, 10). A number of consensus sites for N-Glycosylation are present in the extracellular domains, giving rise to a sugar content of ~7% (for literature see Ref. 55); and a number of consensus sites for **phosphorylation**, present on the cytoplasmic loops, presumably fulfill regulatory functions (56).

Photoaffinity labeling, using lipid-soluble probes, has been used to assign the arrangement of the transmembrane sequences in relation to the lipid bilayer and the putative central ion channel (57-59). From such studies, it has been concluded that the M4 sequence, which is also the least conserved, is the most exposed to the lipid environment, with the M1 and M3 sequences displaying more limited exposure to the lipid environment, and M2 facing the lumen of the ion channel. This assignment of M2 as making the principal contribution to the lining of the ion channel is also supported by labeling by channel blockers and by use of the SCAM technique (see text below).

Various spectroscopic techniques show that the nAChR contains substantial amounts of both a-helices and b-sheets (for literature see Ref. 10). In particular, Naumann et al. (60), using Fourier transform infrared (FTIR) spectroscopy on native receptor-rich membranes, have shown a predominance of b structure, 36 to 43%, and an a-helical content of 32 to 33%. Of particular interest are the putative conformations of the membrane-spanning sequences. Görne-Tschelnokow et al. (61) attacked this problem directly, by performing FTIR spectroscopy on membrane preparations from which the extramembrane domains had been shaved by **proteolysis**. Their data suggested **a** beta-sheet content of ~40% for the transmembrane sequences. Modeling studies also suggested a substantial b-sheet component (62). Various labeling studies, which attempt to correlate the degree of labeling of residues with orientation toward either the ion-channel lumen or the lipid bilayer, and thus with either an a-helical or a b-strand pitch, yield complex results (see, for example, Refs. 9, 10, 59, and 63); and precise assignments will, most likely, have to await a high-resolution 3D protein structure.

1.3. ACh-Binding Site

Identification of the residues comprising the ACh-binding site of the nAChR was approached by affinity labeling. Karlin and co-workers used the same radioactive affinity label that they had used to label the a subunit selectively, a quaternary derivative of maleimide, to identify the residues labeled. Because they had demonstrated that labeling occurred subsequent to reduction of the receptor, it was not surprising that they found that the residues labeled were the adjacent cysteines, Cys192 and Cys193, which apparently form an intrachain disulfide bond in the native nAChR, and which are present only in the a-subunit (64). As predicted, these residues are localized in the sequence that had been assigned to the extracellular domain, and would thus be the natural candidate for the ACh-binding site. The importance of this region for agonist and antagonist binding was confirmed by the observation that short synthetic peptides containing Cys192 and Cys193 (eg, from residue 185 to 196) displayed specific binding to aBgt, albeit with much lower affinity than the native receptor (65). Moreover, the a-subunits of the nAChR of both snakes and of the mongoose, which are resistant to aBgt, display mutations in this region that can provide a structural basis for resistance (66).

Changeux and co-workers conducted an extensive study of the residues labeled by the tertiary photoaffinity label, DDF (67). In addition to Cys192 and Cys193, this probe labeled primarily aromatic residues, including Tyr93, Trp149, Tyr190 and Tyr198, all, again, in the putative cytoplasmic domain. Use of other labeling agents, by other laboratories, broadly confirmed these assignments and identified additional aromatic residues (for literature see Ref. 68). Thus the ACh-binding pocket of the nAChR can be viewed as an “aromatic basket” (16) in which the quaternary group of ACh interacts with these aromatics via the p electron–cation interactions (69) which X-ray crystallographic studies have shown to play a prominent role within the “aromatic gorge” of AChE (70, 71).

Although the studies discussed above indicate a prominent role for the a-subunit in binding of both agonists and antagonists, numerous labeling studies have revealed contributions of adjacent subunits to ligand-binding. These studies have been critically reviewed by Hucho et al. (10). Taken together, the data clearly indicate that the two ACh-binding sites are at the interfaces between the two a-subunits and the g- and d-subunits. This, in turn, implies structural difference between the two sites that can serve to explain nonequivalence of the two binding sites in terms of affinity for both a-neurotoxins (72) and antagonists (73).

1.4. Ion Channel

Pharmacological studies on the nAChR revealed a number of noncompetitive antagonists, both natural and synthetic, that blocked the change in permeability elicited by ACh without inhibiting the binding of ACh itself. It was, therefore, suggested that at least some of these compounds act by entering the ion channel and sterically blocking ion movement through it (for literature see Refs. 9, 10, and 16). Based on the currently held view that the ion channel is the hole in the rosette seen in the electron microscope, such “channel blockers” are believed to exert their action by plugging this hole. Some channel blockers, such as chlorpromazine (74) and trimethylphosphonium (75), bind irreversibly upon UV irradiation; and their labeled derivatives can, accordingly, be used to identify putative elements of the channel lining. Rapid-mixing studies, using nAChR-enriched microsacs, showed that exposure to ACh leads, initially, to greatly increased labeling, followed by diminished incorporation which is consistent with desensitization as measured by ion flux measurements (76). Such labeling studies showed dominant labeling of the residues in the M2 transmembrane sequences of all four subunits, suggesting that they make the principal contribution to the lining of the lumen of the ion channel, in the open state of the channel. One such noncompetitive channel blocker, quinacrine azide, was, however, shown to label amino acid residues in M1 (77).

In parallel to such labeling studies on the purified receptor, use of site-directed mutagenesis, combined with expression in *Xenopus* oocytes (78) and use of the patch-clamp technique, permitted assessment of the contributions of individual amino acid residues to the conductance properties of the ion channel, an approach pioneered by the joint efforts of the Numa and Sakmann laboratories (see, for example, Refs. 79 and 80).

A third approach, developed more recently, is the substituted-cysteine-accessibility method, abbreviated as SCAM (81), which combines site-directed mutagenesis with chemical modification, so as to identify the amino acid residues lining the ion channel and their involvement in function. Thus, residues believed to line the ion channel (primarily from the M2 transmembrane sequence, but also from M1) are replaced one-by-one by cysteine residues, using site-directed mutagenesis, and expressed in *Xenopus* oocytes. The reactivity of their thiol groups with thiol reagents bearing negative or positive charges is examined *in situ*, both in the presence and absence of ACh, thus permitting assessment of their accessibility in both the closed and open states of the channel. Furthermore, these sulfhydryl reagents can be added both intra- and extracellularly, yielding information concerning accessibility of channel-lining residues from both surfaces (63).

These various experimental approaches have led to the identification of residues within the M2 sequences of all five subunits that determine the conductance and selectivity of the nAChR channel. In particular, using nAChR mutants expressed in *Xenopus* oocytes, three rings of negatively charged residues which may be referred to as the extracellular (or outer), the intermediate, and the cytoplasmic (or inner) ring, have been shown to play important roles in determining channel conductance (80). A ring of polar (serine and threonine) residues, named the central ring, is located above the intermediate ring, forming a constriction that may serve as part of the selectivity filter (82, 83). The bulk of the transmembrane sequence of M2 lies between this central ring and the outer ring.

A more detailed topographical picture has been obtained by the SCAM technique, as summarized by Karlin and Akabas (9). Thus, broadly speaking, the residues in M2 of the a-subunit can be fitted to an Amphipathic helix so that, with one exception, all the residues on one face of the helix are labeled in the SCAM protocol; some are equally accessible in the presence and absence of ACh, some are more accessible in its presence, and some are more accessible in its absence. Furthermore, certain residues at the extracellular end of the M1 helix of the a-subunit are also labeled. The pattern of labeling of M2 in the absence of ACh is consistent with an a-helical conformation, except for a short stretch in the middle (aLeu250 to aSer252), while in the presence of ACh it is consistent with an uninterrupted a-helix. The pattern of labeling of M1 cannot be ascribed to a specific conformational motif, although it too is changed in the presence of ACh. Karlin and Akabas (9) hypothesize that a movement of M1 and M2 relative to each other, with a concomitant change in **secondary structure**, may flip open the gate of the channel. More recently, the SCAM technique has also located the gate, using comparative studies in which labeling was carried out from either the extracellular or cytoplasmic sides (63). In the absence of ACh—that is, in the closed state of the channel—there is a barrier to the sulfhydryl agents, when added to either side, reacting with residues aGly240 and to aThr244. ACh binding removes this barrier, which serves as an activation gate. Residues aGly240, aGlu241, aLys242, and aThr244 line a narrow part of the channel in which this gate is located. It should be noted that the second of these residues, aGlu241, belongs to the inner anionic ring, and aThr244 to the central ring, as defined above (80, 82).

1.5. Structural Studies

Despite the extensive studies performed on the characterization of the ACh-binding site and of the ion channel, the question with which all structural and functional studies on the nAChR are ultimately concerned is how binding of ACh is transduced into a permeability change in the ion channel. This is ultimately a problem best addressed by a structural biology approach. In spite of attempts from many laboratories to obtain nAChR crystals that would diffract X-rays (for a published example, see Ref. 84), this has not yet been achieved. Our current structural knowledge is, therefore, derived from the work of Unwin (for a recent summary see Ref. 53). As mentioned above, the postsynaptic membrane of *Torpedo* electric organ contains densely packed, partially crystalline arrays of nAChR (38). When isolated, such membranes have a natural propensity to recrystallize in tubular form (85, 86). Since the early 1980s, Unwin has been using electron microscopy to probe the structure of the nAChR from *Torpedo marmorata* and is now able to compare the receptor in its open and closed states at 9 Å resolution (53). The receptor is revealed as an elongated structure, ~125 Å long; the extracellular portion of each subunit extends ~60 Å above the membrane surface, and the intracellular portions extend ~20 Å from the cytoplasmic surface. A density underlying each receptor most likely represents the cytoskeletal protein rapsyn (see text above), normally present in 1:1 stoichiometry with the receptor (87). A view from above shows the five subunits arranged around a fivefold axis of pseudosymmetry, as predicted. The opening of the putative ion channel in the center is about 20 Å at its entrance, narrowing sharply at the membrane surface. At the current resolution, it is possible to begin to glimpse some elements of secondary structure. Thus in each subunit, in a region about 30 Å away from the extracellular surface, a group of three short rods can be detected, presumably a-helices. The two subunits identified as a-subunits (50) contain cavities shaped by these rods, which may correspond to the ACh-binding pockets. The narrowest portion, corresponding to the pore, appears to be shaped by five bent a-helical rods, each contributed by one of the subunits (Fig. 1, left). The bends in the rods, near the middle of the membrane, are the parts closest to the axis of the pore and may represent the gate. In order to visualize the open state of the nAChR, Berriman and Unwin (88) devised a rapid-freezing device, designed to trap the open state, after application of ACh, by preventing the transition to the desensitized state. Comparison of the ACh-activated receptor with the nonactivated form revealed only slight changes (Fig. 1, right). Concerted twisting motions appeared to occur within the rods lining the putative ACh-binding pockets, which were consistent with the requirement that two ACh molecules, binding simultaneously to both a-subunits, are required to open the channel. These localized disturbances were associated with small rotations extending along the axis of all the subunits, and with a switching of the helices within the pore from the bent shape seen in the nonactivated receptor to a tapered, more open configuration. If it is assumed that the threonine side chains of the central ring, which are believed to serve as the pore (see text above, along with Ref. 83) face into the pore, a minimum diameter of 10 Å can be estimated, comparable to the diameter obtained by use of various organic cations (89). Such a concerted rotation of the transmembrane sequences surrounding the lumen of the putative ion channel is consistent with the data accumulated by the various studies using site-directed mutagenesis and labeling, some of which were discussed above (see, in particular, Refs. 59 and 63).

Figure 1. Simplified diagram of the nAChR in its closed (left) and open (right) states, as suggested by the structural results. An ACh molecule first enters a binding site in one of the a-subunits (rectangle), but significant displacements are blocked by the neighboring subunit, lying between the two a-subunits. Interaction of a second ACh with the other

site then attempts to draw the neighboring subunit out of the way. A concerted localized displacement thereby takes place, initiating small rotations of the subunits along the shaft to the membrane. The rotations disrupt the gate by disrupting the association of a-helices around the pore in the closed state (left), switching over to an alternate configuration in which a widened polar pathway for ion movement is created. (From Ref. 53, with permission.)

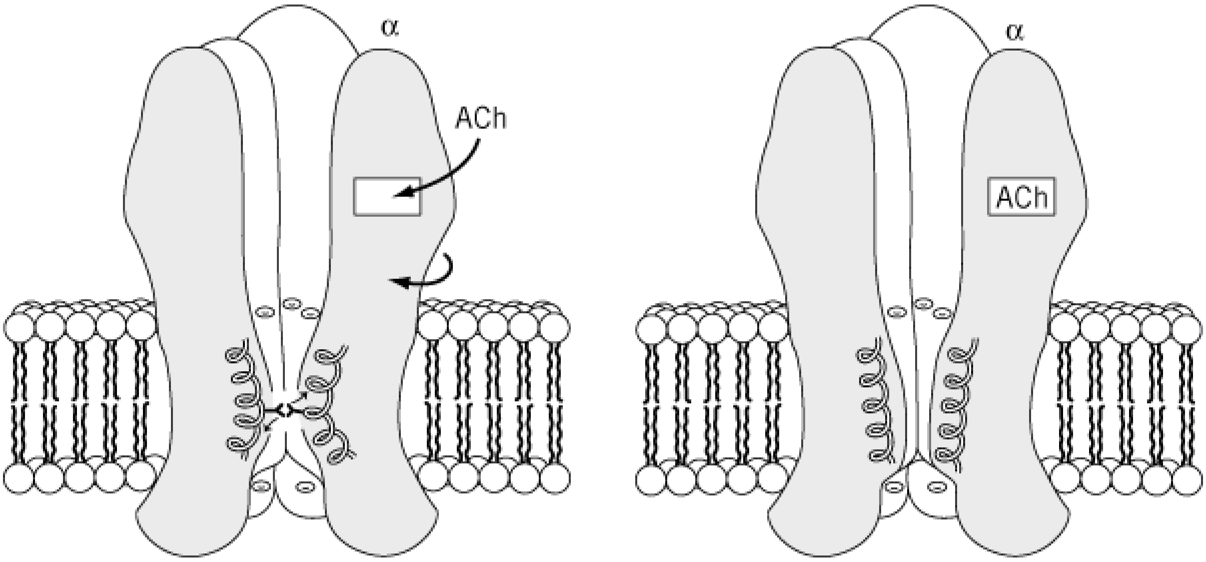

Obviously, when higher-resolution images become available, a more detailed mechanistic description will be feasible, but the conceptual stage appears to have been set.

1.6. Neuronal Nicotinic Receptors

Already in the late 1970s, it was proposed, on the basis of ^{125}I-aBgt-binding studies, that nAChRs were present not only in skeletal muscle, but also in the central nervous system (90, 91). These studies were not the subject of widespread attention, primarily due to the fact that functional correlates were lacking. When, in the mid-1980s, cloning techniques revealed the presence in brain of an nAChR gene family homologous to, but clearly distinct from, those of electric organ and muscle, and widely distributed in different brain areas (92, 93), it became obvious that nAChRs, like muscarinic receptors, must have important functions in brain. For many years, however, the lack of specific agonists and antagonists for a given neuronal nAChR subtype severely hampered the identification of functional nAChRs in various brain areas. These difficulties were further aggravated by the unusually fast kinetics of inactivation of some nAChR subtypes, compared to their peripheral counterpart (for literature, see Ref. 94). Development of techniques permitting rapid application and removal of agonists was necessary to overcome this limitation (see, for example, Refs. 95 and 96).

The cloning approach revealed the existence of a large number of AChR receptor subunits in the brain. In contrast to muscle and electric organ, however, these appear to fall into only two categories, a and b. By now nine a-subunits (97) and nine b-subunits have been described in vertebrate brain (98), and multiple nAChR subunits have also been described in invertebrates such as *Caenorhabditis elegans* (99) and *Drosophila* (100).

As discussed by Sargent (98), the various subtypes of subunits are expressed differentially in one brain region or another. The most recently discovered a9-subunit, for example, has a pattern of expression restricted to cochlear hair cells (97). The pharmacology of neuronal nicotinic receptors in relation to such topics as nicotine addiction (101) and Alzheimer's disease (102) are currently topics of intensive investigation; so too is their involvement in brain plasticity (103) and in behavior, learning, and memory (104, 105). A recent development is the observation that choline serves as a selective agonist for a7 nAChRs in rat hippocampal neurons (106), in line with earlier reports for a7 ectopically expressed in oocytes (107, 108). Because a7 belongs to what appears to be the evolutionarily oldest group of nAChrs (109), it is feasible that choline, rather than ACh, was the primeval transmitter for cholinergic receptors.

Neuronal nAChRs have not yet been purified or expressed in large amounts. Thus, essentially all our knowledge of their functional properties comes from studies in which subunits were expressed singly or in combination, most frequently by injection into *Xenopus* oocytes. Such expression studies were augmented, as for *Torpedo* and muscle nAChRs, by site-directed mutagenesis. These studies have been reviewed in detail by Sargent (98), and only a few points will be discussed here briefly.

Presence of an a-subunit is necessary to obtain a functional receptor; and in the case of the a7-subunit, injection of it alone into oocytes is sufficient for it to form functional oligomers (110). Changeux, Bertrand, and co-workers took advantage of this experimental system to perform expression, combined with site-directed mutagenesis, which showed that the ligand-gated ion channel produced by the a7-subunit closely resembles that of the pentameric muscle and *Torpedo* receptors (see, for example, Ref. 111 and the review in Ref. 16). Direct experimental evidence for a pentameric stoichiometry was provided for the chick nAChR produced in oocytes by expression of the a4 and b2 subunits with radioactive label incorporated into them. The stoichiometry of the subunits in the purified receptor was consistent with an $a4_2b2_3$ pentamer (112). This does not mean, however, that expression of the mRNAs for any mixture of a-subunits, with or without a b-subunit, will produce a functional oligomer. Thus far, only a7 has been shown to produce functional oligomers containing only a subunits. Furthermore, a recent study of Yu and Role (113) has shown that a5 can participate in the function of an ACh-gated ion channel only if it is coexpressed with another a- and a b-subunit. The structural basis for such restrictions with respect to assembly and/or function are, at this stage, unknown. Patrick and co-workers (114) observed, however, that a Cyclophilin is required for expression of functional homo-oligomeric, but not hetero-oligomeric, nAChRs. They raise the possibility that the a-subunits in the homo-pentamer may not assume identical folds. Cyclophilins may thus play a critical role in the maturation of such homo-oligomers, acting directly or indirectly as prolyl *cis/trans* Isomerases or as **molecular chaperones** (115).

Bibliography

1. P. Taylor (1990) In *The Pharmacological Basis of Therapeutics* (A. G. Gilman, T. W. Rall, A. S. Nies, and P. Taylor, eds.), 8th Edition, Pergamon Press, New York, pp. 122–130.
2. V. P. Whittaker (1992) *The Cholinergic Neuron and its Target: The Electromotor Innervation of the Electric Ray Torpedo as a Model*, Birkhäuser, Boston.
3. H. H. Dale (1914) J. Pharmacol. Exp. Ther. **6**, 146–190.
4. R. J. Lefkowitz, B. B. Hoffman, and P. Taylor (1990) In *The Pharmacological Basis of Therapeutics* (A. G. Gilman, T. W. Rall, A. S. Nies, and P. Taylor, eds.), 8th ed., Pergamon Press, New York, pp. 84–121.
5. D. A. Brown et al. (1997) Life Sci. **60**, 1137–1144.
6. S. Numa et al. (1983) Cold Spring Harbor Symp. Quant. Biol. **48**, 57–69.
7. T. Kubo et al. (1986) Nature **323**, 411–416.
8. J. Wess et al. (1997) Life Sci. **60**, 1007–1014.
9. A. Karlin and M. H. Akabas (1995) Neuron **15**, 1231–1244.
10. F. Hucho, V. I. Tsetlin, and J. Machold (1996) Eur. J. Biochem. **239**, 539–557.
11. D. Nachmansohn (1959) *Chemical and Molecular Basis of Nerve Activity*, Academic Press, New York.
12. B. Katz (1966) *Nerve, Muscle and Synapse*, McGraw-Hill, New York.
13. S. C. Froehner (1993) Annu. Rev. Neurosci. **16**, 347–368.
14. Z.-Z. Wang et al. (1996) Cold Spring Harbor Symp. Quant. Biol. **61**, 363–371.
15. J. R. Sanes (1997) Curr. Opin. Neurobiol. **7**, 93–100.
16. J.-P. Changeux (1995) Biochem. Soc. Trans. **23**, 195–205.

17. I. Silman and A. H. Futerman (1987) Eur. J. Biochem. **170**, 11–22.
18. J. Massoulié et al. (1993) Prog. Neurobiol. **41**, 31–91.
19. J. Patrick and J. Lindstrom (1973) Science **180**, 871–872.
20. A. Vincent et al. (1995) J. Physiol. Paris **89**, 129–136.
21. D. Nachmansohn (1955) Harvey Lect. **39**, 57–99.
22. A. Karlin and E. Bartels (1966) Biochim. Biophys. Acta **126**, 525–535.
23. A. Karlin and M. Winnik (1968) Proc. Natl. Acad. Sci. USA **60**, 668–674.
24. I. Silman and A. Karlin (1968) Science **164**, 1420–1421.
25. J.-P. Changeux, T. Podleski, and L. Wofsy (1967) Proc. Natl. Acad. Sci. USA **58**, 2063–2070.
26. R. D. O''Brien and L. P. Gilmour (1969) Proc. Natl. Acad. Sci. USA **63**, 496–503.
27. R. D. O''Brien, L. P. Gilmour, and M. E. Eldefrawi (1970) Proc. Natl. Acad. Sci. USA **65**, 438–445.
28. C. C. Chang and C. Y. Lee (1963) Arch. Int. Pharmacodyn. **144**, 241–257.
29. C. C. Chang and C. Y. Lee (1966) Brit. J. Pharmacol. **28**, 172–181.
30. C. Y. Lee (1972) Annu. Rev. Pharmacol. **12**, 265–286.
31. H. C. Fertuck and M. M. Salpeter (1976) J. Cell Biol. **69**, 144–158.
32. J.-P. Changeux, M. Kasai, and C. Y. Lee (1970) Proc. Natl. Acad. Sci. USA **67**, 1241–1247.
33. R. Miledi, P. Molinoff, and L. T. Potter (1971) Nature **229**, 554–557.
34. E. Karlsson, E. Heilbronn, and L. Widlund (1972) FEBS Lett. **28**, 107–111.
35. A. Karlin and D. A. Cowburn (1973) Proc. Natl. Acad. Sci. USA **70**, 3636–3640.
36. J. A. Reynolds and A. Karlin (1978) Biochemistry **17**, 2035–2038.
37. J. Cartaud et al. (1973) FEBS Lett. **33**, 109–113.
38. J. E. Heuser and S. R. Salpeter (1979) J. Cell Biol. **82**, 150–173.
39. R. R. Neubig, E. K. Krodel, N. D. Boyd, and J. B. Cohen (1979) Proc. Natl. Acad. Sci. USA **76**, 690–694.
40. M. Mishina et al. (1986) Nature **321**, 406–411.
41. M. Kasai and J. P. Changeux (1971) J. Membr. Biol. **6**, 1–80.
42. M. Weber, T. David-Pfeuty, and J. P. Changeux (1975) Proc. Natl. Acad. Sci. USA **72**, 3443–3447.
43. B. Katz and S. Thesleff (1957) J. Physiol. **138**, 63–80.
44. N. Nelson, R. Anholt, J. Lindstrom, and M. Montal (1980) Proc. Natl. Acad. Sci. USA **77**, 3057–3061.
45. G. Boheim et al. (1981) Proc. Natl. Acad. Sci. USA **78**, 3586–3590.
46. C. L. Weill, M. G. McNamee, and A. Karlin (1974) Biochem. Biophys. Res. Commun. **61**, 997–1003.
47. M. A. Raftery, M. W. Hunkapiller, C. D. Strader, and L. E. Hood (1980) Science **208**, 1454–1456.
48. D. S. Wise, J. Wall, and A. Karlin (1981) J. Biol. Chem. **256**, 12624–12627.
49. A. Karlin et al. (1983) J. Biol. Chem. **258**, 6678–6681.
50. E. Kubalek, S. Ralston, J. Lindstrom, and N. Unwin (1987) J. Cell Biol. **105**, 9–18.
51. P. C. Kearney et al. (1996) Neuron **17**, 1221–1229.
52. H. A. Lester (1997) Harvey Lect., **91**, 79–98.
53. N. Unwin (1998) J. Struct. Biol. **121**, 181–190.
54. J.-L. Popot and J.-P. Changeux (1984) Physiol. Rev. **64**, 1162–1239.
55. H. Shoji et al. (1992) Eur. J. Biochem. **207**, 631–641.
56. R. L. Huganir and P. Greengard (1987) Trends Pharmacol. Sci. **8**, 472–477.

57. J. Giraudat, C. Montecucco, R. Bisson, and J.-P. Changeux (1985) Biochemistry **24**, 3121–3127.
58. M. P. Blanton and J. B. Cohen (1994) Biochemistry **33**, 2859–2872.
59. M. P. Blanton et al. (1998) J. Biol. Chem. **273**, 8659–8668.
60. D. Naumann, C. Schultz, U. Görne-Tschelnokow, and F. Hucho (1993) Biochemistry **32**, 3162–3168.
61. U. Görne-Tschelnokow et al. (1994) EMBO J. **13**, 338–341.
62. M. O. Ortells and G. G. Lunt (1996) Prot. Eng. **9**, 51–59.
63. G. G. Wilson and A. Karlin (1998) Neuron **20**, 1269–1281.
64. P. N. Kao et al. (1984) J. Biol. Chem. **259**, 11662–11665.
65. D. Neumann, D. Barchan, M. Fridkin, and S. Fuchs (1986) Proc. Natl. Acad. Sci. USA **83**, 9250–9253.
66. D. Barchan, M. Ovadia, E. Kochva, and S. Fuchs (1995) Biochemistry **34**, 9172–9176.
67. J. Langenbuch-Cachat et al. (1988) Biochemistry **27**, 2337–2345.
68. J.-P. Changeux, J.-L. Galzi, A. Devillers-Thiéry, and D. Bertrand (1992) Q. Rev. Biophys. **25**, 395–432.
69. D. A. Dougherty and D. A. Stauffer (1990) Science **250**, 1558–1560.
70. M. Harel et al. (1993) Proc. Natl. Acad. Sci. USA **90**, 9031–9035.
71. M. Harel et al. (1996) J. Am. Chem. Soc. **118**, 2340–2346.
72. A. Maelicke and E. Reich (1976) Cold Spring Harbor Symp. Quant. Biol. **40**, 231–235.
73. S. E. Pedersen and J. B. Cohen (1990) Proc. Natl. Acad. Sci. USA **87**, 2785–2789.
74. T. Heidmann, R. E. Oswald, and J. P. Changeux (1983) Biochemistry **22**, 3112–3127.
75. F. Hucho, W. Oberthür, and F. Lottspeich (1986) FEBS Lett. **205**, 137–142.
76. T. Heidmann, J. Bernhardt, E. Neumann, and J. P. Changeux (1983b) Biochemistry **22**, 5452–5459.
77. M. DiPaola, P. N. Kao, and A. Karlin (1990) J. Biol. Chem. **265**, 11017–11029.
78. E. A. Barnard, R. Miledi, and K. Sumikawa (1982) Proc. R. Soc. Lond. B **215**, 241–246.
79. K. Imoto et al. (1986) Nature **324**, 670–674.
80. K. Imoto et al. (1988) Nature **335**, 645–648.
81. M. H. Akabas, D. A. Stauffer, M. Xu, and A. Karlin (1992) Science **258**, 307–310.
82. K. Imoto et al. (1991) FEBS Lett. **289**, 193–200.
83. A. Villarroel, S. Herlitze, M. Koenen, and B. Sakmann (1991) Proc. R. Soc. B **243**, 69–74.
84. S. Hertling-Jaweed et al. (1988) FEBS Lett. **241**, 29–32.
85. J. Kistler and R. M. Stroud (1981) Proc. Natl. Acad. Sci. USA **78**, 3678–3682.
86. A. Brisson and P. N. T. Unwin (1984) J. Cell Biol. **99**, 1202–1211.
87. W. J. LaRochelle and S. C. Froehner (1986) J. Biol. Chem. **261**, 5270–5274.
88. J. A. Berriman and N. Unwin (1994) Ultramicroscopy **56**, 241–252.
89. B. N. Cohen, C. Labarca, N. Davidson, and H. A. Lester (1992) J. Gen. Physiol. **100**, 373–400.
90. Z. Vogel and M. Nirenberg (1976) Proc. Natl. Acad. Sci. USA **73**, 1806–1810.
91. J. Patrick and W. B. Stallcup (1977) Proc. Natl. Acad. Sci. USA **74**, 4689–4692.
92. D. Goldman et al. (1987) Cell **48**, 965–973.
93. S. Heinemann et al. (1990) Prog. Brain Res. **86**, 195–203.
94. E. X. Albuquerque et al. (1997) J. Pharmacol. Exp. Ther. **280**, 1117–1136.
95. N. G. Castro and E. X. Albuquerque (1993) Neurosci. Lett. **164**, 137–140.
96. Z.-W. Zhang, S. Vijarayaghavan, and D. K. Berg (1994) Neuron **12**, 167–177.

97. A. B. Elgoyhen et al. (1994) Cell **79**, 705–715.
98. P. B. Sargent (1993) Annu. Rev. Neurosci. **16**, 403–443.
99. J. T. Fleming et al. (1997) J. Neurosci. **17**, 5843–5857.
100. E. D. Gundelfinger (1992) Trends Neurosci. **15**, 206–211.
101. J. A. Dani and S. Heinemann (1996) Neuron **16**, 905–908.
102. H. Schröder et al. (1991) Neurobiol. Aging **12**, 259–262.
103. J.-P. Changeux et al. (1996) Cold Spring Harbor Symp. Quant. Biol. **61**, 343–362.
104. N. Le Novère, M. Zoli, and J. P. Changeux (1996) Eur. J. Neurosci. **8**, 2428–2439.
105. E. D. Levin et al. (1997) Brain Res. Bull. **43**, 295–304.
106. M. Alkondon et al. (1997) Eur. J. Neurosci. **9**, 2734–2742.
107. A. Mandelzys, P. De Koninck, and E. Cooper (1995) J. Neurophysiol. **74**, 1212–1221.
108. R. L. Papke, M. Bencherif, and P. Lippiello (1996) Neurosci. Lett. **213**, 201–204.
109. N. Le Novère and J. P. Changeux (1995) J. Mol. Evol. **40**, 155–172.
110. S. Couturier et al. (1990) Neuron **5**, 847–856.
111. D. Bertrand et al. (1993) Proc. Natl. Acad. Sci. USA **90**, 6971–6975.
112. R. Anand et al. (1991) J. Biol. Chem. **266**, 11192–11198.
113. C. R. Yu and L. W. Role (1998) J. Physiol. **509**, 667–681.
114. S. A. Helekar, D. Char, S. Neff, and J. Patrick (1994) Neuron **12**, 179–189.
115. S. A. Helekar and J. Patrick (1997) Proc. Natl. Acad. Sci. USA **94**, 5432–5437.

Suggestions for Further Reading

116. E. X. Albuquerque et al. (1997) Properties of neuronal acetylcholine receptors: pharmacological characterization and modulation of synaptic function. J. Pharmacol Exp. Ther. **280**, 1117–1136.
117. J.-P. Changeux (1995) The acetylcholine receptor: a model for allosteric membrane proteins. Biochem. Soc. Trans. **123**, 195–205.
118. F. Hucho, V. I. Tsetlin, and J. Machold (1996) The emerging three-dimensional structure of a receptor: the nicotinic acetylcholine receptor. Eur. J. Biochem. **239**, 539–557.
119. A. Karlin and M. H. Akabas (1995) Towards a structural basis for the function of nicotinic acetylcholine receptors and their cousins. Neuron **15**, 1231–1244.
120. P. B. Sargent (1993) The diversity of neuronal nicotinic acetylcholine receptors. Ann. Rev. Neurosci. **16**, 403–443.
121. N. Unwin (1998) The nicotinic acetylcholine receptor of the Torpedo electric ray. J. Struct. Biol. **121**, 181–190.
122. V. P. Whittaker (1992) "The cholinergic neuron and its target: the electromotor innervation of the electric ray *Torpedo* as a model", Birkhäuser, Boston.

Achaete–Scute Complex

A central theme in developmental biology is to understand how the mechanisms that specify particular cell types integrate with those that govern where and when cell type-specific structures form during animal development. Over the better part of the past century, the development of the *Drosophila* nervous system has served as a model with which to unravel the interconnected processes of cell fate specification and pattern formation. The **genes** of the *achaete–scute* complex (AS-C) bridge these two processes. The AS-C is composed of four related genes found within ~90 kbp of DNA in the distal tip of the X-chromosome. The four genes—*achaete* (*ac*), *scute* (*sc*), *lethal of scute* (*l'sc*) and *asense* (*ase*)—all encode for basic **helix-loop-helix** transcriptional activator proteins and were initially identified by mutational analysis. Loss-of-function mutations in the AS-C remove sensory organs in the peripheral nervous system (PNS) and neural structures in the central nervous system (CNS), whereas gain-of-function mutations induce the formation of ectopic neural structures. The "proneural" *ac*, *sc*, and *l'sc* genes are expressed prior to neural precursor formation in precise patterns of cell clusters that forecast where neural precursors will form. During both embryonic and adult development, the primary patterning genes in *Drosophila* act through a large array of cis-acting regulatory regions found within the AS-C to create the stereotyped pattern of AS-C-expressing proneural cell clusters. Within each cluster (equivalence group), a cell communication process mediated by the Notch signaling pathway (lateral inhibition) restricts AS-C gene expression to a single cell. Within this cell, *ac*, *sc* and *l'sc*, either alone or in combination, are thought to activate a cassette of genes that directs this cell to acquire the neural precursor fate. All other cells within the cluster extinguish AS-C gene expression and are directed towards epidermal development. One target of the AS-C proneural genes in neural precursors is *ase*, which promotes the differentiation of neural structures. The AS-C thus links the process of cell fate specification to that of pattern formation: the AS-C genes receive and interpret global positional information through their regulatory regions and translate this information through their function into the formation (and differentiation) of a two-dimensional array of neural structures.

1. Genetic and Molecular Characterization of the *Achaete–Scute* Complex

The embryonic and adult *Drosophila* nervous systems are composed of a variety of different neural structures, each organized in reproducible but distinct patterns. For example, the neural precursors of the embryonic CNS form in orthogonal rows, whereas in the adult PNS large innervated bristles arise in an irregular, yet stereotyped pattern. Each bristle, or sensory organ, forms from a single neural precursor cell that occupies a fixed location in the developing fly. Cell migration is limited in the *Drosophila* PNS and CNS. Thus, the initial neural precursor pattern largely determines the later pattern of neural structures.

Genetic analyses identified a set of four genetic activities, designated the AS-C, located near the distal tip of the X-chromosome critical for the formation, patterning, and differentiation of neural structures (1). Loss-of-function mutations in any one of these genes remove neural structures, although the precise set of structures removed differs for each gene. For example, loss of *l'sc* activity primarily affects the CNS, whereas loss of *ac* or *sc* activity primarily results in PNS defects. Loss of *ase* function removes sensory organs along the wing blade but also causes differentiation defects in other sensory organs. Conversely, mis-expression of any AS-C gene promotes the formation of ectopic neural structures. These analyses suggested that the AS-C promotes the initial commitment of a cell to become a neural precursor and that their gene products are at least partially redundant. Detailed genetic mosaic analyses in the *Drosophila* wing imaginal disc (the larval structure that generates the wing and notum of the adult fly) showed that the activities of *ac* and *sc* define zones of neural competency from which neural precursors arise (2). These zones of neural competency are known as proneural cell clusters and are "equivalence groups" within which all cells can (although only one or a few will) become a neural precursor.

The genes *ac*, *sc*, and *l'sc* are each expressed in a complex and dynamic pattern of cell clusters, each of which quickly resolves to a single cell, the putative neural precursor (Fig. 1). The gene expression patterns of *ac* and *sc* are identical throughout neurogenesis and partially overlap with the expression pattern of *l'sc*. On the other hand, *asense* is expressed exclusively in neural precursors and their progeny. Based on mutant phenotypes and expression patterns, *ac, sc*, and *l'sc* are called proneural genes whereas *ase* is called a neural precursor gene.

Figure 1. Patterning and specification of neural precursors. (**a**) Patterning of AS-C gene expression. Schematic representation of the ectoderm of a *Drosophila* embryo. The expression of the *ac* and *sc* genes in four proneural clusters per hemisegment is shown in red and blue. The activity of the early patterning genes *ftz*, *odd*, *DER*, and *dpp* subdivide the embryo and lead to the activation of *ac/sc* gene expression in reproducible quadrants. For example, the combined action of *ftz* activation and *odd* repression leads to *ac/sc* gene expression in domains that express *ftz* but not *odd* (yellow). Along the D/V axis, *dpp* (light blue) and *DER* (green) restrict *ac/sc* expression to the lateral column. Together, the action of these four genes delimit *ac/sc* gene expression within one proneural cluster, shown in blue. Note that other factors can overcome *DER* mediated repression in the medial column. (**b**) Singling out of a neural precursor. Within each proneural cluster, a single cell (in this example, the central cell) comes to express the AS-C proneural genes to the highest level, and this cell becomes the presumptive neural precursor (dark blue cell). (**c**) Resolution of cell fate within a proneural cluster. The presumptive neural precursor retains proneural gene expression and acts through the *Notch* signaling pathway to remove proneural gene expression in the other cells of the cluster (white). These cells are directed toward epidermal development. (**d**) Neural precursor lineage. Each neural precursor goes through an invariant cell lineage to produce a particular neural structure. The lineage of a sensory bristle of the PNS is shown. The neural precursor divides to yield two differently fated daughter cells, which in turn divide to produce a total of four cells. Each cell acquires a different fate, and together the four cells make up a functional sensory organ—an innervated bristle.

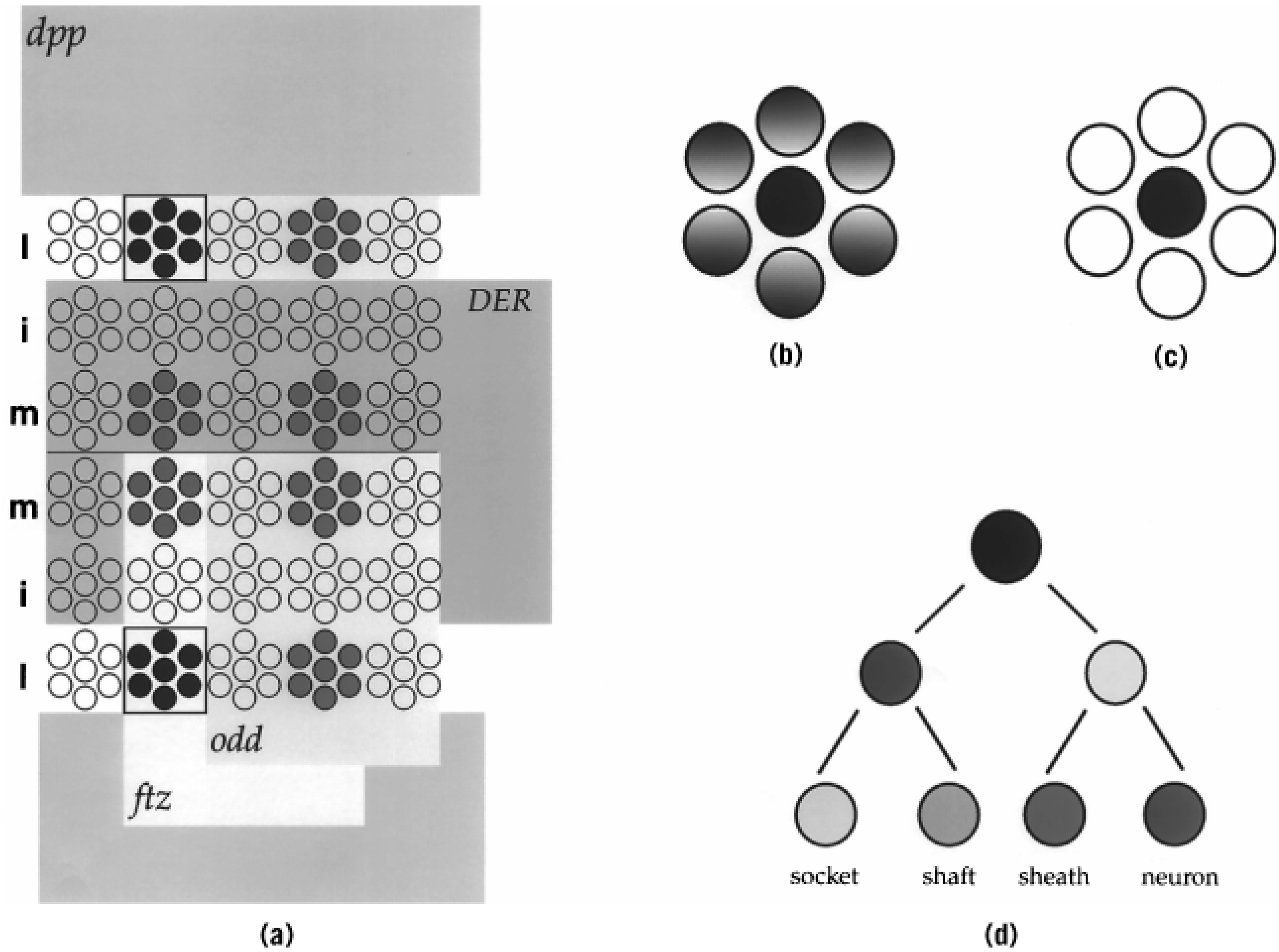

The molecular cloning of the AS-C in the 1980s identified all four genes as encoding putative transcriptional activator proteins that belong to the class B type of basic helix-loop-helix (bHLH) proteins. These four genes are contained within ~90 kbp of DNA, separated from one another by an average of ~30 kbp of DNA replete with *cis*-regulatory regions required to activate different members of the AS-C in complex and partially overlapping patterns (3). Transcriptional activation requires the formation of a heterodimer between A and B class bHLH proteins (4); these heterodimers recognize the core DNA sequence CANNTG, where N is not specified (an 'E' box). An A-class bHLH protein with which AS-C gene products heterodimerize and activate transcription is the product of the *daughterless* (*da*) gene. Heterodimers of one AS-C gene product and Da mediate transcriptional activation of genes expressed throughout proneural clusters and in neural precursors. The *da* gene is expressed ubiquitously throughout *Drosophila* development, and AS-C genes are expressed in complex yet invariant patterns of cell clusters that predict where neural precursors form. Thus, the spatiotemporal specificity of where and when neural precursors develop is a function of the pattern of AS-C gene expression.

2. Cis- and Trans-Regulation of Proneural Gene Expression

Activation of the proneural genes of the AS-C in precise and reproducible patterns of proneural clusters is the first step in the formation of the stereotyped two-dimensional pattern of neural precursors in the *Drosophila* nervous system. The genetic regulatory mechanisms that dictate where and when AS-C expressing proneural clusters form are best understood for the development of the embryonic CNS (5). The anterior/posterior (A/P) and dorsal/ventral (D/V) register of AS-C-expressing cell clusters in the early embryo suggests that the segmentation genes, which segment the embryo along the A/P axis, and the dorsoventral genes, which specify pattern along the D/V axis, function to lay down directly the initial pattern of AS-C proneural clusters. A similar process mediated by ***wingless*** and decapentaplegic (*dpp*), as well as the genes of the *iroquois* complex (6), probably acts directly on the AS-C to create the pattern of AS-C-expressing cell clusters in adult structures.

During development of the embryonic *Drosophila* CNS, the AS-C proneural genes are expressed in an invariant orthogonal pattern of proneural cell clusters. For example, *ac* and *sc* are co-expressed in two rows of cell clusters in the medial and lateral—but not intermediate—columns of each segment. Prior to AS-C gene activation, the activities of different A/P and D/V patterning genes have subdivided the early embryo into an orthogonal pattern of squares, reminiscent of a checkerboard. Each square expresses a unique combination of these patterning genes, and the borders of the AS-C proneural clusters match precisely the limits of these squares (Fig. 1). This suggests a model whereby the combined activities of particular combinations of patterning genes within a square either does or does not activate a member of the AS-C. The composite pattern of AS-C-positive cell clusters would then result from the integration of the activities of each square.

Support for the checkerboard model comes from genetic analyses that assayed the expression of AS-C genes in embryos mutant for various known patterning genes. For example, the anterior border of every fourth transverse row of *ac/sc*-positive cell clusters coincides with the anterior edge of the expression of the *fushi-tarazu* (*ftz*) pair-rule gene, and the posterior border of these proneural clusters abuts the anterior border of the *odd-skipped* (*odd*) pair-rule gene (Fig. 1). In embryos mutant for *ftz*, this row of *ac/sc*-expressing proneural clusters disappears, whereas in embryos mutant for *odd* it expands posteriorly to fill the entire *ftz* domain. Thus, the combined action of *ftz* activation and *odd* repression defines the anterior and posterior boundaries respectively, of proneural clusters in this row. The D/V patterning genes control the mediolateral extent of AS-C proneural clusters. For example, the medial boundary of the lateral column of AS-C proneural clusters abuts the lateral border of the activity of the *Drosophila* epidermal growth factor (EGF) receptor (*DER*), and the lateral boundary of these clusters abuts the medial boundary of *dpp* activity (Fig. 1). In embryos mutant for *DER*, the lateral column of AS-C-expressing proneural clusters expands medially, whereas in *dpp* mutant embryos these clusters expand laterally. Thus, *DER* and *dpp* together restrict *ac/sc* gene expression to the lateral column in the developing CNS. The concerted action of *ftz* and *odd* along the A/P axis, and *DER* and *dpp* along the D/V axis, can account for the activation of *ac/sc* in one eighth of its proneural clusters. Combinations of other patterning genes probably act similarly to initiate AS-C proneural gene expression in the other regions of the developing CNS and PNS.

Scattered throughout the AS-C are regulatory regions that decode the positional information contained within the checkerboard pattern of spatial regulators and translate it into the transcriptional activation of *ac*, *sc*, and *l'sc*. The locations of many of these regulatory regions have been identified through the use of DNA rearrangements within the AS-C and of reporter gene constructs that contain specific genomic regions from the AS-C region (7). For example, *ac* and *sc* share a number of regulatory regions located between the two genes that function to activate *ac* and *sc*, but not *l'sc*, in identical patterns throughout development. It is thought that the gene products of many of the patterning genes act directly through these regulatory regions to create the precise and invariant pattern of AS-C-expressing proneural clusters.

3. Resolution of Proneural Cell Clusters: The Singling out of the Neural Precursor

Within each proneural cluster, AS-C expression quickly becomes restricted to one (or a few) cells (Fig. 1). This cell initiates *ase* expression, enlarges, and segregates as a neural precursor to a position below the proneural cluster from which it arose. All clusters exhibit identical dynamics of proneural gene expression, which directly reflect the cell-fate decisions made by the cells of a cluster. Initially, all cells express one or more of the proneural genes; proneural gene expression confers on all cells the ability to become a neural precursor. Then, via a cell-cell communication pathway mediated by the *Notch* signaling pathway, one cell comes to express the proneural genes to the highest level. This cell is the presumptive neural precursor; it then acts, again through the *Notch* pathway, to inhibit and eventually to extinguish proneural gene expression from all other cells of the cluster (8). The cells that lose proneural gene expression are directed toward the epidermal fate. Thus the fate of cells within a proneural cluster correlates—not with the initial expression of the proneural genes—but rather with the fate of proneural gene expression in that cell: cells that retain proneural gene expression become neural precursors, whereas cells that lose proneural gene expression are directed toward the epidermal fate.

The analysis of the AS-C provides a paradigm for how specific cell fates (and cellular structures) arise in reproducible and invariant patterns, but many questions still remain with respect to the AS-C. For example, roughly half of all CNS neural precursors still form in embryos devoid of AS-C function. Thus other "proneural genes" must exist that promote neural precursor formation in the CNS. In addition, AS-C function is not restricted to the nervous system. The gene *l'sc* mediates the initial selection of muscle progenitor cells in the mesoderm in much the same way that it (as well as *ac* and *sc*) single out neural precursors in the ectoderm. Furthermore, Galant et al (9) recently demonstrated that a butterfly AS-C **homologue** is expressed in, and thus may promote the formation of, the precursors to the pigment-producing scale cells that cover the butterfly wing. Thus, AS-C genes may mediate additional developmental events in *Drosophila* and other animals. Finally, in *Drosophila* the AS-C is an integral unit composed of four structurally related genes. Has the overall genomic structure of the AS-C and the relative position and expression of each AS-C gene been strongly conserved throughout evolution, as is observed for the genes of the **homeobox** clusters? Or does the AS-C and its constituent genes display significant plasticity over evolutionary time? Research on the AS-C has led to an understanding of some of the molecular mechanisms that specify particular cell types and those that determine where and when these cell types form. It is likely that further insights will derive from continued analysis of AS-C expression, regulation, and function.

4. Acknowledgments

I thank Michelle Hresko, Grace Panganiban, Lisa Nagy, and Ellen Ward for their comments. J.B.S is supported by a grant from NINDS (RO1-NS36570), the Cancer Research Fund of the Damon Runyon-Walter Winchell Foundation Award, DRS-9 and by a HHMI Research Resources Program for Medical Schools Junior Faculty Award #76296-538202.

Bibliography

1. A. Garcia-Bellido (1979) Genetics **91**, 491–520.

2. C. Stern (1954) American Scientist **42**, 213–247.
3. S. Campuzano, L. Carramolino, C. V. Cabrera, M. Ruiz-Gomez, R. Villares, A. Boronat, and J. Modolell (1985) Cell **40**, 327–338.
4. C. Murre, P. Schonleber-McCaw, H. Vaessin, M. Caudy, L. Y. Jan, Y. N. Jan, C. V. Cabrera, J. N. Buskin, S. D. Hauschka, A. B. Lassar, H. Weintraub, and D. Baltimore (1989) Cell **58**, 537–544.
5. J. B. Skeath, G. Panganiban, J. Selegue, and S. B. Carroll (1992) Genes Dev. **6**, 2606–2619.
6. J. L. Gomez-Skarmeta, R. Diez del Corral, E. De La Calle-Mustienes, D. Ferres-Marco, and J. Modolell (1996) Cell, **85**, 95–105.
7. J. L. Gomez-Skarmeta, I. Rodriguez, C. Martinez, J. Culi, D. Ferres-Marco, D. Beamonte, and J. Modolell (1995) Genes Dev. **9**, 1869–1882.
8. J. A. Campos-Ortega (1993) In *The Development of Drosophila melanogaster* (M. Bate and A. Martinez-Arias, eds.), Cold Spring Harbor Press, Cold Spring Harbor, NY, pp. 1091–1130.
9. R. Galant, J. B. Skeath, S. Paddock, D. L. Lewis, and S. B. Carroll (1998) Current Biology **8**, 807–813.

Achilles' Cleavage

Achilles' cleavage (AC) is a procedure developed to permit cutting double-stranded **DNA** at a single site (the AC site) in a complex genome (Fig. 1). The AC site is first protected from **methylation** by a sequence-specific DNA-binding protein, and the methylated genome is subsequently cut by a methylation-sensitive restriction enzyme. Other sites in the genome containing the same restriction/methylation site as the AC site are methylated and thus are not cut. The two key components of any AC system are (i) a restriction site that is recognized by both a methylation-sensitive restriction enzyme and its corresponding methyltransferase and (ii) the ability to block methylation of the chosen AC site by sequence-specific binding of a protein to that site. The overlap of the AC site and the recognition sequence for the DNA binding protein can occur naturally, or it can be engineered using recombination or site-directed mutagenesis. These requirements somewhat limit the applications of the AC technique.

Figure 1. Achilles' Cleavage. Diagram of the method used to prevent restriction enzyme digestion at all sites except for the Achilles' cleavage (AC) site. Horizontal lines connected by short vertical lines represent double-stranded DNA. *Hha*I restriction sites are marked by bold vertical lines above the double-stranded DNA. The binding site for the DNA-binding protein is represented by a solid rectangle. The DNA-binding protein is represented by an empty oval. Sites of methylation are indicated by a vertical line and the letter ‘m.’

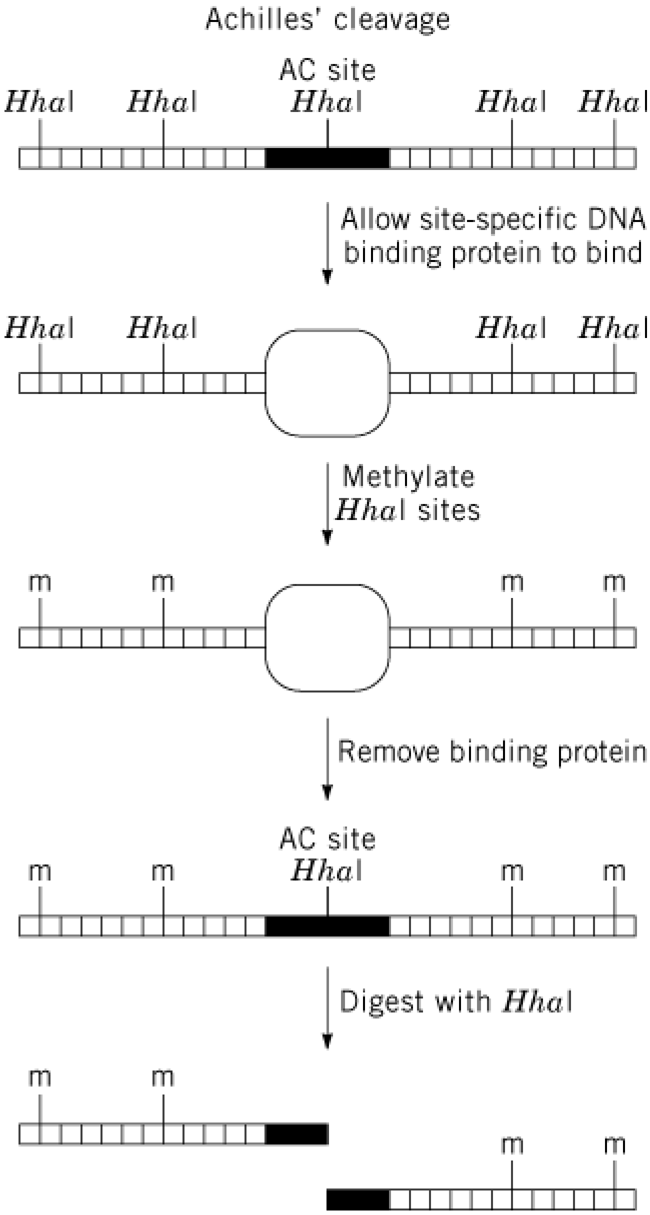

Koob et al. (1) originally developed this procedure using two different **repressor/operator** systems. In one instance, **plasmids** carrying the operator of the lac operon were incubated with the Lac repressor and then methylated by the *Hha* I methyltransferase. Repressor binding prevented methylation of the *Hha* I site located within the *lac* operator. The methyltransferase and the operator protein were subsequently removed, leaving only the unmethylated AC site free to be cut by *Hha* I (1). Variations of the original AC method were also used to demonstrate the ability to make only one or a few cuts in the genomes of **yeast** and *Escherichia coli* (2), to turn frequent-cutting restriction enzymes into rare cutters (3), and to analyze the strength of protein-DNA interactions (4).

1. RecA-AC and RARE

The original AC method was made more universally applicable by using **RecA** protein and a sequence-specific **oligonucleotide** to form the protective complex, obviating the need for a sequence-specific binding protein. Two groups simultaneously developed this procedure, and their protocols were designated RecA-AC (5) and RARE (6). The RecA-AC/RARE technique still requires selection of a cleavage site that is recognized by both a restriction enzyme and its cognate methyltransferase. An oligonucleotide of 40 to 60 nucleotides in length is designed that matches the

DNA sequence containing the cleavage site. In the presence of Mg^{2+} and a non-hydrolyzable ATP analogue [eg, ATP(g-S)], RecA protein will bind to the oligonucleotide, forming a complex. When double-stranded DNA is added, the complex will bind to the matching genomic sequence to form a so-called 'triple-stranded' synaptic complex. This complex protects the cleavage site from methylation. As in the AC procedure, the methyltransferase and the RecA protein are removed after methylation, before the methylation-protected site is cleaved with the appropriate restriction enzyme.

As an alternative, the RecA complex can be used to protect specific restriction sites from restriction enzyme digestion, rather than from methyltransferase. This technique can be useful in some cloning procedures.

The RecA-AC/RARE technique has been used in various genome mapping experiments, for example to map gaps in human contiguous (**contig**) DNA and to map telomeres (7). The ability to cut genomic DNA at a few specific sites allows mapping large pieces of DNA by using pulsed-field gel electrophoresis and **Southern blotting** techniques to size DNA between two cleavage sites, or between a marker and the end of a telomere (7).

The RecA-AC/RARE technique is a useful technique for mapping and manipulating DNA and should continue to prove helpful in large-scale genome analysis studies of the future. One limitation to the technique is the number of sequences recognized by both a restriction enzyme and a methyltransferase. As more restriction enzyme/methyltransferase pairs are isolated or developed, the technique will be come even more useful.

Bibliography

1. M. Koob, E. Grimes, and W. Szybalski (1988) Science **241**, 1084–1086.
2. M. Koob and W. Szybalski (1990) Science **250**, 271–273.
3. J. Kur, M. Koob, A. Burkiewicz, and W. Szybalski (1992) Gene **110**, 1–7.
4. P. M. Skowron, R. Harasimowicz, and S. M. Rutkowska (1996) Gene **170**, 1–8.
5. M. Koob, A. Burkiewicz, J. Kur, and W. Szybalski (1992) NAR **20**, 5831–5856.
6. L. J. Ferrin and R. D. Camerini-Otero (1991) Science **254**, 1494–1497.
7. L. J. Ferrin and R. D. Camerini-Otero (1994) Nature Genet. **6**, 379–383.

Suggestions for Further Reading

8. W. Szybalski (1997) RecA-mediated Achilles" heel cleavage. Curr. Opinion Biotechnol. **8**, 75–81.
9. L. J. Ferrin (1995) Manipulating and mapping DNA with RecA-assisted restriction endonuclease (RARE) cleavage, In *Genetic Engineering, Principles and Methods* (J. K. Setlow, ed.), Plenum Press, New York, Vol. **17**, pp. 21–30.

Acridine Dyes

Acridines are fused linear tricyclic aromatic molecules of planar geometry. Aminoacridine (Fig. 1) was originally developed as a topical antibacterial agent and is one of the most widely used and studied acridines. It is a strong base (pK_a 9.9) due to the resonant amino group and is largely ionized at physiological pH. Acridines are typical DNA-**intercalating** ligands, binding tightly but reversibly to double-stranded DNA by insertion of the aromatic chromophore between adjacent base pairs, with the long axis of the acridine parallel to the base-pair axis, ensuring maximum overlap in the binding site (1, 2). It was originally hypothesized by Brenner et al. (3) that acridine-induced mutations arise through the addition or deletion of a single base pair, an event described as **frameshift mutagenesis**.

Figure 1. Structure of the mutagen 9-aminoacridine.

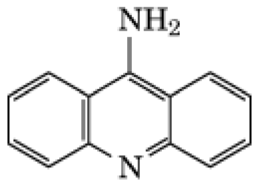

9-Aminoacridine is a strong mutagen in the rII region of **bacteriophage** T4 (4), in the CI gene of lambda phage (5), at various loci in *Escherichia coli* (6), and at the hisC3076 locus in *Salmonella typhimurium* (7). This and related simple acridines cause frameshift mutagenesis, especially in monotonous runs of repeated sequences. In mammalian cells their activity is somewhat weak and variable. They appear not to be causing frameshifts (at least in the most commonly used mammalian assays), but are mutagenic through weak ability to break chromosomes (8).

Substitutions on the acridine ring profoundly affect the mutagenic characteristics of these compounds, which have been divided into seven subgroups according to their distinctive mutagenic characteristics (2). 9-Aminoacridine and related simple compounds form the first group, while proflavine and other 3,6-diaminoacridines form the second group. The 3,6-diamino groups increase DNA binding affinity, and these compounds resemble 9-aminoacridine in having frameshift mutagenic activity, but are also substrates for metabolic activation (9). They are also readily activated by visible light into other products that are mutagenic in the *Salmonella* mutagenicity test (Ames test) (10). Some of these compounds and also the third class of quaternized acridines have considerable affinity for mitochondrial DNA. The fourth group of acridines retain DNA intercalation activity, but also act as topoisomerase II (topo II) poisons (see DNA Topology).

Type II topoisomerases produce double-strand breaks in DNA during replication and transcription, permitting strand passage through the transient break, which is then resealed by the enzyme. The potent antitumor activity of 9-anilinoacridines of the fourth group, such as amsacrine (Fig. 2), is thought to relate to their ability to stabilize the cleavable complex formed between topo II enzymes and DNA, thereby leading to an accumulation of double-strand breaks (11). These DNA breaks also result in these compounds showing strong clastogenic and recombinogenic properties. A clastogen is a physical, chemical or viral agent that produces chromosome breaks and other chromosomal mutagenesis. The fifth group of benzacridines are characterized by a higher susceptibility to metabolic activation, primarily through oxidative mechanisms (12). Benzacridines are primarily base-pair substitution mutagens, producing a spectrum of mutagenic events that is fundamentally different from that produced by other acridines and in which the acridine ring plays only a minor role. The sixth group of acridines, epitomized by those originally developed in the Institute of Cancer Research, Philadelphia, and widely known as ICR compounds (13), all carry an alkylating moiety, usually a nitrogen mustard. These compounds are not only potent frameshift mutagens in various organisms, but also cause base-pair substitution events in mammalian cells (2, 14). Although the nitroacridines can be distinguished as a seventh group, they may alternatively be considered as a subgroup of the previous class, because they can act as either simple acridines or as alkylators, depending upon the position of the nitro substitution and the nitroreductase capability of the organism concerned.

Figure 2. Structure of the 9-anilinoacridine amsacrine.

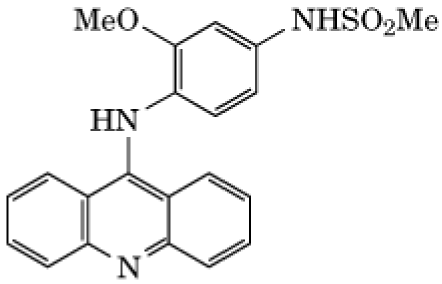

Bibliography

1. L. R. Ferguson and W. A. Denny (1990) Mutagenesis **5**, 529–540.
2. L. R. Ferguson and W. A. Denny (1991) Mutat. Res. **258**, 123–160.
3. S. Brenner, L. Barnett, F. H. C. Crick, and A. Orgel (1961) J. Mol. Biol. **3**, 121–124.
4. A. Orgel and S. Brenner (1961) J. Mol. Biol. **3**, 762–768.
5. T. A. Skopek and F. Hutchinson (1984) Mol. Gen. Genet. **195**, 418–423.
6. S. M. Thomas and D. G. MacPhee (1985) Mutat. Res. **151**, 49–56.
7. L. R. Ferguson and D. G. MacPhee (1983) Mutat. Res. **116**, 289–296.
8. W. R. Wilson, N. M. Harris, and L. R. Ferguson (1994) Cancer Res. **44**, 4420–4431.
9. M. Fukenaga, Y. Mitzuguchi, and L. W. Yielding (1987) Chem. Pharm. Bull. Japan **35**, 792–797.
10. Y. Iwamoto, L. R. Ferguson, A. Pearson, and B. C. Baguley (1992) Mutat. Res. **268**, 35–41.
11. L. R. Ferguson and B. C. Baguley (1996) Mutat. Res. **355**, 91–101.
12. R. E. Lehr, A. W. Wood, W. Levin, A. H. Conney, and D. M. Jerina (1988) In *Polycyclic Aromatic Hydrocarbon Carcinogenesis: Structure–Activity Relationships* (S. K. Yang and B. D. Silverman, eds.), CRC Press, Boca Raton, FL, pp. 31–58.
13. H. J. Creech, R. K. Preston, R. M. Peck, and A. P. O''Connell (1972) J. Med. Chem. **15**, 739–746.
14. L. F. Stankowski, K. R. Tindall, and A. W. Hsie (1986) Mutat. Res. **160**, 133–147.

Acrocentric Chromosome

An acrocentric chromosome has a single centromere that is localized at or near one end of the chromosome (acro = extremity). One of the most common forms of chromosomal translocation occurs when two acrocentric chromosomes fuse at the ends containing the centromeres (1). This is called a Robertsonian event (Fig. 1). This generally leads to the formation of a metacentric chromosome, where the new centromeric region appears at or near the middle of the new chromosome. Robertsonian events lead to a decrease in the apparent number of chromosomes. Much of the variation in the number of chromosomes in the members of a family or genus is related to this type of acrocentric chromosomal fusion. Whereas the number of chromosomal arms remain relatively constant, counting two for a metacentric chromosome and one for an acrocentric, the number of chromosomes can vary widely. For example, most dogs have either 32 to 38 or 18 to 21 autosomes (any chromosome other than the X- or Y-chromosomes), but 34 to 38 chromosomal arms. Those with the greater number of autosomes have larger numbers of acrocentric chromosomes (2, 3). In genomes whose karyotypes contain exclusively acrocentric chromosomes (e.g., that of the house mouse, *Mus musculus*), rapid chromosome identification can be achieved via whole-chromosome painting techniques, e.g., spectral karyotyping (4).

Figure 1. Robertsonian translocation occurs when two acrocentric chromosomes fuse to create a single metacentric chromosome.

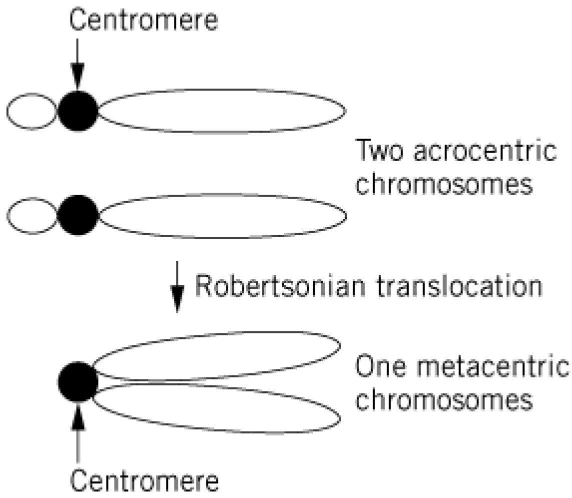

Bibliography

1. W. Robertson, J. Morph. **27**, 179–197 (1916).
2. R.K. Wayne, W.G. Nash, and S.J. O"Brian, Cytogenet. Cell Genet. **44**, 123–133 (1987).
3. R.K. Wayne, W.G. Nash, and S.J. O"Brian, Cytogenet. Cell Genet. **44**, 134–141 (1987).
4. T. Ried, E. Schrock, Y. Ning, and J. Wienberg, Hum. Mol. Genet. **7**, 1619–26 (1998).

Additional Reading

5. Wagner R.P., Maguire M.P., and Stallings R.L., *Chromosomes. A Synthesis*, Wiley-Liss, New York, 1993.

Acrosome

The acrosome is an organelle of the spermatozoon that covers the apical part of the sperm head. This organelle comprises an outer acrosomal membrane, an inner acrosomal membrane, and plasma membranes. The acrosome plays an important role during the early stages of fertilization, in that the acrosome and its associated molecules mediate recognition of the egg to be fertilized. Although acrosome morphology varies with the species, the function of the acrosome and its contents as regulating elements during the early stages of fertilization are fairly similar among species. The acrosome contains **proteolytic** enzymes (see Proteinases) as well as proteins for binding to the zona pellucida and plasma membrane of the Egg (1). Therefore, the associated molecules of the acrosome have been proposed as targets for nonhormonal antifertilization agents.

1. Primary Ligands

The primary ligands are proteins that are located on or close to the acrosome; their function is to ensure that recognition between the gametes is species-specific. This is especially necessary in animals with extracorporal fertilization (eg, frog and sea urchin). On the surface of the acrosomal cap, there is a plethora of adhesion molecules (2), but their origin is not in all cases clear. Sperm adhesins become associated only upon ejaculation (3). Many of these primary ligands, such as galactosyltransferase (4), are lectins and bind to O-linked oligosaccharides and glycans of the ZP3 receptor of the oocyte's extracellular matrix, the zona pellucida (5, 6). Other proteins were discovered that induce metabolic events; a 95-kDa protein was detected that induces **phosphorylation** events (7).

One of the most fascinating events during the early stages of fertilization is the acrosome reaction . After the initial contact of the sperm with the zona pellucida of the oocyte, and under the influence of progesterone (8), a unique event called the acrosome reaction takes place, which is calcium-dependent (9). Although in mammals the acrosome reaction can be induced without zona pellucida glycoproteins, they act in a catalytic manner (10). The acrosome reaction involves exocytosis of the outer membrane, causes the formation of hybrid vesicles, and leads to exposure of the inner contents of the acrosome. In many invertebrates, such as starfish, sea cucumbers, or sea urchin, a polymerization event takes place that results in the formation of actin filaments. In mollusks, the actin filaments are already present in the unreacted spermatozoon and exposed on activation.

Recent investigations report the presence of the **inositol phosphate** system in mammalian sperm. It involves the activation of a sperm **receptor** that stimulates a **G-protein**. This activates phospholipase C, which cleaves subsequently phosphatidyl inositol diphosphate (PIP_2) into **diacylglycerol** and inositol triphosphate (IP_3). IP_3 triggers the release of calcium from intercellular stores, and diacylglycerol activates protein kinasekinase C, which is calcium-dependent. This causes proteins to be phosphorylated and leads subsequently to the acrosome reaction (11). Upon their exposure, the molecules within the acrosome become important for the fertilization process.

2. Secondary Ligands: Acrosin/Proacrosin

A major component of the inner acrosome is the protein proacrosin . This is the best-characterized molecule of those involved in the early stages of fertilization. It is important for local lysis of the zona pellucida and therefore plays a central role at the stage of sperm penetration. Proacrosin is stored as its inactive form, a zymogen. On raising the pH, or on contact with zona pellucida glycoproteins, the zymogen converts into its active proteolytic form, acrosin . This is accomplished by several intramolecular reorganizations (12). Proacrosin is a two-polypeptide chain molecule and, typical of serine proteinases, the heavy chain starts at residue Val24. Major alterations of the molecule involve proteolytic cleavage of the proline-rich C-terminal tail, cleavage of the light chain, and linkage to the heavy chain via disulfide bonds.

Proacrosin is a multifunctional protein; it does not act solely as a proteinase, but is also a fucose-binding protein (13). The molecule shows high binding affinity for fucoidan, heparin, and zona pellucida glycoprotein preparations (14). The primary mechanism of proacrosin binding to the zona pellucida is not only an interaction with carbohydrates, but involves positively charged amino acid residues of the proacrosin and negatively charged sulfate groups of the zona pellucida glycoproteins. **Homology modeling** of proacrosin revealed that the groove for binding to the zona pellucida contains loops in which the positively charged amino acids are located. The active site for proteolytic activity is located in the center, surrounded by the positively charged amino acids. The binding groove and proteolytic center appear to form a single reactive unit, even though they are located on different regions on the polypeptide chain. The proteolytic activity could be blocked without affecting proacrosin's binding characteristics.

The arrangement of the binding site and proteolytic center suggests two major tasks of the enzyme during fertilization. The molecule recognizes the zona pellucida specifically, binds to it, and digests it locally to promote sperm entry through the extracellular matrix. However, there must be further binding and proteolytic proteins involved in fertilization, as mouse **knockout strains** lacking the proacrosin gene did not produce infertile males (15); other molecules must be able to take over the role of proacrosin. On the other hand, male mice with a functionally active proacrosin gene demonstrated a significantly greater fitness in terms of reproductive success in a competition-mating experiment with the proacrosin knockout mice (16). Although proacrosin is the major compound of the acrosomal vesicle, there are further adhesion proteins. Fertilin , formerly designated PH-30, is a molecule that is involved in interactions between the sperm and egg (17, 18).

Bibliography

1. A. P. Aguas and P. Pinto da Silva (1985) J. Cell. Biol. **100**, 528–534.
2. R. Jones (1990) J. Reprod. Fert. Suppl. **42**, 89–105.
3. J. J. Calvete, D. Solis, L. Sanz, T. Diaz-Maurino, W. Schäfer, K. Mann, and E. Töpfer-Petersen (1993) Eur. J. Biochem. **218**, 719–725.
4. X. Gong, D. H. Dubois, D. J. Miller, and B. D. Shur (1995) Science **269**, 1718–1721.
5. S. Kitazume-Kawaguchi, S. Inoue, Y. Inoue, and W. J. Lennarz. (1997) Proc. Natl. Acad. Sci. USA **94**, 3650–3655.
6. R. A. Kinloch, Y. Sakai, and P. M. Wassarman (1995) Proc. Natl. Acad. Sci. USA **92**, 263–267.
7. L. Leyton, P. LeGuen, D. Bunch, and P. M. Saling (1992) Proc. Natl. Acad. Sci. USA **89**, 11692–11695.
8. E. R. Roldan, T. Murase, and Q. X. Shi (1994) Science **266**, 1578–1581.
9. C. Arnoult, R. A. Cardullo, J. R. Lemos, and H. M. Florman (1996) Proc. Natl. Acad. Sci. USA **93**, 13004–13009.
10. C. N. Tomes, C. R. McMaster, and P. M. Saling (1996) Mol. Reprod. Dev. **43**, 196–204.
11. R. Yanagimachi (1994) Mammalian fertilization. In *The Physiology of Reproduction*, 2nd ed. (E. Knobil and J. D. Neill, eds.), Raven Press, New York, pp. 189–317.
12. T. Baba, W. Kashiwabara, K. Watanabe, H. Itoh, Y. Michikawa, K. Kimura, M. Takada, A. Fukamizu, and Y. Arai (1989) J. Biol. Chem. **264**, 11920–11927.
13. E. Töpfer-Petersen and A. Henschen (1987) FEBS Lett. **226**, 68–42.
14. R. Jones and C. R. Brown (1987) Exp. Cell Res. **171**, 505–508.
15. T. Baba, S. Azuma, S. Kashiwabara, and Y. Toyoda (1994) J. Biol. Chem. **269**, 31845–31849.
16. I. M. Adham, K. Nayernia, and W. Engel (1997) Mol. Reprod. Dev. **46**, 370–376.
17. E. A. Almeida, A. P. Huovila, A. E. Sutherland, L. E. Stephens, P. G. Calarco, L. M. Shaw, A. M. Mercurio, A. Sonnenberg, P. Primakoff, and D. G. Myles (1995) Cell **81**, 1095–1104.
18. J. P. Evans, R. M. Schultz, and G. S. Kopf (1997) Dev. Biol. **187**, 94–106.

Suggestions for Further Reading

19. B. T. Storey (1995) Interactions between gametes leading to fertilization: The sperm"s eye view. Reprod. Fertil. Dev. **7**, 927–942. Describes the interactions between the gametes leading to fertilization.
20. E. Töpfer-Petersen and J. J. Calvete (1995) Molecular mechanisms of the interaction between sperm and the zona pellucida in mammals: Studies on the pig. Int. J. Androl. Suppl. 2 **18**, 20–26. Summarizes established similarities and differences between sperm oocyte interactions of mammalian species.

Actin

Actin is one of the most ubiquitous and conserved eukaryotic proteins. While actin was originally isolated and studied as part of the contractile apparatus of muscle (see Thin Filament), we now know that actin is found in virtually all eukaryotic cells and can be the most abundant protein present. Actin forms part of the cytoskeleton in nonmuscle cells and is involved in the maintenance of cell shape as well as cell dynamics and motility. The active form of actin is a helical polymer called F-actin (F for filamentous), assembled from monomeric subunits of G-actin (G for globular). Actin exists in a number of very similar isoforms (88% amino acid identity between yeast cytoplasmic actin and human muscle actin), and these isoforms display tissue, rather than species, specificity (1, 2). Thus, human cytoplasmic actin is much closer in sequence to yeast cytoplasmic actin than it is to human muscle actin. The actin monomer contains 374–376 residues, varying with the isoform, and is about 42k MW.

Actin interacts specifically with over 40 other proteins, and many of these interactions fall into separate classes. There are proteins that control the polymerization state of actin by nucleating, capping, or severing filaments [such as gelsolin, profilin, cofilin, and the b-thymosins (3-7)], proteins that crosslink actin filaments together into gels and bundles [such as a-**actinin**, villin, and fimbrin (8-10)], and proteins that regulate the interactions of **myosin** with actin [such as **tropomyosin**, **troponin**, calponin, and caldesmon (11), (see Thin Filament)]. In addition, many glycolytic enzymes bind actin, and it has been suggested that this provides spatial organization to metabolic processes via an association with the cytoskeleton (12). Other high-affinity interactions, such as between G-actin and the endonuclease DNase I (see DNase 1 Sensitivity) (13), do not lend themselves to simple explanations at this time.

Extensive biochemical, structural, and genetic studies have explored the properties of both G- and F-actin. The most detailed structural information exists for G-actin, since X-ray crystal structures have been obtained for complexes of G-actin with DNase I (13), gelsolin segment 1 (14), and profilin (15). The G-actin structure consists of two domains, each with two subdomains. These domains were originally called the “large” and “small” domains, but this terminology is not appropriate, as we now know that the “large” domain only contains 51% of the mass of the subunit. The N- and C-terminii are both located in the largest subdomain, subdomain-1. Between the two domains is a nucleotide-binding cleft, normally occupied by ATP in G-actin and ADP in F-actin, as well as the high-affinity metal-binding site. The subunit structure of G-actin is homologous to that of yeast hexokinase and the ATP-binding domain of HSC-70, a chaperonin, suggesting a common evolutionary origin for all of these proteins (16). It has been proposed that the bacterial protein FtsA has the same fold (17), which would indicate that FtsA is a prokaryotic ancestor of the eukaryotic actins. It has already been established that the bacterial FtsZ protein has a common structure with eukaryotic tubulins. Since neither hexokinase nor HSC-70 polymerize, it is evident that actin's ability to polymerize does not reside in any unique features of the secondary or tertiary structure, but rather evolved later. Thus, establishing that FtsA has a common subunit structure with actin will not, in and of itself, reveal any information about possible quaternary structures for FtsA.

Electron microscopic observations of F-actin (18-20) have been very useful in defining the orientation of the subunit in the filament, as well as revealing aspects of structural dynamics. X-ray fiber diffraction from oriented gels of F-actin has led to an atomic model for F-actin (21, 22), which provides a starting point for understanding the molecular details of the interactions of actin with many other proteins and ligands. However, many of the atomic details are still underdetermined by the method of fitting the monomeric structure into the filament, since the X-ray fiber diffraction pattern does not introduce all of the constraints needed. We thus have a general picture of the orientation of the subunit in the filament, but still lack information about many of the atomic interactions.

The subunit is oriented in the filament so that the two domains are nearly perpendicular to a plane containing the helix axis (Fig. 1). The resulting filament is about 100 Å in diameter, and subunits are spaced axially by a 27.3 Å rise along the filament axis. The change in the axial rise per subunit is less than .08 Å per subunit (<0.3%) when actin filaments in muscle are placed under full tension (23, 24), establishing that these filaments are relatively inextensible. Nevertheless, this amount of extensibility is enough to complicate the interpretation of muscle mechanics. Subunits are related to their axial neighbors by an ~167° rotation about the filament axis, giving rise to a 59 Å pitch left-handed helix (sometimes called the genetic helix). An interesting property of the actin filament is the ability of subunits to rotate within the helix (25), and it has recently been shown that an actin-binding protein, cofilin, can change the twist of the actin filament by 5° per subunit, without significantly changing the axial rise per subunit (7). The helical geometry of actin also gives rise to two right-handed long-pitch strands containing actin subunits related by a 54.6 Å axial separation. These strands typically have a mean pitch of ~700–760 Å (with the differences in the mean being due to the isoform, preparative conditions, associated proteins and ligands, etc.). The double-stranded character of these helices give rise to “crossovers” in projection at half of the pitch, or about 350–380 Å, but these crossover spacings can be variable due to the angular freedom within the actin filament (25, 26).

Figure 1. The G-actin subunit is shown by a ribbon representation (39) based upon the structure determined by X-ray crystallography (13). The degree of sequence conservation in actin is indicated by the fact that the only residues (45 out of 375) that differ between vertebrate striated skeletal muscle and yeast cytoplasmic actin are indicated by the asterisks. The four subdomains of actin are labeled S1–S4, and the most conserved part of the molecule is subdomain 2, with only 2 substitutions out of 38 residues between these two isoforms. The cleft between the two domains is occupied by ATP and a bound metal (indicated by the sphere). Adapted from Orlova et al. (40).

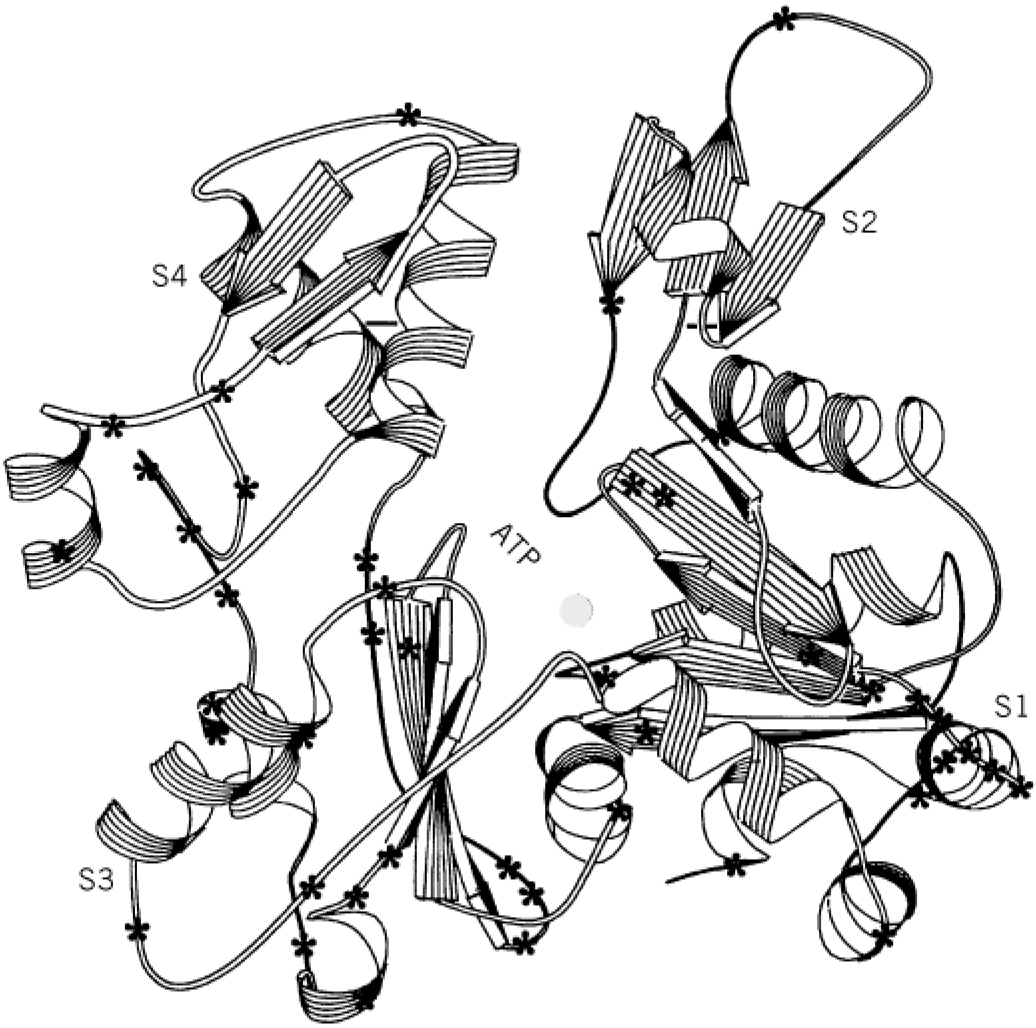

Every subunit in the actin filament is oriented with the same polarity, which gives rise to the overall polarity of the filament. This polarity has been described as the filament having a “barbed” end and a “pointed” end, based upon the morphological polarity that appears in electron micrographs when actin filaments are extensively decorated by the binding of proteolytic fragments of myosin, such as S1 or HMM (heavy meromyosin). This decoration generates a chevron appearance caused by all myosin molecules binding to the actin filament with an angle of about 45°. The morphological polarity has been related to a kinetic polarity apparent during *in vitro* polymerization, since the barbed end is the fast-growing end and the pointed end is the slow-growing end.

The helical symmetry of the actin filament is often described as 13/6 or 28/13, meaning that it has a helical repeat of 13 subunits in 6 turns of the 59 Å helix, or 28 subunits in 13 turns. The helical repeat is the distance that a subunit must be translated axially to bring it into register with another subunit. An ideal 13/6 helix would have crossovers every 355 Å, with each crossover containing a helical repeat, while an ideal 28/13 helix would have crossovers every 382 Å, with two crossovers per helical repeat. However, there is no reason to believe that the helical symmetry needs to be described as a ratio of small integers, as there is an infinitesimally small change in structure from a symmetry of 13/6 to one of 1301/600 (a rotation of ~0.1° per subunit), but the helical repeat changes from 355 Å to 35,517 Å! The actual symmetry of the actin filament is entirely defined by the interactions between one actin subunit and four nearest neighbors (–2 and 2 along the same long-pitch strand, and –1 and +1 on the opposite strand). In the absence of accessory proteins [such as **tropomyosin**, which binds to seven actin subunits along the same long-pitch strand (see Thin Filament)], all changes of state must be propagated by such local interactions. Nevertheless, many *in* *vitro* experimental observations have shown that pure actin (in the absence of accessory proteins) can have long-range cooperative interactions within a filament (20, 27-29).

The flexibility of the actin filament has been studied by many methods, including spectroscopy (30), light microscopy (31), and electron microscopy (32, 33). Most studies have suggested a persistence, or correlation, length of about 6–7 µm. This indicates that an actin filament much shorter than 6–7 µm can be treated as a rigid rod, while a filament much longer than 6–7 µm can be treated as a random coil. The persistence length does not suggest that a 6–7 µm filament is approximated well by a rigid rod, since an actin filament only 0.6 µm in length (one-tenth of the persistence length) will have a characteristic fluctuation of tangents at the two ends of about 25°.

Actin polymerization has been studied *in vitro* in great detail and is induced by raising the salt concentration. As for almost all other protein polymers in the cell, the assembly process involves the noncovalent binding of subunits to each other, such that every subunit (with the exception of subunits at the filament ends) is in the same environment. Probably more is known about the *in vitro* polymerization of actin than for any other protein polymer, but new findings suggest that the *in vivo* regulation of actin assembly involves the interactions with many other proteins and may be greatly different from what occurs *in vitro* (34). Polymerization can occur *in vitro* when the subunit concentration is above the critical concentration, which is the concentration of the monomer that would be at equilibrium with a population of polymers (see Treadmilling). Polymerization *in vitro* also requires that a monovalent salt, such as NaCl, be present at a concentration of ~100 m*M*, or a divalent salt such as $MgCl_2$ be present at ~1 m*M*.

Actin has a single high-affinity metal binding site, which has a greater affinity for Ca^{2+} than for Mg^{2+}. However, due to the much higher concentrations of Mg^{2+} than Ca^{2+} present *in vitro*, it is expected that this site will be occupied by Mg^{2+}. This has been shown experimentally to be true in muscle (35), where the Mg^{2+} concentration is three orders of magnitude higher than the Ca^{2+} concentration. Actin also has 5–10 lower affinity metal binding sites (36). The spontaneous nucleation of actin filaments is often the rate-limiting step in actin polymerization *in vitro*, since the subsequent growth of existing filaments can occur rapidly. Within the cell, however, there is good reason to believe that actin polymerization occurs under the control of other proteins which serve to nucleate and cap growing filaments, and it is possible that spontaneous self-nucleation of actin filaments may never occur.

Actin polymerization is also loosely coupled to the hydrolysis of the bound nucleotide. While almost all attention has been focused on the primary nucleotide-binding site, actin also has a second nucleotide-binding site with mM affinity (37). Since this site is likely to be occupied in cells such as muscle where there exists a millimolar concentration of ATP, it remains to be seen whether this second site plays a physiological role. It is known that the nucleotide hydrolysis is not required for polymerization, since G-ADP actin can polymerize, as can G-actin subunits containing nonhydrolyzable analogs of ATP. The role of ATP hydrolysis is to actually destabilize the filament (38), allowing for depolymerization to occur more readily. ATP hydrolysis lags behind the initial polymerization event and occurs once a subunit is part of the polymer. The cell therefore uses the energy of ATP hydrolysis to allow for the dynamic assembly and disassembly of actin filaments, in contrast to less dynamic components of the cytoskeleton, such as intermediate filaments. The energy of ATP hydrolysis can also be used to drive treadmilling, where there is a unidirectional flux of subunits through a filament.

Bibliography

1. P. A. Rubenstein (1990) BioEssays **12**, 309–315.
2. E. S. Hennessey, D. R. Drummond, and J. C. Sparrow (1993) Biochem. J. **291**, 657–671.
3. E. Ballweber, E. Hannappel, T. Huff, and H. G. Mannherz (1997) Biochem. J. **327**, 787–793.
4. M. F. Carlier and D. Pantaloni (1997) J. Mol. Biol. **269**, 459–467.

5. D. A. Schafer and J. A. Cooper (1995) Ann. Rev. Cell Dev. Biol. **11**, 497–518.
6. L. D. Burtnick, E. K. Koepf, J. Grimes, E. Y. Jones, D. I. Stuart, P. J. McLaughlin, and R. C. Robinson (1997) Cell **90**, 661–670.
7. A. McGough, B. Pope, W. Chiu, and A. Weeds (1997) J. Cell Biol. **138**, 771–781.
8. P. Matsudaira (1991) Trends Biochem. Sci. **16**, 87–92.
9. D. Hanein et al. (1998) Nature Struct. Biol. **5**, 787–792.
10. K. A. Taylor and D. W. Taylor (1994) Biophys. J. **67**, 1976–1983.
11. L. S. Tobacman (1996) Ann. Rev. Physiol. **58**, 447–481.
12. H. R. Knull and J. L. Walsh (1992) Curr. Top. Cell. Reg. **33**, 15–30.
13. W. Kabsch, H. G. Mannherz, D. Suck, E. F. Pai, and H. C. Holmes (1990) Nature **347**, 37–44.
14. P. J. McLaughlin, J. T. Gooch, H. G. Mannherz, and A. G. Weeds (1993) Nature **364**, 685–692.
15. C. E. Schutt, J. C. Myslik, M. D. Rozycki, N. C. W. Goonesekere, and U. Lindberg (1993) Nature **365**, 810–816.
16. K. M. Flaherty, D. B. McKay, W. Kabsch, and K. C. Holmes (1991) Proc. Natl. Acad. Sci. **88**, 5041–5045.
17. P. Bork, C. Sander, and A. Valencia (1992) Proc. Natl. Acad. Sci. **89**, 7290–7294.
18. R. A. Milligan, M. Whittaker, and D. Safer (1990) Nature **348**, 217–221.
19. A. Orlova and E. H. Egelman (1995) J. Mol. Biol. **245**, 582–597.
20. A. Orlova, E. Prochniewicz, and E. H. Egelman (1995) J. Mol. Biol. **245**, 598–607.
21. K. C. Holmes, D. Popp, W. Gebhard, and W. Kabsch (1990) Nature **347**, 44–49.
22. M. Lorenz, D. Popp, and K. C. Holmes (1993) J. Mol. Biol. **234**, 826–836.
23. K. Wakabayashi, Y. Sugimoto, H. Tanaka, Y. Ueno, Y. Takezawa, and Y. Amemiya (1994) Biophys. J. **67**, 2422–2435.
24. H. E. Huxley, A. Stewart, H. Sosa, and T. Irving (1994) Biophys. J. **67**, 2411–2421.
25. E. H. Egelman, N. Francis, and D. J. DeRosier (1982) Nature **298**, 131–135.
26. J. Hanson (1967) Nature **213**, 353–356.
27. F. Oosawa (1983) In *Muscle and Non-Muscle Motility* (A. Stracher, ed.) Academic Press, New York, p. 151.
28. G. Drewes and H. Faulstich (1993) Eur. J. Biochem. **212**, 247–253.
29. A. Muhlrad, P. Cheung, B. Phan, C. Miller, and E. Reisler (1994) J. Biol. Chem. **269**, 11852–11858.
30. T. Yanagida and F. Oosawa (1978) J. Mol. Biol. **126**, 507–524.
31. H. Isambert, P. Venier, A. C. Maggs, A. Fattoum, R. Kassab, D. Pantaloni, and M. F. Carlier (1995) J. Biol. Chem. **270**, 11437–11444.
32. T. Takebayashi, Y. Morita, and F. Oosawa (1977) Biochim. Biophys. Acta **492**, 357–363.
33. A. Orlova and E. H. Egelman (1993) J. Mol. Biol. **232**, 334–341.
34. M. F. Carlier (1998) Curr. Opin. Cell Biol. **10**, 45–51.
35. T. Kitazawa, H. Shuman, and A. P. Somlyo (1982) J. Musc. Res. Cell Motil. **3**, 437–454.
36. M. F. Carlier, D. Pantaloni, and E. D. Korn (1986) J. Biol. Chem. **261**, 10778–10784.
37. P. Kiessling, B. Polzar, and H. G. Mannherz (1993) Biol. Chem. Hoppe-Seyler **374**, 183–192.
38. C. Combeau and M. F. Carlier (1988) J. Biol. Chem. **263**, 17429–17436.
39. P. J. Kraulis (1991) J. Appl. Crystallogr. **24**, 946–950.
40. A. Orlova, X. Chen, P. A. Rubenstein, and E. H. Egelman (1997) J. Mol. Biol. **271**, 235–243.

Suggestions for Further Reading

41. P. Sheterline, J. Clayton, and J. Sparrow (1995) Actin, Protein Profile **2**, 1–103.

42. E. Reisler (1993) Actin molecular structure and function, Curr. Opin. Cell Biol. **5**, 41–47.
43. K. R. Ayscough and D. G. Drubin (1996) Actin: General principles from studies in yeast, Ann. Rev. Cell Dev. Biol. **12**, 129–160.

Actin-Binding Proteins

1. The Actin Microfilament System

Actin was identified more than 50 years ago as an essential element of the force generating apparatus of muscle cells (1, 2). Together with myosin, tropomyosin, and a large number of other proteins, actin filaments constitute sarcomeres, which are ordered serially along contractile myofibrils (3, 4). In the mid 1960s, actin (5) and myosin (6, 7) were recognized as major structural components of the eukaryotic cytoplasm (8-10); for an early review of the field see (11). The unexpected observation that actin was the inhibitor of DNase I (12), and that the DNase inhibitor could be crystallized (13), led to the identification of the actin monomer-binding protein, profilin (14). The properties of profilin seemed to explain how unpolymerized actin could exist at high concentrations in cells without spontaneously polymerizing (15). It is now known that there are several other proteins controlling actin polymerization, and today the family of actin-binding proteins contains over 100 members including proteins that sequester actin monomers (profilins, thymosins), sever (gelsolins), depolymerize (cofilins), and cross-link (villin, fimbrin) actin filaments. Further characterization of the nonmuscle myosins (16), and an increased appreciation of the role of polymerization of actin suggests how cells can extend pseudopods and drag themselves along extracellular matrices (17, 18), and exhibit the high degree of motility seen on the surface of lymphocytes and in malignant cancer cells. This entry will describe general characteristics of actin-binding proteins, the analysis of which in many cases has reached the atomic level.

Actin is an obligatory component of all eukaryotes, and is one of the most highly conserved proteins during evolution. Its sequence has varied less than 10% during the last 1200 million years (19). In mammalian cells, six different isoforms are known, of which the muscle specific a-isoform and the nonmuscle b-isoform are the most studied [for review, see (20)]. On the basis of structural homology an actin-related protein, FtsA, which is involved in cell division, has been recognized in prokaryotes (21). Also, in eukaryotes, there are several actin-related proteins, ARPs (22).

Actin can be kept in a monomeric form only under low salt conditions or in the presence of actin **sequestering** proteins (review 20). Under physiological salt conditions, actin polymerizes into long filaments. In this form, actin participates in force generation and motile activity. The actin filament is polar, with a rapidly growing (+)-end (barbed end) and a slow growing (–)-end (pointed end). In the cell, actin filaments grow by addition of monomers at the (+)-end, which is located at the outer edge of cell surface protrusions: lamellipodia and filopodia. In the submembraneous zone all round the cell, actin filaments are organized into sheets and bundles held together along their lengths by a variety of crosslinking proteins, which differ in length and flexural rigidity.

The myosins vary in structure; some are globular in shape, like myosin I, and do not polymerize, whereas others have a long a-helical, supercoiled, rod domain and can form filamentous superstructures in the cytoplasm (16). Together, actin and myosin transduce chemical free energy of adenosine trisphosphate (ATP) to mechanical work, not just in muscle cells, but in all eukaryotic cells. In different states of organization, the actomyosin system, is responsible for muscle contraction, cell locomotion, and cell division, and for many different local cellular transport processes (4). In nonmuscle cells, the actomyosin system is referred to as the microfilament system.

It is based on the organization of actin filaments, whose formation, organization and activity depend on the activity of a large number of actin-binding proteins, including myosin.

Microfilaments are present in particularly high concentrations in close apposition to the inner leaflet of the lipid bilayer (23-27), where they are directly or indirectly linked to cell surface proteins (receptors and adhesion proteins) continuously probing the extracellular environment. The lipid bilayer of the plasma membrane has been likened with “light machine oil” (28). It is an excellent electrochemical barrier, but it is the dense cortical weave of microfilaments which confers mechanical stability and deformability to the cell surface. Thus, the microfilament system can be viewed as an integral part of the physical barrier that separates the cellular contents from the outside world.

One of the first submembraneous actin-containing superstructures to be characterized was the red blood cell cortical network consisting of actin and the actin-binding proteins **tropomyosin**, spectrin and **band 4.1** (29). Linkage to the plasma membrane is provided by the spectrin-binding protein ankyrin, which binds to the transmembrane anion channel band III, and band 4.1 (an ERM protein, see below), which interacts directly with the transmembrane protein glycophorin. The adaptability of the shape of the red blood cell to the compressive forces present in the low-bore blood capillaries reflects the elastic properties of the spectrin:actin network. In the intestinal epithelium (30, 31, and refs. therein), microvilli on the apical surface of the cell are formed by tightly packed actin filament bundles stabilized by the actin crosslinking proteins villin and fimbrin (Fig. 1). The presence of nonmuscle myosin in these structures suggests that active movement may be involved in the resorptive process.

Figure 1. Structural organization of a microvillus. Among the simplest and best studied cell surface structures are the microvilli on polarized epithelial cells, especially those on cells of the intestinal epithelium. The majority of the proteins involved in the architecture of the microvillus have now been identified and characterized. Most of them are essential for the survival of the organism. In some cases their three-dimensional structure has been determined. It is still unclear how the assembly of the microvillus takes place and how it is controlled, how dynamic microvilli are, and what their contribution to uptake of nutrients is. The construction of a microvillus on apical surface of an intestinal epithelial cell is shown here. Many of the microvillar proteins also occur in other cell surface structures. An exception is villin, which is confined to the microvilli of a few cell types. In addition to villin, the major actin-binding proteins of the microvillar core are ezrin, fimbrin, and myosin-I. Drawing from Fath and Burgess 1995, *Curr. Biol.* **5**, 591–593.

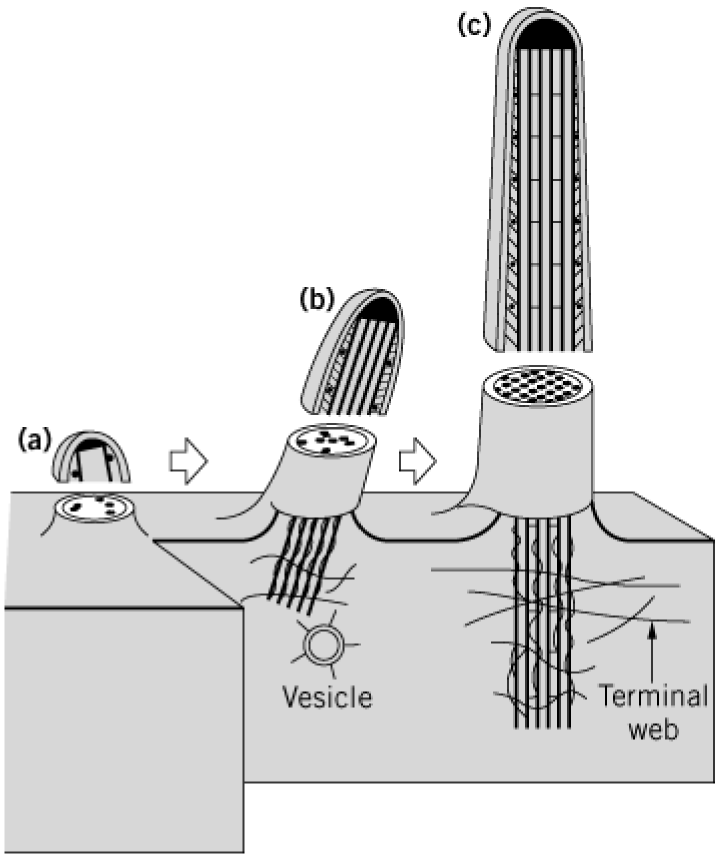

Specializations of the membrane-associated actomyosin system are found in all sensory organs, ie chemomechanical transduction in the actomyosin system is essential to the ability of the organism to perceive perturbations in the environment. For instance, the cellular basis for the sense of hearing lies in the microfilament-rich stereocilia in the hair cells of the inner ear, which convert subtle changes in the ambient air pressure to electrical signals transmitted to the brain via nerve impulses (32). Similarly, the mechanosensory cells in the skin confer the sense of touch (33).

Macrophages, lymphocytes, and neutrophils, which are highly motile cells, exploit the full potential of the cortical microfilament system as they forcibly move through and along extracellular matrices. When macrophages contact foreign invaders, the versatility of the cell cortex allows them to adapt their own surface structures as they engulf the pathogen.

The process of cell migration depends on the coordination of four major events involving microfilament reorganization: extension at the leading edge of membrane lamellae and filopodia, attachment to extracellular structures via transmembrane adhesion molecules, development of intracellular tension, and release of trailing end attachments with retraction of trailing ends (18, 27, 34, 35). The protrusion of lamellae at the advancing edge is driven by polymerization of actin filaments at focal complexes containing their fast growing ends at the plasma membrane, and crosslinking of formed filaments (24, 25, 36, 37). Clustering of transmembrane adhesion proteins, integrins, gives rise to focal adhesion sites (Fig. 2) linking extracellular matrix proteins to bundled actin filaments on the inside of the plasma membrane (38). The importance of the focal adhesions in transmembrane signalling is emphasized by their association with kinases regulating signal transducing protein:protein interactions and enzymes generating second messengers controlling not only the microfilament system, but also gene transcription (39). Several actin-binding proteins are targetted to these sites, contributing to formation of the integrin:actin filament linkage. The association of linkage proteins like talin, tensin, and vinculin appears to be controlled by phosphorylation. Myosin is activated through Ca^{2+}-dependent processes (40, 41), and the regulated deployment of myosin molecules leads to the generation of the forces needed for cell motility and other translocation processes. Release of adhesion at the trailing end of a migrating cell is controlled by Ca^{2+} and is followed by endocytosis of the integrins and their recycling to advancing cell edges (42). Used filaments are depolymerized, a process which involves the actin monomer- and filament-binding protein ADF (or cofilin) (17), and sequestered forms of unpolymerized actin are reformed (see Fig. 3).

Figure 2. Proteins of focal adhesion sites. Adherens junctions comprise both cell:extracellular matrix contacts, exemplified by focal adherens in tissue cultured cells, and intercellular junctions such as the zonula adherens between epithelial cells. The regulated assembly of adherens junctions is essential to a diversity of cellular functions including wound healing, anchorage-dependent cell proliferation, adhesion, and migration. Assembly of an adherens junction may be initiated when an integrin of the b1 subfamily binds to its extracellular matrix ligand, when a cadherin recognizes an identical molecule on a neighboring cell, or when a growth factor activates its receptor. These ligand–receptor interactions result in establishment of a physical connection between the extracellular ligand and the actin cytoskeleton. Efforts to elucidate these linkages have implicated vinculin as one of the connecting molecules in a chain that involves binding of the b1 subunit of integrin to talin, talin to vinculin, vinculin to a-actinin, and a-actinin to filamentous actin. It is now known that vinculin also can bind directly to actin filaments. How the initial ligand–receptor interactions trigger recruitment and organization of the multiple proteins found at an adherens junction is unknown, but recent evidence suggest that the activities of tyrosine kinases, tyrosine phosphatases, protein kinases and members of the Rho family of small GTPases are involved. (Drawing from M. C. Beckerle (1997) *Bioassays* **18**, 949–957)

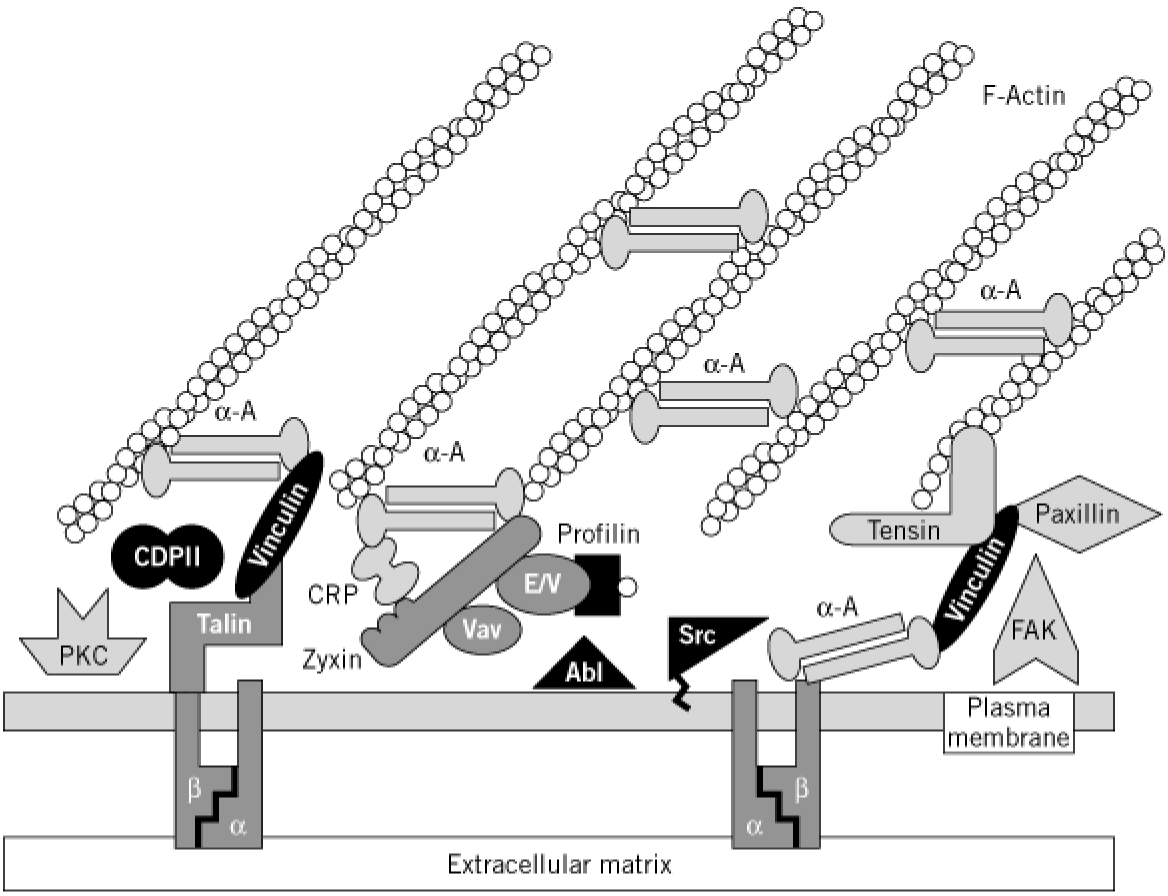

Figure 3. Links between the phosphatidylinositol and the cell motility cycles. Binding of growth factors like platelet-derived growth factor and epidermal growth factor to their cognate receptors activate the kinases activities of the receptors resulting in phosphorylation of a number of tyrosines on the cytoplasmic part of the receptor. This leads to activation of the signal transduction elements Cde42, Rac and Rho which control outgrowth of filopodia, membrane lamellae and the formation of stress fibers, respectively (64). There is only little information so far regarding the

mechanism of activation of these small GTPases and how they relay the signal to the phosphatidylinositol (PI) cycle. Receptor activation is followed by an immediate increase in the activity of kinases that form PtdIns 4,5-bisphosphate (PIP2) and PtdIns 3,4,5-trisphosphate (PIP3). Profilin, gelsolin, CapZ, a-actinin, vinculin, the ERM family of proteins all bind these phosphoinositides, which influence their activity in the microfilament-based cell motility cycle (CM-cycle). Phosphoinositides binding to CapZ or gelsolin unblock the (+)-end of actin filaments allowing incorporation of profilin:actin at that site. Profilin:actin is then dissociated and the actin monomer becomes stably incorported into the growing filament. Cross-linking of filaments by proteins like fimbrin gives rise to the ensembles of filaments seen in membrane lamellae and filopodia which function together with myosin in the contractile phase of cell motility. Calcium ions play important roles in regulating both the actomyosin interaction and the depolymerization of actin filaments. The depolymerization is facilitated by the dephosphorylated form of cofilin and the actin monomer sequestering proteins thymosin and profilin (rev. 163). Another branch of signal transduction from the growth factor receptor activates the gene program that leads to DNA synthesis and cell division. Grb and Sos are small proteins acting as signal transduction elements activating the small GTPases Ras, which in turn activates the serine/threonine kinase Raf. The further signalling pathway is complex invlving mitogen activated protein kinases, MAPKK and MAPK (for review, see *Cell* 1998, **95**, 447–450). Other abbreviations: IP3, inositol trisphosphate; IP2, inositol bisphosphate; IP, inositol monophosphate; DG, diacylglycerol; Pha, phosphatidic acid; CDP-DG, cytidyldiphosphate-diacylglycerol; PI, phosphatidylinositol.

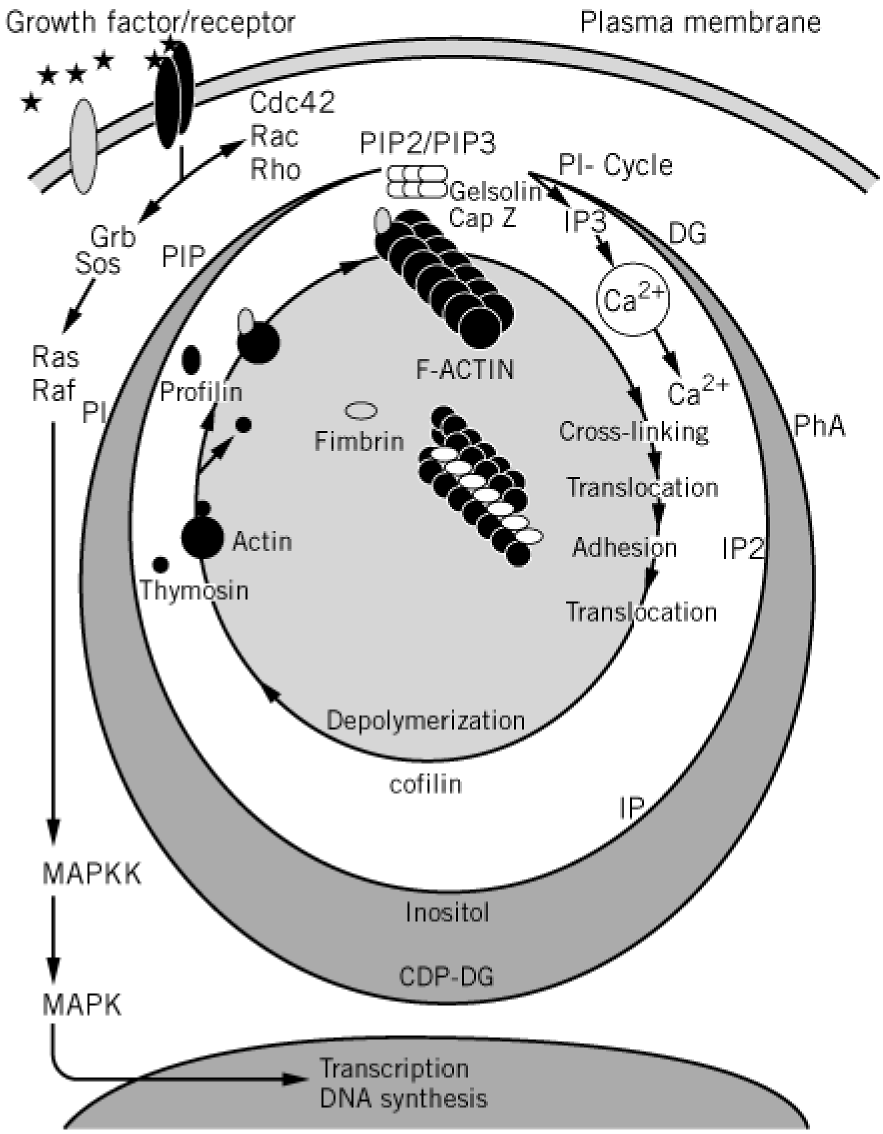

Thus, the combined action of protein factors controlling polymerization, crosslinking and tension development in the cell cortex is initiated by transmembrane signalling. Controlling the timing and position of sites of polymerization at the cell surface is a potent means of regulating shape change. An astonishing variety of well-ordered, yet dynamic, structures are possible, reflecting the mechanical properties and specificities of the different kinds of actin bundling proteins and junctional connectors. Their timed and coordinated formation prevents the appearance of random rigid networks, which would be incompatible with the well-orchestrated movements seen.

2. Signal Transduction and Restructuring of the Actin Microfilament System

Cell surface receptors continuously monitor the extracellular milieu and pass signals to the cytoplasm by generating second messengers of various kinds which either stimulate or inhibit the activity in the microfilament system. Addition of growth factors to serum-starved cultured cells causes the immediate outgrowth of membrane lamellae and filopodia, events that depend on the polymerization and organization of actin. About 60 seconds later, there is a generalized increase in motile activity of the cells, including restructuring of the actin-containing stress fiber system and translocation of the cell. Observations of this kind have been made both with epidermal growth factor (EGF) (43) and platelet-derived growth factor (26). In the case of EGF, a significant fraction of the receptors was found in direct association with microfilaments, and a binding site for actin on the receptor has been identified (44, 45).

The phosphatidylinositol-cycle (PI cycle) is coupled to activation of the microfilament system (46). Ligand-induced, receptor-mediated activation of kinases generate phosphatidyl inositol 4,5-bisphosphate (PtdIns 4,5-P2) and phosphatidyl inositol 3,4,5-trisphosphate (PtdIns 3,4,5-P3) (47, 48), both of which affect the activity of actin-binding proteins. Profilin, gelsolin, a-actinin, vinculin, ERM family of proteins, and myosin all bind PtdIns 4,5-P2, and/or PtdIns 4,5-P3. Stimulation of platelets with low concentrations of thrombin causes a transient increase in polyphosphoinositides during the first 10 sec (49). This is accompanied by an equally transient transformation of unpolymerized actin into filaments. This initial polymerization is over in about 10–20 sec (49). The immediate precursor for this polymerization appears to be profilin:actin, since increased amounts of free profilin appears in cell extracts after stimulation. Within 2 min, these filaments become organized into supramolecular structures by the action of crosslinking proteins stabilizing the protrusions seen on the platelet surface (50-52). Simultaneous activation of phospholipase Cg-1 results in the hydrolysis of PtdIns 4,5-P2, releasing the second messenger inositol trisphosphate, which causes release of Ca^{2+} ions from intracellular Ca^{2+} stores (53). Calcium ions are involved in activation of the actomyosin interaction and thereby force generation.

In addition to connections to the phosphatidyl inositol signal transduction cycle, the microfilament system is linked to the cAMP-dependent signalling system. Agonists causing increasing levels of cAMP often inhibit actin polymerization (54). A connection between adenylate kinase pathways and the actin monomer-binding protein profilin was suggested by genetic studies showing that increased levels of profilin could compensate for the deletion of the C-terminal domain CAP of the cyclase (55, 56). In platelets, the actin-binding protein, vasodilator-stimulated protein VASP is phosphorylated by cAMP- and cGMP-dependent kinases (57), which then correlates with the inhibition of microfilament reorganization.

The proteins involved in controlling the organization and function of the microfilament system are part of multiprotein signal transduction complexes. Several of these proteins have been identified as products of protooncogenes, ie proteins which in mutated form may cause cancer (58, 59). In these signal transduction complexes the proteins are linked together by adaptor modules in linker proteins such as SH2, SH3, and WW domains which recognize specific features of short polypeptide stretches, especially phosphotyrosine-containing and polyproline sequences (60). An example is the oncogene product **Vav** that has several such binding motifs suggesting how it links signal transduction at the cell surface to restructure the cortical cytoplasm (61). Vav possesses many of the homology domains commonly found in signal transduction complexes, comprising a phosphotyrosine-binding SH2 domain, two proline-rich peptide recognizing SH3 domains, a phosphatidyl inositol 4,5-bisphosphate recognizing PH domain, a guanine nucleotide exchange factor DH-domain, two cysteine-rich nuclear transcriptionally important LIM domains, and an actin-binding calponin homology domain. The clearest demonstration that these functional linkages actually lead to nuclear transcription is that the production of Interleukin-2 (IL2) requires Vav-dependent actin cap formation in activated T-cells (62, 63).

Outgrowth of filopodia and membrane lamellae, and the formation of stress fibers, which are manifestations of the activation of the microfilament system by different kinds of ligand:receptor interactions, all depend on the activation of members of the Rho subfamily of small GTPases for their control. The small GTPase Cdc42 appears to control formation of filopodia, Rac controls membrane lamellae and Rho stress fibers (64). There is only little information so far as to how the receptor-mediated transmembrane signal is relayed to the GTPases and what their downstream targets are. It has been shown with permeabilized platelets that ligation of the thrombin receptor, and activated Rac, uncap actin filament (+)-ends through phosphoinositide synthesis (65). Some of the microfilament-controlling, signal transduction elements mentioned below interact with small GTPases. Interestingly, moesin (see below), an actin-binding protein linking actin filaments to transmembrane receptors, is required for Rho and Rac effects on the actin filament system (66).

VASP belongs to a growing collection of related proteins that are involved in stimulation of assembly of actin filaments *in vivo* (67-69). In moving cells, it is found in highly dynamic membrane regions and in integrin-rich adhesion plaques. Molecular cloning of VASP has established that it has both a central proline-rich core, which interacts directly with profilin (68, 70), and an actin-binding site. In cells, the primary site of growth of actin filaments is thought to be at advancing cell edges, and profilin:actin heterodimers are believed to be guided into this site by VASP (71). High concentrations of VASP appear to be targetted to focal adhesion sites by zyxin (72). Zyxin also binds a-actinin and Vav suggesting that orderly assembly of crosslinked actin networks can proceed at these locales. In addition to binding profilin and zyxin, VASP binds to the SH3 domains of the src-family of protein kinases (69), thus integrating signal transduction via phosphorylation with the ordered assembly of cortical structures in locally specialized sites (63). VASP and vinculin complexes can be immunoprecipitated out of cell extracts with either antivinculin or antiVASP antibodies, and recent experiments have demonstrated that the interaction between the two proteins is enhanced by PtdIns 4,5-bisphosphate binding to vinculin (73).

VASP has come to prominence owing to its relevance to the understanding of the movement of the bacterium *Listeria* through the host cell cytoplasm (74). *Listeria* expresses a proline-rich protein on its surface called ActA (zyxin-like), which binds to the modular proline-binding SH3-domain of VASP. Apparently, VASP can attract profilin:actin complexes to sites of polymerization on the surface of the bacterium, generating a propulsive force. There are many examples of pathogenic microorganisms that have acquired host cell genes that code for proteins that modulate the behavior of the microfilament system for the purpose of invasion, locomotion in the cytoplasm, and cell-to-cell spreading.

WASP is a multidomain, actin-binding protein, which is defective in patients afflicted with Wiskott-Aldrich syndrome (75, 76), a disease characterized by severe thromifocytopenia and immunodeficiency. WASP is specific to hematopoietic cells, which in case of WAS have a paucity of surface filopodia and other shape abnormalities (77). The small GTPases Cdc42 and Rac bind directly to WASP (78-80). WASP is also a binding partner for Src family of protein tyrosine kinases (81).

A protein homologous to WASP, N-WASP, is more widely distributed. N-WASP is concentrated at nerve terminal regions in the post synaptic density, and coexpression of Cdc42 and N-WASP induces extremely long actin-based filopodia in cells (82, 83). Its involvement in the formation of membrane lamellae and filopodia may be controlled by phosphoinositides in the plasma membrane. It contains a pleckstrin homology PH domain and a cofilin homology domain. Furthermore, N-WASP has been shown to be essential for the actin polymerization-dependent movement of the bacterium *Shigella flexneri* (84).

WIP is a recently discovered WASP interacting protein that is important for cortical actin assembly (85). WIP contains both profilin- and actin-binding regions, which like in VASP, are near each other in the protein sequence suggesting that they constitute the binding site for a profilin:actin heterodimer to be added to a growing actin filament. The small signal transduction GTPase Cdc42 binds to WASP (78, 79), but not to WIP. Thus, WIP function may be regulated by Cdc42 via WASP. Stimuli that activate Cdc42 may target the WASP-WIP complex to the actin filament system via interactions between the WH1 domain of WASP and the proline-rich ABM1 motifs of structural proteins such as zyxin and vinculin. The presence of SH3 binding motifs in both WIP and WASP, and the capacity to bind to the adaptor protein Nck (86), suggest that the WASP-WIP complex couples additional signaling pathways to the actin filament system.

Formins are profilin and actin-binding proteins from *S. cerevisiae*. They direct the determination of cell polarization and cytokinesis (87 for refs.). In response to a-mating factor, the formin Bni1p forms complexes with the active form of Cdc42, actin, profilin, and actin associated protein Aip3p (88-90). These proteins localize to the tips of mating projections suggesting that the formin is a target for Cdc42, linking the pheromone response pathway to activation of the actin system.

The formin family of proteins is also important in limb and kidney development in vertebrates (91). Mutations in formins lead to defects in the contractile ring formation during cytokinesis, causing the appearance of multinucleated cells. Formins are localized both in the cytoplasm and the nucleus of the cells. FH-proteins, defined by the presence of 'formin homology' regions, are important for a number of actin-dependent processes, including polarized cell growth and cytokinesis. They are large, probably multi-domain, proteins and their function may in part be mediated by an interaction with profilin.

IQGAP is yet another actin-binding, multidomain, regulatory protein (92). It was originally described as a 190-kD protein with extensive sequence similarity to the catalytic domain of RasGaps (91). These proteins control the activity of small regulatory GTPases by stimulating their GTPase activity. Subsequently an IQGAP2 was described as a liver-specific protein with a 62% homology to IQGAP1 (93). However, so far no GAP activity has been found in relation to the GTPases examined. Both IQGAPs have several copies of a ca 50 amino acid long internal repeat (IR), a single WW (SH3-like) domain presumably binding to proline-rich sequences, a number of calmodulin-binding IQ motifs, and a putative actin-interacting calponin homology CH domain. In transient transfection of COS-7 cells with epitope-tagged Cdc42, it was demonstrated that IQGAP is present in the advancing lamellae of motile cells, and a major *in vivo* target of activated Cdc42 (94). The IQGAP1 binds to filamentous actin *in vitro* via its N-terminal domain and cross-links actin filaments in a Cdc42-dependent manner (95). Recently IQGAP1 was implicated in the regulation of E-cadherin-mediated cell-cell adhesion (96).

In fission yeast, *Schizosaccharomyces pombe*, the rng2 gene codes for an IQGAP-related protein, rng2p. The rng2p is located in the actomyosin ring and the spindle pole body and is required for the assembly of the actomyosin ring at cytokinesis (97).

Paxillin is not known as an actin-binding protein, but it is involved in the control of the microfilament system at the adhesion contacts. It was detected as a 68-kD phosphotyrosine-containing protein in RSV-transformed cells, and was later purified from smooth muscle cells (98, 99). Many features of paxillin suggest that it functions in signalling events at the adhesive membrane. It is concentrated at focal adhesions, and it is tyrosine phosphorylated in response to extracellular matrix binding and cell transformation. It binds *in vitro* to the elongated tail domain of vinculin, and thereby links vinculin to the SH3 domain of the $pp60^{csrc}$, a component of focal contacts. Integrins, which are the principal transmembrane proteins at these sites, do not seem to bind directly to paxillin, and paxillin does not seem to bind either a-actinin or actin, but there is evidence for direct association of paxillin to growth factor receptors. Adhesion of cells to an extracellular matrix like fibronectin or laminin via transmembrane integrins results in increased tyrosine phosphorylation of paxillin, and a similar increase in phosphorylation takes place in connection with clustering of integrins in the plane of the membrane with antibodies. This phosphorylation appears to be caused by activation of the focal adhesion-associated tyrosine kinase, pp125^{FAK}, and tyrosine phosphorylation of paxillin and pp125^{FAK} initiated by cell adhesion is accompanied by the appearance of organized actin-containing stress fibres. Mutagenesis of paxillin has identified one of the paxillin LIM domains as being responsible for targetting this protein to focal contacts (100)

Zyxin is a low-abundance phosphoprotein localized at sites of cell-substratum adhesion in fibroblasts (72). It has an architecture of an intracellular signal transducer with a proline-rich domain, a nuclear export signal, and three copies of the LIM motif. LIM is a double **zinc finger** domain found in many proteins that play central roles in regulation of cell differentiation. Zyxin interacts with a-actinin, members of the cysteine rich protein CRP family, proteins that display Src homology 3 (SH3 domains) and Vasp/Ena family members, which in turn bind to both actin and profilin. Zyxin and its partners have been implicated in the spatial control of actin filament assembly as well as in pathways important for cell differentiation. Based on its repertoire of binding partners and its behaviour, zyxin is thought to serve an organizing centre for the assembly of multimeric protein machines that function both at sites of cell adhesion and in the nucleus.

In summary, the major signal transduction pathways and mechanisms of activation have been shown to be linked to the changes in the dynamic restructuring of the actin cortex: the phosphatidyl inositol cycle and the cAMP second messenger systems and the small GTPase coupled signal transduction mechanisms. All of this points to the growing realization that cytoplasmic signal transduction and transcriptional events in the nucleus are so interwoven that discussions of sequential control by one system or the other are oversimplifications. The idea that actin cortical movements are "downstream" events of "upstream" effectors is similarly unjustified, since actively motile cells are required for the generation of the signal itself.

There are perplexing aspects of polymerization-based propulsion of bacterial pathogens, and by implication filopodial extension. WASP and N-WASP have actin-binding sequences. It is not clear what the role of these proteins is in the regulation of actin polymerization at focal growth sites. It is known that the polar actin filaments are oriented such that their fast growing ends are "pushing" against the moving bacterial wall, or against the membranes of the advancing edges of lamellipodia and filopodia. Actin-binding proteins such as WASP are anchored in these nascent growth complexes (to ActA in the case of *Listeria*). The problem is to explain what happens when an incoming actin monomer is presented as a profilin:actin precursor to the end of the growing filament, since it would appear to be blocked by WASP. Another problem is to account for the free energy of ATP hydrolysis that is made available by the actin polymerization reaction.

3. Further Links of Actin Filaments to the Extracellular Matrix

Cortactin is the name of two related proteins p80 and p85, which cross-link actin filaments close to the plasma membrane. Cortactin was first recognized as a substrate for tyrosine-phoshorylation in pp60^{src}-transformed cells, but its presence has also been demonstrated in a variety of nontransformed cells (101). Cortactins have internal repeats of 37 amino acid residues in the N-terminal end of the molecule, which are necessary for their binding to actin filaments. In the C-terminus there is an SH3-domain, and preceding that in the sequence there are proline and serine/threonine rich regions. These latter parts of the molecule are not needed for actin-binding, and their functions remain to be elucidated.

In non-transformed cells, cortactin is normally phosphorylated on serine and threonine, but becomes transiently phosphorylated on tyrosine in response to growth factor stimulation, and on transformation by activated cSrc. In platelets, cortactin becomes transiently tyrosine-phosphorylated in reponse to stimulation with thrombin. However, tyrosine phosphorylation of cortactin does not appear to affect its ability to bind to actin filaments, although it does influence its localization to the cortical actin filament system.

Stimulation of cultured cells with various growth factors and platelets with thrombin results in translocation of cortactin into the actin filament system of advancing lamellae and filopodia (102, 103). Activation of fibroblast growth factor receptor-1 results in an association of the activated receptor with cSrc, and a correlated association of cortactin with SH2 domain of cSrc. The redistribution from the cytoplasm into advancing lamellae (ruffles and lamellipodia) appears to depend on the Rac-1-induced activation of the serine/threonine kinase PAK1, a downstream effector of Rac1 and Cdc42 (104). These GTPases are involved in the control of kinases in the phosphatidyl inositol signalling pathway, and there is evidence that PtdIns 4,5-bisphosphate could be involved in the association of cortactin with the activated microfilament system (105).

Eps8 is a putative actin-binding protein which resembles cortactin in its distribution in the cell (106). It has an unusual Src homology-3 domain in the carboxy terminus, formed by an intertwined dimer of Esp8 molecules which may affect its peptide specificity. Eps8 is mostly localized in the perinuclear region. However, on stimulation of cells with growth factors, it accumulates in the peripheral cell extensions, where it is found colocalized with cortactin and filamentous actin. The Eps8 pool associated with newly formed lamellipodia and membrane lamellae appears to be mostly detergent-insoluble, as is the tyrosine phosphorylated population of Eps8 molecules generated by activation of vSrc kinase, suggesting Eps8 recruitment to specific sites during cell remodeling.

Ezrin, radixin, moesin (ERM) belong to the band 4.1 superfamily on the basis of their homology to the erythrocyte band 4.1, a protein that connects the actin/spectrin network to the erythrocyte membrane protein glycophorin C (31, 107, 108). Like cortactin, the ERM proteins appear to play structural and regulatory roles in stabilizing specialized organizations of actin filaments in connection with the plasma membrane both during development and in adult tissues. They are generally present in microvilli, filopodia, and membrane ruffles, sometimes together, but more often differentially distributed between different types of cells. They link transmembrane proteins with the cortical actin filaments, a process governed by signal transduction involving the Rho-GTPase (109). Ezrin has been shown to bind specifically to nonmuscle b-actin with high affinity (110).

The N-terminal domain of ezrin associates with plasma membrane components, and the C-terminal half connects these structures with the submembranous actin filaments. Purified ezrin exists in an inactive conformation that requires activation to expose sites that allow it to associate with the membrane components and with actin filament (107). It has been shown that binding of ezrin to the transmembrane hyaluronan receptor CD44 (111) requires activation of ezrin by PtdIns 4,5-bisphosphate binding to the N-terminal domain of ezrin (112-114). These are not the only transmembrane proteins binding ERM, since ERM proteins have a membrane location also in cells that do not express CD44. It is now known that ERM proteins, in addition to CD44, also bind to intercellular adhesion molecules, ICAM-1 and ICAM-2. A positively charged amino acid cluster of CD44, CD43, and ICAM2 positioned close to the lipid bilayer has been implicated in the binding (115).

A group of phosphorylated, 50–55 kDa, ezrin-binding protein has been purified from human placenta and bovine brain by affinity chromatography on immobilized N-terminal domains of ezrin or moesin (31). Isolated EBP50 has two peptide-binding PDZ domains in the N-teminal half of the molecule with capacity to bind to cytoplasmic tails of transmembrane proteins. The EBP50 can be coprecipitated with ERM and may serve to bind ERM members to one or more integral membrane proteins.

Cells opened up by the use of the detergent digitonin are still amenable to activation with non-hydrolyzable analogues of GTP. Addition of guanosine 5′-O-(3-thiotriphosphate), GTPgS, to such permeabilized cell models induces assembly of both actin filaments and focal adhesion complexes through activation of endogenous Rho and Rac (66). The sensitivity to GTPgS is lost after a few minutes of incubation, but can be restored by the addition of the actin-binding protein moesin indicating that moesin is required for the effect of Rho and Rac on actin filament system. This is an important step towards the resolution of the signal relay which initiates the reorganization of the microfilament system.

Talin is an elongated, flexible actin-binding protein first recognized in smooth muscle (116, 117) and platelets (118, 119). It is present in focal contacts in tissue cultured cells, in adhesion plaques formed by activated platelets, in myotendinous junctions, and in dense plaques of smooth muscle, but is absent from cell:cell interaction sites (for refs, see 38). In motile cells talin is present in membrane ruffles. It is a major protein in platelets constituting more than 3% of the total protein. In response to activation, it is redistributed to the actin-rich platelet cortex (120). Thus talin is clearly of central importance for the association of actin filaments to membrane components to sites where cells make close contact with extracellular matrix proteins, and it has been shown to interact with the cytoplasmic domains of transmembrane b1-integrin (116, 121).

Talin has a molecular mass of of 270 kD as estimated from the gene sequence (122). It is about 60 nm in length, and appears to be composed of a series of globular domains as judged by electron microscopy (123). In solution, it forms homodimers by antiparallel association of the monomers. It binds to integrin, vinculin, and actin *in vitro*. There are reports that talin can nucleate, cap and cross-link actin filaments, and that its activities may be controlled by phosphorylation by both serine/threonine and tyrosine kinases (124, 125). An N-terminal domain of talin is homologous to ezrin (122), and may be the part of the molecule which associates with membrane lipids. The larger C-terminal domain contains the binding site for vinculin (see (38) and (125) for further refs.). Disruption of the talin gene in embryonic stem cells leads to a disturbance in the formation of vinculin and paxillin-containing focal contacts and cell spreading (126). The talin (–/–) cells do form embryoid bodies, and notably two morphologically distinct cell types have been observed that were able to spread and form focal adhesion-like structures with vinculin and paxillin on fibronectin. Thus, although talin was essential for the expression of b1-integrin, a subset of differentiated cells managed without it. What substitutes for talin in these cells is unclear.

Vinculin is a 117-kD, actin-binding protein found concentrated at all sites of attachment of filamentous actin to transmembrane components of adherens junctions (38, 127-131). At these sites, it enters into multiple interactions with other proteins at the cytoplasmic face of the contacts. It is critically required as a structural component in the formation of the junctions. On ligand-induced clustering of integrins, vinculin is recruited from the cytoplasm to sites of integrin-ligand interaction, where it is a substrate for tyrosine phosphorylation by $pp60^{src}$.

There is electron microscopic evidence that the vinculin molecule can attain different conformational states. It is found either as a compact, globular molecule, or it is unfolded into a globular head with an extended tail (132-134). In the compact globular state, its actin-binding capacity is masked by an intramolecular association of the 95-kD head and 30-kD tail domains. The actin-binding site can be exposed by binding of acidic phospholipids to the protein suggesting that the affinity of vinculin for target molecules is regulated by modulation of the head-to-tail interaction, and that this may be used in the control of the assembly of adherens junctions (73, 135). The phospholipid PtdIns 4,5-bisphosphate binds to two descrete regions of the vinculin tail, disrupts the intramolecular head-tail interaction and induces vinculin oligomerization. The binding of PtdIns 4,5-bisphosphate to vinculin also enhances the association of vinculin to VASP the actin- and profilin-binding protein present in focal adhesion sites. The C-terminal tail region contains a binding site for the focal adhesion protein paxillin (136). Furthermore, vinculin has been identified as part of the cadherin-catenin junctional complex (137-139).

Tensin is a dimer of two 200 kD polypeptide chains. It is found in different types of cell contacts, including focal adhesions, zonula adherens, intercalated discs, and myotendinous and neuromuscluar junctions (140-143). It contains three distinct, actin-binding sites per monomer and appears to cap as well as cross-link actin filaments. Tensin also binds vinculin and possibly tyrosine kinase receptors through a Src homology 2 (SH2) domain (144). It has been suggested that a tensin dimer with its 6 actin-binding sites might wrap around the end of an actin filament, and bind it to a tyrosine kinase receptor through its SH2 domain. Induction of the formation of a focal contact, by the binding of extracellular ligands to integrins, causes tensin to be phosphorylated on tyrosine. Insertin, an actin-binding protein suggested to be involved in the actual incorporation of monomers into filaments, has been recognized as a proteolytic breakdown product of tensin (145).

4. Proteins Controlling Polymerization of Actin

DNase I (mw 31 000) was the first actin monomer-binding protein found (12). However it is doubtful whether DNase I plays a role as an actin monomer-binding protein in the cell. Since the enzyme is produced by acinar cells in the pancreas and secreted into the duodenum, it has been thought of as a digestive enzyme. However, intracellular forms of the enzyme have been observed, and there is evidence that it might be involved in programmed cell death, apoptosis. (146).

The crystallization of DNase I was reported in 1948 by Kunitz (147). The same year Laskowsky and collaborators described the presence of a proteinaceous inhibitor in tissues from vertebrates (148, 149). Two DNase I inhibitors (I and II) were isolated and crystallized in 1966 (13, 150). They were shown to form gelifying high molecular weight aggregates. Searching for the identity of the inhibitors eventually led to the finding that actin was the ubiquitous inhibitor of DNase I (12). Analysis of the crystals of the DNase I inhibitor II revealed that they contained actin together with an equimolar amount of a small protein, now known as profilin (14, 15). Later, the inhibitor I and II were identified as profilin in complex with g-actin and b-actin, respectively (151).

DNase I is a glycoprotein. It forms a stable 1:1 complex with monomeric actin, and when mixed with equimolar amounts filamentous actin, it causes depolymerization of the filaments and formation of the 1:1 complex with actin (152-154). Kabsch and coworkers provided the first insights into the structure of actin by solving the structure of the DNase I:actin complex (155; see special entry on actin). The high resolution structure of DNase I alone and complexed to an oligonucleotide has been reported as well (156, 157). The current model of the actin filament was arrived at using the structure of the actin monomer, as it occurs in the DNase I:actin crystal, together with diffraction data obtained with oriented gels of F-actin (158). This model is claimed to fit well into reconstructions of actin filaments from electron microscopic images (159, 160), and reconstructions of actin filaments with bound actin-binding proteins are interpreted in terms of this model (see below). However, doubts about this model being a relevant representation of the actin filament have been expressed, and an alternative way of deriving a model of F-actin has been suggested from the analysis of the organization of actin monomers in crystals of profilin and actin (161, 162). To ascertain the validity of the current model, independent information about the orientation of the actin monomer in the actin filament needs to be acquired.

Profilin (mw 12 000–15 000) is an abundant actin monomer-binding protein in eukaryotic cells (163, review). (See separate article Profilin.) Particularly high concentrations of profilin are found in lymphoid cells and brain cells. In lymphoid tissues the concentration of unpolymerized actin is about 100 μM and in platelets it may be as a high as 200 μM. In both cases about 50% of the unpolymerized actin can be accounted for by profilin:b-actin and profilin:g-actin isoforms. The remaining unpolymerized actin appears to be sequestered by b-thymosins (see below). For references on specific aspects of profilin, see (164-189).

Observations point at profilin being an important factor in the control of the release of inositol trisphosphate and thus of the generation of Ca^{2+} pulses in the cell. The primary targets for Ca^{2+} regulation in cells is the actomyosin system with global changes in structure and activity as the result. It is now known that many of the microfilament-associated proteins interact with components formed in the phosphatidylinositol-cycle as a result of receptor-mediated activation of the cell, and that these interactions modulate the activity of these proteins vis-a-vis actin. Although the exact physiological roles of these interactions remain to be elucidated, it suggests that the phosphatidylinositol-cycle is directly involved in controlling the microfilament-based motility cycle (see Fig. 3).

Beta thymosins constitute a conserved family of polypeptides (mw 5 000), the members of which were originally isolated from mammalian thymus and thought to be important for the immunoregulatory activities of this organ (190). Homologues of Tb4 have been found also in distantly related organisms (191). The thymosin b4 isoform is abundant in mammalian tissues, and has attracted much attention after the discovery of its association with unpolymerized actin in platelet extracts. It has a poorly defined structure as determined by NMR in solution (192). Binding studies suggested that it binds to the (+)-end of the actin monomer in competition with profilin. However, crosslinking studies imply a more complex interaction involving sites at both ends of the actin molecule (193).

Binding of thymosin b4 to actin monomers inhibits incorporation of actin monomers at both ends of the actin filament. Thymosin b4 has a rather low affinity for actin ($K_d = 5\ \mu M$), but since it is present in high concentrations in cells (in platelets ca 500 µM) it is considered to be the most important actin sequestering protein. In the presence of polymerization-inhibiting concentrations of thymosine b4, addition of profilin overcomes the thymosin effect, due to the higher affinity of profilin for actin ($K_d = 0.25\ \mu M$), and the fact that profilin:actin can add actin monomers onto the fast growing ends of actin filaments (see Profilin).

In vitro, thymosin can be shown to bind also to actin filaments and decrease the critical concentration for actin polymerization (194), and experiments on cultured cells indicate that b-thymosins may not be just actin sequestering factors (195). In the NIH3T3 cell line thymosin b10 is the predominant beta thymosin isoform, being present in about equimolar concentration to proflin and ADF/cofilin. Overexpression of thymosin b10 in these cells led to an increase in the cellular content of polymerized actin without any change in the total actin content of the cells. An intimate relationship with the regulation of the dynamic functioning of the microfilament system is also indicated by the increase in motility caused by overexpressing thymosin b10. Consonant with this an isoform of beta thymosine, thymosin b15, is upregulated in some forms of malignant cells (196).

The ADF/cofilin family of proteins include actin depolymerizing factor, cofilin, destrin, depactin, actophorin (197-199). These proteins are found in all kinds of eukaryotes, and when tested genetically they have proved to be essential. *In vitro*, they can form 1:1 complexes with actin monomers as well as with actin in filamentous form. The structure of the prototype ADF/cofilin, actophorin from *Acanthamoeba* have been solved by crystallography (200) and there are NMR structures of yeast cofilin and destrin (201, 202). It has recently been recognized that an ADF homology domain is present in each member of a newly identified protein family consisting of the ADF/cofilins, the twinfilins, and the drebrin/Abp1s (203).

In the cell, most of the ADF/cofilin is found in the perinuclear area, but there are also significant amounts in highly motile advancing lamella and filopodia, where the reorganization of actin through polymerization/depolymerization is most intensive. The interaction between ADF/cofilin and actin is sensitive to the pH of the medium, and as in the case of profilin, polyphosphoinositides interfer with the ADF:actin interaction. Physiologically, however, the most important mechanism controlling the activity of ADF/cofilin depends on phosphorylation/dephosphorylation of the protein. Phosphorylation of ADF/cofilin at a site near the N-terminus (S3) blocks its binding to actin. In cell extracts about 60% of the protein is phosphorylated, and in connection to receptor-mediated stimulation of cells dephosphorylation of ADF/cofilin takes place. The phosphatase involved in this reaction has not been identified, but a specific protein kinase, LIM kinase, has been found responsible for the *in vivo* phosphorylation of ADF/cofilin (204, 205).

The turnover of actin filaments inside living cells appears to be up to 100-fold faster than in *in vitro* experiments with actin alone. It has now been demonstrated in *in vitro* as well as in *in vivo* experiments that ADF/cofilin can accelerate the turnover of actin filaments (17, 199, 206-208). ADF/cofilin binds with higher affinity to ADP-containing actin, monomeric as well as filamentous, and facilitation of filament growth by active ADF/cofilin is likely to be brought about by increased depolymerisation of the actin filaments at their proximal ADP-containing ends increasing treadmilling activity. Nucleotide exchange, possibly enhanced by profilin, would in this model precede the reallocation of the ATP-containing precursor to the fast growing, distal (+)-end of the population of growing filaments. The presence of ADF in lamellipodia, where filaments are long, argues against a severing function *in vivo*, and the end-specific effects of ADF on filament assembly seen *in vitro* also indicate that the severing activity of ADF/cofilin is less important *in vivo*.

Twinfilin is a newly discovered protein composed of two cofilin-like regions (209). It was identified and characterized as an actin monomer-binding protein in budding yeast. Genes coding for homologous proteins have been recognized also in *Caenorhabditis elegans*, humans and mice. The two halves of the molecule twinfilin I and II resemble the corresponding domain from other species more than they resemble each other. Thus, twinfilins have evolved from a common ancestor and the twinfilins represent a single protein family (199). Twinfilin does not appear to act as an actin filament depolymerizing factor, but there are *in vivo* observations that suggest its involvement in the control of the dynamics of the microfilament system.

4.1. Arp

The first reports describing a family of actin-related proteins, the Arps, appeared a few years ago (2, 209). These are highly conserved proteins that share a 30–60% homology with actin, but are functionally distinct from actin. Two of these actin-related proteins, Arp2 (44 kD) and Arp 3 (47 kD) have attracted a great deal of attenion, since they were discovered to exist in a large complex together with five other proteins (40 kD, 35 kD, 19 kD, 18 kD, and 15 kD) that could be isolated by affinity chromatography on immobilized profilin (210). The Arp2/Arp3 complex has been reported to nucleate actin filament formation, to bind along the sides of actin filaments and to express filament crosslinking activity. A similar complex was identified in searching for factors that initiate actin assembly at the surface of Listeria (211). The Arp2/Arp3 complex is highly conserved among eukaryotes. Null mutations are lethal. It is localized in the cortex of amoebae and yeast and in the lamellipodia of higher eukaryotes (212, 213). In yeast, the Arp2/Arp3 complex is required for the integrity and motility of actin patches and for endocytosis (214). Thus the complex appears to play a major role in actin-based motility.

It has now been demonstrated that the Arp2/Arp3 complex isolated from *Acanthamoeba* binds profilin (215) and to the (–)-ends of actin filaments (168). It is not an efficient nucleator of actin polymerization. Capped filaments grow by the addition of monomers to the (+)-end. The complex can be seen by electron microscopy to attach the (–)-end of one filament to the side of another filament. This suggests that the Arp2/Arp3 complex might control the assembly of a branching network of actin filaments in the advancing lamellae of motile cells. Similar branching of actin filaments have been recognized earlier in electron microscopic pictures of the weave of microfilaments in advancing lamellae in moving keratinocytes (36). The cellular concentrations of the Arp2/Arp3 complex has been estimated to be high enough to cap the (–)-ends of all filaments in a cell. These observations imply that models assuming that actin filaments *in vivo* undergo an ADF/cofilin-aided depolymerization from the (–)-end during motile activity may be too simplistic, since there must also be mechanisms for the controlled uncapping of the (–)-ends of the filaments.

Further studies of the *Listeria* system have shown that the bacterial protein ActA, which is essential for the actin polymerization-dependent propulsion of the bacterium through the cytoplasm, acts synergistically with the Arp2/Arp3 complex *in vitro*. Working together, they eliminate the lag phase in the polymerization of actin and increase the initial rate of assembly 50-fold (216). This activity has been shown to reside in the N-terminal domain of the ActA protein. A cellular protein that corresponds to ActA has not yet been identified, but zyxin has been pointed out as a plausible candidate.

Capping protein Z (CapZ) is a heterodimeric protein, which was first detected in skeletal muscle sarcomers, where it is associated with actin filaments at the Z-line end of sarcomers, i.e. at the (+)-end of the filament (217). *In vitro*, it binds with high affinity ($K_d \approx$ nM) to the (+)-end of actin filaments. A homologous protein that exists in non-muscle cells, capping protein b_2 (CPb_2), is enriched at the edge of the advancing lamellum of spreading platelets. By binding to the (+)-end of actin filaments, it blocks the addition of actin monomers to that end, and since actin filaments *in vivo* appear to grow by assembly primarily at that end, these capping proteins may be important regulators of actin polymerization. The fact that CPb_2 is necessary for the proper organization of actin bundles in the morphogenesis of bristles in *Drosophila*, the view is strengthened that CPb_2, gelsolin in some cases, and Cap G may play active roles in actin-based motility in response to signaling. There is evidence also in this case that polyphosphoinositides are involved in the regulation of the protein.

4.2. Adducin
In erythrocytes there is, in addition to CapZ, a second actin filament (+)-end capping protein, adducin (218, 225). This protein is associated with the short erythrocyte actin filaments (one a,b heterodimer per filament). Adducin has been shown to bind to spectrin:actin complexes in the cell cortex, and promote the binding between these two proteins. It also appears to be able to bind directly to actin filaments and to bundle them. Adducin has a relatively low affinity for the filament (+)-end, but even so it appears to be the capping protein bound to the erythrocyte actin filaments, and not CapZ. Its binding to actin filaments is downregulated by calcium and calmodulin, an effect possibly modulated by reversible phosphorylation of the protein. The complex relationship between adducin and the spectrin:actin network indicates that adducin represents a new type of regulated actin filament-binding and barbed end capping protein. The entire molecule is required for capping activity, and the association of adducin with actin filaments seems to be regulated by Rho-associated kinase and myosin phosphatase.

Gelsolin is an abundant and ubiquitously expressed actin-binding protein, which confers calcium sensitivity to the regulation of the dynamics of the microfilament system (219). (See separate article Gelsolin.) For references on specific aspects of gelsolin, see (219-223).

Tropomodulin is a 43 kD protein that caps the (–)-ends of actin filaments in erythrocyte cortical network and in striated muscle sarcomeres (225). The interaction is particularly tight when tropomyosin is bound simultaneously. It is thought that tropomodulin is important in controlling the length of the actin filaments in these situations.

5. Architectural Elements of the Actin Cortex

The dynamic changes in cell surface morphology and motile behaviour, seen in response to growth hormones and other cell stimulating agents, reflect changes in the formation, organization, and activity of the microfilament system. Actin-binding proteins that cross-link actin filaments into tightly packed bundles and more loosely organized networks are necessary for the formation of the weave of microfilaments seen in membrane lamellae and filopodia and in the rest of the submembraneous zone around the cell. Actin-based surface projections on cells take many forms, such as the elaborate stereocilia of cochlear hair cells, microvilli of intestinal epithelium, and the membrane ruffles and filopodia on moving fibroblasts. The formation of these structures depends on the activity of actin-crosslinking proteins. Important members of this class of proteins belong to the spectrin superfamily which are reviewed in ref. 237.

Villin is closely related to gelsolin, an actin severing protein (described above), but distinguished from gelsolin by the presence of an additional domain comprised of 76-amino acid residues, called the “headpiece” (224-229). The headpiece contains an additional actin-binding site, which confers actin filament bundling activity to the protein. Villin is found in the microvilli of certain types of epithelia. Crosslinking of actin filaments occurs at low Ca^{2+} concentrations. Like gelsolin, villin severs actin filaments in the presence of micromolar concentrations of Ca^{2+}, and after breakage of the actin filament, villin remains bound to the (+)-end of one of the fragments. The actin-binding properties, tissue distribution and expression during cell differentiation suggest that villin is important in organizing the actin filament core of microvilli in epithelial cells forming brush borders. In support of this, villin expressed transiently in transfected fibroblasts, results in loss of stress fibers and appearance of large numbers of microvillar protrusions on the dorsal surface of the cells. Microinjection of high concentrations of villin into cells that normally lack this protein, lose their stress fibres, and incorporate the villin into cell surface microspikes and large microvilli, an activity which was shown to depend on the presence of the C-terminal head piece.

The N-terminal domain of villin (14T) consists of 126 amino acid residues. It binds calcium and actin. The structure of this domain has been determined by NMR (230). The 76-amino acid residue long, C-terminal domain of villin is an actin-binding module that is also used in another actin-bundling protein **dematin** (band 4.9), but whose core domain is unrelated to villin. The 3-dimensional structure of the stably-folded 35 residue long subdomain of the villin headpiece has been determined by NMR (231). It is the smallest autonomously folding protein unit found.

Fimbrin belongs to the plastin family of actin-binding proteins (31, 232, 237). Members of this family are present in all types of eukaryotic cells. Fimbrin is the smallest of the actin crosslinking proteins. It consists merely of an N-terminal EF-domain and two actin-binding domains, each composed of two CH domains. Fimbrin is present together with villin in the microvilli of the intestinal brush border, and in the membrane lamellae and microspikes of most other eukaryotic cell types. A fimbrin-binding site on actin has been suggested from analysis of actin mutations suppressing fimbrin mutations (233). The structure of the N-terminal actin-crosslinking domain of fimbrin has been solved by crystallography (234), and electron cryomicroscopic images of fimbrin-decorated actin filaments has been used to localize the fimbrin-binding site on the surface of the actin filament (235).

In a suggested scenario for the formation of a microvillus (236), the first phase consists of the “streaming” of actin filaments from electron-dense plaques on the apical plasma membrane. These filaments then gathered into loose bundles that extend into rudimentary microvilli. Villin may contribute to an initial bundling of the filaments. Ezrin (see section 3), a protein controlled by tyrosine phosphorylation, links the microvillar actin filaments to the membrane components. During a second phase, the microvilli elongate and become highly organized into a full core of hexagonally-packed actin filaments. This phase correlates in time with the localization of fimbrin to the core of the microvillus. In this way a stable surface protrusion is thought to take form. Similar schemes may apply to the development of surface protrusions on the surface of other types of cells.

ABP-280, filamin, and ABP-120, are all rod-like, dimeric, actin filament crosslinking proteins, where each monomer has an N-terminal actin-binding CH-domain and a long repeat region consisting of tandemly repeated, 100 amino acid residue long, homologous segments (237). The length of the repeat region is different in the different ABPs. The ABP120 was found in *Dictyostelium discoideum*. The vertebrate variants, ABP-280 and filamin, are major cellular proteins, and products of different genes. Filamin is located specifically in the Z-lines structure of the sarcomeres in muscles. ABP-280 is a major cellular protein in non-muscle cells, where it is present in the cell cortex. The function of ABP-280 appears to be to cross-link actin filaments into orthogonal networks. The 3D-structure of the repeat region of ABP-120 (gelation factor, 6 repeats) has been determined by NMR spectroscopy, which shows it to have an immunoglobulin-like fold (226). Both filamin and ABP-280 (24 repeats) share conserved residues that form the core of the gelation factor repetitive segment structure as determined by NMR. This distinguishes these actin crosslinking proteins from the spectrins and a-actinins, which have tandem repeats of an a-helical domain.

On the basis of their actin filament crosslinking activity, depending on the presence of a calponin homology CH domain, and their elongated shape, as seen by electron microscopy, these proteins have been grouped together with the spectrin and fimbrin families into a superfamily. It is true that the actin binding domains of all these proteins are homologous. However, the presence or absence of repeat domains, and the widely different structures of the repeat domains of the spectrin and filamin families, rather suggests that the three families should be considered as separate protein families employing a common actin-binding domain, since it is possible that the different families will turn out to have quite different functions in relation to the actin filament system.

Spectrin (fodrin) was first isolated as part of the matrix proteins of the erythrocyte plasma membrane (237-240). Underneath the lipid bilayer of these cells, and linked to transmembrane proteins glycophorin and the ion channel band 3, there is a regular organization of units consisting of five or six spectrin molecules attached to a short actin filament. The spectrin molecules are attached to spectrins of adjacent units to form a sheet of five- and six-sided polygons. The membrane skeletons, and isolated junctional complexes, reproducibly contain four proteins in the molar ratios of 1 spectrin dimer:2-3 actin monomers:1 band 4.1 protein:0.1–0.5 protein 4.9 (protein designations refer to mobility on gel electrophoresis). In addition tropomyosin, tropomyosin-binding protein and adducin are thought to be part of the junctional complex.

Spectrin consists of two subunits, an a and a b subunit, which form heterodimers, which in turn associate to form tetramers in the membrane lattice. The b-chain has an N-terminal actin binding CH domain and 12 a-helical repeat domains, whose structure has been determined by NMR spectroscopy (241). The a-chain associates in an antiparallel fashion with the b-chain. It has a C-terminal EF-hand domain, which is close to the actin-binding site of the b-chain followed towards the N-terminus by a binding site for protein 4.1, and a Src-like sequence in the middle of the somewhat longer repeat region. Between repeat 11 and 12, there is a calmodulin-binding sequence inserted. The structures of the spectrin repeat, the phosphoinositide-binding pleckstrin (PH) domain, the SH3 domain, and the CH domain have all been determined (241-246).

The spectrin-actin based network of proteins endows the erythrocyte with an exquisite elasticity which makes it possible for it to go through quite drastic shape changes. However, it is clear that the structural role played by the spectrin:actin system is not its sole function. The close relationship between the spectrin-actin system and transmembrane ion channels implies that the range of controlling functions is wider. The spectrin-actin system is not unique to the erythrocytes, but exists also in other tissues and in cells of as widely separated organisms as *Drosophila*, *Acanthamoeba*, *Dictyostelium*, echinoderms, and possibly also in higher plants.

Alfa-actinin is a classical skeletal muscle protein identified a long time ago (237, 247). It is highly enriched at the Z-disc-end of the actin filaments in the sarcomeres of the myofibrils. It is now known also to be an integral part of the microfilament system in nonmuscle cells, where an interaction between transmembrane b1 integrins and a-actinin has been demonstrated (see Fig. 2). There are several isoforms of a-actinin, which are products of three different genes. *In vitro*, it crosslinks actin filaments into regular ladder-like structures. It is therefore thought to contribute to the organization of actin in cells. Alfa-actinin is an elongated homodimer (200-215 kD) with antiparallel arrangement of the two subunits. Each subunit consists of a CH-domain, 4 a-helical domains (“spectrin repeats”), and an EF-hand domain. The binding of nonmuscle a-actinin to actin filaments is modulated by Ca^{2+} binding to the EF-domain, whereas the muscle isoform of a-actinin is insensitive to Ca^{2+}. The 3D-structure of the CH-domain is known by analogy to the structure of the corresponding domain from calponin solved by x-ray crystallography, and the structure of the repeated domain is known by analogy to the known a-helical repeat domain in spectrin, and the EF-hand can be compared with calmodulin.

Alfa-actinin can be extracted from myofibrils without major destruction of the sarcomeric organization of the actin filaments in the myofibril, and when added back to the myofibril preparation it rebinds at the Z-disc. This implies that a-actinin may serve some function, other than a structural, in relation to the actin filaments. In nonmuscle cells, a-actinin is found enriched in spots along stress fibres and in cell adhesion plaques.

Dystrophin is the product of the gene responsible for the X-linked myopathies Duchenne and Becker muscular dystrophy. It is an elongated protein of high molecular weight (430 kD) present in low amounts in muscle and nerve cells. A closely related protein, utrophin, is more widely distributed, and there are many dystrophin/utrophin isoforms produced, due to the operation of alternative promotors and alternative splicing. The structure of these proteins place them in the spectrin/a-actinin family of proteins. They are multidomain proteins; the largest isoform is comprised of 3 N-terminal and 2 internal actin-binding sites, a peptide-binding WW domain, a calcium-binding EF domain, a zinc finger domain. The N-terminal actin binding region has sequence homology with the calponin homology CH domains of the spectrin/a-actinin family of proteins.

Dystrophin/utrophin connect cortical actin filaments with transmembrane proteins, dystroglycans and sarcoglycans, which in turn associate with extracellular matrix proteins, laminin and merosin, respectively. Skeletal muscle dystrophin can be purified from muscle cells as a large multiprotein dystrophin-glycoprotein complex, which stabilizes actin filaments *in vitro* through lateral associations. Both dystrophin and utrophin bind with higher affinity to b- than to a-actin. Comprehensive reviews on the structure and function of the dystrophin/utrophins are found in ref 237, 248.

6. Ion Channel-associated Actin-binding Proteins

The spectrin-actin network in erythrocytes is involved in anchoring ion exchange proteins in the membrane via the linker protein ankyrin, a critical link in maintaining the characteristic biconcave shape of the cell (249). In axons, an interaction between actin, **fodrin**, and ankyrin appears to be responsible for concentrating sodium channels at the nodes of Ranvier (249). At the neuromuscular junction, the clustering of acetycholine receptors appears to be mediated by spectrin, actin, and the **rapsyn/43 kD actin-binding protein** (250). Various lines of evidence suggest that intact actin filaments, and perhaps actin polymerization itself, are required for calcium regulation of the postsynaptic response of NMDA receptors in the central nervous system (251). Postsynaptic excitatory synapses are most often found on the small actin-rich budlike structures, called spines, that protrude from the dendrites of highly arborized neurons such as cerebellar Purkinje cells (252). Dendritic spines have pronounced electron-dense (as seen by electron microscopy) post-synaptic densities, called PSD's, that are the likely sites of proteins linking receptors to actin. Candidate proteins include PSD-95/SAP90, chapsyn/PSD-93, SAP102, and **alpha-actinin-2**. Only alpha-actinin has a demonstrated actin binding affinity, and it has been suggested that clustering for some classes of receptors might be mediated by a looser, more “corral-like”, entrapment mechanism (253). The PSD contains brain dystrophin, an isoform of the muscle protein originally identified as the mutated gene product involved in muscular dystrophy that is known to link transmembrane ion channels to actin filaments (254).

The precise role for actin in the functioning of ion channels is unclear. The provision of clustered anchorage sites may confer cooperativity in the opening of channels, or support the formation of multiprotein complexes capable of integrating different signalling or environmental factors. It is not unlikely that the actin network might passively or actively transmit forces to the channels providing the impetus behind stretch-activated gating phenomena.

7. Myosin as an Actin-binding Protein

The myosins belong to a large superfamily of proteins, which together with actin transduce chemical energy to force generating tension and movements in the eukaryotic cells. Myosin II is the prime partner of actin in the generation of force in muscle, as well as in nonmuscle cells. Generally myosins are thought of as the force generators, and therefore referred to as motor molecules. However, the actual mechanism of force generation is still unknown. Although, the ATP-binding head domain is largely conserved, there are many different molecular forms of myosin serving in as diverse functions as muscle contraction, cell motility, membrane traffic, and sensory perception. Myosin hydrolysis ATP to ADP.Pi still bound to the head domain. Interaction with actin filaments brings about product release, and in the presence of actin filaments, there is a rapid ATP-dependent cycling of heads on and off the actin filaments as ATP is hydrolysed. A current review of the myosin superfamily and their functional involvements is found in ref. 255. For a more detailed account of the structure and function of myosin see the entry on myosin in this encyclopedia.

8. Regulators of the Actomyosin Interaction

The N-terminus of actin is involved in the binding of a large number of actin binding proteins, including myosin (S1), tropomyosin, troponin I, a-actinin, caldesmon, gelsolin, cofilin, actobindin. This actin interface is important for muscle contraction, since it is implicated not only in the activation of the myosin ATPase, but also in the regulation of actomyosin interaction by interacting with troponin I.

Tropomyosin is an elongated, dimeric, coiled-coil a-helical protein that binds along the actin filament (see special entry). The tropomyosin molecule has a sevenfold repeat of nonpolar and polar amino acid residues that bind seven actin monomers in the filament. Multiple genes for tropomyosin and alternative splicing can generate a number of tropomyosins that are differentially expressed during development and in different cell types. Muscle cells express 1–2 and most vertebrate nonmuscle cells 3–8 tropomyosin isoforms. Tropomyosin in complex with the heterotrimeric protein troponin makes muscle contraction Ca^{2+} dependent, but the function of tropomyosin in nonmuscle cells has not been clarified. However, the involvement of tropomyosin in the control of chemomechanical transduction also in nonmuscle cells is indicated by the occurrence of tropomyosin in tightly bundled and contractile organizations of actin filaments (stress fibres). For further information see special entry on tropomyosin.

Troponin is a heterotrimeric protein complex that interacts directly with actin through one of its subunits. Together with tropomyosin it confers calcium sensitivity to muscle contraction in striated muscles (see special entry).

Caldesmon is involved in the regulation of the actomyosin interaction in smooth muscle (256, 257). It inhibits actomyosin ATPase and filament sliding *in vitro* has been shown to bind to subdomain 2 of actin. Three-dimensional image reconstruction of reconstituted thin filaments consisting of actin and smooth muscle tropomyosin, both with and without a caldesmon derivative added has been reported. In filaments containing the caldesmon derivative, tropomyosin was found in a different position as compared to the situation in the absence of the caldesmon. The observations suggest that caldesmon causes changes in the relationship between tropomyosin and the actin filament, which are different from those seen with troponin.

The giant modular protein nebulin (mw 600- 900 kD) spans the whole length of the thin filament of the striated muscle sarcomeres in vertebrates, and has been proposed to function as a “ruler” for control of the length of actin filaments in sarcomeres (258-260). It is thought to bind and stabilize F-actin. It comprises 2-3 % of the myofibrillar protein mass of skeletal muscles. There are tissue and development-specific isoforms. The C-terminal part of human nebulin is anchored in the sarcomere Z-disk and contains an SH3 domain. The nebulin SH3 sequence from several species has been determined and found strikingly conserved. Its 3D-structure has been determined in solution by NMR spectroscopy, and its interaction with poly(L-proline) has been modelled. Nebulin consists of nearly 200 tandem repeats of homologous modules about 35 residues long. These are organized into about 20 tandem superrepeats consisting of 7 different modules, and this superrepeat segment is flanked near the N- and C-termini by single-repeat regions containing 8 modules of the same type. It has been proposed that the 35 residue module is the basic actin-binding domain and that the superrepeats reflect tropomyosin/troponin binding sites along the nebulin molecule. Exactly how the nebulin molecules are linked to actin filaments in the sarcomere of muscle is not yet known. Nebulin promotes actin nucleation and stabilizes actin filaments. Crosslinking experiments have identified the first two residues in actin to be involved in binding nebulin.

9. Future Directions

One of the most remarkable aspects of the contractile apparatus in muscle cells is the capacity of the system to ramp up its power output in response to increased demands for mechanical work. This phenomenon is known as the Fenn Effect, and it suggests that the acto-myosin system can increase its ATPase activity in response to higher imposed loads. It is apparently the lattice organization of filaments into sarcomeres that somehow enables the effect of external loads to be transmitted directly to the proteins producing the biochemical reactions that produce work from ATP hydrolysis. It remains to be seen if the bundles and meshworks found in non-muscle cells display similar, or even more unusual, chemomechanical feedback mechanisms. Muscle cells also perform work at nearly 100% thermodynamic efficiency, and it is interesting to ask whether the free energy transduction pathways in the cytoplasm are equally optimized for their tasks.

The newly discovered connections between the microfilament system and signal transduction raise a host of questions that will be the subject of future research. What roles do mechanical forces play in transmitting signals from the surfaces of cells to their nuclei? What regulates the assembly of these focal sites of signalling potential and what leads to their breakup after a signalling cascade has outlived its usefulness?

The large number of actin-binding proteins obscures the possible branching points that must have occurred during evolution to establish this incredibly diverse dynamical system. The analysis of evolutionary relationships in actin-binding proteins from amoeba, plants, and mammals will be of extraordinary interest for understanding how the immune system and the mammalian nervous system developed as specializations of more primitive motile mechanisms.

Bibliography

1. F. B. Straub (1942) Studies from the Institute of Medical Chemistry, Univ. Szeged **2**, 3–15.
2. F. B. Straub (1942) Studies from the Institute of Medical Chemistry, Univ. Szeged **3**, 23–37.
3. A. G. Engel and C. Franzini-Armstrong (1994) *Myology*, vol. **1**, 2nd edition. McGraw-Hill, Inc. New York.
4. B. Alberts, D. Bray, A. Johnson, J. Lewis, M. Raff, K. Roberts, and P. Walter (1998) *Essential Cell Biology*, Garland Publishing Inc., New York & London.
5. S. Hatano, T. Totsuka, and F. Oosawa (1966) Biochim. Biophys. Acta **127**, 488–498.
6. S. Hatano and M. Tazawa (1968) Biochim. Biophys. Acta **154**, 507–519.
7. M. R. Adelman and E. W. Taylor (1969) Biochemistry **8**, 4964–4975.
8. H. Ishikawa, R. Bishoff, and H. Holzter (1969) J. Cell Biol. **43**, 312–328.
9. E. Lazarides and K. Weber (1974) Proc. Natl. Acad. Sci **71**, 2268–2272.
10. K. Weber and U. Groeschel-Stewart (1974) Proc. Natl. Acad. Sci **71**, 4561–4564.
11. T. D. Pollard and R. R. Weihing (1974) Critical Reviews in Biochemistry **2**, 1–65.
12. E. Lazarides and U. Lindberg (1974) Proc. Natl. Acad. Sci **71**, 4742–4746.
13. U. Lindberg (1966) J. Biol. Chem. **241**, 1246–1248.
14. L. Carlsson, L.-E. Nyström, U. Lindberg, K. K. Kannan, H. Cid-Dresdner, S. Lövgren, and H. Jörnvall (1976) J. Mol. Biol. **105**, 353–366.
15. L. Carlsson, L.-E. Nyström, I. Sundkvist, F. Markey, and U. Lindberg (1977) J. Mol. Biol.

115, 465–483.

16. V. Mermall, P. L. Post, and M. S. Mooseker (1998) Science **279**, 527–533.
17. M.-F. Carlier and D. Pantaloni (1997) J. Mol. Biol. **269**, 459–467.
18. M. D. Welch, A. Mallavarapu, J. Rosenblatt, and T. J. Mitchison (1997) Curr. Opin. Cell Biol. **9**, 54–61.
19. R. F. Doolittle (1995) Philos. Trans. R. Soc. Lond. B. Biol. Sci. **349**, 235–240.
20. P. Sheterline, J. Clayton, and J. Sparrow (1996) *Protein profile; Actin*, 3rd edition. Acad. Press, London.
21. M. Sanchez, A. Valencia, M. J. Ferrandiz, C. Sander, and M. Vicente (1994) EMBO J **13**, 4919–4925.
22. S. Frankel and M. S. Mooseker (1996) Curr. Opin. Cell Biol. **8**, 30–37.
23. J. V. Small and J. E. Celis (1978) Cytobiologie **16**, 308–325.
24. A.-S. Höglund, R. Karlsson, E. Arro, B.-A. Fredriksson, and U. Lindberg (1980) J. Muscle Res. Cell Motil. **1**, 127–146.
25. J. V. Small, G. Rinnerthaler, and H. Hinsen (1981) Cold Spring Harb. Symp. Quant. Biol. **46**, 599–611.
26. K. Mellström, A.-S. Höglund, M. Nistér, C.-H. Heldin, B. Westermark, and U. Lindberg (1983) J. Muscle Res. Cell Motil. **4**, 589–609.
27. J. V. Small, M. Herzog, and K. Anderson (1995) J. Cell Biol. **129**, 1275–1286.
28. G. L. Nicolson, G. Poste, and T-H. Ji (1977) Cell Surface Reviews, vol. **3**., Dynamic aspects of cell surface organization (G. Poste and G. L. Nicolson, eds.), North-Holland, Amsterdam, p. 148.
29. A. Viel and D. Branton (1996) Curr. Opin. Cell Biol. **8**, 49–55
30. M. Arpin, M. Algrain, and D. Louvard (1994) Curr. Opin. Cell Biol. **6**, 136–141.
31. A. Bretscher, D. Reczek, and M. Berryman (1997) J. Cell Sci. **110**, 3011–3018.
32. A. J. Hudspeth (1997) Curr. Opin. Neurobiol. **7**, 480–486.
33. M. Kernan and C. Zuker (1995) Curr. Opin. Neurobiol. **5**, 443–448.
34. M. Abercrombie, J. E. Heysman, and S. M. Pegrum (1970) Exp. Cell Res. **59**, 393–398.
35. G. Albrecht-Buehler and R. M. Lancaster (1976) J. Cell Biol. **71**, 370–382.
36. T. M. Svitkina, A. B. Verkhovsky, K. M. McQuade, and G. G. Borisy (1997) J. Cell Biol. **139**, 397–415.
37. A. Y. Chan, S. Raft, M. Bailly, J. B. Wyckoff, J. E. Segall, and J. S. Condeelis (1998) J. Cell Sci. **111** 199–211.
38. B. M. Jockusch, P. Bubeck, K. Giehl, M. Kroemker, J. Moschner, M. Rothkegel, M. Rüdiger, K. Schlüter, G. Stanke, and J. Winkler (1995) Ann. Rev. Cell Dev. Biol. **11**, 379–416. Review.
39. A. Howe, A. E. Aplin, S. K. Alahari, and R. L. Juliano (1998) Curr. Opin. Cell Biol. **10**, 220–231.
40. J. Kendrick-Jones, R. C. Smith, R. Craig, and S. Citi (1987) J. Mol. Biol. **198**, 241–252.
41. K. M. Trybus (1991) Curr. Opin. Cell Biol. **3**, 105–111.
42. M. A. Lawson and F. R. Maxfield (1995) Nature **377**, 75–79.
43. M. Chinkers, J. A. McKanna, and S. Cohen (1979) J. Cell Biol. **83**, 260–265
44. J. C. den Hartigh, P. M. van Bergen en Henegouwen, A. J. Verkleij, and J. Boonstra (1992) J. Cell Biol. **119**, 349–355
45. M. A. Van der Heyden, P. A. Oude Weernink, B. A. Van Oirschot, P. M. Van Bergen en Henegouwen, J. Boonstra, and G. Rijksen (1997) Biochim. Biophys. Acta **1359 (3)**, 211–221.
46. I. Lassing and U. Lindberg (1985) Nature **314**, 472–474.
47. X. D. Ren and M. A. Schwartz (1998) Curr. Opin. Gent. Dev. **8**, 63–67.

48. C. L. Carpenter, K. F. Tolias, A. C. Couvillon, and J. H. Hartwig (1997) Adv. Enzyme Regul. **37**, 377–390.
49. I. Lassing and U. Lindberg (1990) FEBS Lett. **262**, 231–233.
50. L. Carlsson, F. Markey, I. Blikstad, T. Persson, and U. Lindberg (1979) Proc. Natl. Acad. Sci. USA **76**, 6376–6380.
51. F. Markey, T. Persson, and U. Lindberg (1981) Cell **23**, 145–153.
52. J-H. Hartwig and K. Barkalow (1997) Curr. Opin. Hematol. **4**, 351–356.
53. M. J. Berridge (1993) Nature **361**, 315–325.
54. M. Halbrügge and U. Walter (1993) In *Protein Kinases in Blood Cell Function* (C.-K. Huang and R. I. Sha"afi, eds.), CRC Press, Boca Raton, FL, pp. 245–298.
55. J. Field, A. Vojtek, R. Ballester, G. Bolger, J. Colicelli, K. Ferguson, J. Gerst, T. Kataoka, T. Michaeli, and S. Powers (1990) Cell **61**, 319–327.
56. M. Fedor-Chaiken, R. J. Deschenes, and J. R. Broach (1990) Cell **61**, 329–340.
57. C. Haffner, T. Jarchau, M. Reinhard, J. Hoppe, S. M. Lohman, and U. Walter (1995) EMBO J. **14**, 19–27.
58. A. Ben-Ze"ev (1997) Curr. Opin. Cell Biol. **9**, 99–108.
59. E. Weisberg, M Sattler, D. S. Ewaniuk, and R Salgia (1997) Crit. Rev. Oncog. **8**, 343–358.
60. G. B. Cohen, R. Ren, and D. Baltimore (1995) Cell **80**, 237–248.
61. R. L. Collins, M Deckert, and A. Altman (1997) Immunology Today **18**, 221–224.
62. K. D. Fischer, Y. Y. Kong, H. Nishina, K. Tedford, L. E. Marengere, I. Kozieradzki, T. Sasaki, M. Starr, G. Chan, S. Gardener, M. P. Nghiem, D. Bouchard, M. Barbacid, A. Bernstein, and J. M. Penninger (1998) Curr. Biol. **8**, 554–562
63. L. J. Holsinger, I. A. Graef, W. Swat, T. Chi, D. M. Bautista, L. Davidson, R. S. Lewis, F. W. Alt, and G. R. Crabtree (1998) Curr. Biol. **8**, 563–572.
64. A. Hall (1998) Science **279**, 509–514.
65. J. H. Hartwig, G. M. Bokoch, C. L. Carpenter, P. A. Janmey, L. A. Taylor, A. Toker, and T. Stossel (1995) Cell, **82**, 643–653.
66. D. J. G. Mackay, F. Esch, H. Furthmayr, and A. Hall (1997) J. Cell Biol. **138**, 927–938.
67. M. Reinhard, M. Halbrügge, U. Scheer, C. Wiegand, B. M. Jockusch, and U. Walter (1992) EMBO J. **11**, 2063–2070.
68. C. Haffner, T. Jarchau, M. Reinhard, J. Hoppe, S. M. Lohmann, and U. Walter (1995) EMBO J. **14**, 19–27.
69. F. B. Gertler, K. Niebuhr, M. Reinhard, J. Wehland, and P. Soriano (1996) Cell **87**, 227–239.
70. M. Reinhard, K. Giehl, K. Abel, C. Haffner, T. Jarchau, V. Hoppe, B. M. Jockusch, and U. Walter (1995) EMBO J. **14**, 1583–1589.
71. L. G. Cao, G. G. Babcock, P. A. Rubenstein, and Y. L. Wang (1992) J. Cell Biol. **117**, 1023–1029
72. M. C. Beckerle (1997) BioEssays **19**, 949–956.
73. S. Hüttelmaier, O. Mayboroda, B. Harbeck, T. Jarchau, B. M. Jockusch, and M. Rüdiger (1998) Curr. Biol. **8**, 479–488.
74. I. Lasa and P. Cossart (1996) Trends Cell Biol. **6**, 109–114. Review
75. J. M. J. Derry, H. E. Ochs, and U. Francke (1994) Cell **78**, 635–644.
76. T. Kirchhausen and F. S. Rosen (1996) Curr. Biol. **6**, 676–678.
77. U. Molina, D. M. Kenney, F. D. Rosen, and E. Remold-O"Donnell (1993) J. Exp. Med. **151**, 4383–4390.
78. P. Aspenström, U. Lindberg, and A. Hall (1997) Curr. Biol. **6**, 70–75.
79. M. Symons, J. M. J. Derry, B. Kartak, S. Jiang, V. Lemahieu, F. McCormick, U. Francke, and

A. Abo (1996) Cell **84**, 723–734.

80. R. Kolluri, K. F. Tolias, C. L. Carpenter, F. S. Rosen, and T. Kirchhausen (1996) Proc. Natl. Acad. Sci. USA **93**, 5615–5618.
81. S. Banin, O. Truong, D. R. Katz, M Waterfield, P. M. Brickell, and I. Gout (1996) Curr. Biol. **6**, 981–988.
82. H. Miki, K. Miura, and T. Takenawa (1996) EMBO J. **14**, 5326–5335.
83. H. Miki, T. Sasaki, Y. Takai, and T. Takenawa (1998) Nature **391**, 93–96.
84. S. T. Suzuki, H. Miki, T Takenawa, and C. Sasakawa (1998) EMBO J. **17**, 2767–2776.
85. N. Ramesh, I. M. Anton, J. H. Hartwig, and R. S. Geha (1997) Proc. Natl. Acad. Sci. USA **94**, 14671–14676.
86. I. M. Anton, W. Lu, B. J. Mayer, N. Ramesh, and R. S. Geha (1998) J. Biol. Chem. **273**, 20992–20995.
87. J. A. Frazier and C. M. Field (1997) Curr. Biol. **7**, 414–417.
88. M. Evangelista, K. Blundell, M. S. Longtine, C. J. Chow, N. Adames, J. R. Pringle, M. Peter, and C. Boone (1997) Science **276**, 118–122.
89. J. Petersen, O. Nielsen, R. Egel, and I. M. Hagan (1998) J. Cell Biol. **141**, 1217–1228.
90. N. Watanabe, P. Madaule, T. Reid, T. Ishizaki, G. Watanabe, A. Kakizuka, Y. Saito, K. Nakao, B. M. Jockusch, and S. Narumiya (1997) EMBO J. **16**, 3044–3056.
91. L. M. Machesky (1998) Curr. Biol. **8**, 202–205.
92. L. Weissbach, J. Settleman, M. F. Kalady, A. J. Snijders, A. E. Murthy, Y.-X. Yan, and A. Bernards (1994) J. Biol. Chem. **269**, 20517–20521.
93. S. Brill, S. Li, C. W. Lyman, D. M. Church, J. J. Wasmuth, L. Weissbach, A. Bernards, and A. J. Snijders (1996) Mol. Cell Biol. **16**, 4869–4878.
94. J. W. Erickson, R. A. Cerione, and M. J. Hart (1997) J. Biol.Chem. **272**, 24443–24447.
95. M. Fukata, S. Kuroda, K. Fujii, T. Nakamura, I. Shoji, Y. Matsuura, K. Kawa, A. Iwamatsu, A. Kikuchi, and K. Kaibuchi (1997) J. Biol. Chem. **272**, 29579–29583.
96. S. Kuroda, M. Fukata, M. Nakagawa, K. Fujii, T. Nakamura, T. Ookubo, I. Izawa, T. Nagase, N. Nomura, H. Tani, I. Shoji, Y. Matsuura, S. Yonehara, and K. Kaibuchi (1998) Science **281**, 832–835.
97. K. Eng, N. I. Naqvi, K. C. Wong, and M. K. Balasubramanian (1998) Curr. Biol. **8**, 611–621
98. C. E. Turner, J. R. Glenney Jr., and K. Burridge (1990) J. Cell Biol. **111**, 1059–1068.
99. C. E. Turner (1994) BioEssays **16**, 47–52.
100. M. C. Brown, J. A. Perrotta, and C. E. Turner (1996) J. Cell Biol. **135**, 1109–1123.
101. H. Wu and J. T. Parsons (1993) J. Cell Biol. **120**, 1417–1426.
102. X. Zhan, C. Plourde, X. Hu, R. Friesel, and T. Maciag (1994) J. Biol. Chem. **269**, 20221–20224.
103. K. Ozawa, K. Kashiwada, M. Takahashi, and K Sobue (1995) Exp. Cell Res. **221**, 197–204.
104. S. A. Weed, Y. Du, and J. T. Parsons (1998) J. Cell Sci. **111**, 2433–2443.
105. H. He, T Watanabe, X. Ahan, C. Huang, E. Schuuring, K. Fukami, T. Takenawa, C. C. Kumar, R. J. Simpson, and H. Maruta (1998) Mol. Cell Biol. **18**, 3829–3837.
106. C. Provenzano, R. Gallo, R. Carbone, P. P. Di Fiore, G. Falcone, L. Castellani, and S. Alema (1998) Exp. Cell Res. **242**, 186–200.
107. K. V. Kishan, G. Scita, W. T. Wong, P. P. Di Fiore, and M. E. Newcomer (1997) Nat. Struct. Biol. **4**, 739–743.
108. A. Vaheri, O. Carpén, L. Heiska, T. S. Helander, J. Jääskeläinen, P. Majander-Nordenswan, M. Sainio, T. Timonen, and O. Turunen (1997) Curr. Opin. Cell Biol. **9**, 659–666.
109. R. J. Shaw, M. Henry, F. Solomon, and T. Jacks (1998) Mol. Biol. Cell **9**, 403–419.

110. C. B. Shuster and I. M. Herman (1995) J. Cell Biol. **128**, 837–848.
111. J. W. Legg and C. M. Isacke (1998) Curr. Biol. **8**, 705–708.
112. V. Niggli, C. Andreoli, C. Roy, and P. Mangeat (1995) FEBS Lett. **376**, 172–176.
113. S. Tsukita, S. Yonemura, and S. Tsukita (1997) Trends Biochem. Sci. **22**, 53–58.
114. M. Hirao, N. Sato, T. Kondo, S. Yonemura, M. Monden, T. Sasaki, Y. Takai, S. Tsukita, and S. Tsukita (1996) J. Cell Biol. **135**, 37–51.
115. S. Yonemura, M. Hirao, Y. Doi, N. Takahashi, T. Kondo, and S. Tsukita (1998) J. Cell Biol. **140**, 885–895.
116. K. Burridge and L. Connell (1983) Cell Motil. **3**, 405–417.
117. L. Molony, D. McCaslin, J. Abernethy, B. Paschal, and K. Burridge (1987) J. Biol. Chem. **262**, 7790–7795.
118. N. C. Collier and K. Wang (1982) FEBS Lett. **143**, 205–210.
119. T. O"Halloran, M. C. Beckerle, and K. Burridge (1985) Nature **317**, 449–451.
120. M. C. Beckerle, K. Burridge, G. N. De Martino, and D. E. Croall (1987) Cell **51**, 569–577.
121. A. Horwitz, K. Duggan, C. Buck, M. C. Beckerle, and K. Burridge (1986) Nature **320**, 531–533.
122. D. J. G. Rees, S. E. Ades, S. J. Singer, and R. O. Hynes (1990) Nature **347**, 685–689.
123. J. Winkler, H. Lunsdorf, and B. M. Jockusch (1997) Eur. J. Biochem. **243**, 430–436.
124. V. Niggli, S. Kaufmann, W. H. Goldmann, T. Weber, and G. Isenberg (1994) Eur. J. Biochem. **226**, 951–957.
125. W. H. Goldmann, R. M. Ezzel, E. D. Adamson, V. Niggli, and G. Isenberg (1996) J. Muscle Res. Cell Motil. **17**, 1–5.
126. H. Priddle, L. Hemmings, S. Monkley, A. Woods, B. Patel, D. Sutton, G. A. Dunn, D. Zicha, and D. R. Critchley (1998) J. Cell Biol. **142**, 1121–1133.
127. B. Geiger (1979) Cell **18**, 193–205.
128. B. Geiger, K. T. Tokuyasu, A. H. Dutton, and S. J. Singer (1980) Proc. Natl. Acad. Sci. USA **77**, 4127–4131.
129. B. Geiger (1982) J. Mol. Biol. **159**, 685–701.
130. K. M. Yamada and B. Geiger (1997) Curr. Opin. Cell Biol. **9**, 76–85.
131. S. W. Craig and R. P. Johnson (1996) Curr. Opin. Cell Biol. **8**, 74–85.
132. R. P. Johnson and S. W. Craig (1994) J. Biol. Chem. **269**, 12611–12619.
133. L. Molony and K. Burridge (1985) J. Cell. Biochem. **29**, 31–36.
134. L. M. Milam (1985) J. Mol. Biol. **184**, 543–545.
135. J. Week, S. T. Barry, and D. R. Critchley (1996) Biochem. J. **314**, 827–832.
136. C. K. Wood, C. E. Turner, P. Jackson, and D. R. Critchley (1994) J. Cell Sci. **107**, 709–717.
137. R. B. Hazan, L. Kang, S. Roe, P. I. Borgen, and D. L. Rimm (1997) J. Biol Chem. **272**, 32448–32453.
138. E. E. Weiss, M. Kroemker, A.-H. Rüdiger, B. M. Jockusch, and M. Rüdiger (1998) J. Cell Biol. **141**, 755–764.
139. M. Watabe-Uchida, N. Uchida, Y. Imamura, A. Nagafuchi, K. Fujimoto, T. Uemura, S. Vermeulen, F. van Roy, E. D. Adamson, and M. Takeichi (1998) J. Cell Biol. **142**, 847–857.
140. J. A. Wilkins, M. A. Risinger, and S. Lin (1986) J. Cell Biol. **103**, 1483–1494.
141. S. M. Bockholt, C. A. Otey, J. Glenney Jr., and K. Burridge (1992) Exp. Cell Res. **203**, 39–46.
142. S. H. Lo, P. A. Janmey, J. J. Hartwig, and L. B. Chen (1994a) J. Cell Biol. **125**, 1067–1075.
143. S. H. Lo, E. Weisberg, and L. B. Chen (1994b) BioEssays **16**, 817–823.
144. S. Davis, M. L. Lu, S. H. Lo, S. Lin, J. A. Butler, B. J. Druker, T. M. Roberts, Q. An, and L. B. Chen (1991) Science **252**, 712–715.

145. C. Weight, A. Gaertner, A. Wegner, H. Korte, and H. E. Meyer (1992) J. Mol. Biol. **227**, 593–595.
146. H. G. Mannherz, M. C. Peitsch, S. Zanotti, R. Paddenberg, and B. Polzar (1995) Curr. Top. Microbiol. Immunol. **198**, 161–174.
147. M. Kunitz (1948) Science **108**, 19–20.
148. W. Dabrowska, E. J. Cooper, and M. Laskowski (1945) J. Biol. Chem. **177**, 991–992.
149. E. J. Cooper, M. J. Trautman, and M. Laskowski (1950) Proc. Soc. Exptl. Biol. Med. **73**, 219–222.
150. U. Lindberg (1967) Biochemistry **6**, 323–335.
151. M. Segura and U. Lindberg (1984) J. Biol. Chem. **259**, 3949–3954.
152. S. E. Hitchcock, L. Carlsson, and U. Lindberg (1975) Cell Motility Cold Spring Harbor Symp. pp. 545–559.
153. S. E. Hitchcock, L. Carlsson, and U. Lindberg (1976) Cell **7**, 531–542.
154. H. G. Mannherz, H. Brehme, and U. Lamp (1975) Eur. J. Biochem. **60**, 109–116.
155. W. Kabsch, H. G. Mannherz, D. Suck, E. F. Pai, and K. C. Holmes (1990) Nature **347**, 37–44.
156. C. Oefner and D. Suck (1986) J. Mol. Biol. **192**, 605–632.
157. S. A. Weston, A. Lahm, and D. Suck (1992) J. Mol. Biol. **226**, 1237–1256.
158. K. C. Holmes, D. Popp, W. Gebhard, and W. Kabsch (1990) Nature **347**, 44–49.
159. K. C. Holmes, M. Tirion, D. Popp, M. Lorenz, W. Kabsch, and R. A. Milligan (1993) Adv Exp. Med. Biol. **332**, 15–22.
160. I. Rayment, H. M. Holden, M. Whittaker, C. B. Yohn, M. Lorenz, K. C. Holmes, and R. A. Milligan (1993) Science **261**, 58–65.
161. C. E. Schutt, M. D. Rozycki, J. C. Myslik, and U. Lindberg (1995) J. Struct. Biol. **115**, 186–198.
162. R. Page, U. Lindberg, and C. E. Schutt (1998) J. Mol. Biol. **280**, 463–474.
163. K. Schlüter, B. M. Jockusch, and M. Rothkegel (1997) Biochim. Biophys. Acta **1359**, 97–109.
164. F. Buss, C. Temm-Grove, S. Henning, and B. M. Jockusch (1992) Cell Motil. Cytoskeleton **22**, 51–61.
165. M. Evangelista, K. Blundell, M. S. Longtine, C. J. Chow, N. Adames, J. R. Pringle, M. Peter, and C. Boone (1997) Science **276**, 118–122.
166. N. Watanabe, P. Madaule, T. Reid, T. Ishizaki, G. Watanabe, A. Kakizuka, Y. Saito, K. Nakao, B. M. Jockusch, and S. Narumiya (1997) EMBO J. **16**, 3044–3056.
167. J. Petersen, O. Nielsen, R. Egel, and I. M. Hagan (1998) J. Cell Sci. **111**, 867–876.
168. R. D. Mullins, J. F. Kelleher, J. Xu, and T. D. Pollard (1998) Mol. Biol. Cell **9**, 841–852.
169. V. Magdolen, U. Oechsner, G. Muller, and W. Bandlow (1988) Mol. Cell Biol. **8**, 5108–5115.
170. M. Haugwitz, A. A. Noegel, J. Karakesisoglou, and M. Schleicher (1994) Cell **79**, 303–314.
171. D. A. Kaiser, M. Sato, R. F. Ebert, and T. D. Pollard (1986) J. Cell Biol. **102**, 221–226.
172. A. Lambrechts, J. van Damme, M. Goethals, J. Vandekerckhove, and C. Ampe (1995) Eur. J. Biochem. **230**, 281–286.
173. T. Fujiwara, K. Tanaka, A. Mino, M. Kikyo, K. Takahashi, K. Shimizu, and Y. Takai (1998) Mol. Biol. Cell **9**, 1221–1233.
174. W. Witke, A. H. Sharpe, and D. J. Kwiatkowski (1993) Mol. Biol. Cell **4** 149a.
175. C. Björkegren, M. Rozycki, C. E. Schutt, U. Lindberg, and R. Karlsson (1993) FEBS Lett. **333**, 123–126.
176. C. E. Schutt, J. C. Myslik, M. D. Rozycki, N. C. Goonesekere, and U. Lindberg (1993) Nature **365**, 810–816.
177. E. S. Cedergren-Zeppezauer, N. C. W. Goonesekere, M. D. Rozycki, J. C. Myslik, Z. Dauter,

U. Lindberg, and C. E. Schutt (1994) J. Mol. Biol. **240**, 459–475.
178. K. S. Thorn, H. E. Christensen, R. Shigeta, D. Huddler, L. Shalaby, U. Lindberg, N. H. Chua, and C. E. Schutt (1997) Structure **5**, 19–32.
179. N. M. Mahoney, P. A. Janmey, and S. C. Almo (1997) Nature Struct. Biol. **4**, 953–960.
180. W. J. Metzler, A. J. Bell, E. Ernst, T. B. Lavoie, and L. Mueller (1994) J. Biol. Chem. **269**, 4620–4625.
181. H. Larsson and U. Lindberg (1988) Biochim. Biophys. Acta **953**, 95–105.
182. E. Korenbaum, P. Nordberg, C. Björkegren-Sjögren, C. E. Schutt, U. Lindberg, and R. Karlsson (1998) Biochemistry **37**, 9274–9283.
183. V. K. Vinson, E. M. De La Cruz, H. N. Higgs, and T. D. Pollard (1998) Biochemistry **37**, 10871–10880.
184. D. Pantaloni and M.-F. Carlier (1993) Cell **75**, 1007–1014.
185. M.-F. Carlier and D. Pantaloni (1993) Sem. Cell Biol. **5**, 183–191.
186. F. Markey, H. Larsson, K. Weber, and U. Lindberg (1982) Biochim. Biophys. Acta **704**, 43–51.
187. S. C. Mockrin and E. D. Korn (1980) Biochemistry **19**, 5359–5362.
188. P. J. Goldschmidt-Clermont, L. M. Machesky, S. K. Doberstein, and T. D. Pollard (1991) J. Cell Biol. **113**, 1081–1089.
189. M. Tanaka and H. Shibata (1985) Eur. J. Biochem. **151**, 291–297.
190. U. Lindberg, C. E. Schutt, E. Hellsten, A.-C. Tjäder, and T. Hult (1988) Biochim. Biophys. Acta **967**, 391–400.
191. D. Safer and V. T. Nachmias (1994) BioEssays **16**, 473–479.
192. V. T. Nachmias (1993) Curr. Opin. Cell Biol. **5**, 56–62.
193. M. Czisch, M. Schleicher, S. Horger, W. Voelter, and T. A. Holak (1993) Eur. J. Biochem. **218**, 335–344.
194. D. Safer, T. E. Sosnick, and M. Elzinga (1997) Biochemistry **36**, 5806–5816.
195. M. F. Carlier, D. Didry, I. Erk, J. Lepault, M. L. Van Troys, J. Vandekerckhove, I. Perelroizen, H. Yin, Y. Doi, and D. Pantaloni (1996) J. Biol. Chem. **271**, 9231–9239.
196. H. Q. Sun, K. Kwiatkowska, and H. L. Yin (1996) J. Biol. Chem. **271**, 9223–9230.
197. L. Bao, M. Loda, P. A. Janmey, R. Stewart, P. Anand-Apte, and B. R. Zetter (1996) Nat. Med. **12**, 1322–1328.
198. M. F. Carlier and D. Pantaloni (1997) J. Mol. Biol. **269**, 459–467.
199. J. A. Theriot (1997) J. Cell. Biol. **136**, 1165–1168.
200. A. Moon and D. G. Drubin (1995) Mol. Biol. Cell **6**, 1423–1431.
201. S. A. Leonard, A. G. Gittis, E. C. Petrella, T. D. Pollard, and E. E. Lattman (1997) Nat. Struct. Biol. **4**, 369–373.
202. A. A. Fedorov, P. Lappalainen, E. V. Fedorov, D. G. Drubin, and S. C. Almo (1997) Nat. Struct. Biol. **4**, 366–369.
203. H. Hatanaka, K. Ogura, K. Moriyama, S. Ichikawa, I. Yahara, and F. Inagaki (1996) Cell **85**, 1047–1055.
204. P. Lappalainen, M. M. Kessels, J. M. T. V. Cope, and D. G. Drubin (1998) Mol. Cell Biol. **9**, 1951–1959.
205. S. Arber, F. A. Barbayannis, H. Hanser, C. Schneider, C. A. Stanyon, O. Bernard, and P. Caroni (1998) Nature **393**, 805–808.
206. N. Yang, O. Higuchi, K. Ohashi, K. Nagata, A. Wada, K. Kangawa, E. Nishida, and K. Mizuno (1998) Nature **393**, 809–812.
207. M.-F. Carlier, V. Laurent, J. Santolini, R. Melki, D. Didry, G. X. Xia, Y. Hong, N.-H. Chua, and D. Pantaloni (1997) J. Cell Biol. **136**, 1307–1323.

208. J. Rosenblatt, B. J. Agnew, H. Abe, J. R. Bamburg, and T. J. Mitchison (1997) J. Cell Biol. **136**, 1323–1332.
209. B. L. Goode, D. G. Drubin, and P. Lappalainen (1998) J. Cell. Biol. **142**, 723–733.
210. T. A. Schroer (1994) J. Cell Biol. **127**, 1–4.
211. L. M. Machesky (1997) Curr. Biol. 164–167.
212. M. D. Welch, A. Iwamatsu, and T. J. Mitchison (1997) Nature **385**, 265–269.
213. L. M. Machesky, E. Reeves, F. Wientjes, F. J. Mattheyse, A. Grogan, N. F. Totty, A. L. Burlingame, J. J. Hsuan, and A. W. Segal (1997) Biochem. J. **328**, 105–112.
214. M. D. Welch, A. H. DePace, S. Verma, A. Iwamatsy, and T. J. Mitchison (1997) J. Cell Biol. **138**, 375–384.
215. D. Winter, A. V. Podtelejnikov, M. Mann, and R. Li (1997) Curr. Biol. **7**, 519–529.
216. R. D. Mullins, J. A. Heuser, and T. D. Pollard (1998) Proc. Natl. Acad. Sci. USA **95**, 6181–6186.
217. M. D. Welch, J. Rosenblatt, J. Skoble, D. A. Portnoy, and T. J. Mitchison (1998) Science **281**, 105–108.
218. J. F. Casella, S. W. Craig, D. J. Maack, and A. E. Brown (1987) J. Cell Biol. **105**, 371–379.
219. P. A. Kuhlman, C. A. Hughes, V. Bennet, and V. M. Fowler (1996) J. Biol. Chem. **271**, 7986–7991.
220. H. L. Yin (1987) Bioessays **7**, 176–179.
221. T. Azuma, W. Witke, T. P. Stossel, J. H. Hartwig, and D. J. Kwiatkowski (1998) EMBO J. **17**, 1362–1370.
222. P. J. McLaughlin, J. T. Gooch, H.-G. Mannherz, and A. G. Weeds (1993) Nature **364**, 685–692.
223. L. D. Burtnick, E. K. Koepf, J. Grimes, E. Y. Jones, D. I. Stuart, P. J. McLaughlin, and R. C. Robinson (1997) Cell **90**, 661–670.
224. A. McGough, W. Chiu, and M. Way (1998) Biophys. J. **74**, 764–772.
225. V. M. Fowler (1996) Curr. Opin. Cell Biol. **8**, 86–96.
226. J. Hartwig (1994) Actin-binding proteins 1. Spectrin Superfamily. Protein Profile. **1**, 711–778.
227. A. Bretscher and K. Weber (1979) Proc. Natl. Acad. Sci. USA **76**, 2321–2325.
228. M. S. Mooseker (1985) Annu. Rev. Cell Biol. **1**, 209–241.
229. D. Louvard (1989) Curr. Opin. Cell Biol. **1**, 51–57.
230. J. J. Otto (1994) Curr. Opin. Cell Biol. **6**, 105–109.
231. M. A. Markus, P. Matsudaira, and G. Wagner (1997) Protein Sci. **6**, 1197–1209.
232. C. J. McKnight, P. T. Matsudaira, and P. S. Kim (1997) Nat. Struct. Biol. **4**, 180–184.
233. A. Bretscher and K. Weber (1980) J. Cell Biol. **86**, 335–340.
234. J. E. Honts, T. S. Sandrock, S. M. Brower, J. L. O"Dell, and A. E. M. Adams (1994) J. Cell Biol. **126**, 413–422.
235. S. C. Goldsmith, N. Pokala, W. Shen, A. A. Fedorov, P. Matsudaira, and S. C. Almo (1997) Nat. Struct. Biol. **4**, 708–712.
236. D. Hanein, P. Matsudaira, and D. J. DeRosier (1997) J. Cell Biol. **139**, 387–396.
237. K. R. Fath and D. R. Burgess 1995, Curr. Biol. **5**, 591–593.
238. P. Fucini, C. Renner, C. Herberhold, A. A. Noegel, and T. A. Holak (1997) Nat Struct Biol **4**, 223–230.
239. T. W. Tillack, S. L. Marchesi, V. T. Marchesi, and E. Steers Jr. (1970) Biochim. Biophys. Acta **200**, 125–131.
240. G. L. Nicolson, V. T. Marchesi, and S. J. Singer (1971) J. Cell Biol. **51**, 265–272.
241. V. Bennett (1990) Curr. Opin. Cell Biol. **2**, 51–56.

242. J. Pascual, M. Pfuhl, G. Rivas, A. Pastore, and M. Saraste (1996) FEBS Lett **383**, 201–207.
243. P. Fucini, C. Renner, C. Herberhold, A. A. Noegel, and T. A. Holak (1997) Nat. Struct. Biol. **4**, 223–230.
244. J. Pascual, M. Pfuhl, D. Walther, M. Saraste, and M. Nilges (1997) J. Mol. Biol. **273**, 740–751.
245. M. Nilges, M. J. Macias, S. I. O''Donoghue, and H. Oschkinat (1997) J. Mol. Biol. **269**, 408–422.
246. F. J. Blanco, A. R. Ortiz, and L. Serrano (1997) J. Biomol. NMR **9**, 347–357.
247. K. D. Carugo, S. Banuelos, and M. Saraste (1997) Nat. Struct. Biol. **4**, 175–179.
248. S. Ebashi and F. Ebashi (1965) J. Biochem. **58**, 7–13.
249. S. J. Winder (1997) J. Muscle Res. Cell Motil. **18**, 617–629.
250. V. Bennett (1990) Physiol. Rev. **70**, 1029–1065.
251. Y. Srinivasan, L. Elmer, J. Davis, V. Bennett, and K. Angelides (1988) Nature **333**, 177–180.
252. M. Colledge and S. C. Froehner (1998) Curr. Opin. Neurobiol. **8**, 357–363.
253. C. Rosenmund and G. L. Westbrook (1993) Neuron **10**, 805–814.
254. K. M. Harris and S. B. Kater (1994) Annu. Rev. Neurosci. **17**, 341–371.
255. D. W. Allison, V. I. Gelfand, I. Spector, and A. M. Craig (1889) J. Neurosci. **18**, 2423–2436.
256. T. Kim, K. Wu, J. Xu, and I. B. Black (1992) Proc. Natl. Acad. Sci. USA **89**, 11642–11644.
257. P. A. Huber (1997) Int. J. Biochem. Cell Biol. **29**, 1047–1051.
258. J. M. Squire (1997) Curr. Opin. Struct. Biol. **7**, 247–257.
259. J. Trinick (1992) FEBS Lett. **307**, 44–48.
260. R. Littlefield and V. M. Fowler (1998) Annu. Rev. Cell Dev. Biol. **14**, 487–525.

Actin Polymerization Toxins

Several bacteria release toxins that modify actin or proteins controlling its polymerization (1). A group of *Clostridia spp.* secrete binary toxins, whose most studied member is the C2 toxin released by *Cl. botulinum*. Botulinum C2 toxin is not neurospecific, as are botulinum neurotoxins, but it affects many nonneuronal cells (2). In the intestinal loop model, it induces an acute inflammatory reaction, characterized by the alteration of endothelia and a large increase in vascular permeability. At the same time, epithelial degeneration, exfoliation, and necrosis are also observed. In cultured cells, C2 causes rounding up, with formation of blebs, followed by cell death.

Two polypeptide chains, I (55 kDa) and II (100 kDa), are needed for cell intoxication. Chain I catalyzes the **ADP-ribosylation** of Arg177 of soluble G-actin, a residue located in an area involved in protein-protein contact within the polymerized form, F-actin. The ADP-ribosylated G-actin binds to the barbed end of F-actin and prevents polymerization, whereas depolymerization at the opposite end is unaffected (3). This leads *in vitro* and *in vivo* to the disassembly of actin microfilaments, with cell rounding and release of focal adhesion plaques.

Single-chain enzymes that catalyze the ADP-ribosylation of small G proteins are released by several bacteria (4). They cannot intoxicate cells because they lack the second polypeptide chain, but they are active after cell permeabilization or injection. C3 toxin is released by some strains of *Cl. botulinum*; it catalyzes the specific ADP-ribosylation of Asn-41 of Rho, a small GTP-binding protein involved in the regulation of actin polymerization. C3 induces the depolarization of F-actin, with rounding up and binucleation of injected cells. A different type of Rho modification is caused by cytotoxic necrotizing factors released by *E. coli* strains associated with gastroenteritis, urogenital infections, and septicemia (5). These factors cause cell ruffling, stress fiber formation, and multinucleation, by a covalent modification of Rho protein to lock it in its GTP-bound active form (6).

Clostridia spp. involved in the induction of diarrhea, associated with pseudomembraneous colitis, release in the intestine enterotoxins of very large dimensions (7). They are termed large clostridial toxins (LCTs) because of their size, which is in the range of 250 to 308 kDa. They are organized as A-B toxins, which are cleaved proteolytically into two polypeptide chains, A and B (see Toxins). The carboxyl-terminal part includes segments of 20 to 50 residues repeated 14 to 30 times, which are believed to mediate LCT binding to cell surface **receptors.** Such an organization in the absence of an oligomer of type B gives rise to a multivalent type of cell binding, as in the case of cholera toxin. Binding is followed by internalization of LCTs into coated **vesicles** and then into endosomes. By an unknown mechanism, the amino-terminal catalytic domain of the LCTs is released from the rest of the molecule and translocates into the cytosol, where it catalyzes the transfer of a sugar residue from the corresponding UDP derivative to an actin polymerization controlling protein (7, 8). All LCTs induce rounding of different cells in culture, but the effects of the various LCT toxins can be differentiated by staining actin filaments: *Cl. difficile* and *Cl. novyi* LCTs cause a breakdown of the F-actin microfilaments, whereas *Cl. sordellii* LCT induces the formation of filopodialike structures on the cell surface, with some membrane blebbing 7. This is related to the different protein(s) targeted by the LCTs. All of them modify a threonine residue of small GTP-binding protein(s) of the **Ras** superfamily, in such a way that its GTPase activity is unaltered but it can no longer interact with its effector molecule. This provides a further example of the ability of bacterial toxins to “choose” essential cell targets and to modify essential cell functions.

Bibliography

1. K. Aktories (1997) In *Guidebook to Protein Toxins and Their Use in Cell Biology* (R. Rappuoli and C. Montecucco, eds.), Sambrook and Tooze, Oxford University Press, Oxford.
2. L. L. Simpson (1989) J. Pharmacol. Exp. Ther. **251**, 1223–1228.
3. M. Wille, I. Just, A. Wegner, and K. Aktories (1992) J. Biol. Chem. **267**, 50–55.
4. K. Aktories and A. Wegner (1992) Curr. Top. Microbiol. Immunol. **175**, 115–131.
5. A. Caprioli et al. (1984) Biochem. Biophys. Res. Commun. **118**, 587–593.
6. E. Oswald et al. (1994) Proc. Natl. Acad. Sci. USA **91**, 3814–3818.
7. C. von Eichel-Streiber, P. Boquet, M. Sauerborn, and M. Thelestam (1996) Trends Microbiol. **4**, 375–382.
8. I. Just et al. (1995) Nature **375**, 500–503.

Actinomycin D

Actinomycins are chromopeptide antibiotics produced by various species of streptomycetes (1). They differ only in their content of certain amino acids in their peptide rings (Fig. 1). Actinomycin D, which is active against several forms of cancer, has the distinction of being the first antibiotic discovered (in 1943) to possess useful antitumor activity. It is still used in the clinic for that purpose. It occupies a unique place in the origins of molecular biology for quite a different reason, however, namely its astounding specificity as an inhibitor of DNA-dependent RNA synthesis, which enabled it to play a vital part in the discovery of messenger RNA and helped uncover the early evidence that **transcriptional** regulation of gene expression is fundamental to cell growth and development (2).

The result of its near-absolute specificity for binding tightly to double helical B-form DNA is a total blockade of transcription by **RNA polymerase**, leading to cessation of synthesis of all forms of RNA, stable as well as unstable. Elongation of growing RNA chains is promptly terminated; there is no particular effect on the process of initiation of transcription. Thus actinomycin was used in the 1960s to measure the kinetics of breakdown of pulse-labeled RNA, thought to reflect at least partly the turnover of mRNA, and to establish the requirement for new RNA transcription in such processes as induced enzyme synthesis, mechanisms of steroid hormone and peptide hormone action, and early embryonic development. Replication of DNA **viruses** is usually strongly inhibited by actinomycin, but many RNA viruses are completely insensitive to the antibiotic; this is clear evidence that their life cycles do not require the participation of DNA at any point. Because actinomycin acts essentially identically to block transcription in all cells, once it has gained access to the nucleus, it is equally applicable to the study of gene activity in eukaryotes as well as prokaryotes (it is generally ineffective against gram-negative bacteria simply because of a permeability problem, for if the walls of such cells are digested away, or otherwise weakened, the protoplast is revealed as fully sensitive to the antibiotic).

Figure 1. The structures of the actinomycin antibiotics.

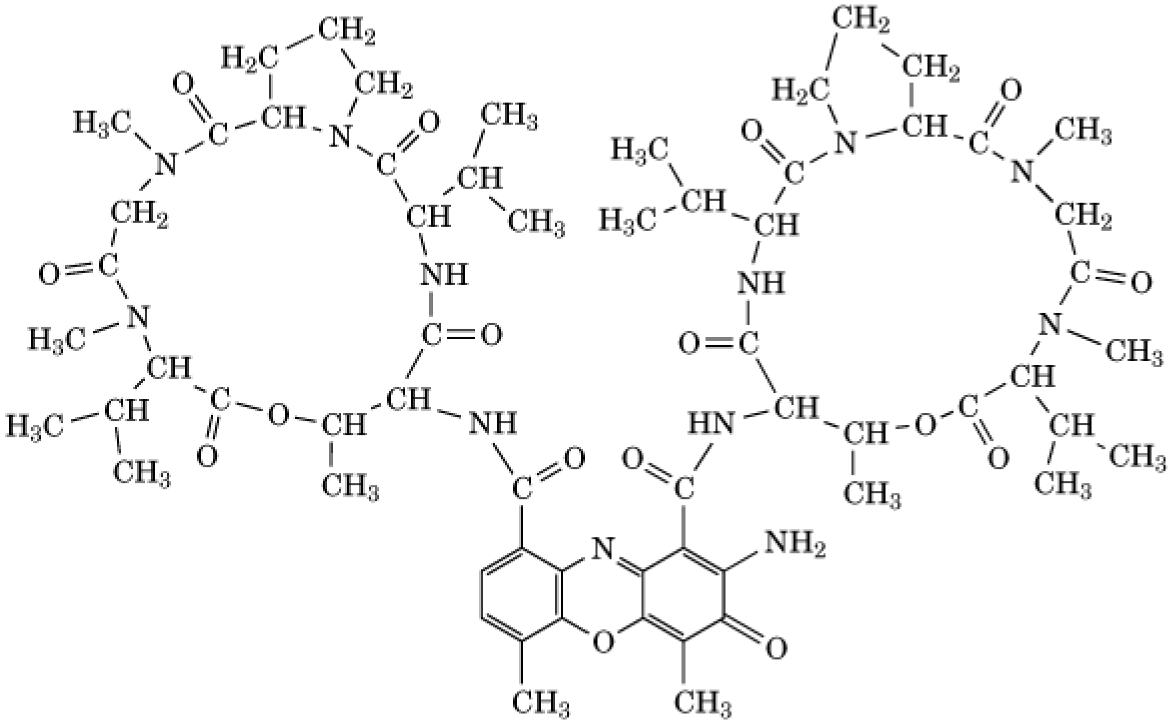

actinomycin D

Actinomycin does not bind to RNA or to single-stranded DNA, and its affinity for double-helical DNA is related to the latter's content of guanine nucleotides; synthetic polynucleotides composed entirely of A · T base pairs do not interact with the antibiotic at all. It took some time to establish the nature of the actinomycin–DNA complex, and for many years the matter was controversial. Eventually the issue was resolved in favor of intercalation as a result of careful structure–activity comparisons (1), binding measurements with a wide variety of synthetic as well as naturally occurring DNAs (3, 4), hydrodynamic experiments with circular DNA (5), X-ray crystallography (6), and high-resolution nuclear magnetic resonance (**NMR**) (7). A landmark was the determination of the structure of a crystalline 1:2 actinomycin:deoxyguanosine complex, which revealed for the first time that the antibiotic has an axis of near-perfect twofold rotational symmetry, which allows it to react with two guanine nucleosides in a symmetry-related fashion (6). This observation immediately suggested plausible intercalation of the phenoxazinone chromophore between two G · C base pairs of DNA at a rotationally symmetrical site centered around a 5′-GpC-3′ step. The strong preference of actinomycin for such sites in DNA was elegantly confirmed by Footprinting experiments a decade later (8, 9). With its tricyclic aromatic chromophore firmly embedded between the base pairs, the cyclic pentapeptide rings of the antibiotic are left neatly filling the minor groove of the distorted B-form helix, where they form numerous additional **van der Waals** contacts that help to stabilize the complex; positioned this way, their intrinsic right-hand twisted disposition with respect to the intercalated chromophore makes perfect sense, and the whole antibiotic molecule occupies a site covering about six base pairs in the minor groove.

Detailed kinetic studies have revealed that both the association and dissociation reactions are complicated and require several rate constants to fit the data (3, 10). The slowest processes are characterized by time constants in the range of minutes, conspicuously slower than those measured for most other DNA-binding drugs, and there is a correlation between the slowest rate constant for the dissociation reaction and the efficiency of inhibition of chain elongation by RNA polymerase. This has led to the notion that reversibly bound actinomycin molecules serve as relatively long-lived blocks to the progression of the transcribing enzyme along its template, providing a partial explanation for the extreme effectiveness of actinomycin as an inhibitor of RNA synthesis. What is not so obvious is why the functioning of DNA as a template in replication should remain unaffected even at much higher concentrations of actinomycin (2).

The critical determinant that enables the antibiotic to recognize its preferred binding sites in DNA seems to be the 2-amino group of the guanine nucleotide, as is also true for numerous other ligands (11). If the 2-amino group is removed from guanines (leaving inosine–cytosine base pairs) and transferred to adenines (forming 2,6-diaminopurine-thymine base pairs), the sites to which actinomycin binds are relocated accordingly (11, 12). The molecular recognition process includes the formation of hydrogen bonds between the purine 2-amino groups and the carbonyl substituents of the L-**threonine** residues in the peptide rings of the antibiotic; there are also hydrogen bonds from the same threonine residues to the N(3) atoms of the purine nucleotides at the binding site (6, 12). Some of the kinetic complexity of the association/dissociation reactions no doubt reflects a "shuffling" process, whereby actinomycin initially interacts with a variety of potential binding sites on the DNA lattice, then migrates one-dimensionally to locate its preferred binding sites marked by a pair of purine 2-amino groups suitably disposed in the minor groove of the double helix (13).

Bibliography

1. J. Meienhofer and E. Atherton (1977) In *Structure–Activity Relationships Among the Semisynthetic Antibiotics* (D. Perlman, ed.), Academic Press, New York, pp. 427–529.
2. E. Reich and I. H. Goldberg (1964) Prog. Nucleic Acid Res. Mol. Biol. **3**, 183–234.
3. W. Müller and D. M. Crothers (1968) J. Mol. Biol. **35**, 251–290.
4. R. D. Wells and J. E. Larson (1970) J. Mol. Biol. **49**, 319–342.
5. M. J. Waring (1970) J. Mol. Biol. **54**, 247–279.
6. H. M. Sobell, S. C. Jain, T. D. Sakore, and C. E. Nordman (1971) Nature New Biol. **231**, 200–205.
7. D. J. Patel (1974) Biochemistry **13**, 2396–2402.
8. M. J. Lane, J. C. Dabrowiak, and J. N. Vournakis (1983) Proc. Natl. Acad. Sci. USA **80**, 3260–3264.
9. M. W. Van Dyke, R. P. Hertzberg, and P. B. Dervan (1983) Proc. Natl. Acad. Sci. USA **79**, 5470–5474.
10. R. Bittman and L. Blau (1975) Biochemistry **14**, 2138–2145.
11. C. Bailly and M. J. Waring (1995) Nucleic Acids Res. **23**, 885–892.
12. S. Jennewein and M. J. Waring (1997) Nucleic Acids Res. **25**, 1502–1509.

13. K. R. Fox and M. J. Waring (1985) Nucleic Acids Res. **14**, 2001–2014.

Suggestions for Further Reading

14. E. F. Gale, E. Cundliffe, P. E. Reynolds, M. H. Richmond, and M. J. Waring (1981) *The Molecular Basis of Antibiotic Action*, 2nd ed., Wiley, London, pp. 314–333.
15. H. M. Sobell (1973) The stereochemistry of actinomycin binding to DNA and its implications in molecular biology. Prog. Nucleic Acid Res. Mol. Biol. **13**, 153–190.

Activation Energy

The kinetic rates of chemical and enzyme-catalyzed reactions depend on temperature. The relationship for this dependence is known as the Arrhenius law:

$$k = Ae^{E/RT} \tag{1}$$

where A and E are constants, R is the gas constant, and T is the absolute temperature in Kelvin units. The activation energy E is the height of the energy barrier that the reaction must exceed to pass from reactants to products. It is usually expressed in kilocalories per mole or in joules per mole. Equation 1 can be expressed as:

$$\log k = \log A - E/(2.303RT) \tag{2}$$

Therefore the magnitude of the activation energy can be obtained from the slope of a plot of the log of a rate constant for a reaction as a function of $1/T$. Many chemical and enzyme-catalyzed reactions increase the rate of reaction by two- to threefold for each 10°C increase in temperature. Although this relationship is useful in explaining the temperature dependence of reactions, it does not explain the rate in the thermodynamic terms of **enthalpy** H **entropy** S, or **free energy** G. This analysis comes from transition state theory. The Arrhenius activation energy does correspond to the standard enthalpy of the reaction in the van't Hoff equation (1).

Bibliography

1. A. Cornish-Bowden (1979) *Fundamentals of Enzyme Kinetics*, Butterworths, London, Boston, pp. 9–12.

Suggestions for Further Reading

2. D. Piszkiewicz (1977) *Kinetics of Chemical and Enzyme-Catalyzed Reactions*, Oxford University Press, New York, pp. 27–52.

Active Site

The folding of a polypeptide chain that produces the final protein structure of an enzyme also leads to formation of the active site. From X-ray crystallography studies, it is apparent that the active site of an enzyme is a groove, cleft, or pocket that has access to the solvent and forms only a small part of the total solvent-**accessible surface** of the protein. The relatively large sizes of enzymes are undoubtedly due to the need to obtain, at the active site, the correct spatial relationships of the amino acid residues that are involved in binding of substrates, catalysis, and the release of products, as well as for any conformational changes associated with these steps. The binding of substrates or inhibitors at the active site pocket of an enzyme involves matching up of the nonpolar groups of the substrate with the nonpolar side-chains of amino acid residues, **hydrogen bonding** between the polar appropriate groups on the substrate with the backbone NH and CO groups within the active site, and even **salt bridge** formation. For substrates, these initial interactions are followed by the conformational changes that lead to the formation of the transition-state complex (see Transition State Analogue) and the chemistry for catalyzing the reaction brought about by reactive groups with the correct alignments. These may be the acidic, basic, and nucleophilic groups of the protein component of the enzyme, or the electrophilic groups of a prosthetic group (see Coenzyme, Cofactor).

Active Site-Directed Irreversible Inhibitors

Active site-directed irreversible inhibitors of enzymes are also known as *active site-direcetd inactivating reagents*, *affinity labels*, and *photoaffinity labels*. They combine the features of a substrate, or substrate analogue, with those of a group-specific reagent, as in affinity labeling, and have been used to determine the amino acid residues that are present in the active site and involved in enzymic catalysis. They are capable of binding specifically and reversibly at the active site of an enzyme and then causing inactivation through time-dependent covalent modification of an adjacent amino acid residue. The functional group of the inhibitor is usually an electrophile that can interact with an appropriately positioned nucleophile of the enzyme, to generate a covalent bond between them. The electrophilic groups include epoxides and a-haloketones. Since these compounds are reactive in solution, they could also cause some nonspecific enzyme modifications.

The action of an active-site directed irreversible inhibitor I can be illustrated by

$$\mathbf{E} + \mathbf{I} \rightleftharpoons \mathbf{EI} \rightarrow \mathbf{E} - \mathbf{I} \qquad (1)$$

where EI represents a Michaelis complex (see Michaelis–Menten Kinetics) and $E - I$ denotes the covalently cross-linked form of the complex. On the basis of this formulation, it would be expected that at the early stages of the interaction, I would behave as a **competitive inhibitor** with respect to the substrate. Examples of the action of an active-site directed irreversible inhibitors are the acetylation of amino acid residues at the active site of prostaglandin synthase by aspirin (acetyl salicylate) (1) and the alkylation by L-**TPCK** (*N*-tosylphenylalanine chloromethyl ketone) of a **histidine** residue at the active site of a-**chymotrypsin** (2).

Photoaffinity labels, such as diazoketones and aryl azides, introduce a greater degree of specificity to the modification of amino acid residues, as they are not reactive in solution. It is only after the reversible interaction of the affinity label at the active site of an enzyme, and exposure of the resulting complex to light of the correct wavelength, that a highly reactive group is formed. Such treatment with diazoketones and aryl azides leads to the formation of carbenes and azines that are extremely reactive and can add across O—H bonds of unionized carboxyl groups or unsaturated carbon–hydrogen bonds (3).

Bibliography

1. G. J. Roth, N. Stanford, J. W. Jacobs, and P. W. Majerus (1977) Biochemistry **16**, 4244–4248.
2. C. Walsh (1979) *Enzymatic Reaction Mechanisms*, W. H. Freeman and Company, San Francisco, Calif., p. 86.
3. V. Chowdry and F. H. Westheimer (1979) Ann. Rev. Biochem. **48**, 293–325.

Active-Site Titrants

For determination of values for the kinetic rate constants and **ligand-binding** stoichiometries associated with an **enzyme**-catalyzed reaction, it is necessary to know the concentration of functional active sites of the enzyme. The latter value cannot be calculated simply from the total concentration of protein and molecular weight of the enzyme; even when the enzyme preparation has been shown to be homogeneous by a variety of techniques, it is possible that inactive enzyme is present. The inactivity could be due to the inability of the enzyme to bind substrate or perform the chemistry of the reaction, or both. Therefore, before undertaking detailed kinetic investigations on any enzyme, it is important to determine the concentrations of the active sites that can both bind the ligands and are active.

The concentration of binding sites can be obtained from data for the reversible inhibition of an enzyme by a tight-binding substrate analogue that gives rise to competitive inhibition. Tight-binding inhibition occurs under conditions where the total inhibitor concentration I_t is comparable to the total enzyme concentration E_t, and a substantial fraction of the inhibitor is bound, so that allowance has to be made for the reduction of free inhibitor concentration as a result of formation of the enzyme-inhibitor complex (1). The variation of the steady-state velocity as a function of the concentrations of I_t and E_t is described by Equation 1:

$$v = \frac{kA}{2(K_a + A)}[\{(K_i' + I_t - E_t)^2 + 4K_i'E_t\}^{1/2} - (K_i' + I_t - E_t)] \quad (1)$$

where k denotes the maximum rate of product formation in terms of moles per mole of enzyme per second, K_a is the Michaelis constant for the substrate present at concentration A, and K_i' represents an apparent inhibition constant whose relationship to the true inhibition constant K_i for the interaction of I with E is given by

$$K_i' = K_i(1 + A/K_a)$$

Equation 1 also applies to multisubstrate reactions, provided that the nonvaried substrates are present at saturating concentrations. When no assumptions are made about the purity of the enzyme, E_t of Equation 1 is replaced by aEx, where a represents the degree of purity of the enzyme and Ex denotes the total protein concentration. Fitting to the modified form of Equation 1 of steady-state velocity data obtained at varying concentrations of I_t and E_t would yield values for K_i' as well as a, which would yield a measure of the concentration of binding sites (2, 3).

The technique of active-site titration is used to determine the concentration of catalytically active enzyme (4, 5). It requires that on mixing enzyme and the titrating substrate, there is an initial rapid burst of product formation because of the accumulation of an enzyme-bound intermediate whose rate of breakdown is much slower than its rate of formation. The procedure can be illustrated by reference to the Uni–Bi reaction:

$$\begin{array}{ccccccc} E & \rightleftharpoons & EA & \rightarrow & EQ & \rightarrow & E \\ + & & & & + & & + \\ A & & EPQ & & P & & Q \end{array}$$

for which P is released before Q, and at a very much faster rate. Specific measurement of the release of P as a function of time would yield a plot (Fig. 1) that consists of curved (burst) and linear sections. The intersection of the extrapolated linear curve with the vertical ordinate would give the concentration of *P* that is equal to the concentration of functional active sites.

Figure 1. Active-site titration curve showing burst formation of a covalent enzyme-intermediate complex.

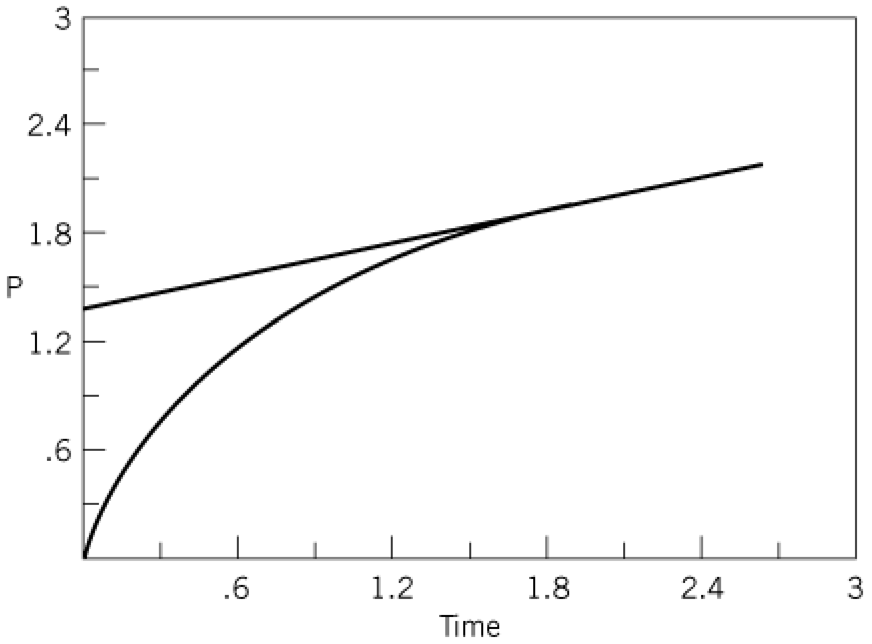

Active-site titrations may be performed with chromogenic or radioactive substrates, and rapid reaction techniques are often required. This is not the case, however, for determination of the active-site concentration of *hexokinase* (6). This can be done by incubating the enzyme with ^{14}C-glucose and ATP complexed with Cr^{3+}, rather than the usual Mg^{2+}, and separating the enzyme-CrADP-glucose-6-phosphate complex on a Sepharose column. In this case, the enzyme undergoes only a single turnover, and the product complex has a half-life of over 10 min, so the amount of ^{14}C associated with the enzyme gives a measure of the active-site concentration (6).

Comparison of the results obtained from tight-binding inhibition and active-site titration studies could yield information about the presence in an enzyme preparation of substantial proportion of sites that can bind substrate, but cannot catalyze the reaction.

Bibliography

1. J. W. Williams and J. F. Morrison (1979) Meth. Enzymol. **63**, 437–467.
2. J. F. Morrison and S. R. Stone (1985) Comments Mol. Cell. Biophys. **2**, 347–368.
3. M. J. Sculley and J. F. Morrison (1986) Biochem. Biophys. Acta **874**, 44–53.

4. A. Fersht (1977) *Enzyme Structure and Mechanism*, W. H. Freeman and Company, San Francisco, Calif., pp. 122–126.
5. F. J. Kezdy and E. T. Kaiser (1970) Meth. Enzymol. **19**, 3–20.
6. K. D. Danenberg and W. W. Cleland (1975) Biochemistry **14**, 28–39.

Adenovirus

The adenoviruses constitute a large group of DNA **viruses**, the *Adenoviridae* family. Genera include *Mastadenovirus* (human, simian, bovine, equine, porcine, ovine, canine, and opossum) and *Aviadenovirus* (birds). Adenoviruses are nonenveloped icosahedral particles of 70 to 100 nm in diameter, with 252 capsomeres, of which 240 are hexons and 12 are penton bases. A projecting fiber attaches to each penton base to form a penton.

Human adenoviruses (Ads) include 47 serotypes, which can be classified into six subgroups, A to F, based on their ability for red-blood-cell agglutination and oncogenicity in rodents, plus their DNA homology. Ads cause respiratory tract infections, conjunctivitis, hemorrhagic cystitis, and gastroenteritis. Highly oncogenic group A (eg, Ad12 and Ad18), weakly oncogenic group B (eg, Ad3 and Ad7), and Ad9 of group D can induce tumors in rodents, but no conclusive evidence has been reported linking adenoviruses with malignant diseases in the human. All Ads that have been tested can transform cultured rodent cells. No infectious virus is present, but viral transforming genes (E1A and E1B) are present and expressed in tumors and in transformed cells induced by adenoviruses.

The viral genome consists of a single linear molecule of double-stranded DNA [MW ~23×10^6, size ~36 kilobase pairs (kbp)], varying somewhat with the type. Human adenovirus type 2 (Ad2), the first to be sequenced completely, has a total of 35,937 bp. The Ad genome has inverted terminal repeats of 103 bp to 163 bp, depending on the type, and two identical replication origins, one in each terminal repeat. A 55-kDa terminal protein (TP) covalently bound to each 5′ end of the viral DNA molecule serves as a primer for protein-primed viral DNA replication. The viral genome carries five early transcription units (E1A, E1B, E2, E3, E4), two delayed early transcription units (IX and IVa2), and one late transcription unit (major late), all of which are transcribed by **RNA polymerase II**. The viral genome also carries one or two (depending on the type) VA genes transcribed by RNA polymerase III. The *E1A, E1B, IX, major late, VA*, and *E3* are on the rightward reading DNA strands (r strand), and others are on the leftward reading DNA strand (l strand).

The E1A is the first transcription unit to be expressed shortly after infection, using cellular transcription factors, encoding two major mRNAs of 12S and 13S. The encoded E1A proteins are required for productive viral replication and play a key role in cell transformation. E1A proteins transactivate early and late viral genes and cellular transcription units, and they bind cellular proteins, including p300, a family member of CBP (CREB binding protein)/p300, plus the RB family members, RB (**retinoblastoma** susceptibility gene product, tumor suppressor), p107, and p130. Binding to these cellular proteins is required for cell transformation. Binding of E1A to RB disrupts the RB · E2F complex to activate a cellular transcription factor, E2F, resulting in the activation of E2F-dependent **cell-cycle**-related genes.

Two major proteins of 19 kDa and 55 kDa, encoded by 13S and 22S messenger RNAs, respectively, are generated from the E1B region. The E1B proteins are required for efficient viral growth and cooperate with E1A products to transform rodent cells, preventing E1A-induced apoptosis. The E1B 19-kDa protein has a functional similarity to the cellular anti-apoptotic Bcl-2, and the E1B 55-kDa protein interacts with **tumor suppressor** and apoptosis-related p53.

Region E2 encodes proteins involved in viral replication, including the viral terminal protein precursor, pTP (coded by *E2B*), viral DNA polymerase (coded by *E2B*), and the DNA-binding protein (coded by *E2A*). None of the *E3* proteins are required for productive infections of adenoviruses in cultured cells, but are important for *in vivo* infections in humans, suppressing host defense mechanisms by cytotoxic T lymphocytes or **tumor necrosis factor**-a. The E4 proteins are involved in transcriptional regulation, preferential transport of viral mRNA, and efficient viral DNA replication. Other functions of the E4 gene, such as transformation with E1A, tumor-suppressor p53 binding, and apoptosis-inhibiting activities, have been recently reported. The Ad9 E4 gene can oncogenically transform rat cells in the absence of the E1A and E1B genes and is required for mammary tumorigenesis.

The transcription of adenovirus late genes is triggered by the onset of viral DNA replication, yielding at least 18 distinct mRNAs by differential poly(A) site utilization and alternative splicing. Viral DNA replication activates a major late **promoter** (MLP) located at 16.4 map units of the viral genome, and one large primary transcript is generated, terminating at 99 map units at the right end of the genome. This transcript is processed to five families of late mRNAs, L1 to L5, based on the use of common poly(A) addition sites. The late mRNAs encode structural polypeptides of the viral particle and proteins involved in polypeptide processing, capsomere assembly, and packaging of the viral genomic DNA.

Adenoviruses are being used as **vectors** for delivery of therapeutic genes to target organs *in vivo*. Recombinant adenoviruses can be constructed by replacing the E1A and E1B genes with foreign ones. The E3 region also can be deleted without significant changes in virus growth. Recombinant adenoviruses can propagate efficiently in 293 cells, which complement the defect. The advantages are that the growth of recombinant viruses does not require host cell division, and a high titer of recombinant viruses can be easily obtained.

Suggestions for Further Reading

T. Shenk (1996) "*Adenoviridae*: The Viruses and Their Replication". In *Fields Virology*, 3rd ed. (B. N. Fields et al., eds.), Lippincott-Raven, Philadelphia, pp. 2111–2148.

M. S. Horwitz (1996) "Adenoviruses". In *Fields Virology*, 3rd ed. (B. N. Fields et al., eds.), Lippincott-Raven, Philadelphia, pp. 2149–2171.

J. Tooze (1981) *DNA Tumor Viruses*, 2nd ed., Cold Spring Harbor Laboratory Press, Cold Spring Harbor, NY, pp. 943–1054.

Adenylate Charge

The adenylate charge, or adenylate energy charge, is a linear measure of the energy stored in the adenylate system ([ATP] + [ADP] + [AMP]) in a living cell. It is analogous to the charge of a storage battery. Its value is defined by the expression:

$$\text{Adenylate charge} = \frac{[\text{ATP}] + 0.5[\text{ADP}]}{[\text{ATP}] + [\text{ADP}] + [\text{AMP}]}$$

The status of the adenylate system is best described by the adenylate charge and appears to be the most ubiquitous regulatory signal in metabolism; it affects the rates of nearly all metabolic conversions and the partitioning of metabolically available substances between oxidation, synthesis of cell substance, and production of storage compounds. In living organisms, the same controls that regulate metabolic partitioning also maintain the value of the adenylate charge near 0.9.

1. Background

Organisms are exquisitely regulated material- and energy-transducing systems. Material from the environment must be converted to the many compounds of which the organism is made, and energy, usually obtained either by absorption of sunlight or from oxidation of foodstuffs, must be converted for use in biosynthesis, movement, and membrane activities. Partitioning of material and energy between those functions must be adjusted continuously to meet the changing needs of the cell or organism. Transduction of energy through the adenylate system is an integral part of each of those functions.

Any system that is not at chemical and physical equilibrium can, in principle, supply energy. The two types of nonequilibrium situations that are mainly used in energy storage and transduction by organisms are (1) difference in electric charge or chemical potential across a membrane (see Membrane Potentials) and (2) a ratio of [ATP] to [ADP] that is far from equilibrium. All cells contain enzyme systems that catalyze transfer of energy between the two.

The energy status of a chemical storage system may be defined by either of two parameters: the molar Gibbs **free energy** change of the relevant chemical reaction or the mole fraction of the higher-energy state of the system. The two are computationally interconvertible but are not linearly related. The molar free energy change is a function of the ratio of activities of the products and reactants of the reaction; the mole fraction is a linear measure of the extent of reaction. In the familiar case of a lead storage battery, the free energy is measured by the voltage and the mole fraction by the charge (measured by a hydrometer in this case).

If a generic energy-transducing reaction is indicated by the type of reaction $A \leftrightharpoons B$, the molar free energy change is given by

$$\Delta G = \Delta G^\circ + RT \ln \left(\frac{[B]}{[A]} \right) \tag{1}$$

and the fractional charge (mole fraction of the more energetic state) by

$$\text{Fractional charge} = \frac{[B]}{[A] + [B]} \tag{2}$$

In the case of a lead storage battery, A is ($2Pb(SO_4) + 2H_2O$) and B is ($Pb + PbO_2 + 2H_2SO_4$). For the metabolic adenylate system, A is ($ADP + P_i$) and B is (ATP).

A system is fully discharged when only A is present and fully charged when it consists of B alone. For intermediate states, the stoichiometrically linear charge function indicates how much work is available as a fraction of that of a totally charged system. [This metabolic use of the term "work" is slightly nonstandard. In thermodynamic terms, the maximum work available is the integrated product of the charge multiplied by the changing value of the Gibbs free energy as the system goes to equilibrium. But the energy of the adenylate system is used stoichiometrically—for example, to affect chemical change or mechanical movement—and charge is therefore proportional to available work, defined in terms of biological effect.] It is because of its stoichiometric nature that the charge function is more relevant in most contexts than the molar free energy change for both storage batteries and the metabolic adenylate system.

If the adenylate system merely alternated between ADP and ATP, the charge function would be the simple ATP mole fraction, [ATP]/([ATP] + [ADP]). Some enzymes, however, couple the use of ATP to synthetic reactions by converting ATP to AMP and pyrophospate, and so the concentration of AMP must also be taken into account.

$$\mathrm{ATP} + \mathrm{H_2O} \leftrightharpoons \mathrm{AMP} + \mathrm{PP_i} \qquad (3)$$

The pyrophosphate is rapidly hydrolyzed enzymically by pyrophosphatase, and this removal of product pulls the reaction forward (increases the numerical value of the negative free energy change).

Accumulation of AMP as a consequence of such reactions would deplete the cell's stores of ATP and ADP and so would be rapidly lethal. That outcome is prevented by the action of adenylate kinase, which catalyzes the phosphorylation of AMP:

$$\mathrm{ATP} + \mathrm{AMP} \leftrightharpoons 2\mathrm{ADP} \qquad (4)$$

The sum of reactions (2) and (3) is conversion of two molecules of ATP to two of ADP. In such cases, a single molecule of ATP, in effect, supplies twice as much metabolic energy to a metabolic reaction as is obtained from action of an ordinary kinase that converts ATP to ADP, but a second molecule of ATP is required to make good the energy balance.

Because of the participation of AMP in metabolic energy transduction, the simple mole fraction of ATP is not an adequate measure of the energy status of the adenylate system. Reaction (3) shows that two molecules of ADP are energetically equivalent to one of ATP. Thus, the linear charge function for the adenylate system (the effective mole fraction of ATP) is seen to be

$$\text{Adenylate charge} = \frac{[\mathrm{ATP}] + 0.5[\mathrm{ADP}]}{[\mathrm{ATP}] + [\mathrm{ADP}] + [\mathrm{AMP}]} \qquad (5)$$

The adenylate charge is the linear measure of the metabolic work available. A system containing only ATP is fully charged, with an adenylate charge value of 1.0, and one containing only AMP is fully discharged, with an adenylate charge of 0. The charge value would be 0.5 if only ADP were present. If reaction (3) catalyzed by adenylate kinase is at equilibrium, the concentrations of ATP, ADP, and AMP are fixed for any particular value of the adenylate charge (Figure 1).

Figure 1. Mole fractions of the components of the adenylate nucleotide system as a function of the adenylate charge. The reaction catalyzed by adenylate kinase is assumed to be near equilibrium, with an apparent equilibrium constant irrespective of differential ionization and magnesium binding) of 0.8.

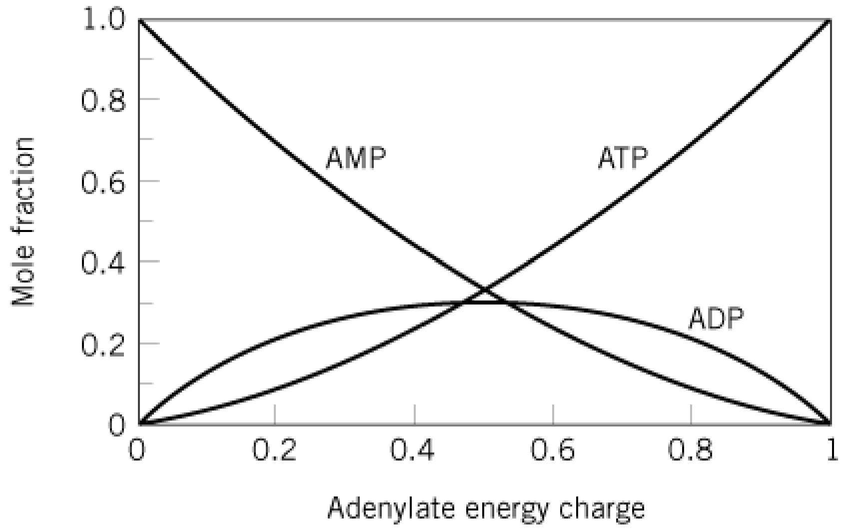

2. Regeneration and utilization of ATP

In aerobic organisms, ATP is regenerated mostly by oxidation of foods or storage compounds to carbon dioxide (see ATP Synthase). In anaerobic organisms, substrates undergo other energy-yielding conversions—for example, fermentation of glucose to ethanol and carbon dioxide—rather than oxidation. Carbohydrates are converted to pyruvate by way of the glycolytic pathway. The pyruvate is oxidized to a derivative of acetic acid, acetyl coenzyme A, which is oxidized to carbon dioxide in the reactions of the citrate cycle, or Krebs cycle. The electrons lost in those oxidations are passed on to oxygen by mediation of a series of membrane-associated enzymes. Those electron transfers are coupled to the conversion of ADP to ATP, thus supplying metabolically available energy to the adenylate system. The routes by which other classes of foods are metabolized feed into this central pathway. Fats are broken down to produce acetyl coenzyme A, which joins the carbohydrate pathway at that point. Amino acids derived from **protein degradation** are metabolized by individual pathways to produce various intermediates of glycolysis or the citrate cycle. Thus, the same central pathways are taken in the utilization of all foods.

Glycolysis and the citrate cycle are also centrally involved in biosynthesis. The biosynthetic pathways leading to the many components of a cell all begin with intermediates of glycolysis or the citrate cycle. That is, 10 or 12 intermediates of these degradative pathways are also the starting points for all synthetic sequences. Each such intermediate occupying a metabolic branchpoint must be partitioned between two competing pathways, one leading to oxidation to carbon dioxide and the other to synthesis of one or more components of the cell. The adenylate system provides energy for the chemical activities of the cell, including biosynthesis, for **active transport** of nutrients and ions across membranes against chemical potential gradients, and for most other biological requirements, including mechanical movement. All those functions are catalyzed or affected by proteins. Proteins involved in those functions have evolved affinities for ATP and ADP (or AMP) that maximize their functional usefulness to the organism. Thus, it is essential that the ratio of ATP to ADP remain virtually constant. The problem would be equivalent to the regulation of voltage by the power supply of a complex electronic device, if it were not so much more complicated.

3. Regulation of the Regeneration and Utilization of ATP

The rate of regeneration of ATP from ADP is regulated in large part by controlling the rate at which substrate is made available to the electron transport phosphorylation system. At least five enzymes that catalyze reactions in glycolysis or the citrate cycle respond sensitively to the status of the adenylate pool and adjust the properties of the catalytic site accordingly. An increase in the energy charge causes a decrease in the rate of the reaction catalyzed by the enzyme, and a decrease in charge causes an increase in rate. This **feedback inhibition** system acts to adjust the rate of regeneration of ATP to meet momentary requirements and thus to stabilize the value of the charge. The multiplicity of control sites may be surprising; a single throttle point would seem to be sufficient to regulate the rate of supply of substrate to the electron transport system. The regulatory requirements are, however, much more complex because the central pathways also supply starting materials for synthesis.

Core metabolism consists of the central pathways by which foodstuffs or storage materials of all types are prepared for oxidation and of branches from those pathways that lead to synthesis of one or more products. The primary function of oxidative pathways is regeneration of ATP from ADP, which puts energy into the adenylate system. Biosynthesis is powered by conversion of ATP to ADP, which removes energy from the adenylate system. Adjustment of the partitioning of resources between these oppositely directed pathways to meet the momentary metabolic needs of the cell or organism is the most central of the regulatory requirements that underlie cellular function and survival. At each branchpoint, the partitioning of resources must respond at least to the energy status of the cell as reflected in the ATP/ADP system and to the momentary need for the end products of the synthetic branch.

At such branchpoints, the next enzyme in the degradative pathway and the first enzyme in the biosynthetic branch compete for the branchpoint metabolite, their common substrate. Maintenance of an appropriate balance between oxidation and biosynthesis requires that both enzymes must be regulated. As well as decreasing the rate of the degradative reaction, an increase in the value of the charge leads to an increase in the rate of the competing reaction that channels the branchpoint metabolite into biosynthesis. Thus, enough substrate is oxidized to maintain the normal status of the adenylate system, and biosynthesis is allowed to the extent that the products are needed and the supply of resources allows.

This partitioning is not affected by turning enzymes on and off but by changing the affinities of the competing enzymes for the substrate, which allows for much more sensitive control. Affinity is usually expressed in terms of the Michaelis constant, $\boldsymbol{K_m}$, the concentration of substrate at which half the catalytic sites bind substrate, leading to a reaction velocity half the maximal rate. Thus, competition between the enzymes is regulated in the most direct and effective way—by modulating their relative abilities to capture the common substrate. The competition is shown generically in Figure 2. Reactions in pathways that lead to degradation of substrate and the regeneration of ATP respond to variation in the energy status of the adenylate pool as indicated by curve *R*, and reactions that direct substrate into biosynthetic pathways that utilize ATP respond as shown by curve *U*. The result is that the value of the energy charge is maintained within a narrow range of values near the intersection of the curves. If the charge drifts upward slightly, the rate of use of ATP in biosynthesis tends to increase and the rate of regeneration of ATP decreases, counteracting the drift. A downward drift has the opposite effect.

Figure 2. Generalized illustration of the effects of the adenylate charge on the rates of reactions in which ATP is regenerated (*R*) and in which ATP is utilized (*U*). Curve *U* was calculated for an enzyme for which the K_m for ATP at the catalytic site is six times that of ADP. Curve U^* represents 80% depression of rate as a consequence of feedback inhibition of the enzyme by the end product of the biosynthetic sequence.

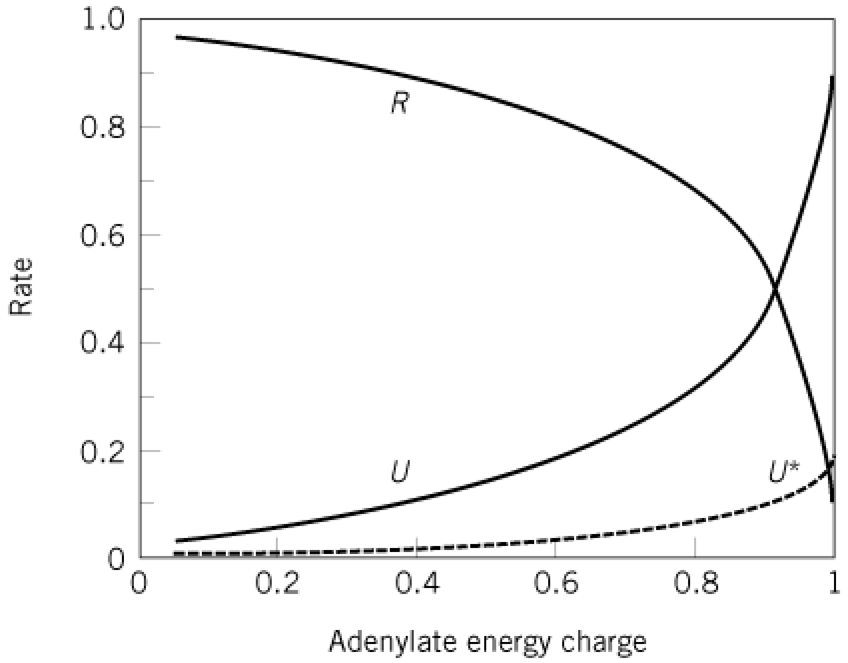

The regulatory interactions illustrated by curves *R* and *U* are necessary but not adequate. By themselves, they would adjust the rate of all biosynthetic sequences similarly and only on the basis of the availability of energy, without regard to the need for the individual products. Those controls are supplemented by product feedback inhibition. The first enzyme in nearly every biosynthetic sequence that has been studied bears a regulatory site that binds the end product of the sequence. When that site is occupied, the conformation of the enzyme changes so as to decrease the affinity for substrate at the catalytic site (increase the K_m) (see Allostery). Thus, as the concentration of end product rises, the fraction of enzyme molecules that bind it increases, the affinity of enzyme for substrate decreases, and the enzyme competes less vigorously for substrate. When the concentration of end product falls—for example, when an amino acid is being used more rapidly for protein synthesis—a smaller fraction of the regulatory sites of the first enzyme involved in its synthesis is occupied by end product. The resulting decrease in K_m causes the substrate to be more successful in its competition with the enzyme that catalyzes the next step in the degradative pathway, and the rate of synthesis increases. Such interactions adjust synthetic rates to meet changing metabolic needs. Curve U^* in Figure 2 illustrates the response of an enzyme when the end product of its sequence is available in adequate amount from external sources. Any response between curve U^* and somewhat above curve *U* is possible. Under ordinary conditions, the response will fluctuate in the vicinity of curve *U* to adjust production to meet metabolic demand. These interactions stabilize the pools of amino acids, assuring that they will neither be depleted when demand for protein is high nor build up to unnecessary or injurious levels when demand is small. Pool levels of other metabolites are regulated similarly.

The curves of Figure 2 thus provide a general overview of the regulation of the central pathways in their roles of regenerating ATP and providing starting materials for biosynthesis (1). The interaction of curves *R* and *U* adjust degradative metabolism and overall biosynthetic rates so as to maintain a nearly constant value of energy charge and, in the process, necessarily cause an appropriate partitioning of resources between degradation and synthesis. Superposition of product feedback inhibition, illustrated by curve U^*, adjusts the rate of each individual synthetic sequence to meet the momentary needs of the organism or cell. Even when the overall rate of biosynthesis is high, the synthetic pathway leading to any given metabolite will be suppressed when that product is in good supply. Thus, the components of this control system act together to assure that the adenylate system, the immediate energy source for nearly all cell activities, is maintained at a high and constant charge, near 0.9 (2), and that the rate of production of each biosynthetic product is determined by interaction between the overall availability of resources and the cell's need for the individual product. Regulation of biosynthetic rates is roughly equivalent to the decisions made by a human consumer who must balance how strongly an item is desired and how readily it can be afforded.

4. Regulatory Properties of Enzymes

Enzymes that show *R*-type responses (see Allostery) catalyze reactions in the pathways that supply substrates for electron transport–linked regeneration of ATP but usually do not involve ATP or ADP directly. Such enzymes have, therefore, evolved regulatory, allosteric sites, distinct from the catalytic site, where ADP or AMP can bind, causing conformational changes that increase the binding affinity for the substrate at the catalytic site. Some such enzymes decrease substrate affinity when ATP binds at a regulatory site. Typically, the nucleotide binds cooperatively to two or more sites, and the effect on K_m is related to the square or higher power of the nucleotide concentration. Such interactions underlie the sensitive response of *R*-type enzymes to variation in the value of the charge (3).

In contrast, ATP and ADP are directly involved in most of the reactions at branchpoints that direct substrate into synthetic sequences. Thus, separate nucleotide-binding regulatory sites are not required. The *U*-type response is a consequence of higher affinity at the catalytic site for ADP, a product of the reaction, than for ATP, a reactant. This reversal of the usual pattern of higher affinity for reactants than for products results in pronounced inhibition by ADP across most of the energy charge range. At a charge of 0.5, for example, when the concentrations of ATP and ADP are approximately equal, ATP would be excluded from most of the catalytic sites because of competition by ADP. The result would be that most of the kinetic response to variation in the ATP/ADP ratio would occur in a rather narrow range near the high end of the energy charge scale. Curve *U* of Figure 2 is calculated for an enzyme for which the value of K_m for ATP is six times that for ADP.

The regulatory stability illustrated by Figure 2 depends on (1) precise evolutionary adjustment of the affinities for adenylates at regulatory sites of *R*-type enzymes and at catalytic sites of *U*-type enzymes and of the conformational links by which binding at those sites causes conformational changes that modulate affinity for substrate at catalytic sites and (2) the relative affinity at catalytic sites of *U*-type enzymes for ATP and ADP. As a consequence of such interactions, the ATP/ADP ratio, or the energy charge, affects reaction rates more strongly than do the absolute concentrations of the adenylate nucleotides. A mutant strain of *Escherichia coli* unable to synthesize adenylate nucleotides grew on adenine-limiting media at essentially normal rates when the intracellular concentrations of ATP, ADP, and AMP were half the normal levels. The energy charge and the ATP/ADP ratio retained their normal values. That mutant, like other organisms that have been studied, did not grow if the energy charge fell slightly below its usual value of about 0.9 (4).

The controls illustrated in Figure 2 should not be confused with thermodynamic or mass-action effects; they are strictly kinetic. The value of the Gibbs free energy change is high and negative for *U*-type reactions under all physiological conditions, as is also true for *R*-type reactions. Thus, degradation of fuels and synthesis of products are both thermodynamically favorable at all times, and evolved kinetic control mechanisms determine which conversions actually occur. The adenylate energy transduction system, which links metabolic sequences and nearly all other cell activities energetically, is ideally placed for the additional role of mediating the regulatory interactions that underlie the integrated activities of cells and organisms.

Bibliography

1. D. E. Atkinson (1972) In *Horizons of Biochemistry* (A. San Pietro and H. Gest, eds.), Academic Press, New York, pp. 83–96.
2. A. G. Chapman and D. E. Atkinson (1977) In *Advances in Microbiological Physiology*, vol. **15**

(A. H. Rose and D. W. Tempest, eds.), Academic Press, New York, pp. 253–308.
3. D. E. Atkinson (1970) In *The Enzymes*, 3rd ed., vol. **1** (P. D. Boyer, ed.), Academic Press, New York, pp. 461–489.
4. J. S. Swedes, R. J. Sedo, and D. E. Atkinson (1975) J. Biol. Chem. **250**, 6930–6938.

Suggestions for Further Reading

5. D. E. Atkinson (1977) *Cellular Energy Metabolism and Its Regulation*, Academic Press, New York. A general discussion of metabolic interactions and regulation. Chapters 4 (pp. 85–107) and 7 (pp. 201–224) are most relevant to the subject of this article.
6. R. H. Garrett and C. M. Grisham (1995) *Biochemistry*, Saunders/Harcourt Brace, New York, Chapters "17" and "25". An excellent general biochemistry textbook with strong coverage of metabolism.

Adenylate Cyclases

The ubiquity of cyclic AMP (cAMP) in regulating **enzymatic** activity and/or **genetic expression** in all kingdoms of life, except for the **archaea** (but see later), accounts for the interest displayed in its mode of synthesis and the vast amount of literature devoted to the enzymes that produce it, the adenylate cyclases. These enzymes, which catalyze synthesis of cAMP from ATP and yield pyrophosphate as a by-product, can be classified into four different classes according to their common features: (1) cyclases related to enterobacterial adenylate cyclases; (2) toxic adenylate cyclases isolated from bacterial pathogens; (3) a large and probably ancient class that comprises cyclases from both eukaryotes and prokaryotes and is strongly related to guanylate cyclases; and (4) one example, presently known only from the eubacteria *Aeromonas hydrophila* and *yersinia pestis*, that differs entirely from all other classes.

0.1. Class I: The Enterobacterial Type

The first complete adenylate cyclase gene, *cya*, was cloned and sequenced from *Escherichia coli*. Work on other enterobacteria, such as *Erwinia chrysanthemi*, *Proteus mirabilis*, *Salmonella typhimurium*, *Yersinia intermedia*, and *Yersinia pestis* demonstrates that both the environment of the genes and the proteins specified are similar in size and overall organization to those of *E. coli* at the corresponding locus (1). Analysis of the *cya* gene from other bacterial species, related to enterobacteria but distinct from them, using genetic complementation of appropriate *cya* defective strains of *E. coli* (and more recently by direct sequencing of whole genomes) reveals that the genes from many other bacteria, in particular *Aeromonas caviae*, *Aeromonas hydrophila*, *Haemophilus influenzae*, *Pasteurella multocida*, and *Vibrio cholerae*, directly synthesize a protein structurally and phylogenetically related to the *E. coli* cyclase (1, 2) (see also the database at `http://www.tigr.org`).

No long stretch of **hydrophobic** amino acid residues is present to explain the membrane-bound localization of the adenylate cyclases. In all cases, the proteins are very rich in cysteine residues, an uncommon feature for proteins located in the cytoplasm or at the cytoplasmic border of the membrane. This might account for the extreme difficulty in purifying the enzymes. In addition, they are also rich in histidine residues, which could indicate that metal ions take part in the folding and/or activity of the polypeptide chain, but no experimental data support this hypothesis. Finally, the protein is made of two functionally well-defined **domains**. The catalytic domain is NH_2-terminal, whereas the glucose-sensitive regulatory domain is COOH-terminal. Comparison of the polypeptide sequence of the catalytic domain of the *E. coli* enzyme with sequences in the protein data libraries do not reveal significant identities with other known proteins. The catalytic domain sequence has been experimentally identified to be about 420 residues. Differences in the amino acid sequence of the *E. chrysanthemi* enzyme often result from the presence of complementary charged residues in place of neutral ones. This suggests that there are more electrostatic interactions (including salt bridges) that stabilize the protein at the lower growth temperature of this bacterium. This observation might be helpful when trying to understand the tertiary structure of the protein, which is still not known.

The carboxy-terminal domain of the protein is involved in regulating of the enzymatic activity, in particular its inhibition by glucose. A component of the phosphorylation cascade that mediates import of glucose in the cell, enzyme IIAGlc, is involved in this regulation, but in a way not yet understood. An aspartate residue (Asp414 in the *E. coli* enzyme) is involved in the process in an unknown way. Tonic inhibition of the catalytic domain by the regulatory domain could be relieved by phosphorylation of this residue, although such phosphorylation has never been demonstrated (3).

0.2. Class II: The Calmodulin-Activated Toxic Class

Whooping cough is caused by the **gram-negative** bacterium *Bordetella pertussis*, which secretes many toxic proteins into the medium, including an adenylate cyclase. In 1980 it was discovered that this enzyme is activated by a host protein, calmodulin, which does not occur in bacteria (4). Two years later, Leppla (5) demonstrated that another toxic adenylate cyclase, secreted by a gram-positive bacterium, *Bacillus anthracis*, the etiological agent of anthrax, is also activated by host calmodulin. These observations stimulated intense efforts, but several years were required before the *cya* genes from either organisms could be cloned. However, in 1988 a simple idea, predating its generalization under the name "two-hybrid system," *in vivo* complementation by a **plasmid** encoding an activator of the function (in this case, calmodulin), permitted the cloning of adenylate cyclase genes coding for the calmodulin-dependent cyclases (6).

Bordetella pertussis adenylate cyclase is synthesized as a large bifunctional polypeptide chain of 1706 amino acid residues. This contrasts with the various low values reported for the molecular weight of the purified protein (from 43 to 70 kDa). The explanation became apparent when it was demonstrated that the N-terminal segment of the protein (400 residues) alone displays calmodulin-activated adenylate cyclase activity, whereas the rest of the molecule is responsible for hemolytic activity and for transporting the toxin. Sequence, molecular genetic, and physiological studies indicate that the adenylate cyclase domain is fused to a polypeptide chain similar to that of the *E. coli* hemolysin toxin. Therefore the name cyclolysin was coined for the toxic adenylate cyclase from *B. pertussis*.

The adenylate cyclase of *B. anthracis* has been named after the symptom it triggers in the infected host, edema factor. It is encoded in a plasmid, together with another toxin, the lethal factor and a carrier protein, the protective antigen, necessary to internalize both the edema factor and the lethal factor into host target cells. The adenylate cyclase (edema factor) protein, 800 amino acid residues long, comprises four regions of different function. The first region is a signal peptide, permits secretion of the protein. The second region corresponds to the domain that binds with the protective antigen. The third region encodes the adenylate cyclase function. It is followed by the fourth region of unknown function. These toxic adenylate cyclases have been subjected to a most thorough biochemical analysis, but they have not yet been crystallized.

In spite of several attempts to isolate other members of this class, until 1998, we knew only three examples of such proteins, isolated from extremely distant bacteria, one gram-positive and two gram-negative (the adenylate cyclase from *B. bronchiseptica* is very similar to the *B. pertussis* enzyme) (7). Several examples of similar proteins have now been discovered in *Pseudomonas aeruginosa*, and in *Yersinia* species. Comparison of the catalytic regions of the *B. pertussis* and *B. anthracis* adenylate cyclases identified four conserved regions that are involved in catalysis, calmodulin binding and activation. The first region comprises a sequence, Gly-XXXX-Gly(Ala)-Lys-Ser, similar to the nucleotide-binding motif found in many ATP- or GTP-binding proteins.

Therefore it was proposed as part of the catalytic site, and *in vitro* mutagenesis substantiated this interpretation. A second region, with the sequence Pro-Leu-Thr-Ala-Asp-Ile-Asp having some similarity in 6-**phosphofructokinase**, is also involved in catalysis, and it was proposed that the aspartate residues present in this region are involved in binding ribose and magnesium-phosphate. Although it is strongly conserved, however, the first proline residue does not seem very important because it could be replaced by a leucine residue without any measurable influence on the activity or calmodulin activation of the wild-type enzyme.

Although many calmodulin-dependent enzymes have been identified, the mechanism of activation by calmodulin is still poorly understood (see Calmodulin). In several cases, limited **proteolysis** releases active, calmodulin-independent forms of the enzymes. Accordingly, it was proposed that the calmodulin-binding domain of these enzymes blocks access of substrates to the active site and that activation results because an inhibitory domain is removed upon binding calmodulin. The most original feature of the *B. pertussis* protein is that it can be split into two separate domains which recover most of the initial activity when combined. This observation, together the with analysis of mutants in the region conserved between the *B. anthracis* and *B. pertussis* enzymes, indicates that these proteins may form a catalytic center from the cooperation of two halves. The function of calmodulin may be to trigger the appropriate conformational movement necessary to form an active catalytic center (3).

0.3. Class III: The “Universal” Class

Adenylate cyclases from multicellular eukaryotes have long remained elusive because purifying the corresponding catalytic subunit is extremely difficult. Following intense work all over the world, however, they have been the first adenylate cyclases to be crystallized and analyzed by X-ray crystallography (see Fig. 1). The activity of these enzymes is subject to a complex regulatory pattern, in particular by GTP-binding proteins. Class III enzymes were first discovered in yeast, but, for convenience, we start with the eubacterial enzymes.

Figure 1. Three-dimensional model of the C1 and C2 domains of the catalytic core of type I adenylate cyclase derived fr the X-ray crystallographic structure of the C2 homodimer of the type II enzyme (19). The polypeptide backbone of the C domain is green and that of C2 is red. The C-terminal nonhomologous segment of C1 is truncated after the a-helix 5 (low right). Only a few side chains in the active site are shown, designated by one-letter abbreviations. When they differed frc the residues in the crystal structure, they were placed according to Liu *et al*. [*Proc. Natl. Acad. Sci.* (1997) **94**, 13414–13419.] ATP was placed as described by Liu *et al*. and modified according to the interactions reported by Tesmer *et al*. [*Science* (1997) **278**, 1907–1916.] The ligand atoms are indicated by C, white; N, blue; O, red; P, green, and Mg, purple. figure is kindly provided by James Hurley. See color insert.

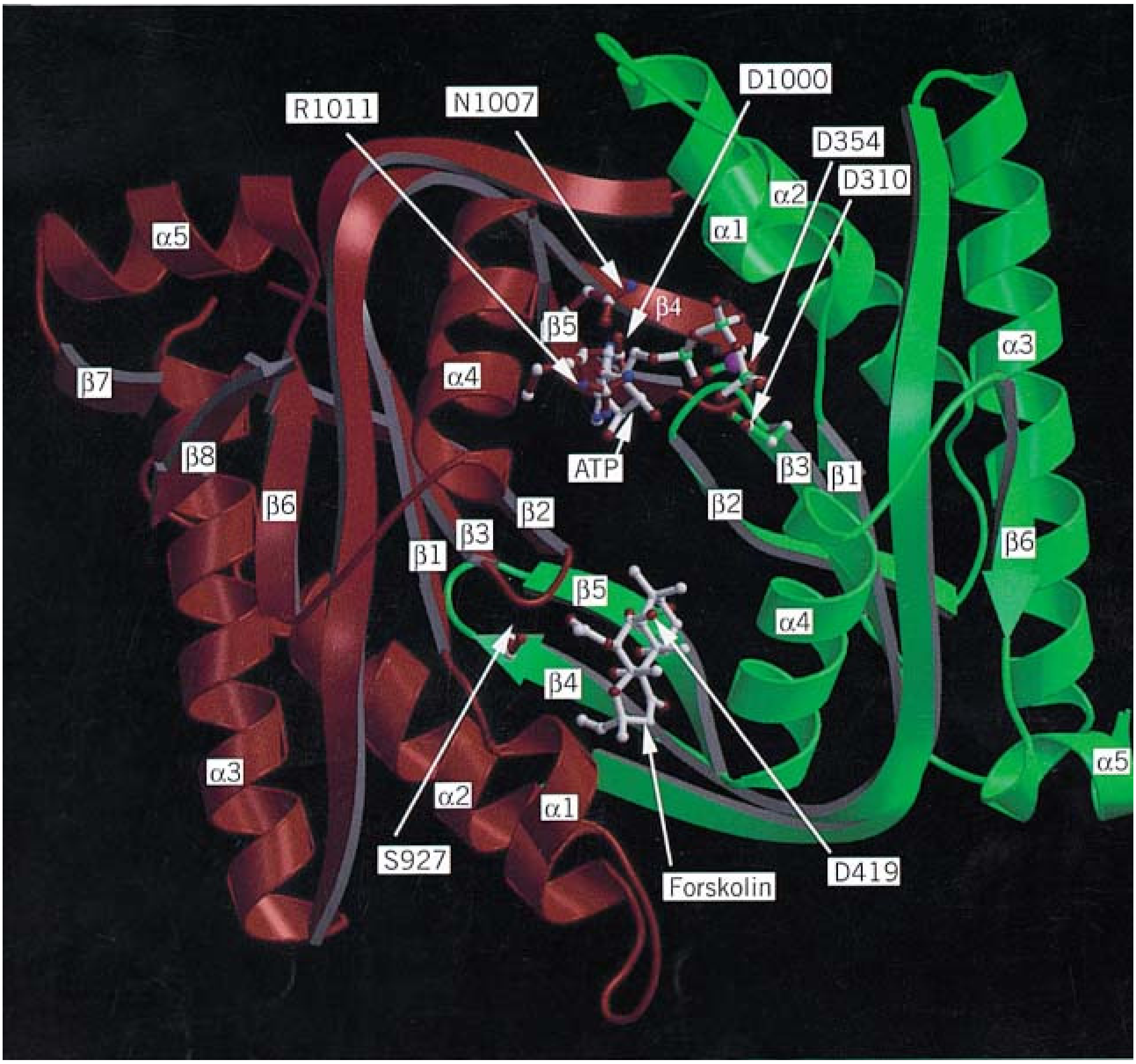

0.3.1. Eubacteria

Class III adenylate cyclases form a very diverse collection in eubacteria, both in length and in regulation. Gram-positive bacteria such as *Corynebacterium liquefaciens* secrete large amounts of cAMP because they have a very active class III adenylate cyclase, which is activated by pyruvate. *S. coelicolor* synthesizes a much less active adenylate cyclase involved in aeromycelium formation. Gram-negative bacteria, such as *Rhizobium meliloti*, synthesize at least two different adenylate cyclases. Disruption of both genes simultaneously does not alter cAMP production and suggests the presence of further enzymes. The gram-negative sliding myxobacterium *Stigmatella aurantiaca*, that exhibits an elaborated differentiation pattern, harbors at least two adenylate cyclase genes, each of them corresponding to class III enzymes. They have been partially purified and are inhibited by adenosine, as are the mammalian enzymes (see later). They comprise two domains. The catalytic domain is carboxy-terminal and the regulatory domain is a likely ion transporter in one case and the phosphorylated moiety of a two-component regulatory system in the other. Many other bacteria possess class III cyclases, in particular **cyanobacteria** (8, 9). These enzymes generally comprise two domains. The catalytic domain is carboxy-terminal. There are no indications that they must oligomerize to be active.

0.3.2. Lower Eukaryotes

Saccharomyces cerevisiae was the first organism from which class III adenylate cyclase genes were cloned and sequenced. The enzyme is activated by the *RAS* gene product (10, 11). Two forms of the enzyme may exist. A long form contains repetitions of a leucine-rich motif that plays a regulatory role and whose significance was recently substantiated and extended. Then it became clear that this eukaryotic adenylate cyclase is completely different from the enterobacterial class because of sequence differences in the catalytic center and also because the organization of the gene is different. The catalytic domain is located at the COOH-terminus in *S. cerevisiae* cyclase, whereas it is found at the NH_2-terminus in *E. coli*. The yeast enzyme remained the only example of its class until Garbers, Goeddel and co-workers (12) recognized that the genes encoding guanylate cyclases that had been cloned from several metazoans were derived from an ancestor common to the yeast adenylate cyclase. Another member of class III was subsequently discovered by Young *et al.* (13), who cloned the adenylate cyclase gene from *Schizosaccharomyces pombe* by hybridization using the catalytic domain gene sequence from *S. cerevisiae* as a probe. Finally, the first higher eukaryote adenylate cyclase gene isolated in Gilman's laboratory (14) from bovine brain displayed features clearly reminiscent of this class. Since then, many other genes or cDNA for adenylate cyclases belonging to this class have been isolated and sequenced from lower eukaryotes: *Saccharomyces kluyveri*, *Trypanosoma brucei* and *T. equiperdum*, *Plasmodium falciparum*, *Neurospora crassa*, and *Dictyostelium discoideum* (3).

0.3.3. Higher Eukaryotes: Nine Types

Many class III adenylate cyclases have been identified in higher eukaryotes, in particular in vertebrates, but the most thorough study is in mammals, where several types differing in their regulatory properties have been identified (15). All are regulated in more or less complex ways by **G-proteins** (16). Mammalian adenylate cyclases are informally grouped into nine types according to their tissue location and activity regulation. All but type 9 are activated by the diterpene forskolin, and some are activated by protein kinase C and/or other regulators. Type 1 enzymes were described as calmodulin-activated enzymes from brain. Type 2 proteins are found in brain, lung and other tissues. Type 3 are abundant in olfactory tissue, and the smaller type 4 enzymes are present in testicular tissue. Adenylate cyclase 1, 2, and 8 are positively regulated by calcium/calmodulin, whereas types 5 and 6 are directly inhibited by calcium. Adenylate cyclase 2 and 4 are sensitive to multiple regulatory effects from diverse receptors (3, 15). Adenylate cyclase 9 mRNA, found in rat brain, is particularly abundant in the hippocampus, cerebellum, and neocortex (17). However, the classification into types is somewhat arbitrary (for example, type 4 can also be calmodulin-activated). They all have overall similar structures. Two phylogenetically related cytoplasmic domains are required for catalysis. All types are connected by an integral membrane domain and have variable integral membrane domains at the NH_2 terminus of the protein. Among their many functions, their role in synaptic plasticity and memory is particularly interesting (18) and will certainly make adenylate cyclases extremely fashionable again.

0.3.4. Three-Dimensional Structure

The diverse origins of class III adenylate cyclases are reflected in the wide variation in their general organizations and molecular weights. The smallest protein is the *R. meliloti* enzyme, which contains only a catalytic domain, although some data suggest that an upstream sequence may yield a much longer protein that has a complex regulatory pattern. The next shortest protein, also bacterial, is the enzyme from *C. liquifaciens*. The yeasts produce long proteins, as do higher eukaryotes (except in the case of the testicular enzyme). In all cases, the catalytic domain is located at the COOH-terminus. The mammalian enzymes consist of twelve hydrophobic membrane-spanning regions that form two distinct domains, two cytoplasmic regions that contain both variable and conserved regions, and, in particular, two well-conserved domains that are responsible for catalysis.

Comparison of the catalytic domain sequences of the class III proteins shows that four amino acid stretches are strongly conserved: (1) (Met/Leu/Ile/Val)-(Met/Leu/Ile/Val)-Phe-(Ala/Thr)-(Asp/Ser)-(Leu/Ile)-X-(Asn/Asp)-(Phe/Ser); (2) (Ile/Val)-Lys-Thr-X-Gly-(Ser/Asp)-(Ala/Ser/Thr)-(Tyr/Phe)-

Met; (3) (Met/Leu/Ile/Val)-(Arg/Lys)-(Met/Leu/Ile/Val)-Gly-(Met/Leu/Ile/Val)-(His/Asn)-X-Gly-X-(Val/Ala)-(Val/Leu)-(Ala/Ser)-Gly; and (4) (Trp/Tyr/Phe)-Gly-(Asn/Asp/Pro)-Thr-Val-Asn-X-Ala-Ser-Arg-(Met/Leu/Ile/Val) (see Fig. 2). Crystallization of the catalytic core of one protein and determination of its structure by X-ray diffraction (19) showed that these regions are part of the organization of the structure (Fig. 1). The crystal structure contains the forskolin-binding site but unfortunately not the nucleotide binding site. As a step toward understanding the evolution and function of class III cyclases, enzymes displaying significant guanylyl cyclase activity that have evolved from an adenylyl cyclase ancestor were isolated. A single amino acid residue change (Gly-Asp-Thr-Val-Asn to Gly-Asp-Thr-Ile-Asn in the region of the fourth a-helix of the catalytic core) alters the nucleotide specificity of the enzyme (20). This corresponds to a pocket situated in a region of the protein that might accommodate the heterocyclic base (19).

Figure 2. Alignment of the amino acid sequences of Class III adenylate cyclases from various organisms. The four regio text are enclosed in the four boxes. Secondary structural elements found in the crystal structure of Fig. 1 are displayed ur corresponding residues of the active site depicted in Fig. 1 are indicated.

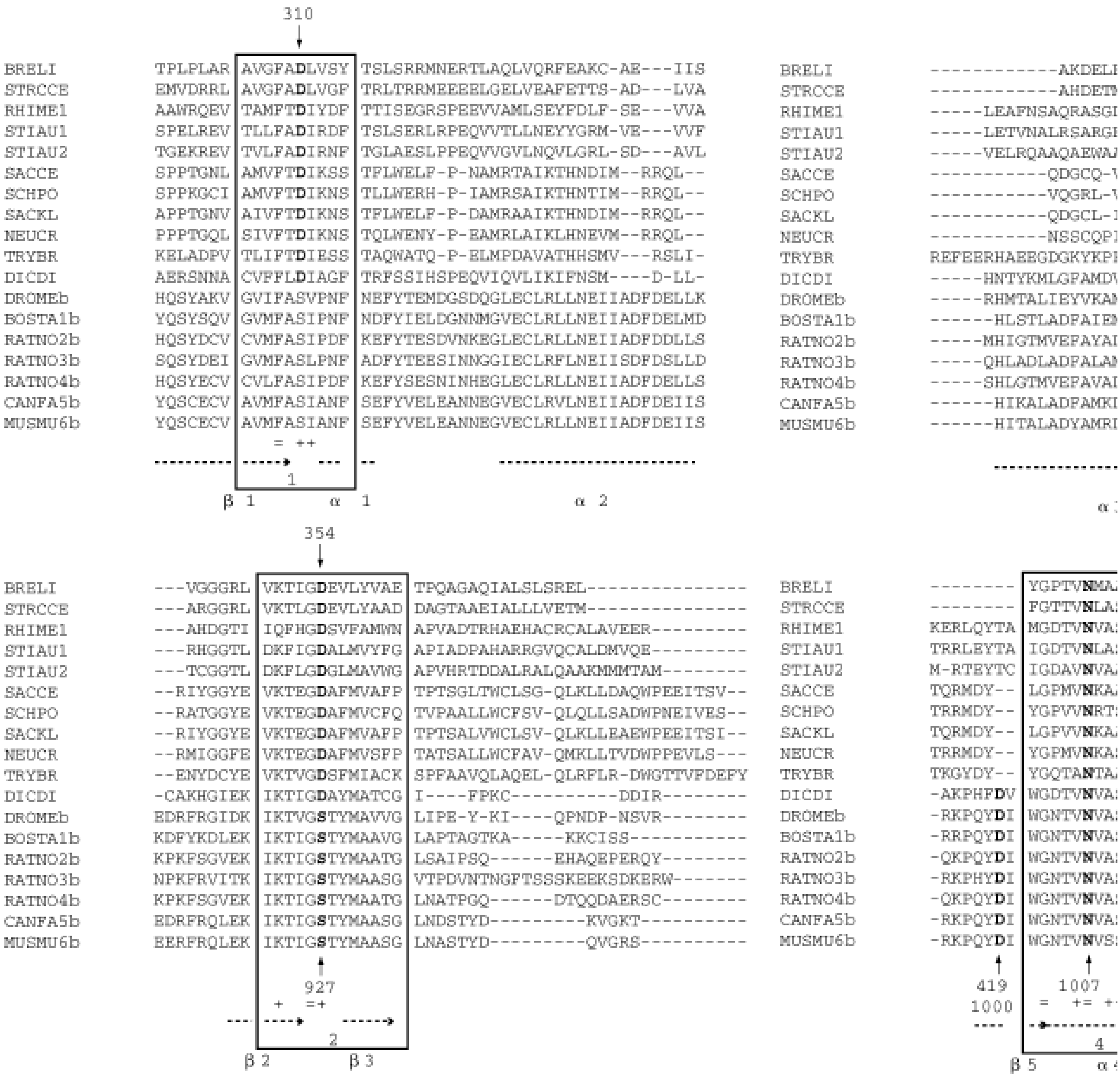

0.4. Class IV Adenylate Cyclases

The preceding three classes of structurally unrelated adenylate cyclases already pose a challenging problem. So it was a surprise that *Aeromonas hydrophila* synthesizes another enzyme, a very small cyclase of 193 residues, which has an optimal temperature for activity of 65°C and is at least ten times more active than the class I adenylate cyclase in the same organism (21). No function has yet been discovered for this protein. As yet, it has been found only in various isolates of *A. hydrophila* and in *Y. pestis* (unpublished). There was one report of the presence of cAMP in Archaea, but this was later proven to be the result of an artifact of the growth culture. Therefore it was interesting to see that the sequence of adenylate cyclase from *A. hydrophila* is significantly similar to a gene product of the archaebacterium *Methanococcus jannaschii*. The gene is expressed in *E. coli*, where it is toxic, but it does not restore cAMP synthesis. Therefore, nothing is yet known about the nature of adenylate cyclases, if they exist, in Archaea, but we may expect that, at some point, they might be discovered and that they would belong to this new class.

Bibliography

1. A. Danchin (1993) Adv. Sec. Mess. Phosphoprot. Res., **27**, 109–161.
2. P. Trotot, O. Sismeiro, C. Vivarès, P. Glaser, A. Bresson-Roy, and A. Danchin (1996) Biochimie **78**, 277–287.
3. O. Barzu and A. Danchin (1994) Prog. Nucleic Acid Res. Mol. Biol. **49**, 241–283.
4. J. Wolff, G. H. Cook, A. R. Goldhammer, and S. A. Berkowitz (1980) Proc. Natl Acad. Sci. USA **77**, 3840–3844.
5. S. H. Leppla (1982) Proc. Natl Acad. Sci. USA **79**, 3162–3166.
6. P. Glaser, D. Ladant, O. Sezer, F. Pichot, A. Ullmann, and A. Danchin (1988) Mol. Microbiol. **2**, 19–30.
7. F. Betsou, O. Sismeiro, A. Danchin, and N. Guiso (1995) Gene **162**, 165–166.
8. M. Kasahara, K. Yashiro, T. Sakamoto, and M. Ohmori (1997) Plant Cell. Physiol. **38**, 828–836.
9. M. Katayama and M. Ohmori (1997) J. Bacteriol. **179**, 3588–3593.
10. T. Kataoka, D. Broek, and M. Wigler (1985) Cell **43**, 493–505.
11. P. Masson, G. Lenzen, J. M. Jacquemin, and A. Danchin (1986) Curr. Genet. **10**, 343–352.
12. M. Chinkers, D. L. Garbers, M. S. Chang, D. G. Lowe, H. Chin, D. V. Goeddel, and S. Schulz (1989) Nature **338**, 78–83.
13. D. Young, M. Riggs, J. Field, A. Vojtek, D. Broek, and M. Wigler (1989) Proc. Natl. Acad. Sci. USA **86**, 7989–7993.
14. J. Krupinski, F. Coussen, H. A. Bakalyar, W.-J. Tang, P. G. Feinstein, K. Orth, C. Slaughter, R. R. Reed, and A. G. Gilman (1989) Science **244**, 1558–1564.
15. J. Hanoune, Y. Pouille, E. Tzavara, T. Shen, L. Lipskaya, N. Miyamoto, Y. Suzuki, and N. Defer (1997) Mol. Cell. Endocrinol. **128**, 179–194.
16. A. Marjamaki, M. Sato, R. Bouet-Alard, Q. Yang, I. Limon-Boulez, C. Legrand, and S. M. Lanier (1997) J. Biol. Chem. **272**, 16466–16473.
17. R. T. Premont, I. Matsuoka, M. G. Mattei, Y. Pouille, N. Defer, and J. Hanoune (1996) J. Biol. Chem. **271**, 13900–13907.
18. M. D. Nielsen, G. C. K. Chan, S. W. Poser, and D. R. Storm (1996) J. Biol. Chem. **271**, 33308–33316.
19. G. Zhang, Y. Liu, A. E. Ruoho, and J. H. Hurley (1997) Nature **386**, 247–253.
20. A. Beuve, E. Krin, and A. Danchin (1993) Compt. Rend. Acad. Sci. Paris **316**, 553–559.
21. O. Sismeiro, P. Trotot, F. Biville, C. Vivarès, and A. Danchin (1998) J. Bacteriol. **180**, 3339–3344.

Adenylylation

Adenylylation is the process in which adenosine-5′-monophosphate (AMP) is covalently attached to a protein, nucleic acid, or small molecule via a phosphodiester or phosphoramidate linkage. Most often, the AMP is derived from ATP, but in some bacterial adenylylation reactions $NADP^+$ is the source. Similarly, deadenylylation is the process in which AMP is removed from the adenylylated molecule. The adenylylation/deadenylylation processes may provide regulatory control of enzyme activity, contribute to intermediate steps in individual enzymatic reaction mechanisms, or occur as intermediate steps along the biosynthetic pathway of cofactors. In this sense, adenylylation is analogous to **phosphorylation**, sulfation, **methylation**, and other intracellular covalent modification reactions for which multiple functions exist. Adenylylation occurs in a wide range of organisms, including bacteria, yeast, and mammals, although it is less common than many other post-translational modification reactions as a source of enzyme regulation. The general chemical reaction for ATP-dependent adenylylation is shown in Figure 1.

Figure 1. General reaction scheme for ATP-dependent adenylylation. R = O or N. The a, b, and g phosphorous atoms are labeled.

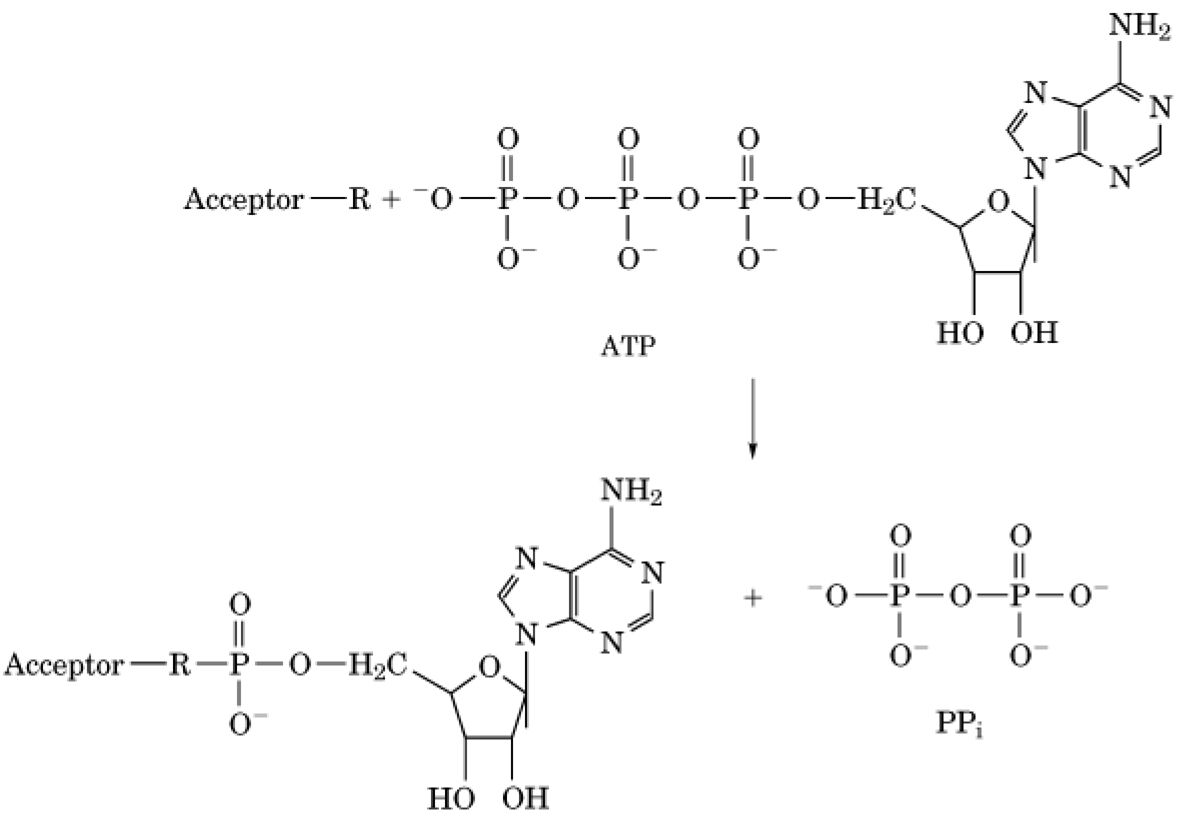

It is important to distinguish adenylylation from the related processes of phosphorylation, adenylation, and **ADP-ribosylation**:

1. Phosphorylation is readily distinguished from each of the other processes by the lack of

incorporation of sugar or adenine in the acceptor.

2. Adenylation results in covalent attachment of ADP via the b-phosphoryl group. Relatively few examples of adenylation are known, and they appear to be limited to adenylation of carbohydrates to yield, for example, glucose-1-ADP.
3. ADP-ribosylation results in a covalent bond between the ribose moiety of NADPH and an acceptor.

These covalent modification reactions also contribute to multiple biological functions, including regulation of enzymatic activity. Analytically, adenylation may be distinguished from adenylylation with the appropriate radiolabeled substrates. Specifically, a-^{32}P-ATP, but not b-^{32}P-ATP or g-^{32}P-ATP, will yield radiolabeled acceptor if adenylylation occurs. Typically, ATP that is radiolabeled with ^{3}H or ^{13}C in the adenine moiety is also used, in separate experiments, to confirm that label incorporated into the acceptor is not a result of phosphorylation, without adenylylation. An additional criterion that is often applied to distinguish adenylylation from phosphorylation is its sensitivity to phosphodiesterases. Phosphodiesterases will cleave the AMP from an adenylylated substrate, but they will not hydrolyze phosphate from phosphorylated protein. Specific examples of molecules that are adenylylated are discussed separately below.

1. Glutamine Synthetase

In all organisms, glutamine synthetase (GS) plays a critical role in intermediary metabolism by catalyzing the ATP-dependent condensation of ammonia with glutamate, to yield glutamine. It was discovered by Stadtman and co-workers (1, 2) that *Escherichia coli* glutamine synthetase exhibited dramatically different kinetic properties when isolated from cultures grown in nitrogen-rich vs. nitrogen-starved media. They demonstrated that the differences in enzymatic activity of GS corresponded to the presence or absence of covalently attached adenylyl groups. Since their initial findings, bacterial GS and associated regulatory enzymes have provided a paradigm for understanding biological regulation of nitrogen assimilation in some prokaryotic organisms. Comparison of the molecular details of adenylylation-dependent regulation of prokaryotic GS remains an active research area. Mammalian and plant GS, in contrast, are not regulated by adenylylation.

Regulation of glutamine biosynthesis is characterized most thoroughly for *E. coli* and includes a complex bicyclic cascade that controls the adenylylation of Tyr397 on the surface of GS. Bacterial GS are dodecameric oligomers with two face-to-face hexameric rings. In the subset of bacterial strains that regulate GS activity via adenylylation, the adenylylation state of GS may vary from 0 to 12 AMPs/GS dodecamer, and the enzymatic activity decreases with increasing extent of adenylylation. The regulatory cascade is summarized in Figure 2. It includes the adenylyl transferase (ATase), a signal transduction enzyme (P_{II}), and a uridylyl transferase (UTase) enzyme that responds directly to nitrogen levels. When the nitrogen levels are low, UTase uridylylates P_{II} at Tyr51 to form P_{II}-UMP. P_{II}-UMP stimulates the deadenylylation activity of ATase, to decrease the proportion of GS in the adenylylated form and thus to increase the rate at which nitrogen is "fixed" in the amino acid glutamine, derived from glutamate by GS. When nitrogen levels are high, the UTase cleaves the UMP from P_{II}-UMP to generate P_{II}. Unmodified P_{II} stimulates the adenylylation activity of ATase, to increase the adenylylation state of GS and reduce its efficiency in converting glutamate to glutamine. The complexity of these regulatory cascades underscores the importance of adenylylation as a mechanism for controlling nitrogen metabolism in some prokaryotes.

Figure 2. Bicyclic cascade for regulation of *E. coli* glutamine synthetase (GS). ATase catalyzes the

adenylylation/deadenylylation of GS; P_{II} stimulates the adenylylation activity, and uridylylated P_{II} (P_{II}-UMP) stimulates the deadenylylation activity. Uridylylation of P_{II} is catalyzed by UTase. UTase uridylylates P_{II} when nitrogen levels are low, and it hydrolyzes the uridylyl group from P_{II}-UMP when nitrogen levels are high.

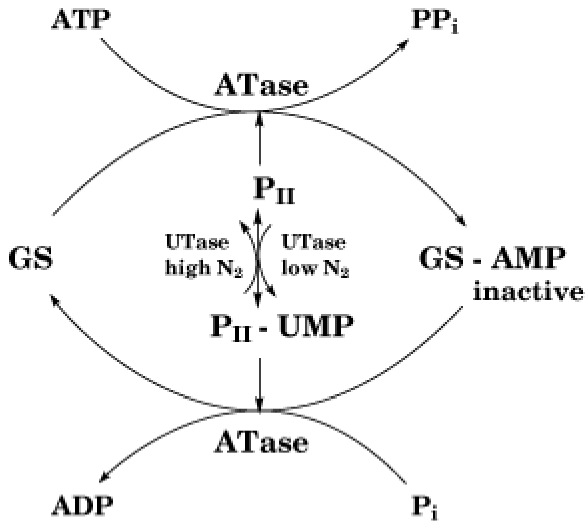

The structural basis for the decrease in enzymatic activity of *E. coli* GS upon adenylylation is not known. Although X-ray crystallography structures are available for the unadenylylated GS from *Salmonella typhimurium* (3, 4), no structure for an adenylylated GS has been determined. Spectroscopic and kinetic analyses indicate that adenylylation causes an increase in the Km (Michaelis constant) for substrates and for the metal cofactors (Mg^{2+} or Mn^{2+}) that are required at each GS active site, although no specific interactions between the adenylyl group and protein residues have been identified (5-7). On the basis of many biophysical criteria and hydrodynamic volume properties, the adenylylated and unadenylylated forms of GS do not differ greatly in conformation (8, 9). Presumably, adenylyl groups attached at Tyr397 of each subunit in dodecameric GS induce subtle changes in the local conformation of the active sites to which they are adjacent. Spectroscopic methods have suggested that the adenine moiety of AMP attached to each subunit within the hexameric ring structure is highly dynamic, and it collides by diffusion with the subunit adjacent to it (10, 11). Thus, specific hydrogen bonds or electrostatic interactions between the adenylyl groups and protein residues may be limited to the phosphate and ribose moieties of AMP. Alternatively, AMP may simply block the enzyme active sites sterically.

Based on sequence comparisons of GS from numerous prokaryotes, and on mutational analysis of the *E. coli* and *Anabaena 7120* GS, a minimal **consensus sequence** including the Tyr 397 to be adenylylated and a properly positioned proline residue are required for efficient adenylylation by ATase. These two residues are indicated in bold in the local sequence of *E. coli* GS: Met-Asp-Lys-Asn-Leu-**Tyr**-Asp-Leu-**Pro**-Pro-Glu-Glu-Ser-Lys. Individual mutation of several residues in this sequence has negligible or modest effects on the rate of adenylylation by ATase. In contrast, replacement of the bold proline nearly abolishes the ATase-catalyzed adenylylation, and substitution of serine by proline at the analogous position in the *Anabaena 7120* is sufficient to make this GS a substrate for ATase from *E. coli* (12, 13).

The *E. coli* Atase has been characterized genetically and biochemically; it is a constitutively expressed 945 amino acid residue protein (~115 kDa) that contains two highly homologous **domains** (8, 14). Genetically engineered N- and 3C-terminal domains that have been expressed separately and purified are both catalytically active. However, the two nonoverlapping constructs exhibit different catalytic activities. The N-terminal domain (residues 1 to 423) catalyzes deadenylylation of GS, requires P_{II}-UMP, and is inhibited by P_{II}. In contrast, the C-terminal domain (residues 425 to 945) catalyzes the adenylylation of GS and is not regulated by P_{II} or P_{II}-UMP. It is striking that P_{II} is required for the adenylylation activity of the full-length ATase, whereas the C-terminal domain by itself is unresponsive to P_{II} or P_{II}-UMP. Presumably, P_{II} and P_{II}-UMP regulate the adenylylation reaction of the C-terminal domain by interacting with the N-terminal domain, or the full-length construct is required to maintain the structural integrity of this regulatory site. In addition, glutamine activates the adenylylation reaction of the C-terminal domain. It also is noteworthy that the adenylylation and deadenylylation reactions catalyzed by ATase are not the reverse of each other. Deadenylylation requires inorganic phosphate (P_i) rather than PP_i, and the reaction product is ADP rather than ATP. In effect, this deadenylylation reaction may be considered formally as transfer of an adenylyl group from GS to P_i, or the adenylylation of phosphate anion. Although the two functional domains of ATase exhibit significant homology at the amino acid level, they have clearly distinct functional properties. The structural basis for these differences remains unknown.

2. DNA Ligases, RNA Ligases, and Related Enzymes

DNA ligases and RNA ligases catalyze the formation of phosphodiester bonds at single strand breaks with adjacent 3′-hydroxyl and 5′-phosphate termini in DNA or RNA, respectively. For bacterial, mammalian, and virus ligases, the first step in the catalytic cycle is the adenylylation of an active-site e-amino group of a lysine side chain (Fig. 3). Mammalian and virally encoded ligases utilize ATP to adenylylate the lysine, whereas bacterial ligases exploit $NADP^+$. A consensus sequence found in ligases from each of these sources that includes the adenylylated Lys, in bold, is -**Lys**-X-(Asp/Asn)-Gly- (15, 16). The phosporamidate bond formed upon adenylylation of the lysine residue is more stable toward hydrolysis than is the phosphoester bond formed upon adenylylation of tyrosine residues or hydroxyl groups of aminoglycosides. Interestingly, a similar consensus sequence is found in messenger RNA-capping enzymes that transfer guanylylate to the 5′-terminus of mRNA, followed by methylation to generate the mature RNA message.

Figure 3. Mechanism for DNA and RNA ligases. The catalytic reaction begins with ATP-dependent adenylylation of the
adenine; E, a ligase.

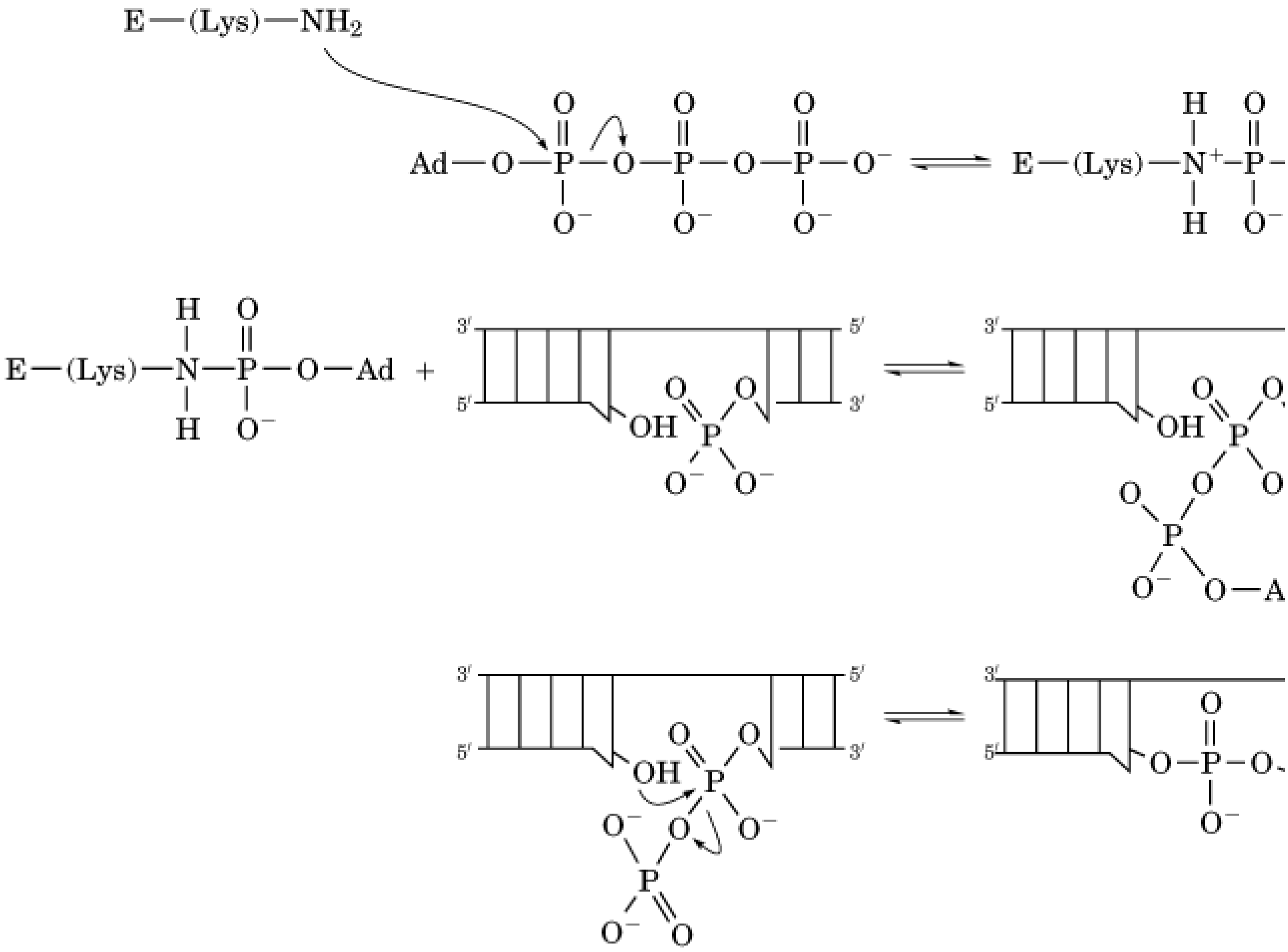

Functionally related RNA 3′-phospho-cyclases have been identified, and they appear to be present in mammals, yeast, enteric bacteria, and archaebacteria. This wide distribution suggests that these enzymes have a critical role, but no physiological function has been determined. As part of the catalytic cycle, the 3′-phosphoryl group on the terminal nucleotide of transfer RNA or **small nuclear RNA** (snRNA) undergoes ATP-dependent adenylylation, to generate a phosphodiester bond. This intermediate is attacked subsequently by the 2′-hydroxyl group to release AMP and produce a terminal cyclic phosphate (17). As with the ligase-catalyzed reactions, this cyclization proceeds via an initial adenylylation reaction.

3. Other Mammalian Proteins

On the basis of radiolabeling experiments, it has been suggested that plasma membrane proteins from liver or parotid glands of rats are adenylylated (18, 19). No function has been ascribed to any of these proteins. The hepatic proteins are glycosylated, and their adenylylation is inhibited by lectins (20). An interesting possibility is that the adenylyl group is attached to these proteins via their carbohydrates. The same proteins are phosphorylated, and it has been suggested that some protein kinases may be capable of catalyzing adenylylation, in addition to phosphorylation. Further studies that demonstrate covalent attachment of adenylyl groups unambiguously are required, and the physiological function for adenylylation of these proteins remains unclear.

4. Aminoglycoside Antibiotics

Several aminoglycoside antibiotics, including tobramycin, gentamycin, and kanamycin, are adenylylated by bacterial nucleotidyl transferases, and this contributes to antibiotic resistance in some strains. The enzymes responsible are not specific for ATP, and they also utilize GTP or UTP, thus resulting in guanylylation or uridylylation as well. These nucleotidyl transferases are **plasmid**-encoded. The adenylylation (nucleotidylylation) site on various aminoglycoside antibiotics differs, but it is most frequently either (a) the 2′- or the 3′-hydroxyl of the 3-aminoglucose ring or (b) the 4′-hydroxyl of the 6-aminoglucose ring. Based on the X-ray crystallography structure of kanamycin nucleotidyl transferase (21), the catalytic mechanism has been proposed to be an in-line displacement of PP_i by the hydroxyl group of the aminoglycoside, with an active-site glutamate residue acting as a general base. The presence of only a few contacts between the adenine ring of ATP and the nucleotidyl transferase active site is consistent with the lack of specificity for the nucleotide substrate.

5. Adenosine-5-Phosphosulfate

An additional example of adenylylation is provided by the biosynthetic pathway of the cofactor 3′-phospho-adenosine-5′-phosphosulfate (PAPS), which is summarized in Figure 4. This cofactor is used by several sulfotransferases in the sulfation of catechols, phenols, and other alcohols. An intermediate formed en route to PAPS is adenosine-5′-phosphosulfate (APS). APS is formed by ATP sulfurylase, in an adenylylation reaction that requires ATP and sulfate ion, SO_4^{2-}, to yield APS and PP_i. The formation of APS is partially rate-limiting in PAPS biosynthesis, and deficiency of ATP-sulfurylase may cause impaired sulfation of proteoglycans required for maintenance of extracellular matrix, cartilage, and connective tissues. Thus, the adenylylation reaction catalyzed by this enzyme may have direct clinical impact, manifested as chondrodysplasias, if it operates inadequately (22).

Figure 4. Biosynthesis of 3′-phospho-adenosine-5′-phosphosulfate (PAPS). The first step in the biosynthetic pathway is adenylylation of sulfate to generate adenosine-5′-phosphosulfate (APS).

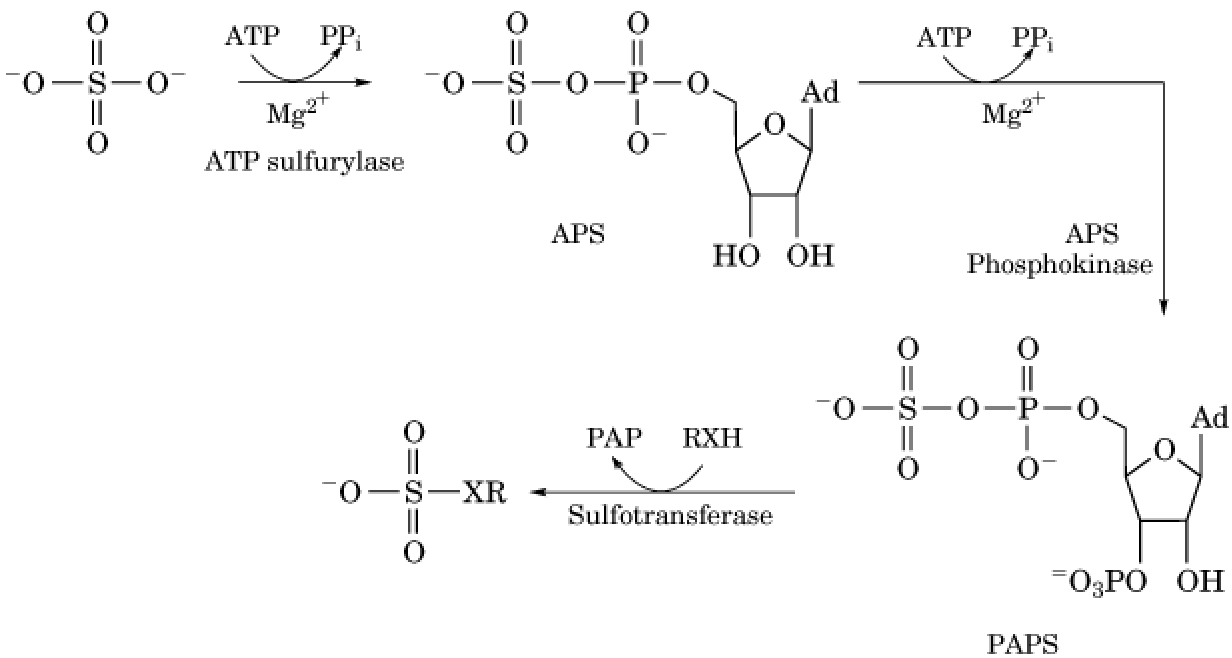

Bibliography

1. B. M. Shapiro, H. S. Kingdon, and E. R. Stadtman (1967) Proc. Natl. Acad. Sci. USA **58**, 642–649.
2. B. M. Shapiro and E. R. Stadtman (1968) J. Biol. Chem. **243**, 3769–3771.

3. R. J. Almassy, C. A. Janson, R. Hamlin, N. H. Xuong, and D. Eisenberg (1986) Nature **323**, 304–309.
4. M. M. Yamashita, R. J. Almassy, C. A. Janson, D. Lasek, and D. Eisenberg (1989) J. Biol. Chem. **264**, 17681–17689.
5. A. Ginsburg, J. Yeh, S. B. Hennig, and M. D. Denton (1970) Biochemistry **9**, 633–648.
6. L. M. Abell and J. J. Villafranca (1991) Biochemistry **30**, 1413–1418.
7. L. P. Reynaldo, J. J. Villafranca, and W. DeW. Horrocks Jr. (1996) Prot. Sci. **5**, 2532–2544.
8. S. B. Hennig and A. Ginsburg (1971) Arch. Biochem. Biophys. **144**, 611–627.
9. W. M. Atkins (1994) Biochemistry **33**, 14965–14973.
10. J. J. Villafranca, S. G. Rhee, and P. B. Chock (1978) Proc. Natl. Acad. Sci. USA **75**, 1255–1259.
11. W. M. Atkins, B. M. Cader, J. Hemmingsen, and J. J. Villafranca (1993) Protein Sci. **2**, 800–813.
12. E. D. Longton, B. M. Cader, J. Hemmingsen, and J. J. Villafranca (1992) In *Biosynthesis and Molecular Regulation of Amino Acids in Plants* (B. K. Singh, H. E. Flores, and J. C. Shannon, eds.), American Society of Plant Physiologists, Rockville, MD, pp. 59–68.
13. J. Hemmingsen (1991) *Doctoral dissertaion*, The Pennsylvania State University, University Park, PA.
14. R. Jaggi, W. C. van Heeswijk, H. V. Westerhoff, D. Ollis, and S. G. Vasudevan (1997) EMBO J. **16**, 5562–5571.
15. T. Lindahl and D. E. Barnes (1992) Annu. Rev. Biochem. **61**, 251–281.
16. A. E. Tomkinson, N. F. Totty, M. Ginsburg, and T. Lindahl (1991) Proc. Natl. Acad. Sci. USA **88**, 400–404.
17. P. Genschik, E. Billy, M. Swianiewicz, and W. Filipowicz (1997) EMBO J. **16**, 2955–2967.
18. E. San Jose, A. Benguria, and A. Villalobo (1990) J. Biol. Chem. **265**, 20653–20661.
19. M. Hara-Yokoyama, H. Sugiya, and S. Furuyama. (1994) Int. J. Biochem. **26**, 1103–1109.
20. E. San Jose, H. J. E. Villalobo, H-J. Gabius, and A. Villalobo (1993) Biol. Chem. Hoppe-Seyler **374**, 133–141.
21. L. C. Pedersen, M. M. Benning, and H. M. Holden (1995) Biochemistry **34**, 13305–13311.
22. A. Superti-Furga (1994) Am. J. Hum. Genet. **55**, 1137–1145.

Suggestions for Further Reading

23.

Reviews of Nitrogen Regulation of GS in Bacteria and GS Evolution

24. J. R. Brown, F. T. Robb, and W. F. Doolittle (1994) J. Mol. Evolution **38**, 566–576.
25. B. Magasanik (1993) J. Cell. Biochem. **51**, 34–40.

Genetic Relationships of Aminoglycoside-Modifying Enzymes, Including Adenylyl Transferases

26. K. J. Shaw, P. N. Rather, R. S. Hare, and G. H. Miller (1993) Microbiol. Rev. **57**, 138–163.

Overview of PAPS Biosynthesis

27. C. D. Klaasen and J. W. Boles (1997) FASEB J. **11**, 404–418.

Adjuvants

The term *adjuvant* designates substances that enhance the immune response without affecting the specificity of recognition. "Adjuvanticity" was first described in the 1920 by Ramon, who made the observation that mineral substances (such as metal salts and aluminum) or crude materials (such as tapioca) considerably augment the immune response to various vaccines. He then invented the name of "substances stimulantes et adjuvantes de l'immunité." When an immune response is monitored by the kinetics of occurrence of circulating antibodies, it can easily be shown that, in the presence of adjuvants, the antibody titer is considerably higher and is maintained for a much longer period of time. Although first discovered over 70 years ago, very little progress has been made in this area, and the mode of action of adjuvants remains somewhat elusive. It is generally accepted that they act essentially in two ways: (*1*) retain the antigen in emulsion or aggregates, depending on the nature of the adjuvant, ensuring a slow but relatively constant release of antigen that may continuously restimulate the immune system; and (*2*) behave as a nonspecific activator of some partners of the immune response, like mobilizing macrophages that are acting as **antigen-presenting** cells or by exerting a polyclonal activation of lymphocytes, which is the case for the bacterial lipopolysaccharide (LPS), a potent polyclonal activator of B cells.

To date, the best and universally used substance is the so-called Freund's complete adjuvant, which is an emulsion prepared with a suspension of killed mycobacteria in mineral oil. Unfortunately, it cannot be used for human purposes and must be strictly confined to laboratory animals. Attempts have been made to isolate active molecules from mycobacteria (and also from many other microorganisms). This resulted in a long list of molecules, from which the muramyl dipeptide (*N*-acetylmuramyl-L-alanyl-D-isoglutamine, or MDP) was the most extensively studied. Endowed with good adjuvant properties, it is still too toxic for human use; and many attempts have been made, and are still being made, to define nontoxic homologues. For vaccination purposes in humans thus far, the old recipes, among which are aluminum hydroxide, aluminum phosphate, or alum precipitate, are still the most widely used.

An interesting advance was made with ISCOM (which stand for immuno-stimulating complex), proposed by Morein et al. (1) ISCOM is a cage-like matrix made up of cholesterol and Quil A, which is a substance extracted from the bark of a tree, *Quillaja saponaria*, that contains, after partial purification, five main components with triterpenoid structures. The matrix spontaneously organizes in the presence of antigen, most often protein isolated from a viral coat envelope. The construction ensures high immunogenicity and is used in a number of animal vaccines.

It is likely that one key event played by adjuvants is at the steps of antigen uptake and processing by antigen-presenting cells. Supporting this idea is the fact that bacterial, or more generally particulate antigens, are far better immunogens than the purified molecules isolated from cells. This constitutes an obvious difficulty for designing sophisticated "pure" vaccines, which would at first sight appear advantageous over using complete bacteria that usually contain toxic components, but that also serve as carrier with an adjuvant effect for the desired antigen. To date, an ideal vaccine would have to reconcile the purity of a recombinant protein with a well-characterized potent adjuvant. We know much about making recombinant proteins, but have at present no convincing pure adjuvant. One interesting approach is to use a living vector, such as vaccinia virus, that has been genetically modified to express a given antigen at the surface of the microorganism. One may also couple a gene expressing the antigen with a gene encoding a **cytokine** that would specifically favor the amplification of a helper T cell compartment. Another possibility is to embed the antigen in liposomes that could be eventually targeted to well-defined cells of the immune system.

All these approaches have been attempted with variable success. To date, one must unfortunately admit that, despite the fantastic progress made in recent years in the understanding of the basic mechanisms that operate in the immune system, no really significant advances have been made in defining more efficient and more rational vaccines.

See also the entries Immune Response, Immunization, and Immunogen.

Bibliography

1. B. Morein, B. Sundquist, S. Höglund, K. Dalsgaard, and A. Osterhaus (1984) Iscom, a novel structure for antigen presentation of membrane proteins from envelopped viruses. Nature, **308**, 457–460.

Suggestion for Further Reading

2. F. R. Vogel (1995) Immunologic adjuvants for modern vaccine formulations. Ann. N.Y. Acad. Sci., **754**, 153–160.

ADP-Ribosylation, Mono

MonoADP-ribosylation is a post-translational modification, catalyzed by ADP-ribosyltransferase (ADPRT), that transfers the ADP-ribose moiety from NAD^+ to a specific amino acid residue of target protein and releases the nicotinamide moiety. To date, four amino acid-specific ADPRT have been reported, specific for arginine, cysteine, diphthamide (a modified form of histidine), and asparagine residues. These transferases were originally discovered as the **cholera**, **pertussis**, and diphtheria toxins and the *Clostridium botulinum* C3 enzyme (1, 2), in the order of amino acid-specificity described above. The native form of such ADP-ribosylating toxins is a heteromultimer, and one of the subunits has ADP-ribosyltransferase activity (1). The catalytic subunit penetrates the host cell with the assistance of the other subunits. The prokaryotic ADPRT modify target proteins, including a variety of GTP-binding proteins, in eukaryotic cells (Fig. 1). This modification leads to alterations in the target protein, and consequently in cell functions (1). The bacterial toxins and C3 enzyme have proven extremely useful in studies on signal transduction pathways in various cell types of eukaryotes. MonoADP-ribosylation must be distinguished from poly-ADP ribosylation.

Figure 1. Target protein and acceptor site for ADP-ribosylation in eukaryotic cells by prokaryotic toxins and C3 enzyme.

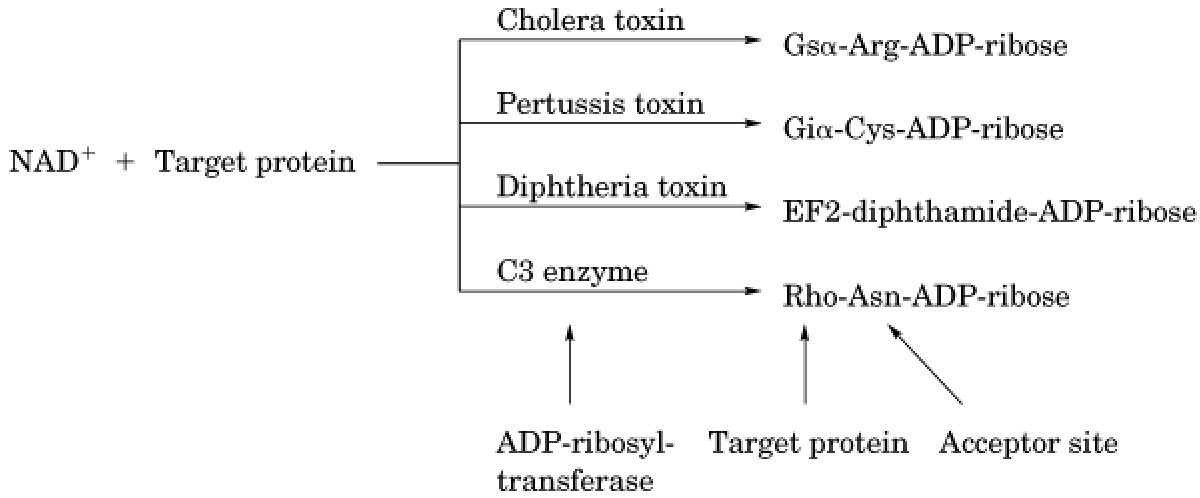

The reversible Arg-specific ADP-ribosylation (Fig. 2), like protein **phosphorylation**, was initially documented as a regulatory mechanism for control of nitrogen fixation in the **photosynthetic** bacteria *Rhodospirillum rubrum* and *Azospirillum braziliense* (3). Endogenous dinitrogenase reductase-ADPRT modifies Arg101 on the target protein, dinitrogenase reductase, resulting in inactivation of the reductase. Recovery from the inactive form is achieved through cleavage of the Arg-ADP-ribose linkage by dinitrogenase reductase-activating glycohydrolase. This is the only example of metabolic regulation through endogenous ADP-ribosylation. Purification, characterization, and molecular cloning of eukaryotic Arg-specific ADP-ribosyltransferase (4-7) and of ADP-ribosyl-Arg hydrolase (8) were reported. By analogy to prokaryotes, metabolic regulation through reversible ADP-ribosylation in eukaryotes has been postulated.

Figure 2. Arg-specific ADP-ribosylation and de-ADP-ribosylation reactions.

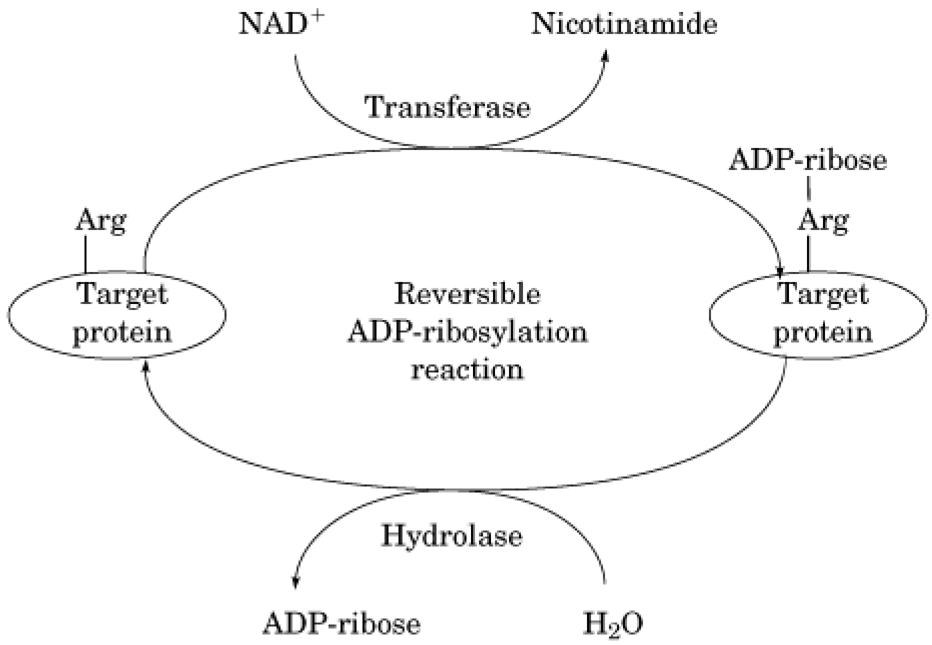

Among the eukaryotic ADPRTs detected, the best-defined one is Arg-specific. Purification and characterization of the ADPRT from turkey erythrocytes (4), rabbit skeletal muscle (9), and chicken peripheral heterophils (polymorphonuclear leukocytes) (5) revealed that these enzymes exhibit different physical and regulatory properties, kinetics, and intracellular localization. Guanidino compounds, such as arginine and agmatine, function *in vitro* as acceptors for Arg-specific ADPRT (4). With b-NAD^+ and arginine as substrate, a-ADP-ribosylated arginine is formed by Arg-specific ADP-ribosyltransferase; and the a anomer, but not the b anomer, is utilized as substrate by ADP-ribosyl-Arg hydrolase (10).

Some of the ADPRTs catalyze NAD glycohydrolysis or auto-Arg-specific ADP-ribosylation, when either water or the enzyme itself serve as acceptor for ADP-ribose (1, 2). Upon incubation of intact cells or cell lysates with [^{32}P]NAD^+, it would appear that the ADP-ribose released from NAD^+ by cellular NAD glycohydrolase is attached to some proteins nonenzymatically (11, 12). Thus, enzymatic and non-enzymatic ADP-ribosylations should be differentiated.

Molecular cloning and expression studies of complementary DNA for Arg-specific ADPRT revealed that the rabbit and human skeletal muscle transferases are glycosylphosphatidylinositol-anchored (GPI-anchored) (6) and that two forms of transferases from chicken bone marrow cells are secreted (7).

The previously known rat and mouse T-cell marker RT6 have significant sequence Homology to the ADPRT. It is now accepted that these proteins are GPI-anchored and possess transferase and/or NAD glycohydrolase activities (13-15).

A common feature of the vertebrate Arg-specific ADP-ribosyltransferase is their resemblance to the transferase from cholera toxin and to *Escherichia coli* heat-labile enterotoxin. Strictly conserved regions around the active site containing two Glu residues (E207 and E209, indicated with an asterisk in Fig. 3) are seen in all Arg-specific ADPRT detected in vertebrates, bacteria, and viruses. On the other hand, RT6.1 and RT6.2 (rat), which have NAD glycohydrolase activity, but not Arg-specific ADPRT, contain Gln in place of Glu207. The recombinant protein of a mutant Gln207Glu-RT6.1 possesses Arg-specific ADPRT activity (16, 17), but alterations in the kinetic parameters of the NAD glycohydrolase reaction are slight (17). Furthermore, the mouse homologues of rat RT6, Rt6.1, and Rt6.2 have Glu207 and ADPRT activity. When the Glu is replaced with Gln, Rt6.1 loses the activity (17).

Figure 3. Comparison of the amino acid sequences of a Glu-rich motif in eukaryotic, prokaryotic, and viral Arg-specific ADP-ribosyltransferases and T-cell antigen RT6. References are cited by the numbers in parentheses. ADPRT: arginine-specific ADP-ribosyltransferase.

```
                                                   *  *
RT6.1                                    202: SFYPDQEEVLIPG    (20)
RT6.2                                    202: SFRPDQEEVLIPG    (13)
Mouse homologue of the rat RT6, Rt6.1    202: SYYTHEEEVLIPG    (21)
                                Rt6.2    202: SSFPREEEVLIPG    (21)
Chicken bone marrow ADPRT1               217: SFFPSEDEVLIPP     (7)
                    ADPRT2               217: SFYPSEDEVLIPP     (7)
Chicken erythroblast ADPRT               217: STFPGEDEVLIPP    (22)
Rabbit skeletal muscle ADPRT             233: SFFPGEEEVLIPP     (6)
Human skeletal muscle ADPRT              233: SFFPGEEEVLIPP    (23)
Cholera toxin                            105: SPHPDEQEVSALG    (24)
E. coli heat-labile enterotoxin          105: SPHPYEQEVSALG    (25)
C. perifringens iota toxin               414: PGYAGEYEVLLNH    (26)
Bacteriophage T2                         583: LGIATEAEVILPR    (27)
```

It has been reported that defects in RT6 expression are associated in various animal models with the pathogenesis of autoimmune insulin-dependent diabetes and systemic lupus erythematosus (18, 19), although a possible mechanism for RT6-mediated protection from these autoimmune diseases is unknown. Definite physiological functions of monoADP-ribosylation in eukaryotes must be established by further investigation.

Bibliography

1. S. F. Carroll and R. J. Collier (1994) Methods Enzymol. **235**, 631–639.
2. F. R. Althaus and C. Richiter (1987) *ADP-Ribosylation of Proteins*, Springer-Verlag, Berlin, pp. 131–194.
3. P. W. Ludden (1994) Mol. Cell. Biochem. **138**, 123–129.
4. J. Moss, S. J. Stanley, and P. A. Watkins (1980) J. Biol. Chem. **255**, 5838–5840.
5. K. Mishima, M. Terashima, S. Obara, K. Yamada, K. Imai, and M. Shimoyama (1991) J. Biochem. **110**, 388–394.
6. A. Zolkiewska, M. S. Nightingale, and J. Moss (1992) Proc. Natl. Acad. Sci. USA **89**, 11352–11356.
7. M. Tsuchiya, N. Hara, K. Yamada, H. Osago, and M. Shimoyama (1994) J. Biol. Chem. **269**, 27451–27457.
8. J. Moss, S. J. Stanley, M. S. Nightingale, J. J. Murtagh Jr., L. Monaco, K. Mishima, H.-C. Chen, K. C. Williamson, and S.-C. Tsai (1992) J. Biol. Chem. **267**, 10481–10488.
9. J. E. Peterson, S.-A. L. Jacquiline, and D. J. Graves (1990) J. Biol. Chem. **265**, 17602–17609.
10. J. Moss, N. J. Oppenheimer, R. E. West Jr., and S. J. Stanley (1986) Biochemistry **25**, 5408–5414.
11. H. Hilz, R. Bredehost, P. Adamietz, and Wielckens (1982) *ADP-Ribosylation Reactions. Biology and Medicine*, Academic Press, San Diego, CA, 207–219.
12. D. Cervantes-Laurean, D. E. Mintaer, E. L. Jacobson, and M. K. Jakobson (1993) Biochemistry **32**, 1528–1534.
13. F. Koch, F. Haag, A. Kashan, and H.-G. Thiele (1990) Proc. Natl. Acad. Sci. USA **87**, 964–967.
14. T. Takada, K. Iida, and J. Moss (1994) J. Biol. Chem. **269**, 9420–9423.
15. F. Koch-Nolte, D. Petersen, S. Balasubramanian, F. Haag, D. Kahlke, T. Willer, R. Kastelein, F. Bazan, and H. G. Thiele (1996) J. Biol. Chem. **271**, 7686–7693.
16. T. Maehama, S. Hoshino, and T. Katada (1996) FEBS Lett. **388**, 189–191.
17. N. Hara, M. Tsuchiya, and M. Shimoyama (1996) J. Biol. Chem. **271**, 29552–29555.
18. D. L. Greiner, E. S. Handler, K. Nakano, J. P. Mordes, and A. A. Rossini (1986) J. Immunol. **136**, 148–151.
19. F. Koch-Nolte, J. Klein, C. Hollmann, M. Kuhl, F. Haag, H. R. Gaskins, E. Leiter, and H.-G. Thiele (1995) Int. Immunol. **7**, 883–890.
20. F. Haag and H.-G. Thiele (1990) Nucl. Acids Res. **18**, 1047.
21. C. Hollmann, F. Haag, M. Schlott, A. Damaske, H. Bertuleit, M. Matthes, M. Kuhl, H. G. Thiele, and F. Koch-Nolte (1996) Mol. Immunol. **33**, 807–817.
22. T. Davis and S. Shall (1995) Gene **164**, 371–372.
23. I. J. Okazaki, A. Zolkiewska, M. S. Nightingale, and J. Moss (1994) Biochemistry **33**, 12828–12836.
24. J. J. Mekalanos, D. J. Swartz, G. D. Pearson, N. Harford, F. Groyne, and M. de Wilde (1983) Nature **306**, 551–557.
25. T. Yamamoto, T. Gojobori, and T. Yokota (1987) J. Bacteriol. **169**, 1352–1357.
26. S. Perelle, M. Gibert, P. Boquet, and M. R. Popoff (1995) Infect. Immun. **63**, 4967.

27. T. Koch and W. Ruger (1994) Virology **203**, 294–298.

Suggestions for Further Reading

28. F. Haag and F. Koch-Nolte (1997) "ADP-Ribosylation in Animal Tissues; Structure, Function, and Biology of Mono(ADP-ribosyl)transferases and Related Enzymes". *Advances in Experimental Medicine and Biology*, Vol. **419**, Plenum Press, NewYork.
29. J. Moss and P. Zahradka (1994) "ADP-Ribosylation: Metabolic Effects and Regulatory Functions". *Molecular and Cellular Biochemistry*, Vol. **138**, Kluwer, Dordrecht, The Netherlands.

Adriamycin

1. Introduction

Adriamycin is the trade name for an anthraquinone-containing antibiotic which also has the international nonproprietary name (INN) of doxorubicin (1) and the NCI internal identification number NSC 123127. It is a member of the anthracycline group of compounds that contain an anthraquinone chromophore and a polycyclic ring system (1). It has good anticancer activity against a wide spectrum of tumors (and still remains as the antitumor agent that has the widest spectrum of anticancer activity) and is one of the most extensively used of the fifty or so chemotherapeutic compounds currently in clinical use (2-4). Its full potential as an anticancer agent has not been reached because of a dose-limiting cardiotoxicity (1-4). Despite enormous effort during the last 30 years to develop more effective and less cardiotoxic derivatives, it remains one of the best, proven anticancer drugs. It also exhibits good antibacterial activity.

2. Structure and Chemistry

Adriamycin consists of a planar tetracyclic ring system linked by a glycosidic bond to daunosamine, an amino sugar (Fig. 1). It is a bright red compound that is normally isolated as the hydrochloride salt, has the chemical composition $C_{27}H_{29}O_{11}\cdot HCl$, a molecular weight of 579.98, and is soluble in water, physiological saline, and methanol (5, 6). The p*K*a of the amino group is 8.2 (5, 6). In neutral aqueous buffers, it self-associates (7), has absorbance maxima at 233, 480, and 530 nm, and at concentrations less than 25 µM has an extinction coefficient of 11,500 $M^{-1}cm^{-1}$ at 480 nm (7). It is fluorescent and can be quantitated in aqueous solutions using excitation and emission wavelengths of 480 and 595 nm, respectively. The solid compound is quite stable if kept in the dark at 4°C and free of moisture. It is photosensitive and therefore solutions must also be kept in the dark at 4°C; even under these conditions, some decomposition will occur in a week or so. It chelates Fe^{3+} with exceedingly high affinity and readily forms the $Fe(Adriamycin)_3$ complex (8).

Figure 1. Structure of Adriamycin and clinically relevant derivatives.

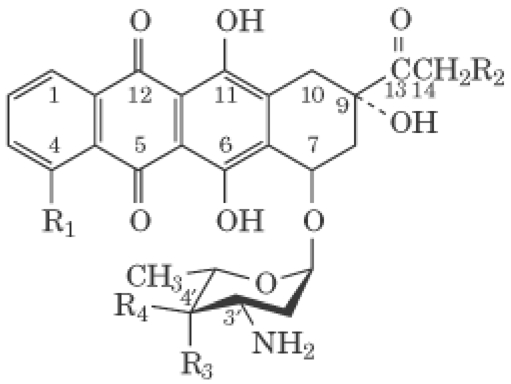

	R_1	R_2	R_3	R_4
Adriamycin	OCH_3	OH	OH	H
Daunomycin	OCH_3	H	OH	H
Epirubicin	OCH_3	OH	H	OH
Idarubicin	H	H	OH	H

3. History

In 1958 a new species of *Streptomyces* was identified in a soil sample taken from southern Italy. A red antibiotic, daunomycin was isolated from this microorganism and exhibited good activity against a range of murine tumors (1). In a search for other potentially more active derivatives of daunomycin, the soil microorganism was subjected to the mutagen *N*-nitroso-*N*-methyl urethane and produced a mutant strain that yielded a modified form of the antibiotic. This new antibiotic (named Adriamycin because of the closeness of the original soil sample to the Adriatic Sea) exhibited both a wider spectrum of activity and an improved anticancer response against animal tumors than daunomycin (1) and was also remarkably successful in treating human tumors. Adriamycin was rapidly introduced into clinical trials in Italy and the United States and was approved for clinical use in the United States in 1974 (1).

4. Clinical Use

4.1. Tumors

Adriamycin is particularly useful for treating solid tumors such as breast, lung, ovarian, and thyroid carcinomas, as well as soft tissue sarcomas (2-4). It is also active against lymphoid and myelogenous leukemia (2-4).

4.2. Dose and Administration

It is normally administered as a bolus at a dosage of 45–75 mg/m^2 every 3–4 weeks, or more recently as a continuous intravenous infusion during 4–5 days (2, 3). It is inactive if administered orally because the glycosidic bond is hydrolyzed in the gastrointestinal tract. For most treatment regimes it is administered as one component of a combination of drugs (2).

4.3. Side Effects

The most significant problem is a cumulative, dose-dependent cardiomyopathy that can lead to heart failure in up to 10% of patients who receive the maximum recommended dose of 550 mg/m^2(2, 3). This cardiotoxicity can be acute (hours to days following treatment) or more commonly, can be delayed by months or even years. The cardiotoxicity appears to be due to the redox activity of the drug (9): Adriamycin can undergo a one electron reduction [catalyzed by a range of enzymes such as microsomal cytochrome P450 reductase, mitochondrial NADH dehydrogenase, cytochrome b5 reductase, and xanthine reductase (10)] leading to production of the semiquinone that generates superoxide in the presence of molecular oxygen, then hydrogen peroxide, and ultimately the extremely reactive and highly toxic hydroxyl radical. These hydroxyl radicals react with any nearby molecule, and hence lead to oxidative damage of critical targets such as DNA and membrane lipids. In most tissues this lethal process is minimized by superoxide dismutase (which converts superoxide to hydrogen peroxide) and catalase (which subsequently converts hydrogen peroxide to water), as well as glutathione peroxidase (which also converts hydrogen peroxide to water). Heart tissues are particularly sensitive to Adriamycin because of their greatly compromised capacity for protection against hydroxyl radicals due to the lack of the bulk hydrogen peroxide detoxifying enzyme catalase and also because Adriamycin inhibits gutathione peroxidase activity (10). Other side effects of Adriamycin therapy are hair loss (alopecia) which usually starts after the first dose of Adriamycin, nausea and vomiting (usually overcome nowadays by appropriate antinausea drugs), and reduction in bone marrow function (with maximum suppression 10–14 days following treatment).

4.4. Pharmacokinetics

The disappearance of Adriamycin in plasma is adequately described by a three-compartment model whose half-lives are approximately 10 min, 3 h, and 30 h (11). The plasma level is rapidly depleted and only 0.2 mM remains (average of nine patients) several hours after administration of a 30 mg/m^2 bolus dose of Adriamycin (12); 0.02 μM remains several hours following a 75 mg dose (either as a bolus or 4 h infusion) to a single patient (13). In contrast, the intracellular concentration of drug was approximately 4 μM and 6 μM, respectively, for these two studies (12, 13). The striking features of these results are that the intracellular concentration of drug is typically 100–1000 times greater than that in plasma (14), and that the intracellular drug pool has an extremely long half-life of 4–5 days (13). The uptake into solid tumors is similar to that of normal tissues (12).

Pharmacology. The major metabolite of Adriamycin involves metabolism of the C9 side chain alcohol to adriamycinol, where the conversion is catalyzed by the ubiquitous cytoplasmic NADPH-dependent aldo-keto reductase (15). Subsequent microsomal glycosidases that are present in most tissues convert adriamycinol into the inactive deoxyadriamycinol aglycon and daunosamine. The aglycon is then demethylated and conjugated to polar groups to yield more hydrophilic metabolites that are excreted mainly in the bile (15).

The drug distribution has been examined in 20 cancer patients where tissue uptake decreased in the following order: liver > lymph nodes > muscle and bone marrow > fat and skin (12). It has long been known that Adriamycin localizes in the nucleus at the subcellular level (16). This has been confirmed recently in single squamous carcinoma cells by quantitative confocal laser scanning microscopy, where the nuclear level was twice that of the cytoplasm 30 minutes after exposure to 1 μg/mL of Adriamycin, and increased even more with time (17). Interestingly, the cytoplasmic drug level was also higher than that of the medium (17), and this is surprising because Adriamycin is taken up into cells by passive diffusion (18). Nuclear localization is readily attributed to the known high affinity of Adriamycin for DNA (see below). The nature of cytoplasmic localization is less clear, but the distribution as a multitude of small patches of fluorescence throughout the cytoplasm (19) is consistent with some degree of mitochondrial localization (because the drug binds to mitochondrial membranes and, to a lesser extent, also to mitochondrial DNA); it is known that there are as many as a thousand mitochondria per cell (20).

4.5. Resistance

When cells in culture are exposed to Adriamycin for an extended period of time, the cells gradually become resistant to the drug. This type of resistance is due primarily to amplification of the multidrug transporter gene *mdr1* that leads to overexpression of a 170-kDa glycoprotein now known as P-glycoprotein (21). This protein forms a pore in the cell membrane and actively pumps Adriamycin (and many other drugs) out of the cell, using ATP as an energy source. In patients treated with Adriamycin, much of the resistance that develops over several months (and diminishes the antitumor effect of the drug) and appears to derive from overexpression of P-glycoprotein. To enhance the usefulness of Adriamycin, there have been some attempts to develop specific inhibitors of this protein. This approach is no longer considered viable because of the multitude of other drug efflux pumps that have been identified in recent times (22).

In addition to the phenomenon of multidrug resistance, other mechanisms of resistance have been identified for Adriamycin, including elevated levels of glutathione and decreased levels of topoisomerase II in cells in culture (although not yet demonstrated in tumors) (21).

5. Interactions with DNA

Numerous studies have shown that Adriamycin binds to DNA with high affinity by intercalating between adjacent base pairs of DNA. In this process the DNA unwinds to accommodate the drug. This is reflected by an increase in the length of small linear fragments of DNA (hence an increase in the viscosity of the solution) or in the loss of a number of negative supercoils for supercoiled DNA such as a plasmid (that results in an initial increase of viscosity and a decrease of the sedimentation coefficient). These processes have been summarized previously (3, 23). The structure of the intercalated species has been fully characterized by X-ray crystal studies of the drug–oligonucleotide complex. The dominant features are that the drug chromophore lies virtually at right angles to the adjoining base pairs and the amino sugar fits snugly into the minor groove of DNA (24, 25).

Earlier binding studies (before about 1980) misinterpreted curved Scatchard plots as indicating more than one class of DNA binding site. It is now known that this curvature which results from the extreme form of negative cooperativity is displayed when the drug binds to DNA, and is fully described by the neighbor-exclusion principle; values for the intrinsic association constant and the number of occluded base pairs are approximately $2 \cdot 10^6\ M^{-1}$ and 3.0 bp, respectively, at near physiological ionic strengths (26, 27). Although this interpretation assumes that the drug intercalates randomly between all possible base pair combinations, this is not strictly correct because there is a slight selectivity of sequence for some sites. Theoretical quantum mechanical calculations indicated the requirement for a three base pair site, and ACG is likely to be the preferred site (28, 29). *In vitro* transcription footprinting studies confirmed the requirement for a triplet site, but showed that the preferred consensus sequence is TCA (where the drug intercalates between C and A) (30), although there was clearly only small energetic differences between this and other triplet sites.

Adriamycin is in rapid equilibrium with DNA. The on-rate is diffusion controlled, and the off-rate is also fast and usually measured by stopped-flow detergent sequestration. This has revealed that Adriamycin has an overall half-life on DNA of approximately 0.5 s at room temperature (31), although by analogy with the structurally similar drug daunomycin, the kinetic processes are likely to be much more complex, especially for longer dissociation times (32).

6. Mechanism of Action

The exact molecular events involved in the mechanism of action of Adriamycin have not yet been resolved. Although many possible mechanisms have been proposed and the problems in identifying the critical factors have been well summarized (33, 34), many potential mechanisms have been identified, including impairment of topoisomerase II activity, bioreductive action of the drug, free radical effects, membrane related effects (33, 34). There is a convincing body of evidence to show that the primary target is DNA (33-35). Some of this evidence is that almost all of the drug in the nucleus (>99.8% of single, living cells is associated with DNA (36); more than 80% of all of the drug present in human tumor biopsies is associated with DNA (37); and increasing drug activity (over three orders of magnitude) correlates with increasing DNA binding, damage, or impairment of DNA template activity (38). Therefore DNA binding appears to be related in some way to the anticancer properties, and at present there are two types of interactions with DNA that appear to relate to the drug action: impairment of topoisomerase II activity and formation of drug–DNA adducts.

6.1. Impairment of Topoisomerase II

When Adriamycin is added to tumor cells in culture, protein-associated double- and single-strand

DNA breaks occur close to nuclear matrix attachment sites where topoisomerase II is localized. This enzyme regulates the topological state of DNA, and the DNA breaks appear to arise from intercalation of the drug at that site, which results in structural distortions that interfere with the re-ligation step of topoisomerase II (2, 39, 40). There are several reasons why this appears to be a major contribution to the mechanism of action of Adriamycin: the activity of the enzyme is reduced in tumor cells which are resistant to Adriamycin (39, 40); a correlation has been shown between the induction of double-strand DNA breaks and the cytotoxicity of Adriamycin in P388 leukemia cells (41); and this type of DNA damage occurs at clinical levels of the drug (39, 40). However, there is also evidence that other factors contribute to the mechanism of action of Adriamycin and that the activity cannot be accounted for solely by impairment of topoisomerase II: some studies failed to detect DNA strand breaks in cell cultures at Adriamycin concentrations where cytotoxic responses were observed (42); topoisomerase II mediated damage is rapidly reversible following removal of the drug (39), whereas it is known that DNA double- strand breaks increase long after removal of the drug (43); some derivatives that induce a high level of double-strand breaks exhibit a low level of cytotoxicity (44); and there is little evidence that topoisomerase II is involved in some tumors (10).

6.2. Adriamycin–DNA Adducts

There have been many reports of Adriamycin–DNA adducts formed by enzymatic, microsomal, or cellular activation of the drug (33, 45, 46), but it was not until 1990 that it became clear from *in vitro* transcription footprinting studies that these adducts formed predominantly at 5′-GC-3′ sequences (47). It was subsequently shown that adducts at these sites behave as an interstrand cross-link (48, 49), although with limited stability [half-life of 5 –40 h depending on the DNA sequence and fragment length (49, 50)]. It is now clear that adducts at GC sequences and interstrand cross-links at GC sequences are one and the same lesion and that the adducts stabilize DNA sufficiently so that they function as “virtual interstrand cross-links” (51-53). The adducts have been well characterized in the solid state by X-ray crystal diffraction (54) and in solution by 2-D NMR (55).

Surprisingly, it has been shown that the adducts are mediated by formaldehyde and involve a characteristically unstable aminal linkage to the N-2 of guanine on one strand of DNA (51-55) (Fig. 2). This unusual adduct exhibits some of the characteristics of an interstrand cross-link because of the additional stability that arises from the intercalated chromophore and from additional hydrogen bonds that are formed to the second DNA strand (51-55). The cross-linkage is unstable to heat and to alkali, and this explains why it has proven so difficult to find this lesion in cells in the past (50). Conditions have been established to isolate these lesions from tumor cells (56-59), and this led to a resurgence in cellular studies of this drug. There is now good evidence that these adducts contribute to the mechanism of action of Adriamycin: the capacity of different derivatives of Adriamycin to form adducts (virtual cross-links) correlates well with their cytotoxicity (57), and gene-specific cross-linking assays have detected sufficient lesions in both the nuclear and mitochondrial genomes to show that this lesion is cytotoxic at clinical levels of the drug (58). Total cellular DNA adducts have also been quantitated directly using $[^{14}C]$Adriamycin (58). Because of the formaldehyde-dependent activation of Adriamycin, formaldehyde-releasing prodrugs that have been examined in combination with Adriamycin lead to as much as a 20-fold increase of Adriamycin–DNA adduct levels and a synergistic cytotoxic response (59).

Figure 2. Structure of Adriamycin–DNA adducts (52, 54, 55). The exact location of H bonds has not been defined and will depend upon the DNA sequence flanking the 5′-[GC-drug-N]3′ binding site (55).

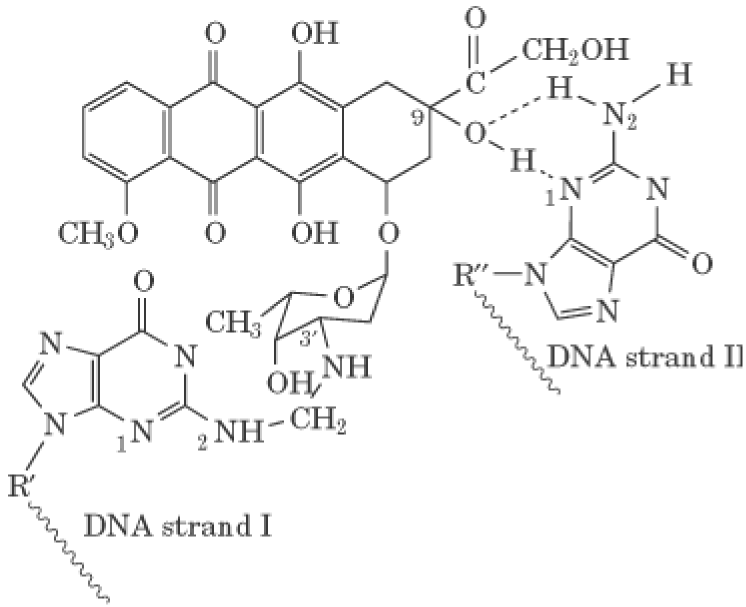

6.3. Other Possible DNA-Related Effects

Two additional DNA-related effects also occur at low drug levels *in vitro*, but at this stage the contribution to the mechanism of action of Adriamycin under clinical conditions is unknown (34): impairment of DNA ligase activity (60): impairment of helicase activity (61).

6.4. Current Status

The evidence at present indicates that there is no single mechanism of action of Adriamycin. Both impairment of topoisomerase II activity (resulting in protein associated double-strand breaks) and formation of interstrand cross-links occur at clinical levels of the drug. It is known that Adriamycin activates the general cellular response to DNA damage in which the tumor suppressor protein p53 is induced, resulting in arrest of the cell cycle and the induction of apoptosis (62). Although it is known that apoptosis occurs at submicromolar concentrations of the drug (63), this response is yet to be fully understood in the context of drug-induced cytotoxicity (64). The development of new derivatives of Adriamycin in the future is likely to rely heavily on an even more detailed understanding of the molecular consequences of the DNA damage induced by this drug.

7. The Search for New Derivatives

Because of the dose-limiting toxicity of Adriamycin, there has been an intense international effort in the past three decades to find new derivatives that have improved anticancer activity and/or reduced cardiotoxicity. This endeavor has been extremely well summarized by Weiss (1). Unfortunately, the outcome from this search has been disappointing. From more than 2000 derivatives tested by 1992 (and perhaps as many as 2500 tested to date), none is substantially superior to Adriamycin for proven clinical anticancer activity. However, several offer advantages for clinical use: idarubicin (lacking the methoxy group at the C4 position) is more amenable to oral administration than Adriamycin; epirubicin is less cardiotoxic and results in less nausea and vomiting than Adriamycin at equimolar doses—it has anticancer activity similar to that of Adriamycin, but reduced side effects have facilitated its wide use as an alternative to Adriamycin. High-dose clinical trials are still in progress with this derivative. One new and encouraging approach that is emerging is the development of “preactivated” forms of the anthracyclines; these formaldehyde-activated derivatives (doxoform, epidoxoform) exhibit increased toxicity to tumor cells, especially to anthracycline-resistant cells (65).

Bibliography

1. R. B. Weiss (1992) Semin. Oncol. **19**, 670–686.
2. V. T. DeVita, S. Hellman, and S. A. Rosenberg (2001) *Cancer: Principles and Practice of Oncology*, 6 ed., Lippincott Williams and Wilkins, Philadelphia.
3. W. B. Pratt, R. W. Ruddon, W. D. Ensminger, and J. Maybaum (1994) *The Anticancer Drugs*, 2 ed, Oxford University Press, New York, pp. 155–165.
4. T. W. Sweatman and M. Israel (1997) In *Cancer Therapeutics, Experimental and Clinical Agents* (B.A. Teicher, ed.), Humana Press, Totowa, NJ, pp. 113–135.
5. F. Arcamone (1982) *Doxorubicin: Anticancer Antibiotics*, Academic Press.
6. R. T. Dorr and D. S. Alberts (1982) In *Current Concepts in the Use of Doxorubicin Chemotherapy* (S.E. Jones, ed.), Farmitalia Carla Erba S.p.A., Milano, Italy, pp. 1–20.
7. J. B. Chaires, N. Dattagupta, and D. M. Crothers (1982) Biochemistry **21**, 3927–3932.
8. A. Garnier-Suillerot (1988) In *Anthracycline and Anthracenedione-Based Anticancer Agents* (J.W. Lown, ed.), Elsevier, Amsterdam, pp. 129–161.
9. J. H. Doroshow (1995) In *Anthracycline Antibiotics: New Analogues, Methods of Delivery, and Mechanisms of Action* (W. Priebe, ed.), American Chemical Society, Washington, DC, pp. 259–267.
10. pp. 160–164 of Ref. 3.
11. p. 378 of Ref. 2.
12. Y. N. Lee, K. K. Chan, P. A. Harris, and J. L. Cohen (1980) Cancer **45**, 2231–2239.
13. P. A. J. Speth, P. C. M. Linssen, J. B. M. Boezeman, J. M. C. Wessels, and C. Haanen (1986) **377**, 414–422.
14. C. E. Myers, E. G. Mimnaugh, G. C. Yeh, and B. K. Sinha (1988) In *Anthracycline and Anthracenedione-Based Anticancer Agents* (J.W. Lown, ed.), Elsevier, Amsterdam, p. 529.
15. pp. 158–160 of Ref. 3.
16. A. DiMarco (1975) Cancer Chemother. Rep. **6**, 91–106.
17. K. Kawai, Y. Minamiya, M. Kitamura, I. Matsuzaki, M. Hashimoto, H. Suzuki, and S. Abo (1997) Cancer **79**, 214–219.
18. M. Dalmark and H. H. Storm (1981) Gen. Physiol. **78**, 349–364.
19. V. Pillay, R. D. Martinus, J. S. Hill, and D. R. Phillips (1998) J. Cell. Biochem. **69**, 1–7.
20. J. W. Shay and H. Werbin (1987) Mutat. Res. **186**, 149–160.
21. pp. 50–66 of Ref. 3.
22. J. S. Lee, S. Scala, Y. Matsumoto, B. Dickstein, R. Robey, Z. Zhan, G. Altenberg, and S. E. Bates (1997) J. Cell Biochem. 513–526.
23. S. Neidle and M. R. Sanderson (1983) In *Molecular Aspects of Anti-Cancer Drug Action* (S. Neidle and M.J. Waring, eds.), Macmillan, London, pp. 35–56.
24. A. H. Wang, G. Ughetto, G. J. Quigley, and A. Rich (1987) Biochemistry **26**, 1152–1163.
25. G. Ughetto (1988) In *Anthracycline and Anthracenedione-Based Anticancer Agents* (J.W. Lown, ed.), Elsevier, Amsterdam, pp. 295–334.
26. F. Barcelo, J. Martorell, F. Gavilanes, and J. M. Gonzalez-Ros (1988) Biochem. Pharmacol. **37**, 2133–2138.
27. E. Stutter, H. Schuetz, and H. Berg (1988) In *Anthracycline and Anthracenedione-Based Anticancer Agents* (J.W. Lown, ed.), Elsevier, Amsterdam, pp. 245–293.
28. K. Chen, N. Gresh, and B. Pullman (1986) Nucleic Acids Res. **14**, 2251–2267.
29. B. Pullman (1991) Anti-Cancer Drug Design **7**, 95–105.
30. H. Trist and D. R. Phillips (1989) Nucleic Acids Res. **17**, 3673–3688.
31. B. Gandecha and J. R. Brown (1985) Biochem. Pharmacol. **34**, 733–736.
32. D. R. Phillips, P. Greif, and R. C. Boston (1988) Mol. Pharmacol. **33**, 225–230.

33. pp. 528–569 of Ref. 14.
34. D. A. Gewirtz (1999) Biochem. Pharmacol. **57**, 727–741.
35. C. Cullinane, A. van Rosmalen, and D. R. Phillips (1994) Biochemistry **33**, 4632–4638.
36. M. Gigli, S. M. Doglia, J. M. Millot, L. Valantini, and M. Manfait (1988) Biochim. Biophys. Acta **950**, 13–20.
37. J. Cummings and C. S. McArdle (1986) Br. J. Cancer **53**, 835–838.
38. L. Valentini, V. Nicolella, E. Vannini, M. Menozzi, S. Penco, and F. Arcamone (1985) Il. Farmaco Ed. Sci. **40**, 377–389.
39. C. Holm, J. Covey, D. Kerrigan, K. W. Kohn, and Y. Pommier (1991) In *DNA Topoisomerases in Cancer* (M. Pomesil and K. Kohn, eds.), Oxford University Press, pp. 161–171.
40. Y. Pommier (1995) In *Anthracycline Antibiotics: New Analogues, Methods of Delivery and Mechanisms of Action*. ACS Symposium Series No. 574, pp. 183–203.
41. G. J. Goldenberg, H. Wang, and G. W. Blair (1986) Cancer Res. **46**, 2978–2983.
42. F. A. Fornari, W. D. Jarvis. M. S. Orr, J. K. Randolph, S. Grant, and D. A. Gerwitz (1996) Biochem. Pharmacol. **51**, 931–940.
43. M. Binaschi, G. Capranico, P. De Isabella, M. Marini, R. Supino, and S. Tinelli (1990) Int. J. Cancer **45**, 347–352.
44. M. Binaschi, G. Capranico, L. Dal Bo, and F. Zunino (1997) Mol. Pharmacol. **51**, 1053–1059.
45. D. R. Phillips (1990) In *Molecular Basis of Specificity in Nucleic Acid-Drug Interactions* (B. Pullman and J. Jortner, eds.), Kluwer Academic, Dordrecht, The Netherlands, pp. 137–155.
46. J. Cummings, L. Anderson, N. Willmott, and J. F. Smyth (1991) Eur. J. Cancer **27**, 532–535.
47. C. Cullinane and D. R. Phillips (1990) Biochemistry **29**, 5638–5646.
48. C. Cullinane, A. van Rosmalen, and D. R. Phillips (1994) Biochemistry **33**, 4632–4638.
49. S. M. Cutts and D. R. Phillips (1995) Nucleic Acids Res. **23**, 2450–2456.
50. A. van Rosmalen, C. Cullinane, S. M. Cutts, and D. R. Phillips (1995) Nucleic Acids Res. **23**, 42–50.
51. D. J. Taatjes, G. Guadiano, K. Resing, and T. H. Koch (1996) J. Med. Chem. **39**, 4135–4138.
52. D. J. Taatjes, G. Guadiano, K. Resing, and T. H. Koch (1997) J. Med. Chem. **40**, 1276–1286.
53. R. A. Luce, S. Th. Sigurdsson, and P. B. Hopkins (1999) Biochemistry **38**, 8682–8690.
54. A. H. Wang, Y. Gao, Y. Liaw, and Y. Li (1991) Biochemistry **30**, 3812–3815.
55. S. M. Zeman, D. R. Phillips, and D. M. Crothers (1998) Proc. Natl. Acad. Sci. USA **95**, 11561–11565.
56. A. Skladanowski and J. Konopa (1994) Biochem. Pharmacol. **47**, 2269–2278.
57. A. Skladanowski and J. Konopa (1994) Biochem. Pharmacol. **47**, 2279–2287.
58. C. Cullinane, S. M. Cutts, C. Panousis, and D. R. Phillips (2000) Nucleic Acids Res. **28**, 1019–1025.
59. S. M. Cutts, A. Rephaeli, A. Nudelman, I. Hmelnitsky, and D. R. Phillips (2001) Cancer Res., in press.
60. G. Ciarrochi, M. Lestingi, M. Fontana, S. Spadari, and A. Montecucco (1992) Biochem J. **279**, 141–146.
61. N. R. Bachur, R. Johnson, F. Yu, R. Hickey, N. Appelgren, and L. Malkas (1993) Mol. Pharmacol. **44**, 1064–1069.
62. G. Zaleskis, E. Berleth, S. Verstovek, M. J. Ehrke, and E. Mihich (1994) Mol. Pharmacol. **46**, 901–908.
63. A. Skladanowski and J. Konopa (1993) Biochem. Pharmacol. **46**, 375–382.
64. R. B. Lock and L. Stribinskiene (1996) Cancer Res. **56**, 4006–4012.
65. D. J. Taatjes and T. H. Koch (2001) Curr. Med. Chem. **8**, 15–29.

Suggestions for Further Reading

66. R. B. Weiss (1992) The anthracyclines: Will we ever find a better doxorubicin? Semin. Oncol. **19**, 670–686. A detailed review of the history of Adriamycin and of the search for new derivatives.

67. D. A. Gewirtz (1999) A critical evaluation of the mechanism of action proposed for the antitumor effects of the anthracycline antibiotics, Adriamycin and daunomycin. Biochem. Pharmacol. **57**, 727–741. An excellent and comprehensive review of possible molecular mechanisms of action of the anthracycline class of anticancer agents.

68. V. T. DeVita, S. Hellman, and S. A. Rosenberg (2001) *Cancer: Principles and Practice of Oncology*, 6 ed., Lippincott Williams and Wilkins, Philadelphia. Contains a concise and current review of Adriamycin and emphasizes cellular and clinical aspects.

Affinity Chromatography

1. The Basic Principle

Affinity chromatography (AC) is a general **chromatographic** method for the selective extraction and purification of biological macromolecules on the basis of their biorecognition (1-3). The method makes use of the specific physiological affinity between a desired macromolecule (M) and one of its physiological ligands (L). The ligand, or its analogue (L′), actually acts as a "bait" and is used to extract or "fish out" a desired macromolecule (M_1) (Fig. 1) from a mixture of macromolecules (M_1; M_2; M_3; M_4; M_5; M_6¼). The other macromolecules have a very low (if any) affinity for L, presumably because they are designed to refrain from interfering *in vivo* with the physiological recognition of L by M.

Figure 1. Schematic representation of the general procedure for an AC purification. For further details, see text.

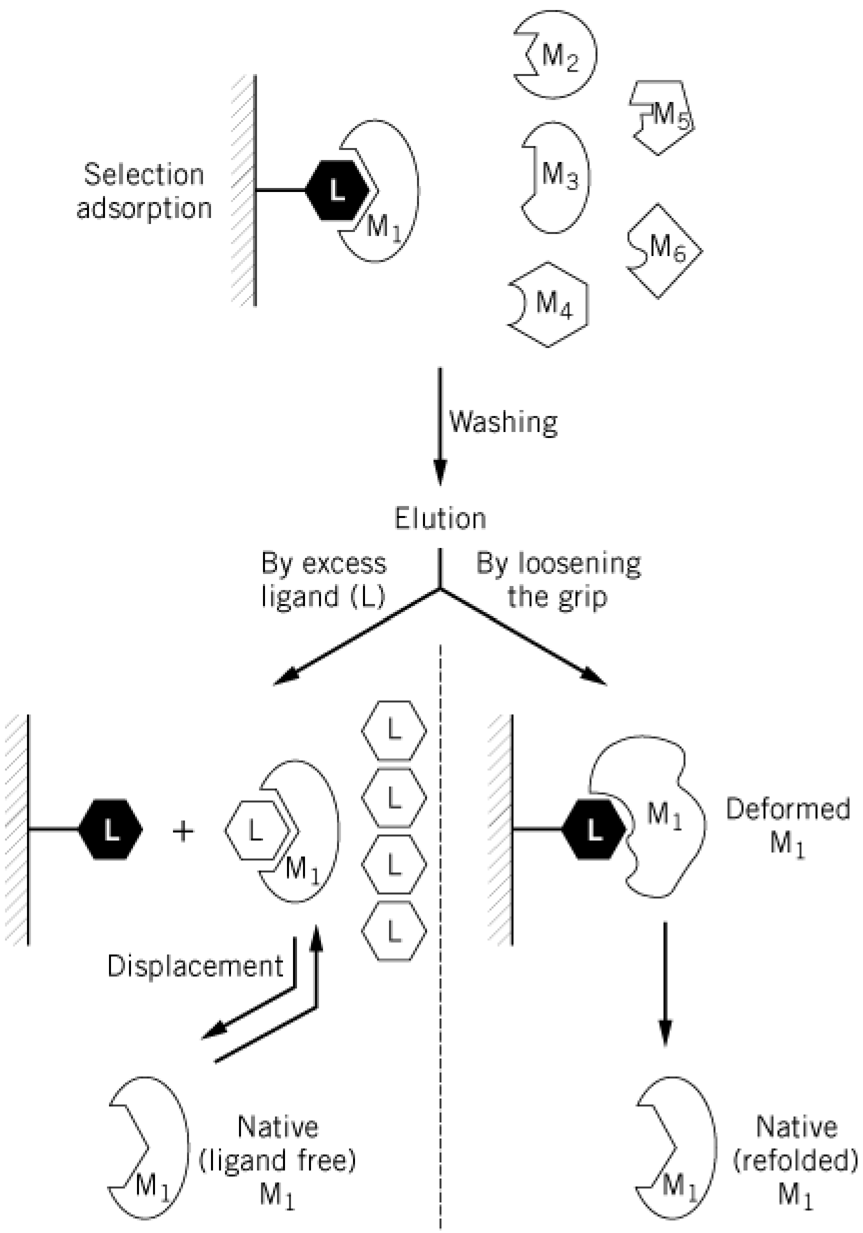

2. General Procedure for an AC Purification: Key Steps

1. *Immobilization (anchoring) of the ligand on an inert carrier*: L is anchored on a carrier to yield an insoluble material, usually in a beaded form. This carrier should be as inert as possible (eg, beaded agarose) to achieve true **active-site**-mediated AC. Also, the attachment point of the ligand should not involve groups that are involved in binding to the macromolecule. Over the years, different carriers and various methods for ligand immobilization were developed. These were reviewed and evaluated by Wilchek et al. (3). In general, the anchoring of L onto an inert carrier involves (i) the introduction of chemically reactive groups to the inert carrier, (ii) the covalent attachment of L to the activated carrier, and (iii) inactivation of the excess of reactive groups (if any) that may remain on the activated carrier after completion of the ligand anchoring step. The immobilized ligand can be used either batchwise or as a column. It may also find other uses—for example, to detect or demonstrate specific protein–protein interactions by the binding of a specific protein. Furthermore, it may use the resulting column material to bind and fish out another protein that interacts with it. Such immobilized ligands have been used also for labeling of cells, for the localization of proteins on cell surfaces, for the demonstration of leakage of enzymes or specific proteins from damaged tissues, and so on.

Historically, the pioneering work of Axén et al. (4) on the CNBr activation of beaded agarose had a great influence on the development of AC and the conversion of this methodology into a most widely used tool in separation science. To this day, beaded agarose continues to be the inert carrier of choice, and its activation with CNBr for ligand binding is still an activation method of choice. A thorough analytical study of the mechanism of activation of agarose by CNBr (5) showed that three major products are formed: a carbamate (chemically inert), a linear or a cyclic imidocarbonate (slightly reactive), and a cyanate ester (chemically very reactive). Analysis of freshly activated agarose showed that 60% to 85% of the total coupling capacity of the agarose is due to the formation of the cyanate esters. They are the ones that actually react and immobilize the ligand (Fig. 2). On the basis of this mechanism of activation by CNBr, it became possible to develop more efficient activation procedures, which are reviewed in Refs. 3 and 6.

Figure 2. The mechanism of the CNBr activation of agarose. (Modified from Ref. 3.)

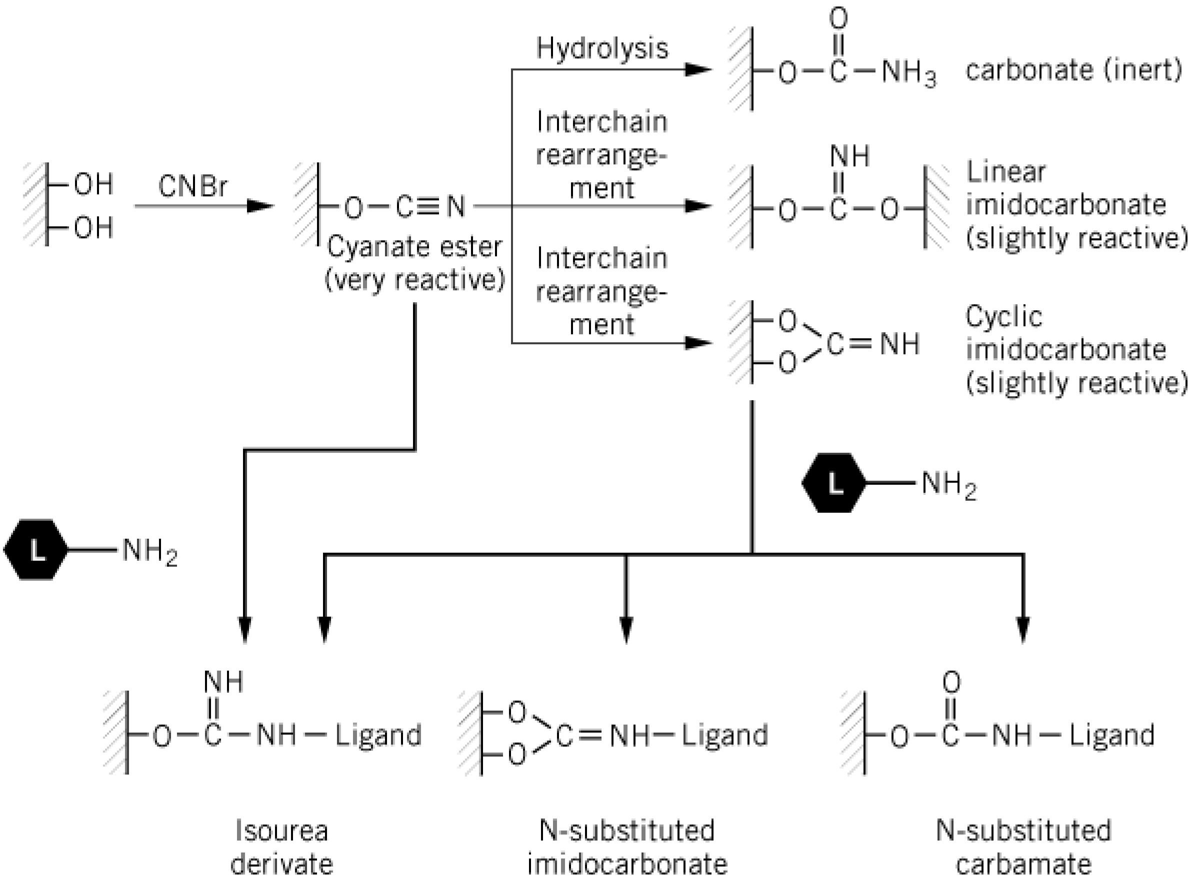

2. *Selective adsorption*. The key selective step in AC is obviously the extraction of the desired macromolecule M, which is singled out and removed by the immobilized L, from the mixture in which it is present. The macromolecule—be it an enzyme, an antibody, a receptor, a hormone, a growth factor, or the like—is selectively bound by the biospecific ligand L, which can be another protein, a peptide, a polynucleotide or a nucleotide, a polysacharide or a carbohydrate, a lipid, a vitamin, or just a metal ion. Functionally, L may be a substrate, a substrate analogue, an inhibitor, an antigen, a coenzyme, a cofactor, or a regulatory metabolite. In many cases, the biospecific ligand used for the immobilization is a structural analogue of the physiological ligand (L′). It is imperative, however, to ensure that it still retains the property of selective binding to M, and ideally to M only. In choosing the ligand for an affinity chromatography column, it is often possible to adjust the grip

of M onto the anchored L, and thus to optimize both the adsorption and the elution steps. It should be noted that the adsorption conditions used (buffer, pH, ionic strength, temperature) should also be carefully chosen to secure an optimal and selective adsorption.

3. *Washing out nonspecifically bound impurities*. This is usually carried out with an excess of the buffer used for selective adsorption.

4. *Elution of the desired macromolecule*. The detachment of M from the column (elution) is one of the most important steps in purification by AC. Obviously, the ideal elution is by a specific displacement of M with an excess of its biospecific ligand (Fig. 1). This procedure preserves the native structure of M by forming the more stable complex of M with its biospecific ligand L. When such elution is achieved, it strongly suggests that true **active-site**-mediated AC is involved. However, very often biospecific ligands fail to elute the desired protein, and nonspecific means have to be applied. These usually include a change in solvent or buffer composition, a change in pH or in ionic strength, the addition of a **chaotropic** or a "deforming" buffer, a change in temperature, or a change in the electric field (**electrophoretic** desorption) (3). All these bring about a deformation of the protein (7, 8), a concomitant loosening of the grip of M for L, and consequently elution. In some cases, the binding of M to the L column is so tight that it is not possible to recover M in a fully active form. If M is an enzyme, this may yield a less active preparation (part of the M molecules may be totally inactive, or all molecules may have a lower affinity for the substrate or a lower turnover number). In some instances, the purified enzyme is fully active, but it may lose its ability to be regulated—for example, if the regulatory domain of M loses its affinity for a regulatory metabolite. Under such circumstances, immobilized ligands with lower affinity for M must be tried. Among the remedies that can be used to improve the elution step, one should note the possibility of binding the ligand to the matrix by means of an easily cleavable form—for example, through an ester bond (9, 10), which can be readily hydrolyzed with a mild base; through a link that includes vicinal hydroxyl groups, which can be readily cleaved with periodate; or through diazo bonds, which can be readily reduced with dithionates (11). It should be remembered, however, that such columns are of limited value, because they can be used only once. Electrophoresis has also been used for elution (12). Because proteins are charged, they will detach from the column and migrate toward the appropriate electrode, if the column with the adsorbed M is exposed to a strong enough electric field. This mild method of elution was successfully applied with high yields in immunoaffinity chromatography and in some AC systems.

3. Interposing an "Arm" Between the Ligand and the Matrix Backbone

While developing the basic principles of AC, it was observed that the purification of M is often improved by interposing a hydrocarbon chain (an "arm" or a "spacer") between L and the matrix backbone (1). It was presumed that such an arm relieves the steric restrictions imposed by the backbone on the ligand, thereby increasing its flexibility and its availability to the protein (13). Such arms were found to improve significantly the extraction of proteins and the efficacy of the purification by AC. Initially, it was assumed that such hydrocarbon arms do not alter the inert nature of the matrix, a condition that obviously has to be ensured to preserve an active-site mediated adsorption of the extracted protein. This assumption seemed reasonable at the time because it had just been shown that at least some water-soluble proteins are quite well described as "an oil drop with a polar coat" (14), implying that the surface of water-soluble proteins is polar and thus not attracted to lipophilic "baits." We now know that such arms, in and of themselves, may bind proteins. In fact, this observation led to the discovery of hydrophobic chromatography.

4. The Limitations of Biospecificity—Interactions that are not Active Site-Mediated

Proteins and their physiological ligands are multifunctional molecules whose functions involve a variety of physical interactions: hydrophobic, **electrostatic**, ion-dipole, and so on. Therefore, it is reasonable to assume that a protein might interact with a column coated with a ligand (very often anchored to the beads at a local concentration much higher than its concentration *in vivo*) not only by means of its active site. While it is sometimes possible to minimize these nonspecific interactions, it is not always possible to avoid such interfering effects, because they may be an intrinsic property of the system. For example, if ATP is linked to a matrix through its amino group or its ribose moiety; the column thus obtained may retain an enzyme having a biospecific site for ATP; but at the same time, this very column would be negatively charged due to its triphosphate groups, and it would have hydrophobic loci due to its adenine residues. Other proteins, in addition to the desired one, may therefore "regard" the column material as an **ion exchanger** by virtue of its triphosphate groups, or as a hydrophobic column by virtue of its adenine moieties. The efficiency of resolution will then depend on the magnitude of the affinity produced by charge–charge or hydrophobic interactions, as compared to the affinity between the active site of the desired macromolecule and its immobilized substrate or effector analogue. With columns of macromolecular ligands (eg, enzyme subunits, antibodies, lectins), the probability of encountering such built-in interfering effects is considerably higher, because their immobilization usually involves different anchoring points. This leads to a heterogeneous presentation of the various regions of the ligand macromolecule. In some of these presentations, the biospecific active site is available for interaction, while in other presentations the active site itself is inaccessible or sterically hindered. Hydrophobic patches in such ligands may be available for interaction not only in the biospecifically functional presentation, but also in other presentations. In fact, the tendency of a lectin such as concanavalin A to adsorb onto hydrophobic substances, in addition to its binding to sugars of the mannosyl configuration, was observed in several laboratories.

5. The Relativity of Biological Recognition: Different Proteins may Share a Taste for a Biorecognition Elements

The occurrence of common biorecognition sites in different enzymes is obvious when they are functionally similar, acting on the same substrate (eg, ATP), or utilizing the same cofactor (eg, NAD). This actually forms the basis for general ligand-affinity chromatography (15). However, common biorecognition elements may also be found with proteins having no apparent functional similarity. For example, the free catalytic subunit of cAMP-dependent protein kinase (**protein kinase A**) is preferentially retarded on immobilized soybean trypsin inhibitor (16). Though initially unexpected, this is actually not surprising; in spite of the fact that **trypsin** and this kinase catalyze two different chemical reactions (hydrolysis of peptide bonds versus a phosphotransferase reaction), these two enzymes do have similar biorecognition elements (or subsites) at their active site: trypsin cleaves peptide bonds adjacent to positively charged amino acid residues (arginine and lysine), while cAMP-dependent protein kinase phosphorylates serine residues that are vicinal (in the sequence of amino acids) to the same positively charged arginine and lysine residues (17-20). Similarly, it was shown (21) that TLCK (a-*N*-tosyl-L-lysine chloromethyl ketone), an affinity labeling reagent originally designed for labeling the active site of trypsin, specifically attacks a thiol group at the active site of the catalytic subunit of cAMP-dependent protein kinase. It seems, therefore, that the retardation of the free catalytic subunit on the immobilized inhibitor is due (at least in part) to an affinity between the inhibitor and recognition subsites at the active site of the enzyme.

Bibliography

1. P. Cuatrecasas, M. Wilchek, and C. B. Anfinsen (1968) Proc. Natl. Acad. Sci. USA **61**, 636.
2. P. Cuatrecasas and C. B. Anfinsen (1971) Annu. Rev. Biochem. **40**, 259.
3. M. Wilchek, T. Miron, and J. Kohn (1984) Methods Enzymol. **104**, 3.
4. R. Axén, J. Porath, and S. Ernbäck (1967) Nature (London) **214**, 1302.
5. J. Kohn and M. Wilchek (1981) Anal. Biochem. **115**, 375.
6. S. B. Mohan and A. Lyddiatt (1997) In *Affinity Separations* (P. Matejtschuk, ed.), IRL Press, Oxford University Press, New York, p. 1.
7. S. Shaltiel, J. L. Hedrick, and E. H. Fischer (1966) Biochemistry **5**, 2108.
8. J. L. Hedrick, S. Shaltiel, and E. H. Fischer (1969) Biochemistry **8**, 2422.
9. R. J. Brown, N. E. Swaisgood, and H. R. Horton (1979) Biochemistry **18**, 4901.

10. P. Singh, S. D. Lewis, and J. A. Shafer (1979) Arch. Biochem. Biophys. **193**, 284.
11. P. Singh, S. D. Lewis, and J. A. Shafer (1980) Arch. Biochem. Biophys. **203**, 776.
12. M. R. Morgan, P. J. Brown, M. J. Lieiand, and P. D. Ocan (1978) FEBS Lett. **87**, 239.
13. P. Cuatrecasas (1970) J. Biol. Chem. **245**, 3059.
14. D. C. Phillips (1966) Sci. Am. November, 78.
15. K. Mosbach (1978) Adv. Enzymol. **46**, 205.
16. E. Alhanaty, N. Bashan, S. Moses, and S. Shaltiel (1979) Eur. J. Biochem. **101**, 283.
17. H. G. Nimmo and P. Cohen (1977) Adv. Cyclic Nucl. Res. **8**, 145.
18. O. Zetterquist et al. (1976) Biochem. Biophys. Res. Comun. **70**, 696.
19. B. E. Kemp, E. Benjamin, and E. G. Krebs (1976) Proc. Natl. Acad. Sci. USA **73**, 1038.
20. P. Daile, P. R. Carnegie, and J. D. Young (1975) Nature **257**, 416.
21. A. Kupfer, V. Gani, J. S. Jimenez, and S. Shaltiel (1979) Proc. Natl. Acad. Sci. USA **76**, 3073.

Affinity Electrophoresis

By analogy to affinity chromatography, it is possible to introduce specific **ligands** for a macromolecule into the gels of gel electrophoresis and to measure the specific retardation of the macromolecule due to its interaction with such a reagent. The advantage of such affinity methods lies in the augmented resolving power conferred by the specificity of the binding interaction.

The procedures used to introduce affinity reagents into gels have varied. In cross electrophoresis, a ligand with a net charge opposite to the species of interest migrates electrophoretically into the gel in the opposite direction. Alternatively, uncharged ligands can simply be added to the gelation mixture. Macromolecular substrates within a gel may serve as immobilized affinity reagents, either by themselves or as carriers of covalently attached affinity groups. The magnitude of the electrophoretic retardation depends on the concentration of the affinity reagent in the gel; quantitative determination of this relationship makes it possible to estimate the apparent association constant for binding of the ligand to the sample. Further information concerning the interaction can be gained from affinity electrophoresis by variation of the buffer composition (eg, the addition of metal ions to the buffer), the pH, or the temperature.

Suggestions for Further Reading

T. C. Bog-Hansen and J. J. Hau (1981) Glycoproteins and glycopeptides (affinity electrophoresis). In *Electrophoresis: A Survey of Techniques and Applications*, Vol. **18B** (Z. Deyl, A. Chrambach, F. M. Everaerts, and Z. Prusik, eds.), Elsevier, Amsterdam, pp. 219–252.

T. C. Bog-Hansen and K. Takeo, eds. (1989) Symposium on affinity electrophoresis. Electrophoresis **10**, 811–870.

K. Takeo (1987) Affinity electrophoresis. Adv. Electrophoresis **1**, 229–280.

Affinity Labeling

Affinity labeling is a strategy to modify chemically an amino acid residue within a specific **ligand-binding** site of an enzyme, either at the active site or at a regulatory, **allosteric** site. In this approach, a reagent is designed that resembles structurally the natural ligand of the enzyme but features in addition a functional group capable of reacting covalently and indiscriminately with many different amino acid residues. The designed reagent is intended to mimic the natural ligand in forming a reversible enzyme-reagent complex analogous to the enzyme-substrate complex and, once directed to that specific site, to react irreversibly with an amino acid residue accessible from that site. In the case of a purified enzyme, such a reagent allows identification of a particular ligand binding site or **domain**, which can be an experimental evaluation of a predicted binding site location based on recognition of a protein motif from its amino acid sequence. Affinity labeling constitutes a valuable starting point for selecting appropriate target sites for subsequent site-directed mutagenesis experiments and is an important tool in probing structure–function relationships in enzymes. If the synthesized reagent has a characteristic absorbance or fluorescence spectrum, affinity labeling offers a means of introducing a chromophore at a specific substrate site to report on the enzyme conformation or on distances between designated sites in the enzyme. For medicinal chemistry, affinity labeling permits mapping of the substrate binding site and establishment of its size, so that inhibitory drugs directed toward that site can be designed more rationally. In the case of a heterogeneous cell preparation or of a complex protein mixture, a specific affinity label can be used to identify a **receptor** protein or to tag a class of macromolecules, such as **nucleotide binding** proteins.

One characteristic of affinity labeling is the initial formation of a reversible enzyme–reagent complex (ER), as indicated below.

$$E + R \underset{k_{-1}}{\overset{k_1}{\rightleftharpoons}} ER \xrightarrow{k_{max}} ER' \tag{1}$$

where E and R represent the free enzyme and reagent, respectively, and ER' is the covalently modified enzyme. The formation of a reversible ER complex is often indicated by a "rate saturation effect" in which the rate constant for modification (k_{obs}) increases as the reagent concentration is elevated until the enzyme site is saturated with reagent; subsequently, the rate constant (k_{max}) is not changed by further increases in reagent concentration (see Kinetics). This kinetic pattern contrasts with the linear dependence on reagent concentration of the rate of a direct bimolecular chemical modification. For an affinity label, k_{obs} can be described by the equation

$$k_{obs} = \frac{k_{max}}{1 + \frac{K_R}{[R]}} \tag{2}$$

where the apparent dissociation constant for the enzyme–reagent complex K_R, is given by $(k_{-1} + k_{max})/k_1$ and where k_{max} is the maximum rate of modification at saturating concentrations of reagent. This type of kinetic behavior is often presented as a double reciprocal plot of $1/k_{obs}$ versus $1/[R]$, based on the equation

$$\frac{1}{k_{obs}} = \frac{1}{k_{max}} + \left(\frac{K_R}{k_{max}}\right)\left(\frac{1}{[R]}\right) \tag{3}$$

Examples of **purine** nucleotide-based affinity labels are shown in Figures 1 and 2. Experiences with their use illustrate the possibilities of affinity labeling.

Figure 1. Comparison of the structures of the natural ligand adenylosuccinate and of the affinity label 6-(4-bromo-2,3-di
5′-monophosphate (6-BDB-TAMP).

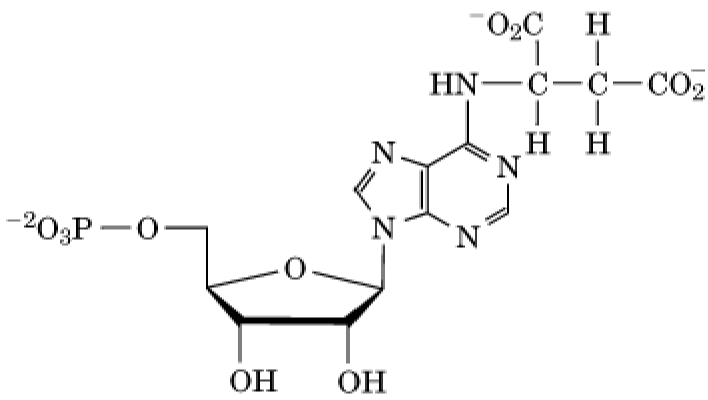

Adenylosuccinate

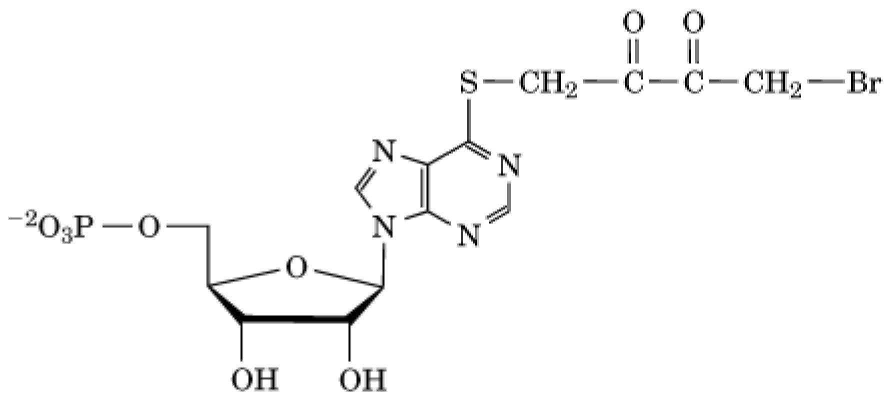

6-BDB-TAMP

Figure 2. Comparison of the structures of the affinity label (**a**) guanosine 5′-0-[S-(4-bromo-2,3- dioxobutyl)thio]phosph
(**b**) the natural ligand GTP.

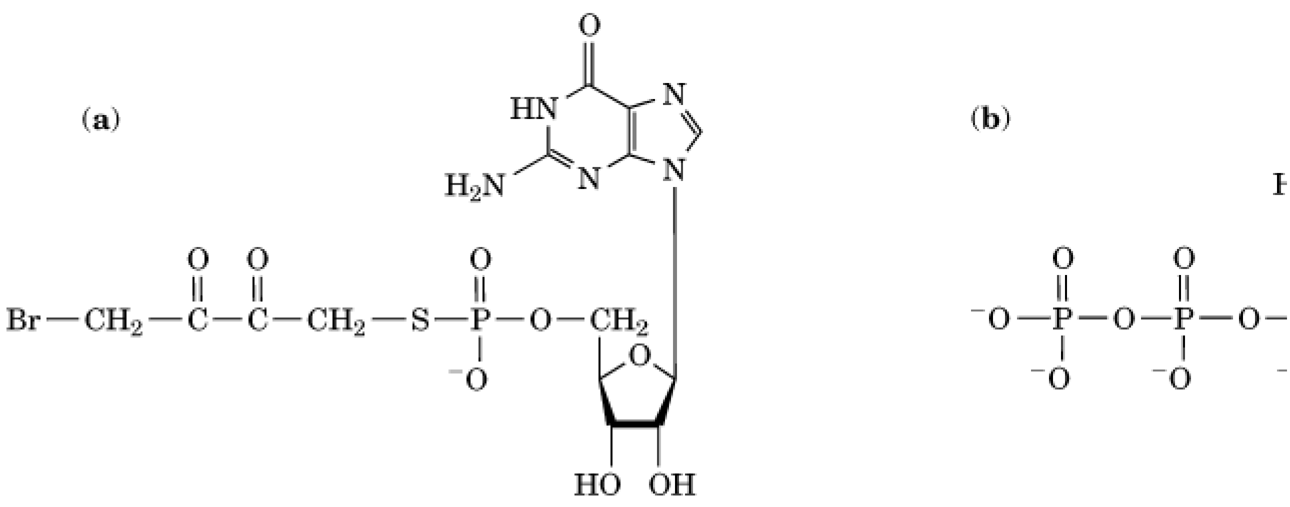

GMPS-BDB

GTP

1. BDB-TAMP

The compound 6-(4-bromo-2,3-dioxobutyl)thioadenosine 5′-monophosphate (6-BDB-TAMP) shown in Figure 1 was synthesized as a reactive nucleotide analogue to target nucleotide binding sites in enzymes (1). The bromoketo group, adjacent to the 6-position of the purine ring, can potentially react with several nucleophiles found in proteins, including those of the side chains of cysteine, histidine, tyrosine, lysine, methionine, **glutamate**, and **aspartate** residues. In addition, the dioxo group provides the possibility of reaction with arginine residues.

As shown in Figure 1, the structure of 6-BDB-TAMP also exhibits a remarkable resemblance to that of adenylosuccinate, a key metabolic intermediate in the conversion of inosine monophosphate to adenosine monophosphate. The last step in that pathway is catalyzed by adenylosuccinate lyase, an enzyme proposed to initiate the cleavage reaction to AMP by attack of an enzymic general base on the b hydrogen of adenylosuccinate. Elimination of the amino group is then facilitated by protonation of the leaving group by an enzymic general acid. Despite this proposal, the key general base and acid of the enzyme had not been identified. The similarity between the structures of adenylosuccinate and 6-BDB-TAMP suggested that the latter would bind irreversibly to the adenylosuccinate site of adenylosuccinate lyase, where the bromodioxobutyl group would be likely to occupy the succinyl subsite at which the critical catalytic steps should occur.

6-BDB-TAMP has recently been confirmed to function as an affinity label of *Bacillus subtilis* adenylosuccinate lyase (2). The initial inactivation rate constant exhibits nonlinear dependence on the concentration of 6-BDB-TAMP, with an apparent reversible K_R = 30 μM prior to irreversible inactivation at pH 7.0 and 25°C. The tetrameric enzyme incorporates about 1 mol of 6-BDB-[^{32}P] TAMP per mol of enzyme subunit on complete inactivation. The substrate adenylosuccinate or the products AMP plus fumarate protect against inactivation and incorporation of radioactive reagent, indicating that 6-BDB-TAMP targets the adenylosuccinate binding site. Purification of the only radioactive peptide labeled by 6-BDB-TAMP led to the identification of His^{141} as the modified amino acid (2). These results indicated that 6-BDB-TAMP is an affinity label of His^{141} in the substrate binding site of adenylosuccinate lyase, where it may serve as a general base accepting a proton from the succinyl group during catalysis (2) (see Histidine (His, H) residues). This study illustrates many of the desirable characteristics of affinity labeling: binding of the reagent by the enzyme prior to modification of a single site under mild conditions, competition between the reagent and the natural ligand (adenylosuccinate), and identification of the modified residue within a protein of known amino acid sequence.

2. GMPS-BDB

A reactive guanine derivative is shown in Figure 2, guanosine 5′-0-[S-4-bromo-2,3-dioxobutylthio] phosphate (GMPS-BDB), which represents a novel class of compounds containing a bromodioxobutyl group linked to the sulfur of a purine nucleotide thiophosphate (3, 4). The reactive moiety of GMPS-BDB is located at a position equivalent to that of the pyrophosphate region of GTP, as illustrated in Figure 2. Thus, it might be expected that GMPS-BDB would act as an affinity label for GTP sites in proteins (see GTP-Binding Proteins).

Adenylosuccinate synthetase catalyzes the first of the two enzymatic reactions in the conversion of IMP: the condensation of IMP and aspartate to form adenylosuccinate, as GTP is hydrolyzed to GDP and inorganic phosphate. The phosphoryl group has been proposed to be transferred to IMP from the terminal phosphate of GTP to form a 6-phosphoryl-IMP intermediate.

GMPS-BDB has been used as an affinity label of adenylosuccinate synthetase from *Escherichia coli*, and it has been demonstrated that inactivation occurs concomitantly with the modification of Arg^{143} of each subunit of the dimeric enzyme (5). The modification of Arg^{143} and the inactivation by GMPS-BDB is prevented by adenylosuccinate or by IMP plus GTP, implying that the reaction target is in the region of the active site. This result pointed to Arg^{143} as a logical target for site-directed mutagenesis; when the positively charged arginine was replaced by the neutral leucine, the expressed mutant enzyme exhibited a significant decrease in its affinity for nucleotides (5).

The crystal structure of *E. coli* adenylosuccinate synthetase has been determined, allowing a comparison to be made between the substrate sites identified by affinity labeling of the enzyme in solution and those assigned within the crystalline form by X-ray crystallography. Arg^{143} from one subunit projects into the putative active site of the second subunit, indicating that both subunits of dimeric adenylosuccinate synthetase contribute to each active site and that Arg^{143} plays an important role in nucleotide binding.

3. AMPS-BDB

The adenosine analogue of GMPS-BDB has also been synthesized: adenosine 5′-0-[S-(4-bromo-2,3-dioxobutyl)thiophosphate] (AMPS-BDB) (4) and can be considered as a reasonable mimic of ADP or ATP. Bovine liver glutamate dehydrogenase is an allosteric enzyme that is reversibly activated by ADP. On incubation of AMPS-BDB with glutamate dehydrogenase, the enzyme reacts covalently, resulting in an irreversibly *activated* enzyme that is no longer responsive to externally added ADP (6). AMPS-BDB appears to function as an ADP substitute that is covalently bound to Arg^{459} within the activator site of the allosteric bovine liver glutamate dehydrogenase (6).

The above are representative examples of enzymes that have been studied using the strategy of affinity labeling. They illustrate how affinity labeling, X-ray crystallography and site-directed mutagenesis can be used as complementary approaches in evaluating the functional role of particular amino acids in a protein.

Bibliography

1. R. F. Colman, Y.-C. Huang, M. M. King, and M. Erb (1984) Biochemistry **23**, 3281–3286.
2. T. T. Lee, C. Worby, J. E. Dixon, and R. F. Colman (1997) J. Biol. Chem. **272**, 458–465.
3. D. H. Ozturk, I. Park, and R. F. Colman (1992) Biochemistry **31**, 10544–10555.
4. S. H. Vollmer, M. B. Walner, K. V. Tarbell, and R. F. Colman (1994) J. Biol. Chem. **269**, 8082–8090.
5. O. A. Moe et al. (1996) Biochemistry **35**, 9024–9033.
6. K. O. Wrzeszczynski and R. F. Colman (1994) Biochemistry **33**, 11544–11553.

Suggestions for Further Reading

7. R. F. Colman (1983) Affinity labeling of purine nucleotide sites in proteins. Ann. Rev. Biochem. **52**, 67–91.
8. R. F. Colman (1990) Site-specific modification of enzyme sites. In *The Enzymes*, 3rd ed., Vol. **19** (D. S. Sigman and P. D. Boyer, eds.), Academic Press, San Diego, Calif., pp. 285–321.
9. R. F. Colman (1997) Affinity labels for NAD(P)-specific sites. Methods Enzymol. **280**, 186–203.
10. R. F. Colman (1997) Affinity labelling. In *Protein Function: A Practical Approach*, 2nd ed. (T. E. Creighton, ed.) Oxford University Press, Oxford UK, pp. 155–183.
11. W. B. Jakoby and M. Wilchek, eds. (1977) Affinity labeling. Methods Enzymol. **46**.

Affinity Maturation

It was observed long ago that the affinities of antibodies increase with time during immunization with a T-dependent antigen. When such an antigen is injected for the first time, it induces the occurrence of low-affinity IgM antibodies, which are rapidly replaced by IgG. This takes place in the first two weeks of the primary response. At the same time, an increase of the average affinity is usually observed. If the same antigen is given a second time, IgG antibodies are subsequently produced at a higher yield, and with an average affinity that is still increasing. This is characteristic of the secondary response, a phenomenon that may be repeated and amplified by multiple administrations of the antigen. This is why long-term immunization schedules are used whenever both high titers and high affinity are wanted. Affinity maturation, which is a unique property of B cells stimulated by T-dependent antigens, is the consequence of (*1*) the clonal organization of lymphocytes, (*2*) the expansion of clones that have been stimulated specifically by the antigen, and (*3*) the presence of a very peculiar mechanism that generates somatic mutations at each cellular division of stimulated B cells.

1. Antibody specificities are spread randomly in the huge collection of clones that represent at any given time the repertoire expressed by B lymphocytes that have rearranged their immunoglobulin genes and thus have IgM at their surface. Clones that are potentially reactive to the antigen proliferate, as the result of the cooperation between T cells and B cells and the phenomenon of **antigen processing** and presentation. This ensures that the first wave of antibodies are generally of low or moderate affinity.

2. As the immunization proceeds, expansion of the B-reactive cell population takes place, giving rapidly growing colonies, termed *germinal centers*, in secondary lymphoid organs (lymph nodes, tonsils, spleen). Germinal centers are highly organized structures that favor cell–cell interactions that will amplify local B-cell division and expansion.

3. At the same time, somatic mutations will be triggered by a mechanism that is **probably** enzyme-driven, but still not completely elucidated. The rate of the mutations that are introduced is of the order of 1×10^3 per base pair and per generation, which is excessively high. As a result of these mutations, some clones will gain affinity, whereas others will lose. One therefore needs mechanisms to select clones of high affinity and eliminate those of lower affinity; otherwise the system would expand indefinitely and explode. Stimulation by antigen will favor the saving and expansion of clones with the highest affinity, whereas apoptosis will operate on cells that did not receive stimuli as they lost recognition ability.

PCR and DNA sequencing at the level of single cells allowed the group of Rajewsky to trace the successive mutations that occurred at each cell division, so that it was possible to reconstruct a genealogical tree of these mutations within the germinal center. Interestingly, hypermutated cells can ultimately follow two types of differentiation: One leads to the terminal plasma cells, which will secrete circulating antibodies, and the other leads to the so-called memory cells that may persist for long periods of time and may be restimulated with great efficiency in the course of another run of immunization.

The extraordinary plasticity and adaptability of the immune system are thus quite remarkable and allow it to respond efficiently to pathogens. Raising memory cells endowed with the ability to produce rapidly high-affinity antibodies is an obvious goal of vaccination.

See also entries Immune Response, Class Switching, and Somatic Hypermutations.

Suggestions for Further Reading

D. M. Tarlinton, A. Light, G. J. Nossal, and K. G. Smith (1998) Affinity maturation of the primary response by V gene diversification. Curr. Top. Microbiol Immunol. **229**, 71–83.

C. J. Jolly, S. D. Wagner, C. Rada, N. Klix, C. Milstein, and M. S. Neuberger (1996) The targeting of somatic hypermutation. Semin. Immunol., **8**, 159–168.

A. Ehlich, V. Martin, W. Muller, and K. Rajewsky (1994) Analysis of the B-cell compartment at the level of single cells. Curr. Biol. **4**, 573–583.

Affinity Selection

A key requirement of combinatorial library approaches is that desirable molecules must be segregated from the remaining library population. Segregation is most often accomplished by affinity partitioning, in which an immobilized target is used to capture interacting molecules from a solution-phase library. Target proteins can be immobilized either using antibodies bound to *Staphylococcus* protein A, using absorption of targets onto wells of plastic microtiter plates, or covalent attachment to a variety of polymeric supports. Alternatively, combinatorial libraries attached to solid supports—for example, one-bead, one-compound (OBOC) libraries—can be used to bind soluble targets. Solid-phase libraries have also been used to screen highly complex targets, such as living cells on which a variety of receptors are expressed (1). In all cases, unbound material is removed by washing, and the bound material is recovered for amplification or identification, depending on the nature of the library.

Plastic pins were used to develop the first peptide-based combinatorial libraries. The pins are arranged such that they fit neatly into a single well of a microtiter plate. Thus, the pin system provides a convenient format for both synthesis and screening. The power of this method derives largely in the ease of handling large numbers of discrete syntheses in parallel. Sequential steps of the synthesis can be carried out by transferring the pin arrays through various microtiter reaction chambers. The peptides are then directly available for affinity screening, either on the solid phase or following cleavage from the solid support.

Lam et al. (2) developed another approach for peptide affinity selection involving split synthesis of peptides on solid support beads (OBOC libraries: see Combinatorial Synthesis). From a pool of millions of beads, a binding reaction is performed using a target molecule such as an antibody, receptor, enzyme, or even whole cells. Beads displaying affinity for the target are isolated, and the peptide on the bead can be microsequenced.

Fodor et al. (3) have developed immobilized combinatorial libraries on silicon microchips. Chip-based addressable libraries of peptides, oligonucleotides, and small organic molecules can be readily prepared. These methods use photolithography to control regions accessible for subsequent chemical modification. This method enables a miniaturized, fully addressable library to be generated on the surface of a silicon chip. The resulting arrays can be screened using standard affinity methods.

The affinity selection methods described above are extremely broad in their applications. Although classical nucleic acid libraries have been screened by **hybridization**, which is a highly specialized type of affinity partitioning, modern DNA and RNA aptamer libraries are screened in identical fashion to other combinatorial libraries by affinity selection over immobilized targets. Although selection strategies have been introduced that are based on properties other than affinity, such methods are highly specialized and are not likely to displace the current reliance on affinity methods for combinatorial screening.

See also Combinatorial Libraries, Libraries, Combinatorial Synthesis, DNA Libraries, Genomic Libraries, cDNA Libraries, Expression Libraries, Peptide Libraries, and Phage Display Libraries.

Bibliography

1. M. E. Pennington, K. S. Lam, and A. E. Cress (1996) Mol. Diversity **2**, 19–28.
2. K. S. Lam, S. E. Salmon, E. M. Hersh, V. J. Hruby, W. M. Kazmierski, and R. J. Knapp (1991) Nature **354**, 82–84.
3. S. P. Fodor, J. L. Read, M. C. Pirrung, L. Stryer, A. T. Lu, and D. Solas (1991) Science **251**, 767–773.

Agarose

Agarose is one of the two most popular materials used to prepare gels for use in gel electrophoresis, the other being polyacrylamide. Agarose is primarily a polymer of molecular weight approximately 120 kDa of agarobiose (an anhydrogalactose-galactose disaccharide). At sufficiently high concentrations and low temperatures, the polymer forms b-helical strands, which interact by **hydrogen bonding** to form the agarose gel; they dissociate at higher temperatures to form agarose solutions. Such thermally controlled gelation is the unique feature of agarose, which provides both a high reproducibility and simplicity of preparing the gel. Since gelation requires noncovalent interactions between the copolymer strands, denaturing agents, such as solutions of urea, prevent gelation.

Agarose is derived from a natural product of oceanic algae, agar. It is processed to reduce the content of acidic groups, primarily sulfate, so as to reduce the degree of electroendosmosis that occurs during electrophoresis. Further industrial processing produces a large number of commercially available agarose fractions distinguished by (1) the degree of electroendosmosis in an electric field, determined by the number of acidic groups; (2) the degree of covalent substitution of the acidic groups with chemical groupings such as hydroxyethyl or vinyl (allyl) groups, which tends to lower the melting point in proportion to the degree of substitution; (3) the addition of linear carbohydrate polymers, such as clarified locust bean gum, to increase the viscosity of the gel and thereby eliminate measurable electroendosmosis.

Most agaroses at concentrations greater than about 0.4% (w/v) form gels at room temperature. Agaroses with unusually high gel strengths can gel at concentrations as low as about 0.05%. The pore sizes of such agarose gels make them ideal for separating **DNA** molecules and **oligonucleotides**; their mobility is determined primarily by their size, as nucleic acids of the same class have the same charge density per nucleotide. The least concentrated gels exhibit mean pore sizes of up to 500 to 1,000 nm, sufficiently large for the penetration of large particles or small viruses (see Particle Electrophoresis). Highly soluble agarose species substituted to a maximum extent by hydroxyethyl groups can be used to prepare gels with concentrations of up to 9 to 10%. Such gels have pores of similar size to those of 3 to 6% polyacrylamide gels, and with greater resolving power for native proteins. Agarose can also be used as a copolymer with polyacrylamide, which provides larger pore sizes than polyacrylamide by itself. The copolymer is produced by adding agarose to the mixture of acrylamide monomers before its polymerization. For the separation by size of DNA fragments, or of other large particles, by capillary zone electrophoresis, solutions of agarose can be used.

The adherence of agarose gels to glass or plastic apparatus walls is very weak, and only horizontally oriented gel electrophoresis apparatus can normally be used. The adherence of agarose to vertical glass surfaces may, however, be strengthened by drying a thin film of agarose onto glass walls; this can permit electrophoresis in vertical glass slabs or tubes. Horizontal thin-layer agarose gels with high Joule heat dissipation capacity, which are therefore amenable to electrophoresis at high field strength without melting, can be formed on hydrophilic surfaces of thin plastic sheets (eg, "Gel-Bond").

For preparative purposes, bands of a macromolecular sample in agarose gels may be recovered by solubilizing the agarose at increased temperature or adding the enzyme agarase. The macromolecule of interest is subsequently separated from the low-molecular-weight agarose fragments by filtration or precipitation methods.

Suggestions for Further Reading

I. C. M. Dea, A. A. McKinnon, and D. A. Rees (1972) Tertiary and quaternary structure in aqueous polyacrylamide systems which model cell wall cohesion: Reversible changes in conformation and association of agarose, carrageenan and galactromannans. J. Mol. Biol. **68**, 153–172.

T. G. L. Hickson and A. Polson (1968) Some physical characteristics of the agarose molecule. Biochim. Biophys. Acta **165**, 43–58.

FMC Corporation (1982) *The Agarose Monograph*, Bioproducts Dept., Rockland, ME.

J. O. Jeppson, C. B. Laurell, and B. Franzen (1979) Agarose gel electrophoresis. Clin. Chem. **25**, 629–638.

P. Serwer (1983) Agarose gels: Properties and use for electrophoresis. Electrophoresis **4**, 375–382.

D. Tietz (1987) Gel electrophoresis of intact subcellular particles. J. Chromatogr. **418**, 305–344.

Agglutination

"Agglutinin" is an obsolete term for an antibody capable of causing cells to come together in macroscopic clumps. Agglutination (clumping) of bacteria by serum was perhaps the earliest observed manifestation of *in vitro* immune reactions. The phenomenon is due to crosslinking of cells through the reaction of multivalent antibody molecules with cell-surface antigens. The quantity of antibody necessary for crosslinking is generally very small, yet the cell masses involved in agglutination generate a response visible to the naked eye. Because of these characteristics, this oldest of techniques remains one of the most sensitive and widely used types of immunoassay.

Agglutination immunoassays can employ cells or synthetic particles. The two broad categories of cell-based agglutination assay are termed "direct" and "passive". In the direct assay, antibodies cause clumping of microbes or blood cells by reaction with surface antigens endogenous to those cells. Typically, the immune status of serum in a test sample will be assessed, based on the highest dilution that will still agglutinate target cells. Direct agglutination assays are widely used to diagnose infectious disease by the presence of specific antibodies in acute or convalescent serum. The "monospot" assay for infectious mononucleosis is an example of this application (1). In passive agglutination immunoassays, the target antigen is exogenous, and is coated covalently or by adsorbtion onto the cells used for the assay. Test samples are then assayed as for the direct agglutination method. Many variants of direct and passive agglutination are in use for research or diagnostic procedures. For example, the test for Rh blood type is a two-step method in which antibodies in the test sample react with endogenous Rh antigen on erythrocytes, then addition of anti-human IgG induces agglutination (2).

Availability of uniformly sized latex particles allowed development of a chemically defined substrate on which to attach antigen or antibody (3). The role of the particles was precisely analogous to that of cells, in that their aggregation in response to antibody–antigen crosslinking generated an optically detectable signal. The advantage of inert particles was in their stability, compared to cells, and in interassay reproducibility. Measurement of agglutination was at first by turbidometry. Development of laser light-scattering techniques have greatly improved the sensitivity of detection (4) and have led to development of automated instruments for quantitation of agglutination reactions.

Bibliography

1. C. L. Lee, I. Davidsohn, and R. Slaby (1968) Am. J. Clin. Pathol. **49**, 3–11.
2. R. R. A. Coombs, A. E. Mourant, and R. R. Race (1945) Br. J. Exp. Pathol. **26**, 255–266.
3. J. M. Singer and C. M. Plotz (1956) Am. J. Med. **21**, 888–892.
4. V. Schulthess, R. J. Cohen, N. Sakato, and G. B. Benedek (1974) Immunochemistry **13**, 955–962.

Agrobacterium

Agrobacterium tumefaciens and *Agrobacterium rhizogenes* are members of the *Agrobacterium* genus of soil **bacteria** responsible, respectively, for tumor formation and hairy root disease in dicotyledenous **plants**. The molecular basis of inducting neoplastic growth in plants has been one of the most intriguing areas of research in plant pathology for more than 50 years. Advances in understanding the molecular basis of tumor formation has led to the development of **vector** systems based on *Agrobacterium* to carry out plant genetic engineering.

Agrobacterium belongs to the *Rhizobiacae* family. Classification of the bacterium has been based on physiological and biochemical criteria, although increasingly the taxonomic structure of the genus has been based on **DNA** analysis of **chromosomal** groups of the differing biovars (1). The best studied members of the genus are *A. tumefaciens* and *A. rhizogenes*. *A. tumefaciens* is the causative agent of crown gall disease. It has a wide, obvious host range, including the majority of dicotyledonous plants and some monocotyledonous plants (2). Practically, crown gall can be a serious disease of fruit crops, including grape vines. The physical basis of crown gall disease is the transfer of a defined region of DNA, transferred or T-DNA, from a **plasmid** maintained in the bacteria, known as the Ti or tumor-inducing plasmid (see Ti Plasmid) to the genome of the infected plant cell. *A. rhizogenes* induces hairy root disease analogously. A T-DNA is transferred from the Ri, or root-inducing, plasmid to the genome of the infected plant cell (see Ri Plasmid). This natural form of plant cell transformation has been adapted and used extensively in creating **transgenic** plants (see Plant Genetic Engineering).

Bibliography

1. H. Bouzar, J. B. Jones, and A. Bishop (1995) In *Agrobacterium Protocols* (K. M. A. Gartland and M. R. Davey, eds.), Humana Press, Totowa, NJ, pp. 9–13.

2. M. DeCleene and J. DeLey (1976) Bot. Rev. **113**, 81–89.

Suggestions for Further Reading

3. K. Kersters and J. De Ley (1984) "Genus III Agrobacterium Conn 1943", In *Bersey''s Manual of Systematic Bacteriology*, Vol **1** (N. R. Krieg and J. G. Holt, eds.), Williams and Wilkins, Baltimore, pp. 244–254.
4. G. Kahl and J. Schell (1982) *Molecular Biology of Plant Tumors*, Academic Press, London.

Alanine (Ala, A)

The amino acid alanine is incorporated into the nascent polypeptide chain during **protein biosynthesis** in response to four **codons**—GCU, GCC, GCA, and GCG—and represents approximately 8.3% of the residues of the proteins that have been characterized. The alanyl residue incorporated has a mass of 71.09 Da, a **van der Waals volume** of 67 Å^3, and an accessible surface area of 113 Å^2. Ala residues are usually relatively variable during divergent evolution, as they are frequently interchanged in **homologous** proteins with serine, threonine, valine, glutamic acid and proline residues.

The Ala side chain is simply a methyl group:

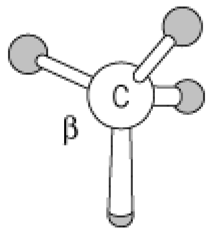

This nonpolar side chain makes Ala residues unreactive chemically, relatively **hydrophobic**, and not very hydrophilic; consequently, 38% of the Ala residues are fully buried in the folded conformations of proteins. There, the methyl side chain undergoes rapid rotations about the C_a–C_b single bond. Ala has the greatest tendency of all the normal amino acid residues to adopt the **alpha-helical** conformation in model **peptides**. It occurs frequently in that conformation in folded protein structures, but at about only half that frequency in beta-sheets and in reverse turns.

Suggestion for Further Reading

T. E. Creighton (1993) *Proteins: Structures and Molecular Properties*, 2nd ed., W. H. Freeman, New York.

Albumins

Albumins are operationally defined as proteins that (1) remain soluble in pure water after dialysis of protein samples such as egg white or blood serum against distilled water and (2) are not precipitated in 50% saturated ammonium **sulfate**. This contrasts with another group of proteins, called globulins, which are precipitated in both distilled water and 50% saturated ammonium sulfate. This operational classification is rather obsolete today, but names like serum albumin, ovalbumin, and lactalbumin have remained. Other albumins include muscle albumin and plant albumins (1).

1. Blood Albumins

Serum albumin and other plasma proteins have been most closely studied, mainly for their medical interest. After the cells have been removed from blood by light centrifugation in the presence of chelating agents such as EDTA, a yellowish fluid called plasma remains. By the addition of Ca^{++}, fibrinogen is converted to fibrin and the clotting process produces a soft gel. Removal of this gel by centrifugation or other methods will leave a clear fluid called serum. Serum thus obtained contains 70 to 80 g/L of total protein, consisting of more than 150 different kinds of proteins. Dialysis of serum against distilled water will precipitate the globulins, while albumins stay in solution. The albumin fraction contains serum albumin as the major protein (2, 3). (see Serum Albumin).

2. Egg Albumins

Egg proteins are first classified into yolk proteins and egg white proteins. Yolk contains proteins called vitellogenin, phosvitin, and lipovitellin, all in association with yolk lipid. Egg white is a reservoir of several kinds of proteins as a protective and nutritious environment for the fetus. Egg white proteins are further divided into albumins and globulins, as for serum proteins. The following is a list of egg white proteins that are not globulins. Descriptions of egg white globulins are found under Globulins.

2.1. Ovalbumin

This is the major **glycoprotein** in the white of eggs, comprising 65% of the total egg white protein, with a molecular weight of 43,000 and isoelectric point (pI) of 4.7. The N-terminal glycine residue is acetylated. Two species containing one or two sites of **phosphorylation** can be separated by electrophoresis. Oligosaccharide containing three moles of N-acetylglucosamine and five moles of mannose is linked to an asparagine residue through an **N-glycosidic** linkage. Treatment of ovalbumin with subtilisin yields a readily crystallizable plakalbumin, named after the platelike appearance of the resulting crystals. Ovalbumin is often used as an effective antigen in immunological studies. The protein has recently been found to have a similar amino acid sequence and three-dimensional structure to a1-antitrypsin of the serpin family (4) (see Ovalbumin).

2.2. Ovotransferrin (or *conalbumin*)

This protein binds ferric ions and is the same as apo-transferrin, but differing in the carbohydrate moiety. In egg white, the protein is present in an almost iron-free form. This protein constitutes about 10% of the egg protein.

2.3. Ovomucoid

Ovomucoid is a glycoprotein (carbohydrate content about 25% by weight) with a molecular weight of 28,000 and constitutes 1.5% of the total egg white protein. It inhibits **trypsin** and **chymotrypsin** but not **plasmin**, thrombin, elastase, or collagenase. Its pI falls in the range 3.9 to 4.5. It remains active in the supernatant after egg white has been coagulated by heat. It has three **homologous** domains connected by linking peptides, each domain being homologous to bovine pancreatic trypsin inhibitor (BPTI). Thus, it is speculated that ovomucoid has evolved by two tandem repeats of the BPTI gene. Carbohydrates are linked to asparagine residues at residue numbers 10, 53, 69, 75, and 175. Similar inhibitors can be purified from the egg white of the quail, goose, and turkey.

2.4. Ovoinhibitor
This is a 48-kDa multiheaded proteinase inhibitor that can simultaneously inhibit trypsin, chymotrypsin, and elastase. Unlike ovomucoid, it also inhibits the proteinases of bacterial origins. It is a glycoprotein with 5 to 10% content of carbohydrate.

2.5. Avidin
This protein occupies a special position in biochemistry in that it is widely used as a probe based on its strong affinity for biotin. Their binding constant reaches $10^{14}\ M^{-1}$ under optimal conditions. Avidin-biotin systems are widely used for labeling macromolecular interacting systems, not only protein–protein interactions, but also systems based on DNA and other macromolecules. Avidin can be substituted by streptavidin, which is of bacterial origin but with a similar activity. Avidin in the egg white is largely free of biotin, and feeding rats with purified avidin as the sole protein source will cause various symptoms known to accompany biotin (vitamin H) deficiency.

2.6. Ovomucin
This is a glycoprotein of high molecular weight responsible for the mucous character of egg white. The treatment of ovomucin with reagents that react with thiol groups reduces the viscous nature of egg white.

3. Plant Albumin

Ricin is an example of plant albumins (from *Ricinus communis*) and has an interesting toxic function. It consists of an A subunit, of 32 kDa, pI of 7.5, and 2.4% carbohydrate, and a B subunit, of 34 kDa, pI of 4.8, and 6.5% carbohydrate. It inactivates the 60S subunit of ribosomes after being internalized into the cell and thus inhibits a peptide elongation step (see Translation). The A subunit carries out the inactivation reaction, while the B subunit, which binds to cell-surface galactose residues, helps the A subunit to be internalized into the cell. Plant albumins are more readily precipitable in 50% ammonium sulfate than animal albumins.

4. Milk Albumins

4.1. a-Lactalbumin
This is a single-chain 14-kDa protein that is the same as the B chain of lactose synthetase in lactating granules. The A chain of lactose synthetase alone catalyzes the synthesis of N-acetylgalactosamine from N-acetylglucosamine and UDP-galactose, but when in association with a-lactalbumin, it uses glucose as a substrate and synthesizes lactose. The amino acid sequence of a-lactalbumin with 143 amino acids (human, bovine, guinea pig) is homologous to that of lysozyme, and its three-dimensional structure is also similar. A recent review of the relationship between lysozyme and lactalbumin is recommended (5) (see also Alpha-Lactalbumin and Lysozymes).

4.2. Lactoferrin
This is an iron-binding protein of 88,000 in humans and 86,000 in cows. It is similar in functional properties to serum transferrin, but immunologically and structurally distinguishable (6).

Bibliography
1. B. Blombäck and L. A. Hanson (1979) *Plasma Proteins*, John Wiley & Sons, New York.
2. M. Perutz (1992) *Protein Structure: New Approach to Disease and Therapy*, W. H. Freeman and Co., New York.
3. T. Peters Jr. (1985) Adv. Prot. Chem. **37**, 161–245.
4. P. E. Stein, G. W. Leslie, J. T. Finch, and R. W. Carrell (1991) Crystal structure of uncleaved ovalbumin at 1.95 Å resolution, J. Mol. Biol. **221**, 942–959.
5. M. A. McKenzie and F. H. White Jr. (1991) Lysozyme and -Lactalbumin: Structure, function, and interrelationships, Adv. Prot. Chem. **41**, 173–315.

6. B. F. Anderson, H. M. Baker, E. J. Dodson, G. E. Harris, S. V. Rumball, J. M. Waters, and E. M. Baker (1987) Structure of lactoferrin at 3.2 Å resolution, Proc. Nat. Acad. Sci. USA **84**, 1769–1773.

Alcohol Dehydrogenase (ADH)

ADH is a type of enzyme that catalyzes the reversible interconversion of an alcohol to an aldehyde/ketone [EC 1.1.1.1]. The substrate specificity is often wide, but it typically includes at least some activity with ethanol. The **coenzyme** is often **NAD$^+$**. ADH was initially purified from yeast (YADH) and from horse liver (LADH), sources from which it is commercially available. It is, however, now known to be widespread, with at least some forms present in **eukaryotes**, **prokaryotes** and **archaeabacteria** in general. It has been well studied at the protein and **DNA** levels from many sources. The "classical" forms of ADH are Zn-containing metalloproteins with subunits of ~40 kDa (~350 to 390 residues) (1). They are now considered part of a larger protein family (see Protein Evolution), known as medium-chain dehydrogenases/reductases (**MDR**) (2).

Although ADH is frequently regarded as well understood, much is still unknown, and novel findings of general interest are constantly obtained:

1. ADH is no longer just an enzyme, but a whole system of great complexity, involving other protein families and a multiplicity of MDR forms.
2. another such family is (short-chain dehydrogenases/reductases) SDR (3). The major ADH of insects is this type, and SDR enzymes are numerous, including **hormone**-converting and regulatory enzymes in humans and all living forms.
3. MDR-ADH occur as different classes (4) and **isozymes**. They exhibit distinct evolutionary patterns, repeated evolutionary origins, and varying properties. At least six classes and eight genes have been discerned in mammals, but these numbers are likely to grow; they differ among species because of recent gene duplications. Expressions differ with organ, tissue, and age, including special fetal forms.
4. Functionally, the ADH system has long been an enigma, but recent results suggest that it has important roles. Metabolically, ADH is associated with aldehyde dehydrogenase, which is part of another large family. Medically, both activities are important in alcohol metabolism and in several disease states but also in vision and in cellular regulation and differentiation (5, 6).

1. MDR-ADH

1.1. Classes in Vertebrates

Mammals and most vertebrates contain different classes of MDR Zn-containing ADH enzymes. These classes differ substantially in substrate specificity and in their immunological, chromatographic, and electrophoretic properties (4). They constitute separate forms that are intermediate in their properties between isozymes and distinctly different enzymes, and they differ in primary structures by about 30% but have closely related conformations (Fig. 1). The classes reflect a series of gene duplications, which occurred largely at early vertebrate times (8). Later duplications in individual lines have given rise to intraclass isozymes. The subunits of isozymes can hybridize into mixed dimers that reflect the subunit mixture, but those of different classes do not.

Figure 1. Structure of human ADH class I (7). The diagram and the modeling of ethanol were made with the program ICM (Molsoft, Metuchen, NJ) from coordinates in the data bank.

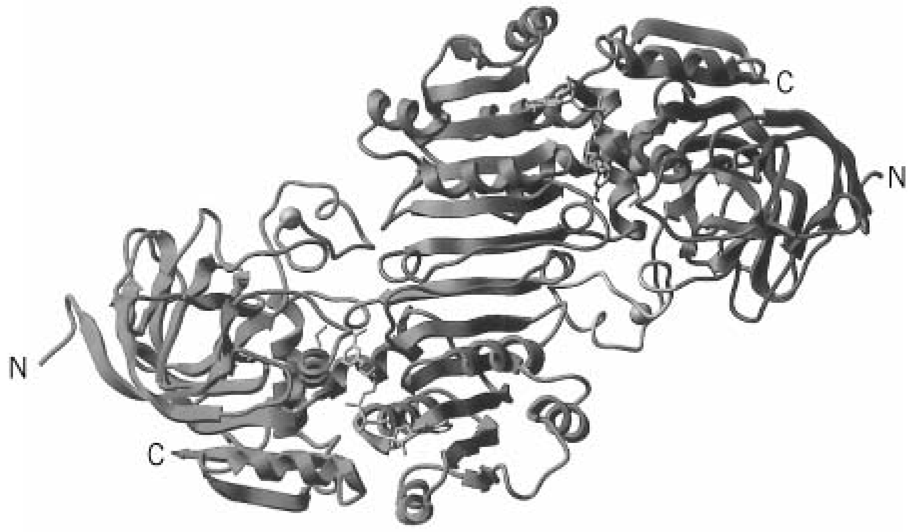

Class I contains the classical ADH enzyme, which is present in large amounts in liver but in lower amounts in many other organs. It is involved in ethanol metabolism and in liver function. It has good enzymatic activity with primary alcohols, cyclohexanol, retinols, and many other alcohols, plus their corresponding aldehydes. Isozymes occur and are largely species specific. The horse ADH subunits E and S derive from two separate genes and the human subunits a, b, and g from three genes. The a subunit is expressed in the fetus and b and g in the adult. The b and g types also exhibit further variability from alleles that have different population distributions in Caucasians and Orientals. This population variation, together with other alleles of the next enzyme of alcohol metabolism (aldehyde dehydrogenase), explains the different sensitivity to ethanol consumption of Caucasians and Orientals.

Class II ADH is highly variable. It is also expressed in the liver but in lower amounts. Thus far it is without a recognized functional role, but in humans it has a higher K_m for ethanol, and hence is of little importance in ethanol metabolism.

Class III ADH is expressed universally in cells and organs, and is identical to glutathione (GSH)-dependent formaldehyde dehydrogenase (EC 1.2.1.1). In the absence of GSH, it is a dehydrogenase toward long-chain alcohols and is largely inactive with ethanol. The $\boldsymbol{K_m}$ for ethanol is >3 M , so there is activity only at high ethanol concentrations. In the presence of GSH, class III ADH is active with the GSH/formaldehyde adduct, hydroxymethyl-GSH, when it functions as a formaldehyde dehydrogenase, producing formic acid.

Class IV ADH is present in the stomach and in skin (epithelia). It is the most ethanol-active form and has been discussed in relation to first-pass ethanol metabolism and to retinol dehydrogenase function. Both roles, however, are far from established.

Little is known about the remaining enzyme classes in vertebrates.

Class III is the evolutionary ancestor, which is apparent from phylogenetic trees (Fig. 2), the rates of change in present forms, and in apparently being the only MDR-ADH in invertebrates. However, final judgment of the phylogeny must await characterization of further forms. Additional gene duplications probably remain to be discovered, and the true evolutionary relationships may be complex, involving both extant and extinct forms.

Figure 2. Evolutionary tree of animal ADH. The deviating class I form of bony fish is indicated by a star. The tree was calculated using ClustalW (2) with corrections for multiple substitutions.

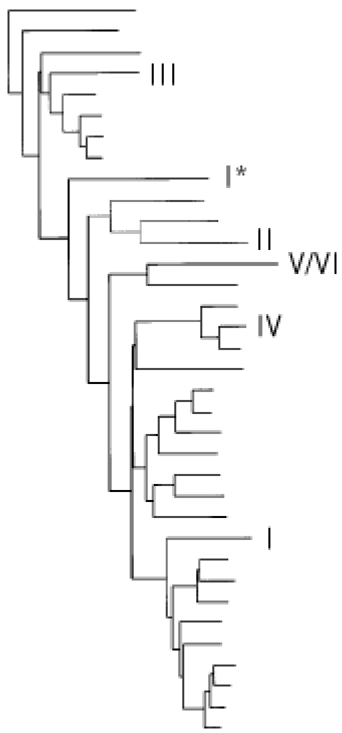

In molecular terms, the classes exhibit different evolutionary patterns. Class III is like an enzyme of basic metabolism, and has relatively constant functional properties among species and variation primarily in the nonfunctional parts of the protein (Fig. 3). Class I is the result of an early gene duplication from class III, whereas class IV in turn diverged from the class I line. Special hybrid forms of class I/III (in fish), II/I (in birds) and IV/I (in amphibians) have been traced and may reflect either the phylogeny or simply additional gene duplications. In short, the ADH system has many interesting evolutionary features (8).

Figure 3. Variable segments in subunits of ADH. Those subunits that vary between class I enzymes affect functional segments, typical of a functionally variable protein. Those subunits variable between class III enzymes affect superficial segments, typical of a functionally constant protein (3).

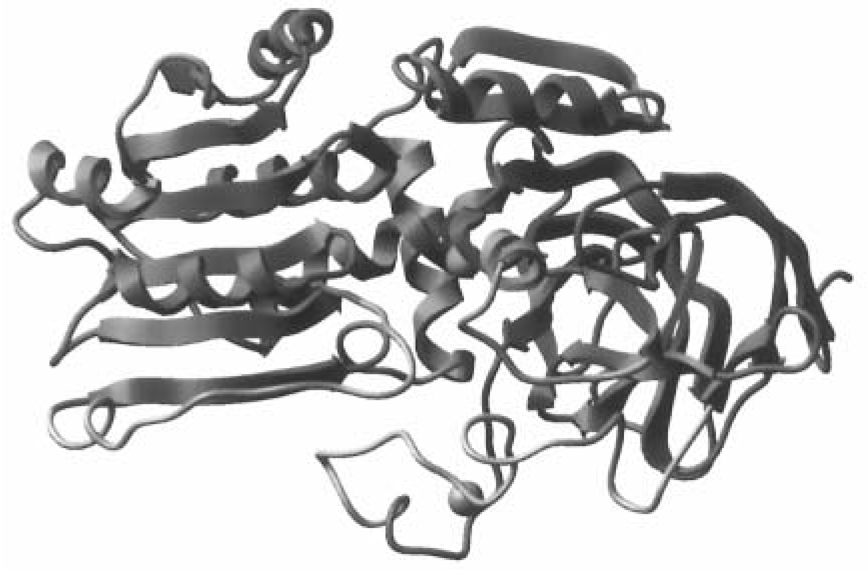

1.2. Yeast, Plants, Other Nonvertebrate Forms

Nonvertebrate MDR-ADH are also frequent and have at least two classes. One is the class III enzyme, which has GSH-dependent formaldehyde dehydrogenase activity, as expected from the ancestral properties noted previously. The other is ethanol-active MDR-ADH: yeast ADH (YADH, from at least three genes) and plant ADH (PADH). YADH has greater ADH activity than LADH because of weaker **coenzyme** binding and consequently a greater turnover rate, because coenzyme dissociation is the rate-limiting step. Although YADH and PADH are related to LADH structurally and functionally, they are products of gene duplications separate from that leading to class I ADH. Combined, all of these ethanol-active forms suggest that ADHs active with alcohol have arisen several times during evolution, probably by functional **convergence**. Presumably all or many of these ethanol-active forms are derived from the ancestral class III line (Fig. 4), but they can differ in quaternary structure. Ethanol-active YADH is a tetramer, whereas yeast class III ADH is a dimer.

Figure 4. Functional convergence toward ethanol dehydrogenases in different lines of living organisms, emphasizing the repeated appearance of ethanol-activity, many separate gene duplications, and an apparent MDR-ancestral nature of class III. Dashed lines indicate unknown relationships, and dotted lines low activity with ethanol. Segment-minus forms lack internal segments (Fig. 1) and are tetrameric. The remaining forms are dimers. Apart from the gene duplications shown, which lead to ethanol-active dehydrogenases, additional branchings lead to cinnamyl ADH (in plants), sorbitol dehydrogenase (in animals), threonine dehydrogenase (in prokaryotes), several reductases (in prokaryotes and eukaryotes), and additional enzymes.

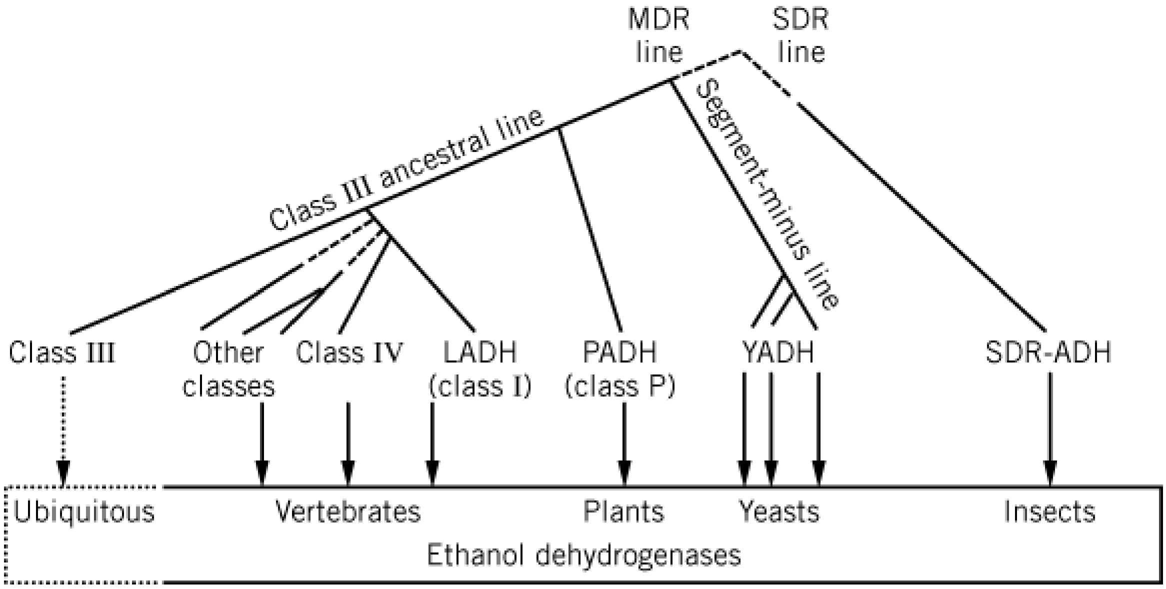

1.3. Function

Liver ADH (class I) is the major metabolic enzyme for ethanol, either ingested or produced in the intestine, and for other alcohols. Overall, the formaldehyde specificity of the ancestral form (class III), the multiplicity of all ADH systems, and the gradual changes in substrate specificity suggest that the whole ADH system is a basic enzyme, together with aldehyde dehydrogenase, in cellular defense reactions against alcohols and aldehydes, converting them to acidic end products. The validity of this general role of ADH is supported by the fact that the only animals apparently lacking ADH (except for formaldehyde-active class III) are marine invertebrates (10), whose environment is low in alcohol and aldehyde levels. The formaldehyde dehydrogenase activity of class III ADH is universal and constant throughout the living world, although the K_m and enzymatic efficiencies are increased in microorganisms. This permits life at higher aldehyde concentrations (11) and suggests a general defense function for the ADH system.

Additional functions of individual classes are likely. Class IV has been discussed relative to its possible role in retinal formation important for rhodopsin and vision (6) and in retinoic acid formation, which important for vertebrate growth and differentiation (5). Similarly, special forms of ADH and aldehyde dehydrogenase are involved in the fatty acid cycle in dermal wax and plasmalogen formation in the central nervous system and are associated with an inborn error of metabolism (Sjögren-Larsson syndrome) affecting the corresponding genes (12).

1.4. Other MDR Enzymes

Many enzymes active on other alcohols or polyols are related to MDR-ADH in structure and origin. Among these are sorbitol dehydrogenase, threonine dehydrogenase, quinone oxidoreductase, the enoyl reductase component of the fatty acid synthesis machinery, and enzymes with undefined functions, like VAT-1 of synaptic membranes (2). These enzymes are similar conformationally and in their overall active-site relationships. But they also differ markedly, including functionally, in that all do not have the active-site zinc typical of MDR-ADH. This suggests that they have different enzymatic mechanisms. Zinc is also absent in quinone oxidoreductase, which is a crystallin in ocular lenses of some animals.

2. SDR-ADH

Insect ADH is the only well known SDR-ADH, but hundreds of other SDR enzymes are known. These enzymes work on hydroxyl groups of a multitude of sugar, steroid, prostaglandin, and other compounds. They also include reductases, with other activities (like double-bond saturation), and enzymes of no less than three of the enzyme classes in general (oxidoreductases, lyases, and isomerases (3)).

3. Other ADH Forms

ADH activity is also known in enzymes other than the MDR and SDR forms, including iron-activated forms (13). Prokaryotes have several different forms, including long-chain alcohol dehydrogenases (14) and methanol dehydrogenases. They may even have MDR relationships, and this definitely applies to other special prokaryotic forms, such as factor-dependent formaldehyde DH (15), which is apparently the equivalent of class III MDR-ADH in **Gram-positive** bacteria.

Bibliography

1. C.-I. Brändén, H. Jörnvall, H. Eklund, and B. Furugren (1975) *The Enzymes*, 3rd ed., chap. "11", pp. 103–190.
2. B. Persson, J. S. Zigler Jr., and H. Jörnvall (1994) Eur. J. Biochem. **226**, 15–22.
3. H. Jörnvall et al. (1995) Biochemistry **34**, 6003–6013.
4. B. L. Vallee and T. J. Bazzone (1983) Curr. Top. Biol. Med. Res. **8**, 219–244.
5. G. Duester (1996) Biochemistry **35**, 12221–12227.
6. A. Simon et al. (1995) J. Biol. Chem. **270**, 1107–1112.
7. T. D. Hurley et al. (1994) J. Mol. Biol. **239**, 415–429.
8. O. Danielsson et al. (1994) Proc. Natl. Acad. Sci. USA **91**, 4980–4984.
9. J. D. Thompson, D. G. Higgins, and T. J. Gibson (1994) Nucleic Acids Res. **22**, 4673–4680.
10. M. R. Fernández et al. (1993) FEBS Lett. **328**, 235–238.
11. M. R. Fernández et al. (1995) FEBS Lett. **370**, 23–26.
12. V. De Laurenzi et al. (1996) Nature Genet., **12**, 52–57.
13. R. K. Scopes (1983) FEBS Lett. **156**, 303–306.
14. T. Inoue et al. (1989) J. Bacteriol. **171**, 3115–3122.
15. P. W. van Ophem, J. Van Beeumen, and J. A. Duine (1992) Eur. J. Biochem. **206**, 511–518.

Suggestions for Further Reading

16. H. Weiner et al., eds. (1987 to 1997) *Enzymology and Molecular Biology of Carbonyl Metabolism*, Vols. **1–6**, Plenum, New York. Up-to-date summaries on ADH and the metabolically-related enzymes. Published biannually from the conference series with the same name, Vol. **6** (1997) now in press.
17. H. Eklund and C.-I. Brändén (1987) Alcohol dehydrogenase. Biol. Macromol. Assembl. **3**, 74–142.
18. W. F. Bosron, T. Ehrig, and T.-K. Li (1993) Genetic factors in alcohol metabolism and alcoholism. Seminars Liver Dis. **13**, 126–135.
19. J. Shafqat et al. (1996) Pea formaldehyde-active class III alcohol dehydrogenase: Common derivation of the plant and animal forms but not of the corresponding ethanol-active forms (classes I and P). Proc. Natl. Acad. Sci. USA **93**, 5595–5599.

Aligning Sequences

The most basic activity in sequence analysis involves aligning protein or nucleotide sequences together. This need arises due to the processes of molecular evolution: gene duplication followed by continual **divergence** of the sequences through the accumulation of mutations over time. Comparative biological analysis, which has long been such a powerful tool for biologists (as exemplified by Linnaeus and Darwin), is arguably even more applicable in sequence analysis than in any other branch of biology, because it can be applied to an enormous number of character states at the level of individual residues in nucleic acid or protein sequences. First, however, related sequences must be correctly aligned before the power of comparative analysis can be brought to bear. Because of the difficulty of aligning highly diverged sequences, and the many applications of sequence alignment, this is one of the most active areas for method development in computational biology.

Alignment tasks generally divide into pairwise sequence alignment and multiple sequence alignment, although the underlying algorithms may share many details. The most sensitive methods for aligning sequences belong to the class of algorithms known as dynamic programming (or minimum string edit) that were initially developed for applications in text comparison. Two of the dynamic programming algorithms most used in biology are usually known as Needleman–Wunsch (1) and Smith–Waterman (2), after the researchers who first applied them to biological sequences. Because these algorithms allow gaps to be inserted at any position in the sequences, they are computationally slow. By contrast, word comparison algorithms, which do not allow gaps, are much faster, but at the expense of accuracy and sensitivity in aligning sequences.

1. Pairwise Sequence Alignment Algorithms

1.1. Dynamic Programming

The basic algorithm works through a two-dimensional matrix in which every residue in one sequence is scored against every residue in the other sequence (1). The algorithm begins in one corner (eg, top left) of the matrix and ends in the opposite corner (bottom right). At each point in the matrix, the algorithm iterates the same set of choices. Typically, it chooses which of three existing paths scores best when extended into the current point: (i) match the residues and continue aligning from the previously aligned residue pair, or (ii) pay the penalty and insert a one-residue gap into sequence X, or (iii) pay the penalty and insert a one-residue gap into sequence Y (see Gap Penalty). The algorithm is guaranteed to find the best path through the matrix, allowing for gaps at any position in either sequence. Scores for matching the residues are taken from residue exchange, or mutation, matrices. For nucleotide sequences, these are usually quite simple: for example, +1 for an *identity*, 0 for a *transition*, and –1 for a *transversion*. For proteins, typical exchange matrices are the more complex 20 * 20 *PAM* (point accepted mutation) matrices introduced by Margaret Dayhoff (3), or subsequently derived PAM series derived from larger alignment datasets (4, 5). A PAM 250 matrix is shown in Figure 1. Gap penalties are used to control the frequency and length of gaps inserted in the sequences. Where appropriate, varying gap penalties in a position-specific manner can improve the alignment.

Figure 1. PAM250 amino acid exchange matrix developed by Gonnet and colleagues (4) and superseding the original D
acids have positive log-odds exchange values while dissimilar pairs have negative values. All positive scores are colored
purple highlights similar pairs of hydrophobic residues, and green indicates similar pairs of hydrophilic residues. The hig
aromatic residues (Phe, Tyr, Trp) and are stronger than exact matches of highly mutable residues such as Ser. The strong
hydrophobic residues and small or negatively charged residues.

C	S	T	P	A	G	N	D	E	Q	H	R	K	M	I
11.5	0.1	–0.5	–3.1	0.5	–2.0	–1.8	–3.2	–3.0	–2.4	–1.3	–2.2	–2.8	–0.9	–1.1
	2.2	1.5	0.4	1.1	0.4	0.9	0.5	0.2	0.2	–0.2	–0.2	0.1	–1.4	–1.8
		2.5	0.1	0.6	–1.1	0.5	0.0	–0.1	0.0	–0.3	–0.2	0.1	–0.6	–0.6
			7.6	0.3	–1.6	–0.9	–0.7	–0.5	–0.2	–1.1	–0.9	–0.6	–2.4	–0.6
				2.4	0.5	–0.3	–0.3	0.0	–0.2	–0.8	–0.6	–0.4	–0.7	–0.8
					6.6	0.4	0.1	–0.8	–1.0	–1.4	–1.0	–1.1	–3.5	–4.5
						3.8	2.2	0.9	0.7	1.2	0.3	0.8	–2.2	–2.8
							4.7	2.7	0.9	0.4	–0.3	0.5	–3.0	–3.8
								3.6	1.7	0.4	0.4	1.2	–2.0	–2.7
									2.7	1.2	1.5	1.5	–1.0	–1.9
										6.0	0.6	0.6	–1.3	–2.2
											4.7	2.7	–1.7	–2.4
												3.2	–1.4	–2.1
													4.3	2.5
														4.0

Residue Identity
Hydrophobic Similarity
Hydrophilic Similarity

Dynamic programming algorithms work through a two-dimensional matrix of area M*N in aligning sequences of lengths M and N. Therefore the computational requirement [usually symbolized as O(MN)] has a constant factor for the calculation, multiplied by the two sequence lengths. To obtain an alignment, the algorithm makes a first pass to determine the end of the highest scoring matched segment and then a second pass working back to obtain the alignment. If only the highest score, but not the actual path, is needed (as in a database search), then only the first pass need be done. Naive implementations that first plot the whole matrix to an array will also use O(MN) memory. Because the algorithm works through the array systematically, however, it is unnecessary to store the whole array in memory. Memory-efficient implementations of the first pass are straightforward, because the alignment is not being kept (6). The second pass, to obtain the alignment, is more complicated, but memory-efficient recursive methods have been developed that have allowed large alignment tasks to be ported to small personal computers, with a small but acceptable loss in calculation speed (7-9).

1.2. Global Alignment

The standard Needleman–Wunsch algorithm (1) finds the optimal full-length alignment for a pair of sequences. Global alignment is appropriate where sequences are known to be both **homologous** and collinear and is therefore often used for multiple alignment of sequence families.

1.3. Best Local Alignment

Variants of the Smith–Waterman algorithm (2) find the optimal alignment that has a positive value for the path for a given pair of sequences. Except for highly related sequences, the best local alignment is a partial match between the sequences. Residue exchanging mutation matrices, such as *PAM*250, provide log-odds scores for the likelihood that a pair of residues will exchange as a result of mutation: Similar residues that exchange easily have positive log scores, while dissimilar residues have negative log scores. The best local alignment is taken as the highest-scoring continuously positive path. This algorithm is appropriate under conditions where sequences are not known to be both fully homologous and collinear—for example, multi*domain* proteins, or DNA regions containing rearrangements. Smith–Waterman type algorithms underlie the most sensitive methods for database searching by sequence homology yet to be devised. Because of the computational cost, they are not applied as often as search methods using ungapped alignment algorithms.

The Waterman–Eggert (10) extension of the algorithm will return sets of suboptimal paths that do not intersect with the optimal path, and in this way it can find repeats in sequences.

1.4. Best Local Ungapped Alignment

Widely used database search tools, such as BLAST (11) and FASTA (12), search for the highest scoring matched regions without allowing for gaps. Word searches and other ungapped alignment methods are much faster than dynamic programming approaches, but at the expense of sensitivity. Thus these methods are likely to miss homologous but divergent matches. To improve the results, FASTA does a second dynamic pass on the set of top hits. For a small reduction in search speed, BLAST2 examines the gap cost between the set of ungapped positive matches between two sequences and returns composite best locally aligned regions, including gaps whenever the score is still positive. The latter algorithm is likely to approach Smith–Waterman sensitivity except for the most unusual alignment circumstances.

2. Multiple-Sequence Alignment

This is a set of homologous protein or nucleotide sequences that have been correctly aligned, allowing for the presence of indels. Figure 2 shows an aligned region for some elongation factor TU sequences.

Figure 2. Part of a multiple alignment of 14 prokaryotic EFTU sequences using the one-letter code for amino acids. Gap
by asterisks are completely conserved, columns marked by colons are strongly conserved, and columns marked by perio
bottom shows the conservation in the columns. Color is an essential aid to sequence analysis and is used here to highligh
properties. Inverted characters indicate poorly matching regions of sequence. Some of these are due to natural sequence
sequence determination causing frameshifted regions: EFTUSPIPL 203–206, EFTUODOSI 234–243, EFTUMYCPN 27
errors may lead to false inferences: If R-285 were completely conserved, it would be a candidate functional residue, whil
incorrectly suggests a surface loop. See color insert.

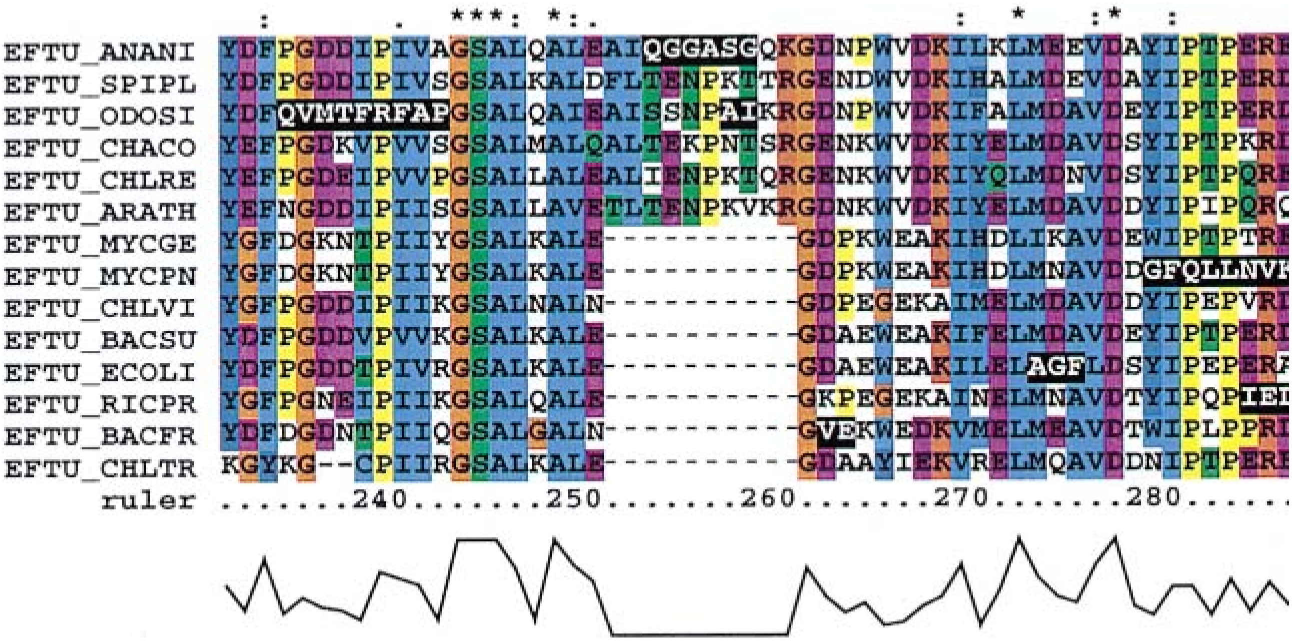

2.1. Uses of Multiple Alignments

Multiple alignments are indispensable in computational biology. They are the basic dataset used to construct phylogenetic trees, which are themselves important computational tools (eg, for weighting sequences by divergence) as well as providing insight into past evolution. They reveal conserved residues that are likely to be structurally or functionally (eg, in catalysis) important and unconserved positions that either are unimportant or have acquired a change of function (Fig. 2). They improve the accuracy of many sequence analysis functions as compared to single sequences, such as **secondary structure prediction** (13), coiled-coil prediction (14), and **transmembrane helix** prediction (15). They are useful as the query input for the most sensitive homology searches (alignment profile (16) and hidden Markov model searches (17)) and can be used to detect divergent homologues that single-sequence queries cannot pick up. They are useful in the detection of **domains** and in defining their boundaries in modular, mosaic proteins (18). Multiple alignments of folded RNAs are a prime resource used in determining their secondary and tertiary structures, by mapping residue conservation and long-distance-coupled mutations (19, 20). DNA multiple alignments are used for identifying conserved signals, such as **promoter** elements and **RNA splice** sites (21).

2.2. Multiple-Alignment Algorithms

So far it has been necessary to adopt heuristic strategies to generate multiple alignments, because formally correct methods have been computationally impractical to implement. The ideal method to align N sequences would be N-dimensional dynamic programming, as this would be guaranteed to find the optimal path (ie, the optimal multiple alignment) in an N-dimensional matrix. Unfortunately the computer time required to align N sequences of length l is $O(l^N)$ and is impractical for more than three or four sequences, although by limiting the search space to likely regions, the MSA program can align up to eight sequences (22). Another broad class of methods, those that iterate toward an optimized score for the alignment, are still computationally intensive but are becoming practical with increasing computer power. These include a number of approaches, some of which may be used in combination, such as global minimization, genetic algorithms, and trained **neural networks** (23, 24). The goal is to harness a good model description of a multiple-sequence alignment with an effective iteration strategy, so as to get high-quality alignments in a practical timescale. In the meantime, widely used alignment programs such as Clustal W (25) follow the heuristical clustered alignment strategy.

2.3. Progressive Clustered Alignment

This two-step approach was introduced by Feng and Doolittle (26) in an attempt to minimize errors in the final multiple alignment, by aligning the most similar sequences first and the most divergent ones last. The set of unaligned sequences are first aligned in pairwise fashion to each other, so that a matrix of the approximate pairwise similarities may be obtained. A matrix-based tree construction method, such as Neighbor-Joining (27), is used to construct a dendrogram linking the sequences according to their observed similarities. Guided by the dendrogram branching order, the sequences are then sequentially aligned together using dynamic programming, beginning with the most closely related sequences and ending by merging the most divergent groups by profile alignment. This procedure minimizes alignment errors, which become more likely with increasing sequence divergence, becoming a problem for proteins less than 25% to 30% identical in sequence. The final alignment should always be examined for misalignment, especially of the more divergent sequences, because such errors are likely to be present in any but the most straightforward multiple alignment task.

The sensitivity of the basic clustered alignment strategy can be improved by several modifications, such as weighting the sequences by divergence and position-specific gap penalties (25). Where tertiary structure information is available, gap penalty masks can be employed to guide the gaps into regions of sequence that are expected to be tolerant of indels (28).

2.4. Profile Alignment

A set of aligned sequences can be aligned to one or more new sequences by treating the group much as a single sequence. The score for one alignment column can be obtained by summing the log-odds residue exchange scores for the observed set of amino acids (16), correcting for sequence relatedness by downweighting similar sequences (25). Conserved alignment columns score more highly than unconserved columns, where the log-odds scores tend to cancel each other. Gap penalties can be lowered at existing indels, because gaps in new sequences are more likely at these positions than at ungapped positions. The improvement in signal to noise provided by the extra information in the alignment means that a profile alignment is more accurate than independent pairwise alignment of the same set of sequences. As well as being used to merge aligned groups in the clustered alignment strategy, profiles provide a sensitive search strategy to find highly divergent homologues and are one of the main sequence analysis tools for identifying protein domain families (18).

2.5. Hidden Markov Model (HMM) Alignment

HMMs are a class of probabilistic models, applicable when the components of a complex linked system behave independently (a so-called Markov chain). Up to a point, this is valid for residue mutations in globular protein sequences, and HMMs are being applied increasingly in multiple-alignment algorithms and profile-type database searches (17, 29). The models are more complex than the widely used PAM model for protein evolution introduced by Margaret Dayhoff (3), providing both advantages and disadvantages. On the plus side, the models provide direct probabilities for evaluating database search matches, which can include multiple matches in a repeated sequence and can formally treat biological complexities such as splice junctions in genomic sequence. On the debit side, the extra parameters lead to more complex optimization problems at several levels. Thus, inexperienced users may set up poorly optimized HMMs while, for program developers, there is a problem as to whether the most appropriate HMMs are being applied to sequence evolution. It is important for the user not to be seduced by technical jargon, but to justify the use of newer methods such as these on the basis of convincing results.

3. Error in Sequence Alignments

Errors are very common and invalidate any conclusions obtained by methods based on sequence alignments (see Fig. 2). The three main sources of error are: the input sequences, mistakes by the user, or alignment algorithm failure. Causes and effects of error are manifold; some major ones are discussed below.

3.1. Errors in the Input Sequences

Experimental errors in determining sequences include double-insert cloning errors, truncated cDNA clones, base insertion or deletion causing translation **frameshifts**, and translation with inappropriate genetic code (eg, for plastid-encoded proteins). Figure 3 shows an example of a frameshift error in a database entry. Algorithm failure during alignment may be induced by sequence error, such as frameshifted regions, in which the sequences are no longer similar, and may induce incorrect gap placement (Fig. 2). Errors in sequences are very common and likely to be present in any sequence family (30, 31).

Figure 3. Frameshifted segment in the *Mycoplasma pneumoniae* EFTU sequence revealed by comparing the DNA to the closely related *Mycoplasma genitalium* EFTU using a dynamic programming three-frame comparison allowing shifts be translation frames (30). Exclamation points mark the frameshift sites. The first frameshift is caused by a base being drop and the second frameshift is caused by a base being added, thereby returning to the original translation frame. See Figure multiple alignment spanning this region.

```
                               ******************************************  **
M.genitalium EFTA 151          AEEVRDLLTSYGFDGKNTPIIYGSALKALEGDPKWEAKIHDLIKA
Translation                    AEEVRDLLTSYGFDGKNTPIIYGSALKALEGDPKWEAKIHDLMNA
M.pneumoniae DNA  619          ggggcgttattgtggaaacaatgtgcagcgggcatggaacgtaag
                               caatgattccagtagaaccttagcctactagacagacataattact
                               aagatcaattccttcgcctttttatagtatttggatgcttagtat


                               **** ****!   ********************************
M.genitalium EFTU 200          IPTPTREVDG+++PFLLAIEDTMTITGRGTVVTGRVERGELKVGQ
Translation                    IPTPEREVD^^^^PFLLAIEDTMTITGRGTVVTGRVERGELKVGQ
M.pneumoniae DNA  765          acacgcgggAAACctttgaggaaaaagcgaggagcggcggtaggc
                               tcccagata    ctttctaactctcgggcttcggtaggatatga
                               tattatagc    gcggacaccggttcttcgtctgtattagaata
```

Further errors can arise in preparing sequence database entries. These can affect any part of the entry and can have particularly unpredictable consequences. However, the most common annotation errors are undoubtedly in predicted translation products and are a consequence of the limited accuracy of current gene prediction algorithms; that is, despite high-quality DNA sequence, the predicted protein sequence might contain artificially translated **introns**, missed exons, or terminal truncations or might be an artificial fusion product of two independent genes. Protein sequence alignments can often help in identifying translation problems.

3.2. Mistakes by the User
Generally these are due to inadequate attention to detail. Erroneous inclusion of nonhomologous sequences in the input set is quite common, particularly if keyword searches are used to extract a set of sequences; there are many examples of unrelated proteins performing equivalent functions, as well as sequences that have functions incorrectly ascribed to them. Another source of error occurs during the alignment process, when parameters may be set poorly. Trial and error is usually needed to find the parameters that best suit a particular group of sequences. For example, insertion of too few or too many gaps may suggest that the gap penalties are not optimal. It is important to take the time to get a basic understanding of how a given program works, or it is unlikely to do the best job.

3.3. Algorithm Failure
Clustered alignment is a heuristic strategy that is not guaranteed to find the optimal multiple alignment. The alignment process is likely to compound errors introduced by the user or in the input sequences. Alignment mistakes will also be made in difficult alignment cases, even when there are no input errors. There are many instances of homologous proteins having diverged over long periods of time, so that they have apparently very little sequence similarity. The “twilight zone” where sequence similarity merges with sequence dissimilarity is in the range 20% to 25% identity. (Five percent identity would be a random match for protein sequence, neglecting residue biases. In practice, given residue biases and gap insertions to maximize the similarity, the expectation for random sequence matches approaches ~15% identity, but higher for short or biased sequences. There is, however, no *a priori* reason why correctly aligned but extremely divergent proteins should not be found with 0% pairwise identity.) Divergent nucleotide sequences are even harder to align, because random similarity is reached at ~25% identity before gaps are added. Wherever possible, alignments need to be checked against additional data available for a sequence family, such as known tertiary structures and whether invariant catalytic residues, or any other known conserved motifs, are correctly aligned.

3.4. Consequences of Errors in Aligned Sequences
Errors in multiple alignments can have disastrous consequences for **phylogenetic** inference on the basis of sequence trees. Sequences with misaligned segments or translation frameshifts are apparently more divergent than they should be from the other sequences. The branch leading to that

sequence will then have a longer length (which erroneously implies a more rapid molecular clock) and the branch point may migrate toward the centre of the tree, giving a false order of divergence. Such incorrect phylogenies may be quite exciting when they seem to refute established viewpoints. Two rules of thumb are useful: (i) Infinitely more wrong tree topologies can be generated than right ones, and (ii) wrong phylogenies are more interesting than right phylogenies. Incautious advocacy of a wrong phylogeny can waste many peoples' time.

Errors also disrupt evaluation of conserved sites in sequences (Fig. 2). Catalytic residues are often absolutely conserved, so a single misaligned sequence may lead to rejection of the correct site. Most conserved residues have a structural role: Structure prediction for protein uses conserved **hydrophobic** residues and, for RNA, conserved base-pairing residues. Misalignments disrupt the conservation periodicities, leading to rejection of the correct structures. Terminally truncated sequences of multidomain proteins can lead to false inferences for the domain boundaries, which are very usefully defined by coincidence with the protein *N*- or *C*-termini.

Bibliography

1. S. B. Needleman and C. D. Wunsch (1970) J. Mol. Biol. **48**, 443–453.
2. T. F. Smith and M. S. Waterman (1981) Adv. Appl. Math. **2**, 482–489.
3. M. O. Dayhoff, R. M. Schwartz, and B. C. Orcutt (1978) In *Atlas of Protein Sequence and Structure*, Vol. **5**, Suppl. 3 (M. O. Dayhoff, ed.), NBRF, Washington, pp. 345–352.
4. S. A. Benner, M. A. Cohen, and G. H. Gonnet (1994) Protein Eng. **7**, 1323–1332.
5. G. Vogt, T. Etzold, and P. Argos (1995) J. Mol. Biol. **249**, 816–831.
6. O. Gotoh (1982) J. Mol. Biol. **162**, 705–708.
7. E. W. Myers and W. Miller (1988) CABIOS **4**, 11–17.
8. J. D. Thompson (1995) CABIOS **11**, 181–186.
9. J. A. Grice, R. Hughey, and D. Speck (1997) CABIOS, **13**, 45–53.
10. M. S. Waterman and M. Eggert (1987) J. Mol. Biol. **197**, 723–728.
11. S. F. Altschul, W. Gish, W. Miller, E. W. Myers, and D. J. Lipman (1990) J. Mol. Biol. **215**, 403–410.
12. W. R. Pearson and D. J. Lipman (1988) Proc. Natl. Acad. Sci. USA **85**, 2444–2448.
13. B. Rost and C. Sander (1993) J. Mol. Biol. **232**, 584–599.
14. A. Lupas, M. Van Dyke, and J. Stock (1991) Science, **252**, 1162–1164.
15. B. Persson and P. Argos (1994) J. Mol. Biol. **237**, 182–192.
16. M. Gribskov, A. D. McLachlan, and D. Eisenberg (1987) Proc. Natl. Acad. Sci. USA, **84**, 4355–4358.
17. S. Eddy (1996) Curr. Opin. Struct. Biol. **6**, 361–365.
18. P. Bork and T. J. Gibson (1996) Methods Enzymol. **266**, 162–184.
19. C. R. Woese, R. R. Gutell, R. Gupta, and H. F. Noller (1983) Microbiol. Rev. **47**, 621–669.
20. F. Michel and E. Westhof (1990) J. Mol. Biol. **216**, 585–610.
21. R. F. Doolittle (1990) *Molecular Evolution: Computer Analysis of Protein and Nucleic Acid Sequences, Methods in Enzymology*, Vol. 183, Academic Press, San Diego, CA.
22. D. J. Lipman, S. F. Altschul, and J. D. Kececioglu (1989) Proc. Natl. Acad. Sci USA **86**, 4412–4415.
23. O. Gotoh (1996) J. Mol. Biol. **264**, 823–838.
24. C. Notredame and D. G. Higgins (1996) Nucleic Acids Res. **24**, 1515–1524.
25. J. D. Thompson, D. G. Higgins, and T. J. Gibson (1994) Nucleic Acids Res. **22**, 4673–4680.
26. D.-F. Feng and R. F. Doolittle (1987) J. Mol. Evol. **25**, 351–360.
27. N. Saitou and M. Nei (1987) Mol. Biol. Evol. **4**, 406–425.

28. A. M. Lesk, M. Levitt, and C. Chothia (1986) Protein Eng. **1**, 77–78.
29. A. Krogh, M. Brown, S. Mian, K. Sjölander, and D. Haussler (1994) J. Mol. Biol. **235**, 1501–1531.
30. E. Birney, J. D. Thompson, and T. J. Gibson (1996) Nucleic Acids Res. **24**, 2730–2739.
31. J. M. Claverie (1993) J. Mol. Biol. **234**, 1140–1157.

Suggestions for Further Reading

32. R. F. Doolittle (1990) *Molecular Evolution: Computer Analysis of Protein and Nucleic Acid Sequences , Methods in Enzymology*, Vol. 183, Academic Press, San Diego, CA.
33. R. F. Doolittle (1996) *Computer Methods for Macromolecular Sequence Analysis, Methods in Enzymology*, Vol. 266, Academic Press, San Diego, CA.
34. D. Sankoff and J. B. Kruskal (1984) *Time Warps, String Edits and Macromolecules: The Theory and Practice of Sequence Comparison*, Addison-Wesley, Reading, MA.
35. M. S. Waterman (1989) *Mathematical Methods for DNA Sequences*, CRC Press, Boca Raton, FL.

Alkaline Phosphatase

Alkaline phosphatases (E.C. 3.1.3.1) belong to a family of orthophosphoric monoester phosphohydrolases that have an alkaline pH optimum. Their genes are very frequently used as a **reporter** gene. Alkaline phosphatase activity is most commonly detected by the hydrolysis of 5-bromo-4-chloro-3-indolyl phosphate (BCIP), which, when coupled to the reduction of nitro blue tetrazolium (NBT), forms a formazan and an indigo dye that together form a strong black/purple precipitate (1). In addition, a number of fluorogenic substrates are also available (1). 4-Methylumbelliferyl phosphate (MUP) gives a blue **fluorescent** product upon hydrolysis, and 2-hydroxy-3-naphthoic acid-2-phenylanilide phosphate (HNPP/Fast Red TR) fluoresces with a broad emission peak between 540 and 590 nm and can be observed using either fluorescein or rhodamine filter sets. Molecular Probes Inc. have also developed a proprietary substrate called ELF-97 (Enzyme Linked Fluorescence-97), in which cleavage of the molecule converts it from a soluble phosphate to an insoluble alcohol, with an accompanying shift from weak blue fluorescence to a bright yellow fluorescence (2).

Human placental alkaline phosphatase (hpAP) is most commonly used as a reporter enzyme in nonradioactive detection systems, where the enzyme is linked to other molecular probes (eg, specific antibodies)—for example, for the detection of proteins and nucleic acids by **Western blot**, Southern blot, and **Northern blot** analysis, and most commonly in in situ hybridization. Elegant studies have also been performed in which hpAP is fused to soluble extracellular domains of receptor molecules, which are then used as probes to detect the sites of ligand production *in vivo* and facilitate the subsequent cloning of the ligand genes (3).

Although animals express a number of alkaline phosphatase genes, the human placental isoform has been developed as a reporter gene, because it can be distinguished from other endogenous isoforms through its high thermostability (4). Thus all background endogenous alkaline phosphatase activities, from embryonic, intestinal, and nonspecific genes, can be minimized by preheating tissue preparations up to 80°C for prolonged periods. hpAP also retains its activity following histological processing for wax imbedding and sectioning tissues. In addition, background from endogenous alkaline phosphatases can be further inhibited by the amino acids L-phenylalanine or L-homoarginine.

hpAP has been used in a wide range of applications, including *in vitro* transfection studies and transgenic studies *in vivo*. The sensitivity of hpAP in transient expression assays is equivalent to that of chloramphenicol acetyltransferase (CAT) (see Reporter Genes). A particularly useful variant of hpAP is a cDNA encoding a secreted form of the protein (5, 6) that allows hpAP activity to be assayed by sampling tissue culture medium, giving the benefit of monitoring changes in gene expression with time. In this system, background activities are further eliminated, because the endogenous isoforms are anchored to the cell membranes and do not contribute to the activity in the culture supernatants.

hpAP is also an effective reporter gene to analyze gene expression *in situ* in tissue preparations. hpAP was first used in retroviral vectors to infect small numbers of cells in developing embryos as a tool to study cell fate and lineage analysis; subsequently, hpAP has been used as a robust reporter gene in transgenic mice (7). Indeed, mice that express high levels of hpAP from a ubiquitously expressed **promoter** thrive with no adverse effects. hpAP is particularly useful to use in combination with a second reporter gene, such as *lacZ* (**beta-galactosidase**), in dual labeling studies, as the common substrates are quite distinct and give different colored products (8).

Bibliography

1. D. A. Knecht and R. L. Dimond (1984) Anal. Biochem. **136**, 180–184.
2. K. D. Larison et al. (1995) J. Histochem. Cytochem. **43**, 77–83.
3. J. G. Flanagan and P. Leder (1990) Cell **63**, 185–194.
4. P. Henthorn (1988) Proc. Natl. Acad. Sci. **85**, 6342–6346.
5. T. T. Yang, P. Sinai, P. A. Kitts, and S. R. Kain (1997) Biotechniques, **23**, 1110–1114.
6. B. R. Cullen and M. H. Malim (1992) Methods Enzymol. **216**, 362–368.
7. S. E. DePrimo, P. J. Stambrook, and J. R. Stringer (1996) Transgenic Res. **5**, 459–466.
8. X. Li, W. Wang, and T. Lufkin (1997) Biotechniques, **23**, 874–878.

Alkylation

Alkyl groups have the general formula $C_n H_{2n+1}$–. Alkylation is a reaction that introduces an alkyl group into a compound. Commonly used alkylating agents are olefins, alkyl halides, and alcohols. Biologically important alkylation occurs on nitrogen and oxygen atoms in polynucleotides. Alkylating agents that cause these reactions are mutagens and carcinogens and include methyl methanesulfonate, dimethyl sulfate, *N*-methyl-*N*-nitrosourea, dimethylnitrosourea, 1-methyl-3-nitro-1-nitrosoguanidine, etc. Some alkylating agents are used as anticancer drugs, including cyclophosphamide, nitrogen mustard and its oxide, and triethylenephosphoramide.

Alkylating agents easily alkylate nucleophiles in proteins such as those on cysteine (1), histidine (2), and methionine (3) residues, amino groups (4), and sometimes tyrosine residues and carboxyl groups (5). The most well-known alkylation is that for blocking free thiol groups of cysteine residues to prevent their oxidation, especially in the course of determining the primary structure of a protein (see Protein Sequencing).

1. Reduction and Alkylation of Proteins

The protein at a concentration of 2% (w/v) is dissolved in 0.5 M **Tris** buffer, pH 8.1, containing 6 M **guanidinium chloride** and 0.002 M EDTA and reduced with **dithiothreitol** (50 mol/mol of disulfide bond) at 30° to 40°C for 4 h under nitrogen (6). Then the solution is cooled to room temperature, and iodoacetamide (100 mol/mol of the original disulfide bond) is added, with the addition of NH_4OH as necessary to maintain a constant pH. Other alkylating agents that can be employed instead are iodoacetic acid, 4-vinylpyridine, N-ethylmaleimide, and ethyleneimine.

Bibliography

1. J. Bridgen (1972) Biochem. J. **126**, 21–25.
2. A. M. Crestfield, W. H. Stein, and S. Moore (1963) J. Biol. Chem. **238**, 2413–2420.
3. J. M. Gleisner and R. L. Blaklay (1975) J. Biol. Chem. **250**, 1580–1587.
4. H. J. Goren and E. A. Barnard (1970) Biochemistry **9**, 974–983.
5. K. Takahashi, W. H. Stein, and S. Moore (1967) J. Biol. Chem. **242**, 4682–4690.
6. M. J. Waxdal et al. (1968) Biochemistry **7**, 1959–1966.

Allelic Exclusion

The clonal selection theory put forward by Burnet (1) and Jerne (2) proposes that each single lymphocyte expresses only one single type of antibody. This theory received its first structural confirmation when it was shown that patients with multiple myeloma, a proliferative disorder of plasma cells, had in their serum a highly elevated level of only one molecular species of immunoglobulin, originating from the corresponding malignant clone. Single-cell experiments performed by the Nossal group in Australia (3) indicated that each cell isolated from mouse **immunized** with *Salmonella* antigens produced only one antibody of one given specificity. These observations were in agreement with the clonal theory, but did not explain by which mechanism this was achieved. An elegant approach to that problem was made with the analysis of allotypes in heterozygous animals. Allotypes, as defined by Oudin (4), are antigenic specificities that are shared by a group of animals within a given species. These genetic markers are **allelic** variants of immunoglobulins that are found on both the heavy and light chains. They have been studied extensively in the rabbits, mice, and humans. In most cases, they are the result of a few amino acid substitutions that confer specific epitopes (or allotopes) that can be recognized by specific antibodies. In a rabbit heterozygous for H- and L-chain allotypes, Oudin showed that any given immunoglobulin molecule always had two identical heavy chains and two identical light chains with respect to the corresponding allotypes. This ensured that the Ig molecule was symmetrical and therefore had two identical antibody combining sites, an obvious prerequisite of the clonal theory. The next step was made at the intracellular level, when Pernis et al. (5) showed with specific anti-allotype antibodies that, in a heterozygous rabbit, any given cell always expressed only one allotype of each heavy or light chain. This suggested that a B cell, although **diploid**, had only one of its two alleles functional, and the phenomenon was termed “allelic exclusion.”

The molecular mechanisms that account for this phenomenon could be understood only when the complex mosaic structures of immunoglobulin (Ig) genes were deciphered. Each Ig heavy or light chain contains an NH_2-terminal variable and a COOH-terminal constant region, each encoded by a multiplicity of gene segments. Diversity of the variable regions, which is directly linked to the necessity to produce a very large number of different antibody molecules with a limited number of genes, is generated by specific mechanisms of gene rearrangements that take place exclusively in lymphocytes. The heavy-chain **variable region** is encoded after the rearrangement of three discrete sets of germline gene segments (V_H, D, J_H), and two for the light chain (V_L, J_L). Gene rearrangements take place sequentially during B-cell differentiation in the bone marrow, in a strictly regulated manner, as initially proposed by Alt and Baltimore. The heavy-chain gene segments rearrange D to J_H and V_H to D–J_H. The gene-segment joinings are random, so only one-third of the rearranged genes have an open reading frame. As soon as one rearrangement is in frame, the corresponding m chain is expressed. Whenever the first rearrangement is successful, the second allele remains in the germline configuration, which indicates that a regulatory mechanism has taken place. It was shown by transfection experiments and by making m transgenic mice that the negative feedback inhibition of the gene rearrangement of the second allele was controlled by the m chain itself, when expressed at the cell surface. It was also shown that, at this "preB stage," the m chain was associated with a surrogate light chain (YL), which is monomorphic and composed of two polypeptide chains encoded by the l5 and VpreB genes. Expression of m–YL has been shown to down-regulate the heavy-chain gene rearrangement, whereas rearrangement of the light chain locus is switched on, in the same random reading frames as above. The final result of this complex sequence of events is that, at each locus, only one allele is functional; the other one either remains in the germline configuration or has an out-of-frame rearranged gene, thereby accounting for the allelic exclusion phenomenon.

See also entries Clonal Selection Theory, Gene Rearrangement, and Antibody.

Bibliography

1. M. F. Burnet (1959) *The Clonal Selection Theory of Acquired Immunity*, Vanderbilt University Press, Nashville, TN.
2. N. K. Jerne (1955) The natural selection theory of antibody formation. Proc. Natl. Acad. Sci. USA **41**, 849–857.
3. G. J. V. Nossal, A Szenberg, G. L. Ada, and C. M. Austin (1964) Single cell studies on 19 S antibody production. J. Exp. Med. **119**, 485–502.
4. J. Oudin (1960) Allotypy of rabbit serum proteins. I. Immunochemical analysis leading to the inoliviolualization of seven main allotypes. J. Exp. Med. **112**, 107–124.
5. B. Pernis, G. Chiappino, A. S. Kelus, and P. G. H. Gell (1965) Cellular localisation of immunoglobulins with different allotypic specificities in rabbit lymphoid tissues. J. Exp. Med. **122**, 853–876.
6. F. Alt (1984) Exclusive immunoglobulin genes. Nature **312**, 502–503.

Suggestions for Further Reading

7. E. ten Boeckel, F. Melchers, and A. G. Rolink (1998) Precursor B cellsshowing H chain allelic inclusion display allelic exclusion at the level of pre-B cell receptor surface expression. Immunity **8**, 199–207.
8. D. Löffert, A. Ehlich, W. Müller, and K. Rajewsky (1996) Surrogate light chain expression is required to establish immunoglobulin heavy chain allelic exclusion during early B cell development. Immunity **4**, 133–144.

Alloantibody, Alloantigen

Alloantigens are **allelic** variants that can induce, when injected into animals of the same species but having a distinct genetic background, the production of the corresponding alloantibodies. The most commonly known example of alloantigens are the blood group substances, which define the basic ABO blood groups in humans. Blood group substances have long been identified as being derived from a polysaccharide core that is found in pneumococcus group XIV, onto which three genes encoding for glycosyl transferases will serially add units that will confer a specific antigenicity to the newly derived molecule. Three genes operate this system in humans: A, B, and H. The H gene is present in all individuals and will add one residue of fucose, leading to the so-called H substance. In individuals who possess the A gene, an additional GalNAC (*N*-acetylgalactosamine) will be added, providing the A substance, which is expressed at the red blood cell surface and confers the A group. In those who have the B gene, a galactose residue is added to H, making the B substance, which is also expressed at the cell surface of red cells in individuals of group B. The A and B genes are codominant, so an individual will express the A, the B, or both the A and B molecules at the red blood cell surface, depending upon what A and B genes are present. If neither the A nor B allele is present, the group will be O. There are many other blood groups in humans, with special reference to the Lewis groups, which are also derived from the same polysaccharide backbone by addition of different units. What is peculiar regarding the ABO blood group system is the fact that individuals who lack the A or the B specificity spontaneously produce alloantibodies directed against the missing substance. So an individual of group A will make anti-B alloantibodies, an individual of group B will produce anti-A, and one of group O will have both. Very severe accidents in blood transfusion would result from the agglutination of the donor red blood cells by the alloantibodies of the recipient. The reverse situation, agglutination of the host red blood cells by antibodies of an incompatible donor, should also be avoided, although accidents are less severe. Antigen compatibility between donor and recipient is therefore a must. ABO compatibility should also be observed in allografts.

Even if the genetic determinism of these alloantigens is straightforward, it still is not clear why the alloantibodies corresponding to the nonexpressed substance(s) are produced. The prevalent explanation is that blood groups cross-react with bacteria normally present in the intestinal flora, which would stimulate the immune system to produce the corresponding crossreacting antibodies. It should be stressed that these “natural” antibodies are of the IgM type, which may be directly related to the fact that they are the result of the stimulation by a T-independent polysaccharide antigen. The titer of alloantibodies varies greatly between individuals, but may be considerably elevated upon an incompatible transfusion.

Another famous case of alloantigen in the blood groups is the Rhesus factor, which was responsible for the dramatic hemolytic disease of the newborn, due to the immunization of an Rh mother against red blood cells of an Rh^+ fetus. This occurs during the delivery because some fetal red cells may enter the maternal circulation and induce the formation of IgG antibodies that will actively cross the placental barrier in a subsequent pregnancy and then provoke lysis of Rh^+ fetus red cells. Treatment involves complete transfusion of the newborn with Rh blood. It has now been generalized to prevent the immunization by injecting the Rh mother with anti-D (anti-Rhesus) antibodies immediately after delivery, to trap the red blood cells from the newborn that would have penetrated the maternal circulation at birth.

Many other alloantigens are known, but alloantibodies are generally not produced unless the antigen is given. This is the case of the major histocompatibility complex (MHC) molecules, which constitute a major problem in transplantation. The name of major histocompatibility complex indicates by itself how these molecules were first discovered as a major target for graft rejection, as the result of a very severe alloimmune response, characterized primarily by the production of cytotoxic T lymphocytes. Many other systems may behave as potential alloantigens, which simply reflects the existence of allelic variants. The case of allotypes of immunoglobulins has been studied particularly by immunologists and has provided remarkable genetic markers for the study of immunoglobulin biosynthesis and diversity at the time.

Suggestion for Further Reading

P. L. Mollison, C. P. Engelfriet, and M. Contreras (1987) *Blood Transfusion in Clinical Medicine*, 8th ed., Blackwell, Oxford, UK.

Allophenic

Allophenic individuals are composed of cells of two different genotypes (often called mosaics or chimeras). Allophenic mice are the basis of the revolution in mouse genetics, allowing mice with specific gene replacements to be generated and studied. Allophenic mice are made by mixing cells from two embryos of different genotypes (1). These new composite embryos are implanted into foster mothers and allowed to develop. The early embryos are able to compensate and form a single individual from the mixture of embryonic cells. The mosaic progeny that result from these manipulations have tissues that contain cells of the two different genotypes. The allophenic mice have also been called tetraparental mice. When the germ cells are also of mixed origin, progeny can be recovered from both genotypes.

The ability to make allophenic mice in the laboratory was first used to study the contributions of cells to individual tissues. The number of cells that give rise to a particular tissue can be estimated from the proportions of the two genotypes in a large number of allophenic mice. The cellular autonomy of mutant phenotypes can be determined by generating allophenic mice between mutant and wild-type mouse embryos. The two cell types usually differ both in the mutant of interest and in some marker genotype, such as an enzyme polymorphism.

Two advances in the technology of allophenic mice have contributed to a revolution in mouse genetics in the last few years. The first advance was the ability to use embryonic teratocarcinoma cells from cell culture as one of the two cell types used to make the allophenic mice (2). The cultured cells are injected into the interior of a normal mouse embryo and are incorporated into the embryo, to form an allophenic mouse. The teratocarcinoma cells are totipotent and can even form germ cells that give rise to the **gametes** for the next generation. The second major advance was the development of techniques for site-directed mutagenesis and gene replacement in mammalian cells in culture (3) (see Gene Targeting). A gene of interest is altered in a specific way in teratocarcinoma cells in culture. A clone of cells with the altered genotype is produced, and cells from the clone are injected into early mouse embryos to produce allophenic mice. These allophenic mice can be studied as mosaic individuals or can be allowed to develop to fertile adults. If some of the germ cells in the adult allophenic mice are derived from the genetically altered teratocarcinoma cells, progeny can be recovered from the gametes produced by the teratocarcinoma cells and used to found a mutant strain of the specific genotype desired. This has led to the production of hundreds of new mouse strains mutant for developmentally important genes. It has also made the construction of mouse models for human disease far easier than in the past. These technologies have been extended from mice to a variety of other mammals; and they could be used to alter the human genome genetically, with far-reaching consequences.

Bibliography

1. B. Mintz (1962) Science **138**, 594.
2. B. Mintz and K. Illmensee (1975) Proc. Natl. Acad. Sci. USA **72**, 3585–3589.

3. M. R. Capecchi (1989) Science **244**, 1288–1292.

Suggestions for Further Reading

4. B. Mintz (1974) Annu. Rev. Genetics **8**, 411–470.
5. R. Jaenisch (1988) Science **240**, 1468–1474.

Allostery

Allostery is used to describe regulatory phenomena in biological systems. The term "allosteric" (other shape) was coined by Monod and coworkers to describe a particular type of regulatory behavior and marks an important synthesis in the development of biochemistry and molecular biology. Since its inception, the term has evolved to describe several related concepts and is used today to describe a variety of phenomena. To some, it is associated with a particular type of regulatory behavior, while to many it is used to describe several different aspects of regulation. The development of the concept, the meanings it has come to have, its application in describing regulatory properties of proteins and enzymes, and recent developments that indicate the need to use it in its original sense are described here.

The allosteric concept was conceived in the early 1960s by Monod and coworkers to describe the properties of regulatory enzymes. In the mid-1950s, several investigators described enzymes whose catalytic properties were dependent on effector molecules other than the substrate. The first well-characterized example of this behavior was the finding by Cori and colleagues that 5′-AMP is required for the *in vitro* catalytic activity of glycogen phosphorylase b from resting skeletal muscle (1). Studies of the regulation of biosynthetic pathways in bacteria showed that the catalytic properties of the first enzyme in a pathway are often modulated by the end product of the pathway, which has a structure different from that of the substrate—for example, isoleucine inhibition of threonine deaminase (see Threonine Operon) (2) and CTP inhibition of aspartate transcarbamoylase (3). The differences in the structures of the substrates and effectors were first noted by Monod and Jacob, who postulated in a seminal paper in 1961 that the effectors bind to separate and distinct sites (4). They coined the term *allosteric site* for the effector binding site to distinguish it from the active site and postulated that the effectors act indirectly by causing changes in the conformation of the enzyme that alter its catalytic site and kinetic properties. In 1963, Monod and coworkers compiled the available data on regulatory enzymes (5). These enzymes all contained more than one subunit per enzyme molecule–that is, dimers, tetramers, and dodecamers. For several of these enzymes, changes in quaternary structure (association–dissociation of the subunits) had been shown to occur upon addition of the effectors. Monod was also aware of unpublished crystallographic results showing that the oxygen-binding sites on hemoglobin are located far from one another and that the distances between the amino acid residues labeled by heavy atoms change upon binding of oxygen (Ref. 6, pp. 577–578). On this basis, the key elements of a general model for the functional structures of regulatory enzymes were formulated:

1. Each molecule of the native enzyme contains multiple subunits with binding sites for substrates and ligands, and the regulatory behavior depends on the relationships between the subunits.
2. No direct interactions between substrate(s) or effectors are required, that is, the effectors act indirectly on the catalytic site.
3. The actions of the effectors are due entirely to a reversible conformational change in the protein that is induced by effector binding.

Monod et al. postulated that protein conformational change is the basis for control and coordination of chemical events in living cells, and Monod considered this to be the "second secret of life" (Ref. 6, p. 576). Structural studies using X-ray crystallography methods support the concepts of this general model.

These concepts were used to develop the concerted model, a specific molecular model for describing regulatory behavior (7). This model was developed as a plausible explanation for the positive cooperativity in the binding of oxygen to hemoglobins. Because the apparent affinity for binding of oxygen changes as its concentration is varied, these are called *homotropic interactions*. The concerted model retains the aspects of the general model with respect to oligomeric structure of the protein, multiple binding sites located far from one another, and conformational changes upon binding of one ligand that are transmitted by protein conformational changes to the other ligand binding sites, thereby altering the binding affinities. This model defines the relations between the conformational changes and ligand binding. The word *concerted* refers to the all-or-none nature of the conformational transition. That is, only two conformations are allowed for the subunits in an oligomer and all of the subunits in a given oligomer have the same conformation. The conformations are denoted by the terms *R-state* and *T-state*, and they differ in affinity for binding ligands. The R-state has the higher affinity for ligands. Positive cooperativity in oxygen binding is explained by a large predominance of the unliganded protein in the T-state with a shift to the R-state upon binding of oxygen. The model was extended to enzymes by assuming that the interactions between the substrate and enzyme are in rapid equilibrium and that all forms of the enzyme have the same V_{max}. At this juncture, the term *allosteric* takes a different meaning. The conformational change between the two states is called an *allosteric transition*. So, in addition to referring to sites for molecules other than the substrate, it refers to interactions between substrate binding sites on different subunits. The concept of the "other shape" is extended to the enzymes, which are termed "allosteric enzymes."

This initial formulation of the concerted model describes homotropic interactions. The original considerations of the allosteric concept were developed to treat cases in which the behavior of one molecule, the substrate, depends on the concentration of another molecule. These are called *heterotropic interactions*. The regulatory enzymes whose properties were catalogued by Monod et al. showed both homotropic and heterotropic effects (5). The phenomenon of desensitization—that is, treatments that result in loss of substrate homotropic interactions and heterotropic interactions, but do not affect catalytic activity, had been described for some of these enzymes. Monod et al. postulated that desensitization means that the molecular basis might be the same for both homotropic and heterotropic interactions. They stated that if this were the case, the concerted model could also be used to describe heterotropic effects—that is, the original allostery. In the model, activating effectors have higher affinity for the R-state, while inhibitory effectors have higher affinity for the T-state. This issue has resulted in great confusion in the use of the model. All subsequent treatments presume that a single allosteric transition is the basis for both homotropic and heterotropic effects. This presumption is particularly evident in structural studies of regulatory proteins, where the terms R-state and T-state dominate discussions.

In the three cases of regulatory proteins that have been examined with care, it is clear that the concerted model fails. More than two states are involved in oxygen binding to hemoglobin (8, 9). Homotropic and heterotropic interactions are not due to the same transition in aspartate transcarbamoylase (10, 11). Although the same T-state is predicted for phosphofructokinase with different inhibitors, experimental results show that the properties of the inhibited forms are different (12). These results argue strongly that the term *allosteric* should be used in a stricter sense to refer to effects of one ligand on the binding of another, independently of assumptions about the mechanism of the interaction.

Bibliography

1. E. H. Fischer, A. Pocker, and J. C. Saari (1971) Essays Biochem. **6**, 23–68.

2. H. E. Umbarger (1956) Science **123**, 848.
3. R. A. Yates and A. B. Pardee (1956) J. Biol. Chem. **221**, 757–780.
4. J. Monod and F. Jacob (1961) CSHSQB **26**, 389–401.
5. J. Monod, J.-P. Changeaux, and F. Jacob (1963) J. Mol. Biol. **6**, 306–329.
6. H. F. Judson (1979) *The Eighth Day of Creation: The Makers of the Revolution in Biology*, Simon & Shuster, New York.
7. J. Monod, J. Wyman, and J.-P. Changeaux (1965) J. Mol. Biol. **12**, 88–118.
8. G. K. Ackers and J. H. Hazzard (1993) Trends Biochem. Sci. **18**, 385–390.
9. J. M. Holt and G. K. Ackers (1995) FASEB J. **9**, 210–218.
10. W. N. Lipscomb (1994) Adv. Enzymol. Rel. Areas Mol. Biol. **68**, 67–151.
11. R. C. Stevens, Y. M. Chook, C. Y. W. N. Cho, Lipscomb, and E. R. Kantrowitz (1991) Protein. Eng. **4**, 391–408.
12. V. L. Tlapak-Simmons and G. D. Reinhart (1994) Arch. Biochem. Biophys. **308**, 226–230.

Alpha-Bungarotoxin and Curare-Mimetic Toxins

The venom of the banded krait snake (*Bungarus multicinctus*) contains a variety of protein toxins that are collectively called bungarotoxins. As is often the case, an animal venom is, in fact, a mixture of different toxins specific for different target molecules. The a-neurotoxins, or curare-mimetic toxins, bind specifically to the acetylcholine receptor with high affinities ($\boldsymbol{K}_d$ in the 10^{-9} to 10^{-12} M range for neuronal and muscular receptors of different species) and prevent the opening of the ion **channel** caused by acetylcholine binding (1, 2). Such inhibition of the transmission of the nerve-muscle impulse results in a flaccid paralysis, which may end in respiratory failure and death.

a-bungarotoxin is the prototype of a large group of monomeric toxins, produced by many snakes, including cobra and sea snakes, and composed of 66 to 74 amino acid residues with four or five disulfide bonds. Their three-dimensional structure is rather flat, with three adjacent b-sheet loops (3) that expose residues essential for receptor binding: Lys-27, Trp-29, Arg-39, and Lys-55 (numbering of erabutoxin) (Fig. 1) (4).

Figure 1. Erabutoxin, a snake toxin that binds to the acetylcholine receptor. Folding of the polypeptide chain shows the typical three-finger folding of curare-mimetic snake toxins. Several residues determine the specific binding and inhibition of the acetylcholine receptor with Lys-27, Trp-29, Arg-33, and Lys 47 playing a major role (4). Reproduced from (2) with permission.

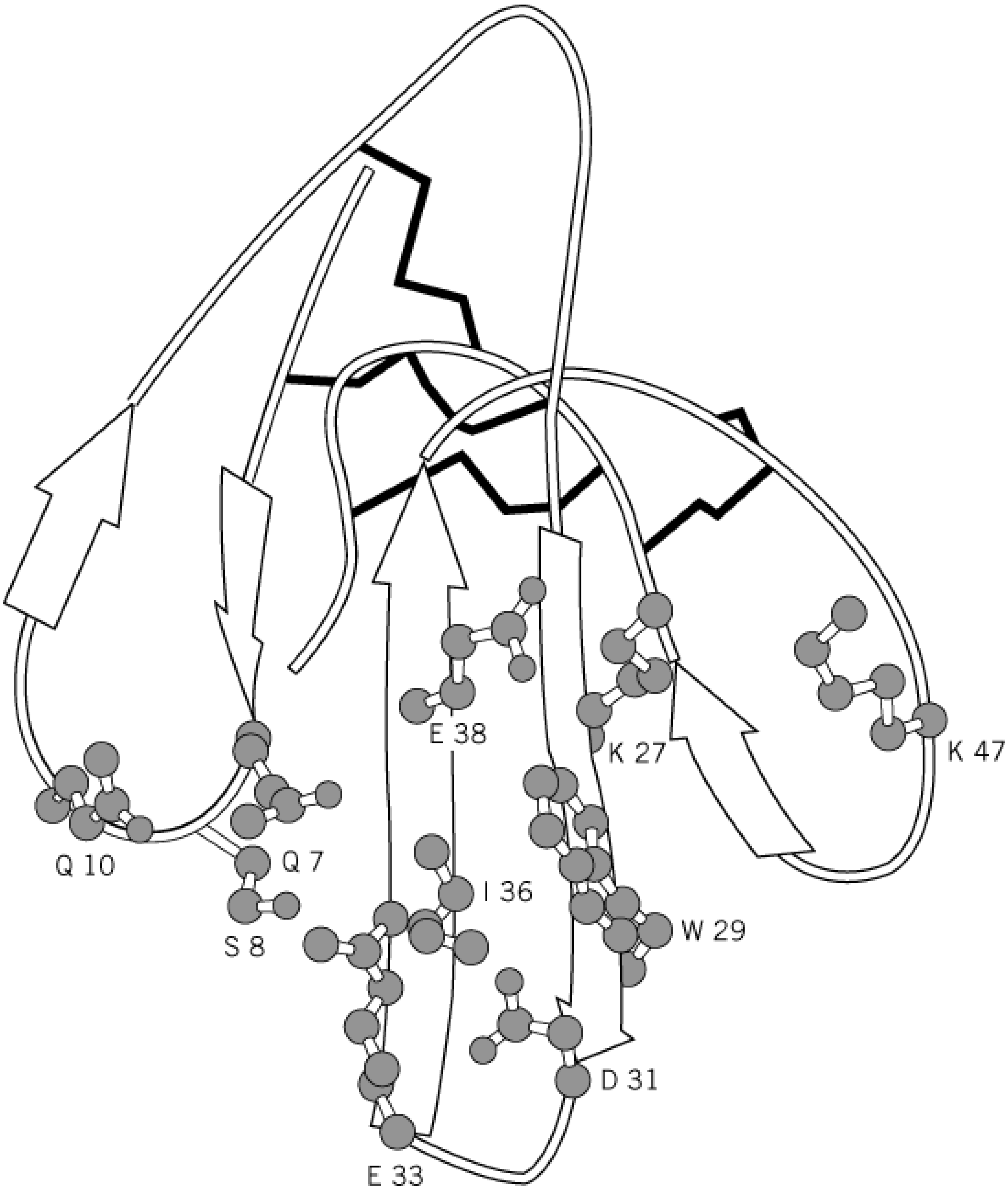

Many species of snakes, including *B. multicinctus*, also produce a-neurotoxins of smaller size. Their polypeptide chains are 60 to 62 residues long but adopt the same three-finger b-sheet fold, stabilized by four disulfide bonds. At variance from the longer a-neurotoxins, these toxins are dimers, but the same three positively charged residues are essential for receptor binding. The corresponding area of the acetylcholine receptor involved in a-neurotoxin binding has not been mapped in detail, but the segment of residues 185 to 199 plays a major role, together with residues 128 to 142.

The various a-neurotoxins bind with a range of affinities and specificities to the multitude of muscular and neuronal acetylcholine receptors; fluorescent and **radiolabeled** toxin derivatives are invaluable tools for the study of the structure and function of such receptors (5).

Bibliography

1. A. L. Harvey, ed. (1991) *Snake Toxins*, Pergamon Press, New York.
2. R. Rappuoli and C. Montecucco (1997) *Guidebook to Protein Toxins and Their Use in Cell*

Biology, Oxford University Press, Oxford, UK.
3. M. D. Walkinshaw, W. Saenger, and A. Maelicke (1980) Proc. Natl. Acad. Sci. USA **77**, 2400–2404.
4. O. Tremeau et al. (1995) J. Biol. Chem. **270**, 9362–9369.
5. A. Devillers-Thiery et al. (1993) J. Membr. Biol. **136**, 97–112.

Alpha-Helix (3_{10}-Helix and Pi-Helix)

The right-handed a-helix is one of two regular types of protein **secondary structure**, the other being the b-strand that forms b-sheets. Helices are formed from consecutive stretches of **residues** of the polypeptide chain and are characterized by a right-handed coiled backbone and a regular repeating pattern of backbone hydrogen bonds. a-Helices are usually depicted as coils or cylinders in protein structure diagrams (Fig. 1). There are 3.6 residues in every turn of a-helix, and for each turn the backbone is translated by 5.4 Å (or 1.5 Å per residue). In protein structures, the average length of an a-helix is 10 residues, although much shorter and longer examples have been observed. The backbone angles are approximately –60° and –50° for f and Y, respectively, corresponding to the allowed region in the lower left of the Ramachandran Plot. The atoms of the polypeptide chain pack closely together in the a-helical conformation, making favorable van der Waals interactions. The side chains of each residue are oriented outward from the axis of the helix, with the Ca–Cb bond pointing toward the *N*-terminal end of the helix.

Figure 1. A typical protein a-helix. (**Left**) The helix is depicted schematically as a coil, and the *N*- and *C*-terminal ends, with their respective partial positive and negative charges, are indicated. (**Right**) The atomic detail of the a-helical structure is shown, with hydrogen bonds between backbone carbonyl oxygens (*i*) and backbone amide nitrogens of residue (*i* + 4) indicated by dotted lines. Nitrogen atoms are shown in blue and oxygen atoms are shown in red. This figure was generated using Molscript (3) and Raster3D (4, 5). See color insert.

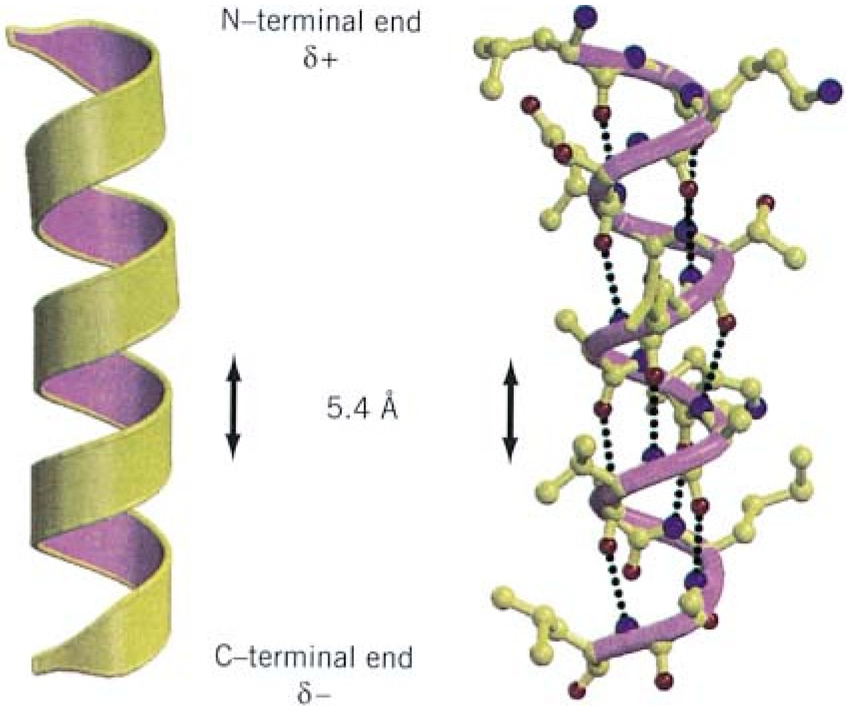

A regular hydrogen bond pattern is formed in the a-helix, corresponding to bonds formed between the backbone carbonyl oxygen of residue (*i*) and the backbone amide of residue (i + 4) in the polypeptide chain, so that there are 13 atoms between each acceptor and donor pair. Thus, apart from the first few amide groups and last few carbonyl oxygen atoms, all the peptide bonds in an a-helix form hydrogen bond interactions. The hydrogen bonds are all oriented in the same direction, as are the dipoles of each of the peptide bonds. Therefore, the helix itself also has a significant dipole moment (a partial positive charge at the *N*-terminus and a partial negative charge at the *C*-terminus), and charged residues that interact with the dipole are often found in the sequence at the appropriate end of a helix (1). For example, the negatively charged Asp residue is highly favored at the *N*-terminus. The helix dipole has also been implicated in protein functions, such as substrate binding and catalysis.

Different amino acids have different tendencies for forming a-helices (2). The amide nitrogen of proline is cyclized with its backbone and thus cannot act as a hydrogen bond donor. Proline residues therefore are not found frequently in a-helices; when they are, they cause irregularities such as kinks and bends in the middle of helices. On the other hand, proline is a preferred residue at the *N*-terminus of the helix where other residues would have an unpaired backbone amide.

The staggered arrangement of side chains around the helix can be visualized in two dimensions through the use of a **helical wheel** (a projection down the axis of the helix). Helices in membrane proteins are often amphipathic, having polar or charged side chains arranged on one side and **hydrophobic** side chains on the opposite side of the helix.

There are several variations to the a-helix conformation of proteins. The 3_{10}-helix is more tightly wound than the a-helix with backbone hydrogen bonds formed between residues (*i*) and (i + 3). Its name is based on its structure, with three residues per turn and 10 atoms between hydrogen bond donor and acceptor (although in real protein structures this geometry may be somewhat distorted). The 3_{10}-helix is usually only observed at the ends of a-helices or in short stretches of 4 to 5 residues. The P-helix is more loosely wound than the a-helix with backbone hydrogen bonds formed between the (*i*) and (i + 5) residues and is very rarely observed in protein structures. The left-handed helix, having the same hydrogen bonding pattern as a-helices but backbone f and Y angles of +60° and

+50° (rather than the –60° and –50° angles of the right-handed a-helix), is not often observed, because this conformation results in steric clashes between backbone and side chain atoms. A glycine residue, however, having only a hydrogen atom as its side chain, can adopt this conformation. The poly(Pro)II helix, with no backbone hydrogen bonds, is also left-handed, with three residues per turn and a translation of 3.12 Å per residue. This helical structure is observed in polyproline and in proline-rich regions of proteins.

[See also Protein Structure and Secondary Structure, Protein.]

Bibliography

1. L. Serrano and A. R. Fersht (1989) Nature **342**, 296–299.
2. J. S. Richardson and D. C. Richardson (1988) Science **240**, 1648–1652.
3. P. J. Kraulis (1991) J. Appl. Crystallogr. **24**, 946–950.
4. E. A. Merritt and M. E. P. Murphy (1994) Acta Crystallogr. **D50**, 869–873.
5. D. J. Bacon and W. F. Anderson (1988) J. Mol. Graphics **6**, 219–222.

Suggestions for Further Reading

6. D. J. Barlow and J. M. Thornton (1988) Helix geometry in proteins. J. Mol. Biol. **201**, 601–619.
7. C. Branden and J. Tooze (1991) *Introduction to Protein Structure*, Garland, New York.
8. W. G. J. Hol, P. T. Van Duijnen, and H. J. C. Berendsen (1978) The -helix dipole and the properties of proteins. Nature **273**, 443–446.
9. J. S. Richardson (1981) The anatomy and taxonomy of protein structure. Adv. Protein Chem. **34**, 167–339.
10. C. Toniolo and E. Bennedetti (1991) The polypeptide 3_{10} helix. TIBS **16**, 350–353.

Alpha-Helix Formation

a-Helices are the most common type of **secondary structure** in globular proteins (see Alpha-Helix (310-Helix and Pi-Helix)). As such, there is intense interest in understanding the factors that contribute to a-helix formation in peptides and proteins (1-4).

All peptide helices unfold with increasing temperature. This indicates that helix formation is an enthalpically favorable process (it proceeds with the release of heat). The main feature of helical structure is the repeating pattern of intramolecular hydrogen bonds formed between atoms in the peptide backbone (> C=O · H—N <). These hydrogen bonds probably provide the main enthalpic stabilization to the helical conformation (5). Opposing this **enthalpy** is the conformational **entropy** of freezing the backbone conformation, because the process of change from a disordered conformation (unfolded peptide or protein) to an ordered one (helix) is unfavorable entropically. This unfavorable entropy is about the same magnitude as the favorable enthalpy; that is, in isolation the helices are at best marginally stable.

Because the a-helix has an (i, i + 4) backbone hydrogen bonding pattern, the first four > N—H and the last four >C=O groups of the helix will not be hydrogen-bonded to a backbone partner. Polar groups that do not form hydrogen bonds to water or other protein groups are destabilizing (see Protein Stability). Therefore it is important that these groups either be hydrated or have other intramolecular partners. The side chain of the first residue of the helix (the “*N*-cap”) often fills this role, if it is able to hydrogen-bond to one or two otherwise unsatisfied backbone >N—H groups. These "capping" hydrogen bonds have been proposed to be important factors in determining where helices begin and end in proteins (6, 7).

The helical conformation has the peptide groups and their associated dipoles aligned in the same direction, whereas in nonhelical forms the dipoles are distributed randomly. As the helix forms, the dipoles on adjacent peptide groups align in an unfavorable fashion (see Electrostatic Interactions). However, when a full turn of the helix is completed, the first hydrogen bond is formed and the peptide groups involved in the hydrogen bond align favorably. This adds to the **cooperativity** of helix formation: Once the first hydrogen bond is formed, it is easier to continue forming the helix. The alignment of the individual peptide group dipoles in a single direction gives rise to a helix *macrodipole* (simply the additive effects of the individual dipoles). The *N*-terminus of the helix has a partial positive charge, while the *C*-terminus carries a partial negative charge. Residues with charged side chains at the ends of a helix can interact favorably or unfavorably with the helix macrodipole, giving rise to an effect known as the *charge–dipole interaction*.

Different amino acid residues have different tendencies to form helices (see Helix–Coil Theory). For example, alanine is found in protein helices much more often than is glycine (8). The intrinsic preference to be in a helical conformation has been termed *helix propensity*. Since this is an intrinsic property, it should be characteristic of a given amino acid and independent of context. However, quantitative measurements of helix propensity in different systems have provided markedly different results (1, 2, 4). This reflects the difficulty of measuring intrinsic properties in complex molecules like proteins and peptides (however, see Ref. 9).

Interactions between side chains can also affect the stability of helices. Side chains three and four residues away from each other in the amino acid sequence will be close in space in a helical conformation. Therefore, electrostatic interactions, hydrogen bonds, or **hydrophobic** contacts between these side chains can contribute to helix stability. Likewise, if interactions are possible in the nonhelical form of the peptide or protein, this can alter the amount of a-helix observed in a peptide or protein. Figure 1 shows examples of various types of side-chain interactions possible in the helix, an estimate of the magnitudes of the contributions of the main factors contributing to helix stability, and comparison of these estimates with the **free energy** provided by typical interactions in proteins.

Figure 1. Interactions involving amino acid side chains that affect the stability of isolated a-helices. (**Top**) Ribbon model of an a-helix, with stabilizing interactions involving (i) hydrogen bonding of the *N*-cap side-chain at the *N*-terminus, indicated here as Asn, (ii) favorable electrostatic interactions of ionized side chains (Asp and Arg shown here) with the helix dipole, and (iii) electrostatic interactions between oppositely charged side chains on adjacent turns of the helix. (**Bottom**) Quantitative estimates of the net stabilizing interactions in an isolated a-helix and in folded globular proteins.

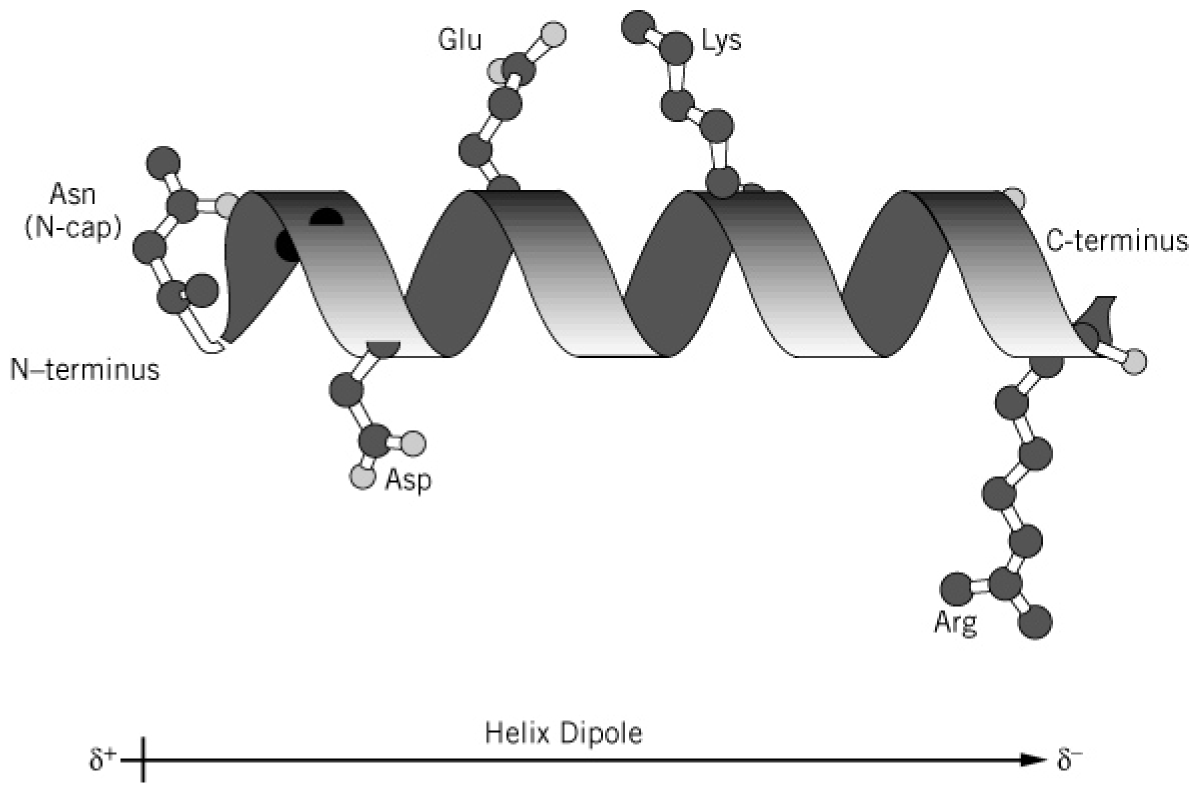

In addition to the stability of helices, their rates of folding and unfolding are of interest as well. The transition from helix to random coil occurs very rapidly, on the order of nanoseconds, two to three orders of magnitude faster than the fastest folding proteins (10).

Bibliography

1. J. M. Scholtz and R. L. Baldwin (1992) Annu. Rev. Biophys. Biomol. Struct. **21**, 95–118.
2. A. Chakrabartty and R. L. Baldwin (1995) Adv. Protein Chem. **46**, 141–176.
3. J. W. Bryson, S. F. Betz, H. S. Lu, D. J. Suich, H. X. Zhou, K. T. O"Neil, and W. F. DeGrado (1995) Science **270**, 935–941.
4. N. R. Kallenbach, P. Lyu, and H. Zhou (1996) In *Circular Dichroism and the Conformational Analysis of Biopolymers* (G. D. Fasman, ed.), Plenum Press, New York.
5. J. M. Scholtz, S. Marqusee, R. L. Baldwin, E. J. York, J. M. Stewart, M. Santoro, and D. W. Bolen (1991) Proc. Natl. Acad. Sci. USA **88**, 2854–2858.
6. L. G. Presta and G. D. Rose (1988) Science **240**, 1632–1641.
7. E. T. Harper and G. D. Rose (1993) Biochemistry **32**, 7605–7609.
8. P. Y. Chou and G. D. Fasman (1978) Adv. Enzymol. **47**, 45–148.
9. J. K. Myers, C. N. Pace, and J. M. Scholtz (1997) Proc. Natl. Acad. Sci. USA **94**, 2833–2837.
10. S. Williams, T. P. Causgrove, R. Gilmanshin, K. S. Fang, R. H. Callender, W. H. Woodruff, and R. B. Dyer (1996) Biochemistry **35**, 691–697.

Suggestion for Further Reading

11. The first four references cited above provide excellent reviews of helix formation in peptides and the relationship between helix formation in peptides and proteins.

Alpha-Lactalbumin

It requires patience to achieve quiet research. The investigation of properties of a-lactalbumin (a-LA) was not worthy of much notice until about 1965, especially from the standpoint of molecular biology. It is only a protein component of the complex enzyme "lactose synthase" and elucidation of its function had made little progress. However, the hidden connection to molecular biology was ferreted out in about 1967 and initiated the great explosion of activity in studying the molten globule (MG) conformation of proteins. These studies of the MG proteins opened a new area of structural biology connected to various physiological functions. Modern molecular biology sometimes requires the MG protein model to understand such physiological processes. The best-characterized MG is that formed by a-LA, and it can easily be prepared. a-LA is now one of the star proteins in molecular biology. The development of research into a-LA has been deeply affected by changing times.

One (a) of three peaks in the **sedimentation velocity** patterns of proteins in the non-casein fraction of skim milk was found responsible for a lactalbumin isolated from milk, which has subsequently been called a-lactalbumin. In the middle-1960s, it was confirmed that lactose is synthesized in the mammary gland UDP-galactose (UDP-Gal) and glucose (Glc) by an enzyme "lactose synthase," which can be resolved into two fractions. One of them is a-LA, and the other is galactosyltransferase (GT). Alone in the Golgi apparatus, but with metal ions such as Mn^{2+}, the latter catalyzes the transfer of Gal to GlcNAc on **glycoproteins**:

$$\text{UDP-GAL} + \text{GlcNAc} \rightarrow \text{Lactosamine-NAc} + \text{UDP} \qquad (1)$$

where NAc is the NAc is the N-acetyl group. a-LA is synthesized in the mammary gland during the lactation. It passes through the Golgi apparatus where it combines with GT and alters its substrate specificity to inhibit reaction 1. A decrease of three of magnitude in the K_m for Glc facilitates the synthesis of lactose instead:

$$\text{UDP-Gal} + \text{Glc} \rightarrow \text{Lactose} + \text{UDP} \qquad (2)$$

1. Structures

a-LA is normally a single polypeptide chain of 123 residues, four disulfide bonds, and a molecular weight of about 14,000 except for rat a-LA, which has 140 residues. About 1970, similarities were noted in the molecular weight and amino acid sequence between a-LA and hen egg white lysozyme (HEWL), a lytic enzyme. Subsequently, it was found that the exon-intron organization of the genes for both proteins are the same 1, 2. These suggested **divergent** evolution of the two proteins from a common ancestral gene, and a-LA was assumed to have a three-dimensional structure similar to that of HEWL, in spite of marked differences in their functions. **X-ray crystallographic** determination of the a-LA structure was not successful for a long time, but the conformations of both proteins in aqueous media were compared. Until 1980, significant differences in their physical behavior were observed:1) An intermediate conformation appears in the unfolding equilibrium of a-LA, but not of HEWL, at intermediate concentrations of **guanidinium chloride** (GdmCl) at a neutral pH, which is also stable at acid pH and is designated the "A-State"; 2) One Ca^{2+} ion is tightly bound to a-LA, but not to HEWL, and stabilizes the native (N) form. Removal of Ca^{2+} from a-LA induces the A-state near room temperature. Figure 1 shows a phase diagram of bovine a-LA for the N-, A-, and U- (unfolded) states in of GdmCl at 25°C, and the unfolding equilibrium has been explained in terms of the three states (3-5). Subsequently, it was shown that the kinetic intermediate of bovine a-LA captured at the early stage of refolding from U has properties similar to the equilibrium A-state. Later, it was reported that a number of proteins including HEWL assume the equilibrium and kinetic intermediate(s) similar to the A-state of a-LA in the molten globule (MG) form, and the MG was considered to be a third physical state of proteins (see Molten Globule). However, the conformational transition of the A to U of a-LA is nonco-operative, and then the folding of a-LA along the multipathway, which is apparently in the two-state type, is proposed (6-8). Also, recently, the kinetic intermediates of folding of a-LA with non-native secondary structures were shown, especially in the apo-form (9).

Figure 1. Phase diagram for the three states (N, A, and U) of bovine a-lactalbumin in a solution of GdmCl at any concentration and pH at 25°C.* The solid curves represent the pH and [GdmCl] where K_{eq}^{NU} K_{eq}^{AU}, or K_{eq}^{NU} is unit. K_{eq}^{ij} is for the conformational transition between *i* and *j*. The other curves represent the pH and [GdmCl] where K_{eq}^{NA} = 10 or 0.1 (---), K_{eq}^{AU} = 10 or 0.1 (-.-), and K_{eq}^{NU} = 10 or 0.1 (-. .-). *K. Kuwajima, Y. Ogawa, and S. Sugai (1983) *J. Biochemistry* (Tokyo) **89**, 759–770.

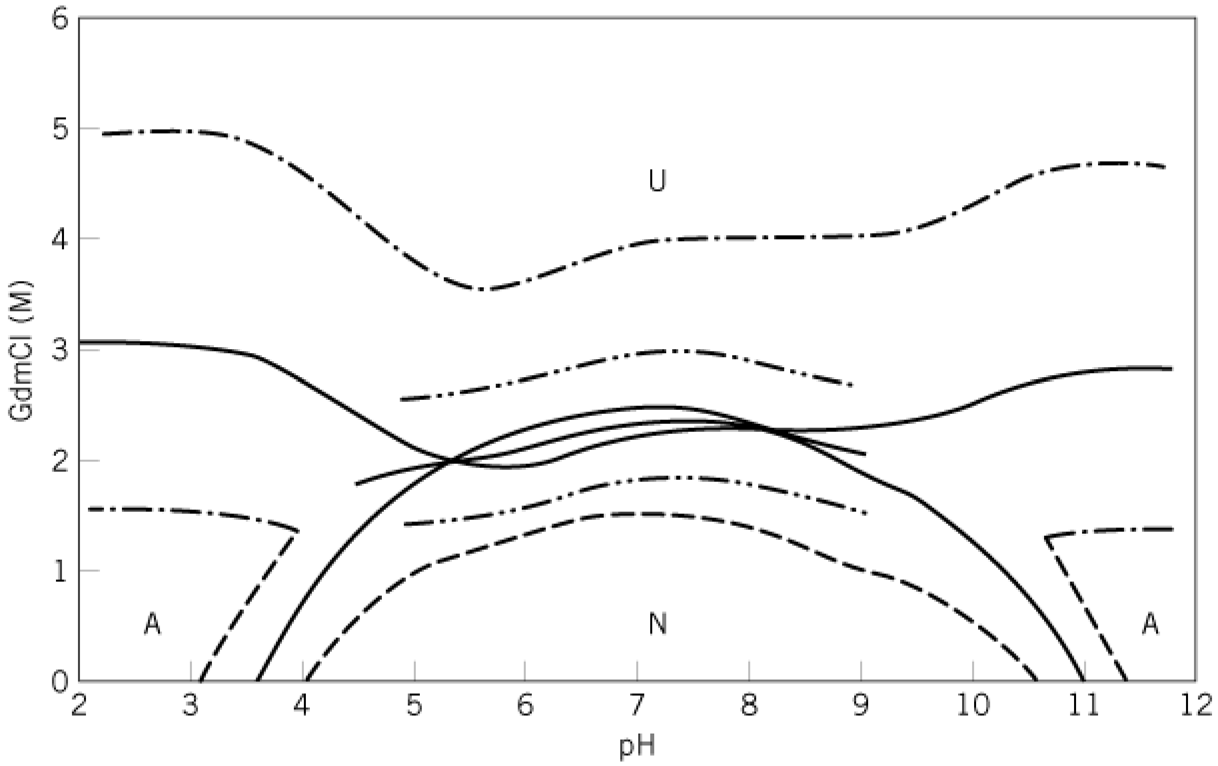

Since 1987, the crystal structures of a-LA from various species (baboon, human, goat, guinea pig, and bovine) and their recombinant and mutant forms have been determined at resolutions of 1.15 to 2.4Å 10-15. The overall features of the authentic forms are similar to those of HEWL. Both structures are divided into two (a and b) sub**domains** by a deep cleft, the a-domain comprises residues 1 to 34 and 86 to 123, and the b-domain includes residues 35 to 85. In baboon a-domain contains four a-helices, A (residues 5 to 11), B (23 to 34), C (86 to 99), and D (105 to 109), plus single turns of 3_{10}-helices (12 to 16,101 to 104, and 115 to 119). The b-domain consists of a three-stranded antiparallel b-sheet (41 to 56), a 3_{10}-helix (76 to 82), and loop regions (Fig. 2). In a-LA from other species, however, the D-helix is replaced by a loop. The C-terminal region is flexible. The conformation and the ligand coordination of a Ca^{2+}-binding site (K_a of 10^9 to $10^{10} M^{-1}$ in the N-state) are observed at the interface of both the domains in all of a-LA. The Ca^{2+}-binding site is composed of three Asp residues at 82, 87, and 88 and peptide carbonyl oxygens at residue 79 and 84 (the other two ligands are water molecules) and is in a slightly disordered, rigid pentagonal bipyramidal form (designated the “a-LA elbow”). The Asp residues are not found in the corresponding region of most lysozymes, but some have the Ca^{2+}-binding site in an a-LA elbow (Table 1), which bind a Ca^{2+} ion in the N-state and are important for studying the evolution of the a-LA family. A Zn^{2+}-binding site was also found in the human a-LA crystal, located at the entrance of the cleft between the two subdomains and coordinated with Glu 49, Glu 116, and two water molecules. Also, the Mn^{2+}-and weak Ca^{2+}-binding sites were also indicated. a-LA binds numerous other metal ions: Na^{+},K^{+},Ba^{2+},Mg^{2+},Co^{2+},Cu^{2+},Pb^{2+},Hg^{2+},Cd^{2+},Sr^{2+},Al^{3+},Tb^{3+},Eu^{3+},Sc^{3+}, and Y^{3}. However, elucidation of their locations and roles in lactose synthesis are awaited. Recently, binding of fatty acids to human a-LA is noted in connection with its function. The structures of a-LA determined by X-ray crystallography and by NMR in solution exhibit two **hydrophobic** clusters of aromatic residues: cluster I of Phe 31, His 32, Tyr 36, and Trp 118 and cluster II of Trp 26, Phe 53, Trp 60, and Trp 104 (16-19). These make up the cores in a-LA by combining with other hydrophobic parts in the a-domain.

Table 1. Comparison of “Equivalent Amino Acid Residues” in Some a-Lactalbumins and Lysozymes at the Calcium-Binding Sites

Protein	Source	Residue[a] 79	82	84	87	88
a-Lactalbumin	Baboon	Lys	Asp	Asp	Asp	Asp
	Human	Lys	Asp	Asp	Asp	Asp
	Bovine	Lys	Asp	Asp	Asp	Asp
	Equine	Lys	Asp	Asp	Asp	Asp
	Wallaby	Lys	Asp	Asp	Asp	Asp
	Guinea pig	Lys	Asp	Asp	Asp	Asp
	Goat	Lys	Asp	Asp	Asp	Asp
	Camel	Lys	Asp	Asp	Asp	Asp
	Rabbit	Asn	Asp	Asp	Asp	Asp
	Rat	Lys	Asp	Gly	Asp	Asp
Lysozyme	Human	Ala	Gln	Asn	Asp	Ala
	Bovine	Glu	Glu	Asp	Lys	Ala
	Hen egg	Ala	Ser	Asp	Ala	Ser
	Equine	Lys	Asp	Asn	Asp	Asp
	Pigeon	Lys	Asp	Asn	Asp	Asp
	Canine	Lys	Asp	Asn	Asp	Asp

[a] Residue numbers for lysozyme are equivalent numbers for human a-lactalbumin.

2. Molten Globule Intermediate

The molten globule of a-LA is compact (a radius of gyration only about 10% larger than that of the N-form) and has N-like secondary structures, but without the specific **tertiary structural** packing interactions. a-LA assumes the following stable MG forms in aqueous media: 1) An equilibrium unfolding state at intermediate concentrations of GdMCl or urea; 2) The acid state; 3) A partially unfolded state obtained by removing of the bound Ca^{2+} at neutral pH and low salt concentrations, and 4) After partial reduction of the disulfide bonds. NMR and amide hydrogen exchange show heterogeneous structures of the MG, an a-domain relatively structured by hydrophobic interactions, and a more unfolded b-domain. Hydrophobic clusters I and II in the native form are somewhat rearranged locally, and some form of the hydrophobic core persists in the MG form and play as nuclei for the folding. The disulfide bond between Cys 6 and Cys 120 in native a-LA can be reduced extremely quickly by thiol agents. The free thiol groups in the three-disulfide intermediate (3SS) of a-LA are easily modified by **iodoacetic acid** or iodoacetoamide and generate carboxymethylated or carboxyamidomethylated 3SS a-LA, respectively. These trapped derivatives of bovine a-LA retain the N-form, with slight changes in the local conformation very near Cys 6 and Cys 120, but they assume the MG form in the absence of Ca^{2+} or at acid pH (20-25). A two-disulfide species and its trapped derivatives can also be obtained by subsequently reducing the 28–111 disulfide bond. The 2SS derivatives have partial MG characteristics. These disulfide intermediates and their derivatives are frequently used as models of partly unfolded proteins in the molecular biology because they are well characterized and easily prepared (26-28).

3. Functions

Lactose synthase (reaction 2) has long been studied to determine the binding sites of the saccharides and of metal ions and the interaction site between GT and a-LA. The structure of a-LA-GT complex has not been determined, but it has been shown by indirect methods such as chemical modification and site-directed mutagenesis that Ca^{2+} and some residues of a-LA adjacent to the cleft including Phe 31, His 32, Ala 106, and Leu 110 are crucial for the function of lactose synthase. The flexible C-terminal region, part of the hydrophobic clusters, and the cleft are essential for the lactose synthase function. The binding sites of a-LA on GT have been tentatively identified. The difference in function between a-LA and lysozyme has been explained by roles of some residues such Tyr 103 in a-LA. Mutations of six residues in the cleft of a-LA to the corresponding ones of lysozyme created a catalytic site of lysozyme in a-LA and hydrolyzed the glycoside bond, as chicken lysozyme (29).

It has been confirmed that **molecular chaperones** bind the protein and assist it folding in the cell. Physicochemical studies *in vitro* indicate that the **chaperonin**GroEL binds apo- or disulfide-reduced a-LA in the MG form, although it scarcely interacts with the N-state of a-LA (30-34). GroEL recognizes the hydrophobic surface exposed on the MG-form. a-LA bound to GroEL is also in the MG-form. a-LA and its disulfide-reduced forms in the MG interact with other chaperones and are frequently used as model substances for studies of protein folding in the cell. The insertion of soluble proteins into membranes and the conformations of the membrane-bound protein have been topics of interest (35-38). The insertion of a-LA into model membranes occurs under conditions that favor formation of the MG with its hydrophobic surface. The inserted a-LA is also in the MG-form, and its association with a lipid bilayer affects the chain mobility of the lipids.

Recently, some multimers of human a-LA prepared from its milk casein fraction were indicated to induce **apoptosis** in cancer cells, leukoma (L210), and lung carcinoma (A549) but not in healthy cells, although the monomeric human a-LA did not induce apoptosis in any cell (39-42). The active **high oligomers** are folding variants of human a-LA, to which fatty acids are bound, and assume the MG form. They were shown to accumulate in the nuclei of sensitive cells and to induce DNA fragmentation. The latter process requires Ca^{2+} ions. a-LA has important biological functions in addition to lactose synthesis.

a-LA is a protein of interesting structure, properties, and functions, and it will be noted in molecular biology in the future.

Bibliography

1. D. C. Phillips et al (1986) Biochem. Soc. Trans. 15, 737–744.
2. P. K. Qasba and S. Kumar (1997) Crit. Rev. Biochem. Mol. Biol. 32, 255–306.
3. K. Kuwajima et al (1976) J. Mol. Biol. 106, 359–373.
4. K. Kuwajima et al (1977) J. Mol. Biol. 114, 241–258.
5. M. Mizuguchi et al (2000) Proteins Struct. Funct. Genet. 38, 407–413.
6. W. Pfeil (1998) Proteins Struct. Funct. Genet. 30, 43–48.
7. M. Nozaka et al (1978) Biochemistry 17, 3753–3758.
8. M. Ikeguchi et al (1998) Protein Sci. 7, 1564–1574.
9. A. Troullier et al (2000) Nat. Struct. Biol. 7, 78–86.
10. R. Acharya et al (1989) J. Mol. Biol. 208, 99–127.
11. R. Acharya et al (1991) J. Mol. Biol. 221, 571–581.
12. R. Acharya et al (1996) Structure 4, 691–703.
13. R. Acharya et al (1998) Biochemistry 37, 4767–4772.
14. K. Harata et al (1999) J. Mol. Biol. 287, 347–358.
15. K. Harata et al (2000) J. Biol. Chem. 275, 37021–37029.
16. A. T. Alexandrescu et al (1992) Eur. J. Biochem. 210, 699–709.
17. A. T. Alexandrescu et al (1993) Biochemistry 32, 1707–1718.
18. C. M. Dobson et al (1999) J. Mol. Biol. 286, 1567–1580.
19. C. M. Dobson et al (1999) J. Mol. Biol. 288, 673–688.
20. J. J. Ewbank and T. E. Creighton (1991) Nature 350, 518–520.
21. J. J. Ewbank and T. E. Creighton (1993) Biochemistry 32, 3677–3707.
22. J. J. Ewbank and T. E. Creighton (1994) Biochemistry 33, 1534–1538.
23. P. S. Kim et al (1995) Trans. R. Soc. London B 348, 43–47.
24. P. S. Kim et al (1996) Biochemistry 35, 859–863.
25. D. F. Moriarty et al (2000) Biochim. Biophys. Acta 1476, 9–19.
26. K. Brew et al (1991) J. Biol. Chem. 266, 698–703.
27. K. Brew et al (1996) Biochemistry 35, 9710–9715.
28. K. Brew et al (1999) Protein Eng. 12, 581–587.
29. Y. Xue et al (2001) Proteins Struct. Funct. Genet. 42, 17–22.
30. M. K. Hayer et al (1994) EMBO J. 13, 3192–3202.
31. C. V. Robinson et al (1994) Nature 372, 646–651.
32. K. Kuwajima et al (1996) J. Mol. Biol. 258, 827–838.
33. K. Kuwajima et al (1996) J. Mol. Biol. 264, 643–649.
34. K. Kuwajima et al (1999) J. Mol. Biol. 293, 125–137.
35. S. Bunuelos and A. Muga (1995) J. Biol. Chem. 270, 29910–29915.
36. S. Bunuelos and A. Muga (1996) FEBS Lett. 386, 21–25.
37. S. Bunuelos and A. Muga (1996) Biochemistry 35, 3892–3898.
38. K. M. Cauthern et al (1996) Protein Sci. 5, 1349–1405.
39. M. Svanborg et al (1995) Proc. Natl. Acad. Sci. U.S.A. 92, 8064–8068.
40. M. Svanborg et al (1999) J. Biol. Chem. 274, 6386–6396.
41. M. Svanborg et al (2000) Proc. Natl. Acad. Sci. U.S.A. 97, 4221–4226.
42. M. Svanborg et al (2001) Eur. J. Biochem. 268, 186–191.

Suggestions for Further Reading

43. L. J. Berliner and D. Johnson (1988) -Lactalbumin and calmodulin, In Calcium Binding

Proteins, Vol. II (M. P. Thompson, ed.), CRC Press, Boca Raton, FL, pp. 79–116.

44. M. J. Kronman (1989) Metal-ion binding and the molecular conformational properties of -lactalbumin. Crit. Rev. Biochem. Mol. Biol. **24**, 565–667.
45. K. Kuwajima (1989) The molten globule state as a clue for understanding the folding and cooperatively of globular protein structure. Proteins: Struct. Funct. Genet. **6**, 87–103.
46. H. A. McKenzie and F. H. White Jr. (1991) Lysozyme and -lactalbumin: Structure, function and interrelationship Adv. Protein Chem. **41**, 171–315.
47. K. Brew and J. A. Grobler (1992) -Lactalbumin Advanced Dairy Chemistry Proteins, Vol. **1** (P. F. Fox, ed.), Elsevier Applied Service London and New York, pp. 191–229.
48. S. Sugai and M. Ikeguchi (1994) Conformational comparison between -lactalbumin and lysozyme. Adv. Biophys. **30**, 37–84.
49. K. Kuwajima (1996) The molten globule state of -lactalbumin. FASEB J. **10**, 102–109.
50. E. A. Permyakov and L. J. Berliner (2000) -Lactalbumin: structure and function. FEBS Lett. **473**, 269–274.

Alternative Splicing

Most eukaryotic **genes** that code for proteins contain noncoding sequences (**introns**) that are interspersed among the coding regions (exons). Transcription of these genes generates so-called pre-mRNA molecules, which are converted to mature mRNAs by a process termed RNA **splicing**. During this process, the introns are precisely excised and the exons are ligated together (see RNA Splicing). The majority of nuclear pre-mRNAs are spliced constitutively; that is, only one mature mRNA species is generated from a single pre-mRNA in all tissues. In some cases however, alternative 5′ and/or 3′ splice sites are used during splicing, resulting in the production of more than one mRNA species from a single pre-mRNA. Alternative splicing has been documented for many eukaryotic genes, and a variety of alternative splicing patterns have been observed, as depicted schematically in Figure 1. The utilization of alternative 5′ and/or 3′ splice sites (also referred to as donor and acceptor sites, respectively) can result in structurally distinct mRNAs by either excluding potential exon sequences or incorporating otherwise noncoding intron sequences. For some pre-mRNAs, alternative splicing is a nonregulated event such that two or more alternatively spliced mRNAs are produced at a given ratio to one another in all cell types. For others, the choice of alternative splice sites is regulated in a tissue-specific or developmental manner. This type of regulation is mediated by trans-acting factors that are differentially expressed in a particular tissue or at a specific time during development (see text below). These *trans*-acting factors may be positive or negative regulators that activate or repress the use of an alternative splice site either directly or indirectly, for example by modulating the affinity of general splicing factors.

Figure 1. Patterns of alternative splicing. Constitutively spliced exons are shown as black boxes, alternatively spliced exons are shown as shaded boxes, and introns are shown as a solid lines between the exons. Transcription start sites are indicated by an arrow, and polyadenylation sites are indicated by p(A). Splicing events are depicted by a dashed line.

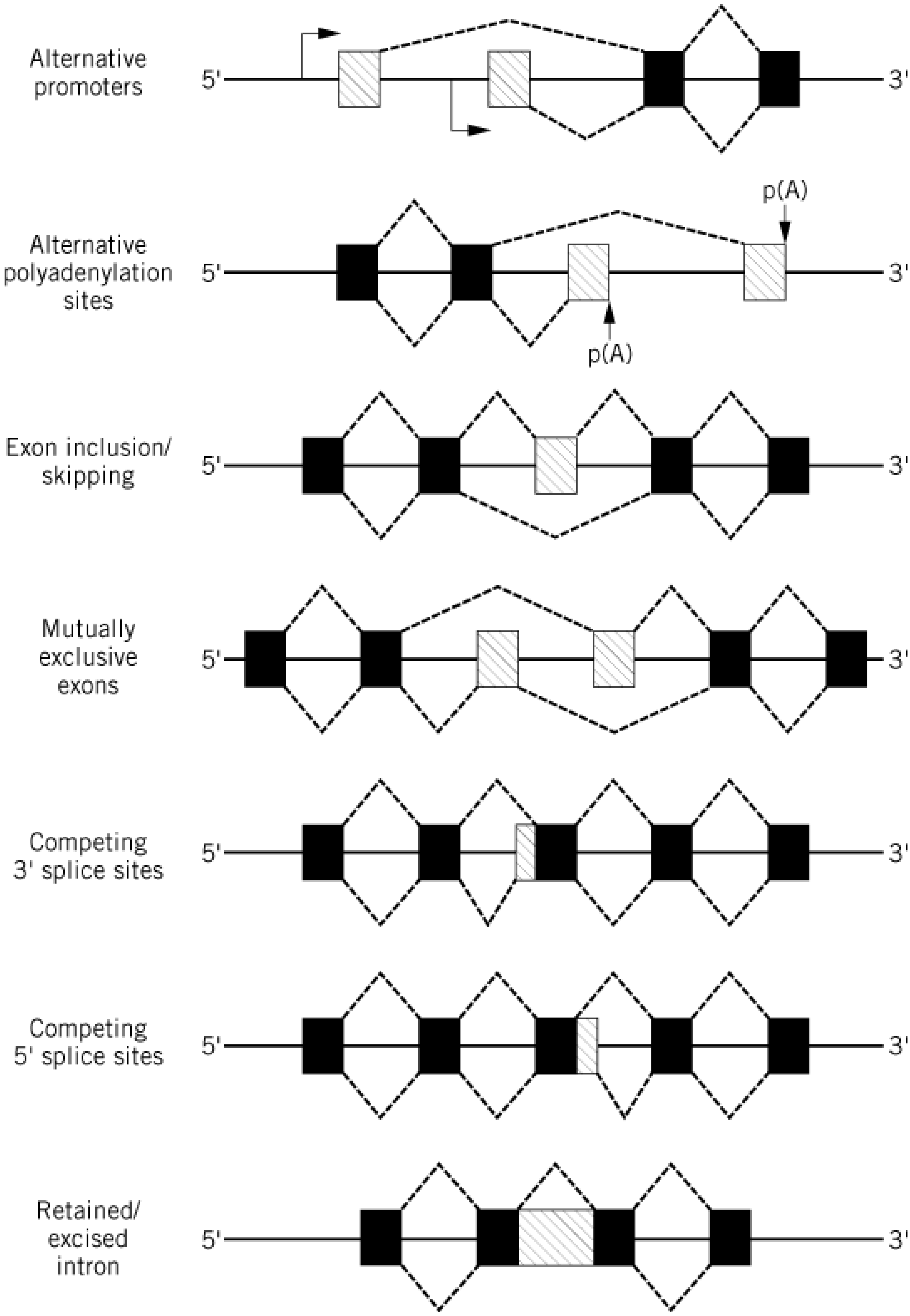

Alternative splicing can lead to both quantitative and qualitative changes in gene expression. Quantitative changes can arise if the alternatively spliced mRNA contains a prematurely truncated open reading frame (ie, due to the presence of a stop codon) or exhibits an altered stability or translation efficiency. In many cases, alternative splicing leads to the production of so-called protein isoforms that are structurally identical in all but a specific region or domain (1). Such structural variants of a given protein often exhibit significant functional differences. Thus, through the generation of multiple protein isoforms, alternative splicing can enhance the phenotypic variability of a single gene.

A central question in both constitutive and alternative splicing that has yet to be clearly resolved is how the correct pairs of 5′ and 3′ splice sites are selected for cleavage and subsequent ligation (see also Splice Sites). Pre-mRNAs contain multiple authentic 5′ and 3′ splice sites, which must be properly paired in order to prevent the random skipping of one or more exon. Furthermore, these sites must be distinguished from other nonauthentic sites that are also repeatedly present in most pre-mRNAs. In the case of alternative splicing, several different factors appear to be responsible for the preferential selection of one splice site over another. Firstly, features of the pre-mRNA itself (so-called cis-acting elements) can influence splice-site utilization. For example, the conserved sequences found at the 5′ and 3′ splice sites and the branch site contribute to splice site selection (see Splice Sites). In recent years it has become clear that the relative strengths of competing splice sites is often a deciding factor in determining which site is used preferentially. The strength of a particular 5′ or 3′ splice site is generally a measure of how efficiently it binds spliceosomal components, such as the U1 and U2 snRNPs or the splicing factor U2AF, which play important roles during the early stages of spliceosome assembly. This in turn is often, but not always, a function of how closely its sequences match the 5′ and 3′ splice site consensus sequences, or a function of the length and uridine content of the polypyrimidine tract, which determines its affinity for U2AF. The selection of weak 5′ and 3′ splice sites, on the other hand, can be enhanced by splicing factors that promote U1 or U2 snRNP binding (eg, SR proteins; see text below). Some 5′ splice sites also activate usage of an upstream 3′ splice site (eg, in the preprotachykinin pre-mRNA); and, vice versa, some 3′ splice sites can promote the use of a downstream 5′ splice site (eg, in the B-tropomyosin pre-mRNA) (2, 3). In the former case, factors bound at the 5′ splice site (the U1 snRNP) enhance the interaction of U2AF with the upstream 3′ splice site via a network of molecular interactions across the exon (4, 5)

In some cases, regions of the pre-mRNA other than the 5′ and 3′ splice sites also contribute to alternative splice-site selection. Purine-rich sequences (so-called splicing enhancers), which are typically located in exons and often bind SR proteins, are known to enhance the use of adjacent 5′ or 3′ splice sites by stabilizing the interactions of spliceosomal components with them (reviewed in Ref. 6). In some instances, intron sequences or sequences in the 3′-untranslated region that regulate polyadenylation have also been shown to influence alternative splicing. Finally, pre-mRNA secondary structure (eg, stem-loop structures) can affect splice-site selection, for example by blocking the interaction of spliceosomal components with a particular splice site (7, 8).

Splice-site selection during alternative splicing is also regulated by *trans*-acting factors. Many of the currently identified *trans*-acting factors also function in constitutive pre-mRNA splicing. In this case, variations in their concentration, or the concentration of factors that compete with them, are thought to lead to tissue-specific modulation of splice-site usage. Foremost in this catagory of factors are members of the evolutionarily conserved SR protein family, which are characterized by an amino-terminal **RNA-binding domain** and a *C*-terminal domain rich in arginine–serine (RS) dipeptides (reviewed in Ref. 9). SR proteins (eg, SF2/ASF and SC35) play essential roles in constitutive nuclear pre-mRNA splicing, particularly at the earliest stages of spliceosome assembly (see Spliceosome). Moreover, in pre-mRNAs that contain multiple 5′ or 3′ splice sites (see Fig. 1), high concentrations of SR proteins generally enhance the use of the more proximal (downstream) 5′ splice site (so-called switching activity) or more proximal 3′ splice site (9, 10). However, apparently due to differences in the affinities of individual SR proteins for different pre-mRNAs, the effect of a particular SR protein on 5′ splice site selection can vary from one pre-mRNA to the next (11, 12). SR proteins appear to act by facilitating the interaction of the U1 snRNP with the 5′ splice site, an initial step for 5′ splice-site recognition, or by promoting the association of U2AF with the 3′ splice site (see Spliceosome). High concentrations of SR proteins can also inhibit exon skipping (Fig. 1), which likewise involves promoting the use of a proximal 5′ splice site. Interestingly, the activity of SR proteins such as SF2/ASF or SC35 in 5′ splice-site selection (but not in constitutive splicing) can be antagonized by the hnRNP proteins A/B (13, 14). High concentrations of these proteins generally favor the use of more distal 5′ splice sites, and the ratio of 5′ splice site usage is determined by the relative amounts of hnRNP A/B and SR protein. Thus, the amount of some alternatively spliced pre-mRNAs can be modulated by varying the cellular concentrations of these proteins (15). SR proteins are also involved in activating weak 5′ and 3′ splice sites that are located adjacent to purine-rich splicing enhancers (reviewed in Refs. 9 and 16). The binding of specific SR proteins to these exon enhancer sequences promotes the interaction of U2AF, and thus the U2 snRNP, with the 3′ splice site or the U1 snRNP with the 5′ splice site.

Trans-acting alternative splicing factors that are expressed in a tissue-, sex- or developmental-specific manner have also been identified. In mammals, concrete, well-understood examples of cell-specific regulators of alternative splicing are currently limited. The best-characterized factors are those responsible for alternative splicing events in the fruit fly *Drosophila melanogaster*. For example, sex determination in fruit flies involves a cascade of alternative splicing events that are regulated by sex-specific proteins (17) (see Fig. 2). In males, splicing of the Sex-lethal (Sxl), transformer (tra) and doublesex (dsx) pre-mRNAs are nonregulated events that appear to require only the general splicing machinery (ie, they represent the so-called default splicing patterns). In females, alternative splice sites are activated by female-specific factors, either directly or indirectly, through the inactivation of the male-specific site. The first of these factors known to act in this cascade is the female-specific Sxl protein, which regulates its own synthesis by an alternative splicing event. In females, Sxl is thought to block (by a currently unknown mechanism) use of the 3′ splice site of the third exon of the Sxl pre-mRNA, which leads to exon 3 skipping (18, 19). Because exon 3 contains a stop codon, functional Sxl protein is produced only from the female-specific Sxl mRNA (Fig. 2). In the next step of this cascade, the Sxl protein inhibits the use of the upstream 3′ splice site of exon 2 of the *tra* pre-mRNA, which in turn activates splicing at a weaker downstream 3′ splice site. Specifically, Sxl has been shown to bind to the stronger polypyrimidine tract of the upstream 3′ splice site and thereby to inhibit the binding of U2AF (20). This results in U2AF binding to the downstream site, for which it has a lower affinity. The resulting exclusion of exon 2, which also contains a stop codon, leads to the production of functional *tra* protein in females. In the last step, the tra protein, in conjunction with tra-2, directly activates use of the weak 3′ splice site of exon 4 of the doublesex pre-mRNA. Tra and Tra-2, both of which contain RS domains, interact with a purine-rich splicing enhancer present in exon 4 and recruit SR proteins, as well as U2AF, to the upstream 3′ splice site (reviewed in Ref. 6). As a result, exon 4 is included in female-specific dsx mRNA, and polyadenylation occurs at the end of this exon. The resulting female dsx protein represses male differentiation, whereas the male protein represses female differentiation. Although in this particular case much has been learned about the molecular mechanisms responsible for splice-site selection, in most cases a clear understanding of the complex processes of alternative splicing awaits further investigation.

Figure 2. Cascade of alternative splicing events in the sex determination pathway of *Drosophila*. For simplicity, only those exons and introns involved in alternative splicing events are shown. In female flies, the sex lethal protein regulates its own synthesis and that of the tra protein by blocking the use of the 3′ splice site of the third and second exons of the sex-lethal and tra pre-mRNAs, respectively. Both of these exons contain a stop codon, as indicated. The tra protein, together with tra-2, interacts with a splicing enhancer in the fourth exon of the double-sex pre-mRNA and activates use of the upstream 3′ splice site. Exons are depicted as numbered boxes, and introns are depicted as solid lines. Dashed lines above the introns represent splicing events in females, and those below indicate splicing events in males. The sex-lethal (sxl), transformer (tra), and tra-2 proteins are indicated by circles. Polyadenylation is indicated by p(A). (Adapted from Ref. 21).

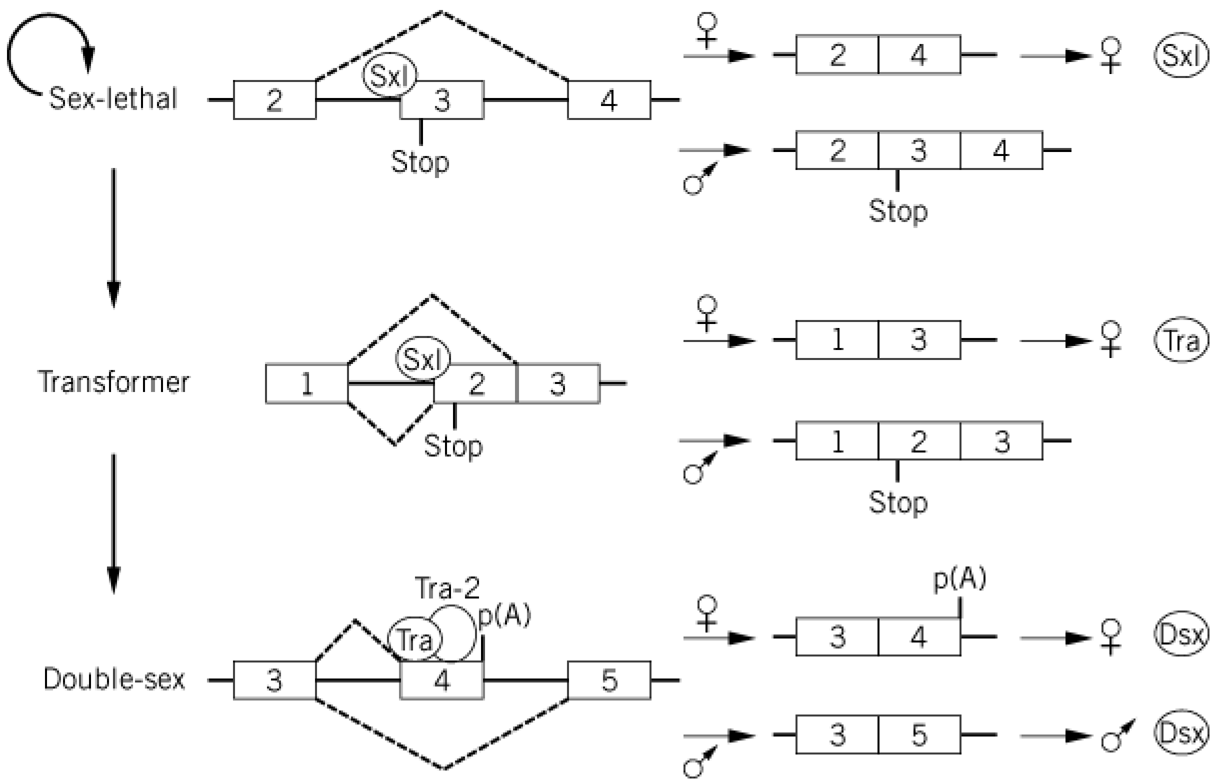

Bibliography

1. R. E. Breitbart, A. Andreadis, and B. Nadal-Ginard (1987) Annu. Rev. Biochem. **56**, 467–495.
2. F. H. Nasim, P. A. Spears, H. M. Hoffmann, H.-C. Kuo, and P. J. Grabowski (1990) Genes Dev. **4**, 1172–1184.
3. T. Tsukahara, C. Casciato, and D. M. Helfman (1994) Nucleic Acids Res. **22**, 2318–2325.
4. B. E. Hoffman and P. J. Grabowski (1992) Genes Dev. **6**, 2554–2568.
5. S. M. Berget (1995) J. Biol. Chem. **267**, 14902–14908.
6. K. J. Hertel, K. W. Lynch, and T. Maniatis (1997) Curr. Opin. Cell Biol. **9**, 350–357.
7. P. A. Estes, N. E. Cooke, and S. A. Liebhaber (1992) J. Biol. Chem. **267**, 14902–14908.
8. P. Sirand-Pugnet, P. Durosay, B. Clouet d" Orval, E. Brody, and J. Marie (1995) J. Mol. Biol. **251**, 591–602.
9. X.-D. Fu (1995) RNA **1**, 663–680.
10. D. S. Horowitz and A. R. Krainer (1994) Trends Gen. **10**, 100–106.
11. A. M. Zahler, K. M. Neugebauer, W. S. Lane, and M. B. Roth (1993) Science **260**, 219–222.
12. A. M. Zahler and M. B. Roth (1995) Proc. Natl. Acad. Sci. USA **92**, 2642–2646.
13. A. Mayeda and A. R. Krainer (1992) Cell **68**, 365–375.
14. X. Yang, M. R. Bani, S. J. Lu, S. J. Rowan, Y. Ben-David, and B. Chabot (1994) Proc. Natl. Acad. Sci. USA **91**, 6924–6928.
15. J. F. Caceres, S. Stamm, D. M. Helfman, and A. R. Krainer (1994) Science **265**, 1706–1709.
16. J. L. Manley and R. Tacke (1996) Genes Dev. **10**, 1569–1579.
17. B. S. Baker (1989) Nature **340**, 521–524.
18. J. I. Horabin and P. Schedl (1993) Mol. Cell. Biol. **13**, 1408–1414.
19. B. Granadino, L. O. F. Penalva, M. R. Green, J. Valcárcel, and L. Sánchez (1998) Proc. Natl. Acad. Sci. USA **94**, 7343–7348.
20. J. Valcárcel, R. Singh, P. D. Zamore, and M. R. Green (1993) Nature **362**, 171–175.

21. M. J. Moore, C. C. Query, and P. A. Sharp (1993) In *The RNA World* (R. F. Gesteland and J. F. Atkins eds.), Cold Spring Harbor Laboratory Press, Cold Spring Harbor, NY, pp. 303–358.

Suggestions for Further Reading

22. Y.-C. Wang, M. Selvakumar, and D. M. Helfman (1997) "Alternative Pre-mRNA Splicing". In *Eukayotic mRNA Processing* (A. R. Krainer, ed.), IRL Press, Oxford, UK, pp. 242–279.
23. B. Chabot (1996) Directing alternative splicing: cast and scenarios. Trends Gen. **12**, 472–478.
24. J. L. Manley and R. Tacke (1996) SR proteins and splicing control. Genes Dev. **10**, 1569–1579.
25. D. C. Rio (1993) Splicing of pre-mRNA: mechanism, regulation and role in development. Curr. Opin. Genet. Dev. **3**, 574–584.

Alu Sequences

The genomes of almost all higher **eukaryotes** contain highly repetitive DNA sequences that are not clustered together. They are distributed throughout the genome, interspersed with longer stretches of DNA with unique (or moderately repetitive) sequences. In the human genome, the majority of such sequences belong to a single family of Sines called the **Alu family** . Each sequence is about 300 base pairs long. Although the many copies present are recognizably related, they are not precisely conserved in sequence. Their name derives from the fact that most contain a single site of cleavage for the **restriction enzyme AluI** near their middle. More than 500,000 Alu sequences are present in the human genome, accounting for 3 to 6% of the total DNA. Any particular segment of DNA of 5000 bp or longer has a high probability of containing at least one Alu sequence. Most Alu sequences are flanked by tandem direct repeats of DNA and move like transposable elements creating target-site duplications when they insert.

On average Alu DNA sequences contain about 80% identity between members of the family, but certain internal regions are more conserved: an internal 40-bp region and two sets of sequences, one near the 5′ end and another one farther down in the transcriptional direction, that are homologous to sequences found in the **promoter** for **RNA polymerase** III.

One end of the Alu DNA segment is defined precisely by comparing several Alu sequences. The other end occurs at, or is adjacent to, a run of A bases of variable length that may or may not be interrupted occasionally by other bases. The internal structure of an Alu sequence is dimeric and may consist of an ancestral duplication of a segment of approximately 150 bp. In some rodents, a major SINE is 130 bp long and has sequence similarities with half of the primate Alu sequences. As in Alu, it is bound on one side by a poly(dA) sequence.

1. Origin

The Alu sequence derives from an internally deleted host cell 7SL RNA gene that encodes the RNA component of the signal-recognition particle (SRP) that functions in **protein biosynthesis** (1, 2). Consequently, an Alu sequence can be considered to be a transposable element or an unusually mobile pseudogene. Alu sequences are transcribed from the 7SL RNA promoter, a polymerase III promoter internal to the transcript, so that it carries the information necessary for its own transcription wherever it moves. However, it needs to borrow a reverse transcriptase to transpose.

2. Evolution

The Alu sequences may be grouped into discrete subfamilies on the basis of their sequences. Distinct families have amplified within the human genome in recent evolutionary history (3). The Human Specific or Predicted Variant subfamily, one of the most recently formed group of Alu sequences, amplified to 500 copies within the human genome sometime after the human/great ape divergence, which is thought to have occurred 4 to 6 million years ago. Comparisons of the sequence and locations of the Alu sequences in different mammals suggest that they have multiplied only recently.

Polymorphism of the Alu family member differs from other types of **polymorphism**, such as Variable Number of Tandem Repeat (VNTR, or minisatellite DNA) or Restriction Fragment Length Polymorphism (RFLP), because individuals share Alu insertions based upon identity by descent from a common ancestor as a result of a single event that occurred one time within the human population (4). In contrast the VNTR and RFLP polymorphisms have arisen multiple times within a population. Alu sequences represent a unique source of human genetic variation and a molecular fossil record of genomic evolutionary history. These sequences are natural landmarks for physical gene mapping and for reconstructing the evolutionary history/expansion of tandemly arrayed gene families (4).

3. Possible Functions

The physiological role of Alu elements is unknown, although it has been proposed that they are involved in DNA replication, regulation of transcription, and transport of signal recognition particle RNA to the nucleus. For example, Alu RNA and proteins that bind to Alu elements have been identified in human cells. In particular, it has been demonstrated that some Alu sequences in human gene regions have been altered in sequence so that they are now important in controlling and enhancing transcription (5). The consensus sequence of one of the major Alu families contains a functional retinoic acid binding element (see Response Element). The random insertion throughout the primate genome of thousands of Alu repeats containing a retinoic acid response element might have altered the expression of numerous genes, thereby contributing to evolutionary potential (6).

Bibliography

1. A. M. Weiner (1980) Cell **22**, 209–218.
2. E. Ullu, S. Murphy, and P. M. Melli (1982) Cell **29**, 195–202.
3. M. A. Batzer et al. (1996) J. Mol. Evol. **42**, 22–29.
4. R. J. Britten (1994) Proc. Natl. Acad. Sci. USA **91**, 6148–6150.
5. R. J. Britten (1996) Proc. Natl. Acad. Sci. USA **93**, 9374–9377.
6. G. Vansant and W. F. Reynolds (1995) Proc. Natl. Acad. Sci. USA **92**, 8229–8233.

Suggestion for Further Reading

7. P. Jagadeeswaran, B.G. Forgeti, and S. M. Weissman (1981) Short interspersed repetitive DNA elements in eucaryotes: Transposable DNA elements generated by reverse transcription of RNA pol III transcripts? Cell **26**, 141–142.

Amber Mutation

An amber mutation is a nonsense mutation that changes a sense **codon** (one specifying an amino acid) into the translational stop codon UAG, causing premature termination of the polypeptide chain during translation. The mutation, the codon, and the mutant are all called amber. Amber mutations arise by single base changes in the codons for eight amino acids (and in the UAA stop codon, although this is not a nonsense mutation). Mutations in the anticodons of the transfer RNAs that read those eight codons, in principle, could give rise to amber suppressors, but suppressors are recovered only if another tRNA exists that reads the codon. In *Escherichia coli*, five amber suppressors that arise by a single base change have been identified. In addition, amber mutations are suppressed by ochre suppressors because of wobble pairing in the third position (5′) of the anticodon. Amber mutations in *E. coli* and its **bacteriophages** are easily identified by their pattern of suppression by known suppressors. In **bacteria**, amber suppressors have relatively mild effects. Many laboratory strains and even natural isolates of *E. coli* carry amber suppressors. This might be surprising, because amber suppressors are expected to prevent the proper termination of many proteins, but amber codons are used relatively infrequently in *E. coli* and related bacteria.

The name amber was originally given to mutants of bacteriophage T4 that grow on *E. coli* strain K12 (l) but not on *E. coli* strain B (1). It turned out that the K12 strain used has an amber suppressor, whereas the B strain does not. The word amber was inspired by Harris Bernstein who participated in the original experiment (Bernstein means amber in German), although published versions of the story disagree on whether the mutants were named after Harris Bernstein himself or his mother (2, 3). It also could be significant that at nearly the same time that amber mutants were being discovered, Seymour Benzer was also analyzing nonsense mutations in the *rII* genes of phage T4 and calling them “ambivalent” (4).

Bibliography

1. R. H. Epstein, A. Bolle, C. Steinberg, E. Kellenberger, E. Boy de la Tour, R. Chevalley, R. Edgar, M. Susman, C. Denhardt, and I. Lielausis (1964) Cold Spring Harbor Symp. Quant. Biol. **28**, 375–392.
2. R. S. Edgar (1966) In *Phage and the Origins of Molecular Biology* (J. Cairns, G. S. Stent, and J. D. Watson, eds.), Cold Spring Harbor Laboratory Press, Cold Spring Harbor, NY, pp. 166–170.
3. F. W. Stahl (1995) Genetics **141**, 439–442.
4. S. Benzer and S. P. Champe (1962) Proc. Natl. Acad. Sci. USA **48**, 1114–1121.

Amber Suppressor

Amber suppressors are mutant tRNAs that translate the UAG (amber) termination codon as a sense codon. Amber mutations cause protein synthesis to terminate prematurely, resulting in inactive, truncated polypeptides. Amber suppressors allow for protein synthesis beyond the translational block resulting in active protein. Hence the term “suppressor;” these mutant tRNAs “suppress” the phenotypes of amber mutations. These suppressors have been extensively used in prokaryotic genetic studies, and in studies of the translational apparatus and mechanisms. For complete discussions of these and other suppressors, see Nonsense Suppression, Suppressor tRNA, and Genetic Suppression.

Ames Test

The *Salmonella*/mammalian **microsome** test for mutagens was originally developed in the laboratory of Bruce Ames (1) and has become sufficiently used and well-recognized to be familiarly described by his name. The assay utilizes several specially constructed strains of *Salmonella typhimurium* that normally require histidine for growth and can be reverted to **prototrophy** by a wide range of different mutagens. The assay requires that test chemicals and bacteria be plated onto a minimal agar petri dish, incorporating trace amounts of histidine and biotin, which are required for growth, to allow all the bacteria to grow through a small number of generations. In the absence of mutagen, a small number of colonies will grow on these plates, whereas mutagenic chemicals may increase this number very considerably. Mutations are scored as the number of revertant colonies per dish, usually as a function of applied dose. The test protocol incorporates homogenates of (usually) rat liver directly into the petri dish, thereby permitting mammalian metabolism of many compounds that require activation before they will interact with cellular DNA.

The DNA sequence around the original mutation has been determined in those strains most commonly used for mutagenicity testing (Table 1). The bacteria have been made more sensitive to mutagens by the introduction of several additional characteristics. Many of the strains carry a deletion in the *uvrB* gene and are defective in the ability for DNA repair. The bacterial cell wall has increased permeability to bulky chemicals because of the *rfa* mutation, and certain introduced **plasmids** may increase the sensitivity of the bacteria to mutation by some types of chemicals. The Ames test was originally developed as a screen for chemical carcinogens (1), but this has only proved appropriate to certain chemical classes (eg, Ref. 2). Nevertheless, because of the enormous number of chemicals tested in this assay, it must still occupy a premier position in testing for mutagenic properties of chemicals.

Table 1. Genotype and Reversion Characteristics of Some *Salmonella typhimurium* Strains Commonly Used for Mutagenicity Testing

		Additional Mutations				
Histidine Mutation	**Strain Number**	**Permeability**	**Repair**	***R*Factor**	**Nature of Mutation**	
hisC3076	TA1537	*rfa*	D*uvrB*	-	WT sequence unknown. Mutant thought to be +1 near CCC	Frameshifts
hisD3052	TA1538	*rfa*	D*uvrB*	-	WT:GAC-ACC-GCC-CGG-CAG¼	Frameshifts
	TA98			pKM101	Mutant:GAC-ACC-GCC-GGC-AGG¼	
HisD6610	TA97	*rfa*	D*uvrB*	PKM101	WT:GTC-ACC-CCT-GAA-GAG-A*TC-GCC Mutant:GTC-	Frameshifts

					ACA-CCC-CCC-TGA (opal)	
hisG46	TA1535	*rfa*	D*uvrB*	-	WT:.......-CTC-¼	Some base-pair substitution events
	TA100			pKM101	Mutant:¼-CCC-¼	Extragenic suppressors
HisG428	TA102	*rfa*		PAQ1	WT:CAG-AGC-AAG-CAA-GAG¼	Transitions and transversions
	TA104				Mutant:CAG-AGC-AAG-TAA (ochre)	Extragenic suppressors
						Small deletions (–3, –6)

Bibliography

1. B. N. Ames, J. McCann, and E. Yamasaki (1975) Mutat. Res. **31**, 347–364.
2. J. Ashby and R. W. Tennant (1994) Mutagenesis **9**, 7–16.

Amidination

Amidination takes place when an amino group is treated with an imide ester.

The reaction proceeds with reasonable yield when conducted under alkaline conditions (pH around 10). Side reactions, such as cross-linking take place at lower pH. Both a- and ε-amino groups can be amidinated, and the basicity of the modified residue increases. The amidinyl groups incorporated are stable in acidic media. The role of amino groups in protein function can be investigated by amidination. Proteins can be readily **radiolabeled** by amidinating with ^{13}C- or ^{3}H-labeled imide ester. Amidination of the ε-amino group on lysine residues is particularly useful in peptide mapping and in determining the primary structure of a protein (see Protein Sequencing). The proteolytic enzyme **trypsin** does not cleave at the modified lysine residues, thereby limiting cleavage to arginine residues. Moreover, amidinyl groups are removed by aminolysis, and the resulting deprotected **peptides** are cleaved further with trypsin.

1. Acetamidination of Proteins

After reduction and alkylation of the protein (100–700 nmol), it is dissolved in a few mL of 0.2 M triethylamine-HCl buffer, pH 10.3, containing 5.0 M guanidinium chloride (GdmCl) (1). Ethyl (or methyl) acetamide hydrochloride is dissolved in an equivalent amount of NaOH solution to maintain a final acetamide concentration of 0.1 to 0.15 M (100-fold molar excess of acetamide over amino groups). The reaction mixture is incubated for 1 hr at 25°C, **dialyzed** against 0.05 M NH_4HCO_3 containing 2.5 M GdmCl, and then against 0.05 M NH_4HCO_3. The protein is finally lyophilized.

2. Deamidination by Methylaminolysis

Acetamidinated protein or peptide (2.7 mg) is dissolved in 1.6 mL of 6 to 9 M urea. Then 0.9 mL of methylamine-formic acid buffer (9.6 M methylamine adjusted with HCOOH to pH 11.5) is added, and the reaction mixture is held for 4 h at 25°C. The final concentration of methylamine is 3.5 M. The reaction mixture is exhaustively dialyzed against deionized water at 4°C or, for peptides, isolated by gel filtration on Sephadex G-10, equilibrated and eluted with 0.1 M NH_4HCO_3.

Bibliography

1. G. C. DuBois et al. (1981) Biochem. J. **199**, 335–340.
2. J. K. Inman et al. (1983) Methods Enzymol. **91**, 559–569.

Amino Acid Analysis

The amino acid compositions of proteins are routinely determined by completely hydrolyzing the peptide bonds of the polypeptide chain, and then determining quantitatively the constituent amino acids that were released.

1. Peptide Bond Hydrolysis

The traditional method of hydrolyzing polypeptide chains has been to incubate them anaerobically in 6 *M* HCl at approximately 110°C for 24–72 h (1). More modern methods use other acids, higher temperatures, and shorter periods of time. Most peptide bonds hydrolyze at similar rates, but those between the large nonpolar amino acid residues, particularly **Val**, **Leu**, and **Ile**, are hydrolyzed more slowly and require longer hydrolysis times or the addition of organic acids such as trifluoroacetic acid. Hydrolysis is presumably hindered sterically by the bulky side chains.

Any chemical procedure that hydrolyzes the peptide bonds of the backbone will also hydrolyze the chemically similar amide side chains of **Asn** and **Gln** residues, to produce the amino acids aspartic acid and glutamic acid, respectively. It is feasible to measure the total number of Asn and Gln residues by measuring the amount of ammonia released during the hydrolysis, but otherwise it is not possible to distinguish between Asp and Asn and between Glu and Gln after hydrolysis of the polypeptide chain. In this case, it is common practice to designate such uncertain residues by the three-letter abbreviations Asx and Glx, and by the one-letter abbreviations B and Z, respectively.

Trp residues are usually destroyed completely by acid hydrolysis, probably as a result of reaction with chlorine produced by oxidation of the HCl. They can be protected by the addition of thiol or sulfonic acid compounds or of phenol to scavenge the chlorine (2). **Tyr** residues are also susceptible to chlorination, but they are usually lost only partially. The thiol groups of **Cys** residues are oxidized and the amino acid partially destroyed by acid hydrolysis; this residue is best analyzed after performic acid oxidation of the protein to convert all the Cys residues to cysteic acid.

Some of the problems with acid hydrolysis can be overcome by using other procedures, such as hydrolysis by alkali or by proteinases. Other amino acids, notably Ser and Thr, are destroyed by alkaline hydrolysis, however, and total proteinase digestion to amino acids is not straightforward. Consequently, acid hydrolysis remains in common use.

2. Quantifying the Amino Acids

The identities and quantities of the various amino acids present in a protein hydrolyzates are normally determined by automated amino acid analyzers. The amino acids are separated chromatographically and quantified as they emerge from the column. Traditional methods used ion-exchange chromatography of the free amino acids, followed by detection with ninhydrin or fluorescent reagents such as fluorescamine. Proline does not react in the usual manner with such reagents, due to absence of an amino group, so special procedures are required to measure it. More rapid and sensitive methods now predominate, in which the amino acids are reacted with suitable reagents prior to the chromatographic separation, rather than after. The favored method at present is to react the amino acids with phenylisothiocyate (see Edman Degradation) and then to separate the colored derivatives by reverse-phase chromatography. With this procedure, a complete quantitative amino acid analysis can be carried out in just a few minutes with only picomole quantities of amino acids (3).

The relative numbers of aromatic residues (**Phe**, **Tyr**, and **Trp**) in intact proteins and peptides can usually be determined from the UV absorbance spectrum under conditions in which the polypeptide chain is fully unfolded so that its spectrum is the sum of its constituent residues (4).

Amino acid analysis does not give directly the number of residues of each amino acid per polypeptide chain. The most accurate result is the molar ratios of the various amino acids. The true molecular weight of the polypeptide chain, in the absence of any non-amino acid moieties, must be known for the amino acid analysis results to be converted to the number of residues of each amino acid per chain. Only with very accurate results, or with very small proteins, are such values usually close to the actual integer values. An alternative procedure is to use progressive chemical modification of one type of amino acid side chain for counting residues.

Bibliography

1. R. L. Hill (1965) Adv. Protein Chem. **20**, 37–107.
2. L. T. Ng et al. (1987) Anal. Biochem. **167**, 47–52.
3. S. A. Cohen and D. J. Strydom (1988) Anal. Biochem. **174**, 1–16.
4. H. Edelhoch (1967) Biochemistry **6**, 1948–1954.

Amino Acids

Twenty amino acids are the building blocks of proteins. They are linked together in a linear polypeptide chain by forming peptide bonds between them, in an order ordained by the nucleotide sequence of the corresponding **gene** for the protein, **translated** from the corresponding messenger RNA.

Nineteen of the amino acids have the general structure

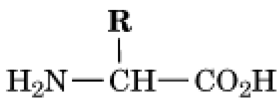

and differ only in the chemical structures of the side chain R. The amino group and the carboxyl group give this class of compounds its name. At physiological pH values, both groups are ionized, and the zwitterion is the common form of the amino acid. The exceptional amino acid, proline, differs in that its side chain is bonded to the nitrogen atom of the amino group, which is then a secondary amine, and proline is an imino acid:

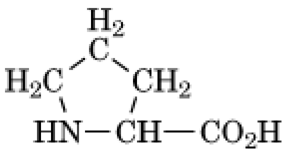

The central a-carbon atom is asymmetric in 19 of the amino acids and is always the L isomer:

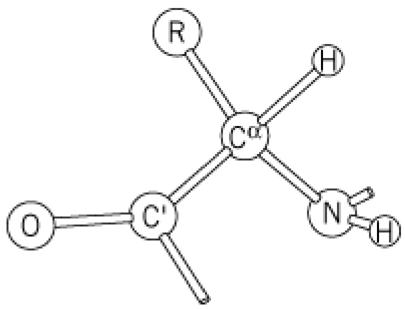

The exception is glycine, in which the side chain is simply another hydrogen atom, so the C^a atom is no longer asymmetric.

The structures of the side chains of the 20 normal amino acids used in protein biosynthesis are described in Figure 1, and their properties are described in individual entries. The central, asymmetric carbon atom is designated as a, and the atoms of the side chains are commonly designated b, g, d, ε and z in order away from the C^a atom. Chemical groups are, however, usually designated by the carbon atom to which they are bonded; hence, the Nz atom of a lysine residue is part of the ε-amino group. A 21st amino acid that is used in protein biosynthesis in only a few instances is selenocysteine. Many variations of these 21 amino acids can be found in proteins as a result of post-translational modifications after synthesis of the polypeptide chain.

Figure 1. The side chains of the 20 amino acids that occur naturally in proteins. Small unlabeled spheres are hydrogen at labeled. Double bonds are black, and partial double bonds are shaded. In the case of proline, the bonds of the polypeptid included and are black. The three- and one-letter abbreviations commonly used appear below the name of the amino acic and threonine have asymmetric centers in their side chains, and only the isomer illustrated is used biologically.

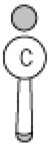

Glycine
Gly
G

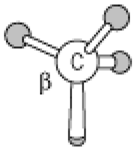

Alanine
Ala
A

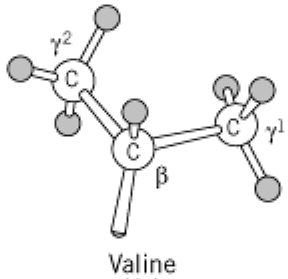

Valine
Val
V

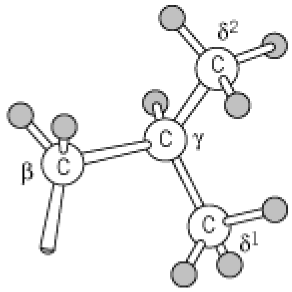

Leucine
Leu
L

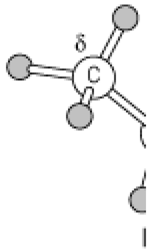

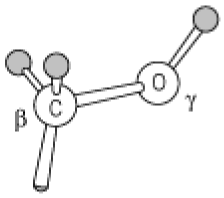

Serine
Ser
S

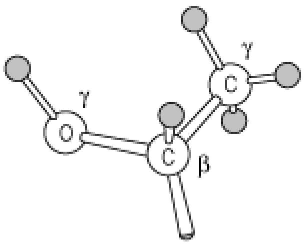

Threonine
Thr
T

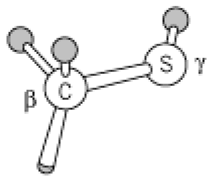

Cysteine
Cys
C

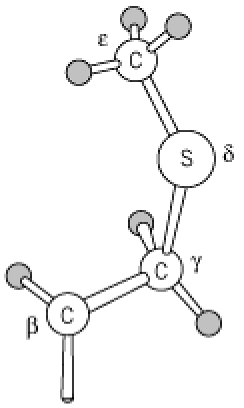

Methionine
Met
M

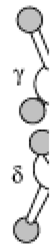

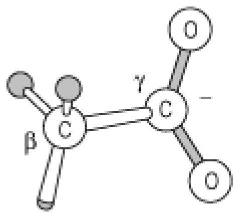

Aspartic acid
Asp
D

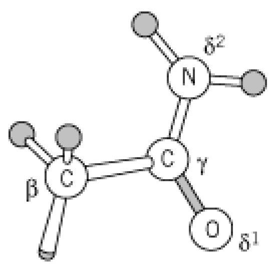

Asparagine
Asn
N

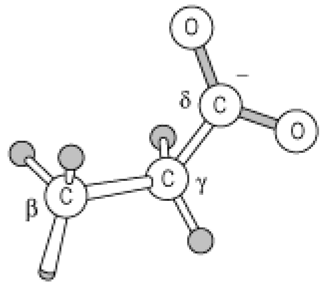

Glutamic acid
Glu
E

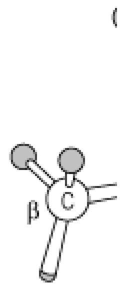

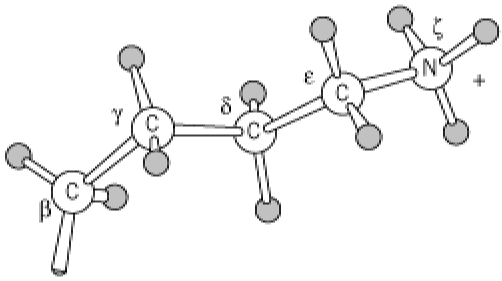

Lysine
Lys
K

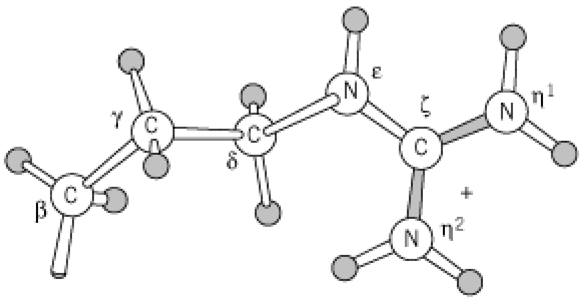

Arginine
Arg
R

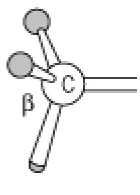

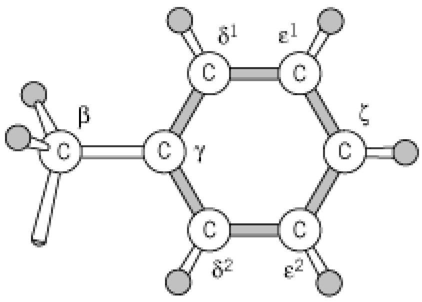

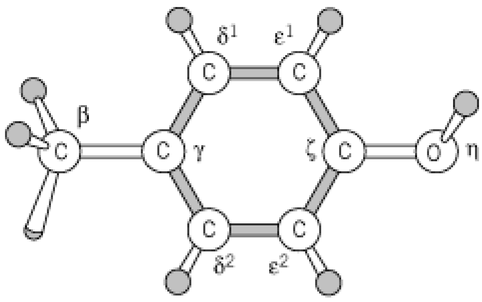

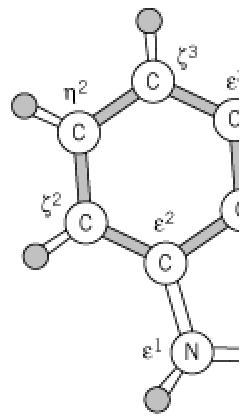

Linking the amino acids into a polypeptide chain involves the condensation of the a-carboxyl group of one with the a-amino group of the next, with the elimination of one water molecule. The remaining amino acid within the polypeptide chain is then known as a *residue*. Each type of residue is frequently designated with either three- or one-letter abbreviations, which are given in Figure 1. The three-letter abbreviations are obvious, but the one-letter are preferred with long sequences, as they save space and are less likely to be confused; for example, Gln, Glu, and Gly can easily be confused, but not Q, E, and G. The sequences of amino acids in proteins are usually written with either abbreviation, starting at the left with the *N*-terminal residue, with the free a-amino group, which is considered the first residue of the polypeptide chain. Amino acid residues in polypeptide chains are properly referred to by changing the ending of their amino acid names, adding or replacing the frequent "-ine" ending with "-yl" (eg, glycyl or alanyl residues), but the amino acid names are commonly used for the residues also. This complication can be minimized by using the one- or three-letter abbreviations. Note that these abbreviations should be used for residues in proteins only, not for the free amino acids.

Depending on the organism and its circumstances, the amino acids are derived from breaking down proteins ingested in feeding and recycling them, and also in some cases by synthesis de novo. In the well-known case of humans, the following amino acids cannot be synthesized and must be obtained from the diet: histidine, isoleucine, leucine, lysine, threonine, tryptophan, and valine. Arginine is synthesized, but not at a rate sufficient during growth. Methionine is required in large amounts to produce cysteine if that amino acid is not supplied adequately; similarly, phenylalanine is required in the absence of tyrosine.

Suggestions for Further Reading

E. J. Cohn and J. T. Edsall (1943) *Proteins, Amino Acids and Peptides*, Van Nostrand-Reinhold, Princeton, NJ.

R. E. Marsh and J. Donohue (1967) Crystal structures of amino acids and peptides, Adv. Protein Chem. **22**, 235–256.

Amino Groups

Amino groups are widely distributed in biological substances such as proteins, **polynucleotides**, polysaccharides, and lipids. They play important roles in electrostatic interactions because of their nucleophilicity and positive charge. The amino groups in the **nucleotides** of nucleic acids are involved in pairing bases. Modification of these groups causes serious errors in nucleic acid replication, translation, and **gene expression**. Amino groups in proteins are important for maintaining their structure and solubility and, sometimes, for manifestating their biological function. In particular, an amino group plays a pivotal role in the enzymes that utilize pyridoxal phosphate derivatives as **coenzymes**.

There are two kinds of amino groups in proteins. One is the N-terminal a-amino group, that has a pK_a of 6 to 8, and the other is the ε-amino group of lysine residues that have pK_a values generally between 8 and 10.5. The N-terminal amino group is very important for elucidating the primary structure of a protein because a free N-terminal amino group is indispensable for Edman

Degradation. N-terminal amino groups in proteins are often protected by acylation as a posttranslational modification. Attaching ubiquitin molecules to the amino groups of proteins induces their degradation . Amino groups are reactive nucleophiles and are widely utilized to immobilize proteins on solid supports for affinity chromatography.

1. Chemical Modification of Amino Groups in Proteins

Many modification methods for amino groups have been invented based on their excellent nucleophilicities (1). An amino group is a strong nucleophile only in its nonprotonated form, so it is most reactive at high pH. Because of the differences in pK_a values between a- and ε-amino groups, the former may be selectively modified by controlling the pH of the reaction medium. Because many amino groups are exposed and not involved in the protein function, modification of amino groups is suitable for introducing reporter groups, such as chromophores, into proteins and for **radiolabeling** them. The number of amino groups present and subsequently the extent of their modification with some modifying reagents, is determined by trinitrophenylation with 2,4,6-**trinitrobenzene sulfonic acid**. The integral number of amino groups present in a protein can be counted. Representative modification methods for amino groups are shown in Table 1.

Table 1. Chemical Modification of Amino Groups of Proteins

Reaction	Reagent	pH
Acylation	Acetic anhydride	5.5–8
	Acetylimidazole	>5
	N-Acetylsuccinimide	>4
	Citraconic anhydride	8.2
	N-Hydroxysuccinimide acetate	6.9–8.5
	Maleic anhydride	6–10
	Succinic anhydride	7–10
Alkylation and arylation	1-Fluoro-2,4-dinitrobenzene	7–11
	Iodoacetic acid	7.5–9
	2,4,6-Trinitrobenzene sulfonic acid	9.5
Amidination	Methyl acetamidate	7–10.5
Carbamylation	Potassium cyanate	>7
Guanidination	1-Guanyl-3,5-dimethylpyrazole nitrate	9.5
	O-Methylisourea	10–11
Reductive alkylation	Formaldehyde + sodium borohydride	8–10

Bibliography

1. T. Imoto and H. Yamada (1989) In *Protein Structure: A Practical Approach* (T. E. Creighton, ed.), IRL Press, Oxford, UK, pp. 247–277.

Aminoacyl tRNA Synthetases

The aminoacyl tRNA synthetases catalyze reactions that establish the rules of the genetic code. For this reason, there is great interest in these enzymes and their **evolutionary** development, which is thought to be closely connected to the establishment of the code. Research on the synthetases has led to the concept of an operational RNA code for amino acids that is imbedded in the acceptor stems of transfer RNA (**tRNA**) (1). The operational RNA code may have played an important role in the assembly of the genetic code and in the overall design of tRNA synthetases.

In the flow of genetic information, messenger RNA (mRNA) is **transcribed** from DNA, and the mRNA, in turn, is the template for protein synthesis (Fig. 1). The triplet **codons** of mRNA interact with the anticodons of tRNA through **complementary base pairing**. Amino acids joined to tRNA are incorporated into the growing polypeptide chain. The algorithm of the genetic code relates each amino acid to a specific trinucleotide codon. The triplet associated with a particular amino acid is determined in the aminoacylation reaction, where a given amino acid is linked to a tRNA bearing the anticodon trinucleotide that corresponds to that amino acid. These aminoacylation reactions are catalyzed by aminoacyl tRNA synthetases.

Figure 1. Flow of genetic information. Messenger RNA is synthesized from DNA. The mRNA has a string of trinucleotide codons that are translated into a polypeptide whose amino acid sequence is determined by the codons, according to the rules of the genetic code. The amino acid that is inserted into the polypeptide is determined by the codon–anticodon interaction with the tRNA that bears the amino acid corresponding to the particular anticodon. Therefore, the genetic code is determined by the linking of a particular amino acid with a particular anticodon triplet within a tRNA. The joining of amino acids to tRNA is catalyzed by aminoacyl tRNA synthetases. Thus, the genetic code is determined at the biochemical level in the aminoacylation reaction. (This figure was provided by Arturo Morales.)

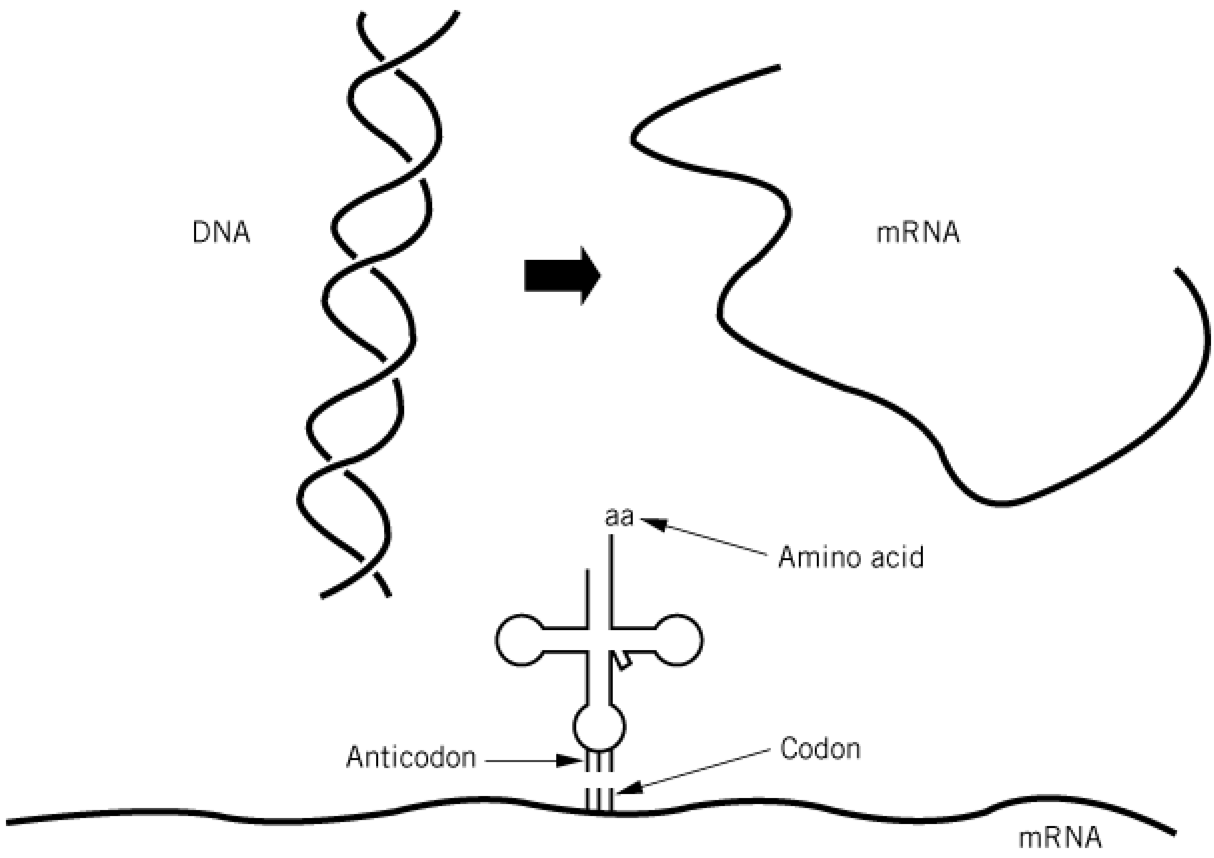

1. Aminoacylation Reaction and the Genetic Code

For most tRNA synthetases, aminoacylation is carried out in a two-step reaction:

$$E + AA + ATP \leftrightarrow E(AA\text{-}AMP) + PP_i \tag{1}$$

$$E(AA\text{-}AMP) + tRNA \leftrightarrow AA\text{-}tRNA + AMP + E \tag{2}$$

In the first reaction, the enzyme, E, uses ATP to activate an amino acid, AA, to yield the firmly bound *aminoacyladenylate* (AA-AMP). In the second step, the activated amino acid is transferred to the 3′-end of the tRNA, where it is connected by an ester linkage to the 2′- or 3′-hydroxyl group (after initial attachment, the amino acid can migrate back and forth between the 2′ and the 3′ positions). While most synthetases can carry out amino acid activation in the absence of tRNA, there are a few exceptions (such as glutaminyl-, glutamyl-, and argininyl-tRNA synthetases) that require the presence of the cognate tRNA for amino acid activation.

Because each of the 20 natural amino acids used in protein synthesis has a corresponding, or **cognate**, aminoacyl tRNA synthetase, there are 20 of these enzymes in each cellular compartment where proteins are synthesized. Each of them must distinguish its amino acid from all others and, at the same time, recognize the cognate tRNA that bears the anticodon corresponding to that amino acid. In **prokaryotes** and in the cytoplasm of **eukaryotes**, there is typically one tRNA synthetase for each amino acid (eukaryotic mitochondria have an additional set of synthetases that are essential for mitochondrial protein synthesis). However, the degeneracy of the genetic code means that there are 61 trinucleotides coding for the 20 amino acids. Reading these 61 triplets requires more than just 20 tRNAs. As a consequence, there are multiple tRNA isoacceptors for many of the synthetases. The synthetases for a particular amino acid must, therefore, recognize and aminoacylate all tRNA isoacceptors for that amino acid. This consideration in itself has important implications.

For example, the codons for serine are sixfold degenerate. In order to read these six codons, the serine tRNA isoacceptors must collectively permute all three anticodon nucleotides. Thus, for a single seryl-tRNA synthetase to aminoacylate all these $tRNA^{Ser}$ isoacceptors, the anticodon is not suitable for discrimination. Direct experiments *in vitro* and the X-ray crystallography structure of the seryl-tRNA synthetase-$tRNA^{Ser}$ complex have demonstrated that, in fact, seryl-tRNA synthetase does not contact the anticodon trinucleotide (2). This observation, and others described below, showed that, for at least some amino acids, the relationship between an amino acid and the triplet of the genetic code is not direct.

2. Classes of Aminoacyl tRNA Synthetases

The synthetases are heterogeneous in quaternary structures and subunit sizes, and this heterogeneity obscured more fundamental relationships between these enzymes. For example, in *Escherichia coli*, the quaternary structures of synthetases include a, a_2, a_4, and a_2b_2 (3). Subunit sizes vary from 303 to 951 amino acid residues (4). The 20 aminoacyl tRNA synthetases are now known to be divided into two classes of 10 enzymes each (Table 1) (8, 9). These classes are based on conserved sequence motifs and the structural architecture of the catalytic domains (8, 9). The classification is also based on the fact that the site of initial amino acid attachment on the tRNA differs between the two classes (8). The classes appear to be fixed in evolution, because there is no example of an enzyme switching classes depending on the organism to which it belongs. Thus, the two classes may have developed early in evolution.

Table 1. Classes of Aminoacyl tRNA Synthetases

Class I	Class II
Arginine	Alanine
Cysteine	Asparagine[0]
Glutamic	Aspartate
Glutamine1	Glycine
Isoleucine	Histidine
Leucine	Lysine
Methionine	Phenylalanine
Tryptophan	Proline
Tyrosine	Serine
Valine	Threonine

Gram-positive bacteria, plant chloroplasts, and animal mitochondria have been shown to have less than 20 tRNA synthetases. Instead, glutamyl-tRNA synthetase catalyzes attachment of glutamic acid to both $tRNA^{Glu}$ and $tRNA^{Gln}$ and, similarly, aspartyl-tRNA synthetases catalyzes attachment of aspartate to both $tRNA^{Asp}$ and $tRNA^{Asn}$. An amidotransferase then catalyzes the amidation of Glu-$tRNA^{Gln}$ to give Gln-$tRNA^{Gln}$, and, likewise, amidation of Asp-$tRNA^{Asn}$ gives Asn-$tRNA^{Asn}$ (5-7).

2.1. Class I

These enzymes are usually monomers and are characterized by an architecture that is similar to that seen in dehydrogenases and other **nucleotide-binding** proteins. This structural motif is a **Rossmann** nucleotide-binding fold, which consists of alternating b-strands and a-helices (Fig. 2) (10-12). In the case of class I tRNA synthetases, the fold is divided into two b_3a_2 halves to give an overall b_6a_4 structure. In this structure, the b-strands are arranged in parallel. A polypeptide of variable length, designated as connective polypeptide 1 (CP1), links together the two halves of the active site (13). In some class I enzymes, this insertion plays a role in translational editing. It also contains some of the residues for binding the synthetase to the tRNA acceptor helix (14).

Figure 2. Design of a class I tRNA synthetase. The nucleotide-binding fold of class I tRNA synthetases consists of alter (cylinders) that form a b_6a_4 structure. A two-dimensional spatial arrangement of these elements is shown at the top, and below. A second domain of variable size occurs after the nucleotide-binding fold. The fold is split into two b_3a_2 halves b *polypeptide 1* (CPI). A second, smaller insertion (CP2) splits the second half of the fold. Two sequence elements were us enzymes. These are known as the *12-residue signature sequence*, which ends in the HIGH tetrapeptides (10, 11) and as t locations in the schematic structure are shown near the label signature sequence and KMSKS. By way of example, an ali sequences of the 10 class I *E. coli* enzymes is shown beneath the schematic figures. Similar alignments can be made for throughout evolution. (This figure was provided by Arturo Morales.)

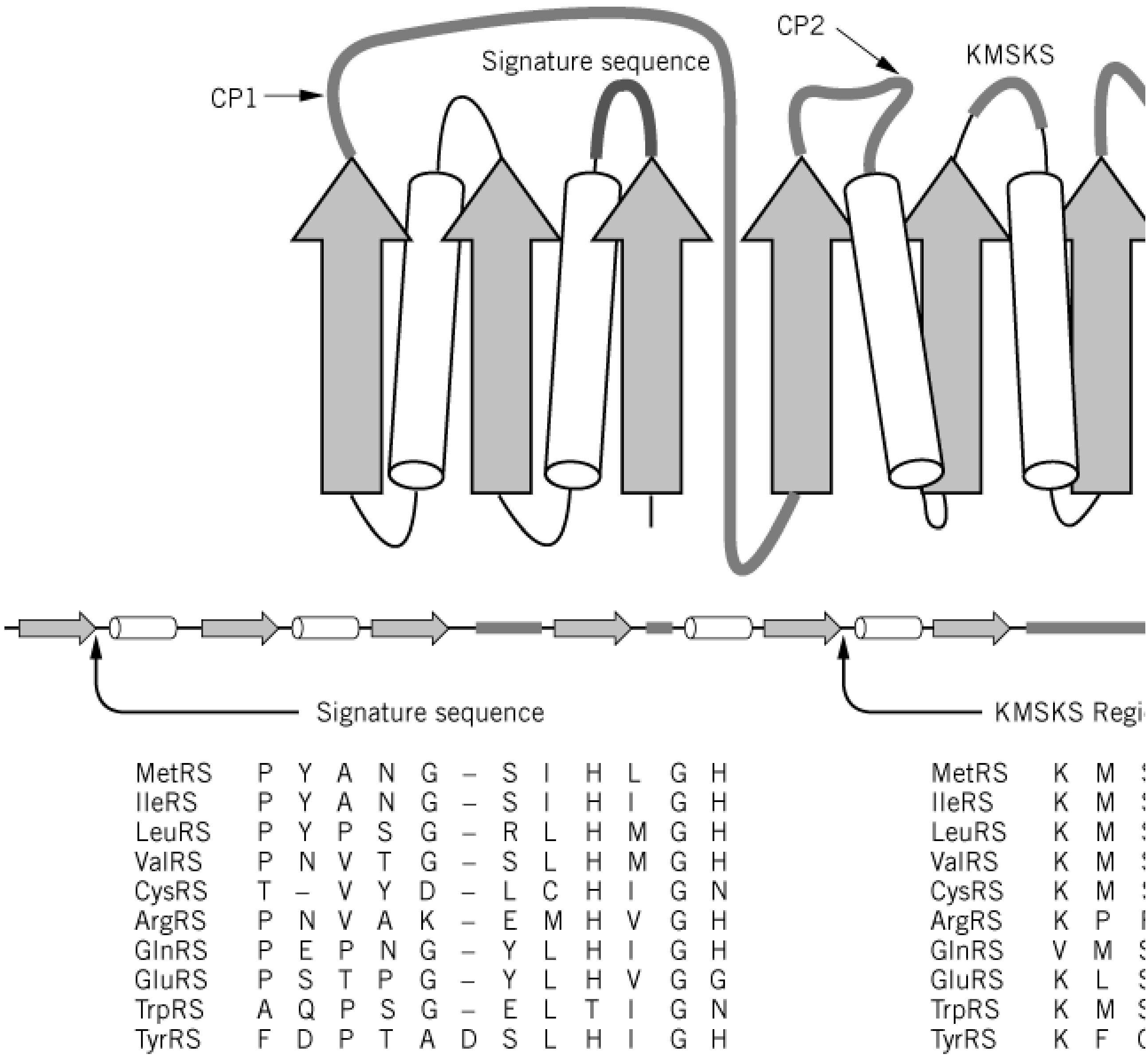

The nucleotide-binding fold contains the site for adenylate synthesis. This catalytic **domain** may be identified by two characteristic sequence motifs, without any knowledge of three-dimensional structure. One motif is the 11–amino acid element known as the signature sequence, which ends in the sequence–His–Ile–Gly–His, or HIGH in one-letter code (10, 11). This element is located in the first half of the nucleotide-binding fold at the end of the first b-strand and the beginning of the first a-helix. It was designated as a signature sequence because it served as a clear signature for a subgroup of related synthetases, before many crystal structures were determined. The second element is the KMSKS motif, located in the second half of the nucleotide-binding fold (15). These elements are critical parts of the active site.

2.2. Class II

The class II enzymes are mostly a_2 dimers. The active sites of class II enzymes have a completely different architecture that harbors three characteristic sequence motifs. The structure consists of a seven-stranded antiparallel b-sheet with three a-helices (9, 16-18) (Fig. 3) (8, 9, 19). The three characteristic sequence motifs are known as motifs 1, 2, and 3. The sequences of these motifs are highly degenerate (8, 9). They consist of a helix–loop–strand, strand–loop–strand, and strand–helix, respectively. All three of these motifs form part of the active site.

Figure 3. Design of a class II tRNA synthetase. The seven-stranded b-sheet with three a-helices is shown. The variable-s
line that may occur on either the *N*- or the *C*-terminal side of the class-defining domain. Three characteristic sequence m
and are distinguished in this illustration by their different shadings. These motifs are highly degenerate in sequence and c
strand–loop–strand (motif 2), and strand–helix. The locations of these motifs in the class-defining domain are shown. Ar
motifs for *E. coli* tRNA synthetases is also shown (8, 19). Note the high degeneracy of these sequence motifs, especially
sequence elements in class I enzymes (Fig. 2). (This figure was provided by Dr. Arturo Morales.)

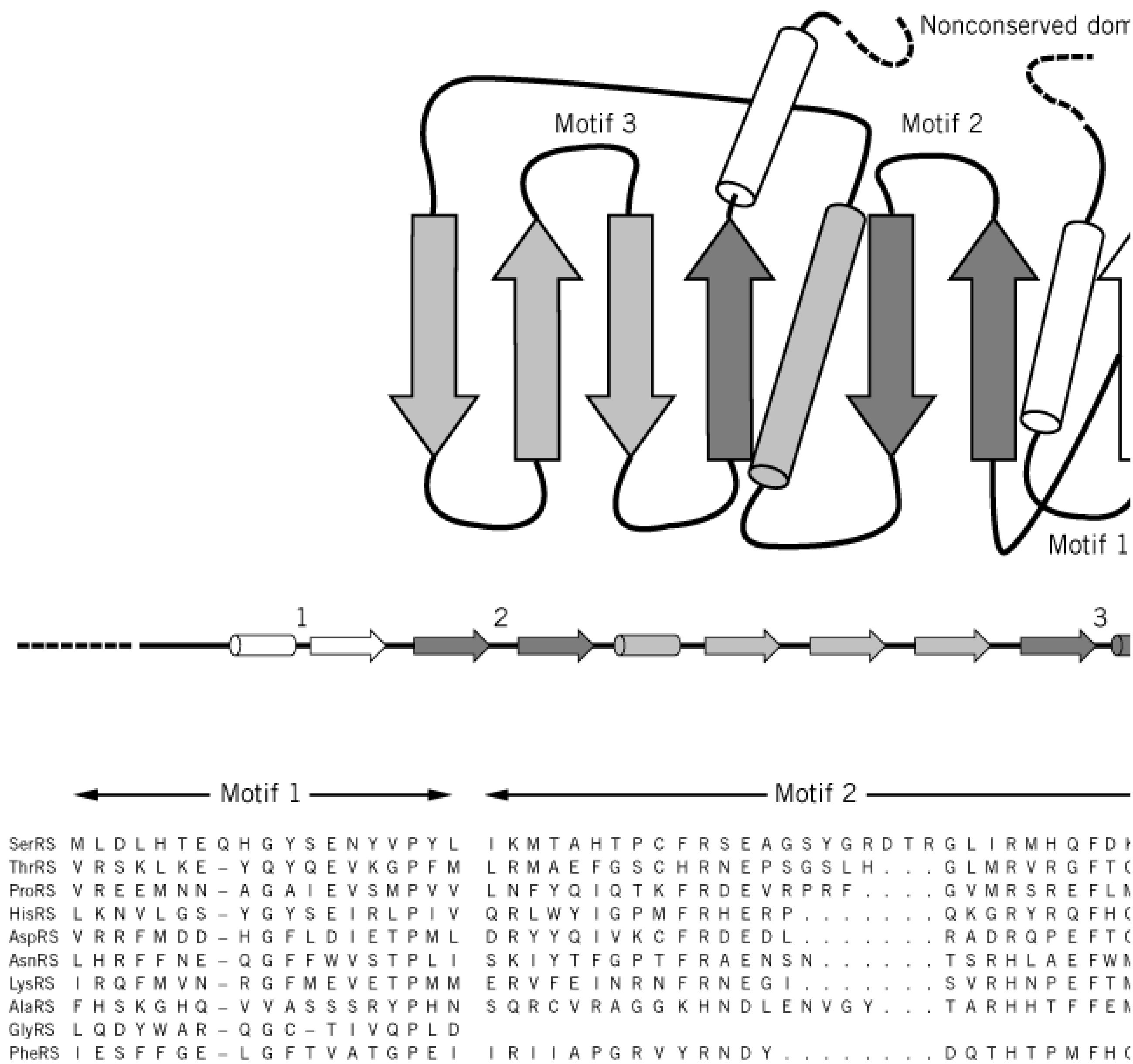

2.3. Amino Acid Attachment

The site of initial amino acid attachment for class I enzymes is the 2′-hydroxyl, whereas the 3′-hydroxyl is used by class II enzymes (20). This distinction is now understood to result from a difference in the ways that the two enzymes approach the end of the tRNA. In particular, class I enzymes approach the end of the tRNA acceptor helix from the minor groove side, while class II enzymes approach from the major groove side (21).

3. Overall Structural Design and the Synthetase-tRNA Complex

The class-defining active-site domain is only a part of the tRNA synthetase structure. Inserted into the active-site domain are sequence motifs that enable the tRNA acceptor helix to bind with its 3′-end near the aminoacyl adenylate. These insertions are typically idiosyncratic to the synthetase. Two examples are the CP1 insertions of class I enzymes and the variable loops of motif 2 of class II enzymes, both of which have a role in docking the acceptor helices to the enzymes. However, in addition to insertions into the active-site domain, all synthetases have a second major domain. This domain, also typically idiosyncratic to the enzyme, provides for contacts with parts of the tRNA that are distal to the amino acid attachment site. For many (but not all) synthetases, this includes contacts with the anticodon. For the class I methionyl- and glutaminyl-tRNA synthetases, this second, anticodon-binding, domain is largely a-helical and largely b-structure, respectively (22, 23). This difference demonstrates that, even for enzymes in the same class, their second domains are completely unrelated. In the case of the class II seryl-tRNA synthetase, an unusual coiled-coil protrudes from the N-terminus of the enzyme. This structure, which is not found in many other class II enzymes, provides for contacts with the variable loop of $tRNA^{Ser}$ (2, 24).

Thus, to a rough approximation, the synthetases comprise two major domains (9, 14, 16, 23, 25-31). The tRNA molecule also comprises two major domains, which consist of the four arms of the cloverleaf secondary structure (Fig. 4). One domain is the acceptor-TyC minihelix, where the amino acid acceptor end and the TyC stem stack together to make a helix of 12 base pairs. The second domain is formed by stacking of the dihydrouridine stem with the anticodon stem. The result is an L-shaped three-dimensional structure where the amino acid acceptor end and the anticodon-containing template-reading-head are segregated into separate structural units (see Transfer RNA).

Figure 4. Examples of crystal structures of class I and class II tRNA synthetases. Regardless of the class to which an enz assigned, its structure can be approximated as comprising two major domains. One is the class-defining active site doma which is shared by all members of the same class. This domain (gray) is thought to be the historical tRNA synthetase. Th second domain (dark gray) is typically idiosyncratic to the synthetase and is not shared by all members of the same class domain was probably added later to the synthetase structure. In these illustrations, the domains have been defined by the obvious visual divisions in the structures and, for that reason, the catalytic domain may extend somewhat beyond the reg contains the class-defining motifs. Some of these enzymes are homodimers; in all cases, only a single subunit is shown. I case of the tyrosyl tRNA synthetase, TyrRS, the structure of the second domain is not complete and therefore is truncate structural representation. Not shown is PheRS (25), which has an a_2b_2 quaternary structure. These structures were determ for GlnRS (14), GluRS (26), MetRS (23), TyrRS (27), TrpRS (28), AspRS (16), LysRS (29), GlyRS (30), HisRS (31), ar SerRS (9). (This figure was provided by Arturo Morales.)

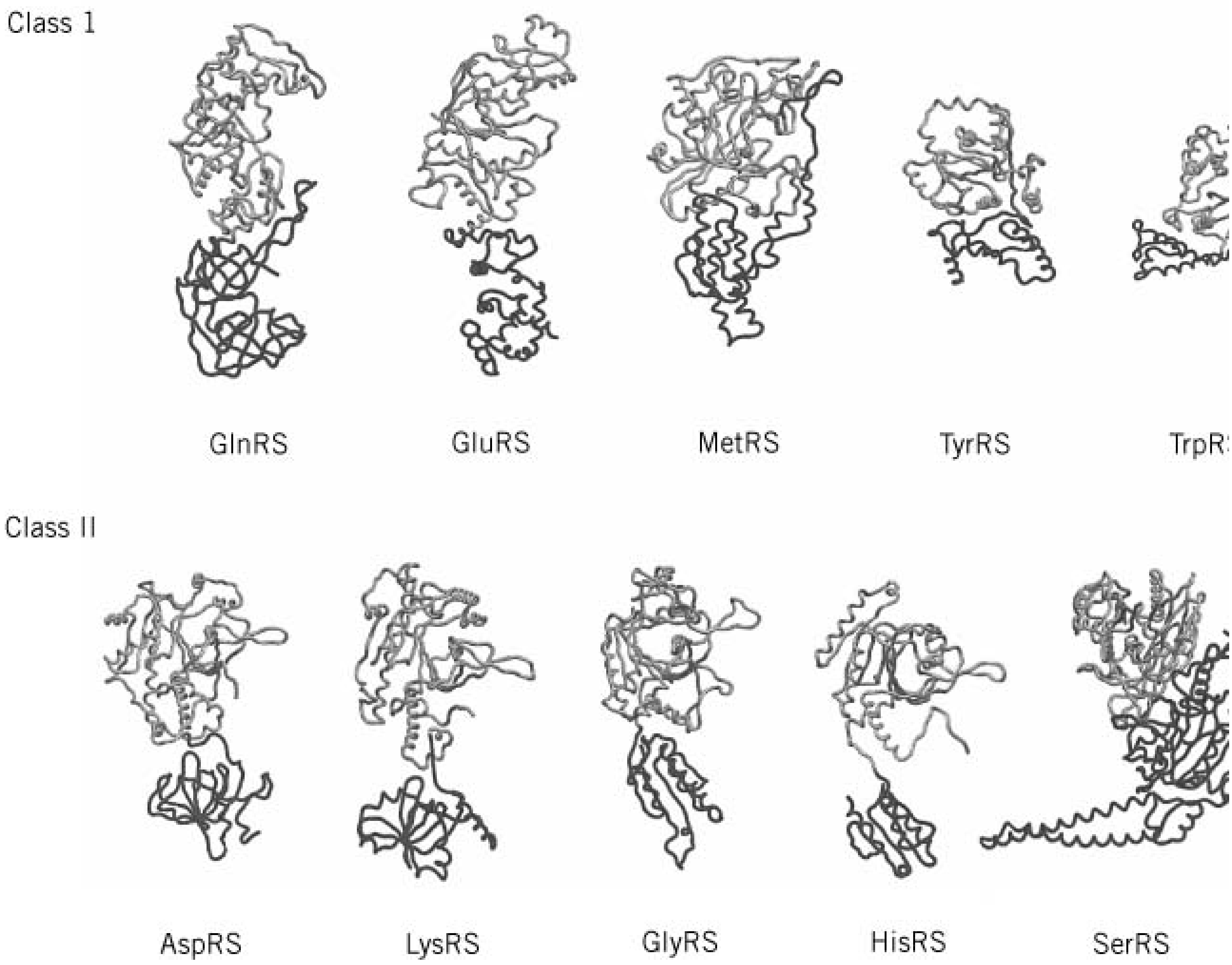

The two major domains of the synthetase make contact with the two domains of the L-shaped tRNA molecule (Fig. 5). The catalytic domain, with insertions containing RNA-binding determinants, interacts with the acceptor-TyC minihelix. The second major domain interacts with the second domain of the tRNA, where interactions may extend as far as the anticodon trinucleotide or may involve contacts with special structures, such as the large variable loop of $tRNA^{Ser}$. The details of the interactions between tRNA and synthetase are described in RNA-binding proteins.

Figure 5. Two major domains of a synthetase interacting with two domains of a tRNA. (**a**) Schematic representation of t domains that segregate the amino acid attachment site into a 12-bp minihelix stem–loop and the anticodon triplet into a s TyC loops are indicated as common landmarks found in most all tRNA. (Adapted from Ref. 32.) (**b**) Domains of a synth of a tRNA. The second domain of the synthetase is shown with a dotted line to indicate that it varies in size and often ex 33.) (**c**) Examples of synthetase-tRNA complexes, with the active-site class-defining domain interacting with the accepto second, idiosyncratic domain of the synthetase interacting with the second domain of the tRNA (5, 16). Separate shades domains. In the case of aspartyl tRNA synthetase, the protein is a dimer. Binding of a single tRNA to the monomer is sh domain interactions. The dimeric complex with two bound tRNA is also shown at the right. (This figure was provided b

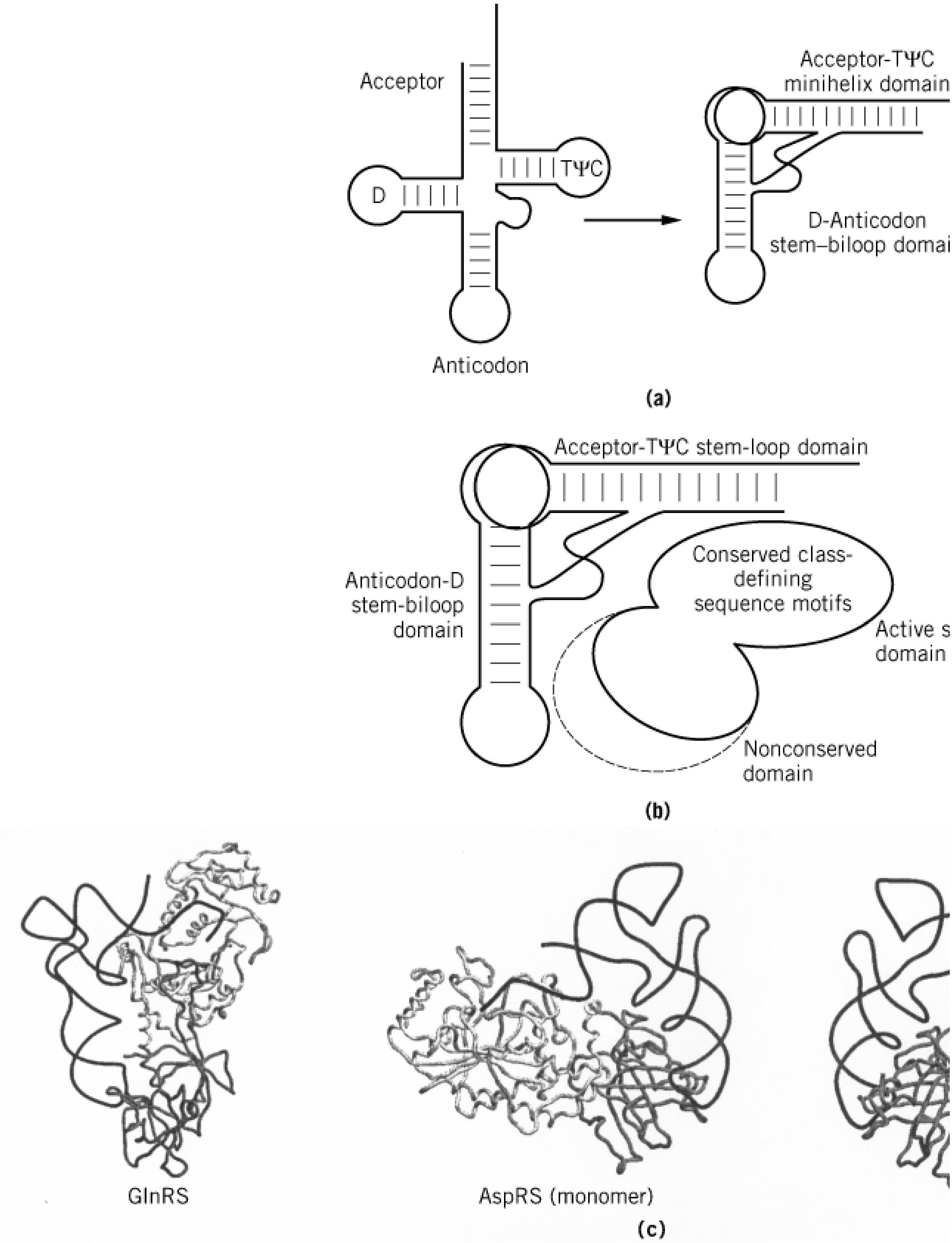

4. Operational RNA Code for Amino Acids

In addition to seryl-tRNA synthetase, alanyl-tRNA synthetase is an example of a synthetase that makes no contact with the anticodon (34). Instead, an acceptor helix G3:U70 **wobble** base pair is a major determinant of the identity of an alanine tRNA (35, 36). Alteration of this base pair to G:C, A:U, I:U, or U:G abolishes aminoacylation with alanine (37-39). Transfer of this base pair into other, nonalanine tRNA confers alanine acceptance on them. Thus, the G3:U70 pair marks a tRNA for charging with alanine.

Because the G3:U70 base pair is located in the acceptor helix, further experiments tested whether the 12-bp acceptor-TyC minihelix by itself would be a substrate for aminoacylation (Fig. 6) (40-42). Not only the minihelix, but also a 7-base-pair(bp) microhelix consisting of just the acceptor stem, is efficiently charged with alanine, provided that it contains the G3:U70 base pair (40, 43). Transfer of this base pair into other microhelices confers alanine acceptance on them. Thus, the charging behavior of the mini- and microhelices reproduces that seen with the full tRNA.

Figure 6. Minihelix and microhelix substrates for aminoacylation. The minihelix is derived from the 12-bp acceptor-TyC domain of the tRNA, while the microhelix is a hairpin helix whose base pairs consist of the 7-bp acceptor stem portion (40). These substrates for aminoacylation are devoid of the anticodon trinucleotides of the genetic code. About 11 examples of aminoacylation of minihelix or microhelix structures have been demonstrated. These substrates have been used to delineate the operational RNA code for amino acids (41). (Adapted from Ref. 42.)

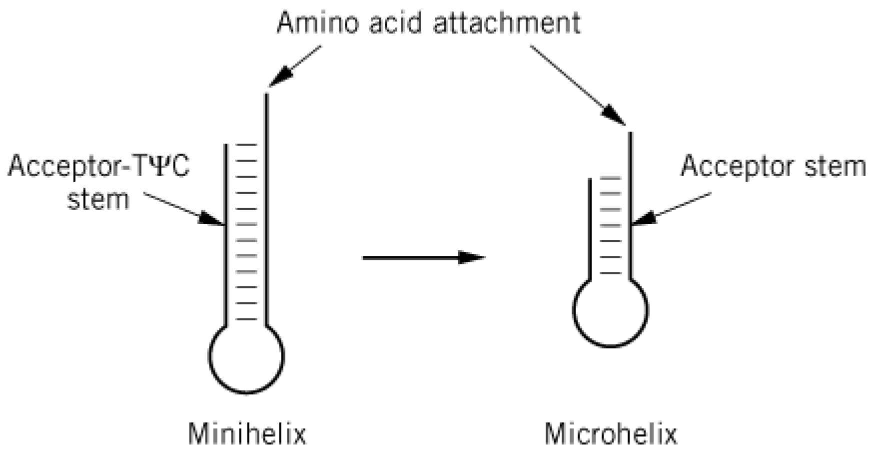

The charging of specific RNA helices has now been demonstrated with at least 11 different tRNA synthetases, even for cases where the anticodon is known to play a significant role in the recognition of the related tRNA (41, 44-47). In the case of histidine, for example, an extra nucleotide at the 5′ end of the acceptor helix is characteristic of and unique to histidine tRNA throughout evolution. RNA microhelices that contain the extra base are charged with histidine (48). Thus, the 5′-appended nucleotide marks a molecule for charging with histidine. The smallest substrates seen to be charged with specific amino acids are stem–loop hairpins with as few as four base pairs stabilized by an RNA **tetraloop** motif (Fig. 7) (49).

Figure 7. RNA tetraloop substrates for aminoacylation. The amino acid that can be charged onto the designated structures is indicated (49). These short helices are stabilized by an RNA tetraloop motif that confers unusual stability to short RNA helices. (Adapted from Ref. 49.)

A	A	A	A
C	C	C	C
C	C	C	C
A	U	$^{-1}$G-C	A
^{1}G-C	^{1}G-C	^{1}G-C	^{1}C-A
G-C	C-G	U-A	G-C
G-U^{70}	G-C^{70}	G-C^{70}	C-G^{70}
C-G	C-G	C-G	G-C
U G	U G	U G	U G
U C	U C	U C	U C
Ala	Gly	His	Met

The charging of microhelix substrates is sometimes considerably less efficient than that for the corresponding tRNA. In each case, however, charging is sequence-specific and depends on two to four nucleotides near the amino acid attachment site. In a fine-structure mapping of the efficiently charged alanine microhelix, a constellation of atoms was identified as critical for the aminoacylation signal. Prominent among these atoms was the exocyclic 2-amino group of G of the G3:U70 base pair. Also important were specific 2′-hydroxyl groups that fell within a 5-Å (Å = 10^{-10} m) radius of the critical 2-amino group (39).

These anticodon-independent aminoacylations of oligonucleotide substrates demonstrate that specific RNA sequences and structures per se, rather than the trinucleotides of the genetic code, correspond to specific amino acids. The relationship between these RNA sequences and structures and particular amino acids constitutes an operational RNA code for amino acids that is distinct from, but related to, the genetic code. This operational RNA code may have predated the genetic code (1).

5. Assembly of the Synthetase-tRNA Complex and Relationship of the Operational RNA Code to the Genetic Code

Several considerations led to the proposal that the minihelix and anticodon-containing second domain of tRNA had distinct origins (1, 50-52). The minihelix, with its amino acid attachment site, is viewed as the historical, or earliest, part of the tRNA. Similarly, the class-defining catalytic domain of tRNA synthetases is thought to be the historical enzyme, with the idiosyncratic second domain added later. Experiments with alanyl-tRNA synthetase have demonstrated that a relatively small piece of the enzyme (containing the active site) can by itself charge an RNA microhelix. This result directly demonstrated a domain–domain interaction between discrete units of the tRNA and the synthetase that may somewhat resemble an evolutionarily earlier system (33, 54).

Thus, the early synthetase may have consisted solely of a domain for adenylate synthesis. Insertions into this domain allowed the docking of RNA substrates near the activated amino acid so that aminoacylation could occur (Fig. 8). Addition of the second domain of the tRNA, with its anticodon-containing template reading head, and of the second domain of the synthetases was a second, later event. This event led to the joining of the operational RNA code to the genetic code. This scheme also suggests that the relationship between a particular amino acid and the triplet of the code is random, and simply depends on which anticodon-containing domain happened to be fused to the minihelix domain of the tRNA.

Figure 8. Assembly of a tRNA synthetase in evolution. A primordial tRNA synthetase is envisioned as interacting with a minihelix-like structure. As the tRNA structure developed, a template reading head (anticodon domain) was added, along with the second domain for the synthetase. (Adapted from Ref. 1.)

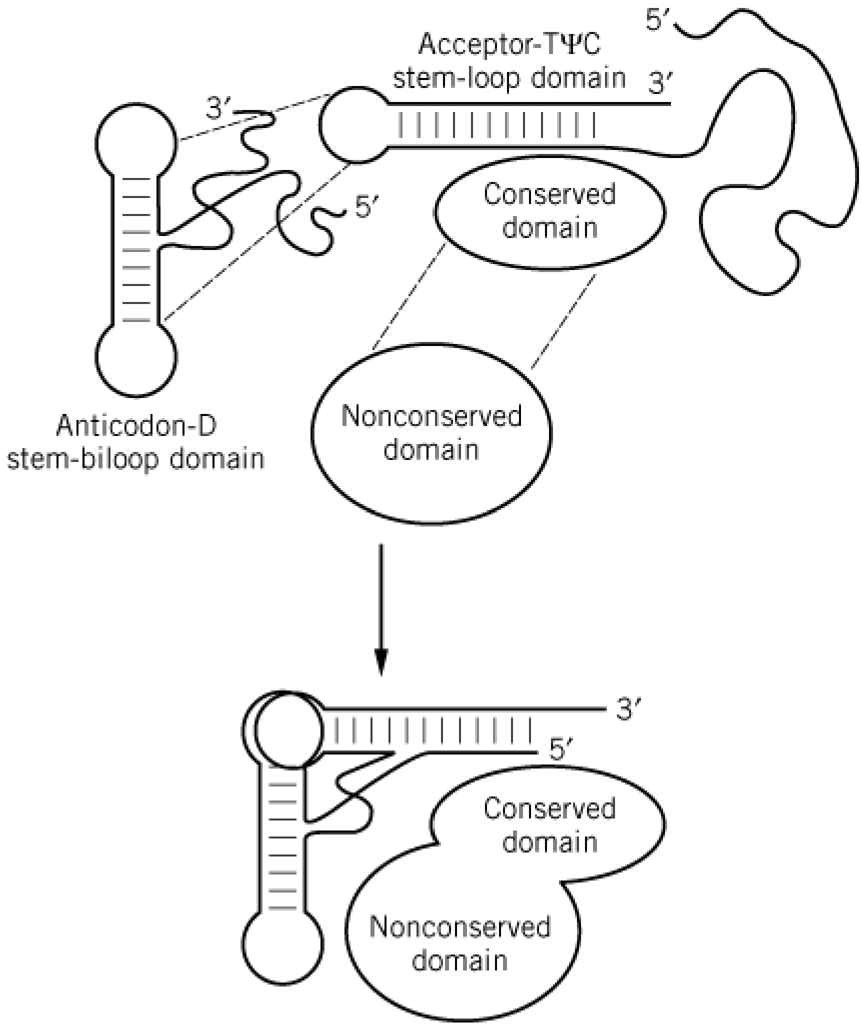

6. Conclusions

The tRNA synthetases may be among the earliest proteins, arising in evolution contemporaneously with the development of the genetic code. The first synthetases may have been **ribozymes** that catalyzed aminoacylation reactions with a specificity that depended on the sequences and structures of the RNA substrates (54, 55). The proteins that replaced these ribozymes were probably small. As a result, they could not extend much beyond the amino acid attachment site and, for that reason, gave rise to a system of interactions that based specificity of aminoacylation on interactions near the end of the acceptor helix. How these charged RNA substrates were used to synthesize specific proteins is a question of great interest.

Bibliography

1. P. Schimmel, R. Giegé, D. Moras, and S. Yokoyama (1993) Proc. Natl. Acad. Sci. USA **90**, 8763–8768.
2. V. Biou, A. Yaremchuk, M. Tukalo, and S. Cusack (1994) Science **263**, 1404–1410.
3. P. Schimmel (1987) Ann. Rev. Biochem. **56**, 125–158.
4. S. A. Martinis and P. Schimmel (1996) in *Escherichia coli and Salmonella* (F. C. Neidhardt Jr.,

ed.), ASM Press, Washington, DC, pp. 887–901.
5. A. Schon, C. G. Kannangara, S. Gough, and D. Söll (1988) Nature **331**, 187–190.
6. A. W. Curnow, M. Ibba, and D. Söll (1996) Nature **382**, 589–590.
7. Y. Gagnon, L. Lacoste, N. Champagne, and J. Lapointe (1996) J. Biol. Chem. **271**, 14856–14863.
8. G. Eriani, M. Delarue, O. Poch, J. Gangloff, and D. Moras (1990) Nature **347**, 203–206.
9. S. Cusack, C. Berthet-Colominas, M. Hartlein, N. Nassar, and R. Leberman (1990) Nature **347**, 249–255.
10. T. A. Webster, H. Tsai, M. Kula, G. A. Mackie, and P. Schimmel (1984) Science **226**, 1315–1317.
11. S. W. Ludmerer and P. Schimmel (1987) J. Biol. Chem. **262**, 10801–10806.
12. C. Hountondji, F. Lederer, P. Dessen, and S. Blanquet (1986) Biochemistry **25**, 16–21.
13. R. M. Starzyk, T. A. Webster, and P. Schimmel (1987) Science **237**, 1614–1618.
14. M. A. Rould, J. J. Perona, D. Söll, and T. A. Steitz (1989) Science **246**, 1135–1142.
15. C. Hountondji, P. Dessen, and S. Blanquet (1986) Biochimie **68**, 1071.
16. M. Ruff, S. Krishnaswamy, M. Boeglin, A. Poterszman, A. Mitschler, A. Podjarny, B. Rees, J. C. Thierry, and D. Moras (1991) Science **252**, 1682–1689.
17. S. Cusack, M. Hartlein, and R. Leberman (1991) Nucl. Acid Res. **19**, 3489–3498.
18. D. Moras (1992) Trends Biochem. Sci. **17**, 159–164.
19. S. Cusack (1993) Biochimie **75**, 1077–1081.
20. P. R. Schimmel and D. Söll (1979) Annu. Rev. Biochem. **48**, 601–648.
21. J. Cavarelli and D. Moras (1993) FASEB J. **7**, 79–86.
22. M. A. Rould, J. J. Perona, D. Söll, and T. A. Steitz (1991) Nature **352**, 213–218.
23. S. Brunie, C. Zelwer, and J. Risler (1990) J. Mol. Biol. **216**, 411–424.
24. S. Cusack, A. Yaremchuk, and M. Tukalo (1996) EMBO J. **15**, 2834–2842.
25. L. Mosyak, L. Reshetnikova, Y. Goldgur, M. Delarue, and M. G. Safro (1995) Nature Struct. Biol. **2**, 537–547.
26. O. Nureki, D. G. Vassylyev, K. Katayanagi, T. Shimizu, S. Sekine, T. Kigawa, T. Miyazawa, S. Yokoyama, and K. Morikawa (1995) Science **267**, 1958–1965.
27. P. Brick, T. N. Bhat, and D. M. Blow (1988) J. Mol. Biol. **208**, 83–98.
28. S. Doublie, G. Bricogne, C. Gilmore, and C. W. Carter Jr. (1995) Structure **3**, 17–31.
29. S. Onesti, A. D. Miller, and P. Brick (1995) Structure **3**, 163–176.
30. D. T. Logan, M.-H. Mazauric, D. Kern, and D. Moras (1995) EMBO J. **14**, 4156–4167.
31. J. G. Arnez, D. C. Harris, A. Mitschler, B. Rees, C. S. Francklyn, and D. Moras (1995) EMBO J. **14**, 4143–4155.
32. J. J. Burbaum and P. Schimmel (1991) J. Biol. Chem. **266**, 16965–16968.
33. D. D. Buechter and P. Schimmel (1993) Crit. Rev. Biochem. Mol. Biol. **28**, 309–322.
34. S. J. Park and P. Schimmel (1988) J. Biol. Chem. **263**, 16527–16530.
35. Y.-M. Hou and P. Schimmel (1988) Nature **333**, 140–145.
36. W. H. McClain and K. Foss (1988) Science **240**, 793–796.
37. S. J. Park, Y.-M. Hou, and P. Schimmel (1989) Biochemistry **28**, 2740–2746.
38. K. Musier-Forsyth, N. Usman, S. Scaringe, J. Doudna, R. Green, and P. Schimmel (1991) Science **253**, 784–786.
39. K. Musier-Forsyth and P. Schimmel (1992) Nature **357**, 513–515.
40. C. Francklyn and P. Schimmel (1989) Nature **337**, 478–481.
41. S. A. Martinis and P. Schimmel (1995) in *tRNA: Structure, Biosynthesis and Function* (D. Söll

and U. L. RajBhandary, eds.), American Society for Microbiology, Washington, DC, pp. 349–370.
42. P. Schimmel (1993) in *The Translation Apparatus* (K. H. Nierhaus, F. Franceschi, A. R. Subramanian, V. A. Erdmann, and B. Wittmann-Liebold, eds.), Plenum Press, New York, pp. 13–21.
43. C. Francklyn, J.-P. Shi, and P. Schimmel (1992) Science **255**, 1121–1125.
44. M. Frugier, C. Florentz, and R. Giegé (1994) EMBO J. **13**, 2218–2226.
45. Y.-M. Hou, T. Sterner, and R. Bhalla (1995) RNA **1**, 707–713.
46. C. L. Quinn, N. Tao, and P. Schimmel (1995) Biochemistry **34**, 12489–12495.
47. M. E. Saks and J. R. Sampson (1996) EMBO J. **15**, 2843–2849.
48. C. Francklyn and P. Schimmel (1990) Proc. Natl. Acad. Sci. USA **87**, 8655–8659.
49. J.-P. Shi, S. A. Martinis, and P. Schimmel (1992) Biochemistry **31**, 4931–4936.
50. A. M. Weiner and N. Maizels (1987) Proc. Natl. Acad. Sci. USA **84**, 7383–7387.
51. H. F. Noller (1993) in *The RNA World* (R. F. Gesteland and J. F. Atkins, eds.), Cold Spring Harbor Laboratory Press, Cold Spring Harbor, NY, pp. 137–156.
52. N. Maizels and A. Weiner (1994) Proc. Natl. Acad. Sci. USA **91**, 6729–6734.
53. D. D. Buechter and P. Schimmel (1995) Biochemistry **34**, 6014–6019; Correction, p. 16352.
54. J. A. Piccirilli, T. S. McConnell, A. J. Zaug, H. F. Noller, and T. R. Cech (1992) Science **256**, 1420–1424.
55. M. Illangasekare, G. Sanchez, T. Nickles, and M. Yarus (1995) Science **267**, 643–647.

Aminopeptidases

Enzymes that catalyze the hydrolytic cleavage of the peptide bond that connects the N-terminal residue to the rest of a peptide, **polypeptide**, or protein are referred to as aminopeptidases (E.C. 3.4.11) (see Peptidases). The products of hydrolysis are, therefore, the released N-terminal amino acid and the remainder of the peptide chain. The latter can, in turn, also be an aminopeptidase substrate; hence these enzymes can release amino acids sequentially, ultimately resulting in complete hydrolysis of the polypeptide (though in practice this is not always observed). The principal determinant of specificity appears to be the free a-**amino group** of the N-terminal residue; hence these enzymes can release most, though not all, of the known amino acids, albeit at different rates. There are some aminopeptidases (eg, methionine aminopeptidase) that are quite limited in specificity. Usually, aminopeptidases can also act on amino acid amides and esters, which provide convenient substrates for routine assays. Some aminopeptidases sequentially remove dipeptides from the N-terminus of substrates, and these are referred to as dipeptidyl-peptidases. Others remove tripeptides and, hence, are tripeptidyl-peptidases.

Many aminopeptidases are zinc **metalloenzymes**, but some are serine proteinases or **thiol proteases**. Of those that require zinc, some have an active site containing a single ion (see Thermolysin), whereas others have a co-catalytic site that involves two closely spaced zinc ions.

Aminopeptidases are widely distributed in various tissues and cells. They can be monomeric (a single polypeptide chain) or have up to 12 subunits. Many are integral components of cell membranes, but they are also found in the **cytosol**. They have a broad range of biological functions, including regulation of hormone concentration, control of the cell cycle, and recovery of amino acids from dietary peptides and proteins (1). All proteins synthesized by **eukaryotic** cells begin at their N-terminus with methionine, and its removal by methionine aminopeptidase is often crucial, not only for biological function of the protein but even for cell survival. Aminopeptidases also play important roles in the food industry—for example, ripening of cheese (2) and production of soy sauce (3).

Aminopeptidases are inhibited by the antitumor antibiotic bestatin [(2*S*,3*R*)-3-amino-2-hydroxy-4-phenylbutanol]-L-leucine, isolated from culture filtrates of *Streptomyces olivoreticuli*. It is a potent inhibitor of bovine lens aminopeptidases, with a K_i of 1.3 nM, and has numerous biological activities when administered to laboratory animals.

Membrane-bound aminopeptidases have often been identified on the basis of some other property, and then, once their amino acid sequence has been established, they are recognized to be aminopeptidases. Thus, the B-lymphocyte differentiation factor BP-1/6C3, whose expression correlates with proliferation and transformation of immature B cells (antibody-producing lymphocytes), has been shown to be identical to glutamyl aminopeptidase, also known as aminopeptidase A (4). Also the myeloid leukemia antigen CD-13 has been identified as aminopeptidase N (5), and the amino acid sequence of leukotriene A4 hydrolase revealed an aminopeptidase-like structure that led to the recognition of its aminopeptidase activity (6). Aminopeptidase N has also been shown to have a function unrelated to its enzymatic activity; that is, it serves as a cell-surface **receptor** for certain coronaviruses that cause upper respiratory infections (7).

The amino acid sequence and three-dimensional structure of leucine aminopeptidase from bovine lens have been determined (8). This is a broad-specificity cytosolic enzyme found in tissues of all organisms. It has a high degree of sequence similarity to several other aminopeptidases, which suggests that they all share similar structures and catalytic mechanisms.

Bibliography

1. A. Taylor (1993) FASEB J. **7**, 290–298.
2. J. Meyer, D. Howald, R. Jordi, and M. Fuerst (1989) Milchwissenschaft **44**, 678–681.
3. T. Nakadai (1988) Nippon Shoyu Kenkyusho Zasshi **14**, 50–56.
4. Q. Wu et al. (1990) Proc. Natl. Acad. Sci. USA **87**, 993–997.
5. T. Inoue et al. (1994) J. Clin. Endocrinol. Metab. **79**, 171–175.
6. J. Z. Haeggstrom, A. Wetterholm, B. L. Vallee, and B. Samuelsson (1990) Biochem. Biophys. Res. Commun. **173**, 431–437.
7. B. Delmas et al. (1992) Nature **357**, 417–420; Yeager et al. ibid. 420–422.
8. S. K. Burley, P. R. David, A. Taylor, and W. N. Lipscomb (1990) Proc. Natl. Acad. Sci. USA **87**, 6878–6882.

Suggestions for Further Reading

9. A. Taylor (1993) Aminopeptidases: towards a mechanism of action. Trends Biochem. Sci. **18**, 167–172.
10. H. Kim and W. N. Lipscomb (1994) Aspartate transcarbamylase from *Escherichia coli*: activity and regulation. Adv. Enzymol. **68**, 153–213.

2-Aminopurine (AP)

AP is a base analogue that is a mutagen in a wide range of systems and species (1, 2) (Fig. 1). Freese (3, 4) originally described A.T → G.C and G.C → A.T transition mutations following AP treatment of **bacteria** and **bacteriophage**. The results were interpreted as resulting from **tautomeric** shifts and changes in base pairing behavior following the incorporation of AP into DNA. AP is readily metabolised to form deoxy-2-aminopurine triphosphate (dAPTP) (5), which may be incorporated opposite thymine during DNA replication, to form an AP.T base pair. During subsequent rounds of replication, incorporation of dCMP opposite the AP would lead directly to an A.T → G.C transition mutation. Law et al. (6) found that a DNA duplex containing AP.C is thermodynamically more stable than a DNA duplex containing A.C. This is in agreement with the suggestion that the rate of insertion of an improper base by a **DNA polymerase** is determined by differences in stability between the newly formed mismatch site and the corresponding normal **Watson–Crick base pair** (7). The probability that transition mutations will occur results from a combination of the likelihood of tautomeric shifting, the availability of the analogues to the DNA replicating machinery, and the discriminatory behavior and fidelity of the DNA polymerases.

Figure 1. Structure of the base analogue 2-aminopurine.

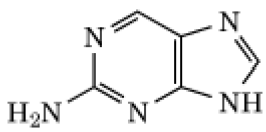

Although best known as a base-pair substitution mutagen, the earliest reports of AP activity focused on the production of unequal, multipolar **mitosis** in mouse tissue culture cells, producing **aneuploid** daughter cells also bearing chromosome mutations (1). AP also causes frameshift mutations—for example, in a set of lacZ mutant variants of *Escherichia coli* (2). *E. coli dam* mutants have reduced ability for methylation of adenine. Many of these mutants also have enhanced sensitivity to AP and increased mutability by this base analogue (8). It appears that AP is partially able to saturate or inactivate the methylation-directed mismatch repair system, allowing the escape from repair of replication errors that lead to frameshift mutation. This results in indirect mutations that can be detected at certain sites (2).

Bibliography

1. A. Ronen (1979) Mutat. Res. **75**, 1–47.
2. C. G. Cupples, M. Cabrera, C. Cruz, and J. H. Miller (1990) Genetics **125**, 275–280.
3. E. Freese (1959a) Proc. Natl. Acad. Sci. USA **45**, 622–633.
4. E. Freese (1959b) J. Mol. Biol. **1**, 87–105.
5. E. G. Rogan and M. J. Bessman (1970) J. Bacteriol. **103**, 622–633.
6. S. M. Law, R. Eritja, M. F. Goodman, and K. J. Breslauer (1996) Biochemistry **35**, 12329–12337.
7. M. F. Goodman, R. L. Hoskins, R. Lasker, and D. N. Mhaskar (1993) Basic Life Sci. **31**, 409–423.
8. B. W. Glickman, P. van den Elsen, and M. Radman (1978) Mol. Gen. Genet. **163**, 307–312.

Aminopterin, Methotrexate, Trimethoprim, and Folic Acid

Aminopterin, methotrexate, and trimethoprim are all analogs of *folic acid* (Fig. 1) that antagonize folate-dependent metabolic pathways (1, 2). Folate is a water-soluble vitamin. Although some bacteria synthesize folate, mammalian cells cannot, and consequently it is an absolute dietary requirement. Reduced folates function as **cofactors** in many metabolic processes common to nearly all cells, such as **thymidylate** and **purine** synthesis and donation of methyl groups (Fig. 2) (1). Folates gain entry into mammalian cells by either the reduced folate carrier (RFC) and/or a hydrophobic membrane-associated folate receptor (FR) found in placental, choroid plexus and kidney cells (3). The FR is unidirectional and, once inside, cellular retention of folate is enhanced by its polyglutamation, catalyzed by the enzyme folylpolyglutamyl synthetase (FPGS) (4). FPGS adds up to six or seven glutamic acid residues via an unusual peptide bond through their g-carboxyl group, rather than the normal a. The number of glutamic acid residues added may play a role in regulating and distributing reduced folates, and in guaranteeing their availability as cofactors. Polyglutamation also increases the affinity of folate for folate-dependent enzymes, such as thymidylate synthase (TS), aminoimidazole carboxamide ribonucleotide and glycinamide ribonucleotide transformylases. The latter two are involved in purine synthesis. In cells synthesizing DNA, 5,10-methylenetetrahydrofolate serves in thymidylate synthesis as a methyl group donor for converting dUMP to dTMP. This is the only reaction in which tetrahydrofolate is partially oxidized to dihydrofolate (1, 4). Dihydrofolate reductase (DHFR) is the critical enzyme involved in converting dihydrofolate back to tetrahydrofolate, thus maintaining reduced folate pools to serve as one-carbon group carriers (see Fig. 2).

Figure 1. (**a**) The structures of folic acid and folate analogs: folic acid and analogs; (**b**) the structure of trimethoprim.

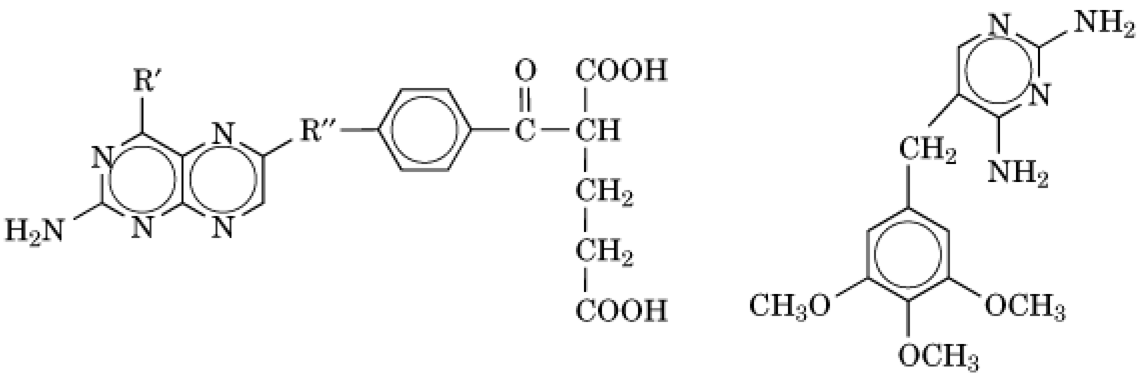

	R′	R″
Folic acid	-OH	$-CH_2NH-$
Methotrexate	$-NH_2$	$-CH_2N(CH_3)-$
Aminopterin	$-NH_2$	$-CH_2NH-$

(a)

(b)

Figure 2. Folate transport, accumulation, and target enzymes. (*1*) folate receptor (FR); (*2*) reduced folate carrier (RFC), which is bidirectional; (*3*) folylpolyglutamyl synthetase (FPGS); (*4*) dihydrofolate reductase (DHFR); (*5*) aminoimidazo

carboxamide ribonucleotide and glycinamide ribonucleotide tranformylases; (*6*) thymidylate synthase (TS); (*7*) passive diffusion of lipid-soluble compounds. FH_4 and FH_4 $(glu)_n$, tetrahydrofolate with and without the added glutamyl residue: FH_2, dihydrofolate; CH_2FH_4, 5,10 methylene-FH_4; 10-CHO-FH_4, 10-formyl FH_4; B_{12}, vitamin B12 [Adapted from Hum and Kamen (1996) *Investigational New Drugs* **14**, 110–111.]

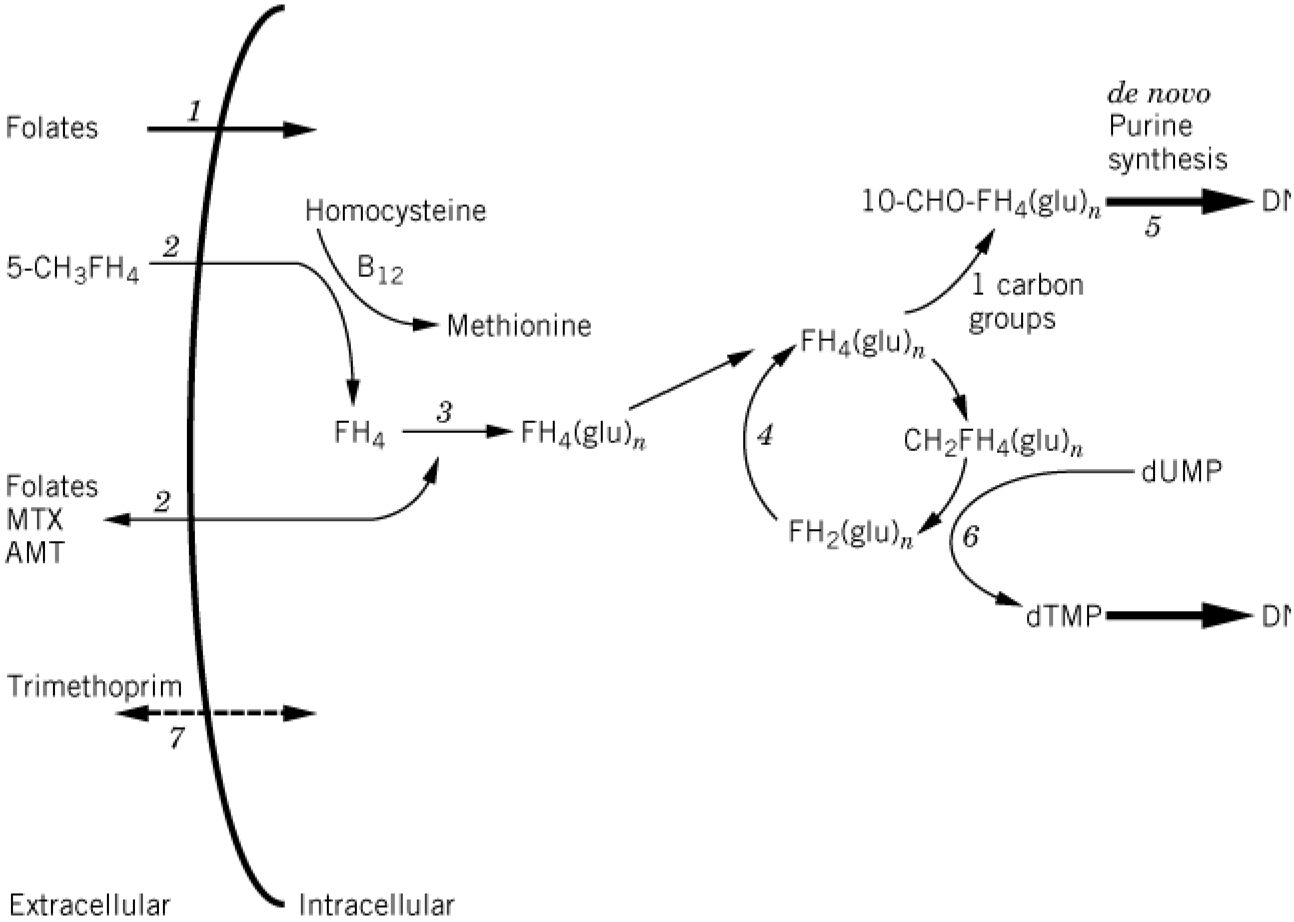

Folate homeostasis is recognized as important. The structure of DHFR has been determined by X-ray crystallography. One proposed mechanism of resistance to methotrexate involves DHFR gene amplification (5-7). The FR is overexpressed in some carcinomas, and its gene has been localized to the 11q13 region (3). Human FPGS has been cloned and mapped to chromosome 9q (4). The complementary DNA for RFC has been **cloned** and the RFC gene localized to the long arm of chromosome 21 (8-11).

1. Methotrexate (MTX)

Folate analogs entered cancer therapy in the 1940s, when aminopterin was successfully used to induce temporary remissions in children with acute lymphoblastic leukemia (ALL) (12). Because of a better therapeutic index, MTX eventually emerged as the antifolate used clinically in treating cancers, such as leukemias, lymphomas, osteosarcoma, breast cancer, choriocarcinoma, head and neck cancers, and nonmalignant disorders, such as arthritis and asthma (4, 13).

Like folates, MTX enters mammalian cells via the RFC. MTX has an apparent **dissociation constant** in the micromolar range, and via the FR has higher affinity in the nanomolar range (3). Cellular retention of MTX is enhanced by polyglutamation, which also enhances the affinity of the drug for enzymes. Once inside the cell, MTX acts as a tight-binding **competitive inhibitor** of DHFR. This leads to an accumulation of dihydrofolate and depletion of the reduced folate pools in cells actively making dTMP via the *de novo* pathway. Accumulated dihydrofolate polyglutamates are also inhibitors of TS and the enzymes involved in the *de novo* synthesis of purines (1). The resulting imbalance of nucleotides causes base substitutions, which lead to errors in DNA synthesis and ultimately to cell death.

2. Aminopterin (AMT)

Aminopterin (AMT) was the first antifolate drug used clinically in childhood ALL (12) (see previous). Although more potent than MTX, in preclinical studies the toxicity of AMT was more severe and more unpredictable (13-15). Transport and metabolic studies *in vitro* have shown that AMT is the preferred substrate (16, 17). This results in greater AMT accumulation at lower concentrations and more complete polyglutamation, leading to improved cellular retention for the cytotoxic effect.

The greater potency of AMT compared to MTX has led to renewed clinical interest. AMT may find a role in treating patients with resistant or refractory malignancies or those patients in whom *in vitro* studies indicate AMT is the better choice on the basis of metabolism and accumulation (16).

3. Trimethoprim

Trimethoprim is an antibacterial agent developed in the 1950s. Studies by Hitchings (2) showed that its mechanism of action is the competitive inhibition of DHFR. Unique to trimethoprim is its much greater affinity (50,000- to 100,000-fold) for bacterial DHFR than for mammalian DHFR (18, 19). Trimethoprim is lipid-soluble and enters cells rapidly without requiring specific transport mechanisms. Its selective toxicity is further enhanced by the ability of folinic acid to reverse even the slight effects of trimethoprim on mammalian cells, whereas bacterial cells, unable to transport folinic acid, are not rescued by folinic acid administration (19, 20). In addition to its antibacterial activity, the drug has activity against *Pneumocystis carinii*, an opportunistic infection of the lungs encountered in severely immunocompromised patients (especially HIV patients).

Bibliography

1. M. C. Hum and B. A. Kamen (1996) Investigational New Drugs **14**, 110–111.
2. G. H. Hitchings (1973) J. Infect. Dis. **128**(suppl), S433–S436.
3. S. Weitman, R. G. W. Anderson, and B. A. Kamen (1994) In *Vitamin Receptors: Vitamins as Ligands in Cell Communities* (K. Dakshinamurti, ed.), Cambridge University Press, Cambridge, UK, pp. 106–136.
4. T. A. Garrow, A. Admon, and B. Shane (1992) Proc. Natl. Acad. Sci. USA **89**, 9151–9155.
5. F. W. Alt et al. (1978) J. Biol. Chem. **253**, 1357–1370.
6. J. R. Bertino (1993) Ode to Methotrexate, J. Clin. Oncology **11**(1), 5–14.
7. E. Chu and C. H. Takimota (1993) In *Principles & Practice of Oncology* (V. T. De Vita, S. Hellman, and S. A. Rosenburg, eds.), Lippincott, Philadelphia, pp. 358–374.
8. J. A. Moscow et al. (1995) Cancer Res. **55**, 3790–3794.
9. P. D. Prasad et al. (1995) Biochem. Biophys. Res. Commun. **206**, 681–687.
10. S. C. Wong et al. (1995) J. Biol. Chem. **270**, 17468–17475.
11. T. L. Yang-Feng et al. (1995) Biochem. Biophys. Res. Commun. **210**(3), 874–879.
12. S. Farber et al. (1948) N. Engl. J. Med. **238**, 787–793.
13. A. Goldin et al. (1955) J. Natl. Cancer Inst. **15**, 1657–1664.
14. F. M. Sirotnak and R. C. Donsbach (1975) Biochem. Pharmacol. **24**, 156–158.
15. F. S. Philips et al. (1973) Cancer Res. **33**, 153–158.
16. A. Smith et al. (1996) Clin. Cancer Res. **2**(1), 69–73.
17. B. G. Rumberger, J. R. Barrueco, and F. M. Sirotnak (1990) Cancer Res. **50**, 4639–4643.

18. Anonymous (1971) Trimethoprim-sulfamethoxazole. Drugs, **1**(1), 8–53.
19. J. J. Burchall (1973) J. Infect. Dis. **128**(suppl), S437–S441.
20. W. Brumfitt and J. M. T. Hamilton-Miller (1980) Brit. J. Hosp. Med. **23**(3), 281–288.

Suggestions for Further Reading

21. J. R. Bertino, B. A. Kamen, and A. Romanini (1997) "Folate antagonists". In *Cancer Medicine* (J. F. Holland, R. C. Bast, D. L. Morton, E. Frei, D. W. Kufe, and R. R. Weicheslbaum, eds.), Williams and Wilkins, Baltimore, pp. 907–922.
22. R. L. Blakley and S. J. Benkovic (1984) *Folates and Pterins: Chemistry and Biochemistry of Folates*, Wiley, New York, Vol. 1.
23. C. H. Takimoto and C. J. Allegra (1995) New antifolates in clinical development, Oncology **9**, 649–659.

Amphipathic

Compounds that contain both highly polar and nonpolar, **hydrophobic** moieties are *amphipathic*. In the presence of water, these compounds tend to aggregate, forming structures that are strongly influenced by the relative extents of the polar and hydrophobic characters of the molecule, with the polar groups acting to shield the hydrophobic moieties from the solvent. In lipids, the hydrophobic group is the hydrocarbon domain of the aliphatic chain (see Lipids and Fatty Acids). Typical examples are (a) the sodium salts of fatty acids, which form micelles in water, and (b) phospholipids, which form bilayers in membranes. The presence of significant amounts of nonpolar amino acids, such as alanine, valine, leucine, isoleucine, proline, methionine, phenylalanine, and tryptophan, make certain proteins amphipathic; these amino acids are believed to increase the accessibility of the proteins to the hydrophobic domain of the membrane bilayer (see Fluid Mosaic Model).

Amphoteric

An amphoteric molecule is one that has both acidic and basic chemical features. For example, proteins are amphoteric electrolytes because they generally have both acidic and basic groups on the side chains of their amino acid residues. Extreme examples of amphoteric molecules are the ampholytes used to establish pH gradients in isoelectric focusing.

Ampicillin

Ampicillin (D[–]-a-aminobenzylpenicillin; Fig. 1) is a member of a growing family of antimicrobial agents known as the semisynthetic penicillins. The semisynthetic penicillins are derivatives of the natural product, 6-aminopencillanic acid, that have been deliberately modified chemically (1). The chemical modifications are introduced to create new compounds with specific desirable properties.

In the case of ampicillin, the addition of the aminobenzyl side chain results in a product with an increased resistance to acidic pH. Thus, ampicillin is medically significant because it was the first penicillin to be administered orally in chemotherapeutic practice. Furthermore, ampicillin exhibits a broader antibacterial spectrum than do the naturally occurring penicillins and is effective against many Gram-negative bacterial species. The outer membrane component of the Gram-negative bacterial cell wall represents a permeability barrier to many antibiotics, including the natural penicillins (2). The broad activity spectrum and the relative low cost of ampicillin have made it an invaluable tool in molecular biology and genetics for studying Gram-negative model organisms, such as *Escherichia coli* and *Haemophilus influenzae*. Applications that employ ampicillin are summarized below.

Figure 1. Structure of ampicillin.

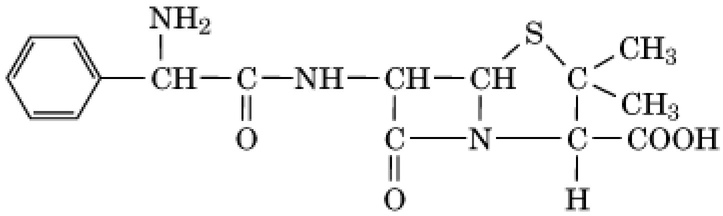

The first application of penicillin in genetics was for the selection of auxotrophic mutants of *E. coli* (3, 4). This technique, penicillin selection, was based on the fact that penicillin kills only actively growing bacteria, whereas nongrowing bacteria are penicillin-tolerant (see Penicillin). Although benzylpenicillin (penicillin G) was employed in the original studies describing this technique, ampicillin would be far more effective for this purpose because of its broad spectrum.

Molecular biologists have extensively exploited genetic elements encoding b-lactamase (see Penicillin-Binding Proteins), especially the enzyme designated TEM-1. TEM-1 is a broad spectrum b-lactamase that confers effective high level resistance to penicillins (5). The gene encoding TEM-1 was incorporated into the first plasmid cloning vectors (6) and has been widely used in cloning vectors since. Ampicillin has been used routinely for the selection and maintenance of bacteria carrying recombinant plasmids encoding b-lactamase, and this is undoubtedly its most common application in molecular biology. For this purpose, ampicillin is incorporated into bacteriological media at final concentrations ranging from about 50–100 µg/mL. For *E. coli*, these levels are about 10–20 times higher than the minimum inhibitory concentration (MIC) of ampicillin. The MIC is defined as the minimum concentration of the antibiotic that is necessary to inhibit bacterial growth.

When a mixture of ampicillin-sensitive and ampicillin-resistant bacteria are plated on solid media containing ampicillin, such as for selection of transformants carrying a b-lactamase-encoded plasmid, it is not uncommon to find large colonies formed by ampicillin-resistant bacteria surrounded by a zone of smaller colonies. The ampicillin-resistant bacteria in the large central colonies produce and secrete b-lactamase. The activity of the secreted b-lactamase creates a zone of reduced ampicillin concentration around the resistant colonies, and this permits the ampicillin-sensitive bacteria in the vicinity to grow. The subsequent growth of the ampicillin-sensitive bacteria results in the formation of the smaller so-called satellite colonies. The satellite colonies normally do not represent a major hindrance in these procedures, because the desired ampicillin-resistant bacteria can be readily purified by streaking on an ampicillin-containing medium. However, the problem of satellite colony formation can be minimized by substituting carbenicillin, another semisynthetic penicillin (see Fig. 1 in Penicillin) for ampicillin in the selection medium at a concentration of 50–100 µg/mL (7). Carbenicillin is less susceptible to hydrolysis by the b-lactamase and is therefore less likely to promote satellite colony formation. It is therefore often used in place of ampicillin.

The b-lactamase gene has also been introduced into plaque-forming and defective derivatives of the *E. coli* bacteriophage Mu (8). These ampicillin-selectable phages have been used for mutagenesis and for the construction of *lac* fusions in applications that take advantage of the ability of Mu to **transpose** randomly.

The concept of transposon mutagenesis has been applied to transposable genetic elements encoding b-lactamases for the generation of random gene fusions that are directly selectable with ampicillin (or carbenicillin). For example, a derivative of Tn*3* designated Tn*3*-HoHo1 (9) is a *lacZ*-containing transposon capable of producing both transcriptional and translational **beta-galactosidase** fusions. Although it was originally developed for studies on Agrobacterium *tumefaciens*, it has been adapted for use in other bacterial genera.

b-Lactamase is a periplasmic enzyme. It has served as an important model for studying protein export to the bacterial periplasm. Urbain et al. (10) have recently developed a technique for quantifying b-lactamase activity in cultures of *E. coli* carrying recombinant plasmids that confer ampicillin resistance. Their assay involved determining the conversion of ampicillin to aminobenzylpenicilloic acid in periplasmic extracts of cells by quantitative high performance liquid chromatography (**HPLC**). The procedure may be useful for investigating the mechanism of b-lactamase translocation. It may also prove useful in studies on protein expression. For example, since b-lactamase is expressed constitutively from ampicillin-selectable recombinant plasmids, its activity could serve as a useful internal standard in protein coexpression studies.

b-lactamase has also been used as a genetic tool for studying membrane proteins, and these applications are based on the fact that b-lactamase is an exported protein (11, 12). A plasmid vector that permits the *in vitro* construction of translational fusions between a gene of interest, encoding either a membrane protein or an exported protein, and the mature form (ie, the exported form) of the TEM b-lactamase has been described (13). Transformants carrying recombinant plasmids with in-frame fusions are ampicillin-selectable. This technique may be used for the analysis of protein export signals or for determining the topological organization of membrane proteins. A strategy for maximizing yields of membrane and exported proteins based on this vector has also been described (14). It is notable that alkaline phosphatase has been used widely for studying protein export signals and for topological mapping of membrane proteins (15). The b-lactamase system is an attractive alternative to alkaline phosphatase for these purposes (13, 14) (see Reporter Genes). For example, b-lactamase fusions are directly selectable (with ampicillin), whereas the identification of alkaline phosphatase fusions is based on phenotypic screening. Moreover, only the periplasmic form of alkaline phosphatase is enzymatically active, whereas both the cytoplasmic and periplasmic forms of b-lactamase are active. Consequently, the cellular location of the b-lactamase fusions can be determined on the basis of the levels of ampicillin resistance; cytoplasmic b-lactamase confers ampicillin resistance only at high cell density, whereas periplasmic b-lactamase confers ampicillin resistance at low cell density. As an extension of these studies, Broome-Smith et al. (16) have constructed a transposable b-lactamase element, designated *TnblaM*, that is equivalent to the transposable alkaline phosphatase element, *TnphoA*. The b-lactamase fusions constructed with *TnblaM* are directly selectable with ampicillin, and this is a major advantage over alkaline phosphatase system, which as already noted is based on phenotypic screening.

Bibliography

1. J. H. C. Nayler (1991) in *50 Years of Penicillin Application. History and Trends*, Public Ltd., Czech Republic, 64–74.
2. H. Nikaido and M. Vaara (1985) Microbiol. Rev. **49**, 1–32.
3. J. Lederberg and N. Zinder (1948) J. Am. Chem Soc. **70**, 467–468.
4. B. D. Davis (1949) Proc. Natl. Acad. Sci. USA **35**, 1–10.
5. N. Datta and M. D. Richmond (1966) Biochem. J. **98**, 204–210.

6. F. Bolivar, R. L. Rodriguez, M. C. Betlach, and H. W. Boyer (1977) Gene **2**, 75–93.
7. F. M. Ausubel, R. Brent, R. E. Kingston, D. D. Moore, S. D. Seidman, J. A. Smith, and K. Struhl (1994) *Current Protocols in Molecular Biology*, Wiley, New York, p.1.8.7.
8. E. A. Groisman (1991) Meth. Enzymol. **204**, 180–212.
9. S. E. Stachel, G. An, C. Flores, and E. W. Nester (1985) EMBO J. **4**, 891–898.
10. J. L. Urbain, C. M. Wittich, and S. R. Campion (1998) Anal. Biochem. **260**, 160–165.
11. J. K. Broome-Smith, M. Tadayyon, and Y. Zhang (1990) **4**, 1637–1644.
12. M. Tadayyon, Y. Zhang, S. Gnaneshan, L. Hunt, F. Mehraein-Ghomi, and J. K. Broome-Smith (1992) Biochem. Soc. Trans. **20**, 598–601.
13. J. K. Broome-Smith and B. G. Spratt (1986) Gene **49**, 341–349.
14. J. K. Broome-Smith, L. D. Bowler, and B. G. Spratt (1989) Mol. Microbiol. **3**, 1813–1817.
15. C. Manoil, J. J. Mekalanos, and J. Beckwith (1989) J. Bacteriol. **172**, 515–518.
16. M. Tadayyon and J. K. Broome-Smith (1992) Gene **111**, 21–26.

Amyloid

Amyloid is an insoluble, proteinaceous, fibrous material associated with a number of prominent disease states (1), which can also form spontaneously *in vitro* from oligopeptides and **denatured** proteins. The disease states in which amyloid has been implicated as an important, or even causal, factor include Alzheimer's disease (see Amyloid Precursor Protein), the transmissible spongiform encephalopathies (see Scrapie), non-insulin-dependent (type II) diabetes, and a number of polyneuropathies. It is thought that the extreme stability of amyloid fibrils permits their progressive accumulation in the extracellular spaces of vital organs whose functioning is thereby inhibited, leading to organ failure and death. The *in vivo* development of amyloid deposits from globular precursor proteins is linked to either genetic mutation, incorrect processing, or the abnormal accumulation of wild-type proteins. Probably the most remarkable feature of amyloid is that its molecular structure appears to be constant and independent of the protein precursors. For example, all amyloids, regardless of the disease involved or the source of the fibrils, share similar morphological (2), tinctorial (3), and structural (4, 5) properties. This implies that amyloid formation is not a simple aggregation process but a structural conversion of globular proteins to a state that can be incorporated into a particular type of fibrous protein structure. The amyloid diseases may therefore be defined as diseases of protein misfolding.

At least 15 different proteins can form amyloid fibrils *in vivo* (1), and recently the involvement of amyloid fibrils in Huntingdon's disease has also been demonstrated (6). In the **electron microscope**, amyloid fibers are about 100 Å (10 nm) in diameter and usually straight or only slightly curved. Closer examination shows the fibrils to be composed of a number of smaller diameter protofilaments, arranged in a more or less parallel array. In those fibrils so far examined, the protofilaments give the fibrils the appearance of hollow cylinders or ribbons when observed in cross section. Although the number, size, and arrangement of these constituent protofilaments appear to differ somewhat, the ribbons may be merely unrolled or unformed cylinders, and hence the variation may not be so great as appears. The molecular structure of the amyloid fibrils has been established by X-ray fiber diffraction. The first diffraction patterns (7, 8) showed the intense 4.7 Å (0.47 nm) meridional and 10 Å (1 nm) equatorial reflections that have been subsequently shown to characterize all amyloid X-ray patterns. These reflections indicate that the molecular structure of amyloid is composed of beta-sheets arranged parallel to the fiber axis, with their constituent beta-strands at right angles to the axis of the fibril (4, 9). This so-called “cross-b” structure is quite different from the more common insect silk **chorions**, whose fibers are formed from b-sheets having their b-strands parallel to the fiber axis. The first use of intense synchrotron X-ray sources on amyloid (10) extended the observable X-ray pattern to 2 Å (0.2 nm) and revealed how this “classic” amyloid model could be reconciled with low-energy twisted b-sheets (11). These new data revealed a previously unobserved repeat distance of 115 Å (11.5 nm) along the fiber axis of the transthyretin amyloid of familial amyloidotic polyneuropathy (FAP), which was proposed (10) to correspond to the repeat distance of a complete helical turn of a twisted b-sheet, whose helix axis was parallel to the fiber axis. The basic helical unit therefore consists of a segment of b-sheet whose 24 b-strands complete one helical turn. This beta-helix model of the molecular structure of the amyloid protofilament is shown in Figure 1. Given that all amyloid fibrils share common morphological, tinctorial, and structural properties, it is reasonable to see the b-helix model as characteristic of all amyloid protofilaments. The b-helix model is distinct from other fibrous proteins, showing that the amyloid structure is unique. Its features enable low energy twisted b-sheets to be incorporated in a linear fibril in such a way that continuous b-type **hydrogen bonding** can be extended over the total length of the fibril. This, together with the opportunity for a continuous **hydrophobic** core to stabilize the b-sheet interactions along the length of the fibril, can be reasonably held to account for the known extreme stability of amyloid fibrils, which is central to their role in disease.

Figure 1. Drawing of one complete turn of the proposed b-helix structure of the amyloid fibril. The arrows represent b-strands and are shaded to represent the different b-sheets. The direction of the arrows has no significance, and no b-strand connections are shown.

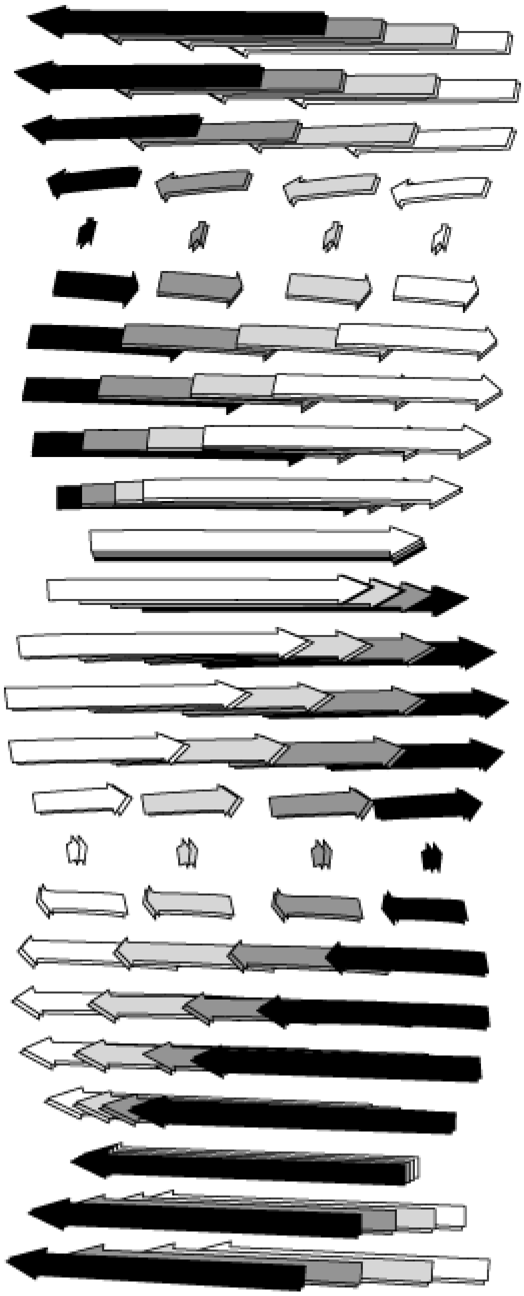

A remarkable property of amyloid fibrils is that they appear to be very similar whatever their source. This has recently been critically tested (5) by showing that the high resolution synchrotron X-ray patterns from eight different amyloids, of both disease and synthetic origins, have the same structural characteristics. This observation suggests that amyloid is a highly stable generic structure capable of accommodating proteins and peptides with a wide range of chain lengths and structures within a common fibrillar form. The repetition of b-strands in the fibril model allows polypeptide chains of different lengths to occupy the same structural framework. For example, a 10-residue peptide could form a single b-strand of the amyloid structure, consistent with the known lower limit on the length of peptides capable of forming amyloid, while longer polypeptide chains could fold back and forward on themselves, thereby forming a number of consecutive b-strands of the amyloid b-sheets. The need for loops of chain of different lengths or conformation between successive b-strands to maximize the b-strand propensity, and to generate a stable hydrophobic core between the b-sheets, is likely to give each fibril a characteristic structure within the core amyloid framework. Thus it is probably realistic to consider amyloids as a closely related family of fibrils, each with its own detailed structural differences, while maintaining a similar overall core structure.

The nature of the processes that convert the globular, soluble protein precursors into amyloid fibrils, known as either *amyloidogenesis* or *fibrillogenesis*, are important, as they underpin the development of amyloid diseases and represent a novel field of scientific investigation. It is evident that some of the proteins forming the predominantly b-structured amyloid fibrils are themselves largely a-helical in their normal soluble states, for example, lysozyme, the prion protein, and the Ab peptide in Alzheimer's disease (see Amyloid Precursor Protein). The nature of this structural rearrangement has been particularly studied in two amyloidogenic proteins: transthyretin (TTR) and lysozyme. Transthyretin amyloidosis is associated with familial amyloidotic polyneuropathy (FAP) and senile systemic amyloidosis (SAA). Both the wild-type protein (SAA) and more than 50 different genetic variants (FAP) (13) give rise to amyloid. That so many variants of transthyretin are amyloidogenic (nearly 40% of all its residues), suggests that the structure of this protein allows a particularly facile transformation into the fibrillar form. As transthyretin is a 55-kDa homotetramer, with the four monomers associating in such a way as to generate a stack of four 8-stranded b-sheets (14), there is a superficial structural similarity with amyloid fibril (10). Nevertheless there is evidence that the tetrameric form of TTR is not a building block for the fibril (15), and the discovery of a molecular hotspot in the pattern of amyloidogenic variants (16) suggests that structural change to the monomer is also required prior to its incorporation into the fibril. It is therefore evident that even all-b proteins, such as TTR, must undergo a significant degree of structural rearrangement to form amyloid.

The human lysozyme molecule (see Lysozymes) has about 35% a-helix and only 10% b-sheet structure, segregated into an a- and a b-domain. Hence the structural changes that must accompany its incorporation into the predominantly b-structured amyloid fibril will need to be extensive. Two genetic variants of human lysozyme are known to form amyloid *in vivo*, Ile56Thr and Asp67His (17). A thorough biophysical study of these variants has highlighted major differences in their stability and folding behavior as compared with the wild type (18). It has generated a possible mechanism of the a- to b-structural transformation of fibril formation of lysozyme, shown in Figure 2, which may be applicable *mutatis mutandis* to other amyloidogenic proteins. Thermal denaturation studies show that the variants unfold at temperatures at least 10°C lower than wild-type lysozyme and, unlike the wild type, do not regain activity when returned to physiological conditions. Fourier transform infrared spectroscopy (see Vibrational Spectroscopy) of Asp67His lysozyme shows a significant gain in b-structure and loss of a-structure in the soluble material, demonstrating that an a-to-b structural interconversion is associated with fibril formation. Detection of an unfolding intermediate displaying the characteristic binding to the hydrophobic dye 1-anilinonaphthalene sulfonic acid (**ANS**) is consistent with a **molten globule**-like intermediate, as shown in Figure 2. Hydrogen exchange shows that the flexibilities of the native folds of the variants have been dramatically increased by the mutations. Inspection of the X-ray crystallography structures of the two variants (18) suggests that the key to both amyloidogenic mutations in human lysozyme lies in the effect they produce at the interface between the a- and b-domains, with the result that domain adhesion may be weakened. Both variant lysozymes unfold dramatically faster than the wild-type protein, because the docking of the two domains, required for achieving the final rigid protein fold (19), is compromised by the presence of a threonine side-chain in the place of the wild-type **hydrophobic** anchoring residue, isoleucine.

Figure 2. Schematic drawing of the possible mechanism of fibril formation in human lysozyme. (—) b-sheet structure; (**—**) a-helical structure. A partly-folded, molten-globule form (II), distinct from the native (I), and denatured (III) forms, self-associates through the b-domain (IV) to initiate fibril formation. This provides a template for further deposition and the development of a b-sheet core structure of the amyloid fibril (V). Undefined structures are shown as broken lines.

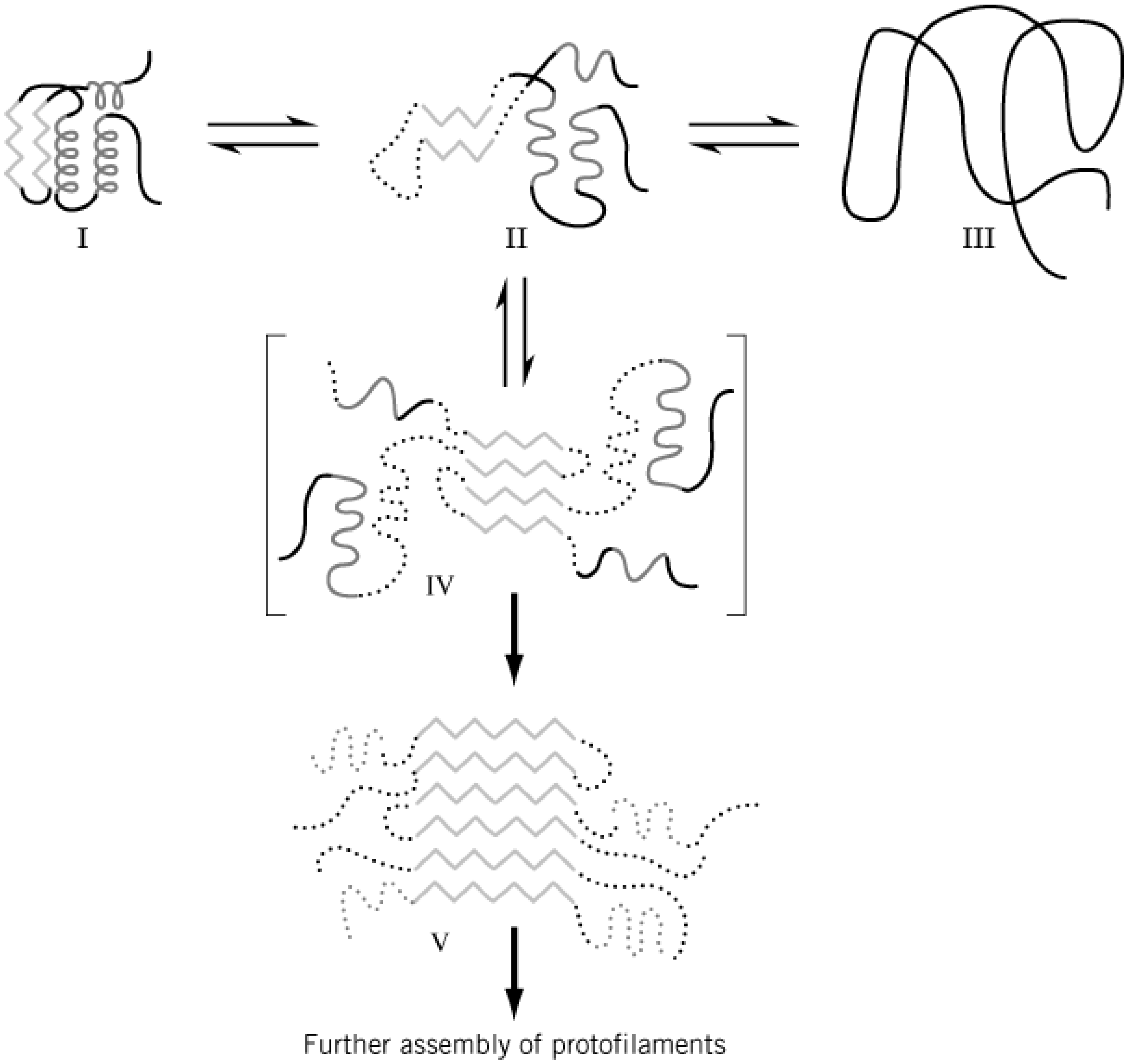

Detailed study of the structure and behavior of variants of lysozyme has led to the proposal that transient populations of amyloidogenic proteins in a molten-globule state that lacks global cooperativity are an important feature of the conversion from a soluble to the fibrillar state (18). These observations lead to a model of the mechanism for amyloid formation for amyloidogenic lysozyme shown in Figure 2. Such a mechanism may also operate for other amyloidogenic proteins. For example, the structure of the 121–231 domain of the prion protein (20) also demonstrates that mutations associated with prion disease are involved in the maintenance of the hydrophobic core, which may be related to the earlier suggestion of a molten globule intermediate in the formation of aggregates in scrapie (21) (see Prion). Recent evidence supports the hypothesis that conformational plasticity is a key feature in prion fibril formation. A similar observation has been made for the Ab protein forming the amyloid in Alzheimer's disease (22) (see Amyloid Precursor Protein). The mechanism for helix-to-sheet conversion in lysozyme, proceeding from soluble forms of the amyloidogenic precursor proteins through transient populations of intermediates with the characteristics of molten globules, and on to intermolecular b-sheet association, seems to parallel the processes in the aggregation of prions and the Ab amyloid peptides, and it may occur generally in the amyloidoses. Studies of these processes is certain to extend our knowledge of **protein folding** behavior into new areas and coincidentally address some of the more intractable diseases of our times.

Bibliography

1. M. B. Pepys (1994) in *Santer''s Immunologic Diseases* (M. M. Frank, K. F. Austen, H. N. Claman, and E. R. Unanue, eds.), Little, Brown & Co., Boston, pp. 637–655.
2. A. S. Cohen, T. Shirahama, and M. Skinner (1981) in *Electron Microscopy of Protein*, Vol. **3** (I. Harriss, ed.), Academic Press, London & New York, pp. 165–205.
3. G. G. Glenner, E. D. Eanes, and D. L. Page (1972) J. Histochem. Cytochem. **20**, 821–826.
4. G. G. Glenner (1980) N. Eng. J. Med. **303**, 1283–1292.
5. M. Sunde, L. C. Serpell, M. Bartlam, P. E. Fraser, M. B. Pepys, and C. C. F. Blake (1997) J. Mol. Biol. **273**, 729–739.
6. E. Scherzinger et al. (1997) Cell **90**, 549–558
7. E. D. Eanes and G. G. Glenner (1968) J. Histochem. Cytochem. **16**, 673–677.
8. L. Bonar, A. S. Cohen, and M. Skinner (1967) Proc. Soc. Exp. Biol. Med. **131**, 1373–1375.
9. J. H. Cooper (1976) in *Amyoidosis* (O. Wehelius and A. Paternak, eds.), Academic Press, London & New York, pp. 61–68.
10. C. C. F. Blake and L. C. Serpell (1996) Structure **4**, 989–998.
11. C. Chothia (1973) J. Mol. Biol. **75**, 295–302.
12. L. C. Serpell, M. Sunde, P. E. Fraser, P. Luther, E. Morris, E. Sandgren, E. Lundgren, and C. C. F. Blake (1995) J. Mol. Biol. **254**, 113–118.
13. M. J. M. Saraiva (1995) Hum. Mutat. **5**, 191–196.
14. C. C. F. Blake, M. J. Geisow, S. J. Oatley, B. Rerat, and C. Rerat (1978) J. Mol. Biol. **121**, 339–356.
15. W. Colon and J. W. Kelly (1992) Biochemistry **31**, 8654–8660.
16. L. C. Serpell, G. Goldsteins, I. Dacklin, E. Lundgren, and C. C. F. Blake (1996) Amyloid: Int. J. Exp. Clin. Invest. **3**, 75–85.
17. M. B. Pepys et al. (1993) Nature **362**, 553–557.
18. D. R. Booth et al. (1997) Nature **385**, 187–793.
19. S. D. Hooke, S. E. Radford, and C. M. Dobson (1994) Biochemistry **33**, 5867–5876.
20. R. Riek, S. Hornemann, G. Wider, M. Billeter, R. Glockshuber, and K. Wüthrich (1996) Nature **382**, 180–182.
21. J. Safar, P. Roller, D. Gajdusek, and C. Gibbs (1994) Biochemistry **33**, 8375–8383
22. C. Soto, E. Castano, B. Frangione, and N. Inestrosa (1995) J. Biol. Chem. **270**, 3063–3067.

Suggestions for Further Reading

23. G. R. Bock and J. A. Goode, eds. (1996) *The Nature and Origin of Amyloid Fibrils*, Ciba Foundation, John Wiley and Sons Ltd., Chichester, UK.
24. L. C. Serpell, M. Sunde, and C. C. F. Blake (1997) The molecular basis of amyloidosis. Cell. Mol. Life Sci. **53**, 871–887.

Amyloid Precursor Protein

At the molecular level, the necessary, and probably sufficient, cause for the brain dysfunction in Alzheimer's disease is the deposition of aggregated forms of the amyloid b-protein (Ab or bA4), a **proteolytic** fragment of the amyloid precursor protein (APP), in the brain parenchyma and vascular system (1). In the Western world, dementia is the most common neurological diagnosis and is the third leading cause of natural death, and Alzheimer's disease is by far the dominant cause of dementia (2). It has been estimated that there are 3 million patients in the United States alone with Alzheimer's disease (3). In addition, older patients with Down's syndrome (trisomy 21) tend to develop a neuropathology that is very similar to that seen in Alzheimer's patients (4) The disease is chronic, progressive, and at present untreatable. The progression of the disease begins with loss of short-term memory and disorientation, followed by complete impairment of memory, judgment, and reasoning. Firm diagnosis of the disease can be given only after postmortem examination of the brain, which is characterized by extensive loss of neurons and particular microscopic lesions, which include what are now called "neurofibrillar tangles" and "senile plaques." The neurofibrillar tangles are composed of paired helical filaments consisting of phosphorylated **tau protein**, which is normally associated with microtubules. The senile plaques are composed mainly of Ab deposited in the brain parenchyma. Also present in the brain is congophilic amyloid angiopathy from the accumulation of the Ab peptide in the walls of blood vessels. The Ab protein in the senile plaques and in the vascular deposits is present in the form of amyloid (5, 6), long, stable fibrils resulting from the accumulation of precursor peptides that adopt a continuous beta-sheet structure. In this regard, Alzheimer's disease is related to Creutzfeldt–Jakob disease (CJD) and other spongiform encephalopathies, which are also characterized by the presence of amyloid deposits, in that case composed of the prion protein. All known risk factors for Alzheimer's disease appear to influence one or more of the following: (1) the concentration of Ab (7); (2) the amount of the longer, more amyloidogenic Ab chains (8, 9); or (3) the initiation of amyloid formation (10). Increases in any of these factors appear to increase the risk of Alzheimer's disease. Study of the origins of the b-amyloid protein from APP, its aggregation into amyloid fibrils, and the identification of genes involved in its inherited susceptibility are therefore central to understanding of, and devising therapies against, the scourge of Alzheimer's disease.

The amyloid precursor protein (APP), is a 110–130-kDa protein with the features of a transmembrane cell-surface **glycoprotein**. It is encoded by a gene localized on chromosome 21 encoded by 18 exons (see Introns, Exons). A family of eight transmembrane glycoproteins is generated by alternative splicing of some of these exons (11). The amino acid sequence predicts that the single transmembrane domain of APP is near the *C*-terminus (Fig. 1) (12). The Ab sequence consists of a maximum 43-residue segment straddling the transmembrane and extracellular portions of the APP chain, and encoded by parts of exons 16 and 17. APP is processed in two distinct pathways : a major nonamyloidogenic route involving **proteolytic** cleavage within the region carrying the Ab segment to separate the extracellular and membrane-bound domains (13): and an amyloidogenic route, shown in Figure 1, leading to the release of the Ab segment (7). The cleaving of the Ab sequence from an internal site in the APP chain implies that two distinct proteolytic events are required to generate the *N*-terminus and the *C*-terminus of the Ab peptide. The proteolytic enzymes involved in processing APP are termed *secretases*: a-secretase for cleavage of APP within the Ab segment, and b- and g-secretases for cleavage of APP at the *N*- and *C*-terminal sides of the Ab segment, respectively. Soluble, *C*-truncated forms of APP are generated by two pathways: (1) by a-secretases cutting within the Ab sequence, thereby precluding the release of Ab (13); and (2) by b-secretases cleaving near the *N*-terminus of Ab producing *C*-terminal fragments containing the complete Ab (14). The generation of intact Ab chains suggests that g-secretases generate the *C*-terminus of b-amyloid from these *C*-terminal fragments of APP after release of the transmembrane domain from the lipid bilayer (7). The identity and location of the secretases have proved elusive, but clearly they are of prime importance in Alzheimer's disease, and targets for therapies.

Figure 1. Schematic diagram of the derivation of the 4-kDa b-amyloid protein (Ab) from the 110–130-kDa amyloid precursor protein (APP) by the action of the a-, b-, and g-secretase enzymes. The probable domain structure of APP has been simplified.

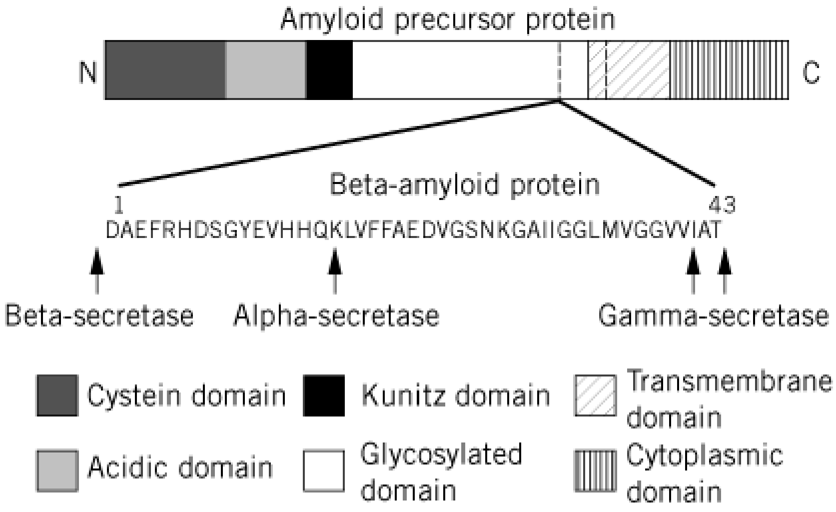

Electron microscope and X-ray fiber diffraction analyses, often using synthetic analogs or fragments of the Ab peptide, have revealed the molecular characteristics of the Ab amyloid fibrils. In the electron microscope, different forms of Ab amyloids are seen at different pH values, but the physiological form appears to be represented by a fibril about 90 Å (9 nm) diameter, composed of five or six parallel protofilaments 25–30 Å (2.5–3 nm) in diameter arranged around a hollow core (15). The X-ray fiber diffraction patterns of Ab amyloid (16, 17) show the usual 4.7 Å (0.47 nm) meridional reflection and 10 Å (1 nm) equatorial reflection that demonstrate that the molecular structure of amyloid consists of paired b-sheets running parallel to the fiber axis, with their constituent b-strands perpendicular to the fiber axis. This structure is very similar to that observed in other amyloids produced from a variety of proteins and peptides (see Amyloid). Some shorter Ab chains, such as residues 11–28, particularly when aligned in a strong magnetic field, form pseudocrystals (18), which give more detailed X-ray diffraction patterns that may be capable of yielding greater structural detail and hence begin to define the features that dispose them to form amyloid.

The discovery that Ab is produced and secreted by cells continuously under normal metabolic conditions, and is present in a soluble form in biological fluids (14, 19), suggests that other factors are involved in Ab amyloidosis. It has been proposed that the isolated Ab protein exists in two forms: a soluble form that may represent a normal host protein and a modified amyloidogenic form (20). These two forms have identical sequences and hence are likely to represent conformation isomers. The soluble form is easily degraded and appears to have an **alpha-helical/random coil** structure: NMR analysis of synthetic Ab 1–40 (21) has shown that residues 15–23 and 31–35 form a-helices, while the rest of the peptide is in a random-coil conformation, and no stable tertiary structure is present. The amyloidogenic form is more resistant to degradation, has a high b-sheet content, and forms the fibrillar aggregates found in brains with Alzheimer's disease. This behavior is very reminiscent of the normal and scrapie forms of the prion protein, which is also an agent for amyloid brain diseases (see Prion, Scrapie, and Amyloid). The existence of two structural forms for the Ab protein implies the possibility that other proteins may be involved in regulating their interconversion. It is known, for example, that in the rare early-onset (30–60 years of age) form of Alzheimer's disease, the disease has been linked to mutations on chromosomes 1 and 14, in addition to chromosome 21, which carries the APP gene. The genes on chromosomes 14 and 1 have been identified with presenilin 1 (22) and presenilin 2 (23, 24), respectively. The two presenilins have 65% amino acid sequence identity, and hydrophobicity plots predict seven transmembrane regions resembling a structural membrane protein. The genetic variants of presenilin 1 allow the secretion of Ab peptides of longer length, and hence more amyloidogenic (25), possibly through a mechanism involving protein sorting and trafficking of APP.

The more common sporadic and familial late onset (>65 years) form of the disease has been linked with mutations on chromosome 19, subsequently narrowed to the ϵ4 allele of the **apolipoprotein** E (apoE) gene (26, 27). These studies have shown that carriers of the ϵ4 allele have an increased risk of developing Alzheimer's disease and that the inheritance of the e4 allele correlates with an increased deposition of Ab amyloid in blood vessels and plaques. The apoE4 **isoform** differs from apoE3, the most common isoform, by an Arg/Cys substitution at position 112. The apoE protein is known to be one of the proteins associated with amyloid deposits (28). It has been found that apoE can form complexes with synthetic Ab analogues and to enhance amyloid fibril formation by Ab *in vitro* (29), possibly by a direct physical interaction. Frangione and his colleagues (30) have made the intriguing proposal that apoE can itself possibly form an amyloid-like structure (there is experimental evidence for this in its *C*-terminal domain), which may be able to induce other proteins such as Ab to misfold into a b-sheet structure that could allow them to be incorporated into a growing amyloid fibril. They term this process "conformational mimicry," and certainly the most recent analyses of *in vivo* amyloid formation characterize it as a disease of protein misfolding, which is possibly **cooperative** (see Amyloid).

Bibliography

1. A. I. Bush, K. Beyreuther, and C. L. Masters (1992) Pharmacol. Ther. **56**, 97–117.
2. A. Ott, M. M. B. Bretaler, and F. van Harskamp (1995) Br. Med. J. **310**, 970–973.
3. R. E. Scully et al. (1993) New Engl. J. Med. **324**, 1255–1263.
4. K. E. Wisniewski, A. J. Dalton, D. R. Crapper-McLachlan, G. Y. Wen, and H. M. Wisniewski (1985) Neurology **35**, 957–961.
5. G. G. Glenner and C. W. Wong (1984) Biochem. Biophys. Res. Comm. **120**, 885–890.
6. C. L. Masters, G. Simms, N. A. Weinman, G. Multhaup, B. L. McDonald, and K. Beyreuther (1985) Proc. Natl. Acad. Sci. USA **82**, 4245–4249.
7. C. Haas and D. J. Selkoe (1993) Cell **75**, 1039–1042.
8. C. Hilbich, B. Kisters-Woike, J. Reed, C. L. Mastrers, and K. Beyreuther (1992) J. Mol. Biol. **228**, 460–473.
9. N. Suzuki et al. (1994) Science **264**, 1336–1340.
10. B. Hymen et al. (1995) Proc. Natl. Acad. Sci. USA **92**, 3586–3590.
11. R. Sandbrink, C. L. Masters, and K. Beyreuther (1994) J. Biol. Chem. **269**, 1510–1517.
12. J. Kang et al. (1987) Nature **325**, 733–736.
13. F. S. Esch et al. (1990) Science **248**, 1122–1124.
14. P. Seubert et al. (1993) Nature **361**, 260–263.
15. P. E. Fraser, J. Nguyen, W. Surewicz, and D. A. Kirschner (1991) Biophys. J. **60**, 1190–1201.
16. D. A. Kirschner, C. Abraham, and D. A. Selkoe (1986) Proc. Natl. Acad. Sci. USA **83**, 503–507.
17. P. E. Fraser et al. (1992) Biochemistry **31**, 10716–10723.
18. H. Inouye, P. E. Fraser, and D. A. Kirschner (1993) Biophys. J. **64**, 502–519.
19. M. Shoji et al. (1992) Science **258**, 126–129.
20. C. Soto, E. Castano, B. Frangione, and N. Inestrosa (1995) J. Biol. Chem. **270**, 3063–3067.
21. H. Sticht, P. Bayer, D. Willbold, S. Dames, C. Hilbich, K. Beyreuther, R. W. Frank, and P. Rosch (1995) Eur. J. Biochem. **233**, 293–298.
22. R. Sherrington et al. (1995) Nature **375**, 754–760.
23. E. Levy-Lahad et al. (1995) Science **269**, 973–977.
24. E. Rogaev et al. (1995) Nature **376**, 775–778.
25. M. Barinaga (1995) Science **268**, 1845–1846.
26. E. H. Corder et al. (1993) Science **261**, 921–923.

27. W. J. Strittmatter (1993) Proc. Natl. Acad. Sci. USA **90**, 1977–1980.
28. T. Wisniewski and B. Frangione (1992) Neurosci. Lett. **135**, 235–238.
29. J. Ma, A. Yee, H. B. Brewer, S. Das, and H. Potter (1994) Nature **372**, 92–94.
30. B. Frangione, E. M. Castaño, T. Wisniewski, J. Ghiso, F. Prelli, and R. Vidal (1996) in *The Nature and Origin of Amyloid Fibrils*, Ciba Foundation Symposium 199 (G. R. Bock and J. A. Goode, eds.), John Wiley and Sons Ltd., Chichester, UK, pp. 132–145.

Suggestions for Further Reading

31. D. J. Selkoe (1994) Normal and abnormal biology of the beta-amyloid precursor protein, Annu. Rev. Neurosci. **17**, 489–517.
32. G. Evin, K. Beyreuther, and C. L. Masters (1994) Alzheimer''s disease amyloid precursor protein, Amyloid: Int. J. Exp. Clin. Invest. **1**, 263–280.

Analogy

Analogy is a similarity caused by factors other than a common genetic ancestry. In general, analogy is a similarity arising by convergent evolution. Therefore, in contrast to homology, analogy between two traits of interest is not based on the sharing of a common ancestor. Originally, the term “analogy” was used mostly for morphological characters. For example, the wings of bats and insects are said to be analogous organs, as they perform the same function in different species, even though they do not show a common underlying plan of structure. It is obvious that the wings of bats and insects were not derived evolutionarily from the same organ in a common ancestor.

When the similarity between two different molecules is found at the level of **nucleotide sequences**, amino acid sequences, and the tertiary structure of proteins, it is important to know whether the similarity is homologous or analogous. In particular, characteristic patterns of amino acids (“amino acid sequence motifs”) and the tertiary structures of protein molecules may exhibit analogy rather than homology. In contrast, any sequence similarities of nucleotides and amino acids are explained mostly by homology, because the probability that the two sequences of interest are similar by chance can be computed easily and is usually extremely small.

Analytical Ultracentrifugation

Analytical ultracentrifugation experiments fall into two different categories, termed **sedimentation velocity** and **sedimentation equilibrium**. However, they are often employed sequentially on a given macromolecule under analysis (Fig. 1), and they yield related, complementary information about the solution behavior of a macromolecule that is of great interest for a variety reasons. The need may be simple, for example, to determine whether a macromolecule aggregates when prepared or stored in various ways, e.g., refrigerated, frozen, or lyophilized. On a much more complex level and much more important in the context of modern protein biochemistry and molecular biology is to detect and measure the interactions of macromolecules with themselves or with other molecules and to relate this to their functional roles. For these studies, the precise analysis of their behavior in solution is necessary. Finally, analytical ultracentrifugation plays an important role in medicine and industry. It is the reference method for analyzing the concentration-dependent solution behavior of recombinant proteins and other macromolecules employed in pharmaceutical/pharmacological research and in structure-based drug design (1).

Figure 1. Typical execution scheme for sedimentation velocity (SV) and sedimentation equilibrium (SE) runs.

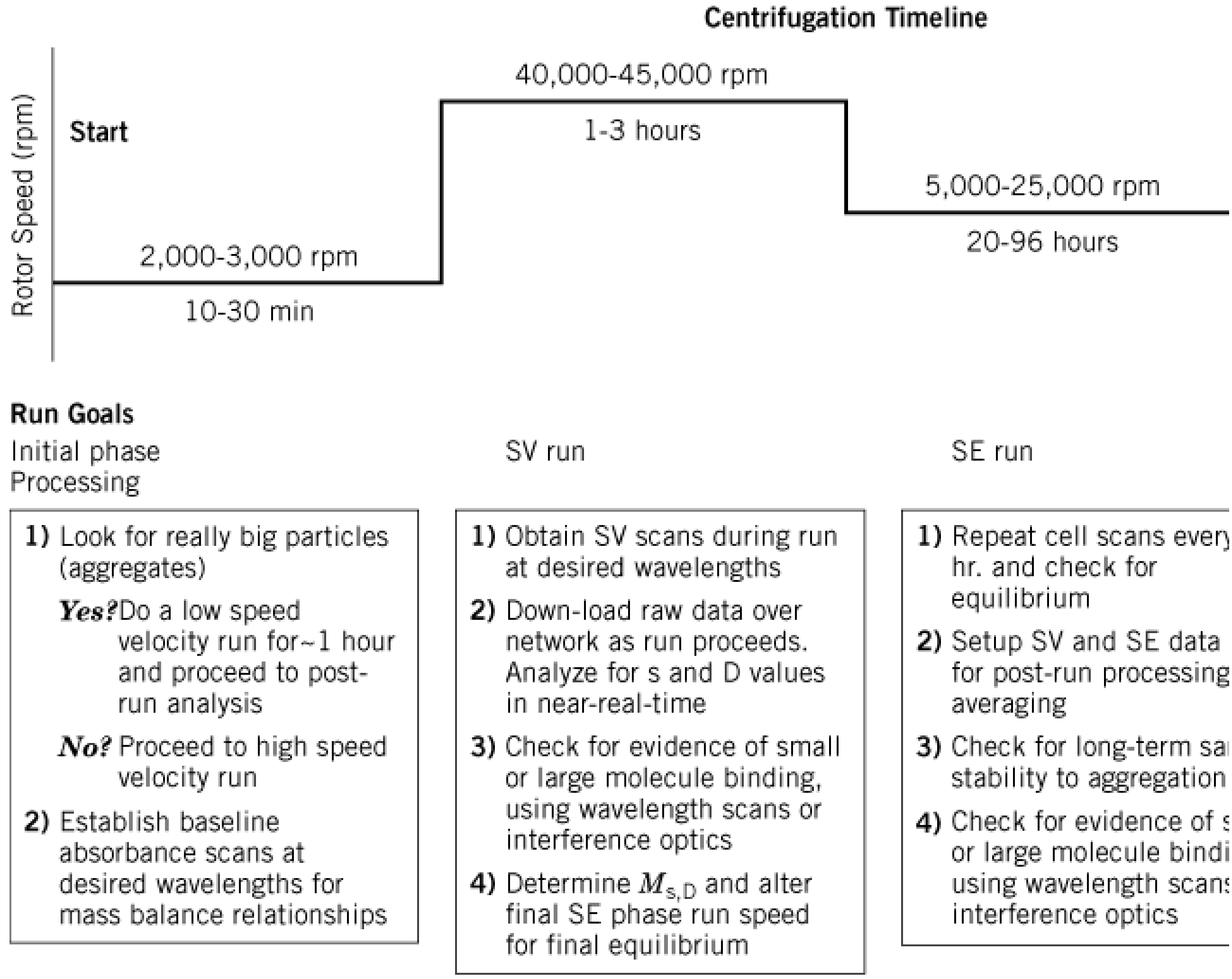

Analytical ultracentrifugation differs from preparative centrifugation in several important respects. First and foremost as the name implies, it is an *analytical* technique. If carefully applied, it can give hydrodynamic information that is precise, accurate, and unobtainable by any other single method. The hydrodynamic parameters (**molecular weights** and sedimentation coefficients) obtained from analytical ultracentrifugation are absolute measurements because the technique is an absolute physical method in the strictest sense. It measures either the intensive or extensive physical properties of solutes directly and requires only knowledge of the rotational rate of the centrifuge rotor, the sample temperature, and the solution density and viscosity (which are extensive properties of the solute–solvent system).

Similarly, calculations of molecular properties from ultracentrifugation data are based on direct, first-principle analyses of solute behavior in solution. Unlike indirect methods, such as static light-scattering, the calculations in analyzing data from the analytical ultracentrifuge do not rely on comparison to a known standard. For example, in static light scattering the scattering behavior of a low molecular weight organic molecule (toluene, for example) is required to calibrate the instrument. Dynamic light scattering provides absolute diffusion coefficients, but the molecular weights estimated from the diffusion coefficients are indirect and depend upon the solution density, viscosity, etc. and on assumptions about molecular dimensions.

Another major difference between preparative centrifugation and analytical ultracentrifugation is that the latter is usually applied to highly purified solute samples. Although samples must be pure, analytical analyses usually require only small amounts of sample material, in the range of 10 to 1000 µg per sample. Finally, although analytical ultracentrifugation is inherently a nondestructive technique, it is not routine to recover or reuse samples that have been analyzed because analytical ultracentrifuge cells and rotors (Figs. 2 and 3), especially those that are most useful for analyzing numerous samples, are not designed for facile sample recovery. Although analytical ultracentrifugation was at one time a useful tool for evaluating the purity of certain biological macromolecules, its use as a simple tool for purity analysis has been superseded by a variety of other bioanalytical techniques. For example, inexpensive SDS-PAGE is routinely the technique of choice for analyzing protein purity during a protein separation protocol and for estimating the molecular weights of polypeptide chains present.

Figure 2. A four-hole analytical ultracentrifuge rotor and a vertically exploded view of the cell assembly with a double-sector, long-channel centerpiece. Sample and reference solutions for analysis (~400 to 500 µl) are introduced into the sealed centerpiece with an appropriate syringe system. Then the cell is placed in the rotor and subjected to centrifugation. Depending upon the analyses performed, it is possible after centrifugation to recover a portion of the sample using the same syringe system (figure courtesy of Beckman Instruments, by permission).

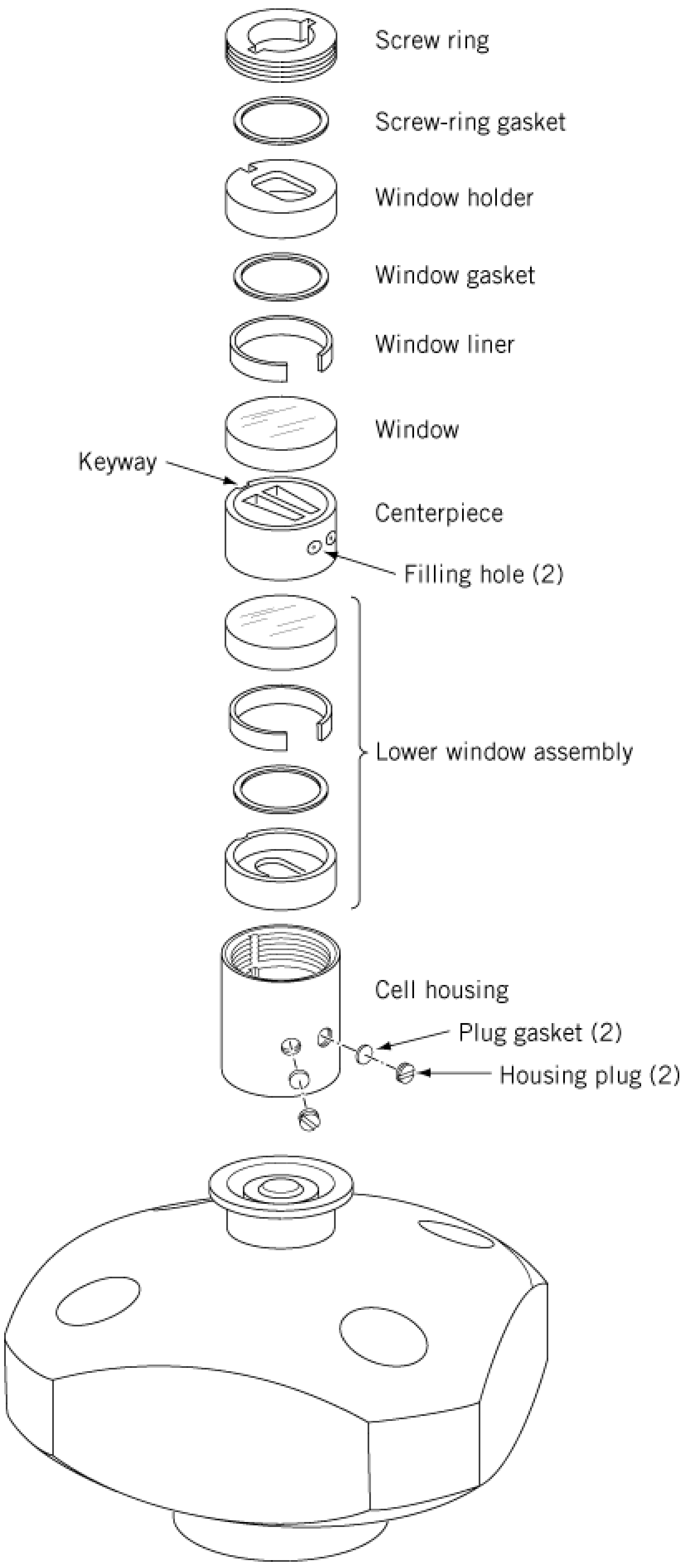

Screw ring
Screw-ring gasket
Window holder
Window gasket
Window liner
Window
Keyway
Centerpiece
Filling hole (2)
Lower window assembly
Cell housing
Plug gasket (2)
Housing plug (2)

Figure 3. Illustrations of centerpieces used in analytical ultracentrifugation. Left, a long-column, double-sector centerpiece used for sedimentation velocity and equilibrium studies that require large data sets. Right, the multichannel centerpiece (or "Yphantis" centerpiece after its inventor, Dr. David Yphantis) used primarily for sedimentation equilibrium studies where analysis of a larger number of samples is desired.

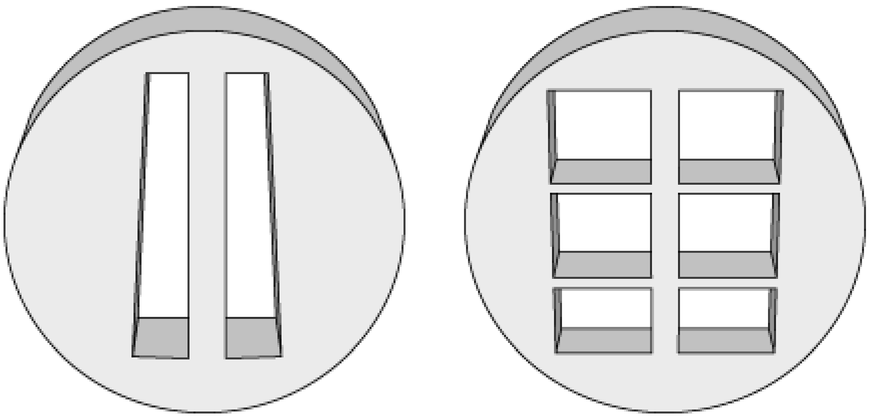

The present (and likely future) value of analytical ultracentrifugation lies in its unmatched ability to provide direct information in two primary areas: (1) the extent to which an otherwise chemically pure sample of a macromolecular solute exhibits monodispersity or polydispersity and (2) the extent to which different chemically pure molecules interact. Because these two questions are fundamental to all areas of modern cellular and molecular biology and biochemistry, analytical ultracentrifugation remains a unique and extremely powerful biophysical tool.

1. The Modern Analytical Ultracentrifuge

The technique requires only small sample volumes, ~20 µl to ~500 µl depending upon the type of centerpiece employed (Figs. 2 and 3). A computer-controlled optical system detects the exact extent and position of the radial displacement of solute molecules at various times during the centrifugation run. Optical detection is accomplished by directly measuring the concentration of the solute as a function of radial position in the sample cell, either by its absorbance or by the change in refractive index, using Rayleigh interference optics. Like dual-beam optical spectroscopy, the technique is also differential in that it employs a sample solution to be measured and a reference solution used to "blank out" or "subtract" a signal background. The only modern, commercially available analytical ultracentrifuges are the XLA/XLI models manufactured by Beckman Instruments, which operate at speeds ranging from ~2,000 to ~50,000 rpm . The precise speed or speed range of operation for an experiment is determined by the type of measurement(s) to be made and depends on the size of the molecules being studied and on the type of sample cell centerpieces, centrifuge rotor, and the data collection system used.

The XLA/XLI analytical ultracentrifuges offer either absorbance-based optical detection (XLA, Fig. 4) or both absorbance and interference-based optical detection (XLI, Fig. 5). In addition to measuring the molecular weights and sedimentation coefficients of individual molecules, their distributions in samples can also be measured. The analytical ultracentrifuge can also be also used for direct determination of **ligand-binding** constants and stoichiometries. Further, when combined with other physical measurements, these instruments are useful for determining the diffusion coefficients and molecular shapes of macromolecules. Thus, changes in shape related to ligand binding or solvent perturbations can also be evaluated.

Figure 4. Absorbance-based optical system of the XLA analytical ultracentrifuge from Beckman Instruments. Light from a high intensity flash lamp passes along an optical tube to a computer-controlled toroidal diffraction grating, which selects the wavelength(s) of observation. Light at the selected wavelength, within the range ~200–800 nm , is focused on the sample cell in the rotor. Light passing through the sample is recorded by the radially tracking photomultiplier. Then the data are analyzed using specialized software on an associated computer (figure courtesy of Beckman Instruments, by permission).

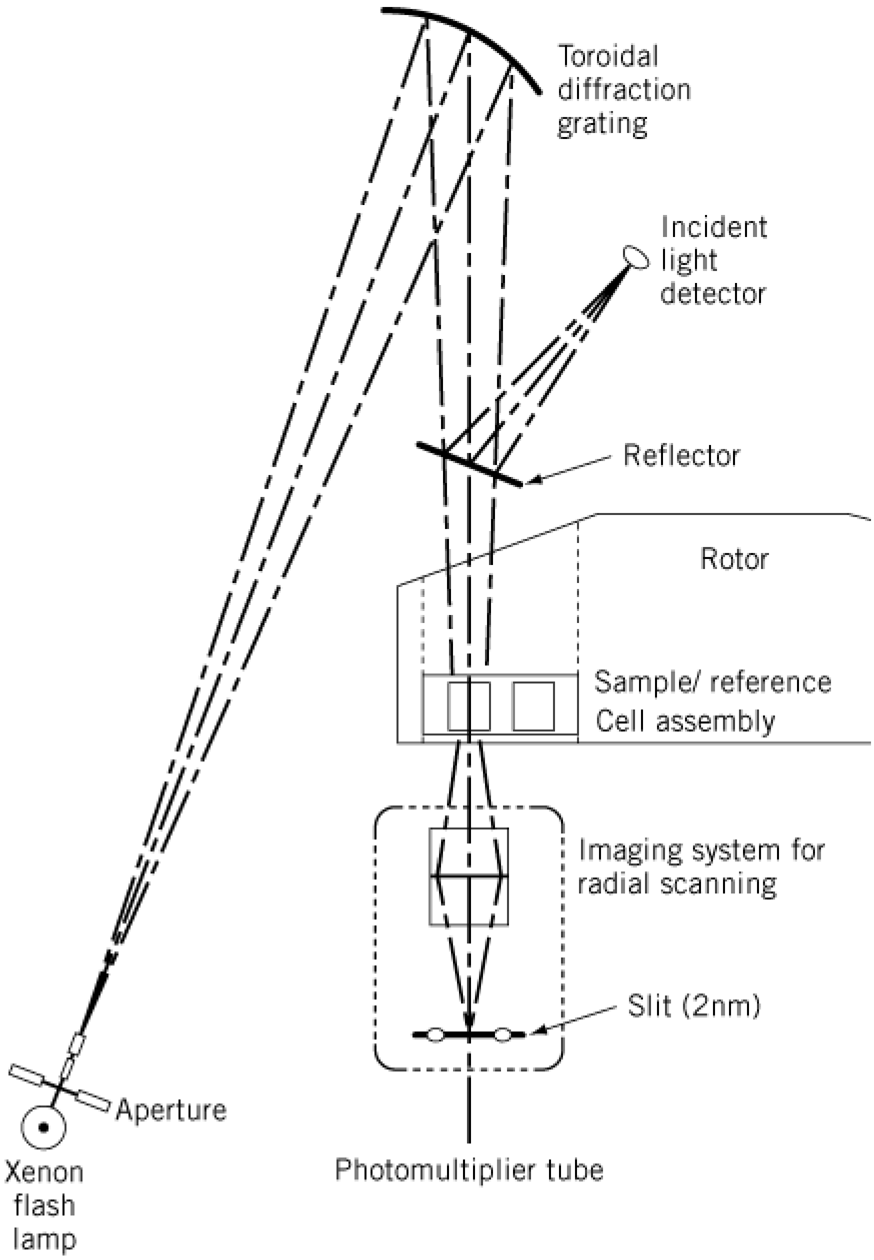

Figure 5. Interference and/or absorbance-based optical system of the XLI ultracentrifuge from Beckman Instruments. The absorbance-based optical system is outlined in Fig. 4. For interference measurements, a laser light source is attached to the absorbance optical tower, and an additional optical path and detector system is employed (lower right quadrant of figure). The interference system uses Rayleigh interference optics and a computer-controlled CCD camera detection system. Data are analyzed using specialized software on an associated computer. Using an eight-hole centrifuge rotor and centerpieces that hold three sample and reference solutions each, it is possible to analyze 21 samples in a single ultracentrifuge run (figure courtesy of Beckman Instruments, by permission).

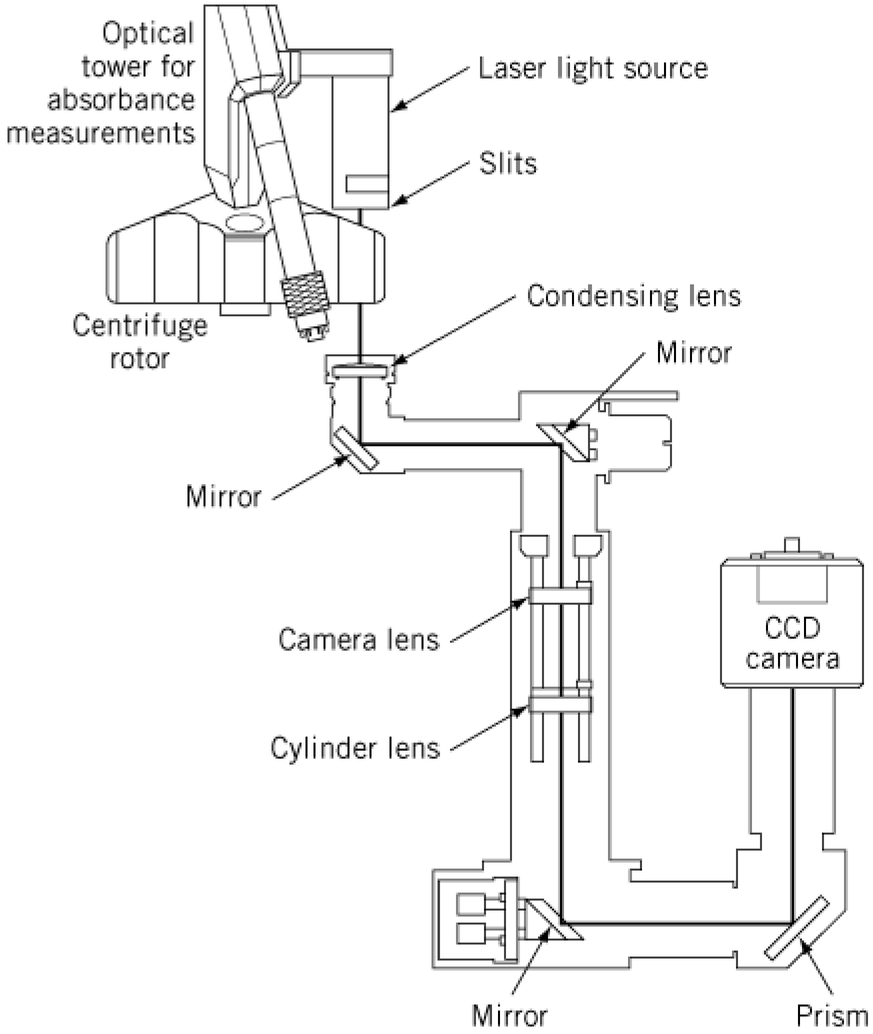

1.1. Choosing an Optical System for Measurements

Although it is often useful to employ both absorbance and optical interference measurements when examining a sample, some considerations make one type of measurement preferable to the other. The possible choices for various types of samples are outlined in Table 1. In addition to the general preferences for detecting various analytes, other important factors influence the choice of detection methods. The relative sensitivities and dynamic ranges of absorbance versus interference detection can be a consideration. The typical useful range for absorbance measurements in a sedimentation equilibrium centrifugation experiment for an "average" protein with an absorbance at 280 nm of 1.0 $(mg/ml)^{-1}(cm)^{-1}$ is in the range of ~10 µg/ml to ~4 mg/ml , when the measurements employ centerpieces with both standard (12 mm) and reduced (3 mm) path lengths. In **sedimentation velocity experiments** using absorbance detection at 280 nm, the practical low end of the concentration range is about 50 to 100 µg/ml. Sensitivity for proteins can be increased by using light with wavelengths in the range of 215 to 240 nm, where the protein peptide backbone absorbs and the absorbance of a protein is typically 3- to 10-fold greater, although this is technically more demanding. Alternatively, the protein may have a natural cofactor chromophore with a large extinction coefficient, or chemical modification can be used to introduce such a chromophore. Optical interference measurements have roughly the same absolute dynamic range as absorbance measurements, but they are routinely more useful in the mid-to-high concentration range, i.e., ~0.1 to ~10 mg/ml .

Table 1. General Preferences in Analytical Ultracentrifugation for Detecting Different Analytes

Analyte	Absorbance Detection	Interference Detection
Carbohydrates	Usually not useful unless solute has appreciable UV or visible absorbance properties	Usually the method of choice
Nucleic acids	Follow absorbance at ~260 nm	Possible, can be used at high analyte concentrations
Organic polymers	Usually not useful unless solute has appreciableUV or visible absorbance properties	Usually the method of choice
Polysaccharides	Usually not useful unless solute has appreciableUV or visible absorbance properties	Usually the method of choice
Proteins	Useful if protein contains Trp and/or Tyr residues, so that it absorbs at 280 nm	Useful if protein lacks Trp and Tyr residues

The selectivity of the detection technique can also be a factor in performing an experiment. The use of this approach is illustrated in Fig. 6 for examining the potential for interactions between the Alzheimer's disease beta-amyloid peptide and the serum C1Q component of the complement system, which other studies had suggested is a trigger for activating the complement cascade and for potential neuronal cell loss. In this work, a 5-kDa peptide was labeled with the chromophore *fluorescein*. Binding of the labeled peptide to a ~150 kDa antifluorescein antibody was used as a positive control to examine the potential for b-amyloid peptide to bind to C1q. The labeled peptide binds to the antibody as expected, but it does not bind to C1q.

Figure 6. Binding of a xanthene-labeled Alzheimer's b-amyloid peptide to an antifluorescein antibody but not to serum complement C1q, as analyzed at sedimentation equilibrium at low speed (5000 rpm). The fluorescein analog, xanthene, absorbs light at 510 nm (solid line), and the proteins absorb light at 280 nm (dotted line). Panel (**a**) shows the radial distributions of labeled peptide alone at 280 and 510 nm (no sedimentation). Panel (**b**) shows the labeled peptide sedimented in the presence of C1q, C1q tended to sediment, but the peptide did not. Panel (**c**) shows the control experiment where the labeled peptide was sedimented in the presence of an anti fluorescein antibody. The peptide binds to the antibody and sediments with a molecular weight equivalent to that of the antibody. These results demonstrate that the monomeric form of the amyloid peptide implicated in Alzheimer's disease is unlikely to bind to complement C1q and thus induce complement-mediated neural cell death (from Ref. 8, with permission).

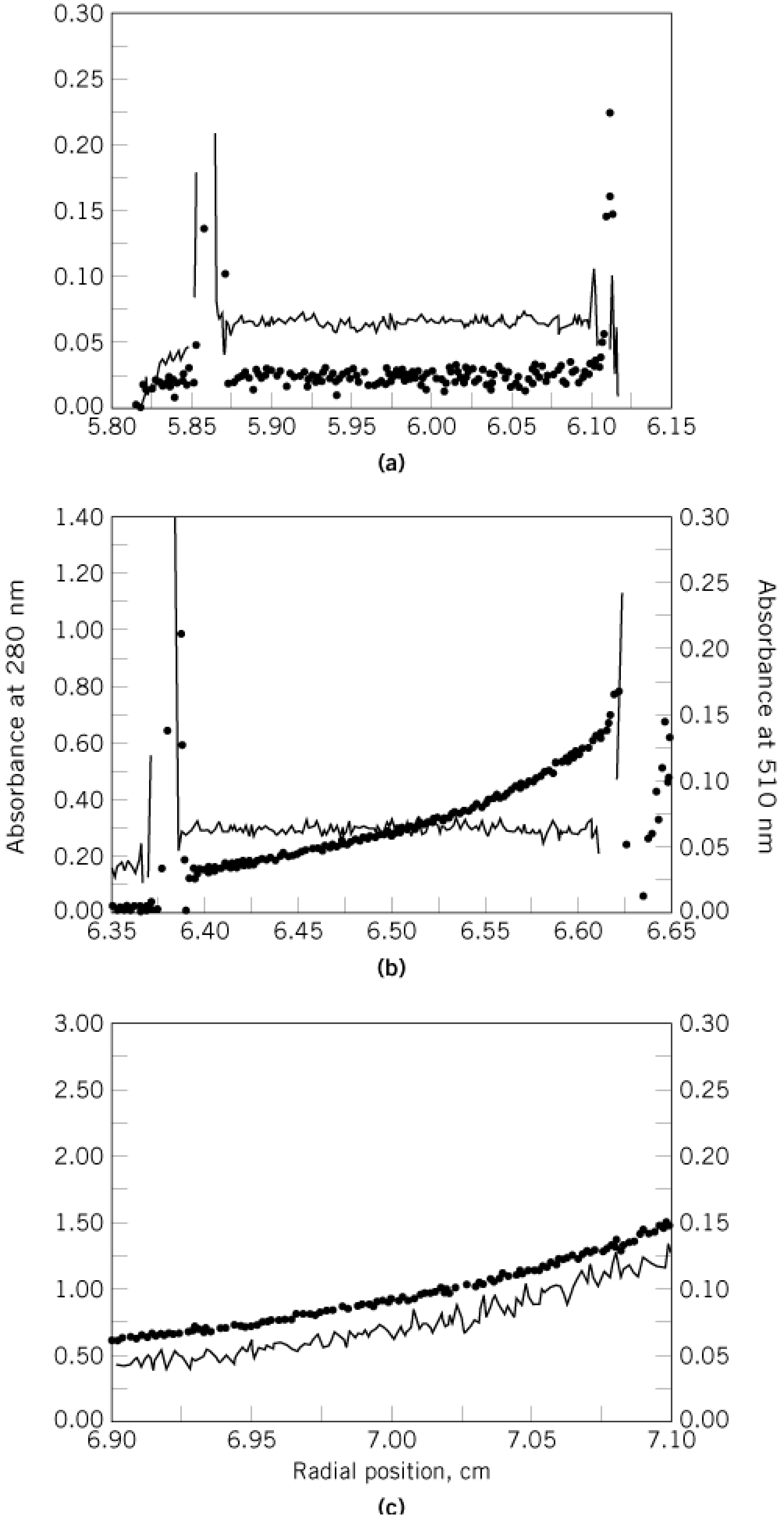

0.30
0.25
0.20
0.15
0.10
0.05
0.00
5.80
5.85
5.90
5.95
6.00
6.05
6.10
6.15
(a)
1.40
1.20
1.00
0.80
0.60
0.40
0.20
0.00
Absorbance at 280 nm
0.30
0.25
0.20
0.15
0.10
0.05
0.00
Absorbance at 510 nm
6.35
6.40
6.45
6.50
6.55
6.60
6.65
(b)
3.00
2.50
2.00
1.50
1.00
0.50
0.00
0.30
0.25
0.20
0.15
0.10
0.05
0.00
6.90
6.95
7.00
7.05
7.10
Radial position, cm
(c)

In analytical ultracentrifugation, another important consideration is sample and reference solution buffer matching. If the solutions are poorly matched, the resulting data are usually poor, even with the extensive signal averaging employed with advanced detectors and software.

Interference detection measurements are based on the change in the refractive index of the solution caused by a solute, which is a function of its concentration. For these measurements, the system records the differential change in the refractive index of the sample versus the reference cell, as a function of radial position. The refractive index of a solution is a function of the mass of all solutes, not of their absorbance or molarity, and it is not possible to distinguish between different solutes. In fact, buffers and salts routinely contribute most of the change in refractive index because they are present in much higher concentrations than the protein. Therefore, interference measurements are extremely sensitive to small mismatches in refractive index between the buffers of the sample and reference solutions. As a result, samples analyzed by interference measurements routinely require exhaustive dialysis. With appropriate sample/reference solution preparation, it is possible to achieve protein concentrations of >100 mg/ml routinely. The only effective upper limit is the intrinsic solubility of the protein itself under the conditions of analysis (rotor velocity, temperature, pH, etc., which can be easily changed). For both absorbance and interference measurements, the lower limit on size is a molecular weight of ~200 Da, and the upper limit is effectively about 30×10^6 Da.

Absorbance optics permit the differential absorbance of two molecules to be employed to distinguish their sedimentation properties (as in Fig. 6). This is not possible with interference optics, however, so it is not possible to distinguish between two different solute molecules with similar masses.

Another feature of interference measurements is their use in a differential mode. Because the interference optical system is double-beam, differential centrifugation experiments can be performed where the protein is present in both cells and a small ligand only in one. Consequently, the signal from the protein is blanked out, leaving only the signal from the ligand. A ligand that binds to the protein (even weakly) is displaced along the radial axis of centrifugal force in the centrifuge cell. Because the protein signal is blanked out, the only change in refractive index observed along the radial (force) axis is caused by the change in radial distribution of the ligand (2, 3).

Absorbance measurements generally have less stringent referencing requirements. In practice it is necessary only that the reference buffer has an absorbance at the wavelength of analysis at which it is electronically possible for the instrument to perform the desired subtraction. Therefore, absorbance measurements are relatively more forgiving for buffer matching in sample/reference preparation. They are not without other intrinsic problems, however, in particular those related to the absorbance of buffers and solute extinction coefficients. Most biologically useful buffers and common solution additives have some characteristic absorbance in the wavelengths used to analyze proteins in solution. Because of the high total sample/reference solution absorbance, it may be difficult or impossible to make the requisite difference absorbance measurements. However, under these conditions protein samples that have been carefully prepared by dialysis but are optically opaque at UV wavelengths, may be routinely analyzed by interference rather than absorbance detection (as above). Finally, one interesting drawback to absorbance measurements, which is routinely neglected in sedimentation equilibrium analyses (in particular), is that the analyte solution extinction coefficient(s) may vary with the composition of the solution, so that its absorbance can change during a centrifugation run. Homo- or heteroassociation processes may alter the protein extinction coefficients, which contributes nonlinear perturbations to the total absorbance. Thus careful analyses require that the radial distributions of molecules undergoing such associations be measured at several wavelengths. Interference measurements, in comparison, are insensitive to these alterations in solute extinction coefficient.

1.2. Monodispersity, Polydispersity, Paucidispersity, and Nonideality

A solute is said to be monodisperse if it exhibits behavior characteristic of a single species in solution. If the solute undergoes indefinite self-association under the solution conditions examined, it is said to exhibit *polydispersity*. If a sample of solute molecules is composed of a mixture of a limited number of species with different chemical compositions, its solution behavior is *poly*disperse, for example, with respect to its molecular weight distribution, but the sample is termed *pauci*disperse. The differences between various types of solute behavior in solution are outlined in Table 2. It is often useful to define molecular weight distributions in terms of the molecular weight averages M_n, M_w, and M_z, which are the number-, weight-, and z-averages, respectively (Table 3). They are valuable for estimating sample homogeneity. A pure solute gives identical values of M_n, M_w, and M_z. Different methods of measurement give different averages.

Table 2. Summary of Types of Solute Hydrodynamic Behavior

Hydrodynamic Characteristic	Example	Sedimentation Velocity Behavior	Sedimentation Equilibrium Behavior	Consequences
Monodisperse	Solute is pure, a single spherelike chemical entity that does not undergo self-interaction	Velocity profiles fit a single-term Lamm equation (see Sedimentation Velocity Centrifugation), and the single sedimenting boundary gives unique values of *s* and *D* during run	Data fit a single exponential term at all rotor speeds and solute concentrations	Molecular weight, *s*, and *D* have minimal or no dependencies on concentration; solute solution behavior is “ideal” or nearly so
Paucidisperse	Sample comprises a small number of chemically distinct solutes, which may or may not interact	Velocity profiles fit a multiple-term Lamm equation, and sedimenting boundaries give multiple values of *s* and *D* during run	Data do not fit a single exponential term at all rotor speeds and solute concentrations	Molecular weight, *s*, and *D* depend on concentration
		It may be possible to resolve separate sedimenting g*	Chances for extracting binding constants for a	

		(s) distributions	macromolecular assembly are usually severely diminished	
Polydisperse	Sample comprises multiple solutes, which may or may not interact	Velocity profiles fit a multiple-term Lamm equation, and sedimenting boundaries give multiple values of s and D during run	Data do not fit a single exponential term at all rotor speeds and solute concentrations	Molecular weight, s, and D depend on concentration, solute solution behavior is usually termed "nonideal"
	Sample is pure, a single spherelike chemical entity that aggregates	It may be possible to resolve separate sedimenting $g^*(s)$ distributions	Depending upon nature of self-association, it may be possible to extract binding constants for a macromolecular assembly process	
Nonideal	Sample comprises a single, highly asymmetric chemical entity that undergoes self-interaction	Velocity profiles fit a multiple-term Lamm equation, and sedimenting boundaries give multiple values of s and D during run	Data exhibit skewed behavior and cannot be fit by conventional analyses	s and D depend on concentration, solute solution behavior is "nonideal"
		It may be possible to resolve separate sedimenting $g^*(s)$ distributions	Usually not possible to extract binding constants for a macromolecular assembly process	

Table 3. Molecular Weight Averages

Type	Equation[a]	Methods to Determine
M_n, number-average	$\frac{\sum_i c_i}{\sum_i (c_i/M_i)}$	Osmotic pressure, sedimentation equilibrium

M_w, weight-average	$\frac{\sum_i C_i M_i}{\sum_i C_i}$	Sedimentation equilibrium; light scattering
M_z, z-average	$\frac{\sum_i C_i M_i^2}{\sum_i C_i M_i}$	Sedimentation equilibrium

[a] C_i is the concentration, and M_i is the molecular weight of the *i*th species in weight per unit volume.

Nonideality is typically observed at high concentrations of a solute and is caused by the effects of excluded volume (versus actual molecular volume) on solute hydrodynamic behavior. The effects of nonideality are small for spherical molecules, because their excluded and actual volumes are essentially equivalent. With such molecules, their hydrodynamic behavior varies in direct proportion to the size of the molecular sphere. When molecules are rodlike, nonideality becomes more pronounced. As the concentration increases, the effect is nonlinear and it is significantly worse at greater ratios of molecular length to width. Intermolecular interactions are another cause of nonideality. For example, electrostatic charge–charge repulsion can be significant at high solute concentrations and low solution ionic strengths. Experimentally, such charge–charge effects are usually reduced by increasing the solution ionic strength. The role of nonideality in sample behavior is identified by performing a series of studies at different solute concentrations and extrapolating the measured hydrodynamic parameters to infinite dilution.

1.3. Other Physical Measurements Necessary to Analyze Ultracentrifuge Data

Calculating results from sedimentation equilibrium and velocity experiments requires several additional physical measurements of the solute and of the solutions employed. To calculate the anhydrous weight-average molecular weight, the density of the solvent and the partial specific volume of the solute must be known.

There are typically two ways to obtain these values. They can be measured with an ultrasonic density meter or pyncnometer or estimated from various tables if the specific buffer and solute chemical compositions are known. For a protein, the approximate partial specific volume is calculated from its amino acid composition (4, 5). The density of a buffer of exact composition can be estimated from an appropriate reference table (for example, from the *CRC Handbook of Chemistry and Physics*). Of the two direct methods for determining solvent densities and solute partial specific volumes, ultrasonic densitometry is preferred because it requires less solute for measurements. It is good experimental practice to measure both the solvent density and the partial specific volume of a solute sample of interest. In the case of proteins, this is particularly true if the studies analyze the tendencies of the proteins to undergo association or conformational changes when bound to a ligand. Such interactions are often accompanied by significant changes in the volume of the protein that are unaccounted for if the specific volumes of the individual amino acids comprising the protein are used in the calculation (6, 7). Additionally, if the protein contains carbohydrate (a **glycoprotein**, for example) or bound lipid (a **lipoprotein**), estimates from reference tables can, at best, be charitably characterized as a guess.

The final physical measurement necessary is the measurement of the solution viscosity . This value can be estimated from tables (5) (as for buffer density), but again it is good experimental practice to measure the solution viscosity directly with a simple, commercially available viscometer.

Bibliography

1. S. W. Snyder, R. P. Edalji, F. G. Lindh, K. A. Walter, L. Solomon, S. Pratt, K. Steffy, and T. F. Holzman (1996) J. Protein Chem. **15**, 763–774.
2. I. Z. Steinberg and H. K. Schachman (1966) Biochemistry **12**, 3728–3747.

3. T. M. Lohman, C. G. Wensley, J. Cina, J. R. R. Burgess, and M. T. Record (1980) Biochemistry **19**, 3516–3522.
4. E. J. Cohn and J. T. Edsall (1943) In *Proteins, Amino Acids, and Peptides as Ions and Dipolar Ions* (ACS Monograph series), Reinhold Publishing, New York, pp. 155–176.
5. H. Durchschlag (1986) In *Thermodynamic Data for Biochemistry and Biotechnology* (H. J. Hinz, ed.), Springer-Verlag, New York, pp. 45–128.
6. H. Durchschlag and R. Jaenicke (1982) Int. J. Biol. Macromol. **5**, 143–148.
7. H. Durchschlag and R. Jaenicke (1982) Biochem. Biophys. Res. Commun. **108**, 1074–1079.
8. S. W. Snyder, G. T. Wang, L. Barrett, U. S. Ladror, D. Casuto, C. M. Lee, G. A. Krafft, R. B. Holzman, and T. F. Holzman (1994) Exp. Neurol. **128**, 136–142.

Suggestions for Further Reading

9. K. E. Van Holde (1971) *Physical Biochemistry*, Prentice–Hall, Inc., Englewood Cliffs, NJ, pp. 70–121. A short, highly readable and concisely illustrated treatment of the mechanical model of centrifugation for the biologist.
10. D. Eisenberg and D. Crothers (1979) "Physical Chemistry with Applications to the Life Sciences", Benjamin–Cummings, Menlo Park, CA, pp. 701–745. An excellent introductory physical chemistry text with a good review of fundamental flow equations and a number of useful examples.
11. C. Tanford (1961) *Physical Chemistry of Macromolecules*, Wiley, New York, pp. 317–456. A classic and still relevant text on the nature of transport processes as applied to biological systems.
12. T. M. Schuster and T. M. Laue (1994) "Modern Analytical Ultracentrifugation: Acquisition and Interpretation of Data for Biological and Synthetic Polymer Systems", Birkháuser, Boston. The most recent compendium of modern data analytical methods and applications pertaining to the new XLA analytical ultracentrifuge.

Androgenesis

Androgenesis is the mode of **reproduction** of **eukaryotes** where both sets of chromosomes of the offspring are of paternal origin. In higher **plants**, androgenesis can be obtained either *in vitro* with anther cultures or with isolated pollen grains. In animals, androgenesis can be obtained only experimentally. A technique similar to that described in the entry **Digynism** can be used, that of pronuclear transplantation: the male **pronucleus** is removed from a fertilized egg and injected into another egg, from which the female pronucleus is then removed, so that now the zygote contains two paternally derived sets of chromosomes.

Rarely, diandric embryos arise spontaneously when a fertilized egg loses its female pronucleus. These embryos are not viable. In humans, their implantation results in a uterine tumor called a hydatiform mole. In spontaneous abortions, diandric embryos are a minority among triploid conceptuses (1).

Diandric embryos are useful for studies of genetic imprinting.

Bibliography

1. D. E. McFadden and J. T. Pantzar (1996) Hum. Pathol. **27**, 1018–1020.

Aneuploidy

An aneuploid cell has one or more complete chromosomes either in excess or less than the normal haploid, **diploid**, or polyploid number characteristic of the species from which the cell derives. In other words, the chromosome number is not a multiple of the haploid cell number of chromosome.

Fluorescence in situ hybridization (FISH) with chromosome-specific probes has been successfully applied to rapidly detect numerical aberrations in metaphase and interphase amniotic cells (1). Aneuploidy arises primarily by the process of **nondisjunction**, probably caused by nonrandom premature centromere division in the first meiotic division of maternal **meiosis**. This varies among chromosomes, however, and a significant proportion of paternal and/or meiosis II errors have been described.

The presence of kinetochores or kinetochore proteins (detected immunochemically) in the **micronuclei** of binucleated cells indicates a cell with a high probability for aneuploidy following **cytokinesis** (2, 3). The relationship between Y-Chromosome aneuploidy in male humans, the number of micronuclei, the status of kinetochore proteins, and aging has been reviewed (4).

Bibliography

1. W. L. Kuo et al. (1991) Am. J. Hum. Genet. **49**, 112–119.
2. D. A. Eastmond and J. D. Tucker (1989) Mutat. Res. **224**, 517–525.
3. B. K. Vig, H. J. Yoo, and D. Schiffmann (1991) Mutagenesis **5**, 361–367.
4. J. Nath, J. D. Tucker, and J. C. Hando (1995) Chromosoma **103**, 725–731.

Suggestion for Further Reading

5. D. K. Griffin (1996) The incidence, origin, and etiology of aneuploidy. Int. Rev. Cytol. **167**, 263–296. An exhaustive review.

Angiogenin

Angiogenin (Ang) is one of a group of proteins that are potent inducers of angiogenesis, the process by which new blood vessels are formed (see Epidermal Growth Factor, Fibroblast Growth Factors, Transforming Growth Factors, Tumor Necrosis Factor). It was first isolated from medium conditioned by human adenocarcinoma (HT-29) cells based on the premise that tumor cells must secrete angiogenic factors in order to attract blood vessels so that they can grow. Ang was identified by its ability to stimulate angiogenesis on the chorioallantois, the outer membrane that surrounds the embryo in fertilized chicken eggs. Subsequently, it was shown to be present in normal human plasma, bovine milk, and bovine and mouse serum. It is a 14-kDa basic protein that has 33%

sequence identity to bovine pancreatic ribonuclease A and is one of several members of the RNase A superfamily of proteins that have unusual biological activities. It is the only angiogenic protein that is a ribonuclease, and the only ribonuclease that is angiogenic. It is an important protein that may be involved in wound healing, is critical for the growth of solid tumors, and has become a target for the treatment of metastatic cancer and other angiogenesis-related diseases. For recent reviews on Ang see Refs. 1 and 2.

1. Protein Chemistry

Human Ang is a single polypeptide chain of 123 amino-acid residues and three disulfide bonds (Fig. 1). All of the main components of the catalytic site (see Active Site) of RNase A are present in Ang, and thus it is not surprising that it has enzymatic activity toward RNA and dinucleotides and which, like that of RNase A, is limited to cleavage after pyrimidines. What is surprising is that this activity is four to six orders of magnitude less than that of RNase A. Nevertheless, it is essential for angiogenic activity. Part of the reason for such low activity was revealed by X-ray crystallography (Fig. 2). The structure of Ang is closely similar to that of RNase A, but with two major differences. On the one hand, the pyrimidine-binding (B_1) component of the catalytic active site was found to be occluded by the side chain of Gln117. On the other, the second (B_2) component of this site is structurally quite different from that in RNase A. In the latter, it is part of an eight-residue disulfide loop that is found in all of the 55 known mammalian members of the ribonuclease superfamily but missing in all of the nine known Ang. Instead, it is replaced by a sequence of residues that interacts with a cell-surface binding protein (see text below). Despite these likely impediments to substrate binding, Ang does catalyze RNA hydrolysis, albeit very weakly.

Figure 1. Amino acid sequence of human angiogenin. The active site histidine (H) and lysine (K) residues are in bold, and the disulfide bridges between cysteine (C) residues are indicated by dotted lines.

<QNDSRYTHFL TQ**H**YDAKPQG RDDRYCESIM RRRGLTSPC**K**

DINTFIHGNK RSIKAICENK NGNPHRENLR ISKSSFQVTT

CKLHGGSPWP PCQYRATAGF RNVVVACENG LPV**H**LDQSIF

RRP

Figure 2. The polypeptide fold for human angiogenin drawn with the program MOLSCRIPT. (From Ref. 9, with permission.)

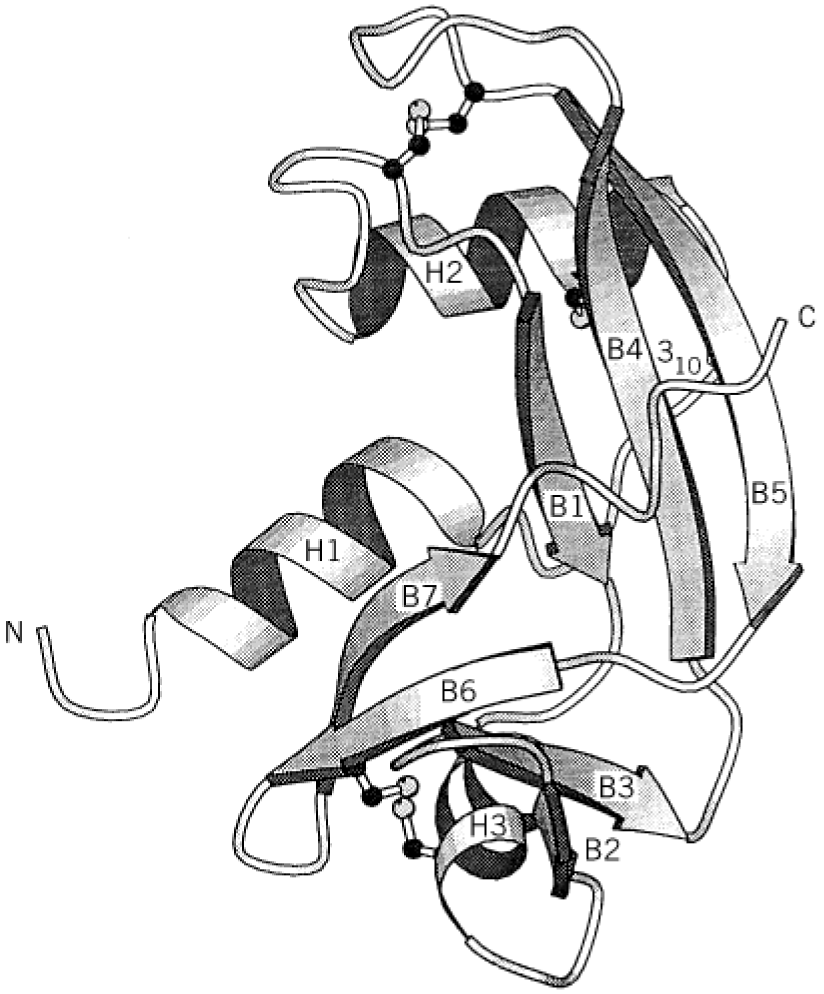

It has been suggested that through evolution Ang was endowed with a unique structure that attenuates its catalytic potency toward RNA in general, but that undergoes a conformational change when Ang is brought together with its specific, yet unidentified, substrate (3). Whether this structural rearrangement activates Ang or merely ensures its specificity is unknown. It may be that the very low activity of Ang is perfectly adequate for carrying out its unique biological function. It should be noted, however, that Ang is an effective inhibitor of cell-free protein synthesis by virtue of its ability to cleave 18S rRNA when this substrate is present in the intact ribosome, and in fact is an even more effective inhibitor than RNase A. When isolated 18S RNA is used as substrate, the activity of Ang is markedly decreased relative to RNase A. This suggests that the activity of Ang depends on the environment of its substrate.

2. Molecular Biology

The human *Ang* gene, localized to chromosome band 14q11, is present as a single copy per haploid genome, with no **introns** in the protein-coding region (1, 2). The gene has been cloned and expressed in both *Escherichia coli* and BHK cells, and well over 40 Ang variants have been prepared in order to explore various aspects of its structure–function relationships. Thus, site-directed mutagenesis of His13, His114, or Lys40 (the equivalents of the catalytic residues His12, His119, and Lys41 in RNase A) abolishes *both* the ribonucleolytic and the angiogenic activity of Ang. Although angiogenically inactive, these variants block the angiogenic activity of native angiogenin. By contrast, an Ang variant in which residues 58 to 70 were replaced by residues 59 to 73 of RNase A had 300- to 600-fold more activity toward RNA substrates but was angiogenically inactive. Thus, ribonuclease activity is essential but not sufficient for angiogenic activity. Moreover, this variant, unlike the active site variants, was unable to block the angiogenic activity of native Ang, suggesting that the mutated region of the protein is involved in cell binding, probably interacting with a cell-surface binding protein. Recall that in RNase A this region of the molecule constitutes the B_2 component of the substrate binding site. In Ang it apparently has evolved into a cell binding site, with loss of catalytic activity but concomitant acquisition of a new biological potential.

3. Cell Biology

Blood vessels are composed of specialized cells known as endothelial cells. It is not surprising, given its function, that ^{125}I-labeled Ang binds to endothelial cells, and it does so in a manner that is characteristic of receptor binding—that is, time- and concentration-dependent, reversible, saturable, and competitive with unlabeled Ang. Yet Ang is a plasma protein (200 to 400 mg/L), and obviously it does not continuously stimulate new blood vessel formation as it circulates through the vasculature. This is explained by the fact that the angiogenin **receptor** is only expressed in sparsely cultured endothelial cells, not in confluent cells (as exist in blood vessels) (4). The receptor, not yet fully characterized, is a 170-kDa transmembrane protein whose presence on the cell surface correlates with the mitogenic activity of Ang. When the receptor is present, the cells respond to Ang by both increased thymidine uptake and cell proliferation. Confluent cells lack the receptor and, hence, do not respond this way to Ang.

Experiments with protein cross-linking reagents have demonstrated that Ang also interacts with a 42-kDa endothelial cell-surface protein that is a member of the actin family (1, 2). On binding Ang, it dissociates from the cell surface as an Ang–actin complex. Remarkably, this complex activates tissue plasminogen activator (tPA) and thus generates plasmin (see Plasminogen). This, in turn, stimulates cell-associated proteolytic activity to degrade the extracellular matrix and thereby facilitates cell migration, an essential feature of the angiogenesis process. Ang also acts as a cell adhesion molecule and, when coated on a plastic surface, mediates the binding of endothelial and tumor cells. *In vivo* it may help direct migrating blood vessels toward Ang-secreting tumor cells.

Addition of Ang to cultured endothelial cells stimulates a transient increase in cellular **diacylglycerol**, seemingly the result of an Ang-induced activation of phospholipase C, as well as an increase in prostacyclin secretion owing to activation of phospholipase A_2. Interpretation of these second messenger responses has not been possible, thus far, largely because the systems are complex and may only be stimulated indirectly by Ang.

4. Nuclear Translocation

Angiogenin undergoes endocytosis by sparsely cultured endothelial cells and is rapidly translocated from the cell surface to the nucleus, where it accumulates in the nucleolus (1, 2). This process is receptor-mediated and regulated by a nuclear localization signal (see Nuclear Import, Export) that involves three basic residues, Arg31-Arg32-Arg33, of Ang. This signal is essential for angiogenesis and suggests that the substrate for the ribonucleolytic activity of Ang is located in the nucleolus, a highly specialized region where biogenesis of ribosomes takes place (see Nucleolus and Ribosomes). One possibility is that the ribonucleolytic activity of Ang enhances the transcription and processing of rRNA. Two enzymatically inactive variants of angiogenin whose cell-binding site is intact also accumulate in the nucleolus when added to endothelial cells, but they are angiogenically inactive. This suggests that not only is nuclear localization essential for the biological activity of Ang but, in addition, the translocated protein must be enzymatically active. This has been confirmed by recent studies in which a DNA aptamer (an oligonucleotide that binds fairly tightly to Ang) that inhibits both the enzymatic and angiogenic activities of Ang is also translocated to nucleus, but only when added to endothelial cells together with Ang. The inhibitor and the protein accumulate in the nucleus in a 1:1 stoichiometric ratio (5).

5. Mechanism of Action

Although Ang may well be involved in a variety of angiogenesis-related situations, its mechanism of action is likely to be quite similar for each of them; hence it is only summarized here in the context of tumor-induced angiogenesis. All tumor cells that have been examined have been found to secrete Ang, and in at least one case, pancreatic cancer, the aggressiveness of the tumor is related to the amount of angiogenin produced (6). Ang secreted by tumor cells migrates through the extracellular matrix until it reaches an endothelial cell. There it combines with cell-surface actin and dissociates as a complex that stimulates the activity of tPA and the formation of plasmin. Degradation of the extracellular matrix—for example, by plasmin-activated matrix metalloproteinases—may stimulate a few endothelial cells to migrate, and this could trigger expression of the Ang receptor. Binding of Ang to the receptor would then, on the one hand, initiate a second-messenger response, perhaps through activation of the above-mentioned phospholipases, and, on the other, promote endocytosis and nuclear localization of Ang. The ribonucleolytic action of Ang within the nucleolus would, together with signals generated via the second messengers, activate processes leading to cell proliferation. The proliferating endothelial cells would migrate through the now degraded extracellular matrix toward the tumor cell from which the Ang was released. The cell-adhesion properties of Ang may be important for ensuring cell migration in the proper direction. At present, this view of the mode of action of Ang is largely speculative, particularly because nothing is known about the events that occur within the nucleus and lead to cell division. Nevertheless, it summarizes current thinking and is a useful basis for further investigation.

6. Tumor Biology

The levels of Ang and its messenger RNA are increased in the tissues and cells of patients with various types of cancers, indicative of an *in vivo* role for Ang in the process of tumor angiogenesis. This being the case, anti-angiogenin agents could have potential importance in the treatment of cancer and other angiogenesis-related diseases. The most potent inhibitor of Ang is a 50-kDa protein originally isolated from placenta as an inhibitor of RNase A, hence known as placental ribonuclease inhibitor (RI) (1, 2). It inhibits Ang with a K_i of 0.7 fM, one of the strongest protein–protein interactions known, and is 60-fold stronger than its inhibition of RNase A. Unfortunately, RI is evidently unstable in extracellular fluids and has not been found to be effective in treating tumors in laboratory animals.

Monoclonal antibodies raised against Ang have been used to treat athymic mice injected with HT-29 colon carcinoma cells, and they reduced the incidence of tumors by up to 65%. Similar results have been observed with other types of tumors, and when used in conjunction with conventional therapeutic agents, a synergistic effect was seen (2). Actin was also tested for its anti-tumor activity, and it too was capable of preventing tumor growth in more than 60% of treated animals. It should be noted that anti-angiogenin agents do not affect the growth of already-established tumors. They are only effective when administered to animals at the same time as the tumor cells. They are thought to act by specific extracellular inactivation of tumor-secreted Ang and the consequent inhibition of tumor angiogenesis. These experiments are important in that they provide clear evidence of a crucial role for angiogenin in the early stages of development of these tumors.

7. Other Biological Properties

One of the major complications associated with regular hemodialysis is the increased morbidity and mortality arising from infections. This has been attributed to dysfunction of polymorphonuclear leukocytes. Indeed, a number of compounds have been isolated from uremic serum and shown to inhibit the biological activity of these white cells. One of these is an inhibitor of leukocyte degranulation that turns out to be Ang (7). Nanomolar concentrations of Ang inhibit both spontaneous and peptide-stimulated degranulation by 60% and 30%, respectively. However, Ang has no other effect on the cellular responses of polymorphonuclear leukocytes, such as chemotaxis, phagocytosis or their peptide-stimulated oxidative respiratory burst.

Ang has also been reported to suppress significantly the proliferation of human lymphocytes stimulated by a mixed-lymphocyte culture or by phytohemagglutinin or concanavalin A (8). A maximal immunosuppressive effect was seen at an Ang dose of 50 to 100 mg/mL. It was thought that this effect might synergize with the effect of Ang on neovascularization of tumors and thereby contribute to tumor development.

8. Conclusions

Ang is now recognized as a pleiotropic molecule capable of inducing several intra- and extracellular activities. It induces most of the individual events in the process of angiogenesis including binding to endothelial cells, stimulating second messengers, mediating cell adhesion, activating cell-associated proteinases, inducing cell invasion, stimulating DNA synthesis and cell proliferation, and organizing the formation of tubular structures from cultured endothelial cells. Characterization of its cellular receptors, elucidation of its mechanism of nuclear translocation, identification of its intranucleolar target substrate, and understanding how these events result in cellular proliferation and blood vessel formation will provide important and novel information that can be utilized for either promoting or inhibiting angiogenesis for therapeutic purposes.

Bibliography

1. J. F. Riordan (1997) "Structure and Function of Angiogenin" In *Ribonucleases: Structures and Functions* (G. D"Alessio and J. F. Riordan, eds.), Academic Press, New York, pp. 445–489.
2. B. L. Vallee and J. F. Riordan (1997) Cell. Mol. Life Sci. **53**, 803–815.
3. R. Shapiro (1998) Biochemistry **37**, 6847–6856.
4. G.-f. Hu, J. F. Riordan, and B. L. Vallee (1997) Proc. Natl. Acad. Sci. USA **94**, 2204–2209.
5. V. Nobile, N. Russo, G.-f. Hu, and J. F. Riordan (1998) Biochemistry **37**, 6857–6863.
6. S. Shimoyama et al. (1996) Cancer Res. **56**, 2703–2706.
7. H. Tschesche, C. Kopp, W. H. Horl, and U. Hempelmann (1994) J. Biol. Chem. **269**, 30274–30280.
8. J. Matousek et al. (1995) Comp. Biochem. Physiol. **112B**, 235–241.
9. P. J. Kraulis (1991) J. Appl. Crystallogr. A **24**, 946–950.

Suggestions for Further Reading

10. F. Bussolino, A. Mantovani, and G. Persico (1997) Molecular mechanisms of blood vessel formation. Trends Biochem. Sci. **22**, 251–256.
11. J. Folkman and P. A. D"Amore (1996) Blood vessel formation: What is its molecular basis? Cell **87**, 1153–1155.

Anhydrides

"Anhydride" means "without water," and many anhydrides are present in nature. Anhydrides are easily hydrated in the presence of water to acids or bases. Inorganic anhydrides include SO_3, P_2O_5, CaO, Na_2O, etc. Acid anhydrides are the most important anhydrides in biochemistry. An acid anhydride [I] is formed by eliminating a molecule of water from two acids (Scheme 1):

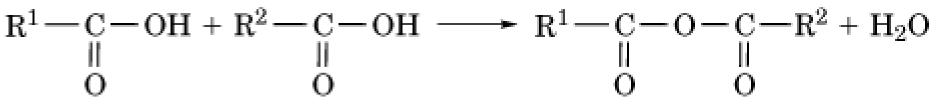

[I] Carboxylic acid anhydride

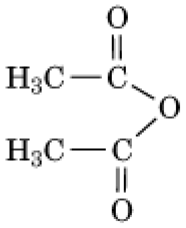

[II] Acetic anhydride

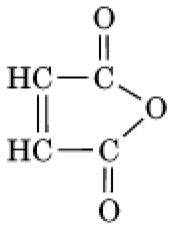

[III] Maleic anhydride

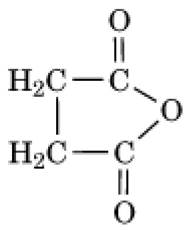

[IV] Succinic anhydride

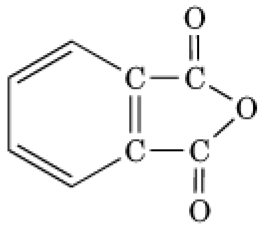

[V] Phthalic anhydride

Adding a molecule of water reverses the reaction. Practically, a carboxylic acid anhydride is prepared by the nucleophilic displacement of chloride ion from acyl chlorides by carboxylate ion.

Acid anhydrides are reactive and are good acylating agents. They react with water to yield acids, with amino groups to yield amides, and with alcohols to yield esters. Acid anhydrides are utilized as reactive intermediates in organic syntheses, such as peptide synthesis, and sometimes as **enzyme-substrate** intermediates. Acid anhydrides are unstable and therefore have large standard **free energies** of hydrolysis. The two terminal phosphate linkages in ATP are anhydride linkages, and acid anhydrides play important roles in bioenergetics (see Adenylate Charge). Acid anhydrides are widely employed for chemical modification of proteins, particularly of amino groups. The acetylation reaction by an acid anhydride with amino groups in a protein proceeds so easily that this reaction is suitable for the **radiolabeling** of a protein with a radioisotope-labeled acid anhydride (1). Acetic anhydride [II], maleic anhydride [III], and succinic anhydride [IV] are frequently employed in chemical reactions and chemical modifications of proteins. Phthalic anhydride [V] is an aromatic anhydride and is a good leaving group.

1. Acetic Anhydride

Acetic anhydride is the most important acid anhydride. Its boiling point is 139.6°C, and it has a characteristic penetrating odor. It is widely employed in organic syntheses. It is used to introduce the acetate group into organic compounds and is called an acetylating agent. To acetyle amino groups in a protein (2), prepare a protein solution (2 to 10%, w/v) in half-saturated sodium acetate. Over a period of 1 h at 0°C, add, in five equal portions, a weight of acetic anhydride equal to that of the protein, and continue stirring for an additional hour.

Bibliography

1. T. N. M. Schumacher, and T. J. Tsomides (1995) In *Current Protocols in Protein Science* (J. E. Coligan et al., eds.), Wiley, pp. 3.3.11–3.3.12.
2. T. Imoto and H. Yamada (1989) In *Protein Structure: A Practical Approach* (T. E. Creighton, ed.), IRL Press, Oxford, UK, pp. 247–277.

8-Anilinonaphthalene-1-Sulfonic Acid

8-Anilinonaphthalene-1-sulfonic acid (ANS) (Fig. 1) and its dimer, 1,1′-bis(4-anilino-5-naphthalenesulfonic acid) (bis ANS) are two widely used "**hydrophobic**" probes in **fluorescence** studies of proteins and membranes (1). These dyes are minimally fluorescent in polar environments, such as aqueous solutions, but their fluorescent emission is dramatically increased in nonpolar environments. An increase in quantum yield (intensity) and a blue shift in the wavelength of maximum emission (l_{max}) is observed when binding to macromolecules.

Figure 1. The structure of 8-anilinonaphthalene-1-sulfonic acid (ANS).

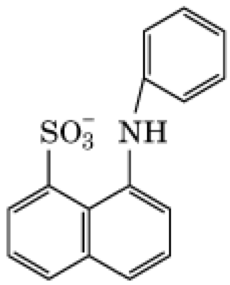

The most common uses of ANS (and bis-ANS) are (1) to monitor conformational changes in proteins (2, 3); (2) to follow the kinetics of **protein folding** and unfolding (4-6); (3) to detect and characterize partially folded intermediates of proteins (both transient and equilibrium) (7, 8); (4) to measure changes in membrane properties (9, 10); (5) to detect the presence of exposed hydrophobic accessible surfaces (11); and (6) to study **ligand binding** through displacement assays (12, 13). Photoincorporation of bis-ANS has been used to locate solvent-exposed hydrophobic regions in proteins (14) and more specifically (1) to investigate **virus** capsid structure and assembly (15, 16); (2) to monitor tubulin assembly and interaction with drugs (17) because bis-ANS specifically inhibits assembly of tubulin (18); (3) to measure distances via fluorescent energy transfer from tryptophan residues to bound ANS (17, 19); (4) to study **enzyme**–substrate interactions (20), including **nucleotide** binding (21); and (5) as a sensitive staining method for proteins in SDS-PAGE (22). ANS has been used to detect conformational changes in a wide variety of functional proteins during ligand binding (ranging from small molecules to DNA) (13, 23).

The advantages of ANS as a probe reflect the simplicity of fluorescence experiments and the sensitivity of ANS to its immediate environment. Although most commonly used in the fluorescent steady-state mode, it has also been used in more complex experiments (6, 25). The **absorbance** spectrum of ANS has maxima at ~270 nm and in the 345 to 380 nm range. The fluorescent emission spectrum is very sensitive to the environment and has a maximum of ~520 nm in water, which becomes progressively blue-shifted with decreasing polarity and reaches 464 nm in very nonpolar environments. A corresponding change occurs in the fluorescent lifetime from ~0.25 ns in water to ~15 ns in hydrophobic environments. The overlap between ANS excitation and tryptophan emission in the vicinity of 350 nm provides a useful donor/acceptor energy transfer system. Although the properties of ANS and bis-ANS are similar, the dimer has substantially higher affinity for many protein sites (26).

It is commonly assumed that ANS and bis-ANS bind to proteins and membranes by hydrophobic interactions mediated by the two aromatic rings, although there is little direct data (such as X-ray crystallography or NMR structures) to support this hypothesis. These dyes are anions over most of the commonly used pH range and electrostatic interactions are also important (possibly even critical) in ANS binding to proteins and membranes (27).

The applications of ANS to biomembrane studies have been summarized (24) and are not presented in any depth here. ANS binds to membranes in the vicinity of the phospholipid polar headgroups. The nonpolar part of the ANS molecule is directed toward the region of the fatty acid side chains, but the ANS does not penetrate very far into the nonpolar region of the bilayer. The binding is very sensitive to the nature of the phospholipids and to the presence of other membrane components, such as cholesterol.

For proteins, it is likely that only those ANS molecules that bind in hydrophobic regions exhibit the characteristic strong fluorescence. The remaining ANS molecules are bound to cationic sites exposed to aqueous solvent and hence are quenched (28). The thermodynamics of ANS binding to a protein have been determined: the binding is enthalpically driven at all temperatures and entropically opposed at temperatures greater than 14°C (27). The self-association of ANS and bis-ANS in water correlates with their tendency to form complexes with proteins (29). Thus care must be taken, especially when working at low pH and high ANS concentrations, to avoid ANS aggregation.

It has been recognized for some time that ANS and bis-ANS are excellent probes for partially folded intermediate states of proteins, such as the molten globule (7-30). Because the dyes do not normally bind significantly to the native states of most proteins nor to the fully **unfolded** states, they are widely used as a diagnostic for the presence of partially folded intermediates. However, ANS and bis-ANS do bind to some native proteins, usually to a specific site, e.g., the heme-binding site in apo-**myoglobin** (31). The predilection of ANS for nonnative conformations has been useful in investigating designed proteins to determine whether they have a rigid, tightly packed core, or are more like a molten globule (32), and in studies to determine the conformational state of substrate proteins interacting with molecular chaperones (33).

Fluorescent changes that correspond to binding and release of ANS during protein folding are frequently used to characterize the kinetics of folding, especially the buildup and decay of transient intermediates (34-36). Differences in partially folded intermediate conformations of proteins are distinguished by differences in the properties of bound ANS (5, 37).

The interpretation of results from ANS probe experiments is not without hazards, in part because the dyes perturb the system under investigation. For example, in experiments to monitor the kinetics of protein folding, the presence of ANS or bis-ANS and their strong affinity for transient intermediates significantly perturb the kinetics of folding (35). Similarly, it is customarily assumed that if ANS or bis-ANS is added to the native protein and binding is observed, it is to the native state. However, when the native state is only nominally predominant, preferential binding of the dye to a partially folded intermediate effectively shifts the equilibrium to favor the intermediate conformation (19). The presence of tight-binding ligands (eg, substrates) to the native state shifts the equilibrium back to the native conformation (19). Another source of potential complications in interpreting results arises from the fact that the dye concentration used in many studies drastically exceeds the protein concentration. It is important to use purified ANS. Most commercial preparations contain some bis-ANS, which produces misleading results because bis-ANS often binds much more tightly than ANS. The bis-ANS is removed by Sephadex LH-20 chromatography (38).

Bibliography

1. L. Stryer (1965) J. Mol. Biol. **13**, 482–495.
2. T. Korte and A. Herrmann (1994) Eur. Biophys. J. **23**, 105–113.

3. H. Tsuruta and T. Sano (1990) Biophys. Chem. **35**, 75–84.
4. G. de Prat Gay et al. (1995) J. Mol. Biol. **254**, 968–979.
5. M. C. Shastry and J. B. Udgaonkar (1995) J. Mol. Biol. **247**, 1013–1027.
6. B. E. Jones, J. M. Beechem, and C. R. Matthews (1995) Biochemistry **34**, 1867–1877.
7. G. V. Semisotnov et al. (1991) Biopolymers **31**, 119–128.
8. Y. Goto and A. L. Fink (1989) Biochemistry **28**, 945–952.
9. A. Azzi (1975) Q Rev. Biophys. **8**, 237–316.
10. M. G. Tozzi-Ciancarelli, C. Di Massimo, and A. Mascioli (1992) Cell. Mol. Biol. **38**, 303–310.
11. M. Cardamone and N. K. Puri (1992) Biochem. J. **282**, 589–593.
12. C. D. Kane and D. A. Bernlohr (1996) Anal. Biochem. **233**, 197–204.
13. I. Taylor and G. G. Kneale (1994) Methods Mol. Biol. **30**, 327–337.
14. J. W. Seale, J. L. Martinez, and P. M. Horowitz (1995) Biochemistry **34**, 7443–7449.
15. A. T. Da Poian, J. E. Johnson, and J. L. Silva (1994) Biochemistry **33**, 8339–8346.
16. J. Secnik et al. (1990) Biochemistry **29**, 7991–7997.
17. A. Bhattacharya, B. Bhattacharyya, and S. Roy (1996) Protein Sci. **5**, 2029–2036.
18. P. Horowitz, V. Prasad, and R. F. Luduena (1984) J. Biol. Chem. **259**, 14647–14650.
19. L. Shi, D. R. Palleros, and A. L. Fink (1994) Biochemistry **33**, 7536–7546.
20. P. M. Horowitz and N. L. Criscimagna (1985) Biochemistry **24**, 2587–2593.
21. R. Takashi, Y. Tonomura, and M. F. Morales (1977) Proc. Natl. Acad. Sci. USA **74**, 2334–2338.
22. P. M. Horowitz and S. Bowman (1987) Anal. Biochem. **165**, 430–434.
23. A. R. Walmsley, G. E. Martin, and P. J. Henderson (1994) J. Biol. Chem. **269**, 17009–17019.
24. J. Slavik (1982) Biochim. Biophys. Acta **694**, 1–25.
25. E. E. Gussakovsky and E. Haas (1995) Protein Sci. **4**, 2319–2326.
26. C. G. Rosen and G. Weber (1969) Biochemistry **8**, 3915–3920.
27. W. R. Kirk, E. Kurian, and F. G. Prendergast (1996) Biophys. J. **70**, 69–83.
28. D. Matulis, R. Lovrien, and T. I. Richardson (1996) J. Mol. Recognition **9**, 433–443.
29. B. Stopa et al. (1997) Biochimie. **79**, 23–26.
30. Y. Goto, T. Azuma, and K. Hamaguchi (1979) J. Biochem. **85**, 1427–1438.
31. E. Bismuto et al. (1996) Protein Sci. **5**, 121–126.
32. S. F. Betz et al. (1996) Fold Des **1**, 57–64.
33. M. Gross et al. (1996) Protein Sci. **5**, 2506–2513.
34. A. F. Chaffotte et al. (1992) Biochemistry **31**, 4303–4308.
35. M. Engelhard and P. A. Evans (1995) Protein Sci. **4**, 1553–1562.
36. O. B. Ptitsyn et al. (1990) FEBS Lett. **262**, 20–24.
37. E. Zerovnik et al. (1997) Eur. J. Biochem. **245**, 364–372.
38. S. S. York, R. C. Lawson Jr., and D. M. Worah (1978) Biochemistry **17**, 4480–4486.

Suggestions for Further Reading

39. C. A. Royer (1995) Fluorescence spectroscopy. Methods Mol. Biol. **40**, 65–89.
40. J. Slavik (1982) Anilinonaphthalene sulfonate as a probe of membrane composition and function. Biochim. Biophys. Acta **694**, 1–25.

Animal Pole, Vegetal Pole

The cell mass of an egg is not uniformly distributed, but it exhibits significant differences in terms of morphology and at the molecular level. In order to describe this polarity, the terms animal pole and *vegetal pole* were invented to describe the two opposite poles of the egg.

Unlike the eggs of insects, which are elliptically shaped, most **oocytes** of amphibians and mammalians exhibit a less pronounced asymmetry. One element of asymmetry is the location of the cell nucleus, which is normally not right in the center of the oocyte, but is more peripheral, sometimes even adjacent to the egg membrane. Due to gravitational forces, the yolk within settles to the bottom of the egg and forms the vegetal pole; consequently, the polarity becomes more apparent when more yolk is present in the egg. Another component causing asymmetry is that **polar bodies** extruded during **meiosis** are frequently located in the region of the animal pole. In ascidians, sperm enters the egg somewhere in the animal hemisphere (1), causing cytoplasmic movements and rotation of the egg cortex. As a consequence, a further distinct region, the *gray crescent*, becomes visible in the fertilized egg. The gray crescent is also visible in amphibians, but is not very apparent in sea urchins. In the egg of *Unio elongatulus*, sperm entry occurs only at the vegetal pole. This is attributed to the presence of a 220-kDa binding protein that is concentrated in a restricted region of the crater region within the vegetal pole (2).

The naming of the two poles, animal and vegetal, is not based on a precise function; rather, the names have arisen from the idea that the “higher” organs evolve in the animal polar region, whereas the vegetal pole was assumed to be destined to form the “lower” organs necessary for reproduction and providing nutrition. The two poles form one of three possible coordinates, and further developmental changes in a number of amphibians correlate with the subsequent dorsal-ventral body axis of the animal. In mammals, the mechanism by which the inner cell mass settles in certain places is not fully understood. However, it was shown in the mouse that the bilateral symmetry of the early blastocyst is normally aligned with the animal-vegetal axis of the zygote. The embryonic-abembryonic axis is oriented orthogonally to the animal-vegetal axis (3).

After a sperm activates the egg, karyogamy of the male and female **pronuclei** occurs, and the egg starts to divide by **mitosis**. Most important, the cell mass does not increase during the first cell divisions; starting from the one cell, two cells are formed, after another round of divisions four cells, then eight cells, 16 cells, and so forth, until a great number of smaller cells are formed at the morula stage. These cells do not all have the same size; the smaller ones are called micromeres, whereas the larger ones are named *macromeres*. During these cleavage steps, there is relatively little **gene expression** from the nucleus of the new individual cells. In other words, the genome of the new cell does not determine its own development after fertilization and karyogamy at these very early stages of development. With regard to the new cells, the regulating elements are external, maternally derived gene products. These substances, mostly **RNA** molecules, are already present in the unfertilized egg, and they are the important factors that determine the fate of the divided cells. This has been shown by a number of experiments. Chemical inactivation or enucleation in embryos has shown that the nucleus is not necessary for the initial rounds of cleavage. Even enucleated egg fragments are able to perform developmental changes, and cross-fertilization experiments revealed that cells follow the maternal pattern of development. These maternally derived gene products are not evenly distributed in the egg, indicating that the animal and vegetal pole are not only a matter of morphological appearance, but are also related to the presence of a concentration gradient of different gene products. This was demonstrated in experiments in which sections of the animal or vegetal pole were excised and recultivated. When micromeres of the vegetal pole at the 16-cell stage were implanted into the animal pole of a donor embryo, a complete second gut developed; the micromeres are capable of changing the fate of neighboring cells (4). Cutting sea urchin eggs at the eight-cell stage into two halves, to produce two embryos each with an animal and a vegetal cell, generates two pluteus capable of normal development. In contrast, cutting the cell into an animal and an vegetal hemisphere causes considerable aberrations from the normal development.

One of the most quoted experiments to show that animal and vegetal pole cells differ significantly involved excision in which the fate of sections at the 64-cell stage were investigated. The individual cells alone were capable of forming only a **blastula**. However, adding at least four micromeres from the vegetal pole could compensate for this defect and lead to a pluteus. Fewer numbers of micromeres resulted in forms intermediate between blastula and normal pluteus. Interestingly, the vegetalization occurs not only after the addition of micromeres, but also when Li^+ ions were provided. At the animal pole, messenger RNA were found that code for cell-surface proteins. These mRNA were found only in the macromeres and mesomeres, not in the micromeres (5). In the vegetal pole region are localized dorsal determinants that are necessary for dorsal axis development in Xenopus. The dorsal determinants move from the vegetal pole to a subequatorial region, where they are incorporated into gastrulating cells (6). However, dorsal development may be also activated by the contact between the cortical dorsal determinant and the equatorial core cytoplasm that are brought together by cortical rotation upon fertilization (7).

Gastrulation is the next morphogenic event, and it starts in the region of the vegetal pole or near to the gray crescent, depending on the species. At least five different epigenic movements are observable in the further process of differentiation: invagination of cells, immigration, delamination, proliferation, and epiboly. This means that, although the polarity of the egg determines the fate of the cells at different positions, further movements and reorganization take place that are necessary for organogenesis in higher mammals. One predominantly epigenic movement is invagination during gastrulation. It was shown that vegetal egg cytoplasm is responsible for the specification of vegetal blastomeres and promotes gastrulation. Vegetal-deficient embryos of *Halocynthia roretzi* fail to enter gastrulation. They are animalized and arrested at the blastula stage. Reimplantation of the vegetal pole cytoplasm into vegetal-deficient embryos caused gastrulation at the site where implantation occurred (8).

Bibliography

1. J. E. Speksnijder, L. F. Jaffe, and C. Sardet (1989) Dev. Biol. **133**, 180–184.
2. R. Focarelli and F. Rosati (1995) Dev. Biol. **171**, 606–614.
3. R. L. Gardner (1997) Development **124**, 289–301.
4. A. Ransick and E. H. Davidson (1993) Science **259**, 1134–1138.
5. M. Di Carlo, D. P. Romancino, G. Montana, and G. Ghersi (1994) Proc. Natl. Acad. Sci. USA **91**, 5622–5626.
6. M. Sakai (1996) Development **122**, 2207–2214.
7. H. Kageura (1997) Development **124**, 1543–1551.
8. H. Nishida (1996) Development **122**, 1271–1279.

Suggestion for Further Reading

9. H. Eyal-Giladi (1997) Establishment of the axis in chordates: Facts and speculations. Development **124**, 2285–2296. A review of the establishment of the axis in chordates.

Ankyrins

Ankyrins are a family of conserved proteins whose prime function is to act as a link between integral membrane proteins and the **spectrin**- or fodrin-based framework lying on the cytoplasmic side of the plasmalemma. The ankyrins were first characterized as those proteins that displayed a strong affinity for spectrin in **erythrocyte** membranes. They are expressed in particularly high levels in vertebrate brain but are also found in tissues such as skeletal muscle, lymphocytes, neutrophils and many epithelial tissues (1); they are also found in such primitive organisms as worms (nematodes) and fruit flies (***Drosophila***). Associations between ankyrins and a diverse selection of membrane proteins such as cell adhesion molecules and **ion channels** (the **anion exchanger**, or band 3 protein, Na^+/K^+ ATPase and the voltage-sensitive **sodium channel**) have been characterized and confirm that a key role of the ankyrins is to mediate interactions between spectrin in erythrocytes (known as fodrin in other cells) and proteins constituting the cell membrane. Deficiencies in ankyrin (as well as spectrin and some other membrane-associated proteins) have been correlated with structurally weak erythrocytes.

Ankyrins from erythrocytes (Ank1) and brain (Ank2) are monomeric proteins with a simple **domain** substructure. Each protein has an *N*-terminal domain (about 89 to 95 kDa) with membrane-binding abilities that can interact with the anion exchanger and tubulin (amongst others). Most of this globular region comprises 24 tandem quasi-repeats of a 33-residue motif. Because six such repeats appear to represent the smallest structural entity, it is possible that there are four subdomains within the *N*-terminal domain. It has also been suggested that the 33-residue structures, while folding up in a common manner, could position nonconserved residues on surface sites that would enable them to interact with a wide range of different protein ligands, rather than with a single ligand multiple times. The sequence of the 33-residue motif is very similar to those found in transcription factors, in cell-cycle control proteins, and in proteins regulating tissue differentiation. The second domain of ankyrin (about 62 kDa) can be subdivided into two parts; the first is acidic, proline-rich, and about 80 residues in length. In erythrocytes it links the cytoplasmic domain of the transmembrane anion exchanger to b-spectrin at about the midpoint of the tetrameric structure that b-spectrin forms with a-spectrin (see Spectrin). The second portion is basic and much larger (almost 500 residues). It contains the consensus sequence (Arg–Arg–Arg–Lys–Phe–His–Lys/Arg) that is also required for spectrin- or fodrin-binding. It is also much more highly conserved in sequence than the acidic 80-residue subdomain. The *C*-terminal domain is about 70 kDa in both Ank1 and one variant of Ank2, but about 290 kDa in an **isoform** of Ank2 that is generated by alternative splicing. The smaller isoform of Ank2 (molecular weight about 220 kDa) is common in adult rats, while the larger one (about 440 kDa) is expressed highly in neonatal animals. Furthermore, the 220-kDa protein is found widely in the brain (neuron cell bodies, dendrites and glia), whereas the 440-kDa protein seems to be found specifically in unmyelinated axons and dendrites (2). In both Ank1 and Ank2, the *C*-terminal domain has a regulatory role arising from its ability to modulate the binding affinities of both the membrane-binding and spectrin-binding domains. The sequences of the *C*-terminal domains differ in size, and the overall homology is not high, although there are some regions of similarity.

Ank3, which is the major ankyrin in kidney, is found in most epithelial cells, axons and muscle cells and has many structural similarities to Ank1 and Ank2. It too has an *N*-terminal domain (89 kDa) containing a 33-residue repeat with the **consensus sequence** (Asp/Asn–Gly–apolar–Thr–Pro/Ala–Leu–His–apolar–Ala–Ala–X–X–Gly–His/Asn–apolar–X–Val/Ile–Val/Ala–X–apolar–Leu–Leu–X–X–Gly–Ala–X–Apolar/Pro–Asn/Asp–Ala–X–Thr–Basic), a 65-kDa domain with spectrin-binding ability, and a *C*-terminal domain (56 kDa) with regulatory attributes (2). Interestingly, however, multiple transcripts are expressed, some of which lack the repeat domain at the *N*-terminal end of the molecule. It is possible that these ankyrins are involved in intracellular vesicle stabilization, sorting, or targeting (2).

Bibliography

1. V. Bennett and D. M. Gilligan (1993) The spectrin-based membrane skeleton and micron-scale organization of the plasma membrane. Annu. Rev. Cell Biol. **9**, 27–66.
2. L. L. Peters, K. M. John, F. M. Lu, E. M. Eicher, A. Higgins, M. Yialamas, L. C. Turtzo, A. J.

Otsuka, and S. E. Lux (1995) Ank3 (epithelial ankyrin), a widely distributed new member of the ankyrin gene family and the major ankyrin in kidney, is expressed in alternatively spliced forms, including forms that lack the repeat domain. J. Cell Biol. **130**, 313–330.

Annealing, Nucleic Acids

When two complementary nucleic acid strands are mixed under conditions favoring complex formation, the fully associated duplex is the lowest free-energy state of the system. The annealing process involves formation and disruption of partially **base-paired** regions and expansion of those regions as the system samples progressively more extensively base-paired intermediate states on the path to the lowest energy fully base-paired state. This lowest energy state may not be achieved due to kinetically trapped structures.

Denaturation of short oligonucleotide duplexes is a thermodynamically and kinetically reversible process. When the solution is cooled after melting of the duplex, the optical and hydrodynamic properties of oligonucleotide duplexes return to the initial values. The denaturation of synthetic polymers of repeating sequence are optically reversible, which indicates that most bases are in intact base pairs. However, the hydrodynamic properties display hysteresis. The change in hydrodynamic properties is due to the formation of branched structures comprised of hairpin loops and concatenated aggregates. Natural DNAs display hysteresis in both optical and hydrodynamic properties, indicating failure of a significant fraction of the bases to find a partner base and the presence of a nonlinear structure.

When two nucleic acid polymers encounter each other during hybridization or renaturation, the probability of an exact match of base pairs in the initial complex is very small. Instead, small stretches of duplex are nucleated. These complexes may grow if the sequences of the two strands permit. If there is sufficient thermal energy, ie, sufficiently high temperature, the nucleated regions will form and disassociate as the system seeks the lowest free-energy state. If there is not sufficient thermal energy, unproductive complexes will dominate, and the equilibrium configuration will not be achieved. Conversely, if there is too much thermal energy, formation of the duplex regions will be disfavored, and the strands will separate.

This leads to a common strategy of duplex formation. The annealing process is optimized by incubation at the "melting" temperature, T_m, followed by slow cooling to permit the facile reorganization of the duplex regions, to optimize sequence alignment.

Intramolecular hairpins and internal loops in single-stranded nucleic acid polymers present a significant impediment to annealing (Fig. 1). These structures form rapidly compared to duplex structures. The rate constant for hairpin formation is 10^5–10^7 s^{-1} , meaning the structures form on the microsecond timescale. The second-order rate constant for oligonucleotide duplex formation is 10^5–10^7 M^{-1} s^{-1}. Therefore, at the low concentration of annealing experiments, duplexes form on a time scale of seconds or longer. Intramolecular structures are at a lower energy than is the fully unfolded single-stranded structure. These competing structures must be unfolded for the annealing process to proceed toward the formation of the complementary duplex. The activation energy associated with this unfolding process is large, so that at temperatures well below the T_m of these single-stranded structures, the rate of duplex formation is very slow.

Figure 1. Intramolecular structures formed by nucleic acid single strands.

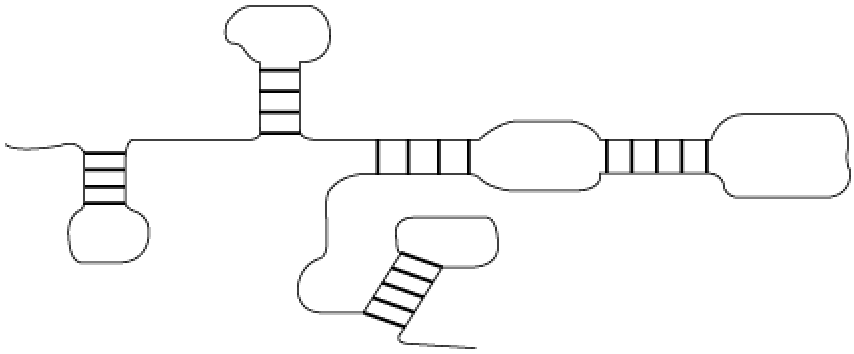

Defects in the alignment of base sequences (Fig. 2), including hairpins and internal loops, as well as mismatches and bulges, can occur in duplexes. Here the activation energy, and thus the time required for conversion, is even greater than for single-stranded structures. Because the alphabet of nucleic acids contains only four letters, there are regions of nucleotide sequence complementarity even in random sequences. These regions may form nucleation complexes that cannot be extended, resulting in large numbers of nonproductive intermediate states. In highly repetative sequences, large numbers of such structures may be formed. Under permissive conditions, they are readily interconvertable, and the proper sequence alignment can be achieved.

Figure 2. Misalignment structures in nucleic acid duplexes.

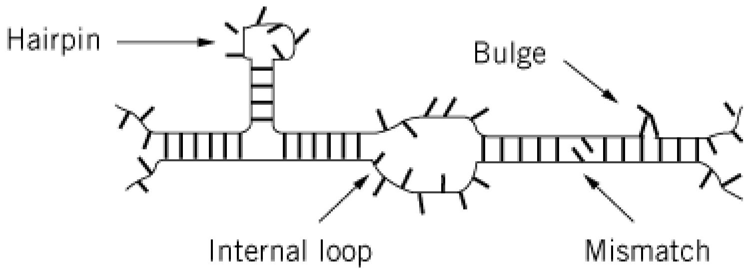

In contrast to polymers where sequence alignment dominates the kinetics of annealing, formation of short oligonucleotide duplexes is dominated by the frequency of encounter of the complementary strands. Once nucleation occurs, the pairing of the remaining bases is rapid.

Short oligonucleotide duplexes can form without appreciable competing structures. However, competition between the duplex and single-stranded hairpin structures can occur with oligonucleotides of appropriate sequence. The *unfolded single-strand-to-hairpin* and *unfolded single-strand-to-duplex* equilibria are in competition. The two equilibria differ in molecularity, so they can be distinguished experimentally by the concentration dependence. The hairpin structure will be favored at low concentration; and the duplex, at high strand concentration. The salt concentration also affects these equilibria. Because of its lower charge density, the hairpin is favored at low salt concentrations. Therefore, a combination of salt and oligonucleotide concentration can be used to isolate one of the structures.

Because the formation of a complex involves more than one nucleic acid strand, the concentration and the length of the constituent strands also influence the stability of the nucleic acid complex. There is a complex interplay between the length and concentration in determining complex stability. Two events contribute to the formation and stabilization of the complex. The nucleation event (Fig. 3), in which the strands make initial productive contacts, is a multimolecular (bimolecular for duplex formation) process that depends on strand concentration. The propagation process (Fig. 4), also called zipping, in which the prenucleated base-paired chain is extended, is a pseudomonomolecular process. Formally more than one strand is involved, but the formation of a closed base pair adjacent to a preformed base pair is effectively a monomolecular process analogous to extension of a hairpin.

Figure 3. The nucleation event. The number of strands that are interacting changes. The process is bimolecular and depends on strand concentration.

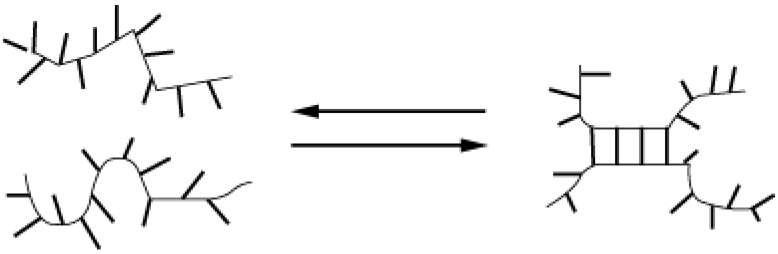

Figure 4. The propagation (zipping) event. The number of strands in the complex does not change; therefore, the process is pseudomonomolecular.

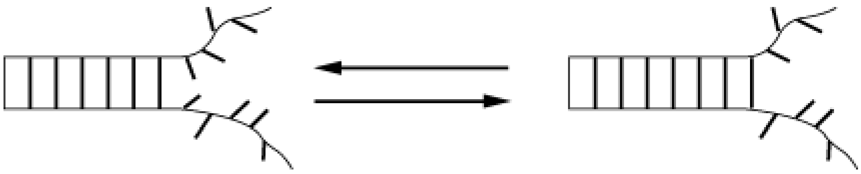

For short oligonucleotides, the nucleation event dominates complex formation. The concentration dependence of the stability is simple and described adequately by the conventional mass-action model. For polymeric complexes, nucleation accounts for a relatively small part of the total stabilizing free energy. The concentration dependence of complex formation disappears for polymeric nucleic acids. For complexes of intermediate length, both nucleation and propagation make nontrivial contributions to complex formation and stability. The concentration dependence of intermediate length complex stability is reduced relative to that for short complexes of short oligonucleotides, but not vanishing as for polymers.

Suggestion for Further Reading

V. A. Bloomfield, D. M. Crothers, and I. Tinoco (1974) *Physical Chemistry of Nucleic Acids*, Harper & Row, New York.

Annexins

Annexins are a family of structurally homologous, calcium- and membrane-binding proteins from eukaryotic sources including animals, plants, protists, and fungi. More than twenty distinct annexins have been characterized. Annexin homologues, notably 14-3-3 proteins, have also been identified through sequence similarities. Intracellularly, annexins vary in their organ, tissue, cell, and subcellular distribution and localization, and some annexins also occur extracellularly. The mechanism of release of annexins into the extracellular milieu is unclear because annexins lack **signal sequences**. Depending on the source, some annexins constitute a significant proportion (>1%) of total cell protein. Though their *in vivo* functions are not yet established, annexins have been implicated in many processes, including cell proliferation and differentiation, signal transduction, membrane trafficking and secretion, **vesicle** aggregation, cell adhesion, interactions with cytoskeletal elements, apoptosis, anticoagulation, phospholipase A_2 inhibition, and **ion channel** activity or regulation. **Phosphorylation** may regulate some annexin-mediated processes. At least two annexins are major substrates for the tyrosine kinases, epidermal growth factor receptor, and retrovirus-encoded protein tyrosine kinase pp60v-src. Phosphorylations through other **tyrosine kinases** or **serine/threonine kinases**, for example, protein kinase C and cAMP-dependent protein kinase A, also have been observed.

Before annexins were recognized as a family, the proteins were identified in many laboratories by their calcium-dependent binding to particulate fractions or hydrophobic chromatographic column matrices. Initially these proteins were given diverse names, which reflected either their source or putative function, including lipocortins, calpactins, endonexins, placental anticoagulant proteins (PAPs), chromobindins, calcimedins, and calelectrins. Subsequent sequence analysis revealed that many of these proteins have a common identity. The general term *annexin* subsequently was adopted in reference to their common ability to *annex to* membranes. In common nomenclature, individual annexins are designated by Roman numerals for example, annexin VII.

1. Macromolecular Interactions

The binding of calcium ions to annexins is relatively weak, with **dissociation constants** K_d in the millimolar-to-micromolar range. Complexation with membranes or other proteins increases their calcium-binding affinities. *In vitro*, annexins bind lanthanides and divalent cations, such as strontium, barium, and zinc. Calcium-dependent binding to membranes is high-affinity, and K_d is in the nanomolar range, whereas phospholipid monomers are bound poorly. In many systems, the annexin-membrane association is reversible upon addition of calcium chelators. In other systems, annexins behave more like integral membrane proteins. Typically, acidic phospholipids, such as phosphatidylserine, are strongly preferred by annexins, whereas binding to pure phosphatidylcholine membranes has not been observed. Such phospholipid binding preferences may target annexins to specific locations. The strong response of annexin V to extracellular exposure of phosphatidylserine is widely used as the basis of flow cytometric assays to detect membrane phospholipid asymmetry in apoptosis and other cellular processes.

In addition to their membrane lipid-binding properties, some annexins interact with other proteins. Some annexins interact with members of the **EF-hand** family, which suggests structural complementarity between the two protein families.

Annexins II and XI each form heterocomplexes in which the heavy chain is an annexin and the light chain resembles S-100 protein. Extracellular annexins have been described as cell surface **receptors** for some **viruses** (1, 2) and matrix proteins, such as collagen (reviewed in Ref. 3) and tenascin C (4). Annexin II is identified as a co-receptor for **plasminogen**/tissue plasminogen activator (reviewed in Ref. 5). Calcium-dependent lectin activity has been identified in some annexins that bind to specific sialoglycoproteins and glycosoaminoglycans, such as heparin (6, 7). The biological importance of this interaction is not yet understood, but it may be related to cell surface function.

2. Primary Structures and Molecular Evolution

Annexin sequences are comprised of two regions, a variable N-terminal region and a conserved C-terminal core region. The core region consists of four or eight canonical repeats of approximately 70 amino acid residues. Sequence homology exists between repeats within an individual annexin and between annexins. The sequence data suggest that gene duplication and subsequent gene fusion produced a four-**domain** ancestral precursor. Further gene fusion of two four-domain annexins produced annexin VI, which is unique in its possession of eight repeats. The core region is associated with the calcium-dependent phospholipid-binding properties of annexins. Each repeat contains a highly conserved stretch of amino acid residues with a **consensus** calcium-binding sequence (Lys/Arg)-Gly-X-Gly-Thr-X_{38}-(Asp/Glu).

The variable N-terminal regions of annexins exhibit little homology and confer the distinct functional properties of individual annexins. Here the **intron**-exon structures are not highly conserved, whereas they are in the core region. The N-terminal region in annexins may consist of only a few amino acid residues or hundreds. Annexins VII (synexin) and XI have the largest and most hydrophobic N-terminal regions. These may considerably modify the properties of these proteins that arise from the common annexin core. In many annexins, phosphorylation sites occur within the N-terminal regions, as do some protein–protein interaction sites.

3. Crystal Structures of Annexins

Annexin crystal structures reveal a highly conserved **alpha-helical** fold in the C-terminal core region characteristic of this family. Each basic repeating unit is made up of five a-helices, four of which run antiparallel, in a four-helix bundle and the fifth helix is perpendicular. The four-domain annexin structure is nearly planar, and the domains are arranged as a symmetrical array. The eight-domain annexin VI resembles two four-domain annexin structures that are approximately perpendicular to each other and are linked by a long, a-helical segment (8, 9). Most annexin crystal structures lack the variable N-terminal domains, which are intentionally truncated or lost through proteolysis. The only exception to date, that of full-length annexin I, reveals an unexpected juxtaposition between helices in the N-terminus and core domains, a finding that may suggest a mechanism for membrane aggregation (10).

In annexin crystal structures, numerous bound calcium ions are observed in loops along one surface of the protein molecule. These loops have structural motifs that are distinct from those in EF-hand proteins or C2-domain proteins. There are several structural motifs for these calcium-binding sites. The site corresponding to the consensus calcium-binding sequence has the highest affinity for calcium and structurally resembles a type of site observed in phospholipase A_2. Other sites bind lanthanides more strongly than calcium. Annexin V (Fig. 1) adopts two distinct molecular conformations, depending on whether a tryptophan side chain in the third domain extends outward from the protein surface or lies buried within the protein core. Spectroscopic and biochemical evidence indicates that the two states are interrelated and may describe a calcium-dependent conformational change that influences membrane binding. The crystal structures of annexin V complexes with calcium and phospholipid head group analogs indicate that calcium ions are involved directly in the attachment to membranes (11).

Figure 1. Ribbon diagram of annexin V (10). N-terminus as labeled, calcium ions as filled spheres.

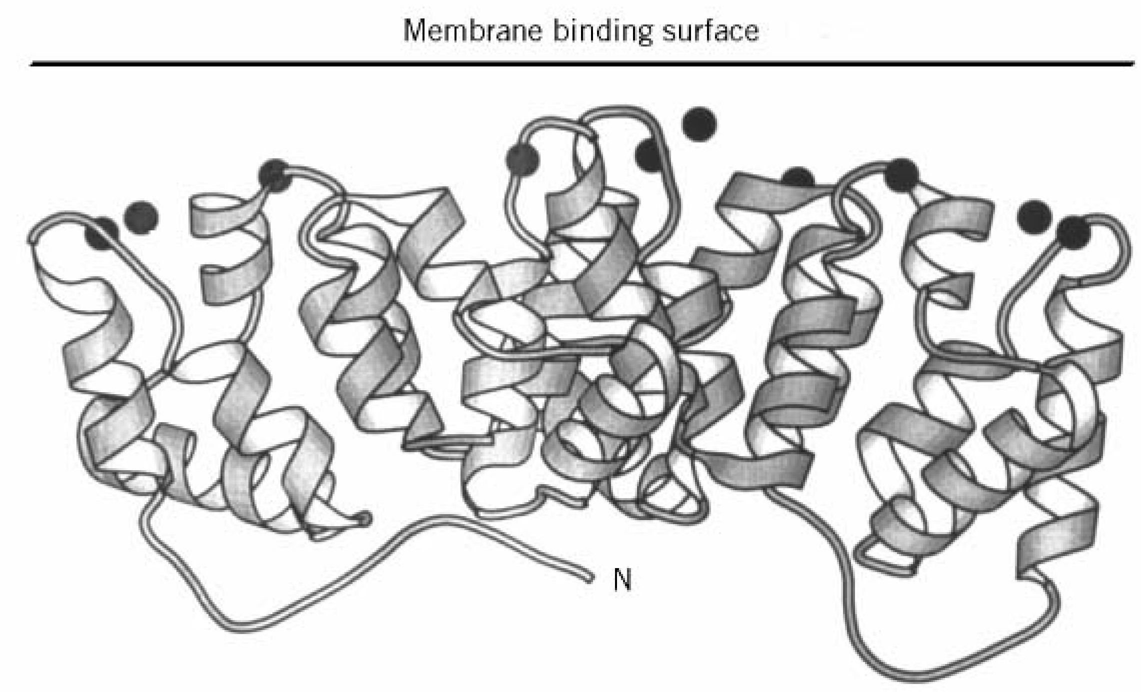

4. Membrane-Bound Annexins

The membrane-bound structures of two annexins have been investigated by electron microscopy, and there is little evidence that the protein penetrates into the lipid bilayer. The molecular structures of membrane-bound annexins are essentially the same as in their crystals, except that the molecules reorient themselves so that their calcium-binding sites are in contact with the membrane (8, 12, 13). Several annexins exhibit calcium-dependent self-association and/or form two-dimensional arrays on membrane surfaces, a property that may underlie their biological functions (14, 15).

Structure-based mechanisms for annexin function have been proposed, but are not fully established. Two hypotheses have been presented to explain the annexin-induced calcium channel activity observed *in vitro*. In the "microscopic electroporation" model described for annexin V, the peripheral binding of the protein changes the electrostatic properties of the membrane (16). The calcium ion is translocated to the **cytosol** through a putative central pore in the annexin molecule. In an alternative model of calcium channel activity, based on hydra annexin XII, the protein hexamer inserts into the bilayer and creates a transmembrane structure resembling an inverted micelle (17, 18). Experimental data have been offered to support both hypotheses, but the mechanism and physiological relevance of the channel activity remains controversial. Mechanistic models in which annexins restrict access to membrane phospholipids and/or surfaces have been proposed to explain their inhibition of phospholipase A_2 (19) and thrombin (14), and various models have been suggested for processes, such as vesicle aggregation and membrane fusion. The *in vivo* functions of annexins remain under intensive investigation.

Bibliography

1. K. Hertogs et al. (1993) Virology **197**, 549–557.
2. J. F. Wright, A. Kurosky, and S. Wasi (1994) Biochem. Biophys. Res. Commun. **198**, 983–989.
3. K. von der Mark and J. Mollenhauer (1997) Cell. Mol. Life Sci. **53**, 539–545.
4. C. Y. Chung and H. P. Erickson (1994) J. Cell. Biol. **126**, 539–548.
5. K. A. Hajjar and J. S. Menell (1997) Ann. N.Y. Acad. Sci. **811**, 337–349.

6. K. Kojima et al. (1996) J. Biol. Chem. **271**, 7679–7685.
7. G. Kassam et al. (1997) J. Biol. Chem. **272**, 15093–15100.
8. J. Benz et al. (1996) J. Mol. Biol. **260**, 638–643.
9. H. Kawasaki, A. Avila-Sakar, C. E. Creutz, and R. H. Kretsinger (1996) Biochim. Biophys. Acta **1313**, 277–282.
10. A. Rosengarth, V. Gerke, and H. Luecke (2001) J. Mol. Biol. **306**, 489–498.
11. M. A. Swairjo et al. (1995) Nat. Struct. Biol. **2**, 968–974.
12. A. Oloffson, V. Mallouh, and A. Brisson (1994) J. Struct. Biol. **113**, 199–205.
13. D. Voges et al. (1994) J. Mol. Biol. **238**, 199–213.
14. H. A. M. Andree et al. (1992) J. Biol. Chem. **267**, 17907–17912.
15. C. Pigault et al. (1994) J. Mol. Biol. **236**, 199–208.
16. P. Demange et al. (1994) Trends Biochem. Sci. **19**, 272–276.
17. H. Luecke et al. (1995) Nature **378**, 512–515.
18. S. E. Moss (1995) Nature **378**, 446–447.
19. F. F. Davidson and E. A. Dennis (1989) Biochem. Pharmacol. **38**, 3645–3651.

Suggestions for Further Reading

20. J. Mollenhauer and others (1997) Annexins, Cell. Mol. Life Sci. **53**, 506–555. A multiauthor review with nine concise articles on selected topics, including some material not reviewed elsewhere (eg, plant annexins). Up-to-date reviews on annexin genetics and molecular structure; phosphorylation; collagen-binding; and the roles of annexins in apoptosis, secretion, cancer, and autoimmune diseases.
21. B. A. Seaton, ed. (1996) *Annexins: Molecular Structure to Cellular Function*, R. G. Landes, Austin TX. Sixteen chapters covering a wide range of topics, including comprehensive reviews on annexin gene and molecular structure; biology of annexins I and XI; annexins in phagocytic leukocytes; nematode annexins; annexin binding to phospholipids and lipid assemblies; roles in membrane trafficking; calcium-independent annexin functions, including annexin/protein interactions; annexin functions involving phospholipid membrane asymmetry and clinical applications; and current experimental approaches to understanding annexin function.
22. P. Raynal and H. B. Pollard (1994) Annexins: A novel family of calcium- and membrane-binding proteins in search of a function, Biochim. Biophys. Acta **1197**, 63–93. A comprehensive survey covering most aspects of putative annexin function.
23. M. A. Swairjo and B. A. Seaton (1994) Annexin structure and membrane interactions: *a* molecular perspective, Ann. Rev. Biophys. Biomol. Struct. **23**, 193–213. Review with emphasis on structural and biophysical aspects of annexin-membrane associations and effects on lipid bilayer.

Anomalous Dispersion

If an atom is hit by an X-ray beam, as in X-ray crystallography, it scatters the beam in all directions. The scattered radiation can have the same wavelength as the primary beam (Rayleigh or coherent or elastic scattering) or a longer wavelength (Compton or incoherent or inelastic scattering). For diffraction, only the coherent part of the scattering is of interest. Incoherent scattering simply increases the background.

Electrons in an atom are bound by the nucleus and are, in principle, not free electrons. However, they can be regarded as such if the frequency of the incident radiation w is large compared with the natural absorption frequencies w_n of the scattering atom, or if the wavelength of the incident radiation is short compared with the absorption edge wavelength. This is normally true for the light atoms but not for the heavy atoms (Table 1).

Table 1. The Position of the Ka-Edge for Some Elements

Atomic number	**6**	**16**	**26**	**34**	**78**
Element	C	S	Fe	Se	Pt
Ka edge (Å)	43.68	5.018	1.743	0.980	0.158

If the electrons in an atom are regarded as free electrons, the atomic scattering amplitude (atomic scattering factor in units of electron scattering) is a real quantity *f* because the electron cloud is centrosymmetric. If they are not free electrons, the atomic scattering factor becomes an imaginary quantity, the scattering amplitude per electron:

$$f(\text{per electron}) = \frac{E_0 e^2}{mc^2} \times \frac{\omega^2}{\omega^2 - \omega_n^2 - i\kappa_n\omega} \qquad (1)$$

where E_0 is the amplitude of the electric vector of the incident beam, and k_n is a damping factor for the *n*th orbit (K or L or ¼). For w > w_n, Eq. (1) approaches $f = E_0e^2/mc^2$, the scattering amplitude of a free electron (1-3).

In practice, the complex atomic scattering factor, called $f_{\text{anomalous}}$, is separated into three parts: $f_{\text{anomalous}} = f + f' + if''$. f is the contribution to the scattering if the electrons were free electrons, f' is the real part of the correction to be applied for non-free electrons, and f'' is the imaginary correction. $f + f'$ is the total real part of the atomic scattering factor. Values for f, f' , and f'' are always given in units equal to the scattering by one free electron and are listed in Ref. 3. Because the anomalous contribution to the atomic scattering factor is mainly due to the electrons close to the nucleus, the value of the correction factors diminishes slowly as a function of the scattering angle, slower than for *f*.

Anomalous scattering causes a violation of Friedel's law: I(h k ℓ) is no longer equal to *I*(h k ℓ). This fact can be used profitably for determining the absolute configuration (4). Moreover, it can assist in the structural determination of proteins.

Bibliography

1. R. W. James (1965) *The Optical Principles of the Diffraction of X-rays*, G. Bell and Sons, London, p. 135.
2. H. Hönl (1933) Ann. der Physik, 5. Folge **18**, 625–655.
3. International Union of Crystallography (1995) *International Tables for Crystallography*, Vol. **C** (A. J. C. Wilson, ed.), Kluwer Academic Dordrecht, Boston, London.

4. J. M. Bijvoet, A. F. Peerdeman, and A. J. van Bommel (1951) Nature **168**, 271–271.

Suggestions for Further Reading

5. J. Drenth (1999) *Principles of Protein X-ray Crystallography*, Springer, New York.

Antennapedia Complex

The antennapedia complex (ANT-C) is a group of tightly linked **genes** that is found in the proximal portion of the right arm of the third chromosome of *Drosophila melanogaster*. The most prominent members of the complex produce striking **homeotic** transformations in adult flies carrying mutations in these genes. Thus mutations in the *Antennapedia* (*Antp*) locus cause a transformation of the antenna of the adult fly into a leg, while lesions in the *proboscipedia* (*pb*) gene cause the adult mouth parts to develop into legs rather than the normal palps used in feeding. The existence of the homeotic ANT-C was originally proposed based on the tight linkage of the *proboscipedia* (*pb*), *Sex combs reduced* (*Scr*), and *Antennapedia* (*Antp*) loci. Subsequent genetic analyses have shown that two other homeotic loci, *labial* (*lab*) and *Deformed* (*Dfd*), are also members of the complex. The homeotic loci of the ANT-C are involved in the specification of segmental identity in the posterior head (gnathocephalic) and anterior thoracic regions of the embryo and adult. Moreover, the linear order of the homeotic loci in the complex, *lab*, *pb*, *Dfd*, *Scr*, and *Antp*, corresponds to the anterior–posterior order of altered segments (intercalary, mandibular, maxillary, labial, and thoracic) found in animals bearing mutations in each of the resident loci. Taken together, the results of mutational analyses indicate that members of the complex are necessary to repress head development in the thorax (*Antp*) and elicit normal segmental identity in the anterior thorax (*Scr*) and posterior head (*Scr*, *Dfd*, *pb*, and *lab*).

A similar group of homeotic genes called the Bithorax Complex (BX-C) is found more distally on the third chromosome. This set of three homeotic genes (*Ultrabithorax*, *abdominal-A*, and *Abdominal-B*) acts in a similar fashion to the ANT-C, but in the posterior of the thorax and in the abdomen. The ANT-C is distinguished from the BX-C not only by virtue of the domain of action of its homeotic loci (anterior versus posterior) but also by the presence of loci that are not overtly homeotic in character. Two of these, *fushi tarazu* (*ftz*) and *zerknullt* (*zen*), have been shown to affect segment enumeration (*ftz*) and the formation of dorsal structures (*zen*) in the early embryo. A third nonhomeotic gene is bicoid (*bcd*). Mutations in this locus result in female sterility and maternal effect lethality. Eggs laid by *bcd* females fail to develop normal anterior ends and instead produce mirror-image duplications of structures normally produced at the posterior terminus of the embryo.

In addition to these genetically defined loci, several other genes have been found in the ANT-C by molecular mapping. The first of these is a cluster of cuticle-protein-related genes that map between the *lab* and *pb* loci. Eight small (about 1 kbp) transcription units make up the cluster, and all have sequence similarities to known cuticle protein genes. These genes (*cc1* through *cc8*) are also apparently regulated by ecdysone in imaginal discs. Deletion of the entire cluster has no apparent effect on the development or cuticle morphology of embryos, larvae, or adults. The second molecularly identified gene is the *Amalgam* (*Ama*) transcription unit. The encoded protein places the gene in the immunoglobulin superfamily and, like the cuticle cluster, the locus can be deleted from the genome with no discernible effect on the organism. Finally, there is the *zen2* or *z2* transcription unit that resides immediately adjacent to the *zen* gene. This locus is similar in structure and sequence to *zen*, but like *Ama* and the *cc* genes has no discernible function.

The entire complex has been **cloned** and sequenced and shown to cover 335 kbp of genomic DNA. The most distal transcription unit is *Antp*, which covers the distalmost 100 kbp of the complex and is made up of eight exons. Proximally, the next 75 kbp contain the *Scr* and *ftz* loci. The distal 50 kbp of this interval contain sequences necessary for *Scr* expression, as well as the two exons of the *ftz* locus and its associated regulatory elements. The proximal 25 kbp contain the three identified exons of the *Scr* transcription unit. The five exons of the *Dfd* gene are found in the central portion of the next-most-proximal 55-kbp interval. The *Dfd* transcription unit covers only 11 kbp of this region, and the 20-kbp interval flanking the gene proximally is the location of cis-acting regulatory elements for the locus. The next 25-kbp interval contains four of the nonhomeotic transcription units that help distinguish the ANT-C and BX-C. The distalmost is *Ama*, next *bcd*, and finally *zen* and *z2*. The *z2*, *zen*, and *Ama* transcription units are all relatively small (1 to 2 kbp) and comprise two exons each. The *bcd* gene is somewhat larger (3.6 kbp) and is made up of four exons. Immediately proximal to the *z2* transcription unit (about 1 kbp from its 3′ end) is the 5′ end of *pb*, which extends over the next 35 kbp of genomic DNA and contains nine exons. The next 25 kbp of the complex contain the cuticle cluster and its eight identified transcription units. The final 25 kbp are the sites of the *lab* gene, which is made up of three exons. Despite the nonhomeotic nature of three of the smaller transcription units (*zen*, *bcd*, and *ftz*) resident in the complex, these loci are tied to the larger homeotic genes of the region by the nature of their protein products. All five of the large homeotics (*Antp*, *Scr*, *Dfd*, *pb*, and *lab*), and the three small genes, have a **homeobox** motif, and their protein products are found in the **nuclei** of the cells in which they are expressed. Thus eight of the genes in the ANT-C encode regulatory proteins that act as transcription factors. The *z2* gene also contains a homeobox; however, the biological significance of the gene is not known, as deletions of this transcription unit have no discernible effect. The cuticle-like genes and *Ama* do not contain a homeobox.

The reasons for the clustering of these developmentally significant loci of similar function are not known. The existence of common or overlapping regulatory elements, the need to insulate regulatory sequences from chromosomal position effect, and the possibility of higher-order chromatin structures for proper expression have all been proposed. Whatever the reason, the homeotic complex structure has a long evolutionary standing. Similar clusters are found in vertebrates, an observation consistent with a very early origin of these genes, probably predating the separation of protostomes and deuterostomes.

Suggestions for Further Reading

M. Affolter, A. Schier, and W. J. Gehring (1990) Homeodomain proteins and the regulation of gene expression, Curr. Opin. Cell Biol. **2**, 485–495.

M. D. Biggin and McGinnis W. (1997) Regulation of segmentation and segmental identity by Drosophila homeoproteins: the role of DNA binding in functional activity and specificity, Development **124**, 4425–4433.

A. Dorn, M. Affolter, W. J. Gehring, and W. Leupin (1994) Homeodomain proteins in development and therapy, Pharmacol. & Therap. **61**, 155–183.

D. Duboule and G. Morata (1994) Colinearity and functional hierarchy among genes of the homeotic complexes, Trends Genet. **10**, 358–364.

R. Finkelstein and N. Perrimon (1991) The molecular genetics of head development in Drosophila melanogaster, Development **112**, 899–912.

W. J. Gehring, M. Affolter, and T. Burglin (1994) Homeodomain proteins, Ann. Rev. Biochem. **63**, 487–526.

G. Gellon and W. McGinnis (1998) Shaping animal body plans in development and evolution by modulation of Hox expression patterns, BioEssays **20**, 116–125.

G. Jurgens and V. Hartenstein (1993) "The terminal regions of the body pattern". In *The Development of Drosophila melanogaster* (M. Bate and A. Martinez Arias, eds.), Cold Spring Harbor Laboratory Press, pp. 687–746.

T. C. Kaufman, M. A. Seeger, and G. Olsen (1990) Molecular and genetic organization of the Antennapedia gene complex of *Drosophila melanogaster*, Adv. Genet. **27**, 309–362.

P. A. Lawrence and G. Morata (1994) Homeobox genes: their function in Drosophila segmentation and pattern formation, Cell **78**, 181–189.

R. S. Mann (1997) Why are Hox genes clustered? BioEssays **19**, 661–664.

W. McGinnis and R. Krumlauf (1992) Homeobox genes and axial patterning, Cell **68**, 283–302.

G. Morata (1993) Homeotic genes of *Drosophila*, Curr. Opin. Genet. Dev. **3**, 606–614.

A. Popadic, A. Abzhanov, D. Rusch, and T. C. Kaufman (1998) Understanding the genetic basis of morphological evolution: the role of homeotic genes in the diversification of the arthropod bauplan, Int. J. Dev. Biol. **42**, 453–461.

B. T. Rogers and T. C. Kaufman (1997) Structure of the insect head in ontogeny and phylogeny: a view from *Drosophila*, Int. Rev. Cytol. **174**, 1–84.

Antibiotic Resistance

In the 1940s, the clinical use of antibiotics first curbed the widespread threat of deadly bacterial infection. These drugs effectively inhibited bacterial growth that had gone unchecked for decades. Antibiotics did not, however, eradicate the threat of bacterial infection. In fact, the widespread use of antibiotics gave a selective advantage to bacteria that had antibiotic resistance. Many strains of bacteria have developed antibiotic resistance, or insensitivity to antibiotic drugs, in response to antibiotic selection pressures. Now, bacteria employ a myriad of resistance mechanisms to circumvent the best efforts of antibiotic researchers and clinicians. Only with the development of new and potent antibiotics and the appropriate use of existing antibiotics will researchers regain control over this resilient lifeform, bacteria.

1. A Historical Perspective

The development of antibiotics as therapeutic agents began in the late 1930s to combat the most common cause of death, infectious disease. In the preantibiotic era, any infection could prove mortal. Subsequently, over 150 different antibiotics have been synthesized or discovered, and these drugs are used to treat bacterial infections, such as pneumonia, malaria, and tuberculosis (1, 2).

Antibiotics are a collection of natural products and synthetic compounds that kill bacteria. Naturally occurring antibiotics are isolated from molds, yeasts, and bacteria. These organisms use antibiotics as defense mechanisms to kill other bacteria. Alternatively, synthetic antibiotics are developed by understanding the architecture and function of bacteria (see Fig. 1). Some bacteria have cell walls, and many effective antibiotics, such as penicillin, bacitracin, and cephalosporin, inhibit the synthesis of this cell wall. The bacterial machinery for **protein biosynthesis** differs from that of many host organisms and, therefore, is a good target for antibiotics, such as tetracycline and chloramphenicol. Additionally, antibiotics, such as **rifampin** and quinolones, specifically inhibit DNA replication in bacteria (1).

Figure 1. Mechanisms of action of some common antibiotics. A schematic of some basic functions of bacterial cells to which antibiotics are targeted. The X indicates an inhibition of that function by the antibiotics noted (see text for details).

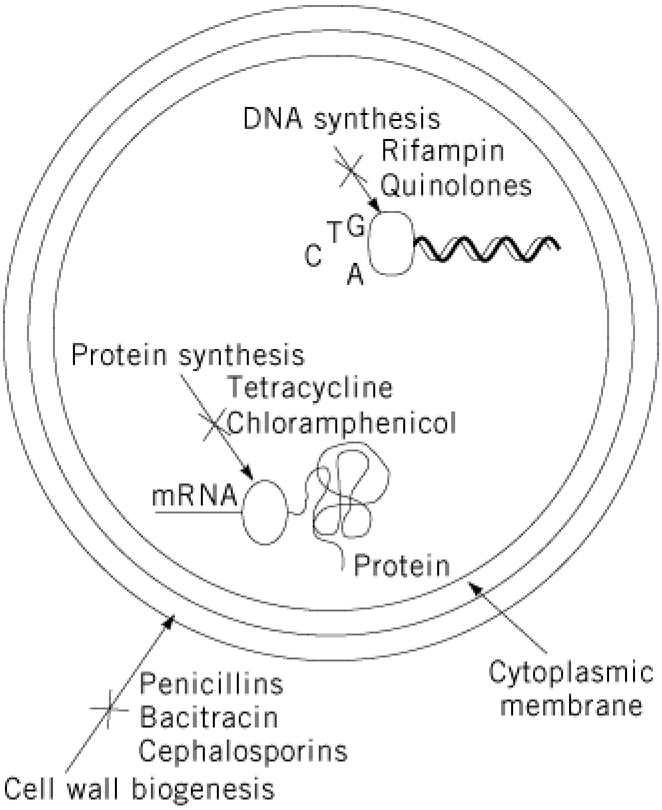

Antibiotics were considered the “wonder drugs” of their time, and in retrospect, this highly favored opinion resulted in their overuse. Antibiotics were commonly prescribed by physicians to cure and to appease their patients. Some patients would have genuine bacterial infections, for which antibiotic treatment is appropriate, whereas others would request antibiotics for viral infections that are not susceptible to these drugs. In addition, individuals who have suppressed immune systems, such as AIDS patients or organ transplants patients, would harbor bacteria that acquire resistance more easily. Antibiotics were also used prophylactically in agriculture and aquaculture industries to keep livestock healthy (3).

By the late 1960s, infectious disease appeared to be under control by the use of a variety of antibiotics. However, antibiotics simply depressed the propagation of bacteria. They did not eradicate it. Nonetheless, research in human health changed its focus from infectious diseases to chronic diseases, and new antibiotics were no longer being developed (2, 4). Many microbiologists warned the human health community that bacteria were potent, infectious pathogens that should not be underestimated. Bacteria have survived for more than three billion years despite numerous environmental changes on earth, and industrial wastes, insecticides, and herbicides. Obviously, the mechanisms bacteria use to survive and adapt to these adversities were very effective.

2. The Origins of Antibiotic Resistance

Even before the first clinical application of antibiotics, antibiotic resistance, the ability of bacteria to evade the deleterious effects of antibiotics, was postulated. In 1940, Abraham and Chain identified a bacterial enzyme that inactivates one of the first antibiotics, penicillin. Then, any bacterium that produces this enzyme would be resistant to penicillin (5). Moreover, microorganisms that use an antibiotic as defense mechanisms would require immunity to that antibiotic. This inherent resistance to a particular antibiotic was defined as a naturally-occurring trait called intrinsic resistance. A few strains of bacteria with intrinsic resistance to a particular antibiotic would not constitute a clinical threat because many diverse antibiotics are available. However, the ability of bacteria to propagate this antibiotic resistance to other strains of bacteria had been underestimated.

The exchange of genetic information between bacteria of the same strain is a common, yet typically slow process. Mechanisms of exchange include (1) **conjugation**—a single DNA strand from one bacterium enters another bacterium and is replicated as a part of that genome, (2) **transduction**—foreign DNA is introduced into bacteria by transducing bacteriophages, and (3) transformation—autonomously replicating circular DNA plasmids are obtained by bacteria (1). Originally, it was believed that these genetic exchange mechanisms were restricted to bacteria of the same strain. However, a new method of gene exchange, using integrons, was recently identified (6, 7).

Integrons are independent, mobile elements that encode **genes** for protein functions, and encode additional DNA to guarantee the integron's expression and integration into the bacterial genome. Integrons effectively generate widespread antibiotic resistance by donating antibiotic resistance genes to any strain of bacteria. Ironically, it is widely believed that integrons evolved only recently in response to antibiotic selection pressure. In other words, the use of antibiotics advanced the widespread occurrence of antibiotic resistance.

In addition to the acquisition of genes by the exchange of genetic information, bacteria also have a high mutation rate that allows them to respond to the selective pressure of antibiotics by using their own genome. For example, if bacteria were subjected to tetracycline, a random mutation in the 30S ribosome to weaken tetracycline binding would be advantageous and, therefore, would be perpetuated by the survival of the tetracycline-resistant bacteria (1). It has also been postulated that **housekeeping genes**, like acyltransferases, may have mutated to gain the ability to modify and inactivate aminoglycoside antibiotics (8-10).

The widespread phenomenon of antibiotic resistance has developed from the promiscuity of bacteria and their genomes. Initially, intrinsic antibiotic resistances were isolated incidents, but the threat of antibiotics has been readily circumvented using the acquisition of antibiotic resistance genes and the high mutational frequency of individual bacteria.

3. Mechanisms of Antibiotic Resistance

Using both newly acquired genes and their own mutated genes, bacteria utilize three basic mechanisms to support antibiotic resistance. Enzymes that degrade antibiotics inside the cell are key players in antibiotic resistance. Bacteria can also alter their permeability barriers to keep antibiotic concentrations below toxic levels inside the cell. Furthermore, the cellular targets of antibiotics can be modified to evade the effects of the antibiotics. These mechanisms of antibiotic resistance are distinct, but all are obtained through the acquisition or mutation of genes.

3.1. Enzymatic Inactivation of Antibiotics

Degradative enzymes are a common mechanism by which bacteria become resistant to antibiotics. Such enzymes chemically modify antibiotics so that they no longer function. The genes for these degradative enzymes are obtained by acquisition of exogenous genes or mutation of endogenous genes. The expression of these genes also governs the level of antibiotic resistance in bacteria.

b-Lactamases are common examples of degradative enzymes that generate antibiotic resistance. b-Lactamases inactivate b-lactam antibiotics, a structurally similar group of penicillin-like antibiotics, all of which have a b-lactam ring structure. b-Lactamases are typically grouped into two major classes, penicillinases and cephalosporinases, based on their substrate affinity (11, 12). In addition to b-lactamases, other enzymes also degrade different antibiotics, such as the aminoglycosides, gentamycin, tobramycin, and amikacin.

All b-lactam antibiotics function similarly. Their b-lactam ring structure inhibits the final step of bacterial cell wall synthesis. Bacterial cell walls are constructed of alternating *N*-acetylglucosamine and *N*-acetyl-muramic acid residues that form long peptidoglycan chains, and the final step in cell wall synthesis involves the enzymatic crosslinking of these peptidoglycan chains by a transpeptidase. Because the b-lactam bond resembles a portion of the peptidoglycan chains, this transpeptidase can mistake a b-lactam antibiotic for its natural substrate and hydrolyze the b-lactam bond. This hydrolysis covalently links the b-lactam drug to the transpeptidase and renders it nonfunctional (13) (see also Penicillin-Binding Proteins).

Although b-lactamases are effective at degrading some antibiotics, their mere presence is not sufficient to cause clinically relevant antibiotic resistance. In fact, these enzymes are found ubiquitously in almost all bacteria, and in some blue-green algae and mammalian tissues. b-lactamases must be present in sufficient quantities to degrade the b-lactam antibiotics effectively before they inhibit cell wall synthesis. The cellular concentration of a b-lactamase depends on its gene expression, and b-lactam antibiotics are inducers of b-lactamase expression. Furthermore, particular b-lactamases have variable affinities for b-lactam antibiotics. Therefore, the degree of antibiotic resistance due to b-lactamases is based on a combination of the ability of the b-lactam antibiotic to induce the expression of b-lactamase, and its ability to be a substrate for b-lactamase (14).

As researchers began to understand this mechanism of antibiotic resistance, more effective b-lactam antibiotics were developed. The early cephalosporins, like penicillin and amoxicillin, are extremely sensitive to b-lactamases, because these b-lactam antibiotics are potent inducers of b-lactamase expression and good substrates for the b-lactamase. In contrast, the more recently developed antibiotic, imipenem, is a strong inducer of b-lactamase expression but maintains its antibiotic activity because it is a poor substrate for most b-lactamases (15). In addition to these new antibiotics, combination therapies are also being implemented to combat antibiotic resistance. Such therapies are comprised of a b-lactam antibiotic together with b-lactamase inhibitors, like clavulanic acid, sulbactam, and tazobactum (16).

3.2. Altered Permeability Barriers: Pore Proteins and Efflux Systems.
The bacterial cell membrane is the major permeable barrier separating the outside of the cell from the inside. The fluidity of the membrane is generally balanced to include most nutrients, while excluding many toxins. Adjusting this fluidity impedes the function of the membrane. Therefore, bacteria cannot protect themselves by changing the fluidity of their membrane. Instead, bacteria have additional structures that surround the cytoplasmic membrane or form pores through it. The alteration of these structures to exclude antibiotics is another mechanism of antibiotic resistance.

Gram-positive and Gram-Negative Bacteria have distinct structures that surround their cytoplasmic membranes. Most Gram-positive bacteria have thick cell walls that are mechanically quite strong, although very porous. Although the cell wall helps Gram-positive bacteria retain their shape, it does not exclude most antibiotics and, therefore, is not a good barrier. Thus, Gram-positive bacteria are relatively susceptible to the influx of antibiotics. Alternatively, a more effective barrier, a second lipid bilayer or membrane, surrounds Gram-negative bacteria. This outer membrane is partially composed of a lipid, lipopolysaccharide (LPS), that is not commonly found in cytoplasmic membranes. The distinguishing feature of LPS is its decreased fluidity, which makes the LPS bilayer an efficient barrier that prevents the permeation of most **hydrophobic** antibiotics into Gram-negative bacteria (17).

Enveloped by effective barriers, bacteria use pore-forming proteins, called porins, to obtain nutrients from outside the cell. Porins are transmembrane proteins that function as nonspecific, aqueous channels, and allows nutrients to diffuse across the membrane. Porins generally exclude antibiotics because they are narrow and restrictive. Most antibiotics are large, uncharged molecules that cannot easily traverse the narrow porin channels that are lined with charged amino acid residues. However, some antibiotics enter the bacteria through porins, and the deletion or alteration of these porins to exclude particular antibiotics is linked to antibiotic resistance.

Because bacteria cannot develop barriers that are impermeable to all molecules, some toxins do diffuse into bacteria along with nutrients. Therefore, bacterial cell membranes also contain transport proteins that cross the membranes and use energy to remove toxins. They are called active efflux systems, and some are directly identified as another significant cause of antibiotic resistance.

Many active efflux systems resemble other transport proteins that catalyze the efflux of common, small molecules, like glucose or cations, and it is likely that mutation has modified them to transport antibiotics. Based on their overall structure, mechanism, and sequence homologies, these transport proteins are classified into four families: (1) the major facilitator family; (2) the resistance nodulation division family; (3) the staphylococcal multidrug resistance family; and (4) the ATP-binding cassette (ABC) transporters. Of these four families, only the ABC transporters use the chemical energy generated from the hydrolysis of ATP to drive molecules across the membrane. Members of the three other families use an electrochemical proton gradient, or proton-motive force, as the source of energy (18, 19).

Some active efflux systems exclude a variety of unrelated toxins from the cell. These multidrug resistance (MDR) efflux systems in bacteria are comparable to those found in mammalian cells (see Drug Resistance). An example of a bacterial MDR efflux system is the Bmr transporter that transports drugs which have diverse chemical structures and physical properties and include cationic dyes, rhodamine-6G, ethidium bromide, and the antibiotics netropsin, puromycin, and fluoroquinone (20). Other MDR efflux systems characterized in bacteria include NorA in *Staphylococcus aureus*, MexB in *Pseudomonas aeruginosa*, and EmrB in *Escherichia coli*. If MDR efflux systems occur extensively in bacteria as the source of many antibiotic resistances, they pose a far more formidable challenge than more specific mechanisms of resistance.

3.3. Modification of the Antibiotic's Target

Antibiotics inhibit bacterial growth by inactivating different key proteins that are essential for bacterial survival (see Fig. 1). However, the antibiotic sensitivity of these target proteins can be altered. Typically, antibiotic targets are altered by reducing their affinity for the antibiotic. Bacteria accomplish this change in affinity several ways. Bacteria acquire exogenous DNA for a mutated target protein that no longer interacts with the antibiotic, yet retains the original target protein's function. Alternatively, bacteria's endogenous genes can be mutated to achieve the same end. In contrast, DNA for novel modifying enzymes can be acquired to alter the antibiotic target posttranslationally, reducing its affinity for the antibiotic.

Altering an antibiotic's target protein directly at the DNA level is a common mechanism of target modification. An example of this modification is the mutation of genes for penicillin-binding proteins (PBPs). PBPs are transpeptidases, previously discussed, that catalyze the final step in bacterial cell wall synthesis. These PBPs have high affinity for penicillin and its derivatives, and the binding of penicillin permanently inactivates PBPs. Originating from both endogenous and exogenous DNA sources, mutated PBPs can have a lower affinity for penicillin. Therefore, PBPs are resistant to the antibiotic, yet still provide a crucial function in bacterial cell wall synthesis (21, 22). Another example of target modification via mutated DNA is a single amino acid mutation in the quinolone resistance-determining region of the **DNA gyrase** gene, gyrA, that can provide up to a 20-fold increase in quinolone resistance (23).

In addition to using mutated antibiotic targets, bacteria can acquire new genes that produce proteins that, in turn, alter antibiotic targets. A well-studied example is the resistance of Staphylococci to **erythromycin**. It is known that Staphylococci have acquired genes to produce a protein that methylates a residue on the 23S ribosome. The 23S ribosome is the target of erythromycin, but methylated 23S ribosome has a low affinity for erythromycin. This exogenous gene is expressed and prevents the binding of erythromycin to the ribosomes, making the bacteria erythromycin-resistant (24).

Bibliography

Bibliography

1. H. C. Neu (1992) Science **257**, 1064–1073.
2. J. Travis (1994) Science **264**, 360–362.
3. M. Castiglia and R. A. J. Smego (1997) J. Am. Pharm. Assoc. **NS37**, 383–387.
4. G. H. Cassell (1997) FEMS Immunol. Med. Microbiol. **18**, 271–274.
5. E. P. Abraham and E. Chain (1940) Nature **146**, 837.
6. H. W. Stokes and R. M. Hall (1989) Mol. Microbiol. **3**, 1669–1683.
7. C. M. Collis, G. Grammaticopoulos, J. Briton, H. W. Stokes, and R. M. Hall (1993) Mol. Microbiol. **9**, 41–52.
8. T. Udou, Y. Mizuguchi, and R. J. J. Wallace (1989) FEMS Microbiol. Lett. **48**, 227–230.
9. K. J. Shaw et al. (1992) Antimicrob. Agents Chemother. **36**, 1447–1455.
10. P. N. Rather, E. Orosz, K. J. Shaw, R. Hare, and G. Miller (1993) J. Bacteriol. **175**, 6492–6498.
11. M. H. Richmond and R. B. Sykes (1973) Adv. Microb. Physiol. **9**, 31–88.
12. K. Bush (1989) Antimicrob. Agents Chemother. **33**, 259–276.
13. A. Tomasz (1979) Annu. Rev. Microbiol. **33**, 113–137.
14. D. M. Livermore (1993) J. Antimicrob. Chemother. **31** (suppl. A), 9–21.
15. J. Y. Jacobs, D. M. Livermore, and K. W. M. Davy (1984) J. Antimicrob. Chemother. **14**, 221–229.
16. K. Coleman et al. (1994) J. Antimicrob. Chemother. **33**, 1091–1116.
17. P. R. Cullis and M. J. Hope (1985) In *Biochemistry of Lipids and Membranes* (D. E. Vance and J. E. Vance, eds.), Benjamin and Cummings, New York, Chap. "2".
18. S. B. Levy (1992) Antimicrob. Agents Chemother. **36**, 695–703.
19. K. Lewis, D. C. Hooper, and M. Ouellette (1997) ASM News **63**, 605–610.
20. A. A. Neyfakh, V. E. Bidnenko, and L. B. Chen (1991) Proc. Natl. Acad. Sci. USA **88**, 4781–4785.
21. B. G. Spratt and K. D. Cromie (1988) Rev. Infect. Dis. **10**, 699–711.
22. J. M. Ghuysen (1991) Annu. Rev. Microbiol. **45**, 37–67.
23. G. A. Jacoby and A. A. Medeiros (1991) Antimicrob. Agents Chemother. **35**, 1697–1704.
24. R. Leclercq and P. Courvalin (1991) Antimicrob. Agents Chemother. **35**, 1267–1272.

Suggestions for Further Reading

25. A short news article: J. Davies (1996) Bacteria on the rampage, Nature **383**, 219–220.
26. Two well written reviews in an excellent anthology: 1. A. Bauernfeind and N. H. Georgopapadalou (1995) In *Drug Transport in Antimicrobial and Anticancer Chemotherapy* (N. H. Georgopapadalou, ed.), Dekker, New York, Vol. 17, pp. 1–19. 2. R. E. W. Hancock (1995) In *Drug Transport in Antimicrobial and Anticancer Chemotherapy* (N. H. Georgopapadalou, ed.), Dekker, New York, Vol. 17, pp. 289–306.
27. Three exhaustive articles in a single issue of *Science* devoted to antibiotic resistance: 1. J. Davies (1994) Inactivation of antibiotics and the dissemination of resistance Genes, Science **264**, 375–382. 2. H. Nikaido (1994) Prevention of drug access to bacterial targets: Permeability barriers and active efflux systems, Science **264**, 382–388. 3. B. G. Spratt (1994) Resistance to antibiotics mediated by target alterations, Science **264**, 388–393.

Antibody

Antibodies are specific proteins, termed immunoglobulins, that are produced by B cells upon stimulation with antigens, which may be proteins, polysaccharides, nucleic acids, and so on, either in soluble form or as part of complex cellular organisms, such as bacteria, parasites, **viruses**, eukaryotic cells of animal or plant tissues, and pollens. In fact, the immune system is so built as to have the potential to make antibodies against any macromolecule of the living world. It was reported at the end of the nineteenth century by von Behring and Kitasato that a group of guinea pigs immunized against a sublethal dose of diphtheria toxin became resistant to diphtheria, whereas another group that received tetanus toxin resisted further challenge with a normally lethal dose of tetanus toxin. This key experiment showed that the protection was specific toward the immunizing agent. Thus, one master word in immunology is specificity, and this immediately raises the problem of what immunologists call the repertoire. How is it possible to make the billions of different molecules that are potentially necessary to assume specific recognition of an obviously astronomical number of potential antigens? What structures are recognized on an antigen? What are the structural bases for antibody specificity? All these are basic questions that have been solved progressively during the past 40 years.

The protein nature of antibodies was established by M. Heidelberger in 1928, by showing that protein nitrogen was present in a specific antigen–antibody precipitate in which the antigen was a polysaccharide, which must have originated from the antibody part of the precipitate. Progress in the knowledge of the structure of antibodies paralleled the emergence of new technological tools in biochemistry and in molecular biology. Analytical ultracentrifugation performed by Kabat and Tiselius at the end of the 1930 indicated that antibodies were found in several classes of sizes, mostly with sedimentation coefficients of between 19S and 7S. **Electrophoretic** characterization of serum, also studied by Kabat in the same period, revealed that antibodies were located in the globulin part of the spectrum, mostly in the slowest moving g-globulin fraction. This name remained in use for years until it was replaced by a more generic one, that of immunoglobulins. Immunoglobulins are thus defined as the immune proteins synthesized specifically by B cells. They are expressed in two forms: (*1*) as integral membrane proteins at the surface of B lymphocytes, where they represent the B-cell receptor (BCR), by analogy with the T-cell receptor (TCR) expressed at the surface of T cells; and (*2*) as a soluble form, secreted in the bloodstream by the plasma cells, which represent the terminal stage of differentiation of the B lineage. This soluble form is what immunologists call circulating antibodies, or simply antibodies.

A main difficulty encountered in studying antibody structure was due to their extraordinary heterogeneity, which deserves some comments. As a rule, when an antigen such as hemoglobin or serum albumin, or in fact any protein, is used as an immunogen, a large array of antibodies with discrete fine specificities is synthesized. At the surface of a protein, many discrete regions are recognized by as many distinct antibodies. These regions are called *antigenic determinants*, or epitopes. For a protein of molecular weight 50 kDa, there are 10, 20, or more epitopes that could be identified by distinct antibodies. But antibody heterogeneity is not limited to the mosaic of epitopes. It may be shown that in fact one given epitope may be recognized by slightly different antibodies, and this contributes an extraordinary multiplication of the heterogeneity. This results from the clonal organization of lymphocytes, as originally proposed by Burnet (1). B lymphocytes (and T cells as well) are organized as discrete clones, each of which makes one and only one type of antibody molecule. In humans, the average population of lymphocytes at any given time is of the order of 10^{12}, of which approximately one-fifth are B cells and four-fifths are T cells. These B cells make about 10^{20} molecules of circulating immunoglobulins, a number that can be calculated from the Ig concentration in serum (10 mg/mL). The size of one clone is largely dependent on the immunization state and can vary from one single resting cell to several thousand or more. What happens when an animal is being immunized is that all clones that happen to interact somewhat with any potential epitope of the administered antigen will proliferate, expand, and synthesize as many different antibodies, thereby contributing to a very great heterogeneity. This of course made it very difficult, if not impossible, to study the fine structure of antibody molecules, especially when considering their amino acid sequences. A bias was brought to this by the existence of multiple myeloma in humans, or its equivalent as experimentally induced plasmacytoma in the mouse. These are lymphoproliferative disorders that affect plasma cells. As a result of the malignancy, one clone will expand specifically so that, very rapidly, it will become the major B-cell clone expressed in the body. The corresponding immunoglobulin will be secreted in excessively large amounts, and this provides a homogeneous material available for structural studies. An obvious drawback with this material is that the antibody specificity is generally unknown, which prevents its use for the study of **antigen–antibody interactions**. This difficulty was turned around when Kohler and Milstein (2) succeeded in making somatic hybrids between myeloma cells and normal B lymphocytes from hyperimmunized mice. These hybridomas combined the properties of myeloma cells, which can grow indefinitely in culture or upon transplantation in syngeneic strains of mice, with the clones of immunized lymphocytes that could be selected for a known antigenic specificity, leading to the fantastic expansion of "monoclonal antibodies" (mAbs). Monoclonal antibodies were not only suitable for detailed structural analysis of antibodies, including determination of the three-dimensional protein structure of antibody–antigen complexes. They also allowed access, through the hybridoma cells, to isolation of messenger RNA encoding Ig polypeptide chains and the corresponding complementary DNA, and thus to the complete gene organization of the three main Ig gene loci.

The basic structure of antibodies, elucidated from the pioneer work of Porter in England (3) and Edelman in the United States (4), is given by that of the IgG molecule—known initially as 7S-g-globulin. It is a symmetrical molecule, containing two identical heavy chains (H, 52 kDa) and two identical light chains (L, 23 kDa), which are either **kappa** (k) **or lambda** (l) **chains**. Each H–L pair contains one combining site for the antigen, so the conventional H_2 L_2 IgG molecule is bivalent. The symmetry of the molecule is in agreement with the clonal selection theory, which postulated that each B cell expressed one and only one antibody specificity. This basic model could be extrapolated to other antibody classes, which differ from each other in the nature of their heavy chains and the degree of polymerization of the basic H_2L_2 unit. Five classes have thus been described in higher vertebrates: IgG, IgM, IgA, IgD, and IgE, having the corresponding g, m, a, d, and e heavy chains, respectively. IgM are expressed as H_2L_2 monomers at the cell surface of B cells, but are pentamers in the serum. IgA is mostly a dimer, whether other classes remain as monomers. The diversification of classes allows the antibodies to assume two types of function: (*1*) antigen recognition, common to all classes, and (*2*) biological or effector functions, such as **complement** fixation, active transplacental transfer, or fixation to various cell types, which amplify the action of antibodies and generally favor the elimination of a pathogen.

The functional duality of antibody molecules was clearly established in the late 1950 by Porter (5), who succeeded in cleaving the IgG antibody by papain, a proteinase, which led to the isolation of two identical fragments that were antigen binding, or Fab, and one Fc fragment that did not recognize the antigen but fixed the first component of the complement cascade. Structural support for this organization was clearly demonstrated by Hilschmann in 1965 (6), who reported the first amino acid sequence of two monoclonal human light chains. This is another example of the importance of monoclonal materials in this saga of the determination of the antibody structure. The work was performed on Bence-Jones proteins, which are free light chains isolated from the urine of patients with multiple myeloma. They are the result of a dysbalanced synthesis between the monoclonal heavy and light chains by the malignant plasma cells. Because of their smaller size, they pass the renal barrier and are thus easily isolated in large amounts from patient's urine. The major discovery was that the Bence-Jones light chains, or Ig light chains, were composed of one NH_2-terminal half of 110 amino acid residues that profoundly differed between two patients, whereas the COOH-terminal half, also of 110 residues, was identical. This gave clear evidence for the existence of a huge structural diversity in antibodies, providing a unique basis for antibody specificity. Further extensive work indicated that heavy chains had also a variable region of similar size and a much longer constant region. The antibody combining site could thus be visualized as resulting from a contribution of both the V_H and the V_L regions. A more detailed analysis, computed by Kabat (7), indicated that within the V **variable regions**, subregions of hypervariability could be identified around positions 30, 50, and 100, which were later proven to participate directly in making up the antibody combining site. Three hypervariable regions, also called *complementarity determining regions* (CDR), were identified on each heavy and light chain, and their fine analysis revealed an extraordinary diversity that certainly could account for the expected huge repertoire of antibodies necessary to accommodate the potential repertoire of epitopes of the living world. Direct proof that the CDRs were implicated in antigen recognition came first from affinity labeling experiments, until a final confirmation was provide by X-ray crystallography analysis of crystals of antigen–antibody complexes. In fact, crystals were prepared from the Fab fragment of an antilysozyme antibody, combined with lysozyme, because the complete IgG antibody molecule contains a floppy "hinge" region that prevents crystallization. This structure, obtained by the group of Poljak (8), presented in Figure 1, indicates that about 20 amino acid residues of the antibody participate in binding the antigen, plus a similar number of residues from the antigen. On average, the area of interaction of the two partners is of the order of 600 $Å^2$. Care should be taken in attempts to generalize this model to all other antigen-antibody pairs, because the size and shape of the antibody combining site varies greatly from one system to another. This variation is reflected in the wide variation of the association constants K_A, between 10^5 and 10^{12} M^{-1} . The interactions between antigen and antibody are exclusively non covalent and involve primarily salt bridges, van der Waals interactions, and hydrogen bonds. The contributions of **enthalpy** and **entropy** vary immensely from one system to another, stressing again, if needed, the fantastic diversity potential of antibody molecules.

Figure 1. Three-dimensional structure of a lysozyme–Fab antilysozyme, showing the amino acid contributions from the heavy chain (upper part of Fab) and from the light chain (lower part). The antigen is on the right, and the Fab is on the left. (**a**, **b**) Side views. (**c**) Front view of the interacting residues of the antibody combining site (left) and epitope (right). (From Ref. 1, with permission from R. Poljak.)

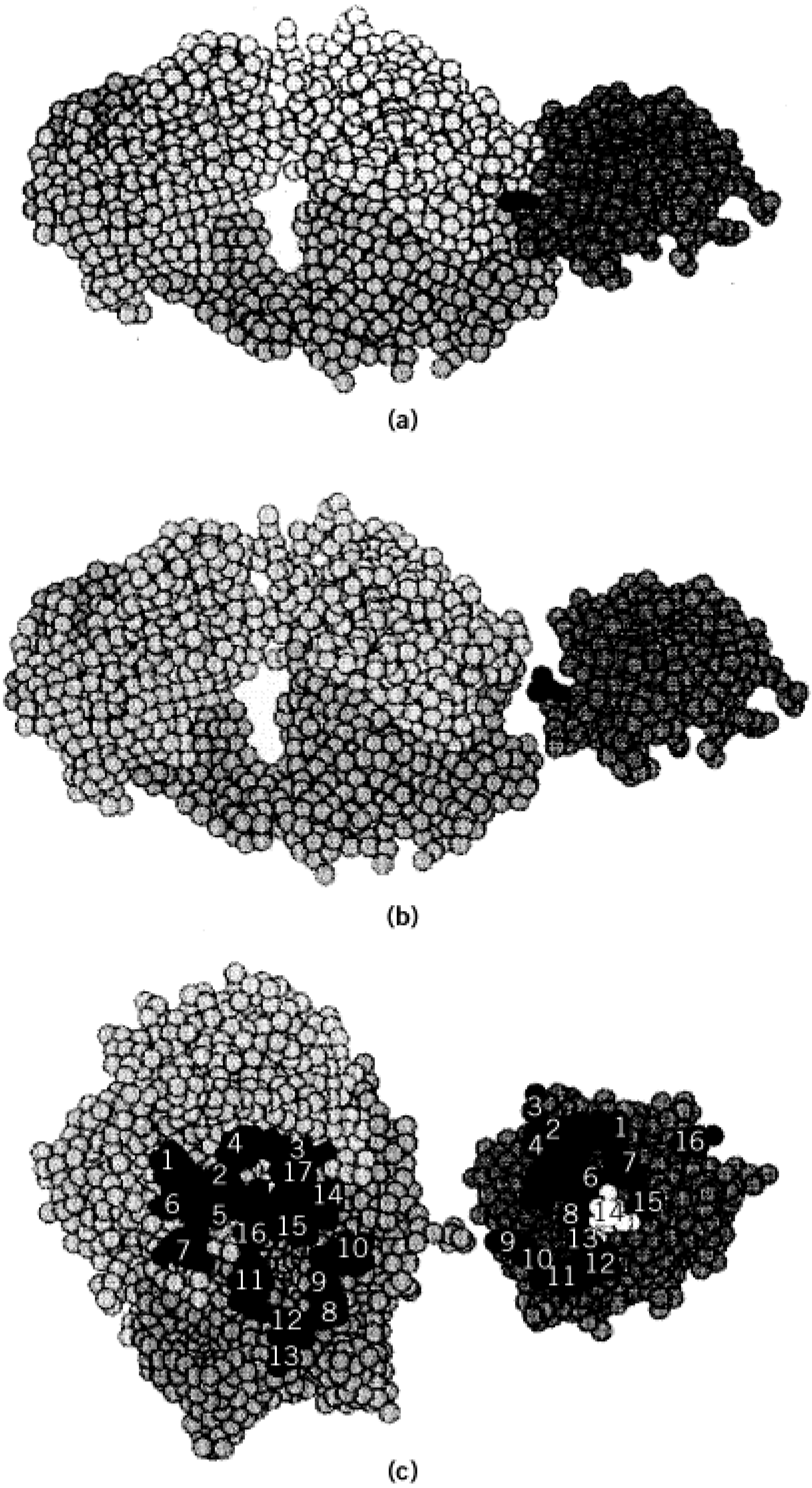

Ultimately, the main problem that the immune system has to face is how to generate such a huge diversity with a number of genes that must necessarily be limited. At the time of the first data concerning the amino acid sequences of the light chains, many hypotheses were put forward to account for this diversity. There were two extremes: One considered that the diversity was exclusively the result of somatic hypermutations, whereas the other claimed that everything was encoded at the germline level, arguing that, provided that any light chain might pair with any heavy chain, 10,000 L-chain genes and 10,000 H-chain genes might generate 10^8 antibodies, a number that was already considered reasonable. Besides the fact that 20,000 genes would represent a large portion of the genome, this theory did not account for the conservation of the constant regions, a very serious objection that led Dreyer and Bennet (9) to propose that genes encoding the V and the C regions were separate in the germline. This was shown to be the case when the basic principles of the Ig gene organization were elucidated by the elegant experiments of Tonegawa in 1978 (10). In brief, V and C regions are encoded by separate regions within each of the three H, K, and L Ig loci, with a small number of **C genes** and a large number of V genes (Fig. 2). In addition, the V regions are in fact encoded by a mosaic of two gene segment clusters for the light chains (V_L and J_L) and three for the heavy chains (V_H, D, and J_H). Random combination of these elements takes place exclusively during B-cell differentiation and leads to a large collection of clones expressing various combinations from the basic gene mosaic. Diversity is further amplified greatly by other mechanisms, including somatic hypermutation. As a result, the number of distinct B-cell clones present at any time certainly far exceeds that necessary, especially in view of antigen–antibody recognition being partly degenerate.

Figure 2. Schematic organization of the three Ig gene loci in (**a** mice and (**b**) humans. The IGK, IGL, and IGH loci, codi the k light chain, the l light chain, and the heavy chain, respectively, are located on mouse chromosomes 6, 16, and 12 ar human chromosomes 2, 22, and 14, respectively.

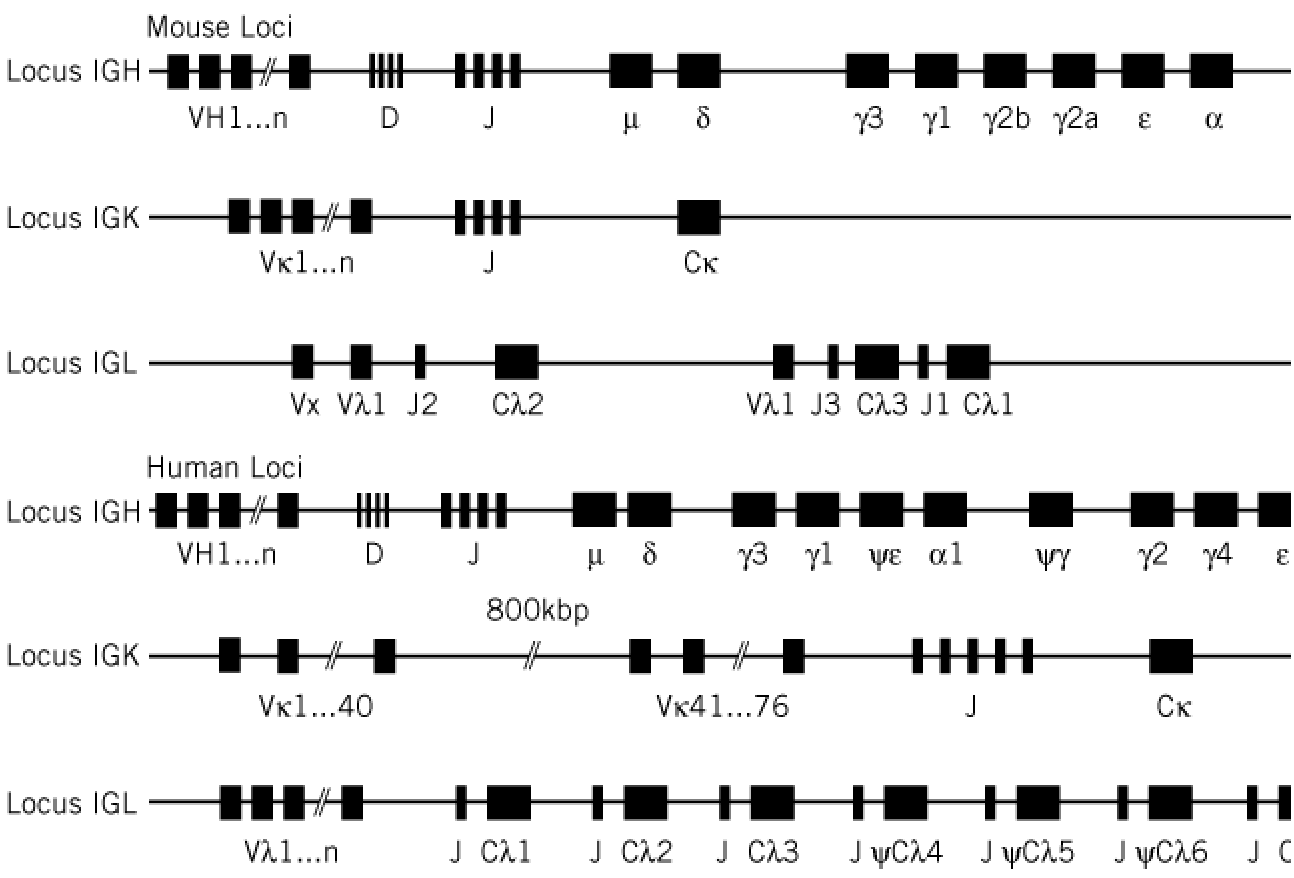

See also entries B Cell, Immunoglobulin, Clonal Selection Theory, Gene Rearrangement, and Repertoire.

Bibliography

1. M. F. Burnet (1959) *The Clonal Selection Theory of Acquired Immunity*. Vanderbilt University Press, Nashville, TN.
2. B. Köhler and C. Milstein (1975) Continuous culture of fused cells secreting antibody of

predefined specificity. Nature **256**, 495–499.
3. J. B. Fleischman, J. B. Pain, and R. R. Porter (1962) Reduction of gammaglobulins. Arch. Biochem. Biophys. Suppl. **1**, 174–180.
4. G. M. Edelman and M. D. Poulik (1961) Studies on structural units of the -globulins. J. Exp. Med. **113**, 861–884.
5. R. R. Porter (1959) The hydrolysis of rabbit gammaglobulin and antibodies by cristalline papain. Biochem. J. **73**, 119–126.
6. N. Hilschmann and L. Craig (1965) Amino acid sequence studies with Bence-Jones proteins. Proc. Natl. Acad. Sci. **53**, 1403–1409.
7. T. T. Wu and E. A. Kabat (1970) An analysis of the sequences of the variable regions of the Bence-Jones proteins and mycloma light chains and their implications for antibody complementarity. J. Exp. Med. **132**, 211–250.
8. A. G. Amit, R. A. Mariuzza, S. E. V. Phillips, and R. J. Poljak (1986) Three-dimensional structure of an antigen–antibody complex at 2.8 A resolution. Science **233**, 747–753.
9. W. J. Dreyer and J. C. Bennett (1965) The molecular basis of antibody formation: a paradox. Proc. Natl. Acad. Sci. USA **54**, 864–869.
10. S. Tonegawa (1983) Somatic generation of antibody diversity. Nature, **302**, 575–581.

Suggestions for Further Reading

11. G. M. Edelman, B. A. Cunningham, W. E. Gall, P. D. Gottlieb, U. Rutishauser, and M. J. Waxdal (1969) The covalent structure of an entire gamma G immunoglobulin molecule. Proc. Natl. Acad. Sci. USA **63**, 78–85.
12. F. Alt, T. K. Blackwell, and G. D. Yancopoulos (1987) Development of the primary antibody repertoire. Science **238**, 1079–1087.

Antibody–Antigen Interactions

Binding of antigens has long been a central paradigm for molecular recognition. In addition, the biological nuances of antigen recognition have such profound ramifications for medicine that the study of antibody–antigen interactions remains a key branch of molecular immunology. In this entry we first describe the structural chemistry of antigen binding, then follow with aspects of antibody–antigen interaction that lead to unique biological phenomena.

1. Chemical Aspects of Antibody–Antigen Interaction

1.1. General Properties

The chemical interactions between antibody and antigen do not differ substantially from other protein–ligand interactions. Hydrogen bonds, van der Waals interactions, and sometimes salt bridges are used to form the antibody-antigen contact. Extremely close steric complementarity between antibody and antigen surfaces seems to be a common characteristic of interfaces (1). Gaps between the opposing antibody and antigen surfaces are sometimes filled by water molecules (2). The association constant for antibody–antigen interactions ranges from 10^5 to 10^{12} M^{-1}, with typical values for protein antigens around 10^8–10^9 M^{-1} (3). Rate constants for binding low molecular weight haptens can be as high as 10^8 $M^{-1}s^{-1}$. Reactions with macromolecular antigens are slower, $\leq 10^6$ $M^{-1}s^{-1}$, except for highly charged antigens, which sometimes enhance the rate through electrostatic interactions (4). In most cases, antigen binding does not cause easily observed changes in the binding site of an antibody. In some cases, conformational changes in the antibody are intrinsic to the binding mechanism. These changes can be caused subsequent to antigen binding, termed an "induced fit" mechanism (5); alternatively, antigen can bind selectively to one of several preexisting antibody conformations (6). Generalizations about the nature of the antibody–antigen interaction are hazardous, as is clear from the observation that the same antibody can bind one ligand through a few strong contacts and another ligand through many weak interactions (7).

1.2. Combining Site Structure and Function

Comparative studies showed that antibody variability was concentrated in three short stretches of sequence within each variable domain (8). These regions were postulated to confer antigenic specificity on an antibody molecule, and were termed "complementarity-determining residues" (CDRs). X-ray crystallographic studies confirmed that the CDRs, although noncontiguous in the antibody primary structure, formed loops that were adjacent to each other in three-dimensional space (9). The position of CDRs within an IgG molecule is shown in Figure 1. Structural studies on antibody–antigen complexes have confirmed that the CDRs form the vast majority of intermolecular contacts. Non-CDR residues can also form contacts, however, and in some cases not all CDRs participate in the interaction with antigen (10). Of the six CDRs, heavy chain CDR3, formed at the genetic level by joining of a D segment to V_H and J_H, is the most structurally diverse, and usually the most energetically significant in binding antigen. (See Immunoglobulin Structure.)

Figure 1. Position of CDRs (dark lines) within an IgG molecule.

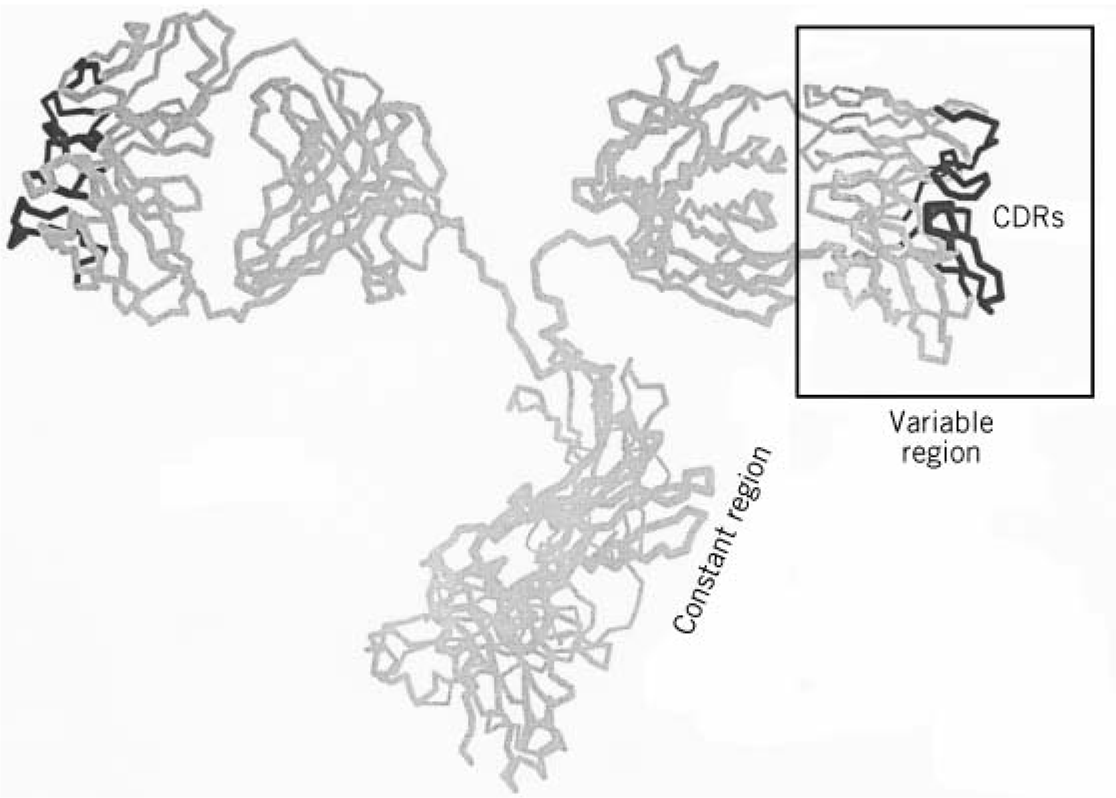

1.3. Antigenicity

Antibodies bind to structurally precise surfaces on protein antigens (11). These surface areas can be composed of a contiguous length of polypeptide chain or from several parts of a chain that are separate in primary structure but adjacent in three-dimensional space. The only true prerequisite for a portion of a protein to be recognized as an antigen is surface **accessibility**, although other factors, such as hydrophilicity and mobility, are often considered in predicting antigenicity from protein sequence (12). In the case of peptide–antibody complexes, about 7–10 peptide residues fit in the binding site of the antibody and form an ordered structure, even if the free peptide itself is not strongly ordered in solution (13). Sometimes a bound peptide structure resembles the conformation of the same sequence in an intact protein, a phenomenon that underlies the utility of peptide vaccines (14).

2. Biological Aspects of Antibody–Antigen Interaction

2.1. T-Dependent and T-Independent Immune Responses

"Normal" immune responses depend on the participation of T cells. In outline, antibody-producing B cells capture antigen (protein or protein–hapten conjugate) on their surface, internalize and fragment the antigen, and represent short peptide fragments on the cell surface, embedded in the binding groove of major histocompatibility complex (MHC) molecules. T-cells recognize the peptide–MHC combination and produce signals that cause B cells to enter pathways of proliferation and differentiation (15). Molecular genetic processes activated at the immunoglobulin loci include heavy-chain class switching and somatic hypermutation, leading to production of soluble IgG, IgE, and IgA of high affinity. T-independent antigens include virtually all nonprotein macromolecules. B-cell proliferation and differentiation also occur in a T-independent response, but chain switching and somatic mutation are difficult to detect. Structural attributes of antibodies in a T-independent response are that they are of the IgM isotype, contain germline (unmutated) **variable region** sequences, and show low antigen affinity.

2.2. Maturation of the Immune Response

Antibodies isolated soon after an initial antigen exposure, termed "primary response antibodies", differ from those obtained later in the response or after a second administration of antigen. This transformation of the antibody repertoire, which leads to progressive increases in the affinity for antigen (16), is termed "maturation of the immune response." The structural basis of this phenomenon has been determined from studies of immune responses to haptens, and can be outlined as follows. Contact with antigen induces a process within lymphocytes that introduces point mutations in the variable regions of antibody genes (17). Most mutations have a neutral or deleterious effect on antigen affinity (18). However, some mutations improve the interaction with antigen. Higher affinity confers a selective advantage on lymphocytes that express this mutation, which may be competing with nearby lymphocytes for a limited amount of antigen. Selected lymphocytes proliferate and can undergo further rounds of mutation and selection. Maturation of the immune response leads to improved affinity universally in anti-hapten responses. The same progressive affinity increase is presumed to occur with protein antigens, but unequivocal evidence for this is lacking.

The diversity of the initial repertoire is determined by germline variable gene diversity and processes involved in gene rearrangement. At a structural level, antibody diversity is concentrated around the center of the antigen combining region. Somatic mutation acts to form the mature repertoire, which for protein antigens will show association constants in excess of $10^8\ M^{-1}$. Somatic point mutations can occur anywhere in the variable region, but those selected during maturation are in general located in a band immediately peripheral to the area of diversity expressed in the early repertoire (19).

2.3. Anti-idiotype Antibodies

"Idiotype" is an immunological word that corresponds in structural terms to the unique CDRs of an individual antibody. If an antibody (Ab1) is used to **immunize** an animal, its CDRs can be recognized as a foreign structure, even in an animal of the same species. An antibody that reacts with the CDRs of Ab1 will be made, termed an **anti-idiotype** antibody (Ab2). The anti-idiotype can be used in the same way to generate an anti-anti-idiotype (Ab3). In a theory of immune regulation (20), if Ab1 is complementary to an antigen and Ab2 is complementary to Ab1, then the binding site of

Ab2 should resemble the initiating epitope on the antigen. ***In vivo***, Ab2 is then said to carry an “internal image” of the antigen. This chain of alternating complementary recognition properties is diagrammed in Figure 2).

Figure 2. Chain of complementary binding activities within an idiotype network.

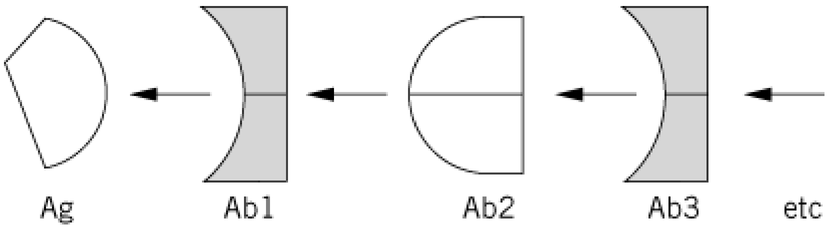

Structural studies have investigated the extent to which the internal image model is accurate. No gross structural similarity between an antigen and Ab2 is necessary for both molecules to bind to Ab1 with high affinity. However, the structure of an antilysozyme (Ab1) complexed with an Ab2 showed that many of the Ab1 residues used for binding lysozyme were also used to bind Ab2 (21). Furthermore, many Ab2 atoms contacting Ab1 occupied positions analogous to contact atoms in lysozyme, and intermolecular hydrogen bonds and even water molecules at the interface were conserved between the Ab1:lysozyme and Ab1:Ab2 complexes. Thus Ab2 can mimic an antigen through close chemical complementarity with Ab1, even in the absence of sequence or structural homology. In the case of Ab3 molecules, structural similarity to Ab1 is unequivocal, although not surprising. CDR sequences are often nearly identical between Ab1 and Ab3, and the structure of an antigen:Ab3 complex shows chemical complementarity as stringent as would be expected at the interface between antigen and an antibody raised directly (22).

2.4. Heterophile Antibodies and Molecular Mimicry

An antibody that reacts with an antigen to which the host has not been exposed is termed a “heterophile antibody” (23). The origin of heterophile antibodies is obscure; no antigen has been unambiguously identified that in a natural situation causes heterophile antibodies to appear. Structurally, heterophile antibodies tend to be low affinity IgM that react with carbohydrate antigens. Some heterophile antibodies, termed “natural antibodies,” appear to arise spontaneously and persist for the lifetime of the organism. The heterophile antibodies that determine ABO blood group compatibility are of this type. In other cases, appearance of heterophile antibodies clearly results from infection. For example, infectious mononucleosis in humans reproducibly induces antibodies specific for an antigen on sheep red blood cells (24). The supposition in such cases is of a process of “molecular mimicry”: a pathogen-specified product is made during infection that possesses sufficient structural similarity to the heterophile antigen that heterophile antibodies are induced (25). When the reactivity induced is to a self-antigen normally subject to immune **tolerance** mechanisms, autoimmune disease may result. For example, streptococcal respiratory infection is the immediate antecedent of rheumatic fever, an autoimmune attack on the heart and vascular tissue. A carbohydrate structure on the bacterial surface is thought to mimic structural glycoproteins in heart valves and vessels (26). Experimental induction of autoimmune diseases by immunization supports this type of antibody–antigen interaction as an initiating mechanism for autoimmunity (27).

2.5. Polyreactive or Polyspecific Antibodies

Polyreactive antibodies do not fit the standard paradigm of one antibody recognizing a single antigen. Instead, a single polyreactive antibody can recognize a panel of many antigens that bear no obvious chemical similarity to each other. Many polyreactive antibodies are IgM, and others are IgG and other isotypes and can bind antigens with high affinity. For example, a set of hybridomas screened for simultaneous reactivity with tubulin, actin, myosin, and single- and double-stranded

DNA showed a median antibody affinity for all five antigens of $10^7\ M^{-1}$ (28). The molecular basis of polyreactivity is unknown. Numerous V genes have appeared in polyreactive antibodies, and there is as yet no characteristic sequence motif that predicts polyreactivity. Nevertheless, sequence studies implicated heavy-chain CDR3 as a major determinant of polyreactivity (29). Structure–function studies comparing a polyreactive and monoreactive anti-insulin with similar sequences confirmed that polyreactivity was associated with heavy-chain CDR3 (30). This CDR loop is presumed to adopt multiple conformations to accommodate different antigens, but crystallographic data on the three-dimensional structure of polyreactive antibodies are lacking.

Bibliography

1. A. G. Amit, R. A. Mariuzza, S. E. V. Phillips, and R. J. Poljak (1986) Science **233**, 747–753.
2. T. N. Bhat, G. A. Bentley, G. Boulot, M. I. Green, D. Tello, W. Dall"Acqua, H. Souchon, F. P. Schwarz, R. A. Mariuzza, and R. J. Poljak (1994) Proc. Natl. Acad. Sci. USA **91**, 1089–1093.
3. I. Pecht (1982) "Dynamic aspects of antibody function", in *The Antigens* (M. Sela, ed.), Academic Press, New York, Vol. **6**, pp. 1–68.
4. C. S. Raman, R. Jemmerson, B. T. Nall, and M. J. Allen (1992) Biochemistry **31**, 10370–10379.
5. J. M. Rini, U. Schulze-Gahmen, and I. A. Wilson (1992) Science **255**, 959–965.
6. D. Lancet and I. Pecht (1976) Proc. Natl. Acad. Sci. USA **73**, 3548–3553.
7. W. Dall"Acqua, E. R. Goldman, E. Eisenstein, and R. A. Mariuzza (1996) Biochemistry **35**, 9667–9676.
8. T. T. Wu and E. A. Kabat (1970) J. Exp. Med. **132**, 211–250.
9. R. J. Poljak, L. M. Amzel, H. P. Avey, B. L. Chen, R. P. Phizackerly, and F. Saul (1973) Proc. Natl. Acad. Sci. USA **70**, 3305–3310.
10. D. R. Davies, E. A. Padlan, and S. Sheriff (1990) Annu. Rev. Biochem. **59**, 439–473.
11. D. C. Benjamin, J. A. Berzofsky, I. J. East, F. R. N. Gurd, C. Hannum, S. J. Leach, E. Margoliash, J. G. Michael, A. Miller, E. M. Prager, M. Reichlin, E. E. Sercarz, S. J. Smith-Gill, P. E. Todd, and A. C. Wilson (1984) Annu. Rev. Immunol. **2**, 67–101.
12. J. A. Berzofsky (1985) Science **229**, 932–940.
13. R. Stanfield and I. A. Wilson (1995) Curr. Opin. Struct. Biol. **5**, 103–113.
14. R. A. Lerner (1982) Nature **299**, 592–596.
15. A. Lanzavecchia (1985) Nature **314**, 537–539.
16. H. N. Eisen and G. W. Siskind (1964) Biochemistry **3**, 996–1008.
17. M. G. Weigert, I. M. Cesari, S. J. Yonkovich, and M. Cohn (1970) Nature **228**, 1045–1047.
18. C. Chen, V. A. Roberts, and M. B. Rittenberg (1992) J. Exp. Med. **176**, 855–866.
19. I. M. Tomlinson, G. Walter, P. T. Jones, P. H. Dear, E. L. L. Sonnhammer, and G. Winter (1996) J. Mol. Biol. **256**, 813–817.
20. N. Jerne (1974) Ann. Inst. Pasteur (Immunol) **125C**, 373–389.
21. B. A. Fields, F. A. Goldbaum, X. Ysern, R. J. Poljak, and R. A. Mariuzza (1995) Nature **374**, 739–742.
22. K. C. Garcia, S. V. Desiderio, P. M. Ronco, P. J. Verroust, and L. M. Amzel (1992) Science **257**, 528–531.
23. J. Forssmann (1911) Biochem. Z. **37**, 78–115.
24. J. R. Paul and W. W. Bunnell (1932) Am. J. Med. Sci. **183**, 90–104.
25. R. T. Damian (1964) Am. Naturalist **98**, 129–149.
26. J. B. Zabriskie, K. C. Hsu, and B. C. Seegal (1970) Clin. Exp. Immunol. **7**, 147–159.
27. R. S. Fujinami and M. B. A. Oldstone (1985) Science **230**, 1043–1045.
28. L. Diaw, C. Magnac, O. Pritsch, M. Buckle, P. M. Alzari, and G. Dighero (1997) J. Immunol. **158**, 968–976.

29. C. Chen, M. P. Stenzel-Poore, and M. B. Rittenberg (1991) J. Immunol. **147**, 2359–2367.
30. Y. Ichiyoshi and P. Casali (1994) J. Exp. Med. **180**, 885–895.

Suggestions for Further Reading

31. E. A. Padlan (1994) Anatomy of the antibody molecule, Mol. Immunol. **31**, 169–217. (A superb, comprehensive review of antibody structure and function.)
32. FASEB J. **9**, 1–147 (1994). An entire issue devoted to structural immunology, including reviews and research papers.
33. Immunol. Rev. **163**, "Molecular anatomy of the immune response" (1998). (An entire volume of reviews of structural immunology.)

Antibody-Conjugated Toxins

Soon after the discovery of the high specificity of antibody binding, Paul Ehrlich proposed to exploit such specificity to redirect and restrict the activity of toxins to pathological tissues such as tumors (1-3). Such "magic bullets" could be developed only long after his proposal because of the need of antibodies of well-defined specificity, such as monoclonal antibodies, and to improve the understanding of the biochemistry and mechanism of the action of toxins. Such conjugates have been prepared by linking one of the many available cell-killing plant or bacterial toxins via a **disulfide** or thioether bond to an antibody specific for a cell surface antigen of cancer and noncancer cells. Chimeric toxins have also been prepared by fusing a toxin gene to a gene encoding a hormone, growth factor, or **cytokine** with the intention of depleting receptor-rich cell populations (1-3). In general, it is important that the linkage between the two immunotoxin parts be easily cleaved on or inside cells. Moreover, to restrict immunotoxin binding only to the cells to be intoxicated, the portion of the toxin determining its intrinsic specificity (the B subunit) must be either deleted or inactivated mutationally, and the F_c portion of the antibody must be removed. In this respect, **ribosome**-inactivating plant toxins lacking the B subunit have been frequently used. To avoid unspecific binding to F_c-receptor bearing cells, the toxin can be linked to the $F(\mathrm{ab})_2$ portion of a monoclonal antibody. An additional problem may be presented by the presence of circulating antitoxin antibodies elicited in previous vaccination protocols (eg, anti**diphtheria**) or during the treatment with the immunotoxin. In the latter case, one can use another immunotoxin made with the same antibody and an immunologically unrelated toxin.

Several antibody-conjugated toxins are very effective in killing target cells in culture or in isolated dispersed tissues, ie, bone marrow, but are less effective *in vivo*, because of the lack of accessibility of the cancer cells in solid tumors. However, protocols are being developed to overcome these problems and exploit the potentials of immunotoxins to reach small cancer populations that are undetected by physical and surgical methods (3).

Bibliography

1. S. Olsnes, K. Sandvig, O. W. Petersen, and B. van Deurs (1989) Immunol. Today **10**, 291–295.
2. D. A. Vallera (1994) Blood **83**, 309–317.
3. G. R. Trush, L. R. Lark, and E. S. Vitetta (1996) Ann. Rev. Immunol. **14**, 49–71.

Anticodon

The anticodon of transfer RNA (tRNA) is in the central part of the linear RNA sequence, at positions 34, 35, and 36. This triplet of nucleotides forms transitory base pairs with three nucleotide codons of the **messenger** RNA (mRNA) during **protein biosynthesis**. These codon/anticodon interactions enable the mRNA to direct the order of incorporation of amino acids into the polypeptide chain. These interactions occur on the small subunit of the ribosome. The presence of the anticodon in the seven-membered central loop of tRNA led to the designation of this subdomain as the anticodon loop. The anticodon stem plus the loop constitute the anticodon arm (stem and loop), which contributes to one branch of the L-shaped 3D structure of tRNA. In this structure, the anticodon is about 80 Å from the amino acid acceptor end of the tRNA (see Fig. 1 of Transfer RNA). Besides its fundamental contribution to translation of the genetic information through complementary pairing to the codon, the anticodon of tRNA may contain important identity elements, recognized by cognate aminoacyl-tRNA synthetases, which lead to specific aminoacylation of the tRNA. Besides the anticodon, other members of the loop and of the nearby stem, including modified nucleotides, also contribute both to the efficiency and specificity of aminoacylation.

Codon–anticodon interaction occurs basically through classic **Watson–Crick base pairs**. However, additional types of interactions allow **wobble** to occur between the third base of the codon and the first base of the anticodon (1). The original wobble rules suggested that the first nucleoside of the anticodon can pair with more than one nucleoside at the third position of the codon. Thus, anticodons with a U at the first position could interact with codons having either A or G at the third position. Those presenting a G at position 34 could interact with codons terminating with U or C. More interestingly, tRNA presenting an inosine (deaminated adenosine) at position 34 could recognize codons terminating with either C, U, or A. For example, yeast $tRNA^{Ala}$, anticodon 5′-IGC-3′, interacts with three codons: 5′-GCC-3′, 5′-GCU-3′, and 5′-GCA-3′.

Numerous data accumulated over the years led to revised wobble rules (2, 3), which reflect new possible interactions between classic bases and take into account the vast occurrence of modified nucleosides in the anticodons of tRNA, especially those at the wobble position (residue 34, first position of the anticodon). One minor tRNA, *Escherichia coli*, $tRNA^{Ile}2$, has a methionine anticodon CAU. However, in the mature tRNA, C34 is modified by covalent attachment of lysine on position 2 of the pyrimidine ring, converting it to lysidine or a “k2C” base. Lysidine at the wobble position leads to recognition of the isoleucine-specific codon 5′-AUA-3′ instead of the methionine codon AUG. Interestingly, this modification is also required for specific recognition of the tRNA by isoleucyl-tRNA synthetase (see discussion below). Other examples of modification at position 34 that contribute to the specificity of codon–anticodon recognition have been reported. This is also true for nucleotide 37, at the 3′ side of the anticodon triplet. Many different modified purine nucleosides have been identified at this position, and these modifications contribute to the fidelity of protein synthesis. For example, hypermodification of A to i6A (*N*-6-isopentenyladenosine), t6A (*N*-6-threonylcarbamoyladenosine), and their derivatives, stabilizes the relatively weak A-U and U-A base pairing between the third position of the anticodon and the first position of the codon. The presence of the hypermodified nucleoside ms2i6A (*N*-6-(D-2-isopentenyl)-2-methylthioadenosine), in contrast, prevents codon misreading by *E. coli* $tRNA^{Phe}$. Modifications introduce conformational flexibility or rigidity that restrict or enlarge the number of potential base pairs. Thus the molecular mechanism by which modified bases alter codon recognition are largely structural in nature.

UAG (**amber**), UAA (**ocher**), and UGA (opal) codons do not code for an amino acid, because there are no tRNA with corresponding anticodons. Known as **nonsense codons**, they normally signal termination of translation, but such codons can be created by mutation, when they cause premature termination of protein synthesis. Interestingly, nonsense **suppressor** tRNA, with mutations in the anticodon, can recognize and "suppress" nonsense mutations by inserting a specific amino acid during translation (4). The first suppressor tRNA identified was a tyrosine-specific tRNA in which a single base substitution converted the anticodon from GUA (Tyr) to CUA (amber). Conversion of a classic tRNA to an efficient suppressor RNA may also involve mutations outside the anticodon. Suppressor tRNA have been used as a tool in the search of tRNA identity elements *in vivo* and as a way of inserting desired amino acids at specific sites in proteins.

The anticodon triplet specifies which amino acid the tRNA will insert in response to a codon and is, of course, directly correlated with the amino acid bound to the -CCA end. A simple analysis of the genetic code, however, reveals that the anticodon is not a common signal for synthetase recognition. For example, there are six different serine codons and, consequently, the potential for six different anticodon sequences in serine-specific tRNA. This great variability in isoacceptor tRNA precludes a common signal in the anticodon for recognition by seryl-tRNA synthetase, but it is clear that anticodon nucleotides, as well as other nucleotides within the anticodon loop, are critical for which amino acids are charged by aminoacylation (5-10).

Single-point mutations at any anticodon nucleotide of yeast $tRNA^{Phe}$ or yeast $tRNA^{Asp}$ lead to severe losses in aminoacylation efficiency (11, 12). A simple anticodon switch changes the aminoacylation specificity of methionine and valine tRNA (13). Depending on the tRNA, one, two, or three anticodon nucleotides may be involved in tRNA specificity. Position 35 is required for charging of arginine, both 35 and 36 are important for valine or threonine, and 34, 35, and 36 are involved in specificity for Asn, Asp, Cys, Gln, Ile, Lys, Met, Phe, Trp, and Tyr. In *E. coli* $tRNA^{Gln}$, residue 35 is of greater importance than residues 34 and 36. In yeast $tRNA^{Asp}$, nucleotides 34 and 35 contribute more than do nucleotide 36. Transplantation of anticodons into noncognate tRNA results in increases of four to six orders of magnitude in aminoacylation of the chimeric tRNA with the amino acid corresponding to the transplanted anticodon. Since it does not preclude aminoacylation of the chimeric tRNA with the original amino acid, however, it is clear that additional identity elements elsewhere in the tRNA structure dictate amino acid specificity (see Transfer RNA). The extent and the relative contribution of the different nucleotides of the anticodon to this specificity varies. The losses in specificity for yeast $tRNA^{Asp}$ are about 500-fold, while those for *E. coli* $tRNA^{Val}$ are 100,000-fold.

Other nucleotides within the anticodon domain often contribute to amino acid specificity. Residue 38 is involved in yeast $tRNA^{Asp}$, and both residues A37 and U38 are involved in *E. coli* $tRNA^{Gln}$. An original approach to anticodon domain function uses the *in vitro* synthesis of minihelices (shortened forms of tRNA) mimicking isolated anticodon stem and loop domains. These minihelices possess identity elements and were tested for stimulation of aminoacylation rates of the acceptor stem as substrate and/or for inhibition of full-length tRNA charging (14). Yeast valyl-tRNA (15) and *E. coli* isoleucine-tRNA (16) anticodon minihelices stimulated, up to threefold, the aminoacylation of an acceptor arm minihelix by cognate aminoacyl-tRNA synthetase. The isolated anticodon domain of $tRNA^{fMet}$ binds to *E. coli* methionyl-tRNA synthetase (17).

The anticodon domain is further implicated in discrimination between initiator and elongator forms of tRNA (18) and in alternate functions of tRNA, such as initiation of **reverse transcription** in retroviruses (19) (see Transfer RNA).

Bibliography

1. F. H. C. Crick (1966) J. Mol. Biol. **19**, 548–555.
2. S. Yokoyama and S. Nishimura (1995) in *tRNA: Structure, Biosynthesis, and Function* (D. Söll and U. L. RajBhandary, eds.), American Society for Microbiology, Washington, DC, pp. 207–223.
3. K. Watanabe and S. Osawa (1995) in *tRNA: Structure, Biosynthesis, and Function* (D. Söll and

U. L. RajBhandary, eds.), American Society for Microbiology, Washington, DC, pp. 225–250.
4. H. Ozeki, H. Inokuchi, F. K. M. Yamao, H. Sakano, T. Ikemura, and Y. Shimura (1980) in *Transfer RNA: Biological Aspects* (D. Söll, J. Abelson, and P. Schimmel, eds.), Cold Spring Harbor Laboratory, New York, pp. 341–362.
5. L. Kisselev (1985) Prog. Nucleic Acid Res. Mol. Biol. **32**, 237–266.
6. L. Pallanck, M. Pak, and L.-H. Schulma (1995) in *tRNA: Structure, Biosynthesis, and Function* (D. Söll and U. L. RajBhandary, eds.), American Society for Microbiology, Washington DC, pp. 371–394.
7. R. Giegé, J. D. Puglisi, and C. Florentz (1993) Prog. Nucleic Acid Res. Mol. Biol. **45**, 129–206.
8. W. H. McClain (1993) J. Mol. Biol. **234**, 257–280.
9. M. E. Saks, J. R. Sampson, and J. N. Abelson (1994) Science **263**, 191–197.
10. W. H. McClain (1995) in *tRNA: Structure, Biosynthesis, and Function* (D. Söll and U. L. RajBhandary, eds.), American Society for Microbiology Press, Washington, DC, pp. 335–347.
11. J. R. Sampson, A. B. DiRenzo, L. S. Behlen, and O. C. Uhlenbeck (1989) Science **243**, 1363–1366.
12. J. Putz, J. D. Puglisi, C. Florentz, and R. Giegé (1991) Science **252**, 1696–1699.
13. L. H. Schulman and H. Pelka (1988) Science **242**, 765–768.
14. S. A. Martinis and P. Schimmel (1995) in *tRNA: Structure, Biosynthesis, and Function* (D. Söll and U. L. RajBhandary, eds.), American Society for Microbiology Press, Washington, DC, pp. 349–370.
15. M. Frugier, C. Florentz, and R. Giegé (1992) Proc. Natl. Acad. Sci. USA **89**(9), 3990–3994.
16. O. Nureki, T. Niimi, T. Muramatsu, H. Kanno, T. Kohno, C. Florentz, R. Giegé, and S. Yokoyama (1994) J. Mol. Biol. **236**, 710–724.
17. T. Meinnel, Y. Mechulam, S. Blanquet, and G. Fayat (1991) J. Mol. Biol. **220**, 205–208.
18. N. Mandal, D. Mangroo, J. J. Dalluge, J. A. McCloskey, and U. L. RajBhandary (1996) RNA **2**, 473–482.
19. C. Isel, J.-M. Lanchy, S. F. J. Le Grice, C. Ehresmann, B. Ehresmann, and R. Marquet (1996) EMBO J. **15**, 917–924.

Anti Conformation

Anti is used as a prefix to describe the relative orientation of two substituents on adjacent atoms of a molecule when their torsion angle is about 180° (1) (see Conformation). In addition to its formal usage, *anti* has become broadly used to describe the orientation of the **nucleic acid** bases relative to the ribose ring when describing the torsion angle about the glycosidic bond (2). The glycosidic bond torsion is defined by the relative positions of the four atoms surrounding this bond, O4′—*C*1—N9 (1—*C*4(2)) for the purine (pyrimidine) nucleosides (3). When C4 is not over the ribose ring, the conformation is *anti*, corresponding to torsion angles of –80 to –180 and 100 to 180°. Conformations where the purine ring is over the sugar are *syn* and correspond to torsion angles of –80 to 100°. These conformations for adenine are shown in Figure 1.

Figure 1. The *anti* and *syn* conformations of dAMP are shown. The bonds defining the glycosidic torsion angle are darkened for emphasis in both conformers. In the *anti* conformer, the torsion is 110° , and in the *syn* conformer the

torsion angle is +60.

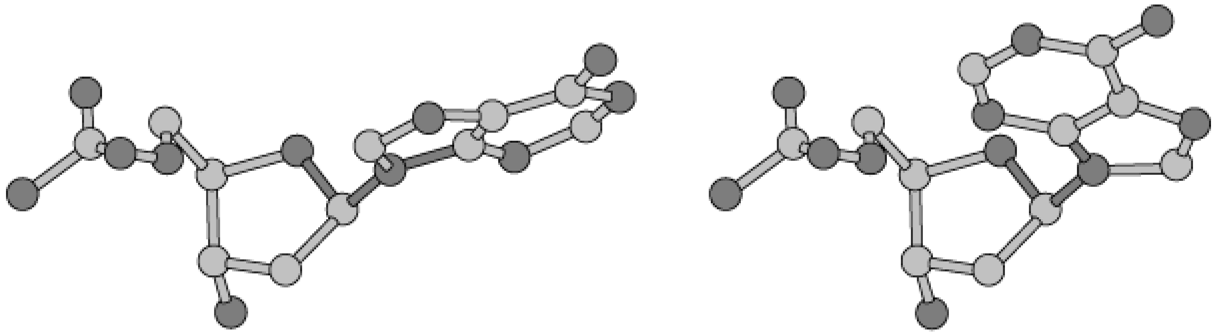

anti dAMP   *syn* dAMP

Bibliography

1. W. Klyne and V. Prelog (1960) Experientia **16**, 521.
2. A. E. V. Haschemeyer and A. Rich (1967) J. Mol. Biol. **27**, 369–384.
3. IUPAC-IUB Commission on Biochemical Nomenclature (1983) Eur. J. Biochem. **17**, 193–201.

Suggestions for Further Reading

4. C. R. Cantor and P. R. Schimmel (1980) *Biophysical Chemistry, Part I: The Conformation of Biological Macromolecules*, W. H. Freeman, San Francisco, CA.
5. E. L. Eliel et al. (1967) *Conformational Analysis*, Wiley-Interscience, New York.
6. W. Saenger (1984) *Principles of Nucleic Acid Structure*. "Springer Advanced Texts in Chemistry" (C. R. Cantor, ed.), Springer-Verlag, New York.

Antifreeze Proteins

Antifreeze proteins (AFPs) adsorb specifically to the surface of ice. By doing so, they inhibit its growth and cause a nonequilibrium depression of the freezing point below the colligative melting/freezing point (1). This depression, which is referred to as thermal hysteresis (°C), helps organisms to avoid or resist freezing when they encounter ice at temperatures below their colligative freezing points. For example, in polar and cold temperate marine environments bony fishes (teleosts) can encounter icy seawater at its freezing point of ≈ –1.9°C, which is over 1°C colder than their colligative freezing point of ≈ –0.7°C. Those fishes that have adapted to this environment produce high concentrations of AFP in their blood (10–25 mg/mL) that can depress their freezing point by the crucial 1°C needed for survival. For practical reasons, AFPs (sometimes known as thermal hysteresis proteins) have been best characterized in fish, but have also been found in insects, plants, and bacteria that encounter subzero conditions. Not all of these organisms resist freezing. In those that do freeze, AFPs may enhance their freeze tolerance by keeping ice crystals from growing (recrystallizing) in the frozen state (2). Recrystallization of ice occurs as the melting temperature is approached and ice becomes more dynamic. It is effectively inhibited by very low AFP concentrations (µg/mL). Although there are reports of AFPs neutralizing ice nucleators (3) and of having protective effects on cells above 0°C (4), the two well-established functions of macromolecular antifreezes, thermal hysteresis and inhibition of ice recrystallization, are related activities that depend on AFP interaction with ice by an absorption-inhibition mechanism.

1. Inhibition of Ice Growth

In ice, each water molecule makes four tetrahedrally oriented hydrogen bonds to neighboring molecules, and the resulting ice lattice has an underlying hexagonal symmetry. When an aqueous solution is cooled in the presence of an ice crystal, water adds preferably to the atomically rough prism surfaces of the crystal much faster than to the two smoother basal planes. At slight undercooling below the freezing point, the prism surfaces are curved, and the ice grows radially as a disk (Fig. 1). Most solutes are swept aside by the expanding ice front. However, AFPs with a specific affinity for an ice surface plane become adsorbed to that surface and cause growth inhibition that further defines the surface plane and typically shapes the ice crystal into a hexagonal bipyramid. The basis for growth inhibition at the surface of ice is that water is forced to add to the lattice between the bound AFP (1, 5). These submicroscopic ice fronts are constrained to grow with a surface curvature that makes it thermodynamically unfavorable for water to join the lattice, which in turn leads to a local depression of the freezing point below that of the bulk solvent. Rather than completely covering the surface, AFPs have been likened to buttons on a mattress (Fig. 1d).

Figure 1. i) In the absence of AFP, a single ice crystal from the melt will grow fastest along the crystallographic *a* axes to form a disk with curved prism surfaces. ii) View of disk perpendicular to i) with *c* axis perpendicular to the page. iii) AFP adsorption to any aspect of the prism surface will force the crystal to become a hexagonal bipyramid. iv) The inset shows a section of the surface illustrating the submicroscopic ice front curvature between bound AFPs.

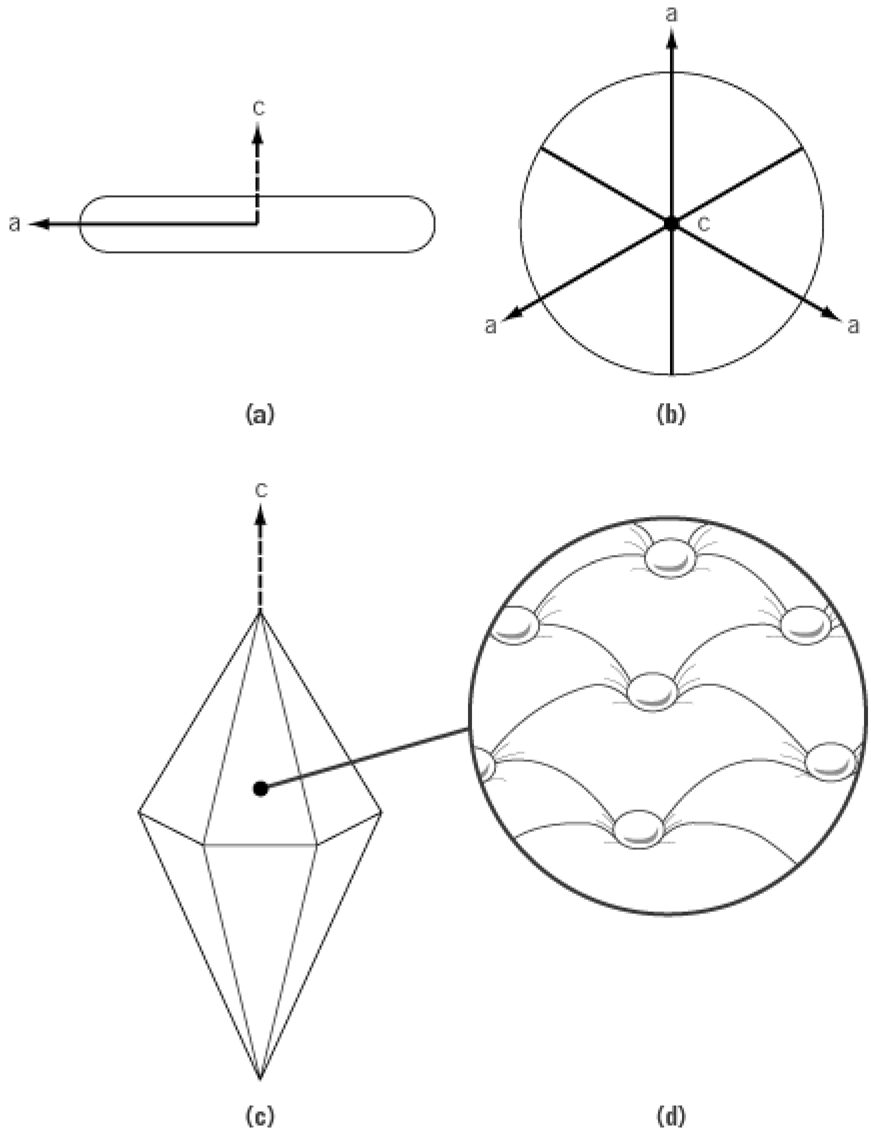

The relationship between thermal hysteresis and AFP concentration is nonlinear. Thermal hysteresis increases hyperbolically with increasing AFP concentration and approaches a plateau value of between 1 and 1.5°C for fish AFPs and 5 to 6°C for insect AFPs. If the temperature falls below the nonequilibrium freezing point at moderate to high AFP concentrations, the ice crystal will grow uncontrollably. At low AFP concentrations and moderate undercooling, the ice front will overgrow bound AFPs. This phenomenon has been used to deduce the ice surface to which AFPs bind by growing ice in a dilute AFP solution and then allowing it to sublime (ice etching) (5). The position of the AFP residue etch on the ice indicates its binding plane and, in some cases, its orientation of binding on that plane.

2. Adsorption of AFPs to Ice

One of the most intriguing features of AFPs is their structural diversity. In fish, there are at least five unrelated types, which are also different from insect AFPs (Fig. 2). It is likely that additional types will be discovered. They are so different that it has not been possible to identify a shared sequence or structural motif that could explain their common ice-binding activity. An added complication is that they bind to different ice surface planes (6). Early models for binding of AFPs to ice relied on a hydrogen-bonding match to the ice lattice (5, 7). However, it has been argued that hydrogen bonding of AFPs to liquid water is energetically favored over binding to ice (8). Also, correct identification of the ice-binding sites now shows them to be more hydrophobic than originally thought (9). One structural feature that AFPs have in common is an extensive region of intimate surface complementarity between the AFP and ice. Thus the energetic contributions to binding could include van der Waals interactions over the AFP–ice interface, some hydrogen bonds, and an entropic component from not having to solvate the AFP and ice surfaces in contact (10)

Figure 2. AFP structures. The 3D structures of Type I AFP from winter flounder (1WFA); Type II AFP from sea raven (2AFP); Type III AFP from ocean pout (1MSI); beetle AFP (1EZG); and moth AFP were solved by X-ray crystallography or nuclear magnetic resonance. The approximate masses of the proteins are indicated in kDa.

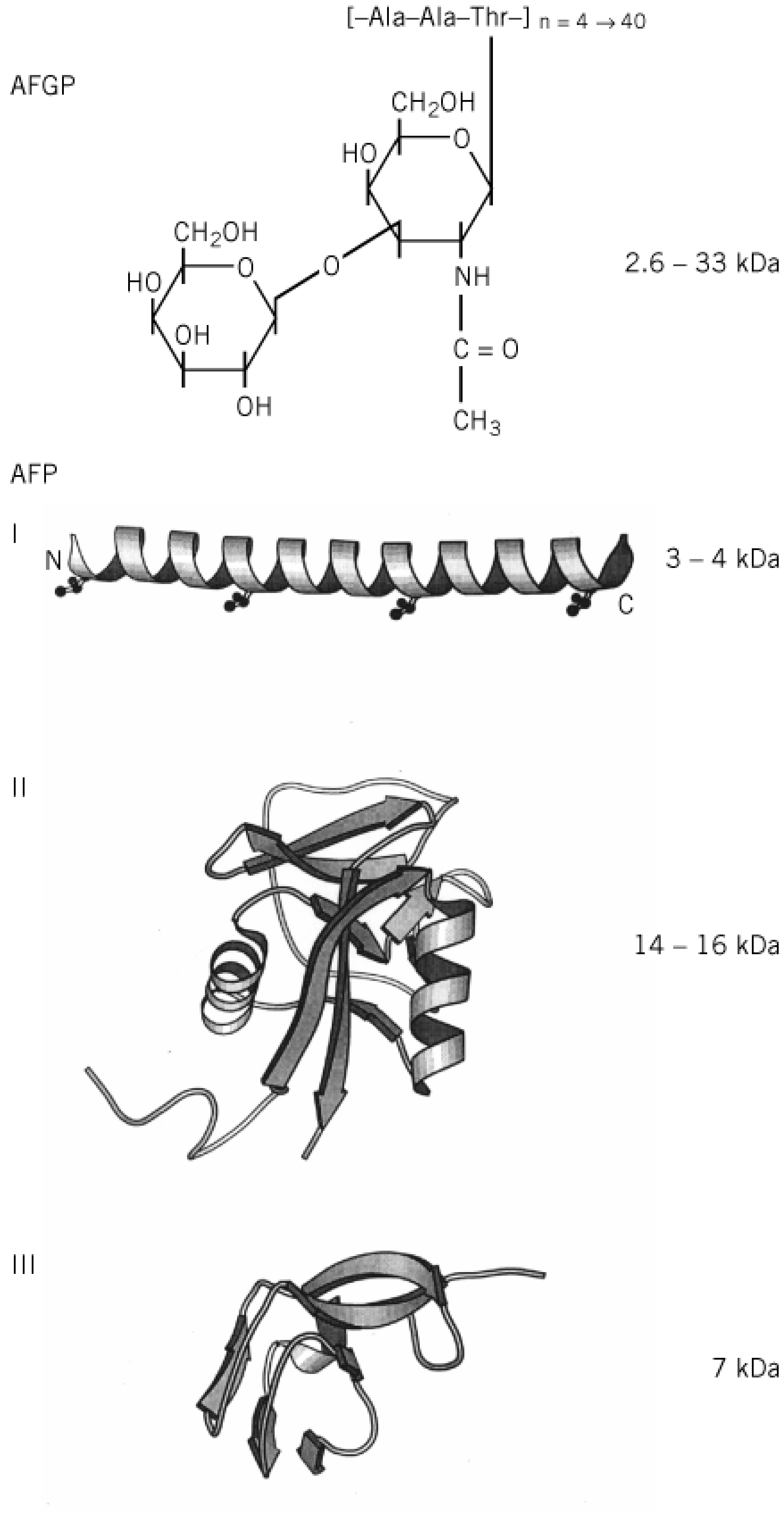

3. Evolution of AFPs

Fish AFPs have been classified into five different types. Antifreeze **glycoproteins** (AFGPs) are polymers of the tripeptide repeat Ala-Ala-Thr with a disaccharide (b-D-galactopyranosyl-(1→3)-2-acetamido-2-deoxy-a-D-galactopyranose) attached to the Thr. Type I AFP is an alanine-rich single a-helix. Type II AFP is a globular protein with sequence homology and structural similarity to the carbohydrate recognition domain of calcium-dependent lectins. Type III AFP is a smaller protein with a unique ß-sandwich fold that is homologous to a portion of sialic acid synthase. The most recently discovered (Type IV) AFP has homology to apolipoprotein E and is thought to be a helix-bundle protein.

It is clear that the different AFP types have distinct origins, which suggests that they have been independently co-opted as antifreezes relatively recently in the 175-million-year radiation of the bony fishes (11). Indeed, there are now several examples of very closely related fishes producing different AFP types and at least one clear example of distantly related fishes producing the same type through **convergent** evolution (12). This pattern of recent evolution is reinforced by the observation that AFP gene families show evidence of extensive **amplification**, often with the AFP genes organized as tandem repeats and with substantial variation in gene dosage (13). The diversity of AFP types is also reflected in their expression and processing. AFP genes are either constitutively expressed or are regulated by a variety of cues, including temperature, photoperiod, and hormonal cycles (14). Fish AFPs are typically produced in the liver as pre-proteins for secretion into the serum with or without a pro-sequence. The small antifreeze glycoproteins are produced from a large polyprotein by both **proteolysis** and glycosylation (12). In winter flounder, the external tissues, skin, scales, fins, and gills produce **isoforms** representing a subclass of Type I AFP that appears to lack a signal sequence (15).

Not unexpectedly, plant and insect AFPs are also different. AFPs from winter rye appear to be homologs of three types of extracellular plant pathogenesis-related sequences, namely endochitinases, endoglucanases, and thaumatin-like proteins (16), and carrot AFP is related to polygalacturonase inhibitor (17). These similarities reinforce the links between AFPs and sugar/polysaccharide-binding proteins. Plant AFPs appear to be more active in ice recrystallization inhibition than thermal hysteresis, whereas insect AFPs show considerably more thermal hysteresis activity than fish AFPs. AFPs from moths and beetles have distinct origins, and yet they both form ß-helices with similar threonine-rich ice-binding sites (18, 19). In some terrestrial insects that can resist freezing at temperatures down to –30°C, AFPs may be part of a suite of cryoprotective mechanisms that include elevated polyol levels and the elimination of ice nucleators that would interfere with supercooling.

4. Conclusion

Although adsorption-inhibition is the generally accepted mechanism of AFP action, the energetics of tight binding to ice are not yet fully understood. Other areas of current research include the basis for the hyperactivity of insect AFPs, activities of AFPs other than thermal hysteresis, and applications for AFPs in conferring freeze tolerance/resistance to unprotected organisms.

Bibliography

1. P. W. Wilson (1993) Cryo-Letters **14**, 31–36.
2. C. A. Knight, A. L. DeVries, and L. D. Oolman (1984) Nature **308**, 295–296.
3. A. Parody-Morreale, K. P. Murphy, E. DiCera, R. Fall, A. L. DeVries and S. J. Gill (1988) Nature **333**, 782–783.
4. B. Rubinsky, A. Arav, and G. L. Fletcher (1991) Biochem. Biophys. Res. Commun. **180**, 566–571.
5. C. A. Knight, C. C. Cheng and A. L. DeVries (1991) Biophys. J. **59**, 409–418.
6. C. C. Cheng and A. L. DeVries (1991) *Life Under Extreme Conditions* (G. di Prisco, ed.), Springer-Verlag, Berlin, pp. 1–14.
7. D. Wen and R. A. Laursen (1992) Biophys. J. **63**, 1659–1662.

8. A. D. J. Haymet, L. G. Ward, and M. M. Harding (1999) J. Am. Chem. Soc. **121**, 941–948.
9. J. Baardsnes, M. E. Houston, Jr., H. Chao, R. S. Hodges, C. M. Kay, and P. L. Davies (1999) FEBS Letters **463**, 87–91.
10. F. D. Sönnichsen, C. I. DeLuca, P. L. Davies and B. D. Sykes (1996) Structure **4**, 1325–1337.
11. G. K. Scott, G. L. Fletcher, and P. L. Davies (1986) Can. J. Fisheries Aquatic Sci. **43**, 1028–1034.
12. L. Chen, A. L. DeVries, and C. H. C. Cheng (1997) Proc. Natl. Acad. Sci. USA **94**, 3817–3822.
13. C. L. Hew, N. C. Wang, S. Joshi, G. L. Fletcher, G. K. Scott, P. H. Hayes, B. Buettner, and P. L. Davies (1988) J. Biol. Chem. **263**, 12049–12055.
14. P. L. Davies, C. L. Hew, and G. L. Fletcher (1988) Can. J. Zool. **66**, 2611–2617.
15. Z. Gong, K. V. Ewart, Z. Hu, G. L. Fletcher, and C. L. Hew (1996) J. Biol. Chem. **271**, 4106–4112.
16. W. C. Hon, M. Griffiths, A. Mlynraz, Y. C. Kwok, and D. S. C. Yang (1995) Plant Physiol. **109**, 879–989.
17. D. Worrall, L. Elias, D. Ashford, M. Smallwood, C. Sidebottom, P. Lillford, J. Telford, C. Holt, and D. Bowles (1998) Science **282**, 115–117.
18. Y.-C. Liou, A. Tocilj, P. L. Davies, and Z. Jia (2000) Nature **406**, 322–324.
19. S. P. Graether, M. J. Kuiper, S. M. Gagne, V. K. Walker, Z. Jia, B. D. Sykes, and P. L. Davies (2000) Nature **406**, 325–328.

Suggestions for Further Reading

20. M. Griffith and K. V. Ewart (1995) Antifreeze proteins and their potential use in frozen foods. Biotechnol. Adv. **13**, 375–402.
21. Y. Yeh and R. E. Feeney (1996) Antifreeze proteins: structures and mechanisms of function. Chem. Rev. **96**, 601–617.
22. P. L. Davies and B. D. Sykes (1997) Antifreeze proteins. Curr. Opin. Struct. Biol. **7**, 828–834.
23. K. V. Ewart, Q. Lin, C. L. Hew (1999) Structure, function and evolution of antifreeze proteins. Cell. Mol. Life Sci. **55**, 271–283.
24. J. G. Duman (2001) Antifreeze and ice nucleator proteins in terrestrial arthropods. Annu. Rev. Physiol. **63**, 327–357.
25. G. L. Fletcher, C. L. Hew, and P. L. Davies (2001) Antifreeze proteins of teleost fishes. Annu. Rev. Physiol. **63**, 359–390.

Antigen

The historical definition of an antigen, given for many years in immunology textbooks, is a rather circular one, because it describes the antigen as a foreign substance that induces upon penetration in an animal (or a human being) the production of an antibody with which it will combine specifically, *in vivo* or *in vitro*. This classical antibody response is a characteristic of vertebrates. Although not basically wrong, this definition necessitates some comments addressing three points: (*1*) antibody, (*2*) induction, and (*3*) foreignness.

1. Antibody

When this definition was proposed, the immune response was characterized solely by the production of antibodies. When it was realized, in the 1960, that the specific functions of the immune system relied on two distinct types of lymphocytes, B cells and T cells, it became clear that the immune response could no longer be limited to the production of antibodies. B and T cells “recognize” the antigen, but in very different ways. B cells express immunoglobulins at their surface, whereas T cells express the so-called T-cell receptor (TCR). By extension, surface immunoglobulins are also given the name of B-cell receptor (BCR), by analogy with the TCR. Once stimulated by an antigen, in combination with other signals (**cytokines**), the B cells differentiate into plasma cells that will express a soluble form of immunoglobulins, also known as *antibodies* or *circulating antibodies*, because they are free in the bloodstream. Immunoglobulins and TCR are constructed on the same general pattern, but are encoded by discrete sets of **genes**. They interact with the antigen in very different manners. The immunoglobulins—or antibodies—interact directly with a nativeform of the antigen, through a small portion of this antigen called the *antigenic determinant* or epitope. The TCR does not recognize the antigen as a whole, but interacts witha fragment of it, which results from **antigen processing** and presentation. This has been well studied for **protein** antigens, which are cleaved into peptides (the processing step) in the so-called antigen-presenting cells (macrophages, dendritic cells, etc.), which will then reexpress these peptides at their surface, in close association with molecules encoded by genes of the major histocompatibility complex (MHC) (presentation step). Finally, the TCR will bind to both the peptide and the MHC-presenting molecule. The peptide derived from the antigen and that interacts with the corresponding TCR is describedas the “T-epitope.”

2. Induction

For a long period of time, in fact until it became possible to work on the chemistry of antibodies in the beginning of the 1960, immunochemists centered their interest on the most accessible partner of the antigen–antibody complex—that is, the antigen, for which simple models of well-defined structure could be worked out. Although somewhat frustrating for a physiologist (this would be like an enzymologist exclusively studying substrates), this approach shed light on the exquisite specificity of recognition by the immune system, thanks mostly to the pioneering work of Landsteiner (1) and the discovery of haptens. Haptens are small molecules that are unable to stimulate the immune system, but may bind to an antibody. To produce this antibody, the hapten had to be conjugated to a protein that served as a carrier, conferring the property of stimulating the immune system. This observation clearly indicated that induction and recognition were two separate properties of an antigen. To clarify this, it was proposed to distinguish antigenicity from immunogenicity and, consequently, an antigen from an immunogen. Antigenicity describes the chemical structures that condition interaction with an antibody or with a TCR, whereas immunogenicity defines the properties of a molecule to induce an immune response. This distinction is far from pure semantics. A protein, considered as a typical “natural” immunogen, has the dual characteristics of a carrier, which is involved in processing and presentation, and of a hapten (in fact a mosaic of haptens) represented by the B epitope. This duality is of central importance for the immune system, in that it implies a close cooperation between B, T, and antigen-presenting cells. In most cases, an antibody response requires cooperation with the T-cell compartment, leading to the distinction of T-dependent antigens, as opposed to T-independent ones, which can stimulate B cells directly without this T-cell “help.”

3. Foreignness

At the end of the nineteenth century, the first antigens that were identified were pathogens: bacteria, **viruses**, parasites, or toxins of various origins. It was soon realized that pathogenicity and immunogenicity were not linked and that a huge variety of cells or molecules could induce an immune response, providing that they were foreign to the animal it was injected into. Furthermore, this requirement of foreignness was strengthened by the famous aphorism “horror autotoxicus” put forward in 1901 by Ehrlich, to indicate that the immune system could not be stimulated by self-components, leading to the concept that it was a master of self–nonself discrimination. Due to independent observations of Grubb, Oudin, and Kunkel (2-4), it became apparent that this distinction between self and nonself was not as clear as initially thought. Oudin described three types of antigenic specificities, termed *isotypy*, *allotypy*, and *idiotypy*. Isotypy refers to those specificities that are characteristic of one molecule of one given animal species, for instance the mouse serum albumin. An antibody raised against albumin of one given mouse will react with the albumin of anymouse. Allotypy defines antigenic specificities that are shared by a group of individuals within a given species, as initially shown by Oudin for the rabbit immunoglobulins. This is the case of the human blood groups, for which people of, say, group A share this specificity. Allotypy simply reflects the existence of epitopes (or allotopes) that are encoded by allelic variants (see Alloantibody, Alloantigen). The last type of specificity, idiotypy, is more subtle, and is inherent to the molecules of the immune system itself. It was initially described by Oudin as the characteristics of one antibody molecule, synthesized by one given animal and specific for one given antigen. So, if a rabbit is given antigen X, it will produce an anti-X antibody (or Ab1). If a second rabbit, expressing the same immunoglobulin allotypes, is immunized against the anti-X antibody, it will produce an anti-anti-X antibody (or Ab2). Ab1 is an idiotype, Ab2 an **anti-idiotype**, and the antigenic specificities recognized on Ab1 by Ab2 are called the *idiotopes*. Because it was later shown that Ab1 and Ab2 could be produced as discrete waves within the same animal, it was clearly realized that the self–nonself distinction was not so obvious. The horror autotoxicus dogma had also to be revisited when it was shown by Avrameas, and extended by Coutinho (5), that a low level of natural autoantibodies was consistently present in every individual, as well as autoreactive T-cell clones. Such natural antibodies have no pathogenic effect,as opposed to those identified in certain autoimmune diseases, for reasons that are still not completely understood.

The term *antigen* covers a huge number of structures, from cells and macromolecular complexes, to relatively small molecules, the lower limit in molecular weight being of the order of a few thousand. Ultimately, and whatever the source of the materials considered, proteins and, to a lesser extent, polysaccharides are the main antigens. Proteins are representative of the T-dependent antigens, which implies processing and presentation. Depending upon their size, the potential number of discrete epitopes of one given antigen may vary from a very small number to several tens, in roughly linear proportion with the exposed area of the molecule. Polysaccharides behave most frequently as T-independent antigens. They are frequently constituents of the bacterial surface and are thus important for the preparation of vaccines against these microorganisms. Another example of polysaccharide antigens is given by the major blood groups in humans. Some macromolecular complexes, such as bacterial lipopolysaccharides, have been studied extensively because they also behave as polyclonal potent mitogenic activators of B cells. Nucleic acids are considered poor immunogens, although they clearly constitute a target for autoantibodies in systemic lupus erythematosus, a severe autoimmune disease. More recently, DNA has been tentatively used as a vaccine, in the form of expression vectors encoding a protein that acted secondarily as an immunizing antigen.

Detailed analysis of the antigenic determinants or epitopes of natural antigens is a difficult task and has necessitated the use of models, among which the most extensively studied in the 1960s and 1970s were polysaccharides by the group of Kabat at Columbia University (6). Based on the binding inhibition of dextran (a polymer of glucose) to anti-dextran antibodies by oligosaccharides of various lengths, the range of size of an epitope, and hence that of the corresponding antibody combining site, was estimated to be between 3 and 6 monosaccharide units. A similar approach was taken by the group of Sela at the Weizmann Institute, with synthetic peptides that mimicked the structure of natural proteins. Direct analysis of natural peptide epitopes with the corresponding antibody was made much later by X-ray crystallography and gave a clear picture of the organization of the antibody combining site. The central message is that there is a huge diversity in size and form of natural epitopes. At the surface of a protein, the number of amino acid residues that interact with the antibody combining site varies from a few to about 20. The variation in both size and number of epitopes at the antigen surface contribute a large part of the heterogeneity of the immune response.

See also entries Antigen Processing, Presentation, Epitope, Immunogen, Idiotypes, and

Superantigens, Xenogeneic.

Bibliography

1. K. Landsteiner and J. van der Scheer (1936) On cross-reactions of immune sera to azoproteins. J. Exp. Med. **63**, 325–339.
2. R. Grubb (1956) Agglutination of erythrocytes coated with incomplete anti-Rh by certain rheumatoid arthritic sera and some other sera. Acta Path. Microbiol. Scand. **39**, 195–197.
3. J. Oudin (1960) Allotypy of rabbit serum proteins. I. Immunochemical analysis leading to the individualization of seven main allotypes. J. Exp. Med. **112**, 107–124.
4. M. Harboe, C. K. Osterland, and H. G. Kunkel (1962) Genetic characters of human -globulins in myeloma proteins. J. Exp. Med. **116**, 719–738.
5. A. Coutinho, M. D. Kazatchkine, and S. Avrameas (1995) Natural autoantibodies. Curr. Opin. Immunol. **7**, 812–818.
6. E. A. Kabat (1956) Heterogeneity in extent of the combining regions of human antidextran. J. Immunol. **77**, 377–380.

Suggestions for Further Reading

7. Y. Paterson (1991) The structural basis of antigenicity. Intern. Rev. Immunol. **7**, 121–218.
8. M. van Regenmortel (1989) Structural and functional approaches to the study of protein antigenicity. Immunol. Today **10**, 266–271.

Antigen Processing, Presentation

Antigen processing and presentation are crucial steps for recognition of protein antigens by T cells. The T-cell receptor (TCR) will not bind a protein directly, as do immunoglobulins, but only as peptides derived from the original protein (processing step) and bound to class I or class II molecules of the major histocompatibility complex, or MHC (presentation step). This applies to helper as well as to effector cytotoxic T lymphocytes and therefore condition severy aspect of the T-dependent immune response. These functions strictly condition immunogenicity and correlate well with the dichotomy between carrier and hapten that had indicated long ago that the hapten part of the complex was recognized as such by the B cell, but was unable to initiate an immune response unless conjugated to a carrier protein (see Antigen). Later it was shown that carrier recognition involved the T helper cell but was also strictly dependent on MHC molecules (MHC restriction). Antigen processing and presentation take place in specialized cells and involve a number of molecules, most of which are encoded by genes of the MHC.

The antigen-presenting cells that are most efficient and most extensively studied are the dendritic cells and the epidermal Langerhans cells. They originate from $CD34^+$ bone marrow precursors and migrate to different tissues. They express FcR e I and FcRII, as well as class I and class II molecules of MHC (in humans, HLA-DR). They internalize the antigen by the **endosomal** pathway and, after processing, reexpress at the cell surface antigen-derived peptides associated with class I molecules. Alternatively, they may present peptides associated with class I MHC after macropinocytosis. They may become interdigitated cells and migrate to secondary lymphoid organs, where they present peptides specifically to CD4 T cells. B cells also behave as antigen-presenting cells, and this is of major importance for the antibody response induced by a T-dependent antigen, because it conditions the necessary direct interaction between T and B cells. Finally, macrophages and monocytes also can present antigens, in addition to their other functions.

There are two main pathways for antigen processing and presentation. One involves association with MHC class I molecules and presentation to CD8 T lymphocytes, while the other involves MHC class II molecules and interaction with CD4 lymphocytes.

1. Class I Pathway

MHC Class I molecules are composed of one a polypeptide chain of 43 kDa that forms a heterodimer with the b2 microglobulin. A peptide binding site, which accommodates nonapeptides, is shared by the first two **domains** of the a chain. There is a huge degeneracy in peptide recognition by one such site, as expected from the low number of different MHC molecules expressed in any individual. Class I molecules are specialized in the presentation of endogenous proteins, synthesized *in situ* by a virus or any intracellular bacteria or parasite. Processing starts as a fraction of these cytosolic proteins are hydrolyzed in the proteasome, a **proteinase**-rich complex involved in **protein degradation**. The resulting peptides will be transported by the specialized TAP gene products to class I molecules in the endoplasmic reticulum. The class I peptide complex will pass through the Golgi apparatus, where the a chain becomes glycosylated before being included in a **secretory vesicle** and finally expressed at the plasma membrane. Interaction with the CD8 T cell involves the TCR, which makes contact with amino acid residues of both the peptide and the class I molecule, whereas CD8 binds solely to the MHC molecule. In addition to this specific interaction, many other cell adhesion molecules contribute to this "immunological synapse," as immunologists sometimes call it.

2. Class II Pathway

MHC class II molecules are composed of two chains, a and b, each containing two domains. The peptide binding site is shared by the a1 and b1 domains. The ab heterodimer associates with the Ii (CD74) invariant chain that prevents any association of an endogenous peptide with the class II molecule. After glycosylation during passage through the Golgi, the complex is packed in the class II vesicles that fuse with endosomes, where the invariant Ii chain is hydrolyzed, leaving only the CLIP peptide still associated with the ab heterodimer. The last step, controlled by HLA-DM molecules, involves an exchange between CLIP and a peptide derived from an exogenous protein antigen. The complex of peptide and class II molecules may now be expressed at the cell surface. A fraction of the class II molecules is reinternalized and may bind new peptides, before being reexpressed at the cell surface. The size of peptides that bind to the class II molecule may vary from between 10 and 30 amino acid residues. Interaction with T cells is somewhat similar to the case previously described, except that it involves essentially CD4 T cells.

CD4 T cells are helper cells that will either (a) interact with the T effector compartment and promote the emergence of cytotoxic T cells or (b) interact with B cells that will ultimately produce antibodies. The latter interaction is of particular interest, because the B cell will act as both a presenting cell and an antibody-producing cell. The T-cell–B-cell interaction is initiated because the B cell presents peptides derived from the specific antigen that had been internalized after binding to the surface immunoglobulin. The antigenic peptide–class II complex will trigger the interacting TCR and activate the T-cell CD3 signaling module. Critical molecules are then produced by the T cell, amongst which are soluble cytokines and one membrane ligand, CD40L, which will bind to its receptor, the CD40 molecule, which is constitutively expressed on the B cell. This is the major signal that will ultimately activate the final phase of differentiation of the B cell and provide the key to clonal expansion and antibody production.

See also entries B Cell, Antibody, T Cell, T-Cell Receptor (TCR), Antigen, Immunogen, and Immune Response.

Suggestions for Further Reading

J. L. Whitton (1998) An overview of antigen presentation and its central role in the immune response. Curr. Top. Microbiol. Immunol. **232**, 1–13.

R. M. Steinman and J. Banchereau (1998) Dendritic cells and the control of immunity. Nature **392**, 245–252.

Antigenic Variation

Antigenic variation is a sophisticated molecular mechanism that allows parasites, **viruses**, and some bacteria to escape the immune response of the invaded host, by changing the nature of their expressed surface antigens. Classical examples are (a) **trypanosomes** amongst parasites and (b) **influzenza virus**.

Trypanosomes are infectious agents transmitted by glossinas and are responsible for severe tropical diseases, such as sleeping sickness in humans. Trypanosomes express surface **glycoproteins** that induce an immune response in the host. Although at any given time one trypanosome expresses one surface glycoprotein, it may switch to the expression of another one, having a slightly different structure. There are large numbers of these different forms (up to 1000), called **variable surface glycoproteins** (VSG), each being encoded by a distinct **gene**. There are two known mechanisms that account for the successive expression of different VSG genes. One is transposition that brings a gene that was present initially as part of one of several gene clusters, scattered on different chromosomes, to one telomere end. As a consequence of the transposition, that gene is expressed, until another one becomes functional. An alternative mechanism is a change in the control of transcription of expression sites. As the structure varies from one VSG to another, there is a permanent change in antigenicity of the parasite population, thereby ensuring escape from the immune mechanisms of the host. Although a large number of genes are potentially active, only a limited fraction is used, so that the repertoire of different VSGs expressed in one host remains limited; this may explain the appearance of chronic immunity in tropical populations.

Viruses use a different mechanism to escape the immune system. One example is that of influenza A, which expresses two surface antigens, hemagglutinin and neuraminidase. It is well known that new variants always arise, sometimes being highly dangerous as they spread rapidly. New variants are the result of mutations, which induce *antigenic drift*, and exchange of genetic material between different virus strains, leading to *antigenic shift*, which has a more drastic impact on spreading of the virus. Antigenic variation of viruses is a major drawback in preventing infection (see Virus Infection, Animal). One approach is to prepare modified strains by site-directed mutagenesis and thus produce vaccines that might anticipate their natural variation.

A more recent problem of antigenic variation is that by HIV, which mutates rapidly, leading to the rapid accumulation of numerous variants within the same patient and providing a particularly efficient way for the virus to escape the immune system. Added to the fact that lymphocytes themselves area major target for this virus, this stresses the unusual danger of this virus.

Suggestions for Further Reading

G. A. Cross, L. E. Wirtz, and M. Navarro (1998) Regulation of vsg expression site transcription and swtiching in Trypanosoma brucei. Mol. Biochem. Parasitol. **91**, 77–91.

S. Subbarao and G. Schochetman (1996) Genetic variability of HIV-1. AIDS **10** (Suppl. A), S13–S23.

Anti-Idiotype Immunoglobulins

Every biologist is familiar with the fact that injection of an antigen into an animal induces an immune response that results, among other things, in the production of specific antibodies. So, if a mouse is given antigen X, it will produce the corresponding anti-X antibody. If we now purify this anti-X antibody and inject it into a mouse of the same strain, (ie, expressing the same **allotypes** as the first mouse), the second mouse will produce an antibody that will react with the anti-X antibody and that represents an anti-anti-X antibody. This defines the idiotypic specificities, which were first described independently in the 1960s by Oudin (1) in the rabbit and by Kunkel (2) in humans. These specificities are located on the **variable regions** of both the heavy and the light chains and are the result of epitope(s) [in this case we use the term of idiotope(s)], related at least in part to the antibody combining site of anti-X. It was shown subsequently that this game could be played one step further: If we now inject a third mouse with the anti-anti-X molecule, the mouse will make anti-anti-anti-X antibodies. Immunologists proposed a simplified nomenclature that reads

$$X \neg Ab1 \neg Ab2 \neg Ab3 \cdots$$

where Ab1 is the idiotype, Ab2 is the anti-idiotype, and Ab3 is the anti-anti-idiotype. This constitutes the so-called idiotypic cascade. One observation of particular interest, independently made by the groups of Oudin in Paris and Urbain (3) in Bruxelles, was that some antibodies in the Ab3 population behaved like Ab1, in that they could interact with antigen X, which the animal had never "seen." This led them to consider that Ab2 had structures resembling X, because it could induce the formation of antibodies (Ab3) that behaved as anti-X. Ab2 was thus considered an "internal image" of the antigen. The observation was generalized by Jerne (4), once it was shown that this cascade could take place spontaneously within the same animal and that the level of expression of each antibody could be modulated (up or down, depending upon the experimental conditions). Jerne proposed that the entire population of antibodies of a given individual were organized as a huge network of interactions, leading to a dynamic equilibrium of B lymphocytes. This was called the *idiotypic network*.

Modulation of the repertoire of B cells expressed at any given time by injection of either partner of the cascade was thoroughly investigated during a number of years. Particular attention was paid to the diverse roles exerted by the Ab2 antibodies, because it was demonstrated that two subpopulations, termed Ab2b and Ab2a, had completely antagonistic regulatory effects, resulting either in the production of Ab3 antibodies that were Ab1-like, or in the down regulation of Ab1. Ab2b are anti-idiotype antibodies that contain a typical internal image and are therefore able to stimulate the production of anti-X antibodies, without disposing of the original antigen. This led to the development of numerous attempts to make "idiotypic vaccines." The second type of population, Ab2a, recognizes idiotopes that are outside the antibody combining site of Ab1, and they appeared quite suitable to repress undesirable antibodies (ie, autoantibodies that have a pathogenic effect in autoimmune diseases).

The theoretical interest of idiotypic vaccines is to function as surrogate for antigens that are difficult to use for immunization, either because they are difficult to isolate, are poorly immunogenic, or present a potential hazard. Many attempts have been made, especially for **viruses**, including HIV, and parasites such as schistosomiasis. Antibodies were generally produced, but it turned out that in most (if not all) cases they were poorly neutralizing, and the protective effect *in vivo* was too low relative to the high efficiency that is expected from an acceptable vaccine.

Down-regulation of pathogenic autoantibodies encountered in autoimmune disease has also been extensively investigated, and it is still currently used in therapeutics. In fact, one uses immunoglobulin preparations assembled from very large pools of donors that are administered intravenously (IVIg). Although experimental arguments are compatible with the presence of anti-idiotypes, many other factors may account for the down regulation of the patient antibodies.

Finally, an interesting application of the internal image is the isolation of cellular receptors by Ab2b that mimic the corresponding ligand. Numerous examples have been reported and successfully used; the first was the Ab2b of the insulin cascade, which was shown to activate the insulin receptor of the b islet of pancreas. Adrenergic receptors or T3 and T4 thyroid hormone receptors are other examples. This could facilitate receptor isolation by the use of immunoadsorbents prepared with these anti-idiotypic internal image antibodies.

See also entries Autoantibody, Autoimmunity, Idiotypes.

Bibliography

1. J. Oudin and M. Michel (1969) Idiotypy of rabbit antibodies. Comparison of idiotypy of various kinds of antibodies formed in the same rabbit against S. typhi. J. Exp. Med. **130**, 619–629.
2. H. G. Kunkel, M. Mannick, and R. C. Williams (1963) Individual antigenic specificity of isolated antibodies. Science **140**, 1218–1220.
3. J. Urbain, M. Wilker, J. D. Frannsen, and C. Collignon (1977) Idiotypic regulation of the immune system by the induction of antibodies by anti-idiotypic antibodies. Proc. Natl. Acad. Sci. USA **74**, 5126–5129.
4. N. K. Jerne (1974) Towards a network theory of the immune system. Ann. Immunol. **125 C**, 373–389.

Suggestions for Further Reading

5. C. A. Bona (1996) Internal image concept revisited. Proc. Soc. Exp. Biol. Med. **213**, 32–42.
6. R. J. Poljak (1994) An idiotope-anti-idiotope complex and the structural basis of molecular mimicking. Proc. Natl. Acad. Sci. USA **91**, 1599–1600.

Antiparallel Beta-Barrel Motifs

Antiparallel b-barrel motif is a general term that describes several protein motifs observed in protein structures that have in common a barrel-shaped b-sheet structure formed from antiparallel beta-strands. These include the b-barrel, the **Greek key** barrel (formed from two Greek key motifs), and the **jelly roll** barrel (Fig. 1). The different motifs have different connections between the strands in the barrel. Other types of antiparallel b-barrels include the interleukin-1 motif and the **neuraminidase** superbarrel. All these protein barrels comprise only antiparallel b-strands and are therefore classified as all-b structural **domains**. They therefore differ significantly from the TIM barrel, which is classified as an a/b domain and is formed from a parallel b-barrel surrounded on the exterior by a-helices.

Figure 1. Schematic representation of the up and down (or b-meander), Greek key, and jelly roll topologies.

Antiparallel b-barrels can be formed from each of these three protein motifs, which represent different ways of linking consecutive b-strands together into a b-sheet.

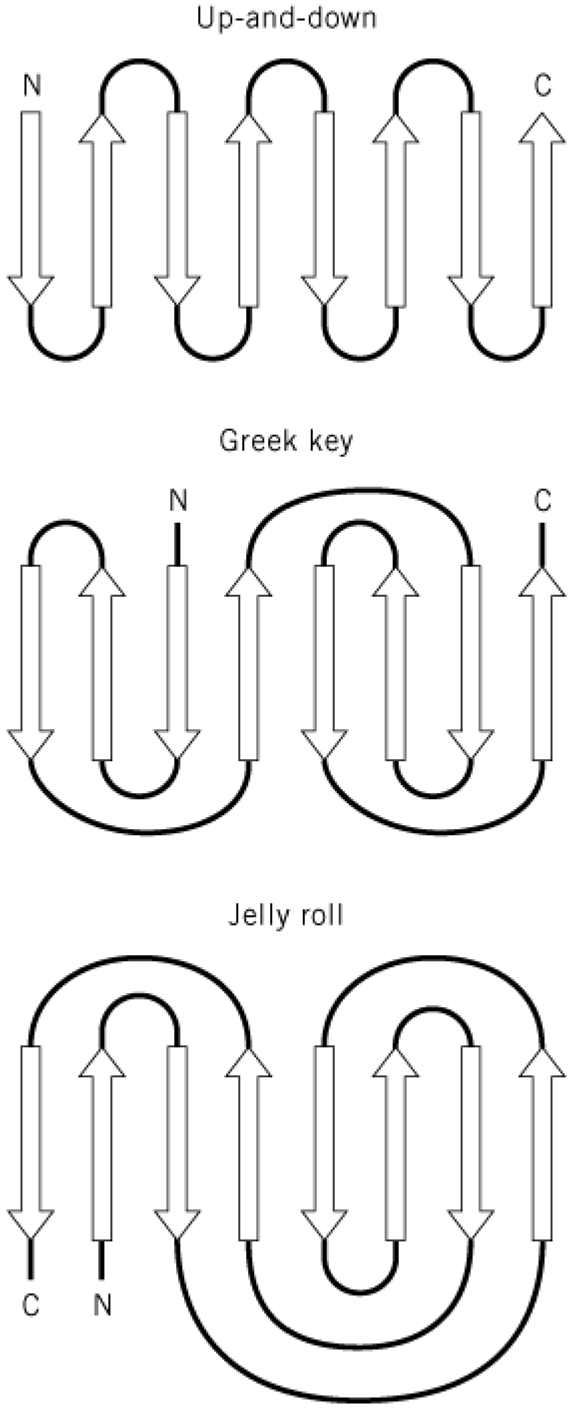

[See also b-Barrel, Greek Key Motif, Jelly Roll Motif, and TIM Barrel.]

Antisense Oligonucleotides

Antisense oligonucleotides are used to **hybridize** to a specific **RNA** molecule *in vivo* and thereby to inhibit its subsequent use. In most cases, the target RNA is a messenger RNA (mRNA), which cannot then be translated into a protein. All that is required is knowledge of the gene's nucleotide sequence, so that an antisense oligonucleotide with the complementary sequence can be synthesized. In this way, the expression of one **gene** can be blocked, and the consequent observed effects help to elucidate the physiological role of the gene and its product.

Selection of the sites in a RNA molecule at which optimal antisense activity may be induced is complex, dependent on the terminating mechanism and influenced by the chemical class of the oligonucleotide. Each RNA displays a unique pattern of sites of sensitivity. Within the phosphorothioate oligodeoxynucleotide class, studies have shown that antisense activity can vary from undetectable to 100% by shifting an oligonucleotide by just a few bases in the RNA target (1, 2). Significant progress has been made in developing general rules that help to define potentially optimal sites in RNA species, but to a large extent this must be determined empirically for each RNA target and every new chemical class of oligonucleotides.

1. Therapeutic Uses

Besides being useful for characterizing the roles of genes, antisense oligonucleotides have the potential for therapeutic use to regulate the expression of certain genes or to block an infection by a pathogenic **bacterium** or **virus**. The therapeutic use of oligonucleotides represents a new paradigm for drug discovery, because oligonucleotides have not been studied before as potential drugs and they are being used to intervene in processes that have not been considered sites at which drugs might act. The affinity and the specificity of binding derive from the hybridization of two oligonucleotides and therefore are theoretically much greater than can be achieved with small molecules. Furthermore, the rational design of the nucleotide sequence of antisense oligonucleotide is much more straightforward than the design of small molecules interacting with proteins. Finally, it is possible to consider the design of antisense drugs to treat a very broad range of disorders, including those not amenable to other types of treatment.

This use of antisense oligonucleotides is still in its infancy, and the initial enthusiasm must be tempered by appropriate reservations concerning practical aspects. To be useful as a drug, an antisense oligonucleotide must be much more stable than ordinary nucleic acids, and it must be able to reach its desired site of action, the interior of a cell. Questions about the technology reduce to, can oligonucleotide analogs be created that have appropriate properties to be drugs? Specifically, what are the pharmacokinetic, pharmacological, and toxicological properties of these compounds and what are the scope and potential of the medicinal chemistry of oligonucleotides? Answers to many of these questions are available now.

2. Phosphorothioate oligodeoxynucleotides

To address the problem of stability, nonconventional oligonucleotides not susceptible to degradation or to hydrolysis by nucleases have been designed. Of the first generation of oligonucleotide analogs, the phosphorothioate class is best understood and has produced the broadest range of activities (3). Phosphorothioate oligonucleotides differ from normal in that one of the nonbridging oxygens in the phosphate group is replaced by a sulfur. The resulting compound is negatively charged, chiral at each phosphorothioate, and much more resistant to nucleases than a phosphodiester bridge.

2.1. Hybridization

The hybridization of phosphorothioate oligonucleotides to DNA and RNA has been thoroughly characterized. The melting temperature (T_m) of a phosphorothioate oligodeoxynucleotide bound to RNA is lower than for a corresponding phosphodiester oligodeoxynucleotide by approximately 0.5° C per nucleotide. Compared to RNA duplex formation, a phosphorothioate oligodeoxynucleotide has a T_m approximately 2.2°C lower per nucleotide. This means that, to be effective *in vitro*, phosphorothioate oligodeoxynucleotides must be relatively long, typically at least 17 to 20 nucleotides, and invasion of double-stranded regions of the target RNA is difficult (4-7).

2.1.1. Interactions with Proteins

Phosphorothioate oligonucleotides bind to proteins. These interactions can be (3) nonspecific, sequence-specific, or structure-specific, each of which may have different characteristics and effects. Nonspecific binding to a wide variety of proteins has been demonstrated, most thoroughly with serum albumin. The affinity of such interactions is low. The **dissociation constant** (K_d) for albumin is approximately 200 µM, about the same as for its binding of aspirin or penicillin (8-10). Phosphorothioates also interact with **nucleases** and **DNA polymerases**; they are slowly metabolized by both endo and **exonucleases** and are **competitive inhibitors** of these enzymes (11). In an RNA–DNA duplex, phosphorothioates are substrates for ribonuclease H (RNaseH) (12). At higher concentrations, phosphorothioates inhibit the enzyme, presumably by binding as a single strand (11). Again, the oligonucleotides are competitive antagonists for the DNA–RNA substrate.

Phosphorothioates are competitive inhibitors of DNA polymerase a and b with respect to the DNA template and **noncompetitive inhibitors** of DNA polymerases g and d (12). They are also competitive inhibitors for the **reverse transcriptase** of HIV and inhibit its associated RNase H activity (13, 14). They bind to the cell surface protein CD4 and to protein kinase C (15). Phosphorothioates inhibit various viral polymerases (16), and they also cause potent, nonsequence-specific inhibition of RNA splicing (17).

2.1.2. In Vivo Pharmacokinetics

Binding of phosphorothioate oligonucleotides to serum albumin and alpha-2 macroglobulin provides a repository for these drugs in the serum and prevents their rapid renal excretion. Because serum protein binding is saturable, however, intact oligomer may be found in urine with high doses (18, 19), eg, 15 to 20 mg kg^{-1} administered intravenously to rats. Phosphorothioate oligonucleotides are rapidly and extensively absorbed after parenteral administration, as much as 70% within 4 h (20, 21). Distribution of phosphorothioate oligonucleotides from blood after absorption or intravenous administration is extremely rapid. Distribution **half-lives** are less than one hour (18-20, 22). Clearance from the blood and plasma exhibits complex kinetics, with a terminal elimination half-life of 40 to 60 h in all species except man, where it may be somewhat longer (21). Phosphorothioates distribute broadly to all peripheral tissues, although no evidence for significant penetration of the blood brain barrier has been reported. Liver, kidney, bone marrow, skeletal muscle, and skin accumulate the highest amounts (20, 22). Liver accumulates the drug most rapidly (20% of a dose within 1 to 2 hours) and also eliminates it most rapidly (eg, the terminal half-life from liver is 62 h and from renal medulla 156 h). Within the kidney (23), oligonucleotides are probably filtered by the glomerulus, then reabsorbed by the proximal convoluted tubule epithelial cells, perhaps mediated by interactions with specific proteins in the brush border membranes. At relatively low doses, clearance of phosphorothioate oligonucleotides is caused primarily by metabolism (19, 20, 22), mediated by exo- and endonucleases.

2.1.3. Pharmacological Activities

Phosphorothioates also have effects inconsistent with the antisense mechanism for which they were designed. Some of these effects are sequence- or structure-specific. Others result from nonspecific interactions with proteins. These effects are particularly prominent in *in vitro* tests for antiviral activity, when high concentrations of cells, viruses, and oligonucleotides are often incubated together (24, 25). Human immune deficiency virus (HIV) is particularly problematic, because many oligonucleotides bind to the gp120 protein (26). Moreover, uncertainty as to the mode of action of antisense oligonucleotides is certainly not limited to antiviral or just *in vitro* tests (27-29). These observations indicate that, before drawing conclusions, careful analysis of dose-response curves, direct analysis of target protein or RNA, and inclusion of appropriate controls are required. In addition to interactions with proteins, other factors can contribute to unexpected results, such as overrepresented sequences of RNA and unusual structures that may be adopted by oligonucleotides

(26).

A relatively large number of reports of *in vivo* activities of phosphorothioate oligonucleotides have now appeared documenting activities after both local and systemic administration (30). However, for only a few of these reports have sufficient studies been performed to draw relatively firm conclusions concerning the mechanism of action by directly examining target RNA levels, target protein levels, and pharmacological effects, using a wide range of control oligonucleotides and examining the effects on closely related isotypes (31-34). Thus, there is a growing body of evidence that phosphorothioate oligonucleotides induce potent systemic and local effects *in vivo*, suggesting highly specific effects difficult to explain via any mechanism other than antisense.

2.1.4. Toxicological Properties

Phosphorothioate oligonucleotides are not toxic in themselves, but their use is limited by side effects. In rodents, this is immune stimulation (35, 36). In monkeys, it is sporadic reductions in blood pressure associated with bradycardia, which is often associated with activation of C-5 **complement** involving activation of the alternative complement pathway (37). All phosphorothioate oligonucleotides tested to date induce these effects, although there are slight variations in potency depending on their sequence and/or length (36, 38, 39). A second prominent toxicological effect in the monkey is on blood clotting. The mechanisms responsible for these effects are probably very complex, but preliminary data suggest that direct interactions with thrombin are at least partially responsible (40).

In man, the toxicological profile differs. When ISIS 2922 is administered intravitreally to patients with cytomegalovirus retinitis, the most common adverse event is anterior chamber inflammation, which is easily managed with steroids. A relatively rare and dose-related adverse event is morphological changes in the retina associated with loss in peripheral vision (41). ISIS 2105, a 20-mer phosphorothioate designed to inhibit the replication of human papilloma viruses that cause genital warts, has been administered intradermally at doses as high as 3 mg/wart weekly for three weeks. Essentially no toxicities have been observed (42).

2.1.5. Therapeutic Index

An attempt to put the toxicities and their dose-response relationships into a therapeutic context is shown in Fig. 1. This is particularly important because considerable confusion has arisen concerning the potential utility of phosphorothioate oligonucleotides for selected therapeutic purposes as a result of unsophisticated interpretation of toxicological data. As can be readily seen, the immune stimulation induced by these compounds is particularly prominent in rodents and unlikely to be dose-limiting in humans. Nor have hypotensive events in humans been observed to date. This toxicity occurs at lower doses in monkeys than in man and certainly is not dose-limiting in man. On the basis of present experience, the dose-limiting toxicity in man is likely to result from blood clotting abnormalities, associated with peak plasma concentrations well in excess of 10 μg/ml. Thus, it phosphorothioate oligonucleotides have a therapeutic index that supports their evaluation for a number of therapies.

Figure 1. Plasma concentrations of ISIS 2302 at which various activities are observed. These concentrations are those of intact ISIS 23902 and were determined by extracting and analyzing plasma by capillary zone electrophoresis.

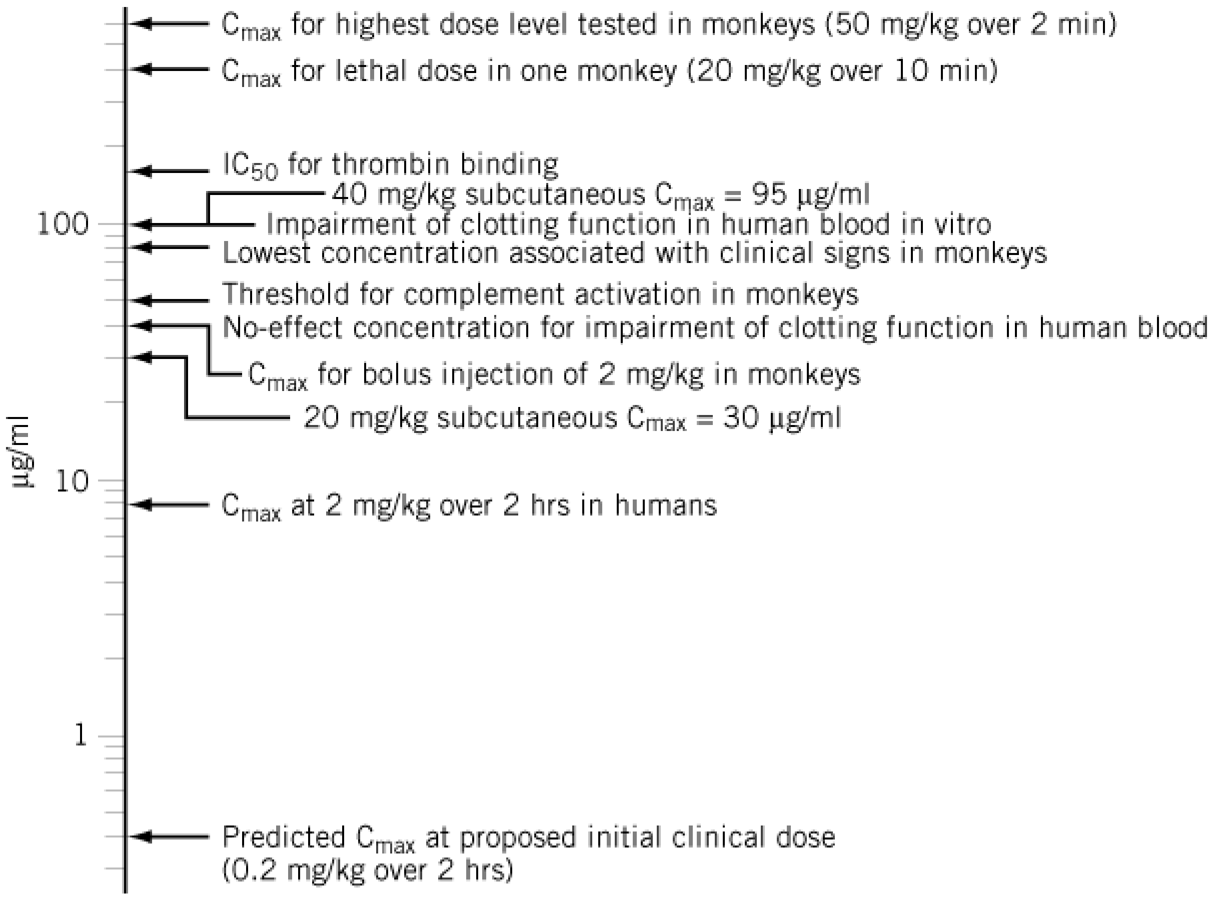

2.1.6. Clinical Activities

Significant therapeutic benefit has been reported in patients with cytomegalovirus retinitis treated locally with fomivirsen (43). ISIS 2302 administered every other day for one month also resulted in statistically significant improvement for five to six months in patients with steroid-dependent Crohn's disease in a randomized, double-blind placebo, controlled trial (44).

2.2. Medicinal Chemistry of Oligonucleotides

The core of any rational drug discovery program is medicinal chemistry. Although the synthesis of modified **nucleic acids** has been a subject of interest for some time (see DNA Synthesis), the intense focus on the medicinal chemistry of oligonucleotides dates perhaps no more than the past five years. Modifications have been made to the base, sugar, and phosphate moieties of oligonucleotides (Fig. 2). The subjects of medicinal chemical programs include approaches to (3) create enhanced and more selective affinities for RNA or duplex structures, the ability to cleave nucleic acid targets, enhanced nuclease stability, (4) cellular uptake and distribution, and *in vivo* tissue distribution, metabolism, and clearance. Arguably, the most interesting modifications to date are those that alter the sugar moiety (45) and the backbon. Modifications such as 2′ methoxyethoxy enhance affinity for RNA, potency *in vivo*, provide a dramatic increase in stability, and reduce the potency for blood clotting and inflammatory effects. Also of interest are a number of modifications that replace the phosphate or the entire phosphate sugar backbone. Several novel chemical classes are being evaluated in animals and will shortly be studied in man, so it seems likely that a variety of chemical classes with differing properties will be available in the near future.

Figure 2. Isis oligonucleotide modifications.

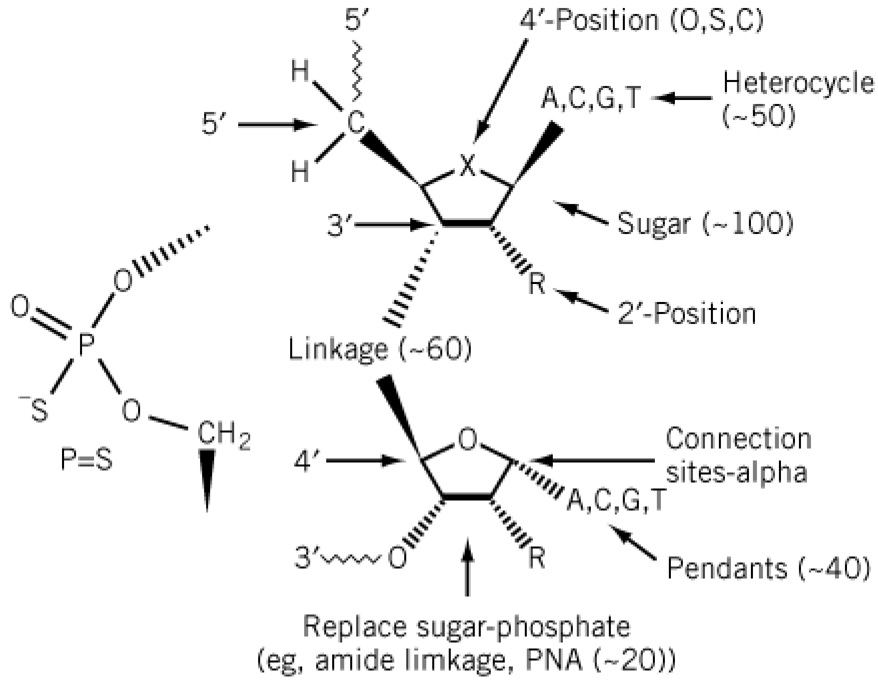

Bibliography

1. M. Y. Chiang et al. (1991) J. Biol. Chem. **266**, 18162–18171.
2. C. F. Bennett and S. T. Crooke (1996) "Oligonucleotide-based inhibitors of cytokine expression and function". In *Therapeutic Modulation of Cytokines* (B. Henderson, and M. W. Bodmer eds.), CRC Press, Boca Raton, pp. 171–193.
3. E. De Clercq, F. Eckstein, and T. C. Merigan (1969) Science **165**, 1137–1140.
4. W. F. Lima et al. (1992) Biochemistry **31**, 12055–12061.
5. T. Vickers et al. (1991) Nucleic Acids Res. **19**, 3359–3368.
6. B. P. Monia et al. (1993) J. Biol. Chem. **268**, 14514–14522.
7. B. P. Monia et al. (1992) J. Biol. Chem. **267**, 19954–19962.
8. S. T. Crooke et al. (1996) J. Pharmacol. Exp. Ther. **277**(2), 923–937.
9. R. W. Joos and W. H. Hall (1969) J. Pharmacol. Exp. Ther. **166**, 113–118.
10. S. K. Srinivasan, H. K. Tewary, and P. L. Iversen (1995) Antisense Res. Dev. **5**(2), 131–139.
11. S. T. Crooke et al. (1995) Biochem. J. **312**(2), 599–608.
12. W. Y. Gao et al. (1992) Mol. Pharmacol. **41**, 223–229.
13. C. Majumdar et al. (1989) Biochemistry **28**, 1340–1346.
14. Y. Cheng, W. Gao, and F. Han (1991) Nucleosides Nucleotides **10**, 155–166.
15. C. A. Stein et al. (1991) Acquired Immune Defic. Syndr. **4**, 686–693.
16. C. A. Stein and Y. C. Cheng (1993) Science, **261**, 1004–1012.
17. D. Hodges and S. T. Crooke (1995) Mol. Pharmacol., **48**, 905–918.
18. S. Agrawal, J. Temsamani, and J. Y. Tang (1991) Proc. Natl. Acad. Sci. USA **88**, 7595–7599.
19. P. Iversen (1991) Anticancer Drug Des. **6**(6), 531–8.
20. P. A. Cossum et al. (1994) J. Pharmacol. Exp. Ther. **269**, 89–94.
21. S. T. Crooke et al. (1994) Clin. Pharm. Ther. **56**, 641–646.
22. P. A. Cossum et al. (1993) J. Pharmacol. Exp. Ther. **267**, 1181–1190.
23. J. Rappaport et al. (1995) Kidney Int. **47**, 1462–1469.

24. R. F. Azad et al. (1993) Antimicrob. Agents Chemother. **37**(9), 1945–1954.
25. R. W. Wagner et al. (1993) Science **260**, 1510–1513.
26. J. R. Wyatt et al. (1994) Proc. Natl. Acad. Sci. USA **91**, 1356–1360.
27. C. M. Barton and N. R. Lemoine (1995) Br. J. Cancer **71**, 429–437.
28. T. L. Burgess et al. (1995) Proc. Natl. Acad Sci USA **92**, 4051–4055.
29. M. Hertl, L. M. Neckers, and S. I. Katz (1995) J. Invest. Dermatol. **104**, 813–818.
30. S. T. Crooke (1995) *Therapeutic Applications of Oligonucleotides*, R. G. Landes, Austin, TX.
31. N. M. Dean and R. McKay (1994) Proc. Natl. Acad. Sci. USA **91**, 11762–11766.
32. N. M. Dean et al. (1996) Cancer Res. **56**(15), 3499–3507.
33. B. P. Monia et al. (1995) Nature Med. **2**(6), 668–675.
34. B. Monia et al. (1996) J. Biol. Chem. **24**(14), 14533–14540.
35. S. P. Henry et al. (1997) Toxicology **116**(1–3), p. 77–88.
36. S. P. Henry et al. Antisense Nucleic Acid Drug Dev., In Press.
37. S. Henry et al. J. Pharmacol. Exp. Ther., In Press.
38. K. G. Cornish et al. (1993) Pharmacol. Commun., **3**, 239–247.
39. W. M. Galbraith et al. (1994) Antisense Res. Dev. **4**(3), 201–206.
40. S. Henry, W. Novotny, and J. Leeds. Submitted.
41. S. L. Hutcherson et al. (1995) Abstracts of the SFO, CA, *35th ICAAC*, p. 204.
42. J. M. Glover et al. (1996) Pharmacol. Exp. Ther., In Press.
43. D. S. Boyer et al. (1997) In *AAO Annual Meeting*, San Francisco.
44. B. R. Yacyshyn et al. N. Engl. J. Med., Submitted.
45. Y. S. Sanghvi, and P. D. Cook (1994) Symposium Series No. 580 American Chemical Society, Washington, DC, p. 232.

Suggestions for Further Reading

46. S. T. Crooke and B. Lebleu (1993) *Antisense Research and Applications*, CRC Press, Boca Raton.
47. S. T. Crooke (1992) Ann. Rev. Pharmacol. Toxicol. **32**, 329–376.
48. S. T. Crooke (1993) FASEB J. **7**, 533–539.
49. S. M. Freier (1993) "Hybridization considerations affecting antisense drugs", In *Antisense Research and Applications* (S. T. Crooke and B. Lebleu, eds.), CRC Press, Boca Raton, pp. 67–82.
50. S. T. Crooke (1995) *Therapeutic Applications of Oligonucleotides*, R. G. Landes, Austin.

Antisera

Antisera have long been the major reagent in immunology, and this field was for years known as serology. An antiserum is the serum of an animal that has been **immunized** against an antigen, or more commonly hyperimmunized, to get the highest possible titer of the desired antibodies. Very clearly, vaccination and serotherapy were the first great miracle in fighting against pathogens, long before the discovery of antibiotics. From a medical standpoint, antisera were used to fight quickly against a pathogen or a toxin, because vaccination takes a long time to generate a host immune response. There are several concerns regarding the use of antisera for therapy in humans or in animals. First, one has to be certain that protection is indeed ensured by antibodies and not exclusively by cell-mediated immunity. This is not a trivial matter, because there are only a limited number of instances in which protection is due primarily to antibodies. Second, the use of antisera from a foreign animal species (heterologous antisera) will induce a strong immunization of the host against all the injected antigens. This results in the appearance, within a week or two, of a local and generalized syndrome, called *serum sickness*, that may include urticaria, local edema, rashes, arthralgia, fever, lymphadenopathy, and, ultimately, severe glomerulonephritis resulting from the formation of immune complexes. This was observed when serotherapy with horse serum was extensively used in humans, especially against **diphtheria** or tetanus. Diphtheria, a bacterial disease, can now be cured with antibiotics, and children undergo a regular schedule of vaccination that actively prevents the disease. Tetanus remains a very severe disease, with an elevated rate of mortality. Serotherapy is still used because antibodies are extremely effective against the toxin; nevertheless, everyone should be revaccinated every 10 years, because this provides the best and safest protection.

Heterologous antisera should be used only in very exceptional occasions—for example, after bites from highly dangerous snakes. Heterologous antisera are being systematically replaced, when appropriate, by purified immunoglobulins, preferentially of human origin. Intravenous immunoglobulins (IVIgs) are used to correct severe immunodeficiencies of the B-cell compartment. For example, this is the case with X-linked agammaglobulinemia (Bruton disease), which is transmitted genetically through the mother and occurs in young boys. This disease is due to a variety of mutations of the BTK gene (for Bruton tyrosine kinase) that result in an early blockage of B-cell differentiation. IVIgs are also used to help patients with chronic or transient hypoglobulinemia. Whenever the deficiency is severe and would necessitate a lifelong treatment, an allogenic bone marrow graft is performed, which restores the immune system of the patient. IVIgs are also used in therapy of autoimmune diseases, although the mechanisms are not absolutely understood, but may be due in part to a reequilibration of the idiotype network. Specific purified antibody of human origin can be prepared in some selected cases. The most popular preparation is the anti-D (Rhesus) immunoglobulins that are used worldwide for prevention of the hemolytic disease of the newborn (see Alloantibody, Alloantigen).

With the start of organ transplantations, many attempts were made to prevent rejection by blocking the immune system of the recipient. Antilymphocyte serum, prepared in rabbits or in horses, has been used but had the usual limitation linked to the induction of serum sickness mentioned above. It could, however, help for a transient difficult acute period of rejection. It has been replaced by a monoclonal antibody, prepared in the mouse and directed against the CD3 (signaling module) of the T-cell receptor. Used for a short period of time, it proved efficient in down-modulating the immune response of the host, with limited risk of immunization against the heterologous immunoglobulin. Genetic engineering has also been proposed to minimize immunization against heterologous determinants. One classical approach is to insert the six specific hypervariable regions of a murine monoclonal antibody in place of the corresponding regions of a human antibody framework, using protein engineering. This engineered antibody is certainly less immunogenic, but it still is, because of the idiotype determinants that cannot be avoided. Fully engineered human monoclonal antibodies would certainly be ideal for human use. This goal is being worked on actively by pharmaceutical companies. Its is not yet practical, and no one has yet succeeded in making stable “natural” human monoclonal antibodies.

Besides the roles in human therapy mentioned above, antisera remain of course reagents of choice for experimental purposes. They may be used to identify new molecules and to purify them with techniques like immunoaffinity chromatography or **immunoprecipitation**, which are powerful tools to isolate rare components, such as membrane proteins, receptors, hormones, or diverse ligands. Monoclonal antibodies have tended to replace antisera, which is partly unfortunate and sometimes a mistake, because conventional antisera can be exquisitely specific and are very efficient, potent tools, with a mosaic of specificities that may of great help to the molecular biologist.

See also entries Immunization and Immunogen.

Suggestion for Further Reading

E. Harlow and D. Lane, eds. (1988) *Antibodies: A Laboratory Manual*, Cold Spring Harbor Laboratory Press, Cold Spring Harbor, NY.

Antitermination Control of Gene Expression

Bacteria have evolved many different complex mechanisms to control both transcription and translation of **genes** in response to environmental changes. In many cases, transcription is controlled at the level of initiation by DNA-binding proteins that either inhibit (repressors) or stimulate (activators) initiation. In addition, transcription can be regulated at the level of elongation. In some cases, transcription of a gene or operon will terminate prematurely in the absence of the action of a positive regulatory molecule. In these cases, antitermination factors allow transcription to read through termination signals and to generate full-length transcripts.

Two fundamentally different mechanisms for antitermination have been described. In one case, RNA polymerase is modified so as to allow it to read through transcription terminators. This type of mechanism controls phage development (1) and expression of rRNA operons (2). The second mechanism, covered in this chapter, involves trans-**acting factors** that interact with **RNA** and prevent formation of the terminator structure. This mechanism is very similar to **attenuation**, but antitermination can be distinguished from attenuation in that the action of the regulatory molecule results in transcription readthrough, with the default pathway being premature termination. In attenuation, the action of the regulatory molecule induces transcription termination, and the default pathway is readthrough.

Three distinct mechanisms that regulate gene expression by antitermination will be reviewed here. These mechanisms differ primarily in the type of biomolecule used as the regulator. The first mechanism uses antiterminator proteins that are activated to bind RNA targets in response to environmental stimuli. In the second mechanism, transfer RNA is used as the regulator. In this case, the degree of aminoacylation (or charging) of the tRNA is used to sense the availability of the cognate amino acid within the cell, to induce expression of genes involved in metabolism of this amino acid. Finally, in the case of the **Escherichia coli** tryptophanase operon, it appears that ribosomes are used as the regulatory molecule. Thus, bacteria have evolved a large number of mechanisms to use different biomolecules to all perform the same task—that is, to alter the conformation of the nascent mRNA to signal RNA polymerase whether it should terminate prematurely or continue transcription of the particular structural gene(s).

1. RNA-Binding Protein-Mediated Antitermination: The Sac/Bgl Family of Antiterminator Proteins

Expression of several catabolic operons in bacteria is regulated by antitermination involving RNA-binding proteins. These proteins prevent formation of Rho-independent transcription terminators in the nascent mRNA upstream of the regulated gene(s) (3). One such system in *E. coli* and several in *Bacillus subtilis*, appear to be highly related based on similarities of their antiterminator proteins as well as their RNA targets. In addition, several other systems function similarly but appear to have arisen independently. A general model for this mechanism is shown in Figure 1.

Figure 1. A general model for antitermination control by the Sac/Bgl family of antiterminator proteins. Under noninducing conditions, transcription starts at the promoter (designated by the arrow) and terminates prematurely, often in a leader region prior to the structural genes. In the presence of inducer, the antiterminator protein is activated to bind to the RAT (ribonucleic antiterminator) RNA. This binding stabilizes an RNA secondary structure involving the RAT, which prevents formation of the overlapping terminator, and transcription continues into the structural genes.

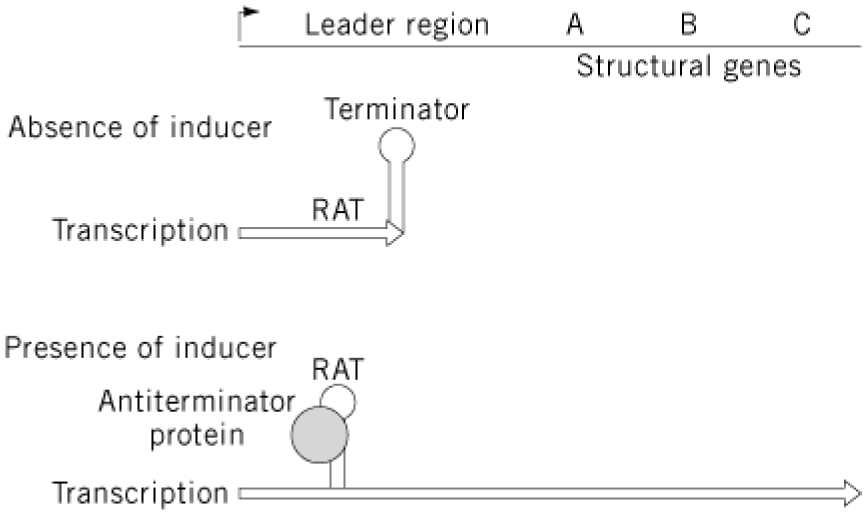

1.1. The *E. coli bgl* Operon

The *E. coli bglGFB* operon encodes all the functions necessary for the regulated uptake and utilization of aromatic b-glucosides. The operon is cryptic in wild-type strains but can become functional through spontaneous mutations. When functional, expression of this operon is regulated by antitermination mediated by the BglG protein in response to the levels of b-glucosides (4). In the absence of inducer, BglG does not bind RNA, and most transcripts terminate at one of two Rho-independent transcription terminators present in the leader region upstream of *bglG* and between *bglG* and *bglF*. When b-glucoside levels are high, BglG binds to an RNA target, named RAT for ribonucleic antiterminator, just upstream of the terminators. This binding stabilizes an alternative antiterminator RNA structure, which prevents formation of the terminator, thus allowing transcription to continue and the operon to be expressed.

The RNA-binding activity of BglG is regulated by **phosphorylation** mediated by BglF. In the absence of b-glucosides, BglF phosphorylates BglG, which prevents it from dimerizing and binding to the RAT (5). In the presence of b-glucosides, BglF dephosphorylates BglG, which now dimerizes and binds to the RAT. Phosphorylation of both b-glucosides and BglG is accomplished by transfer of the phosphate group from the same phosphorylated residue, Cys24, in BglF (6). These results suggest that, under conditions in which b-glucoside levels are high, the phosphate group can be transferred from BglG back to Cys24 in BglF. A model has been proposed in which unliganded BglF phosphorylates BglG, and b-glucoside binding induces BglF to undergo a conformational change that activates it to dephosphorylate BglG.

A similar system for b-glucoside utilization exists in the related **Gram-negative** enteric bacterium *Erwinia chrystanthemi*, although in this case the *arb* operon is not cryptic (7). ArbG shows high sequence similarity to BglG, suggesting that it functions analogously in antitermination control of the *E. chrystanthemi arb* genes. Antitermination also appears to control b-glucoside operons in several Gram-Positive Bacteria as well. A putative b-glucoside (*bgl*) operon has also been identified in *B. subtilis* and may be regulated by a similar antitermination mechanism (8). In addition, a protein, BglR, with homology to BglG also controls b-glucoside usage in *Lactococcus lactis* (9).

1.2. The *B. subtilis sac* Genes

Expression of two sucrose utilization operons in *B. subtilis*, *sacPA* (10) and *sacB* (11), is induced by sucrose via transcription antitermination mediated by the RNA-binding proteins SacT and SacY, respectively. SacT and SacY show extensive sequence similarity to each other, as well as to BglG from *E. coli*. The antitermination mechanisms that control these genes also appear to be quite similar to that described above for the *E. coli bgl* operon. Rho-independent transcription terminators exist in leader regions upstream of both *sacPA* and *sacB* and prevent transcription of the structural genes in the absence of the inducer, which is sucrose. In the presence of sucrose, SacT and SacY are activated to bind RAT sequences in the *sacPA* and *sacB* leader transcripts, respectively, and allow transcription to read through into the structural genes (12). Like BglG in *E. coli*, both of these antiterminator proteins are phosphorylated. In the case of SacY, phosphorylation negatively regulates RNA-binding activity and appears to be mediated by SacX (13). SacT is phosphorylated by HPr, a component of the phosphoenolpyruvate **phosphotransferase system**, but the role of this phosphorylation in sucrose-mediated antitermination is less clear (12).

Recently, the protein structure of the RNA-binding domain of SacY has been determined by both NMR (14) and X-ray crystallography (15). The domain exists as a dimer, with each monomer consisting of a four-stranded antiparallel beta-sheet. Several amino acid residues have been identified through genetic, biochemical, and preliminary NMR studies as being important for RNA binding. These residues are clustered on the surface of one side of the protein structure (15).

1.3. Other Examples of Bgl/Sac Type Antiterminators

In addition to the *bgl* and *sac* systems described above, several other operons are regulated by RNA-binding antiterminator proteins with homology to BglG, SacY, and SacT. LicT regulates the *licS* gene, which is involved in b-glucan utilization in *B. subtilis* (16). There is also a RAT sequence overlapping a potential Rho-independent terminator upstream of *licS*.

In *Lactobacillus casei*, the lactose (*lac*) operon is regulated in response to lactose levels by LacT, which shows sequence homology to the other members of the Bgl/Sac family of antiterminators (17). The 5′-leader region of the *lac* mRNA contains a region with sequence similarity to the RAT sequence, as well as a potential stem-loop structure resembling a Rho-independent terminator.

1.4. Antiterminators with No Similarity to the Bgl/Sac Family

Several other systems are regulated by RNA-binding antiterminator proteins that are unrelated to those of the Bgl/Sac family; furthermore, these proteins do not appear to be related to each other. These regulatory systems thus appear to have arisen independently.

In *B. subtilis*, both the *glp* regulon, which is involved in usage of glycerol-3-phosphate, and a histidine-utilization (*hut*) operon are regulated by RNA-binding antiterminator proteins; GlpP (18) and HutP (19), respectively. The amino acid sequences of these antiterminator proteins are not similar to any other antiterminator proteins. Further, the mechanisms by which these antiterminator proteins function appear to be different from those described above, because there are no clear antiterminator RNA secondary structures near the terminators in these operons.

The amidase (*ami*) operon of *Pseudomonas aeruginosa* is regulated by antitermination in response to short-chain aliphatic amides, such as acetamide. The *amiR* gene encodes an antiterminator protein (AmiR), which is negatively regulated by AmiC, apparently through formation of an AmiC-AmiR complex (20). Acetamide destabilizes the AmiC-AmiR complex, leading to antitermination and expression of the operon. AmiR interacts with an RNA target in the 5-leader region of the *ami* mRNA that contains a Rho-independent terminator. However, no clear antiterminator RNA secondary structure is predicted. AmiR binding has been suggested to function in antitermination by interfering directly with formation of the terminator stem-loop structure (20).

In addition to all the catabolic operons described above, one anabolic operon has been shown to be regulated by antitermination. Expression of the *nas* operon of *Klebsiella pneumoniae*, which encodes enzymes required for nitrate assimilation in this bacterium, is induced by nitrate or nitrite. The NasR protein mediates transcription antitermination through a terminator in the leader region of the operon (21). This protein shows weak homology with AmiR in the carboxyl-terminal region.

2. Transfer RNA-Mediated Antitermination

An interesting variation on the antitermination mechanism involves the use of tRNA as the regulatory molecule. This mechanism regulates a large number of aminoacyl-tRNA synthetase genes in Gram-Positive Bacteria (22, 23) and several amino acid biosynthetic operons, including the *ilv-leu*, in *B. subtilis* (24, 25), and the *his* and *trp* operons in *Lactococcus lactis* (26). Expression of these genes is induced specifically by starvation for the corresponding amino acid. In the case of the amino acid operons, insufficient levels of the amino acid leads to increased expression of the corresponding biosynthetic operon. For the aminoacyl-tRNA synthetase genes, increasing the level of the synthetase is thought to allow more efficient charging of the cognate tRNA when the corresponding amino acid pool is low.

A long (approx. 300-nucleotide) untranslated leader region exists upstream of the structural gene(s) of these operons that contains several conserved features, including three stem-loop structures preceding a Rho-independent transcription terminator. Hence, in the absence of the inducing signal, transcription terminates prematurely in the leader region prior to the coding sequences. In addition to the conserved secondary structures, there is an important conserved 14-nucleotide sequence known as the T-box present in each leader region; hence these genes are known as the T-box family. An alternate arrangement of the leader region involving base-pairing between a portion of the T-box and a conserved sequence in the 5′ side of the terminator stem has been proposed to form an antiterminator structure that allows transcription to read through into the structural genes (Fig. 2) (27).

Figure 2. Model for antitermination control by tRNA. Under conditions with adequate levels of the cognate amino acid (aa), the charged tRNA does not interact with the leader region, and the terminator forms. Under conditions of starvation for the appropriate amino acid, the uncharged tRNA interacts with the leader region via base-pairing between the anticodon and the specifier sequence, and by base-pairing between the CCA sequence at the acceptor end of the tRNA with the side bulge of the antiterminator in the leader. These interactions stabilize formation of the antiterminator conformation of the leader transcript, resulting in induction of expression of the gene. The tRNA is shown as the shaded cloverleaf structure, and a boxed “A.A.” attached to the tRNA indicates it is aminoacylated. Adapted from T. M. Henkin (1996) *Annu. Rev. Gen*. **30**, 35–57.

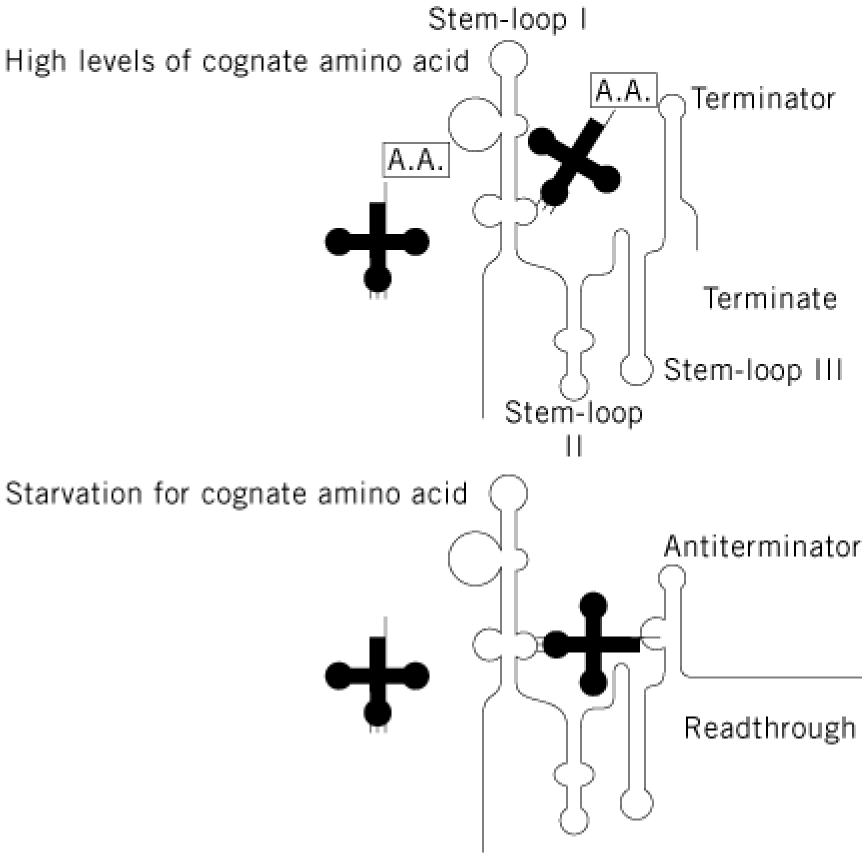

Another important conserved feature of the leader region of these genes is the presence of a triplet sequence corresponding to a codon for the appropriate amino acid for each operon. For example, in *tyrS*, which encodes tyrosyl-tRNA synthetase, the leader contains a UAC tyrosine codon, while the ilv-leu operon leader contains a CUC leucine codon. This triplet is always present in a bulged sequence in Stem-loop I (Fig. 2) and has been shown to be critical for induction in several systems. It was the presence of these triplets that led to the hypothesis that tRNAs play a role in this regulatory mechanism. This triplet was designated the "specifier sequence" because, in the case of the *B. subtilis tyrS* gene, altering the sequence to correspond to a codon for another amino acid switched induction to respond to starvation for the new amino acid (27). Other experiments demonstrated that translation of this codon was not involved in induction and that uncharged tRNA was the inducer (27). In addition, a second interaction between the CCA sequence at the 3′ end of the uncharged tRNA and the complementary UGG sequence in the T-box have been shown to be important (28).

A model for tRNA-regulated antitermination regulation is presented in Fig. 2. Under starvation conditions for the corresponding amino acid, the cognate uncharged tRNA interacts with two sites in the leader region, to induce formation of the antiterminator structure and allow transcription to read through into the coding region. Aminoacylation of this tRNA is predicted to interfere with the interaction at the CCA end and prevent the charged tRNA from binding; the leader transcript then folds into the conformation with the terminator, halting transcription. It is not known if factors in addition to tRNA are required for antitermination. To date, however, it has not been possible to reconstitute tRNA-mediated antitermination in vitro, and several other lines of evidence also suggest that other factors may be involved in this mechanism (23).

In addition to the antitermination mechanism described above, processing of the leader RNA has been shown to play a role in regulating expression of the *B. subtilis thrS* gene (29). Cleavage occurs in the loop of the antiterminator near the T-box sequence and is more efficient under threonine starvation conditions, suggesting that bound tRNA induces both antitermination and RNA processing. This processing increases the stability of the mRNA, which would allow for increased translation and production of the threonyl-tRNA synthetase. Thus induction of expression of this gene in response to threonine starvation occurs at both the level of transcription antitermination and mRNA stability.

3. The *E. coli* Tryptophanase Operon

E. coli and several other microorganisms have the capacity to degrade tryptophan as a source of carbon, nitrogen, and/or energy (30). The degradative tryptophanase operon (*tnaCAB*) of *E. coli* is regulated by catabolite repression (31) and by an antitermination mechanism. Antitermination involves translation of a ***cis***-*acting* 24-residue leader peptide (*tnaC*) containing a critical Trp codon (32, 33), one or more RNA polymerase pause sites between *tnaC* and *tnaA* (34), and Rho termination factor (34). While the precise antitermination mechanism responsible for controlling the *tna* operon is not firmly established, all of the data are consistent with the following model (Fig. 3) (35). During growth in a medium lacking both tryptophan and a catabolite-repressing carbon source, transcription initiation is efficient. As transcription proceeds, translation of the leader peptide occurs as soon as the coding sequence becomes available. Once the translating ribosome reaches the UGA stop codon, ribosome release exposes a *rut* (Rho utilization) site that immediately follows the stop codon. Rho then binds to the *rut* site and begins to translocate in the 3′-direction, until it encounters paused RNA polymerase, ultimately leading to transcription termination upstream of *tnaA*. When cells are growing with inducing levels of tryptophan, TnaC, or a complex of TnaC with an unidentified protein, prevents ribosome release at the *tnaC* stop codon, thereby masking the *rut* site and, hence, blocking Rho interaction with the transcript. Eventually RNA polymerase would overcome the pause signal and transcribe the structural genes encoding tryptophanase (*tnaA*) and a tryptophan **permease** (*tnaB*). This model assumes that there is a fundamental difference between the TnaC peptide, or the TnaC peptide-protein complex, in cells growing with or without tryptophan. It was proposed that such a complex under inducing conditions would prevent ribosome release (35), reminiscent of characterized translation attenuation mechanisms (36). The tryptophanase operon of *Proteus vulgaris* is thought to be regulated by a mechanism essentially identical to that of *E. coli* (37).

Figure 3. Model of *E. coli tna* operon regulation. Under noninducing conditions (no extracellular tryptophan), ribosome dissociation at the *tnaC* stop codon exposes a *rut* site, allowing Rho binding. Rho translocates to the paused RNA polymerase, leading to transcription termination. Under inducing conditions (extracellular tryptophan), ribosome stalling at the *tnaC* stop codon prevents Rho association, leading to transcription readthrough. See text for details. Adapted from C. Yanofsky, K. V. Konan and J. P. Sarsero (30).

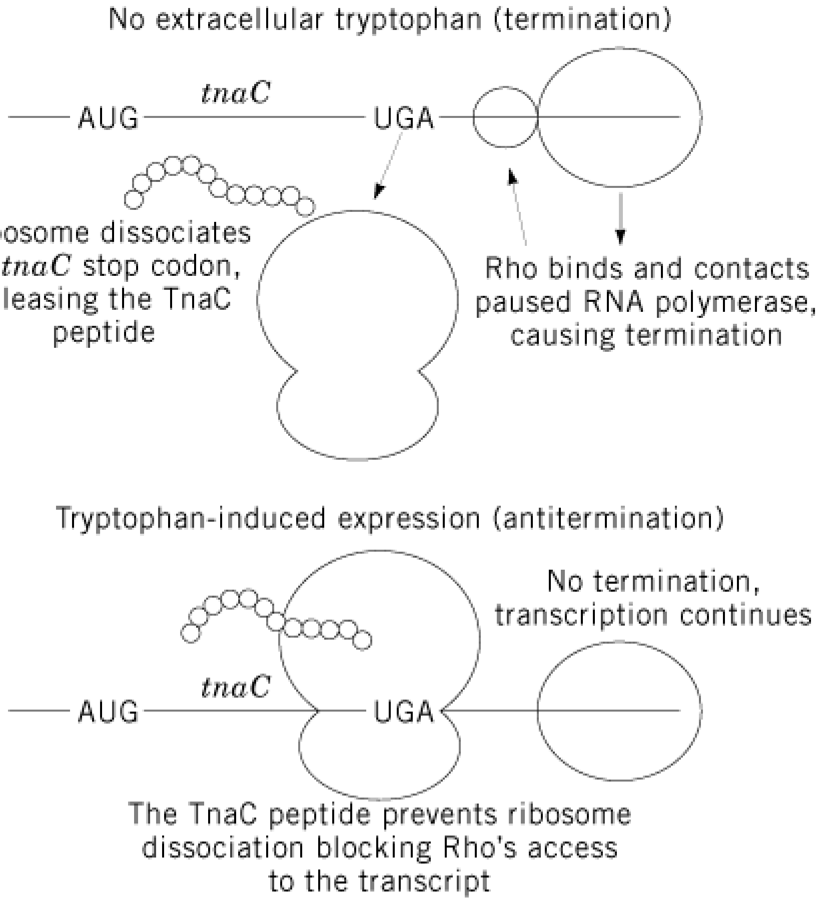

Bibliography

1. D. I. Freidman and D. L. Court (1995) Mol. Microbiol. **18**, 191–200.
2. C. Condon, C. Squires, and C. L. Squires (1995) Microbiol. Rev. **59**, 623–645.
3. B. Rutberg (1997) Mol. Microbiol. **23**, 413–421.
4. S. Mahadevan and A. Wright (1987) Cell **50**, 485–494.
5. O. Amster-Choder and A. Wright (1990) Science **249**, 540–542.
6. Q. Chen, J. C. Arents, R. Bader, P. W. Pestma, and O. Amster-Choder (1997) EMBO J. **16**, 4617–4627.
7. M. El Hassount, B. Henrissat, M. Chippaux, and F. Barras (1992) J. Bacteriol. **174**, 765–777.
8. D. Le Coq, C. Lindner, S. Krüger, M. Steinmetz, and J. Stulke (1995) J. Bacteriol **177**, 1527–1535.
9. J. Bardowski, D. S. Ehrlich, and A. Chopin (1994) J. Bacteriol. **176**, 5681–5685.
10. M. Debarbouille, M. Arnaud, A. Fouet, A. Klier, and G. Rapoport (1990) J. Bacteriol. **172**, 3966–3973.
11. A. M. Crutz, M. Steinmetz, S. Aymerich, R. Richter, and D. Le Coq (1990) J. Bacteriol. **172**, 1043–1050.
12. M. Arnaud, M. Debarbouille, G. Rapoport, M. H. Saier Jr., and J. Reizer (1996) J. Biol. Chem. **271**, 18966–18972.
13. M. Idelson and O. Amster-Choder (1998) J. Bacteriol. **180**, 1043–1050.
14. X. Manival, Y. Yang, M. P. Strub, M. Kochoyan, M. Steinmetz, and S. Aymerich (1997) EMBO J. **16**, 5019–5029.
15. H. van Tilbeurgh, S. Manival, S. Aymerich, J. M. Lhoste, C. Dumas, and M. Kochoyan (1997)

EMBO J. **16**, 5030–5036.
16. K. Schnetz, J. Stulke, S. Gertz, S. Krüger, M. Krieg, M. Hecker, and B. Rak (1996) J. Bacteriol. **178**, 1971–1979.
17. C. A. Alpert and U. Siebers (1997) J. Bacteriol. **179**, 1555–1562.
18. E. Glatz, R. P. Rutberg, and B. Rutberg (1996) Mol. Microbiol. **19**, 319–328.
19. L. Wray Jr. and S. Fisher (1994) J. Bacteriol. **176**, 5466–5473.
20. S. A. Wilson, S. J. M. Wachira, R. A. Norman, L. H. Pearl, and R. E. Drew (1996) EMBO J. **15**, 5907–5916.
21. J. T. Lin and V. Stewart (1996) J. Mol. Biol. **256**, 423–435.
22. T. M. Henkin (1994) Mol. Microbiol. **13**, 381–387.
23. C. Condon, M. Grunberg-Manago, and H. Putzer (1996) Biochimie **78**, 381–389.
24. J. A. Grandoni, S. A. Zahler, and J. M. Calvo (1992) J. Bacteriol. **174**, 3212–3219.
25. J. A. Grandoni, S. B. Fulmer, V. Brizio, S. A. Zahler, and J. M. Calvo (1993) J. Bacteriol. **175**, 7581–7593.
26. P. Renault, J. J. Godon, C. Delorme, G. Corthier, and S. D. Erlich (1995) Dev. Biol. Stand. **85**, 431–441.
27. F. J. Grundy and T. M. Henkin (1993) Cell **74**, 475–482.
28. F. J. Grundy S. M. Rollins, and T. M. Henkin (1994) J. Bacteriol. **176**, 4518–4526.
29. C. Condon, H. Putzer, and M. Grunberg-Manago (1996) Proc. Natl. Acad. Sci. USA **93**, 6992–6997.
30. C. Yanofsky, K. V. Konan, and J. P. Sarsero (1996) Biochimie **78**, 1017–1024.
31. J. L. Botsford and R. D. DeMoss (1971) J. Bacteriol. **105**, 303–312.
32. P. Gollnick and C. Yanofsky (1990) J. Bacteriol. **172**, 3100–3107.
33. K. Gish and C. Yanofsky (1995) J. Bacteriol. **177**, 7245–7254.
34. V. Stewart, R. Landick, and C. Yanofsky (1986) J. Bacteriol. **166**, 217–223.
35. K. V. Konan and C. Yanofsky (1997) J. Bacteriol. **179**, 1774–1779.
36. P. S. Lovett and E. J. Rogers (1996) Microbiol. Rev. **60**, 366–385.
37. A. V. Kamath and C. Yanofsky (1997) J. Bacteriol. **179**, 1780–1786.

Suggestions for Further Reading

38. T. M. Henkin (1996) Control of transcription termination in prokaryotes. Ann. Rev. Gen. **30**, 35–57. A comprehensive review of the mechanisms of gene regulation by controlling transcription termination in bacteria.
39. T. Platt (1998) "RNA structure transcription elongation, termination and antitermination". In *RNA Structure and Function* (R. W. Simons and M. Grunberg-Manago, eds.), Cold Spring Harbor Laboratory Press, Cold Spring Harbor, NY, pp. 541–574. A more in-depth look at the processes involved in transcription and regulation of transcription termination.
40. M. Steinmetz (1993) "Carbohydrate catabolism: pathways, enzymes, genetic regulation, and evolution". In *Bacillus subtilis and Other Gram-positive Bacteria: biochemistry, physiology, and molecular genetics*. (A. L. Sonenshein, J. A. Hoch, and R. Losick, eds.), American Society for Microbiology, Washington, DC, pp. 157–170. A more in-depth look at the Sac systems in *B. subtilis*.

Antithrombin

Antithrombin is a proteinase inhibitor of the serpin family that is the principal anticoagulant in human plasma; it is also known as antithrombin-III. It is composed of a single polypeptide chain of 432 amino acid residues, with four carbohydrate side chains (see N-Glycosylation). It has a reactive-center peptide bond between Arg393 and Ser394 that provides a specific target for thrombin, factor Xa, and other proteinases of the blood clotting system. Antithrombin is present in plasma at a concentration of nearly 100 mg/L and circulates in a relatively inactive form, being activated conformationally by the binding of heparin. Genetic deficiency or dysfunction of antithrombin is a significant cause of familial thromboembolic disease.

Suggestions for Further Reading

S. T. Olson and I. Björk (1992) "Regulation of thrombin by antithrombin and heparin cofactor II", in *Thrombin, Structure and Function* (L. J. Berliner, ed.), Plenum Press, New York, pp. 159–217.

L. Jin, J. P. Abrahams, R. Skinner, M. Petitou, R. N. Pike, and R. W. Carrell (1997) The anticoagulation activation of antithrombin by heparin, Proc. Natl. Acad. Sci. USA **94**, 14683–14688.

a_1-Antitrypsin

a_1-Antitrypsin is a proteinase inhibitor of the **serpin family** that consists of a single polypeptide chain of 294 amino acid residues and four carbohydrate side chains (see N-Glycosylation). It also known as a_1-proteinase inhibitor. Present at a concentration of 1 g/L, it is the predominant proteinase inhibitor in human plasma in terms of concentration. Its reactive-center peptide bond between Met358 and Ser359 specifically targets the elastases that are involved in connective tissue remodeling. Genetic deficiency of a_1-antitrypsin is relatively common and predisposes to the development of the lung disease emphysema, with an associated risk of liver cirrhosis (see Serpins).

Suggestions for Further Reading

R. W. Carrell, J.-O. Jeppsson, C.-B. Laurell, S. O. Brennan, M. C. Owen, L. Vaughan, and D. R. Boswell (1982) Structure and variation of human $_1$-antitrypsin, Nature **298**, 329–334.

R. Mahadeva and D. A. Lomas (1998) $_1$-Antitrypsin deficiency, cirrhosis and emphysema, Thorax **53**, 501–505.

AP Endonucleases

AP endonucleases are enzymes that cleave the phosphodiester bond on either side of an AP site in DNA and are involved in base excision repair. Enzymes that cleave the phosphodiester bond to the 3′

side are referred to as type I AP endonucleases, and those that cleave the phosphodiester bond 5′ to the AP site are type II AP endonucleases. Whether or not a bona fide type I AP endonuclease exists that is not associated with DNA glycosylase activity is not known. However, type II AP endonucleases, which cleave AP sites by hydrolysis, have been found in many organisms and have been characterized.

1. AP Lyases (Class I AP Endonucleases)

Type I AP endonucleases are also DNA glycosylases, and it appears that the same active site is involved in both the glycosylase and AP endonuclease activities. However, it has also been demonstrated that cleavage of AP site occurs by b-elimination, which involves abstraction of a hydrogen from the C2′ position of the deoxyribose. Because this is a lyase reaction, and not a hydrolyase reaction, the type I AP endonucleases are referred to as AP lyases (1).

Endonuclease III and 8-oxoguanine glycosylase are examples of this class of enzymes (1, 2). The a-NH_2 group of the *N*-terminal amino acid residue forms a Schiff base with the ring-opened form of the deoxyribose, eventually leading to cleavage of the deoxyribose–phosphate bond without water addition. Following elimination of the base by glycosylase action, the enzyme remains attached to DNA through a protonated Schiff base intermediate where the C1′ of the sugar is covalently bound to the nitrogen of the *N*-terminal a-amino group of the protein (3). b-Elimination of this intermediate, followed by hydrolysis of the Schiff base, results in cleavage of the phosphodiester bond and generation of a *trans* a–b-unsaturated aldehyde on the 5′ side, and a 5′-phosphate on the 3′ side, of the cleavage, which is concomitant with the release of the enzyme. When the AP lyase activity is associated with a glycosylase activity, the two reactions are, for the most part, coupled (2). In these instances, it is natural to assign a physiological role to the AP lyase. However, cleavage of an AP site on the 3′ side occurs readily even in the absence of enzymes and can be accelerated by alkaline pH and by basic proteins such as histones and cytochrome *c*. Hence the assignment of AP lyase activity to a protein in the absence of an associated glycosylase activity is virtually impossible.

2. AP Endonucleases (Class II AP Endonucleases)

These enzymes hydrolyze the phosphodiester bond 5′ to an AP site. AP endonuclease IV in *E. coli*, which has a **homologue** in yeast and humans, is the only example of a "pure" AP endonuclease—that is, an endonuclease with only hydrolysis activity 5′ to an AP site and with no significant activity on any other substrate. However, the best-characterized AP endonuclease is the *E. coli* exonuclease III and its homologues in eukaryotes, including yeast, Drosophila, and mammals. In contrast to the pure AP nuclease endonuclease IV, the exonuclease III, as the name implies, has exonuclease activity as well.

2.1. Exonuclease III/Rrp1/APE

The prototype of this group of enzymes, exonuclease III, has several activities, including **ribonuclease** H, 3′ to 5′ exonuclease, and type II AP endonuclease. The enzyme is specific for double-stranded DNA. It is a simple polypeptide chain of 30 kDa with no cofactor. The X-ray crystallography structure of an enzyme–substrate complex demonstrates that the base is flipped out of the double helix, into the active site of the enzyme (4). The *E. coli* enzyme is a potent 3′ to 5′ exonuclease. The exonuclease activity has a preference for blunt double-stranded termini, but it can initiate exonuclease action from a nick as well. An activity related to the 3′ to 5′ exonuclease function is the ability of the enzyme to remove deoxyribose fragments, including 3′-phosphoglycolate esters and 3′-phosphate, from the 3′ termini of DNA strand breaks generated by attack of reactive oxygen species on DNA. Exonuclease III-defective mutants are extremely sensitive to H_2O_2 and ionizing radiation, which most probably kills cells through the strand breaks introduced by reactive oxygen species. As a rule, these are not clean breaks with 3′-OH and 5′-P termini. Instead, they most often contain either 3′-phosphate or fragmented deoxyribose, which must be processed further before they can be utilized by **DNA polymerases** to fill in the gap created by the DNA damage. These structures are removed efficiently by exonuclease III, but not by endonuclease IV.

The *Drosophila* exonuclease III homologue is a monomer of 75 kDa. The 250-amino-acid-residue *C*-terminal region of the protein is homologous to the exonuclease III family of AP endonucleases. However, the *N*-terminal 400 residues are not related to any known sequence, and the function of this putative **domain** is unknown at present. The *Drosophila* enzyme was initially isolated as an activity that catalyzes strand transfer and was thought to perform a **RecA**-like function in this organism, hence the name Rrp1 (Recombination related protein 1). However, later work has not confirmed a role for this protein in recombination. The enzyme has a potent type II AP endonuclease activity, but its 3′ to 5′ exonuclease activity is rather modest compared to the *E. coli* enzyme and is only 10^{-2} to 10^{-3} of the AP endonuclease activity. Whether the *N*-terminal 400 residues play any role in recombination or in DNA repair is not known at present.

The human AP endonuclease (APE/HAP1/APEX) is highly homologous (90% to 95% sequence identity) to the enzymes from bovine and rodent sources. These enzymes are 35-kDa monomers and are clearly related to *E. coli* exonuclease III. The mammalian enzymes have potent type II AP endonuclease and 3′-phosphoglycol aldehyde esterase activities necessary for denuding a “jagged” 3′ terminus caused by direct attack of reactive oxygen species or by direct hit by ionizing radiation. In contrast to exonuclease III, however, the 3′ to 5′ exonuclease activity of mammalian type II AP endonucleases is rather weak and undetectable with certain 3′ sequences. The structure of human AP endonuclease indicates that it flips out the deoxyribose moiety into the active site (5), as is observed also in the *E. coli* exonuclease III.

A unique property of mammalian APE proteins is their capacity to reduce critical cysteine residues in certain transcription factors and by doing so activate these transcription factors. In fact, the human APE was also purified as a factor that activates the AP-1(Jun/Fos) transcription factor and was named Ref (for reducing factor 1) before the realization that it is identical to APE. The APE cysteine residue involved in this reduction reaction is located in the NH_2-terminal region and plays no role in the AP endonuclease activity of this protein. In addition to Jun and Fos, other transcription factors, including USF, NF-kB, c-Myb, and v-Rel, are activated by reduction of an oxidized cysteine by APE *in vitro* (5). However, the physiological role of these *in vitro* activities is currently not known.

Mouse APE **knockout** mutants are lethal at the embryonic stage. This could be due to either (a) the importance of base excision repair for survival of the organism or (b) disruption of an activating mechanism for important transcription factors.

2.2. Endonuclease IV

The *E. coli* endonuclease IV, Nfo, is a monomer of 30 kDa that cleaves 5′ to AP sites in a reaction that is independent of divalent metal ions such as Mg^{2+} . It also has potent 3′-PGA diesterase and 3′-phosphatase activities but does not have exonuclease function. Although Nfo^{-} mutants are not especially sensitive to H_2O_2, they are hypersensitive to killing by the oxidative agents bleomycin and *t*-butylhydroperoxide, indicating that endonuclease IV acts on a subclass of oxidative DNA lesions that are not processed efficiently by exonuclease III. The importance of Nfo in cellular defense against oxidative stress is underscored by the fact that this is the only DNA repair enzyme that is induced by oxidative stress as part of the SoxRS regulon.

The Nfo homologue in yeast, Apn1, is the major AP endonuclease in this organism. Apn1 is a monomer of 40 kDa with 31% sequence identity with the *E. coli* Nfo endonuclease. The biochemical properties of Apn1 are very similar to those of Nfo, and indeed the expression of Apn1 in *E. coli* corrects the oxidant-sensitive phenotype of *nfo* mutants, but not the H_2O_2 sensitivity.

Bibliography

1. V. Bailly and W. G. Verly (1987) Biochem. J. **242**, 565–572.
2. M. L. Dodson, R. D. Schrock, and R. S. Lloyd (1993) Biochemistry **32**, 8284–8290.
3. R. P. Cunningham, H. Asahara, J. F. Bank, C. P. Scholes, J. C. Salerno, K. Surerus, E. Munck, J. McCracken, J. Peisach, and M. H. Emptage (1988) Biochemistry **28**, 4450–4455.
4. C. D. Mol, C. F. Kuo, M. M. Thayer, R. P. Cunningham, and J. A. Tainer (1995) Nature **374**, 381–386.
5. M. A. Gorman, S. Morera, D. G. Rothwell, E. de la Fortelle, C. D. Mol, J. A. Tainer, I. D. Hickson, and P. S. Freemont (1997) EMBO J. **16**, 6548–6558.

Suggestions for Further Reading

6. B. Demple and L. Harrison (1994) Repair of oxidative damage to DNA: enzymology and biology. Annu. Rev. Biochem. **63**, 915–948.
7. P. W. Doetsch and R. P. Cunningham (1990) The enzymology of apurinic/apyrimidinic endonucleases. Mutation Res. **236**, 173–201.
8. E. Seeberg, L. Eide, and M. Bjoras (1995) The base excision repair pathway. Trends Biochem. Sci. **20**, 391–397.
9. R. J. Roberts (1995) On base flipping. Cell **82**, 9–12.

AP Sites (Apurinic/Apyrimidinic Sites)

AP (apurinic/apyrimidinic) sites are deoxyribose residues in the DNA that have lost the purine or pyrimidine bases.

1. Occurrence

AP sites are generated by a variety of mechanisms:

1.1. Spontaneous Base Loss

The glycosylic bond joining the base to the deoxyribose in the DNA backbone is relatively unstable and is cleaved, even under physiological conditions, at a rate incompatible with life. It is estimated that at normal pH and temperature there are base losses at rates of about 10^{-12} s^{-1} for double-stranded DNA and 10^{-10} s^{-1} for single-stranded DNA. This means that humans (with about 1.2×10^{10} bp per diploid cell) lose about 1 base per minute per cell, or, taking into account that there are about 10^{13} cells in the human body, lose 1.5×10^{16} bases from their DNA daily. The rate of base loss is greatly accelerated by heat and low pH. Because of higher susceptibility of their N9 atom to nucleophilic attack, the purine bases are hydrolyzed at a rate about 100-fold faster than are pyrimidines (1). In fact, because of this unique property of purines, one of the procedures for chemical DNA sequencing reactions consists of heating the DNA at acidic pH, followed by cleavage of the resulting AP site by alkali treatment.

1.2. Ionizing Radiation

Ionizing radiation most often causes base reduction, oxidation, or fragmentation. In particular, a urea residue attached to the deoxyribose is a relatively common product of ionizing radiation and, for all practical purposes, may be considered an AP site. Such radiation causes base loss by either (a) generating reactive oxygen species that attack and destroy bases or (b) direct hits by ionizing radiation.

1.3. Glycosylases

There are about a dozen DNA glycosylases with varying degrees of specificity for bases with minor modifications: uracil glycosylase, 3-methyladenine DNA glycosylase, 8-oxoguanine DNA glycosylase, and glycosylases that act on mismatches, such as T-G glycosylase, specific for the T residue, and A-G glycosylase, specific for the A residue. These enzymes release the modified, abnormal, or mismatched bases by hydrolyzing the glycosylic bond linking the base to the deoxyribose. Most of the glycosylases have dual enzymatic activities in that, after cleaving the glycosylic bond, they also cleave the phosphodiester bond by b-elimination. However, some, such as uracil glycosylase, are “pure” glycosylases with no such associated AP lyase activity.

2. Consequences

AP sites in DNA are, in fact, very unstable. Even at physiological pH and temperature, the abasic sugar can be eliminated by b–d elimination. The presence of the divalent metal ions that would be expected in biological fluids greatly accelerates the cleavage reaction. The reaction may be further accelerated by basic proteins, such as cytochrome *c*. Consequently, AP sites as such do not constitute an important lesion interfering with cell survival. In contrast to b-elimination, however, which occurs readily under a variety of conditions, the d-elimination reaction, which in combination with b-elimination would release the abasic deoxyribose from DNA, does not occur at physiologically relevant rates. AP endonucleases hydrolyze the phosphodiester bond 5 to the AP site, and *Escherichia coli* cells that lack this enzyme are sensitive to agents that generate AP sites or fragmented deoxyribose residues.

Bibliography

1. T. Lindahl (1976) Nature **259**, 64–66.

Suggestions for Further Reading

2. B. Demple and L. Harrison (1994) Repair of oxidative damage to DNA: enzymology and biology. Annu. Rev. Biochem. **63**, 915–948.
3. E. Seeberg, L. Eide, and M. Bjoras (1995) The base excision repair pathway. Trends Biochem. Sci. **20**, 391–397.

Apoptosis

Wyllie et al. initially used the term “apoptosis” in a paper in 1972 to describe a newly observed form of cell death (1). The discovery of apoptosis has revolutionized many areas of modern biology, especially those areas concerned with disease development (2). This is primarily because apoptosis is an active form of cell death that, unlike necrosis, is critical for the maintenance of tissue homeostasis (3, 4). Thus, cell populations are numerically controlled through not only differentiation and proliferation, but also the physiological loss of cells through apoptosis. Critically, this implies that a cell which loses the capacity to apoptose, or a cell which becomes inappropriately sensitive to death stimuli, can lead to perturbations in cell number regulation and, ultimately, disease development.

Cells undergoing apoptosis are evident in all tissues in response to diverse stimuli. In healthy tissues, apoptosis accounts for all the cell deaths occurring in response to normal physiological signals. Apoptosis (often referred to as programmed cell death in a developmental context) occurs at many stages of embryonic development, eg, during the formation of digits from a solid limb paddle, where interdigital cells between the digits die (5). Single apoptotic cells are evident in healthy proliferating tissues such as small gut crypts and the dermis of the skin (4). Moreover, apoptosis is also seen during endocrine-induced atrophy of tissues, in cell-mediated immunity, in development of the nervous system, and in the "necrotic" oxygen-starved cores of solid tumors (6).

Morphologically, an apoptotic cell is very different from a necrotic cell (1, 6, 7); see Figure 1. One of the most prominent and easily identifiable stages of apoptosis involves the nucleus. Chromatin condenses and forms aggregates near the nuclear membrane, which becomes convoluted, whereas the nucleolus becomes enlarged and appears abnormally granular. The chromatin is also subject to the actions of an activated **endonuclease** that cleaves the DNA into 300- to 50-kbp fragments initially, and 180-bp fragments subsequently (8). Changes in the cytoplasm are also evident at this time; the cell shrinks visibly, adherent cells round up, and distinct protuberances or membrane blebs are discernible. **Organelles** within the shrunken cytoplasm still look normal, except for dilation of the endoplasmic reticulum. These "blebbing" cells exclude vital dyes, indicating no structural failure in the cell membrane. It is at this point in the apoptotic process, which may only take 10 to 30 minutes, that apoptotic cells *in vivo* are **phagocytosed**, by either their nearest neighbors or professional macrophages (9). Thus, apoptosis occurring in single cells *in vivo* is very easily overlooked due to its rapid progression. Cells in the later stages of apoptosis, especially those *in vitro*, form apoptotic bodies as a result of pinching off of the highly convoluted blebbing areas of the cell. These apoptotic bodies are phagocytosed or, in situations where there is much cell death, the unphagocytosed apoptotic cells undergo secondary necrosis, characteristically swelling and loosing membrane integrity.

Figure 1. A comparison of apoptosis and necrosis.

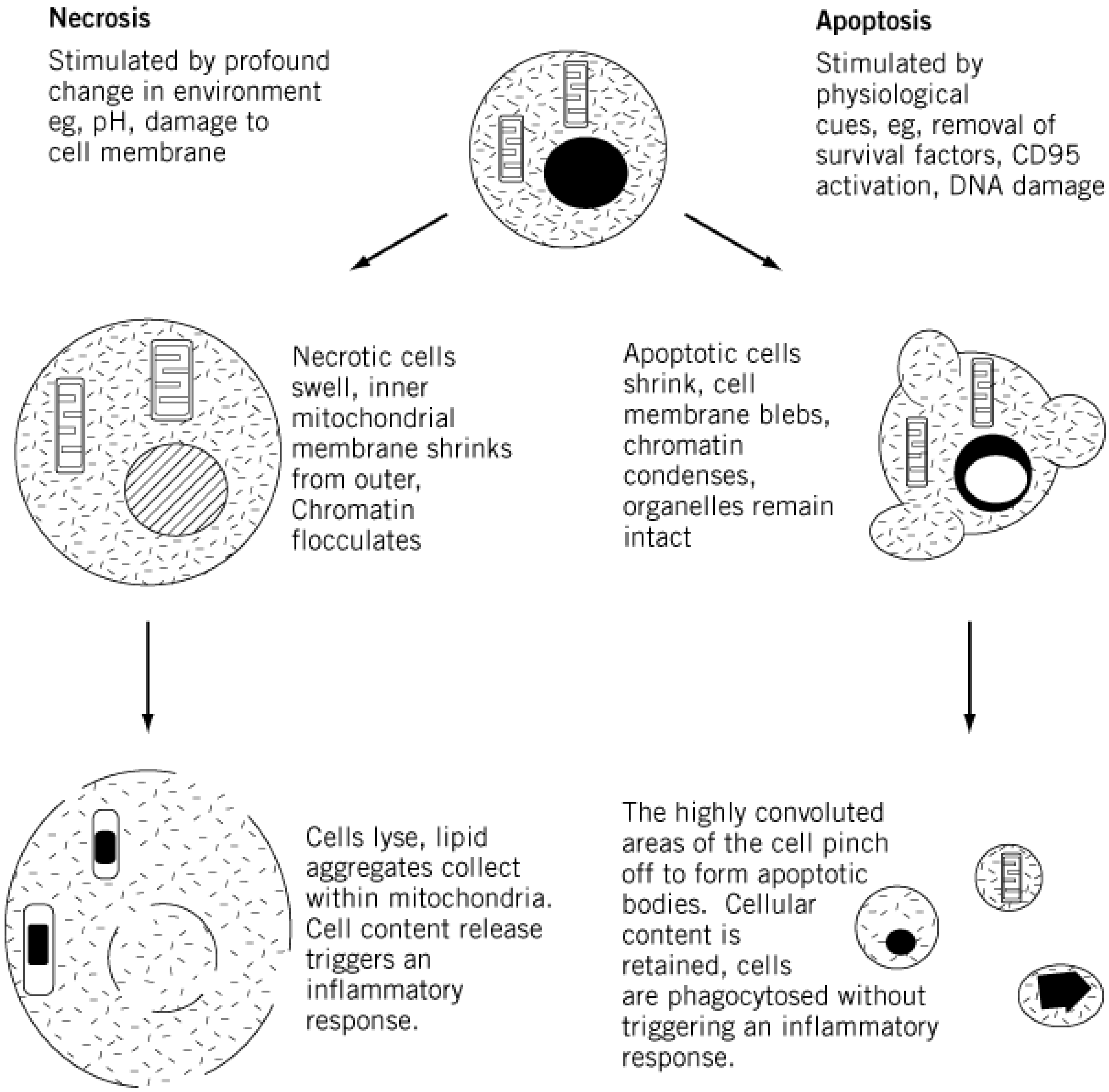

1. Removal of Apoptotic Cells

A critical part of the apoptotic pathway is the efficient recognition and phagocytosis of apoptotic cells. The rapid disposal of apoptotic cells does not elicit an immune response, consistent with apoptosis being the “no-nonsense” pathway for the disposal of unwanted cells. A breakdown in either the communication between macrophage and apoptotic cell or in the pathway of apoptosis itself may be two of the mechanisms through which chronic inflammatory disorders occur. Recognition of apoptotic cells by professional macrophages is mediated partly by $a_v b_3$ integrin (the *vitronectin* receptor) and the CD36 ligand. Between these two molecules on the external surface of the cell sits a **glycoprotein** containing the sequence -R-G-D- (-Arg-Gly-Asp-), *thrombospondin*, which acts as a molecular bridge to bind to an unknown anionic site on the apoptotic cell (10-12). Apoptotic cells also express surface phosphatidylserine, which binds to an as yet uncharacterized macrophage **receptor** (13, 14). The recognition of apoptotic cells mediated by the vitronectin receptor, CD36 ligand, and thrombospondin is confined to monocyte-derived macrophages. Recognition of apoptotic cells through the expression of phosphatidylserine, which is flipped onto the cellular surface due to the inactivation of an ATP-dependent flipase, is utilized primarily by inflammatory macrophages (9, 15). Four other molecules have been implicated in apoptotic cell recognition systems: (1) the 61D3-antigen found on human macrophages, (2) ICAM-3, found on the surface of human B cells (16), (3) the ABC1 transporter (17), and (4) the macrophage scavenger receptor (18). As mentioned previously, the interaction between apoptotic cells and macrophages does not elicit an inflammatory response, unless the apoptotic cells start to undergo secondary necrosis. Under these circumstances, other macrophage receptors are employed, and inflammatory **cytokines** are released (19). This change from "silent" death to one that activates the immune system may be a method of recruiting more phagocytes to the site of cell death to cope with the increasing number of corpses.

2. Regulation of Apoptosis and Cell Viability

The discovery that apoptosis is an active form of cell death which is transiently suppressable by both inhibitors of protein and RNA synthesis suggested that the cell needed to synthesize new proteins prior to its death [reviewed in (20)]. This sparked an enthusiastic hunt for a critical cell death gene that had to be translated prior to death. No such gene has been found, but many genes that regulate apoptosis have been identified as a result.

A cell can be triggered to undergo apoptosis in response to diverse stimuli, with each stimulus activating different pathways involving **gene expression**, as well as post-translational modification. The discovery that apoptosis can be suppressed by the presence of specific survival factors, either cytokines or proteins expressed within the cell, suggested that regulation of cell viability was paramount to the function of the cell (21). Indeed, it appears that apoptosis represents a default pathway in all cells (22). If a cell does not receive the correct survival stimulus, it will die; consequently, cells within multicellular organisms are maintained in a viable state by a constant supply of survival factors.

Once a cell is triggered to apoptose, activation of a common set of destruction proteins, irrespective of the stimulus involved, precipitates the morphological changes that we call apoptosis. Overall, the apoptotic pathway can be divided into three phases:

1. The *decision phase*, in which the cell receives a stimulus and, depending on both its internal and external environments, may or may not be triggered to die.
2. The *commitment phase*, in which the cell is committed to death and cannot recover.
3. The *execution phase*, in which the decision to die has been made and the activated apoptotic machinery leads to the morphological changes that define an apoptotic cell.

3. The Decision Phase of Apoptosis

The decision phase can be compared to that of a judge hearing the evidence during a trial. The evidence presented comes from many different sources: genes, cytokines, toxic chemicals, DNA damage, and the presence of viral and bacterial infection. Only once all the evidence is heard will the sentence be passed. The genes that modulate the decision phase are many and varied. Some are more commonly associated with the regulation of the cell cycle, such as *c*-**myc**, *cdc25*, *c-fos*, p53 and *rb* (**retinoblastoma**), whereas others are members of recently identified gene families, such as the *bcl-2* family. **Cytokines** can either trigger or delay apoptosis. Tumor necrosis factor a (TNFa) and CD95 ligand (CD95L, FasL, Apo-1L) are two examples of cytokines that trigger apoptosis upon binding to their receptors (23), whereas the addition of factors such as **interleukin**-3 (IL-3) (24) or ***insulin**-like growth factor 1* (IGF-1) suppresses death (25). Conversely, removal of anti-apoptotic cytokines also induces cell death (26, 27). Both viruses and bacteria trigger apoptosis upon infection of a cell, suggesting that the cell commits suicide to prevent the invading pathogen from spreading. However, both viruses and bacteria have evolved mechanisms that manipulate this response. Adenovirus, eg, has three genes required for productive infection: E1A, E1Bp19, and p55. E1A stimulates the infected cell to proliferate; however, this stimulus concomitantly triggers apoptosis. E1Bp19 and p55 delay the host cell from triggering cell death, thereby facilitating virus production (28, 29).

Alternatively, some bacteria such as *Shigella flexneri* actively promote the death of the cell by triggering the execution machinery (30-32). This allows the early release of the bacteria and triggers an immune response, which damages the surrounding tissue and aids the passage of the bacteria into its target cells.

3.1. Oncogenes, Tumor Suppressor Genes, and Apoptosis

In terms of suppressing tumorigenesis, long-lived organisms like humans need to limit the chances of their component cells acquiring mutations that lead to increased proliferative capacity and eventual clonogenic outgrowth. This is, in part, limited by restricting the types of cells with proliferative capacity. Many adult cell lineages exist in a senescent or postreplicative state. Moreover, for those cells that must retain the capacity to divide, apoptosis provides a “safety net.” Genes that are involved in proliferation are also involved in cell death; in fact, the two processes appear inexorably linked. This paradoxical coupling of two opposing biological processes was first realized through work on the pervasive oncogene *c-myc* (33) but has since been confirmed for several mitotic genes (34).

3.2. *c-myc* and Apoptosis

The protein product of the *c*-**myc** gene, c-Myc, is both necessary and sufficient to ensure fibroblast proliferation; in the presence of **mitogen**, all cells in cycle express c-Myc. Fibroblasts remain in cycle as long as mitogens and c-Myc are present, but only remain viable in the presence of additional survival factors. In the absence of such survival factors, cycling cells expressing deregulated Myc undergo apoptosis. This response to oncogene deregulation is thought to protect the organism against cells that acquire mutations in c-Myc. Mutant cells that continuously express c-Myc will proliferate, but since the survival factor *in vivo* is thought to be limiting, the mutant cells will die once the supply of factor is exhausted (25, 35). Thus, small proto-tumors may well arise *in vivo*, but they should regress due to lack of survival signals. If, however, another mutation has occurred producing a cooperating anti-apoptotic lesion, the mutated cells will survive. Several genes that cooperate with *myc* during tumorigenesis are anti-apoptotic. For example, v-Abl, which is a very good suppressor of apoptosis in response to many stimuli, will render haemopoietic cells cytokine-independent for growth and survival (36, 37). *bcl-2*, a gene initially identified through its translocation in the t(14:18) mutation found in follicular lymphoma (38), will cooperate with *myc*, suppressing the apoptotic signal induced through Myc expression (39, 40). The outcome of this cooperation *in vivo* is lymphoma, as seen in both double *bcl-2/Eμ-myc* **transgenic** mice (41, 42) and in human patients with the t(14:18) translocation (43, 44).

3.3. Bcl-2, an Anti-apoptotic Oncogene

The potent ability of Bcl-2 to suppress apoptosis triggered in response to a number of diverse stimuli prompted much research into its biochemical function. This function is still relatively obscure, but several members of the Bcl-2 family of proteins have been identified as a result (45-47). Bcl-2's form and functionality have been conserved throughout multicellular evolution, as exemplified by Ced-9, its counterpart in the nematode *C. elegans*, and the Adenovirus E1Bp19 protein (48). Ten or so members of this family now exist, and all share defined regions of homology, although not all act to suppress apoptosis (Table 1). The pro-apoptotic members of the family (Bax, Bak, and Bcl-x_S (49-53)) share three regions of homology, BH-1, -2, -3, whereas the anti-apoptotic members (Bcl-2 and Bcl-x_L) have a fourth region of homology, known as BH-4 (54, 55). Removal of the BH-4 **domain** from either Bcl-2 or Bcl-x_L results in a loss of protective function. Family members can dimerize with themselves and with one another, and these interactions are important for their function (56, 57). For example, Bcl-2 preferentially binds to the pro-apoptotic family member Bax, whereas Bcl-x_L binds to Bak. If the number of Bax homodimers in the cell exceeds the number of Bcl-2 homodimers or Bax/Bcl-2 heterodimers, then the cell is more likely to undergo apoptosis (47). However, it is not clear which forms of these proteins are dominant for determining life or death. A second set of Bcl-2-associated proteins has been identified that influences cell survival through interaction with Bcl-2 family members, but whose members do not have all, if any, of the BH regions (Table 2) (45, 46). Bag-1, eg, has no homology to Bcl-2, but binds to it and augments the protective function of Bcl-2 (58). Bad, on the other hand, has homology to the family and binds Bcl-2, an interaction that disrupts Bcl-2's binding with Bax, leading to cell death (59, 60).

Table 1. Pro-apoptotic and Anti-apoptotic Members of the Bcl-2 Family[a]

Bcl-2 Family Inhibitors	Bcl-2 Family Promotors
Bcl-2 (mammalian)	Bax (mammalian)
Bcl-xL (mammalian)	Bak (mammalian)
Bcl-w (mammalian)	Bcl-xS (mammalian)
Mcl-1 (mammalian)	
A1 (mammalian)	
NR-13 (mammalian)	
E1B p19 (viral)	
BHRF1 (viral)	

[a] Anti-apoptotic members contain up to 4 Bcl-2 homology (BH) domains and the transmembrane (TM) domain, whereas pro-apoptotic members contain only BH 1-3 and the TM domain, except for Bcl-x_s that contains only BH4, BH3, and the TM domain. Members of this gene family have been conserved throughout evolution with homologues existing in nematodes, mammals, and viruses (46, 47, and references therein].

Table 2. Proteins That Bind to Bcl-2 Family Members and Regulate Their Function[a]

Bcl-2-like Inhibitors of Apoptosis	Bcl-2-like Promotors of Apoptosis
Bag-1 (no BH domains)	Hrk (BH 3, TM domain)
Bra (BH 2 and BH 3)	Bik (BH 3, TM domain)
Raf-1 (no BH domains)	Bid (BH 3)
	Bim (BH 3, TM domain
	Bad (BH 1, 2, 3, no hydrophobic tail)

[a] A variety of proteins interact with Bcl-2 proteins. Some contain the BH domains that influence their function, such as Bid, Bim, Bik, whereas others have no homology with Bcl-2, but still bind and influence its function (46, 47, and references therein].

Both Bcl-x_L and Bcl-2 have effects on cell-cycle transition (61). Cells expressing either gene exhibit a longer-than-average time to reenter the cell cycle after arresting in G_0, suggesting that Bcl-x_L and Bcl-2 interact with components of the cell-cycle machinery.

3.4. Tumor Suppressor Genes and Apoptosis

Tumor suppressor gene products suppress unrestrained cell proliferation through their specific inhibitory effects on the cell cycle and are implicated in the development of neoplasia following their loss or functional inactivation. One tumor suppressor gene product, p53, induces apoptosis in some tumor cell lines. p53 is a short-lived protein that is stabilized in the presence of DNA damage and triggers cell-cycle arrest, presumably to facilitate DNA repair (62). If the DNA damage is too great to repair, apoptosis is triggered, earning p53 the title "guardian of the genome" (63). At present, it is unclear if p53's induction of apoptosis is effected through its upregulation of $p21^{Waf\text{-}1/Cip\text{-}1}$, leading to cell-cycle arrest (64), through some other p53-regulated gene, or is independent of p53 transcriptional activity (65). Bax, the pro-apoptotic Bcl-2 homologue, is transcriptionally regulated by p53, but not all apoptotic cell deaths induced by p53 stabilization require Bax expression (66). The role of p53 as a sensor of DNA damage was neatly illustrated by examining apoptosis in thymocytes from p53-knockout mice (67, 68). p53 null thymocytes undergo death by apoptosis as normal, except when treated with agents that damage DNA, such as etoposide or irradiation. Therefore, in the absence of p53, the cell is neither instructed to leave the cell cycle and repair the damaged DNA, nor to die. Cells therefore progress through subsequent cycles with damaged and mutated DNA. The role of p53 in inducing apoptosis in circumstances in which DNA damage is not evident is at present unclear, although in p53 knockout mice there is no evidence of a defect in tissue homeostasis due to ineffective cell death when cytokines become limiting (67, 68).

A second tumor suppressor gene implicated in control of apoptosis is the **retinoblastoma** (*rb*) gene (69-71). The absence of the functional gene product, Rb, results in massive apoptosis in the haemopoietic and nervous system possibly due to the cells being constantly in cycle and unable to arrest or terminally differentiate. This makes it impossible for cells to establish appropriate survival signals and cell:cell contacts. Loss of both p53 and Rb function results in rapid tumor progression (72), suggesting that cells which have overcome restraints upon cell-cycle progression can also escape apoptosis, underlining the link between cell proliferation and cell death.

3.5. Cytokine Signaling Pathways and Apoptosis

Although a wealth of information is available about the signal transduction pathways activated by cytokines and growth factors in many cell types, surprisingly little is known about how apoptosis (and conversely cell viability) is modulated. Initially, many of the factors now referred to as *survival factors* were considered solely to stimulate cells to proliferate. Thus, many of the identified signal transduction pathways are involved in proliferation but not necessarily survival. For survival signals, two pathways can exist. Cells can be stimulated to survive by one specific pathway. Loss of this signal upon removal of the cytokine may simply trigger cell death due to negation of the first signal. However, removal of the cytokine may trigger another independent signaling pathway. Only now are these different possibilities being investigated.

3.5.1. Survival Signals

Cytokines with very different actions activate substantially overlapping signaling circuits, many of which appear to be required, but are not solely responsible, for regulating cell survival. However, even with these complex signaling networks, it is possible to gather some information about survival signals. For example, apoptosis stimulated by the withdrawal of **nerve growth factor** (NGF) in phaeochromocytoma (PC12) cells involves the induction of the AP-1 transcription factor c-Jun proximal to the time when neurons become committed to apoptosis. Activation of c-Jun requires phosphorylation by the protein kinase JNK (MKK4) that is, in turn, activated by MAP kinase (73) (see Phosphorylation, Protein). In contrast, the suppression of apoptosis by NGF in the same cells may involve a discrete survival signaling pathway routed through **Ras** (74), Raf, and MAP kinase (73). Hence, in this case, the induction of apoptosis and promotion of survival may be independent informational processes, rather than mere negation of one other.

In some documented cases, the ability of anti-apoptotic cytokines to suppress apoptosis does not depend on the synthesis of new genes or proteins, indicating that survival is mediated by posttranslational mechanisms. IGF-1 (25), a potent inhibitor of apoptosis in many cell types, and epidermal growth factor (EGF) (75) are reported to suppress apoptosis effectively in cells treated with inhibitors of RNA and protein synthesis. The suppression of apoptosis in such instances must be effected by means of preexisting molecular machinery. One possible candidate signal is the activation of PI-3 kinase (PI3-K) through Ras, whose inhibition blocks the ability of NGF to mitigate apoptosis (76). However, specificity is absent, since PI3-K is activated in many signaling pathways in response to signals that do not suppress apoptosis. IGF-1 also signals via PI3-K, and the pro- and anti-apoptotic signaling pathways for this cytokine have been identified. PI3-K can be activated by its upstream effector Ras, and it can activate several downstream pathways, including the ribosomal protein $p70^{S6K}$, the **Rho** family polypeptide Rac, and the serine/threonine protein kinase PKB/Akt. Of these downstream effectors, PKB/Akt is anti-apoptotic in fibroblasts expressing c-Myc and in other cell types in the absence of survival factors, whereas the Ras-mediated Raf signaling pathway is pro-apoptotic (77-79). These findings underscore the pleiotropic nature of intracellular signaling. Signals emanating from GTP-Ras trigger a plethora of potential biological outcomes, some of which promote apoptosis and some of which suppress it. The net outcome for Ras activation is presumably dictated by downstream interactions that potentiate or mitigate other signals.

3.5.2. Killer Cytokines

Apoptosis can also be triggered by certain **cytokines**, such as TNFa and CD95 ligand. These two pathways represent the best understood triggers of apoptosis, since their activation pathways are essentially mapped. CD95 ligand and TNFa bind and activate their specific receptors on the surface of the cell (80). The TNF type 1 and CD95 (Fas, Apo-1) receptors are functionally similar; both are transmembrane receptors that contain a region within their cytoplasmic tail which is necessary for the initiation of the apoptotic response (81-83). This region of homology is called the *death domain* (DD). Several adaptor proteins bind to this domain and can trigger apoptosis by directly linking to the downstream effector caspase machinery (23). Alternatively, in the case of TNFR1, the adaptor proteins can also activate NFkB signaling pathways (84). CD95-induced cell death, eg, results in the association of the ***d**eath-**i**nduced* ***s**ignaling **c*** *omplex* (DISC) (80). Upon binding of its ligand, the CD95 receptor trimerizes and binds to its death domain the protein *Fas-associated death domain* (FADD), also known as MORT1 (85, 86). FADD contains a C-terminal DD and, at its N-terminus, a *death effector domain* (DED), so called because the expression of this domain is required to trigger CD-95-induced apoptosis. The DED domain of FADD binds to the DED in caspase-8, a protein also called FLICE (FADD-like ICE, where ICE is "interleukin converting enzyme") (87, 88). The thiol proteinase domain of FLICE, located at its C-terminus, is activated upon binding FADD, and FLICE then activates the *caspase cascade* by cleaving downstream caspases (89) (see Caspases). CD95-triggered apoptosis can be suppressed by expression of the anti-apoptotic proteins Bcl-2 and Bcl-x_L (90) or by proteins that inhibit the interaction of FLICE with FADD (91). Thus, the binding of CD95 ligand to the receptor and recruitment of FADD occur within the decision phase of apoptosis. The commitment of cells to CD95-induced apoptosis does not appear to occur until FLICE is recruited to the DISC, cleaved, and therefore activated. TNFR1 exhibits a similar pathway involving an overlapping set of adaptor proteins (23).

4. The Commitment Phase of Apoptosis

As yet, it is unclear what commits a cell to undergo apoptosis. To a certain degree, the final trigger must be cell autonomous, because cells that have received the same stimulus do not all enter apoptosis at the same time; cells may die within 10 minutes of the signal or within 3 days. Initially, the caspases were proposed to act at this point, with their activation leading to certain death (92-94) Although exogenous expression of pro-caspases leads to cell death, this death is again stochastic and can be suppressed by the addition of IGF-1 (95) or thiol proteinase inhibitors such as the poxvirus protein CrmA and **baculovirus** inhibitor p35 (96, 97). Surprisingly though, not all caspase inhibitors suppress cell death. In the case of c-Myc-induced or Bax-induced apoptosis, the addition of tetrapeptide caspase inhibitors based on the pro-IL-1b cleavage site does not prevent cells from becoming committed to die (98, 99). Thus, even when caspases are inhibited, the cell still undergoes commitment, but it takes much longer to progress through the morphological changes of apoptosis (99). This result suggests caspases are required for the rapid execution phase of apoptosis, but not necessarily for commitment.

The unknown entity in mammalian cells is the putative homologue of the *cell death gene 4* (Ced-4) (see Programmed Cell Death). Ced-4 is required for cell death in *C. Elegans* and appears to function upstream of Ced-3, suggesting that Ced-4 may be involved in commitment (100). Recent data have shown that Ced-9, Ced-3, and Ced-4 bind one another, with Ced-4 being the critical intermediate (101-104). Without Ced-4 expression, Ced-9 does not interact with Ced-3. The expression of Ced-4 in mammalian cells produces a similar reaction between Bcl-x_L and the Ced-3 homologue, FLICE (caspase-8) (101). Whether Ced-4 is a killer of mammalian cells is also not clear, but Ced-4 expression is toxic to yeast (104). In the fission **yeast** *Schizosaccharomyces pombe*, Ced-4 localizes to condensed chromatin and induces caspase-independent death in this apoptotically naïve cell model. Cell death is suppressed upon the expression of Ced-9, which causes relocalization of Ced-4 to the membrane of the nucleus and to the endoplasmic reticulum. These data strongly suggest that Ced-9 suppresses Ced-4-induced death by binding to it. This, in turn, implies that the disruption of the Bcl-x_L/ Ced-4-“like protein” and FLICE interaction in mammalian cells may commit the cell to death.

5. The Execution Phase of Apoptosis

The execution phase describes the stage where the cells morphologically change and exhibit all the characteristics of apoptosis. Not all the agents responsible for these changes have been identified, but activation of the endonuclease occurs at this stage, as does activation of the *ced-3* homologues, the caspases. Overall, the caspase pathway can be thought of as a packaging process that carries out the rapid dismantling of the cell. Cells still die in the absence of caspase activity, but death is significantly prolonged (99). The cleavage of caspase substrates such as Poly-(ADP ribose) polymerase (PARP), the catalytic subunit of DNA protein kinase, and nuclear lamins [reviewed in (105)], in concert with an endonuclease, allow the nucleus and chromatin to be degraded efficiently. This saves the dying cell energy and facilitates the maintenance of membrane integrity, which in turn prevents release of the cell contents, which would stimulate an immune response.

Other effectors of the execution phase are not so well documented. Both ceramide and reactive oxygen species are found in apoptotic cells, but their exact roles are not clear (110-114): They may well be a consequence of death, rather than an effector. Changes in mitochondria also occur within apoptotic cells (115-117). Selective release of **cytochrome *c*** from the mitochondria appears to trigger apoptosis through activation of the caspases. A membrane permeability transition also occurs where the pores that regulate traffic between the mitochondrial outer and inner membranes become disrupted (117). However, it is unclear exactly when this change occurs within an individual cell undergoing apoptosis, making it difficult to assign these changes to a particular phase within the apoptotic pathway.

Overall, the execution phase is one where caspases and endonucleases are active and the cell is dismantled, progressing through the series of morphological changes that originally defined the process of apoptosis. Execution ends with the efficient and rapid phagocytosis of the corpse.

6. Summary

Apoptosis is an active form of cell death indistinguishable from programmed cell death that occurs during invertebrate and vertebrate development. Apoptosis is thought to be the default state of all cells; hence, cells must receive a survival signal in order to remain viable. Apoptosis is triggered in response to a diverse set of stimuli and plays a critical role in the maintenance of tissue homeostasis. Mutations that disrupt the apoptotic pathway are pivotal in the development of many diseases, including degenerative brain disorders and cancer.

Bibliography

1. A. H. Wyllie, J. F. Kerr, and A. R. Currie (1972) Cellular events in the adrenal cortex

following ACTH deprivation. J. Pathol. **106**, 1.

2. C. B. Thompson (1995) Apoptosis in the pathogenesis and treatment of disease. Science **267**, 1456–1462.
3. G. Evan, E. Harrington, A. Fanidi, H. Land, B. Amati, and M. Bennett (1994) Integrated control of cell proliferation and cell death by the *c-myc* oncogene. Phil. Trans. R Soc. Lond. B **345**, 269–275.
4. M. D. Jacobson, M. Weil, and M. C. Raff (1997) Programmed cell death in animal development. Cell **88**, 347–354.
5. J. R. Hinchliffe and D. A. Ede (1973) Cell death and the development of limb form and skeletal pattern in normal and wingless (ws) chick embryos. J. Embryol. Exp. Morphol. **30**, 753–772.
6. A. H. Wyllie, J. F. Kerr, and A. R. Currie (1980) Cell death: The significance of apoptosis. Int. Rev. Cytol. **68**, 251–306.
7. J. F. Kerr, A. H. Wyllie, and A. R. Currie (1972) Apoptosis: A basic biological phenomenon with wide–ranging implications in tissue kinetics. Br. J. Cancer **26**, 239–257.
8. A. H. Wyllie (1980) Glucocorticoid-induced thymocyte apoptosis is associated with endogenous endonuclease activation. Nature **284**, 555–556.
9. J. Savill, V. Fadok, P. Henson, and C. Haslett (1993) Phagocyte recognition of cells undergoing apoptosis. Immunol. Today **14**, 131–136.
10. J. Savil, I. Dransfield, N. Hogg, and C. Haslett (1990) Vitronectin receptor-mediated phagocytosis of cells undergoing apoptosis. Nature **343**, 170–173.
11. J. Savill, N. Hogg, Y. Ren, and C. Haslett (1992) Thrombospondin cooperates with CD36 and the vitronectin receptor in macrophage recognition of neutrophils undergoing apoptosis. J. Clin. Invest. **90**, 1513–1522.
12. Y. Ren, R. L. Silverstein, J. Allen, and J. Savill (1995) CD36 gene transfer confers capacity for phagocytosis of cells undergoing apoptosis. J. Exp. Med. **181**, 1857–1862.
13. V. A. Fadok, D. R. Voelker, P. A. Campbell, D. L. Bratton, J. J. Cohen, P. W. Noble, D. W. Riches, and P. M. Henson (1993) The ability to recognize phosphatidylserine on apoptotic cells is an inducible function in murine bone marrow-derived macrophages. Chest **103**, 102s.
14. V. A. Fadok, D. R. Voelker, P. A. Campbell J. J. Cohen, D. L. Bratton, and P. M. Henson (1992) Exposure of phosphatidylserine on the surface of apoptotic lymphocytes triggers specific recognition and removal by macrophages. J. Immunol. **148**, 2207–2216.
15. V. A. Fadok et al. (1992) Different populations of macrophages use either the vitronectin receptor or the phosphatidylserine receptor to recognize and remove apoptotic cells. J. Immunol. **149**, 4029–4035.
16. P. K. Flora and C. D. Gregory (1994) Recognition of apoptotic cells by human macrophages: Inhibition by a monocyte/macrophage-specific monoclonal antibody. Eur. J. Immunol. **24**, 2625–2632.
17. M. F. Luciani and G. Chimini (1996) The ATP binding cassette transporter ABC1 is required for the engulfment of corpses generated by apoptotic cell death. Embo. J. **15**, 226–235.
18. N. Platt and S. Gordon (1995) Role of the murine scavenger receptor in the recognition of apoptotic thymocytes by macrophages. J. Cell Biochem. Suppl. **19B**, 300.
19. M. Stern, J. Savill, and C. Haslett (1996) Human monocyte-derived macrophage phagocytosis of senescent eosinophils undergoing apoptosis. Mediation by alpha v beta 3/CD36/thrombospondin recognition mechanism and lack of phlogistic response. Am. J. Pathol. **149**, 911–921.
20. N. J. McCarthy, C. A. Smith, and G. T. Williams (1992) Apoptosis in the development of the immune system: Growth factors, clonal selection and bcl-2. Canc. Metas. Rev. **11**, 157–178.
21. G. I. Evan, L. Brown, M. Whyte and E. Harrington (1995) Apoptosis and the cell-cycle. Curr. Opin. Cell Biol. **7**, 825–834.

22. M. Raff, B. Barres, J. Burne, H. Coles, Y. Ishizaki, and M. Jacobson (1993) Programmed cell death and the control of cell survival: Lessons from the nervous system. Science **262**, 695–700.
23. S. Nagata (1997) Apoptosis by death factor. Cell **88**, 355–365.
24. M. K. Collins, J. Marvel, P. Malde, and A. Lopez-Rivas (1992) Interleukin 3 protects murine bone marrow cells from apoptosis induced by DNA damaging agents. J. Exp. Med. **176**, 1043–1051.
25. E. Harrington, A. Fanidi, M. Bennett, and G. Evan (1994) Modulation of Myc-induced apoptosis by specific cytokines. Embo. J. **13**, 3286–3295.
26. G. T. Williams, C. A. Smith, E. Spooncer, T. M. Dexter, and D. R. Taylor (1990) Haemopoietic colony stimulating factors promote cell survival by suppressing apoptosis. Nature **343**, 76–79.
27. R. C. Duke and J. J. Cohen (1986) IL-2 addiction: Withdrawal of growth factor activates a suicide program in dependent T cells. Lymphokine Res. **5**, 289–299.
28. E. White, P. Sabbatini, M. Debbas, W. Wold, D. Kusher, and L. Gooding (1992) The 19-kilodalton Adenovirus E1B transforming protein inhibits programmed cell death and prevents cytolysis by tumour necrosis factor . Mol. Cell. Biol. **12**, 2570–2580.
29. E. White, R. Cipriani, P. Sabbatini, and A. Denton (1991) Adenovirus E1B 19-kilodalton protein overcomes the cytotoxicity of E1A proteins. J. Virol. **65**, 2968–2678.
30. A. Zychlinsky, B. Kenny, R. Menard, M. C. Prevost, I. B. Holland, and P. J. Sansonetti (1994) IpaB mediates macrophage apoptosis induced by *Shigella flexneri*. Mol. Microbiol **11**, 619–627.
31. K. Thirumalai, K. S. Kim, and A. Zychlinsky (1997) IpaB, a *Shigella flexneri* invasin, colocalizes with interleukin-1 beta-converting enzyme in the cytoplasm of macrophages. Infect. Immun. **65**, 787–793.
32. A. Guichon and A. Zychlinsky (1996) Apoptosis as a trigger of inflammation in *Shigella*-induced cell death. Biochem. Soc. Trans. **24**, 1051–1054.
33. G. Evan et al. (1992) Induction of apoptosis in fibroblasts by *c-myc* protein. Cell **63**, 119–125.
34. M. Zonig and G. I. Evan (1996) Cell cycle: On target with Myc. Curr. Biol. **6**, 1553–1556.
35. E. Harrington, A. Fanidi, and G. Evan (1994) Oncogenes and cell death. Curr. Opin. Genet. Dev. **4**, 120–129.
36. C. A. Evans, L. P. Owen, A. D. Whetton, and C. Dive (1993) Activation of the Abelson tyrosine kinase activity is associated with suppression of apoptosis in hemopoietic cells. Cancer Res. **53**, 1735–1738.
37. J. L. Cleveland, M. Dean, N. Rosenberg, J. Y. Wang, and U. R. Rapp (1989) Tyrosine kinase oncogenes abrogate interleukin-3 dependence of murine myeloid cells through signaling pathways involving c-myc: Conditional regulation of c-myc transcription by temperature-sensitive v-abl. Mol. Cell. Biol. **9**, 5685–5695.
38. Y. Tsujimoto, L. R. Finger, J. Yunis, P. C. Nowell, and C. M. Croce (1984) Cloning of the chromosome breakpoint of neoplastic B cells with the t(14;18) chromosome translocation. Science **226**, 1097–1099.
39. A. Fanidi, E. Harrington, and G. Evan (1992) Cooperative interaction between *c-myc* and *bcl-2* proto-oncogenes. Nature **359**, 554–556.
40. R. Bissonnette, F. Echeverri, A. Mahboubi, and D. Green (1992) Apoptotic cell death induced by *c-myc* is inhibited by *bcl-2*. Nature **359**, 552–554.
41. A. Strasser, A. W. Harris, M. L. Bath, and S. Cory (1990) Novel primitive lymphoid tumours induced in transgenic mice by cooperation between *myc* and *bcl-2*. Nature **348**, 331–333.
42. T. J. McDonnell and S. J. Korsmeyer (1991) Progression from lymphoid hyperplasia to high-grade malignant lymphoma in mice transgenic for the t(14;18). Nature **349**, 254–256.
43. S. J. Korsmeyer, T. J. McDonnell, G. Nunez, D. Hockenbery, and R. Young (1990) Bcl-2: B cell life, death and neoplasia. Curr. Top. Microbiol. Immunol. **166**, 203–207.

44. Y. Tsujimoto, J. Cossman, E. Jaffe, and C. M. Croce (1985) Involvement of the bcl-2 gene in human follicular lymphoma. Science **228**, 1440–1443.
45. J. C. Reed (1997) Double identity for proteins of the Bcl-2 family. Nature **387**, 773–776.
46. M. D. Jacobson (1997) Apoptosis: Bcl-2-related proteins get connected. Curr. Biol. **7**, R227–R281.
47. E. Yang and S. J. Korsmeyer (1996) Molecular thanatopsis: A discourse on the BCL2 family and cell death. Blood **88**, 386–401.
48. G. Williams and C. Smith (1993) Molecular regulation of apoptosis—genetic-controls on cell-death. Cell **74**, 777–779.
49. Z. Oltvai, C. Milliman, and S. Korsmeyer (1993) Bcl-2 heterodimerizes in vivo with a conserved homolog, Bax, that accelerates programed cell death. Cell **74**, 609–619.
50. L. Boise et al. (1993) *bcl*-x, a *bcl-2*-related gene that functions as a dominant regulator of apoptotic cell death. Cell **74**, 597–608.
51. T. Chittenden, E. Harrington, R. O"Connor, G. Evan, and B. Guild (1995) Induction of apoptosis by the Bcl-2 homologue Bak. Nature **374**, 733–736.
52. M. Kiefer, M. Brauer, V. C. Powers, J. Wu, S. Umansky, L. Tomei, and P. Barr (1995) Modulation of apoptosis by the widely distributed Bcl-2 homologue Bak. Nature **374**, 736–739.
53. S. Farrow et al. (1995) Cloning of a novel *bcl-2* homologue by interaction with adnovirus E1B 19K. Nature **374**, 731–733.
54. B. S. Chang, A. J. Minn, S. E. Muchmore, S. W. Fesik, and C. B. Thompson (1997) Identification of a novel regulatory domain in Bcl-xL and Bcl-2. Embo J. **16**, 968–977.
55. S. W. Muchmore, M. Sattler, H. Liang, R. P. Meadows, J. E. Harlan, H. S. Yoon, D. Nettesheim, B. S. Chang, C. B. Thompson, S. L. Wong, S. L. Ng, and S. W. Fesik (1996) X-ray and NMR structure of human Bcl-xL, an inhibitor of programmed cell death. Nature **381**, 335–341.
56. X.-M. Yin, Z. Oltvai, and S. Korsemeyer (1994) Bh1 and bh2 domains of Bcl-2 are required for inhibition of apoptosis and heterodimerization with Bax. Nature **369**, 321–323.
57. T. Sato, S. Irie, S. Krajewski, and J. C. Reed (1994) Cloning and sequencing of a cDNA encoding the rat Bcl-2 protein. Gene **140**, 291–292.
58. S. Takayama et al. (1995) Cloning and functional-analysis of *bag-1*—a novel *bcl-2*-binding. Cell **80**, 279–284.
59. E. Yang, J. P. Zha, J. Jockel, L. H. Boise, C. B. Thompson, and S. J. Korsmeyer (1995) Bad, a heterodimeric partner for Bcl-xL and Bcl-2, displaces Bax and promotes cell death. Cell **80**, 285–291.
60. J. Zha, H. Harada, E. Yang, J. Jockel, and S. J. Korsmeyer (1996) Serine phosphorylation of death agonist BAD in response to survival factor results in binding to 14-3-3 not BCL-X(L) Cell **87**, 619–628 (see comments).
61. L. O"Reilly, D. Huang, and A. Strasser (1996) The cell death inhibitor Bcl-2 and its homologues influence control of cell cycle entry. Embo. J. **15**, 6979–6990.
62. M. B. Kastan, O. Onyekwere, D. Sidransky, B. Vogelstein, and R. W. Craig (1991) Participation of p53 protein in the cellular response to DNA damage. Cancer Res. **51**, 6304–6311.
63. D. P. Lane (1992) Cancer. p53, guardian of the genome. Nature **358**, 15–16 (news; comment).
64. W. El-Deiry et al. (1993) *WAF1*, a potential mediator of p53 tumor suppression. Cell **76**, 817–825.
65. C. Caelles, A. Helmberg, and M. Karin (1994) p53-dependent apoptosis in the absence of transcriptional activation of p53-target genes. Nature **370**, 220–223 (see comments).
66. C. Yin, C. M. Knudson, S. J. Korsmeyer, and T. Van Dyke (1997) Bax suppresses

tumorigenesis and stimulates apoptosis in vivo. Nature **385**, 637–640.

67. S. W. Lowe, E. M. Schmitt, S. W. Smith, B. A. Osborne, and T. Jacks (1993) p53 is required for radiation-induced apoptosis in mouse thymocytes. Nature **362**, 847–849 (see comments).
68. A. R. Clarke et al. (1993) Thymocyte apoptosis induced by p53-dependent and independent pathways. Nature **362**, 849–852 (see comments).
69. A. Clarke et al. (1992) Requirement for a functional *Rb-1* gene in murine development. Nature **359**, 328–330.
70. E.-H. Lee et al. (1992) Mice deficient for Rb are nonviable and show defects in neurogenesis and haematopoiesis. Nature **359**, 288–294.
71. T. Jacks, A. Fazeli, E. Schmitt, R. Bronson, M. Goodell, and R. Weinberg (1992) Effects of an *Rb* mutation in the mouse. Nature **359**, 295–300.
72. H. Symonds et al. (1994) p53-dependent apoptosis suppresses tumour growth and progression *in vivo*. Cell **76**, 703–711.
73. Z. Xia, M. Dickens, J. Raingeaud, R. Davis, and M. Greenberg (1995) Opposing effects of ERK and JNK-p38 MAP kinases on apoptosis. Science **270**, 1326–1331.
74. C. D. Nobes and A. M. Tolkovsky (1995) Neutralizing anti-p21ras Fabs suppress rat sympathetic neuron survival induced by NGF, LIF, CNTF and cAMP. Eur. J. Neurosci. **7**, 344–350.
75. A. Geier, R. Beery, M. Haimsohn, R. Hemi, Z. Malik, and A. Karasik (1994) Epidermal growth factor, phorbol esters, and aurintricarboxylic acid are survival factors for MDA-231 cells exposed to adriamycin. In Vitro Cell Dev. Biol. Anim. **30a**, 867–874.
76. R. Yao and G. M. Cooper (1995) Requirement for phosphatidylinositol-3 kinase in the prevention of apoptosis by nerve growth factor. Science **267**, 2003–2006.
77. S. Kennedy, A. Wagner, S. Conzen, J. Jordan, A. Bellacosa, P. Tsichlis, and N. Hay (1997) The PI 3-kinase/akt signaling pathway delivers an anti-apoptotic signal. Genes & Devel. **11**, 701–713.
78. H. Dudek et al. (1997) Regulation of neuronal survival by the serine-threonine protein-kinase akt. Science **275**, 661–665.
79. A. Kauffmann-Zeh, P. Rodriguez-Viciana, E. Ulrich, C. Gilbert, P. Coffer, and G. Evan (1997) Suppression of c-Myc-induced apoptosis by Ras signalling through PI 3-kinase and PKB. Nature **385**, 544–548.
80. P. Krammer, I. Behrmann, P. Daniel, J. Dhein, and K.-M. Debatin (1994) Regulation of apoptosis in the immune sustem. Curr. Opin. Immunol. **6**, 279–289.
81. S. Nagata and P. Golstein (1995) The Fas death factor. Science **267**, 1449–1456.
82. L. Tartaglia, T. Ayres, G. Wong, and D. Goeddel (1993) A novel domain within the 55 kd TNF receptor signals cell death. Cell **74**, 845–853.
83. N. Itoh and S. Nagata (1993) A novel protein domain required for apoptosis. Mutational analysis of human Fas antigen. J. Biol. Chem. **268**, 10932–10937.
84. M. Rothe, V. Sarma, V. W. Dixit, and D. V. Goeddel (1995) Traf2-mediated activation of NF-kappa-b by TNF receptor-2 and CD40. Science **269**, 1424–1427.
85. M. Boldin, E. Varfolomeev, Z. Pancer, I. Mett, J. Camonis, and D. Wallach (1995) A novel protein that interacts with the death domain of Fas/Apo1 contains a sequence related tothea death domain. J. Biol. Chem. **270**, 7795–7798.
86. A. M. Chinnaiyan, K. O"Rourke, M. Tewari, and V. M. Dixit (1995) FADD, a novel death domain-containing protein, interacts with the death domain of Fas and initiates apoptosis. Cell **81**, 505–512.
87. M. Muzio et al. (1996) FLICE, a novel FADD homologous ICE/CED-3–like protease, is recruited to the CD95 (Fas/Apo-1) death-inducing signaling complex. Cell **85**, 817–827.
88. M. Boldin, T. Goncharov, Y. Goltsev, and D. Wallach (1996) Involvement of MACH, a novel

MORT1/FADD-interacting protease, in Fas/APO-1- and TNF receptor-induced cell death. Cell **85**, 803–815.

89. A. Chinnaiyan and V. Dixit (1996) The cell-death machine. Curr. Biol. **6**, 555–562.
90. X. Zhang et al. (1996) Up-regulation of Bcl-xL expression protects CD40-activated human B cells from Fas-mediated apoptosis. Cell Immunol **173**, 149–154.
91. M. Thome et al. (1997) Viral FLICE inhibitory proteins (FLIPs) prevent apoptosis induced by death receptors. Nature **386**, 517–521.
92. E. Alnemri, D. Livingston, D. Nicholson, G. Salvesan, N. Thornberry, W. Wong, and J. Yuan (1996) Human ICE/CED-3 protease nomeclature. Cell **87**, 171.
93. Y. Lazebnik, A. Takahashi, G. Poirier, S. H. Kaufmann, and W. Earnshaw (1995) Characterization of the execution phase of apoptosis *in vitro* using extracts from condemned-phase cells. J. Cell Sci. **19**, 41–49.
94. A. Takahashi and W. Earnshaw (1996) Ice-related proteases in apoptosis. Curr. Opin. Gen. & Dev. **6**, 50–55.
95. Y. Jung, M. Miura, and J. Yuan (1996) Suppression of interleukin-1 beta-converting enzyme-mediated cell death by insulin-like growth factor. J. Biol. Chem. **271**, 5112–5117.
96. V. Gagliardini, P. A. Fernandez, R. K. Lee, H. C. Drexler, R. J. Rotello, M. C. Fishman, and J. Yuan (1994) Prevention of vertebrate neuronal death by the crmA gene. Science **263**, 826–828.
97. N. Bump et al. (1995) Inhibition of ICE family proteases by baculovirus antiapoptotic protein p35. Science **269**, 1885–1888.
98. J. Xiang, D. Chao, and S. Korsmeyer (1996) Bax-induced cell death may not require interleukin-1ß-converting enzyme-like proteases. Proc. Natl. Acad. Sci. USA **93**, 14559–14563.
99. N. McCarthy, M. Whyte, C. Gilbert, and G. Evan (1997) Inhibition of Ced-3/ICE-related proteases does not prevent cell death induced by oncogenes, DNA damage, or the Bcl-2 homologue Bak. J. Cell. Biol. **136**, 215–227.
100. J. Yuan and H. R. Horvitz (1992) The *Caenorhabditis elegans* cell death gene ced-4 encodes a novel protein and is expressed during the period of extensive programmed cell death. Development **116**, 309–320.
101. A. M. Chinnaiyan, K. O"Rourke, B. R. Lane, and V. M. Dixit (1997) Interaction of CED-4 with CED-3 and CED-9: A molecular framework for cell death. Science **275**, 1122–1126 (see comments).
102. M. S. Spector, S. Desnoyers, D. J. Hoeppner, and M. O. Hengartner (1997) Interaction between the *C. elegans* cell-death regulators CED-9 and CED-4. Nature **385**, 653–656.
103. D. Wu, H. D. Wallen, and G. Nunez (1997) Interaction and regulation of subcellular localization of CED-4 by CED-9. Science **275**, 1126–1129 (see comments).
104. C. James, S. Gschmeissner, A. Fraser, and G. Evan (1997) Ced-4 induces chromatin condensation in *S. pombe* and is inhibited by direct physical association with Ced-9. Curr. Biol. **7**, 246–252.
105. M. Whyte (1996) ICE/Ced-3 proteases in apoptosis. Trends Cell Biol. **6**, 245–248.
106. A. Fraser, N. McCarthy, and G. I. Evan (1996) Biochemistry of cell-death. Curr. Opin. Neurobiol. **6**, 71–80.
107. T. Fernandes Alnemri et al. (1996) In-vitro activation of CPP32 and Mch3 by Mch4, a novel human apoptotic cysteine protease containing 2 FADD-like domains. Proc. Natl. Acad. Sci. USA **93**, 7464–7469.
108. Y. A. Lazebnik, A. Takahashi, R. D. Moir, R. D. Goldman, G. G. Poirier, S. H. Kaufmann, and W. C. Earnshaw (1995) Studies of the lamin proteinase reveal multiple parallel biochemical pathways during apoptotic execution. Proc. Natl. Acad. Sci. USA **92**, 9042–9046.
109. A. Fraser and G. Evans (1996) A license to kill. Cell **85**, 781–784.

110. P. J. Hartfield, G. C. Mayne, and A. W. Murray (1997) Ceramide induces apoptosis in PC12 cells. FEBS Lett. **401**, 148–152.
111. S. C. Wright, H. Zheng, and J. Zhong (1996) Tumor cell resistance to apoptosis due to a defect in the activation of sphingomyelinase and the 24 kDa apoptotic protease (AP24). Faseb. J. **10**, 325–332.
112. P. Santana et al. (1996) Acid sphingomyelinase-deficient human lymphoblasts and mice are defective in radiation-induced apoptosis. Cell **86**, 189–199.
113. G. J. Pronk, K. Ramer, P. Amiri, and L. T. Williams (1996) Requirement of an ICE-like protease for induction of apoptosis and ceramide generation by REAPER. Science **271**, 808–810.
114. M. Jacobson and M. Raff (1995) Programmed cell-death and *bcl-2* protection in very-low oxygen. Nature **374**, 814–816.
115. R. M. Kluck, E. Bossy Wetzel, D. R. Green, and D. D. Newmeyer (1997) The release of cytochrome c from mitochondria: A primary site for Bcl-2 regulation of apoptosis. Science **275**, 1132–1136 (see comments).
116. J. Yang, X. Liu, K. Bhalla, C. N. Kim, A. M. Ibrado, J. Cai, T. I. Peng, D. P. Jones, and X. Wang (1997) Prevention of apoptosis by Bcl-2: Release of cytochrome c from mitochondria blocked. Science **275**, 1129–1132 (see comments).
117. G. Kroemer, N. Zamzami, and S. A. Susin (1997) Mitochondrial control of apoptosis. Immunol. Today **18**, 44–51.

Suggestions for Further Reading

118. M. D. Jacobson (1997) Apoptosis: Bcl-2-related protein get connected. Curr. Biol. **7**(5), R277–R281. An up-to-date review on the pathway of apoptosis.
119. M. D. Jacobson, M. Weil, and M. C. Raff (1997) Programmed cell death in animal development. Cell **88**, 347–354.
120. M. Sluyser, ed. (1996) *Apoptosis in Normal Development and Cancer*, Taylor and Francis, London.
121. E. Yang and S. J. Korsmeyer (1996) Molecular thanatopsis: A discourse on the Bcl-2 family and cell death. Blood **88**, 386–401.

ara Operon

The pentose sugar L-arabinose is distributed widely as a component of **plant** polysaccharides in pectins, gums, and cell walls. It is also present in smaller amounts in the cell walls of some **bacteria**. Thus it is likely that, in its natural environment in the vertebrate intestine, the bacterium *Escherichia coli* periodically encounters arabinose released through degradation of these polymers (1). Not surprisingly, *E. coli*, like many other bacteria and fungi, has *ara* **genes** that encode the enzymes and **transport** proteins necessary to utilize L-arabinose as a source of carbon and energy.

The *ara* genes of *E. coli* have been of exceptional importance to biology for several reasons. If the lac operon is the exemplar of regulation of **gene expression** by **repression of expression**, the *ara* operon is the counterpart as the model for positive control of gene expression, even though more complete analysis has revealed that each has both positive and negative features. (An operon is one gene or a linear sequence of related genes that are transcribed as one unit from a common initiation point [see Transcription]. The transcript is then **translated** into protein products corresponding to the separate genes.) The first clear example of DNA looping as a feature of transcription control was the *ara* operon. The hypothesis of positive control of the *ara* operon was a challenge to establishment scientists, and its validation was the end of a fascinating story in the history of science. Moreover, the details of the operon are complex and interesting in themselves.

1. *ara* Operon of *Escherichia coli*

The classical *ara* operon of the bacterium *Escherichia coli* comprises three genes, *araBAD* (Fig. 1). This and four other operons, *araC, araE, araFGH*, and *araJ*, are uniquely associated with metabolism of L-arabinose (Table 1). Each set of genes is under control of the activator protein AraC, the product of the *araC* gene. The function of each gene is known, except for *araJ*, which may encode a protein that processes or transports an arabinose-containing polymer, or pumps potentially toxic arabinosides from the cell.

Figure 1. The positions of the *araBAD* operon and the *araC* regulatory gene on the *E. coli* chromosome. Transcription o
nucleotide-pair region between *araB* and *araC*. Nucleotide location on the *E. coli* chromosome is shown beneath the gen
the three inverted repeat REP sequence pairs that are assumed to produce three self-paired hairpin structures in the mRN
entire chromosome contains approximately 4,639,221 nucleotide pairs. The primary sequence information is in Refs. 24

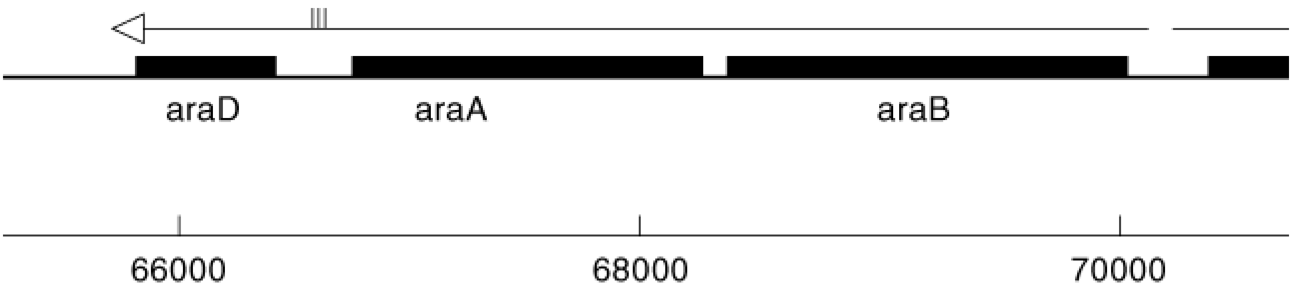

Table 1. *ara* Genes and Gene Products

Gene	Location on the *E. coli* chromosome (minutes)[a]	Size of gene (amino acid codons)	Activity of product
araA	1.4	500	L-arabinose isomerase
araB	1.5	566	L-ribulokinase
araC	1.5	292	AraC regulatory protein
araD	1.4	231	L-ribulose-5-phosphate-4-epimerase
araE	64.2	472	L-arabinose transport, low affinity
araF	42.8	329	L-arabinose transport, high affinity
araG	42.7	504	L-arabinose transport,

			high affinity
araH	42.6	329	L-arabinose transport, high affinity
araJ	8.5	394	Transport or processing of polymer? Efflux of toxic arabinosides?

[a] Location is based on a 100 minute circular chromosome.

1.1. Uptake and Utilization of Arabinose

Two independent systems deliver arabinose from the environment across the cell membrane into the cell. *araE* encodes a membrane protein that mediates arabinose uptake via proton **symport** and is the lower affinity transporter (K_M = 50 µM) (2). The *araFGH* operon encodes a **periplasmic** arabinose-binding protein (*araF*), a probable ATPase subunit (*araG*), and a membrane protein (*araH*), which together mediate ATP-driven arabinose transport. This transporter shows higher affinity for arabinose (K_M = 1 µM) than AraE, but lower capacity (2, 3).

Internal arabinose is converted in three steps to D-xylulose-5-phosphate, a metabolyte in the pentose-phosphate shunt pathway and one that is not unique to arabinose metabolism. The enzyme mediating the first step, L-arabinose isomerase, has a low affinity for arabinose with a KM (Michaelis constant) of 60 mM (4); this suggests that cells growing on arabinose have a very high internal arabinose concentration (5). The glucose-specific phosphotransferase enzyme IIA^{Glc} when unphosphorylated inhibits the isomerase (unpublished results cited in 6) This inhibition may be one of the causes of the preferential use of glucose when both arabinose and glucose are in the environment.

The product of isomerase activity, L-ribulose, is converted to L-ribulose-5-phosphate by L-ribulokinase, and the phosphorylated compound is converted in turn to xylulose phosphate by the epimerase encoded by *araD*. Arabinose inhibits growth of *araD* mutants on other nutrients, presumably because accumulation of a high concentration of ribulose phosphate is toxic. Thus secondary mutants lacking isomerase or kinase activity as the result of *araA, araB*, or *araC* mutation, and therefore not forming ribulose phosphate, can be selected by plating an *araD* population on broth plates containing arabinose (7).

1.2. Regulation of *ara* Operon Expression

In the absence of arabinose, the *ara* genes are essentially not expressed, except for the regulatory gene, *araC*. On exposure to L-arabinose, all of the *ara* genes are activated, transcription of *araBAD* begins within five seconds, and the Ara proteins appear within several minutes, allowing growth on the sugar (5). The true inducer has been shown by X-ray crystallography of the inducer-AraC protein complex to be -L-arabinose (8). L-lyxose also induces the *ara* genes (9). However induction of the *ara* genes by lyxose is unlikely to occur in nature because L-lyxose is rare. *araC* mutants have been obtained that are inducible by D-fucose or by -methyl-L-arabinoside, normally inhibitors of induction (1, 10, 11).

In vivo studies using cells lacking both arabinose transport systems showed the K_M for induction by arabinose to be unexpectedly high, nearly 10 mM (11), although, as noted above, the internal arabinose concentration is likely to be higher than this during growth on arabinose because of the low affinity of the isomerase for the pentose. The high concentration-dependence of induction suggests that there might be natural selection against a mutant isomerase with a better affinity for arabinose.

Complementation studies showed that the *presence* of AraC protein is necessary for *araBAD* gene expression (12, 13), a discovery unanticipated by those who believed all gene activation resulted from *removal* of repressors. Later, AraC was shown to be required for expression of the other *ara* operons as well (except for *araC*). *araC* is the prototype for a large family of regulatory genes that share sequence similarity in the DNA binding region and are homologous and presumably related through evolution (14).

Cyclic AMP (3¢,5¢-cyclic AMP, cAMP) bound to cyclic AMP receptor protein (CRP) is also a positive regulator for all the *ara* operons. Expression of many genes is controlled by availability of CRP-cAMP; lack of expression due to low CRP-cAMP is referred to as catabolite repression. *In vitro* transcription of *araBAD* mimics that *in vivo* in that it requires both the AraC and CRP regulatory proteins with their bound ligands. Analysis of transcription *in vitro*, and further *in vivo* studies, have given a broad understanding at the molecular level of control of *araBAD* transcription although details remain to be determined (5).

The AraC protein structure has two domains connected by a flexible polypeptide linker. The *N*-terminal domain binds arabinose and is responsible for formation of the active dimeric form of the protein. The *C*-terminal domain binds DNA at specific sites, with similar sequences, upstream of each *ara* operon. In the regulatory region between the divergently transcribed *araBAD* and *araC* operons (Fig. 1), there are five sites at which AraC can bind (Fig. 2).

Figure 2. Activation of transcription of the *araBAD* operon by arabinose. CRP refers to CRP-cAMP, and P refers to RNA polymerase. AraC protein is shown as a dimer bound to $I_1$and O_2in the absence of arabinose and to $I_1$and I_2in the presence of arabinose. I_1, I_2, O_1 (a double site), and $O_2$are all potential binding sites for the AraC protein and conform to the consensus sequence 5¢;-TAGCN$_7$TCCATA-3¢ (reading in the direction of the arrows) (16) although there is considerable variation among sites. Note how the mode of pairing of the dimers differs depending on the presence of arabinose (5, 8). On addition of arabinose, transcription of *araBAD* is initiated and expression of *araC* is increased (bottom). After a few minutes AraC-arabinose dimers are thought to bind to O_1 and O_2 so as to form a new DNA loop and reduce *araC* transcription to that characteristic of cells in the absence of arabinose (not shown).

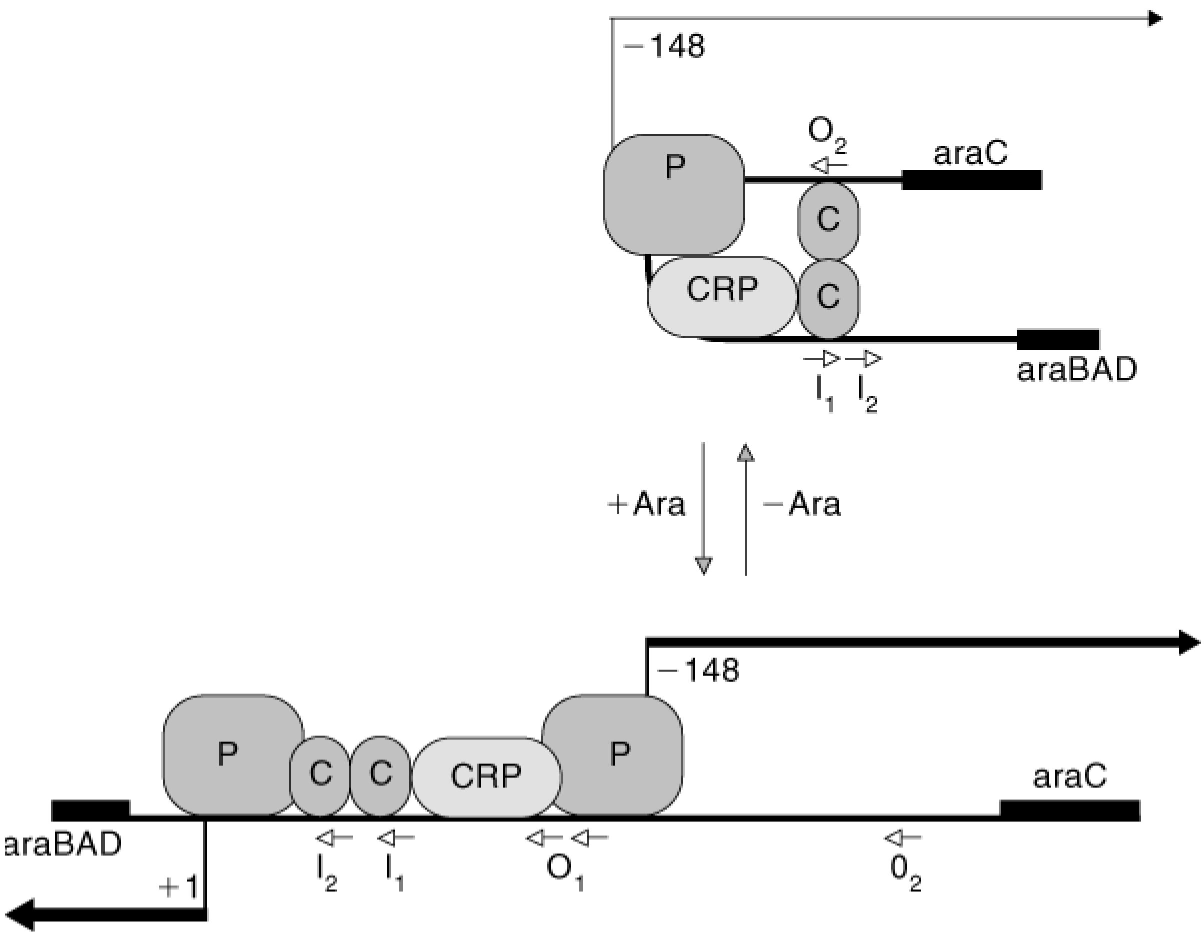

In the absence of arabinose, the two DNA-binding domains of the AraC dimer are oriented so that they can not readily bind both of the adjacent I sites at the same time. Instead, the AraC dimer contacts I_1 and O_2, thereby forming a DNA loop within the region between *araB* and *araC* (Fig. 2) (15). On addition of arabinose, the dimer undergoes a conformational shift such that the two DNA-binding domains preferentially bind I_2I_1 (Fig. 2) (16). The presence of AraC at I_2 stimulates addition of **RNA polymerase** and open complex formation, and transcription of *araBAD* commences, if CRP-cAMP is present (5). Although this model was proposed and refined before detailed structural information was available, X-ray crystallographic studies of the AraC *N*-terminal domain and linker support the model (8).

Addition of arabinose also affects expression of *araC*. When the I_1-O_2 loop is opened, transcription of *araC* is accelerated (Fig. 2). After a few minutes, AraC-arabinose dimers are thought to reform DNA loops, this time by bridging O_1 and O_2 (17, 18). O_1-O_2 looping does not regulate *araBAD* transcription, but interferes with RNA polymerase binding and initiation at the *araC* promoter; this reduces the rate of *araC* transcription to that characteristic of cells in the absence of arabinose (5).

araC is controlled by CRP-cAMP as well. CRP-cAMP binding increases, but is not essential for, *araC* transcription; it is necessary for substantial expression of the other *ara* operons.

The mechanism by which AraC-arabinose, CRP-cAMP, and RNA polymerase interact to trigger transcription is not clear. Bound CRP-cAMP helps to open the I_1I_2 repression loop on addition of arabinose, but it probably activates RNA polymerase binding or initiation as well, either by direct contact or indirectly through contact with AraC (5). (CRP-cAMP does not aid AraC binding.)

Several kinds of CRP-cAMP-independent mutants have been obtained. One class (*rpoD*) has an altered RNA polymerase **sigma factor**-70 subunit (19), while another (*araC*) is altered in AraC itself (20). Other mutants (*araI*) are transcribed by RNA polymerase independently of the AraC or CRP proteins, and they result from changes at the RNA polymerase binding site in the *araBAD* promoter (21).

2. Other Mechanisms for Arabinose Degradation

The pathway for arabinose degradation that is common to *E. coli* and many other bacteria is not the sole means for utilizing L-arabinose in the biological world, nor is the regulatory model described above the only means for control of *ara* enzyme synthesis. At least five different pathways exist (1), and different regulatory systems are found even among organisms using the same pathway. Although the work on other organisms is still at an early stage, it is known that the **gram-positive** bacterium, ***Bacillus*** *subtilus*, utilizes the same degradatory pathway for arabinose utilization as *E. coli* but appears to use a simple repressor as the means of control of *ara* gene expression (22). The fungus ***Aspergillus*** uses a completely different pathway for arabinose utilization and, not surprisingly, appears to have different control systems as well (23). It will be remarkable if the *ara* genes in these other organisms are regulated by the simple repressors once hypothesized for the *ara* genes in *E. coli*.

Bibliography

"*ara* Operon" in , Vol. 1, pp. 187–190, by Robert B. Helling, University of Michigan, Department of Biology, Ann Arbor, Michigan; "*ara* Operon" in (online), posting date: January 15, 2002, by Robert B. Helling, University of Michigan, Department of Biology, Ann Arbor, Michigan.

1. M.E. Doyle (1974) Ph.D thesis, The University of Michigan, University Microfilms, Ann Arbor, MI, 71 pp.
2. R. Schleif (1969) J. Mol. Biol. **46**, 185–196.
3. R.W. Hogg (1977) J. Supramol. Struct. **6**, 411–417.
4. J.W. Patrick and N. Lee (1968) J. Biol. Chem. **243**, 4312–4318.
5. R. Schleif (2000) Trends in Genetics **16**, 559–565.
6. C. Hoischen et al. (1996) J. Bacteriol. **178**, 6082–6086.
7. H. Boyer, E. Englesberg, and R. Weinberg (1962) Genetics **47**, 417–425.
8. S.M. Soisson et al. (1997) Science **276**, 421–425.
9. E. Ibanez et al. (2000) J. Bacteriol. **182**, 4625–4627.
10. S. Beverin, D.E. Sheppard, and S.S. Park (1971) J. Bacteriol. **106**, 107–112.
11. M.E. Doyle et al. (1972) J. Bacteriol. **110**, 56–65.
12. R.B. Helling and R. Weinberg (1963) Genetics **48**, 1397–1410.
13. E. Englesberg et al. (1965) J. Bacteriol. **90**, 946–957.
14. M.-T. Gallegos et al. (1997) Microbiol. Mol. Biol. Rev. **61**, 393–410.
15. K. Martin, L. Huo, and R. Schleif (1986) Proc. Nat. Acad. Sci. USA **83**, 3654–3658.
16. N. Lee, C. Francklyn, and E. P. Hamilton (1987) Proc. Nat. Acad. Sci. USA **84**, 8814–8818.
17. E. P. Hamilton and N. Lee (1988) Proc. Nat. Acad. Sci. USA **85**, 1749–1753.
18. L. Huo, K. J. Martin, and R. Schleif (1988) Proc. Nat. Acad. Sci USA **85**, 5444–5448.
19. J.C. Hu and C.A. Gross (1985) Mol. Gen. Genet. **199**, 7–13.
20. L. Heffernan, R. Bass, and E. Englesberg (1976) J. Bacteriol. **126**, 1111–1131.
21. A.H. Horwitz, C. Morandi, and G. Wilcox (1980) J. Bacteriol. **142**, 659–667.
22. L. J. Mota, L. M. Sarmento, and I. Sa-Nogueira (2001) J. Bacteriol. **183**, 4190–4201.
23. G.J.G. Ruijter et al. (1997) Microbiol. **143**, 2991–2998.

24. R.G. Wallace, N. Lee, and A.V. Fowler (1980) Gene **12**, 179–190.
25. N. Lee et al. (1986) Gene **47**, 231–244.

Suggestions for Further Reading

26. J. Beckwith (1987) "The operon: an historical account". In *Escherichia coli and Salmonella typhimurium. Cellular and Molecular Biology* (F.C. Neidhardt, J.L. Ingraham, K.B. Low, B. Magasanik, M. Schaechter, and H.E. Umbarger, ed.), American Society for Microbiology, Washington, DC, pp. 1439–1443. (Describes the difficulty in achieving acceptance of the model of positive control.)
27. J. Gross and E. Englesberg (1959) Determination of the order of mutational sites governing L-arabinose utilization in *Escherichia coli* B/r by transduction with phage P1bt. Virology **9**, 314–331. (This is the research paper in which the initial studies with the *ara* operon are described. It has served as a model guiding analysis of many other genes.)
28. R. Schleif (1993) "Induction, repression and the *araBAD* operon". In *Genetics and Molecular Biology*, 2nd ed., Johns Hopkins University Press, pp. 359–383. (Systematic description of the arabinose genes and enzymes, and how it has been studied. Thoughtful and stimulating, with problems (and answers at the end of the book).
29. R. Schleif (2000) Regulation of the L-arabinose operon of *Escherichia coli*. Trends in Genetics **16**, 559–565. (Recent review of control of transcription of the *ara* genes focusing on the AraC protein and its structural changes.)

Arabidopsis

Arabidopsis thaliana (L.) Heynh is a dicotyledonous plant that is ideally suited for molecular-genetic studies. It is generally accepted as a model for unraveling the molecular mechanisms involved in plant growth and development, biochemical pathways, cell biology, physiology, and pathogenic interactions. Minimal genomic DNA content, few repetitive DNA sequences, and small gene families account for its technical and biological simplicity. *Arabidopsis* is a natural diploid amenable to laboratory-scale genetic experiments. It is small (15 cm to 30 cm) and is grown at high density (100 plants per 0.5 m^2) without seed contamination. It has a short life cycle (6 weeks to 3 months), high seed production by self-fertilization (up to 10,000 seeds per plant), is mutagenized easily, and with its 200 different ecotypes is a natural source of genetic variation. International coordination of *Arabidopsis* research has resulted in fast exchange of material, methodology, and information and in the creation of large-scale research programs, such as the genome-sequencing and expressed-sequence tag (EST) projects. The completion of the entire genome sequence was a milestone in plant biology because for the first time a molecular overview has been obtained of common and different pathways between plants and other eukaryotes. Moreover, every plant gene is now accessible for functional analysis. In the post-genomic era *Arabidopsis* research maintains its pioneering position in the field of plant science.

1. History

The first botanical description of *Arabidopsis* by Johannes Thal goes back to 1577. In 1907, Laibach studied the continuity of the chromosomes (5 per haploid genome) by using the plant, and he was the first to emphasize the advantages of the species for genetic analyses (1). In 1976, Bennett and Smith showed that *Arabidopsis* has the smallest nuclear DNA content of the angiosperms analyzed. In that period, extensive chemical and irradiation mutagenesis of the plant was performed (2). Koornneef *et* *al.* (3) published the first genetic map containing 76 morphological markers. In the mid eigthies, Meyerowitz and coworkers demonstrated the small size and low complexity of the genome, which provoked a general interest in using the plant as an experimental model (4). In 1988, efficient transformation methods opened the potential of transgenic research in the species (5). At the same time, saturation mutagenesis of the genome by insertion of heterologous DNA was initiated and resulted in large collections that became available to the scientific community (6). In 1989, the US National Science Foundation launched the 'Multinational Coordinated Long Range Plan for Arabidopsis Genome Research', steered by an international board of scientists, with the aim of promoting *Arabidopsis* as a model system for plants, in analogy to other models such as *Drosophila melanogaster* and *Caenorhabditis elegans*. The major achievements of this initiative were a seed and DNA stock centers (The Arabidopsis Biological Resource Center [Ohio State University, Colombus, OH, USA] and the Nottingham Arabidopsis Stock Centre [University of Nottingham, Loughborough, UK]), a database, and joint efforts for physical mapping and sequencing of the genome and for gene identification. The *Arabidopsis* genome sequencing project was initiated in Europe at the end of 1993, followed by an American and a Japanese initiative. This international consortium, the Arabidopsis Genome Initiative completed the entire sequence by the end of 2000 (7).

2. Classification, Geographical Distribution, and Ecotypes

Arabidopsis thaliana is an annual herb of the mustard family (Brassicaceae, previously named Cruciferae), has bisexual flowers, and is typified by a cross-shaped corolla, tetradynamous stamen (four long and two short ones), and capsular fruit (siliques). The genus *Arabidopsis* consists of 27 species and has been classified under a new tribe, the Arabidae, based on classical morphological and molecular phylogenetic studies. *Arabidopsis* is a facultative long-day plant, meaning that long days accelerate the initiation of flowering. It originated from Eurasia and North Africa, but is now a common weed in the temperate regions of the Northern Hemisphere. Its broad geographical distribution resulted in natural variation. Approximately 200 ecotypes (wild populations) have been registered. These ecotypes represent a natural source of heritable variation: for instance, differences are observed in flowering time, response to cold, fresh weight production, and pathogen resistance. Among ecotypes, a DNA sequence polymorphism of up to 1.4% in low-copy DNA has been measured. Deletions, insertions, and substitutions have occurred. Frequently used ecotypes are Columbia, Niederzenz, Wassilewskija, and the laboratory strain Landsberg *erecta*. The Columbia ecotype was used as standard for the genome sequence, whereas other ecotypes are preferred for mutagenization. DNA polymorphisms are exploited in F2 populations for mapping and quantitative trait locus (QTL) analyses.

3. Genome Structure and Organization

The size of the nuclear genome of *Arabidopsis* was estimated to be between 50 to 150 Mb as determined by reassociation kinetics (see C-Value), flow cytometry, or electron microscopy. From recent physical mapping data, this size was refined to 100 to 140 Mb, which is 3- to 400-fold smaller than that of other members of the angiosperms.

In 2000, the genome sequence of *Arabidopsis* was published, covering 115.4 megabases of the 125-megabases genome (7). A whole genome duplication as well as lateral gene transfer from a cyanobacterial-like ancestor appears to be part of the evolution of the *Arabidopsis* genome. The *Arabidopsis* genome consists for 80% of single- and low-copy DNA. Four classes of highly repeated DNA have been identified, which represent only 10% of the genome and are located mainly at the telomeres and around the centromeres. Ribosomal DNA accounts for 6% of the genome and is localized at the top of chromosomes 2 and 4. In addition to the genomic sequencing, more than 30,000 redundant *Arabidopsis* ESTs have been sequenced and submitted to public databases. Comparison of EST data with data of the genome sequencing program indicates that approximately 60% of the genes are represented by an EST.

From the sequence data, several conclusions can be drawn on gene organization and DNA composition: the gene density is one gene every 4.5 kb, the average gene length is 2 kb, genes have between 0 to 30 introns, 25,498 predicted transcripts encode proteins of approximately 11,000 families, and roughly 30% of the genes could not be assigned to functional categories. The gene families are either dispersed or in tandem arrays; long stretches (approximately 120 kb) of unique or low-copy DNA are interspersed with short stretches of a few kb of moderately repeated DNA; the GC content of the DNA is 35%, and methylation occurs in 6% of the cytosine bases.

The availability of the genome sequences of *Arabidopsis* and several other organisms allows comparisons at the genome level. For example, *Arabidopsis*, *Drosophila* and *C. elegans* have a similar amount of approximately 11,000 to 15,000 different protein types, indicating that this is the minimal number of proteins needed for a functional multicellular organism. Basic processes, such as translation, appear to be conserved across kingdoms, whereas more specialized processes use proteins that differ between plants and animals. These include membrane channels and transporters, components of signal transduction pathways, and transcription factors (8). Plants contain roughly 150 unique protein families (7).

Information on the genome project and on research in general on *Arabidopsis* is centralized in "The Arabidopsis Information Resource" (TAIR) database. A home-page on the Internet (`http://www.arabidopsis.org/home.html`) provides a lot of information on ongoing research (genetic and physical maps, genome sequence information, links to public databases, seed and DNA stock centers, etc.).

4. Genetics and Physical Mapping

Based on metaphase staining and genetic linkage group analyses, the haploid chromosome number is 5, ranging in size from 13.4 Mb to 25.4 Mb. The genetic map comprises more than 460 loci. The ratio of physical to genetic distance between markers on average is 200 kb per cM. However, from the physical map construction of chromosome 4, recombination hot spots (30–50 kb/cM) and low spots (≥550 kb/cM) were found (9). Many tools are available to map a mutation, for example, recessive visible markers, codominant embryo-lethal markers, dominant selectable markers on the located T-DNA and *Activation/Dissociation* insertions, restriction fragment length polymorphism (RFLP)-derived or PCR-based molecular markers, such as microsatellites, insertion/deletions (INDEL), and single nucleotide polymorphisms (SNP). Several molecular marker maps have been constructed based on RFLP, rapid amplified polymorphic DNA, or amplified fragment length polymorphism (AFLP) as well as on different mapping populations. A combined map, made by statistical integration, gives an approximate position and order for the markers. Recombinant inbred (RI) lines, derived from a cross between Columbia and Landsberg *erecta* (10), have been used to locate 1265 molecular markers to date. The physical map consists of contigs of DNA clones that are correlated with the mapped markers. Currently, YAC, bacterial artificial chromosome (BAC), and phage P1 artificial chromosome (PAC) contig maps are available that cover the entire genome.

5. Scientific Advances and Applications

The molecular-genetic approach in *Arabidopsis* research together with cell biology tools, such as confocal microscopy, laser cell ablation, and dye-loading have led to major breakthroughs in plant developmental biology (11-13). Tremendous progress has been made in understanding the molecular control of meristem identity in vegetative meristems, during flower initiation and flower organ formation, embryo development, and pattern formation during embryogenesis, root development, epidermal cell fate specification in root hair, and trichome formation. Genes have been identified that are involved in hormone perception, biosynthesis, and signal transduction. The first hormone receptor for plants has been characterized in *Arabidopsis* (14). Much of the molecular insights into light perception and signal transduction, cell cycle regulation, and in disease resistance in higher plants comes from studies in *Arabidopsis* (15-17). Biochemical items, such as cell wall biology, are being explored. Within the next 10 years, the function of every gene will be determined. This will be achieved by reverse genetics techniques, such as knockouts and targeting-induced local lesions in genomes (TILLING) (18), to create allelic diversity and by implementation of genome-wide methods, such as transcript profiling and microarrays. In general, biological processes will be analyzed by genomics and bioinformatics tools in order to identify all the molecular components involved.

The *Arabidopsis* genes and mutants are resources that are exploited to isolate orthologs from other species and to test their functional conservation (19), or that are used for the genetic modification of even distantly related crop plants (20). The molecular markers within contigs in *Arabidopsis* have been used for comparative mapping with *Brassica* spp. Colinearity in 5- to 10-cM regions has been demonstrated between the *Arabidopsis* genome and that of *Brassica nigra* (21). This implies that information and markers obtained from the physical mapping in *Arabidopsis* can be applied to syntenic genomic regions in mustard crops to analyze important traits in breeding programs. Microarrays of *Arabidopsis* have proven to be useful for the analysis of transcription profiles of developing seeds in related species, such as *Brassica* (22), and will be a great help in the study of seed biology in engineered plants. It is to be predicted that *Arabidopsis* will be used as a reference system to accelerate knowledge accumulation in crop species. DNA sequence analysis showed the presence of genes in the *Arabidopsis* genome that suggest the existence of secondary metabolism pathway in this plant (7). Hence, *Arabidopsis* might be a helpful tool to unravel these pathways in medicinal plants.

Bibliography

"Arabidopsis" in , Vol. 1, pp. 190–192, by Mieke Van Lijsebettens, Nancy Terryn, and Marc Van Montagu, Ghent University, Departments of Molecular Genetics and Plant Genetics, Flanders Interuniversity Institute for Biotechnology (VIB), K.L. Ledeganckstraat 35, Gent, Belgium, B-9000, milij@gengenp.rug.ac.be; "Arabidopsis" in (online), posting date: January 15, 2002, by Mieke Van Lijsebettens, Nancy Terryn, and Marc Van Montagu, Ghent University, Departments of Molecular Genetics and Plant Genetics, Flanders Interuniversity Institute for Biotechnology (VIB), K.L. Ledeganckstraat 35, Gent, Belgium, B-9000, milij@gengenp.rug.ac.be.

1. F. Laibach (1943) Bot. Archiv **44**, 439–455.
2. G.P. Rédei (1975) Ann. Rev. Genet. **9**, 111–127.
3. M. Koornneef et al. (1983) J. Hered. **74**, 265–272.
4. R.E. Pruitt and E.M. Meyerowitz (1986) J. Mol. Biol. **187**, 169–183.
5. D. Valvekens, M. Van Montagu, and M. Van Lijsebettens (1988) Proc. Natl. Acad. Sci. USA **85**, 5536–5540.
6. K.A. Feldmann (1991) Plant J. **1**, 71–82.
7. Arabidopsis Genome Initiative (2000) Nature **408**, 796–815.
8. J.L. Riechmann et al. (2000) Science **290**, 2105–2110.
9. R. Schmidt et al. (1995) Science **270**, 480–483.
10. C. Lister and C. Dean (1993) Plant J. **4**, 745–750.
11. C. van den Berg et al. (1997) Nature **390**, 287–289.
12. M.F. Yanofsky et al. (1990) Nature **346**, 35–38.
13. J.A. Long et al. (1996) Nature **379**, 66–69.
14. G.E. Schaller and A.B. Bleecker (1995) Science **270**, 1809–1811.
15. J.L. Dangl (1995) Cell **80**, 363–366.
16. C. Lin et al. (1995) Science **269**, 968–970.
17. A. Hemerly et al. (1992) Proc. Natl. Acad. Sci. USA **89**, 3295–3299.
18. C.M. McCallum, L. Comai, E.A. Greena, and S. Henikoff (2000) Nature Biotechnol. **18**, 455–457.
19. V.F. Irish and Y.T. Yamamoto (1995) Plant Cell **7**, 1635–1644.

20. D. Weigel and O. Nilsson (1995) Nature **377**, 495–500.
21. U. Lagercrantz, J. Putterill, G. Coupland, and D. Lydiate (1996) Plant J. **9**, 13–20.
22. T. Girke et al. (2000) Plant Physiol. **124**, 1570–1581.

Suggestions for Further Reading

23. J. Bowman (1994). *Arabidopsis: an Atlas of Morphology and Development*, Springer-Verlag, New York, NY.
24. C. Koncz, N.-H. Chua and J. Schell (1992). *Methods in Arabidopsis Research*, World Scientific, Singapore.
25. J.M. Martínez-Zapater and J. Salinas (1998). *Arabidopsis Protocols* (Methods in Molecular Biology Series), The Humana Press, Totowa, NJ.
26. E.M. Meyerowitz and C.R. Somerville (1994). *Arabidopsis* (Cold Spring Harbor Monograph Series, Vol. **27**), Cold Spring Harbor Laboratory Press, Cold Spring Harbor, NY.

Arginine (Arg, R)

The amino acid arginine is incorporated into the nascent polypeptide chain during **protein biosynthesis** in response to six **codons**—CGU, CGC, CGA, CGG, AGA, and AGG—and represents approximately 5.7% of the residues of the proteins that have been characterized. The arginyl residue incorporated has a mass of 156.19 Da, a **van der Waals volume** of 148 Å^3, and an accessible surface area of 241 Å^2. Arg residues have average conservation during divergent evolution; they are interchanged most frequently in **homologous** proteins with lysine, the other basic residue.

The Arg side chain consists of three nonpolar methylene groups and the strongly basic d-guanido group:

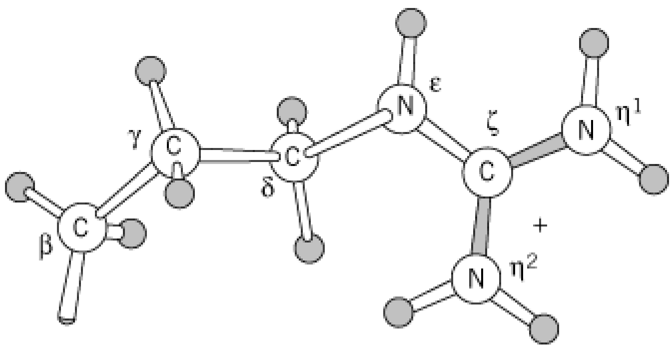

With a pK_a value usually of about 12, the guanido group is ionized over the entire pH range in which proteins exist naturally. The ionized guanido group is planar as a result of resonance:

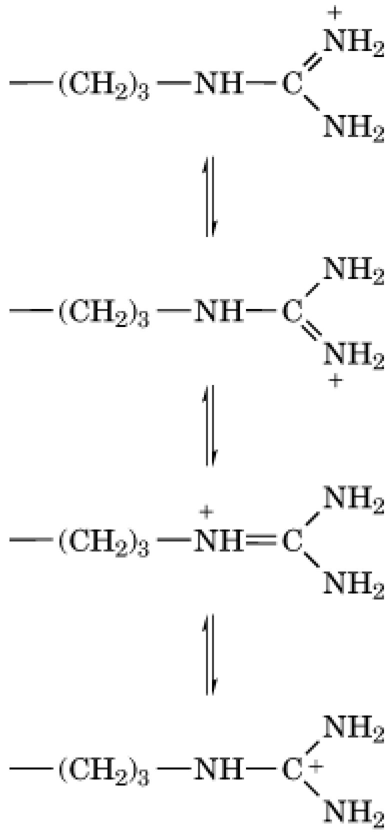

and the positive charge is effectively distributed over the entire group. In the protonated form, the guanido group is unreactive, and only very small fractions of the nonionized form are present at physiological pH values. The guanido groups of Arg residues are almost invariably at the surfaces of native protein structures, and virtually no Arg residues are fully buried, but the nonpolar part of the side chain, and the adjoining polypeptide backbone, are frequently buried within the interior. Arg residues favor the *alpha*-**helical** conformation in model peptides and also occur most frequently in that **secondary structure** in folded protein structures.

Proteinases frequently cleave polypeptide chains adjacent to Arg residues, as in the processing of pro-hormones, such as pro-**insulin**, at pairs of basic residues.

The guanido group can form heterocyclic condensation products with 1,2- and 1,3-dicarbonyl compounds, such as phenylglyoxal, 2,3-butanedione, and 1,2-cyclohexanedione:

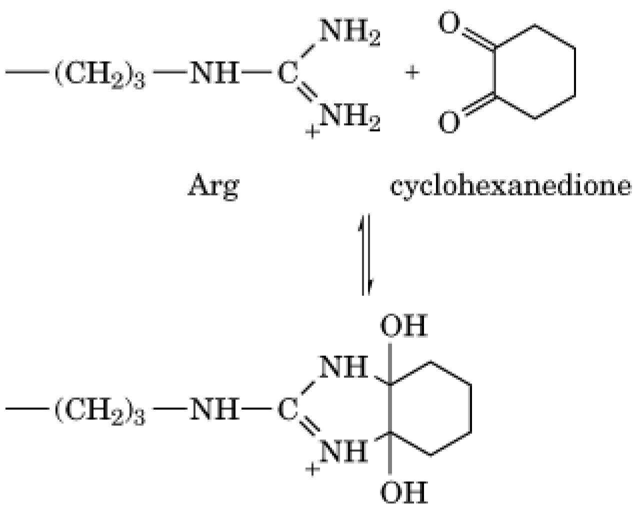

These reactions occur readily because the distance between the two carbonyl groups of the reagents closely matches that between the two unsubstituted nitrogen atoms of the guanido group. The adduct formed can be stabilized further by the presence of borate, which complexes with the adjacent hydroxyl groups.

The guanido group can be cleaved by hydrazine (H_2NNH_2) to produce the side chain of ornithine:

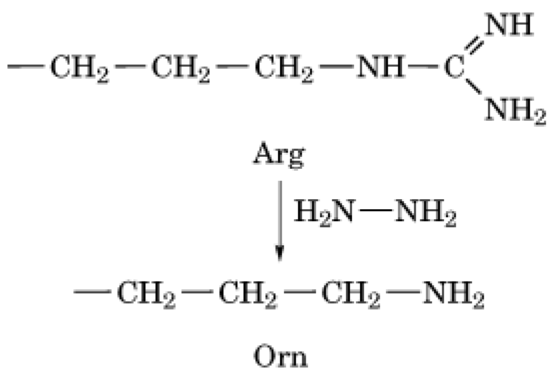

This reaction is, however, often accompanied by cleavage of the polypeptide backbone.

Suggestions for Further Reading

E. L. Smith (1977) Reversible blocking at arginine by cyclohexanedione, Meth. Enzymol. **47**, 156–161.

A. Honegger et al. (1981) Chemical modification of peptides by hydrazine, Biochem. J. **199**, 53–59.

R. B. Yamasaki et al. (1980) Modification of available arginine residues in proteins by *p*-hydroxyphenylglyoxal, Anal. Biochem. **109**, 32–40.

Ascaris

Ascaris is a genus of large animal parasitic nematodes. Common species include *Ascaris equorum*, a horse parasite, *Ascaris suum*, a pig parasite, and *Ascaris lumbricoides*, which parasitizes humans. Adult ascarid nematodes, which reside in the host intestine, range from several inches to several feet in length, and females can produce more than 2 million eggs per day. Fertilized eggs are released into the environment by defecation, where they remain dormant until ingested by another host. The acidic environment of the stomach and the increase in temperature trigger resumption of embryonic development, resulting in first-stage (L1) juveniles (often termed *larvae*) inside the egg shell. After molting once, the larvae hatch from the egg as second-stage (L2) juveniles. Like all nematodes (*q.v.*), Ascaris molts through three more juvenile stages (L3–L4) and then to a sexually mature adult. Stages in the parasitic life cycle are tissue-specific: The L2 burrows through the wall of the small intestine and is carried via the bloodstream or lymphatic system to the lungs, bronchi, and trachea. It molts to L3 and migrates up the trachea and down the esophagus, returning to the small intestine where it molts to L4 and then, about two to three months after the initial infection, to a mature adult that begins producing eggs. About 25% of the human population is infected by *Ascaris lumbricoides*, primarily in developing countries. Ascaris infections are generally debilitating but not life-threatening, although heavy infections can cause severe complications resulting from intestinal obstruction, peritonitis, or allergic reaction.

As an experimental organism, Ascaris was important to early embryologists and cytologists such as Theodor Boveri and Otto zur Strassen in the 1890s, who took advantage of several favorable properties of the early embryos that are still exploited by present-day researchers. The embryos are obtainable in large numbers from gravid females; they are transparent, facilitating observation by light microscopy; they can be stored in their original dormant state and their development initiated synchronously by high temperature or acid shock; and the pattern and timing of their embryonic cleavages, like those of most nematodes (*q.v.*), are invariant from embryo to embryo, with many cell fates apparently determined as the cells are born. The species studied most extensively by Boveri, *Ascaris megalocephala*, has the additional advantage of having only one large chromosome, which was convenient for cytological studies. Ascaris also has the peculiarity that there is chromosome fragmentation and diminution in all of the **somatic** precursor cells as they separate from the **germ line** in the early embryo. Although later work has shown that most of the discarded DNA does not include coding sequences, this feature allowed Boveri to demonstrate that cytoplasmic components specific to the germ line were responsible for maintaining chromosomal integrity in these cells, which supported the view that nonrandomly segregating cytoplasmic determinants were responsible for dictating early cell fates.

In the modern era, Ascaris has also become an important system for research in neurobiology. Part of the rationale behind Sydney Brenner's choice of the small free-living soil nematode *Caenorhabditis elegans* (see Caenorhabditis) for genetic and ultrastructural analysis of a simple nervous system and its development was the hope that Ascaris, only distantly related but much more suitable for electrophysiology because of its larger size, would allow functional analysis of a homologous nervous system. This hope has been largely realized: The two nervous systems appear to be very similar in both structure and function, and information from each has been valuable in understanding the other.

Suggestion for Further Reading

G. O. Poinar (1983) *The Natural History of Nematodes*, Prentice-Hall, Englewood Cliffs, NJ, p. 323.

Asexual

The term “asexual” means without sex; it is an adjective applied to multicellular organisms with missing or atrophied sexual organs and to forms of reproduction that do not involve the fusion of male and female gametes (see Asexual Reproduction).

The initial concept of sex referred to diploid, multicellular species in which new individuals are produced by the fusion of two haploid gametes, a sperm and an ovum (sexual reproduction). Individuals of many of these species may be classified into two sexes, *male* and *female*, depending on whether they are able to produce sperm or ova (eggs), respectively. This is the situation in most animals and in dioecious plants. The sex of an individual may be determined genetically or by the environment. Individuals are *asexual* if the organs that produce gametes are missing or atrophied; *intersexual* if their sexual organs are intermediate or ambiguous; or ***hermaphrodite*** if they have both kinds of sexual organs, whether they are functional or not. Hermaphroditism is prevalent in many species of plants, whether both pollen and ova are produced in the same *hermaphrodite* flowers, or in separate flowers of the same plant (*monoecious* plants).

These concepts cannot be transferred to unicellular organisms without some modifications. The haploid cells that predominate in the life cycles of many unicellular eukaryotes can often be classified into different **mating types**, sometimes more than two, with the criterion that only those of different mating type are able to fuse and form diploids. This situation is called *heterothallism*. The mating types of the lower eukaryotes are sometimes called sexes, even though cells of different mating types are not homologous to sperm and ova of the animals.

In the situation called *homothallism*, diploid cells may be formed by the fusion of two genetically identical haploid cells. This would happen if there were a single mating type or if haploid cells change their mating type when they find no partner of the opposite one, as occurs in the homothallic strains of the yeast *Saccharomyces*.

Asexual bacteria are unable to transfer or receive DNA via conjugation (see Hfr'S And F-Primes; F Plasmid).

Asexual Reproduction

Asexual reproduction includes all forms of reproduction that do not involve the fusion of male and female gametes. The asexual reproduction of a cell consists in the formation of genetically identical daughter cells; in the eukaryotes, this implies nuclear division via mitosis. Multicellular organisms are formed through repeated cycles of asexual reproduction from an initial zygote (see Development and Embryology). The daughter cells need not be completely identical, because cells with the same genotypes may differ in the quantitative distribution of transcription factors (see Differentiation). The genotypes of the daughter cells may differ because of mutation, mitotic recombination, chromosomal nondisjunction, and other infrequent events.

There are two kinds of *asexual* reproduction of multicellular organisms, namely, parthenogenesis and vegetative reproduction. Parthenogenesis imitates sexual reproduction, in that embryogenesis is apparently normal, but without participation of a male gamete. Haploid individuals are produced through the parthenogenetic development of a normal female gamete. **Diploid** individuals are produced through the fusion of the haploid nuclei of a female gamete and a neighboring haploid cell, such as the synergids of plants and the polar bodies of animals. Other diploid individuals are produced through the parthenogenetic development of a diploid cell after failure of meiosis. In vegetative reproduction, individuals are derived from one or many somatic cells. It is a common natural process in many plants and lower animals, and it is the only multiplication mechanism in some of them.

Artificial interventions permit new forms of asexual reproduction. These include (a) the production of haploid plants from the culture of anthers and (b) the production of diploid animals through the replacement of the nucleus of the ovum by a somatic nucleus. Vegetative reproduction and ameiotic parthenogenesis lead to the formation of *clones*, which are sets of individuals with identical genotype. Clonal propagation is usually carried out through vegetative reproduction from a single cell or a group of identical cells.

The parasexual cycle may be seen as a form of asexual reproduction in the lower eukaryotes and in cultured cells of multicellular organisms. Haploid cells, not necessarily of different **mating type**, fuse to form heterokaryons, and the nuclei of the heterokaryon fuse to produce diploid nuclei; these revert to haploidy, not by meiosis, but by random chromosome losses during mitosis, accompanied by mitotic recombination.

The sexual processes of bacteria imply the conjugation of two compatible cells and the transfer of part of the genetic information of one to the other (see Hfr'S And F-Primes; F Plasmid). Formally similar are asexual processes in which some genetic information from a cell is transferred to another via a **virus** or via naked DNA (see Transformation). These processes are not exclusive to the prokaryotes.

In evolutionary terms and in comparison with the various sexual processes, asexual reproduction has advantages of speed, economy, and the conservation of certain genotypes that may be lost or made less frequent after meiosis (see Heterosis, and Aneuploidy). The main drawback of asexual reproduction is the limited creation of new genetic variation (see Genetic Diversity).

Asparagine (Asn, N)

The amino acid asparagine is incorporated into the nascent polypeptide chain during **protein biosynthesis** in response to six **codons**—CGU, CGC, CGA, CGG, AGA, and AGG—and represents approximately 4.4% of the residues of the proteins that have been characterized. The asparaginyl residue incorporated has a mass of 114.11 Da, a **van der Waals volume** of 96 $Å^3$, and an accessible surface area of 158 $Å^2$. Asn residues are those most variable during divergent evolution; they are interchanged frequently in **homologous** proteins with serine, aspartic acid, lysine, and histidine residues.

The side-chain of Asn residues is the same as that of aspartic acid, except that the carboxyl group has been converted to the amide:

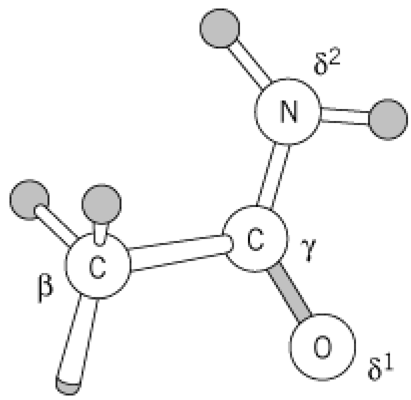

Both amino acids occur naturally and are incorporated directly into proteins during their biosynthesis; Asn residues do not arise from amidation of Asp in proteins. The amide side chain does not ionize and is not very reactive chemically. It is polar, however, because it is both a hydrogen bond donor and acceptor. The amide group is labile at extremes of pH and at high temperatures, and Asn residues can **deamidate** to Asp. The Asn residue is especially labile at alkaline pH because its side chain is sterically suited to interact with the —NH— group of the following residue in the polypeptide chain, to form transiently a cyclic succinimidyl derivative (see Deamidation). This derivative can undergo racemization and hydrolysis to cleave the polypeptide chain or to produce a mixture of D and L isomers of Asp and isoAsp residues. In an isoAsp residue, the normal backbone peptide bond is through the side-chain carboxyl group rather than the usual a-carboxyl. The deamidation reaction of Asn residues occurs 30–50 times more rapidly if the following residue is **Gly**, because the absence of a side chain there favors succinimide formation, and —Asn—Gly— sequences are especially prone to deamidation. The rate depends on the polypeptide conformation, however, because only some conformations permit succinimide formation. If the succinimide ring reacts with hydroxylamine instead of water, peptide cleavage results. Therefore, Asn—Gly peptide bonds are readily cleaved by incubation with hydroxylamine.

Asn residues are the site of N-glycosylation of proteins, one of the most prevalent post-translational modifications. The Asn residue that is so glycosylated always occurs in a characteristic sequence: —Asn—Xaa—Ser—, —Asn—Xaa—, Thr—, or —Asn—Xaa—Cys—, where Xaa can be any residue except **Pro**, which also cannot immediately follow the tripeptide sequence.

Suggestions for Further Reading

S. J. Wearne and T. E. Creighton (1989) Effect of protein conformation on rate of deamidation: ribonuclease A, Proteins Struct. Funct. Genet. **5**, 8–12.

W. J. Chazin et al. (1989) Identification of an isoaspartyl linkage formed upon deamidation of bovine calbindin D_{9k} and structural characterization by 2D ^{1}H NMR, Biochemistry **28**, 8646–8653.

P. Bornstein and G. Balian (1977) Cleavage at Asn-Gly bonds with hydroxylamine, Meth. Enzymol. **47**, 132–144.

F. Wold (1985) Reactions of the amide side-chains of glutamine and asparagine *in vivo*, Trends Biochem. Sci. **10**, 4–6.

Aspartate Transcarbamoylase

Aspartate transcarbamoylase (carbamoylphosphate:L-aspartate carbamoyl-transferase, ATCase, EC 2.1.3.2) is a ubiquitous enzyme of **pyrimidine** biosynthesis in which it catalyzes the first unique step in the *de novo* synthetic pathway:

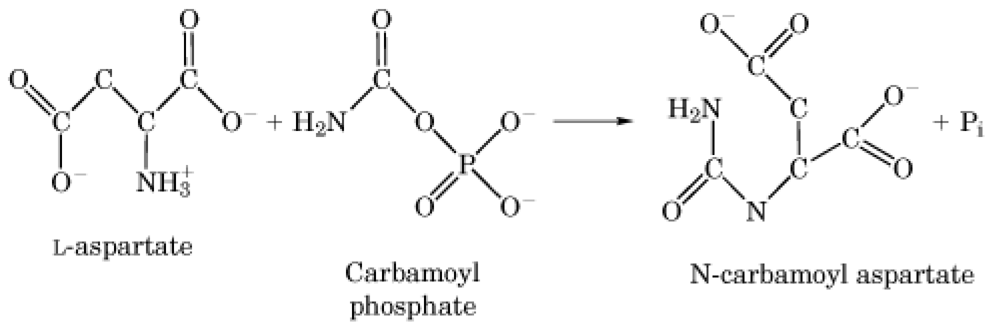

1. The *Escherichia coli* Paradigm

Although the enzyme exists in a variety of oligomeric and multifunctional complexes in various organisms, the most studied ATCase is that of *Escherichia coli*. It is a structurally complex, **allosterically** regulated enzyme containing two catalytic trimers associated with three regulatory dimers, $2(c_3){:}3(r_2)$ (Fig. 1). The catalytic polypeptide chain is encoded by the *pyrB* **gene**, whereas *pyrI* encodes the regulatory polypeptide. These genes are preceded by two tandem **promoters**, designated P_1 and P_2, and an open reading frame encoding a 44-residue leader polypeptide, *pyrL*. Promoter P_2 has been identified as the physiologically significant promoter (see Fig. 2).

Figure 1. Structure of the intact *E. coli* ATCase viewed along the 3-fold axis (**a**) and along the approximate 2-fold axis (

located within the catalytic trimer. The allosteric sites are located within the regulatory dimers. The PDB file 8at1 was us

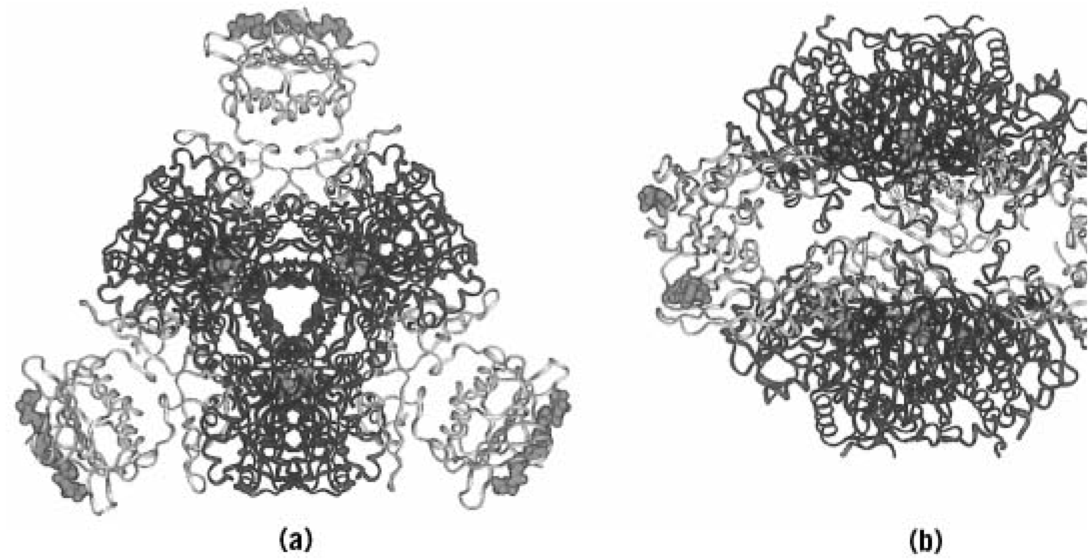

Figure 2. Genetic organization of the *E. coli pyrLBI* operon. The position of the three cistrons on the chromosome is sho positions of three hairpin structures adopted by the messenger RNA. The sequence around the first two is shown below. *pause hairpin*, flanked on each side by uridine-rich sequences. The second is the *terminator hairpin*, encoded by the atte

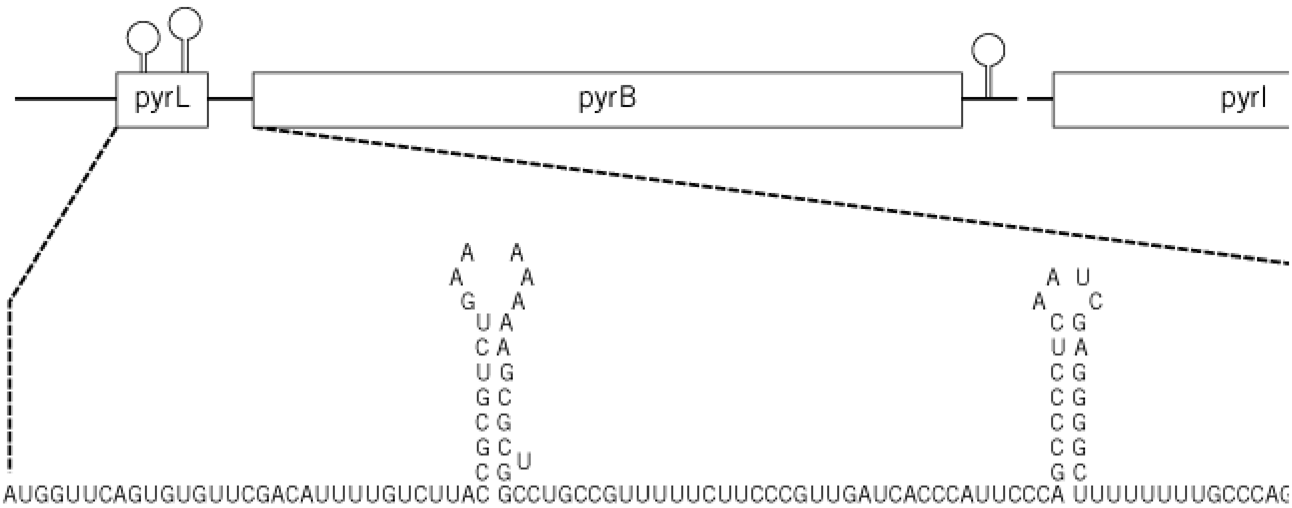

The *pyrLBI* operon is located on the linkage map of *E. coli* at 97 minutes and unlinked to any of the genes or small operons of the other six enzymes involved in pyrimidine biosynthesis. The expression of these genes is noncoordinately regulated by the intracellular levels of uridine or cytidine nucleotides, with the expression of the *pyrBI* operon negatively regulated over 300-fold. Most of this regulation (50-fold) occurs through a UTP-sensitive **attenuation** control mechanism, whereas attenuator-independent mechanisms are responsible for approximately a 6.5-fold range of regulation, including a pyrimidine-sensitive **transcriptional** initiation mechanism, and **stringent** control by ppGpp (1). According to the current model for attenuation control, transcriptional termination at the *pyrBI* attenuator (a **rho**-independent transcriptional terminator) is regulated by the relative rates of transcription and translation within the *pyrBI* leader region. Low intracellular levels of UTP cause **RNA polymerase** to pause at the uridine-rich region in the leader transcript (this pausing is enhanced by NusA, a general transcription factor that increases the efficiency of termination). This allows time for a ribosome to initiate translation and catch up to the stalled RNA polymerase before it transcribes the attenuator region. As RNA polymerase eventually makes its way through the attenuator, the adjacent translating ribosome blocks formation of the *terminator hairpin*. This permits RNA polymerase to read through into the *pyrBI* structural genes, with translation terminating before the *pyrB* initiation codon. When intracellular levels of UTP are high, RNA polymerase does not pause during the transcription of *pyrL*. Without this pausing, the ribosomes cannot catch up to RNA polymerase before it transcribes the attenuator. This allows formation of the RNA hairpin, thus terminating transcription prior to the structural genes.

In addition to the genetic regulation of *pyrLBI*, the gene product ATCase also exerts significant control over the rate of pyrimidine biosynthesis (2). This is achieved by allosteric modification of the enzymatic activity in response to substrate concentration (**homotropic** cooperativity) and the nucleotide end products of both the purine and pyrimidine pathways (**heterotropic** regulation; see Tables 1 and 2). In the oligomeric complete enzyme, catalysis proceeds by a preferred order mechanism, with carbamoyl phosphate binding before aspartate and N-carbamoyl-L-aspartate leaving before inorganic phosphate. Homotropic cooperativity is induced by aspartate in the presence of a saturating concentration of carbamoyl phosphate and involves a structural transition of the enzyme consistent with a two-state, **concerted model**. As aspartate is bound, the enzyme shifts from the **T-state**, characterized by low activity and low affinity for substrates, to the **R-state** with high activity and high affinity for substrates. The kinetic consequence of this positive cooperativity is a sigmoidal substrate saturation curve (Fig. 3). Heterotropic activation is caused by the purine ATP, whereas the pyrimidine end products CTP and UTP **feedback inhibit** the enzyme. The pattern of inhibition exhibited by pyrimidine nucleotides is synergistic: CTP inhibits ATCase activity approximately 60% and UTP has minimal effect, while CTP in combination with UTP inhibits ATCase activity >95% (3). CTP, ATP, and UTP bind competitively, with different affinities, to a common allosteric site. CTP binds the most tightly with a pattern consistent with two classes of three sites each, whose **dissociation constants** differ by a factor of 20 ($K_{d\text{-CTP}}$: 5 to 20 µM). The binding of ATP follows a pattern similar to that of CTP with two classes of affinity sites, except that ATP binding is an order of magnitude weaker than that of CTP ($K_{d\text{-ATP}}$: 60 to 100 µM). The binding of UTP appears to be limited to three sites ($K_{d\text{-UTP}}$: 800 µM), although there may be a second class of sites too weak to be measured. Interestingly, the binding of CTP to three sites appears to enhance the binding of UTP to the remaining three sites almost 100-fold, resulting in a predicted K_d for UTP in the presence of CTP of 10 µM (4). These biochemical binding characteristics are well suited to the physiological requirements of the pathway: Although the intracellular concentration of CTP (500 µM) and UTP (900 µM) is 3- to 6-fold lower than that of ATP (3 to 5 *mM*), their stronger binding can effectively displace ATP at the allosteric sites of the enzyme.

Figure 3. Substrate saturation profile of the *E. coli* ATCase. The velocity of the enzyme at varying concentrations of asp

presence of no allosteric effectors •, the activator ATP °, the inhibitor CTP ▼, and both pyrimidine end-products CT

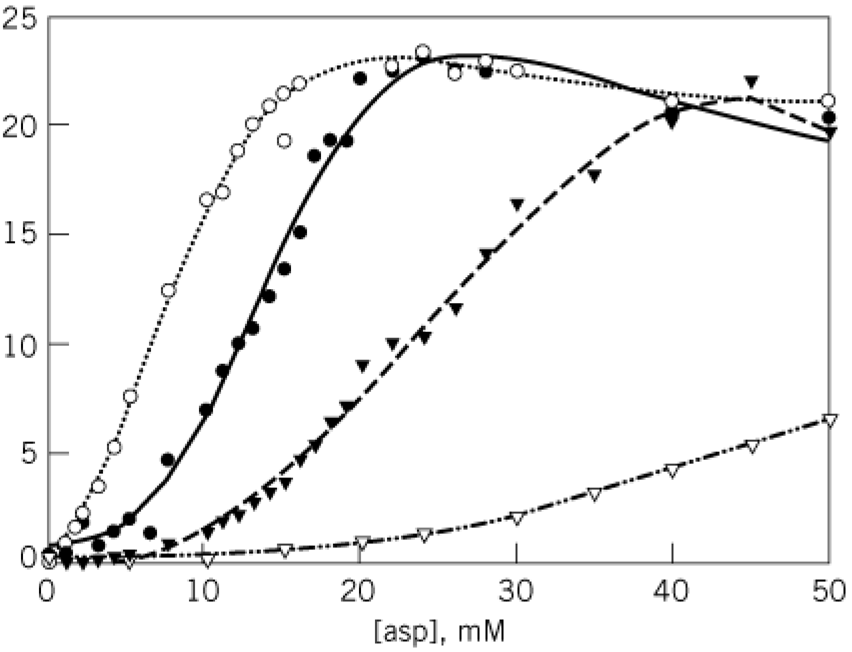

Physiological Significance of Catalytic Characteristics of the *E. coli* Aspartate Transcarbamoy

Catalytic Characteristic	Functional Consequence
• Ordered substrate binding (CP→Asp)	• Places catalytic emphasis on aspartate
• Cooperative aspartate binding	• Allows large changes in catalytic activity with onl of physiological substrate concentrations
• Distinct regulatory and catalytic subunits	• Increased sophistication in the allosteric modulatic activity
• Presence of shared active sites and catalytictrimers	• Facilitates modulation of catalytic activity with sul movements
• T→R structural transition	• Provides for dramatic differences in aspartate bind modulation of catalytic capacity at physiological lev

Table 2. Physiological Significance of Allosteric Characteristics of the *E. coli* Aspartat

Allosteric Characteristic	Functional Consequence
• Allosteric inhibition by CTP	• 50–70% inhibition of activity by nucleotide balance new synthesis with utilization
• Synergistic inhibition by UTP and CTP	• UTP and CTP are both end-products of the b pathway and the synergism provides 90–95% activity
• Competitive allosteric activation by ATP	• ATP competes with CTP and UTP for the sa thus balancing intracellular purine and pyrimi pools
• Competitive allosteric inhibition by	• Allows for displacement of ATP (activation)

CTP and CTP + UTP	(CTP or CTP + UTP)
• Negative cooperativity in binding CTP	• Permits modulation of enzymatic activity ov of inhibitor concentration
• Communication of allosteric signals across protein–protein interfaces	• Facilitates modulation of allosteric signal
• Asymmetry of the holoenzyme	• Provides two distinct classes of allosteric bir a single enzyme

Comparison of the X-ray crystallography structures of the enzyme has revealed that each of the catal independently folding structural **domains**: the carbamoyl phosphate (CP) domain and aspartate (Asp sites are located at the interface between the CP and Asp domains of one catalytic chain and the CP chain. Likewise, the regulatory chains are composed of two structural domains: the zinc-binding (Zn domain. Differences between the two states of the enzyme have been identified by comparison of the inhibitor (CTP) and the R-state structure binding a bisubstrate analogue [N-(phosphonacetyl)-L-aspa change in quaternary structure involves substantial conformational rearrangements as the catalytic tr mutually reorient 10° around the 3-fold axis, while each regulatory dimer rotates 15° around the 2-fc binding, the two domains of each catalytic chain (Asp and CP) undergo domain closure, whereas the chain (Allo and Zn) undergo domain separation. Site-directed mutagenesis studies have shown that c domains is important for the formation of the high-affinity, high-activity R-state, which is required t conformation needed for catalysis, and for homotropic cooperativity.

Figure 4. Domain organization of the *E. coli* ATCase illustrated with one catalytic chain (C1) and its associated regulat composed of two independently folding domains: the aspartate-binding (Asp) domain and carbamoyl phosphate-bindin regulatory chain is composed of the zinc-binding (Zn) domain and nucleotide-binding (allosteric) domain. This R1:C1 u MOLSCRIPT programs.

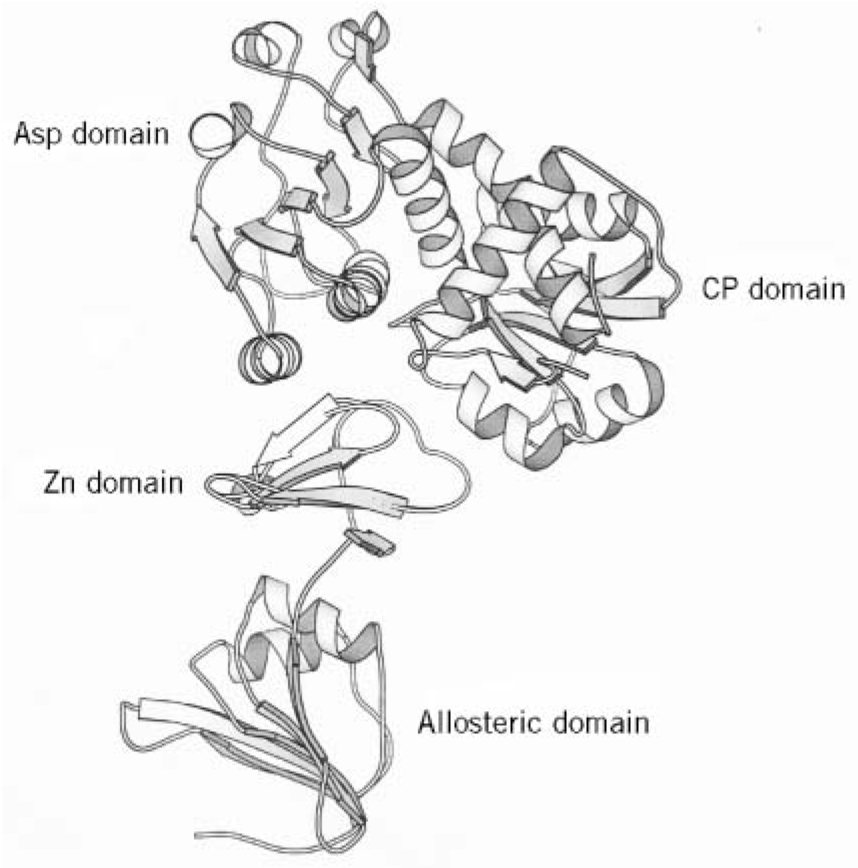

In addition to these studies, well over 100 site- and region-specific mutations have been created in th studies, along with the many structural and biochemical analyses, have contributed to our understanc active-site and allosteric site locations, identifying interactions important to the stabilization of the T catalytically significant residues. More recently, site-directed mutagenesis studies have been directec mechanism. Mutations have been created that can effectively separate the homotropic from the heter from inhibition, and CTP inhibition from CTP + UTP synergism. Although the mechanism of alloste current mutagenesis and structural studies are attempting to identify and differentiate between possit discreet pathways for each nucleotide signal, (2) complex and multiple interlocking pathways, or (3) energy changes.

2. Diversity of Aspartate Transcarbamoylase

2.1. Prokaryotes

With the exception of some anaerobic protozoan parasites, all examined organisms are capable of *de* and have been found to possess the enzyme aspartate transcarbamoylase. The earliest classification c and Jones in 1969 (16), based on enzyme size and response to nucleotides, partitioned the enzyme in ATCases are the largest ATCases found in bacteria and were initially described for the pseudomona ATCases of *E. coli* and other members of the *Enterobacteriaceae*; whereas (3) class C is the class w until recently was restricted to **Gram-positive** bacteria such as *Bacillus* (Fig. 5). The class A ATCas in size, and the intact enzyme exists as two catalytic trimers of 35 kDa in dodecameric association w chains ($2A_3$:$3D_2$). In *P. putida*, this 45-kDa chain has been shown to be a nonfunctional homologue the third enzyme in *de novo* pyrimidine biosynthesis immediately following ATCase in the biosynth

Figure 5. Organization of the first three enzymes and genes of pyrimidine biosynthesis: glutamine amidotransferase (G
DHOase. Although multiple examples are known for each category, the examples selected to represent each class are fr
subtilis (13), *S. cerevisiae* (9), and hamster (14). The genetic organization is represented according to the following: Bo
enzyme designations above and gene designations below. Noncoding DNA that joins genes transcribed into polycistron
segments. Overlapping genes are represented by overlapping boxes. Although all seven cistrons of *pyr* metabolism are
organization of only the first three is shown here.

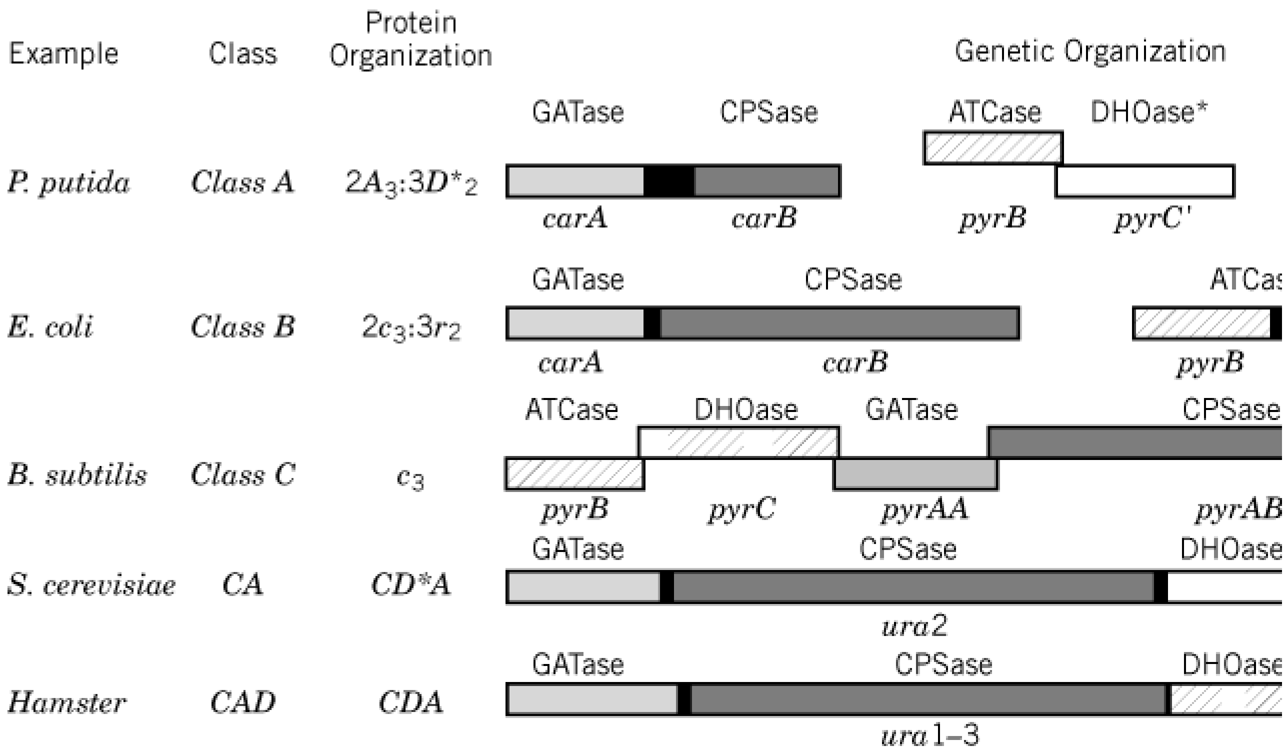

The *Bacillus subtilis* enzyme at 100 kDa is a typical class C enzyme and corresponds in size, archite
catalytic trimer of the *E. coli* enzyme. Class C enzymes are composed of three identical polypeptide
34 kDa each and have no associations with other enzymes in the pathway. Furthermore, these enzym
regulatory subunit nor the attendant allosteric regulation. As a consequence of the active site being s
catalytic chains, the class C homotrimer may be considered the catalytic core of the bacterial ATCas
pyr genes are scattered around the chromosome and are not coordinately regulated, all seven *B. subti*
the same operon and transcribed on a single messenger RNA. The 3′ ends of the reading frames over
downstream open reading frames for all **cistrons** in the cluster except *pyrB* and the preceding ORF1.
repressed by pyrimidines, and expression of aspartate transcarbamoylase has been shown to decline
sporulation. The mechanisms for the nutritional and developmental regulation of *pyr* gene expressio
been elucidated.

Although the class B enzymes appeared to be restricted to the *Enterobacteriaceae*, recent studies sug
(7) may also contain very similar c_6:r_6 enzymes. The *E. coli* ATCase provides the textbook example
inhibition by pathway end-products CTP and UTP, and activation by the end-product of the parallel
ATP. However, the various ATCases from different tribes of the *Enterobacteriaceae* display diverge
inhibition or activation. For example, while CTP serves as an allosteric feedback inhibitor in the *E. c*
effect or serve as an allosteric activator in other *Enterobacteriaceae* (Table 3). Some of these diverg
the basic regulatory paradigm of inhibition by pathway end-products as a mechanism to conserve en
of unneeded products. Nonetheless, the discovery of CTP + UTP synergistic inhibition provided a co
the allosterically regulated enzymes: Since the concentration of ATP in actively growing cells is 2 to
continually activated by ATP unless CTP or CTP + UTP are present to reduce the activated enzyme
in which CTP is an activator, the combination of CTP and UTP always serves as an effective antago

Table 3. Classification and Allosteric Characteristics of Bacterial Aspartate Tra

ATCase Class Characteristics	Bacterial Species[a]	Alloster
ATCase A	*Pseudomonas fluorescens*	No activation UMP Inhibition
	Acintobacter calcoaceticus	
	Azomonas agilis	
	Azotobacter vinelandii	
ATCase B1 (I)[b]	*Escherichia coli*	ATP activation
	Salmonella typhimurium	CTP, CTP + UTP
ATCase B2 (IV)	*Yersinia intermedia*	ATP activation CTP, UTP inhibiti
ATCase B3 (V)	*Erwinia carnegiana*	No activation
	Erwinia herbicola	sCTP[c], CTP + UT
ATCase B4 (IV)	*Yersinia entercolitica*	ATP activation No inhibition
ATCase B5 (IV)	*Yersinia kristensenii*	No activation
	Yersinia frederiksenii	No inhibition
ATCase B6 (II)	*Aeromonas hydrophila*	CTP, ATP activati
	Serratia marcescens	CTP + UTP antag
ATCase B7 (III)	*Proteus vulgaris*	CTP, ATP activati CTP + UTP Inhibi
ATCase C	*Bacillus subtilis*	None
	Streptococcus faecalis	
	Staphylococcus epidermidis	

[a] Class A and C examples are from (15).

[b] Tribal classifications (given in parentheses) are according to Bergey's *Manual of Determinative Ba* subgroups of the ATCase class B enzymes.

[c] sCTP indicates only slight inhibition by CTP (>20%).

Due to the oligomeric nature of the class B enzymes, it has been possible to form hybrids by combin enzyme with the regulatory subunits of different enzymes that have diverged allosteric patterns. The have demonstrated that the regulatory dimer determines the nature of the allosteric control of ATCas chimeric proteins have been constructed by intragenic fusion of the CP domain with the Asp domain Allo domain) forming several novel protein structures. In one instance, this type of protein engineeri chimeric enzyme by fusion of the domains of the hamster ATCase cDNA and the bacterial *pyrB* gen active ATCase trimers that, although unstable, could marginally satisfy physiological requirements.

Table 4. The Regulatory Chain of Class B ATCases Dictates the Allosteric

Source of subunit		Response to Effectors[a]	
Catalytic Subunit	Regulatory Subunit	ATP	CTP
E. coli	*E. coli*	+	–
	S. marcescens	+	+
	P. vulgaris	+	+
S. marcescens	*E. coli*	+	–
	S. marcescens	+	+
	P. vulgaris	+	+
P. vulgaris	*E. coli*	+	–
	S. marcescens	+	+
	P. vulgaris	+	+

[a] + = activation; – = inhibition.

2.2. Eukaryotes

The ability to form chimeric proteins opens the possibility that intragenic fusions could provide a me development of new proteins by the fusion of domain modules. Among the biosynthetic pathways of examples of single polypeptides that carry multiple enzymatic activities. Eukaryotic ATCases provic examples of a multienzymatic protein. In lower eukaryotes, such as **yeast**, the first enzyme in the pat *synthetase* (CPSase), and ATCase are physically linked, forming the CD*A protein fusion complex. *cerevisiae* and *S. pombe*, the enzyme architecture includes four domains; three functional domains c *amidotransferase* (GLNase), CPSase, ATCase activities, and one dihydrorotase-like (D*; DHOase) c the third enzymatic activity of the pyrimidine biosynthetic pathway just following ATCase. This stru the architecture previously discussed for the class A prokaryotic enzymes, which possess a domain v DHOase. The regulation of this complex includes the feedback inhibition of both CPSase and ATCa though the carbamoylphosphate produced by GLNase/CPSase is tightly channeled to ATCase and a the GLNase/CPSase alone should be sufficient to regulate pyrimidine metabolism.

In higher eukaryotes, the CA complex is associated with a functional DHOase domain producing a n (physically arranged in a CDA sequence). This complex provides the central metabolic control for p CPSase subjected to allosteric inhibition by UTP and activation by 5-phosphoribosyl 1-pyrophospha regulatory and catalytic functions involve a single polypeptide chain, the multifunctional complex m structure. A series of **proteolytic** and genetic truncation studies over the last 15 years have provided structure of CAD is well-defined and simple: Each enzymatic domain is separated from the others by polypeptide linker, and each domain can function in the absence of the other activities.

There are a number of proposals regarding the evolutionary role of the multienzymatic architecture. channeling occurs between CPSase and ATCase of the bifunctional CD*A complex. Channeling of s successive enzymatic activities are carried out on the same protein complex and could conceivably p advantage by limiting the loss of intermediate products. However, this is not always the case, as the freely releases the products of CPSase and ATCase, whereas ATCase and DHOase can readily utiliz outside the enzymatic complex. In the case of CAD and similar enzymatic complexes, coordinate **ge** alternative regulatory advantage for the evolution and maintenance of large enzymatic complexes. T complexes would provide for a smaller number of independent genes to regulate and simplify the co subcellular localization of multiple enzymatic activities.

In summary, the *de novo* biosynthetic pathway involves the set of reactions that supplies UMP from metabolic pathways: aspartate, glutamine, ATP, PRPP and carbon dioxide. The *de novo* pyrimidine enzymatic steps from carbamoyl phosphate synthetase (CPSase) to orotidylate decarboxylase (OMP evolution has developed a variety of regulatory controls and genetic organizations. Independent of it ATCase provides an important regulatory component of *de novo* pyrimidine biosynthesis in all free- maintaining homeostasis in intracellular nucleotide pools is an essential consideration for metabolisr enzymological regulation mechanisms are critical for balancing the nucleotide precursors of DNA/R

Bibliography

1. C. Liu, J. P. Donahue, L. S. Heath, and C. L. Turnbough Jr. (1993) J. Bacteriol. **175**, 2363–2369
2. J. C. Gerhart and A. B. Pardee (1962) J. Biol. Chem. **237**, 891–896.
3. J. R. Wild, S. J. Loughrey, and T. C. Corder (1989) Proc. Natl. Acad. Sci. USA **86**, 52–56.
4. P. England and G. Hervé (1993) Biochemistry **31**, 9725–9732.
5. R. P. Kosman, J. E. Gouaux, and W. N. Lipscomb (1993) Proteins **15**, 147–176.
6. H. Ke, W. N. Lipscomb, Y. Cho, and R. B. Honzatko (1988) J. Mol. Biol. **204**, 725–747.
7. C. Purcarea, G. Hervé, M. M. Ladjimi, and R. Cunin (1997) J. Bacteriol. **179**, 4143–4157.
8. M. Lollier et al. (1995) Curr. Genet. **28**, 138–149.
9. L. Jaquet et al. (1995) J. Mol. Biol. **248**, 639–652.
10. M. J. Schurr et al. (1995) J. Bacteriol. **177**, 1751–1759.
11. T. A. Hoover et al. (1983) Proc. Natl. Acad. Sci. USA **80**, 2462–2466.
12. C. D. Pauza, M. J. Karels, M. Navre, and H. K. Schachman (1987) Proc. Natl. Acad. Sci. USA **7**
13. C. L. Quinn, B. T. Stephenson, and R. L. Switzer (1991) J. Biol. Chem. **266**, 9113–9127.
14. J. P. Simmer et al. (1989) Proc. Natl. Acad. Sci. USA **86**, 4382–4386.
15. M. J. Kenny, D. McPhail, and M. Shepherdson (1996) Microbiology **142**, 1873–1879.
16. M. R. Bethell and M. E. Jones (1969) Arch. Biochem. Biophys. **134**, 352–365.

Suggestions for Further Reading

17. J. N. Davidson et al. (1993) The evolutionary history of the first three enzymes in pyrimidine bi 157–164.
18. E. R. Kantrowitz and W. N. Lipscomb (1990) *Escherichia coli* aspartate transcarbamoylase: The concerted allosteric transition. Trends Biochem. Sci. **15**, 53–59.
19. W. N. Lipscomb (1996) Aspartate transcarbamoylase from *Escherichia coli*: Activity and regula 151.
20. H. K. Schachman (1993) Aspartate transcarbamoylase. Curr. Opin. Struct. Biol. **3**, 960–967.
21. J. R. Wild and M. E. Wales (1990) Molecular evolution and genetic engineering of protein dom transcarbamoylase. Ann. Rev. Microbiol. **44**, 93–118.

Aspartic Acid (Asp, D)

The amino acid aspartic acid is incorporated into the nascent polypeptide chain during **protein biosynthesis** in response to only two **codons**—GAU and GAG—and represents approximately 5.3% of the residues of the proteins that have been characterized. The aspartyl residue incorporated has a mass of 115.09 Da, a **van der Waals volume** of 91 $Å^3$, and an accessible surface area of 151 $Å^2$. Asp residues are frequently changed during divergent evolution; they are interchanged in **homologous** proteins most frequently with asparagine and glutamic acid residues.

The side chain of Asp residues is dominated by its carboxyl group:

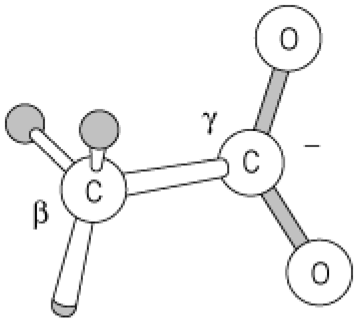

This carboxyl group is normally no more reactive than are those of corresponding organic molecules, such as acetic acid. Its intrinsic pK_a value is close to 3.9, so Asp residues are ionized and very polar under physiological conditions; consequently, very few Asp residues are buried in folded protein structures, and nearly all have at least the carboxyl group on the surface. The pK_a can be shifted in folded proteins, however, and either the ionized or nonionized form can be used in the protein's function. For example, carboxyl proteinases have one active-site carboxyl group function in the ionized form, and another when nonionized. Asp carboxyl groups have a weak intrinsic affinity for Ca^{2+} ions, and they are used in many calcium-binding proteins.

Asp residues differ from Glu only in having one methylene group, rather than two, so it might be thought that they would be very similar chemically and functionally in proteins, but this is not so. The slight difference in length of the side chains causes them to have different tendencies in their chemical interactions with the peptide backbone, so they have markedly different effects on the conformation and chemical reactivity of the peptide backbone. For example, Asp residues favor the *alpha*-**helical** conformation much less than Glu residues. In folded protein structures, Asp residues occur most frequently in reverse turns, whereas Glu residues are most frequently found in a-helices. The polypeptide chain can be cleaved relatively easily at Asp residues, because the side-chain carboxyl group participates in the reaction. —Asp—Pro— peptide bonds are especially labile in acid, because the carboxyl group interacts with the unique tertiary N atom of the Pro residue.

Suggestions for Further Reading

M. Landon (1977) Cleavage at aspartyl-prolyl bonds, Meth. Enzymol. **47**, 145–149.

T. E. Creighton (1993) *Proteins: Structures and Molecular Properties*, 2nd ed., W. H. Freeman, New York.

Aspartyl Proteinase Inhibitors, Protein

The synthetic peptide aspartyl proteinase inhibitors [see Proteinase Inhibitors, Protein] are among the most intensively designed molecules. The principal recent reason for this is that HIV proteinase inhibitors turned out to be successful drugs for fighting AIDS. In contrast, the protein inhibitors of aspartyl proteinases are very little studied. It is difficult to believe that this neglect is a result of the rare occurrence of such inhibitors in nature. The activation of zymogens of aspartyl proteinases (pepsinogen) has been a problem of long-standing interest. The propeptide is clearly a pepsin inhibitor. Much more potent and typical is the pepsin inhibitor from the roundworm (*Ascaris lumbricoides*). The determination of the three-dimensional structure of its complex with pepsin is now in progress and may awaken this long-dormant field. A large number of reports deal with cathepsin D inhibitors classified as members of the soybean trypsin inhibitor (Kunitz), or STI family, [see Soybean Trypsin Inhibitor (Kunitz), STI, (Kunitz)]. Many of the cathepsin D inhibitors are also said to inhibit trypsin, but the details of their interaction either with cathepsin D or with trypsin have been little studied.

Asymmetric Unit

The asymmetric unit is the fundamental structure that is repeated in crystals of macromolecules (see Crystallography**;** X-Ray Crystallography). Depending on the symmetry of the crystallographic lattice, each particle is present in multiple copies in the unit cell of the crystal. Only if symmetry is absent (space group P1) is a single copy present in the unit cell. In this case, the entire unit cell is an asymmetric unit. But if the unit cell has symmetry elements, it can be divided into identical parts related by this symmetry. Such a part, called the asymmetric unit, does not contain any crystallographic symmetry element. In Fig. 1, a projection of the unit cell in space group P2 is drawn. The twofold axes are perpendicular to the plane of the drawing. This unit cell has two asymmetric units. If the structure of the asymmetric unit is known, the structure of the entire crystal can be reproduced by applying the crystallographic symmetry.

Figure 1. Projection of a unit cell in space group P2 that has twofold axes (black ellipses) perpendicular to the plane of the drawing. The circles are particles related by the symmetry. The symmetry divides the unit cell into two exactly equal parts. Therefore, this cell has two asymmetric units.

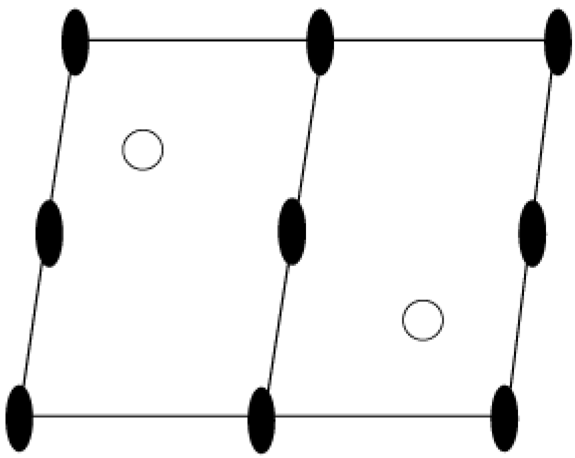

Bibliography

1. International Union of Crystallography (1992) *International Tables for Crystallography*, Vol. **A** (T. Hahn, ed.), Kluwer Academic, Dordrecht, Boston, London.

Suggestions for Further Reading

2. J. P. Glusker, M. Lewis, and M. Rossi (1994) *Crystal Structure Analysis for Chemists and Biologists*, VCH, New York, Weinheim, Cambridge.
3. J. Drenth (1999) *Principles of Protein X-ray Crystallography*, Springer, New York.

Atomic Force Microscopy

Binnig, Quate, and Gerber developed a scanning probe technique known as atomic force microscopy (AFM) and as *scanning force microscopy*. Unlike its predecessor, scanning tunneling microscope (STM), AFM also images nonconducting samples, such as biological specimens, in a liquid environment at molecular and even atomic resolution. Currently, structural information about biological materials at the molecular level is obtained from other **microscopic** techniques, including electron microscopy, electron crystallography, X-ray crystallography, nuclear magnetic resonance (NMR) spectroscopy, and vibrational spectroscopy. These techniques require extensive sample preparation and unfavorable operating environments, and they are unsuitable for providing real-time functional information. Molecular function is studied by various molecular biological, biochemical, and electrophysiological techniques, but it is difficult to combine both structural and functional studies in one technique. Moreover, these techniques provide incomplete information about the surfaces of biological macromolecules, the very sites of their interactions with other molecules. In contrast, AFM images the surfaces of biological specimens, where most of the regulatory biochemical and other signals are directed. Other microscopic techniques also image surfaces, for example, the **scanning electron microscope** (SEM), but AFM images living cells and molecules in a liquid environment at comparable and often greater resolution.

1. Principle of Operation

AFM is based on the general physical principle that the interactive force between two bodies is inversely proportional to some power of the distance separating them and on the physicochemical natures of the interacting bodies. A tip that is sharp on the molecular scale is attached to a cantilevered spring: As it is moved across the surface of the specimen, it is deflected by the interactive forces between the atoms of the tip and those of the specimen (see Fig. 1 of Scanning Probe Techniques). Because the spring constant of the commonly used cantilevers (10^{-1} to 10^{-2} N/m) is much smaller than the intermolecular vibrational spring constant of the atoms in the specimen (10 N/m), the cantilever senses exquisitely small forces exerted by the individual sample atoms. The tip's deflection is a measure of the forces sensed by the cantilever, which are transduced to generate molecular images.

In practice, a microfabricated cantilevered tip is pressed against a sample surface by a small tracking (loading) force. The tip is raster-scanned in the x-y plane over the specimen by moving the sample beneath the tip or by moving the tip over the sample. The sample's vertical position (z) is also monitored. The three planes of movement are controlled by a piezoelectric xyz scanner, and the information about the three coordinates is used to create the image (Fig. 1). The cantilevered tip is brought sufficiently close to touch the sample (known as “contact” mode), or it oscillates at a finite distance (>a few nanometers) from the surface (“noncontact” mode). A noncontact mode microscope has the advantage that it does not perturb the sample, but the lateral resolution in these microscopes is poor, and hence they are not commonly used for biological imaging.

Figure 1. Schematic illustration of the operating principle of multimodal atomic force microscopes. (**a**) Schematic of the combined scanning ion conductance and atomic force microscope. A pipette serves as the probe: A laser beam reflecting from a mirror glued to the back of the pipette provides the deflection signal for the topographic image as the pipette is moved across the surface. The electrode has a nanometer-sized hole. Electrodes within the pipette and in the bath measure electrical currents (R. A. Proksch, R. Lal, P. K. Hansma, G. Morse, and G. Stucky (1996) *Biophys. J.* **71**, 2155–2157). (**b**) A combined light and atomic force microscope. The first focal point is located inside the upper portion of the piezoelectric scanner. After the positions of the lenses are adjusted, the scanning focused spot accurately tracks the cantilever, and the zero-deflection signal from the four-segment photodiode is independent of the position within the scan area. One of the key advantages of this new AFM is that there is optical access to the sample from above and below. Thus, the new AFM can be combined with an optical microscope of high numerical aperture. The other key advantage is that the sample is stationary during scanning and can be large, so that techniques for on-line perturbations and recordings are easily incorporated. For details, see P. K. Hansma, B. Drake, D. Grigg, C. B. Prater, F. Yasher, G. Gurley, V. Elings, S. Feinstein, and R. Lal (1994) *J. Appl. Phys*. **76**, 796–799; R. Lal and S. A. John (1994) *Am. J. Physiol*. **256**, C1–C21.

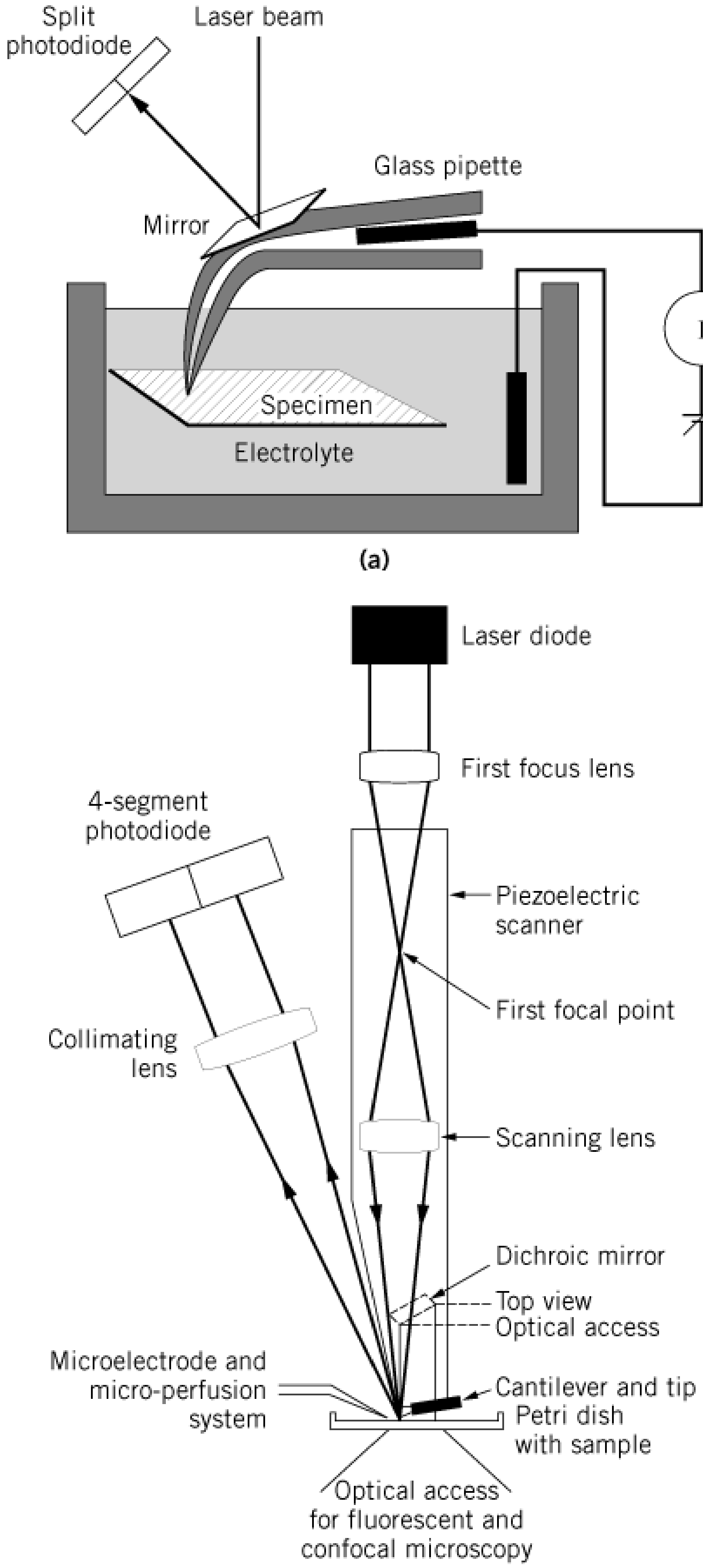
Split photodiode
Laser beam
Glass pipette
Mirror
I
Specimen
Electrolyte
(a)
Laser diode
First focus lens
4-segment photodiode
Piezoelectric scanner
First focal point
Collimating lens
Scanning lens
Dichroic mirror
Top view
Optical access
Microelectrode and micro-perfusion system
Cantilever and tip
Petri dish with sample
Optical access for fluorescent and confocal microscopy

(b)

The deflective force is translated into a detectable signal in several ways. The most common is by an optical lever system (Fig. 1). A monochromatic laser beam reflects from the upper face of the cantilever, the angular direction of which changes as the cantilevered tip undergoes deflections. The reflected beams are captured and converted into electrical signals by position-sensitive multisegmented photodetectors. Such an optical lever amplifies the cantilever's deflection as much as a thousandfold, so deflections even less than a nanometer are measured.

1.1. Modes of Operation

Using an appropriate feedback system, the cantilever's deflection is kept constant or left to respond freely to the sensed forces. In the constant deflection mode (also called "constant force mode"), the feedback loop changes the height of the sample (to maintain the constant deflection) by adjusting the voltage applied to the z portion of the xyz piezoelectric scanner. The amount of z change corresponds to the sample's topological height at each point in the x-y raster. Combining the information from the three coordinates generates the 3-D image.

In the variable deflection mode ("constant height mode"), the feedback loop is open so that the cantilever deflection is proportional to the change in the tip–sample interaction, that is the force sensed by the cantilever. The surface image is constructed from the deflection information. It is called the constant height mode because the z component of the piezoelectric scanner does not change appreciably. This is usually unsuitable for a sample with large surface corrugation (e.g., cells), because the force fluctuations, and thus the cantilever's deflections, are enormous and often result in disengagement of the tip from the sample.

"Error mode" imaging relies on the imperfection in the feedback loop to operate in the constant-deflection mode. The error signal is amplified to yield contour information in the z plane. In the error mode, the feedback loop gathers high-frequency information that is normally not acquired in the constant deflection mode. This high-frequency information provides details of sharp contour changes (edges) in the sample. Measurements of actual height in error mode imaging are not accurate, however, in contrast to the other modes of operation. The main advantage of error mode operation is that imaging occurs without exerting high forces on the sample.

In "tapping mode" imaging, the cantilever is oscillated at very high frequency, normally near its resonance frequency, as it scans the sample. As the tip approaches the sample surface, its oscillatory amplitude decreases because of energy loss when the tip "taps" the surface. The amplitude of the cantilever oscillation is detected and used by the feedback system to adjust the tip–sample distance for constant amplitude. This ensures a much shorter tip–sample contact time, and smaller lateral forces are exerted on the cantilever. In this way, this mode has been successfully used for imaging delicate and individual macromolecules. The disadvantage of this mode of operation is that the vertical imaging force can be large, thus increasing the possibility of sample damage.

1.2. Sample Preparation

AFM is used to image specimens in aqueous, semiaqueous, or dry conditions. The imaging condition is normally chosen to maintain the specimen in as near a lifelike condition as possible. Where resolution takes priority over the physiological condition, however, the investigator is not as constrained. Imaging conditions also influence the choice of substrate, the stability of the specimen with respect to the tip interaction, and the preservation of the specimen with respect to its physiological or biochemical functions. At present, investigators rely on an empirical approach to find a suitable method, and probably will for some time to come. When it "works", the search stops for the "ideal support" or buffer.

The physicochemical characteristics of the sample determine or suggest ways under which it can be imaged. Problems encountered are as simple as getting the sample to attach to the support. Techniques for sample support include drying down of samples and adsorption to specially prepared surfaces. For example, imaging of **plasmid** DNA is vastly improved in to both resolution and consistency, under propanol, which increases the humidity and produces a more hydrated condition. This allows reducing the tip-tracking force exerted on the sample to <1 nN , thus decreasing sample deformation.

The interaction of the sample with the support determines the magnitude of the imaging force. If the sample does not adhere tightly to the support, low tracking forces must be used for imaging, or the tip literally sweeps the sample from the support. Originally, graphite (**hydrophobic** and uncharged), mica (hydrophilic and negatively charged), and glass (usually negatively-charged) were the supports most routinely used. These supports can also be modified chemically to adjust their hydropathy, charge density, and polarity. Today the repertoire has expanded greatly, and examples include gold treated with a variety of agents for DNA imaging. Gold supports maintained under potential (voltage) control have been used for DNA imaging with the **scanning transmission microscope**, and they may also prove useful for AFM.

The specimen support can also be modified or coated chemically so that it acts as a **ligand** for the sample and thus orients the specimen in a defined way. It is also possible to use artificial systems to generate constraints where there were none before. Examples include imaging isolated **cholera toxin** molecules incorporated into synthetic phospholipid bilayers, followed by covalent cross-linking or imaging the vaccinia virus protrusion out of living cells held by a suction pipette.

1.3. Forces in AFM
Interactive forces that deflect the cantilevered-tip are attractive or repulsive, and they vary depending on the mode of operation and the conditions used for imaging.

In contact mode imaging, the tip is deflected mainly by the repulsive forces from the overlapping electron orbitals of the atoms of the tip and sample. The dominant attractive force is a van der Waals interaction due primarily to the nonlocalized dipole–dipole interactions among atoms of the tip and specimen. When imaging in air, (attractive) surface tension is also present because of adsorbed water layers. For imaging in fluids, electrostatic interactions between charges on the specimen and the tip (occurring either naturally or induced by to polarization), osmotic pressure due to charge movements and rearrangements, and structural forces due to hydration, solvation, or adhesion enable a reduction in the net imaging force although both the meniscus and surface tension forces are abolished.

The interplay of local forces determines the stability of the specimen and the resolution. Theoretically the force should be $\leq 10^{-10}$ N for nonperturbed biological imaging. The sensitivity of AFM is sufficient to record small interactive forces, including the breaking of hydrogen bonds. Imaging in contact mode under liquid, but with a net attractive rather than repulsive force, increases the resolution significantly and has produced true atomic resolution, even with an imaging force of 10^{-11} N. As explained below, however, successful imaging of cells, membranes, and isolated proteins has been obtained with forces as large as 10^{-7} N.

In principle, any movement of the tip caused by its interaction with the sample in the x, y, or z directions provides information about the specimen's topography. To date, most information has been obtained from z deflections. Improvements in hardware and software have, however, allowed recording movements in the zy or zx planes and measurement of lateral forces for image generation. The contribution of lateral forces to image contrast generation can be substantial.

1.4. Resolution in AFM
1.4.1. Spatial Resolution
The limit of spatial resolution for AFM is not well defined because, unlike conventional microscopies, the images are formed by reconstructing the contours of interacting forces between the specimen and tip. The operating resolution in AFM is defined as the minimum size of two adjacent features that can be distinguished clearly. By selecting a small scan size and suitable operating conditions, one can distinguish two structures that are less than a nanometer apart. Image processing

tools used to define resolution in X-ray crystallography and electron microscopy studies may not give correct results for AFM. The operating resolution can be divided into three categories:

1. Instrumental resolution: The lateral resolution is about 1 Å and is determined by the limitations of the hardware. The vertical resolution is 0.1 Å, and hence molecular perturbations on a sample surface can be imaged.
2. Target resolution: The lateral resolution achieved depends on the characteristics of the tip, the operating environment, and the nature of the specimen. For crystalline solid specimens and many inorganic materials, atomic resolution of 1 to 2 Å has been achieved.
3. Resolution in biological specimens: The nature of the biological samples and their preparation play a key role in determining the resolution limits. For the surface of a living cell, the resolution is relatively poor (~10 nm) but greater than that by light microscopy and comparable to that by scanning electron microscopy. In a biological specimen whose the density of particles is high and mobility is limited (e.g., proteins in a membrane), the resolution is comparable to that of a crystalline specimen.

1.4.2. Temporal Resolution

Temporal resolution is limited by the maximum speed at which a specimen can be scanned and still have the tip accurately track surface features. Preliminary studies suggest that the scan speed should be ≤2.2 μm/s for 1 nm spatial resolution on soft and deformable biological materials imaged in aqueous solution. Thus, membrane macromolecules whose dimensions are 10 nm × 10 nm (such as **channels** and **receptors**) divided into 10 × 10 pixels (with pixel size ~1 nm) require about 45 to 50 ms to image. However, if only a single line is scanned, the image can be repeated every 4 to 5 ms. Measuring at a single point, rather than scanning, increases the temporal resolution significantly, and hence it is possible to obtain spatial information at very short time intervals. The temporal resolution also depends on the mode of operation (constant deflection or constant height mode), operating environment (solvents, pH, viscosity, elasticity), and the nature of the interactions between tip and sample. In the constant-height mode, the scan speed is limited by the speed with which the deflection of the cantilever changes in reacting to surface features. In the constant deflection mode, the scan speed is limited by how the speed with which the piezo scanner changes its z component. There is ultimately a limit to the temporal resolution imposed by the low-pass filter used to eliminate sampling noise. These filters typically have a cutoff frequency of ~15 kHz , corresponding to a time resolution of 67 μs.

Temporal resolution also depends on the material being imaged. Individual molecules at molecular resolution require faster scan speeds than cells at lower resolution. Molecular movements of biological macromolecules can be correlated with their lateral diffusion constant. Lipids in a bilayer have a typical diffusion constant of 10^{-8} cm^2/s , corresponding to a mean velocity of ~2 μm/s. The proteins embedded in natural biomembranes have diffusion constants many orders of magnitude lower (e.g., the acetylcholine receptor in myoblast patches has a diffusion constant <3.0×10^{-12} cm^2/s. Thus it is quite possible to obtain images at molecular resolution of proteins and other macromolecules that are properly anchored in a lipid bilayer or immobilized on a substrate.

1.5. Identity of Imaged Structure

Although AFM provides molecular-resolution surface information for crystalline and amorphous materials, it is often difficult to define the nature of individual components, especially if the specimen contains a heterogeneous population of structures. This is the case with most biological systems, except in favorable systems like membranes that contain a crystalline patch of similar protein molecules. For mixed macromolecules, it is essential to compare the information obtained from AFM with that from alternative or complementary techniques, such as structural probes of electron microscopy and X-ray crystallography, biochemical and immunological binding assays, pharmacological labeling, and electrophysiological measurements.

1.6. Examples of AFM Imaging

1.6.1. Cells and Cellular Processes

AFM images cellular and subcellular structures in physiological conditions at a resolution far exceeding that of optical microscopes. Living cells have been imaged in aqueous conditions with a resolution as small as 10 nm. By applying a larger imaging force, intracellular **organelles** and cytoskeleton networks have also been examined (Fig. 2). The ability to view structures beneath the plasma membrane is puzzling. Two possible mechanisms are (1) the tip penetrates the bilayer and images the substructure or (2) the plasma membrane drapes around the cytoskeletal fibers and the tip images the contour of the plasma membrane. If the "drape" model is correct, these observations give wonderful demonstrations of the flexibility of biological membranes and a potential tool for measuring the "drape characteristics" of natural and synthetic membranes.

Figure 2. Images obtained with AFM. (**a**) Error-mode AFM image of a fixed atrial cell. The cytoskeletal network and ce nucleus are visible. [S. Shroff, D. Saner, and R. Lal (1995) *Am. J. Physiol*. **269**, C286–292.] (**b**) AFM error mode image a freeze-fracture replica of atrial tissue. Details can be identified in the mitochondrion and in the atrial granules and vesicles. Scale Bar: 1 mm. [L. Kordylewsky, D. Saner, and R. Lal (1994) *J. Microsc*. **173**, 173–181.] (**c**) Error-mode AF image of a neurite outgrowth in PC-12 cells treated with **nerve growth factor** and dibutyryl cyclic AMP. For details, se R. Lal, B. Drake, D. Blumberg, D. Saner, P. K. Hansma, S. Feinstein (1995) *Am. J. Physiol*. **269**, C275–C285. (**d**) Lamb DNA under propanol using a regular silicon nitride tip. Note the sharp bends in the strands and a fairly regular series of lumps along the strands, 6 to 8 nm apart. The strand width is 7 to 9 nm, greater than expected, which may result from the relatively large size of the tip. Scan size is 1000 nm × 1000 nm (courtesy H. Hansma, H. G. Hansma, R. L. Sinsheimer, M Q. Li, and P. K. Hansma (1992) *Nucleic Acids Res*. **20**, 3585–3590). (**e**) AFM height mode image of a single connexon (gap junction hemichannel) imaged on its cytoplasmic face. The subunit structure, a central pore, and the spacing betwee connections are apparent [S. A. John, D. Saner, J. Pitts, M. Finbow, and R. Lal (1997) *J. Struct. Biol*. **120**, 22–31).] (**f**) High-resolution AFM imaging of a single acetylcholine receptor expressed in *Xenopus* oocytes. The channel has a diameter of ~10.5 nm , and the five subunits (~1 to 1.5 nm in diameter) that have a central pore-like structure are shown. The protrusion of one unit is not apparent in the image [R. Lal (1998) *Scanning Microsc*. **10**, 81–96].

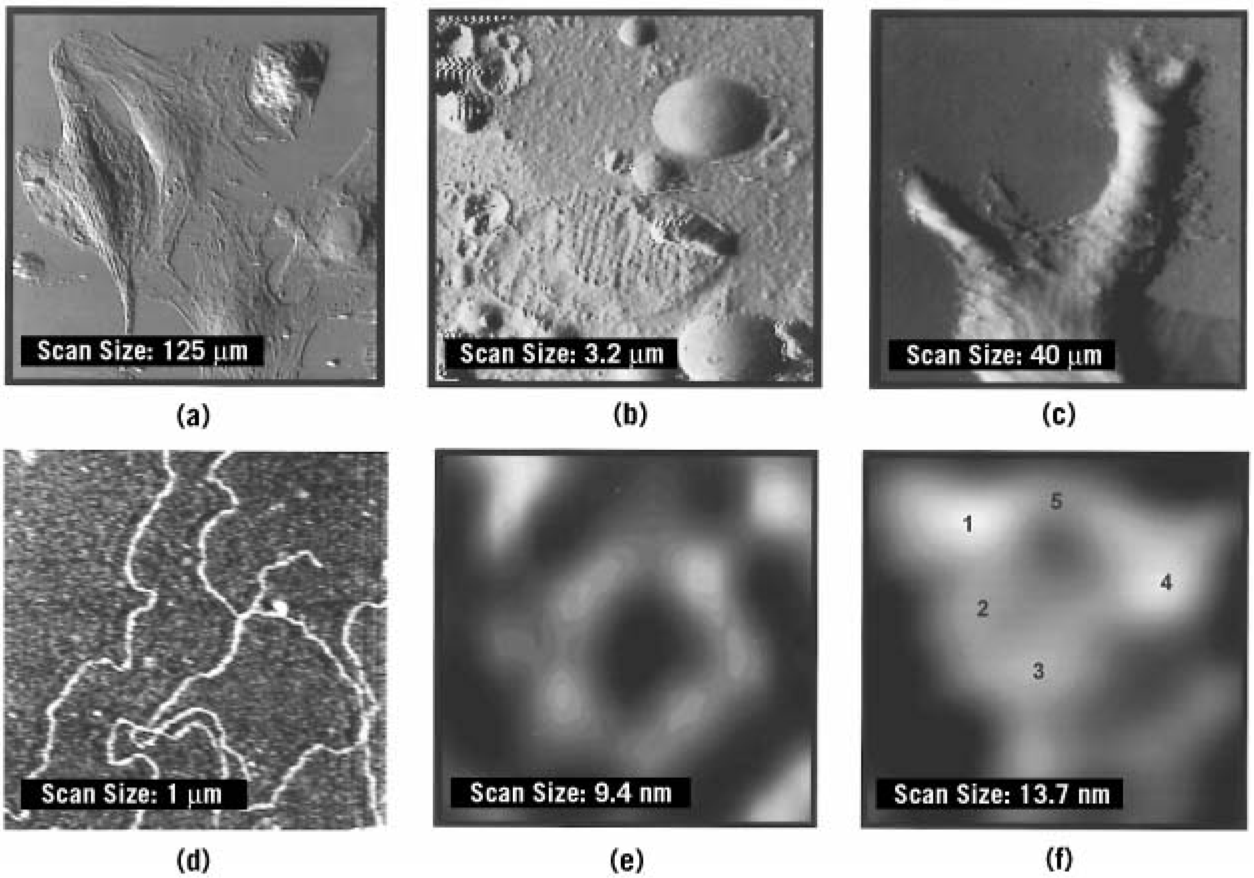

In AFM imaging, the scan area can be varied from the micron to nanometer range, and hence it is possible to image features ranging from whole cells to individual macromolecules, such as **ion channels** and receptors (Fig. 2). In air-dried, hydrated Xenopus oocytes in which acetylcholine receptor proteins are expressed, the characteristic pentameric subunit structure of the expressed receptor has been observed after removing of the follicle layer. This technique of imaging expressed proteins on or in the surface of the plasma membrane of oocytes will shortly enable the characterization of a myriad of ion channels and receptors expressed in an appropriate expression system.

The major factor limiting resolution in imaging a cell surface is the mobility of the upper plasma membrane, plus the mobility of the macromolecules within the plasma membrane: the lower membrane is anchored to the substrate. Improvements in resolution may be made by (1) increasing the surface rigidity (e.g., suction of cells onto patch pipettes and thus reducing the lateral mobility of proteins); (2) by imaging with low forces (e.g., attractive force mode imaging or magnetic tapping imaging).

1.6.2. Membranes and Membrane Proteins

Imaging membranes, both native and reconstituted, has received wide attention because of their flattened 2-D sheet-like structure and the ease in preparing them. Purified membrane proteins, such as bacteriorhodopsin, gap junctions, acetylcholine receptor, and the hexagonally packed intermediate (HPI) layer from *Drosophila radiodurans*, have been imaged in aqueous conditions without fixation (Fig. 2). These membrane proteins have been characterized extensively by alternative techniques, such as electron microscopy and electron and X-ray crystallography. The results from AFM studies agree remarkably with those from other techniques. In addition, AFM images provide a direct observation of membrane polarity. For example, extracellular and cytoplasmic surfaces of gap junctions are distinguished unambiguously. The thickness measurement in AFM study is also direct and often very precise.

Synthetic membranes (Langmuir–Blodgett) and reconstituted vesicles have been imaged at molecular resolution. Images of Langmuir–Blodgett films provide direct measurement of lipid membrane thickness, obtained previously by indirect methods and theoretical extrapolations, because the height resolution in AFM is subnanometer. AFM images of Langmuir–Blodgett films show individual polar head groups and their molecular arrangement, including their long-range packing. An advantage of studying these membranes with AFM is that one can change the lipid composition on-line and study lipid–lipid interactions, lipid fluidity, and lipid–protein interactions. AFM images of proteins that are naturally embedded within membranes and form 2-D crystalline arrays and images of LB films provide some of the best evidence that the imaging of biological specimens generally agrees with that by electron microscopy, with the advantage, of course, that AFM imaging occurs in nearly physiological environments. It is also worth noting that such a correlation adds weight to the interpretation of images gathered by electron microscopy.

Proteins immobilized by synthetic membranes have also been imaged. Bacterial porins are one of the best-studied channel-forming membrane proteins. Porins reconstituted as 2-D crystals in lipid vesicles have been imaged in a liquid environment. AFM images at molecular resolution show the trimeric structure of porins illustrated by X-ray crystallography and electron microscopic single-particle reconstruction. In addition, recent studies show that molecular resolution can be obtained on noncrystalline specimens in liquid media. This opens a new avenue for studying the molecular structure of biological macromolecules (e.g., ion channels, receptors) that are easily expressed in an appropriate expression systems, such as the *Xenopus* oocyte, or simply isolated and anchored properly on suitable substrates. For example, purified **cholera toxin** molecules incorporated into synthetic phospholipid bilayers by covalent cross-linking, observed at molecular resolution, have the expected pentameric structure. Other membrane proteins imaged by AFM include the hexagonally packed intermediate (HPI) layer of *Drosophila radiodurans*, Na^+, K^+-**ATPase**, vacuolar **proton**

pumps (V-H^+-ATPase), and Ca^{2+}-ATPase.

As mentioned before, AFM imaging of whole cell membranes has also been achieved. Acetylcholine receptor expressed in *Xenopus* oocytes has been observed. **Calcium channels** have been localized on the calyx-type nerve terminal of fixed chick ciliary ganglion in culture by imaging **avidin**-coated 30-nm gold particles incubated with w-**conotoxin** GVIA linked to biotin, although the molecular structure of individual calcium channels was not reported. The interchannel spacing of 40 nm was noticed, which may reflect the spatial limitation due to tagging with 30-nm gold particles. Individual calcium channels have much smaller diameters. Other membrane channels, such as **sodium channels**, **potassium channels**, and gap junctions, are 6 to 10 nm in diameter. Isolated cellular organelles have been imaged with AFM, including nuclear pore complexes, ~134 nm in outer diameter, with a central pore-like trough.

1.6.3. Isolated Macromolecules, such as DNA, Amino Acids, and Proteins
Imaging isolated macromolecules is challenging because it is difficult to find suitable surfaces to which to anchor the molecules for repeatable and reliable imaging. The recent development of cryo-AFM shows good promise for obtaining high-resolution images of isolated macromolecules. Images at molecular resolution have been obtained of DNA at the **plasmid** and **chromosomal** levels, polyamino acids, isolated proteins, and ligand–receptor complexes. Large protein fibers, such as actin and microtubules, have also been imaged at molecular resolution, and it was possible to discern individual actin molecules. Isolated protein molecules show dynamic changes while imaging with the AFM. For example, when glycogen phosphorylase *b* binds to phosphorylase kinase, the dimensions and shapes of the proteins change noticeably.

Imaging DNA and nucleic acids has been appealing for many reasons. Given their well-known geometry and easy availability, they are readily identified and hence used for calibration and for studies of the interaction between tip and sample. Intriguingly, this may also open a door for structure-based sequencing and mapping of DNA AFM. However, DNA sequencing AFM will require an order-of-magnitude improvement in resolution (to ~2 to 3 Å). This increase may come from improvements in hardware and software, but methods to prepare DNA in extended conformations will probably be just as important in improving resolution.

Images of double-stranded DNA at molecular resolution (2 to 3 nm), in which the helical pitch and turns could be deciphered, have been obtained in air and liquid. Occasional images at higher resolution showing individual base pairs have also been obtained. Single-stranded DNA, though, has proven more intractable to image at any molecular resolution.

Images of complexes of DNA and protein A deposited onto mica show single proteins bound to the end of the DNA strands. In addition some single protein molecules bind to up to four DNA strands per protein molecule. When **RNA polymerase** binds to DNA, AFM images show that the modified DNA is bent at marked angles where the polymerase binds. One appeal of these approaches is in searching for DNA-binding proteins and, intriguingly, perhaps to image the effects of **topoisomerase** on DNA.

1.6.4. Imaging Dynamic Processes
AFM, unlike other molecular level imaging systems, allows imaging in an aqueous environment. In an elegant set of studies, AFM was used to visualize real-time surface processes on vaccinia virus *pox viridae*-infected monkey kidney cells. Real-time changes in surface morphology and the exocytosis of enveloped virus and proteins were observed over a period of 19 hours. In contrast, cells not infected with virus showed no appreciable change in surface morphology. The real-time contractile activity of cultured atrial myocytes was also imaged. As the concentration of calcium increased, cells underwent rapid contraction, and a corresponding shortening in cytoplasmic fibers (perhaps cross-bridges) was observed.

Dynamic studies have been conducted on isolated proteins, such as formation of glycogen phosphorylase-phosphorylase kinase complexes, antibody–antigen interactions, dynamics of immunoglobulin adsorption, and binding of streptavidin to a biotinylated lipid bilayer. Real-time polymerization of **fibrin**, a protein important in blood clotting, shows that the polymer chain grows by the fusion of many short chains, rather than by successive addition of monomers to a few long chains. A change in Langmuir–Blodgett film morphology has been observed as trace amounts of a fluorescent dye are added, suggesting that the perturbation of molecular conformation by the tracer molecules may not be as insignificant as is commonly believed.

AFM can be used for *in situ* studies of the growth of protein 3-D crystals in their native solution environment and of the role of nucleation centers, lattice defects, and saturation level. These studies may provide clues for growing the 3-D crystals essential for high-resolution X-ray crystallography.

1.7. Structure-Function Studies

AFM can be combined with other techniques, which opens the possibility, as various biochemical, pharmacological, and other perturbations are introduced on-line, of real-time dynamic studies for direct structure–function correlations at the molecular level. For example, "single cell" experiments have been reported where electrical activity and AFM images were obtained from *Xenopus* oocytes expressing acetylcholine receptor. Electrical recording of acetylcholine-sensitive current and labeling by specific binding of **a-bungarotoxin** were also conducted in parallel. The receptor density calculated from the AFM studies correlates well with that from electrical measurements and toxin binding, but the clustering of acetylcholine receptor differs from the uniform distribution of the expressed receptors that is commonly assumed in electrophysiological studies. A correlation between patch-clamp electrical recording and AFM of transcription factor IID (TFIID) interactions with the nuclear pore complex has also been reported, showing unplugging of the nuclear pore complex accompanied by prolonged electrical current through the channel, perhaps reflecting the reopening of the channels. A combined AFM and patch-clamp study measured the electrical current in the membrane patches excised from *Xenopus* oocytes and attached to the pipette tip, while imaging the surface topology with AFM. Although the resolution of such a study is limited, it nevertheless shows the promise of direct structure-function studies of membrane macromolecules. Another study simultaneously measured images of bacteriorhodopsin in purple membranes adsorbed onto a lipid monolayer, ion transport through the membrane, and the electrical properties of the membrane. A recent study simultaneously measured the surface structure of nuclear pore filters and electrical current passing across the filter through pores of different diameters. For such a study, a scanning ion-conductance microscope was developed that records electrical activity, while imaging the 3D-structures of various membranes (Fig. 1).

Imaging force can be varied considerably during experiments. Such a feature has been used to nanomanipulate protein and membrane structures, and two different conformations of membrane proteins have been reported.

As already mentioned, action is at biological surfaces. The potential for rapidly characterizing and cataloguing the structures of synthetic peptides opens vistas for synthesizing drugs that can interact with "similar surfaces" within the body. Because AFM measures the force of an interaction between substrate and cells, interactions of a ligand or agonist should be measurable if well-defined molecules are placed on the tip of the AFM. Then it may be possible to use this ligand as a probe to determine the presence or absence of a receptor in impure, natural preparations. Perhaps more importantly, it may be possible to measure the interactive forces between agonist and receptor. This information will prove useful in designing of drug inhibitors or mimics.

1.8. Analysis of Micro-mechanical Properties

Contrast mechanism and image formation in AFM reflect a sum of many local forces and the micromechanical properties of the specimen. As the choice of specimen is shifted from rigid and hard materials (such as mica, graphite, tungsten) to soft and deformable biological materials, the dominating micro-mechanical properties shift from pure frictional to viscoelastic. Frictional forces on the atomic scale have been measured between two silica surfaces, two thin films, and between tungsten and graphite. By using local frictional force contours, fluorinated and hydrocarbon regions were distinguished in a Langmuir–Blodgett film. The hydrocarbons and fluorocarbons had separate domain structures: hydrocarbons as circular domains, fluorocarbons as the surrounding flat films. The frictional force was higher in the fluorinated region than in the hydrocarbon region. Such compositional studies provide a mechanism to identify individual components in a multicomponent sample like a cell membrane.

The viscoelastic properties of several soft, deformable biological materials, including cells, has also been obtained by a technique called *force mapping*. Such a study can be undertaken during on-line pharmacological and biochemical perturbations. In each imaging pixel, the tip is brought into proximity with the surface until a preset deflection is reached. The tip then retracts to its original position, and this process is repeated in every pixel. A height image is obtained from the amount of vertical piezo movement necessary at each point to obtain the preset deflection of the cantilever. For each pixel, a deflection versus distance curve is stored, which can be fitted to different models to obtain properties, such as the elastic modulus of the sample surface. Usually, the tip apex is approximated by a semisphere or a cone and the specimen by a spherical or planar model, depending on the shape of the features on the surface.

Thus, AFM is an imaging tool and also a system for analyzing micromechanical properties of cells, subcellular organelles, and macromolecules. It may be possible to study localized viscoelastic properties of molecular motor units, the distribution and propagation of contraction waves in a muscle cell, and the correlation between the calcium concentration wave and electrical propagation. One can also induce local shearing (frictional) force or pressure to assess the effects on the vascular system (mimicking the role of blood flow-induced shearing on vasorelaxation) or to distinguish pressure- or shear-sensitive ion channels in plasma membranes.

1.9. Simultaneous Multimodal Imaging

The simple design of AFM allows integrating it with other techniques, such as light fluorescence microscopy, laser confocal microscopy, and near-field scanning optical microscopies. Such integrated systems permit simultaneous multimodal imaging and provide independent verification with appropriately labeled markers. For example, using appropriately labeled **fluorescent** signals, one can identify specific areas and then use AFM to obtain high-resolution details.

1.9.1. Combined AFM and Light Fluorescence Microscope

Although conventional AFMs are ideal for high-resolution imaging, they could not be combined with large-aperture optical microscopes. In a few AFMs, however, the cantilever moves and the sample is stationary, permitting the addition of optical microscopes that have high numerical apertures. The most promising of these AFMs has the scanned-cantilever mode in which the cantilever position is accurately tracked by a scanned focused spot (Fig. 1) and is incorporated into an inverted fluorescence microscope. This combined fluorescence and force microscope has been used to image **immunolabeled** membranes and whole cells (Fig. 2). Fluorescent labels show remarkable correspondence among AFM images and the specificity of the molecules: such correspondence that one can obtain structural information at molecular resolution on biological macromolecules present individually or in small clusters, long as they have detectable fluorescent signals.

1.9.2. Combined Atomic Force Microscope and Confocal Microscope

Early combined AFM and laser-scanning confocal microscopes (LSCM) included features like a stationary sample stage, an AFM with an optical tracking system for the scanned cantilever, and either a scanned-beam or tandem design confocal microscope. The limitations of such systems include a limited scan range of both the AFM and confocal images. The scan range of the independently scanned confocal spot is limited to the size of the field of view of the objective and off-axis optical aberrations, and the scanned-cantilever AFMs with optical level detection require optical tracking of the cantilever for a large scan range. The latter constraint was overcome by the scanned-cantilever (tip) design with an optical tracking feature (the features explained previously in the combined AFM-fluorescence microscope), where the sample is scanned by a piezo system and the AFM tip and objective remain stationary. The AFM registers the topography of the sample surface, and the LSCM laser scans the surface to obtain fluorescent data on the same scan area. Although the AFM scan size is increased in this improved design, the confocal scan size is still limited by the objective. Moreover, although the AFM images are of the sample surface, the confocal image plane may not be the sample surface, but anywhere within the confocal slice, which could be no more than 100 nm thick.

A new combined AFM and LSCM allows simultaneous imaging of the sample surface in both modes, in addition to the conventional confocal imaging through the sample thickness. The salient features of such a combined microscope include a scanned-sample approach wherein the specimen is scanned above an inverted microscope objective with a fixed optical path for fluorescent LSCM imaging. An AFM positioned directly above the sample simultaneously measures the surface topography. Therefore, in this design the confocal spot and AFM cantilever remain stationary. Optical cantilever tracking is not required, and the confocal spot can be centered in the microscope's objective. The AFM feedback system ensures that the focal point is on or near the surface of the specimen, so that when the cantilever is positioned at the confocal spot, the LSCM and AFM images are acquired in direct registration, allowing image features to be easily correlated.

In this combined multimodal system, the confocal plane can be selected from the topmost region on a specimen surface or anywhere through its depth, so it is quite possible to follow, for example, cytoplasmic signal transduction processes leading to changes in the cellular plasma membrane surface conformations.

1.9.3. Combined Atomic Force Microscopy and Electrophysiological Recording

A combined tapping-mode AFM and a scanning ion-conductance microscope have been developed recently (Fig. 1). One of the salient features of this combined microscope is a bent glass pipette used as both the force sensor and the conductance probe. The force-sensing capability allows measuring of the pipette deflection, which then is used to create surface images in both regular contact mode and tapping mode. The conductance-measuring capability allows recording the electrical current flow across pores in a suitable specimen. Using such a microscope, it is possible to image the structures of channels and receptors and to measure their functional states (conducting vs. non-conducting) (Fig. 3).

Figure 3. Examples of AFM multimodal imaging. (**a**) and (**b**) Simultaneous immunofluorescence and atomic force microscopy of amyloid b peptide (AbP) reconstituted into liposomes. All liposomes, with or without AbP, were imaged with AFM (**a**), a few are shown at higher magnification in the inset. The liposomes were treated with anti-AbP antibody and subsequently identified with fluorescein-conjugated second antibody. The AbP-carrying liposomes showed strong fluorescence signals (**b**). [S. K. Rhee, A. P. Quist, and R. Lal (1998) *J. Biol. Chem.* **273**, 13379–13382]. (**c**), (**d**) and (**e**) Adhesion sites between a *Xenopus* retinal glial cell (XR1 cell line) and extracellular matrix material in a cell culture. The fluorescent images show the location of b-**integrin** (**c**) and f-actin (**d**) fibers detected by immunofluorescence, and the tapping mode AFM image (**e**) reveals the 3-D architecture of the focal point after removing of the cell body [R. Lal and R. Proksch (1997) *Int. J. Imaging Syst. Technol.* **8**, 293–300]. (**f**) and (**g**): Simultaneously combined AFM and fluorescence-confocal microscopic images. The sample was a suspension of fluorescently labeled latex beads that were dried into a gel on a plastic diffraction grating. The lines of the grating are visible in the topographic AFM image (**f**) but not in the confocal fluorescent image (**g**). The two images allow distinguishing a nonfluorescent particle (left arrow) from a fluorescent particle (right arrow), although both appear as raised bumps in the AFM image. [P. E. Hillner, D. A. Walters, R. Lal, H. G. Hansma, and P. K. Hansma (1995) *J. Micro. Soc. Am*. **1**, 123–126]. (**h**) and (**i**): Simultaneously combined AFM and scanning ion-conductance microscope (SICM) electrophysiology. (**h**) shows a tapping mode AFM image of a nucleopore membrane, and (**i**) shows the associated ionic conductivity image obtained by tapping mode SICM. Note that there are some differences in the pores detected by the two procedures. For example, the area circled in white shows a groups of pores that appear to be deep in the AFM image and highly conductive in the SICM image. The area circled in grey contains a large pore that appears deep in the AFM image but is nonconductive in the SICM image. The scale bars at the bottom are intensity-coded. Brighter is a greater height in the AFM image and a greater conductance in the SICM image. [R. A. Proksch, R. Lal, P. K. Hansma, G. Morse, and G. Stucky (1996) *Biophys. J.* **71**, 2155–2157.]

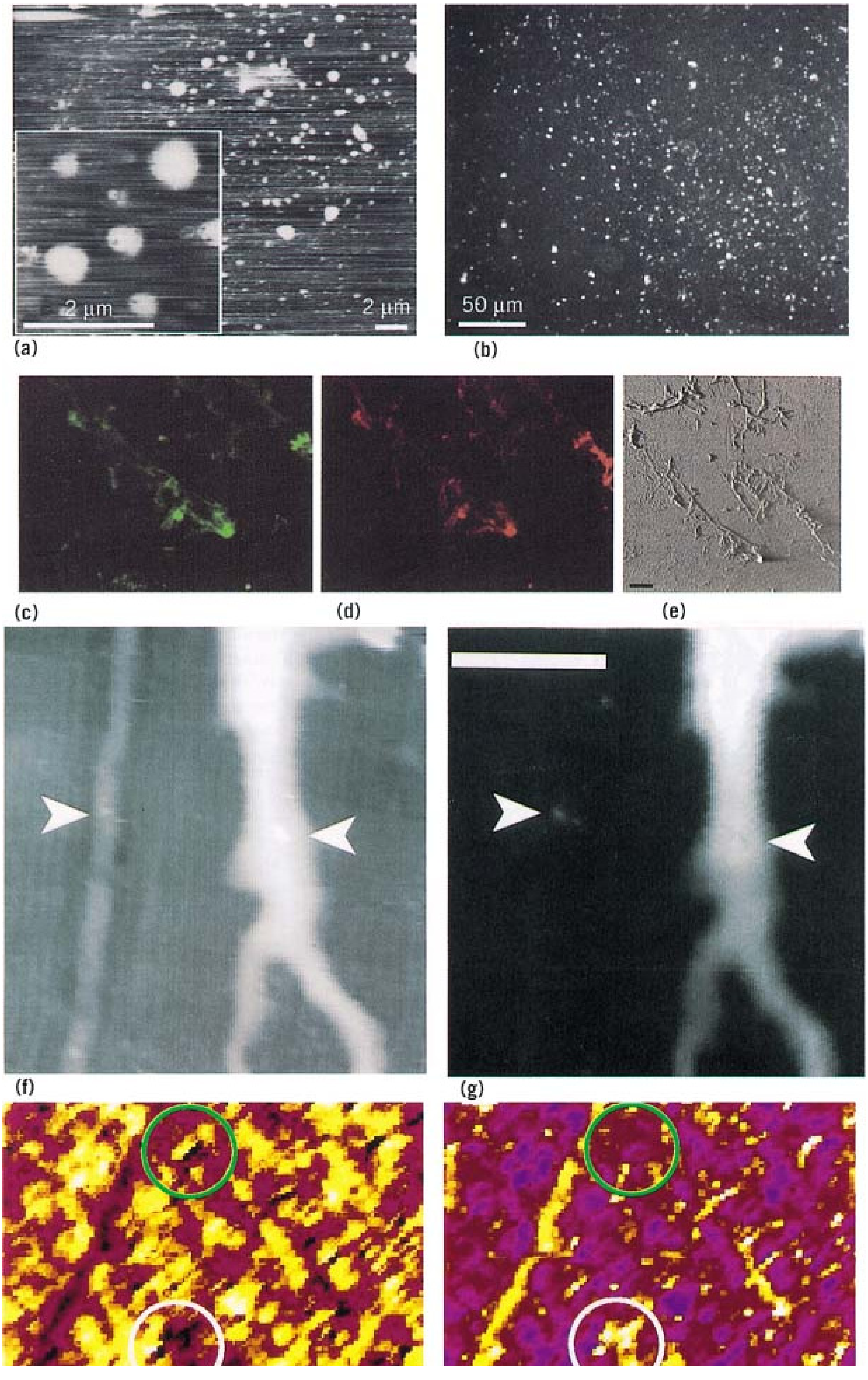

2 µm
2 µm
(a)
50 µm
(b)
(c)
(d)
(e)
(f)
(g)

Another approach is combining AFM with the patch-clamp technique in the same experiment. Such a combined technique records electrical current in the excised membrane patches from *Xenopus* oocytes that are attached to the patch pipette tip, while simultaneously observing the surface topology with AFM. Also, The membrane surface is also deformed by applying pressure through the patch pipette and observing the lateral displacement of features. However, the resolution is limited to about 10 nm.

Suggestions for Further Reading

G. Binnig, C. F. Quate, and C. Gerber (1986) Atomic force microscope, Phys. Rev. Lett. **56**, 930–933.

B. Drake, S. A. C. Gould, A. L. Weisenhorn, H. G. Hansma, P. K. Hansma, C. F. Quate, C. B. Prater, T. R. Albrecht, and D. S. Cannell (1989) Imaging crystals, polymers, and processes in water with the atomic force microscope, Science **243**, 1586–1589.

P. K. Hansma, V. B. Elings, C. E. Bracker, and O. Marti (1988) Scanning tunneling microscopy and atomic force microscopy—application to biology and technology, Science **242**, 209–216.

E. Henderson, P. G. Haydon, and D. S. Sakaguchi (1992) Actin filament dynamics in living glial cells imaged by atomic force microscopy, Science **257**, 1944–1946.

P. E. Hillner, D. A. Walters, R. Lal, H. G. Hansma, and P. K. Hansma (1995) Combined atomic force and confocal laser scanning microscope, J. Micro. Soc. Am. **1**, 123–126.

J. H. Hoh, R. Lal, S. A. John, J. P. Revel, and M. F. Arnsdorf (1991) Atomic force microscopy and dissection of gap junctions, Science **253**, 1405–1408.

R. Lal (1998) Imaging molecular structure of channels and receptors with an atomic force microscope, Scanning Microsc. **10**, 81–96.

R. Lal and S. A. John (1994) Biological applications of atomic force microscopy, Am. J. Physiol. Cell Physiol. **266**, C1–C21.

R. Lal and R. Proksch (1997) Multimodal imaging with atomic force microscopy: Combined atomic force, light fluorescence, and laser confocal microscopy and electrophysiological recordings of biological membranes, Int. J. Imaging Syst. Technol. **8**, 293–300.

F. Ohnesorge and G. Binnig (1993) True atomic resolution by atomic force microscopy through repulsive and attractive forces, Science **260**, 1451–1456.

B. N. J. Persson (1987) The atomic force microscope—can it be used to study biological molecules, Chem. Phys. Lett. **141**, 366–368.

R. A. Proksch, R. Lal, P. K. Hansma, D. Morse, and G. Stucky (1986) Imaging the internal and external pore structures of membrane in fluid: Tapping mode scanning ion conductance microscopy, Biophys. J. **71**, 2155–2157.

D. Sarid (1991) *Scanning Force Microscopy: With Applications to Electric, Magnetic and Atomic Forces*, Oxford University Press, New York.

Y. Z. Zhang, S. Sheng, and Z. Shao (1996) Imaging biological structures with the cryoatomic force microscope, Biophys. J. **71**, 2168–76.

ATP Synthase

ATP synthase, also called F_0F_1 ATPase, or simply F-ATPase, is the universal protein that terminates oxidative phosphorylation by synthesizing ATP from ADP and phosphate. Nearly identical proteins are found in eukaryotic mitochondria and bacteria, and they all operate on the same principle. Electron-driven ion **pumps** set up concentration and electrical gradients across a membrane (see Chemiosmotic Coupling and Proton Motive Force). ATP synthase utilizes the energy stored in this electrochemical gradient to drive nucleotide synthesis. It does this in a surprising way by converting the electromotive force into a rotary torque that promotes phosphate binding and liberates ATP from the catalytic site where it was formed. Remarkably, this process can be reversed in certain circumstances. ATP hydrolysis can drive the engine in reverse, so that F-ATPase functions as a proton pump. Indeed, the vacuolar V-ATPases, the most ubiquitous intracellular proton pumps, are structurally similar to ATP synthase and operate according to the same principles.

ATP synthase is composed of at least eight subunit types, whose stoichiometries are denoted by the subscripts (a_3, b_3, g, d, ε, a, b_2, c_{12}), that combine into two distinct regions. The geometric arrangement of the subunits is shown schematically in Fig. 1(a). The soluble F_1 portion consists of a hexamer, a_3b_3. This hexamer is arranged in an annulus about a central shaft consisting of the coiled-coil g subunit. Subunits d and ε are also generally isolated with F_1. The F_0 portion consists of three transmembrane subunits, a, b_2, and c_{12}. The 12 copies of the c-subunit form a disk into which the g and ε subunits insert. The remainder of F_0 consists of the transmembrane subunits a and b_2. The latter is attached by the d subunit to an a subunit, so that it anchors the a subunit to F_1. Thus there are two "stalks" connecting F_0 to F_1, gε and b_2d.

Figure 1. Schematic diagram of the subunit organization of ATP synthase (1). (**a**) The a_3b_3 hexamer and a portion of the g shaft. The lower part of g has not been resolved. The c-subunit consists of 12 pairs of transmembrane a-helices, and the a subunit consists of six transmembrane a-helices. The ε subunit abuts c and g and interacts with the DELSEED region of b. The a subunit is attached to an a subunit via the b and d subunits. (**b**) The proton motive force at the a–c interface leads to the functional subdivision into two counterrotating assemblies, usually denoted as the "rotor" and "stator." The rotor consists of subunits c_{12}-g-ε, and the stator consists of subunits a-b_2-d-a_3b_3.

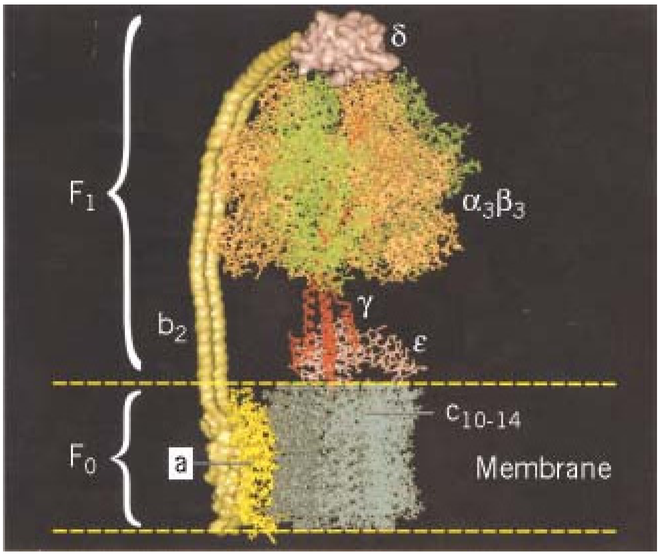

The key to understanding how ATP synthase carries out its catalytic and synthetic roles lies in this geometric organization. The entire protein can be divided into two operational regions denoted suggestively as the "rotor" and the "stator" for reasons that derive from the rotary mechanism by which the protein operates (Fig. 1b). Indeed, it turns out that ATP synthase has two rotary engines in one. The F_0 motor converts transmembrane electrochemical energy into a rotary torque on the g shaft, and F_1 uses ATP hydrolysis to turn the g shaft in the opposite direction. Because they are connected, one drives the other in reverse. When F_0 dominates, the rotor turns clockwise (looking upward in Fig. 1), so that F_1 synthesizes ATP. When F_1 dominates, so that F_0 is driven counterclockwise, it can pump protons against an electrochemical gradient. Deciphering how this remarkable dual energy transduction works is one of the great triumphs of modern chemistry.

1. ATP Synthesis in F_1 is Driven by Rotation of the g-Shaft

We begin with the F_1 motor, because we now know precisely what it looks like. This is due to John Walker and the X-ray crystallography group at Cambridge, who worked out the exact structure of the a_3b_3 hexamer and most of the g shaft (1). A stereo view of the structure is shown in Fig. 2. Walker was awarded the Nobel Prize in 1997 because his structure revealed essential asymmetries in the molecule's structure that were the key to understanding how it worked. In the early 1980's, Paul Boyer at UCLA proposed the surprising theory that, in the catalytic sites of F_1, ATP is in chemical equilibrium with its reactants, ADP and phosphate (2). So the formation of ATP is essentially without cost energetically. However, because each ATP hydrolyzed under cellular conditions liberates about 12 kcal/mol, this energetic price must be paid at some point. Boyer proposed that F_1 pays this price in the mechanical work necessary to liberate the nucleotide from the catalytic site. Further, release of product (ATP) proceeds sequentially and cyclically around the a_3b_3 hexamer because the synthetic reactions are synchronized in a fixed-phase relationship by rotation of the g shaft and cooperative coupling between the three catalytic sites. Boyer's “binding change” mechanism neatly fits the Walker structure, and Boyer shared the 1997 Nobel Prize. A schematic diagram of the binding change mechanism is shown in Fig. 3.

Figure 2. Stereo pair showing the molecular structure of the F_1 subunit run through center, coils extending out from mid in light gray, and the two coils of the g subunit medium gray. Its asymmetrical structure is evident. In the b subunit: the s is in dark gray, and the lower hinge segment is medium gray. The structure of the ε subunit (not shown) is known, but it the g and c subunits.

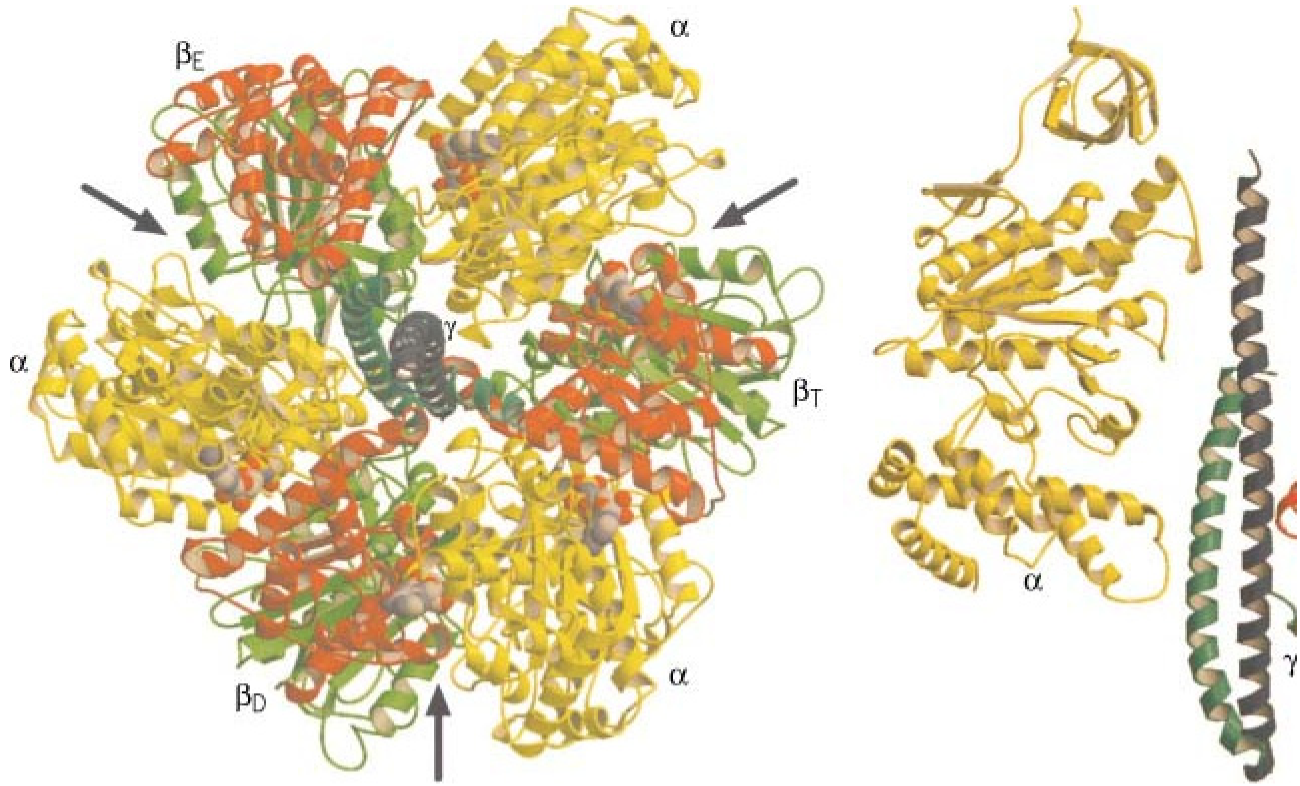

Figure 3. The binding change mechanism. Notation for site occupancies: T = ATP bound, DP = ADP • P_i bound, D = A] numbered clockwise. The lengths of the arrows indicate the relative binding affinities. (**a**) The system starts with either ((b_1, b_2, b_3) = (D, T • D • P, D). (**b**) Clockwise rotation of g increases the binding affinity of ADP in b_1, traps ATP in b_2, a (**c**) Further rotation of g traps ADP and allows P_i binding in b_1, releases the tightly bound ATP and allows ADP binding

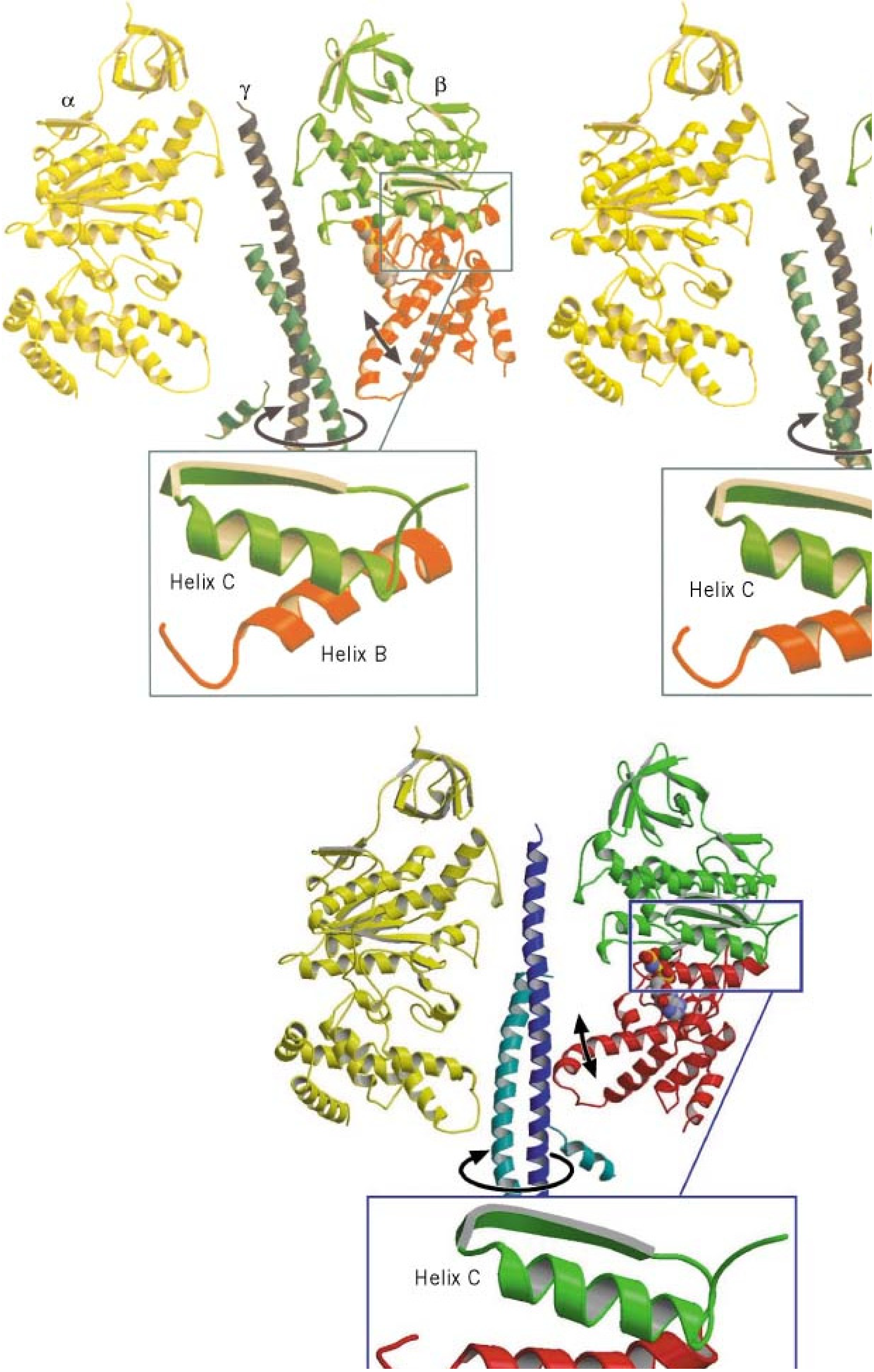

α
γ
β
Helix C
Helix B
Helix C
Helix C

There are actually six nucleotide-binding sites on the a_3b_3 hexamer. All lie at the interfaces between the a and b subunits. The catalytic sites lie mostly in the b subunit, whereas the noncatalytic sites lie mostly in the a subunit. The role of the noncatalytic sites is uncertain, but they may help to hold the hexamer together. Each catalytic site traverses the synthetic cycle sequentially:

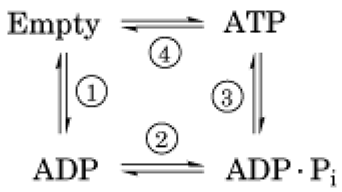

In steps 1 and 2, a site binds ADP and phosphate (not necessarily in that order). While trapped in the catalytic site in step 3, the reactants (ADP and P_i) and product (ATP) are in chemical equilibrium. Step 4 requires the input of mechanical torque from F_0 on g to trap the reactants in the ATP state and to pry open the site, releasing the tightly bound ATP. Most of the 12 kcal/mol price of synthesis is paid in step 4. The way in which this works is found in the shape of the a_3b_3 hexamer and the g shaft.

The g subunit is asymmetric and bowed. It fits into a central annulus in a_3b_3, which is itself asymmetric (Fig. 4). At the top of the a_3b_3 hexamer is a **hydrophobic** "sleeve" in which the g shaft rotates. Further down, however, the annulus is offset from the center, so that as g rotates clockwise, it sequentially pushes outward on each catalytic site. In addition, the ε subunit is located eccentrically and attached to the g and c subunits, so that as g rotates, it comes into contact sequentially with each b subunit in a conserved region called the DELSEED sequence (named for the single-letter abbreviation of its constituent amino acid residues). Together, this asymmetrical rotation exerts stress on the catalytic site, loosening its grip on ATP, so that thermal fluctuations can free it into solution.

Figure 4. Cross section of F_1 showing the conformational changes in the b subunits that drive rotation of g. The a subunit is on the left and the stationary barrel region of b is on the right. During the hydrolytic cycle, the lower segment of b undergoes a hinge-bending motion that rotates it about 30° inward. This motion pushes on the eccentric g coiled coil, causing it to rotate within the barrel bearing. During synthesis, the rotation of g pushes on each catalytic site. The panels show three snapshots of the motion during a 180° rotation. Movies of the rotational sequence can be downloaded from the authors' World Wide Web site: (site currently unavailable)

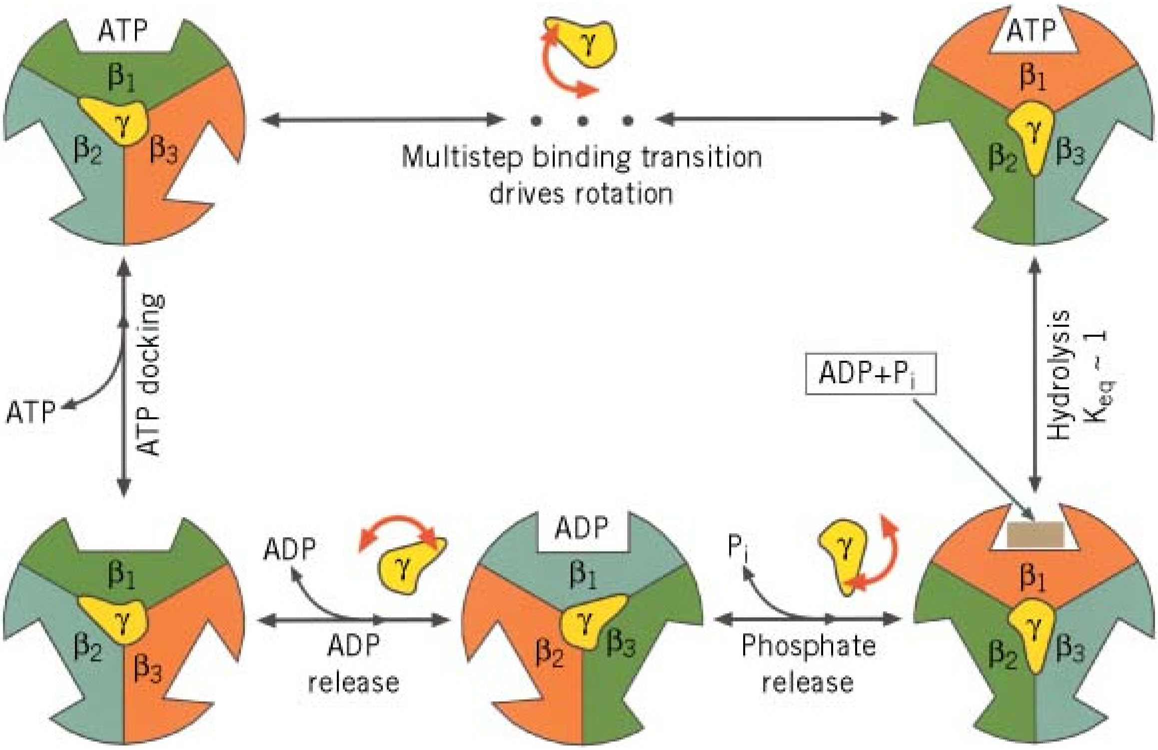

(3). These interactions may mediate phosphate- and nucleotide-binding, the necessary precursors to synthesis. In addition, the catalytic sites are elastically coupled, so that the occupancy of one site affects the affinity of the other two sites. The consequence of this coupling is that when ATP concentrations are low enough so that only one site is occupied, hydrolysis proceeds much more slowly than when more than one site is occupied.

Together with the F_1 molecular structure, the binding change model strongly supports the idea that catalysis involves rotation of the g subunit. However, dramatic visual confirmation was provided by *in vitro* experiments in which the a_3b_3g subunits were isolated and attached to a bead. A fluorescently tagged actin filament was attached to the g shaft, and when ATP was supplied, the filament could be clearly seen rotating. In fact, a complete revolution takes place in three steps and consumes a single ATP per step (4).

The viscous drag on the actin filament was estimated, which allowed computing the torque developed by the F_1 motor and comparing it with the **free energy** available from ATP hydrolysis. The startling result was that the motor generates an average torque of more than 40 piconewton nanometers (40×10^{-12} N $\times$ 10^{-9} m), more than six times the maximum force developed by kinesin or myosin. More impressively, the motor operates near 100% mechanical efficiency, this precludes any sort of heat engine, which would be limited by the Carnot efficiency (4). Several models have been proposed that address the issue of torque generation and efficiency (4-6).

The energy to drive this motion derives from the hydrolytic cycle of ATP at the catalytic site. Moreover, the conformational change that drives the hydrolysis motor must be nearly the reverse of the motion that frees ATP from the catalytic site during synthesis. Examination of the structure reveals that the major conformational change is a hinge-bending motion in the b subunits. The bottom portion of each b subunit below the nucleotide-binding site rotates inward approximately 30°, during which it pushes on the bowed g subunit, turning it much like one cranks an automobile jack (Fig. 4).

2. F_0 Converts Proton Motive Force into Rotary Torque

Currently, there have been no direct observations of rotation in the F_0 portion of ATP synthase (7). However, current thinking is that the F_0 assembly converts the energy contained in the transmembrane proton motive force into a rotary torque at the interface of the a and c subunits (Fig. 1). This torque turns the rotor (the c, g, and ε subunits), which couples to the F_1 synthetic machine.

The c assembly consists of 12 subunits, each consisting of two transmembrane alpha-helices (8). There is one essential acidic amino acid (Asp61 in the *Escherichia coli* ATP synthase) which binds protons. Because variants of ATP synthase can operate on sodium rather than protons, the interaction between the c subunit and the translocated ion has the property of an electrostatic carrier mechanism (9).

The a subunit consists of six transmembrane a-helices that contain at least one essential basic residue (Arg210 in *E. coli*) (8, 10). The electrostatic interaction of these rotor and stator charges is essential for torque generation, and several proposals have been put forward for the way this could work (11-14). Whatever the mechanism, the F_0 motor must generate a torque sufficient to liberate three ATP's from the three catalytic sites in F_1 for each revolution. If the proton flux through the stator is tightly coupled to the rotation of the c subunit, then a rotation of 2p/3 carries four protons down the electromotive potential of 230 mV typical of the mitochondrial inner membrane (14). This is sufficient to account for the mechanical energy required for synthesis of one ATP.

Under anaerobic conditions, the ATP synthase of the bacteria *E. coli* can reverse its operation, hydrolyzing ATP and turning the c subunit backward so that it functions as a proton pump. This is not surprising because the F-ATPases are structurally similar to the most common proton pumps, the vacuolar, or V-ATPases (7). These pumps may have been the **evolutionary** precursors of ATP synthase (15). A striking difference between the two is that the F-ATPases have 12 acidic rotor charges, whereas the V-ATPases have six. It can be shown that this enables the V-ATPases to function more efficiently as ion pumps at the expense of relinquishing their capability to synthesize ATP.

3. Summary

Both the F_1 and F_0 motors can operate in both directions. F_1 is a hydrolytically driven three-piston engine that can be driven in reverse to synthesize ATP from ADP and phosphate. F_0 is an ion-driven rotary engine that can be driven in reverse to function as an ion pump. The F-ATPases are structurally similar to and presumably evolutionarily related to the V-ATPase ion pumps (15). It is thought that most ion pumps function by an “alternating access” mechanism, whereby an ion is first bound strongly on the dilute side, then energy is supplied to move the ion so that it communicates with the concentrated side and weakens its binding affinity (16). In contrast with other ion pumps, however, the F and V-ATPases accomplish this by a rotary mechanism that is driven indirectly by nucleotide hydrolysis, rather than by direct phosphorylation (17). It is thought that the F_0 motor is also related to the bacterial **flagellar** motor. Both can operate on sodium, although the flagellar motor has eight or more “stators” and develops far more torque than F_0 (18, 19).

The mechanism driving the F_1 hydrolytic motor may carry hints for other nucleotide hydrolytically fueled motors, such as kinesin, myosin, and dynein. However, important structural differences may make the comparison difficult (4). For example, the motors previously mentioned all “walk” along a polymer track to which they bind tightly during a portion of their mechanochemical cycle. The power stroke of the F_1 motor is driven by the b subunit, which pushes on the g shaft, but does not bind tightly to it, that is, it does not “walk” around the g shaft. Moreover, no other motor operates with nearly the efficiency of the F_1 motor, implying that there are important entropic steps in other motors that are absent in the F_1 motor.

Bibliography

1. J. Abrahams, A. Leslie, R. Lutter, and J. Walker (1994) Nature **370**, 621–628.
2. P. Boyer (1993) Biochim. Biophys. Acta **1140**, 215–250.
3. M. Al-Shawi, C. Ketchum, and R. Nakamoto (1997) J. Biol. Chem. **272**, 2300–2306.
4. K. Kinosita, R. Yasuda, H. Noji, S. Ishiwata, and M. Yoshida (1998) Cell **93**, 21–24.
5. F. Oosawa and S. Hayashi (1986) Adv. Biophys. **22**, 151–183.
6. H. Wang and G. Oster (1998) Nature **396**, 279–282.
7. M. Finbow and M. Harrison (1997) Biochem. J. **324**, 697–712.
8. R. H. Fillingame (1997) J. Exp. Biol. **200**, 217–224.
9. P. Dimroth (1997) Biochim. Biophys. Acta **1318**, 11–51.
10. R. H. Fillingame (1996) Curr. Opinion Struct. Biol. **6**, 491–498.
11. S. B. Vik and B. J. Antonio (1994) J. Biol. Chem. **269**, 30364–30369.
12. W. Junge, H. Lill, and S. Engelbrecht (1997) Trends Biochem. Sci. **22**, 420–423.
13. G. Kaim, U. Matthey, and P. Dimroth (1998) EMBO J. **17**, 688–695.
14. T. Elston, H. Wang, and G. Oster (1998) Nature **391**, 510–514.
15. R. Cross and L. Taiz (1990) FEBS Lett. **259**, 227–229.
16. B. Alberts, D. Bray, J. Lewis, M. Raff, K. Roberts, and J. Watson (1994) *Molecular Biology of the Cell*, Garland, New York.
17. S. Khan (1997) Biochim. Biophys. Acta **1322**, 86–105.
18. H. Berg (1995) Biophys. J. **68**, 163s–166s.
19. K. Muramoto, I. Kawagishi, S. Kudo, Y. Magariyama, Y. Imae, and M. Homma (1995) J. Mol. Biol. **251**, 50–58.

Suggestions for Further Reading

20. P. Boyer (1993) The binding change mechanism for ATP synthase—some probabilities and possibilities. Biochim. Biophys. Acta **1140**, 215–250.
21. J. Weber and A. E. Senior (1997) Catalytic mechanism of F1-ATPase. Biochim. Biophys. Acta **1319** (1), 19–58.

ATP-Binding Motif

The ATP-binding motif, also called the *Walker motif*, is a structural protein motif that is frequently found in proteins that bind ATP or GTP. It can usually be identified from just the primary structure of a protein using a fingerprint sequence that characterizes proteins as ATP or GTP-binding (see GTP-Binding Proteins). Walker et al. (1) identified two regions of sequence conservation: the A region has a stretch of small **hydrophobic** residues followed by [Gly/Ala]━X━X━Gly━X━Gly━Lys━Thr/Ser, where X is any residue. The second region of sequence conservation also has a stretch of small hydrophobic residues, this time ending in a conserved **aspartate** residue. In the three-dimensional structures of proteins having the ATP-binding motif, such as adenylate kinase, the hydrophobic residues of the A-region form a buried b-strand, and the glycine-rich region forms a loop, called the P-loop, that interacts with the phosphate of the bound nucleotide. The second conserved region codes for another hydrophobic b-strand, and the conserved aspartate is required for binding the magnesium ion that usually accompanies nucleotides bound to proteins.

The ATP-binding motif represents a common, but not the only, mode of interaction between proteins and ATP/GTP. For example, it is structurally distinct from the actin fold of proteins such as actin, hsp70, and hexokinase, which bind and hydrolyze ATP or GTP and where a conformational change is implicated in nucleotide binding (2).

[See also Nucleotide-Binding Motif and P-Loop.]

Bibliography

1. J. E. Walker, M. Saraste, M. Runswick, and N. Gay (1982) EMBO J. **1**, 945–951.
2. W. Kabsch and K. C. Holmes (1995) FASEB J. **9**, 167–174.

Suggestions for Further Reading

3. G. E. Schulz (1992) Binding of nucleotides by proteins. Curr. Opin. Struct. Biol. **2**, 61–67 (Excellent review of nucleotide binding motifs.)

ATPase

Any enzyme that catalyzes the hydrolysis of ATP to ADP and inorganic phosphate (P_i) is classified as an ATPase. In some cases, the phosphate is transiently transferred to the protein before its release as a product. The hydrolysis of ATP liberates much energy, so this reaction is usually coupled to another, energetically unfavorable reaction. Three major types of ATPase are associated with membranes that couple ATP hydrolysis to the translocation of specific ions across a membrane: P-, V-, and F-ATPases.

P-ATPases have a relatively simple polypeptide composition (one or two subunits) and are phosphorylated as part of their catalytic cycle. Examples of P-ATPases are (*1*) the Na^+, K^+ – ATPase of the plasma membrane of animal cells; (*2*) the H^+ – ATPase of the plasma membranes of **yeast**, **fungi**, and plants; and (*3*) the Ca^{2+} – ATPase of the sarcoplasmic reticulum (the endoplasmic reticulum of muscle). The plasma membrane Na^+, K^+ – ATPase and H^+ – ATPase function to generate and maintain the plasma membrane electrical potential difference (inside negative), as well as the ionic disequilibria across that membrane. Ca^{2+} – ATPases function in Ca^{2+} homeostasis (see Calcium Signaling).

V-ATPases have a much more complicated polypeptide composition than do P-ATPases and are not phosphorylated during catalysis. V-ATPases are found on the membranes within the interiors of **eukaryotic** cells (endomembranes), including membranes from vacuoles (from which the “V” is derived), **lysosomes**, **Golgi**, **secretory vesicles**, **clathrin**-coated vesicles, and, in some instances, plasma membranes. V-ATPases are H^+ – ATPases that show some similarity to the proton-linked ATP synthases. The function of V-ATPases is to catalyze proton transport into the endomembrane interior compartments at the expense of ATP hydrolysis. Acidification of the interior of endomembranes is required for some of their functions. In **archaebacteria**, an enzyme with similarity to V-ATPases functions as an ATP synthase.

F-ATPases (also known as "F_1–F_0") have a complex polypeptide composition and, as in V-ATPases, there is no phosphorylated intermediate in the reaction mechanism. In non**photosynthetic** eukaryotes, the F-ATPase is found exclusively on the inner membrane of mitochondria, whereas in green plants and algae there are two distinct F-ATPases; one in mitochondria and the other on the thylakoid membrane of chloroplasts. In bacteria, F-ATPase is present in the plasma membrane. ATPases couple the flow of protons (or Na^+ in some cases) to ATP hydrolysis and synthesis. The activity of the F-ATPases is very tightly regulated. Several mechanisms combine to prevent wasteful ATP hydrolysis by F-ATPase, but to allow rapid ATP synthesis at the expense of electrochemical proton (or Na^+) potentials generated by proton translocation linked to electron transport (see Chemiosmotic Coupling). F-ATPases operate *in vivo* as ATP synthases; consequently, the term *ATP synthase* is preferred to *F-ATPase* when referring to the entire enzyme. The catalytic portion of the ATP synthase may be readily removed from coupling membranes and purified as a large 400-kDa water-soluble protein. Such preparations may have high ATPase activity and are called "F_1" or "F_1-ATPase" (see ATP Synthase).

Attenuation Of Transcription

The ability to modulate **gene** expression in response to changing environmental signals is crucial for the survival of all organisms. Virtually every stage involved in the synthesis, function, and degradation of macromolecules is a potential target for one or more regulatory events (1). Regulatory mechanisms have been identified for all three stages of transcription (initiation, elongation, and termination). Several postinitiation regulatory mechanisms have been categorized as transcription attenuation mechanisms. Transcription attenuation can be defined as any mechanism that utilizes transcription pausing or transcription termination to modulate expression of downstream genes. For the purpose of this article, however, the definition will be restricted to situations in which the action of the regulatory molecule promotes transcription termination, with the default situation being transcriptional readthrough. There are also related **antitermination** mechanisms in which the action of the regulatory molecule promotes transcriptional readthrough.

Once transcription of a gene is initiated, the transcription elongation complex and its nascent transcript are potential targets for regulation. As transcription proceeds, the nascent transcript may fold into specific secondary and tertiary structures that signal the transcribing **RNA polymerase** to pause or terminate transcription before reaching the structural genes (1). Transcription attenuation mechanisms allow the organism to modulate the extent of transcriptional readthrough past the terminator structure in response to changing environmental signals, thereby regulating expression of the downstream genes. As will be seen, several different transcription attenuation mechanisms have been identified.

1. Transcription Attenuation of Biosynthetic Operons of Enteric Bacteria

Transcription attenuation was the first demonstration that organisms can exploit RNA structure to modulate gene expression. The first attenuation mechanism was elucidated by Charles Yanofsky and his coworkers for the *Escherichia coli* tryptophan biosynthetic operon (*trpEDCBA*; see TRP Operon) (2). In addition, many other amino-acid biosynthetic operons in enteric bacteria are regulated by transcription attenuation (eg, *his*, *leu*, *ilv*, *pheA*). In each case, the genetic information required for transcription attenuation is encoded within a 150–300-bp leader region located between the **promoter** and the first structural gene of the operon (1). Because the salient features of transcription attenuation are conserved in each system, the *E. coli trp* operon will be discussed, and the key differences with respect to other operons will be pointed out where appropriate.

Transcription initiation of the *E. coli trp* operon is regulated by TrpR, a **DNA-binding** repressor protein. Once transcription starts, the elongating transcription complex is subject to control by transcription attenuation (1). The combined actions of repression (80-fold) and transcription attenuation (eight-fold) result in approximately 600-fold regulation in response to changing concentrations of intracellular tryptophan (3). A simplified model of the *E. coli trp* operon transcription attenuation mechanism is depicted in Figure 1 (4). The 141-nucleotide leader transcript can form three overlapping RNA secondary structures, referred to as the pause structure, the antiterminator, and a Rho-independent terminator. In addition, the nascent *trp* leader transcript contains a small open reading frame that encodes a 14-amino acid residue leader peptide. Soon after transcription of the *trp* operon is initiated, a secondary structure (structure1:2) forms in the nascent transcript that signals RNA polymerase to pause. The paused RNA polymerase complex allows sufficient time for a ribosome to initiate translation of the leader peptide. The translating ribosome then disrupts the paused RNA polymerase complex, and transcription resumes, with the ribosome closely following the molecule of RNA polymerase, thereby coupling transcription and translation. At this point, two different outcomes can occur, depending on the level of tryptophan in the cell. Under conditions of limiting tryptophan, the level of charged transfer RNA $tRNA^{Trp}$ is low. As a result of the low tryptophanyl-$tRNA^{Trp}$ concentration, the translating ribosome stalls at one of two tandem Trp **codons** strategically placed within the leader peptide coding sequence. Ribosome stalling at the Trp codons effectively uncouples transcription and translation. As transcription proceeds, therefore, the antiterminator structure (structure 2:3) forms and prevents formation of the overlapping Rho-independent terminator (structure 3:4), resulting in transcriptional readthrough into the *trp* structural genes. Under conditions of tryptophan excess, the level of charged $tRNA^{Trp}$ is sufficiently high to allow efficient translation of the tandem Trp codons, and the ribosome continues to the end of the leader peptide. When the ribosome reaches the leader peptide stop codon, it physically blocks formation of the antiterminator structure, thereby promoting terminator formation and, hence, termination of transcription, before RNA polymerase reaches the *trp* structural genes. Thus, expression of the *trp* operon is decreased when the cell has an adequate supply of tryptophan. As can be seen by the above example, the regulatory signal is charged $tRNA^{Trp}$, and the sensory event is the capacity to translate a short peptide-coding sequence (1). The transcription attenuation mechanisms for several other amino acid biosynthetic operons, such as the *his*, *phe*, and *leu* operons, are essentially identical to that for the *trp* operon, except that the leader peptides contain seven His (5), seven Phe, and four Leu codons (6), respectively.

Figure 1. Model of transcription attenuation for the *E. coli trp* operon. RNA polymerase pauses following formation of the pause structure provides time for a ribosome to initiate translation of the leader peptide. Under tryptophan-limiting conditions, the ribosome stalls at the tandem Trp codons, resulting in transcription readthrough. Under conditions of tryptophan excess, the ribosome reaches the leader peptide stop codon. This ribosome position blocks formation of the antiterminator, leading to terminator formation and transcription termination. (See text for details.) Adapted from Landick and Yanofsky (4).

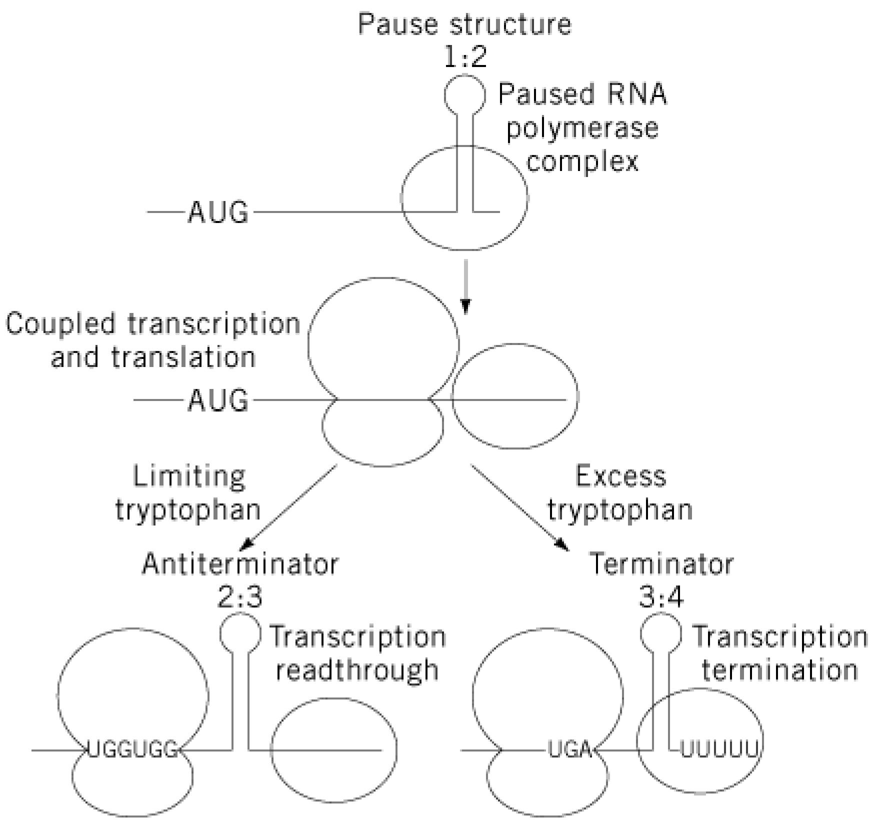

Expression of the *E. coli* pyrimidine biosynthetic operon, *pyrBI*, is also regulated by transcription attenuation (7, 8). In this case, the concentration of UTP serves as the regulatory signal, in conjunction with a UTP-dependent pause signal consisting of an RNA hairpin and several U residues just after the hairpin. A transcription terminator exists approximately 60 nucleotides downstream of the pause structure, but the leader transcript does not have the potential to form an antiterminator structure. Finally, there is a 44-residue leader peptide encoded by an open reading frame beginning prior to the pause signal and extending past the terminator. The model for this attenuation mechanism is as follows: When there is a deficiency of UTP, the transcribing RNA polymerase pauses at the leader pause site. This provides time for a ribosome to initiate translation of the leader peptide, which results in coupled transcription and translation. As transcription proceeds, the translating ribosome prevents formation of the transcription terminator, allowing transcription of the structural genes. However, pausing is inefficient when the cell contains an adequate supply of UTP. In this case, RNA polymerase transcribes and recognizes the terminator before the ribosome reaches this segment of the leader transcript, thus halting transcription in the leader region prior to the structural genes.

2. Transcription Attenuation of Gram-Positive Biosynthetic Operons

The transcription attenuation mechanisms that have been identified for the *trp* and *pyr* operons in the **Gram-positive bacterium** *Bacillus subtilis* differ dramatically from those described for the enteric bacteria. Most notably, ribosomes and tRNA molecules are not involved. Instead, sequence-specific RNA-binding proteins are responsible both for sensing the level of tryptophan or UMP in the cell and, ultimately, for the decision to terminate transcription or to readthrough into the structural genes.

Expression of the *trpEDCFBA* operon of *B. subtilis* is regulated by TRAP, the *trp* RNA-binding attenuation protein (9, 10). TRAP is composed of 11 identical subunits arranged in a single ring (11). Tryptophan binding between each adjacent subunit in a cooperative manner activates TRAP to bind RNA (11). Transcription initiation of the *trp* operon appears to be constitutive, occurring 203 nucleotides upstream of the first structural gene. A transcription attenuation model for the *B. subtilis trp* operon is depicted in Figure 2. The *B. subtilis trp* leader transcript contains inverted repeats that can form mutually exclusive antiterminator and Rho-independent terminator structures (12), although there is no apparent transcription pause signal in this case. When cells are growing in excess tryptophan, tryptophan-activated TRAP binds to 11 closely spaced (G/U)AG repeats present in the *trp* leader transcript (11, 13). Recent studies have shown that TRAP binds to these repeats by wrapping the RNA around the protein ring, with the bases of the (G/U)AG repeats interacting with several amino acid residues on adjacent subunits in the protein (14). TRAP binding blocks formation of the antiterminator, which allows formation of the overlapping terminator structure. Thus, transcription halts in the leader region prior to the *trp* structural genes. Under conditions of limited tryptophan, TRAP is not activated and does not bind to the *trp* leader transcript. Thus, as transcription proceeds, the antiterminator forms, allowing transcription readthrough into the *trp* structural genes (9, 12).

Figure 2. Model of transcription attenuation of the *B. subtilis trp* operon. The large boxed letters designate the complementary strands of the terminator and antiterminator RNA structures. Small rectangles represent the GAG and UAG repeats involved in TRAP binding; these triplet repeats are also outlined in the sequence of the antiterminator structure. Numbers indicate the residue positions relative to the start of transcription. Nucleotides 108 to 111 overlap between the antiterminator and terminator structures and are shown as outlined letters. The TRAP protein is represented as an 11-subunit ring, and the bound RNA is shown forming a matching circle on binding to TRAP, with each triplet repeat interacting with one subunit. From Antson et al. (11).

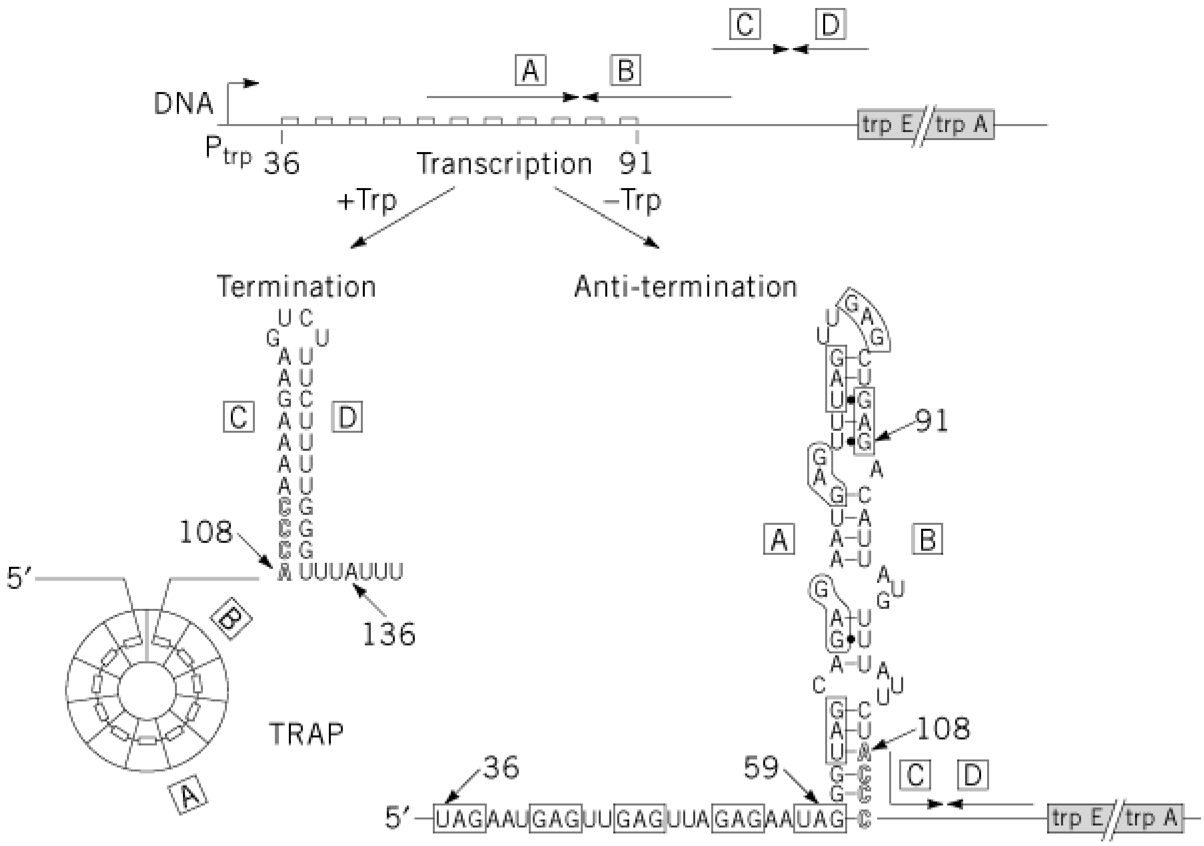

Expression of the *B. subtilis pyr* operon is also controlled by transcription attenuation mediated by an RNA-binding protein. This operon encodes 10 polypeptide chains involved in de novo synthesis of pyrimidines (15, 16). Transcription attenuation occurs in response to UMP levels through the action of PyrR, which is encoded by the first gene of the operon (17). There are several novel features of the attenuation mechanism that controls this operon. In contrast to the systems described previously, the *pyr* operon contains three attenuators: one located in the 5′-untranslated leader region, the second between the first and second genes, and the third between the second and third genes of the operon. Each attenuator can form three alternative RNA secondary structures. In addition to terminator and antiterminator structures similar to those described previously, a structure called the anti-antiterminator can form upstream of, and overlapping, the antiterminator. In the presence of UMP, PyrR is activated to act at each of the three attenuators to promote transcription termination and downregulate expression of the operon. In contrast to the mechanism by which TRAP controls attenuation in the *trp* operon, PyrR binding does not interfere directly with formation of the antiterminator structure, but rather functions by stabilizing the anti-antiterminator, which thereby indirectly stabilizes the terminator (18). The nature of the binding sites for PyrR and TRAP reflects the different effects these proteins have on RNA structure when they bind. TRAP binds to an entirely single-stranded site (19, 20), whereas PyrR binds to a stem-loop structure (21).

Another novel feature of this system is that PyrR is not only an RNA-binding regulatory protein, it is also an enzyme, uracil phosphoribosyltransferase (UPRTase), which catalyzes formation of UMP from uracil and 5-phosphoribosyl-1-pyrophosphate. The physiological role of this enzyme is not clear, as *B. subtilis* has an additional UPRTase that has been shown to be more important for UMP synthesis. The structure of PyrR in the absence of UMP shows two oligomeric forms of the protein, one as a dimer and the other as a hexamer (21). Both forms appear to exist in solution, but PyrR is thought to bind RNA as a dimer. Neither the amino acid sequence nor the structure of PyrR show significant similarity to TRAP. Thus it appears that these two similar attenuation mechanisms evolved independently.

3. Antisense RNA-Mediated Transcription Attenuation

Antisense RNA control of gene expression has been documented for many prokaryotic genes, some of which involve an interesting form of transcription attenuation (22-24). For example, the copy number of the *Streptococcus agalactiae* plasmid pIP501 is regulated by antisense RNA-mediated transcription attenuation (23, 24). The antisense RNA (RNA III) inhibits expression of *repR*, the gene encoding the essential RepR initiator protein, by binding to the nascent *repR* leader transcript (RNA II). This interaction promotes formation of a Rho-independent terminator upstream of the *repR* coding sequence. Interaction of RNA III with RNA II is initiated by the formation of a “kissing complex” between single-stranded loops of both molecules, followed by propagation of the RNA helix. In the absence of RNA III interaction, formation of the transcriptional terminator is prevented, and expression of *repR* can proceed normally. A model illustrating this mechanism is depicted in Figure 3.

Figure 3. Model of plasmid-encoded *repR* transcription attenuation. Interaction of RNA III with the nascent RNA II (*repR*) transcript promotes terminator formation and transcription termination. In the absence of RNA III interaction, refolding of the nascent transcript blocks formation of the terminator, leading to transcription readthrough. (See text for details.) Adapted from Brantl and Wagner (24).

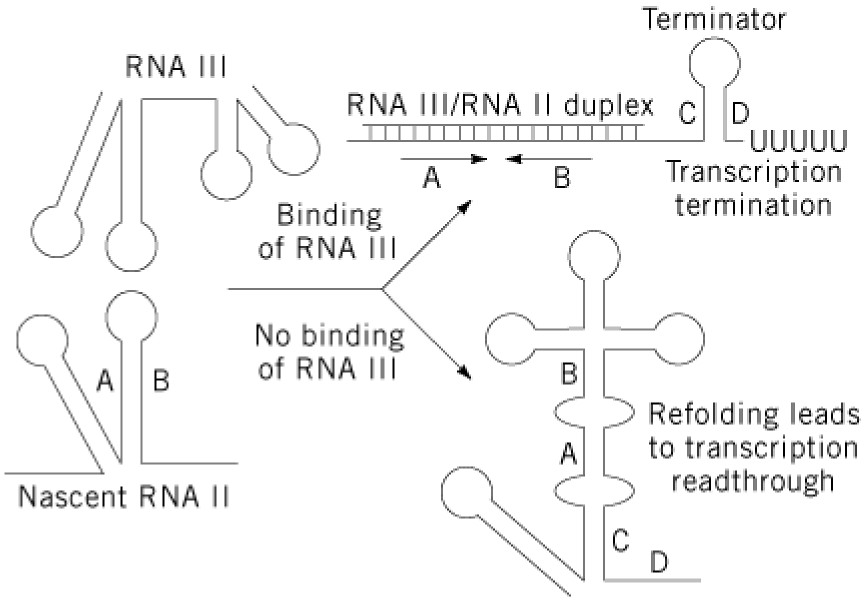

4. Transcription Attenuation of Eukaryotic Genes

Expression of many eukaryotic genes is also regulated at the level of elongation of transcription by processes similar to attenuation (for reviews see 25, 26). In many cases, the action of an inducer protein is required to release the stalled RNA polymerase II elongation complex. In several systems, including *c-myc* (27-31), *N-myc* (32), *c-fos* (33), and adenosine deaminase (34), potential stem-loop structures, similar to prokaryotic transcription terminators, have been identified near the sites of attenuation. However, the precise transcription attenuation mechanisms of these systems are not known.

The best-characterized eukaryotic system involving control of transcription elongation is transcriptional activation of **HIV**-1 by the transactivator protein Tat (35). In this system, transcription initiates at the HIV-1 promoter in the viral long terminal repeat (LTR). In the absence of Tat, transcription terminates prematurely prior to the structural genes. Tat recognizes an RNA target called TAR, located near the 5′-end of the viral transcript (36, 37)). After binding to TAR, Tat interacts with several host cell proteins to enhance the processivity of RNA polymerase II and allow expression of the HIV-1 genes. Transcriptional pausing of RNA polymerase II just downstream of the TAR RNA structure was recently demonstrated. This could allow time for Tat to interact with TAR before RNA polymerase terminates prematurely (38). Interestingly, the pause signal is an RNA stem-loop similar to those seen in attenuation control in enteric bacterial systems.

Bibliography

1. C. Yanofsky (1988) J. Biol. Chem. **263**, 609–612.
2. C. Yanofsky (1981) Nature **289**, 751–758.
3. C. Yanofsky, R. L. Kelley, and V. Horn (1984) J. Bacteriol. **158**, 1018–1024.
4. R. Landick and C. Yanofsky (1987) In Escherichia coli *and Salmonella typhimurium: cellular and molecular biology* (F. C. Neidhardt, J. L. Ingraham, K. B. Low, B. Magasanik, M. Schaechter, and H. E. Umbarger, eds.), American Society for Microbiology, Washington, DC, pp. 1276–1301.
5. S. W. Artz and D. Holzschu (1983) In *Amino Acids: Biosynthesis and Genetic Regulation* (K. M. Herrmann and R. L. Summerville, eds.), Addison-Wesley Publishing Co., Reading, Mass, pp. 379–404.
6. P. W. Carter, J. M. Bartkus, and J. M. Calvo (1986) Proc. Natl. Acad. Sci USA **83**, 8127–8131.

7. K. L. Roland, F. E. Powell, and C. E. Turnbough (1985) J. Bacteriol. **163**, 991–999.
8. S. P. Lynn et al. (1987) J. Mol. Biol. **194**, 59–69.
9. P. Babitzke and C. Yanofsky (1993) Proc. Natl. Acad. Sci. USA **90**, 133–137.
10. J. Otridge and P. Gollnick (1993) Proc. Natl. Acad. Sci. USA **90**, 128–132.
11. A. A. Antson et al. (1995) Nature **374**, 693–700.
12. H. Shimotsu, M. I. Kuroda, C. Yanofsky, and D. J. Henner (1986) J. Bacteriol. **166**, 461–471.
13. P. Babitzke, J. T. Stults, S. J. Shire and C. Yanofsky (1994) J. Biol. Chem. **269**, 16597–16604.
14. M. Yang et al. (1997) J. Mol. Biol. **270**, 696–710.
15. C. G. Lerner, B. T. Stephenson, and R. L. Switzer (1987) J. Bacteriol. **169**, 2202–2206.
16. C. L. Quinn, B. T. Stephenson, and R. L. Switzer (1991) J. Biol. Chem. **266**, 9113–9127.
17. R. J. Turner, Y. Lu, and R. L. Switzer (1994) J. Bacteriol. **176**, 3708–3722.
18. Y. Lu, R. J. Turner, and R. L. Switzer (1996) Proc. Natl. Acad. Sci. USA **93**, 14462–14467.
19. P. Babitzke, J. Yealy, and D. Campanelli (1996) J. Bacteriol. **178**, 5159–5163.
20. S. Xirasagar, M. B. Elliott, W. Bartolini, P. Gollnick, and P. Gottlieb (1998) J. Biol. Chem. **272**, 19863–19869.
21. D. R. Tomchick, R. J. Turner, R. L. Switzer, and J. L. Smith (1998) Structure **6**, 337–350.
22. R. P. Novick, S. Iordanescu, S. J. Projan, J. Kornblum, and I. Edelman (1989) Cell **59**, 395–404.
23. S. Brantl, E. Birch-Hirschfeld, and D. Behnke (1993) J. Bacteriol. **175**, 4052–4061.
24. S. Brantl and E. G. H. Wagner (1994) EMBO J. **13**, 3599–3607.
25. D. L. Bently (1995) Curr. Opin. Genet. Dev. **5**, 210–216.
26. S. Wright (1993) Mol. Biol. Cell. **4**, 661–668.
27. D. Eick and G. W. Bornkamm (1986) Nucl. Acids. Res. **14**, 8331–8346.
28. T. K. Kerpola and C. M. Kane (1988) Mol. Cell Biol. **8**, 4389–4394.
29. L. London, R. G. Keene, and R. Landick (1991) Mol. Cell Biol. **11**, 4599–4615.
30. N. Mechti et al. (1986) Nucl. Acids. Res. **14**, 9653–9666.
31. S. Wright, L. F. Mirels, M. Clara, B. Calayag, and J. M. Bishop (1991) Proc. Natl. Acad. Sci. USA **88**, 11383–11387.
32. L. Xu, Y. Meng, R. Wallen, and R. A. DePhino (1995) Oncogene **11**, 1865–1872.
33. R. Treisman (1986) Cell **46**, 567–574.
34. V. Ramamurthy et al. (1990) Mol. Cell. Biol. **10**, 1484–1491.
35. K. A. Jones (1997) Genes and Dev. **11**, 2593–2599.
36. B. Berkhout, R. H. Silverman, and K. T. Jeang (1989) Cell **59**, 273–282.
37. C. Dingwall et al. (1989) Proc. Natl. Acad. Sci. **86**, 6925–6929.
38. M. Palangat, T. I. Meier, R. G. Keene, and R. Landick (1998) Mol. Cell. **1**, 1033–1042.

Suggestions for Further Reading

39. P. Babitzke (1997) Regulation of tryptophan biosynthesis: Trp-ing the TRAP or how *Bacillus subtilis* reinvented the wheel. Mol. Microbiol. **26**, 1–9. (A recent review covering TRAP-mediated regulation of the *B. subtilis trp* genes.)
40. R. Landick and C. L. Turnbough (1992) "Transcriptional attenuation". In *Transcriptional Regulation*, (S. L. McKnight and K. R. Yamamoto, eds.) Cold Spring Harbor Laboratory Press, Cold Spring Harbor, NY, pp. 407–446. (An in-depth review of attenuation, particularly amino acid operons in enteric bacteria.)
41. T. M. Henkin (1996) Control of transcription termination in prokaryotes. Ann. Rev. Gen. **30**, 35–57. (A review covering control of transcription termination in prokaryotes.)

Autoantibody

Autoantibody is a very misleading term for certain antibodies, because it covers very different situations. This probably is largely due to Ehrlich's initial proposals, formulated at the beginning of the twentieth century, of the *horror autotoxicus* dogma, leading later to the discrimination between self and nonself (1). If one sticks to this view, one must consider that autoantibodies escape from the dogma and produce a pathological situation, as is the case for autoimmune diseases. Two main observations have led us to revisit this view: one is the existence of idiotypes and **anti-idiotypes**, and the other is the presence of the so-called natural autoantibodies.

It was proposed by Jerne (2) that immunoglobulins are organized as a large idiotypic network in which Ig molecules regulate each other by their interactions. Another, more pragmatic approach would be to consider that the millions of different Ig molecules present at any given time in one individual provide a sufficient number of different specificities to recognize any potential epitope, including those expressed by the immunoglobulins themselves, and more generally by any self-**epitope**, unless subject to strict negative selection during differentiation, leading to an absolute tolerance state, which would be in agreement with Ehrlich's concept. Is this the case? During B-cell differentiation, before leaving bone marrow as immature B lymphocytes, newly formed cells are screened against the local environment, and self-aggressive cells are eliminated, providing the major basis for B-cell tolerance. But this is not an all-or-none phenomenon. It is believed to be relatively flexible, based on the average affinity of IgM molecules expressed at the surface of immature B cells. This view leaves open the possibility that immature B cells circulating in the periphery have retained some autoreactive potential against a possible self antigen.

The next question is, Are there natural immunoglobulins endowed with properties of recognition of self molecules? The answer is undoubtedly yes and is supported by many observations, especially those from the groups of Avrameas and Coutinho (3). Natural antibodies in whole serum were first described as having the essential characteristic of being polyreactive, a conclusion that was not *a priori* surprising because of their polyclonality. When analysis at the **monoclonal** level was made possible with the hybridoma technology, it was realized that most natural antibodies had a wide recognition spectrum, as observed from their patterns of binding to many different molecules used for systematic screening. Most natural antibodies were IgM, and complementary DNA sequencing of their V_H and V_L regions revealed that they contained very few mutations, indicating that they reflected transcription of germline **genes**. Affinity measurements revealed moderate but significant association constants. Natural monoclonal autoantibodies thus seem best defined as primarily germline-encoded and polyreactive. Polyreactivity contains in itself the possibility of having both anti-self and anti-nonself specificities. Presumably due to their relatively modest affinities, low concentration, and, of course, the fact that they passed the screen for potentially aggressive anti-self specificities, these antibodies qualify as harmless and may be regarded as the pool of basic circulating immunoglobulins of wide spectrum, endowed with a high connectivity, and constituting the primary germline idiotypic network. By contrast, aggressive autoantibodies found in the serum of patients suffering autoimmune diseases generally contain mutated sequences and are often of isotypes other than IgM.

One may thus consider active immunization as bringing a transient perturbation of the background of the natural equilibrium, leading to the emergence of clones that acquire a greater affinity and an increased specificity through the occurrence of somatic hypermutations.

See also entries Autoimmunity, Autoimmune Diseases, Idiotypes.

Bibliography

1. P. Ehrlich (1900) The Croonian lecture: On immunity. Proc. Roy. Soc. Lond. (Biol.) **66**, 424.
2. N. K. Jerne (1974) Towards a network theory of the immune system. Ann. Immunol. **125C**, 373–389.
3. A. Coutinho, M. D. Kazatchkine, and S. Avrameas (1995) Natural autoantibodies. Curr. Opin. Immunol. **7**, 812–818.

Suggestion for Further Reading

4. A. Coutinho, M. D. Kazatchkine, and S. Avrameas (1995) Natural autoantibodies. Curr. Opin. Immunol. **7**, 812–818.

Autoimmune Diseases

Autoimmunity is not pathologic *per se* because natural autoantibodies, natural autoreactive T-cell clones, and the connected idiotypes and **anti-idiotypes** are part of the basic organization of the immune system. Autoimmune diseases (AIDS) are the consequence of a major failure in the regulation of the immune system, as the emergence of self-reactivity becomes aggressive and harmful to the organism. They represent a major cause of morbidity, and their incidence increases with aging.

The primary causes of autoimmune diseases (AIDS) are still very poorly understood, and the precise target of the autoimmune reactions is not always known. In some cases, one organ, and eventually one target molecule, can be identified. Examples of these are myasthenia gravis, in which antibodies directed against the acetylcholine receptor have been identified, or autoimmune thyroiditis, where the presence of autoantibodies directed against receptors for thyroid stimulating hormone have been documented. Such antibodies may have very different impacts upon binding. Some may act as a mimic of the hormone and therefore activate thyrocytes, thereby inducing hyperthyroidism, which is characteristic of Graves' disease. Conversely, others will block receptor activation, leading to a hypothyroidism state, as seen in Hashimoto's disease. Another example of an organ-specific AID is insulin-dependent diabetes mellitus, in which the cellular target is the b islets of the endocrine pancreas. Some AIDs appear to be not organ-specific, such as systemic lupus erythematosous, when a number of autoantibodies are directed against a large variety of antigens, including DNA and nucleoproteins.

Several characteristics generally underline the occurrence of AIDs: (a) In most cases there is a genetic predisposition, with a frequent linkage to certain major histocompatibility complex (MHC) haplotypes; (b) they are chronic diseases that persist for years; and (c) although the molecular target of autoantibodies or autoreactive T-cell clones may be identified, this does not clarify the nature of the initial antigen, if any.

Linkage to an MHC haplotype is indicated by the increase of the relative risk for a given AID to occur. The most spectacular example is that of ankylosing spondylitis, a very severe arthritis that most frequently affects hips, for which 95% of patients are HLA-B27. This indicates a relative risk of about 70 (ie a $B27^+$ individual has 70 times greater chance to have the disease than the average population). This AID is also particularly interesting because it has been observed that microorganisms such as *Klebsiella* share an identical sequence of six amino acid residues, Gln—Thr

—Asp—Arg—Glu—Asp (QTDRED), with an epitope of the HLA27 molecule. It was postulated that this AID might be the consequence of an epitope mimicry, an infection with *Klebsiella* inducing an immune response that subsequently would cross-react with the HLA epitope of the host. A similar hypothesis was proposed for rheumatoid arthritis, a very common rheumatological disorder that may develop for years, because it was found to be associated with certain DR4 alleles expressing the Gln —Lys—Arg—Ala—Ala (QKRAA) sequence. A similar sequence was found in Hsp 70, which might provide another example of epitope mimicry as the starter for the initial immunization.

The V_H and V_L regions of autoantibodies isolated from AID patients have been sequenced extensively, with the hope of detecting significant differences from natural, nonaggressive autoantibodies. Frequently, dominant expression of some V_H and/or V_L is observed, as in the case of anti-DNA autoantibodies isolated from lupus patients. In most occasions, but not always, these antibodies have mutated **variable regions**, as opposed to the germline sequences generally found in natural antibodies. The significance of this remains unclear, however, primarily because the autoantibodies developed by a rather large number of AID patients seem to be only passive witnesses of an autoimmune response, rather than being involved in pathogenesis, which is frequently attributed to cytotoxic T lymphocytes.

Numerous animal models have been defined and extensively studied. Many have stressed the importance of the genetic background, such as the obese strain of chickens that develop a hereditary spontaneous autoimmune thyroiditis that is quite similar to Hashimoto's disease. Another example is the nonobese diabetic (NOD) mice that develop an autoimmune diabetes, which spontaneously develops an insulitis that becomes full insulin-dependent diabetes mellitus at 7 months of age. New Zealand black (NZB) mice and other strains that spontaneously develop a systemic lupus erythematosous-like syndrome are another example. These models are interesting because they provide a possible key to understanding the genetic basis for the equivalent human diseases. Other approaches are centered more on attempts to isolate antigens that might induce an AID-like syndrome. An example of this is experimental autoimmune encephalomyelitis, which is a possible model for multiple sclerosis; it can be induced upon injection of myelin basic protein, from which encephalitogenic peptides and precise epitopes have been described. This disease can also be transferred with lymphocytes but not by serum, pointing to the role of cell-mediated immunity in this AID. Interestingly, T cells with a suppressive activity have also been identified, offering the possibility of modulating the immune system negatively by this approach. Such a treatment is eagerly awaited for most AIDs, particularly multiple sclerosis. Thus far, primarily nonspecific immunosuppressive agents are used, with the obvious problem of generating severe secondary effects.

See also entries Autoantibody and Idiotypes.

Suggestions for Further Reading

G. Del Prete (1998) The concept of type-1 and type-2 helper T cells and their cytokines in humans. Int. Rev. Immunol. **16**, 427–455.

C. C. Goodnow (1997) Balancing immunity, autoimmunity and self-tolerance. Ann. NY. Acad. Sci. **815**, 55–66.

E. G. Spack (1997) Treatment of autoimmune diseases through manipulation of antigen presentation. Crit. Rev. Immunol. **17**, 529–536.

Autoimmunity

The immune system is able to discriminate between self and nonself, but there are often ambiguities with this formulation. First, it certainly is intended to stress the fact that the immune system is designed for the important role of fighting against external pathogens, whereas it should be harmless for the components of the organism. There are two ways to be harmless. One is simply not to "show off," the second is to be present, but silent. Immunologists long lived with the idea originally put forward by Ehrlich in 1901 of the *horror autotoxicus*, thus considering that autoantibodies, and more generally autoimmunity, could not exist. This was even strengthened by Burnet, when he proposed the clonal selection theory, based on the elimination of autoreactive lymphocytes (the so-called "forbidden clones"), leading to immune **tolerance**. On these bases, autoimmunity may only be considered to be a pathological deviation, with the emergence of autoimmune diseases. Discovery of the interactions between idiotype and **anti-idiotype** and of the existence of natural antibodies endowed with auto reactivity made it necessary to reconsider the problem.

A long debate has taken place for years between immunologists, first on the existence, and then on the nature, of natural antibodies and their possible autoimmune properties. Identification of "natural" monoclonal antibodies that were polyspecific clarified the situation, because it was demonstrated that these antibodies contained **variable (V) regions** of both the heavy and the light chains that were mostly not mutated, and like the germline gene from which they were derived. As a result, these antibodies could be considered the first circle of antibody defense, with some polyspecificity that is the best witness of a certain degeneracy of recognition by the immune system. Deliberate immunization will stimulate clones that have the best affinity for the antigen, and this affinity will be amplified by the mechanism of somatic hypermutation, as the specificity becomes more precise. To be polyspecific immediately implies that both auto- and xenospecificities may be found, as was shown using a large panel of random antigens for screening. Autoimmunity has also been described in the T-cell population and is subject to the same comments, with the exception that T cells do not mutate upon antigenic stimulation.

The entire repertoire expressed at a given time by the immune system is probably best visualized as a large network of interacting molecules that regulate each other. Deliberate immunization would result in transient perturbation of this equilibrium. Deviation to the production of aggressive B- and T-cell clones would thus be a central alteration of this equilibrium, ensuring some leakiness for the negative selection of potentially aggressive clones.

See also entries Autoantibody, Autoimmune Diseases, Idiotypes.

Suggestions for Further Reading

C. Goodnow (1996) Balancing immunity and tolerance: deleting and tuning lymphocyte repertoires. Proc. Natl Acad. Sci. USA **93**, 2264–2271.

S. Lacroix-Desmazes, L. Mouthon, S. H. Spalter, S. Kaveri, and M. Kazatchkine (1996) Immunoglobulins and the regulation of autoimmunity through the immune network. Clin. Exp. Rheumatol. **14** (Suppl. 15), S9–S15.

R. J. Cornall, C. C. Goodnow, and J. G. Cyster (1995) The regulation of self-reactive B cells. Curr. Opin. Immunol. **7**, 804–811.

Autonomous Controlling Elements

Transposable elements are discrete pieces of DNA that can move between nonhomologous positions in the genome. When Barbara McClintock discovered transposable elements in maize, she called them controlling elements, emphasizing that they could affect gene expression, in addition to being able to move from place to place within the genome (1). She discovered two classes of elements; one she termed *activator* (Ac), which could itself translocate within the genome. She also determined that Ac encoded a product that could promote the movement of a second class of elements called *dissociation* (Ds). In the presence of Ac, Ds could move and cause chromosome breaks that altered the expression of nearby genes, but was unable to move in the absence of Ac. Ds elements are so-named because their translocation could be associated with chromosome breakage.

We now know that Ac is an intact transposable element encoding a recombinase, a transposase, that promotes element translocation and has special sequences at the termini of the element upon which the transposase acts to promote translocation. Such intact elements are said to be “autonomous” because they can translocate without the assistance of another element. Ds, by contrast, is a nonautonomous element. It doesn't encode a transposase itself and is thus dependent on the presence of other Ac elements to supply a transposase to promote its transposition. Ds is actually an Ac element that has undergone internal deletions that have removed the transposase gene but have left intact the special terminal sequences on which transposase acts intact (Fig. 1). Thus the terminal sequences of Ds are the same as the terminal sequences of Ac, so that the Ac transposase can promote the translocation of Ds (2); there are several different Ds elements that contain different extents of the internal, nonterminal sequences. The deletions are thought to result from abortive repair of the gapped donor site after element excision (2-4).

Figure 1. Autonomous and nonautonomous elements. A schematic representation on an intact (autonomous) Ac element is shown (top line). It encodes a transposase formed from several exons (not shown) and special recombination sequences at the ends of the element. The arrows represent short perfect inverted repeats and the oval other repeated sequences; these are not shown to scale. Only some of the subterminal repeats are necessary for transposition. Various deletion derivatives of Ac are shown (lines 2–5); these internal deletions make the element dependent on an intact Ac for transposase and hence for translocation.

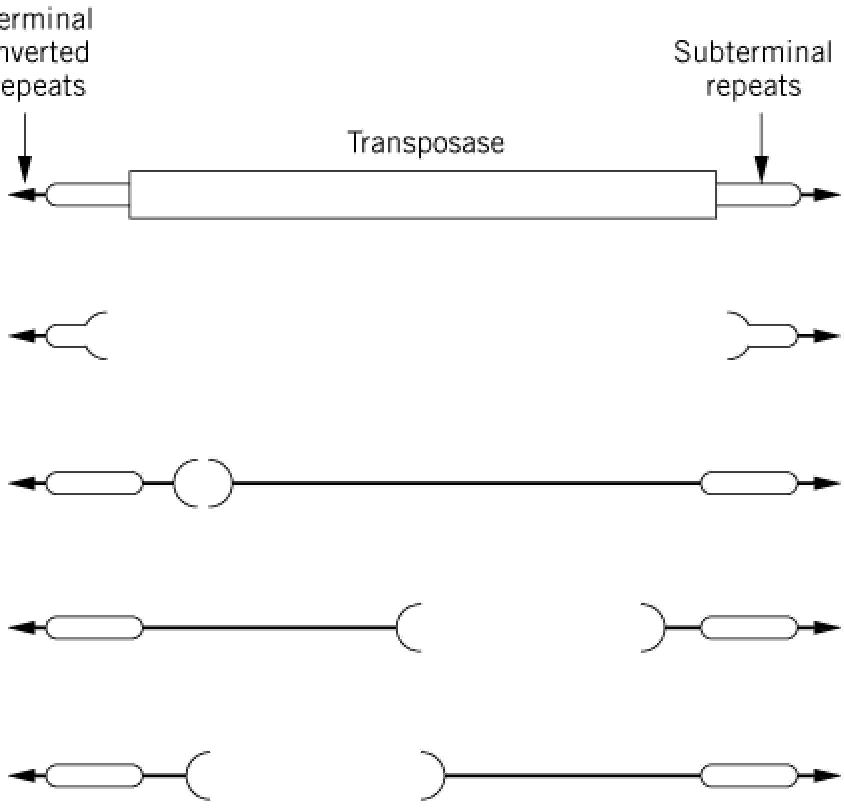

Ds Elements

Virtually all bacterial elements that have been observed are autonomous; that is, encode a transposase and have cognate terminal sequences. Nonautonomous and autonomous elements are frequently observed in other organisms such as *Drosophila*, Caenorhabditis *elegans*, and plants (5).

Bibliography

1. B. McClintock (1956) Cold Spring Harbor Symp. Quant. Biol. **21**, 197–216.
2. E. Rubin and A. A. Levy (1997) Mol. Cell. Biol. **17**, 6294–6302.
3. E. S. Coen, T. P. Robbins, J. Almeida, A. Hudson, and R. Carpenter (1989) In *Mobile DNA* (D. A. Berg and M. M. Howe, ed.), American Society for Microbiology, Washington, DC, pp. 413–436.
4. W. R. Engels, D. M. Johnson-Schlitz, W. B. Eggleston, and J. Sved (1990) Cell **62**, 515–525.
5. H. Saedler and A. Gierl (1996) Curr. Top. Microbiol. Immunol. **204**, 27–48.

Autonomously Replicating Sequences

The chromosomes of **yeast** contain many genomic segments at which DNA replication is ordinarily initiated. On average, one is found every 40 kb in the *Saccharomyces cerevisiae* genome. These regions can act as the **origin of replication** for a circular **plasmid**. When such a segment is linked to a nonreplicative DNA fragment, it can confer on that fragment the ability to replicate autonomously as a plasmid in a yeast cell in the S-phase of the cell cycle. This construction is called an *autonomously replicating fragment* (ARS).

An ARS-containing DNA fragment can **transform** yeast cells at much higher frequencies than a fragment without an ARS, because it can replicate autonomously without undergoing a rare homologous recombination before its **genes** can be expressed. In contrast to the latter transformants, however, those formed with an ARS-containing DNA are extremely unstable and lose the transforming DNA even under selective conditions. For unknown reasons, they tend to remain associated with the mother cell without being evenly distributed to the daughter cell upon division.

ARS have been found in *Saccharomyces cerevisiae* and but also in other yeasts, such as *Candida maltosa*, *Hansenula polymorpha*, *Kluyveromyces lactis*, and *Schizosaccharomyces pombe*. They are not restricted to yeasts and have also been described in other lower **eukaryotes**, such as *Aspergillus nidulans* and *Entamoeba histolytica*, and even in at or near potential replicative origins from *Drosophila*, Chinese hamster, and humans.

Autoradiography

Autoradiography is the technique of recording an image of a preparation containing beta-particle emitting radioactivity, using photographic film, X-ray-sensitive film, an emulsion, or other radiation-sensitive medium. The samples are placed directly against the film for a period of time to allow radioactive emissions from the sample to interact with the film emulsion and create an image. A photographic emulsion is a suspension of crystals of silver bromide embedded in gelatin. When crystals of silver bromide are struck by charged-particle or photon radiation, the silver atoms are ionized and form an invisible latent image. After exposure to the sample, the photographic grains in the emulsion are fixed using standard photographic developing, which removes silver bromide that has not been ionized. After the emulsion is developed, each small aggregate of reduced silver atoms becomes a visible dark spot on the emulsion; collectively, they make up the photographic image.

Production of a visible silver grain requires a number of ionization events, so the photographic response is not exactly linear to the amount of radiation present. Preflashing the film with a uniform low intensity of light “primes” each grain of silver to become reduced and visible after absorbing just one or a very few additional beta particles from the sample. This increases substantially the sensitivity of the film and also makes the photographic response more directly proportional to the amount of radiation in the sample. The signal-to-noise ratio is often increased by exposing the film to low temperatures. The sensitivity can also be enhanced by using scintillation screens that emit visible light on encountering a beta particle; the light is recorded by the film (see Fluorography).

Autoradiography has a large number of practical applications in the biological, chemical, and physical sciences, because it provides both qualitative and quantitative information (eg., images and amounts present). It may be used to image large, small, and microscopic specimens, including sectioned whole organisms, organs, tissues, cellular structures, and nucleic acids that contain some radiolabeled compound. An example of a whole-animal autoradiograph is shown in Figure 1. Cells may be autoradiographed either in culture as a monolayer, on a glass slide, or on thinly sectioned living tissues from an animal organ or tumor. Microautoradioagraphy involves coating the sample directly with a radiation-sensitive emulsion; cellular constituents that have incorporated the radiolabel can be clearly identified. Autoradiography is used with electrophoresis or chromatography to image radiolabeled macromolecules and other separated chemicals for quantitative analysis. For example, autoradiography is useful for indicating the position of hybridized nucleic acids on Southern blots and **Northern blots**, and of proteins on **Western blots.**

Figure 1. Whole-body autoradiograph of a rat that had been injected with indium-111 chloride. Courtesy of B. Anders Jönsson, Lund University, Sweden.

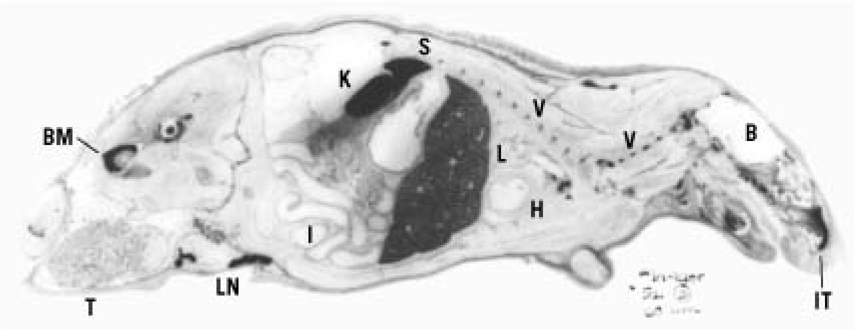

1. Historical Development

The first autoradiograph, or **autoradiogram**, was made in 1859 by Crookes, who placed uranium rocks on photographic plates (1). Crookes would not understand the process by which the images were created until 37 years later when he visited the laboratory of Henri Becquerel. Bequerel discovered gamma rays from naturally radioactive uranium salts in 1896 when he placed uranium together with photographic plates that had been placed inside black paper to protect them from sunlight (1). This discovery closely followed the discovery of X rays by Wilhelm Roentgen in 1895 using a Crookes electron tube.

The French photographer Nicéphore Niepce had observed the darkening of silver grains on photographic plates by uranium in 1867, but he did not recognize any practical applications of this phenomenon (2). Although George de Hevesy, the pioneer of radioactive tracers, had used bismuth isotopes in animals in 1923, the first autoradiographs of radioactively labeled animal tissues were made in 1924 by Lacassagne in France (1-3). Lacassagne fed polonium-210 to rabbits and later placed thin sections of rabbit kidney tissues in paraffin blocks against photographic plates. Gettler made the first autoradiographs of human tissues from deceased persons who had ingested radium chloride in 1933 (1).

The earliest images were of poor quality. Autoradiographic techniques were improved by Leblond, who, in 1943, showed the microdistribution of iodine-131 in cells (1, 2). In 1946, Bélanger and Leblond (4) developed a method for locating radioactive elements in tissues by covering histological sections with a photographic emulsion. In 1954, Gabriel introduced techniques for identifying radioiodine using human serum albumin zone paper electrophoresis (1). In 1953, techniques were developed for labeling nucleic acids and studying kinetics of cell mitosis and division (5). High resolution techniques have more recently been employed for study of other metabolic and pharmacokinetic processes in molecular biology.

2. Film-Less Autoradiography

Modern trends in autoradiography involve replacing high speed X-ray film with radiation detector systems, laser scanners, and computer-based imaging systems. A variety of radiation-detecting crystals and phosphors have been developed for this purpose. Storage phosphor screens are more sensitive, by a factor of about 20–100 for beta-emitting radionuclides (2), and they are reusable. The exposure time is also much less, by a factor of about 10, over conventional X-ray film, and samples may be processed at room temperature and without a darkroom or chemicals for film developing. Applications of filmless autoradiography include **two-dimensional gels**, Southern blots, **Northern**

blots, immunoblots, and quantitative polymerase chain reaction (**PCR**) (2).

Microchannel array detectors have been introduced to replace both X-ray films and phosphor screens (8). The new instruments are faster (by a factor of ~10) and have greater image resolution than do phosphor screens for detecting latent images from hybridization studies using macromolecules labeled with carbon-14, sulfur-35, phosphorus-32, and iodine-125 from flat gels, blots, membranes, tissue slices, and other flat specimens.

Bibliography

1. M. Brucer (1990) *A Chronology of Nuclear Medicine*, Heritage Publications Inc., St. Louis, MO.
2. R. Wegmann, N. Balmain, S. Ricard-Blum, and S. Guha (1995) Cell. Mol. Biol. **41**, 1–20.
3. A. Lacassagne, J. Lattes, and J. Lavedan (1925) J. Radiol. Electr. **9**, 1–14.
4. L.-F. Bélanger and C. P. Leblond (1946) Endocrinology **39**, 386–400.
5. A. Howard and S. R. Pelc (1970) Heredity **6** (suppl.), 261–273.
6. J. G. Gall and M. Pardue (1969) Proc. Natl. Acad. Sci. USA **63**, 378–383.
7. E. M. Southern (1975) J. Mol. Biol. **98**, 503–517.
8. Packard Instrument Company (1993) *Enter the New Era of Instant Autoradiography: The InstantImager™*, promotional literature from Packard Instrument Company, Meriden, Conn.

Suggestions for Further Reading

9. G. A. Boyd (1955) *Autoradiography in Biology and Medicine*, Academic Press, New York.
10. E. J. Hall (1994) *Radiobiology for the Radiologist*, 4th ed., J. B. Lippincott Company, Philadelphia, pp. 92–95, 397–402.
11. J. C. Kaplan and M. Delpech (1989) “"Biologie Moléculaire et Médecine"”, in *Médecine et Sciences Flammarion*, Paris, p. 610.
12. D. LeGuellec and J. -Y. Sire (1991) in *Microscopie électronique. Cryométhodes, Immunocytologie, Autoradiographie, Hybridation in situ* (G. Morel, ed.), INSERM, pp. 299–304.
13. R. Wegmann, N. Balmain, S. Ricard-Blum, and S. Guha (1995) Cell. Mol. Biol. **41**, 1–20.

Autosome

An autosome is any chromosome other than the sex chromosomes. For example, the human genome has 24 chromosomes, including 22 autosomes plus the X- and the Y-chromosomes. This is described as the haploid set. If a cell contains a complete haploid set of chromosomes, it is described as euploid. If the chromosome set is altered by duplication or deletion then the cell is **aneuploid**. If a cell contains two sets of genomes per nucleus, it is **diploid**, and if it contains more than two, it is described as polyploid.

Organisms that have a largely vegetative existence, such as some **fungi** and **algae**, have mainly haploid cells. In metazoans the **gametes**, such as the **spermatozoa** and **oocytes** in humans, are haploid. Sexual **reproduction** involves the fusion of two haploid gametes to form a diploid egg in an animal. The vast majority of the cells in an animal that develop from an egg are diploid. Thus there are two active copies of each autosome in most animal cells. In **plants**, a polyploid state is common where the number of genomic copies in somatic cells may range from 3 to 10 (1). The number of genomic copies can actually be **polymorphic** within a particular species (2). Thus plants are relatively insensitive to the number of copies of a particular **gene** in a given cell. This is not the case with animals, where somatic cells are almost always diploid. The only exceptions are those animals with **parthenogenetic** life styles in which either males or females develop as a default state from an unfertilized egg. In general, animal cells cannot accommodate more than two copies of a particular chromosomal region.

Aneuploidy occurs when parts of chromosomes or whole chromosomes are absent from the genome. In humans the nondisjunction of homologous chromosomes during **meiosis** or of sister chromatids during **mitosis** can lead to aneuploidy. When a chromosome is in excess of the normal euploid number, the condition is called hyperploidy. For example, a hyperploid state in humans occurs when there are three copies of a particular chromosome, a condition known as trisomy. All human autosomes except chromosome 1 have been found as trisomies (3). Most trisomic embryos are spontaneously aborted, but live births occur with trisomies of chromosomes 13, 18, and 21 (4). The most common human trisomy to reach term is that of chromosome 21, resulting in Down's syndrome. These children are mentally retarded, predisposed to cancer and have a shortened life span. Presumably the deleterious effects of three copies of chromosome 21 follow from an imbalance in the expression of one or several sets of genes on chromosome 21 relative to the other genes on the other chromosomes in the cell.

Experiments in *Drosophila melanogaster* indicate that changes in the dosage of a single gene might be tolerated, but a deletion that includes several genes or a large section of a chromosome is likely to cause sterility (5). Surprisingly in trisomies of *D. melanogaster* involving whole chromosome arms, many of the duplicated autosomal genes express only diploid levels of gene product. The expression of genes outside the duplicated region is also affected, however, indicating the pleiotropic effects of altering gene copy number. An interesting aspect of sexual reproduction requiring the use of two distinct haploid gametes is that there are two copies of each autosome in a diploid cell, whereas there are be one or two copies of each sex chromosome. **Dosage compensation** is the phenomenon whereby the **transcriptional** activity of genes on the sex chromosome is adjusted to similar levels independent of the number of copies, so that it is constant relative to the activity of a gene on an autosome (see X-Chromosome Inactivation).

Humans, again have two X-chromosomes in one sex (female) and one X-chromosome in the other (male). To achieve dosage compensation, an entire X-chromosome is silenced in female diploid cells. This process is called X-chromosome inactivation and results in the formation of the Barr body. The capacity to monitor the activity of genes on autosomes relative to the sex chromosomes has facilitated the discovery of novel mechanisms of regulating genes at the level of whole chromosomes.

Bibliography

1. J. E. Averett (1980) "Polyploidy in plant taxa: summary". In *Polyploidy* (W. H. Lewis, ed.), Plenum, New York.
2. K. Irifune (1990) J. Sci. Hiroshima Univ. **23**, 163–181.
3. T. J. Hassold (1986) Trends Genet. **2**, 105–109.
4. E. B. Hook, B. B. Topol, and P. K. Cross (1989) Am. J. Hum. Genet. **45**, 855–861.
5. D. L. Lindsley et al. (1972) Genetics **71**, 157–184.

Suggestion for Further Reading

6. M. S. Clark and W. J. Wall (1996) *Chromosomes. The Complex Code*, Chapman and Hall, London.

Auxins

1. History

Auxins were the first class of plant hormones to be discovered. Initial observations by Charles Darwin and his son Francis on the phenomenon of bending of canary grass coleoptiles toward a unilateral source of light (known as phototropism) led the foundation for a series of experiments that culminated in the discovery of the first phytohormone (1). The active substance was isolated from oat coleoptiles by Went in 1926 (2) and later identified and named auxin (from the Greek "to increase"). By analogy with the animal hormone concept from Bayliss and Starling (3), plant physiologists interpreted auxin as a phytohormone.

2. Biosynthesis and Metabolism

The most abundant natural auxin is indole-3-acetic acid (IAA). It is mainly synthesized in the shoot apex and in young leaves. Other substances with auxin activity that are found in plants are indole-3-butyric acid, 4-chloro-indole-acetic acid, and phenyl acetic acid (4, 5); these compounds are active only at higher concentrations, and their roles in development remain largely unknown. Multiple pathways exist for auxin biosynthesis; some of these are dependent on tryptophan, while others are independent (Fig. 1). In certain species, different routes are operational (6), whereas in others, essentially all of the IAA is derived from tryptophan (7). Three possible routes for tryptophan-dependent IAA synthesis have been proposed (4, 5), which include indole-3-acetonitrile, tryptamine, and indole-3-pyruvic acid as the respective intermediates. Genes encoding tryptophan decarboxylase (which catalyzes the conversion of tryptophan to tryptamine) and nitrilase (forming IAA from indole-3-acetonitrile) have been cloned (8-10). The route via indole-3-acetonitrile has been found primarily in Brassicaceae. Likewise, the tryptamine pathway is not supposed to be of general importance, because tryptamine is not universally present in plants. A unique tryptophan-dependent pathway via indole-3-acetamide is used by bacteria and by plant cells that are transformed with ***Agrobacterium*** *tumefaciens*. The corresponding genes have been used to alter the IAA levels in **transgenic** plants (11).

Figure 1. Auxin biosynthesis in higher plants. (Based on Ref. 4.)

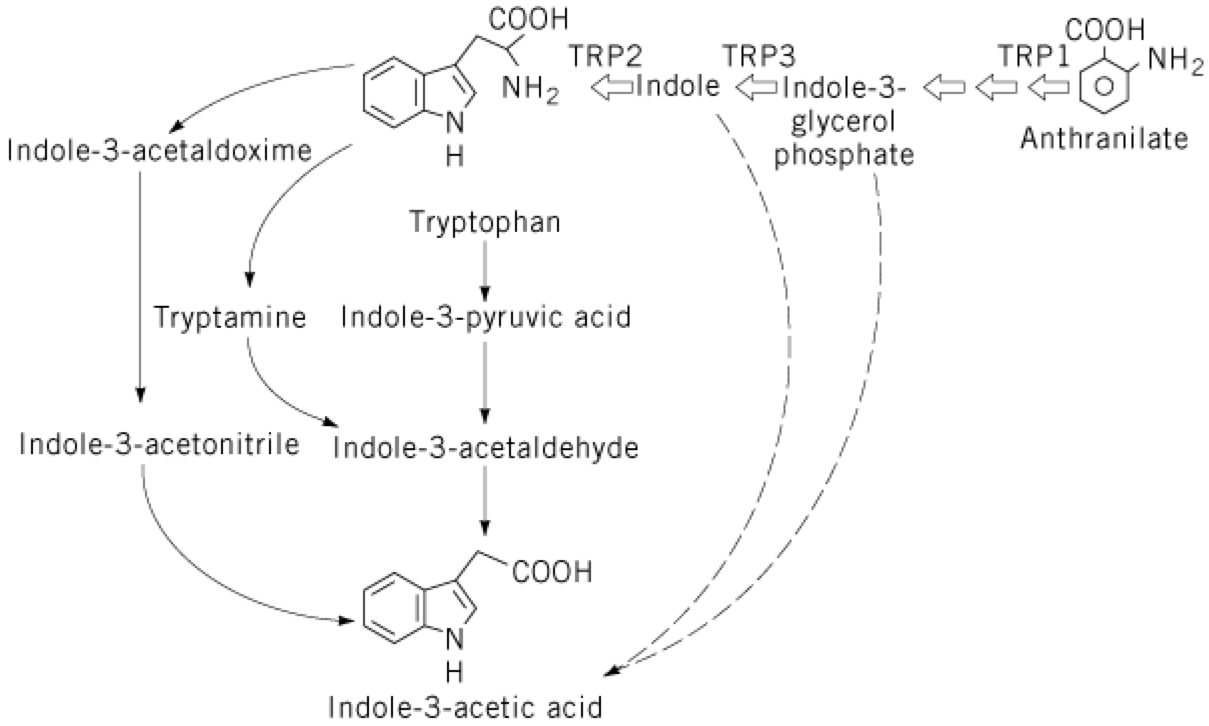

Tryptophan-auxotroph mutants have revealed the existence of a tryptophan-independent pathway for IAA biosynthesis. Both maize (12) and Arabidopsis (13) tryptophan mutants overproduce IAA or IAA conjugates, respectively. On the other hand, mutants that block tryptophan biosynthesis before indole-3-glycerol phosphate have a **phenotype** suggestive of auxin deficiency (14). Based on these observations, IAA was proposed to be synthesized through a tryptophan precursor, either indole or indole-glycerol phosphate, thereby bypassing tryptophan (4). An auxin-overproducing mutant that accumulates both free and conjugated auxins has been isolated (15, 16). The wild-type gene product might inhibit auxin biosynthesis and shows similarity to aminotransferases (17).

Of all the auxin present in plant tissues, 95% resides in conjugated form, coupled to amino acids, **peptides**, or proteins via amide bonds, or to sugars via ester linkages (18). The role of these conjugates is diverse: the storage of free IAA (released by hydrolysis), its transport, and eventually its catabolism. A genetic approach was used to characterize a hydrolase that catalyzes the formation of free IAA from IAA-Leu (10). The *ILR1* (*IAA-leucine resistant 1*) **gene** encodes a protein with similarity to a bacterial aminoacylase that catalyzes amide cleavage.

3. Transport

Another important aspect determining auxin levels is transport of the hormone. Auxin transport can be either (a) polar, basipetally directed, and active or (b) nonpolar and inactive (19). The latter occurs through phloem tissue. Polar transport is probably involved specifically in processes of apical dominance, vascular differentiation, and shoot–root communication. Evidence exists for the presence of influx and efflux carriers, although protonated auxin can enter cells by simple diffusion. Proton–auxin **symport**, energized by the plasma membrane **proton pump**, allows a more rapid uptake than by diffusion. The AUX1 protein has been suggested to represent an auxin uptake carrier (20), based on its similarity to amino acid uptake carriers, which also function as symporters. Although several mutants have been characterized that show growth defects similar to those upon treatment with polar transport inhibitors (21), only one of them appears to be a candidate for the auxin efflux carrier. The PIN1 (*pin formed 1*) gene product shows the characteristics of a transmembrane protein (22). The corresponding mutant displays abnormal cotyledon development, together with twisted, narrow leaves with branching midveins. Auxin transport is reduced at all stages of development (23).

Recently, factors that may modulate auxin transport have been characterized (24, 25). Both the loci *RCN1* (*ROOT CURLING on NPA1*) (coding for a protein phosphatase A regulatory subunit) and *MP1* (*MONOPTEROS1*) (coding for a homologue of the auxin response factor ARF1) (26) (see text below) have been isolated based on their altered response to auxin transport inhibitors. Mutations in the *MP1* gene interfere with vascular strand formation and with initiation of the body axis in the embryo (27).

4. Signal Perception and Transduction

The perception and transduction of the auxin signal remains largely enigmatic (Fig. 2). Two different approaches have been followed toward the identification of putative auxin receptors: (a) the characterization of auxin-resistant mutants and (b) the isolation of auxin-binding proteins (28, 29). Because auxin is present both intra- and extracellularly, a site of perception may be needed on both sides of the membrane. Although many auxin-binding proteins have been identified, none has been proven to function as an internal receptor at the molecular level. In contrast, an external receptor has been characterized. There is evidence that auxin causes changes in the plasma membrane potential via stimulation of the proton ATPase and modulation of **ion channels**. These rapid responses result from auxin binding to a protein named ABP1 (auxin-binding protein 1). Thus far, it is unknown whether ABP1 mediates cell growth. Although ABP1 possesses a *C*-terminal signal for retention in the endoplasmic reticulum (ER) and largely resides in the ER, it does not seem to bind auxin in this cellular compartment. Instead, ABP1 can reach the cell surface by a yet unknown mechanism, as demonstrated by immunolocalization experiments (30). It is hypothesized that ABP1 is retained at the membrane periphery by interaction with a docking protein, because ABP1 does not contain a potential membrane-spanning domain. The nature of the docking protein is undefined, but biochemical evidence supports the concept of a **G-protein**-coupled receptor (GCR) (31). These receptors contain seven transmembrane domains and are directly coupled to heterotrimeric G proteins. A possible effector could be phospholipase A_2, which produces lysophospholipids and free fatty acids. The former have been proposed to act as second messengers that can activate the plasma membrane proton ATPase (32, 33). However, G-protein-coupled receptors may activate different G proteins in different cell types, as has been shown in animal cells (34), and therefore may control a downstream branched transduction pathway. At least one report suggests the involvement of a MAP kinase cascade in the initiation of cell division by auxin in cell cultures (35).

Figure 2. A model for auxin signal transduction. PL, phospholipids; PLA_2, phospholipase A_2; LPC, lysophospholipids; FA, fatty acids. (Modified from Refs. 29 and 39.)

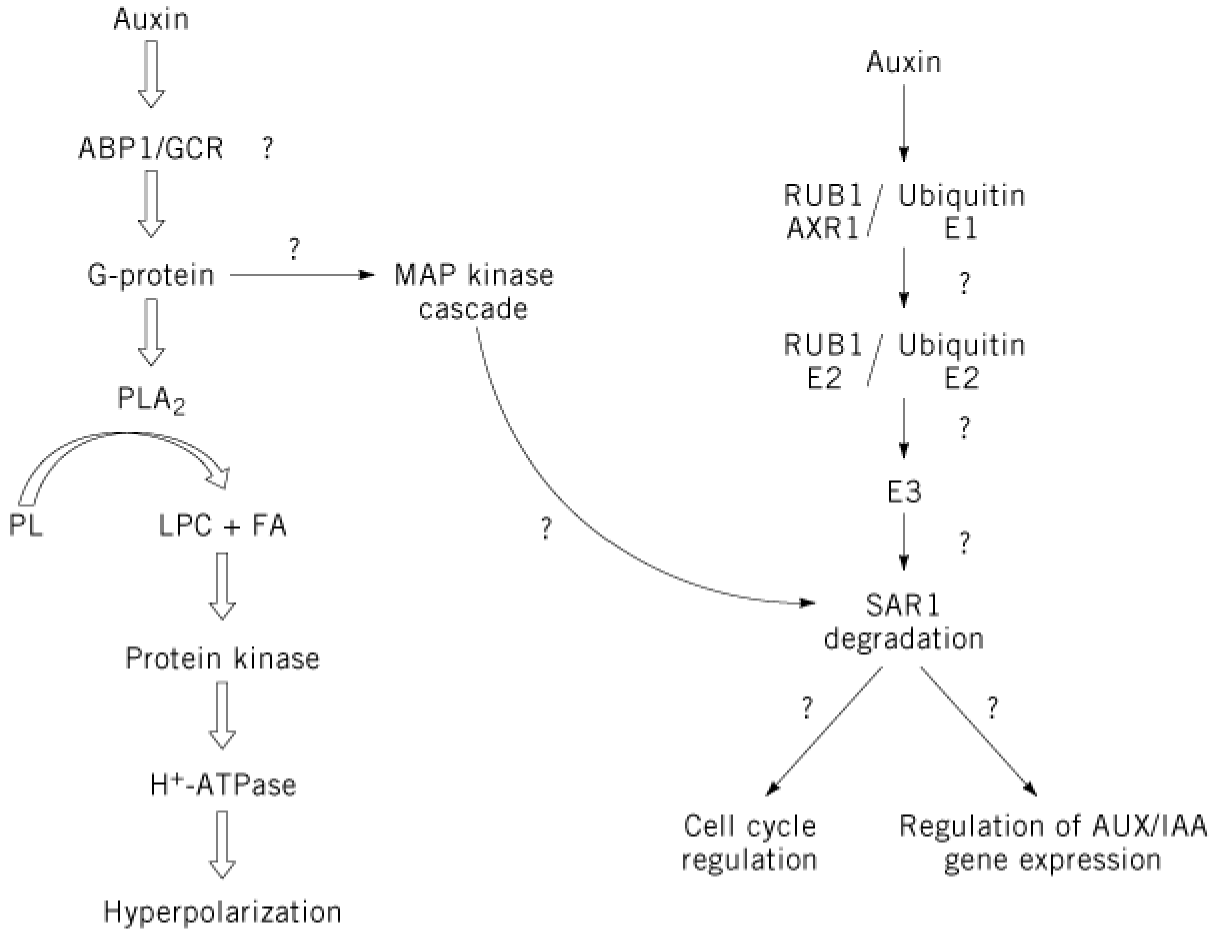

The second approach to molecular characterization of auxin signal transduction involves the isolation and characterization of auxin-resistant mutants. At least seven loci were identified by screening for resistance to auxin-induced root growth inhibition (21). AXR1 (auxin resistant 1) probably plays a role at an early stage in the signaling chain, because the recessive *axr1* mutant cannot respond to auxin in all the assays tested. The *AXR1* gene encodes a protein with homology to the amino-terminal half of the **ubiquitin**-activating enzyme E1 (36). Thus, a central part of the mechanism of auxin action appears to play a regulatory role in protein degradation. Recently, two genes of *Saccharomyces cerevisiae* were found to be similar to *AXR1* (37). One of these regulates the stability of key components of cell cycle regulation, such as the **cyclin**-dependent kinase inhibitor Sic1p, through conjugation of the ubiquitin-like protein RUB1 to CDC53p, a component of a E3 ubiquitin—protein ligase complex (37). The speculation that *AXR1* plays a role in cell cycle control is considerably strengthened by the characterization of the *tir1* (*transport inhibitor response 1*) locus, a semidominant mutation that also confers auxin resistance (38). Sequence analysis revealed similarity between TIR1 and F-box proteins found in E3 ubiquitin-protein ligase complexes in yeast. The product of the *SAR1* (*suppressor of auxin resistance*) gene has been proposed as a candidate target for AXR1-dependent ubiquitin degradation (39). The *sar1* mutant was identified as a suppressor of the Axr1 phenotype (40). SAR1 may function as a repressor of *AUX/IAA* genes, or it may be involved in cell cycle regulation (40). The mostly root-specific *axr4* mutation probably defines an AXR1-independent path. Double-mutant analysis indicates that at least two interacting pathways exist, in which AXR4 and AUX1 define a first route while AXR1 defines a second one (41).

5. Downstream Targets

Ultimately, the auxin signal leads to induction or repression of a series of target genes, some of which are responsive in a few minutes (42, 43). The products of these primary response genes are likely candidates to play a role in auxin-stimulated growth. The induction of the early genes is independent of *de novo* **protein biosynthesis**, implying that **post-translational processes** control the activity of factors that affect their expression. The transcriptional activation of early genes is based on the presence of auxin-responsive, cis-acting, response elements (AuxREs). Two auxin response-element domains were defined in the *Pisum sativum IAA4* and *IAA5* genes, one of which acts as an auxin switch while the other acts as an enhancer element. The former AuxRE is present in the promoter of *AUX/IAA*, *SAUR* (*small auxin-upregulated mRNAs*, and auxin-inducible 1-aminocyclopropane-1-carboxylate synthase genes. An alternative AuxRE is found in the promoter of the *GH2* and *GH4* genes. Essentially, this element consists of a G-box motif, binds bZIP factors, and is generally responsive to stress signals. The biological role of most of the auxin early-response gene products remains to be elucidated. Nevertheless, based on similarities with proteins of known functions, it is proposed that *GH2* and *GH4* genes are **glutathione-*S*-transferases**. *AUX/IAA* polypeptide chains are short-lived nuclear proteins that probably function as an auxin switch in a secondary phase of signal transduction (42), implying that their target gene products probably mediate auxin responses. Thus, the *AUX/IAA* polypeptides might be involved in homo- and heterodimerization with auxin response factors, such as ARF1, that bind to AuxREs (26, 44). The *IAA17* and *AXR3* genes are identical (44). *Axr3* is a dominant auxin-resistant mutant with extremely resistant roots, although the general phenotype of the mutant resembles auxin hypersensitivity (45).

6. Effects

Depending on temporal and spatial factors, a particular subset of downstream target genes is activated and results in one of many described effects. Auxin has been implicated in a variety of growth and developmental processes, such as cell division, stem and root elongation, leaf expansion, formation of adventitious and lateral roots, induction of vascular tissue, apical dominance, tropisms, flowering, and fertility (46).

Bibliography

1. C. Darwin and F. Darwin (1881) *The Power of Movement in Plants*, Appleton-Century-Crofts, New York.
2. F. W. Went (1927) Proc. Kon. Nederl. Akad. Wetensch. **30**, 10–19.
3. W. M. Bayliss and E. H. Starling (1902) Proc. R. Soc. **69**, 352–353.
4. J. Normanly, J. P. Slovin, and J. D. Cohen (1995) Plant Physiol. **107**, 323–329.
5. B. Bartel (1997) Annu. Rev. Plant Physiol. Plant Mol. Biol. **48**, 51–66.
6. L. Michalczuk, T. J. Cooke, and J. D. Cohen (1992) Phytochemistry **31**, 1097–1103.
7. K. Bialek, L. Michalczuk, and J. D. Cohen (1992) Plant Physiol. **100**, 509–517.
8. V. De Luca, C. Marineau, and N. Brisson (1989) Proc. Natl. Acad. Sci. USA **86**, 2582–2586.
9. D. Bartling, M. Seedorf, A. Mithöferr, and E. W. Weiler (1992) Eur. J. Biochem. **205**, 417–424.
10. B. Bartel and G. R. Fink (1995) Science **268**, 1745–1748.
11. H. J. Klee and C. P. Romano (1994) Crit. Rev. Plant Sci. **13**, 311–324.
12. A. D. Wright, M. B. Sampson, M. G. Neuffer, L. Michalczuk, J. P. Slovin, and J. D. Cohen (1991) Science **254**, 998–1000.
13. R. L. Last, P. H. Bissinger, D. J. Mahoney, E. R. Radwanski, and G. R. Fink (1991) Plant Cell **3**, 345–358.
14. R. L. Last and G. R. Fink (1988) Science **240**, 305–310.
15. W. Boerjan, M.-T. Cervera, M. Delarue, T. Beeckman, W. Dewitte, C. Bellini, M. Caboche, H. Van Onckelen, M. Van Montagu, and D. Inzé (1995) Plant Cell **7**, 1405–1419.
16. J. J. King, D. P. Stimart, R. H. Fisher, and A. B. Bleecker (1995) Plant Cell **7**, 2023–2037.
17. M. Gopalraj, T.-S. Tseng, and N. Olszewski (1996) Plant Physiol. **111** (Suppl.), 114 (469).
18. J. Normanly (1997) Physiol. Plant. **100**, 431–442.

19. T. L. Lomax, G. K. Muday, and P. H. Rubery (1995) In *Plant Hormones* (P. J. Davies, ed.), Kluwer Dordrecht, pp. 509–530.
20. M. J. Bennett, A. Marchant, S. T. May, H. G. Green, S. P. Ward, P. A. Millner, A. R. Walker, B. Schulz, and K. A. Feldmann (1996) Science **273**, 948–950.
21. O. Leyser (1997) Physiol. Plant. **100**, 407–414.
22. L. Galweiler, E. Wisman, A. Yephremov, and K. Palme (1996) P307
23. K. Okada, J. Ueda, M. K. Komaki, C. J. Bell, and Y. Shimura (1991) Plant Cell **3**, 677–684.
24. C. Garbers, A. DeLong, J. Deruére, P. Bernasconi, and D. Söll (1996) EMBO J. **15**, 2115–2124.
25. C. S. Hardtke and T. Berleth (1998) EMBO J. **17**, 1405–1411.
26. T. Ulmasov, G. Hagen, and T. J. Guilfoyle (1997) Science **276**, 1865–1868.
27. G. K. H. Przemeck, J. Mattsson, C. S. Hardtke, Z. R. Sung, and T. Berleth (1996) Planta **200**, 229–237.
28. H. Barbier-Brygoo (1995) Crit. Rev. Plant Sci. **14**, 1–25.
29. H. Macdonald (1997) Physiol. Plant. **100**, 423–430.
30. J. Deikman and M. Ulrich (1995) Planta **195**, 440–449.
31. P. A. Millner, D. A. Groarke, and I. R. White (1996) Plant Growth Regul. **18**, 143–147.
32. G. F. E. Scherer and B. André (1993) Planta **191**, 515–523.
33. H. Yi, D. Park, and Y. Lee (1996) Physiol. Plant. **96**, 359–368.
34. E. J. Neer (1995) Cell **80**, 249–257.
35. T. Mizoguchi, Y. Gotoh, E. Nishida, K. Yamaguchi-Shinozaki, N. Hayashida, T. Iwasaki, H. Kamada, and K. Shinozaki (1994) Plant J. **5**, 111–122.
36. H. M. O. Leyser, C. A. Lincoln, C. Timpte, D. Lammer, J. Turner, and M. Estelle (1993) Nature **364**, 161–164.
37. D. Lammer, N. Mathias, J. M. Laplaza, W. Jiang, Y. Liu, J. Callis, M. Goebl, and M. Estelle (1998) Genes Dev. **12**, 914–926.
38. M. Ruegger, E. Dewey, W. M. Gray, L. Hobbie, J. Turner, and M. Estelle (1998) Genes Dev. **12**, 198–207.
39. W. M. Gray and M. Estelle (1998) Curr. Opin. Biotechnol. **9**, 196–201.
40. A. Cernac, C. Lincoln, D. Lammer, and M. Estelle (1997) Development **124**, 1583–1591.
41. C. Timpte, C. Lincoln, F. B. Pickett, J. Turner, and M. Estelle (1995) Plant J. **8**, 561–569.
42. S. Abel and A. Theologis (1996) Plant Physiol. **111**, 9–17.
43. Y. Takahashi, S. Ishida, and T. Nagata (1995) Plant Cell Physiol. **36**, 383–390.
44. D. Rouse, P. Mackay, P. Stirnberg, M. Estelle, and O. Leyser (1998) Science **279**, 1371–1373.
45. H. M. O. Leyser, F. B. Pickett, S. Dharmasiri, and M. Estelle (1996) Plant J. **10**, 403–413.
46. P. J. Davies (1995) *Plant Hormones: Physiology, Biochemistry and Molecular Biology*, Kluwer, Dordrecht, The Netherlands.

Auxotroph

An auxotroph is a mutant that requires a factor for growth that is not required by the **wild-type**. The opposite of an auxotroph is a **prototroph**, an organism that grows in minimal medium containing only inorganic salts and a carbon source (plus an additional energy source if the organism is an

autotroph). Typical auxotrophic mutations are in genes encoding biosynthetic enzymes for amino acids, vitamins, and **nucleotides**. Some organisms are natural auxotrophs. For example, humans require that all vitamins and several amino acids be supplied in their food. In contrast many, but not all, free-living **microorganisms**, such as *Escherichia coli*, are prototrophs. A specific auxotrophic **phenotype** is called an auxotrophy, eg, an arginine auxotrophy, and the mutant is called an arginine auxotroph.

Avidin

Avidin is a minor **glycoprotein** component of egg white that binds the vitamin biotin with the largest **association constant** known ($\mathbf{K_a} \sim 10^{15}\ M^{-1}$) for a **ligand**–protein interaction (1). Its function in egg white is not known precisely, although protective or antibiotic activities have been suggested. It gained importance not because of its natural functionality, but because of its utility as a tool in molecular biology [see Avidin-Biotin System]. Together with its bacterial relative streptavidin and in complex with biotin, avidin has become one of the most important tools in molecular biology because of its myriad of applications in many fields of biology, biotechnology, and even chemistry (2). Originally, the avidin-biotin complex was introduced to localize, detect, and isolate biologically active molecules (3, 4), but over the years it has became a standard system for replacing radioactivity in immunoassays, for DNA probes, and for various clinical and medical applications (5, 6).

The avidin molecule forms a very stable tetramer that consists of four identical monomers. The monomer is glycosylated at asparagine-17 and is strongly basic (isoelectric point of about 10.5) due to a surplus of arginine and lysine residues. The relatively high molar **absorption** ($A^{1\%}_{[280\ nm]} = 1.54$) reflects the four tryptophan and one tyrosine residue per monomer. The molecular mass of the glycosylated tetramer is about 62,400 Da. When the oligosaccharide residue is removed, the estimated mass is 57,120 Da.

Each avidin monomer binds one molecule of biotin. The binding is considered to be kinetically noncooperative among the subunits (7), although one of the tryptophan residues from a neighboring monomer is inserted physically into the binding site and thus contributes to binding biotin and to the enhanced stability of the tetrameric structure (8). Avidin also binds to the dye HABA (4′-hydroxyazobenzene-2-carboxylic acid), but the association constant (ca. $10^6\ M^{-1}$) is considerably lower than that of the avidin-biotin complex.

The unusually strong binding and the many uses of the system caused scientists to try to understand the molecular basis for this interaction. Moreover, since its inception, many groups have sought to improve various components of the system or the system as a whole. Concurrently, structure-function studies have been implemented, in which early results show the importance of aromatic amino acids in the biotin-binding sites of both avidin and streptavidin. The final structural proof is the determination of the crystal structure of both proteins (Fig. 1), which shows that their overall fold, organization into the tetramer, and content and position of amino acids in the binding sites are all similar (8-10).

Figure 1. Ribbon diagrams of the avidin–and streptavidin–biotin monomers, showing the eight strands of the b-barrel. The biotin molecule is shown in a ball-and-stick model.

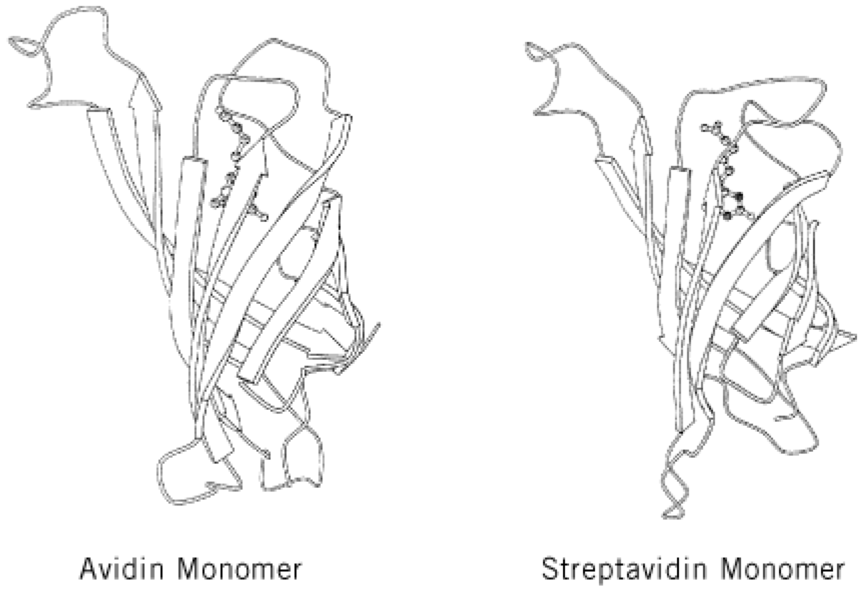

The avidin monomer forms a b-barrel, composed of eight antiparallel b-strands, connected sequentially by loops. The biotin-binding site is a **hydrophobic** pocket that, in the absence of biotin, contains five molecules of structured water. The combined structure of these water molecules emulates that of biotin itself, and as a consequence, they prevent the binding pocket from collapsing. The water molecules are expelled upon binding of biotin. Because no conformational change occurs during complex formation, the binding has a gain of **free energy**. In fact, the avidin-biotin system can be considered a natural host–guest complex. It is clear that any change of this “ideal system” leads to reduced affinity. Indeed, site-directed mutagenesis or chemical modification of residues in the binding site have reduced the affinity constant. An example is the nitration of the essential binding-site tyrosine (11), which decreases the association constant to ~10^{10} M^{-1} , and renders the binding reversible at alkaline pH. Another example is the site-directed modification of tryptophan 120 in streptavidin to phenylalanine, which is also accompanied by a loss in affinity (12).

Different modifications of avidin were introduced over the years, including Extravidin, Neutralite avidin, and Lite avidin (13). Extravidin and Neutralite avidin are avidins in which the arginine residues were modified, whereas the oligosaccharide moieties were removed from Lite and Neutralite avidins. These derivatives are useful in many applications, because avidin, being a basic glycoprotein, is subject to a variety of extraneous nonspecific or undesired binding, particularly to DNA. Similar qualities of genetically engineered forms of avidin are possible because avidin was successfully expressed in a eukaryotic host (14, 15). This should enable preparation of different derivatives of avidin with high affinities, provided that the binding site residues are preserved. It seems that the nonbinding-site residues can be altered extensively.

Bibliography

1. N. M. Green (1975) Adv. Protein Chem. **29**, 85–133.
2. M. Wilchek and E. A. Bayer (1989) Trends Biochem. Sci. **14**, 408–412.
3. E. A. Bayer and M. Wilchek (1978) Trends Biochem. Sci. **3**, N237–N239.
4. E. A. Bayer and M. Wilchek (1980) Methods Biochem. Anal. **26**, 1–45.
5. M. Wilchek and E. A. Bayer (1984) Immunol. Today **5**, 39–43.
6. M. Wilchek and E. A. Bayer (1988) Anal. Biochem. **171**, 1–32.
7. M. L. Jones and G. P. Kurzban (1995) Biochemistry **34**, 11750–11756.
8. O. Livnah, E. A. Bayer, M. Wilchek, and J. L. Sussman (1993) Proc. Natl. Acad. Sci. USA **90**,

5076–5080.
9. W. A. Hendrickson, A. Pähler, J. L. Smith, Y. Satow, E. A. Merritt, and R. P. Phizackerley (1989) Proc. Natl. Acad. Sci. USA **86**, 2190–2194.
10. P. C. Weber, D. H. Ohlendorf, J. L. Wendoloski, and F. R. Salemme (1989) Science **243**, 85–88.
11. E. Morag, E. A. Bayer, and M. Wilchek (1996) Biochem. J. **316**, 193–199.
12. T. Sano and C. R. Cantor (1995) Proc. Natl. Acad. Sci. USA **92**, 3180–3184.
13. E. A. Bayer and M. Wilchek (1994) In *Egg Uses and Processing Technologies* (J. S. Sim, and S. Nakai, eds.), CAB International, Wallingford, UK, pp. 158–176.
14. K. J. Airenne, P. Sarkkinen, E.-L. Punnonen, and M. S. Kulomaa (1994) Gene **144**, 75–80.
15. K. J. Airenne, C. Oker-Blom, V. S. Marjomäki, E. A. Bayer, M. Wilchek, and M. S. Kulomaa (1997) Protein Express. Purif. **9**, 100–108.

Suggestions for Further Reading

16. M. Wilchek and E. A. Bayer, eds. (1990): *Avidin-Biotin Technology*, Methods Enzymol., Vol. **184**, Academic Press, San Diego, p. 746.
17. N. M. Green (1990) Avidin and streptavidin, Methods Enzymol. **184**, 51–67.

Avidin-Biotin System

The avidin-biotin system has become one of the major mainstays in biochemical analysis and has far-reaching application in biotechnology, industry, and clinical medicine (1). The general idea of the avidin-biotin system is that biotin, a low molecular weight vitamin, can be chemically coupled to other low or high molecular weight molecules (e.g., proteins, hormones, **DNA** molecules, etc.). The biotin moiety is still recognized by avidin or streptavidin, either as the native protein or in derivatized form containing any one of a number of reporter groups or probes. The principle of this system is illustrated in Fig. 1.

Figure 1. Overview of the avidin-biotin system and the two major strategies for the various applications. In both approa desired experimental system is combined with a biotinylated binder molecule. Approach A involves direct interaction wi probe. In approach B, avidin is a sandwich between the biotinylated binder and the biotinylated probe. Various targets, b the applications are listed.

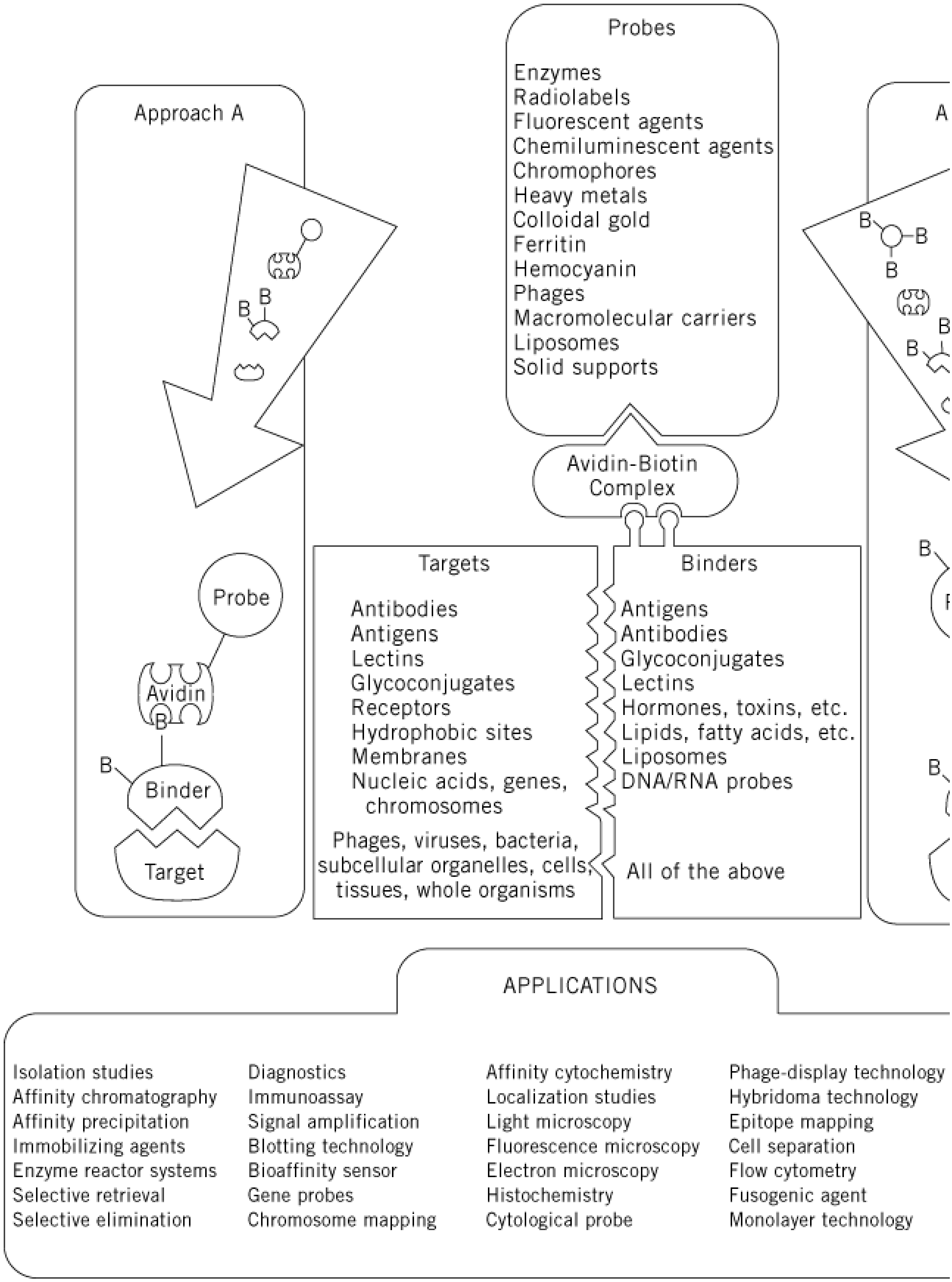

The avidin-biotin system has become a “universal” tool in most of the fields of the biological sciences, because of studies that commenced in the mid 1970s and the constant development that has continued until today (2-6). The system has been applied for a wide variety of purposes (Fig. 1) and has recently been adapted for clinical use for the localization, imaging, and therapy of cancer (7). The binder and the target can be any of the components listed in Figure 1. What is required for this system is the capacity to biotinylate a binding entity so that the specificity and activity of the binding function is retained. For different approaches to biotinylation and the reagents used for binding to different functional groups, see Biotin. As can be seen, most of the functional groups on biological molecules can be modified with biotin.

Because of its charge neutrality and lack of **glycosylation**, streptavidin is generally preferred over egg-white avidin in many applications, although new derivatives of avidin (e.g., Neutravidin) may prove advantageous and less expensive [see Avidin and Streptavidin). The final component added to the system is the probe. The various probes and their potential uses are shown in Fig. 1. The probes are prepared in two ways. They are chemically conjugated directly to avidin or streptavidin (Fig. 1, Approach A) and are **fluorescent**, **radioactive**, or other types of macromolecules (proteins, polysaccharides, etc.). A second approach is to biotinylate the probes and to interact them with streptavidin under subsaturating ratios, thus leaving extra binding sites vacant (Fig. 1, Approach B). More recently, **fusion proteins** have been prepared of streptavidin with different enzymes and native fluorescent proteins.

In many cases, such as **affinity chromatographic** applications, more reversible binding of biotin to avidin would be a distinct advantage. In this context, streptavidin has a critical disadvantage in that the interaction between its subunits is very strong, and it cannot be used when reversibility of the interaction is desired. This is in contrast to avidin, from which an immobilized monovalent form can be produced (8), and the immobilized avidin monomer binds biotinylated compounds reversibly (9).

Site-directed mutagenesis and chemical modification studies are currently being performed on both avidin and streptavidin to understand better their interaction with biotin, the interaction between their subunits, and, perhaps eventually, for better application in the previously-mentioned systems (10, 11). In this regard, the single, critical tyrosine residue of the binding sites of avidin and streptavidin was **nitrated**, and the tetrameric structures of the resultant “nitro avidin” and “nitro streptavidin” were retained (12). The biotin-binding property also had sufficiently high affinity for a variety of applications, including affinity chromatography, enzyme immobilization, and **phage-display** technology (13, 14). The major difference between the nitro avidins and the native molecules is that biotinylated compounds are released by competition with free biotin, and then the latter is liberated by treating the column with basic solutions (pH 10), thereby regenerating the original biotin-binding capacity of the nitro avidin affinity column. Reduced or altered binding characteristics are also conferred on the binding sites of avidin or streptavidin by site-directed mutagenesis of selected binding site residues, such as tryptophans.

Today, the avidin/streptavidin-biotin system is a real necessity in most fields of biological study.

Bibliography

1. M. Wilchek and E. A. Bayer, eds. (1990) *Avidin-Biotin Technology Methods in Enzymology*, Vol. **184**, Academic Press, San Diego.
2. E. A. Bayer and M. Wilchek (1978) Trends Biochem. Sci. **3**, N237–N239.
3. E. A. Bayer and M. Wilchek (1980) Methods Biochem. Anal. **26**, 1–45.
4. M. Wilchek and E. A. Bayer (1984) Immunol. Today **5**, 39–43.
5. M. Wilchek and E. A. Bayer (1989) In *Protein Recognition of Immobilized Ligands* (T. W. Hutchens, ed.), Alan R. Liss, New York, pp. 83–90.
6. E. A. Bayer and M. Wilchek (1996) In *Immunoassay* (E. P. Diamandis and T. K. Christopoulos, eds.), Academic Press, San Diego, pp. 237–267.
7. G. Paganelli, P. Magnani, A. G. Siccardi, and F. Fazio (1995) In *Cancer Therapy with Radiolabeled Antibodies* (D. M. Goldenberg, ed.), CRC Press, Boca Raton, FL, pp. 239–254.

8. N. M. Green and E. J. Toms (1973) Biochem. J. **133**, 687–700.
9. K. P. Henrikson, S. H. G. Allen, and W. L. Maloy (1979) Anal. Biochem. **94**, 366–370.
10. A. Chilkoti, P. H. Tan, and P. S. Stayton (1995) Proc. Natl. Acad. Sci. USA **92**, 1754–1758.
11. A. Chilkoti, B. L. Schwartz, R. D. Smith, C. J. Long, and P. S. Stayton (1995) Bio/Technology **13**, 1198–1204.
12. E. Morag, E. A. Bayer, and M. Wilchek (1996) Biochem. J. **316**, 193–199.
13. E. Morag, E. A. Bayer, and M. Wilchek (1996) Anal. Biochem. **243**, 257–263.
14. M. E. M. Balass, E. A. Bayer, S. Fuchs, M. Wilchek, and E. Katchalski-Katzir (1996) Anal. Biochem. **243**, 264–269.

Suggestion for Further Reading

15. M. D. Savage, G. Mattson, S. Desai, G. Nielander, S. Morgensen, and E. J. Conklin (1992) *Avidin-Biotin Chemistry: A Handbook* Pierce Chemical Co., Rockford, Ill.

Azurin

Azurins are proteins of bacterial origin that belong to the family of cupredoxins (ie, blue single-copper proteins) as is plastocyanin (1). Azurins consist of a single polypeptide chain that contains ca. 128 amino acid residues (~14 kDa molecular weight) (2). Several X-ray crystallography studies of azurins isolated from various bacteria, as well as of single-site mutated forms, have yielded high-resolution, three-dimensional protein structures (Fig. 1) (1, 3-6). The protein consists of eight b-strands that form a b-sandwich (barrel) structure. A segment between b-strands 4 and 5 lies outside this barrel and contains a short **a-helix** (residues 55 to 67). The copper ion is bound about 7 Å below the protein's surface and is coordinated by five ligands: three equatorial ones [a cysteine(112) thiolate and two imidazoles (His46 and His117)] and two weak ligands in axial positions (the carbonyl O atoms of Gly45 and Met121). This configuration (the carbonyl O atom in Gly45 excepted), is conserved in all known structures of "blue" type 1 (T1) copper sites determined thus far (1).

Figure 1. The three-dimensional structure of azurin. The copper center with its ligands is seen near the top of the molecule. The disulfide bond is found at the opposite end of the molecule.

These protein–metal interactions yield a copper site that has a distorted, trigonal bipyramidal geometry, which may explain the stabilization of the Cu(I) state relative to Cu(II) (7) (see Redox Enzymes). Structure-imposed Cu → L p-backbonding has been proposed to account further for stabilization of the cuprous state, because strong p-interaction with the d_p orbitals results in an increase of the ligand field strength. The oxidation/reduction potentials of the Cu(II)/Cu(I) in azurins (~310 mV) are higher than is generally observed for copper complexes. Studies of several mutant forms in which Met121 is replaced, demonstrated that large **hydrophobic** residues raise the Cu(II)/(I) potential, whereas negatively charged ones lower it (8): The span in reduction potential going from Glu121 to Leu121 azurin is 300 mV, or about half the range of the potentials for the naturally occurring T1 sites. The large increase in reduction potentials caused by substitutions involving bulky hydrophobic side chains at position 121 is rationalized by exclusion by such side chains of water from the metal site or simply by providing a low dielectric environment for the copper ion. In contrast, negatively charged hydrophilic residues or water are expected to stabilize the copper ion in the more positively charged +2 state and thus lower the potential, as is indeed observed. Smaller effects on the reduction potential were observed when mutations were made in other positions. It should be emphasized, however, that a thiolate copper ligand *per se* is not a prerequisite for high reduction potentials (8).

As with all other cupredoxins, azurins are also spectroscopically characterized by an intense blue color and a uniquely narrow hyperfine coupling in the electron paramagnetic resonance (EPR) spectrum (see Electron Paramagnetic Resonance). The intense blue color is due to a

$\pi S \rightarrow Cu(d_{x^2-y^2})$ligand-to-metal charge transfer involving the thiolate ligand as the electron donor; it has a molar extinction coefficient of 4000 to 6000 $M^{-1}cm^{-1}$ (9). This is more than 100 times larger than what is found for simple Cu(II) complexes. A second characteristic property associated with the blue (T1) Cu (II) is an EPR spectrum displaying a hyperfine splitting in the $g_{||}$ region, due to interaction of the Cu(II) nuclear and electron spins, which is unusually narrow (~0.008 cm^{-1}), or approximately 50% smaller than those of inorganic copper complexes. This is attributed to delocalization of the unpaired $Cu(d_{x^2-y^2})$electron onto the Cys(S) *p*p orbital, thus reducing the nuclear–electron interaction (10). The unique spectroscopic properties of the T1 site are most likely related to the electron-mediating function of cupredoxins, and this relationship is a central issue in studies of biological electron transfer proteins (11).

Recent experimental investigations of the electron transfer mechanism by azurin have in part been directed toward the intramolecular process in single-site mutated forms of the proteins (12-14). This was motivated by the finding that azurin provides a useful model system for studies of long-range, intraprotein electron transfer (LRET). One way by which this reaction can be induced is from the half-reduced disulfide bond to the Cu(II) ion (12, 14). Another one is by attaching an extraneous redox center to the protein (11, 13). Results of these studies yielded insights into the mechanisms of intramolecular electron transfer in proteins and the parameters that determine the degree of electronic coupling between electron donor and acceptor. Effective electron transfer in proteins requires minimal reorganization of the redox centers as a result of the process. As described above, the metal ion in the blue copper proteins is coordinated to a site that is intermediate between the preferred geometries for Cu(II) (tetragonal planar) and Cu(I) (tetrahedral) (6). Furthermore, the relatively high reduction potentials provides an increased driving force. Finally, the tightly knit, antiparallel b-sheet structure of azurin probably improves the electronic coupling between the reaction partners through the protein matrix.

Bibliography

1. E. T. Adman (1991) Adv. Protein Chem. **42**, 145–198.
2. L. Ryden and J.-O. Lundgren (1976) Nature **261**, 344–346.
3. E. T. Adman and L. H. Jensen (1981) Isr. J. Chem. **21**, 8–12.
4. H. Nar, A. Messerschmidt, and R. Huber (1991) J. Mol. Biol. **218**, 427–447.
5. W. E. B. Shephard, B. F. Anderson, D. A. Lewandoski, G. E. Norris, and E. N. Baker (1990) J. Am. Chem. Soc. **112**, 7817–7819.
6. A. Messerschmidt, L. Prade, S. J. Kroes, J. Sanders-Loehr, R. Huber, and G. W. Canters (1998) Proc. Natl. Acad. Sci. USA **95**, 3443–3448.
7. C. S. St. Clair, W. R. Ellis Jr., and H. B. Gray (1992) Inorg. Chim. Acta **191**, 149–155.
8. T. Pascher, B. G. Karlsson, M. Nordling, B. G. Malmström, and T. Vanngård (1993) Eur. J. Biochem. **212**, 289–296.
9. H. B. Gray and E. I. Solomon (1981) In *Copper Proteins*, Vol. **3** (T. G. Spiro, ed.), Wiley, New York, pp. 1–39.
10. W. E. Antholine, P. M. Hanna, and D. R. McMillin (1993) Biophys. J. **64**, 267–272.
11. A. J. Di Bilio et al. (1997) J. Am. Chem. Soc. **119**, 9921–9922.
12. O. Farver, L. K. Skov, G. Gilardi, G. van Pouderoyen, G. W. Canters, S. Wherland, and I. Pecht (1996) Chem. Phys. **204**, 271–277.
13. J. J. Regan et al. (1995) Chem. Biol. **2**, 489–496.
14. O. Farver and I. Pecht (1997) J. Biol. Inorg. Chem. **2**, 387–392.
15. T. J. Mizoguchi, A. J. Di Bilio, H. B. Gray, and J. H. Richards (1992) J. Am. Chem. Soc. **114**, 10076–10078.

B Cell

Specific recognition by the immune system is mediated fundamentally by B and T lymphocytes. These cells derive from the hematopoietic stem cells through discrete differentiation pathways, although both originate in the bone marrow (and in the liver during embryonic and fetal life) (see Hematopoiesis). T cells mature in the thymus, whereas B cells continue to differentiate in the bone marrow itself. B cells express immunoglobulins that directly interact with native epitopes—that is, subregions of an antigen with a well-defined three-dimensional structure. Surface immunoglobulins are associated with a signaling module made of a Iga-Igb heterodimer to form the B-cell receptor (BCR). In contrast to the BCR, T-cell receptors (TCRs) do not interact directly with native epitopes, but they identify peptides derived from the original antigen as presented by molecules encoded by genes of the major histocompatibility complex (MHC).

Both the B and the T cells have to face the repertoire problem—that is, how to generate extremely large number of different immunoglobulins and TCRs to meet the requirements of recognizing an extraordinary large number of discrete epitopes. A theoretical approach suggests that this number might be as large as 10^{17}. Because the total number of lymphocytes in a human adult averages 10^{12} (roughly divided into one-fifth B cells and four-fifths T cells), and taking into account that they are clonally organized, the number of BCRs and/or TCRs expressed at one given time appears much less than 10^{17}, which implies some basic degeneracy in the immune recognition system. Nevertheless, the number of different structures must still be quite large, which therefore raises the problem of how to generate such a large repertoire with, necessarily, a limited number of genes. This is the main challenge for B cells (and T cells as well), to which the way they differentiate brings the answer.

During fetal life, B lymphocytes differentiate in the liver and then in the bone marrow, which remains active throughout life. The first steps of B-cell differentiation take place in the bone marrow, which is a primary lymphoid organ, and drives precursors derived from the hematopoietic stem cells to the immature B lymphocytes. This period of differentiation is antigen-independent and is essentially devoted to generation of the basic immunoglobulin repertoire, which is the result of a complex sequence of events that involve multiple gene rearrangements. Immature B lymphocytes migrate to secondary lymphoid organs, namely spleen, lymph nodes, tonsils, and gut-associated lymphoid tissues, including Peyer's patches. Further differentiation necessitates antigen encounter and a number of complex cellular interactions, among which cooperation between the B and T cells plays a major role. A second round of diversity is then generated, which results mostly from somatic mutations, and the final steps of differentiation, including isotype switching, lead to the emergence of plasma cells and memory B cells. Two discrete lineages of B cells have been well-characterized in the mouse and are designated B1 and B2. B1 cells express the CD5 marker, have a low level of surface IgD, and are mostly encountered in peritoneal and pleural cavities. They seem preferentially responsible for autoantibody synthesis. B2 cells represent the major and conventional B-cell population.

1. From the Hematopoietic Stem Cell to the Immature B Cell

All differentiation events that drive the emergence of the various lineages (granulocytes, erythrocytes, monocytes, megakaryocytes, **lymphocytes**) derive from a common hematopoietic stem cell that originates in the bone marrow. The B lineage presumably initiates from a precursor common to the B and the T lymphocytes. The main features of the molecular and cellular events that take place in the bone marrow and lead to B cell commitment are indicated in Figure 1. Three major subpopulations define the B lineage: proB, preB, and immature B cells. The successive steps of differentiation proceed from the periphery toward the center of the bone marrow and may be followed in several ways: (a) acquisition and/or loss of surface antigens (especially CD markers) identified by monoclonal antibodies, (b) identification of cytoplasmic proteins and/or messenger RNA transcripts, and (c) analysis of the gene rearrangement status for each of the three Ig gene loci: H, L, and K.

Figure 1. B-cell differentiation in humans. Early steps of B-cell differentiation take place in the bone marrow and are an
The major discrete steps that lead from the hematopoietic stem cell (HSC) to the immature B lymphocyte are identified t
gene rearrangements, by the presence of cytoplasmic markers, and by the expression of characteristic markers at the cell
early stages that go from HSC to the early proB cell encompass several precursors that are not yet completely defined. T
deoxynucleotidyl transferase, responsible for generating N diversity; YL, surrogate light chain that combines with the Ig
the preB receptor. Late events of B-cell differentiation, which take place in the periphery, are antigen-dependent. The ge
organization plays a key role in mounting a T-dependent B-cell response, during which affinity is tuned upon the acquisi
mutations and the biological functions of the antibodies are adapted by isotype switching. Ultimately, this differentiation
cells that secrete antibodies and in memory B cells that are involved in secondary responses. Each step of differentiation
by various CD surface markers, as indicated.

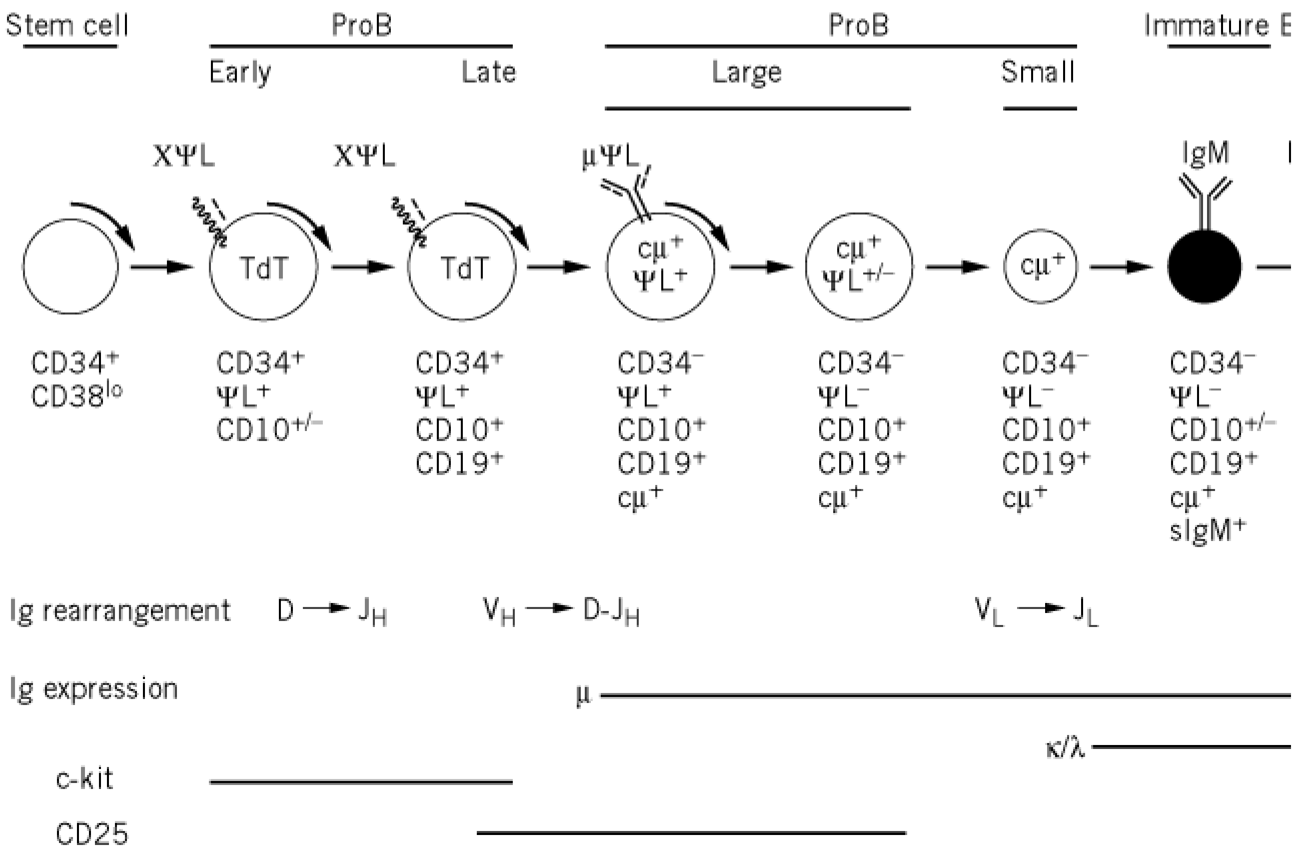

The first steps of differentiation involve a sequence of direct interactions of the precursors with the stromal cells, ensured by various sets of **cellular adhesion molecule**s (CAMs). The VLA4 integrin expressed at the cell surface of the precursors interacts with stromal VCAM1, and the resulting early proB cells now express Kit, a receptor that binds the stem cell factor of stromal cells. This interaction triggers proliferation of the proB cells, which will continue to differentiate through other stimuli. Late proB cells are stimulated by a soluble growth factor also of stromal origin, **interleukin-**7 (IL-7), which drives proliferation of preB cells. As these steps of differentiation proceed, the cells are dividing, and Ig gene rearrangements that generate the basic repertoire take place in a sequential fashion. CD marker characterization indicates that CD34, which is already expressed in the hematopoietic stem cells, remains present at the surface of precursors and proB cells. Late proB cells can be characterized by the coexpression of CD34 with CD19, which is a very specific marker of the

B lineage because it is found on all subsequent stages, with the exception of the plasma cells. CD10, also known as the common acute lymphocytic leukemia antigen (CALLA), is expressed up to the immature B-cell stage a seems expressed slightly before CD19. Other markers are expressed as differentiation proceeds, such as CD20, CD21, CD22, CD23, and CD24.

2. The Basic Ig Repertoire Develops in the Bone Marrow as B Cells Differentiate

As already stated, the main feature of B-cell differentiation is the acquisition of the basic repertoire of immunoglobulins that becomes expressed as IgM on immature B cells. IgM has the classical H_2L_2 organization, and both the H and L chains have variable and constant regions. The variable regions of the heavy and light chains interact in the antibody combining site, which is responsible for specific antigen recognition. Heavy and light chains are encoded by genes that are localized on three discrete gene clusters, H, k and l, located on chromosomes 14, 2, and 22, respectively. The unique feature of Ig gene organization is that they must be rearranged by the specific recombinases RAG1 and RAG2 (for recombinase activating genes) before becoming functional. The first recombination event, DH to JH, takes place in the early proB cells (see Fig. 1) and is rapidly followed by the rearrangement of one of the V_H segments to D-J. Another enzyme, terminal deoxynucleotidyl-transferase, is also active in proB cells, for which it represents an additional cytoplasmic marker. This enzyme adds nucleotides in a random fashion during the joining of D to J and of V to D-J rearrangements. ProB cells that have rearranged the IgV_H locus must “make” two decisions. One is to remain monoclonal with respect to H-chain production, the second is to activate rearrangement of the light chains. Both events are regulated by the m chain itself, which must be in its membrane form. Once the first allele of the IgH locus has completed the rearrangement process, the resulting gene may be functional or not, depending upon whether the recombination has generated a sequence of nucleotides with an open reading frame. Because of the triplet organization of the genetic code, this happens only once every three rearrangements. If the first rearrangement is out of frame, the second allele will recombine, with the same probability of success. A second failure will lead to cell death. Conversely, once a functional gene has been generated, the resulting heavy chain will exert a negative feedback on a further rearrangement of the IgH locus, ensuring monoclonal expression of the m chain. Much evidence suggests that the heavy chain must be expressed at the cell surface to regulate these events. Expression of the m chain at the cell surface requires that it associate with another partner, which resembles the light chain, and for this reason it is named YL or surrogate light chain. First described in the mouse and then identified in humans, the surrogate light chain is composed of two polypeptide chains, encoded by the l-like (or l5 in the mouse) and the VpreB genes, part of the regular IgL locus. The m-YL complex becomes expressed at the surface of what is now a large preB cell, which also expresses CD10 and CD19, but no longer CD34. The cell is able to undertake light-chain gene rearrangements, which occur in the order k→l. The recombination process is regulated in the same manner as that of the heavy chains, so there is only one light chain that is expressed in any given cell, either k or l (see l) Light Chains). The negative feedback on further rearrangements of the light chain genes is exerted by the complete IgM, which is now expressed at the surface of the immature B cell and has replaced the mYL complex. At this point, the Iga–Igb module is associated with the preB cell complex, strongly suggesting that the mYL complex might be considered a “preB” receptor.

3. Immature B Cells are Selected Before Leaving the Bone Marrow

Before leaving the bone marrow, immature B cells that express surface IgM are confronted with the local “self” antigenic environment. They are particularly sensitive to triggering by multivalent antigens, resulting in their clonal deletion by apoptosis. Alternatively, soluble self antigens do not cause the immature B cells to die, but instead induce an anergic state that does not seem to prevent the cells migrating to the periphery. It should be noted, however, that this negative selection has a threshold that leaves a fraction of autoreactive cells going to the periphery. These cells are responsible for the presence in the bloodstream of natural autoantibodies that must be of some physiological relevance. Once validated by this “quality control,” immature B cells circulate to the periphery through blood vessels and lymphatic system, colonize the secondary lymphoid organs, and actively recirculate. They now have become mature B cells, expressing both IgM and IgD isotypes at their surface.

4. Final Steps of B-Cell Differentiation Take Place in the Periphery and are Antigen-Dependent

The B lymphocytes that are now circulating in the periphery are nondividing, short-lived cells. To achieve their ultimate differentiation, they must be triggered by an antigen, most often T-cell-dependent (Fig. 1). Within the first days after antigenic stimulation and T-cell help, activated B cells may mature to plasma cells that have an abundant endoplasmic reticulum and secrete immunoglobulins. Activated B cells may also evolve to colonize the primary follicle of a lymph node and generate a germinal center, where they interact with follicular dendritic cells, divide rapidly, switch to another isotype, most frequently IgG, and start to accumulate somatic hypermutations that considerably amplify diversity and affinity. Clones of high affinity will be positively selected by antigen and can now progress toward plasma cell differentiation or become long-lived B memory cells.

5. Conclusions

Differentiation of B cells is a highly sophisticated process that takes place continuously in the bone marrow and results in the constant emergence of a very large repertoire of immunoglobulins, expressed both as membrane B-cell receptors (BCRs) and soluble antibodies. The numerous molecular events that lead from the hematopoietic stem cell to the mature B cell are under constant selective pressure, implying a high level of cell death. Therefore, the available repertoire appears, at any given time, to be a compromise between the necessary economy in the gene number, compensated by the recombination processes, and an unavoidable wastage due to the stochastic aspects of gene rearrangements and to the negative selection of clones having a high affinity for self components.

See also entries Antibody, Clonal Selection Theory, Gene Rearrangement, Immunoglobulin, and Repertoire.

Suggestions for Further Reading

P. D. Burrows and M. D. Cooper (1997) B cell development and differentiation. Curr. Opin. Immunol., **9**, 239–244.

Y. J. Liu and C. Arpin (1997) Germinal center development. Immunol. Rev., **156**, 111–126.

H. Karasuyama, A. Rolink, and F. Melchers (1996) Surrogate light chain on B cell development. Adv. Immunol, **63**, 1–41.

A. Galy, M. Travis, D. Cen, and B. Chen (1995) Human T, B, natural killer and dendritic cells arise from a common bone marrow progenitor cell subset. Immunity **3**, 459–473.

J. Banchereau and F. Rousset (1992) Human B lymphocytes: phenotype, proliferation, and differentiation. Adv. Immunol. **52**, 125–262.

L. A. Herzenberg and A. B. Kantor (1993) B-cell lineages exist in the mouse. Immunol. Today **14**, 79–83.

B_{12} (Cobalamin)

Cobalamins are complex organometallic cofactors containing a central cobalt atom that is coordinated equatorially to four nitrogen atoms provided by the corrin ring. The two cofactor forms of this vitamin are *adenosylcobalamin* (AdoCbl) and *methylcobalamin* (MeCbl). A variety of other forms have been described in which the upper ligand is a water, *glutathione*, or cyano group, but the physiological significance of these forms is unknown. In nature, this cofactor is found in association with two enzyme subfamilies, the AdoCbl-dependent *isomerases* that catalyze 1,2 rearrangement reactions and the MeCbl-dependent *methyltransferases* that catalyze transmethylation reactions. Members of both subfamilies are fairly prevalent in the bacterial world, where the isomerases are involved in fermentative pathways, and the methyltransferases are involved in pathways leading to methionine, acetate, or methane. In mammals, only two B_{12}-dependent enzymes are known, the cytoplasmic *methionine synthase* and the mitochondrial *methylmalonyl-CoA mutase*. In this review, the molecular biological aspects of B_{12} biosynthesis, enzymology and diseases will be discussed briefly.

1. B_{12} Biosynthesis

The structural cousins, vitamin B_{12}, heme, and chlorophyll, are constructed from a common template that is derived from the precursor, 5-aminolevulinic acid. Methylation at C2 converts the common intermediate, uroporphyrinogen III, to precorrin-1 and commits it to B_{12} biosynthesis. Thereafter, a biosynthetic assembly line, which includes a series of methylations, ring contraction (between rings A and D), cobalt insertion, alkylation, amidations, and nucleotide loop assembly reactions, takes the cofactor to its final form. Two separate pathways lead to corrin ring biosynthesis in the aerobic and anaerobic worlds (for reviews, see Refs. 1-4). They run parallel at some steps and diverge at others. A unique structural feature of B_{12} is the presence of a nucleotide loop that terminates in dimethylbenzimidazole, which can serve as the lower axial ligand to cobalt. The pathways leading to the assembly of dimethylbenzimidaole in aerobic and anaerobic organisms are distinct, but their details remain to be elucidated (5). The **genes** encoding corrin biosynthesis functions have been **cloned** from *Pseudomonas denitrificans*, where they are organized in clusters scattered along the genome (reviewed in Ref. 3) and from *Salmonella typhimurium*, where they are clustered at 41 min (reviewed in Ref. 2). The transcription factor PocR regulates the transcription of the cobalamin biosynthetic and propanediol utilization (dependent on a B_{12} enzyme) genes in *S. typhimurium* (6, 7).

2. B_{12} Enzymes

The cofactor role of AdoCbl was first described by Barker and co-workers in glutamate mutase (8), followed a few years later by the discovery of MeCbl in methionine synthase (9). B_{12}-dependent enzymes catalyze chemically difficult reactions and manipulate the reactive cobalt–carbon bond in radically different ways (reviewed in Ref. 10). In the methyltransferase subfamily, cobalamin is the initial acceptor of the methyl group donated from substrates such as methyltetrahydrofolate and methanol, and alkyltransfer to and from the cobalamin occurs *via* heterolytic cleavage of the cobalt–carbon bond. In the isomerases, the cobalt–carbon bond is broken homolytically, as the enzymes catalyze 1,2 rearrangement reactions. The migration of a diversity of groups, ranging from carbon (in methylmalonyl-CoA mutase, glutamate mutase, and methylene glutarate mutase) to nitrogen (in ethanolamine ammonia lyase and b-lysine mutase) and oxygen (in diol dehydrase), is catalyzed by the isomerases. The genes encoding a number of methyltransferases and isomerases have been cloned and the structures of the B_{12}-binding domain of the *Escherichia coli* methionine synthase (11) and of the *Propionibacterium shermanii* methylmalonyl-CoA mutase (12) have been determined. In both enzymes, the cofactor is bound in an extended conformation in which the intramolecular base, dimethylbenzimidazole, is removed from the cobalt and replaced by a **histidine** residue donated by the protein. Another important member of the B_{12} family of enzymes is ribonucleotide reductase, which converts ribonucleotides to deoxyribonucleotides (13). The reaction mechanisms of B_{12}-dependent enzymes are discussed in a number of reviews (10, 14-18).

3. B_{12}-Related Diseases

Functional B_{12} deficiency can result from either nutritional insufficiency or from genetic defects (19, 20). It is manifested clinically by a combination of symptoms including hematological and neurological abnormalities, methylmalonic aciduria and homocystinuria, depending on whether one or both B_{12}-dependent enzymes is affected. The genetic defects or inborn errors of cobalamin metabolism can result from impairments in uptake, transport, or enzymatic function and are inherited as autosomal recessive traits. Cobalamin absorption and transport abnormalities resulting from impairments in intrinsic factor, its receptor, or in transcobalamin (TC) II have been described. The cDNA encoding human intrinsic factor (21) and TC II (22) have been cloned and mapped, and genetic defects in TC-II in patient cell lines have been identified (23).

Intracellular cobalamin metabolism is complex, compartmentalized, and dependent on several enzymes. Defects in the early steps following internalization of TC II/cobalamin affect both MeCbl and AdoCbl syntheses and fall into the *cbl* C, D, and F genetic complementation groups. The identities of the proteins encoded by these loci and their precise functions are unknown. MeCbl synthesis is specifically compromised in *cbl*G and *cbl*E patients. Cloning of the cDNA encoding methionine synthase (24-26) and identification of mutations correlated with the *cbl*G phenotype (25, 27) indicate that this locus represents methionine synthase. AdoCbl synthesis is specifically impaired in *cbl*A, B, and *mut* patients. The defect in *cbl*B and *mut* patients is in cobalamin adenosyltransferase and methylmalonyl-CoA mutase, respectively. The cDNA encoding methylmalonyl-CoA mutase has been cloned (28), and a number of pathogenic mutations have been described (29).

Bibliography

1. A. Battersby (1994) Science **264**, 1551–1557.
2. A. I. Scott (1994) Tetrahedron **50**, 13315–13333.
3. F. Blanche, B. Cameron, J. Crouzet, L. Debussche, D. Thibaut, M. Vuilhorgne, F. J. Leeper, and A. R. Battersby (1995) Angew. Chem. Int. Ed. Engl. **34**, 383–411.
4. A. I. Scott (1996) Pure Appl. Chem. **68**, 2057–2063.
5. P. Renz (1998) In *Vitamin B_{12} and B_{12} Proteins* (B. Kraeutter, D. Arigoni, and B. T. Golding, eds.), Wiley-VCH, Weinheim, Germany.
6. T. A. Bobik, M. Ailion, and J. R. Roth (1992) J. Bacteriol. **174**, 2253–2266.
7. M. R. Rondon and J. C. Escalante-Semerena (1992) J. Bacteriol. **174**, 2267–2272.
8. H. A. Barker, H. Weissbach, and R. D. Smyth (1958) Proc. Natl. Acad. Sci. USA **44**, 1093–1097.
9. J. R. Guest, S. Friedman, D. D. Woods, and E. L. Smith (1962) Nature **195**, 340–342.
10. R. Banerjee (1997) Chem. Biol. **4**, 175–186.
11. C. L. Drennan, S. Huang, J. T. Drummond, R. Matthews, and M. L. Ludwig (1994) Science **266**, 1669–1674.
12. F. Mancia, N. H. Keep, A. Nakagawa, P. F. Leadlay, S. McSweeney, B. Rasmussen, P. Bösecke, O. Diat, and P. R. Evans (1996) Structure **4**, 339–350.
13. S. Licht, G. J. Gerfen, and J. Stubbe (1996) Science **271**, 477–481.
14. C. L. Drennan, R. G. Matthews, and M. L. Ludwig (1994) Curr. Opin. Struct. Biol. **4**, 919–929.
15. B. T. Golding and W. Buckel (1997) In *Comprehensive Biological Catalysis* (M. L. Sinnott, ed.), Vol. **4**, Academic Press, London.
16. B. Babior (1988) Biofactors **1**, 21–26.

17. J. Stubbe (1988) Biochemistry **27**, 3893–3900.
18. R. G. Matthews, R. V. Banerjee, and S. W. Ragsdale (1990) Biofactors **2**, 147–152.
19. W. A. Fenton and L. E. Rosenberg (1995) *Inherited Disorders of Cobalamin Transport and Metabolism*, McGraw-Hill, New York, pp. 3111–3128.
20. M. I. Shevell and D. S. Rosenblatt (1992) Can. J. Neurol. Sci. **19**, 472–486.
21. B. K. Dieckgraefe, B. Seetharam, L. Banaszak, J. F. Leykam, and D. H. Alpers (1988) Proc. Natl. Acad. Sci. USA **85**, 46–50.
22. O. Platica, R. Janeczko, E. V. Quadros, A. Regec, R. Romain, and S. P. Rothenberg (1991) J. Biol. Chem. **266**, 7860–7863.
23. L. Qian, E. V. Qaudros, and S. P. Rothenberg (1997) Meth. Enzymol. **281**, 269–281.
24. Y. N. Li, S. Gulati, P. J. Baker, L. C. Brody, R. Banerjee, and W. D. Kruger (1996) Human Mol. Genet. **5**, 1851–1858.
25. D. Leclerc, E. Campeau, P. Goyette, C. E. Adjalla, B. Christensen, M. Ross, P. Eydoux, D. S. Rosenblatt, R. Rozen, and R. A. Gravel (1996) Human. Mol. Genet. **5**, 1867–1874.
26. L. H. Chen, M.-L. Liu, H.-Y. Hwang, L.-S. Chen, J. Korenberg, and B. Shane (1997) J. Biol. Chem. **272**, 3628–3634.
27. S. G. Gulati, P. Baker, B. Fowler, Y. Li, W. Kruger, L. C. Brody, and R. Banerjee (1996) Human Mol. Genet. **5**, 1859–1866.
28. R. Jansen, F. Kalousek, W. A. Fenton, L. E. Rosenberg, and F. D. Ledley (1989) Genomics **4**, 198–205.
29. F. D. Ledlay and D. S. Rosenblatt (1997) Human Mutation **9**, 1–6.

Suggestion for Further Reading

30. R. Banerjee, ed. (1999) *Chemistry and Biochemistry of* B_{12}, Wiley, New York.

B-Cell Receptor (BCR)

Immunoglobulins can exist as membrane proteins, expressed at the surface of B cells. When B cells differentiate in the bone marrow from the initial hematopoietic stem cells, they reach a stage, called *immature B lymphocytes*, that is characterized by the presence of IgM at the cell surface (Fig. 1). This IgM, which is a basic m2k2 or m2l2 monomer, is anchored into the membrane bilayer by an extra portion at the COOH-terminus of the heavy chains that is not present in the soluble form. Differences in length result simply from the alternative splicing of membrane exons (see Introns, Exons) present in the germline. The **transmembrane** region is terminated by only three amino acid residues located in the cytoplasm of the B cell.

Figure 1. Schematic representation of the B-cell receptor (BCR). The BCR is composed of one antigen binding module, the surface IgM, connected to the signaling module, a heterodimer containing the Iga and Igb, encoded by the MB-1 and B-29 genes, respectively. Note the Ig domain organization of the ectodomains of the Iga and Igb chains that contain in their cytoplasmic part the ITAM (immunoreceptor tyrosine-based activation motif) motifs that play a central role in signaling by contacting intracellular protein tyrosine kinases.

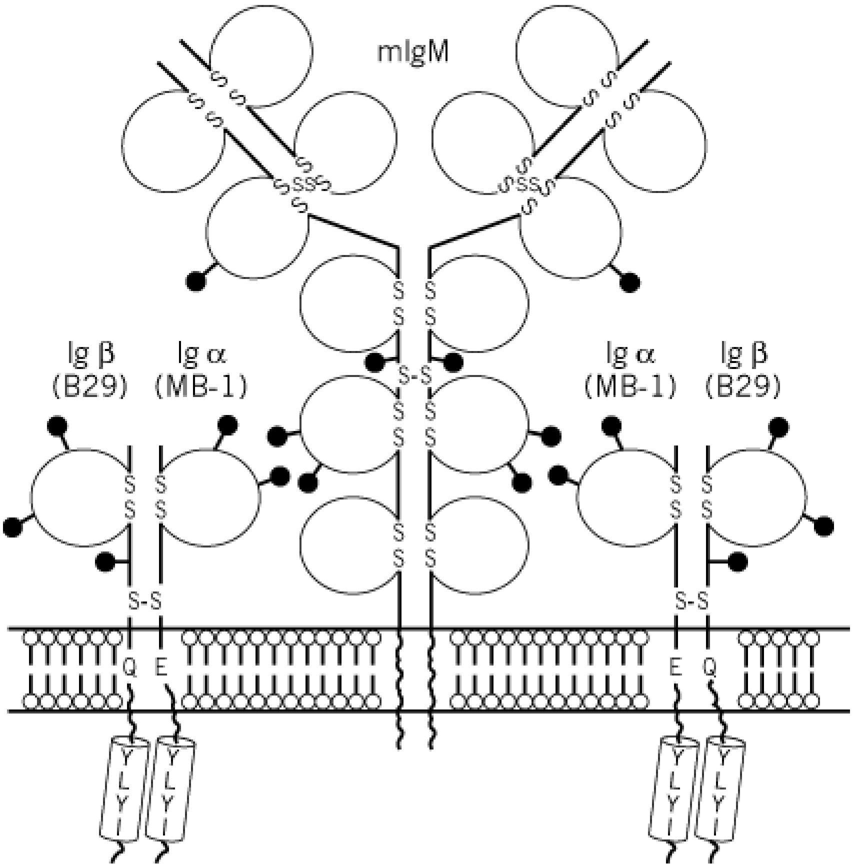

Because the surface Ig clearly acts as a B-cell receptor (BCR) upon triggering by the antigen, the necessity of a signaling module, similar to CD3 in T cells, is apparent. This was indeed the case. The BCR-activating module is a heterodimer composed of one Iga and one Igb chain (also designated as CD79 a and b), each of which has an external Ig-like domain, a transmembrane portion, and an cytoplasmic region that contains several signaling motifs, called *immunoreceptor tyrosine-based activation motif* (ITAM). ITAM were first described on polypeptide chains of CD3 and consist of two Tyr—X—X—Leu/Ile sequences separated by a stretch of seven amino acid residues. They are found in a number of signal transduction modules associated with most crucial receptors of the immune system, such as the T-cell receptor (TCR), BCR, and FcR. Upon stimulation of BCR with cross-linking antigens, ITAM interact with protein **tyrosine kinases** of the **src** family ($p59^{fyn}$, $p53^{lyn}$, $p56^{lyn}$, $p55^{lck}$), leading to the translocation of $p72^{syk}$ to the membrane and activation of the **ras** pathway and **phospholipase C**g2. As a consequence, the BCR is internalized, which is the first step of processing of antigens by B cells. Full activation of B cells require other signals, involving molecules other than the BCR.

Suggestion for Further Reading

M. Reth (1995) The B cell receptor complex and co receptors. Immunol. Today **16**, 310–313.

B-DNA

B-DNA is the predominant type of DNA structure under physiological conditions. The B-DNA double helix is right-handed, with its base pairs perpendicular to the helix axis that passes through the center of the base pairs. The major groove and minor groove are roughly equivalent in depth, 8.5 and 7.5 Å, respectively, whereas the width of the major groove is ~12 Å and that of the minor groove is ~6 Å.

The first X-ray crystallography structure of B-DNA (Fig. 1A) was that of a dodecamer sequence d $(CGCGAATTCGCG)_2$ that contains the EcoRI **restriction** sequence GAATTC (1). There are a number of interesting structural features associated with this B-DNA structure. A distinctive feature is that the minor groove is narrower at the AATT region of the double helix than the CGCG ends. The narrow minor groove at the AATT region is filled by a spine of water molecules that form hydrogen bonds to both the O2 of thymines and the N3 of adenines, although this spine of waters has been reinterpreted recently using a higher resolution structural analysis as a spine of waters on sodium ions (2). Additionally the base pairs in the central AATT region of the helix have high propeller twist angles. The propeller twisting enhances the stacking of the bases along each strand of the double helix, and the AT base pairs are in general less restrictive to propeller twisting because of fewer hydrogen bonds than the GC base pairs (3). Lastly, the sugar pucker of the deoxyribose ring favors the C2′-*endo* conformation, although a range of conformations from C1′-exo to O4′-*endo* is also present. This may reflect the greater flexibility associated with B-DNA structures.

Figure 1. Examples of the structure of B-form DNA. (**a**) Crystal structure of the double-stranded dodecamer d (CGCGAATTCGCG) (Protein Data Base BDL084), with the water molecules in the minor groove shown as spheres. (**b**) Crystal structure of the double-stranded d(CGCAAATTTGCG)-distamycin A complex (Protein Database GDL003). The drug displaces the waters in the minor groove. (**c**) Crystal structure of the double-stranded decamer d (CCAGGCCTGG) (Protein Database BDJS30), with the waters bound to the minor groove shown as spheres. See color insert.

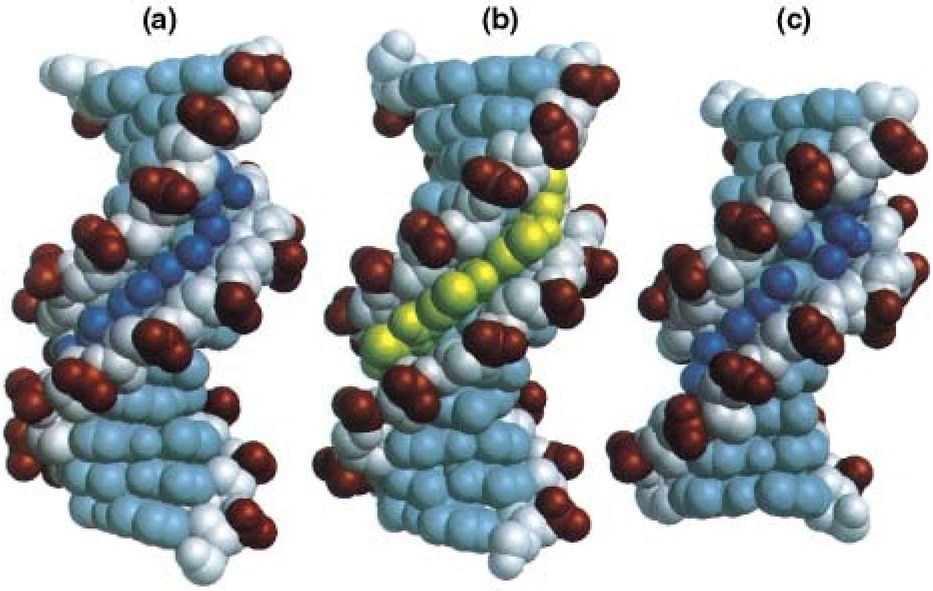

The narrow minor groove region associated with the A-T sequences in B-DNA affords an excellent binding site for the minor groove-binding drugs, such as distamycin A, netropsin, Hoechst 33258, Hoechst 33342, and DAPI. The crystal structure and solution structures of the complexes of several DNA oligonucleotides with those minor groove-binding drugs, most of them in 1–1 drug-to-duplex complexes (Fig. 1B), have been determined (4, 5). Those structures revealed that the drug replaces the spine of hydration in the narrow minor groove and stabilizes the DNA structure, without perturbing the overall conformation significantly. The narrow minor groove associated with the central AATT base pairs is essential for the 1–1 binding mode of drugs. The binding energy derives in part from the gain in **entropy** associated with the displacement of the water molecules. The sequence preference for A-T regions by minor groove-binding drugs is due to the greater negative electrostatic potential at the bottom of the minor groove at A-T regions. Finally the presence of N2 amino groups of guanines provides both a charge and a steric hindrance to drug binding.

NMR study of the binding of distamycin A (a pyrrole-containing anti-tumor antibiotic) to DNA containing A-T sequences revealed a more complex pattern. Distamycin A can bind DNA not only in a 1–1 drug/duplex complex but also in a 2–1 mode, with two distamycins bound to the minor groove in an antiparallel, side-by-side manner (6). The latter binding mode requires that the minor groove width at the binding site be expanded so as to accommodate two drug molecules, reflecting the flexibility of B-DNA. This new finding has stimulated an active study in the design of new minor groove-binding compounds that can bind to all four base pairs, (A-T, T-A, C-G, and G-C), with high specificity. It was found that compounds with imidazole-containing units do not have a great discriminating power regarding the recognition toward G/C versus A/T base pairs. However, compounds that combine the imidazole units with the pyrrole units can be designed to possess excellent sequence-specific binding properties. Rules for such designs have been proposed recently (7).

Additional work on the high-resolution crystal structures of several DNA decamer oligonucleotides with “mixed” sequences, including d(CCAGGCCTGG) (Fig. 1C), showed that the minor groove width of those structures in general is wider, but with some variations. Those DNA decamers have a slightly narrow or wide minor groove, depending on the sequence. In general, the A-T regions have a narrower minor groove than the G-C regions. The hydration structure in the groove is dependent on the groove width. It was noted that a single spine of water molecules along the floor of the minor groove is associated with a narrow minor groove, whereas a ribbon of double water molecules, bridging the base edge N or O atom to the O4′ atoms of the sugar ring, is associated with the wide minor groove.

Bibliography

1. R. M. Wing, H. R. Drew, T. Takano, C. Broka, S. Tanaka, K. Itakura, and R. E. Dickerson, (1980) Nature **287**, 755–758.
2. X. Shui, L. McFail-Isom, G. G. Hu, and L. D. Williams (1998) Biochemistry **37**, 834–8355.
3. C. R. Calladine (1982) J. Mol. Biol. **161**, 343–352.
4. M. Coll, C. A. Frederick, A. H.-J. Wang, and A. Rich (1987) Proc. Natl. Acad. Sci. USA **84**, 8385–8389.
5. H. Robinson, Y.-G. Gao, C. Bauer, C. Roberts, C. Switzer, and A. H.-J. Wang (in press) Biochemistry, and references cited therein.
6. J. G. Pelton and D. E. Wemmer (1989) Proc. Natl. Acad. Sci. USA **86**, 5723–5727.
7. S. White, J. W. Szewczyk, J. M. Turner, E. E. Baird, and P. E. Dervan (1998) Nature **391**, 468–471.

Backbone

Backbone, or main chain, is the general term used to describe the connecting chain in polymers. Different kinds of polymers have different chemical backbones. For example, in proteins the backbone is a polypeptide chain, but **nucleic acids** have a sugar phosphate backbone. The backbone of a polymer, which may adopt a regular structural conformation, is the constant or repeating part of the polymer, as opposed to the attached side chains, which can be variable.

[See also Polymer and Side Chain.]

Suggestions for Further Reading

L. Mandelkern (1983) *An Introduction to Macromolecules*, Springer-Verlag, New York.

P. Munk (1989) *Introduction to Macromolecular Science*, Wiley-Interscience, New York.

Bacteriocins

Broadly defined, bacteriocins are substances produced by one **bacterium** that adversely affect another. Most of them are **peptide antibiotics** that are synthesized on ribosomes, as in normal **protein biosynthesis**. Others, such as bacitracin and **gramicidin**, are synthesized in bacteria by multienzyme complexes or sequential enzyme reactions (1). In a strict sense, bacteriocin is an abbreviation of bacterial toxin (with antibacterial activity). Many bacterial toxins act against **eukaryotic** cells and are not called bacteriocins. Some of them, however, like **diphtheria**, tetanus or **cholera** toxins, resemble bacteriocins, such as colicins or pyocins, in having domain structures that convey the binding and toxic activities specific to each molecule (2, 3). The current basis for allocating a name to the agent responsible for bacteriocinlike activity produced by **Gram-positive** or -negative bacteria is to adopt some derivation of either the genus or species name of the producer strain, together with an alphabetical and/or numerical code designation specifying that strain. To avoid confusion, bacteriocins that have the same amino acid sequence, irrespective of the species of origin, should have the same name, that first published. There is a wide variety of locations of the genetic determinants of bacteriocins. They can be encoded by conjugative or nonconjugative **plasmids**, by conjugative transposons, or be encoded on the chromosome (4).

Because of the different cell-wall structures of gram-positive or -negative bacteria, their bacteriocins have evolved differently in size and specificity. In gram-negative bacteria, the outer membrane necessitates receptor-mediated antagonistic activities, and very specific proteins are produced with domains for receptor binding, translocation, and activity (see Colicins). In contrast, gram-positive bacteria possess a multilayered peptidoglycan wall without an outer membrane. This favors peptides of small size that penetrate the murein network without receptor binding and specific translocation. Consequently, bacteriocins produced by gram-positive bacteria have a broad host range and are sometimes active on taxonomically unrelated genera. Thus, many of the bacteriocinlike agents produced by gram-positive bacteria kill species other than those likely to have the same ecological niche. Production of antibiotic peptides is the rule in gram-positive bacteria. Proteins the size of colicins are hardly ever encountered. In general the structures of these peptides must be stabilized by posttranslational modifications.

Presently there is a burgeoning interest in bacteriocins because of the possible applications in the food industry (particularly lactic acid bacteria) and as a strategy for preventing certain infectious diseases. This review gives the general features of the main classes of bacteriocins and emphasizes the common features that are beginning to emerge.

An organism that produces a peptide antibiotic must be able to (1) synthesize the antibiotic, (2) export the antibiotic into the extracellular medium, (3) protect itself from the action of the antibiotic, and (4) interact with the sensitive cell and interfere with its growth or survival. This interaction may or may not require entry of the antibiotic into the cell. Such entry is characteristic of some of the better-characterized ribosomally synthesized low molecular weight bacteriocins. For a detailed description of these bacteriocins, the reader is referred to the Suggestions for further reading.

1. Classes of Bacteriocins

A list of representative examples of lantibiotic and non-lantibiotic bacteriocins, together with their organisms of origin and mode of action is presented in Table 1. Four distinct classes of bacteriocins from lactic acid bacteria have been defined (5).

Table 1. Representative Examples of Lanthionine-Containing Bacteriocins

Bacteriocin	Type	Mass	Organism of Origin	Mode of Action (References)
Nisin A	L-A	3353	*Lactococcus lactis*	Pore formation (8)
Pep5	L-A	3488	*Staphylococcus epidermis*	Pore formation (44)
Subtilin	L-A	3317	*Bacillus subtilis* ATCC 6633	Pore formation (45)
Epilancin K7	L-A	3032	*Staphylococcus epidermis*	Pore formation (46)
Epidermin	L-A	2164	*Staphylococcus epdermis*	Pore formation (47)
Gallidermin	L-A	2164	*Staphylococcus gallinarum*	Pore formation (48)
Lacticin 481	L-A	2901	*Lactococcus lactis*	Pore formation (49)
Streptococcin A-FF22	L-A	2795	*Streptococcus pyognes*	Pore formation (50)
Salivaricin A	L-A	2315	*Streptococcus salivarus*	Pore formation (51)
Mutacin	L-A	3245	*Streptococcus mutans*	Pore formation (52)
Lactocin S	L-A	3764	*Lactobacillus sake*	Pore formation (36)
Carnocin U149	L-A	4635	*Carnobacterium piscicola*	Pore formation (53)
Cytolysin L1	L-A	4164	*Enterococcus faecalis*	Pore formation (54)
Cinnamycin	L-B	2042	*Streptomyces cinnamoneus*	Membrane disorganization (55)
Duramycin	L-B	2014	*Streptomyces cinnamoneus*	Membrane disorganization; pore formation (55)
Mersacidin	L-B	1825	*Bacillus* sp.	Cell-wall synthesis (56)
Actagardine	L-B	1890	*Actinoplanes* sp.	Cell-wall synthesis (57) inhibition

Class I The lantibiotics (lanthionine-containing peptides) are small antibiotic peptides that are distingu content of dehydro and thioether amino acids (lanthionine and 3-methyl-lanthionine) (6). Two their distinctive ring structure. Type A comprises screw-shaped, amphipathic molecules that ha two to seven net positive charges. Type B consists of more globular molecules that have molec charge or a net negative charge. The lantibiotics include a growing list of modified peptides tha bacilli, lactococci, lactobacilli, staphylococci, streptococci, and streptomyces (Fig. 1). The func twofold. First, these small peptide molecules are less likely to achieve stable conformations by they are generally extremely heat stable. Unusual cross-links like the thioether bridge from lan retain their proper folded structure despite their small size (7). Secondly, unusual sidechains, su repertoire of chemical reactivity that is be important for the biological activity of these peptide

Figure 1. Primary structure of representative lantibiotics. Abbreviations used: dhA, didehydroalanine; dhB, dide ß-methyl lanthionine; Ala-NH-Lys, lysinoalanine; Asp-OH, hydroxyaspartic acid.

Nisin A

Subtilin

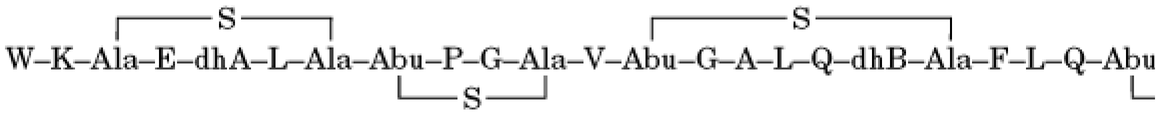

Pep5

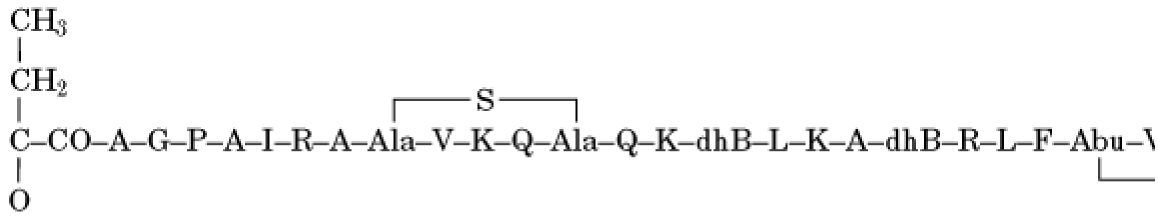

Epidermin

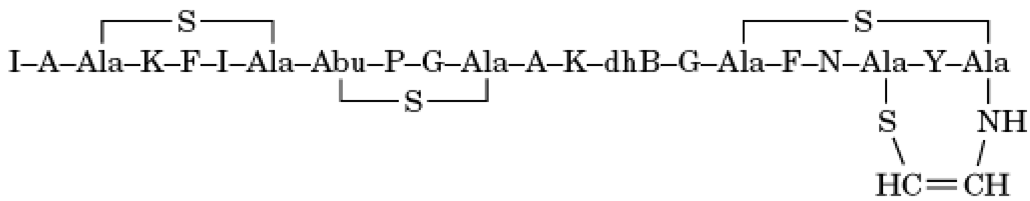

Cinnamycin

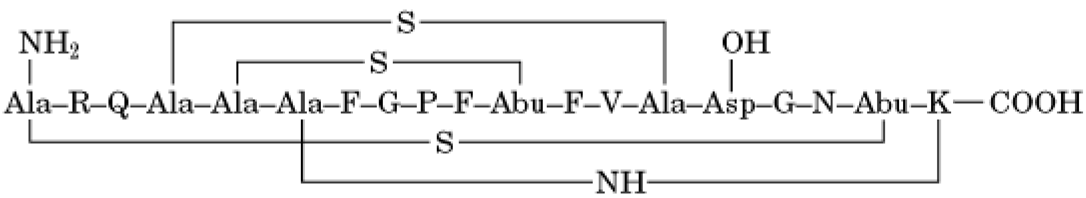

Mersacidin

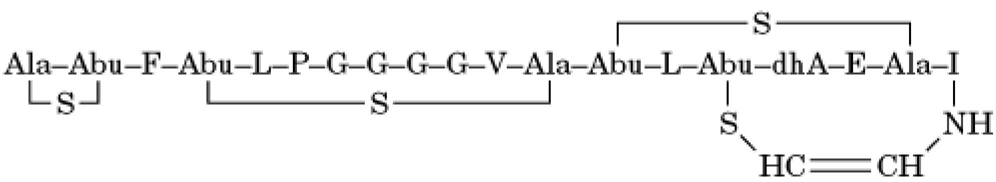

Class II These bacteriocins are small (<10 kDa), relatively heat stable, non-lanthionine-containing pept been subdivided into Class IIa, *Listeria*-active peptides with the N-terminal consensus sequenc IIb, poration complexes requiring two different peptides for activity; Class IIc, thiol-activated j for activity. Unmodified peptide antibiotics (not containing lanthionine) share several characte prepeptide that has an N-terminal extension (**leader peptide**). Leader peptides are amphiphilic hydrophobic region of the **sec**-dependent exported proteins (see **protein targeting**). The leade particularly at the proteolytic processing site, where two glycine residues are found at position (4, 9). The processed, active bacteriocins contain a substantial amount of **hydrophobic** amino Accordingly, the plasma membrane is the target of most of these bacteriocins. Flanking region **gene** of non-lantibiotic peptides contain additional **open reading frames** for which a function demonstrated or postulated on the basis of sequence homologies. Such genes code for immunit proteins consisting of a histidine kinase and the respective regulator, and for proteins with sign family. Some of these genes have an operon-like organization.

Class III	These bacteriocins are large (>30 kDa) heat-labile proteins that include many bacteriolytic ext muramidases) that mimic the physiological action of bacteriocins.
Class IV	These are complex bacteriocins that contain essential lipid or carbohydrate moieties in additio purified antibacterial components is still necessary to confirm that the presence of the addition biological activity of these molecules, thereby justifying the establishment of this class IV.

1.1. Microcins

An additional class of bacteriocins comprises a family of antibiotic substances called "microcins" produced by diverse members of the *Enterobacteriacae* (10). They are distinguished from the majority of colicins by much lower molecular weight (<10 kDa) and because their synthesis is not induced by conditions that lead to induction of the **SOS repair** pathway. Instead, they are synthesized during the stationary phase, similar to that observed with most conventional antibiotics (11). The microcins were operationally defined as substances produced by gram-negative bacteria that pass through a cellophane membrane and inhibit the growth of an indicator *Escherichia coli* strain (12). Several substances known to be ribosomally synthesized fall within this group. The best known of these antibiotics peptides are microcin C7, microcin B17, and colicin V. Microcin C7 is a heptapeptide containing modifications at both the N- and C-termini that block protein synthesis *in vivo* and *in vitro* (13). Microcin B17 (Mcc B17) is a 43-residue peptide containing posttranslational modifications at the peptide backbone including serine, cysteine, and glycine residues, that result in thiazole and oxazole rings (14). Mcc B17 has much in common with lantibiotics because it is derived from a precursor peptide that is posttranslationally modified; 26 out of the 43 residues are glycine. Mcc B17 inhibits DNA replication and induces the SOS response (15). The target of this antibiotic is a DNA gyrase (16) (see DNA Topology). Colicin V (ColV) was first described in 1925 in the first report of an antibiotic substance produced by *E. coli* (17). It has a molecular weight of only 6000. The structure of mature colicin V is not totally known, even regarding side-chain modifications or N-terminal processing. Colicin V kills sensitive cells by disrupting their membrane potential (18).

2. Biosynthesis and Posttranslational Modifications

Generally the low molecular weight bacteriocins of gram-positive bacteria are first formed in an inactive precursor form that has a leader peptide. Following a variety of posttranslational modification reactions, the C-terminal propeptide domain is cleaved from the N-terminal leader sequence to yield the mature antimicrobial molecule. These prepeptides range from 18 to 30 amino acid residues and are not highly homologous except near the cleavage site. The prepeptides of all non-lanthionine-containing bacteriocins characterized thus far have two Gly residues at positions –2 and –1 relative to the processing site and b-turn promoting residues near the cleavage site. Possible functions of the prepeptide include (1) stabilizing the propeptide during translation; (2) keeping the bacteriocin inactive, particularly after completion of modifications and thus helping to protect the producing strain; (3) allowing recognition of the ABC transporter system; (4) directing the precursor through a specific recognition motif toward biosynthetic enzymes (modification enzymes); (5) interacting with the propeptide region to stabilize a conformation that is essential for correct modification and thioether formation. There is evidence that the modifications of lantibiotics are made at the prepeptide stage. Cross-similarities between leaders of the modified and unmodified bacteriocins indicate that the overall features of leader peptides are important during regulation, synthesis, and generation of the immunity of peptide bacteriocins, regardless of whether or not they are modified.

Table 2. Non-Lanthionine-Containing Bacteriocins

	Mode of Action

Bacteriocin	Type	Mass	Organism of Origin	(References)
Pediocin PA-1	NLC	4600	*Pedicoccus acido lantici* PAC 1.0	Pore formation (58)
Mesentericin Y-105	NLC	3666	*Leuconostoc mesenterides* Y105	Pore formation (59)
Carnobacteriocin A	NLC	5100	Carnobacterium piscicola LV17A	? (60)
Sakacin A	NLC	4308	*Lactobacillus sake* LB706	? (61)
Lactacin F	NLC	5600	*Lactobacillus* sp.	Pore formation (62)
Lactococcin A	NLC	5800	*Lactococcus lactis* (cremoris)	Pore formation (63)

The primary amino acid sequences of the propeptide components of many of the low molecular weight bacteriocins produced by gram-positive bacteria are known now. One important feature of the bacteriocins of gram-positive bacteria is their cysteine content. Those in which one or more cysteine residues are linked to dehydrated serine and threonine residues to form the thioether-linked amino acids lanthionine and methyl-lanthionine are called lantibiotics as previously mentioned (Fig. 1). Alternatively, bacteriocins in which pairs of cysteine residues undergo modification to form disulfide bonds are called cystibiotics (cysteine-containing antibiotics). A third subgroup of the bacteriocins, of which lactococin B is an example, are designated thiolbiotics, because they contain only a single cysteine residue that must be present in the reduced **thiol** form to be active (19). At neutral pH, many of the low molecular weight bacteriocins are cationic. This is a unifying feature of lantibiotic and non-lanthionine containing bacteriocins and may have some significance for their activity.

Little is known about the posttranslational modification reactions and the biosynthetic enzymes involved in the maturation of lantibiotics. The lantibiotic B and C genes (designated *Lan*B and *Lan*C, as stipulated by the 1st and 2nd International Workshops on Lantibiotics) are probably involved in the maturation pathways, because mutation studies indicate that the gene products are essential for producing functional lantibiotics. The products of these genes, designated LanB and LanC, but also known as NisB and NisC, respectively, may be involved in the dehydration and thioether bond formation. Limited similarity was reported between LanB and *E. coli* IlvA, a threonine dehydratase, thus suggesting a similar function (20). This leads to the hypothesis that LanC and other similar proteins are involved in the enzyme-catalyzed formation of thioether bonds from the dehydrated residues and cysteine. Another modification enzyme that has been identified is EpiD, which is encoded by the epidermin gene cluster located on the 54-kb plasmid pTu32 (21). EpiD has no homologue in other lantibiotic gene clusters, and it catalyzes the biosynthesis of the C-terminal aminovinylcysteine residue of epidermin (22).

3. Extracellular and Maturational Release

After biosynthesis, class I and II bacteriocins are released to the extracellular medium. For each bacteriocin there is a relatively specific membrane protein system whose function is to translocate a precursor form of the antibiotic across the cytoplasmic membrane to the outside of the cell. The secretion of several peptide bacteriocins is mediated by dedicated transmembrane translocators belonging to the ATP-binding cassette (ABC) transporter superfamily (23-26). The transporters are encoded in the same operons as the bacteriocin structural gene or on a neighboring operon. The C-terminal ATP-binding domain and the N-terminal hydrophobic integral membrane domain are expressed as a single polypeptide or as separate polypeptides. Recently, strong evidence has been reported that, very likely, all precursor peptides of the lantibiotic and non-lantibiotic bacteriocins that have leader peptides of the double glycine type (see above) are processed by their dedicated ABC-transporters, concomitant with export (27). It has also been proposed that the N-terminal domains of bacteriocin transporters are essential for initial recognition and subsequent proteolytic processing. These new proteolytic enzymes are thiol proteinases. In fact, genes for potential ABC transporters have been found in all the known lantibiotic gene clusters. The lantibiotic transporters range in size from 535 to 714 amino acid residues and generally have the ATP-binding **domain** and the membrane-spanning domain in the same single protein. Sometimes a second ABC transporter system has been identified, which is not essential for production but participates in producer self-protection, thus providing some type of additional immunity (28). Although the leader sequence of the double-glycine type may be cleaved concomitant with export by the ABC-transporter itself, this is not the general case.

The ABC transporters have thiol proteinase activity, and putative proteinase genes (designated P) have been described for the leader peptides of other lantibiotics. These gene products share similarities with **subtilisin**-like serine proteinases. For example, the *Nis*P gene encodes an extracellular serine proteinase with a C-terminal extension anchoring it on the outer side of the cytoplasmic membrane (29). With nisin, it has been shown that cleavage of the leader peptide is not a prerequisite for export by the ABC-transporter, and this conclusion may be extended to other peptides with antimicrobial activity (30).

A detailed maturational pathway has been proposed for nisin (31). First the inducing signal (which could be nisin itself) activates the transcription at the *nis*A promoter (which has features also found in other positively regulated **promoter** sequences) via a two-component response-regulator system (32). This results in the production of pre-nisin containing free cysteines and no dehydrated residues. The pre-nisin is directed, presumably by virtue of the leader peptide, to a membrane-located complex containing the modifying enzymes LanB (probably involved in dehydration) and LanC (probably involved in thioether bonds, as previously mentioned). At this stage, the leader helps to maintain the peptide in an inactive form. Subsequently, the precursor nisin is translocated via the ABC exporter NisT at the expense of ATP hydrolysis. Finally, precursor nisin is activated by proteolytic cleavage by the extracellular protease NisP attached to the outside of the cell envelope. The role of the leader is still not fully understood, apart from its function in producing an inactive conformation. In particular, it is not known how it functions in targeting the pre-lantibiotic to the maturation and export proteins, what its fate is after cleavage, and how it contributes to processes, such as self protection, after it has been cleaved off.

This proposed sequence of events may also apply to other lantibiotics. However, additional intracellular conversions are required in specific modification reactions, such as those involving the N- and C-termini of epidermin (33), lantibiotic Pep5, epilamin K7 (34, 35), and lactocin S (36). In these cases it is likely that the leader peptide cleavage occurs intracellularly.

4. Modes of Action

The various structural properties of the subgroups of bacteriocins are reflected in their three different modes of action. The primary activity of Class I type A lantibiotics is based on forming voltage-dependent, short-lived pores in the cytoplasmic membrane (37, 38). The peptides rapidly induce leakage of ions and small metabolites from bacterial cells and a collapse of the electrochemical proton gradient, leading to cessation of biosynthetic processes and eventually to cell death. Type A lantibiotics require a membrane potential of between 50 and 100 mV for pore formation, depending on the individual peptide. It is assumed that pores are formed by a transiently associated peptide oligomer in a transmembrane orientation (barrel stave model), as suggested for alamethicin. The susceptibility toward a particular peptide of different bacterial species, or even of strains within one species, varies much more than one would expect on the basis of the pore-formation model. *In vivo* pore formation or pore stability may be positively or negatively influenced by such factors as phospholipid composition of the membrane, interactions of the peptides with integral membrane components, or the presence of surface layers. The models may need to be refined, and pore formation may depend on local perturbation of the bilayer (39). In addition, the peptides could exert secondary effects that contribute to bactericidal activity, such as autolysis of cells by activating cell-wall hydrolyzing enzymes (40).

The antibacterial effects of class I type B lantibiotics are rather weak. They bind to the head groups of phospholipids, preferentially to phosphoethanolamine, which may cause membrane permeabilization and allow the release of cations and other small solutes. Duramycin also induces the formation of complex pores (41). Mersacidin and actagardine are distinguished from other type B lantibiotics by their mode of action. Both interfere with cell-wall biosynthesis in gram-positive bacteria, which may eventually offer new possibilities in antimicrobial therapy (42).

Generally, the bactericidal action of class II bacteriocin against sensitive cells is produced principally by destabilizing membrane function, such as energy transduction, rather than disrupting the structural integrity of the membrane. This effect results from the energy-independent dissipation of the proton motive force and loss of the permeability barrier of the cytoplasmic membrane. It contrasts with the energy-dependent bactericidal action of the lantibiotics. In addition, before pores are formed, all of the non-lanthionine containing bacteriocins interact with membrane-associated receptor proteins, in contrast to class I lantibiotic bacteriocins.

5. Immunity of Bacteriocin-Producing cells

One of the definitive features of bacteriocin-producing cells is their ability to resist the action of their own inhibitory substances through a specific immunity mechanism. Such a mechanism is based on dedicated peptides or proteins called immunity proteins, which specifically antagonize the bacteriocin. For nisin and subtilisin, their antagonist proteins of 245 and 165 amino acid residues, respectively, display the features of bacterial lipoproteins and are similar in amino acid sequence. Despite the high degree of similarity of these lantibiotics, there is no cross-immunity between producing cells. In other cases, as with pepS, the immunity is much more closely related to the immunity systems of unmodified bacteriocins, which are short, have only 69 residues, and have a hydrophobic N-terminal segment and a strongly hydrophilic C-terminal part.

Currently, there are no clues to the mechanism of the immunity phenomenon. The proposed location of the peptides outside the cell and the observation that the cytoplasmic membrane of immune clones is not depolarized by externally added bacteriocin suggest that the bacteriocins are directly antagonized by the immunity peptide, like colicin A, for example (43).

Bibliography

1. H. Kleinhauf and H. von Döhren (1990) Eur. J. Biochem. **192**, 1–15.
2. M. Kageyama, M. Kobayashi, Y. Sano, and H. Masaki (1996) J. Bacteriol. **178**, 103–110.
3. H. Bénédetti and V. Géli (1996) In *Handbook Biological Physics* (W. N. Konings, H. R. Kaback, and J. S. Lolkema eds.), Elsevier, Amsterdam, The Netherlands, Vol. **2**, pp. 665–691.
4. H. G. Sahl (1994) In *Antimicrobial Peptides* (Ciba Foundation Symposium 186), Wiley, Chichester, pp. 27–53.
5. T. R. Klaenhammer (1988) Biochimie **70**, 337–349.
6. G. Jung (1991) Angew. Chem. Int. Ed. Engl. **30**, 1051–1068.
7. E. Gross and J. L. Morell (1967) J. Amer. Chem. Soc. **53**, 2791–2792.
8. E. Gross and J. L. Morell (1971) J. Amer. Chem. Soc. **93**, 4634–4635.
9. W. M. de Vos, O. P. Knipers, J. R. van der Meer, and R. J. Siezen (1995) Mol. Microbiol. **17**, 427–437.
10. F. Baquero and F. Moreno (1984) FEMS Microbiol. Lett. **23**, 117–124.

11. J. F. Martin and A. L. Demain (1980) Microbiol. Rev. **44**, 230–251.
12. C. Asensio, C. Perez-Diaz, M. C. Martinez, and F. Baquero (1976) Biochem. Biophys. Res. Commun. **69**, 7–14.
13. R. Kolter and F. Moreno (1992) Ann. Rev. Microbiol. **46**, 141–163.
14. A. Bayer, S. Freund, C. Nicholson, and C. Jung (1993) Angew. Chem. Int. Ed. Engl. **32**, 1336–1339.
15. M. Herrero and F. Moreno (1986) J. Gen. Microbiol. **132**, 393–402.
16. J. L. Vizan, C. Hernandez-Chico, I. del Castillo, and F. Moreno (1991) EMBO J. **10**, 467–476.
17. A. Gratia (1925) C.R. Soc. Biol. **93**, 1040–1041.
18. C. Yang and J. Konisky (1984) J. Bacteriol. **158**, 757–759.
19. G. Bierbaum and H. Sahl (1991) In *Nisin and Novel Antibiotics* (G. Jung and H. G. Sahl, eds.), Escom Publishers, Leiden, The Netherlands, pp. 386–396.
20. Z. Gutowski-Eckel, C. Klein, K. Siegers, K. Bohm, M. Hammelmann, and K. D. Entian (1994) Appl. Environ. Microbiol. **60**, 1–11.
21. N. Schnell, G. Engelke, R. Augustin, F. Rosenstein, F. Götz, and K. D. Entian (1991) In *Nisin and Novel Antibiotics* (G. Jung and H. G. Sahl, eds.), Escom Publishers, Leiden, The Netherlands, pp. 269–276.
22. T. Kupke, S. Stefanovic, H. G. Sahl, and F. Götz (1992) J. Bacteriol. **174**, 5354–5361.
23. L. Gilson, H. K. Mahanty, and R. Kolter (1990) EMBO J. **9**, 3875–3884.
24. M. S. Gilmore, R. A. Segarra, and M. C. Booth (1990) Infect. Immunol. **58**, 3914–3923.
25. J. D. Marugg, C. F. Gonzalez, B. S. Kunka, A. M. Ledeboer, M. J. Pucci, M. Y. Toonen, S. A. Walker, L. C. Zoetmulder, and P. A. Vandebergh (1992) Appl. Environ. Microbiol. **58**, 2360–2367.
26. G. W. Stoddard, J. P. Petzel, M. J. van Belkum, J. Kok, and L. L. McKay (1992) Appl. Environ. Microbiol. **58**, 1952–1961.
27. L. S. Havarstein, H. Holo, and I. F. Nes (1994) Microbiol. **140**, 2393–2389.
28. K. Venema, G. Venema, and J. Kok (1995) Trends Biochem. Sci. **3**, 299–304.
29. J. R. van der Meer, J. Polman, M. M. Beerthuyzen, R. J. Siezen, O. P. Kuipers, and W. M. de Vos (1993) J. Bacteriol. **175**, 2578–2588.
30. J. R. van der Meer, H. S. Rollema, R. J. Siezen, M. M. Bethuyzen, O. P. Kuipers, and W. M. de Vos (1994) J. Biol. Chem. **269**, 3555–3562.
31. W. M. de Vos, O. P. Kuipers, J. R. van der Meeer, and R. Siezen (1995) Mol. MIcrobiol. **17**, 427–437.
32. W. M. de Vos and G. F. Simons (1994) In *Genetics and Biotechnology of Lactic Acid Bacteria* (M. J. Gasson and W. M. de Vos, eds.), Backie Academic, Glasgow, pp. 52–105.
33. T. Kupke, C. Kempter, V. Gnan, G. Jung, and F. Götz (1994) J. Biol. Chem. **269**, 5653–5659.
34. M. Reis, M. Eschbach-Bludau, M. Iglesias-Wind, T. Kupke, and H. G. Sahl (1994) Appl. Environ. Microbiol. **60**, 2876–2883.
35. M. van de Kamp, H. W. van den Hooven, R. N. Konings, C. W. Hilbers, C. W. van de Ven, G. Bierbaum, H. G. Sahl, O. P. Kuipers, R. J. Seizen, and W. M. de Vos (1995) Eur. J. Biochem. **230**, 587–600.
36. M. Skangen, J. Nissen-Meyer, G. Jung, S. Stefanovic, K. Sletten, C. I. Mortreveldt-Abilgaard, and I. F. Nes (1994) J. Biol. Chem. **269**, 27183–27185.
37. H. G. Sahl (1991) In Nisin and novel lantibiotics *Proceedings of the First International Workshop on Lantibiotics* (G. Jung and H. G. Sahl, eds.), Leiden, Escom Publishers, pp.347–359.
38. R. Benz, G. Jung, and H. G. Sahl (1991) In Nisin and novel lantibiotics *Proceeding of the First International Workshop on Lantibiotics* (G. Jung and H. G. Sahl, eds.), Leiden, Escom

Publishers, pp. 359–372.
39. A. J. Driessen, H. W. van den Hooven, W. Kuiper, M. van de Kamp, H. G. Sahl, R. N. Konings, and W. Konings (1995) Biochemistry **34**, 1606–1614.
40. G. Bierbaum and H. G. Sahl (1987) J. Bacteriol. **169**, 5452–5458.
41. T. Sheth, R. M. Henderson, S. B. Hlady, and W. A. Cuthbert (1992) Biochim. Biophys. Acta **1107**, 179–185.
42. S. Chatterjee, D. Chatterjee, K. Jani, H. Blumbach, B. Ganguli, N. Klesel, M. Limbert, and G. Seibert (1992) J. Antibiot. **45**, 839–845.
43. D. Espesset, D. Duché, D. Baty, and V. Géli (1996) EMBO J. **15**, 2356–2364.
44. R. Kellner, G. Jung, and H. G. Sahl (1991) In *Nisin and Novel Lantibiotics* (G. Jung and H. G. Sahl, eds.), Escom Publishers, Leiden, The Netherlands, pp. 141–158.
45. E. Gross, H. H. Kitz, and E. Nebelin (1973) Hoppe-Seyler"s Z. Physiol. Chem. **354**, 810–812.
46. M. van de Kamp, L. Horstink, H. W. van den Hooven, R. N. Konings, C. W. Hilbers, A. Frey, H. G. Sahl, J. W. Metzger, and F. J. van de Ven (1995) Eur. J. Biochem. **227**, 757–771.
47. H. Allgaier, G. Jung, R. Werner, U. Schneider, and H. Zähner (1986) Eur. J. Biochem. **160**, 9–22.
48. R. Kellner, G. Jung, T. Hörner, H. Zähner, N. Schnell, K. Entian, and F. Götz (1988) Eur. J. Biochem. **177**, 53–59.
49. J. C. Piard, C. Delorme, M. Novel, M. Desmageaud, and G. Novel (1993) FEMS Microbiol. Lett. **112**, 313–318.
50. R. W. Jack, A. Carne, J. Metzger, S. Stefanovic, H. G. Sahl, G. Jung, and J. R. Tagg (1994) Eur. J. Biochem. **220**, 455–462.
51. K. F. Ross, C. Ronson, and J. R. Tagg (1993) Appl. Environ. Microbiol. **59**, 2014–2021.
52. J. Novak, P. W. Canfield, and E. J. Miller (1994) J. Bacteriol. **176**, 4316–4320.
53. G. Stoffels, J. Niessen-Meyer, A. Gudmundsdottir, K. Sletten, H. Halo, and I. F. Nes (1992) Appl. Environ. Microbiol. **58**, 1417–1422.
54. M. S. Gilmore, R. A. Serraga, M. C. Booth, C. P. Bogie, L. R. Hall, and D. B. Clewell (1994) J. Bacteriol. **176**, 7335–7344.
55. A. Fredenhagen, F. Märki, G. Fendich, W. Märki, J. Gruner, J. van Oostrum, F. Raschdorf, and H. H. Peter (1991) In *Nisin and Novel Lantibiotics* (C. Jung and H. G. Sahl eds), Escom Publishers, Leiden, The Netherlands, pp. 131–140.
56. H. Kogler, H. Bauch, H. W. Fehlhaber, C. Griesinger, W. Schubert, and V. Teetz (1991) In *Nisin and Novel Lantibiotics* (G. Jung and H. G. Sahl, eds.), Escom Publishers, Leiden, The Netherlands, pp. 159–170.
57. N. Zimmermann, N. S. Freud, A. Fredenhagen, and G. Jung (1993) Eur. J. Biochem. **216**, 419–428.
58. M. L. Chikindas, M. J. Garcia-Garcera, A. J. Driessen, A. M. Ledeboer, J. Niessen-Meyer, I. F. Nes, T. Abee, W. N. Konings, and G. Venema (1993) Microbiology **59**, 3577–3584.
59. A. Maftah, T. Renault, C. Viguoles, Y. Hechard, P. Bressolier, M. Ratineaud, Y. Cenatiempo, and R. Julian (1993) J. Bacteriol. **175**, 3232–3235.
60. R. W. Woboro, T. Henkel, M. Sailer, K. L. Roy, J. C. Vederas, and M. E. Skiles (1994) Microbiology **140**, 517–526.
61. A. Holck, L. Axelson, S. S. E. Birkeland, T. Aukrust, and H. Bloom (1992) J. Gen. Microbiol. **138**, 2715–2720.
62. P. Muriana and T. R. Klaenhammer (1991) J. Bacteriol. **173**, 1779–1788.
63. H. Holo, O. Niessen, and I. F. Ness (1991) J. Bacteriol. **173**, 3879–3887.

Suggestions for Further Reading

64. R. James, C. Lazdunski, and F. Pattus, eds. (1992) *Bacteriocins, Microcins and Lantibiotics*, NATO ASI Series, Springer-Verlag, Berlin, Vol. **H65**.
65. R. W. Jack, J. R. Tagg, and B. Ray (1995) Bacteriocins of gram-positive bacteria, Microbiol. Rev. **59**, 171–200.
66. T. R. Klaenhammer (1993) Genetics of bacteriocins produced by lactic acid bacteria, FEMS Microbiol. Rev. **12**, 39–86.
67. F. Moreno, J. L. San Millan, C. Hernandez-Chico, and R. Kolter (1995) Microcins, Biotechnology, **28** 307–321.
68. H-G. Sahl, R. W. Jack, and G. Bierbaum (1995) Biosynthesis and biological activities of lantibiotics with unique post-translational modifications, Eur. J. Biochem. **230**, 827–853.

Bacteriorhodopsin

Bacteriorhodopsin is a small (26 kDa) integral membrane protein, the prototype of seven-helical **G-protein**–linked **receptors**, that upon illumination transports protons across the membrane. It forms extended two-dimensional hexagonal arrays in the cytoplasmic membrane of **halobacteria**. Its transmembrane a-helices surround the **prosthetic group** retinal, which is linked via a Schiff Base to Lys216 near the middle of helix G and lies at a small angle to the membrane plane. Photoisomerization of the retinal from all-*trans* to 13-*cis* sets off a sequence of thermal reactions (the "photocycle") in which the interaction of the retinal and the protein causes proton transfers between various donor and acceptor groups. Together, these transfers result in the complete translocation of a proton from the cytoplasmic to the extracellular surface, thus generating a transmembrane electrochemical gradient for protons. The proton gradient is utilized in the way usual in **bacteria** for the synthesis of ATP, the uptake of nutrients (amino acids) and K^+, and the transport of Na^+ out of the cells (see Proton Motive Force).

Bacteriorhodopsin forms trimers that assemble in the two-dimensional hexagonal array that constitutes the patches termed "**purple membrane**." The purple membrane contains only bacteriorhodopsin and lipids, and the regular crystalline lattice made it possible to determine its structure by cryo-**electron crystallography** at 7 Å (1) and then 3 Å (2) resolution. The protein was also crystallized from a lipid cubic phase, and its structure has now been determined by X-ray crystallography at 2.5 Å resolution (3). The protein consists of seven transmembranous a-helices, with short interhelical loops and short N and C termini. Three of the helices, B, C, and D, are normal to the plane of the membrane and the other four, A, E, F, and G, are inclined at various small angles to the perpendicular (Fig. 1). The retinal is bound to the ε**-amino group** of Lys216, forming a protonated Schiff base near the middle of helix G, and its polyene chain lies at about 23° from the membrane plane. Thus the Schiff base divides the protein into extracellular and cytoplasmic halves.

Figure 1. Structure of bacteriorhodopsin (1), and the pathway of proton transport. The seven transmembranous a-helices are shown, along with only the all-*trans* retinal and the most important residues. The curved arrows identify the proton transfers that occur at different times in the photocycle (see text) and add up to the complete transport of a proton from the cytoplasmic (upper) to the extracellular surface of the membrane.

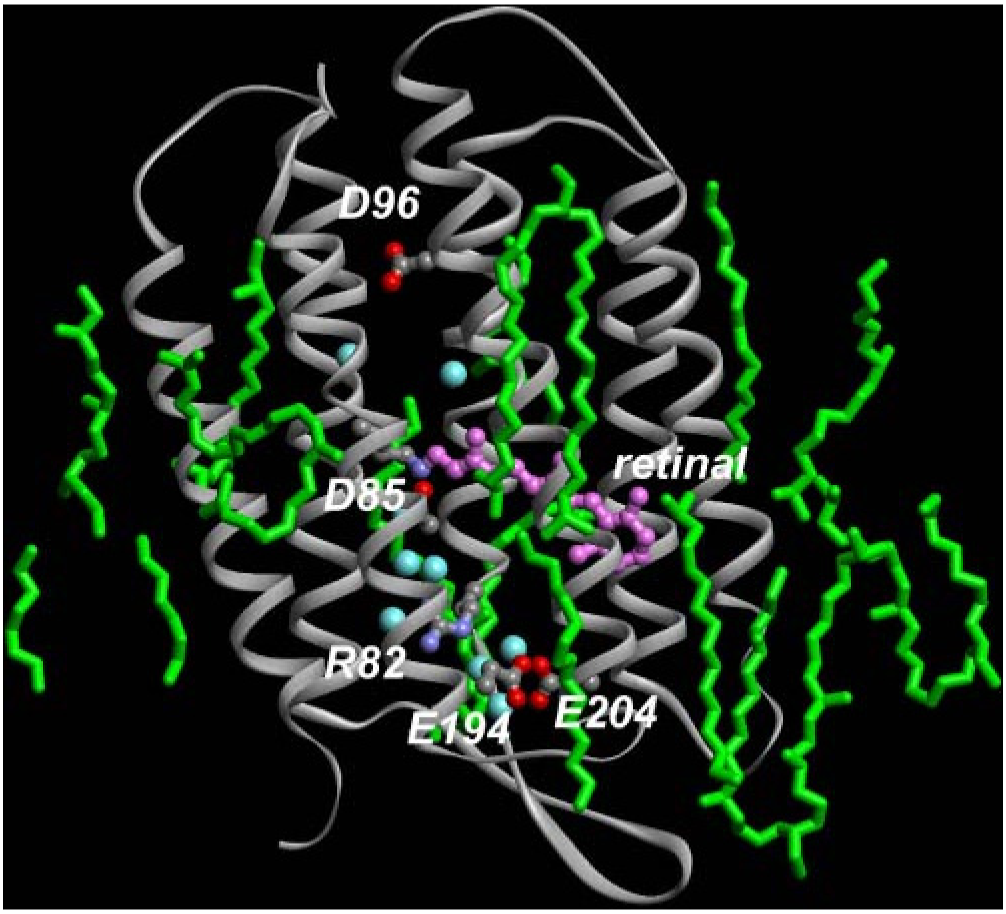

The trajectory of the transported proton from one surface to the other is through proton-conductive "half-channels" through each of the two halves of the molecule. Identification of the residues that participate in the two half-channels has been the objective of much research in the past few years. The extracellular half-channel is quite complex and contains polar and hydrogen-bonding residues. Many of them play roles in the release of protons to the extracellular surface. Asp85 and Asp212 are anionic residues located near the Schiff base. A possible pathway for protons leads from Asp85, via Arg82, Glu204, and Glu194, to the extracellular surface and is consistent with functional studies. Another plausible pathway is through Glu9 or Glu74, but the results of mutagenesis indicate that these two residues are dispensable. The cytoplasmic half-channel is simpler. It contains mostly **hydrophobic** residues between the retinal and Asp96, which is the proton donor in the reprotonation of the Schiff base. Thr46 is close enough to interact with Asp96, and mutagenesis confirms its significant role in the proton donor and acceptor function of Asp96. Acidic residues at the cytoplasmic aqueous interface include residues 36, 38, 102, and 104. It has been suggested that they form a "funnel" at the surface that directs protons into the cytoplasmic half-channel (2). Although immobilization of the protein in the purple membrane is responsible for the well-known, extraordinary thermal and photostability of bacteriorhodopsin, neither the trimeric arrangement of the monomers nor the rigid lattice structure have functional roles in the transport activity (4). Thus, availability of the structure of bacteriorhodopsin, even at the current limited resolution, has generated considerable insights into the proton transport mechanism and has provided the framework for mechanistically interpreting a wealth of spectroscopic information.

The chromophore with all-*trans*, 15-*anti* retinal has a broad **absorption** band with a maximum at 568 nm. This is considerably red-shifted from that of retinal in isolation (380 nm) or a retinal analog with a protonated Schiff base (440 nm). This red-shift results primarily from the diffuse counterion to the charged Schiff base, which comprises principally Asp85 with a contribution from Asp212, which is several angstroms removed and providing only partial compensation of the charge (5). The all-*trans* chromophore exists in thermal equilibrium with the 13-*cis*, 15-*syn* configuration, which absorbs at 555 nm. Sustained illumination converts the retinal to 100% all-*trans*, 15-*anti*, known as "light-adaptation" (6). The photoreaction of this isomer is normally active in transport.

The photocycle of the all-*trans* chromophore is described by the intermediate states J, K, L, M, N, and O, their substates, and the sequence of their interconversions (Fig. 2). Each intermediate is characterized by a distinct absorption maximum in the visible wavelength region, numerous vibrational bands of the retinal in the infrared and Raman region and of the protein in the infrared region (see Vibrational Spectroscopy). The kinetics of the photocycle describe the sequence and the energetics of the chemical reactions that translocate protons across the membrane. In the K intermediate, which arises on the nanosecond timescale after decay of the excited state, the retinal assumes a twisted 13-*cis*, 15-*anti* configuration, as indicated by high-amplitude hydrogen-out-of-plane vibrations. Its absorption maximum is red-shifted by 30 to 40 nm from the initial state. It is converted in about one microsecond into the L state, which absorbs at 540 to 550 nm. In L, the polyene of the retinal is more relaxed, but other changes begin to appear in the protein in both the extracellular and cytoplasmic regions (7). The Schiff base forms stronger hydrogen bonds that are correlated with structural changes of bound water detected in the infrared wavelength region. One of these water molecules is bound to the Schiff base, Asp85, and Asp212 and may play a role in the pK_a shifts that result in proton transfer from the Schiff base to Asp85. The hydrogen bonding of two other water molecules near Asp96 are also affected in L, suggesting that the structural changes near the Schiff base are transmitted all the way across the protein to the cytoplasmic region.

Figure 2. The photocycle of bacteriorhodopsin. The intermediate states are shown, and the isomeric configuration of the retinal is indicated. The Schiff base is protonated in all but the M states.

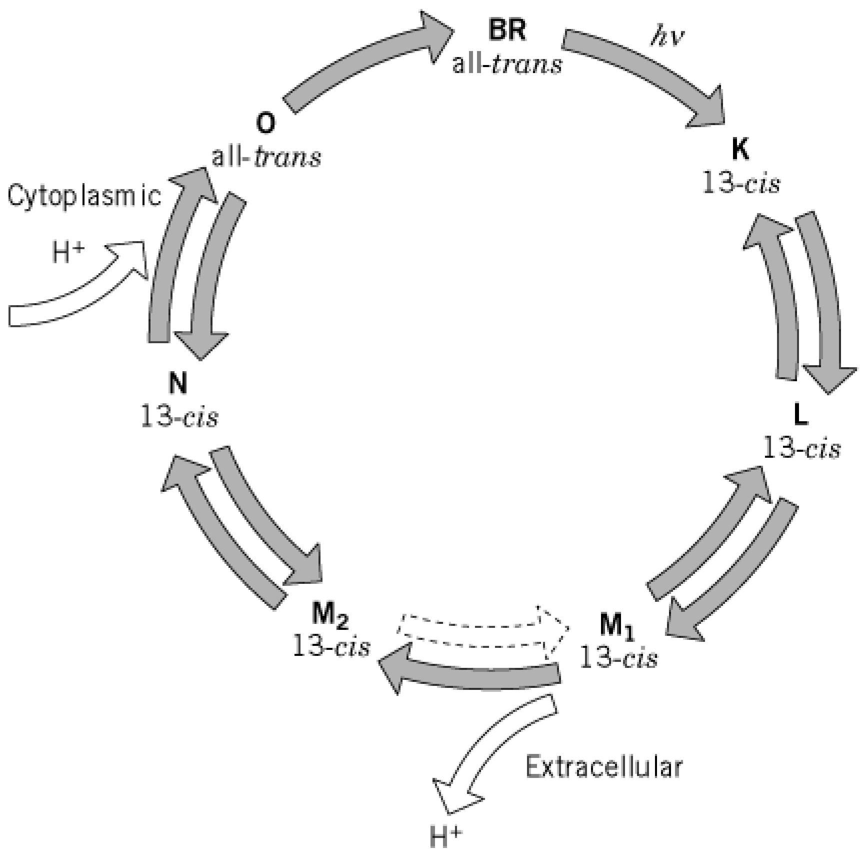

The M state is formed by transfer of a proton from the retinal Schiff base to Asp85 (8). It has a strongly blue-shifted absorption maximum at 410 nm. The kinetics of this conversion, measured at visible and infrared wavelengths, suggest that L is in equilibrium with an early M state, M_1, and that the mixture of L and M_1 decay together to form the late M state, M_2 (9-11). At pH > 6 this occurs in a unidirectional reaction, and thus L disappears as M_2 is formed. At pH < 6, however, the $M_1 \rightarrow M_2$ reaction is not unidirectional, and both L and M_1 remain present and coexist with M_2 because at the higher pH a proton dissociates from a site in the extracellular region that interacts with Asp85. This site is either Glu204 or depends on the carboxyl group of Glu204. Its proton is passed to Glu194 and is released from there to the extracellular surface. The anomalous titration properties of Asp85 indicate that the nature of the interaction between the proton affinities of this aspartate residue and the proton release site is such that either may be protonated but not both (12, 13). When Asp85 becomes protonated by the Schiff base, the pK_a of the proton release group is lowered, and the proton dissociates. When this proton is released to the bulk solution at a pH greater than the pK_a for the release, the pK_a of Asp85, in turn, is driven higher, and deprotonation of the Schiff base becomes complete. This prevents reprotonation of the Schiff base from the extracellular direction.

Reprotonation of the Schiff base is from the cytoplasmic direction by Asp96 (8, 14), which produces the N intermediate that absorbs near 560 nm but with a lower extinction than the initial state. Large-scale protein conformational changes in N are evident from a pair of negative and positive difference features in the infrared spectrum that originate from a shift of the amide I band (15). Electron and X-ray diffraction studies of the M and the N states, measured either at various times after flash illumination and freezing or in a photostationary state at ambient temperature, indicate considerable changes of conformation at the cytoplasmic surface. The most conspicuous of these is an outward tilt of the cytoplasmic end of helix F (16). Its occurrence in the M intermediate may be transitory during the M → N conversion of the unperturbed wild-type photocycle, but this feature is clearly observable when M is stabilized in the wild-type or in mutant forms of the protein. The movement of helix F as a rigid body is confirmed by distance measurements using pairs of spin labels (17). The effects of osmotic agents, humidity, and in-plane cooperativity in the purple membrane lattice on the M → N reaction and on the protein conformation change suggest that the rationale of the helical tilt is to increase the hydration of the cytoplasmic region and thereby to decrease the pK_a of Asp96. Thus, Asp96 becomes a proton donor to the Schiff base. The tilt of helix F is recovered during decay of the N state, presumably recovering the initial high pK_a of Asp96 and causing its reprotonation from the cytoplasmic surface.

Reisomerization of the retinal to all-*trans* occurs in the N → O transition (18). This is made possible by the lowered barrier-to-bond rotation in the polyene chain upon protonation of the Schiff base. Residues that contact the chain near the 9-methyl and 13-methyl groups, such as Trp182 (19) and Leu93 (20), facilitate the reisomerization, probably through steric interactions that transmit residue displacements in the protein to the retinal and vice versa. The O state has a strongly red-shifted maximum at visible wavelengths, at least partly because Asp85 is still protonated. Consequently, the main component of the counterion to the protonated Schiff base is lacking. Large-amplitude hydrogen-out-of-plane vibrations indicate that, as in the K state, the retinal chain is twisted. These features disappear in the final O → BR reaction, which appears to be limited by the rate of proton transfer from Asp85 to the still unprotonated proton release site (21). As expected from the recovery of the low initial pK_a of Asp85, this reaction is unidirectional under all conditions, and it ensures the full repopulation of the initial state and also the functioning of the **proton pump** against large transmembranous proton gradients.

Bacteriorhodopsin is one of three types of similar retinal proteins in halobacterial membranes. Their functions are all based on the photoisomerization of all-*trans* retinal to 13-*cis*, 15-*anti* and the protein reactions that accompany the thermal reisomerization. Halorhodopsin is an inwardly-directed, light-driven chloride ion pump. It lacks Asp85 and Asp96, and the retinal Schiff base does not deprotonate during the photocycle (22). Sensory rhodopsins I and II are receptors for phototactic behavior (23). A profound similarity in the mechanisms of these proteins with different functions is indicated by the fact that their activities are interconvertible with minimal perturbations. Thus, the Asp85Thr mutant of bacteriorhodopsin binds chloride, exhibits a photocycle similar to that of halorhodopsin, and transports chloride from the extracellular to the cytoplasmic direction (24). Halorhodopsin, in turn, transports protons when the weak acid, azide, is added, by binding near the Schiff base and functioning as a proton acceptor (25). Sensory rhodopsin I transports protons like bacteriorhodopsin when the transducing protein that is normally tightly bound to it is genetically deleted (26, 27).

Bibliography

1. N. Grigorieff et al. (1996) J. Mol. Biol. **259**, 393–421.
2. Y. Kimura et al. (1997) Nature **389**, 206–211.
3. E. Pebay-Peyroula, G. Rummel, J. P. Rosenbusch, and E. M. Landau (1997) Science **277**, 1676–1681.
4. N. A. Dencher and M. P. Heyn (1979) FEBS. Lett. **108**, 307–310.
5. K. Nakanishi et al. (1980) J. Am. Chem. Soc. **102**, 7945–7947.
6. G. S. Harbison et al. (1984) Proc. Natl. Acad. Sci. USA **81**, 1706–1709.
7. A. Maeda et al. (1997) J. Biochem. (Tokyo) **121**, 399–406.
8. M. S. Braiman et al. (1988) Biochemistry **27**, 8516–8520.
9. L. Zimányi et al. (1992) Biochemistry **31**, 8535–8543.
10. S. Dickopf and M. P. Heyn (1997) Biophys. J. **73**, 3171–3181.
11. B. Hessling, J. Herbst, R. Rammelsberg, and K. Gerwert (1997) Biophys. J. **73**, 2071–2080.
12. S. P. Balashov, E. S. Imasheva, R. Govindjee, and T. G. Ebrey (1996) Biophys. J. **70**, 473–481.
13. H. T. Richter, L. S. Brown, R. Needleman, and J. K. Lanyi (1996) Biochemistry **35**, 4054–4062.
14. K. Gerwert, B. Hess, J. Soppa, and D. Oesterhelt (1989) Proc. Natl. Acad. Sci. USA **86**, 4943–4947.
15. M. S. Braiman, O. Bousché, and K. J. Rothschild (1991) Proc. Natl. Acad. Sci. USA **88**, 2388–2392.
16. S. Subramaniam, M. Gerstein, D. Oesterhelt, and R. Henderson (1993) EMBO J. **12**, 1–8.
17. T. E. Thorgeirsson et al. (1997) J. Mol. Biol. **273**, 951–957.
18. S. O. Smith et al. (1983) Biochemistry **22**, 6141–6148.
19. O. Weidlich et al. (1996) Biochemistry **35**, 10807–10814.
20. J. K. Delaney, G. Yahalom, M. Sheves, and S. Subramaniam (1997) Proc. Natl. Acad. Sci. USA **94**, 5028–5033.
21. H. T. Richter et al. (1996) Biochemistry **35**, 15461–15466.
22. D. Oesterhelt (1995) Israel J. Chem. **35**, 475–494.
23. W. D. Hoff, K. H. Jung, and J. L. Spudich (1997) Annu. Rev. Biophys. Biomol. Struct. **26**, 223–258.
24. J. Sasaki et al. (1995) Science **269**, 73–75.
25. G. Váró, L. S. Brown, R. Needleman, and J. K. Lanyi (1996) Biochemistry **35**, 6604–6611.
26. R. A. Bogomolni et al. (1994) Proc. Natl. Acad. Sci. USA **91**, 10188–10192.
27. U. Haupts, C. Haupts, and D. Oesterhelt (1995) Proc. Natl. Acad. Sci. USA **92**, 3834–3838.

Suggestions for Further Reading

28. T. G. Ebrey (1993) "Light energy transduction in bacteriorhodopsin". In *Thermodynamics of Membranes, Receptors and Channels*, (M. Jackson, ed.), CRC Press, Boca Raton, FL, pp. 353–387.

29. J. K. Lanyi (1993) Proton translocation mechanism and energetics in the light-driven pump bacteriorhodopsin. Biochim. Biophys. Acta **1183**, 241–261.
30. J. K. Lanyi and G. Váró (1995) The photocycles of bacteriorhodopsin. Israel J. Chem. **35**, 365–386.
31. R. A. Mathies, S. W. Lin, J. B. Ames, and W. T. Pollard (1991) From femtoseconds to biology: Mechanism of bacteriorhodopsin''s light-driven proton pump. Ann. Rev. Biophys. Biophys. Chem. **20**, 491–518.
32. D. Oesterhelt, J. Tittor, and E. Bamberg (1992) A unifying concept for ion translocation by retinal proteins. J. Bioenerg. Biomembr. **24**, 181–191.

BAL 31 Nuclease

The enzymes commonly referred to as BAL 31 nuclease have been widely used for manipulation of nucleic acids, most frequently through their ability to shorten both strands of double-stranded DNA from the ends in a controllable manner. Other activities include endonucleolytic attack on double-stranded DNA in response to the presence of a variety of covalent and noncovalent alterations in DNA structure (eg, DNA-carcinogen adducts and junctions between right- and left-handed helical regions) and highly processive unidirectional exonucleolytic degradation of single-stranded DNA.

1. Source and Some Physical Properties

BAL 31 is the strain designation given the original isolates of the marine bacterium that produces the nucleases, which was originally determined to be a species of *Pseudomonas* (1) but was reclassified as *Alteromonas espejiana* (2). The **nuclease** activity was discovered adventitiously as a contaminant in preparations of the *Alteromonas* bacteriophage PM2, but these enzymes proved to be bacterial products secreted into the culture medium (3, 4). The common name also appears as BAL31 and BAL-31; all should be used when searching electronic databases.

The bulk of the nuclease activity in culture supernatants is owing to two molecularly and kinetically distinct forms, both of which are active as single polypeptide chains (5). The smaller of these, designated the "slow" (S) form, is produced by **proteolysis** of the larger, "fast" (F) form, which in turn derives from an even larger precursor that has not been characterized (6). *Alteromonas espejiana* copiously produces extracellular proteinase activity (6), which accounts for the progressive conversion of larger to smaller species in the culture fluid as growth proceeds. At least the S species is not a fully homogenous protein, because its N-terminal amino acid is not unique; either the presumed endoproteolytic event that generates this species from the F form does not occur at a unique site or there is exoproteolytic activity as well. Conversion of the F form to a species indistinguishable in molecular size and catalytic properties from the S form can be done by proteolysis *in vitro* (6).

The American Type Culture Collection strain of this organism (ATCC 29659) is suitable for production of the nucleases. No overproducing strains, either of *Alteromonas* itself or of heterologous hosts containing **cloned** nuclease **genes**, have been reported. Purification procedures that effect separation of the S and F forms have been described (5) and modified (6). BAL 31 nuclease is available commercially from several sources, but these products are mixtures of the S and F species. A partial amino acid sequence of an internal fragment produced by cleavage with cyanogen bromide has been obtained (7). This new sequence did not have significant homology with any reported sequences. Some physical properties of the S and F forms are presented in Table 1 (5).

Table 1. Some Physical Properties of F and S Forms of BAL 31 Nuclease

Molecular Weight (kDa)	Isoelectric pH	Molar Absorption Coefficient(10^5 liter/mol-cm)	Weight Absorption Coefficient(dl/g-cm)
F 109.0	4.2	1.10 ± 0.09	10.2 ± 0.8
S 85.0	4.2	1.00 ± 0.03	11.7 ± 0.3

2. Reactions Catalyzed

Five activities appear to account for the degradation—ultimately to mononucleotides—of DNA: (1) a 5′ → 3′ exonuclease activity that acts on single-stranded DNA in a highly processive manner (ie, many nucleotides are removed in a single productive enzyme-substrate encounter) (8); (2) a 3′ → 5′ directed exonuclease activity that acts only on duplex structures, leaving a 5′-terminated single-stranded "tail" (9); (3) an endonuclease activity against single-stranded DNA, (much slower than the exonuclease activity on single-stranded DNA [8]), that is also elicited by a variety of covalent or noncovalent distortions or lesions in duplex DNA (3-5, 10-14); (4) an exonuclease activity that can excise a small number of nucleotides starting from the site of a strand break (nick) in duplex DNA (15), which is inferred to be 5′ → 3′-directed; and (5) an activity that can remove short 3′-terminated tails from otherwise duplex DNA. The F and S forms differ greatly in the rates of removal of nucleotides, at given molar concentrations of DNA ends and enzyme, via the 3′ → 5′ exonuclease action on double-stranded DNA, which led to their "fast" and "slow" designations (5). The two forms have comparable kinetic behavior toward single-stranded DNA (5, 8).

The BAL 31 nucleases also catalyze the terminally directed hydrolysis of double-stranded RNA and degrade RNA that contains nonduplex structure (16). Whether an analog of the endonuclease activity on altered duplex DNA exists has not been determined, except that cleavage probably occurs in response to a strand break in duplex RNA.

The 5′ → 3′ exonuclease activity on single-stranded DNA is highly processive, as the nucleases are able to degrade DNA polymers of nearly 500 nucleotides in length completely without dissociation of enzyme from substrate (8). The much larger (5,400-nucleotide) f**X174** DNA did not appear to be degraded processively, however, so there may be limits to the number of nucleotides removed in a single productive enzyme-substrate encounter (5). The values of V_{max} and the turnover number (k_{cat}), on the basis of the rates of internucleotide bond hydrolysis, are similar for the 500-nucleotide polymer described above and the minimal DNA substrate, a dinucleotide diphosphate (8). The kinetic data appear to require a **facilitated diffusion** mechanism for the activity on macromolecular substrates, in which nuclease molecules bind randomly and diffuse along the contour of the chain until a 5′ end is located, at which time catalysis can begin (8). This apparently was the first example of a requirement for facilitated diffusion in an enzymatic reaction.

The 3′ → 5′ exonuclease activity on duplex DNA and the 5′ → 3′ exonuclease activity on single-stranded DNA can account for the progressive reduction in the length of duplex DNA. Above certain nuclease concentrations, short 5′-terminated single-stranded tails from the 3′ → 5′ exonuclease activity are evident in partial digests (9). If 3′-terminated tails are present, they cannot be more than a few nucleotides in length. The 5′ tails have a limiting length, at the higher enzyme concentrations examined, of about 7 nucleotide residues when about 100 nucleotides are removed by the 3′ → 5′ exonuclease activity. Up to 50% of the ends could be joined in DNA Ligase reactions under conditions favoring the joining of fully base-paired ends. This indicates that the 5′ → 3′ exonuclease activity on single-stranded DNA can terminate at the junction between single- and double-stranded regions, to leave fully based-paired ends on a significant fraction of molecules in a partially digested population. **DNA polymerase**-mediated repair, to render ends with 5′-terminated tails fully base-paired, markedly increased the fraction of ends joinable by DNA ligase, as expected (9).

As the nuclease concentrations were decreased below those mentioned above, the average length of the single-stranded tails per 100 nucleotides removed increased dramatically, and the ligase-mediated joining of ends in the absence of polymerase-mediated repair became undetectable. This apparent dependence on the concentration of the enzyme of the relative velocities of two exonuclease reactions that it catalyzes has not been explained. The velocity of the overall reaction to shorten DNA, as measured by the hyperchromicity associated with the hydrolysis of internucleotide bonds, is proportional to enzyme concentration, as expected (17). Repair of ends generated at the low nuclease concentrations noted above with DNA polymerase rendered a high percentage of the molecules ligatable (9).

There must be an activity that can remove short 3′-terminated protruding single-stranded tails from duplex DNA, because the nuclease readily degrades such starting substrates (9). No evidence exists, however, for 3′ terminally directed hydrolysis of single-stranded DNAs (8).

The value of the Km(Michaelis constant), in terms of the molar concentration of DNA ends, for the overall exonucleolytic shortening of duplex DNA by the S form is so large that it is not practical for the substrate concentration to approach it in actual reactions. Consequently, the enzyme velocity is directly proportional to substrate concentration over the accessible range (18). A value for this K_m was reported in earlier work (5), but it appears to have been determined under conditions for which the substrate concentration did not exceed that of the enzyme, violating a premise of Michaelis-Menton-based kinetics. Kinetic parameters (V_{max} per unit concentration of nuclease and K_m) for the length reduction of duplex DNA by the F form can be measured accurately, because the K_m value is much lower than for the S form and lies in the range of experimentally accessible concentrations of DNA ends. More recent values (18) are in reasonable agreement with the earlier data (5).

These kinetic parameters for the F nuclease depend on the length of the DNA substrate (7) (not determinable for the S form as noted). This has been shown (7) to be consistent with a model in which nonspecific binding of the nuclease away from the ends is followed by a “search” process to form a productive enzyme-substrate complex, with the enzyme bound to a terminus, as for the degradation of single-stranded DNA. However, such a mechanism is not required by the kinetics as in the case of single-stranded DNA (noted in the text above).

The kinetics of length reduction of duplex DNA are also dependent on its guanine + cytosine(G + C) content (7, 18). This is significant in the case of the S form of the nuclease, for which the rate of nucleotide removal from DNA ends decreases over fourfold over the range of 37–66 mole% G + C residues. This dependence is somewhat less for the F enzyme. Data are available to predict these effects of DNA base composition on the kinetics (18).

In contrast to the high processivity for the 5′ → 3′ exonuclease action on single-stranded DNA noted earlier, the 3′ → 5′ exonuclease is quasi-processive, removing only about 18 and 28 nucleotide residues per productive binding event for the S and F enzymes, respectively (9).

The length reduction of duplex RNA (16) presumably proceeds by a similar mechanism but has not been characterized. The BAL 31 nucleases are the most efficacious enzymes known for the controlled length reduction of duplex DNA, and they are apparently the only enzymes that can catalyze this reaction for duplex RNA.

Duplex DNA is not attacked endonucleolytically (away from an end) at a significant rate unless there is some alteration of the duplex structure. Hence, nonsupercoiled, closed circular duplex DNA (form I° DNA) is extremely resistant to attack by the BAL 31 nucleases (11, 13, 14). The very limited attack on form I° DNA at high enzyme concentrations and long incubations (14), plus the kinetic parameters for exonucleolytic degradation of linear duplex DNA, lead to estimates of the relative rates of introduction of endonucleolytic breaks to exonucleolytic scissions of 8×10^{-11} and 7×10^{-12} for the S and F enzymes, respectively.

Negative supercoiling in closed circular DNA can elicit the endonuclease activity (12). In the majority of molecules of such supercoiled DNA, an endonucleolytic event (cleavage in one strand) is followed by the removal, in a processive manner, of several nucleotides (6.5 and 2.8 nucleotides for the F and S forms, respectively) from the initially nicked strand, to yield a gapped circular DNA intermediate (15). A fraction contain only a strand break, and no nucleotides are excised. The percentage of molecules with no nucleotides removed is significantly lower for the F nuclease than for the S species. The nicks and gaps are bounded by 5′-phosphoryl and 3′-hydroxyl termini. It is assumed that other alterations that result in endonucleolytic attack give rise to such gapped circular intermediates.

The removal of a small number of nucleotides could be accomplished exonucleolytically, starting from the site of the initial nick. Or, there could be a second endonucleolytic cut a few nucleotides away from the first one; the short oligonucleotide between endonucleolytic breaks would dissociate at room temperature to leave a gap. Available evidence supports the exonucleolytic mechanism. It was reasoned that the presumed exonucleolytic activity producing the gaps should be 3′ → 5′–directed, as the exonucleolytic activity attacking base-paired ends has this characteristic. However, this proved to be inconsistent with the results of further experiments carried out assuming the 3′ → 5′ mode of attack; the 5′ → 3′ attack is thus inferred. Because this activity operates on nominally duplex DNA, it might be expected that it could remove nucleotides in a 5′ → 3′ direction from fully based-paired ends, to leave 3′-terminated single-stranded ends. It was noted that, if these are present, they could not be more than a few nucleotides in length, but this does not rule out very limited activity comparable to that producing the gaps.

The nicked and gapped circular DNA intermediates are then converted to linear duplex DNA by a second endonucleolytic event in the other strand, which requires a second encounter with a nuclease molecule (15). The resulting linear duplex DNA is further degraded by the mechanism noted in the text above. As expected, circular duplex DNA containing a nick introduced by means other than BAL 31 nuclease action is converted to linear duplex DNA, with the occurrence of gaps of the average sizes noted above in most of the circular molecules before their linearization (15).

3. Effects of Solvent Variables and Denaturing Agents

Both Ca^{2+} and Mg^{2+} at concentrations above 10–12 mM are required for maximum activity on both single- and double-stranded substrates (9). All activities are optimal near neutral pH (4, 9). The nucleases are remarkably resistant to inactivation at elevated salt concentrations (4, 10). The reaction buffer in which most of the work described above was done contained 0.6 M NaCl). This salt tolerance is not surprising, considering that sea water is the natural milieu of these extracellular enzymes.

High concentrations of agents that normally **denature** proteins fail to eliminate the nuclease activities. Single-stranded DNA is degraded at 40% of the maximum rate in 6.5 M urea (4), and substantial activity on this substrate was found in the presence of 6 M **guanidinium** chloride. Crude preparations maintained activity against both single- and double-stranded substrates in the presence of 5% (w/v) SDS (3). At least a portion of the structure of the S nuclease does not become disrupted under the stringent denaturation conditions used for denaturing SDS-PAGE (6).

The nucleases are not remarkably resistant to thermal inactivation, as the half-life for disappearance of the activity on single-stranded DNA is only 3–5 minutes at 50°C (7). However, tests on preparations stored at 4°C imply that most of the activity should be retained for years in a buffer containing 5 mM Mg^{2+} and Ca^{2+} (4). Commercial preparations are often supplied in 50% (v/v) glycerol for storage at –20°C , under which conditions they should retain full activity indefinitely.

4. Applications

By far the most extensive use of the BAL 31 nucleases, represented by hundreds of literature citations, has been the controlled length reduction of linear duplex DNA. The bulk of these reports describe the production of deletion mutants and/or the elucidation of sequences required for a particular biological activity of a (usually) cloned DNA segment. Cloned sequences can be deleted unidirectionally by cleavage of the vector containing the cloned insert at a unique restriction site on one side of the insert (see Restriction Enzymes), carrying out a partial BAL 31 degradation, releasing the shortened insert from the shortened vector by use of a restriction site on the other side of the insert, and ligation to an intact linearized vector DNA (19).

Numerous reports have appeared of BAL 31 nuclease-mediated identification of **telomeric** sequences, which occur at the ends of linear eukaryotic chromosomes and hence are degraded first by the exonuclease in intact DNA; Yao and Yao (20) and De Lange and Borst (21) apparently represent the earliest work. Where these DNAs are too large to isolate as intact molecules in solution, in situ lysis in agarose has been used (22) so that the initial substrate DNA is largely intact.

The progressive removal of sequences from duplex ends allows the determination of the restriction map of a DNA, either naturally linear or linearized at a unique site, by noting the order in which fragments from subsequent digestion with the restriction enzyme in question disappear from gel electrophoresis patterns of progressively shortened aliquots (19, 23). This technique is greatly enhanced if unidirectional deletions can be done, as noted above (19), as ambiguity arising from loss of sequences from both ends of the fragment is eliminated. The sites of bound proteins, including nucleosomes, and interstrand crosslinks that block the exonuclease can be elucidated because intact duplex sequences between such sites will not be attacked (24, 25).

The endonuclease activity that cleaves in response to alterations in duplex structure has been used in several laboratories to detect such alterations. This attack will be followed by cleavage of the other strand and exonucleolytic attack from the ends thus generated, as noted in the text above. Where chemical modification is done, form I° DNA is used (this requires that the modification does not introduce nicks), and the rate of its loss on incubation with nuclease is monitored. Some of the chemical lesions that give rise to endonucleolytic attack are pyrimidine dimers and possibly other photoproducts of ultraviolet irradiation, adducts with carcinogens such as *N*-acetoxy-*N*-2-acetylaminofluorene and *N*-methyl-*N*-nitrosourea, interstrand cross-links produced by reaction with nitrous acid, apurinic sites, and adducts with Hg^{2+} and Ag^{+} ions (11, 13, 14). Strand breaks were noted in the text above as eliciting cleavage of the opposite strand. Noncovalent alterations eliciting endonucleolytic attack include moderate degrees of negative supercoiling and very high degrees of positive supercoiling (12), junctions between right-handed B-DNA and left-handed Z-DNA regions (10), the presence of unpaired nucleotides in one strand of an otherwise duplex DNA (26), and cruciform structures resulting from the extrusion of inverted repeated sequences under supercoiling stress (27, 28). **Matrix attachment sites** for **nucleolar** DNA are apparently sensitive to the nuclease (29). Finally, the lack of sensitivity of form I° DNAs has been used to help identify such species in DNA populations (30).

Bibliography

1. R. T. Espejo and E. S. Canelo (1968) J. Bacteriol. **95**, 1887–1891.
2. K. Y. Chan, L. Baumann, M. M. Garza, and P. Baumann (1978) J. Syst. Bacteriol. **28**, 217–222.
3. H. B. Gray, Jr., D. A. Ostrander, J. L. Hodnett, R. J. Legerski, and D. L. Robberson (1975) Nucleic Acids Res. **2**, 1459–1492.
4. H. B. Gray, Jr., T. P. Winston, J. L. Hodnett, R. J. Legerski, D. W. Nees, C.-F. Wei, and D. L. Robberson (1981) In *Gene Amplification and Analysis* (J. G. Chirikjian and T. S. Papas, eds.), Elsevier North-Holland, New York, pp. 169–203.
5. C.-F. Wei, G. A. Alianell, G. H. Bencen, and H. B. Gray, Jr. (1983) J. Biol. Chem. **258**, 13506–13512.
6. C. R. Hauser and H. B. Gray, Jr. (1990) Arch. Biochem. Biophys. **276**, 451–459.
7. T. Lu (1992) *Some physical and catalytic properties of BAL 31 nuclease, Ph.D. dissertation*, University of Houston, Houston, Texas.
8. T. Lu and H. B. Gray, Jr. (1995) Biochim. Biophys. Acta **1251**, 125–138.
9. X.-G. Zhou and H. B. Gray, Jr. (1990) Biochim. Biophys. Acta **1049**, 83–91.
10. M. W. Kilpatrick, C.-F. Wei, H. B. Gray, Jr., and R. D. Wells (1983) Nucleic Acids Res. **11**, 3811–3822.
11. R. J. Legerski, H. B. Gray, Jr., and D. L. Robberson (1977) J. Biol. Chem. **252**, 8740–8746.
12. P. P. Lau and H. B. Gray, Jr. (1979) Nucleic Acids Res. **6**, 331–357.
13. C.-F. Wei, G. A. Alianell, H. B. Gray, Jr., R. J. Legerski, and D. L. Robberson (1983) In *DNA Repair: A Laboratory Manual of Research Procedures* (E. C. Friedberg and P. C. Hanawalt, eds.), vol. **2**, pp. 13–40.
14. C.-F. Wei, R. J. Legerski, G. A. Alianell, D. L. Robberson, and H. B. Gray, Jr. (1984) Biochim. Biophys. Acta **782**, 404–414.
15. A. Przykorska, C. R. Hauser, and H. B. Gray, Jr. (1988) Biochim. Biophys. Acta **949**, 16–26.
16. G. H. Bencen, C.-F. Wei, D. L. Robberson, and H. B. Gray, Jr. (1984) J. Biol. Chem. **259**, 13584–13589.
17. X.-G. Zhou (1989) *Ethidium bromide-mediated renaturation of denatured closed circular DNAs in alkaline solution: mechanistic aspects and fractionation of closed circular DNAs on a molecular weight basis. Some catalytic properties and mechanism of exonuclease action of BAL 31 nuclease, Ph.D. dissertation*, University of Houston, Houston, Texas.
18. H. B. Gray, Jr. and T. Lu (1993) In *Enzymes of Molecular Biology* (M. M. Burrell, ed.), Humana Press, Totowa, New Jersey, pp. 231–251.
19. C. R. Hauser and H. B. Gray, Jr. (1991) Gene Anal. Tech. Appl. **8**, 139–147.
20. M.-C. Yao and C. H. Yao (1981) Proc. Natl. Acad. Sci U.S.A. **78**, 7436–7439.
21. T. De Lange and P. Borst (1982) Nature **299**, 451–453.
22. R. F. Wintle, T. G. Nygaard, J. A. Herbrick, K. Kvaloy, and D. W. Cox (1997) Genomics **40**, 409–414.
23. R. J. Legerski, J. L. Hodnett, and H. B. Gray, Jr. (1978) Nucleic Acids Res. **5**, 1445–1464.
24. W. A. Scott, C. F. Walter, and B. L. Cryer (1984) Mol. Cell. Biol. **4**, 604–610.
25. W.-P. Zhen, O. Buchardt, H. Nielsen, and P. E. Nielsen (1986) Biochemistry **25**, 6598–6603.
26. D. H. Evans and A. R. Morgan (1982) J. Mol. Biol. **160**, 117–122.
27. L. H. Naylor, H. A. Yee, and J. H. van de Sande (1988) J. Biomol. Struct. Dyn. **5**, 895–912.
28. N. M. Morales, S. D. Coburn, and U. R. Muller (1990) Nucleic Acids Res. **18**, 2777–2782.
29. O. V. Iarovaia, M. A. Lagarkova, and S. V. Razin (1995) Biochemistry **34**, 4133–4138.
30. E. Cuzzoni, L. Ferretti, C. Giordani, S. Castiglione, and F. Sala (1990) Mol. Gen. Genet. **222**, 58–64.

Suggestions for Further Reading

31. H. B. Gray, Jr., T. P. Winston, J. L. Hodnett, R. J. Legerski, D. W. Nees, C.-F. Wei, and D. L. Robberson (1981) "The extracellular nuclease from *Alteromonas espejiana*: an enzyme highly specific for nonduplex structure in nominally duplex DNA", In *Gene Amplification and Analysis* (J. G. Chirikjian and T. S. Papas, eds.), Elsevier North-Holland, New York, pp. 169–203.
32. H. B. Gray, Jr. and T. Lu (1993) "The BAL 31 nucleases (EC 3.1.11)", In *Enzymes of Molecular Biology* (M. M. Burrell, ed.), Humana Press, Totowa, New Jersey, pp. 231–251.

Balbiani Ring

The polytene chromosomes of insects have extraordinary utility in the investigation of **chromosomal** structure and function. Polytene chromosomes display the phenomenon of puffing in which the chromatin associated with chromosomal bands is decondensed. In the larval salivary glands of the midge *Chironomus*, several puffs become very large and are described as *Balbiani rings* . Balbiani is the cytologist who discovered polytene chromosomes in 1881. The visible aspect of a puff is essentially the complex of **RNA** and protein that accumulates as a result of vigorous **transcriptional** activity. Among the gene products encoded by the Balbiani rings are the glue proteins required to attach the midge pupa to its substrate. All of the Balbiani ring genes are expressed coordinately and maximally during the second larval instar. Then they show differential expression in prepupae (1). The most detailed ultrastructural analysis has been performed on Balbiani ring 2 in chromosome IV of *Chironomus tentans*. Although the polytene chromosome band itself contains more than 470 kbp of DNA, the major gene is 37 kbp long and contains two very well-defined transcription units that are differentially expressed at the prepupal stage. Electron microscopy detects the first engaged **RNA polymerase** molecule at the approximate start site of transcription and the last RNA polymerase at the site of termination (2, 3). Within each puff, the Balbiani ring gene forms a loop of transcriptionally active chromatin with attached ribonucleoprotein complexes. As synthesis proceeds, the nascent transcripts fold up into compact ribonucleoprotein complexes that head toward the **nuclear pores** when they are exported to the cytoplasm. Each 37-kb pre-mRNA transcript is processed in the nucleus by staged association with specific proteins (4).

Contour measurements of chromosomal structure in the puff indicate that the chromatin is fully extended into an array of nucleosomes 10 nm in diameter at the site of transcription, whereas once transcription is completed, chromatin coils back up into a 30-nm diameter fiber, which is then finally packaged into a supercoiled loop. Upstream of the start site of transcription is a region free of nucleosomes, presumably corresponding to the **promoter**, and compacted chromatin fibers are further upstream and downstream of the gene. Immunologic analysis allows defining the structural components of chromatin on active and inactive segments of the Balbiani ring. Surprisingly, proteins, such as histone H1 and the core histones, remain on chromatin even while it is actively transcribed (5). Thus keen observation allows a rather complete ultrastructural picture of the transcription process.

Bibliography

1. U. Lendahl and L. Weislander (1987) Develop. Biol. **121**, 130–138.
2. B. Bjorkroth, C. Ericsson, M. M. Lamb, and B. Daneholt (1988) Chromosoma **96**, 333–340.
3. C. Ericsson et al. (1989) Cell **56**, 631–639.
4. H. Mehlin, B. Daneholt, and U. Skoglund (1992) Cell **69**, 605–613.
5. C. Ericsson, U. Grossbach, B. Bjorkroth, and B. Daneholt (1990) Cell **60**, 73–83.

Suggestion for Further Reading

6. B. Daneholt (1997) A look at messenger RNP moving through the nuclear pore. Cell **88**, 585–588.

Barnase and Barstar

Barnase is a **ribonuclease** secreted by the bacterium ***Bacillus*** *amyloliquefaciens*. It is a small protein of 110 amino acid residues with no disulfide bonds or nonpeptide components (see Protein Structure). As such, it was recognized in the early 1960s to be an ideal subject for the then-emerging study of **protein folding**. Its specific inhibitor, barstar, is produced intracellularly by the same organism and is an equally simple and even smaller protein of only 89 residues. Together they form a two-subunit complex in which the active site of barnase is buried, providing a model system for the study of protein–protein interactions. The system has contributed substantially to our understanding of how proteins fold and interact and has potential for further uses.

The three-dimensional structures of both proteins and their complex have been determined (Fig. 1) (1). The genes for both proteins have been **cloned** into **plasmid vectors** in ***Escherichia*** *coli* and the expressed products obtained in high yield. Expression of barnase alone is lethal, so simultaneous expression of barstar is necessary for production of barnase.

Figure 1. Molscript (1) representation of the structures (**a**) barstar and (**b**) barnase in their complex.

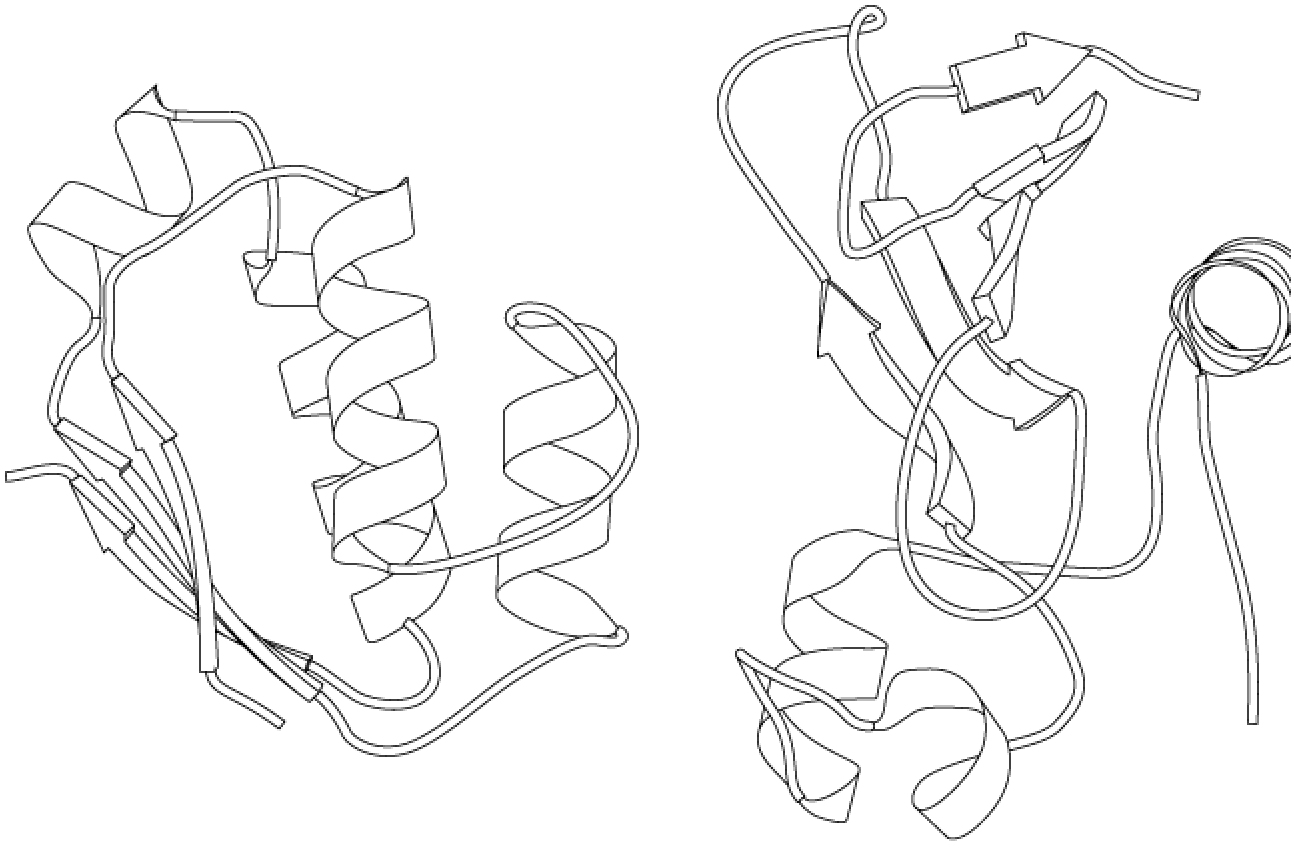

(a) (b)

The catalytic mechanism of barnase and its relatives is essentially the same as that of the pancreatic ribonuclease family (see **Ribonuclease A**), with a histidine and a glutamic acid residue acting respectively as proton donor and acceptor, in place of the two histidines of the latter. The barnase active site lies in a broad groove on the side of the b-sheet opposite the major **a-helix** (see Fig. 1). In the complex, which has a **dissociation constant** on the order of 10^{-14} M, barstar completely blocks the active site, with most of its contacts involving its second helix and an adjacent loop. An aspartic acid carbonyl group of barstar occupies the position of the attacked phosphate group of substrate RNA. The rate at which barnase and barstar associate is controlled largely by charged groups, positive on barnase, negative on barstar. Mutation to alanine of any of these charged residues reduces binding but increases the stability of each protein, indicating the evolutionary balance between function and stability.

Both barnase and barstar may be unfolded reversibly by heat or by **denaturants** such as urea or **guanidinium chloride** (see **Protein unfolding**). Both fold and unfold in a highly **cooperative** two-state manner; that is, only the native and unfolded states are significantly occupied at **equilibrium** under most conditions. During the kinetics of folding, however, barnase passes through an observable intermediate state. In this it exemplifies the behavior of most larger proteins or protein **domains** (see **Protein folding**). Barstar, on the other hand, appears to collapse more directly to the folded state, as do most other smaller proteins. Studies of barnase folding, using kinetic and equilibrium techniques and site-directed mutagenesis, have traced the order in which its parts come together to form the native fold and have estimated the free energies of various interactions in several states that occur during folding.

Barnase is a member of a large family of microbial ribonucleases that share the same basic tertiary structure but have quite divergent sequences; this provides a wider system for approaching the central problem of how the fold is determined by the sequence (see Protein Structure Prediction).

The homologous ribonucleases of the *Streptomyces* share less than 25% sequence identity with barnase, but the structure of the active-site region is so well conserved that these enzymes are also inhibited by barstar, with dissociation constants as low as 2×10^{-12} *M*; consequently, coexpression of barstar permits the high level expression of the cloned genes for these enzymes as well. As the *Streptomyces* also produce barstar homologues, it seems clear that the extreme structural conservatism of the active site of the ribonucleases is based on the strict requirement of strong binding to the inhibitor.

Separate from the continuing application of barnase and barstar as small model proteins to general problems of protein structure and chemistry are more recent uses of their genes that take advantage of the toxic effect of barnase expression in tissues of heterologous organisms. Under control of a specific **promoter**, expression of the barnase gene can ablate cells under conditions or in tissues where the promoter is turned on. This property is being applied, for example, in studies of development, strategies against **viruses**, design of a conditionally lethal selective **cloning vector**, and, most spectacularly, in the development of male-sterile **plants**. In the last instance, male sterility can be reversed by inclusion of the barstar gene.

There have been several efforts at **computer simulation** of aspects of barnase folding and unfolding, and more can be expected. The continued application of directed mutagenesis, physical chemistry, and computer modeling to the folding mechanisms of barnase and barstar and their homologues will provide insight into the manner in which the sequences of these two interdependent families of proteins determine their native folds. *In vivo* use of the barnase gene, with its lethal effect limited to specific conditions or tissues, will be useful to developmental biologists and should have many practical applications in agriculture and possibly in medicine as well.

Bibliography

1. P. Kraulis (1991) J. Appl. Crystallog. **24**, 946–950.

Suggestions for Further Reading

2. R. W. Hartley (1997) "Barnase and Barstar", in *Ribonucleases, Structure and Functions* (G. D"Alessio and J. F. Riordan, eds.), Academic Press, New York, pp. 51–100. (Contains an exhaustive bibliography through 1995.)
3. A. Matouschek, L. Serrano, and A. R. Fersht (1994) "Analysis of protein folding by protein engineering", in *Mechanisms of Protein Folding* (R. H. Pain, ed.), IRL Press, Oxford, pp. 137–159.

Barr Body

In eutherian (placental) mammals, **dosage compensation** mechanisms operate in female cells to silence one of the two **X-chromosomes**, so that female cells have as many X-chromosome-derived transcripts as male cells containing a single X-chromosome. This **X-chromosome inactivation** process was first proposed by Mary Lyon (1961) and is known as the **Lyon hypothesis** (1). Female mammalian embryos begin development with two active X-chromosomes, but very early in embryogenesis almost all of the genes on one of the two X-chromosomes become inactivated Random X-Inactivation). Although the initial choice between inactivation of the maternal or paternal X-chromosome is random, once established in a repressed state the same X-chromosome are inactivated after every cell division. The inactivation process occurs over the entire chromosome, and practically all of the genes on the chromosome are silenced. This transcriptional inactivation is concomitant with the chromosome taking on the appearance of **heterochromatin** and also becoming late replicating during **S phase** (see Facultative Heterochromatin). Only a small fraction of the inactive X-chromosome, including the genes located in the pseudoautosomal region at Xp22.3, escapes the global silencing process (2). The inactive chromosome remains in the nucleus and can be detected cytologically as a *Barr body* in somatic cells (3). The Barr body is found only in cells containing more than one X-chromosome, if cells are trisomic for the X-chromosome, two Barr bodies will be detected. The staining procedures used to detect Barr bodies argue for a global difference in chromatin condensation (4). Differences in staining of heterochromatin compared to transcriptionally competent **euchromatin** may be caused by differences in compaction or differences in the association of many more accessory proteins in heterochromatin (5).

The use of advanced microscopy and molecular **cytogenetics**, in which fluorescent ***in situ* hybridization** is used to "paint" chromosomal territories, has recently allowed detailed dissection of chromosomal organization (see Denaturation Mapping. Light microscopic optical serial sectioning of the active and inactive X-chromosome territories reveal that they occupy similar volumes. However, reconstructed active X-chromosomes have a flatter shape and a more extended, folded surface area than the inactive X-chromosome (6). The conclusion is that the differential staining properties of the Barr body are caused mainly by the association of a distinct group of accessory proteins and RNA with this inactive chromosome (see X-Chromosome Inactivation).

Even on the active X-chromosome, most of the chromatin is not transcriptionally active. Thus, on both the inactive and the active X-chromosomes, the great majority of the chromatin is maintained in a folded state typical of a transcriptionally repressed state. There are, however, global differences in chromatin organization between active and inactive X-chromosomes. The inactive X chromosome has high overall nucleosomal density—i.e., it carries a higher "concentration" of all histones, including the unusual variant macroH2A, than all autosomes or the active X (7). This likely contributes to the optical density of the Barr Body as visualized microscopically. The Barr body contains methylated DNA, hypoacetylated histones, a specialized structural RNA (Xist), and is late replicating during the S phase. Association with Xist RNA is an important causal factor in X-inactivation, and somehow leads to the selective hypermethylation of the inactive X, which results in deacetylation of chromatin assembled over it and transcriptional quiescence. The three-dimensional distribution in the nucleus of Xist RNA coincides with the chromosomal territory occupied by the inactive X-chromosome (8). Even after removing bulk chromatin in the preparation of a nuclear matrix (which is responsible for the overall morphology of the nucleus), the Xist RNA remains in the matrix. This is consistent with the hypothesis that Xist RNA has a structural role in establishing the inactive X-chromosome territory. The Barr body still has a great deal to teach scientists about the molecular mechanisms that establish and maintain nuclear compartments.

Bibliography

1. M.F. Lyon, Nature **190**, 372–373 (1961).
2. C.M. Disteche, Trends Genet. **11**, 17–22 (1995).
3. M.L. Barr and E.G. Bertram, Nature **163**, 676–677 (1949).
4. S.M. Gartler and A.D. Riggs, Annu. Rev. Genet. **17**, 155–190 (1983).
5. S.W. Brown, Science **151**, 417–425 (1966).
6. R. Eils et al., J. Cell Biol. **135**, 1427–1440 (1996).
7. Perche P.Y. et al., Curr. Biol. **10**, 1531–1534 (2000).
8. C.M. Clemson, J.A. McNeil, H.F. Willard, and J.B. Lawrence J. Cell Biol. **132**, 259–275 (1996).

Additional Reading

9. CremerT. et al., Role of chromosome territories in the functional compartmentalization of the

cell nucleus, Cold Spring Harbor Symp. Quant. Biol. **58**, 777–792 (1993).
10. BirdA.P. and WolffeA.P., Cell **99**, 451–454 (1999).
11. PanningB. and JaenischR., Cell **93**, 305–308 (1998).
12. CsankovskyG., NagyA., and JaenischR., J. Cell Biol. **153**, 773–783 (2001).

Base Excision Repair

Base excision repair is the DNA repair system for abnormal bases in DNA, such as uracil, hydroxymethyluracil, and hypoxanthine, and for nonbulky base modifications, such as thymine glycol and hydrates, 8-hydroxyguanine, O^4-methylthymine, and 3-methyladenine (Fig. 1). The abnormal bases and simple base lesions are removed from DNA by the combined actions of DNA glycosylases (1-3) and AP (apurinic/apyrimidinic) endonucleases. The basic reaction carried out by glycosylases is the cleavage of the glycosylic bond joining the base to deoxyribose. Some of the glycosylases cleave both the glycosylic bond and the phosphodiester bond 3′ to the resulting AP site in a more or less concerted reaction. Hence, DNA glycosylases have been classified either as "pure" glycosylases or as glycosylase/AP lyases. AP endonucleases are also classified as either 3′- or 5′-AP endonucleases. All 3′-AP endonucleases are lyases that cleave the phosphodiester bond by b-elimination. The 5′-AP endonucleases carry out true hydrolysis.

Figure 1. Repair of 3-methyl adenine by base excision repair. Methyladenine DNA glycosylase cleaves the glycosylic bond of the alkylated base; this releases the alkylated base and leaves an AP site. An AP lyase and an AP endonuclease cleave 3′ and 5′, respectively, of the AP site, releasing the abasic sugar. The resulting gap is filled in by Pol I in *E. coli* and by Pol b or Po ld and e in humans, to produce repair patches of 1 to 10 nucleotides.

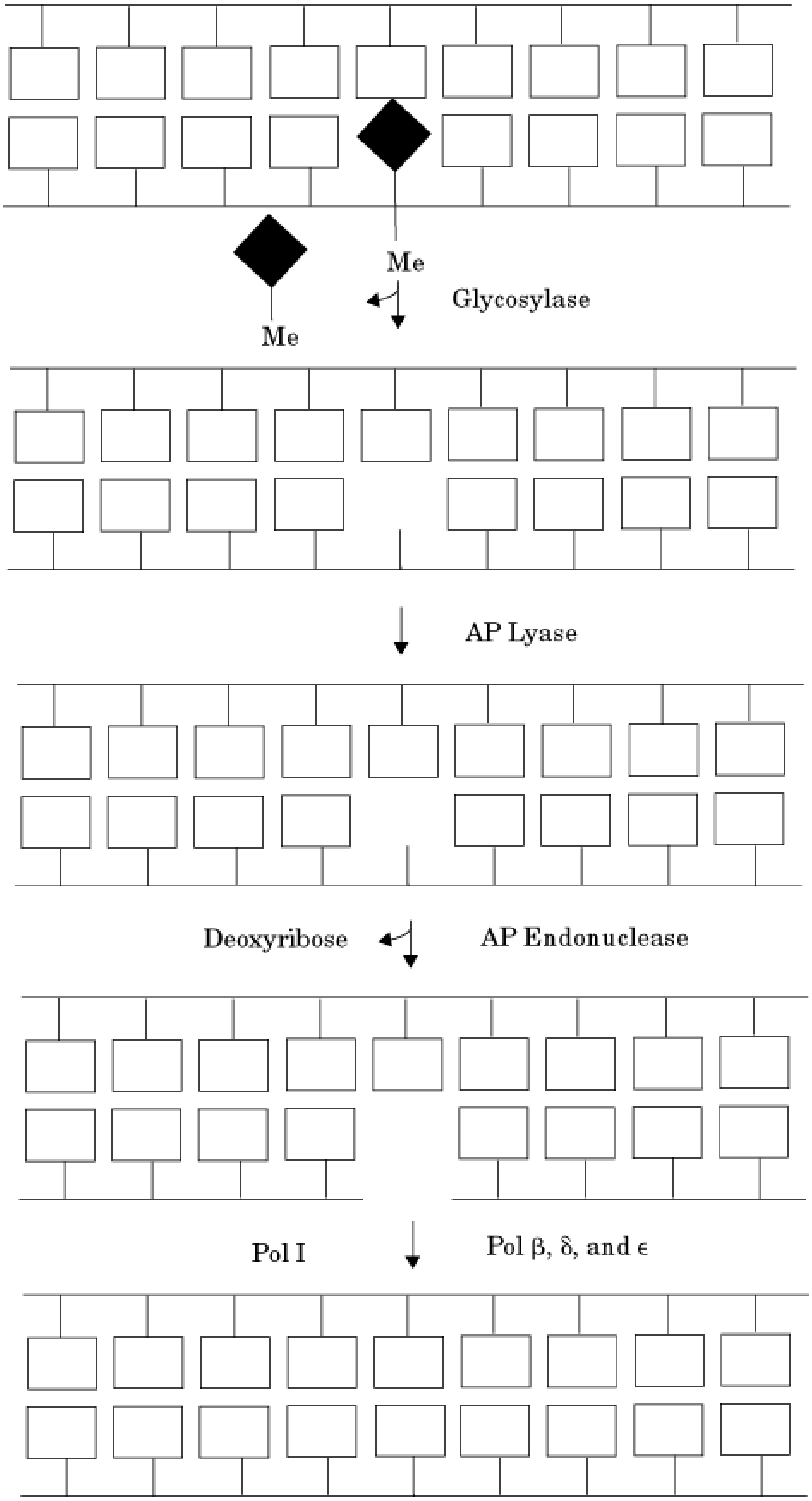

The combined actions of glycosylase, AP lyase, and AP endonuclease/exonuclease creates a one- to two-nucleotide gap in the damaged strand. This gap is filled in by **DNA polymerase** I in *Escherichia* *coli*, and mostly by DNA polymerase b (4) and to a lesser degree by DNA polymerases d and ε in yeast and humans (5). The resulting nick is ligated by DNA Ligase in *E. coli*, and in eukaryotes by the ligase I– (6) or ligase III–XRCC1 complex (7). Depending on the polymerase/ligase combination involved in filling in and sealing the gap, a repair patch of 1 to 10 nucleotides may be produced.

Bibliography

1. T. Lindahl (1974) Proc. Natl. Acad. Sci. USA **71**, 3649–3653.
2. T. Lindahl (1976) Nature **259**, 64–66.
3. J. Laval (1977) Nature **269**, 828–832.
4. R. W. Sobol, J. K. Horton, R. Kohn, H. Gu, R. K. Singhal, R. Prasad, K. Rajewsky, and S. H. Wilson (1996) Nature **379**, 183–186.
5. Z. Wang, X. Wu, and E. C. Friedberg (1993) Mol. Cell. Biol. **13**, 1051–1058.
6. R. Prasad, R. K. Singhal, D. K. Srivastava, J. T. Molina, A. E. Tomkinson, and S. H. Wilson (1996) J. Biol. Chem. **271**, 16000–16007.
7. K. W. Caldecott, C. K. McKeown, J. D. Tucker, S. Ljungquist, and L. H. Thompson (1994) Mol. Cell. Biol. **14**, 68–76.

Suggestions for Further Reading

8. B. Demple and L. Harrison (1994) Repair of oxidative damage to DNA: enzymology and biology. Annu. Rev. Biochem. **63**, 915–948.
9. E. Seeberg, L. Eide, and M. Bjoras (1995) The base excision repair pathway. Trends Biochem. Sci. **20**, 391–397.

Base Pairs

DNA exists predominantly as an antiparallel double-stranded helix. The two strands are helically coiled, which maximizes the exposure of the negatively charged sugar–phosphate backbone to water and shields the **hydrophobic** aromatic bases in the middle from water. Figure 1 shows the Watson–Crick base pairs in which the specificity of base pairing is provided by hydrogen bonds. The complementary arrangements of hydrogen bond donors and acceptors allow the Watson–Crick base pairing of guanine with cytosine (G:C) and adenine with thymine (A:T). The two C1′ atoms within a G:C base pair and an A:T base pair are equidistant (~10.5 Å). It should be noted that other types of base pairs are also known to exist, and they often are involved in unusual DNA structures.

Figure 1. Schematic illustration of the A:T and G:C Watson–Crick base pairs. Hydrogen bonds are shown as dashed line Hydrogen bond donors (gray arrow) and acceptors (white arrow) of the bases are shown. Note that the bases can pair in more than one way. Hydrophobic edges of the base pairs are emphasized by gray shade. The major and minor groove edges of the base pair are shown.

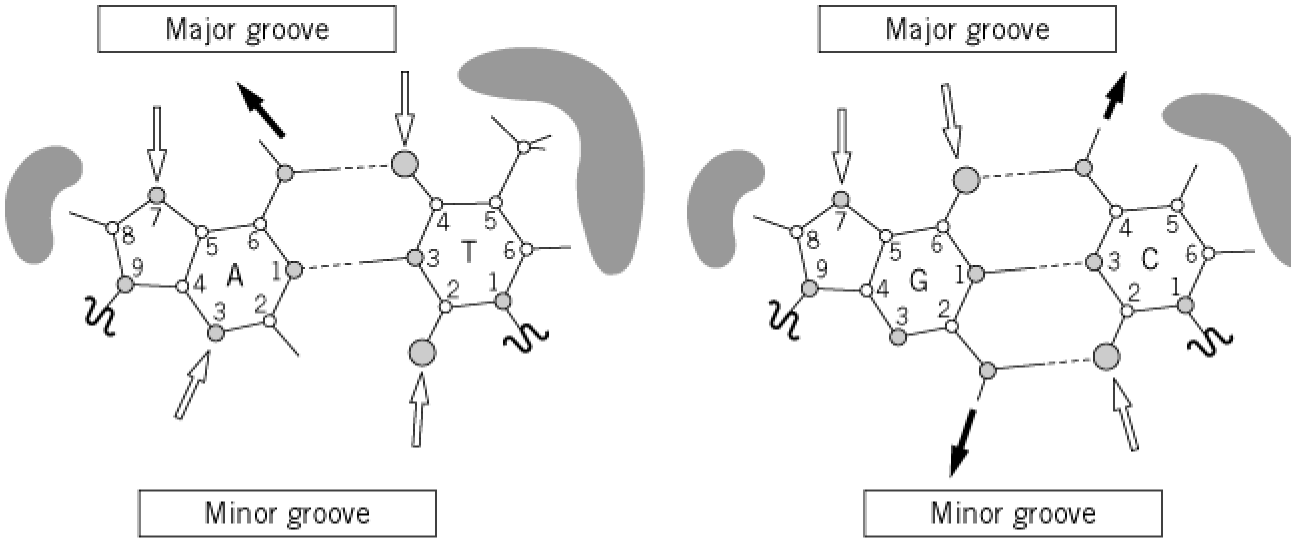

Bases in a DNA double helix are stacked on top of each other. The stacking interaction is stabilized by the electronic p━p interaction of the aromatic rings, and it also minimizes the exposure of the bases to the solvent. The base stacking has preferred interactions, depending on the characteristic dipole–dipole interactions between adjacent base pairs. Thus, the stacking patterns vary with the helix type and the particular base–base step. In B DNA, the 5′-purine-*p*-pyrimidine-3′ (Pu-Py) base-pair step has a good stacking overlap, and is thus more stable, whereas the 5′-pyrimidine-*p*-purine-3′ (Py-Pu) base-pair step has a poor stacking overlap, and is thus less stable (Figure 2). Such differences in stacking energy have strong implications in the bendability of DNA associated with protein binding. It has been noted that DNA sequences with Py-Pu steps in B-DNA are deformed more easily; therefore steps such as CpG, TpA, or TpG (=CpA) are often associated with kinked DNA structures.

Figure 2. Stacking interactions in B-DNA (left) and Z-DNA (right) showing Pu-Py step stacking (top) and Py-Pu step stacking (bottom). The circle shows the position of the helix axis. Note that the Py-Pu steps (including CpG, TpA, and CpA (=TpG)) in B-DNA have very small stacking interactions, causing those steps to be easily deformed.

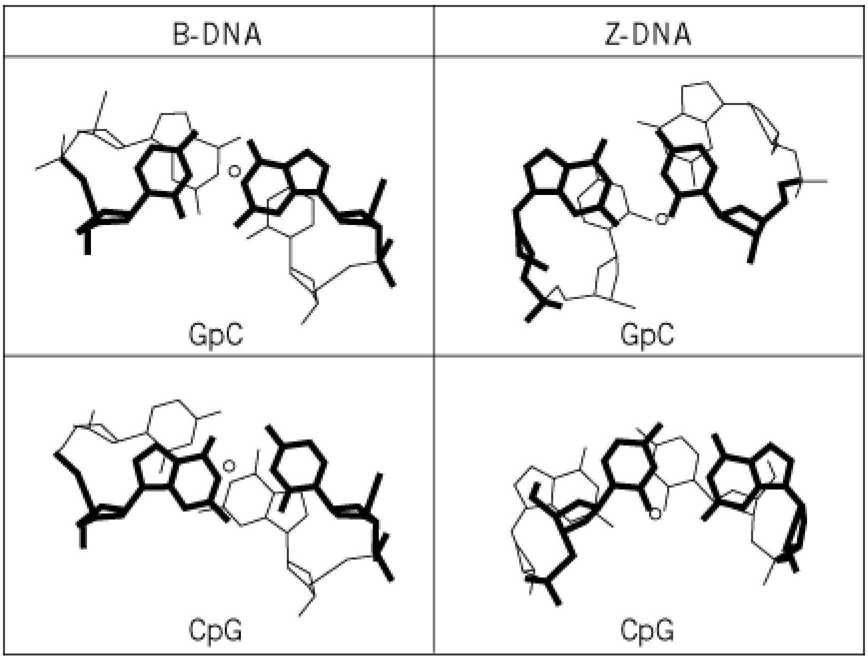

Through the high resolution X-ray structures of DNA oligonucleotides, it has been found that base pairs within a DNA duplex (or other structures) have significant departures from a strict coplanar geometry. The conformational parameters associated with the DNA base pairs are defined in Figure 3. For a more complete definition, the reader is referred to the Cambridge Convention (1).

Figure 3. Definitions of various base pair conformations. (upper two rows) or two successive base pairs (bottom row). In the top row the motions of the bases are coordinated, while in the middle row their motions are opposed. The left, center, and right columns describe rotations about the *z*, *y*, and *x* axes, respectively. The standard coordinate frame is defined at the upper left.

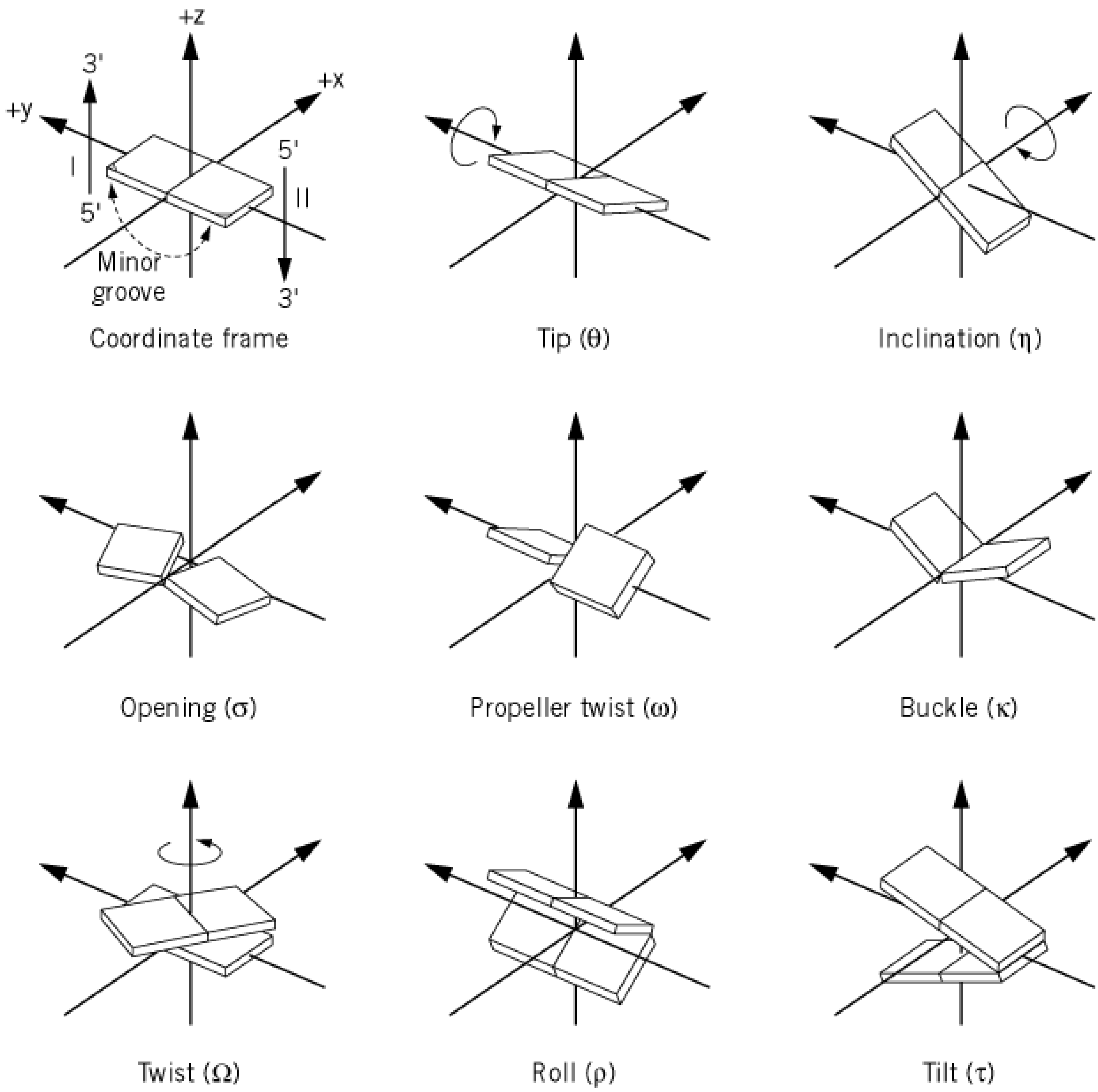

Bibliography

1. R. E. Dickerson et al. (1989) EMBO J. **8**, 1–4.

Base-Pair Substitution

These mutations of DNA affect only one base pair at a time, possibly producing either amino acid substitutions or chain termination codons in a gene (see Genetic Code). Amber (UAG), ochre (UAA), and UGA codons will all terminate polypeptide synthesis (see Stop Codons). Amino acid substitutions often produce leaky and/or **temperature-sensitive** mutations, whereas chain-terminating mutants are usually nonleaky. It has been suggested that there is an important difference between the consequences of frameshift and base-pair substitution mutations in diploid organisms. Frameshifts are often **recessive**, whereas base-pair substitution mutations may exert partial **dominance** (1).

Freese (2) divided base-pair substitutions into two classes, *transitions* and *transversions*. Transitions are mutations in which the purine–pyrimidine orientation is conserved; that is, a purine is replaced by another purine, a pyrimidine by another pyrimidine. The eight possible transversion mutations in double-stranded DNA are: A.T ↔ T.A; T.A ↔ G.C; G.C ↔ C.G; C.G ↔ A.T. Transition mutations have the purine–pyrimidine orientation conserved, as in A.T ↔ G.C or C.G ↔ T.A.

Transitional mutations have been traditionally considered to be due to **tautomerism** of nucleotides. All of the four common DNA bases can exist in tautomeric forms, of which the biologically most interesting involve keto–enol pairs for thymine and guanine and amino–imino pairs for cytosine and adenine. The tautomer, although obeying the usual purine–pyrimidine pairing rules, is capable of hydrogen bonding with a base that is normally noncomplementary. If this occurs and is not repaired, it will lead directly to base-pair substitution mutagenesis in subsequent cell generations. Some base analogues are highly mutagenic, presumably through direct incorporation into DNA through mispairing with a normal base in a tautomeric form (see 2-Aminopurine (AP), 5-Bromouracil). Some DNA alkylating chemicals may be mutagenic through adding an alkyl group onto a normal nucleotide base, thereby affecting its base-pairing properties in subsequent rounds of replication (see Dimethyl Sulfate (DMS)). Such premutagenic events will be fixed at a low level during subsequent rounds of replication, typically leading to transition mutations of various types.

Bibliography

1. C. Wills (1968) Proc. Natl. Acad. Sci. USA **61**, 937–944.
2. E. Freese (1959) Brookhaven Symp. Biol. **12**, 63–73.

Bence-Jones Proteins

By the middle of the nineteenth century, a British physician made a curious observation on the urine of a patient suffering from a bone disease (in fact, a multiple myeloma). Perhaps because his name was Dr. Watson, this practitioner was curious. So, once back home he heated the urine and observed the formation of a precipitate at 60°C, which redissolved upon boiling. Because he was also clever, he realized that this was not normal, but could not provide any explanation. He thus sent a sample to a member of the faculty in London, Dr. Henry Bence-Jones, who not only confirmed the fact but also gave the answer. The mysterious substance was tagged as "hydrated albumin deutoxide." Dr. Watson was certainly pleased with the answer, but was forgotten. Dr. Bence-Jones became immortal, although the nature of the Bence-Jones protein (BJP) remained a puzzle until it was solved by Edelman and Gally (1), who showed, more than a century later, that BJP were the free form of the monoclonal immunoglobulin light chain that is associated with a heavy chain in the corresponding myeloma protein.

BJPs have been of great interest for quite a while because they are present in large amounts in urine of most patients with multiple myeloma, thus providing a simple source of monoclonal materials, perfectly suitable for structural analysis of light chains, including amino acid sequencing. The first two sequences were obtained by Hilschmann and Craig in (2) in 1965 for two BJPs of the k isotype, giving the first evidence that immunoglobulin chains contained **variable** and **constant** regions. In normal physiological situations, the synthesis rates of the heavy and light chains are similar, whereas they are most often imbalanced in malignant conditions. In most cases of multiple myeloma, an excess of light chain is produced and secreted, quite often as **disulfide-bonded** dimers, causing an associated kidney disease. The presence of BJP is still a valid sign for the diagnosis and prognosis of multiple myeloma.

In the mouse, an equivalent disease may be induced, at a frequency dependent upon the strain, with a high response in BALB/c, as shown by Potter (3). In the mouse too, BJPs are present in the urine of animals that develop a plasmacytoma. Because the tumor may be transplanted for generations and produce unchanged myeloma proteins and BJP, this provided most of the materials that allowed the immunologists to solve the basic features of immunoglobulin structure and to open the way to monoclonal antibodies, as well as the key to Ig genes and thus to the elucidation of the genetic basis for antibody diversity.

See also entries Antibody, Immunoglobulin, and l) Light Chains.

Bibliography

1. G. M. Edelman and J. A. Gally (1962) The nature of Bence-Jones proteins. Chemical similarities to chains of myeloma globulins and normal -globulins. J. Exp. Med. **116**, 207–227.
2. N. Hilschmann and L. Craig (1965) Amino acid sequence studies with Bence-Jones proteins. Proc. Natl. Acad. Sci. USA **53**, 1403–1409.
3. J. L. Fahey and M. Potter (1959). Bence-Jones proteinemia associated with a transplantable mouse plasma cell neoplasm. Nature **184**, 654–655.

Suggestion for Further Reading

4. R. A. Kyle (1994) The monoclonal gammopathies. Clin. Chem. **40**, 2154–2161.

Beta-Bulge

The b-bulge is a term used to define a specific **secondary structure** feature of protein structures, where the regular hydrogen bond interactions and backbone conformation of the b-sheet are disrupted by the presence of an extra residue. The additional residue is usually located on a b-strand at one edge of the b-sheet, where the bulge is more easily accommodated within the structure of the protein (Fig. 1). b-Bulges occur frequently, and often there are two or more per protein (1). In some cases, b-bulges have been found to be conserved in the structures of related proteins, where they may play a functional role. The more general role of the b-bulge is to alter the direction of the b-strand, so that it may be considered a type of turn. However, the change in direction of the polypeptide chain is not as pronounced as that caused by other types of turns.

Figure 1. Example of a classic b-bulge in an antiparallel b-sheet. Three b-strands of the antiparallel b-sheet are shown. The normal twist of the b-sheet is clearly accentuated by the b-bulge, caused by an additional residue in the middle b-strand at the edge of the b-sheet. The close-up view of the b-bulge **(right)** shows residue X from the b-strand forming backbone hydrogen bonds (shown as dashed lines) with two residues (1 and 2) from the outer b-strand. For clarity, side-chain atoms have been removed, backbone nitrogen atoms and backbone oxygen atoms are shown as dark spheres. This figure was generated using Molscript (3) and Raster3D (4, 5).

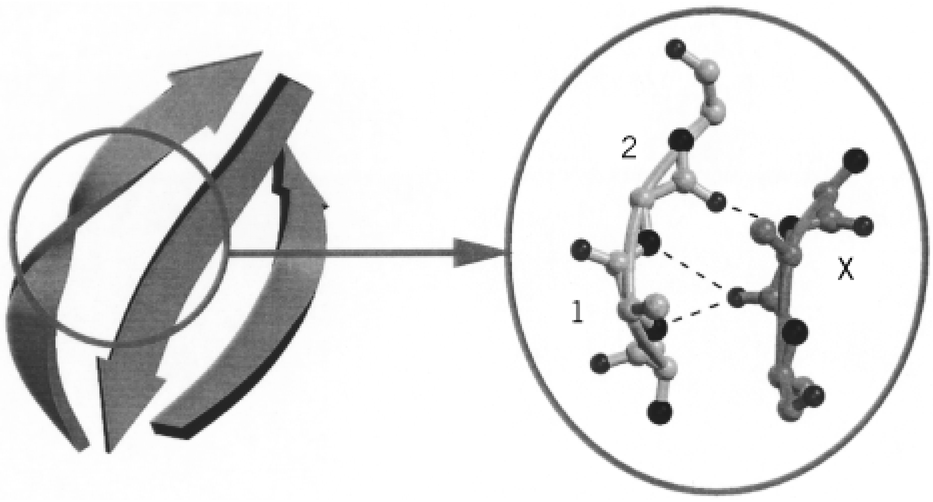

A b-bulge is that region between two consecutive b-type hydrogen bonds that includes two residues (called positions 1 and 2) on one b-strand opposite a single residue (position X) on the other b-strand (2). There are several different classes of b-bulge, most (90%) occurring between antiparallel b-strands. The two most common are the classic and the G1, accounting for about 80% of b-bulges. In the classic b-bulge, the residue at position 1 has backbone dihedral angles (f = –100, y = –25) (see Ramachandran Plot), closer to those of an a-helical than to a b-strand conformation, but residue 2 has angles closer to the b-strand conformation (f = –180 and y = 160). In the G1 b-bulge, the residue at position 1 has a positive f value (f = 85 and y = 0) and is therefore almost always glycine (thus the name G1). The residue at position 2 of the G1 class has dihedral angles corresponding to b-strand (y = –90 and y = 150). The G1 b-bulge often occurs in combination with a type II b-turn (which requires a glycine at position 3). Compared to the usual b-sheet structure, a b-bulge disrupts the alternating side chain placement on one of the b-strands and increases the right-handed twist of the b-strand from the usual 10° to 35° to 45°.

[See also Beta-Sheet.]

Bibliography

1. A. W. E. Chan, E. G. Hutchinson, D. Harris, and J. M. Thornton (1993) Protein Sci. **2**, 1575–1590.
2. J. S. Richardson, E. D. Getzoff, and D. C. Richardson (1978) Proc. Natl. Acad. Sci. USA **75**, 2574–2578.
3. P. J. Kraulis (1991) J. Appl. Crystallogr. **24**, 946–950.

4. E. A. Merritt and M. E. P. Murphy (1994) Acta Crystallogr. **D50**, 869–873.
5. D. J. Bacon and W. F. Anderson (1988) J. Mol. Graphics **6**, 219–222.

Beta-Galactosidase of *Escherichia Coli*

Exploration of the lactose (*lac*) system of *Escherichia coli* was started in the late 40s at the Pasteur Institute in Paris by Jacques Monod and his collaborators. As a result, most of the major concepts of **gene expression** and regulation were established with this system (see Lac Operon). The major gene product of the *lac* operon is b-galactosidase, the enzyme that splits lactose into glucose and galactose and the product of the *lac*Z gene. In addition to its importance for studies of enzyme induction, this protein has become very useful as a reporter gene in very many studies of **gene expression**.

1. Characterization

Because of its importance in genetic studies of *lac* operon, *E. coli* b-galactosidase was purified and characterized by several groups in the early 50s (9, 10). It could be easily measured quantitatively because of a chromogenic substrate, *o*-nitrophenyl-b-D-galactoside (ONPG). The enzyme is a hydrolytic transglucosidase and accounts for up to 5% of the total protein in haploid, fully induced or constitutive strains of *E. coli*. The purified enzyme was crystallized, although its three-dimensional structure had to wait 40 years to be solved (see later). Several procedures for producing large amounts of enzyme have been described (reviewed in Ref. 6). b-galactosidase is a particularly stable enzyme. It can be stored in 40% ammonium sulfate for several years at 4 °C without significant loss of activity. In buffered solution, the enzyme is stable at 37 °C for several weeks. At 57 °C the half-life of heat inactivation is 10 min (11). Active enzyme is recovered with 100% yield after **denaturation** with 8 M urea, and fairly good recovery is possible after treatment by 6 M **guanidinium chloride** (12).

b-Galactosidase is specific for the b-D-galactopiranoside configuration and cleaves the bond between the anomeric carbon (C1) and the glycosyl oxygen (10). The enzyme acts as a hydrolase, but also as a transferase. The galactosyl moiety can be transferred to monosaccharides, oligosaccharides, alkyl alcohols, and phenols and also to **mercaptoethanol**. b-Galactosidase also transfers the galactosyl moiety from the C4 position to the C6 position of glucose to form *allolactose*, which is the natural **inducer** of the *lac* operon (13). b-Galactosidase requires Mg^{2+} and Na^{+} ions for maximal activity (9), but the reason for needing these cations is still unclear.

That b-galactosidase is a tetramer of four identical subunits, possessing one active site per subunit, is well documented, and the tetramer is the only active form of the enzyme. Because of its high turnover number (about 6000 moles of ONPG hydrolyzed/sec/mole of enzyme, one molecule of b-galactosidase per bacterial cell can be accurately measured. Several residues (Glu 461, Met 502, Tyr 503, Glu 537) have been identified as important for catalytic function or to be near the active site (14, 15). These residues are found in the three-dimensional structure in close proximity to one another and form a pocket likely to be the substrate-binding site (16).

The amino acid sequence of b-galactosidase, determined before DNA **sequencing** techniques had been developed, was the longest protein sequence ever determined (17). According to this sequence, the protein contains 1021 amino acid residues and a subunit molecular weight of 116,248. Subsequently, the nucleotide sequence of the *lacZ* gene was also determined (18), from which it was predicted that b-galactosidase consists of 1023 residues, with a molecular weight of 116,353 per subunit. It is quite remarkable that the amino acid sequence deduced from the DNA sequence differs only in ten amino acid residues from that obtained by amino acid sequencing of such a large protein.

There is also a **homologue** of b-galactosidase, evolved b-galactosidase (EBG). Normally *E. coli* does not grow on lactose when the *lacZ* gene is deleted. However, cells with *lacZ* deletions were selected that grow on lactose and produce a new b-galactosidase, called EBG (19). The *ebgA* gene maps at 66 min on the *E. coli* chromosome, whereas that for *lacZ* maps at 8 min. The active EBG protein is a hexamer containing 964 residues per monomer. The sequence identity between the *ebgA* and *lacZ* genes at the DNA nucleotide level (50%) exceeds that at the amino acid level (30%). This led to the conclusion that the two genes descended by **divergence** from a common ancestral gene. b-galactosidase and EBG do not cross-react with antisera prepared against each type of protein.

2. b-Galactosidase Complementation

The term complementation has been generally used in genetics for the phenomenon by which a biological function lost or altered by a mutation is restored through mutual compensation by two differently altered mutant genes. In the case of *intracistronic complementation*, where the two mutations occur within different copies of the same **cistron**, it is generally accepted that the repair of function occurs at the level of the protein product of the gene and involves the interaction of differently altered polypeptide chains (see Interallelic Complementation). Such complementation involves noncovalent interaction of polypeptide chains and may occur by reassociation of differently altered subunits of an oligomeric protein or by interaction between fragments of a single polypeptide chain. Studies of b-galactosidase complementation contributed to elucidating the structure of the enzyme and to understanding the mechanism of the specific recognition, reassociation, and folding of proteins (for reviews, see Refs. 20, 21).

2.1. Complementation Between Point Mutants

Jacob and Monod (8) showed that heterogenotes carrying different *lacZ*$^{-}$ point mutants may become *lacZ*$^{+}$ by complementation. *In vitro* studies carried out by Perrin (22) showed that many of the inactive proteins containing these point mutations exhibit monomeric structures, but cross-react immunologically with b-galactosidase. In contrast, the active, complemented, b-galactosidase had a sedimentation coefficient like tetrameric wild-type 16 S, although it was more heat-labile. The restoration of enzyme activity in this type of complementation can be accounted for by a mechanism suggested by Crick and Orgel (23), repair of lesions by reassociation of differently altered subunits.

Some inactive b-galactosidase proteins with point mutations exist as dimers. A specific class of these mutants can be activated up to 1000 times by specific antibodies raised against wild-type b-galactosidase (24, 25). The activating antibody directs the formation of active tetramers. In a strict sense this is not a complementation reaction, but the kinetics of activation are similar to those of complementation between point mutant proteins *in vitro*: In both cases, the appearance of b-galactosidase activity is a relatively slow process, requiring about 300 min at 37 °C.

2.2. Complementation Between Deletion Mutants

The isolation of deletion mutants of the *lacZ* gene involving quite large genetic segments (26) led to the discovery of a new type of intracistronic complementation (for a review, see Ref. 27). Inactive *lacZ* deletion mutants, lacking part of the gene corresponding to either the amino- or the carboxy-terminal region of the b-galactosidase polypeptide chain, would complement another inactive deletion mutant containing the region missing in the first. The N- and C-terminal regions involved in the two distinct classes of complementation are known as the a and w regions, respectively (Fig. 1). Both a- and w-complementation represent noncovalent reassociation of complementary fragments of the b-galactosidase subunit polypeptide chain, which then can reassemble into an enzymatically active tetrameric structure. a- and w-complementation takes place *in vivo* in partial diploids and *in vitro*, with extracts of relevant mutant strains.

Figure 1. Diagrammatic representation of the *lacZ* gene. The figures and letters above the solid line indicate the position of point mutations in the *lacZ* gene: *o*, operator; *y*, structural gene of Lac permease. The figures below the line represent recombination frequencies, as determined by crosses between two point mutants. The lines below indicate the extent of various deletions: M 15 isolated by Beckwith (28); A 238 and W 4680, isolated by Cook and Lederberg (29); all others by Jacob, Ullmann and Monod (26). Reprinted from (20) by permission of Cold Spring Harbor Laboratory.

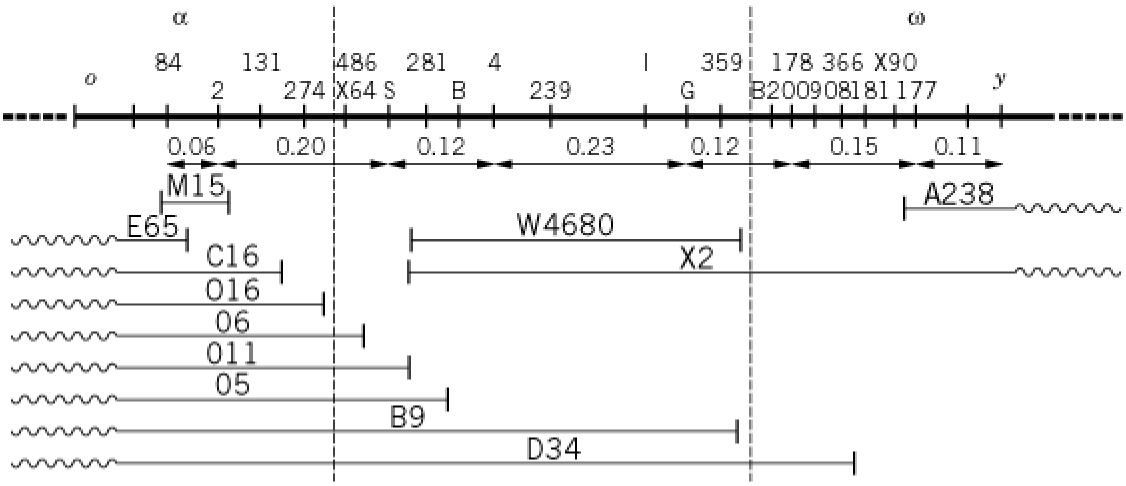

2.3. a-Complementation

All mutants that have their promoter-proximal segment (a-segment) intact are a-donors. All genes that contain partial deletions of the N-terminus not extending beyond a barrier (which is located by the dashed line in Figure 1 between mutants 274 and X64) are a-acceptors when the proteins they produce are mixed with that of an a-donor (30). The time course of *in vitro* a-complementation is relatively slow and reaches a plateau in about 3 h. The a-complemented enzyme, like wild-type b-galactosidase, is a tetramer but is less stable to heat or urea treatment. The equilibrium constant for the complementation reaction was estimated to be approximately 1 to 2 × $10^9 M^{-1}$ (21). Given the slow association rate constant, one can predict a very low dissociation rate, indicating that the complementation process is virtually irreversible under physiological conditions.

The most unusual property of the a-peptide is its high temperature resistance in 6 M guanidinium chloride. Bacterial extracts of *lacZ* strains containing a-donors liberate soluble a-peptides after boiling in this denaturant (30) or after autoclaving in its absence (31). The smallest a-peptide still capable of complementation has a size of about 7400 Da. Upon cleavage of b-galactosidase with **cyanogen bromide**, Langley et al. (32) isolated and sequenced a peptide that has a-donor activity corresponding to residues 3 to 92 of the polypeptide chain.

The best studied a-acceptor is the M15 protein, produced by the *lacZ* mutant DM15 isolated by Beckwith (28) and shown genetically to be a small deletion in the early part of the gene (Fig. 1). The M15 protein lacks residues 11 through 41 of b-galactosidase and is a dimer (33). It has a trace level of enzyme activity and can be significantly activated by addition of anti-b-galactosidase antibodies (34), up to 15% of that obtained by a-complementation.

The nature of the a-complementation process and its probable pathway have been studied extensively (21). It is believed that the a-peptide modifies the quaternary structure of the a-acceptor by causing its tetramerization and consequently the recovery of enzymatic activity. The three-dimensional structure of b-galactosidase (16) fully confirms this prediction by showing that the a-peptide segment of the polypeptide chain participates in forming specific subunit contacts (see later).

2.4. w-Complementation

All mutants that have their promoter-distal region (w-region) intact are w-donors. They complement w-acceptors that are products of deletion or point mutants in the w-region (27) (Fig. 1), which represents about one-third of the total genetic length of *lacZ*. The purified w-peptide has a molecular weight of 40,000 Da (35). The kinetics of w-complementation are faster than those of a-complementation and reach a maximum extent in about 1 h. Although w-peptide is reversibly **renatured** from 8 M urea or 6 M guanidinium chloride, it is highly heat-labile.

w-Acceptor proteins active in complementation have not been obtained in pure form. In crude bacterial extracts (36, 37), w-acceptor exists in different forms of aggregation, depending on the ionic strength. At low ionic strength it is probably a tetramer that dissociates at high ionic strength, most probably into monomers. Both forms are active in complementation. The w-complemented enzyme is a tetramer, like the wild type, and exhibits very similar catalytic properties. The main difference appears after denaturation in 8 M urea. Recovery of its enzyme activity after renaturation does not exceed 5%, whereas it is practically 100% with wild-type enzyme. Moreover, the w-peptide is recovered quantitatively from the complemented enzyme after urea treatment (11).

One of the most remarkable features of w-complementation is the high affinity and specificity that the peptide fragments exhibit. They reassociate even at high dilution and in the presence of a large excess of foreign proteins. The yield of complementation is considerably increased in the presence of a b-galactosidase substrate analog or in the presence of anti-b-galactosidase antibodies (36, 37). Comparing wild-type and w-complemented b-galactosidase, Goldberg (38) proposed a model for the tertiary structure of the two monomers. After having shown that the active, complemented enzyme involves reassociation into a tetrameric structure of four w-acceptor polypeptides with four w-peptides, he showed that both w and acceptor are folded to form compact globular structures, close to those of the corresponding segments of the complete polypeptide within the native enzyme. This “globule model” involves the notion that large polypeptide chains contain several distinct **domains** that assemble specifically to give the polypeptide chain its final tertiary structure. The well-defined compact w-domain is apparent within the native monomer in the three-dimensional structure of b-galactosidase (16), which also shows an unstructured 10-residue exposed segment that joins the w-domain to the rest of the chain. This explains, *a posteriori*, why mild proteolytic treatment of the wild-type b-galactosidase liberates significant amounts of w-peptide (11).

3. Three-Dimensional Structure

The structure of tetrameric b-galactosidase was solved by X-ray crystallography at 2.5 Å resolution by B.W. Matthews et al. (16). It is the longest polypeptide chain for which an atomic structure has been determined. The crystal structure shows that b-galactosidase is a tetramer with dimensions of roughly 175 × 135 × 90 Å along the respective twofold axes. The constituent monomers interact through two different monomer–monomer contacts. The b-galactosidase monomer consists of five compact domains and a relatively extended 50-residue N-terminal segment, corresponding to the a-peptide, which contributes to the activating interface (Fig. 2). The monomer is relatively flat and elongated and has approximate dimensions of 50 × 100 × 40 Å. The first domain consists of residues 52 to 217, the second of residues 220 to 334, the third of residues 334 to 627, the fourth of residues 627 to 736, and the final fifth domain, corresponding to the w peptide, of residues 737 to 1023. Topologically, the second domain is identical to the fourth domain. The modular structure of the monomer corroborates earlier findings (37, 38), which suggested that the folding of this rather long polypeptide chain is facilitated by each domain acting as an independent unit.

Figure 2. Three-dimensional structure of b-galactosidase. (**a**) Ribbon representation of the b-galactosidase tetramer showing the largest face of the molecule. Contacts between red/green and blue/yellow dimers form the long interface. Contacts between the red/yellow and blue/green dimers form the activating interface. Formation of the tetrameric particle results in two deep clefts that run across opposite faces of the molecule. Each contains two active sites. (**b**) Ribbon diagram of the blue/green dimer viewed down the molecular two-fold axis, showing the composition of the activating interface. Residues 1 to 50 from each chain, which form the a-complementation region (see text), are shown

in red. The interface includes contacts between the respective complementation peptides, between two a-helices from the respective monomers that pack together to form a four-helix bundle and between an extended loop (residues 272 to 288) from each monomer that reaches across the interface and extends into the active-site region of the neighboring monomer, stabilizing the active site structure. (**c**) Stereo ribbon diagram of the b-galactosidase monomer showing the domain organization of the chain. Residues corresponding to successive domains are colored in successive spectral colors. See color insert.

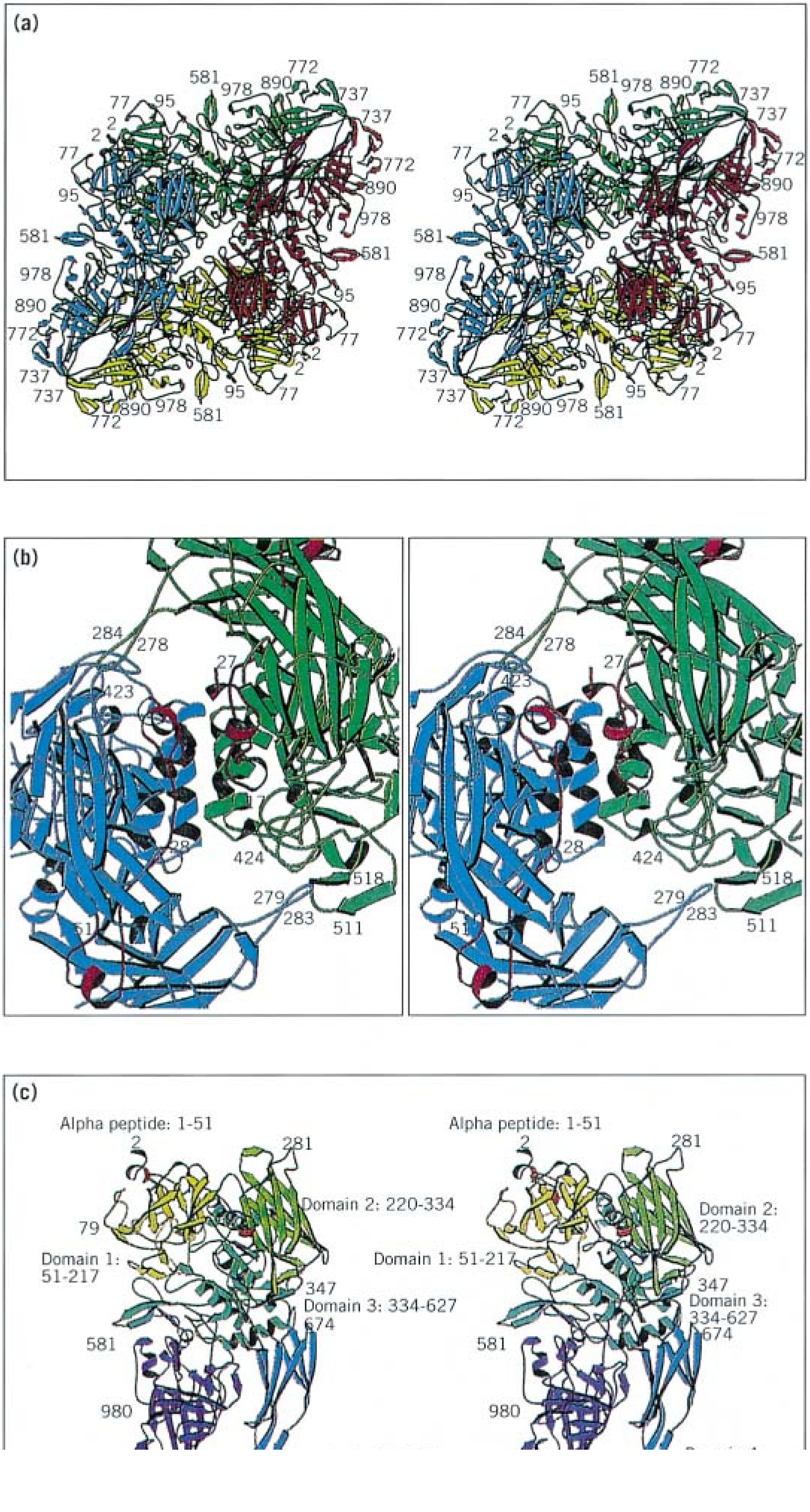
(a)
581
978
890
772
737
737
77
95
2
2
77
95
772
890
978
581
581
978
890
772
737
737
772
890
978
581
95
77
2
2
77
95
(b)
284
278
27
423
28
424
518
279
283
511
(c)
Alpha peptide: 1-51
2
281
Domain 2: 220-334
79
Domain 1:
51-217
347
Domain 3: 334-627
674
581
980
Alpha peptide: 1-51
Domain 2:
220-334
Domain 1: 51-217
Domain 3:
334-627

At present, no structure of a complex of b-galactosidase with a substrate or analog is available, so the specific interaction sites between enzyme and substrate are not known. Nevertheless, earlier biochemical studies (14, 15) concluded that residues important for catalytic function or near the active site (Glu461, Met502, Tyr503, Glu537) are found close to one another and located around a deep pit within the third domain, which is postulated to be the substrate-binding site. Residues from distant regions of the sequence (Trp568, Trp999) also contribute to the active site.

The X-ray structure of b-galactosidase provides a structural rationale for both a- and w-complementation. The N-terminal segment, representing the a peptide, participates in forming a subunit interface, which in turn allows formation of the active site, made up of elements from two different subunits. The w-fragment, corresponding to the fifth domain of the subunit, exhibits a specific topology. Rotation of this domain by more than 90° positions Trp 999 at the active site in the vicinity of the third domain.

4. b-Galactosidase as a Tool

The b-galactosidase of *E. coli* is one of the most commonly used enzymes in molecular biology for several reasons: (*1*) numerous genetic and biochemical aspects of the *lac* system are known; (*2*) several indicator media are available for detecting lactose metabolism and monitoring Lac^+ and Lac^- bacteria; (*3*) the assay procedure based on o-nitrophenyl-b-D-galactoside (ONPG) hydrolysis is exquisitely sensitive; (*4*) the protein is highly stable and easy to purify; and (*5*) the availability of substituted galactoside derivatives permits selecting and screening *lac* mutants exhibiting a variety of phenotypes. For example, the chromogenic noninducing and colorless substrate, 5-bromo-4-chloro-3-indolyl-b-D-galactoside (X-Gal), forms an insoluble blue dye upon hydrolysis, thus providing a sensitive test for b-galactosidase in solid media. X-Gal also discriminates between strains that produce high and low levels of b-galactosidase, allowing detection of plaque-forming **bacteriophages** that carry the *lacZ* gene.

5. b-Galactosidase Fusions

The observation that the N-terminal 23 residues of b-galactosidase can be replaced with other amino acids without affecting enzymatic activity enabled Müller-Hill and Kania (39) to obtain fusions between *lacI* and *lacZ* genes that produce a hybrid protein that has both Lac repressor and b-galactosidase activities. Several genetic methods have been developed to construct *lac* fusions that produce hybrid genes which specify hybrid proteins. Subsequently, *in vitro* construction of hybrid genes facilitated obtaining a variety of fusions (40). A number of commercially available vectors exist for constructing *lacZ* fusions *in vitro*. They contain a *lacZ* gene truncated at the 5′-end and preceded by a synthetic oligonucleotide containing multiple restriction enzyme cleavage sites, a *polycloning* site. Thus, if a 5′-coding sequence is cloned into one of these sites so that transcription and translation are restored across *lacZ*, a hybrid protein with b-galactosidase activity is produced. The sensitive detection of this activity with X-Gal has made b-galactosidase one of the most commonly used *in vivo* **reporter enzymes**. Using the *lacZ* gene as a reporter provides a sensitive method to detect genes subject to specific regulatory signals or to study the mechanism localizing a protein to a given cellular compartment. The regulation, identification, and localization of many proteins of various origins have been uncovered by using the b-galactosidase activity of fusion proteins as a marker.

During the last few years, a number of new eukaryotic expression vectors that produce b-galactosidase fusion proteins have been designed. They are currently being used to analyze developmentally regulated genes, transgenic expression, tissue-specific expression, and a number of other aspects involved in embryogenesis or developmental biology. This approach has been facilitated by using replication-defective retroviral vectors that encode the *lacZ* gene (41), which has become a widely used cell lineage marking system. The labeled cells are easily identified by histochemical staining, using X-Gal or **immunofluorescence** with antibodies raised against b-galactosidase.

b-galactosidase fusions provide a unique and versatile experimental tool. The hybrid proteins are easy to purify (42) and can be used as antigen to raise antibodies against the target gene product. In addition, because there is no restriction on the size of the target gene DNA fused to *lacZ* and because many hybrid proteins retain all or a portion of the activity of the target gene product, these fusions provide a means to identify functional domains within the target gene product.

5.1. a-Complementation

Perhaps the most widely exploited property of b-galactosidase is a-complementation, described previously. Whereas the region of the foreign protein that can replace the N-terminus of b-galactosidase is more or less random in hybrid fusion proteins, replacements in the a-peptide for a-complementation are more restrictive. That insertion of a few amino acid residues does not always interfere with complementation capacity (43) was widely used during the late 70s to develop new cloning vectors, now commercially available. Indeed, a-complementation has become one of the most commonly used methods for identifying bacterial colonies containing recombinant DNA.

The first vector based on a-complementation was developed by Messing et al. (44). Within the major intergenic region of the filamentous bacteriophage M13, they inserted the *lac* regulatory region and the DNA sequence that codes for the first 146 amino acids of b-galactosidase that have a-complementation capacity. When infected with these phages, bacteria that produce the M15 a-acceptor protein produce active b-galactosidase by complementation and form blue plaques in the presence of the chromogenic substrate X-Gal. Insertion of foreign DNA into the a region of M13 interferes with a-complementation and gives rise to recombinants that form pale blue or colorless plaques. This simple test has made cloning in filamentous bacteriophages a routine procedure. The insertion of a series of synthetic restriction enzyme sites into the a-region provides a variety of targets for cloning foreign DNA fragments. Insertion of these polycloning sites, representing up to 18 extra amino acid residues, into the a-region has practically no effect on a-complementation capacity. Insertion of additional DNA into a cloning site, however, generally abolishes a-complementation and creates recombinant bacteriophages that produce colorless plaques when grown on X-Gal plates (*blue/white screen*). The great advantage of using vectors generated from single-stranded DNA phage, like M13, is that one obtains both the double-stranded replicative form from the infected bacteria and the single-stranded DNA, from the progeny phage. The latter is frequently used as a template for sequencing with the dideoxy-mediated chain-terminating **Sanger method** (45) and also for *in vitro* mutagenesis. Many other vectors that permit identification of recombinant clones based on a-complementation have been designed subsequently. The most commonly used are the pUC vectors (46).

Recently, Mohler and Blau (47) adapted intracistronic complementation of the *lacZ* gene for use in eukaryotic cells. By constructing replication-defective **retroviral** vectors that express a-donors and a-acceptors and w-donors and w-acceptors, complementation of the relevant *lacZ* mutants in mammalian cells permits analyzing cell fusion and detecting colocalized interacting proteins within single intact cells. a- and w-complementation can be exploited for a wide range of studies, including **transgenic** animals that express complementing *lacZ* mutants from two **promoters** of interest, which then could reveal cell lineages in which the products of both genes coincide spatially and temporally. In line with these results, Rossi et al. (48) applied b-galactosidase complementation to monitor protein–protein interactions in intact eukaryotic cells.

Given the wide range of applications for b-galactosidase during the last decades, one can anticipate that further development of the b-galactosidase fusion and complementation systems will contribute to our understanding of many features of cellular regulation and organization.

Bibliography

1. M. Cohn, J. Monod, H. R. Pollock, S. Spiegelman, and R. Stanier (1953) Nature **172**, 1096–1097.
2. J. Monod, G. Cohen-Bazire, and M. Cohn (1951) Biochem. Biophys. Acta **7**, 585–599.
3. J. Lederberg and E. L. Tatum (1946) Cold Spring Harbor Symp. Quant. Biol. **11**, 113–114.
4. E. L. Wollman, F. Jacob, and W. Hayes (1956) Cold Spring Harbor Symp. Quant. Biol. **21**, 141–162.
5. H. W. Rickenberg, G. N. Cohen, G. Buttin, and J. Monod (1956) Ann. Inst. Pasteur **91**, 829–857.
6. I. Zabin and A. V. Fowler (1978) In *The Operon* (J. H. Miller and W. S. Reznikoff, eds.), Cold Spring Harbor Laboratory, Cold Spring Harbor, New York, pp. 89–121.
7. A. B. Pardee, F. Jacob, and J. Monod (1959) J. Mol. Biol. **1**, 165–178.
8. F. Jacob and J. Monod (1961) J. Mol. Biol. **3**, 318–356.
9. M. Cohn (1957) Bact. Rev. **21**, 140–168.
10. K. Wallenfels and O. P. Malhotra (1961) Adv. Carbohydrate Chem. **16**, 239–298.
11. A. Ullmann, F. Jacob, and J. Monod (1968) J. Mol. Biol. **32**, 1–13.
12. A. Ullmann and J. Monod (1969) Biochem. Biophys. Res. Commun. **35**, 35–42.
13. C. Burstein, M. Cohn, A. Kepes, and J. Monod (1965) Biochem. Biophys. Acta **95**, 634–639.
14. M. Ring and R. E. Huber (1990) Arch. Biochem. Biophys. **283**, 342–350.
15. C. G. Cupples, J. H. Miller, and R. E. Huber (1990) J. Biol. Chem. **265**, 5512–5518.
16. R. H. Jacobson, X-J. Zhang, R. F. DuBose, and B. W. Matthews (1994) Nature **369**, 761–766.
17. A. V. Fowler and I. Zabin (1977) Proc. Natl. Acad. Sci. USA **74**, 1507–1510.
18. A. Kalnins, K. Otto, U. Rüther, and B. Müller-Hill (1983) EMBO J. **2**, 593–597.
19. H. W. Stokes, P. W. Betts, and B. G. Hall (1985) Mol. Biol. Evol. **2**, 469–477.
20. A. Ullmann and D. Perrin (1970) In *The Lactose Operon* (J. R. Beckwith and D. Zipser, eds.), Cold Spring Harbor Laboratory, Cold Spring Harbor, New York, pp. 143–172.
21. I. Zabin (1982) Mol. Cell. Biochem. **49**, 87–96.
22. D. Perrin (1963) Cold Spring Harbor Symp. Quant. Biol. **28**, 529–532.
23. F. H. C. Crick and L. E. Orgel (1964) J. Mol. Biol. **8**, 161–165.
24. B. Rotman and F. Celada (1968) Proc. Natl. Acad. Sci. USA **60**, 660–667.
25. E. Conway de Macario, J. Ellis, R. Guzman, and B. Rotman (1978) Proc. Natl. Acad. Sci. USA **75**, 720–724.
26. F. Jacob, A. Ullmann, and J. Monod (1965) J. Mol. Biol. **31**, 704–719.
27. A. Ullmann, D. Perrin, F. Jacob, and J. Monod (1965) J. Mol. Biol. **12**, 918–923.
28. J. R. Beckwith (1964) J. Mol. Biol. **8**, 427–430.
29. A. Cook and J. Lederberg (1962) Genetics **47**, 1335–1353.
30. A. Ullmann, F. Jacob, and J. Monod (1968) J. Mol. Biol. **24**, 339–343.
31. S. L. Morrison and D. Zipser (1970) J. Mol. Biol. **50**, 359–371.
32. K. E. Langley, A. V. Fowler, and I. Zabin (1975) J. Biol. Chem. **250**, 2587–2592.
33. K. E. Langley, M. R. Villarejo, A. V. Fowler, P. J. Zamenhof, and I. Zabin (1975) Proc. Natl. Acad. Sci. USA **72**, 1254–1257.
34. R. S. Accolla and F. Celada (1976) FEBS Lett. **67**, 299–302.
35. M. E. Goldberg and S. J. Edelstein (1969) J. Mol. Biol. **46**, 431–440.
36. A. Ullmann and J. Monod (1970) in *The Lactose Operon* (J. R. Beckwith and D. Zipser, eds.), Cold Spring Harbor Laboratory, Cold Spring Harbor, New York, pp. 265–272.
37. F. Celada, A. Ullmann, and J. Monod (1974) Biochemistry **13**, 5543–5547.

38. M. E. Goldberg (1969) J. Mol. Biol. **46**, 441–446.
39. B. Müller-Hill and J. Kania (1974) Nature **249**, 561–563.
40. T. J. Silhavy and J. Beckwith (1985) Microbiol. Rev. **49**, 398–418.
41. J. R. Sanes, J. L. R. Rubenstein, and J-F. Nicolas (1986) EMBO J. **5**, 3133–3142.
42. A. Ullmann (1984) Gene **29**, 27–31.
43. U. Rüther, M. Koenen, K. Otto, and B. Müller-Hill (1981) Nucleic Acids Res. **9**, 4087–4098.
44. J. Messing, B. Gronenborn, B. Müller-Hill, and P.H. Hofschneider (1977) Proc. Natl. Acad. Sci. USA **74**, 3642–3646.
45. F. Sanger, S. Nicklen, and A. R. Coulson (1977) Proc. Natl. Acad. Sci. USA **74**, 5463–5467.
46. J. Vieira and J. Messing (1982) Gene **19**, 259–268.
47. W. A. Mohler and H. M. Blau (1996) Proc. Natl. Acad. Sci. USA **93**, 12423–12427.
48. F. Rossi, C. A. Charlton, and H. M. Blau (1997) Proc. Natl. Acad. Sci. USA **94**, 8405–8410.

Suggestions for Further Reading

49. *The Lactose Operon* (1970). (J. R. Beckwith and D. Zipser, eds.), Cold Spring Harbor Laboratory, Cold Spring Harbor, New York, 437 pages.
50. A. Ullmann (1992) Complementation in -galactosidase: From protein structure to genetic engineering, BioEssays **14**, 201–205.
51. B. Müller-Hill (1996) *The lac Operon. A Short History of a Genetic Paradigm*, Walter de Gruyter. Berlin, New York.

Beta-Glucuronidase

b-Glucuronidase (E.C. 3.2.1.31; GUS) is the most widely used reporter gene in plant molecular biology (1). The *gusA* gene cloned from *Escherichia coli* encodes a 68-kDa b-glucuronidase that forms a stable homotetramer and catalyzes the hydrolysis of a large number of glucuronides, in which D-glucuronic acid is conjugated through a b-*O*-glycosidic linkage to any aglycone. b-Glucuronidase has emerged as the reporter gene of choice to be used in plants, because there is very little or no endogenous glucuronidase activity across the phyla. This minimizes the detection of background activity and allows very small quantities of GUS to be detected. GUS activity may be followed in cell lysates or *in situ*. The major use of GUS has been to study gene expression patterns in transgenic plants by expressing GUS under the control of regulatory sequences of interest. A second use has been to monitor the intracellular fate of chimeric proteins by generating GUS fusion genes. For example, GUS has been fused to gene leader sequences that target the fusion gene to different organelles and allow intracellular trafficking of proteins to be studied (2).

GUS activity may be detected using a variety of substrates. As in the case of **beta-galactosidase** and X-gal, GUS expression is most commonly detected using histochemical substrates, such as X-GlcU (5-bromo-4-chloro-3-indolyl b-D-glucuronide), which gives a dark blue precipitate upon hydrolysis. Alternative substrates include 5-bromo-6-chloro-3-indolyl b-D-glucuronide, 6-chloro-3-indolyl b-D-glucuronide, and indoxyl b-D-glucuronide that give magenta, pink, and blue precipitates, respectively (3). The variety of substrates also makes GUS a valuable component of dual (or multiple) reporter gene systems; for example, GUS and *lacZ* expression could be detected in the same tissues by using substrates that give different colored histochemical precipitates. In addition to histochemical substrates, a number of fluorescent and chemiluminescent substrates have been developed that are analogous to the substrates for b-galactosidase, such as CFDG-GlcU (Molecular Probes Inc.) and 4-methylumbelliferyl b-D-glucuronide (MUGlcU) (4).

In the case of *lacZ*, problems may be encountered in loading substrates into cells; to load FDG, for example, cells must undergo a moderate osmotic shock that can affect cell viability. In the case of GUS, however, a second gene, *gusB*, may be expressed that encodes a **permease** that actively takes up and transports glucuronide substrates into the cell. In addition to substrates that allow reporter gene visualization, a number of other bioactive molecules can be conjugated to glucuronides, which could then be released by hydrolysis in GUS-expressing cells. Thus, combined use of gusA and gusB increases the use of the reporter gene, from merely indicating gene expression to controlling a specific cell manipulation (1).

Bibliography

1. R. A. Jefferson (1989) Nature **342**, 837–838.
2. R. A. Jefferson, T. A. Kavanagh, and M. W. Bevan (1987) EMBO J. **6**, 3901–3907.
3. G. A. Hull and M. Devic (1995) Methods. Mol. Biol. **49**, 125–141.
4. C. E. Olesen, J. J. Fortin, J. C. Voyta, and I. Browstein (1997) Methods Mol. Biol. **63**, 61–70.

Beta-Helix

A b-helix is a type of protein motif or **domain** found in a very few protein structures. It is characterized by an unusual parallel b-sheet topology formed from three parallel b-sheets wound together into a right-handed helical structure (Fig. 1). The b-strands in each b-sheet are short, having only 2 to 5 residues. Each coil of the b-helix has the same three-dimensional arrangement of a group of **secondary structure** elements and is thus similar to other coiled repeating structures, such as the b-roll, composed of two parallel b-sheets forming a b-helix, and the leucine-rich repeat of **ribonuclease inhibitor** that is composed of repeating a-helices and b-strands forming a horseshoe-shaped structure. In the b-helix, the side chains of repeating residues are packed into the center of the helix and interact with one another to form, for example, "asparagine ladders," "serine stacks," and/or "aromatic stacks."

Figure 1. Orthogonal views of the b-helix of pectate lyase E (1), showing the three parallel b-sheets. For clarity, only the b-strand secondary structure (as purple arrows) and loops connecting the strands (yellow) are shown. Short helical regions and the *N*- and *C*-terminal loops have been removed. This figure was generated using Molscript (2) and Raster3D (3, 4). See color insert.

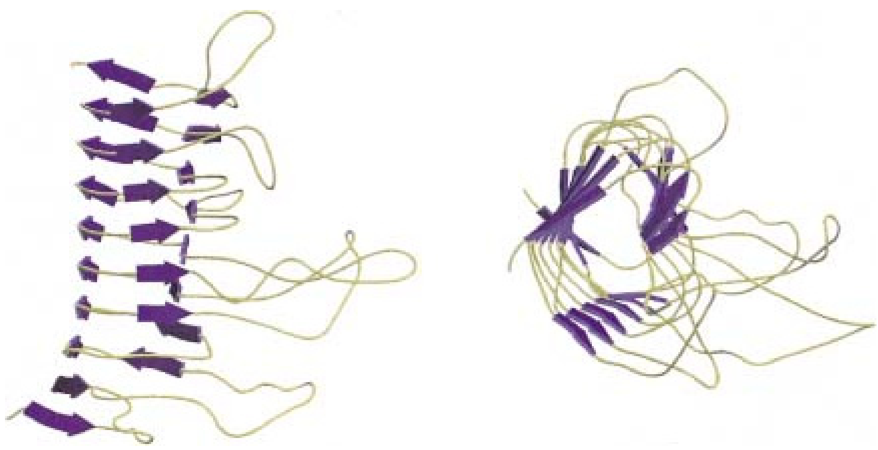

[See also Beta-Sheet, Protein Motif, Domain, Protein, and Protein Structure.]

Bibliography

1. M. D. Yoder, S. E. Lietzke, and F. Jurnak (1993) Structure **1**, 241–251.
2. P. J. Kraulis (1991) J. Appl. Crystallogr. **24**, 946–950.
3. E. A. Merritt and M. E. P. Murphy (1994) Acta Crystallogr. **D50**, 869–873.
4. D. J. Bacon and W. F. Anderson (1988) J. Mol. Graphics **6**, 219–222.

Suggestions for Further Reading

5. M. D. Yoder and F. Jurnak (1995) The parallel -helix and other coiled folds. FASEB J. **9**, 335–342.
6. C. Kisker et al. (1996) A left-handed -helix revealed by the crystal structure of carbonic anhydrase from the archaeon bacteria *Methanosarcina thermophila*. EMBO J. **15**, 2323–2330.

Beta-Lactamases

b-Lactamases constitute one of the oldest known mechanisms of bacterial antibiotic resistance and one of the most widely distributed. The enzymes hydrolyze b-**lactam** antibiotics, such as penicillin, rendering them inactive (Fig. 1).Most of these enzymes also react with other cyclic structures, such as g-lactams and isatoic anhydride derivatives (1), and some have low reactivity with simple esters, peptides, and depsipeptides. Richmond and Sykes (2) and Bush (3) classified b-lactamases according to their catalytic activity and apparent substrate specificity, which remains the most useful classification for the clinical microbiologist. Today, the ready availability of b-lactamase amino acid sequences obtained from their **genes** provides the basis for a structural classification first proposed by Ambler (4). There are two types of b-lactamase:

1. those with a serine residue at their active site that is transiently acylated by the b-lactam substrate during hydrolysis (Richmond and Sykes groups I and II; Ambler class A, plus the more recently distinguished classes C and D); for an example, see Serine Proteinase.
2. those with metal ion cofactors, which are Zn(II) in the physiological state, and with apparently no acyl-enzyme intermediate (Richmond and Sykes group III; Ambler class B) (see

Metalloproteinases).

The serine b-lactamases include enzymes that have both narrow and broad substrate specificities and are sensitive, to varying degrees, to b-lactam **enzyme-activated inhibitors**. This group is the more abundant and currently poses the greater clinical problem. The metallo-b-lactamases are active on a broad spectrum of b-lactam substrates and are much less sensitive to the mechanism-based inhibitors, although they can be inhibited by metal-ion chelating agents. This group has been relatively scarce in nature, but its prevalence is rising because of the increased use of b-lactam antibiotics that resist hydrolysis by serine b-lactamases.

Figure 1. The reaction catalyzed by b-lactamases.

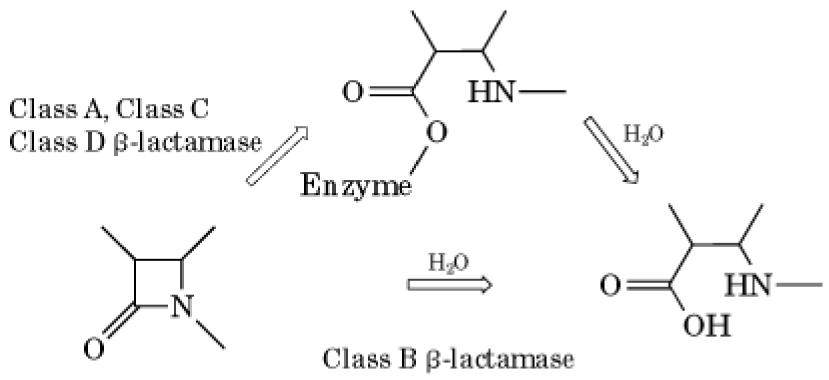

1. Serine b-lactamases

Sequence comparisons of the active serine enzymes indicate six major groups:

1. The class A b-lactamases: Richmond and Sykes Group II enzymes; Bush groups 2a (penicillinases), 2b (broad spectrum b-lactamases), 2b′ (extended broad spectrum b-lactamases), 2c (carbenicillinases), 2e (cephalasporinases). This group also includes a few proteins identified as D-Ala-D-Ala carboxypeptidases (DAC).
2. The class C b-lactamases: Richmond and Sykes and Bush Group 1, together with three proteins from *Streptomyces*, *Nocardia*, and *Bacillus subtilis*, identified as carboxypeptidase/transpeptidases.
3. The Class D b-lactamases from gram-negative bacteria (Bush Group 2d oxacillinases), together with b-lactam receptor proteins from gram-positive bacteria.
4. The bifunctional transglycosylase/transpeptidase, class A penicillin-binding proteins (PBP).
5. The monofunctional transpeptidase, class B PBP.
6. D-Ala-D-Ala carboxypeptidases (DAC).

The last three groups are biosynthetic enzymes of the bacterial cell wall that react with D-Ala-D-Ala.

All six groups have three sets of conserved residues in common, which comprise the active site of the enzyme (see later). The first comprises the sequence Ser-X-X-Lys, where X is any residue and the serine residue is the one that is transiently acylated by substrates and the only residue that is absolutely conserved in all of the proteins. The second has either a serine (class A) or a tyrosine residue (in class C and class D b-lactamase groups), followed after one residue by an asparagine (except in one class D b-lactamase). The third conserved segment is usually Lys-Thr-Gly, but only the glycine residue is absolutely conserved. Sequence analyses have suggested that b-lactamase activity may have arisen several times by a process of evolutionary **convergence**.

Three-dimensional structures of class A enzymes from *Staphylococcal aureus* (5), *Bacillus cereus*

(6), *B. licheniformis* (7), *Streptomyces albus* (8), and *Escherichia coli* TEM-1 (9, 10) have been published, which include only two of the five activity groups of class A enzymes. Structures of the class C b-lactamases from *Citrobacter freundii* (11) and *Enterobacter cloacae* (12) have been published, and this group is extended by the homologous structure of the transpeptidase domain of the *Streptomyces* carboxypeptidase/transpeptidase (13). The overall structures of all of these enzymes and a DAC are similar. The core of each molecule is a five-stranded, antiparallel b-sheet flanked on one side by three a-helices and on the other by a larger, more diverse a/b domain (see Protein Structure). The active site lies between the two domains and is bound by one edge of the b-sheet. As shown in Figure 2, the conserved residues listed previously make up the active site regions and occupy very similar positions in all of the structures (Figure 2). Even the alternative serine and tyrosine residues in the second conserved segment of class A (DAC) and class C (DAC), respectively, have their hydroxyl groups in the same positions; see Ser 130 and Tyr150 in Fig. 2 a and b, respectively. Major differences between the two classes of enzymes that are believed to have functional consequences occur in the area that serves as a recognition pocket for the side chain of the substrate. The class A enzymes have a loop (the W loop) that forms the base of the acyl amino side-chain binding pocket. This loop includes residues Glu166 and Asn170, which localize and activate a water molecule for attack on the ester bond of the substrate (14, 15). The projection of this loop into the active site also limits the scope for binding bulky acyl side chains, which was exploited in developing b-lactamase-resistant antibiotics, such as methicillin.

Figure 2. Comparison of the similar active-site regions of b-lactamases of class A (a) and class C (b). The residues are identified with the one-letter code. The lack spheres are water molecules observed crystallographically that are probably hydrogen-bonded (dashed lines) to various groups of the protein. The active-site serine residue that is acylated in the catalytic reaction is S70 in (a) and S64 in (b).

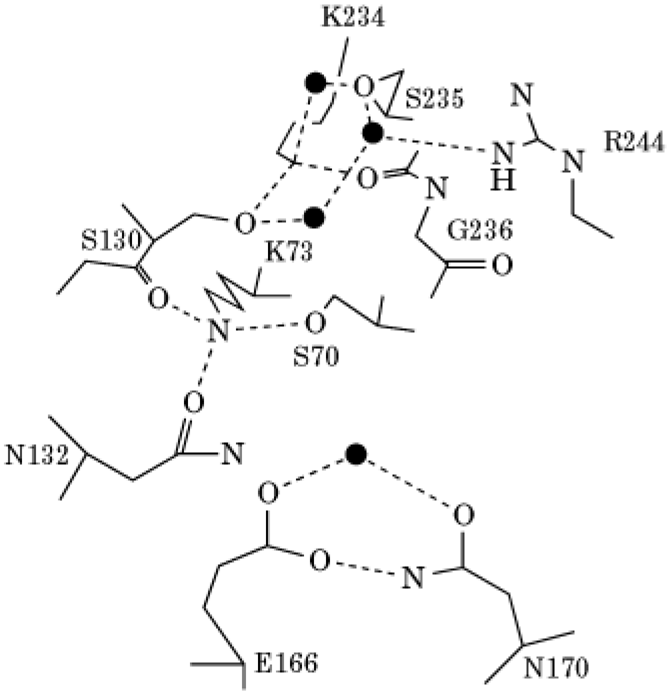

(a)

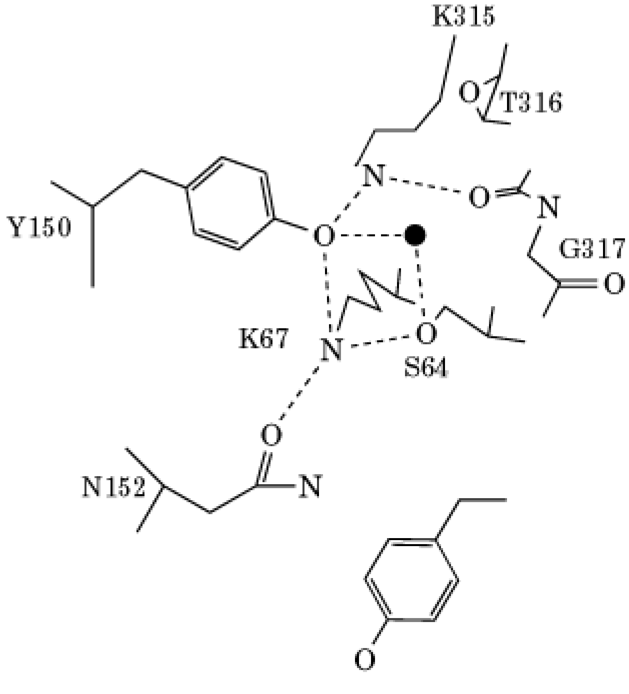

(b)

Evolutionary accumulation of peripheral mutations that modify the conformation of the W loop and of neighboring surface loops that define the edges of the side-chain recognition pocket has led to the appearance of enzymes that belong to groups 2b′, 2c, and 2e that have extended substrate recognition profiles (16). In the class C enzymes, the water molecule that attacks the ester of the acyl intermediate is located on the opposite side of the plane of the ester and is activated by direct interaction with components of a hydrogen-bonded relay formed by the conserved residues. Identification of the individual residues involved in activating of the water has not yet been achieved, although Tyr150 has been implicated (11). The class C enzymes have a deeper, more **hydrophobic** side-chain binding pocket, lined by Tyr122, that enables them to bind substrates with large 7-acyl amino side chains.

Conformational changes during the b-lactamase reaction have been proposed for the class A, C, and D b-lactamases on a variety of grounds. With simple substrates, NMR and circular dichroism spectroscopy have suggested changes in the structure accompanying acyl-enzyme formation (17, 18). A number of substrates show nonstoichiometric bursts of hydrolysis (19), and a conformation change leading to a substrate-induced inactivation has been invoked (1, 20). These observations in solution contrast with the finding of very few differences in the structures of the free enzyme and the acyl-enzyme complex determined by X-ray crystallography (9, 11). An unambiguous description of the reaction mechanism must wait until these observations can be reconciled.

2. Metallo-b-lactamases

Sequence comparisons suggest that there are four groups of this type of b-lactamase that are not closely related, but share similarities with a protein from the actinorhodin biosynthetic gene cluster of *Streptomyces*. A few residues involved in binding the metal ion cofactors are absolutely conserved within this diverse group. Three structures are available, that representing two of the major subgroups of metallo-b-lactamases (Fig. 3). All three structures are similar overall to each other, but not to the serine b-lactamases, and the core of each molecule is formed from two antiparallel b-sheets, each with additional parallel strands and flanked by a-helices. The structure of *Bacillus cereus* b-lactamase II was solved with Cd(II) in place of the natural Zn(II) metal ion (21). One Cd(II) ion is bound tightly, with a dissociation constant of about 1 µM, by the side chains of three histidine and one cysteine residue (22-24). In the homologous enzyme from *Bacteroides fragilis*, one Zn(II) ion is similarly coordinated by three histidine side chains, as in the *B. cereus* enzyme, but the fourth ligand is a water molecule that is shared with a second Zn(II) ion (25). The second zinc ion is further coordinated by three other side chains, those of His, Cys, and Asp residues. Two more Cd(II) ions are located in the *B. cereus* structure, but the coordination of one of them is much weaker (23), so it may not be physiological. Early stoichiometries determined for the binding of Zn(II) and Cd(II) suggested that two ions per molecule are bound (22). The second Cd(II) ion is bound by two Asp residues and lies only 10 Å from the tightly bound ion (Fig. 3), where it might modulate the catalytic activity. It is believed that the water molecule complexed with the two Zn(II) ions in the *B. fragilis* enzyme is activated to form hydroxide for attack on the b-lactam ring, and a corresponding water molecule is probably activated by the tightly bound ion in the *B. cereus* enzyme.

Figure 3. Comparison of the similar active-site regions of metallo-b-lactamases from *Bacillus cereus* (a) and *Bacteriodes fragilis* (b). The shaded spheres are the two metal ions, cadmium (II) in (a) and zinc (II) in (b), and the smaller solid spheres are water molecules observed crystallographically.

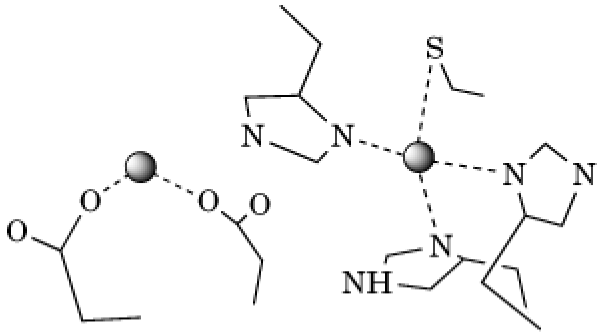

(a)

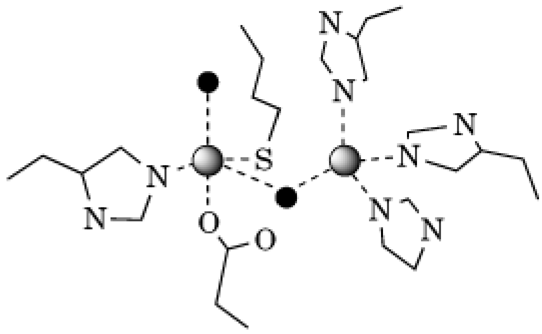

(b)

3. Inhibition

The important role of b-lactamases in antibiotic resistance has led to the development of specific b-lactamase inhibitors that can be used to protect b-lactamase-sensitive antibiotics. For the serine b-lactamases, several classes of mechanism-based inhibitors have been discovered, and several inhibitor proteins are known (26). In many cases, the mechanism of action of the small-molecule inhibitors is not clear, and only two classes have been used in combination with antibiotics.

Clavulanic acid has been widely used clinical application. It is selective for the class A and class D b-lactamases. Opening of the b-lactam ring of clavulanic acid by the initial attack of the b-lactamase triggers a series of chemical rearrangements in the inhibitor moiety (Fig. 4) that results in an acyl-enzyme that is resistant to attack by water and may even be cross-linked by the inhibitor moiety (27).

Figure 4. Suggested mechanism for the reaction of TEM-2 class A b-lactamases with clavulanic acid (27).

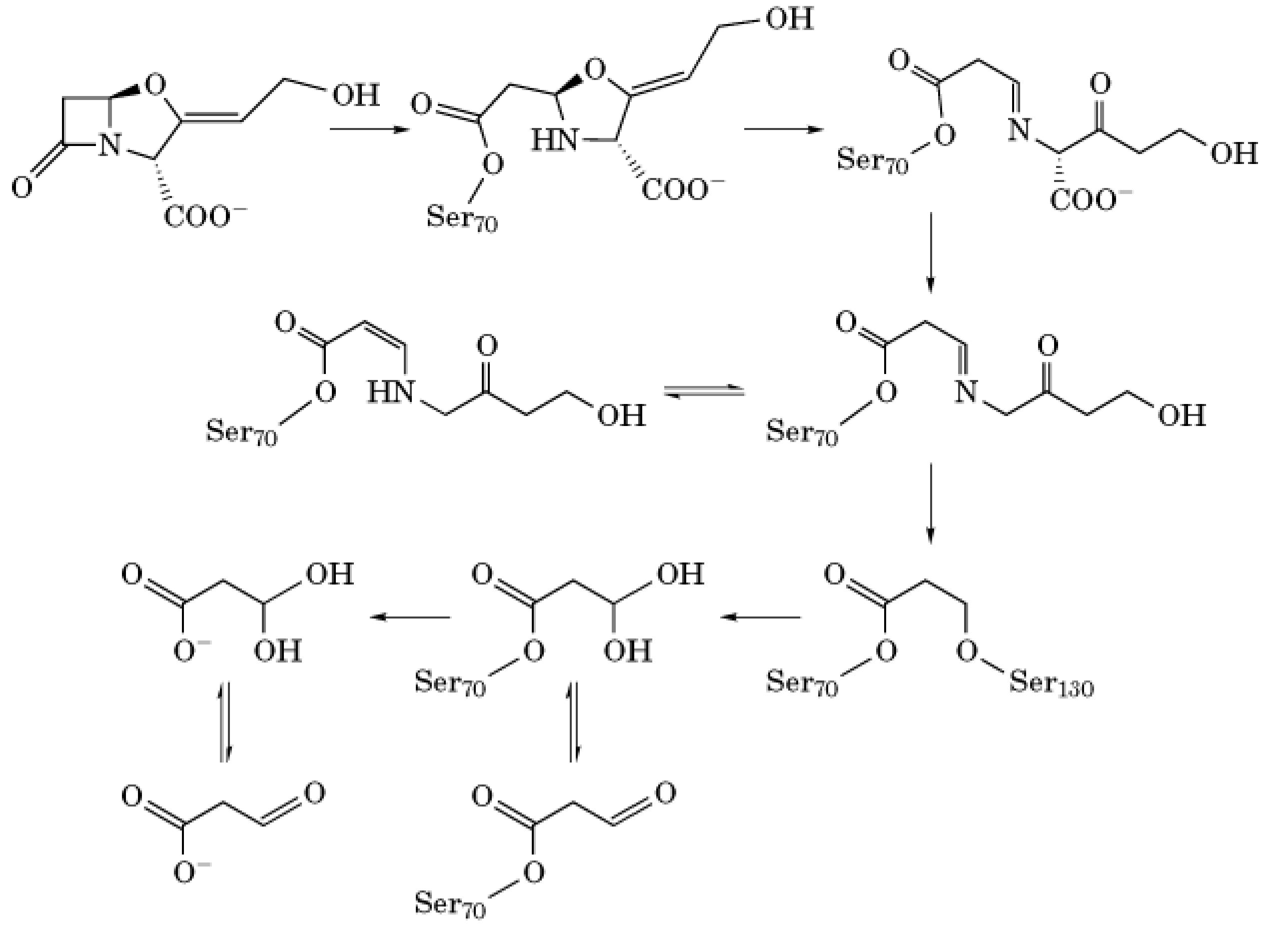

The penam sulfone acids *sulbactam* and *tazobactam* are also used clinically as b-lactamase inhibitors. As with clavulanic acid, a series of chemical rearrangements are provoked by the reaction with b-lactamase. Although sulbactam and tazobactam are relatively selective for class A and class D b-lactamases, analogs that have increased activity against class C b-lactamases have been reported (28).

4. Regulation of Biosynthesis

Expression of chromosomal b-lactamase in *Bacillus* and of **plasmid**-encoded b-lactamases in staphylococci is under the control of a typical repressor protein (Blal and Mecl, respectively) and a second regulatory protein (BlaR and MecR, respectively). The BlaR and MecR regulatory proteins are similar. Both are integral membrane proteins that have a b-lactam-binding **domain** homologous to the class D serine b-lactamases (29). The predicted topology of the polypeptide in the membrane is three to five membrane-spanning **a-helices**, and the N-terminus in the cytoplasm and the b-lactam-binding domain is on the outer surface of the membrane, where it could act as a **receptor** for b-lactams.

Expression of chromosomal class C b-lactamases in Enterobacteriaceae from the *amp*C gene is under the control of the *amp*D, *amp*E, *amp*G, and *amp*R gene products. AmpR protein is a typical transcription activator that is lost in organisms, such as *E. coli*, that have constitutive AmpC production. AmpR responds to the binding of 1,6-anhydro-*N*-acetylmuramyl-[L]-alanyl-[D]-glutamyl-*meso*-diaminopimelic acid (MurNAc tripeptide) produced by breakdown of the peptidoglycan of the cell wall (30). The three other proteins are involved in transmembrane signaling for induction of the b-lactamase. Inactivation of AmpD results in massive overproduction of b-lactamase, whereas loss of either AmpE or AmpG activity results in a total block of induction.

AmpD is an amidase that cleaves the tripeptide from the MurNAc tripeptide, thus inactivating it as an inducer. It is thought that AmpG is an integral membrane protein that acts as a transporter for the MurNAc tripeptide, whereas it has been suggested that AmpE, also an integral membrane protein, provides energy for its uptake (31).

Bibliography

1. M. G. P. Page (1993) Biochem. J. **295**, 295–304.
2. M. H. Richmond and R. B. Sykes (1973) Adv. Microb. Physiol. **9**, 31–88.
3. K. Bush (1989) Antimicrob. Agents Chemother. **33**, 264–270, 271–276.
4. R. P. Ambler (1980) Phil. Trans. R. Soc. Lond. **B239**, 321–331.
5. O. Herzberg and J. Moult (1987) Science **236**, 694–701.
6. B. Samaraoui, B. Sutton, R. Todd, P. Artimyuk, S. G. Waley, and D. Phillips (1986) Nature **320**, 378–380.
7. P. C. Moews, J. R. Knox, O. Dideberg, P. Charlier, and J.-M. Frère (1990) Proteins: Struct. Function Genet. **7**, 156–171.
8. O. Dideberg, P. Charlier, J. P. Wery, P. Dehottay, J. Dusart, T. Erpicum, J.-M. Frère, and J.-M. Ghuysen (1987) Biochem. J. **245**, 911–913.
9. N. C. J. Strynadka, H. Adachi, S. E. Jensen, K. Johns, A. Sielecki, C. Betzel. K. Sutoh, and M. N. G. James (1992) Nature **359**, 700–705.
10. C. Jelsch, L. Mourey, J. M. Masson, and J.-P. Samama (1992) Proteins: Struct. Function Genet. **16**, 364–383.
11. C. Oefner, A. D''Arcy, J. J. Daly, K. Gubernator, R. L. Charnas, I. Heinze, C. Hubschwerlen, and F. K. Winkler (1990) Nature **343**, 284–288.
12. E. Lobkovsky, P. C. Moews, J. Liu, H. Zhao, J.-M. Frère, and J. R. Knox (1993) Proc. Natl. Acad. Sci. USA **90**, 11257–11261.
13. J. A. Kelly and A. P. Kuzin (1995) J. Mol. Biol. **254**, 223–236.
14. R. M. Gibson, H. Christensen, and S. G. Waley (1990) Biochem. J. **272**, 613–619.
15. W. A. Escobar, A. K. Tan, and A. L. Fink (1991) Biochemistry **30**, 10783–10787.
16. G. A. Jacoby and A. A. Medeiros (1991) Antimicrob. Agents Chemother. **35**, 1697–1704.
17. M. Jamin, C. Damblon, A. M. Baudin-Misselyn, F. Durant, G. C. K. Roberts, P. Charlier, G. Llabres, J.-M. Frère. (1994) Biochem. J. **301**, 199–203.
18. P. Taibi-Tonche, I. Massova, S. B. Vakulenko, S. A. Lerner, and S. Mobashery (1996) J. Am. Chem. Soc. **118**, 7441–7448.
19. A. Samuni and N. Citri (1975) Biochem. Biophys. Res. Commun. **62**, 7–11.
20. S. G. Waley (1991) Biochem. J. **279**, 87–94.
21. B. J. Sutton, P. J. Artymiuk, A. E. Cordero-Borboa, C. Little, D. C. Phillips, and S. G. Waley (1987) Biochem. J. **248**, 181–188.
22. R. B. Davies and E. P. Abraham (1974) Biochem. J. **143**, 129–135.
23. G. S. Baldwin, A. Galdes, A. O. Hill, B. E. Smith, S. G. Waley, and E. P. Abraham (1978) Biochem. J. **175**, 441–447.
24. A. Carfi and O. Dideberg (1995) EMBO J. **14**, 4919–4921.
25. N. O. Concha, B. A. Rasmussen, K. Bush, and O. Herzberg (1996) Structure **4**, 823–836.
26. N. C. J. Strynadka, S. E. Jensen, K. Johns, H. Blanchard, M. Page, A. Matagne, J.-M. Frère, and M. N. G. James (1994) Nature **368**, 657–660.
27. R. P. A. Brown, R. T. Aplin, and C. J. Schofield (1996) Biochemistry **35**, 12421–12432.
28. H. G. F. Richter, P. Angehrn, C. Hubschwerlen, M. Kania, M. G. P. Page, J.-L. Specklin, and F. K. Winkler (1996) J. Med. Chem. **39**, 3712–3722.
29. T. Kobayashi, Y. F. Zhu, N. J. Nicholls, and J. O. Lampen (1987) J. Bacteriol. **169**, 3873–3878.

30. J. T. Park (1995) Mol. Microbiol. **17**, 4521–426.

31. S. Lindquist, M. Galleni, F. Lindberg, and S. Normark (1989) Mol. Microbiol. **3**, 1091–1102.

Suggestion for Further Reading

32. M. I. Page, ed. (1992) *The Chemistry of -Lactams* Blackie Academic & Professional, Glasgow. An excellent coverage of all aspects of the interaction of -lactamases with substrates and inhibitors. Particularly useful chapters are " -Lactamase: mechanism of action" by S. G. Waley (pp. 198–228) and " -Lactamase: Inhibition" by R.F. Pratt (pp. 229–271).

Beta-Lactoglobulin

b-Lactoglobulin is the major whey protein in the milk of ruminants, and it has also been reported in milk from many other species, although not human, lagomorph, or rodent. Where found, genetic variants have also been reported in most cases. Isolation of whey protein from bovine milk is straightforward (1), and its concentration is 2 to 3 g/L. Consequently, the protein has been used since its first isolation in 1934 as a convenient, small, soluble protein with which to develop and calibrate new techniques. For example, it is used as a component of standard mixtures for isoelectric focusing and SDS-PAGE and a calibration sequence for automatic sequenators (see Protein Sequencing). The extensive literature on b-lactoglobulin, largely that from the domestic cow, can be broadly divided into studies related to the molecule as a protein and those related to its importance to the dairy industry. Reviews of both abound (2-6).

The polypeptide chain of the protein contains about 160 residues. That of ruminant species is dimeric, and in other species it is monomeric. Figure 1 shows some of the known sequences from the SWISSPROT database (7). Disulfide bonds link cysteines 66 to 160 and 106 to 119. The asterisks show structurally conserved regions that were recognized following the structural determination first of the homologous plasma *retinol-binding protein* and then of bovine b-lactoglobulin (8, 9). These motifs define a widely distributed family called the *lipocalins* (10, 11), whose structure is an eight-stranded antiparallel b-barrel with $(+1)_8$ topology (see Beta-Sheet) and with an **a-helix** on the outer surface. The structure of b-lactoglobulin is shown in Fig. 2 (12). The family relationship has also been observed in the gene sequences, which show similar arrangements of **introns** and **exons** (13). The 400 bp upstream of the **open reading frame** controls the high level of expression and its restriction to the mammary gland (14). This has led to successful use of the b-lactoglobulin operon in transgenic technology (15).

Figure 1. Sequences of mature b-lactoglobulins with the totally conserved residues in bold. The sites of possible genetic shown in the bovine sequence in italics, and changes in the bovine B variant are shown above. The N-terminal sequence (34). The asterisks show the structurally conserved regions indicative of the lipocalin family.

```
******************

BOVINE A   LIVTQTMKGL DIQKVAGTWY SLAMAASDIS LLDAQSAPLR VYVE
PIG I      VEVTPIMTEL DTQKVAGTWH TVAMAVSDVS LLDAKSSPLK AYVE
HORSE II   TDIPQTMQDL DLQEVAGRWH SVAMVASDIS LLDSESVPLR VYVE
DONKEY     TNIPQTMQDL DLQEVAGKWH SVAMAASDIS LLDSEEAPLR VYIE
DOG I      IVVPRTMEDL DLQKVAGTWH SMAMAASDIS LLDSETAPLR VYIQ
CAT I      ATVPLTMDGL DLQKVAGMWH SMAMAASDIS LLDSETAPLR VYVQ
DOLPHIN    VSVIRTMEDL DIQRVAGTWH SVAMAASDIS LLDTEEAPLR VNVE
KANGAROO   VENIRSKNDL GVEKFVGSWY LREAAKT--- -MEF-SIPLFDMDIK
MONKEY     IDSPQTMQDV DLPKLAGTWH SMAMAA....


               G
BOVINE A   WENDECAQKK IIAEKTKIPA VFKIDALNEN --KVLVLDTD YKKY
PIG I      RENDKCAQEV LLAKKTDIPA VFKINALDEN --QLFLLDTD YDSH
HORSE II   GANHACVERN IVAQKTEDPA VFTVNYQGER --KISVLDTD YAHY
DONKEY     GENKGCAEKK IFAEKTESPA EFKINYLDED --TVFALDSD YKNY
DOG I      WEDGRCAEQK VLAEKTEVPA EFKINYVEEN --QIFLLDTD YDNY
CAT I      WEDNRCVEKK VLAEKTECAA KFNINYLDEN --ELIVLDTD YENY
DOLPHIN    RDKNGCVKEK IIAEKTEIPA VFKINFLNEN --KIFVLDSD YTNY
KANGAROO   -KTDRCVEKK LLLKKTKKPT EFEIYISSES SYTFCVMETD YDSY


            A    ***************
BOVINE A   VCQCLVRTPE VDDEALEKFD KALK-ALPMH IRLSFNPTQL EEQC
PIG I      VCQSLARTLE VDDQIREKFE DALK-TLSVP MRI--LPAQL EEQC
HORSE II   VCQYLARTQK VDEEVMEKFS RALQ-PLPGR VQIVQDPSGG QERC
DONKEY     VCQYLARTQM VDEEIMEKFR RALQ-PLPGR VQIVPDLTRM AERC
DOG I      MCQCLARTLE VDENVMEKFN RALK-TLPVH MQLLN-PTQA EEQC
CAT I      VCQCLTRTLK ADNEVMEKFD RALQ-TLPVH VRLFFDPTQV AEQC
DOLPHIN    TCAYLARTLQ VDDGVMEKFN KAIKPALPMH IRL-FSPTQL EEQC
KANGAROO   ACAHYVRRIE -ENKGMNEFK KILR--T-LA MPYTVIEVRT RDMC
```

Figure 2. A MOLSCRIPT (35) diagram of the dimer of b-lactoglobulin showing the fold of the main chain.

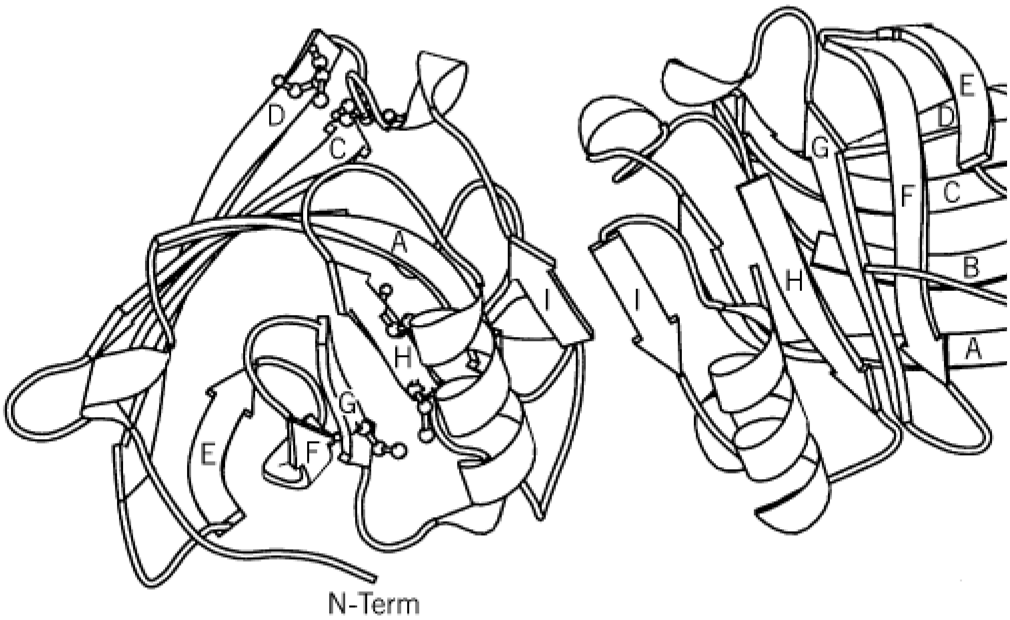

No definite function has yet been ascribed to b-lactoglobulin, but its presence in a family containing mostly small, secreted proteins that transport **hydrophobic** molecules perhaps implies that its function, other than the obvious nutritional one, is associated with the transport or uptake of fatty acids or retinol, both of which it binds (16, 17). Indeed, over 20 different **ligands** have been reported that have **association constants** varying between 5×10^7 and 4×10^2M (3). By analogy with other lipocalins, the binding site should be in the central pocket formed by the b-strands, but there is no definitive evidence that this is the case. Recently it has been shown that palmitate and retinol can bind independently and simultaneously (18).

Some physical parameters of the protein are summarized in Table 1. The bovine protein is stable down to pH 2, and conformational studies have shown that there are several pH-dependent changes between pH 2 and pH 9 (19, 20). At the extremes of pH, the dimer dissociates, and it aggregates above pH 8.5 to 9.0. The conformational change between pH 6 and 8 leads to increased reactivity of the free cysteine residue, perhaps triggered by the titration of a carboxyl group with a pK_a of 7.3. An association of four dimers forms an octamer at 5°C and pH 4.5 mainly in the A variant. This probably results from a carboxyl–carboxylate interaction involving the Gly64Asp change between the most common B and A genetic variants of b-lactoglobulin (21).

Table 1. Selected Fundamental Parameters of Bovine b-Lactoglobulin

Number of amino acids	162
A variant	Asp64, Val118
B variant	Gly64, Ala118
Relative molecular mass	18,400
Sedimentation coefficient ($S°_{20w}$)	2.83×10^{13} s^{-1}
Diffusion coefficient	7.70×10^{-7} cm^2s^{-1}
Stokes' radius	2.68 nm
Radius of gyration	2.17 nm

Axial ratio	2:1
Dipole moment	730 Debye
Absorbance at 280 nm	0.96 (1.0 g/l solution, 1 cm cell)

The complex behavior during refolding from urea between 2° and 25°C is ascribed to **disulfide interchange**. Cys106 pairs with either Cys119 or Cys121, and the former is the native (22, 23). It is not yet clear whether this also explains the partially folded form observed at pH 2, where the protein is predominantly a monomer (24). Refolding from **guanidinium chloride** at low pH shows a transient increase in helical content (25), an effect that is stabilized in ethanolic solution (26).

b-Lactoglobulin has been cloned and expressed both in *Escherichia coli* and in **yeast**, allowing creation of **site-directed mutations** (27) for probing the solution properties (28) or modifying the thermal denaturing behavior (29). Thermal denaturation is of particular interest to the dairy industry because heating milk is the basis of much processing and also the genetic variants exhibit different behavior (30). In addition, protein concentration, pH, temperature, ionic strength, dielectric constant, and buffer type all contribute to the denaturing behavior. Differential scanning **calorimetry** and thermal aggregation studies show that the A variant is less stable than the B variant (31), but studies at lower protein concentration show that the reverse is true (32). Thermal aggregation also involves intermolecular disulfide interchange, presumably initiated by the free thiol group (33).

Bibliography

1. R. Aschaffenburg and R. Drewry (1957) Biochem. J. **65**, 273–277.
2. J. M. A. Tilley (1960) Dairy Sci. Abstr. **22**, 111–125.
3. R. L. J. Lyster (1972) J. Dairy Res. **39**, 279–318.
4. S. G. Hambling, A. S. McAlpine, and L. Sawyer (1992) In *Advanced Dairy Chemistry I*. (P. F. Fox, ed.), Elsevier, Amsterdam, pp. 141–190.
5. M. McSwiney, H. Singh, O. Campanella, and L. K. Creamer (1994) J. Dairy Res. **61**, 221–232.
6. J. E. Kinsella and D. M. Whitehead (1987) Adv. Food Nutr. Res. **33**, 343–438.
7. A. Bairoch and B. Boeckmann (1994) Nucleic Acid Res. **22**, 3578-
8. M. Newcomer et al. (1984) EMBO J. **3**, 1451–1454.
9. M. Z. Papiz et al. (1986) Nature **324**, 383–385.
10. S. Pervaiz and K. Brew (1987) FASEB J. **1**, 209–214.
11. D. R. Flower (1996) Biochem. J. **318**, 1–14.
12. S. Brownlow et al. (1997) Structure, **5**, 481–495.
13. S. Ali and A. J. Clark (1988) J. Mol. Biol. **189**, 415–426.
14. J. P. Simons, M. McClenaghan, and A. J. Clark (1987) Nature **328**, 530–532.
15. A. L. Archibald et al. (1990) Proc. Natl. Acad. Sci. USA **87**, 5178–5182.
16. A. A. Spector and J. E. Fletcher (1970) Lipids **5**, 403–411.
17. F. D. Fugate and P. S. Song (1980) Biochim. Biophys. Acta **652**, 28–42.
18. M. Narayan and L. J. Berliner (1997) Protein Sci. **7**, 150–157.
19. C. Tanford, L. G. Bunville, and Y. Nozaki (1959) J. Am. Chem. Soc. **81**, 4032–4036.
20. S. N. Timasheff, L. Mescanti, J. J. Basch, and R. Townend (1966) J. Biol. Chem. **241**, 2496–2501.
21. J. Witz, S. N. Timasheff, and V. Luzzati (1964) J. Am. Chem. Soc. **86**, 168–173.
22. H. A. McKenzie, G. B. Ralston, and D. C. Shaw (1972) Biochemistry **11**, 4539–4547.

23. T. E. Creighton (1980) J. Mol. Biol. **137**, 61–80.
24. L. Ragona et al. (1997) Folding and Design **2**, 281–290.
25. D. Hamada, S. Segawa, and Y. Goto (1996) Nature Struct. Biol. **3**, 868–873.
26. E. Dufour, H. C. Bertrand, and T. Haertlé (1993) Biopolymers **33**, 589–598.
27. C. A. Batt, L. D. Rabson, D. W. S. Wong, and J. E. Kinsella (1990) Agric. Biol. Chem. **54**, 949–955.
28. Y. Katakura, M. Totsuka, A. Ametani, and S. Kaminogawa (1994) Biochim. Biophys. Acta **1207**, 58–67.
29. C. A. Batt, J. Brady, and L. Sawyer (1994) Tr. Food Sci. **5**, 261–265.
30. E. Jakob and Z. Puhan (1992) Int. Dairy J. **2**, 157–178.
31. X. L. Huang, G. L. Catignani, and H. E. Swaisgood (1994) J. Agric. Food Chem. **42**, 1276–1280.
32. G. I. Imafadon, K. F. Ng-Kwai-Hang, V. R. Harwalkar, and C.-Y. Ma (1991) J. Dairy Res. **74**, 2416–2422.
33. S. P. F. M. Roefs and K. G. Dekruif (1994) Eur. J. Biochem. **226**, 883–889.
34. N. Azuma and K. Yamauchi (1991) Comp. Biochem. Physiol. **99B**, 917–921.
35. P. J. Kraulis (1991) J. Appl. Cryst. **24**, 946–950.

Suggestions for Further Reading

36. L. Banaszak, N. Winter, Zh. Xu, D. A. Bernlohr, S. Cowan, and T. A. Jones (1994) Lipid-binding proteins—a family of fatty-acid and retinol transport proteins, Adv. Protein Chem. **45**, 89–151.
37. L. K. Creamer (1995) Effect of sodium dodecyl sulphate and palmitic acid on the equilibrium unfolding of bovine -lactoglobulin Biochemistry **34**, 7170–7176.
38. P. F. Fox (1995) *Heat Induced Changes in Milk*, 2nd ed., International Dairy Federation, Brussels.
39. T.-R. Kim et al. (1997) High level expression of bovine -lactoglobulin in *P. pastoris* and characterization of its physical properties, Prot. Eng. **10**, 133.
40. H. A. McKenzie (1971) " -Lactoglobulins". In *Milk Proteins—II*. Academic Press, New York. pp. 257–330.
41. B. Y. Qin et al. (1998) Structural basis of the Tanford transition of bovine -lactoglobulin, Biochemistry. **37**, in press.
42. R. Townend, T. T. Herskovits, S. N. Timasheff, and M. J. Gorbunoff (1969) The state of amino acid residues in -lactoglobulin Arch. Biochem. Biophys. **129**, 567–580.

Beta-Meander

The b-meander is a protein motif frequently observed in protein structures. It has a particular type of antiparallel b-sheet structure, with a very simple topology in which two or more b-strands that are consecutive in sequence are also adjacent to one another in the three-dimensional structure (Fig. 1). b-Meanders are equivalent to multiply linked **hairpins**.

Figure 1. Schematic representation of a b-meander consisting of four b-strands (shown as arrows).

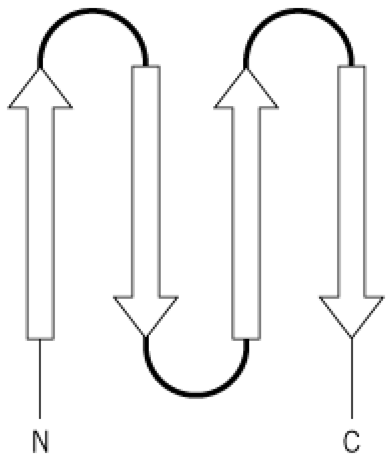

[See also Beta-Sheet.]

Beta-Pleated Sheet

b-Pleated sheet is an alternative name for b-sheet, a type of **secondary structure** occurring in protein structures. The name arises from the pleated nature of the sheet and the individual b-strands when viewed from the side.

[See also Beta-Sheet.]

Beta-Sheet

The b-sheet is a **secondary structure** component of protein structure, comprising two or more adjacent b-strands linked by hydrogen bonds. In contrast to the coiled backbone of the **a-helix**, the structure of a b-strand is characterized by an extended backbone conformation, corresponding to the favorable upper left region of the Ramachandran Plot. b-Sheets are formed by a side-by-side arrangement of b-strands, with backbone hydrogen bonds between adjacent strands linking the sheet together. The side chains of consecutive residues on a b-strand do not interact with each other, but lie alternately above and below the sheet, giving a pleated appearance to the b-sheet backbone (the b-sheet is sometimes referred to as a b-pleated sheet).

b-Strands are often depicted as arrows in protein structure diagrams, with the direction of the arrow running from the N-terminal end to the C-terminal end of the b-strand. When packed together in a b-sheet, the b-strands may all be oriented in the same direction (parallel b-sheet) or in alternating directions (antiparallel b-sheet). In some cases, the b-strands will be a mixture of parallel and antiparallel (mixed b-sheet). The backbone hydrogen bonding patterns of parallel and antiparallel b-sheet structures differ (Fig. 1). In the parallel b-sheet, hydrogen bonds are evenly spaced along the b-strand and point at an angle to the other strand. The antiparallel b-sheet has alternately wide and narrow spacings between adjacent hydrogen bonds. The average backbone angles for parallel and antiparallel b-sheets also vary, with f of –119° and Y of 113° for parallel structures and f of –139° and Y of 135° for antiparallel structures (see Ramachandran Plot). Most b-sheets have a right-handed twist of about 10°. The regular hydrogen bonding pattern and backbone angles of b-sheets are sometimes disrupted at the edges by the formation of a b-bulge, accentuating the twist to 35° to 45°.

Figure 1. b-Sheet structure in proteins. Schematic representation of parallel and antiparallel b-sheets, with each strand of the sheet depicted as an arrow having direction from the *N*-terminal to the *C*-terminal end. In the lower half of the figure, the atomic detail of the b-sheet structure is shown, with hydrogen bonds between backbone carbonyl oxygen atoms and amide nitrogen atoms indicated by dotted lines. Note the approximately equal spacing of hydrogen bonds in the parallel b-sheet compared with the alternating wide and narrow spacing in the antiparallel b-sheet. For clarity, only Cb atoms of side chains are shown. Nitrogen atoms and oxygen atoms are shown as dark spheres. This figure was generated using Molscript (1) and Raster3D (2, 3).

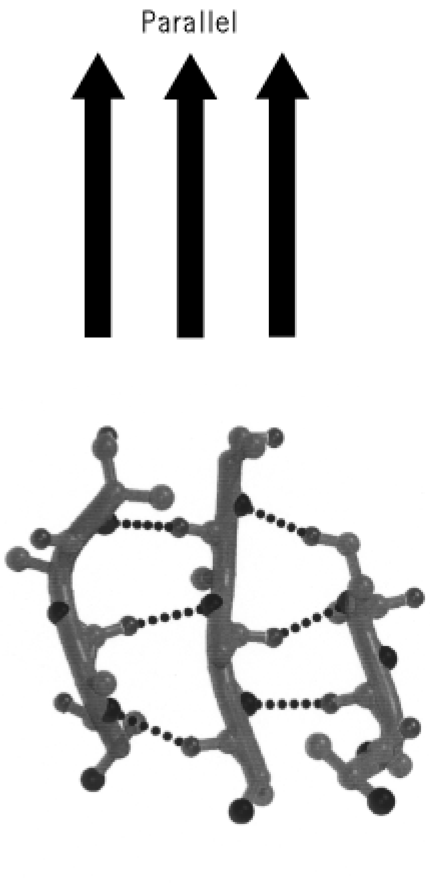

Because a b-sheet can be formed from sections of polypeptide chain that are distant from each other in the primary structure, many different types of b-sheet have been identified in protein structures. The b-meander is a simple antiparallel b-sheet topology where b-strands that are consecutive in sequence are also located adjacent to one another in the three-dimensional structure. The adjacent b-strands in a b-meander are often connected by **hairpin** turns. Other types of antiparallel b-sheet structure include the jelly roll motif, the Greek key motif, and the b-barrel. The b-helix is formed from parallel b-sheets.

[See also Protein Structure and Secondary Structure, Protein.]

Bibliography
1. P. J. Kraulis (1991) J. Appl. Crystallogr. **24**, 946–950.
2. E. A. Merritt and M. E. P. Murphy (1994) Acta Crystallogr. **D50**, 869–873.
3. D. J. Bacon and W. F. Anderson (1988) J. Mol. Graphics **6**, 219–222.

Suggestions for Further Reading
4. C. Branden and J. Tooze (1991) *Introduction to protein structure*, Garland, New York.
5. T. E. Creighton (1993) *Proteins: Structures and Molecular Properties*, W. H. Freeman, New York.
6. J. S. Richardson (1981) The anatomy and taxonomy of protein structure. Adv. Protein Chem. **34**, 167–339.

Beta-Strand

A b-strand is one of the two regular types of **secondary structure** (the other being the a-helix) that is commonly observed in protein structures. The b-strand is characterized by an extended backbone conformation. The b-strand is not stable as a discrete structural unit by itself, but is stable only when it associates through hydrogen bond interactions with adjacent b-strands to form a b-sheet.

[See also Beta-Sheet and Secondary Structure, Protein.]

Beta-Turns

A b-turn is a type of nonregular **secondary structure** in proteins that causes a change in direction of the polypeptide chain. In the b-turn, a hydrogen bond is formed between the backbone carbonyl oxygen of one residue (i) and the backbone amide NH of the residue three positions further along the chain ($i + 3$) (Fig. 1) (1). This (i) to ($i + 3$) interaction distinguishes b-turns from g-turns, which have an (i) to ($i + 2$) hydrogen bond. There are several different types of b-turns, classified according to the backbone dihedral angles of the two intervening residues, ($i + 1$) and ($i + 2$). The type I and II turns are the most common, together accounting for about two-thirds of all b-turns, but they have very different amino acid preferences (2). Type I turns prefer Asn, Asp, or Ser in the (i) position; Asp, Ser, Thr or Pro in ($i + 1$); Asp, Ser, Asn, or Arg in ($i + 2$); and Gly, Trp, or Met in ($i + 3$). In contrast, type II turns have a preference for Pro at position ($i + 1$), Asn or Gly at position ($i + 2$) and Gln or Arg at ($i + 3$) (2). Other b-turn types include type I′ (related to type I by inversion of the sign of the f and y angles of the Ramachandran Plot), II′ (related to type II in the same way), IV, VIa, VIb, and VIII. Types I′ and II′ are almost exclusively found in **hairpins**; that is, they usually connect two adjacent antiparallel b-strands. The type IV b-turn is a miscellaneous type that includes any (i) to ($i + 3$) hydrogen-bonded turn in a protein structure where the f and y angles are different (by >40°) from the values that define the other b-turn types (Table 1). Types VIa and VIb have a proline *cis*-peptide bond at the ($i + 2$) position; in type VIa the proline adopts a backbone conformation close to that of a-**helical** residues, whereas in type VIb the proline has a conformation similar to that of residues in a b-strand.

Figure 1. Schematic representations of a b-turn in a protein structure. (**Left**) The b-turn is shown connecting two b-strands in a hairpin motif. (**Right**) The detailed atomic structure of the b-turn is shown. Residues are numbered 1 to 4 for (*i*) to (*i* + 3). The hydrogen bond between the backbone carbonyl oxygen of residue 1 and the backbone amide nitrogen of residue 4 is shown as a dotted line. This example is a type I b-turn, because the backbone angles for the (*i* + 1) residue are f = –63° and y = –33°; and for the (*i* + 2) residue, f is –86° and y = –3°. Oxygen atoms and nitrogen atoms are shown as dark spheres. This figure was generated by Molscript (3) and Raster3D (4, 5).

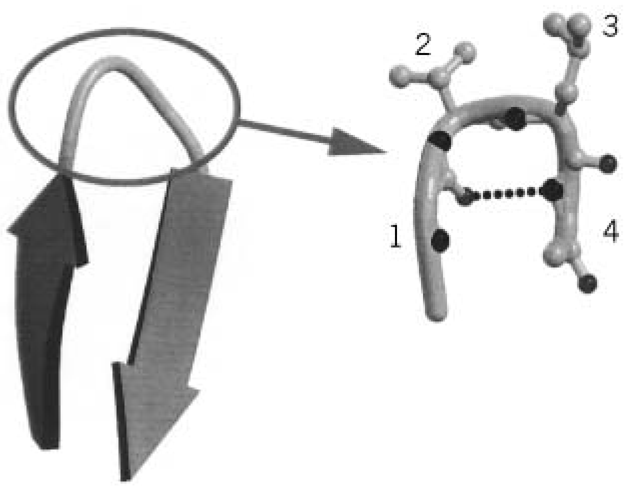

Table 1. Classification of Beta-Turn Types

	Backbone Dihedral Angles of Central Residues			
Beta-Turn Type	**f*i* + 1**	**y*i* + 1**	**f*i* + 2**	**y*i* + 2**
I	–60°	–30°	–90°	0°
I′	60°	30°	90°	0°
II	–60°	120°	80°	0°
II′	60°	–120°	–80°	0°
IV	Any (*i*) to (*i* + 3) hydrogen-bonded turn having angles that differ by more than 40° from those of other b-turn types			
VIa	–60°	120°	–90°	0°
VIb	–120°	120°	–60°	0°
VIII	–60°	–30°	–120°	120°

[See also Secondary Structure, Protein, Turns, Gamma-Turns, and Omega Loop.]

Bibliography
1. J. S. Richardson (1981) Adv. Protein Chem. **34**, 167–339.
2. C. M. Wilmot and J. M. Thornton (1988) J. Mol. Biol. **203**, 221–232.
3. P. J. Kraulis (1991) J. Appl. Crystallogr. **24**, 946–950.
4. E. A. Merritt and M. E. P. Murphy (1994) Acta Crystallogr. **D50**, 869–873.
5. D. J. Bacon and W. F. Anderson (1988) J. Mol. Graphics **6**, 219–222.

Bicoid

Mutational analysis in the fruitfly *Drosophila melanogaster* has demonstrated that many aspects of anteroposterior patterning are already programmed in the oocyte by maternal gene activity (1, 2). During embryonic development, cells within an embryonic field receive positional information and are instructed by the concentration gradient of morphogens (3). Historically, the graded distribution of the Bicoid protein (Bcd) has provided the first evidence for the existence of such a morphogenetic gradient. Maternally derived *bcd* messenger RNA is localized to the anterior pole of the oocyte, where it serves as the source for the Bcd concentration gradient. Then, Bcd acts as a concentration-dependent activator of transcription and as a **translational repressor**. However, Bcd is only part of a wider regulatory network of maternal determinants, and its presence might actually be restricted to dipteran flies.

0.1. Anterior Localization of the Maternal Determinant *Bicoid*

Evidence for an anterior organizing center has been obtained by experimental embryology, for example, the removal and transplantation of polar cytoplasm (4) (see Organizer). The nature of the patterning agents has been identified as RNA-containing particles (5). Genetic experiments have shown that the anterior morphogenetic function requires the activity of the *bicoid* maternal gene (*bcd*). Mothers homozygous mutant for *bcd* are normal, but all of their progeny lack head, thorax, and some abdominal structures. Instead posterior terminal structures are duplicated at the anterior (Fig. 1; (6)). Cloning of the *bcd* **gene** revealed that *bcd* is expressed during oogenesis and that its mRNA is localized to the anterior tip of the oocyte and early embryo (Fig. 2) (7). This localization depends on the presence of the *bcd* 3′-UTR, which contains a specific structure recognized by factors that carry it to the anterior pole along the polarized microtubule array of the oocyte (8).

Figure 1. Phenotype of *bcd* embryos. Mothers homozygous mutant for *bcd* lay embryos that develop cuticles lacking all head structures (hs), thorax (T1, T2, T3), and two abdominal segments (A2, A4). Furthermore, the posterior structures like the spiracles (sp) are duplicated at the anterior.

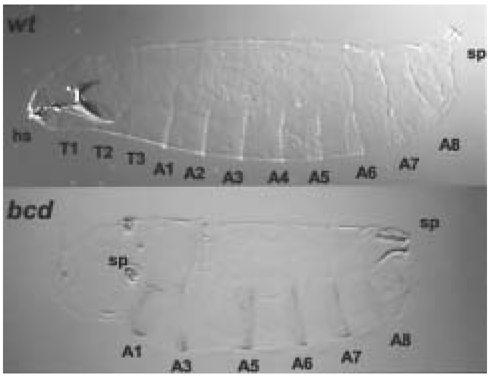

Figure 2. mRNA and protein expression of bcd and cad. The *bcd* mRNA is localized at the most anterior tip of the embryo. Its translation and diffusion of its protein product lead to the formation of the Bcd morphogenetic gradient. Maternal *cad* mRNA is distributed throughout the embryo, but its translation is blocked by the Bcd protein. This leads to the formation of a posterior to anterior gradient of the Cad protein.

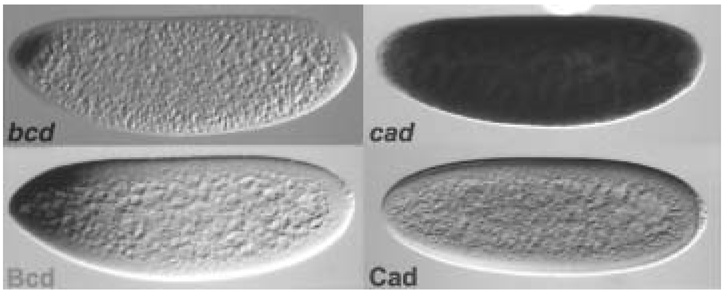

0.2. The Morphogenetic Gradient of the Bicoid Transcription Factor
After egg deposition, the anteriorly localized *bcd* mRNA starts to be **translated**, producing a source of the Bcd protein. Then, Bcd **diffuses** passively in the syncytial environment of the blastoderm embryo and generates an anteroposterior concentration gradient whose high point is at the anterior pole of the embryo and whose low point is near the posterior pole (Fig. 2; (9, 10)). Decreasing or increasing the copy number of the *bcd* gene changes the slope of the Bcd gradient and, consequently, changes the fate map of the early embryo. This suggests that anterior positional values are specified by Bcd in a concentration-dependent manner (9, 10).

The Bcd protein contains a homeodomain (7) that does not belong to any specific class (see Homeobox Genes). It is characterized by a **lysine** residue at residue 50 (Lys50) of the homeodomain that determines its **DNA-binding** specificity (14). Bcd functions as a transcriptional activator in cell culture and in yeast (11-13). The morphogenetic gradient of Bcd differentially activates the first zygotically active segmentation genes, the gap genes. At high concentrations of Bcd, the head gap genes *orthodenticle* (*otd*), *empty spiracles* (*ems*), and *buttonhead* (*btd*) are activated (15-18), whereas lower levels of Bcd are required to activate *hunchback* (hb), which is expressed in a broad anterior domain (Fig. 3; (13)). A detailed study of the proximal *hb* **promoter** suggested that the affinity of Bcd binding sites in the promoters of the different target genes determines at which threshold level, and therefore at which position along the anterior-posterior axis, these genes are activated (19, 20). The ability of Bcd to activate target genes differentially provided the first molecular explanation of how a morphogen might act.

Figure 3. Expression pattern of *bcd* target genes. *bcd* is a maternal gene that controls the expression of the zygotic gap

target genes. The morphogenetic gradient of Bcd protein differentially activates head (*otd, ems*, and *btd*) or thoracic (*hb*) gap genes.

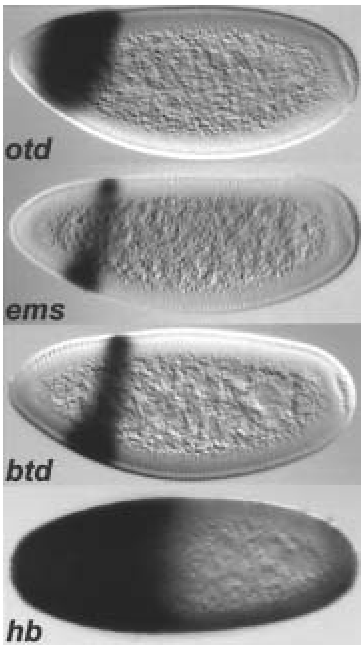

Although Bcd is a DNA-binding protein, it also controls translation of the *caudal* gene (*cad*). *cad* is a gene required for posterior development, and its function is evolutionarily conserved in diverse organisms, including vertebrates (21). Maternal *cad* mRNA is ubiquitously distributed (22-24). Its translation is blocked at the anterior of the embryo by *bcd*, leading to a posterior-to-anterior gradient of the Cad protein (Fig. 3). *cad* is expressed ectopically in *bcd* mutant embryos throughout the embryo. Bcd binds to a sequence in the 3′-untranslated region of the *cad* mRNA (25-27). Like DNA binding, Bcd's RNA binding is conferred by the homeodomain and depends on the presence of Lys50 in the homeodomain. The Bcd homeodomain is the only one that binds RNA (25, 27).

0.4. Bicoid is Integrated into a Network of Maternal Determinants

Bcd is not the only maternal morphogen involved in anteroposterior patterning. A morphogenetic gradient of the Hunchback protein (Hb) creates the correct polarity in the embryo in the absence of *bcd*. The anteroposterior Hb gradient is established by translational repression of ubiquitous maternal mRNA by the *nanos* posterior determinant (28-30). Bcd and Hb are redundant for abdominal segmentation because high levels of maternal Hb rescue the abdominal phenotype of *bcd* mutant embryos (28, 29) and the activation of the central gap gene *Krüppel*. At the anterior of the embryo, Bcd and Hb synergize to activate the anterior gap genes (31). Because each morphogen has instructive functions on its own, both must be removed from the embryo to disrupt the polarity of the embryo completely. In more posterior regions, Bcd is also redundant with *cad* for activating the gap gene *knirps* (32). This shows that *bcd* function is partially redundant with other maternal functions. It should be noted that maternal *hb* and *cad* functions are not essential for viability in the presence of *bcd*. It is likely that they represent remains of ancestral systems that patterned the embryo before the appearance of *bcd*.

At the anterior pole of the embryo, Bcd function is influenced by the activity of the terminal system, which involves locally activating the Torso (Tor) **receptor tyrosine kinase** (33). Tor activity leads to two opposite effects on Bcd function. Tor activity increases the activator function of Bcd by lowering the threshold level of Bcd where target genes are activated (18, 34, 35). At the anterior pole, however, Bcd function is blocked in a Tor-dependent manner, and most *bcd* target genes retract from the anterior pole where Bcd concentration is the highest (36). The effect of *tor* activity on Bcd function might be mediated by *tor*-dependent phosphorylation of Bcd (36), or it may be indirect and may involve other factors (34).

0.5. Evolutionary Considerations on Bicoid

There are several reasons to believe that the critical functions of *bcd* in patterning the anteroposterior axis of the *Drosophila* embryo (Fig. 4) may not be conserved throughout evolution. *bcd* is unlikely to represent an ancestral morphogen. No *bcd* homologous genes have been identified outside higher dipterans (38), despite its homeobox and its specific location in the Hox cluster (7). Moreover, *bcd* shows an unusually high rate of **divergence** for a homeobox gene (39), and its function is not even conserved within higher dipterans (38, 40). Therefore, it is reasonable to assume that *bcd* is the result of recent gene duplication in the Hox cluster of dipterans and that it evolves relatively freely. Therefore, although the role of Bcd in *Drosophila* represents a striking example of a powerful morphogenetic **transcriptional factor**, it is likely that this function is not conserved in other insects and may exist only to allow the *Drosophila* embryo to develop quickly.

Figure 4. Morphogenetic functions of the Bcd gradient. The Bcd gradient differentially activates zygotic target genes (dark boxes) in head and thorax anlagen. The Bcd gradient also leads to the formation of the Cad protein gradient by blocking translation of its mRNA.

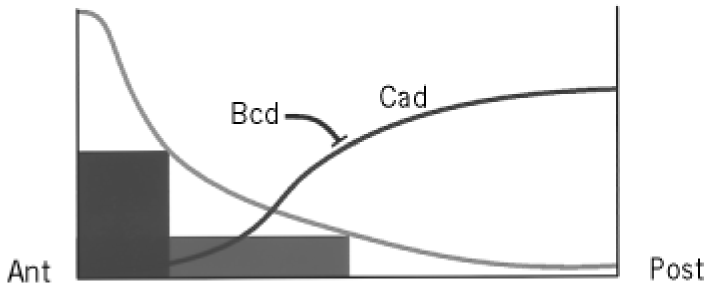

Bibliography

1. C. Nüsslein-Volhard and E. Wieschaus (1980) Nature **287**, 795–801.
2. C. Nüsslein-Volhard, H. G. Frohnhofer, and R. Lehmann (1987) Science **238**, 1675–1681.
3. L. Wolpert (1969) J. Theor. Biol. **25**, 1–47.
4. K. Sander (1969) *Advances in Insect Physiology* (J. E. Treherne, M. J. Berridge, and V. B. Wigglesworth, eds.), Academic Press. Vol. **12**, pp. 125–235.
5. K. Kalthoff (1979) *Determinants of Spatial Organization* (S. Subtelney and I. R. Konisberg, eds.), Academic Press, N.Y., pp. 97–126.
6. H. G. Fröhnhofer and C. Nüsslein-Volhard (1986) Nature **324**, 120–125.
7. T. Berleth, M. Burri, G. Thoma, D. Bopp, S. Richstein, G. Frigerio, M. Noll, and C. Nüsslein-Volhard (1988) EMBO J. **7**, 1749–1756.
8. D. Ferrandon, L. Elphick, C. Nüsslein-Volhard, and D. St Johnston (1994) Cell **79**, 1221–1232.
9. W. Driever and C. Nüsslein-Volhard (1988) Cell **54**, 95–104.
10. W. Driever and C. Nüsslein-Volhard (1988) Cell **54**, 83–93.
11. S. D. Hanes and R. Brent (1989) Cell **57**, 1275–1283.
12. W. Driever, J. Ma, C. Nüsslein-Volhard, and M. Ptashne (1989) Nature **342**, 149–154.
13. G. Struhl, K. Struhl, and P. M. Macdonald (1989) Cell **57**, 1259–1273.
14. J. Treisman and C. Desplan (1989) Nature **341**, 335–337.
15. D. Dalton, R. Chadwick, and W. McGinnis (1989) Genes and Devel. **3**, 1940–1956.
16. R. Finkelstein and N. Perrimon (1990) Nature **346**, 485–488.
17. U. Walldorf and W. J. Gehring (1992) EMBO J. **11**, 2247–2259.

18. E. A. Wimmer, M. Simpson-Brose, S. M. Cohen, C. Desplan, and H. Jäckle (1995) Mechanisms of Development **53**, 235–245.
19. W. Driever, G. Thoma, and C. Nüsslein-Volhard (1989) Nature **340**, 363–367.
20. G. Struhl (1989) Nature **338**, 741–744.
21. V. Subramanian, B. I. Meyer, and P. Gruss (1995) Cell **83**, 641–653.
22. M. Mlodzik and W. J. Gehring (1987) Cell **48**, 465–478.
23. M. Mlodzik, A. Fjose, and W. J. Gehring (1985) EMBO J. **4**, 2961–2969.
24. P. M. MacDonald and G. Struhl (1986) Nature **324**, 537–545.
25. R. Rivera-Pomar, D. Niessing, U. Schmidt-Ott, W. J. Gehring, and H. Jäckle (1996) Nature **379**, 746–749.
26. J. Dubnau and G. Struhl (1996) Nature **379**, 694–699.
27. S. K. Chan and G. Struhl (1997) Nature **388**, 634.
28. G. Struhl, P. Johnston, and P. A. Lawrence (1992) Cell **69**, 237–249.
29. M. Hülskamp, C. Pfeifle, and D. Tautz (1990) Nature **346**, 577–580.
30. C. Schülz and D. Tautz (1995) Development **121**, 1023–1028.
31. M. Simpson-Brose, J. Treisman, and C. Desplan (1994) Cell **78**, 855–865.
32. R. Rivera-Pomar, X. Lu, N. Perrimon, H. Taubert, and H. Jackle (1995) Nature **376**, 253–256.
33. N. Perrimon and C. Desplan (1994) Trends in Biochemical Sciences **19**, 509–513.
34. Q. Gao, Y. Wang, and R. Finkelstein (1996) Mechanisms of Development **56**, 3–15.
35. U. Grossniklaus, K. M. Cadigan, and W. J. Gehring (1994) Development **120**, 3155–3171.
36. E. Ronchi, J. Treisman, N. Dostatni, G. Struhl, and C. Desplan (1993) Cell **74**, 347–355.
37. Y. Bellaïche, R. Bandyopadhyay, C. Desplan, and N. Dostatni (1996) Development **122**, 3499–3508.
38. R. Schöder and K. Sander (1993) Roux"s Arch. Dev. Biol. **203**, 34–43.
39. R. Sommer and D. Tautz (1991) Development **113**, 419–430.
40. F. Bonneton, P. J. Shaw, C. Fazakerley, M. Shi, and G. A. Dover (1997) Mechanisms of Development **66**, 143–156.

Suggestions for Further Reading

41. P. A. Lawrence (1992) *The Making of a Fly, The Genetics of Animal Design*, Blackwell Scientific Publications.
42. P. A. Lawrence and G. Struhl (1996) Cell **85**, 951–961.
43. D. St Johnston (1995) Cell **81**, 161–170.
44. D. St Johnston and C. Nüsslein-Volhard (1992) Cell **68**, 201–219.

Bifunctional Crosslinking Reagents

1. Terminology

If a bifunctional chemical crosslinking agent is designed so that its two reactive groups are identical, it is referred to as a *homobifunctional* reagent; if its two reactive groups are different, it is a *heterobifunctional* reagent. If one or both reactive groups of the crosslinker become so only as the result of a photochemical reaction caused by exposing the reagent to light of an appropriate wavelength, then the crosslinking reagent is photoactivatable, photoreactive, photosensitive, or **light-activated (caged)**. The portion of the crosslinking reagent other than, and usually between, its two reactive groups is referred to as the *spacer arm*, or *crossbridge*. If the spacer arm contains a covalent bond that can be easily broken (by an oxidant, reductant, base, etc), then the crosslinker is termed *cleavable*; otherwise, it is classified as *noncleavable*. With most chemical crosslinkers, a portion of the reagent is incorporated into the final crosslinked complex; however, there is a special class of reagents that facilitate crosslinking without being incorporated into the final covalent complex. These reagents are referred to as *zero-length* crosslinkers, because the groups they crosslink are not separated by a spacer arm.

2. Variables in the Design of Crosslinking Reagents

By varying the chemical and physical properties of the reactive groups and spacer arm of a crosslinking agent, one can obtain crosslinkers with different properties and uses. A heterobifunctional reagent, with its two different types of reactive groups, allows for different selectivities in the functional groups that become crosslinked, compared to a homobifunctional reagent containing a pair of the same reactive groups. The selectivity shown by the reactive groups of crosslinkers for the side chains of particular amino acids mirrors the selectivity of those reactive groups when used as monofunctional reagents in the chemical modification of proteins, from which crosslinking is an outgrowth.

A number of variables pertain to spacer arms: (*1*) the length of the crossbridge, as in the case of bisimidoesters (Table 1) with different numbers of methylene groups in the spacer arm; (*2*) its geometry, which in the case of the phenylenebismaleimides (Table 1) also causes an increase in length, progressing from *ortho* to *para*; (*3*) its chemical nature, especially the number of charged or polar groups on the spacer arm, which influences the crosslinker's solubility properties and uses. For example, membrane proteins would more likely be crosslinked by bifunctional reagents that are **hydrophobic**, rather than hydrophilic. Reporter groups (chromophores, radioactive tracers, etc) can also be incorporated into spacer arms to facilitate quantification of the extent of protein modification, studies on the crosslinked complex, or identification of the crosslinked components. Incorporation into the spacer arm of cleavable bonds, such as disulfide bonds, is also useful in the identification of crosslinked components, especially by diagonal methods (1).

Table 1. Examples of Bifunctional Crosslinkers

Compound	Structure	Class
Homobifunctional		
1. *N,N′-p*-Phenylenebismalemide	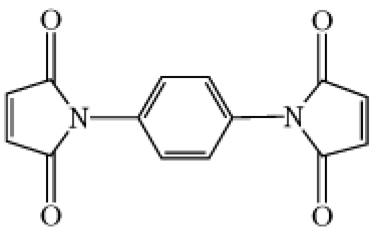	Bismalemide
2. *N,N′*-Ethylene-bis (iodoacetamide)		Bishaloacetylamide

	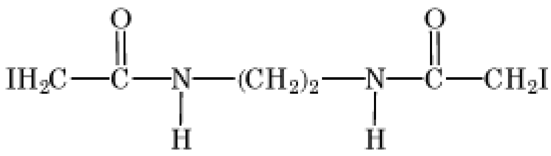	
3. Dimethylsubermidate	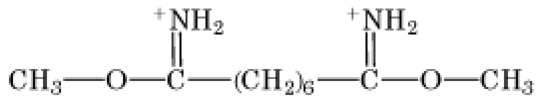	Bisimidoester
4. *N*-Hydroxysuccinimidylsuberate	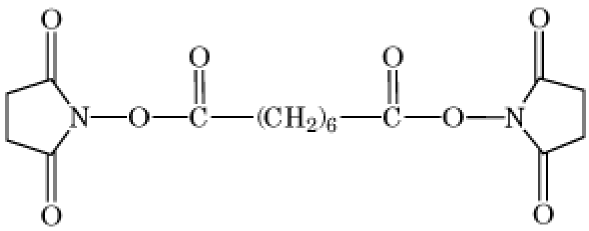	*N*-Hydroxysuccinimi
5. Glutaraldehyde	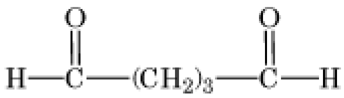	Dialdehyde
Heterobifunctional		
6. *N*-Succinimidyl-3-maleimidopropionate	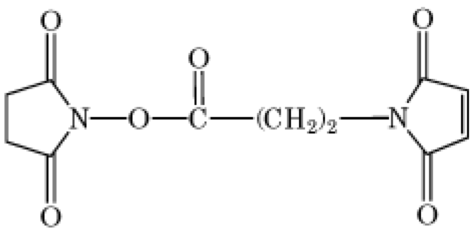	*N*-Hydroxysuccinimide
7. *N*-5-Azido-2-nitrobenzoyloxysuccinimide	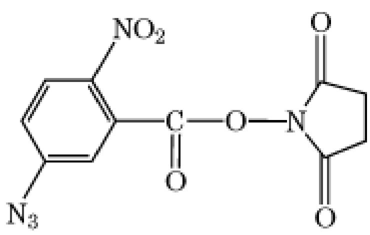	Arylazide/N-hydroxy ester

3. Examples of Bifunctional Crosslinkers

The compounds listed in Table 1 are representative of some of the most frequently used chemical classes of crosslinking reagents, but they represent only a small fraction of the literally hundreds of bifunctional crosslinking reagents that have been described in the scientific literature. The widely used *N*-substituted bismaleimides are selective for thiol groups, especially at pH values near neutrality, where amino groups are predominantly protonated. This class of crosslinkers is available with many different spacer arms, having large variations in length and solubility, or having chromophores or cleavable bonds incorporated. The alkylating bishaloacetyl crosslinkers are also selective at neutral pH for sulfhydryl groups, but they will also react with imidazole side chains of some **histidine** residues under this condition. It should be remembered that few reagents used to modify proteins chemically are absolutely specific for any given amino acid side chain; on the other hand, high selectivity can often be achieved empirically through varying the pH, reaction time, and concentrations of reactants.

The bisimidoesters were among the earliest used crosslinkers and are also available with a variety of spacer arms. These compounds preferentially react at alkaline pH with amino groups, with which they form amidine bonds, retaining the positive charge of the original amine. A more frequently used class of amine-selective reagents is the N-hydroxysuccinimide esters, which produce an amide-crosslinked product that is relatively stable in aqueous solution. The *N*-hydroxysuccinimide ester group is frequently combined with maleimide, such as in compound 6 of Table 1, to produce heterobifunctional crosslinkers with selectivity toward crosslinking amino and sulfhydryl groups. Another common class of heterobifunctional crosslinkers contains at one end a photoactivatable group, which is generally assumed to be nonselective for the functional groups it modifies. For this class of reagents, the two-step reaction protocol is particularly useful, with the chemical reaction being carried out first in the absence of activating radiation, followed by irradiation of the photosensitive group to bring about crosslinking. The arylazide shown in Table 1 (compound 7) is an example of a photosensitive crosslinker that is widely used. The bis-homobifunctional aldehyde glutaraldehyde (Table 1, compound 5) is perhaps the most frequently used chemical crosslinker.

Bibliography

1. J. A. Cover, J. M. Lambert, C. M. Norman, and R. R. Traut (1981) Biochemistry **20**, 2843–2852.

Suggestions for Further Reading

2. S. S. Wong (1993) *Chemistry of Protein Conjugation and Cross-Linking*, CRC Press, Boca Raton, FL. (An outstanding book describing all aspects of the chemistry and uses of bifunctional reagents in crosslinking and conjugation, with an extensive bibliography for each chapter.)
3. Annual products catalog of Pierce Chemical Co., Rockford, IL. [Contains structures, helpful information, and specific uses (with references) for a large number of bifunctional reagents.]

Binding

Total binding B_L is the number of ligand molecules that at any moment are in contact with (occupy sites on) the accessible surface of a protein molecule. It is related to preferential binding (as measured by equilibrium dialysis) by

$$B_L = \left(\frac{\partial m_L}{\partial m_{pr}}\right)_{T,\mu_w,\mu L} + \frac{m_L}{m_w} B_w \tag{1}$$

where B_L and B_w are the numbers of ligand and water molecules, respectively, that are in contact with the protein surface.

When the interactions are weak, the ligand must be used at high concentration (eg, 1 *M* sucrose, 3 *M* glycerol, 8 *M* urea). As a consequence, the total binding is *not* given by equilibrium dialysis, as the last term of Eq. (1) (binding of water) becomes significant. Total binding can be measured by nonthermodynamic techniques that respond to contacts between ligand molecules and protein [(1)]. Such techniques include **calorimetric** titration, which detects the heat of protein–ligand contact, or spectroscopic techniques (eg, **fluorescence** or **uv absorbance**) that detect spectral perturbations each time a ligand–protein contact is made. If the total hydration is known from other techniques, then total binding can be derived from dialysis equilibrium results by the application of Eq. (1).

Bibliography

1. S. N. Timasheff (1995) In *Protein-Solvent Interactions* (R. B. Gregory, ed.), Marcel Dekker, New York, Chap. "11".

Bioinformatics

Bioinformatics is a new branch of molecular biology, also kown as computational biology. Computational physics and computational chemistry have emerged as third branches in their respective disciplines, after the experimental and theoretical branches, due largely to the advance of computational capabilities in modern computers. In contrast, bioinformatics has emerged in molecular biology as the result of advances in experimental technology, especially in the high-throughput DNA sequencing, which is generating a vast amount of **gene** and protein sequence data. Since initiation of the Human Genome Project in the late 1980s, bioinformatics has become an integral part of the coordinated efforts to sequence the entire genomes of a number of organisms from **bacteria** to human. Consequently, bioinformatics is a data-driven discipline requiring large-scale databases and associated technologies for data management and interpretation. This contrasts with the model-driven, theory-based approaches in computational physics and computational chemistry.

Bioinformatics covers a diverse range of topics, which broadly have two roles. First, bioinformatics is widely used in experimental projects, such as in determining the optimal **genetic mapping** strategy and how best to assemble raw sequence data, and in the storing and handling information and materials. Secondly and more important, the major task of bioinformatics is to develop new databases and new computational technologies that will help to understand the biological meaning encoded in the sequence data. Interpretation of sequence data cannot be achieved by numerical calculations based on first-principle equations, which are virtually nonexistent in biology, but it requires using and processing empirical knowledge acquired from experimental data. This is what human experts would do if the amount of data and knowledge were manageable in size. Thus, bioinformatics was born from the marriage of molecular biology, in the age of massive data production, with artificial intelligence, which is a mature branch of computer science, to automate knowledge processing.

Table 1 summarizes topics in bioinformatics for interpretating of sequence data. The methods of computer science have been used traditionally in artificial intelligence applications, such as speech recognition and natural language processing, but they are also quite effective in solving problems in molecular biology. There is a rough distinction between how data are organized and consequently what kinds of computational methods are used in the three categories of Table 1. In the first category of similarity searches, the database is a collection of all the known primary data, such as the sequence database and the structure database, which are the repositories of all reported sequences and three-dimensional structures, respectively, of **nucleic acids** and proteins. A basic operation in this category is comparing of individual sequences or structures to detect any similarity. For example, to understand the functional implications of a newly determined gene or protein sequence, it is customary to perform a sequence similarity, or homology, search, comparing the query sequence with each of the sequences in the database. If any similar sequence is found in the database, the query sequence is assumed to have a similar or related function. This reasoning is based on the empirical observation that homologous sequences generally share similar functions and similar 3-D structures, because they arose from a common evolutionary ancestor and because of functional constraints.

Table 1. Bioinformatics for Interpretation of Sequence Data

Problems in BiologicalScience		Methods in Computer Science
Similarity search	Pairwise sequence alignment	Dynamic programming
	Sequence similarity search	Simulated annealing
	Multiple sequence alignment	Genetic algorithms
	RNA secondary structure prediction	Other optimization algorithms
	3-D protein structure alignment	
Structure/function prediction	Motif extraction	Discriminant analysis
	Functional site prediction	Neural network
	Cellular localization prediction	Hidden Markov model
	Coding region prediction	Formal grammar
	Transmembrane segment prediction	Other pattern recognition and learning algorithms
	Protein secondary structure prediction	
	3-D protein structure prediction	
	3-D RNA structure prediction	
Molecular classification	Superfamily classification	Clustering algorithms
	Fold classification	
	Ortholog/paralog grouping of genes	

The procedure of comparing two sequences is a problem of sequence alignment, which is a major topic in sequence analysis. Given a similarity measure of amino acids or nucleotides, the problem of obtaining the best sequence alignment is equivalent to optimizing a given score function that represents the overall similarity. There are variations in how the optimal alignment is made, either globally for the entire sequences or locally to detect localized regions, how many sequences are aligned at a time, and which similarity measure is to be used. By allowing insertions and deletions (indels), the number of possible alignments grows exponentially as the number and length of the sequences to be compared increases. Thus, the sequence alignment problem is a typical combinatorial optimization problem in computer science. Although the alignment of two or three sequences can be solved rigorously by using dynamic programming algorithms (1), which effectively evaluate all possibilities, multiple alignment of many sequences requires heuristic algorithms to obtain approximate solutions. Furthermore, to search large databases effectively for similar sequences, heuristic algorithms such as FASTA (2) and BLAST (3) have been developed for rapidly identifying regions of two sequences that are similar locally. Other extensions of the sequence alignment algorithms include analysis of a single RNA sequence to predict any **secondary structure** (see RNA Structure Prediction) and compare two 3-D protein structures.

When humans try to interpret a sentence written in a foreign language, they use dictionaries and a knowledge of grammar. However, the process of using a homology search to interpret a sentence written in the DNA language is like comparing it with all the sentences written in the past and checking precedents as to how they were interpreted. Sequence interpretation would become more efficient if our knowledge of sequence-functional relationships were more advanced. The second and third categories in Table 1 involve such reorganizations of the primary data. In the second category of structure/function prediction, the primary data are classified into a group based on a given criterion, such as functional identity, and higher level knowledge is abstracted from this group. This is based on our empirical observation that the function of a protein molecule is usually exerted at a functional site in its three-dimensional structure, which is usually a **ligand-binding** site for other molecules, and that the site is formed by one or more linear polypeptide segments that have conserved sequence patterns. These conserved patterns are called sequence motifs, and they can be extracted, for example, by multiple alignment of a set of sequences that have the same function. A motif search against a library of known motifs is widely used as an alternative method for interpreting sequence data, when no similar sequences have been found by a homology search. However, the bioinformatics problem here is not how to search the known motifs, but how best to extract and define new motifs effectively. Thus, the problem is related to machine learning in computer science, where a higher level concept or a generalized pattern is abstracted from a set of given examples.

Although the second category in Table 1 is targeted at a specific function and a specific group of sequences, the third category of molecular classification represents a more global analysis, where the grouping is attempted with all the available data, and the relationship among groups, which is often hierarchical, is examined. For example, all known protein sequences can be hierarchically classified into families and superfamilies according to their level of sequence similarity. Because complete genome sequences are available, it has become possible to establish similarity relationships of all **genes** within species (paralogous genes) and across species (orthologous genes). These analyses are carried out by clustering algorithms, and the similarity score is used as a measure of the closeness of two sequences. In practice, however, there are biological difficulties, notably due to the abundance of multi**domain**, multifunctional proteins, which make automatic clustering a complicated task.

Molecular biology has been dominated by a reductionist approach where, starting from a selected functional aspect of life, such as metabolism, signal transduction, or development, molecular components and their interactions are identified experimentally. In contrast, sequencing an entire genome identifies a complete set of genes and proteins in an organism, but it does not tell how they should be interrelated to form a functioning, living system. This is where a synthetic approach based on bioinformatics will play an increasingly more dominant role in the basic research into understanding life and in the applied research into biomedical relevance. Table 2 summarizes the role of bioinformatics relative to the level of abstraction in nature. At the molecular level, an amino acid residue is represented by a symbol, for example, C for cysteine, which is a compound consisting of carbon, hydrogen, nitrogen, oxygen, and sulfur atoms. When comparing two amino acid sequences, only the one-dimensional connection of symbols is considered biologically relevant, neglecting any atomic details. At a higher level of abstraction, which may be called a network level, a gene or a protein is represented by a symbol, for example, Ras for an **oncogene** product. A primary concern here is the Ras signal transduction pathway, which is generated by a network of interacting molecules. Bioinformatics is relatively well established at the molecular level, such as in the sequence and structure databases and in the computational methods to analyze them. To step up to a higher level, however, it is necessary to develop new databases and new computational technologies, such as a network database containing all the wiring-diagram information about genes and molecules, plus the algorithms to analyze them. This direction would eventually lead to *in silico* reconstruction of a biological organism.

Table 2. Level of Abstraction

Level	Constituents	Entity	Informatics
Subatomic level	Elementary particles	Atom	Computational physics
Atomic level	Atoms	Amino acid, etc.	Computational chemistry
Molecular level	Amino acids, nucleotides, etc.	Protein, gene, etc.	Bioinformatics
Network level	Proteins, genes, etc.	Molecular pathway, molecular assembly	

Bibliography

1. S. B. Needleman and C. D. Wunsch (1970) J. Mol. Biol. **48**, 443–453.
2. W. J. Wilbur and D. J. Lipman (1983) Proc. Natl. Acad. Sci. USA **80**, 726–730.
3. S. F. Altschul et al. (1990) J. Mol. Biol. **215**, 403–410.

Biopolymer

Biopolymers, sometimes referred to as biological macromolecules, are polymers of biological importance such as proteins, **nucleic acids**, and carbohydrates. Like all polymers, biopolymers are formed by joining together many copies of repeating units to form long chains that have a repeating or constant backbone and variable side chains. The repeating units of proteins are the 20 naturally occurring amino acids that form a polypeptide chain. Nucleic acids are formed from **nucleotides** and have a sugar-phosphate backbone with **purine** or **pyrimidine** side chains.

[See also Polymer and Macromolecule.]

Suggestions for Further Reading

A. G. Walton and J. Blackwell (1973) *Biopolymers*, Academic Press, New York.

P. Munk (1989) *Introduction to Macromolecular Science*, Wiley-Interscience, New York.

Biotin

Biotin is a vitamin (vitamin H) and a growth factor, first isolated by Kögl in 1935 (1). Its structure (Fig. 1) was established by du Vigneaud in 1942 (2, 3).

Figure 1. The structure of biotin.

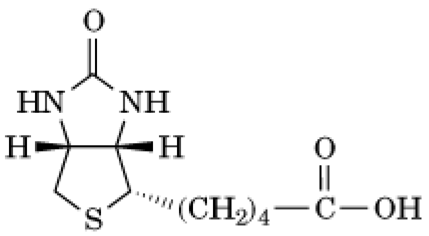

Biotin is a prosthetic group for a family of "biotin-requiring" enzymes (carboxylases, decarboxylases and transcarboxylases) (4). These multisubunit enzymes contain two types of active sites, one wherein a molecule containing a carboxylic acid group serves as a donor of the carboxyl group and the second wherein another molecule acts as an acceptor. The biotin moiety is attached through a lysine residue in a particular sequence (Ala-Met-Lys-Met) that is exposed on the surface of a special type of biotin-binding subunit. The biotin group participates as a transient carrier to which the carboxyl group is bound covalently in the process of being transferred from the donor to the acceptor molecule. The biotin moiety of the enzyme is readily available for binding to avidin, which inactivates the enzyme. After serving their respective function, the biotin-requiring enzymes undergo degradation, whereby e-N-biotinyl lysine (termed biocytin) is released into the circulation. There the enzyme biotinidase hydrolyzes biocytin to regenerate biotin and lysine. A rare mutation in the gene in humans causes a deficiency in the level of this enzyme in the blood stream, which, in turn, causes a disease due to a deficiency of biotin (5).

Biotin attained true fame when it was recognized that the high-affinity interaction between avidin and biotin can be applied for a variety of biotechnological and biomedical purposes (as described in Avidin-biotin system)(6, 7). The varied application of this system is usually achieved upon coupling biotin covalently to different biologically active binder molecules, antibodies, hormones, **DNA**, etc. The binding of biotin to either avidin or streptavidin greatly enhances the stability of these proteins, such that the avidin–biotin or streptavidin–biotin complex is essentially irreversible. Because both proteins primarily recognize the ureido ring of the biotin molecule, the carboxylic acid side-chain can be modified almost at will, and the resultant derivatives can be used to incorporate biotin covalently into virtually any other molecule (Fig. 2).

Figure 2. Selected approaches using different biotin-containing reagents for biotinylating functional groups on proteins.

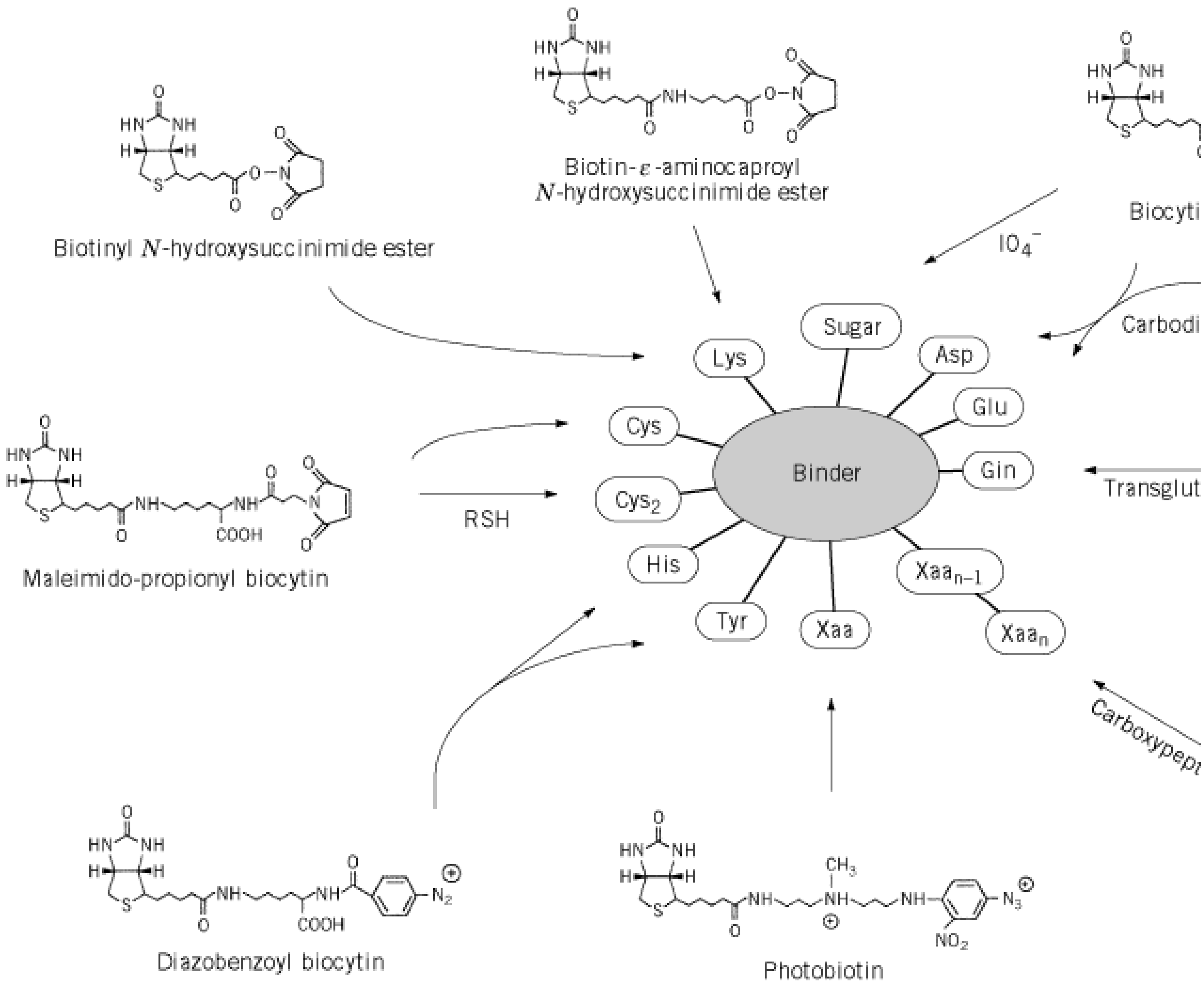

Both polyclonal and monoclonal antibodies have been produced against biotin. Comparing the sequence of the V_H region of a monoclonal anti-biotin preparation (8) with the sequences of avidin and streptavidin revealed an astonishing similarity in their binding sites, indicating that such functional elements are conserved in nature for a given purpose, irrespective of the protein type.

Bibliography

1. F. Kögl and B. Z. Tönnis (1936) Physiol. Chem. **242**, 43–73.
2. V. du Vigneaud, D. B. Melville, K. Folkers, D. E. Wolf, R. Mozingo, J. C. Kereszteolf, and S. A. Harris (1942) J. Biol. Chem. **146**, 475–485.
3. V. du Vigneaud, K. Hoffman, and D. B. Melville (1942) J. Amer. Chem. Soc. **64**, 188–189.
4. J. Moss and M. D. Lane (1971) Adv. Enzymol. **35**, 321–372.
5. B. Wolf, G. S. Heard, J. R. McVoy, and R. E. Grier (1985) Ann. N.Y. Acad. Sci. **447**, 252–62.
6. E. A. Bayer and M. Wilchek (1978) Trends Biochem. Sci. **3**, N237–N239.
7. E. A. Bayer and M. Wilchek (1980) Methods Biochem. Anal. **26**, 1–45.
8. H. Bagci, F. Kohen, U. Kuscuoglu, E. A. Bayer, and M. Wilchek (1993) FEBS Lett. **322**, 47–50.

Suggestion for Further Reading

9. M. Wilchek and E. A. Bayer, eds. (1990) *Avidin-Biotin Technology, Methods Enzymol.* Vol. **184**, Academic Press, San Diego.

Biotin Repressor

All genes for the biosynthesis of biotin of *Escherichia coli* are grouped in a single operon located at 17 min on the chromosome, except for except for *bioH*, which is located at 75 min. The genes of the operon *bioA*,*BFCD* are transcribed divergently from a single regulatory region located between the *bioA* and the *bioB* genes. Transcription in both directions is corepressed by biotinyl-5′-adenylate and the biotin repressor. The following table shows the respective function of these genes:

bioC and bioH	Unidentified steps in pimeloyl CoA biosynthesis
bioF	7-Keto-8-aminopelargonic acid synthetase
bioA	7,8-Diaminopelargonic acid synthetase
bioD	Dethiobiotin synthetase
bioB	Biotin synthase (introduction of the S atom)

No precise information is available on the function of the *bioC* and *bioH* genes, other than that a mutation in either gene results in no excretion of a known intermediate in the pathway. Therefore the products of these genes have been assigned to some early steps before 7-keto-8-aminopelargonic acid synthesis. All biotin genes are coordinately repressed when biotin is added to the growth medium in excess of 1 ng/Ml.

The biotin repressor is a very interesting bifunctional protein of 321 amino acid residues, which acts at two different levels. In addition to its repressor function, it is endowed with acetyl CoA carboxylase biotin holoenzyme synthetase activity, which activates biotin to biotinyl-5′-adenylate and transfers the biotin to acceptor proteins. As soon as these proteins are totally biotinylated, biotinyl-5′-adenylate accumulates and serves as the corepressor of the biotin operon. This is a case of an enzyme synthesizing its own repressor, a unique property thus far among DNA-binding proteins. Mutations in the corresponding gene (*birA*) inactivate the repressor function partially or totally and also alter the enzymatic function. This repressor binds to a 40-bp symmetrical biotin **operator** site to prevent transcription of the biotin biosynthetic genes. The structure of the repressor is highly asymmetrical and consists of three **domains**. The N-terminal domain is mostly **alpha-helical**, contains a helix–turn–helix motif and is loosely connected to the remainder of the molecule. The central domain consists of a seven-stranded mixed beta-sheet, with a-helices covering one face. The other side of the sheet is largely exposed to the solvent and contains the enzyme's active site. The C-terminal domain comprises a six-stranded antiparallel b-sheet sandwich. The location of biotin is consistent with mutations affecting enzymatic activity.

Two molecules of the monomeric repressor bind cooperatively to one molecule of operator in the nanomolar concentration range. The data suggest that one molecule of repressor monomer binds to each of the two operator half sites and that they form a dimer only after they bind. Because the complex between repressor and DNA has not yet been crystallized, details of its structure remain an open question.

BiP (Hsp70)

The acronym BiP stands for binding protein, and it is the only member of the hsc,hsp70 family known to occur in the lumen of the endoplasmic reticulum (ER) of mammalian cells. It was identified originally as an ER protein that increases in amount when cells are starved of glucose (1) and subsequently as a protein that binds noncovalently to the heavy (H) chains of immunoglobulins as they enter the ER lumen (2). The alternative term of "Grp78" stands for **glucose-regulated protein** with an apparent subunit mass of about 78 kDa. BiP is now regarded as having a general **molecular chaperone** role for transport in the ER lumen and for protein folding in vivo. BiP proteins are highly conserved in mammals, and there is 67% identity between mouse BiP and a homologue in the ER lumen of *Saccharomyces cerevisiae* called "Kar2p" (3). Like all hsc,hsp70 proteins, BiP exhibits a weak ATPase activity.

1. Structure

BiP is encoded in a nuclear gene located on human chromosome 9q34, and cDNA from mammalian species indicate a primary translation product of 635 amino acid residues, including an 18-residue *N*-terminal signal sequence for ER targeting and the *C*-terminal tetrapeptide **KDEL sequence** for ER retention (GenBank accession numbers M19645 and M17169). The *N* and *C* termini contain clusters of acidic residues thought to be involved in Ca^{2+} binding (4). No crystal structure is available for mammalian BiP, but a structure is known for the *N*-terminal 45-kDa fragment of bovine hsc70, which retains the ATPase activity (5), and for the *C*-terminal polypeptide-binding domain of the *Escherichia coli* hsp70 homologue called **DnaK** (6). Purification protocols for BiP utilize affinity chromatography on ATP columns (7). Recombinant hamster BiP has been purified from *E. coli* cells (8) and is marketed by StressGen Biotechnologies Corporation, as are polyclonal antibodies to rodent BiP. *In vivo* BiP exists in interconvertible oligomeric and monomeric forms and is subject to **phosphorylation** on serine and threonine residues, as well as to **ADP-ribosylation**. However, only monomeric, unmodified species of BiP are found in complexes with unfolded or unassembled polypeptides (9).

2. Function

BiP binds transiently to a range of newly synthesized secretory proteins, as they traverse the ER membrane and enter the ER lumen, and more permanently to misfolded, underglycosylated, or unassembled proteins whose transport from the ER is blocked (10); it does not bind to native, folded proteins. The binding is reversed by the addition of ATP and is believed to exert a molecular chaperone function by preventing premature folding and/or aggregation; this function is achieved by the shielding of potentially interactive **hydrophobic** surfaces during the time when BiP is bound. There is also evidence that the BiP homologue in yeast functions as a molecular motor protein to promote the transport of proteins across the ER membrane (11). This transport function requires the binding of the BiP homologue to the *J* domain of the yeast ER membrane protein Sec63p (12) (see also text later in this article). Studies of the binding of synthetic peptides and bacteriophage peptide libraries show that the optimum peptide length for binding is seven to eight residues, with extensive sequence diversity but a marked preference for hydrophobic residues (13, 14). These observations support the idea that BiP binds to a wide range of sequences that normally occur inside fully folded proteins. A computer program is available that scores potential BiP binding sites in protein sequences (14); it has been used to map such sequences in immunoglobulin heavy chains to the regions that interact with light chains (15).

3. Interaction with Other Chaperones

Cytosolic hsc,hsp70 proteins in the bacterial and eukaryotic cytosol interact with other chaperones of the DnaJ (or hsp40) family that contain *J* domains (see DnaK/DnaJ Proteins). The yeast BiP homologue, Kar2p, interacts with two other ER proteins that contain *J* domains: Sec63p, a membrane protein involved in protein translocation across the ER membrane (16); and Scj1p, a lumenal protein (17). BiP also binds either sequentially or simultaneously with chaperones such as **calnexin** and Grp94 during the folding in the ER of proteins such as immunoglobulin light (L) chains (18), thyroglobulin (19), vesicular stomatitis virus G protein (20), and major histocompatibility complex class II chains (21). BiP is thus one component in a complex set of interactions in the ER lumen between different chaperones and polypeptide chains that are folding.

4. Induction of BiP

BiP is an abundant protein under normal growth conditions, constituting about 5% of the ER lumenal proteins, but its amount increases greatly under conditions that result in the accumulation of proteins within the ER lumen that are unable to fold correctly. These conditions include the biosynthesis of mutant chains, glucose starvation, and treatment with amino acid analogs, drugs that inhibit glycosylation, and calcium **ionophores** (22). The **promoters** of BiP genes in mammals contain several cis-acting regulatory elements required for high basal-level expression and for inducibility (22, 23).

Bibliography

1. J. Pouyssegur, R. P. C. Shiu, and I. Pastan (1977) Cell **11**, 941–947.
2. I. G. Haas and M. Wabl (l983) Nature **306**, 387–389.
3. K. Normington, K. Kohno, Y. Kozutsumi, M. J. Gething, and J. Sambrook (l989) Cell **57**, 1223–1236.
4. D. R. J. Macer and G. L. E. Koch (1988) J. Cell. Sci. **91**, 61–70.
5. K. M. Flaherty, C. DeLuca-Flaherty, and D. B. McKay (1990) Nature **346**, 623–628.
6. X. Zhu, X. Zhao, W. F. Burkholder, A. Gragerov, C. M. Ogata, M. E. Gottesman, and W. A. Hendrickson (l996) Science **272**, 1606–1614.
7. P. J. Rowling, S. H. McLaughlin, G. S. Pollock, and R. B. Freedman (1994) Protein Exp. Purif. **5**, 331–336.
8. J. Wei and L. M. Hendershot (1995) J. Biol.Chem. **270**, 26670–26676.
9. P. J. Freiden, J. R. Gaut, and L. M. Hendershot (1992) EMBO J. **11**, 63–70.
10. M. J. Gething, S. Blond-Elguindi, K. Mori, and J. F. Sambrook (1994) in *The Biology of Heat Shock Proteins and Molecular Chaperones* (R. I. Morimoto, A. Tissieres and C. Georgopoulos, eds.), Cold Spring Harbor Laboratory Press, Cold Spring Harbor, pp. 111–135.
11. S. Panzner et al. (1994) Cell **81**, 561–570.
12. J. L. Brodsky and R. Schekman (1993) J. Cell Biol. **123**, 1355–1363.
13. G. C. Flynn, J. Pohl, M. T. Flocco, and J. E. Rothman (1991) Nature **353**, 726–730.
14. S. Blond-Elguindi, S. E. Cwirla, W. J. Dower, R. J. Lipshutz, S. R. Sprang, J. F. Sambrook, and M. J. Gething (1993) Cell **75**, 717–728.
15. G. Knarr, M. J. Gething, S. Modrow, and J. Buchner (1995) J. Biol. Chem. **270**, 27589–27594.
16. D. Feldheim, J. Rothblatt, and R. Schekman (1992) Mol. Cell. Biol. **12**, 3288–3296.
17. G. Schlenstedt, S. Harris, B. Risse, R. Lill, and P. A. Silver (1995) J. Cell Biol. **129**, 979–988.
18. J. Melnick, J. L. Dul, and Y. Argon (1994) Nature **370**, 373–375.
19. P. S. Kim and P. Arvan (1995) J. Cell Biol. **128**, 29–38.

20. C. Hammond and A. Helenius (1994) Science **266**, 456–458.
21. M. S. Marks, R. N. Germain, and J. S. Bonifacino (1995) J. Biol. Chem. **270**, 10475–10481.
22. A. S. Lee (1992) Curr. Opin. Cell Biol. **4**, 267–273.
23. W. W. Li, L. Sistonen, R. I. Morimoto, and A. S. Lee (1994) Mol. Cell. Biol. **14**, 5533–5546.

Suggestion for Further Reading

24. D. N. Herbert, J. F. Simons, J. R. Peterson, and A. Helenius (1995) Calnexin, calreticulin and BiP/Kar2p in protein folding, Cold Spring Harbor Symp. Quant. Biol. **60**, 405–415.
25. F.-U. Hartl (l996) Molecular chaperones in cellular protein folding, Nature **381**, 571–580.
26. J. L. Brodsky (1996) Post-translational protein translocation: not all hsc70s are equal, Trends Biochem. Sci. **21**, 122–126.
27. M.-J. Gething, ed. (1997) *Molecular Chaperones and Protein Folding Catalysts*, Oxford University Press, Oxford (this volume contains much detailed information about BiP).

Bisubstrate Analogue

Bisubstrate analogues were developed originally for mechanistic studies on enzymes that catalyze reactions with two substrates or products. However, they have also proved to be of value in studies on enzymes by X-ray crystallography. Bisubstrate analogues are characterized by the fact that they embody in a single molecule the structural features of each of the two substrates (or products). Hence, it was expected that they would bind simultaneously at the binding sites for the two substrates, and therefore more tightly than the individual substrate molecules, and act as potent enzyme inhibitors. They have also been referred to as transition state analogues, but such a classification seems inappropriate.

Two early, and now classical, examples of bisubstrate enzyme inhibitors are P^1, P^5-di-(adenosine-5′) pentaphosphate (AP_5A) and *N*-phosphonoacetyl-L-aspartate (PALA), whose structures are given in Figure 1. AP_5A was developed as an inhibitor of adenylate kinase, which is a monomeric enzyme that catalyzes the reaction:

$$MgATP^{2-} + AMP^{2-} \rightleftharpoons MgADP^{-} + ADP^{3-}$$

The reaction conforms to a rapid equilibrium, random **kinetic mechanism**, which implies that the enzyme possesses two distinct nucleotide-binding sites within its active site. One is for either $MgATP^{2-}$ or $MgADP^{-}$ and the other is for ADP^{3-} or AMP^{2-}. Irrespective of whether they are substrates or products, the moieties bound by the enzyme include two adenosine moieties and four phosphate moieties, whereas AP_5A differs only in having five phosphate groups linked covalently. AP_5A is a potent inhibitor of the adenylate kinase reaction, with the apparent inhibition constant K_i value being in the nanomolar region; the inhibition is competitive with respect to both MgATP and AMP, as would be expected (1, 2). Binding studies indicate that the stoichiometry of binding is 1:1 and the **dissociation constant** is 15 nM (3). The binding affinity is reduced seven-fold in the absence of Mg^{2+}. It is of interest that the binding to adenylate kinase of AP_4A, which is the equivalent of covalently linking ATP to AMP, or ADP to ADP, is almost 3,000-fold weaker. An increase in the number of phosphoryl groups to six also reduces the binding affinity by 400-fold. The crystal structures of three adenylate kinases and enzyme–AP_5A complexes were solved well ahead of the spatial assignment of the substrate binding sites. A review of the problems associated with the determination of the structural relationship between the two nucleotide binding sites of adenylate kinase has been presented (4).

Figure 1. Examples of bisubstrate analogues. (**a**), P^1, P^n-di(adenosine-5′) *n*-phosphate, where $n = 4$ (AP_4A), 5 (AP_5A), or 6 (AP_6A). (**b**), *N*-phosphonoacetyl-L-aspartate (PALA).

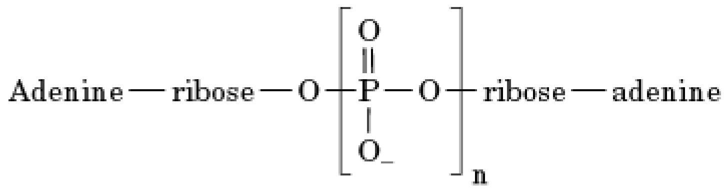

(a)

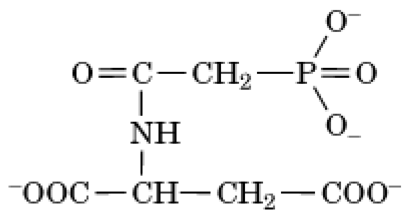

(b)

AP_5A also acts as a strong inhibitor of ATP:NMP phosphotransferase from *Dictyostelium discoideum*, which utilizes either UMP or CMP as the acceptor of a phosphoryl group from ATP (5). Binding studies indicate that the dissociation constant of the enzyme-AP_5A complex is 160 µM. However, the corresponding bisubstrate analogue with uridine replacing one adenine nucleotide (UP_5A) is a more potent inhibitor and binds with a dissociation constant of 3 nM. The enzyme has been co-crystallized with UP_5A.

PALA has been used extensively for kinetic and structural studies on aspartate transcarbamoylase **(ATCase)**, which catalyzes the reaction:

$$\text{Carbamoyl phosphate} + \text{aspartate} \rightleftharpoons \text{carbamoylaspartate} + P_i$$

PALA is considered an analogue of the two substrates linked covalently. The intact ATCase enzyme consists of both catalytic and regulatory units, does not show Michaelis–Menten kinetics, and is subject to **allosteric** control by nucleoside triphosphates. However, it is possible to prepare an active trimer of just the catalytic subunits that shows Michaelis–Menten kinetics and is not subject to allosteric control. This form of enzyme has been very useful for elucidating fundamental information about the catalytic sites and mechanism of action of ATCase. Investigations with the catalytic trimer have shown that one molecule of PALA binds to each subunit of the trimer (6) and the inhibition is linear competitive with respect to carbamoyl phosphate and linear noncompetitive relative to aspartate (7). Additional kinetic data have indicated that the kinetic mechanism for the aspartate transcarbamoylase reaction is essentially ordered, with carbamoyl phosphate being the first substrate to add; this explains the inhibition pattern. The pH-independent K_i value for the enzyme-PALA complex is 7.2 nM, which is three orders of magnitude lower than the dissociation constant for the corresponding enzyme-carbamoyl phosphate complex (7).

PALA has also played an important role in the demonstration that the co-operativity observed with intact ATCase can be explained in terms of a two-state allosteric **concerted model** (8). Thus, the binding of up to three molecules of PALA to the intact enzyme, which has six active sites, leads to activation, even though PALA is occupying active sites, as a result of displacing the equilibrium between the T (inactive) and R (active) forms of the enzyme toward R. Only with greater occupancy is PALA inhibitory. Structural studies support the idea that PALA is a true bisubstrate analogue of the substrates for the enzyme (9).

Bibliography

1. G. E. Lienhard and I. I. Secemski (1973) J. Biol. Chem. **248**, 1121–1123.
2. P. Feldhaus, T. Frohlich, R. S. Goody, M. Isakov, and R. H. Schirmer (1975) Eur. J. Biochem. **57**, 197–204.
3. J. Reinstein, I. R. Vetter, I. Schlichting, P. Rosch, A. Wittinghofer, and R. S. Goody (1990) Biochemistry **29**, 7440–7450.
4. M.-D. Tsai and H. Yan (1991) Biochemistry **30**, 6806–6818.
5. L. Wiesmuller, K. Scheffzek, W. Kliche, R. S. Goody, A. Wittinghofer, and J. Reinstein (1995) FEBS Lett. **363**, 22–24.
6. G. R. Jacobson and G. R. Stark (1973) The Enzymes **9**, 225–308.
7. J. L. Turnbull, G. L. Waldrop, and H. K. Schachman (1992) Biochemistry **31**, 6562–6569.
8. L. E. Parmentier, M. H. O"Leary, H. K. Schachman, and W. W. Cleland (1992) Biochemistry **31**, 6598–6602.
9. W. N. Lipscomb (1994) Adv. Enzymol. **68**, 67–151.

Bithorax Complex

The homeotic genes of the bithorax complex (BX-C) have been the subject of many landmark discoveries in the field of **developmental** biology. Homeotic genes were first identified in *Drosophila* by mutations that affect their expression. These mutations lead to spectacular effects on the morphology of the fly; they cause the development of a specific body structure (ie, segment, antenna, leg, wing) at the place where another structure normally develops. The first homeotic mutations, *bithorax* (*bx*) and *bithoraxoid* (*bxd*), were described in 1923 by Bridges and Morgan (1). For example, in flies homozygous for *bxd* mutations, their first abdominal segment (A1) develops like a copy of the segment immediately adjacent anteriorly—namely, the third thoracic segment (T3). Thus, the role of the bxd^+ function is to assign the identity of A1. In the late 1940s, Ed Lewis pioneered the field of developmental genetics by discovering the existence of additional homeotic mutations near *bx* and *bxd*. Although these mutations seem to affect different body segments of the thorax and abdomen, their complementation patterns turned out to be rather complex. Because they all mapped at the same genetic and cytological position, Lewis decided to name the locus the bithorax complex (BX-C). The work of Lewis was compiled in a milestone article in 1978 (2) in which he describes a series of homeotic mutations of BX-C that affect the identities of the third thoracic segment and all of the abdominal segments. Mutations in any of them transform the considered segment into a copy of the segment immediately anterior. Remarkably, genetic mapping revealed that these mutations are arranged on the chromosome in the same order along the anteroposterior axis as the segments they affect. By combining three mutations, Lewis produced flies with four wings instead of two (transformation of T3 into T2). Because such animals look like more ancestor forms of insect, Lewis proposed that homeotic genes played an instrumental role in evolution. The correspondence between the order of the genes on the chromosome and the order of the segments on the body of the fly has now attained almost mystical status and has turned out to be true also of the vertebrate homologues of BX-C. The Nobel Prize Committee has recognized this pioneering works by awarding its 1995 Nobel Prize of Medicine to Ed Lewis and two other *Drosophila* geneticists (Y. Nusslein-Volhard and E. Wieschaus).

In 1978, BX-C was the first *Drosophila* gene **cloned** from the chromosome without any prior knowledge of the products. To clone what turned out to be a large complex, Bender, Spierer, and Hogness developed the method of **chromosome walking** (3). Finally, in 1983, the molecular characterization of the BX-C led to the discovery of the homeobox in the laboratories of W. Gehring and of M. Scott (4, 5).

1. Molecular Genetics of BX-C

Figure 1 summarizes the molecular genetics of the BX-C. The complex covers 300 kbp of DNA, which are represented by the thin horizontal line marked off in kb (6, 7). Above the DNA line are represented the sites of the homeotic mutations that affect the identities of each of the segments under the control of the BX-C. The vertical arrows represent the sites of chromosomal rearrangement breaks, the triangles the sites of insertion of transposons, and the horizontal lines the extent of deletions. Expression studies and analysis of the homeotic **phenotypes** in embryos have revealed that the unit transformed in each of these nine classes of mutations does not correspond to body segments; instead, it is composed of the posterior part of one segment and the anterior compartment of the next segment. These units are named parasegments (PSs) (8). For example, *bxd* mutations cause the transformation of the posterior part of T3 (pT3) and the anterior part of A1 (aA1) into p (T2) and aT3. This corresponds to the transformation of parasegment 6 (PS6) into PS5. The mutations affecting parasegment identity form nine discrete entities that, as predicted by Lewis, are aligned on the chromosome in the same order as the parasegments in which they act on the body of the fly (*abx/bx*, *bxd/pbx*, *iab-2* through *iab-8*). These mutations define nine PS-specific functions, and the arrows point toward the parasegments of the adult fly that are most affected in each class of mutations (Fig. 1). For reasons that will become clear later, it is worthwhile noting that all the mutations affecting the PS-specific functions are due to chromosomal rearrangements (more than 100 have been mapped). Thus, it seems impossible to affect these functions by point mutations, and it is unlikely that they correspond to individual **genes** coding for distinct proteins.

Figure 1. Genetic map of the bithorax complex (BX-C). The 300 kilobases of DNA that compise the complex are indica bottom line, which is marked off in 10^4 base pairs. Above the DNA line are represented the sites of the homeotic mutatic affect the identities of each of the segements under control of BX-C. The vertical arrows represent the sites of chromosoı rearrangement breaks, the triangles the sites of insertion of transposons, and the horizontal lines the extent of deletions. T parasegments (PS5 to PS13, 14) that each part of the complex controls are indicated above, in the adult fly. The three tra units (*Ubx*, *abdA*, and *AbdB*) are indicated below the DNA; in each case, transcription occurs from right to left. The exor indicated by the thick horizontal lines, the introns by the thin V's connecting them. H indicates the homeobox domain. Tl alternative promoters a and g are indicated for *AbdB*. Mutations that affect the transcription units are indicated below the

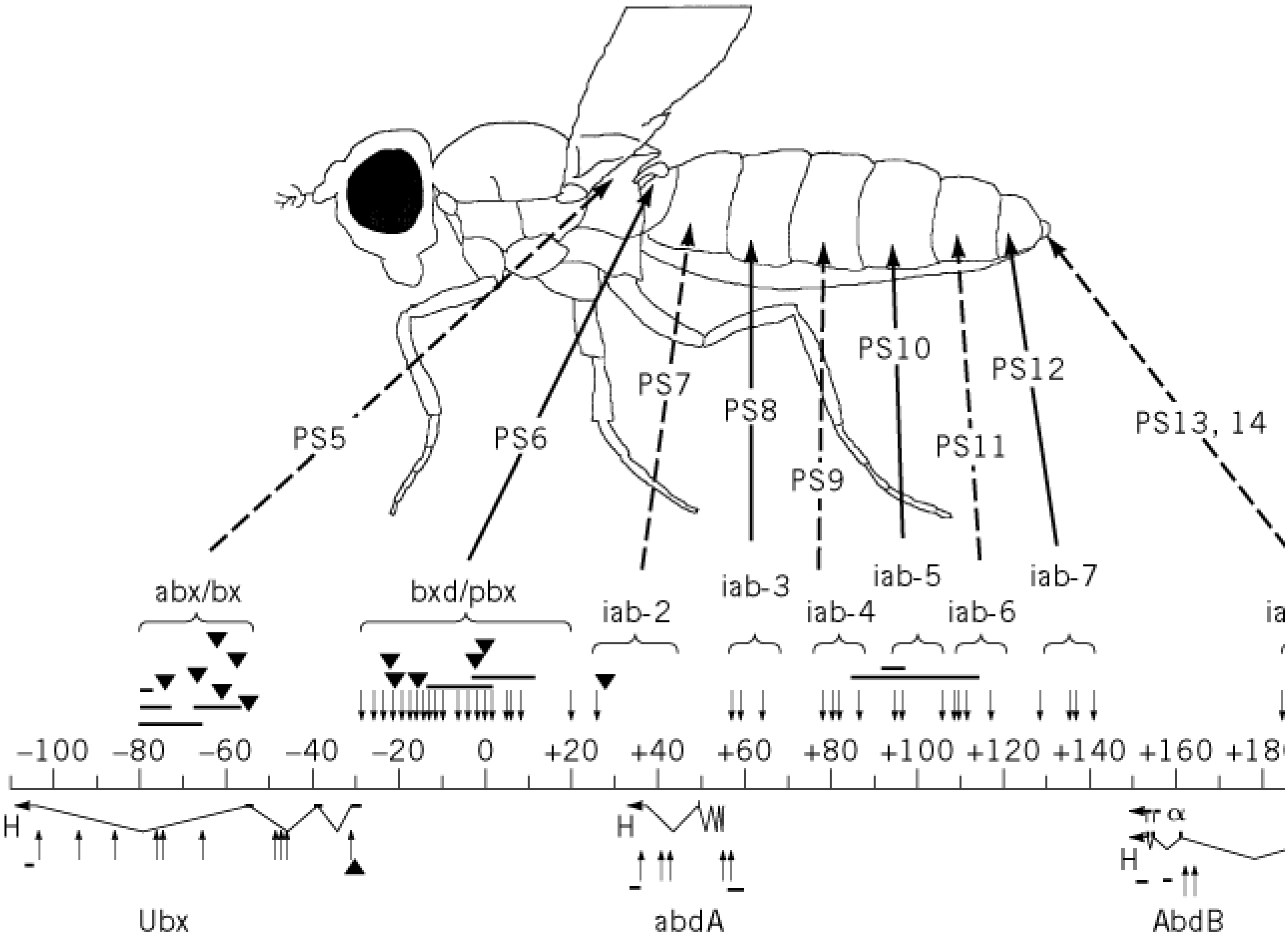

Northern blots and the isolation and sequencing of complementary DNA revealed the existence of only three transcription units *Ubx*, *abd-A*, and *Abd-B*. These three transcriptions units are all transcribed from right to left (of Fig. 1) and contain a **homeobox** sequence at their 3′ end. The *Ubx* transcription unit covers 7O kb of DNA and can generate 12 different transcripts by alternative splicing and polyadenylation. Translation of these messenger RNAs yields a family of six proteins characterized by constant amino- and carboxy-proximal regions of 247 and 99 amino acid residues, respectively. The latter homeobox sequence is encoded by the 3′-terminal common exon. The members of this family are distinguishable by a short variable region that links the constant regions and consists of different combinations of three optional elements of 9, 17, and 17 residues (9-11). The spectrum of RNA products changes with time and tissue. It has been demonstrated that the *Ubx* protein containing the portion coded by the second microexon is not expressed in the nervous system (12). However, the different **isoforms** of the *Ubx* product are not all essential, since a mutation that eliminates the second microexon (and thus four isoforms) has no effect on fly viability and development (13).

The *abd-A* transcription unit is spread over a 20-kb region of DNA, and the mature *abd-A* transcript is composed of at least eight exons (14). As in *Ubx*, the *abd-A* transcription unit contains a microexon, but no alternative splicing generating multiple forms of the *abd-A* product has been detected thus far. The homeobox homology is found near the middle of the 330-residue protein. Analysis of the sequence of the whole BX-C (15) indicates that the open reading frame extends further upstream from the published ATG initiation codon, raising the possibility that *abd-A* may be slightly larger than originally thought. In as much as this upstream open reading frame is conserved in *Tribolium*, it is likely that *abd-A* consists of 590 residues (16).

Finally, the *Abd-B* transcription unit consists of three classes of transcripts that are generated by the use of three alternate **promoters** and differential spicing (Fig. 1). While the alpha class of transcripts produces a protein of 55 kDa, the beta and gamma forms produce a product of 30 kDa that is truncated at the *N*-terminus (17, 18).

Mutations that affect the *Ubx*, *abd-A*, and *Abd-B* transcription units (shown below the DNA line in Fig. 1) are all lethal at the embryo stage of development, and cuticle analysis of the dead embryos detects homeotic transformations. In *Ubx* mutants, PS5 and PS6 are transformed into PS4. If such an embryo could survive, it would give rise to a fly with T3 and A1 transformed into T2 (ie, a fly with three pairs of wings). Homozygous *abd-A* embryos have PS7, 8, and 9 transformed into PS6 (in the adult this would correspond to a transformation of A2, A3, and A4 into A1). Finally, *Abd-B* mutations have PS10, 11, 12, and 13 transformed into PS9 [A5–A8 transformed into A4 (2, 7, 19, 20)].

2. Expression

The genetic and molecular data that have been described thus far appear to conflict. On the one hand, genetic analysis reveals the existence of nine parasegment-specific functions that are responsible for the identity of PS5 to 13, which will form the posterior thorax and the abdominal segments of an adult fly. On the other hand, molecular studies indicate that BX-C encodes only three protein products. This apparent discrepancy was solved when antibodies directed against the *Ubx*, *abd-A*, and *Abd-B* products became available, allowing determination of which part of the embryo these genes are expressed. A first observation derived from these studies is that each of the *Ubx*, *abd-A*, and *Abd-B* genes are expressed in domains composed of several parasegments. *Ubx* is expressed from PS5 to 13 (9, 21), *abd-A* from PS7 to 12 (14, 22), and *Abd-b* from PS10 to 14 (23, 24). Second, the expression patterns are complex, intricate, and dynamic. Comparisons of the expression patterns between wild-type embryos and those carrying mutations in the PS-specific functions revealed that the latter correspond to large *cis*-regulatory regions that are responsible for construction of the complex expression patterns of *Ubx*, *abd-A*, and *Abd-B*. The *abx/bx* and *bxd/pbx cis*-regulatory regions are responsible for UBX expression in PS5 and 6, respectively (21, 25, 26). The *iab-2*, *iab-4*, and *iab-4 cis*-regulatory regions control expression of *Abd-A* in PS7, 8, and 9, respectively, while *iab-5*, *iab-6*, *iab-7*, and *iab-8* are responsible for the pattern of ABD-B expression (initiated from the a promoter) in PS10 to 13 (14, 24, 27). PS14 expresses a truncated form of ABD-B, resulting from transcription initiated from the b and g promoters.

3. BX-C Regulation

BX-C gene regulation can be divided into two phases, initiation and maintenance. During the early phases of embryogenesis, when parasegment identity is initially selected, the PS-specific *cis*-regulatory regions are the targets of the **gap gene** and pair-rule gene products (28-31). These gap and pair-rule proteins activate the *cis*-regulatory regions in successively more posterior parasegments.

The gap and pair-rule gene products are present only transiently during early development. The fact that homeotic genes are expressed throughout development implies the existence of a mechanism that maintains the activity state of each of the *cis*-regulatory regions. This maintenance system requires the **Polycomb** *group* (*Pc-G*) and the **trithorax** *group* (*trx-G*) genes (32-34). While the products of the *Pc-G* function as negative regulators, the products of the *trx-G* act as positive regulators. The products of the *Pc-G* exert their regulatory effects by interacting with specific elements in each of the *cis*-regulatory domains called *polycomb*-**response elements** (35-39). There may be equivalent or overlapping *trx* response elements for the *trx-G* proteins (36, 40). Though their precise mode of action is unknown, the products of the *Pc-g* and *trx-g* are thought to stabilize the expression patterns in each parasegment by imprinting an inactive or active chromatin conformation of the PS-specific *cis*-regulatory subregions (33, 41, 42).

4. Regulatory Elements of BX-C

Molecular studies using reporter gene constructs have revealed the existence of elements within the PS-*cis*-regulatory units that seem to be responsible for the initiation and maintenance phases of BX-C regulation. Some DNA fragments are able to initiate expression of a *Ubx-lacZ* reporter gene in the proper parasegments during early embryonic development (28, 30, 43, 44). In most cases, however, these patterns are not maintained, and expression expands into more anterior parasegments around the time when BX-C regulation would switch to the maintenance mode. Other BX-C DNA fragments are capable of retaining the appropriate parasegmental restrictions in lacZ expression after the gap and pair-rule gene products disappear. These fragments contain "maintenance elements," also known as *Pc-g* response elements because their activity depends on *Pc-g* gene products (35-39, 43, 44). Finally, a third type of regulatory elements that has been identified in experiments with *Ubx-lacZ* reporter constructs are tissue- or cell-type-specific enhancers. They induce *lacZ* expression in specific tissue or cell types, with no restriction along the anteroposterior axis.

Many observations suggest that the PS-specific *cis*-regulatory units are organized into functionally independent domains. This is best illustrated by the expression patterns of "enhancer trap" transposons integrated in different domains of the complex (45, 46). These enhancer traps are subject to regulatory elements located within the same domain, but they are insensitive to regulatory elements in adjacent domains. The autonomy of each domain is ensured by elements that are believed to function as boundaries. Two such regulatory elements, *Mcp* and *Fab-7*, have been identified. *Mcp* is located between the *iab-4* and *iab-5 cis*-regulatory units or domains, while *Fab-7* is located between *iab-6* and *iab-7* (46-50).

5. Concluding Remarks

Molecular analysis of the BX-C has confirmed most of the predictions that Lewis had foreseen in his 1978 model. He had initially envisioned activation of a new gene product in each parasegment. It is now clearly established that there are only three major groups of related protein products encoded by BX-C (UBX, ABD-A, and ABD-B). Discrete genetic units exist, however, that are sequentially activated in each parasegment. These units function as transcription regulatory regions (PS-specific *cis*-regulatory regions). The complex *cis*-regulation that they mediate results in a very intricate pattern of expression, both between and within parasegments. Each parasegment is a mosaic of cells expressing different homeotic products. Under the direction of these proteins, different cells adopt different fates, yielding the complex array of pattern elements that characterizes a given parasegment (or segment). The PS-specific *cis*-regulatory regions are large (*bxd* is spread over more than 30 kb; see Fig. 1) and can act from remote distances on their target promoters (*iab-5* is localized 50 kb away from its target *Abd-B* promoter). These properties suggest that the structure of the chromatin plays an important role to allow such long-distance interactions. Chromatin structure is also evoked by the properties of the *Pc-G* gene. The products of these *Pc-G* genes function as cellular memory to maintain the repressed state of the homeotic genes in body regions where they have not been activated during early development. There are analogies between the *Pc-G* repression and **mating-type** silencing in yeast or heterochromatic position-effect variegation in *Drosophila*. Though little is known at the molecular level, these analogies suggest that *Pc-G* repression involves the formation of a complex of Pc-G proteins leading to a chromatin structure that is refractory to transcription. The finding of boundary elements insulating adjacent PS-specific *cis*-regulatory regions has led to a model in which the sequential activation the *cis*-regulatory regions would be due to the stepwise opening of chromosomal domains (45, 46, 49, 51). Although no molecular clues exist to support such a model, it provides a rationale for the remarkable correspondence between the genomic organization of the BX-C and the anteroposterior axis of the fly. A similar model has been discussed recently in the case of the clusters of homeotic genes in mice, the Hox clusters (52).

Bibliography

1. C. B. Bridges and T. Morgan (1923) Carnegie Inst. Washington Publ. **327**, 137.
2. E. B. Lewis (1978) Nature **276**, 565–570.

3. W. Bender, P. Spierer, and D. S. Hogness (1983) J. Mol. Biol. **168**, 17–33.
4. W. McGinnis, M. S. Levine, E. Hafen, A. Kuroiwa, and W. J. Gehring (1984) Nature **308**, 428–433.
5. M. P. Scott and A. J. Weiner (1984) Proc. Natl. Acad. Sci. USA **81**, 4115–4119.
6. W. Bender, M. Akam, F. Karch, P. A. Beachy, M. Peifer, P. Spierer, E. B. Lewis, and D. S. Hogness (1983) Science **221**, 23–29.
7. F. Karch, B. Weiffenbach, M. Peifer, W. Bender, I. Duncan, S. Celniker, M. Crosby, and E. B. Lewis (1985) Cell **43**, 81–96.
8. A. Martinez-Arias and P. Lawrence (1985) Nature **313**, 639–642.
9. P. A. Beachy, S. L. Helfand, and D. S. Hogness (1985) Nature **313**, 545–551.
10. M. B. O"Connors, R. Binari, L. A. Perkins, and W. Bender (1988) EMBO J. **7**, 435–445.
11. K. Kornfeld, R. B. Saint, P. A. Beachy, P. J. Harte, D. A. Peattie, and D. S. Hogness (1989) Genes & Dev. **3**, 243–258.
12. R. Weinzierl, J. M. Axton, A. Ghysen, and M. Akam (1987) Genes & Dev. **1**, 386–397.
13. A. Busturia, I. Vernos, J. Casanova, and G. Morata (1990) EMBO J. **9**, 3551–3555.
14. F. Karch, W. Bender, and B. Weiffenbach (1990) Genes Dev. **4**, 1573–1587.
15. C. H. Martin, C. A. Mayeda, C. A. Davis, C. L. Ericsson, J. D. Knafels, D. R. Mathog, S. E. Celniker, E. B. Lewis, and M. J. Palazzolo (1995) Proc. Natl. Acad. Sci. USA **92**, 8398–8402.
16. T. D. Shippy, S. J. Brown, and R. E. Denell (1998) Dev. Genes Evol. **207**, 446–452.
17. M. Zavortink and S. Sakonju (1989) Genes Dev. **3**, 1969–1981.
18. S. E. Celniker, D. J. Keelan, and E. B. Lewis (1989) Genes Dev. **3**, 1424–1436.
19. E. Sanchez-Herrero, I. Vernos, R. Marco, and G. Morata (1985) Nature **313**, 108–113.
20. J. Casanova, E. Sanchez-Herrero, A. Busturia, and G. Morata (1987) EMBO J. **6**, 3103–3109.
21. R. A. H. White and M. Wilcox (1985) Nature **318**, 563–567.
22. A. Macias, J. Casanova, and G. Morata (1990) Development **110**, 1197–1207.
23. M. DeLorenzi, N. Ali, G. Saari, C. Henry, M. Wilcox, and M. Bienz (1988) EMBO J. **7**, 3223–3231.
24. S. E. Celniker, S. Sharma, D. J. Keelan, and E. B. Lewis (1990) EMBO J. **9**, 4277–4286.
25. C. Cabrera, J. Botas, and A. Garcia-Bellido (1985) Nature **318**, 569–571.
26. R. A. H. White and M. E. Akam (1985) Nature **318**, 567–569.
27. E. Sanchez-Herrero (1991) Development **111**, 437–449.
28. S. Qian, M. Capovilla, and V. Pirrotta (1991) EMBO J. **10**, 1415–1425.
29. J. Muller and M. Bienz (1992) EMBO J. **11**, 3653–3661.
30. M. J. Shimell, J. Simon, W. Bender, and M. B. O"Connor (1994) Science **264**, 968–971.
31. F. Casares and E. Sanchez Herrero (1995) Development **121**, 1855–1866.
32. A. Shearn (1989) Genetics **121**, 517–525.
33. R. Paro (1990) Trends Genet. **6**, 416–421.
34. J. Simon, A. Chiang, and W. Bender (1992) Development **114**, 493–505.
35. J. Simon, A. Chiang, W. Bender, M. J. Shimell, and M. O"Connor (1993) Dev. Biol. **158**, 131–144.
36. C. S. Chan, L. Rastelli, and V. Pirrotta (1994) EMBO J. **13**, 2553–2564.
37. B. Christen and M. Bienz (1994) Mech. Dev. **48**, 255–266.
38. A. Chiang, M. B. O"Connor, R. Paro, J. Simon, and W. Bender (1995) Development **121**, 1681–1689.
39. S. Poux, C. Kostic, and V. Pirrotta (1996) EMBO J. **15**, 4713–4722.
40. H. Strutt, G. Cavalli, and R. Paro (1997) EMBO J. **16**, 3621–3632.

41. V. Pirrotta and L. Rastelli (1994) Bioessays **16**, 549–556.
42. J. Simon (1995) Curr. Opin. Cell Biol. **7**, 376–385.
43. J. Simon, M. Peifer, W. Bender, and M. O"Connor (1990) EMBO J. **9**, 3945–3956.
44. J. Muller and M. Bienz (1991) EMBO J. **10**, 3147–3155.
45. K. McCall, M. B. O"Connor, and W. Bender (1994) Genetics **138**, 387–399.
46. M. Galloni, H. Gyurkovics, P. Schedl, and F. Karch (1993) EMBO J. **12**, 1087–1097.
47. H. Gyurkovics, J. Gausz, J. Kummer, and F. Karch (1990) EMBO J. **9**, 2579–2585.
48. F. Karch, M. Galloni, L. Sipos, J. Gausz, H. Gyurkovics, and P. Schedl (1994) Nucleic Acids Res. **22**, 3138–3131.
49. J. Mihaly, I. Hogga, J. Gausz, H. Gyurkovics, and F. Karch (1997) Development **124**, 1809–1820.
50. J. Mihaly, I. Hogga, S. Barges, M. Galloni, R. Mishra, K. Hagstrom, M. Müller, P. Schedl, L. Sipos, J. Gausz, H. Gyurkovics, and F. Karch. (1998) CMLS, **54**, 60–70.
51. M. Peifer, F. Karch, and W. Bender (1987) Genes Dev. **1**, 891–898.
52. T. Kondo, J. Zákány, and D. Duboule (1998) Molec. Cell **1**, 289–300.

Biuret Reaction

Proteins form biuret-like compounds (structure **I**) in alkaline solution by losing a proton from the nitrogen atoms of the peptide bonds. In strong alkaline solution and Cu^{2+}, this compound forms a blue colored complex (structure **II**). This color reaction is called the biuret reaction. The sensitivity of the reaction is not very great, but the color yield is similar from protein to protein. Thus, this reaction has been employed to quantify proteins in widely varying samples.

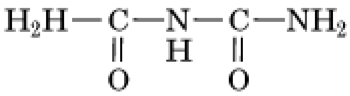

[I] Biuret; carbamylurea

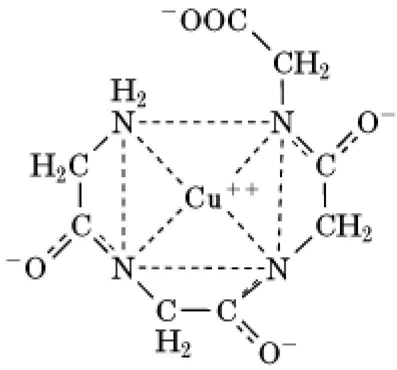

[II] A kind of biuret compound; copper glycine peptide complex under alkaline conditions

According to the method of Gornall et al. (1), 1 to 10 mg of protein is determined by **absorbance** at 540 nm after incubation with biuret reagent ($CuSO_4$, potassium sodium tartrate, NaOH) for 30 min at 20° to 25°C. An improved biuret method by Westley and Lambeth (2), which removes the free Cu^{2+} ion with an ion-exchange resin and adds Na-diethyldithiocarbonate as a coloring reagent, detects 0.05 to 1 mg of protein. A simple and sensitive micro-biuret method was developed by Itzhaki and Gill (3), where UV absorbance at 310 nm is employed to quantify protein.

Bibliography

1. A. G. Gornall, C. S. Bardawill, and M. M. David (1949) J. Biol. Chem. **177**, 751–766.
2. J. Westley and J. Lambeth (1960) Biochim. Biophys. Acta **40**, 364–366.
3. R. F. Itzhaki and D. M. Gill (1964) Anal. Biochem, **9**, 401–410.

Blastoderm

The blastoderm is an embryo at the stage that consists of a single cell layer. This cell layer is formed by the cleavage divisions of the fertilized zygote, largely under the control of maternally deposited gene products.

Suggestions for Further Reading

B. I. Balinsky (1975) *An Introduction to Embryology*, 4th ed., W. B. Saunders, Philadelphia, p. 5.

S. Shostak (1991) *Embryology: An Introduction to Developmental Biology*, Harper Collins, New York.

S. F. Gilbert (1997) *Developmental Biology*, Sinauer Associates, Sunderland, MA.

L. Wolpert et al. (1998) *Principles of Development*, Oxford University Press, Oxford, U.K.

J. M. W. Slack (1991) *From Egg to Embryo: Regional Specification in Early Development*, 2nd ed., Cambridge University Press, Cambridge, U.K.

Blastomere

After fertilization, the zygote begins the cleavage divisions. During the cleavage divisions, the cells of the embryo are called *blastomeres*.

Suggestions for Further Reading

B. I. Balinsky (1975) *An Introduction to Embryology*, 4th ed., W. B. Saunders, Philadelphia, p. 5.

S. Shostak (1991) *Embryology: An Introduction to Developmental Biology*, Harper Collins, New York.

S. F. Gilbert (1997) *Developmental Biology*, Sinauer Associates, Sunderland, MA.

L. Wolpert et al. (1998) *Principles of Development*, Oxford University Press, Oxford, U.K.

J. A. Moore (1972) *Heredity and Development*, Oxford University Press, New York.

Blastopore

The blastopore is a line of invagination on amphibian embryos for gastrulation (1). After fertilization, the amphibian zygote divides to form a mass of cells called blastomeres. The upper surface is called the *animal pole*, and the lower surface is called the *vegetal pole*. During gastrulation, the cells at the vegetal pole move inside the embryo, and the cells of the animal pole are left to form the outer surface of the embryo. The animal cells left at the surface will form the ectoderm, including the nervous system. The cells that move inside during gastrulation form the mesoderm and endoderm.

The process of gastrulation begins with the formation of a small indentation between the animal and vegetal poles on one side of the embryo. This small indentation is the beginning of formation of the blastopore. As gastrulation proceeds, the blastopore expands laterally to form a crescent, and eventually it encircles the entire embryo as gastrulation proceeds. The vegetal cells and the marginal cells between the vegetal and animal cells invaginate through the blastopore and form a second layer inside the embryo. As gastrulation continues, the blastopore shrinks to cover the remaining vegetal cells, called the *yolk plug*. When the blastopore almost completely covers the yolk plug, organogenesis begins. Interactions between various groups of cells during gastrulation cause cells to become determined to form various organs and structures. The determination of cells caused by interactions with their neighboring cells is called *developmental induction*. One of the most well-known examples is the organizer region of the amphibian embryo that specifies the determination of the nervous system. This is the dorsal lip of the blastopore and is often called the *Spemann organizer*, because it was first characterized by Hans Spemann (2).

Bibliography

1. B. I. Balinsky (1975) *An Introduction to Embryology*, 4th ed., W. B. Saunders, Philadelphia, pp. 161–164.
2. H. Spemann (1938) *Embryonic Development and Induction*, Yale University Press, New Haven.

Suggestions for Further Reading

3. S. Shostak (1991) *Embryology: An Introduction to Developmental Biology*, Harper Collins, New York.
4. S. F. Gilbert (1997) *Developmental Biology*, Sinauer Associates, Sunderland, MA.
5. L. Wolpert et al. (1998) *Principles of Development*, Oxford University Press, Oxford, U.K.
6. J. A. Moore (1972) *Heredity and Development*, 2nd ed., Oxford University Press, New York.

Bleomycin

Bleomycin (BLM), discovered in 1962, is a family of low-molecular-weight metalloglycopeptides

(M_r approximately 1500) produced by *Streptomyces verticillus* and isolated from the culture media of *S. verticillus* as copper complexes (1-3). It is widely used as an anticancer antibiotic in patients. BLM acts as a limited endonuclease and produces a variety of lesions in DNAs by a mechanism involving free radical attack on deoxyribose in both DNA strands. BLM damages DNAs in ways that mimic ionizing radiation. The detailed knowledge of the complicated chemistry of BLM and its interactions with DNA *in vivo* and *in vitro* drives much of its use in applications to molecular biology. BLM and structurally related analogues are considered radiomimetic and oxidative DNA-cleaving reagents, and as such they are utilized as chemical tools to study and understand the activities of this class of agents. Tools of molecular biology are also employed to understand the chemical, biological, and clinical aspects of the mechanism of action of BLMs. In addition, broadly used cloning strategies in several organisms use a gene conferring resistance to BLM and structurally related analogues as a selectable marker. Phleomycin (PLM) is used as the selective agent and is available in commercial formulations. BLM causes multiple changes to cells and is cytocidal, and its cytotoxicity is high where there is no or only a limited barrier to BLM reaching cellular targets. BLM effectively kills all types of cells tested. Cellular resistance is conferred in several ways, including protection by nucleosomes in chromatin, DNA repair, metabolic inactivation of BLM, BLM-resistance proteins, and restricted entry of BLM. An overview of resistance mechanisms was recently published (4).

1. Structure and Activated Complex

The structurally complex BLMs contain a metal-binding domain and a **DNA-binding** domain (Fig. 1). BLMs require metals and oxygen species for their activity (5-9). The metal-binding domain is also the site of oxygen activation and is attached to a disaccharide group; it binds redox-active transition metals, such as Fe(II), Co(II), Cu(II), Ni(II), and Zn(II). The most stable BLM–O_2–metal complex is formed with cobalt (8). When a BLM-Fe(II)-O_2 complex binds to DNA and the Fe(II) oxidizes to Fe(III), the complex attacks the C4′ position of DNA deoxyribose (10-13). The complex thereby behaves as a limited endonuclease.

Figure 1. Structures of bleomycins and phleomycins (16, 117-119).

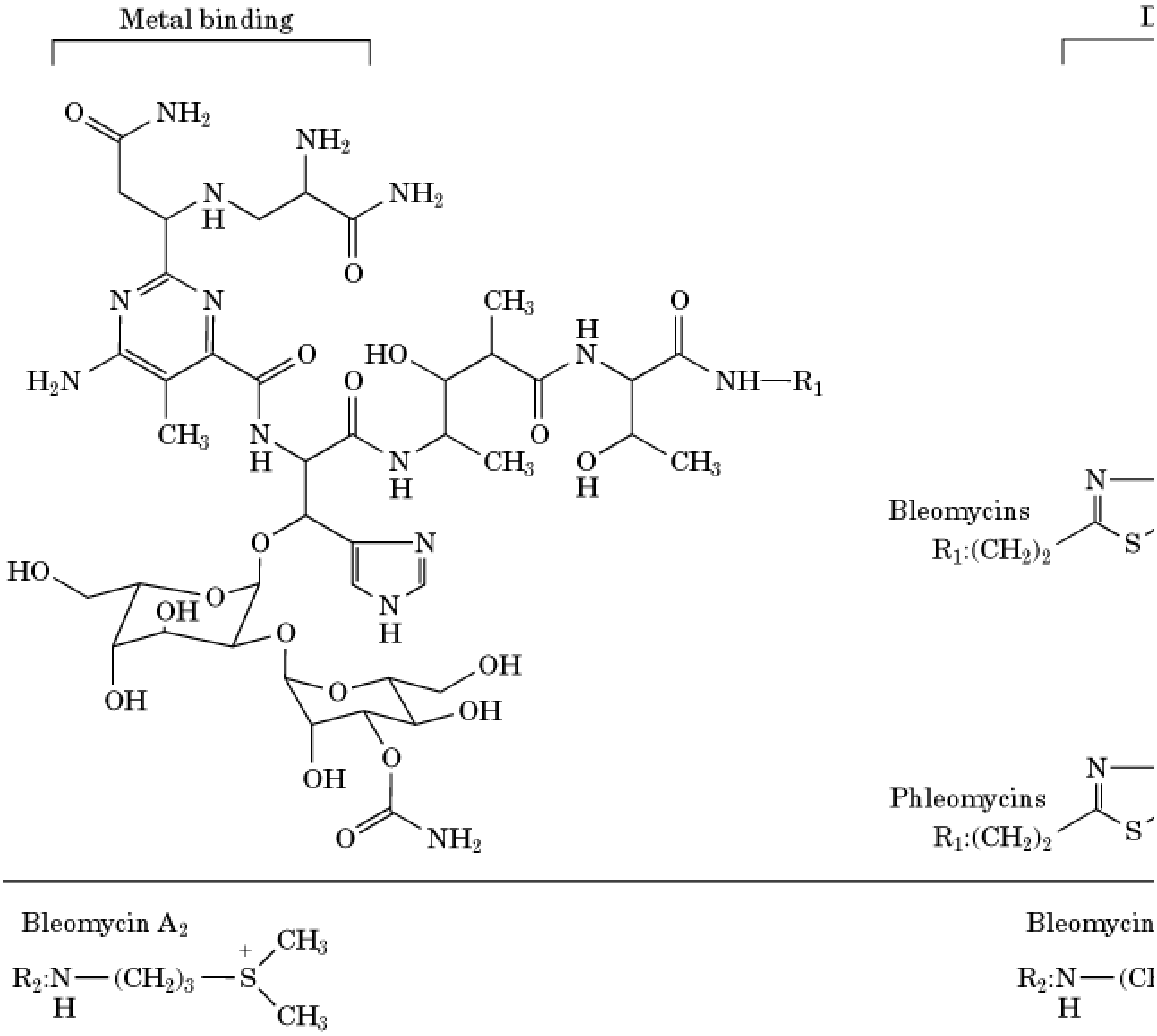

The coplanar bithiazole moiety partially intercalates into the minor groove between bases of DNA. The cationic *C*-terminal amines are also involved in interactions with nucleic acids. The terminal amines in BLM A_2 and BLM B_2 are dimethylsulfonium propylamine and agmatine, respectively, and are similar in length and bear one positive charge (Fig. 1). BLM B_2 produces considerably more DNA breaks and killing than BLM A_2 over a wide range of chemical concentrations (14). Without the terminal amine, the BLM molecule no longer cleaves DNA or possesses antitumor activity.

BLM and structurally related PLM (15) differ in the oxidation state of their sulfur heterocycles (Fig. 1). One of the two conjugated thiazole rings of the BLM bithiazole is modified by hydrogenation to 4,5-dihydrothiazole (thiazoline) in PLM (16, 17). In addition, the *C*-terminal amines in clinical preparations of BLMs differ chemically and quantitatively from prepared mixtures of PLMs. Tallysomycin is closely related to BLM (18, 19).

2. Anticancer Use

BLM is an important therapeutic agent that is useful as a single agent in treating several human cancers and is widely used in combination chemotherapy and radiotherapy. The water-soluble product used in cancer treatment, Blenoxane, is a family of 11 metal-free congeners differing in their terminal amines. The clinical mixture (20) is comprised mainly of BLM A_2 [approximately 55% to 70% (usually 68% to 69%)] and BLM B_2 (approximately 25% to 32%). The effectiveness of BLM as an anticancer agent is associated with its ability to produce lesions in DNA (21, 22).

BLM is principally used in patients with lymphoma or a variety of solid tumors. It has been included in regimens for treating malignant and peripheral T-cell lymphomas, as well as in combination BEP chemotherapy (BLM, etoposide, cisplatin) for metastatic testicular teratoma and Hodgkins and non-Hodgkins lymphoma. BLM is also used in the chemotherapy and management of Kaposi's sarcoma (eg, pulmonary, gastrointestinal, epidemic, disseminated), as well as with vincristine in combination chemotherapy for epidemic Kaposi's sarcoma. BLM does not cause bone-marrow, hepatic, or renal toxicities, nor does it cause cardiosuppression. Pulmonary fibrosis is a side effect of BLM treatment that limits its use. The molecular mechanism of lung fibrosis is being investigated, but is not fully known. Patients with genetic susceptibility are particularly susceptible to lung fibrosis (23, 24). In animal models, taurine (25) or taurine and niacin (26) counter BLM-induced lung fibrosis. The newer BLM derivatives, peplomycin and liblomycin, were developed because of their lower pulmonary toxicity and broader antitumor spectrum in animal studies (27).

3. Mechanism of Action on Nucleic Acids

3.1. Chemical Action on DNA: DNA Damage

The unique chemical action of BLMs in the presence of oxygen and Fe(II) catalytically cleaves double-stranded DNA *in vivo* and *in vitro*. Single- and double-stranded breaks are produced, leaving 5′-phosphate- and 3′-phosphoglycolate-termini (11, 28-32). The most genotoxic and lethal lesions for cells are double-stranded breaks. BLM recognizes 5′-phosphoguanylyl(3′,5′)thymidine or 5′-phosphoguanylyl(3′,5′)cytosine sequences most frequently, releasing the pyrimidines when they are located to the 3′ side of guanosine (28-30, 33-36) and leaving DNA alkali-labile (32, 37). While cleavage at the first site is G-Py-specific, the second nucleophilic attack by a BLM–Fe(II)–O_2 complex on the opposite DNA strand is not a sequence-specific cleavage and instead is probably targeted by the structural perturbation of the DNA at the first cleavage site (38, 39). Deoxyribose degradation also produces 3-(pyrimidin-1′-yl)-2-propenal and 3-(purin-9′-yl)-2-propenal (11, 31, 40) and oligonucleotide 3′-(phosphoro-2-*O*-glycolic acid) derivatives (11, 31, 41). DNA strand breaks are stoichiometric with the production of base propenals (42).

3.2. Preferential Cleavage between Nucleosomes

BLM preferentially cleaves **linker regions** of chromatin between nucleosomes (43-47). The enhanced resistance of DNA bound to nucleosomes seems to be related to the necessity of a conformational change for BLM binding and intercalation. In yeast, internucleosomal cleavage and DNA degradation (46) and killing (48) are less pronounced in logarithmic phase cells than in cells that are in stationary phase. The cellular and molecular basis for this may relate to the highly effective use of BLM on particular solid tumors.

3.3. Bleomycin and Phleomycin

PLM was discovered before bleomycin, but was too toxic in patients to be used as an anticancer drug. PLM is also substantially more effective than BLM on a per mole basis in yeast in producing cell killing (48), DNA breaks in intracellular DNAs (49), release of nucleosomes from chromatin (45), and genetic changes (50). Thus, the DNA lesions produced by the BLM and PLM could differ in their nature or frequency, or they could be processed differently by the cells. The mechanisms of BLM and PLM interaction with DNA *in vitro* also appear to differ (51-54). PLM exhibits a higher requirement than BLM for ferrous ions (49). Bithiazole intercalation in DNA is thought to be necessary for producing double-stranded, but not single-stranded, breaks *in vitro* (52). Accordingly, BLM produces more double-strand breaks than PLM in PM2 phage DNA (52, 54). Cu(II)BLM, but not Cu(II) PLM, intercalates (51). BLM, but not PLM, degrades relaxed DNA to a greater extent than either positively or negatively **superhelical** DNA (54). On the other hand, BLM and PLM cleave DNA *in vitro* at similar preferred sites at similar frequencies (55, 56) and produce comparable numbers of DNA breaks under some conditions (57, 58).

3.4. RNA

BLM cleaves a variety of RNAs. The most studied have been transfer RNA and tRNA precursors. In contrast to DNA cleavage, BLM-induced RNA cleavage is usually wholly or predominately at a single site, often at a junction between single- and double-stranded RNA regions (59-62).

4. DNA Repair

4.1. Biochemical and Genetic Evidence for Radiomimetic Properties

The cellular processes that repair BLM-induced DNA lesions are not entirely known. The most important mechanisms for the repair of BLM-induced DNA damage are recombinational repair, base-excision repair, and post-replication repair. BLM and ionizing radiation produce similar lesions in DNA, although BLM produces a narrower spectrum of products than ionizing radiation. DNA breaks are introduced approximately linearly with increasing concentrations of BLM (14) and ionizing radiation (63). Some of the chromosomal lesions produced after either BLM treatments or ionizing irradiation can be ligated immediately and lead to a quick component of DNA rejoining, but other lesions require more time for processing before the termini of the DNA molecules become substrates for ligation (14, 63-65). For example, the unusual phosphoglycolate must be removed by the DNA 3′-repair diesterase activity of apurinic and apyrimidinic endonuclease (66, 67). After extension of the remaining DNA strand by one nucleotide, DNA ligase resynthesizes intact DNA molecules by forming a phosphodiester bond between adjacent 3′-hydroxyl and 5′-phosphoryl termini (14). Rapid and slower components of DNA rejoining have been identified in several laboratories. An ultrarapid phase of cellular recovery accompanies rapid repair in human cells (64, 68), suggesting that some of the cytotoxic treatment effects of BLM could be counteracted in the clinic and reduce chemotherapeutic effectiveness.

The importance of DNA repair is shown by the many studies in various organisms of mutants hypersusceptible to killing by BLM and defective in repair of DNA lesions. All *rad* mutations of *Saccharomyces cerevisiae* (69-72) that confer hypersensitivity to killing by BLM analogues also confer cross-sensitivity to ionizing radiation (73-78), so pathways are shared for the repair of chromosomal damage by bleomycins and ionizing radiation. Moreover, mutant strains with altered resistance to lethal effects of BLM have been isolated and characterized in several laboratories, and direct selection for mutations conferring hypersensitivities to lethal effects of BLM resulted in mutants exhibiting cross-hypersensitivities to ionizing radiation.

4.2. Genetic Recombination and Mutation

Mechanisms of recombination are important for DNA repair and rejoining recombinant DNA. BLM is recombinogenic and mutagenic (38, 50, 79-85). The amount of recombination or mutation caused by BLM depends upon the assay system and treatment conditions. BLM was found to be weakly mutagenic to mitochondrial DNA (86).

5. Additional Cellular Targets

5.1. Membrane

The plasma membrane restricts BLM internalization in some mammalian cells (87, 88). This could be due to the polar and charged groups on the BLM molecule. Membrane damage by BLM (68, 89) or cell electropermealization (88) circumvents this restriction.

5.2. Cell Wall

BLM molecules are readily taken up into yeast cells, but are not equally distributed from cell to cell (89). BLM initially localizes to cell walls, causes cell wall and membrane damage, and aids the enzymatic conversion of cells to spheroplasts (75, 89-91). BLM alters the anchorage of several mannoproteins in the cell wall matrix of intact cells or isolated cell walls, and it disrupts essential cell wall polymers. These activities facilitate the entry of BLM into yeast cells.

5.3. BLM Hydrolase

BLM hydrolase hydrolyzes and inactivates BLM. The enzyme is a thiol proteinase that has DNA-binding and peptide-cleavage domains. It binds DNA and RNA. BLM hydrolase activity protects cells from BLM toxicity, but limits the use of BLM in cancer chemotherapy. Although its normal cellular function is unknown, the enzyme is present in diverse organisms, including humans (92-96) and yeast (97-100). Expression of the yeast BLM hydrolase in mammalian cells results in resistance to BLM (101). A member of a galactose regulatory system (102, 103), yeast BLM hydrolase binds to nicked double-stranded DNA, single-stranded DNA, and RNA, without sequence specificity (104). This enzyme associates with plasma membranes and is in the cytosol (105). Human BLM hydrolase was recently shown to exhibit endopeptidase activity (106). This enzyme is thought to play a role in the development of resistance to BLM during chemotherapy (95, 107-109).

5.4. BLM Resistance Proteins

Several proteins in microorganisms that produce BLM or structural analogues actually confer resistance to these products. Vectors bearing genes encoding these proteins confer high levels of resistance to BLM and related antibiotics and are used as cloning vehicles. The proteins bind and form stable complexes with BLM with high specificity, thereby preventing BLM from complexing with DNA. One of these proteins is encoded by the *Streptoalloteichus hindustanus* (*Sh*) *ble* gene (110-112) found on the Tn5 bacterial transposon, along with additional genes encoding resistance to other antibiotics. Expression of the *Sh ble* gene in transgenic mice reduced BLM toxicity in the mice and protected against lung fibrosis (113, 114). High levels of the protein were detected in lungs, kidney, and spleen.

5.5. Multiple Targets and Cytotoxicity

Multiple cellular targets of BLM are expected because of the chemical mechanism of action of the molecule and because some of the BLM-hypersensitive mutants isolated in different organisms do not exhibit hypersensitivity to lethal effects of radiation. Multiple cellular enzymes are important for surviving the toxicities of BLM, and deficiencies in their function could reduce chances of survival. The relationship and significance of each cellular target of BLM to cellular toxicity are not known. Why BLM causes apoptosis in some types of cells and not in others is also unknown. BLM is not considered apoptotic at low concentrations. Far less is known about targets of BLM in cells than about the chemical mechanism of action of BLM *in vitro* on defined substrates.

Additional factors modulate BLM activity. Generally, BLM preferentially affects mitotic cells in the G2-M phase of the cell cycle. BLM is unlikely to be a useful agent to study meiosis because of the abundant lesions the molecule produces in DNA. Intracellular metal ion concentrations and pH also modulate BLM activities (48, 115, 116). Studies elucidating the roles of the multiple targets of BLM and factors that modulate BLM activities will improve our understanding and efficacious uses of the widely studied BLM family of related compounds.

Bibliography

1. H. Umezawa, K. Maeda, T. Takeuchi, and Y. Okami (1966) J. Antibiotics **19**, 200–209.
2. H. Umezawa, Y. Suhara, T. Takita, and K. Maeda (1966) J. Antibiotics **19**, 210–215.
3. H. Umezawa (1976) GANN **19**, 3–36.
4. W. S. El-Deiry (1997) Curr. Opin. Oncol. **9**, 79–87.
5. E. A. Sausville, J. Peisach, and S. B. Horwitz (1976) Biochem. Biophys. Res. Commun. **91**, 871–877.
6. R. M. Burger, J. Peisach, and S. B. Horwitz (1981) J. Biol. Chem. **256**, 11636–11639.
7. R. M. Burger, S. J. Projan, S. B. Horwitz, and J. Peisach (1986) J. Biol. Chem. **261**, 15955–15959.

8. J. Stubbe and J. Kozarich (1987) Chem. Rev. **87**, 1107–1136.
9. P. C. Dedon and I. H. Goldberg (1992) Chem. Res. Toxicol. **5**, 311–332.
10. R. M. Burger, J. Peisach, and S. B. Horwitz (1981) Life Sci. **28**, 715–727.
11. L. Giloni et al. (1981) J. Biol. Chem. **256**, 8608–8615.
12. J. W. Sam and J. Peisach (1993) Biochemistry **43**, 1488–1491.
13. L. F. Povirk, Y. H. Han, and R. J. Steighner (1989) Biochemistry **28**, 5808–5814.
14. C. W. Moore (1990) Biochemistry **29**, 1342–1347.
15. K. Maeda, H. Kosaka, K. Yagishita, and H. Umezawa (1956) J. Antibiotics **9**, 82–85.
16. T. Takita et al. (1972) J. Antibiotics **25**, 197–199.
17. D. A. McGowan, U. Jordis, D. K. Minster, and S. M. Hecht (1977) J. Am. Chem. Soc. **99**, 8078–8079.
18. H. Kawaguchi et al. (1977) J. Antibiotics **30**, 779–788.
19. M. Konishi et al. (1977) J. Antibiotics **30**, 789–805.
20. C. Crooke and W. Bradner (1976) J. Med. **7**, 333–425.
21. S. K. Carter, S. T. Crooke, and H. Umezawa (1978) *Bleomycin, Current Status and New Developments*, Academic Press, New York.
22. S. M. Hecht, ed. (1979) *Bleomycin: Chemical, Biochemical and Biological Aspects*, Springer-Verlag, New York.
23. C. K. Haston, C. I. Amos, T. M. King, and E. L. Travis (1996) Cancer Res. **56**, 2596–2601.
24. R. P. Marshall, R. J. McAnulty, and G. J. Laurent (1997) Int. J. Biochem. Cell. Biol. **29**, 107–120.
25. R. E. Gordon, R. F. Heller, and R. F. Heller (1992) Adv. Exp. Med. Biol. **315**, 319–328.
26. G. Gurujeyalakshmi, M. A. Hollinger, and S. N. Giri (1998) Am. J. Respir. Cell. Mol. Biol. **18**, 334–342.
27. T. Takita and T. Ogino (1987) Biomed. Pharmacother. **41**, 219–226.
28. A. D. D"Andrea and W. A. Haseltine (1978) Proc. Natl. Acad. Sci. USA **75**, 3608–3612.
29. M. Takeshita, P. Grollman, E. Ohtsubo, and H. Ohtsubo (1978) Proc. Natl. Acad. Sci. USA **75**, 5983–5987.
30. A. P. Grollman and M. Takeshita (1980) Adv. Enzymol. Regul. **18**, 67–83.
31. N. Murugesan et al. (1985) Biochemistry **24**, 5735–5744.
32. H. Sugiyama, C. Xu, N. Murugesan, and S. M. Hecht (1985) J. Am. Chem. Soc. **107**, 4101–4105.
33. M. Takeshita and P. Grollman (1979) In *Bleomycin: Chemical, Biochemical and Biological Aspects* (S. Hecht, ed.), Springer-Verlag, New York, pp. 207–221.
34. C. K. Mirabelli, C.-H. Huang, A. W. Prestayko, and S. T. Crooke (1982) Cancer Chemother. Pharmacol. **8**, 57–65.
35. C. K. Mirabelli et al. (1982) Cancer Res. **42**, 2779–2785.
36. V. Murray and R. F. Martin (1985) J. Biol. Chem. **260**, 10389–10391.
37. J. C. Wu, J. W. Kozarich, and J. Stubbe (1983) J. Biol. Chem. **258**, 4694–4697.
38. R. J. Steighner and L. F. Povirk (1990) Proc. Natl. Acad. Sci. USA **87**, 8350–8354.
39. L. F. Povirk, Y.-H. Han, and R. J. Steighner (1989) Biochem. **28**, 8508–8514.
40. R. M. Burger, A. R. Berkowitz, J. Peisach, and S. B. Horwitz (1980) J. Biol. Chem. **255**, 11832–11838.
41. S. Uesugi et al. (1984) Nucleic Acids Res. **12**, 1581–1592.
42. R. M. Burger, J. Peisach, and S. B. Horwitz (1982) J. Biol. Chem. **257**, 8612–8614.
43. M. T. Kuo and T. C. Hsu (1978) Nature **271**, 83–84.

44. M. T. Kuo and T. C. Hsu (1978) Chromosoma **68**, 229–240.
45. C. W. Moore, (1988) Cancer Res. **48**, 6837–6843.
46. C. W. Moore, C. S. Jones, and L. A. Wall (1989) Antimicrob. Agents Chemother. **33**, 1592–1599.
47. K. Sidik and M. J. Smerdon (1990) Biochem. **29**, 7501–7511.
48. C. W. Moore (1982) Cancer Res. **42**, 929–933.
49. C. W. Moore (1989) Cancer Res. **49**, 6935–6940.
50. J. F. Mc.Koy et al. (1995) Mutat. Res. DNA Repair **336**, 19–27.
51. L. F. Povirk, M. Hogan, N. Dattagupta, and M. Buechner (1981) Biochem. **20**, 665–671.
52. C.-H. Huang, C. K. Mirabelli, Y. Jan, and S. T. Crooke (1981) Biochem. **20**, 233–238.
53. C.-H. Huang, A. W. Prestayko, and S. T. Crooke (1982) Biochem. **21**, 3704–3710.
54. C.-H. Huang, C. K. Mirabelli, S. Mong, and S. T. Crooke (1983) Cancer Res. **43**, 2849–2856.
55. M. Takeshita et al. (1981) Biochem. **20**, 7599–7606.
56. J. Kross, W. D. Henner, S. M. Hecht, and W. A. Haseltine (1982) Biochem. **21**, 4310–4318.
57. H. Suzuki et al. (1969) J. Antibiot. **22**, 446–448.
58. R. Stern, J. A. Rose, and R. M. Friedman (1974) Biochemistry **13**, 307–312.
59. B. J. Carter et al. (1990) Proc. Natl. Acad. Sci. USA **87**, 9373–9377.
60. A. Huttenhofer, S. Hudson, H. F. Noller, and P. K. Mascharak (1992) J. Biol. Chem. **267**, 24471–24475.
61. L. L. Guan et al. (1993) Biochem. Biophys. Res. Commun. **191**, 1338–1346.
62. M. V. Keck and S. M. Hecht (1995) Biochemistry **34**, 12029–12037.
63. C. W. Moore (1982) J. Bacteriol. **150**, 1227–1233.
64. C. W. Moore and J. B. Little (1985) Cancer Res. **45**, 1982–1986.
65. C. W. Moore (1988) J. Bacteriol. **170**, 4991–4994.
66. A. W. Johnson and B. Demple (1988) J. Biol. Chem. **263**, 18017–18022.
67. J. Laval (1996) Pathol. Biol. **44**, 14–24.
68. C. W. Moore, A. W. Malcolm, K. N. Tomkinson, and J. B. Little (1985) Cancer Res. **45**, 1978–1981.
69. J. Game (1993) Semin. Cancer Biol. **4**, 73–83.
70. S. Prakash, P. Sung, and L. Prakash (1993) Annu. Rev. Genet. **27**, 33–70.
71. E. C. Friedberg (1995) *DNA Genes and Mutagenesis*. ASM Press, Washington, D.C.
72. D. Ramotar and J.-Y. Masson (1996) Mol. Cell. Biochem. **158**, 65–75.
73. C. W. Moore (1978) Mutat. Res. **51**, 165–180.
74. C. W. Moore (1980) J. Antibiot. **33**, 1369–1375.
75. C. W. Moore (1982) Antimicrob. Agents Chemother. **21**, 595–600.
76. C. W. Moore (1991) J. Bacteriol. **173**, 3605–3608.
77. D. J. Keszenman, V. A. Salvo, and E. Nunes (1992) J. Bacteriol. **174**, 3125–3132.
78. C. H. He, J.-Y. Masson, and D. Ramotar (1996) Can. J. Microbiol. **42**, 1263–1266.
79. M. A. Hannan and A. Nasim (1978) Mutat. Res. **53**, 309–316.
80. M. A. Hannan, A. Nasim, and T. Brychcy (1978) Mutat. Res. **58**, 107–110.
81. B. K. Vig and R. Lewis (1978) Mutat. Res. **55**, 121–145.
82. C. W. Moore (1978) Mutat. Res. **58**, 41–49.
83. A. Severgnini, O. Lillo, and E. Nunes (1991) Environ. Mol. Mutagen. **18**, 102–106.
84. L. F. Povirk and M. J. F. Austin (1991) Mutat. Res. **257**, 127–143.
85. L. F. Povirk et al. (1994) J. Mol. Biol. **243**, 216–226.

86. L. R. Ferguson and P. M. Turner (1988) Eur. J. Cancer Clin. Oncol. **24**, 591–596.
87. G. Pron, J. Belehradek, Jr., S. Orlowski, and L. M. Mir (1994) Biochem. Pharmacol. **48**, 301–310.
88. L. M. Mir, O. Tounekti, and S. Orlowski (1996) Gen. Pharmacol. **27**, 745–748.
89. C. W. Moore, R. Del Valle, J. F. Mc.Koy, A. Pramanik, and R. E. Gordon (1992) Antimicrob. Agents Chemother. **36**, 2497–2505.
90. R. Beaudouin et al. (1993) Antimicrob. Agents Chemother. **37**, 1264–1269.
91. S. T. Lim, C. K. Jue, C. W. Moore, and P. N. Lipke (1995) J. Bacteriol. **177**, 3534–3539.
92. S. Akiyama et al. (1981) Biochem. Biophys. Res. Commun. **101**, 55–60.
93. J. S. Lazo, S. M. Sebti, and A. E. Filderman (1987) In *Metabolism and Mechanism of Action of Anti-cancer Drugs* (G. Powis and R. A. Prough, eds.), Taylor and Francis, London, pp. 194–210.
94. C. Nishimura, H. Suzuki, N. Tanaka, and H. Yamaguchi (1989) Biochim. Biophys. Acta **1012**, 29–35.
95. S. M. Sebti et al. (1989) Biochemistry **28**, 6544–6548.
96. S. E. Montoya, R. E. Ferrell, and J. S. Lazo (1997) Cancer Res. **57**, 4191–4195.
97. N. G. Kambouris, D. J. Burke, and C. E. Creutz (1992) J. Biol. Chem. **267**, 21570–21576.
98. C. Enenkel and D. H. Wolf (1993) J. Biol. Chem. **268**, 7036–7043.
99. U. Magdolen, G. Müller, V. Magdolen, and W. Bandlow (1993) Biochim. Biophys. Acta **1171**, 299–303.
100. H. E. Xu and S. A. Johnston (1994) J. Biol. Chem. **269**, 21177–21183.
101. A. Pei, T. P. Calmels, C. E. Creutz, and S. M. Sebti (1995) Mol. Pharmacol. **48**, 676–681.
102. L. Joshua-Tor, H. E. Xu, S. A. Johnson, and D. C. Rees (1995) Science **269**, 945–950.
103. W. Zheng, H. E. Xu, and S. A. Johnston (1997) J. Biol. Chem. **272**, 30350–30355.
104. W. Zheng and S. A. Johnston (1998) Mol. Cell. Biol. **18**, 3580–3585.
105. I. Niemer, G. Müller, and G. Strobel (1997) Curr. Genet. **32**, 41–51.
106. R. P. Koldamova, I. M. Lefterov, V. G. Gadjeva, and J. S. Lazo (1998) Biochemistry **37**, 2282–2290.
107. D. Drocourt, T. Calmels, J. P. Reynes, M. Baron, and G. Tiraby (1990) Nucleic Acids Res. **18**, 4009.
108. D. Bromme et al. (1996) Biochemistry **35**, 6706–6714.
109. A. A. Ferrando, A. Velasco, E. Campo, and C. Lopez-Otin (1996) Cancer Res. **56**, 1746–1750.
110. A. Gatignol, M. Baron, and G. Tiraby (1987) Mol. Gen. Genet. **207**, 342–348.
111. A. Gatignol, M. Dassain, and G. Tiraby (1990) Gene **91**, 35–41.
112. D. Drocourt et al. (1990) Nucl. Acids Res. **18**, 4009.
113. P. L. Tran et al. (1997) J. Clin. Invest. **99**, 608–617.
114. J. Weinbach et al. (1996) Cancer Res. **56**, 5659–5665.
115. C. W. Moore and D. A. Vossler (1980) Biochim. Biophys. Acta **610**, 425–429.
116. C. W. Moore (1994) Antimicrob. Agents Chemother. **38**, 1615–1619.
117. T. Takita et al. (1972) J. Antibiot. **25**, 755–758.
118. H. Naganawa, Y. Muraoka, T. Takita, and H. Umezawa (1977) J. Antbiot. **30**, 388–396.
119. T. Takita et al. (1978) J. Antibiot. **31**, 801–804.

Suggestions for Further Reading

120. R. M. Burger (1998) Cleavage of nucleic acids by bleomycin. Chem. Rev. **98**, 1153–1170. (Reviews the chemical mechanism of bleomycin action.)

121. S. M. Hecht (1994) RNA degradation by bleomycin, a naturally occurring bioconjugate. Bioconjugate Chem. **5**, 513–526. (Reviews and compares mechanisms of cleavage of DNAs and RNAs.)
122. J. S. Lazo and S. M. Sebti (1997) Bleomycin. Cancer Chemother. Biol. Response Modif. **17**, 40–45. (Together with earlier reviews in this series by the same authors, this article provides overview of clinical uses of bleomycin and mechanisms of tumor resistance to bleomycin cytotoxicity.)
123. D. H. Petering, Q. Mao, W. Li, E. DeRose, and W. E. Antholine (1996) Metallobleomycin–DNA interactions: structures and reactions related to bleomycin-induced DNA damage. Met. Ions Biol. Syst. **33**, 619–648. (Reviews mechanisms of interactions of metallobleomycin and DNA in cells and *in vitro*.)
124. L. F. Povirk (1996) DNA damage and mutagenesis by radiomimetic DNA-cleaving agents: bleomycin, neocarzinostatin and other enediynes Mutat. Res. **355**, 71–89. (Summarizes the chemical action and relationship of DNA lesions to types of mutations produced by radiomimetic antibiotics.)

Blood Clotting

The clotting or coagulation of blood is necessary for the maintenance of vascular integrity, and is therefore essential to survival. Cessation of bleeding can be achieved within minutes, involving both cellular and soluble protein components present in blood. The overall function of the blood coagulation system is the rapid amplification of a small initial stimulus via a series of sequential reactions that activate various zymogens and pro-cofactors of serine proteinases, culminating in the generation of thrombin, which proteolytically converts fibrinogen to fibrin. Fibrin monomers subsequently polymerize to form the insoluble fibrin clot. The major enzymatic components of the coagulation pathways are a series of **homologous** serine proteinases whose function is determined primarily by differences in the organization of their *N* terminal, noncatalytic **domains**. Most of the reactions are catalyzed by complexes between these serine proteinases, nonenzymatic protein cofactors, and serine proteinase zymogens that are assembled on phospholipid surfaces in the presence of calcium ions. These complexes are able to catalyze activation of the proteinase zymogen by limited **proteolysis** at rates up to 10^6-fold greater than those in the absence of cofactor/phospholipid. The proteinase product of one reaction then participates in another analogous complex, thus providing the amplification, as well as the multiple levels at which both positive and negative regulation can be exerted.

Figure 1 shows the two classical pathways of blood coagulation, termed the *intrinsic* and *extrinsic* pathways. These were originally envisaged as elegant, essentially linear sequences of reactions, but **feedback inhibition** reactions and cross-reactions between the two pathways are now known to be important and to provide further amplification. The terminology used to describe the two pathways of blood coagulation is somewhat counterintuitive, tending to imply the opposite to what is now known to be the physiological clotting mechanism. Genetic deficiencies in the extrinsic pathway lead to severe bleeding tendencies, but initiation of this pathway *in vitro* requires components in the form of tissue extracts (containing tissue factor and phospholipid) that are not present in blood. By contrast, the physiological role of the “intrinsic” pathway is unclear, as genetic deficiencies in its components do not give rise to bleeding disorders, but all the components are present in blood, and it can be initiated by simply removing blood from the circulation. This is due to contact with a negatively charged surface, such as glass, giving the pathway its alternative name of “contact activation," and involves proteinases and cofactors quite distinct from those of the extrinsic pathway.

Figure 1. The proteolytic reactions of the blood clotting pathways. The zymogen/proteinase pairs are shown in black with the "forward" reactions as solid lines, the cofactors are shown in blue with the positive feedback reactions as dashed blue lines. The proteolytic negative feedback reactions are shown in red. The complexes initiating the two pathways of coagulation are boxed: the factor VII–tissue factor complex and the contact activation complex that assembles on high molecular-weight kininogen (HMWK). The Roman numeral system used for the coagulation proteinases and cofactors is based loosely on the order in which they were discovered, with the exceptions of the first four components fibrinogen, prothrombin, tissue factor–phospholipid complex, and Ca^{2+}. The proteolytically activated forms of these factors are denoted by a subscript "a," for example, factor X_a. Additional nonproteolytic inhibitory mechanisms exist, the principal of which are the serpin antithrombin (an inhibitor of most of the Gla-proteinases) and tissue factor pathway inhibitor (TFPI), a Kunitz-type proteinase inhibitor of factors VII_a and X_a.

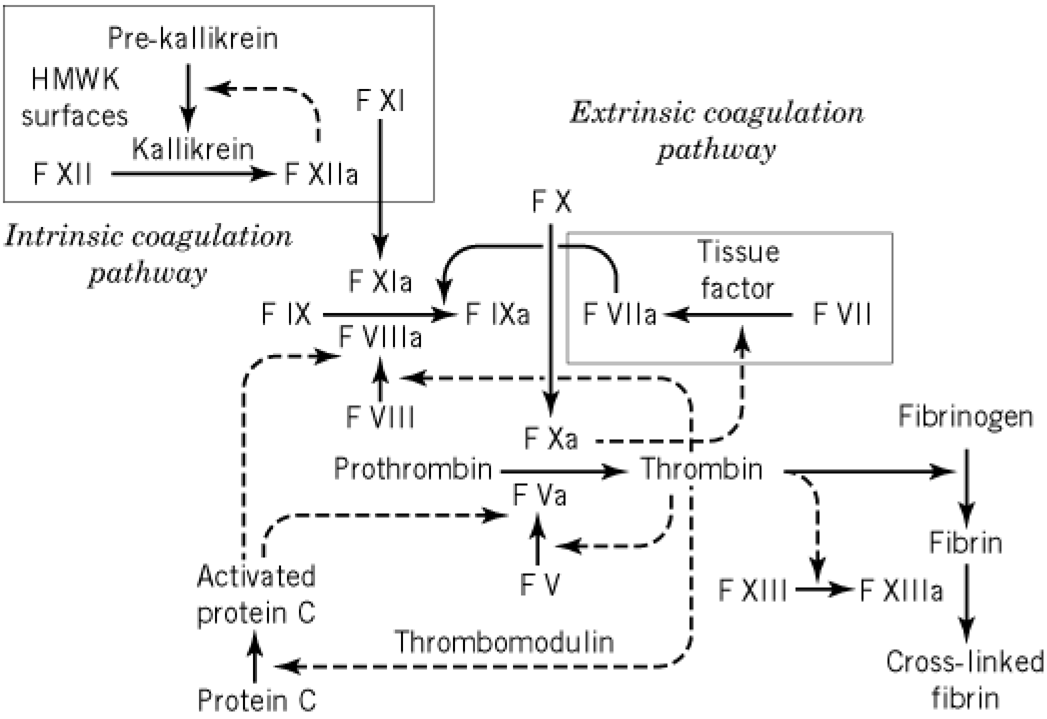

A complete description of the coagulation system and the many proteolytic and inhibitory reactions that lead to its exquisite functional regulation is beyond the scope of this article. We will therefore focus on two key proteolytic steps that are representative of the two types of multicomponent complexes of the extrinsic pathway and that demonstrate the fundamental interactions and mechanisms underlying catalysis of the proteolytic reactions of blood coagulation; one requiring proteolytically activated soluble cofactors, the other requiring integral membrane protein cofactors that do not require proteolytic activation.

1. Regulation of Blood Clotting by Complexes Involving Soluble Protein Cofactors

The only proteolytic reaction common to both pathways is the activation of prothrombin, the final serine proteinase zymogen of the coagulation cascade. Factor X_a (i.e., activated factor X) is the proteinase component of the "prothrombinase complex" that catalyzes the generation of thrombin. Both zymogen and active proteinase have an *N*-terminal "Gla domain," which contains g-carboxyglutamic acid residues. The Gla domain is also present in prothrombin (as well as factors VII and IX, and protein C, the so-called vitamin K–dependent or Gla proteinases); it binds Ca^{2+} and participates in binding to negatively charged phospholipid surfaces, which *in vivo* are provided principally by activated platelets. Therefore, both enzyme and substrate bind to phospholipid surfaces, with **dissociation constants** of 0.1–1 μ*M* (1). The cofactor of the prothrombinase complex is factor V_a, which is generated by thrombin-catalyzed limited proteolysis of factor V, providing one of the major feedback activation reactions. Factor V_a also binds to negatively-charged phospholipid surfaces, but with a much lower dissociation constant of ~ 5 nM (2). It does not contain a Gla domain, and binds through a different mechanism involving partial insertion of the protein into the lipid bilayer; it is often viewed as a membrane binding site for factor X_a. The latter thus incorporates into the complex by both protein–phospholipid and protein–protein interactions. Kinetic experiments suggest that the two phospholipid-bound components associate by lateral diffusion, but the interactions involved are complex and to some extent **cooperative**. Although prothrombin also binds to phospholipid, it is not clear whether the relevant substrate is phospholipid-bound prothrombin or prothrombin in the solution phase but at a high local concentration in the vicinity of the membrane surface, which can be several orders of magnitude above that in bulk solution. The kinetic effect of prothrombin binding to phospholipid is a reduction in the apparent Km (Michaelis constant) for prothrombin activation ("apparent" as the K_m does not reflect the true concentration at the phospholipid–surface interface). This is of physiological significance, since the K_m falls from ~ 100 μM to < 1 μM (3), compared to a concentration of 1.4 μ*M* in blood plasma. In addition to this effect, the catalytic rate constant, k_{cat}, for prothrombin activation is greatly increased, primarily as a consequence of the X_a–V_a interaction (Table 1). This suggests that the active-site environment of the proteinase is significantly affected by complex formation, although the molecular basis of this effect is not known. The prothrombinase complex also helps to achieve maximum catalytic advantage by ordering the sequence of the two proteolytic cleavages required for prothrombin activation (see Thrombin).

Table 1. Effect of Various Components of Prothrombinase Complex on Kinetic Parameters for Prothrombin Activation[0]

Components	K_m, μ*M*	k_{cat}, s^{-1}	Relative Rates
X_a Ca^{2+} PL V_a	0.2	30	100
X_a Ca^{2+} PL	0.06	0.04	0.42
X_a Ca^{2+} V_a	34	6.2	0.12
X_a Ca^{2+}	84	0.01	0.00009
X_a	131	0.01	0.00005

Source: Data taken from Rosing et al. (3).

The phospholipid-bound complex of factor IX_a (proteinase) and factor $VIII_a$ (cofactor) that activates factor X has molecular and functional characteristics very similar to those of the prothrombinase complex. Factor VIII shares homology with factor V and is also activated by thrombin; factor IX has the same domain structure as factor X and is also activated by factor VII_a. There is evidence that the phospholipid-binding properties of these proteinase–zymogen components enable the proteinase product of one complex to be transferred to the subsequent complex as its enzyme without dissociation from the membrane, thereby giving a further catalytic advantage (4).

2. Regulation of Blood Clotting by Complexes Involving Integral Membrane Proteins

Two integral membrane proteins with quite distinct and contrasting functions are involved in the regulation of blood coagulation: tissue factor and thrombomodulin, which are involved, respectively, in the initiation and termination of coagulation. Blood coagulation subsequent to injury of the vasculature is initiated by the exposure of tissue factor, a nonenzymatic cofactor widely expressed by cells of the subendothelium of blood vessels (although its expression can also be induced in endothelial cells and monocytes). Tissue factor binds factor VII_a, a Gla-proteinase, with high affinity (K_d = 1–5 n*M*) (5). The structure of this complex has been determined by X-ray crystallography (6); the extracellular part of tissue factor is composed of two homologous C2-type **immunoglobulin**-like modules, and the protein is most closely related to the IFNg receptor, a member of the class 2 **cytokine** receptors (see Interferons). Factor VII_a is engaged in multiple contacts with both of the tissue factor modules.

The classical substrate for factor VII_a in this complex is factor X, but it is now known that factor IX is also a physiologically relevant substrate (7) (see Hemophilia). Activation of these substrates, and the subsequent incorporation of their activated forms into their cognate complexes, thus propagates the initial stimulus proteolytically. In contrast to factors V and VIII, tissue factor is constitutively active as a cofactor and does not require proteolytic processing. However, factor VII does need proteolytic activation for the complex to be active, and what initially catalyzes this cleavage and thus constitutes the initial proteolytic event in the coagulation cascade has not been a trivial problem to address, because of the extraordinary sensitivity of the system to proteolytic activation, and it remains a topic of controversy. Proposals have included (*1*) that factor VII is not a true zymogen and possesses a significant degree of intrinsic proteolytic activity, (*2*) induction of activity in factor VII by tissue factor, (*3*) autoactivation of factor VII, (*4*) and activation of factor VII by trace amounts of activated proteinases. Although not demonstrated unambiguously, mechanism 4 appears to be favored, as factor VII can be activated by factors VII_a, IX_a, X_a, and thrombin *in vitro*. These may be generated by the contact activation system, alternative mechanisms, or "leakage" of the system, but in such low amounts that they are insignificant in the absence of tissue factor. The principal activator of factor VII once the system is initiated is considered to be factor X_a (8). Tissue factor has little or no effect on factor VII activation, but assembly of the tissue factor complex increases factors IX and X activation by up to 10^4-fold (9). Both the kinetic mechanisms and the molecular interactions responsible for this effect are analogous to those described for the prothrombinase complex, which involves the optimal presentation of the zymogen substrate to the catalytically efficient proteinase:cofactor complex for maximum catalytic advantage.

The other integral membrane protein of the coagulation system, thrombomodulin, is expressed by endothelial cells and acts as a cofactor for the proteolytic activation of the negative regulator of the coagulation system, protein C (10). Activated protein C (a Gla-proteinase) proteolytically inactivates the procoagulant cofactors factors V_a and $VIII_a$. In common with the principal feedback activation reactions, thrombin is again involved. But in this case, rather than proteolytically activating the cofactor, it is the enzymatic component of the thrombomodulin complex; thus thrombin can fully modulate its own generation. The interaction with thrombomodulin dramatically alters the substrate specificity of thrombin, such that protein C activation is increased 10^4-fold, while its activity toward factor V and fibrinogen is diminished (1). Although protein C can bind phospholipid through its Gla domain, this interaction plays only a minor part in these effects and, because thrombin lacks a Gla domain, protein–protein interactions are the major determinants in thrombomodulin complex anticoagulant function, in contrast to the procoagulant complexes described above.

Bibliography

1. C. T. Esmon, N. L. Esmon, and K. W. Harris (1982) J. Biol. Chem. **257**, 7944–7947.
2. S. Krishnaswamy and K. G. Mann (1988) J. Biol. Chem. **263**, 5714–5720.
3. J. Rosing, G. Tans, J. W. Govers-Riemslag, R. F. Zwaal, and H. C. Hemker (1980) J. Biol. Chem. **255**, 274–283.
4. K. G. Mann, M. E. Nesheim, W. R. Church, P. Haley, and S. Krishnaswamy (1990) Blood **76**, 1–16.
5. R. F. Kelley, K. E. Costas, M. P. O"Connell, and R. A. Lazarus (1995) Biochemistry **34**, 10383–10392.
6. D. W. Banner, A. D"Arcy, C. Chene, F. K. Winkler, A. Guha, W. H. Konigsberg, Y. Nemerson, and D. Kirchhofer (1996) Nature, **380**, 41–46.
7. K. A. Bauer, P. M. Mannucci, A. Gringeri, F. Tradati, S. Barzegar, B. L. Kass, H. ten Cate, A. S. Kestin, D. B. Brettler, and R. D. Rosenberg (1992) Blood **79**, 2039–2047.
8. S. Butenas and K. G. Mann, (1996) Biochemistry **35**, 1904–1910.
9. M. Zur and Y. Nemerson (1980) J. Biol. Chem. **255**, 5703–5711.
10. C. T. Esmon (1995) FASEB J. **9**, 946–955.

Suggestion for Further Reading

11. K. G. Mann, R. J. Jenny, and S. Krishnaswamy (1988) Cofactor proteins in the assembly and expression of blood clotting enzyme complexes. Annu. Rev. Biochem. **57**, 915–956.

Blot Overlays

Regardless of whether a blot contains immobilized **DNA**, **RNA** or protein (see Blotting), it is ultimately reacted with a specific probe that defines the type of **ligand-binding** interaction being studied (see Southern Blots (DNA Blots), RNA Blots (Northern Blots), and Protein Blots (Western Blots)). **Radiolabeled** probes are detected by autoradiography, and the radioactive complexes are quantified by computer-digitized imaging or simply by excising out the bands and “counting” the radioactivity. Often the primary probe itself is not easily detectable, so a secondary probe is used, such as an antibody against the first probe conjugated to an enzyme, or avidin or streptavidin when the primary probe is biotinylated (see Avidin-Biotin System). When using an enzyme-conjugated probe, one must ensure that the quencher or blocking reagent used on the blot has no interfering enzymatic activity. For example, hemoglobin should not be used when horseradish peroxidase is employed as the detection system.

1. DNA Probes

Traditionally, Southern and RNA blots of DNA and RNA, respectively, are probed with single-stranded DNA or double-strand DNA that has been **denatured**. The probes are usually radioactive, so that any duplex formed upon **hybridization** of the probe to a nucleic acid on the blot is detected by autoradiography. The rationale of such experiments is to identify the position of the immobilized nucleic acid in the electrophoretogram that is complementary to the sequence of the probe, so that they hybridize by **Watson-Crick base pairing**. The conditions for hybridization, the *stringency*, are regulated according to the degree of homology and complementarity between the probe and the target (1, 2). DNA is also used to probe protein blots, a procedure that has been named “Southwestern blotting.” As expected, this type of experiment is designed to reveal specific interactions between defined DNA sequences and the DNA-binding proteins that bind them, such as transcription factors (3). DNA probing of *colony* or *plaque* blots is a routine approach in recombinant DNA cloning (4).

2. Immunoblotting

The original application of protein blots was for identifying a particular antigen in a protein gel pattern by probing the blot with its corresponding antibody (5). Detecting the immunocomplex is often accomplished by using a secondary probe, for example, a goat antimouse IgG conjugated to an enzyme, such as horseradish peroxidase, when a murine monoclonal antibody is used for the primary probe. The sensitivity of these assays is increased by combining **immunoprecipitation** prior to gel electrophoresis. Thus, a crude sample of proteins is first immunoprecipitated with relevant antibodies, and the precipitated proteins are subsequently resolved by electrophoresis, blotted, and probed with a monoclonal antibody of interest. The use of antibodies to probe colony or plaque blots is very effective in screening expression libraries (6).

3. Lectin Blotting

To identify **glycoproteins**, lectins can be used to probe protein blots (7). A radioactive or enzyme-conjugated lectin is employed as the probe. A particular case of interest is the fact that the enzyme horseradish peroxidase is itself a glycoprotein. Thus, for example, a blot can be probed with the mannose-specific lectin concanavalin *A*, washed and further incubated with horseradish peroxidase directly (8). The multivalent concanavalin A binds to blotted glycoproteins containing mannose and subsequently also binds to the horseradish peroxidase without the need for chemical conjugation. When using lectins, ensure that the quencher used does not itself contain sugar.

4. Ligand Blotting

Blotting is usually considered for detecting antigens or nucleic acid hybrids, but it is also a very powerful way to identify all sorts of protein–protein interactions, even interactions involving nonpeptide ligands. Thus when studying any **receptor**, one should consider probing protein blots with any corresponding ligands that are detectable (9). In such experiments, it is usually advisable not to boil the protein sample or subject it to disulfide bond reduction before electrophoresis. Furthermore, the blot can be incubated in solutions that promote renaturation of the immobilized proteins. Omission of methanol from the transfer buffers used in electroblotting is also helpful for retaining functional conformations of the blotted protein. Ligand blotting has been used successfully to identify peptides that bind to hormones, **cytoskeletal** components, neurotoxins, nucleotides, calmodulin, and even ions such as Ca^{2+} (9-11) (Fig. 1).

Figure 1. Neurotoxin overlays of protein blots. *Escherichia coli* transformed with pATH2 expression **vectors** containing DNA inserts corresponding to the neurotoxin binding site (lanes 3 and 4) or not (lanes 1 and 2) were induced for gene expression (lanes 2 and 4) or not (lanes 1 and 3). Then samples of all four treatments were resolved by SDS-PAGE and stained with Coomassie brilliant blue (**a**) or blotted onto nitrocellulose membrane filters and probed using radioactive neurotoxin. Then the washed filters were autoradiographed (**b**). The arrows indicate the position of the fusion protein containing the toxin binding site.

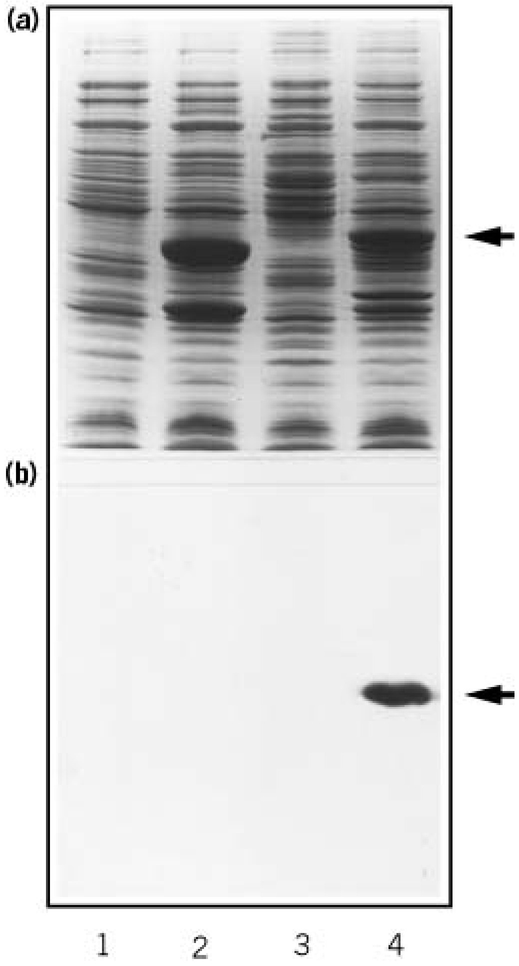

5. Cell Blotting

Blots have even been probed with intact cells, which has proven useful for identifying interactions between proteins and cells (12). Furthermore, bacteria can be used to probe a blot, and the interaction with a protein is detected by subsequently allowing the bacteria to grow on the surface of the blot, so that colonies are observed at the site of the immobilized protein (13). **Viruses** have also been used to probe blots to detect their corresponding receptor proteins.

In summary, one should consider probing blots with selected ligands any time bimolecular interactions are to be analyzed. Surveying literature databases using specific conjugations, such as "ligand-blot", "calmodulin-blot" or "cell-blot," as key words usually produces results that provide the imaginative investigator with starting points from which to proceed.

Bibliography

1. J. Meinkoth and G. Wahl (1984) Anal. Biochem. **138**, 267–284.
2. L. G. Davis, M. D. Dibner, and J. F. Battey (1986) *Basic Methods in Molecular Biology*, Elsevier, New York, pp. 62–65.
3. C. N. Flytzanis (1994) In *Protein Blotting: A Practical Approach* (B. S. Dunbar, ed.), IRL Press, Oxford, UK, pp. 163–168.
4. Ref. 2 pp. 227–229.
5. H. Towbin and J. Gordon (1984) J. Immunol. Methods **72**, 313–340.
6. T. V. Huynh, R. A. Young, and R. W. Davis (1986) In *DNA Cloning, A Practical Approach*,

Vol. **1** (D. M. Glover, ed.), IRL Press, Oxford, UK, pp. 49–78.
7. S. Bar-Nun and J. M. Gershoni (1994) In *Cell Biology; a laboratory handbook*, Vol **3** (J. E. Celis, ed.), Academic Press, San Diego, pp. 323–331.
8. J. C. S. Clegg (1982) Anal. Biochem. **127**, 389–394.
9. J. M. Gershoni (1988) Methods of Biochemical Analysis **33**, 1–58.
10. P. Hossenlopp and M. Binoux (1994) In *Protein Blotting: A Practical Approach* (B. S. Dunbar, ed.), IRL Press, Oxford, UK, pp. 169–188.
11. A. Vieira, R. G. Elkin, and K. Kuchler (1994) In *Cell Biology: A laboratory handbook*, Vol. **2** (J. E. Celis, ed.), Academic Press, San Diego, pp. 314–321.
12. E. G. Hayman, E. Engvall, E. A"Hearn, D. Barnes, M. Pierschbacher, and E. Rouslahti (1982) J. Cell Biol. **95**, 20–23.
13. J. M. Gershoni (1987) Protein blotting: a tool for the analytical biochemist, Adv. Electrophoresis **1**, 141–176.

Blotting

Blotting is a method in which a macromolecule is immobilized on a blotting matrix and subsequently probed with a detectable ligand to determine whether the macromolecule binds that specific **ligand**. The immobilized macromolecule can be **DNA**, **RNA** or protein, in which case one generates DNA blots (Southern blots), RNA blots (Northern blots) (1), or protein blots (Western blots) (2, 3). Blots of lipids have also been produced (4). The macromolecule can be applied to the blotting matrix directly (dot blot), or it can be derived and eluted from an electrophoretic gel (gel blot) or even from a **bacterial** colony or **bacteriophage** plaque (colony blot).

1. Typical Blot Analysis

The most common application of blotting involves a complex mixture of DNA, RNA, or protein to be resolved by using a standard gel electrophoresis procedure, such as agarose gel separation of DNA fragments or RNA or SDS-PAGE of protein samples. After electrophoresis, the gel is dismantled from its cassette or glass plates, etc., and a sheet of an appropriate blotting matrix (eg, a nitrocellulose membrane filter; see Blotting Matrices) is cut to size and applied to the surface of the gel. The transfer of the resolved polynucleotides or peptides is accomplished via a procedure called "blotting", and the blotted macromolecules adsorb to the surface of the matrix while retaining their relative positions, thus creating a faithful replica of the original electrophoretic pattern. The "blot" thus produced is subsequently incubated with a ligand probe, which might be **radioactive** for detection via autoradiography or conjugated to an enzyme whose activity is detectable (see Blot Overlays). Extensive washing of the blot removes the excess probe from that which is specifically associated with the immobilized macromolecule and remains bound. Subsequent detection of the retained ligand in the complex formed identifies the relevant bimolecular interaction.

2. Methods for Blotting

2.1. Dot Blotting
This is the simplest method of applying a sample to be tested (5, 6). The sample can be an unfractionated polynucleotide or protein mixture in solution. A small volume (typically 2 to 5 µl) is applied directly to the surface of a dry blotting matrix by micropipetting the sample onto the matrix or by using commercial vacuum manifolds that enable the application of larger sample volumes

(e.g., 100 µl to 1 ml) by filtration. Such manifolds often create focused and uniform dots or thin slots of sample, thus leading to the terms "dot blots" or "slot blots", respectively. Typically, an 8cm × 12 cm piece of blotting matrix contains as many as 96 different dots that correspond to the geometry of a standard 96-well **ELISA** plate. Once created, the dot blot is processed and probed as any other blot (see Southern Blots (DNA Blots), RNA Blots (Northern Blots), Protein Blots (Western Blots), and Blot Overlays). The advantages of the dot blot procedures are that they do not require any separation process and thus do not subject the sample to undue chemical modifications that could, for example, **denature** a protein sample (although some denaturation of protein occurs upon adsorption to the matrix). Moreover, dot blots are simple, cheap and quick. Where quantification is intended, direct dot blotting ensures maximal yields of sample recovery. Obviously, however, chromatography or electrophoresis is necessary to resolve a complex sample to ascribe the signal to a specific component.

2.2. Gel Blots

Gel electrophoresis is routinely employed to resolve macromolecules of DNA, RNA, or protein. Agarose gels and **polyacrylamide gels** can be blotted, and the common goal is to elute the "bands" efficiently from the gel to be immobilized on the surface of the blotting matrix, so as to generate a faithful replica of the electrophoretic pattern. This can be accomplished in a number of ways:

1. Diffusion blotting simply relies on the fact that the macromolecules in the gel spontaneously **diffuse** out of the gel (7). Consequently, blots are produced when a blotting matrix is simply applied to one or both sides of the gel. This approach is usually time-consuming (24 to 72 h) and of low efficiency, but it produces two equal copies simultaneously.
2. Convection blotting (also called capillary transfer) is the process of eluting the resolved macromolecules by mass flow of buffer through the gel. This is the original procedure introduced by Edwin Southern for transferring DNA restriction fragments from agarose gels onto nitrocellulose membrane filters (thus the term Southern blotting) (8). In this method, the gel is placed on top of a paper wick, which draws buffer from a reservoir. The gel is covered with a piece of blotting matrix that, in turn, is covered by a stack of paper towels or absorbent paper and a weight that ensures uniform pressure over the surface of the gel. The stack of paper towels draws a continuous flow of buffer vectorially through the gel, and with it the polynucleotides or peptides, which are eluted and deposited on the surface of the blotting matrix (9).
3. Vacuum blotting is an elaboration of blotting by convection in which the flow is accelerated by employing negative pressure (i.e., suction). Positive pressure has also been used to enhance blotting.
4. Electroblotting is achieved by applying an electric field so as to elute the proteins or polynucleotides from their corresponding gels by electrophoresis. This technique has been used primarily for proteins because binding DNA and RNA to nitrocellulose requires high salt conditions that are incompatible with electroblotting. Electroblotting of nucleic acids is possible, however, with alternative blotting matrices, such as nylon membranes. A variety of commercial apparatus equipment and home-made systems are available, including those that generate gradient electric fields and provide different elution efficiencies to compensate for differences in the molecular mass of the polymers to be eluted (10, 11). Electroblotting is performed by using tank systems, which require 2 to 4 liters of transfer buffer, or semidry blotting systems, which conserve buffer and are flexible because different buffers can be employed for the anode and cathode (12).
5. Direct blotting is an elaboration of electroblotting in which a conveyor belt passes the blotting matrix by the exposed bottom of the polyacrylamide gel during electrophoresis. As the proteins or DNA fragments reach the bottom of the gel, they are deposited directly onto the slowly moving blotting matrix and generate a blot. The resolution of the bands is modulated by regulating the conveyor belt speed (13).

2.3. Colony Blots

At times it is necessary to identify a specific bacterial colony or phage that contains DNA of interest or expresses a particular protein. Libraries of **recombinant DNA**-containing bacteria or lambda phage expression libraries are used to produce colony or plaque blots to be processed and screened like any other blot. The library of bacteria or phage is plated on agar after suitable incubation, and replicas are produced by simply placing a sheet of blotting matrix, such as nitrocellulose membrane or nylon membrane, onto the colony- or plaque-containing surface. The matrices pick up sufficient material from each colony or plaque at precisely the same relative position corresponding to that on the original agar plate. Then the colony blots are processed, for example, by standard DNA filter hybridization, immunoblotting, or ligand blotting (14, 15) (Fig. 1).

Figure 1. Bungarotoxin overlay of bacterial colonies. *Escherichia coli* were transformed with a pATH2 expression **vector** containing a DNA insert coding for a fragment of the a subunit of the nicotinic acetylcholine receptor. This fragment is responsible for the receptor's binding of the neurotoxin a-**bungarotoxin**. The bacteria were plated to a density of approximately 200 colonies per agar plate (**a**) and expression was induced. A replica of the plate was produced by using a nitrocellulose filter disc, which was processed for overlay with radio-**iodinated** a-bungarotoxin. The filter was subsequently washed and autoradiographed, illustrating those colonies that contain the relevant DNA fragment (**b**) (for details see Ref 15).

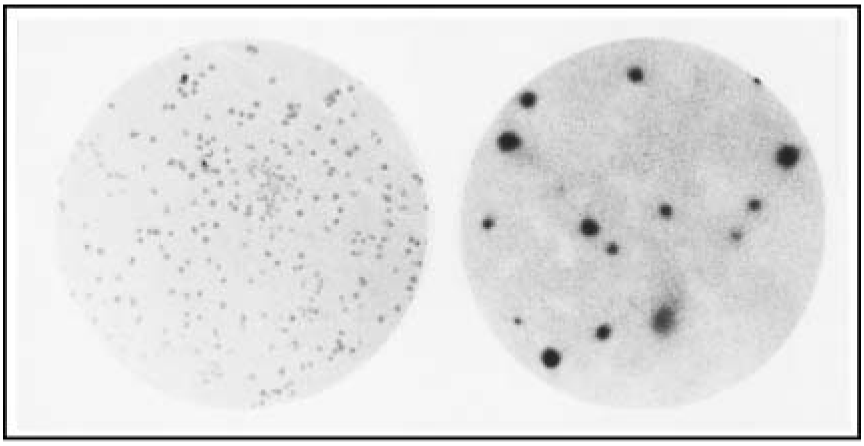

(a) (b)

Bibliography

1. J. Meinkoth and G. Wahl (1984) Anal. Biochem. **138**, 267–284.
2. J. M. Gershoni and G. E. Palade (1983) Anal. Biochem. **131**, 1–15.
3. H. Towbin and J. Gordon (1984) J. Immunol. Methods **72**, 313–340.
4. T. Taki, S. Handa, and D. Ishikawa (1994) Anal. Biochem. **221**, 312–316.
5. J. M. Gershoni (1988) Methods Biochem. Anal. **33**, 1–58.
6. L. G. Davis, M. D. Dibner, and J. F. Battey (1986) *Basic Methods in Molecular Biology*, Elsevier, New York, pp. 147–149.
7. B. Bowen, J. Steinberg, U. K. Laemmli, and H. Weintraub (1980) Nucleic Acids Res. **8**, 1–20.
8. E. M. Southern (1975) J. Mol. Biol. **98**, 503–517.
9. Ref. 6 pp. 62–65.
10. M. Bittner, P. Kupferer, and C. F. Morris (1980) Anal. Biochem. **102**, 459–471.
11. J. M. Gershoni, F. E. Davis, and G. E. Palade (1985) Anal. Biochem. **144**, 32–40.
12. G. Jacobson (1994) In *Protein Blotting: A Practical Approach* (B. S. Dunbar, ed.), IRL Press, Oxford, UK, pp. 53–72.
13. S. Beck (1993) Methods Mol. Biol. **23**, 219–223.
14. Ref. 6 pp. 185–189.

15. J. M. Gershoni (1987) Proc. Natl. Acad. Sci USA **84**, 4318–4321.

Blotting Matrices

Blotting is the process of transferring macromolecules from **electrophoretic** gels to immobilizing matrices, called blotting matrices. The variety of matrices available for blotting is quite diverse, and the characteristics of each directly affects the ultimate result and quality in different blot analyses [see Blotting, Southern Blots (DNA Blots), Protein Blots (Western Blots), RNA Blots (Northern Blots), and Blot Overlays]. Generally, two kinds of blot matrices are used: (1) chemically modified paper filters and (2) microporous membrane filters. Although filters are used, blotting depends on chemical adsorption of transferred molecules to the filter material itself, rather than filtration per se, where separation is achieved by size exclusion. Thus porosity is less important than the chemical composition, density, and thickness of the material. After binding of the desired ligand, normally the remaining binding sites on the matrix are blocked with a neutral compound, known as a quencher or blocking reagent.

1. Paper Filters

Initially, it was thought that transferred molecules would be best suited for blotting if they were covalently bound to the blotting matrix. This led to chemically modified paper filters that contained active moieties to bind DNA, RNA, and protein covalently. For example, **cyanogen bromide** (CNBr)-activated paper was produced (1), as was diazobenzyloxymethyl (DBM) paper, which was the most popular filter of this type (2). These filters covalently immobilize the blotted macromolecules, but they are cumbersome to handle, have the fibrous texture characteristic of blotting paper, and therefore are rarely used today.

2. Membrane Filters

Microporous membrane filters have become the matrices of choice for blotting. These materials are thin films of synthetic polymers with very fine, uniform surfaces. Filters with average porosities of 0.2 to 0.45 µm are extremely suitable for all types of blotting. A variety of materials exist, and each offers unique advantages.

2.1. Nitrocellulose
Nitrocellulose is by far the most commonly used blotting matrix. It binds DNA, RNA, and protein reasonably well, although the mechanism is not clear (3, 4). **Hydrophobic** interactions definitely play a role, and the salt conditions are critical, particularly for the adsorption of RNA. Nitrocellulose is often produced as a mixed ester with cellulose acetate, which reduces to some extent its binding capacity for proteins. The advantages of nitrocellulose are that it binds protein well and affords very good signal-to-background ratios in Western blotting assays. It allows staining of the immobilized protein patterns with such dyes as Ponceau S and Amido black. It becomes brittle, however, after baking at 80°C (typical for Southern and Northern blotting), which reduces the repeated use of these filters. Furthermore, nitrocellulose is less resistant to various organic solvents, such as methanol (5).

2.2. Nylon Membranes
Nylon membranes were introduced initially as an alternative to nitrocellulose for protein blotting (5), and subsequently they were applied in RNA and DNA transfers (4). These membranes are usually derivatives of nylon 66 and often are modified with positive charges. They have proven exceptional

binders of DNA, RNA, and protein, but at times this presents some difficulty by producing high backgrounds, particularly in protein blotting. These filters are mechanically stable and thus can be reprobed numerous times without lossing band definition or sensitivity.

2.3. Polyvinyl Difluoride

Polyvinyl difluoride (PVDF) membrane filters have a special application in blotting where subsequent chemical manipulation of the immobilized macromolecule is desired. A case in point is the use of these membranes in protein blots, where the individual bands are excised out of the blot and subjected to Edman Degradation for N-terminal amino acid sequencing of the resolved and blotted polypeptide chains (6, 7).

Bibliography

1. L. Clarke, R. Hitzman, and J. Carbon (1979) Methods Enzymol. **68**, 436–442.
2. J. C. Alwine, D. J. Kemp, and G. R. Stark (1977) Proc. Natl. Acad. Sci. USA **74**, 5350–5354.
3. A. De Maio (1994) In *Protein Blotting: A Practical Approach* (B. S. Dunbar, ed.), IRL Press, Oxford, UK, pp. 11–32.
4. J. Meinkoth and G. Wahl (1984) Anal. Biochem. **138**, 267–284.
5. J. M. Gershoni and G. E. Palade (1982) Anal. Biochem. **124**, 396–405.
6. M. A. Mansfield (1994) In *Protein Blotting: A Practical Approach* (B. S. Dunbar, ed.), IRL Press, Oxford, UK, pp. 33–52.
7. C. Eckerskorn and F. Lottspeich (1993) Electrophoresis **14**, 831–838.

Blunt-End Ligation

Blunt-end ligation is covalently joining two or more double-stranded **DNA** fragments with flush ends by the enzyme DNA Ligase (1). Many restriction enzymes produce blunt ends, when they cleave both polynucleotide chains at the same site, and some **cohesive ends** are converted to blunt ends by the fill-in reaction. Blunt end ligation is a much less efficient reaction than ligation of DNA fragments with cohesive ends. One technique for overcoming the low efficiency of blunt-end ligation is ligating a short oligonucleotide **linker fragment** to the DNA ends that are to be joined (2). Because a large molar concentration of the linker can be added to the reaction, its ligation to the ends of the DNA occurs more readily than joining of the ends themselves. Linkers are designed to contain a unique restriction site so that the ligation mixture is digested with the corresponding enzyme to create cohesive ends, which can be joined by conventional ligation.

The efficiency of blunt-end ligation is greatly increased by carrying out the reaction in the presence of 15% polyethylene glycol, 6,000 MW (PEG), although only linear molecules are produced in this reaction. Circular **plasmids** are required for efficient transformation of *Escherichia coli*. An efficient way of producing circular molecules from the linear product of blunt-end ligation is including a bacteriophage P1 lox recombination site in one of the molecules being ligated (3). After ligation, the DNA is treated with Cre recombinase, which by recombination between the lox sites produces a circular molecule from a linear molecule that contains two lox sites. This type of molecule is created when the molecule without a lox site is ligated to two molecules with a lox site, one at each end.

It is possible to amplify the products of a low-efficiency ligation containing the desired insert by **PCR**, using primers that bind to vector DNA on each side of the cloning site. The PCR product of the expected size is purified and recloned. This results in transformants from ligations that give no positive colonies on direct transformation (4).

Bibliography

1. T. Maniatis, E. F. Fritsch, and J. Sambrook (1982) *Molecular Cloning; a Laboratory Manual*, 2nd ed., Cold Spring Harbor Press, Cold Spring Harbor, NY.
2. G. J. Bhat, M. J. Lodeg, P. J. Myler, and K. D. Stuart (1991) Nucleic Acids Res. **19**, 398.
3. A. C. Boyd (1993) Nucleic Acids Res. **21**, 817–821.
4. H. W. Son and E. Lolis (1995) BioTechniques **18**, 644–650.

Suggestion for Further Reading

5. A. E. T. Konson and D. S. Levin (1997) Mammalian DNA ligases, Bioessays **19**, 893–901; a review of DNA ligases.

Bohr Effect

Bohr et al. (1) discovered that the oxygen dissociation curve of blood shifts to higher partial pressures of oxygen in the presence of increasing concentrations of carbon dioxide by lowering the oxygen affinity of hemoglobin. This effect, it was concluded, results from the concomitant decrease in pH, and the effect of pH on the oxygen affinity of hemoglobin has subsequently been known as the Bohr effect. It was subsequently discovered that CO_2 also lowers the oxygen affinity of hemoglobin (Hb) directly by binding to its a-amino groups, forming carbamino compounds (2, 3):

$$O_2 - Hb - NH_2 + CO_2 \leftrightarrow Hb - NHCOOH + O_2 \tag{1}$$

The original observations of Bohr et al. (1) are now known as the "classical Bohr effect," which is a composite of the specific effects of H^+ and CO_2.

The CO_2 content of blood is reduced upon oxygenation of hemoglobin at a constant CO_2 pressure (4). This phenomenon, known as the "classical Haldane effect," is a combination of the oxygen-linked dissociation of the carbamino groups (Eq. 1) and release of protons

$$Hb(H^+)_\delta + O_2 \leftrightarrow HbO_2 + \delta\ H^+ \tag{2}$$

followed by dehydration of bicarbonate:

$$H^+ + HCO_3^- \leftrightarrow H_2CO_3 \leftrightarrow CO_2 + H_2O \tag{3}$$

The release of protons upon oxygenation or their uptake upon deoxygenation of hemoglobin is known as the "Haldane effect."

The Bohr effect and the Haldane effect are thermodynamically equivalent (5) because they are linked functions (6). Whatever effect oxygen binding has on the affinity of hemoglobin for protons, changes in the pH must have the same effect on the affinity of hemoglobin for oxygen:

$$\left(\frac{\delta H^+}{\delta Y}\right)_{pH} = \left(\frac{\delta \log Po_2}{\delta pH}\right)_Y \quad (4)$$

where H^+ is the number of protons bound per heme group, Y is the fraction of hemoglobin binding sites occupied by O_2, and P_{O2} is the partial pressure of O_2. The left-hand side of Eq. 4 is known as the "Haldane coefficient," and the right-hand side is the "Bohr coefficient." They give the magnitude of the Haldane and Bohr effects, which must be the same.

These effects are physiologically important for efficient and regulated transport of O_2 and CO_2 in opposite directions (see Hemoglobin). When the shape of the oxygen dissociation curve expressed by Y versus log P_{O2} is independent of changes in pH, at least within the range $0.1 < Y < 0.9$, Eq. 4 is simplified to

$$\delta = \frac{\Delta \log P_{50}}{\Delta pH} \quad (5)$$

where P_{50} is the P_{O2} at Y = 0.5 and d is the Bohr coefficient, which is independent of the degree of O_2 binding. The Bohr coefficient expresses the number of protons (per heme group) bound to hemoglobin upon full oxygenation and is the same as d of Eq. 2.

d is negative above pH 6.3, and protons are released upon oxygenation of hemoglobin, whereas d is positive at lower pH values, and protons are taken up upon oxygenation. These two phenomena are known respectively as the "alkaline" and "acid" Bohr effects. At physiological pH 7.4, human adult hemoglobin A (HbA) has d = –0.6 in the presence of 0.1 *M* NaCl. This value is halved in the absence of Cl^-.

The Bohr effect arises from changes in the pK_a values of particular ionizable groups of hemoglobin as a result of changes in their environment upon binding oxygen. The group primarily responsible for the alkaline Bohr effect of human HbA is the imidazole side chain of the C-terminal His146 of the b chain. Its pK_a value changes from 8.0 to 7.1 upon oxygenation, contributing the greater part of the alkaline Bohr effect in the absence of Cl^-. In the presence of Cl^-, binding of these ions to several ionizable groups that line the central cavity of the hemoglobin molecule, including the a-amino groups of the a chains and the ε-amino groups of Lys82 of the b chains, affects the protonation of those groups. Consequently, the release of Cl^- ions upon binding of oxygen produces an additional, Cl^--dependent Bohr effect (7). It is thought that His143 of the b chains is one of the groups responsible for the acid Bohr effect (8), but the others are still unidentified.

The term "Bohr effect" is sometimes used for pH-dependent binding of other ligands, such as CO_2 and alkylisocyanides, to hemoglobin. It is also used for pH-dependent ligand binding to oxygen-binding proteins other than hemoglobin.

Bibliography

1. C. Bohr, K. A. Hasselbalch, and A. Krogh (1904) Skand. Arch. Physiol. **16**, 402–412.
2. J. K. W. Ferguson and F. J. W. Roughton (1934) J. Physiol. (London) **83**, 87–102.
3. J. V. Kilmartin and L. Rossi-Bernardi (1969) Nature **222**, 1243–1246.
4. J. Christiansen, C. C. Douglas, and J. S. Haldane (1914) J. Physiol. (London) **48**, 244–277.
5. I. Tyuma and Y. Ueda (1975) Biochem. Biophys. Res. Commun. **65**, 1278–1283.
6. J. Wyman (1964) Adv. Protein Chem. **19**, 223–286.
7. M. F. Perutz, G. Fermi, C. Poyart, J. Pagnier, and J. Kister (1993) J. Mol. Biol. **233**, 536–545.

8. M. F. Perutz, J. V. Kilmartin, K. Nishikura, J. H. Fogg, P. J. G. Butler, and H. S. Rollema (1980) J. Mol. Biol. **138**, 649–670.

Suggestions for Further Reading

9. J. V. Kilmartin and L. Rossi-Bernardi (1973) Interaction of hemoglobin with hydrogen ions,carbon dioxide, and organic phosphates, Physiol. Rev. **53**, 836–890.
10. I. Tyuma (1984) The Bohr effect and the Haldane effect in human hemoglobin, Jpn. J. Physiol. **34**, 205–216.

Bowman–Birk Inhibitors

Bowman–Birk proteinase inhibitor is a member of a widely studied family of serine proteinase inhibitors, protein. Most such inhibitors consists of a single polypeptide chain of 65–80 amino acid residues containing two homologous regions, each with a reactive site. In some Bowman–Birk inhibitors, both sites are specific for trypsin; in others, one is specific for trypsin and one for chymotrypsin; and, in still others, one is for trypsin and one for elastase. Ternary complexes of one inhibitor and two enzyme molecules are commonly found. The polypeptide chain is crosslinked by seven disulfide bridges, some within the homology regions, others between them, endowing the inhibitor with great stability.

Suggestion for Further Reading

T. Ikenaka and S. Norioka (1986) "Bowman–Birk family serine proteinase inhibitors". In *Proteinase Inhibitors* (A. Barrett and G. Salveson, eds.), Elsevier New York, 361–374.

BPTI (Bovine Pancreatic Trypsin Inhibitor)

Bovine pancreatic trypsin inhibitor, BPTI (Kunitz), is also called trypsin kallikrein inactivator, TKI, aprotinin, and Trasylol™. It is the first protein inhibitor of proteinases [see Proteinase Inhibitors, Protein] to be isolated and characterized by Moses Kunitz as an inhibitor of bovine trypsin. It was independently discovered as a kallikrein inactivator. BPTI was the first protein proteinase inhibitor to be sequenced. Shortly afterward, sequencing the kallikrein inactivator revealed the identity of the two inhibitors. They consist of 58 amino acid residues, crosslinked by three disulfides. Lys^{15} is at the P_1 position of the reactive site. The K_I for BPTI-bovine b trypsin interaction, 5×10^{-14} M, is often—probably incorrectly—referred to as the strongest of the proteinase–protein proteinase inhibitor interactions. BPTI is also extremely stable. Its T_m at neutral pH is 103°C. BPTI was the first protein proteinase inhibitor to have its three-dimensional structure determined both in free form and in complex with bovine b trypsin. It has been—and still is—widely used in Europe as a drug to avoid postsurgical complications. For this use, it is isolated from bovine lungs. BPTI has been the first superbly characterized small protein that was widely available. Therefore, it became the favorite substance of many protein researchers. It was the first protein to have its three-dimensional structure determined by nuclear magnetic resonance (NMR). It served as the object of numerous molecular dynamics and structure prediction calculations. It was the first protein for which the pattern of closure of disulfide bridges was studied in detail. BPTI (Kunitz) gave its name to a widely studied family of standard-mechanism canonical protein inhibitors of serine proteinases.

Suggestion for Further Reading

W. Gebhard, H. Tschesche, and H. Fritz (1986) "Bowman–Birk family serine proteinase inhibitors". In *Proteinase Inhibitors* (A. Barrett and G. Salveson, eds.), Elsevier New York, 375–388.

Bragg Angle

The Bragg angle is important for analyzing the diffraction from crystals in X-ray crystallography. W.L. Bragg noted that X-ray diffraction by a crystal can be understood without going into the details of diffraction theory (1). The process is similar to ordinary reflection of light from a mirror. In the crystal, the mirrors are the lattice planes. They are the planes constructed through the lattice points, which are the corners of the unit cells. Within a set, the planes are parallel and equidistant with perpendicular distance *d* (Fig. 1). q, the reflective angle, is called the Bragg angle. The beams reflected from the upper and the lower lattice plane are in phase and reinforce each other if the difference in path lengths of the two beams, which is given by the path A–B–C, is an integral number of the wavelength l. The path difference is also equal to 2*d* sin q. This results in Bragg's law: 2*d* sin q = n l, where *n* is an integer, 1, 2 3, etc.

Figure 1. Bragg's view on X-ray diffraction. The incident beam is reflected by lattice planes. *d* is their distance, and q is the reflective angle.

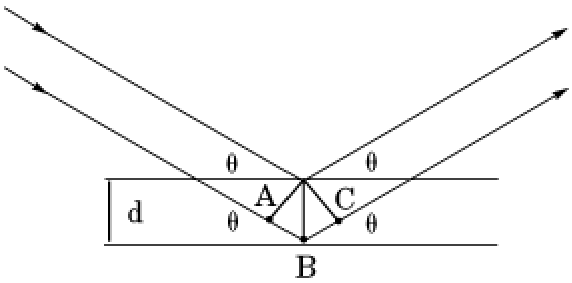

Bibliography

1. W. L. Bragg (1913) Proc. Cambridge Phil.Soc. **17**, 43–57.

Suggestions for Further Reading

2. J. P. Glusker, M. Lewis, and M. Rossi (1994) *Crystal Structure Analysis for Chemists and Biologists*, VCH Publishers, New York, Weinheim, Cambridge.
3. J. Drenth (1999) *Principles of Protein X-ray Crystallography*, Springer, New York.

Brassinosteroids

1. History

Unlike the five other “classical” plant hormones, which were all discovered more than 35 years ago, brassinosteroids (BRs) have been identified only recently. In 1979, Grove et al. (1) reported on the first growth-promoting steroid from plants. The substance was isolated from *Brassica napus* (rapeseed) pollen and was called *brassinolide*. Brassinolide was found in minute quantities in pollen grains; about 250 kg of pollen were needed to obtain only 10 mg of the pure compound. BRs are widely present in angiosperm families, but are also found in gymnosperms, ferns, and green algae (2).

Recently, BRs have gained recognition as true plant hormones (3). Genetic experiments provided evidence that they are indispensable for normal plant growth. A second breakthrough in our knowledge of BRs owes to the recent elucidation of the entire biosynthetic pathway (2, 4) (Fig. 1).

Figure 1. Brassinosteroid biosynthesis in higher plants. Steps mediated by DET2, DWF4, and CPD in *Arabidopsis* are indicated. (Adapted from Ref. 7.)

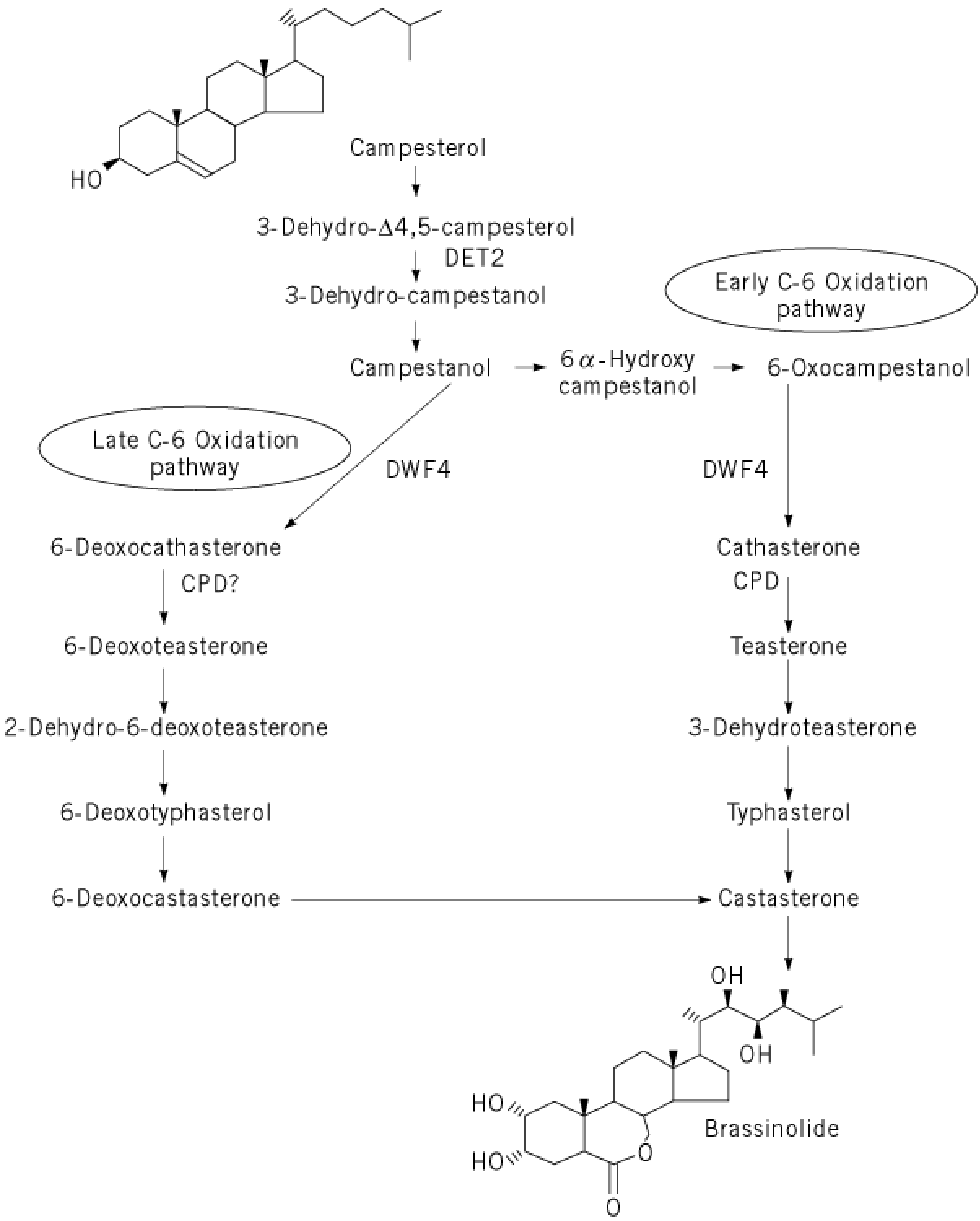

2. Biosynthesis and Metabolism

Brassinosteroids are unique as plant hormones because they are structurally related to the insect molting hormone ecdysone and to mammalian steroid hormones. More than 40 BRs occur naturally, all of which share a common 5a-cholestane skeleton. The relative activities of the BRs increase according to their position in the biosynthetic pathway: brassinolide is most active, whereas early precursors up to 6-oxocampestanol are virtually inactive (5). Hydroxylation at position C22 is critical for biological activity.

Brassinolide is synthesized from campesterol via two pathways (2) (Fig. 1). These pathways were established by classical labeled-precursor feeding experiments. Campesterol is derived essentially from the mevalonate pathway. Initially, the double bond in the B ring of campesterol is reduced to campestanol (6) over 3-hydro-D4,5-campesterol and 3-dehydro-campestanol. From campestanol, two possible routes lead to brassinolide. In this branch, campestanol can be oxidized on C6 to yield 6-oxocampestanol, with 6a-hydroxycampestanol as an intermediate.

The first branch is called the early C6-oxidation pathway and seems ubiquitous in higher plants. 6-Oxocampestanol is subsequently hydroxylated at position 22 on the side chain (7), resulting in cathasterone, and further hydroxylated at position 23, to yield teasterone (4). This step is followed by epimerization of the hydroxyl function on C3, yielding typhasterol, with 3-dehydroteasterone as an intermediate (8, 9). Typhasterol is further hydroxylated on C2, resulting in castasterone that is finally converted to brassinolide by lactamization of the B ring (10). Two steps in the early C6-oxidation pathway appear to be rate-limiting: (a) the formation of cathasterone from 6-oxocampestanol and (b) the final conversion of castasterone to brassinolide (2).

A second possible route from campestanol to castasterone is the so-called late C6-oxidation path, with 6-deoxo brassinosteroids as intermediates. The latter compounds are the least active BRs and were therefore considered to be dead-end products. The second biosynthetic path has been discovered only recently; it was demonstrated in cultured cells and seedlings of *Catharanthus roseus*, as well as in seedlings of rice and tobacco (11, 12). Recent evidence indicates that 6-deoxoteasterone is formed from campestanol via 6-deoxocathasterone, by subsequent hydroxylations (7). This step is followed by an epimerization to yield 6-deoxotyphasterol, comparable to the conversion from teasterone to typhasterol in the early oxidation pathway. Finally, 6-deoxotyphasterol is hydroxylated at position 2, forming castasterone.

Compelling evidence for an essential role for BRs in plant growth and development came from recent genetic studies in Arabidopsis *thaliana* (3, 13). The *det2* (*de-etiolated 2*), *dwf4* (*dwarf4*), *cpd* (*constitutive photomorphogenesis and dwarfism*), and *dim* (*diminuto*) mutants identify different steps in BR biosynthesis (7, 14-17). All of these mutants display drastic **phenotypic** effects that can be reverted by application of brassinolide. In the light, the plants are smaller than wild type because of reduced cell size, the leaves are darker green, apical dominance is reduced, and the plants are less fertile. In the dark, a de-etiolation phenotype is observed, characterized by short and thick hypocotyls, open and expanded cotyledons, and formation of primary leaves. This phenotype is accompanied by derepression of light-regulated genes, with the exception of the *dim* mutant, where a normal repression of light-regulated genes is observed in the dark (18). Collectively, these observations support the existence of cross-talk between the light and BR signaling pathways. The four **genes** corresponding to the above-mentioned loci have been **cloned** recently. The *DET2* gene product shares similarity with mammalian steroid 5a-reductases. Definite proof for its function was given by two experiments that support functional conservation between mammalian and plant steroid 5a-reductases (19). When expressed in human embryonic kidney cells, DET2 catalyzed 5a-reduction of several animal steroid substrates. In addition, *det2* mutants could be rescued by expression of human steroid 5a-reductases. The *CPD* and *DWF4* genes were cloned by T-DNA tagging, and both encode cytochrome P450 monooxygenases that share homology with steroid hydroxylases (7, 15). Feeding studies indicated that DWF4 acts as a 22a-hydroxylase (7), whereas CPD functions as a 23a-hydroxylase (15). It is reasonable to assume that each enzyme would play a role in both branches of BR biosynthesis, although there is yet no evidence that CPD uses 6-deoxocathasterone as a substrate. Finally, the *DIM* gene encodes a protein with a putative FAD-binding domain and a nuclear localization motif (see Nuclear Import, Export) (18, 20). Feeding experiments indicate that *dim* mutations affect a step before typhasterol formation, so it might be involved in epimerization of teasterone (13).

As is the case for most other plant hormones, glucosylation plays a role in deactivation of BRs. Some of these conjugates may serve as a storage form, as for instance the C23-glucosylated brassinolide and esters at position C3 (21, 22). Permanent inactivation of BRs is achieved by C25 and C26 hydroxylation, as well as by cleavage of the side chain (13). It should be noted that transport of BR storage forms is facilitated after glucosylation, as a result of their increased hydrophilicity. Transport of labeled BRs has been shown to occur from root to shoot, probably via xylem (23). It is not yet clear, however, whether this also plays a role in determining the endogenous levels of BRs.

3. Signal Perception and Transduction

The conservation of steroid-like compounds as signaling molecules across several phyla including fungi, invertebrates, and vertebrates made it tempting to speculate on the existence of soluble nuclear BR receptors in plants (24, 25). Two BR-insensitive mutants, *bri1* (*brassinosteroid insensitive 1*) and *cbb2* (*cabbage 2*), have been isolated in *Arabidopsis* (16, 26). In both mutants, hormone insensitivity is specific to BRs, and neither one can be rescued by external BR application. Expression of BR-regulated genes was abolished in BR-insensitive mutants (16). *Bri1* and *cbb2* mutations result in dramatic effects on development, including an exacerbated dwarfism, bushy phenotype, dark green and thickened leaves, and male sterility. In addition, de-etiolation of dark-grown seedlings was observed (26). *Bri1* and *cbb2* are alleles of a single locus, and the corresponding gene has been cloned using a map-based approach (27). Surprisingly, BRI1 does not share similarity with **steroid receptors**, but belongs to the class of receptor-like transmembrane kinases (28). Members of this family have an *N*-terminal extracellular leucine-rich repeat (LRR); there are 25 such repeats in BRI1, with a unique stretch of 70 amino acid residues between the 21st and 22nd LRR. These are followed by a transmembrane domain and an internal **serine/threonine kinase** domain that relays the signal. Other LRR kinases include proteins that influence meristem size and organ formation, such as clavata1, erecta, and Xa21, which confers resistance against *Xanthomonas oryzae pv. Oryzae* in rice (29-31). The *BRI1* gene is ubiquitously expressed in plant tissues in light and dark, consistent with a presumed role as a BR receptor in different cell types (27). The BRI1 protein could bind BR either directly or indirectly, via a protein intermediary. Although none of the previously identified LRR kinases can bind nonproteinaceous ligands, the island of 70 unique amino acid residues in the LRR of BRI1 could serve the purpose of directly binding BR. Mutation of this region severely affects BRI1 activity. In animal systems, LRR kinases are known to form homo- or heterodimers upon ligand binding, thereby activating the intrinsic kinase activity (28). Heterodimerization of BRI1 and XA21, or other LRR domains of disease resistance proteins, could control cross-talk between BR and pathogenic signaling (27).

4. Downstream Targets

To date, genes involved in the primary response to BR have not been identified. Likewise, cis-acting sequences or trans-acting factors involved in the BR response remain to be characterized. In contrast, the expression of at least 50 genes was altered upon treatment of soybean hypocotyls and epicotyls with BR for 2 to 17 h (32, 33). One of these genes was cloned, and the predicted polypeptide chain shared similarity with xyloglucan endo-*trans*-glycosylases (XETs) (34). The gene was termed *BRU1* (*BR up-regulated*) and is not responsive to either auxin or gibberellin. Its recombinant product catalyzed endo-*trans*-glycosylation *in vitro* (35). The *in vivo* function of *BRU1* is thus to control expansion growth, either by cell-wall loosening or by integration of newly synthesized xyloglucans in the wall (36).

In *Arabidopsis*, the *TCH4* (*touch 4*) gene encodes an active XET, and its transcriptional activation is maximal within 2 h of BR treatment (37). XET is encoded by a multigene family in the *Arabidopsis* genome. Some family members, such as *TCH4*, are responsive to BR and auxin, but not to gibberellins, whereas others, such as *meri5* (*meristem 5*), are regulated by gibberellins, less generally by BR, and not by auxin (16). Certain *XET* genes do not respond to BR. The *XET* gene family thus appears to be differentially regulated by a combination of hormonal and environmental cues (such as light, heat, cold, and touch) (38). In Situ Hybridization of soybean epicotyl cross sections with a *BRU1* probe revealed highest gene expression in vascular tissues (phloem cells and xylem parenchyma), as well as in the cortical starch sheath layer (35). In contrast to the rather restricted action of auxin on cell elongation, BRs have been shown to have an effect both on epidermal and internal tissues (39). Nevertheless, the action is more profound on internal tissues, correlating well with the spatial expression pattern of *BRU1*. Comparative kinetic analysis of auxin and BR action indicates that auxin possibly initiates cell wall elongation at the epidermis, whereas BR continues to stimulate elongation of both outer and inner layers (39-41). BRs thus seem to have a prolonged effect on cell elongation. Brassinolide application results in a predominantly transverse orientation of cortical microtubules, allowing expansion in the longitudinal direction (42).

5. Effects

The final effects of BRs result from expression of an array of secondary response genes, mentioned above. A multitude of BR functions in plant development are known, including leaf bending and unrolling, stem elongation, root inhibition, xylogenesis, and pollen tube growth (5). It is clear that several of these activities may result from cross-talk with light and other hormonal signaling cascades.

Bibliography

1. M. D. Grove, G. F. Spencer, W. K. Rohwedder, N. Mandava, J. F. Worley, J. D. Warthen, G. I. Steffens, J. L. Flippen-Anderson, and J. C. Cook (1979) Nature **281**, 216–217.
2. S. Fujioka and A. Sakurai (1997) Physiol. Plant. **100**, 710–715.
3. S. D. Clouse (1996) Curr. Biol. **6**, 658–661.
4. S. Fujioka, T. Inoue, S. Takatsuto, T. Yanagisawa, T. Yokota, and A. Sakurai (1995) Biosci. Biotech. Biochem. **59**, 1543–1547.
5. T. Yokota (1997) Trends Plant Sci. **2**, 137–143.
6. H. Suzuki, T. Inoue, S. Fujioka, T. Saito, S. Takatsuto, T. Yokoto, N. Murofushi, T. Yanagisawa, and A. Sakurai (1995) Phytochemistry **40**, 1391–1397.
7. S. Choe, B. P. Dilkes, S. Fujioka, S. Takatsuto, A. Sakurai, and K. A. Feldmann (1998) Plant Cell **10**, 231–243.
8. H. Suzuki, S. Fujioka, S. Takatsuto, T. Yokota, N. Murofushi, and A. Sakurai (1994) J. Plant Growth Regul. **13**, 21–26.
9. H. Suzuki, T. Inoue, S. Fujioka, S. Takatsuto, T. Yanagisawa, T. Yokota, N. Murofushi, and A. Sakurai (1994) Biosci. Biotech. Biochem. **58**, 1186–1188.
10. T. Yokota, Y. Ogino, N. Takahashi, H. Saimoto, S. Fujioka, and A. Sakurai (1990) Agric. Biol. Chem. **54**, 1107–1108.
11. Y.-H. Choi, S. Fujioka, A. Harada, T. Yokota, S. Takatsuto, and A. Sakurai (1996) Phytochemistry **43**, 593–596.
12. Y.-H. Choi, S. Fujioka, T. Nomura, A. Harada, T. Yokota, S. Takatsuto, and A. Sakurai (1997) Phytochemistry **44**, 609–613.
13. M. Szekeres and C. Koncz (1998) Plant Physiol. Biochem. **36**, 145–155.
14. J. Li, P. Nagpal, V. Vitart, T. C. McMorris, and J. Chory (1996) Science **272**, 398–401.
15. M. Szekeres, K. Németh, Z. Koncz-Kálmán, J. Mathur, A. Kauschmann, T. Altmann, G. P. Rédei, F. Nagy, J. Schell, and C. Koncz (1996) Cell **85**, 171–182.
16. A. Kauschmann, A. Jessop, C. Koncz, M. Szekeres, L. Willmitzer, and T. Altmann (1996) Plant J. **9**, 701–713.
17. R. Azpiroz, Y. Wu, J. C. LoCascio, and K. A. Feldmann (1998) Plant Cell **10**, 219–230.
18. T. Takahashi, A. Gasch, N. Nishizawa, and N.-H. Chua (1995) Genes Dev. **9**, 97–107.
19. J. Li, M. G. Biswas, A. Chao, D. W. Russell, and J. Chory (1997) Proc. Natl. Acad. Sci. USA **94**, 3554–3559.
20. A. R. Mushegian and E. V. Koonin (1995) Protein Sci. **4**, 1243–1244.
21. H. Suzuki, S. K. Kim, N. Takahashi, and T. Yokota (1993) Phytochemistry **33**, 1361–1367.

22. S. Asakawa, H. Abe, N. Nishikawa, M. Natsume, and M. Koshioka (1996) Biosci. Biotech. Biochem. **60**, 1416–1420.
23. N. Nishikawa, S. Toyama, A. Shida, and F. Futatsuya (1994) J. Plant Res. **107**, 125–130.
24. M. Beato, P. Herrlich, and G. Schutz (1995) Cell **83**, 851–857.
25. S. D. Clouse (1996) Plant J. **10**, 1–8.
26. S. D. Clouse, M. Langford, and T. C. McMorris (1996) Plant Physiol. **111**, 671–678.
27. J. Li and J. Chory (1997) Cell **90**, 929–938.
28. D. M. Braun and J. C. Walker (1996) Trends Biochem. Sci. **21**, 70–73.
29. S. E. Clark, R. W. Williams, and E. M. Meyerowitz (1997) Cell **89**, 575–585.
30. W.-Y. Song, G.-L. Wang, L.-L. Chen, H.-S. Kim, L.-Y. Pi, T. Holsten, J. Gardner, B. Wang, W.-X. Zhao, L.-H. Zhu, C. Fauquet, and P. Ronald (1995) Science **270**, 1804–1806.
31. K. U. Torii, N. Mitsukawa, T. Oosumi, Y. Matsuura, R. Yokoyama, R. F. Whitier, and Y. Komeda (1996) Plant Cell **8**, 735–746.
32. S. D. Clouse and D. Zurek (1991) In *Brassinosteroids: Chemistry, Bioactivity and Applications*, ACS Symposium Series, Vol. **474** (H. G. Cutler, T. Yokota, and G. Adam, eds.), American Chemical Society, Washington, D.C., pp. 122–140.
33. S. D. Clouse, D. M. Zurek, T. C. McMorris, and M. E. Baker (1992) Plant Physiol. **100**, 1377–1383.
34. D. M. Zurek and S. D. Clouse (1994) Plant Physiol. **104**, 161–170.
35. S. D. Clouse (1997) Physiol. Plant. **100**, 702–709.
36. D. J. Cosgrove (1997) Plant Cell **9**, 1031–1041.
37. W. Xu, M. M. Purugganan, D. H. Plisensky, D. M. Antosiewicz, S. C. Fry, and J. Braam (1995) Plant Cell **7**, 1555–1567.
38. W. Xu, P. Campbell, A. K. Vargheese, and J. Braam (1996) Plant J. **9**, 879–889.
39. R. Tominaga, N. Sakurai, and S. Kuraishi (1994) Plant Cell Physiol. **35**, 1103–1106.
40. M. Katsumi (1985) Plant Cell Physiol. **26**, 615–625.
41. D. M. Zurek, D. L. Rayle, T. C. McMorris, and S. D. Clouse (1994) Plant Physiol. **104**, 505–513.
42. K. Mayumi and H. Shibaoka (1995) Plant Cell Physiol. **36**, 173–181.

Brefeldin A

Brefeldin A (BFA) is a fungal metabolite that is a powerful tool for dissecting membrane traffic and organelle dynamics. It is named after *Penicilium brefeldianum*, which produces it. BFA is a macrolide antibiotic with a molecular weight of 280.36 Da and the structure

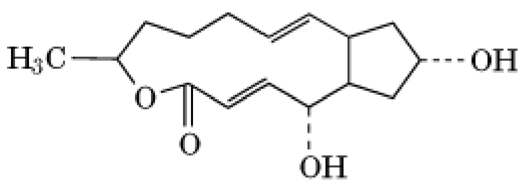

BFA is normally used on cells in culture at concentrations of 1 to 10 µM. As first discovered by Misumi et al. (1), BFA primarily inhibits secretion, without significantly affecting endocytosis. It does not affect protein biosynthesis significantly, does not deplete cellular ATP levels, and does not affect **cytoskeletal** elements. The unique feature of BFA, which distinguishes it from other inhibitors of protein traffic, is that it causes coalescence of organelles. Within minutes of BFA application, the Golgi apparatus fragments and fuses with the endoplasmic reticulum (ER), which does not fragment (2), leading to mixing of the two compartments.

The effects of BFA are completely reversible. Retrograde movement of Golgi proteins into the ER occurs via long, tubulovesicular processes extending out of the Golgi along microtubules. This retrograde traffic pathway can be separated into two distinct phases: movement of Golgi proteins into the intermediate compartment between the ER and Golgi complex, followed by cycling between the modified ER and the intermediate compartment (3). Remarkably, many Golgi enzymes are still active in this environment and can modify proteins in the ER (4).

One of the important uses of BFA-induced redistribution has been the functional demarcation of compartments along the secretory pathway (5). It is clear that BFA affects the early Golgi compartments, the *cis* and medial cisternae. Whether BFA also affects the *trans*-most cisternae of the Golgi stack and the *trans*-Golgi network seems to be dependent on tissue and cell type. Thus, in pancreatic acinar cells, exit from the Golgi complex and formation of **secretory granules** are not BFA-sensitive (6), while in other cells the formation of secretory granules is inhibited (7). Secretion of preformed secretory granules is not inhibited by BFA. Thus, the effects of BFA point to a common mechanism in the traffic of proteins that follow either the constitutive or the regulated pathways of exocytosis.

BFA's effects are not limited to the Golgi apparatus and are reiterated throughout the **endosome**/**lysosome** system. BFA treatment induces tubulation of these compartments (8). Similar to the mixing of the Golgi with the ER, the *trans*-Golgi network mixes with the recycling endosomal system. Remarkably, this mixed system remains partly functional, with normal cycling between plasma membrane and endosomes, but with impaired traffic between endosomes and lysosomes (8). This suggests that the vesicle-budding mechanisms (see below) in the endocytic pathway are similar to, yet distinct from, those in the exocytic pathway. Furthermore, these observations reinforce the plasticity of the endocytic pathway, which is largely functional even when some traffic steps are inhibited.

The major effects of BFA on protein traffic are explained by its ability to prevent binding of cytosolic coat proteins onto membranes (9). The target of BFA's action is a **nucleotide exchange factor** for **ADP-ribosylation** factor (ARF), a small GTP-binding protein. BFA inhibits the ability of Golgi membranes to catalyze the exchange of GTP onto ARF specifically, thereby preventing ARF from interacting with the membrane. As a result, the association of the coat protein b-COP with the Golgi membrane is inhibited (10, 11). b-COP is a subunit of a cytosolic protein complex, the coatomer, that reversibly associates with Golgi membranes and controls vesicular transport.

One possible mode of ARF action is via its ability to stimulate phospholipase D in Golgi membranes (12). Phospholipase D converts phospholipids into phosphatidic acid and thus can alter the lipid content of membranes. Stimulation of the Golgi-associated phospholipase D activity is BFA-sensitive, suggesting a possible link between transport events and the underlying architecture of the lipid bilayer.

The pathogenic bacterium *Staphylococus aureus* mimics the action of BFA and disassembles the Golgi apparatus (13, 14). This effect is mediated by the secretion of EDIN (epidermal-cell differentiation inhibitor), an extracellular enzyme that ADP-ribosylates Rho GTPase. As a result, all the manifestations of BFA treatment are reproduced. Thus, the regulatory circuit of coat-membrane assembly may involve more than one small GTP-binding protein. In addition to the effects of the small GTP-binding proteins, heterotrimeric G proteins of the Gi/Go subfamily also contribute to the regulation of the cycle of coatomer binding (15, 16). Activation of heterotrimeric G proteins promotes binding of b-COP to Golgi membranes and antagonizes the effect of BFA.

Several BFA-resistant cell lines exist, including the PtK1 rat kangaroo cell line, a derivative of monkey kidney Vero cells, and two derivatives of the human epidermoid carcinoma KB cell line (17). The BFA resistance is dominant and is due to a Golgi-associated factor that is **homologous** to the target of BFA in cells that are sensitive to the drug. In Golgi membranes from BFA-resistant PtK1 cells, the basal phospholipase D activity is high and insensitive to BFA (12), suggesting a mechanism for the drug resistance. Another mechanism may involve a member of the ATP-binding cassette superfamily of transport proteins, as suggested by BFA-resistant mutants in yeast (18).

The ability of BFA to affect budding of **clathrin**-coated vesicles from the *trans*-Golgi network (observed in many, but not all cells) is mediated through the rapid and reversible redistribution of g-adaptin (19). This component of the clathrin coat is specific to Golgi-derived coated vesicles and is absent from plasma membrane-derived coated vesicles. The kinetic and pharmacological similarities between BFA's effects on g- adaptin and b-COP underscore the biochemical similarities between membrane budding mechanisms that are mediated by various coat complexes.

The effects of BFA are readily reversible, and this reversibility is due partly to its detoxification. The mechanism of BFA detoxification was studied in CHO cells and is mediated by the **glutathione *S*-transferase** system via conversion of the antibiotic to its **glutathionyl** and **cysteinyl** derivatives, followed by secretion (20).

BFA affects cellular compartmentalization not only via protein traffic, but also through lipid metabolism (21). Its main effect on lipids is enhanced hydrolysis of sphingomyelin, a key regulator of cell proliferation and differentiation. Sphingomyelin is produced from ER-derived ceramide and is delivered to other membranes, presumably via the same trafficking system used for proteins. The effect of BFA on the level of sphingomyelin seems to be a result of the mixing of cellular membranes. BFA treatment also increases the rate of sphingomyelin biosynthesis from phosphatidylcholine, and this effect may be related to the above-mentioned action on phospholipase D. In this context, it is noteworthy that C6 ceramide, a cell-permeable ceramide analogue, partially restores BFA sensitivity in a BFA-resistant cells (22).

The various effects of BFA on a number of cellular membranous organelles indicate both the common and distinct mechanisms that operate to sort membrane components. BFA seems to inhibit a common key step in the mechanism of vesicle budding, namely, regulation of the nucleotide status of different small G proteins. The BFA-sensitive G proteins are each endowed with organelle specificity, coupled perhaps to tissue specificity, which explains the variable sensitivity of membranes to BFA. On the other hand, the use of BFA has also revealed a physiological connection between cellular signal transduction pathways and the traffic of membrane lipids and proteins through the cell.

Bibliography

1. Y. Misumi, Y. Misumi, K. Miki, A. Takatsuki, G. Tamura, and Y. Ikehara (1986) J. Biol. Chem., **261**, 11398–11403.
2. J. Lippincott-Schwartz, L. C. Yuan, J. S. Bonifacino, and R. D. Klausner (1989) Cell **56**, 801–813.
3. J. Lippincott-Schwartz, J. G. Donaldson, A. Schweizer, E. G. Berger, H. P. Hauri, L. C. Yuan, and R. D. Klausner (1990) Cell **60**, 821–836.
4. N. E. Ivessa, C. De Lemos-Chiarandini, Y. S. Tsao, A. Takatsuki, M. Adesnik, D. D. Sabatini, and G. Kreibich (1992) J. Cell Biol. **117**, 949–958.
5. R. D. Klausner, J. G. Donaldson, and J. Lippincott-Schwartz (1992) Cell Biol. **116**, 1071–1080.
6. L. C. Hendricks, S. L. McClanahan, G. E. Palade, and M. G. Farquhar (1992) Proc. Nat. Acad. Sci. USA **89**, 7242–7246.
7. S. G. Miller, L. Carnell, and H. H. Moore (1992) J. Cell Biol. **118**, 267–283.

8. J. Lippincott-Schwartz, L. Yuan, C. Tipper, M. Amherdt, L. Orci, and R. D. Klausner (1991) Cell **67**, 601–616.
9. L. Orci, M. Tagaya, M. Amherdt, A. Perrelet, J. G. Donaldson, J. Lippincott-Schwartz, R. D. Klausner, and J. E. Rothman (1991) Cell **64**, 1183–1195.
10. J. G. Donaldson, J. Lippincott-Schwartz, G. S. Bloom, T. E. Kreis, and R. D. Klausner (1990) J. Cell Biol. **111**, 2295–2306.
11. J. G. Donaldson, D. Finazzi, and R. D. Klausner (1992) Nature **360**, 350–352.
12. N. T. Ktistakis, H. A. Brown, P. C. Sternweis, and M. G. Roth (1995) Proc. Nat. Acad. Sci. USA **92**, 4952–4956.
13. M. Sugai, C. H. Chen, and H. C. Wu (1992) J. Biol. Chem. **267**, 21297–21299.
14. M. Sugai, C. H. Chen, and H. C. Wu (1992) Proc. Nat. Acad. Sci. USA **89**, 8903–8907.
15. J. G. Donaldson, R. A. Kahn, J. Lippincott-Schwartz, and R. D. Klausner (1991) Science **254**, 1197–1199.
16. N. T. Ktistakis, M. E. Linder, and M. G. Roth (1992) Nature **356**, 344–6.
17. N. T. Ktistakis, M. G. Roth, and G. S. Bloom (1991) J. Cell Biol. **113**, 1009–1023.
18. T. G. Turi and J. K. Rose (1995) Biochem. Biophys. Res. Commun. **213**, 410–418.
19. M. S. Robinson and T. E. Kreis (1992) Cell **69**, 129–138.
20. A. Bruning, T. Ishikawa, R. E. Kneusel, U. Matern, F. Lottspeich, and F. T. Wieland (1992) J. Biol. Chem. **267**, 7726–32.
21. C. M. Linardic, S. Jayadev, and Y. A. Hannun (1992) J. Biol. Chem. **267**, 14909–14911.
22. T. Oda, C. H. Chen, and H. C. Wu (1995) J. Biol. Chem. **270**, 4088–4092.

Suggestions for Further Reading

23. R. D. Klausner, J. G. Donaldson, and J. Lippincott-Schwartz (1992) Brefeldin A: insights into the control of membrane traffic and organelle structure. J. Cell Biol. **116**, 1071–1080.
24. J. Lippincott-Schwartz, L. C. Yuan, J. S. Bonifacino, and R. D. Klausner (1989) Rapid redistribution of Golgi proteins into the ER in cells treated with brefeldin A: evidence for membrane cycling from Golgi to ER. Cell **56**, 801–813.
25. N. T. Ktistakis, H. A. Brown, P. C. Sternweis, and M. G. Roth (1995). Phospholipase D is present on Golgi-enriched membranes and its activation by ADP ribosylation factor is sensitive to brefeldin A. Proc. Natl. Acad. Sci. USA **92**, 4952–4956.

5-Bromouracil

Litman and Pardee (1) found that three **thymine** analogues (5-bromouracil, 5-chlorouracil and 5-iodouracil) were all incorporated fairly efficiently into the **DNA** of **bacteriophage** T4, and all were powerful mutagens in this organism. Further studies on 5-bromouracil (BU) mutagenesis by Freese (2, 3) were important in defining transition and transversion mutations and distinguishing these events from frameshift mutation. All the mutants induced by BU could be reverted by either BU or 2-aminopurine, although spontaneous and **acridine**-induced mutants could not. The BU-induced mutations were suggested to be transitions, because it was considered that the most likely effect of incorporating this base analogue into DNA would be to induce mispairing with guanine, by a mechanism that was unknown at that time (3). Mispairings with guanine do occur and can lead to BU mutagenesis (for example, as shown in Fig. 1).

Figure 1. Mechanism of generation of transition mutation by 5-bromouracil (BU) after DNA replication. The presence of BU in one DNA strand in place of the original thymine (T), causes guanine (G) to be inserted in the complementary position upon DNA replication, instead of the original adenine (A).

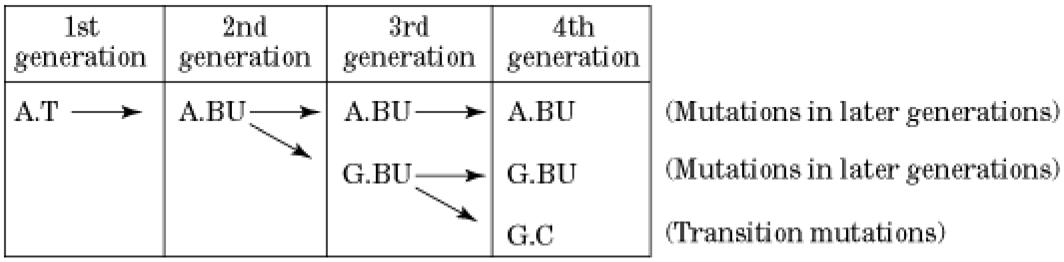

There is some evidence that ionization of bromouracil leads to a high probability of mispairing with guanine and that ionized structures are more likely to be involved in this type of mutagenesis than a neutral wobble-pairing structure containing the favored keto structures of BU (4). Goodman et al. (5) suggested that BU may exhibit substantially different base-pairing behavior depending upon whether it is present as a template base or as a deoxyribonucleoside triphosphate substrate. They interpreted differences in mutagenesis by this base analogue in different organisms and different systems as due partly to the relative size of and imbalance of the deoxynucleoside triphosphate pools. Classic interpretations of BU mutagenesis invoke direct base mispairing, and this is likely to be involved in the mutagenesis seen in bacterial and bacteriophage systems. However, studies in **yeast** (6) suggest that the majority of BU-induced mutants do not occur at the site where BU is incorporated. Szyszko et al. (7) have identified uracil as a major lesion after BU incorporation into DNA of *E. coli*, presumably because of dehalogenation of incorporated BU. They suggested that this would be followed by formation of apyrimidinic sites by the enzyme uracil-DNA glycosylase, followed by single-stranded nicks. Efficient BU mutagenesis is dependent upon various DNA repair gene functions, suggesting a major role for SOS response repair in many of the BU-induced mutations (8).

Bibliography

1. R. M. Litman and A. B. Pardee (1956) Nature **178**, 529–531.
2. E. Freese (1959) Proc. Natl. Acad. Sci. USA **45**, 622–633.
3. E. Freese (1959) Brookhaven Symp. Biol. **12**, 63–73.
4. H. Yu, R. Eritja, L. B. Bloom, and M. F. Goodman (1993) J. Biol. Chem. **268**, 15935–15943.
5. M. F. Goodman, R. L. Hopkins, R. Lasken, and D. N. Mhaskar (1985) Basic Life Sci. **31**, 409–423.
6. V. Noskov, K. Negishi, A. Ono, A. Matsuda, B. Ono, and H. Hayatsu (1994) Mutat. Res. **308**, 43–51.
7. J. Szyszko, I. Pietrzykowska, T. Twardowski, and D. Shugar (1983) Mutat. Res. **108**, 13–27.
8. I. Pietrzykowska, M. Krych, and D. Shugar (1985) Mutat. Res. **149**, 287–296.

Buffers

1. Basic Principles

The term *buffer* solution usually refers to a solution that minimizes changes in pH when hydrogen ions (hydrons, H^+) are added to the solution or removed from it. (As discussed in reference1, IUPAC has approved *hydron* to designate a hydrogen cation when a term independent of hydrogen isotope is desired.) Such a solution is therefore said to buffer the pH. Solutions can also be designed to buffer other species, particularly metal ions, as will be described below.

Because the concentration of hydrogen ions in biological media is low, usually about 0.1 µM, it could be greatly changed by the production or consumption of very small quantities of hydrogen ions in chemical reactions. This is what makes buffering commonly necessary in experiments in molecular biology. The principle of a buffer is simple. Relative to the low concentration of free hydrogen ions, the buffer consists of much higher concentrations of both a base, A^-(ie, a substance that can combine reversibly with the hydrons), and its conjugate acid, HA, which is formed when the base combines with a hydron. Hence the equilibrium

$$HA \rightleftarrows H^+ + A^- \tag{1}$$

is established. Subsequently, any addition of H^+ causes a much smaller increase in its free concentration, $[H^+]$, because some of the hydrons are used up in making more HA to displace this equilibrium to the left. Likewise, any fall in $[H^+]$ is diminished because it leads to the dissociation of HA.

2. Simple Theory

Users of buffers need to be aware of many features of their action if they are not to make mistakes that can easily ruin their experiments. For this, a little theory of buffer solutions is required.

2.1. Dissociation of Water

Water spontaneously dissociates into one hydrogen ion and one hydroxide ion:

$$H_2O \rightleftarrows H^+ + OH^- \tag{2}$$

Because of the equilibrium, the product $[H^+][OH^-]$ is constant; its value, about 10^{-14} M^2, changes only slightly with temperature. Both the hydrons and the hydroxide ions will be largely hydrated, reversibly combined with one or more water molecules. In this article, the term *acid* is used in the sense of a Brønsted acid, a substance that can donate a hydron, and *base* is used to mean a Brønsted base, a substance that can combine with one. If no such acid or base is added to pure water, the values of $[H^+]$ and $[OH^-]$ are equal, namely, 10^{-7}M, ie, 0.1 µM. Given that the pH is defined as

$$pH = -\log_{10}[H^+] \tag{3}$$

the pH is 7. The pH scale is useful in water over about the range 0 to 14, over which $[H^+]$ varies from 1 M to 10^{-14} M, and $[OH^-]$ from 10^{-14} M to 1 M.

2.2. The pK_a and the pH

The acid HA will have a dissociation constant, K_a, the equilibrium constant for reaction (1), which is defined as

$$K_a = \frac{[H^+][A^-]}{[HA]} \tag{4}$$

Rearranging this to find $[H^+]$ gives

$$[H^+] = \frac{K_a[A^-]}{[HA]} \tag{5}$$

and taking the negative logarithm of each side to find the pH [eq. (3)] gives

$$pH = pK_a - \log\frac{[A^-]}{[HA]} \tag{6}$$

if we define pK_a as $-\log K_a$. This is known as the Henderson–Hasselbalch equation, and it is fundamental for understanding buffer action and how single groups titrate.

Figure 1 shows the fractional concentration of the base, ie, $[A^-]/([HA] + [A^-])$, as a function of pH. The first point to note is that, when the pH = pK_a,$\log([A^-]/[HA] = 0$, and so $[A^-]/[HA] = 1$, and $[A^-]$ is 0.5 of its maximal value. Hence, the pK_a is the pH at which the acid is half-dissociated. When the pH is one unit above the pK_a, $\log([A^-]/[HA]) = 1$, and so $[A^-]/[HA] = 0$, and hence $[A^-]$ is 10/11, ie, 0.91, of its maximal value as shown; when the pH is two units above the pK_a, $\log([A^-]/[HA]) = 2$, and so $[A^-]/[HA] = 100$ and, hence, $[A^-]$ is 100/101, ie, 0.99 of its maximal value. Similarly, when the pH is one unit below the pK_a, $\log([A^-]/[HA]) = -1$, and so $[A^-]/[HA] = 0.1$, and $[A^-]$ is 0.091 of its maximal value; when the pH is two units below the pK_a, $[A^-]$ is 0.01 of its maximal value. These figures illustrate that comparing the pH with the pK of a substance instantly indicates how much of the substance or group is in its hydronated and unhydronated forms. All simple acids follow the curve of Figure 1; they differ only in their pK_a values.

Figure 1. The dependence of the fractional concentration of the basic form of a monobasic acid on the pH. The vertical axis shows the concentration of A^- expressed as a fraction of the sum of the concentrations of A^- and HA. Vertical lines mark: (1) pH = $pK_a - 1$, when $[A^-] = 0.1[HA]$, so the fractional concentration of A^- is 1/11; (2) pH = pK_a, when $[A^-] = [HA]$, so the fractional concentration of A^- is 1/2; (3) pH = $pK_a + 1$, when $[A^-] = 10[HA]$, so the fractional concentration of A^- is 10/11.

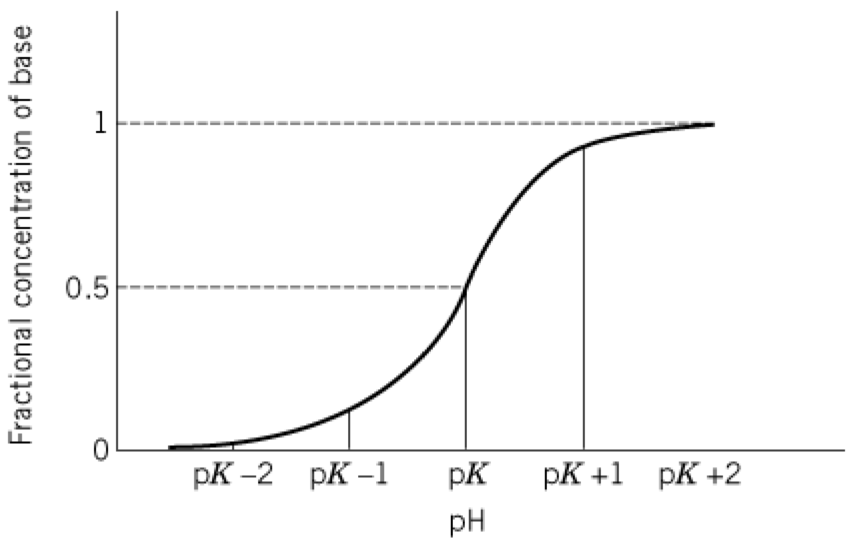

2.3. Theory of Buffering

With properly buffered solutions, both [A^-] and [HA] will be much greater than [H^+] and [OH^-]. In this case, any H^+ produced in a reaction converts A^- into HA, and any H^+ taken up dissociates from HA to convert it into A^-. To see the consequences of this, it is convenient to modify the Henderson–Hasselbalch equation as follows:

$$\mathrm{pH} = \mathrm{p}K_\alpha - \log\frac{[\mathrm{A}^-]}{[\mathrm{HA}]} = \mathrm{p}K_\alpha - \log[\mathrm{A}^-] + \log[\mathrm{HA}] \tag{7}$$

For good buffering, it is necessary for *both* [A^-] and [HA^-] to be large enough so the logarithm of neither is changed enough to produce an unacceptable change in pH when some of one is converted into the other.

This means that there are two basic requirements for a buffer: (1) It must be sufficiently concentrated (in terms of the total of [A^-] + [HA^-]), and (2) the pH must not be too far from the pK_a of the buffer so that the concentrations of *both* A^- and HA will be large. It is the second of these that is most often forgotten. If the pH and pK_a differ by one unit, only 1/11 of the total buffer concentration will be in the minor form.

This point may be illustrated by the example of a worker who wondered why mercaptoethanol and **iodoacetate** inhibited his enzyme when neither one by itself did so. He was using more than 10 mM of each reagent in a 10-mM Tris buffer of pH 7. Hence, the 10-mM H^+ released when the mercaptoethanol and iodoacetate reacted exceeded by tenfold the concentration of free Tris, which was less than 1 mM in a solution far below its pK_a of 8.1.

To a first approximation, dilution does not affect the pH of a buffer solution because it does not affect the ratio [A^-]/[HA^-]. There are, however, two qualifications to this conclusion. First, it is assumed that the dissociation constant of the buffering acid is unaltered whereas, in fact, it is likely to change with ionic strength (see below). It is also assumed that dilution is not so extreme that either [A^-] or [HA^-] become comparable to [H^+] or [OH^-]. In any case, dilution decreases the concentrations of both A^- and HA; hence dilution makes the solution a worse buffer in that a given amount of conversion of one form into the other will produce a larger change in the ratio.

3. Practical Points

3.1. pH Measurement

Methods of measuring pH are outside the scope of this article but the process is important because reproducibility of buffer preparation often depends on it (see below). The most common method uses a glass electrode. This method depends on dipping the electrode into the solution to be tested in such a way that an electrical cell is created and that the potential given by this cell depends on the pH of the solution. Normally, a layer of thin glass separates the solution under test from one containing one of the electrodes of the cell. This glass is selectively permeable to hydrons, so that the potential across it depends on the pH of the solution. Provided that the other junction potential between this solution and the other electrode is negligible—a condition approached by a bridge containing concentrated KCl—the potential should reliably indicate the pH.

Such pH meters require calibration, and standard buffers are used for this. The makers normally give reliable instructions for calibrating the electrode, but some of these are easily overlooked. The first concerns the temperature. The pH standards have pH values that may themselves vary with temperature. Standardization is valid at only one particular temperature, and it cannot be assumed that an electrode standardized at one temperature gives a meaningful reading at a different one. The pH range specified by the makers of the apparatus should also be noted. Glass membranes may be slightly permeable to Na^+, so that when $[H^+]$ is low, as in alkaline solution, even a slight sensitivity to Na^+ may cause overestimation of $[H^+]$ and hence too low an estimate of a high pH.

3.2. Specifying a Buffer Solution

Buffer solutions are often specified in a conventional way, such as 0.2-M sodium acetate buffer, pH 4.8. The concentration given should refer to the sum of the two forms of the buffering species, designated here as $[AcO^-]$ and [HOAc] in the case of acetate buffer, but such a specification does not make fully clear how this solution has been obtained. It might have been prepared by (1) mixing the appropriate amounts of sodium acetate and acetic acid, as calculated from the p*K* and the Henderson–Hasselbalch equation, (2) adding 0.2-M sodium acetate to 0.2-M acetic acid until a pH of 4.9 was reached, or (3) adding strong NaOH to 0.2-M acetic acid to reach pH 4.9, on the assumption that the volume added diluted the acetic acid negligibly. It would not have been appropriate, however, to have added strong HCl to 0.2-M sodium acetate, as this would have produced NaCl in addition to the buffering species.

Measuring pH is not straightforward, especially in view of the effects of temperature on the measurements (see above); for reproducibility, especially between different laboratories, it is much safer to specify the concentration of *each* form of the buffering substance, given that weighing material out with an accuracy of 1% to 2% is easy. Even an error of 2% in each would change the pH by only log(1.04), ie, by 0.017 of a pH unit. Hence, it would be better to describe the buffer just mentioned as 0.12-M sodium acetate, 0.08-M acetic acid (pH 4.8), thus adding the pH for information rather than as part of the definition.

3.3. Effects of Temperature

Users should remember that the pH of a buffer may change with temperature. This is because the dissociation constant of the buffering acid, like any other equilibrium constant, depends on temperature if the dissociation has an appreciable **enthalpy** change, D*H*. Dissociations of carboxylic acids and phosphoric acid have low values of D*H*, and so this effect is small with buffers based on them, but the dissociation of ammonium to ammonia and a hydron is accompanied by a large heat intake (ie, D*H* is positive), and increasing temperature promotes dissociation, ie, lowers the pK_a. Hence, the pH of a buffer that uses an amino group decreases on heating. The effect is quite large, a fall of 0.028 per degree Celsius.

The importance of this needs to be considered in each experiment. If a user wished the glutamate residues of an enzyme to be hydronated to the same extent in an experiment at 0 °C as they would be in a buffer of pH 7 at 20 °C, it would be wrong to use an amino buffer with a pH of 7 at 20 °C and simply cool it. Cooling would raise the pH of the buffer, but not the pK_a of the residues, so these residues would dissociate more on cooling. But this would be a proper procedure if the experimenter was concerned with the state of the lysine residues because their pK_a would rise with that of the buffering amine so that their degree of hydronation would remain the same.

3.4. Effects of Concentration

The dissociation constants referred to above are those actually exhibited by the buffering species in the solution being used; ie, they are not idealized values extrapolated to standard conditions of ionic strength and temperature. They therefore change with ionic strength and the addition of other components to the solution, eg, organic solvents or deuterium oxide. Many experiments may require a solution with a particular ionic strength or particular concentrations of specified ions. Remember that these may affect the apparent value of the p*K* of the buffering species.

An acid and its conjugate base differ by one H^+ and therefore by one charge. Typically, they will have charges 0 and –1, or +1 and 0. If, however, one of the forms has more than unit charge, positive or negative, the p*K* will have a greater dependence on ionic strength. The most commonly used buffer to which this applies is phosphate buffer, where the acid is $H_2PO_4^-$ and its conjugate base is the doubly charged HPO_4^{2-}. This makes its pK_a particularly sensitive to ionic strength. For example, a solution of 0.2-M phosphate may increase its pH by over 0.2 of a unit on tenfold dilution.

Many chemical reactions are catalyzed by acids or bases, so that an increased buffer concentration can accelerate them even at a fixed pH. This should be borne in mind when altering buffer concentrations. It is not very common for enzyme-catalyzed reactions because natural selection often ensures that if such catalysis accelerates the reaction, a corresponding acidic or basic group will be present in the enzyme to provide it.

3.5. Volatile Buffers

Separation methods such as chromatography and electrophoresis often require a buffered solution. This solution needs appreciable ionic strength (in ion-exchange chromatography to give a constant competition for the sites of the exchanger, in electrophoresis to give a constant conductivity and therefore electric field) that is negligibly affected by the substances being separated. Because it is convenient to be able to remove the buffer at the end of the procedure, a volatile buffer that can be removed by evaporation is desirable. The two forms of the buffering substance must differ in charge, however, so that one at least will have a net charge and hence be nonvolatile. Nevertheless, volatile buffers can be prepared by mixing a volatile acid with a volatile base, provided that their pK_a values are not greatly separated. An example is a mixture of pyridine (pK_a 5.2) and acetic acid (pK_a 4.8). On mixing, some of the acetic acid dissociates to acetate and hydronates some of the pyridine to pyridinium. Hence, the pH will be given by

$$\mathrm{pH} = 5.2 + \log\frac{[\text{pyridine}]}{[\text{pyridinium}]} = 4.8 + \log\frac{[\text{acetate}]}{[\text{acetic acid}]} \tag{8}$$

The concentrations of pyridinium ($C_5H_5N^+$-H) and acetate (AcO^-) ions will be equal, because each acetic acid molecule that dissociates to acetate forms one pyridinium ion. As the solution is evaporated off, water, pyridine (C_5H_5N) and acetic acid (AcOH) evaporate, and so the equilibrium

$$\mathrm{AcO^- + C_5H_5N^{-}\text{-}H \rightleftarrows AcOH + C_5H_5N} \tag{9}$$

is displaced to the right to replace the un-ionized forms as they are removed.

Ammonium bicarbonate forms a useful buffer of this type. Although it is highly volatile in solution, it is not volatile when dry, as it has a stable crystal lattice. Hence to allow ammonium and bicarbonate to react to form ammonia and carbon dioxide, it may be necessary after one drying to add a little water and then dry it again. Alternatively, triethylammonium bicarbonate, prepared from triethylamine and carbon dioxide, may be used, as it does not form nonvolatile crystals. Ammonium acetate and ammonium formate have been used in this way (2), but the procedures for drying them are complicated because their pK_a values are so far apart that there is very little of the un-ionized forms at equilibrium.

3.6. Appropriate pK_a Values

Biological material usually has a pH near 7, and it is not always easy to find a buffering species with the desired pK_a. Carboxylic acids possess values that are too low, whereas amines have values that are too high. A large number of the commonly used buffers are amines with electron-attracting substituents, which make the lone pair of electrons on the nitrogen atom less available and so lower the atom's pK_a. Examples include:

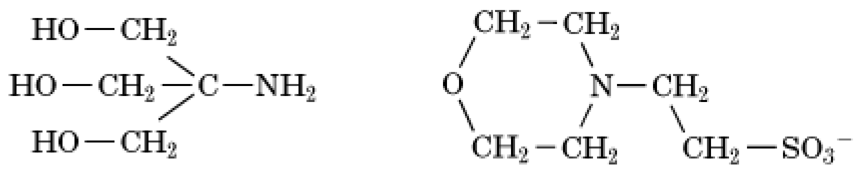

Tris 2-Morpholinoethanesulfonic acid

(**10**)

with pK_a values of 8.1 and 6.2, respectively (see Tris Buffer). Phosphate Buffers are commonly used because they have a convenient pK_a of about 7 between $H_2PO_4^-$ and HPO_4^{2-}. Their main disadvantages are their propensity to support fungal and algal growth and the sensitivity of their pK_a to ionic strength (see above).

3.7. The Need for Buffers
It should be remembered that it is pointless to add a buffer if the components of the reaction mixture are already highly buffering. Glycolytic intermediates, for example, are phosphate esters, and adjusting them to a pH near 7 creates a buffered solution.

3.8. Chemical Reactivity
It is often important to use buffering species that will not react chemically under the conditions of an experiment. Hence an experiment to acylate amino groups of proteins should use a buffer whose basic component has as low a nucleophilic reactivity as possible. Exclusion of primary amines, such as Tris, may be all that is needed. But extreme conditions may demand introduction of steric hindrance; eg, 2,6-dimethylpyridine has a pK_a close to that of pyridine but vastly less nucleophilic reactivity because the methyl groups have little steric effect on protonation of the nitrogen atom but greatly slow its reaction with larger molecules.

Another form of reactivity is the possibility of precipitating desired components in the solution, eg, cations such as Ca^{2+}, by phosphate. Occasionally, reactivity may even be of advantage. Urea is often used as a protein **denaturant** but, if kept for long in concentrated solution, especially at raised temperatures, its equilibration

$$NH_2—CO—NH_2 \rightleftarrows NH_4^+ + CNO^- \qquad (11)$$

can produce about 20-mM cyanate (CNO^-) from 8 M urea (3). The harm in this is the reverse reaction, because the cyanate can carbamoylate lysine residues in proteins, forming *uncharged* ureas and destabilizing the folded protein. This process is minimized if ammonium ions are present in the buffer as they compete with the protein for the cyanate.

3.9. “Good” Buffers
A number of buffers were recommended by Good and colleagues (4) for a variety of reasons. The most important was that both acidic and basic forms were charged and, therefore they could not rapidly permeate biological membranes. If **organelles** are suspended in a buffer without this feature, acetate, for example, molecules of acetic acid, but not acetate ions, may penetrate them and lower the internal pH below that of the external buffer. Many of the Good buffers have strongly acid groups, such as sulfonate, $—SO_3^-$. An example is 2-morpholinoethanesulfonate (eq. **10**); its sulfonate group renders it impermeant even when its nitrilo group is un-ionized. Other desirable characteristics of buffering species are also listed (4). For many purposes, transparency at UV wavelengths is necessary.

Under other circumstances, the possession of a further charge can be a disadvantage. Ideally, buffers for ion-exchange chromatography possess only one species with a charge opposite in sign to that of the exchanger so that the equilibration of the exchanger can be followed by pH changes; for example, a buffer cation cannot adsorb to, or desorb from, the exchanger except by exchange with H^+, which changes the pH.

4. Metal-Ion Buffers

The free concentration of many metal ions in biological media is very low, and it may be necessary to buffer it. The principles are exactly the same as those that apply to buffering $[H^+]$. Some compound that binds the metal ion is introduced in roughly equal concentrations of the free and metal-bound forms. A substance that buffers in the correct concentration range can be chosen from a tabulation of binding constants (5).

A complication is that many of the compounds that ligate metal ions with suitable affinity also bind hydrons, resulting in competition between the cations for the ligand. This means that the affinity of the ligand for the metal ion varies with pH. The complex of the buffering species with the metal ion is often a chelate, so that two or more ligating groups are involved. Hence, the competition is not a simple 1:1 replacement, and the pH dependence of the net affinity may be complex.

Bibliography

1. J. F. Bunnett and R. A. Y. Jones (1988) Pure Appl. Chem. **60**, 1115–1116.
2. C. H. W. Hirs, S. Moore, and W. H. Stein (1952) J. Biol. Chem. **195**, 669–683.
3. G. R. Stark, W. H. Stein, and S. Moore (1960) J. Biol. Chem. **235**, 3177–3181.
4. N. E. Good and S. Izawa (1972) Methods Enzymol. **24**, 53–68.
5. R. M. Smith and A. E. Martell (1974-89) *Critical Stability Constants*, vols. **1–6**, Plenum Press, New York.

Suggestion for Further Reading

6. R. J. Beynon and J. S. Easterby (1996) *Buffer Solutions: The Basics*, IRL Press Oxford, U.K. This gives not only an excellent account but also WWW addresses for programs to calculate buffer compositions (`http://www.bi.umist.ac.uk/buffers.html`) and other help on the Internet.

bZip Domain

The bZip DNA binding domain and the closely related **helix-loop-helix** (HLH) domain are found in many eukaryotic transcription factors. Both bind in the major groove of DNA and have the capability of forming homo- or heterodimers with proteins of the same class. The simplest of these domains is the bZip domain which, when bound to DNA, forms a continuous a-helix. The lower basic part of this helix (the b of bZip) forms sequence specific contacts with DNA whereas the upper part can dimerize with an appropriate partner through the formation of a leucine zipper. The dimer thus has the appearance of a pair of scissors binding to a palindromic DNA sequence in which each half-site is exposed on the opposite face of DNA. The helix-loop-helix domain binds to DNA in a similar manner with the difference that the a-helix involved in dimerization is separated from the DNA binding a-helix by a short loop.

Buoyant Density

The buoyant density of a macromolecule is its effective density in solution. It is defined relative to the fluid medium in which it resides and/or through which it is sedimented (see Centrifugation). The dimensions of buoyant density are in cm^3/g. If a macromolecule is sedimented through a fluid column in which the density of the column is adjusted so that it spans a gradient of density *both* less than *and* greater than the macromolecule, the macromolecule moves to a fixed position in the fluid column (see Density Gradient Centrifugation). At this position the density of the macromolecule is equal to that of the solvent. This is an equilibrium position that is independent of time. This process or technique is termed density gradient sedimentation-equilibrium, equilibrium banding or isopycnic gradient centrifugation. These techniques have uses that range from the analysis of macromolecule solvation to the separation of both living cells and subcellular **organelle** systems (1). Recently the evaluation of macromolecular values of buoyant density have been been employed in a variety of research situations including (1) the analysis of viral infectivity during therapy (2, 3); (2) the nature of circulating immune complexes of **viruses** (4); (3) as a preselection method for **PCR** methods (5).

Bibliography

1. S. Daenen, W. Huiges, E. Modderman, and M. R. Halie (1993) Leukemia Res. **17**, 37–41.
2. A. Nagasaka, S. Hige, T. Matsushima, J. Yoshida, Y. Sasaki, I. Tsunematsu, and M. Asaka (1997) J. Med. Virol. **52**, 190–194.
3. T. Kanto, N. Hayashi, T. Takehara, H. Hagiwara, E. Mita, M. Naito, A. Kasahara, H. Fusamoto, and T. Kamada (1995) J. Hepatol. **22**, 440–448.
4. M. Hijikata, Y. K. Shimizu, H. Kato, A. Iwamoto, J. W. Shih, H. J. Alter, R. H. Purcell, and H. Yoshikura (1993) J. Virol. **67**, 1953–1958.
5. R. J. Carrick, G. G. Schlauder, D. A. Peterson, and I. K. Mushahwar (1992) J. Virol. Meth. **39**, 279–290.

Suggestions for Further Reading

6. C. H. Chervenka (1973) A Manual of Methods for the Analytical ultracentrifuge, Spinco Division, Beckman Instruments, Inc. Palo Alto, CA. *The classic manual of methods for the original model E analytical ultracentrifuge*. Although the mechanical components related to model E have been superseded by the modern XLA and XLI analytical ultracentrifuges, the methods themselves are still applicable.
7. R. Hinton and M. Dobrota (1980) *Laboratory Techniques in Biochemistry and Molecular Biology: Density Gradient Centrifugation* (T. S. Work and E. Work, eds.), North-Holland, New York. A somewhat dated, but useful, compendium of techniques for preparative density gradient centrifugation.

C Genes of Immunoglobulins

C genes encode for the constant (C) regions of immunoglobulin (Ig) heavy and light chains and therefore define the isotypes of H (g, m, a, d and l) and L (k, l) chains. The simplest structure is that of the Ck gene, which is unique in both the human and mouse species. It encodes for the entire constant region of the k chain. In humans, the Ck gene has three **allelic** variants based on single amino acid substitutions at two positions, which constitute the Km allotypes. The Ck gene is separated from the Jk region by a noncoding region of 1.2 kbp that contains a k enhancer. A second enhancer region is present in the 3′ flanking region. The organization of the Cl genes is somewhat more complicated, and there are some minor differences between humans and mouse. In both cases, they are present as tandem duplications of a JlCl unit, in which each J gene is separated from the C gene by a noncoding sequence of about 1 kbp. There are four discrete tandems in the mouse, Jl1Cl1 to Jl4Cl4, of which only three are functional. In humans, four functional tandem JC pairs are present, in addition to three pairs of pseudogenes. An enhancer region is present 3′ of the coding region in both species. In humans, the IgK and IgL loci are located at **chromosomal** positions 2p12 and 22q11, respectively.

The heavy-chain constant gene locus, located at 14q32 in humans, spans over 200 kbp. The detailed organization of the individual human CH genes is given in Figure 1. Some characteristic features may be identified. First, each isotype is encoded by a mosaic of exons (see Introns, Exons) that precisely reflects the **domain** structure of the Ig. The constant region of Cm is encoded by four exons, Cm1 to Cm4, corresponding to the four constant domains of the m chain, whereas in the case of the Cg isotypes one of the exons encodes the hinge region. Second, each isotype encoding C gene has additional membrane exons (one or two, depending on the isotype) that encode the transmembrane section and the short COOH-terminal cytoplasmic tail. Coding units that make secreted or membrane heavy chains result from alternative splicing and terminate at two distinct polyadenylation sites (see Fig. 1). The overall CH region also contains two pseudogenes. It will be noticed that a switch region is located at 5′ of each set of C genes, with the exception of the d locus, which accounts for the coexpression of IgM and IgD at the surface of mature B cells.

Figure 1. Organization of human heavy-chain constant region genes. Exons encoding discrete constant domains (CH), hinge regions (H), or transmembrane portion of surface heavy chains (M) are represented by open squares or rectangles. Polyadenylation sites are indicated by a dot. (From Ref. 1, with permission; adapted from Ref. 2.)

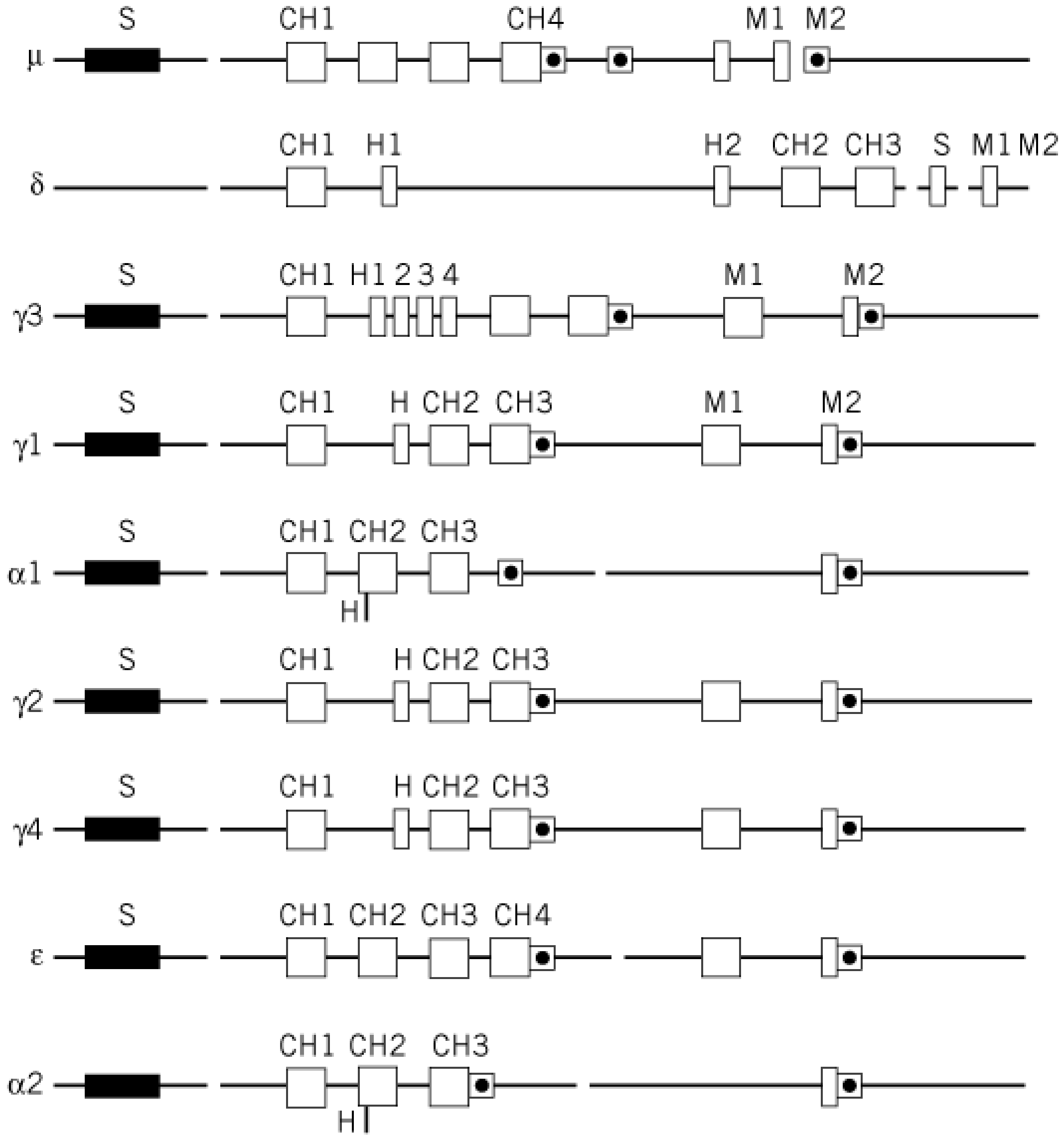

A final remark should be made regarding the general organization of the regulating elements that control IgH gene expression. **Promoter** regions are present at 5′ of each V gene and will be discussed elsewhere. Enhancers are split into two regions; one is located at 5′ of the Sm switch region, so that with each switching event it will control the newly adjacent isotype gene; the other is located at 3′ of the entire IgCH locus and may thus control whatever gene is to be turned on.

See also entries Antibody, Class Switching, Isotype, and Switch Region.

Bibliography

1. J.-P. Revillard (1998) In *Immunologie*, De Boeck Université, Paris-Bruxelles, p. 57.
2. J. D. Capra and J. D. Duker (1989) J. Biol. Chem. **264**, 12745.

Suggestions for Further Reading

3. V. Giudicelli et al. (1997) IMGT, the international ImMunoGeneTics database. Nucleic Acids Res. **25**, 206–2011.
4. T. Honjo, F. W. Alt, and T. H. Rabbitts (1989) *Immunoglobulin Genes*, Academic Press, New York.

5. F. Matsuda and T. Honjo (1996) Organization of the human immunoglobulin heavy chain locus. Adv. Immunol. **62**, 1–29.

C-Banding

The procedure of C-banding is used to highlight regions of constitutive heterochromatin. In man, sites of C-banding include the centromeres of all of the chromosomes and large segments of heterochromatin in chromosomes 1, 3, 9, 16 and the Y-Chromosome. The DNA sequences in constitutive heterochromatin are highly **repetitive** and include many satellite DNA sequences that are thought to be genetically inert. The distribution of satellite DNA sequences in chromosomes varies considerably from species to species and can even provide information that is specific to a particular individual.

C-banding involves the depurination of DNA in the chromosomes by treatment with hydrochloric acid. The sugar-phosphate backbone of DNA remains intact. Treatment with hydrochloric acid (0.2 M) is halted before depurination is complete (a treatment of several minutes). Then the chromosomes are incubated for several minutes with either sodium hydroxide (0.07 M) or barium hydroxide (0.07 M). This **denatures** the DNA, which aids solubilization. Then the chromosomes are washed overnight with 2 × SSC (0.3 M NaCl plus 0.03 M trisodium citrate) at 66°C. This warm salt wash breaks the sugar-phosphate backbone and allows DNA fragments to dissolve. Then the chromosomes are stained with **Giemsa**. Staining relies on the retention of intact nucleoprotein complexes in the highly compacted heterochromatin.

C-banding of metaphase chromosomes is greatly enhanced in resolution by two methodological improvements: first, by using chromosomes isolated early in **metaphase**, when the contraction of chromatin is incomplete; second, by the use of a sophisticated microscopic technique known as epi-illumination, in which the chromosome is viewed from the same side as it is illuminated. This provides enhanced contrast between stained and unstained bands.

Suggestion for Further Reading

R. P. Wagner, M. P. Maguire, and R. L. Stallings (1993) *Chromosomes. A Synthesis*. Wiley-Liss, New York.

C-Terminus

The *C*-terminus is the term for one end of the polypeptide chain of a protein. Proteins are polymers formed by condensation of the amino groups and carboxyl groups of amino acids. That end of the polypeptide chain having an uncondensed or “free” carboxyl group is called the carboxyl terminus, or ***C*-terminus** (Fig. 1). By convention, the *C*-terminus is the last residue in the protein sequence or primary structure. Similarly, the other end of the polypeptide chain, having an uncondensed or free amino group, is termed the amino terminus, or ***N*-terminus**, and by convention it is the first residue in the protein sequence. The *C*-terminal carboxyl group is usually negatively charged at physiological pH.

Figure 1. Schematic representation of a protein, showing the *C*-terminus as the last residue in the polypeptide chain. The square brackets indicate the repeating part of the chain (the backbone), and the R group denotes the variable side chain of each amino acid residue. The *N*-terminus is the first residue in the chain.

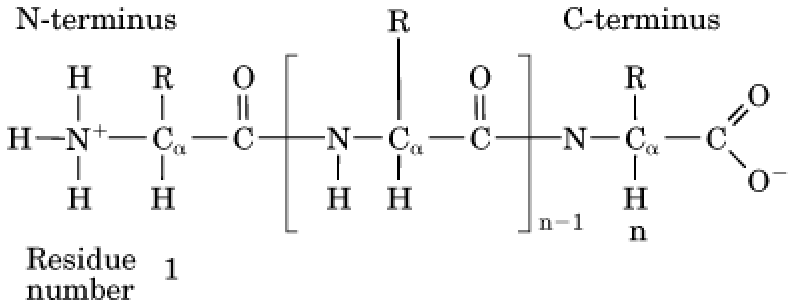

The *C*-terminal carboxyl group can be changed by post-translational modification such as **amidation**. An amidated *C*-terminus is more common in smaller proteins, or peptides, including hormones and toxins, and may be important for biological function or stability. Another important covalent modification that occurs only at the *C*-terminal residue is the attachment of membrane anchors to secure an otherwise water-soluble protein to a hydrophobic membrane. Proteins can be degraded by carboxypeptidases that specifically hydrolyze the *C*-terminal peptide bond.

[See also N-Terminus and Polypeptide Chain.]

C-Value

The *C*-value is the long-used term for the mystery, or paradox, of the wide range of genome sizes present among **eukaryotes**. They range from 13 Mbp (megabase pairs, 1.3×10^7) for **yeast** to 1.7×10^{11} bp for *Amphiuma*, or the mudpuppy, a urodele amphibian. The units used above, the number of nucleotide pairs in one haploid set of DNA, should be used consistently. In much of the literature, the amount of DNA per cell is expressed in picograms (1 pg is 9.8×10^8 nucleotides), and the classic tables are often in error due to the limited accuracy of the methods used. The most accurate genome sizes are those for which complete nucleotide sequences are available; for example, the yeast genome has 13,105,020 bp (base pairs), give or take a small uncertainty because not all copies of repeated sequences (see Repetitive DNA) have been sequenced. The smallest bacterial genome accurately known from sequence is that of Mycoplasma *genitalium*, with 580,073 bp. Viruses have even smaller genomes, but they are not free-living and depend on their hosts for much of the required information. A part of the range in DNA content is apparently due to the different requirements of different species for genetic information, but that is not all there is to it, by any means.

The familiar fruit fly, **Drosophila**, is a complete animal, with all of the necessary structures, and it is not surprising that it has more DNA than yeast, which has an apparently simpler structure. The genome of *Drosophila melanogaster* is about 170 Mbp. It is easy to imagine that more genes and associated regulatory systems are needed to program the development and specify the complex structure of an animal. That is clearly true, but life is not so simple. The yeast genome has little space between its **genes** and almost no **introns**, and it is this compactness of organization that accounts for the relatively small size of its genome. The Drosophila genome, and plant and animal genomes in general, do not share this very compact organization, although some are more compact than others. They typically have large intergenic spaces, and most of the genome is not made up of genes and regulatory systems and has no known function. Most mammals, including humans, have about 3×10^9 bp, and it is not obvious why we require 20 times more DNA than does *Drosophila*. Some believe it is required for the brain, but humans have no more DNA than do mice. It is not reasonable that the mudpuppy requires almost 50 times more genetic information than we do, and its large genome must have some other explanation. One might expect that the very large urodele genomes are burdened with repeated sequences, and they do have a larger fraction of repeated sequences (90%) than *Drosophila* (30%). That is not the only source of the large genome size, however, since the so-called single-copy DNA is also very large in absolute quantity in the large urodele genomes. The genome sizes of single-celled protozoa range from about 1.0×10^9 to 1.0×10^{12}, but that information does nothing to reduce the mystery.

The "*C*-value paradox" remains as paradoxical as when it was first observed. It is known that a more compact genome is typically more compact in many features, such as smaller introns and smaller amounts of repeated sequences. Natural selection forces controlling genome size must exist, but remain unknown. How genomes have evolved is not well known, but it seems that there have been events of growth, some due to doubling of the entire set of chromosomes, others due to increases in the interspersed repeated sequences. Extraordinary reductions in DNA have also occurred in some species, while closely related species have retained their large genomes. There is a correlation between genome size and cell size, but it is not known how the two are connected, although cell size does affect metabolic rates. All that can be said is that genome size is not a parameter that is understood, although it is nevertheless intimately connected with gene structure and organization. That mammals have a quite uniform genome size is evidence for selective forces that control the *C*-value. Some geneticists consider the extra DNA in large genomes as a possible limitation in searching for genomic and regulatory function and have favored organisms with relatively small genomes, such as the puffer fish (*Fugu rubripes*) and a weed (Arabidopsis *thaliana*). Of course, the small genomes do reduce the amount of work required to determine the complete genome sequence.

Suggestions for Further Reading

T. Cavalier-Smith, ed. (1985) *The Evolution of Genome Size*, John Wiley & Sons, Chichester, U.K.

B. John and G. L. G. Miklos (1988) *The Eukaryote Genome in Development and Evolution*, Allen & Unwin, London.

CAAT Box

A CAAT box is a *cis*-acting regulatory element in transcription that contains the sequence 5′-CCAAT-3′ at its core and is bound by one or more different transcription factors. These include but are not limited to C/EBP and various members of the CTF/NF1 family of proteins. Because of the multiplicity of transcription factors that recognize a CAAT box, it is usually not possible to determine the identity of the particular factor that regulates expression of a gene by simple sequence inspection. CAAT boxes are found upstream of a number of genes transcribed by **RNA polymerase** II and increase the transcriptional rate of the gene above the level that could be achieved by the transcriptional core machinery in the absence of a CAAT box. These *cis*-acting sequence elements are generally found upstream of the TATA box, but their exact position relative to it is variable, and they may be found in either orientation relative to the direction of transcription from the downstream initiation site.

Cadherins

The cadherins are a family of **transmembrane** proteins that regulate cell–cell adhesion in a Ca^{2+}-dependent manner during **embryogenesis** and as the animal matures (1). Three general groups of cadherins exist within the superfamily: (i) the “classical” cadherins, (ii) the desmosomal cadherins, and (iii) the protocadherins (1). The classical cadherins, of which there are more than 40 examples, display much conservation in their structures. The sequences of their cytoplasmic domains may be as much as 90% identical for proteins within the same species and up to 60% between widely divergent species. In contrast, there is more variation in sequence within the extracellular domains, and 30% to 60% identity is common. These cadherins are located at the adherens junction and at other points of contact between cells that lack a highly organized structure. The desmosomal cadherins, on the other hand, are the Ca^{2+}-dependent cell adhesion molecules found in **desmosomes**. Within the desmosomal cadherins there are two subclasses: the desmogleins and the desmocollins. **Isoforms** of both have been characterized. The desmogleins and desmocollins are structurally distinct, implying different roles *in vivo*. The third group of cadherins, the protocadherins, are more variable in their structures, and their claim for inclusion in the cadherin family lies with the repeating structures in their extracellular domains that are similar to those displayed by the classical and desmosomal cadherins. The protocadherins also have cell adhesion properties, which again link them to the cadherin family.

Cadherins are classified as Type I integral **membrane glycoproteins** (ie, their *N*-termini lie on the extracellular side of the cell membrane) and, with one exception (glycosylphosphatidylinositol-anchored T-cadherin), each molecule contains a single a**-helica**l transmembrane-spanning region (M) separating the cytoplasmic from the extracellular domain (1). The extracellular domain generally contains four quasi-repeating motifs (E1, E2, E3, and E4), each about 112 residues long and with one or two potential Ca^{2+}-binding sites per repeat (Fig. 1). A (partial) fifth domain of quite variable length has been designated the *extracellular anchor* (EA). Some at least of the first four repeats participate in an antiparallel overlap with similar domains in cadherin molecules emanating from other cells, thus facilitating homotypic assembly under Ca^{2+} control. Other proteins are also believed to be involved in this interaction. Details of the conformation of a cadherin repeat have recently been obtained using nuclear magnetic resonance (NMR) and X-ray diffraction methods (2, 3). These repeats are also important in determining the specificity of adhesion between the different cadherins. The cytoplasmic domain, which is able to bind a variety of proteins, contains a substructure that shows considerable variations in size between different members of the cadherin family. Consider, for example, human desmoglein and human *N*-cadherin (4). Both display a proline-rich region (albeit of different lengths) termed the *intracellular anchor* (IA), followed by a highly charged region (C1). This represents the full extent of the human *N*-cadherin sequence, in contrast to human desmoglein, which contains a further 320 residues. The C1 domain, being highly conserved between *N*-cadherin and desmoglein, is likely to be involved in interactions with cytoskeletal microfilaments and other key proteins in the cytoplasm, such as plakoglobin. The remaining part of human desmoglein can be subdivided into a 59-residue proline-rich domain (C2), a region with novel 29-residue repeats (C3) that contain a high density of putative **phosphorylation** sites, and a *C*-terminal domain (C4) that is quite divergent in sequence between human and cow, for example. The first half of domain C4 (known as C4a) is very nonpolar and contains two partial repeats of length 28 residues that are rich in glycine residues. They are not related to the 29-residue repeat seen in domain C3. Subdomain C4b is clearly basic in character, in contrast to all of the other cytoplasmic domains, which are acidic. A model of the spatial arrangement of desmoglein in the desmosome has been proposed (4).

Figure 1. Comparison of the domain structures of human desmoglein 1 (HDSG1), desmoglein 3 (HDSG3), desmocollin 3 (HDSC3), and *N*-cadherin (NCAD). This illustrates the structural similarities between the classical cadherins and those in the desmosomes. The transmembrane a-helical segment (M) separates the extracellular domains E1 to E4 and the extracellular anchor EA from the intracellular anchor IA and the intracellular domains C1 to C4. Putative calcium-binding domains in the E domains are shown as shaded rectangles. The two desmocollin 3 forms result from alternative splicing. The black rectangle represents 11 amino acids at the *C*-terminal end that are unique to the shorter structure. (From Ref. 5, with permission.)

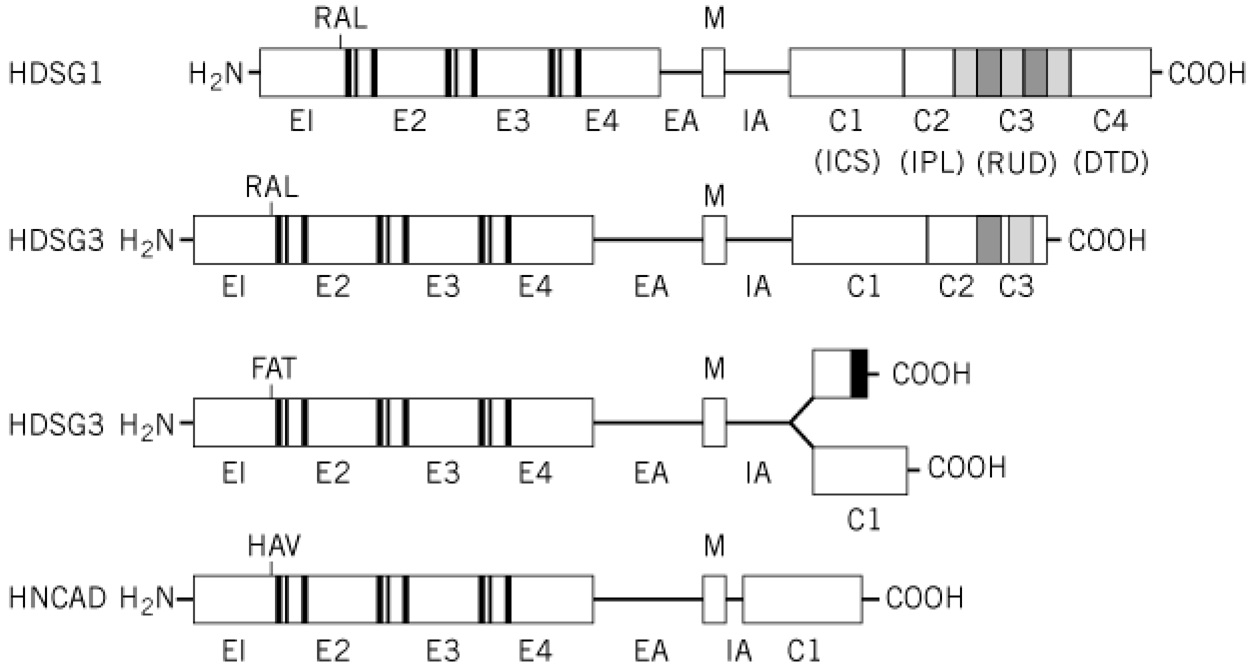

Bibliography

1. J. A. Marrs and W. J. Nelson (1996) Cadherin cell adhesion molecules in differentiation and embryogenesis. Int. Rev. Cytol. **165**, 159–205.
2. M. Overduin, T. S. Harvey, S. Bagby, K. I. Tong, P. Yau, M. Takeichi, and M. Ikura (1995) Solution structure of the epithelial cadherin domain responsible for selective cell adhesion. Science **267**, 386–389.
3. L. Shapiro, A. M. Fannon, P. D. Kwong, A. Thompson, M. S. Lehmann, G. Grubel, J.-F. Legrand, J. Als-Nielsen, D. R. Colman, and W. A. Hendrickson, (1995) Structural basis of cell-cell adhesion by cadherins. Nature (London) **374**, 327–337.
4. L. A. Nilles, D. A. D. Parry, E. E. Powers, B. D. Angst, R. M. Wagner, and K. J. Green (1991) Structural analysis and expression of human desmoglein: a cadherin-like component of the desmosome. J. Cell Sci. **99**, 809–821.
5. A. P. Kowalczyk, T. S. Stappenbeck, D. A. D. Parry, H. L. Palka, M. L. A. Virata, E. A. Bornslaeger, L. A. Nilles, and K. J. Green (1994) Structure and function of desmosomal transmembrane core and plaque molecules. Biophys. Chem. **50**, 97–112.

Suggestions for Further Reading

6. K. J. Green and J. C. R. Jones (1996) Desmosomes and hemidesmosomes: structure and function of molecular components. FASEB J. **10**, 871–881.
7. M. Takeichi (1995) Morphogenetic roles of classic cadherins. Curr. Opin. Cell Biol. **7**, 619–627.
8. O. Huber, C. Bierkamp, and A. Kemier (1996) Cadherins and catenins in development. Curr. Opin. Cell Biol. **8**, 685–691.

Caenorhabditis

Caenorhabditis is a genus of primarily free-living soil nematodes. The free-living species *Caenorhabditis elegans* has become well known after being chosen by Sydney Brenner in the 1960s for a concerted genetic, ultrastructural, and molecular analysis of animal development (1). A few other Caenorhabditis species have been characterized in less detail, largely for comparison, but the findings summarized in this article are for *C. elegans* unless otherwise indicated.

C. elegans was chosen for a variety of features, including its short life cycle and **hermaphroditic** mode of development (facilitating genetic analysis), its anatomical and cellular simplicity (<1000 somatic cells in the adult hermaphrodite), and its transparency and small size (facilitating light microscopy of developing animals and ultrastructural analysis, respectively). Its genome size has turned out to be relatively small as well (100 Mb), making molecular biology convenient. An entire field of *C. elegans* biology has grown out of Brenner's original investigations. As a result of this effort and the relative simplicity of “the worm,” as it is sometimes referred to, *C. elegans* is now the most completely understood metazoan in terms of genetics, ultrastructure, development, and physiology, and it has taken its place with the fruit fly ***Drosophila*** and the laboratory mouse as one of the most important model organisms for research biology (2, 3). Its entire cell lineage from zygote to adult has been determined; its ultrastructure including the complete connectivity of its nervous system has been described in detail; an extensive genetic map has been assembled; and DNA sequencing of its entire genome will be completed in 1998. It is beautifully suited for the genetic approach: identifying **genes** required for any biological process of interest by mutations that affect it, molecularly characterizing these genes after isolation by positional cloning, and eventually studying the biochemical functions of the corresponding gene products. As in all organisms, the genetic control of development and physiology is still only beginning to be understood in *C. elegans*. The rapidly accumulating detailed knowledge of the worm's biology, as well as the recent realization that many developmental and physiological mechanisms are remarkably conserved throughout the animal kingdom, make *C. elegans* a powerful experimental system for investigating a variety of the most important questions in current biological research.

1. General Description

C. elegans inhabits soil in most parts of the world and feeds on soil **bacteria**. The adults are about 1 mm in length, and the two sexes, hermaphrodites and males, are morphologically distinguishable (Fig. 1). The hermaphrodites produce both eggs and sperm and can self-fertilize. Males can mate with hermaphrodites to give cross progeny; hermaphrodites cannot fertilize each other. A hermaphrodite can produce about 300 self progeny, in addition to cross progeny if mated. Embryos begin development in the hermaphrodite uterus and are laid at the gastrulation stage. They hatch as first-stage juveniles (L1 larvae), which as in all nematodes grow through three subsequent larval stages punctuated by molts, before a final molt to the sexually mature adult. The adult reproductive period lasts for about 4 days, after which the animals live for an additional 2 weeks.

Figure 1. Anatomy of hermaphrodite and male *C. elegans* adults. Major structural features mentioned in the text are labe Hermaphrodite. (**b**) Male. (**c**) Hermaphrodite, bright-field photomicrograph. Scale bar 0.1 mm. P, pharynx; I, intestine; C vulva; DG, distal gonad. (**d**) Hermaphrodite, cross section through the anterior, viewed toward the anterior. *d*, *v*, *l*, *r*, dor muscle; h, hypodermis; I, intestine; g, gonad; pc, pseudocoelom; nc, nerve cord. Note the treads (alae) on the left and rig

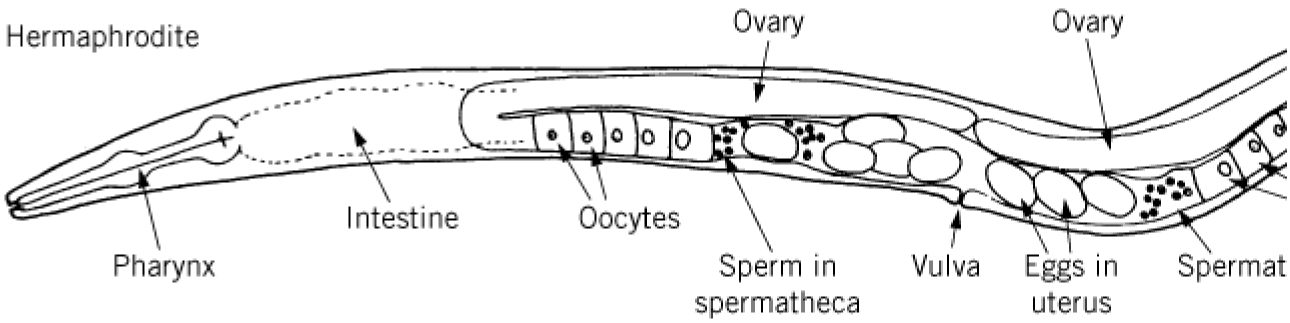

(a)

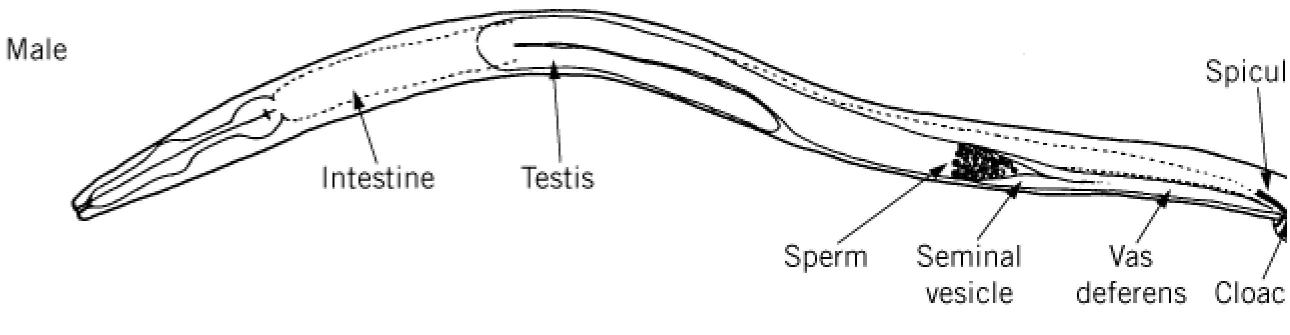

(b)

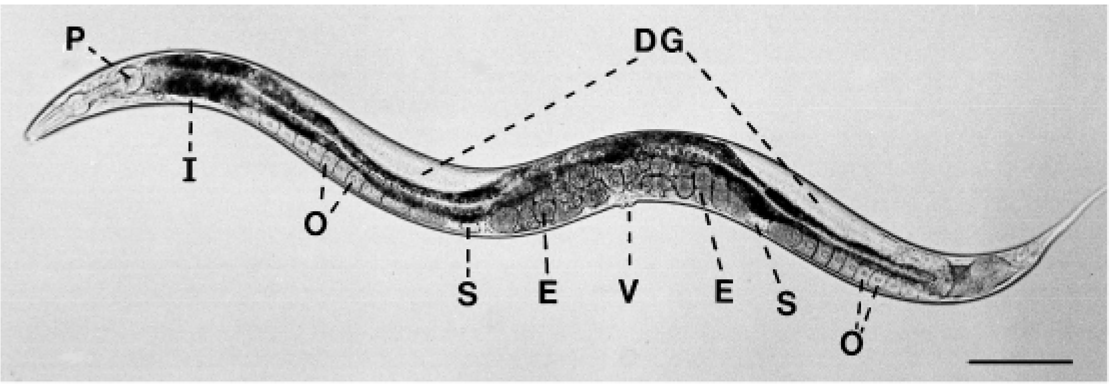

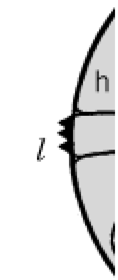

(c)

C. elegans is one of the simplest metazoans and has fixed numbers of **somatic cells**: 959 in the adult hermaphrodite and 1031 in the adult male. In the laboratory it can be cultured conveniently on agar plates spread with *Escherichia coli* bacteria, or in liquid culture when larger quantities are desired for biochemical work. Individual animals can be observed and transferred from plate to plate with a platinum wire “worm pick” under a dissecting microscope, which is sufficient for scoring many mutant phenotypes. Taking advantage of the animal's transparency throughout the life cycle, it is possible to follow individual cells during development at higher magnification using a compound microscope, preferably equipped with Nomarski differential interference-contrast optics (see Microscopy).

2. Genetics and the Genome

C. elegans is **diploid**, with five autosomes (I–V) and a sex chromosome (X). Hermaphrodites are XX and males XO; sex is determined by the X chromosome to autosome ratio. Males arise spontaneously in self-fertilizing hermaphrodite populations at a frequency of about 0.2%, as the result of X chromosome **nondisjunction**.

The haploid genome size of *C. elegans* is 100 Mb, about 10 times that of **yeast**, one-half that of *Drosophila*, and one-thirtieth that of mammals. Based on frequency of predicted coding units in the genomic DNA sequence, which is now nearly complete, the estimated total number of functional **genes** is about 13,000. Over 1000 genetic loci have been identified by mutation following chemical mutagenesis and mapped to the six linkage groups. Positional cloning of mutationally identified genes is facilitated by an extensive physical map of overlapping clones, which is anchored to the genetic map at many locations. The DNA sequence of the entire genome will soon be completely known.

3. Anatomy

C. elegans has the typical nematode body plan (see Nematodes): an outer tube of hypodermis with attached musculature and neurons, surrounding an interior space (the *pseudocoelom*), which contains the gut and, in adults, the gonad (see Fig. 1). The hypodermis secretes a three-layered, **collagenous** cuticle that is shed and replaced at each larval molt (see text below). Four bands of body-wall muscles run the length of the animal. The neuromuscular system bends the body only in the dorsal–ventral direction, so that the animal always lies on one side or the other on a solid surface. Specialized hypodermal cells on each side secrete “treads,” known as *alae*, on which the worm moves. The digestive system consists of a muscular pharynx in the head, which crushes bacteria and pumps them into the intestine, which empties at the anus near the tail. An excretory system controls the hydrostatic pressure on which the worm depends to maintain its body shape.

The entire nervous system of the hermaphrodite consists of only 302 neurons and 56 supporting and glial cells. The major ganglion is the nerve ring at the base of the pharynx, which sends processes down ventral and dorsal nerve cords to a secondary ganglion in the tail. Motor neurons from the cords enervate the body-wall muscles. Sensory neurons extend into the nerve ring from chemoreceptors and touch receptors in the head. Hermaphrodites have specialized neurons that control egg-laying (see text below); males lack these but have additional neurons that provide input from sensory structures in the tail and control male mating behavior.

The hermaphrodite reproductive system is comprised of a bilobed gonad, with one lobe extending anteriorly and one posteriorly from the uterus near the middle of the animal. The gonad consists of a somatic sheath surrounding the germ cells and has several specialized regions. The distal arm of each lobe contains **mitotically** dividing germ-cell **nuclei** in a common **cytoplasm**. The nuclei enter **meiosis** as they move away from the distal tip. The earliest nuclei to mature differentiate into sperm during the fourth larval stage; at the molt to adulthood the germ line switches sex, and subsequent meiotic nuclei are recruited to form **oocytes** as they round the bend into the proximal arm, which contains the oviduct. At the proximal end of the oviduct is the spermatheca, containing stored sperm, through which the oocytes pass and become fertilized on their way to the uterus. A muscular vulva connects the uterus to the outside and serves as the egg-laying apparatus. In the male, the gonad is single lobed and produces only sperm, which are stored in the vas deferens and released through the cloaca in the tail. The fan-shaped male tail is specialized for mating, which is accomplished by deposition of sperm through the hermaphrodite vulva into the uterus, where they move to the spermatheca and compete for oocytes with the resident hermaphrodite sperm.

4. Fertilization and Embryonic Development

Following fertilization, a tough chitinous egg shell forms around the zygote, and embryonic cleavage begins. The spheroidal embryos, about 70 µm in length, are viable if dissected out of the hermaphrodite at this time, but normally they remain in the uterus for about 2 h until the onset of gastrulation, when they are laid through the vulva. Gastrulation is simple; only 53 cells move from the exterior to the interior, but the result is a triploblastic embryo with outer ectodermal precursor cells that will form the hypodermis and nervous system, inner endodermal precursors that will form the gut, and in between a layer of mesodermal precursors that will give rise to muscles and the somatic gonad. By 6 h after fertilization, midway through embryogenesis, the embryo consists of about 600 cells. At this point, cell proliferation essentially ceases and a process of morphogenesis begins which literally squeezes the spheroidal embryo into the shape of a worm as organogenesis proceeds internally and cuticle is formed externally. During this time about 40 cells undergo programmed cell death and are engulfed by neighboring cells. At the end of embryogenesis the worm, about 3.5 times the length of the original embryo, digests the shell from the inside and hatches out of the egg.

The process of **embryogenesis** is essentially invariant at the cellular level. It proceeds by a stereotyped series of **cell divisions** (Fig. 2), whose timing and relative spatial orientations are the same in every embryo. This feature and the transparency of the embryo made it possible for John Sulston and his colleagues to trace out the entire embryonic cell lineage from fertilization to hatching, so that the ancestry of each of the 558 cells in the L1 is known (4). Most cells are born close to their final locations; only about 12 cells undergo long-range migrations during embryogenesis.

Figure 2. Early divisions in the *C. elegans* embryonic cell lineage, showing cells and tissues derived from each of the major branches. The vertical axis shows time after fertilization and total number of cells in the embryo. Horizontal lines indicate times of cell divisions. P_0 through P_4 are germ line cells; the cells named AB, MS, E, C, and D are somatic founder cells for the various branches of the lineage. The number of cells of each different type produced in each branch is indicated. Note that many cells are programmed to die during embryonic development, especially in the AB and MS branches.

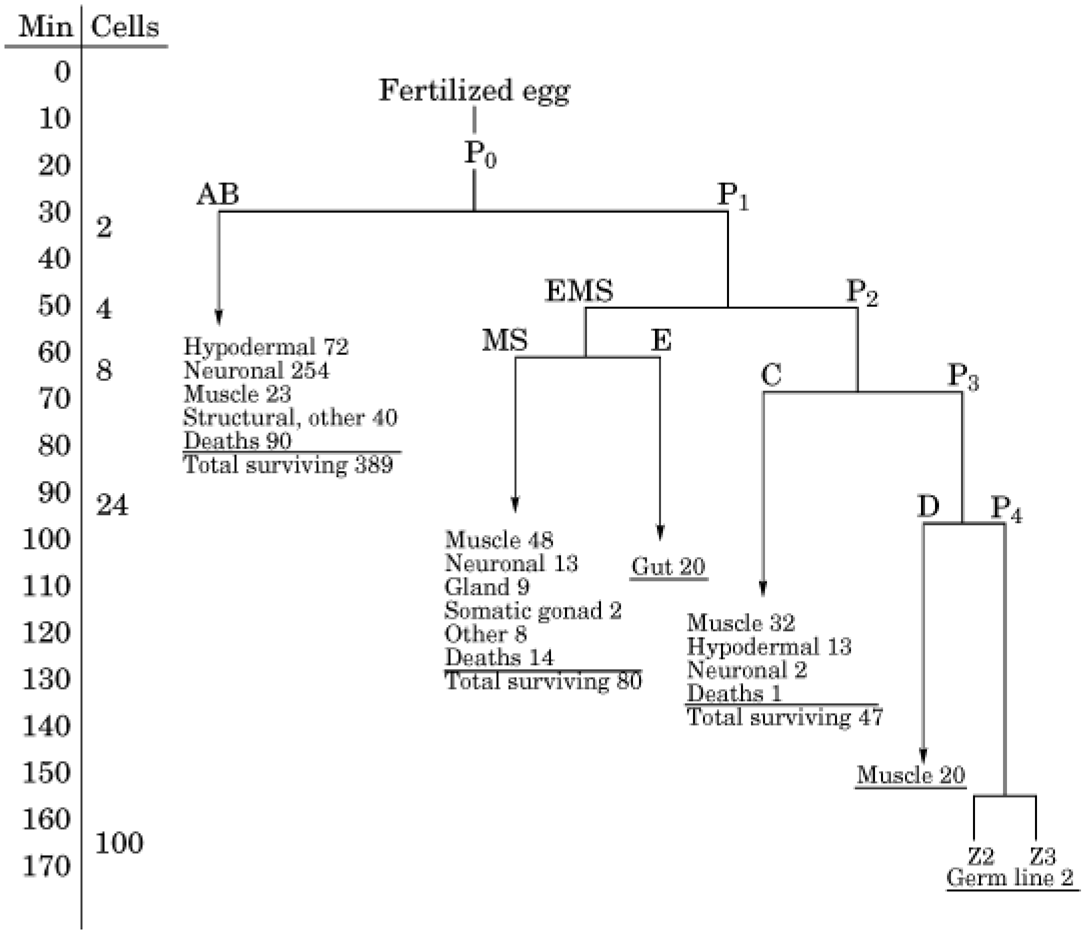

Genetic and molecular analysis of the cleavage stage has revealed that cell fates in the early embryo (Fig. 2) are determined by a combination of maternally derived factors, which segregate asymmetrically to specific cells during cleavage, and cell-signaling mechanisms by which certain cells induce new cell fates in their neighbors. This patterning process appears to proceed by evolutionarily conserved mechanisms that are common to all embryos; for example, the signaling pathways so far known to be employed include several that are also important for insect and vertebrate development, such as the *wingless* (Wnt), and ***Notch*** pathways (5).

5. Larval Development

5.1. Larval Stages

After hatching as an L1, the worm grows through three more larval stages, L2–L4 (Fig. 3), separated by molts at which a new cuticle is secreted by the underlying hypodermis and the old one shed. The newly hatched L1, 250 μm long with 558 cells in the hermaphrodite and 560 in the male, includes functional digestive, neuromuscular, and neurosensory systems and a gonad primordium consisting of two somatic and two germ-line cells. Most of the cells in the L1 divide no further during larval development. However, 55 are *blast* cells that undergo additional divisions during larval development to produce, primarily, the adult reproductive structures and the neurons that control them: the hermaphrodite and male gonads, the vulva and egg-laying muscles in the hermaphrodite, and the sex muscles and specialized tail mating structures in the male. Additional motor neurons are also produced in the nerve cords for finer control of the body-wall muscles. As in the embryo, the invariance of these processes, the transparency of all stages, and the small number of cells involved made it possible to map the larval cell lineages in both sexes from L1 to adulthood (6). Consequently, the entire cell ancestry of *C. elegans* is known, from fertilized egg to adult.

Figure 3. The *C. elegans* life cycle. Clock circle indicates hours of development after fertilization at 25°C. Eggs containing developing embryos are laid at about 2 h. The L1 larvae, hatching at about 14 h, undergo four more molts at the times indicated as they grow to adulthood. See text for further explanation.

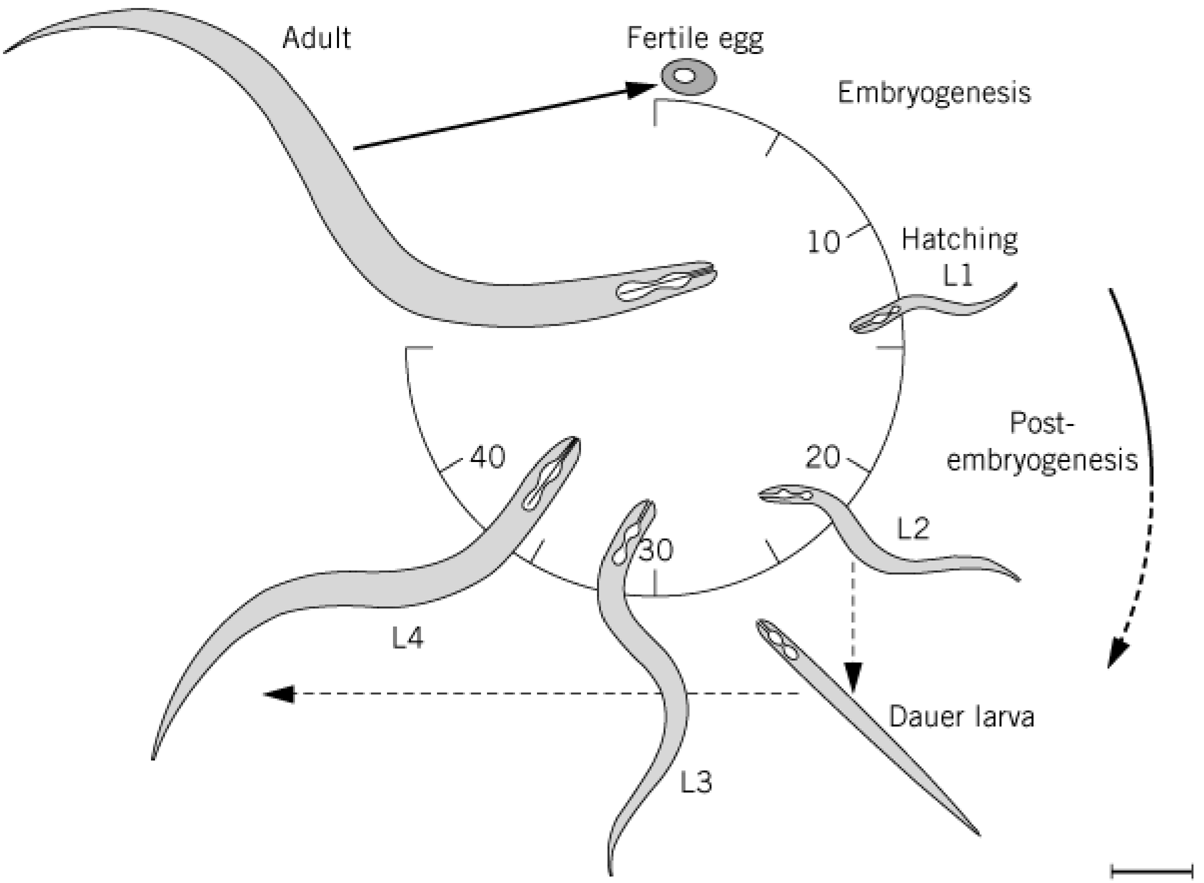

5.2. Cell Interactions during Larval Development

Elaboration of larval structures involves cell interactions, again occurring by evolutionarily conserved signaling pathways such as those involving homologues of Notch, Wnt, epidermal growth factor (EGF), and transforming growth factor (TGF)-b-superfamily ligands as the signaling molecules. Application of the genetic approach to the process of vulval development, for example, has revealed details of a ***ras***-based pathway by which the developing gonad signals underlying hypodermal cells to differentiate using an EGF-like ligand. The molecular components are very similar to those of *ras* pathways found in mammalian cells, in which conversion of *ras* to an **oncogene** causes a variety of cancers, and the *C. elegans* pathway has become an important model system for cancer research.

Cell interactions during larval development also include guidance cues by which several cells, including the growing axonal processes of motorneurons and the distal tip cells of the enlarging hermaphrodite gonad, find their way along the basement membrane of the pseudocoelom en route to their final destinations. Again, application of the genetic approach in *C. elegans* has shown that this process is accomplished by a conserved mechanism: The so-called *netrin* ligands and their **receptors** that guide these cells in the worm are remarkably similar to the molecules that guide axonal growth from the neural floor plate to the spinal cord in developing avian and mammalian embryos, making *C. elegans* a potentially useful model system for study of nerve regeneration.

The cell divisions and molts in larval development occur in a precisely timed sequence. Again, application of the genetic approach has identified many of the genes in the timing mechanism and is providing new information on how developmental clocks function.

5.3. The Dauer Larva

Like most free-living nematodes, *C. elegans* can molt to an alternative form of the L3, called a *dauer larva* (German for "enduring larva") when conditions are unsuitable for reproduction. Dauer larvae, often simply called dauers, do not feed, are relatively resistant to drying, and can live for up to a year if desiccation is prevented. If conditions improve, they can molt to the L4 stage and resume the normal developmental pathway, with no change in subsequent lifespan. Dauer development is triggered by lack of food and overcrowding, signaled by a pheromone of unknown nature that stimulates chemosensory structures in the head. This process is of interest for at least two reasons. First, the signaling mechanism involves homologues of ligands, receptors, and downstream components of the evolutionarily conserved TGF-b pathway, which is of widespread importance but not fully understood in mammalian development. Second, entry into the pathway of dauer development appears to turn off genes that normally limit the *C. elegans* lifespan to less than 3 weeks, allowing the dauer to live much longer. This finding, and the experimentally convenient short normal lifespan, make *C. elegans* an exciting model system for studying genetic control of aging, which is under active investigation (7).

6. Behavior and the Nervous System

C. elegans can move forward or backward and change direction, by coordinated flexing of its body-wall muscles. It is touch-sensitive, moving forward in response to a touch on the tail and backward in response to a touch on the head. Chemosensors in the head, connected by sensory neurons to the ring ganglion, can detect a variety of ions as well as volatile odorants and elicit either an attractive or repulsive response (see Chemotaxis). For example, *C. elegans* is attracted to Na^+ , K^+ , Cl^- , and several alcohols and ketones; it is repelled by Cu^{2+} , acid pH, D-tryptophan, and benzaldehyde. Males are attracted by a pheromone of unknown nature that is produced by hermaphrodites. Although some of its relatives have photoreceptors, *C. elegans* does not appear to respond to light or use it as a sensory cue. It does, however, sense and respond to temperature and will move to a preferred point in a temperature gradient.

Is an animal with only 302 neurons capable of learning? Simple conditioning experiments suggest that *C. elegans* not only can habituate to several stimuli, but also is capable of associative learning, that is, learning to use a normally neutral stimulus to predict the arrival of a second more significant stimulus. For example, if presence of food is paired with one of two equally attractive ions and absence of food with the other during conditioning, the conditioned animals will preferentially move toward a source of the paired ion when tested subsequently in the absence of food, and this preference lasts up to 7 h after training. In addition, *C. elegans* not only can sense a temperature gradient, but also can "remember" the temperature at which it has previously fed and move to the same temperature when placed in a new gradient without food. The genetic approach should allow the genes involved in learning and memory in *C. elegans* to be identified and the mechanisms of the proteins they encode to be elucidated.

C. elegans does not show obvious circadian rhythms, but it exhibits much higher frequency (ultradian) rhythms, such as a regular defecation cycle that is repeated about once every 45 s when the animal is feeding, regardless of the temperature. As in other organisms, the mechanisms of the temperature-compensated molecular clocks that control such cycles (like the human heartbeat) are just beginning to be understood. Application of the genetic approach to cyclical behaviors in *C. elegans* is identifying the genes and proteins that control ultradian rhythms.

7. Current Investigation and Online Information about *C. elegans*

Knowledge about *C. elegans* genetics, development, and behavior is accumulating rapidly in several areas of currently exciting biological research, some of which are mentioned above. These include mechanisms of pattern formation in development, origins of left–right asymmetry in animal body plans, cell fate determination, programmed cell death, cell migration and guidance, developmental timing mechanisms, physiological sensory mechanisms, organization of animal genomes, and animal evolution.

As a supplement to the references listed below, much current knowledge of *C. elegans* is accessible electronically on the World Wide Web. A convenient access site can be found at `http://eatworms.swmed.edu`.

Bibliography

1. S. Brenner (1974) Genetics **77**, 71–94.
2. W. B. Wood et al. (eds.) (1988) *The Nematode Caenorhabditis elegans*, Cold Spring Harbor Laboratory Press, Cold Spring Harbor, NY.
3. D. L. Riddle, T. Blumenthal, B. J. Meyer, and J. R. Priess (eds.) (1997) *C. elegans II*, Cold Spring Harbor Laboratory Press, Cold Spring Harbor, NY.
4. J. Sulston, E. Schierenberg, J. White, and J. Thomson (1983) Dev. Biol. **100**, 64–119.
5. R. Schnabel and J. R. Priess (1997) In *C. elegans II* (D. L. Riddle, T. Blumenthal, B. J. Meyer, and J. R. Priess, eds.), Cold Spring Harbor Laboratory Press, Cold Spring Harbor, NY, pp. 361–382.
6. J. Sulston and H. Horvitz (1977) Dev. Biol. **56**, 110–156.
7. C. Kenyon (1997) In *C. elegans II* (D. L. Riddle, T. Blumenthal, B. J. Meyer, and J. R. Priess, eds.), Cold Spring Harbor Laboratory Press, Cold Spring Harbor, NY, pp. 791–813.

Suggestions for Further Reading

8. S. Brenner (1974) The genetics of *Caenorhabditis elegans*. Genetics **77**, 71–94. (The classic paper in which Brenner first presented his rationale, descriptions of morphological and behavioral mutants, and preliminary genetic analysis of *C. elegans*.)
9. D. L. Riddle, T. Blumenthal, B. J. Meyer, and J. R. Priess (eds.) (1997) *C. elegans II*, Cold Spring Harbor Laboratory Press, Cold Spring Harbor, NY. (The sequel to the previous reference book. A good up-to-date summary of current knowledge about *C. elegans*.)
10. J. Sulston and H. Horvitz (1977) Post-embryonic cell lineages of the nematode *Caenorhabditis elegans*. Dev. Biol. **56**, 110–156. (The first extensive cell lineaging of *C. elegans*, describing all the cell lineages during larval development.)
11. J. Sulston, E. Schierenberg, J. White, and J. Thomson (1983) The embryonic cell lineage of the nematode *Caenorhabditis elegans*. Dev. Biol. **100**, 64–119. (The monumental paper in which Sulston and his co-workers published the complete embryonic cell lineage of *C. elegans*.)
12. W. B. Wood (1988) In *The Nematode Caenorhabditis elegans* (W. B. Wood and the community of *C. elegans* researchers, eds.), Cold Spring Harbor Laboratory Press, Cold Spring Harbor, NY, pp. 1–16. (The introductory chapter to a useful general reference on *C. elegans*.)

Caged ATP

The synthesis of caged ATP (caged ADP and caged phosphate) and many of the properties that make these reagents useful in a variety of biological applications were first published in 1978 (1). The driving force for the development of such a reagent was the desire to be able to introduce ATP rapidly (and synchronously) at sites of biological interest at a desired time. A pulse of ATP would be released by **light activation** and would then initiate the processes being studied (Fig. 1). In contrast to affinity labeling, here the ATP analogue should not bind to its site prior to activation and ATP is released freely in solution. The strategy employed was an approach that had previously been used in synthetic organic chemistry (ie, photodeprotection). In the chemical applications, a desired functionality in a molecule was modified and protected from a variety of reagents and conditions during a multistep synthesis, to be deprotected at a later step by a light-activated process. In biological applications, the caged substrates are "protected" from their receptor, enzyme, or binding site by the chromophoric moiety, and following the pulse of light they are released to their biological target.

Figure 1. Basis of photorelease of a caged substrate. The biological ligand (L) or substrate is rendered inactive by the attachment of a photocleavable chromophore (x). Following photoactivation the ligand is released accompanied by the modified chromophore, or photofragment.

$$\mathrm{L{-}X} \xrightarrow{h\nu} \mathrm{L + X'}$$

The properties of molecules appropriate for the study of biological systems are subject to more constraints than those used in synthetic organic chemistry. Much of the subsequent work on various caged ATP molecules and other caged compounds has been aimed at refining or improving their basic properties to expand the areas of application or overcome a particular limitation. The design requirements for a caged ATP are illustrative of the needs of any caged biological ligand or substrate (2).

The basic requirements for a biologically useful caged ATP (and for most other caged compounds) are as follows: (i) The activating light must be at wavelengths long enough to avoid damage to biological material (usually greater than 300 nm). (ii) The photorelease process must be as efficient as possible; that is, the quantum yield (ratio of molecules of product obtained to molecules of caged compound excited) must be as high as possible. (iii) The photorelease process should be as rapid as possible, relative to the rate of the process of interest; this has been achieved in the tens of microseconds to millisecond range, at normal temperatures and pH values. (iv) The photoreleased fragment, which usually is the modified chromophore, should not be harmful to biological materials (see text below). (v) The **absorbance** of the caged compound should be reasonably high at the exciting wavelength or wavelength range. Initially it was thought that too high an absorbance might lead to nonuniform release of substrate across the depth of an illuminated sample. Interestingly, for the recent application of multiphoton excitation, very high absorbances are an advantage. (vi) Prior to photolysis, the caged substrate should neither bind to nor interact with the biological material of interest. In many respects, the first caged ATP reported and subsequently used (but the second synthesized) fulfilled many of these requirements. In a variety of systems, one or other of these properties has been less than ideal, and this has led to various variations on the original structure in attempts to provide an improved caged ATP.

1. Synthesis and Photochemical Properties of Caged ATP

The initial synthesis of caged ATP was based on a strategy of first preparing caged phosphate and then coupling this to ADP. This had the advantage that the photochemical lability, quantum yield, and so on, could be first characterized, using caged phosphate and the readily assayed free substrate, inorganic phosphate (1). This route suffered from the following disadvantages: (i) It was less direct than was desirable to achieve a gamma ^{32}P-labeled caged ATP for a variety of **phosphorylation** studies, and (ii) it was not generally applicable to a wide range of phosphate-bearing biological ligands that might be desirable to cage. It would be better to have a more universal caging moiety that could be readily attached to the nucleotide or other organophosphates. These disadvantages were overcome by the development of a synthesis by Trentham and co-workers, who were able to attach the protecting 2-nitrobenzyl-based chromophore directly to the terminal phosphate of ATP, using a diazoprecursor (3). This was based on an approach that had been used by others to prepare a photosensitive cyclic AMP phosphotriester analogue (4). This method was used to prepare a wide array of caged phosphorylated biological ligands, including GTP, ADP, inositol trisphosphate, and so on (3).

The quantum yield for the first successful caged ATP was 0.54 and has not been bettered by subsequent analogues. The first caged ATP that was synthesized, the primary 2-nitrobenzyl analogue, yielded on photolysis some ATP, but only very low levels, even though photolysis was complete. It was hypothesized that this was due to a reaction between ATP and the released photofragment (2-nitrosobenzaldehyde), so that a chemically modified ATP resulted (1). The 2-nitrophenylethyl analogue (from the secondary benzyl alcohol) then became the molecule of choice, because photolysis yielded the less reactive 2-nitrosoacetophenone and free ATP in high yield (Fig. 2). This is the caged ATP that has been used most frequently in biological studies. The absorbance properties of caged ATP are simply the sum of the spectra of the 2-nitrobenzyl moiety and of ATP. This results in a long tail of absorbance that extends to above 350 nm. This has enabled illumination above 300 nm to be employed (using lasers or flash-lamps) so that photodamage due to absorption by most biological samples is avoided.

Figure 2. Photolysis of caged ATP. Photolysis of caged ATP produces a proton, free ATP, and the photofragment, 2-nitrosoacetophenone.

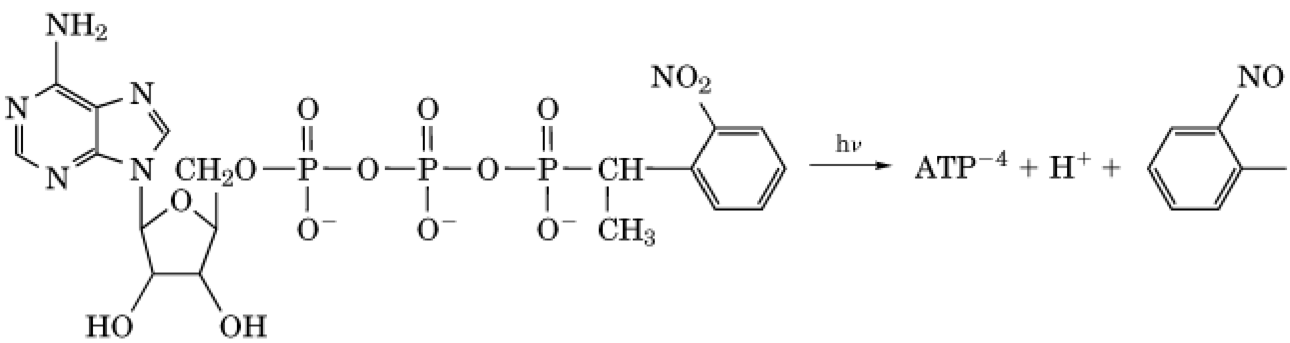

2. Mechanism and Kinetics of Photorelease

Although the earliest studies showed that ATP release could be achieved in a subsecond time frame, ideas about the kinetics of the release process and the likely mechanism were initiated by the report of McCray et al. in 1980 (5). From this work it was apparent that the rate of release of ATP from caged ATP was pH-dependent and in the millisecond time range.

Importantly, it was also pointed out in this work that there was a chromophoric intermediate on the reaction pathway, identified tentatively as an aci-nitro intermediate. The intermediacy of this type of chromophore has proven useful in later mechanistic studies of the photorelease of caged substrates, because it is central to almost all photorelease processes in which the protecting moiety is a 2-nitrobenzyl residue. Another tool that has been useful in mechanistic studies, and profitably used by Trentham and colleagues, is the reaction of the photoreleased nitrosoketone with thiol groups. This reaction had been initially employed by Kaplan et al. (1) to protect biological samples against any damaging effects of the photofragment, because it was known that nitrosoketones react readily with thiols. It was shown that the inhibition of the Na,K-ATPase enzyme due to the actions of the photofragment could be prevented by the simultaneous presence of **dithiothreitol** (DTT) or similar reagents. Furthermore, the protecting thiol had to be present in amounts at least stoichiometric with the released photofragment. In many subsequent applications, it has become routine to include reduced glutathione or DTT in the reaction media to mop up the released photofragment. Trentham and colleagues (6) used the rapid rate of this reaction to examine the release rates of the photofragment. This proved valuable because with caged ATP, as with many photoreleased biological substrates, it is often difficult to identify a biological process that is sufficiently fast to be used unambiguously as a bioassay to determine the photorelease rate of substrate. It should be emphasized, however, that for all new caged substrates it is essential to measure the release rate of the photoproduct of interest and not merely the rate of decay of an intermediate on the release pathway. There have been several reports of biphasic decay of putative aci-nitro intermediates when their breakdown was followed using transient ultraviolet spectroscopy (7, 8).

The most recent estimates (obtained from time-resolved infrared spectroscopy) of the formation of free ATP following the photolysis of caged ATP are about 220 s^{-1} at pH 7 and 22°C, a rate that is the same as the aci-nitro anion intermediate decay rate (9). An outline of the steps involved in the photolysis pathway are shown in Figure 3.

Figure 3. Scheme of breakdown of caged-ATP following excitation. The release rate of ATP is controlled by dark reactions that follow photoexcitation and relaxation to ground states. A detailed study of the products and intermediates has been made using time-resolved infrared spectroscopy and isotopomers of caged ATP (6).

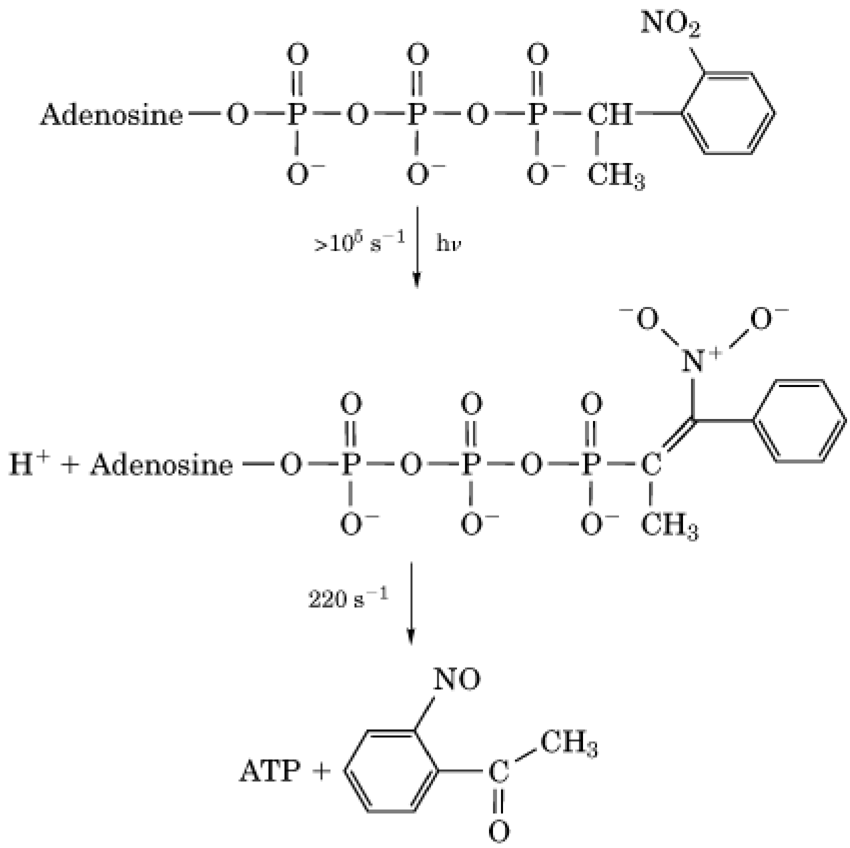

3. Other Caged ATP Structures

The most familiar caged ATP is P^3-(1-(2-nitrophenyl)ethyl) adenosine 5′-triphosphate. Variations on the basic theme have been made in the hope of increasing the long wavelength absorbance of the molecule or of speeding the rate of release. Unfortunately, no molecule yet reported has achieved this aim while simultaneously maintaining the relatively high quantum yield. Most attempts have involved variations in the chromophore, while maintaining the same nitrobenzyl photochemical cleavage mechanism (10). Recently potentially useful alternative photochemistries have begun to be exploited, but as yet no generally useful molecule has emerged (11-13).

4. Biological Applications of Caged ATP

The two areas where caged ATP has been used most extensively are in studying the mechanism of **active transport** by **ion pumps** and in the mechanism of muscle contraction and its regulation. In single turnover studies of the Na,K-ATPase (see text below), Forbush showed that caged ATP did in fact bind with low affinity to the enzyme prior to photolysis (14). This leads to extra complications in kinetic modeling of events following photolysis. Subsequently, similar effects have been noted in muscle fibers (15). Such observations suggest that a caged ATP with a bulkier chromophore might reduce the pre-photolysis binding.

5. Studies on Ion Pumps

The ion pumps are P-type ATPases that couple the transport of ions against their electrochemical potential gradient to the hydrolysis of ATP. This family of membrane proteins includes the Na pump or Na,K-ATPase, the Ca pump [from intracellular membranes (SERCA) or plasma membranes (PMCA)], **proton pumps** from a variety of organisms such as yeast, bacteria, and so on, and a range of heavy metal pumps that transport Cu, Cd, Ni, and so on, across cellular membranes throughout the animal and plant kingdom (16). The studies on ion pumps that have used caged ATP illustrate well several of the different advantages of this experimental strategy. These proteins carry out a series of biochemical transformations that are thought to accompany the transport of cations across the membrane. These transformations arise from the intermediate involvement of a phosphoenzyme, which is formed by transferring the terminal phosphate of ATP to the protein at an early step in the cycle, and from the protein to water in a later step. These kinase and **phosphatase** activities are linked to ion binding, translocation, and ion release steps (17). In order to probe the cation activation of some of these processes, it was necessary in the case of the Na pump to be able to initiate the pump cycle in a sealed system. This was required because the activating and inhibitory cations have very asymmetric effects, depending on whether they act at the extracellular or intracellular surface. The strategy employed was to trap caged ATP within resealed human erythrocyte ghosts. The extracellular medium could then be altered at will, and the Na pump process could be initiated by illumination of the ghost suspension and release of intracellular ATP from caged ATP. This enabled characterization of the side effects of activating and inhibiting cations on the transphosphorylation reactions under genuine initial rate conditions (18, 19). The essential properties of the photorelease strategy here were the stability of caged ATP during experimental procedures, until ultraviolet irradiation, when ATP could be released in good yield synchronously inside the cells in suspension. The possibility of releasing ATP from caged ATP in a rapid synchronous fashion within an ordered structure was also exploited in structural studies of the Ca pump in oriented multilayers where diffraction before and after the release of ATP from caged ATP showed movements of the protein mass relative to the membrane structure during the reaction cycle (20). Such studies would not have been possible without the photorelease approach.

Ion pumps transfer charge during their reaction cycle across cell membranes; and electrophysiological measurements of such movements, along with their analysis, have been a central area of study. In recent years, Bamberg and co-workers (21) and Apell and co-workers (22) have initiated the use of caged ATP in a novel experimental system to analyze the mechanistic consequences of these phenomena in a variety of ion pumps. These workers have used black lipid membranes and have either attached or fused to them biomembrane fragments or vesicles containing ion pumps. Following the rapid, synchronous release of ATP from caged ATP in the medium bathing the membranes, the current-carrying and charge translocating steps can be analyzed with a conventional electrophysiological measuring system (23, 24). Such studies have probed the basis of the electrogenic nature of the Na pump and of the electrically neutral basis of the gastric proton pump, for example (25). Recent studies have dissected out the electrical properties of the bacterial active K transporter, the Kdp-ATPase of *Escherichia coli* (26).

5.1. Regulation and Control of Muscle Contraction

An adequate understanding of the mechanism of muscle contraction can only be achieved from experiments in a fairly intact and complex tissue. This is because the structure of the muscle fiber and its organization is an inherent feature of its function. The sliding filament model for the molecular basis of muscle contraction is the prevailing paradigm in this field, and its central feature is this relationship (27, 28). Thus it is necessary to be able to perform high-resolution kinetic studies in an ordered array of macromolecules. Recent efforts have been aimed at understanding the precise steps in the ATP hydrolysis cycle carried out by myosin that lead to the generation of force during contraction. Caged ATP has found application in detailed studies on the kinetics of ATP hydrolysis, structural changes in the fiber organization associated with contraction and relaxation (at the macroscopic and molecular levels), spectroscopic measurements on muscle fibers, and the process of relaxation associated with Ca pumping by the sarcoplasmic reticulum. Studies in all these areas have received considerable impetus by the introduction of the photorelease strategies. It has been shown that it is possible to photorelease ATP (or other substrates) in chemically skinned muscle fibers in the millisecond time range and to cause the synchronized initiation of biochemical processes that produce contraction (or relaxation) in the bundle of fibers (29, 30). Prior to this technology, such experiments were limited by the diffusional delays that were inherent in mechanically adding substrate and allowing it to diffuse into the fiber to its site of action. Initial studies that employed this approach to analyze the kinetics of the mechanical processes have now been greatly extended; by using covalently attached chromophoric reporters or paramagnetic reporters, the kinetics of conformational changes in the myosin protein can be monitored (31, 32). As well as such structural studies, it has also been possible to carry out time-resolved diffraction studies of fibers in a synchnotron beam prior to and following the release of caged ATP within the fiber (33, 34). These applications use the highly ordered skeletal muscle system to understand the basis of muscle contraction and relaxation. In smooth muscle, the contractile system has evolved to a highly complex level of cellular regulation, and many signal transducing systems and effectors play a role in regulating smooth muscle activity (35). In this area, the photorelease of caged ATP (and a variety of second messengers) continues to be a highly fruitful strategy. Recent studies by the Somlyos and their group provide a wide range of applications of this technology to the smooth muscle system (36, 37).

5.2. Other Systems

Since 1980 to the present time (early 1999) there have been more than 200 articles published using caged ATP, and many more using related substrates. These have extended from difference Fourier structural determinations of proteins with or without bound substrates (38, 39), to the cellular effects of occupancy of receptors (40). Structural biology of macromolecules, especially proteins, continues to provide enormous insights into molecular biological processes, and it is in this area that several interesting applications have great potential. The possibility of obtaining not merely a static picture of a protein at atomic resolution, but also one that contains dynamic information, is enticing. The accessibility of high-intensity radiation sources and a revival of interest in the Laue Diffraction method have made fast X-ray crystallography studies an attainable goal. The idea that such measurements could be made with protein crystals before and after laser-induced release of caged substrates within a crystal has received recent attention; and although many of the technical difficulties (uniformity of release, fate of photofragment, local heating effects) have not been overcome, this approach offers great promise for the future (41, 42). The number of physiological systems that have begun to be probed using caged ATP continues to increase; recent additions to this group include L-type Ca channel modulation (43), single kinesin molecules in optical traps (44), ATP-sensitive K channels in cholinergic interneurons (45), sea-urchin sperm **flagella** motility (46), and limulus photoreceptors (47).

6. Summary

The introduction of the photorelease strategy that followed the description of caged ATP has now been extended to a wide array of biological substrates, including nucleoside phosphates, cyclic AMP, cyclic GMP, protons, Ca^{2+}, Mg^{2+}, peptides, inositol phosphates, sugars, amino acids, neurotransmitters, toxins, and so on. In almost all cases, the photochemical process has the same basis as the original caged ATP strategy; along with a wide array of biological substrates, the approach can now be employed to probe systems that range in complexity from single protein crystals to brain slices.

Bibliography

1. J. H. Kaplan, B. Forbush III, and J. F. Hoffman (1978) Biochemistry **17**, 1929–1935.
2. G. P. Hess (1999) (this encyclopedia).
3. J. W. Walker, G. P. Reid, J. A. McGray, and D. R. Trentham (1988) J. Am. Chem. Soc. **110**, 7170–7177.
4. J. Engels and E.-J. Schlaeger (1977) J. Med. Chem. **20**, 907–911.
5. J. A. McCray, L. Herbette, T. Kihura, and D. R. Trentham (1980) Proc. Natl. Acad. Sci. USA **77**, 7237–7241.
6. A. Barth et al. (1997) J. Am. Chem. Soc. **119**, 4149–4159.
7. J. E. T. Corrie (1993) J. Chem. Soc., Perkins Trans **1993**, 2161–2166.
8. G. C. R. Ellis-Davies, J. H. Kaplan, and R. J. Barsotti (1996) Biophys. J. **70**, 1006–1016.
9. A. Barth et al. (1995) J. Am. Chem. Soc. **117**, 10311–10316.
10. J. F. Wootton and D. R. Trentham (1989) NATO ASI Series C **272**, 277–296.
11. J. E. Baldwin et al. (1990) Tetrahedron **46**, 6879–6884.
12. R. S. Givens et al. (1993) J. Am. Chem. Soc. **115**, 6001–6012.
13. J. E. T. Corrie and D. R. Trentham (1992) J. Chem. Soc., Perkins Trans I, 2409–2417.
14. B. Forbush III (1984) Proc. Natl. Acad. Sci. USA **81**, 5310–5314.
15. J. Sleep, C. Hermann, T. Barman, and F. Travers (1994) Biochemistry, **33**, 6038–6042.
16. S. Lutsenko and J. H. Kaplan (1995) Biochemistry **34**, 15607–15613.
17. J. H. Kaplan (1985) Annu. Rev. Physiol. **47**, 534–544.
18. J. H. Kaplan and R. J. Hollis (1980) Nature **288**, 587–589.
19. J. H. Kaplan (1982) J. Gen. Physiol. **80**, 915–937.
20. D. Pascolini et al. (1988) Biophys. J. **54**, 679–688.
21. K. Fendler, E. Grell, M. Haubs, and E. Bamberg (1985) EMBO J. **4**, 3079–3085.
22. R. Borlinghaus, H.-J. Apell, and P. Lauger (1987) J. Membr. Biol. **97**, 161–178.
23. E. Bamberg, H.-J. Butt, A. Eisenrauch, and K. Fendler (1993) Q. Rev. Biophys., **26**, 1–25.
24. I. Wuddel and H.-J. Apell (1995) Biophys. J. **69**, 909–921.
25. M. Stengelin, K. Fendler, and E. Bamberg (1993) J. Membr. Biol. **132**, 211–227.
26. K. Fendler, S. Drose, K. Altendorf, and E. Bamberg (1996) Biochemistry, **35**, 8009–8017.
27. A. F. Huxley and R. Niedergerke (1954) Nature **173**, 971–973.
28. H. E. Huxley and J. Hanson (1954) Nature **173**, 973–976.
29. Y. E. Goldman, M. G. Hibberd, J. A. McCray, and D. R. Trentham (1982) Nature **300**, 701–705.
30. E. Homsher and N. C. Millar (1990) Annu. Rev. Physiol. **52**, 875–896.

31. J. W. Tanner, D. D. Thomas, and Y. E. Goldman (1992) J. Mol. Biol. **223**, 185–203.
32. C. L. Berger, F. C. Svensson, and D. D. Thomas (1989) Proc. Natl. Acad. Sci. USA **86**, 8753–8757.
33. K. J. V. Poole, G. Rapp, Y. Maeda, and R. S. Goody (1988) Adv. Exp. Med. Biol. **226**, 391–404.
34. K. Horiuti et al. (1994) J. Biochem. **115**, 953–957.
35. A. P. Somlyo and A. V. Somlyo (1994) Nature **372**, 231–236.
36. A. P. Somlyo and A. V. Somlyo (1990) Annu. Rev. Physiol. **52**, 857–874.
37. B. Zimmerman et al. (1995) J. Biol. Chem. **270**, 23966–23974.
38. A. J. Scheidig et al. (1995) J. Mol. Biol. **253**, 132–150.
39. C. Raimbault et al. (1997) Eur. J. Biochem. **250**, 773–782.
40. G. D. Housley, N. P. Raybould, and P. R. Thorne (1998) Hear. Res. **119**, 1–13.
41. J. Hadju and L. N. Johnson (1990) Biochemistry **29**, 1669–1678.
42. I. Schlichting et al. (1990) Nature **345**, 309–314.
43. B. O"Rourke, P. H. Backx, and E. Marban (1992) Science **257**, 245–248.
44. M. Higuchi, E. Muto, Y. Inoue, and T. Yanagida (1997) Proc. Natl. Acad. Sci. USA, **94**, 4395–4400.
45. K. Lee, A. K. Dixon, T. C. Freeman, and P. J. Richardson (1998) J. Physiol. **510**, 441–453.
46. T. Tani and S. Kamimura (1998) J. Exp. Biol. **201**, 1493–1503.
47. M. N. Faddis and J. E. Brown (1992) J. Gen. Physiol. **100**, 547–570.

Calcium Signaling

Calcium ion is an important second messenger involved in cell signaling and signal transduction. Most calcium in cells is sequestered in intracellular vesicles, the endoplasmic reticulum (ER) or mitochondria, where it is stored for release when needed. Small, localized increases in calcium result from its regulated release from the ER, which is produced by inositol trisphosphate, IP_3. IP_3 is produced by the **hormone**-dependent hydrolysis of phosphoinositides, to produce **inositol phosphates**, including IP_3. The IP_3 binds to a specific ER protein, a specialized **calcium channel** with four identical subunits, each with a single membrane-spanning segment and a single IP_3-binding site (1). The binding of IP_3 to this receptor results in a stereospecific release of calcium from the ER.

IP_3-sensitive calcium channels are expressed ubiquitously in tissues. However, the process of regulated calcium release is most tightly regulated in endocrine and neuronal cells, and it is often involved in coupling stimulus to secretion, which is usually a calcium-dependent process. Calcium release from the ER is oscillatory in nature. Increases in intracellular calcium are modulated not by increases in the amount of the ion released, but instead by the frequency of the oscillations. This may explain why the release of some hormones is pulsatile.

One of the critical targets in calcium signaling is CAM kinase, a multigene family of protein kinases that are sensitive to regulation by calcium/calmodulin. There are at least four members of this protein kinase family, with differences in distribution and substrate specificity. CAM kinases appear to be especially critical to modulation of signaling in the central nervous system (2).

Bibliography
1. M. J. Berridge (1993) Nature **361**, 315–325.
2. P. I. Hanson and H. Shulman (1992) Annu. Rev. Biochem. **61**, 229–601.

Calcium-Binding Proteins

Calcium-binding proteins (CaBPs) are a key component linking the inorganic and organic systems that produce biological activities. Calcium is one of the most abundant inorganic elements in nature and is ubiquitous throughout biology, playing roles at the organismal, cellular, and molecular levels. Calcium is an essential component of shells and bones, where it is essentially deposited in crystals to create macroscopic support structures. At the cellular level, Ca^{2+} is one of the crucial currencies of most living organisms, acting as a second messenger in a wide range of key intracellular and extracellular systems. Calcium-binding proteins play important roles in mediating each of these effects. These proteins can be grouped into four primary categories: (*1*) intracellular proteins involved in Ca^{2+}-mediated signal transduction, (*2*) enzymes, (*3*) extracellular cell surface and extracellular matrix proteins, and (*4*) proteins containing g-carboxyglutamic acid (Gla) residues. Although a variety of structural motifs bind Ca^{2+} , all involve oxygen atoms of the protein backbone or side chains, reflecting the intrinsic affinity of Ca^{2+} for oxygen atoms.

1. Intracellular Calcium-Signaling Proteins

1.1. EF-Hand Calcium-Binding Proteins

This family is the most extensively studied class of CaBPs. These proteins are characterized by a highly conserved helix–loop–helix motif termed the EF-Hand Motif, which consists of a 12-residue Ca^{2+}-binding loop flanked by two alpha-helices. Almost all EF-hand CaBPs are composed of pairs of EF-hands. This pairing of Ca^{2+}-binding sites is presumed to stabilize the protein conformation, increase the Ca^{2+} affinity of each site over that of isolated sites, and provide a means for cooperativity in Ca^{2+} binding. The cooperativity between sites allows for an “all or nothing” response to Ca^{2+}-binding, which is crucial for the function of these CaBPs as intracellular Ca^{2+} sensors.

Calmodulin and troponin C are the best known members of this family of CaBPs. They each have two largely independent domains connected by a flexible linker. Each domain contains two EF-hands, so these proteins each bind four Ca^{2+} ions. In the resting cell, they exist in an inactive state, with either Mg^{2+} or no ion bound. When the intracellular Ca^{2+} concentration rises in response to a signal, the proteins bind Ca^{2+}. This induces a dramatic conformational change, exposing a large **hydrophobic** surface within each domain that can interact with target proteins. There are many other CaBPs thought to function in a similar manner including caltractin and the calmodulin-like domain of plant Ca^{2+}-dependent protein kinase.

Less is known about the S100 proteins, another large and important subfamily of EF-hand CaBPs. The proteins in this subfamily are composed of two EF-hands each, the first of which is a variant version with a 14-residue binding loop, termed a pseudo-EF-hand. The ligands in the pseudo EF-hand are mainly carbonyl oxygens of the peptide backbone, whereas the canonical 12-residue loop coordinates Ca^{2+} primarily with oxygen atoms of side chains. Many S100 proteins are found as hetero- or homodimers, and they exhibit tissue-specific expression patterns. While these proteins are thought to be involved in signal transduction, the molecular mechanism of this function is not known, nor have any target proteins been positively identified. However, the expression of S100 proteins is deregulated in some diseases, including cancer, rheumatoid arthritis, and Down's syndrome, and antibodies against these proteins are commonly used as markers for screening for these diseases.

Most EF-hand CaBPs are directly involved in intracellular calcium signal transduction. However, at least three fulfill other cellular requirements. Parvalbumin and calbindin D_{9k} (an S100 protein) are thought to play roles in Ca^{2+} buffering and in Ca^{2+} uptake and transport, respectively. These and other members of the EF-hand protein family are active in various aspects of intracellular Ca^{2+} homeostasis. The diversity of the roles of EF-hand CaBPs is further illustrated by the recent structure of BM-40, a glycoprotein found in the extracellular matrix (1), which was shown to contain two EF-hands. Prior to this discovery, the EF-hand motif was thought to be unique to intracellular CaBPs. This diversity in function of the EF-hand CaBPs provides evidence of very extensive evolutionary optimization of the fit between the EF-hand CaBP fold and the calcium ion.

1.2. Annexins

The annexin family is a second important class of intracellular CaBPs. The exact function of the proteins in this family is unknown, but they do exhibit an intriguing Ca^{2+}-dependent high-affinity binding to phospholipids (see Membranes). Annexins bind a large number of Ca^{2+} ions with high cooperativity. They assist transport of Ca^{2+} ions across membranes *in vitro*, although the physiological relevance has not yet been established. The mechanism of membrane binding is not known. The current model involves the Ca^{2+} ions acting as “glue” by simultaneously interacting with the protein and the membrane (2).

2. Ca^{2+}-Binding Enzymes

Two well-known enzymes exhibit Ca^{2+}-dependent translocation to the membrane fraction, presumably through a mechanism similar to that used by the annexins. Some **isoforms** of protein kinase C bind to phospholipids with high affinity in the presence of Ca^{2+} (2). The intracellular group IV phospholipase A_2 also requires Ca^{2+} for membrane association (3).

Many other enzymes require Ca^{2+} ions for stability. This includes many **serine proteases**: members of both the **trypsin** and the subtilisin families have been found to bind Ca^{2+}. These proteases each bind one to three Ca^{2+} ions, which are required for structural stability but do not directly participate in catalysis. In most cases, the Ca^{2+} ions are coordinated by ligands dispersed throughout the structure. Trypsin is an exception, however, and binds Ca^{2+} using a single 12-residue surface loop. The use of Ca^{2+} ions to stabilize the protein fold is not unique to the serine proteases. Another example of an enzyme that uses Ca^{2+} in this manner is thermolysin, a Zn^{2+}-dependent protease.

In other enzymes, the Ca^{2+} ions are directly involved in catalysis. This includes the secreted forms of phospholipase A_2, in which the required Ca^{2+} ion is thought to be involved in transition state stabilization (4). **Staphylococcal nuclease**, a secreted protein that catalyzes DNA and RNA hydrolysis, also relies on Ca^{2+} for catalysis. The structure of this protein shows Ca^{2+} bound in the active site, where it is thought to be used to polarize the phosphate at the scissile phosphoester bond (5, 6).

3. Extracellular Cell Surface and Extracellular Matrix Ca^{2+}-binding Proteins

3.1. Cadherins

These are tissue-specific cell adhesion molecules that are strongly Ca^{2+}-dependent (see Cadherins). At the levels of Ca^{2+} found in the extracellular milieu, cadherins bind several Ca^{2+} ions. A major conformational change is seen when Ca^{2+} is removed from these proteins. The resulting change to the apo state conformation is thought to prevent cadherins from interacting with each other.

3.2. C-Type Lectins

The C-type lectins are a Ca^{2+}-dependent class of lectins, which mediate many cell surface carbohydrate recognition events. Selectins, concanavalin A, and mammalian mannose-binding protein are examples of this type of CaBP. The structure of mannose-binding protein shows that Ca^{2+} is directly involved in binding the carbohydrate to this protein. In concanavalin A, on the other hand, the Ca^{2+}-binding site is $1.0–1.4 \times 10^{-9}$ m from the carbohydrate binding site; Ca^{2+} does not participate directly in binding the carbohydrate, but instead stabilizes the protein structure. It is not known whether selectins use Ca^{2+} directly in carbohydrate binding or to stabilize the fold required for carbohydrate recognition.

3.3. EGF Modules

A subset of EGF motifs present as **domains** in a number of proteins contain b-hydroxy–aspartic acid residues and have Ca^{2+}-binding activity. This type of EGF motif is found in some proteins involved in the blood clotting cascade and also in the extracellular matrix protein fibrillin. Fibrillin has 54 EGF modules, 43 of which are thought to bind Ca^{2+}. It is thought that Ca^{2+} is important in maintaining the structure of the fibrillin monomers and also in allowing the monomers to aggregate into microfibrils. A sheath of these microfibrils covers and stabilizes the elastin fibers that give tissues such as skin, blood vessels, and lungs their needed elasticity.

4. Gla-Containing Proteins

The Gla-containing proteins contain g-carboxyglutamic acid residues. This is a glutamic acid residue that has been carboxylated in a vitamin K–dependent process. These proteins are found in the bones and teeth, in the kidney, and in the blood. Osteocalcin (bone Gla-protein) and matrix Gla-protein are found in bone. They are believed to be involved in the mineralization of this tissue (7). Similar proteins are thought to be involved in the mineralization of teeth. In the kidney, the Gla-containing protein nephrocalcin inhibits the nucleation, aggregation, and growth of calcium oxalate crystals. An abnormal form of this protein is found in the urine of people suffering from kidney stones. However, it is not entirely clear whether this defect is responsible for the growth of kidney stones (8).

By far the best studied of the Gla-containing proteins are those found in blood. The majority of Gla-containing proteins are zymogen forms of serine proteases involved in the blood clotting (coagulation) cascade. These proteins are: pro**thrombin**, factor VII, factor IX, factor X, protein C, protein S, and protein Z. The protease domains of these proteins are very similar to the pancreatic digestive proteases **trypsin**, **chymotrypsin**, and elastase. The Gla-containing coagulants require Ca^{2+} binding in order to bind to phospholipids. This Ca^{2+}-dependent phospholipid binding is responsible for the membrane association properties required for the function of the proteins. Ca^{2+} binding also appears to be necessary for the formation of the native conformation of the Gla domain (9).

The Gla-containing coagulants have two classes of metal ion binding sites. There are approximately three higher affinity sites that are not metal ion–specific, and three to four lower affinity sites, which are specific for Ca^{2+}. Only Sr^{2+} can substitute for Ca^{2+} in both types of binding site.

The high resolution three-dimensional structure of the Gla domain of prothrombin, with seven Ca^{2+} ions bound (10), reveals the Gla domain to involve nine to 10 turns of alpha-helix, in three separate helices. Seven Ca^{2+} ions interact with 24 oxygen atoms from 16 of the 18 carboxylate groups of the nine Gla residues that are ordered in the structure. A 10th Gla residue is disordered and does not participate in Ca^{2+} binding. The coordination geometries of the Ca^{2+} ions do not correspond to any idealized polyhedra. Five of the Ca^{2+} ions are involved in a polymeric array with 18 of the liganding oxygen atoms. Four of these Ca^{2+} ions are completely buried in the protein. This complex structure is thought to nucleate the folding of the Gla domain, and is essentially electrically neutral. The complexity and irregularity of this structure explains the selectivity for Ca^{2+} ions. Ca^{2+} is able to adopt different and distorted coordination geometries. Mg^{2+}, on the other hand, is fairly rigid in its requirement for six ligands, and cannot accommodate the unusual network of ligands in the Gla domain. The remaining two metal ion sites in the Gla domain of prothrombin are solvent accessible, and carry a net charge of about +0.5 each. Because of the positive charge, these sites are thought to be involved in neutralizing the negatively-charged phospholipids, allowing the protein to associate with membranes.

Bibliography

1. E. Hohenester, P. Maurer, C. Hohenadl, R. Timpl, J. N. Jansonius, and J. Engel (1996) Nature Struct. Biol. **3**, 67–73.
2. M. D. Bazzi and G. L. Nelsestuen (1993) Cell. Signal. **5**, 357–365.
3. J. Y. Channon and C. C. Leslie (1990) J. Biol. Chem. **265**, 5409–5413.
4. E. A. Dennis (1994) J. Biol. Chem. **269**, 13057–13060.
5. P. J. Loll and E. E. Lattmam (1989) Prot. Struct. Funct. Genet. **5**, 183–201.
6. F. A. Cotton, E. E. Hazen, and M. J. Legg (1979) Proc. Natl. Acad. Sci. USA **76**, 2551–2555.
7. M. F. Young, J. M. Kerr, K. Ibaraki, A.-M. Heegaard, and P. G. Robey (1992) Clin. Orthoped. Rel. Res. **281**, 275–294.
8. F. L. Coe, Y. Nakagawa, J. Asplin, and J. H. Parks (1994) Miner. Electrolyte Metab. **20**, 378–384.
9. J. W. Suttie (1993) FASEB J. **7**, 445–452.
10. M. Soriano-Garcia, K. Padmanabhan, A. M. de Vos, and A. Tulinsky (1992) Biochemistry **31**, 2554–2566.

Suggestions for Further Reading

11. M. Celio, ed. (1996) *Guidebook to the Calcium-Binding Proteins*, Oxford University Press, Oxford.
12. H. Kawasaki and R. H. Kretsinger (1995) *Protein Profile; Calcium-Binding Proteins 1: EF-hands*, Vol. **2**, Academic Press, London (a good general source for information about EF-hand proteins).
13. S. Liemann and A. Lewit-Bentley (1995) Annexins: a novel family of calcium- and membrane-binding proteins in search of a function, Structure **3**, 233–237.
14. P. Maurer, E. Hohenester, and J. Engel (1996) Extracellular calcium-binding proteins, Curr. Opin. Cell Biol. **8**, 609–617.
15. C. A. McPhalen, N. C. J. Strynadka, and M. N. G. James (1991) Calcium-binding sites in proteins: a structural perspective, Adv. Protein Chem. **42**, 77–144.
16. L. J. Van Eldik, J. G. Zendegui, D. R. Marshak, and D. M. Watterson (1982) Calcium-binding proteins and the molecular basis of calcium action, Intern. Rev. Cytol. **77**, 1–61. (A review of Gla-containing proteins, Ca^{2+}-binding enzymes, and EF-hand proteins.)

Calmodulin

Calmodulin is the quintessential member of the **EF-hand** family of calcium-binding proteins and functions as a key mediator in numerous signal transduction pathways. It is an acidic protein (isoelectric point of 4.2) of molecular weight 16.8 kDa that is found in most eukaryotic cells, from yeast to humans. It is composed of two largely independent globular **domains** connected by a flexible central a-helix. The affinity of calmodulin for Ca^{2+} is fine-tuned to respond to intracellular calcium signals. Conformational changes within each of the domains induced by the binding of Ca^{2+} leads to the transduction of the Ca^{2+} signal.

1. Biological Function

Calmodulin is a signal transduction protein. It has been implicated in the control of a wide range of cellular functions, including cell proliferation, smooth muscle contraction, the regulation of **ion channels**, long-term potentiation and memory, and exocytosis. Furthermore, it has recently been found inside the nucleus, where it is thought to be involved in the regulation of DNA replication, **gene expression**, and DNA repair. In a resting cell with basal levels of Ca^{2+} , calmodulin exists in the inactive apo state. When a calcium signal is initiated and the intracellular levels of Ca^{2+} increase, calmodulin binds Ca^{2+} ions. This causes the protein to undergo a dramatic conformational change that exposes a large **hydrophobic** patch on the protein. This newly exposed hydrophobic surface then interacts with various cellular proteins, modulating their activity and thereby transducing the calcium signal.

Protein kinases and **phosphatases** are among the best studied of calmodulin's targets. These enzymes are activated by the release of an autoinhibitory **domain** that is bound to the active site in the resting state. Ca^{2+}-loaded calmodulin activates these proteins by binding to a site near to or overlapping with the autoinhibitory domain, causing the auto-inhibitory domain to dissociate from the active site. Myosin light chain kinase and calcium-calmodulin-dependent protein kinase II are two well-known examples of this class of calmodulin-regulated proteins. Calmodulin also regulates proteins involved in the generation of other second messengers, such as calmodulin-dependent cyclic nucleotide phosphodiesterase and nitric oxide synthase. The mechanism of regulation of these enzymes is thought to be very similar to that used to regulate the kinases and phosphatases. Calmodulin has also been shown to interact with proteins of the cytoskeleton and their regulatory proteins, such as spectrin and brush border myosin. However, the biological significance of these interactions is still unclear.

Recently, interactions between apocalmodulin and targets such as neuromodulin and unconventional myosins have been described. These interactions are thought to be mediated by an “IQ motif” (with the consensus sequence IQXXXRGXXXR, where X is any amino acid) in the target (see Protein Motif). This motif and its interaction with a Ca^{2+}-free EF-hand calcium-binding protein was first described in myosin (1, 2). The functional significance of the interaction of proteins containing the IQ motif with apocalmodulin is not clear. It has been suggested, however, that perhaps neuromodulin, which is associated with the plasma membrane, functions as a trap for calmodulin, sequestering it near the membrane in the absence of the activating calcium signal (3).

2. Ion-Binding Properties

Calmodulin binds four calcium ions, with a **dissociation constant** of about 10^{-6} *M*. Binding is selective for Ca^{2+}; calmodulin does not bind Mg^{2+} or monovalent ions with appreciable affinity. The binding of Ca^{2+} is also highly **cooperative**, which is very important for calmodulin's biological function as a calcium sensor, because it allows for a tightly controlled "all or nothing" response to the calcium signal: the four binding events all occur within a very narrow range of Ca^{2+} concentration. If these binding events were spread over a large range of Ca^{2+} concentrations, calmodulin would be at least partially activated over the entire range. The system would therefore lack the required sharp separation between the activate and inactive states.

3. Structure

Calmodulin is a largely helical protein composed of four EF-hand motifs organized into two independent globular domains, each of which contain two EF-hands. The two domains are connected by a long, flexible central a-helix, giving the protein a dumbbell-like appearance (Figure 1a). This quaternary structure is relatively similar in the apo- and Ca^{2+}-loaded states of the protein. However, significant conformational changes occur within the individual domains on Ca^{2+} binding (Fig. 1b). In the apo state, each domain occupies the "closed" conformation (4-6). In this conformation, the four helices in the domain are nearly antiparallel, with interhelical angles near 180°. In Ca^{2+}-loaded calmodulin, each domain occupies an "open" conformation in which the four a-helices are nearly perpendicular to each other (7, 8). Each domain exposes a hydrophobic surface of about 1.25×10^{-8} m^2 in this open conformation (5).

Figure 1. Ribbon representations of the three-dimensional conformations of $(Ca^{2+})_4$-calmodulin in the (**a**) absence and (**b**) presence of a target peptide. The peptide-free diagram was constructed using the coordinates of 1CLL (8). The two domains at the ends of the central a-helix consist of two EF-hand motifs. The diagram of $(Ca^{2+})_4$-calmodulin and the peptide analog of the myosin light chain kinase was constructed using the coordinates of 2BBM (10). The bound peptide is depicted darker than calmodulin.

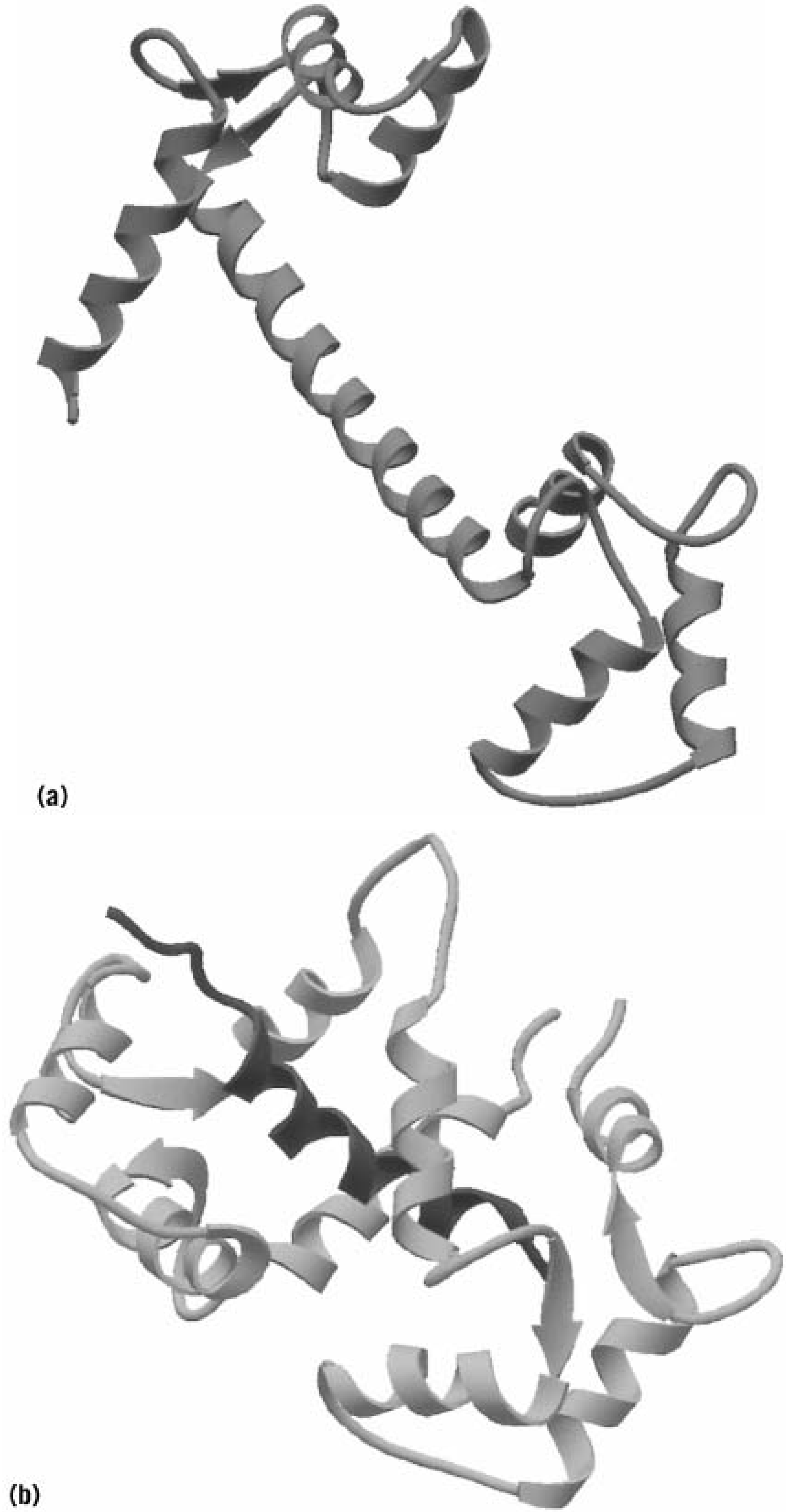

(a)

(b)

4. Interactions with Target Peptides

The biophysical characterization of the interaction between calmodulin and its targets is often studied using small peptides (10–20 amino acid residues) derived from the calmodulin-binding domain of target enzymes. Calmodulin binds to these target peptides extremely tightly, with dissociation constants ranging from 10^{-7} to 10^{-11} M. The peptides adopt an amphiphilic helical conformation, and tend to have a bulky hydrophobic residue at either end, often (but not always) spaced 12 residues apart. However, the sequences of the target peptides are not highly similar. Calmodulin is able to bind so tightly to such a wide array of targets because of its own plasticity. The flexible central a-helix connecting its two domains can function as an "expansion joint," allowing calmodulin to bind to peptides with different numbers of residues between the two bulky hydrophobic anchors. Furthermore, **van der Waals** interactions, which can be rather nonspecific, tend to dominate as the critical components stabilizing the interaction between calmodulin and the peptides. Hydrogen bonds, which are more structurally specific, are not as important in these interactions. The adaptability of the peptide binding surface of calmodulin may be further aided by its high proportion of methionine residues. Methionine is an unusually flexible and polarizable amino acid, which may allow calmodulin to mold its peptide-binding surface to meet the requirements of many different peptide sequences (9, 10).

High resolution three-dimensional structures of three complexes of calmodulin and peptides derived from target enzymes have been reported (11-13). These structures show that the relative disposition of the two domains of calmodulin is altered by the binding of a target peptide, but there is little change within the Ca^{2+}-activated domains themselves. The calmodulin–peptide complex forms a well-packed ellipsoid, which contrasts sharply with the dumbbell shape of calmodulin observed in the absence of target (Fig. 1). The two domains of calmodulin essentially wrap around the target peptide, forming a hydrophobic tunnel in which the peptide binds. As of yet, there are no structures of calmodulin bound to an entire target protein. It is thought, however, that the mode of binding to the target sequence on the intact enzyme will be very similar to that seen in the calmodulin–peptide complexes.

Bibliography

1. Xie, D. H. Harrison, I. Schlichting, R. M. Sweet, V. N. Kalabokis, and A. G. Szent-Gyorgyi (1994) Nature **368**, 306–312.
2. A. Houdusse and C. Cohen (1996) Structure **4**, 21–32.
3. Y. Liu and D. R. Storm (1990) Trends Pharmacol. Sci. **11**, 107–111.
4. H. Kuboniwa, N. Tjandra, S. Grzesiek, H. Ren, C. B. Klee, and A. Bax (1995) Nature Struct. Biol. **2**, 768–776.
5. M. Zhang, T. Tanaka, and M. Ikura (1995) Nature Struct. Biol. **2**, 758–767.
6. B. E. Finn, J. Evenäs, T. Drakenberg, J. P. Waltho, E. Thulin, and S. Forsén (1995) Nature Struct. Biol. **2**, 777–783.
7. Y. S. Babu, C. E. Bugg, and W. J. Cook (1988) J. Mol. Biol. **204**, 191–204.
8. R. Chattopadhyaya, W. Meador, A. Means, and F. Quiocho (1992) J. Mol. Biol. **228**, 1177–1192.
9. H. J. Vogel and M. Zhang (1995) Mol. Cell. Biochem. **149/150**, 3–15.
10. K. T. O"Neil and W. F. DeGrado (1990) Trends Biochem. Sci. **15**, 59–64.
11. M. Ikura, G. M. Clore, A. M. Gronenborn, G. Zhu, C. B. Klee, and A. Bax (1992) Science **256**, 632–638.
12. W. E. Meador, A. R. Means, and F. A. Quiocho (1992) Science **257**, 1251–1255.
13. W. E. Meador, A. R. Means, and F. A. Quiocho (1993) Science **262**, 1718–1721.

Suggestions for Further Reading

14. O. Bachs, N. Agell, and E. Carafoli (1994) Calmodulin and calmodulin-binding proteins in the nucleus, Cell Calcium **16**, 289–296 (a review of the current knowledge about calmodulin"s nuclear functions).
15. A. Crivici and M. Ikura (1995) Molecular and structural basis of target recognition by

calmodulin, Annu. Rev. Biophys. Biomol. Struct. **24**, 85–116 (an exhaustive review of interactions between calmodulin and its targets).
16. R. D. Hinrichsen (1993) Calcium and calmodulin in the control of cellular behavior and motility, Biochim. Biophys. Acta **1155**, 277–293.
17. L. J. Van Eldik and D. M. Watterson, eds. (1997) *Calmodulin and Signal Transduction*, Academic Press, San Diego (a book containing articles about many aspects of calmodulin"s function and structure).
18. C. B. Klee and E. Carafoli, eds. (1997) *Calcium as a Cellular Regulator*, Oxford University Press, Oxford.

Calnexin/Calreticulin

Calnexin (also known as *p88*, *IP90*, and *CATCHER*) is a membrane-bound **molecular chaperone** present in the endoplasmic reticulum (ER) that binds selectively to many monoglucosylated **glycoproteins** that fold in this compartment during synthesis by ribosomes bound to the cytosolic face of the ER membrane. Calreticulin is a soluble homologue of calnexin, with the same glycan specificity, but occurs in the ER lumen. Together with other proteins, calnexin and calreticulin provide a means for improving the efficiency of protein folding and assembly in the ER compartment and form part of the quality-control system that ensures that only correctly folded and assembled proteins are transported from the ER compartment along the pathway followed by secretory proteins (1). Unlike some other molecular chaperones, calnexin and calreticulin are not **stress response** proteins, do not exhibit ATPase activity, and appear to recognize glucose residues in core glycans rather than **hydrophobic** surfaces in partially folded polypeptides (1). In some cell types, calreticulin also occurs in the nucleus and cytosol, where it binds to steroid hormone receptors and integrin molecules, respectively; these interactions may indicate roles for calreticulin in **gene expression** and cell signaling.

1. Discovery

An 88-kDa protein termed *p88* was found in transient association with class I **major histocompatibility** molecules synthesized by several murine lymphoma cell lines (2). Newly synthesized-class I heavy chains bound rapidly to p88 before they associated with b_2-microglobulin chains. In mutant cells that lack microglobulin, the incompletely assembled class I molecules exhibited prolonged interaction with p88 and were correspondingly impaired in their transport to the **Golgi** stacks (3). Moreover, microglobulin and peptides derived from the cytosol need to be assembled with the heavy chain before the latter can be released from p88. These findings led to the proposal that p88 is a molecular chaperone that promotes assembly of class I molecules by retaining intermediates in the ER until complete complexes are formed.

Independent **pulse-chase** experiments on a human ER protein termed *IP90* showed that it transiently associates with many newly synthesized proteins, including the T-cell receptor (TCR), the B-cell antigen receptor, and class I molecules (4, 5). The binding of IP90 to TCR complexes lacking a chains was prolonged, consistent with a retention role for this protein in the ER for incompletely assembled complexes (6). Subsequently, p88 and IP90 were found to be identical with the Ca^{2+}-binding phosphoprotein calnexin (4-7), a protein originally identified as one of several proteins labeled by **phosphorylation** of canine pancreatic **microsomes** with [g-^{32}P]-GTP (8).

2. Structure

Calnexin is a type I nonglycosylated integral membrane protein of 573 amino acid residues, with a predicted molecular weight of 65,400 and with its substrate-binding domain in the lumen of the ER. It has a cytosolic tail of 89 residues that is phosphorylated and contains a *C*-terminal RKPRRE (━Arg━Lys━Pro━Arg━Arg━Glu) sequence that acts as an ER-retention signal (9). It also possesses four **domains** with high sequence similarity to calreticulin, the major calcium-binding protein of the ER lumen. Calreticulin contains 400 amino acid residues (46,000 molecular weight), which include both a KDEL ER-retrieval sequence and a strongly negatively charged region involved in Ca^{2+} binding at its *C* terminus (10). Both calnexin and calreticulin appear to function as monomers.

3. Function

Calnexin and calreticulin are both lectins that specifically recognize glycoproteins that contain monoglucosylated core glycans; they do not recognize glycans containing two, three or no glucose residues (11, 12). When nascent chains of glycoproteins enter the ER lumen, a core glycan containing three terminal glucose residues is added en bloc to specific asparagine sidechains (see N-Glycosylation). This addition of glycan may have evolved initially to make folding intermediates more soluble under the conditions of high protein concentration that characterize the ER lumen. These glucose residues are then rapidly removed one at a time by glucosidases I and II in the ER lumen. Another lumenal enzyme called UDP-Glc:glycoprotein glucosyltransferase then adds back one glucose residue. Thus glycans containing single terminal glucose residues can arise either as intermediates in the glucose-trimming process or after regeneration by the transferase. Such monoglucosylated glycans then bind to calnexin and calreticulin. In the case of pancreatic ribonuclease B, this binding occurs solely through the glycan and does not involve additional recognition of the protein moiety by the lectins (13, 14), but such additional recognition may occur in the case of other proteins (11, 15).

The function of the binding of calnexin and calreticulin to monoglucosylated glycoproteins appears to be to assist their correct folding by preventing aggregation of partially folded or misfolded chains and ensuring retention of the latter until they are degraded (see DNA Degradation In Vivo). Evidence for this conclusion comes from experiments in which proteins unable to fold correctly because of mutation remain bound to these chaperones for much longer than normal proteins and are eventually degraded (16-18). Additional possible roles include the suppression of formation of nonnative disulfide bonds (19) and the premature assembly of oligomers (18).

The distinction between correctly folded and partially folded chains is not made by these lectins but by the glucosyltransferase. This enzyme has the unusual property of distinguishing, by an unknown mechanism, between subtly different protein conformations; it adds glucose to the core glycan only if the protein attached to this glycan is not correctly folded (20, 21). Such reglucosylated glycoproteins will then bind back to calnexin and calreticulin. The removal and addition of the terminal glucose residue then continues until the protein has folded sufficiently to be no longer recognized by the transferase. The binding of calnexin to ribonuclease B *in vitro* is dynamic, indicating that the binding is readily reversible; glucosidase II cannot remove terminal glucose residues while calnexin is bound to the glycoprotein (14).

Calnexin and calreticulin associate with a wide range of proteins in the ER, including soluble secretory proteins, extracellular matrix molecules, **ion channels**, membrane **receptors**, and various glycoproteins of **viruses**. They also retain misfolded proteins that accumulate in some ER-storage diseases such as cystic fibrosis and a1-antitrypsin deficiency (22). Addition of glucosidase inhibitors to cells results in reduced rates of secretion of many glycoproteins, presumably due to the inhibition of their binding to the chaperones (23). All these observations support the view that the functions of calnexin and calreticulin are important for cell function. Nevertheless, viable mammalian cell lines are known that lack either glucosidase I or II or calnexin, while mutants of *Saccharomyces cerevisiae* that lack genes for any one of these three proteins show no growth defect. However, mutants of *Saccharomyces pombe* that lack calnexin are not viable. Both species of *Saccharomyces* appear to lack calreticulin. These discrepancies may indicate some redundancy and overlap of function amongst the chaperones in the ER compartment, which include BiP, hsp90, and protein disulfide isomerase, as well as calnexin and calreticulin (1).

Bibliography

1. A. Helenius, E. S. Trombetta, D. N. Hebert, and J. S. Simons (l997) Trends Cell Biol. **7**, 193–200.
2. E. Degen and D. B. Williams (1991) J. Cell Biol. **112**, 1099–1115.
3. E. Degen, M. F. Cohen-Doyle, and D. B. Williams (1992) J. Exp. Med. **175**, 1653–1661.
4. F. Hochenstenbach, V. David, S. Watkins, and M. B. Brenner (1992) Proc. Natl. Acad. Sci. USA **89**, 4734–4738.
5. K. Galvin et al. (1992) Proc. Natl. Acad. Sci USA **89**, 8452–8456.
6. V. David, F. Hochstenbach, S. Rajagopalan, and M. B. Brenner (1993) J. Biol. Chem. **268**, 9585–9592.
7. N. Ahluwalia, J. J. M. Bergeron, I. Wada, E. Degen, and D. B. Williams (1992) J. Biol. Chem. **267**, 10914–10918.
8. I. Wada, D. Rindress, P. H. Cameron, W.-J. Ou, J. J. Dohery, D. Louvard, A. W. Bell, D. Dignard, D. Y. Thomas, and J. J. M. Bergeron (1991) J. Biol. Chem. **266**, 19599–19610.
9. M. Michalak, R. E. Milner, K. Burns, and M. Opas (1992) Biochem. J. **285**, 681–692.
10. B. Sonnichsen, J. Fullefrug, P. Nguyen, W. Diekmann, D. G. Robinson, and G. Mieskes (1994) J. Cell Sci. **107**, 2705–2717.
11. F. E. Ware, A. Vassilakos, P. A. Petersen, M. R. Jackson, M. A. Lehrmann, and D. B. Williams (1995) J. Biol. Chem. **270**, 4697–4704.
12. R. G. Spiro, Q. Zhu, V. Bhoyroo, and H.-D. Soling (1996) J. Biol. Chem. **271**, 11588–11594.
13. A. R. Rodan, J. F. Simons, E. S. Trombetta, and A. Helenius (1996) EMBO J. **15**, 6921–6930.
14. A. Zapun, S. M. Petrescu, P. M. Rudd, A. R. Dwek, D. Y. Thomas, and J. J. M. Bergeron (1997) Cell **88**, 29–38.
15. D. B. Williams (1995) Biochem. Cell Biol. **73**, 123–132.
16. C. Hammond and A. Helenius (1994) Science **266**, 456–458.
17. D. F. Qu, J. H. Teckman, S. Omura, and D. H. Perlmutter (1996) J. Biol. Chem. **271**, 22791–22795.
18. D. N. Hebert, B. Foellmer, and A. Helenius (1996) EMBO J. **15**, 2961–2968.
19. W. Chen, J. Helenius, I. Braakman, and A. Helenius (1995) Proc. Natl. Acad. Sci. USA **92**, 6229–6233.
20. M. C. Sousa, M. A. Ferrero-Garcia, and A. J. Parodi (1992) Biochemistry **31**, 97–105.
21. S. E. Trombetta and A. J. Parodi (1992) J. Biol. Chem. **267**, 9236–9240.
22. P. J. Thomas, B. Qu, and P. L. Pederson (1995) Trends Biochem. Sci. **20**, 456–459.
23. V. Gross, T. Andus, T. A. Tranhl, R. T. Schwartz, K. Decker, and P. C. Heinrich (1983) J. Biol. Chem. **258**, 12203–12209.

Suggestions for Further Reading

24. C. Hammond and A. Helenius (1993) A chaperone with a sweet tooth, Curr. Biol. **3**, 884–886.
25. J. J. M. Bergeron, M. B. Brenner, D. Y. Thomas, and D. B. Williams (1994) Calnexin: a membrane-bound chaperone of the endoplasmic reticulum, Trends Biochem. Sci. **19**, 124–128.
26. C. Hammond and A. Helenius (1995) Quality control in the secretory pathway, Curr. Opinion

Cell Biol. **7**, 523–529.
27. D. B. Williams and T. A. Watts (1995) Molecular chaperones in antigen presentation, Curr. Opin. Immunol. **7**, 77–84.
28. M.-J. Gething, ed. (1997) *Molecular Chaperones and Folding Catalysts*, Oxford University Press, Oxford (contains detailed articles on calnexin and calreticulin).
29. S. Dedhar (1994) Novel functions for calreticulin: interactions with integrins and modulation of gene expression? Trends Biochem. Sci. **19**, 269–271.
30. M. G. Coppolino, M. J. Woodside, N. Demaurex, S. Grinstein, R. St-Arnaud, and S. Dedhar (1997) Calreticulin is essential for integrin-mediated calcium signalling and cell adhesion, Nature **386**, 843–847.

5′ Cap

The 5′cap is characteristic of all **RNAs** transcribed by RNA polymerase II, and it is added to the nascent transcript soon after transcriptional initiation. Many lines of evidence suggest that the cap contributes to many aspects of RNA metabolism, including RNA stability (1), pre-mRNA **splicing** (2, 3), polyadenylation (4), U **small nuclear RNA** (snRNA) export (5), and translation of messenger RNA (6). The influence of the cap on RNA metabolism, in both the nucleus and the cytoplasm, is mediated by cap-binding proteins.

The cap consists of an inverted 7-methyl guanosine nucleotide linked by a 5′-5′-triphosphate linkage to the first template-encoded nucleotide of the RNA, to give the following structure: $m^7G(5')ppp(5')N$. The cap modification is one of the earliest covalent modifications detected on a nascent RNA transcript, and it occurs cotranscriptionally (7). The actual capping reaction requires the sequential action of several enzymatic activities and is well understood (see Fig. 1). The capping enzyme possesses an RNA 5′-triphosphatase activity, which converts the 5′ terminal triphosphate of the RNA to a diphosphate. RNA guanylyltransferase then catalyzes the transfer of GMP, derived from GTP, to the diphosphate, resulting in the formation of the G(5′)ppp(5′)N cap. This cap structure is the substrate for methylation by RNA (guanine-7)-methyltransferase, which converts it to the monomethylated cap structure. In the absence of cap methylation, the reaction is reversible. The genes encoding the capping enzyme and methylase are essential in the **yeasts** *Saccharomyces cerevisiae* and *Schizosaccharomyces pombe*, underlining the importance an intact cap for viability (8-10). The cause of death in these mutants is probably due to cumulative defects in the various processes in which the cap is involved, such as RNA stability and **splicing** (11).

Figure 1. The capping reaction at the 5′ nucleotide (N) of an RNA transcript: (*1*) the 5′-triphosphate of the nascent transcript is hydrolyzed by RNA 5′-triphosphatase to a diphosphate; (*2*) mRNA guanylyltransferase adds the cap from GMP (which is derived from GTP). The cap is then methylated on the N-7 (position 7 nitrogen) of guanosine by mRNA (guanine-7) methylase.

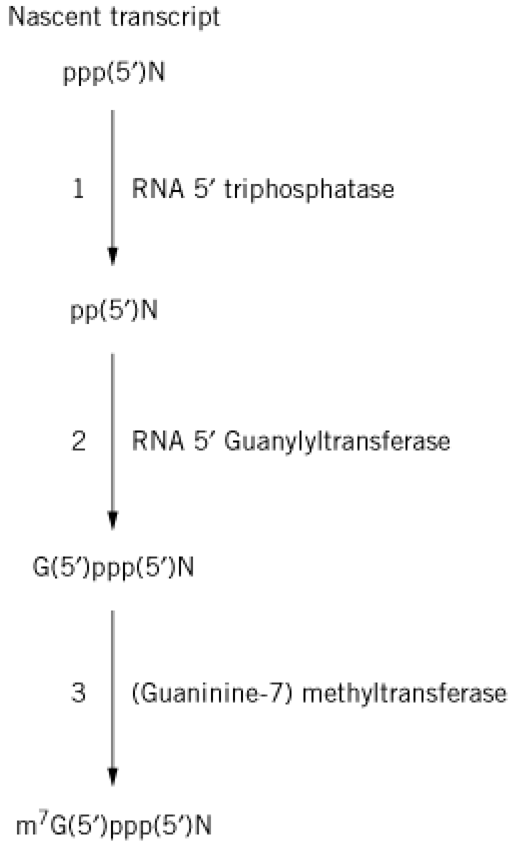

Bibliography

1. Y. Furuichi, A. LaFiandra, and A. J. Shatkin (1977) Nature **266**, 235–239.
2. M. Konarska, R. Padgett, and P. Sharp (1984) Cell **38**, 731–736.
3. A. Krainer, T. Maniatis, B. Ruskin, and M. Green (1984) Cell **36**, 993–1005.
4. C. Cooke and J. C. Alwine (1996) Mol. Cell. Biol. **16**, 2579–2584.
5. J. Hamm and I. W. Mattaj (1990) Cell **63**, 109–118.
6. A. Shatkin (1985) Cell **40**, 223–224.
7. M. Salditt-Georgieff, M. Harpold, S. Chen-Kiang, and J. E. Darnell Jr. (1980) Cell **19**, 69–78.
8. S. Shuman and B. Schwer (1995) Mol. Microbiol. **17**, 405–410.
9. Y. Shibagaki, N. Itoh, H. Yamada, S. Nagata, and K. Mizumoto (1992) J. Biol. Chem. **267**, 9521–9528.
10. B. Schwer and S. Shuman (1994) Proc. Natl. Acad. Sci. USA **91**, 4328–4332.
11. B. Schwer and S. Shuman (1996) RNA **2**, 574–583.

Suggestions for Further Reading

12. J. D. Lewis, S. Gunderson, and I. W. Mattaj (1995) The influence of 5¢ and 3¢ end structures on pre-mRNA metabolism, J. Cell Sci. Suppl. **19**, 13–19.
13. J. D. Lewis and E. Izaurralde (1997) The role of the cap structure in RNA processing and nuclear export, Eur. J. Biochem. **247**, 461–469.

Cap-Binding Proteins

Most of the functions in the nucleus and cytoplasm of the cap of messenger RNA (mRNA) are mediated by cap-binding proteins (CBP), which show highly specific binding to the cap structure, $m^7G(5')ppp(5')N$. Two major cap-binding activities have been characterized in **eukaryotes**. The first is the nuclear cap-binding complex (CBC), which plays a role in pre-mRNA **splicing** (1-3), polyadenylation (4), and U **small nuclear RNA** (snRNA) export (5). The second, eIF4E (6), is part of a trimeric complex, eIF4F, which is required for cap-dependent translation of mRNA.

CBC was initially identified in nuclear extracts from HeLa cells as an activity that bound specifically to a normal 7-methyl guanosine-5′-capped RNA. Purification of the activity showed that it was a heterodimeric complex comprising two subunits; CBP80 and CBP20 (1). Neither protein alone can bind specifically to the 5′cap—only as a heterodimer. Current evidence has shown that CBC is required for efficient (*1*) pre-mRNA splicing, (*2*) polyadenylation, and (*3*) the export of RNA polymerase II–transcribed U snRNA (see below).

CBC is required for efficient splicing of the cap-proximal **intron**, where its major function is to facilitate the binding of U1 snRNP to the cap-proximal 5′ splice site (3) (see Gene Splicing). Experiments in the yeast *Saccharomyces cerevisiae* and in HeLa splicing extracts have demonstrated that this function of CBC is conserved in evolution (2, 7).

A role for CBC in polyadenylation has also been demonstrated *in vitro* (4): (see Polyadenylation). Depletion of CBC from HeLa cell polyadenylation extracts results in a reduction in the efficiency of polyadenylation. Further analysis of this defect demonstrated that CBC was required for efficient cleavage of the pre-mRNA, but not for the polyadenylation reaction itself.

Nucleocytoplasmic transport of some classes of RNA, specifically the 5′capped uracil-rich (U) snRNAs, is facilitated by CBC. Antibodies raised against one of the subunits, CBP20, can specifically inhibit the interaction of CBC with the cap and, as a consequence, inhibit the export of these U snRNAs from the nucleus to the cytoplasm (5).

The other CBP, eIF4E, is required for cap-dependent translation of mRNA in the cytoplasm, and it can bind directly to the cap as a monomer (6). In order to function in translation, eIF4E has to assemble with two other polypeptide chains in a heterotrimeric complex of eIF4A, eIF4G, and eIF4E, to form a complex known as eIF4F. This trimeric complex binds to the cap of mRNAs and complexes with a second translational initiation complex, eIF3, which has an RNA helicase activity. This helicase activity is thought to unwind **secondary structure** in the mRNA and to allow the cap-dependent association of the 40S **ribosomal** subunit with the mRNA. The 40S subunit then scans for the initiation codon complexes with the 60S ribosomal subunit to initiate translation.

Bibliography

1. E. Izaurralde, J. Lewis, C. McGuigan, M. Jankowska, E. Darzynkiewicz, and I. Mattaj (1994) Cell **78**, 657–668.
2. J. Lewis, D. Görlich, and I. Mattaj (1996) Nucl. Acids Res, **24**, 3332–3336.
3. J. D. Lewis, E. Izaurralde, A. Jarmolowski, C. McGuigan, and I. W. Mattaj (1996) Genes Devel. **10**, 1683–1698.
4. S. M. Flaherty, P. Fortes, E. Izaurralde, I. W. Mattaj, and G. M. Gilmartin (1997) Proc. Nat. Acad. Sci. USA **94**, 11893–11898.
5. E. Izaurralde, J. Lewis, C. Gamberi, A. Jarmolowski, C. McGuigan, and I. W. Mattaj (1995) Nature **376**, 709–712.
6. N. Sonnenberg, M. Rupprecht, W. Merrick, and A. Shatkin (1979) Proc. Natl. Acad. Sci. USA

75, 4345–4349.
7. H. Colot, F. Stutz, and M. Rosbash (1996) Genes Devel. **10**, 1699–1708.

Suggestions for Further Reading

8. J. D. Lewis and E. Izaurralde (1997) the role of the cap structure in RNA processing and nuclear export, Eur. J. Biochem. **247**, 461–469.
9. W. Merrick and J. Hershey (1996) in J. Hershey, M. Mathews, and N. Sonnenberg, eds., *Origins and Targets of Translational Control*, Cold Spring Harbor Laboratory Press, Cold Spring Harbor, New York, pp. 1–29.

Capillary Zone Electrophoresis

Capillary zone electrophoresis (CZE) is electrophoresis in very thin capillaries. It is an analytical separation method that is compatible with high field strength (200 to 800 V/cm) and small samples (micrograms to nanograms). The high field strength makes the separation rapid and gives high resolving power (1). The very small capillary diameter, less than 0.2 mm, counteracts dispersion of the zone, presumably through interaction of the analyte with the inner wall of the capillary. The sample is detected by its absorbance or fluorescence as it proceeds past a stationary detector at the end of the migration path.

The inner walls of the silicate capillary carry negatively charged groups, so electroendosmosis is significant; this can be used for the purpose of separation, but it is usually suppressed by coating the inner wall with a polymer such as polyacrylamide gel or dextran. Separations based predominantly on size and shape differences are achieved in CZE in the presence of soluble polymers to produce a **molecular sieve** effect. A variety of uncharged hydrophilic polymers in a wide range of molecular weights are available for that purpose (2-4). Although providing high resolving power (see Gel Electrophoresis), gels are less applicable to CZE because the gelation process may introduce air bubbles and inhomogeneities within the capillary; also, a gel-filled capillary can only be used once or a few times, while polymer solutions can be replaced easily. One drawback of CZE is that the analyte bands are enclosed within the tube and therefore are unavailable for detection by immunological, hybridization, and staining techniques. However, the eluate of CZE can be subjected to mass spectrometry to provide molecular weights of the species detected, in addition to their mobilities (5).

Bibliography

1. F. Foret and P. Bocek (1989) Adv. Electrophoresis **3**, 273–347.
2. K. Ganzler, K. S. Greve, A. S. Cohen, B. L. Karger, A. Guttman, and N. C. Cooke (1992) Anal. Chem. **64**, 2665–2671.
3. M. C. Ruiz-Martinez, J. Berka, A. Belenkii, F. Foret, A. W. Miller, and B. L. Karger (1993) Anal. Chem. **65**, 2851–2858
4. D. Tietz, A. Aldroubi, H. Pulyaeva, T. Guszczynski, M. M. Garner, and A. Chrambach (1992) Electrophoresis **13**, 614–615.
5. D. Figeys, I. van Oostveen, A. Ducret, and R. Aebersold (1996) Anal. Chem. **68**, 1822–1828.

Suggestions for Further Reading

6. P. Gebauer and P. Bocek (eds.) (1995) Symposium on capillary electrophoresis theory. Electrophoresis **16**, 1985–2174.
7. P. D. Grossman and J. C. Colburn (1992) *Capillary Electrophoresis*, Academic Press, New York, pp. 1–352.
8. B. L. Karger (ed.) (1993) Symposium on capillary electrophoresis. Electrophoresis **14**, 371–560.

Capsids, Viral

The capsids of **viruses**—the protein part of the virus particle (virion) that surrounds and protects the nucleic acid genome—have been the subject of intense study by biochemists and structural biologists for over 50 years (see Virus Structure). Capsids are also noteworthy in that they provide one of the few examples in which the detailed properties of a biological system have been predicted successfully from "first principles." This entry describes the principles on which we understand capsid structure—that is, what we expect capsids to be like and why we expect that, and then describes the ways in which real viruses do or do not follow those expectations.

A **gene** of double-stranded DNA can encode a protein of only about 1/20 the mass of the gene itself. As a consequence, if a virus is to encode its own capsid (and in almost all cases, viruses do so), it will only be able to make enough protein to produce a useful sized capsid if it can use multiple copies of the protein(s) encoded in its genes. Crick and Watson (1), who made the first concrete proposal for how proteins might be arranged in virus capsids, assumed that the capsids would be made of multiple identical virus-encoded protein subunits. They also made another assumption, based on a prominent property of proteins, namely that proteins are very specific in the interactions they make with other molecules, presumably including other proteins in the structure of a virus capsid. They assumed that the identical protein subunits would be packed into the capsid structure in such a way that they all made the identical set of contacts with their neighbors—so-called **equivalent packing**. Mathematically, there are only two general ways to satisfy these assumptions when packing asymmetric objects like proteins; these are to arrange the protein subunits with helical symmetry or to arrange them with one of the cubic symmetries. Helical symmetry is easily visualized: The subunits are arranged in a helical array as if they were on successive steps of a spiral staircase. Formally, each subunit is related to the preceding one by a characteristic rotation and a translation in the direction of the helix axis. "Cubic" symmetry refers to a small group of symmetries characterized by having multiple axes of rotational symmetry. These correlate with the five classical Platonic solids, which have these symmetry axes. Besides the cube, from which the entire group of symmetries takes its name, the Platonic solids include the tetrahedron, the octahedron, the dodecahedron, and the icosahedron. Of these, the icosahedron allows (or more properly, arranging protein subunits according to the five-, three-, and twofold rotational symmetry axes of an icosahedron) allows the largest structure to be made with a given size of subunit for any of the group. More to the point, of this group of symmetries, it is icosahedral symmetry that is used by real viruses.

1. Helical Symmetry

Many viruses can be shown to have helical symmetry. The best studied of these is the well-known tobacco mosaic virus (TMV), which has a virion with only one type of protein subunit, present in something over 2000 copies and arranged in a simple helix with 16.33 subunits per turn. There is in principle no limit on how long a helical structure such as this can be, but in TMV it is limited during assembly by the length of the genomic RNA. In the mature virion, the single-stranded RNA genome follows the helix of the proteins and lies in the groove between successive layers of the helix on the inside of the helical tube, three nucleotides per protein subunit. A domain of each subunit closes over this groove after the RNA has entered it during assembly and effectively seals off the RNA from the solvent (2).

Structurally somewhat more complex examples of helically symmetric viruses are the filamentous bacteriophages, such as phage M13. The major protein subunit of these viruses is arranged in what might best be described as a small number of helices running in parallel up a cylindrical tube. The circular single-stranded DNA genome of these viruses is stretched the length of the helical tube. The filamentous phages have small numbers of copies of additional virus-encoded proteins present on the ends of the virions. These have roles in virion assembly and in **virus infection** (3).

Many enveloped viruses, for example, influenza virus, have their genome—single-stranded RNA in the case of Influenza—wrapped in a helical array with a virus-encoded protein. The resulting flexible nucleoprotein rods are enclosed in the viral envelope, one such structure for each of the eight different genome segments in the case of influenza.

2. Icosahedral Symmetry and Quasi-Equivalent Packing

An icosahedron (Fig. 1) has 20 faces, each an equilateral triangle. Its symmetry is defined by axes of rotational symmetry, each passing through the center of the icosahedron: five-fold axes passing through the corners, three-fold axes passing through the centers of the faces, and twofold axes passing through the centers of the edges. Strictly speaking, an icosahedral virus capsid is not an icosahedron; instead, its protein subunits are related to each other by the symmetry axes of an icosahedron. However, thinking of the protein subunits as lying on the surface of an icosahedron provides a convenient way to visualize and discuss the structure of the capsid, as well as a reasonable approximation to the truth. To make an icosahedrally symmetric capsid, we place three identical protein subunits on each face of the icosahedron, symmetrically arrayed about the center. These subunits will necessarily also find themselves in symmetrical relations with their fellows around all the five-, three-, and twofold axes of the icosahedron, and inspection of a model of such a structure shows that all of the subunits lie in equivalent relationships to their neighbors.

Figure 1. An icosahedron.

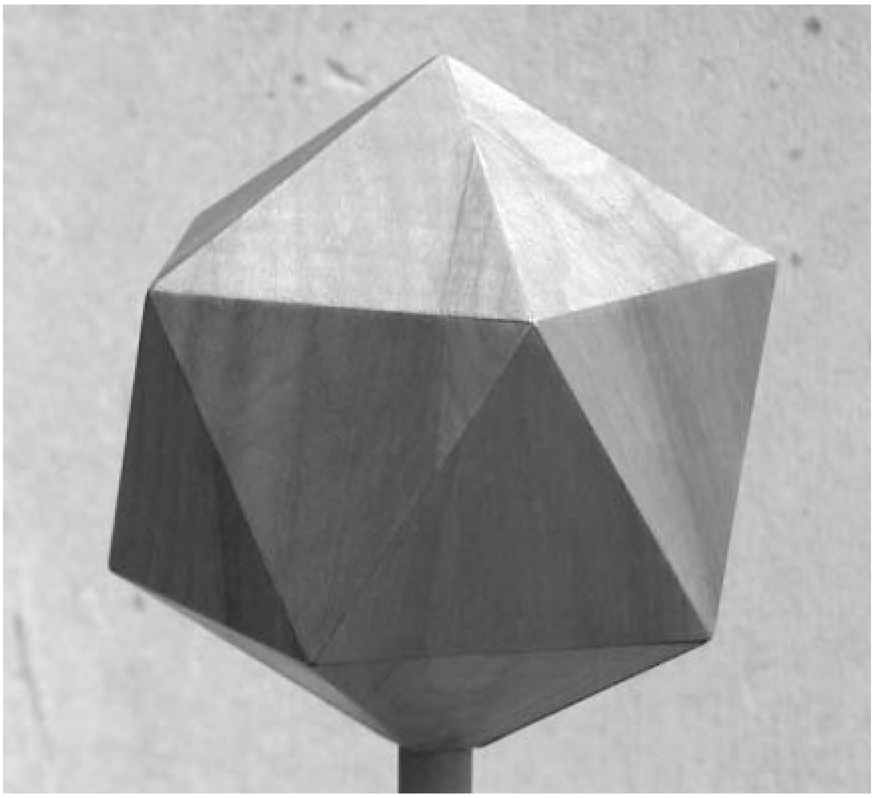

Current knowledge of virus structure allows us to see that some small virus capsids—for example, the Parvoviruses—can be adequately described as such 60-subunit icosahedrally symmetric structures. However, it was already clear by about 1960 that the majority of “spherical” viruses are too large and have too many subunits to be so described. Because there is mathematically no way to make a larger structure while preserving strict equivalence in subunit packing, it was not clear that this way of describing capsid structure would be applicable to most viruses. However, Caspar and Klug (4) proposed a clever extension of Crick and Watson's ideas that has provided a framework for understanding and describing the great majority of spherical virus capsids. Caspar and Klug introduced the idea of “quasi-equivalence” in protein subunit packing. In a nutshell, they suggested that if the requirement for equivalence were relaxed—but not abandoned entirely—it would be possible to make much larger capsids with identical protein subunits, containing multiples of 60 subunits.

A simple way to imagine the process of making a larger capsid is to start with a 60-subunit capsid as described above, group the subunits together into the pentamers that surround each corner (fivefold axis) of the icosahedron, and move those pentamers away from the center to a larger radius. Caspar and Klug's insight was that there are certain ways to fill the resulting spaces between the pentamers with *hexamers* of the same subunit that preserve, at least approximately, the geometrical packing arrangements among all of the subunits in the structure.

A more systematic way to describe this process, shown in Figure 2, is to consider constructing an icosahedron from a piece of paper that has a hexagonal lattice of “protein subunits” printed on it. (Experience has shown, in fact, that the most effective way to understand the concepts described here is to actually take scissors in hand and to construct and examine some capsid models.) The simplest way to make an icosahedron from such a sheet of paper is to cut out 20 of the small triangles in the lattice that each contain three subunits, and join them together into an icosahedron. This icosahedron will have 60 subunits, equivalently packed, and will be identical to the 60-subunit structure described above. It is possible, however, to cut larger triangles out of the paper and use them as the faces of the icosahedron; as long as the corners of these larger triangles fall on the intersection points of the lattice, the resulting icosahedron will be biologically sensible and geometrically acceptable. The figure shows an example of such a larger triangle encompassing four of the small unit triangles. If 20 of these are cut out and assembled into an icosahedron, the structure will have $4 \times 60 = 240$ protein subunits. The subunits in this case are not all equivalently packed—some are in pentamers and some in hexamers, and there are other subtle differences in their geometrical relationships to their neighbors—but the basic relationships between subunits are nonetheless preserved: They are quasi-equivalent. The faces of this icosahedron are said to be “triangulated” into the four unit triangles, and the structure as a whole is said to have a “triangulation number” (T) of 4. The figure also shows a somewhat more complex way of defining the icosahedral face, in which the edges of the icosahedral face are not parallel to the lattice lines. In the example shown, the area of the face is equal to the area of seven small triangles, and the corresponding icosahedron is given the triangulation number 7. More generally, the triangulation number of any icosahedron can be calculated from the formula $T = h^2 + hk + k^2$, where h and k are the number of steps along the lattice in the **h** and **k** directions required to go from one corner of the icosahedral face to another. The “allowed” triangulation numbers derived in this way are a subset of the integers and form an infinite series that starts 1, 3, 4, 7, 9, 12, 13,¼.

Figure 2. A hexagonal lattice of protein subunits with indications of how they can be fit into a strictly equivalent virus capsid ($T = 1$) or into two different kinds of quasi-equivalent capsids ($T = 4$, $T = 7$). The irregular wedge-shaped objects, of which three are packed into each small triangle, represent protein subunits. The bold triangles show the faces of the capsid icosahedron for the three indicated triangulation numbers. The **h** and **k** unit vectors are used to calculate the triangulation number, as described in the text.

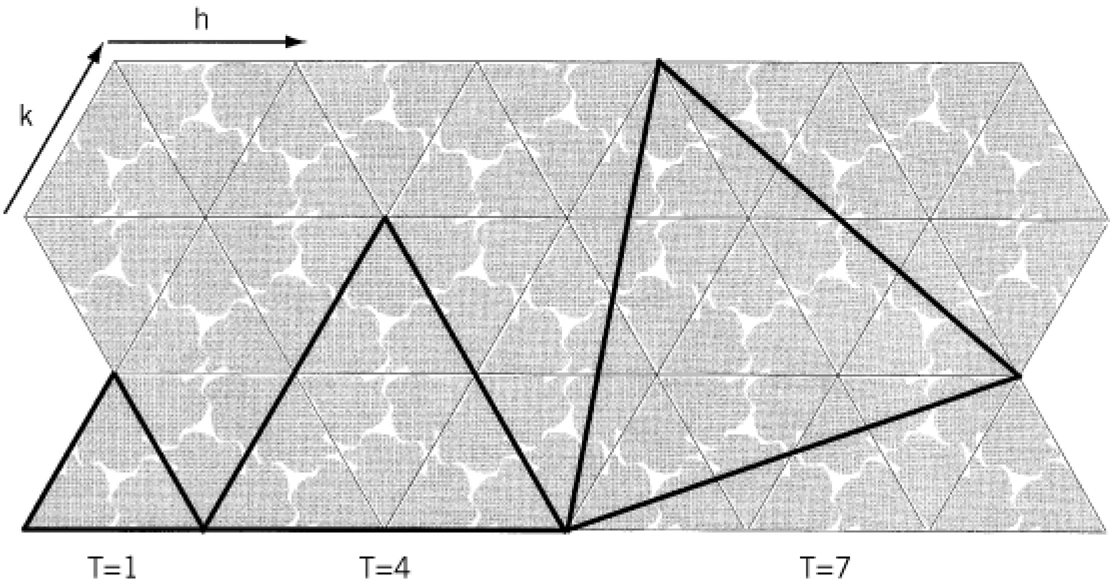

3. Icosahedral Virus Capsids in Nature

As the structures of actual virus capsids have been determined in increasing numbers and in increasing detail over the past 30 years, the general predictions of the Caspar and Klug theory have largely been confirmed. At the same time, there are now many examples of "variations on the theme"—features of the structures that are not explicitly predicted by the theory, but are not at odds with its basic concepts. In addition, there are at least two examples of structures that should not have occurred. The definitive test of how the capsid structure is organized is a high-resolution structure by X-ray crystallography; however, it is often possible to get useful information from lower resolution structural measurements. For example, the hexamers and pentamers of the capsid subunit often cluster in such a way that they can be seen by electron microscopy as a distinct morphological unit, called a **capsomere**. Examining the geometrical relationships among the capsomeres on the surface of a capsid can lead to a good idea of the triangulation number of the capsid.

Parvoviruses, as mentioned above, have 60-subunit $T = 1$ structures (5). The same is true for the small f**X174, bacteriophage**, but in this case there are two proteins present in 60 copies each, rather than only one (6). Here we can think of the heterodimer as the basic building block, with 60 copies of that heterodimer arranged with $T = 1$ icosahedral symmetry.

$T = 3$ capsids, the first group that requires that quasi-equivalence be invoked, are especially well-populated, with examples from plant, animal, and bacterial viruses. Tomato bushy stunt virus (TBSV), the first of this group to be solved to atomic resolution, conforms quite well to the expectations of the theory, having 180 chemically identical subunits, each of which occupies one of three similar but nonidentical positions in the $T = 3$ lattice (7). One set of subunits in TBSV, those occupying the "C" position, send an end of their polypeptide chain toward the threefold symmetry axes, where they intertwine with the corresponding parts of the two symmetrically related subunits. This was the first of what are now several examples of capsid proteins interdigitating and intertwining with their neighbors; this is presumed to provide mechanical strength to the capsid. Poliovirus (a Picornavirus) has a structure very similar to that of TBSV, including the positioning of subunits and even the fold of the polypeptide chains within those subunits, but in this case the three quasi-equivalent positions are occupied by three similar but chemically distinct proteins (8). We might imagine that two of the three coding regions encoding these three proteins were the result of gene duplication in an ancestral virus that, like TBSV, had only one capsid protein gene. A slightly different variation on this theme is found in Cauliflower Mosaic virus (a Comovirus), in which the three quasi-equivalent positions are occupied by two proteins, one of which consists of two very similar **domains**, each occupying one of the three quasi-equivalent positions. These last two examples can be regarded either as slightly noncanonical $T = 3$ structures or as $T = 1$ structures made of 60 copies of the heterotrimer (Picornavirus) or heterodimer (Comovirus).

Many capsid structures with larger triangulation numbers have been identified and characterized. Among these are lambda phage, **P22 phage**, bacteriophage HK97, and others ($T = 7$), **T4 phage** and Reovirus ($T = 13$), Herpesvirus ($T = 16$), and Adenovirus ($T = 25$). The largest triangulation number that has been definitively determined is that of the algal virus PBCV1 ($T = 169$). A particularly instructive example is provided by bacteriophage P2 and its satellite phage P4. The P2 capsid protein assembles into a $T = 7$ shell; but in the presence of P4, which does not encode its own capsid protein, the P2 capsid protein assembles into a $T = 4$ structure, just big enough to enclose the P4 genome. This is accomplished through the agency of a P4-encoded protein that associates transiently with the P2 capsid protein during assembly and directs it into the $T = 4$ geometry (9).

Although these large viruses all fit into the general picture envisioned by Caspar and Klug, they are replete with exceptions and extensions to the original picture, and these variations all expand our view of how capsids can be constructed. For bacteriophage T4 and Adenovirus, the proteins that make the pentamers at the five-fold symmetric corners of the capsid are encoded by a different gene from the proteins at the six-fold positions in the remainder of the capsid. This is analogous to the Picornavirus example above and presumably reduces the amount of conformational or bonding versatility demanded of any one protein, at the relatively minor expense of encoding an additional protein. In T4, the major component of the capsid, which occupies the hexamer positions, is, as expected, a hexamer, but in Adenovirus these positions are occupied by *trimers* of the “hexon protein” (10). However, the hexon protein is organized into two similarly folded domains, and the structure of the trimeric hexon is very close to a sixfold symmetric arrangement of those domains.

Some viruses—particularly but not exclusively some of the double-stranded DNA phages—have prolate capsids, which have a standard icosahedral arrangement of subunits, except that the shell is elongated along one of the fivefold axes of symmetry and an extra band of hexamers is inserted around the equator. Thus bacteriophage T4 has an elongated $T = 13$ capsid, and bacteriophage f29 has an elongated $T = 4$ capsid. These structures pose interesting questions with regard to how their length is specified and accurately achieved, but they cause no serious problems for the idea of quasi-equivalent packing.

Most viruses have other capsid subunits in addition to the main, icosahedrally packed, subunit protein. In some cases, these are present in equimolar amounts with the main subunit and packed with the same symmetry. Thus phages l and T4 have well-studied examples of such “decoration proteins”; Herpesvirus has a protein clustered as trimers that fits this description, but is systematically absent from positions immediately surrounding the pentamers. Proteins in this category are known in some cases to provide additional strength and stability to the capsid. Structurally, they can be regarded simply as additional domains of the main capsid protein, albeit ones that are encoded by separate genes and generally join the structure at a different time.

Many capsids also have “minor” proteins that are not arrayed with icosahedral symmetry. The portal protein of the double-stranded DNA phages, for example, forms a grommet-like 12-subunit oligomer that replaces a pentamer at one of the five-fold corners of the icosahedral shell and provides an attachment site for the six-fold symmetric helical tail (11). Adenovirus has a trimeric spike extending out from the shell along each of its five-fold symmetry axes.

The first radical deviation from the expectations of the Caspar–Klug ideas was found in the virion of Papovavirus SV40. The capsomeres of SV40 visible by electron microscopy are arranged as expected for a $T = 7$ structure. However, all of the capsomeres are pentamers of the VP1 subunit (12), including the 60 capsomeres situated at positions of sixfold local symmetry, which would be expected to be hexamers in order to interact quasi-equivalently with their environment. The subunits adapt to this extraordinary state of affairs by having the part of the polypeptide chain that contacts the neighboring capsomere located on a flexible arm corresponding to the *C*-terminus of the subunit. The *C*-terminal arm leaves its home subunit at dramatically different angles in different cases, allowing it to interact with its neighbor in essentially the same way in each case. This it does by invading the structure of the neighbor and forming one strand of a b-sheet structure in that subunit. This might be regarded as a form of quasi-equivalent interaction, but of a sort requiring a much more radical subunit flexibility than envisioned by Caspar and Klug.

Another surprising arrangement of subunits is found in fungal virus L-A and bacteriophage f6. These capsids have 120 identical protein subunits, not one of the "allowed" numbers. These are $T = 1$ structures, built of 60 asymmetric homodimers. The unexpected feature of this arrangement is that the two chemically identical subunits occupy nonequivalent positions. Nonetheless, these capsids, as for those of SV40, evidently function well enough to have survived natural selection (ie, very well indeed), and an understanding of their structures enlarges our view of the capabilities of proteins.

Bibliography

1. F. Crick and J. D. Watson (1956) Nature **177**, 473–475.
2. J. N. Champness et al. (1976) Nature **259**, 20–24.
3. L. Makowski and M. Russel (1997) In *Structural Biology of Viruses* (W. Chiu, R. M. Burnett, and R. L. Garcea, eds.), Oxford University Press, New York, pp. 352–380.
4. D. Caspar and A. Klug (1962) Cold Spring Harbor Symp. Quant. Biol. **27**, 1–24.
5. J. Tsao et al. (1991) Science **251**, 1456–1464.
6. R. McKenna, L. Ilag, and M. Rossmann (1994) J. Mol. Biol. **237**, 517–543.
7. A. J. Olson, G. Bricogne, and S. C. Harrison (1983) J. Mol. Biol. **171**, 61–93.
8. J. Hogle, M. Chow, and D. Filman (1985) Science **229**, 1358–1365.
9. O. Marvik et al. (1995) J. Mol. Biol. **245**, 59–75.
10. R. M. Burnett (1997) In *Structural Biology of Viruses* (W. Chiu, R. M. Burnett, and R. L. Garcea, eds.), Oxford University Press, New York, pp. 209–238.
11. C. Basinet and J. King (1985) Annu. Rev. Microbiol. **39**, 109–129.
12. R. L. Garcea and R. C. Liddington (1997) In *Structural Biology of Viruses* (W. Chiu, R. M. Burnett, and R. L. Garcea, eds.), Oxford University Press, New York, pp. 187–208.

Suggestions for Further Reading

13. W. Chiu, R. M. Burnett, and R. L. Garcea (eds.) (1997) *Structural Biology of Viruses* Oxford University Press, New York.
14. B. N. Fields, D. M. Knipe, and P. M. Howley (eds.) *Virology* (1996) Lippincott-Raven, Philadelphia.
15. J. E. Johnson and J. A. Speir (1997) J. Mol. Biol. **269**, 665–675.
16. J. E. Johnson and A. J. Fisher (1994) In *Encyclopedia of Virology*, Vol. **1** (R. G. Webster and A. Granoff, eds.), Academic Press, London, pp. 1573–1586.

Carbon Isotopes

Carbon is element number 6 in the periodic table and has valence states of 2, 3, or 4 (1). Thirteen isotopes of carbon have been identified (2), ranging in atomic mass number from ^{8}C (half-life = 3 × 10^{-22} s) to ^{20}C (half-life = 0.01 s) (see Radioactivity and Radioisotopes). Two stable isotopes of carbon are found in nature: ^{12}C at 98.9%, and ^{13}C at 1.1% abundance.

The most important radioactive isotope of carbon is ^{14}C (half-life = 5730 years). Carbon-14 decays by beta-minus emission to nitrogen-14, which is stable. Carbon-14 decay yields one beta particle, with an energy of 0.156 MeV maximum, 0.0495 MeV on average. Carbon-14 is produced naturally in the earth's atmosphere by cosmic ray interactions with stable nitrogen-14 according to the reaction $^{14}N(n,p)^{14}C$. Atmospheric $^{14}CO_2$ is inhaled by animals and respired by plants in photosynthesis, incorporating small amounts of carbon-14 in all living organisms. Consequently, carbon-14 dating is useful for determining the age of organic matter such as wood and archeological specimens. Hundreds of different organic molecules have been labeled with carbon-14 as a tracer for studying biochemical processes and are available from commercial suppliers.

Another radioactive isotope, carbon-11 (half-life = 20.38 min), is used in nuclear medicine diagnostics with positron-emission tomography. Carbon-11 decays by beta-plus (positron) emission to boron-11, which is stable. Carbon-11 decay yields 0.98 beta particles, with an energy of 0.960 MeV maximum, 0.386 MeV on average. Positron emission is characterized by twin 0.511-MeV photons that result from the annihilation of a positron and an electron and allow it to be detected externally. Carbon-11 is produced by proton accelerators according to the reaction $^{11}B(p,n)^{11}C$. Carbon-11 positrons are useful for ^{11}C-acetate (3) and ^{11}C-palmitate (3) metabolism kinetic imaging in the assessment of heart disease (4).

Carbon-13 is very useful in studies involving nuclear magnetic resonance (NMR), because it gives an NMR signal, whereas the more abundant isotope, carbon-12, does not.

Carbon-14 was first produced artificially for metabolism studies in 1939. At present, it is produced commercially by neutron irradiation of beryllium nitride or aluminum nitride according to the reaction $^{14}N(n,p)^{14}C$. The low cross section of this reaction and the long half-life of carbon-14 results in low specific activities, which can make carbon-14 labeling of organic materials quite difficult.

Carbon-14 labeling of organic molecules has numerous applications in the biomedical sciences. Examples include studies of glucose metabolism and conversion to $^{14}CO_2$, galactose oxidation, carbohydrate metabolism, the Krebs cycle, **nucleic acid** synthesis and **hybridization**, autoradiography, or fluorography, and for studying many other biochemical pathways. Among the most important carbon-14 compounds used in biochemistry and metabolism studies are the carbon dioxides and monoxide, carboxyl-labeled acids, methanols, cyanides, carbides, formic acids, and cyanamides (5). Carbon-14 is detected by beta-particle liquid scintillation counting, autoradiography, and fluorography.

Bibliography

1. D. R. Lide and H. Pr. Frederikse, eds. (1995) *CRC Handbook of Chemistry and Physics*, CRC Press, Boca Raton, Fla.
2. Knolls Atomic Power Laboratory (1966) *Chart of the nuclides*, 15th ed., available from General Electric Company, San Jose, Calif.
3. H. R. Schön, H. R. Schelbert, A. Najafi et al. (1982) Am. Heart J. **103**, 532–547.
4. T. L. Rosamond, D. R. Abendschein, B. E. Sobel et al. (1987) J. Nucl. Med. **28**, 1322–1329.
5. *The Radiochemical Manual*, 2nd ed. (1966) Amersham, Bucks, England.

Suggestions for Further Reading

6. J. R. Catch (1961) *Carbon-14 Compounds*, Butterworths, London.

7. J. C. Harbert, W. C. Eckelman, and R. D. Neumann, eds. (1996) *Nuclear Medicine: Diagnosis and Therapy*, Thieme Medical Publishers, Inc., New York.

Carbonic Anhydrase

The enzyme carbonic anhydrase (CA) catalyses the reversible hydration of carbon dioxide to bicarbonate and a proton, using a catalytic zinc ion bound at the active site (1, 2). Carbonic anhydrases are of interest because of their varied metabolic roles, efficient catalytic mechanisms, and high metal ion specificity. The enzyme is found in animals, plants, and bacteria, where it plays roles in respiration, photosynthesis, and CO_2 fixation. Three genetically distinct families of CA proteins have been identified: aCA isozymes, found in all animals; bCA, commonly found in plants and bacteria; and gCA, found in a variety of bacteria (3). Of these classes of CA proteins, the a-CA family is the best characterized. This article provides a brief overview of the metabolic roles and genetic structure of the a-CA human isozymes and describes the catalytic reaction mechanism and metal-binding properties of the high activity, well-characterized human a-CA isozyme II (CAII). Recent work on the b- and g-CA enzymes, which catalyze CO_2 hydration using radically different protein structures, is summarized.

1. Metabolic Function and Genetic Structure of Human a-CA Isozymes

Carbonic anhydrase II (CAII) was first discovered in 1933 in human erythrocytes (4), where it facilitates CO_2 transport in respiration by converting CO_2, released as a metabolic by-product from tissues, to bicarbonate. Bicarbonate is carried by the bloodstream to pulmonary capillaries, where its conversion back to CO_2 is catalyzed by CA for release by the lung. CAII is also expressed in many other tissues, including ocular epithelium, where it plays a role in maintaining intraocular pressure (5). A human genetic disease in which CAII is nonfunctional indicates that this isozyme is also crucial for bone resorption and kidney function (6). Furthermore, the inhibition of CAII by aromatic sulfonamides (RSO_2NH_2) is used clinically to treat glaucoma and altitude sickness (5). Additionally, at least six more CA human **isozymes** with varied activities and locations have been discovered (5). The cytosolic isozymes CAI, CAIII, and CAVI are expressed in high concentrations in red blood cells, **muscle** cells, and salivary glands, respectively. CAIV is a membrane-bound isozyme important for regulating bicarbonate levels in the kidney, whereas CAV is a mitochondrial isozyme. CAVI is secreted by the salivary glands. The exact physiological role of several of these isozymes is still under investigation.

The genomic structure of the human CA isozymes lends insight into their evolution and regulation of their transcription. CAI, CAII, and CAIII have been mapped to chromosome 8q22, CAV and VII to chromosome 16, CAIV to chromosome 17q, and CAVI to chromosome 1 (3). This chromosomal mapping, along with comparisons of DNA sequence homologies, indicates that gene duplication events over 450 million years ago led to distribution of the CA isozymes on four different chromosomes; further gene duplications occurred later, resulting in closely linked isozymes CAI, CAII, and CAIII on one chromosome, and CAIV and VI on another (3). The structures of the various human CA genes currently are being studied to determine the mechanism of their tissue-specific expression. CAI has an unusually long 5′-**untranslated region** containing two **promoters** that direct expression of CAI in erythroid cells and in the colon (7). Other CA genes are also likely to have complex structures to direct their expression in different locations and developmental stages.

2. Catalytic Mechanism and Zinc-Binding Properties of Human CAII

Carbonic anhydrase II is the most thoroughly characterized and most highly active of the CA isozymes, catalyzing the hydration of CO_2 with a rate constant of ~ 10^6 s^1 (1). The crystal structure of CAII reveals a tightly bound zinc ion coordinated by the nitrogen atoms of three protein histidine residues, His94, His96, and His119, located at the bottom of a deep active site cleft (Fig. 1) (8). At physiological pH, a hydroxide ion is also bound by zinc, completing the tetrahedral geometry of the metal site. Residue Thr199 forms a hydrogen bond with the zinc hydroxide, orienting it for efficient catalysis. Catalysis occurs in two main steps (1), initiated by nucleophilic attack of the hydroxide ion on the carbonyl carbon of CO_2 to form bicarbonate.

$$\text{E-ZnOH}^- + \text{CO}_2 + \text{H}_2\text{O} \leftrightarrow \text{E-ZnHCO}_3^- + \text{H}_2\text{O} \leftrightarrow \text{E-ZnOH}_2 + \text{HCO}_3^- \quad (1)$$

Water displaces bicarbonate, and the product is released. In the second, rate-limiting step in catalysis (Eq. (2)), the catalytically active enzyme species is regenerated by transfer of the product proton from the zinc-water to protein residue His64. This residue is exposed to solvent and transfers the proton to buffer B:

$$\text{E-ZnOH}_2 + \text{B} \leftrightarrow {}^+\text{H-E-ZnOH}^- + \text{B} \leftrightarrow \text{E-ZnOH}^- + \text{BH}^+ \quad (2)$$

This proton shuttle is essential for rapid catalysis, as transfer of the proton to buffer is much faster than transfer to water. Carbonic anhydrase is one of the few biological systems in which proton transfer can be studied (9).

Figure 1. The crystal structure of human CAII determined by X-ray crystallography (8). It reveals a twisted b-sheet structure in which three histidine residues coordinate the catalytic zinc ion. Figure generated using MOLSCRIPT (13).

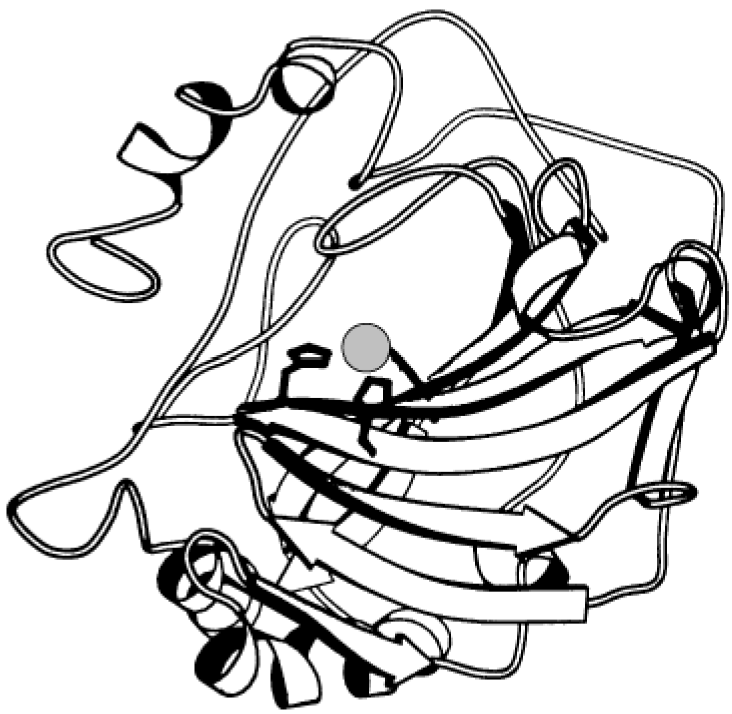

Just as the active site of CA has evolved for rapid catalysis, the protein structure is optimized for tight, specific binding of the zinc ion, with a K_d of ~ 2 pM (2, 10) (see Zinc-Binding Proteins). CAII binds only Cu^{2+}, and Hg^{2+} with comparable affinity, and neither of these metals confers catalytic activity to the enzyme (10). CAII has a much lower affinity, with a K_d of nanomolar, for metals such as Co^{2+}, Mg^{2+}, Cd^{2+}, and Ni^{2+}, and only the Co^{2+}-substituted enzyme is active. As the metal binding properties of this protein have been studied extensively, CAII is often used as a model for creating novel metal sites in proteins.

Studies in which site-directed mutagenesis has been used to alter the nature of conserved residues in the zinc site (2) reveal the importance of several factors for high metal affinity. First, in almost all CAII variants studied, the zinc ion retains tetrahedral geometry even if the surrounding protein structure must be rearranged to accommodate new side-chain positions. Second, the distance between the metal and ligand is crucial. Third, conserved residues that form hydrogen bonds with the histidine zinc ligands each contribute modestly to zinc affinity but play a large role in controlling the rates of metal equilibration (2, 11). The histidine ligands, the residues that form hydrogen bonds to these ligands, and the surrounding protein structure contribute to the reactivity and binding properties of the zinc ion.

3. Genetically Distinct CA Families Arose Through Functional Convergence

Examples of the b-CA and g-CA carbonic anhydrase families are only now being discovered and characterized. In an amazing example of evolutionary functional **convergence**, these protein families are completely unrelated genetically to one another and to the a-CA family, yet these enzymes catalyze the same reaction using a catalytic zinc ion (3). The structure determined by X-ray crystallography of a g-CA isolated from **archaebacteria** (12) reveals a trimeric protein containing three active sites; in each active site, a zinc ion is bound at the monomer interface by three histidine residues from different polypeptide chains. As in a-CA proteins, the zinc is bound in tetrahedral geometry, the fourth ligand being a solvent molecule. In this case, a glutamic acid residue located near the zinc ion in g-CA may be the functional analog of Thr199 in human CAII. No structure of b-CA has been solved yet, but phylogenetic and spectroscopic data suggest that the zinc ion may be coordinated by glutamate or cysteine residues rather than histidine (3).

4. Summary

In recent years, the techniques of site-directed mutagenesis and X-ray crystallography have greatly expanded our knowledge of the relationships between protein structure and function in human CAII (2). The structure of CAII appears to have evolved for maximum catalytic activity and metal affinity. Applying these methods to the carbonic anhydrase enzymes that have evolved independently to catalyze the same reaction will give further insight into how protein structure can dictate the reactivity and affinity of metals.

Bibliography

1. D. N. Silverman and S. Lindskog (1988) Acc. Chem. Res. **21**, 30–36.
2. D. W. Christianson and C. A. Fierke (1996) Acc. Chem. Res. **29**, 331–339.
3. D. Hewett-Emmett and R. E. Tashian (1996) Mol. Phylogenet. Evol. **5**, 50–77.
4. W. C. Stadie and H. O"Brien (1933) J. Biochem. **103**, 521–529.
5. S. J. Dodgson, R. E. Tashian, G. Gros, and N. D. Carter (1991) *The Carbonic Anhydrases: Cellular Physiology and Molecular Genetics*, Plenum Press, New York.
6. W. S. Sly et al. (1983) Proc. Natl. Acad. Sci. USA **80**, 2752–2756.
7. H. J. M. Brady et al. (1991) Biochem. J. **277**, 903–905.
8. K. Hakansson, M. Carlsson, L. A. Svensson, and A. Liljas (1992) J. Mol. Biol. **227**, 1192–1204.
9. D. N. Silverman (1995) Meth. Enzymol. **249**, 479–503.

10. S. Lindskog and P. O. Nyman (1964) Biochim. Biophys. Acta **85**, 462–474.
11. C.-C. Huang et al. (1996) Biochemistry **35**, 3439–3446.
12. C. Kisker et al. (1996) EMBO J. **15**, 2323–2330.
13. P. Kraulis (1991) J. Appl. Crystallogr. **24**, 946–950.

Suggestions for Further Reading

14. D. W. Christianson (1991) Structural biology of zinc. Adv. Prot. Chem. **42**, 218–355.
15. S. J. Dodgson, R. E. Tashian, G. Gros, and N. D. Carter (1991) *The Carbonic Anhydrases: Cellular Physiology and Molecular Genetics*, Plenum Press, New York.
16. W. S. Sly and P. Y. Hu (1995) Human carbonic anhydrases and carbonic anhydrase deficiencies. Ann. Rev. Biochem. **64**, 375–401.
17. R. E. Tashian (1992) Genetics of the mammalian carbonic anhydrases. Adv. Gen. **30**, 321–356.

Carboxyl Groups

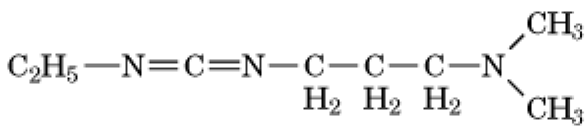

[I] EDC

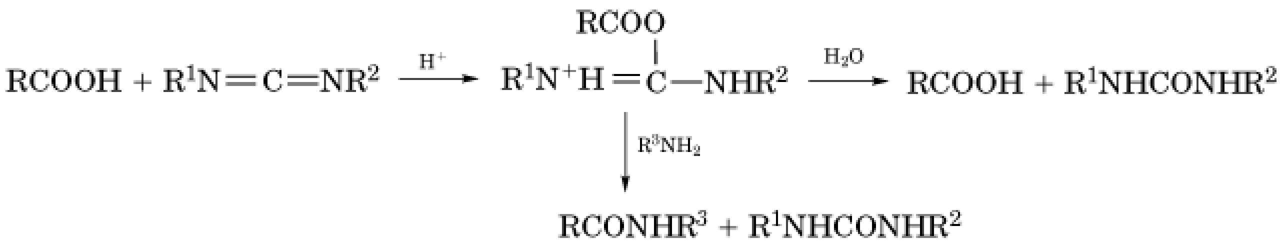

A carboxyl group has the formula —COOH. Among compounds that have a carboxyl group are carboxylic acids. A carboxyl group shows relatively weak acidity. Many carboxylic acids are found in nature as free acids or in the form of esters, amides, or salts. Biologically important acids are those found in the metabolic pathways of glycolysis, fatty acids, amino acids, and so on. A carboxylic acid reacts with a base to form a salt and can be reduced to an aldehyde and an alcohol. A carboxylic acid forms an ester with an alcohol, an amide with an amine, and an acid anhydride with an carboxylic acid [see Anhydrides]. Carboxyl groups are not very reactive, and some catalyst or activation processes are required for their reactions.

There are three kinds of carboxyl groups in proteins, the C-terminal a-carboxyl, the b-carboxyl of aspartic acid, and the g-carboxyl of glutamic acid. They have intrinsic pK_a values of 3.8, 4.0, and 4.4, respectively. Carboxyl groups are often employed as catalytic groups in enzymes, and they often play critical roles in **ligand binding**. Thus, carboxyl groups are important in protein chemistry.

1. Chemical Modification of Carboxyl Groups in Proteins

Esterification and amidation are the usual chemical modifications of carboxyl groups (1). Carboxyl groups in proteins are esterified by treating the dry protein with methanol-HCl. However, this method is drastic and not suitable for selective modification of carboxyl groups. Trialkyloxonium salts, such as triethyloxonium tetrafluoroborate, are commonly used for mild esterification of carboxyl groups in proteins (2). Diazoacetyl compounds, such as diazoacetamide, methyl diazoacetate, and *N*-diazoacetylglycinamide, react with carboxyl groups at acidic pH to form esters. Other reagents, such as acid halogen compounds and ethyleneimine have also been used to esterify the carboxyl groups in proteins.

Carboxyl groups are amidated with simple amines after activating the carboxyl groups with water soluble carbodiimides, such as 1-ethyl-3-(3-dimethylaminopropyl) carbodiimide (EDC) [**I**]. At pH 4.75 to 5, the reaction proceeds as in Scheme 1. Exhaustive amidation is achieved by using high concentrations of both amine (1 M) and EDC (0.1 M) at pH 4.75 under **denaturing** conditions (3). Limited amidation is possible using low concentrations of amine (0.1 M) and EDC (2.6 mM) under mild conditions at pH 5.0 (4). Isoxazolium salts, including Woodward's Reagent K (2-ethyl-5-phenylisoxazolium 3′-sulfonate), can be used in the place of EDC at pH 3 to 5. Amidation is also achieved by ammonolysis of the esters in liquid ammonia at –55°C. In this case, selective amidation is possible starting with a selectively esterified protein (5).

Bibliography

1. T. Imoto and H. Yamada (1989) In *Protein Structure: A Practical Approach* (T. E. Creighton, ed.), IRL Press, Oxford, U.K., pp. 247–277.
2. S. M. Parsons et al. (1969) Biochemistry **8**, 700–712.
3. T.-Y. Lin and D.E. Koshland Jr. (1969) J. Biol. Chem. **244**, 505–508.
4. H. Yamada et al. (1981) Biochemistry **20**, 4836–4842.
5. R. Kuroki et al. (1986) J. Biol. Chem. **261**, 13571–13574.

Carboxyl Proteinase

The carboxyl proteinases (E.C. 3.4.23) are also known as *aspartyl proteinases* or *acid proteinases*, so called because the mechanism by which they catalyze the hydrolysis of peptide bonds in proteins (see Proteinases) involves the participation of two carboxyl groups, usually provided by the side chains of two aspartic acid residues (1). The prototypical member of this large family of structurally-related enzymes is the gastric proteinase, **pepsin**, which is optimally active at acid pH. Other members include *rennin* (*chymosin*) from the fourth stomach of the calf; *renin*, a kidney enzyme found in blood plasma; cathepsin D, found in **lysosomes**; numerous fungal enzymes, such as penicillopepsin; and a number of retroviral proteinases from retroviruses, including the human immunodeficiency virus HIV proteinase that is the target of the proteinase inhibitors used in the treatment of acquired immune deficiency syndrome (AIDS). Pepsin and renin illustrate the range of specificity exhibited by proteinases in general and carboxyl proteinases in particular. Pepsin cleaves multiple bonds in virtually all proteins found in the diet, whereas renin cleaves a single bond in its only known biological substrate, *angiotensinogen*—the precursor of *angiotensin*.

Carboxyl proteinases occur in all **eukaryotic** organisms and are important for protein processing and degradation. They are generally synthesized as inactive precursors that spontaneously activate under acidic conditions. Protein and peptide substrates bind to the active site of these enzymes, and one of the carboxylate groups (in the case of pepsin, it is from Asp32) activates a water molecule to attack the carboxyl group of the peptide bond that is to be cleaved (Figure 1). The other carboxyl group, which is protonated (in pepsin, it is Asp215), donates a proton to the peptide nitrogen atom to form an activated intermediate that dissociates into the products. It is believed that this general mechanism pertains to all of the carboxyl proteinases.

Figure 1. Schematic representation of the mechanism of action of carboxyl proteinases. The substrate (top line) binds to the active site of the enzyme [represented by the carboxyl groups of Asp32 and Asp215 (porcine pepsin numbering)] to form an enzyme-substrate complex. P_1 and P'_1 are the sidechains of the main specificity-determining amino acid residues that contribute the -CO- and -NH- groups to the peptide bond that will be hydrolyzed. The carboxylate group of Asp 32 promotes the attack of a water molecule on the carbonyl carbon of the peptide bond, to form a tetrahedral intermediate that is stabilized by transfer of a proton from Asp 215. The intermediate undergoes rearrangement to form a product complex, which subsequently dissociates, thereby regenerating the original enzyme.

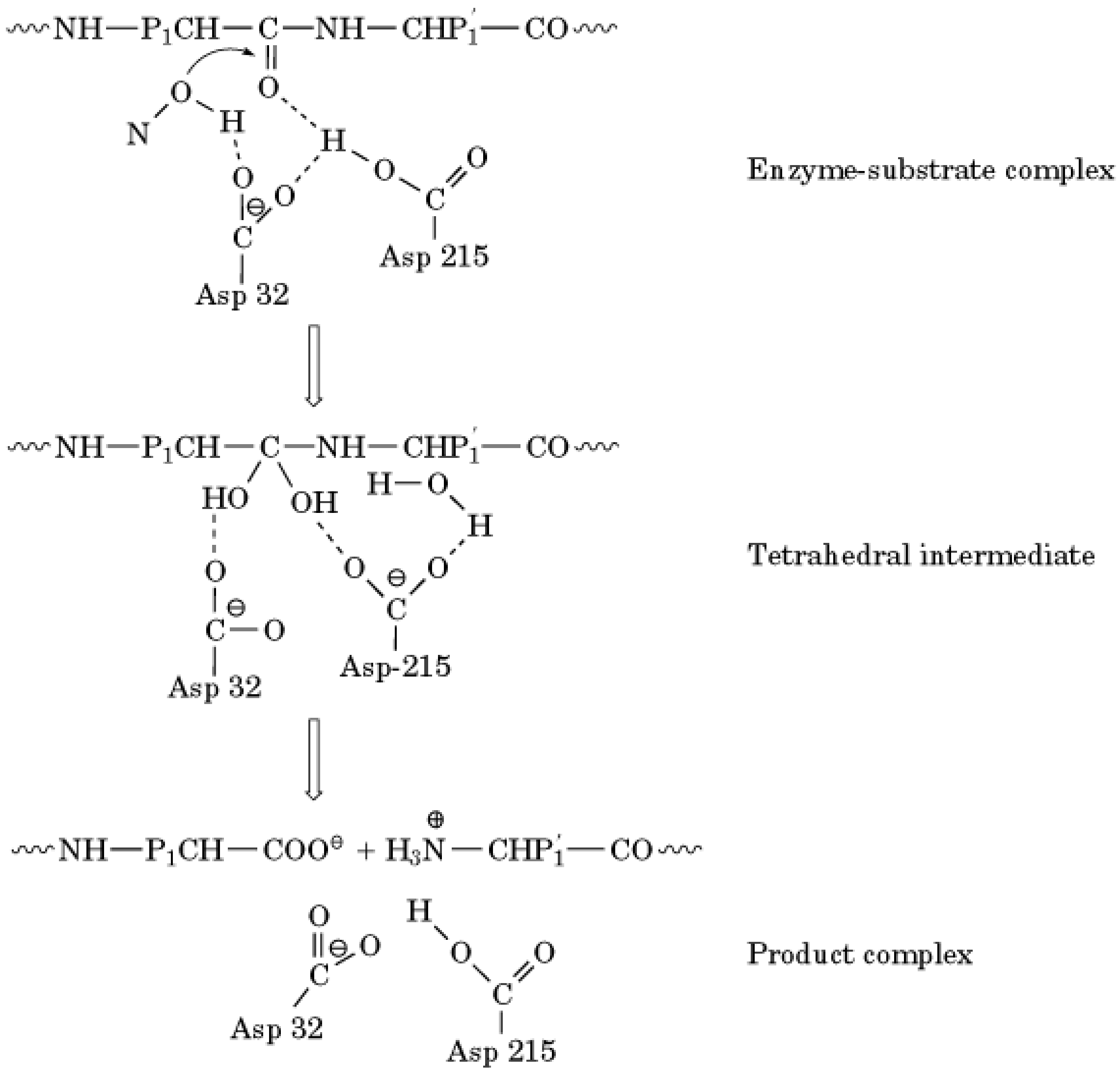

It is interesting that in carboxyl proteinases such as pepsin and renin, both catalytic carboxyl groups are present in the same molecule. In the retroviral proteinase from HIV-1, which only contains 99 amino acids, two molecules form a dimer with a single active site containing one catalytic aspartic acid from each subunit. The larger mammalian and microbial carboxyl proteinases contain approximately 325 residues and appear to have **homologous** amino- and carboxyl-terminal **domains** that likely evolved from an early gene duplication and **fusion** event. Each domain contributes a catalytically active aspartic acid residue.

A characteristic feature of carboxyl proteinases is their susceptibility to inhibition by pepstatin, an acylated pentapeptide analogue produced by **Streptomyces**. Recently a number of carboxyl proteinase inhibitors have been found useful for the treatment of AIDS, particularly when used in conjunction with other viral enzyme inhibitors. Carboxyl proteinase inhibitors have also been proposed for the treatment of malaria. Two such proteinases are believed to be essential for degradation of hemoglobin in the red blood cell phase of the life cycle of the parasite.

Bibliography

1. D. R. Davies (1990) Annu. Rev. Biophys. Biophys. Chem. **19**, 189–215.

Carboxypeptidases

Enzymes that catalyze the hydrolytic cleavage of the carboxyl-terminal amino acid residue from an oligo- or polypeptide chain are called carboxypeptidases.

One group of these enzymes uses a catalytic mechanism analogous to that of the serine proteinases and, in fact, are inhibited by the prototypical serine proteinase inhibitor, diisopropylfluorophosphate (DIFP). These enzymes are found in the **vacuoles** of higher **plants** and **fungi** and in the **lysosomes** of animal cells, and they presumably participate in intracellular **protein degradation**. Many fungi also secrete serine carboxypeptidases. *Carboxypeptidase Y* (E.C. 3.4.16.1) is a serine carboxypeptidase present in yeast vacuoles (1). It is a very useful enzyme for determining the amino acid sequence of peptides and proteins (see Protein Sequencing), because it can release all C-terminal amino acids, including proline. Moreover, it is active in the presence of **denaturants**, such as urea or sodium dodecyl sulfate (**SDS**), and in the pH range from 4 to 7.

The other group contains metallocarboxypeptidases, which have a zinc ion at the catalytic site (2). The best known of these are the pancreatic enzymes, carboxypeptidases A and B, which are synthesized as largely inactive zymogens, procarboxypeptidases A and B, and stored in the zymogen granules of the pancreatic acinar cells. On ingestion of a meal, they are released into the duodenum through the pancreatic duct, become activated by the action of trypsin, and help digest dietary proteins and peptides. The specificity of carboxypeptidase A (E.C. 3.4.17.1) is toward aromatic and bulky **hydrophobic** amino acids, nicely complementary to that of **chymotrypsin**, which generates peptides with just such amino acids at their C-termini. Similarly, the specificity of carboxypeptidase B (E.C. 3.4.17.2) is toward peptides with the C-terminal basic amino acids arginine and lysine, which can be generated by the action of **trypsin**. The combined action of these endo- and exopeptidases ensures optimum formation of essential amino acids. Carboxypeptidase N circulates in plasma and is a peptidyl-L-arginine hydrolase that is thought to be responsible for the degradation of bradykinin and other hormones.

An important dipeptidyl carboxypeptidase, *angiotensin converting enzyme* (ACE), cleaves C-terminal dipeptides from a variety of substrates, most notably angiotensin I and bradykinin. The former reaction generates angiotensin II, a potent vasopressor, and the latter inactivates a vasodilator. This dual effect on blood pressure has led to the widespread use of ACE inhibitors as antihypertensive agents.

Bibliography

1. K. Breddam (1986) Carlsberg Res. Commun. **51**, 83–128.

2. F. X. Aviles et al. (1993) Eur. J. Biochem. **211**, 381–389.

Carcinogen

Translated literally, the term “carcinogen” means giving rise to carcinomas, or epithelial malignancies. In practice, “carcinogen” is used to describe any physical or chemical agent that increases the incidence of tumors in animal models or in human populations. Chemical carcinogens are a diverse group of agents with a range of properties. Much of the early work on carcinogenesis in animal models identified two stages: tumor initiation, thought to involve a mutational event, and tumor promotion, which probably did not. Although this classification of events is still useful in animal studies, it is now recognized as an oversimplification. Cancer develops through a series of stages, which have been exceptionally well-characterized in certain cancers such as those of the colon (1). (An historic perspective on the development of understanding the nature of carcinogenesis is given by Harris (2)). Many of the steps in carcinogenesis involve either mutations or epigenetic changes, with cells gaining a selective advantage and undergoing clonal expansion as a result of activation of **protooncogenes** and/or inactivation of tumor suppressor genes. “Epigenetic” is defined as “all processes relating to the expression (transcription and translation) and the interaction of the genetic material. Epigenetic mechanisms may act at three levels of cell organization: (1) Turn genes off or modulate **protein biosynthesis**, (2) regulate the translation of messenger RNA into proteins, and (3) regulate the topographic distribution and function of proteins.” (3). Metastatic spread of the cancer involves the activation of further oncogenes controlling various aspects of cell adhesion and movement. A scheme showing some of the events involved in various stages of cancer development is shown in Figure 1.

Figure 1. Factors involved in the various stages of carcinogenesis.

INITIATION →	PROMOTION →	PROGRESSION →	METASTASIS
Mutation (exogenous and endogenous factors)	Increased cell turnover (growth factors, hormones, non-genotoxic chemicals)	Genetic instability (mutation of 'normal' oncogenes, suppressor gene loss, chromosomal rearrangements)	Tumor invation (activation of enes for angiogenesis, cell adhesion, proteolysis)

Mutagenicity is the major mechanism for the activation of proto-oncogenes, and most carcinogens are also mutagens. Miller and Miller (4) claimed that the property in common to all the diverse carcinogens is that they either interact directly with DNA or can be metabolically activated to nucleophilic intermediates that are reactive with DNA. While this is certainly true for most carcinogens, there is increasing recognition that not all carcinogens are DNA reactive. For example, inhibitors of topoisomerase II enzymes have been shown to induce human cancers (5), and these act to cause DNA breaks indirectly by poisoning the enzyme (see DNA Topology). A number of carcinogens may act through epigenetic mechanisms. There is also a class of carcinogens that have no action at all on the genetic material (eg, **peroxisome** proliferators, which are thought to work through **receptor** binding and modification of fatty acid metabolism (6)).

While there is no doubt that mutagenic mechanisms are involved in carcinogenesis, there is considerable doubt as to the relative roles of exogenous and endogenous mutagens in the development of human cancers. Exogenous mutagens include alkylating chemicals such as nitrogen mustards and nitrosamines, usually encountered in cancer therapy, and industrial chemicals such as vinyl chloride, dimethyl sulfate, and bis(chloromethyl) ether. Prominent endogenous mutagenic processes include oxy-radical DNA damage, DNA depurination, **DNA polymerase** infidelity, and deamination of 5-methylcytosine.

Bibliography

1. B. Vogelstein, E. R. Fearon, S. R. Hamilton, S. E. Kern et al. (1988) N. Engl. J. Med. **319**, 525–532.
2. C. C. Harris (1991) Cancer Res. **51** (Suppl.), 5023s–5044s.
3. R. Reiger, A. Michaelis, and M. M. Green (1991) *Glossary of Genetics: Classical and Molecular*. Springer-Verlag, New York.
4. E. C. Miller and J. A. Miller (1966) Pharmacol. Rev. **18**, 805.
5. L. R. Ferguson and B. C. Baguley (1994) Environ. Mol. Mutagen. **24**, 245–261.
6. S. Green (1995) Mutat. Res. **333**, 101–109.

Casein

Several kinds of phosphoproteins collectively called casein constitute 80% of the protein of cow's milk and 40% of that of humans. Casein is made up of all 20 kinds of amino acids, which is an important characteristic from a nutritional point of view. Skim milk, which is the milk left after the cream is removed, is brought to pH 4.7 to form a precipitate that contains the casein. The supernatant is called whey and contains 20% of the total protein. Electrophoresis at alkaline pH separates casein into the a, b, and g fractions. The a fraction is further separated into a_{s1} and a_{s2}, the common subscript *s* signifying sensitivity to precipitation by the addition of calcium and k-casein. Both a_s-casein and b-casein are precipitated with Ca^{++}, whereas k-casein is not. In milk, these caseins constitute micelles (calcium caseinate-phosphate complex) of a diameter in the range of 30 to 300 nm. The a- and b- caseins are rich in phosphate, mainly in the form of O-phosphoserine residues, and they form a calcium complex that is not soluble, but precipitated. When surrounded by the hydrophilic parts of k-casein in milk, however, it is soluble as large complexes. The g-casein fraction is a heterogeneous mixture primarily of proteolytic fragments of b-casein.

Bovine b-casein contains 209 amino acid residues (with a molecular weight of 23,600) and is very hydrophobic. Five phosphoserine residues are found in the N-terminal region. In milk, the phosphoserine residues are associated with Ca^{++} ions, forming calcium caseinate. b-casein and its partial hydrolysis products present in milk do not have definite three-dimensional structures. They are considered to have a random coil structure that is easily digestible, an advantage of casein as a nutritional protein. The relative casein composition of bulk milk is given in Table 1.

Table 1. Average Casein Composition of Bovine Bulk Milk Samples

Casein Type	Weight %
a_{s1}	38.1
a_{s2}	10.2
b	35.7
k	12.8
g	3.2
Total	100.0

The fourth stomach of ruminating animals (abomasum) contains a proteolytic enzyme called *chymosin*, which liberates a glycopeptide from k-casein at neutral pH. The remaining molecule, called para-casein, reacts with Ca^{++} and then forms an insoluble curd, the source of cheese. The enzyme preferentially cleaves the peptide bond between Phe105-Met106 of k-casein to produce para-k-casein. Humans do not have chymosin, but **pepsin** in the stomach converts k-casein to para-casein to start the digestion of milk in the infant stomach. Chymosin and pepsin are structurally related.

The casein micelle has a complex structure, and the relative disposition of the four subspecies of casein, and especially that of k-casein, has long been the focus of discussion. Since chymosin preferentially digests k-casein, this casein is thought to be on the periphery of the micelle. Recent **electron micrographs** of variously treated micelles show granular structures covering the surface, prompting a suggestion that a casein micelle is composed of smaller-sized submicelles. The idea of a submicellar structure has actually been a long standing one from reconstitution experiments, and by incorporating various observations, a currently accepted model of casein micelles is presented by Holt (1), as reproduced in Figure 1.

Figure 1. Structural model of casein micelles. Reproduced from (1) (Fig. 13, p. 108) with permission.

Secretory vesicles of casein micelles are found abundantly in mammary secretory cells. After the casein proteins are synthesized, they undergo O-glycosylation and **phosphorylation** before being secreted. These changes occur in concert with lactose synthesis by the enzyme known as lactose synthetase. All the enzymes involved in glycosylation, phosphorylation, and lactose synthesis can tolerate Ca^{++} concentrations in the range of 1 *mM*. Accumulation of Ca^{++} in the mammary gland cell, together with phosphorylation of some serine residues, is necessary for the formation of casein micelles.

Bibliography

1. C. Holt (1992) Structure and stability of bovine casein micelles, Adv. Prot. Chem. **43**, 63–151.

Caspases

Caspases are proteinases involved in apoptosis and programmed cell death. They are mammalian **homologues** of the Ced-3/interleuking-1b converting enzyme (ICE) products of cell death genes (1). The caspase family in mammalian cells currently numbers 14, as shown in Figure 1. They are thiol proteinases that are synthesized as inactive pro-proteins that are processed to a pro-domain and two subunits of approximately 10 and 20 kDa in size. The pro-caspases are inert until proteolytic cleavage of the pro-domain and/or the p10 subunit from the p20 subunit. Caspases share a conserved active-site sequence, -Gln-Ala-Cys-Arg-Gly- (QACRG) or -Gln-Ala-Cys-Gln-Gly- (QACQG), and cleave their substrates at the peptide bond after an aspartate residue; hence, their name- **c**ysteine **asp**artate-specific protein**ases** (1, 2). Caspases cleave specific substrates during apoptosis and are required for the rapid degradation of the cell (2-6); however, none is thought to be critical for apoptosis to occur.

Figure 1. The mammalian caspase family. The various members have been arranged in a phylogeny on the basis of their relative amino acid sequence homologies. The members of the Ced-3-like family of caspases are thought to be the downstream effectors of apoptosis and to be activated in a caspase cascade by the apical members represented by caspases 2, 8, 9, and 10 (1).

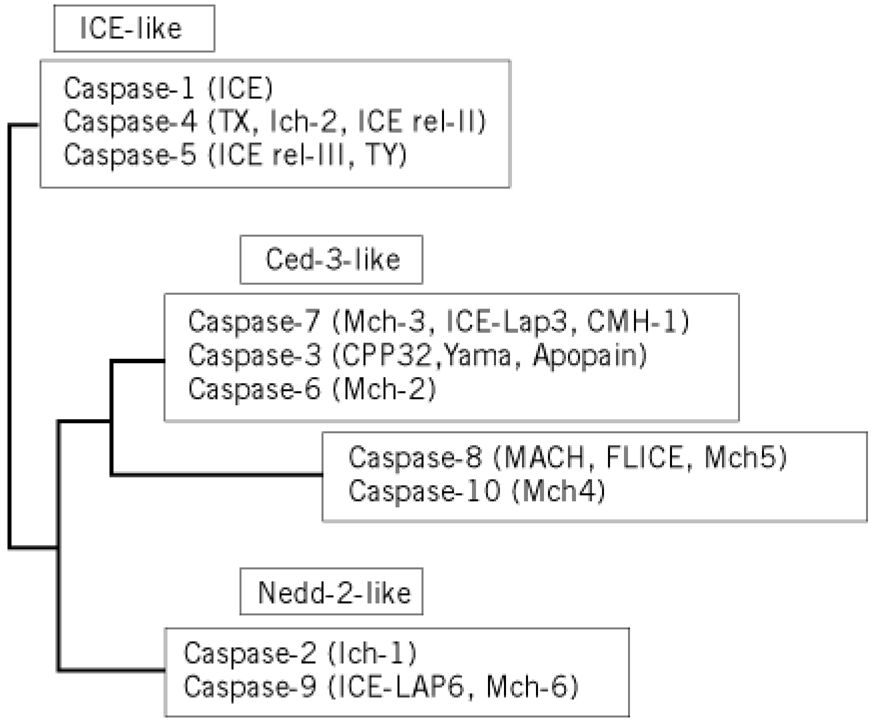

Caspases can be divided into subgroups, with each sharing a specific substrate specificity beyond the overall caspase requirement for Asp at the P1 position of the substrate (see Proteinases). Caspases 1, 4, and 5, for example, preferentially cleave after -Tyr-Val-Ala-Asp- (YVAD) sequences and have not been shown to be critical for apoptosis to occur. Caspases 3 and 6, however, are active during cell death and cleave primarily substrates with the sequence -Asp-Xaa-Xaa-Asp- (DxxD). Caspases 2, 8, and 10 are different again and are thought to activate primarily the downstream caspases, such as caspase 3 and 6 (7). This suggests that caspases act in a hierarchy, with activated upstream caspases cleaving downstream caspases and activating them in turn, to generate a *caspase cascade* (4, 8). The apical caspases are proposed to be those with large pro-domains such as caspases 2, 8, and 10. The pro-domains contain a protein structure that facilitates their interaction with other proteins leading to caspase activation, as seen in CD95 (Fas/Apo-1)-induced apoptosis (9).

Bibliography

1. E. Alnemri, D. Livingston, D. Nicholson, G. Salvesan, N. Thornberry, W. Wong, and Yuan, J. (1996) Human ICE/CED-3 protease nomenclature. Cell **87**, 171.
2. A. Takahashi and W. Earnshaw (1996) Ice-related proteases in apoptosis. Curr. Opin. Gen. Dev. **6**, 50–55.
3. A. Chinnaiyan and V. Dixit (1996) The cell-death machine. Curr. Biol. **6**, 555–562.
4. Y. Lazebnik, A. Takahashi, G. Poirier, S. H. Kaufmann, and W. Earnshaw (1995)

Characterization of the execution phase of apoptosis *in vitro* using extracts from condemned phase cells. J. Cell. Sci. **19**, 41–49.
5. M. Whyte (1996) ICE/Ced-3 proteases in apoptosis. Trends Cell Biol. **6**, 245–248.
6. A. Fraser, N. McCarthy, and G. I. Evan (1996) Biochemistry of cell death. Curr. Opin. Neurobiol. **6**, 71–80.
7. T. Fernandes Alnemri, R. C. Armstrong, J. Krebs, S. M. Srinivasula, L. Wang, F. Bullrich, L. C. Fritz, J. A. Trapani, K. J. Tomaselli, G. Litwack, and E. S. Alnemri (1996) *In vitro* activation of CPP32 and Mch-3 by Mch-4, a novel human apoptotic cysteine protease containing 2 FADD-like domains. Proc. Natl. Acad. Sci. USA **93**, 7464–7469.
8. Y. A. Lazebnik, A. Takahashi, R. D. Moir R. D. Goldman, G. G. Poirier, S. H. Kaufmann, and W. C. Earnshaw (1995) Studies of the lamin proteinase reveal multiple parallel biochemical pathways during apoptotic execution. Proc. Natl. Acad. Sci. USA **92**, 9042–9046.
9. A. Fraser and G. Evan (1996) A license to kill. Cell **85**, 781–784.

Cassette Mutagenesis

Cassette mutagenesis involves replacing a wild-type **DNA** sequence with synthetic double-stranded oligonucleotides in order to introduce one or more mutations (1-6). The technique allows saturation of a target amino acid codon with mutations, and can be used to probe the role of that particular residue in a protein and the effect of specific point mutations in it. In their description of the method, Wells et al. (4) synthesized single-stranded oligonucleotides containing different codons over the target in separate pools. Oligonucleotide-**site-directed mutagenesis** procedures are used to generate **restriction sites** that closely flank the target codon in the **plasmid** containing the gene of interest. Use of the appropriate restriction endonucleases permits insertion of the synthetic duplex cassettes. These are designed to restore fully the wild-type coding sequence except over the target codon, and also to eliminate one of the restriction sites. This latter point is important for selection of the clones containing the mutant cassette.

Several variations on the original technique have been developed for specific purposes. For example, Reidhaar-Olsen and Sauer (5) described a combinatorial method, in which they randomized two or three positions by oligonucleotide cassette mutagenesis, selected for functional protein and then sequenced to determine the spectrum of allowable substitutions at each position. They applied the method repeatedly in order to examine the role of different substitutions on the DNA-binding domain of **lambda repressor**. Kegler-Ebo et al. (6) described codon cassette mutagenesis as a way of depositing single codons at specific sites in double-stranded DNA. Using this method, a series of 11 cassettes is sufficient to insert all possible amino acids at any constructed target site.

Bibliography

1. S. Green (1955) Mutat. Res. **333**, 101–109.
2. M. D. Matteuci and H. L. Heyneker (1983) Nucleic Acids Res. **11**, 3113–3121.
3. J. B. McNeil and M. Smith (1985) Mol. Cell. Biol. **5**, 3545–3551.
4. J. A. Wells, M. Vasser, and D. B. Powers (1985) Gene **34**, 315–323.
5. J. F. Reidhaar-Olsen and R. T. Sauer (1988) Science **241**, 53–57.
6. D. M. Kegler-Ebo, G. W. Polack, and D. DiMaio (1994) Methods Mol. Biol. **57**, 297–310.

Catabolite Repression

The ability of glucose to inhibit the synthesis of certain enzymes, referred to as the *glucose effect*, was recognized in **bacteria** at an early date by Monod (1). He observed that when *Escherichia coli* encounters both glucose and lactose, for example, it metabolizes the glucose first and represses the use of lactose, resulting in biphasic growth (diauxie). This phenomenon is due to the repressive effect of glucose on the synthesis of enzymes required for the metabolism of other sugars. Later, the term catabolite repression was introduced as a general name for the glucose effect because compounds closely related to glucose elicited varying degrees of repression of glucose-sensitive enzymes, and the catabolites derived from the repressing compound were assumed to cause the glucose effect (2). Studies on catabolite repression up to the early 1970s brought about the discovery of a positive control system of transcription by cyclic AMP (cAMP) and the cyclic AMP receptor protein (CRP) (also called the catabolite gene activator protein, (CAP)) and led to the concept that catabolite repression is caused by reduction of the level of intracellular cAMP (3). We now know that multiple and different mechanisms are operating, depending on the growth conditions and the target operons, and that the cAMP-dependent mechanism is just one aspect of catabolite repression. Ironically, the preferential utilization of glucose over lactose, the prototype of catabolite repression, is not due to the reduction of the cAMP-CRP complex (4, 5).

Sometimes the term catabolite repression has been used to describe the glucose effect that is independent of the operon-specific regulator, such as the Lac repressor. Here, we shall use it as a general name for the glucose effect as originally defined. According to this view, which is apparently generally accepted, catabolite repression includes all forms of the glucose effect, regardless of their mechanisms. We also concentrate on catabolite repression in *E. coli*. Although several mechanisms of glucose catabolite repression are now understood in *E. coli*, a common feature is that glucose causes catabolite repression ultimately by modulating the activity of transcription factors involved in the regulation of target operons.

1. cAMP–CRP Complex

The best characterized mechanism of catabolite repression involves the regulation of the intracellular concentration of the cAMP–CRP complex. It is well known that the presence of glucose in the growth medium lowers the intracellular cAMP level under certain conditions (3, 6). Cyclic AMP is synthesized from ATP by the enzyme adenylate cyclase. Although the mechanism of regulation of the cAMP level remains elusive, glucose is thought to decrease cAMP by decreasing the level of the phosphorylated form of enzyme IIA^{Glc}, which is involved in the activation of adenylate cyclase. IIA^{Glc} is one of the enzymes of the phosphoenolpyruvate-dependent carbohydrate **phosphotransferase system** (PTS) and is directly responsible for the **active transport** and phosphorylation of glucose (7). Recently, it was discovered that the concentration of CRP is also lowered by the presence of glucose and that this is an additional factor contributing to catabolite repression (8). The decreased CRP is a consequence of the complex autoregulation of expression of the *crp* gene (9). It should be noted that the reduction in the cAMP-CRP level by glucose is usually rather moderate (in the range of several-fold).

2. Inducer Exclusion

The second mechanism of catabolite repression is inducer exclusion, by which glucose lowers the intracellular concentration of inducers necessary for the induction of catabolic operons (7). The target of glucose signaling in inducer exclusion is operon-specific regulators, such as the Lac repressor. The dephosphorylated enzyme IIA^{Glc}, which accumulates in the presence of glucose, binds to and inactivates (for example) the Lac permease, resulting in an increase of the active unliganded Lac repressor (see Lac Operon). Inducer exclusion is a mechanism by which glucose inhibits more strictly the expression of target operons.

3. Catabolite Repressor/Activator Protein

The third mechanism of catabolite repression is mediated by the catabolite repressor/activator (Cra) protein, which acts as a global regulator of genes encoding enzymes of central carbohydrate metabolism (10). The unliganded form of Cra binds to the operator regions of target operons, causing either activation or inhibition of transcription. The presence of glucose or other PTS sugars produces glycolytic catabolites, such as fructose-1-phosphate, which bind to the Cra protein and cause it to dissociate from the target DNA, resulting in either catabolite repression or catabolite activation.

4. Relationships between the Various Mechanisms

While multiple mechanisms of catabolite repression have been identified in *E. coli*, their signaling pathways appear to be interrelated to each other. For example, the PTS plays a pivotal role in the regulation of the intracellular concentrations of cAMP, inducer, and glycolytic catabolites. In addition, it is particularly important to realize that the contribution of each mechanism varies, depending on growth conditions and the target genes. For example, the Cra-mediated mechanism may play no role in catabolite repression of the *lac* operon, because this operon is not under the control of Cra. An unexpected finding is that the presence of glucose in the lactose medium does not affect the intracellular cAMP level (4). This means that catabolite repression mediated by the reduction in cAMP never happens in glucose–lactose diauxie. The presence of unliganded Lac repressor through inducer exclusion is the principal mechanism for this historical phenomenon (4, 5). Figure 1 illustrates the present understanding of catabolite repression in the glucose–lactose system.

Figure 1. Mechanism of catabolite repression in the glucose-lactose system (4). When both lactose and glucose are present, glucose is transported and phosphorylated by the glucose PTS (IIA^{Glc} + IICB^{Glc}), increasing the concentration of the nonphosphorylated form of IIA^{Glc}, which prevents the uptake of lactose by inhibiting the Lac permease activity. Thus, the concentration of *lac* inducer is very low in the presence of glucose, so the Lac repressor is active and represses transcription of the *lac* operon. It should be noted that glucose does not affect the binding of cAMP–CRP to the promoter, because the levels of cAMP and CRP are not reduced by the presence of glucose.

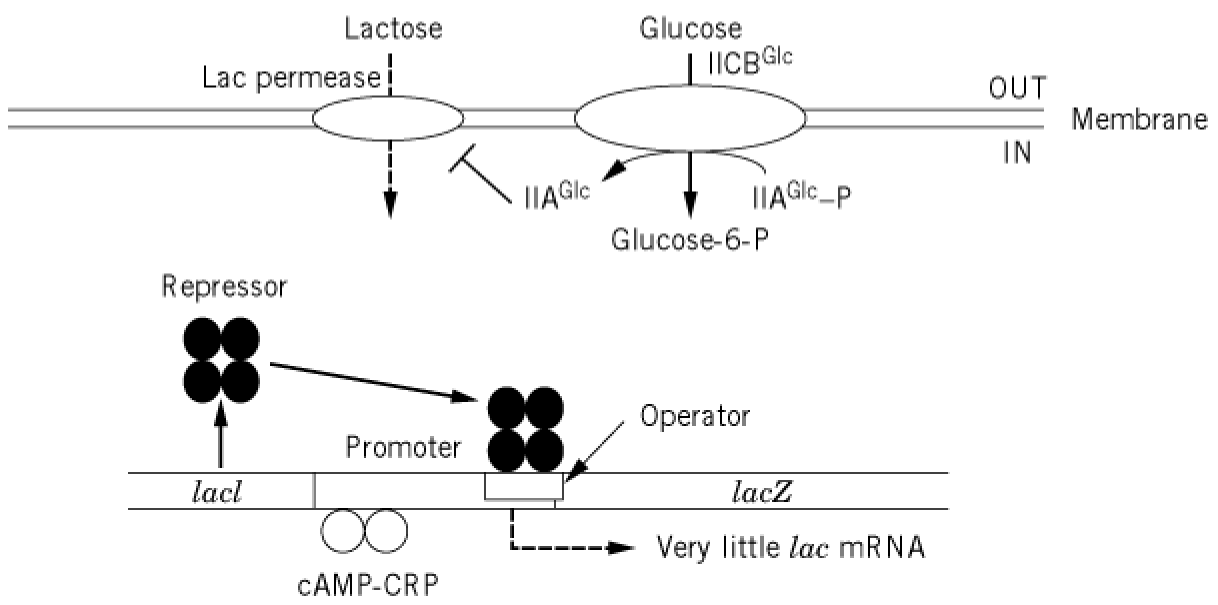

There are more stories yet to be elucidated before catabolite repression in *E. coli* is fully understood. Further diversity in the mechanism of catabolite repression is known in **Gram-positive** bacteria (11).

Bibliography

1. J. Monod (1947) Growth **11**, 223–289.
2. B. Magasanik (1961) Cold Spring Harbor Symp. Quant. Biol. **26**, 249–256.
3. I. Pastan and R. Perlman (1970) Science **169**, 339–344.
4. T. Inada, K. Kimata, and H. Aiba (1996) Genes to Cells **1**, 293–301.
5. K. Kimata, H. Takahashi, T. Inada, P. Postma, and H. Aiba (1997) Proc. Natl. Acad. Sci. USA **94**, 12914–12919.
6. R. S. Makman and E. W. Sutherland (1965) J. Biol. Chem. **240**, 1309–1314.
7. P. W. Postma, J. W. Lengeler, and G. R. Jacobson (1993) Microbiol. Rev. **57**, 543–594.
8. H. Ishizuka, A. Hanamura, T. Kunimura, and H. Aiba (1993) Mol. Microbiol. **10**, 341–350.
9. H. Ishizuka, A. Hanamura, T. Inada, and H. Aiba (1994) EMBO J. **13**, 3077–3082.
10. M. H. Saier and T. M. Ramseier (1996) J. Bacteriol. **178**, 3411–3417.
11. C. J. Hueck and W. Hillen (1995) Mol. Microbiol. **15**, 395–401.

Suggestions for Further Reading

12. B. Magasanik (1970) "Glucose effects: inducer exclusion and repression", in *The Lactose Operon*, J. Beckwith and D. Zipser, eds., Cold Spring Harbor Laboratory Press, Cold Spring Harbor, New York, pp. 189–220.
13. A. Ullmann and A. Danchin (1983) Role of cAMP in bacteria, Adv. Cyclic Nucleotide Res. **15**, 1–53.
14. N. D. Meadow, D. K. Fox, and S. Roseman (1990) The bacterial phosphoenolpyruvate:glycose phosphotransferase system. Annu. Rev. Biochem. **59**, 497–542.
15. M. H. Saier Jr., T. M. Ramseier, and J. Reizer (1996) "Regulation of carbon utilization", in *Escherichia coli and Salmonella typhimurium: Cellular and Molecular Biology*, F. C. Neidhardt, R. Curtiss III, J. L. Ingraham, E. C. C. Lin, J. K. B. Low, B. Magasanik, W. S. Reznikoff, M. Riley, M. Schaechter, and H. E. Umbarger, eds., American Society for Microbiology, Washington, DC, pp. 1325–1343.

Catalase

Catalase, also called *hydroperoxidase*, is a protective enzyme that has been studied for over a century; the concept of a specific protein catalyzing (hence the name *catalase*) the degradation of hydrogen peroxide to oxygen and water first appeared in 1900 (1). Removal of H_2O_2, as shown in the following reaction, avoids unwanted side reactions and prevents the formation of the even more reactive hydroxyl radical:

$$2\ H_2O_2 \rightarrow 2\ H_2O + O_2 \qquad (1)$$

Although the removal of these reactive oxygen species is not essential for growth, catalases do enhance long-term survival in an aerobic environment (2).

A number of developments have spawned considerable interest in the enzyme and spurred extensive studies of both the enzyme and its genes. The first was the simplicity of the "drop test" assay, which involves the visual monitoring of oxygen evolution after the application of a drop of 30% H_2O_2 to the edge of a bacterial colony. Such ease of **phenotypic** scoring has resulted in extensive use of the enzyme as a diagnostic tool for microbiological strain identification. Catalases have been found to be synthesized as part of a variety of **stress response** systems, resulting in their frequent use as indicators of stress response activation. More recently, the catalase–peroxidase family has gained notoriety from its role as the *in vivo* activator of isoniazid into an effective antibiotic in *Mycobacterium tuberculosis* (3). Loss of the enzyme through mutation results in isoniazid resistance, one of the reasons for the increasing spread of tuberculosis.

1. Assay

Two quantitative assay methods are commonly used for catalase activity. One involves the measurement of oxygen evolution using an oxygraph equipped with a Clark electrode (4); the second is a spectrophotometric assay of H_2O_2 by its **absorbance** at 240 nm (5). The two assay procedures produce comparable values in reasonably clear protein solutions, but the oxygraph protocol has the advantage that it can be used for catalase determinations in whole-cell suspensions and in quite turbid extracts. Catalase activity can be visualized on polyacrylamide gels following electrophoresis under nondenaturing conditions (6), producing a clear band in a brown background. This same visualization procedure can be easily modified to visualize peroxidase activities as brown bands on a clear background.

2. Classification

Because of the protection afforded against active oxygen species by catalases, most aerobic organisms produce at least one catalase from among the three main classes of the enzyme. The largest class includes the "typical," heme-containing, monofunctional catalases with either small (~60 kDa) or large (>80 kDa) subunits. The next largest class includes the bifunctional catalase–peroxidases, which are also heme-containing but with sequence similarity to plant and fungal peroxidases. The third and, to date, smallest class includes the non-heme- or Mn-containing catalases. Small-subunit, monofunctional catalases have been found in prokaryotes and eukaryotes but not in an archael species, and the large-subunit catalases are restricted to fungi and bacteria. The catalase-peroxidases are found in **prokaryotes** and **archaebacteria**, and the non-heme-containing enzymes have been found only in bacteria (7).

3. Reaction

Catalases and peroxidases both degrade H_2O_2 but, whereas catalase employs H_2O_2 as both electron donor and acceptor (reaction 1), a peroxidase uses organic substrates as the electron donor to reduce H_2O_2:

$$H_2O_2 + RH_2 \rightarrow 2\ H_2O + R \tag{2}$$

The catalase-peroxidases catalyze both reactions 1 and 2 at significant rates.

The well-characterized catalytic reaction pathway is a two-step process. First, H_2O_2 is converted to water and an oxyferryl species, compound I, with the iron in the +5 oxidation state but with part of the charge delocalized in a heme cation radical:

$$Heme\text{—}Fe^{III} + H_2O_2 \rightarrow heme\text{—}Fe^{V} = O(cpd\ I) + H_2O \quad (3)$$

Then compound I reacts with a second molecule of H_2O_2 to produce water and molecular oxygen:

$$Heme\text{—}Fe^{V} = O + H_2O_2 \rightarrow heme\text{—}Fe^{III} + O_2 + H_2O \quad (4)$$

In the absence of a suitable substrate for the reduction of compound I, other intermediates can be formed such as the catalytically inactive compound II.

4. Structure and Properties

Detailed structural information is now available for all three types of catalases. Small- and large-subunit catalases share a common highly conserved core sequence of about 350 residues organized in a b-barrel structure (see Beta-Sheet). This is illustrated in Figure 1 (8, 9), which compares the small subunit of *Proteus mirabilis* catalase (Fig. 1**a**) and the large subunit of *Escherichia coli* HPII (Fig. 1**b**). An *N*-terminal extension of 10–90 residues (colored red in Fig. 1B) and a *C*-terminal extension of 150–170 residues (colored white in Fig. 1**b**), the latter organized in a flavodoxin-like structure, are added to the core structure in the large-subunit enzyme. The tetrameric organization of small-subunit enzymes is sufficiently stable to resist denaturation by organic reagents and to retain activity over a broad pH range from 4 to 11. In large-subunit enzymes, the extended sequences allow the amino terminus of one subunit to be overlapped or trapped by the carboxyl terminus of an adjacent subunit (10), and this interweaving further enhances the resistance of the tetramer to denaturation by heat, **SDS**, and urea.

Figure 1. Comparison of the structures of the small subunit of *Proteus mirabilis* catalase (**a**) (8) and the large subunit of *E. coli* HPII catalase (**b**) (9). The conserved b-barrel core structure is colored blue in both subunits. The 78 additional residues at the *N* terminus of HPII in (**b**) are colored red, and the 195 additional residues at the *C* terminus of HPII in (**b**) are colored white. See color insert.

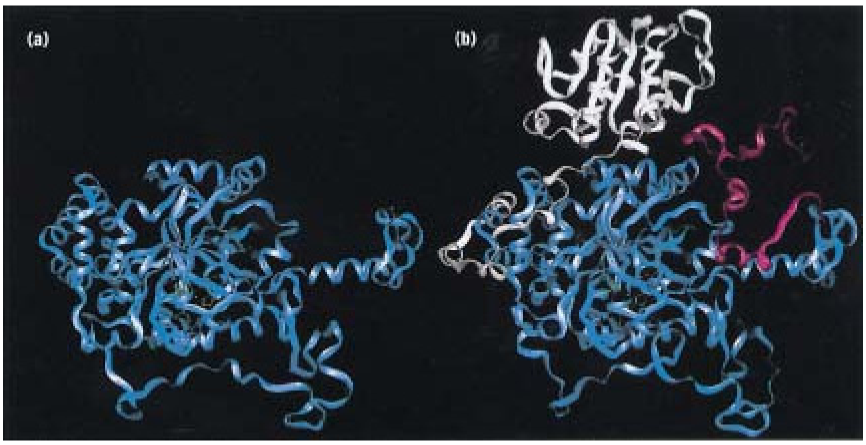

Besides size, the small- and large-subunit catalases have two other characteristic differences. The first is that small-subunit enzymes contain heme *b*, which in large-subunit enzymes is converted to a *cis*-hydroxy g-spirolactone heme *d* and flipped 180°. The second is that small-subunit, but not large-subunit, catalases contain NADPH (11), which is postulated to have a role in the reduction of inactive compound II. A number of unusual modifications have been identified in catalases, including

1. A methionine sulfone in the active site of the *P. mirabilis* enzyme (12)

2. A blocked cysteine residue in HPII from *E. coli* (13)
3. A histidine–tyrosine bond in HPII

The narrow channel leading to the deeply buried active site of catalases limits access to small substrates and inhibitors, and results in a 10-fold higher apparent $\boldsymbol{K}_{\mathbf{m}}$ for H_2O_2 compared to the non-heme-containing catalases and catalase–peroxidases. Within the catalase active site, a histidine residue immediately above the heme, and an asparagine residue situated to one side, orient the H_2O_2 over the heme iron (12) to facilitate a very fast reaction in both small- and large-subunit enzymes [k_{cat} @ $3.5 \times 10^5\ s^{-1}$ (15) and $1.2 \times 10^5\ s^{-1}$, respectively] as compared to the catalase–peroxidases and non-heme-containing catalases [k_{cat} @ $1.6 \times 10^4\ s^{-1}$ (16) and $3.9 \times 10^5\ s^{-1}$ (17), respectively].

5. Cloning and Expression

The number of catalase enzymes in a given organism varies: one in animals, one or two in **fungi**, one to three in plants, and zero to three in bacteria. The availability of catalase-deficient hosts, the ease of assay, and the development of protocols using oligonucleotide and **PCR** probes have facilitated the cloning and characterization of over 90 catalase genes. Most of the isolated genes are from plants and bacteria, with a small number from fungi and animals. A **phylogenetic** comparison of the core protein sequences has revealed separate branches for the small-subunit enzymes from bacterial, plant, animal, and fungal sources, and one additional branch containing the large-subunit enzymes from both fungal and bacterial origins.

The most detailed studies of catalase gene expression have been carried out in plants and bacteria. In maize, catalase expression is tied to developmental changes during kernel development and seed germination and to environmental factors such as light and growth regulators (18). A multitude of species-specific mechanisms control catalase and catalase–peroxidase expression in bacteria, but two common threads are evident among these expression patterns involving induction either by an active oxygen species such as H_2O_2 or in stationary phase. In most cases, the control mechanisms can be rationalized as either protective responses to oxidative stress or as a means of enhancing long-term survival during metabolic limitation (7, 19).

Bibliography

1. O. Loew (1900) U.S. Dept. Agriculture Rpt. 65, Govt. Printing Office, Washington, DC.
2. M. R. Mulvey, J. Switala, A. Borys, and P. C. Loewen (1990) J. Bacteriol. **172**, 6713–6720.
3. J. S. Blanchard (1996) Annu. Rev. Biochem. **65**, 215–239.
4. M. Rorth and P. K. Jensen. (1967) Biochim. Biophys. Acta **139**, 171–173.
5. A. G. Hildebrandt and I. Roots (1975) Arch. Biochem. Biophys. **171**, 385–397.
6. E. M. Gregory and I. Fridovich. (1974) Anal. Biochem. **58**, 57–62.
7. P. C. Loewen (1997) In J. G. Scandalios, ed., *Oxidative Stress and the Molecular Biology of Antioxidant Defenses*, Cold Spring Harbor Laboratory Press, Cold Spring Harbor, NY, pp. 273–308.
8. P. Gouet, H. M. Jouve, and O. Dideberg (1995) J. Mol. Biol. **249**, 933–954.
9. J. Bravo, N. Verdaguer, J. Tormo, C. Betzel, J. Switala, P. C. Loewen, and I. Fita (1995) Structure **3**, 491–502.
10. W. R. Melik-Adamyan, V. V. Barynin, A. A. Vagin, V. V. Borisov, B. K. Vainshtein, I. Fita, M. R. N. Murthy, and M. G. Rossmann (1986) J. Mol. Biol. **188**, 63–72.
11. H. N. Kirkman and G. F. Gaetani (1984) Proc. Natl. Acad. Sci. USA **81**, 4343–4347.
12. A. Buzy, V. Bracchi, R. Sterjiades, J. Chroboczek, P. Thibault, J. Gagnon, H.-M. Jouve, and G.

Hudry-Clergeon (1995) J. Protein Chem. **14**, 59–72.
13. S. Sevinc, W. Ens, and P. C. Loewen (1995) Eur. J. Biochem. **230**, 127–132.
14. I. Fita and M. G. Rossmann (1985) J. Mol. Biol. **185**, 21–37.
15. A. Deisseroth and A. L. Dounce (1970) Physiol. Rev. **50**, 319–375.
16. A. Claiborne and I. Fridovich (1979) J. Biol. Chem. **254**, 4245–4252.
17. Y. Kono and I. Fridovich (1983) J. Biol. Chem. **258**, 6015–6019.
18. J. G. Scandalios (1992) in J. G. Scandalios, ed., *Molecular Biology of Free Radical Scavenging Systems*, Cold Spring Harbor Laboratory Press, Cold Spring Harbor, NY, pp. 117–152.
19. H. Schellhorn (1994) FEMS Microbiol. Lett. **131**, 113–119.

Catalysis

Catalysis by enzymes starts with the collision between the enzyme E and its substrate A to form an enzyme-substrate complex EA:

$$\begin{array}{ccc} \mathrm{E + A \rightleftharpoons EA \rightleftharpoons EA^*} & \rightleftharpoons & \mathrm{EP^* \rightleftharpoons EP \rightleftharpoons E + P} \\ [\text{ collision clamping }] & \text{conversion} & [\text{ unclamping dissociation }] \\ \text{binding} & \text{catalysis} & \text{release} \end{array}$$

This is a second-order reaction, as it involves two reactants, and the collision rate is equal to $k[E_t][A_t]$, where k is a second-order rate constant. There is a distinct limit to the value of k, as it cannot exceed the diffusion rate (see Diffusion-Controlled Reactions and Turnover Number). Nonproductive complexes can also form as a result of the interaction of a substrate with an enzyme. If the structure of a substrate is complementary to that of the active site of the enzyme, the interaction rate is high and the binding tight. If, however, this is not the case, some of the binding energy has to be utilized to facilitate the interaction through a conformational change or clamping reaction on the enzyme. Binding is the product of the initial interaction and the subsequent conformational change.

After being bound to the enzyme, the substrate must undergo activation. That is, a proportion of the total number of substrate molecules in the ground state must be raised to the transition state. This is a short-lived, unstable species with a structure intermediate between that of the substrate and the product. These activated molecules can fall back to the ground state or be converted to EP^* at a rate that is independent of the structure of the reactants. The activation energy barrier for the conversion of ground-state molecules to transition-state molecules is very much lower for an enzyme-catalyzed reaction than for either a noncatalyzed reaction or chemically catalyzed reaction. In the activated state, the substrate is bound more tightly to the enzyme than it is in the ground state (see Transition State Analogue). If such tighter binding did not occur, there would be no catalysis. In fact, the increase in rate is proportional to the increase in binding. It is for this reason that transition state analogues are potent inhibitors of enzymes. After formation of the EP^* complex, the enzyme undergoes another conformational or unclamping reaction to release the product into the bulk medium and regenerate the free form of enzyme. Such regeneration is an essential part of enzymic catalysis.

Bibliography

1. D. D. Hackney (1990) The Enzymes **19**, 1–36.

Catalytic Antibodies

The concept of *catalytic antibodies* owes its origin to Pauling and Jencks, who proposed that an antibody normally differs from an enzyme by its inability to bind selectively and to stabilize the transition state of a chemical reaction. An antibody that did happen to be specific for a transition state should therefore function like an enzyme and promote chemical catalysis of the corresponding reaction (1). Advances in chemical synthesis and in hybridoma technology to produce monoclonal antibodies have enabled the exploitation of the diversity and affinity of the immune repertoire to develop catalytic antibodies that are elicited against transition state analogues. The binding sites of these antibodies are anticipated to bind substrates structurally related to the transition state and to process them to products through a pathway lower in free energy, and therefore more rapid, than the normal one that occurs in the absence of antibody. By clever design of appropriate transition state analogues, "tailor-made catalysts" should be created to catalyze reactions with no enzymic counterparts. Challenge of the immune system with a transition state analogue to induce a catalytic antibody is a necessary, but not a sufficient, condition to generate an effective catalyst; factors other than high affinity for the transition state, such as precise orientation of catalytic residues and the effective release of reaction products at the active site, also contribute to the overall catalytic efficiency of an antibody. Strategies have evolved to design transition state analogue immunogens that would solicit catalytic functions within the antibody combining site for efficient catalysis.

1. Reactions Catalyzed by Antibodies

There are now approximately 100 reactions that have been catalyzed by antibodies (1-3). These reactions include (*1*) pericyclic processes (oxy-Cope rearrangement, Diels–Alder condensation, Claisen rearrangement), (*2*) elimination reactions (decarboxylation, dehydration, *syn* elimination of HF from fluoroketones, E2 (biomolecular) elimination of benisoxazole), (*3*) hydrolyses (carbonate esters, esters, amide, lactones, enol ethers), (*4*) bond-forming reactions (lactonization, peptide synthesis, cationic cyclization, aldol condensation), and (*5*) redox reactions (ketone reduction, epoxidation, sulfoxide oxidation). Antibodies can catalyze, with high stereo- and regiospecificity, reactions that may not generally be catalyzed by enzymes. This property has appeal in the potential application of antibody catalysis to commercial synthetic and medical uses, such as pharmaceutical synthesis and prodrug activation.

2. The Nature of the Catalytic Site

The active sites of catalytic antibodies elicited by a given immunogen exhibit high sequence homologies and are often structurally convergent (4). These sites harbor shallow clefts complementing the structural and electronic features of the immunogen. The positioning of active site residues in the binding pocket is accomplished by somatic mutation of the germline ancestral antibody arising from an immunological response (5). The germline antibody undergoes a substantial amount of induced-fit conformational change on binding the immunogen. By the process of affinity maturation, the active site residues in the mature antibody become preoriented such that a rigid binding pocket is generated for optimal binding (lock-and-key fit).

3. Nature of Catalysis

Catalysis by antibodies is like that by enzymes, in that it exhibits Michaelis–Menten kinetics in which substrate binding precedes a chemical transformation, followed by dissociation of the product. Kinetic characterization experiments (6) indicate that the antibody-catalyzed reaction recapitulates a number of characteristics expected of an enzyme, but the chemical transformation step is often rate-limiting. The rate enhancement is generally less than that observed for enzymes catalyzing similar reactions. Transition state analogues are only approximations of the true transition state, and they also do not demonstrate the extremely tight binding to enzymes that is predicted theoretically (see Transition State Analogue). Furthermore, antibodies catalyze reactions primarily through restrictions on the translational and rotational movement of substrates, and only to a lesser extent through the active-site acid/base or nucleophilic catalysis that occurs in enzymes. The difference in catalytic efficiency between antibody and enzyme can also be attributed in part to the latter's ability to provide more extensive electrostatic interactions and hydrogen bonding during catalysis through conformational mobility (7).

4. Generation of Catalytic Antibodies

The recovery of catalytic antibodies relies on an efficient means of sampling the immune repertoire and screening for effective catalysts. The murine immune repertoire is estimated to have a diversity of 10^8, and it can be further expanded by immunization. The majority of catalytic antibodies have been derived from hybridomas that generally capture only 0.01% of the immune repertoire. The development of recombinant antibody fragments as combinatorial libraries consisting of $\geq 10^6$ members in **lambda** and in M13 phage has increased the access to the immune repertoire and possibly the recovery of catalytic antibodies. The diversity of an antibody combinatorial library, and potentially the yield of efficient catalytic antibodies, can be further expanded by polypeptide chain-shuffling experiments in which the heavy-chain fragment of a catalytic antibody is allowed to cross with a library of light-chain fragments elicited by the same immunoglobulin, and vice versa (8).

5. Screening for Catalytic Antibodies

Catalytic antibodies have been identified by their high affinities for the appropriate haptens, as well as their catalytic activities for the desirable reactions. Given the often low activity of catalytic antibodies, sensitive but specific methods have been developed for identifying the catalyst. CatELISA is based on screening for the presence of antibody-catalyzed reaction products using product-specific antibodies as primary antibody indicators in enzyme-linked immunosorbent assay (ELISA) (9). An alternative method depends on the catalytic release of a reactive species that can be trapped via covalent modification of the phage-displayed antibody, which then permits the recovery of DNA encoding catalytic antibody clones from the phage particles (10). Another method involves the recovery of antibody clones that sustain growth of **microorganisms**, such as **yeast** or bacterial auxotrophs, through catalysis of essential biological pathways (11). The host organisms, however, may also impose an additional selection on what catalytic antibodies can be recovered from the screen, since the host will not survive expression of antibodies that are toxic.

Bibliography

1. R. A. Lerner, S. J. Benkovic, and P. G. Schultz (1991) Science **252**, 659–667.
2. S. J. Benkovic (1992) Annu. Rev. Biochemistry **61**, 29–54.
3. J. R. Jacobsen and P. G. Schultz (1995) Curr. Opin. Struct. Biol. **5**, 818–824.
4. J. B. Charbonnier et al. (1997) Science **275**, 1140–1142.
5. G. J. Wedemayer et al. (1997) Science **276**, 1665–1669.
6. J. D. Stewart et al. (1994) Proc. Natl. Acad. Sci. USA **91**, 7404–7409.
7. M. R. Haynes et al. (1994) Science **263**, 646–652.
8. B. Posner et al. (1994) Trends Biochem. Sci. **19**, 145–150.
9. D. S. Tawfik et al. (1993) Proc. Natl. Acad. Sci. USA **90**, 373–377.

10. K. D. Janda et al. (1997) Science **275**, 945–948.
11. Y. Tang, J. B. Hicks, and D. Hilvert (1991) Proc. Natl. Acad. Sci. USA **88**, 8784–8786.
12. J. A. Smiley and S. J. Benkovic (1994) Proc. Natl. Acad. Sci. USA **91**, 8319–8323.

Catalytic Triad

The term *catalytic triad* is used to describe the arrangement of amino acid residues in the active sites of serine proteinases that underlies their mechanism of enzyme action. It was first applied to the active site of **chymotrypsin** when the structure of that enzyme was determined by X-ray crystallography (1). Earlier studies had shown that chymotrypsin could be inactivated by chemical modification of one of its serine residues with the nerve gas, diisopropylfluorophosphate (DIFP). Examination of the enzyme structure revealed that the hydroxyl group of this serine, residue 195, was “activated” by the imidazole group of histidine 57, which in turn was “activated” by the carboxyl group of **aspartate** 102 (Fig. 1). Originally described as a *charge relay system*, these three residues are more commonly called a *catalytic triad*.

Figure 1. The catalytic triad, the hydrolytic apparatus of serine proteinases. It consists of the side chains of an aspartic acid, a histidine, and a serine residue (eg, residues 102, 57 and 195, respectively, in bovine chymotrypsin). In the absence of substrate, the imidazole group of the histidine is unprotonated, but it potentiates the nucleophilic properties of the hydroxyl side chain of the serine. When substrate binds to the active site, the serine proton is transferred to the imidazole group and the oxygen attacks the carbonyl group of the substrate. The resulting positively charged imidazole is stabilized by interaction with the negative charge of the aspartate carboxyl group. The activated serine is also highly reactive toward inhibitors such as PMSF and DIFP.

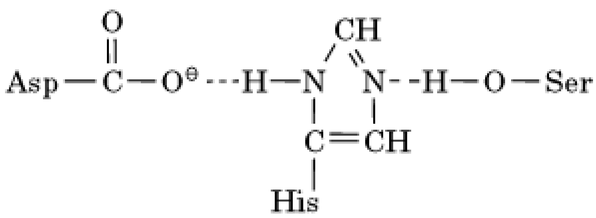

Similar triads have been observed in both the chymotrypsin and subtilisin evolutionary families of serine proteinases (2), as well as in other hydrolytic enzymes (3). It is remarkable that the bacterial serine proteinase subtilisin has the same geometrical arrangement of aspartate, histidine, and serine residues as chymotrypsin, but all other structural aspects of the two proteins are quite different. This is a classic example of **convergent** evolution. The activated serine interacts with the carbonyl carbon atom of the peptide bond to be hydrolyzed, forming an oxyanion intermediate, which is converted to an acylated serine with release of the amine component of the peptide. Subsequent hydrolysis of the acylenzyme occurs by the reverse reaction in which water substitutes for the activated serine.

Bibliography

1. D. M. Blow (1976) Acc. Chem. Res. **9**, 145–152.
2. T. A. Steitz and R. G. Schulman (1982) Annu. Rev. Biochem. Biophys. **11**, 419–444.
3. D. M. Blow (1990) Nature **343**, 694–695.

Cathepsins

The term *cathepsin* is derived from the Greek word meaning “to digest” and is used to describe a broad range of intracellular proteinases that serve important biological functions. Two major pathways have been identified that control the degradation of cellular proteins. One operates within the **cytoplasm** and is called the **ubiquitin**-mediated pathway. The other functions within specific cellular compartments, especially the **lysosomes**, but also in endosomes and the endoplasmic reticulum. Lysosomes are the major site of intracellular protein degradation (1). They are amply endowed for this function because they contain as many as 20 different proteolytic enzymes and as many other hydrolytic enzymes (eg, **phosphatases**, lipases, **nucleases**, and sulfatases) (1).

The lysosomal proteinases are called *cathepsins*. They are single-chain proteins that range in molecular mass from 20 kDa to about 40 kDa. Typically they have a broad substrate specificity, are optimally active at somewhat acidic pH, and belong to either the thiol proteinase or carboxyl proteinase classes. For no particular reason, they have been designated by letters as cathepsins B, L, H, M, N, S, and T, all of which are thiol proteinases or, more commonly, *cysteine proteinases*; and cathepsins D and E, which are carboxyl (or *aspartyl*) proteinases (2). All of these are endopeptidases, enzymes that cleave peptide bonds in the internal part of a protein. In addition, there are several lysosomal *exopeptidases*, including *cathepsin C*, which removes dipeptides from the amino-terminus of polypeptide chains and is therefore a dipeptidyl aminopeptidase, and at least two carboxycathepsins that are carboxypeptidases. Cathepsin G is a chymotrypsin-like serine proteinase found in neutrophils, and cathepsin R is another serine proteinase found in the endoplasmic reticulum.

The lysosomal cathepsins have been considered to be the most active proteinases in the body, because they degrade four times as much protein as the pancreatic and gastric proteinases combined (3). Much of this is essentially turnover of cytosolic proteins to balance **protein synthesis** and maintain homeostasis. However, cathepsins are also important components of the **immune system**: In order for a foreign protein to generate an antibody response, it must be taken up by a specialized **antigen-presenting** cell and degraded within endosomes. The resultant peptide fragments are then “presented” on the cell surface, where they trigger antibody production (4).

Bibliography

1. F. Authier, B. I. Posner, and J. J. M. Burgeron (1994) In *Cellular Proteolytic Systems* (A. J. Ciechanover and A. L. Schwartz, eds.), Wiley-Liss, New York, pp. 89–113.
2. J. S. Bond and P. E. Butler (1987) Annu. Rev. Biochem. **56**, 333–364.
3. A. J. Barrett and H. Kirschke (1981) Methods Enzymol. **80**, 535–561.
4. C. V. Harding (1994) In *Cellular Proteolytic Systems* (A. J. Ciechanover and A. L. Schwartz, eds.), Wiley-Liss, New York, pp. 163–180.

Caudal Protein

Caudal protein (Cad) was identified originally as a **homeodomain** protein in *Drosophila*, but **homologues** have subsequently been found in vertebrates as well. It belongs to the superfamily of **DNA-binding** homeodomain transcription factors. Caudal messenger RNA, which is supplied by the mother in the unfertilized egg; is required for proper segmentation of posterior segments in insects and for the development of the posterior lineage in vertebrates. In *Drosophila*, Caudal has been shown to bind to **promoter** elements and to activate directly the transcription of several segmentation genes. In this process, it cooperates with other transcriptional activators of segmentation genes, eg, Bicoid (another homeodomain protein). At the preblastoderm stage, Caudal protein forms a gradient, which is generated by **translational repression** caused by Bicoid binding to the *cad* mRNA. Although this early function appears to be specific to *Drosophila* (and other long-germ-band insects), the zygotic function of Caudal, specification of the most posterior segments in insects or posterior cell lineage in vertebrates, appears to be conserved throughout the animal kingdom.

The *caudal* (*cad*) gene of *Drosophila* was first isolated as a **homeobox**-containing gene by cross-hybridization to the homeobox of ***Ultrabithorax*** (*Ubx*) and others (1, 2). The *cad* homeodomain shares 58% identity with that of *ftz*, and 53% and 52%, respectively, with those of *Antp* and *Ubx*. During *Drosophila* development, *cad* is expressed both maternally and zygotically. The maternal expression is detected in the **germ line** in nurse cells during **oogenesis**, and its mRNA accumulates in the developing **oocyte**. At the end of oogenesis, the *cad* mRNA is distributed evenly throughout the oocyte. No Cad protein is detected during oogenesis. Cad protein is first detected beginning with nuclear division cycles 6 or 7, just prior to the formation of the syncitial blastoderm. From this stage on to the 13 nuclear cycle, the distribution of Cad protein forms a concentration gradient throughout the embryo and along the anterior-posterior axis, with its maximum at the posterior end. The *cad* mRNA remains uniformly distributed throughout the cytoplasm to the 12 nuclear cleavage; subsequently, it follows the protein gradient, when it is then distributed as a concentration gradient itself. Nevertheless, the protein gradient precedes the mRNA gradient by several nuclear cycles, so that the mRNA gradient is not relevant for the generation of its protein gradient (see below). Following the final nuclear cleavage during cellularization of the blastoderm, the maternally-derived *cad* mRNA disappears, and with it the protein translated from it (1-3).

Formation of the protein gradient from the initially uniformly distributed mRNA is generated by translational repression in the anterior regions of the embryo. Another maternally provided homeodomain protein, Bicoid, binds the *cad* mRNA and prevents its translation (4, 5). This is the only reported example of a homeodomain protein controlling the expression of another homeodomain factor at the level of its mRNA by translational repression. Caudal protein also accumulates in the pole cells during their formation and is present there for several hours of embryogenesis. There is no *de novo* expression in the pole cells, however, and all the protein present was synthesized from the maternally provided mRNA. Formation of the Caudal protein gradient does not depend on zygotic gene expression. In older unfertilized eggs, an anterior-posterior gradient is detected that is similar to that normally present in embryos of the same stage (2, 3). Maternally expressed Caudal has also been reported in other insects, such as *Bombyx mori* (6).

Zygotic expression of Caudal protein in *Drosophila* begins during cellularization of the blastoderm as a stripe in the posterior region of the embryo corresponding to the anlagen of the most posterior segments (the presumptive abdominal segments A9/A10, parts of the telson) and the hindgut. At the extended-germ-band stage, and throughout the rest of embryogenesis, *cad* is expressed in posterior midgut cells, the Malpighian tubules, the anal plate and, at weaker levels, during germ-band extension in pair-rule-like stripes (1-3). In third instar larvae, *cad* is expressed in the Malpighian tubules, the posterior midgut, the gonads of both sexes, and in the anlagen of the anal plates and the hindgut, within the genital (3). Most aspects of the zygotic expression are conserved in those vertebrates that have been analyzed (7-10).

In *Drosophila*, the function of the Caudal transcription factor is required for segment specification in the thoracic and abdominal regions by regulating the transcription of several segmentation genes (11-14). Embryos lacking both maternal and zygotic Cad protein are severely shortened, with variable deletions of many of the thoracic and abdominal segments. Zygotically provided protein can, however, largely rescue these defects. Ectopic expression of Caudal protein throughout the embryo at the blastoderm stage leads to **phenotypes** that are somewhat opposite to the phenotypes observed in *cad*-defective embryos (15). Analysis of the cis-acting elements of several segmentation genes has demonstrated that Cad is directly activating transcription of *fushi tarazu* (11) and other segmentation genes (12-14). Caudal acts in concert with Bicoid, and is partially redundant, in controlling the expression of the downstream targets, the segmentation genes (12, 13).

Embryos from wild-type mothers that lack zygotic function display an absence of parts of the most posterior segments, the terminalia; in particular, the anal tuft, parts of the anal pads, and the terminal sense organs, all structures that are derived from a cryptic tenth abdominal segment, are deleted (2). The isolation and developmental expression analysis of Caudal homologues in vertebrates (7-10) has suggested that this aspect of Caudal function, specification of most posterior segments or posterior lineage in vertebrates, has been conserved throughout evolution. Based on the expression patterns of some of the vertebrate Caudal homologues, additional roles for this subfamily of homeodomain transcription factors have been proposed; eg, participation in rostrocaudal axial patterning or in the development and regeneration of the liver (16, 17). However, all the assumptions of Caudal function (s) in vertebrate development are based purely on the respective expression patterns, and no loss-of-function mutants have been reported to date. Thus, all these proposed roles of vertebrate Caudal homologues await confirmation by the analysis of specific mutants, eg, **knockout** mice, or the potential identification of mutants in other model systems, such as the zebrafish.

Bibliography

1. M. Mlodzik, A. Fjose, A. Gehring, and W. J. Gehring (1985) EMBO J. **4**, 2961–2969.
2. P. M. MacDonald and G. Struhl (1986) Nature **324**, 537–545.
3. M. Mlodzik and W. J. Gehring (1987) Cell **48**, 465–478.
4. J. Dubnau and G. Struhl (1996) Nature **379**, 694–699.
5. R. Rivera-Pomar, D. Niessing, U. Schmidt-Ott, W. J. Gehring, and H. Jäckle (1996) Nature **379**, 746–749.
6. X. Xu, P. X. Xu, and Y. Suzuki (1994) Development **120**, 277–285.
7. A. Frumkin, Z. Rangini, A. Ben-Yehuda, Y. Gruenbaum, and A. Fainsod (1991) Development **112**, 207–219.
8. A. Frumkin et al. (1993) Development **118**, 553–562.
9. J. S. Joly et al. (1992) Differentiation **50**, 75–87.
10. F. Beck, T. Erler, A. Russell, and R. James (1995) Dev. Dyn. **204**, 219–227.
11. C. Dearolf, J. Topol, and C. Parker (1989) Nature **341**, 3430–3433.
12. R. Rivera-Pomar, X. Lu, N. Perrimon, H. Taubert, and H. Jäckle (1995) Nature **376**, 253–256.
13. C. Schulz and D. Tautz (1995) Development **121**, 1023–1028.
14. T. Hader et al. (1998) Mech. Dev. **71**, 177–186.
15. M. Mlodzik, G. Gibson, and W. J. Gehring (1990) Development **109**, 271–277.
16. A. V. Morales, E. J. de la Rosa, and F. Pablo (1996) Dev. Dyn. **206**, 343–353.
17. U. Doll and J. Niessing (1996) Eur. J. Cell Biol. **70**, 260–268.

Suggestions for Further Reading

18. R. Rivera-Pomar and H. Jäckle (1996) From gradients to stripes in *Drosophila* embryogenesis: filling in the gaps. Trends Genet. **12**, 478–483.
19. D. Duboule (1994) *Guidebook to Homeobox Genes*. Sambrook and Tooze Publication, Oxford

University Press, Oxford, U.K.

Cauliflower Mosaic Virus

Cauliflower mosaic virus (CaMV) was the first plant **virus** shown to have a DNA genome and the first shown to **replicate** by **reverse transcription**. The virus is found worldwide but only causes significant losses locally. It is transmitted by aphids in the externally borne or stylet-borne manner (see Virus Infection, Plant) and encodes a helper factor that is required for transmission. It has a narrow host range, being restricted primarily to the Cruciferae. CaMV is the type member of the Caulimovirus genus, which contains 11 species and 6 possible members.

This virus has had a significant impact on plant virology and plant molecular biology. The unravelling of the reverse transcription replication mechanism led to the concept of *pararetroviruses* (1, 2). The virus is an important source of gene regulatory elements, which have been used extensively in the genetic manipulation of plants.

1. Virus Structure

CaMV particles are isometric, about 50 nm in diameter (**Fig.** 1). Although the virus particles have been crystallized, X-ray crystallography did not yield detailed information, most probably because of the heterogeneity of the coat protein (3) The structure has been shown by cryoelectron microscopy and three-dimensional **image reconstruction** to comprise three concentric layers of solvent-excluded density (4). The outermost layer is made up of a total of 420 coat protein subunits arranged in $T = 7$ **icosahedral symmetry**; it is the first example of a $T = 7$ virus that obeys the stoichometric rules of icosahedral symmetry. The DNA genome is distributed in layers II and III, together with some of the viral coat protein. The viral coat protein is expressed from **open reading frame** IV (see below) as a 58-kDa precursor molecule that is processed **proteolytically** to several molecular sizes, the major ones being 42 and 37 kDa. The protein in virions is **glycosylated** and **phosphorylated**, and the virions also contain minor amounts of the products of open reading frames III and V.

Figure 1. External structure of cauliflower mosaic virus, viewed down a local five-fold axis.

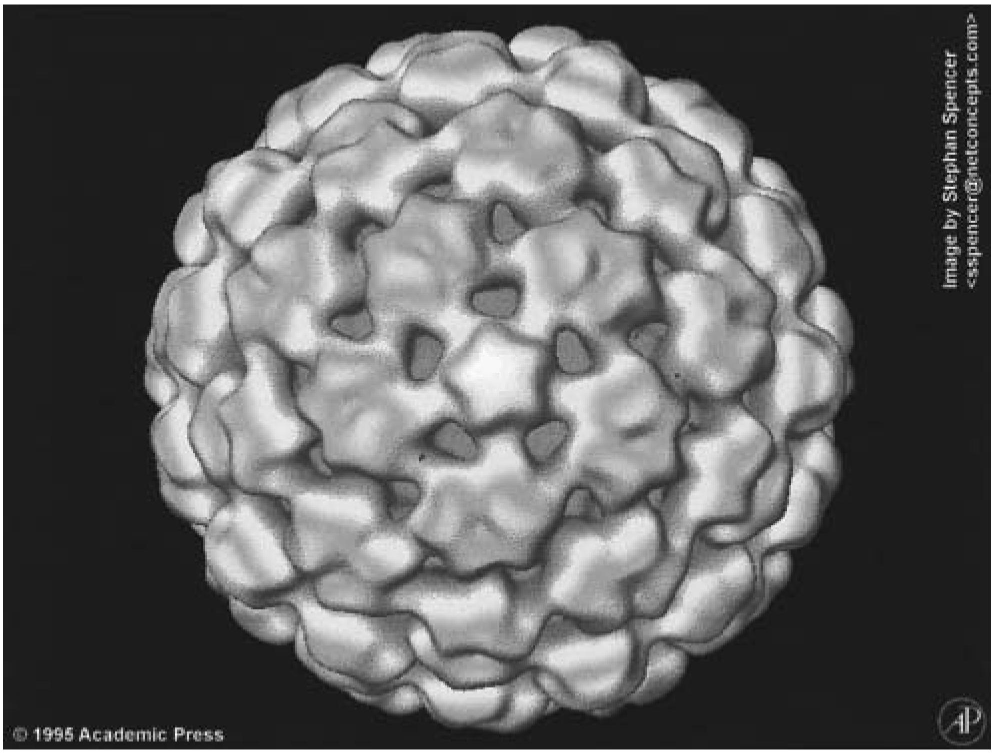

CaMV particles are very stable and are only dissociated at high pH (5) or by digestion of the coat protein with proteinases.

2. Viral Genome

Each virus particle contains a single molecule of circular double-stranded DNA of 8 kbp. The DNA of most isolates of CaMV has three discontinuities (D1, D2, and D3 in Fig. 2), one in one strand (the a strand) and two in the other (yielding the b and g strands); one strain has only two discontinuities, one in each strand. The discontinuities have an unusual structure, with a fixed 5′ DNA nucleotide (with sometimes one or two ribonucleotides attached) and variable 3′ end, overlapping the 5′ end by 10 to 30 nucleotides. They are the sites of the priming of (+)- and (–)-strand DNA replication, and this unusual structure results from viral replication (see below). The DNA has a twisted conformation that, because of the discontinuities, cannot be **supercoiled**, the constraining forces being unknown.

Figure 2. Genome organization of CaMV. The double-stranded DNA genome is represented by the thick double circle, with the discontinuities shown as ●. The promoters for the 35S and 19S transcripts are indicated by ⊠, and the positions of the transcripts are shown by the outer arcs. The inner arcs are the open reading frames I to VIII.

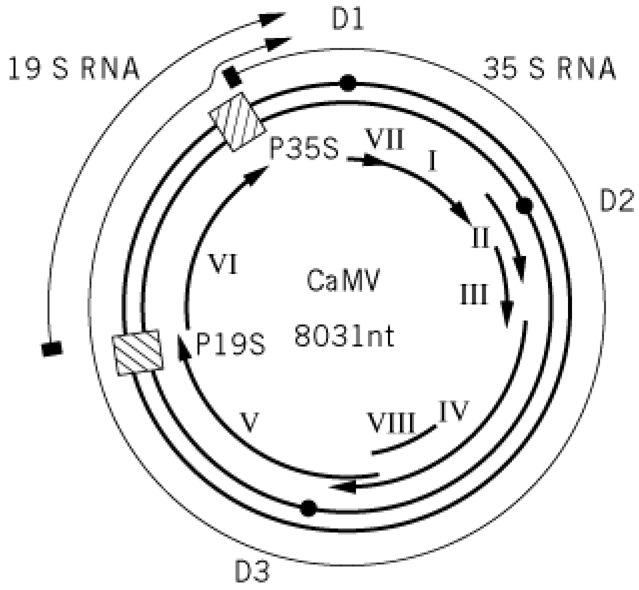

CaMV DNA has six, or possibly eight, open reading frames (ORFs) on the complement to the a strand (**Fig.** 2). ORF I product (37 kDa) is involved in the cell-to-cell movement of the virus, and ORF II product (18 kDa) is the aphid transmission protein (see Virus Infection, Plant). The product of ORF III is a protein of 15 kDa that is processed to 11 kDa and thought to be involved in packaging the DNA genome (6). ORF IV encodes the viral coat protein, which contains the "cys" motif C^{ys-} X_2C^{ys-} X_4 H^{is-} X_4C^{ys-} characteristic of retrovirus *gag* or nucleoproteins and a highly basic lysine-rich region. The viral polymerase (reverse transcriptase +ribonucleaseH) is encoded by ORF V (79 kDa). The product of ORF VI forms the matrix of the inclusion bodies in which virus particles are found embedded in the **cytoplasm** of infected cells. It has several functions, including being the site of the reverse transcription phase of viral replication (7), involved in virus assembly (8), a transactivator during viral expression (see below), and a symptom determinant. No products have been found for ORFs VII and VIII, and it is uncertain whether they are expressed.

3. Transcription and Translation

CaMV DNA is transcribed asymmetrically from the a strand to give a more-than-genome length transcript (the 35S RNA), with a terminal repeat of 180 nucleotides and subgenomic transcript (the 19S RNA) that is the messenger RNA for ORF VI (Fig. 2); the transcripts are **polyadenylated**. There are suggestions of other transcripts, such as one for ORF V (9), but these have not been characterized. **Splicing** events between the leader sequence and an acceptor site in ORF II (10) are essential for virus infectivity. It is possible that these events might form the mRNA for expression of ORF III and, possibly, ORFs IV and V.

The **promoter** for the 35S RNA is well characterized and widely used in the expression of transgenes in plants. It directs constitutive, high-level expression in most tissues of most plant species. The promoter has a modular structure, with regions that control the tissue specificity of expression [reviewed in 11). Nuclear factors have been identified that bind to specific regions of the promoter. The 19S promoter is much weaker than the 35S promoter and is less well characterized.

The CaMV genome also contains the signal sequence for the polyadenylation of both the 35S and 19S transcripts. Due to the terminal repeat, the transcription of the 35S RNA has to pass this signal the first time it is encountered and recognize it the second time. It is thought that the bypass is due to the proximity of the promoter (12).

Translation of the 35S RNA is effected by several unusual mechanisms [reviewed in (11) and further refined in (10)). The leader sequence upstream of ORFI is long (>600 nucleotides) and contains several **AUG** start codons, which could inhibit downstream translation. However, this leader sequence is folded into a complex stem-loop structure, which enables small ribosomal subunits to “shunt” from the 5′ to 3′ end of the leader sequence without scanning the sequence in between; this then opens up ORFI. Translation of downstream ORFs on this polycistronic message is dependent on the presence of a **transactivator**, which is the product of ORF VI, and possibly on the splicing mechanism described above. This process of transactivation seems to enable ribosomes that have translated one ORF to remain competent to translate the next ORF downstream.

4. Viral Replication

The replication cycle of CaMV (Fig. 3) has been studied in much detail, but there are are still several aspects that are not fully understood. Virus particles enter the uninfected cell and are unencapsidated by an unknown mechanism. The viral DNA genome enters the nucleus, where the discontinuities are sealed and the molecule associates with histones forming a minichromosome (Fig. 3, step 2). This is the template for transcription by the host DNA-dependent **RNA polymerase**, giving the 35S and 19S RNAs, which pass to the cytoplasm (Fig. 3, step 3). The 19S RNA is translated to yield the inclusion body protein. The 35S RNA has two functions, being the mRNA for at least the products of ORFs I and II and the template for the reverse transcription phase of replication. There is some evidence that this phase of replication takes place in viruslike particles in the inclusion bodies (7). The first event in reverse transcription is the annealing of the 3′ end of $tRNA^{met}_{init}$ to a site, that of discontinuity 1 (D1), about 600 nucleotides from the 5′ end of the 35S RNA (Fig. 3 step 4). This acts as a primer for the synthesis of a-strand DNA toward the 5′ end of the template. RNaseH activity removes the RNA moiety of the DNA–RNA duplex thus formed and leaves DNA (Fig. 3, step 5) that, because of the terminal repeat of the 35S RNA, is complementary to the 3′ end of the template. Thus, a strand switch is effected, and synthesis of the a strand DNA continues (Fig. 3, step 6). The digestion of the RNA by RNaseH leaves purine-rich regions at the positions of discontinuities 2 and 3 (D2 and D3), which act as primers for the synthesis of the b and g strands (Fig. 3 steps 7 and 8). When the oncoming strand of (+)-strand DNA reaches the next priming site, it displaces the primer and some newly synthesized DNA, resulting in the triple-strand discontinuity described above. A second strand switch occurs at the tRNA priming site between the oncoming a and g strands, allowing the synthesis of the g strand to continue and making discontinuity 1.

Figure 3. Replication cycle of CaMV. Step 1: The input DNA containing discontinuities 1–3 (D1–D3) passes to the nucleus where it forms minichromosomes (step 2). These are the template for the transcription of the 35S RNA (step 3) with terminal repeats r, which moves to the cytoplasm. Priming of the 35S RNA occurs by the annealing of the 3′ end of $tRNA^{met}_{init}$ to the primer binding site (PBS) on the 35S RNA and leads to the synthesis of (–)-strand DNA (step 4). RNaseH removes the RNA of the RNA DNA duplex, leaving the complement to the terminal repeat sequence R (step 5). This anneals to the 3′ end of the 35S RNA, and DNA synthesis continues (step 6). RNAseH activity leaves purine-rich regions ●, which act as primers for (+)-strand DNA synthesis (steps 7 and 8). The oncoming strand displaces the primer sequence, thus giving the characteristic discontinuities, and a second strand-switch is effected at D1 to complete the molecule.

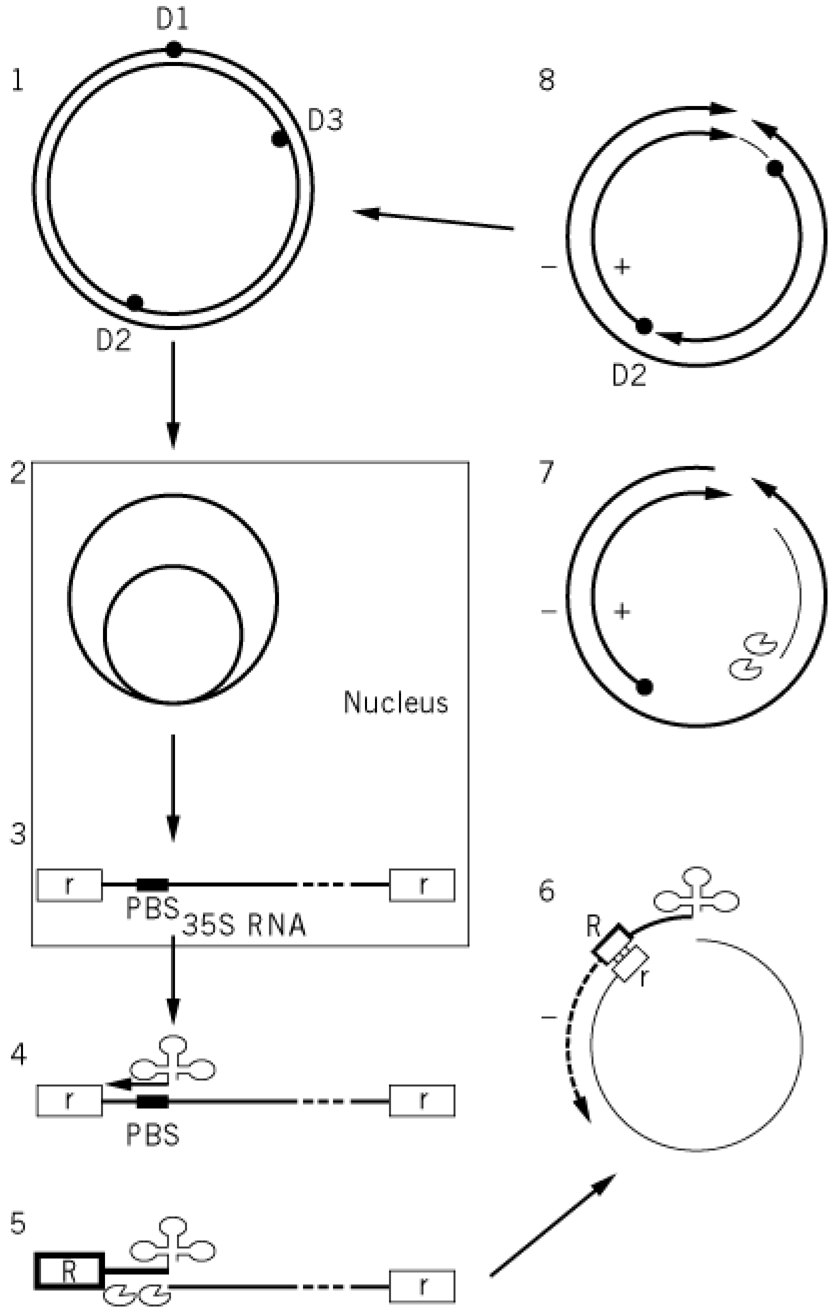

Bibliography

1. R. Hull and H. Will (1989) Trends Genet. **5**, 357–359.
2. H. Temin (1989) Nature **339**, 254–255.
3. Z. X. Gong, H. Wu, R. H. Cheng, R. Hull, and M. G. Rossmann (1990) Virology **179**, 941–945.
4. R. H. Cheng, N. H. Olson, and T. S. Baker (1992) Virology **186**, 655–668.
5. R. Al Ani, P. Pfeiffer, G. Lebeurier, and L. Hirth (1979) Virology **93**, 175–187.
6. J. L. Mougeot, T. Guidasci, T. Wurch, G. Lebeurier, and J. M. Mesnard (1993) Proc. Natl. Acad. Sci. USA **90**, 1470–1473.
7. C. M. Thomas, R. Hull, J. A. Bryant, and A. J. Maule (1985) Nucl. Acids Res. **13**, 4557–4576.
8. A. Himmelbach, Y. Chapdelaine, and T. Hohn (1996) Virology **217**, 147–157.
9. A. L. Plant, S. N. Covey, and D. Grierson (1985) Nucl. Acids Res. **13**, 8305–8321.
10. Z. Kiss-László, S. Blanc, and T. Hohn (1995) EMBO J. **14**, 3552–3562.

11. H. M. Rothnie, Y. Chapdelaine, and T. Hohn (1994) Adv. Virus Res. **44**, 1–67.
12. H. Sanfaçon and T. Hohn (1990) Nature (Lond.) **346**, 81–84.

Suggestion for Further Reading

13. R. J. Shepherd (1994) "Caulimoviruses". In *Encyclopedia of Virology* (R. G. Webster and A. Granoff, eds.), Academic Press, London, pp. 223–226.

cDNA Libraries

In contrast to genomic libraries, which contain raw DNA sequences harvested from an organism's chromosomes, cDNA libraries are composed of processed nucleic acid sequences harvested from an organism's **RNA** pools (see Complementary DNA (cDNA)). cDNA can be prepared from any RNA source, including in RNA and noncoding RNA, isolated from single cell organisms, cultured metazoan cells, and isolated tissues. cDNA libraries provide a powerful means of examining cell- and tissue-specific gene expression. For example, mammalion cDNA libraries contain only the fraction of sequences that are expressed in the subject tissues at the time of harvest, typically in the range of 10% of the **genes** carried by the genome. Also, cDNA is typically prepared enzymatically from **polyadenylated** mRNA, a population of RNA that has previously undergone post-transcriptional editing and removal of any intervening sequences (**introns**). Whereas genes in genomic DNA are often interrupted by numerous introns, the copy of a gene in a cDNA or mRNA commonly contains an uninterrupted sequence encoding the gene product. Thus, cDNA inserts are directly expressible as both RNA and protein gene products. Vectors used in cDNA libraries often contain expression elements that mediate transcription and translation of the cloned cDNAs.

In constructing cDNA libraries, the goal is usually to represent full-length protein coding sequences for all of the mRNAs expressed in the subject cells or tissue. Thus, it is essential to preserve the integrity of cellular mRNA during extraction and purification protocols. Libraries made from fragmented RNA will not preserve the full open reading frame, rendering the resultant partial clones less useful. Unfortunately, RNA tends to be a transient species by design, as cells have developed complex post-transcriptional mechanisms to regulate gene expression through mRNA decay. The problem is worse in certain tissues, such as pancreas, that secrete large amounts of degradative enzymes as part of their normal function. Though troublesome, the RNA decay problem can be overcome through specialized procedures that seek to inactivate **ribonuclease** enzymes concomitantly with RNA extraction from intact tissue.

Once total RNA is extracted from the subject tissue, the mRNA fraction is purified by annealing to oligodeoxythymidine (oligo-(dT)) cellulose. Oligo-(dT) is a short polymer that hybridizes specifically to polyadenylate. Because the majority of cellular mRNAs are **polyadenylated**, affinity chromatography over oligo-(dT) cellulose provides a simple means to remove contaminating RNA species, such as ribosomal and transfer RNAs, which do not contain poly A tails. The purified mRNA is then annealed to oligo-(dT), which serves as a primer that can be extended by the enzyme **reverse transcriptase** (RT). RT extension thus generates **antisense** DNA copies of the purified mRNA species. Under appropriate conditions, RT can be induced to complete a second-strand DNA synthesis, using the first DNA strand as a template. The result is a collection of double-stranded DNA copies of the parental mRNA population (hence the “c” in “cDNA”). The double-stranded DNA population can then be cloned into an appropriate plasmid or bacteriophage vector to constitute a cDNA library.

cDNA libraries may be screened either by **hybridization** to the cloned inserts or by detection of RNA or protein expression products encoded by the cDNA inserts. Hybridization screening is similar in principle for both genomic and cDNA libraries and uses synthetic oligonucleotide probes or gene probes derived from existing clones. The probes are labeled with radioactivity or a fluorescent tag and then annealed to the total nucleic acids contained within a population of bacterial colonies or viral plaques. Colonies or plaques that contain nucleic acids complementary to the probe can then be detected and purified. Protein expression libraries can be screened based on affinity to antibodies, proteins, nucleic acids, or small-molecule ligands. In addition, functional properties can be screened for, such as catalysis or induction of transcription of a reporter gene.

Useful information regarding tissue-specific patterns of gene expression can be ascertained through screening cDNA libraries. By definition, a cDNA population is derived from the fraction of genes expressed in a given tissue through sampling the mRNA pool. These expressed sequences can be sampled and characterized in brute force fashion by high-throughput random sequencing of cDNA clones isolated from a library. It is not necessary to determine the full-length cDNA sequence in order to derive useful information from this approach. The partial sequences obtained are entered into an Expressed Sequence Tag (EST) database where the frequency of each partial sequence (known as a "tag") can be scored (1). In this manner, it is possible to determine the expression level of individual genes for any tissue. Furthermore, investigators that identify a gene product of interest in the EST database are already one step ahead on their sequencing efforts, because much of the open reading frame may already be in the public database. Finally, it is possible to request many EST clones from the I.M.A.G.E. Consortium (Integrated Molecular Analysis of Genomes and their Expression; `http://www-bio.llnl.gov/bbrp/image/image.html`), providing an easy source of genetic material for subcloning projects.

The concept of ESTs as quantitative indicators of gene expression levels has been further refined through a new method termed Serial Analysis of Gene Expression (SAGE) (2). SAGE provides a means of tagging every mRNA in the cell with a small, intrinsic nine-nucleotide sequence that is essentially unique to each transcript. In addition, SAGE provides a means to eliminate artifacts arising through processing and polymerase chain reaction (PCR) amplification of the original cDNA, thereby rendering the method highly quantitative. Finally, SAGE enables high throughput sequencing of the nine-nucleotide tags on a scale sufficient to quantify several hundred thousand cDNA species for a given tissue (3). Although the sequence information obtained from a single SAGE tag is minimal, it is usually sufficient to identify the transcript via hybridization or database searching methods. SAGE is being conducted on a large scale through the Cancer Genome Anatomy Project (CGAP; (site currently unavailable)), with the goal of rendering in detail the molecular differences between various normal tissues and tumors, in order to understand better the molecular basis of cancer. Ultimately the CGAP database, among others, will provide the capability of performing "virtual" **Northern blots**, in which any sequence segment can be screened through WWW-based databases to ascertain all known sequence, genetic, and biological information associated with mRNAs containing the sequence segment.

Tissue- or cell-specific gene expression can also be studied through specialized cDNA libraries derived from the subset of genes that are differentially expressed between two preparations of mRNA (4). For example, a cell culture line can be treated with a hormone, such as dexamethasone, and RNA can be prepared from samples of the cell culture before and after treatment. cDNAs prepared from the pretreatment population can then be used to remove selectively any complementary mRNAs from the post treatment preparation through a process known as subtractive hybridization. The majority of the mRNA species remaining in the post treatment pool should be those transcripts that were synthesized as a direct result of hormone treatment. These specific mRNAs can then be converted into cDNA and cloned into a suitable library vector, to constitute a differential cDNA library. Screening or sequence tagging a subtractive library greatly increases the efficiency of characterizing tissue-specific or stimulus-specific differences in gene expression.

See also Combinatorial Libraries, Libraries, Combinatorial Synthesis, Affinity Selection, DNA

Libraries, Genomic Libraries, Expression Libraries, Peptide Libraries, and Phage Display Libraries.

Bibliography
1. M. D. Adams, M. Dubnick, A. R. Kerlavage, R. Moreno, J. M. Kelley, T. R. Utterback, J. W. Nagle, C. Fields, and J. C. Venter (1992) Nature **355**, 632–634.
2. V. E. Velculescu, L. Zhang, B. Vogelstein, and K. W. Kinzler (1995) Science **270**, 484–487.
3. L. Zhang, W. Zhou, V. E. Velculescu, S. E. Kern, R. H. Hruban, S. R. Hamilton, B. Vogelstein, and K. W. Kinzler (1997) Science **276**, 1268–1272.
4. J. S. Wan, S. J. Sharp, G. M. Poirier, P. C. Wagaman, J. Chambers, J. Pyati, Y. L. Hom, J. E. Galindo, A. Huvar, P. A. Peterson, M. R. Jackson, and M. G. Erlander (1996) Nat Biotechnol **14**, 1685–1691.

Cell Adhesion Molecules

Cell adhesion molecules play central roles in embryonic development, tissue organization, and overall maintenance of the structure and form of multicellular organisms (1, 2) They provide the physical links between cells and other cells, and between cells and the extracellular matrix. Adhesion molecules are also involved in dynamic cell interactions, such as during tissue morphogenesis, cell migration, immunological and inflaemmatory responses, and possibly memory formation (1, 3-7). Adhesive proteins are also intimately involved in intracellular signaling processes that regulate cell growth, differentiation, gene regulation, and prograemmed cell death (8-13).

Cell adhesion molecules mediate adhesive interactions by forming specific protein-protein interactions or between proteins and complex carbohydrates. In addition, cell adhesion molecules frequently link directly to multimolecular protein complexes on the cytoplasmic face of the plasma membrane, which, in turn, mediate interactions with the cytoskeleton and signal transduction pathways (3, 9-13). Consequently, these cell adhesion and signaling complexes not only link cells with other cells and the extracellular matrix but also help to integrate extracellular physical information with the major signal transduction pathways within cells (see Integrins). For example, they appear to transduce information from inputs as diverse as transient contacts with other cells, binding of different connective tissue molecules, and tension or torsion at the cell surface. Each of these inputs connects to intracellular signaling pathways, such as phosphorylation cascades (9-12).

1. Types of Adhesion

The physical linkages involved in cell adhesion are provided by adhesion molecules that function as parts of general adhesion systems or in specialized adhesive structures. For example, epithelial cells can adhere to other cells along broad expanses of plasma membrane using general-purpose adhesive molecules such as cadherins (14-16). They can also adhere to each other by specialized adhesive structures, such as adherens junctions, desmosomes, and tight junctions (1). Each type of specialized junctional complex requires specific adhesion molecule components, which can include specialized cadherins and other proteins. Fibroblasts can also form complexes with other cells, but they most characteristically adhere to extracellular matrix. Cell-to-matrix adhesions can be broad and flat, as when epithelial cells adhere via integrins to basement membranes, or they can involve specialized structures that include hemidesmosomes or the focal contacts of fibroblastic and endothelial cells. The protein complexes involved in cell-to-matrix adhesion contain different complements of adhesive, cytoskeletal, and signal transduction molecules than those involved in cell-to-cell adhesion (1, 13, 15). This entry will first provide a general overview of specific types of cell adhesion proteins, then briefly discuss how they are integrated into cytoskeletal and signaling networks.

2. General Features of Cell Adhesion Proteins

Cell adhesiveness is generally based on the specific binding of a protein to another molecule at the cell surface. When adhesion results from binding of an adhesion molecule to the same type of protein on a neighboring cell, the interaction is termed '*homophilic*.' The cadherin family is a major mediator of such homophilic interactions (14-16) (see Cadherins). Cadherins form complexes in which both intercellular and lateral binding interactions cooperate to create tightly packed adhesion complexes that mediate adhesion with high avidity.

In many systems, however, adhesiveness involves binding of a receptor to a specific ligand. In cell-to-cell adhesion, the target protein of an adhesion receptor can be a "counter-receptor" or a complex carbohydrate on a protein anchor in the plasma membrane. In cell-to-matrix interactions, a plasma membrane adhesion protein such as an integrin can bind to an extracellular matrix protein that is itself considered to be an adhesive protein. For example, the protein bound could be a fibronectin or a laminin, which are complex, multifunctional proteins involved in both cell adhesion and anchorage to structural components of the extracellular matrix (2, 15, 17).

Consequently, there are two broad classes of adhesion molecules or receptors (Fig. 1). One class is bound to the plasma membrane, often as a transmembrane protein (Fig. 1). This type of molecule is generally a receptor, a homophilic adhesion molecule, or a counterreceptor. It often consists of an extracellular domain containing one or more cell-interaction domains or sites, as well as a stalk region, a hydrophobic transmembrane domain, and (usually) a cytoplasmic domain or tail. This type of molecule is often also involved in transmembrane transmission of signals.

Figure 1. Schematic diagram of a generalized transmembrane adhesion molecule consisting of an extracellular domain, transmembrane segment, and cytoplasmic domain. See text for discussion.

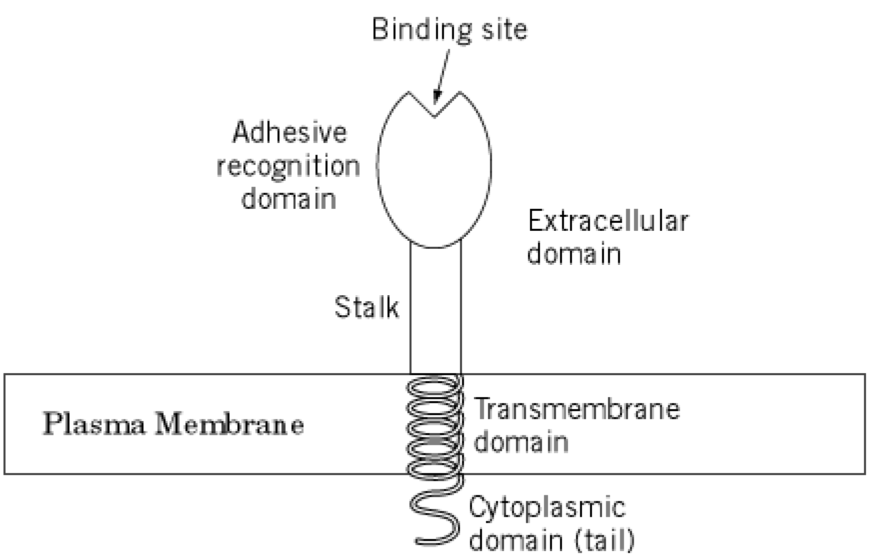

The second broad class of adhesion molecules consists of proteins that are often classified as cell surface or extracellular matrix proteins (see Extracellular Matrix), but that contain domains or sites involved in cellular adhesion (Fig. 2). Molecules in this class include fibronectins, laminins, vitronectin, tenascins, thrombospondins, and the collagens. All contain one or more cell-binding domains, which consist of a primary recognition motif consisting of a short peptide sequence (eg, Arg—Gly—Asp), and sometimes a synergy site that provides a substantial increase in receptor-binding specificity and affinity. As discussed below, many of these proteins also contain a variety of other functional domains.

Figure 2. Schematic suemmary of common features of extracellular matrix adhesion molecules. Linear arrays of structural and functional domains provide a series of specific binding sites. See text for further discussion.

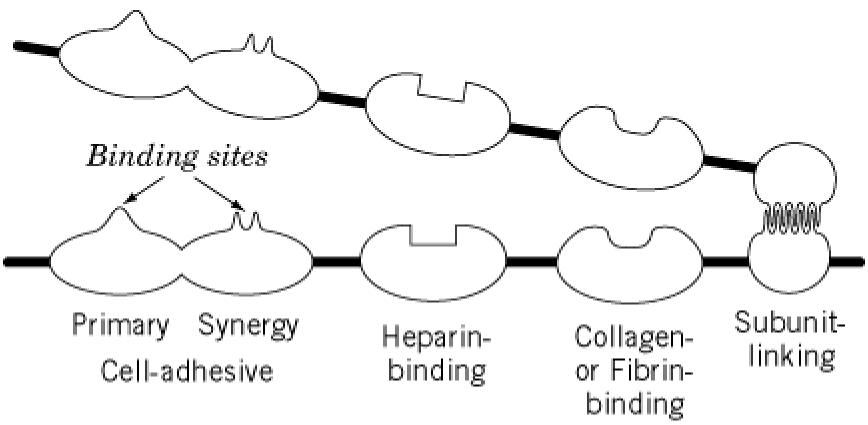

In general, adhesion molecules frequently have the following properties (1-3, 6, 14-16, 18-25):

- Composed of multiple repeats of protein motifs, such as the immunoglobulin (Ig) motif, the epidermal growth factor (EGF) repeat, or the fibronectin motif.
- Specialized functional domains, including a domain for formation of dimers or higher polymers.
- Moderate affinity, for example, with dissociation constants (K_d) in the range of 10^{-6}–$10^{-7}M$ for fibronectin, and even as weak as $10^{-4}M$ for leukocyte adhesion molecules that mediate rolling adhesion. In contrast, many well-known protein—protein interactions have affinities with $K_d = 10^{-9}$–10^{-11} M.
- High avidity after clustering. Adhesion molecules often form functional clusters or aggregates in the plane of the plasma membrane, which causes them to develop strong total avidity due to the cooperation of the otherwise weak binding of individual molecules.
- Regulation by activation, such as the "inside-out" signaling that increases the affinity of integrins in platelet activation and leukocyte adhesion, or regulation by phosphorylation of the cadherin system.

3. Specific Cell Adhesion Molecules

The broad class of adhesion molecules embedded in the plasma membrane contains several large groups of proteins that share common structural motifs, especially the Ig motif (Fig. 3). Cadherins represent a large superfamily of proteins involved in homophilic cell-to-cell adhesive interactions (14-16) (see Cadherins). Cadherins bind to cadherins of the same type on other cells via cell interaction sites that can include the recognition sequence His—Ala—Val. Besides the "classic" cadherins, such as E-cadherin and N-cadherin, there are a number of other types of cadherins, as the highly specialized cadherins termed *desmocollins* and *desmogleins* found exclusively on desmosomes, which link cells together at these particularly strong attachment sites connected to intermediate filaments such as keratins or vimentin. Cadherins are quite sensitive to depletion of calcium in the surrounding medium, accounting for the ability of calcium chelators such as EDTA to dissociate tissues into component cells. Although desmosomal cadherins are present in epithelia of all ages, cadherins appear to be of particular importance during embryonic development, when they mediate cell—cell adhesion and help define tissues by their propensity to bind primarily to cadherins of the same type, rather than to other cadherins on unrelated cell types (14-16). These specific adhesive interactions result in cell sorting to form tissue regions of closely related cells.

Figure 3. Examples of cell adhesion protein complexes linking plasma membranes of one cell (top) with another (botton are listed. Adhesion molecules comprising repeating immunoglobulin motifs include cadherins, NCAM, fasciculins, VC the plasma membrane. Cadherins appear to exist as dimers that form lateral and intercellular connections. Selectins bind carbohydrates in certain mucins. CD2, CD48, and CD58 contain only two Ig repeats. Myelin protein zero (P_0) forms hon spaced plasma membranes.

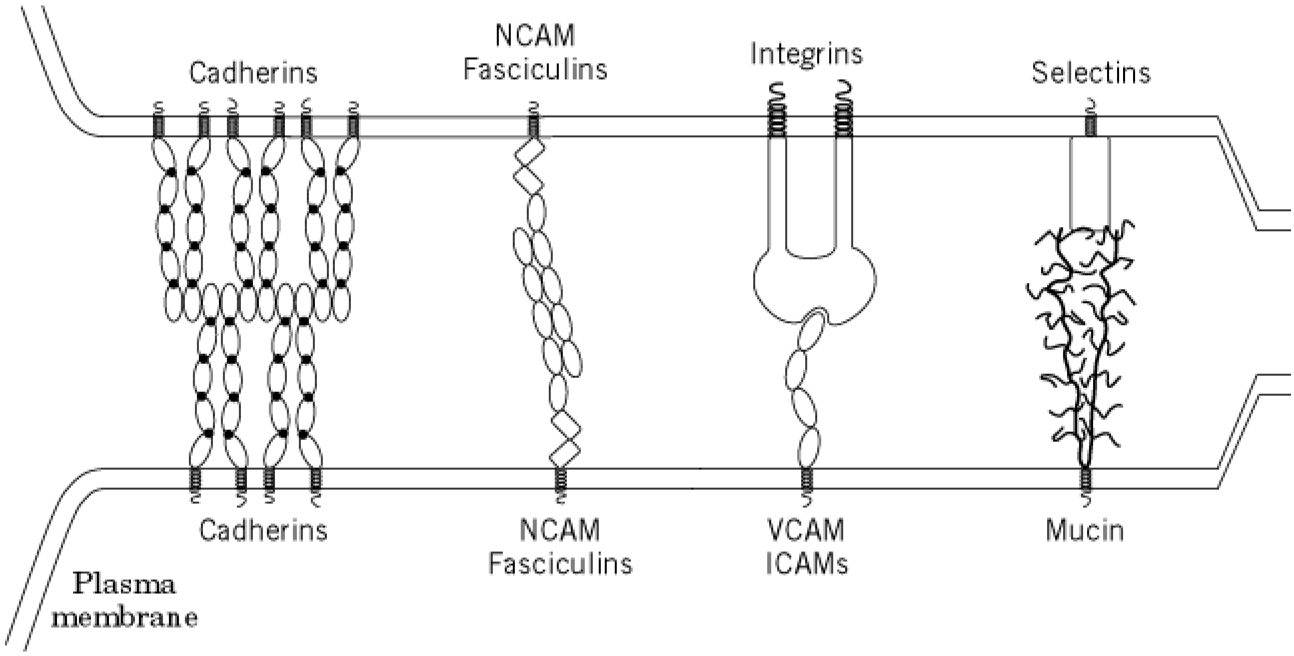

Integrins are major cell-surface receptors for a host of extracellular matrix proteins, as well as “counterreceptors” on other cells (8) (see Integrins). There are more than 20 types of integrin subunits. Genetic absence of most integrin subunits leads to disease or death, often in the embryo or near the time of birth. Integrins are heterodimers of one a and one b subunit, each of which provides adhesive specificity. They have a highly distinctive appearance, with a bulbous head domain contributed by each subunit, a binding site that also appears to involve part of each subunit, and two spindly legs (Fig. 3). The legs penetrate through the plasma membrane and usually terminate in rather short cytoplasmic domains. Although short, these cytoplasmic tails can mediate a remarkable range of signaling events (see text below). Integrin functions are also often inhibited by depletion of divalent cations.

Although cell adhesion molecules (CAMs) and counterreceptors are structurally related by their use of the Ig motif, and they often even share the -CAM designation, they can differ functionally (Fig. 3). Molecules such as NCAM are homophilic adhesive molecules that bind to the same type of molecule on adhering cell surfaces (22). In contrast, counterreceptors such as the ICAMs and VCAM have specialized peptide recognition sites that are bound specifically by integrins such as LFA-1 (CD11a/CD18 or a_1b_2) or VLA-4 (a_4b_1). The functions and sites of expression of these molecules differ widely. For example, molecules such as NCAM are implicated along with cadherins in embryonic developmental events, such as axonal bundling and guidance, whereas the ICAM counterreceptors are present as targets for binding by cells in the blood circulation. Levels of counterreceptors on the cell surface can often also be regulated rapidly in response to cytokines.

A new family of transmembrane proteins termed *ADAMs*, which are membrane proteins with a disintegrin and a metalloproteinase domain (26), contain a proteinase-like domain, as well as an integrin recognition site in the disintegrin domain. A member of this family is present on sperm and may play a role in adhesive interactions, but the functions of other members of this rapidly growing family remain to be characterized. Syndecans are cell-surface heparan sulfate proteoglycans, with a protein core that crosses the plasma membrane and terminates in a cytoplasmic tail. Syndecans appear to function as "coreceptors," mediating signaling in association with a primary adhesion molecule (27, 28). For example, syndecans bind to fibronectin at the same time that cell surface integrins bind to a cell-binding domain of fibronectin, and these binding partners cooperate during formation of the specialized adhesion sites known as focal contacts. Syndecans have several other signaling functions as well, and they can to interact with both cytoskeletal proteins and protein kinase C (27, 28).

4. Extracellular Adhesion Molecules

The second major class of adhesive molecules exists extracellularly, and its members are generally targets for cell-surface adhesion receptors such as the integrins. A gallery of such molecules is presented in Figure 4, showing functional binding sites for recognition by cell-surface receptors and domains for binding to a variety of ligands. Many contain one or more heparin-binding domains, which are used to bind to heparan sulfate proteoglycans in the extracellular matrix or in cell-surface syndecan molecules. Many also contain other types of binding domains for extracellular molecules, such as for collagen/gelatin, fibrin, entactin (nidogen), and fibulin (Figs. 2 and 4). Many of these molecules are both large and multimeric, with a specific domain for covalent cross-linking to other subunits. Finally, most of these proteins are either alternatively spliced or encoded by a set of closely related genes, thereby generating a number of isoforms. A number of reviews provide details about these complex proteins (see Extracellular Matrix and Refs. 2, 18-22).

Figure 4. Composite of six examples of cell adhesion molecules of the extracellular matrix: (**a**) Fibronectin, (**b**) Laminir Vitronectin, (**d**) Thrombospondin, (**e**) Tenascin, (**f**) Nidogen (entactin). These molecules vary widely in size and shape, a organized into functional binding domains. Specific molecular or cell-binding sites are labeled.

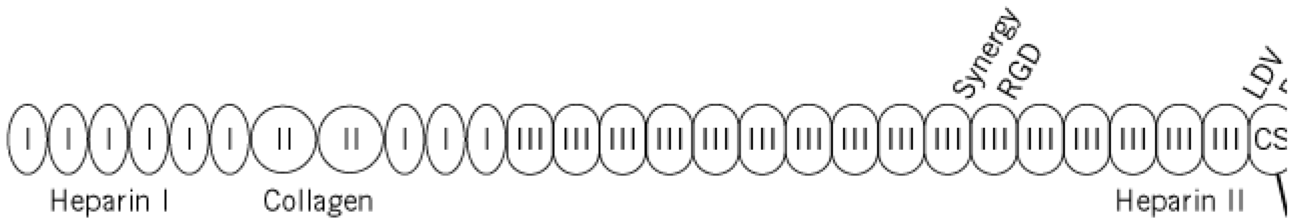

(a)

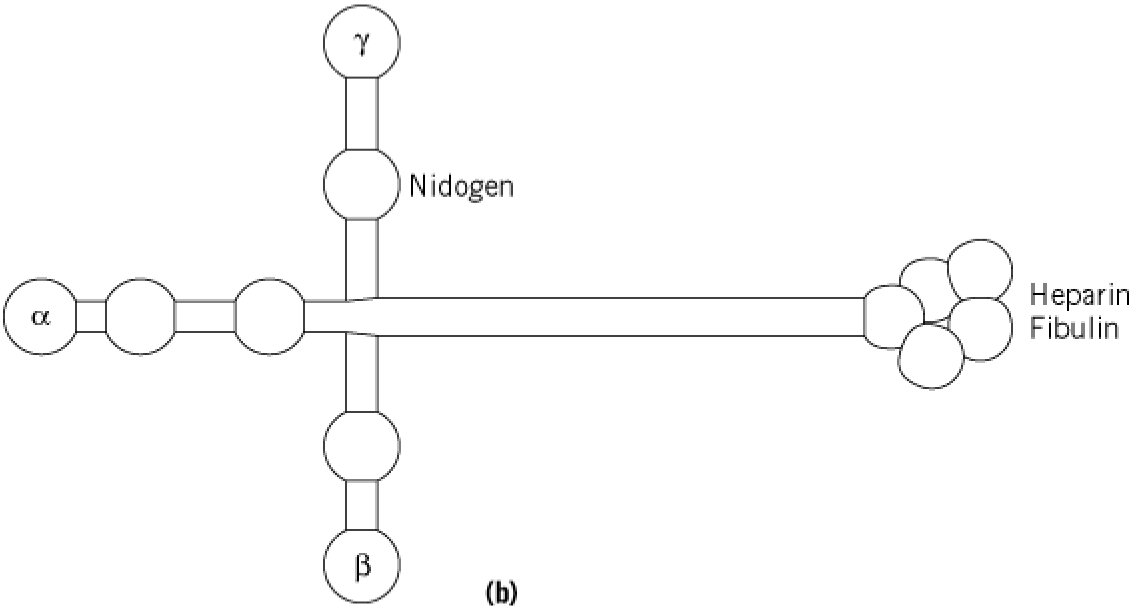

(b)

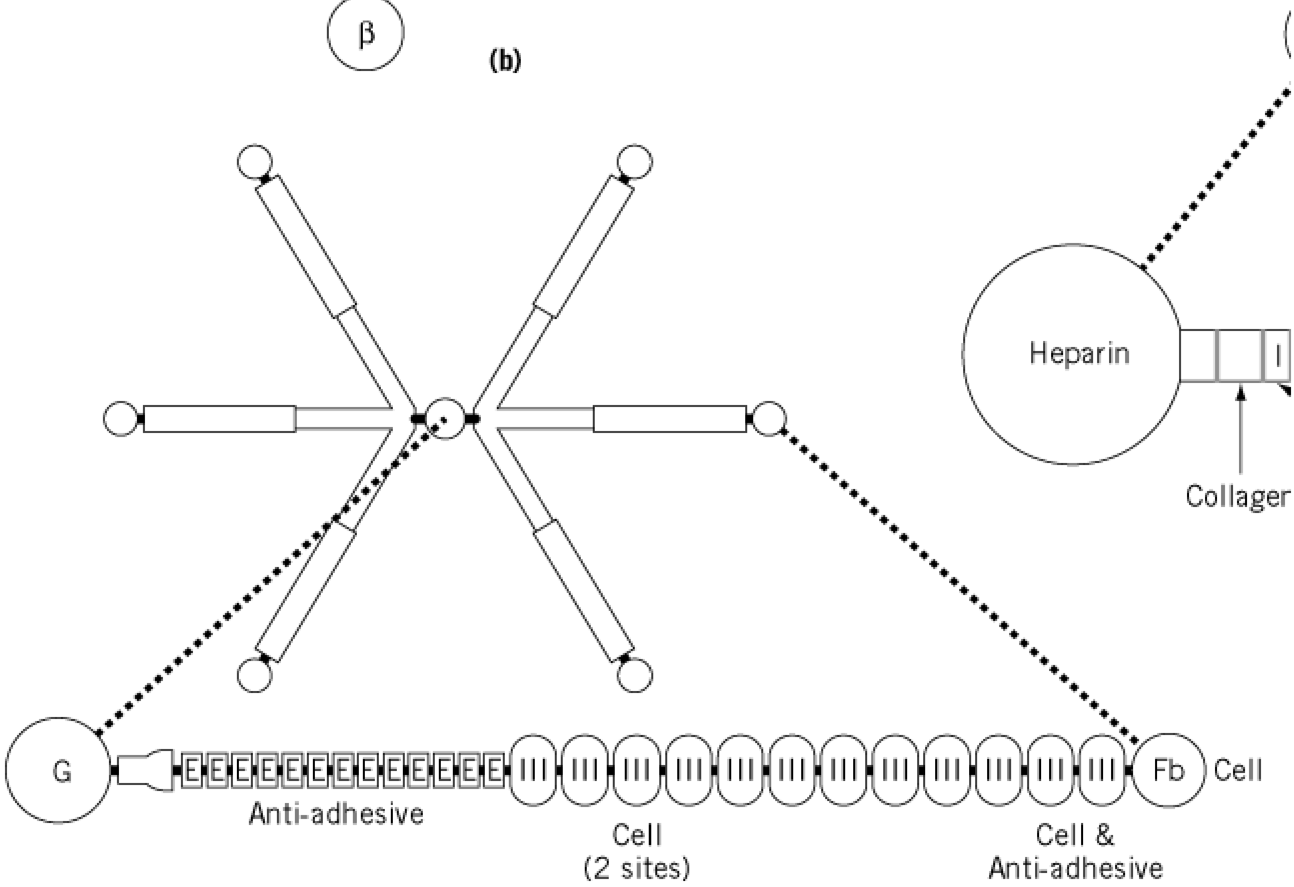

(e)

5. Peptide Adhesive Recognition Sites

A striking characteristic of a number of cell adhesion molecules is their frequent use of short peptide recognition sites (Refs. 18, 23-25, 29-31 and references cited therein). Short peptides with these sequences can at least partially mimic the binding function of intact molecules to adhesion receptors. Examples include Arg–Gly–Asp (RGD) and Leu–Asp–Val (LDV), which can bind directly to certain integrin receptors. Nevertheless, binding can be 25- to 200-fold more active in larger peptides or proteins, such as in association with a "synergy" site that functions synergistically with the primary adhesive peptide site (30). Some peptide recognition sites appear to be "cryptic" in the intact molecule, and may be active only in small fragments of the protein, such as after proteolysis. Table 1 lists the putative peptide recognition sequences in cell adhesion molecules. It is important to stress that a number of adhesion molecules also function by adhering to other proteins over much broader intermolecular contact areas, via multiple molecular contacts and with no simple peptide motif, in analogy to classic high affinity noncovalent protein–protein interactions (19). It is nevertheless striking that so many cell adhesion molecules use simple, specific, peptide adhesive-recognition motifs.

Table 1. Adhesive Recognition Sequences

Protein and Peptide Name	Recognition Sequence
Fibronectin	
Cell-binding determinant	G*RGD*S
Synergy site	PHS*R*N
Potential synergistic sites	RNS, SDV
CS1 site of IIICS domain	DELPQLPHPNLHGPEI*LDV*PS
CS5 site of IIICS domain	*REDV*
FN-C/H-I	YEKPGSPPREVVPRPRPGV
FN-C/H-II	KNNQKSEPLIGRKKT
FN-C/H-III	YRYRYTPKEKTGPMKE
FN-C/H-IV	SPPRRARVT
FN-C/H-V	WQPPRARI
Type III5 site	KLDAPT
E1	TD*IDAP*S
Laminin a_1 chain	
PA22.2 (IKVAV)	SRARKNAAS*IKVAV*SADR
RGD site	RGDN
GD-1	KATPMLKMRTSFHGCIK
GD-2	KEGYKVRLDLNITLEFRTTSK
GD-3	KNLEISRSTFDLLRNSYGVRK
GD-4	DGKWHTVKTEYIKRKAF
GD-6	KQNCLSSRASFRGCVRNLRLSR

AG-10	NRWH*SIYITR*FG
AG-32	TWY*KIAFQRN*RK
AG-73	RKR*LQVQLSIR*T
Laminin b_1 chain	
YIGSR	*YIGSR*C
PDSGR	*PDSGR*
F9 (RYVVLPR)	*RYVVLPR*PVCFEKGKGMNYVR
LGTIPG	*LGTIPG*
Integrin a_2b_1 binding site	YGYYGDALR
B-7	AFGVLALWGTRV
B-133	DSITKYFQMSLE
B-160	VILQQSAADIAR
Laminin b_2 chain	
LRE site	*LRE*
Laminin g_1 chain	
P20	RNIAEIIKDI
C-16	KAFDIT*YVRL*KF
C-28	TD*IRVTLN*RLNTF
C-64	SE*TTVKYIFR*LHE
C-68	T*SIKIRGTY*SER
Fibrinogen	
RGD sites	*RGD*S and *RGD*F
g chain peptide	HHLGGA*KQAGDV*
Integrin a_Mb_2 binding site	K*RLD*GGS
von Willebrand factor	
RGD site	*RGD*S
GPIb site	CQEPGGLVVPPTDAP plus LCDLAPEAPPPTLPP
Asp-514—Glu-542	DLVFLLDGSSRLSEAEF- EVLKAFVVDemmE
Vitronectin	*RGD*V
Entactin/nidogen	SIGF*RGD*TC
Fertilin	*TDE*
Circumzooite protein	*VTCG*
Thrombospondin	
(CD36-binding motif)	CS*VTXG*
Heparin-binding motif	¼*YSXY*
N-Terminal domain site	VDAVRTEKGFLLLASLRQ*MKKTRG*-TLLALERKDHS
GAG-independent site	FQGVLQNVRFVF
4NIs	*RFYVVMWK*
Collagen type I	
RGD sites	*RGD*TP and S*RGD*TG

DGEA site	*DGEA*
Collagen type IV	
IV-H1	GVKGDK*GNPGWPGAP*
Hep-I	TAGSCLRKFSTM
Hep III	GEFYFDLRLKGDK
a_3(IV) 185–203	CNYY*SNS*YSFWLASLNPER
a_2b_1 binding site	FYFDLR
Amyloid P component	FTLCPR
Amyloid precursor protein	*RHDS*
Bone sialoprotein	EP*RGD*NYR (cyclic)
L1	PSITW*RGD*GRDLQEL
ICAM-1	
JF9	VLYGPRLDERDAPGNWTW- PENSQQTPMC
ICAM40-51	KELLLPGNNRKV
Cyclic peptide 1	PSKVILPRGGC (cyclic)
a_Lb_2 binding site	LET, IET
LLG-C4	CPCF*LLG*CC (cyclic)
ICAM-2	GKSFTIECRVPTVEP
NCAM	KYSFNYDGSE
VCAM-1	
Domain 1 C-D loop	Q*IDS*P (cyclic peptide with terminal Cs)
(binding motifs)	IDSP, GNEH, KLEK
N-Cadherin	LRA*HAV*DVNG
Myelin protein 0 (P_0)	YSDNGTF
Ninjurin	PPRWGLRNRPIN
Leishmania pg63	¼*SRYD*¼
Streptavidin	*GRYDS*[a]

[a] See Refs. 14, 16, and 22 for additional information.

Two key sites of membrane adhesion molecules that allow them to function as signal transduction receptors are their ligand-binding domains and their cytoplasmic domains. The ligand-binding domains are of obvious importance in binding to extracellular molecules, but their roles are more intriguing in at least some cases. There appear to be separable functions for ligand occupancy, specifically, for filling the binding site with a ligand or an antibody, as opposed to receptor clustering (which can be induced by a multivalent ligand, such as fibrils of fibronectin or collagen). These two inputs can cooperate in promoting accumulation of specific cytoskeletal proteins, such as a-actinin and actin, which are thought to be crucial for forming strong adhesions (32). Even though they lack intrinsic enzymatic activities, integrins appear to be able to function as signaling receptors and as regulators of actin cytoskeletal organization by recruiting other molecules to their cytoplasmic domains. Integrins can reportedly bind directly to certain cytoplasmic proteins directly, such as to talin, a-actinin, and focal adhesion kinase, perhaps regulated by ligand occupancy on the outside of the cell. Integrin clustering appears to play a central role in forming large intracytoplasmic complexes of over 30 molecules that can serve as signaling centers, such as for MAP kinase activation (Fig. 5; Refs. 9-13, 32).

Figure 5. Integrin adhesion and signaling complex formed after cell adhesion molecule interactions. Binding of a ligand and aggregation of adhesion receptors in the plane of the plasma membrane results in the formation of multimolecular complexes that can contain over 30 cytoskeletal and signal transduction molecules, which link to the actin-containing cytoskeleton and mediate intracellular signaling.

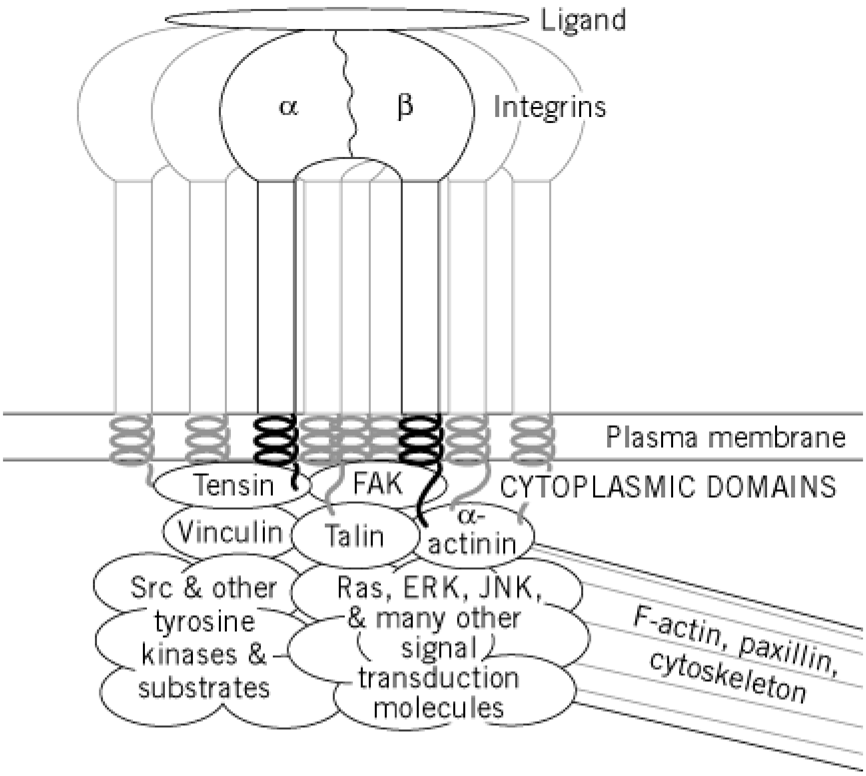

6. Major Functions of Cell Adhesion Molecules Beyond Adhesiveness

Cell adhesion molecules and receptors can be intuitively understood as mechanisms for attaching cells to other cells, for permitting cell adherence to extracellular matrix molecules, and for mediating traction during cell migration. It has become clear, however, that they also play critical roles in cellular signaling. In fact, their signaling functions may be of equal biological importance. A current view is that “adhesion” proteins are actually “cell-interaction” proteins that have multiple functions involving the bidirectional transfer of information at the cell surface. In fact, some of these proteins, such as thrombospondin and tenascin, can have antiadhesive activities in certain situations and can modulate a host of cellular functions. Even classic “adhesive” proteins, such as fibronectin, can have a bewildering range of activities, mediated by integrin binding, that range from activating or modulating nearly every known maemmalian signal transduction pathway. These pathways include tyrosine phosphorylation by tyrosine kinases, mitogen-activated protein kinases (MAP kinases), Ca^{2+} and H^{+} fluxes, inositol phosphate pathways, and protein kinase C, which prevent apoptosis and activate specific gene transcription (9-12).

This same theme of complex formation, binding of cytoskeletal proteins such as actin, and accumulation of signaling molecules also appears to occur for cell-to-cell adhesion molecules (14-16, 22). Cadherin cytoplasmic domains interact with catenins, which then link to the actin cytoskeleton. In addition, however, the binding of b-catenin to cadherins can titrate its cytoplasmic levels; b-catenin molecules that are not bound by cadherins can enter the nucleus and regulate gene expression (3). A variety of other signaling pathways exist in cell-cell and cell-matrix adhesion systems. Although much more remains to be learned about precise pathways and overall integration of the many cytoplasmic effects of cell adhesion molecules, it is clear that adhesion molecules are crucial components of the basic regulatory mechanisms of cells and provide dynamic links to the external environment.

Bibliography

1. B. Alberts et al., in *Molecular Biology of the Cell*, 3rd, ed., Garland Publishing, New York , 1994, pp. 949–1009.
2. E.D. Hay, ed., *Cell Biology of Extracellular Matrix*, Plenum Press, New York 1991.
3. B.M. Gumbiner, Cell **84**, 345–357 (1996).
4. S.F. Gilbert, *Developmental Biology*, Sinauer Associates, Sunderland, Mass., 1994.
5. R.O. Hynes and Q. Zhao, J. Cell Biol. **150**, F89–96 2000).
6. G.M. Edelman and J.P. Thiery, *The Cell in Contact: Adhesions and Junctions as Morphogenetic Determinants*, John Wiley & Sons, New York, 1985.
7. D.L. Benson, L.M. Schnapp, L. Shapiro and G.W. Huntley, Trends Cell Biol. **10**, 473–482 (2000).
8. R.O. Hynes, Cell **69**, 11–25 (1992).
9. E.A. Clark and J.S. Brugge., Science **268**, 233–239 (1995).
10. M.A. Schwartz, M.D. Schaller, and M.H. Ginsberg, Annu. Rev. Cell Devel. Biol. **11**, 549–599 (1995).
11. A.E. Aplin, A.K. Howe, and R.L. Juliano, Curr. Opin. Cell Biol. **11**, 737–744 (1999).
12. F.G. Giancotti and E. Ruoslahti, Science **285**, 1028–1032 (1999).
13. K.M. Yamada and B. Geiger, Curr. Opin. Cell Biol. **9**, 76–85 (1997).
14. M. Takeichi, Annu. Rev. Biochem. **59**, 237–252 (1990).
15. B.M. Gumbiner, J. Cell Biol. **148**, 399–404 (2000).
16. U. Tepass et al., Nat. Rev. Mol. Cell Biol. **1**, 91–100 (2000).
17. S.K. Sastry and K. Burridge, Exp. Cell Res. **261**, 25–36 (2000).
18. K.M. Yamada, J. Biol. Chem. **266**, 12809–12812 (1991).
19. C. Chothia and E.Y. Jones, Annu. Rev. Biochem. **66**, 823–862 (1997).
20. R. Gonzalez-Amaro and F. Sanchez-Madrid, Crit. Rev. Iemmunol. **19**, 389–429 (1999).
21. M.J. Humphries, Biochem. Soc. Trans. **28**, 311–339 (2000).
22. H. Kamiguchi and V. Leemmon, Curr. Opin. Cell Biol. **12**, 598–605 (2000).
23. S. Ayad, *The Extracellular Matrix Factsbook*, 2nd ed., Academic Press, San Diego 1998.
24. T. Kreis and R. Vale, *Guidebook to the Extracellular Matrix, Anchor, and Adhesion Proteins*, Oxford University Press, New York 1999.
25. C. Isacke and M. A. Horton, *The Adhesion Molecule Factsbook*, Academic Press, San Diego 2000.
26. J. Schlondorff and C.P. Blobel, J. Cell Sci. **112**, 3603–3617 (1999).
27. J.R. Couchman and A. Woods, J. Cell Sci. **112**, 3415–3420 (1999).
28. A.C. Rapraeger, J. Cell Biol. **149**, 995–998 (2000).
29. E. Ruoslahti, Annu. Rev. Cell Devel. Biol. **12**, 697–715 (1996).
30. S. Aota, M. Nomizu, and K. M. Yamada, J. Biol. Chem. **269**, 24756–24761 (1994).
31. M. Nomizu et al., Arch. Biochem. Biophys. **378**, 311–320 (2000).
32. K.M. Yamada and E.H.J. Danen, in J. S. Gutkind, ed., *Signaling Networks and Cell Cycle Control*, Humana Press, Totowa, NJ, 2000, pp. 1–25.

Additional Reading

33. Alberts B. et al., "Cell junctions, cell adhesion, and the extracellular matrix", in *Molecular Biology of the Cell*, 3rd ed., Garland Publishing, Inc., New York, pp. 949–1009 1994.
34. Hay E.D., ed., *Cell Biology of Extracellular Matrix*, Plenum Press, New York 1991.
35. Chothia C. and Jones E.Y., Annu. Rev. Biochem. **66**, 823–862 (1997).
36. Gumbiner B.M., Cell **84**, 345–357 (1996).

Another excellent source of current information on adhesion molecules is found each year in issue number 5 of *Current Opinion in Cell Biology*. These annual issues are devoted to “cell-to-cell contact and extracellular matrix,” and provide useful updates in the field.

Cell Cycle

A dramatic change in how we understand the progression of the eukaryotic cell cycle, from phenomenological to biochemical, occurred in the late 1980s. The cell cycle consists of four main phases: G1, S, G2, and M. DNA replication occurs in S phase, and the chromosomes are segregated to daughter cells during mitosis (M phase). The so-called gap phases (G1 and G2) are defined simply as the periods separating DNA replication and mitosis. The length of the cell cycle ranges from just a few minutes in certain early embryos (which don't need to increase their mass between divisions), to 1.5 h in budding yeast, to approximately one day in typical mammalian tissue culture cells. In mammalian cells, the durations of S phase (~7 h) and mitosis (~1 h) are relatively inflexible, whereas the lengths of the gap phases can vary greatly. The length of G1 is particularly variable and is sensitive to the levels of nutrients and growth factors. In general, once a cell progresses past the “Restriction Point” in G1, it becomes committed to complete the cell cycle. A convergence of research in yeast, marine invertebrates, and frogs led to a phenomenal growth in our mechanistic understanding of how all eukaryotic cells regulate these events and the transitions between them. The basic machinery controlling the cell cycle consists of a subfamily of protein kinases, termed cyclin-dependent kinases (Cdk's). These enzymes are in turn regulated by a number of mechanisms, including transcription, inhibitory and activating **phosphorylations**, binding to inhibitory proteins, and **ubiquitin**-mediated protein degradation. Checkpoints that prevent the execution of one cellular event before a prior step has been completed further modulate cell cycle progression.

1. Historical Threads: Yeast Genetics, MPF, and Cyclins

Genetic studies of the cell cycle in the yeasts *Saccharomyces cerevisiae* and *Schizosaccharomyces pombe* illuminated important principles underlying the logic of cell cycle control and identified many of its key players. Screens were performed for conditional temperature-sensitive mutations, causing cells to arrest quickly with uniform morphologies, indicative of defects in executing individual cell cycle steps. Analysis of a large collection of such *cdc* (cell division cycle) mutants from *S. cerevisiae* placed them into series of dependent and independent pathways (1). For example, inactivation of *CDC28* causes cells to arrest at “START” (equivalent to the restriction point of mammalian cells) and blocks pathways leading to formation of the bud, DNA replication, and duplication of the spindle pole body. Inactivation of genes acting after *CDC28* can block one of these pathways, while the other two continue. A similar screen in the distantly related yeast *Schizosaccharomyces pombe* successfully identified the most proximal regulators of the G2 to mitosis transition (Fig. 1) (2). *cdc*2^+ was found to be the key regulator of entry into mitosis and to encode a protein kinase. Inactivation of *cdc*2^+ causes cells to arrest in G2, whereas its premature activation leads to early entry into mitosis. Genetic analysis indicated that the *cdc*25$^+$ gene product functioned in a pathway leading to activation of Cdc2 and that the product of *wee*1$^+$ functioned in a pathway leading to inhibition of Cdc2. Sequence analysis of these genes indicated that both *cdc*2$^+$ and *wee*1$^+$ encoded protein kinases, but initially shed little light on the function of Cdc25 (see text below).

Figure 1. Regulation of the G2-to-mitosis transition in *Schizosaccharomyces pombe*. *cdc*2$^+$ is required for this transition. In the absence of its activity, cells arrest in G2. *cdc*25$^+$ is a positive regulator of *cdc*2$^+$, and its inactivation also gives a G2 arrest. In contrast, wee1$^+$ negatively regulates *cdc*2$^+$, and its inactivation leads to premature activation of Cdc2 and entry of cells into mitosis at an unusually small size (a "wee" phenotype).

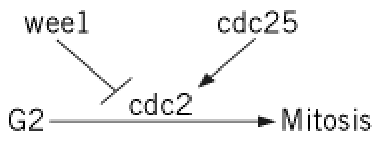

Two other lines of research provide essential historical threads leading to our current understanding of the cell cycle. The first involves maturation promoting factor (MPF), which was originally defined as a developmental factor found in the cytoplasm of metaphase-arrested frog eggs that could induce oocytes to proceed through meiosis and to "mature" into eggs following its injection into their cytoplasm (3). Subsequent research found that MPF activity is present in all eukaryotic cells during M phases (meiosis or mitosis). Thus, MPF is a universal regulator of entry into mitosis. The second thread concerns the cyclins. The first cyclins were found during studies of translational control before and after fertilization of sea urchin eggs conducted as part of the Physiology course at the Marine Biological Laboratory in Woods Hole (4). These proteins were synthesized continuously, and they accumulated until their abrupt degradation during mitosis. This pattern of accumulation hinted that cyclins might play an important role during the cell cycle. Later work showed that the injection of cyclin messenger RNA led to the maturation of frog oocytes, suggesting that cyclins, like MPF, functioned as positive regulators of the G2-to-mitosis transition (5).

Work on cyclins, MPF, and the yeast *cdc* genes came to an explosive convergence in the late 1980s with the purification of MPF and the identification of its subunits as homologs of *cdc*2$^+$ and cyclin (6-9). Thus, this key regulator of entry into mitosis was a protein kinase (Cdc2) whose activity was controlled at least in part via the cyclic accumulation and degradation of a regulatory subunit (cyclin). The activity of Cdc2 is typically assayed by its ability to **phosphorylate** a convenient substrate, histone H1. Cdc2 is a workhorse master regulator. Rather than sitting at the apex of a large regulatory pathway, Cdc2 generally phosphorylates the downstream-most targets of mitotic regulation. For example, its direct phosphorylation of nuclear lamins causes the disassembly of the lamin-containing filaments of the nuclear lamina (10, 11).

2. Regulation of Cdc2 Activity: Phosphorylation and Cyclin Degradation

In addition to cyclin binding, enzymes such as Cdc2 are regulated by multiple phosphorylations (12, 13) (see Fig. 2). Cdc2 is negatively regulated via phosphorylation of Thr14 and Tyr15. (The amino acid positions in this section refer to the phosphorylation sites in human Cdc2.) These sites are phosphorylated by Wee1 (the negative regulator of Cdc2 identified genetically in *Schizosaccharomyces pombe* (see Fig. 1)) and by Wee1-like protein kinases (Mik1 in *Schizosaccharomyces pombe* and the membrane-bound Myt1 protein in vertebrates). Dephosphorylation of these inhibitory sites is carried out by Cdc25 proteins, genetically identified activators of Cdc2 that share distant similarity to protein **tyrosine phosphatases**. Finally, activating phosphorylation of Cdc2 occurs on Thr161 within the so-called T-loop and is carried out by the Cdk-activating kinase (CAK). Dephosphorylation of Thr161 has not been as well studied. It occurs following cyclin degradation, possibly by a phosphatase termed KAP. Two feedback loops operate as cells enter mitosis and lead to the inhibition of Wee1-like enzymes and the stimulation of Cdc25, thus ensuring the abrupt and irreversible transition from G2 to mitosis. The roles of cyclin binding and activating phosphorylation have been studied using X-ray crystallography of Cdk2 (14-16), a close relative of Cdc2. Monomeric Cdk2 is inactive for two major reasons. First, residues that interact with the phosphates of ATP are out of position, resulting in the misalignment of the g-phosphate of ATP for phosphoryl transfer. Second, the T-loop is positioned so that it would physically prevent protein substrates from gaining access to the site of catalysis. Binding to cyclin relieves this steric block and moves residues that interact with ATP into their proper positions. The cyclin A-Cdk2 complex is about 1% active. Full activation requires activating phosphorylation (on Thr160 in Cdk2), which alters the positions of some T-loop residues and creates an acidic patch for the binding of optimal substrates containing a key basic residue.

Figure 2. Activation of Cdc2. Monomeric Cdc2 is unphosphorylated and inactive. Binding to cyclin induces its phosphorylation on inhibitory sites (Thr14 and Tyr15) by Wee1-like protein kinases and its phosphorylation on an activa site (Thr161) by CAK. The transition into mitosis is accompanied by two feedback loops involving stimulation of Cdc25 (the phosphatase acting on Thr14 and Tyr15) and inhibition of Wee1-like enzymes, resulting in the abrupt and irreversib activation of Cdc2 and entry into mitosis. The degradation of cyclin by the ubiquitin system toward the end of mitosis le to the inactivation of Cdc2 and its dephosphorylation, probably by a phosphatase called KAP.

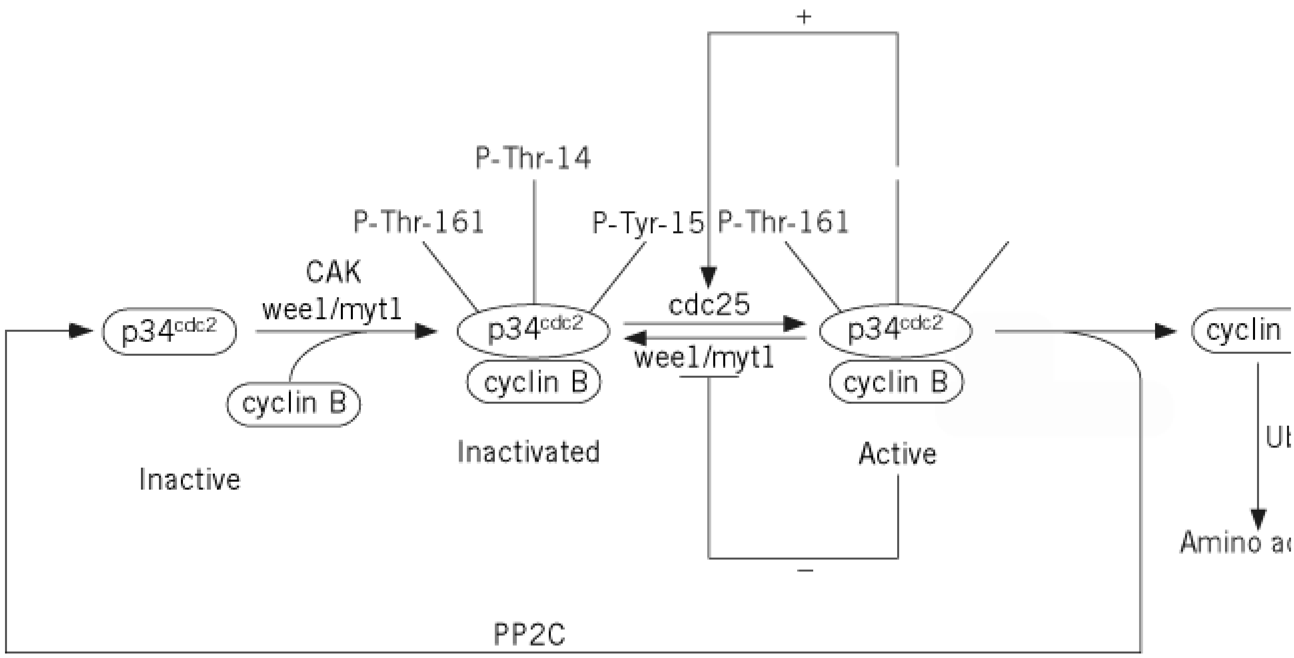

One of the irreversible ratchet steps in the cell cycle is the degradation of cyclins by the ubiquitin system (17). Ubiquitin is a 76-residue protein whose covalent attachment to proteins can target them for **proteolysis** by the proteasome, a huge multiproteinase unwinding and degrading machine. Ubiquitin is activated by its ATP-dependent covalent attachment to an enzyme called E1. E1 then transfers ubiquitin to one of many E2 enzymes. The E2s can ubiquitinate substrates, often with the help of an E3. The E3s may be the most diverse and interesting components of this system. Some E3s receive the covalently bound ubiquitin; others serve as matchmakers that bring together a substrate and the appropriate E2. For the mitotic cyclins, the E3 was first termed the cyclosome, though it is now generally termed the *anaphase promoting complex* (APC), an 8- to 12-subunit complex. The APC is the regulated component of the ubiquitin system for the degradation of the mitotic cyclins and serves as the target for checkpoint signals (see below) that can block cyclin degradation. The ubiquitin-dependent degradation of cyclins that act earlier in the cell cycle generally does not require the APC and has been best studied in *S. cerevisiae*.

3. Relatives: Cdks and Cyclins

Both Cdc2 and the mitotic cyclins are members of large families of related proteins, many of which function in cell cycle regulation. The Cdc2 relatives are termed Cdks (for cyclin-dependent kinases) and the cyclin relatives are designated by letter. The different cyclins accumulate at various times during the cell cycle and pair with a limited subset of the Cdks to execute their respective functions. The major cyclin–Cdk complexes and their functions are shown in Table 1. Complexes of D-type cyclins with Cdk4 and Cdk6 function in progression through G1 and are the first kinases to phosphorylate the cell-cycle inhibitor retinoblastoma protein (Rb). The cyclin E–Cdk2 complex stimulates the initiation of DNA synthesis, and the cyclin A–Cdk2 complex is generally thought to promote passage through S phase. Cyclin B partners with Cdc2 to promote the G2-to-mitosis transition. All of these complexes are regulated by phosphorylations on sites equivalent to those used in Cdc2. In addition to these enzymes, a large number of cyclin–Cdk complexes function in processes other than cell cycle regulation, including transcription and neuronal differentiation. In general, the regulatory subunits of these Cdks are stable proteins and are classified as cyclins only on the basis of sequence similarity.

Table 1. Functions of Cyclin–Cdk Complexes Involved in Cell Cycle Control

Catalytic Subunit	Major Cyclin Partner	Function
Cdc2	Cyclin B	G2 to M
Cdk2	Cyclin A	S
Cdk2	Cyclin E	G1 to S
Cdk4	Cyclin D	G1
Cdk6	Cyclin D	G1

4. Cdk Inhibitors

In addition to cyclin binding and phosphorylation, Cdks are also regulated by the binding of inhibitory proteins (18). These can be divided into two classes: the CIP/KIP family (consisting of $p21^{CIP1}$, $p27^{KIP1}$, and $p27^{KIP2}$) and the INK4 family (consisting of $p15^{INK4b}$, $p16^{INK4a}$, $p18^{INK4c}$, and $p19^{INK4d}$). The CIP/KIP proteins bind preferentially to the cyclin–Cdk complex and cause its inactivation. These proteins bind to numerous Cdks, but show a preference for Cdk2. In contrast, the INK4 proteins bind preferentially to monomeric Cdks (inhibiting the binding of cyclin) and are specific for Cdk4 and Cdk6. Cdk inhibitors play very important roles both in cell cycle progression (particularly in responses to growth factors) and during development. One of the best-studied roles for a Cdk inhibitor involves the regulation of the initiation of DNA synthesis in *S. cerevisiae* by Sic1p. Entry into S phase in *S. cerevisiae* requires the activity of complexes containing an S-phase cyclin (Clb5p or Clb6p) and the budding yeast Cdk, Cdc28p. These complexes are inhibited by Sic1p. Degradation of Sic1p by the ubiquitin system is triggered following the phosphorylation of Sic1p by Cdc28p bound to G1 cyclins, thereby freeing the Clb5p and Clb6p complexes to initiation DNA replication (19).

5. Checkpoints

Among the key mechanisms for ensuring the orderly progression of cell cycle events are checkpoints, which monitor the completion of certain events and prevent the execution of subsequent events if the monitored event has not been completed (20, 21). For example, checkpoints can block entry into mitosis if the DNA is damaged or has not been fully replicated, or they can block exit from mitosis if the spindle has not been properly assembled. In *S. cerevisiae* a checkpoint even monitors whether a bud has formed. One of the defining features of a checkpoint sensor is that it is not part of the machinery being sensed and that it is dispensable, though only for the short term. The checkpoint that provides the paradigm for all others involves the sensing of **DNA damage** and unreplicated DNA by Rad9p in *S. cerevisiae*. A number of yeast *cdc* mutants cause G2 arrests that are dependent on this checkpoint. For example, inactivation of *CDC9*, which encodes DNA Ligase, leads to G2 arrest if *RAD9* is functional. In contrast, inactivation of *CDC9* in a *rad9* mutant does not lead to an immediate arrest. Instead, cells progress into mitosis and continue through a couple of cell cycles, until they arrest as microcolonies. The G2-arrested *RAD9* cells remain viable while they attempt to repair their DNA, whereas the *rad9* cells rapidly lose viability as they proceed through the checkpoint. Unperturbed wild-type cells grow normally in the absence of this checkpoint. The importance of checkpoints to a proper cell cycle and to human health is underscored by the p53 protein. p53 is the most frequently mutated protein in human cancers and functions as part of a checkpoint responding to DNA damage by transcriptionally inducing the p21 Cdk inhibitor (22), thereby blocking cell cycle progression. The absence of this checkpoint leads to genomic instability (the accumulation of further mutations, loss of chromosomes, etc.) and a greatly increased risk of tumor formation.

Bibliography

1. J. R. Pringle and L. H. Hartwell (1981) In *The Molecular Biology of the Yeast Saccharomyces* (J. Strathern, E. Jones, and J. Broach, eds.), Cold Spring Harbor Laboratory Press, Cold Spring Harbor, NY, pp. 97–142.
2. P. Nurse (1990) Nature **344**, 503–508.
3. Y. Masui and C. L. Markert (1971) J. Exp. Zool. **177**, 129–146.
4. T. Evans, E. T. Rosenthal, J. Youngblom, D. Distel, and T. Hunt (1983) Cell **33**, 389–396.
5. K. I. Swenson, K. M. Farrell, and J. V. Ruderman (1986) Cell **47**, 861–870.
6. W. G. Dunphy, L. Brizuela, D. Beach, and J. Newport (1988) Cell **54**, 423–431.
7. J. Gautier, C. Norbury, M. Lohka, P. Nurse, and J. Maller (1988) Cell **54**, 433–439.
8. J. C. Labbé, J. P. Capony, D. Caput, J. C. Cavadore, J. Derancourt, M. Kaghad, J. M. Lelias, A. Picard, and M. Dorée (1989) EMBO J. **8**, 3053–3058.
9. J. Gautier, J. Minshull, M. Lohka, M. Glotzer, T. Hunt, and J. L. Maller (1990) Cell **60**, 487–494.
10. M. Peter, J. Nakagawa, M. Dorée, J. C. Labbé, and E. A. Nigg (1990) Cell **61**, 591–602.
11. G. E. Ward and M. W. Kirschner (1990) Cell **61**, 561–577.
12. M. J. Solomon (1993) Curr. Opin. Cell Biol. **5**, 180–186.
13. M. J. Solomon and P. Kaldis (1998) In *Results and Problems in Cell Differentiation*, Vol. **22**: Cell Cycle Control (M. Pagano, ed.), Springer, Heidelberg, pp. 79–109.
14. J. L. DeBondt, J. Rosenblatt, J. Jancarik, H. D. Jones, D. O. Morgan, and S.-H. Kim (1993) Nature **363**, 595–602.
15. P. D. Jeffrey, A. A. Russo, K. Polyak, E. Gibbs, J. Hurwitz, J. Massagué, and N. P. Pavletich (1995) Nature **376**, 313–320.
16. A. A. Russo, P. D. Jeffrey, and N. P. Pavletich (1996) Nat. Struct. Biol. **3**, 696–700.
17. R. W. King, R. J. Deshaies, J.-M. Peters, and M. W. Kirschner (1996) Science **274**, 1652–1659.
18. T. J. Soos, M. Park, H. Kiyokawa, and A. Koff (1998) In *Results and Problems in Cell*

Differentiation, Vol. **22**: Cell Cycle Control (M. Pagano, ed.), Springer, Heidelberg, pp. 111–131.
19. R. M. Feldman, C. C. Correll, K. B. Kaplan, and R. J. Deshaies (1997) Cell **91**, 221–230.
20. L. H. Hartwell and T. A. Weinert (1989) Science **246**, 629–634.
21. S. J. Elledge (1996) Science **274**, 1664–1672.
22. J. W. Harper, G. R. Adami, N. Wei, K. Keyomarsi, and S. J. Elledge (1993) Cell **75**, 805–816.

Suggestions for Further Reading

23. W. G. Dunphy, ed. (1997) *Methods in Enzymology*, Vol. **283**: Cell Cycle Control, Academic Press, San Diego, CA.
24. D. O. Morgan (1997) Cyclin-dependent kinases: engines, clocks, and microprocessors. Annu. Rev. Cell Dev. Biol. **13**, 261–291.
25. A. Murray and T. Hunt (1993) *The Cell Cycle*, W. H. Freeman, New York.
26. M. Pagano, ed. (1998) *Results and Problems in Cell Differentiation*, Vol. **22**: Cell Cycle Control, Springer, Heidelberg.

Cell Death

It is not initially obvious why cell death should be considered important. The death of single-celled organisms, such as **amoeba** or **bacteria**, has no apparent advantage for the individual cell. However, in multicellular organisms damage to an individual cell can have repercussions for the whole animal. It therefore makes biological sense to dispose of this cell and replace it with a healthy one. Cells become damaged in a variety of different ways, but for long-lived, multicellular animals, the greatest risk is from a damaged cell that has acquired an **oncogenic** mutation leading to unrestricted clonal growth. To minimize this risk, several pathways have evolved that limit the expansion of somatic cells, one of which is cell death.

Tissue size is restricted by several different methods, not all of which actually require the physical loss of the cell. The problem facing multicellular organisms is how to maintain the capacity to divide and replace damaged cells while minimizing the risk of mutation leading to enhanced growth potential. One way around this problem is to make tissues post-replicative, as occurs in the central nervous system (CNS). All the neurons within the CNS are produced during embryogenesis and are then maintained throughout the life span of the organism. For some tissues, however, such an approach is not practical due to persistent physical damage to the cells, such as occurs in the epithelial lining of the gut or skin. Here, cells are continuously produced by a select number of proliferating stem cells. The daughter cells they produce move upward, away from the basement membrane, terminally differentiate, and are eventually shed. Because these cells are continuously replaced, any damaged cell should be automatically eliminated. Tissue size is also restricted by the need for vascularization. If there is no blood supply, only a small proportion of cells can be maintained by the diffusion of solutes, which is one of the reasons why many solid tumors have central necrotic zones.

For tissues that require a significant number of cells in cycle, the risk of mutation is minimized by both senescence and cell death. Senescence is a pathway that is invoked once cells have undergone a specific number of doublings, causing them to arrest permanently. Cells in this senescent state are unable to reenter the cell cycle (1). Thus, a cell that does acquire a mutation allowing constant proliferation is limited in its capacity to divide, restricting clonal outgrowth [see Senescence]. Finally, cells can be triggered to die when no longer required, or when damaged. This "programmed cell death" is essential for the maintenance of tissue homeostasis and is invoked in disparate situations including DNA damage, absence of survival signals, and oncogene activation (2, 3) [see Programmed Cell Death and Apoptosis]. Thus, multicellular organisms are protected against somatic mutation by a number of independent mechanisms that act in concert to limit the potential for neoplastic transformation.

1. The Meaning of Cell Death

The concept that cell death is fundamentally important for restricting cell population expansion took some time to be accepted for several reasons. Dead cells are not obvious in healthy tissues, whereas they are abundant in areas of damaged tissue, such as ischemic heart tissue resulting from myocardial infarction, allowing dead cells to be fundamentally associated with disease. Only during embryogenesis are dying cells seen in abundance, but these were generally regarded as cells deleted as a result of overproduction during development. In addition, death is seen as a bad outcome in human terms, a misconception that has allowed human anthropomorphic confusions to outweigh scientific evidence. More recently, however, several of these objections have been overruled, allowing cell death to become an accepted, essential daily process.

Early investigators of both invertebrate and vertebrate development observed that developmental cell deaths occurred in response to several biological cues and could be suppressed by inhibitors of both protein and RNA synthesis (4, 5), suggesting a requirement for macromolecular synthesis (6, 7). Moreover, they made the important connection that these cell deaths were an essential part of the developmental program of the organism concerned; hence the term "programmed cell death" (PCD) (8). It is now possible in less complex invertebrate models, such as the nematode *Caenorhabditis elegans*, to map both the fate of all individual cells within the developing organism and the genes that dictate these fates (9) [see Programmed Cell Death].

For vertebrates, the importance of cell death was not appreciated until the detailed characterization of the form of cell death termed apoptosis (10). The programmed cell deaths observed during development are identical to apoptotic cells in mammalian tissues, suggesting that a regulated form of cell death has been conserved throughout evolution (11, 12). From these early observations, our understanding of apoptosis/PCD has grown to include a complex pathway that is both morphologically and biochemically distinct from classical necrosis or accidental cell death. Necrosis is a passive event, in which cells that become irreversibly damaged, and therefore useless, die (13, 14). This form of cell death, which requires no input from the dying cell, occurs in cells subject to physical disruption or severe toxic stress. Conversely, apoptosis/PCD describes a pathway of events in which the cell is actively involved. Due to the active nature of apoptosis, which is triggered by many physiological and toxic stimuli, this form of cell death is sometimes referred to as "cell suicide." Overall, the importance of "active" cell death is underlined by the fact that death is the default state for all cells. Hence, all cells are programmed to die, unless signaled to survive (15).

The importance of cell death in the regulation of tissue homeostasis is paramount. The number of proliferating cells determines the cell population number, as does the number of differentiating cells and the number of dying cells. Research over the last 20 years has graphically shown how cells that have mutations which disrupt their capacity to undergo apoptosis in response to physiological stimuli are involved in the etiology of several diseases, including Alzheimer's, AIDS, and cancer (16).

Aside from the three pathways of death described above, the "death" of a cell does not always result in the loss of viability or cellular function. Within a cell population, few cells are actually proliferating, many are in a resting state outside of the cell cycle, known as **GM_0** phase. Certain cells can reenter the cell cycle given the appropriate stimuli, but cells that enter a permanent G_0 state do not respond to these proliferation signals. Cells in the latter state are termed senescent and can complete all normal functions except division (1) [see Senescence]. Cells that escape the confines of senescence are able to proliferate continuously and, more important, the mutations that lead to the evasion of senescence are common and perhaps mandatory in tumor cells (17).

Thus, the description “cell death” encapsulates several diverse processes. This can involve the physical loss of the cells through apoptosis/PCD or, in some circumstances, necrosis. Alternatively, cell death can refer to a genetic death, where cells no longer retain the ability to replicate, but continue to survive. Which method of cell death is induced depends on several factors, including the cell's internal environment, its external environment, and its developmental history. It is not yet clear whether the genes that regulate apoptosis/PCD and senescence overlap. For example, genes such as p53 and **retinoblastoma** appear to be required for the regulation of apoptosis and senescence, but it is not clear whether these genes perform similar or different roles in each pathway. Indeed, cells that have evaded the first signal to senesce enter *crisis*, which is defined as the point at which the culture exhibits both apoptosis and proliferation. This suggests that there must be some overlap in the control of different types of cell death, and this may enable one type of cell death to be employed when another either is not suitable or is not able to be induced.

Bibliography

1. C. A. Afshari and J. C. Barrett (1996) "Molecualr genetics of in vivo cellular senescence". In *Cellular Aging and Cell Death* (N. J. Holbrook, G. R. Martin, and R. A. Lockshin, eds.), Wiley-Liss, New York, pp. 109–122.
2. A. J. Hale, C. A. Smith, L. C. Sutherland, V. E. Stoneman, V. Longthorne, A. C. Culhane, and G. T. Williams (1996) Apoptosis: Molecular regulation of cell death. Eur. J. Biochem. **237**, 884.
3. S. J. Martin, and D. R. Green (1995) Apoptosis and cancer: The failure of controls on cell death and cell survival. Crit. Rev. Oncol. Hematol. **18**, 137–153.
4. J. R. Tata (1966) Requirement for RNA and protein synthesis for induced regression of the tadpole tail in organ culture. Dev. Biol. **13**, 77–94.
5. R. A. Lockshin (1969) Programmed cell death. Activation of lysis by a mechanism involving the synthesis of protein. J. Insect Physiol. **15**, 1505–1516.
6. A. Glucksmann (1965) Cell death in normal development. Arch. Biol. Liege **76**, 419–437.
7. P. G. Clarke and S. Clarke (1996) Nineteenth century research on naturally occurring cell death and related phenomena. Anat. Embryol. Berl. **193**, 81–99.
8. R. A. Lockshin and C. M. Williams (1964) Programmed cell death. II. Endocrine potentiation of the breakdown of the intersegmental muscles of silkmoths. J. Insect Physiol., **10**, 643.
9. R. E. Ellis, J. Y. Yuan, and H. R. Horvitz (1991) Mechanisms and functions of cell death. Ann. Rev. Cell Biol. **7**, 663–698.
10. A. H. Wyllie, J. F. Kerr, and A. R. Currie (1972) Cellular events in the adrenal cortex following ACTH deprivation. J. Pathol. **106**, ix.
11. M. D. Jacobson, M. Weil, and M. C. Raff (1997) Programmed cell death in animal development. Cell **88**, 347–354.
12. A. Fraser, N. McCarthy, and G. I. Evan (1996) Biochemistry of cell-death. Curr. Opin. Neurobiol. **6**, 71–80.
13. B. F. Trump, J. M. Valigorsky, J. H. Dees, W. J. Mergner, K. M. Kim, R. T. Jones, R. E. Pendergrass, J. Garbus, and R. A. Cowley (1973) Cellular change in human disease. A new method of pathological analysis. Hum. Pathol. **4**, 89–109.
14. A. H. Wyllie, J. F. Kerr, and A. R. Currie (1980) Cell death: The significance of apoptosis. Int. Rev. Cytol. **68**, 251–306.
15. M. C. Raff (1992) Social controls on cell survival and cell death. Nature **356**, 397–400.
16. C. B. Thompson (1995) Apoptosis in the pathogenesis and treatment of disease. Science **267**, 1456–1462.
17. W. E. Wright and J. W. Shay (1996) "Mechanisms of escaping senescence in human diploid

cells". In *Celluar Aging and Cell Death* (N. J. Holbrook, G. R. Martin, and R. A. Lockshin, eds.), Wiley-Liss, New York, pp. 153–166.

Suggestions for Further Reading

18. N. J. Holbrook, G. R. Martin, and R. A. Lockshin (1996) *Cellular Aging and Cell Death*. Vol. **16**, Modern Cell Biology (J. B. Harford, series ed.), Wiley-Liss, New York. A good introductory text to both senescence and cell death.
19. M. Sluyser (1996) *Apoptosis in Normal Cancer and Development*, Taylor & Francis, London. This book covers all aspects of apoptosis, giving both a physical discription of the process and covering all the molecular aspects of the pathway.

Cell Fusion, Cell Hybrids

Fusions of both the external and intracellular membranes of cells are important for differentiation and development. Moreover, enveloped **viruses** infect cells via fusion of their envelopes with cell or endosome membranes.

Cell fusion is the process of fusion of the membranes of two or more cells and results in the formation of cells with multiple **nuclei**. It occurs at various stages of the natural development of organisms, such as in the first step of fertilization of an **oocyte** with sperm and in myotube formation by fusion of myoblasts during differentiation of skeletal muscles. Artificial cell fusion can be induced by the addition of a high concentration of Sendai virus, an enveloped virus of the paramyxovirus group, as was demonstrated in 1957–63 (1-3). This finding coincided with cell biology's beginning focus on the culture of **somatic cells** of birds and mammals. In 1961, Barski et al. (4) reported the appearance of hybrid cells after a few months of mixed culture of two different mouse cancer cell lines. These hybrid cells had a single nucleus containing chromosomes from both parent cell lines, and their appearance was considered to be due to the spontaneous fusion of cells of the two cell lines.

Sendai virus proved to be an important development in this field because it has some useful characteristics for the fusion of somatic cells:

1. Its targets are sialoglycoproteins and sialolipids, which are present in the cell membranes of almost all mammalian and fowl cells. Consequently, it can induce the fusion of a wide range of cells (3).
2. Its cell fusion activity is not affected by procedures that inactivate the viral genome, such as exposure to ultraviolet (UV) light. Thus, fused cells could be prepared under conditions inhibiting virus growth, using a UV-inactivated virus.
3. There is no species specificity in its fusion of cells, so interspecific heterokaryons can be induced easily (5, 6), unlike in the case of fertilization.
4. The frequency of virus-induced hybrid formation is at least 1000 times greater than that of spontaneous hybridization.

Littlefield reported in 1964 (7) further progress in methods for the selection of hybrid cell clones, by fusing two different mutants defective in the **salvage pathway** for nucleotide biosynthesis and culturing them in a medium containing **aminopterin**, which inhibits *de novo* nucleotide synthesis. One of the mutant cell lines that were fused lacked **thymidine kinase**, the other **hypoxanthine-**

guanine phosphoribosyl transferase. The only cells that could grow from the mixed culture were fused cells that had acquired mutual complementation of the two mutant defects. Based on these new techniques, the field of *somatic cell genetics* was established in the 1960s.

That the chemical fusogen **polyethylene glycol** is effective for the fusion of protoplasts of **plant** cells was first reported in 1974 (8). With this fusogen, hybrid plants, such as the "pomato," can be prepared in cultures of somatic hybrid cells. Moreover, *electroporation* (see Transfection) was found to be useful as a physical method for cell fusion in the 1980s (10, 11). Cell fusion by these two methods does not require viral receptors, so they have made possible the fusion of cells from all kinds of organisms.

In the early stage of somatic cell genetics in the 1960s and 70s, many reports provided important information on some basic phenomena in cell biology, permitting a focus on molecular biology in the next stage of the 1980s and 90s. The main findings were as follows:

1. Immediately after multinucleated cell formation by artificial cell fusion, some nuclear proteins derived from the parents are rapidly transferred and mixed between the various nuclei. This tends to induce synchronization of the stage of DNA replication of the nuclei after the fusion of randomly growing cells. The degree of this synchronization is greatest in cells with only two nuclei and decreases sharply with an increasing number of nuclei in polykaryocytes (12, 13). This may be why almost all randomly isolated hybrid cells have in their nucleus one set of chromosomes derived from each parent. As a special case, the fusion of cells in **mitosis** with cells in interphase causes the rapid dissolution of the nuclear membrane of the interphase cells, followed by the condensation of its chromosomes, a process named *chromosomal pulverization* (14) or *premature chromosome condensation* (15). Reactivation of dormant nuclei from chick erythrocytes was demonstrated upon their fusion with cultured mammalian cells (16, 17). In the case of cell neoplastic transformation by tumor viruses, induction of Simian Virus 40 (SV40) production was observed after the fusion of SV40-transformed nonproducer hamster cells with monkey cells, which are a permissive host for SV40 (18). Later, a similar observation was reported on the fusion of Rous sarcoma virus (RSV)-transformed rat cells with chicken cells (a permissive host of RSV) (19). In the case of cell differentiation, the distinction between luxury and household functions of cells was observed by the formation of hybrids of cells with different phenotypes (20). The findings were important for choosing the correct combination of cells for hybridization of differentiated cells. In 1974, Köhler and Milstein (21) reported that monoclonal antibodies could be prepared from hybrid cells (hybridomas) of B cells and **myelomas** (tumor cells obtained from B cells). This method of preparing monoclonal antibodies is now a major technique in molecular, cell, and developmental biology, and in medicine.
2. Weiss and Green (22) observed that the chromosomal balance is unstable in interspecific man/mouse hybrids and human chromosomes disappear randomly during serial passage in culture. Based on this finding, mapping of the human chromosomes became possible (23) and was followed by the technique of direct in situ hybridization of the chromosomes with complementary DNA.
3. In 1972, Bootsma and colleagues (24) demonstrated that genetic complementation groups in a hereditary disease, *xeroderma pigmentosum*, could be classified by the cell fusion technique. This was the first successful genetic analysis of a human hereditary disease.

1. Mechanism of Cell Fusion

Artificial cell fusion using the various fusogens mentioned above has been established as a routine laboratory method. These fusogens, viral, chemical, and physical, have different modes of action on cell membranes, but induce similar changes in the cell membrane for fusion of the lipid bilayers. In general, **glycoproteins** are distributed on cell surfaces, with their **hydrophobic** domains embedded in the lipid bilayer of the cell membrane, their hydrophilic domains exposed to the outside, while their intracytoplasmic domains are associated with the cytoskeletal system. Water molecules are also associated with the outside of cell membranes. These structures on the exteriors of cells inhibit the close contact of lipid bilayers of neighboring cell membranes, which is essential for cell fusion. Close contact of membranes requires on the cell membrane surface the transient appearance of areas from which glycoproteins are excluded. All the fusogens can induce such areas.

Sendai virus has two glycoproteins: HN with **receptor** binding and destroying activities, and F with fusogenic activity that is essential for fusion. The first step in cell fusion is the attachment of the virus to cell surfaces and agglutination of the cells, which is produced by HN activity. The second step is insertion of the fusogenic domain of F into the lipid bilayer. This domain is located at the N-terminus of F and consists of 15 relatively hydrophobic residues (25); it has the unique characteristic of trapping cholesterol molecules in its tertiary structure at 37°C (26). The amino acid sequence of this domain is well conserved in paramyxoviruses.

Simultaneous removal of cholesterol molecules from multiple sites in the cell membrane by the attachment of several hundred virus particles perturbs the cell membrane and causes breakdown of the normal barrier to ions. At this stage, calcium ions from the medium promptly penetrate the cell and induce changes in cell structures, such as separating the connection between the cytoplasmic domains of membrane proteins and the cytoskeletal system (see Calcium Signaling). Macromolecules can also **diffuse** through the cell membrane, and membrane fluidity increases, so that membrane proteins can move more freely in the lipid bilayer. This results in clustering of intramembrane domains of the proteins (demonstrable as cold-induced clustering) and the appearance of areas with no membrane proteins. The appearance of these areas is followed by close attachment of the lipid bilayers of neighboring cells, due to strong hydrophobic interactions, and cell fusion (27).

Polyethylene glycol is reported to induce clustering of membrane proteins similar to that induced by Sendai virus (28). Electroporation by electric pulses causes pores to be formed in cell membranes that may allow Ca^{2+} ions into the cytoplasm, as is also caused by Sendai virus. Thus, the fundamental mechanisms of these three fusogens appear to be similar.

It is known that calcium ions (29) and an energy (ATP) supply (2) are required for cell fusion. In the absence of either one, cells rapidly degenerate and fusion is greatly decreased. Evidence suggests that calcium ions associate directly with phospholipid molecules to normalize the perturbed membrane structure and promote a connection between the two lipid bilayers, in addition to acting in the cytoplasm as mentioned above. Why does cell fusion require an energy supply? In simple terms, cell fusion would be expected to produce a favorable decrease in **free energy**, by changing from a number of small vesicles to one large one, in which case an energy supply would not be necessary. Energy may be required for the removal of excess calcium ions introduced into the cytoplasm during cell fusion, but not for the membrane fusion itself. On culture of fused cells, the calcium ions are rapidly sequestered in **organelles** of the cells, and their level in the cytoplasm returns to normal. If the supply of energy is delayed, the cells degenerate.

2. Supplement

1. In the case of Sendai virus, cell-to-cell fusion is also possible as a result of viral envelope fusion itself, if one virus envelope fuses with the membranes of two different cells. But envelope fusion is slower than that induced by a high concentration of the virus and is observed to occur after completion of cell-to-cell fusion. Finally, as a result of viral envelope fusion, many viral glycoproteins are integrated into the fused cell surfaces, which are excluded from the cell surface by internalization by coated vesicles in culture (30) (see Clathrin).

Polykaryocytes (syncytia) are often observed in pathological tissues infected by an enveloped virus, such as paramyxoviruses, retroviruses and the Herpes virus. This polykaryocyte formation may occur by cell fusion via viral envelope fusion. Newly synthesized viral glycoproteins are distributed massively on the surfaces of infected cells, which consequently are quite similar to the viral envelope, and they may fuse with neighboring noninfected cells, as in viral envelope fusion.

2. Enveloped viruses cause infection by fusion of their envelopes either (a) with cell membranes at neutral pH or (b) with endosome membranes at acidic pH after their internalization from the cell surface. Infections by paramyxoviruses, retroviruses, and the Herpes virus are of the first type and induce syncytia formation *in vivo* and *in vitro*. Influenza virus is of the second type and does not induce syncytia *in vivo*, but the viral envelope can fuse with cell membranes under acidic conditions *in vitro*. This is because the influenza fusogenic glycoprotein (HA, or hemagglutinin) is not functional at neutral pH, but becomes functional under acidic conditions by a conformational change, forming trimers (31).

The fusogenic glycoproteins of various enveloped viruses differ, but all of them contain a hydrophobic domain that can interact with the lipid bilayer of cellular membranes. In some cases, the glycoproteins of the viruses are known to be synthesized in an inactive form in which their hydrophobic domain is hidden and then activated by **proteolytic** cleavage exposing this domain. This was first demonstrated by Homma (32) with the Sendai virus. In this virus, the F glycoprotein is synthesized as an inactive form F_0 and is then cleaved to F_1 and F_2, with the fusogenic domain being exposed at the N-terminus of F_1. The glycoprotein (gp160) of human immunodeficiency virus (HIV) a retrovirus, is cleaved to gp120 and gp41, and the fusogenic domain is exposed at the N-terminus of gp41 (33). The HA glycoprotein of influenza virus is also activated by the cleavage of inactive HA_0 to HA_1 and HA_2, with the hydrophobic domain being exposed at the N-terminus of HA_2 (34) and becoming functional by trimer formation under acidic conditions.

3. Application of Fusogenic Reactions to Cell Engineering

Various biotechniques for the reconstitution of cells or introduction of macromolecules into cells have been developed using the unique characteristics of the interactions of fusogens with cell membranes. Introduction of macromolecules such as DNA, RNA, and proteins from the medium into the cytoplasm has become possible by perturbation of the cell membrane. Electroporation is usually used for that purpose (35), but treatment of the cells with Sendai virus can also be used (36).

Another technique for the introduction of macromolecules is based on the mechanism of infection of Sendai virus with cell membranes. In 1979, Uchida et al. (37) reported on the reassembly of viral envelopes as artificial **vesicles**, with HN and F glycoproteins embedded in their surface and any macromolecules present trapped inside. These pseudovirus particles containing the macromolecules instead of viral nucleocapsids will introduce those macromolecules into a cell that they “infect.” This technique is especially useful *in vivo*. Subsequently, modifications have been made to simplify the preparation procedure, using spontaneous fusion of the UV-inactivated virus with simple, artificial liposomes containing the desired macromolecules. Using such a preparation, the human hepatitis B virus genome has been introduced into rat liver cells *in vivo* to induce hepatitis (38). This technique is useful for drug delivery *in vivo* and gene therapy (39).

Reconstruction of cells was first reported by Veomett et al. in 1974 (40). On incubation with cytochalasin, cells could be separated into *nucleoplasts* (enclosed by cell membranes but lacking cytoplasm) and *cytoplasts* (without a nucleus). Viable cells could be reconstituted by the fusion of nucleoplasts with cytoplasts. Heterologous combinations could also be constituted. This technique has been expanded to the preparation of cloned animals. Introduction of nuclei from somatic cells at the early stages after cleavage of fertilized eggs into enucleated eggs, by Sendai virus-mediated fusion, is reported to result in a high frequency of development of animals (41).

Bibliography

1. Y. Okada, T. Suzuki, and Y. Hosaka (1957) Med. J. Osaka Univ. **7**, 709–717.

2. Y. Okada (1962) Exp. Cell Res. **26**, 98–128.
3. Y. Okada and J. Tadokoro (1963) Exp. Cell Res. **32**, 417–430.
4. G. Barski, S. Sorieul, and F. Cornfert (1961) J. Natl. Cancer Inst. **26**, 1269–1277.
5. H. Harris and J. F. Watkins (1965) Nature **205**, 640–646.
6. Y. Okada and F. Murayama (1965) Exp. Cell Res. **40**, 154–158.
7. J. Littlefield (1966) Exp. Cell Res. **41**, 190–196.
8. K. N. Kao and M. R. Michayluk (1974) Planta **115**, 355–367.
9. G. Melchers, M. D. Sacristan, and A. A. Holder (1978) Carlsberg Res. Commun. **43**, 203–218.
10. M. Senda, J. Takeda, S. Abe, and T. Nakamura (1979) Plant Cell Physiol. **20**, 1441–1443.
11. U. Zimmermann and J. Vienken (1982) J. Membrane Biol. **67**, 165–182.
12. T. Yamanaka and Y. Okada (1966) Biken"s J. **9**, 159–175.
13. T. Yamanaka and Y. Okada (1968) Exp. Cell Res. **49**, 461–469.
14. H. Kato and A. A. Sanderberg (1968) J. Nat. Cancer Inst. **41**, 1117–1123.
15. P. N. Rao and R. T. Johnson (1972) J. Cell Sci. **10**, 495–513.
16. H. Harris (1965) Nature **206**, 583–588.
17. N. R. Ringertz (1974) In *Somatic Cell Hybridization* (R. L. Davidson and F. de la Cruz, eds.), Raven Press, New York, pp. 239–264.
18. P. Gerver (1966) Virology **28**, 501–509.
19. J. Svoboda, O. Machala, and I. Holzanek (1967) Acta Virol. **13**, 155–157.
20. R. L. Davidson and K. Yamamoto (1968) Proc. Nat. Acad. Sci. USA **60**, 894–901.
21. G. Köhler and C. Milstein (1975) Nature **256**, 495–497.
22. M. C. Weiss and H. Green (1967) Proc. Nat. Acad. Sci. USA **58**, 1104–1111.
23. R. J. Klebe, T. Chen, and F. H. Ruddle (1970) Nat. Acad. Sci. USA **66**, 1220–1227.
24. E. A. de Weerd-Kastelein, W. Keijzer, and D. Bootsma (1972) Nature New Biol. **238**, 80–83.
25. M. J. Gething, J. M. White, and M. D. Waterfield (1978) Proc. Nat. Acad. Sci USA **75**, 2737–2740.
26. K. Asano and A. Asano (1985) Biochem. Int. **10**, 115–122.
27. J. Kim and Y. Okada (1981) Exp. Cell Res. **132**, 125–136.
28. D. S. Roos, J. M. Robinson, and R. L. Davidson (1983) J. Cell Biol. **97**, 909–917.
29. Y. Okada and F. Murayama (1966) Exp. Cell Res. **44**, 527–551.
30. J. Kim and Y. Okada (1982) Exp. Cell Res. **140**, 127–136.
31. I. A. Wilson, J. J. Skehel, and D. C. Wiley (1981) Nature (Lond.) **289**, 366–373.
32. M. Homma (1971) J. Virol. **8**, 619–629.
33. J. M. McCune et al. (1988) Cell **53**, 55–67.
34. S. G. Lazarowitz and P. W. Choppin (1975) Virology **68**, 440–454.
35. U. Zimmermann, J. Vienken, and G. Pilwat (1980) Bioelectrochem. Vioenerg. **7**, 553–574.
36. K. Tanaka, M. Sekiguchi, and Y. Okada (1975) Proc. Nat. Acad. Sci. USA **72**, 4071–4075.
37. T. Uchida et al. (1979) Biochem. Biophys. Res. Commun. **87**, 371–379.
38. K. Kato et al. (1991) J. Biol. Chem. **266**, 3361–3364.
39. V. J. Dzau, M. J. Mann, R. Morishita, and Y. Kaneda (1996) Pro. Nat. Acad. Sci. USA **93**, 11421–11425.
40. G. Veomett, D. M. Prescott, J. Shay, and K. R. Porter (1974) Proc. Nat. Acad. Sci. USA **71**, 1999–2002.
41. J. McGrath and D. Solter (1983) Science **220**, 1300–1302.

Suggestions for Further Reading

42. N. Düzgunes, ed. (1993) *Membrane Fusion Technique*, Part B, Methods in Enzymology, Vol. **221**, Academic Press.
43. N. Düzgunes and F. Bronner, eds. (1988) *Membrane Fusion in Fertilization, Cellular Transport, and Viral Infection*, Current Topics in Membranes and Transport, Vol. **32**, Academic Press.
44. J. Wilschut and D. Hoekstra, eds. (1991) *Membrane Fusion*, Marcel Dekker, Inc.

Cell Junctions

A cell junction is a cell surface structure observed by electron microscopy that mediates cellular interactions. Cell junctions are of two types, those that mediate cell–cell interactions and those that mediate cell–substratum interactions. In the former category, the cells of vertebrates possess four principal types, all of which are represented at the lateral surfaces of simple epithelial cells, such as those that line the intestine and kidney tubules (Fig. 1). The four principal types of cell–cell junction are (i) the tight junction or zonula occludens (pl. zonulae occludentes); (ii) the intermediate junction or zonula adherens (pl. zonulae adherentes); (iii) the **desmosome** or macula adherens (pl. maculae adherentes); (iv) the gap junction or nexus. The principal type of cell–substratum junction is the hemidesmosome, which is present in contact with the basement membrane in the basal cells of stratified epithelia, such as epidermis, in some simple epithelial cells, especially amnion, and mammary epithelium. Cells that are well spread in culture exhibit a second type of cell–substratum junction, the focal adhesion or focal contact (Fig. 1). This is a region where the lower cell surface is most closely apposed to the culture substratum (separation 10 to 15 nm). It is not clear whether the focal contact has a strict equivalent *in vivo*, but its study has made an extensive and important contribution to the understanding of cell adhesion. The basic structures of the principal types of cell junctions were elucidated by electron microscopy in the 1960s (1-3). Since then, a substantial amount of detailed knowledge of the molecular composition of each junctional type has been revealed.

Figure 1. Generalized simple epithelial cell showing cell junctions and other adhesion mechanisms. The lateral surface mediates cell–cell interactions via adhesive junctions, the zonula adherens (intermediate junction) and the desmosome, and communicating gap junctions that allow small molecules to be exchanged between the cytoplasm of adjacent cells. The tight junction, or zonula occludens, restricts and regulates paracellular permeability. The basal surface mediates adhesion to the basement membrane. Hemidesmosomes are present in some simple epithelia but are most numerous in epidermis. Integrin and non-integrin receptors for several matrix components are present here. When cells are cultured, many of these become localized in focal contacts, small areas where adhesion to the substratum is strongest. (From *Journal of Cell Science*, with permission of the Company of Biologists.)

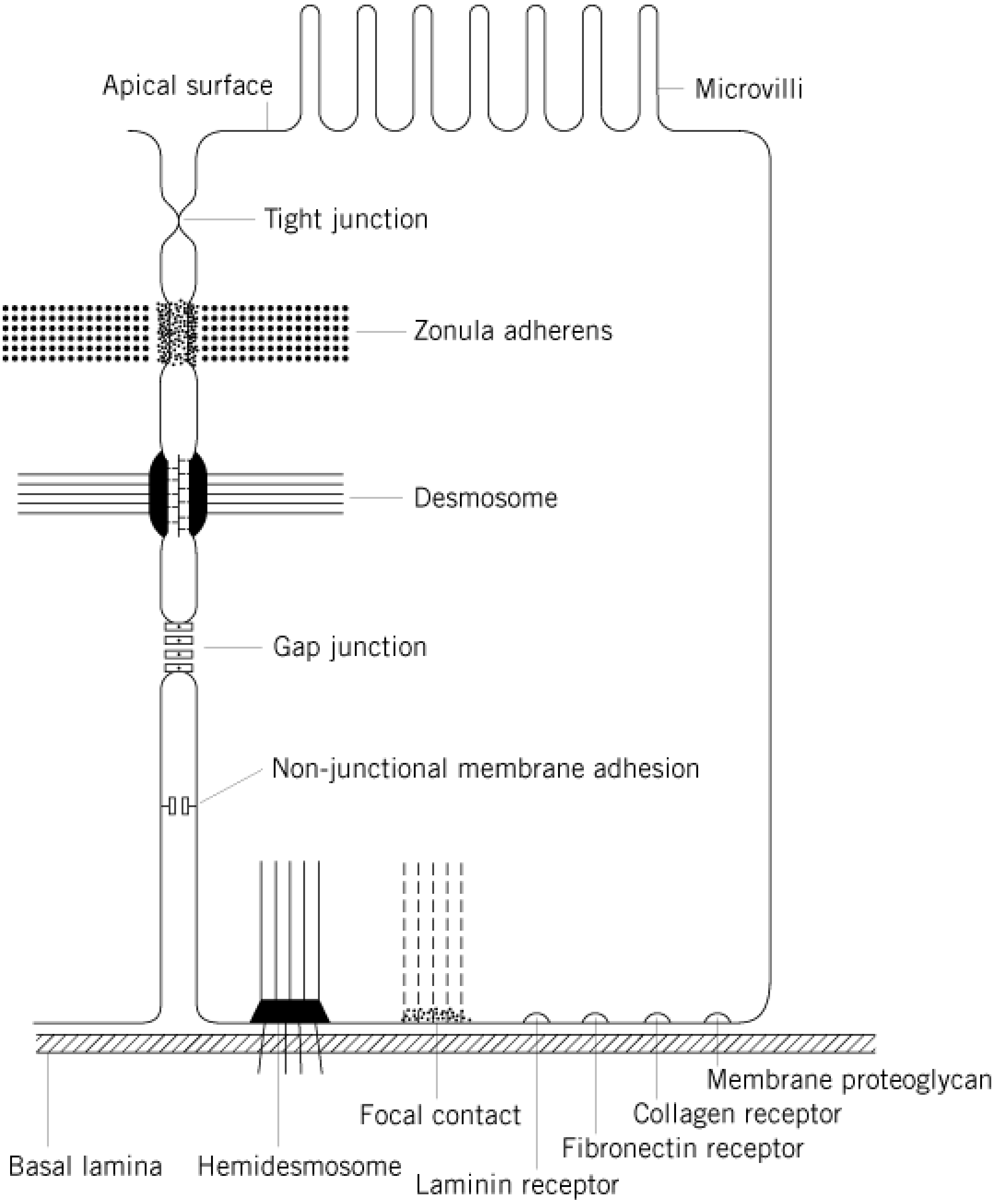

The intermediate junction, the desmosome, the hemidesmosome, and the focal contact are primarily adhesive junctions that bind cells to each other or to their substratum. Each represents a cell-surface site at which cell adhesion molecules (see Cell Surface Adhesion Receptors) are concentrated. In desmosomes and intermediate junctions, the adhesion molecules are specific types of cadherins (4, 5); in hemidesmosomes and focal contacts, they are integrins (6). These junctions also represent cell-surface attachment points for elements of the cytoskeleton. In desmosomes and hemidesmosomes, the associated cytoskeletal elements are intermediate filaments, also known as tonofilaments. These are important in providing structural continuity throughout a tissue. This continuity is disrupted in certain **autoimmune** and genetic diseases of desmosomes (eg, pemphigus) (7), hemidesmosomes (eg, bullous pemphigoid, junctional epidermolysis bullosa) (8), or intermediate filaments (eg, epidermolysis bullosa simplex) (9). Such diseases result in structural disruption of the epidermis and/or mucosal tissues, with effects ranging from mild to lethal. In intermediate junctions and focal contacts, the cytoskeletal elements are actin filaments, also known as microfilaments. The actin filaments associated with focal contacts are organized into large bundles, called stress fibers, of several micrometers in length. During animal development, morphogenetic events such as gastrulation and neural tube rolling involve gross changes in cell shape that appear to be caused by contraction of submembranous microfilament rings associated with zonula adherens-type junctions (10, 11). More limited contractile activity of such rings may be involved in regulation of the permeability of tight junctions, with which zonulae adherentes are frequently closely associated in the simple epithelial junctional complex, a region where junctions are concentrated at the extreme apicolateral interface between the cells.

Transduction of signals across the plasma membrane is a vital function in the regulation of normal cell behavior in both developing and adult organisms. Many adhesion receptors have now been shown to transduce signals, either from inside the cell to outside regulating the function of the receptors themselves, or from outside to inside regulating signalling pathways and gene expression in response to adhesive stimuli. Such signal transduction is an additional important function of adhesive junctions (12).

The principal function of the tight junctions is to occlude the paracellular channels of epithelia, thereby restricting intercellular leakage of molecules between the distinct biological compartments separated by the epithelium (13). Tight junctions are also important in forming tight seals between some endothelial cells, such as those of the blood–brain barrier. Their sealing properties arise because they are zonular in nature, encircling the entire apicolateral margins of simple epithelial cells, and because there is direct contact between the plasma membranes of adjacent cells. Tight junctions are also important in maintaining the composition of the different membrane domains of epithelial cells, because they prevent diffusion of molecules within the outer leaflet of the plasma membrane, thereby restricting them to either the apical or the basolateral domain (14). This property is sometimes referred to as the “fence” function of tight junctions, and their occluding properties are described as a “gate” function.

Gap junctions, so-called because they exhibit a regular plasma membrane separation of 2 nm, are punctate membrane sites that provide hydrophilic channels for direct cell-to-cell communication (15). They permit diffusion of molecules of less that 1000 daltons between cells. These ubiquitous junctions are important in both excitable and nonexcitable tissues. In the former they facilitate direct transmission of electrical impulses, while in the latter they mediate a phenomenon called metabolic cooperation, and they may also transmit signaling molecules such as **calcium** and **inositol phosphates** between cells. Their function is essential in embryonic development (16) and in the normal functioning of adult tissues—for example, in coordination of the contraction of cardiac muscle and smooth muscle in the uterus during parturition (17, 18).

Gap junctions appear to be widespread in the animal kingdom, being present even in primitive organisms such as *Hydra*. Intermediate junctions have also been clearly demonstrated in invertebrates (eg, in *Drosophila*). The occurrence of desmosomes and tight junctions in invertebrates is much less clear. Desmosome-like structures are clearly present in insects—for example, between the apposed epithelia of the upper and lower surface of the wing blade in *Drosophila*. However, these desmosome-like structures appear to be associated with microtubules rather than intermediate filaments, and their adhesion may be mediated by integrins rather than cadherins. Tight junctions are absent from insects, which instead possess septate junctions, structures that have a ladder-like ultrastructural appearance between adjacent plasma membranes and which, like tight junctions, appear to restrict paracellular permeability (19).

Bibliography

1. M. G. Farquhar and G. E. Palade (1963) J. Cell Biol. **17**, 375–412.
2. D. E. Kelly (1966) J. Cell Biol. **28**, 51–72.
3. J-P. Revel and M. Karnovsky (1967) J. Cell Biol. **33**, 7–12.
4. J. L. Holton et al. (1990) J. Cell Sci. **97**, 239–246.

5. P. J. Koch et al. (1990) Eur. J. Cell Biol. **53**, 1–12.
6. A. Sonnenberg et al. (1991) J. Cell Biol. **113**, 907–917.
7. J. R. Stanley (1995) In “Cell adhesion and human disease.” Ciba Found. Symp. **189**.
8. R. E. Burgeson and A. M. Christiano (1997) Curr. Opin. Cell Biol. **9**, 651–658.
9. W. H. I. McLean and E. B. Lane (1995) Curr. Opin. Cell Biol. **7**, 118–125.
10. T. E. Schroeder (1970) J. Embryol. Exp. Morphol. **23**, 427–462.
11. P. Karfunkel (1971) Dev. Biol. **25**, 30–56.
12. C. Rosales et al. (1995) Biochem. Biophy. Acta. **1242**, 77–98.
13. J. L. Madara and K. Darmsathaphorn (1985) J. Cell Biol. **101**, 2124–2133.
14. K. Simons (1990) In *Morphoregulatory Molecules* (G. M. Edelman, B. A. Cunningham, and J.-P. Thiery, eds.), Wiley, New York, pp. 341–356.
15. N. B. Gilula, O. R. Reeves, and A. Steinbach (1972) Nature **235**, 262–265.
16. A. E. Warner, S. C. Guthrie, and N. B. Gilula (1984) Nature **311**, 127–131.
17. W. C. Cole and R. E. Garfield (1985) In *Gap Junctions* (M. V. L. Bennett and D. C. Spray, eds.), Cold Spring Harbor Laboratory Press, Cold Spring Harbor, NY, pp. 215–230.
18. E. C. Beyer, D. L. Paul, and D. A. Goodenough (1987) J. Cell Biol. **195**, 2621–2629.
19. P. J. Bryant (1994) In *Molecular Mechanisms of Epithelial Cell Junctions: From Development to Disease* (S. Citi, ed.) R. G. Landes, Austin, TX, pp. 1–21.

Suggestions for Further Reading

20. D. R. Garrod and J. E. Collins (1992) "Intercellular Junctions and Cell Adhesion in Epithelial Cells". In “*Epithelial Organization and Development*” (T. P. Fleming, ed.), Chapman and Hall, London, pp. 1–52. (A source of reference to the early literature.)
21. D. R. Garrod, M. A. J. Chidgey, and A. J. North (eds.) (1998) *Adhesive Interactions of Cells*, JAI Press, Greenwich, CT. (Reviews on desmosomes by the editors, tight junctions by S. Citi, and adherens junctions and focal contacts by A. Ben-Ze"ev, as well as other reviews in cell adhesion.)
22. D. A. Goodenough, J. A. Goliger, and D. L. Paul (1996) Annu. Rev. Biochem. **65**, 475–502. (A thorough review of gap junctions.)
23. L. Barradori and A. Sonnenberg (1996). Curr. Opin. Cell Biol. **8**, 647–656. (An introduction to the literature on hemidesmosomes.)

Cell Line

When a primary cell culture (see Tissue Culture) is subcultured, it becomes a cell line. This implies that multiple lineages of cells, not necessarily distinct from each other, coexist in the culture (1). Serial subculture, while maintaining these parallel lineages, will tend to show convergence towards whatever common **phenotype** is best adapted to the culture conditions being employed, as the cell type with the greatest proliferative ability will predominate. The cell line may be finite and die out after a fixed number of population doublings, or become a continuous cell line (see Immortalization) (Fig. 1). Cell lines, particularly continuous cell lines, can become a valuable resource, particularly if preserved in liquid nitrogen after appropriate characterization and validation. Many continuous cell lines are currently available, with wide-ranging properties, including drug resistance markers, inducibility for specific enzymes, estrogen sensitivity, cornification, blood vessel formation, hemoglobin synthesis, myogenesis, and transfection susceptibility (Table 1). Finite cell lines with distinct phenotypic properties are also becoming available through the development of serum-free selective media (2-4). (see Serum Dependence) and can be derived in the laboratory or purchased from commercial suppliers.

Figure 1. Effect of continued culture passage on cumulative cell number, assuming that no cells are discarded. The curve shows the initial decline due to selection, then exponential growth during the replicative phase, and then growth arrest and eventual deterioration following senescence, in a finite cell line, or continued proliferation, often at an enhanced rate, following transformation. Reproduced from Freshney's *Culture of Animal Cells, A Multi-Media Guide*, 1999, Wiley-Liss, N.Y.

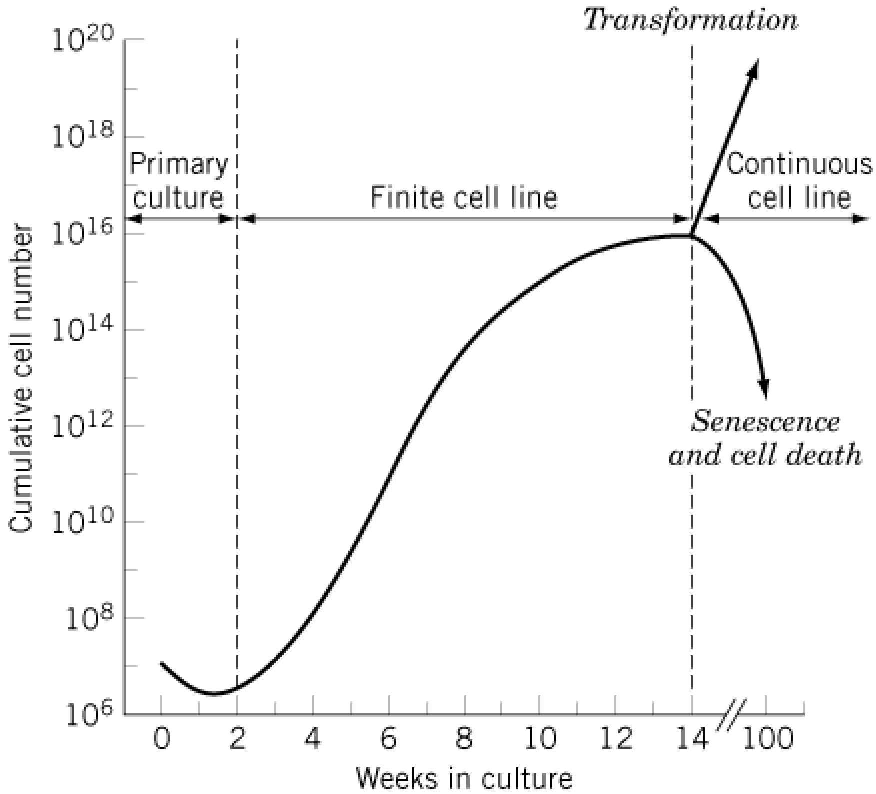

Table 1. Cell Lines in Common Use[a]

Cell line	Morphology	Origin	Age	Status	Ploidy	Characteristics	Referei
MRC5	Fibroblast	Human lung	Embryonic	Normal	Diploid	Susceptible to human viral infection	Jacobs (1970) *Nature* **2:** 168
WI38	Fibroblast	Human lung	Embryonic	Normal	Diploid	Susceptible to human viral infection	Hayflick Moorhea (1961) *E: Cell Res.* 585

IMR90	Fibroblast	Human lung	Embryonic	Normal	Diploid	Susceptible to human viral infection	Nichols e (1977) *Science* **1** 60
A2780	Epithelial	Human ovary	Adult	Neoplastic	Aneuploid	Chemosensitive with resistant variants	Tsuruo et (1986) *Jp Cancer R* **77**, 941
A549	Epithelial	Human lung	Adult	Neoplastic	Aneuploid	Synthesizes pulmonary surfactant	Giard et a (1972) *J. Natl.Can Inst.* **51**,
A9	Fibroblast	Mouse subcutaneous	Adult	Neoplastic	Aneuploid	HGPRT-ve: deriv. L929	Littlefiel (1964) *Nature* **2** 1142
BHK21-C13	Fibroblast	Syrian hamster kidney	NB	Normal	Aneuploid	Transformable by polyoma virus	Macpher and Stok (1962) *Virology* 147
BRL3A	Epithelial	Rat liver	NB	Normal		Produce IGF-II	Coon (19 *J. Cell Bi* **39**, 29a
Caco-2	Epithelial	Human colon	Adult	Neoplastic	Aneuploid	Transports ions and amino acids	Fogh (19 *J. Natl. Cancer I* **58**, 209
CHANG liver	Epithelial	Human liver	Embryonic	Normal?	Aneuploid	HeLa contaminated	Chang (1 *Proc. Soc Exp.Biol. Med.* **87**,
CHO-K1	Fibroblast	Chinese hamster ovary	Adult	Normal	Diploid	Simple karyotype	Puck et a (1958) *J. Exp. Med* **108**, 945
EB-3	Lymphocytic	Human	Juvenile	Neoplastic	Diploid	EB virus + ve	Epstein a Barr (196 *Lancet* **1**,
GH1, GH3	Epithelial	Rat	Adult	Neoplastic	Aneuploid	Produce growth hormone	Yasumur al. (1966 *Science* **1** 1186
HeLa	Epithelial	Human cervix	Adult	Neoplastic	Aneuploid	G6PD type A	Gey et al (1952) *Cancer R* **12**, 364
HeLa-S3	Epithelial	Human cervix	Adult	Neoplastic	Aneuploid	High plating efficiency; will grow well in suspension	Puck and Marcus (1955) *Pr Natl. Aca*

							Sci. USA 432
Hep-2	Epithelial	Human larynx	Adult	Neoplastic	Aneuploid	HeLa contaminated⟨su⟩d	Moore et (1955) *Cancer R* **15**, 598
HT-29	Epithelial	Human colon	Adult	Neoplastic	Aneuploid	Differentiation inducible with NaBt	Fogh and Trempe (1975) in *Human Tumor C in vitro*, J Fogh, ed. Academi Press, Ne York, p.
KB	Epithelial	Human oral	Adult	Neoplastic	Aneuploid	HeLa contaminated	Eagle (19 *Proc. Soc Exp. Biol (N.Y.)* **89** 362
L1210	Lymphocytic	Mouse	Adult	Neoplastic	Aneuploid	Rapidly growing; suspension	Law et al (1949) *J. Natl. Car Inst.* **10**,
L5178Y	Lymphocytic	Mouse	Adult	Neoplastic	Aneuploid	Rapidly growing suspension	
L929	Fibroblast	Mouse	Adult	Normal	Aneuploid	Clone of L cell	Sanford e (1948) *J. Natl. Car Inst.* **9**, 2
LS	Fibroblast	Mouse	Adult	Neoplastic	Aneuploid	Grow in suspension: deriv. L929	Paul and Struthers (unpublis
MCF7	Epithelial	Human breast pleural effusion	Adult	Neoplastic	Aneuploid	Estrogen recep +ve	Soule et a (1973) *J. Natl.Can Inst.* **51**,
P388D	Lymphocytic	Mouse	Adult	Neoplastic	Aneuploid	Grow in suspension	Dawe and Potter (19 *Am. J. Pa* **33**, 603; Koren et (1975) *J. Immunol.* **114**, 894
S180	Fibroblast	Mouse	Adult	Neoplastic	Aneuploid	Cancer chemotherapy screening	Dunham Stewart (1953) *J. Natl. Car Inst.* **13**,
STO	Fibroblast	Mouse	Embryonic	Normal	Aneuploid	Used as feeder	Bernstein

						layer for embryonal stem cells	(1975) *P Natl. Aca Sci. USA* 1441
3T3-L1	Fibroblast	Mouse, Swiss	Embryonic	Normal	Aneuploid	Adultipose differentiation	Green an Kehinde (1974) *C* **1**, 113
3T3 A31	Fibroblast	Mouse BALB/c	Embryonic	Normal	Aneuploid	Contact inhibited; readily transformed	Aaronsor and Toda (1968) *J. Physiol.* ' 141
NRK49F	Fibroblast	Rat kidney	Adult	Normal	Aneuploid	Induction of suspension growth by transforming growth factors	DeLarco Todaro (1978) *J. Physiol.* ! 335
Vero	Fibroblast	Monkey kidney	Adult	Normal	Aneuploid	Viral substrate and assay	Hopps et (1963) *J. Immunol.* 416
ZR-75-1	Epithelial	Human breast, ascites fluid	Adult	Neoplastic	Aneuploid	ER-ve, EGFr +ve	Engel (1! *Cancer R* **38**, 3352

[a] Modified from R. I. Freshney *Culture of Animal Cells*, 1994, 3rd ed., Wiley-Liss, N.Y., p. 151.

1. Origin of Cell Lines

Regenerating tissues *in vivo* are made up of a small, self-repopulating, stem cell pool, an expandable pool of proliferating **progenitor cells**, and a nonproliferating differentiated cell pool. On demand, cells leave the stem cell pool and enter the progenitor compartment, where expansion is regulated to meet the current demand in the differentiated cell compartment. When cells enter the differentiated cell compartment, this may be an irreversible process, as seen with erythrocytes, keratinocytes, and neurons; or it may be reversible, as seen with hepatocytes, endothelial cells, and fibrocytes. Cell lines can be derived from any tissue with a proliferating compartment, or from cells that can re-enter a proliferating compartment. It is possible that cell lines will contain stem cells, but, except for hemopoietic cells (see Hematopoiesis), markers are unavailable to determine this. As many cell lines express lineage markers and can, under appropriate conditions, differentiate, it seems most likely that they are derived from the progenitor cells of the tissue.

As cell lines are derived from random outgrowth or from disaggregated cells, multiple lineages of cells will be present. The purity of the culture will be determined by how well these lineages are matched, that is, derived from cells with the same phenotypic fate, or are derived from cells with dissimilar fates. In practice, the selective pressure exerted by the medium will tend to limit the cell population to cells of like phenotype with similar survival capacity, and cells that proliferate less rapidly will gradually be overgrown. It is possible that cells within one phenotypic group have different proliferative capacities but interactions between them produces a uniform proliferative rate in the entire population.

2. Finite Cell Lines

When a cell line is generated at the first subculture of a primary culture, its lifespan is determined, initially, by the environmental conditions. If the conditions are inadequate, the cell line will die out within one or two subcultures, but if the medium, substrate, and other conditions are satisfactory, then the cell line may progress through several serial subcultures. The ultimate limit to the number of subcultures will be determined by the potential regenerative life-span of the cells (see Senescence; Immortalization). Most cell lines from normal tissues will undergo a fixed number of population doublings (Fig. 1), given by the product of the number of passages and the estimated number of doublings per passage (5). These are known as finite cell lines. Normal human skin fibroblasts will usually achieve around 50–60 population doublings and then enter senescence. Senescent cells no longer proliferate, may be partially differentiated, and can remain viable for several months. Cultures of finite cell lines must, therefore, be stored frozen at an early passage level, thawed when required, and used between predetermined passage levels, usually between 10 and 30, to ensure an adequate and consistent supply.

3. Continuous Cell Lines

Some cell lines, such as those derived from mice or from tumors of many species, are not limited by a finite lifespan. They progress either by smooth transition to an immortal cell line (see Immortalization) or undergo neoplastic transformation at some stage and, instead of dying out after a set number of population doublings, continue to proliferate unchecked. Some cultures show evidence of selection and go through a period called *crisis*, when most cells in the population die out by senescence, but a transformed subpopulation survives, usually with an enhanced growth rate, increased cloning efficiency, loss of contact inhibition, acquisition of anchorage-independent growth, ability to grow to a higher saturation density, and increased tumorigenicity in animals (see: Neoplastic Transformation).

There are a large number of continuous cell lines in existence, many of which are banked in repositories such as the American Type Culture Collection (ATCC) or the European Collection of Animal Cell Cultures (ECACC). They form a valuable resource of vigorously growing cultures, capable of unlimited expansion, but are subject to several caveats.

1. Their origin must be validated before use. Acquisition from a reputable cell bank, or the originator, will usually guarantee this, but there are many instances of continuous cell lines being cross-contaminated by other, more vigorously growing cell lines such as HeLa Cells (6-8). The identity of a cell line needs to be confirmed prior to extensive use. This is done most effectively by performing a DNA fingerprinting, but it is also possible by immunotyping, **isoenzyme** analysis, or chromosome analysis.

2. The cells must be shown to be free from infection. Continuous cell lines form an ideal substrate for mycoplasma, which can grow undetected in the culture (9). Again, most reputable cell banks will be able to demonstrate that cell lines being distributed are mycoplasma-free, but stocks still need regular checks every 1 or 2 months to ensure that they remain uninfected.

3. Continuous cell lines are genetically unstable. They are usually aneuploid (the chromosomal complement differs in number, and by chromosomal rearrangements, from the donor) and heteroploid (contain subpopulations with differing chromosomal constitutions). This is reflected in their phenotypic diversity, including variations in morphology, enzyme activity, antigenic expression, and growth characteristics. It is normal practice to clone such populations, select a clone with the required properties, and cryopreserve sufficient ampoules (12–100) for future use. Cultures are generally maintained for a limited period, usually about 3 months, and then replaced from frozen stock.

4. Subculture

Subculture, or passage, is the transfer of a culture from one vessel to another, usually using **trypsin** to dislodge the cells from the substrate and dissociate them from each other. If the cell line is proliferating, then subculture will also imply diluting the cell concentration achieved at the end of the culture period, to a new seeding concentration to initiate a new culture. Growth from seeding until the next subculture is known as a growth cycle, which is repeated each time the culture is passaged. A series of growth cycles constitute serial propagation, and this should not normally proceed beyond about 3 months without replacing stock from the freezer (see above).

Each growth cycle is composed of a lag phase (Fig. 2), where the cells are recovering from trypsinization, synthesizing new extracellular matrix, adhering to the substrate, spreading, repolymerizing the actin microfilament cytoskeleton, and responding to signaling from extracellular matrix adhesions and cytoskeletal rearrangements, which leads to expression of cyclins and, eventually, reentry to the cell cycle. When the cells start to divide, they enter the exponential or "log" phase of the growth cycle and will continue exponential growth until all the available growth surface is occupied or the medium is exhausted. If the medium is limiting, it is customary to replace it half way through the exponential phase of growth. When all the available growth surface is occupied, the culture is said to be *confluent* and will require to be subcultured again. If the culture is allowed to progress beyond confluence, growth will slow down, as a result of density limitation of growth (see Contact Inhibition), and the culture enters the plateau phase of the growth cycle. If the cells are normal and respond to normal growth control signals, there will be little evidence of cell proliferation or cell loss in plateau, specifically, minimal turnover. If, however, the cells are transformed, they will continue to proliferate for several cell generations after reaching confluence and reach a higher saturation density at plateau, due to deficiencies in contact inhibition of cell motility and density limitation of cell proliferation (10, 11). Even in plateau, there will be continued cell proliferation, although at a lower level than in exponential growth, balanced by increased cell loss from apoptosis, resulting in a greater turnover than occurs in normal cells in plateau.

Figure 2. Phases in the growth cycle of cultured cells following subculture. Modified from Freshney's *Culture of Animal Cells, A Multi-Media Guide*, 1999, Wiley-Liss, N.Y.

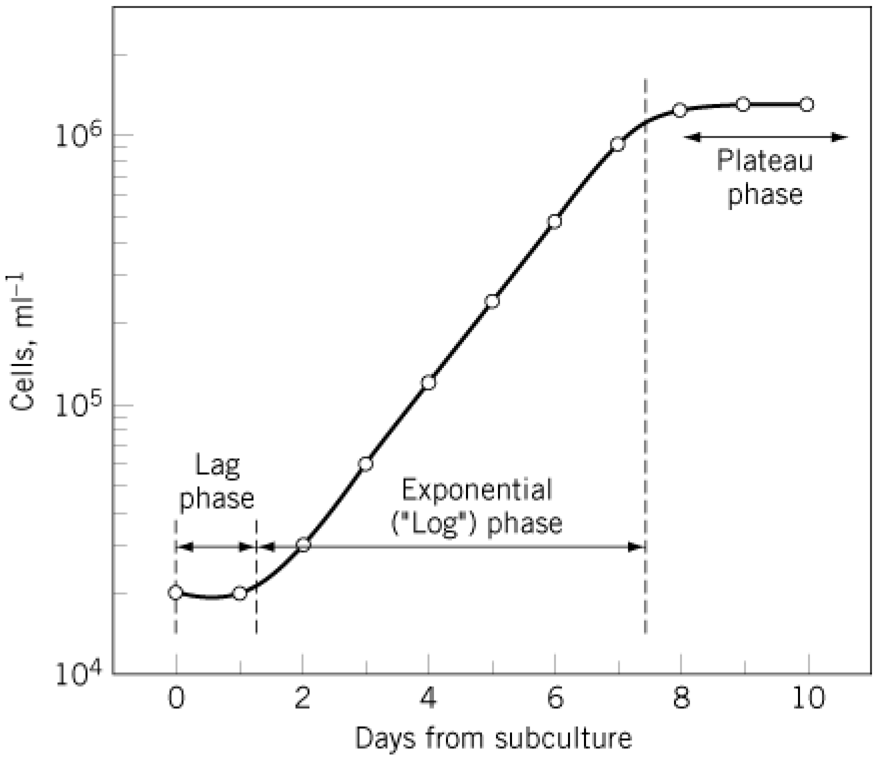

The numerical parameters that can be derived from the growth curve are the duration of the lag period, the doubling time in mid–log phase, and the saturation density in plateau. The last will depend on the feeding regimen and, if cell kinetics are being determined, should be measured under nonlimiting medium conditions. Where these parameters are consistent, they can be used to calculate the split ratio, the degree of dilution required to reinitiate a new growth cycle with a short lag period and to achieve the appropriate density for subculture at a convenient time in the future, usually around one week. The split ratio should be a power of 2 when handling finite cell lines. This allows an approximate calculation of the number of generations that have elapsed since the last subculture; for instance, a split ratio of 8 would imply that the cells had undergone 3 population doublings in each growth cycle. Split ratios are less useful with continuous cell lines. They are not needed to determine the stage in the life cycle of the cell line, as it is immortal, and the population doubling time is so much shorter that split ratios of the order of 1–100 are required to produce a week-long growth cycle. At this level of dilution, it is more advisable to determine the cell concentration at each subculture and to dilute to give the seeding concentration that will allow growth to the next subculture in a suitable interval, say, one week.

5. Selective Culture

Alterations in the choice of medium and/or substrate will determine which cells survive in primary and early passage cultures. Most selective media are serum-free (see Serum Dependence), and recipes are available for the culture of many different cell types, including fibroblasts, epithelial cells (epidermal, mammary), glial cells, melanocytes, endothelial cells, and smooth muscle Table 2. Selection of a purified cell culture, with defined characteristics, by cloning, use of a selective medium, or physical separation, allows the resultant culture to be called a *cell strain*.

Table 2. Examples of Selective Media[a]

Cells or Cell Line	Medium	Reference
Fibroblasts	MCDB 202	McKeehan et al. (1977) *In Vitro* **13**, 399.
Fibroblasts	MCDB 110	Bettger et al. (1981) *Proc. Natl. Acad. Sci. USA* **78**, 5588.
Keratinocytes	MCDB 153	Tsao et al. (1982) *J. Cell Physiol.* **110**, 219
Bronchial epithelium	LHC	Lechner and LaVeck (1985) *J. Tissue Cult. Meth.* **9**, 43
Mammary epithelium	MCDB 170	Hammond et al. (1984) *Proc. Natl. Acad. Sci. USA* **81**, 5435
Prostate epithelium (rat)	WAJC 401	McKeehan et al. (1982) *In Vitro* **18**, 87.
Prostate epithelium (human)	WAJC 404	McKeehan et al. (1984) *Cancer Res.* **44**, 1998
Glial cells		Michler-Stuke and Bottenstein (1982) *J. Neurosci. Res.* **7**, 215
Melanocytes		Naeyaert et al. (1991) *Br. J. Dermatol.* **125**, 297

Small cell lung cancer	HITES	Carney et al. (1981) *Proc. Natl. Acad. Sci. USA* **78**, 3185
Adenocarcinoma of lung		Brower et al. (1986) *Cancer Res.* **46**, 798
Colon carcinoma		Van der Bosch et al. (1981) *Cancer Res.* **41**, 611
Endothelium	MCDB 130	Knedler and Ham (1987) *In Vitro* **23**, 481

[a] Modified from R. I. Freshney *Culture of Animal Cells*, 1994, 3rd ed., Wiley-Liss, New York.

6. Characterization

Cell morphology and growth characteristics are simple criteria for characterization. Spindle-shaped cells are usually considered to be fibroblast-like, without necessarily implying that they are known to be of the fibrocyte lineage. Similarly, cells that grow in patches of polygonal, or pavement-like, cells with distinct boundaries between the cells are said to be epithelial-like, although numerous other cell types can assume a similar morphology. Characterization of a cell strain employs such criteria as (*1*) identification of the type of intermediate filament protein (eg, cytokeratin subtype in different epithelial cells, desmin in muscle cells, glial fibrillary acidic protein in astrocytes, and neurofilament protein in neurons and some neurendocrine cells) (12); (*2*) expression of cell-surface antigens, such as epithelial membrane antigen (13); (*3*) enzymes, such as tyrosine aminotransferase and its inducibility by glucocorticoids in hepatocytes (14); (*4*) marker chromosomes (15); (*5*) **isoenzymes** (16); and (*6*) the **DNA fingerprint** (17, 18). The same criteria may be used to characterize a cell line, but would give only an average for the population in a cell strain.

7. Cell Banks

Most of the cell lines in common use are lodged in cell banks containing records of their identifying characteristics. Cell lines or strains that have been characterized and shown to be free of mycoplasma can be submitted to a cell bank for safe-keeping, with or without authority to distribute to other users. Cell lines may be obtained from cell banks for a set charge (Table 3) (19).

Table 3. Cell Banks[a]

United States and Canada	American Type Culture Collection (ATCC), 12301Parklawn Drive, Rockville, MD 20852
	National Institute of General Medical Sciences (NIGMS), Human Genetic Mutant Cell and National Institute on Ageing Cell Culture Repositories, Coriell Institute for Medical Research, Copewood Street, Camden, NJ 08103
	Repository for Human Cell Strains, and Cell Repository for Neuromuscular Diseases, Children's Hospital Research Instsitute, McGillUniversity, 2300 rue Tupper Street, Montreal, Quebec H3H 1P3, Canada

Europe	European Collection for Animal Cell Cultures (ECACC), PHLS/CAMR, Porton, Salisbury, England
	European Collection for Biomedical Research,Dept. Cell Biology and Genetics, Erasmus University, P.O. Box 1783, Rotterdam,Netherlands
	Collection Nationale des Cultures des Microorganismes,Institute Pasteur, 25 rue du Dr. Roux, F-75724 Paris Cédex 15, France
	Human Genetic Cell Repository, Hospices Civilsde Lyon, Hôpital Debrousse, 29 rue Soeur Bourier, F-69322 Lyon Cédex05, France
	Tumorbank, Institut für Experimentelle Pathologie (dkfz), Deutsche Krebsforschungszentrum, in Neuenheimer Feld 280, Postfach 101949, D-6900 Heidelberg 1, Germany
	Centro Substrati Cellulari, Instituto Zooprofilattico Sperimentale della Lombardia, e dell'Emilia, Via A.Biandri 7, I-25100 Brescia, Italy
	National Bank for Industrial Microorganisms and Cell Cultures (NBIMCC), Blvd. Lenin 125 BL 2, V floor, Sofia, Bulgaria
	National Collection of Agricultural and Industrial Microorganisms (NCAIM), Dept. Microbiology, University of Horticulture, Somloiut 14-16, H-1118 Budapest, Hungary
Japan	Japanese Cancer Research Resources Bank (JCRB), National Institute of Hygienic Sciences, Kami-Yoga, Setagaya-Ku, Tokyo
	General Cell Bank, Institute of Physical andChemical Research of RIKEN, 2-1 Hirosawa, Wako, Saitama, 351-01
Australia	Commonwealth Serum Laboratories, 45 Poplar Road,Parkville, Victoria 3052

[a] Modified from R. I. Freshney, *Culture of Animal Cells*, 1994, 3rd ed., Wiley-Liss, New York.

Information on cell lines is also available through a number of data banks (20) such as ATCC ⟨www.atcc.org⟩ and ECACC ⟨www.ecacc.org.uk⟩.

Bibliography

1. W. I. Schaeffer (1990) In Vitro Cell. Dev. Biol. **26**, 97–101.
2. D. W. Barnes, D. A. Sirbasku, and G. H. Sato, eds. (1984) *Methods for Serum-Free Culture of Epithelial and Fibroblastic Cells*, Alan R. Liss, New York, pp. 3–24.
3. R. Maurer (1992) in *Animal Cell Culture, a Practical Approach*, 2nd ed. R. I. Freshney, ed., IRL Press at Oxford University Press, Oxford pp. 15–46.

4. D. W. Jayme and D. F. Gruber (1994) in *Cell Biology, a Laboratory Handbook*, J. E. Celis, ed., Academic Press, Nw York, pp. 18–24.
5. L. Hayflick, P. S. Moorhead (1961) Exp. Cell Res. **25**, 585–621.
6. C. S. Stulberg, W. D. Peterson, Jr., and W. F. Simpson, (1976) Am. J. Hematol. **1**, 237–42.
7. W. A. Nelson Rees, D. W. Daniels, and R. R. Flandermeyer (1981) Science **212**, 446–452.
8. R. J. Hay (1991) Dev. in Biol. Stand. **75**, 193–204.
9. G. T. McGarrity, D. G. Murphy, and W. W. Nichols eds., *Mycoplasma Infection of Cell Cultures*, Plenum Press, New York, pp. 87–104.
10. R. Dulbecco and J. Elkington (1973) Nature **246**, 197–199.
11. B. Westermark (1974) Int-J. Cancer **12**, 438–451.
12. F. C. S. Ramaekers, J. J. G. Puts, A. Kant, O. Moesker, P. H. K. Jap, and G. P. Vooijs (1982) Cold Spring Harbor Symp. Quant. Biol. **46**, 331–339.
13. E. Heyderman, K. Steele, and M. G. Ormerod (1979) J. Clin. Pathol. **32**, 35–39.
14. T. Ikeda, N. Sawada, M. Satoh, and M. Mori (1998) J. Cell. Physiol. **175**, 41–49.
15. T. R. Chen (1988) Cytogen. Cell Genet. **48**, 19–24.
16. K. G. Steube, D. Grunicke, and H. G. Drexler (1995) In Vitro Cell. Dev. Biol. **31**, 115–119.
17. G. N. Stacey, B. J. Bolton, D. Morgan, S. A. Clark, and A. Doyle (1992) Cytotechnology **8**, 13–20.
18. G. Stacey, B. Bolton, A. Doyle, and B. Griffiths (1992) Cytotechnology **9**, 211–216.
19. A. Doyle, R. Hay, and B. E. Kirsop, eds. (1990) *Living Resources for Biotechnology*, Cambridge Univ. Press, Cambridge, U.K., pp. 1–15.
20. A. Doyle, R. Hay, and B. E. Kirsop, eds. (1990) *Living Resources for Biotechnology*, Cambridge Univer. Press, Cambridge, England, pp. 17–49.

Cell Lineage

The daunting complexity of vertebrate organisms has led investigators to adopt a reductionist approach to their investigation. This approach is based on the assumption that an otherwise impossibly complicated system can be effectively understood through an analysis of its constituent cells and molecules. A reductionist concept of development envisions the process as the assembly of elementary units in many combinations and permutations, unfolding over time in stages that escalate progressively in their complexity. The transition from one stage to the next is influenced by the conditions that prevailed during the earlier period. Developmental biology thus seeks to infer the mechanisms of morphogenesis and histogenesis from the properties, activities, and responses of the precursors that give rise to the various lineages of the cells of the body.

That the concept of lineage should be an important one in developmental biology is something of a paradox. In a simplistic sense, it seems odd that lineage can be a meaningful issue, when all of the cells of an animal descend from a single precursor, the fertilized zygote. Distinct lineages, however, arise very early in embryogenesis. Formation of a body plan in lower vertebrates, including amphibia, is a process that begins in the oocyte, continues after fertilization and cleavage, and is finally completed at gastrulation (1, 2). Polarity in the oocyte causes cytoplasmic constituents to be distributed asymmetrically in the egg and newly formed blastula (3-6). This asymmetric distribution establishes different lineages in blastomeres, which do not each inherit identical cytoplasmic determinants from their predecessors. The resulting differential inheritance creates cellular differences between the blastomere-derived lineages and allows cells to interact with one another (7, 8). Regional inequalities and cellular interactions may then be expressed as functional differences between cells in different locations. These processes form an ordered cascade that leads to the establishment of a pattern of small groups of like cells that follow a developmental agenda common to themselves, but different from those followed by other small groups of cells located elsewhere in the embryo (4). Functional differences between cells located in particular sites in the developing embryo are necessary for the differential cellular behaviors that underlie morphogenetic movements, like gastrulation and neurulation (9-11). It is also these different cellular loci, and the progeny to which they give rise, that provide developmental meaning to the concept of lineage.

In mammals, the establishment of lineages is delayed relative to that in amphibian embryos. Early cleavage cells of mammalian embryos appear to be identical to one another and totipotent (12). Each of the blastomeres of a two-cell embryo is capable of generating a complete adult, and will do so if the embryo is split (13, 14). Destruction of a single blastomere, moreover, may not prevent the normal development of a mature animal. **Chimeric** animals can also be constructed by combining morulae (15). It is thus unlikely that localized determinants play a role in mammalian development prior to or during the eight-cell stage. The pattern of cell diversification must be generated at subsequent stages, through the interactions of cells with one another and with their microenvironment.

1. Lineage as a Pedigree

Lineage, understood as a set of cells for which the ancestry can be traced back to a single progenitor, can possibly be delineated in simple transparent embryos, such as that of Caenorhabditis *elegans* by direct observation (16, 17). Cells can be recognized and followed from egg to adult in a living embryo as they divide, migrate, differentiate, and/or die. Keeping track of the cells is facilitated by the fact that nematode development is virtually invariant. Because the process is so constant, it is possible to predict the fates of descendant cells from their positions on the lineage tree. It is, of course, not possible to use similar direct observation by itself to determine the pedigrees of the cells of an adult mammal. Not only are the numbers of cells in a mammalian embryo too large to permit the progeny of unmarked individual cells to be followed, the details of cell lineage in mammals may also show random variations, even between genetically identical individuals. Lineage can possibly be followed in mammals by marking individual precursor cells in one or another location, for example, with a replication-deficient retrovirus that carries the gene encoding *Escherichia coli* **beta-galactosidase** (18-20). The activity of the bacterial enzyme or the protein can then be detected histochemically or immunocytochemically, respectively, thereby permitting all of the cells of the clone that ultimately develops from the single virus-infected progenitor to be identified. This type of analysis has been especially powerful in studies of the development of the central nervous system (CNS).

Studies of *C. elegans* have been particularly important in establishing that the terminally differentiated cells of an adult animal do not necessarily constitute the lineal descendants of a single founder cell (16, 17, 21). Different phenotypic classes of cells (with the exception of intestinal and germ cells) in *C. elegans* thus arise from several founder cells, which themselves are found on different arms of the lineage tree. The descendants of a single primitive embryonic precursor, therefore, may become cells of the hypodermis, musculature, and nervous system of the mature animal (21). Lineage in the straightforward pedigree sense thus does not predict the commitment of multipotent precursor cells to a specific phenotype. That choice, the moment when a cell's fate has become determined, may be made long before the terminally differentiated phenotype becomes evident in the appearance of the cell, and may be shared by cells originating from more than a single progenitor (22). Determination in this sense implies that a cell has undergone a lasting and autoperpetuating change that will forevermore distinguish that cell and its progeny from other kinds of cell and will commit the determined cell and its descendants to a common specialized developmental program. Cells may become determined either before, or when, they overtly differentiate (display their ultimate phenotype in a detectable manner); moreover, all of the cells that are determined to follow a shared developmental program do not necessarily arise from a common precursor, and multipotent precursor cells may divide asymmetrically so that not all of their progeny are identically determined. The observation that cells of a particular terminally differentiated phenotype may not share an origin from a single "founder" has led the concept of lineage to acquire a meaning distinct from its linkage to cellular pedigrees.

2. Lineage and Determination

Cells of embryos that share a determined fate, as well as those that descend from a common founder, are often referred to as members of a common lineage. For example, the multipotent stem cells that are found in the neuroepithelium of the neural tube are self-sustaining, but they also give rise to progeny determined to be neurons or glia; following determination, the cells are said to be developing in neuronal or glial lineages (23). Lineage is used to denote their common determined phenotype, not their origin from a common precursor. The neuroepithelial stem cells proliferate in response to the actions of defined mitogens, including epidermal growth factor (EGF) and fibroblast growth factor (FGF), and differentiate as neurons or glia under the influence of a variety of microenvironmental factors. Factors that have been found under at least some circumstances (*in vitro* or *in vivo*) to promote the restriction of subsets of central nervous system stem cells to the glia lineage include sonic hedgehog (Shh) (24), ciliary neurotrophic factor (CNTF) (25), leukemia inhibitory factor (LIF) (25), and bone morphogenetic protein 4 (BMP4) (26).

The generation of the phenotypic diversity of cells in various brain regions occurs in stages, progressing from pluripotentiality to lineage restriction (a phenomenon that prevents cells from giving rise to certain types of progeny), to the determination of specific phenotypes, and finally to the manifestation of the features of the terminally differentiated cells (27). Because of their responsiveness to their microenvironment, transplanted stem cells can integrate into a variety of brain regions, and thus potentially may provide a tool for treating the diseased or injured brain (23). The progenitor cells of the vertebrate brain, however, are themselves heterogeneous and thus members of different lineages (27). These differences help to explain how and when neuroepithelial cells begin to respond to the molecular signals provided by their microenvironment. Environmental factors, be they mitogens, trophic growth factors, or morphogens, can only affect cells that have prepared themselves to be affected. To respond to an extracellular factor, the responding cell must have previously acquired the relevant receptors. Most of the stem cells of the vertebrate nervous system express the intermediate filament protein, nestin (23, 25). Lineages of progenitors, however, can be defined by the expression in common of molecular properties that distinguish the cells of the lineage from other progenitors in the neuroepithelium; such lineage-defining molecular traits include expression of the ***achaete/scute*** family of basic helix–loop–helix (bHLH) transcription factors, **EGF receptors**, ventricular zone gene 1 (*vzg-1*), and the embryonic neural cell adhesion molecule (E-NCAM) (27). Progenitors in different locations may respond differently to the gliogenesis-promoting factors noted above.

3. Lineages in the Development of the Neural Crest

A source of precursor cells in developing vertebrates that has been extremely valuable for studies of the role(s) of cell lineage in development has been the neural crest (28, 29). This is a transitory structure that appears during embryogenesis and disappears as its component cells disperse, migrating through the embryo to give rise to a wide variety of terminally differentiated cell types (30, 31). The lineages of cells as diverse as melanocytes, fibroblasts, endocrine cells, smooth and skeletal muscle, cartilage, bone, meningeal cells, Schwann cells, satellite cells, enteric glia, autonomic, enteric, and sensory neurons can all be traced back to the neural crest. A great deal of investigation has been devoted to understanding when crest-derived cells become determined, and what factors cause them to become so. Considerable evidence indicates that at least some of the cells of the premigratory crest are pluripotent. Clones of these cells give rise in culture to several different classes of terminally differentiated cells (32-35). Lineage studies that have marked (by microinjection) individual cells of the premigratory crest (36, 37), as well as early-migrating crest-derived cells (38), have shown that progeny of the marked precursors reach different destinations and thus give rise to a variety of cell types. Furthermore, cultures of stem cells can be prepared from the neural crest (39, 40), just as they can from the neuroepithelium of the neural tube (23, 25).

Although it is clear that the neural crest contains multipotent cells, the population of cells in the premigratory crest is actually heterogeneous. Some of the cells, even in the premigratory crest itself, are already determined (41). Cells determined to develop in the melanocytic lineage, for example, migrate selectively along the dorsolateral pathway (42). Among the uncommitted cells, there appears to be a progressive loss of developmental potential that occurs as a function of age (28, 29, 43). Whether the loss of developmental potential is simply determined by the age of the cells, or by the signals the cells receive as a result of their position in the embryo, has yet to be determined.

Some of the crest-derived cells that arrive in the organs that lie at the ends of their migratory pathways are still multipotential when the crest-derived cells arrive. The bowel has been carefully investigated in this regard and is a good model to illustrate the role of lineages in neural crest development (44). Two techniques have been employed to investigate the developmental potential of the crest-derived cells that colonize the gut. One, back-transplantation, consists of placing a segment of avian gut that has received a complement of émigrés from the neural crest in a migration pathway of a younger host embryo (45, 46). When this is done, crest-derived cells leave the grafts and remigrate in their new hosts. Where they go depends on where the grafts are placed. If the grafts are situated so as to replace the host's crest in locations that normally provide crest-derived émigrés for the bowel, the donor cells migrate to the host's gut and participate in forming the enteric nervous system (ENS). On the other hand, if the grafts are placed anywhere else in the embryo, the enteric crest-derived cells of the donor fail to migrate to the host's bowel. Instead, they migrate to peripheral nerves, sensory, and sympathetic ganglia. Donor cells that arrive in sympathetic ganglia become catecholaminergic sympathetic neurons, even though catecholaminergic neurons are not found in the enteric ganglia of the avian gut. Donor cells that find themselves in peripheral nerves develop as Schwann cells, even though the ENS contains glia rather than Schwann cells. Enteric crest-derived cells thus learn nothing from their previous journey to the bowel and evidently remember nothing of it. Crest-derived cells from the donor gut, however, never give rise to muscle, melanocytes, or connective tissue, indicating that they have lost at least some of developmental potential of their ancestors; nevertheless, they remain pluripotent to the extent that they are able to give rise to cell types that they would not have done had they been left *in situ*.

Clonal analysis of crest-derived cells isolated from the embryonic avian (47) or fetal mammalian bowel (48, 49) has also suggested that the population of crest-derived émigrés that colonizes the gut is a heterogeneous mixture of multipotent and determined cells. One or more terminally differentiated types of cells may be found in clones arising from individual precursors. None of the clones developing *in vitro* from enteric crest-derived cells contain melanocytes, endocrine cells, or skeletal muscle, although some contain smooth muscle. The heterogeneity of the crest-derived cell population that colonizes the bowel is reflected in the birthdays of the different types of enteric neuron (50). Some of these cells, containing acetylcholine or serotonin, are born very early in embryonic life, beginning in the mouse at E8.5, an age that precedes the arrival in the bowel of even the most precocious of enteric neurons. The crest-derived population that arrives in the gut, therefore, must contain a mixture of already-determined postmitotic neurons, as well as the undetermined pluripotent precursors that were revealed by the experiments involving back-transplantation and clonal analysis described above. On the other hand, other types of enteric neuron, such as those that contain calcitonin gene-related peptide (CGRP), do not even begin to leave the mitotic cycle until after the last serotonergic neurons have been born. The fact that the timing of the birthdays of enteric neurons is a function of their phenotypic class was among the earliest observations to suggest that multiple lineages of crest-derived precursors participate in the formation of the ENS. It is at least plausible that neurons in the same lineage might be born at similar times.

Confirmation of the idea that the ENS is formed by multiple lineages of crest-derived precursors came from a study that combined an *in vitro* investigation of enteric neuronal development with an analysis of the effects of the targeted deletion of the mash-1 transcription factor (51). It had previously been known that cells in the developing mammalian (but not avian) bowel are transiently catecholaminergic (TC) (52-55), and that these cells are derivatives of the neural crest (56-58). The TC cells were found not to be neurons, because they proliferate (56, 57, 59), although it was postulated that the TC cells might be neural precursors. That hypothesis was confirmed, and the disappearance of TC cells was found to occur not because they die, but because they lose their catecholaminergic properties as they acquire the characteristics of their terminally differentiated phenotype (56).

When it was discovered that TC cells express the same cell-surface differentiation antigens as precursors in the sympathoadrenal lineage, it was proposed that enteric and sympathetic neurons arise from a common lineage of crest-derived progenitors (60, 61). This idea was furthered by the demonstration that *mash-1* is expressed during the development of both sympathetic and enteric neurons (62, 63). On the other hand, knockout of *mash-1* is accompanied by the loss of almost the entire sympathetic nervous system (the superior cervical ganglion is spared), while the development of the ENS (except for that of the esophagus, which is lost) is merely delayed (63, 64).

The shared features expressed by sympathoadrenal and ENS precursors made it possible to test the hypothesis that sympathetic and enteric neurons are derivatives of a common precursor lineage. **Complement**-mediated lysis of all of the cells isolated from the bowel that express **antigens** common to the sympathoadrenal lineage reduces the numbers of enteric neurons developing *in vitro*, but it does not prevent their formation (51). No serotonergic neurons develop *in vitro* following lysis of TC cells, although neurons expressing CGRP appear normally. The cells in the developing bowel that express *mash-1* were found to be TC cells, and the knockout of *mash-1* in mice was demonstrated to result in the complete loss of early-developing serotonergic neurons, while late-born CGRP-containing cells appear on schedule. The apparent delay in timing of the formation of the ENS in *mash-1* knockout mice is thus due to the selective loss of the early-developing lineage of enteric neurons. These observations established for the first time that the ENS is, in fact, derived from at least two lineages of crest-derived precursors. One of these, which may be common to the precursors of sympathoadrenal cells, obligatorily expresses *mash-1*, gives rise to neurons that are born early, and is the origin of all of the serotonergic neurons of the bowel. The other lineage is never catecholaminergic, does not express *mash-1*, gives rise to neurons that are born late, and is the origin of peptidergic enteric neurons, including those that contain CGRP.

Since the discovery of the role of *mash-1* in the development of one lineage of enteric neurons, additional lineages or sublineages of enteric neuronal precursor have been discovered. All of the crest-derived cells that colonize the bowel appear to express $p75^{NTR}$, the common neurotrophin receptor (44, 56, 65). The cells (from the vagal and sacral regions of the neural crest) evidently also express Ret (66, 67), which must be stimulated by its functional ligand, glial cell line-derived neurotrophic factor (GDNF) (68-70). Actually, in order to stimulate Ret, GDNF has to form a complex with an a-component, GFRa-1 (71-73). If Ret (74, 75), GDNF (69, 76), or GFRa-1 (77) are knocked out, there are no neurons or glia in the entire bowel below the esophagus and in the immediately adjacent region of the stomach. GDNF is a mitogen for early crest-derived enteric neuronal precursors and later supports their development as neurons (78-80). Because the defect in the *mash-1* knockout mice is much more limited than that seen after the elimination of Ret or the components of its ligand complex, it follows that the *mash-1*-dependent lineage is a subset of a larger lineage of GDNF-dependent precursors.

More limited sublineages have been identified by the dependence of subsets of enteric neurons on other growth factor/receptor complexes, such as a still-to-be identified neuropoietic cytokine that activates the alpha component of the receptor for CNTF (65). Other factors, such as NT-3/TrkC (81) and **laminin**-1 (82, 83), have been identified that promote the development of enteric neurons, but these factors do not define particular lineages. Endothelin-3 (ET-3) and its preferred receptor, endothelin B (ET_B), also appear to be necessary for a subset of enteric neurons (84, 85). This factor/receptor complex, however, does not appear to define a particular lineage of enteric neurons. When either ET-3 (84) or ET_B (85) is knocked out in mice, the terminal colon becomes aganglionic, just as it does in humans with Hirschsprung's disease, some of whom also display ET-3 (86) or ET_B (87) mutations. The lesion that results from deletion of ET-3 or ET_B thus is geographically restricted, but within the affected zone all lineages of crest-derived enteric neurons are affected. ET-3 has been found to inhibit enteric neuronal development, and it has been postulated to act by preventing the premature differentiation of enteric neurons before their crest-derived have completed their colonization of the gut (78, 88).

4. Summary

The concept of lineage is used in two ways in describing development. In the pedigree sense, lineage is used to refer to the descendants of a common progenitor. Sharing a lineage defined as a pedigree, however, does not necessarily mean that the descendants of the common progenitor share the same developmental program or fate. Lineage as a pedigree is thus independent of the determination of its members. In a second developmental sense, the term *lineage* is used to refer to cells that do follow a common developmental program, regardless of whether these cells trace their ancestry back to a single shared precursor. Usually they do not. Identity of determination thus is now the common denominator that defines lineage.

Bibliography

1. J. B. L. Bard (1990) *Morphogenesis: The Cellular and molecular processes of Developmental Anatomy*, Cambridge University Press, Cambridge, U.K.
2. J. P. Trinkaus (1984) *Cells into Organs: The Forces That Shape the Embryo*, 2nd ed., Prentice-Hall, Engelwood Cliffs, NJ.
3. M. R. Rebagliati et al. (1985) Cell **42**, 769–777.
4. J. B. Gurdon (1992) Cell **68**, 185–199.
5. J. P. Vincent, G. F. Oster, and J. C. Gerhart (1986) Dev. Biol. **113**, 484–500.
6. M. Kirchner, J. Newport, and J. Gerhart (1985) Trends Genet. **1**, 41–47.
7. S. C. Guthrie and N. B. Gilula (1989) Trends Neurosci. **12**, 12–16.
8. J. D. Hardin and L. Y. Cheng (1986) Dev. Biol. **115**, 490–501.
9. H. Spemann (1938) *Embryonic Development and Induction*, Yale University Press, New Haven, CT.
10. W. C. Smith et al. (1993) Nature **361**, 547–549.
11. K. W. Y. Cho et al. (1991) Cell **66**, 1111–1120.
12. R. L. Gardner (1985) Philos. Trans. R. Soc. Lond. (Biol.) **312**, 163–178.
13. S. J. Kelly (1977) J. Exp. Zool. **200**, 365–376.
14. A. K. Tarkowski (1959) Nature **184**, 1286–1287.
15. A. McLaren (1976) *Mammalian Chimeras*, Cambridge University Press, Cambridge, U.K.
16. C. Kenyon (1985) Philos. Trans. R. Soc. Lond. (Biol.) **312**, 21–38.
17. J. E. Sulston and H. R. Horvitz (1977) Dev. Biol. **56**, 110–156.
18. D. D. Galileo et al. (1990) Proc. Natl. Acad. Sci. USA **87**, 458–462.
19. C. Walsh and C. Reid (1995) Ciba Found. Symp. **193**, 21–40.
20. J. G. Parnavelas, M. C. Mione, and A. Lavdas (1995) Ciba Found Symp. **193**, 41–58.
21. J. E. Sulston, E. Schierenberg, and J. G. White (1983) Dev. Biol. **100**, 64–119.
22. B. Christ, H. J. Jacob, and M. Jacob (1977) Anat. Embryol. **150**, 171–186.
23. R. McKay (1997) Science **276**, 66–71.
24. D. M. Orentas and R. H. Miller (1996) Dev. Biol. **177**, 43–53.

25. K. K. Johe et al. (1997) Genes Dev. **10**, 3129–3140.
26. R. E. Gross et al. (1996) Neuron **17**, 595–606.
27. L. Lillien (1998) Curr. Opin. Neurobiol. **8**(1), 37–44.
28. N. M. Le Douarin and E. Dupin (1993) J. Neurobiol. **24**, 146–161.
29. D. J. Anderson (1989) Neuron **3**, 1–12.
30. N. M. Le Douarin (1982) *The Neural Crest*, Cambridge University Press, Cambridge, U.K.
31. N. M. Le Douarin (1986) Science **231**, 1515–1522.
32. K. Ito, T. Morita, and M. Sieber-Blum (1993) Dev. Biol. **157**, 517–525.
33. M. Sieber-Blum and A. M. Cohen (1980) Dev. Biol. **80**, 96–106.
34. M. Sieber-Blum et al. (1993) J. Neurobiol. **24**(2), 173–184.
35. A. Baroffio, E. Dupin, and N. M. Le Douarin (1988) Proc. Natl. Acad. Sci. USA **85**, 5325–5329.
36. M. Bronner-Fraser and S. E. Fraser (1988) Nature **335**, 161–164.
37. M. Bronner-Fraser and S. Fraser (1989) Neuron **3**, 755–766.
38. S. E. Fraser and M. Bronner-Fraser (1991) Development **112**, 913–920.
39. D. L. Stemple and D. J. Anderson (1993) Dev. Biol. **159**, 12–23.
40. D. Stemple and D. J. Anderson (1992) Cell **71**, 973–985.
41. P. D. Henion and J. A. Weston (1997) Development **124**(21), 4351–4359.
42. C. A. Erickson and T. L. Goins (1995) Development **121**, 915–924.
43. D. J. Anderson (1993) Annu. Rev. Neurosci. **16**, 129–158.
44. M. D. Gershon (1997) Curr. Opin. Neurobiol. **7**, 101–109.
45. T. P. Rothman et al. (1990) Development **109**, 411–423.
46. T. P. Rothman et al. (1993) Dev. Dyn. **196**, 217–233.
47. F. Sextier-Sainte-Claire Deville, C. Ziller, and N. M. Le Douarin (1994) Dev. Biol. **163**, 141–151.
48. L. Lo and D. J. Anderson (1995) Neuron **15**(3), 527–539.
49. L. Lo, L. Sommer, and D. J. Anderson (1997) Curr. Biol. **7**, 440–450.
50. T. D. Pham, M. D. Gershon, and T. P. Rothman (1991) J. Comp. Neurol. **314**, 789–798.
51. E. Blaugrund et al. (1996) Development **122**, 309–320.
52. P. Cochard, M. Goldstein, and I. B. Black (1978) Proc. Natl. Acad. Sci. USA **75**, 2986–2990.
53. G. M. Jonakait et al. (1979) Proc. Natl. Acad. Sci. USA **76**, 4683–4686.
54. G. Teitelman, T. H. Joh, and D. J. Reis (1978) Brain Res. **158**, 229–234.
55. M. D. Gershon et al. (1984) J. Neurosci. **4**, 2269–2280.
56. G. Baetge, J. E. Pintar, and M. D. Gershon (1990) Dev. Biol. **141**, 353–380.
57. G. Baetge and M. D. Gershon (1989) Dev. Biol. **132**, 189–211.
58. G. Baetge, K. A. Schneider, and M. D. Gershon (1990) Development **110**, 689–701.
59. G. Teitelman et al. (1981) Dev. Biol. **86**, 348–355.
60. D. J. Anderson et al. (1991) J. Neurosci. **11**, 3507–3519.
61. J. F. Carnahan, D. J. Anderson, and P. H. Patterson (1991) Dev. Biol. **148**, 552–561.
62. F. Guillemot and A. L. Joyner (1993) Mech. Dev. **42**, 171–185.
63. F. Guillemot et al. (1993) Cell **75**, 463–476.
64. L. Lo et al. (1994) Perspect. Dev. Neurobiol. **2**, 191–201.
65. A. Chalazonitis et al. (1998) Dev. Biol. **198**(2), 343–365.
66. V. Pachnis, B. Mankoo, and F. Costantini (1993) Development **119**, 1005–1017.
67. P. L. Durbec et al. (1996) Development **122**, 349–358.

68. P. Durbec et al. (1996) Nature 381–793.
69. S. Jing et al. (1996) Cell **85**, 1113–1124.
70. M. Trupp et al. (1996) Nature **381**, 785–789.
71. M. Trupp et al. (1997) J. Neurosci. **17**, 3554–3567.
72. A. M. Davies et al. (1997) Neuron **19**, 485.
73. J. Widenfalk et al. (1997) J. Neurosci. **17**, 8506–8519.
74. A. Schuchardt et al. (1994) Nature **367**, 380–383.
75. J. J. S. Treanor et al. (1996) Nature **382**, 80–83.
76. M. Sénchez et al. (1996) Nature **382**, 70–73.
77. G. Cacalano et al. (1998) Neuron **21**, 53–62.
78. C. J. Hearn, M. Murphy, and D. Newgreen (1998) Dev. Biol. **197**, 93–105.
79. R. O. Heuckeroth et al. (1998) Dev. Biol. **200**(1), 116–129.
80. A. Chalazonitis et al. (1998) Dev. Biol. **204**, 385–406.
81. A. Chalazonitis et al. (1994) J. Neurosci. **14**, 6571–6584.
82. T. P. Rothman et al. (1996) Dev. Biol. **178**, 498–513.
83. A. Chalazonitis et al. (1997) J. Neurobiol. **33**, 118–138.
84. A. G. Baynash et al. (1994) Cell **79**, 1277–1285.
85. K. Hosoda et al. (1994) Cell **79**, 1267–1276.
86. P. Edery et al. (1996) Nat. Genet. **12**(4), 442–444.
87. E. G. Puffenberger et al. (1994) Cell **79**, 1257–1266.
88. J. J. Wu, T. P. Rothman, and M. D. Gershon (1997) Neurosci. Abst. **23**, 24.

Suggestions for Further Reading

89. B. Alberts et al. (1994) *Molecular Biology of the Cell*, 3rd ed., Garland Publishing, New York, pp. 1037–1107.
90. N. M. Le Douarin and E. Dupin (1993) J. Neurobiol. **24**, 146–161.
91. L. Lillien (1998) Curr. Opin. Neurobiol. **8**(1), 37–44.

Cell Surface Adhesion Receptors

Cell surface adhesion receptors are molecules that mediate cell adhesion by binding to other molecules on the surface of an adjacent cell or to a component of the extracellular matrix. Many adhesion receptors have been described. Most of them belong to one of a small number of families of related molecules in which individual members share the same basic molecular structure. The principal families are the cadherins, the immunoglobulin (Ig) superfamily, the integrins, and the selectins (Fig. 1) as follows.

Figure 1. Diagram showing the generalized molecular structures of the four principal families of cell-surface adhesion receptors. (From Ref. 7, with permission of BMJ Publishing Group.)

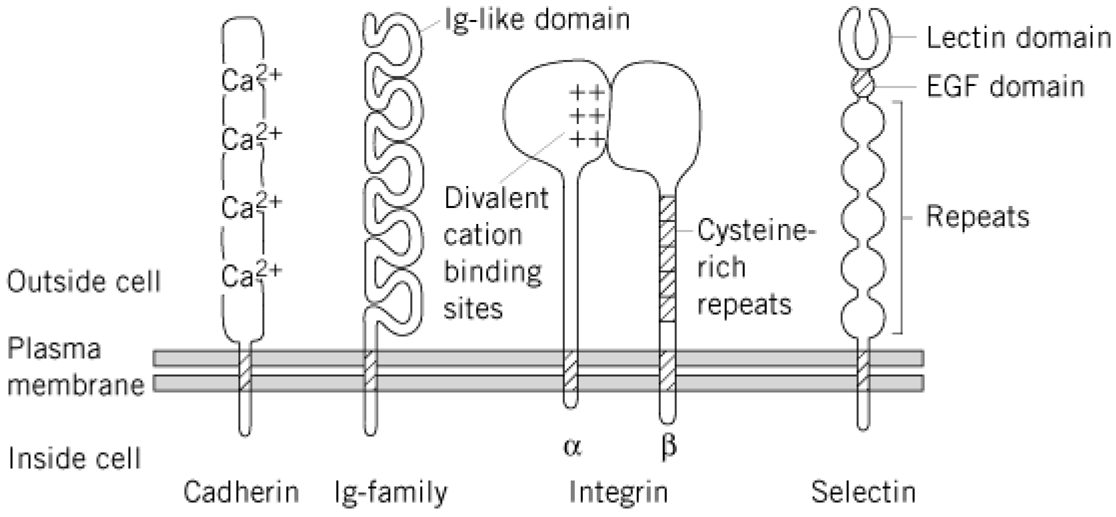

1. Cadherins

In most tissues, a major contribution to intercellular adhesion is made by calcium-dependent cell adhesion molecules knows as cadherins (1). In general, these are simple transmembrane glycoproteins. The extracellular domain has an adhesion site toward the *N*-terminal region and several **calcium-binding** sites. Adhesive binding is mainly homophilic: a cadherin molecule on one cells binds to another cadherin molecule of the same type on the next cell. Linkage of the cytoplasmic **domain** to the cytoskeleton through proteins known as catenins is necessary for cadherin function. The best characterized is epithelial cadherin, E-cadherin. This appears very early in development, when it is involved in compaction of the eight-cell embryo and cell polarization. In adult epithelia—for example, intestinal epithelium—it is present on the lateral cell surfaces but is concentrated in intercellular junctions, known as the zonulae adherentes (see Cell Junctions; Intermediate Junction), which ring the apicolateral margins of cells. These junctions are characterized by a cortical ring of cytoskeleton, the major component of which is actin. Cadherins are also present in the nervous system, where they play an essential role in neural development.

The adhesive glycoproteins of the other major intercellular junctions of epithelia, the **desmosomes** are also members of the cadherin family (2). Their extracellular domains are very like those of cadherin, but their cytoplasmic domains differ, being specialized for forming desmosomal plaques and, thereby, attachment to the keratin intermediate filament cytoskeleton, rather than to actin.

2. Immunoglobulin Superfamily

Another major group of cell-to-cell adhesion molecules are members of the Ig superfamily. Their extracellular portions are characterized by the presence of at least one, and usually multiple, immunoglobulin-like domains (3, 4). Included in this group are several nervous system cell adhesion molecules, such as the neural cell adhesion molecule (N-CAM), L-1, and TAG, which are involved in neuronal guidance and fasciculation. Several members of the immunoglobulin family are concerned with antigen recognition and adhesion in T cells. These include the following: the T-cell receptor (CD3) and its co-receptors CD4 and CD8, which together recognize the complexes of antigen peptide and major histocompatibility complexes on other cells; the major histocompatibility complex molecules themselves; and lymphocyte function related antigen 2 (LFA-2 or CD2), a receptor for another immunoglobulin-like molecule, LFA-3, expressed on other cells. Another group of immunoglobulin-like cell adhesion molecules includes the so-called intercellular adhesion molecules, ICAM-1, -2, and -3, which are more widely expressed, for example, on epithelial and endothelial cells, and V-CAM on endothelial cells. These are involved in the inflammatory response.

The immunoglobulin superfamily is large and diverse, probably because the basic structure of the immunoglobulin domain is versatile and readily adaptable to different binding functions (see Immunoglobulin Structure). Among these molecules, however, the T cell receptor and the immunoglobulins themselves have somatically-variable domains necessary for antigen recognition. Members of the superfamily are even present in insects, where they are involved in nerve connections; the association of immunoglobulin-like domains in cellular recognition preceded the immune system in evolution.

3. Integrins

Both cell-to-cell and cell-to-matrix receptors are contained within this large family of adhesion molecules. Integrins are heterodimers consisting of one a chain and one b chain, both of which are necessary for adhesive binding (5). Seventeen different a chains and eight different b chains are now known. Integrins may be classified into subfamilies according to which b subunit is involved in the complex. Thus b1 integrin may associate with one of nine different a subunits, to give a series of matrix receptors of differing specificity. The b2 integrins, on the other hand, are a family of cell-to-cell adhesion molecules of lymphoid cells with three alternative a subunits. The classification is made more complicated because some a subunits can associate with different b subunits (for example, a6b1 and a6b4).

Some integrins are apparently quite specific in their ligand-binding properties—for example, a5b1 for the Arg–Gly–Asp tripeptide sequence of fibronectin—whereas others are promiscuous—for example, avb3, once regarded as the vitronectin receptor, also binds fibronectin, fibrinogen, von Willebrand factor, thrombospondin, and ostepontin. An interesting example is a4b1, which binds both the IIICS domain of fibronectin and V-CAM on endothelial cells. To complicate matters further, individual cell types usually express multiple integrins. A good example to consider here is the blood platelets that express predominantly aIIbb3 (GPIIb/IIIa), which binds fibrinogen, fibronectin, von Willebrand factor, and vitronectin, but also lesser amounts of aVb3, a5b1, a2b1 (collagen), and a6b1 (laminin).

4. Selectins

Most cellular interactions seem to entail homophilic or heterophilic protein–protein interactions. However, the selectins constitute a family of cell adhesion proteins that bind to carbohydrate. Selectins have **lectin**-like carbohydrate-binding domains at their extracellular *N*-terminal extremities (6). One of these, L-selectin (L = leucocyte) is a “homing receptor,” mediating regionally specific adhesion of lymphocytes to endothelium in peripheral lymph nodes. This molecule is also involved in the adhesion of neutrophils to endothelium during the inflammatory response. Two other members of this family, E-selectin (E = endothelial) and P-selectin (P = platelet), also participate in the inflammatory response. E-selectin is unregulated on endothelial cells over a period of hours after stimulation by inflammatory mediators. P-selectin is contained within Wiebel–Palade bodies of endothelial cells and platelet a granules, from which it is rapidly mobilized on activation, mediating adhesion to neutrophils and monocytes.

Bibliography

1. M. Takeichi (1990) Cadherins: a molecular family important for selective cell–cell adhesion. Annu. Rev. Biochem. **59**, 237–252.
2. D. R. Garrod, M. A. J. Chidgey, and A. J. North (1996) Curr. Opin. Cell Biol. **8**, 670–678.
3. T. A. Springer (1990) Nature **346**, 425–434.
4. G. M. Edelman and K. L. Crossin (1991) Annu. Rev. Biochem. **60**, 155–190.
5. R. O. Hynes (1992). Cell **69**, 11–25.
6. M. P. Bevilaqua and R. M. Nelson (1993) J. Clin. Invest. **91**, 379–387.
7. D. R. Garrod (1997). "Cell to cell and cell to matrix adhesion". In *Basic Molecular and Cell*

Biology, 3rd ed., D. S. Latchman (ed.) BMJ Publishing Group, pp. 79–96.

Suggestions for Further Reading

8. D. R. Garrod, M. A. J. Chidgey, and A. J. North (eds.) (1999) *Adhesive Interactions of Cells*, JAI Press, Geenwich, CT. (A series of up-to-date reviews on cell adhesion receptors and intercellular junctions.)
9. "Cell adhesion and human disease." Ciba Found. Symp. **189**. (A valuable collection of reviews on cell adhesion molecules and their involvement in human disease.)
10. M. Hortsch and C. S. Goodman (1991) Annu. Rev. Cell Biol. **7**, 505–557. (Adhesion receptors in *Drosophila*—the invertebrate situation.)

CEN Sequences

Autonomously replicating sequences (ARS) are not stable *in vivo* during cell division and cannot be used readily as plasmid **vectors**. But, if certain DNA sequences that function as centromeres in yeast (CEN sequences) are grafted onto a **plasmid** already containing an ARS, the resulting vector plasmid is stabilized and segregates accurately during **mitosis** and **meiosis**. The CEN sequences are necessary for attaching chromosomes to the **mitotic spindle**, presumably through some specific connector proteins that join the microtubules to the centromere. In addition, CEN sequences can be used to construct linear chromosomes by preventing circularization by the addition of **telomeric** sequences that are normally at the end of chromosomes (1, 2).

Conserved features of *Saccharomyces cerevisiae* CEN SEQUENCES are confined to a region of about 120 bp. The highly conserved 8 bp at the left (PuTCACPuTG, where Pu = purine) constitute the left boundary of a functional CEN sequence. The right boundary lies within or just beyond the 25 bp at the right, with the consensus sequence TGT-T-TG–TTCCGAA—AAA, where - indicates no specific base. A mutant that lacks the left conserved element can still assemble into a centromere that is partially functional in mitosis and well functioning in meiosis. The sequences between the two conserved terminal DNA elements are not essential for centromere function. Their lengths can be increased by 50% or their sequence from 6 to 12% in GC content without measurable changes in mitotic or meiotic segregation of plasmids carrying such CEN mutations (3). The right boundary sequence appears to be a binding site for a protein, as evidenced by various inactive mutations, especially in the central CCG sequence, and by an exonuclease blocking assay (4). The left element, which carries the **palindromic** sequence CACPuTG, binds the **helix–loop–helix motif** protein CPF1 (5).

Bibliography

1. L. Clarke and J. Carbon (1980) Nature **287**, 504–509.
2. C–L Hsiao and J. Carbon (1981) Gene **15**, 157–166.
3. L. Panzeri et al. (1985) EMBO J. **4**, 1867–1874.
4. R. Ng., J. Ness and J. Carbon (1986) Basic Life Sci. **40**, 479–492.
5. R. Niedenthal, R. Stoll, and J. H. Hegemann (1991) Mol. Cell. Biol. **11**, 3545–3553.

Suggestion for Further Reading

6. L. Clarke and J. Carbon (1985) "The structure and function of yeast centromeres," Ann. Rev. Genet. **19**, 29–57.

Centrifugation

Centrifugation is a technique often employed during isolation or analysis of various cells, **organelles**, and biopolymers, including proteins, **nucleic acids**, lipids, and carbohydrates dissolved or dispersed in biologically relevant solvents (ie, typically aqueous buffers). It is also applicable to synthetic macromolecules dispersed or dissolved in nonaqueous, organic solvents. In this technique, the sample (comprising a liquid phase and a solute) is placed in a suitable vessel, and the vessel is spun in a centrifugal rotor. The centrifugal force created by the spinning rotor causes the solute sample to sediment out of solution (typically, though not always, toward the base of the vessel) (Fig. 1). The centrifugal force applied to the sample is akin to gravitational force (acceleration) and is measured in gravities, as in $n \times G$ (the gravitational constant G equals 6.6720×10^{-11} N-m^2/Kg^2). The extent to which the sample sediments toward the base of the vessel is a function of a series of complex interacting factors related to the properties of the solute alone and of the system as a whole (solvent and solute) (Fig. 1, Tables 1 and 2).

Figure 1. A schematic diagram of a centrifugation experiment.

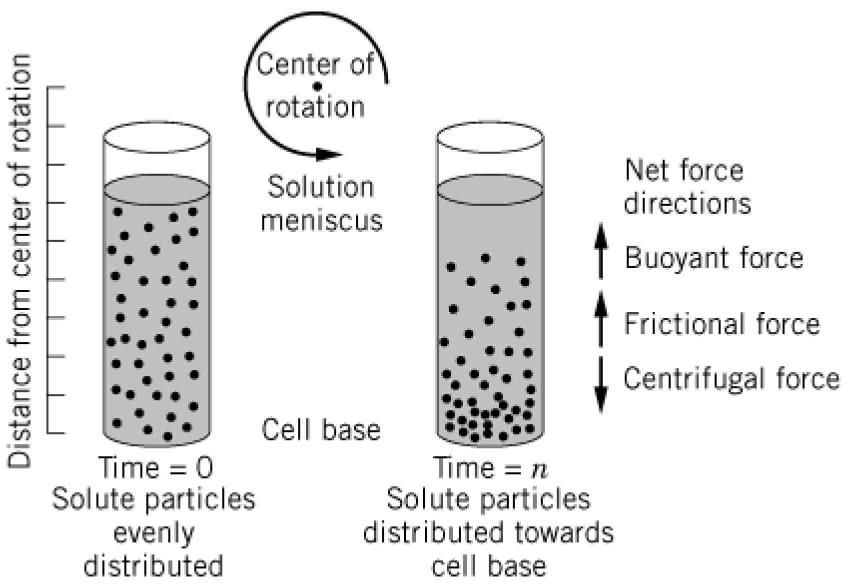

Table 1. The Forces Involved in Centrifugation

Proportionality Constant or Force Equation	Cause or Definition	Dimensions

Centrifugal force = w^2rm	Centrifugation of solute of mass, *m*	(g-cm) (radians/sec)
Buoyant force = $-w^2rm_s$	Solvent of mass m_s; displacement by sedimenting solute	(g-cm) (radians/sec)
Frictional force = $-fv$	Resistance to movement of solute particle at velocity *v* through solvent	$g\text{-}cm/sec^2$

Table 2. General Proportionality and Descriptive Constants for Centrifugation

Term	Definition	Dimensions
Angular velocity = w = (2r/60) × rpm	$2\pi\left(\frac{\text{radians}}{\text{revolution}}\right)\left(\frac{\text{revolutions}}{\text{min}}\right)\left(\frac{1\text{min}}{60\text{sec}}\right)$	radians/sec
Frictional coefficient = *f* = 6phr$_s$	Stokes' law frictional coefficient for a sphere of equivalent radius r_s in a solvent of viscosity h.	g/sec
Diffusion coefficient *D*	Defined by Fick's first law (see Refs. 1 and 2) for an ideal solution at infinite dilution as D = RT/N*f*, e.g., 1 Fick = 10^7 cm^2/sec	cm^2/sec
Sedimentation coefficient *s*	The velocity of sedimentation per unit of centrifugal force	sec
Solution density r	Mass per unit volume	g/cm^3
Solution viscosity h	The resistance to change within a fluid, a type of internal friction	poise or dyne-sec/cm^2
Solute partial specific volume *v*	The change in volume per unit mass	cm^3/g
Solute buoyant density	Effective density determined by isopycnic centrifugation in a specific gradient medium	g/cm^3
Avagadro's number *N*	6.022×10^{23}	$mole^{-1}$
Gas constant *R*	8.314×10^7	ergs/K-mole

The factors that define the entire sedimenting system include (1) the rate w at which the rotor spins; (2) the length of time for which the centrifugal force is applied; (3) the solvent density r; and (4) the system temperature *T*. The factors specific to the sedimented solute include (1) the radial distance *r* of the solute from the central axis of rotation; (2) the solute partial specific volume *v*; (3) the solute diffusion coefficient *D*; (4) the solute **frictional coefficient** *f*; and (5) the solute sedimentation coefficient *s*. During centrifugation (Fig. 1), the centrifugal force is opposed by buoyant density and frictional forces. Under these conditions it can be shown that the rate of sedimentation of the solute molecules of weight-average molecular weight M_w and moving as a radial boundary r_b is defined by

$$\text{Boundary velocity} = v = \frac{M_w(1-\bar{v}\rho)}{Nf}\omega^2 r_b. \tag{1}$$

Operationally, the technique can be divided into preparative and analytical modes, which differ principally in whether the actual recovery of the materials that have been centrifugally separated is desired or practical (Fig. 2).

Figure 2. Common preparative and analytical methods used in centrifugation.

Preparative Isolation and Recovery of Solute(s)	Solute Analytical Information
Common Methods	Common Methods
Selective pelleting	Sedimentation velocity
Density gradient separations	Sedimentation equilibrium
Rate zonal	
Flotation	
Isopynic	

1. Preparative Centrifugation and Ultracentrifugation

Preparative centrifugation (Fig. 2) is routinely employed in isolating, separating, and purifying a variety of biological and cellular/subcellular components. Some examples include chromatin, coated vesicles (see Clathrin), cytosolic proteins, DNA, **Golgi**, inclusion bodies, **lipoproteins**, **lysosomes**, **Microorganisms**, **Microsomes**, mitochondria, myelin, **nuclei**, **glycoproteins**, **RNA**, **Peroxisomes**, plasma membranes, **polysomes**, proteoglycans, ribosomes, synaptosomes, and **viruses**. Preparative centrifugation has two primary modes of separation. Solutes can be selectively pelleted from solution, as described here, or they can be subjected to separation along a solution density gradient (see Density Gradient Centrifugation).

1.1. Selective Pelleting or Differential Centrifugation

Clearing macromolecular components from solution is probably the most commonly employed preparative centrifugation technique. In this method the sample is subjected to centrifugation, usually, though not necessarily, at a constant rotor velocity. Over time, a pellet of sedimented material is deposited along the most radially distant wall of the tube containing the sample (Table 3). At a sufficiently high rotor speed (and therefore high centrifugal force), virtually all macromolecular solute components heavier than the solvent are pelleted out of solution over time. Because it is possible to select a variety of rotor velocities, sample tube dimensions, rotor types, centrifugation run times, etc., it is often possible to accomplish a significant level of purification by pelleting alone because the method of separation relies on the differential sedimentation rates of small and large solute components. For example, large components are typically removed by sedimentation at low speeds for short periods of time. If the supernatant from such a centrifugation is placed in a new container and centrifuged again at a higher rotor velocity for an appropriate period of time, it is possible to collect another distribution of particles from solution, this time of smaller dimensions than the first. Therefore repeating this process yields a series of pelleted samples with distributions of solute molecules, each of which have accumulated under conditions differing only in their centrifugal forces and thus have different sedimentation rates. Most samples of biological interest are complex mixtures of interacting solutes in solution at widely different concentrations. Because the size, shape, and concentration distributions of these components are routinely broad, together they exhibit very broad distributions of sedimentation rates. Thus the technique of solute pelleting, though widely applied, is only rarely sufficient to purify a single component completely. Typically it is used to selectively enrich, often to a high degree, a preparation of cellular or subcellular components in a single component. For small biological solutes, such as soluble cytosolic proteins prepared by a protein isolation procedure, pelleting is routinely employed along with differential precipitation (**salting out**) using ammonium sulfate (see Sulfate Salts) to yield highly enriched, sedimented precipitates of the desired protein components.

Table 3. Descriptive Constants for Preparative Centrifugation

Term	Definition
Clearing factor, k	time (hours) = $k/s, s$ = *svedbergs*; the value of k varies with each rotor type and compares the relative rotor efficiencies for pelleting
Clearing time, t	t = k/s (see clearing factor, above); the time required to pellet a particle to the base of the tube
Flotation Coefficient, f_s	For particles which float in a particular solution in a centrifugal field, it is similar to the sedimentation coefficient, units are in sec.
Relative centrifugal force or (RCF)	RCF = $1.12r\,(\text{rpm}/1000)^2$, where r is in mm; the ratio of the centrifugal force at a specific rotation rate in rpm for a particular rotor at a particular radius r from the center of rotation of that rotor to the gravitational force of the Earth at sea level.
Square-root speed reduction law	$[\text{Maximum allowed rotor speed} = \dfrac{\text{Desired speed}}{\sqrt{\dfrac{\text{Max allowed solution density}}{\text{actual solution density}}}}$ Used to calculate the permissible rotor speed in rpm when using nonprecipitating gradient materials at densities greater than the manufacturer permits in a rotor

Pelleting is also of great use when applied to harvesting viruses or cells from various growth media. When cells or viruses are used to produce various recombinant proteins of pharmaceutical interest, centrifugal harvesting is often employed to capture the biological component from the (usually large) fermentation broth. In these applications, a preparative centrifuge and rotor capable of accepting a continuous flow into and through the rotor are employed. The centrifugal force applied to the sample stream as it passes through the rotor is adjusted to permit selective pelleting of cells within the centrifuge rotor. The cell-depleted broth passes out of the rotor/centrifuge and into a receiver vessel, and, then the harvested cells are recovered from the centrifuge rotor.

Bibliography

1. K. E. Van Holde (1971) *Physical Biochemistry*, Prentice Hall, Englewood, Cliffs, NJ, pp. 70–121.

2. H. Fugita (1962) *Mathematical Theory of Sedimentation Analysis*. Academic Press, New York.

Suggestions for Further Reading

3. K. E. Van Holde (1971) *Physical Biochemistry*, Prentice–Hall, Englewood Cliffs, NJ, pp. 70–121. A short, highly readable and concisely illustrated treatment of the mechanical model of centrifugation for the biologist.
4. D. Eisenberg and D. Crothers (1979) *Physical Chemistry with Applications to the Life Sciences*, Benjamin–Cummings, Menlo Park, CA, pp. 701–745. An excellent introductory physical chemistry text with a good review of fundamental flow equations and a number of useful examples.
5. C. Tanford (1961) *Physical Chemistry of Macromolecules*, Wiley, New York, pp. 317–456. A classic and still relevant text on the nature of transport processes as applied to biological systems.

Centromeres

The centromere (kentron = center; meros = part) is the region of the mitotic chromosome that participates in chromosomal movement. The mitotic spindle attaches to a specialized structure at the centromere known as the kinetochore. The motor responsible for the movement of the chromosomes toward the spindle poles during mitosis is also located at the centromere. Morphologically, centromeres are distinguished by their appearance at metaphase and anaphase as constrictions in the chromatin and by their heterochromatin staining pattern. A chromosome without a centromere is described as acentric. It does not segregate properly during cell division and is rapidly lost in successive cell cycles.

Centromeres occupy different positions in chromosomes, and they are useful markers. Chromosomes with a single centromere are called monocentric. Chromosomes with centromeres near one end are called acrocentric, those with the centromere visible at or near the middle are metacentric, and those with the centromere truly at the end are telocentric. The monocentric chromosomes found in most metazoan plants and animals almost always have centromeres embedded in segments of heterochromatin. Some organisms, such as plants in the genus *Luzula*, have holocentric chromosomes with diffuse centromeres. In these chromosomes the spindle attaches to the centromeric heterochromatin that is distributed along the entire length of the chromosome (1). Mammalian tissue culture cells occasionally develop chromosomes with multiple centromeres (2). A chromosome with two centromeres is called dicentric. Dicentric chromosomes are often the result of chromosome breakage followed by fusion. A dicentric chromosome normally breaks at anaphase, when the centromeres are pulled in opposite directions. The holocentric chromosomes found in certain plants have developed as yet unknown mechanisms to avoid this problem.

Centromeres represent highly specialized chromosomal organelles. The simplest types of centromeres are found in the yeast *Saccharomyces cerevisiae*. The presence of these centromeric sequences, together with the autonomously replicating sequences that serve to direct DNA replication within exogenous plasmid DNAs allow these small minichromosomes to be stably maintained through cell division. The centromeric sequence allows the minichromosomes to be segregated in mitosis and meiosis with accuracy. Maintenance of minichromosomes through cell division also provides a simple assay for the definition of functional centromeric sequences in yeast.

All of the yeast centromeres are functional as small segments of DNA about 1,000 base pairs (1 kbp) or less in length. Nucleosomes are assembled in specific positions on these DNA sequences, and they contain a specialized histone H3 molecule (Cse4p) (16). Within each segment of centromeric DNA are similar nucleotide sequences. In the middle of the centromeric DNA is a 220-bp segment that constitutes the centromeric core, that contains the minimal sequence necessary for centromeric function. Only a single spindle fiber attaches to a yeast centromere (4). If this attachment is to the core, then the nucleoprotein complex assembled on the core also functions as a kinetochore.

Mammalian centromeres are considerably more complex than those in *S. cerevisiae*. Early experiments on the centromere of the human Y-chromosome established that much more DNA is required for the chromosomal segregation function than in yeast. Over 300 kbp of DNA, including 200 kbp of a-satellite DNA, are required to generate a functional centromere, suggesting the epigenetic—i.e., meta-DNA—mechanisms establish centromere location in cells of metazoa (17), a notion supported by the appearance of neo-centromeres in mammalian cells over nonrepetitive DNA (18). For native centromeres, however, deletion of the a-satellite DNA makes the centromere inactive (5).

The centromere can be broken up into three distinct structures, the kinetochore and the central and pairing domains (Fig. 1). The protein constituents of the centromere have been identified primarily through the use of autoantibodies from patients with rheumatic disease. These include the inner centromeric proteins (INCENP) and the CENP A, B, and C proteins. Immunological staining reveals that the INCENPs are in the pairing domain. The central domain contains dense chromatin known as constitutive heterochromatin. The kinetochore is anchored to this heterochromatin (Fig. 1). The DNA within this heterochromatin is composed primarily of various families of repetitive DNA (satellite DNA).

Figure 1. An expanded view of the centromere of a mammalian chromosome. The centromere is a bipartite structure. The central axis between the pairing domains is indicated by the dashed line. The relative positions of heterochromatin, the INCENPS, and CENPS are indicated within the kinetochore and the central and pairing domains.

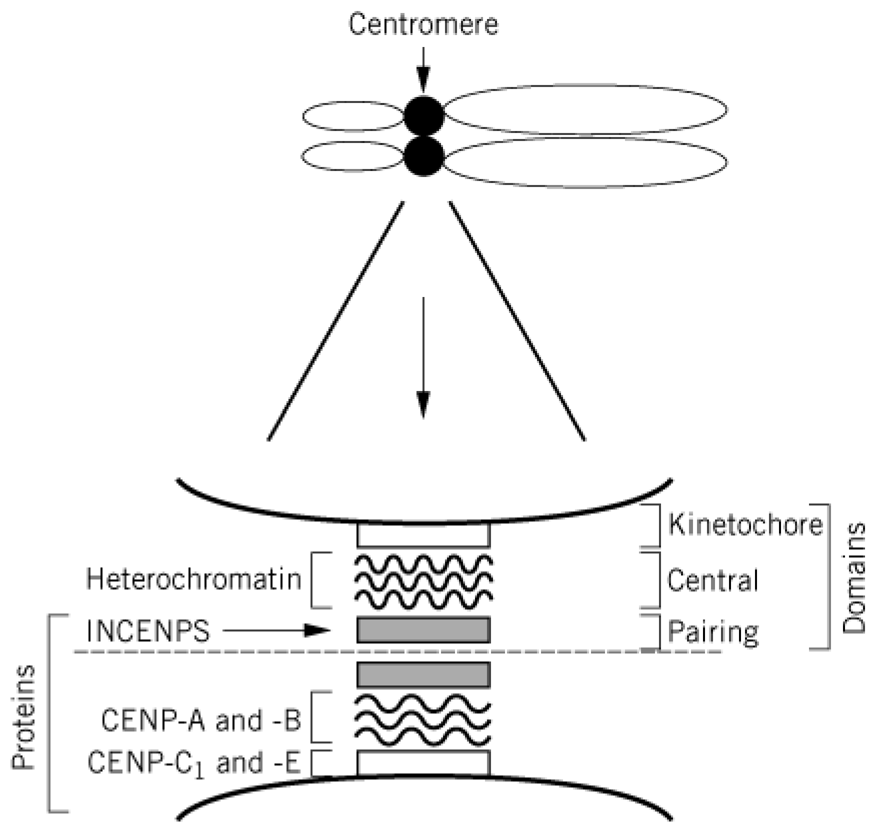

The a-satellite family of DNA sequences (which comprises 5% of the human genome) is probably present at the centromeres of all human chromosomes. The basic repeat 171 bp long, occurs in large arrays up to 3×10^6 bp long. The a-satellite repeats assemble a specialized chromatin structure that provides many insights into the molecular nature of constitutive heterochromatin. It has been long that nucleosomes are positioned with respect to the nucleotide sequence found in a-satellite DNA so that histone-DNA contacts would begin and end at particular sites (6). An important point is that a single nucleosome is believed to exist on every 171 bp repeat. In modified form, this DNA sequence also provides the foundation for crystallization of the nucleosome more (7). Several interesting specialized chromosomal proteins also associate with a-satellite DNA. A 10-kDa protein, high mobility group protein (HMG-I/Y) binds to a-satellite DNA specifically *in vitro* (8). The HMG-I/Y protein binds selectively in the minor groove of the double helix, associating with runs of six or more AT base pairs. In addition HMG-I/Y also probably recognizes certain secondary structural features of the DNA molecule. CENP-B specifically recognizes a 17-bp DNA sequence (5′ CTTCGTTGGAA CGGGA 3′) in a subset of a-satellite DNA repeats. The DNA-binding domain of CENP-B is necessary and sufficient for localization to the centromere in vivo (9). CENP-B contains anionic regions rich in aspartic and glutamic acid residues, which are characteristic of many proteins that interact with chromatin. CENP-B is found throughout the centromeric heterochromatin beneath the kinetochore plates (see Kinetochore). Although the exact functions of CENP-B in heterochromatin are not known, it may play a role in the higher order folding of centromeric chromatin through self-assembly mechanisms. Although CENP-B is found at all mammalian centromeres examined, the CENP-B recognition element is not found in all a-satellite DNA (10). It is possible that CENP-B can also be targeted to centromeres through interactions with other protein components.

CENP-A is also specifically associated with centromeric DNA and is especially interestin because it shares homology with core histone H3. Recent sequence analysis has revealed that CENP-A is a very specialized H3 variant (11). Each core histone and CENP-A have two domains, and amino-terminal tail domain that lies on the outside of nucleosomal DNA and a carboxyl-terminal, histone-fold domain that is involved in protein—protein interactions and in wrapping the DNA. CENP-A has a highly divergent amino-terminal tail domain and a relatively conserved carboxy-terminal, histone-fold domain. The targeting of CENP-A to centromeric DNA is directed by the histone-fold domain, and it is very likely that a highly specialized, dedicated chromatin assembly mechanism exists to enable the selective heterodimerization of CENP-A with histone H4 over centromeric DNA (19). Although the exact mechanism by which this is achieved is still unknown. Characterization of a CENP-A homologue in yeast (CSE4, Ref. 3) establishes that this specialized histone is essential for normal chromosomal segregation during mitosis. Genetic evidence suggest that CSE4 heterodimerizes with histone H4 (19). This establishes that specialized nucleosomal structures are present at the centromere, in addition to the presence of positioned nucleosomes. Clearly, the centromere represents a highly differentiated chromosomal domain even at the most fundamental level of chromatin structure.

CENP-C is a large 107-kDa protein that is highly hydrophilic and basic (pI = 9.4) (13). CENP-C is concentrated in a narrow band immediately below the inner kinetochoric plate at the interface between the chromosome and the kinetochore (Fig. 1). CENP-C binds DNA directly and is required for normal kinetochoric assembly. CENP-C is found only at the active centromere of a stable dicentric chromosome, suggesting a direct role in centromeric function (14). Other components of the centromere include CENP-E, which resembles microtubule-binding motor proteins. CENP-E is a 312-kDa polypeptide chain with a tripartite structure consisting of globular domains at the N- and C-termini, separated by a 15,000-residue a-helical domain that is predicted to form coiled-coils. CENE-E colocalizes to the centromere and kinetochore during metaphase, but it is released from the centromere at the onset of anaphase, when it is degraded. CENE-E functions as a kinetochoric motor during the early part of mitosis (15) (See Kinetochore). The proper cohesion between centromeres on sister chromatids prior to the metaphase-anaphase transition in mitosis, and centromere nondisjunction on sister chromatids during meiosis I are essential for proper chromosome behavior. Both are effected by the preferential association of the cohesion complex (120) with centromeres (16, 21); in addition to the cohesins, in metazoa, noncohesion proteins as MEI-S322 also associate with the centromere and mediate kinetochore assembly as well as sister chromatid cohesion during meiosis (22).

The assembly of the centromere and the mechanisms of kinetochoric association with chromatin offer perhaps our best opportunity to understand the construction of a specialized chromosomal domain at the biochemical level.

Bibliography

1. S. Pimpinelli and C. Goday, Trends Genet. **5**, 310–313 (1989).
2. B.K. Vig and N. Paweletz, Chromosoma **96**, 275–283 (1988).
3. S. Stoler, K.C. Keith, K.E. Curnick, and M. Fitzgerald-Hayes, Genes Dev. **8**, 573–586 (1995).
4. J.B. Peterson and H. Ris, J. Cell Sci. **22**, 219–226 (1976).
5. C. Tyler-Smith, R. Oakley, and Z. Larin, Nat. Genet. **5**, 368–375 (1993).
6. R.T. Simpson, Prog. Nucl. Acids Res. Mol. Biol. **40**, 143–184 (1991).
7. K. Luger et al., Nature **389**, 251–260 (1997).
8. M.J. Solomon, F. Strauss, and A. Varshavsky Proc. Natl. Acad. Sci. U.S.A. **83**, 1276–1280 (1986).
9. A.F. Pluta et al., Science **270**, 5191–5194 (1995).
10. I.G. Golberg et al., Mol. Cell Biol. **16**, 5156–5168 (1996).
11. K.F. Sullivan, M. Hechenberger, and K. Masri, J. Cell Biol **127**, 581–592 (1994).
12. M.M. Smith et al., Mol. Cell Biol. **16**, 1017–1026 (1996).
13. H. Saitoh et al., Cell **70**, 115–125 (1992).
14. J. Tomkiel et al., J. Cell Biol. **125**, 531–545 (1994).
15. K.D. Brown, K.W. Wood, and D.W. Cleveland, J. Cell Sci. **109**, 961–969 (1996).
16. K.F. Sullivan, Curr. Opin. Genet. Dev. **11**, 182–188 (2001).
17. G.H. Karpen and R.C. Allshire, Trends Genet. **13**, 489–496 (1997).
18. A.E. Barry et al., Hum. Mol. Genet. **8**, 217–227 (1999).
19. L. Glowczewski et al., Mol. Cell Biol. **20**, 5700–5711 (2000).
20. A.V. Strunnikov, Trends Cell Biol. **8**, 454–459 (1998).
21. T. Tanaka, M.P. Cosma, K. Wirth, and K. Nasmyth, Cell **98**, 847–858 (1999).
22. J.M. Lopez, G.H. Karpen, and T.L. Orr-Weaver, Curr. Biol. **10**, 997–1000 (2000).

Čerenkov Radiation

Čerenkov radiation, or the Čerenkov effect, is the visible bluish-white light surrounding a radioactive source observed in a pool of water. The phenomenon was first reported by the Russian physicist P. A. Čerenkov in 1934 (1), who was one of several scientists who observed the glow of light in close proximity to intense gamma-radiation sources. This effect is the reason why radiation sources are said to “glow in the dark.” Its importance for molecular biology is that it is routinely used to measure the amount of the isotope ^{32}P in a sample (see Radioactivity and Phosphorous Isotopes).

The Čerenkov effect can be explained by classic electromagnetic theory and principles of optic science. Analysis of Čerenkov radiation has shown fundamental relationships between the velocity of charged particles, light, the intensity of the light, and its wavelength spectrum (2). Only a small fraction (<0.1%) of the charged-particle radiation is emitted by the absorbing medium as coherent light. According to Jelley (3), who provided the first scientific explanation for the Čerenkov effect, the observed light results from charged particles traversing a transparent dielectric medium, one that does not conduct electricity. Charged particles are produced in the absorbing medium (water) when gamma radiation from the radioactive source interacts with the absorber. These charged particles produce local polarization along their path in the dielectric. Light in the visible spectrum is emitted when the polarized molecules in the medium return to their rest state soon after passage of the charged particle. If the velocity of the charged particles is less than that of light in the same medium, the light emitted from molecules in the dielectric is overridden and not observed. However, if the velocity of the charged particles is greater than that of light in the dielectric, a wavefront of light is produced from individual molecules in the dielectric, and the emission is reinforced by constructive interference. The Čerenkov effect is analogous to the bow wave from a ship that travels faster than the velocity of the surface waves, or to the shock wave trailing a supersonic aircraft passing though air. In other words, if the velocity v of a charged particle traversing a transparent dielectric material of refractive index n (= bc) exceeds the velocity of light (c/n) in the medium, or v > c/n and b > 1/n, then Čerenkov radiation is emitted at an angle x relative to the particle direction, where x = arccos (1/bc). The velocity c of light in a vacuum is 2.997×10^{10} cm/s, and b = v/c. The Čerenkov photons form a conical wavefront of half-angle (90° – x) behind the particle.

The polarization effect actually decreases the energy lost by a charged particle that traverses a condensed medium, whereas the production of Čerenkov radiation increases the loss of energy by the particle. The visible spectrum is produced at a frequency interval of about 3×10^{14} Hz. Applications of Čerenkov radiation theory have been developed for detecting single high energy charged particles, measuring the energy of charged particles, and determining angles of incidence.

The light pulses emitted by charged particles traveling in a transparent medium can be collected and counted by modern scintillation counters. The amount of light produced in water is small compared to that produced in the presence of a scintillator, but it can be detected from beta-emitting radionuclides if their energy is greater than the threshold energy of 265 keV. The average energy of phosphorous-32 beta particles is 695 keV, so the majority of emitted beta particles can be detected.

Bibliography

1. P. A. Čerenkov (1934) Compt. Rend. Acad. Sci. URSS **2**, 451.
2. I. Frank and I. Tamm (1937) Compt. Rend. Acad. Sci. URSS **3**, 109.
3. J. V. Jelley (1953) Atomics **4**, 81.

Suggestions for Further Reading

4. F. H. Attix (1986) *Introduction to Radiological Physics and Radiation Dosimetry*, Wiley, New York.
5. W. J. Price (1958) *Nuclear Radiation Detection*, 2nd ed., McGraw-Hill, New York.

Chain-Termination (Dideoxy) DNA Sequencing

The relative length of a DNA chain is determined easily and accurately by gel electrophoresis, and the most common types of DNA sequencing use methods that map sequence information to DNA chain lengths. For chain-termination DNA sequencing, this is done by synthesizing the complement of the DNA using a **DNA polymerase** under conditions that terminate synthesis at sites where only one of the four bases occurs. Thus, all sequencing experiments are done in three steps. First, a single pure DNA segment is isolated for sequencing. Second, this DNA is used as a template for synthesis catalyzed by a **DNA polymerase** with mixtures of normal and chain-terminating nucleotides. Finally, the products of this synthesis are separated according to size by gel electrophoresis. Numerous variations on each of these steps are commonly used.

1. Isolation of Specific Segments of DNA

Most of the techniques of molecular biology rely on isolating specific segments of DNA, and sequencing is no exception. In fact, the first practical application of chain-termination sequencing relied on cloning specific DNA segments using vectors derived from **M13 bacteriophage**. These bacteriophages contain a single-stranded DNA **chromosome** that accommodates inserts of more than 5000 bases. Isolating the single-stranded DNA in pure form from these phages is simple and inexpensive, so these vectors are still commonly used. Similarly, virtually all plasmid vectors are commonly used for DNA sequencing, and essentially any clone of up to about 200 kb can be sequenced by cycle sequencing techniques, provided sufficient DNA can be purified. Another popular way of isolating DNA for sequencing is by using the polymerase chain reaction (**PCR**). With nested PCR primers, it is now relatively simple to amplify segments of **genomic** DNA for direct sequencing in a matter of hours.

2. Chain Termination Reactions

Chain termination reactions require the isolated template DNA, a suitable primer, 2′-deoxynucleoside triphosphates (dNTPs), 2′,3′-dideoxynucleoside triphosphate (ddNTP) chain terminators, and a DNA polymerase. The most critical component is the DNA polymerase. Many DNA polymerases have been used for sequencing, including those from eubacteria, such as the DNA polymerase I (**Klenow fragment**) of *Escherichia coli*, **reverse transcriptases** from retroviruses, such as avian myeloblastosis virus, polymerases from bacteriophage, such as **T7 phage** DNA polymerase, and polymerases from archaea, such as *Thermococcus litoralis*. Virtually all of these have been genetically or chemically modified to eliminate exonuclease activities or to improve reaction rates with the ddNTPs.

The most recent examples of polymerases specifically engineered for DNA sequencing are enzymes derived from *Thermus aquaticus*, Taq DNA polymerase. Two regions of this polymerase are modified to produce particularly effective polymerases for DNA sequencing. First, *Taq* DNA polymerase has 5′-3′ exonuclease activity, which degrades sequencing primers. The first 300 amino acid residues at the N-terminus of this enzyme are required for this exonuclease activity. Portions of this **domain** can be deleted, or the activity can be eliminated by point mutation. Secondly, normally *Taq* DNA polymerase is relatively inefficient at using ddNTPs. As discovered by Tabor and Richardson, this can be improved more than 10^4-fold by changing residue Phe667 to Tyr. This modification improves ddNTP usage, and it also greatly improves the quality of the sequence data obtained. Native *Taq* DNA polymerase produces sequencing bands that vary in intensity more than 15-fold, depending on the nearby sequence. In contrast, Tyr667 polymerase produces bands that vary in intensity by less than threefold. This makes interpretating the results of the electrophoretic separation much more accurate. A number of polymerases that have this modification are now commercially available, as is T7 DNA polymerase, which naturally has a tyrosine at the corresponding position.

3. Cycle Sequencing

Cycle sequencing is the process of using repeated cycles of thermal denaturation and polymerization to produce greater amounts of product in a DNA sequencing reaction. The amount of product DNA increases linearly with the number of cycles. (This distinguishes it from PCR, which uses two primers so that the amount of product increases exponentially with the number of cycles.) During each cycle, the thermostable DNA polymerase extends the annealed primer molecules, typically at 60° to 70°C. The mixture is heated above the melting temperature of DNA (95°C), dissociating the extended primer from the template. Then, the mixture is cooled, allowing another molecule of primer (which is present in excess) to anneal to the limited supply of template. Further cycles of extension and denaturation result in producing much more extended primer than the amount of template used. This improves the sensitivity of the sequencing experiment, and it also allows ready use of double-stranded templates for sequencing. Generally, cycle sequencing works much more reliably over a wider range of template concentrations than noncycled protocols. This accounts for its nearly universal application for large-scale DNA sequencing projects.

4. Methods for Labeling DNA Sequences

The products of the chain termination reactions must be labeled for all practical DNA sequencing methods. The original label was a-^{32}P dATP that was simply added to the chain-termination reaction. Newly synthesized DNA was labeled with radioactive phosphorous, and detected by simple autoradiography. More recently, the lower energy isotopes ^{33}P and ^{35}S (in the form of a-thio-dATP) have been used because they generate autoradiograms with higher resolution. These offer the advantage of using less total radioactivity than other methods. In addition, only specifically terminated, elongated DNA chains are labeled and therefore visualized by autoradiography, which eliminates the background bands and stops normally observed on DNA sequencing autoradiograms and results in extremely clean sequence data.

Automated, **fluorescent** DNA sequencing methods were introduced in 1987 and have become essential tools for large-scale sequencing efforts. The sequence products used by these automated systems are labeled by fluorescent primers (dye primers) or fluorescent dideoxynucleotides (dye terminators). These have been used in single-color detection instruments, and in four-color multiplex instruments in which the four bases are distinguished by color. Recent innovations include fluorescent dye-labeled DNA primers that exploit fluorescent **energy transfer** to optimize the absorption and emission properties of the label. These primers carry a fluorescein derivative at the 5′-end as a common donor and rhodamine derivatives attached to a modified thymidine within the primer sequence as acceptors. Adjustment of the donor–acceptor spacing by placing the modified thymidine in the primer sequence allows generating four primers. All have strong absorption at a common excitation wavelength (488 nm) and efficient fluorescent emission at 525, 555, 580, and 605 nm. These improve the sensitivity and accuracy of the automated sequencing system.

Fluorescent dye-labeled ddNTP terminators have also been used extensively for DNA sequencing, and those that use the energy-transfer principle are also commercially available. Like the radio-labeled terminators, they have the advantage of labeling only specifically terminated, elongated DNA chains, so that background bands are eliminated.

5. Electrophoresis and Automated Sequencing

The high-resolution separation of DNA fragments by size is essential for all sequencing methods. For radioactively labeled DNA sequencing experiments, this is done by using gels cast in glass plates that are 0.2 to 0.4 mm thick, 40 to 80 cm long, and wide enough to accommodate 32 to 96 samples. Typically, the gels are 4 to 8% polyacrylamide cross-linked with *N*,*N*′-methylene bisacrylamide (see Polyacrylamide) and contain tris borate buffer (0.089 M, pH 8.3) and 7 to 8 M urea. After electrophoresis for 2 to 18 hours, the gels must be removed from the glass plates for autoradiography and reading of the sequence of 200 to 400 nucleotides. Because these gels are cumbersome to make and use, considerable effort has been made to improve separation methods. The most commonly used methods involve a sensitive fluorescent detection instrument that continuously monitors the migration of fluorescent-labeled DNA past a fixed position on the gel. The results are collected and evaluated directly by computer, producing finished sequence information. This saves considerable labor in "reading" the sequence from the gels and improves the resolution sufficiently to read 500 or more bases routinely from a single sequence experiment. Noncross-linked "gels" have also been introduced that run in 50 to 100 micron diameter, 40 to 70 cm long capillaries with fluorescent detection. The efficient heat transfer of these electrophoresis media allow faster, high-resolution separations.

Suggestions for Further Reading

C. W. Fuller and M. A. Reeve (1995) Thermo sequenase - A novel thermostable polymerase for DNA sequencing, Nature **376**, 796–797.

J. Ju et al. (1995) Design and synthesis of fluorescence energy transfer dye-labeled primers and their application for DNA sequencing and analysis, Anal. Biochem. **231**, 131–140.

L. G. Lee et al. (1992) DNA sequencing with dye-labeled terminators and T7 DNA polymerase: Effect of dyes and dNTPs on incorporation of dye-terminators, and probability analysis of termination fragments, Nucleic Acids Res. **20**, 2471–2483.

J. Messing (1983) Bacteriophage M13 vectors for DNA sequencing, Methods Enzymol. **101**, 33–38.

G. M. Prober et al. (1987) system for rapid DNA sequencing with fluorescent chain-Terminating Dideoxynucleotides, Science **238**, 336–341.

B. B. Rosenblum et al. (1997) New dye-labeled terminators for improved DNA sequencing patterns, Nucleic Acids Res **25**(22), 4500–4504.

F. Sanger, S. Nicklen, and A. R. Coulson (1977) DNA sequencing with chain terminating inhibitors, Proc. Natl. Acad. Sci. USA **74**(12), 5463–5467.

L. M. Smith et al. (1986) Fluorescence detection in automated DNA sequence analysis, Nature **321** (6071), 674–679.

S. Tabor and C. C. Richardson (1995) A single hydroxyl moiety in Pol I-T DNA polymerase is responsible for distinguishing between deoxy- and dideoxyribonucleotides, Proc. Natl. Acad. Sci. USA **92**, 6339–6343.

P. B. Vander Horn et al. (1997) Thermo sequenase DNA polymerase and *T. acidophilum* pyrophosphatase: New thermostable enzymes for DNA sequencing, BioTechniques **22**, 758–765.

Chaotropes: Kosmotropes

Compounds that increase and decrease, respectively, the aqueous solubility of proteins are classified as chaotropes and kosmotropes (1). Therefore, the Hofmeister series of ions may be divided into these two categories. For the series of anions, solubilization in water is promoted in the order

$$SCN^- > CLO_4 > I^- > Br^- > Cl^- > F^- > HPO_4^{2-} > SO_4^{2-}$$

Those on the left-hand side of Cl^- generally increase the solubility; they are called *chaotropes*.

Those on the right-hand side of Cl^- act as salting-out agents; they are called *kosmotropes*. Chaotropes are **water**-structure breakers; kosmotropes, to the contrary, are water-structure makers. A similar division may be made about the Na^+ ion in the cationic Hofmeister series. In the salts, the predominant effect is that of anions. An important characteristic is that the effects are additive for all the species in the solution.

Organic molecules also affect water structure and can be classified as chaotropes and kosmotropes. Thus, urea, glycine, formamide, and acetamide are chaotropes. Organic kosmotropes are sucrose, polyols, the methylacetamines, methyl formamides, and methyl ureas. Except for sugar and the polyols, caution must be exercized in using organic kosmotropes, since their action may reverse itself at high concentration.

The mechanism of action of these molecules in stabilizing or destabilizing protein structure, and as a corollary in acting as **salting in** or **salting out** agents, is related to their effects on the orientation of water molecules through polar interactions with the water hydrogen bond donor and acceptor properties. By perturbing or strengthening the interactions between water molecules (maximization of hydrogen bond formation), these molecules exercise their chaotropic or kosmotropic actions. At interfaces, the water structure is already perturbed by the nonavailability at the surface of other water molecules for hydrogen bond formation. This is true for the water–air interface. Similar perturbations may occur at interfaces with proteins and other biological entities—hence, the effect on their properties. Control of reactions by the chaotropic/kosmotropic effect is very widespread in biological systems. Its principal diagnosis is that the compound which affects a particular process must be present at a high concentration (local concentration for cell compartments and organelles).

Bibliography

1. K. D. Collins and M. W. Washabaugh (1985) Quart. Rev. Biophys. **18**, 323–422.

Chaperonin

The chaperonins are a family of **molecular chaperone** found in all types of cell whose function is to assist the correct folding of certain polypeptide chains that have been either newly synthesized or generated from native proteins by environmental stresses that cause partial unfolding.

1. Nomenclature

The term *chaperonin* was suggested by Sean Hemmingsen (1) to describe a family of highly sequence-related molecular chaperones found in chloroplasts, mitochondria, and **eubacteria** such as *Escherichia coli*. This term was proposed to simplify the existing complex nomenclature for different members of this family whose close relationship was only realized when cDNA for the chloroplast chaperonin was sequenced (1). The term was subsequently extended to distant homologues found in **archaebacteria** and the eukaryotic cytosol (2, 3). The two subfamilies of the chaperonin family are referred to as follows:

1. The GroE or group I subfamily, found in chloroplasts and other plastids, mitochondria, and all eubacteria
2. The TCP-1 or group II subfamily, found in archaebacteria and the eukaryotic cytosol

The GroE terminology reflects the fact that the eubacterial protein was first identified by genetic studies in four laboratories in 1972/73 as a bacterial protein required for the replication of **bacteriophage** such as lambda in *E. coli* (4). “Gro” refers to phage growth, and the suffix “E” refers to the observation that the phage growth defect is overcome when the phage carries a mutation in the head gene E. The TCP-1 terminology is derived from the identification of a protein called the *t*-complex polypeptide encoded by the mouse T locus (5). The mitochondrial members of the GroE subfamily are sometimes referred to as “hsp60” proteins, but this terminology should not be used to describe the chaperonins as a whole, since the eukaryotic TCP-1 members and the chloroplast GroE members are not **heat shock** proteins.

Table 1 presents a suggested nomenclature and useful abbreviations for members in both subfamilies, and lists other names that are used. Some authors confine the abbreviation “cpn60” to the GroE subfamily, but this restriction is inconsistent with the fact that the TCP-1 members share with the GroE members subunit molecular masses of approximately 60 kDa.

Table 1. Nomenclature of the Chaperonins

Preferred Name	Other Names	Useful Abbreviations
GroE subfamily		
Eubacterial chaperonin 60	GroEL (*E. coli*), 65-kDaantigen	Eu cpn60
Eubacterial chaperonin 10	GroES (*E. coli*), cochaperonin	Eu cpn10
Mitochondrial chaperonin 60	hsp60, mitonin, HuCha60	Mt cpn60
Mitochondrial chaperonin 10	hsp10, cochaperonin	Mt cpn10
Chloroplast chaperonin 60	Rubisco subunit binding protein	Ch cpn60
Chloroplast chaperonin 10	chaperonin 21, cochaperonin	Ch cpn10, Ch cpn21
TCP-1 subfamily		
Cytosolic chaperonin 60	*t*-Complex polypeptide 1, chaperonin-containing TCP-1, TCP-1 ring complex	Cyt cpn60, TCP-1, CCT, TRiC
Archaebacterial chaperonin 60	Thermophilic factor 55, thermosome	Ar cpn60, TF55

2. Function

The main function of the chaperonins is to assist the folding of certain newly synthesized polypeptide chains into their biologically active conformations (see Protein Folding In Vivo). They achieve this end, not by providing steric information required for each chain to fold correctly, but by sequestering each partially-folded chain in a protected compartment generated by the oligomeric structure of the chaperonin molecule. In this compartment, each chain can continue to fold to a point where aggregation with other partially folded chains is no longer a problem (6-9). This aggregation arises because some proteins fold via intermediate states that expose **hydrophobic** surfaces transiently and are thus subject to intermolecular interactions with similar states. This aggregation effect can sometimes be observed when chemically denatured proteins refold spontaneously in dilute solution *in vitro* (see Protein Folding In Vitro), but its magnitude is expected to be enhanced in the intact cell because of the phenomenon of macromolecular crowding, or excluded volume, thus increasing the effective concentrations of these states by two or three orders of magnitude (8, 9). It should be stressed that, although the chaperonins increase the yield of correctly folded proteins by minimizing aggregation, they do not increase the rate of folding above that achieved by the fastest folding fraction of spontaneously refolding chains that manage to avoid aggregation.

The best evidence for this view of chaperonin function comes from genetic and **pulse-chase** labeling studies with living cells. Several proteins imported into the mitochondria of yeast cells form aggregates when the function of the mitochondrial chaperonin is impaired by mutation (10), whereas about 30% of newly synthesized soluble cytoplasmic proteins in *E. coli* cells become either insoluble or inactive when cpn60 function is switched off by means of a temperature-sensitive mutation (11). *In vitro* studies of the ameliorating effect of added GroE proteins on the aggregation of various pure denatured proteins during their refolding after removal of denaturant are consistent with this antiaggregation role (12-14). *In vitro* studies also suggest that a side effect of this antiaggregation role is the partial unfolding of nonaggregated chains that have become kinetically trapped in misfolded conformations, thus allowing these chains another chance to fold correctly (15); it is not clear how important such an effect may be *in vivo*. In addition, the GroE chaperonins in eubacteria and mitochondria (16) and the TCP-1 chaperonins in the archaebacteria (17) are stress proteins that prevent and reverse the denaturation of some fully folded proteins by stresses such as high temperature.

It must be emphasized that the actual spectrum of proteins that use chaperonin function to fold correctly in intact cells is not known, but preliminary calculations and observations suggest that it is probably a minority in the case of both the GroE chaperonins (9, 18) and the TCP-1 chaperonins (7). Genetic evidence derived from the study of yeast mutants suggests that a major function of the eukaryotic TCP-1 is to assist the folding of tubulin and actin (19), consistent with the observation that newly synthesized chains of actin and tubulin can be isolated from pulse-labeled cells of **CHO** cells in the form of complexes with TCP-1 chaperonin oligomers (20). *In vitro* protein refolding experiments also suggest that the substrate specificities of the GroE chaperonins and the TCP-1 chaperonins are different (6).

3. Structure

The chaperonins occur as large oligomeric structures consisting of two stacked rings of subunits, each about 55–60 kDa in size, surrounding a central cavity or cage in which the protein substrate binds; each subunit catalyzes the slow hydrolysis of ATP to ADP. The GroE chaperonins have seven subunits per ring, whereas the TCP-1 chaperonins have eight or nine. The subunit sequence identity between members of the GroE subfamily is in the range 42–76%, whereas that between members of the TCP-1 subfamily is around 30–40%, but the identity between the subfamilies is much less (15–20%) and is confined to regions corresponding to the ATPase domain in GroE cpn60. The evolutionary implications of these similarities are under debate (7, 21).

A convenient abbreviation for the chaperonin(s) is cpn(s). Thus the subunits of the ring can be called *cpn60 subunits*, and the oligomer can be called *cpn60*. The GroE subfamily also contains another type of oligomeric ring made of seven smaller 10-kDa subunits, called *cpn10*, because there is a slight similarity between the cpn10 subunit sequence and part of the cpn60 subunit sequence (21). GroE cpn60 and cpn10 oligomers bind to each other in 1:1 and 1:2 ratios in the presence of either ATP or ADP, and these binary complexes play an essential role in the protein folding function of these molecules (8, 9). The chloroplast cpn10 oligomer is unusual in that each subunit consists of two copies of a cpn10 sequence fused head to tail and thus is often referred to as *cpn21* (22).

The TCP-1 oligomers found in the eukaryotic cytosol are much more variable than those found in either the archaebacteria or the GroE subfamily, since subunits of the latter consist of only one or two sequences, whereas the former have at least eight different, but related, subunit sequences in each ring (6, 7, 23). For this reason, the eukaryotic TCP-1 oligomers are also called *CCT complexes*, for chaperonin-containing TCP-1 complexes, or *TriC* for TCP-1 ring complexes (see Table 1). The TCP-1 chaperonins do not appear to contain cpn10-like members.

The best-studied chaperonins are the cpn60 and cpn10 oligomers from *E. coli*, termed GroEL and GroES, respectively. GroEL has been extensively studied by both negative stain and cryoelectron microscopy (24, 25) and by X-ray crystallography of a double mutant form (26). GroEL is a cylindrical structure containing a central cavity about 50 Å in diameter (Fig. 1a). Each subunit consists of (*1*) an apical domain to which the protein substrate and GroES bind; (*2*) an equatorial domain that protrudes into the central cavity, which contains the ATPase site and is responsible for most of the intersubunit interactions; and (*3*) an intermediate domain that contains potential hinge sites responsible for the considerable movements of the other two domains revealed by electron microscopy (24, 25). These conformational changes result from the binding of nucleotide and GroES to the GroEL (26) cylinder. The crystal structure of GroES shows a dome-shaped structure with a hydrophilic inner surface that fits over one end of the GroEL cylinder (24, 27, 28) (see also Fig. 1b,c), creating a large enclosed dome-shaped space about 65 × 80 Å in size, inside which the protein substrate continues to fold (29-32) (see also Fig. 1c,d).

Figure 1. Structure and function of the chaperonin system. (**a**,**b**) Space-filling representations showing a top and side view, respectively, of the crystal structure of a double mutant form of GroEL (26). Two adjacent subunits are colored with the apical domains in red and purple, the intermediate domains in orange and yellow, and the equatorial domains in blue and green, respectively. Free passage between the GroEL rings is obstructed by *N*- and *C*-terminal residues not resolved in the crystal structure. (**b**) side view of GroES (28) at the top; two adjacent domains and a single mobile loop that is structured in the GroES crystal due to crystal packing are colored. The loop regions normally protrude from the base of GroES downward toward the GroEL. (**c**) Asymmetrical GroEL/GroES complexes as revealed by cryoelectron microscopy (45). Note the upward and outward movement of the apical GroEL domains interacting with GroES. (**d**) Model of the GroEL/GroES reaction cycle in assisting protein folding (30); see text for details. The term *unfolded protein* refers to a partially folded intermediate that is represented by the light pink spheres; folded protein is represented by the dark pink sphere, while the hatched spheres represent a mixture of folded and partially- folded proteins expected in a population of GroEL molecules. At step 4, GroES may associate with either the protein-containing ring of GroEL or with the opposite empty ring; the latter possibility is not shown. Reprinted from *Nature* 381, 571–580 (1996), with permission; copyright (1996) Macmillan Magazines Ltd. See color insert.

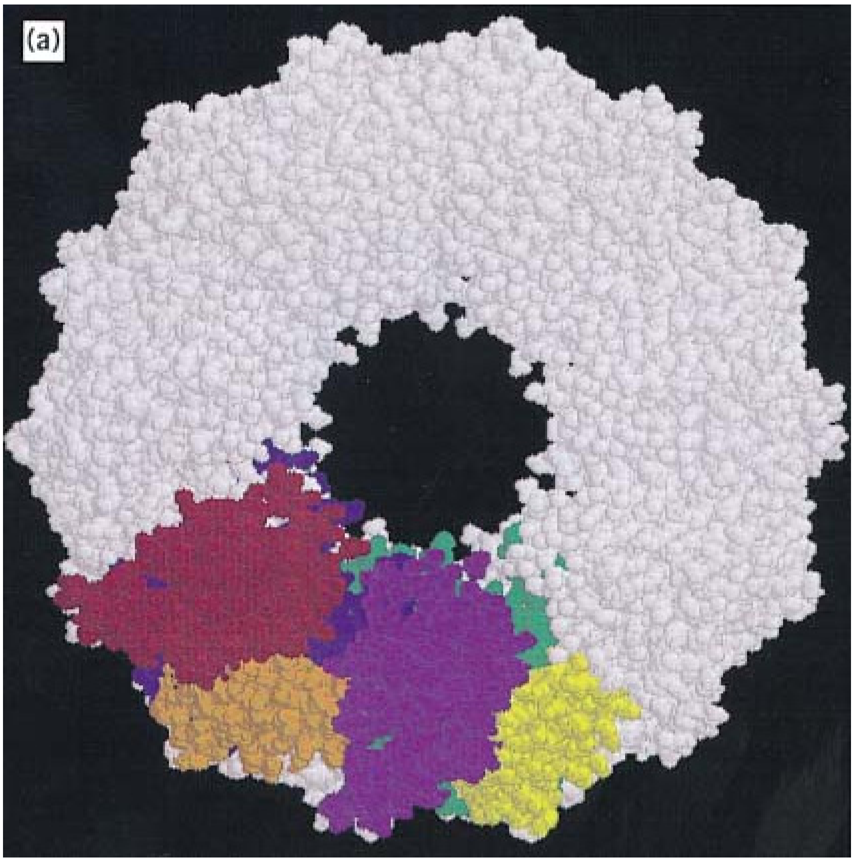

Figure 1. (*continued*) Structure and function of the chaperonin system. (**a**,**b**) Space-filling representations showing a top and side view, respectively, of the crystal structure of a double mutant form of GroEL (26). Two adjacent subunits are colored with the apical domains in red and purple, the intermediate domains in orange and yellow, and the equatorial domains in blue and green, respectively. Free passage between the GroEL rings is obstructed by *N*- and *C*-terminal residues not resolved in the crystal structure. (**b**) side view of GroES (28) at the top; two adjacent domains and a single mobile loop that is structured in the GroES crystal due to crystal packing are colored. The loop regions normally protrude from the base of GroES downward toward the GroEL. (**c**) Asymmetrical GroEL/GroES complexes as revealed by cryoelectron microscopy (45). Note the upward and outward movement of the apical GroEL domains interacting with GroES. (**d**) Model of the GroEL/GroES reaction cycle in assisting protein folding (30); see text for details. The term *unfolded protein* refers to a partially folded intermediate that is represented by the light pink spheres; folded protein is represented by the dark pink sphere, while the hatched spheres represent a mixture of folded and partially- folded proteins expected in a population of GroEL molecules. At step 4, GroES may associate with either the protein-containing ring of GroEL or with the opposite empty ring; the latter possibility is not shown. Reprinted from *Nature* 381, 571–580 (1996), with permission; copyright (1996) Macmillan Magazines Ltd. See color insert.

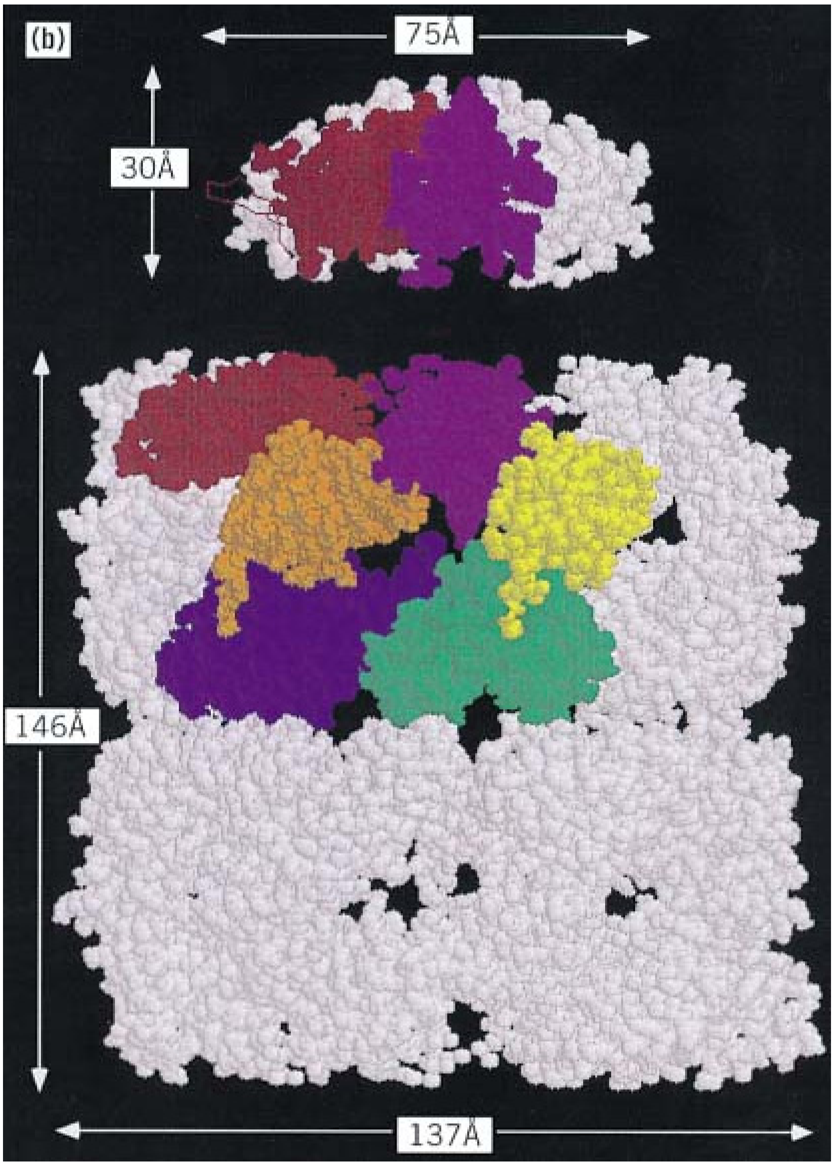

Figure 1. (*continued*) Structure and function of the chaperonin system. (**a**,**b**) Space-filling representations showing a top and side view, respectively, of the crystal structure of a double mutant form of GroEL (26). Two adjacent subunits are colored with the apical domains in red and purple, the intermediate domains in orange and yellow, and the equatorial domains in blue and green, respectively. Free passage between the GroEL rings is obstructed by *N*- and *C*-terminal residues not resolved in the crystal structure. (**b**) side view of GroES (28) at the top; two adjacent domains and a single mobile loop that is structured in the GroES crystal due to crystal packing are colored. The loop regions normally protrude from the base of GroES downward toward the GroEL. (**c**) Asymmetrical GroEL/GroES complexes as revealed by cryoelectron microscopy (45). Note the upward and outward movement of the apical GroEL domains interacting with GroES. (**d**) Model of the GroEL/GroES reaction cycle in assisting protein folding (30); see text for details. The term *unfolded protein* refers to a partially folded intermediate that is represented by the light pink spheres; folded protein is represented by the dark pink sphere, while the hatched spheres represent a mixture of folded and partially- folded proteins expected in a population of GroEL molecules. At step 4, GroES may associate with either the protein-containing ring of GroEL or with the opposite empty ring; the latter possibility is not shown. Reprinted from *Nature* 381, 571–580 (1996), with permission; copyright (1996) Macmillan Magazines Ltd. See color insert.

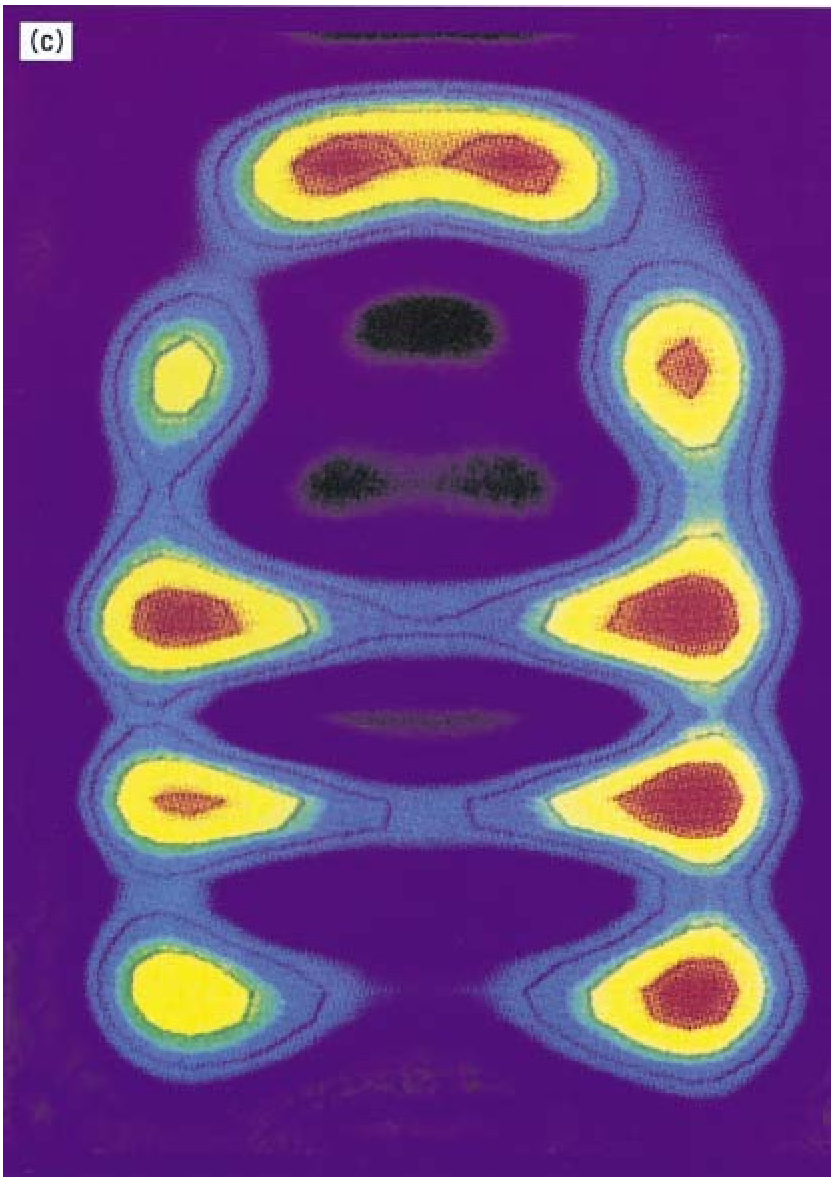

Figure 1. (*continued*) Structure and function of the chaperonin system. (**a**,**b**) Space-filling representations showing a top and side view, respectively, of the crystal structure of a double mutant form of GroEL (26). Two adjacent subunits are colored with the apical domains in red and purple, the intermediate domains in orange and yellow, and the equatorial domains in blue and green, respectively. Free passage between the GroEL rings is obstructed by *N*- and *C*-terminal residues not resolved in the crystal structure. (**b**) side view of GroES (28) at the top; two adjacent domains and a single mobile loop that is structured in the GroES crystal due to crystal packing are colored. The loop regions normally protrude from the base of GroES downward toward the GroEL. (**c**) Asymmetrical GroEL/GroES complexes as revealed by cryoelectron microscopy (45). Note the upward and outward movement of the apical GroEL domains interacting with GroES. (**d**) Model of the GroEL/GroES reaction cycle in assisting protein folding (30); see text for details. The term *unfolded protein* refers to a partially folded intermediate that is represented by the light pink spheres; folded protein is represented by the dark pink sphere, while the hatched spheres represent a mixture of folded and partially- folded proteins expected in a population of GroEL molecules. At step 4, GroES may associate with either the protein-containing ring of GroEL or with the opposite empty ring; the latter possibility is not shown. Reprinted from *Nature* 381, 571–580 (1996), with permission; copyright (1996) Macmillan Magazines Ltd. See color insert.

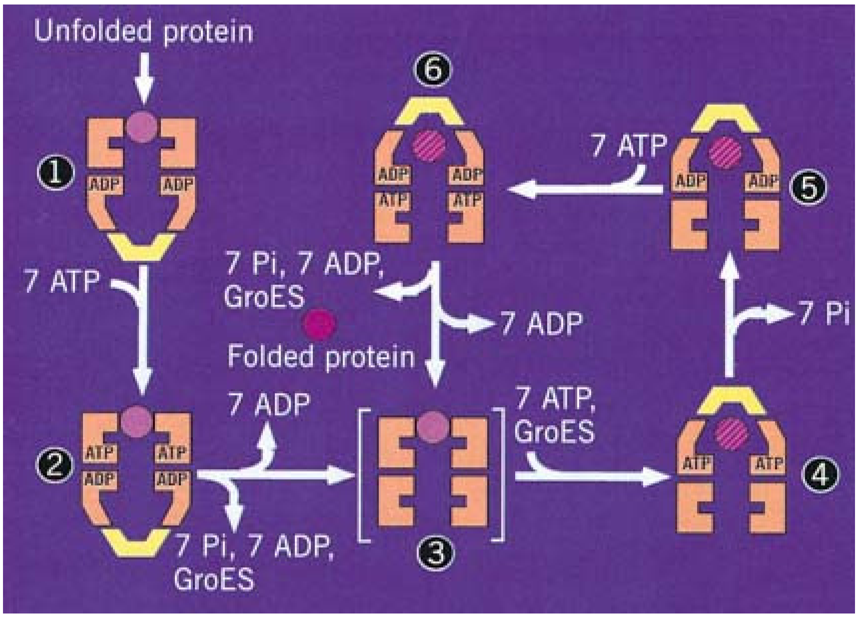

No crystal structure for any TCP-1 chaperonin is yet available, but electron-microscopic studies suggest that the general architecture and overall domain structure of the TCP-1 cylinder resembles that of GroEL (33, 34). The archaebacterial chaperonin was originally termed thermophilic factor 55, because it is virtually the only protein made by thermophilic archaebacteria under heat-shock conditions (35), but it is now termed the *thermosome* (36). Thermosomes generally contain eight subunits per ring, but there are several reports that a significant subset of particles contain nine subunits per ring, while the chaperonins of some *Sulfolobus* species appear all to contain nine subunits per ring (37). The thermosomes of *Pyrodictium*, *Thermoplasma*, and *Sulfolobus* consist of two different but related subunits of almost identical molecular mass (33). Electron-microscopic image analysis suggests that the two types of subunit in the thermosome of *Thermoplasma acidophilum* alternate within each ring, generating a four-fold symmetry (38).

Averaged electron-microscopic images of the mammalian TCP-1 particle reveal a ringlike structure with eightfold quasi-rotational symmetry with a central channel (33). Primary structures of eight distinct types of related subunit have been determined by cloning and sequencing of mouse cDNA; these types share about 30% amino acid residue identity. A striking observation is that the sequence of each type is more highly conserved among different eukaryotic species than are the sequences between types in any one species; in mammals the sequence identity is over 96% for each type of subunit, and around 60% between yeast and mouse. These observations have prompted the conclusion that each type of subunit diverged early in evolution, has changed only slowly during the evolution of eukaryotes, and thus may have a specific function in binding subsets of sequences in substrate proteins and/or other molecular chaperones (6, 7). Consistent with this suggestion is the observation that the different types of subunit in each TCP-1 chaperonin ring deviate most from one another in the sequences of the apical domains, where the protein substrate binds.

4. Mechanism of Action

The molecular details of how the chaperonins function have, and continue to be, studied by means of *in vitro* protein refolding experiments using defined components, but such experiments suffer from the disadvantage that the conditions under which they are performed are different in important respects from those operating during protein folding in the intact cell (9, 18). Thus it is not surprising that this field is subject to intense debate between people supporting different views (39). Since the chaperonins evolved to fold proteins inside cells,and not inside test tubes, it is essential when evaluating the validity of these views to define those aspects of chaperonin action observed *in vitro* that are mechanistically essential to improve the yield of correctly folded protein, when extrapolated as far as possible to *in vivo* conditions. In our opinion, the model outlined in Figure 1d best meets this criterion for the GroE chaperonins (30, 40).

In this model, newly synthesized polypeptide chains are released from ribosomes in the form of partially folded intermediates that may contain bound molecular chaperones of the hsp70/DnaJ families (see Protein Folding In Vivo). The latter chaperones prevent aggregation and premature folding before each chain is complete. Such intermediates are commonly referred to as *unfolded proteins*, but in fact they often are molten globules. These partially folded, compact intermediates lose the hsp70/DnaJ chaperones by an uncharacterized mechanism that results in each intermediate molecule binding by hydrophobic interactions to the apical domains at one end of a GroEL cylinder; the other end of the cylinder is occupied by GroES as a result of ADP binding to the GroEL ring proximal to the GroES (see Fig. 1d, step 1). The binding of polypeptide and the hydrolysis of ATP by the ring not occupied by GroES causes the GroES and the ADP to dissociate (step 2). GroES and ATP then rebind with equal probability to either ring (not both rings), resulting in 50% of the bound polypeptide being encapsulated inside the cavity capped by GroES (step 4). This rebinding of GroES results in the displacement of the bound polypeptide into the cavity, where it can continue to fold; it is for this reason that this model has been dubbed the ”Anfinsen cage” model to stress the idea that the protein in the cavity folds in a similar, but not necessarily identical, manner to that by which it folds in a protein renaturation experiment of the type pioneered by Anfinsen (41, 42). Thus one essential difference between chaperonin-assisted protein folding *in vivo* and spontaneous protein refolding *in vitro* is that the former process segregates each chain into the protected compartment provided by the GroEL/GroES cylinder to avoid the problem of aggregation.

The time available for this protected folding is set by the time it takes each ring of GroEL to hydrolyze seven ATP molecules. This hydrolysis is positively cooperative in each ring, and two rounds take about 10 s at 37°C (steps 4 and 5). The GroES then dissociates, and the protein is free either to diffuse into the cytosol or to rebind to the apical domains of the same GroEL cylinder (step 6). Rebinding occurs only if sufficient hydrophobic residues are still exposed on the surface of the compact intermediate. The cycle of release into the cage then repeats until the protein is folded sufficiently to the point where aggregation with other partially folded proteins is no longer a problem for the cell. The number of reaction cycles will vary, depending on the rate at which a given protein can fold when released into the cavity. Even with a single type of protein substrate, the population of folding chains will not be in synchrony or occupy the same number of cycles, since some chains fold more rapidly than others of the same sequence (see Protein Folding In Vitro). Usually only a fraction of the polypeptide chains fold to completion in a single cycle of GroES binding and unbinding, depending on the intrinsic rate of folding of a particular polypeptide and its tendency to become trapped in misfolded states. Rebinding of these intermediates to the apical domains of GoEL results in partial unfolding in preparation for a subsequent folding trial (30). This unfolding function distinguishes the GroEL/ES machinery from a simple folding cage,which acts solely to prevent intermolecular aggregation.

Uncertainties about this model include the fate of the 50% of polypeptide bound to the GroEL ring not capped by GroES; such polypeptides would be prone to aggregation and degradation if released into the cytosol. Release of such polypeptides *in vitro* is reduced in the presence of high concentrations of synthetic polymers that mimic the macromolecular crowding, excluded volume effect present in the cytosol (40). However, some release of partially folded chains may be essential *in vivo* because of the danger that proteins that are unable to fold correctly as a result of mutation will clog up the GroEL apical domains; an escape route for such molecules may be provided by release from the ring not capped by GroES.

Another problem concerns the significance of GroEL molecules with GroES bound to each end of the cylinder that have been observed *in vitro* (43). The ratio of total GroES subunits to total GroEL subunits in extracts of *E. coli* cells is equimolar, consistent with such GroES/GroEL/GroES complexes occurring *in vivo*, where their formation may be favored by the effect of macromolecular crowding on protein association. Nevertheless, such complexes are not mechanistically essential, at least as deduced from *in vitro* refolding experiments, nor can they be permanent if the compact intermediates are to enter the GroEL cavities.

Another limitation imposed by this model is the size range that can be accommodated inside the cage, which is likely to have an upper limit around 60 kDa. Larger proteins than this, up to about 150 kDa, exist inside bacterial cells and even larger ones in the cytosol of eukaryotic cells. A GroES equivalent to cap the TCP-1 chaperonin oligomer has not been identified, so it is possible that the latter assists protein folding in a manner somewhat different from that for the GroE chaperonins. There is evidence that, unlike GroEL,the mammalian TCP-1 chaperonin binds to chains of actin being synthesized by extracts of reticulocytes before the chains have been released from the ribosomes (44).

There are four known intracellular compartments in which proteins fold that do not appear to contain any type of chaperonin: the endoplasmic reticulum lumen, the intermembrane **mitochondrial** space, the intrathylakoidal lumen, and the **periplasmic** space of **Gram-negative** bacteria. Additionally, the eukaryotic cytosol seems to lack a general chaperonin, since the TCP-1 chaperonin appears to be restricted to a small subset of protein substrates, including actin and tubulin. Thus it is certainly not the case that the folding of all proteins in all cells involves the chaperonins. Given that the intracellular environment strongly favors aggregation, it is likely that the chaperonin-independent proteins utilize the assistance of other types of molecular chaperone for their folding. This assistance may also apply to proteins larger than 60 kDa that cannot fit into the chaperonin cage. For these proteins, the cotranslational and sequential folding of protein **domains** may circumvent the requirement for a sequestered folding compartment.

It is also possible that some chaperonins have roles additional to those discussed above with respect to protein folding, since there are sporadic reports of chaperonin-like molecules occurring on the cell surface in both prokaryotic and eukaryotic cells and in the blood serum, as well as stimulating **cytokine** production by animal cell cultures. The bacterial chaperonins are also the major immunogens in all human bacterial infections, and their possible roles in protective immunity and autoimmune disease is an active area of research (45).

5. Note Added in Proof

The cage mechanism for chaperonin-assisted protein folding is strongly supported by recent structural and functional data. The crystal structure of the asymmetrical GroEL:GroES complex with bound ADP shows that the cage is sufficient to accept proteins up to at least 70 kDa and that the wall of the cage provides a hydrophilic environment permissive for folding (Z. Xu et al. *Nature* **388**, 741–750, 1997). Crystal structures of the archaean thermosome suggest that in this chaperonin the folding cage is closed by loop sequences that emanate from the apical domains of the chaperonin subunits, explaining the lack of a separate GroES-like factor (M. Klumpff et al. *Cell* **91**, 263–270, 1997; L. Ditzel et al. *Cell* **93**, 125–138, 1998). A single ring mitochondrial chaperonin is fully functional in protein folding in a GroES-dependent manner *in vivo* (K. L. Nielsen et al. *Mol. Cell* **2**, 93–99, 1998). The size range of GroEL substrate proteins and their kinetics of interaction *in vivo* are consistent with the cage mechanism (K. L. Ewalt et al. *Cell* **90**, 491–500, 1997). Oligomeric GroEL with an intact central cavity is essential for the maintenence of growth of *E. coli* (F. Weber et al. *Nature Struct. Biol.* **11**, 977–985, 1998).

Bibliography

1. S. M. Hemmingsen, C. Woolford, S. M. van der Vies, K. Tilly, D. T. Dennis, G. C. Georgopoulos, R. W. Hendrix, and R. J. Ellis (1988) Nature **333**, 330–334.
2. R. S. Gupta (1990) Biochem. Int. **20**, 833–841.
3. R. J. Ellis (1990) Science **250**, 954–959.
4. C. Georgopoulos, D. Ang, K. Liberek, and M. Zylicz (1990) in R. I. Morimoto, A. Tissieres,

and C. Georgopoulos, eds., *Stress Proteins in Biology and Medicine*, Cold Spring Harbor Laboratory Press, New York, pp. 191–221.

5. L. Silver, K. Artzt, and D. Bennett (1979) Cell **17**, 275–284.
6. H. Kubota, G. Hynes, and K. Willison (1995) Eur. J. Biochem. **230**, 3–16.
7. K. R. Willison and A. L. Horwich (1996) in R. J. Ellis, ed., *The Chaperonins*, Academic Press, San Diego, pp. 108–136.
8. F. U. Hartl (1996) Nature **381**, 571–580.
9. R. J. Ellis and F. U. Hartl (1996) FASEB J. **10**, 20–26.
10. E. M. Hallberg, Y. Shu, and R. L. Hallberg (1993) Mol. Cell Biol. **13**, 3050–3057.
11. A. L. Horwich, K. B. Low, F. A. Fenton, I. N. Hirshfield, and K. Furtak (1993) Cell **74**, 909–917.
12. P. Goloubinoff, J. P. Christeller, A. A. Gatenby, and G. H. Lorimer (1989) Nature **342**, 884–889.
13. J. Buchner, M. Schmidt, M. Fuchs, R. Jaenicke, R. Rudolph, F. X. Schmid, and T. Kiefhaber (1991) Biochemistry **30**, 1586–1591.
14. J. Martin, T. Langer, R. Boteva, A. Schramel, A. L. Horwich, and F.-U. Hartl (1991) Nature **352**, 36–42.
15. G. S. Jackson, R. A. Staniforth, D. J. Halsall, T. Atkinson, J. J. Holbrook, A. R. Clarke, and S. G. Burston (1993) Biochemistry **32**, 2554–2563.
16. J. Martin, A. L. Horwich, and F. U. Hartl (1992) Science **258**, 995–998.
17. A. Guagliardi, L. Cerchia, S. Bartolucci, and M. Rossi (1994) Protein Sci. **3**, 1436–1443.
18. R. J. Ellis (1996) in R. J. Ellis, ed., *The Chaperonins*, Academic Press, San Diego, pp. 1–25.
19. D. Ursic, J. C. Sedbrook, K. L. Himmel, and M. R. Culbertson (1994) Mol. Biol. Cell **5**, 1065–1080.
20. H. Sternlicht, G. W. Farr, M. L. Sternlicht, J. K. Driscoll, K. R. Willison, and M. B. Yaffe (1993) Proc. Natl. Acad. Sci USA **90**, 9422–9426.
21. R. S. Gupta (1996) in R. J. Ellis, ed., *The Chaperonins*, Academic Press, San Diego, pp. 27–64.
22. U. Bertsch, J. Soll, R. Seetharam, and P. V. Viitanen (1992) Proc. Natl. Acad. Sci. USA **89**, 8696–8700.
23. K. F. Liou and K. R. Willison (1997) EMBO J. **16**, 101–106.
24. A. M. Roseman, S. Chen, H. White, K. Braig, and H. R. Saibil (1996) Cell **87**, 241–251.
25. O. Llorca, S. Marco, J. L. Carrascosa, and J. M. Valpuesta (1997) J. Struct. Biol. **118**, 31–42.
26. K. Braig, Z. Otwinowski, R. Hegde, D. C. Boisvert, A. Joachimiak, A. L. Horwich, and P. B. Sigler (1994) Nature **371**, 578–586.
27. S. C. Mande, V. Mehra, B. Bloom, and W. G. J. Hol (1996) Science **271**, 203–207.
28. J. F. Hunt, A. J. Weaver, S. J. Landry, L. Gierasch, and J. Diesenhofer (1996) Nature **379**, 37–42.
29. J. Martin, M. Mayhew, T. Langer, and F. U. Hartl (1993) Nature **366**, 228–233.
30. M. Mayhew, A. C. R. da Silva, J. Martin, H. Erdjument-Bromage, P. Tempst, and F. U. Hartl (1996) Nature **379**, 420–426.
31. J. S. Weissman, H. S. Rye, W. A. Fenton, J. M. Beecham, and A. L. Horwich (1996) Cell **84**, 481–490.
32. S. Chen, A. M. Roseman, A. S. Hunter, S. P. Wood, S. G. Burston, N. A. Ranson, A. R. Clarke, and H. R. Saibil (1994) Nature **371**, 261–264.
33. T. Waldmann, E. Nimmesgern, M. Nitsch, J. Peters, G. Pfeifer, S. Muller, J. Kellermann, A. Engel, F. U. Hartl, and W. Baumeister (1995) Eur. J. Biochem. **227**, 848–856.
34. V. A. Lewis, G. M. Hynes, D. Zheng, H. Saibil, and K. Willison (1992) Nature **358**, 249–252.

35. B. M. Phipps, A. Hoffmann, K. O. Stetter, and W. Baumeister (1991) EMBO J. **10**, 1711–1722.
36. B. M. Phipps, D. Typke, R. Hegerl, S. Volker, A. Hoffmann, K. O. Stetter, and W. Baumeister (1993) Nature **361**, 475–477.
37. S. Marco, D. Urena, J. L. Carrascosa, T. Waldmann, J. Peters, R. Hegerl, G. Pfeifer, H. Sack-Kongehl, and W. Baumeister (1994) FEBS Lett. **341**, 152–155.
38. M. Nitsch, M. Klumpp, A. Lupas, and W. Baumeister (1997) J. Mol. Biol. **267**, 142–149.
39. A. C. Clarke and P. A. Lund (1996) R. J. Ellis, ed., in *The Chaperonins* Academic Press, San Diego, pp. 168–212.
40. J. Martin and F. U. Hartl (1997) Proc. Natl. Acad. Sci. USA **94**, 1107–1112.
41. R. J. Ellis (1994) Curr. Biol. **4**, 633–635.
42. R. J. Ellis (1996) Fold. Des. **1**, R9–R15.
43. Z. Torok, L. Vigh, and P. Goloubinoff (1996) J. Biol. Chem. **271**, 16180–16186.
44. J. Frydman and F. U. Hartl (1996) Science **272**, 1497–1502.
45. A. R. M. Coates (1996) in R. J. Ellis, ed., *The Chaperonins* Academic Press, San Diego, pp. 268–296.

Suggestions for Further Reading

46. R. J. Ellis, ed. (1996) *The Chaperonins*, Academic Press, San Diego (this is the first book devoted to the chaperonins and contains 10 chapters by different authors covering, as well as the main topics discussed above, other aspects such as gene regulation, gene accession numbers, primary structures, and immunological and medical implications).
47. M.-J. Gething, ed. (1997), *Molecular Chaperones and Protein Folding Catalysts*, Oxford University Press, Oxford (this book contains detailed information about the chaperonins, as well as other molecular chaperones).

Chemical Modification

Chemical modification is one of the most useful methods of identifying the functional groups of a protein. Chemical modification is also used for labeling proteins with reporter groups to monitor their conformations for **radiolabeling** and to increase their stability. If proteins are modified chemically under mild conditions, the modifications occur to the native conformation, and the modified proteins usually retain their native conformations. However, conformational changes in the modified proteins sometimes occur, and one must be careful about checking the conformation of the modified proteins, especially when they lose their functions. One must also be careful about the side reactions that often accompany otherwise specific chemical modifications.

It is possible to modify chemically the residues of aspartic acid, glutamic acid, histidine, lysine, arginine, methionine, tryptophan, tyrosine, and cysteine, and less easily serine, threonine, asparagine, and glutamine, but it is not possible to modify specifically glycine, alanine, valine, leucine, isoleucine, phenylalanine, and proline residues.

Residues that participate in the function are usually **accessible** to the **solvent** and consequently susceptible to reaction with a chemical reagent. The residues that show different reactivity in the presence and absence of a **ligand** are important for the function. A good method for discriminating the functional residues after modification involves analyzing the responsible residues within the proteins retained by an appropriate affinity column [see Affinity Chromatography]. Affinity labeling is a sophisticated way of modifying active site residues selectively. Modification with a **suicide substrate** is a very good method for modifying catalytic residues specifically.

The stability of a protein can be altered by chemical modification (see Protein Stability). Proteins are stabilized by introducing additional stabilizing forces such as **hydrophobic** forces, electrostatic interactions, and hydrogen bonds. Intra- or intermolecular **cross-links** are also effective for stabilizing proteins, as is attaching polymers to their surfaces.

Amino groups are reactive nucleophiles that can be modified by many chemical reactions, including acylation, amidination, and guanidination. Carboxyl groups can be modified after activation with **carbodiimides** or by esterification. Tyrosine residues are modified by nitration with tetranitromethane, **iodination**, or **acetylation** with acetylimidazole. The thiol group is the strongest nucleophile among all of the functional groups of amino acids, so there are many reagents that react specifically with it. Among these reactions are metal binding with *p*-mercurylbenzoate (PCMB); mixed-disulfide formation with disulfide reagents, such as 5,5′-dithiobis(2-nitrobenzoic acid) (DTNB, or Ellman's reagent) or dithiodipyridine; alkylation with **iodoacetate**, methyl iodide, ethyleneimine or ***N*-ethylmaleimide**, cyanylation with 2-nitro-5-thiocyanobenzoic acid (NTCB), and oxidation with many oxidants. Reduction of the disulfide bonds of proteins and alkylation of the resulting thiol groups is an important step in protein chemistry. The imidazole group of histidine residues can be modified with diethylpyrocarbonate, or they can be photooxidized in the presence of photosensitizing dyes. The sulfur of methionine residues can be oxidized to the sulfoxide by air or by oxidants, or alkylated with agents like methyl iodide under acidic conditions. The latter reaction can be reversed by thiols, so an isotopic label can be introduced in 50% of the terminal methyl group of methionine residues using labeled methyl iodide. The guanido group of arginine residues forms heterocyclic condensation products with 1,2- and 1,3-dicarbonyl compounds, such as phenylglyoxal, 2,3-butanedione, and 1,2-cyclohexanedione. The indole ring of the tryptophan residue can be modified with various oxidants, such as *N*-bromosuccinimide, iodine, or ozone, or by electrophilic reagents, such as 2-hydroxy-5-nitrobenzylbromide or 2-nitrophenylsulfenylchloride.

Suggestions for Further Reading

C.H.W. Hirs (ed.) (1967) Modification reactions. Specific modification reactions, Methods Enzymol. **11**, 481–711.

C.H.W. Hirs (ed.) (1972) Modification reactions. Specific modification reactions, Methods Enzymol. **25**, 387–671.

C.H.W. Hirs and S.N. Timasheff (eds.) (1977) Chemical modification, Methods Enzymol. **47**, 407–498.

C.H.W. Hirs and S.N. Timasheff (ed.) (1983) Chemical modification. Active-site labeling, Methods Enzymol. **91**, 549–642.

T. Imoto and H. Yamada (1989) "Chemical modification". In *Protein Structure: A Practical Approach* (T. E. Creighton, ed.), IRL Press, Oxford, U.K., pp. 247–277.

Chemical Shift

A nuclear magnetic resonance (NMR) spectrum of the protons (hydrogen atoms), ^{13}C, or other nuclei of a molecule typically features groups of signals displayed over a range of frequencies. The frequencies can ultimately be related to the Larmor (resonance) frequencies of the nuclei under study. The frequencies of absorbed or emitted energy represented in, for example, the proton NMR spectrum are different for protons in structurally or chemically distinct environments. Chemical shift refers to the sensitivity of the Larmor frequency to the covalent structure of which the observed nucleus is part, sensitivity to the intra- and intermolecular interactions present, and sensitivity to other sample variables, such as temperature, concentration, and pressure. The chemical shift is an important aspect of the NMR experiment because it ultimately provides a unique "signature" for each spin of a molecule of interest.

Atomic nuclei such as ^1H, ^{13}C, and ^{15}N, which have the property referred to as spin, take up certain quantum-mechanically allowed orientations when they are in a magnetic field. In the magnetic field, these nuclei undergo a precessional motion around the direction of the magnetic field. The frequency of this motion (n) is characteristic of the type of nucleus and its local chemical environment and can be expressed as

$$\nu = \gamma B_o(1 - \sigma)/2\pi$$

where g is the gyromagnetic ratio of the nucleus, B_o is the magnitude of the laboratory magnetic field, and s is the chemical shielding parameter, or screening constant. (The precessional frequency is also dependent on possible scalar and dipolar coupling interactions between nuclei; in terms of energy these are smaller influences on the precessional frequency and are neglected for the present discussion [see scalar coupling].) Chemical and structural information is implicit in the value of the shielding parameter; it is the purpose of NMR experiments to measure nuclear precessional frequencies and thus define the values of s for nuclear spins of a sample. The shielding parameter is dimensionless and typically is in the range $1 - 1000 \times 10^{-6}$. Values for s are conveniently discussed in terms of parts per million (ppm).

The chemical shift, as represented by the shielding parameter (s), for a given spin in a molecule depends principally on the chemical bonds that hold the spin to the molecule. The carbon atom of a methyl group has a shielding parameter that is about 180 ppm different from the shielding parameter of the carbon atom of a carbonyl group, primarily because the local electronic structures about the two carbons are so different (see NMR (Nuclear Magnetic Resonance)). Because local electronic structures for a given chemical group tend to be similar from molecule to molecule, the shielding parameters for the molecules' nuclei tend to fall into narrow, identifiable bands. Thus constructing correlation tables that reliably indicate the approximate expected values of the shielding parameters of each nucleus in a molecule is possible. Organic chemistry textbooks generally contain such tables.

Shielding parameters also subtly reflect the entire electronic structure of a molecule and the electronic structures of solvent molecules or other solutes that are present in a sample. The tertiary structures of biopolymers result in characteristic effects on the shielding parameters of their component nuclei (1, 2).

When considered in detail, it becomes apparent that the value of the shielding parameter is dependent on the orientation of the molecule in a magnetic field. That is, s is anisotropic and must be represented by a tensor. In gases and most liquid samples, rotational and translational motions of the molecules are rapid, and molecules change their positions and orientations rapidly in the magnetic field. Consequently, in these samples the value of the shielding parameter detected experimentally is the average of all possible orientations of the molecule. If the motions of the molecules in a sample are restricted, as would be the case in solids or in liquid crystalline solutions that are partially ordered, a range of s values will be detected for a given nucleus.

By convention, NMR spectra are displayed so that shielding parameters (or their equivalents) increase from left to right along a chemical shift axis. That is, the NMR absorption or emission signals for nuclei with the largest shielding parameter appear to the right in the spectrum, whereas nuclei with smaller shielding parameters appear progressively to the left. Also, by convention the algebraic signs of the numbers along the shielding parameter axis are the negatives of the actual number. Finally, measuring absolute values of shielding parameters with confidence is impractical. The NMR signal from a convenient material is thus chosen as a standard or reference signal, and shielding parameters are measured relative to this signal. Therefore, a signal appearing in a proton NMR spectrum at the position labeled 7 ppm has a shielding parameter that is 7 ppm smaller than the shielding parameter that is characteristic of the reference signal, arbitrarily assigned 0 ppm.

Bibliography

1. D. S. Wishart and B. D. Sykes (1994) Methods Enzymol. **239**, 363–392.
2. S. S. Wijmenga, M. Kruithof, and C. W. Hilbers (1997) J. Biomol. NMR **10**, 337–350.

Suggestions for Further Reading

3. R. J. Abraham, J. Fisher, and P. Loftus (1988) *Introduction to NMR Spectroscopy*, Wiley, New York.
4. F. A. Bovey (1988) *Nuclear Magnetic Resonance Spectroscopy*, Academic, San Diego.
5. R. K. Harris (1983) *Nuclear Magnetic Resonance Spectroscopy: a physicochemical view*, Pitman, Marshfield, Mass.
6. S. W. Homans (1992) *A Dictionary of Concepts in NMR*, Clarendon, Oxford.
7. R. Kitamaru (1990) *Nuclear Magnetic Resonance: principles and theory*, Elsevier, New York.
8. R. S. Macomber (1998) *A Complete Introduction to Modern NMR Spectroscopy*, Wiley, New York.
9. C. H. Yoder and C. D. Schaeffer Jr. (1987) *Introduction to Multinuclear NMR*, Benjamin/Cummings, Menlo Park.
10. The NMR literature is replete with theoretical and experimental studies of chemical shielding effects. A database of proton, carbon, and nitrogen chemical shifts in proteins in maintained (http://www.bmrb.wisc.edu).

Chemiluminescence

Chemiluminescence is the production of light via a chemical reaction. As in all luminescence, the source of the light is the decay of an electron from a higher energy excited state to the ground state. In chemiluminescence, the reactants are generally in their ground-state configuration, but one or more of the products is formed with an electron in a high-energy orbital (the product molecule is formed in an excited state). Thus, chemiluminescence is the conversion of chemical energy (Gibbs **free energy**) to radiant energy (light). A necessary precondition for chemiluminescence is that the change in free energy for the reaction be sufficiently large to produce one of the products in an excited-state configuration.

Perhaps the simplest example of a chemiluminescent reaction is the thermal dissociation of the cyclic peroxide tetramethyl 1,2-dioxetane to two molecules of acetone (Fig. 1). The free energy of the transition state of the reaction is about 90 kcal/mol above the ground state for the acetone products. This is sufficient energy for one of the acetone molecules to be produced in an electronically excited state. When this molecule decays to the ground state, a photon of light is emitted.

Figure 1. Simple example of a chemiluminescent reaction, the thermal dissociation of the cyclic peroxide tetramethyl 1,2-dioxetane to two molecules of acetone.

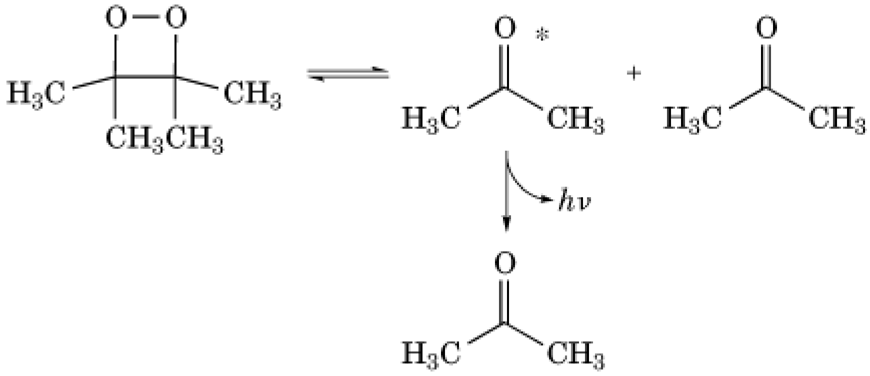

In many cases, a chemiluminescent reaction is carried out in the presence of a dye. The energy from the excited state of the reaction product is transferred to the dye, so that the reaction product is in the ground state and the dye is now in an electronically excited state. The dye will then decay to the ground state and emit a photon of a different color, depending on the chemical structure of the dye. Thus, a reaction that produces UV light may be coupled with a dye that emits in the visible region in order to provide useful illumination. A second reason for coupling a chemiluminescent reaction with a dye is to increase the lifetime of the light emission. Many chemiluminescent reactions are over quickly, and the light is released in a brief, intense flash. If, however, the reaction is coupled with a phosphorescent dye (see Luminescence), the radiant energy is transferred to the dye and is then released at a much slower rate, producing a longer-lasting, but less intense glow. This is the basis of such commercial products as the glow-stick for emergency lighting, as well as the luminescent novelty necklaces or other items often seen at carnivals. An example of the of reaction used in these devices is shown in Figure 2.

Figure 2. Chemiluminescent reaction coupled with a phosphorescent dye. The radiant energy from the chemical reaction is transferred to the dye and is then released at a much slower rate, producing a longer-lasting, but less intense glow. This is the basis of such commercial products as the glow-stick for emergency lighting and luminescent necklaces and other novelty items.

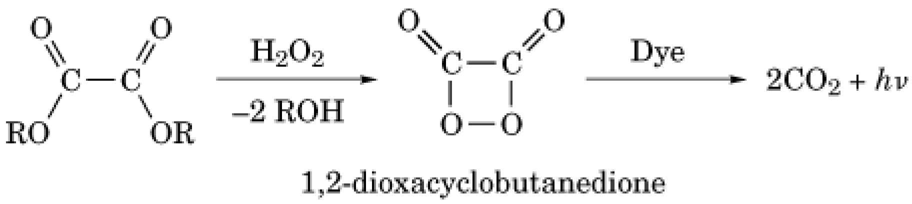

Chemiluminescent reactions are common in living organisms, where they are known as bioluminescent reactions. In some natural systems, energy from the chemical reaction will be passed to "antenna proteins," which serve the same functions as dyes in the strictly chemical reaction (see Luciferases And Luciferins).

Suggestion for Further Reading

J. D. Roberts and M. C. Caserio (1977) *Basic Principles of Organic Chemistry*, 2nd ed., W. A. Benjamin, Menlo Park, CA, pp. 1371–1418.

Chemiosmotic Coupling

Many forms of energy are interconverted by living systems. Chemical energy may be used to drive mechanical processes, to generate osmotic and electrical gradients, and even to emit light. In photosynthesis, light energy is converted to chemical energy and is used indirectly to drive the thermodynamically unfavorable synthesis of ATP from ADP and P_i. In oxidative metabolism in mitochondria and some bacteria, ATP synthesis is driven by the energy released by oxidation of metabolites. During the 1950s, it was clearly established that both oxidative phosphorylation and photosynthetic phosphorylation are dependent on electron transport. How electron transport could be linked to the formation of a phosphoanhydride bond in ATP was a major question in bioenergetics for the next two decades.

Oxidation–reduction reactions are clearly quite different in character from the removal of the elements of water from ADP and P_i to form ATP. Yet, there is not doubt that these two processes are coupled to one another. In biochemical parlance, two reactions are said to be coupled when they share a common intermediate. The nature of the intermediate common to electron transfer and to ATP synthesis was elusive. In 1961 in a short, entirely theoretical article, Peter Mitchell proposed a radically different idea for coupling (1). Rather than a chemical intermediate linking electron transport and phosphorylation, as was then generally thought, Mitchell suggested that transmembrane electrochemical proton potentials $\Delta\tilde{\mu}_{H^+}$could couple the two reactions. In addition, Mitchell realized that specific **active transport** systems could be linked to $\Delta\tilde{\mu}_{H^+}$.

1. The Chemiosmotic Hypothesis

The postulates of the chemiosmotic hypothesis (1-3) in brief are as follows:

1. Membranes that catalyze oxidative phosphorylation (the inner mitochondrial membrane and some bacterial plasma membranes) and photosynthetic phosphorylation (chloroplast thylakoids and plasma membranes of some bacteria) are poorly permeable to protons.
2. Electron transport generates $\Delta\tilde{\mu}_{H^+}$by vectoral transport of electrons and protons.
3. An ATPase is driven in reverse (ATP synthesis) by the energetically favorable flow of protons down their electrochemical potential.
4. Coupling membranes contain specific exchange metabolite transport systems that may be linked to the $\Delta\tilde{\mu}_{H^+}$.

Before considering these postulates in further detail, we will define $\Delta\tilde{\mu}_{H^+}$. The chemical potential of a substance, m, is the free energy of a system per mole. The energetics of the movement of an ion across a membrane has two components: chemical (osmotic) and electrical. Chemical work must be done to generate a concentration (actually activity) gradient and electrical work, to generate the charge imbalance (the membrane potential). The combined electrochemical potential is $\tilde{\mu}$. Just as is the case for Gibbs free energy, *G*, it is the change in electrochemical potential ($\Delta\tilde{\mu}$) that is of interest. In general, at constant temperature and pressure

$$\Delta\tilde{\mu} = RT\ln[x^{z+}]_a/[x^{z+}]_b + zF\Delta\psi \qquad (1)$$

where R is the gas constant (8.3 kJ K^{-1} mol^{-1}); T, the absolute temperature; ln, $\log_e$; x^{z+}, a cation of z positive charges; a and b, two compartments separated by a membrane; z, the charge on the cation; F, Faraday's constant (96.5 kJ mol^{-1} V^{-1}); and Dy, the membrane potential. For protons, $z = 1$, and Equation 1 becomes

$$\Delta\tilde{\mu}_{H+} = RT\ln[H^+]_a/[H^+]_b + F\Delta\psi \tag{2}$$

or

$$\Delta\tilde{\mu}_{H+} = 2.30RT\log[H^+]_a/[H_+]_b + F\Delta\psi \tag{3}$$

or, since pH = –log[H^+],

$$\Delta\tilde{\mu}_{H+} = 2.30RT(pH_b - pH_a) + F\Delta\psi \tag{4}$$

or

$$\Delta\tilde{\mu}_{H+} = 2.30RT(\Delta pH) + F\Delta\psi \tag{5}$$

Mitchell preferred to express Equation 5 in electrical units and coined the term "proton motive force" (pmf or Dp), which is simply $\Delta\tilde{\mu}_{H+}$ divided by F:

$$\Delta p = \Delta\tilde{\mu}_{H+}/F = 2.30RT/F(\Delta pH) + \Delta\psi \tag{6}$$

As forms of energy may be interconverted, so may their units. In some ways it makes sense to consider the energetics of proton gradients in electrical units. Proton fluxes across energy-coupling membranes are analogous to electric circuits. Some people prefer to use $\Delta\tilde{\mu}_{H+}$, others Dp. Since the two terms are readily interconvertible, this usage, although potentially confusing, is not a problem. At 25°C, Equation 5 may be written

$$\Delta\tilde{\mu}_{H+} = 5.69\,\Delta pH + 96.5\Delta\psi \tag{7}$$

where $\Delta\tilde{\mu}_{H+}$ is also given in kilojoules per mole and Dy is expressed in volts. The proton motive force (in millivolts) may be expressed as

$$\Delta p = 59\,\Delta pH + \Delta\psi \tag{8}$$

where Dy is also given in millivolts.

As in any thermodynamic analysis, sign conventions are very important to keep straight for $\Delta\tilde{\mu}_{H+}$. Consider a topologically closed phospholipid bilayer vesicle (Fig. 1). This vesicle has an inside aqueous compartment, a, and an external compartment, b, the suspending medium. DpH is defined as $pH_{out} - pH_{in}$, which is 2.0 units for the case shown in Figure 1. A charge difference (Dy) where the inside of the membrane is more positive than the outside is defined as having a positive sign. Suppose Dy is +100 mV. From the data given in Figure 1. the $\Delta\tilde{\mu}_{H+}$ or Dp may be calculated as $\Delta\tilde{\mu}_{H+}$ = 5.69(2) + 96.5(0.1) = 21.0 kJ mol^{-1} or Dp = 59(2) + 100 = 218 mV. Notice the sign of the answers, which are positive numbers. These values give the energy cost per mole ($+\Delta\tilde{\mu}_{H+}$ or +Dp) to generate the electrochemical protein potential or Dp. The flow of protons down their electrochemical potential is exergonic, and the absolute magnitudes of $\Delta\tilde{\mu}_{H+}$ and Dp are the same, but the sign changes. This statement is equivalent to saying that if a chemical reaction has a positive DG value in the forward reaction, the reverse reaction must have a negative DG of the same absolute magnitude.

Figure 1. $\Delta\tilde{\mu}_{H^+}$Across a vesicular membrane. DpH is defined as pH_{out} (compartment *b*) $-pH_{in}$ (compartment *a*), and Dy as positive since the inside of the membrane is more positive than the outside.

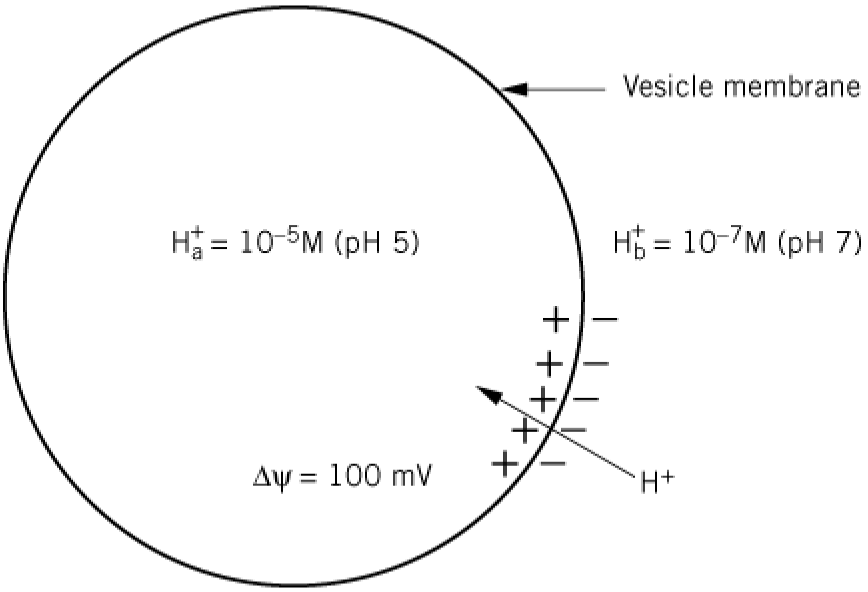

The essence of chemiosmotic coupling is that exergonic electron transport by the respiratory and photosynthetic electron chains is obligatorily linked to transmembrane proton flux, resulting in the generation of $\Delta\tilde{\mu}_{H^+}$. The flow of protons down their electrochemical potential provides the driving force for ATP synthesis. There is compelling evidence in support of these proposals.

2. Evidence in Support of the Chemiosmotic Coupling Hypothesis

As Mitchell predicted (1-3), the mitochondrial, bacterial, and chloroplast membranes that couple ATP synthesis to electron transport are poorly permeable to protons, except when proton-linked processes, such as ATP formation, occur at high rates. Proton transport was shown to be linked to electron transport in mitochondria (4), chloroplasts (5), and bacteria (6). The measurements of the magnitudes of $\Delta\tilde{\mu}_{H^+}$across these membranes turned out to be difficult, but in most instances, $\Delta\tilde{\mu}_{H^+}$values approaching 20 kJ mol^{-1} (Dp ~ 200 mV) have been measured during steady state, rapid electron transport. As predicted by Mitchell, lipophilic weak acids (eg, 2,4-dinitrophenol) could collapse the $\Delta\tilde{\mu}_{H^+}$by shuttling protons across the membrane. ATP synthesis is also inhibited by these reagents, which are termed “uncouplers” because they uncouple electron flow and ATP synthesis.

When Mitchell proposed the chemiosmotic hypothesis, the understanding of biological membrane structure, especially how proteins may be integrated into membranes, was rudimentary. We take for granted today that membrane proteins may be plugged into the lipid bilayer in an asymmetric manner (see Membranes). But in the 1960s Mitchell's proposals for membrane protein asymmetry, transmembrane electron transport, and membrane sidedness were novel. Although not all of Mitchell's predictions turned out to be correct (cytochrome oxidase, for example, translocates protons via a mechanism that Mitchell did not foresee), many were. His model for proton and electron transport in thylakoid membranes is compared to a much more recent view in Figure 2. There is a remarkable similarity between the two schemes.

Figure 2. Schemes for electron and proton transport in chloroplast thylakoid membranes. In (**a**) Mitchell's early scheme (2) is illustrated with the membrane in the horizontal position more commonly used by others. In (**b**) a modern interpretation of electron and proton transport in thylakoids is given. The similarity between the two schemes is remarkable. Note in particular the transmembrane electron transport by photosystem II (PS II) and photosystem I (PS I), the oxidation of water to $2H^+$ and 1/2 O_2 inside (the thylakoid lumen) and proton translocation coupled to plastoquinone (PQ) oxidation/reduction. These elements are essentially the same in the two schemes. Cytochrome *b* (Cyt b) was not properly placed by Mitchell. In (**b**) Mn stands for the manganese of the oxygen evolving complex, Qa and Qb, for the bound plastoquinone electron acceptors of PS II; P_{680} and P_{700}, for the reaction center chlorophylls; Cyt f, for cytochrome f; PC, for plastocyanin; A_0, for the primary electron acceptor in PSI; FeS, for iron–sulfur electron transport proteins; Fd, for ferredoxin. Ferredoxin–$NADP^+$ oxidoreductase and the FeS protein of the cytochrome b6f complex were omitted for clarity.

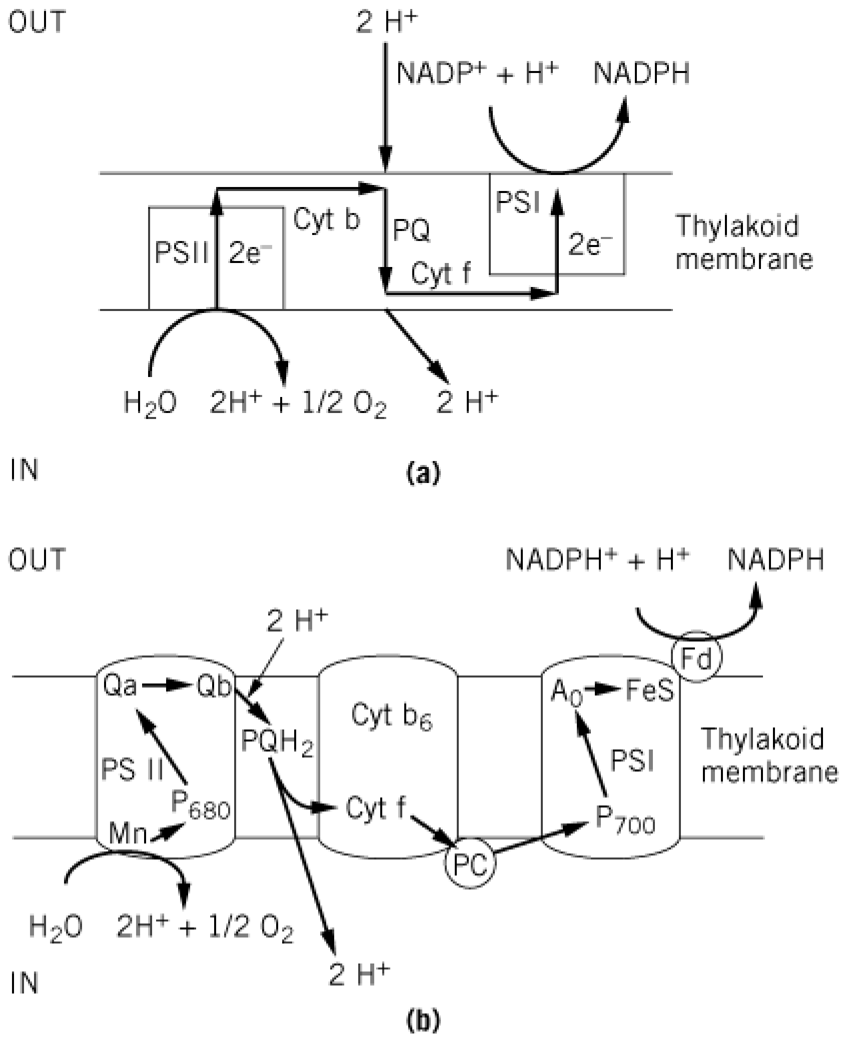

As illustrated in Figure 3 (7), the sidedness of the chloroplast thylakoid membrane is opposite that of mitochondria and bacteria (8). As a result of photoelectron transport, thylakoids accumulate protons from the stroma. In contrast, oxidative electron transport in mitochondria and bacteria cause protons to be ejected from the mitochondria or bacteria. The steady state Dy across the thylakoid membrane is very low, and the DpH is high (as much as 3.5 units). The DpH component of the $\Delta\tilde{\mu}_{H^+}$ in mitochondria and bacteria is, however, usually small, and Dy is high. These observations make sense when it is realized that the mitochondrial matrix and bacterial cytoplasm are the internal compartments bounded by the coupling membranes. The pH of these compartments must be controlled to allow the numerous enzymes they contain to function. In contrast, the thylakoid lumen contains no metabolic enzymes. Electrical neutrality in thylakoids is maintained by Cl^- flux.

Essentially, thylakoids accumulate HCl in the light.

Figure 3. Sidedness of coupling membranes. Mitochondrial and bacterial (*E. coli*) electron transport is coupled to the ejection of protons, whereas in thylakoids, protons are accumulated. Note that, in bacteria and chloroplasts, ATP is generated within the same compartment in which it is used. In contrast, most of the ATP synthesized within mitochondria is exported to the cytoplasm. From Ref. 47, with permission.

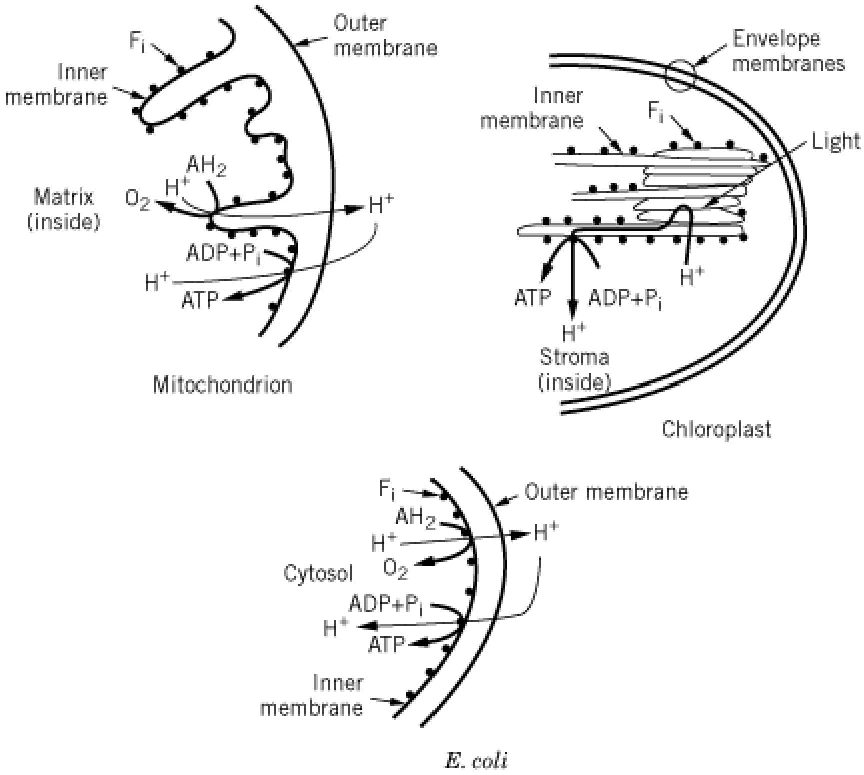

Dramatic evidence in favor of the chemiosmotic hypothesis was obtained in André T. Jagendorf's laboratory during the mid-1960s (9, 10). Simply by adjusting the pH of thylakoid suspensions to pH 4 and rapidly raising the pH to 8.0 in the presence of ADP + P_i, relatively large amounts of ATP are formed *in the dark.* ATP synthesis induced by acid to base transitions is abolished by uncouplers and reagents that block ATP synthesis. Later, it was shown (11) that artificially generated electric fields could also generate ATP. In mitochondrial vesicles, Thayer and Hinkle (12) showed that the rate of D*p*-driven ATP synthesis is as fast or faster than that coupled to electron transfer.

The membrane of the halophilic bacterium, *Halobacter halobium* (*salinarium*) elaborates purple patches composed entirely of bacteriorhodopsin. Bacteriorhodpsin is a light-dependent proton pump that, when incorporated into lipid membranes, can generate substantial $\Delta\tilde{\mu}_{H^+}$(12). When the enzyme from bovine heart mitochondria that catalyzes ATP synthesis was coreconstituted with bacteriorhodopsin, vesicles were obtained that catalyzed light-dependent, uncoupler-sensitive ATP formation (14).

Mitchell's proposal that ATP synthesis is accomplished by driving a proton-linked ATPase in reverse was also novel. By the time Mitchell was developing the chemiosmotic hypothesis, it had been clearly established that the energy of ATP hydrolysis could be used to generate ion gradients. For example, the Na^+ and K^+ concentration gradients and Dy across mammalian plasma membranes are generated by an ATPase, the Na^+,K^+-ATPase. If, Mitchell reasoned, an ATPase acts as an ion pump, might an ATPase operate in reverse to utilize the $\Delta\tilde{\mu}_{H^+}$generated by electron transport to drive ATP synthesis? Work on “coupling factors” during the 1960s established that mitochondria and chloroplasts contain an enzyme that is required for ATP synthesis that could under appropriate conditions also hydrolyze ATP (15). The catalytic part of what is now known as “ATP synthase” is called “F”$_1$ and is an extrinsic membrane protein. F_1 may be removed from the membrane and is very water-soluble. (See article on ATP Synthase.)

Mitochondrial ATP synthesis and hydrolysis are strongly inhibited by the antibiotic, oligomycin. The ATPase activity of F_1, after its removal from the inner mitochondrial membrane, is insensitive to oligomycin—an observation that seemed incompatible with a role of F_1 in oxidative phosphorylation. Racker then showed that a crude detergent fraction of mitochondrial inner membranes contain a factor that confers sensitivity to oligomycin to F_1. This factor was called “F_0”; F_0 is not a coupling factor, and it is improper to denote F_0 as “F zero” or “F naught.” Kagawa and Racker (16) pioneered the isolation and purification of the entire ATPase complex, $F_1 - F_0$, which could be incorporated into phospholipid vesicles that catalyzed energy-linked activities. Similar studies were carried out with the chloroplast ($CF_1 - CF_0$) and bacterial enzymes.

Mitchell predicted that F_0 contains a mechanism for transmembrane proton movement. Removal of CF_1 was shown (17) to greatly enhance the proton permeability of the thylakoid membrane. *N*,*N*′-Dicyclohexylcarbodiimide (DCCD) at low concentrations inhibits ATP synthesis and ATP hydrolysis by $F_1 - F_0$ (17). DCCD acts by blocking proton conductance by F_0 and, in thylakoids, restores net light-dependent proton uptake and high $\Delta\tilde{\mu}_{H^+}$ to membranes from which CF_1 had been removed. The DCCD reacts with an Asp or Glu residue in a very hydrophobic, 8-kDa polypeptide of F_0 (18).

The evidence that $F_1 - F_0$ is a proton-translocating ATPase/ATP synthase is overwhelming. Phosphorylation driven by imposed DpH or Dy is abolished by specific inhibitors of either F_1 or F_0 function. As described above, F_0 conducts protons rapidly, and blocking F_0 proton transport also inhibits ATP synthesis. ATP hydrolysis by $F_1 - F_0$ is linked to proton translocation. In thylakoids ATP hydrolysis in the dark can generate $\Delta\tilde{\mu}_{H^+}$ values of significant magnitude to drive some ATP synthesis. This ATP-dependent ATP synthesis is very sensitive to inhibition by uncouplers. The $\Delta\tilde{\mu}_{H^+}$ generated by ATP hydrolysis can drive electron transport in reverse (19), a process that is blocked by ATP synthase inhibitors and uncouplers. Other evidence that the electron-transport chain and ATP synthase are linked via $\Delta\tilde{\mu}_{H^+}$ includes the facts that phosphorylation decreases the magnitude of $\Delta\tilde{\mu}_{H^+}$ and stimulates the rate of electron transport. Specific inhibition of ATP synthesis increases the $\Delta\tilde{\mu}_{H^+}$ and slows electron transport. Uncouplers strongly decrease $\Delta\tilde{\mu}_{H^+}$ and inhibit ATP synthesis, but stimulate electron transport. An extensive analysis of the coupling between photosynthetic electron transport and ATP synthesis in the steady state gave results strongly indicating that $\Delta\tilde{\mu}_{H^+}$ is the intermediate linking the two processes.

3. Metabolite Transport and Motility

Mitchell's fourth postulate, that coupling membranes contain specific exchange transport systems, has also received broad experimental support, especially for mitochondrial and bacterial coupling membranes. The chloroplast thylakoid membrane does not appear to contain metabolite transporters. ATP is synthesized in chloroplasts within the same compartment (the stroma) in which it is utilized in photosynthesis (see Fig. 3). The inner membrane of the envelope, not the thylakoid membrane, is the permeability barrier of the chloroplast. In contrast, the inner membrane of the mitochondrion and the plasma membrane of bacteria are both coupling membranes and permeability barriers. In these membranes, transport must coexist with ATP synthesis.

Most of the ATP generated by oxidative phosphorylation in mitochondria is exported to the cytoplasm and is hydrolyzed to drive cellular processes. Mitochondria must contain mechanisms to export ATP and import ADP and P_i. In addition, mitochondria will take up pyruvate, di- and tricarboxylic acids, and some amino acids. Cation exchangers are also present. Many of these transporters utilize the $\Delta\tilde{\mu}_{H^+}$established by the electron transport chain (Fig. 4). A few transporters will be briefly considered in this article, with emphasis on ADP/ATP and P_i transporters in mitochondria. (see Mitochondria).

Figure 4. Proton circuits in the mitochondrial inner membrane. Electron transport ejects protons from the mitochondrion, resulting in the formation of $\Delta\tilde{\mu}_{H^+}$. A number of processes including ATP synthesis, ADP/ATP exchange transport, P_i – OH^- exchange transport, and the uptake of certain metabolites (illustrated by pyruvate uptake in exchange for OH^-) are linked to the $\Delta\tilde{\mu}_{H^+}$.

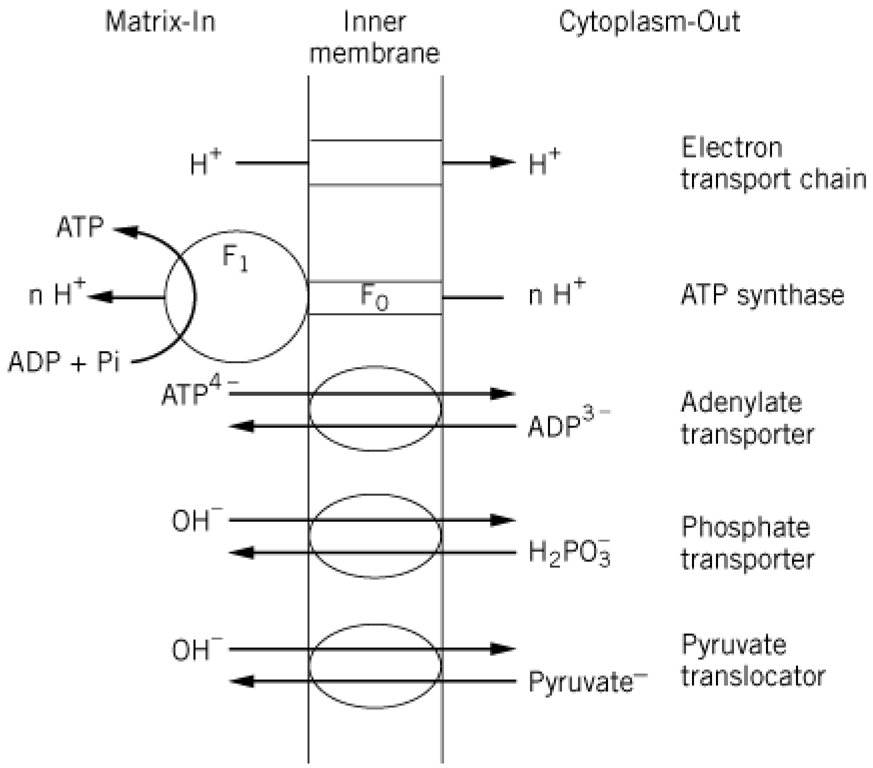

At physiological pH, ADP exists as ADP^{3-}, and ATP as ATP^{4-}. The inner membrane contains a well-characterized transporter, known as the *adenine nucleotide translocator* (20). This transporter catalyzes the counterexchange translocation of ADP^{3-} and ATP^{4-}. The one-for-one exchange transport (**antiport**), with ATP^{4-} exported from the mitochondrion and ADP^{3-} imported, is electrogenic; there would be the net transfer of one negative charge out of the mitochondrion per transport event. The Dy across the mitochondrial inner membrane is outside positive. Thus, ATP^{4-}/ADP^{-3} exchange transport would be promoted in the direction of ATP export and ADP import by the Dy generated by electron flow.

P_i accumulation by mitochondria is also catalyzed by a transporter. P_i is either cotransported with H^+ or counter-exchanged for OH^-. Since the form of P_i that is preferentially transported is $H_2PO_4^-$, one-for-one transport of P_i with either H^+ (**symport**) or OH^- (antiport) is electrically neutral and is not affected by Dy. P_i transport is, however, linked to DpH. The pH of the matrix of respiring mitochondria is about 0.5 unit more alkaline than that of the cytoplasm. Either OH^- antiport or H^+ symport would favor P_i uptake into mitochondria. This mechanism and the rapid utilization of P_i by oxidative phosphorylation assure that the P_i is delivered to the mitochondrial matrix from the cytoplasm. The transport of ATP/ADP and P_i by mitochondria costs the equivalent of one proton/ATP synthesized. Pyruvate, the end product of aerobic glycolysis, is transported into mitochondria via an electrically neutral counterexchange with $OH^{-\prime}$, and its transport, like that of P_i, is linked to DpH.

Bacteria have the potential to carry out the active transport of a large number of compounds, including sugars and amino acids (21). Transport may be linked to the $\Delta\tilde{\mu}_{H^+}$generated by electron transport, or, under anaerobic conditions, by ATP hydrolysis by $F_1 - F_0$. The best-studied example of $\Delta\tilde{\mu}_{H^+}$-dependent active transport in bacteria is the lactose transporter (lac **permease**) of *Escherichia coli* (22). Lactose uptake is obligatorily linked to H^+ uptake into the cell, at a probable stoichiometry of one lactose to one proton. The bacterium maintains, by either electron transport or ATP hydrolysis, a negative Dy (outside positive), and, depending upon the conditions, a negative DpH (inside alkaline). The flow of protons down the $\Delta\tilde{\mu}_{H^+}$provides the driving force for the accumulation of lactose to concentrations in excess of 1,000 times that of the medium. In addition to proton-linked transport systems, bacteria contain ABC (ATP binding cassette) transporters (23) that utilize ATP for transport to metabolites or ions directly, as well as the phosphotransferase system (24) that utilizes phosphoenolpyruvate as both an energy source and a source of phosphate for the transport and concurrent phosphorylation of some sugars.

The concepts developed by Mitchell for metabolite and ion transport were subsequently found to apply to membranes other than coupling membranes. The plasma membranes of higher plant cells, yeast, and fungi contain an enzyme that is structurally, functionally, and mechanistically related to the Na^+, K^+-ATPase of animal cell plasma membranes. This enzyme, the H^+-ATPase (25), is the primary ion pump in plant, yeast, and fungal plasma membranes. ATP hydrolysis pumps protons out of the cells, generating the transplasma membrane $\Delta\tilde{\mu}_{H^+}$. The DpH component in plant cells is 1.0–2.0 pH units, whereas Dy may be in excess of –200 mV. The active transport across the plasma membrane is driven by the energetically favorable flow of protons down the $\Delta\tilde{\mu}_{H^+}$. As is the case for lactose transport in *E. coli*, specific transporters that mediate the translocation of metabolites across the membrane are obligatorily coupled to H^+ transport. An important example of H^+: metabolite cotransport (symport) in plants is the active loading of sucrose (26) into the phloem. As a consequence of sucrose: H^+ cotransport, the sucrose concentration within the phloem may be as high as 0.5 *M*.

An entirely new class of H^+-ATPases was discovered during the 1980s and characterized in the 1990s (27). The members of this class are called “V-ATPases,” in which the V stands for *vacuolar*. All eukaryotic cells contain V-ATPases. In plant and yeast cells, the V-ATPase is present on the vacuolar membrane and in the Golgi apparatus. In animal cells, V-ATPases are present in **clathrin**-coated vesicles, chromaffin granules (adrenal medulla), Golgi membranes, **lysosomes**, synaptic vesicles, and, in some specialized cells, the plasma membrane. The V-ATPases are structurally much more complex than plasma membrane H^+-ATPases, and, although the V-ATPases large subunits have some sequence similarity to the a and b subunits of F_1, V-ATPases and $F_1 - F_0$ ATPases are distinct.

The function of V-ATPases is to hydrolyze ATP and to pump protons from the cytoplasm into the internal aqueous compartment of endomembranes. The interiors of vacuoles and lysosomes are more acidic than that of the cytoplasm. Metabolite and ion fluxes are linked to the $\Delta\tilde{\mu}_{H^+}$generated by the V-ATPase. A Ca^{2+}/H^+ exchange transporter has, for example, been found in the vacuolar membrane of higher plants (28). Acidification of the vesicles that are formed by receptor-mediated endocytosis is required for dissociation of the ligand from its receptor (29).

The V-ATPase of eukaryotes never functions as an ATP synthase. Even in the best of conditions *in vitro*, imposed proton gradients will not cause the pump to reverse. The H^+-ATPase of **archaebacteria** (eg, *Halobacter salinarium* [*halobium*], (30)) more closely resembles V-ATPases than $F_1 - F_0$. Yet, the V-ATPase (sometimes called "A-ATPase" for Archeon), of the archeon can make ATP at the expense of the $\Delta\tilde{\mu}_{H^+}$generated by the light-dependent bacteriorhodopsin proton pump. Eukaryotes tailored the V-ATPase to fit their needs.

In addition to its utilization in ATP synthesis and membrane transport, $\Delta\tilde{\mu}_{H^+}$can be converted to mechanical energy in the form of motility of bacteria with **flagella** such as *E. coli* and *Bacillus subtilis*. Flagellar rotation is driven by $\Delta\tilde{\mu}_{H^+}$, rather than directly by ATP. Starved *B. subtilis* is immotile, but motility may be restored in transient manner by the artificial imposition of Dy. DpH (inside alkaline) is also capable of driving flagellar motion (31).

4. Sodium Electrochemical Potential

The electrochemical sodium ion potential, $\Delta\tilde{\mu}_{Na^+}$, is given by

$$\Delta\tilde{\mu}_{Na^+} = RT\ln[Na^+]_a/[Na+]b + F\Delta\psi \qquad (9)$$

where *R*, *T*, ln, Dy, and *F* are as defined in Equation 1. In some bacteria, $\Delta\tilde{\mu}_{Na^+}$is exploited for ATP synthesis, active transport, and motility. In addition, Na^+/metabolite cotransport systems are present in animal cells. Transporters within the plasma membrane of these cells link the translocation of the substrates (eg, amino acids) to the flux of Na^+ down the $\Delta\tilde{\mu}_{Na^+}$generated by the Na^+, K^+-ATPase (32). In bacteria, part of the $\Delta\tilde{\mu}_{H^+}$generated by respiration may be converted to $\Delta\tilde{\mu}_{Na^+}$by counterexchange transport of Na^+ for H^+. In some bacteria, Na^+ translocation may be linked to metabolism or electron transport without the involvement of $\Delta\tilde{\mu}_{H^+}$. For example, in *Propionigenium modestum*, the anaerobic decarboxylation of succinate to form propionate is coupled to the transport of Na^+ out of bacterium, generating a $\Delta\tilde{\mu}_{Na^+}$(33). In **halophiles**, Na^+ transport has been shown to be driven by electron transport through the NADH dehydrogenase region of the electron transport chain.

Vesicles of the *P. modestum* plasma membrane catalyze ATP-dependent Na^+ transport, and an imposed $\Delta\tilde{\mu}_{Na^+}$drives ATP synthesis (34). The membrane contains a Na^+-ATPase (ATP synthase) that is analogous to the $F_1 - F_0$ ATP synthase of coupling membranes. It is interesting to note that F_0 subunits of the *P. modestum* Na^+-ATPase confer to F_1 from *E. coli* the ability to translocate Na^+ (35). One archeon, *Methanosarina mazei* Gö 1, contains an $F_1 - F_0$ that uses $\Delta\tilde{\mu}_{Na^+}$and a V-ATPase ($V_1 - V_0$) that uses $\Delta\tilde{\mu}_{H^+}$(36). It is clear, therefore, that proton transport per se is not required for ATP synthesis by $F_1 - F_0$. This observation makes mechanisms of ATP synthesis in which translocated protons are directly involved in catalysis very unlikely. $\Delta\tilde{\mu}_{Na^+}$may also be the driving force for motility in some marine bacteria.

5. Pyrophosphate and Energy Coupling

Pyrophosphate (PP_i) is merely two P_i molecules joined by an anhydride bond:

$$2\ HPO_4^{2-} + 2H^+ \leftrightarrow H_2P_2O_7^{2-} + H_2O$$

The equilibrium for this reaction lies far to the left; at pH 7 and 25°C, the standard free-energy change for (PP_i) synthesis from 2 P_i is about +16.7 kJ mol^{-1}. PP_i is a product of several biosynthetic reactions, including aminoacyl tRNA synthesis, fatty-acid activation, and DNA and RNA synthesis. These reactions occur with equilibrium constants close to 1 and are freely reversible. By coupling these reactions to PP_i hydrolysis, the reactions are pulled in the synthetic direction. Cells contain soluble pyrophosphatases that hydrolyze PP_i to 2 P_i.

Other roles for PP_i in plants have recently been elucidated. The vacuolar membrane contains a pyrophosphatase (37) that couples pyrophosphate hydrolysis to inward proton translocation. Both the V-ATPase and the pyrophosphatase contribute significantly to the $\Delta\tilde{\mu}_{H^+}$ across the vacuolar membrane. Thus, some of the energy of PP_i hydrolysis is conserved by generation of the $\Delta\tilde{\mu}_{H^+}$. In addition, PP_i may be utilized as a phosphoryl donor, as an alternative to ATP, in glycolysis.

In the photosynthetic bacterium, *Rhodospirillum rubrum*, a pyrophosphatase, and $F_1 - F_0$ ATPase (ATP synthase) exist within the same membrane (38). Net PP_i synthesis driven by the photoelectron transport chain of the bacterium has been observed. PP_i synthesis is inhibited by proton ionophores (uncouplers), but not by reagents that block ATP synthesis by interacting with F_1. Membrane vesicles (chromatophores) from *R. rubrum* are oriented so that the catalytic sites of both the ATP synthase and the pyrophosphatase face the outside. ATP hydrolysis by these vesicles in the dark is coupled to inward H^+ translocation, resulting in the generation of substantial $\Delta\tilde{\mu}_{H^+}$ values. It is even possible to detect ATP-dependent pyrophosphate synthesis that is also uncoupler-sensitive. ATP hydrolysis and pyrophosphate synthesis are linked by the $\Delta\tilde{\mu}_{H^+}$.

6. Concluding Remarks

The four postulates of the chemiosmotic coupling hypothesis have received broad experimental support. Coupling membranes are poorly permeable to H^+. Electron transport results in the generation of $\Delta\tilde{\mu}_{H^+}$ at values that are consistent with the energetic demands of ATP synthesis. An ATPase is present that is reversible and can make ATP, provided the magnitude of $\Delta\tilde{\mu}_{H^+}$ is sufficient, or hydrolyze ATP if the $\Delta\tilde{\mu}_{H^+}$ is low. Artificially imposed $\Delta\tilde{\mu}_{H^+}$ can drive ATP synthesis at rates as least as fast as in oxidative or photosynthetic phosphorylation. $\Delta\tilde{\mu}_{H^+}$ is energetically and kinetically competent to be the intermediate common between electron transport and ATP synthesis. The fourth postulate, the existence of exchange transporters and their possible coupling to the $\Delta\tilde{\mu}_{H^+}$, has had a tremendous impact on the field of metabolite transport, not only in mitochondria but also in many other membranes. In part, the chemiosmotic hypothesis had its origins in Mitchell's long-standing interest in active transport in bacteria. The chemiosmotic hypothesis provided a new theoretical basis for the interpretation of transport experiments. Very early on, Mitchell proposed that membrane proteins may be organized in specific orientations within membranes and that electron transfer may in part occur across membranes. For his remarkable insights and experimental contributions, Peter Mitchell was awarded the Nobel Prize in Chemistry in 1978.

That H^+ (or Na^+) translocation is coupled to ATP synthesis and hydrolysis is generally accepted. Some evidence suggests that under some circumstances, the protons translocated during electron transport need not equilibrate with the bulk aqueous phase prior to their passage through $F_1 - F_0$ to make ATP. Because of the high buffering capacity of the interior of thylakoids, 50 ms or more of illumination may be required to generate DpH values of magnitudes sufficient to drive ATP synthesis. When the generation of Dy by proton transport is prevented, permeant buffers should delay the onset of ATP synthesis by increasing the internal buffering capacity. The delay is not as long as it should be, if it is assumed that the added buffer is uniformly distributed throughout the internal volume of the thylakoids (39, 40). These and other observations kept alive the localized proton theory of R. J. P. Williams (41). According to this theory, dubbed "microchemiosmosis" by Mitchell, protons are trapped in localized regions of the membrane that are not necessarily in equilibrium with each other. The transmembrane bulk phase $\Delta\tilde{\mu}_{H^+}$ was proposed to be used only for energy storage.

It is difficult to design experiments that provide unequivocal support for the localized proton hypothesis. If protons may be delivered to the ATP synthase without equilibrating with the bulk aqueous phase, some barrier must exist to prevent equilibration. Disruption of thylakoid structure has been suggested to convert the coupling mechanism from localized to delocalized (ie, chemiosmotic). It would thus be very difficult to establish the nature of the barrier. Results of a number of other reported experiments at first glance seem at odds with the chemiosmotic hypothesis. In most cases, flaws in the methods used or in the interpretation of the results can explain the apparent discrepancy.

The chemiosmotic hypothesis has stood the test of time. During the past few years, much has been learned about the structure of some of the proton and electron translocators of coupling membranes. Yet, we know little about how cytochrome oxidase pumps protons or how the ATP synthase exploits the $\Delta\tilde{\mu}_{H^+}$ to drive ATP synthesis. The emphasis of bioenergetics has shifted away from *what* couples electron transport to ATP synthesis to *how* the proton translocating elements work.

Bibliography

1. P. Mitchell (1961) Nature **191**, 144–148.
2. P. Mitchell (1966) *Chemiosmotic Coupling in Oxidative and Photosynthetic Phosphorylation*, Glynn Research, Bodmin, Cornwell, England.
3. P. Mitchell (1979) *Les Prix Nobel en 1978, Nobel Foundation*, Stockholm, pp. 142–143.
4. P. Mitchell and J. Moyle (1965) Nature **298**, 147–151.
5. J. S. Neuman and A. T. Jagendorf (1964) Arch Biochem Biophys. **107**, 109–119.
6. P. Mitchell (1962) J. Gen. Microbiol. **29**, 144–148.
7. R. E. McCarty (1985) Bioscience **35**, 27.
8. P. C. Hinkle and R. E. McCarty (1978) Sci. Am. **238**, 104–123.
9. A. T. Jagendorf and E. Uribe (1966) Proc. Natl. Acad. Sci. USA **55**, 170–177.
10. A. T. Jagendorf (1967) Fed. Proc. **26**, 1361–1369.
11. H. T. Witt (1979) Biochim. Biophys. Acta **505**, 355–427.
12. W. S. Thayer and P. C. Hinkle (1975) J. Biol. Chem. **250**, 5330–5335.
13. W. Stoekenius (1985) Trends Biochem Sci. **10**, 483–485.
14. E. Racker and W. Stoeckenius (1974) J. Biol. Chem. **249** 662–663.
15. E. Racker (1976) *A New Look at Mechanisms in Bioenergetics*, Academic Press, New York.
16. Y. Kagawa, A. Kandrach, and E. Racker (1973) J. Biol. Chem. **248**, 676–684.
17. R. E. McCarty and E. Racker (1967) Brookhaven Symp. Biol. **19**, 202–212.
18. K. J. Cattell, C. R. Lindop, I. G. Knight, and R. B. Beechey (1971) Biochem. J. **125**, 169–177.
19. B. Chance and G. Hollunger (1961) J. Biol. Chem. **258**, 1474–1486.
20. M. Klingenberg (1989) Arch. Biochem Biophys **270**, 1–14.
21. R. D. Simoni and P. W. Postman (1975) Annu. Rev. Biochem. **44**, 523–554.
22. H. R. Kaback (1986) Annu. Rev. Biophys. Chem. **15**, 279–319.
23. C. F. Higgins (1992) Annu. Rev. Cell Biol. **8**, 67–113.
24. N. D. Meadow, D. K. Fox, and S. Roseman (1990) Ann. Rev. Biochem. **59**, 497–542.
25. R. Serrano (1990) in C. Larsson and I. M. Moller, eds., *The Plant Plasma Membrane: Structure, Function and Molecular Biology*, Springer-Verlag, New York, pp. 127–153.
26. N. Sauer (1992) in D. T. Cooke and D. T. Clarkson, eds., *Transport and Receptor Proteins of Plant Membranes: Molecular Structure and Function*, Plenum Press, New York, pp. 67–75.

27. N. Nelson (1989) J. Bioenerg. Biomembr. **21**, 533–571.
28. K. S. Schumaker and H. Sze (1986) J. Biol. Chem. **261**, 12172–12178.
29. I. Melman (1992) J. Exp. Biol. **172**, 39–45.
30. K. Ihara, T. Abe, K.-I. Sugimura, and Y. Mukohata (1992) J. Exp. Biol. **172**, 475–485.
31. S. Matsuura, J. Shioi, and Y. Imae (1977) FEBS Lett. **82**, 187–190.
32. E. J. Collarini and D. L. Oxender (1987) Annu. Rev. Nutr. **7**, 75–90.
33. P. Dimroth (1991) Bioessays **13**, 463–468.
34. W. Hilpert, B. Schink, and P. Dimroth (1984) EMBO J. **3**, 1665–1670.
35. W. Laubinger, G. Dekers-Hebestreit, N. Altendorf, and P. Dimroth (1990) Biochemistry **25**, 5458–5463.
36. R. Wilms, C. Frieberg, E. Wegerk, I. Meier, F. Mayer, and V. Müller (1996) J. Biol. Chem **271**, 18843–18852.
37. P. A. Rea, Y. Kim, V. Sarafian, R. J. Poole, J. M. Davies, and D. Sanders (1992) Trends Biochem. Sci. **17**, 348–353.
38. P. Nyring, B. F. Nore, and A. Strid (1991) Biochemistry **30**, 2883–2887.
39. R. D. Horner and E. N. Moudrianakis (1983) J. Biol. Chem. **258**, 11643–11647.
40. R. A. Dilley, S. M. Theg, and W. A. Beard (1987) Annu. Rev. Plant Physiol. **38**, 347–389.
41. R. J. P. Williams (1969) Curr. Top. Bioenerg. **3**, 79–156.

Suggestions for Further Reading

42. W. A. Cramer and D. B. Kraff (1990) *Energy Transduction in Biological Membranes. A Text of Bioenergetics*, Springer-Verlag, New York.
43. G. D. Greville (1969) A scrutiny of Mitchell"s chemiosmotic hypothesis of respiratory chain and photosynthetic phosphorylation, Curr. Top. Bioenerg. **3**, 1–78 (a very clear and useful review of the state of chemiosmotic coupling in the early days).
44. D. G. Nichols and S. J. Ferguson (1992) *Bioenergetics*, Academic Press, London.
45. R. N. Robertson (1968) *Protons, Electrons, Phosphorylation and Active Transport*, Cambridge University Press, London (in this slender volume, the author describes thoughts about charge separations and ion fluxes that predated the chemiosmotic hypothesis).
46. V. P. Skulachev and P. C. Hinkle, eds. (1982) *Chemiosmotic Proton Circuits in Biological Membranes*, Addison-Wesley, London.

Chemokines

Chemokines are small secreted proteins, generally 8 to 15 kDa in mass, that were originally identified by their ability to stimulate chemotaxis and/or activate leukocytes (lymphocytes, neutrophils, eosinophils, mast cells, monocytes, and macrophages). They are now known to be multifunctional and to be secreted by many different cell types in response to various stimuli (for reviews see Refs. 1-5). In inflamed tissues, they may induce effector functions such as the generation of an oxidative burst or the secretion, from storage granules, of proteinases (by neutrophils and monocytes), histamine (by basophils), and cytotoxic proteins (by eosinophils). Chemokines activate **cell-surface receptors** to promote adhesion of circulating leukocytes to the vascular endothelium and subsequently to facilitate extravasation (diapedesis) of the adherent leukocyte into adjacent tissue, the source of the chemokine. They have proinflammatory effects and can give rise to acute or chronic inflammatory responses; some have been shown to be involved in movement and activation of cells in both angiogenesis/vasculogenesis and neural pathfinding, thus implicating them in aspects of development not directly involved in the immune response.

1. Chemokine Structure and Chromosome Location

The chemokine family (at least 40 members have been identified in humans) consists of four classes distinguished by the positioning of four conserved cysteine residues near the N-terminus of the protein. These four cysteine residues define a distinct structural motif based on the two disulfide bonds (C16C3, C26C4) that they form. All the chemokines possess a central b-pleated sheet region consisting of three antiparallel beta-strands (a Greek key motif) followed in most cases by a C-terminal alpha-helix. There is evidence that the chemokines can form dimers and higher oligomers, but whether this is important for their function is controversial (2). The N-terminal sequence of the chemokines is of particular importance in determining their specificity. Alteration or removal of one or a few amino acid residues can dramatically affect their activity or target cell specificity. This provides the opportunity for the specificity of a chemokine to be altered by local factors subsequent to its secretion.

The CXC or a-class chemokines possess a single residue between the first and second cysteines. This family can be further subdivided by the presence or absence of the amino acid sequence Glu-Leu-Arg (ELR) preceding the first cysteine. This sequence is recognized by chemokine receptors on specific cell types, and thus, has functional implications. The CC or b-class chemokines have no residues between the first and second cysteines. Some members of this group have two additional cysteine residues that form a third disulfide bond (6).

Two additional chemokines have been identified that do not fit into either the CC or CXC classes. The g class is missing both the first and third cysteines. This C chemokine has lymphotactin as its prototype member. The d class possesses a CXXXC motif, and thus far is represented only by fractalkine/neurotactin. This atypical membrane-bound CXXXC chemokine has, on the C-terminal side of the b-sheet sequences, a long glycosylated mucin structure, followed by a transmembrane segment and a short C-terminal cytoplasmic **domain**. The chemokines, with their alternative names, are listed in Table 1 by class.

Table 1. Human Chemokines and Their Receptors

Chemokine (and Alternative Names)	Receptors
ELR + CXC	
IL-8	CXCR1, R2
GROa (MGSA-a)	CXCR2, R1
GROb (MGSA-b,MIP-2a)	CXCR2
GROg (MIP-2b)	CXCR2
ENA-78	CXCR2
LDGF-PBP	CXCR2
GCP-2	CXCR2
Non-ELR CXC	
PF4	Unknown, GAGs[a]
Mig	CXCR3
IP-10	CXCR3, GAGs[a]

ITAC	CXCR3
SDF-1a/b	CXCR4
BCA-1/BLC	CXCR5
CC	
MIP-1a (LD78a)	CCR1, CCR5, CCR9
MIP-1b (Act-2, HC21)	CCR1, CCR5, CCR9
MDC (STCP-1)	CCR4
TECK	Unknown
TARC	CCR4
RANTES	CCR1, CCR3, CCR4, CCR5
HCC-1	CCR9
HCC-4 (NCC-4, LEC)	Unknown
DC-CK1 (PARC, MIP-4, AMAC-1)	Unknown
MIP-3a (LARC, Exodus)	CCR6
MIP-3b (ELC)	CCR7
MCP-1	CCR2, CCR9
MCP-2	CCR2, CCR9
MCP-3	CCR2, CCR9
MCP-4	CCR2, CCR3, CCR9
Eotaxin	CCR3, CCR9
Eotaxin-2/MPIF-2	CCR3
Six CysteineCC	
I-309	CCR8
MIP-5/HCC-2(Lkn-1)	CCR1, CCR3
MPIF-1 (CKb-8)	Unknown
6Ckine (SLC,Exodus-2, TCA-4)	CCR7, CXCR3
Others	
Lymphotactin (SCM-1)	XCR1
CX3C (Fraktalkine, Neurotactin)	CX3CR1
Multiple Chemokines	DARC (Duffy antigen)

[a] GAG = Glycosyl amino glycan.

Members within a class are linked both by their structural similarities and by their location in the human genome. Although there are exceptions in each class, members of the CXC group generally map to the chromosomal locus 4q13. CC chemokines are found primarily on chromosomes 7, 8, 9, and 17. Chromosomal location may provide a useful tool in identifying new members of the g and d classes.

2. Chemokine Expression

Chemokines are expressed by virtually all cell types. Regulation of chemokine expression is complex and highly dependent on specific signaling pathways. Cells can express chemokines constitutively or in response to stimulation by, for example, **interleukin**-1 (IL-1), interleukin-4, tumor necrosis factor a, **interferon**-g (IFN-g), or pathogenic agents such as endotoxin (lipopolysaccharide). Low molecular-weight fragments (200 kDa) of the glycosaminoglycan hyaluronan (resulting from tissue destruction, for example) can enhance expression of some chemokines (eg, MIP-1, RANTES, or MCP-1) in specific macrophage types (eg, bone marrow-derived macrophages or elicited peritoneal macrophages) (7). Depending upon the situation, the expression of these same chemokines can be either suppressed or enhanced by inflammatory mediators, such as IL-10 or IFN-g (8).

One well-characterized example of induction of chemokines is provided by the macrophage. Macrophages can be stimulated to produce-chemokines during T cell-directed delayed type hypersensitive reactions in tissues by contact with activated T cells displaying CD40L. Kornbluth et al. (9) found that, although LPS was also a potent inducer of chemokines, the macrophage-stimulating lymphokines IFN-g and GM-CSF (granulocyte macrophage colony stimulating factor) produced by activated T cells were not good inducers.

3. Chemokine Receptors

Chemokines bind to seven-transmembrane-spanning G-protein-coupled receptors (see Heterotrimeric G Proteins) whose sequence homology is distinct from that of other such receptors. The interaction of a chemokine with its receptor can activate diverse signaling pathways, depending upon the specific signaling elements expressed by the target cell. Chemokine receptors are named on the basis of the cysteine motif that they recognize, and most will bind more than one chemokine ligand in that group. Likewise, a particular chemokine can interact with more than one receptor. Table 1 lists the chemokines and their respective receptors. Some receptors are expressed constitutively by particular cell types, whereas the expression of others may require an inducing signal. Thus CCR1 and CCR2 are constitutively expressed by monocytes, but are expressed by lymphocytes only after stimulation by IL-2 (10). Some chemokine receptors are expressed by nonhematopoietic cells, eg, endothelial cells, neurons, astrocytes, and epithelial cells. This emphasizes recent findings that chemokine receptors may have other important functions besides that of leukocyte chemotaxis. The Duffy antigen receptor, the determinant of the Duffy blood group, is found on a variety of cells, including erythrocytes and endothelial cells, as well as cells of the nervous system. It is unusual in its ability to bind both CC and CXC chemokines without eliciting any known biologic response. Possibly it serves to store or scavenge chemokines (11).

Specific chemokines generally act on specific subsets of leukocytes as a function of the receptors expressed by the cell (Table 2). Most CXC chemokines containing the ELR sequence are chemotactic for neutrophils, whereas non-ELR chemokines generally attract lymphocytes. Neutrophils express the CXCR1 receptor, which is stimulated by IL-8 and granulocyte chemotactic protein-2 (GCP-2), and the CXCR2 receptor, which responds to IL-8, GCP-2, the LPS-induced CXC chemokine (LIX), the neutrophil-activating peptide-2 (NAP-2), the epithelial cell-derived neutrophil activating peptide 78 (ENA-78), and the growth-regulated oncogenes, GRO-a, GRO-b and GRO-g. IL-2-stimulated lymphocytes express CXCR3, the receptor for MIG, IP-10, ITAC, and 6Ckine.

Table 2. Primary Expression of Chemokine Receptors[a]

Receptor (Alternative Names)	Primary Expression
CCR1	Monocytes, eosinophils, activated T cells
CCR2	Monocytes, eosinophils, activated T cells
CCR3	Basophils, eosinophils, subset of Th2, monocytes
CCR4	Activated T lymphocytes

CCR5	Monocytes, T lymphocytes
CCR6 (GPR-CY4, DRY6, CKR-L3)	T and B lymphocytes, bone marrow-derived dendritic cells
CCR7 (EBI1)	Activated T and B lymphocytes
CCR8 (Ter1, CemR1)	Monocytes, T lymphocytes
CCR9 (D6)	Bone marrow, T lymphocytes, monocytes
CXCR1 (IL-8RA)	Polymorphonuclear cells (PMNs, neutrophils)
CXCR2 (IL-8RB)	Polymorphonuclear cells (PMNs, neutrophils)
CXCR3	Activated T lymphocytes
CXCR4 (LESTR,HMSTR,Fusin)	Monocytes, T lymphocytes, PMNs
CXCR5 (BLR-1)	B cells
XCR1 (GPR5)	Unknown
CX3CR1 (V28)	Neurons, endothelial cells
DARC (Duffy antigen)	Red blood cells, postcapillary endothelial cells

[a] This table lists cell types that have been widely accepted as expressors of chemokine receptors. It should be noted that many other cell types express these receptors as well.

Eosinophils, basophils, monocytes, NK cells, and T cells respond to members of the family of CC chemokines. These include monocyte chemoattractant proteins (MCP-1, -2, -3, -4, and -5), macrophage inflammatory protein-1a and -1b (MIP-1a, MIP-1b), RANTES (regulated on activation, normal T expressed and secreted), eotaxin-1 and -2, and I-309. Receptors for these chemokines expressed by eosinophils are CCR1 (recognized by MCP-3 and -4; MIP-1; RANTES) and CCR3 (recognized by MCP-3 and -4; eotaxin-1 and -2; RANTES). Basophils express CCR3 and CCR2, which is activated by all the MCPs. Receptors expressed on monocytes are CCR1, 2, 5, and 8. Ligands for CCR5 include MIP-1a, MIP-1b, and RANTES, whereas the ligand for CCR8 is I-309. Activated T cells express CCR1, CCR2, CCR4 (recognized by TARC, the thymus and activation-regulated chemokine), CCR5, and CCR7, whose ligand is MIP-3 and 6Ckine (3, 4).

4. Chemokine Signaling

The ability of pertussis toxin to suppress many of the chemokine-induced signals suggests that the heterotrimeric G_{abg} proteins mediating chemokine signaling belong to the G_i group, which is defined by their ability to inhibit adenylate cyclase. Activation of the G_i protein leads to replacement of GDP with GTP and dissociation into a_i•GTP and bg subunits, both membrane-associated. Downstream mediators of general G_{abg} signaling may include the ***src*** of nonreceptor protein **tyrosine kinases**, phosphatidylinositol 3-kinase (PI3-K), phospholipase C, protein kinase C species, and the Ras-Raf-MEK-ERK kinase cascade (12, 13). Phospholipase C hydrolyzes phosphatidylinositol 4,5-bisphosphate to produce inositol trisphosphate, a mobilizer of intracellular Ca^{2+}, and **diacylglycerol**, which, together with Ca^{2+}, activates protein kinase C (see Second Messengers and Calcium Signaling). Activation of phospholipase D, which generates phosphatidic acid, and phospholipase A2, which releases **arachidonic acid**, may be direct or indirect downstream effects of chemokine stimulation. Immediate effects (within seconds) on cell behavior are generally mediated by reversible changes in protein **phosphorylation** of **cytoskeletal** proteins, directed in part by the small Gtpases Rho, Rac and Cdc42, thereby affecting the polymerization and depolymerization of actin, which underlies the extension and retraction of lamellipodia, implementors of leukocyte migration (3). Longer term changes are effected by **transcriptional** or **posttranscriptional** changes in gene expression.

Evidence for specific signaling intermediates includes the following: The response of neutrophils to chemoattractants can be suppressed by inhibitors of tyrosine phosphorylation, possibly acting on members of the *src* of nonreceptor protein tyrosine kinases (12). In human T lymphocytes, RANTES induces PI3-K; also, wortmannin, which is a potent PI3-K inhibitor, can inhibit RANTES-induced T-lymphocyte responses (14). In a T-cell hybrid, MCP-1 mobilized intracellular Ca^{2+} concentrations, stimulated Ca^{2+} import, and transiently increased tyrosine phosphorylation of the ERKs by a pertussis toxin-sensitive process (15). In human monocytes, Yen et al. (16) obtained evidence for a putative G_q-mediated pathway, distinct from the pertussis toxin-sensitive G_i-dependent pathway, which activated ERK2 via a protein kinase C-dependent process that probably did not require Ras. Both the G_i and the proposed G_q pathways were required for a chemotactic response to MCP-1. MIP-1 activation of the CCR5 receptor expressed in a transfected murine pre-B lymphoma cell line led to phosphorylation and activation of a protein **tyrosine kinase**, known variously as RAFTK, Pyk2, or CAK-b, that is related to focal adhesion kinase (17). The cytoskeletal protein paxillin became phosphorylated and associated with RAFTK, and the downstream signaling kinases JNK/SAPK and p38 also appeared to be stimulated. Thus, chemokines have the ability to activate a variety of signal transduction mechanisms that connect the extracellular environment with the cytoskeleton.

5. Chemokine Functions

As part of the immune defense system, lymphocytes patrol the body, continually surveying it for pathogens or cells expressing abnormal surface antigens (11, 18). They move from the blood stream into tissues and then back into the blood stream via the lymphatic circulation. Granulocytes and monocytes exit the blood stream, but cannot recirculate. Extravasation is a coordinated multistep process that requires a series of complex changes in the activity of molecules on the cell's surface as it undergoes the transition from a freely floating cell to a weakly adherent rolling cell, and then to a strongly adherent stationary cell able to insinuate itself between the endothelial cells and penetrate the underlying stroma. Chemokines help drive this process and, as noted in Table 3, determine what types of cells infiltrate into the tissues in various inflammatory diseases. Imai et al. (19) report that the MDC and TARC chemokines, which are produced by dendritic cells in the thymus, act via the CCR4 receptor to recruit and activate T lymphocytes in the thymus. DC-CK1, another C-C chemokine derived from dendritic cells, is a chemoattractant for naive T cells (20). In allergic diseases such as asthma, expression of eotaxin and monocyte chemoattractant proteins appear particularly important in stimulating the accumulation and activation of eosinophils and mast cells, leading to histamine release and the allergic response (21). Similar events are thought to occur in rhinitis and atopic dermatitis.

Table 3. Chemokine Involvement in Inflammatory Diseases

Inflammatory Disease	Infiltrate	Chemokines Involved
Acute respiratory distress syndrome	Neutrophils	IL-8, GRO-a,b,g, ENA-78
Asthma	Eosinophils, T-cells,	MCP-1,4, MIP-1a,

	monocytes, basophils	Eotaxin, Rantes
Bacterial pneumonia	Neutrophils	IL-8, ENA-78, GRO-a,b,g
Sarcoidosis	T-cells, monocytes	IP-10, MIP-1a, MCP-1, Rantes
Glomerulonephritis	Monocytes, T-cells, neutrophils	MCP-1, GRO
Rheumatoid arthritis	Monocytes, neutrophils	IL-8, MCP-1, IL-8, ENA-78
Osteoarthritis	Monocytes, neutrophils	MIP-1b, IL-8
Atherosclerosis	T-cells, monocytes	IL-8, IP-10, Rantes, MCP-1
Inflammatory bowel disease	Monocytes, neutrophils, T-cells, eosinophils	MCP-1, IL-8, ENA-78, Eotaxin
Psoriasis	T-cells, neutrophils	MCP-1, MIG, IL-8, Rantes, MIP-1
Bacterial meningitis	Neutrophils, monocytes	IL-8, GRO-a, MCP-1, MIP-1a,b
Viral meningitis	T-cells, monocytes	MCP-1, IP-10
Multiple sclerosis	T-cells	Rantes, IP-10, MIP-1a
Seasonal allergic rhinitis	Eosinophils	Eotaxin, Rantes, IL-8, MIP-1, MCP-1
Periodontal disease	Monocytes, PMNs	IL-8, MCP-1

Subsets of lymphocytes express different surface molecules that allow them to target different tissues in the body. Extravasation of the lymphocyte from the blood stream is initiated when a free flowing lymphocyte becomes tethered to the endothelium such that it can still roll in the direction of flow. Rolling of leukocytes is controlled in part by the interaction of selectins with specific sialylated carbohydrate determinants. L-selectin, expressed by lymphocytes, monocytes, neutrophils, and eosinophils, interacts with receptors such as CD34 on the activated endothelium. P-selectin and E-selectin molecules are expressed by activated endothelial cells and bind structures related to the tetrasaccharide sialyl Lewis antigens on the leukocyte surface. Thrombin and histamine can mobilize P-selectin from intracellular stores, whereas up-regulation of E-selectin requires induction by inflammatory agents such as IL-1, tumor necrosis factor, or LPS. This interaction appears to result in activation of leukocyte 1 and 2 integrins, enabling them to bind to ligands of the immunoglobulin superfamily (eg, VCAM-1, the ICAMs; see Cell Adhesion Molecules) either expressed constitutively by the endothelial cells or induced by inflammatory agents. Various subsets of lymphocytes rolling on an ICAM-1 monolayer can be induced to arrest within one second by SDF-1, 6Ckine, MIP-3, or MIP-3; adhesion, which can be prevented by pertussis toxin, is transient, lasting some 5 to 8 minutes (22).

In inflammatory diseases, it is likely that sentinel cells at the site of inflammation produce chemokines that induce the strong interactions required to elicit leukocyte invasion. Chemokine expression has been demonstrated in glomerulonephritis, asthma, inflammatory bowel disease, and allogenic transplant rejection (2, 4). Because multiple inflammatory mediators are generally elaborated at sites of inflammation, the task of determining which is responsible for any particular pathogenic response is difficult. Although there is considerable redundancy built into the system, some chemokines predominate in some forms of injury. For example, IL-8 is a major causative factor associated with reperfusion injury and acid-induced pneumonitis, which is the consequence of neutrophil invasion and the release of inflammatory mediators (23).

Angiogenesis (see Angiogenin), the induction of synthesis of new blood vessels, typically with reference to the vascularization of a tumor, is a complex response affected by many factors, including chemokines. Although the specific role of chemokines in angiogenesis is unclear, evidence has suggested that CXC chemokines possessing the ELR motif generally promote angiogenesis, whereas those lacking the ELR motif tend to inhibit it (24). Mice lacking either SDF-1 or the counterpart receptor CXCR4 are defective in formation (vasculogenesis) of the large vessels supplying the intestinal tract (25). Vessels supplying the small intestine were missing major branches, and this led to hemorrhaging. Likewise, the vascular supply to the stomach in these mice was bereft of all large arteries and veins.

Many functions regulated by chemokines in the immune system, including cell migration and adhesion, as well as cytoskeletal reorganization, are important in the development and function of the nervous system. Defects in brain development in the CXCR4-deficient mouse (and its counterpart, the SDF-1 deficient mouse) are likely to be harbingers of other developmental and brain-specific functions of chemokines (26). The CXCR4-deficient mouse is embryonic-lethal, although with some animals surviving to term. The most prominent defects are found in the development of the cerebellum, where the granule neurons migrate prematurely. Since the radial glial cells are preserved in these animals, the evidence is consistent with an inhibitory role of SDF-1 on granule cell migration. This inhibition could occur by blocking the action of a migratory-promoting substance, or by altering adhesion molecules on the cell surface of the radial glial cell or the granule neuron. Since some of the guidance cues for this migratory process have been identified, it is of obvious importance to investigate if SDF-1 has any action to modulate the expression or conformation of these proteins.

Additional evidence for central nervous system actions of chemokines has been provided by the **transgenic** (see Transgenic Technology) expression of chemokines under the influence of the myelin basic protein **promoter**. Directed expression of the murine chemokine KC stimulated neutrophil infiltration of the brain at various sites (27). Likewise, overexpression of MCP-1 in both thymus and brain led to infiltration of either MAC-1, F4/80, or macrophages and monocytes, respectively (28). These studies demonstrate that each organ is capable of recruiting mononuclear cells under specific conditions.

6. Viral Adaptation to Chemokines

Viruses often exploit endogenous cell surface receptors, including chemokine receptors, in the initial stages of infection. For example, mice deficient in MIP-1 as the result of a targeted gene disruption (**knockout** mice) exhibit attenuated responses to certain viral infections (Coxsackie virus, influenza virus). Several of the chemokine receptors serve as entry mechanisms for various strains of HIV. Roger (29) has reviewed the role of chemokine receptors and the HLA **haplotype** in the development of AIDS. The CCR5 receptor appears to be the preferred coreceptor for macrophage-tropic, nonsyncytium-forming HIV-1 strains, whereas the CXCR4 receptor (fusin) primarily services the syncytium-inducing, T-cell-line-tropic HIV-1 strains (30). Some HIV isolates can utilize both receptors, while a few other variants appear to have acquired the ability to co-opt other chemokine receptors as coreceptors for virus infection. Individuals with mutations in chemokine receptors may exhibit considerable resistance to infection or to progression of the disease. One mutation in particular should be noted. People homozygous for a deletion mutation in the CCR5 gene (CCR5 d32) are resistant to infection by the virus; heterozygotes for the same mutation had a significantly slower onset of disease (31). Chemokines can also affect the progression of an HIV infection. SDF-1, a ligand for CXCR4, inhibits HIV entry into cells (32, 33), and the CC chemokines MIP-1a, MIP-1b, and RANTES, all ligands for CCR5, likewise seem to retard HIV-1 infection (34).

7. Conclusion

The chemokine field is evolving rapidly. Although the initial focus has been on the role of chemokines in the immune system, future directions for chemokine research lie in elucidating chemokine expression and function in other organs and during development. Importantly, the involvement of chemokines and their receptors in many disease processes makes them primary targets for drug development.

8. Acknowledgments

Research in the authors' laboratories has been supported by the National Institutes of Health.

Bibliography

1. N. W. Schluger and W. N. Rom (1997) Current Opin. Immunol. **9**, 504–508.
2. B. J. Rollins (1997) Blood **90**, 909–928.
3. M. Baggiolini (1998) Nature **392**, 565–568.
4. A. D. Luster (1998) New England J. Med. **338**, 436–445.
5. A. Zlotnick, J. Morales, and J. A. Hedrick (1998) Adv. Immunol. in press.
6. A. Pardigol et al. (1998) Proc. Natl. Acad. Sci. USA **95**, 6308–6313.
7. C. McKee et al. (1996) J. Clin. Invest. **98**, 2403–2413.
8. M. R. Horton et al. (1998) J. Immunol. **160**, 3023–3030.
9. R. S. Kornbluth, K. Kee, and D. D. Richman (1998) Proc. Natl. Acad. Sci. USA **95**, 5205–5210.
10. P. Loetscher, M. Seitz, M. Baggiolini, and B. Moser (1996) J. Exp. Med. **184**, 569–577.
11. M. B. Furie and G. J. Randolph (1995) Amer. J. Pathol. **146**, 1287–1301.
12. G. M. Bokoch (1995) Blood **86**, 1649–1660.
13. J. S. Gutkind (1998) J. Biol. Chem. **273**, 1839–1842.
14. L. Turner, S. G. Ward, and J. Westwick (1995) J. Immunol. **155**, 2437–2444.
15. P. M. Dubois et al. (1996) J. Immunol. **156**, 1356–1361.
16. H.-h. Yen, Y. Zhang, S. Penfold, and B. J. Rollins (1997) J. Leukoc. Biol. **61**, 529–532.
17. R. K. Ganju et al. (1998) Blood **91**, 791–797.
18. T. A. Springer (1994) Cell **76**, 301–314.
19. T. Imai et al. (1998) J. Biol. Chem. **273**, 1764–1768.
20. G. J. Adema et al. (1997) Nature **387**, 713–717.
21. B. Lamkhioued et al. (1997) J. Immunol. **159**, 4593–4601.
22. J. J. Campbell et al. (1998) Science **279**, 381–384.
23. H. G. Folkesson, et al. (1995) J. Clin. Invest. **96**, 107–116.
24. R. M. Strieter et al. (1995) J. Leukocyte Biol. **57**, 752–762.
25. K. Tachinaba et al. (1998) Nature **393**, 591–594.
26. Y-R. Zou et al. (1998) Nature **393**, 595–599.
27. M. E. Fuentes et al. (1995) J. Immunol. **155**, 5769–5776.
28. M. Tani et al. (1996) J. Clin. Invest. **98**, 529–539.
29. M. Roger (1998) FASEB J. **12**, 625–632.
30. Y. Feng, C. C. Broder, P. E. Kennedy, and E. A. Berger (1996) Science **272**, 872–877.
31. M. W. Smith et al. (1997) Science **277**, 959–965.
32. C. C. Bleul (1996) Nature **382**, 829–833.
33. E. Oberlin et al. (1996) Nature **382**, 833–835.
34. D. Zagury et al. (1998) Proc. Natl. Acad. Sci. USA **95**, 3857–3861.

Chemotaxis

Chemotaxis is the movement of a motile cell in response to chemical changes in the environment, and it implies a directional sense. In most cases where **bacteria** migrate up concentration gradients of attractants, direction is not sensed directly. The small size of bacteria would make spatial comparisons of concentration unreliable. Instead, bacteria usually sense temporal changes in concentration by using chemoreceptors, **transducer proteins** that bind or release attractants and repellents. This temporal measurement allows the cells to alter motion of their **flagella** briefly so that a "biased random walk" brings the bacteria to the right destination (1, 2) (Fig. 1). Eukaryotic cells carry out chemotaxis by an unrelated mechanism, and they are much larger and probably do sense direction.

Figure 1. Motion of peritrichous bacteria. (**a**) Random walk in an isotropic medium. (**b**) Biased random walk in a gradient of an attractant or repellent.

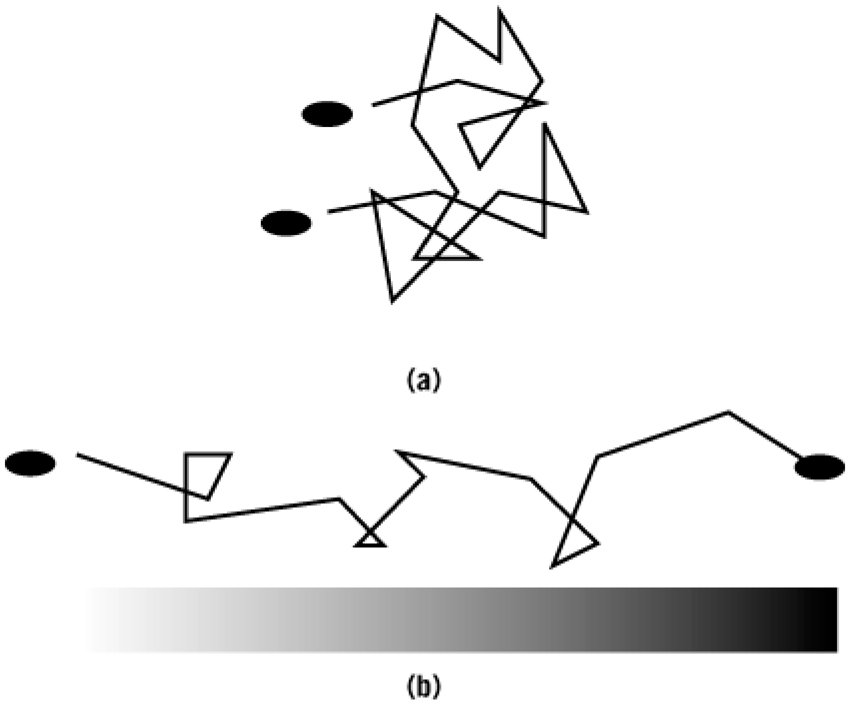

1. Bacteria

There are three main types of motile bacteria: 1) the peritrichous (flagella over the surface), 2) the polar (flagella at one or both poles), and 3) the gliding bacteria, which lack flagella.

The peritrichous bacteria, such as ***Escherichia coli*** and ***Bacillus** subtilis*, normally swim smoothly by rotating their flagella counterclockwise (looking along the flagella toward the cell body) and tumble by rotating their flagella clockwise, which discoordinates the bundle of flagella. Chemotaxis in *E. coli* occurs when the cell happens to move toward higher attractant concentrations. It decreases the probability of tumbling and, thus, increases the tendency to travel up the attractant gradient (1).

This decreased probability of tumbling results (Fig. 2) because the attractant molecules bind to methylated chemoreceptors to cause a brief inactivation of the cytoplasmic CheA **kinase** (see **Transducer proteins**). Consequently, there is less phosphorylated CheA (CheA-P) and less CheY-P (2) (see **Phosphorylation**). CheY-P dissociates from the switch that controls flagellar rotation, so that smooth swimming ensues. The enhanced smooth swimming is short-lived because CheZ hydrolyzes the phosphoryl group from CheY, and the CheR **methyltransferase** increases the degree of methylation of the chemoreceptor and restores the prestimulus activity of CheA (3) (see also Methylation, Protein). Thus, there is an inverse relation between the levels of CheY-P and termination of a smooth swimming event.

Logically, it seems plausible that bacteria moving by chance toward *lower* attractant concentrations would show an increased tendency to tumble and, hence, to begin heading in another direction. In the case of *E. coli*, however, there is no demonstrable increased tendency for these bacteria to tumble compared with bacteria in an isotropic medium (1). Interestingly, CheY-P cannot affect rotational direction of the flagella by itself. Fumarate needs to be released or synthesized for switching to occur (4) and also promotes tumbling (5). The connection between CheY-P and fumarate in controlling direction of flagellar rotation has not been elucidated.

The role of CheY-P is less clear in the case of polar bacteria, such as *Caulobacter crescentus* and ***Pseudomonas*** *aeruginosa.* When these bacteria move by chance toward lower concentrations of attractant, they reverse motion by rotating their flagella in the opposite direction, to head back up the gradient. If repellent is added, however, they show a series of reversals of motion. This result implies that CheY-P does not govern the *direction* of rotation of the flagella but instead causes repeated reversals of behavior. Such an event might ensue if binding of CheY-P to the switch reduces the energy of activation of switching the flagellar rotational direction. In the absence of binding, the energy of activation is presumed to be so high that reversals are very infrequent. In the case of *Halobacterium salinarium,* negative stimuli cause significant increases in the concentrations of free fumarate in the cytoplasm (4).

Other bacteria, like *Sinorhizoboium meliloti,* a **Gram-negative** bacterium phylogenetically rather distant from *E. coli*, rotate their flagella unidirectionally. In this case, the CheA/CheY system also exists with the complication that there are two species of CheY. CheY2-P is the major species that affects flagellar movement, and it acts by slowing flagellar rotation (6). Some bacteria, such as *Rhodobacter sphaeroides*, have multiple copies of many of the *che* genes (7).

Figure 2. Diagram of the mechanism of chemotaxis in *Escherichia coli*. Open arrows indicate control of the designated reaction or signaling step. At the *top*, the attractant (Att) binds to its transmembrane chemoreceptor, which is methylated on Glu residues. The methyl groups are depicted as closed black circles. This binding decreases the phosphorylated form of the protein CheA (*center*), which decreases phosphorylation of the proteins CheY and CheB. Dephosphorylated CheB is much less active in removing the methyl groups from the chemoreceptor, so CheR restore them. Phosphorylated CheY dissociates from the switch that controls flagellar rotation, and smooth swimming ensues. CheZ hydrolyzes the phosphoryl group from CheY, ending the response to the attractant.

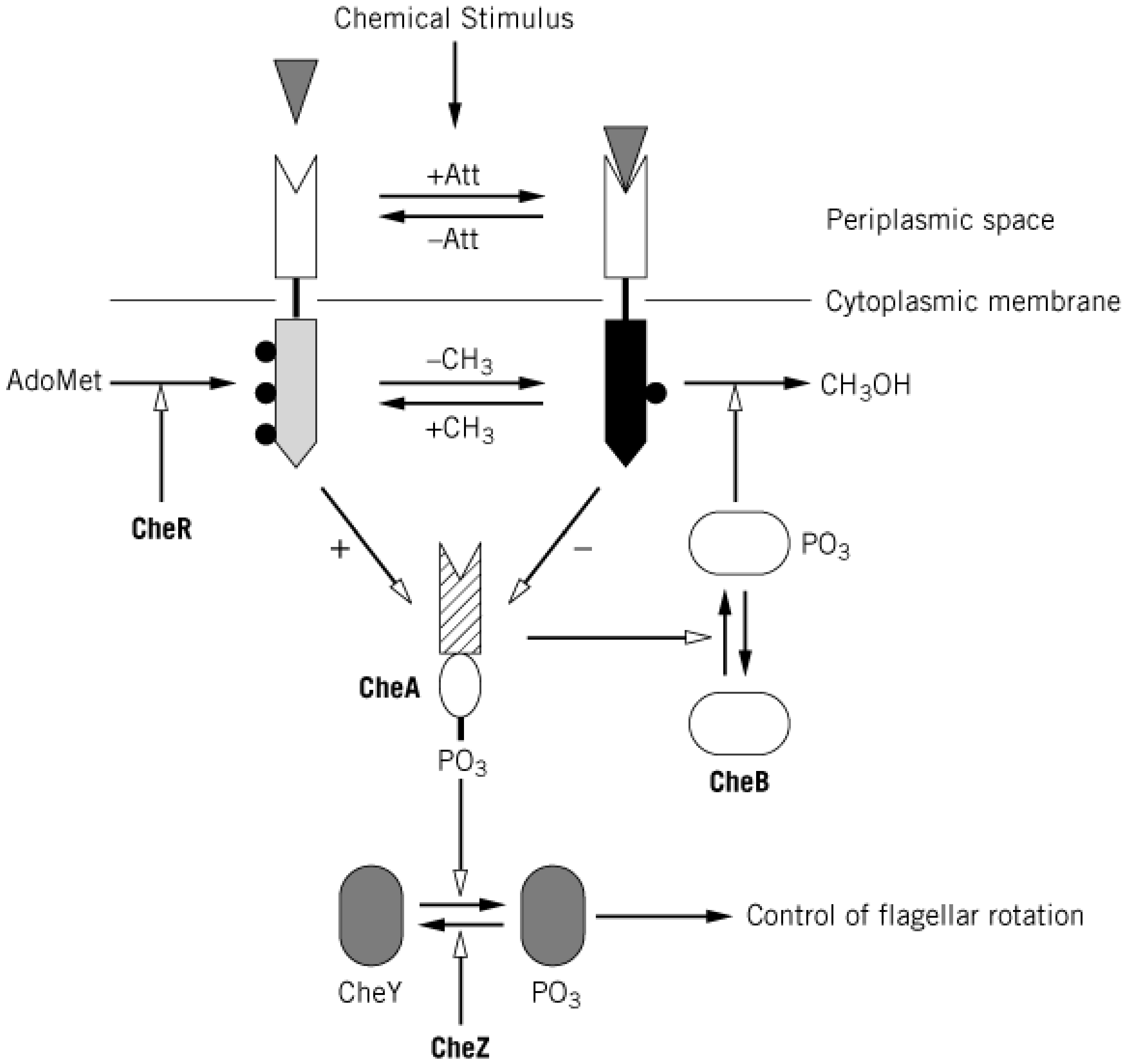

Thus, it appears that the basic system involving the two-component couple CheA and CheY is universal, but how it functions varies for different groups of organisms.

The potential role for CheY-P is still less clear in the case of the gliding bacteria. One of them, *Myxococcus xanthus*, has two motility systems, the S (social) system powered by extrusion and retraction of pili from the ends and the A (adventurous) system, powered by a mechanism of unknown structure along the sides. The former coordinates cells and, unless the agar concentration is quite low, requires cell contact for movement. The frequency and pole at which pili activity occurs is governed by the Frz proteins, which are homologous to the chemotaxis proteins in flagellated cells. However, none of the genes encode a single-domain CheY (8, 9).

One issue that has existed for many years has been whether the rotation of multiple flagella are coordinated or independent. The finding that bundles of flagella located 50 mm apart on *Spirillum volutans* were observed switching synchronously within 10 ms implies electrical coordination of direction of the flagellar rotation (1). In contrast, certain mutant strains of ***Salmonella*** *typhimurium* show random and uncorrelated switching of their flagellar direction when observed under partially de-energized conditions (10). *E. coli* filamentous cells switch their flagella asynchronously although biases of nearby, but not distant, motors were correlated (11). In *H. salinarium*, an **archaeon,** the rotational direction of flagellar bundles on each end is also uncoordinated, and cells were frequently observed to be immobilized because the bundles at both ends worked against each other. Thus, there is no general rule governing flagellar coordination. Indeed, the mechanism by which an electrical connection could work, as in *S. volutans*, is obscure.

2. Eukaryotes

Chemotaxis in eukaryotes occurs by an unrelated mechanism. The process is best known from studies in the aggregating slime mold ***Dictyostelium*** *discoidium* and in leucocytes; it is probably quite similar in both. In the slime mold, chemotaxis plays a role in feeding and in the aggregation that precedes **differentiation** and **sporulation**. Chemotaxis in *Dictyostilium* involves apparent polarization of the cell to form pseudopodia or lamellipodia at the leading edge at the highest concentration of attractant molecules. Polarization and formation of pseudopodia are concerted events regulated by G protein-coupled/serpentine **cyclic AMP** (cAMP) receptors (cARs) along the surface of the organism. During aggregation, cAMP is produced and binds to a cAR, which activates a heterotrimeric **G-protein**. **Guanylate cyclase** is activated by operation of this G-protein, thereby producing cGMP. cGMP activates a cGMP-dependent protein kinase, which regulates myosin II heavy and light chain kinases and may also help regulate the actin cytoskeleton. Phosphorylation of the myosin heavy chain causes it to depolymerize so that pseudopod extension can only occur locally. Posteriorly, contraction occurs and pseudopod formation is blocked. At the same time cAMP binding to its receptor leads to activation of phosphatidylinositol-3 kinase. The product, phosphoinositol-3,4,5-triphosphate, attracts PH (pleckstrin homology) proteins, including the kinase Akt/PKB, to the localized region where the local amount of cAMP-bound receptor is highest. Another PH domain protein is CRAC. It is required for receptor activation of adenylyl cyclase (see below), which then propagates the cAMP signal to neighboring cells. This membrane localization lasts only 5 to 8 s; however, that is long enough to produce an "activation domain" as a focus for multiple pathways needed for chemotaxis, pseudopod extension, and cell polarization. F-actin is assembled primarily there. Actin polymerization is activated by formation of an Arp2/3 protein complex. Nucleation is induced by Arp2/3 interaction with WASp and Scar adaptor proteins. These proteins provide the structural linkage to the activated cAR through the activated form of Rac and Cdc42, which are regulated by the G protein G_{bg}. Pseudopod formation also requires actin crosslinking and filament growth regulated by actin binding proteins (12, 13).

Binding of cAMP to the receptors transiently activates both adenylyl cyclase and ERK2 MAP kinase. A rise in internal cAMP activates protein kinase A such that it inhibits ERK2 and leads to loss of ligand binding by the receptor. ERK2 also phosphorylates the cAMP diesterase REG A that reduces the internal concentration of cAMP. A secreted membrane-associated phosphodiesterase reduces the external cAMP concentrations, and the cells become sensitive again. These features account for spontaneous oscillations of external cAMP production of about 6 min that permit chemotactic migration of cells toward centers during the aggregation process (14).

Bibliography

1. H. C. Berg (1975) Annu. Rev. Biophys. Bioeng. **4**, 119–136.
2. J. B. Stock and M. G. Surette (1996) In *Escherichia coli and Salmonella, Cellular and Molecular Biology*, 2 ed. (F. C. Neidhardt, ed.), ASM Press, Washington, DC, Vol. **I**, pp. 1103–1129.
3. J. S. Parkinson (1993) Cell **73**, 857–871.
4. R. Barak and M. Eisenbach (1996) Curr. Top. Cell. Reg. **34**, 137–158.
5. K. Prasad, S. R. Caplan, and M. Eisenbach (1998) J. Mol. Biol. **280**, 821–828.
6. V. Sourjik and R. Schmitt (1996) Mol. Microbiol. **22**, 427–436.
7. J. P. Armitage Adv. Microbiol. Physiol. **41**, 229–289.
8. H. Sun, D. R. Zusman, and W. Shi (2000) Curr. Biol. **10**, 1143–1146.
9. M. J. Ward and D. R. Zusman (1997) Mol. Microbiol. **24**, 885–893.
10. R. M. Macnab and D. P. Han (1983) Cell **32**, 109–117.

11. A. Ishihara, J. E. Segall, S. M. Block, and H. C. Berg (1983) J. Bacteriol. **155**, 228–237.
12. R. A. Firtel and R. Meili (2000) Curr. Opin. Genet. Develop. **10**, 421–427.
13. R. A. Firtel and C. Y. Chung (2000) BioEssays **22**, 603–615.
14. M. T. Laub and W. F. Loomis (1998) Mol. Biol. Cell **12**, 3521–3532.

Suggestions for Further Reading

15. J. J. Falke and S. H. Kim (2000) Structure of a conserved receptor domain that regulates kinase activity: the cytoplasmic domain of bacterial taxis receptors. Curr. Opin. Struct. Biol. **10**, 462–469.

Chimera

Spemann (1, 2) was the first to employ the term "chimera" and to consider the great potential for surgically created chimeric embryos in the analysis of **developmental** mechanisms. The chimera method has frequently involved imaginative experimental procedures by which cells of one species are grafted into another. Any animal thus composed of different cell populations that derive from more than one fertilized egg should be considered as a chimera. This type of animal can currently be constructed in amphibians, birds, and mammals.

Many fundamental concepts of embryology have been at least partly formulated on the basis of results of cell or tissue transplants between two different embryos, usually separate species of amphibians. The most spectacular transplantation experiments, published by Spemann and Mangold in 1924 (3), demonstrated the organizing power of the dorsal lip of the blastopore during gastrulation by interspecific transplantations of this area. More recently, a model of lens induction was developed by using chimeric eyes (4). The technical advantages of producing amphibian chimeras are straightforward, owing to the independence of the embryos from their parents. They are easily accessible and receptive to foreign tissue, even across species barriers. All these qualities are not shared by higher vertebrates, such as birds and mammals. Nonetheless, bird embryos have several advantages over other vertebrate embryos, making certain interesting approaches feasible. The greatest advantage is continual accessibility within the egg throughout the developmental period. Another is the ease with which the various rudiments can be delineated, and thus removed and replaced, with extreme precision. An avian chimera obtained by combining quail and chick cells has been the most successful method, having provided a continual source of new data about developmental mechanisms for almost 30 years (5, 6). With the advent of the quail-chick nuclear marker, which is particularly simple to employ, easy to identify, and endowed with great resolving power, avian chimeras have been used to study the ontogeny of the nervous system, the development of the hematopoietic and immune systems, and the formation of muscles and skeleton. Quail heterochromatin in the nucleus is concentrated around the nucleolus. This creates a large, deeply staining mass that is easily distinguishable from the diffuse heterochromatin of chick cells. Moreover, there are some antigens that are quail-specific and not detectable in chick cells. These phenomena allow individual quail cells to be readily distinguished, even when most of the cell population is chick.

Although the avian embryo is a practical model, perfectly suitable for tissue graft experiments after the incubated egg is opened, it is difficult to undertake this type of investigation in the mammalian fetus *in utero*. Nonetheless, it has become routine to remove postimplanted mammalian embryos from the uterus, manipulate them, and return them to a foster mother for further development. Thus, chimeric mice are the result of two or more early-cleavage (usually 4- or 8-cell) embryos that have been artificially aggregated to form a composite embryo. Since each cell is able to produce any component of the body, the construction of the chimeric mouse has very important consequences for the study of mammalian ontogeny. A very powerful application of this technique is the transfer of genes into every cell of the mouse embryo. During mouse development, there is a stage when only two cell types are present: outer cells, which will form the fetal portion of the placenta, and inner cells, which will give rise to the embryo itself. These inner cells are known as embryonic stem cells because each in isolation can generate all the cells of the embryo (7, 8). These cells can be grown in culture, where they are treated to incorporate new DNA. The new embryonic stem cells can then be injected into another early-stage mouse embryo, resulting in a chimeric mouse. Mice that derive from these animals are **transgenic** mice. Our understanding of regulatory mechanisms in mammalian development is improving increasingly rapidly as a result of the construction of these genetically modified mice. A combination of the tools of developmental genetics with those of embryology should lead to real advances in the study of such mechanisms. In this field, our group has pioneered the grafting of embryonic tissues from transgenic mice into the chick embryo (9, 10). Owing to these interspecies grafting experiments, it is possible to monitor factors that regulate the expression of a particular gene *in vivo*. The value of this technique is greatly increased when a reporter gene is used to follow the changes in gene expression of the grafted cells. The possibility of conducting grafts until late stages of *in vivo* development allows the behavior of wild and mutant mouse cells to be observed at any developmental stage and location.

1. Amphibian Chimera

Using amphibians, Spemann and Mangold (3) improved our understanding of the specification of the nervous system by transplanting dorsal blastopore lip tissue from an early gastrula into the ventral ectoderm of another gastrula. They used differently pigmented embryos from two species of newt: darkly pigmented *Triturus taeniatus* and nonpigmented *Triturus cristatus*. On the basis of color, it was easy to distinguish host and donor tissues. The dorsal blastopore lip tissue from early *Triturus taeniatus* gastrula, once transplanted into an early *Triturus cristatus* gastrula in the region, would normally become ventral epidermis. In fact, the donor tissue did not become belly skin but invaginated and formed a secondary embryo, face to face with its host. The more recent use of nuclear markers has allowed Spemann's results to be confirmed (11). Such chimeras elegantly demonstrate the organizing power of the dorsal lip of the blastopore in amphibian gastrula, since whole secondary embryos formed under the influence of the transplanted tissue.

Considerable advances have also taken place in the field of differentiation and organogenesis through the use of amphibian chimeras. The more common examples are those involving the interaction of epithelia with adjacent mesenchyme. After being separated, embryonic epithelium and mesenchyme can be recombined in different ways (12). In a classic experiment, Spemann and Schotté (13) transplanted flank ectoderm from an early frog gastrula into the region of newt gastrula destined to become part of the mouth. Similarly, the presumptive flank ectodermal tissue of newt gastrula was placed into the presumptive oral regions of frog embryos. The structures of the mouth region differ greatly between salamander and frog larvae. The *Triturus* salamander larva has club-shaped balancers beneath its mouth, whereas frog tadpoles produce mucus-secreting glands and suckers. Frog tadpoles also have a horny jaw without teeth, whereas the salamander has a set of calcareous teeth in its jaw. The larvae resulting from the transplants were chimeras. The salamander larvae had froglike mouths, and the frog tadpoles had salamander teeth and balancers. In other words, the mesodermal cells instructed the ectoderm to make a mouth, but the ectoderm responded by making the only mouth it “knew” how to make. Thus, instructions sent by mesenchymal tissue can cross species barriers, although the response of the epithelium is species-specific. Thus, organ-type specificity is usually controlled by the mesenchyme within a species, but species specificity is usually controlled by the responding epithelium.

The cells that form the lens are derived from a region of head ectoderm in contact with optic vesicles of the anterior neural plate. Servetnick and Grainger (14) removed animal cap ectoderm from various gastrula stages and then transplanted them into the presumptive lens region of neural-plate-stage embryos. Ectoderm from early gastrula showed little or no competence to form lenses, but ectoderm from slightly later stages was able to. By the end of gastrulation, this ability to respond to the neural plate signal had been lost. This competence was found to be inherent within the ectoderm itself and not induced by other surrounding tissues. These observations showed that only mid- to late-gastrula ectoderm is able to respond to signals from the anterior neural plate. It has recently been demonstrated that the transcription factor Pax6 may play a role in the determination processes of eye tissue (see Pax Genes).

2. Avian Chimera

When portions of quail embryo are grafted into a similar region of chick embryo, the cells become integrated into the host and participate in the construction of the appropriate organs. This grafting is done while the embryo is still inside the egg, and the chick that hatches is a "chimera," having a portion of its body composed of quail cells (15). The quail is usually chosen as a donor because it is easier to identify quail cells among chick cells than the reverse.

The ontogeny of the peripheral nervous system is one of the fields in which the use of avian chimeras is the most fruitful. This system arises almost entirely from the neural crest, a transient structure that develops at the neural tube apex. To follow the fate of chick neural tube-bearing neural crests, a segment is replaced by a homologous quail fragment. This method has permitted the diverse range of neural crest potentialities to be well-described, and the list of neural crest derivatives well-defined (6).

In relation to its origin, neural crest not only participates in the formation of spinal and cranial sensory ganglia, sympathetic and parasympathetic ganglia and plexuses, and Schwann cells of the peripheral nerves, but it also gives rise to endocrine and paraendocrine cells (calcitonin-producing cells, carotid body type-I cells, adrenomedullary cells) and pigment cells. The construction of an avian chimera has demonstrated the contribution of the cephalic neural crest to mesectodermal derivatives. For example, nasal and maxillary processes are built up partly by crest cells of mesencephalic origin. The mesencephalic crest cells also form the cephalic skeleton, the upper and lower jaws, the palate, and the tongue. The rhombencephalic crest participates in formation of the pre-optic region and the hyoid arch skeleton. In addition to cartilage and bone, the cephalic neural crest takes part in other derivatives of the head and neck, such as dermis and connective tissue.

Brain development has also been characterized by the use of the quail-chick chimera technique (16). Quail-chick brain chimeras can hatch and survive without showing impaired movement or locomotion, which indicates that functional synapses have been established between host and donor neurones, as well as between donor neurones and host muscles. Moreover, the normal behavior of the chimeras demonstrates that proper neuronal connections develop in the brain, which means that quail axons recognize local signals for growth and directionality in the chick environment, as they do in normal development. An interesting application of the chimeras is illustrated by chicks with transplanted quail mesencephalic-diencephalic brain areas, which then exhibit quail vocalization (17). Another important issue is the elucidation of when and where groups of cells in the brain make commitments to particular development pathways. Genes with spatially restricted expression are of particular interest, since they may indicate the existence of committed groups of cells that are important in pattern formation, but are not discernible on the basis of morphology. An example is provided by the **zinc-finger** gene *Krox-20*, which has restricted domains of expression in the early neural plate. *Krox-20* is expressed in the early neural epithelium, first in one stripe, and then in two stripes in the hindbrain. Subsequently, *Krox-20* is expressed in two alternating segments (rhombomeres) in the hindbrain. The generation of stripes of *Krox-20* expression in the early neural plate suggests that rhombomeric precursor cells are committed prior to the morphological appearance of the rhombomere.

Hox homeotic gene expression is seen along the dorsal axis, from the anterior boundary through to the tail. Direct evidence for hindbrain plasticity comes from quail-chick chimera experiments showing that anterior-to-posterior transpositions can reprogram Hox expression and induce a transformation in cell fate (18). The quail-chick system has also shown that environmental cues play a significant role in maintaining the Hox code in the neuroepithelium.

Chimeric experiments involving the muscles of the body, limbs, and skeleton have also been carried out in birds. For development, somites are the primitive metameric structures of the vertebrate body from which arise the vertebrae that surround the spinal cord, the muscles and connective tissue holding the vertebrae, the dermal layer of the skin of the back, and the limb musculature. All these data were obtained by constructing a chimeric embryo after interspecific grafts of somites between quail and chick embryos (19, 20). The somites appear as pairs of epithelial spheres that bud off from the unsegmented paraxial mesoderm in a craniocaudal direction. They become polarized into a ventral mesenchymal compartment, the sclerotome, which yields the dorsal skeleton, and a dorsal epithelial component, the dermomyotome, from which striated muscle and dermis arise. By constructing a quail-chick chimera after interspecific exchanges of medial or lateral halves of newly-formed somites, Ordhal and Le Douarin (21) determined that, regardless of the somites, cells farthest from the neural tube (ie, lateral) migrate to form the body wall and limb musculature.

The interspecies graft method in birds has contributed considerably to understanding the control mechanisms of somite patterning. This method demonstrates that specification of the somite is accomplished by the interaction of different tissues that form its environment. In fact, the newly formed somite is composed mostly of unspecified cells, and the determination of somite compartments toward the different lineages is regulated by environmental cues. The ventral-medial portion of the somite is induced to become the sclerotome by factors, especially *Sonic hedgehog* protein, that are secreted from the notochord and neural tube floor plate. If portions of the notochord, the source of Sonic **hedgehog**, are transplanted next to other regions of the somite, those regions also become sclerotome cells. These sclerotome cells express a new transcription factor, Pax1, which activates cartilage-specific genes and is necessary for the formation of vertebrae (22). In similar ways, the myotome is induced by two distinct signals. The muscles surrounding the body axis, which arise from the medial portion of the somite, are induced by factors from the dorsal neural tube, probably members of the *Wnt* family (23, 24). The muscles derived from the lateral portion of the somite, which form the musculature of the limbs and body wall, are probably induced through the combination of Wnt proteins from the epidermis with bone morphogenetic protein-4 (BMP4) protein from the lateral plate mesoderm (25). These factors cause the myotome cells to express particular transcription factors, MyoD and Myf5, that activate muscle-specific genes. The dermatome differentiates in response to another factor secreted by the neural tube, neurotrophin 3 (NT-3) (26).

3. Mammalian Chimera

The laboratory mouse is by far the most popular mammal used to construct chimeras for developmental studies. Mice offer a large variety of genetically well-characterized strains that provide scope for using genetic markers. Moreover, they breed throughout the year and thus continually supply embryos. The most convenient time for manipulation of a mammalian embryo is before its implantation. During the first three to four days of gestation, mouse embryos have not yet formed an attachment in the mother's reproductive tract and can thus be explanted, manipulated, and then retransplanted into another mouse to continue their development. Chimeric mice are generally formed by the fusion of two early embryos that organize to produce a single mouse with two distinct cell populations.

A skeletal muscle cell (myotube) is an elongated cell containing many nuclei. It has been widely debated whether this cell is derived from the fusion of several mononucleated precursor cells (myoblasts) or from a single cell that undergoes nuclear division without cell division. Evidence for the fusion process has been provided by mouse chimeric constructions. Mintz and Baker (27) fused mouse embryos from two strains that produce different types of the dimeric enzyme isocitrate dehydrogenase: one strain makes the A subunit and the other B. If myotubes are formed from one cell whose nuclei divide without cytokinesis, the dimeric enzyme will be purely AA or BB. If, however, myotubes are formed by fusion between cells, some might code for the B subunit and others for A, in which case the molecules of the enzyme will be hybrid (AB). Electrophoresis can separate these three types (see Isozyme, Isoenzyme). The presence of the hybrid AB enzyme in extracts of skeletal muscle tissue confirms the fusion model.

The study of mutations that impair development or function has long been recognized as a valuable means of elucidating the normal role of genes in such processes. Genetically chimeric animals consisting of mixtures of mutant and wild type cells can be of considerable value for studying the genes that are primarily implicated in developmental mechanisms. Methods of manipulating mouse embryos and transferring genes into every embryonic cell are now standard procedures. In recent years, an extraordinary increase in the use of these methods has led to numerous exciting prospects.

The most widely used method to produce transgenic mice is to inject **cloned** DNA into a pronucleus of a fertilized egg. Although this method has been used primarily for studies of **gene expression**, an unexpected benefit is the frequent integration of the injected DNA into genes, causing insertional mutations. Experimental infection of embryos by retroviruses has also been developed as a method for gene transfer. As in the case of spontaneous infection, this approach has resulted in insertional mutations. An additional approach to producing transgenic mice involves genetic modification of tissue culture lines of embryonic stem cells, followed by their re-incorporation into growing embryos. By applying somatic cell genetic techniques to these cells while in culture, both random and selected insertional mutations have been produced. Another method for assaying the function of a gene is to eliminate it from the genome of the whole organism. Very recent studies, using strategies to inactivate genes by homologous recombination in embryonic stem cells, with the subsequent generation of germ-line chimeras, have made this scenario possible and thereby initiated a new era in mammalian developmental biology.

The power of this technology can be illustrated by the *int-1* gene, which is expressed during central nervous system development in a temporally and spatially restricted fashion. Following inactivation of the gene by homologous recombination in embryonic stem cells, germ-line chimeras were obtained and bred to derive homozygous *int-1*-deficient mice. These homozygous mice were not viable, because specific regions of the brain were missing. This experiment indicates that *int-1* is an essential gene for early development and suggests that its expression might determine the fate of a cell. The *Hox a-3* gene has been found to control segment-specific gene expression in Drosophila, but what is its role in mammals? Chisaka and Capecchi (28) used gene targeting to determine the function of *Hox a-3* in the development of the mouse. Homozygous mutants of *Hox a-3* were found to have severe anomalies in development of the hindbrain and in mesectodermal neural crest derivatives and to lack thyroid, parathyroid, and thymus glands. These studies clearly open up new avenues for the study of mammalian development at the molecular level and will certainly be instrumental in unraveling the molecular networks responsible for the functioning of a multicellular organism.

4. Mammalian Avian Chimera

In chimeras, the analysis of cell lineages depends on the ability to distinguish between cells of different origins. Markers are required to trace the developmental fate of cells and to recognize them at all ages in chimeric embryos. In mammals, genetic manipulations appear to be valuable means of elucidating the normal role of genes and identifying altered cells. Furthermore, the environment of the chimera allows these cells to survive and to display their phenotype. In chimeras, identification of all the descendants of genetically modified cells has thus far provided a reliable and sensitive means of measuring alterations in embryogenesis. In conjunction with an *in situ* marker, this may help in determining the cell type and the nature of the functions affected by the particular mutant. Extremely sensitive labeling is possible with transgenic mouse lines since cells that integrate foreign DNA, such as a reporter gene encoding for *Escherichia coli* b-galactosidase, are detectable by simple histochemical revelation, which can be used to differentiate grafted cells from host cells. Currently, the major means of exploring this genetic tool is by *in vitro* experiments in which mutant-induced tissue is cultured with wild-type tissue. The culture system is efficient in tissue development for only limited periods, however, and the media used may affect the tissue outcome. *In vivo* micromanipulation remains the most powerful means of studying the fates of cells, their origins, and the cell-cell interactions that govern development. Since implantation of mouse embryo is particularly unsuitable for *in vivo* manipulation, chick embryo is used as the site for developing mouse embryonic cells. Studies in such chimeras provide considerable information on the lineage and the differentiation of mouse embryonic cells, since *in ovo* grafted mouse cells are accessible throughout chick host embryogenesis. Moreover, these results are indicative of the information to be obtained through genetic manipulations in conjunction with embryonic tissue transplantation. It has been clearly demonstrated that *in ovo* transplantation provides a suitable environment for the development of mammalian cells and that the information supplied by this environment is capable of promoting mouse cell differentiation.

Chimeras were prepared by transplanting somites from nine-day postcoitum mouse embryos into two-day-old chick embryos at different axial levels. Mouse somitic cells then differentiated *in ovo* into dermis, cartilage, and skeletal muscle, as they normally do in the course of development, and were able to migrate into chick host limb. To trace the behavior of somitic myogenic stem cells more closely, somites arising from mice bearing a transgene of the desmin gene linked to a reporter gene coding for *E. coli* b-galactosidase were grafted *in ovo*. Interestingly, the transgene was rapidly expressed in myotomal muscles derived from implants. In the limb muscle mass, positive cells were found several days after implantation. This method facilitates investigation of the mechanisms of mammalian development, allowing the normal fate of implanted mouse cells to be studied and providing suitable conditions for identification of descendants of genetically modified cells.

Chimeras were also prepared by transplanting fragments of neural primordium mouse embryos into chick embryos at different axial levels. Mouse neuroepithelial cells differentiated and organized to form the different cellular compartments normally constituting the central nervous system. The graft entered into the development of the peripheral nervous system through migration of neural crest cells associated with mouse neuroepithelium. Depending on the graft level, mouse crest cells participated in the formation of various derivatives, such as head components, sensory ganglia, orthosympathetic ganglionic chain, nerves, and neuroendocrine glands. Knock-out mice with the tenascin genes inactivated, which express LacZ instead of tenascin and show no tenascin production (29), were used specifically to follow Schwann cells lining nerves derived from the implant. Together with the previous results on somite development, this study shows that the chick embryo constitutes a privileged environment, facilitating access to the developmental potentials of normal or defective mammalian cells. It allows study of the histogenesis and precise timing of formation of a known structure, as well as the implications of a given gene at all equivalent mammalian embryonic stages.

Bibliography

1. J. Spemann (1901) Arch. Entwicklungsmech. Org. **12**, 224–264.
2. J. Spemann (1921) Arch. Entwicklungsmech. Org. **48**, 533–570.
3. J. Spemann and H. Mangold (1924). Arch. Mikrost. Anat. Arch. Entwicklungsmech. **100**, 599–638.
4. J. J. Henry and R. M. Grainger (1987) Dev. Biol. **124**, 200–214.
5. N. M. Le Douarin (1969) Bull. Biol. Fr. Belg. **103**, 435–452.
6. N. M. Le Douarin (1982) *The Neural Crest*, Cambridge University Press, London and New York.
7. R. L. Gardner (1968) Nature **220**, 596–597.
8. L. A. Moustafa and R. L. Brinster (1972) J. Exp. Zool. **181**, 193–202.
9. J. Fontaine-Pérus, V. Jarno, C. Fournier Le Ray, Z. L. Li, and D. Paulin (1995) Development **121**, 1705–1718.

10. J. Fontaine-Pérus, P. Halgand, Y. Chéraud, T. Rouaud, M. E. Velasco, C. Cifuentes-Diaz, and F. Rieger (1997) Development **124**, (16), 3025–3036.
11. R. L. Gimlick and J. Cook (1983) Nature **306**, 471–473.
12. J. W. Saunders Jr, J. M. Cairns, and M. T. Gasseling (1957) J. Morphol. **101**, 57–88.
13. H. Spemann and O. Schotté (1932) Naturwissenschaften **20**, 463–467.
14. M. Servetnick and R. M. Grainger (1991) Development **112**, 177–188.
15. N. M. Le Douarin and M. A. Teillet (1973) J. Embryol. Exp. Morphol. **30**, 31–48.
16. N. M. Le Douarin (1993) TINS **16**, 64–72.
17. E. Balaban (1988) Proc. Natl. Acad. Sci. USA **85**, 3657–3660.
18. A. Grappin-Botton, M. A. Bonnin, L. A. McNaughton, R. Krumlauf, and N. M. Le Douarin (1995) Development **121**, 2707–2721.
19. A. Chevallier, M. Kieny, A. Mauger, and P. Sengel (1977) *Vertebrate Limb and Somite Morphogenesis*, Cambridge University Press, Cambridge, pp. 421–432.
20. B. Christ, H. J. Jacob, and M. Jacob (1977) Anat. Embryol. **150**, 171–186.
21. C. P. Ordhal and N. Le Douarin (1992) Development **114**, 339–353.
22. C. A. Smith and R. S. Tuan (1996) Teratology **52**, 333–345.
23. A. E. Münsterberg, J. Kitajewski, D. A. Bumcroft, A. P. McMahon, and A. Lassar (1995) Genes Dev. **9**, 2911–2922.
24. H. M. Stern, A. M. C. Brown, and S. D. Hauschka (1995) Development **121**, 3675–3686.
25. O. Pourquié et al. (1996) Cell **86**, 461–471.
26. G. Brill, N. Kahane, C. Carmeli, D. Von Schack, Y. A. Barde, and C. Kalcheim (1995) Development **121**, 2583–2594.
27. B. Mintz and W. W. Baker (1967) Proc. Natl. Acad. Sci. USA **58**, 592–598.
28. O. Chisaka and M. R. Capecchi (1991) Nature **350**, 473–479.
29. Y. Saga, J. Yagi, Y. Ikawa, T. Sakakura, and S. Aizawa (1992) Genes Dev. **6**, 1821–1838.

Suggestions for Further Reading

30. E. Dupin, C. Ziller, and N. M. Le Douarin (1998) "The Avian Embryo as a Model in Development Studies: Chimeras and *in vitro* Clonal Analysis," Curr. Top. Dev. Biol. **36**, 1-35.15
31. N. Le Douarin, F. Dieterlen Lièvre, and M. A. Teillet (1996) "Quail-Chick Transplantations" Methods Cell Biol. **51**, 23–59.

Chiral and Chiral Center

The word chiral is derived from the Greek word "cheir" for "hand." It was first used to describe any molecule that could not be superimposed on its mirror image, like left and right hands, by Lord Kelvin (1). This supplanted the less precise term dissymetrical used by Pasteur (2). The nonsuperimposable mirror image isomers are enantiomers. The physical property that differentiates enantiomers is the direction that they rotate plane polarized light. Thus, the two enantiomers are differentiated as either dextro(+) or levo(–) rotatory, depending on whether the rotation of the polarized light is clockwise or counterclockwise, respectively. Solutions containing an excess of one of the enantiomers are said to be optically active. A solution containing exactly equal concentrations of both enantiomers is called racemic (see Racemic And Racemization).

The most common structural element that generates chiral molecules is the presence of a tetrahedral atom with four different substituents, by definition a chiral center. The a-carbon of the a-amino acids (Fig. 1), except for glycine, and the hydroxymethylene carbons of carbohydrates are all chiral centers. The mirror images of chiral molecules have different absolute configurations, which are uniquely identified by the rules proposed by Cahn et al. (3) (see Configuration).

Figure 1. The enantiomers of alanine, which are mirror images. Note that the a-carbon is chiral because of the four different substituents. The (L) and (D) designate the absolute configuration of the chiral center, whereas the (+) and (–) indicate which direction an aqueous solution of the enantiomer will rotate the plane of polarized light.

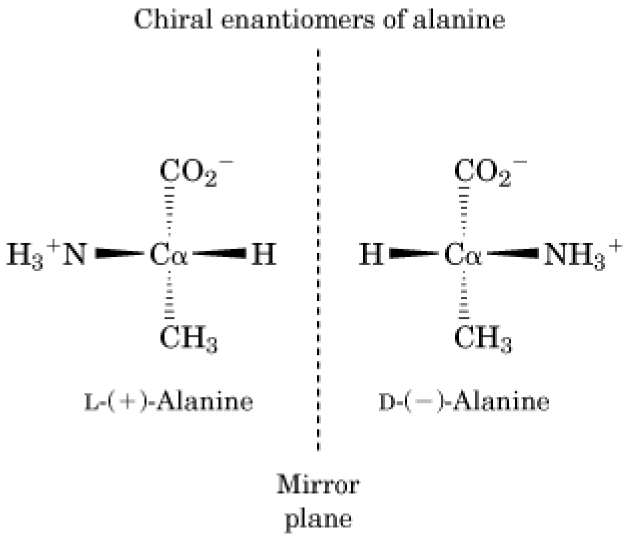

Possessing a tetrahedral chiral center is not required for chirality, nor is the presence of a chiral center proof that the molecule will be chiral. Other arrangements of atoms can generate nonsuperimposable mirror images. One example of biochemical importance is the hexacoordinate complexes of metal ions, such as the Mg ATP complex (4). Other chiral molecular structures have been surveyed by Testa (5). A molecule with an internal mirror plane may have chiral centers but not be chiral. These are meso compounds. Because of their internal symmetry, these molecules can be superimposed on their mirror image. The **diastereomeric** form of tartaric acid, which has two chiral centers, but a mirror plane between C2 and C3, provides an example of a meso compound (Fig. 2).

Figure 2. Meso tartrate, which contains two chiral centers C2 and C3, but is not chiral because there is an internal plane of symmetry. Note that, unlike the enantiomers of alanine, these mirror images can be superimposed by a 180° rotation.

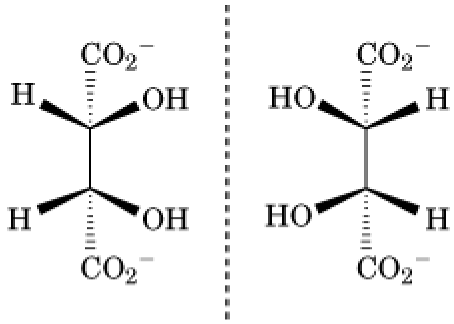

Meso form of tartrate

Bibliography

1. L. Kelvin (1894) Boyle Lect. J. Oxford Univ. Junior Sci. Club (May 25), 25.
2. L. Pasteur (1853) Pharmacol. J. **XIII**. 111.
3. R. S. Cahn, C. K. Ingold, and V. Prelog (1966) Angew. Chem. Int. Ed. **5**, 385–415.
4. E. A. Merritt et al. (1978) Biochemistry **17**(16), 3274–3278.
5. B. Testa (1982) In *Stereochemistry* (C. Tamm, ed.), Vol. **3**, Elsevier, Amsterdam, pp. 1–48.

Suggestions for Further Reading

6. J. March (1985) *Advanced Organic Chemistry*, Wiley-Interscience, New York, pp. 82–100.
7. K. Mislow (1966) *Introduction to Stereochemistry*, W. A. Benjamin, New York, pp. 50–60.

Chironomus

The subfamily chironomini includes Chironomus and related genera that by some estimates contain over 5000 species. Because of this diversity, many studies of chironomids focus on environmental biology and systematics. But it was the giant polytene chromosomes of salivary gland cells and the bright red color of the larvae of these ubiquitous flies that first drew the attention of experimental biologists more than 100 years ago.

The alternating dark bands (chromomeres) and light bands of the polytene chromosomes are punctuated by puffed regions, the largest of which were named Balbiani rings to honor their discovery by E. G. Balbiani in 1881. The possible relationship between chromomeres and genetic loci on the one hand, and between puffs and gene activity on the other, excited the interest of cytologists and geneticists. One of these, W. Beermann, examined the morphology of chromosomes in four cells in the “special lobe” of the salivary glands of larvae that were derived from a cross between *C. tentans* and *C. pallidivitattus*. He was able to correlate the production of prominent secretion granules by these cells with the presence of a specific chromosome puff in both the hybrid and in *C. pallidivitattus*, and showed that the puff was absent from the special cell chromosomes in *C. tentans*, which do not contain the secretion granules. C. Pelling later demonstrated that polytene chromosome puffs selectively incorporated radioactive uridine, firmly establishing that they are sites of active gene transcription. The sequential appearance of some, and the disappearance of other chromosome puffs during development could be mimicked by treating cultured late-stage larval salivary glands with the steroid hormone, 20-hydroxyecdysone. Thus, the same hormone that signals molting and metamorphosis in insects also controls the differential transcription of genes encoded by responsive puffs (see Ecdysone).

In a prodigious feat of molecular isolation that predates molecular cloning by almost a decade, J. E. Edstrom and his colleagues used micro manipulation to dissect individual Balbiani rings. A very large (75S) mRNA (messenger RNA) encoding a polypeptide of about 850 kDa was extracted from pooled Balbiani ring 2 isolates. This and other salivary gland secretory proteins encoded by the major Balbiani rings are extruded through the larval mouth and spun together with benthic detritus to make tabular houses. The stickiness of *Chironomus* “silk” results from the aggregation properties of interacting secretory polypeptides from the major Balbiani rings, and several studies focus on those aspects of structure that could explain the adhesive properties of these unusual biopolymers. In *C. tentans*, each major Balbiani ring encodes polypeptides with internal repetitive domains. The core repeat of one of these domains has four cysteine residues in invariant positions; a subrepeat region contains tandem *basic-pro-acidic* residue motifs. This arrangement might encourage protein strand alignment and polymerization of the “silk”. In other studies, B. Daneholt and colleagues have capitalized on the large size of the Balbiani Ring gene transcripts to investigate messenger ribonucleoprotein (mRNP) assembly and transport through nuclear pores; polytene chromosome centromere and telomere evolution, replication, and function are also areas of active research.

Recent studies have used expression of a chironomid/drosophilid ecdysone receptor (ultraspiracle) gene to understand hormone receptor domain function. Still other seek to define sex-determining genes and proteins, and to characterize diverse transposable elements in chironomids. A significant number of reports have focused on *Chironomus* globin gene structure, polymorphism, and evolution. The rest of this article deals with developmental and functional studies of *Chironomus* hemoglobins and with the structure, organization, and evolution of the many globin genes in this large multigene family.

1. *Chironomus* Hemoglobin Structure and Function

The red pigment so visible through the larval integument was identified as hemoglobin by E. R. Lankester in 1872. In 1932, T. Svedberg et al. used their then-new technique of sedimentation velocity ultracentrifugation to estimate the molecular weight of hemoglobin from *Chironomus* (and other invertebrates); chironomid hemoglobins “weighed in” at 32 kDa. Physiological studies focused on the unusually high oxygen affinity of the hemoglobin (compared to its vertebrate counterparts) and on how it facilitated oxygen supply to larval tissues in a relatively hypoxic benthic habitat.

Chironomus hemoglobin is actually a mixture of many hemoglobin proteins synthesized and secreted by larval fat body. Long before the first chironomid globin gene was cloned, much was known about the structure of these proteins. In contrast to the tetrameric vertebrate hemoglobins (see Hemoglobin), chironomid hemoglobins do not show cooperative binding of oxygen, existing either as monomers or homo-dimers under physiological conditions (Svedberg’s 32 kDa “hemoglobin” was presumably a mixture of homodimers). Over the course of a decade, the amino acid sequences of 12 *C. thummi* globins were determined in the laboratory of G. Braunitzer. Since none is truly similar in sequence to its vertebrate counterparts, alignments of chironomid and vertebrate globin sequences were only possible because they share several amino acids at crucial positions known to be involved in binding the heme group. On the other hand, comparison of the three-dimensional structure of a monomeric chironomid hemoglobin (determined by X-ray crystallography) with that of vertebrate globins reveals many shared structural features, including similarly organized a-helical domains and a characteristic hydrophobic heme pocket. These observations clearly indicate that similar molecular functions and three-dimensional structures can be attained in different proteins despite considerable differences in primary structure. The differences in primary structure between globins of very different organisms reflects adaptation to species-specific oxygen requirements over long evolutionary periods.

Whereas at least two *C. thummi* globin genes encode identical polypeptides (1), pairwise comparisons of amino acid sequences reveal remarkably dissimilar globins. These differences have also been ascribed to evolutionary specialization of different hemoglobins that now serve different respiratory functions (2). However, the physiological roles of individual hemoglobins are at best only poorly understood. *In vivo* determinations of larval O_2 binding and storage abilities under different conditions of oxygen tension necessarily represent a function of the aggregate set of hemoglobins present at the time of measurement. As expected, the O_2 affinities determined for purified hemoglobins that are present in different proportions in the hemolymph are not easily related to the aggregate *in vivo* data. What does emerge from such experiments is a loose correlation of the generally high oxygen affinities of the hemoglobins and the benthic, often oxygen-depleted habitat of larvae.

Larvae live in the mud at the bottom of freshwater ponds and lakes, developing in burrows constructed to detritus cemented by the sticky secreted salivary gland proteins discussed above. Moreover, chironomids can withstand the oxygen stress of polluted or eutrophic waters, often comprising more than 80% of all animal individuals. This tolerance is due in part to the high concentrations of hemolymph hemoglobin. Zebe (3) suggested that hemoglobins of *C. thummi* may not be required for oxygen delivery at higher partial pressures (oxygen needs under these conditions are presumably satisfied by diffusion). Rather, because they can bind O_2 at low partial pressures (50 to 10 torr), the hemoglobins allow continued respiration in times of severe oxygen deficit, when they become physiologically significant. From this, one might predict that oxygen stress will favor larval production of hemoglobins with particularly high O_2 binding affinities. Homodimeric hemoglobins have higher O_2 affinities than the monomeric hemoglobins and do indeed rise in concentration in response to circadian and seasonal declines in O_2 availability and water quality, where they may be more involved in O_2 transport under these conditions than monomeric hemoglobins. With a more pronounced Bohr effect than monomeric hemoglobins, dimeric hemoglobins may also allow response to more immediate changes in oxygenation conditions due to local fluctuations in pH.

Overall hemoglobin levels reach their highest concentrations in the hemolymph of *C. thummi* in the fourth, or last larval stage (instar). Although it is likely that newly synthesized hemoglobins function mainly in respiration, hemolymph hemoglobin is also taken up by developing oocytes and deposited in yolk granules during oogenesis in pupae (4, 5). This hemoglobin undoubtedly serves a nutrient rather than a respiratory function during embryogenesis. At the same time, developing eggs may contain hemoglobins of their own making. Cross-reactive antihemoglobin antibodies tagged with colloidal gold particles are localized over rough endoplasmic reticulum in young embryos, suggesting that hemoglobin synthesis begins at embryogenesis (6). Hemoglobins first accumulate sufficiently to become visible as a red pigment in the blood of second instar larvae. Thereafter, hemoglobin synthesis is cyclic, being high during the instar and declining at each molt. Hemoglobin synthesis occurs for the last time just after pupariation, ceasing sometime in the pupal stage, by which time most existing hemoglobins are degraded. Hemoglobins have disappeared and are virtually undetectable several hours after adult emergence, at which time the adult flies have a fully developed tracheal respiratory system. Once again, in spite of these observations, it is not possible to state with certainty the physiological role played by any given hemoglobin at any given moment. As we will see, this issue may be moot for many of the hemoglobins, since there is reason to believe that much of the structural variation between hemoglobins has not been selected to perform a unique physiological function, but instead is the result of neutral evolution.

2. Developmental Regulation of *Chironomus* Hemoglobin Synthesis

While cyclic hemoglobin production is tied to molting, it should also come as no surprise that the synthesis of individual members of such a large family of hemoglobins is regulated differentially during development. For example, polyacrylamide gel electrophoresis (PAGE) of *C. thummi* fourth instar hemolymph reveals two hemoglobins that are absent in electrophoretic separations of third instar larval hemolymph. Another hemoglobin, detectable in embryo homogenates by electrophoresis and immunoblotting, is undetectable in last instar larval hemolymph. In S1 nuclease protection assays performed to follow specific globin gene expression during development, transcripts of the ct-1, ct-4, ct-7B4, and ct-7B5 globin genes (ct-, ctp-, ctn-, and kc- are prefixes for *C. thummi, C. piger, C. tentans,* and *K. cornishi* globins and globin genes.) are detected at high levels in 3rd instar *C. thummi* larvae (7). Transcripts of each of these globin genes decline to undetectable levels immediately after molting to the fourth instar, reappearing 24 hr later, along with two new fourth-instar–specific globin transcripts (ct-3, ct-6). The expression of each of these globin mRNAs was tracked further during fourth instar development. The results of these experiment indicate that globin transcript steady-state levels follow one of two kinetic patterns. Transcripts of the ct-3 and ct-6 genes rise from very low or undetectable levels after the molt, and then remain elevated through 8 days of the instar. Globin mRNAs expressed in both instars also rise from low or undetectable levels just after the molt. But unlike the specific globin mRNAs, they reach maximum levels after 2 to 3 days and then decline to near basal levels. The absence of detectable globin transcripts just after the third to fourth instar molt is consistent with the observation that the rate of synthesis of hemoglobins of cultured larval tissues exposed to the molting hormone 20-hydroxyecdysone (20HE) is very much reduced. Like other steroid hormones, 20HE binds to an intracellular receptor, which then binds to a hormone response element(s), directly controlling the transcription of adjacent genes. Such direct action on globin is unlikely, since a search in DNA lying between or flanking any *C. thummi* globin gene sequences published or recorded in international DNA sequence databases failed to detect 20HE response elements. As yet unidentified factors must mediate the hormone-induced repression of hemoglobin synthesis during molting. There is no evidence at all for a role for 20HE in the selective repression of "non–stage-specific" globin mRNA levels during the fourth instar, indicating the action of still other factors in the selective silencing of some but not all globin genes.

3. *Chironomus* Globin Gene Structure and Organization

At the same time as the differential expression of hemoglobins or globin transcripts was being described, many more globin genes were being characterized. Known *C. thummi* genes exceed the number needed to account for the 12 hemoglobins that were first isolated. The loci of individual and clustered globin genes were mapped by *in situ* hybridization of cloned DNAs to polytene salivary gland chromosomes, and as noted, the expression of many globin genes including several for which no protein product has yet been isolated, has been shown. Table 1 summarizes some key properties of cloned globin genes characterized thus far. Genes that are clearly inactive include ct-13RT (which suffered insertion of a retroposon in coding DNA; see Fig. 1), ct-V (with an inappropriately located stop codon), and ctn-ORFB (with its coding region truncated at the 5' and 3' ends). With these exceptions, all of the known chironomid globin genes possess the structural prerequisites of active genes, including appropriately located TATA (promoter)and AATAAA (polyadenylation) signals, an open reading frame, and a stop codon. In addition to the first of full-length globin genes in Table 1, many partial genes (8, 9) amplified by PCR from numerous species (eg, for globins 2b, 7, and 9) are probably active. When compared to vertebrate (eg, human) globin genes, a striking difference is that the latter are separated by thousands of nucleotides, whereas chironomid globin genes are often separated by less than 500 nucleotides. Another difference is that chironomid globin genes lack the hallmark structure of three exons separated at conserved positions by two introns that characterize vertebrate (and even plant) globin genes. Instead, different chironomid globin genes are either intronless or contain a single introns at divergent locations. The growing database of chironomid globin genes from several species, their unusual structure, and their organization have sparked considerable interest in the evolution of this unique multigene family.

Figure 1. Intron acquisition by chironmid globin genes. Relative times of independent acquisition of introns at different locations ("type 1" vs "type 2") by ancestral globin genes in the "*pseudothummi*" and "*plumosus*" phylogenetic groups are suggested. Only *C. dorsalis*, the oldest member of the "*pseudothummi*" group, has intronless orthologues of the

intron-bearing genes. Phylogenetic clusters are taken from Guryev et al. 2001 (9). The evolutionary history of intron-bearing and intronless orthologous gene clusters *C. thummi* and its distant relative, *C. tentans* is also shown. ct-, ctn-, and ORF ("open reading frame") designations are deleted to save space. Arrows above the genes indicate direction of transcription. Ancestral genes are designated in italics. Details are explained in the text.

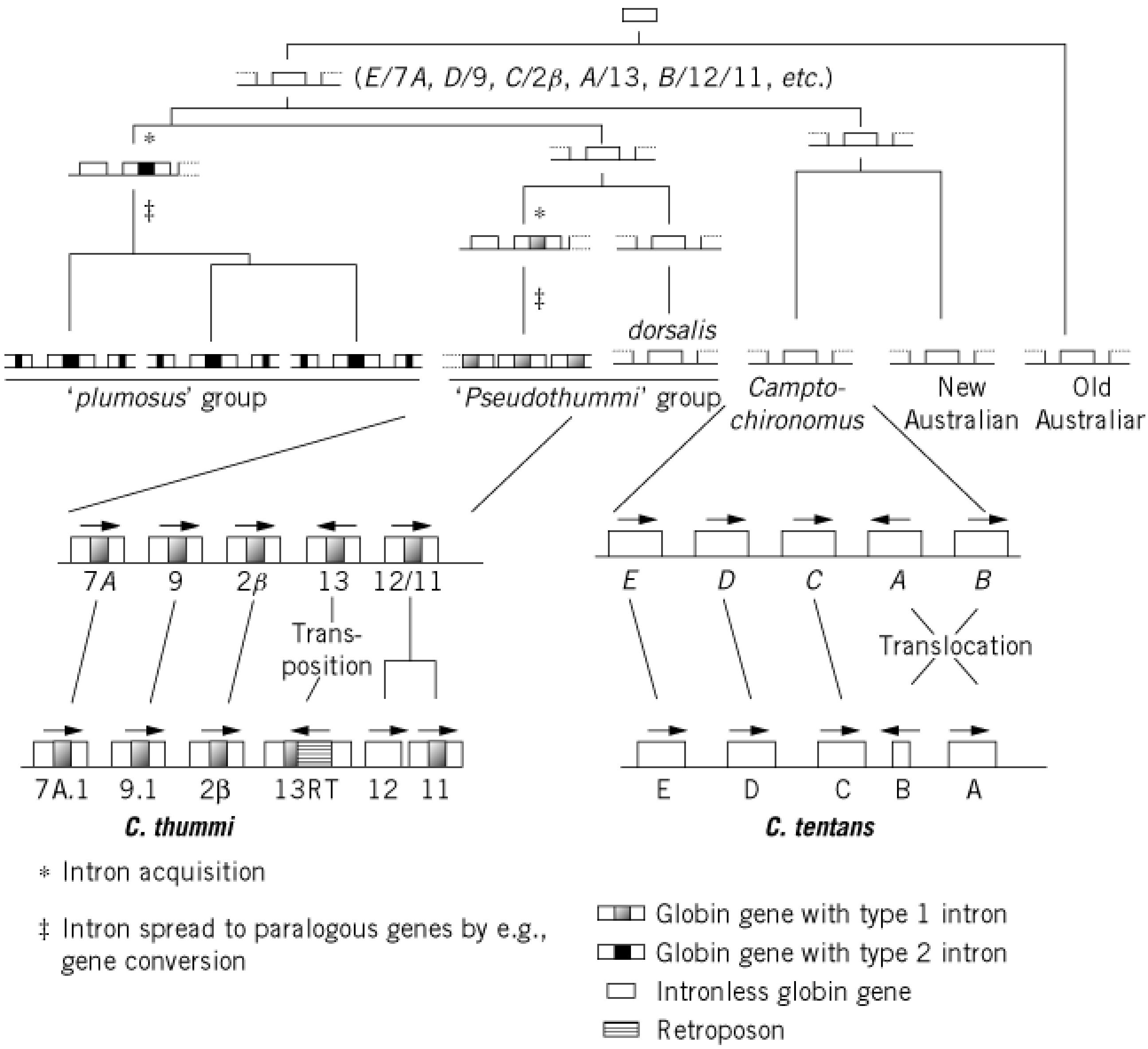

Table 1. Chironomid Globin Genes

Organism	Gene	Protein Product	Status[a]	Homologues	locus[b]	Comments
C. thummi	ct-1	I	active	—	F2b3	Allele of ct-1A; intronless; aa sequence avail.
	ct-1A	IA	active	—	F2b3	Allele of ct-1;

					intronless; aa sequence avail.
ct-3-1	III	*	—	A1B2	Intronless; * 3-1 &/or3-2 = avail. aa sequence
ct-3-2	III	*	—	A1B2	Intronless, *3-1 &/or3-2 = avail. aa sequence
ct-4-1	IV	*	—	A1B2	Intronless, *4-1 &/or4-2 = avail. aa sequence
ct-4-2	IV	*	—	A1B2	Intronless, *4-1 &/or4-2 = avail. aa sequence
ct-E	Putative	Putative	—	A1B2	Intronless
ct-6	VI	Active	—	F2b3	Intronless; aa sequence avail.
Not found	VIIB-1	Active	—	—	aa sequence avail.
Not found	VIIB-2	Active	—	—	aa sequence avail.
ct-7B3	VIIB-3	Active	—	N.D.	Intronless; protein product assumed
ct-7B4	VIIB-4	Active	—	F2b3	Intronless; protein product assumed
ct-7B5	VIIB-5	Active	—	F2b3	Intronless; protein product assumed
ct-7B6	VIIB-6	Active	—	F2b3	Intronless; protein product assumed
ct-7B7	Putative	Putative	—	F2b3	Intronless; protein product assumed

ct-7B8	Putative	Putative	—	F2b3	Intronless; protein product assumed
ct-7B9	Putative	Putative	—	F2b3	Intronless; protein product assumed
ct-7B10	Putative	Putative	—	F2b3	Intronless; protein product assumed
ct-7B9/5	Putative	Putative	—	N.D.	Intronless chimera; protein product assumed
ct-Y	Putative	Active	—	F2b3	Partial DNA sequence, RT-PCR product
ct-W	Putative	Active	—	F2b3	Intronless; protein product assumed
ct-V	None	Inactive	—	F2b3	Stop codon in middle of coding region
ct-Z	Putative	Active	—	F2b3	Intronless; protein product assumed
ct-7A.1	VIIA	Active	—	F2b3	Central intron; aa sequence avail.
ct-9.1	IX	Active	—	F2b3	Central intron; aa sequence of allele avail.
ct-2b	II2b	Active	—	F2b3	Central intron; aa sequence avail.
ct-13RT	None	Inactive	—	F2b3	Central intron; retrposon insertion in coding DNA; may be transcribed

	ct-12	Putative	Putative	—	F2b3	Intronless
	ct-11	Putative	Putative	—	F2b3	Central intron
C. piger	ctp-7B4	Putative	Putative	ct-7B4	F2b3	Intronless; protein product assumed
	ctp-7B5	Putative	Putative	ct-7B5	F2b3	Intronless; protein product assumed
	ctp-7B6	Putative	Putative	ct-7B6	F2b3	Intronless; protein product assumed
	ctp-7B7	Putative	Putative	ct-7B7	F2b3	Intronless; protein product assumed
	ctp-7B8	Putative	Putative	*	F2b3	Intronless; protein product assumed; * chimera of ct-like 7B8 and 7B10 genes;
	ctp-Y	Putative	Putative	ct-Y	F2b3	Intronless; protein product assumed
	ctp-W	Putative	Putative	ct-W	F2b3	Intronless; protein product assumed
	ctp-V	Putative	Putative	ct-V	F2b3	Intronless; protein product assumed
	ctp-Z	Putative	Putative	ct-Z	F2b3	Intronless; protein product assumed
C. tentans	ctn-ORFE	Putative	Putative	ct-7A.1	—	Intronless; protein product assumed
	ctn-ORFD	Putative	Putative	ct-9.1	—	Intronless; protein product

					assumed
	ctn-ORFC	Putative	Putative ct-2	—	Intronless; protein product assumed
	ctn-ORFB	None	Inactive *ct-11/12	—	Intronless; may be transcribed; * ancestor to ct-11 and ct-12
	ctn-ORFA	Putative	Putative ct-13RT	—	Intronless; protein product assumed
C. pallidivittatus	cpa-3-1	Putative	Putative ct-3-1	—	Intronless; protein product assumed
	cpa-3-2	Putative	Putative ct-3-2	—	Intronless; protein product assumed
	cpa-4-1	Putative	Putative ct-4-1	—	Intronless; protein product assumed
	cpa-4-2	Putative	Putative ct-4-2	—	Intronless; protein product assumed
	cpa-E	Putative	Putative cpa-E	—	Intronless; protein product assumed
	cpa-F	Putative	Putative ?	—	Intronless; protein product assumed
K. cornishi	kc-7BA	Putative	Putative ?	—	Intronless; protein product assumed
	kc-7BB	Putative	Putative ?	—	Intronless; protein product assumed
	kc-7BC	Putative	Putative ?	—	Intronless; protein product assumed

kc-7BD	Putative	Putative ?	—	Intronless; protein product assumed
kc-7BE	Putative	Putative ?	—	Intronless; protein product assumed
kc-7BF	Putative	Putative ?	—	Intronless; protein product assumed
kc-7BG	Putative	Putative ?	—	Intronless; protein product assumed

[a] Active genes have been shown to be transcribed and/or translated, or to correspond to an identified globin polypeptide.

[b] Positions mapped to polytene salivary gland chromosomes of *C. thummi*; See Ref. 44 for the mapping of the same genes to the salivary gland chromosomes of other chironomid species.

4. Evolution of *Chironomus* Globins

Phylogenetic analyses support an early origin of monomeric hemoglobins about 500 million years ago and the appearance of homodimeric hemoglobins about 250 to 300 million years ago, corresponding roughly with the origin of Diptera. Recently, a search of the *Drosophila* genome database using a chironomid globin gene query found a distant relative, designated a neuroglobin because it was expressed in brain tissue in *D. melanogaster*; and mouse and human neuroglobins have since been characterized (10-13). The chironomid globin gene family has experienced many of the same evolutionary events as their multigene families, such as point-mutational inactivation, translocations, gene loss, gene conversion, etc. They also support two somewhat unorthodox hypotheses. One that has received much attention in recent years, is that eukaryotic genes can acquire introns, complete with correctly placed intron/exon junctions and splicing signals. The other hypothesis is that much of the diversity of hemoglobin structure in *Chironomus* has arisen by neutral evolution rather than by functional adaptations of the proteins. There is resistance to ascribe to neutral evolution those mutations causing even minor differences in amino acid sequence between the products of homologous genes in different species or paralogous genes in the same organism. Such differences between globin genes in *Chironomus*, and between the products of multigene family members in general, are widely thought to be the result of adaptive selection. However, evidence from the different chironomid globins and globin genes suggest that many were not selected for their adaptive value, but exist instead as a neutral consequence of positive selection of the expression of high levels of hemoglobin from multiple genes.

4.1. Origin of A Central Intron

By the time the first chironomid globin genes were cloned in 1984, the sequencing of vertebrate globin genes had become a cottage industry. Each new report presented a globin gene with the same mosaic structure: three exons and two introns, the latter always interrupting the coding DNA at the same location. In a prophetic para (14), Go analyzed X-ray diffraction data for a vertebrate globin and concluded that in addition to the outer introns, the ancestral globin gene had a third intron in the center of the gene such that the entire gene was separated into four exons of similar length, each coding for a separate structural domain. Go's prediction was fulfilled shortly thereafter with the report of the first plant (legume) globin gene, which had a centrally located intron in addition to two introns at the same position as those in the vertebrate globin genes. Apparently the structure of plant globin genes represents the ancestral state. Many of the first chironomid globin genes to be reported were intronless, a condition presumably due to the reverse transcription of a completely processed transcript and reinsertion of the complementary DNA into the genome. The discovery of the *C. thummi* ct-2b and ct-9.1 genes (15), and of several other invertebrate globin genes with a central intron, however, raised questions about the origin of chironomid globin gene introns. Unlike the conservation of location of the outer vertebrate globin gene introns, the location of central introns is not conserved across kingdoms or phyla, and none is at the position predicted by Go. Could they, like the outer introns in globin genes, still be descendants of an ancestral intron? Gilbert suggested that introns at nonconserved locations have moved by "intron sliding." Others have argued that the discordant location of nitrons is more easily explained if introns can be acquired by previously uninterrupted genes. Hankeln et al. (8) reported that the globin genes of some species have a "central" intron at a slightly different location that those of other species. A chironomid mitochondrial gene phylogeny groups flies with an intron at one location ("type 1") on the "*pseudothummi*" branch, and groups those with an intron at the other location ("type 2") on a separate "*plumosus*" evolutionary branch (8, 16, 17). The phylogeny supports the separate acquisition of an intron by the homologous genes after divergence of the two lineages (Fig. 1). Several plausible mechanisms for intron acquisition have been suggested. In considering these, Kao et al. (15) offered a mechanism whereby a chironomid globin gene containing a centrally located ¼AGGT¼ tetramer (to provide donor and acceptor splice sites) could have acquired a central intron by a simple gene duplication, accompanied (or followed) by deletion of all but the DNA presently found in the intron. A mechanism proposed by Hankeln et al. (8), where introns are acquired by a reversal of the splicing reaction, might explain intron insertion in globin genes lacking these AGGT splice site precursors. An intron once acquired by a single gene might spread to nearby related genes by gene conversion (8); see Fig. 2).

Figure 2. Evolutionary history of orthologous gene clusters in *C. thummi* and its sibling subspecies, *C. piger*. ct-, and ctp
save space. Arrows above the genes indicate direction of transcription. Ancestral genes are designated in italics. Shaded
recent duplications, losses, and fusions.

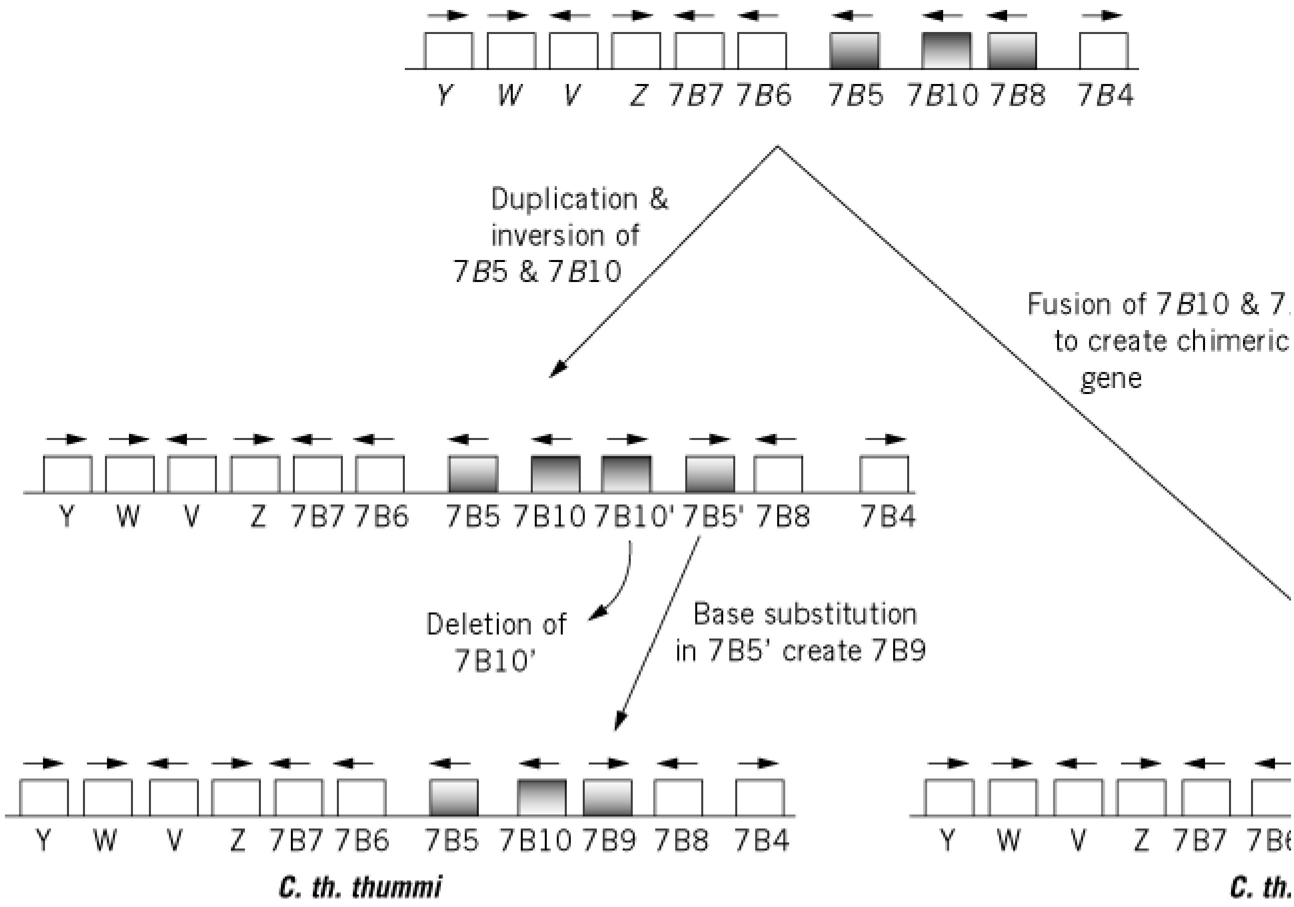

4.2. Evolution of a Globin Multigene Family

The DNA sequences of orthologous globin gene clusters in different chironomid species support the adaptive selection of a high globin gene copy number and the essentially neutral evolution of individual globin genes. The ctp-Y, ctp-W, ctp-V, and ctp-Z genes, and five ctp-7B genes in *C. piger* (18), and the ctp-Y, ctp-W, ctp-V, and ctp-Z genes, and seven ctp-7B genes of sibling species *C. thummi* (1) are a case in point. The phylogenetic study summarized in Figure 2 traces the evolutionary history of the two clusters, showing the seven genes that are clearly homologous, and a series of gene duplications and deletions necessary to explain the current sequence and organization of the clusters. Pairwise comparisons show that at the nucleotide level, homologous globin genes or logical gene pairs (ie, genes of indeterminate orthology, but sharing immediate common ancestry) in the two species share from 96.7% to 99.2% identity. In three cases, homologous genes in each species code for identical polypeptides, despite several millions of years of species divergence. Within *C. thummi*, the ct-7B5, ct-7B6, ct-7B9, and ct-7B10 paralogous genes are also very similar, as shown by the amino acid differences in the pairwise comparisons shown below:

	7B6	**7B10**	**7B5**	**7B9**
7B8	6	4	6	6
7B6		2	1	1
7B10			2	2
7B5				0

In addition to identical paralogues (ct-7B5, ct-7B9), sequencing of an independent genomic clone revealed a gene identical ct-7B5 (19). Designated ct-7B9/5 because its 5’ and 3’ flanking DNA are similar to the 5' and 3' regions of ct-7B9 and ct-7B5, respectively, it probably arose by intrachromosomal crossing over between oppositely oriented ct-7B9 and ct-7B5 in a looped (bent) chromosome structure (with deletion of most or all of ct-7b10). Since the recombination point is in fact external to the transcribed region of the gene, 7B9/5 must simply be another ct-7B5 gene or allele. The recombined region (without ct-7B10) may be an independent gene locus or an allelic haplotype. Clearly the 7B globin gene subfamily predates the *thummi/piger* divergence. The ability of *C. thummi* and *C. piger* to lose different descendants of an ancestral cluster by gene fusion, and the overall similarity of paralogous genes, implies that any small differences that accumulate in the genes before or after fusions and corrections are evolutionarily inconsequential. The 7B gene cluster seems to have undergone periodic expansion and contraction (gene duplication, deletion), while maintaining the ability to encode identical or nearly identical globins for millions of years. The best explanation for this phenomenon is that the few differences that accumulate between 7B genes are the result of random drift (neutral evolution), but that the cluster itself has experienced positive selection of a high number of copies of globin genes as a means to ensure the synthesis of large amounts of hemoglobin.

Whereas the orthologous globin gene clusters in *C. thummi* and *C. piger* illustrate early evolutionary events in the life of a multigene family, globin gene clusters in *C. thummi* and *C. tentans* are separated by 60 million years of evolution (16, 20). The extent paralogous and homologous genes sequences are much less similar to each other (except for a region of the ct-2b and ct-9A genes that underwent partial gene correction, homogenizing intronic and exonic DNA in the middle of the two genes). The divergence of the *C. thummi* and *C. tentans* gene clusters offers a wider window through which to test the concept of gene copy number selection. Figure 1 summarizes evolution of these genes after acquisition and spread of a "type 1" intron in one of the clusters. The ancestral *C. thummi* gene cluster must have had five intron-bearing genes before a gene duplication created ct-11 and ct-12. ct-12 has since lost its intron, and both ct-11 and ct-12 have been diverging for some time (16). In contrast, the *C. tentans* cluster contains only intronless homologues, originally ascribed to multiple intron losses from intron-bearing ancestors (16, 20). Figure 1 reflects more recent phylogenetic evidence that some or all of the genes in these clusters arose early in the genus, and that the *C. tentans* genes never acquired an intron in the first place (9). A difference in the organization of the orthologous genes between *C. thummi* and *C. tentans* is explained if a translocation is assumed between ctn-A and ctn-B (or vice-versa in *C. thummi*). Of special note, the recent inactivation of a different (non homologous) gene in each cluster suggests that not all globin genes in a cluster are indispensable, even after 60 million years of evolution. In *C. thummi*. ct-13RT suffered the insertion of a retroposon into coding DNA in exon I. This occurred very recently, because the rest of the coding region, the intron, and the flanking DNA containing promoter and polyadenylation motifs are all still intact. Recent retroposition is supported by the observation that ct-13RT is actually an allele coexisting with a normal, uninterrupted ct-13 allele (17). In *C. tentans*, the ctn-ORFB gene was truncated at both the 5' and 3' ends. Again, this event must have occurred very recently, because the gene retains all other attributes of a viable, transcribable gene. The phylogenetic analyses of the orthologous *C. thummi* and *C. tentans* gene clusters supports the recent inactivation of the ct-13RT allele and the ctn-ORFB genes, and the likelihood that accumulated amino acid differences between many (if not all) homologous and paralogous genes are the result of neutral evolution. If the greater diversity of the *tentans* and *thummi* genes cannot be completely explained as the positive adaptation of structurally diverse hemoglobins, then their maintenance, like that of the large number of 7B genes in *thummi* and *piger*, must be the result of positive gene copy number selection favoring high levels of hemoglobin synthesis.

In sum, the evolution of *Chironomus* globin genes spans more than 250 million years, in which time individual sequences within and across species have accumulated many amino acid substitutions. Some especially diverged hemoglobins may have evolved to serve unique functions, for example in environments that undergo cyclic changes in oxygenation. The specific expression of some globins during development might reflect habitant (and therefore, oxygenation) differences as larvae first descend from the waters' surface to the benthos, and later ascend to the surface at the time of eclosion. On the other hand, differences between many of the globin genes may be neutral, selection favoring the proliferation of a large family of genes encoding proteins of physiologically similar function. Kimura (21) suggested that duplicated genes accumulating neutral change are preadapted, later becoming substrates for positive adaptation after speciation. A consequence of high gene copy number selection is that some of the many functionally redundant globin genes can serve as raw materials for Darwinian selection, which could explain the evolution and spread of more than 5000 species of Chironomous to diverse habitats.

Bibliography

1. P. M. Trewitt, R. A. Luhm, F. Samad, S. Ramakrishnan, W-Y. Kao, and G. Bergtrom (1995) J. Mol. Evol. **41**, 313–328.
2. M. Goodman, J. Pedwaydon, J. Czelusniak, T. Suzuki, T. Gotoh, L. Moens, F. Shishikura, D. Walz, and S. Vinogradov (1988) J. Mol. Evol. **27**, 236–249.
3. E. Zebe (1991) Comp. Biochem. Physiol. **99A**, 525–529.
4. P. M. Trewitt, D. R. Boyer, and G. Bergtrom (1986). J. Insect Physiol. **32**, 963–969.
5. C. R. Myers, G. Bergtrom, S. M. Crook, D. R. Boyer, M. L. P. Collins (1986). J. Histochem. Cytochem. **34**, 221–226.
6. C. R. Myers, M. L. P. Collins, M. Agresti, and G. Bergtrom (1986) J. Insect Physiol. **32**, 845–851.
7. D. A. Saffarini, P. M. Trewitt, R. A. Luhm, and G. Bergtrom (1991) Gene **101**, 215–222.
8. T. Hankeln, H. Freidl, I. Ebersberger, J. Martin, and E. R. Schmidt (1997) Gene **205**, 151–160.
9. V. Guryev, I. Makarevitch, A. Blinov, and J. Martin. (2001) Mol. Phyl. Evol. **19**, 9–21.
10. T. Burmester, T. Hankeln (1999) Mol. Biol. Evol. **16**, 1809–1811.
11. T. Burmester, B. Weich, S. Reinhardt, T. Hankeln (2000) Nature 407, 520–523.
12. M. Couture, T. Burmester, T. Hankeln, D. L. Rousseau (2001) J. Biol. Chem. (in press).
13. J. T. Trent III, R. A. Watts, M. S. Hargrove (2001) J. Biol. Chem. (in press).
14. M. Go (1981) Nature **291**, 90–92.
15. W-Y. Kao, P. M. Trewitt, and G. Bergtrom (1994) J. Mol. Evol. **38**, 241–249.
16. M. C. Gruhl, W.-Y. Kao, and G. Bergtrom (1997) J. Mol. Evol. **45**, 499–508.
17. M. C. Gruhl, S. V. Scherbik, K. G. Aimanova, A. Blinov, J-L. Diez, and G. Bergtrom (2000) Gene **252**, 153–163.
18. T. Hankeln, C. Luther, P. Rozynek, E. R. Schmidt (1991). In *Structure and Function of Invertebrate Oxygen Carriers* (S. Vinogradov and O. H. Kapp, eds.), Springer Verlag, New York, pp. 287–296.
19. W.-Y. Kao and G. Bergtrom (1995) Gene **153**, 241–249.
20. P. Rozynek, M. Broecker, T. Hankeln, E. R. Schmidt (1991) In *Structure and Function of Invertebrate Oxygen Carriers* (S. Vinogradov and O. H. Kapp, eds.), Springer Verlag, New York, pp. 287–296.
21. M. Kimura (1991) Jpn. J. Genet. **66**, 367–386.

Suggestions for Further Reading

22. W. Beermann (1963) Cytological aspects of information transfer in cellular differentiation. Am. Zool. 23–32.
23. S. T. Case and L. Wieslander (1992) Secretory proteins of Chironomous salivary glands: structural motifs and assembly characteristics of a novel biopolymer. Results Probl. Cell Differ. **19**, 187–226.
24. B. Daneholt (2001) Assembly and transport of a premessenger RNP particle. Proc. Natl. Acad. Sci. U.S.A. **98**, 7012–7017.
25. B. N. Green, A. R. Kuchumov, T. Hankeln, E. R. Schmidt, G. Bergtrom, and S. N. Vinogradov (1998) An electrospray ionization mass spectroscopic study of the extracellular hemoglobins

from *Chironomus thummi thummi*. Biochim. Biophys. Acta. **1383**, 143–150.
26. R. Lewin R (1984) Surprise finding with insect globin genes. Science **226**, 328.
27. P. A. Osmulski and W. Leyko (1991) "The structure and function of vhironomus hemoglobins". In *Structure and Function of Invertebrate Oxygen Carriers* (O. H. Kapp, and S. N. Vinogradov, eds.), Springer-Verlag, New York, pp. 305–312.
28. J. H. Rogers (1989) How were introns inserted into nuclear genes? Trends. Genet. **5**, 340–343.
29. A. Stoltzfus and W. F. Doolittle (1993) Slippery introns and globin gene evolution. Curr. Biol. **3**, 215–217.
30. A. Stoltzfus, D. F. Spencer, M. Zucker, J. M. Logsdon, Jr., and W. F. Doolittle (1995) Introns and the origin of protein-coding genes. Science **268**, 1366–1367.

Chloramphenicol

Chloramphenicol is a bacteriostatic agent that inhibits the growth of many species of Gram-positive and Gram-negative bacteria; it was the first broad-spectrum antibiotic to be used clinically. Originally obtained from cultures of the soil bacterium *Streptomyces venezuelae*, chloramphenicol inhibits bacterial **protein biosynthesis** by interfering with the intrinsic catalytic activity of the peptidyl-transferase of the ribosome during the elongation phase of translation.

Eukaryotic cells are generally not affected by chloramphenicol. Nevertheless, the clinical application of this drug for the treatment of systemic infections has been severely curtailed, primarily because of the haematotoxicity associated with its use. Chloramphenicol continues to be used topically, particularly in the treatment of eye infections. The emergence of chloramphenicol-resistant bacteria, apparently in response to the selective pressure exerted by the drug (see Antibiotic Resistance), has also restricted the use of chloramphenicol in the treatment of bacterial infections.

Chloramphenicol resistance is frequently encountered in many genera of bacteria. Several mechanisms of resistance have been described: (i) modification of the target, the bacterial ribosome; (ii) alteration in the permeability of the bacterial cell, leading to low intracellular antibiotic concentrations; and (iii) enzymatic modification of the antibiotic. Resistance most commonly occurs as the result of inactivation of chloramphenicol by chloramphenicol acetyltransferase (CAT). This enzyme is of value to molecular biologists, because it can be assayed with specificity and sensitivity.

Chloramphenicol is used today in molecular biology primarily as a component of selective media for genetic studies, to distinguish chloramphenicol-resistant from chloramphenicol-susceptible bacteria. Chloramphenicol is also an essential component of CAT assays, which are used to study gene regulation, generally in eukaryotic cells. Finally, chloramphenicol provides a tool with which to investigate the peptidyl-transferase center of the bacterial ribosome.

1. Chemistry

Chloramphenicol [D(–)-*threo*-2-dichloroacetamido-1-*p*-nitrophenyl-1,3-propanediol; Fig. 1] has two asymmetric carbon atoms. Of the four stereoisomers, only one, the D-threo isomer, has antibacterial activity. This compound can be produced on an industrial scale by chemical synthesis or by fermentation. Chloramphenicol is poorly soluble in water, but dissolves readily in organic solvents (eg, methanol).

Figure 1. Chemical structure of chloramphenicol [D(–)-*threo*-2-dichloroacetamido-1-*p*-nitrophenyl-1,3-propanediol].

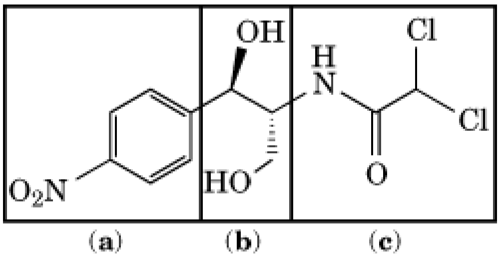

Derivatives having a wide range of para substituents are active; therefore, this part of the molecule is not involved in specific drug–target interactions. The propanediol moiety, the site of the D-threo configuration, is essential for activity. Acetylation of one or both hydroxyl groups inactivates the drug. Removal of the dichloroacetamido side chain virtually eliminates biological activity, although substitution by a number of groups does not render the drug inactive. Some substituents reduce activity against intact bacteria, but enhance the inhibition of cell-free protein synthesis (1). Apparently, these derivatives are not taken up by the bacterial cell as efficiently as the parent compound.

2. Antibacterial Spectrum

Chloramphenicol is a broad-spectrum antibiotic, active against archaebacteria and both gram-positive and gram-negative bacteria. Organisms that fall within its spectrum include *Bacillus anthracis*, *Brucella abortus*, *Corynebacterium diphtheriae*, *Escherichia coli*, *Hemophilus influenzae*, *Klebsiella pneumoniae*, *Neisseria meningitidis*, *Salmonella* spp., *Serratia marcescens*, *Staphylococcus aureus*, *Streptococcus* spp., and so on (2).

Chloramphenicol inhibits translation in bacterial cells, intact chloroplasts, and intact mitochondria. Some of the toxic side effects associated with chloramphenicol may arise from the effect of the drug on mitochondrial metabolism. Translation by mammalian cells, yeast, and protozoa is not inhibited by chloramphenicol.

3. Mode of Action

Chloramphenicol inhibits bacterial peptidyl-transferase, the enzymatic reaction by which one more amino acid is added to the growing polypeptide chain. During the elongation phase of protein biosynthesis in bacteria, chloramphenicol "freezes" **polysomes** on the messenger RNA, thereby fixing the peptidyl-tRNA to the ribosomes (3). Chloramphenicol competes for binding to the 50S subunit of the bacterial ribosome with molecules that specifically bind to the A site of the peptidyl-transferase center (aminoacyl-tRNA and its analogues, eg, CACCA-Leu) and is, therefore, thought to bind next to, or within, the A site of the peptidyl-transferase center (4). In contrast, no competition is observed with substrates that bind at the P site (peptidyl-tRNA analogues, eg, CACCA-LeuAc or AcPhe-tRNA). Furthermore, neither the dinucleotide ApC nor amino acids block the binding of chloramphenicol, whereas both puromycin and the dinucleotide CpA do (5). Thus, the drug presumably binds in the same region of the A site as the universally conserved CCA part of aminoacyl-tRNA.

The peptidyl-transferase assay in which peptide bonds are formed between a peptidyl-tRNA and puromycin on the 50S subunit (the "puromycin reaction") has been used to unravel the mechanism of action of chloramphenicol (6) (Fig. 2). Chloramphenicol blocks this reaction, provided that the donor peptidyl-tRNA, bound at the P site, is short (eg, AcPhe-tRNA). In this case, chloramphenicol appears to disturb the correct positioning of the nascent peptide during its synthesis, thereby causing the premature release of the peptidyl-tRNA from the ribosome. Chloramphenicol does not, however, affect the puromycin reaction when a larger peptidyl-tRNA—for example, Ac(Phe)$_2$-tRNA—is used as donor (7). It is likely, therefore, that chloramphenicol interferes with the binding of the terminal CCA of the aminoacyl-tRNA at the A site and also interferes with the entry of the nascent polypeptide into the "tunnel" that normally guides it away from the peptidyl-transferase center.

Figure 2. The puromycin reaction. A peptidyl-tRNA analogue [eg, Ac[^{14}C]Phe-tRNA) bound to the ribosomal P site of 50S ribosomal subunit reacts with puromycin (an aminoacyl-tRNA analogue) bound to the A site of the peptidyl-transferase center. The resulting peptidyl-puromycin (eg, Ac[^{14}C]Phe-puromycin) is falling of the 50S subunit and can b separated from the substrate (Ac[^{14}C]Phe-tRNA) by extraction.

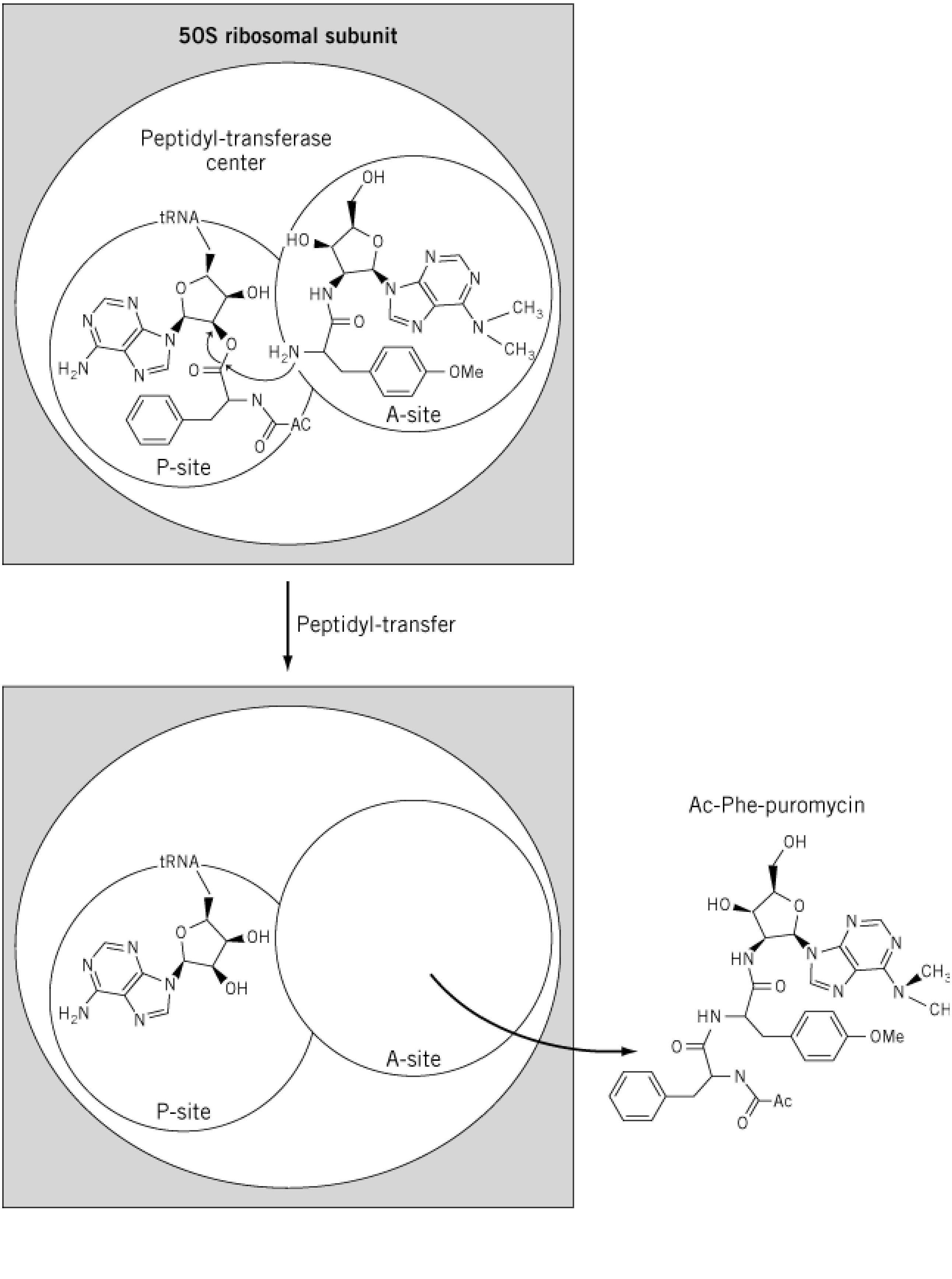

Chloramphenicol inhibits protein synthesis in bacterial extracts with varying potencies depending on the template employed. In particular, synthesis promoted by poly(U) is markedly more resistant to chloramphenicol than that promoted by poly(C) or poly (A) (8). Synthesis occurring with a natural mRNA (eg, MS2 phage RNA) is usually very sensitive to chloramphenicol. The precise reason for the template-dependence is not known. Chloramphenicol may inhibit poly(U)-dependent poly(Phe) synthesis less than it does the synthesis of other polypeptides because the structures of D-threo chloramphenicol and L-phenylalanine are similar (Fig. 3). Competition between these molecules during poly(Phe) synthesis may involve steric hindrance between their phenyl groups and, consequently, chloramphenicol may be chased from the ribosome. Nevertheless, this does not explain why the same template dependence is also observed with several other peptidyl-transferase inhibitors that differ chemically from chloramphenicol and, in particular, that do not have a phenyl group (e.g, the group B streptogramins and the macrolides). Further experiments are needed to elucidate this phenomenon in greater detail.

Figure 3. Structural similarity of D(–)-*threo* chloramphenicol and L-phenylalanine. Competition between these molecules during poly(Phe) synthesis may involve steric hindrance between their phenyl groups.

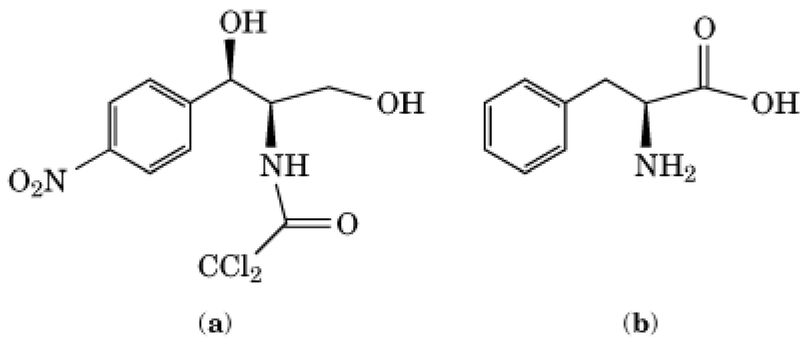

4. Ribosomal Binding Site

Chloramphenicol has a single high-affinity binding site located on the 50S ribosomal subunit ($K_d = 2 \times 10^{-6}$ M), as well as one or more low-affinity sites, at least one of which is located on the 30S subunit ($K_d = 2 \times 10^{-4}$ M) (9). A number of 50S proteins were labeled in affinity-labeling experiments, including L1, L2, L11, L16, L19, and L27 (10). Most of these proteins are located in or next to the peptidyl-transferase center of the ribosome, and several can be affinity-labeled with other antibiotics that interact with this center (**erythromycin**, puromycin, lincosamides, streptogramins).

That the peptidyl-transferase domain is the primary binding site of chloramphenicol was confirmed by RNA footprinting experiments, in which bases of 23S rRNA were compared in antibiotic-free or chloramphenicol-bound ribosomes for their reactivity to chemical probes. Chloramphenicol protected bases A2059, A2062, A2451, and G2505 and enhanced the reactivity of A2058 (11). Protection of A2070 and U2506 has also been observed (12). All these nucleotides are located in the central loop of domain V of 23S rRNA (Fig. 4). Additionally, several mutations of RNA that confer resistance to chloramphenicol have been identified in the same domain (Fig. 4; see references in Ref. 12).

Figure 4. Interaction of chloramphenicol with the central loop of domain V of 23S rRNA. The secondary structure of the central loop of domain V in *E. coli* 23S rRNA is derived from phylogenetic sequence comparisons. Differences in the accessibility of bases to chemical reagents in the presence and absence of chloramphenicol (footprints) are shown in red (–, protection of base; +, enhanced activity). Mutations leading to chloramphenicol resistance are indicated by arrows, and the corresponding organisms are indicated in brackets. All of the eukaryotic mutations were characterized for mitochondrial rRNA. (Figure derived from Refs. 11 and 12.)

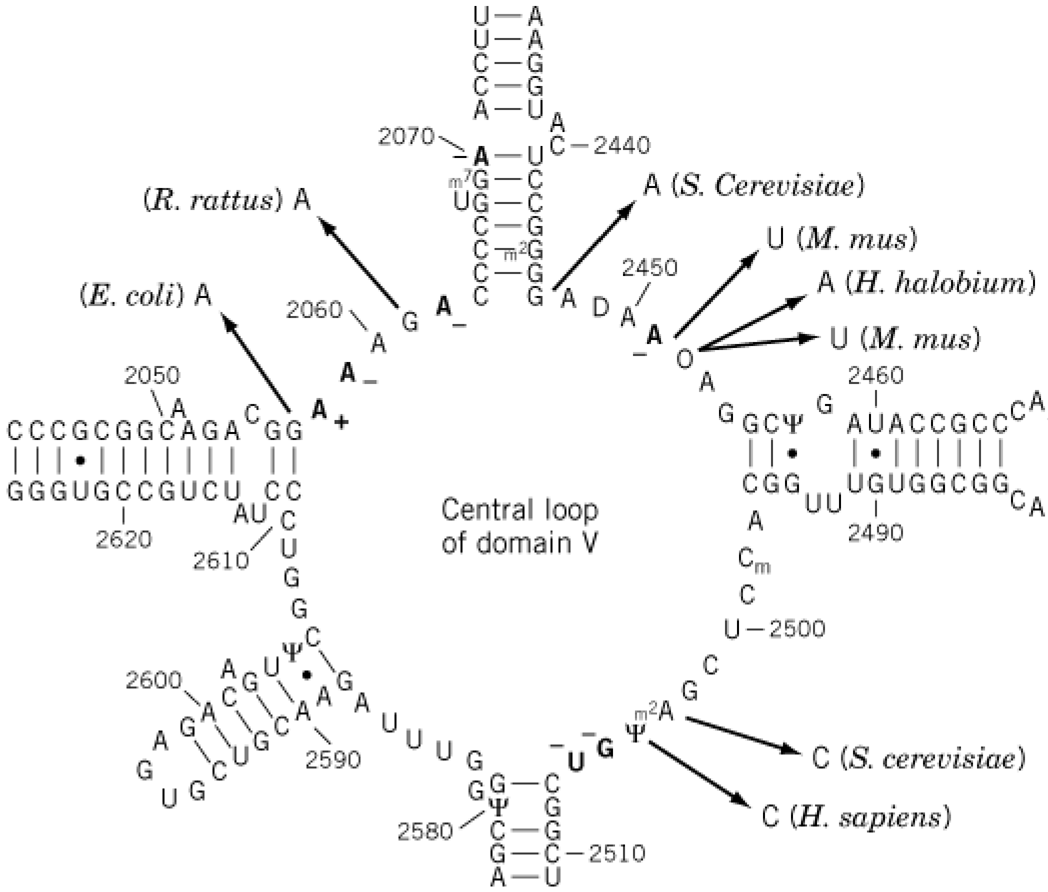

5. Cold-Shock Induction

Shifting growing *E. coli* from 37°C to 20°C inhibits cellular growth and shuts down protein biosynthesis. To compensate for the stress produced by the temperature shift, the levels of (p)ppGpp drop and the synthesis of a subset of proteins is induced; this induction is known as **cold-shock**. Certain inhibitors of protein synthesis, including chloramphenicol, specifically induce the synthesis of the cold-shock proteins in the absence of a temperature shift (13). Ribosomal inhibitors have, in fact, been classified according to their ability to elicit a cold-shock- or a heat-shock-like response. Inhibitors in whose presence the A site of the peptidyl-transferase center is occupied, either by the antibiotic or by an aminoacyl-tRNA (chloramphenicol, erythromycin, fusidic acid, spiramycin, **tetracycline**), produce a cold-shock-like response. In contrast, inhibitors in whose presence the A site of the peptidyl-transferase remains empty (kanamycin, streptomycin) produce a heat-shock-like response.

6. Chloramphenicol Resistance

6.1. Modification of the Bacterial Ribosome
Several mutations in 23S rRNA confer resistance to chloramphenicol. The residues at which these mutations occur (residues G2057, G2061, G2447, A2451, C2452, A2503, U2504; *E. coli* numbering) are located in the peptidyl-transferase loop of 23S rRNA (Fig. 4), which is in accordance with their proposed binding site.

6.2. Alteration in Permeability to Chloramphenicol
Protein synthesis in *S. venezuelae* cells that have begun to produce chloramphenicol becomes insensitive to the antibiotic. There is no modification of the ribosome in these cells; instead, the antibiotic is excluded from the cytoplasm during biosynthesis. The amino acid sequence deduced

from the gene conferring resistance (*cml*) is markedly similar to those of chloramphenicol-resistance genes from *Streptomyces lividans*, *Rhodococcus fascias*, and other bacteria. These polypeptides contain 12 **hydrophobic** regions characteristic of membrane-associated **transport** proteins and are related to a known family of efflux proteins (14).

6.3. Enzymatic Modification of Chloramphenicol

The most common mechanism of chloramphenicol resistance is inactivation by the enzyme chloramphenicol 3′-*O*-acetyltransferase (CAT), encoded by the *cat* gene. The biological and immunological properties of three types of CAT (I, II, III) have been described. The structure of CAT III has been determined by X-ray crystallography, as well as its tertiary complex with chloramphenicol and CoA (15). The enzyme is a trimer; its active sites lie at each of the interfaces between adjacent subunits. CAT catalyzes the transfer of an acetyl moiety from acetyl-CoA to the 3′-hydroxyl of chloramphenicol. The initial product of the reaction, 3-acetyl chloramphenicol, can undergo nonenzymatic intramolecular rearrangement to 1-acetyl chloramphenicol. The latter compound is a substrate for a second round of enzymatic acetylation at the 3-hydroxyl, which yields 1,3-diacetyl chloramphenicol as the final product (Fig. 5). Neither the monoacetylated nor the diacetylated derivative binds to the bacterial ribosome; both, therefore, are devoid of antibiotic activity.

Figure 5. Enzymatic inactivation of chloramphenicol. CAT, chloramphenicol 3′-*O*-acetyltransferase; CPT, chloramphen
CML, chloramphenicol hydrolase.

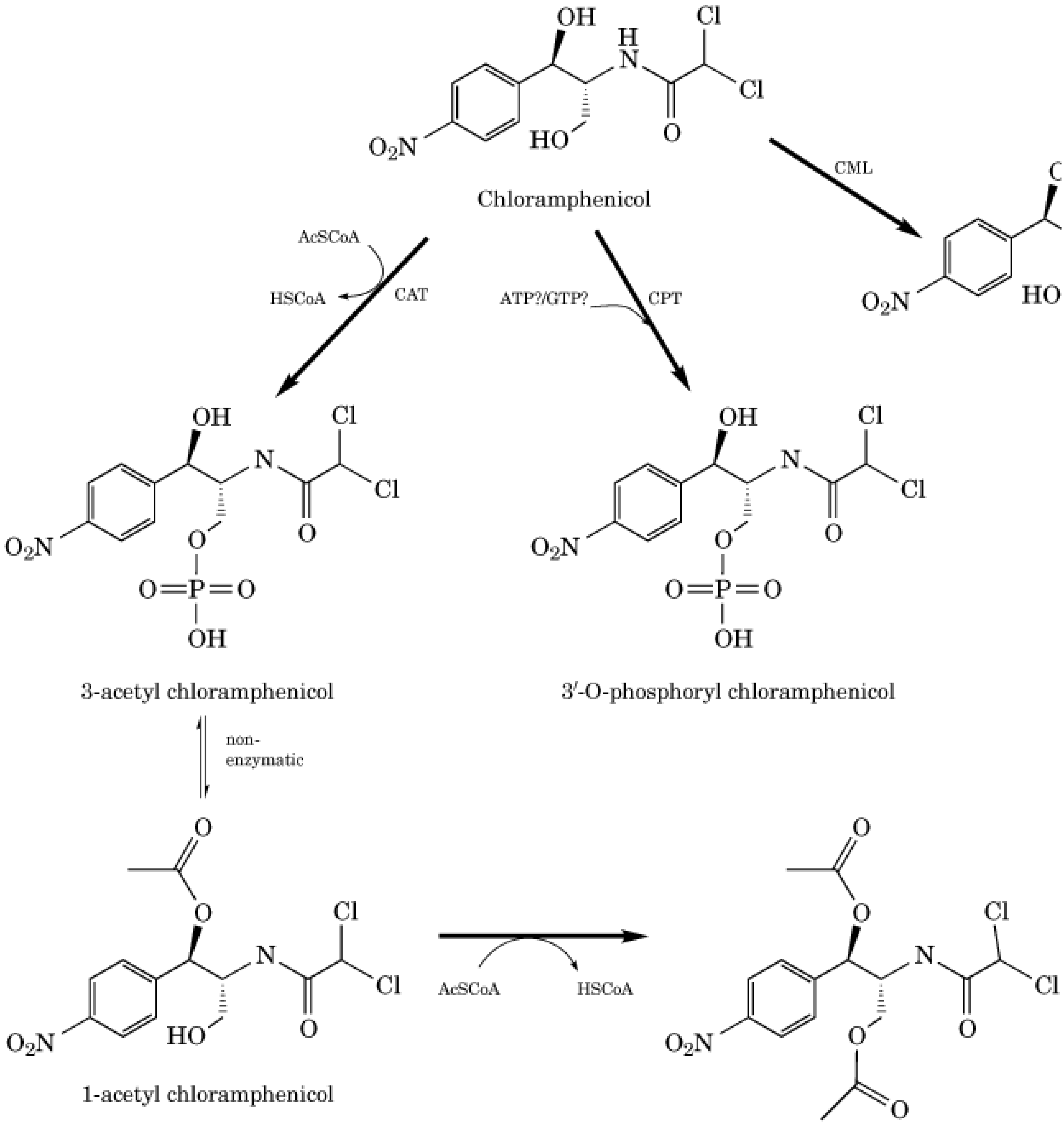

Recently, a second chloramphenicol 3′-*O*-modifying gene was discovered (16). This enzyme, chloramphenicol 3′-*O*-phosphotransferase (CPT) phosphorylates chloramphenicol, yielding 3′-*O*-phosphochloramphenicol, which binds only very weakly to ribosomes and thus does not inhibit translation.

Chloramphenicol is also inactivated by chloramphenicol hydrolase, which hydrolyzes the amide bond (17) (Fig. 5). This enzyme, encoded by the *cml* gene, was first isolated from the mycelium of a chloramphenicol-producing strain of *Streptomyces*. A similar enzyme has been obtained from several other bacteria, including *E. coli*.

6.4. Induction of Chloramphenicol Resistance by Translational Attenuation

Chloramphenicol resistance by enzymatic modification in both Gram-positive and Gram-negative bacteria can be either constitutive or inducible. What is unusual about inducible chloramphenicol resistance is that it occurs by translational attenuation, rather than by transcriptional **attenuation**. The ribosome-binding site for the resistance determinant is sequestered in a secondary "hairpin" structure situated within the encoding mRNA; a short, translated open reading frame, termed the leader, lies upstream of this structure. In the absence of the antibiotic, the secondary structure is maintained, the ribosome does not translate the mRNA that constitutes the hairpin, and the resistance gene is not translated. In the presence of the antibiotic, the ribosome stalls at the leader sequence and the secondary structure relaxes, allowing the *cat* (or *cml*) determinant to be translated (18) (Fig. 6).

Figure 6. Chloramphenicol resistance by translational attenuation. RBS, ribosomal binding site; 30S, small ribosomal subunit; 70S, entire bacterial ribosome.

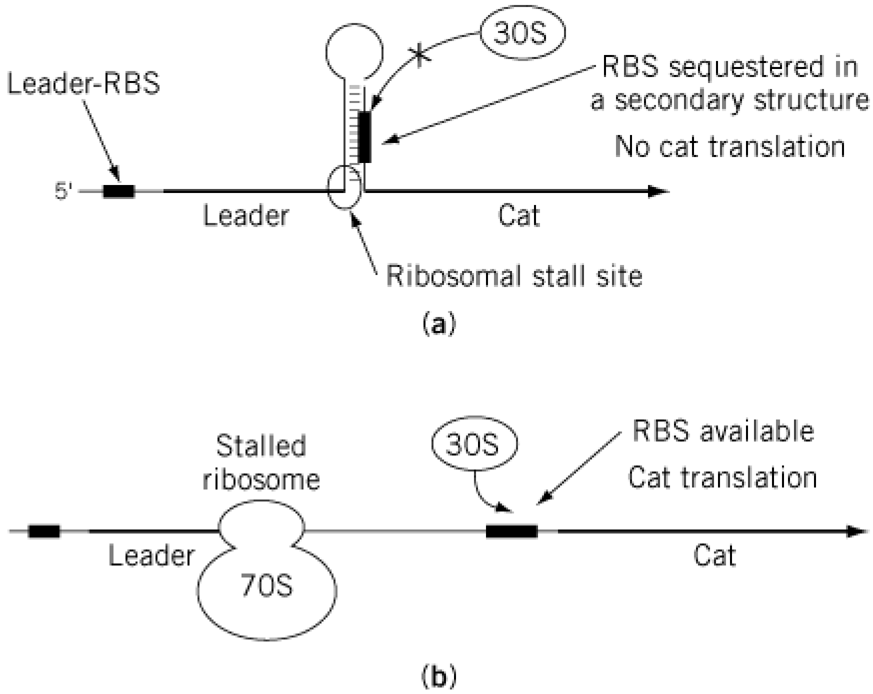

7. The Use of CAT in Molecular Biology

CAT is a gene product that can be assayed with specificity and sensitivity, and consequently it is of considerable value to molecular biologists. When the *cat* gene is fused to heterologous regulatory signals, gene expression can be determined by measuring the CAT activity. Eukaryotes lack endogenous CAT activity, and the amount of CAT activity correlates well with the amount of mRNA transcribed, so the CAT assay has proved to be a powerful tool for investigating and quantifying gene expression in eukaryotic cells. Conventional CAT assays involve the incubation of cell extracts with radioactively labeled chloramphenicol, chromatographic separation of the reaction products, and autoradiography. The recent use of **fluorescent**, rather than radioactive, substrates has dramatically speeded up and simplified the CAT assay (19).

Bibliography

1. O. Pongs (1979) In *Antibiotics* Vol. **1** (F. H. Hahn ed.), Springer-Verlag, Heidelberg, Germany, pp. 26–56.
2. A. A. Yunis (1988) Annu. Rev. Pharmacol. Toxicol. **28**, 83–100.
3. E. Cundliffe and K. McQuillen (1967) J. Mol. Biol. **30**, 137–143.

4. D. Nierhaus and K. H. Nierhaus (1973) Proc. Natl. Acad. Sci. USA **70**, 2224–2228.
5. M. L. Celma, R. E. Monro, and D. Vazquez (1971) FEBS Lett. **13**, 247–251.
6. R. R. Traut and R. E. Monro (1964) J. Mol. Biol. **10**, 63–72.
7. H.-J. Rheinberger and K. H. Nierhaus (1990) Eur. J. Biochem. **193**, 643–650.
8. Z. Kucan and F. Lipmann (1964) J. Biol. Chem. **239**, 516–520.
9. J. L. Lessard and S. Pestka (1972) J. Biol. Chem. **247**, 6909.
10. B. S. Cooperman, C. J. Weitzmann, and C. L. Fernandez (1990) In *The Ribosome: Structure, Function, & Evolution* (W. E. Hill et al., eds.), American Society for Microbiology, Washington, D.C., pp. 491–501.
11. D. Moazed and H. F. Noller (1987) Biochimie **69**, 879–884.
12. C. Rodriguez et al. (1995) J. Mol. Biol. **247**, 224–235.
13. P. A. Lagosky and F. N. Chang (1981) J. Biol. Chem. **256**, 11651–11656.
14. H. Nikaido and M. H. Sailer Jr. (1992) Science **258**, 936–942.
15. A. G. W. Leslie (1990) J. Mol. Biol. **213**, 167.
16. R. H. Mosher et al. (1995) J. Biol. Chem. **270**, 27000–27006.
17. V. S. Malik and L. C. Viking (1971) Can. J. Microbiol. **17**, 1287–1290.
18. P. S. Lovett (1996) Gene **179**, 157–162.
19. C. K. Lefevre et al (1995) Biotechniques **19**, 488–493.

Suggestions for Further Reading

20. E. F. Gale, E. Cundliffe, P. E. Reynolds, M. H. Richmond, and M. J. Waring (1981) Chloramphenicol. In *The Molecular Basis of Antibiotic Action*, 2nd ed. Wiley, New York, pp. 460–468.
21. F. E. Hahn (1983) Chloramphenicol. In *Antibiotics*, Vol. **VI** (F. H. Hahn, ed.), Springer-Verlag, Berlin, pp. 34–45.
22. L. C. Vining and C. Stuttard (1995) Chloramphenicol. Biotechnology **28**, 505–530.

Chloramphenicol Acetyltransferase

The **enzymic** mechanisms by which bacteria modify biologically active molecules are limited by two constraints: (i) the structure–activity correlations for each class of chemical agent and (ii) the metabolic repertoire available to the bacteria. In the case of chloramphenicol (Cml), which has a number of vulnerable functional groups, there are several possibilities. Each functional group of Cml (Fig. 1) contributes to its effectiveness as an inhibitor of ribosomal peptidyltransferase activity (1), and there are examples (reviewed in Ref. 2) of enzyme-mediated resistance to Cml due to dehalogenation, nitro group reduction, hydrolysis of the amide bond, and modification of the hydroxyl groups by phosphorylation (3) or acetylation (2, 4, 5). Nonetheless, after more than four decades of medical and veterinary use, the preponderant enzymic modification mechanism for Cml resistance in bacteria of clinical importance is that of *O*-acetylation of the 3-hydroxyl group, catalyzed by chloramphenicol acetyltransferase (CAT) (Fig. 1).

Figure 1. The mechanism of acetylation of the 3-hydroxyl group of chloramphenicol by acetyl-CoA as catalyzed by

CAT. The two substrates and the His195 residue of CAT are shown (**top**). Within the transition state or tetrahedral intermediate (**bottom**), His195 has abstracted a proton from the 3-hydroxyl group, to generate an "oxyanion" intermediate that has attacked the carbonyl of acetyl-CoA. The intermediate and transition state are stabilized by hydrogen bonding with the side-chain hydroxyl group of Ser148 of CAT.

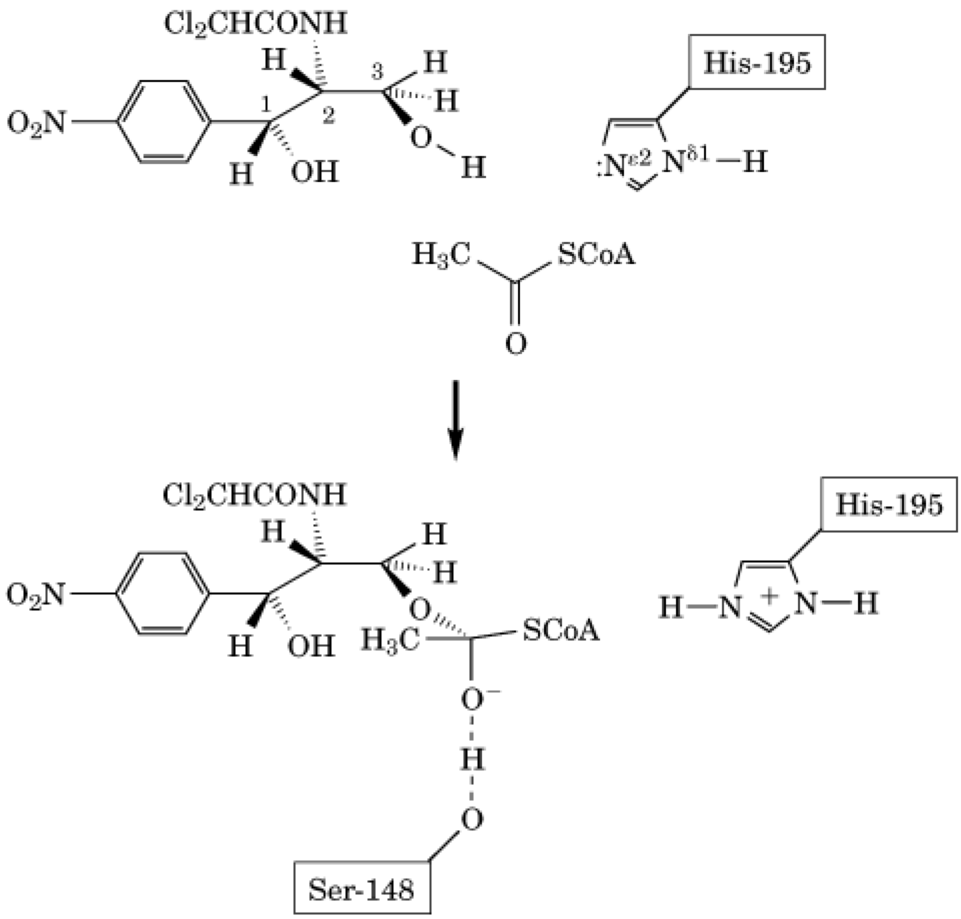

Genes for CAT are widespread among gram-positive and gram-negative bacteria; the *cat* gene in each case is either chromosomal or carried by a mobile genetic element, such as a plasmid or transposon. More important biochemically are the properties of representative variants within the CAT "family" and the pattern of conservation of the primary structure, deduced from nucleotide sequences of its genes, which in turn is related to its three-dimensional protein structure, substrate specificity, and catalysis.

All CAT polypeptide chains are in the range 24 to 26 kDa and normally exist in solution as compact and very stable *homo*-trimers. However, some CAT variants associate *in vivo* and *in vitro* to give hybrids, functional a_2b and ab_2 *hetero*-trimers with physical and catalytic characteristics reflecting the properties of the parental trimers (6). Because natural isolates of Cml-resistant bacteria may occasionally harbor more than one *cat* gene, it is possible in such instances that the intracellular CAT pool will include both parental and hybrid trimers.

The extent of structural variation within the CAT family can be appreciated from a comparison of the deduced primary structures for the products of known *cat* determinants, which yields a lower limit of 28% identity for the most divergent pair of known sequences. Only ~11% of the amino acid residues appear to be identical in all CAT variants, comprising not only residues with side chains that are involved in catalysis and substrate binding, but also those that contribute to critical structural elements necessary for the precise folding and stable packing of the polypeptide chains. A reference point for understanding the variety in primary structures of CAT variants is the type III enzyme

(CAT_{III}), for which a wealth of information is available, including the tertiary structure at high resolution (7, 8) and the structural determinants for the binding of each substrate (2, 4, 5, 7, 8). However, the type I enzyme (CAT_I) may be the most widely distributed variant, because it is specified by many "F-like" R plasmids of gram-negative bacteria, by transposon *Tn9* (9), and by promoter-less *cat* "cassettes," constructed in the laboratory for insertion "downstream" of the noncoding sequences of other genes, to study the regulation of their expression (see Reporter Genes). Type II CAT (CAT_{II}), notable among "enteric" CATs for its particular sensitivity to inhibition by reagents that react with thiol groups and by its association with *Haemophilus influenzae* (10), is less commonly encountered. CAT_I has the remarkable properties of a high affinity for triphenylmethane dyes, such as crystal violet (reviewed in Ref. 2), and the ability to bind a steroidal antibiotic (fusidic acid) both tightly and specifically (11). The latter property is sufficient to confer resistance to fusidate in mutant strains of *Escherichia coli* that were selected for their sensitivity to the antibiotic prior to the introduction of the gene for CAT_I. A plausible mechanism is the effective sequestration of fusidate by high levels of CAT_I, thereby impeding access of the antibiotic to its cellular target, ribosomal elongation factor G. The structural basis for the curious binding of fusidate, which is competitive with respect to Cml, has been deduced by protein engineering and X-ray crystallography (11). Of the eight residues in the Cml binding pocket of CAT_{III} that differ from those of CAT_I, only four appear to be responsible for the former's low affinity (K_i = 279 µM) for fusidate. Replacement of each of the four with their counterparts in CAT_I is sufficient to confer upon CAT_{III} an affinity for fusidate (K_i = 5.4 µM) that approaches that of wild-type CAT_I (K_i = 1.5 µM).

The catalytic machinery of CAT_{III} comprises a number of amino acid side chains (as well as backbone atoms and ordered water molecules) that make precise contacts with one another or with a substrate molecule. The homo-trimers have rotational symmetry at the molecular threefold axis, and consequently have three identical active sites, so only atoms in a single monomer need be addressed. Nonetheless, each of the structurally and functionally equivalent active sites lies deep in the interfacial clefts between subunits. Central to catalysis (12) is His195, which arises from one face of each cleft to supply the general base (N^{e2} in Fig. 1) to deprotonate the C3 hydroxyl of Cml, producing an "oxyanion" intermediate that in turn attacks the carbonyl (C2) carbon of acetyl CoA to yield a tetrahedral intermediate (Fig. 1). Essential for the stabilization of the latter, *en route* to the transition state for the reaction, and confirmed by site-directed mutagenesis (13), is a negatively charged hydrogen bond (Fig. 1) between the oxyanion and the hydroxyl of Ser148, another residue conserved in all CATs. A neighboring participant in catalysis is Thr174, also conserved, which is hydrogen-bonded to a water molecule that in turn probably makes two hydrogen bonds with the putative tetrahedral intermediate (Fig. 1), one to the 1-hydroxyl of Cml and the other to the 3-oxygen of the intermediate. Two additional conserved residues (Arg18 and Asp199) facilitate catalysis via a network of hydrogen bonds with His195, anchoring the side chain of the latter in a novel conformation that allows it to fulfill its general base role (7, 8, 13-15).

Chloramphenicol becomes acetylated on its 1-hydroxyl group also, albeit at a rate much slower than the 3-acetyl derivative is generated (16). The equations below, all of which are reversible, indicate the transformations involved in the two reactions, indicating that in both cases CAT acetylates only the 3-hydroxyl:

$$\text{chloramphenicol} + \text{acetyl-CoA} \rightleftharpoons \text{3-acetyl chloramphenicol} + \text{CoA} \quad (1)$$

$$\text{3-acetyl chloramphenicol} \rightleftharpoons \text{1-acetyl chloramphenicol} \quad (2)$$

$$\text{1-acetyl chloramphenicol} + \text{acetyl-CoA} \rightleftharpoons \text{1,3-diacetyl chloramphenicol} + \text{CoA} \quad (3)$$

Reaction 2 is a nonenzymic acetyl migration, slow and reversible, which yields at equilibrium a mixture of mono-acetyl products. The 1-acetyl Cml so formed is available for a second round of enzymic acetylation at the C3 position, yielding 1,3-diacetyl Cml. Reaction 3 is ~150-fold less efficient than reaction 1, almost certainly due to an unfavorable "fit" of the substrate at the active site because of the bulky 1-acetyl substituent (17). In any case, the sluggish final step (reaction 3) is of little microbiological significance, because both mono-acetyl derivatives of Cml are already devoid of significant antimicrobial activity, making the rate of reaction 1 the prime determinant of the Cml-resistance phenotype.

In summary, the precise geometry and chemical properties of both substrate binding sites (for Cml and acetyl CoA) and of the catalytic center of CAT_{III} each contribute to its extraordinary efficiency, with a turnover number of 600 s^{-1} (25°C) with a K_m for Cml of 12 μM (~4 μg/mL), reassuringly close to the concentrations at which it inhibits most bacteria of clinical importance. A derived kinetic parameter, the so-called specificity constant (k_{cat}/K_m), which combines a measure of substrate affinity with one for catalytic competence, is actually the second-order rate constant for productive collisions of an enzyme with its substrate(s). The value for CAT_{III} and Cml ($5 \times 10^7\ s^{-1}M^{-1}$) approaches that of well-characterized enzyme reactions that are limited by diffusion of the reactants (typically 10^8 to $10^9\ s^{-1}M^{-1}$) and hence at the limit of evolutionary development. By such criteria, CAT_{III} has evolved to a state approaching "perfection" in biological catalysis (18), wherein a fine balance has been struck between rate acceleration (k_{cat}) and specificity (and affinity) for substrate (K_m). Although it is not clear how the specificity and catalytic efficiency of CAT_{III} (and related variants) have evolved, the acetyltransferase (E2p) of the pyruvate dehydrogenase complex, which generates acetyl-CoA for central metabolism, has a three-dimensional structure that is virtually identical to that of CAT, as well as the same mechanism of catalysis, but the two proteins have very few identities in primary structure—only those involved with the active site (19).

It is of interest that there is a large family of "xenobiotic" *O*-acetyltransferases (XATs) with a range of specificities for natural products; several of these enzymes have a low affinity for Cml and hence were first detected as effectors of low-level resistance to the antibiotic (20). All appear to be trimeric but have no sequence homologies with members of the *bona fide* CAT family described above. One such XAT (with CAT activity) has been studied by X-ray crystallography (21) and shown to have a tertiary structure quite different from that of CAT, but the catalytic mechanism may well involve general base catalysis involving a conserved histidine residue.

Bibliography

1. E. F. Gale et al. (1981) *The Molecular Basis of Antibiotic Action*, 2nd ed., Wiley, London, pp. 462–468.
2. W. V. Shaw (1983) CRC Crit. Rev. Biochem. **14**, 1–46.
3. R. H. Mosher et al. (1995) J. Biol. Chem. **27**, 27000–27006.
4. W. V. Shaw (1992) Sci. Progress (Oxford) **76**, 565–580.
5. W. V. Shaw and A. G. W. Leslie (1991) Annu. Rev. Biophys. Biophys. Chem. **20**, 363–386.
6. P. J. Day, I. A. Murray, and W. V. Shaw (1995) Biochemistry **34**, 6416–6422.
7. A. G. W. Leslie (1990) J. Mol. Biol. **213**, 167–186.
8. A. G. W. Leslie, P. C. E. Moody, and W. V. Shaw (1988) Proc. Natl. Acad. Sci. USA **85**, 4133–4137.
9. N. E. Alton and D. Vapnek (1979) Nature **282**, 864–869.
10. I. A. Murray, J. V. Martinez-Suarez, T. J. Close, and W. V. Shaw (1990) Biochem. J. **272**, 505–

510.
11. I. A. Murray et al. (1995) J. Mol. Biol. **254**, 993–1005.
12. A. Lewendon et al. (1994) Biochemistry **33**, 1944–1950.
13. A. Lewendon, I. A. Murray, W. V. Shaw, M. R. Gibbs, and A. G. W. Leslie (1990) Biochemistry **9**, 2075–2080.
14. A. Lewendon et al. (1988) Biochemistry **27**, 7385–7390.
15. A. Lewendon and W. V. Shaw (1993) J. Biol. Chem. **268**, 20997–21001.
16. J. Ellis, C. R. Bagshaw, and W. V. Shaw (1995) Biochemistry **34**, 16852–16859.
17. I. A. Murray et al. (1991) Biochemistry **30**, 3763–3770.
18. W. J. Albery and J. R. Knowles (1976) Biochemistry **15**, 5631–5640.
19. A. Mattevi et al. (1993) Biochemistry **32**, 3887–3901.
20. I. A. Murray and W. V. Shaw (1997) Antimicrob. Agents Chemother. **41**, 1–6.
21. T. W. Beaman, M. Sugantino, and S. L. Roderick (1998) Biochemistry **37**, 6689–6696.

Chloroplast

A distinctive feature of chloroplasts of **plants** and **algae** is their extensive, internal, green, chlorophyll-containing membrane system, called thylakoid membranes, where the primary reactions of photosynthesis occur. This system of photosynthetic reaction centers converts light energy into chemical energy, which is used to drive cellular metabolism. Besides their important role in photosynthesis, chloroplasts are also involved in several biochemical pathways, such as the biosynthesis of amino acids, fatty acids, tetrapyrroles including chlorophyll and heme, carotenoids, isoprenoids and pyrimidines. Chloroplasts are also involved in carbon metabolism and in nitrogen and sulfur assimilation (1). Like mitochondria, chloroplasts possess their own genetic system, which cooperates closely with the nucleus in biosynthesizing numerous organellar components. Chloroplasts represent one type of plastid derived from colorless proplastids in the meristematic cells of plant leaves and shoots, which have only a rudimentary internal membrane system (1). Light profoundly affects the development of proplastids. They differentiate into chloroplasts in the presence of light, whereas in its absence they differentiate into etioplasts, which lack chlorophyll and contain a prolamellar body. Upon subsequent illumination, the prolamellar body gives rise to lamellae of the thylakoid membrane. Depending on the plant tissues, the developmental stage, and the environmental conditions, proplastids also differentiate into chromoplasts in petals or fruits, into leucoplasts in roots, or into amyloplasts in tubers in which starch is accumulated. Proplastids also develop into elaioplasts in glands, certain fruits and seeds, where they are involved in synthesizing lipids, terpenoids, carotenoids, and carbohydrates. Although these various plastid forms have rather distinct morphologies, plastid differentiation is reversible to a large extent, because chloroplasts develop from leucoplasts or amyloplasts, and viceversa. During transitions from chloroplasts to the other plastid forms, the expression of most organellar genes is reduced, whereas specific nuclear genes encoding plastid proteins are activated (1, 2). An important point is that all plastid types contain an internal membrane system that is crucial for their interconversion.

1. Thylakoid Membranes and the Photosynthetic Apparatus

The internal thylakoid membrane system consists of appressed and non-appressed flattened membrane vesicles, called grana and stroma lamellae, respectively (Fig. 1). The primary reactions of photosynthesis are catalyzed by four major protein-pigment complexes of the thylakoid membrane:

(i) photosystem II and (ii) photosystem I, and their associated chlorophyll antennae, (iii) the cytochrome b6/f complex, and (iv) the ATP synthase (Fig. 1; see also Photosynthesis). Briefly, light energy is captured by the antennae and channeled to the reaction centers of photosystem II and photosystem I. The energy is used to energize an electron in chlorophyll and to create a stable charge separation across the membrane. This triggers a series of oxido-reductions along the photosynthetic **electron-transfer** chain. At one end of this chain, water is oxidized by photosystem II with concomitant evolution of oxygen and release of protons into the lumen. Then electrons are transferred to plastoquinone, to the cytochrome b6/f complex, which acts as a **proton pump**, and to the soluble electron carrier plastocyanin in the thylakoid lumen. At the other end of the chain, photosystem I oxidizes plastocyanin upon light absorption and transfers electrons to ferredoxin and then to NADP to form NADPH. The resulting pH gradient is used by the fourth complex, ATP synthase, to produce ATP on the stromal side. This enzyme also functions in the opposite direction by hydrolyzing ATP to pump protons into the thylakoid lumen and thus generate a pH gradient. Because the abundance of the thylakoid membrane complexes facilitates their biochemical analysis and because the state of the redox cofactors is monitored readily by **spectroscopic** techniques, the thylakoid membrane has been studied intensively and represents one of the best-studied membrane systems.

Figure 1. Photosynthetic complexes in the thylakoid membrane of chloroplasts. PSII (photosystem II) is located within the appressed grana region, whereas PSI (photosystem I) is located within the nonappressed stroma lamellae. The photosynthetic electron transfer chain is shown starting with water as electron donor to PSII, to plastoquinone (PQ), to the cytochrome b6/f complex (cytb6/f), to the soluble electron transfer protein plastocyanin (PC), to PSI, to ferredoxin (Fd), to ferredoxin-NADP oxidoreductase (FNR), and to NADP as final electron acceptor. Electron flow is coupled to proton translocation into the lumen. The resulting pH gradient across the thylakoid membrane drives ATP synthesis. Both ATP and NADPH are used for CO_2 fixation.

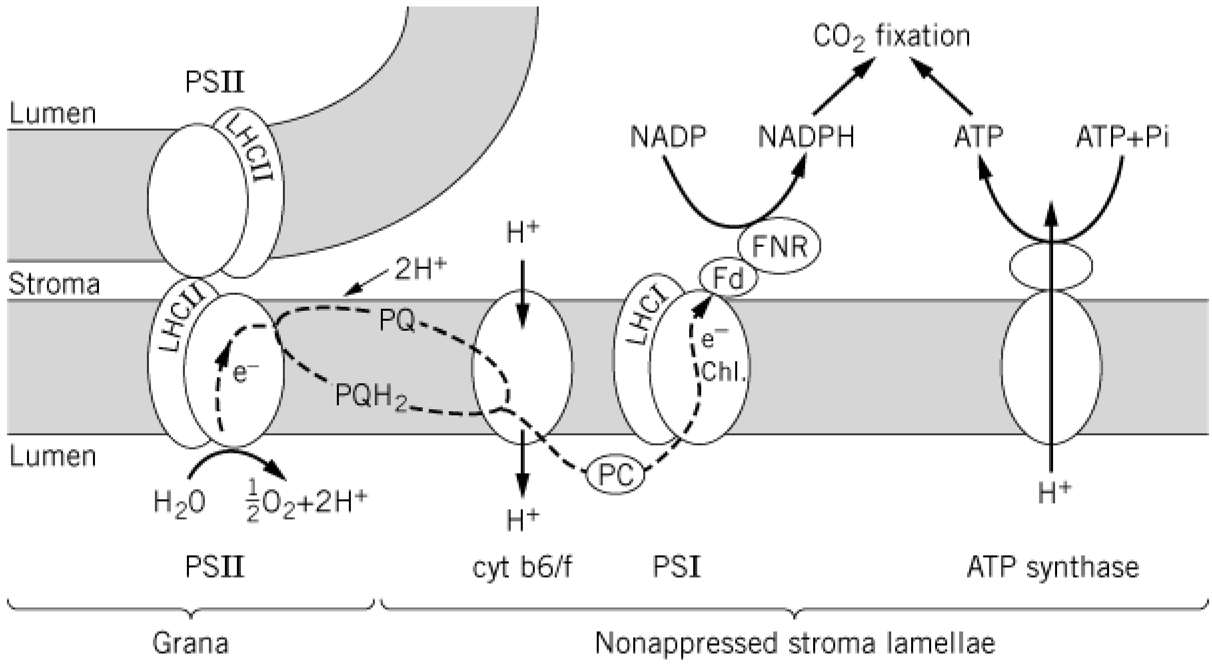

Each of the four photosynthetic complexes contains numerous protein subunits, some of which are encoded by the chloroplast genome, whereas others are encoded by the nuclear genome (Table 1; Fig. 2). The two principal reaction center polypeptides of photosystems I and II are highly **hydrophobic** and contain 11 and 5 transmembrane a-helices, respectively, to which most of the redox cofactors and several chlorophylls are bound with an asymmetrical distribution across the thylakoid membrane. This asymmetry is crucial for the vectorial electron transport in the membrane.

The distribution of these complexes is unequal between the appressed (grana) and nonappressed thylakoid membrane regions (3). Photosystem II is localized predominantly in the grana regions, whereas photosystem I and the ATP synthase complex are found exclusively in the nonappresssed regions. The cytochrome b6/f complex is present in both the grana and nonappressed regions. Destacking and restacking of thylakoid membranes are induced experimentally by decreasing and then increasing again the cation concentration. Remarkably, the lateral segregation of the photosynthetic complexes between grana and stromal membranes is lost upon destacking because of random mixing, but it is restored upon restacking the membranes (4).

Figure 2. Biosynthesis of the photosynthetic apparatus and protein traffic in the chloroplast. Photosynthetic complexes consist of nucleus- and chloroplast-encoded subunits. The former are synthesized as precursors on cytosolic 80S ribosomes and targeted to the chloroplast. Upon import into the organelle, the N-terminal stromal transit peptide domain is cleaved, and the protein is directed to the stroma, to the envelope, or to the thylakoids. In the latter case, the protein contains an additional cleavable thylakoid targeting domain. Several posttranscriptional steps in the chloroplast, such as RNA stability, processing, splicing, editing, and translation, plus the assembly of protein complexes, require the action of numerous nucleus-encoded factors. Chlorophyll, the major pigment of the thylakoid membrane is synthesized entirely in the chloroplast. Synthesis starts from d-aminolevulinic acid (ALA) and involves several steps in common with heme biosynthesis until protoporphyrin IX (proto IX). One of the last steps of chlorophyll synthesis, conversion of protochlorophyllide (Pchlide) to chlorophyllide (Chlide), requires light in land plants. Chlorophyll synthesis is tightly coordinated with the synthesis of its apoproteins. Expression of nuclear genes of photosynthetic proteins is strongly stimulated by light. Some of the chlorophyll precursors influence, directly or indirectly, expression of nuclear genes involved in photosynthesis.

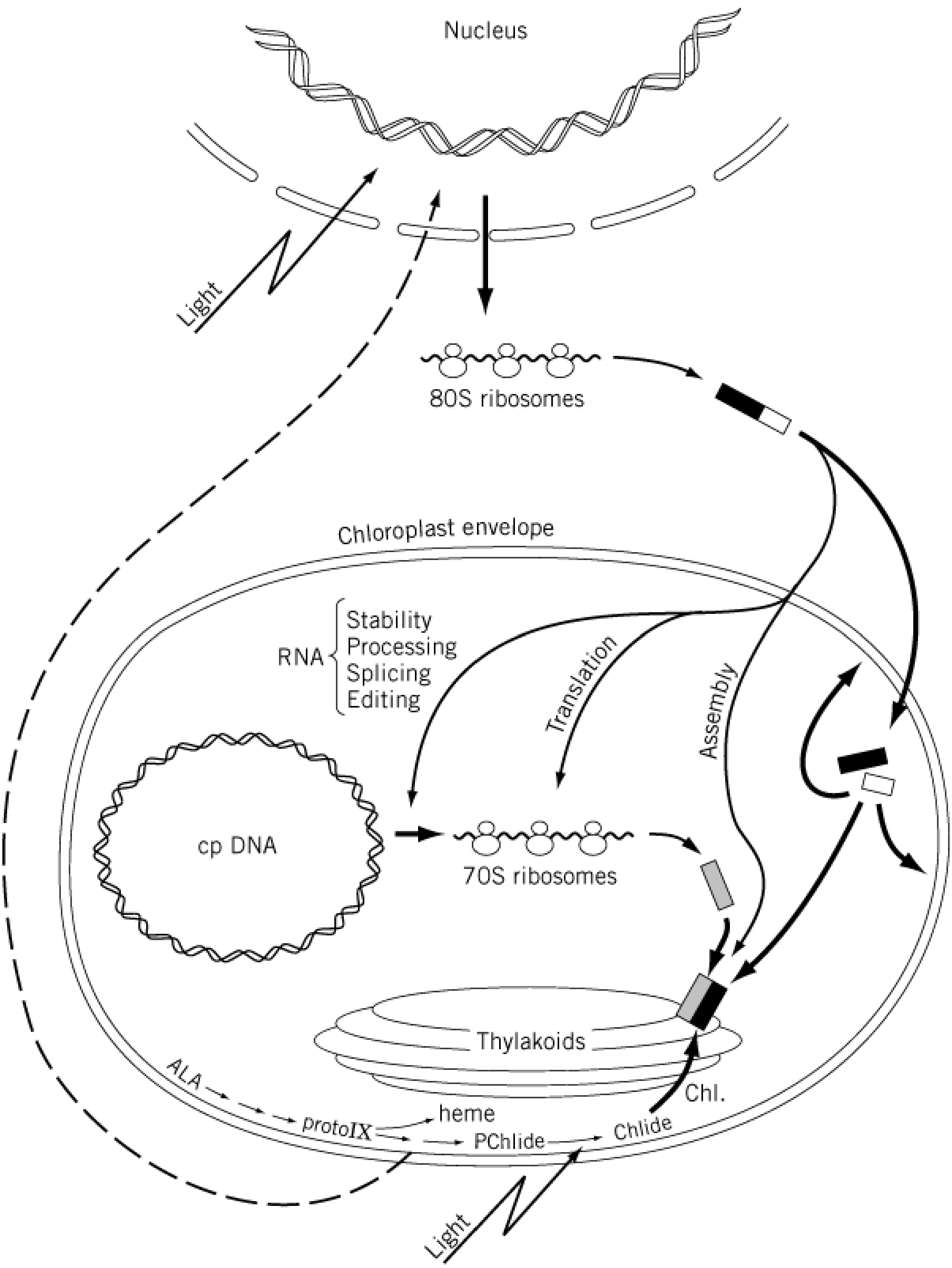

Table 1. Informational Content of Chloroplast DNA from Land Plants and Green Algae

	Number in Chloroplast

Genes Involved in	(Nucleus)[a]
Photosynthesis	
Photosystem II	14 (5)
Photosystem I	5 (8)
Cytochrome b6/f complex	5 (2)
ATP synthase	6 (3)
Ribulose biphosphate carboxlase/oxygenase	1 (1)
NADH dehydrogenase [b]	11
Light-independent chlorophyll synthesis [c]	3
CO_2 uptake[d]	1
Protein Biosynthesis	
Ribosomal RNAs	4
Ribosomal proteins	20
tRNAs	30–31
RNA polymerase subunits	4
Other Functions	
ClpP subunit of ATP-dependent protease	1
ORFs of unknown function	10–20

[a] The number of chloroplast-encoded subunits of photosynthetic complexes. The numbers in parenthesis refer to the number of nucleus-encoded subunits.

[b] These genes are found only in the chloroplast genomes of land plants.

[c] The number of chloroplast genes involved in light-independent chlorophyll synthesis and CO_2 uptake. These genes are found only in the chloroplast genomes of gymnosperms, liverwort, and Chlamydomonas.

[d] This gene is involved in CO_2 uptake.

Other dynamic changes in thylakoid membrane organization occur when plants and algae are subjected to light of different wavelengths that is preferentially absorbed by either photosystems II or I. Under these conditions, part of the chlorophyll antenna is displaced from one photosystem to the other, so as to achieve balanced light absorption and hence optimal functioning of the two photosystems (5). Thus when photosystem II is preferentially activated, the plastoquinone pool is reduced. This leads to the activation of a protein kinase associated with the cytochrome b6/f complex, to the phosphorylation of the light-harvesting complex (LHCII), and to the concomitant movement of part of the photosystem II antenna to photosystem I. If photosystem I is preferentially activated, LHCII is dephosphorylated, and it returns to photosystem II in the grana regions.

1.1. Stroma and Carbon-Fixation Cycle

The ATP and NADPH produced by the primary light reactions of photosynthesis are used as sources of energy and reducing power to drive the reactions of the carbon fixation cycle, which convert CO_2 into glyceraldehyde 3-phosphate, a precursor to sugars, amino acids, and fatty acids. Although these reactions are also called the “dark reactions,” the enzymes involved are inactivated in the dark and need to be reactivated by light through the reducing power generated by photosynthesis. The key reaction, which involves converting one atom of inorganic carbon, as CO_2, into organic carbon, is catalyzed by the enzyme **ribulose 1,5 bisphosphate carboxylase** (Rubisco), a large stromal enzyme that works only sluggishly (6). Therefore, it is required in large amounts and is thought to be the most abundant protein on earth. This enzyme also has an oxygenase activity, which predominates if the concentration of CO_2 is low. Under these conditions it catalyzes the first step of a pathway called photorespiration, which ultimately liberates CO_2 and thereby reverses the photosynthetic reaction. In addition, the stroma includes a large number of proteins involved in several important metabolic pathways (amino acid and fatty acid synthesis, sulfur and nitrogen assimilation). The chloroplast transcription and translation systems are also contained in this compartment.

1.2. Chloroplast DNA and Its Informational Content

Chloroplasts together with mitochondria, are the only cellular organelles containing their own apparatus for **protein biosynthesis**. It consists of chloroplast **DNA**, **RNA polymerase**, enzymes involved in RNA metabolism, ribosomes, transfer RNA, and several translation factors. Chloroplast ribosomes resemble those of **bacteria** and have similar ribosomal RNA and proteins and sensitivity to a similar spectrum of **antibiotics**. The circular chloroplast DNA molecules range in size between 70 kb and 400 kb (7) and are present in about 100 copies per chloroplast. A typical mesophyll cell contains close to 100 plastids and thus about 10,000 chloroplast DNA circles. A dozen chloroplast genomes from several vascular plants and algae have been sequenced. These sequences have revealed the existence of about 120 chloroplast genes in plants and green algae. They include about 50 genes that encode components of the transcriptional apparatus (subunits of RNA polymerase) and of the translational apparatus (ribosomal RNA, ribosomal proteins, transfer RNA, and translation factors). About 40 genes are involved in photosynthesis, and they encode some of the subunits of photosystems I and II, the cytochrome b6/f complex, ATP synthase and Rubisco (see Table 1). The other subunits of these complexes are encoded by the nuclear genome, translated on cytosolic ribosomes, and imported posttranslationally into the chloroplast. The genes involved in the plastid protein synthesizing system and in photosynthesis have been conserved during evolutionary **divergence** of the chloroplast genomes of plants and green algae. The remaining chloroplast genes, however, have not been universally conserved. Eleven genes encoding subunits of NADH dehydrogenase are present in the chloroplasts of plants, but not in algae. Whereas the role of the mitochondrial NADH dehydrogenase in respiration is well understood, the function of the chloroplast enzyme has not yet been elucidated. It could be involved in a chlororespiratory pathway by reducing the plastoquinone pool in the dark, which is ultimately oxidized by molecular oxygen via unknown redox components (8).

In most plants, one of the last steps of the chlorophyll synthesis pathway, the conversion of protochlorophyllide into chlorophyllide, is light-dependent. In green algae and **gymnosperms**, an alternative light-independent pathway for chlorophyll synthesis is mediated by three chloroplast genes that are absent in **angiosperms**. The sequences of chloroplast genomes have revealed additional genes whose functions are still unknown.

The chloroplast genomes of nongreen algae contain twice as many genes as those of higher plants. Additional genes include those required for photosynthesis that are nucleus-encoded in plants and green algae, genes involved in the synthesis of fatty acids, amino acids, and pigments, genes required for **protein folding** and transport, and additional genes of unknown function (9). The smallest plastid genome identified, that of the white parasitic plant *Epifagus virginiana*, is only 70 kbp in size. It has lost all the genes involved in photosynthesis, and the remaining genes encode mostly components of the plastid protein synthesizing system.

It is generally admitted that plastids originated as the result of an endosymbiotic event in which a **prokaryotic** photosynthetic organism, probably similar to a **cyanobacterium**, invaded a primitive **eukaryotic** cell. Strong support for this endosymbiotic hypothesis arises from the considerable similarity between the transcriptional and translational systems of prokaryotes and plastids. It is thought that during evolution genetic information from the intruder was gradually lost and transferred to the nucleus of the host. The question thus arises why chloroplast DNA has been maintained. One possibility is that this evolutionary plastid genome size reduction is still in progress and has not yet reached its final stage. Another possibility is that the plastid protein synthesizing apparatus is essential for synthesizing the large hydrophobic polypeptides of the photosynthetic reaction centers, which cannot be translocated across the plastid envelope membrane. A third recently advanced hypothesis is that the presence of the plastid protein synthesizing system is essential to allow a rapid response of plastid gene expression to environmental changes (10).

1.3. Chloroplast Gene Expression

Two distinct RNA polymerases are present in the chloroplasts of higher plants. One is similar to its bacterial homologue, and its subunits are encoded by chloroplast genes. This enzyme transcribes primarily genes involved in photosynthesis, which are expressed at a high level. The second plastid RNA polymerase is nucleus-encoded and is required for expressing the nonphotosynthetic plastid functions necessary for plant growth (11). Many chloroplast genes are organized in large transcription units. These units are transcribed into large precursor transcripts, which then are processed into individual messenger RNA (mRNA) molecules. Chloroplasts contain RNA **splicing** systems, because several plastid genes contain **introns**, mostly group II and group I, which have a characteristic secondary structure (12). These introns have also been found in mitochondrial genes, and some of them are **self-splicing**. Splicing in the chloroplast is rather complex, as in the case of the *psaA* gene encoding one of the reaction center polypeptides of photosystem I in the green alga *Chlamydomonas*. This gene consists of three coding regions (**exons**) that are widely separated on the chloroplast genome and are flanked by group II intron sequences (13). They are transcribed individually, and maturation of the *psaA* mRNA depends on two trans-splicing reactions in which the separate transcripts of the three exons are spliced together. A particularly intriguing feature is that one of the introns is split into three parts (14). This has interesting evolutionary implications because it is thought that group II introns represent the precursors of nuclear introns and their associated splicing factors. In this view, the split chloroplast intron may represent an intermediate between group II and nuclear introns. The chloroplast genetic system has evolved at a rather slow rate and could have therefore maintained some ancient gene organization.

Another unusual feature of chloroplast RNA metabolism is RNA **editing** in vascular plants (15). Editing in chloroplasts is a posttranscriptional process in which specific C residues of a primary transcript are changed to U. Editing has important implications for interpreting DNA genomic sequence data. As an example, an ACG triplet may be edited to AUG, thereby creating a new initiation codon, which could not be identified in the DNA sequence. Alternatively, an editing event may change an internal codon and thus change the corresponding amino acid predicted by the DNA sequence. Therefore, sequencing of chloroplast genomes may not allow identifying of all of the plastid genes.

Because the subunits, redox cofactors, and pigments of photosynthetic complexes are synthesized by two distinct genetic systems, the process has to occur in a coordinated way (Fig. 2). Genetic studies with ***Chlamydomonas*** and **maize** have indeed revealed the existence of highly complex interactions between nucleus and chloroplast (16). A large number of nuclear genes are involved in chloroplast gene expression. They encode factors targeted to the chloroplast that act at different posttranscriptional steps, such as RNA processing, RNA stability, RNA splicing, translation, and the assembly of photosynthetic complexes. Light strongly enhances some of these steps, especially translation. Several translational activators have been identified, which act at the level of initiating translation. Translation in the chloroplast occurs on chloroplast ribosomes, which are often closely associated with the thylakoid membrane. Cotranslational insertion into the thylakoid membrane has been proposed for the hydrophobic reaction center polypeptides. In addition, synthesis of chlorophyll and its apoproteins needs to be strictly coordinated, because free chlorophyll is highly photoreactive and causes serious damage to the cell.

1.4. Chloroplast-Nuclear Cross talk

Chloroplast function and development depend to a large extent on the nucleus. A large number of nuclear genes encode chloroplast structural components and enzymes and are involved in regulating chloroplast gene expression. Reciprocally, chloroplasts also influence nuclear gene activity. This is apparent in mutant plants with defective chloroplasts, where nuclear genes of proteins involved in photosynthesis are no longer expressed. As an example, when carotenoid synthesis is inhibited, chloroplasts rapidly bleach in strong light because chlorophyll is photooxidized in the absence of carotenoids (17). Under these conditions, expression of nuclear genes that code for several abundant chloroplast proteins involved in photosynthesis is specifically repressed. A block in chloroplast protein synthesis has a similar effect (18). These observations imply the existence of a plastid-derived factor that directly or indirectly influences nuclear gene activity. There are mutants of Arabidopsis in which the transduction of this plastid-derived signal to the nucleus is affected (19). The nature of the plastid factor is still unknown in plants, although studies with *Chlamydomonas* suggest that some porphyrin compounds, which act as intermediates in the chlorophyll biosynthetic pathway, are involved in this response (Fig. 2, 20).

1.5. Protein Sorting in the Chloroplast

Chloroplasts are bounded by an envelope that consists of the outer and inner membranes. The outer membrane is freely permeable to ions and small molecules, whereas the inner membrane is highly selective and contains specific translocators and **permeases** that allow regulated metabolic transport between cytosol and stroma. The envelope also contains the protein import system.

From just the modest size of the plastid genome, it is clear that the majority of the chloroplast proteins are encoded by nuclear genes and imported into the chloroplast. Six chloroplast compartments can be distinguished: (1) the outer envelope membrane, (2) the intermembrane space, (3) the inner envelope membrane, (4) the stroma, (5) the thylakoid membrane, and (6) the lumen. Nucleus-encoded proteins destined to the chloroplast are synthesized as precursor proteins containing, in most cases, a transient N-terminal transit peptide (21). Transit peptides are both necessary and sufficient to import a polypeptide into the chloroplast. Transit peptides of stromal proteins consist of 30 to 120 residues in only a poorly conserved sequence. The only distinguishing feature is that they are rich in hydroxylated amino acids and deficient in acidic residues. Recognition of the protein import **receptor** by the transit peptide is followed by translocation of the precursor protein in an extended conformation across the two envelope membranes. ATP and GTP are the sole energy sources for this process, which also requires the participation of several factors to unfold protein on the outside and to refold protein on the inside of the organelle. Several **molecular chaperones** play an important role in the proper folding of the polypeptides that enter the chloroplast (21). Translocation of the precursor of protochlorophyllide oxidoreductase, an enzyme involved in the last step of chlorophyll synthesis, also requires the presence of its substrate, protochlorophyllide, inside the plastid (22). This raises the possibility that the substrate drives the translocation by inducing or stabilizing folding of the enzyme on the stromal side of the envelope.

Thylakoid precursor proteins contain a bipartite transit peptide. The first domain targets the protein to the stroma, and the second hydrophobic domain, which resembles the **signal sequences** of **secretory proteins**, acts as the thylakoid targeting domain. Surprisingly, there are four pathways for protein translocation into or across the thylakoid membrane (21). The first corresponds to the bacterial protein secretion system and uses **Sec proteins** homologous to the bacterial SecA and SecY proteins. The second uses a system involving a signal recognition particle. The third pathway is rather unique because it uses only the trans-thylakoid pH gradient as an energy source (see Chemiosmotic Coupling). The fourth pathway involves spontaneous insertion of certain proteins into the thylakoid membrane.

Insertion of proteins into the chloroplast envelope occurs by several routes. Some nucleus-encoded polypeptide chains lack a cleavable transit peptide and are inserted directly into the outer and inner membranes. Other envelope membrane proteins containing a cleavable transit peptide use the general import pathway. At least one inner membrane envelope protein is encoded by the chloroplast genome, so it must contain an appropriate targeting signal.

1.6. Chloroplast Engineering

A major breakthrough in chloroplast research in 1988 was the development of an efficient method for genetically **transforming** chloroplasts of the green alga *Chlamydomonas* (23), which was subsequently adapted to higher plants (24). In this method, tungsten or gold particles are coated with DNA and bombarded into cells with a particle gun (see Transfection). Upon entry of the particles into chloroplasts, the DNA is released and integrated into the chloroplast chromosome by homologous recombination. The existence of an efficient chloroplast homologous recombination system and the development of selectable markers for chloroplast transformation have opened the door to manipulating the chloroplast genome. In particular, this new technology allows directed chloroplast gene disruption, a powerful tool for elucidating the role of genes of unknown function. It has also permitted site-directed mutagenesis of specific residues of photosynthetic reaction center polypeptides so as to gain new insights into their structure-function relationship, and it has been very useful for studying chloroplast gene expression. Chloroplast transformation has important applications for plant biotechnology and protein engineering. Because the chloroplast genome is present in multiple copies, up to 10,000 per cell, new genetic information introduced into plastids is amplified. In principle, this opens the possibility of expressing foreign proteins of commercial interest in large quantities. The expression of foreign genes in the chloroplast compartment offers the additional advantage of considerably reducing the risk of transfer of new genetic material to the environment because the chloroplasts from the male parent are not transmitted to the progeny in most crop plants.

Bibliography

1. N. W. Gillham (1994) *Organelle Genes and Genomes*. Oxford University Press, New York.
2. J. K. Hoober (1984) *Chloroplasts*. Plenum Press, New York.
3. J. Olive and O. Vallon (1991) J. Electron. Microsc. Technol. **18**, 360–374.
4. G. Ojakian and P. Satir (1974) Proc. Natl. Acad. Sci. USA **21**, 2052–2056.
5. J. F. Allen (1992) Biochim. Biophys. Acta **1098**, 275–335.
6. R. J. Spreitzer (1993) Ann. Rev. Plant Physiol. Plant Mol. Biol. **44**, 411–434.
7. M. Sugiura (1996) In *Molecular Genetics of Photosynthesis*. (B. Andersson, A. H. Salter, and J. Barber, eds.), Oxford University Press, Oxford, New York, pp 58–74.
8. P. Bennoun (1982) Proc. Natl. Acad. Sci. USA **79**, 4352–4356.
9. M. Reith and J. Munholland (1995) Plant Mol. Biol. Rep. **13**, 333–342
10. J. Allen (1995) J. Theor. Biol. **165**, 609–631.
11. L. A. Allison, L. D. Simon, and P. Maliga (1996) EMBO J. **15**, 2802–2809.
12. M. Sugita and M. Sugira (1996) Plant Mol. Biol. **32**, 315–326.
13. U. Kück, Y. Choquet, M. Schneider, M. Dron, and P. Bennoun (1987) EMBO J. **6**, 2185–2195.
14. M. Goldschmidt-Clermont et al. (1991) Cell **65**, 135–143.
15. H. Kössel et al. (1993) In *Plant Mitochondria*, A. Brennicke and U. Kück (eds.), VCH, Weinheim, Germany, pp. 93–102.
16. J.-D. Rochaix (1992) Ann. Rev. Cell Biol. **8**, 1–28.
17. W. Taylor (1989) Ann. Rev. Plant Physiol. Plant Mol. Biol. **40**, 211–233.
18. J. Gray (1996) In *Membranes: Specialized Functions in Plants*, M. Smallwood, J. P. Knox, and D. J. Bowles, eds., Bios Scientific Oxford, pp. 441–455.
19. R. E. Susek, F. M. Ausubel, and J. Chory (1993) Cell **74**, 787–799.
20. U. Johanningmeier and S. H. Howell (1984) J. Biol. Chem. **259**, 13541–13549.
21. K. Cline and R. Henry (1996) Annu. Rev. Cell Dev. Biol. **12**, 1–26.
22. S. Reinbothe, S. Runge, B. Reinbothe, B. von Cleve, and K. C. Apel (1995) Plant Cell **7**, 161–172.
23. J. E. Boynton et al. (1988) Science **240**, 1534–1538.

24. P. Maliga (1993) Trends Biotechnol. **11**, 101–107.

Suggestions for Further Reading

25. N. W. Gillham (1994) *Organelle Genes and Genomes*, Oxford University Press, New York.
26. J. K. Hoober (1984) *Chloroplasts*, Plenum Press, New York.

CHO Cells

1. Origin

CHO cells were originated as a cell line by Theodore Puck in 1958 (1) from the Chinese hamster, *Cricetulus griseus*. CHO/Pro cells requiring proline for growth were subsequently derived by nutritional selection. The parental cells were treated with bromodeoxyuridine (see 5-Bromouracil) in proline-deficient medium and then exposed to the near-visible UV from a fluorescent light. This killed the growing cells, but not those that required proline. Proline-requiring clones were then grown up by feeding the surviving cells with proline-rich medium. CHO/Pro^{-} was subcloned by dilution cloning, and cell line CHO/Pro-K1 was isolated. The current designation of this cell line in common use is CHO-K1, and it still has a requirement for proline, which is present in Ham's F12, the medium usually recommended for its propagation. It is listed in the American Type Culture Collection (ATCC) catalogue as CCL-61 (Fig. 1).

Figure 1. Confluent culture of CHO-K1 cells. Phase contrast, Olympus CK microscope, 20× objective.

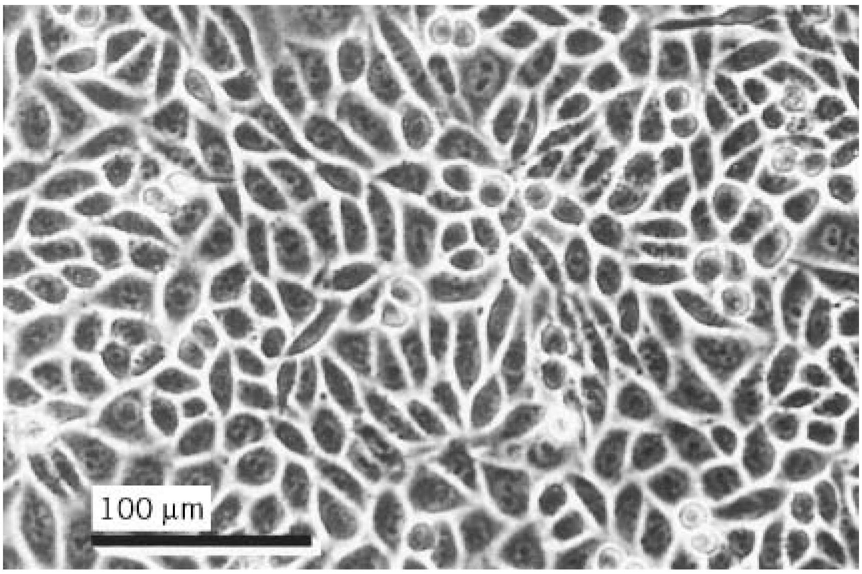

2. Properties

CHO-K1 (Fig. 1) is a continuous cell line and near-**diploid** with 20 chromosomes ($2C = 22$). It has a very short doubling time of around 15 h, making it popular as a host for transfection and biotechnology. The plating efficiency is also very high, and can be 100% under optimal conditions, so these cells have always been popular for clonogenic survival studies of nutritional mutants and radiation survival. Chinese hamster cells originally became popular for genetic studies because of their relatively small number of readily distinguishable chromosomes, but the advent of chromosome banding techniques and chromosome painting by fluorescence in situ hybridization makes the distinction of individual chromosomes easier in many other species.

CHO-K1 cells, although transformed, still retain nutrient-dependent G_1 cell-cycle blockade. Isoleucine deprivation blocks the cells in G_1, and its restoration generates a synchronous population (2).

3. Usage

CHO-K1 cells have been used in cell-cycle control and signaling (3) and are used extensively in biotechnology (4). They are used frequently in DNA transfection (5) and virally mediated DNA transfer (6). They can be maintained in suspension culture to generate large numbers of cells or product. Using methotrexate-induced co-amplification with cotransfected dihydrofolate reductase, they have been used for production of **interferon**-g (7) and pro**thrombin**-2 (8). They have been adapted to grow in serum-free medium (9) (see Serum Dependence). Together with V79 cells, another Chinese hamster cell line, they have been used extensively in genotoxicity studies (10).

Bibliography

1. T. T. Puck, S. J. Cieciura, and A. Robinson (1958) J. Exp. Med. **108**, 945–956.
2. K. D. Ley and R. A. Tobey (1970) J. Cell. Biol. **47**, 453–459.
3. G. Tortora, S. Pepe, C. Bianco, V. Damiano, A. Ruggiero, G. Baldassarre, C. Corbo, Y. S. Chochung, A. R. Bianco, and F. Ciardiello (1994) Intl. J. Cancer **59**, 712–716.
4. K. B. Konstantinov (1996) Biotechnol. Bioeng. **52**, 271–289.
5. S. Subramanian and F. Srienc (1996) J. Biotechnol. **49**, 137–151.
6. T. Schoneberg, V. Sandig, J. Wess, T. Gudermann, and G. Schultz (1997) J. Clin. Invest. **100**, 1547–1556.
7. V. Leelavatcharamas, A. N. Emery, and M. Al-Rubeai (1994) Cytotechnology **15**, 65–71.
8. G. Russo, A. Gast, E. J. Schlaeger, A. Angiolillo, and C. Pietropaolo (1997) Protein Express. Purif. **10**, 214–225.
9. M. J. Keen and N. T. Rapson (1995) Cytotechnology **17**, 153–163.
10. H. F. L. Mark, R. Naram, T. Pham, K. Shah, L. P. Cousens, C. Wiersch, E. Airall, M. Samy, K. Zolnierz, R. Mark, K. Santoro, L. Beauregard, and P. H. Lamarche (1994) Ann. Clin. Lab. Sci. **24**, 387–395

Cholera Toxin and Enterotoxins

Cholera toxin (CLT) and the closely similar heat-labile enterotoxins (LTs) are released by toxigenic strains of *Vibrio cholerae* and *Escherichia coli*, respectively, the causative agents of epidemic diarrheas (1). These bacteria attach firmly to the apical portion of the intestinal epithelium and produce several toxins, including CLT or LT, encoded by genes contained in a transferable virulence cassette (2). Five B subunits (103 residues) are secreted into the bacterial **periplasm**, where they assemble into a pentamer that binds the A chain. A is then proteolytically cleaved at a single point to generate the catalytic A1 chain (192 residues) linked via a disulfide bond to the A2 peptide (3, 4)

(Fig. 1). The structural organization of these enterotoxins is shared by *Shiga* toxins (other enterotoxins, which cause bloody diarrheas and necrosis of intestinal epithelium and are produced by *Shiga spp.* and *E. coli spp.*) and pertussis toxin (3-6). The B pentamer has the shape of an irregular cylinder with a flat surface and convoluted bottom surface. The five B monomers are arranged around a 5-fold axis in the oligomer-binding fold, recently identified in a set of oligonucleotide- and oligosaccharide-binding proteins (7). Each monomer contains five b-strands in an antiparallel beta-sheet and one alpha-helix. The five helices form a central pore hosting the carboxyl-terminal segment of A2, which emerges on the other side with a Lys/Arg-Asp-Glu-Leu motif that may be important in cell penetration (8). The amino-terminal half of A2 forms a long a-helix, rising from the flat surface, involved in interaction with A1. Thus, very few protein–protein contacts exist between A1 and B. The convoluted oligomer B surface, distal from A1, forms five sugar-binding sites on the outside edge of the cylinder (1, 3, 4).

Figure 1. Structural organization of cholera toxin and related toxins, showing a cross section of the molecule of cholera toxin and the *E. coli* heat-labile enterotoxins (1, 3, 4). A is composed of two polypeptide chains: A1, endowed with ADP-ribosyltransferase activity, and A2, which consists of a long a-helix, involved in interaction with A1, followed by a structureless segment that penetrates the small central hole of the B pentamer. Each of the five B subunits forming the B oligomer has a binding site for the oligosaccharide portion of the ganglioside G_{M1}. Thus, cholera toxin binds to the membrane via multiple interactions, with the catalytic A1 subunit pointing away from the membrane, with little protein–protein contact between A1 and B.

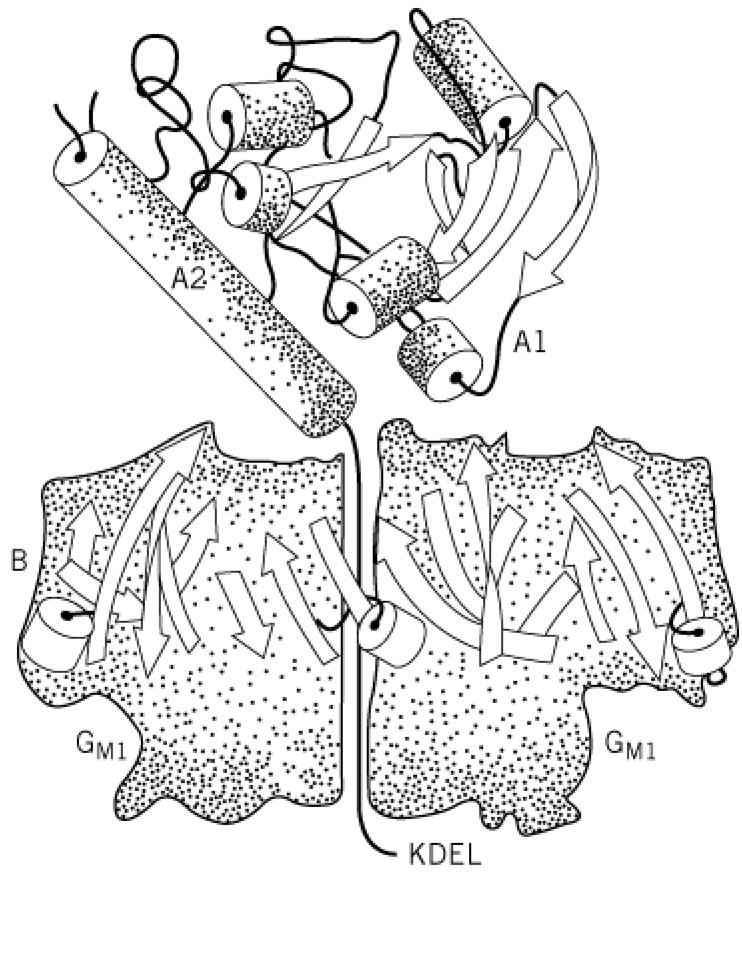

The structure of A1 shows a cleft where NAD binds and Arg-7 and Glu-112, two residues essential for activity, are located (9). Each B subunit of CLT or LTs possesses a single binding site specific for the oligosaccharide portion of a ganglioside (10), and one molecule of toxin binds five glycolipid molecules. Oligosaccharide binding affinity is rather low, but a high affinity of the toxin for the cell ($\boldsymbol{K_d}$ of the order of 10⁻10) is obtained because of the pentavalent binding. This strategy of multivalent binding to obtain a strong cell association is displayed by other bacterial toxins and viruses (11).

The target of CLT and LTs is localized on the basolateral membrane; therefore, these toxins have to transcytose through the cell to display their activity. Available evidence indicates that CLT and LTs are internalized inside apical endosomes that may recycle the glycolipid–toxin complex to the surface or deliver it to later endosomes. As a result of the binding of the **KDEL sequence** of the A subunit to a KDEL **receptor**, the toxin moves retrogradely through the **Golgi** cisternae, and some toxin molecules are then expected to be sorted into basolateral endosomes that fuse with the basolateral membrane (8). At some stage of this intracellular trafficking, these toxins have to be reduced and the A1 subunit has to translocate from the lumenal to the cytosolic side of the membrane to interact with their target on the cytosolic face of the basolateral membrane. Structural and membrane photolabeling data indicate that oligomer B does not penetrate the lipid bilayer (1, 10, 12), but A1 inserts in the membrane upon reduction of the A1━A2 interchain disulfide bond. Hence, it is likely that as soon as the disulfide bridge is reduced, A1 "rolls over" oligomer B and inserts into the membrane. This is at variance from postulated mechanism of membrane penetration of other toxins, whose protomer B plays an active role in the insertion of the catalytic subunit. Neither the chemical nature of the reducing agent nor the intracellular stage at which this step takes place are known.

The A1 subunits of CLT and LTs catalyze the transfer of ADP-ribose from NAD to an Arg residue present in the LRX**R**VXT conserved sequence of the a subunit of the G_S, G_t, and G_{olf} large trimeric GTP-binding proteins involved in the coupling of cell surface receptors to the adenylate cyclase (13). Such modification results in a permanent activation of this latter enzyme and a large increase in cellular cyclic AMP (cAMP) level, which initiates a cascade of signal transduction pathways. A1 ADP-ribosylating activity is enhanced by a group of cytosolic or membrane GTP-binding proteins, termed ARF (ADP-ribosylating factors), present in eukaryotic cells (14). ARF are strongly conserved from yeast to humans and are involved in the control of membrane trafficking and protein transport inside cells (15).

The increased cAMP level brought about by CLT or LTs in the enterocyte has a series of consequences, but the inhibition of a **sodium channel** and activation of a **chloride channel** localized on the apical membrane appear to be very relevant to diarrhea. In fact, a decreased sodium reabsorption and increased chloride secretion cause an osmosis-driven loss of water into the intestine. Also important in cholera is the activation of entero-chromaffim cells, which respond to the cAMP increase with release of VIP (vasointestinal peptide), which further lowers intestinal water reabsorption and inhibits muscle cells with an alteration of intestinal peristalsis.

Bibliography

1. B. D. Spangler (1992) Microbiol. Rev. **56**, 622–647.
2. M. K. Waldor and J. J. Mekalanos (1996) Science **272**, 1910–1914.
3. T. Sixma et al. (1993) J. Mol. Biol. **230**, 890–918.
4. R. G. Zhang et al. (1995) J. Mol. Biol. **251**, 563–573.
5. M. E. Fraser, M. M. Chernaia, Y. V. Kozlov, and M. N. G. James (1994) Nature Struct. Biol. **1**, 59–64.
6. P. E. Stein et al. (1994) Structure **2**, 45–57.
7. A. G. Murzin (1993) EMBO J. **12**, 861–867.
8. W. I. Lencer et al. (1995) J. Cell Biol. **131**, 951–962.
9. M. Domenighini, C. Magagnoli, M. Pizza, and R. Rappuoli (1994) Mol. Microbiol. **14**, 41–50.
10. E. A. Merritt et al. (1994) Protein Sci. **3**, 166–175.
11. G. Menestrina, G. Schiavo, and C. Montecucco (1994) Mol. Aspects Med. **15**, 81–193.
12. M. Tomasi and C. Montecucco (1981) J. Biol. Chem. **256**, 11177–11181.

13. D. M. Gill and M. J. Woolkalis (1991) Methods Enzymol. **195**, 267–280.
14. J. Moss and M. Vaugham (1991) Mol. Microbiol. **5**, 2621–2627.
15. J. E. Rothman and F. T. Wieland (1996) Science **272**, 227–234.

Chorion Genes and Proteins

The outer eggshell of those numerous insects whose embryos develop externally is known as the *chorion*, and it must be mechanically robust in order to provide the environment in which the egg can develop successfully. The chorion must also have a structure that minimizes water loss, while still permitting the gas exchange vital for embryonic respiration. In ***Drosophila*** the chorion consists of an outer exochorion, an endochorion, a thin inner chorionic layer, a wax layer and the vitelline membrane. The endochorion has the most important structural and gas-transporting roles *in vivo* (1). The wax and inner chorionic layers act as the waterproofing agent for the egg. Proteins in the chorion undergo extensive post-translational modifications and consequent peroxidase-catalyzed cross-linking of two or three tyrosine residues, which results in a significant increase in the mechanical stability of the entire structure. In contrast to the chorion in the *Drosophila*, however, the gypsy moth and other Lepidoptera have a chorion with an outer “sieve” layer (30 nm thick) overlying about 50 to 60 lamellae of variable thickness (but each about 0.2 µm thick on average). The innermost region of the chorion (ie, that beneath the lamellar region) is called the *trabecular layer* and has a thickness of about 0.5 µm (2). Lamellar substructures of this general type are not found outside Ditrysia. An individual lamella consists of a fibrous layer in which fibrillar elements reported to be about 3 to 4 nm in diameter lie parallel to the surface. The orientation of the lamellae change in a relatively systematic manner from one lamella to the next, thus generating a liquid crystal-like, cholesteric phase ultrastructure. These and other observations reveal that the *Drosophila* and silk moths show remarkable similarities, but equally remarkable differences. For example, they share regulatory elements that direct chorion **gene expression** to the follicular epithelium at the end of **oogenesis** (2). In contrast, they differ in their structural **gene** sequences, their **chromosomal** organization, their chorionic ultrastructures, and their modes of morphogenesis.

The chorion in general is a very complex structure and, in some cases at least, contains a hundred or more different proteins. The proteins in silk moths, however, all have similarities in sequence and fall within either the a or b branches of the chorion superfamily. These proteins in turn are encoded by numerous duplicated genes, all of which contain a single **intron**. Fortunately, the chorion genes too fall into one of a small number of families - A, B, and C. Each family contains multiple genes that occurred during evolution by gene duplication and sequence **divergence**. The families themselves are related and constitute a superfamily with A genes in one branch and B and C in the other. The A and B genes, which exist in pairs in divergent orientation in the chromosome, are coordinately expressed and **transcribed** in opposite directions under the direction of a bidirectional **promoter**. The chorion genes in *Drosophila* are quite different from those in silkmoths with regard to sequence and organization. In particular, the *Drosophila* genes are tandemly orientated, and each has its own unidirectional promoter that is temporally unique.

Proteins in the mature silkmoth chorion are usually small (10 to 20 kDa) and have *N*- and *C*-terminal **domains** that are variable in sequence and structure. These regions endow the protein with specific functional and structural attributes. Quasi-repeats are not uncommon (3): In *Drosophila* the dipeptide (Gly━His) is repeated five times towards the *N*-terminal end of s36 and nine times in the *C*-terminal region of s38; a hexapeptide repeat based on tyrosine is found in the *C*-terminal region of s36. Peptide repeats of the form (Cys━Gly), (Cys━Gly━Gly), and (Gly━Tyr━Gly━Gly━Leu) are found in the case of silkmoths. Unlike the chorion proteins in *Drosophila*, a central domain is largely conserved in the a and b families of the silkmoth proteins. This is characterized by tandem repeats. In the case of the a family, the central domain is 52 residues in length and displays a six-residue quasi- repeat with a **consensus sequence** (Gly—X—Val/Ile—Y—Val/Ile—Z), where X is generally a charged or large polar residue, Y is variable, and Z is commonly Ala, Gly or Cys. The b family also displays a similar but different six-residue quasi-repeat. The predicted **secondary structure** of both hexapeptide repeats is that of an antiparallel b-strand terminated by a b-turn. Interestingly, the occurrence of valine and isoleucine residues two apart in the a repeat places them on the same side of the b-sheet in a manner analogous to that in feather keratin. Depending on the precise form of the b-turns, one face of the twisted b-sheet would be almost entirely apolar and could give rise to a b-barrel structure in which the apolar residues would be located internally. In the case of the gypsy moth Ld15 protein (and the 292a protein of *A. polyphemus*), both penta- and hexapeptide quasi-repeats are found with consensus sequences of (Gly—Leu—X—Pro/Gly—Tyr), (Tyr—Gly—X—X—Gly/Ala), and (Gly—X—Val—X—apolar—Ala/Gly) (2). *Drosophila* chorion proteins s36 and s38, on the other hand, contain three consecutive large apolar residues in a quasi-repeat, and these are likely to form a b-strand. They are followed by three to seven residues rich in proline and basic amino acids that are likely to form a connecting b-turn or loop. These few examples illustrate that although there are significant variations in the detail of the sequence repeats, the antiparallel b-sheet conformation that is predicted to occur in all cases would seem to be a constant feature of all the chorion proteins. The paired organization of the moth chorion genes may imply that the a and b members of the chorion superfamily interact with one another to form the core of the structure, thus leaving the *N* - and *C*-terminal regions in an external location where they are able to provide other important functional properties.

Bibliography

1. A. C. Spradling (1993) "Developmental Genetics of Oogenesis". In *The Development of Drosophila melanogaster*, Vol. **1**, (M. Bate and A. M. Arias, eds.), Cold Spring Harbor Laboratory Press, Cold Spring Harbor, NY, pp. 1–70.
2. R. F. Leclerc and J. C. Regier (1993) Choriogenesis in the Lepidoptera: morphogenesis, protein synthesis, specific mRNA accumulation, and the primary structure of a chorion cDNA from the gypsy moth. Dev. Biol. **160**, 28–38.
3. S. J. Hamodrakas, A. Batrinou, and T. Christophoratou, Structural and functional features of *Drosophila* chorion proteins s36 and s38 from analysis of primary structure and infrared spectroscopy. (1989) Int. J. Biol. Macromol. **11**, 307–313.

Suggestions for Further Reading

4. F. C. Kafatos, G. Tzertzinis, N. A. Spoerel, and H. T. Nguyen (1995) "Chorion Genes: An Overview of Their Structure, Function and Transcriptional Regulation". In *Molecular Model Systems in the Lepidoptera* (M. R. Goldsmith and A. Wilkins, eds.) Cambridge University Press, Cambridge, England, pp. 181–215.
5. T. L. Orr-Weaver (1991) *Drosophila* genes: cracking the eggshell"s secrets. Bioessays **13**, 97–105.

Chromatid

A chromatid is one of the two adjacent strands of a chromosome that are generated as a result of chromosomal duplication. The two chromatids are held together at the centromere and become visible during **mitosis** (Fig. 1, see top of next page). Chromosomal dynamics during the cell cycle are conveniently discussed in terms of the appearance and behavior of chromatids. It is during **interphase** that DNA is replicated (**S-phase**). Before the S-phase there is a gap known as G1, when the chromosomes are considered to be unineme, meaning that a single duplex DNA molecule runs the entire length of the chromosome (see Lampbrush Chromosomes). The amount of DNA in G1 per haploid genome is called the C-value. A **diploid** cell has a 2C DNA content. After the S-phase, in the gap known as G2, the chromosomes have duplicated and there is a 4C DNA content. Now each chromosome consists of two unineme sister chromatids. Mitosis begins at the end of G2. Whereas the chromosomes are too diffuse and decondensed to be visualized when somatic cells are in the interphase, during mitosis the chromosomes and chromatids become visible. Mitosis can be divided into four stages. During **prophase**, the chromatin in the chromosomes begins to condense so that they appear as morphologically indistinct, diffuse threads. At the end of the prophase, the chromosomes become well separated. Now each chromosome is distinctly double-stranded, consistent with two sister chromatids joined at the centromere. In the metaphase the chromosomes are maximally contracted and align on a plane, known as the metaphase plate. The metaphase plate is midway between the **spindle poles** and represents an integral component of the **mitotic spindle**. In the **anaphase**, the pairing region within the centromere dissolves (see Centromeres). This allows the mitotic spindle to pull the two sister chromatids apart. Each pole receives a complete set of chromatids, representing all of the chromosomes. Finally in **telophase** the mitotic spindle breaks down, and the nuclear membrane is reassembled around the chromosomes. The chromosomes progressively decondense and cease to be visible by light microscopy.

Figure 1. Chromosomal dynamics during the cell cycle. (**a**) At the end of mitosis and in G1, there are two copies of each chromosome, called homologous chromosomes, in a diploid cell. (**b**) At the end of the S-phase and in G2, each chromatid in each chromosome has been duplicated, creating two sister chromatids joined at the centromere. (**c**) During the anaphase of mitosis the two sister chromatids separate and move to opposite spindle poles.

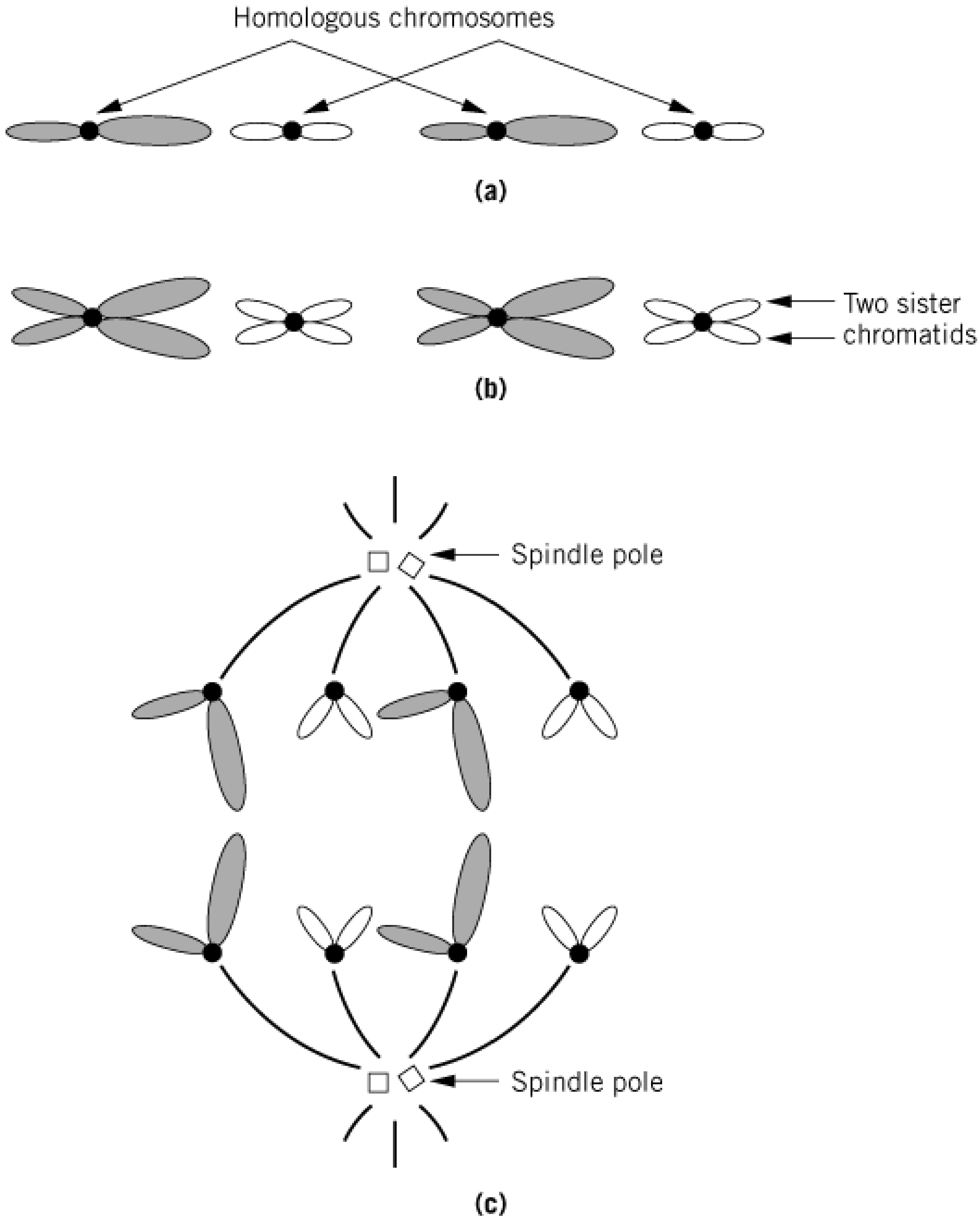

Sister chromatids also interact during **meiosis**, which represents the cell division, chromosomal and chromatid segregation events associated with **gamete** formation. There are two cell divisions during meiosis. Once again chromosomal dynamics are best described in terms of the segregation of chromatids. Initially, the chromosomes replicate, then the cell enters the first meiotic cell division. Homologous chromosomes are attracted to each other, forming stable pairs held together by the synaptonemal complex (see Homologous Chromosomes). Thus each structure consists of two chromosomes, each containing two sister chromatids. Recombination occurs between the maternal- and paternal-derived chromosomes. Sites of such genetic **crossing over** are called **chiasmata**. Chiasmata represent sites of physical breakage and reunion between nonsister chromatids. They generally encompass a few hundred to a few thousand base pairs of DNA. Finally, each pair of chromosomes separates. At the start of the second meiotic cell division, each chromosome consists of two chromatids joined by a centromere. Then the chromatids are aligned on a metaphase plate attached to a spindle. The centromere splits, and the two sister chromatids move to opposite poles. Then nuclei are reformed in each of the four haploid daughter cells. Thus for both mitosis and meiosis the mechanics of chromosome condensation, recombination, and segregation emphasize the fate of individual chromatids.

Suggestions for Further Reading

A. T. C. Carpenter (1987) Gene conversion, recombination nodules, and the initiation of meiotic synapsis. BioEssays **6**, 232–236.

G. J. Gorbsky (1992) Chromosome motion in mitosis. BioEssays **14**, 73–80.

G. S. Roeder (1990) Chromosome synapsis and genetic recombination: Their roles in meiotic chromosome segregation. Trends Genet. **6**, 385–389

Chromatin

Chromatin is the complex of histones and DNA, associated with smaller amounts of other proteins, into which the chromosomal DNA of all eukaryotes is organized. As well as being a means of packing DNA in an orderly fashion, chromatin structure plays a crucial role in the regulation of gene expression, both activation and repression. Three books contain much useful information about chromatin structure and function (1-3); for the most up-to-date information in many areas of this rapidly moving field, the reader will be referred to recent articles and reviews.

1. Overview

Chromatin has a beaded appearance in the electron microscope at low ionic strength, arising from a regularly repeating structure (4). The repeating unit is the nucleosome, which contains ~166 to 240 bp of DNA, of which ~166 bp is wound in two left-handed superhelical turns around an octameric complex of the four core histones (H3, H4, H2A, and H2B) and stabilized by one molecule of histone H1; the nucleosome also includes a variable length of linker DNA (~0 to 76 bp) that connects neighboring nucleosomes. The octamer is organized as a central $H3_2H4_2$ tetramer, which has a rather flat, twisted horseshoe shape, flanked above and below by an H2A–H2B dimer. The details of the organization of histone and DNA in the core of the nucleosome are revealed in the high-resolution structure of the 146-bp nucleosome core particle (which contains no linker DNA and no H1) recently determined by X-ray crystallography (5). The globular domain of histone H1 binds asymmetrically, bridging a point near the dyad and an entering or exiting DNA double helix (6) (see Nucleosome for further details); the basic *C*-terminal domain interacts with the linker DNA, partially neutralizing its charge. The array of nucleosomes is known as a nucleosome filament, or the 10-nm filament (10 nm being the diameter of the nucleosome). The amount of DNA contained in the repeating unit, which reflects the length of linker DNA, is determined from the sizes of the DNA in the chromatin fragments liberated by incomplete digestion with micrococcal nuclease (**Staphylococcal nuclease**), which cuts in the linker. A series of fragments, usually visualized as a "ladder" of bands in gel electrophoresis, occurs at multiples of the unit repeat size. This is commonly about 200 bp (when there is a linker length of 200 – 166 = 34 bp), but it may be as long as ~240 bp (in sea urchin sperm), or as short as ~166 bp (essentially no linker DNA) in yeast and in mammalian cerebral cortex neurons (the glial cells in the same tissue have a repeat length of about ~200 bp). The repeat length measured in this way is the average for the tissue or cell population under examination; there will be local variations about this mean (see Linker DNA). Packaging of the DNA in nucleosomes achieves about a sixfold length compaction of the DNA, and further packing is achieved by salt-dependent, histone H1-assisted folding of the 10-nm nucleosome filament into a 30-nm filament. Much evidence supports a simple helical coiling of the nucleosome filament into a "solenoid" with six nucleosomes per turn, but there are other models (see text below). Most of the chromatin in the cell is in the form of a 30-nm filament throughout most of the cell cycle, and at interphase appears to be looped onto the nuclear matrix; at mitosis, the 30-nm filament is subjected to further levels of folding to give the highly dense metaphase chromosome in which the overall length compaction of the DNA is about 10,000-fold.

The 30-nm filament is not a suitable template for transcription by the large eukaryotic **RNA polymerases** and clearly has to be unfolded first; formation of an "open" ("transcriptionally competent") chromatin state is an essential prerequisite for transcription. This involves acetylation of the basic *N*-terminal regions of the core histones, which appear to play a role in chromatin folding, and some depletion of histone H1. It has recently become clear that acetylases are targeted to particular regions of the chromosome through recruitment, directly or indirectly, by gene regulatory proteins bound to specific DNA sequences at **promoters** or upstream activating sequences. Cells appear to contain many acetylase (and deacetylase) activities, which function as components of multiprotein complexes (see Histone Acetylation). Even in the 10-nm filament form, nucleosomes may act as blocks to the formation of transcription initiation complexes by occluding promoters, which may include strategically positioned nucleosomes. It is now clear that the cell has specialized energy-dependent mechanisms that are required for "remodeling" some promoters, so that they become accessible to transcription factors, as well as mechanisms for facilitating RNA chain elongation. These mechanisms also involve multiprotein complexes, which may have subunits in common with acetylases and deacetylases. Chromatin is thus both an effective means of packing and the target for an integrated network of machines that modify it. There is a wealth of genetic evidence showing that the growing list of factors that regulate transcription includes both *bona fide* chromatin components (eg, histones) and proteins that modify chromatin (eg, acetyltransferases and deacetylases). An unexpected discovery was that a structural motif found in all the core histones is also found in a number of components of the transcription initiation factor TFIID (see Histone Fold), as well as in some histone acetyltransferase complexes (see Histone Acetylation), suggesting a structural and evolutionary link between chromatin and the assemblies that act upon it. Another surprising finding has been that histone H1 may have a specific gene regulatory role, in addition to its role in packaging and as a general repressor (see Histones).

2. Nucleosome Positioning and Mobility

Histones package the whole of the genome and therefore appear to be largely indifferent to DNA sequence. Locally, the position of a nucleosome is determined by the underlying DNA sequence and, in particular (because the DNA, which is normally rigid, is bent around the octamer surface), by the local bendability of DNA, which is sequence-dependent. Analysis of the DNA sequences of bulk nucleosome core particles shows that A and T di- and trinucleotides are likely to occur where the minor groove faces inward, and G and C di- and trinucleotides where the minor groove faces out. This is because the minor groove of AT-rich DNA is naturally narrow and so, by having A and T where the minor groove faces in, the compression of the groove that occurs on wrapping the DNA around the octamer is readily accommodated (7). The dinucleotide periodicity is on average 10.2 bp, exactly the average structural periodicity given by the X-ray crystal structure of the nucleosome core particle (see Nucleosome). The helical periodicity in solution is 10.6 bp, so the DNA is overtwisted in the nucleosome, presumably to achieve the match between the structural and sequence periodicities that underlie the rules that govern rotational positioning of the octamer with respect to the DNA sequence (the orientation of a face of the duplex with respect to the histone octamer surface). This is thus determined by the local bendability (flexibility toward curvature) of the DNA, which is determined by the properties of the individual base steps. A rotationally positioned duplex shows a characteristic 10-nucleotide pattern of nicking by DNase I, as each strand rises from the surface about every 10 nucleotides. Translational positioning, on the other hand (the basis of which is not well understood), refers to the choice of a particular stretch of DNA by the histone octamer, rather than other stretches of the same length translated forward or backward along the DNA by about 10 bp, which would allow the same rotational setting. The abundance of AA/TT dinucleotides separated by roughly 10 bp led to the construction of fragments with alternating A/T and C/C sequences [(A or T)$_3$NN(G or C)$_3$NN]$_n$—the so-called TG pentamer—that indeed formed very stable nucleosomes (8). Selection of naturally occurring 146-bp DNA sequences with a high affinity for the histone octamer revealed (in addition to the A/T, G/C periodicity) that sequences with repeated TATAAACGCC motifs ("phased TATA" sequences) formed nucleosomes that were even more stable, suggesting that high-affinity binding is aided by flexible sequences (9); selection from longer (220 bp) synthetic DNA sequences also revealed a signal (CTAG) that favored high-affinity binding (10). Such sequences, even if they occurred infrequently in the genome, could have important implications for chromatin organization and regulation, as could sequences that are refractory to nucleosome formation (eg, TGGA repeats identified in a negative-selection approach (11). It seems likely that the signals discovered for rotational positioning *in vitro* (7) also function *in vivo*, as revealed by analysis of the complete genome sequences of the yeast *Saccharomyces cerevisiae* and the nematode *Caenorhabditis elegans* (12), where dinucleotide periodicities are compatible with nucleosomal constraints. Analysis of 168-bp chicken erythrocyte chromatosome sequences [ie, containing H5(H1] shows that the statistical preferences of the octamers for particular sequences are slightly modulated (13), presumably in order to optimize the stability of the octamer–DNA–H1 ternary complex. This would be reflected in slight differences in translational positions of nucleosomes in the presence of H5(H1), which might have functional consequences (eg, in exposing or revealing short DNA sequences in an H1-dependent manner). An additional feature of chromatosomal DNA is the frequent occurrence of AGGA within half a double helical turn of one terminus, imposing asymmetry on the chromatosome. Whether this is related to the asymmetric binding of H1 to the nucleosome remains to be seen. The rules for nucleosome organization on DNA sequences have recently been reviewed (14).

Although histones can, in general, package DNA essentially irrespective of sequence, but capitalize on the local bendability of DNA to promote a better fit on the octamer surface, some DNA sequences have a particularly high affinity for the octamer, leading to a "positioned nucleosome" in which a particular translational position is preferred. Nucleosome reconstitution experiments show that the H3–H4 tetramer alone is sufficient to confer positioning on a defined DNA sequence (15, 16). Positioned nucleosomes have been identified *in vivo* by nucleosome mapping techniques and *in vitro* in nucleosome reconstitution experiments on defined DNA sequences. The rules for nucleosome positioning *in vivo* are not well understood: When the TG pentamer (see above) was introduced into yeast, it appeared to exclude nucleosomes rather than provide optimal positioning (17), showing that a strong rotational setting is not sufficient for positioning *in vivo*. Positioned nucleosomes may act as a boundary (18) and determine the positions of several neighboring nucleosomes on either side. More than one positioned nucleosome separated at less than a nucleosome's length of DNA would serve to keep the region clear of histones (eg, at promoters) for the binding of sequence-specific proteins with various gene regulatory or structural roles. At the inducible yeast *PHO5* promoter, events leading to promoter remodeling and transcription of the *PHO5* gene, which encodes a phosphatase, are initiated in response to low phosphate levels by binding of the transcription factor PHO4 to a site between two positioned nucleosomes in a set of four over the promoter (19) (see text below). Positioned arrays of nucleosomes, essential for the functioning of the promoter, are also found in many other cases—for example, the mouse mammary tumor virus (MMTV) major late promoter (20) (see also Ref. 2). It has recently become apparent (21) that nucleosome positioning is the probable explanation for the differential regulation of *Xenopus* oocyte and somatic 5S genes *in vivo* (22), where the oocyte genes are repressed and the somatic genes remain active when H1 accumulates after the mid-blastula transition. Sequence differences between the two types of gene mean that the oocyte nucleosome occludes the TFIIIA binding site and binds H1 preferentially (so the gene is turned off), whereas the converse is broadly true for the somatic gene, which remains active.

A nucleosome core can be reconstituted on to DNA *in vitro* by dialysis of an equimolar mixture of the histone octamer (or H3–H4 tetramers and H2A–H2B dimers) and DNA from high ionic strength (eg, 2 M NaCl) to low ionic strength. Even in cases where there are strong nucleosome positioning signals in the DNA, octamers on different fragments will occupy a population of less favorable minor translational positions in addition to a major position, all with the same rotational setting of the DNA. For example, on the *Xenopus borealis* somatic 5S rRNA gene, which is regarded as a strong positioning sequence, octamers can occupy 10 different positions (six being predominant), all related to each other by the 10 bp helical periodicity of the DNA, which must be caused by a strong rotational signal in the DNA sequence (21). The occupancy of less favorable octamer positions on a DNA sequence is higher at low temperatures (eg, 4°C), when the octamers are trapped, than if the temperature is then shifted to 37° (23). The change in positions populated demonstrates that nucleosomes have an intrinsic mobility, which could be useful, for example, in remodeling of promoters. In the presence of H1, nucleosome mobility is greatly reduced (24, 25); conversely, loss of H1 might enable nucleosomes to move, for example, to expose binding sites for gene regulatory proteins.

3. Higher-Order Structure: The 30-nm Filament

The 10-nm nucleosome filament, which represents the first level of chromatin structure, is the form in which chromatin exists at low ionic strength (eg, >20 mM) *in vitro*. As the ionic strength is increased, the 10-nm filament condenses into a 30-nm (diameter) filament, visible by electron microscopy. Most of the chromatin in the nucleus is in this form. The folding is a consequence of ionic-strength induced screening of the residual negative charge on the linker DNA (26), much of the charge having already been neutralized by the basic tail(s) of histone H1 and, probably, the basic *N*-terminal tails of at least some of the core histones, and results in new interactions (eg, nucleosome-nucleosome) within the higher-order structure.

Various models have been proposed for the 30-nm filament (27), some of which are shown in Figure 1. All agree on a radial distribution of nucleosomes with their faces parallel to the filament axis, but they differ fundamentally in the path taken by the linker DNA, whether bent, curved, or straight. The evidence on this point is conflicting (see Linker DNA). The evidence for the various models has been extensively reviewed (28-31). Much evidence supports the original "solenoid" model (32), which proposes a simple helical coiling of the nucleosome filament, with about six nucleosomes per turn at physiological ionic strength, and necessarily bent linker DNA (Fig. 1a). [The details are easily modified to accommodate the asymmetric, rather than symmetric, location of the globular domain of H1 near the dyad (6); see text above.] The solenoid places the dyads of the nucleosomes, histone H1, and the linker DNA between nucleosomes, on the inside of the solenoid; H1 has indeed been shown to be located within the 30-nm filament (33). However, other models have been proposed, such as the helical-ribbon model (34, 35) (Fig. 1b), which invokes straight linkers and is based on the zigzag appearance of the nucleosome filament in electron micrographs, and these too would be compatible with an internal location of H1. The coiled linker model (36), like that shown in Fig. 1c, which is related to the solenoid, is not necessarily compatible, because the dyads of the nucleosomes, and hence H1, are alternately inside and outside the solenoid for some linker lengths (eg, in chicken erythrocyte chromatin).

Figure 1. Some models of chromatin higher-order structure. The 30 filament is shown as (**a**) a solenoid (32), (**b**) a helical ribbon (34), and (**c**) as a helical conformation with coiled linkers (36). In (**a**) and (**b**) the most condensed structures are shown at the top, and the extended structures present at low ionic strength at the bottom. (From Refs. 32, 34, and 36, respectively, with permission.)

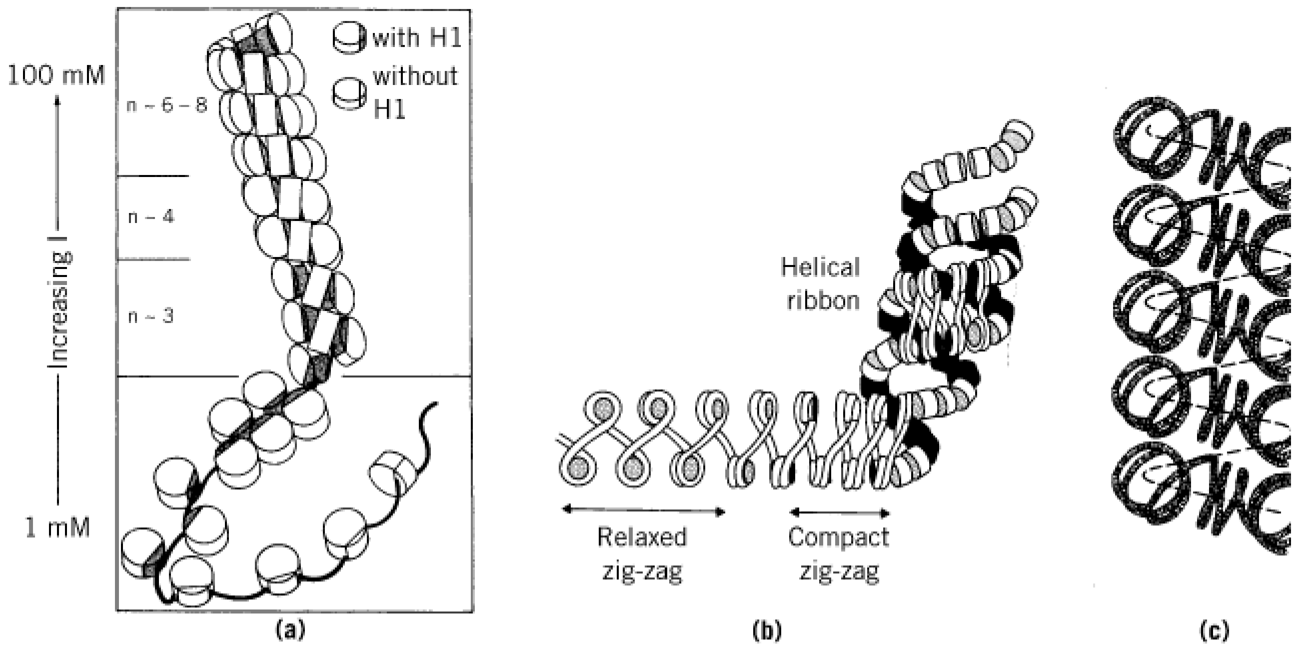

Whatever the model that best describes the spatial relationships between nucleosomes in the higher-order structure, the 30-nm filament in the cell nucleus is unlikely to be completely regular, partly because of local heterogeneity in linker length along the filament within the average value, partly due to the presence of different histone variants or subtypes, and so on. The 30-nm filament is also a dynamic structure that undergoes thermal "breathing", and this property is probably central to gene regulation through control of chromatin folding. The stability of the 30-nm filament is relevant to the ease with which it may be unpackaged for transcription and appears to be increased by special variants of H1 (such as H5 and spH1 in the condensed chromatin of nucleated erythrocytes and sea urchin sperm, respectively) (37), and it is probably decreased in regions of transcriptionally competent chromatin by (partial) loss of H1 (eg, Ref. 38) and by acetylation of the core histone *N*-terminal tails (see Histone Acetylation).

4. Chromatin and Transcription

In eukaryotes, transcription works in a chromatin context (39, 40). Some genes are active in all cell types, whereas others are active only in specific cell types. Active genes in higher eukaryotes have a chromatin structure characterized by a greater sensitivity (7- to 10-fold) to the endonuclease DNase I than the bulk of the chromatin in the nucleus (1, 2). This state precedes active transcription and marks "transcriptional competence"; it is the first step in control of transcriptional activity. DNase I sensitivity is probably due to (partial) relaxation of the 30-nm filament toward the 10-nm filament state, which is probably facilitated by partial loss of linker histones and acetylation of the core histone *N*-terminal tails (41) (see Histone Acetylation). DNase I sensitivity associated with a particular gene extends well beyond the coding region and encompasses an entire chromosomal domain (eg, tens of kilobases) and includes all the regulatory elements (eg, enhancers) for the genes (2). The boundaries of these chromosomal domains have been characterized in only a few cases, and no common feature is apparent. In at least some instances, the boundaries act as "insulators", preserving the structural and functional autonomy of the domain and also blocking the influence of regulatory elements from the outside (42). Short localized regions, termed DNase I hypersensitive sites (typically a few hundred base pairs), in the genome show a much higher sensitivity to DNase I than described above (43). These are due to the absence of a canonical nucleosome and the presence of gene regulatory (sequence-specific) proteins. They often occur within a domain of general DNase I sensitivity, coinciding with promoters or enhancers, and may also occur at the boundaries of chromosomal domains. Hypersensitive sites at promoters may be constitutive or inducible, depending on the gene, and are often flanked by “positioned nucleosomes”.

The presence of a nucleosome at a promoter generally inactivates it (39). Promoters therefore either have to be kept clear of nucleosomes, or one or more nucleosomes has to be perturbed or disrupted to permit assembly of a preinitiation complex and recruitment of RNA polymerase. Promoters may be kept clear either by flanking positioned nucleosomes or by the presence of sequence-specific proteins that bind during replication—for example, the Grf2 protein in yeast, which binds to an extended region of DNA and precludes nucleosome formation (39). The promoters that are packaged in nucleosomes have to be opened up (“remodeled”) in order to permit assembly of a preinitiation complex. The nature and extent of the disruption required to open up a promoter is unclear and may be different in different cases, perhaps depending on where the factor-binding sequences are within a nucleosome (eg, whether they can be exposed simply by loss of H1 or by loss of an H2A-H2B dimer, or whether they also require disruption of the central tetramer in the core of the nucleosome; see Ref. 2). It does not appear to result in complete histone loss. Promoter remodeling and disruption *in vivo* appears to require the action of energy-dependent “chromatin remodeling machines” (see text below) which may be recruited to particular promoters in response to the initial signal for activation, and possibly also histone acetyltransferases (see Histone Acetylation).

In vitro many transcription factors have been shown to be able to can bind to their cognate sites on the surface of a nucleosomes, albeit with lower affinity than to free DNA. The effects can be accounted for by transient “site exposure” as the interactions between the octamer and DNA fluctuate (44); this model predicts that binding of factors to multiple juxtaposed binding sites on the same nucleosome will be cooperative (45), as indeed already observed. Binding occurs without global displacement of the DNA, which will remain anchored at sites not bound by transcription factors. Consistent with this, a recent report shows that the erythroid transcription factor GATA-1 causes extensive disruption of histone–DNA contacts in nucleosome core particles containing GATA-1 sites, except over 50 bp around the dyad that serves to anchor the DNA (46). The complex is stable in solution, and the disruption is reversed on removal of GATA-1. The inherent flexibility of the nucleosome, and the fact that many promoters have clusters of factor-binding sites, suggests that this mechanism of gaining access to binding sites within nucleosomes at promoters could have physiological relevance.

At some inducible promoters, the binding site for the transcription factor that initiates the remodeling events is already exposed, in the linker between two nucleosomes in a short positioned array, rather than within a nucleosome. This is the situation at the *PHO5* promoter in yeast (19). Activation of the promoter in response to low phosphate relies on the accessibility in the uninduced state of a (weak) binding site for a transcription factor (Pho4) in the 70-bp gap between two of the four positioned nucleosomes at the promoter (Fig. 2). Binding of Pho4 leads to disruption of two nucleosomes on either side of the binding site and exposure of a second, stronger Pho4 binding site, as well as binding sites for another transcription factor, Pho2, which binds cooperatively with Pho4. The nature of the disruption is not clear but is reflected in the accessibility to a restriction enzyme of a site normally incorporated into a nucleosome and probably involves a “remodeling complex” (see text below). In other cases, a nucleosome at a promoter may be beneficial or even essential for activation of transcription. In the mouse mammary tumor virus (MMTV) long terminal repeat (LTR) promoter, six positioned nucleosomes place two glucocorticoid response elements in rotational positions (see text above) on one of the nucleosomes, such that they are accessible to glucocorticoid receptor binding in response to hormone; the two sites are also in close proximity on one face of the nucleosome. The binding site for the transcription factor NF1 is occluded until the nucleosomes are disrupted or perturbed in response to receptor binding (20). In a slightly different scenario, wrapping DNA around a nucleosome may bring into proximity two sites outside the nucleosome core, which are separated by about a nucleosome repeat length of DNA. There are several instances of this (2)—for example, the *Drosophila hsp*26 promoter (47), where a critical nucleosome upstream of the start site of transcription performs such a scaffolding role and brings binding sites for **heat shock** transcription factors into proximity with each other and with TFIID, to create a preset promoter, with bound RNA polymerase, waiting only for the binding of heat shock transcription factor to induce it.

The positioned nucleosome is flanked by binding sites for the GAGA protein, which appears to play a crucial role in the architecture of the promoter, by helping to determine the position of the nucleosome (2).

Figure 2. The yeast *PHO5* promoter: chromatin structure in the uninduced (+Pi) and induced (–Pi) states. Large open circles (–1 to –4): the four positioned nucleosomes that are disrupted and become "transparent" upon induction. Small circles: Pho4 binding sites [UASp1 (open) and UASp2 (filled)]. T: TATA box. The thick horizontal line marks the beginning of the coding sequence. From Ref. 75, with permission.

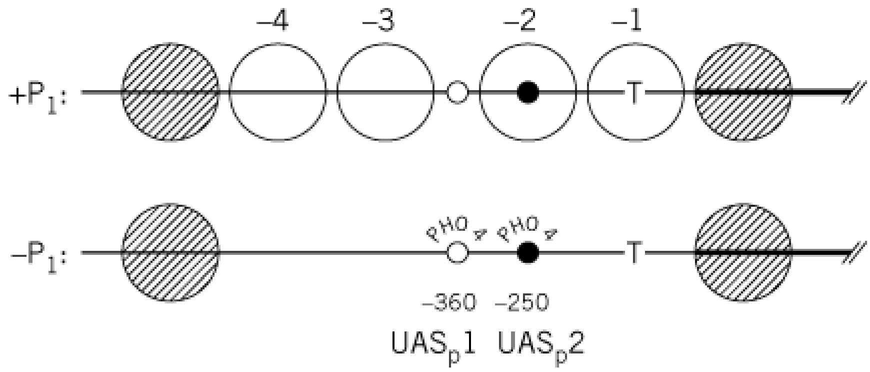

In contrast to initiation, transcriptional elongation can proceed through nucleosomes *in vivo*. In a model system using SP6 polymerase and a single nucleosome, the histone octamer is displaced during elongation (39) and then rebinds upstream of its initial position; the mechanism proposed is transferred from in front of the advancing polymerase to behind it, via a DNA loop that is displaced (48). However, no such studies have yet been carried out with the large eukaryotic RNA polymerases. The indications are that a reconstituted nucleosome array presents a block to elongation by RNA polymerase II, which may be relieved by an energy-dependent mechanism (see next section).

5. Chromatin Remodeling Machines

Exciting discoveries in the last couple of years have revealed several multiprotein complexes (molecular masses ranging from 0.5 to 2 MDa) in *Drosophila*, yeast, and human cells that are able to remodel repressive chromatin in an ATP-dependent manner to permit transcription initiation at promoters *in vitro*. These include three complexes derived from a *Drosophila* embryo extract: NURF (*nu*cleosome *r*emodeling *f*actor), CHRAC (*chr*omatin *a*ccessibility *c*omplex) and ACF (*A*TP-dependent *c*hromatin assembly and remodeling *f*actor); the S*accharomyces cerevisiae* SWI-SNF (*swi*tching-*s*ucrose *non**f*ermenting) and related RSC (*r*emodeling the *s*tructure of *c*hromatin) complexes; and SWI/SNF-related complexes in human cells and *Drosophila*. They have been comprehensively discussed in a number of recent reviews (49-53) that cite the original literature. They all contain an ATPase activity; in the case of the three *Drosophila* complexes, this is the same ISWI (*i*mitation *SWI*2) subunit. The various complexes were purified initially using a range of functional assays to follow the purification, and they appear to be functionally and mechanistically distinct; they are likely to differ in their modes of nucleosomal perturbation. NURF (four protein subunits) was purified as a factor required for ATP-dependent remodeling of chromatin templates so that the GAGA protein is able to bind (GAGA binds to GA-rich sites in several *Drosophila* heat-shock promoters, such as the *hsp*26 promoter, already mentioned); and it facilitates transcriptional activation. Interestingly, the 55-kDa subunit of NURF (which contains "WD repeats," which are protein-interaction motifs) is also found in the *Drosophila* chromatin assembly factor dCAF-1 (54), and human homologues are components of histone acetylase and deacetylase complexes (see Histone Acetylation). CHRAC (five subunits) was purified as a factor that generated ATP-dependent accessibility of sites in a chromatin template, reconstituted *in vitro*, to restriction enzymes. It is also able to generate a regular array from an irregular array of nucleosomes and has been described as an energy-dependent nucleosome spacing factor; it may therefore play a role in chromatin assembly (see text below) (where newly assembled nucleosomes are initially deposited in an irregular array that "matures" to give a regular spacing), although a spacing activity might, of course, also promote transcription factor binding. The third *Drosophila* complex, ACF (four subunits), was also purified as an ATP-dependent nucleosome spacing factor in a fractionated system and plays a role in nucleosome assembly; it can also mediate transcription-factor-mediated chromatin disruption in much the same way as NURF. SWI/SNF (9 to 12 subunits) facilitates transcription factor binding, and both SWI/SNF and RSC (15 subunits) disrupt the repeating 10-nucleotide cleavage pattern given by DNase I on mononucleosomes, showing disruption of the rotational setting of the DNA on the octamer surface. In yeast, the SWI/SNF complex is not abundant and not essential for viability, whereas the RSC complex is abundant and essential. SWI/SNF appears to be necessary for the transcription of only a small subset of genes, and in an *in vitro* system the dependence of transactivation on SWI/SNF activity is much reduced if there are multiple binding sites for the activator on the same nucleosome (55). It is possible that *in vivo* the SWI/SNF complex is needed only for remodeling of weak promoters. Altered forms of mononucleosomes generated by both SWI/SNF (56, 57) and RSC (58) complexes have recently been reported. They retain a full complement of histones and have altered physical properties that would be consistent with either a heavily modified mononucleosome or a dinucleosome. The SWI/SNF products have a higher affinity for transcription factors than unmodified nucleosomes. Much remains to be done to (a) elucidate the mechanisms by which the various chromatin remodeling machines act on chromatin, (b) define the roles of the various subunits, and (c) establish which mechanisms, *in vivo*, play a role in promoter disruption for transcription initiation, and whether others are primarily involved in reversing such disruption or in nucleosome assembly, and so on. The relationship between these complexes and the large acetylase, and deacetylase, complexes (see Histone Acetylation) also remains to be clarified, although the indications are that they cooperate in the remodeling of certain promoters.

The foregoing account has dealt solely with complexes that disrupt chromatin at promoters, allowing transcription initiation complexes to form. The transcriptional machinery also confronts nucleosomes during RNA chain elongation. Experiments on a reconstituted array of nucleosome cores show that the passage of eukaryotic RNA polymerase II is blocked by a nucleosome core and that a heterodimeric protein isolated from human cells will facilitate RNA chain elongation in a chromatin context. The protein has been designated FACT (*fa*cilitates *c*hromatin *t*ranscription) (59) and appears to be a DNA-binding protein, one subunit being an HMG-box protein. Little is yet known about it how it might work, but its action is not ATP-dependent. The *in vitro* assays show a rather modest extension of the transcript (50 to 150 nucleotides) before FACT stalls, and it is not yet clear whether FACT is designed to work only on the promoter-proximal nucleosome or needs cofactors for its normal action, or whether the modest extension is merely due to a technical limitation of the experiment. The chromatin template contains closely packed nucleosome cores (no linker DNA, no H1), and if octamer transfer via a loop of DNA is required, as demonstrated in model systems (48) (see text above), this may not be possible here.

6. Chromatin and Repression

There are hierarchies of repression, through chromatin structure, as there are of transcriptional activation. The most basic level, promoter occlusion by a nucleosome, was discussed above. Superimposed on this is repression through folding of the nucleosome filament into a 30-nm filament (whether this occurs in yeast is unclear). The higher-order structure is stabilized by a hypoacetylated state of the *N*-terminal tails of the core histones (see Histone Acetylation). In organisms other than yeast and *Drosophila*, DNA **methylation** is known to contribute to gene repression through chromatin structure, and a **5-methylcytosine**-binding protein (MeCP2) has recently been reported to recruit deacetylases (60, 61). This could favor a more stable 30-nm filament, which might be further stabilized by the tighter binding of H1 to methylated DNA (62). The 30-nm filament is not a template for transcription, and in some cases, 30-nm filament stabilization (eg, by specialized linker histone variants) and packing in the nucleus may be at least major players in general repression. This may be the situation in mature nucleated erythrocytes (eg, of birds, fish, and amphibia), where H1 is largely replaced by histone H5 and where there is a global and terminal shutdown of transcription; and in sea-urchin sperm, where highlycondensed chromatin is linked to the presence of sperm-specific H1. Other more complex mechanisms of repression also exist, however, resulting in heterochromatin. The essence of these mechanisms—although they differ in many respects in, for example, yeast and *Drosophila,* where they have been extensively studied—is the assembly, over particular chromosomal regions, of repressive multiprotein complexes that interact with chromatin. In the case of *Drosophila* at least, the chromatin is probably in the form of the 30-nm filament, and the mechanisms add an additional layer of repression for genes whose permanent inactivation is crucial and where inappropriate expression cannot be tolerated.

Yeast chromosomes are too small to allow heterochromatin to be seen cytologically, but nonetheless some chromosomal regions show many of the features of heterochromatin in more complex eukaryotes (replication late in S phase, localization at the nuclear envelope, and position effects on gene expression that are inherited **epigenetically**). In *Saccharomyces cerevisiae*, such regions occur at the silent mating type loci, *HML* and *HMR*, and at telomeres (the ends of the chromosomes; genes placed here are repressed) and have been extensively studied by genetic analysis (63). In each case, a multiprotein complex of Sir2, Sir3, and Sir4 proteins (Sir = *s*ilent*i*nformation*r*egulator information regulator) interacts with the *N*-terminal regions of histones H3 and H4. At the telomeres, which contain the sequence $[C_{1-3}A]_n$, the **silencers** consist of multiple binding sites for RAP1 (*r*epressor *a*ctivator *p*rotein 1), whereas silencers at *HML* and *HMR* consist of binding sites for ABF1 (*A*RS-*b*inding *f*actor 1), the *o*rigin *r*ecognition *c*omplex (ORC) and RAP1. Residues 16 to 29 of H4 are required for interaction with Sir3 and Sir4 and for silencing, presumably by providing interactions necessary for stabilization of the multiprotein complex. In addition, although the core histones at the silenced loci in yeast are hypoacetylated, there is a specific requirement for Lys12 in acetylated form, possibly for interaction with Sir3 (63). In the current model for telomeric repression, RAP1 binds to the telomeric repeats, initiating polymerization of Sir3/Sir4 over the adjacent chromatin domain, the binding of the Sir proteins being mediated by interaction with the H3 and H4 *N*-termini, possibly stabilized by acetylation of H4 at Lys12. Other repressive mechanisms in yeast also involve the *N*-terminal tails of H3 and H4 (64).

Extensive genetic studies of heterochromatin have also been carried out in *Drosophila*. Genes brought into juxtaposition with heterochromatin (eg, at centromeres) may be silenced in a subset of cells that normally express the gene—an effect known as position effect variegation (PEV) (2). Chromatin structure is altered in variegating genes, as shown by the properties of the *hsp*26 transgene inserted at various chromosomal locations; the heterochromatic *hsp*26 gene has a noninducible promoter and is packaged in an unusually regular nucleosomal array (65). Modifiers of PEV, identified genetically, are either (a) structural proteins that are components of multimeric protein complexes that interact with chromatin or (b) proteins that could play indirect roles in regulating the formation of chromatin—for example, by modifying histones or DNA. One such protein is the histone deacetylase RPD3 (see Histone Acetylation). However, mutations in this protein that increase acetylation *increase* PEV, rather than decreasing it, as might be expected; this is probably because of the requirement for acetylation at Lys12, as in yeast heterochromatin, against a background of general histone hypoacetylation. The multiprotein complexes that affect PEV, and presumably stabilize chromatin higher-order structure, contain (a) HP1 (heterochromatin protein 1), which binds to chromatin but not to DNA, and (b) the protein termed Su(var)3–7, which interacts with HP1 and chromatin (65). The principles underlying PEV in *Drosophila* seem also to apply to the stable inactivation of **euchromatic** genes needed for maintaining differential expression of developmental regulators (eg, the homeotic genes that control the segmental identity of the insect body). Locally silenced heritable chromatin structures are generated by the assembly of multiprotein complexes that contain members of the Polycomb group (Pc-G) of proteins, which are homologues of HP1 and contain a “chromodomain” (66). The Pc-G genes are responsible for maintaining long-range repression of homeotic genes over multiple enhancers in the later stages of *Drosophila* development. Like HP1, Pc-G proteins appear not to bind DNA. However, specific DNA sequences that recruit Polycomb group proteins and associated silencing factors [Polycomb response elements; (PREs)] have been identified and appear to be essential for stabilizing determined expression states, which are usually (but not invariably) repressive (see Ref. 66). Various models have been proposed for the mechanism of repression, including propagation of a repressive array of interacting proteins over chromosomal domains (the "spreading model" by analogy with the "spreading" effect of heterochromatin into euchromatin in PEV), an alternative model has been proposed in which clusters of Pc-G proteins interact cooperatively with each other to create tethered loop domains of chromatin which ensure repression (67). Mammalian homologues of HP1-like proteins have been found, as have interacting partners, and it seems likely that the same mechanism of silencing, by assembly into repressive heterochromatin, may be used to regulate some developmentally pivotal mammalian genes whose leaky expression would be disastrous for the cell.

Mammalian X-Chromosome Inactivation is an extreme case of heterochromatin formation over a whole chromosome. The precise molecular basis is not known, but there are some notable features of the chromatin composition: hypoacetylation of histone H4; the presence of an unusual H2A variant, macroH2A (see Histones); heavy methylation of the DNA; and the presence of an unusual large untranslated RNA, termed Xist, which is expressed from the inactive X-chromosome, and which is of prime importance in an early event in X-inactivation (68). It would not be too surprising if X-inactivation turned out to have at least some features in common with telomeric and position effect variegation in yeast and *Drosophila*.

7. Replication-Linked Chromatin Assembly

During S-phase of the cell cycle in eukaryotes, it is not just the DNA that undergoes replication, but the chromatin as a whole. Chromatin assembly is tightly coupled to DNA replication and the passage of the replication fork. It involves assembly of nucleosomes on daughter strands, followed by conversion of an initially irregularly spaced array of nucleosomes to a regular array—a process known as maturation. There has been recent progress in understanding the participants in both of these processes. Assembly involves, in equal amounts, both old (parental) histones in preexisting nucleosomes, which are recycled, and newly synthesized histones, which are apparently randomly segregated on to the two nascent duplexes. The temporal order of deposition of newly synthesized histones on to DNA reflects the structural organization of the nucleosome; it begins with the deposition of H3 and H4 to form the central organizing tetrameric core, followed by H2A and H2B as two dimers, and finally addition of H1.

The newly synthesized H4 deposited at the replication fork is diacetylated, at lysines 5 and 12, in all species so far examined (see Histone Acetylation). Newly synthesized H3 is apparently also modified (acetylated or phosphorylated?), although perhaps not in all cell types. The role, if any, played by acetylation *per se* in the assembly process is not well understood. Acetylation is transient and is erased by deacetylases shortly after deposition of histones on to the DNA; one possibility might be that any tendency for premature formation of internucleosome contacts is avoided by the acetylation (see Nucleosome). The deposition of acetylated H3 and H4 involves the participation of chromatin assembly factor 1 (CAF-1), (69), which acts as a core histone **molecular chaperone**. It forms a stable complex with newly synthesized acetylated H3 and H4 and somehow targets them specifically to the replication fork (70); the histone chaperone NAP1 appears to handle H2A and H2B in *Drosophila* (71). Other proteins may also be involved in the assembly process. CAF-1 purified from human cells contains three subunits, indicated by their mass in kDa: p48, p60, and p150; homologues exist in yeast and *Drosophila*. The small subunit (p48) of human CAF-1 is homologous to the regulatory subunit (p46) of the human B-type histone acetyltransferase (responsible for deposition-related acetylation); both subunits bind to histone H4 and, significantly, at a site that is accessible only in the free histone and not in chromatin (as shown by the structure of the nucleosome core particle; see Nucleosome). Strikingly, similar subunits also occur in chromatin remodeling machines (eg, the p55 subunit of *Drosophila* NURF) as noted, as well as in histone deacetylases (see Histone Acetylation), leading to the suggestion that these subunits target the various complexes to their histone substrates in a manner that is regulated by nucleosomal DNA (72). They are members of the highly conserved family of proteins that contain "WD repeats," multiple distinctive sequence motifs that appear to be involved in protein–protein interactions. Because the site of interaction of CAF-1 with H4 is accessible only in the free histone, CAF-1 would have to be displaced before nucleosome assembly could occur; the interactions appear to be disrupted by ACF (*A*TP-requiring *c*hromatin assembly and remodeling *f*actor; see text above). ACF was initially identified as a factor capable of regularly spacing an irregularly spaced nucleosome array (51) and would be well-suited to this role during the maturation step of chromatin assembly. It is also potentially able to participate in the remodeling of nucleosomes that accompanies transcriptional activation (see text above: chromatin remodeling machines).

8. Chromatin Reconstitution

Reconstitution *in vitro* of chromatin from its component parts, like any complex biochemical structure, would allow questions to be asked about structure–function relationships. Reconstitution of the nucleosome core is straightforward. It is achieved by gradual dialysis of a 1:1 molar ratio of histone octamer and 146 bp DNA from 2M NaCl to low salt (eg, 10 mM NaCl). Nucleosome core particles (see Nucleosome) for X-ray crystallography were made in this way. The histones can be presented either as the intact octamer or as a 1:1 molar ratio of H2A–H2B dimers and $(H3)_2(H4)_2$ tetramers.

Long "chromatin" reconstituted *in vitro* by mixing histones at high ionic strength (eg, 2M NaCl), and then dialyzing to low ionic strength, shows close packing of octamers, irrespective of the presence of H1, which has no effect because it is the last histone to bind in this procedure. In attempts to determine what cellular factors determine nucleosome spacing (nucleosome repeat length), several cell-free extracts, from *Xenopus* eggs and oocytes and from *Drosophila* embryos, have been developed that will assemble plasmid DNA, irrespective of sequence, into "physiologically" spaced chromatin in an ATP-dependent fashion, independent of replication. Nucleosome spacing (and hence linker length) is increased by H1. The earliest extracts were from *Xenopus* eggs, which contain a large maternal histone pool, and led to the discovery of two acidic histone chaperone proteins, nucleoplasmin and N1/N2, which facilitated chromatin assembly in this system. Work on the *Xenopus* system is summarized in Ref. 2 (Section 3.4.2). The true role of these proteins may be storage of the large histone pool in the egg. Whether similar proteins exist in somatic cells is unclear, although nucleoplasmin-like proteins have been reported. The *Drosophila* embryo extracts are the same ones that led to the discovery of CHRAC (53) and ACF (51) (see text above: Chromatin remodeling) which themselves have nucleosome spacing activity. Spacing may also have an electrostatic component, involving neutralization of charges on linker DNA (73), and a connection between nucleosome spacing and formation of higher-order structure, which is also ionic strength dependent, has been suggested.

A well-defined *in vitro* system starting with pure components, which has recently been further explored (74), will also assemble "properly spaced" chromatin, in an H1-dependent, ATP-independent manner. Irregularly spaced octamers are first deposited on the DNA by dialysis from high to low NaCl concentration, and then a more regularly spaced array is generated by incubation at "physiological ionic strength" (150 mM NaCl) with H1(H5) in the presence of polyglutamate (which probably binds histones reversibly and allows equilibrium to be reached in the histone positions on the DNA). Interestingly, the system is sensitive to the DNA sequence, and regular nucleosome arrays were generated on only about half of the ~2-kbp cloned chicken genomic sequences tested; the sequences tested (by **Southern blotting**) behaved in essentially the same way in chicken liver nuclei. It is argued (74) that genomic chromatin is a mosaic of less well-ordered regions and regular regions that are about 10 nucleosomes long and contain a nucleosome positioning sequence (or sequences), which effectively acts as a boundary (18) against which linker-histone-dependent nucleosome alignment can occur. It is possible that egg, oocyte, and embryo extracts, which appear to be indifferent to DNA sequence as well as ATP-dependent, are designed to assemble chromatin through rapid cycles of cell division, and not to be responsive, for example, to genomic signals that may be necessary to specify arrays of nucleosomes compatible with gene expression and regulation in somatic cells.

Bibliography

1. K. van Holde (1988) *Chromatin*, Springer-Verlag, New York.
2. A. P. Wolffe (1995) *Chromatin; Structure and Function*, 2nd ed., Academic Press, New York.
3. S. C. R. Elgin (ed.) (1995) *Chromatin Structure and Gene Expression* [Frontiers in Molecular Biology series (B. D. Hames and D. M. Glover, eds.)], Oxford University Press, Oxford, U.K.
4. R. D. Kornberg (1977) Annu. Rev. Biochem. **46**, 931–954.
5. K. Luger, A. W. Mader, R. K. Richmond, D. F. Sargent, and T. J. Richmond (1997) Nature **389**, 251–260.
6. Y.-B. Zhou et al. (1999) Nature (in press).
7. A. A. Travers (1987) Trends Biochem. Sci. **12**, 108–112.
8. T. E. Shrader and D. M. Crothers (1989) Proc. Natl Acad. Sci. USA **86**, 7418–7422.
9. H. R. Widlund et al. (1997) J. Mol. Biol. **267**, 807–817.
10. P. T. Lowary and J. Widom (1998) J. Mol. Biol. **276**, 19–42.
11. H. Cao, H. R. Widlund, T. Simonsson, and M. Kubista (1998) J. Mol. Biol. **281**, 253–260.
12. J. Widom (1996) J. Mol. Biol. **259**, 579–588.
13. S. Muyldermans and A. A. Travers (1994) J. Mol. Biol. **235**, 855–870.
14. A. Travers and H. Drew (1999) Biopolymers (in press).
15. J. J. Hayes, D. J. Clark, and A. P. Wolffe (1991) Proc. Natl. Acad. Sci. USA **88**, 6829–6833.
16. C. Spangenberg et al. (1988) J. Mol. Biol. **278**, 725–739.
17. S. Tanaka, M. Zatchej, and F. Thoma (1992) EMBO J. **11**, 1187.
18. R. D. Kornberg and L. Stryer (1988) Nucleic Acids Res. **16**, 6677–6690.
19. J. Svaren and W. Horz (1997) Trends Biochem. Sci. **22**, 93–97.
20. T. Archer, M. G. Cordingley, R. G. Wolford, and G. L. Hager (1991) Mol. Cell. Biol. **11**, 688–698.
21. G. Panetta et al. (1999) J. Mol. Biol. (in press).
22. P. Bouvet, S. Dimitrov, and A. P. Wolffe (1994) Genes Dev. **8**, 1147–1159.
23. G. Meersseman, S. Pennings, and E. M. Bradbury (1992) EMBO J. **11**, 2951–2959.
24. S. Pennings, G. Meersseman, and E. M. Bradbury (1994) Proc. Natl. Acad. Sci USA **91**, 10275–10279.
25. K. Ura, J. J. Hayes, and A. P. Wolffe (1995) EMBO J. **14**, 3752–3765.
26. D. J. Clark and T. Kimura (1990) J. Mol. Biol. **211**, 883–896.
27. G. Felsenfeld and J. D. McGhee (1986) Structure of the 30 nm fibre. Cell **44**, 375–377.
28. J. Widom (1989) Annu. Rev. Biophys. Biophys. Chem. **18**, 365–395.
29. K. van Holde and J. Zlatanova (1996) Prog. Nucleic Acid Res. Mol. Biol. **52**, 217–259.
30. V. Ramakrishnan (1997) Crit. Rev. Eukaryot. Gene Expr. **7**, 215–230.
31. J. Widom (1998) Annu. Rev. Biophys. Biomol. Struct. **27**, 285–327.
32. F. Thoma, T. Koller, and A. Klug (1979) J. Cell Biol. **83**, 403–427.
33. V. Graziano, S. E. Gerchman, D. K. Schneider, and V. Ramakrishnan (1994) Nature **368**, 351–354.
34. C. L. F. Woodcock, L.-L. Frado, and J. B. Rattner (1984) J. Cell Biol. **99**, 42–52.
35. C. L. Woodcock and R. Horowitz (1995) Trends Cell Biol. **5**, 272–277.
36. J. D. McGhee, J. M. Nickol, G. Felsenfeld, and D. C. Rau (1983) Cell **33**, 831–841.

37. J. O. Thomas, C. Rees, and P. J. G. Butler (1986). Eur. J. Biochem. **154**, 343–348.
38. R. T. Kamakaka and J. O. Thomas (1990). EMBO J. **9**, 3997–4006.
39. R. D. Kornberg and Y. Lorch (1992) Annu Rev. Cell Biol. **8**, 563–589.
40. G. Felsenfeld (1992) Nature **335**, 219–224.
41. T. R. Hebbes, A. W. Thorne, and C. Crane-Robinson (1988) EMBO J. **7**, 1395–1402.
42. P. Geyer (1997) Curr. Opin. Genet. Dev. **7**, 242–248.
43. S. Elgin (1988) J. Biol. Chem. **263**, 19259–19262.
44. K. J. Polach and J. Widom (1995) J. Mol. Biol. **254**, 130–149.
45. K. J. Polach and J. Widom (1996) J. Mol. Biol. **258**, 800–812.
46. J. Boyes et al. (1998) J. Mol. Biol. **279**, 529–544.
47. G. H. Thomas and S. C. R. Elgin (1988) EMBO J. **7**, 2191–2201.
48. V. M. Studitsky, D. J. Clark, and G. Felsenfeld (1994) Cell **76**, 371–382.
49. T. Tsukiyama and C. Wu (1997) Curr. Opin. Genet. Dev. **7**, 182–191.
50. M. J. Pazin and J. T. Kadonaga (1997) Cell **88**, 737–740.
51. T. Ito, J. K. Tyler, and J. T. Kadonaga (1997) Genes to Cells **2**, 593–600.
52. B. Cairns (1998) Trends Biochem. Sci. **23**, 20–25.
53. P. D. Varga-Weisz and P. B. Becker (1998) Curr. Opin. Cell Biol. **10**, 346–353.
54. M. A. Martinez-Balbas, T. Tsukiyama, D. G. Dula, and C. Wu (1998) Proc. Natl. Acad. Sci. USA **95**, 132–137.
55. R. T. Utley, J. Cote, T. Owen-Hughes, and J. L. Workman (1997) J Biol. Chem. **272**, 12642–12649.
56. J. Coté, C. L. Peterson, and J. L. Workman (1998) Proc. Natl. Acad. Sci USA **95**, 4947–4952.
57. G. Schnitzler, S. Sif, and R. E. Kingston (1998) Cell **94** 17–27.
58. Y. Lorch, B. R. Cairns, M. Zhang, and R. D. Kornberg (1998) Cell **94**, 29–34.
59. G. Orphanides et al. (1998) Cell **92**, 105–116.
60. X. Nan et al. (1998) Nature **393**, 386–389.
61. P. L. Jones et al. (1998) Nat. Genet. **19**, 187–191.
62. M. A. McArthur and J. O. Thomas (1996) EMBO J. **15**, 1705–1714.
63. M. Grunstein (1998) Cell **93**, 325–328.
64. M. Grunstein (1997) Nature **389**, 349–352.
65. L. L. Wallrath (1998) Curr. Opin. Genet. Dev. **8**, 147–153.
66. G. Cavalli and R. Paro (1998) Curr. Opin. Cell Biol. **10**, 354–360.
67. V. Pirrotta (1998) Cell **93**, 333–336.
68. A. M. Keohane, J. S. Lavender, L. P. O"Neill, and B. M. Turner (1998) Dev. Genet. **22**, 65–73.
69. S. Smith and B. Stillman (1989) Cell **58** 15–25.
70. A. Verreault, P. D. Kaufman, R. Kobayashim, and B. Stillman (1996) Cell **87**, 95–104.
71. T. Ito, M. Bulger, R. Kobayashi, and J. T. Kadonaga (1996) Mol. Cell. Biol. **16**, 3112–3124.
72. A. Verreault, P. D. Kaufman, R. Kobayashi, and B. Stillman (1997) Curr. Biol. **8**, 96–108.
73. T. A. Blank and P. B. Becker (1995) J. Mol. Biol. **252**, 305–313.
74. K. Liu and A. Stein (1997) J. Mol. Biol. **270**, 559–573.
75. P. D. Gregory and W. Horz (1998) Eur. J. Biochem. **251**, 9–18.

Suggestions for Further Reading

76. S. C. R. Elgin (1996) Heterochromatin and gene regulation in *Drosophila*. Curr. Opin. Genet. Dev. **6**, 193–202.

77. G. Felsenfeld (1996) Chromatin unfolds. Cell **86**, 13–19.
78. E. P. Geiduschek (1998) Chromatin transcription: clearing the gridlock. Curr. Biol. **8**, R373–R375.
79. P. D. Gregory and W. Horz (1998) Chromatin and transcription. Eur. J. Biochem. **251**, 9–18.
80. P. Kaufman (1996) Nucleosome assembly: the CAF and the HAT. Curr. Opin. Cell Biol. **8**, 369–373.
81. R. E. Kingston, C. A. Bunker, and A. N. Imbalzano (1996) Repression and activation by multiprotein complexes that alter chromatin structure. Genes Dev. **10**, 905–920.
82. K. Struhl (1998) Histone acetylation and transcriptional regulatory mechanisms. Genes Dev. **12**, 599–606.

Chromatofocusing

Biological macromolecules differ in their compositions of **buffering** groups, such as amino acids and **purine** or **pyrimidine** bases, thus giving each biomolecule its own unique charge properties. Generally, at low or acidic pH values, most biomolecules have a net positive charge, whereas at a higher or basic pH they carry a net negative charge. Of course, at a certain pH, the isoelectric pH or isoelectric point (p*I*), these biomolecules do not possess a net electric charge. This unique isoelectric pH provides the basis for the selectivity of chromatofocusing in **chromatographically** separating biomolecules.

Chromatofocusing is a special kind of technique classified within the ion-exchange chromatography of biomolecules. A weak ion-exchange matrix and a pH gradient are used in chromatofocusing, instead of a strong ion exchanger and a salt gradient as in normal ion-exchange chromatography. This technique was first described theoretically and experimentally demonstrated by Sluyterman and co-workers (1, 2). They proposed that a pH gradient could be produced in an ion-exchange column packed with an appropriate ion-exchange resin with good buffering capacity. Although a pH gradient in a column can be produced in a manner similar to that of a salt gradient by using two different pH buffers in a mixing chamber of a gradient maker, a pH gradient can be created internally in the column by taking advantage of the buffering capacity of the weak ion-exchange resin. In practice, a certain pH buffer is used to equilibrate a column packed with a weak ion exchanger. Then another buffer with a different pH is passed through the column, which generates a pH gradient in the column. If such a pH gradient is used to elute biomolecules bound to the ion-exchange resin, the biomolecules elute in order of their isoelectric pH.

The mechanism of chromatofocusing is based on the buffering action of the charged groups on the ion-exchange resin and on the fact that a biomolecule has a net negative charge at a pH above its isoelectric point. In a descending pH gradient, a single molecular species exists in three charged states—negative, neutral, and positive. When a positively charged column (ie, packed with an anion exchange resin) is equilibrated with a starting buffer of high pH, biomolecules that become negatively charged are initially retained on the column. When an elution buffer of lower pH is passed through the column, a pH gradient develops and the individual molecules continuously change their charged states. The molecules at the rear of the sample zone are the first to be titrated by the low-pH buffer. These molecules become positively charged when the pH is less than their p*I*, so that they are repelled from the column matrix and are carried rapidly to the front of the sample zone, because of the high velocity of the moving buffer. In traveling to the front of the sample zone, the molecules encounter an increase in pH and are titrated from their positive form to neutrality and back to their negative form. Once the molecules become negatively charged again, they readsorb on the matrix and again fall back to the rear of the sample zone. The cycle between the front and rear of the sample zone results in "focusing" (ie, a continuous narrowing of this zone) until the molecules elute from the column. At this point, the pH of the column effluent is approximately the same as p*I* of the components eluting.

Chromatofocusing is an analytical or preparative technique for separating biomolecules according to their p*I*. The details of this technique relating to column packing, sample preparation, and sample application used in this technique are similar to those for affinity chromatography. A detailed operational protocol is beyond the scope of this article, so the interested reader is directed to other reviews (3, 4).

There are a number of advantages in using chromatofocusing. In this technique, a biomolecule is not subjected to a pH greater than its p*I*, and the resulting focusing effects concentrate the sample into a sharp, highly resolved band. One of the great benefits of chromatofocusing is its ease of operation. No gradient-forming devices or mixers are required. The pH gradient is formed with a single isocratic eluent. Chromatofocusing is used widely in research as the method of choice for resolving **isozymes** and molecular species with very similar charge characteristics, such as transferrin, ferritin, and hemoglobins [see refs. in 3-5].

Bibliography

1. L. A. A. Sluyterman and O. Elgersma (1978) J. Chromatogr. **150**, 17–30.
2. L. A. A. Sluyterman and J. Wijdenes (1978) J. Chromatogr. **150**, 31–44.
3. L. Giri (1990) in *Guide to Protein Purification* (M.P. Deutscher, ed.), *Methods in Enzymology 182*, Academic Press, New York, pp. 380–392.
4. T. W. Hutchens (1989) in *Protein Purification: Principles, High Resolution Methods, and Applications* (J.-C. Janson, and L. Rydén, eds.), VCH, New York, pp. 149–174.
5. Pharmacia (1985) *FPLC Ion Exchange and Chromatofocusing-Principles and Methods*, Offsetcenter AB, Uppsala, Sweden.

Chromatography

Chromatography constitutes a family of closely related methods for separating and analyzing a wide variety of chemicals. Today, despite developments in analytical chemistry that link scientists to many modern and extremely sophisticated devices, the classic methodology of chromatography still plays a very important role among analytical techniques. It is almost impossible to imagine a laboratory without chromatographic equipment. Quality control, product purification, and basic research are some of the fields in which chromatography is used.

1. Definition

The term chromatography, first used by Tsvet (1872–1919), a Russian botanist, derived from the two Greek words *Khromatos* (color) and *graphos* (written). He used the term chromatography to describe his studies on pigment separation using a chalk column (1, 2), thus defining chromatography as a method by which the components of a mixture were separated on an adsorbent column in a flowing system (1, 2). The International Union of Pure and Applied Chemistry (IUPAC) has further defined chromatography as

A method, used primarily for separation of the components of a sample, in which the components are distributed between two phases, one of which is stationary while the other moves. The stationary phase may be a solid, or a liquid supported on a solid, or a gel. The stationary phase may be packed in a column, spread as a layer , or distributed as a film, etc.; in these definitions chromatographic bed is used as a general term to denote any of the different forms in which the stationary phase may be used. The mobile phase may be gaseous or liquid (3).

2. Historical Perspective

Although some phenomena that form the basis of chromatographic methods have been known for a long time, Tsvet is generally referred to as the father of chromatography. In 1906, he described the separation of plant pigments by column liquid chromatography using over 100 adsorption media (1, 4, 5). During the next forty years after Tsvet's work, there were some important developments in the field. For example, Kuhn et al. published two papers in 1931 on separating carotenoids on a calcium carbonate column (6, 7). Kuhn, Karrer, and Ruzicka applied the chromatographic technique to their own fields of interest and were awarded the Nobel prize (1937, 1938, and 1939, respectively) for their contributions to chromatography. Tiselius (8) and Claesson (9) developed the now classical procedures involving the continuous observation of optical properties of solutions flowing out of chromatographic columns. Tiselius was awarded the Nobel prize in 1948 for his research on "Electrophoresis and Adsorption Analysis". The introduction of gradient elution in 1952 (10) was an important contribution to all column chromatographic methods.

Chromatograpic developments greatly accelerated after the famous paper by Martin and Synge appeared in 1941 (11). They presented the invention of liquid-liquid (or partition) chromatography in columns and in planar form (paper chromatography). They also provided a theoretical framework for the basic chromatographic process. Martin and Synge were awarded the Nobel prize in 1952 for this work. When thin layers of supported silica gel were introduced as an alternative for paper in the late 1950s (12, 13), the field of **thin-layer chromatography** (TLC) was born and became so popular that it has largely replaced the older technique. Another main development in the progress of chromatography was the introduction of gas-liquid chromatography (GLC) by James and Martin (14), which had an unprecedented impact on the analytical chemistry of organic compounds. Porath and Flodin introduced **size-exclusion chromatography** in 1959 (15), allowing easy separation of macromolecules. Modern liquid chromatography (**HPLC**) was introduced in the early 1970s, permitting the efficient separation of a wide range of components.

The theory of chromatography was first studied by Wilson (16), who discussed the quantitative aspects in terms of diffusion, adsorption rate, and isothermal nonlinearity. The plate theory was first presented by Martin and Synge (11) and was further explored by Craig (17) and Gluechauf (18). In this theory, chromatography is described in terms closely analogous in its mode of operation to distillation and extraction fractionating columns. Lapidus and Admunson (19), followed by van Deemter and co-workers (20), developed the rate theory, an alternative to the plate theory. In this theory, column efficiency was described as a function of the mobile-phase's flow rate and diffusion properties and the stationary-phase particle size. In 1959, Giddings published another paper on this topic (21), and the rate theory has since become the backbone of chromatographic theory. In 1963, Giddings (22) pointed out that, if the efficiencies of gas chromatography were to be achieved in liquid chromatography, particle sizes of 2 to 20 μm were required. This prediction was found to be correct with the development of HPLC systems. Numerous detailed descriptions of chromatographic theory exist in the literature. Notable examples include a monograph edited by Jönsson (23) and the excellent reviews of Snyder (24) and Horváth and Melander (25).

This is only a small glimpse of the historical development of chromatography. The book *75 Years of Chromatography—A Historical Dialogue* (26), which describes many of the individuals who deserve credit for developing this technique, can be consulted for more complete accounts.

3. Retention Mechanism Classification

There are three common ways to classify chromatographic methods. The first and most popular classification is based on the mechanisms of retention, the manner in which the analyte interacts with the stationary phase. In this classification, chromatography may be divided into the five following basic types:

3.1. Adsorption Chromatography
This technique is based on competition for neutral analytes between the mobile phase (gas or liquid) and a neutral solid adsorbent. Therefore, analytes with **polar groups** are retained longer by a polar adsorbent, and nonpolar analytes interact better with a nonpolar stationary phase. In this type of chromatography, the analytes are simultaneously in contact with both the stationary phase and the mobile phase.

3.2. Partition Chromatography
This technique is based on competition for neutral analytes between the mobile phase (gas or liquid) and a neutral liquid or liquid-like stationary phase (the latter is usually called a “bonded-phase” when long alkyl chains or their derivatives are bonded to a matrix and behave like a liquid). In partition chromatography, the analyte is transferred from the bulk of one phase into the bulk of the other, so that the analyte molecules are surrounded only by molecules of one phase. Separation in partition chromatography is achieved by differences in the partition coefficients of the analytes between the mobile and stationary phases.

3.3. Ion-Exchange Chromatography
This technique is based on the electrostatic interaction between a charged solute and an oppositely charged solid stationary phase. Separation in ion-exchange chromatography is achieved by the differing affinities of ions in solution for oppositely charged ionic groups in the stationary phase. Ion-exchange chromatography is applicable to any solute that acquires a charge in solution. Thus, even carbohydrates, which are largely uncharged below pH 12, are separated by this type of chromatography at sufficiently high pH.

3.4. Size-Exclusion Chromatography
This technique is based on the sieving principle and is variously known as gel chromatography, **gel filtration** and gel-permeation chromatography (see Size Exclusion Chromatography). In this technique, the stationary-phase particles have a wide range of pore sizes, causing the stationary phase to behave like a molecular sieve. Small molecules permeate the pores, and large bulky molecules are excluded. Thus, the solutes are separated on the basis of molecular weight and size, and the larger ones elute first.

3.5. Affinity Chromatography
This technique is based on the unique biological specificity of **ligand-binding** interactions (ie, the lock-and-key mechanism) (see Affinity Chromatography). The ligand is covalently bonded to the matrix that forms packing material for the column. Separation is achieved after the applied macromolecule becomes specifically, but not irreversibly, bound to the ligand. The macromolecule is eluted by altering the composition or pH of the eluent so as to weaken its interaction with the ligand, thus promoting dissociation and facilitating elution of the retained compounds.

Many other types of chromatography, such as **hydrophobic-interaction**, **chiral**, ion-pair, and **salting-out** chromatography, are also frequently used. Furthermore, in practical chromatography intermediate or mixed types are often used. So, although one dominant mechanism is presented, the chromatographic modes are not mutually exclusive. To know more about the relationships of different chromatographic modes, see a schematic diagram by Saunders (27).

4. Development Procedure Classification

The second classification is based on the development procedure, the mechanism by which the sample is removed from the column, and therefore depends on the nature of the mobile phase. This classification was introduced by Tiselius (8) in 1940. There are three chromatographic modes in the classification: (1) elution development, (2) displacement development, and (3) frontal analysis. The principles of each mode are illustrated by Braithwaite and Smith (28). In practice, only elution development and to a lesser extent displacement development are commonly used.

5. Fractionation Phase Classification

The third classification is based on the phases between which the fractionation process takes place. In chromatography, one phase is held immobile or stationary, and the other one (the mobile phase) is passed over it. Therefore chromatography is mainly divided into two large groups named according to the state of aggregation of the mobile phase, liquid chromatography and gas chromatography. Further groupings can be made by naming both the mobile and stationary phases, thus liquid-liquid, liquid-solid , gas-liquid, and gas-solid chromatography have been named. More recently, supercritical fluids have been used as mobile phases, and these techniques have been named supercritical fluid chromatography, irrespective of the state of the stationary phase.

Bibliography

1. M. S. Tsvet (1906) Ber. Deut. Botan. Ges. **24**, 316.
2. M. S. Tsvet (1906) Ber. Deut. Botan. Ges. **24**, 384.
3. *Recommendations on Nomenclature for chromatography, Rules Approved 1973*, IUPAC Analytical Chemistry Division Commission on Analytical Nomenclature (1974) Pure Appl. Chem. **37**, 447.
4. M. S. Tsvet (1910) *Khromofilly v Rastitel"nom i Zhivotnom Mire Tipogr*. Varshavskago Uchebnago Okruga, Warsaw.
5. H. H. Strain and J. Sherma (1967) J. Chem. Educ. **44**, 238–242.
6. R. Kuhn and E. Lederer (1931) Ber. **64**, 1349.
7. R. Kuhn, A. Winterstein, and E. Lederer (1931) Hoppe Seyler"s Z. Physiol. Chem. **197**, 141–160.
8. A. Tiselius (1940) Ark. Kemi. Mineral. Geol. **14B**, 22.
9. S. Claesson (1946) Ark. Kemi. Mineral. Geol. **23A**, 1.
10. R. S. Alm, R. J. P. Williams, and A. Tiselius (1952) Acta Chem. Scand. **6**, 826–836.
11. A. J. P. Martin and R. L. M. Synge (1941) Biochem. J. **35**, 1358–1368.
12. E. Stahl et al. (1956) Pharmazie **11**, 633.
13. E. Stahl (ed.) (1962) *Thin Layer Chromatography*, Academic Press, New York.
14. A. T. James and A. J. P. Martin (1952) Biochem. J. **50**, 679–690.
15. J. Porath and P. Flodin (1959) Nature **183**, 1657–1659.
16. J. N. Wilson (1940) J. Am. Chem. Soc. **62**, 1583–1591.
17. L. C. Craig (1950) Anal. Chem. **22**, 1346–1352.
18. E. Glueckauf (1955) Trans. Faraday Soc. **51**, 34–44.
19. L. Lapidus and N. R. Amundson (1952) J. Phys. Chem. **56**, 984–988.
20. J. J. van Deemter, F. J. Zuiderweg, and A. Klinkenberg (1956) Chem. Eng. Sci. **5**, 271.
21. J. C. Giddings (1959) J. Chem. Phys. **31**, 1462—1467.
22. J. C. Giddings (1963) Anal. Chem. **35**, 2215–2216.
23. J. Å. Jönsson (ed.) (1987) *Chromatographic Theory and Basic Principles (Chromatographic Science Series 38)*, Marcel Dekker, New York.
24. L. R. Snyder (1992) in *Chromatography* (E. Heftmann, ed) (J. Chromatogr. Library, Vol. **51A**), Elsevier, Amsterdam, pp. A1–A68.
25. C. Horváth and W. R. Melander (1983) in *Chromatography* (E. Heftmann, ed.) (J. Chromatogr. Library, Vol. **22A**), Elsevier, Amsterdam, pp. A27–A135.

26. L. S. Ettre and A. Zlatkis (1979) *75 Years of Chromatography-A Historical Dialogue* (L.S. Ettre and A. Zlatkis, eds.) (J. Chromatogr. Library, Vol. **17**), Elsevier, Amsterdam.
27. D. L. Saunders (1975) in *Chromatography*, 3rd ed. (E. Heftmann, ed), Van Nostrand Reinhold, New York, p. 81.
28. A. Braithwaite and F. J. Smith (1985) *Chromatographic Methods*, 4th ed., Chapman and Hall, New York, p. 8.

Chromocenter

The salivary gland nuclei of *Drosophila melanogaster* contain polytene chromosomes. These specialized chromosomes essentially contain duplicated repeats of the **DNA** in the entire chromosome. Polytene chromosomes are fused at their centromeres to form the chromocenter . This specialized chromosomal domain in *Drosophila* consists of constitutive heterochromatin. The DNA sequences within the chromocenter consist of two types of repeats. One type that is assembled into a-heterochromatin is composed of highly repeated simple DNA sequences, whereas the second, b-type is more complex. Structural components of heterochromatin at the chromocenter have been identified (1). The best-characterized protein that accumulates selectively at the chromocenter is known as heterochromatin protein 1 (HP1). Antibodies to HP1 colocalize with the type of DNA repeat found in b-heterochromatin called the Dr.D element (2). This is at the edges of the chromocenter in what is termed pericentric heterochromatin.

HP1 contains a protein motif that is found in other chromatin binding proteins and is known as the chromodomain (for chromatin organization modifier). Recent studies have established that the chromodomain family of proteins comprises more than 40 members (3) that can be subdivided into two major groups. Proteins, such as HP1, contain both an amino-terminal chromodomain and a carboxy-terminal “shadow” chromodomain (4). The amino-terminal chromodomain directly binds to heterochromatin, whereas the carboxy-terminal “shadow” chromodomain determines nuclear localization and assists in binding to chromatin (5). The second group of proteins relies on interactions with other proteins to target association with particular chromatin domains (6). The structure of the chromodomain was recently determined using NMR (7). The chromodomain has strong homology to two archaebacterial DNA-binding proteins. However, the eukaryotic chromodomain does not interact with DNA and is involved in protein-protein interactions. Each chromodomain consists of an amino-terminal, three-stranded, antiparallel beta sheet that folds against a carboxy-terminal alpha-helix. The presence of both a chromodomain and a shadow chromodomain are thought to allow proteins, such as HP1, to function as adapters in assembling large multicomponent proteins.

The chromocenter is a useful chromosomal domain for identifying the structural components of heterochromatin and potentially for actually understanding how heterochromatin is organized at a molecular level. The formation of the chromocenter indicates how similar nucleoprotein complexes that share common structural components can self-associate. It provides a nice example of a specialized nuclear compartment that is assembled so that depends on protein–nucleic acid interactions.

Bibliography

1. T. C. James and S. C. R. Elgin (1986) Mol. Cell Biol. **6**, 3862–3872.
2. G. L. G. Miklos, M.-T. Yamamota, J. Davies, and V. Pirotta (1986) Proc. Natl. Acad. Sci. USA

85, 2051–2055.
3. E. V. Koonin, S. B. Zhou, and J. C. Lucchesi (1995) Nucl. Acids Res. **23**, 4229–4233.
4. R. Aasland and A. F. Stewart (1995) Nucl. Acids Res. **23**, 3168–3173.
5. J. S. Platero, T. Hartnett, and J. C. Eissenberg (1995) EMBO J. **14**, 3977–3986.
6. A. Lorentz, K. Ostermann, O. Fleck, and H. Schmidt (1994) Gene **143**, 1–8.
7. L. J. Ball et al. (1997) EMBO J. **16**, 2473–2481.

Chromogenic Substrate

A chromophore is any light-absorbing group (see Absorption Spectroscopy), and a *chromogenic* substrate is one that is acted on by an enzyme so as to increase or decrease the absorption of light at a particular wavelength as substrate is converted to product. An example of a naturally occurring chromogenic substrate is **NADH**, which absorbs light strongly at 340 nm. The absorbance decreases as NADH is oxidized by a pyridine nucleotide-dependent dehydrogenase, because NAD does not absorb substantially at 340 nm. Artificial chromogenic substrates have been used extensively for kinetic studies on a range of enzymes. *p*-Nitrophenylphosphate is hydrolyzed by **phosphatases** to release *p*-nitrophenol, which has a yellow color in alkaline solution. The increase in absorbance with hydrolysis is measured at 400 nm. *p*-Nitrophenylesters are used in a similar manner to measure the activity of *esterases*. Phenazine methosulfate is used as a convenient means of determining the activity of flavoprotein enzymes, as the oxidized form of the electron acceptor is yellow and the reduced form is colorless. An extensive list of artificial, chromogenic substrates has been recorded (1).

Bibliography

1. R. M. C. Dawson, D. C. Elliott, W. H. Elliott, and K. M. Jones (1986). *Data for Biochemical Research*, Clarendon Press, Oxford, pp. 350–377.

Chromomere

Chromomeres represent discrete structures in chromosomes that are visible under the light microscope in mitotic or meiotic **prophase** (see Chromatid). Electron microscopy and staining indicate that chromomeres represent regions of move complex, higher order structure than the 30-nm chromatin fiber (1). It has been suggested that they represent sites of the preferential chromatin compaction that occurs early in the prophase, coincident with the separation of sister chromatids (2). However, electron microscopic images of native chromatin in the **interphase** nuclei at physiological ionic strengths reveal that chromomeres may be identical to globular clusters of nucleosomes [(superbeads)] that probably represent local coiling of the 30-nm fiber. It is also possible to detect bead-like discontinuities in the chromatin fiber in sectioned nuclei. Under certain conditions, these superbeads are remarkably uniform and contain between 8 and 48 nucleosomes. This suggests that chromomeres represent discrete structural units (3). The failure to find a ubiquitous organization of chromatin into chromomeres or superbeads, however, indicates that all chromatin does not adopt this form of higher order structure in interphase nuclei *in vivo*. This irregularity may in fact represent the true state of affairs within the nucleus, because, clearly, eukaryotic DNA is not packaged into structures of a crystalline order and stability.

Chromomeres are useful for discriminating between different chromosomes. They are arranged in a specific and consistent pattern along each chromosome. In lampbrush chromosomes, chromomeres occur where there are long regions of inactive chromatin that are consequently compacted into higher order structures.

Bibliography

1. D. E. Comings (1978) Ann. Rev. Genet. **12**, 25–45.
2. G. F. Bahr and P. M. Larsen (1974) Adv. Cell. Mol. Biol. **3**, 192–215.
3. H. Zentgraf and W. W. Franke (1984) J. Cell Biol. **99**, 272–286.

Chromosomes

Chromosomes are the nucleoprotein complexes that provide the structural framework for the expression of **genes** and mediate the transfer of genetic information from generation to generation. The nuclei, mitochondria, and chloroplasts of all cells, both **eukaryotes** and **prokaryotes**, plus **viruses**, all contain chromosomes. These various chromosomes can vary greatly in size, from very large (see Polytene Chromosome, Lampbrush Chromosomes) to very small (see Double Minute Chromosome; Minichromosome). All chromosomes contain **DNA**, which can be packaged by different proteins to assemble a nucleoprotein complex. The DNA in the chromosomes of a eukaryotic cell nucleus is packed with small basic proteins known as histones. The most striking property of every chromosome within the eukaryotic cell nucleus is the length of each molecule of DNA incorporated and folded into it. The human genome of 3×10^9 bp would extend over a meter if unraveled and straightened, yet it is compacted into a nucleus only 10^{-5} m in diameter. It is an astonishing feat of engineering to organize such a long linear DNA molecule within ordered structures that can reversibly fold and unfold within the chromosome.

The basic architectural matrix of the chromosomes found within eukaryotic cell nuclei is chromatin. All of the DNA in the nucleus of a somatic cell is packaged into chromatin by the histone proteins, together with other DNA-binding proteins. In specialized **germ cells**, such as sperm, protamines can replace the histones as the primary means of packaging DNA. There is considerable specialization in the type of chromatin assembled in different regions of a chromosome, depending on its functional requirements. Chromatin containing genes that are being expressed in a cell is called euchromatin. A large chromosomal region that contains inactive genes is assembled into facultative heterochromatin. Specialized chromosomal structures that contain very few genes but have other essential architectural roles in the chromosome are assembled into constitutive heterochromatin. The centromere is an essential structure containing constitutive heterochromatin that mediates segregation of the chromosomes. The molecular motors that drive this process are found within the kinetochore that is attached to the centromeric heterochromatin. Other heterochromatic domains are at the ends of chromosomes in specialized structures known as telomeres. Within the telomere are many reiterated terminal repeat sequences resulting from the activity of the enzyme telomerase. The telomere protects the end of the chromosome from degradation, fusion, and progressive loss of DNA during chromosomal **duplication**.

The position of the centromere relative to the rest of the chromosome provides an important reference point for describing different types of chromosomes. Chromosomes can be **metacentric**, with a centromere near the middle of the chromosome, or **acrocentric**, when it is near the end of the chromosome, or even potentially **telocentric**, when it is at the very tip. Most eukaryotic chromosomes are **monocentric**, having a single centromere, but some are **holocentric** and have multiple centromeric domains. Holocentric chromosomes have specialized mechanisms for segregating chromosomes during **cell division** that differ from those found in most plant and animal cells.

In animal cells, the presence of multiple centromeres in a single chromosome is often the product of chromosomal rearrangements. Such events usually occur as a result of chromosomal damage and can involve **duplications**, **inversions**, and translocations. A **dicentric** chromosome contains two centromeres following one of these rearrangements, whereas an **acentric** chromosome lacks a centromere entirely. Isochromosomes might also be formed, where a chromosome contains multiple identical chromosomal arms. All of these rearrangements lead to major problems for segregating chromosomes during the cell division of **meiosis** and **mitosis**. Chromosomal damage can be very useful in mapping the positions of genes relative to each other by methodologies that apply somatic cell genetics (see Radiation Hybrid).

Each **diploid** cell receives two sex chromosomes, either two X-chromosomes in females or one X- and one Y-Chromosome in males, plus two copies of each of the other chromosomes, known as autosomes. Each pair of autosomes consists of two homologous chromosomes, one from the father and one from the mother in humans. Immediately after mitotic division, each chromosome consists of a single DNA molecule. This single molecule of DNA is assembled into a chromatid, which duplicates during the **S-phase** of the cell cycle to form two sister chromatids. Then these sister chromatids are segregated to the two daughter cells at mitosis. In meiosis, haploid germ cells are created. This involves segregating of homologous chromosomes at the first meiotic division before the sister chromatids are segregated at the second meiotic division. Because homologous chromosomal regions are aligned during meiosis, chromosomal rearrangements can lead to major problems in segregating homologous chromosomal material. This can lead to multivalent chromosomes, whereas a normal meiosis would produce only bivalent chromosomes.

For organisms that undergo sexual reproduction, special sex chromosomes exist. In humans, these are known as the X- and Y-chromosomes. Female cells contain two X-chromosomes, whereas male cells contain a single X-chromosome and a Y-chromosome. Mary Lyon proposed that **gene expression** from the two X-chromosomes in a female cell should be the same as that from the single X-chromosome in a male cell (see Lyon Hypothesis). This is accomplished by silencing one of the two X-chromosomes in a female cell (see X-Chromosome Inactivation; Random X-Inactivation). The silenced X-chromosome is converted to a Barr body made up of facultative heterochromatin. X- and Y-chromosomes share some limited regions of homology that mediate their pairing and subsequent segregation during meiosis.

An important aspect of chromosomal biology involves mapping individual genes on chromosomes, which facilitates diagnosing particular diseases. A wealth of mapping procedures exist. These make up the field of cytogenetics, which is based on visualizing chromosomes. Mapping procedures involve using particular stains for the DNA and protein components of the chromosome (see C-Banding; G Banding). In recent times, these methodologies have been supplemented with high-resolution denaturation mapping techniques. Then all of the stained chromosomes of a particular cell that make up the karyotype can be displayed formally as an ideogram.

At a more refined level, structure at the level of chromosome and chromatin also determines the functions of particular genes. It has long been known from visualizating the large polytene chromosomes that individual chromosomal **domains** exist. Individual domains like the Balbiani rings contain chromatin that reversibly changes structure to reflect different functional states. Balbiani rings appear as **puffs** when they are being **transcribed**. Other regions of the polytene chromosome, known as interbands, contain the regulatory DNA sequences that control the appearance of puffs. Chromosomal rearrangements can lead to positioning genes next to large domains of constitutive heterochromatin. Placing a gene next to the chromocenter in *Drosophila*, where the centromeres fuse together, **represses** expression of the gene. This position effect indicates that structurally specialized domains of chromosomes exist and presents a major problem for biotechnology and gene therapy in expressing foreign DNA in target cells.

Nucleases like **DNase I** have been very useful in mapping regulatory DNA in the chromosome. The **locus control regions**, enhancers, and **promoters** that control gene expression exist as sites that are **hypersensitive** to digestion by DNase I. These elements often control the expression of clusters of contiguous genes that have related functions in the cell. Sites with extreme DNase I sensitivity are also found at the regulatory elements controlling the initiation of DNA replication at the **origin of replication**. The **terminally redundant** regulatory elements of retroviruses are also assembled into nucleoprotein complexes that retain accessibility to DNase I.

Chromosomes are fascinating structures around which much of modern medicine and biotechnology revolves. They also provide the foundation for considering basic molecular mechanisms that control gene expression and for considering the forces that facilitate evolution. Genes require a chromosomal environment to be maintained throughout the generations and within which to realize their full regulatory potential.

Chymotrypsin, Chymotrypsinogen

Chymotrypsin (E.C. 3.4.21.1) is a mammalian digestive serine proteinase, of the **trypsin** family, that is synthesized in the acinar cells of the pancreas in the form of an inactive precursor, *chymotrypsinogen*. This zymogen is stored, along with other digestive enzymes and enzyme precursors, in pancreatic granules, whose contents are released into the duodenum when the pancreas is stimulated by the hormones cholecystokinin and acetylcholine, which are secreted in response to eating a meal.

Chymotrypsinogen is a single polypeptide chain of 245 amino acid residues that becomes enzymatically active on **proteolytic** cleavage of the peptide bond that connects Arg15 and Ile16. This cleavage is catalyzed by another pancreatic enzyme, **trypsin**, which in turn is generated from its zymogen precursor, trypsinogen, by enterokinase, an intestinal serine proteinase. Cleavage of the Arg15—Ile16 bond results in a reorganization of the protein structure, alignment of the catalytic triad, and generation of a substrate binding site (1). Other proteolytic cleavages accompany activation of chymotrypsinogen, but only the one cited is crucial for generating enzymatic activity.

The biological function of chymotrypsin is to digest dietary proteins in the small intestine. It catalyzes the cleavage of peptide bonds in which the carbonyl group is supplied primarily by aromatic or bulky **hydrophobic** amino acids (tyrosine, tryptophan, phenylalanine, leucine, isoleucine, methionine). These residues become the C-termini of the product peptides and are subsequently removed by digestion with carboxypeptidase A. The catalytic mechanism of chymotrypsin and other serine proteinases is described elsewhere (see Serine Proteinase).

Numerous chymotrypsin-like enzymes generally referred to as *chymases* have been identified in various animal tissues, particularly in mast cells, neutrophils, and lymphocytes (2). The biological functions of these enzymes are not well understood, but a chymase isolated from human heart is a major angiotensin II -forming enzyme (3). The *prostate-specific antigen*, which is used in the diagnosis of prostate cancer, is a serine proteinase with limited chymotrypsin-like activity (4).

Being a serine proteinase, chymotrypsin is inhibited by diisopropylfluorophosphate (DIFP) and also by numerous, naturally occurring **serine proteinase inhibitors** and serpins (5), as well as many small synthetic peptide analogues or active site reagents (6).

Bibliography

1. R. M. Stroud, A. A. Kossiakoff, and J. L. Chambers (1977) Annu. Rev. Biophys. Bioeng. **6**, 177–193.
2. J. A. Nadel (1991) Ann. N. Y. Acad. Sci. **629**, 319–331.
3. Y. Liao and A. Husain (1995) Can. J. Pharmacol. **11**(Suppl. F), 13F–19F.
4. A. M. el-Shirbiny (1994) Adv. Clin. Chem. **31**, 99–133.
5. J. Potempa, E. Korzus, and J. Travis (1994) J. Biol. Chem. **269**, 15957–15960.
6. J. C. Powers et al. (1989) J. Cell. Biochem. **39**, 33–46.

Suggestions for Further Reading

7. R. M. Stroud (1974) A family of protein-cutting enzymes. Sci. Am. **231**, 24–88.
8. T. A. Steitz and R. G. Shulman (1982) Crystallographic and NMR studies of the serine proteases. Annu. Rev. Biophys. Bioeng. **11**, 419–444.

Cilia and Eukaryotic Flagella

Cilia and eukaryotic flagella are long (10 µm to 40 µm), narrow, membrane-bounded structures that contain a highly ordered, stable microtubule array, consisting of nine fused outer doublet microtubules surrounding a central pair of singlet microtubules. These microtubules are firmly anchored at the base of the cilium or flagellum in basal bodies. The microtubules of cilia and flagella are extremely stable, and their movement is not complicated by dynamics. In addition to the tubulin backbone, these microtubules contain a large and diverse array of microtubule-associated proteins (MAPs), most of which have not been characterized, and several forms of dynein, a large multicomponent ATP-transducing mechanochemical motor protein. The various MAPs create and maintain the stable axoneme structure, and the dynein is responsible for creating the movement. The movements of cilia and flagella involve bending of these long organelles, which is caused by the sliding of stable double-microtubule pairs past each other. Sliding is effected by the dynein motors; the base of the motor is attached permanently to the A microtubule of one outer doublet pair, and the head, which contains the motor **domain**, transiently attaches and detaches to the B subfiber of an adjacent outer doublet pair. The dynein motor "walks" along the B subfiber toward the minus end, creating the movement. The dynein-mediated sliding of outer double-microtubules occurs in a fashion similar to filament sliding in muscle contraction, in which actin filaments and myosin filaments slide past each other through the action of the ATP-transducing myosin motor "heads."

Circadian Rhythms and Clocks in Fungi

Circadian clocks are ubiquitous and present in organisms as distantly related as **fungi** and mammals. Classically defined as rhythms that persist under constant environmental conditions, circadian clocks control daily rhythms that correlate with changes in the external environment. Most likely, circadian rhythms were selected early in evolution for conferring an evolutionary advantage on the organisms containing them.

To compare the properties of circadian rhythms among different organisms, the concept of circadian time (CT) was developed. The circadian day is divided into 24 equal parts, each one circadian hour. By convention, CT0 is subjective dawn, and CT12 represents subjective dusk. The normal circadian cycle in *Neurospora* can be reset in a time-dependent manner by external signals (a property called entrainment) such as light (1) or temperature (2).

Lower eukaryotes are ideal models for clock study because of their genetic and biochemical tractability. *Neurospora crassa* is such an example. Circadian rhythms in *Neurospora* are easily observed with the use of specialized growth tubes called ***race tubes***. When wild-type strains of *Neurospora* are inoculated on one side of a race tube, the organism initiates a rapid vegetative growth toward the opposite side. After growth for a day in constant light, the position of the growth front is marked, and the culture is transferred to constant dark. The light-to-dark transfer synchronizes the culture on CT12 (subjective dusk). Monitoring of the growth front every 24 h reveals a typical pattern of alternate conidial and aconidial bands, whose frequency permits the determination of both period length and phase of the rhythm. The *Neurospora* circadian rhythm has a period of 22 h at 24 °C. This period does not change significantly between 18°C and 30°C, as demanded by the circadian definition of a rhythm (a phenomenon called temperature compensation).

Three general questions drive research in fungal chronobiology: What is the biochemical and/or genetic basis for the clock? How does the clock gets its input from its extracellular and extraorganismal environment? How is time, as paced by the clock, transduced within the cell?

1. The Clock

The central oscillator of the *Neurospora* clock is the *frq* locus. Originally identified by chemical and ultraviolet mutagenesis, mutations at this locus alter the normal circadian clock of the cell but have no severe morphological defects in growth or development (3, 4). Cloning of the *frq* locus elucidated a complex pattern of gene transcription (3, 5). Two overlapping transcripts of 4 and 4.5 kb were identified, both containing long leader sequences, with several upstream open reading frames. These transcripts have been predicted to encode a putative 989-amino-acid-residue protein. Recent data, however, support the existence of two forms of FRQ (6). The long form ($FRQ^{1–989}$) starts at the first in-frame ATG start codon, whereas the short form ($FRQ^{100–989}$) starts at the third in-frame ATG of the longest reading frame in the region (6). Temperature regulates the ratio of FRQ forms by favoring the use of different initiation codons at different temperatures. For example, the long form of FRQ ($FRQ^{1–989}$) is favored at high temperatures, whereas at lower temperatures the short form of FRQ ($FRQ^{100–989}$) is predominant. These similar but functionally distinct forms of the clock protein FRQ represent a novel adaptive mechanism designed to keep the *Neurospora* clock running over a wide range of temperatures (6). Despite its fine regulation, the biochemical function of FRQ remains unknown (7). However, the presence of a nuclear localization signal [required for FRQ activity (8)], a weak **helix–turn–helix** DNA-binding domain (9), and a conserved acidic region strongly suggest the involvement of FRQ in transcription. As predicted for protein regions important for function, all of these FRQ transcription-factor-like signatures are conserved in FRQ homologues isolated from other distantly related fungal species (10).

The autoregulatory feedback cycle controlled by *frq* takes one day to complete. This loop involves the transcriptional activation and repression of the *frq* locus. Starting with low levels of *frq* transcript and protein (dawn), *frq* transcripts begin to rise, reaching a peak accumulation 4 to 5 h later [just before noon—(8)]. The maximal level of FRQ protein can only be observed 4 to 6 h later (relative to the peak in *frq* mRNA). This time lag is probably due to post-transcriptional regulation of *frq* mRNA or FRQ protein. Synthesized FRQ protein enters the nucleus (8) and acts rapidly, either directly or indirectly, to repress *frq* (11). The repressing activity of FRQ remains until the protein begins to be **phosphorylated**, linking the activity of unknown protein kinases to the clock. Phosphorylation of FRQ increases its turnover (12), until its scarcity allows positive factors like *white collar-1* (*wc-1*) and *white-collar-2* (*wc-2*) (1, 7) to restart the cycle (see text below).

2. Input

Light and temperature are among the most important environmental stimuli controlling circadian rhythmicity. The light-dependent signal transduction pathway is thought to involve an as yet uncharacterized flavin-dependent blue-light photoreceptor (13, 14). When wild-type strains of *Neurospora* grown in the dark receive a pulse of light, the levels of *frq* mRNA increase. Two global regulatory genes, *wc-1* and *wc-2*, have been established to be involved directly or indirectly in the induction and maintenance of *frq* mRNA levels following this light treatment. For example, the light response observed in wild-type strains (ie, the increase in *frq* mRNA levels) cannot be detected in strains mutant in *wc-1*, but it is normal in strains mutant in *wc-2*. Interestingly, the products of both loci (*wc-1* and *wc-2*) are required for the maintenance of high-level expression of *frq* mRNA in the light. Therefore, the pulse of light positively stimulates *frq* mRNA levels in an FRQ-independent, WC-dependent manner (1, 15). Moreover, the light dosage positively correlates with the amount of *frq* mRNA, and, depending when this pulse of light is perceived, it can reset the clock, thereby phase advancing or phase delaying the conidiation rhythms of the organism. Complete elucidation of the roles of WC-1 and WC-2 on *frq* gene expression will be essential for a complete understanding of the signal transduction pathway responsible for clock input.

3. Output

Genes whose rhythmic regulation equals the period of the strain under study are said to be part of the output component of the oscillator (ie, they execute the commands given by the master oscillator and establish the cellular rhythm). To be defined as such, loss-of-function mutations in these classes of genes must not affect the functioning of the clock. With this rationale in mind, a systematic search for clock-controlled genes (*ccg*) was carried out in *Neurospora* (16). Most, but not all, of the *ccg* genes identified were found to be induced during the asexual **sporulation** pathway. The ones that were not were postulated to be involved in other developmental pathways (eg, sexual sporulation) or other unknown output pathways (7). Although rhythmically regulated, the levels and amplitude of expression differ among different clock-controlled genes. In addition, their expression pattern in both frq^+, and *frq* changes from gene to gene [ie, some genes are repressed, while others are derepressed or unchanged (7)]. To date, a direct link between *frq* (the central master oscillator) and *ccg* (the foot soldiers) has not been established, despite being an area of active investigation. It is not surprising to find that the *ccg* identified have nothing or very little in common. For example, *ccg-1* codes for a small polypeptide of 71 amino acid residues with no known homologues in other organisms (17), despite its elevated level of expression (18), whereas *ccg-12*, encodes copper metallothionein (18). See Refs. 18 and 19 for a complete description of *ccg* genes. While the mechanisms of circadian rhythms are incompletely understood at this time, it remains undeniable that the molecular strategies employed by fungi are an excellent model system with which to study similar systems in higher eukaryotes.

Bibliography

1. S. K. Crosthwaite, J. J. Loros, and J. C. Dunlap (1995) Cell **81**, 1003–1012.
2. Y. Liu, M. Merrow, J. J. Loros, and J. C. Dunlap (1998) Science **281**, 825–829.
3. J. C. Dunlap (1996) Annu. Rev. Genet. **30**, 579–601.
4. J. F. Feldman (1982) Annu. Rev. Plant Physiol. **33**, 583–608.
5. C. R. McClung, B. A. Fox, and J. C. Dunlap (1989) Nature **339**, 558–562.

6. Y. Liu, Y. Garceau, J. J. Loros, and J. C. Dunlap (1997) Cell. **89**, 477–486.
7. D. Bell-Pedersen (1998) Microbiol. **144**, 1699–1711.
8. C. Luo, J. J. Loros, and J. C. Dunlap (1998) EMBO J. **17**, 1228–1235.
9. M. T. Lewis, L. Morgan, and J. F. Feldman (1996) Mol. Gen. Genet. **253**, 401–414.
10. M. Merrow and J. C. Dunlap (1994) EMBO J. **13**, 2257–2266.
11. M. W. Merrow, N. Y. Garceau, and J. C. Dunlap (1997) Proc. Natl. Acad. Sci. USA **94**, 3877–3882.
12. N. Y. Garceau, Y. Liu, J. J. Loros, and J. C. Dunlap (1997) Cell **89**, 469–476.
13. E. Klemm and H. Ninnemann (1979) Photochem. Photobiol. Rev. **4**, 207–265.
14. J. Paietta and M. L. Sargent (1981) Proc. Natl. Acad. Sci. USA **78**, 5573–5577.
15. S. K. Crosthwaite, J. J. Loros, and J. C. Dunlap (1997) Science **276**, 763–769.
16. J. J. Loros, S. A. Denome, and J. C. Dunlap (1989) Science **243**, 385–388.
17. J. J. Loros (1995) Semin. Neurosci. **7**, 3–13.
18. D. Bell-Pedersen, M. Shinohara, J. J. Loros, and J. C. Dunlap (1996) Proc. Natl. Acad. Sci. USA **93**, 13096–13101.
19. D. Bell-Pedersen, N. Garceau, and J. J. Loros (1996) J. Genet. **75**, 387–401.

Circular Chromosome

All **Hfr strains** (for high frequency of recombination) of *Escherichia coli* originate from F^+ strains (males, possess the *F* sex factor). When mated with F^- recipients (females), they generate about a thousand times more recombinants than the equivalent F^+ strain under identical conditions (1). The recombinants obtained inherit a particular segment of the donor chromosome exclusively (1). The way in which *Hfr* donors transfer their chromosome to recipients was elucidated by violent agitation of a mixture of mating Hfr and F^- in a high-speed mixer. The mating was interrupted at different time intervals and the mixture was plated for detection of recombinants. It was found that recombinants acquire different selected characters from the donor cell at different times. The order in which these characters appear is the order of their arrangement on the chromosome. The only reasonable interpretation of these results is that the effect of agitation is a rupturing of the chromosome during the transit from the donor to recipient bacteria. Only those genes that have already penetrated the recipient bacteria at the time of treatment can appear in recombinants. Thus, the strain Hfr used comprises a homogeneous population of donor bacteria, all of which transfer their chromosome in the same specifically oriented and linear way, so that a particular extremity, designated O (for origin), is always the first to penetrate the recipient bacteria (2, 3).

A number of Hfr stains of independent origin were analyzed with respect to the markers they transferred to recipients and to the orientation of the transfer. The outcome was remarkable and unforeseen. Although all of the bacteria of any one Hfr strain transfer a given set of markers in a particular sequence, different strains transfer different chromosomal segments, parts of which may overlap. Some strains transfer their genes in a direction reverse to others. The relationship of the various genes to one another however, is the same irrespective of the Hfr strain used to map them. This gives an unequivocal general linkage map for *E. coli*, consisting of a single linkage group. Each strain transfers its chromosome as a linear, oriented structure with a specific head and tail, for example,

Y CBAZO OBAZY

_______---------________, or ____ -------- ________

Another strain can always be found which transfers genes A and Z as closely linked markers, for example,

ZY CBAO

__________----- _______

Thus, in spite of this linear transfer, it is impossible to define any extremities on the chromosome. It is concluded that the chromosome of *F*+ donors is originally continuous or circular and that Hfr strains arise by opening up the circle at a point characteristic for each Hfr type to yield a linear, transferable structure (3).

The circular nature of the *E. coli* chromosome has been confirmed by gentle liberation and dispersion of its DNA and visualization by autoradiography or by electron microscopy. Therefore there is indisputable, direct evidence that this chromosome is indeed a continuous, circular thread of double-stranded DNA (4, 5).

References

1. F. Hayes (1953) Cold Spring Harbor. Symp. Quant. Biol. **18**, 75–93.
2. E. L. Wollman and F. Jacob (1955) C. R. Acad. Sc. Paris **240**, 2449–2451.
3. E. L. Wollman and F. Jacob (1958) Ann. Inst. Pasteur **95**, 641–666.
4. J. Cairns (1962) J. Mol. Biol. **4**, 407–409.
5. J. Cairns (1963) Cold Spring Harbor Symp. Quant. Biol. **28**, 43–46.

Suggestion for Further Reading

6. F. Jacob and E. L. Wollman (1961) *Sexuality and the Genetics of Bacteria*, Academic Press, New York, pp. 164–165.

Circular Dichroism

Circular dichroism (CD) is a form of spectroscopy that uses circularly polarized light and is highly sensitive to the conformations of molecules. Because of this conformational sensitivity, CD is one of the most widely used techniques for characterizing the conformations of proteins, **nucleic acids**, and carbohydrates, and for monitoring conformational transitions induced by temperature, solvent composition, **ligand binding**, etc.

The principal conformations of polypeptide chains—alpha-helix, beta-sheet, b-turns, and the so-called unordered conformation—all have distinctive CD spectra that permits these **secondary structures** to be readily recognized in their pure forms or in simple combinations. Even in globular proteins, which represent complex mixtures of these and other conformations, in most cases the CD spectrum can be analyzed to provide reasonably accurate estimates of the fraction of residues in the various secondary structures. CD signals due to aromatic side chains and nonprotein chromophores provide sensitive probes of protein tertiary structures and of protein–ligand interactions. In the field of nucleic acids, CD also provides valuable information about the nature of the secondary and higher order structures detecting the binding of small molecules and proteins. CD has more restricted application to carbohydrates and polysaccharides, but it has some important applications to studies of carbohydrate conformation.

In addition to its pronounced sensitivity to conformation, CD has other advantageous features. Only small amounts of material are required, comparable to those required for a UV-visible absorption spectrum, and it is relatively easy to survey a broad range of conditions of temperature, pH, ionic strength, and solvent composition. Moreover, the cost of the instrumentation is moderate, and it is easy to operate and maintain. The principal limitation of CD is that it provides lower resolution structural information than X-ray crystallography or NMR spectroscopy. A CD signal can rarely be assigned to a specific residue or group in a macromolecule. Whereas CD gives an estimate of the fraction of residues in a globular protein that are in a-helical segments, it cannot provide information on their location in the sequence. These limitations, however, are outweighed by the conformational sensitivity and other experimental advantages of CD.

1. Fundamentals of Circular Dichroism

1.1. Definition of Circular Dichroism

Circular dichroism is a type of spectroscopy in which the difference in absorption of right- and left-circularly polarized light is measured. In circularly polarized light (cpl), the vector **E** describing the electric field of the light, rotates about the direction of propagation once in each period or wavelength of the light. As seen by an observer looking toward the light source, the electric vector may rotate in either a clockwise sense, corresponding to right-circularly polarized light (rcpl), or in a counterclockwise sense, corresponding to left-circularly polarized light (lcpl). At a given instant, the tip of the electric vector of rcpl follows a right-handed helix in space, whereas the tip of the electric vector of lcpl follows a left-handed helix. Therefore, cpl is **chiral**, and rcpl and lcpl are related as mirror images, that is, they are **enantiomeric**. Because of their enantiomeric character, it is to be expected that rcpl and lcpl interact differently with a chiral molecule, giving rise to differences in optical properties for a chiral molecule measured with rcpl and lcpl.

CD is defined as the difference in absorbance of rcpl and lcpl:

$$\mathrm{CD} = \Delta A = A_1 - A_r = \epsilon_1 c \ell - \epsilon_r c \ell = (\epsilon_1 - \epsilon_r) c \ell = \Delta\epsilon_M c \ell \qquad (1)$$

Here A_l and A_r are, respectively, the absorbances for lcpl and rcpl; c is the molar concentration of the chiral species; ℓ is the pathlength of the sample cell (in cm); e$_1$ and e$_r$ are the molar extinction coefficients of the chiral species for lcpl and rcpl, respectively; and De $_M$ is the molar CD, commonly called simply the CD.

To facilitate comparisons of the CD of proteins or nucleic acids of very different molecular masses, it is nearly universal practice to normalize the CD by dividing the molar CD by the number of amino acid or nucleotide residues, yielding the mean residue CD,

$$\Delta\epsilon = \Delta\epsilon_M / n_r = \Delta A / c_r \ell \qquad (2)$$

where n_r is the number of residues and c_r is the molar concentration of residues. Near-UV CD spectra of proteins are reported as either molar CD or mean residue CD, and visible CD spectra are usually reported as molar CD of the protein or the molar CD per visible chromophore, for example, per heme in vertebrate hemoglobins. The reader must always carefully check the basis for reporting CD spectra in the literature.

Although nearly all CD instrumentation measures DA and hence yields De most directly, many instruments are calibrated in units of ellipticity, an angular unit based on an earlier method for measuring CD. The molar ellipticity is defined as

$$[\theta]_{\mathrm{M}} = 100\theta/c\ell \tag{3}$$

where q is the measured ellipticity in degrees and *c* and ℓ have the same meaning as before. Molar ellipticity is directly proportional to molar CD:

$$[\theta]_{\mathrm{M}} = 3298\Delta\epsilon_{\mathrm{M}} \approx 3300\Delta\epsilon_{\mathrm{M}} \tag{4}$$

Mean residue ellipticity [q] is defined by analogy to mean residue CD and is commonly used for reporting protein CD data in the far UV and for CD of DNA and RNA.

1.2. Instrumentation (1)

Measurement of CD requires high sensitivity because the difference between e_l and e_r is small in comparison with their average value $e = (e_l + e_r)/2$, which corresponds to the molar absorbance coefficient measured with unpolarized light. Typically, De/e is of the order of 10^{-3} to 10^{-4}. To achieve adequate signal-to-noise ratios, CD spectrophotometers use a modulation technique. The light incident on a sample is switched between left- and right-circular polarization at a specific frequency. The difference in the sample response to the two forms of circularly polarized light is detected directly by selecting the part of the response that has a frequency component matching that of the modulation of the incident light.

Figure 1 shows a highly schematic representation of a CD spectrophotometer. Light from the source L is dispersed in the monochromator MC, and then a narrow band of wavelengths passes through the linear polarizer lP. The polarizer splits the unpolarized monochromatic beam into two linearly polarized beams, one polarized in the *x* direction, the other in the *y* direction (*z* is the direction of propagation). Then one of the two linearly polarized beams passes through the photoelastic modulator (PEM), which consists of a plate made of a transparent, optically isotropic material bonded to a piezoelectric quartz crystal. When an alternating electric field is applied, the light emerging from the PEM switches from lcpl to rcpl and back with the frequency of the applied electric field, typically about 50 kHz. If the sample S exhibits CD, the amount of light absorbed varies periodically with the polarization of the incident light, and so the intensity of light that reaches the photomultiplier PM exhibits sinusoidal intensity variations at the frequency of the field applied to the PEM. Thus, the photomultiplier output consists of a signal with a small alternating current (ac) component superimposed on a direct current (dc) component. The ac component is filtered out and amplified. The ratio of the ac to the dc component is directly proportional to the circular dichroism of the sample, and this quantity is recorded as a function of wavelength to provide a CD spectrum.

Figure 1. A block diagram of a CD spectrophotometer. L is the light source, MC the monochromator, P the polarizer, PEM the photoelasic modulator, S the sample, and PM the photomultiplier.

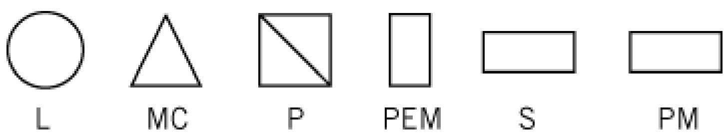

CD is most commonly measured in the visible and ultraviolet regions of the spectrum. Commercially available instruments are used in the 180 to 700-nm region. Some commercial instruments permit measurements to 170 nm, at the edge of the vacuum UV, or to 1000 nm, in the near infrared (IR). Xenon arc lamps, quartz optics, and photomultiplier tubes are used for the light source, the dispersing and polarizing elements, and the detectors, respectively.

CD is also observed in IR absorption bands, associated with vibrational transitions (see Vibrational Spectroscopy). This type of CD is called vibrational circular dichroism (VCD) (2). Some VCD instruments use the same type of layout as that shown in Fig. 1, although the light sources, dispersing and polarizing optics, and detectors are necessarily different. In addition, VCD instruments have been constructed that utilize the Fourier transform principle.

In recent years, CD has been widely used to measure the kinetics (3) of conformational changes in proteins and nucleic acids, especially in investigating protein folding in vitro and unfolding. Reactions on the timescale of a minute or longer are readily measured by using manual mixing and conventional CD instrumentation. A conventional CD instrument coupled to a stopped-flow mixing device permits measurements of reactions with halftimes down to a few milliseconds. Still faster reactions, triggered by temperature or pressure jumps, or by laser or electron pulses, require specialized CD instrumentation (4) that does not utilize the modulation technique. Such instruments have been constructed for nanosecond and picosecond timescales.

1.3. Theoretical Background (5)

The connection between theory and experiment in CD spectroscopy is provided by a quantity called the rotational strength, *R*. Experimentally, the rotational strength is proportional to the area under a CD band, that is, the integral

$$R \propto \int (\Delta\epsilon/\lambda) d\lambda \approx (\lambda_{\max})^{-1} \int \Delta\epsilon d\lambda \qquad (5)$$

The integral is taken over a CD band attributable to a single electronic or vibrational transition. CD bands are generally rather sharp, so it is a satisfactory approximation to replace the l^{-1} factor in the integrand of Eq. 5 by $\lambda_{\max}^{-1}$, where l_{max} is the wavelength at which the CD band has maximal intensity.

The rotational strength is related to molecular properties by the equation

$$R = \mathrm{Im}\{\mu_{0a} \cdot \mathbf{m}_{a0}\}, \qquad (6)$$

where Im indicates the imaginary part of a complex quantity. The first factor in the curly brackets is the electric dipole transition moment for the transition from the ground state 0 to the excited state a. The second factor is the magnetic dipole transition moment of the transition. Qualitatively, $\mathbf{m}_{0a}$ can be interpreted as the linear displacement of charge associated with the transition, and $\mathbf{m}_{a0}$ as the circular displacement of charge. Therefore a non zero rotational strength requires that the transition have both a linear and a circular displacement of charge and that the axis of the circulation not be perpendicular to the linear displacement. This corresponds to a helical motion of electronic charge, where the sense of the helix is determined by the relative orientation of $\mathbf{m}_{0a}$ and $\mathbf{m}_{a0}$ and this determines the sign of the CD band.

1.4. Related Phenomena

Phenomena that depend upon differences in the interaction of a sample with left- and right-circularly polarized light are called chiroptical phenomena. CD is the most widely used chiroptical phenomenon in molecular biology, but others are important for historical reasons or have specialized applications. The first chiroptical phenomenon discovered was optical rotation (OR), the rotation of the plane of polarization of plane-polarized light as it passes through a chiral medium. The angle through which the plane is rotated, commonly measured at 589 nm (the Na D line), is still widely used in organic chemistry to characterize chiral molecules. OR was also used in protein chemistry, but was supplanted in the 1950s by optical rotatory dispersion (6) (ORD), the wavelength dependence of OR, and in the 1960s by CD. The specific rotation a of a sample is defined as

$$[\alpha] = 10\alpha/c'\ell \tag{7}$$

where a is the angle through which the plane of polarization is rotated by the sample, ℓ is defined as in Eq. (1), and c' is the concentration of the chiral substance in g/mL. Molar rotation and mean residue rotation are defined by analogy to the corresponding CD parameters. It should be noted that refraction is a scattering phenomenon and occurs at all wavelengths, not just in absorbance bands. For this reason, OR and ORD can be measured at visible wavelengths for substances that absorb only in the ultraviolet.

2. Proteins

2.1. General Aspects

In the far UV, the peptide groups of the backbone generally dominate the CD spectrum. The peptide group has two electronic transitions in the normally accessible far UV. These are the np^* transition near 220 nm and the pp^* transition near 190 nm in secondary amides and 200 nm in tertiary amides (X-Pro peptide groups). The np^* transition is weak in absorbance, but it gives rise to strong CD bands. The pp^* transition is associated with strong absorbance and CD. Because of the strong electric dipole transition moment, pp^* transitions in neighboring peptide groups interact with each other, giving rise to two or more absorbance and CD bands. This phenomenon, called exciton splitting , is most clearly seen in the a-helix CD spectrum, described later.

The aromatic side chains of **Phe, Tyr,** and **Trp** residues have strong absorbance bands in the far UV that contribute to the CD spectrum (7). In most cases, their contribution is small compared to those of the much more numerous peptide groups. For some proteins, however, aromatic CD bands are clearly discernible.

In the near UV, the CD spectrum of proteins is dominated by the aromatic and disulfide transitions. The near-UV CD bands of the aromatic side chains are generally relatively sharp and have a characteristic fine structure due to vibrational effects. In proteins with a small number of aromatic side chains, the near-UV CD bands can frequently be assigned to one of the three types of aromatic side chains and in some cases, through site-directed mutagenesis, to specific residues in the sequence. The CD bands due to the disulfide bond are generally distinguishable from aromatic CD bands by their much greater width.

For proteins containing only the normal amino acids, there are no CD bands at wavelengths above 300 nm. Many **prosthetic groups**, **coenzymes**, transition-metal ions, and other ligands have absorbance bands in this wavelength region, and these are associated with CD bands in complexes with proteins.

2.2. Secondary Structure Analysis

The various types of secondary structure (see Secondary Structure, Protein) in proteins have characteristic CD spectra, as established by studies of model oligo- and polypeptides. Figure 2 shows CD spectra of a-helix, b-sheet, unordered polypeptides, and b-turns. The a-helix has the most distinctive and strongest CD spectrum with two negative bands of comparable magnitude at ca. 222 and 208 nm and a stronger positive band near 190 nm. The 222 nm band results from the np^* transition of the amide group, whereas the 208 and 190 nm bands both arise from the amide pp^* transition. The latter two bands are from exciton splitting of the pp^* transitions in the amide groups that are held in a well-defined helical geometry. Interactions between the transition dipole moments in a very long helical array give rise to three absorbance bands, one at 208 nm polarized parallel to the helix axis, and two bands at 190 nm, polarized in the two independent directions perpendicular to the helix axis. For a right-handed a-helix, the parallel band is associated with the negative CD band at 208 nm, and the perpendicular bands with the positive CD band at 190 nm. The CD of the a-helix is largely, but not completely, independent of the solvent and of the sequence of amino acids. Aromatic residues (Phe, Tyr, Trp) modify the a-helix CD spectrum, especially if they constitute a sizeable fraction of the residues. In homopolymers of aromatic amino acids, the a-helix CD spectrum is modified beyond recognition.

Figure 2. (**a**) CD spectra of model polypeptides in three conformations: a-helix (——), poly(Glu), pH 4.5 (33); b-sheet (– – – –), poly(Lys-Leu), 0.5 M NaF, pH 7.4 (34); and unordered (· · · · · ·), poly(Lys-Leu) in salt-free aqueous solution (34). (**b**) CD spectra of model peptides in two b-turn conformations: Type I b-turn (– – – –), cyclo(L-Ala-L-Ala-Aca), where Aca is e-aminocaproyl; Type II b-turn (——), cyclo(L-Ala-D-Ala-Aca). Spectra acquired in water at 22°C (35).

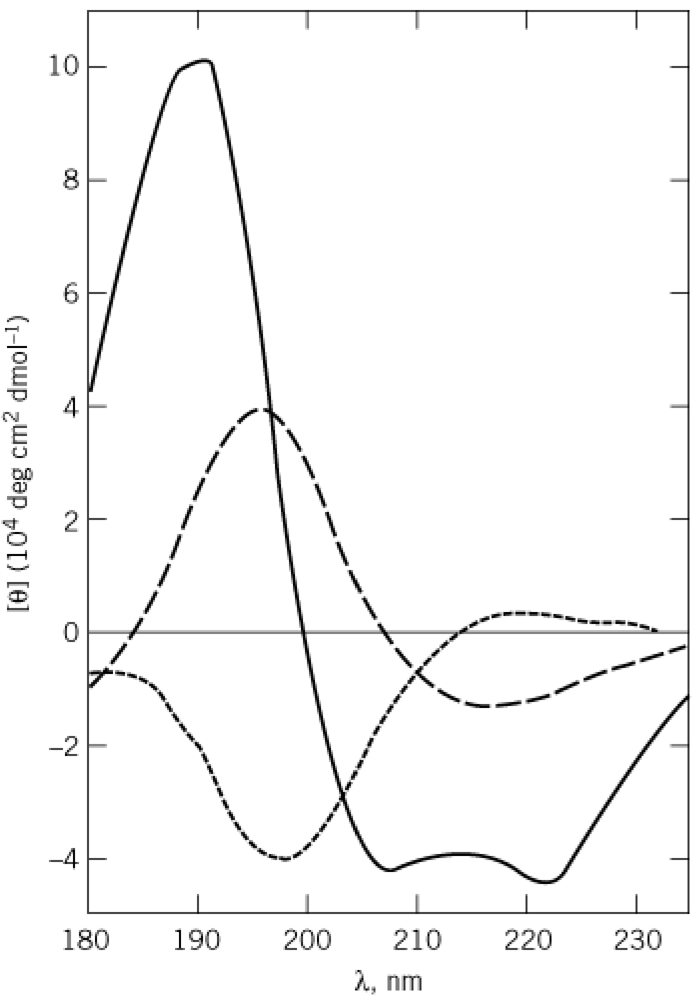

10
8
6
4
2
0
−2
−4
[θ] (10^4 deg cm^2 dmol^−1)
180
190
200
210
220
230
λ, nm

(a)

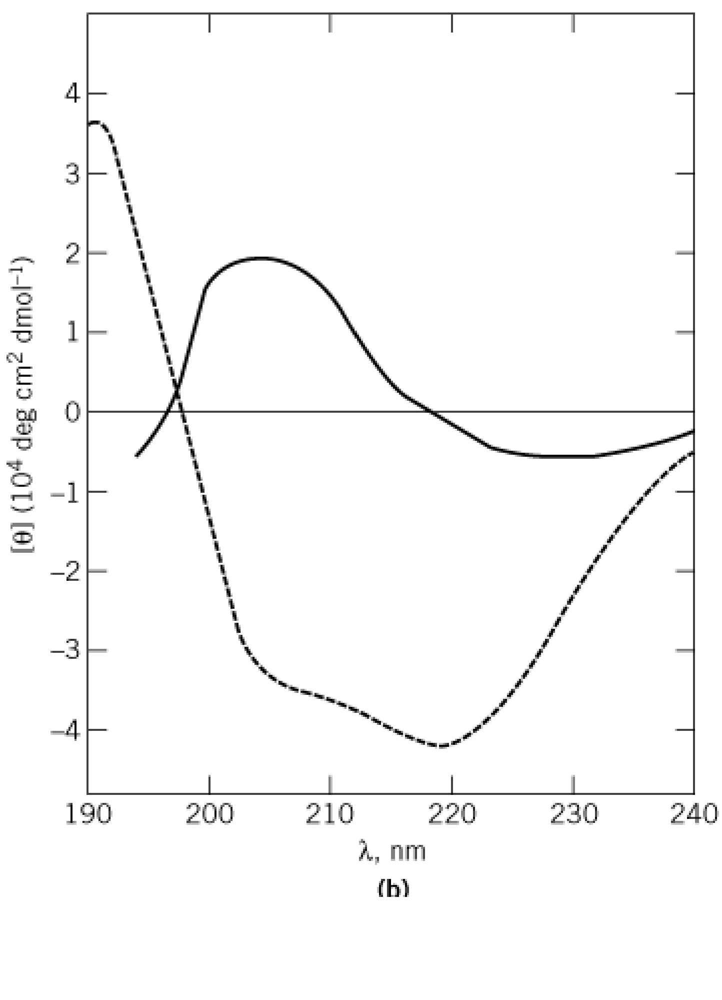

4
3
2
1
0
−1
−2
−3
−4
[θ] (10^4 deg cm^2 dmol^−1)
190
200
210
220
230
240
λ, nm

(b)

The CD of b-sheets is more variable than that of a-helices. A negative band near 217 nm and a positive band in the 195 to 200-nm region are characteristic of b-sheets (Fig. 2). Theory (8) predicts that the absolute value of the ratio of the ellipticity at the positive maximum near 197 nm to that at the negative maximum near 217 nm increases with increasing twisting of the sheet, and is larger for parallel than for antiparallel twisted sheets. The relative amplitude of the 217 nm and 197 nm bands varies considerably among model systems, ranging from ~1.7 for the antiparallel b-sheet formed in poly(Lys) by heating to 52°C at pH 11.1 to 8.3 for the parallel b-sheet of Boc(Val)$_7$OMe in trifluoroethanol.

Several types of b-turn can be distinguished, but only two fundamental types are common in proteins: the type I turn (and its variant, type III), which can accommodate any L-amino acid at either of the positions in the turn, and the type II turn, which usually has a Gly at the second residue of the turn. The CD characteristics of b-turns vary in accordance with the range of conformations. However, studies of cyclic peptides with well-defined b-turns indicate that type I turns have a-helix-like CD spectra, with negative maxima at ~220 and 210 nm and a positive band near 190 nm, whereas type II turns have a CD spectrum like that of a b-sheet, but with the maxima shifted 5 to 10 nm to longer wavelengths, that is, the negative band in the 220 to 225-nm region, and the positive band between 200 and 210 nm (Fig. 2).

All models for unordered random coil polypeptides have a strong negative band near 200 nm (Fig. 2), but some have a long-wavelength positive band and others a negative shoulder at longer wavelengths. The resemblance of the CD spectra of charged poly(Lys) and poly(Glu) to that of poly (Pro) II led to the proposal that these polypeptides are not truly unordered but contain short segments of the poly(Pro)II helix. The current view (9) of unordered polypeptides is that those peptides with a negative shoulder in the 210- to 220-nm region have amino acid residues predominantly in the a-helix and b-sheet regions of conformational space (see Ramachandran Plot) and those with a positive long-wavelength band have a substantial fraction of residues in the poly(Pro)II conformation. The latter systems undergo a noncooperative transition to the former as the temperature increases.

2.2.1. Protein Secondary Structure

Early applications of OR and ORD to the analysis of helix content in proteins have been reviewed (10). Initially, protein CD data were analyzed by fitting the CD spectra of the protein to a linear combination of data for model polypeptides, such as those shown in Fig. 2. However, such methods generally gave poor results because the CD spectra of globular proteins are too complex to be adequately represented by a simple linear combination of homopolymer spectra. Many methods for analyzing protein CD data to obtain secondary structure have been proposed (11, 12). Two features are essential for satisfactory results. First, a basis set of proteins of known secondary structure is needed to calibrate the method by providing information on the CD contributions of the various types of secondary structure existing in real protein structures. Second, it is necessary to allow flexibility in weighting the proteins in this basis set when analyzing each protein. Several methods incorporating these features provide useful estimates of the fraction of a-helix, b-sheet, b-turn, and unordered conformations (11-14). VCD and IR absorption spectra (See Vibrational Spectroscopy) in the amide I region also provide estimates of the secondary structure content of globular proteins by using analytical methods similar to those used for electronic CD (15). Combinations of electronic CD, VCD and IR absorption can also be used.

The methods used for analyzing the secondary structure of proteins should be applied with caution to peptides, because globular proteins are used to calibrate these methods. The CD measured at 220 or 222 nm has frequently been used to determine the helix content of peptides. The difference in CD between the 217 nm negative maximum and the positive maximum near 195 nm, characteristic of b-sheets, has been utilized to quantify the b-strand conformation of peptides (16).

2.2.2. Tertiary Structure of Proteins

Far-UV CD spectra of proteins have been used to assign proteins to the broad classes of all-a, all-b, a + b, and a/b by cluster analysis (17). Aromatic side-chain bands (7) in both the near and far UV have been used as markers to identify tertiary structures. The **T-state** (deoxy) conformation of hemoglobins has a strong negative CD band at 287 nm, whereas the **R-state** (liganded) conformation has weak negative or positive CD at this wavelength. The magnitude of the negative CD band at 250 to 255 nm correlates with the T → R transition in insulin. Tertiary structural changes in the **chymotrypsinogen** → chymotrypsin conversion are associated with a reorientation of the Trp 175 - Trp 215 pair, leading to a large change in the 225 nm Trp CD band.

2.2.3. Protein Folding

One of the major aims in equilibrium studies of protein folding (see Protein Folding In Vitro) is detecting intermediates. If equilibrium intermediates are not detectable, the folding/unfolding process is said to be two-state because only the fully folded and fully unfolded forms are present at significant levels. If only these forms are present, the extent of unfolding is the same regardless of the physical property used to monitor it. CD is especially useful in this regard because the far-UV and near-UV CD measure primarily the secondary and tertiary structures, respectively. If the extent of unfolding measured by these two probes is identical within experimental error, the process is likely to be two-state. On the other hand, lack of coincidence of the unfolding curves measured in these two spectral regions is evidence that one or more intermediates exist.

A type of folding/unfolding intermediate observed in a number of proteins is called the molten globule. This intermediate is nearly as compact as the native protein and has a secondary structure content comparable to that of the native protein. However, the side chains are quite mobile and are not locked into a well-defined tertiary structure. CD is one of the most useful techniques for identifying the molten globule form of proteins. The CD spectrum of a molten globule is similar to that of the native protein in the far UV and reflects a substantial amount of a-helix and/or b-sheet but has only weak features in the near UV because the aromatic side chains do not have well-defined positions and conformations.

Another aspect of equilibrium protein folding studies in which CD has played a major role is investigating the effect of sequence on the stability of intact proteins and peptide segments. Here, the far UV is used to follow the **denaturation** profiles of the wild-type protein and of a series of mutant forms in which specific residues have been altered. From reversible thermal denaturation studies, changes in the free energy of unfolding, DDG_{unf}, can be obtained that measure the effect of the amino acid substitution upon the net stability of the protein and thus shed light on the effects of steric bulk, **hydrophobic** character, and charge effects. There have also been numerous CD studies of model peptides that adopt the helix conformation to examine systematically the effects of amino acid substitutions on a-helix stability (18). Similar studies have recently been reported for b-sheet-forming peptides and protein fragments (19).

Kinetic studies of protein folding by CD have been limited to stopped-flow methods and thus to the millisecond timescale. During the so-called dead time of the experiment, many proteins studied thus far (20) acquire a substantial fraction of a-helix and b-sheet, as evidenced by $[q]_{220}$ values that are generally closer to those of the native form than to the fully unfolded form. By contrast, the CD in the near-UV detected immediately after the dead time is essentially that of the unfolded form. These results generally have been interpreted as resulting from a so-called burst phase in which a molten globule-like intermediate is formed on the timescale of milliseconds or less. Then subsequent slower processes lead to additional formation or remodeling of the secondary structure and formation of the tertiary structure.

2.2.4. Membrane Proteins

The study of membrane proteins in their native environment poses problems for CD. Two kinds of potential artifacts must be avoided. Strongly scattering suspensions of membrane fragments exhibit preferential scattering of rcpl or lcpl, which manifests itself as an apparent CD signal that distorts the true CD of the membrane protein. The particulate character of membrane fragments also distort the CD signals because of the CD analog of Duysens' flattening (21), which occurs in samples with a highly inhomogeneous distribution of absorbing chromophores that is associated with clustering of the chromophores. Methods have been devised that correct for or avoid each of these difficulties, but in the flattening effect, they require that the membrane protein be transferred from the native membrane to small unilamellar vesicles that have, on average, no more than one protein molecule per vesicle. Alternatively, these artifacts are circumvented by solubilizing the membrane protein in a nonionic detergent. This poses some risk of inducing conformational changes in the protein, although nonionic detergents are usually relatively benign.

2.2.5. Protein–Ligand Interactions

CD is widely used to characterize ligand binding to proteins and yield binding constants, stoichiometry, and information about conformational changes in the ligand and/or protein, in favorable cases. If the ligand absorbs at wavelengths above 300 nm, it is convenient to monitor the corresponding CD bands. This is especially so if, as in many cases, the ligand is achiral or a rapidly interconverting racemate. In such cases, the free ligand contributes no background CD, and only the bound ligand contributes to the CD signal. This is effectively so even in chiral ligands, such as NADH, FMN, FAD, in which the chromophore is conformationally mobile in the free form and therefore has only a weak CD signal. Ligand binding is also studied at shorter wavelengths, where protein CD bands are normally studied, either as induced ligand CD bands or as a perturbation of the aromatic and peptide CD bands. These perturbations arise either through direct interactions with the ligand or through changes in the tertiary or secondary structure induced upon ligand binding.

The use of CD to determine **dissociation constants** (K_d) is straightforward, but there are limitations to the range of dissociation constants that can be determined accurately. To provide an accurate analysis, the concentration of the species being monitored must be comparable to the K_d. Given the typical magnitudes of CD, this requires $K_d >$ ca. 1 µM for successful measurements by conventional CD. Fluorescence-detected CD (22) may extend this range to ca. 10 nM.

If $K_d <$ ca. 1µnM, CD cannot be used to measure reversible dissociation, but the protein–ligand complex dissociates negligibly at µM concentrations and above. Studies of such complexes are very fruitful because the ligand serves as a tightly but noncovalently bound spectroscopic probe, capable of reporting conformational changes in the protein. Heme proteins (23) and flavoproteins are important examples. The CD signals from such proteins are highly sensitive to oxidation state, spin state (in heme proteins), and to substrate, inhibitor, and allosteric effector binding.

3. CD of Nucleic Acids

3.1. General Aspects (24)

The **purine** and **pyrimidine** bases of **DNA** and **RNA** are largely responsible for the CD spectra of nucleic acids in the wavelength range normally studied (180 to 300 nm). The sugar and phosphate groups do not absorb significantly above 200 and 180 nm, respectively. From the standpoint of CD, their main function is maintaining the relative geometries of the bases. Each base has a characteristic set of pp* transitions in the 180- to 300-nm region. The corresponding absorbance and CD bands are relatively broad. All five natural bases have one or two moderately intense pp* bands near 260 nm and several more intense bands in the 180- to 200-nm region. In addition, each base is expected to have several np* transitions in the 180- to 300-nm region, but these bands absorb weakly. Though potentially strong in CD, few np* bands have been identified, and the CD spectra of nucleosides, nucleotides, and polynucleotides are dominated by pp* contributions.

The CD spectra of nucleosides and nucleotides are relatively weak compared to those of polynucleotides. In the monomer, only base–sugar and base–phosphate interactions contribute, and the CD is averaged over a broad range of conformations. By contrast, oligo- and polynucleotide CD spectra are dominated by base–base interactions, and the range of conformations is usually narrower.

The CD spectra of oligonucleotides differ markedly from the sum of the constituent monomer spectra. This is illustrated by the spectra of ApA and pA (Fig. 3). The large difference is attributed to coupling of the pp* transitions in the two bases, another example of exciton coupling. This led to a model in which the adenine rings are stacked in a right-handed helix, like two successive bases in A-RNA or A-DNA. In fact, the CD of ApA closely resembles that of poly(A), except that it is only about half as large. This model is supported by theoretical calculations of the CD and more recently by NMR. Interestingly, although the CD spectra of dA, dAp, and dpA are similar to one another and to those of the riboA monomers, the CD spectrum of d(ApA) is quite different from that of ApA and reflect a difference in the geometry of base stacking.

Figure 3. Near-UV CD spectra of the dinucleoside monophosphate ApA (——)and the mononucleotide pA (– – – –). Spectra obtained in 0.1 M Tris, 0.1 M NaCl, pH 7.4 at 5.5°C for ApA and at 20°C for pA (36).

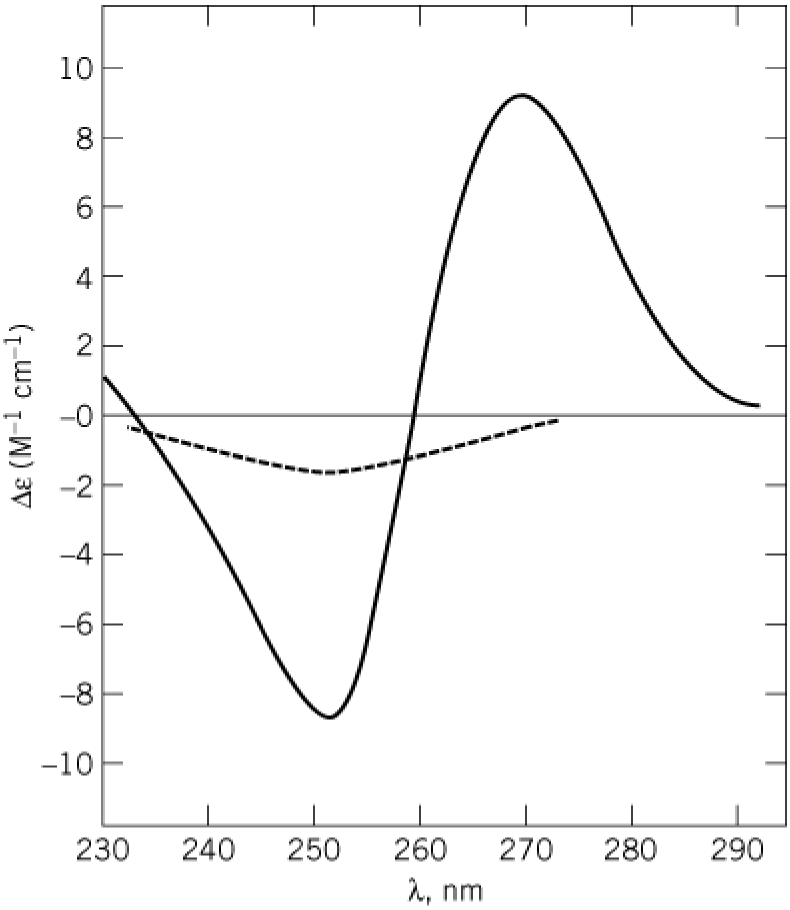

The CD of nucleotide trimers can be described in most cases by the equation

$$[\theta]_{\mathrm{ApBpc}} = (2[\theta]_{\mathrm{ApB}} + 2[\theta]_{\mathrm{BpC}} - [\theta]_{\mathrm{Bp}})/3 \tag{8}$$

This model assumes that (1) nearest neighbor bases stack similarly in dimers and in higher oligomers and (2) only nearest neighbor interactions are significant for CD. The model works reasonably well for higher oligomers and for trimers and has been extended to double-stranded oligonucleotides of DNA and RNA. The same model has been used to derive nearest neighbor frequencies for DNA and

RNA from base-composition and CD data.

3.1.1. Secondary Structure

The CD of a DNA is highly diagnostic of its secondary structure. The B-DNA conformation normally found in aqueous solution has a positive CD band near 275 nm and a negative band of similar magnitude near 245 nm, as shown in Fig. 4. A pair of closely spaced bands of opposite sign is called a couplet, and it is characterized by the sign of its long-wavelength component as a positive or negative couplet. A couplet in which the two lobes are of very similar amplitude is called a conservative couplet. In the far UV, the B-DNA spectrum has a positive couplet with peaks near 190 and 175 nm that is nearly an order of magnitude more intense than the near-UV bands.

Figure 4. The CD spectra of *E. coli* DNA in the B form at low ionic strength (10 mM sodium phosphate buffer, – – – ––), the A form (0.67 mM sodium phosphate buffer, 80% trifluoroethanol, – · –), and the B form at high ionic strengths (6 M NH_4F, ——) (37). (Reprinted with permission from Ref. 37, © 1985, Wiley-Liss.)

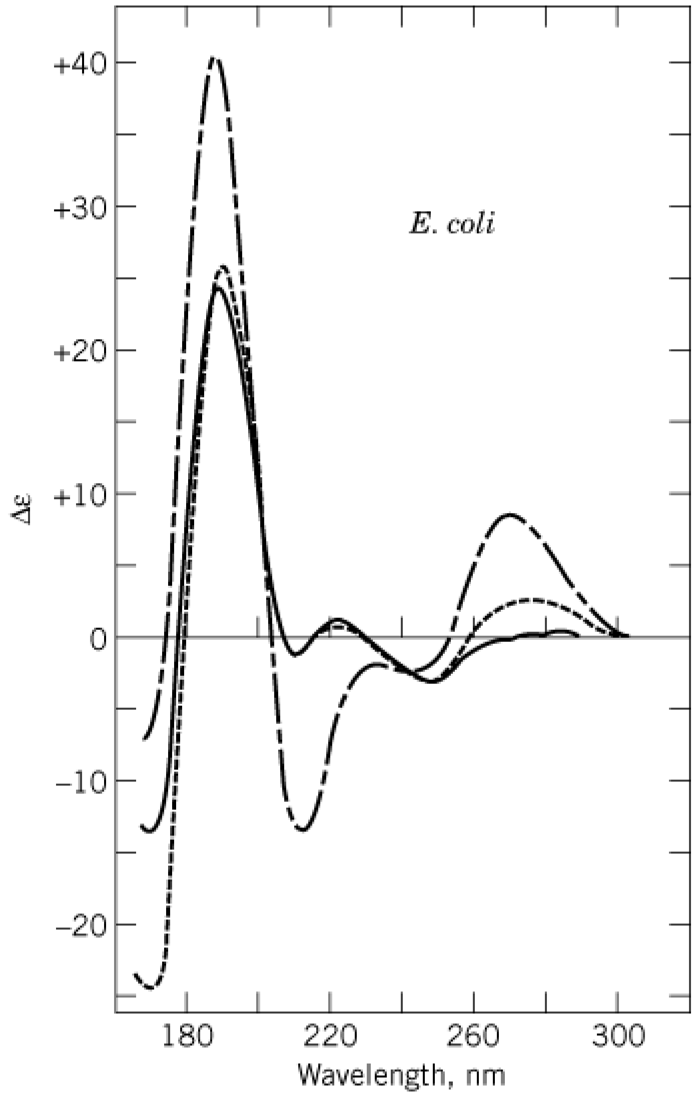

The A-form of DNA (see A-DNA) is favored by low water activity and is induced by adding alcohols. In the near UV, the B → A transition is marked by a large increase in the positive band and a decrease in the magnitude of the 245 nm band. Therefore, the A-DNA CD spectrum is distinctly nonconservative. A strong negative band near 210 nm is also a characteristic feature of the A-DNA spectrum in contrast to the weak negative band in the B-DNA spectrum. Below 200 nm, a positive couplet is observed as in B-DNA, but the couplet is asymmetrical.

The B- and A-forms of DNA are both right-handed double helices. As expected, the left-handed Z form of DNA (see Z-DNA) has a very different CD spectrum, as shown for Z-form poly[d(G-C)] in Fig. 5. The near-UV bands for the Z-form are opposite in sign to those for the B-form and are shifted to longer wavelengths. The strong bands in the far UV are also reversed in sign and are red-shifted relative to those for the B-form. (Note that the CD spectrum of poly[d(G-C)] in the B-form differs from that of natural or "random-sequence" DNA. This is generally true for DNAs with simple di- and trinucleotide repeating sequences, in which specific features of geometry and electronic interactions are not averaged.) The reversed signs of the near-UV CD in the Z-form of poly[d(G-C)] were the first indications of a dramatically different conformation for this copolymer at high salt concentrations, but subsequent studies have shown that the signs of the near-UV CD bands do not reliably indicate helix sense for the double helix. However, the signs of the far-UV CD bands correlate with the helix sense in all known cases: a positive band between 180 and 192 nm for right-handed A-and B-forms and a negative band between 185 and 200 nm for the left-handed Z-form (25). Near-UV CD is widely used to monitor B → Z transitions in DNA.

Figure 5. CD spectra of poly[d(GC)] in three conformations. B form (10 mM sodium phosphate buffer, ...); A form (0.67 M sodium phosphate buffer, 80% trifluoroethanol, — — ——); Z form (10 mM sodium phosphate buffer, 2 M $NaClO_4$, ——) (38). (Reprinted with permission from Ref. 38, © 1985, IRL Press.)

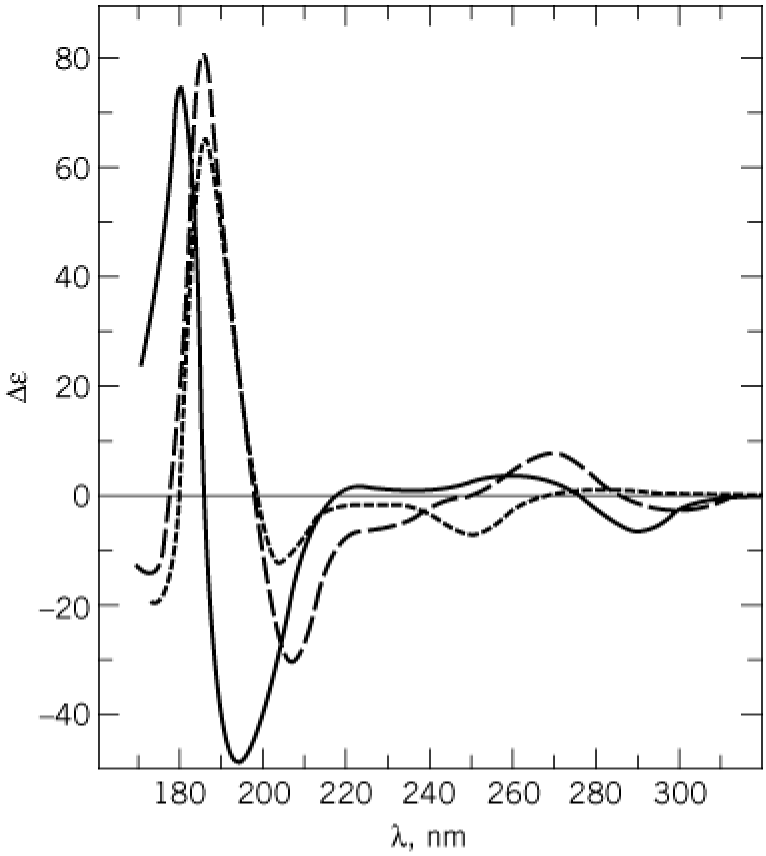

tive to ionic strength. At ionic strengths comparable to physiological, the conservative CD pattern shown in Fig. 4 is observed. As ionic strength increases, the 275 nm band is selectively diminished, and at 6 M NH_4F, it nearly vanishes (Fig. 4). By contrast, the 245 nm band undergoes little change. Studies with closed circular DNA show that changes in ionic strength from ca. 0.1 M to 6 M change the number of base pairs per turn from ca. 10.4 to 10.2. The DNA in chromatin has a CD spectrum similar to that in 6 M NH_4F, indicating that it is a somewhat underwound form of B-DNA.

Double-stranded RNA is nearly always found in the A-form, and never in the B-form. Z-form RNA has been observed for poly[r(G-C)], but the conditions required to drive it into this form are more stringent than for the deoxy copolymer. A-form RNA has a CD spectrum similar to that of A-DNA, except that a weak negative band is commonly observed near 290 nm on the long-wavelength side of the 260 nm band. As with DNAs, the far-UV CD is diagnostic of the helix sense in double-stranded RNA, and the correlation between the sign of the far-UV couplet and the helix sense is the same.

In both RNA and DNA, the single-stranded forms have CD spectra that qualitatively resemble the double-stranded forms because base stacking has a much greater influence on the CD than does base pairing. Stand separation eliminates the latter but does not affect stacking significantly. Thermal denaturation of DNA leads to relatively small CD changes in the near UV but substantially larger far-UV CD changes. CD is also useful in characterizing **triplex** (26) forms of DNA and RNA.

3.1.2. Tertiary Structure

Supercoiling of DNA leads to readily detectable changes in the CD spectrum (27). The positive 275-nm band of B-DNA becomes more positive for negative superhelical supercoiling and conversely for decreased negative superhelical densities. For superhelical densities in the normal range, the CD changes are directly proportional to the superhelical density.

Although there is no evidence that the CD of RNA is directly sensitive to tertiary structure, it is sensitive to sequence and base pairing. Thus, CD has been used to test alternative models of RNA tertiary structure that differ in secondary structure distribution (28).

3.1.3. Ligand Binding to Nucleic Acids

Complexes of DNA and RNA with dyes, antibiotics, and other small ligands (See Intercalation) give rise to induced CD in the ligand absorption bands and to changes in the nucleic acid CD bands (29). These changes permit the determination of dissociation constants and stoichiometries for complexes of such small ligands with DNA and RNA. In some cases, additional structural information about the ligand or nucleic acid conformation is obtained.

CD is widely used to study DNA-protein and RNA-protein interactions (30). A very useful feature of CD in such studies is that the nucleic acid generally dominates the CD spectrum in the 260-nm region, whereas the protein dominates in the 200- to 240-nm region. Because each of these regions responds to the conformation of the dominant component, CD is of great value in monitoring conformational changes upon complex formation. Nonspecific protein–nucleic acid complexes often have dissociation constants in the micromolar range where CD is well suited for measuring K_d values. Specific protein–nucleic acid complexes usually have K_d s that are smaller by several orders of magnitude at physiological ionic strengths. In some cases, the K_d is shifted into the measurable range by increasing the ionic strength. Even if the binding is too tight to permit measuring the K_d by CD, conformational changes in the protein and/or nucleic acid are detected and characterized by CD. CD is also well suited for measuring the kinetics of protein–nucleic acid complex formation.

4. Carbohydrates

Circular dichroism has important applications in studying carbohydrates (31), although these are more limited than for proteins and nucleic acids. Of the chromophores common in carbohydrates, only the amide (N-acetyl sugars) and carboxyl groups (uronic acids) have CD bands above

200 nm. The hydroxyl, ether, acetal, and ketal chromophores that are most typical have their first longest wavelength CD bands near the short-wavelength limit of conventional CD instruments, near 180 nm. Higher energy transitions are studied only with vacuum UV instruments, but they are usually obscured by solvent absorption, so studies are limited to thin solid films. For these reasons, optical rotation and ORD measurements in the near UV and visible regions continue to play an important role in studying carbohydrates.

Monomeric sugars have been investigated extensively, and sector rules relating the signs of CD bands near 170 nm to the conformation of the sugar have been derived. A useful model relating the optical rotation at the Na D line to the conformation of a sugar has been developed. This model is useful in testing features of the conformational energy surface in disaccharides. In the study of polysaccharides, CD and optical rotation have been used to characterize order-disorder, single- to multistranded, and sol to gel transitions (32).

Bibliography

1. W. C. Johnson Jr. (1996) In *Circular Dichroism and the Conformational Analysis of Biomolecules* (G. D. Fasman, ed.), Plenum Press, New York, pp. 635–652.
2. T. A. Keiderling (1996) In *Circular Dichroism and the Conformational Analysis of Biomolecules* (G. D. Fasman, ed.), Plenum Press, New York, pp. 555–598.
3. K. Kuwajima (1996), in *Circular Dichroism and the Conformational Analysis of Biomolecules* (G. D. Fasman, ed.), Plenum Press, New York, pp. 159–182.
4. J. W. Lewis, R. A. Goldbeck, D. S. Kliger, X. Xie, R. C. Dunn, and J. D. Simon (1992) J. Phys. Chem. **96**, 5243–5254.
5. R. W. Woody (1996) In *Circular Dichroism and the Conformational Analysis of Biomolecules* (G. D. Fasman, ed.), Plenum Press, New York, pp. 25–67.
6. K. Imahori and N. A. Nicola (1973) In *Physical Principles and Techniques of Protein Chemistry* (S. J. Leach, ed.), Academic Press, New York, Part C, pp. 357–444.
7. R. W. Woody and A. K. Dunker (1996) In *Circular Dichroism and the Conformational Analysis of Biomolecules* (G. D. Fasman, ed.), Plenum Press, New York, pp. 109–157.
8. M. C. Manning, M. Illangasekare, and R. W. Woody (1988) Biophys. Chem. **31**, 77–86.
9. R. W. Woody (1992) Adv. Biophys. Chem. **2**, 37–79.
10. P. Urnes and P. Doty (1961) Adv. Protein Chem. **16**, 401–544.
11. W. C. Johnson Jr. (1990) Proteins: Struct. Funct. Genet. **7**, 205–214.
12. N. Sreerama and R. W. Woody (1994) J. Mol. Biol. **242**, 497–507.
13. S. Yu. Venyaminov and J. T. Yang (1996) In *Circular Dichroism and the Conformational Analysis of Biomolecules* (G. D. Fasman, ed.), Plenum Press, New York, pp. 69–107.
14. N. J. Greenfield (1996) Anal. Biochem. **235**, 1–10.
15. V. Baumruk, P. Pancoska, and T. A. Keiderling (1996) J. Mol. Biol. **259**, 744–791.
16. L. Zhong and W. C. Johnson Jr. (1992) Proc. Natl. Acad. Sci. USA **89**, 4462–4465.
17. S. Yu. Venyaminov and K. S. Vassilenko (1994) Anal. Biochem. **222**, 176–184.
18. J. M. Scholz and R. L. Baldwin (1992) Ann. Rev. Biophys. Biomol. Struct. **21**, 95–118.
19. D. L. Minor Jr. and P. S. Kim (1994) Nature **367**, 660–663.
20. H. Roder and G. A. Elöve (1994) In *Mechanisms of Protein Folding* (R. H. Pain, ed.), IRL Press, Oxford, pp. 26–54.
21. L. M. N. Duysens (1956) Biochim. Biophys. Acta **19**, 1–12.
22. D. H. Turner (1978) Meth. Enzymol. **49**, 199–214.
23. Y. P. Myer and A. J. Pande (1978) In *The Porphyrins* (D. Dolphin, ed.), Academic Press, New York, Vol. **3**, pp. 271–322.

24. W. C. Johnson Jr. (1996) In *Circular Dichroism and the Conformational Analysis of Biomolecules* (G. D. Fasman, ed.), Plenum Press, New York, pp. 433–468.
25. J. H. Riazance, W. C. Johnson Jr., L. P. McIntosh, and T. M. Jovin (1985) Nucleic Acids Res. **15**, 7627–7636.
26. D. M. Gray, S.-H. Hung, and K. H. Johnson (1995) Meth. Enzymol. **246**, 19–34.
27. S. Brahms, S. Nakasu, A. Kikuchi, and J. G. Brahms (1989) Eur. J. Biochem. **184**, 297–303.
28. K. H. Johnson and D. M. Gray (1991) Biopolymers **31**, 385–395.
29. C. Zimmer and G. Luck (1992) Adv. DNA Sequence-Specific Agents **1**, 51–88.
30. D. M. Gray (1996) In *Circular Dichroism and the Conformational Analysis of Biomolecules* (G. D. Fasman, ed.), Plenum Press, New York, pp. 469–500.
31. E. S. Stevens (1996) In *Circular Dichroism and the Conformational Analysis of Biomolecules* (G. D. Fasman, ed.), Plenum Press, New York, pp. 501–530.
32. E. R. Morris, D. A. Rees, D. Thom, and E.J. Welsh (1977) J. Supramol. Struct. **6**, 259–274.
33. W. C. Johnson Jr. and I. Tinoco Jr. (1972) J. Am. Chem. Soc. **94**, 4389–4390.
34. S. Brahms and J. Brahms (1980) J. Mol. Biol. **138**, 149–178.
35. J. Bandekar, D. J. Evans, S. Krimm, S. J. Leach, S. Lee, J. R. McQuie, E. Minasian, G. Nemethy, M. S. Pottle, H. A. Scheraga, E. R. Stimson, and R. W. Woody (1982) Int. J. Peptide Protein Res. **19**, 187–205.
36. K. E. van Holde, J. Brahms, and A. M. Michelson (1965) J. Mol. Biol. **12**, 726–739.
37. W. C. Johnson Jr. (1985) Meth. Biochem. Anal. **31**, 62–125.
38. J. H. Riazance, W. A. Baase, W. C. Johnson Jr., K. Hall, P. Cruz, and I. Tinoco Jr. (1985) Nucleic Acids Res. **13**, 4983–4989.

Suggestions for Further Reading

39. G.D. Fasman (1996) *Circular Dichroism and the Conformational Analysis of Biomolecules*, Plenum Press, New York.
40. W.C. Johnson Jr. (1985) Circular dichroism and its empirical application to biopolymers, Meth. Biochem. Anal. **31**, 62–125.
41. K. Nakanishi, N. Berova, and R.W. Woody (1994) *Circular Dichroism: Principles and Applications*, VCH, New York.
42. D.W. Sears and S. Beychok (1973) "Circular dichroism", In *Physical Principles and Techniques of Protein Chemistry* (S. J. Leach, ed.), Academic Press, New York, Part C, pp. 445–593.
43. R.W. Woody (1995) Circular dichroism, Meth. Enzymol. **246**, 34–71.

Cis Configuration

The prefix *cis* has been used in chemistry to indicate "on the same side" (1). The original use came from describing stereoisomers of molecules with a ring or containing carbon–carbon double bonds. When similar substituents are on the same side of the ring or double bond, the configuration is referred to as *cis*, and when they are on opposite sides, they are referred to as ***trans***. The C2 and C3 hydroxyl groups of the furanose form of **ribose** are *cis*. The conformation about a single bond may also be noted as *cis* or *trans*, particularly when all the substituents lie in a plane. The *cis* conformation of a peptide bond has both a-carbons on the same side of the *N*—*C* amide bond (see Cis/Trans Isomerization). The notation **s-*cis*** (2) is used to emphasize that the conformation about a single bond is being described, as in *s*-1-*cis* retinal. These different uses of the chemical prefix *cis* are shown in Figure 1.

Figure 1. The various uses of the prefix *cis* are shown. The common feature is that the prefix denotes "on the same side."

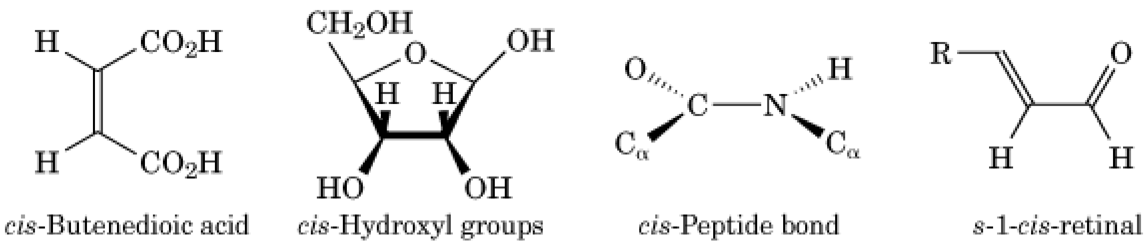

Bibliography
1. A. Baeyer (1888) Liebig''s Annalen der Chemie **CCXLV**, 137.
2. R. Mullikan (1942) Rev. Mod. Phys. **14**, 265–267.

Suggestions for Further Reading
3. E. L. Eliel (1962) *Stereochemistry of Carbon Compounds*, McGraw-Hill, New York, pp. 318–371.
4. J. March (1985) *Advanced Organic Chemistry*, 3rd ed., Wiley-Interscience, New York, pp. 109–115.

***Cis*-Acting**

This term is used in the context of regulation of gene transcription to denote DNA sequences that have to be physically joined to the **genes** in question to influence their activity. Trans-acting sequences, on the other hand, exert their regulatory effects regardless of whether or not they are present on the same chromosome as the regulated gene. *Trans*-acting genes generally encode proteins that bind to *cis*-acting DNA sequences.

Cis-acting sequences were classically identified as a result of their mutation, either silencing or activating the controlled gene, depending on whether the *cis*-acting sequence provided a binding site for **RNA polymerase** or other necessary **transcriptional factor** or for a repressor protein. These two kinds of *cis*-acting sequences, respectively positive and negative in their effect, were first identified in the *Escherichia coli* Lac operon, where they were called the **promoter** and **operator** sequences. With the development of recombinant DNA technology, it became possible to detect protein-binding sites in DNA without mutation (e.g., by footprinting or gel retardation assays), and then to determine their effects on transcription by "engineered" deletions.

Cis-acting sequences that act otherwise than by providing binding sites for regulatory proteins are comparatively uncommon, but two quite different examples should be mentioned. In bacterial operons, a mutation that causes premature translational termination of an upstream gene can cause a drastic reduction in the expression of genes in the same operon further downstream. This is a strictly *cis*-acting effect, acting within a single unit of transcription. The mechanism is explained under Lac Operon.

The second example is from female mammals where one of the two X-chromosomes in each cell lineage is largely inactivated with the notable exception of one gene, active only in the otherwise "silent" X, that is transcribed into a long RNA molecule called Xist. This transcript, which does not encode a protein, plays an essential role in silencing the rest of the chromosome. It acts only in *cis* and remains associated with the chromosome from which it is transcribed without effect on the other, active, X-chromosome (see X-Chromosome Inactivation).

X-chromosome inactivation involves propagating a certain type of condensed and transcriptionally inactivating chromatin structure, generally called heterochromatin, which, in most chromosomes, is restricted to certain segments. In *Drosophila melanogaster*, heterochromatin exerts a *cis*-effect in suppressing gene activity when, as a result of segmental chromosomal rearrangement, it is brought close to genes not normally associated with it. The multiprotein heterochromatin complex spreads along the chromosome, inactivating the genes in its path with a probability that decreases with distance (see Position Effect). Genes that are normally close to heterochromatin are apparently insulated in some way against this effect.

Cis-Dominance

Dominance, in the genetic sense, is a property of one form (**allele**) of a **gene** relative to another allele of the same gene, said to be recessive. Where dominant and **recessive alleles** are present together, the dominant, not the recessive, registers its effect on the organism. Most mutant alleles have lost part or all of their activity and then are usually recessive. When mutant alleles are dominant it is usually because they are hyperactive or have been freed from some normal constraint. The term *cis*-dominant means that the mutation is in an element that has to be physically joined to the gene to exert its effect (ie, in *cis*), not separated from it on another chromosome.

Insofar as a gene is, by definition, an integrated (*cis*-acting) unit of genetic function, any part of a dominant allele, including its coding sequence, could be said to be *cis*-dominant. But, in practice, the term (if it is used at all) is usually reserved for DNA sequences that govern gene activity in *cis* from outside the transcribed or translated sequence.

The concept of *cis*-dominance arose from the classical work of Francois Jacob and Jacques Monod at the Pasteur Institute in Paris on the utilization of the sugar lactose by the bacterium *E. coli* (see Lac Operon). Lactose utilization by the bacterium depends on two proteins, the enzyme b-**galactosidase**, which cleaves lactose to glucose and galactose, and a membrane protein, b-galactoside permease, needed for uptake of lactose into the cell. These proteins are normally synthesized by *E. coli* only in the presence of lactose in the growth medium, or a lactose analogue, that acts as an **inducer**.

Two classes of mutations result in failure to grow on lactose as a carbon source: *lacZ* mutants lack b-galactosidase and *lacY* mutants lack the permease. *LacZ* and *lacY* are two genes that are closely linked (together with a third, seemingly inessential gene *LacA*) in what was later shown to be a single unit of transcription, or operon, transcribed in the sequence Z - Y - A.

Two other kinds of mutants differ from wild type in producing b-galactosidase and permease **constitutively**, that is, whether inducer is present or not. They were mapped respectively in a separate gene, *LacI*, closely linked to *LacZ*, and in a so-called **operator** segment (*o*) at the end of *LacZ* that overlaps the LacZ transcription start point. The *LacI* constitutive mutants (*LacI*–) are recessive to wild type (*LacI*+), which is interpreted as meaning that *LacI*+ encodes a transcriptional repressor and that the repressor function is nullified by inducer. The wild-type operator segment (*o*+) was given the hypothetical role of binding to the *LacI* repressor, blocking *lac* operon transcription. The operator-constitutive mutants (o^c) are interpreted as changes in the DNA sequence of the operator so that it no longer bound the repressor. The inducer was thought to act by binding to the repressor protein and changing its conformation, so that it is no longer bound to the operator (see Fig. 1). All of these elements of the model have since been confirmed by molecular analysis.

Figure 1. The regulation of the *Escherichia coli lac* operon and two kinds of mutations that have dominant effects: $LacI^s$ (noninducible), dominant both in *cis* and in *trans*; and o^c (constitutive), dominant only in *cis*. The partial diploids for testing dominance (items 5–8) were made by introducing F′ plasmids that carry a second copy of the *lac* segment of the bacterial genome. o^c is resistant to the wild type ($LacI^+$) repressor and also to the $LacI^s$ superrepressor. $LacI^-$ mutants, not shown here, are constitutive and recessive. Information from Refs. 1 and 2.

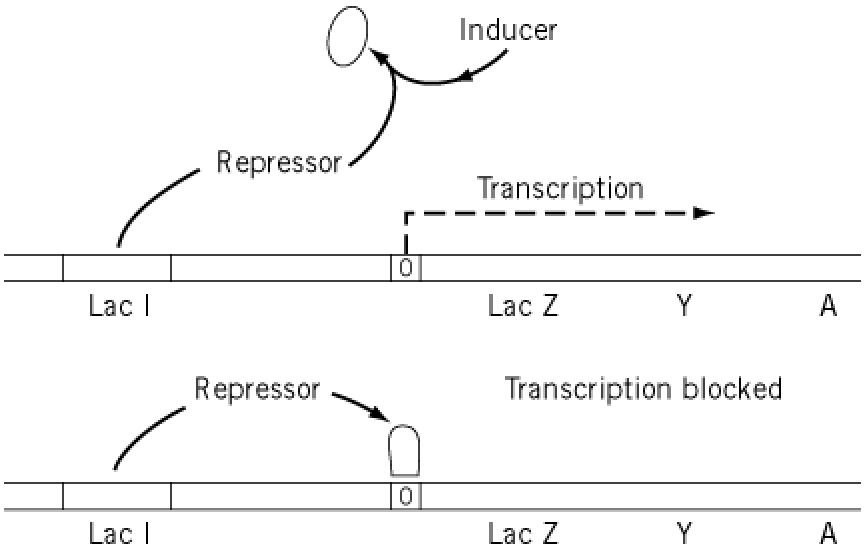

		Lac Z (β-galactosidase) activity	
		No inducer	With inducer
1	[$I^+ O^+ Z^+$]	–	+
2	[$I^+ O^c Z^+$]	+	+
3	[$I^s O^+ Z^+$]	–	–
4	[$I^+ O^+ Z^-$]	–	–
5	[$I^+ O^+ Z^-$ / F′ $I^+ O^c Z^+$]	+	+
6	[$I^+ O^+ Z^+$ / F′ $I^+ O^c Z^-$]	–	+
7	[$I^s O^+ Z^+$ / F′ $I^+ O^+ Z^-$]	–	–
8	[$I^s O^+ Z^-$ / F′ $I^+ O^c Z^+$]	+	+

The tests for dominance were made in partial diploids (merodiploids) that have a second copy of the *Lac* operon brought into the cell as part of an plasmid. Some of the key results are shown in the table of Fig. 1. The formal demonstration of *cis*-dominance comes from the comparison of items 5 and 6. The *trans* merodiploid, $o^{+}LacZ^{-}/o^{c}\ LacZ^{+}$, is constitutive, but the *cis* merodiploid, $o^{+}LacZ^{+}/o^{c}$ $LacZ^{-}$, in inducible.

The *cis*-dominance of o^{c} is readily understandable. There is no way in which the binding of a protein to one piece of DNA could affect the transcription of an unconnected piece. The operator segment is an integral part of the *lac* operon and cannot function when separated from it. On the other hand, *LacI* is a separate and functionally autonomous gene that acts on *LacZ* in *trans* just as well as in *cis*.

Mutations of the rather uncommon $LacI^{s}$ type change the repressor into a superrepressor that is insensitive to inducer and confers noninducibility. Its dominance over $LacI^{+}$ (both in *cis* and in *trans* - see item 7 in Fig. 1) is due to the *LacI* repressor functioning as a **dimer**. In mixed $LacI^{+}/LacI^{s}$ protein dimers, the noninducibility of the $LacI^{s}$ component is imposed on the whole.

The concept of *cis*-dominance was important at a time when the idea that gene sequences had regulatory as well as structurally determining functions was just emerging. Monod and Jacob found that *LacI* acts in *trans* on *LacZ* (and *LacY*) activity and the *o* segment acts only in *cis*. Today it is recognized that the activities of most genes are regulated by multiple *trans*-acting proteins, encoded by other genes, that bind to DNA sequences (**promoters**, enhancers, **silencers**) that act in *cis*. But it is questionable whether *cis*-dominance is an appropriate term in reference to all these *cis*-acting transcriptionally controlling sites. Dominance implies that there are recessive alleles over which the dominance can be demonstrated, which is seldom the case, and the *cis-trans* comparison, which could provide the evidence that the effect applies only in *cis*, is hardly ever available.

One dominant mutation, in ***Drosophila***, for which the *cis-trans* comparison has been made in Contrabithorax (*Cbx*), which maps close to the ***Ultrabithorax*** (*Ubx*) gene and extends its activity in the embryo in an anterior direction. Here the effect of *Cbx* is strong in flies of constitution *Cbx* + / + *Ubx* (*Ubx* being a virtually null allele) but weak, though still significant, in *Cbx Ubx*/ ++. In the latter genotype, the *Cbx* regulator is separated from the gene that it regulates. *Cbx* can be called *cis*-dominant, but the observation that it also has a small effect in *trans* is interesting. E. B. Lewis (3) showed that this and other *trans* effects to do with *Ubx* depend on the close pairing of homologous chromosomes that is a special feature of several *Drosophila* tissues.

The concept of *cis*-dominance is an important part of molecular biological history, even though the current usefulness of the term is rather limited. The principle of *cis*-acting controls of gene activity, to which the concept led, is now a commonplace and essential part of molecular biology.

Bibliography

1. J. R. Beckwith (1970) In *The Lactose Operon* (J. R. Beckwith and D. Zipser, eds.), Cold Spring Harbor Laboratory Press, Cold Spring Harbor, New York, pp. 1–26.
2. F. Jacob and J. Monod (1961) On the regulation of gene activity. Cold Spring Harbor Symp. Quant. Biol. **26**, 193–209.
3. E. B. Lewis (1955) Am. Nat. **89**, 73–89.

Cis/Trans Isomerization

The distinction between the *cis* and *trans* isomers of a molecule originates from a geometry-based classification of molecular structures. When the two substituents X and Y are on the same side of the structural unit [Fig. 1(**a**)] the isomer is *cis*. It is designated *trans* in the opposite arrangement. Ambiguities in the designation of the isomers are avoided by using the more sophisticated *E*/*Z* nomenclature, which often has *E* for the *cis* form and *Z* for the *trans* form. The interconversion between the isomers, the *cis*/*trans* isomerization, occurs by rotation about the central linkage [Fig. 1 (**a**)]. There is a barrier to rotation quantified by the **free energy** of activation DG‡ that is proportional to a first-order rate constant k_{obs}, where k_{obs} = ($k_{cis\text{ to }trans}$ + $k_{trans\text{ to }cis}$ for the reversible isomerization. The bond order of the central linkage correlates with the magnitude of the energy barrier DG‡. It ranges from high values of DG‡ > 100 kJ/mol for double bonds, via an intermediate range for linkages having a partial double bond character, down to low values in the range of $k_B T$ (where k_B is the Boltzmann constant and T the absolute temperature) for C–C single bonds. Under ambient conditions, a rotational barrier >90 kJ/mol indicates that the individual isomers are not readily interconverted, and they may exhibit quite distinct chemical properties. A corresponding DG‡ value has been used to discriminate semantically between different conformations (barrier to rotation <90 kJ/mole) and configurations of a molecule.

Figure 1. (**a**) General representation of *cis/trans* isomerism (**b**) *Cis/trans* isomerism of a prolyl peptide bond.

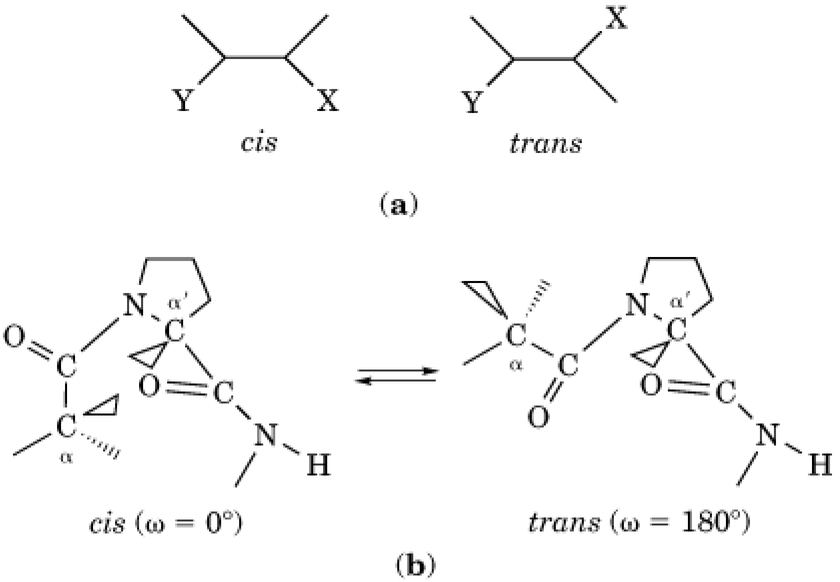

In a polypeptide chain, both the amide -CONH- and the **imide** ━CON < peptide groups are intrinsically competent to undergo *cis*/*trans* isomerization by rotation about the torsion angle w of the peptide bond (see Ramachandran Plot). Among the gene-encoded amino acids, the imide peptide bond is exclusively formed by proline residues. Because the lone electron pair of the nitrogen atom is delocalized over the peptide bond, the C–N linkage has a partial double-bond character. Typically, this destabilizes twisted conformations but stabilizes planar arrangements (*trans*, w = 180° *cis*, w = 0°) of the two a-C atoms adjacent to the peptide bond [Fig. 1(**b**)]. The *cis*/*trans* isomerization of the -CONH- moiety is relatively fast (half-time <1 at room temperature) and leads to a very small percentage of *cis* isomer, ≫1%, at equilibrium. In contrast, the peptidyl-proline moiety (in the following referred to as a prolyl bond) often has *cis/trans* isomers in comparable amounts. Steric constraints, which favor a *trans* arrangement in the case of -CONH-, are similar in both isomers for prolyl bonds, and the *cis* isomer generally occurs in about 20% of the prolyl peptide bonds. There is a relatively high rotational barrier $DG^{‡}$ of about 80 kJ/mol for the prolyl bond. The combination of a substantial population of both isomers and their slow interconversion implies that *cis* prolyl bonds have considerable influence on biochemical reactions of the polypeptide backbone.

In the absence of a folded conformation, polypeptide chains can theoretically form 2^n *cis*/*trans* isomers, where *n* is the number of prolyl bonds in the molecule. In simple cases, as with a four-proline octapeptide derived from the prolactin **receptor**, all of the possible isomers have been detected and quantified in solution (1). Structural formation in the peptide chain, however, reduces the number of isomers substantially. A particular prolyl bond in native proteins is usually either *cis* or *trans* in all the molecules, although *cis*/*trans* isomerization in the native structure has been observed for a few proteins by **NMR** methods in solution. In the latter case, structural alterations propagate through the backbone around the isomeric proline residue, which can be accompanied by distinct biological activities of the isomeric proteins (2, 3). Depending on the polypeptide structure, the **half-time** for prolyl bond isomerization ranges from seconds to hours.

From stereochemical considerations, the peptidyl transferase center on the ribosome is thought to be constructed for synthesizing all peptide bonds in the *trans* conformation. However, in native, globular proteins of known three-dimensional structure, about 5 to 6% of prolyl peptide bonds are *cis* (4, 5). When proline-containing proteins are unfolded in the presence of high concentrations of **denaturants**, such as urea or **guanidinium chloride** (GdmCl), the random coil polypeptides generally equilibrate slowly to a mixture of numerous *cis*/*trans* isomers. For the fraction of unfolded molecules that have one or more nonnative isomers of a prolyl bond, subsequent **refolding** of the protein has to start from different conformational states. If the *cis*/*trans* isomerization is slower than refolding, slow kinetic phases of folding may be apparent when the time course of refolding is monitored. For that reason, *cis/trans* isomerization is the rate-limiting step in folding for some proteins. It is generally most easily detectable when there is a *cis* prolyl bond in the native state, because then a large fraction of unfolded molecules has the incorrect isomer (6, 7).

Chemical catalysis of prolyl bond isomerization is rare. Most organic solvents and micelles or phospholipid **vesicles**, cause a moderate decrease in the rotational barrier. The rate constants are independent of the pH value in the physiological range, unless dissociable groups are located adjacent to proline. An increased rotational barrier results from the O-protonation of the peptide bond in acidic solution, characterized by a $pK_a = –1$. In strong acids, N-protonated species become populated ($pK_a = –7$) that accelerate *cis/trans* isomerization (8). Many relationships between the peptide structure and prolyl bond isomerization have been elucidated. For example, when measured in oligopeptides, the increased barrier to rotation caused by aromatic amino acids that precede the proline residue is accompanied by an increase in the *cis* population of up to 40%, whereas small aliphatic side chains in the same position lead to lower $DG^{‡}$ values in conjunction and lower *cis* contents of 5 to 10% (9).

The conformational constraints on the polypeptide backbone induced by the prolyl *cis/trans* isomerization restrict bimolecular recognition processes. Conformational selectivity was demonstrated by the hydrogen bond directed preferential binding of proline peptides in the *cis* conformation to b-cyclodextrins (10) and to a synthetic, multidentate terephthaloyl amide (11). For the recognition of opioid peptides of the dermorphin type by m- and ∂-receptors, specificity for the *cis* conformers was suggested (12). In a biological context, it may be important that endoproteinases, such as **chymotrypsin**, **trypsin**, thrombin and clostripain cannot readily cleave a peptide bond adjacent to a *cis* prolyl moiety, even if the isomeric bond occupies a position remote from the scissile bond (13, 14). Due to this conformational specificity, the rate of the *cis* to *trans* isomerization of the prolyl bond limits the rate of proteolysis for good substrates in the presence of high protease concentrations, and this is a useful assay for isomerization. Even *in vivo*, the time course of bradykinin (Arg-Pro-Pro-Gly-Phe-Ser-Pro-Phe-Arg) degradation by pulmonary endothelial peptidases is controlled by the conformational specificity of the proteinases (15).

Bibliography

1. K. D. Oneal et al. (1996) Biochem. J. **315**, 833–844.
2. A. P. Hinck, E. S. Eberhardt, and J. L. Markley (1993) Biochemistry **32**, 11810–11818.
3. J. Kordel, S. Forsen, T. Drakenberg, and W. J. Chazin (1990) Biochemistry **29**, 4400–4409.
4. M. W. MacArthur and J. M. Thornton (1991) J. Mol. Biol. **218**, 397–412.
5. D. E. Stewart, A. Sarkar, and J. E. Wampler (1990) J. Mol. Biol. **214**, 253–260.
6. J. F. Brandts, H. R. Halvorson, and M. Brennan (1975) Biochemistry **14**, 4953–4963.
7. F. X. Schmid (1986) Methods Enzymol. **131**, 70–82.
8. H. Sigel and B. R. Martin (1982) Chem. Rev. **82**, 385–426.
9. R. K. Harrison and R. L. Stein (1992) J. Amer. Chem. Soc. **114**, 3464–3471.
10. M. Lin et al. (1995) Anal. Chim. Acta **307**, 449–457.
11. C. Vicent, S. C. Hirst, F. Garciatellado, and A. D. Hamilton (1991) J. Amer. Chem. Soc. **113**, 5466–5467.
12. R. Schmidt et al. (1995) Int. J. Peptide Protein Res. **46**, 47–55.
13. G. Fischer, H. Bang, E. Berger, and A. Schellenberger (1984) Biochim. Biophys. Acta **791**, 87–97.
14. S. Meyer, M. Drewello, and G. Fischer (1996) Biol. Chem. **377**, 489–495.
15. M. P. Merker and C. A. Dawson (1995) Biochem. Pharmacol. **50**, 2085–2091.

Suggestions for Further Reading

16. T.E. Creighton, ed. (1992) *Protein Folding*, W.H., New York; A book written by specialists that summarizes proline-limited protein folding in the context of other folding events.
17. B. Testa (1982) "The geometry of molecules: basic principles and nomenclature", In *Stereochemistry* (C. Tamm, ed.) Elsevier Biomedical Press, Amsterdam, New York, Oxford, pp. 1–47.

Clamp Loaders, Processivity Complex

Chromosomal **replicases**, the **DNA polymerases** that replicate chromosomes, are multiprotein complexes characterized by the high processivity of their DNA synthesis. These replicating machines polymerize thousands of nucleotides without dissociating from the template. The replicases of the three well-characterized systems (***Escherichia*** *coli*, **eukaryotes**, and **bacteriophage** T4), which span the evolutionary spectrum, are similar in function, structure, and overall organization. Their remarkable processivity is achieved by a ring-shaped processivity factor (or "**sliding clamp**") that binds the polymerase catalytic unit and tethers it to the DNA. Another complex of accessory proteins is required to load the clamp onto the DNA. The sliding clamp does not have any affinity for DNA and, therefore, other proteins are needed to assemble the clamp around the DNA. The accessory protein complex ("clamp loader"; also called a "molecular matchmaker") binds to the primer terminus and **couples** ATP hydrolysis to the assembly of the ring around the DNA primer. Therefore, the replicase can be thought of as having three components: (1) a polymerase, (2) a clamp loader complex that assembles the clamp around DNA and (3) a DNA sliding clamp (Table 1).

Table 1. Three-Component Structures of Chromosomal Replicases

	DNA Polymerase	Clamp loader	Sliding Clamp
Eukaryotes	pold (3 subunits)	RF-C complex (5 subunits)	PCNA
E. coli	Core polymerase (3 subunits)	g-complex (5 subunits)	b-subunit
Phage-T4	gp43	gp44/62	gp45

1. The Clamp Loaders

The three best-studied replicases are the *E. coli* DNA polymerase III holoenzyme (polIII), the eukaryotic polymerase d (pold), and the replicase of phage T4. These three multisubunit complexes share structural and functional similarities (reviewed in Refs. 1-3). The clamp loaders for these systems are the g-complex of prokaryotes, the replication factor-C (RF-C) complex (also called Activator-1) of eukaryotes, and a complex of the products of gene 44 and gene 62 (gp44/62) of phage T4. The g-complex is composed of five subunits called g, d, d′, c and y. RF-C is also a five-subunit complex, composed of one large and four small subunits (p140, p40, p38, p37, and p36). gp44/62 contains only two polypeptides gp44 and gp62. In the complex, a tetramer of gp44 is tightly associated with one gp62. Interestingly, the three clamp loaders share amino acid similarities among the subunits (4, 5).

A detailed mechanism by which these clamp loaders operate in assembling the sliding clamp around DNA is not yet known. The basic steps of the loading process, however, have been elucidated (Fig. 1). In general, the clamp loader recognizes the 3′ end of the junction between the single strand and duplex DNA (primer/template) and uses ATP hydrolysis to assemble the clamp around the primer. The status of the clamp loader after assembling the clamp around DNA is not yet clear. It has not yet been determined whether the clamp loader leaves the clamp on the DNA, where it interacts with the polymerase to initiate processive DNA synthesis, or if the clamp loader is also needed to assist binding the polymerase to the clamp (the different features of each clamp loader are discussed later).

Figure 1. A model for clamp loader activity. The clamp loader recognizes the 3′ terminus of a primer and assembles the sliding clamp around the DNA. Following assembly, the clamp interacts with the polymerase and tethers it to the DNA f processive DNA synthesis.

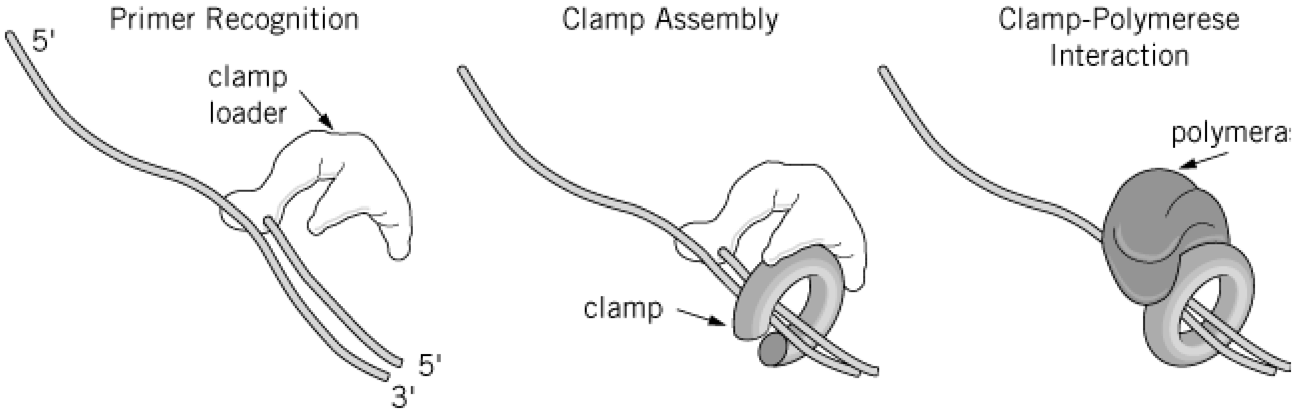

In prokaryotes and eukaryotes, the clamp loader also functions as a clamp unloader (6). Upon completion of an Okazaki fragment, the polymerase rapidly dissociates from the clamp (7-9), leaving the clamp on the DNA (10). The clamps of polIII (the b subunit) and pold [proliferating cell nuclear antigen (PCNA)] are relatively stable on DNA (6, and references therein). Therefore, it was postulated that the sliding clamp remains assembled around the DNA when the synthesis of an Okazaki fragment is complete. During lagging strand synthesis, a new sliding clamp is needed for the synthesis of each Okazaki fragment. In *E. coli* about 10 times more Okazaki fragments are formed during replication than there are b-subunits within the cell. In human cells, the number of Okazaki fragments formed during one round of chromosomal replication has been estimated to be 100 times greater than the amount of PCNA. Therefore, recycling of the clamp (b and PCNA) is needed to fulfill the requirement for a constant supply of clamps for further DNA synthesis. In phage T4, the clamp readily dissociates from DNA upon completion of an Okazaki fragment. Thus, the clamp loader has a dual function during DNA replication: (1) loading of the sliding clamp onto DNA to initiate processive DNA synthesis and (2) recycling the clamps on the lagging strand.

1.1. g-Complex

The g-complex is composed of five subunits (g, d, d′, c, y) (reviewed in Ref. 11). The genes encoding them have been identified, and the purified proteins have been used to study the function of the individual subunits and subassemblies of the g-complex (discussed later). Four of the subunits (d, d′, c and y) are encoded by unique genes. The g-subunit is formed from the same gene (*dnaX*) that encodes t (another subunit of polIII) by an efficient translational **frameshift** mechanism that produces g in an amount equal to t (reviewed in Ref. 12). As a result, the g-subunit consists of the N-terminal 430 residues of t followed by a unique C-terminal Glu residue. In addition, the g-and d′-subunits show amino acid sequence similarity.

No one subunit alone can assemble the b sliding clamp around DNA (11 and references therein). At low ionic strength, a combination of g and d assemble b onto DNA, but the reaction is feeble. The d′-, c- and y-subunits are needed for an efficient loading reaction under physiological conditions (13).

The g-complex has only weak affinity for single-stranded and duplex DNA, and it exhibits weak DNA-dependent ATPase activity, but the ATPase activity is stimulated by the sliding clamp (b-subunit) (14). The best DNA effector for the ATPase activity is a singly primed template, indicating an interaction between the g-complex and the primer/template junction. The g-subunit is the only subunit of the g-complex with an ATP-binding motif, and it binds ATP (15). Furthermore, mutation of the ATP-binding site of g within the g-complex destroys the ATPase activity and the ability to assemble the b-ring onto DNA. The g-subunit, however, lacks significant ATP hydrolysis activity even in the presence of DNA (14, 15), and the d- and d′-subunits are required for ATPase activity, implying that the gdd′ complex recognizes DNA. The g-complex binds b in the presence of ATP. The d subunit interacts with b, with a strength similar to that of the entire g-complex (16), indicating that b binds the g-complex mainly through the d-subunit. Interestingly, however, the interaction between the b-subunit and d does not depend on ATP (whereas the g-complex requires ATP to bind the clamp). These apparently contradictory observations can be explained if the d subunit is buried within the g-complex and ATP induces conformational changes that lead to the interaction of d with b (16). The g-complex also interacts with single-stranded DNA binding protein (SSB) via the c subunit (11). These interactions are important for efficient clamp assembly at physiological ionic strength.

The results obtained with the individual subunits and their subassemblies demonstrate the basic features of the g-complex action during loading of the clamp onto DNA (Fig. 1). Upon binding of ATP, the g-complex undergoes conformational changes leading to interaction of the d-subunit with b. The g-complex recognizes a primed template, aided by the interaction between c and SSB. Assembly of the ring around the DNA primer stimulates the ATPase activity of the g-complex. ATP hydrolysis results in conformational changes such that d is again buried within the g-complex leaving the clamp around the DNA primer. Now the clamp interacts with the polymerase to initiate processive DNA synthesis (Fig. 1).

1.2. Replication Factor-C (RF-C)

RF-C was first isolated from human 293 cells as an essential replication factor for the *in vitro* replication of simian virus-40 (SV-40) (17). The factor was purified later from different sources, including yeast and human cell lines (18 and references therein), based on its ability to stimulate processive DNA synthesis by pold in the presence of PCNA and ATP.

Purified RF-C is a five-subunit complex (p140, p40, p38, p37, and p36). The genes that encode all RF-C subunits from yeast and humans have been identified (4, 5 and references therein), and all are essential in yeast. Although encoded by different genes, they show extensive amino acid sequence similarities in the central region of the protein (reviewed in Ref. 5).

Early biochemical studies determined the role of RF-C as a clamp loader of PCNA and suggested a mode of action during the assembly reaction (Fig. 1). RF-C binds preferentially to single-strand/duplex DNA (template/primer) junction in the presence of ATP (19, 20). PCNA interacts with the RF-C/DNA complex. The DNA-dependent ATPase activity of RF-C is stimulated by the binding of PCNA. The hydrolysis of ATP leads to conformational changes within the RF-C, which locks the PCNA sliding clamp around the DNA. Then the clamp interacts with the polymerase to initiate processive DNA synthesis (Fig. 1).

Biochemical analysis of RF-C individual subunits and the protein–protein interactions within the RF-C complex is underway (eg, 21, 22). Purified proteins, subcomplexes and mutational analysis have shed light on the function of the individual subunits and subassemblies of the RF-C complex. Although each subunit contains an ATP-binding motif, only p40 binds ATP (20). Yeast p36 (23) and a subcomplex of human RF-C (p36-p37-p40) exhibit DNA-dependent ATPase activity. The DNA-binding activity resides within the large subunit (p140) (20), although the p37 subunit also binds DNA weakly. All of the subunits, except p37, bind PCNA (24-26). The intact complex, however, is needed for the assembly of PCNA around the DNA and, to date, no subunit combination analyzed performs this task. Unloading is probably a simpler mechanism, as the p40 subunit is sufficient to unload PCNA from DNA and also interacts with pold (26). The role of this interaction in DNA synthesis, however, is not yet clear. RF-C also interacts with SSB. The interaction between RF-C and SSB might be needed for the assembly of the clamp, as demonstrated for the *E. coli* g-complex.

1.3. gp44/62

Similar to the g-complex and RF-C, the clamp loader of phage T4, the gp44/62 complex, is also composed of five subunits (Table 1). In this case, however, only two polypeptides form the pentamer, where a tetramer of gp44 binds a single subunit of gp62 (27). Like the clamp loader of eukaryotes and prokaryotes, the gp44/62 complex exhibits ATPase activity that is stimulated by the sliding clamp (gp45) and by DNA (28, reviewed in Ref. 29). A DNA structure that resembles a template/primer junction is the best effector for stimulating ATPase activity (27). Cross-linking and protein-DNA footprinting assays demonstrate that the clamp loader interacts with DNA in the absence of gp45, but these interactions are relatively weak, and the clamp is needed for binding to DNA (reviewed in Refs. 29, 30). Studies with individual subunits of the gp44/62 complex revealed that the gp44 exhibits the ATPase activity, whereas gp62 interacts with the clamp (31).

The exact mechanism of action of the gp44/62 complex is not yet fully understood. The overall features of its activity, however, have been determined and are similar to those of the g-complex and RF-C (Fig. 1). The gp44/62 complex interacts with gp45 in an ATP-dependent manner. The complex recognizes the primer terminus, which stimulates the ATPase activity of the clamp loader, bringing about conformational changes that lock the clamp around the primer and allow it to interact with the polymerase to initiate processive DNA synthesis.

2. Concluding Remarks

The polymerases responsible for replicating chromosomal DNA during cell division are multiprotein complexes. The processivity of these enzymes relies on a ring-shaped protein that encircles DNA and tethers the catalytic unit to DNA for processive DNA synthesis. The mechanisms by which the clamp loaders assemble the ring around DNA and disassemble them from DNA are only beginning to be understood. The complexity of this mechanism is inferred from the observation that it requires the coordinate activity of several polypeptides in eukaryotes, prokaryotes, and phage T4. Future studies are needed to elucidate the mechanisms by which the clamp loaders operate in the loading and unloading reactions. Purification of the clamp loader complexes and the individual subunits will enable further analysis of these mechanisms.

Bibliography

“Clamp Loaders, Processivity Complex” in , Vol. 1, pp. 472–474, by Zvi Kelman, University of Maryland, Biotechnology Institute, Rockville, MD and Lori M. Kelman, Montgomery College, Germantown, MD; “Clamp Loaders, Processivity Complex” in (online), posting date: January 15, 2002, by Zvi Kelman, University of Maryland, Biotechnology Institute, Rockville, MD and Lori M. Kelman, Montgomery College, Germantown, MD.

1. B. Stillman (1994) Cell **78**, 725–728.
2. Z. Kelman and M. O"Donnell (1994) Curr. Opinion Genet. Dev. **4**, 185–195.
3. B. Stillman (1996) *DNA Replication in Eukaryotic Cells*. M. L. DePamphilis, ed., CSH Laboratory Press, Cold Spring Harbor, NY, pp. 435–460.
4. M. O"Donnell, R. Onrust, F. B. Dean, M. Chen, and J. Hurwitz (1993) Nucleic Acids Res. **21**, 1–3.
5. G. Cullmann, K. Fien, R. Kobayashi, and B. Stillman (1995) Mol. Cell. Biol. **15**, 4661–4671.
6. N. Yao, J. Turner, Z. Kelman, P. T. Stukenberg, F. Dean, D. Shechter, Z.-Q. Pan, J. Hurwitz, and M. O"Donnell (1996) Genes to Cell **1**, 101–113.
7. C. A. Wu, E. L. Zechner, and K. J. Marians (1992) J. Biol. Chem. **267**, 4030–4044.
8. P. T. Stukenberg, J. Turner, and M. O"Donnell (1994) Cell **78**, 877–887.
9. K. J. Hacker and B. M. Alberts (1994) J. Biol. Chem. **269**, 24221–24228.
10. A. Yuzhakov, J. Turner, and M. O"Donnell (1996) Cell **86**, 877–886.
11. Z. Kelman and M. O"Donnell (1995) Ann. Rev. Biochem. **64**, 171–200.
12. C. S. McHenry (1988) Ann. Rev. Biochem. **57**, 519–550.
13. M. O"Donnell and P. S. Studwell (1990) J. Biol. Chem. **265**, 1179–1187.
14. R. Onrust, P. T. Stukenberg, and M. O"Donnell (1991) J. Biol. Chem. **266**, 21681–21686.
15. Z. Tsuchihashi and A. Kornberg (1989) J. Biol. Chem. **264**, 17790–17795.
16. V. Naktinis, R. Onrust, L. Fang, and M. O"Donnell (1995) J. Biol. Chem. **270**, 13358–13365.

17. T. Tsurimoto and B. Stillman (1989) Mol. Cell. Biol. **9**, 609–619.
18. U. Hubscher, G. Maga, and V. N. Podust (1996) *DNA Replication in Eukaryotic Cells*, M. L. DePamphilis (ed.), CSH Laboratory Press, Cold Spring Harbor, NY, pp. 525–543.
19. S.-H. Lee, A. D. Kwong, Z.-Q. Pan, and J. Hurwitz (1991) J. Biol. Chem. **266**, 594–602.
20. T. Tsurimoto and B. Stillman (1991) J. Biol. Chem. **266**, 1950–1960.
21. F. Uhlmann, J. Chi, H. Flores-Rozas, F. B. Dean, J. Finkelstein, M. O"Donnell, and J. Hurwitz (1996) Proc. Natl. Acad. Sci. USA **93**, 6521–6526.
22. V. N. Podust and E. Fanning (1997) J. Biol. Chem. **272**, 6303–6310.
23. X. Li and P. M. Burgers (1994) Proc. Natl. Acad. Sci. USA **91**, 868–872.
24. M. A. McAlear, E. A. Howell, K. K. Espenshade, and C. Holm (1994) Mol. Cell. Biol. **14**, 4390–4397.
25. M. Chen, Z.-Q. Pan, and J. Hurwitz (1992) Proc. Natl. Acad. Sci. USA **89**, 2516–2520.
26. Z.-Q. Pan, M. Chen, and J. Hurwitz (1993) Proc. Natl. Acad. Sci. USA **90**, 6–10.
27. T. C. Jarvis, L. S. Paul, and P. H. von Hipple (1989) J. Biol. Chem. **264**, 12709–12716.
28. J. R. Piperno and B. M. Alberts (1978) J. Biol. Chem. **253**, 5174–5179.
29. M. C. Young, M. K. Reddy, T. C. Jarvis, E. P. Gogol, M. K. Dolejsi, and P. H. von Hippel (1994) *Molecular Biology of Bacteriophage T4*. (J. D. Karam, ed.), American Society for Microbiology, Washington, DC, pp. 313–317.
30. N. G. Nossel (1994) *Molecular Biology of Bacteriophage T4*. (J. D. Karam, ed.), American Society for Microbiology, Washington, DC, pp. 43–53.
31. J. Rush, T.-C. Lin, M. Quinones, E. K. Spicer, I. Douglas, K. R. Williams, and W. H. Konigsberg (1989) J. Biol. Chem. **264**, 10943–10953.

Suggestions for Further Reading

32. U. Hubscher, G. Maga, and V. N. Podust (1996) "DNA replication accessory proteins", In *DNA Replication in Eukaryotic Cells*. (M. L. DePamphilis, ed.), CSH Laboratory Press, Cold Spring Harbor, NY, pp. 525–543.
33. Z. Kelman and M. O"Donnell (1994) DNA replication enzymology and mechanisms, Curr. Opinion Genet. Dev. **4**, 185–195.
34. M. O"Donnell (1992) Accessory protein function in the DNA polymerase III holoenzyme from *E. coli*. BioEssays **14**, 105–111.
35. B. Stillman (1996) "Comparison of DNA replication in cells from prokarya and eukarya", In *DNA Replication in Eukaryotic Cells* (M. L. DePamphilis, ed.), CSH Laboratory Press, Cold Spring Harbor, NY, pp. 435–460.
36. M. C. Young, M. K. Reddy, and P. H. von Hippel (1992) Structure and function of the bacteriophage T4 DNA polymerase holoenzyme, Biochemistry **31**, 8675–8690.

Class Switching

Upon stimulation with an immunogen, the circulating antibodies belong first to the IgM isotype, before being replaced by immunoglobulins of another class (most frequently an IgG in the bloodstream). This phenomenon is known as isotype switching (or switch) and is the consequence of a gene rearrangement that takes place in the centrocytes, located in the light zone of the germinal center. As a result, the V–D–J rearranged section of the mature B cell, which was initially associated with a Cm constant region to make a complete m chain, will now become associated with the constant region of another isotype. This gene rearrangement involves recognition sequences termed "switch regions" that are located at 5′ of each constant CH gene (with the exception of the d chain gene). These regions are very similar in sequence and are presumably recognized by an enzyme system, which has not been identified to date, but does not involve recombinase. As a result of this recombination event, the portion of DNA localized between the two switch regions concerned is deleted. The light-chain genes are not affected by the isotype switching, so the antibody combining site is unaffected. In other words, isotype switching has changed the Ig isotype without modifying the specificity of the cell. It has simply conferred on the antibody a distinct biological function, which will amplify the physiological action of the immune system in a number of ways, such as to fight more appropriately against pathogens, ensure fetal protection through transplacental transfer, be expressed in secretions, and so on, depending upon the selected isotype. Isotype switching is another example of a mechanism that necessitates interaction between T cells and B cells and makes use of two sets of molecules. One involves CD40 ligand (CD40-L) and CD40, expressed at the cell surfaces of T_H and B lymphocytes, respectively, and ensuring direct contact between the cells. The second signal is provided by the T_H cell and is a **cytokine** that is released as a soluble factor in the immediate proximity of the B cell. Depending upon the nature of the cytokine, and therefore on the type of interacting T cell, the switch mechanism will generate a discrete isotype. For example, secretion of **interleukin**-4 (IL-4) will favor a switch toward the IgE class, whereas transforming growth factor b1 will induce switching to IgA.

See also entries Antibody, Immune Response, Immunoglobulin, Isotype, Switch Region.

Suggestions for Further Reading

J. Stavnezer (1996) Immunoglobulin class switching. Curr. Opin. Immunol. **8**, 199–205.

T. Honjo and T. Kataoka (1978) Organisation of immunoglobulin heavy-chain genes and allelic deletion model. Proc. Natl Acad. Sci. USA **75**, 2140–2144.

Clathrin

Clathrin is the major component of purified **coated vesicles** (1), intracellular structures that derive from coated membrane involved in endocytosis and **receptor** recycling.

Clathrin-mediated endocytosis (2, 3) is the major route for the uptake of specific macromolecules into cells for example, **low density lipoprotein** carrying cholesterol and transferrin bearing iron. Such macromolecules are concentrated from the surrounding cellular fluid by binding to the receptors exposed on the surface of cells. The receptors, in turn, have features in their cytoplasmic tails that enable them to cluster into clathrin-coated pits and thus be endocytosed efficiently in small vesicles. (Fig. 1). The vesicles, in addition, carry other molecules that target them to an internal compartment, the endosome, and allow them to fuse with the endosomal membrane, thus delivering the cargo of nutrients into the lumen for use by the cell. Meanwhile, the coat proteins and receptors are recycled through the endosomal compartment and back to the plasma membrane. The coat proteins diffuse through the cytoplasm to reform coated pits there for a further round of endocytosis.

Figure 1. Endocytosis promoted by a round of clathrin assembly and recycling. [Taken from B.M.F. Pearse and R.A.

Crowther (1987) *Ann. Rev. Biophys. Biophys. Chem.* **16**, 49–68.] (1) Cytoplasmic clathrin triskelions and adaptors (containing specific 100 kDa adaptins and associated subunits) are triggered to assemble on the membrane in a reaction involving GTP-binding proteins with a selection of receptors to form a coated pit(2). The coated pit invaginates as further receptors and coat proteins assemble(3). Pinching-off the completed coated vesicle(4) requires dynamin to promote fusion in the neck region. Uncoating follows, releasing the vesicle (5), which carries molecules primed for fusion with the endosome(6), and the soluble coat components, which recycle(1).

A similar coated vesicle cycle takes place in many nerve terminals. In this case, the cycle replenishes the synaptic vesicle population, whose efficient fusion with the presynaptic membrane, on stimulation, depends on, among other molecules, synaptobrevin, syntaxin, and munc18 (29-32).

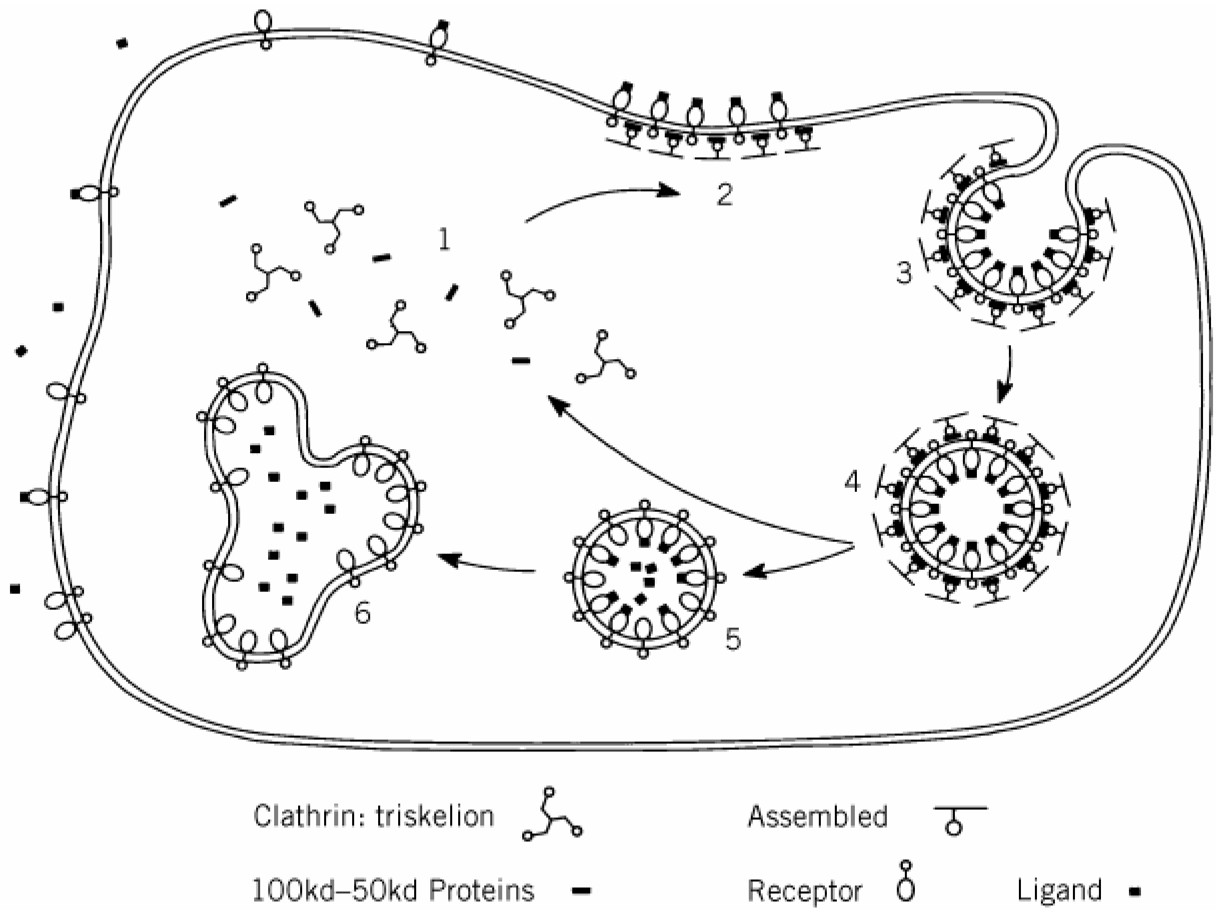

This system of budding coated vesicles is used again and again throughout cellular biology. Thus clathrin-coated vesicles are involved in **antigen presentation** in immunology (4) in delivering receptors and signaling molecules at the right place and time during development (5) and in recycling synaptic vesicle components in nerve synapses (6). In essence, clathrin and its associated proteins provide a mechanism for efficient recycling of specific receptors that are controlled in various ways. Other non-clathrin coated vesicle systems that contain a spectrum of related molecules and certain quite distinct coat components mediate sorting and recycling steps throughout the secretory pathway (7, 8). Clathrin-coated vesicles are more particularly associated with sorting specific molecules from the trans **Golgi** network into the pre-lysosomal/endosome network in addition to their endocytic function.

Unfortunately, **viruses** [eg, influenza virus (9)] exploit the endocytic system to infect cells, and various other pathogens and foreign substances do damage to cells by this route. Defects in the system are also the root cause of certain medical conditions, for example, familial hypercholesterolaemia (2), and I-cell disease (10).

1. Clathrin

The function of clathrin is to form the strong outer, or cytoplasmic, surface of the coat, a remarkable honeycomb of hexagons and pentagons (Fig. 2). This flexible, structural network accommodates extensive areas of flattish membrane or encloses a range of vesicles, the smallest of which (250 Å diameter) is contained within a truncated icosahedron composed of 20 hexagons and 12 pentagons (for review, see Ref. 11).

Figure 2. Field of unstained placental coated vesicles in ice. Hexagonal barrels (H), tennis ball structures (T), larger coats containing vesicle (V), and ferritin (F) are indicated. Scale bar 200 nm. [Taken from G.P.A. Vigers, R.A. Crowther, and B.M.F. Pearse (1986) *EMBO Journal* **5**, 529–534.]

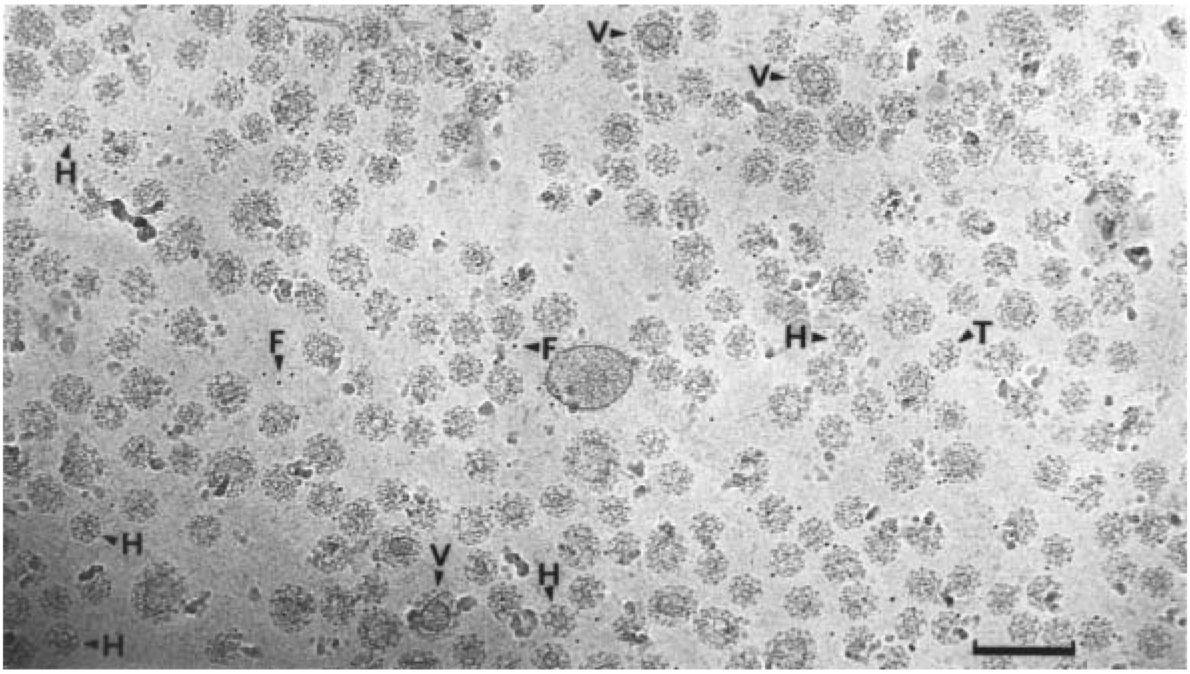

The modular design of the clathrin molecule is extraordinary and unexpected [Fig. 3(**a**)]. The overall shape is that of a triskelion (12, 13). Three heavy chains (180 kDa) and three light chains (one LCa and 2 LCb) form the three-legged structure. The C-termini of the heavy chains come together to form the hub of the structure, and the N-termini are in the terminal domains of the extended legs. The light chains are located along the proximal leg regions, possibly contributing in some way to the geometry at the vertex. Beyond the light chains, the heavy chains exhibit a kink, and the distal ends bend yet again to form a more globular terminal domain.

Figure 3. (**a**) Schematic drawing showing the modular structure of the triskelion. (**b**) Packing diagram showing how triskelions (lacking terminal domains for simplicity) form a hexagonal lattice. (**c**) Three-dimensional map of a clathrin cage containing 12 pentagons and 8 hexagons, computed from electron micrographs of unstained specimens embedded in vitreous ice. Each triskelion leg runs from one vertex along two neighboring polygonal edges and then turns inward. Its terminal domain forms the inner shell of density. [Taken from B.M.F. Pearse and R.A. Crowther (1987) *Ann. Rev. Biophys. Biophys. Chem.* **16**, 49–68.]

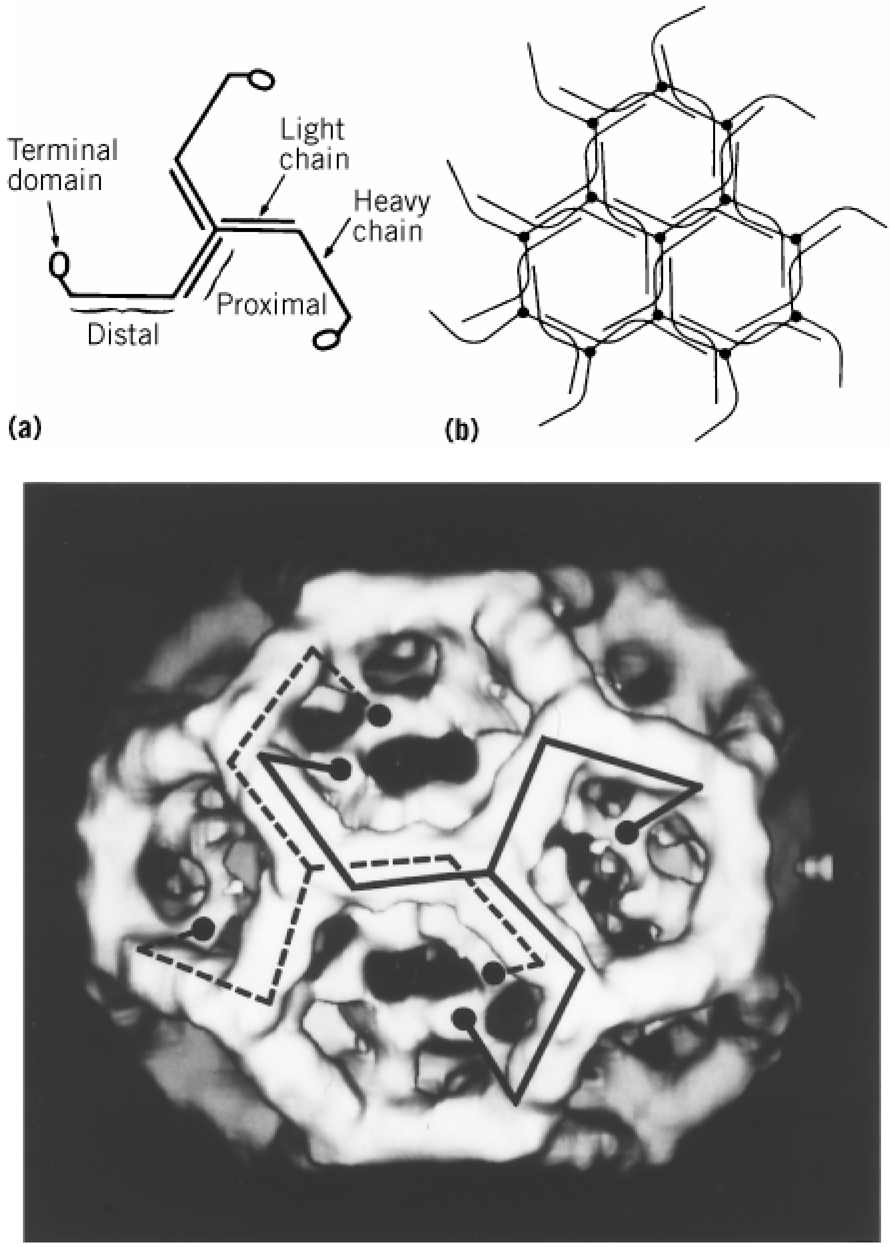

The packing arrangement of the triskelions (lacking terminal domains for simplicity) to form a hexagonal lattice is shown in Fig. 3(**b**). The profiles of two complete triskelions are shown at adjacent vertices of a clathrin cage in the form of a hexagonal barrel in Fig. 3(**c**).

In vitro in artificial conditions, clathrin exhibits its versatility as a construction molecule (Fig. 4). Among other small particles, clathrin makes cubes [Fig. 4(**c**)] a variant of the normal cage (14). In turn the cubes pack together to form remarkable arrays that resemble the foundations of buildings [Fig. 4(**a**) and (**b**)].

Figure 4. The most astonishing type of clathrin aggregate produced *in vitro* is an open square packing of cubes in a pattern reminiscent of the foundations of an ancient building visualized by (**a**) unidirectional shadowing; (**b**) negative staining in uranyl acetate (bar 0.2 μm); (**c**) comparison of cubes with cages, showing from left to right, two-fold, three-fold, and two four-fold views of the cube plus cages of the hexagonal barrel and truncated icosahedron type (football). The edge of the cube is more than twice as long as the vertex to vertex distance in the cages. Bar, 0.1 μm. [Taken from P.K. Sorger, R.A. Crowther, J.T. Finch, and B.M.F. Pearse (1986) *J. Biol.* **103**, 1213–1219.]

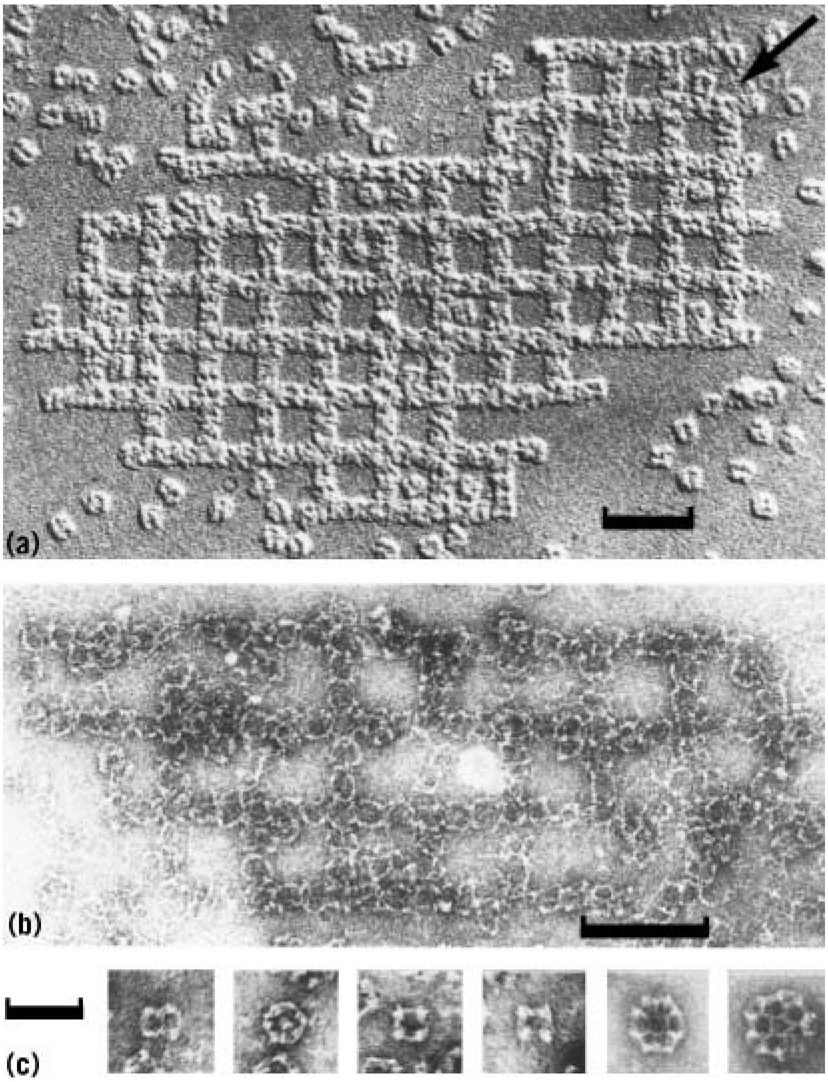

cDNAs coding for clathrin heavy chains and light chains have been **cloned** and sequenced (15, 16). The sequences suggest that part of the light chains form a coiled-coil structure with a corresponding part of the heavy chain to form the proximal legs. Extensive studies of the interaction between light chains and heavy chains, using antibodies and **mutational** analysis, have provided further evidence for the positioning of the light chains along the proximal leg, studies also indicate that the C-termini of the light chains occur at the vertex, where they might influence the structural angles involved in cage assembly (see, eg, Ref. 17). Now the prospects are good for obtaining crystals suitable for determining the high-resolution structure by X-ray crystallography from material produced by expressing parts of the triskelion (e.g., the hub region) in E. coli (17).

An interesting problem is how spurious clathrin cage formation is prevented in the cytoplasm or indeed how clathrin triskelions are disassembled from the coat structure after vesicle budding but are not prevented from forming coated pits. Recently, other attendant "**chaperone**" proteins, hsp70c and cofactor auxilin, have been found, which modulate cage assembly in the cytoplasm (18).

Cloning of clathrin genes has also led to further exploration of the role of clathrin by gene knockout and mutation. Deletion of the clathrin gene in yeast makes various strains very sick, slow growing, or dead. In those that survive, membrane organization is affected. In particular, the processing of pre-pro-a-factor by the kex2 endoproteinase is disrupted, leading to secretion of the immature a-factor and failure in sexual reproduction, and endocytosis of specific molecules, for example, kex2, is reduced, and the cells fill with abnormal vacuoles (19). In a temperature-sensitive mutant of clathrin, transient defects have been observed in sorting to the vacuole. The picture emerging (20) is not dissimilar to that observed in mammalian cells, that is, clathrin is involved in specific sorting steps both in the trans Golgi region and during endocytosis at the plasma membrane. These are the sites where the characteristic coated structures, now confirmed as clathrin-coated pits, were seen in abundance in early **electron microscope** pictures of fixed cell sections (21, 22). In a more complex creature, the slime mold, *Dictyostelium discoideum* (23), failure of clathrin heavy chain expression in cells impairs endocytosis and causes a lack of endosomes and contractile vacuoles, leading to defects in osmoregulation. Such cells also cannot follow the developmental program.

In *Drosophila melanogaster*, the clathrin heavy chain gene is essential (24). However, in flies, a dramatic effect is caused by the shibire mutation. This is a temperature-sensitive mutation in the molecule, now known to be **dynamin**, that is required for budding off a clathrin-coated vesicle (25, 26). At the nonpermissive temperature, the flies drop down as if dead. They cannot recycle their synaptic vesicle components in synapses and therefore cease to fly. However, when cooled down again, they start to fly as usual. These results confirm and extend the original electron microscope observations of abundant clathrin-coated vesicles in nerve synapses (27) and particularly the neuromuscular junction (28). Recent studies have identified many more components in the synaptic vesicle cycle (6) and explored their role by genetic manipulation in *Drosophila* and *Caenorhabditis elegans* [see Fig. 1; (29-32)].

In the worm, *C. elegans*, clathrin-mediated sorting has been implicated in the development of the vulval region (5). This study suggests that even apparently quite subtle perturbations in sorting by the coated vesicle system have profound effects in the development of a complex organism.

Recently, a second clathrin heavy-chain gene (CLTD) has been identified in humans, which has its maximal level of expression in skeletal muscle (33). This gene was found in the region commonly deleted in velo-cardio-facial syndrome (VCFS). Based on the location and expression pattern of CLTD, the suggestion is that **hemizygosity** at this locus plays a role in the etiology of one of the VCFS-associated **phenotypes**.

In summary, the clathrin molecule is an extraordinary building unit that has an intricate packing arrangement and forms coated structures of striking beauty. It carries out an important function.

The assembly properties of clathrin with the coated structures and vesicles it encloses have allowed purifying and identifying many of the other functional components involved. Chief among these are the clathrin adaptors, heterotetrameric complexes that coassemble with clathrin to form the vesicle coat.

1.1. Clathrin Adaptors

Two distinct types of clathrin adaptor complexes have been identified (3, 34). One of these (the PM-adaptor) consists of an a-adaptin (~100 kDa) combined with b-adaptin (~100 kDa) and two smaller subunits, AP50 and AP17. This adaptor is found by **immunofluorescence** with a monoclonal antibody against a-adaptin mainly in plasma-membrane-coated pits. In contrast, the second, the Golgi adaptor, consists of g-adaptin (~95 kDa) combined with b′-adaptin and two other subunits, AP47 and AP20, and is found by immunofluorescence using a monoclonal antibody against g-adaptin in coated pits in the trans Golgi network (Fig. 5).

Figure 5. Immunofluorescence localization of clathrin in fibroblasts showing coated pits on the plasma membrane and in
Robinson and B.M.F. Pearse (1986) *J. Cell Biol.* **102**, 48–54.]

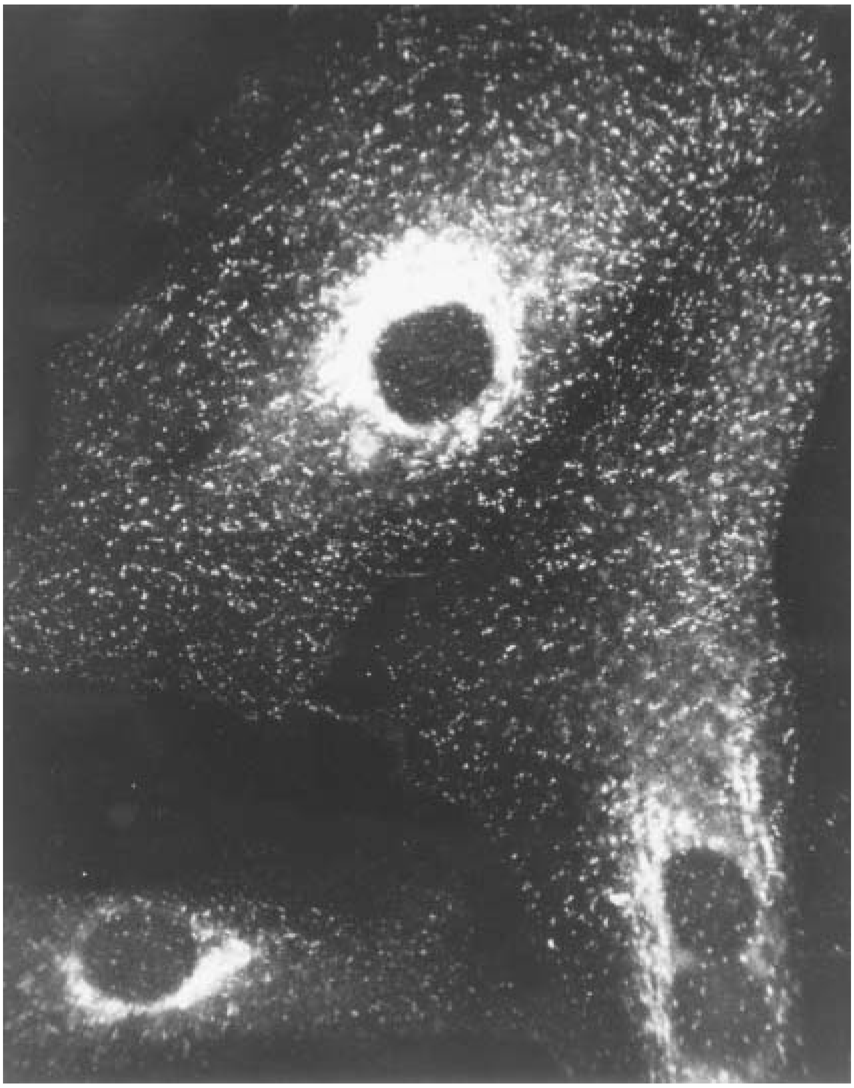

Then the problem immediately arises of how these different adaptor coat complexes assemble on the others. In fact, the problem increases as new related adaptors (35), coats and coatomer complexes (7, the intracellular membrane system. The problem is still incompletely understood, although numerous identified in the cytoplasm and on membranes by a combination of **yeast** genetics and biochemistry. ways in the assembly of particular coated vesicles, their budding, and the control of membrane traffi earlier control proteins identified in post-Golgi membrane transport is Sec4, a small **GTP-binding** p range of GTP-binding proteins have been implicated throughout the recycling system, including Rab sense, **Rho** (38) and heterotrimeric G-proteins (39). For instance, distinct Rab proteins take up a cha particular membrane compartments in the cell and are found in coated pits on those membranes (40) the kinetics of fusion of vesicles from one compartment with another (41), although precisely how th is unclear. ARF, on the other hand, has been implicated in coat binding to membranes notably in the dynamins are concerned with actual budding of coated vesicles, as previously mentioned (see Fig. 1)

When clathrin-coated vesicles assemble on a membrane, they concentrate certain specific receptors i other membrane proteins behind. These specific receptors are recognized by features in their cytopla find its own characteristic **steady-state** distribution throughout the sorting system because each rece sequence. There is no single, defined, clear-cut sequence indicating that a receptor will assemble effi Nevertheless, at least in endocytosis, mutational analysis has pinpointed certain small groups of resid receptors that constitute primary sequence 'features' which allow the normal accumulation of their r Typically, such a 'feature' contains four residues, the first and probably most important of which is t residues (one or both of which is often charged) followed by a bulky aliphatic residue. Such tetrapep with the AP50 subunit of the plasma membrane adaptor (44). However, as more examples are studie possible signals exist and that other factors, such as phosphorylation of receptor tails, play a role in p

(46).

One of the most investigated examples of a receptor that is routed via clathrin-coated vesicles contai network (TGN) is the cation- independent mannose 6-phosphate/IGF-II receptor (MPR). The MPR r lumenal sorting signals, **mannose 6-phosphate**-containing sugar chains on **lysosomal** enzymes, and as cargo inside coated vesicles on their way to lysosomes (47, 48). The MPR has a 163-residue cyto features involved in directing the receptor along its complex, intracellular, recycling pathway, includ Tyr-Lys-Tyr-Ser-Lys-Val (49, 50). The tail region containing these residues, apparently, also acts as lysosomal enzymes, separately or in combination with the C-terminal region (51).

Both types of coated vesicle adaptors bind to the MPR tail. Recognition by the plasma membrane ad the tyrosine residues important for the endocytosis signal, but these same mutations do not abolish s adaptor (52). There is also evidence that the Golgi adaptor preferentially binds to the MPR tail when addition to these cytoplasmic features that determine the routing of the MPR, the extracellular doma play some role in the precise steady-state distribution of the receptor, at least in CV1 and COS cells (

1.2. Clathrin Coats

A low (~50 Å) resolution three-dimensional map of a clathrin coat has been generated from electron in vitreous ice (Fig. 6) (see Electron Imaging). The major components of the coat, clathrin, and adap from purified coated vesicles and separated. Three types of particles were reassembled from these pr clathrin cage itself. The second was derived from the first by partial trypsin digestion to remove the t triskelions, and the third was the complete coat containing both clathrin and adaptors. Maps of each computer imaging tilted specimens of several examples of individual particles of the three different t the incomplete structures from those of the complete coat, three different layers of the overall coat w coded in the image presented (Fig. 6). Thus the outer polyhedral clathrin lattice is highlighted in red, **domains** extends into the structure (green), and the adaptors form an inner shell (blue). These particl the absence of a vesicle, and in fact are actually too small to accommodate a vesicle. Probably the sn contain a vesicle is a truncated icosahedron, which can also be reconstituted as a coat. If purified coa projection they exhibit the same coat thickness composed of three shells of density, whereas the vesi of high density contained within the coat. Now a higher (~20 Å) resolution version of the coat struct types of hexagonal barrel preparations and the equivalent icosahedral specimens by using improved highly developed imaging techniques currently available. This will allow further identification of sm especially if combined with specific antibodies to decorate those domains. It is also possible to gene vesicles from their cytoplasmic constituents and membranes enriched in relevant proteins in physiol exciting prospect as it may lead to a greater understanding of the specificity underlying the assembly locate some of the controlling elements in the structure.

Figure 6. See color insert section. Clathrin encapsulates coated vesicles, the organelles responsible for uptake of essent especially across the placenta in mammals and into oocytes in chickens). (**a**) A three-dimensional map of a clathrin coa specimens reassembled from their constituent protein complexes. Colors highlight the outer polyhedral clathrin lattice (domains (green) revealed in (**b**) and an inner shell of adaptors (blue) exposed in (**c**). These three maps led to the descrip LEGO model. (Courtesy of G.P.A. Vigers, R.A. Crowther, and B.M.F. Pearse from data presented in *EMBO J.* (1986) 5

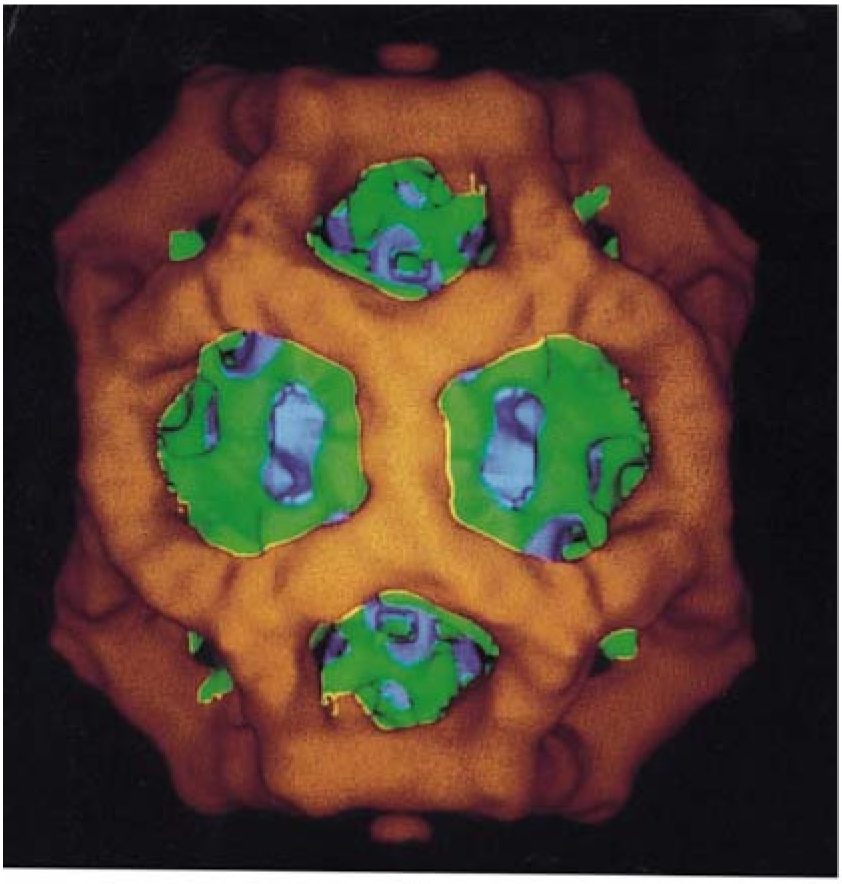

(a)

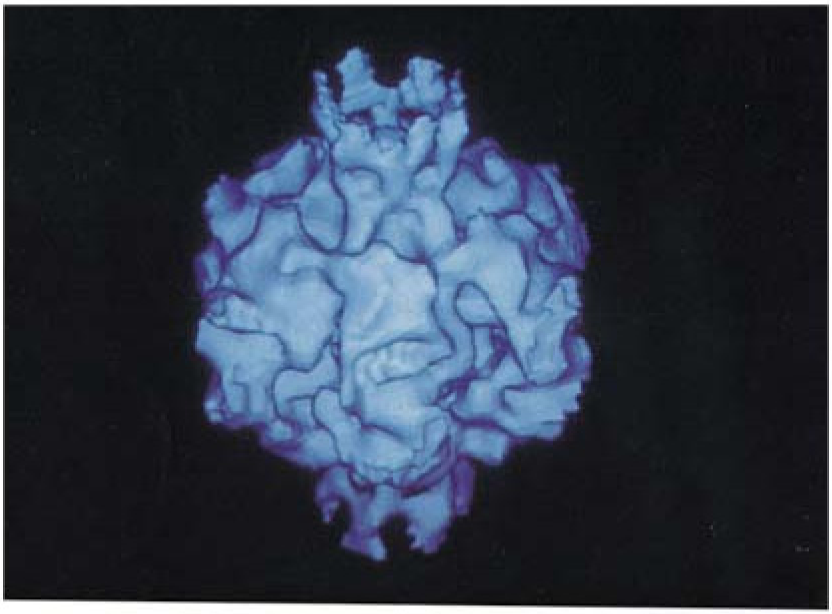

(c)

Bibliography

1. B. M. F. Pearse (1975) J. Mol. Biol. **97**, 93–98.
2. J. L. Goldstein, M. S. Brown, R. G. W. Anderson, D. W. Russell, and W. J. Schneider (1985) A
3. B. M. F. Pearse and M. S. Robinson (1990) Ann. Rev. Cell Biol. **6**, 151–171.

4. P. R. Wolf and H. L. Ploegh (1995) Ann. Rev. Cell Dev. Biol. **11**, 267–306.
5. J. Lee, G. D. Jongeward, and P. W. Sternberg (1994) Genes Dev. **8**, 60–73.
6. P. R. Maycox, E. Link, A. Reetz, S. A. Morris, and R. Jahn (1992) J. Cell Biol. **118**, 1379–1388.
7. R. Schekman and L. Orci (1996) Science **271**, 1526–1533.
8. J. E. Rothman and F. T. Wieland (1996) Science **272**, 227–234.
9. T. Stegmann, R. W. Doms, and A. Helenius (1989) Ann. Rev. Biophys. Biophys. Chem. **18**, 187
10. S. Kornfeld (1986) J. Clin. Invest. **77**, 1–6.
11. B. M. F. Pearse and R. A. Crowther (1987) Ann. Rev. Biophys. Biophys. Chem. **16**, 49–68.
12. E. Ungewickell and D. Branton (1981) Nature **289**, 420–422.
13. T. Kirchhausen and S. C. Harrison (1981) Cell **23**, 755–761.
14. P. K. Sorger, R. A. Crowther, J. T. Finch, and B. M. F. Pearse (1986) J. Cell Biol. **103**, 1213–12
15. A. P. Jackson, H. Seow, N. Holmes, K. Drickamer, and P. Parham (1987) Nature **326**, 154–159.
16. T. Kirchhausen, S. C. Harrison, E. Ping Chow, R. J. Mattaliano, K. L. Ramachandran, J. Smart, Acad. Sci. USA **84**, 8805–8809.
17. S. Liu, M. Wong, C. S. Craik, and F. M. Brodsky (1995) Cell **83**, 257–267.
18. E. Ungewickell, H. Ungewickell, S. E. H. Holstein, R. Lindner, K. Prasad, W. Barouch, B. Mart (1995) Nature **378**, 632–635.
19. G. S. Payne and R. Schekman (1989) Science **245**, 1358–1365.
20. E. Conibear and T. H. Stevens (1995) Cell **83**, 513–516.
21. T. F. Roth and K. R. Porter (1964) J. Cell Biol. **20**, 313–332.
22. D. S. Friend and M.G. Farquhar (1967) J. Cell Biol. **35**, 357–376.
23. T. J. O''Halloran and R. G. W. Anderson (1992) J. Cell Biol. **118**, 1371–1377.
24. C. Bazinet, A. L. Katzen, M. Morgan, A. P. Mahowald, and S. K. Lemmon (1993) Genetics **134**
25. T. Kosaka and K. Ikeda (1983) J. Cell Biol. **97**, 499–507.
26. H. Damke, T. Baba, A. M. van der Bliek, and S. L. Schmid (1995) J. Cell Biol. **131**, 69–80.
27. E. G. Gray and R. A. Willis (1970) Brain Res. **24**, 149–168.
28. J. E. Heuser and T. S. Reese (1973) J. Cell Biol. **57**, 315–344.
29. A. DiAntonio and T. L. Schwarz (1994) Neuron **12**, 909–920.
30. K. Broadie, A. Prokop, H. J. Bellen, C. J. O''Kane, K. L. Schulze, and S. T. Sweeney (1995) Neu
31. Y. Fujita, T. Sasaki, K. Fukui, H. Kotani, T. Kimura, Y. Hata, T. C. Sudhof, R. H. Scheller, and **271**, 7265–7268.
32. E. M. Jorgensen, E. Hartwieg, K. Schuske, M. L. Nonet, Y. Jin, and H. R. Horvitz (1995) Nature
33. H. Sirotkin, B. Morrow, R. DasGupta, R. Goldberg, S. R. Patanjali, G. Shi, L. Cannizzaro, R. Sh Kucherlapati (1996) Human Molecular Genetics **5**, 617–624.
34. S. Ahle, A. Mann, U. Eichelsbacher, and E. Ungewickell (1988) EMBO J. **7**, 919–929.
35. F. Simpson, N. A. Bright, M. A. West, L.S. Newman, R. B. Darnell, and M. S. Robinson (1996)
36. P. Cosson, C. Démolliére, S. Hennecke, R. Duden, and F. Letourneur (1996) EMBO J. **15**, 1792–
37. A. Salminen and P. J. Novick (1987) Cell **49**, 527–538.
38. C. Lamaze, T. Chuang, L. J. Terlecky, G.M. Bokoch, and S. L. Schmid (1996) Nature **382**, 177–
39. R. H. Kehlenbach, J. Matthey, and W. B. Huttner (1994) Nature **372**, 804–809.
40. P. Chavrier, R.G. Parton, H. P. Hauri, K. Simons, and M. Zerial (1990) Cell **62**, 317–329.
41. V. Rybin, O. Ullrich, M. Rubino, K. Alexandrov, I. Simon, M. C. Seabra, R. Goody, and M. Zer
42. A. Peyroche, S. Paris, and C. L. Jackson (1996) Nature **384**, 479–481.
43. P. Chardin, S. Paris, B. Antonny, S. Robineau, S. Béraud-Dufour, C. L. Jackson, and M. Chabre
44. W. Boll, H. Ohno, Z. Songyang, I. Rapoport, L. C. Cantley, J. S. Bonifacino, and T. Kirchhause

5795.
45. I. V. Sandoval and O. Bakke (1994) Trends Cell Biol. **4**, 292–297.
46. A. Pelchen-Matthews, I. J. Parsons, and M. Marsh (1993) J. Exp. Med. **178**, 1209–1222.
47. S. Kornfeld (1992) Ann. Rev. Biochem. **61**, 307–330.
48. J. Klumperman, A. Hille, T. Veenendaal, V. Oorschot, W. Stoorvogel, K. von Figura, and H. J. (
997–1010.
49. P. Lobel, K. Fujimoto, R. D. Ye, G. Griffiths, and S. Kornfeld (1989) Cell **57**, 787–796.
50. M. Jadot, W. M. Canfield, W. Gregory, and S. Kornfeld (1992) J. Biol. Chem. **267**, 11069–1107
51. K. F. Johnson and S. Kornfeld (1992) J. Cell Biol. **119**, 249–257.
52. J. N. Glickman, E. Conibear, and B. M. F. Pearse (1989) EMBO J. **8**, 1041–1047.
53. R. Le Borgne, A. Schmidt, F. Mauxion, G. Griffiths, and B. Hoflack (1993) J. Biol. Chem. **268**,
54. E. Conibear and B. M. F. Pearse (1994) J. Cell Science **107**, 923–932.

Cleveland Map

This method of peptide mapping involves generating of protein fragments via limited **proteolysis**, usually in the presence of **SDS**, followed by electrophoretic separation in SDS-PAGE. The resulting one-dimensional peptide patterns are characteristic of the protein substrate and are used to evaluate structural relationships between proteins and to aid identification of individual polypeptide chains. The technique is named after the first author of a 1977 publication describing the procedure (1), and many variants of this method have subsequently been presented (2).

After initial separation and excision from a primary gel, the protein substrate is digested in solution or, typically, in the stacking zone of the SDS-PAGE "mapping gel." The solution approach relies on purifying the protein by conventional chromatographic procedures or preparative SDS-PAGE followed by excision and electroelution from the gel (3). Protein preparation in SDS-containing gels is feasible because the subsequent digestion is performed in the presence of SDS. Frequently, SDS-PAGE isolation of the protein is possible at an early stage of purification, which is important when only a small amount of the protein is available. For Cleveland mapping, the efficient approach is to place the gel slice that contains the protein band of interest directly into a well of a second SDS/polyacrylamide gel and to add a suitable proteolytic enzyme. After electrophoresis just long enough for the protein substrate to migrate out of the gel piece and enter the stacking zone with the proteinase, the power is temporarily switched off and the gel left for digestion to take place. When the power is turned on again, the fragments of the protein substrate are separated from the proteinase and are mapped in the resolving gel. This procedure is preferred when handling small amounts of protein because of the direct transfer between primary and secondary gels.

The original Cleveland protocol (1) involved brief staining of the primary gel with Coomassie Brilliant Blue, followed by rapid destaining and excision of the band corresponding to the protein substrate. Because fixation of the protein is undesirable due to the electrotransfer, negative staining with 1 M KCl may be an alternative and has been used for subsequent electroblotting and sequence analysis (4). The excised gel piece is equilibrated in buffer containing 0.1% (w/v) SDS to unfold the protein substrate and to obtain a suitable pH of 6.8 for stacking gel electrophoresis and digestion (1). Often, 5 to 10 µg of protein substrate is required for application onto the primary gel to generate a proteolytic pattern detectable by Coomassie Blue staining, but the minimum amount can be substantially lowered if **silver staining fluorescence** techniques or **radiolabeling** are used to visualize the peptide map.

After equilibration, the gel piece that contains the protein is placed in a well of the "mapping gel," and, in the original protocol, overlaid with a solution of the appropriate proteinase in the same buffer. In later protocols, loading of the proteinase below the gel piece is suggested to avoid a variable depth of enzyme solution around the gel piece (2). Once a narrow stack has formed after the initial period of current, usually when the tracking dye (e.g., bromphenol blue) is approaching the bottom of the stacking gel, the power is turned off for 30 to 60 min. This is normally sufficient for the proteinase to cleave susceptible peptide bonds, which typically generates 10 to 20 fragments of 50- to 70-kDa proteins (1). It is crucial that the proteolytic enzyme is active in 0.1% SDS (up to 0.5% for in-solution digestions). Suitable enzymes are **trypsin**, a-**chymotrypsin**, and papain, in addition to the popular V8 proteinase from *Staphylococcus aureus*. All are added in proportions corresponding to an enzyme to substrate ratio in the range of 1:10 to 1:50 (w:w). After digestion, electrophoresis is resumed, and the resulting fragments are resolved, typically in a 15 or 20% acrylamide gel of the discontinuous type (Fig. 1). A unique proteolytic pattern is obtained for each protein substrate and for each individual proteinase. This discriminating feature makes Cleveland mapping useful as a tool for visually judging the similarity between proteins.

Figure 1. One-dimensional Cleveland maps of albumin (A,D,G), tubulin (B,E,H), and alkaline phosphatase (C,F,I), generated by cleavage with papain (A–C), *Staphylococcus aureus* V8 proteinase (D–F), and chymotrypsin (G–I), followed by SDS-PAGE in a 20% (w/v) acrylamide gel. Each combination of protein substrate and proteinase gives a unique pattern. From Ref. 1 with permission.

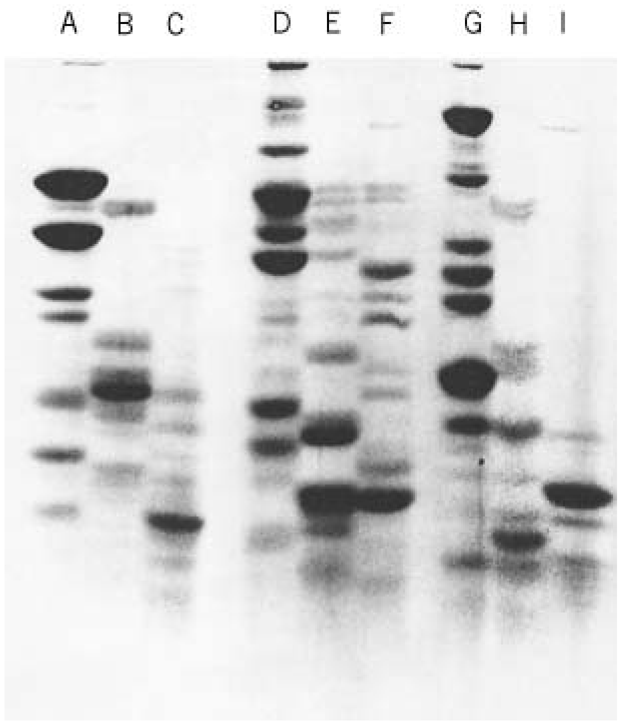

In addition to enzymes, specific chemical cleavage is employed where the protein substrate within a gel is treated in a test tube. Suitable reagents are **cyanogen bromide** for cleavage after methionine residues, *N*-chlorosuccinimide for cleavage at tryptophan, **hydroxylamine** for cleavage at Asn-Gly peptide bonds, and formic acid for cleavage at Asp-Pro bonds. As for the size of the protein substrates, the method is generally applicable to polypeptide chains in the range 10 to 100 kDa.

Peptide fragments smaller than 10 kDa are difficult to resolve into informative peptide maps, although separating such small peptides is possible by using different SDS-PAGE systems. An alternative is to recover small fragments separately by size exclusion chromatography for subsequent peptide mapping by reverse-phase **HPLC**. This can be useful also for proteins large than 10 kDa in order not to waste small fragments (5).

Bibliography

1. D. W. Cleveland et al. (1977) J. Biol. Chem. **252**, 1102–1106.
2. W. J. Gullick (1986) In *Practical Protein Chemistry: A Handbook* (A. Darbre, ed.), Wiley, Chichester, U.K., pp. 207–225.
3. M. W. Hunkapiller et al. (1983) Methods Enzymol. **91**, 227–236.
4. T. Bergman and H. Jörnvall (1987) Eur. J. Biochem. **169**, 9–12.
5. T. Bergman et al. (1991) J. Protein Chem. **10**, 25–29.

Clonal Selection Theory

At the beginning of the twentieth century, Ehrlich was the first to propose that antibodies did exist prior to the introduction of antigen or immunogen and that antigenic stimulation only promoted amplification of molecules of the appropriate specificity. This proposal was quite pertinent, because it contained several key ideas, proven correct some 70 years later. One is the selective process of a preexisting repertoire, the other is that immunoglobulins (Igs) may exist as surface or secreted molecules. The only aspect that was not verified is that Ehrlich imagined a cell to express many different antibodies. After a long period during which hapten analysis indicated the exquisite precision of antibody–antigen interactions, it seemed impossible that antibody structures might preexist to recognize laboratory artifacts, like the haptens being studied. This resulted in the template theory of antibody formation, which required the presence of antigen prior to the synthesis of the corresponding antibodies. Revival of the selection theory was proposed in 1955 by Jerne, but it took another 4 years before the final form of the “clonal selection theory” was put forward by Burnet. The essence of the theory was that antibody specificities were preformed, but in a clonally distributed manner, so that one cell makes only one antibody of one given specificity. This was crucial to provide a mechanism accounting for acquisition of discrimination between self and nonself, after the observation on induction of immunological **tolerance** by the group of Medawar in 1953,when it was demonstrated that tolerance was an acquired phenomenon, resulting from a contact between the immature immune system and the self antigens during gestation or the perinatal period. Burnet most simply explained tolerance by a deletion of those clones that could interact with self components, leading to the concept of “forbidden clones.” Once the basic anti-nonself repertoire established, an antigen was seen as merely selecting and amplifying the cell population of clones expressing the corresponding specific antibodies.

Many investigators worked to define models that would prove the clonal theory, and the literature is amply documented on this point, with many very elegant approaches, such as those based on limiting dilutions, either *in vitro* or *in vivo* after transfer in irradiated mice. The ultimate proof came from molecular analysis, first at the protein level on myeloma proteins and then when the mechanism of gene rearrangement of Ig **genes** was elucidated, under the control of allelic exclusion. Some exceptions to the clonal expression of Ig molecules have been periodically reported. Some were not exceptions, as in the case of lymphocytes coexpressing multiple isotypes that, in fact, share identical V_H and V_L regions, and therefore having the same specificity. Upon reactivation of the recombinase genes upon immunization, for example, a transient coexpression of different V genes may occur, leading to secondary gene rearrangements. But this rarely results in long-term production of antibodies of different specificities. The clonal theory is widely accepted and considered proven, and the fantastic use of monoclonal antibodies is (for most biologists) daily living proof of its pertinence.

See also entries Allelic Exclusion, Antibody, Gene Rearrangement, and Immunoglobulin.

Suggestions for Further Reading

M. F. Burnet (1959) *The Clonal Selection Theory of Acquired Immunity*, Vanderbilt University Press, Nashville, TN.

K. Rajewsky (1996) Clonal selection and learning in the antibody system. Nature **381**, 751–758.

M. Nussenzweig et al. (1987) Allelic exclusion in transgenic mice that express the membrane form of immunoglobulin. Science **236**, 816–819.

Cloning

The word "cloning" has several different meanings. For example, it is possible to clone cells, that is, to cause cells to reproduce themselves so as to make a population of identical cells. In molecular biology, any piece of **DNA** can be cloned—inserted into a **vector** that replicates in a host to produce many copies of the same recombinant vector. It is also possible to clone **genes**. Gene cloning is the process of identifying and isolating a specific gene of interest. Cloning genes is a major focus of molecular biology, and the ability to clone genes has revolutionized biology. Once a gene is identified and cloned into an appropriate vector, it can be manipulated in many different ways. Cloning dramatically amplifies the DNA so that it can be **sequenced**. A cloned gene inserted into an expression system creates an organism that produces up to 25% of its total protein or more as the gene product, allowing large-scale production of the protein (1). A cloned gene can be mutated, and the mutated form inserted back into an organism that lacks a functional copy of the gene (2). This allows structure-function analysis of the gene product. A cloned gene or set of genes can be introduced into a new host to create a new metabolic pathway or to modify an existing pathway (3).

In many cases, gene cloning is carried out by fragmenting the **genomic** DNA from the organism containing the gene of interest and inserting the fragments into self-replicating DNA molecules (vectors) using recombinant DNA techniques; **transforming** the resultant population of recombinant molecules, which comprise a DNA library, into a host organism, screening or selecting the transformants to identify cells that contain the desired DNA, and isolating the vector DNA.

1. Preparation of DNA for Cloning

Genomic DNA must be fragmented before cloning into a suitable vector. It is important to have fragments that contain the gene intact. One way to ensure this is to use a restriction enzyme that makes frequent cuts in the DNA under conditions of partial digestion (so that only some of the sites are cleaved) so as to obtain fragments of the desired size. The restriction enzyme *Sau*3A is often used because it has a four-base recognition sequence and therefore cuts DNA at many sites in the genome. Additionally, it produces cohesive, sticky ends that ligate with BamHI, a site often present in polylinkers. Mechanical shearing also fragments the DNA, but sheared DNA cannot be cloned directly. First, the ragged ends must be filled in and polylinkers added.

Because small fragments of DNA **ligate** to a vector more readily than large fragments, the DNA to be cloned is often fractionated by sucrose density gradient centrifugation (see Sedimentation Velocity Centrifugation) to obtain DNA of the desired size (pp. 2.85–2.86 of Ref. 4). It is important to set up the conditions for ligation so that most of the recombinant molecules produced contain only a single DNA fragment. This means that nearly equal numbers of vector molecules and fragment molecules should be present and that the total DNA concentration should not be too high (~40 µg of vector DNA per mL).

It is necessary to produce a large enough number of transformants or recombinant **bacteriophage** to have a high probability that a fragment carrying the intact gene is present in the population. The exact number depends on the size of the genome from which the gene is being cloned (the larger the genome, the more transformants need to be screened) and the size of the inserts (the larger the insert size, the fewer transformants need to be screened). A major problem in cloning is restriction enzymes in the host, which can degrade foreign DNA. Mutant strains of *Escherichia coli* are available that lack restriction enzymes, and these are best for constructing large libraries for screening or selection. Once a gene is cloned, restriction enzymes in a host are not usually a problem because large amounts of DNA overcome the restriction barrier (5).

Prokaryotic genes are usually cloned from genomic DNA, whereas **eukaryotic** genes are often cloned from complementary DNA (cDNA), which is prepared by copying messenger RNA with **reverse transcriptase.** Most eukaryotic genes contain **introns**, which prevent them from being expressed in prokaryotes, but the introns are not in the cDNA. The cDNA clone is often used as a probe to isolate the gene from a genomic library. The genomic clone can be sequenced to identify the nature and location of the introns and the upstream and downstream sequences of the gene.

2. Cloning Vectors

There are four general types of vectors that are used in *E. coli*: **plasmids**, phage, **cosmids** or bacterial artificial chromosomes (BACs):

1. Plasmids have the advantage that they are smaller than the other vectors and usually give larger amounts of vector DNA from a given volume of culture because of their high **copy number**.
2. Phage vectors allow larger sized inserts of foreign DNA, so that a smaller number of **plaques** are needed to give a high probability that the entire genome of the organism is present in the library that is being screened. Furthermore, phage systems give more plaques per weight of DNA than plasmids give colonies, and plaques are easier to screen than colonies because they are smaller and more uniform. Phage T4 vectors allow cloning inserts as large as 120 kbp (6), whereas phage P1 vectors allow 80-kbp inserts (7), and lambda phage vectors allow up to 40-kbp inserts (pp. 2.2 to 2.125 of Ref. 4). Once a positive plaque is identified, the insert DNA is subcloned into a plasmid vector to take advantage of the greater amplification and ease of DNA preparation associated with plasmid vectors.
3. Cosmid vectors combine features of the preceding two classes because they can be packaged into phage but also replicate as plasmids. They also allow inserts up to 40 kbp (8).
4. Bacterial artificial chromosomes are based on the single-copy **F factor** plasmid and accept >300-kbp DNA fragments (9). Another important system for cloning very large DNA pieces is **yeast artificial chromosomes** (YAC). YACs accept fragments over 200 kbp and are used in genome sequencing and positional cloning of genes (10). Although **yeast** is not as easy to work with as *E. coli*, it is useful for studying eukaryotic genes that cannot be expressed in *E. coli.*

3. Identifying the Gene of Interest

Screening is usually the most difficult step, and there are many different approaches available. The simplest method is to complement a mutant gene in a host organism (see Complementation), which allows direct selection of the desired clone (11). A powerful example of direct selection is cloning a **transposon-tagged** gene where selection is for antibiotic resistance encoded in the transposon.

Another approach is to screen transformant colonies for the gene product, either with specific antibodies (pp. 12.11–12.29 of Ref. 4) or by an enzymatic assay (12). This requires a sensitive, specific assay because foreign genes are often expressed at a low level, and enzymes from the host organism must not interfere with the assay. In addition, the gene to be cloned needs to be expressed in the host organism.

The most general screening approach is to transfer the colonies to a filter, lyse the cells, **denature** the DNA on the filter and **hybridize** a labeled nucleic acid probe to the filter (see Southern Blots (DNA Blots)). The probe pairs with complementary sequences in the DNA on the filter, and the colony to which the probe hybridizes is visualized by the label. There are various methods to design or obtain an oligonucleotide probe that specifically hybridizes to the desired gene.

If one wants to clone the gene coding for a known protein, it is possible to sequence the protein, usually at its N-terminus (see Edman Degradation), and to use reverse translation to determine the probe sequence. However, sequences from internal peptides produced by specific cleavage of the polypeptide chain (eg, by an **arginine**-specific proteinase or by **cyanogen bromide** cleavage at **methionine residues**) are also used if the N-terminus is blocked or if the N-terminal sequence is unsuitable for reverse translation (pp. 11.44–11.57 of Ref. 4).

Another method is using a segment of the DNA from the gene of a closely related organism as the hybridization probe (13). A modification of this approach is looking at **homologous** sequences from a set of organisms to identify highly conserved regions that are used to design an oligonucleotide probe specific for the desired gene. It is important to choose organisms with DNA base compositions close to that of the organism from which the gene is to be cloned.

With the large amount of genomic and cDNA sequence information (see Expressed Sequence Tag) becoming available in computer databases, genes of interest are frequently identified during database searches. Hybridization probes are designed from the sequence information and used to screen a library or to amplify the gene directly.

An ingenious way of selecting for a full-length clone in a phage vector, when a partial clone is available, is inserting the sequence next to the *sup*F gene in a plasmid, infect *rec*A$^+$ cells carrying the plasmid with the phage library, and plate the resulting phage on an *E. coli* strain, where only phage containing *sup*F grows (14). Recombination between the complementary sequences introduces the *sup*F only into the desired phage.

4. Positional Cloning of a Gene Identified by its Mutant Phenotype

Often genes are identified because they have an interesting **phenotype** when mutated. The mutation is mapped by using DNA-based markers. The most closely linked marker is used as a hybridization probe to screen a YAC, BAC, or cosmid library, thus initiating a **chromosome walk** to the gene (15). Once a library clone is identified that is deemed to contain the gene of interest, it is subcloned into a vector used to transform the mutant. The subclone containing the gene is identified by its ability to complement the mutant phenotype.

4.1. Potential Problems with Library-Based Cloning

One problem with direct selection is potential contamination of the library with host DNA, which leads to cloning a host gene, rather than the gene from the original organism. Therefore it is necessary to show that genes isolated by complementation are from the desired organism, which can be done by a Southern blot. Other potential cloning problems are that some DNA fragments cannot be cloned because they contain a poison sequence. DNA fragments containing **repeated DNA** sequences are often unstable, because they recombine easily. So *rec*A mutant strains of *E. coli* are often used as a host for cloning to minimize recombination (16).

A major problem in cloning a DNA fragment that has identical ends (cohesive or blunt) is recircularization of vector molecules that do not contain an insert because the two ends of the cut vector are also identical. This gives a high background of transformants or plaques lacking an insert. One method of minimizing this problem is treating the cut vector with calf alkaline phosphatase to remove its 5′ phosphate groups (pp. 1.60–1.62 of Ref. 4). Dephosphorylated vector molecules cannot circularize, but they ligate to the 5′-phosphate groups on the DNA fragments to be cloned. The resulting recombinant molecule circularizes, producing a circular molecule with a single-stranded nick in each strand. These molecules give transformants. It is necessary to completely inactivate the alkaline phosphatase before the DNA to be cloned is added to the vector. The dephosphorylation reaction must be run under conditions that remove most 5′-phosphate groups but do not inactivate the plasmid, so the reaction has to be monitored carefully.

Another method of dealing with the problem of vector molecules lacking inserts is blue-white screening. Many *E. coli* vectors contain an N-terminal portion of the **beta-galactosidase** gene that codes for the a-fragment that complements the inactive b-fragment. A polylinker is introduced into the b-galactosidase gene so that the a-fragment is inactivated when a DNA molecule is ligated into the polylinker. The ligation mixture is transformed into an *E. coli* host that produces the b-fragment, and the transformants are plated on selective plates. The colonies that contain an insert are white, whereas colonies without an insert are blue (pp. 1.85–1.86 of Ref. 4).

When a probe that hybridizes to the gene to be cloned is available, the cloning process is simplified by using the probe to identify an appropriately sized restriction fragment that contains the gene by using Southern blots run on digests of a number of restriction enzymes. The appropriately sized fragments are eluted from a preparative agarose gel electrophoresis run on genomic DNA digested with the chosen restriction enzyme. The fragments are ligated into a vector cut with a compatible restriction enzyme, and the resulting transformants are screened with the probe. This process significantly reduces the number of colonies or plaques that need to be screened (1 of 40 positive vs. 1 of 1,000 for a *Thermomonospora fusca* gene) (17).

5. PCR to Clone Genes

Whenever sequence information is available for a gene, it is possible to design **PCR** primers that amplify all or part of a gene directly from DNA isolated from the desired organism. The PCR product is used as a probe to screen for the clone, or the PCR product is cloned.

6. Insertional Mutagenesis

Transposons (see Transposon Tagging) and retroviruses are used as insertional mutagens to “tag” genes. If a previously identified transposon or retrovirus inserts into a gene, the sequence of the transposon or retrovirus is used as a tag to identify the host DNA flanking the insertion. Techniques, such as IPCR, plasmid rescue, and library screening (using the element as a probe) are all successful in identifying flanking DNA from a “tagged” individual.

7. Cloning Tissue- or Treatment-Specific Genes

In some cases, researchers do not want to identify a specific gene, but instead they are interested in a certain class of gene, for example, liver-specific genes or genes induced by a hormone. There are numerous methods for identifying such specific types of gene, including subtractive hybridization, differential display, database analysis, and analysis of microarrays (see Expressed Sequence Tag).

8. Immunochemical Methods

Another method for cloning a gene, where the protein has been identified previously, is using an antibody that recognizes the protein to immunoprecipitate **polysomes** making the protein and then to isolate its mRNA. The mRNA produces a cDNA copy that is cloned. The cDNA clone is also used as a probe to isolate a genomic clone.

9. Conclusion

There are a large number of ways to clone a gene or set of genes of interest. The method used depends on what materials are available, such as protein sequence, antibodies to the protein coded for by the gene, gene sequence information, useful libraries for screening, or a “tagged” or “untagged” mutation in the gene of interest. The purpose of cloning a gene is to generate large amounts of DNA for further analysis, such as sequencing or mutational analysis. A cloned gene is also useful for producing the protein or for **antisense** studies, and in some cases it is used to disrupt the endogenous gene by homologous recombination. A cloned gene is also useful as a probe in **gene expression** studies. Cloning a gene is one of the first steps to understanding its function.

Bibliography

1. C. Gellissen and L. P. Hollenberg (1997) Gene **190**, 87–97.
2. S. N. Ho, H. D. Hunt, R. M. Horton, J. K. Pullen, and L. R. Pease (1989) Gene **77**, 51–59.
3. R. A. Dixon, C. J. Lamb, S. Masoud, V. J. H. Sewalt, and N. L. Paiva (1996) Gene **179**, 61–71.
4. J. Sambrook, E. F. Fritsch, and T. Maniatis (1989) *Molecular Cloning; a Laboratory Manual*, Cold Spring Harbor Laboratory Press, Cold Spring Harbor, NY.
5. G. G. Wilson and N. E. Murray (1991) Annu. Rev. Genet. **25**, 585–562.
6. V. B. Rao, V. Thaker, and L. W. Black (1992) Gene **113**, 25–33.
7. J. C. Pierce and N. L. Sternberg (1992) Methods Enzymology **216**, 549–574.
8. N. Fairweather (1997) Methods Mol. Biol. **68**, 137–148.
9. B. A. C. Shizuya, B. Birren, U.-J. Kim, V. Mancino, T. Slepak, Y. Tarhiri, and M. Simon (1992) Proc. Natl. Acad. Sci. USA **89**, 8794–8797.
10. D. T. Burke, G. F. Carle, and M. V. Olson (1987) Science **236**, 806–812.
11. D. Mazel, E. Loic, S. Blanchard, W. Savrin, and P. Marliere (1997) J. Mol. Biol. **266**, 939–949.
12. R. M. Teather and P. J. Wood (1982) Appl. Environ. Microbiol. **43**, 777–780.
13. J. Agnan, C. Korch, and C. Selitrennikoff (1997) Fungal Genet. Biol. **21**, 292–301.
14. A. J. Hanzlik, M. M. Osemlak-Hanzlik, and D. M. Kurnit (1992) Gene **122**, 171–174.
15. S. D. Tanksley, M. W. Ganal, and G. B. Martin (1995) Trends Genet. **11**, 63–68.
16. A. C. M. Radding (1982) Annu. Rev. Genet. **16**, 405–437.
17. S. Zhang, G. Lao, and D. B. Wilson (1995) Biochemistry **34**, 3386–3395.

Suggestions for Further Reading

18. D. M. Glover (1985) *DNA Cloning; a Practical Approach*, Vol. **2**, IRL Press, Washington, D.C., describes methods for cloning into microorganisms other than *E. coli.*
19. D. M. Glover and B. D. Hanes (1995) *DNA Cloning: a Practical Approach*, IRL Press, New York, describes methods for introducing genes into mammalian cells and mammals.
20. D. W. S. Wong (1997) *The ABCs of Gene Cloning*, Chapman and Hall, New York; an overview of cloning.

ClpAP and ClpXP Proteinases

These large ATP-dependent proteinases are involved in **protein degradation** in prokaryotes. Each enzyme is composed of two subcomplexes, both of which are essential for ATP-dependent **proteolysis**. (A similar enzyme system is also found in chloroplasts of plant.)

1. ClpP

The ClpP proteolytic component is a serine proteinase composed of 14 identical subunits, organized in two seven-membered rings. The rings enclose a central chamber where the active sites are localized. To be degraded, proteins must enter this chamber through openings in the rings. By itself, ClpP can hydrolyze small peptides but not polypeptides. To degrade proteins, this proteolytic component must associate with either of two homologous ATPase complexes (ClpA or ClpX), which determine the substrate specificity.

2. ClpA and ClpX

ClpA and ClpX complexes are hexameric rings that associate with each end of the ClpP to form a four-ring active enzyme. These ATPases bind different types of polypeptides, probably unfold them, and facilitate their entry into ClpP for degradation.

Suggestion for Further Reading

S. Gottesman, M. R. Maurizi, and S. Wickner (1997) Regulatory subunits of energy-dependent proteases. Cell **91**, 435–438.

Coding Strand

This is an ambiguous term, and perhaps best avoided. Because **DNA** is double-stranded and only one strand of the DNA of a **gene** is usually **transcribed** to make **RNA**, there is a distinction between the transcribed and the nontranscribed strand at any point in the genome. Using the useful terminology "upstream"/"downstream" to refer to the direction in which the gene is transcribed and translated, the nontranscribed DNA strand runs upstream to downstream in the chemical direction 5′ to 3′, whereas the complementary transcribed strand has the opposite 3′ to 5′ polarity. The transcript RNA runs 5′ to 3′, like the nontranscribed DNA strand. Thus, the nontranscribed DNA strand matches the mRNA in its base sequence (with thymine replacing uracil), not the transcribed strand which has the back-to-front complements of the codons, as explained in Figure 1. Consequently, in predicting encoded amino acid sequence of the encoded protein from a gene DNA sequence, one uses the sequence of the nontranscribed DNA strand because this is the strand from which the codons can be read directly. For this reason, the nontranscribed strand is sometimes called the coding strand.

Some workers, however, adopt the opposite convention because, after all, the transcribed strand provides the information for the codon sequence of the mRNA. Therefore, it is best to eschew the coding versus noncoding terminology and to distinguish the two DNA strands as transcribed versus nontranscribed.

It should be remembered that both strands of a particular segment of DNA can be transcribed, though probably never in the same cell type and at the same time. This may be the case, for example, when genes are "nested" within the introns of other genes (see Gene Structure).

Codon Usage and Bias

The genetic code is degenerate, in the sense that (except for methionine and tryptophan) a given amino acid can be specified by either two, three, four, or six alternative **codons**. When the same amino acid is specified by three, four, or six codons, they cannot all be recognized by the same transfer RNA anticodon, and so in these cases at least two or three distinct transfer RNAs must carry the same amino acid (isoaccepting) but with different anticodons (see Transfer RNA and Aminoacyl tRNA Synthetases).

Not all codons for a particular amino acid are used equally frequently. Generally, strong biases favor some codons and are against others, and different codons are favored in different organisms (Table 1). Some genes within an organism show much greater codon usage bias than others, and there is a strong correlation between the degree of bias shown by a gene and its level of expression in terms of the amount of encoded protein produced. For example, in all organisms where the matter has been examined, the genes that encode ribosomal proteins, which are always relatively abundant, are among the most highly biased. The excellent correlation in *Escherichia coli* between codon bias and level of protein product is shown in Fig. 1. This suggests that the preferred codons are more efficiently translated than the relatively rarely used codons.

Figure 1. Frequency of using favored ("optimal") codons in *E. coli* genes plotted against the quantity of the gene protein products. From Ref. 1 by permission.

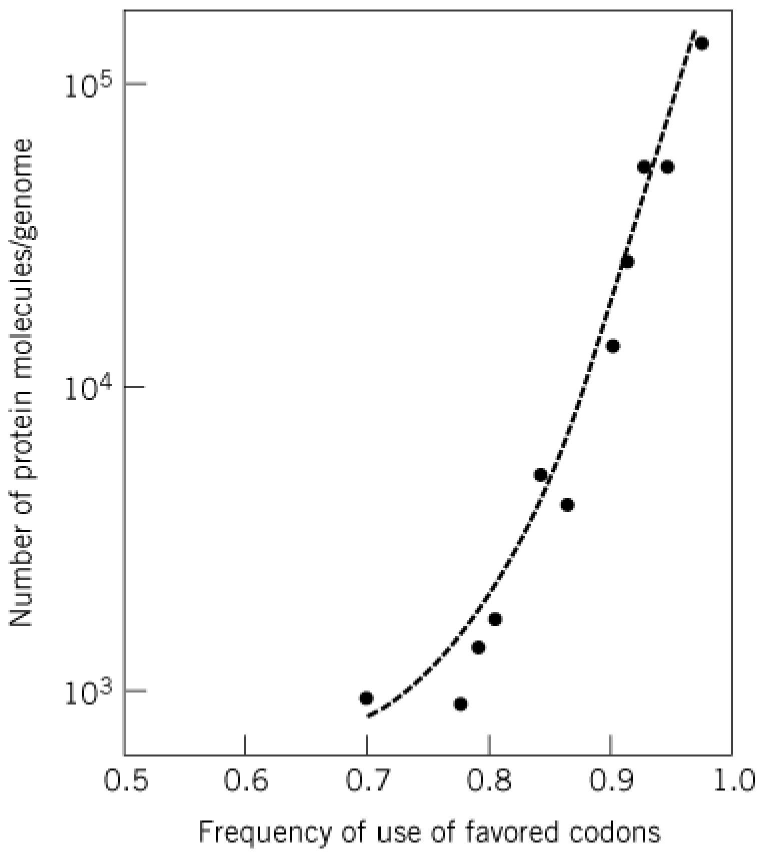

Table 1. Codon Bias in Different Organisms[a]

Amino Acid	Possible Codons	Favored [and Disfavored] Codons: *Drosophila*	*Saccharomyces*	*Escherichia coli*
Leucine	CUU CUC CUA CUG UUA UUG	CUG	UUG	**CUG**
Arginine	CGU CGC CGA CGG AGA AGG	CGU CGC	AGA	CGU CGC
Proline	CCU CCC CCA CCG	CCC	CCA	CCG
Glutamine	CAA CAG	**CAG**	**CAA**	CAG
Lysine	AAA AAG	**AAG**		
Alanine	GCU GCC GCA GCG	GCC	GCU,GCC	
Valine	GUU GUC GUA GUG	*[GUA]*	GUU GUC	*[GUC]*
Glycine	GGU GGC GGA GGG	*[GGG]*	**GGU**	GGU GGC
Serine	UCU UCC UCA UCG AGU AGC	*[AGU]*	UCU UCC	UCU UCC AGC
Threonine	ACU ACC ACA ACG	ACC	ACU ACC	ACC,ACU
Isoleucine	AUU AUC AUA	AUC	AUU AUC	AUC
Asparagine	AAU AAC	**AAC**	AAC	**AAC**
Phenylalanine	UUU UUC	**UUC**	UUC	UUC
Tyrosine	UAU UAC	UAC	UAC	UAC
Glutamic acid	GAA GAG	**GAG**	GAA	GAA
Cysteine	UGU UGC	**UGC**	UGU	
Histidine	CAU CAC	CAC		CAC
Aspartic acid	GAU GAC			

[a] *Drosophila* data from a pool of 15 high-expression genes (3); *E. coli* and *Saccharomyces* from pools of highly expressed genes (1, 2). The codons indicated show strong majority usage (heavy type indicates 90%) except those italicized in brackets where the bias is strongly against. Blanks indicate no strong bias or insufficient data.

Different translation efficiencies of different codons is largely accounted for by a number of factors, pointed out by Ikemura ("Ikemura's rules"), the first of which is that when different isoaccepting tRNAs are present at very different concentrations, the favored codons will be those that are serviced by the most abundant tRNAs. There is evidence for this generalization from *E. coli, Saccharomyces* (1, 2) and *Drosophila* (3). Where a particular amino acid has both codon bias and unequal concentrations of isoaccepting tRNAs, the rule holds virtually without exception. For example, the favored arginine codons in *E. coli* are CGU and CGC, whereas AGA is strongly favored in *Saccharomyces*. In the former organism, the tRNA that has anticodon GCI (I for inosine) recognizing CUC/U is present at several-fold higher concentration than that recognizing AGA, with anticodon UCU* (U* is a modified uridine), whereas in yeast the tRNA inequality is very much the opposite.

The different relative abundances of tRNAs do not, however, explain codon usage bias when it operates between codons served by the same isoaccepting tRNA. Here the bias can be explained in terms of Ikemura's other rules, which account for the fact that an anticodon may pair more comfortably with one codon than with another, even though it recognizes both. Thus an anticodon that has a thiolated uridine or 5-carboxymethyl uridine in the 5′ position (the "wobble" pairing position, see Anticodon) prefers a 3′ A in the codon over 3′ G (rule 2); 5′ inosine (I) prefers U or C to A, even though it pairs with all three (rule 3); and codon-anticodon interactions dependent on the relatively weak A–U or T–A pairings in both of the first two positions work best with a stronger G–C or C–G pairing in the third (rule 4). Examples from *E. coli* consistent with these rules are the biases in favor of GAA over GAG (rule 2), CGU or CGC over CGA (rule 3) and AUC over AUU (rule 4) (1).

1. Effects of Altering Codons

If the more rarely used codons really are translated relatively slowly, one would expect that their introduction into normally highly expressed genes would decrease protein yields. This prediction has been tested experimentally, and substantial effects have indeed been found, especially when multiple and contiguous rare codons have been introduced into the upstream ends of open reading frames. Hoekema et al. (4) carried out a total replacement of the normal codons by synonymous infrequently used codons in the upstream third of the normally highly expressed *Saccharomyces PGK1* (phosphoglycerate kinase) gene and found a tenfold reduction in enzyme yield. There was also a threefold reduction in the level of **messenger mRNA**. In the gene encoding glutamate dehydrogenase, in *Neurospora crassa*, a double frameshift mutant that generated three successive rare codons, numbers 54 to 56 of a 453-codon sequence, brought about a threefold reduction in enzyme without appreciable effect on mRNA level (5). And in *E. coli*, the insertion of an additional mRNA segment containing five contiguous rare AGG arginine codons 24 bases downstream of the initiation codon of *lacZ* (**b-galactosidase**) reduced the enzyme yield by 90% in the early exponential phase and virtually to zero thereafter. Another insertion, identical except that AGG was replaced by the favoured CGU codon (6), had little effect. However, when the distance between the inserted AGG-containing sequence and the initiation codon was increased by additional insertions, the yield of b-galactosidase increased almost linearly with distance, as if the rare codons have maximum effect when translation is just starting and progressively less effect as it proceeds. The mechanism of such distance-dependence is unclear. Chen and Inouye (6), reviewing the positions of rare codons in *E. coli* genes, noted that they fall within the first 25 codons after the initiating AUG and suggested that their function is to modulate the rate of translation. This would only be a regulating mechanism if there were some means of increasing or decreasing the effect, for instance, by adjusting the levels of the least abundant tRNAs. But there is as yet no evidence for this.

If rare codons have strong negative effects on the protein yields of genes, they may be an obstacle to the expression of **transgenes** in alien host cells. A codon that is abundant in the donor organism may be rare in the recipient. Therefore, to obtain a good yield of a foreign protein, it may be necessary to adjust the coding sequence of the introduced gene by *in vitro* DNA manipulation. Perhaps the best example of successful application of this idea is provided by the work of Cormack *et al.* (7), who wished to confer on the fungus *Candida albicans* the ability to produce the green fluorescent protein (GFP) native to the jellyfish *Aequoria victoria*. Introduction of the natural GFP gene into *Candida* on a replicating plasmid **vector** resulted in the formation of some GFP mRNA in the fungus, but no detectable GFP. Replacing the single CUG codon with CUU, in case the *Candida* coding idiosyncracy of translating CUG as serine rather than leucine (8) was responsible for the failure, brought no improvement. But when all the *Aequoria* codons that are comparatively rare in *Candida* were replaced by codons that are common in the fungus, introduction of the transgene produced an abundance of GF protein. The level of GFP mRNA was also considerably increased, which suggests, as does the yeast *PGK1* example mentioned before (4), that blocked translation, and hence failure to cover the mRNA with ribosomes, may expose the mRNA to enzymic degradation.

Bibliography

1. T. Ikemura (1985) Mol. Biol. Evol. **2**, 13–34.
2. P. M. Sharp, T. M. F. Tuohy, and K. R. Mosurski (1986) Nucleic Acids Res. **14**, 5125–5143.
3. D. C. Shields, P. M. Sharp, D. G. Higgins, and F. Wright (1988) Mol. Biol. Evol. **5**, 704–716.
4. A. Hoekema, R. A. Kastelein, M. Vasser, and H. A. de Boer (1987) Mol. Cell. Biol. **7**, 2914–2924.
5. J. A. Kinnaird and J. R. S. Fincham (1991) J. Mol. Biol. **221**, 733–736.
6. G.-F. T. Chen and M. Inouye (1990) Nucleic Acids Res. **18**, 1465–1473.
7. B. P. Cormack et al. (1997) Microbiology **143**, 303–311.
8. M. A. S. Santos and M. F. Tuite (1995) Nucleic Acids Res. **23**, 1481–1486.

Coenzyme, Cofactor

The term cofactor has been used as a general term to indicate that a compound was required, in addition to the enzyme, for a reaction to proceed and that the compound remained unchanged at the end of the reaction. Cofactors were considered to be either activators, such as metal ions, or *coenzymes* , organic molecules that participated in enzymic reactions. **NAD** and NADP were named originally as Coenzyme I (CoI) and Coenzyme II (CoII), respectively, because in studies on metabolic reactions they appeared to function as electron carriers. They certainly perform that role in coupled reactions, such as those catalyzed by glyceraldehyde-3-phosphate dehydrogenase and lactate dehydrogenase:

$$\begin{aligned}&\text{Glyceraldehyde-3-phosphate} + \text{NAD} + P_i\\&\rightleftharpoons \text{1,3-bis glycerophosphate} + \text{NADH} + \text{H}^+\end{aligned} \tag{1}$$

$$\text{Pyruvate} + \text{NADH} + \text{H}^+ \rightleftharpoons \text{lactate} + \text{NAD} \tag{2}$$

with the sum of reactions (1) and (2) being

$$\begin{aligned}&\text{Glyceraldehyde-3-phosphate} + P_i + \text{pyruvate}\\&\rightleftharpoons 1,3\text{-bis glycerophosphate} + \text{lactate}\end{aligned} \tag{3}$$

However, this is not the role of NAD/NADH when functioning as substrates for a dehydrogenase reaction. Similar comments can be made about Coenzyme A (CoA), which functions as an acyl carrier, and Coenzyme Q (CoQ, ubiquinone), which acts as an electron carrier. In this connection, it is of interest that nucleoside phosphates, such as ATP, are not usually classified as carriers of phosphoryl groups.

Other compounds that have been considered as coenzymes are biotin, flavin adenine di- and mono-nucleotide (**FAD**, **FMN**), lipoic acid, pyridoxal phosphate, and thiamin pyrophosphate. Biotin, lipoic acid, and pyridoxal phosphate are bound covalently to carboxylases, acyl transferases, and aminotransferases, respectively. FAD may, or may not, be bound covalently to oxidases. The interaction of thiamin pyrophosphate with decarboxylases is noncovalent, although the binding is tight.

It would seem preferable to consider a compound as a coenzyme only under conditions where it is functioning as a carrier and not when it is simply a substrate for a single enzyme. Compounds that are covalently or tightly bound to an enzyme might better be regarded as **prosthetic groups**. The features that these compounds have in common are the helping groups that they provide to enzymes. These groups possess chemical attributes that the enzymes do not have and that are essential for catalysis.

Cohesive, Sticky Ends

Cohesive ends are short single-stranded sequences of **DNA**, usually 1 to 3 bases long, that are produced at the end of a double-stranded DNA molecule by the action of a type II restriction enzyme that makes staggered cuts in a symmetrical, **palindromic** sequence (1). For example, *Pst*1 cuts the sequence 5′ ..CTGCAG.. to give the ends ..C and TGCAG.. . The two ends 3′ ..GACGTC.. ..GACGT.. C.. produced in this way are complementary, so they bind together by base pairing and allow DNA Ligase to repair the break. Furthermore, any fragment cut by an enzyme of this type binds to any other DNA fragment cut by the same enzyme or to one that creates the same cohesive ends. When the cohesive ends ligated together are cut by enzymes that have different recognition sequences, the new sequence is not cut by either enzyme. In the case of *Bam*HI, 5′ ..GGATCC.. and *Sau*3a, ..GATC.., which produce the same sticky ends ..CCTAGG.. ..CTAG..but have different length recognition sites, the sequence created can always be cut by *Sau*3a but can be cut only by *Bam*HI if the sequence cut by *Sau*3a is a *Bam*HI site. Some restriction enzymes recognize degenerate sequences, so that only when both DNA fragments cut with this type of enzyme have the same sequence do they pair and allow ligation. Depending on the position of the cuts in the two strands, either a 5′-strand or the 3′-strand, creating a 5′-overhang or a 3′-overhang is possible, but each enzyme produces only one type.

Cohesive ends are also present on some **bacteriophages**. For example, on lambda phage they are 12 bases long and are produced by staggered cutting of a symmetrical sequence site (cos site) by a phage enzyme during DNA packaging (2).

Bibliography

1. G. G. Wilson and N. E. Murray (1991) Ann. Rev. Genet. **25**, 585–562.
2. O. Yang, A. Hanagan, and C. E. Catalano (1997) Biochem. **36**, 2744–2752.

Coiled-Coils

A coiled-coil is a generic name for any helical structure that has an axis that is itself helical. A general feature of all such coiled-coil conformations is that the handedness of coiling alternates at successive levels of structure, in line with the well-established practice employed by ropemakers over the centuries. This maximizes the interactions between strands and minimizes relative slippage. There are two particularly well-known classes of coiled-coil structures in biological structures: (i) the a-fibrous proteins and (ii) the collagens. The structure of each will be described.

a-Fibrous proteins display a characteristic **heptad** quasi-**repeat** of the form $(a–b–c–d–e–f–g)_n$, where about 75% of the *a* and *d* are positions are occupied by nonpolar residues such as leucine, isoleucine, and valine (1, 2). These sequences adopt a right-handed a-**helical** conformation with about 3.6 residues per turn. Because the apolar residues in the heptad repeat are 3.5 residues apart, on average, it follows that they will form an apolar stripe on the surface of the a-helix, and this will wind around the helix in a left-handed manner (3). In an aqueous environment, apolar residues tend to pack as closely together as possible to shield each other from the water and, in doing so, provide the **hydrophobic** driving force for assembly. This can be facilitated in this case by two or more a-helices coming together, optimizing the packing of the apolar residues along their interface (so-called knobs-into-holes packing) and winding around one another to generate a left-handed coiled-coil structure (Fig. 1). Favorable electrostatic interactions can also be made between the chains, which help to specify both the relative chain direction and the axial displacement between the chains (1). The interchain ionic interactions occur predominantly between oppositely charged residues in positions *e* and *g* of different chains. Calculations and experimental observations on two-stranded a-helical coiled-coils have shown that the strands are parallel (rather than antiparallel) and in axial alignment. The types of apolar residues in positions *a* and *d* are important in specifying the number of chains in the coiled-coil molecule (see Leucine Zippers). Two-stranded coiled-coils occur in muscle **myosin**, intermediate filaments, plectin, streptococcal M proteins, centrophilin, kinesin, b-giardin, and a host of other proteins. Three-stranded structures are found in the laminins, fibrinogen, the spectrin superfamily of proteins, bacteriophage leg proteins such as gp17, cartilage matrix protein, mannose-binding protein, macrophage scavenger receptor protein, and many others. Four-stranded ropes are found in the silks of the bees, wasps, and ants (*Hymenoptera aculeata*), as well as in globular proteins (such as the **four-helix motif**). Five-stranded coiled-coils have recently been described in HIV capsid protein and in collagen oligomeric matrix protein (COMP) (Fig. 2). As Cohen and Parry (3) have pointed out, it is not the bending of the axis of the a-helix in the supercoiled conformation that is crucial but rather the way in which it permits systematic apolar side-chain interactions to be made. It must also be pointed out that many sequences show discontinuities in their heptad substructures. A recent study by Brown et al. (4) has shown that all such (short) discontinuities can be classified as either “stutters” or “stammers”; these correspond to deletions of three and four residues, respectively, from an otherwise continuous repeat. Physically, a stutter results in a region in which the coiled-coil undergoes a degree of local underwinding to generate a longer supercoil pitch length, whereas the stammer causes a degree of local overwinding, thus giving rise to a shorter supercoil pitch length. The latter is likely to be stereochemically more difficult to achieve. The former has been observed experimentally. A coiled-coil is not confined to fibrous proteins with long rod-like domains as seen in myosin, intermediate filaments, and desmoplakin (for example), but occurs commonly in globular proteins in the form of a-helical bundles. These are generally short in length (say 3 to 10 heptads) and contain anything from two or three a-helices to sizable bundles containing six or even more. The same underlying heptad repeat is present, but it becomes less easy to recognize as the helix length decreases.

Figure 1. The structures of two-stranded coiled-coils. (Left) The backbone model of the two-stranded coiled-coil from a portion of the *N*-terminal end of **tropomyosin**. Two right-handed a-helices coil around each other in a left-handed manner. (Center) A space-filling model of the same structure with the strands shown separated. The apolar residues are shown in black. (Right) The two strands brought together. The apolar residues are interlocked in a systematic way along the axis of the coiled-coil and are shielded from water as a result. (From Ref. 9 with permission.)

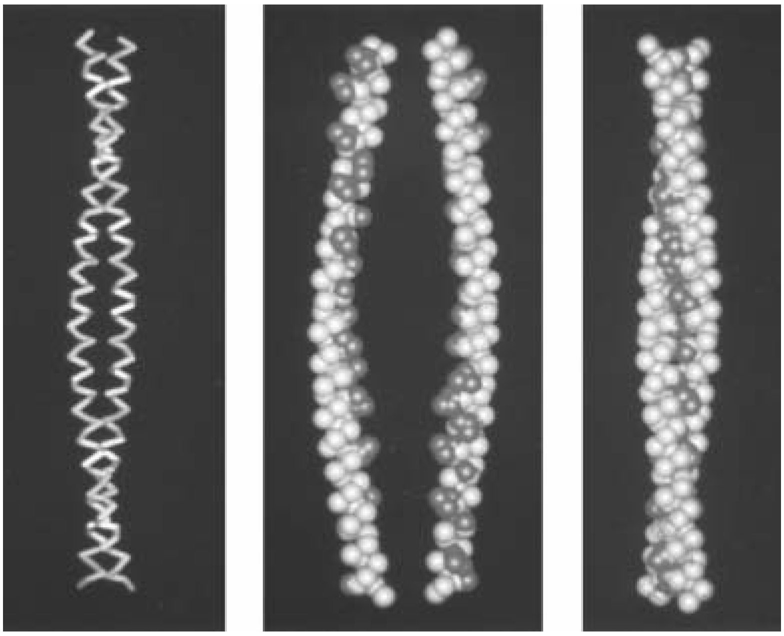

Figure 2. The five-stranded coiled-coil oligomerization domain of cartilage oligomeric matrix protein (COMP). Each of the a-helices forms about one-third of a complete turn over the length of the structure. The N-terminal end is at the bottom of the page. (Courtesy of R. A. Kammerer.) See color insert.

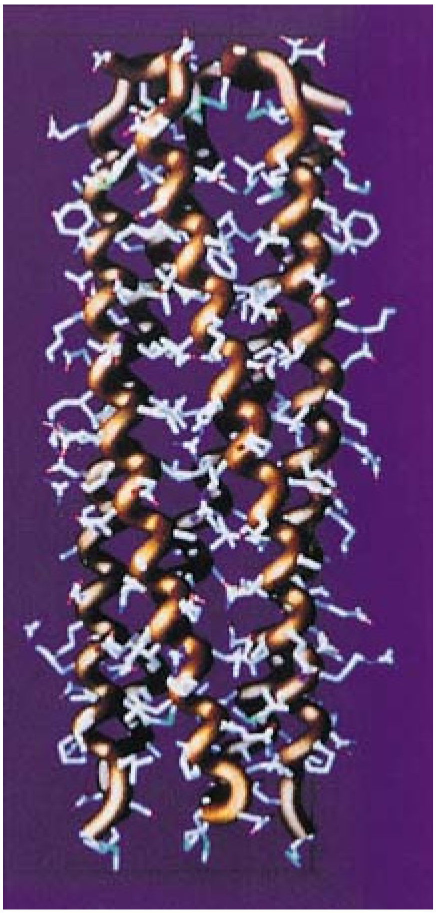

The a-chains in collagen contain a triplet repeat of the form (Gly—X—Y)$_n$, where X and Y can be almost any amino acid residue but are commonly proline and hydroxyproline, respectively. The chain folds up into a left-handed helical structure that is very similar to that seen in polyglycine II and polyproline II. Three a-chains then aggregate in parallel with a one-residue relative axial displacement between chains to generate a right-handed, triple-helical structure in which the glycine residues lie along the axis of the molecule (see Collagen). This class of conformation was originally formulated by Ramachandran and Kartha (5) and Rich and Crick (6) and has subsequently been refined by Fraser et al. (7, 8). The structure has 10 repeating units in three turns, a unit rise of 0.2894 nm, and a pitch length of 0.9647 nm. The individual a-chains have a pitch length of 8.68 nm. The conformation is stabilized by a single hydrogen bond per triplet between the peptide NH group of a glycyl residue and the peptide carbonyl group of an X residue in another chain. Furthermore, water molecules bridge the glycyl NH to the C=Oof a prolyl residue in another chain and the OH group of a hydroxyprolyl residue in the same chain. The diameter of a collagen molecule is about 1.4 nm. Its length varies from one type of collagen to another, but for a Type I collagen molecule its length is close to 300 nm. The molecule thus has a high axial ratio in excess of 200.

Bibliography

1. J. F. Conway and D. A. D. Parry (1990) Structural features in the heptad substructure and longer range repeats of two-stranded -fibrous proteins. Int. J. Biol. Macromol. **12**, 328–334.
2. J. F. Conway and D. A. D. Parry, Three-stranded -fibrous proteins: the heptad repeat and its implications for structure. Int. J. Biol. Macromol. **13**, 14–16.
3. C. Cohen and D. A. D. Parry (1986) -Helical coiled-coils—a widespread motif in proteins. Trends Biochem. Sci. **11**, 245–248.
4. J. H. Brown, C. Cohen, and D. A. D. Parry (1996) Heptad breaks in -helical coiled coils: stutters and stammers. Proteins Struct. Funct. Genet. **26**, 134–145.
5. G. N. Ramachandran and G. Kartha (1955) Structure of collagen. Nature (London) **176**, 593–595.
6. A. Rich and F. H. C. Crick (1961) The molecular structure of collagen. J. Mol. Biol. **3**, 483–506.
7. R. D. B. Fraser, T. P. MacRae, and E. Suzuki (1979) Chain conformation in the collagen molecule. J. Mol. Biol. **129**, 463–481.
8. R. D. B. Fraser, T. P. MacRae, A. Miller, and E. Suzuki, (1983) Molecular conformation and packing in collagen fibrils. J. Mol. Biol. **167**, 497–521.
9. C. Cohen and D. A. D. Parry (1990) -Helical coiled-coils and bundles: how to design an -helical bundle. Proteins Struct. Funct. Genet. **7**, 1–15.

Suggestions for Further Reading

10. C. Cohen and D. A. D. Parry, -Helical coiled-coils and bundles: how to design an -helical bundle. (1990) Proteins Struct. Funct. Genet. **7**, 1–15.
11. R. D. B. Fraser and T. P. MacRae (1973) *Conformation in Fibrous Proteins and Related Synthetic Polypeptides*, Academic Press, London.
12. A. Lupas (1996) Coiled-coils: new structures and new functions. Trends Biochem. Sci. **21**, 375–382.

Cointegrative Vectors

Cointegrative vectors were the first type of **vector** developed for transferring foreign **DNA** from the bacterium Agrobacterium to **plant** cells, for use in plant genetic engineering (1). Although cointegrative vectors may be relatively difficult to work with in practice, compared with the alternative binary vectors, they offer **plasmid** stability in the **bacterial** cell.

The general concept of using cointegrative vectors relies on homologous recombination within *Agrobacterium* to introduce into a modified T-DNA the DNA to be transferred to the plant cell. First, the DNA to be transferred is introduced into an intermediate cloning vector based on an *Escherichia coli* plasmid. The intermediate vector that contains the foreign DNA is introduced by conjugation into *Agrobacterium* that contains the cointegrative vector. The cointegrative vector is a Ti plasmid from which the T-DNA genes that encode oncogenic function have been removed and/or replaced with a sequence that is also contained in the intermediate vector. The intermediate vector is not stable in *Agrobacterium*. Homologous recombination between the intermediate vector and the cointegrative vector results in transferring the foreign DNA to the cointegrative vector. These vectors are designed so that once the foreign DNA, is integrated into the cointegrative vector, it is located between its border sequences. The most generally used cointegrative vector system is the “split-end vector system” (2)

Bibliography

1. P. Zambryski et al. (1983) EMBO J. **2**, 2143–2150.
2. R. Fraley et al. (1985) Bio/Technology **3**, 629–635.

Suggestions for Further Reading

3. R. Walden (1988) *Genetic Transformation in Plants*, Prentice-Hall, Englewood Cliffs, NJ.
4. F. F. White (1993) "Vectors for gene transfer in higher plants". In *Transgenic Plants*, Vol. **1** (D. Kung and R. Wu, eds.), Academic Press, San Diego, pp. 15–48.

Colchicine

Colchicine (Fig. 1), a compound obtained from the autumn crocus, *Colchicum autumnale*, is an ancient drug that has been used for centuries for the treatment of gout (1). Its use in molecular biology began in the mid-1930s when its potent ability to inhibit eukaryotic cell proliferation at mitosis was discovered. Since then, colchicine has had a remarkable history as an experimental tool for characterizing the biochemical properties of tubulin, the protein subunit of microtubules, for characterizing the diverse processes in eukaryotic cells that are dependent upon drug-sensitive microtubules, and for studying the polymerization and dynamics properties of microtubules. For example, colchicine has been used to determine the role of microtubules in mitosis, protein **secretion**, axonal transport, and the development and maintenance of asymmetric cell shape. It has also been used extensively as a cytogenetic tool to determine chromosome numbers in karyotypes. Also, radiolabeled colchicine was used as an affinity marker to effect the first purification of tubulin from brain (2).

Figure 1. Structure of colchicine.

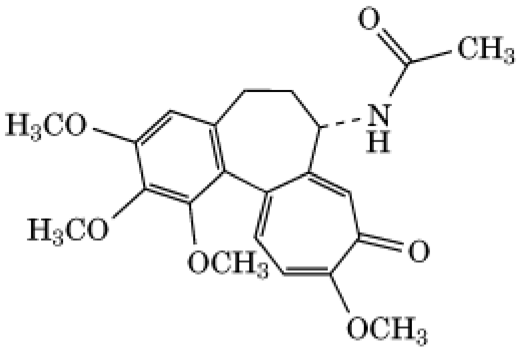

1. Colchicine Binding to Tubulin

The binding of colchicine to tubulin is not a simple process (3-6). The binding reaction is slow and highly temperature-dependent. Binding is extremely slow at 0°C, and 2 to 3 h is required to reach equilibrium at 37°C. The activation energy for the forward reaction is high, ~20 kcal/mol. The kinetics of binding are biphasic. The initial step is the formation of a reversible preequilibrium complex that is followed by a slow step in which conformational changes in tubulin lead to the formation of a final-state tubulin-colchicine (TC) complex. Although the binding of colchicine to tubulin is noncovalent, the final state TC complex is very poorly reversible.

Colchicine binds to tubulin at a single site with a dissociation constant in the range of 0.02 µM to 5 µM. Colchicine has very different affinities for tubulin isolated from different sources. For example, colchicine binds strongly to vertebrate brain tubulin, but it binds very weakly to plant, fungal, and yeast tubulins. Also, there are different tubulin isotypes, and colchicine binds differently to the isotypes purified from same tubulin source (7). Despite intensive investigation, the precise location in tubulin of the colchicine-binding site is not clear. The binding site is thought to reside in the b-tubulin subunit, near residues Cys 354 and Cys 241, close to the intradimer interface.

The binding of colchicine to tubulin induces conformational changes in tubulin, as well as in colchicine (6, 8, 9). For example, the binding of colchicine to tubulin quenches the intrinsic tryptophan **fluorescence** of tubulin, indicating that it induces a small change in the tertiary structure of the protein. It also perturbs the far-ultraviolet circular dichroism spectrum of tubulin, indicating that it changes the **secondary structure** of the protein. In addition, colchicine binding to tubulin strongly increases the intrinsic GTPase activity of tubulin, increases the affinity of the ab dimer association by threefold, changes the exposure of thiol groups in tubulin, and, under certain conditions, induces tubulin to self-assemble into nonmicrotubule polymeric structures. Tubulin is also subject to a time- and temperature-dependent irreversible decay of its protein structure. Binding of colchicine to tubulin slows the rate of decay. The concept that colchicine undergoes conformational changes upon binding to tubulin is evident from the development of colchicine-tubulin fluorescence and the change of the colchicine circular dichroism spectrum upon binding to the protein.

2. Inhibition of Microtubule Polymerization by Colchicine

Colchicine inhibits microtubule polymerization at concentrations that are far below the total concentration of tubulin (10, 11), indicating that colchicine inhibits microtubule polymerization by acting at the microtubule ends. In order to produce its potent actions on microtubule polymerization, colchicine must first form a TC complex. Substoichiometric concentrations of TC-complex only partially depolymerize microtubules, and relatively low concentrations of TC-complex can stabilize microtubules against dilution-induced disassembly (12). These studies support the hypothesis that the TC-complex forms a stabilizing “cap” at the end of the microtubule. Also, the TC-complex can form copolymers with unliganded tubulin when microtubules are assembled in the presence of TC complex (13).

3. Kinetic Suppression of Microtubule Dynamics

Microtubules exhibit two kinds of nonequilibrium dynamics: treadmilling and dynamic instability (see Microtubules). Recent studies have revealed that colchicine and other compounds that depolymerize microtubules (see Vinblastine) strongly suppress these dynamics at relatively low concentrations in the absence of appreciable microtubule depolymerization. Colchicine was found some years ago to suppress treadmilling *in vitro* and the rate of microtubule disassembly upon dilution of the microtubules [now called "kinetic capping" (11, 12)]. However, its stabilizing effects on dynamics were only fully appreciated with the introduction of real-time differential-interference contrast video microscopy, which enabled one to visualize directly in real time the stabilizing action of the drug on the growing and shortening dynamics of individual microtubules (14). Small numbers of incorporated TC complexes strongly suppress the rates and extents of growing and shortening and greatly increase the percentage of time that the microtubules spend in an attenuated state. In addition, the TC complex strongly suppresses the catastrophe frequency and increases the rescue frequency. At low submicromolar concentrations, TC complex suppresses the dynamics without reducing the polymer mass. Significant reduction of polymer mass requires relatively high TC complex concentrations. However, the surviving microtubules are extremely stable. Colchicine appears to suppress microtubule dynamics by binding at the microtubule ends, most probably by inducing a conformational change and/or by steric hindrance at the ends.

Bibliography

1. P. Dustin (1984). *Microtubels*, Springer-Verlag, Berlin, pp. 1–482.
2. R. C. Weisenberg, G. G. Borisy, and E. W. Taylor (1968) Biochemistry **7**, 4466–4478.
3. G. G. Borisy and E. W. Taylor (1967) J. Cell. Biol. **34**, 525–533.
4. L. Wilson and M. Friedkin (1967) Biochemistry **6**, 3126–3135.
5. B. Bhattacharyya and J. Wolff (1974) Proc. Natl. Acad. Sci. USA **71**, 2627–2631.
6. D. L. Garland (1978) Biochemistry **17**, 4266–4272.
7. R. F. Luduena (1983) Mol. Biol. Cell **4**, 445–457.
8. J. M. Andreu and S. N. Timasheff (1982) Biochemistry **21**, 6465–6476.
9. T. David-Pfeuty, C. Simon, and D. Pantaloni (1979) J. Biol. Chem. **254**, 11696–11702.
10. J. B. Olmsted and G. G. Borisy (1973) Biochemistry **12**, 4282–4289.
11. R. L. Margolis and L. Wilson (1977) Proc. Natl. Acad. Sci. USA **74**, 3466–3478.
12. R. L. Margolis, C. T. Rauch, and L. Wilson (1980) Biochemistry **19**, 5550–5557.
13. H. Sternlicht and I. Ringel (1979) J. Biol. Chem. **254**, 10540–10550.
14. D. Panda, J. E. Daijo, M. A. Jordan, and L. Wilson (1995) Biochemistry **34**, 9921–9929.

Suggestions for Further Reading

15. O. J. Eigsti and P. Dustin Jr. (1955) *Colchicine, in Agriculture, Medicine, Biology, and Chemistry*, The Iowa State College Press, Ames, IA.
16. L. Wilson and K. W. Farrell (1986) Ann. NY Acad.Sci. **466**, 690–708.
17. S. B. Hastie (1991) Pharmacol. Ther. **512**, 377–401.
18. L. Wilson and M. A. Jordan (1994) in *Microtubules*, J. S. Hyams and C. W. Lloyd, eds., Wiley-Liss, New York, pp. 59–83.
19. A. Vandecandelaere, S. Martin, M. Schilstra, and P. Bayley (1994) Biochemistry **33**, 2792–2801.

Cold-Sensitive Mutants

Cold-sensitive mutants are a class of **conditional lethal mutants** that cannot grow at a temperature below the organism's normal optimum. The low temperature may be lethal because the mutant form of the protein loses its function or because it forms inappropriate or inhibitory interactions with other proteins. Finding and characterizing second-site revertant mutations that **suppress** the cold-sensitive phenotype identifies protein–protein interactions (see Temperature-Sensitive Mutation).

Colicins

Colicins produced by and active against coliform **bacteria** constitute a subset of the bacteriocins generated by many groups of bacteria. They have been a subject of interest since very early in this century. In 1925, Gratia demonstrated that *Escherichia coli* strain V (virulent in experimental infection) in liquid media produces a heat-stable substance that in high dilution inhibits the growth of *E. coli* (1). This protein was designated as colicin V. It has now been shown that it fits better with the description of the so-called "microcins" (see Bacteriocins) (2). Then a whole series of colicins produced by *E. coli* and closely related members of Enterobacteriacae were discovered. Mainly as a result of the influence and efforts of Fredericq (3), knowledge of the colicins advanced at a great rate, and more than 20 different types were identified on the basis of their action against a set of specific resistant (generally receptor-deficient) mutants (Table 1). In contrast to the bacteriocins from **Gram-positive** bacteria that kill species other than those that are likely to have the same ecological niche, colicins are active only against *E. coli* and closely related bacteria (there is a similar relationship between the cloacins and *Enterobacter cloacae*, the klebicins and *Klebsiella* species, and the pyocins and pseudomonacae). A characteristic feature of colicinogenic bacteria is to be specifically immune to the colicin they make but not to other colicins. A large number of colicins have now been identified, and each has been characterized by the corresponding specific immunity protein. Colicins are **plasmid**-encoded, and each plasmid also bears an immunity protein, thus ensuring that plasmid carriers are protected from the colicin they themselves produce. There is probably a selective advantage for Enterobacteriacae to produce a colicin because 30 to 40% of natural isolates of *E. coli* carry colicinogenic plasmids (4). The colicins exert their lethal effect through a single-hit mechanism (5). There was some controversy about the meaning of this terminology, but now there is a consensus that sensitive cells are killed by a single event, implying that a single molecule kills, although not every one does.

Table 1. Characteristics of Colicins

Colicin	Colicin Activity Group		Receptor	Translocation System
E2,E7,E8,E9	A	DNase	BtuB	TolA, B, Q, R

E3,E6,DF13	A	RNase	BtuB	TolA, B, Q, R
E1	A	Pore-forming	BtuB	TolC, TolA, TolQ
A	A	Pore-forming	BtuB	OmpF, TolA, B, Q, R
N	A	Pore-forming	OmpF	OmpF, TolA, Q
K	A	Pore-forming	Tsx	OmpF, OmpA, Tol A, B, Q, R
Col5	B	Pore-forming	Tsx	TolC, TonB, ExbB, D
Col10	B	Pore-forming	Tsx	TolC, TonB, ExbB, D
Ia,Ib	B	Pore-forming	Cir	TonB, ExbB, D
D	B	Inhibition of protein synthesis	FepA	TonB, ExbB, D
M	B	Inhibition of synthesis of murein and LPS	FhuA	TonB, ExbB, D

Colicins are soluble proteins of 29 to 70 kDa (for colicin V, see previous). Their amino acid sequence is known, and they share the property of being linearly organized in three **domains** that have specific functions. They are also highly asymmetrical molecules and have axial ratios of 8 to 10 (6, 7). Another common feature is that their production is induced by exposure of colicinogenic bacteria to agents like UV light and genotoxic chemicals, such as mitomycin C, that elicit the SOS response. After induction, they are produced in large amounts, so they provide useful model systems to study fundamental biological problems, such as protein–protein interactions, polypeptide translocation and insertion across and into membranes, functioning of voltage-gated pores, etc.

The classification of colicins reflects bacterial rather than colicin properties. According to its activity spectrum against a variety of mutants, a particular colicin is unambiguously assigned to one of two groups, A and B (8, 9). Group B colicins are inactive on strains that have a lesion in the *tonB* gene but are active against strains mutant in *tolA* and *tolB* genes. Group A colicins show the opposite specificity. Now we know that group A colicins (A, E1 to E9, K, L, N, and cloacin DF13) and filamentous **bacteriophage** (f1, fd, and M13) need the Tol proteins to penetrate into cells (9-11). Group B colicins (B, D, Ia, Ib, M, 5, and 10) and phages T1 and F80 need TonB and its associated proteins (8, 9). In all cases studied so far, the determinants for colicinogeny are located on plasmids (Table 1) of two different types: small multicopy plasmids or large low-copy-number plasmids that generally correspond to the A and B groups of colicins. In general, group A colicins are encoded by small plasmids and are actively released to the extracellular medium, whereas group B colicins are encoded by large plasmids and are very poorly secreted.

At least three hypotheses have been proposed to explain the evolution of colicin plasmids: (1) positive selection of diversity, (2) recombinational shuffling, and (3) transposition (12). The different colicins may have evolved by DNA recombination of fragments encoding different colicin domains (see later). This is best exemplified by the common uptake route for colicins B and D, which have a highly homologous N-terminal and central polypeptide sequence (defining the translocation and receptor domains respectively; see later) but very different C-terminal domains with different types of activities (13).

1. Genes for Colicins and Associated Proteins

Regardless of the plasmid type, the genes for the colicin, immunity, and lysis (when there is one) are always clustered (14). The difference between immunity to the enzymatic colicins and to the channel-forming colicins and colicin M (whose target is the cytoplasmic membrane) is reflected in the regulation of their synthesis and the arrangement of the various colicin operons. In enzymatic colicins, the immunity gene is transcribed in the same direction as the colicin and lysis genes (15-17), whereas for the channel-forming colicins and for colicin M, immunity is encoded on the opposite DNA strand and is thus transcribed in the direction opposite to the colicin and lysis genes (18-20). Enzymatic colicin and cognate immunity genes form an operon under the control of an SOS **promoter** (see later). Thus, induction of colicin synthesis results in increasing the amount of immunity protein synthesized, but the presence of a terminator causes partial transcription arrest upstream of the lysis gene. In contrast, inducing the synthesis of pore-forming colicins from their SOS promoter does not result in a concomitant increase in the immunity protein. The immunity is constitutively expressed from a weak promoter (19, 21-23). The situation is similar for the murein-synthesis-inhibiting colicin M and its immunity gene (24).

Colicin production is inducible and suicidal. Under normal conditions, very few cells produce colicin because the expression is repressed by the LexA repressor and is switched on only during the SOS response normally associated with repairing damaged DNA. This means that, in culture, colicin production is inducible in a growing population of cells by mutagens (UV light, mitomycin C). This induction is very efficient. In the absence of mutagens, LexA exhibits a very tight repression (25) and ensures that only a small proportion of cells go down the dead-end road of colicin expression and export. Once they have done so, it is important to the plasmid clone as a whole that the sacrificial cells produce as much colicin as possible. This maximizes selection against non-plasmid-bearing cells. Meanwhile, the silent preservation of many identical copies of the same plasmid in immune cells ensures no significant loss of the plasmids in the producer cell.

2. Extracellular Release of Colicins

Most of the colicins (group A, but not group B) are actively released into the growth medium. Their release mechanism differs from that of proteins secreted by Gram-negative bacteria (see Protein Secretion):

1. they do not contain an N-terminal or C-terminal signal sequence like **Sec**-dependent exported polypeptides or those depending on ABC transporters;
2. their release depends on the function of a lytic protein (variously called *kil*, *lys*, *brp*) whose gene is part of the colicin operon, downstream of the colicin gene;
3. they are released from the host cell some time after synthesis;
4. their extracellular release is not specific, and quasi-lysis proteins have various effect on cells in addition to causing the release of assorted proteins and small molecules (26).

The lysis genes encode short proteins produced in a precursor form with a **signal sequence** and a typical cysteine lipid-modification consensus box, implying that the precursor undergoes the following posttranslational modifications: (1) acylation of the cysteine residue, (2) cleavage of the signal sequence by signal peptidase II, and (3) fatty acylation of the amino group of the now N-terminal acylated cysteine. The maturation and processing of lysis proteins occurs slowly, so every intermediate form can be observed. Both the mature form and the signal sequence accumulate in *E. coli* after processing (27, 28). The addition of globomycin to *E. coli* cells stops processing of lysis protein precursors and inhibits colicin release (29). Acylation is essential for quasi-lysis (29, 30). The mature lysis proteins activate the normally dormant phospholipase A in the outer membrane of colicin-producing cells, thus causing production of lysophospholipids, quasi-lysis, and colicin release (31). However, lysis proteins must also affect the permeability of the inner membrane (32). The lysis protein must reach a critical concentration within the cells before quasi-lysis and colicin release, which also indicates that the lysis protein directly affects the inner membrane. Local modifications in the structure of the bilayer are induced by interactions with lipopeptide micelles, as previously suggested in the case of Iturin A and bacillomycin L (33).

3. Mechanism of Entry and Domain Organization of Colicins

Colicins bind to specific receptors in the bacterial outer membrane, from where they are translocated to, and eventually through, the inner membrane to reach their targets. Consistent with these three steps, their polypeptide chains are linearly organized into three domains: the *N*-terminal domain is involved in the translocation step, the central domain is responsible for receptor binding, and the C-terminal domain carries the lethal activity (Fig. 1). The boundaries of these domains were defined first by limited **proteolytic** digestion (34-36), then by genetic engineering (37, 38), and from sequence homologies between colicins with the same type of lethal activity and using the same receptors (E-type, for example) or the same translocation pathways. Even colicin M, which has a molecular mass of 29 kDa, has three functional domains (24).

Figure 1. The mechanism of colicin Ia attachment and translocation. The outer membrane (OM) receptor for colicin Ia consists of Cir, TonB, and accessory plasma membrane (PM) proteins ExbB and ExbD. The translocation domain (blue), receptor binding domain (green), and channel-forming domain (red) separated by a pair of helices (gray), each 16 nm long, are indicated in colicin Ia. The TonB box of colicin Ia may compete with the TonB box of Cir for linkage to TonB. The channel-forming C domain reaches the plasma membrane, where it forms an ion-conducting channel by subsequent insertion and rearrangement of helices within the membrane (not shown). The translocation T domain may remain near the periplasmic surface of the outer membrane during channel activity. However, the presence of the 16 nm-long T3 helix indicates an alternative possibility in which the T domain crosses the periplasmic space (P) to participate in channel formation *in vivo*. The location of the TonB box on the upper surface of the T domain of sequence Glu(E)-Ile(I)-Met(M) Ala(A)-Val(V) is indicated, reading right to left, as EIMAV. The arrows indicate the locations of the TonB box in the receptor and colicin Ia. Reproduced from (68) with permission.

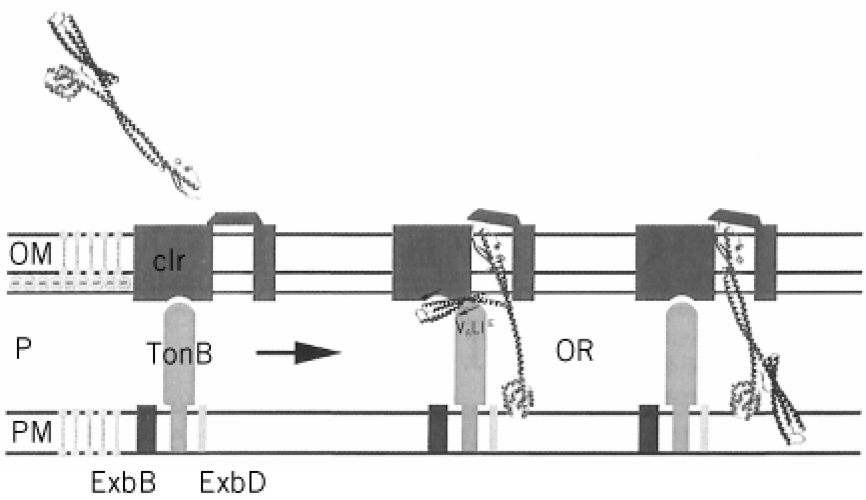

To enter the cells, colicins have borrowed multiprotein systems used by sensitive cells for important biological functions. These proteins include porins, **vitamin B_{12}**, siderophore, nucleoside receptors, and multiprotein systems that cooperate with these proteins. The group A and group B colicins correspond to two different pathways of entry beyond receptor binding: the TonB and the Tol pathway. The receptors for the various colicins are given in Table 1. The protein most frequently used is BtuB, the vitamin B_{12} receptor, which defines the so-called E-type colicins (E2 to E9) (12). High-affinity receptors or iron siderophores are also used by many colicins. The nucleoside Tsx porin and the major porin OmpF are also receptors (Table 1). Depending on the colicin class, the colicin receptors function cooperatively with either the Ton B system or the Tol system.

The *tol* locus was originally defined as comprising four loci, *tol A*, *B*, *Q*, *R*, on the basis of group A colicin tolerance (39). These genes are organized in two operons that comprise three additional genes called *orf*1, *orf*2 and *pal* (40), whose gene products are not directly involved in colicin uptake. However, one of them, the Pal protein (peptidoglycan associated protein), a **lipoprotein** of the outer membrane, interacts with TolB (41). Both *tol* and *pal* mutants have an altered outer membrane (39). The only soluble Tol protein is TolB, which is principally located in the **periplasm** (42) but is linked to the outer membrane through interaction with Pal. The other Tol proteins are associated with the cytoplasmic membrane. TolQ contains three membrane-spanning segments, and TolA and TolR are anchored to this membrane by their *N*-terminal regions. All three proteins interact through membrane-spanning a-helices (43, 44). There is yet no direct evidence that TolB interacts with membrane-associated Tol proteins, but each of the Tol proteins cofractionates with a membrane fraction accounting for the presumed contact sites between the inner and outer membranes of *E. coli*. In colicin A-treated cells, the toxin was also found in this fraction, and the relative amount of Tol proteins was doubled, suggesting that the colicin itself may recruit more Tol proteins at the contact sites (45, 46).

Although both TolB and TolR are required to take up most group A colicins, neither is required for colicin E1, which in contrast requires the so-called TolC protein, a minor outer membrane protein that forms pores *in vitro* (47) and is also involved in secreting hemolysin (48) and colicin V (49). OmpF, another porin, is required for translocating many group A colicins (A, E-type, N) (50, 51). The N-terminal domain of group A colicins contains all the information needed for the translocation step (52) beyond receptor binding, including binding to OmpF (or TolC for colicin E1) and to Tol proteins like TolA (53) and TolB (54). There are about 1000 translocation sites for colicin A per bacterium (55). In addition, it has been shown that: (1) unfolding occurs upon receptor binding (55), (2) the N-terminal domain interacts with Tol proteins, (3) the polypeptide chain spans the entire cell envelope after inserting the pore-forming domain (56), and (4) a reduced constriction of the lumen of the OmpF pore prevents translocation of colicin A and N (57). A hypothetical model of colicin translocation based on these results has been presented (11, 58).

Group B colicins are imported into sensitive cells through high-affinity siderophore receptors and the Ton B pathway. The Ton B system consists of a complex of proteins TonB-ExbB-ExbD, which facilitates the flow of energy from the cytoplasmic to the outer membrane for the energy-dependent transport of ferric siderophores and of vitamin B_{12}. ExbB and ExbD are physically and functionally homologous to TolQ and TolB (59). Ton B, like Tol A, has its N-terminal anchor in the cytoplasmic membrane and spans the periplasm (60). It has been proposed that an energized conformation of TonB, like FepA or FhuA, opens channels in the outer membrane, which act as receptors for the ferric siderophores. Until recently, each of the group B colicins studied uses a Ton B-dependent receptor, but it has now been reported that a new colicin (colicin 10) uses the Ton B system and binds to a Ton B-independent receptor Tsx. Colicin 10 also requires TolC for its uptake (61). Thus the interaction between the colicin receptor and Ton B is not obligatory if TolC is involved. This situation may be comparable to that of the group A colicin E1, which does not need TolB or TolR but does need TolC.

The high-affinity receptors for siderophores and vitamin B_{12} contain a pentapeptide motif close to the N-terminus, called the “Ton B box” (62). Mutations in the Ton B box reduce receptor activity dramatically. They are also **suppressed** by mutations in TonB (63), indicating physical and functional interactions between TonB and the receptors. Group B colicins, such as colicins B and D, which bind to the FepA receptor, and colicin M, which binds to the FhuA receptor, also contain a TonB box sequence close to the N-terminus. This indicates that these colicins interact directly with TonB during translocation. Mutations in the TonB box of colicin B affect its uptake and are suppressed by secondary substitutions clustered in TonB (63). A similar situation is observed with TonB, FhuA, and colicin M. These results suggest that group B colicins need to interact with TonB to be translocated, just as group A colicins need to interact with Tol proteins. Both the N- and C-terminal domains of the protein also interact with the inner membrane and therefore are protected from proteolytic degradation (64). This suggests that the Y-shaped structure (65) allows colicin Ia to span the entire cell envelope, as previously reported with colicin A (66). The receptor-binding domain would be the only part remaining exposed outside the cells.

A molecular model of colicin M uptake has been proposed (24). After first binding to FhuA in the outer membrane, colicin M is taken up in an energy-coupled process through the action of the TonB protein, which is anchored to the inner membrane and spans the periplasmic space. TonB binds to FhuA, inducing the release conformation of FhuA, which, in turn, results in the vectorial translocation of colicin M across the outer membrane. TonB itself has two conformations, energized and unenergized. Energization of TonB takes place in the cytoplasmic membrane. Induction of the receptor release conformation consumes energy, so TonB dissociates from the FhuA receptor and has to be reenergized to induce the next round of colicin M uptake. Because both FhuA and colicin M contain a TonB box, the TonB protein most likely interacts with both of them sequentially. The role of ExbB and D is still unclear. They are involved either in energy transduction (cycling of the TonB conformational change) from the cytoplasmic membrane to TonB or in stabilizing TonB, which is physically and functionally unstable (24, 67, 68).

The 626-residue colicin Ia is about 21 nm long and consists of three functional domains separated by a pair of a-helices 16 nm long. A central domain at the bend of the hairpinlike structure mediates binding to the outer membrane receptor. A second domain mediates translocation across the outer membrane via the TonB pathway. The TonB box recognition motif of colicin Ia is on one side of three 8 nm-long helices arranged as a helical sheet. The third domain, made up of 10 a-helices, is the pore-forming domain (see below). The two exceptionally long 16 nm a-helices enable colicin Ia to span the periplasmic space between the outer and inner membranes (Fig. 1) (68). This type of structure, which will very likely be found in each colicin, strongly suggests how these toxins exploit the machinery of the target cell to get across the periplasmic space (Fig. 1).

4. Mode of Action of Colicins

The biochemical effects of colicins on sensitive bacteria fall into four classes: (1) the RNase colicins typified by colicin E3, (2) DNase colicins typified by colicins E2 and E9, (3) pore-forming colicins like colicin E1, and the still unique colicin M, which inhibits cell wall biosynthesis (24).

4.1. RNase Colicins
The two most extensively studied members of this class are colicin E3 and cloacin DF13 (derived from a strain of *Enterobacter cloacae* closely related to *E. coli*). The 11 kDa and 12 kDa C-terminal segments of these bacteriocins cleave the 16S ribosomal RNA, either in isolation or in intact 30S ribosomal subunits, which explains their inhibitory effect on protein synthesis (69). Colicins E5 and E6 have the same type of activity (70). Although they are highly homologous in their RNase regions (71), colicins E3, E5, E6, and cloacin DF13, each have a specific immunity protein. No structures are yet available for any of these RNase domains.

4.2. DNase Colicins
In 1970, it was shown that colicin E2 causes both single- and double-strand breaks in the DNA of sensitive cells (72), and three new types of DNase colicins were subsequently described (colicin E7, E8, and E9). The sequential identity between the various DNase domains is greater than 80% (71), yet each is inhibited by a specific immunity protein. This is similar to the situation in the RNase-type colicins. Structural and biophysical analysis of the DNase immunity protein complexes has been aided by the *E. coli* overexpression systems developed by Wallis et al. (73-75).

4.3. Pore-Forming Colicins
Pore-forming colicins constitute the largest group. Colicin V must be set apart in this class because it fits the definition of microcins better than that of colicins (2). Pore-forming colicins dissipate the membrane potential (76-80), which causes a series of metabolic effects, such as inhibition of **active transport** and of protein and nucleic acid synthesis, decrease of the internal ATP concentration (see

Adenylate Charge), and leakage of potassium ions (81-85). Cell death results from the depletion of the ATP pool following efflux of phosphate through the channel and ATP hydrolysis (86). Ten pore-forming colicins have been identified thus far. Sequential homologies indicate that they should be separated into two groups: (1) E1, 5, Ia, Ib and (2) A, B, and N (87), differing mainly in a segment containing the loop between helices 8 and 9, as defined in the X-ray crystal structure of the C-domain of colicin A (88). The structures of soluble forms of the channel domains of colicins A, Ia and E1, are known to varying extents (89-92). The pore-forming domain is composed of a bundle of 10 a-helices arranged in three layers in a novel protein fold (93). The N-terminal layer (helices 1 and 2) is connected to another layer consisting of two pairs of amphipathic helices (helices 3 + 4 and 6 + 7), and a single helix (helix 5) connects the two helix pairs. The middle layer is composed of helices 8 and 9, which form a **hydrophobic** hairpin buried in the core of the molecule (Fig. 1). The external sides of the peripheral helices are hydrophilic, which explains the paradox of how the same protein domain exists either in a water-soluble form or in a membrane-inserted state (see later). Because the C-terminal domain of colicins is easily purified by proteolytic digestion of the whole colicins or by genetic engineering, many biophysical studies have been carried out to improve our understanding of this step in the action of pore-forming colicins (for a review, see Suggestions for further reading).

Schein et al. (78) were the first to demonstrate that colicin A forms well-defined channels in planar lipid bilayers that permit ions to cross the membrane (94, 95). Pore-forming colicins form channels of 10 to 30 picosiemens (pS), which correspond to 10^7 ions/sec/channel. These channels are characterized by their sensitivity to the electrical potential across the membrane. The gating voltage (corresponding to the activation or to the inactivation of 50% of the channels) varies for a given colicin. Values are +21, +50, and +70 mV for colicins N, A, and E1, respectively. There are multiple membranes states at the single-channel level. With colicin E1, channels of 10 pS are initially observed. With increased activation in 1 M KCl, channels of 20, 40, and 60 pS with substates appear, and flickering is observed. Similar observations with other colicins suggested the existence of many closed, open, and inactivated states. Thus, the concept of a single-membrane-inserted conformation appears to be incorrect, although a simplified model with a single or a few membrane-inserted forms has been very helpful.

The channel properties of the C-domain and of whole colicin are qualitatively similar for colicin E1, but not for colicins A (96) and Ia (97). Differences are ascribed to the influence of the other domains on the pore-forming domain in the intact molecule. The pores are permeable to cations and anions, but the rates at which they are transported are low (98). There is a relative preference for cations versus anions that is modulated by the pH and the lipid composition (99, 100). Using the relative permeabilities of large organic cations and anions and taking into account their asymmetrical shapes, the size of the channel diameter was estimated at only 0.4–0.5 nm. This implies strong interactions between permeable ions and the side chains of residues exposed in the channel lumen (100).

The transition of pore-forming colicins from a water-soluble to a membrane-inserted state involves large structural changes, which is of interest in the context of **protein folding**, protein translocation, and protein insertion into membranes. From studies with model membrane systems, a likely sequence of events for membrane insertion and pore formation has been proposed for colicins A and E1 (see Suggestions for Further Reading). Briefly, the C-domain first binds to the outer face of the cytoplasmic membrane. The negative charge density plays a part in the binding and the kinetics of insertion (101, 102). After binding, but before insertion, the pore-forming domain must have lost the tertiary structure of the water-soluble form and adopted primarily a **molten globular** conformation, which is still compact and has kept its native secondary structure (87, 103, 104). As mentioned later, the interaction of the N-terminal and central domains with the translocation machinery might trigger the appearance of a molten globular conformation of the channel domain *in vivo* (105). The topology of the membrane-inserted state has been extensively studied, mainly with the pore-forming domains of colicins E1, A, and Ia. The membrane-bound state involves insertion of the hydrophobic helical hairpin formed by H8 and H9 into the bilayer. In contrast to colicin A, which is more dependent on electrostatic interactions, the protein would lie flat on the membrane surface. The hydrophobic hairpin could not insert because the density of charged residues on the membrane surface is too high (103).

The polypeptide translocation involved in voltage-dependent gating has been studied through three main experimental approaches: (1) By using lipophilic radiolabeled probes, Merill and Cramer (106) demonstrated that a 42-residue region of colicin E1 corresponding to helices 5 and 6 was labeled in the presence, but not in the absence, of a membrane potential in a vesicle system with **valinomycin**-induced diffusion potential. Another segment corresponding to the hydrophobic hairpin was strongly labeled in the presence or absence of membrane potential. (2) The existence of a drastic change triggered by a transnegative membrane potential *in vivo* was also demonstrated by disulfide-bond engineering (107). The same technique further showed that a-helices 1, 2, 3, and 10 remain at the membrane surface after application of a membrane potential. (3) Colicin Ia with biotin, conjugated to specific cysteine residues introduced by site-directed mutagenesis, were inserted into a lipid bilayer, and the channels were opened or closed by varying the membrane potential. Then streptavidin was added on the *cis*- or *trans*-side of the membrane. The results demonstrated (108) that a region of the pore-forming domain of colicin Ia reversibly flips across the membrane, implying a large conformational change when potential is applied. A region of at least 68 residues is able to flip back and forth with channel opening and closing. Several open, channel structures probably exist (109).

4.4. Inhibition of Murein Biosynthesis

Colicin M is unique among the colicins in that it inhibits murein biosynthesis (110) by interfering with the dephosphorylation of C_{55}-polyisoprenyl pyrophosphate, which leads to cell lysis (111). It also has a much shorter polypeptide chain than other colicins (29 kDa as compared to 40 to 70 kDa). Yet, it has the same basic design of three functional domains (see previous). The largest part of the C-terminal domain of colicin M resides in the cytoplasmic membrane because the carrier lipid and pyrophosphatase activity were found in the membrane fraction (112). Colicin M does not penetrate deeply into the cytoplasmic membrane but acts mostly at the periplasmic side of this membrane (24). Furthermore, cytoplasmic colicin M does not kill the cells, and only external colicin M, after its import through the energy-dependent TonB system (see previous), has access to the target in the cytoplasmic membrane. A chimeric protein of colicin M linked to a signal peptide directing the C-domain to the periplasm (the outer face of inner membrane) causes cell lysis. The amount of colicin M at the target was so high that immunity broke down (24).

5. The Systems Immune to Colicins

The immunity of colicinogenic cells to the action of the colicin they produce was first noted by Fredericq in 1957 (113). The cell relies for its survival on the immunity protein. The individual cell is safe from its own colicin when that gene is carried on the same plasmid as the *imm* gene. Much progress with regard to the specificity determinants has been made during recent years on the basis of the immune activity, especially for nuclease-type and pore-forming colicins.

5.1. Immunity Against RNases

The determinants for specificity of colicin-immunity interactions with colicins E3, E6 and cloacin DF13 are likely to reside in a limited number of amino acid residues, eight in the nuclease domains and up to nine in the corresponding immunity proteins (114, 115). These determinants are located in the N-terminal regions of both the RNase domain and the immunity protein. A single residue either in Im3 or in Im6 is critical for defining the specificity (116). Other residues are also likely to be involved in the interaction but have more peripheral roles in defining specificity. The 84-residue Im3 (117) is folded into a four-stranded antiparallel b-sheet connected by loops and a single short a-helix, in marked contrast to the structure of a DNase-specific immunity protein Im9 (118), which contains four a-helices. The specificity-determining residues of Im3 at the two main positions are exposed and line one face of the b-sheet (117). No structures are yet available for any RNase domains.

5.2. Immunity Against DNases

The sequences of the DNase domains of colicins E2, E7, E8, and E9 are more than 80% identical, yet they have specific immunity proteins. Site-directed mutagenetic studies identified six Col E9 residues in the C-terminal DNase domain as possible specificity determinants (119). The sequences of Im2, Im7, Im8, and Im9 are 58% identical but are not homologous to the RNase-type immunity proteins. Two amino acid residues were identified as specificity determinants of Im8 and Im9 by using homologous recombination (74) and site-directed mutagenesis (118, 120).

Further structural and biophysical studies of DNase-immunity protein complexes have shown that the DNase E9-Im9 complex is extremely stable (like the Col E9-Im9 complex) with a $\boldsymbol{K_d}$ of 9.3×10^{-17} M, one of the highest affinities ever measured for a protein interaction (121). The association of the nuclease with the Im9 protein is essentially **diffusion-controlled**, involves electrostatic steering, and follows a two-step mechanism in which the proteins form an initial encounter complex before undergoing a conformational change to yield the final stable complex (121). Although there is no cross-reactivity between DNase-type colicins (E2, E7, E8, and E9) and noncognate immunity proteins under normal levels of expression, biophysical studies indicated that the latter bind to the DNase domain of colicin E9 and inhibit its activity (122). The K_d values range from 10^{-17} M (IM9) to 10^{-4} M. Consistent with this result, overexpressing each of the noncognate *Im* genes in bacteria results in significant levels of cross-reactivity toward the ColE9 toxin, and the order of *in vivo* cross-reactivity (Im9 > Im2 > Im8 > Im7) mirrors exactly the measured *in vivo* affinities (122). The specificity for the DNase-Im complexes is controlled through the dissociation constant, which is more than 10^6-fold faster for the noncognate Im proteins. The Im9 fold consists of a distorted antiparallel four-helix bundle in which the second helix (from the N-terminus) is the main specificity determinant (118, 120). The surface regions of Im9 that interact with the DNase include the two central helices of the molecule, and the binding surface is heavily negatively charged, consistent with a positively charged partner DNase domain (118).

5.3. Immunity to Pore-Forming Colicins

The immunity proteins directed against nuclease-type colicins described previously are expressed at a level similar to that of their cognate colicins. In contrast, the proteins immune to pore-forming colicins are expressed constitutively at very low levels (10^2 to 10^3 molecules per cell). Another major difference is that these proteins protect the cells against external colicin because the membrane potential has the wrong orientation for colicin activity from the inside. Thus the immunity is directed against colicins produced by other cells.

Membrane vesicles from cells immune to colicin Ia are depolarized by colicin E1, but not Ia (123), which first indicated a cytoplasmic membrane localization for these types of immunity proteins. In addition, the construction of hybrids between colicins Ia and Ib, A and E1, or A and B, demonstrated that, independent of the translocation pathway, immunity is directed specifically against the C-terminal, pore-forming domain (19, 52, 124). ImmA has four transmembrane a-helices, and both the N- and C-termini are located in the cytoplasm (125). The shorter ImE1 has three transmembrane a-helices. The N- and C-termini are on the cytoplasmic and periplasmic sides of the membrane, respectively (127). These orientations are in agreement with the inside-positive prediction rule (128).

As with Im proteins directed against nucleases, there is no cross-reactivity between homologous immunity proteins directed against homologous A, B, or N colicins. Similarly, overproduction of the immunity protein leads to partial cross-reactivity (124). The main determinant for specific immunity recognition is located in the hydrophobic hairpin of the channel domain of the colicin (124, 129). Either the whole bacteriocin or the C-terminal domain of pore-forming colicins produced in the cytoplasm of *E. coli* are devoid of cytotoxicity. However, when the C-terminal domain is fused to a signal sequence, the channel is inserted and functional, and cell death follows. This could be inhibited by coproduction of the cognate immunity protein (130, 131). The cytotoxocity of the hybrid protein is independent of the uptake machinery normally used, demonstrating that the C-domain alone forms the channel *in vivo*, as in *in vitro*. The interaction of ImA with colicin A requires the immunity protein to assemble functionally but does not require the channel to be in the open state (131). In other words, the immunity protein interacts with the hydrophobic helical hairpin, as first suggested by the studies mentioned previously (124). This interaction was demonstrated directly using an epitope-tagged immunity protein (131). Site-directed mutagenetic studies of ImA indicate that a role for polar regions of ImA cannot be excluded, in addition to the intramembrane helix–helix interactions. Two roles are proposed for the hydrophilic loops in this protein: (1) they may stabilize its interactions with the channel on both sides of the membrane; (2) they may be required for the functional assembly of the transmembrane helices of ImA (132). The colicin E1 immunity protein tolerates a higher degree of substitution than ImA (127).

5.4. Immunity to Colicin M

Like the protein it inhibits, the immunity to colicin M is unique when compared with other Im proteins. It prevents colicin M from inhibiting murein synthesis. This 14 kDa protein has been localized in the cytoplasmic membrane, and a substantial portion is exposed to the periplasmic space. There is indirect evidence that the colicin M-immunity interaction occurs at the periplasmic side of the cytoplasmic membrane (133).

Bibliography

1. A. Gratia (1925) C.R. Soc. Biol. **93**, 1041–1041.
2. R. Kolter and F. Moreno (1992) Ann. Rev. Microbiol. **46**, 141–163.
3. P. Fredericq (1963) Ann. Rev. Microbiol. **11**, 7–22.
4. M. Riley and D. Gordon (1992) J. Gen. Microbiol. **138**, 1345–1352.
5. F. Jacob, L. Siminovitch, and L. Wollman (1952) Ann. Inst. Pasteur **83**, 295–315.
6. J. Konisky (1982) Ann. Rev. Microbiol. **36**, 125–144.
7. D. Cavard, P. Sauve, F. Heitz, F. Pattus, C. Martinez, R. Dijkman, and C. Lazdunski (1988) Eur. J. Biochem. **172**, 507–512.
8. J. K. Davis and P. Reves (1975) J. Bacteriol. **123**, 96–101.
9. J. K. Davis and P. Reeves (1975) J. Bacteriol. **123**, 102–117.
10. R. Nagel del Zwaig and S. E. Luria (1967) J. Bacteriol. **94**, 1112–1123.
11. C. Lazdunski (1995) Mol. Microbiol. **16**, 1059–1066.
12. M. A. Riley (1993) Mol. Biol. Evol. **10**, 1048–1059.
13. U. Ross, E. E. Harkness, and V. Braun (1989) Mol. Microbiol. **3**, 891–902.
14. S. Luria and J. Suit (1987) In *Escherichia coli* and *Salmonella typhimurium* (F. E. Neidhardt, ed.), ASM, Washington, DC, pp. 1615–1624.
15. H. Masaki and T. Ohta (1985) J. Mol. Biol. **82**, 217–227.
16. S. T. Cole, B. Saint-Joanis, and A. P. Pugsley (1985) Mol. Gen. Genetics **198**, 465–472.
17. K. F. Chak and R. James (1985) Nucleic Acids Res. **13**, 2519–2530.
18. P. T. Chan, H. Ohmori, J. I. Tomizawa, and J. Lebowitz (1985) J. Biol. Chem. **260**, 8925–8935.
19. J. A. Mankovich, C. H. Hsu, and J. Konisky (1986) J. Bacteriol. **168**, 228–236.
20. J. Morlon, M. Chartier, M. Bidaud, and C. Lazdunski (1988) Mol. Gen. Genetics **211**, 231–243.
21. R. Lloubes, D. Baty, and C. Lazdunski (1986) Nucleic Acids Res. **14**, 2621–2636.
22. A. P. Pugsley (1988) Mol. Gen. Genetics **211**, 335–341.
23. S. Zhang, L. Yan, and G. Zubay (1988) J. Bacteriol. **170**, 5460–5467.
24. V. Braun, S. Gaisser, C. Glaser, R. Harkness, T. Ölschager, and J. Mende (1992) In *Bacteriocins, Microcins and Lantibiotics* (R. James, C. Lazdunski, and F. Pattus, eds.), Springer-Verlag, Berlin, Heidelberg, NATO ASI Series, Vol. **65**, pp. 119–125.
25. R. Lloubes, M. Granger-Schnarr, C. Lazdunski, and M. Schnarr (1991) J. Mol. Biol. **217**, 421–

428.
26. D. Cavard and B. Oudega (1992) In *Bacteriocins, Microcins and Lantibiotics* (R. James, C. Lazdunski, and F. Pattus, eds.), Springer-Verlag, Berlin, Heidelberg, NATO ASI Series, Vol. **65**, pp. 297–305.
27. B. Oudega, A. Ykema, F. Stegehuis, and F. de Graaf (1984) FEMS Microbiol. Lett. **22**, 101–108.
28. D. Cavard, R. Lloubes, J. Morlon, M. Chartier, and C. Lazdunski (1985) Mol. Gen. Genet. **199**, 95–100.
29. D. Cavard, D. Baty, S. P. Howard, H. Verheij, and C. Lazdunski (1987) J. Bacteriol. **169**, 2187–2194.
30. A. P. Pugsley and S. T. Cole (1987) J. Gen. Microbiol. **133**, 2411–2420.
31. A. P. Pugsley and M. Schwartz (1984) EMBO J. **3**, 2393–2397.
32. S. P. Howard, D. Cavard, and C. Lazdunski (1991) J. Gen. Microbiol. **137**, 81–89.
33. R. Maget-Dana, F. Heitz, M. Ptak, F. Peypoux, and M. Guinaud (1985) Biochem. Biophys. Res. Commun. **129**, 965–971.
34. Y. Ohno-Iwashita and K. Imahori (1980) Biochemistry **19**, 652–659.
35. F. de Graaf and B. Oudega (1986) Curr. Top. Microbiol. Immunol. **125**, 183–205.
36. R. Dreher, V. Braun, and B. Wittman-Liebold (1985) Arch. Microbiol. **140**, 343–346.
37. D. Baty, M. Frenette, R. Lloubes, V. Géli, S. P. Howard, F. Pattus, and C. Lazdunski (1988) Mol. Microbiol. **2**, 807–811.
38. M. Frenette, H. Bénédetti, A. Bernadac, D. Baty, and C. Lazdunski (1991) J. Mol. Biol. **217**, 2509–2514.
39. R. Webster (1991) Mol. Microbiol. **5**, 1005–1011.
40. A. Vianney, M. Michelle Muller, T. Clavel, J. C. Lazzaroni, R. Portalier, and R. E. Webster (1996) J. Bacteriol. **178**, 4031–4038.
41. E. Bouveret, R. Derouiche, A. Rigal, R. Lloubes, C. Lazdunski, and H. Bénédetti (1995) J. Biol. Chem. **270**, 11071–11077.
42. M. Isnard, A. Rigal, J. C. Lazzaroni, C. Lazdunski, and R. Lloubes (1994) J. Bacteriol. **176**, 6392–6396.
43. R. Derouiche, H. Bénédetti, J. C. Lazzaroni, C. Lazdunski, and R. Lloubes (1995) J. Biol. Chem. **270**, 11078–11084.
44. J. C. Lazzaroni, A. Vianney, J. L. Popot, H. Bénédetti, S. Samatey, C. Lazdunski, R. Portalier, and V. Géli (1995) J. Mol. Biol. **246**, 1–7.
45. J. P. Bourdineaud, S. P. Howard, and C. Lazdunski (1989) J. Bacteriol. **171**, 2458–2465.
46. G. Guiard, P. Boulanger, H. Bénédetti, R. Lloubes, M. Besnard, and L. Letellier (1993) J. Biol. Chem. **269**, 5874–5880.
47. R. Benz, E. Maier, and I. Gentscher (1993) Zbl Bakt **278**, 187–196.
48. C. Wandersman and P. Deleplaire (1990) Proc. Natl. Acad Sci. USA **87**, 4776–4780.
49. L. Gilson, H. Mahanty, and R. Kolter (1990) EMBO J. **9**, 3875–3884.
50. H. Bénédetti, M. Frenette, D. Baty, R. Lloubes, V. Géli, and C. Lazdunski (1989) J. Gen. Microbiol. **135**, 3413–3420.
51. J. P. Bourdineaud, H. P. Fierobe, C. Lazdunski, and J. M. Pagès (1990) Mol. Microbiol. **4**, 1737–1743.
52. H. Bénédetti, M. Frénette, D. Baty, R. Lloubes, M. Knibiehler, F. Pattus, and C. Lazdunski (1991) J. Mol. Biol. **217**, 429–439.
53. H. Bénédetti, C. Lazdunski, and R. Lloubes (1991) EMBO J. **10**, 1989–1995.
54. E. Bouveret, A. Rigal, C. Lazdunski, and H. Bénédetti (1997) Mol. Microbiol., **23**, 909–920.
55. D. Duché, D. Baty, M. Chartier, and L. Letellier (1994) J. Biol. Chem. **269**, 24820–24825.

56. H. Bénédetti, R. Lloubes, C. Lazdunski, and L. Letellier (1992) EMBO J. **11**, 441–447.
57. D. Jeanteur, T. Schirmer, D. Fourel, V. Simonet, G. Rummel, C. Widner, J. P. Rosenbusch, F. Pattus, and J. M. Pagès (1994) Proc. Natl. Acad. Sci. USA **91**, 10675–10679.
58. H. Bénédetti, L. Letellier, R. Lloubes, V. Géli, D. Baty, J. M. Pagès, and C. Lazdunski (1992) In *Dynamics of Membrane Assembly* (J.A.F. Op den Kamp, ed.), NATO ASI Series, Springer-Verlag, Berlin, Vol. **63**, pp. 316–332.
59. K. Eick-Helmerich and V. Braun (1995) J. Bacteriol. **171**, 5117–5126.
60. K. Postle (1990) Mol. Microbiol. **4**, 2019–2925.
61. H. Pils and V. Braun (1995) Mol. Microbiol. **16**, 57–67.
62. E. Schramm, J. Mende, V. Braun, and R. M. Kemp (1987) J. Bacteriol. **169**, 3350–3357.
63. V. Braun (1995) FEMS Microbiol. Rev. **16**, 295–307.
64. S. F. Mel, A. M. Falick, A. L. Burlingame, and R. M. Stroud (1993) Biochemistry **312**, 9473–9479.
65. P. Ghosh, S. Mel, and R. M. Stroud (1994) Nature Struct. Biol. **1**, 597–604.
66. H. Bénédetti, R. Lloubes, C. Lazdunski, and L. Letellier (1992) EMBO J. **11**, 441–447.
67. K. Postle and J. Skare (1988) J. Biol. Chem. **263**, 11000–11007.
68. M. Wiener, D. Freymann, P. Ghosh, and R. Stroud (1997) Nature **385**, 461–464.
69. K. Jakes (1982) In *Molecular Action of Toxins and Viruses* (P. Cohen and S. von Heinegen, eds.), Elsevier, Amsterdam.
70. M. Mock and A. P. Pugsley (1982) J. Bacteriol. **150**, 1069–1076.
71. P. C. K. Lau, M. Parsons, and T. Uchimura (1992) In *Bacteriocins, Microcins and Lantibiotics* (R. James, C. Lazdunski, and F. Pattus, eds.), Springer-Verlag, Berlin, pp. 353–378.
72. P. S. Ringrose (1970) Biochim. Biophys. Acta **213**, 320–334.
73. R. Wallis, A. Reilly, A. Rowe, G. Moore, R. James, and C. Kleanthous (1922) Eur. J. Biochem. **207**, 687–695.
74. R. Wallis, G. R. Moore, C. Kleanthous, and R. James (1992) Eur. J. Biochem. **210**, 925–930.
75. R. Wallis, A. Reilly, K. Barnes, C. Abell, D. Campbell, G. Moore, R. James, and C. Kleanthous (1994) Eur. J. Biochem. **220**, 447–454.
76. J. Weiss and S. Luria (1978) Proc. Natl. Acad. Sci. USA **75**, 2483–2487.
77. H. Tokuda and J. Koninsky (1978) Proc. Natl. Acad. Sci. USA **76**, 6167–6171.
78. S. Schein, B. Kagan, and A. Finkelstein (1978) Nature **276**, 159–163.
79. W. Cramer, J. Dankert, and Y. Uratami (1983) Biochim. Biophys. Acta **737**, 173–193.
80. J. P. Bourdineaud, P. Boulanger, C. Lazdunski, and L. Letellier (1990) Proc. Natl. Acad. Sci. USA **87**, 1037–1041.
81. K. Fields and S. Luria (1969) J. Bacteriol. **97**, 57–63.
82. K. Fields and S. Luria (1969) J. Bacteriol. **97**, 64–77.
83. A. Kopecky, D. Copeland, and J. Lusk (1975) Proc. Natl. Acad. Sci. USA **72**, 4631–4634.
84. C. Plate, J. Suit, A. Jetten, and S. Luria (1974) J. Biol. Chem. **19**, 6138–6143.
85. J. Gould and W. Cramer (1977) J. Biol. Chem. **252**, 5491–5497.
86. G. Guihard, H. Bénédetti, M. Besnard, and L. Letellier (1994) J. Biol. Chem. **268**, 17775–17780.
87. C. Lazdunski, D. Baty, V. Géli, D. Cavard, J. Morlon, R. Lloubes, P. Howard, M. Knibiehler, M. Chartier, S. Varenne, M. Frenette, J. L. Dasseux, and F. Pattus (1988) Biochim. Biophys. Acta **947**, 445–464.
88. M. Parker, F. Pattus, A. Tucker, and D. Tsernoglou (1989) Nature **337**, 93–96.
89. M. Parker, J. Postna, F. Pattus, A. Tucker, and D. Tsernoglou (1992) J. Mol. Biol. **224**, 639–657.

90. P. Ghosh, S. Mel, and R. Stroud (1994) Nat. Struct. Biol. **1**, 597–504.
91. P. Elkins, H. Y. Song, W. Cramer, and C. Stauffacher (1994) Proteins Struct. Funct. Genet. **19**, 150–157.
92. M. Wormald, A. Merril, W. Cramer, and R. Williams (1990) Eur. J. Biochem. **191**, 155–161.
93. L. Holm and C. Sander (1993) FEBS Lett. **315**, 301–306.
94. F. Pattus, D. Cavard, R. Verger, C. Lazdunski, and H. Schindler (1983) in *Physical Chemistry of Transmembrane Ion Motions* (G. Spach, ed.), Elsevier, Amsterdam, pp. 407–413.
95. F. Pattus, D. Massote, H. Wilmsen, J. Lakey, D. Tsernoglou, A. Tucker, and M. Parker (1990) Experientia **96**, 180–192.
96. M. Collarini, G. Amblard, C. Lazdunski, and F. Pattus (1987) Eur. Biophys. J. **14**, 147–153.
97. P. Gosh, S. Mel, and R. Stroud (1993) J. Membrane Biol. **134**, 85–92.
98. L. Raymond, S. Slatin, and A. Finkelstein (1985) J. Membrane Biol. **84**, 173–181.
99. J. Bullock (1992) J. Membrane Biol. **125**, 255–257.
100. J. Bullock, E. Kolen, and J. L. Shear (1992) J. Membrane Biol. **128**, 1–16.
101. F. van der Goot, N. Didat, F. Pattus, W. Dowhan, and L. Letellier (1993) Eur. J. Biochem. **213**, 217–221.
102. G. van der Goot, J. Gonzalez-Manas, J. Lakey, and F. Pattus (1991) Nature **354**, 408–410.
103. J. Lakey, G. van der Goot, and F. Pattus (1994) Toxicology **87**, 85–108.
104. M. Parker and F. Pattus (1993) Trends Biochem. Sci. **18**, 391–395.
105. D. Duché, D. Baty, M. Chartier, and L. Letellier (1994) J. Biol. Chem. **269**, 24820–24825.
106. A. Merill and W. Cramer (1990) Biochemistry **29**, 8529–8534.
107. D. Duché, M. Parker, J. Gonzalez-Manas, F. Pattus, and D. Baty (1994) J. Biol. Chem **269**, 6332–6339.
108. S. Slatin, X-Q. Qiu, K. Jakes, and A. Finkelstein (1994) Nature **371**, 158–161.
109. X. Q. Qiu, K. Jakes, P. Kienker, A. Finkelstein, and S. Slatin (1996) J. Gen. Physiol. **107**, 313–328.
110. K. Schaller, J. Höltje, and V. Braun (1982) J. Bacteriol. **152**, 994–1000.
111. R. Harkness and V. Braun (1989) J. Biol. Chem. **264**, 6177–6182.
112. G. Siewert and J. Strominger (1967) Proc. Natl. Acad. Sci. USA **57**, 767–773.
113. P. Fredericq (1957) Ann. Rev. Microbiol. **11**, 7–21.
114. H. Masaki, S. Yajima, A. Akutsur-Koide, T. Ohta, and T. Uozumi (1992) In "*Bacteriocins, Microcins and Lantibiotics*" (R. James, C. Lazdunski, and F. Patus eds.), Springer-Verlag, Berlin, pp. 379–395.
115. A. Akutso, H. Masaki, and T. Ohta (1989) J. Bacteriol. **171**, 6430–6436.
116. H. Masaki, A. Akutsu, T. Uozumi and T. Ohta (1991) *Gene* **107**, 133–138.
117. S. Yajima, Y. Muto, S. Yokoyama, H. Masaki, and T. Uozumi (1992) Biochemistry **31**, 5578–5586.
118. M. Osborne, A. L. Breez, L. Y. Lian, A. Reilly, R. James, C. Kleanthous, and G. Moore (1996) Biochemistry **35**, 9505–9512.
119. M. Curtis and R. James (1991) Mol. Microbiol. **5**, 2727–2733.
120. M. Osborne, L-Y. Lian, R. Wallis, A. Reilly, R. James, C. Kleanthous, and G. Moore (1994) Biochemistry **33**, 12347–12355.
121. R. Wallis, G. Moore, R. James, and C. Kleanthous (1995) Biochemistry **34**, 13743–13750.
122. R. Wallis, K. Y. Leung, A. Pomoner, H. Videler, G. Moore, R. James, and C. Kleanthous (1995) Biochemistry **34**, 13751–13759.
123. C. Weaver, A. Redborg and J. J. Konisky (1981) J. Bacteriol. **148**, 817–828.
124. V. Géli and C. Lazdunski (1992) J. Bacteriol. **174**, 6432–6437.

125. V. Géli, D. Baty, and C. Lazdunski (1988) Proc. Natl. Acad. Sci. USA **85**, 689–693.
126. V. Géli, D. Baty, F. Pattus, and C. Lazdunski (1989) Mol. Microbiol. **3**, 679–687.
127. H. Song and W. Cramer (1991) J. Bacteriol. **173**, 2935–2943.
128. G. von Heijne (1992) J. Mol. Biol. **225**, 487–494.
129. Y. Zhang and W. Cramer (1993) J. Biol. Chem. **268**, 1–8.
130. D. Espesset, Y. Corda, K. Cunningham, H. Bénédetti, R. Lloubes, C. Lazdunski, and V. Géli (1994) Mol. Microbiol. **13**, 1121–1131.
131. D. Espesset, D. Duché, D. Baty, and V. Géli (1996) EMBO J. **15**, 2356–2364.
132. D. Espesset, P. Piet, C. Lazdunski, and V. Géli (1994) Mol. Microbiol. **10**, 1111–1120.
133. T. Ölschläger, A. Turba, and V. Braun (1991) Mol. Microbiol. **5**, 1105–1111.

Suggestions for Further Reading

134. H. Bénédetti and V. Géli (1996) "Colicin transport, channel formation and inhibition". In *Handbook of Biological Physics* (W. Konings, H. Kaback, and J. S. Lolkema, eds.), Elsevier, Amsterdam, Vol. **2**, pp. 665–691.
135. W. Cramer, J. Heymann, S. Schendel, B. Deriy, F. Cohen, P. Elkins, and C. Stauffacher (1995) Structure-function of the channel-forming colicins. Ann. Rev. Biophys. Biomol. Struct. **24**, 611–641.
136. R. James, C. Kleanthous, and G. Moore (1996) The biology of E colicins: Paradigms and paradoxes. Microbiology **142**, 1569–1580.
137. A. P. Pugsley (1984) The ins and outs of colicins: Part 1. Production and translocation across membranes. Part 2. Lethal action, immunity and ecological implications, Microbiol. Sci. **1**, 168–175 and 203–205.
138. V. Braun, H. Pilsl, and P. Grob (1994) Colcins: Structures, modes of action, transfer through membranes and evolution. Arch. Microbiol. **161**, 199–206.

Collagen

Proteins of the *collagen* family are the major components of the extracellular matrix and facilitate the formation and maintenance of a multicellular system. Collagens serve as solid-state regulators for cellular function and as scaffolding of the tissue architecture, particularly in large vertebrates. They contain many proline and glycine residues and a distinct **secondary structure**: the polyproline II-like helix, which is distinct from the a-helix, b-sheet and turn secondary structures in other protein structures. This regular secondary structure arises because the sequences the collagen polypeptide chain consist largely of the repeated sequence Gly━X━Y, with abundant proline residues at the X positions and rich in *hydroxyproline* (Hyp) residues at the Y positions. Three polyproline II-like helices constitute the supersecondary structure of the collagenous triple helix, which is stabilized through hydrogen bonds nearly perpendicular to triple helical axis (see Triple-Helical Proteins). The collagen protein family includes all the structural proteins of the extracellular matrix with triple-helical collagenous **domains** in their molecular architecture.

The collagen superfamily is classified into groups (Table 1) according to their molecular and/or supramolecular structures. The molecular structures of the collagenous proteins can be depicted with ball-and-stick models (Fig. 1). The balls represent noncollagenous or globular domains, without abundant glycine and proline residues, while the sticks show the collagenous triple helices. Some of the triple-helical domains, including that of the type IV collagen, have interruptions in the Gly━X

—Y triplets, in that glycine residues do not always occupy every third position.

Figure 1. Molecular architecture of collagen superfamily depicted with ball and stick models (stick = collagenous, triple-helical domain; ball = noncollagenous domain).

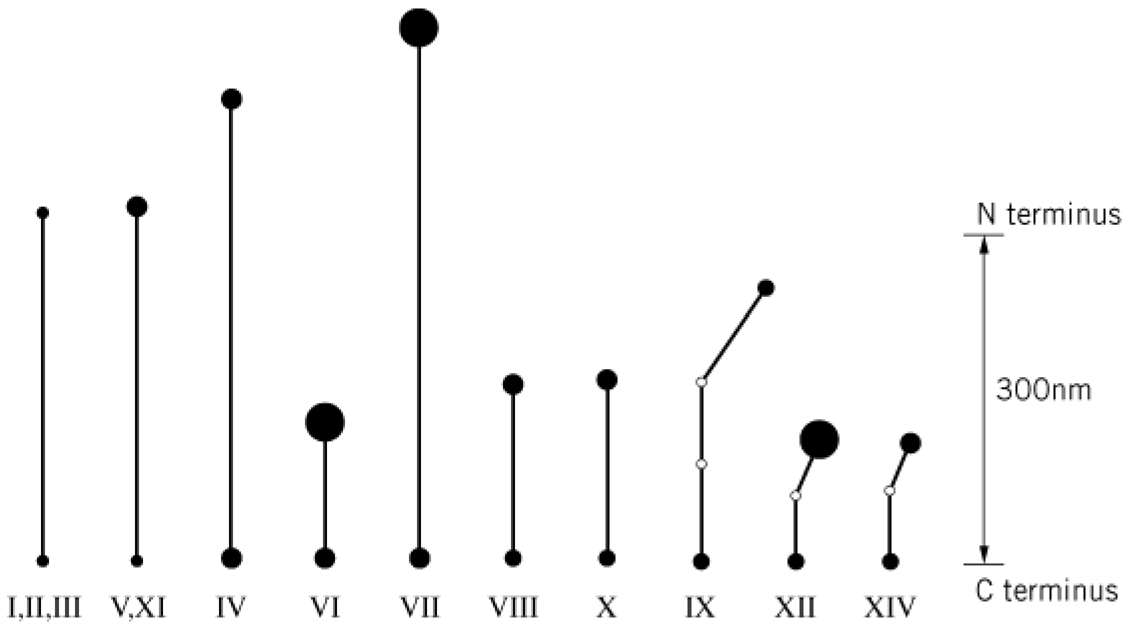

Table 1. Collagen Classification

Family	Types of Molecuels or Chains
Fibrillar collagen	Type I, type II, type III, type V, type XI
Meshwork-forming collagen	a1, a2, a3, a4, a5, and a6 chains of type IV
Fibril associated collagen with type interruptedtriple helices (FACIT)	Type IX, type XII, type XIV, type XVI
Collagen with long triple helix	Type VII
Collagen with short triple helix	Type VIII, type X, type VI
Membrane associated collagen	Type XVII
Others	Type XIII, type XV, type XVIII, type XIX

The structure, assembly, and supramolecular aggregation of type I collagen is the prototype from which has developed our understanding of collagenous structure, particularly the fibrillar collagens. Type I collagen is one of the major components of the fibrous collagens that occur in the greatest amounts. The structure and characteristic properties of triple-helical domains have been deduced from the study of type I collagen, together with comparative studies of other types of collagen. Unless otherwise mentioned, the description of collagen triple helices given below is based primarily on the information obtained through the studies type I collagen. These properties are generally shared with the triple-helical domains in other collagen types, especially regarding the characteristic features distinct from a-helix or b structure in noncollagenous proteins. However, most recent studies suggest that the triple-helical regions have structures and properties specific for each type, particularly in their intermolecular interactions. The characteristic features of the various collagen types are due to differences in the distribution of charged residues along the triple helix, content of glycosylated hydroxylysine and bulky **hydrophobic** residues, as well as imperfection of the Gly—X—Y repeat, which is a prerequisite for the triple-helical conformation.

1. Collagenous Triple Helix; Common and Specific Features among Different Types of Collagen

1.1. Shape and Structure of the Triple-Helical Domains

A variety of physicochemical studies, including direct visualization of individual molecules by rotary shadowing techniques in the **electron microscope**, have demonstrated the rod-like nature of the collagen triple-helical domain. The molecules of type I collagen have a length of about 300 nm (Fig. 1) and a diameter of about 1.4 nm. The rod is neither rigid nor randomly flexible, but appears to possess an intermediate level of semiflexibility.

Details of the three-dimensional structure of the collagen triple helix were established by model building to fit X-ray fiber diffraction data. Frequent occurrence of proline and hydroxyproline residues (which together account for approximately two-ninths (~22%) of the amino acid residues) favor a polyproline II-like conformation. The axial distance between one amino acid and the next in the polyproline II-like helical structure is 0.286 nm, close to twice that in the a-helix (0.15 nm). The triple-helical structure of the synthetic peptide (Pro—Pro—Gly)$_{10}$ was also determined by X-ray crystallography. The overall helical symmetry is left-handed, with 10 residues per three turns (108°/residue) or 7 residues per two turns (103°/residue), with a pitch of 2.9 nm. The three polyproline II-like helical chains are further coiled about a central axis, to form a right-handed helix (Fig. 2). The occurrence of glycine as every third residue gives rise to a polymer of repeating tripeptide units with the formula of (—Gly—X—Y—).

Figure 2. Collagenous triple helix. (**a**) Gly—Pro—Hyp repeated sequence of a chain in a model of part of one a chain in the collagenous triple helix. Both NH and CO groups project perpendicular to the fibrillar axis (C, black; N, blue; O, red; H, gray). (**b**) Backbone of the collagenous triple helix. (**c**) Gly—Pro—Hyp trimer (*left*). Note that there is a groove on the surface of the helix. A part of human type III collagen molecule, [a1(III)]$_3$ in the sequence of GITGARGLAGP (*right*). Note that all the residues except Gly project to the outer surface of the molecule (C, yellow; N, blue; O, red; H, white). See color insert.

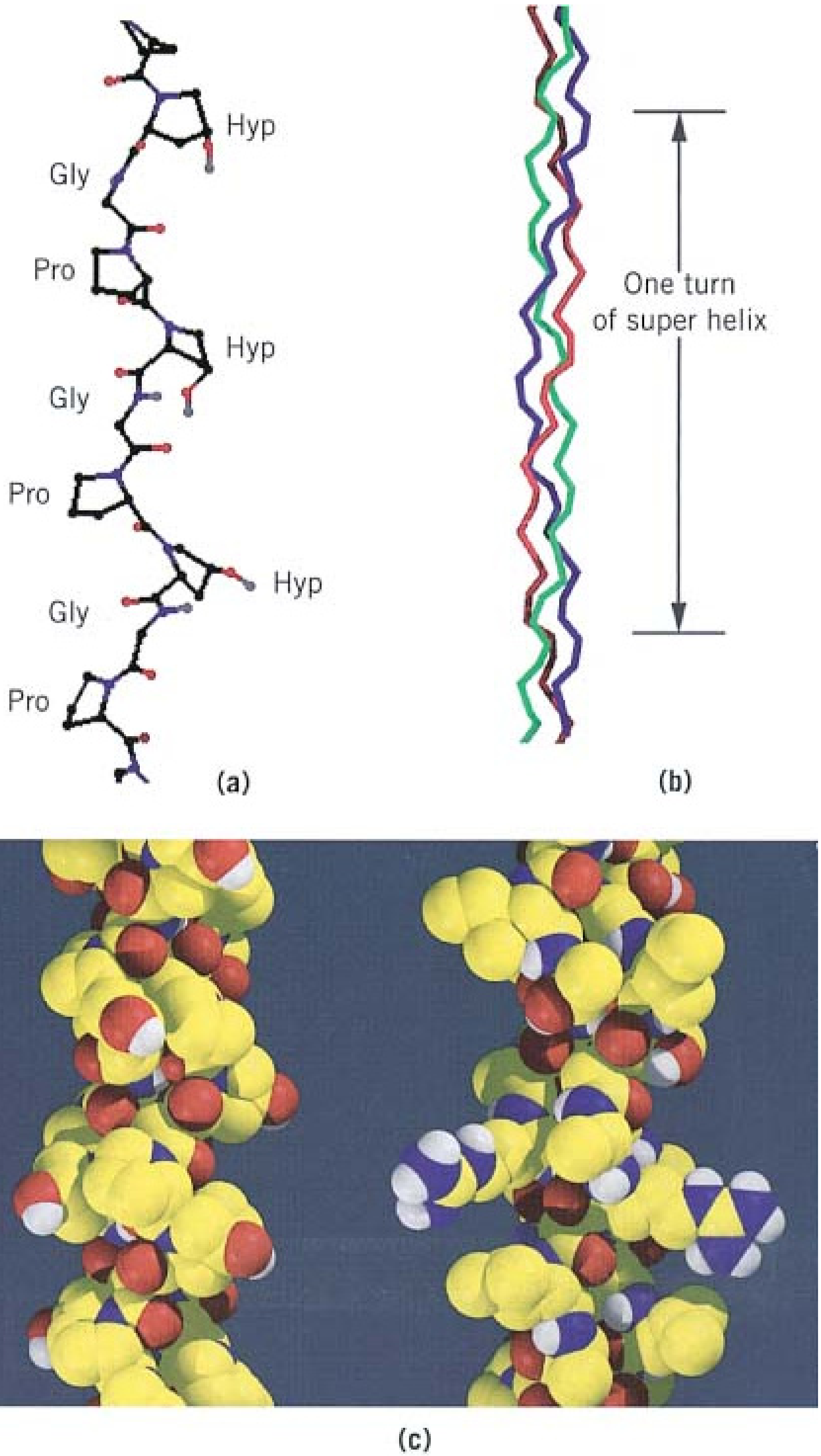

1.2. Thermal Stability of the Triple-Helical Conformation

Flexibility of the collagenous triple helix may vary along the chain. Collagen triple helices of different types have varying flexibility, depending on what residues occupy the X and Y positions. Yet the thermal stability in terms of the helix-to-coil transition temperature (see Helix–Coil Theory) is similar, regardless of the type of collagen, in the same animal or animal tissues. The collagenous domains are heat-stable up to the upper limit of animal body temperature. Heat denaturation of collagenous domains starts around 37°C in mammalian collagens (Fig. 3). The most recent study on the denaturation temperature of the bovine type IV collagen triple-helical domain indicated that the domain also has denaturation temperature above 37°C. This suggests that interruptions in the triplet repeats do not greatly decrease the thermal stability.

Figure 3. Denaturation temperature of collagen triple helix. The temperature was raised stepwise by 1.5°C at intervals of 20 min, and the specific viscosity (h_{sp}) was measured. Pepsin-treated acid-soluble collagen from calf skin (0.8 mg/mL) was dissolved in 0.15 *M* potassium phosphate buffer, pH 6.8, and 1 *M* glucose. Open circles indicate the specific viscosity of the native collagen solution with increasing temperature; filled circles correspond to the values of the denatured collagen solution when the temperature was lowered the same way as it was raised. The broken line is drawn through the values 5% less in the specific viscosity compared with that expected for the native collagen solution. The triangle (T_m) corresponds to the denaturation temperature obtained by the conventional method of taking the midpoint of the curve.

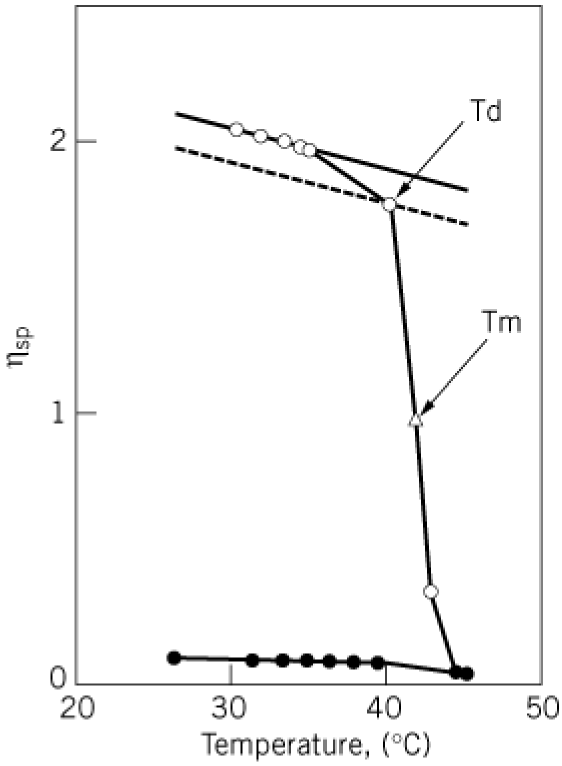

1.3. Primary Sequence Required for the Triple-Helical Conformation

The characteristic primary structure of polypeptides adopting collagenous triple-helical structures consists of repeats of the sequence Gly━X━Y, where Gly represents glycine and X or Y represents any other amino acid residue. Glycine is the only amino acid that can pack tightly at the center of the triple-stranded collagen monomer, where it provides HN groups for hydrogen bonding to O=C━ groups in the peptide bonds of the other chains (Fig. 4). The stability of the triple-helical conformation is due in part to these hydrogen bonds, which are aligned nearly perpendicular to the helical axis. Interruptions of the Gly━X━Y repeats decrease the stability of the conformation. Substitution of a glycine residue occurring within the sequence Gly━X━Y of triple-helical domains destabilizes and disrupts the helical conformation. In the triple helix, the side chains of all the X and Y residues are exposed on the surface of the triple helix.

Figure 4. A schematic drawing illustrating direct interchain hydrogen bonding between (Gly)NH··CO(Pro in X position) the collagenous triple-helix. The three charms (a, b, and c) with repeated Gly-Pro(x)-Pro(y) sequence, eg, -Ga-Xa-Ya, -C Yb-.

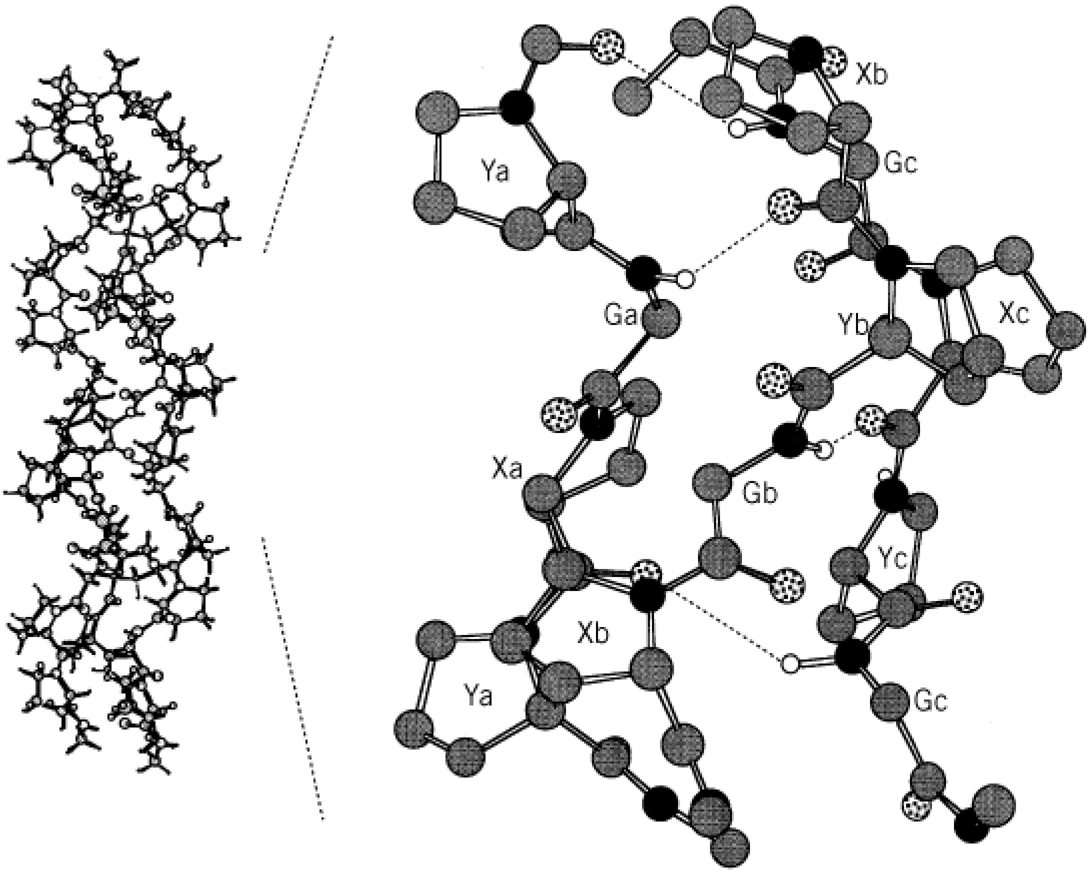

1.4. Proline Residues at Position X and Hydroxyproline Residues at Position Y
The helical conformation of individual a chains arises largely as a result of steric repulsion between
proline residues in the X position (approximately 120 residues per a1(I)) and 4-hydroxyproline resid
the Y position (approximately 100 residues per a1(I) chain) and because the five-membered rings of
imino acids are rigid and limit rotation about the peptide N—C bond. The proline and hydroxyprolin
residues also stabilize the triple helix. The contribution to helix stability from the pyrrolidine rings o
and hydroxyproline is thought to be entropic, in that these residues may not acquire as much freedon
denaturation as other residues. Another interpretation for contribution of the pyrrolidine rings to the
stability of triple-helical conformation is related to the fact that these side chains are located on the s
of the triple helix. Pyrrolidine rings are surprisingly favorable in contact with water. Furthermore,
hydroxylation of the proline residues before Gly or Y positions increases the thermal stability greatly
although hydroxyproline residues at X positions or after Gly decrease the stability. Whether the hydr
group is at the 3 or 4 position of proline residues also influences greatly the thermal stability of the tr
helical conformation.

The amino acid sequence responsible for the formation and stability of the collagenous triple helix is
susceptible to **proteolysis** by collagenases. The sequence specifically recognized by bacterial collage
usually in sequences such as ━GlyXYGlyProYGlyXHypGlyXY━. Cleavage occurs at the amino si
Gly residues.

1.5. Resistance of the Triple-Helical Domains to Pepsin or Other Proteinases
The intact triple-helical domain is generally resistant to most proteinases. However, when heated abo
physiological temperatures, it undergoes a helix-to-coil transition and, once melted, becomes suscep
degradative enzymes. Protein consisting primarily of collagenous domains stays in solution at acidic
the collagenous domains have generally been isolated by **pepsin** treatment of otherwise insoluble tis
a number of triple helices of recently discovered collagen family members, the occurrence of glycine
every third residue is occasionally interrupted. The interrupted sites are speculated to lower the stabi
the triple helix and might form kinks in the rod-like triple helix. Thus, collagen helix that is otherwis
unsusceptible to many proteinases might become susceptible at the interrupted sites of Gly━X━Y r

Thus, type IV collagen may be degraded gradually at the interrupted sites of glycine—X—Y triplets being liberated from the aggregates with pepsin treatment.

1.6. Other Amino Acid Residues at Positions X and Y

All sides chains at positions X and Y protrude out along the surface of the triple helix. Consequently contribute to the hydrophilicity, ionization, hydrophobicity (see Fig. 5), and steric roughness of the p **molecular surface**, including the size of the groove of the triple helix (Fig. 2). Charged groups, toge with their neighboring sequences, may also affect the stability of the triple helix, presumably due to differential contributions from water of hydration on the surface.

Figure 5. Hydrophobic residues in collagen polypeptide chains. The content of hydrophobic residues in collagenous do (indicated as filled circles) is relatively low compared to the globular proteins. However, they projected to the surface o triple helix, while the globular protein keeps most of the hydrophobic residues inside.

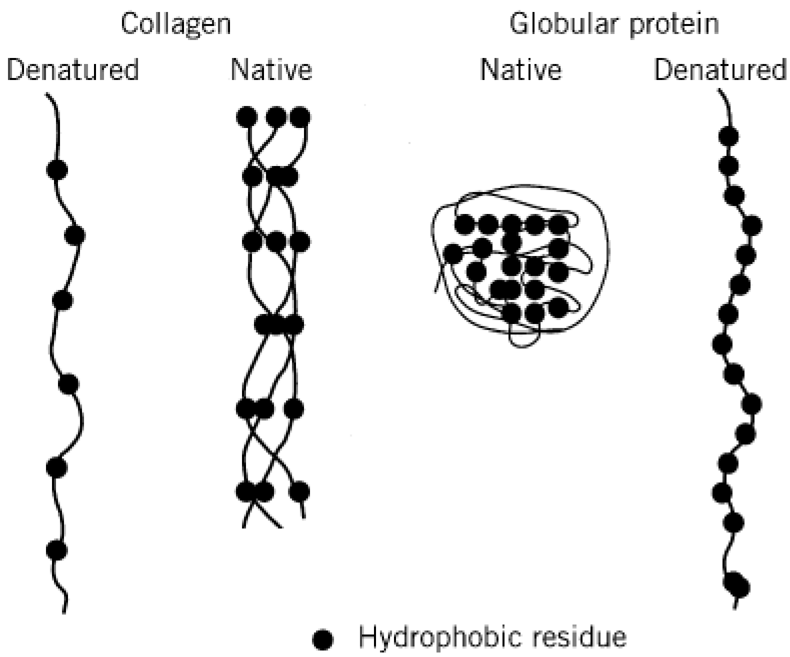

The amino acid residues other than proline or hydroxyproline residues at positions X and Y can prov another classification of the collagen protein family. In general, the collagenous triple-helical domai contain a higher content of basic (arginine + lysine) than of acidic (aspartate + glutamate) residues, r in a basic isoelectric point. Two groups of collagens can be classified on the basis of their relative co of arginine and lysine: the high arginine group (Arg/Lys > 1) and the low arginine group (Arg/Lys < greater content of Lys residues may result in a greater content of hydroxylysine residues, which furth provides a possibility for additional **glycosylation**. A high content of glycosylated hydroxylysine sho contribute greatly to the surface roughness of the triple-helical domains. Another general feature abo amino acid composition of collagens is the low content of hydrophobic amino acid residues. The inte the triple helix is not stabilized by hydrophobic interactions, but they are strong between triple helice because all the hydrophobic residues are exposed on the surface of the triple helix. The content of la hydrophobic residues in the collagenous triple helices also classifies the collagenous proteins into tw groups. One group contains a high ratio of Ala/hydrophobic amino acids (Val, Leu, Ile, Phe, and Me the other group contains a low ratio.

2. Classification of Collagens Based on the Primary Sequence

In the fibrillar collagens, the triple-helical conformation occurs throughout 95% of the length of the ı monomer (Fig. 3). Thus, of the 1057 residues in the a1(I) chain of human collagen, 1014 occur in re Gly—X—Y triplets. The *N*-terminal 17 residues and the *C*-terminal 26 residues (referred to as *telop* do not have glycine as every third residue. The type I collagen helical molecule is a heterotrimer con two identical a1(I) chains and one a2(I) chain. The a1(I) and a2(I) chains are very similar, but their p structures are coded by separate genes and are sufficiently different for the chains to be separated by exchange chromatography and by SDS-PAGE. The a-chains each contain over 1000 amino acid resi have molecular weights of approximately 95,000.

The existence of a family of collagenous proteins in the connective tissues of vertebrates was first id when cartilage collagen (type II) was found to be genetically distinct from the type I collagen of skir and tendon. A third collagen (designated type III) was detected in skin. More than 30 different colla polypeptides have been found in the extracellular matrix in the form of at least 19 different collagen (designated from I to XIX; see Table 2).

Table 2. Polypeptide Chain Composition of Genetically Distinct Collagen Types

Type	Known a chains	Known or Putative Chain Compositionsof Molecules at Present	Length of Triple-Helical Domain (nm)	Main or Known Distribution	Aggregate Structure of PurifiedProtein or that Estimated with Immunohistochemical study, etc.
Fibrillar Collagen					
I	a1(I)	$[a1(I)]_2a2(I)$	300	Almost all connective tissues without hyalinecartilage	Fibril
	a2(I)	$[a1(I)]_3$?			
II	a1(II)	$[a1(II)]_3$	300	Cartilage	Fibril
III	a1(III)	$[a1(III)]_3$	300	Almost similar to type I	Fibril
V	a1(V)	$[a1(V)]_2a2(V)$	300	Almost similar to type I, adult cartilage	Fibril
	a2(V)	a1(V)a2(V)a3(V)			
	a3(V)	$[a1(V)]_3$?			
XI	a1(XI)	a1(XI)a2(XI)a3 (XI)	300	Cartilage	Fibril
	a2(XI)				
	a3(XI)				
V/XI	a1(XI)	$[a1(XI)]_2a2(V)$	300	Vitreous body	Fibril
	a2(V)				
FACIT (Fibril-AssociatedCollagen with Interrupted Triple-Helices)					
IX	a1(IX)	a1(IX)a2(IX)a3		Surface of the	Aggregated with fibrillar

		(IX)		cartilage fibril	collagen periodicallyon the cartilage collagen fibrils
	a2(IX)				
	a3(IX)				
XII	a1(XII)	[a1(XII)]$_3$		Tissues rich in type I	
XIV	a1 (XIV)	[a1(XIV)]$_3$		Tissues rich in type I	
XVI	a1 (XVI)	[a1(XVI)]$_3$			
Others					
VI	a1(VI)	a1(VI)a2(VI)a3 (VI)	100	Almost all connective tissues	Beaded microfibril
	a2(VI)	[a1(VI)]$_2$a2(VI)			
	a3(VI)				
VII	a1(VII)	[a1(VII)]$_3$?	420	Anchoring fibril	Short dimer
VIII	a1 (VIII)	[a1(VIII)]$_3$	150	Basement membrane of endothelial cell	Hexagonal array
	a2 (VIII)	[a1(VIII)]$_2$a2 (VIII), [a2(VIII)]$_3$			
X	a1(X)	[a1(X)]$_3$	130	Hypertrophic cartilage	Hexagonal array
XIII	a1 (XIII)	[a1(XIII)]$_3$?			
XV	a1(XV)	[a1(XV)]$_3$?	150		
XVII	a1 (XVII)	[a1(XVII)]$_3$			
XVIII	a1 (XVIII)	[a1(XVIII)]$_3$?			
XIX	a1 (XIX)	?			FACIT?
Meshwork-Forming Collagen					
IV	a1(IV)	[a1(IV)]$_2$a2(IV)	350	Basement membrane	Polygonal meshwork
	a2(IV)	a3(IV)a4(IV)a5 (IV), [a3(IV)]$_2$a4 (IV)		Sinusoid	
	a3(IV)	[a5(IV)]$_2$a6(IV)?			
	a4(IV)				
	a5(IV)				
	a6(IV)				

The collagen numbering system (with Roman numerals for each collagen type and Arabic numerals individual a-chains) to some extent reflects the relative abundance of the various collagens, in that g the more abundant collagens were identified earliest. In addition to these collagens, there exists a nu secreted proteins that contain collagenous amino acid sequences and short triple-helical conformatio as the **complement** component Clq, acetylcholine esterase, lung surfactant protein, conglutinin, seru mannose-binding protein, scavenger receptors (AR-I and AR-II), and MARCO. The collagenous seq in these proteins contribute to their distinctive structures and functions. Since they have no known st role in the extracellular matrix, however, they are not classified as collagens.

From the data derived from amino acid and gene sequencing, collagen molecules can be grouped int groups shown in Figure 1 and Table 1. Fibrillar collagen molecules are characterized by an uninterru helical domain of approximately 300 nm. They are synthesized as procollagens comprised of three p chains that undergo processing to a chains and subsequently assemble into collagen fibrils and fibers Fibrillar collagen molecules (ie, types I, II, III, V, and XI) exhibit several common structural feature reflect the highly conserved exon–intron structure of the genes.

Polygonal meshwork-forming collagens (type IV collagen polypeptides) have large triple- helical do (>160 kDa) with a length of >350 nm. Their primary structures are characterized by imperfections in ━Gly━X━Y━ triplet sequence. These interruptions are a particular feature of type IV collagen, in the helical domain contains more than 20 short stretches of non-helix-forming amino acids.

Short triple-helical collagen molecules and (types VI, VIII, X) contain interruptions in the helical do (as in types IX, XII, and XIV). Collagen types VIII and X show remarkable homology and might ha similar roles in tissues. Type XII and type XIV collagens have similarities to type IX collagen in the domain structures. A portion of these triple-helical domains have the potential to interact with fibrill collagen. Thus, these three types of collagen, plus type XVI, comprises a group of fibril-associated c with interrupted triple helices (FACIT collagens).

An alternative approach for classifying the collagens depends on supramolecular structures that migh related to their physiological function. Individual collagen types may themselves represent a family of related collagenous structures in the extracellular matrix. Type IV collagen is a family of six hom a chains (a1, a2, a3, a4, a5, and a6), and type V/XI is a family of 6 a chains: a1(V), a2(V), a3(V), a1((XI) and a3(XI).

3. Self-assembly into Supramolecular Structure (Fibrillar Aggregates or Polygonal Meshworks)

3.1. Lateral Interactions Between Triple-Helical Domains

The collagen triple helix is essentially a one-dimensional molecule, with its near-constant axial sepa between amino acid residues throughout the triple-helical domain. This has permitted a direct correl structural data obtained by electron microscopy with chemical sequence data. Lateral association of collagenous triple-helical domains, to form fibrils, is a common feature of the collagen family. Fibri self-assemble spontaneously from solutions of extracted type I collagen when the pH, temperature, a strength are adjusted to physiological values. This lateral association appears to be promoted by elev temperature, suggesting that **hydrophobic interactions** are the principal driving force (Fig. 6). Fibri formation is controlled to a large extent by the amino acid sequence of the collagen and, in particula distribution of polar and hydrophobic residues that are exposed on the surface of the triple-helical do Hydroxylysine and glycosylated hydroxylysine residues might be a most potent candidate involved i limiting the lateral growth of the collagenous domains. The residues on the surface of collagen triple may well be bulky enough to cause steric hindrance in the lateral association of the triple-helical do (Fig. 15, see later). The situation would be particularly pronounced in the triple-helical domains of t and type IV collagens, which respectively contain more than 20 and 50 glycosylated hydroxylysine r in a single polypeptide.

Figure 6. Lateral association of triple-helical domains. Triple-helical domain is highly hydrated at 4°C. At physiological temperature such as 37°C, water molecules on the hydrophobic domains will be dehydrated. Collagen molecules accomp lateral association of the triple-helical domains through the exposed hydrophobic regions.

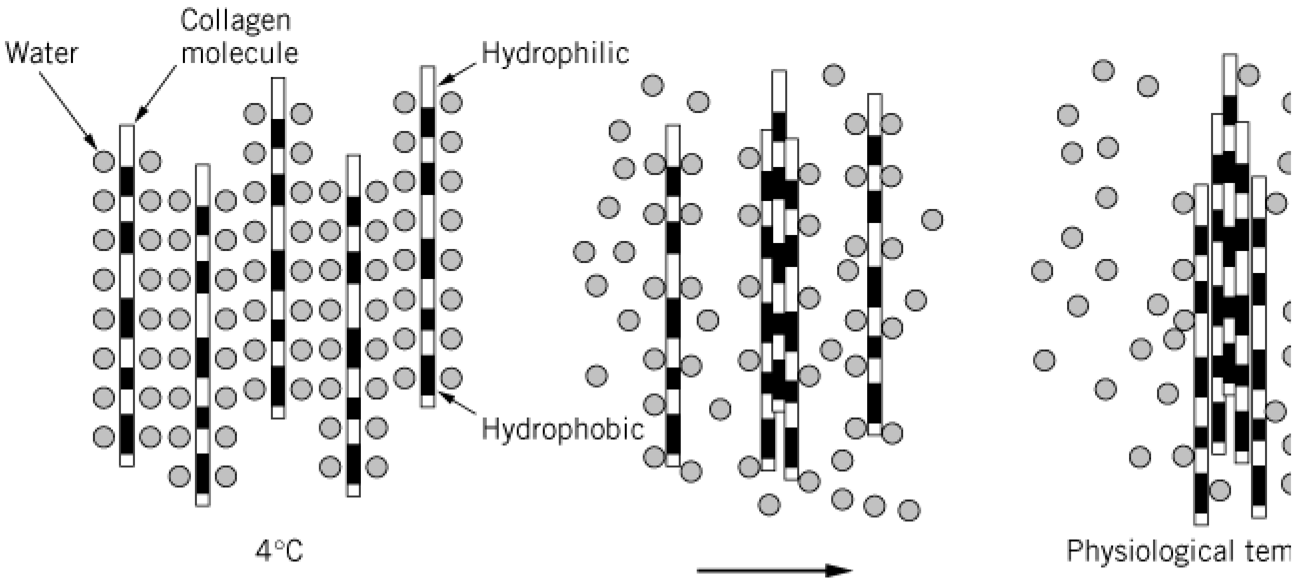

There is stringent control over lateral growth of the collagen fibrils *in vivo*, in that the distributions o fibrillar diameter are sharp in a wide range of extracellular matrices of various tissues. That type I cc can be organized in fibrils with different diameters may indicate the involvement of other regulatory elements. Heterotypic fibrils containing molecules of type III and type V, in addition to type I, collag molecules may predominate *in vivo*. The presence of the **propeptide** of type III procollagen, for exa the surface of collagen fibrils has led to the suggestion that this peptide may have a role in limiting tl diameter. Type V collagen was shown to form banding fibrils with finite diameter (Fig. 7). It has bee postulated that the type V collagen can form hybrid fibrils with the type I collagen. The responsible in the type V collagen appears to be the triple-helical domain, since pepsin-treated type V collagen f only fine fibrils. This finding suggests that type V collagen functions as one of the regulatory elemer fibril diameter, since the triple-helical domain of type V collagen forms D-period banded fibrils, witl potent ability to limit the lateral growth.

Figure 7. Reconstituted type V collagen fibrils. Purified pepsin-treated type V collagen from human placenta with the cl composition of $[a1(V)]_2a2(V)$ forms the banded fibrils with finite thickness. The periodicity of the banding pattern is approximately 65 nm. Fibril thickness is 35 nm in average.

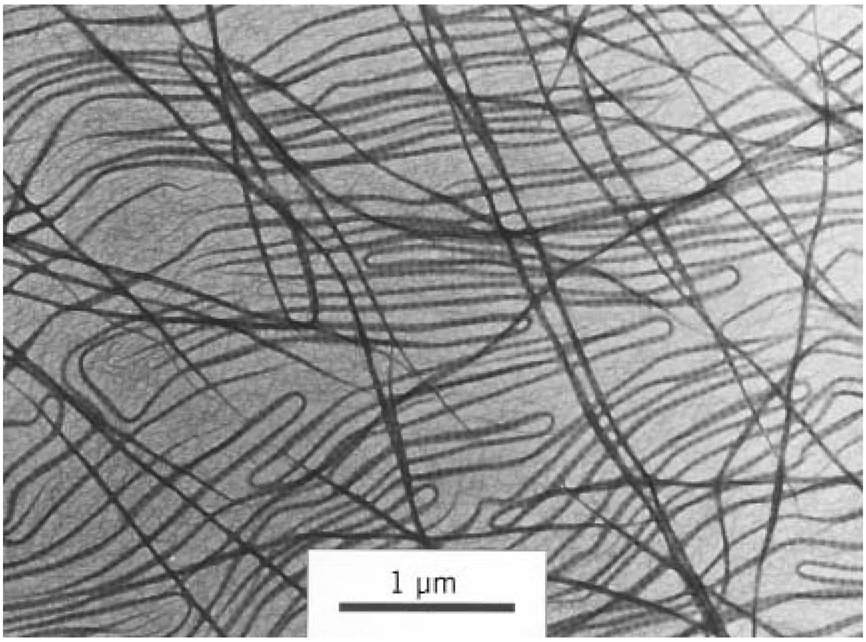

3.2. D-Staggered Lateral Association

The fibrillar structures with banded patterns are accounted for by the specific parallel and mutually staggered alignment of the triple-helical domains of the fibrillar collagens (Fig. 8). The sequence of hydrophobic and charged residues distributed along the triple helix provide maximum electrostatic and hydrophobic interactions between the neighboring molecules. The reconstituted fibrils exhibit a cross-striated banding pattern in the electron microscope, demonstrating conclusively that the aggregation of collagen molecules into axially ordered fibrillar structures is basically a self-assembly process, where the information for association is contained within the assembling molecules themselves.

Figure 8. D-staggered array of type I collagen in banded fibrils.

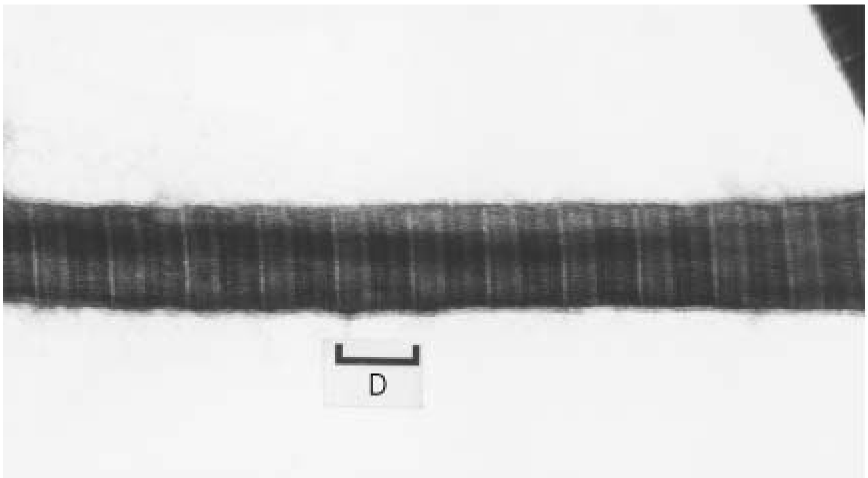

It has been recognized for over 30 years that the cross-striated periodic structure of the native collagen fibril is a consequence of the assembly of molecules in a parallel array, but mutually staggered (ie, axially displaced with respect to one another) by approximately one-quarter of their length—often, which is referred to as the *quarter-staggered array*. The periodicity of the cross-striations in the fibril is explained by the fact that each collagen monomer has eight highly charged regions 67 nm apart that appear under appropriate conditions as stained bands.

The banded period (the D period) is confirmed by low-angle X-ray scattering of rat-tail tendon fibrils, and the overall length of a fibrillar collagen monomer is 4.4 D units (when D = 234 amino acids, the length of one cross-striation period is 67 nm). Within a collagen fibril, the molecules are staggered by integral multiples of the distance D (Fig. 8).

3.3. Collagen Supramolecular Aggregates in Tissues

The organization and arrangement of the collagen fibrils and polygonal meshwork in tissues are subject to considerable variation. Fibrillar collagen, type I collagen in particular, provides the major mechanical strength of skin, tendon, bone, dentine, cornea, sclera, and so on. The fibrillar collagen types form long, unbranched, banded fibrils with a characteristic periodicity of 60–70 nm. The fibrillar aggregate of collagen is classified as a quasi-crystal, because of its highly symmetrical insoluble structure built up of essentially identical subunits. Especially in tendon, type I collagen accounts for approximately 90–95% of the dry weight of the tissue and is present as large, highly orientated fibers. All the fibrillar units are arranged in large parallel bundles, with the average diameter of the fibrils varying between 50 and 500 nm. In dermis, where type I collagen accounts for 80–90% of the collagenous proteins, the fibrils form a coarse network partially oriented in the plane of the skin, with the average diameter of the fibrils between 40 and 100 nm. The orthogonally arranged and precisely packed fibrils in corneal stroma are of particular interest, since the arrangement may well be related to tissue transparency. In the cornea, which has a high content of type V and type I collagens, the collagen fibrils have a uniform diameter of approximately 25 nm. Concentric circles of collagen fibrils in cortical bone provides another type of organization and arrangement.

The skeletal structure of the basal lamina has a special three-dimensional meshwork with an average pore size of about 18 nm. Isolated type IV collagen can reconstitute into polygonal meshwork (Fig. 9) with an average pore size also of about 18 nm (Fig. 10). This suggests that the self-assembled supramolecular structure of the type IV collagen is formed primarily through the lateral interactions of the triple-helical domain, which has kinks or bending points due to interruptions of the Gly—X—Y repeat.

Figure 9. Polygonal meshwork structure of type IV collagen aggregates. Bar in lower right corner is equal to 100 nm. Arrowheads indicate globules presumably formed through NCl domains.

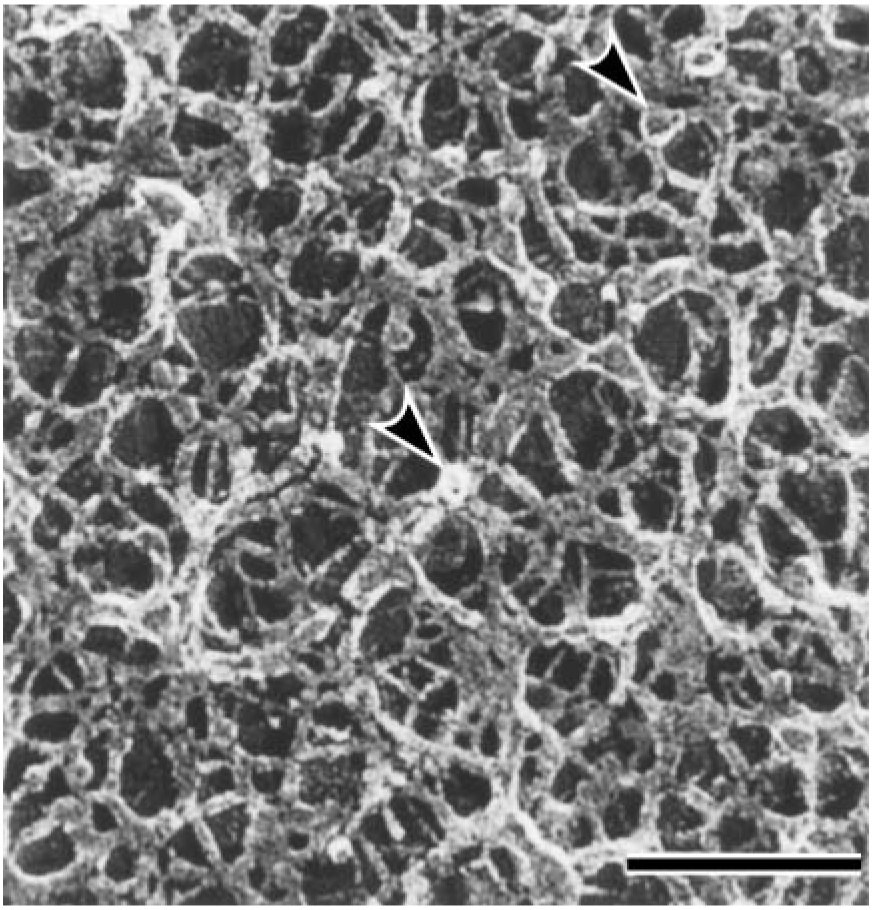

Figure 10. Histograms of the distances between two branching points of polygonal meshwork of type IV collagen aggregates.

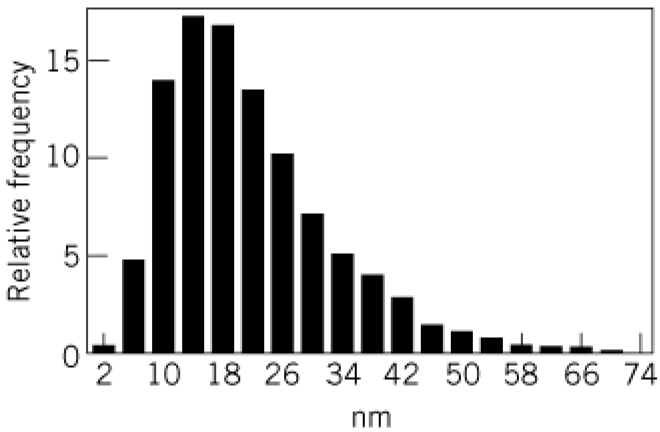

4. Biosynthesis and Chain Assembly of Collagen

Biosynthesis of the collagen molecule is a complex process that begins with transcription of the individual collagen **genes** and culminates in the chains assembled into collagen molecules (Fig. 11). This biosynthetic process involves a number of co- and posttranslational modifications unique to collagenous sequences. Intracellular modifications of the newly synthesized polypeptide chains result in the formation of triple-helical molecules. At least 10 different enzymes have been implicated in the posttranslational processing of the collagen molecule. The biosynthesis of type I collagen can be regarded as a useful model exemplifying many of the common features of collagen biosynthesis. The nonfibrillar collagens may, however, deviate from the general scheme.

Figure 11. Schematic drawing of the complex process of biosynthesis of collagen. Collagen translation products are directed into the endoplasmic reticulum by the *N*-terminal signal peptide that is the cleaved from the polypeptide chain by signal peptidase. Individual procollagen chains undergo complex enzyme-catalyzed post-translational modifications prior to the completion of chain assembly and the folding of the triple helix. Hydroxylation of Lys and Pro and attachment of sugars to hydroxylysine (Hyl) are characteristic post-translational modifications of collagenous polypeptides.

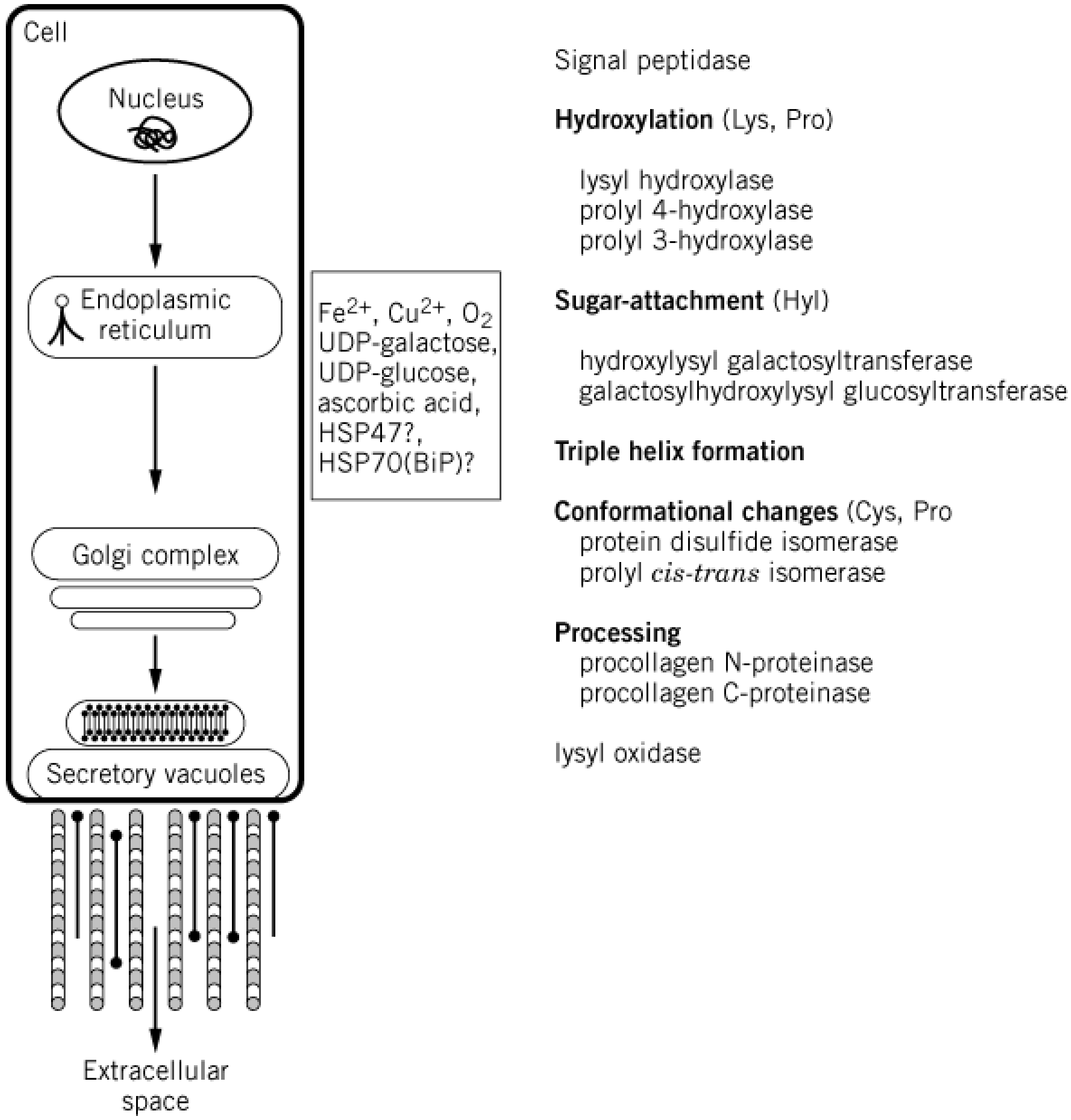

4.1. Pre-procollagen mRNA Translation

The pre-proa collagen chains that are the primary translation product contain hydrophobic *N*-terminal **signal sequences** of 22–26 amino acid residues, similar to those in most other secreted proteins and are essential for targeting of nascent polypeptides to the endoplasmic reticulum (see Protein Secretion). During or shortly after translocation, the signal sequence is removed by the signal peptidase on the luminal side of the endoplasmic reticulum membrane.

Hydroxylation of proline and lysine residues of the newly synthesized collagen polypeptide chains results in the formation of procollagen molecules containing an array of hydroxyproline and hydroxylysine residues. This hydroxylation is produced by collagen-specific enzymes within the cell (see Hydroxylation (Lysine, Proline)).

4.2. Helix Formation and Secretion

The assembly of three polypeptides into a triple-helical collagen molecule is a complex process initiated by association of the three *C*-terminal **propeptides** (in the case of type I collagen), which involves chain alignment, nucleation, and propagation into the triple-helical conformation. Requiring the *C* terminus of the polypeptide chain, chain association and alignment (in the case of type I collagen) takes place only as the chains near full elongation, and folding may proceed in the *C*- to *N*-terminal direction. Association of the *C* termini is stabilized by disulfide bond formation catalyzed by the enzyme protein disulfide isomerase (PDI). Assembly of the triple helical molecule might be limited by cis–trans isomerization (Fig. 12) of the peptide bonds preceding proline residues, which is catalyzed by a cytosolic enzyme, peptidylprolyl cis–trans isomerase (PPI). Formation of the triple-helical conformation appears to preclude further enzymatic post-translational modifications. The procollagen in a triple-helical conformation is ready to be secreted into the extracellular space.

Figure 12. *Cis–trans* isomerization of Ala-Pro peptide bonds. H atoms are not shown.

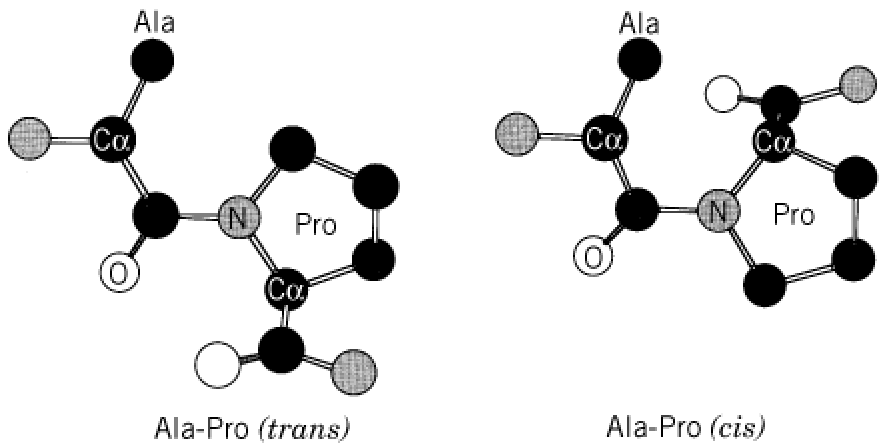

Stable triple helix formation requires 4-hydroxyproline in the Y position of a high proportion of —Gly—X—Y— triplets (at least 100 of the 1000 amino acids of the helical domain of type I collagen) (see Hydroxylation (Lysine, Proline)). The normal rate of procollagen secretion is apparently dependent on triple-helical conformation. If triple helix formation is prevented by inhibiting prolyl hydroxylase (by the use of a,a′-dipyridyl or by limiting the availability of the cofactors Fe^{2+} or O_2), the nonhelical proa(I) chains first accumulate within endoplasmic reticulum.

4.3. Extracellular Polymerization

Fibril formation involves the specific enzymatic cleavage of the procollagen *N*- and *C*-terminal propeptides in the extracellular space (Fig. 13), and these enzymes must therefore play a key role in regulating the aggregation. Such processing is characteristic of the fibrillar collagens and may not be a universal prerequisite for the assembly of all collagen types. The cleavage of the *N*- and *C*-terminal propeptides from the procollagen I molecule at specific peptide bond cleavage sites is achieved by two specific neutral metalloproteinases—procollagen *N*-proteinase and procollagen *C*-proteinase—both of which require Ca^{2+} for activity and are inhibited by metal chelators. These enzymes act essentially only on molecules in the triple-helical conformation. Type I procollagen *N*-proteinase cleaves the *N*-terminal propeptides of types I and II procollagens between a proline and a glutamine residue. A separate enzyme is involved in the processing of the *N*-propeptide of type III procollagen. The type I procollagen *C*-terminal proteinase cleaves the *C*-terminal propeptides of both the proa1(I) and proa2(I) procollagen chains at an Ala—Asp bond. Most recently, procollagen *C*-proteinase was found to be BMP-1(bone morphogenetic protein-1), and recombinant BMP-1 was shown to act as procollagen *C*-proteinase. The enzyme is also able to cleave the *C*-terminal propeptides of type I procollagen homotrimer, type II procollagen, type III procollagen, and other proteins, including laminin-5 and prolysyl oxidase.

Figure 13. Processing of type I procollagen to fibril formation.

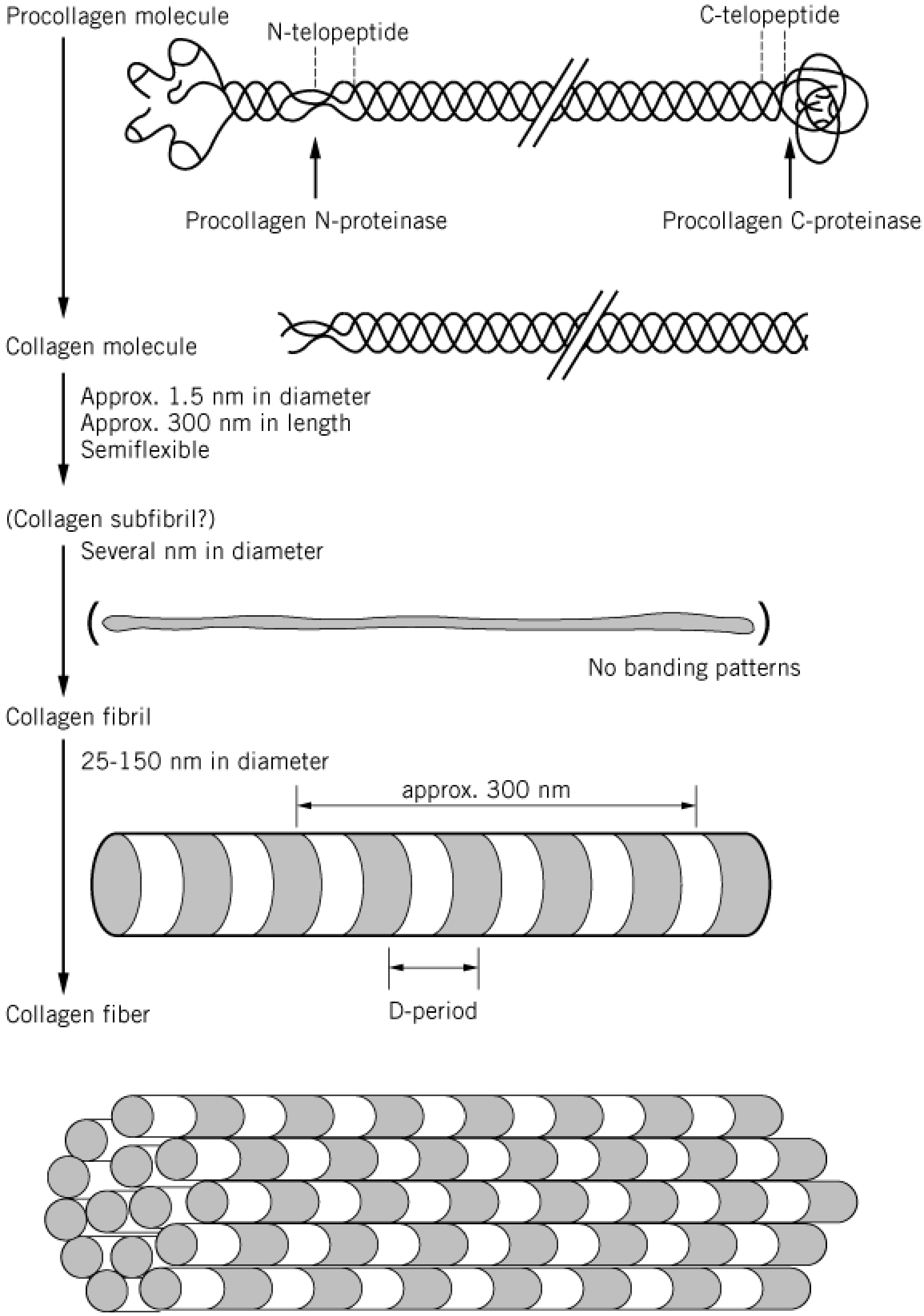

4.4. Crosslinking of Type I Collagen in the Fibrils

Covalent crosslinking of type I collagen in the fibrils involves oxidative deamination of specific lysine or hydroxylysine residues in the nonhelical (telopeptide) regions at the ends of the triple helix. Thus, lysyl and hydroxylysyl aldehydes are generated by lysyl oxidase (protein lysine 6-oxidase) (Fig. 14). The catalytic activity of lysyl oxidase is dependent on strict steric requirements (in the case of type I collagen, the quarter-stagger arrangement of molecules in the fibril) and on the sequence of amino acids surrounding the "target" lysyl/hydroxylysyl residues. The recombinant enzyme was produced as a proenzyme, which could be processed for activation by BMP-1 or procollagen *C*-proteinase.

Figure 14. Oxidative deamination and crosslinking of lysine or hydroxylysine residues. The oxidative deamination, Schiff base formation, and Amadori rearrangements take place *in vivo*. The last step, treatment with sodium borohydride, is carried out in the laboratory to stabilize the crosslinks for chemical analysis.

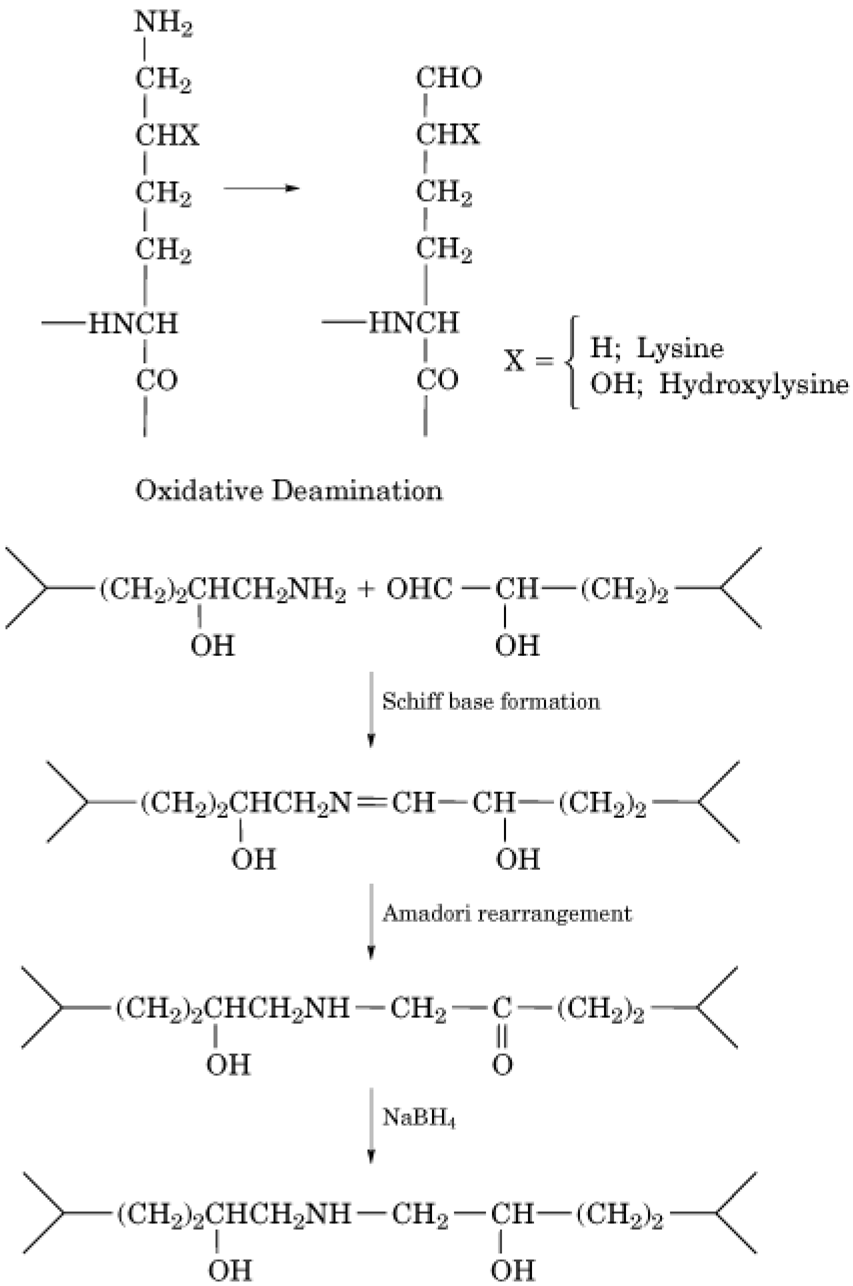

The majority of covalent crosslinks stabilizing the fibrillar collagens involve the telopeptides and, consequently, pepsin treatment of insoluble, crosslinked fibrils tends to release the triple-helical domain, which can be recovered in its native conformation.

5. Posttranslational Modifications of Proline and Lysine Residues

Hydroxylation of proline and lysine residues is a post-translational modification that is specific to collagen (see Hydroxylation (Lysine, Proline)). The reason for hydroxylation of proline residues at the 3 position is not known, but the presence of an appropriate number of 4-hydroxyproline residues in the —Y— position of —Gly—X—Y— is a crucial determinant of the stability of the triple helix under physiological conditions. The hydroxyl group forms hydrogen bonds that contribute to the thermal stability. The transition temperature (thermal denaturation temperature; melting temperature, T_m) of triple helices formed *in vitro* by nonhydroxylated collagen is about 25°C, which is 15°C lower than the fully hydroxylated collagen triple helix (Fig. 3). The importance of hydroxylysine may be inferred from the inherited connective tissue disorder, Ehlers–Danlos syndrome type VI, in which lysyl hydroxylase deficiency results in impaired crosslink formation and consequent susceptibility to mechanical disruption of tissues.

5.1. Glycosylation of Hydroxylysine Residues

Vertebrate collagen molecules contain the monosaccharide galactose and the disaccharide glucosyl–galactose. The glycosides are covalently linked through the hydroxyl group to hydroxylysine residues within the triple-helical domains (see Figs. 15 and 16).

Figure 15. Glycosylated hydroxylysine residues on the surface of the collagen triple helix. The molecular model of a portion (36 residues/chain) of human type V collagen, $[a1(V)]_2a2(V)$, was built up by the McMolw (Molecular Images Software, San Diego, CA, USA) and Chem3D (CambridgeSoft Corporation, Cambridge, MA, USA) programs, using the 2CLG file of the Protein Data Bank, which is the theoretical model of the $(Gly—Pro—Hyp)_4$ trimer. The two lysine residues of the two a1(V) chains are either left unchanged (*left*) or changed to glulcosylgalactosylhydroxylysine (*right*). The glycosylated hydroxylysine residues are evidently bulkier than other residues.

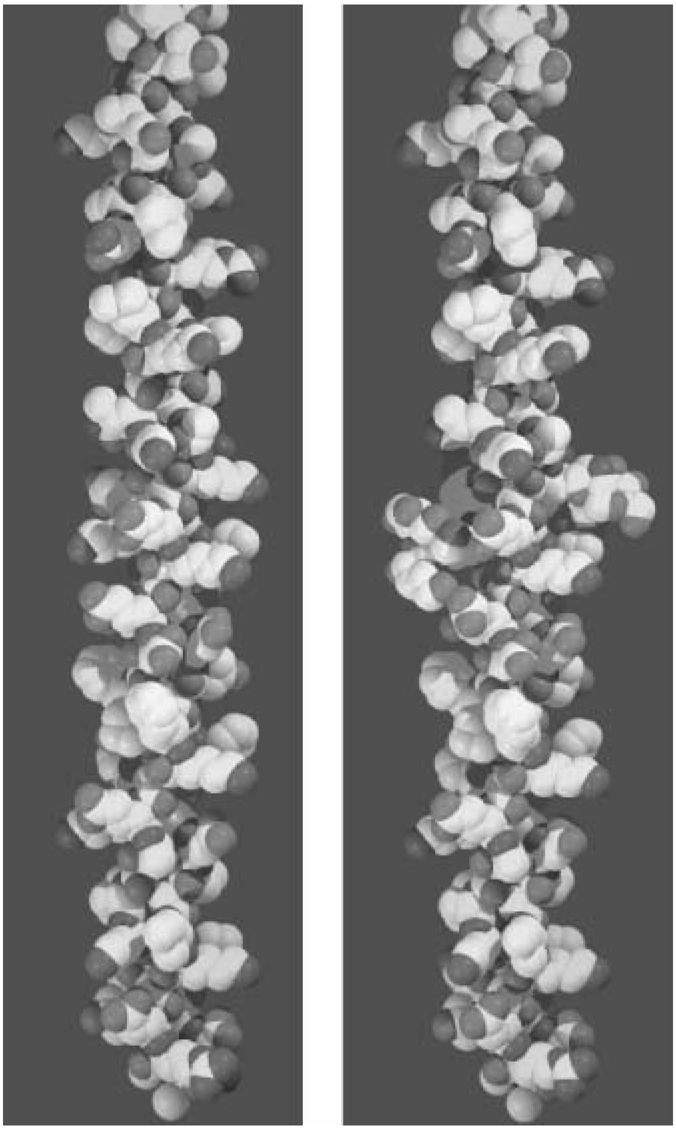

Figure 16. Attachment of galactose and glucose groups to hydroxylysine residues of collagen. (**a**) Enzymatic steps in coupling the two sugars; (**b**) stereo view (direct) of glucosylgalaclosylhydroxylysine. H atoms are not shown.

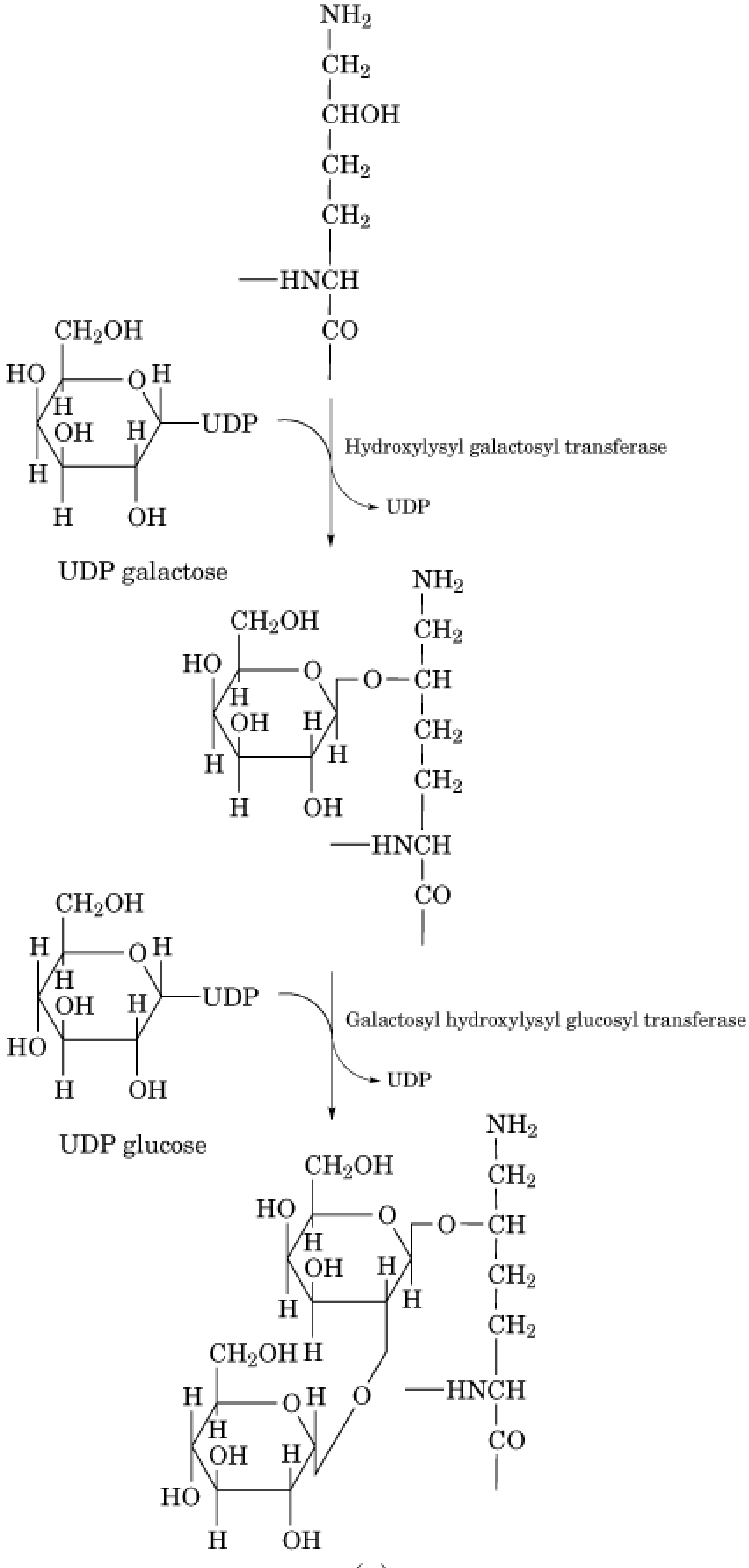
Hydroxylysyl galactosyl transferase
UDP
UDP galactose
Galactosyl hydroxylysyl glucosyl transferase
UDP
UDP glucose

(**a**)

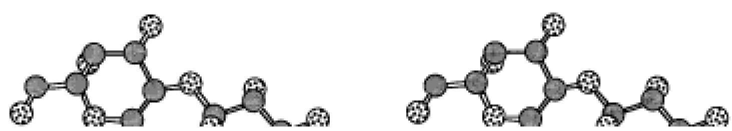

This glycosylation is unique to collagen, and its extent is variable both between collagen types and within the same collagen in different tissues and at different ages. A potential biological role of the specific carbohydrate units would be the regulation of the lateral assembly of the triple-helical domains. An inverse relationship exists between carbohydrate content and collagen fibril diameter, suggesting that the steric hindrance to the formation of highly ordered fibrils might be caused by the bulky glycosylated hydroxylysine residues. The glycosylation of hydroxylysine residues within the triple helix proceeds through the action of two isolated enzymes: hydroxylysyl galactosyl transferase (UDP galactose: 5-hydroxylysine–collagen galactosyltransferase) and galactosyl hydroxylysyl glucosyl transferase (UDP glucose: 5-hydroxylysine-collagen glucosyltransferase). Galactose is transferred to hydroxylysine residues by the former enzyme, while glucose is transferred to galactosyl-hydroxylysine residues by the latter enzyme. The carbohydrates are provided in both reactions by the appropriate UDP-glycosides. Both enzymes require a divalent cation (preferably Mn^{2+}) for the activity. A free e-amino group in the substrate hydroxylysyl residue and a nonhelical polypeptide conformation are requirements for both transferases. The reactions are more favorable with longer peptides. Hydroxylysyl galactosyl transferase can bind at least two manganese ions per molecule of active enzyme.

Suggestions for Further Reading

B. Brodsky (1995) FASEB J. **9**, 1537–1546.

E. Adachi, I. Hopkinson, and T. Hayashi (1997) Basement-membrane stromal relationships: interactions between collagen fibrils and the lamina densa. Intl. Rev. Cytolo. **173**, 73–156.

P. Yurchenco, D. E. Birk, and R. P. Mecham, eds. (1994) *Extracellular Matrix Assembly and Structure*, Academic Press, San Diego.

J. F. Bateman, S. R. Lamandé, and J. A. M. Ramshaw (1996) "Collagen superfamily", in *Extracellular Matrix*, Vol. **2**, W. D. Comper, ed., Harwood Academic Publishers, Amsterdam.

C. M. Kielty, I. Hopkinson, and M. E. Grant (1992) "Collagen", in *Connective Tissue and Its Heritable Disorders*, R. M. Royce and B. Steinmann, eds., Wiley, New York.

Colony-Stimulating Factors

Colony-stimulating factors (CSFs) are **glycoproteins** that stimulate the proliferation, differentiation, and survival of hematopoietic (blood) cells and also activate mature myeloid cell functions. CSFs were first described in the 1960s as activities in various conditioned media that stimulated the growth of colonies of bone marrow cells in semisolid cultures. These colony-forming cells are the precursors of our red and white blood cells (see Hematopoiesis). Purification and characterization of these activities were difficult with the biochemical techniques available because they were present in conditioned media in very low concentrations and also because they were heterogeneous, largely due to variable glycosylation. Eventually, in the late 1970s and 1980s, four different murine CSFs were purified, followed by their human counterparts. These were called

1. Multi-CSF or interleukin-3 (IL-3)
2. Granulocyte-macrophage (GM)-CSF
3. Granulocyte (G)-CSF
4. Macrophage (M)-CSF, or CSF-1

Since then, the development of molecular biology has led to the cloning of CSF complementary DNAs and the production of purified recombinant proteins, facilitating *in vitro* and *in vivo* studies of their activities. All four CSFs have been tested in clinical trials, and both G-CSF and GM-CSF are used in clinical practice to elevate leukocyte levels in a variety of situations. In addition to these CSFs, many interleukins and growth factors have been described that stimulate or co-stimulate bone marrow cell colony growth. The most important of these are the early-acting stem cell factor (SCF) and FLT3/FLK-2 ligand (FL) (1), the erythroid lineage stimulator erythropoietin, and the megakaryocyte and platelet stimulator thrombopoietin (TPO). Recently, TPO has been found to have multilineage activities (2).

1. Biochemical Characteristics

The CSFs belong to a family of **cytokines** that have little sequence identity but were predicted to be similar in structure (3). The protein structures of all four have now been determined, although for IL-3 a mutant molecule with enhanced stability was used, rather than the native molecule (4). They are all **four-helix bundles** with up–up–down–down connectivity. IL-3, G-CSF, and GM-CSF are monomeric secreted proteins, but the soluble form of M-CSF is a **disulfide-bonded** homodimer produced by **proteolytic** cleavage of cell-membrane molecules. Other characteristics are given in Table 1.

Table 1. Biochemical Characteristics of the CSFs

	IL-3		GM-CSF		G-CSF		M-CSF	
Property	Hu	Mu	Hu	Mu	Hu	Mu	Hu	Mu
Amino acids	133	140	127	124	174 (177)[a]	178	224/406/522[a]	519
M_r (kDa)								
Predicted	15.1	15.7	16.3	16	19	19	60	61
Expressed	14–30	28	18–33	18–33	22	25	45–90[b]	45–90[b]
Glycosylation								
N-linked	2	4	2	2	0	0	4	3
O-linked	ND	ND	2	ND	1	1	1	1
Disulfides	1	2	2	2	2	2	7–9	7–9
a-Helix type	Short		Short		Long		Short	
Cross-species activity[c]	–	–	–	–	+	+	+	–

[a] Different forms resulting from alternative splicing.

[b] Disulfide-bonded dimer of proteolytically cleaved transmembrane protein.

[c] Between human and murine. Data derived from Refs. 4, 18, and 19.

2. CSF Genes and Their Expression

The cloning of **genomic** DNA encoding the CSFs and analysis of the regions 5′ of the genes has resulted in a better understanding of the control of CSF expression (see Table 2). A single messenger RNA species is transcribed for IL-3 and GM-CSF, whereas a minor **alternatively spliced** mRNA is produced for human G-CSF that results in a three-amino-acid-residue insertion in the protein after residue Leu35 and a 20-fold reduction in activity. Transcription of M-CSF mRNA is more complex, with four species resulting from alternative splicing of the 10 exons (see Introns, Exons). The largest two differ only in the 3′ untranslated region and encode identical 522-residue **transmembrane** proteins. The smaller two result from splicing out of part of exon 6, which results in loss of the proteolytic cleavage site from the protein produced from the 1.6-kb **transcript** and expression of a stable transmembrane protein (5). The DNA regions upstream of the coding regions contain **promoter** and enhancer elements that have been partially characterized and shown to respond to CSF inducers such as tumor necrosis factor (TNF), IL-1, lipopolysaccharide (LPS), and antigens. The control of CSF gene expression is not understood completely, but it involves control of mRNA stability by elements in the 3′ untranslated region of the mRNAs, as well as control of transcription.

Table 2. Characteristics of the Genes Encoding the CSFs

	IL-3		GM-CSF		G-CSF		M-CSF	
Property	**Hu**	**Mu**	**Hu**	**Mu**	**Hu**	**Mu**	**Hu**	**Mu**
Size (kbp)	2.2	2.7	2.5	2.5	2.5	2.5	20	20
Chromosomal location	5q23-31	11A5-B1	5q21-31	11A5-B1	17q11-22	11D-E2	1p13-21	3F3
Number of exons	5	5	4	4	5	5	10	10
Alternative splicing	No	No	No	No	Yes	No	Yes	Yes
mRNA species (kb)	0.9	0.9	0.78	0.78	1.5	1.5	4, 2.3, 2.0, 1.6	4, 2.6, 1.4
Promoter elements	AP-1, ELF-1, NIP[a], NF-IL-3, CRE, CK-1, CK-2, GC		CK-1, CK-2, IgkB, GC, AP-1, ELF-1		PU box, CK-1, NF-IL-6, octamer, GPE-3,CK-2		SP-1, AP-1, AP-2, NF-1, NF-IL-6, CK-1,CK-2	

[a] Repressor element. Data from Refs. 18 and 19.

3. CSF Production

Many cell types have been shown to produce CSFs *in vitro* in response to various stimuli, such as bacterial products (LPS) and inflammatory cytokines (TNF, IL-1), but the role of CSFs in maintaining white blood cell levels in normal healthy individuals is not entirely clear (see later). Whether unstimulated cells produce CSFs is still debated (6). GM-CSF, G-CSF, and M-CSF are produced by macrophages, endothelial cells, fibroblasts, and stromal cells. In addition, T lymphocytes produce GM-CSF, M-CSF (in humans), and IL-3. Mast cells have been shown to produce IL-3 and GM-CSF. Other cell types have been reported to produce GM-CSF and IL-3, but these studies have yet to be confirmed.

4. CSF Receptors

The CSF receptors are transmembrane proteins belonging to the cytokine receptor class I family, except for the M-CSF receptor, which is a tyrosine kinase receptor. The class I receptors contain a structurally conserved module called the cytokine-binding **domain** (CBD), the hemopoietin domain, or the cytokine receptor homology domain. This module comprises two fibronectin type III domains with four conserved cysteine residues in the *N*-terminal domain and a conserved Trp━Ser━X━Trp━Ser sequence in the *C*-terminal domain. Ligand binding causes dimerization or oligomerization of the receptors, which initiates signal transduction. The IL-3 and GM-CSF receptors form heterodimers of a ligand-specific a-chain and a common b-chain that is also shared with the IL-5 receptor. In the mouse, there is an additional b-chain that is unique to the IL-3 receptor. The G-CSF and M-CSF receptors form homodimers. Receptor dimerization activates tyrosine kinases (intrinsic in the M-CSF receptor, cytoplasmic **JAK** kinases for the other receptors) that **phosphorylate** the receptors, providing binding sites for other signaling molecules that are in turn activated by phosphorylation of tyrosine residues and, in some cases, serine or threonine. Ultimately, these signaling cascades lead to alterations in gene transcription, but the components of the biochemical pathways are still being defined (reviewed in Refs. 7-9).

The CSF receptors are expressed at low levels on hematopoietic cells, usually a few hundred receptors per cell. IL-3 receptors are expressed on neutrophil, eosinophil, and macrophage lineages, on mast cells, and on undifferentiated blast cells. GM-CSF receptors are expressed on neutrophil, eosinophil, and macrophage lineages. G- and M-CSF receptor expression is more restricted; G-CSF receptors are present on neutrophils and at a low level on macrophages, and M-CSF receptors are found on macrophages, osteoclasts, and placental trophoblasts. Recent studies have detected expression of receptors on purified stem-cell populations. Human $CD34^+$ cells expressed SCF, FL, G-CSF, and, at a low level, GM-CSF receptors (10). Murine stem cell populations expressed IL-1a, IL-3, IL-6, and G-CSF receptors (11).

5. Biological Activity

5.1. *In Vitro*

All four of the CSFs stimulate the proliferation and differentiation of bone-marrow progenitors to form colonies in semisolid agar. The type of mature cells in the colonies varies with the stimulator (see Fig. 1). IL-3 was otherwise called multi-CSF because it stimulates the largest number of different cell lineages. Colonies of granulocytes, macrophages, eosinophils, megakaryocytes, undifferentiated blast cells, and mixed cell lineages are obtained. In liquid cultures, proliferation of mast cells is strongly stimulated by IL-3, and some types of B lymphocytes are reported to respond. GM-CSF stimulates growth of granulocytic, macrophage, and eosinophil colonies. Production of dendritic cells, which are important **antigen-presenting** cells in the immune response, is stimulated by GM-CSF. G-CSF and M-CSF are more lineage restricted, producing mainly granulocytic and macrophage colonies, respectively. The CSFs can give enhanced or synergistic responses when used in combination with each other and with other interleukins and growth factors. Some effects of CSFs on nonhematopoietic cells have been reported. G- and GM-CSF can stimulate proliferation of endothelial cells. Placenta-derived cells and oligodendrocytes proliferate in response to GM-CSF. M-CSF stimulates proliferation of trophoblast cells and may be important in pregnancy.

Figure 1. Schematic representation of hematopoiesis and the CSFs and other cytokines required for mature cell production. IL, interleukin; FL, FLT3/FLK-2 ligand; SCF, stem cell factor; TPO, thrombopoietin. GM-CSF and IL-3 stimulate cells inside the dotted line box.

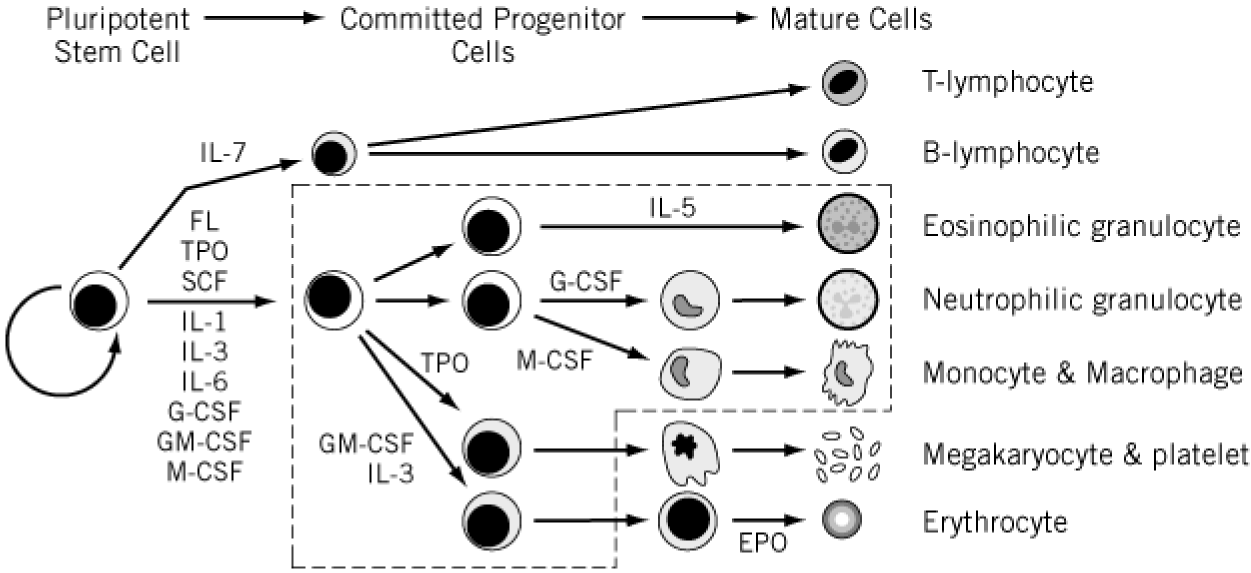

5.2. *In Vivo*

The effects of CSFs *in vivo* have been determined both by injection in mice and humans and by analysis of CSF-deficient mice created by gene targeting and, in the case of M-CSF, a naturally occurring mutation. Injection of IL-3 or GM-CSF elevates circulating levels of neutrophils, monocytes, and eosinophils. G-CSF causes a greater elevation of neutrophils than does IL-3 or GM-CSF, but only a weak increase in monocytes and no effect on other lineages. M-CSF causes a selective elevation of monocytes. The magnitude of these increases depends on the dose of CSF administered. It is interesting that in response to infection, circulating IL-3 or GM-CSF are not usually detected, whereas G-CSF and, to a lesser extent, M-CSF are frequently elevated in serum. These observations suggest that IL-3 and GM-CSF may be important in local inflammatory responses in the tissues rather than in a systemic response to infection.

The importance of the CSFs in maintaining basal hematopoiesis has been assessed by analysis of CSF-deficient mice. For IL-3, GM-CSF, and G-CSF, gene “knockout” mice were created by introduction of a defective version of the gene of interest into embryonic stem cells by homologous recombination. The embryonic stem cells were injected into blastocysts to create chimeric mice that were then bred to create heterozygous and homozygous deficient mice. For M-CSF, mice with a naturally occurring point mutation (*op*/*op*) that resulted in a frameshift in the sequence and a loss of M-CSF production were discovered. The IL-3- and GM-CSF-deficient mice were able to produce normal levels of circulating blood cells and bone marrow progenitors. The GM-CSF-deficient mice developed pulmonary alveolar proteinosis and increased pulmonary infections, presumably as a consequence of defective pulmonary macrophage function. Recent studies in IL-3-deficient mice have shown that IL-3 is important for elevation of basophils and mast cells in response to a parasitic infection (12) and for some delayed-type hypersensitivity (T-lymphocyte-dependent) responses (13). G-CSF defective mice were neutropenic, with neutrophil numbers reduced to 20–35% of wild-type control mice. Bone marrow cellularity was normal, but some granulocytic and macrophage progenitors were reduced in number. These mice were more susceptible to a bacterial infection (*Listeria monocytogenes*) than wild-type mice. Young M-CSF-deficient mice have osteopetrosis, a severe macrophage and osteoclast deficiency resulting in failure of teeth eruption and overgrowth of bone that occludes the marrow cavity and reduces marrow cellularity. Unlike the other CSF-deficient mice, the *op/op* mice overcome their defects with age, which suggests that other cytokines may be able to compensate for the lack of M-CSF. Thus, the CSF-defective mice have shown that each CSF has a unique function *in vivo*. GM-CSF and IL-3 are not required for steady-state hematopoiesis. G- and M-CSF are required for normal neutrophil and macrophage production, respectively. All four CSFs contribute in different ways to control of infection. They may have other nonunique functions that are not revealed in the deficient mice because of compensatory activities of other cytokines. These may be detected in future studies of multiply deficient mice.

6. Myeloid Leukemia

Acute and chronic myeloid leukemias (AMLs and CMLs) are clonal diseases of bone marrow cells in which the predominant cell types are granulocytes and macrophages, although leukemic cells of other lineages are also found. There are potentially two ways in which CSFs could be involved in leukemia: They may be required for the proliferation of the leukemic cells, and they may cause differentiation and clonal extinction of the leukemia. In semisolid agar cultures, CML cells will produce colonies of normal appearance containing granulocytes, macrophages, and eosinophils. The colony growth is dependent on CSF stimulation, and all four CSFs are active. In contrast, AML cells produce small clones with little maturation, and growth is very variable from patient to patient. The cells are responsive to CSFs to a variable extent, and in a proportion of patients (<30%) there is colony growth in the absence of CSFs. The colonies do not contain clonogenic cells that are able to form further colonies in secondary cultures. The leukemic stem cells have not been identified, and their dependence on CSFs is unclear. Whether autocrine production of CSFs by leukemic cells is important is also unknown, with the exception of leukemic monocytes, which produce CSFs like their normal counterparts. Lopez and colleagues have produced a GM-CSF antagonist that induced remission in a murine model of juvenile myelomonocytic leukemia (14). Although there are some leukemic cell lines that differentiate and cease proliferation in response to CSFs *in vitro*, many cell lines are not suppressed by CSFs. There may be defects in the signal transduction pathways that prevent differentiation. In a small number of patients with congenital neutropenia who develop AML, a mutation in the G-CSF receptor expressed by the leukemic cells has been described that prevents differentiation in response to G-CSF (15). However, it is not known whether this mutation contributed to the development of AML.

7. Clinical Use of CSFs

The use of chemotherapy in cancer treatment is limited by its toxicity, primarily neutropenia. Both G-CSF and GM-CSF have been tested extensively in clinical trials and shown to reduce neutropenia, allowing the intensification of chemotherapy doses. Clinical trials have not yet shown, however, whether dose intensification improves survival. G-CSF has fewer side effects and is more effective at elevating neutrophil levels than GM-CSF and thus is usually the CSF of choice, but GM-CSF may be more effective in reducing infectious complications (16). In high-dose chemotherapy followed by autologous bone marrow transplantation, both CSFs reduced the time taken for recovery to ≥500 cells/mm^3 by about one week and, in some trials, reduced the duration of hospital stay. G-CSF (and GM-CSF) treatment increased the levels of circulating progenitor and stem cells so that G-CSF-mobilized peripheral blood progenitor cells are now used instead of bone marrow cells for reconstitution after high-dose chemotherapy. This treatment results in more rapid recovery than bone marrow transplantation.

Patients with congenital neutropenia or idiopathic chronic neutropenia respond to G-CSF treatment with elevation of neutrophil levels, resulting in fewer infections and less time in hospital. A few of these patients (3% in Ref. 17) develop myelodysplasia or leukemia, but at present there is no evidence whether G-CSF increases the frequency of these cases. Despite initial concerns that treatment of leukemia patients with CSFs might exacerbate the disease, there is no evidence that this occurs. Neutrophil recovery has occurred more rapidly in leukemia patients receiving G-CSF or GM-CSF after chemotherapy, but reduction in duration of hospital stay was not usually observed.

There have been fewer clinical trials with M-CSF and IL-3. M-CSF appears to improve recovery from fungal infections and is approved in Japan for use in allogeneic transplantation, induction therapy of AML, and dose-intensive therapy of ovarian cancer. IL-3 given after chemotherapy reduced the recovery time from leukopenia and elevated the levels of neutrophils, monocytes, and eosinophils. In the future, it is likely that combinations of cytokines will be tested.

Bibliography

1. Y. Yonemura, H. Ku, S. D. Lyman, and M. Ogawa (1997) Blood **89**, 1915–1921.
2. G. P. Solar, W. G. Kerr, F. C. Zeigler, D. Hess, C. Donahue, F. J. de Sauvage, and D. L. Eaton (1998) Blood **92**, 4–10.
3. J. F. Bazan (1990) Immunol. Today **11**, 350–354.
4. Y. Feng, B. K. Klein, and C. A. McWherter (1996) J. Mol. Biol. **259**, 524–541.
5. M. Baccarini and E. R. Stanley (1990) In *Growth Factors, Differentiation Factors, and Cytokines* (A. Habenicht, ed.), Springer-Verlag, Berlin, pp. 188–200.
6. F. H. M. Cluitmans, B. H. J. Esendam, J. E. Landegent, R. Willemze, and J. H. F. Falkenburg (1995) Blood **85**, 2038–2044.
7. T. Hara and A. Miyajima (1996) Stem Cells **14**, 605–618.
8. B. R. Avalos (1996) Blood **88**, 761–777.
9. L. R. Rohrschneider, R. P. Bourette, M. N. Lioubin, P. A. Algate, G. M. Myles, and K. Carlberg (1997) Mol. Reprod. Dev. **46**, 96–103 (Abstract).
10. A. W. Roberts, M. Zaiss, A. W. Boyd, and N. A. Nicola (1997) Exp. Hematol. **25**, 289–305.
11. W. J. McKinstry, C. Li, J. E. J. Rasko, N. A. Nicola, G. R. Johnson, and D. Metcalf (1997) Blood **89**, 65–71.
12. C. S. Lanz, J. Boesiger, C. H. Song, N. Mach, T. Kobayashi, R. C. Mulligan, Y. Nawa, G. Dranoff, and S. J. Galli (1998) Nature **392**, 90–93.
13. N. Mach, C. S. Lanz, S. J. Galli, G. Reznikoff, M. Mihm, C. Small, R. Granstein, S. Beissert, M. Sadelain, R. C. Mulligan, and G. Dranoff (1998) Blood **91**, 778–783.
14. P. O. Iversen, I. D. Lewis, S. Turczynowicz, H. Hasle, C. Niemeyer, K. Schmiegelow, S. Bastiras, A. Biondi, T. P. Hughes, and A. F. Lopez (1997) Blood **90**, 4910–4917.
15. F. Dong, R. K. Brynes, R. K. Tidow, K. Welte, B. Lowenberg, and I. P. Touw (1995) N. Engl. J. Med. **333**, 487–493.
16. J. Nemunaitis (1997) Drugs **54**, 709–729.
17. D. C. Dale, M. A. Bonilla, M. W. Davis, A. M. Nakanishi, W. P. Hammond, J. Kurtzberg, W. Wang, A. Jakubowski, E. Winton, P. Lalezari, W. Robinson, J. A. Glaspy, S. Emerson, J. Gabrilove, M. Vincent, and L. A. Boxer (1993) Blood **81**, 2496–2502.
18. D. Metcalf and N. A. Nicola (1995) *The Hemopoietic Colony-Stimulating Factors. From Biology to Clinical Applications*, Cambridge University Press, Cambridge, England.
19. R. Callard and A. Gearing (1994) *The Cytokine Facts Book*, Academic Press, London.

Suggestions for Further Reading

20. G. J. Lieschke (1997) CSF-deficient mice—what have they taught us? Ciba Foundation Symposium **204**, 60–77. A detailed analysis of CSF deficient mice.
21. D. Metcalf (1998) Lineage commitment and maturation in hematopoietic cells: the case for extrinsic regulation. Blood **92**, 345–348.
22. T. Enver, C. M. Heyworth, and T. M. Dexter (1998) Do stem cells play dice? Blood **92**, 348–351. Two sides of the debate about hematopoietic lineage commitment.
23. S. S. Watowitch, H. Wu, M. Socolovsky, U. Klingmuller, S. N. Constantinescu, and H. F. Lodish (1996) Cytokine receptor signal transduction and the control of hematopoietic cell development. Annu. Rev. Cell Dev. Biol. **12**, 91–128.
24. *References 18 and 19 above. Reference 18 gives a detailed, well referenced description of the four CSFs. Reference 19 is less detailed, but covers other cytokines in addition to the original four.*

Combinatorial Libraries

Few fields have emerged as rapidly as the technologies collectively referred to as combinatorial chemistry. The origins of combinatorial “thinking” as applied to biological problems can be traced to our understanding of the immune system. Humoral immunity is based on the generation of billions of different antibody molecules through unique **gene recombination** events. Upon exposure to a foreign immunogen, the subset of the antibody repertoire with specificity for the invader is clonally expanded. During expansion, the active antibody subpool undergoes additional recombination and mutation events, and the most active variants are further selected. This process is reiterated until mature antibody molecules are produced that are highly optimized against the foreign antigen. In essence, antibody repertoires are combinatorial libraries—collections of related but distinct molecules representing different combinations of genetic elements. The recognition of these facts preceded the creation of the first combinatorial library, which was based upon the synthesis and screening of large numbers of synthetic peptides in order to identify selected antigenic determinants of a viral pathogen (1). Given the parallels between the immune system and combinatorial libraries, it is not surprising that the original application of this emerging technology was in the derivation of immunogens capable of stimulating immune protection in animals not yet exposed to certain pathogens.

The hallmarks of a combinatorial approach are the generation and use of complex compound mixtures to identify molecules with desirable properties. Four basic operations underpin combinatorial approaches: (i) generation of libraries containing related but diverse compounds, (ii) selection of molecules with desirable properties from the library, (iii) characterization of the selected molecules, and (iv) amplification of the identified products. Depending upon the chemical composition of the library, the selected molecules may require amplification before structure determination. For example, DNA libraries can be amplified using the polymerase chain reaction (**PCR**) before the final products are identified by sequencing. Synthetic peptides and small molecules cannot be amplified per se and must be subjected to structural elucidation, and then resynthesized for subsequent use. Regardless of the library composition, the four operations enumerated above can be applied in an iterative fashion to progressively refine the selected compounds.

Several entries in this volume deal with the application of combinatorial approaches to complex biological problems. Issues central to the implementation of combinatorial technologies in biological systems will be described below, including cognitive aspects of library design, practical aspects of library construction, basic issues in affinity selection and library screening, and discussions of different library types and their applications. The breadth of the topic Combinatorial Libraries is so expansive that it is impossible to cover any topic in great detail. The entries entitled Libraries, Combinatorial Synthesis, and Affinity Selection are intended to provide a generic introduction to the principles underlying combinatorial operations. The remaining entries, DNA libraries, Genomic libraries, cDNA libraries, Expression libraries, Peptide libraries, and Phage display libraries, provide more specific details regarding the major types of combinatorial libraries in widespread use. Small molecule synthesis or drug discovery applications are not dealt with in detail, although many basic concepts from these fields are presented. The reader is referred to the suggested reading list for additional discussion of these related topics.

See also Libraries, Combinatorial Synthesis, Affinity Selection, DNA Libraries, Genomic Libraries, cDNA Libraries, Expression Libraries, Peptide Libraries, Phage Display Libraries.

Bibliography

1. H. M. Geysen, R. H. Meleon, and S. J. Barteling (1984) Proc. Natl. Acad. Sci. USA **81**, 3998–4002.

Suggestions for Further Reading

2. J. D. Watson (1987) *Molecular Biology of the Gene*, 4th ed., Benjamin-Cummings, Menlo Park, CA.
3. J. Sambrook, E. F. Fritsch, and T. Maniatis (1989) *Molecular Cloning: A Laboratory Manual*, 2nd ed., Cold Spring Harbor Laboratory Press, Cold Spring Harbor, NY.
4. D. J. Kenan, D. E. Tsai, and J. D. Keene (1994) Trends Biochem. Sci **19**, 57–64.
5. J. N. Abelson, ed. (1996) *Combinatorial Chemistry*, Vol. **267**, Methods in Enzymology, Academic Press, San Diego.
6. L. A. Thompson and J. A. Ellman (1996) Chem. Rev. **96**, 555–600.
7. B. K. Kay, J. Winter, and J. McCafferty (1996) *Phage Display of Peptides and Proteins*, Academic Press, San Diego.

Combinatorial Synthesis

The diversity of a molecular library may be derived from natural sources, or it may be created through specialized techniques in synthetic chemistry. Traditionally, synthetic chemists focus on preparing individual compounds, paying careful attention to stereochemical control and to achieving the greatest possible yield and purity. This often requires the use of highly specialized reactions and can be a painstakingly slow process. In contrast, chemists engaged in combinatorial organic synthesis employ transformations that are more general in scope and can be applied to the simultaneous preparation of many chemically distinct compounds. In exchange for the ability to prepare many compounds in a short time frame, compromises are accepted that may result in sacrificing, within acceptable limits, yield and purity of individual reaction products. This entry deals with the basic issues faced in preparing and screening synthetic combinatorial libraries and some of the relevant technologies and methods. No attempt has been made to provide exhaustive coverage of the rapidly expanding range of chemistries now amenable to library synthesis, nor have we attempted to cover the application of combinatorial chemistry as it applies directly to the field of drug discovery. See Combinatorial Libraries.

Combinatorial chemistry seeks to create all possible combinations of a set of building blocks and then extract the identity of members that exhibit a desired property. Thus, if a traditional synthesis involves incorporating building block A, followed by B, and then C to give the desired compound A–B–C, then the analogous combinatorial synthesis would employ a set of monomers, A_1–A_n, followed by a second set of monomers, B_1–B_n, and then a third set of monomers, C_1–C_n, giving all possible combinations of $(A_{1\text{ to }n})$–$(B_{1\text{ to }n})$–$(C_{1\text{ to }n})$. Such processes can be described as n^k sets, where n is the number of building blocks used in each cycle of synthesis and k is the total number of synthetic cycles. The number of individual species generated by these approaches become vast very quickly. For example, a relatively short DNA library of 100 random nucleotide positions has a theoretical complexity of 4^{100}, or 1.6×10^{60} different sequences. This number exceeds the number of protons in the sun. Complexities of more realistic peptide libraries using the 20 amino acids incorporated into proteins are as follows: A library of all possible tripeptides will contain 8000 (20^3) distinct peptide sequences; a library of all possible tetrapeptides will contain 160,000 (20^4) distinct peptide sequences; and a library of all possible pentapeptides will contain 3,200,000 (20^5) distinct peptide sequences. Specialized methods are required to prepare, assay, and elucidate the identity of active compounds from collections of this size. In order to facilitate product purification, compounds are typically synthesized while covalently attached to inert solid supports, including polymeric pins or resin beads, although other materials have been used. Use of solid phase synthesis enables many reactions to be carried out simultaneously using parallel arrays of individual reaction chambers. If each reaction yields a single product, the result is a library of spatially discrete compounds. This approach has the advantage that the identity of compounds can be ascertained immediately, based on the position in the synthetic array and the associated synthetic history. The initial application of this approach was reported by Geysen et al. for synthesis of peptide libraries (1); however, many variations have been reported since then, involving a wide range of chemistries. Although convenient and straightforward to implement, the number of compounds that can be synthesized and screened using this approach is limited by the physical dimensions of the arrays to approximately 10,000 different species. Miniaturization and photolithographic masking techniques have enabled arrays containing more than 100,000 compounds to be synthesized on silica chips (2). Although this has been applied to a variety of chemistries, it is perhaps most widely recognized as the DNA chip technology of Affymetrix (3). Unfortunately, this approach requires highly specialized instrumentation for the photolithographic masking, as well as for assay of the resulting arrays.

The synthesis of larger libraries requires pooling methods that overcome the size limitations of spatial arrays (4). Pooling methods employ mixtures of reactants at each synthetic step (5). For example, in random DNA oligonucleotide synthesis, two or more deoxyribonucleotide phosphoramidites are introduced during each coupling cycle. One major problem with mixture synthesis is that variation in reactivity can result in some building blocks being under- or overrepresented in the final compound pool. At least in some cases, the initial concentration of reactants can be adjusted to correct for these variations in reactivity. A more attractive approach, first introduced by Furka, is the “split synthesis” strategy (6). Briefly, a portion of synthesis resin is “split” or divided into equal portions and placed into individual reaction vessels (Fig. 1). Each vessel receives a single building block in large excess, which drives the reaction to completion. The resin from all the vessels is then recombined, mixed thoroughly, and then redistributed. A second set of building blocks is then introduced. This process is repeated the desired number of cycles, to produce all possible combinations of the desired building blocks. Because each resin bead is exposed to a single building block at each step, there will be only one compound (but many copies) attached to each bead. This has led to the term one-bead, one-compound (OBOC) libraries (7, 8).

Figure 1. Schematic flow of a split synthesis. The resin is first divided into *n* equal portions. Following deprotection, each resin batch is reacted with a different monomer from set A. The resin is pooled, mixed, and divided into equal portions. After deprotection, individual monomers from set B are coupled. The process is repeated, and monomers from set C are added. Each final reaction batch is held separately for subsequent assay.

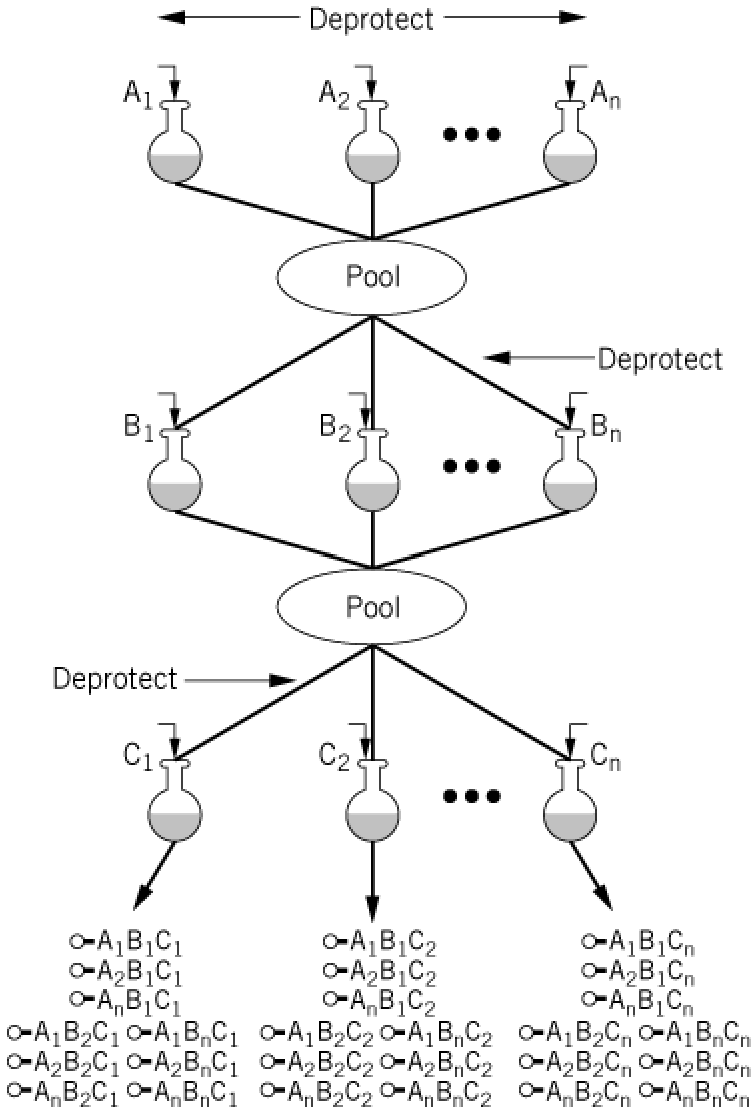

Compound identification is straightforward for spatially discrete libraries; however, identifying active species in the large and complex mixtures that result from pooling strategies presents a formidable problem. Typically, each member of a pool is present in a quantity that, although sufficient for determining biological activity, is insufficient for isolation and structure determination by standard analytical methods. As a result, strategies to identify the active members must be built into the synthetic schemes and closely coupled to the types of assays that will be performed with a particular library.

Compounds can be identified from soluble libraries using deconvolution strategies such as those introduced by Houghten (9, 10). This approach relies on cycles of synthesis and screening to focus progressively in on active species. An initial library is prepared in which one position of diversity is held constant. Each individual pool of compounds contains a different building block at the constant position but a mixture of building blocks at the remaining positions of diversity. Screening identifies the pool and therefore the optimal building block at the defined location. A second library is then synthesized in which all members have the optimal building block at this first position, but each pool contains a different building block at a second position of diversity. This process is repeated until the preferred building block for each position is determined. The chief disadvantage of this approach is that it is a laborious and time-consuming process. Moreover, this strategy does not guarantee that the most potent library member will be identified since selection of a “preferred” building block depends on the cumulative activity of a pool. Selection of a particular building block could, therefore, result from the presence in a pool of a relatively few number of potent compounds or a large number of relatively poor inhibitors.

Several strategies have been developed that allow the active members of a library to be determined without requiring cycles of synthesis and screening. The method of positional scanning (11) involves synthesizing a series of combinatorial libraries, each fixing a single position of diversity. Synthesis of each library is divided such that each component pool is prepared using a single building block at the defined position, while the remaining positions are synthesized using mixtures of building blocks. Although this method does not require resynthesis, it does require additional synthetic effort to prepare a complete set of scanning libraries, and the total number of syntheses is greater than for deconvolution approaches. Moreover, because each position is defined independently, there is an increased chance of missing the most active members in the library.

Orthogonal pooling strategies also avoid the resynthesis burden of deconvolution methods (12). In this approach, two separate libraries are synthesized such that any given pool of the first library has only one compound in common with any pool of the second library. Determining the common species between positive pools from the two libraries reveals the identity of active compounds. The chance for misidentifying the optimal building block at any given position is avoided by this approach, but there is a considerable synthetic burden, as well as compound tracking issues.

The second general assay format is designed to measure the interaction of a target (enzyme, receptor, cell, etc) with compounds while they remain attached to the solid support used for library synthesis. Geysen pioneered this approach for assaying libraries of peptides arrayed on pins (1); however, the full potential was realized only when it was coupled to screening of OBOC libraries (8). Because each resin bead in an OBOC library carries a single library compound and the beads are physically distinct, each bead behaves as an isolated assay system. Briefly, a target is incubated with a pool of beads. The excess target is removed by washing, leaving behind only target that associates specifically with a compound attached to a resin bead. The active compounds are identified following visualization of those beads to which the target specifically interacts.

Specialized techniques are required to identify the compounds attached to individual beads, because each bead can carry at most a few nanomoles of compound, which is insufficient for structure determination except in a few rare cases (eg, peptides). These methods seek to “tag” or “encode” the beads with the synthetic history in a manner that is easily deciphered (13, 14). The code is introduced either prior to library synthesis or following each cycle of building block addition. In the latter case, the chemistries for library synthesis and code synthesis must be mutually compatible, which is one of the major obstacles in the development and utilization of this approach. Examples of encoding methods include the use of peptides read by Edman Degradation (15), nucleic acids read by PCR amplification and sequencing (16), several small molecule chemical classes identified by various analytical methods (17, 18), nonradioactive isotopic tags read by mass spectrometry (19), and radioisotopes encapsulated within the solid-phase support (20, 21). The development of encoding methods is an active area of research because the split synthesis method is currently the only tractable approach to preparing large libraries in which all possible compounds are represented.

See also Combinatorial Libraries, Libraries, Affinity Selection, DNA Libraries, Genomic Libraries, cDNA Libraries, Expression Libraries, Peptide Libraries, and Phage Display Libraries.

Bibliography

1. H. M. Geysen, R. H. Meleon, and S. J. Barteling (1984) Proc. Natl. Acad. Sci. USA **81**, 3998–4002.
2. S. P. Fodor, J. L. Read, M. C. Pirrung, L. Stryer, A. T. Lu, and D. Solas (1991) Science **251**, 767–773.
3. A. C. Pease, D. Solas, E. J. Sullivan, M. T. Cronin, C. P. Holmes, and S. P. Fodor (1994) Proc. Natl. Acad. Sci. USA **91**, 5022–5026.

4. C. Pinilla, J. Appel, S. Blondelle, C. Dooley, B. Dörner, J. Eichler, J. Ostresh, and R. A. Houghten (1995) Biopolymers (Peptide Sci.) **37**, 221–240.
5. H. M. Geysen, S. J. Rodda, and T. J. Mason (1986) Mol. Immunol. **23**, 709–715.
6. A. Furka, F. Sebestyen, M. Asgedom, and G. Dibo (1991) Int. J. Pept. Protein Res. **37**, 487–493.
7. K. S. Lam, M. Lebl, and V. Krchnak (1997) Chem. Rev. **97**, 411–448.
8. K. S. Lam, S. E. Salmon, E. M. Hersh, V. J. Hruby, W. M. Kazmierski, and R. J. Knapp (1991) Nature **354**, 82–84.
9. C. T. Dooley, N. N. Chung, B. C. Wilkes, P. W. Schiller, J. M. Bidlack, G. W. Pasternak, and R. A. Houghten (1994) Science **266**, 2019–2022.
10. S. E. Blondelle, E. Takahashi, P. A. Weber, and R. A. Houghten (1994) Antimicrob. Agents Chemother. **38**, 2280–2286.
11. R. A. Houghten, C. Pinilla, S. E. Blondelle, J. R. Appel, C. T. Dooley, and J. H. Cuervo (1991) Nature **354**, 84–86.
12. B. Deprez, X. Williard, L. Bourel, H. Coste, F. Hyafil, and A. Tartar (1995) J. Am. Chem. Soc. **117**, 5405–5406.
13. S. Brenner and R. A. Lerner (1992) Proc. Natl. Acad. Sci. USA **89**, 5381–5383.
14. K. D. Janda (1994) Proc. Natl. Acad. Sci. USA **91**, 10779–10785.
15. J. M. Kerr, S. C. Banville, and R. N. Zuckermann (1993) J. Am. Chem. Soc. **115**, 2529–2531.
16. M. C. Needels, D. G. Jones, E. H. Tate, G. L. Heinkel, L. M. Kochersperger, W. J. Dower, R. W. Barrett, and M. A. Gallop (1993) Proc. Natl. Acad. Sci. USA **90**, 10700–10704.
17. M. H. J. Ohlmeyer, R. N. Swanson, L. W. Dillard, J. C. Reader, G. Asouline, R. Kobayashi, M. Wigler, and W. C. Still (1993) Proc. Natl. Acad. Sci. USA **90**, 10922–10926.
18. Z.-J. Ni, D. Maclean, C. P. Holmes, M. M. Murphy, B. Ruhland, J. W. Jacobs, E. M. Gordon, and M. A. Gallop (1996). J. Med. Chem. **39**, 1601–1608.
19. H. M. Geysen, C. D. Wagner, W. M. Bodnar, C. J. Markworth, G. J. Parke, F. J. Schoenen, D. S. Wagner, and D. S. Kinder (1996) Chem. Biol. **3**, 679–688.
20. K. C. Nicolaou, X.-Y. Xiao, Z. Parandoosh, A. Senyei, and M. P. Novz (1995) Angew. Chem. Int. Ed. English **34**, 2289–2291.
21. E. J. Moran, S. Sarshar, J. F. Cargill, M. M. Shahbaz, A. Lio, A. M. M. Mjalli, and R. W. Armstrong (1995) J. Am. Chem. Soc. **117**, 10787–10788.

Competence

Competence is the condition of bacterial cells that enables them to take up naked **DNA**. When this DNA can integrate into the chromosome by recombination or, in the case of **plasmids**, establish itself in the cytoplasm, the cells are said to be transformed (see Transformation). Competence is manifested by several species of bacteria—representatives of 29 different genera according to a recent count (1)—but far from all. Even in transformable strains, competence generally depends on the establishment of a particular physiological state. Four species have served as the major experimental models for studies of competence, and we shall therefore confine discussion largely to these: *Bacillus subtilis, Streptococcus pneumoniae* ("pneumococcus"), *Haemophilus influenzae*, and *Neisseria gonorrhoeae*. In view of the universal utility of *Escherichia coli*, which does not acquire competence naturally, we shall also review briefly the artificial induction of competence in this species.

The basic mechanism of DNA uptake appears to be the same in all naturally transformable organisms. Duplex DNA binds to the cell surface, and is then processed so that just one of the two strands passes through a specialized transmembrane channel into the cytoplasm, where it undergoes recombination with the resident chromosome. In **gram-negative** bacteria, a means of first passing through the outer membrane is also needed. The systems that regulate the uptake process, however, as well as the environmental stimuli to which these systems respond, appear to be more idiosyncratic, presumably reflecting the very different natural habitats in which the capacity to take up DNA is induced. Furthermore, the regulatory pathways of competence intersect with those of other metabolic activities. It is with the regulation of competence that this entry is chiefly concerned, the uptake process itself being deferred largely to the entry Transformation. We begin with the bacterium for which most is known at both the mechanistic and regulatory levels.

1. *B. subtilis*

B. subtilis survives and grows in many environments, but its natural reservoir is the soil. It was early appreciated that competence in this bacterium is a phenomenon induced by decelerating growth (2), such as occurs at the transition from exponential to stationary phase or upon depleting the medium of amino acids. Dependence of competence on transition to the stationary phase appears to reflect inhibition of competence by added amino acids (3). Prototrophs in minimal medium can attain competence in exponential phase (4). We now know that it is just one of a number of late-growth responses, which also include excretion of degradative enzymes, antibiotic production, development of motility, and **sporulation** (5). Regardless of the many overlapping inputs from these other pathways, induction of competence is mediated by a single transcriptional activator, the ComK protein (6). This protein stimulates expression of the genes that encode the 12 components of the DNA-uptake machine identified to date (7-9). These genes are distributed among four polycistronic transcription units, *com G*, *C*, *E* and *F*, which specify the DNA-binding apparatus and its assembly, as well as the functions that translocate a single strand of DNA into the cytoplasm. The **nuclease** that degrades the other strand has not been identified. ComK also stimulates (a) the synthesis of **RecA**, which catalyzes the final step of transformation, (b) the recombination of the imported strand with the chromosome, and (c) the synthesis of AadAB, a nuclease/DNA helicase that assists the process.

Several intersecting metabolic currents determine the net level of active ComK at a given moment, and hence the degree of competence. Some of these are indicated in Figure 1. What is remarkable about this system is that positive input from all these factors is necessary for high levels of competence; the absence of any one of them diminishes activation of ComK or reduces transcription of its gene. Stochastic variability, leading to limits on one or more of these factors, may explain why in *B. subtilis* cultures, unlike those of other species, only about 10% of the cells become competent, even with optimum inducing treatments. The special condition of these cells is underscored by assorted observations of their relatively quiescent metabolic state and reduced buoyant density (4).

Figure 1. Competence induction in *B. subtilis* and *S. pneumoniae*. The pathways are drawn to emphasize similarities anc
are thought to be the main participants. M indicates the membrane, OUT indicates the medium, and IN indicates the cytc
and in the text; OBL denotes oligopeptide-binding lipoprotein.; cin stands for competence induction; + indicates stimulai
activity, – indicates repression or inhibition; question marks indicate factors not yet identified or presumed activities not
transcripts. *B. subtilis*: The ComX pheromone is a peptide of 10 amino acid residues that is cleaved from the longer *com.*
a *comQ*-dependent pore to act at a surface domain of the membrane protein, ComP, causing the latter to phosphorylate it
ComP, the sensor of a two-component regulatory system, in turn phosphorylates ComA, converting it to a transcriptiona
Another short (4–7 residue) peptide, competence stimulating factor [CSF (12)], is cleaved from a precursor during expor
through an oligopeptide **permease** pore and to protect ComA ~ P from inactivation by inhibiting a **phosphatase** (12, 13)
ComK from a complex in which it is normally sequestered by the chaperone-like MecA and MecB proteins, liberating it
competence genes (17, 18). *ComG* specifies the DNA-binding apparatus, the *comC* gene product is responsible for proce
ComG complex in the membrane (9), *comE* encodes the DNA translocation functions, and *comF* appears to specify a me
stranded DNA into the cytoplasm (8). The *recA* and *addAB* genes encode recombination functions. ComK also stimulate
amino acids in the medium is mediated by the CodY protein, which represses transcription of *comS* and *comK* (3). The s

involve the freeing of an activator of *comK* transcription, SinR (19). *S. pneumoniae*: Competence stimulating peptide (CS
peptide, probably generated by removal of the **signal sequence** from the ComC prepeptide during secretion by a specific
activates the sensor–regulator protein pair, ComD–ComE, and the resulting ComE ~ P protein stimulates transcription of
transmits the CSP signal to the known late competence genes, as well as, presumably, others not yet identified (*cin* genes
ComD homologue interacts directly with CSP (25). Because CSP ultimately stimulates transcription of its own gene, init
wholesale induction of the culture, effectively synchronizing competence development. The *comC, D*, and *E* genes const
coregulation. The importation of other peptides appears to modulate competence induction (27-29). Strains mutant for th
AliAB develop competence at much lower cell densities than the wild type, suggesting that importation of peptides serve
that the peptides repress *comCDE* transcription until exhausted at higher cell densities.

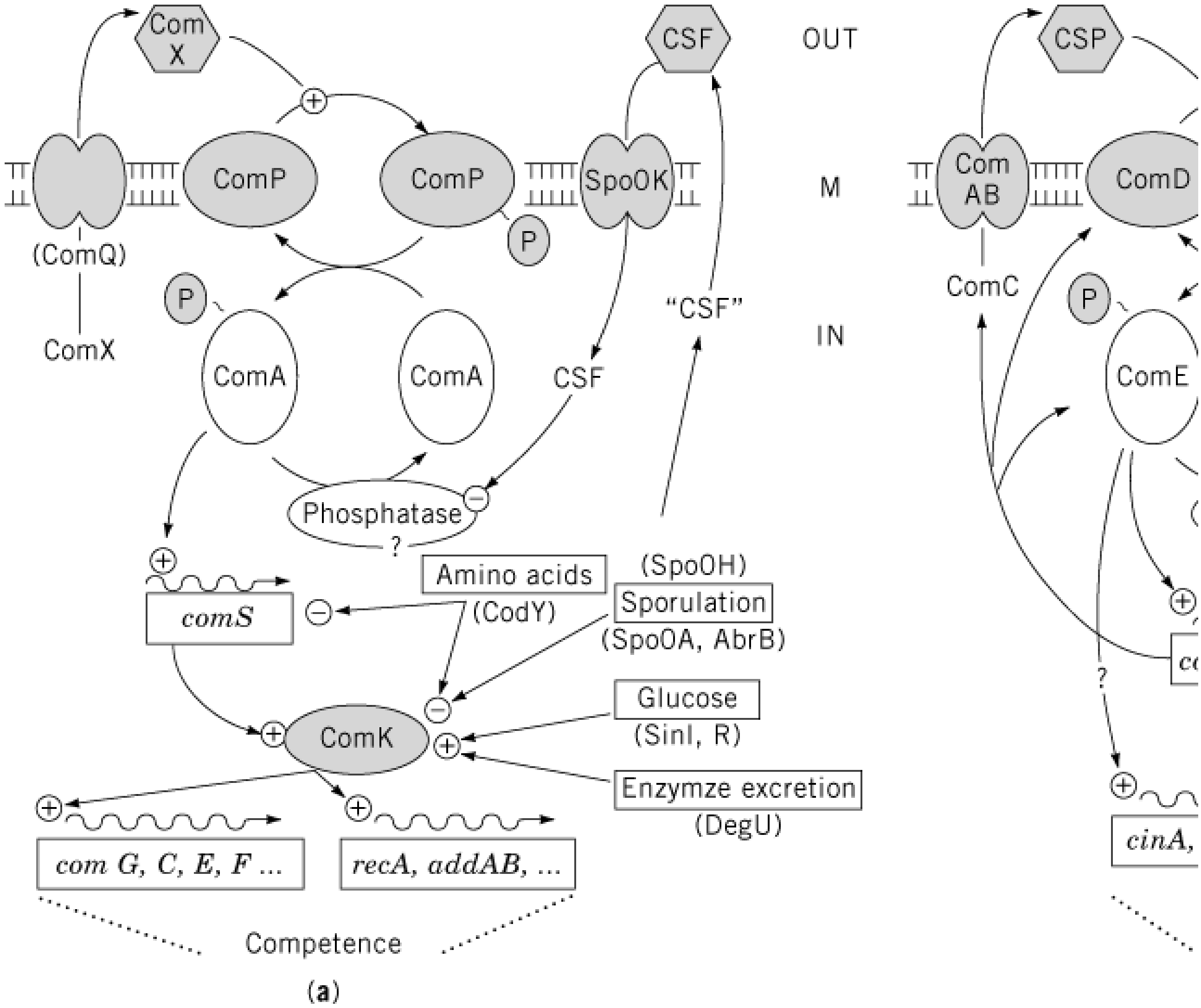

The finding that competence was attained earlier in cultures growing in medium already used for growth of cells to the competent state implied that extracellular signaling molecules promote development of competence (10), and this proved to be the case. Two such molecules are known, both generated by the cell and exported to the medium. The ComX pheromone interacts with the cell-surface protein ComP to initiate a cascade of interactions that culminate in competence (11, 12). Competence stimulating factor (CSF) is probably imported to stimulate this pathway. These interactions are shown in Figure 1 and described in the legend. It is possible that the apparent redundancy of competence-inducing function reflects only the co-opting of the CSF sporulation factor to protect the primary product of the competence-specific pathway, the phosphorylated form of ComA, ComA ~ P (13). Unlike ComX, which seems to be specific for competence, CSF production is intimately linked with the system that regulates sporulation; transcription of its gene requires the Spo0H sigma factor and is stimulated, indirectly, by the Spo0A ~ P transcription regulator. Grossman (14) has suggested that CSF is also a signaling molecule for sporulation.

The external actions of ComX pheromone and of CSF have led to the suggestion that these factors communicate cell-density information to the system that regulates competence (14). ComA thus serves as a depot for these signals, and in its phosphorylated form it sends them on by activating transcription of *comS* (12, 15-18).

This general induction pathway is also subject to nutritional signals: amino acids via CodY (3), and glucose via SinI and SinR (19). How these, as well as signals from the sporulation and enzyme secretion pathways (AbrB, DegU ¼), are integrated to allow the cell to decide whether to commit itself to competence remains an intriguing issue.

2. *S. pneumoniae*

This organism is an obligate parasite of the respiratory tract. In contrast to *B. subtilis, S. pneumoniae* readily attains competence during exponential growth in rich medium. Moreover, all the cells become competent, albeit briefly. Competence in *S. pneumoniae* does share with that of *B. subtilis*, however, an association with a distinct physiological state. This takes the form of altered surface properties, cessation of cell-wall synthesis, increased cell-wall fragility, and release of DNA into the medium. The onset of competence is very sensitive to culture conditions: temperature, the nature of the medium buffer, the concentrations of magnesium and calcium, and pH. In low-pH medium, there is only one peak of competence, at high cell density, whereas in high-pH medium there is a succession of peaks (20).

The competence induction pathway of *S. pneumoniae* shows notable similarities to that of *B. subtilis*, as depicted in Figure 1. Induction of competence is mediated by an extracellular signaling molecule, the competence stimulating peptide (CSP) (21-23), and this initiates the induction cascade via a sensor-regulator protein pair (24-26). Induction is also modulated by imported peptides (27, 28), though in this case the effect is negative (29).

Several proteins other than those shown in Figure 1 make their appearance at competence, some of them associated with the membrane (30); but the only one demonstrated to have a clear role in transformation, indeed in competence itself, is the RecA protein, which mediates homologous recombination (31).

S. pneumoniae cultures exhibit a particular aspect of competence that, though detected long ago (32), has received little attention. Filtrates of cultures that have passed their peak of competence prevent development of competence when added to another culture, suggesting that a specific inhibitor of competence is secreted into the medium. Such a factor might be induced at competence just in order to turn it off again, accounting for the brevity of the competence peak.

3. *H. influenzae*

H. influenzae lives in the mucus of the respiratory tract, where it may be exposed to large amounts of naked DNA (33). Only its own DNA, however, is taken up with high efficiency. This selectivity results from the presence throughout the genome of numerous copies of a short, specific base sequence, the uptake-signal sequence (USS), which is recognized by the uptake apparatus (34, 35). The outer membranes of competent cells extrude vesicles, termed *transformasomes* (or "blebs"), which encapsulate the DNA and then release it into the **periplasm** to allow transport into the cell (36-38). As in *B. subtilis*, growth-inhibiting conditions, such as transient anaerobiosis, nutritional downshift, and approach to stationary phase, induce competence. The level of competence attained varies and can be close to 100% of the population. Nevertheless, there appears to be no cell density sensing involved, each cell developing competence independently. *H. influenzae* cells implanted in the rat peritoneum rapidly develop the capacity to import DNA added with the inoculum and manifest other changes characteristic of the competent state (39).

Several factors important to the development of competence in *H. influenzae* have been identified, but the picture remains fragmented. Of crucial importance is the intracellular level of cyclic AMP (cAMP). Competence was abolished by mutations in the cyclic AMP receptor protein (CRP) and adenylate cyclase (Cya) genes, but could be restored to a *cya* mutant by addition of cAMP (40, 41). The cell senses sugar availability through a carbohydrate phosphotransferase system that increases cAMP synthesis in response to declining sugar availability: Mutations in two genes specifying components of this system, *ptsI* and *crr*, caused partial loss of competence, a deficiency that can be compensated for by added cAMP (42, 43). Competence in *H. influenzae* thus responds directly to nutritional state.

Some clues as to how cAMP might act in competence induction have recently emerged. Notably, cAMP stimulates transcription from a divergent **promoter** region of two genes essential for transformation, *tfoX* and *rec-1*. *TfoX* was originally identified by a mutation, *sxy*-1, that increased transformation 100-fold (44). Null mutations in the gene eliminated DNA binding and transformation, whereas overexpression of *tfoX* caused constitutive competence (45, 46), implying that TfoX is a positive regulator of competence. The finding that TfoX is needed for expression of other competence genes (*com101A*, *dprA*, and *rec-2*) (46, 47) supports this suggestion and hints at a central role in competence similar to that played by the ComK regulator of *B. subtilis*. Whereas *tfoX* transcription normally increases only as cells approach stationary phase, addition of cAMP to a log-phase culture causes an immediate stimulation (46).

On the other hand, transcription of *rec-1*, which encodes the general recombination enzyme that is analogous to RecA of *E. coli*, is only weakly stimulated by cAMP-CRP (48). It is, however, induced by single-stranded DNA, as befits its function of integrating transforming DNA. This common property of Rec proteins has been proposed to endow Rec-1 with another quite distinct function, that of triggering competence. Induction of competence in *H. influenzae* may be associated with the conversion of up to 5% of the chromosomal DNA to single-stranded form. Observing that overproduction of Rec-1 led to early development of competence, Stuy (49) suggested that formation of Rec-1/single-stranded DNA complexes might induce competence gene expression, as the equivalent complexes induce the SOS regulon in *E. coli*. The idea remains untested.

Several new proteins appear in the outer membrane at competence. Some of them, rather than being synthesized *de novo*, are redistributed from the inner membrane. One mutant that fails to do this also fails to bind DNA. It carries a lesion in the gene *por*, which encodes a periplasmic disulfide oxidoreductase, suggesting the need to assemble or fold **disulfide bond**-containing proteins (50) (see Protein Disulfide Isomerase). Two proteins probably involved in conducting DNA into the cytoplasm are induced at competence: Rec-2, which shares homology with the presumed transmembrane channel protein ComEC of *B. subtilis*, and DprA (47).

There is as yet no indication that *H. influenzae* competence responds to a specific extracellular signal. If it does, it now seems unlikely to do so via a sensor-regulator protein pair, such as ComP-ComA in *B. subtilis*: Mutation of the genes encoding four such systems, as deduced from the genome sequence, failed to affect competence (43). What is clear is that the identity and function of most of the components of the competence regulatory system are still unknown, and that the true place of the known ones in the system likewise remains to be shown.

4. *N. gonorrhoeae*

Unlike the bacteria already discussed, for which competence is a transitory response to growth conditions, transformable *Neisseria* strains are competent at all phases of growth (51). An early indication (52) that competence could be induced by a **proteinase**-sensitive factor present in conditioned medium has not been confirmed. The transformation mutants so far reported are defective in one or more of the individual functions known to be involved in transformation-pili and proteins for DNA binding, transport, and recombination (53-55), but none have suggested the existence of competence factors or regulators. The competent state may be so integrated into the general physiology of *Neisseria* that a specific regulatory system is not needed, or the regulatory elements are essential and therefore missed in mutant hunts. Transformation of cells in culture is influenced by pH and by the concentrations of mono- and divalent cations (53), but these factors probably affect DNA-cell envelope interactions directly, rather than by regulating competence gene output.

5. *E. coli*

In 1970, Mandel and Higa (56) discovered that *E. coli* could be induced to take up DNA by treatment of the cells with Ca^{2+} ions. Although this artificial competence has been a key technique in molecular genetics, its basis is not understood. Suspension of *E. coli* cells in cold $CaCl_2$ solution is known to induce the formation of transmembrane pores consisting of an outer shell of polyhydroxybutyrate, connected by Ca^{2+} to an inner sheath of polyphosphate (57). The role of these pores is unclear, because their internal diameter appears to be too small to allow the passage of double-stranded DNA. They do, however, have marked effects on temperature-induced membrane fluidity, and it is possible that, by anchoring an otherwise mobile membrane, they create tension that opens holes elsewhere in the membrane to admit the DNA (57, 58).

6. Summary

One of the most striking aspects of research on competence to emerge in recent years is the interrelationships between the proteins and regulatory factors involved and those of other phenomena previously considered distinct, perhaps the clearest example being *B. subtilis* sporulation (14). Indeed, acquisition of competence is usually accompanied by other major physiological changes. Because of this, and because our knowledge of competence is based largely on laboratory observation, it is fair to question whether DNA uptake itself is relevant in natural bacterial habitats. In fact there are good reasons for thinking that it is, and this issue is taken up in the entry Transformation.

Bibliography

1. M. G. Lorenz and W. Wackernagel (1994) Microbiol. Rev. **58**, 563–602.
2. C. Anagnostopoulos and J. Spizizen (1961) J. Bacteriol. **81**, 741–746.
3. P. Serror and A. L. Sonenshein (1996) J. Bacteriol. **178**, 5910–5915.
4. D. Dubnau (1993) In *Bacillus subtilis and Other Gram-Positive Bacteria* (A. L. Sonenshein, J. A. Hoch, and R. Losick, eds.), ASM, Washington, D.C., pp. 555–584.
5. D. C. Dooley, C. T. Hadden, and E. W. Nester (1971) J. Bacteriol. **108**, 668–679.
6. D. van Sinderen and G. Venema (1994) J. Bacteriol. **176**, 5762–5770.
7. D. van Sinderen, A. Luttinger, L. Kong, D. Dubnau, G. Venema, and L. Hamoen (1995) Mol. Microbiol. **15**, 455–462.
8. D. Dubnau (1997) Gene **192**, 191–198.
9. Y. S. Chung and D. Dubnau (1994) Mol. Microbiol. **15**, 543–551.
10. H. Joenje, M. Gruber, and G. Venema (1972) Biochim. Biophys. Acta **262**, 189–199.
11. R. Magnuson, J. Solomon, and A. D. Grossman (1994) Cell **77**, 207–216.
12. J. Solomon, R. Magnuson, A. Srivastava, and A. D. Grossman (1995) Genes Dev. **9**, 547–558.
13. J. Solomon, B. Lazazzera, and A. D. Grossman (1996) Genes Dev. **10**, 2014–2024.
14. A. D. Grossman (1995) Annu. Rev. Genet. **29**, 477–508.
15. N. M. Nakano and P. Zuber (1991) J. Bacteriol. **173**, 7269–7274.
16. J. Hahn and D. Dubnau (1991) J. Bacteriol. **173**, 7275–7282.
17. L. Kong and D. Dubnau (1994) Proc. Natl. Acad. Sci. USA **91**, 5793–5797.

18. T. Msadek, F. Kunst, and G. Rapoport (1994) Proc. Natl. Acad. Sci. USA **91**, 5788–5792.
19. U. Bai, I. Mandic-Mulic, and I. Smith (1993) Genes Dev. **7**, 139–148.
20. J. D. Chen and D. A. Morrison (1987) J. Gen. Microbiol. **133**, 1959–1967.
21. A. Tomasz and J. L. Mosser (1966) Proc. Natl. Acad. Sci. USA **55**, 58–66.
22. L. S. Havarstein, G. Coomaraswami, and D. A. Morrison (1995) Proc. Natl. Acad. Sci. USA **92**, 11140–11144.
23. L. S. Havarstein, D. B. Diep, and I. F. Nes (1995) Mol. Microbiol. **16**, 229–240.
24. E. V. Pestova, L. S. Havarstein, and D. A. Morrison (1996) Mol. Microbiol. **21**, 853–862.
25. L. S. Havarstein, P. Gaustad, I. F. Nes, and D. A. Morrison (1996) Mol. Microbiol. **21**, 965–971.
26. Q. Cheng, E. A. Campbell, A. M. Naughton, S. Johnson, and H. R. Masure (1997) Mol. Microbiol. **23**, 683–692.
27. G. Alloing, P. de Philip, and J.-P. Claverys (1996) J. Mol. Biol. **241**, 44–58.
28. B. J. Pearce, A. M. Naughton, and H. R. Masure (1994) Mol. Microbiol. **12**, 881–892.
29. G. Alloing, B. Martin, C. Granadel, and J.-P. Claverys (1998) Mol. Microbiol. **29**, 75–83.
30. M. N. Vijayakumar and D. A. Morrison (1986) J. Bacteriol. **165**, 689–695.
31. B. Martin, P. Garcia, M.-P. Castaniè, and J.-P. Claverys (1995) Mol. Microbiol. **15**, 367–379.
32. A. Tomasz and R. D. Hotchkiss (1964) Proc. Natl. Acad. Sci. USA **51**, 480–487.
33. L. Matthews, S. Spector, L. Lemm, and J. Potter (1963) Am. Rev. Respir. Dis. **88**, 199–204.
34. K. L. Sisco and H. O. Smith (1979) Proc. Natl. Acad. Sci. USA **76**, 972–976.
35. D. B. Danner, R. A. Deich, K. L. Sisco, and H. O. Smith (1980) Gene **11**, 311–318.
36. M. Kahn, M. Concino, R. Gromkova, and S. H. Goodgal (1979) Biochem. Biophys. Res. Commun. **87**, 764–772.
37. R. A Deich and L. C. Hoyer (1982) J. Bacteriol. **152**, 855–864.
38. M. E. Kahn, G. Maul, and S. H. Goodgal (1982) Proc. Natl. Acad. Sci. USA **79**, 6370–6374.
39. M. Dargis, P. Gourde, D. Beauchamp, B. Foiry, M. Jaques, and F. Malouin (1992) Infect. Immun. **60**, 4024–4031.
40. M. S. Chandler (1992) Proc. Natl. Acad. Sci. USA **89**, 1626–1630.
41. I. R. Dorocicz, P. M. Williams, and R. J. Redfield (1993) J. Bacteriol. **175**, 7142–7149.
42. L. P. Macfadyen, I. R. Dorocicz, J. Reizer, M. H. Saier Jr., and R. J. Redfield (1996) Mol. Microbiol. **21**, 941–952.
43. M. L. Gwinn, D. Yi, H. O. Smith, and J. F. Tomb (1996) J. Bacteriol. **178**, 6366–6368.
44. R. J. Redfield (1991) J. Bacteriol. **173**, 5612–5618.
45. P. M. Williams, L. A. Bannister, and R. J. Redfield (1994) J. Bacteriol. **176**, 6789–6794.
46. J. J. Zulty and G. J. Barcak (1995) Proc. Natl. Acad. Sci. USA **92**, 3616–3620.
47. S. Karudapuram and G. J. Barcak (1997) J. Bacteriol. **179**, 4815–4820.
48. J. J. Zulty and G. J. Barcak (1993) J. Bacteriol. **175**, 7269–7281.
49. J. H. Stuy (1989) In *Genetic transformation and expression* (L. O. Butler et al., eds.), Intercept Inc., Andover, pp. 85–112.
50. J.-F. Tomb (1992) Proc. Natl. Acad. Sci. USA **89**, 10252–10256.
51. P. F. Sparling (1966) J. Bacteriol. **92**, 1364–1369.
52. A. Siddiqui and I. D. Goldberg (1975) Biochem. Biophys. Res. Commun. **64**, 34–42.
53. G. D. Biswas, T. Sox, E. Blackman, and P. F. Sparling (1977) J. Bacteriol. **129**, 983–992.
54. G. D. Biswas, S. A Lacks, and P. F. Sparling (1989) J. Bacteriol. **171**, 657–664.
55. I. J. Mehr and H. S. Seifert (1997) Mol. Microbiol. **23**, 1121–1131.
56. M. Mandel and A. Higa (1970) J. Mol. Biol. **53**, 159–162.

57. R. N. Reusch and H. L. Sadoff (1988) Proc. Natl. Acad. Sci. USA **85**, 4176–4180.
58. C. E. Castuma, R. Huang, A. Kornberg, and R. N. Reusch (1995) J. Biol. Chem. **270**, 12980–12983.

Suggestions for Further Reading

59. J. M. Solomon and A. D. Grossman (1996) Who"s competent and when: regulation of natural genetic competence in bacteria. Trends Genet. **12**, 150–155. A brief but comprehensive review, providing access to the important literature.
60. A. D. Grossman (1995) Genetic networks controlling the initiation of sporulation and the development of genetic competence in *Bacillus subtilis*. Annu. Rev. Genet. **29**, 477–508. A review of competence development in *B. subtilis* and its interconnections with sporulation and nutritional state.
61. J.-P. Claverys, A. Dintilhac, I. Mortier-Barrière, B. Martin, and G. Alloing (1997) Regulation of competence for genetic transformation in *Streptococcus pneiumoniae*. J. Appl. Microbiol. Symp. Suppl. **83**, 32S–42S. A review of competence regulation in this pathogen, emphasizing the influence of peptide transport and other factors.

Competitive Inhibition

Analogues of the substrate of an enzyme can often bind at the same place within the enzyme's active site as the substrate but are not acted on by the enzyme. They are inhibitors of the enzyme, giving rise to dead-end inhibition, and they usually compete with the substrate, giving rise to competitive inhibition .

1. Linear

The simplest type of competitive inhibition occurs when an inhibitor combines reversibly at the active site of the same form of the enzyme as the substrate. The inhibitor may be a structural analogue of the substrate or a product of that substrate. In the following scheme, the inhibitor I combines reversibly with the free enzyme to form a dead-end EI complex that can only

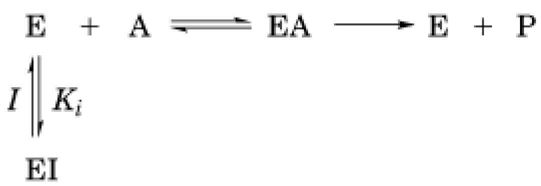

dissociate back to the components from which it was formed. Therefore, the interaction of E and I is at thermodynamic equilibrium, and the inhibition constant K_i is a **dissociation constant**. The general equation that describes this type of inhibition is shown in Equation 1:

$$v = \frac{VA}{K_a(1 + I/K_{is}) + A} \tag{1}$$

where v is the observed velocity of the reaction, V the maximum velocity, K_a the Michaelis constant for the substrate present at concentration A, I the concentration of inhibitor, and K_{is} the apparent inhibition constant. For a single-substrate reaction, K_{is} would be equal to K_i. The double-reciprocal form, Lineweaver–Burk plot, of the equation for linear competitive inhibition (Eq. 2):

$$\frac{1}{v} = \frac{K_a}{V}\left(1 + \frac{I}{K_{is}}\right)\frac{1}{A} + \frac{1}{V} \tag{2}$$

indicates that a primary plot of $1/v$ against $1/A$ at different concentrations of I would yield a family of straight lines that intersect at the same point on the vertical ordinate (Fig. 1). This is the signature of competitive inhibition; sufficiently high concentrations of substrate can compete successfully with the inhibitor. The slope of each curve is given by Equation 3:

$$\text{Slope} = \frac{K_a}{VK_{is}}I + \frac{K_a}{V} \tag{3}$$

A plot of slope against inhibitor concentration would yield a straight line that intersects the abscissa at the point where $I = -K_{is}$. Since this secondary plot should be linear, the inhibition would be classified as linear competitive . Although values for K_{is} can be obtained by such graphical procedures, it is preferable to obtain its value by an overall fit of the primary data to the general equation by use of a least-squares fitting method (1).

Figure 1. Primary double-reciprocal plot for linear competitive inhibition.

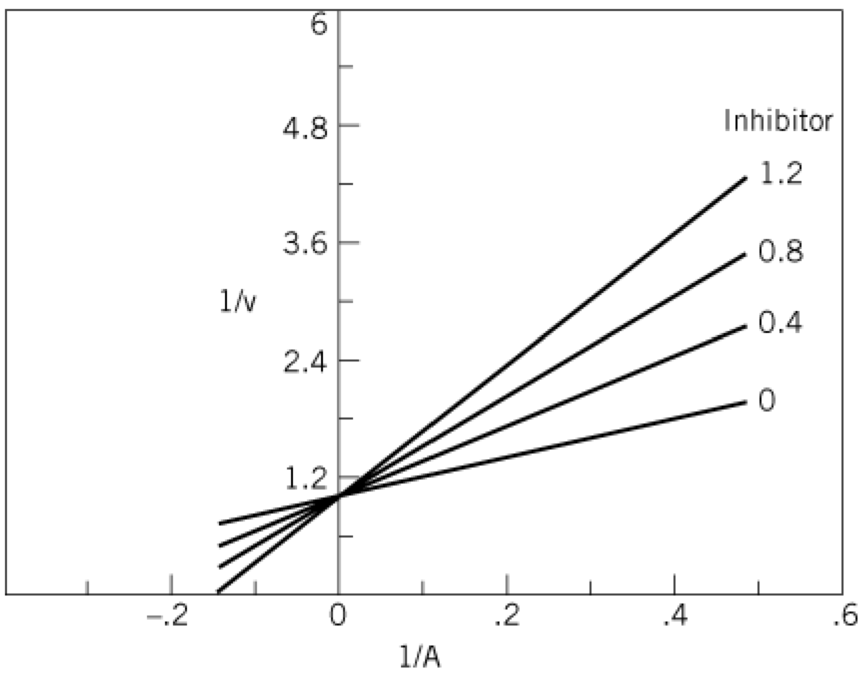

When two substrates are involved in a reaction, the value determined directly for K_{is} may be only an apparent constant, with its value dependent on the concentration of the nonvaried substrate (see Lineweaver–Burk Plot). In this case, it would also have to be stated that the inhibitor was linear competitive with respect to a particular substrate.

Linear competitive inhibition will also be observed with a two-substrate reaction when the inhibitor is an analogue of the first substrate to add in an equilibrium ordered mechanism, A, and the second substrate to add, B, is varied (Fig. 2). The inhibition by I with respect to A will be linear competitive because both A and I compete directly for the same form of enzyme (E). The inhibition by I with respect to B will also be linear competitive, even though I and B combine with different enzyme forms, because the reaction between E and A in an equilibrium-ordered mechanism is at thermodynamic equilibrium. Thus, increasing concentrations of B will ultimately reduce the concentrations of both EA and E to zero, so that no free enzyme remains to interact with I.

Figure 2. Equilibrium-ordered mechanism for which inhibition by *I* would be linear competitive with respect to both substrates.

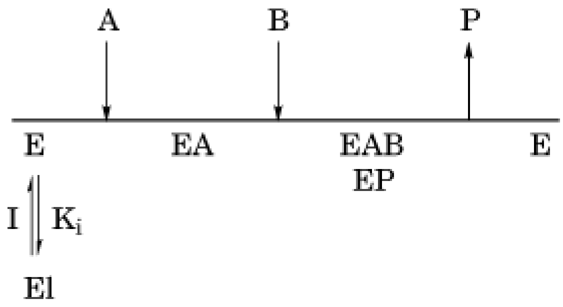

2. Hyperbolic

This type of inhibition occurs when an inhibitor binds reversibly at a site on the enzyme, other than the active site, so as to make it more difficult for the substrate to combine at the active site. Thus, the inhibitor and substrate can be present on the enzyme at the same time. The reactions involved can be illustrated as follows:

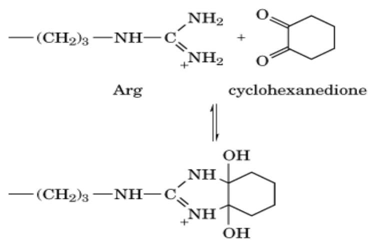

where K_{is} and K_{id} denote dissociation constants for EI and EIA, respectively. It is a thermodynamic requirement that the affinity of the substrate A for the E and EI forms differs, so that

$$K_A = K_a \frac{K_{id}}{K_{is}}$$

For the inhibition to be competitive, the presence of the inhibitor on the enzyme must not affect the rate of product formation. The general equation that describes hyperbolic competitive inhibition is given in Equation 4:

$$v = \frac{VA[1 + \frac{I}{K_{id}}]}{K_a(1 + \frac{I}{K_{id}}) + A} \tag{4}$$

which can be arranged in double-reciprocal form as

$$\frac{1}{v} = \frac{K_a}{V}\left[\frac{1+\frac{I}{K_{is}}}{1+\frac{I}{K_{id}}}\right]\frac{1}{A} + \frac{1}{V} \qquad (5)$$

This is an equation of a straight line for a plot of $1/v$ against $1/A$, but it is apparent that the slopes of the lines will vary as a hyperbolic function of the concentration of I and the intercept of the curves with the vertical ordinate is independent of I. For a plot of slope as a function of I, the curve would be a concave-down, nonrectangular hyperbola, with limiting values of K_a/V and $K_aK_{id}/(VK_{is})$ at zero and infinite concentrations of I, respectively. Values for K_{id} and K_{is} may be obtained from a plot of 1/(slope$_o$ – slope$_i$ against $1/I$, where slope$_o$ and slope$_i$ are slopes of the primary plot in the absence and presence of inhibitor, respectively. Values for K_{is} and K_{id} are best obtained by an overall least-squares fit of the data to the equation that describes hyperbolic competitive inhibition (1).

It should be noted that the same kinetic mechanism would apply if I were an activator that enhances the combination of the substrate with the enzyme. In this case, the plot of slope against I would yield a concave-up, nonrectangular hyperbola (2).

Bibliography

1. W. W. Cleland (1979) Meth. Enzymol. **63**, 103–138.
2. V. L. Schramm and J. F. Morrison (1970) Biochemistry **9**, 671–677.

Competitive Labeling

Competitive labeling is a method of chemical modification for determining the pK_a and the reactivity of functional groups in proteins. The extent of modification of a particular protein group at various pH values is compared to that of the same group in a standard compound. This gives the reactivity of the protein group relative to its intrinsic reactivity, and the pH-dependence gives the p K_a value. These data reflect the **accessibility** of the group in the folded protein, which provides information about the chemical reactivity of the group and its environment in the folded protein. This indirectly gives conformational information about the protein. Conformational transitions associated with function, association, and **ligand binding** can be monitored with this method.

Competitive labeling was originally employed in a study of the amino groups in elastase (1). A mixture of elastase and phenylalanine (the standard compound) was acetylated with a small amount of ^{3}H-labeled acetic anhydride (see Anhydrides). It is important that the amount of the labeling agent is less than that of the groups being modified. Under these conditions, the relative amounts of label in the standard and in the specific protein group will depend upon their relative ionization and reactivities. The fraction of the reactive, nonionized form of the amino group (a_i) and the ratio of reactivity ($r = k_i/k_{standard}$) of the ith group are derived from the known pK_a of the standard ($a_{standard}$) and the measured ratio of labeling:

$$\alpha_i r = \alpha_{\text{standard}}(\text{label on } i\text{th group/label on standard}) \qquad (1)$$

The label on the ith group could be determined by the radioactivity of the appropriate peptide separated by peptide mapping. The values on the right side of the equation are obtained experimentally at each pH and are plotted against pH. The values of the pK_a and of r of the protein group are obtained by theoretical curve fitting.

Besides using acetic anhydride to react with amino groups, 1-fluoro-2,4-dinitrobenzene has been used to react with amino groups and with histidine and tyrosine residues, and **iodoacetate** with thiol groups. A small agent is most suitable for this purpose of modification. Double labeling with ^{3}H-label, followed by ^{13}C-labeling after **denaturation** gives a much more sensitive analysis. In this case, the same group in the denatured protein is the standard.

Bibliography

1. H. Kaplan, K. J. Stevenson, and B. S. Hartley (1971) Biochem. J. **124**, 289–299.

Suggestion for Further Reading

2. N.M. Young and H. Kaplan (1989) "Chemical characterization of functional groups in proteins by competitive labelling". In *Protein Structure: A Practical Approach* (T.E. Creighton, ed.), IRL Press, Oxford, U.K., pp. 225–245.

Complement Fixation

Complement is a set of serum proteins that undergo a sequential series of cleavage and association reactions in response to antibody–antigen complexes. If these complexes occur on a cell surface, complement reactions can cause cell lysis (1). The lysis of erythrocytes is particularly easy to detect visually, due to the release of hemoglobin, and this lysis forms the principle for a type of immunoassay. Antibody–antigen complexes in solution cause complement reactions to occur without cell lysis. Since the complement reactions are stoichiometric and the products short-lived, these non-cell-associated complexes deplete a portion of the complement proteins, a process termed “complement fixation.” This depletion reduces the lysis observed when the complement is subsequently added to antibody-coated erythrocytes.

Key reagents for complement fixation assays, all available commercially, are complement, erythrocytes, and hemolytic antibody (2, 3). Guinea pig serum is usually used as a source of complement, since guinea pig complement reacts with antibodies of most experimentally significant mammalian species. Sheep erythrocytes, washed free of serum components, are used for lysis. Hemolytic antibody is obtained by immunizing rabbits with sheep erythrocyte membranes. The erythrocytes are sensitized in preparation for complement lysis by incubation with the hemolytic antibody. Once amounts of complement and sensitized erythrocytes appropriate for easy detection of lysis are determined, the reagents can be used to measure the interaction of an antibody–antigen pair (4). The antibody and antigen to be tested are incubated for a set time in the presence of complement. Standards containing known amounts of antibody and antigen are incubated simultaneously. Sensitized erythrocytes are next added, and lysis is measured after further incubation, by spectrophotometric determination of hemoglobin. Diminished lysis relative to a control indicates that the antibody–antigen pair in question has formed an aggregate and induced complement reactions to occur in solution, reducing the amount of complement available to lyse cells. Results observed with the standards are used to calibrate the correspondence between antibody–antigen complex formation and lysis. Because antibody–antigen aggregates are the most active species in fixing complement, bell-shaped response curves result when percent complement fixed is plotted against added antibody or antigen. Complement fixation is most efficient at roughly equivalent amounts of antibody and antigen, whereas either component in excess will favor formation of binary and ternary complexes that do not fix complement well. Consequently, several concentrations of antigen or antibody must be tested to establish whether the observed response lies on the increasing or decreasing slope of the standard curve.

As an analytical technique, complement fixation is sensitive to nanogram quantities of antigen, but is subject to reagent variation and interference by chemical components of the sample. A notable value, however, is in study of cross-reactivity between structurally similar antigens. Proteins that differ slightly in sequence give easily measured differences in complement fixation ability when they are probed with a single antiserum. This effect is so regular that complement fixation by homologous antigens can be used to establish the evolutionary relationship between closely related species (5, 6).

Bibliography

1. J. Bordet and O. Gengou (1901) Ann. Inst. Pasteur **15**, 289–302.
2. M. M. Mayer (1961) "Complement and complement fixation", in *Experimental Immunochemistry*, Thomas, Springfield, IL, pp. 133–240.
3. L. Levine and H. Van Vunakis (1967) Meth. Enzymol. **11**, 928–936.
4. E. Wasserman and L. Levine (1961) J. Immunol. **87**, 290–295.
5. E. M. Prager and A. C. Wilson (1971) J. Biol. Chem. **246**, 5978–5989.
6. A. B. Champion, E. M. Prager, D. Wachter, and A. C. Wilson (1974) "Microcomplement fixation", in *Biochemical and Immunological Taxonomy of Animals*, C. A. Wright, ed., Academic Press, London, pp. 397–416.

Complement System

1. Introduction

After the discovery of humoral immunity, Hans Buchner found that if fresh serum possessing an antibacterial antibody was added to bacteria, the bacteria were quickly lysed. However, if the serum was heated to 56°C, the lytic capacity of the serum was lost. He also demonstrated that the loss of lytic capacity could be restored by using unheated nonimmune serum in conjunction with heated immune serum. These studies were extended by others, including Jules Bordet, who concluded that serum contained two components necessary for cellular lysis. These two components are heat-stable antibodies and a heat-labile component that “complements” the lytic function of antibodies. He reasoned that antibodies had two binding sites, one for antigen and the other for heat-labile substance that was given the name ***complement***.

Complement is now known not to be a single component, but it consists of at least 20 chemically and immunologically distinct plasma proteins capable of interacting with one another in a highly regulated manner to provide at least four main biological functions. First, ***cytolysis*** is mediated by the association, or polymerization, of specifically activated complement components on the surface of targets cells. These components form pores that disrupt the integrity of the lipid membrane, and the cell is killed by osmotic lysis. Second, antibody and antigen combine to form ***immune complexes*** that, unless removed, can result in damage of body tissues. The binding of complement proteins prevent the damage from immune complexes by mediating their solubilization and clearance. Third, the ***opsinization*** of foreign particles is mediated by the binding of complement proteins (opsonins). Phagocytic leukocytes bear receptors for these complement proteins, so that opsinized particles are cleared from the body by phagocytosis. Finally, through the activation of complement, **proteolytic** fragments are released whose function are to ***mediate inflammation***. These fragments, or "anaphylatoxins," can act on several target cells such as neutrophils, smooth muscle, and vascular endothelium, as well as organ systems of the body.

The complement proteins are normally present in the circulation and are produced primarily by the liver and other extrahepatic sources, such as macrophages and fibroblasts. Some of the components are produced as functionally inactive proteinases that are activated only when proteolytically cleaved themselves by previously activated complement proteins. Complement activation occurs only at localized sites under specific conditions. The binding of specific antibody to antigen can initiate complement activation through what is called the ***classical pathway***. Additionally, in the absence of antibody, some complement components are directly activated by binding to the surfaces of infectious agents, such as bacteria, **fungi**, and **viruses**, through what is called the **alternative pathway**.

2. Overview of the Complement System

Individual proteins of the complement system are present in the serum as functionally inactive molecules. The individual precursor proteins are designated numerically, such as C1, C2, up to C9. Other proteins involved with the complement system have retained their common, or trivial, names such as properdin, factor B, and factor H. Individual components must be activated sequentially and specifically for the complement cascade to progress and mediate inflammation and lysis of foreign organisms. The activation of complement is a dynamic process that allows the proteins of the system to interact functionally and is not a static singular event.

An overview of the operation of the complement system is shown in Figure 1, and biochemical and physical information of the proteins involved in the complement system are listed in Table 1. A protein called C3 is the central component of the complement system. The alternative and classical pathways are two parallel, but entirely independent, mechanisms that lead to the formation of C3 ***convertases*** whose function is to cleave C3 into C3a and C3b. In the classical pathway, initial events involve binding of specific antibody to antigen. This antigen–antibody complex binds complement C1 and sequentially activates complement proteins C4 and C2, leading to the formation of the C4b2b complex that functions as the ***classical pathway C3 convertase***. In contrast, activation of complement via the alternative pathway occurs independent of antigen–antibody complexes. Instead, alternative pathway activation is dependent on activators that allow the formation and deposition of the C3bBb complex (**alternative pathway C3 convertase**) on their surfaces. Activators of the alternative pathway include many bacteria, fungi, and viruses. Both classical and alternative convertases can cleave additional C3, generating more C3b (see Fig. 1). The binding of additional C3b to these C3 convertases changes them conformationally to ***C5 convertases***, which specifically cleave C5. Once cleaved, both the alternative and classical pathways share the same terminal steps. These steps do not involve the proteolytic cleavage of additional components but instead involve the sequential binding of components C6, C7, C8, and C9. This terminal assembly leads to the formation of the ***membrane attack complex*** (**MAC**), resulting in the osmotic lysis or cytolysis of bacteria or other affected cells.

Figure 1. Schematic representation of the alternative and classical activation of the complement pathway leading to the assembly of the membrane attack complex.

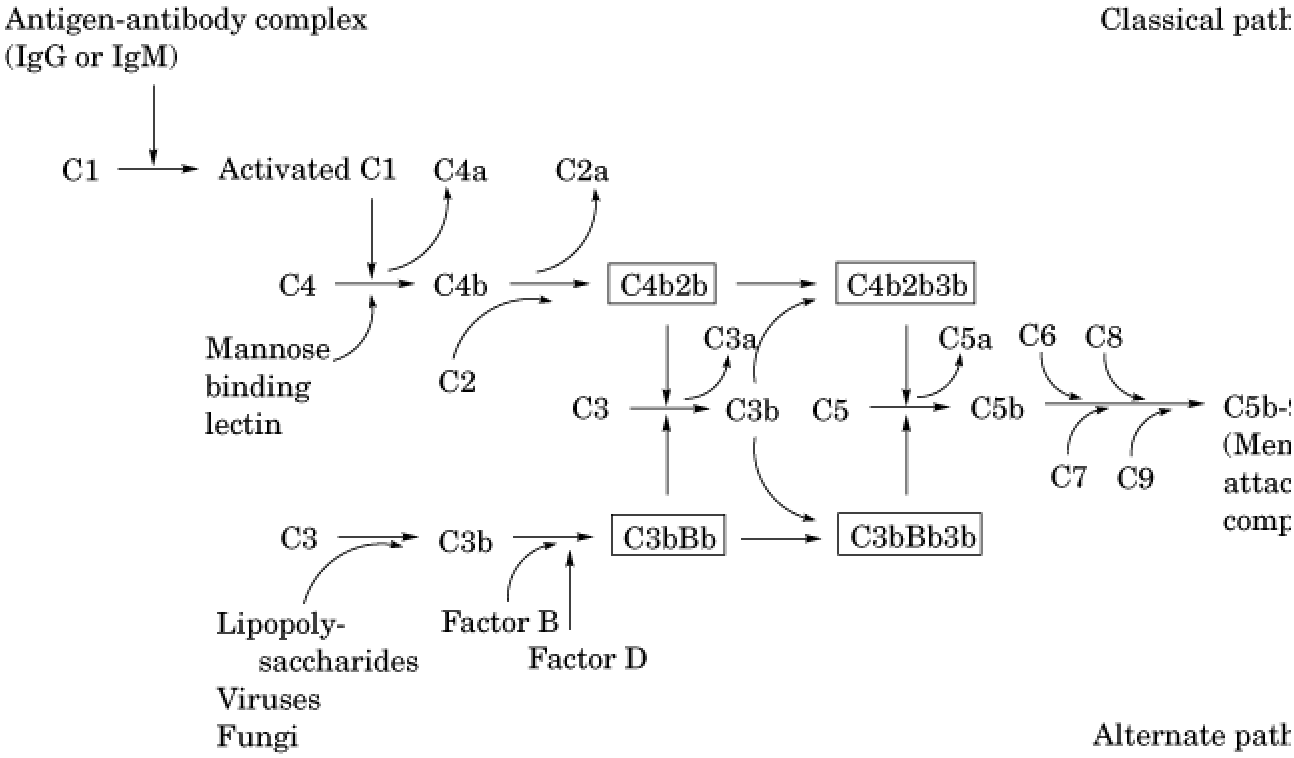

Table 1. Protein Components of the Classical and Alternative Pathways[a]

Component	Serum Concentration, µg/mL	Molecular Weight	Number of Polypeptide Chains	mRNA[b] Size, kb	Chromosome Location	Gene[b] Size, kb
			Classical Pathway			
C1q	75	410,000	6 of A at 24,000	0.52	1	2.5
			6 of B at 23,000	1	1	2.6
			6 of C at 22,000	1.6	1	3.2
C1r	34	85,000	Single chain	2	12	10.5[c]
C1s	30	85,000	Single chain	2	12	10.5[c]
C4	450	210,000	a-Chain, 93,000; b-chain, 75,000; g-chain, 33,000	5.3	6	16
C2	25	95,000	Single chain	2.9	6	18
C3	1500	195,000	a-Chain, 110,000; b-	5.2	19	41

			chain, 75,000			
C5	75	180,000	a-Chain, 115,000; b-chain, 75,000	5.5	9	80
C6	60	128,000	Single chain		5	85
C7	60	121,000	Single chain	3.9	5	78
C8	80	150,000	a-Chain, 64,000;	2.5	1	70
			b-chain, 68,000;	2.6	1	40
			g-chain, 22,000	1	9	1.8
C9	58	79,000	Single chain	2.4	5	80
Mannose binding Lectin	1	~ 600,000	Multimer of 32,000	3.5	10	7
			Alternative Pathway			
Properdin	25	220,000	4 at 56,000	1.6	X	6.4
Factor B	225	100,000	Single chain	2.9	6	6
Factor D	1	25,000	Single chain	1	4	2.5[d]
			Inhibitors—Soluble			
Factor I	34	105,000	46,000	2.4	4	63
Factor H	500	150,000	Single chain	4.4	1	7
C1 inhibitor	275	105,000	Single chain	1.8	11	17
C4 binding protein	150	560,000	6, a-Chain, 70,000; 1,	2.5	1	40
			b-chain, 45,000	1	1	10
S protein	500	83,000	Single chain	1.6	17	5.3
			Membrane—Inhibitors and Receptors			
DAF (CD55)		70,000	Single chain	3.1	1	40
MCP (CD46)		58,000–63,000	Single chain	4.2	1	43
CR1 (CD35)		190,000–280,000	Single chain	7.3–13	1	130–160
CR2 (CD21)		140,000	Single chain	5	1	20
CR3 (CD11b/CD18)		260,000	a-Chain, 165,000;	4.1	16	55
			b-chain, 95,000	3	21	32
CR4 (CD11c/CD18)		245,000	a-Chain, 150,000;	4.7	16	25
			b-chain, 95,000	3	21	32
MIRL (CD59)		18,000	Single chain	0.6–6.0	1	27
C5aR (CD88)		42,000	Single	3.0	19	9

			chain[e]			
C3aR		50,000	Single chain[e]	3.0	12	8

[a] All data for proteins listed are for human complement components.
[b] Approximate size.
[c] C1r size estimated from proximity and homology to C1s.
[d] Complete factor D cDNA hybridizes within a 2.5-kb genomic fragment.
[e] Single chain with 7-transmembrane domains.

During activation, through either the classical or alternative pathway, various cleavage products mediate a variety of biological functions. As discussed, cytolysis is mediated through the membrane attack complex. Opsinization and subsequent phagocytosis by leukocytes is mediated primarily through C3b, a cleavage fragment of C3 that binds receptors for C3b. Cleavage products of C3, C4, and C5 (C3a, C4a, and C5a anaphylatoxins) mediate inflammatory events and the recruitment and activation of leukocytes.

3. Assembly and Activation of the Classical Pathway

The classical pathway is activated by antigen–antibody complexes or aggregated immunoglobulin acting on complement component C1 (Table 1). C1 consists of three distinct protein molecules, C1q, C1r, and C1s, which are held together by Ca^{2+}-dependent bonds. C1 is present in serum as a firm C1q-C1r-C1s complex, while individual C1 components are found only in pathologic conditions. C1 contains one molecule of C1q and two molecules of both C1r and C1s.

A molecule of C1q is comprised of 18 polypeptide chains of three distinct types (A, B, and C) which are twisted together comprising one subunit. Each C1q molecule is then made up of such six subunits connected together; once assembled, its structure is similar to that of collagen. The C1q molecule bears the sites that enable the entire C1 molecule to bind the Fc region of IgM and IgG immunoglobulin molecules. A single C1 molecule can bind about six IgG molecules. After binding to Ag-Ab complexes, C1q undergoes a conformational change that causes C1r to activate itself by a limited self-cleavage.

Activated C1r cleaves a single peptide bond in C1s, which then acquires enzymatic activity of its own. This newly generated enzyme is a serine esterase type and mediates the cleavage of component C4. With the activation of the C1s enzyme, the initial process is complete, and the earlier reactants, including antibody, antigen, C1q, and C1r, are no longer needed.

C4 is composed of three nonidentical polypeptide chains and is synthesized as a single-chain precursor in a beta–alpha–gamma orientation. C1 cleaves a single bond on the C4 alpha chain leading to the production of C4a and C4b. This cleavage leads to the formation of a labile binding site in the larger fragment of C4b, which enables it to bind to the activating surface (activator). The C4b alpha chain, like C3, contains an internal ***thioester*** bond formed between a glutamic acid and cysteine residue. Cleavage of the alpha chain of C4 is followed by stress-induced hydrolysis of the thioester bond. This permits the reactive acyl group of the glutamyl residue to form a covalent bond with a reactive hydroxyl or amino group on the surface of the activator.

C2 cleavage by C1s also generates a labile binding site of unknown chemical composition in the larger C2b fragment, which allows it to bind to C4b. Mg^{2+} ions are required for the formation of the C4b2b complex. Formation of the C4b2b complex is not very efficient, as the majority of C2 and C4 molecules entering into this reaction lose their labile binding sites before achieving union with membranes or with each other and diffuse away as inactive reaction products. The newly formed C4b2b is a proteolytic enzyme that assumes the role of continuing the complement reaction cascade, so earlier activating components are no longer required. The C4b2b complex is also called the **classical C3 convertase**, which acts to cleave C3.

The substrate for C4b2b is C3, which is synthesized as a single chain of beta–alpha orientation that is processed after translation. The larger, alpha chain, is cleaved at a single site located near the amino terminus. The smaller resulting fragment C3a (9000 M_r (relative molecular mass) is a biologically potent peptide that mediates inflammation and will be discussed later. A labile binding site is generated in the larger fragment C3b, which enables the molecule to attach to membranes at sites near, but distinct from, those utilized by antibody and C4b2b. Often described as the "lynchpin," C3 is the precursor of several biologically active fragments that function by association with the other proteins of the complement system leading to lysis of the target cell cell via either classical or alternative pathways. C3 has numerous distinct binding sites, one of which is the thioester domain that allows the molecule to bind covalently to target sites and particles, such as immune complexes and membrane surfaces.

The chemical site of the C3 thioester has the sequence Gly-Cys-Gly-Glu-Glu-Asn with the Cys and second Glu residues joined by a thioester bond, specifically a b-cysteinyl–g–glutaminyl thioester bond. This thioester bond is present in the C3d domain of the alpha chain. With the cleavage of C3 into C3a and C3b, the thioester undergoes a stress-mediated hyrdolysis, and the reactive acyl group of the glutamyl residue forms a covalent bond with a reactive hydroxyl or amino group on the activator surface. A major amount of reactive C3 fails to achieve binding with activators as most of these reactive thioesters have reacted with water.

The attachment of C3b to membranes in the vicinity of C4b2b molecules leads to the generation of the last enzyme of the classical pathway, C4b2b3b, **or the classical C5 convertase**. To this end, the classical pathway has finished the initial steps of activation. From here, the C5 convertase acts on C5 to initiate steps in the forming of the MAC.

4. Activation of the Classical Pathway

The activation of the classical pathway can occur by one of two ways: activation through the use of immunoglobulin or through nonimmunoglobulin activation by cleavage of C1. Immunoglobulin activation of the classical pathway involves the use of antibodies belonging to subclasses IgG_1, IgG_2, and IgG_3, as well as IgM, are capable of initiating the classical pathway. Immunoglobulins IgG_4, IgA, IgD, and IgE are inactive in this regard. Among the three listed above, IgG_3 is the most active in interacting with C1, then IgG_1 and IgG_2. Activation occurs when the first component C1 binds to a site in the Fc region of the IgG or IgM. Only one molecule of bound IgM is capable of initiating the activation of the classical pathway; however, it is estimated that six molecules of IgG are required.

Nonimmunologic activation of the classical pathway can be accomplished by diverse substances such as DNA, certain viruses, and **trypsin**-like enzymes, by direct proteolytic attack on the C1 molecule. Of particular interest are lectins that also act as a nonimmunological activator of the classical pathway. Mannose binding lectin (MBL) is a serum protein found in all mammals and is regulated as an acute-phase protein. MBL is capable of binding carbohydrate moities present on many microorganisms and subsequently capable of activating the classical pathway through C4 without the need for specific antibody or C1q.

5. Alternative Complement Pathway or Properdin Pathway

The alternative pathway may be activated immunologically by aggregates of human IgA and by certain complex polysaccharides, fungi, viruses, bacterial lipopolysaccharides, and trypsin-like enzymes. This system was originally described as the properdin system, a group of proteins involved in resistance to infection, but distinct from complement. The proteins of the alternative pathway, C3, factor B, factor D, and properdin (factor P) perform the functions of activation, recognition, and amplification of the pathway, resulting in the formation of the activator bound C3/C5 convertase. The alternate pathway system was found to be involved in the destruction of certain bacteria, neutralization of some viruses, and red blood cell of (RBC) lysis from patients with paroxysmal nocturnal hemoglobinuria.

6. Activation of the Alternate Pathway

Alternate pathway activation initially proceeds in a manner different from that for the classical pathway. The exact mechanism by which the first C3b molecule is produced is still controversial. However, it is clear that antibody is not required since mixtures of only highly purified alternative pathway proteins behave as well as serum. The ultimate aim of the proteins, C3, factor B, factor D, and properdin is the initiation, recognition, and amplification of the pathway that results in the formation of the activator bound **C3/C5 convertases**. The first requirement for activation is the presence of C3, which participates in the initiation and amplification of the pathway. It is generally accepted that activated C3 (but not-yet cleaved) [C3*] reacts with proenzyme B, and this complex is then cleaved by factor D, yielding two fragments, Ba and Bb. Bb then attaches to C3b forming the alternative pathway C3 convertase. The C3 convertase is able to cleave additional C3 into C3a and C3b. While most C3b remains in the fluid phase, some binds to various cell surfaces. Thus C3b is continuously generated and is deposited on the surface of the activator. The alternative C3 convertase is unstable and decays rapidly unless another alternative pathway member, **properdin**, binds to the C3 convertase and stabilizes it. Properdin binding of C3bBb extends its functional half-life eightfold. The function of the C3 convertase is to produce enough meta-stable C3 to deposit on the surface of surrounding particles. Surface-bound C3b then interacts with factor B and is activated by D to form more C3bBb. This enzyme is capable of cleaving large amounts of C3, and forms more C3bBb (C3bBb3b); thus, a positive feedback mechanism is formed that amplifies the initial stimulus. Many of the C3b molecules bind to the surface of the activator in close proximity to these enzymes, forming C3bBb3b or the alternative pathway C5 convertase. Like its counterpart in the classical pathway (C4b2b3b), the function of C3bBb3b is to proteolytically cleave C5 and initiate the assembly of the membrane attack complex.

7. The Membrane Attack Complex: C5–C9 Reaction

The terminal portion of the complement sequence is known as the MAC (complex). C5–C9 must become membrane bound for damage to occur. This complex may attach to a cell bearing the activation enzymes of the classic or alternate pathways, or it may attach to a bystander cell. The MAC is initiated by the cleavage of C5 by the alternative and classical C5 convertases.

Similar to C3, pro-C5 is secreted in a beta–alpha orientation prior to post translational modification. C5 shares sequence homology with C3 and C4, including the domain corresponding to the thioester region; however, C5 lacks the essential cysteine and glutamic acid residues necessary for thioester formation. Assembly of the MAC initiates with the cleavage of C5. Cleavage at residue 74 of the alpha chain, results in the generation of C5a anaphylatoxin and C5b (Table 1), where C5b can then bind C6. C6 is a single chain peptide that, when bound to C5b, remains loosely attached to the membrane until the addition of C7. Once a single C7 has bound the C5b6, the resulting complex is highly lipophilic and inserts into the lipid bilayer. When inserted, the C5b67 complex serves as a high affinity integral membrane receptor for a single C8 molecule. C8 is composed of three nonidentical polypeptide chains and has an interesting structure in that the alpha and gamma chains are covalently linked by one or more disulfide bonds and the beta chain is joined to the alpha–gamma chains by noncovalent forces. The C5b-8 becomes stably attached to the membrane by insertion of the C8 gamma chain into the lipid bilayer. With this early “MAC” formed, cellular leakage can occur at this stage. The cytolytic process is greatly accelerated by the attachment of C9, the final complement component. The C9 monomer polymerizes at the site of the C5b-8 complex. As few as 4 C9 molecules can result in lysis for many microorganisms. However, when the MAC contains as many 12 to 15 C9 molecules, the "poly-C9" forms a pore in the membrane and permits passive exchange of cytoplasmic contents with the extracellular media with subsequent osmotic lysis. The pores have an internal diameter of about 110 Å and appear similar in structure to those formed by lytic T cells when the related protein **perforin** is deposited on target cells.

8. Control Mechanisms of the Complement System

Given the lytic potential of the complement system, uncontrolled activation can lead to the formation of the MAC on normal tissues and significant generation of C3a, C4a, and C5a anaphylatoxins. Multiple fluid phase and membrane bound proteins tightly regulate both the alternative and classical pathways by acting at specific steps during activation. In addition, the uncontrolled activation of the complement cascade is also prevented by the necessity of specific activators, such as antibody–antigen complexes, as well as the lability of the activated complement components such as C3b. Deficiencies in regulatory proteins result in unregulated complement activation and are apparent in various disease conditions. An overview of the regulation complement pathway activation by both membrane-bound and soluble inhibitors are shown in Figure 2. The biochemical and physical information of these inhibitors are listed in Table 1.

Figure 2. Regulation of classical and alternative complement pathway activation by membrane and soluble inhibitors. Principal components and C3/C5 convertases are retained from Figure 1. Regulators of complement activation are showı italics.

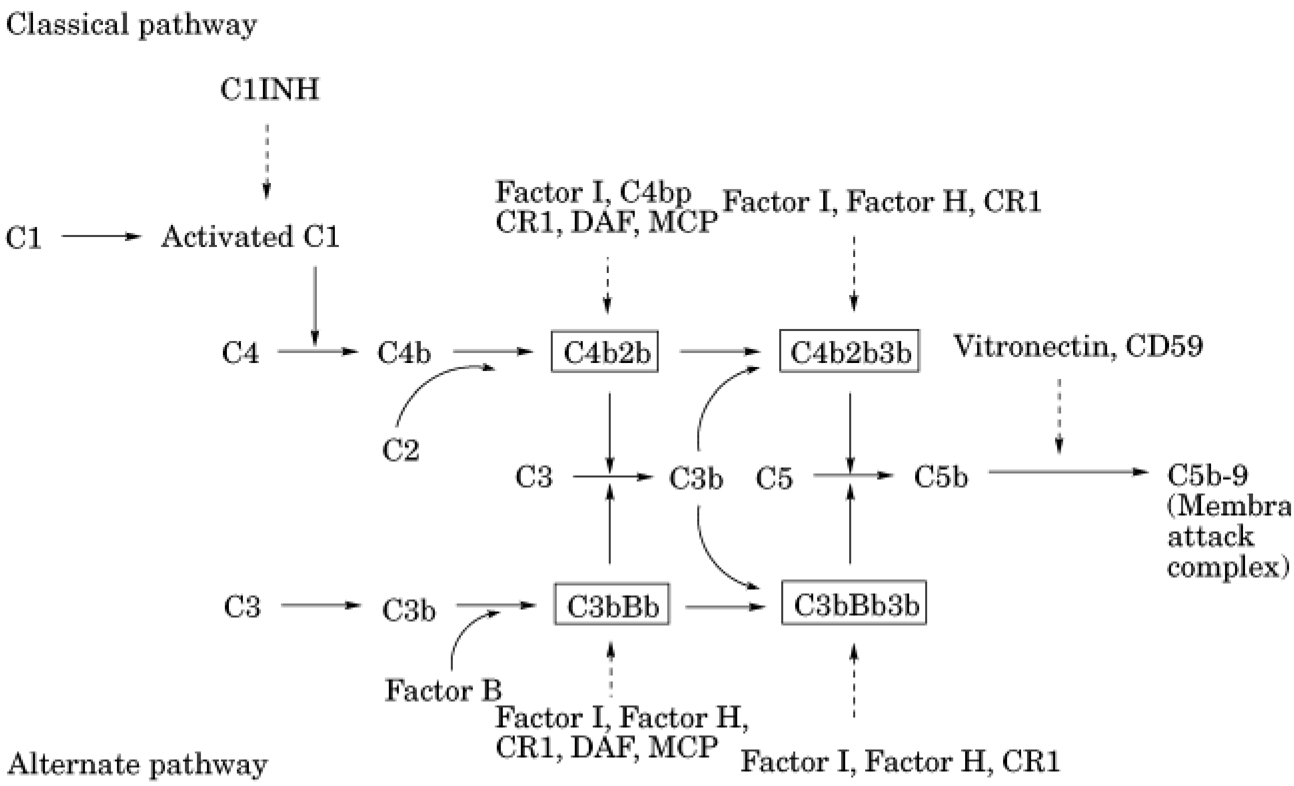

9. Classical Pathway Inactivators

A protein celled ***C1 inhibitor*** (**C1INH**) acts to inhibit the initiation of the classical pathway. C1INH is a member of the serine protease inhibitor family and acts by blocking C1r and C1s of the C1 complex. As with other serpins, such as a_1-antitrypsin, C1INH uses a "bait" sequence that mimics the normal substrates of C1r and C1s. However, when C1INH is cleaved by C1r or C1s, it forms a covalent ester linkage that inhibits cleavage of C4 and C2, thus inhibiting the progression of the classical pathway. Most of the C1 in the serum is already bound to C1INH. On specific binding of C1 to antigen–antibody complexes, C1INH is released allowing classical pathway activation to proceed.

Other means to control the classical pathway involve interfering with the formation of the C3 convertase. Such inhibition can be mediated either through interfering with the assembly of the convertase or in promoting the dissociation of the convertase. Three proteins called ***C4-binding protein*** (***C4 bp***), ***complement receptor type I*** (***CR1***) (also known as CD35), and ***decay accelerating factor*** (***DAF***) (also known as CD55) function as inhibitors of the classical pathway by binding to C4b. In doing so, they compete with C2 for C4b and thus inhibit the formation of the classical C3 convertase. In binding C4b, they also promote the dissociation of the C3 convertase. All three proteins are structurally similar and are homologous members of a family of proteins called the regulators of complement activity (RCAs).

Another way that the C3 convertase can be inhibited is by the cleavage of C4b by a protein called **factor I**. Factor I is a serine esterase that cleaves C4b into two additional fragments: C4c and C4d. C4d remains bound to the original activating surface; however, it is unable to contribute to the formation of the classical C3 convertase. Cleavage of C4b by factor I can only occur in the presence of a "cofactor." The proteins that can serve a cofactor for factor I cleavage include CR1, C4b, and membrane cofactor protein (MCP), or CD46. MCP is also a member of the RCA family but does not possess decay accelerating activity.

10. Alternative Pathway Inactivators

Regulation of the alternative pathway is also accomplished by several circulating and membrane bound proteins, many of which also act on the classical pathway. In analogous fashion, the inhibition of convertase activity through either decay acceleration or by providing cofactor activity for factor I are the major ways in which this is accomplished.

Factor H is a soluble serum protein that possesses decay-accelerating activity that is specific for the Bb fragment of the alternative pathway. By competitively binding Bb, the formation of the alternative C3 covertase is impaired. Factor H is also a member of the RCA family and in binding Bb can also promote the dissassembly of the alternative C3 convertase.

In addition to its role in inhibiting the classical pathway activation, factor I can also cleave C3b using factor H, MCP, and CR1 as cofactors. The resulting fragment of C3b (iC3b) is unable to participate in the formation of the alternative C3 convertase.

11. Inactivators of the Membrane Attack Complex

With the alternative and classical pathways activated, the potential for normal or bystander host cells to be subjected to lysis is significant. Excessive cell lysis is normally prevented by a number of proteins that act to inhibit the formation of the membrane attack complex.

A membrane bound protein that is capable of inactivating the membrane attack complex is the ***membrane inhibitor of reactive lysis*** (***MIRL***), more commonly known as ***CD59***. CD59 is broadly expressed among different cell types and is probably the most important molecule in minimizing damage to bystander cells. It is thought that CD59 acts by binding C8 and C9 and thus inhibits the polymerization of C9 as well as the insertion of the MAC into the membrane.

As discussed above, when C7 binds C5b6, the resulting complex is lipophilic and it inserts into the membrane. This process of membrane insertion is inhibited by **S protein**, also known as **vitronectin**, a protein related to fibronectin and laminin. The S protein is thought to function by binding the C5b67 complex before it inserts into the membrane.

12. Complement Receptors and Biological Consequences of Complement Activation

Through the activation of the complement cascade, through either the classical or alternative pathways, numerous complement derived fragments are generated. Many of these fragments possess biological activities that are mediated through the use of specific receptors.

In addition to regulating the activation of complement, ***CR1 (CD35)*** serves as a high affinity receptor for C3b and C4b. CR1 functions as a receptor for C3b- and C4b-coated particles wherein macrophages ingest and remove these coated particles. Another receptor, ***CR2 (CD21)***, is expressed primarily on B cells, dendritic cells, and epithelial cells. CR2 is known to specifically bind iC3b and C3dg—both factor I–generated cleavage products. In addition, CR2 is also known as the Epstein–Barr virus receptor. ***Mac-1*** or ***CR3 (CD11b/CD18)*** is related to the integrin family and is a specific receptor for the factor I cleavage product of C3b, iC3b. CR3 is expressed on many different cells derived from the bone marrow including neutrophils, mononuclear phagocytes, mast cells and natural killer (NK) cells. The primary role of CR3 is the phagocytosis and clearance of iC3b-coated particles. **CR4 (CD11c/CD18)**, like CR3, is also a member of the integrin family and also binds iC3b as well as C3dg.

The cleavage of C3, C4, and C5 results in the production of **C3a**, **C4a**, and **C5a anaphylatoxins**. These hormone-like peptides mediate a variety of cellular and biochemical responses from leukocytes, including the generation of bacteriocidal superoxide radicals, proteolytic enzyme release from intracellular granules, cellular aggregation, smooth muscle contraction, and phagocytosis. In addition, C5a induces chemotaxis, or the migration, of leukocytes into areas of complement activation. The induction of chemotaxis was thought to be unique for C5a; however, recent findings suggest that C3a may be chemotactic for eosinophils, a cell whose function is mediating allergic reactions. These anaphylatoxins mediate their effects through specific receptors that are coupled to GTP-binding proteins and whose signal transduction can be abrogated by pertussis toxin. The C3a and C4a receptors have been found to be expressed on mast cells, basophils, lymphocytes, and smooth muscle cells. The C5a receptor has been found on mast cells, basophils, neutrophils, monocytes/macrophages, endothelial cells, smooth muscle, liver parenchyma, and epithelial lining of lung as well as astrocytes and microglia of the central nervous system. Of the three anaphylatoxins, the most potent is C5a in mediating biological effects. C3a is approximately 20-fold less potent, while C4a is about 2500-fold less potent than C5a. C5a has been shown to stimulate the release of tumor necrosis factor (TNF) from mast cells as well as stimulating P-selectin (CD62P) expression on vascular endothelium to promote neutrophil binding.

13. Complement Genes and Relationships

On the basis of sequence homologies, many of the complement proteins can be grouped together as members of families. Members of these families share structural and/or functional similarities by which relationships can be assessed.

One of the more defined families is that of the regulators of complement activity (RCAs) as previously discussed. Factor H, CR1, CR2, DAF, C4 bp, and MCP are all members of the RCA, and all share the ability to bind both C3b and C4b. At the peptide level, all members of this family possess multiple, tandemly arranged repeated structures called short consensus repeats (SCRs). Each SCR is 65–70 amino acids long with 11–14 conserved amino acid residues. The composition and number of SCRs each of these members contain vary, but structurally and functionally they form the foundation by which this family is based. The genes encoding H, CR1, CR2, DAF, C4 bp, and MCP are found within an 800-kb genomic segment on the long arm of chromosome 1.

Another group of complement genes that are linked together are C2, factor B, and C4 that all map within the major histocompatibility complex of both humans and mice. In the human, these complement genes, often called the Class III genes, map between the Class II HLA-DR and Class I B loci of chromosome 6. Similar to the Class I and Class II genes, the Class III genes are polymorphic as multiple alleles exist for each of these genes.

Complement components C3, C4, and C5 constitute a structurally homologous family of proteins that includes a_2-**macroglobulin** and pregnancy zonal protein. All except C5 are characterized by the presence of an interal thioester bond allowing these proteins to covalently bind with cell surfaces or other proteins. However, unlike the RCA family, C3, C4, and C5 reside on separate chromosomes (Table 1).

14. Pathologies Related to the Complement System

The complement cascade is a potent and powerful system whose function is the destruction of target cells and infectious agents. Unwanted deposition of complement as well as the production of significant quantities of inflammatory mediators can result in substantial damage to normal healthy tissues. The regulatory mechanism of the MAC and alternative and classical pathways establishes a fine balance between activation and inhibition so as to protect autologous cells but allow the destruction of foreign agents. Deficiencies in nearly any component of the complement system compromise the health of an individual by tipping the balance one way or another. In a general sense, complement deficiencies can be due to the absence of a component due to structural defect in the gene, or the production of a component that is incapable of functioning in its specific role in the cascade. Table 2 summarizes complement deficiencies, the resulting abnormalities, and associated pathologies.

Table 2. Complement Deficiencies and Associated Clinical Abnormalities

Component	Biological Defect	Associated Disease
	Classical Pathway	
C1q, C1r, C1s	Defective classical pathway	Systemic lupus erythematosis (SLE), bacterial infections
C4, C2	Defective classical pathway	SLE, bacterial infections, glomerulonephritis
C3	Defective classical and alternative pathways	Bacterial infections, glomerulonephritis
	Alternative Pathway	
Properdin, factor D	Defective alternative pathway	Bacterial infections
	Membrane Attack Complex	
C5, C6, C7, C8	Defective MAC assembly	Recurrent neisserial infections
	Inhibitors	
Factor I, factor H	Deregulation of complement activation Consumption of C3	Bacterial infections
CR3 (CD11b/CD18)	Impaired opsinization	Bacterial infections

C1 inhibitor	Deregulation of classical pathway	Hereditary angioneurotic edema (HANE)
DAF (CD55)	Deregulated C3 convertase	Paroxysmal nocturnal hemoglobinuria
MIRL (CD59)	Impaired MAC regulation	Paroxysmal nocturnal hemoglobinuria

Deficiencies in alternative and classical pathway components usually manifest clinically in recurrent bacterial infections. The most serious deficiencies are those in C3. Given its role in opsinization, phagocytosis, and lysis of bacteria, homozygous deficiencies in C3 often prove fatal. In contrast, C9 deficient individuals cannot effectively generate MAC formation, yet these patients have minimal or no associated pathology as the addition of C8 to the C5b-7 complex can result in osmotic lysis of target cells. Individuals deficient in the early classical pathway components (C1, C2, and C4) are impaired in their ability to solubilize and clear immune complexes, resulting in local inflammation associated with autoimmune diseases such as ***systemic lupus erythematosus (***SLE***)***.

Patients that are deficient in the terminal complement components (C5 through C9) have impaired ability to assemble the MAC. Of particular interest is that these patients seem to have a propensity for Neisseria bacterial infections suggesting that cytolysis may be the major defense mechanism against these bacteria.

Deficiencies in the soluble and membrane bound regulatory components of complement result in abnormal activation and deposition of complement. Defects in C1INH results in a condition called ***hereditary angioneurotic edema*** (***HANE***), in which the intermittent accumulation of edema (swelling) in the skin and mucosa occurs. The exact mechanism of how the edema occurs is not known; however, without C1INH to inhibit non-specific C1 activation, C2 and C4 are readily cleaved and their by products are implicated. Deficiencies in the expression of phosphytidylinositol-linked membrane proteins result in a condition called ***paroxysmal nocturnal hemoglobinuria*** (*PNH*), where patients suffer from recurrent bouts of intravascular hemolysis. As DAF and CD59 are PI-linked, they also serve to inhibit C3 convertase formation. However, erythrocytes are especially sensitive to lysis as they do not possess membrane bound form of CD59 as other cell types do.

15. Summary

The proteins of the complement system consists of at least 20 chemically and immunologically distinct plasma proteins that can dynamically interact with one another in a highly regulated manner. The complement system can be activated by using either of two converging initiation pathways: the classical pathway, which is activated by antibody–antigen complexes; and the alternative pathway, which is activated by the surface of invading organisms. This interaction of proteins results in (*1*) the lysis of target cells and bacteria, (*2*) the binding and clearance of immune complexes throughout the body, (*3*) the binding of complement based proteins to foreign particles and subsequently cleared by phagocytosis, and (*4*) the generation of inflammatory mediators to enhance the humoral and cellular immune response. The activation of complement is tightly regulated so as to protect host cells from nonspecific attack deposition while allowing the destruction of foreign agents. Deficiencies in complement components of either pathway or in regulatory components are associated with recurrent bacterial infections and autoimmune diseases.

16. Acknowledgments

This is publication 133-IMM from the Institute of Molecular Medicine for the Prevention of Human

Diseases, University of Texas-Houston Health Science Center. This work was supported by GM56050 (DLH) and AI25011 (RAW). This article is dedicated to the memory of Dr. Hans Müller-Eberhard.

Suggestions for Further Reading

A. K. Abbas, A. H. Lichtman, and J. S. Pober (1994) *Cellular and Molecular Immunology*, 2nd ed., Saunders, Philadelphia.

H. Müller-Eberhard (1986) The membrane attack complex, Annu. Rev. Immunol. **4**, 503–528.

H. Müller-Eberhard (1988) Molecular organization and function of the complement system, Annu. Rev. Biochem. **57**, 321–347.

R. A. Wetsel and H. R. Colten (1990) in *Inheritance of Kidney and Urinary Tract Diseases*, A. Spitzer and E. D. Avner, eds., Kluwer Academic, Chapter "18", pp. 401–429.

G. D. Ross, ed. (1986) *Immunobiology of the Complement System*, Academic Press, San Diego, CA.

K. Rother and G. O. Till, eds. (1988) *The Complement System*, Springer-Verlag, New York.

K. Rother and U. Rother, eds. (1986) *Hereditary and Acquired Complement Deficiencies in Animals and Man, Progress in Allergy*, Vol. 39, Karger.

Complementary DNA (cDNA)

The base-pair complementarity between a **gene** and its **transcript** leads to the formation of a DNA–RNA hybrid under experimental conditions that favor specific **hybridization**. Pioneering work by Gillespie and Spiegleman that made use of the complementarity between viral genomic DNA and RNA in infected cells (1) helped establish the beginnings of a new technology for the detection of specific RNA molecules hidden among an RNA background, in this case of viral RNA among host cell RNA. The potential advantages of *complementary DNA* (cDNA) as a probe for RNA detection were recognized before techniques existed to make specific cDNA conveniently for tagging genes. The great abundance in the genome of extra, nontranscribed DNA, which is a common feature of higher organisms, complicates the use of genomic DNA as a cDNA probe. Some time after the first references to cDNA, a **DNA polymerase** activity that depends on the presence of an RNA template was observed in RNA **viruses** (2, 3). This discovery, in addition to extending our knowledge of RNA virus replication intermediates, led to the identification and isolation of a previously unknown form of DNA polymerase called *reverse transcriptase* and to the identification of buffer conditions that allow some DNA-dependent DNA polymerases to use a DNA-primed RNA template to form a DNA product (4, 5). Largely due to the discovery of reverse transcription and the technical advantages it provides for *in vitro* cDNA synthesis, cDNA has become a fundamental research tool for use with higher organisms.

1. cDNA Copies of messenger RNA

Transcriptionally active genes represent only a relatively small fraction of the total host genomic DNA in higher organisms, only 3% in human cells, with the noncoding or nonexpressed DNA representing the majority of the genome. Reverse transcribed cDNA synthesized under carefully controlled conditions is a faithful and stable double-strand DNA copy of cellular RNA and is trimmed of excess genomic sequence. A full-length cDNA molecule made from messenger RNA (mRNA) contains only the protein-coding region of an expressed gene, together with the adjacent untranslated regulatory sequences; it lacks any unexpressed gene or genomic sequences not contained in the mature mRNA, such as **introns** (Fig. 1).

Figure 1. Schematic representation of cDNA synthesis from mRNA. Transcriptionally active genes are transcribed, resulting in pre-mRNA that is processed to the mature form. Nuclear processing includes the removal of intervening sequences (IVS, introns) and addition of a 5′ m_7G cap and 3′ poly dA tail. Different gene activities result in different mRNA abundance shown as A, B, or C. After mRNA isolation and reverse transcription, a population of DNA–mRNA hybrid molecules are formed where the DNA is anti-sense in relation to the mRNA. Second-strand synthesis produces a cDNA population in which the more active gene is represented more than the less active gene.

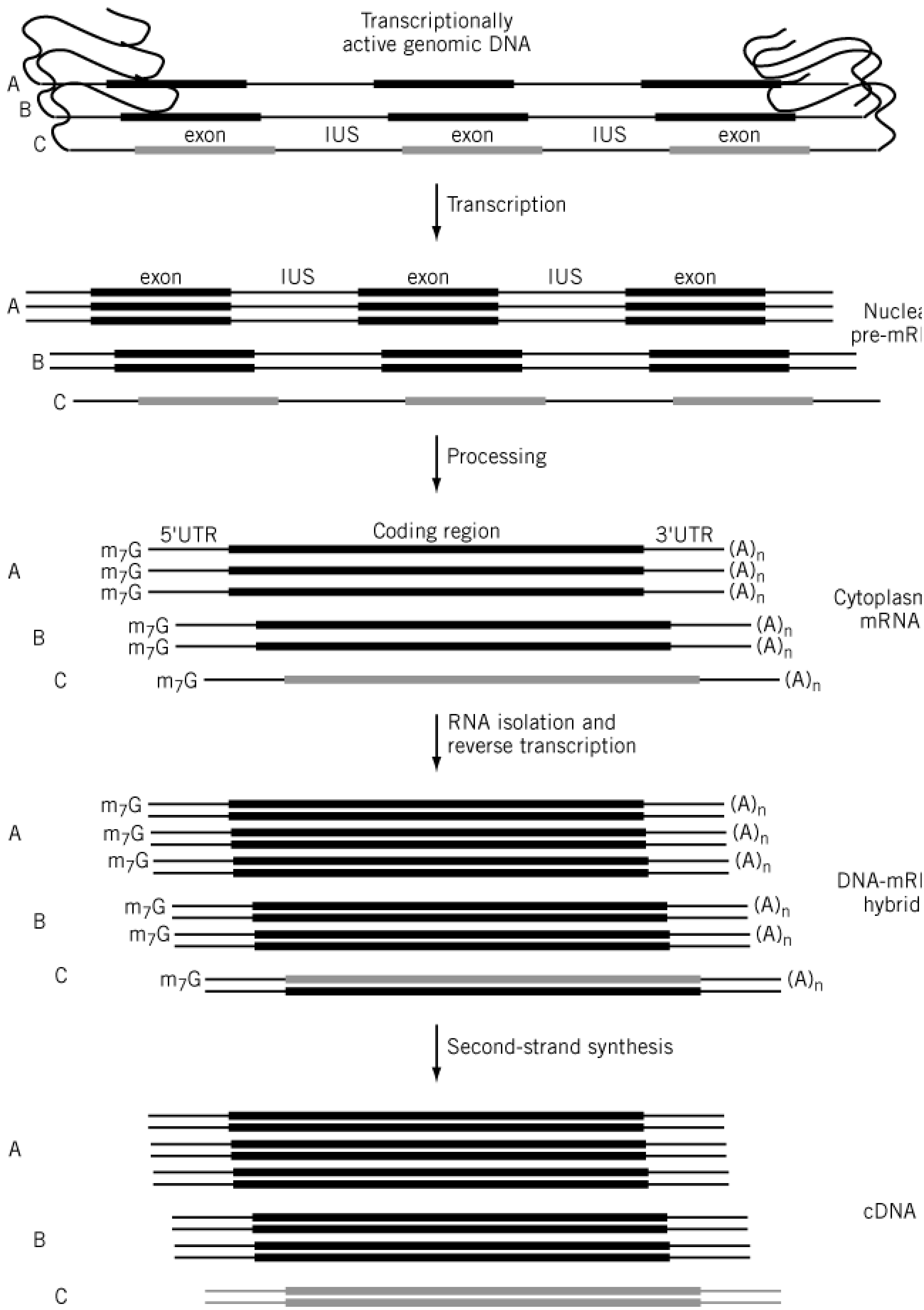
Transcriptionally active genomic DNA
A
B
C
exon
IUS
exon
IUS
exon
Transcription
exon
IUS
exon
IUS
exon
A
Nuclea
pre-mRI
B
C
Processing
5'UTR
Coding region
3'UTR
m7G
(A)n
A
B
C
Cytoplasn
mRNA
RNA isolation and
reverse transcription
A
B
C
DNA-mRI
hybrid
Second-strand synthesis
A
B
C
cDNA

For research that involves mRNA, the preparation of cDNA not only provides a DNA strand complementary to RNA, but it also serves to minimize the technical problems of working directly with RNA, which is chemically unstable at alkaline pH and susceptible to notoriously stable and ubiquitous cellular ribonucleases. A further advantage of cDNA is that in many applications it is integrated into a **prokaryotic** DNA **vector to** form recombinant DNA capable of autonomous replication when **transformed** into a host organism with a favorable genetic background. Engineered vectors with a variety of features are available for many different methods of cDNA analysis. As recombinant DNA, cDNA may be amplified through culturing of the host cells. Because each transformed host cell receives a single recombinant vector, clonal lines of host cells differing only in the recombinant vector received are established. As a copy of total cellular mRNA, however, cDNA is a complex mixture representing the complexity of the template mRNA used to direct its synthesis. Thus, cDNA integrated into a vector, transformed into a host, and cultured represents a complex mixture or **library** of transcripts, a cDNA library. The use of cDNA frequently requires the selection of a single **clone** or cDNA copy from a library, since the analysis of expression from a single gene is often the desired aim. The efficient selection of a previously uncharacterized cDNA clone from an entire cDNA library poses a major technical challenge. Selection of a new cDNA is complicated by the lack of any previous information to assist in the selection process. Often, the selection might start with little information other than observations about the encoded function of the desired cDNA clone or atypical cellular characteristics that could be associated with it.

As a stable copy of RNA, a single selected cDNA clone may be transcribed through vector signals to regenerate the RNA, which may in turn be used for synthesis of the encoded protein, either within a host cell or through the use of **protein biosynthesis *in vitro*** system. The purity of RNA or protein prepared from a single cDNA clone is absolute, thus justifying the effort to prepare a cDNA library and select a desired clone. This is an alternative to the task of biochemical purification of a protein from a tissue or cell extract. A purified cDNA in a regulated protein expression system may be used to provide a continuous renewable protein source for analysis of the structure, activity, or any characteristic of the encoded protein. Also, the effect that a cDNA's expression has on a relevant **eukaryotic** cell line may provide information about the biological role of the encoded function. Thus, cDNA-directed protein expression not only provides a source of pure protein for either *in vitro* or *in vivo* analyses, but it may also provide a method of cloning (selection) of a cDNA from a cDNA library. Many selections of new cDNAs start without protein or gene sequence information, but instead rely on the detection of the function or biological effect. This process is known as direct expression or functional cloning. Any direct expression cloning method mimics the classic genetic methods of rescue or complementation and so could be considered genetics in the absence of mating. To describe functional cloning in a general way, an altered host cell's **phenotype** or measured activity is restored to the wild-type when the genetic material encoding the host's deficiency is supplied. Although experimental approaches that rely on classic genetic methods have produced much information about cellular processes, they depend on good genetic systems to which the genetic material can be delivered. Systems that lend themselves to an imposed manipulation and selection, generally single-cell organisms with a short generation time, are best for this purpose. A myriad of eukaryotic cell cultures that have been purposefully altered or carefully isolated from the affected organs of diseased patients and that show an atypical phenotype have been widely used as host cells for functional cloning. The applications for the functional cloning of new cDNAs from higher organisms also depend on a selectable phenotype or activity to isolate the host cell that harbors the relevant genetic material. As an example, the anchorage-dependent phenotype of nearly all primary tissue cells is not exhibited by many tumor cells that will grow in suspension (6). When the genetic material used is cDNA, the details of the selection method must be designed so that the cDNA library contains the cDNA encoding the deficient host activity, and so that the cDNA is incorporated into the host cells and expressed functionally. With expression of a cDNA library in eukaryotic host cells, the selection of a desired clone depends on acquisition of a new phenotype. In the example of the anchorage-independent phenotype exhibited by some tumor cells, the induction of the anchorage dependency allows selection for a cDNA-encoded activity related to the anchorage phenotype and possibly to the cause of tumor formation (7, 8). For any selection where the desired cDNA is of an mRNA that is in low abundance, the selection will require a large-scale transformation of host cells, in order to produce even a single positive clone.

Acquiring a cDNA opens up many types of experimental approaches for the analysis of gene expression and studies of the protein encoded by the cDNA. As an example, protocols are available to target a single codon in a cDNA for site-directed mutagenesis. By using available methods to express the altered cDNA, the effects of the mutation on the encoded protein's activity may be measured, and in this way, a structure–function relation is probed.

Although the methods to prepare and make use of cDNA are advanced and commercially available, it remains a challenge to select a completely new cDNA clone from a cDNA library. This may limit the uses of cDNA technology to better characterize known cellular processes rather than uncharacterized cellular processes. The successful recovery of a novel cDNA depends on a specific selection strategy that ultimately will test each cDNA for an encoded activity. The task of individually testing each clone in a cDNA library is nearly overwhelming. If a screening method designed to test each cDNA in a collective manner cannot be designed, it forces the need for biochemical methods to purify the protein activity in order to provide enough sequence information to obtain the cDNA by more conventional methods, such as library screening with a sequence probe or selective **PCR** library amplification with degenerate oligonucleotide primers. Evolving methods of protein expression have demonstrated the potential of cDNA selection as a possible alternative to protein purification. However, functional cloning may not always be possible. An alternative approach, which can temporarily bypass the challenge presented by the need to design or apply a new isolation strategy for each new cDNA, is to randomly isolate and analyze cDNA clones first and then subsequently to identify the encoded function. The use of sequence information derived from randomly selected cDNA samples has become part of the Human Genome Project as a way of providing an aid for the physical mapping of expressed genes, as gene tags (9, 10). The cDNA sequences obtained are collected into the expressed sequence tag (EST) database, which is a collection of nonrepetitious human cDNA sequences of randomly selected cDNAs from 250 cDNA libraries from RNA isolated from 37 distinct human organs and tissues (11). The EST information is providing genetic markers for physical gene mapping and also information about the expression pattern of the mapped genes as the cell lineage is known for each sample analyzed. Some hints about the encoded function of the mapped genes may be revealed by the expression pattern. Furthermore, the large volume of sequence information produced by random sequencing may be compared to the available sequence information of the growing number of fully sequenced genes, in order to identify the presence of conserved protein domains with established activities in a process that has come to be known as *functional genomics* (12, 13). This process of extending available information about function to randomly acquired new sequence information, which necessarily requires a unified, large-scale approach, will undoubtedly contribute greatly to the identification of the encoded functions of previously unknown human genes.

2. Preparation of cDNA

2.1. Isolation of RNA Template

The preparation of cDNA begins with the isolation of the RNA that will serve as a template to direct the cDNA synthesis. Since cDNA is representative of the RNA template, an inciteful choice of a cellular source of RNA, such as a tissue that is known or at least thought to contain the specific mRNA of interest, is important. In some cases, the RNA might be tested for the presence of an RNA of interest. In a simple case, the RNA sample could be analyzed prior to use for cDNA preparation by use of a sequence probe. This sort of analysis requires, of course, some definite sequence information about the mRNA of interest. In a more complex case, when no sequence information about the mRNA is available, but detection of the encoded protein is possible, the RNA source could be analyzed for the ability to direct synthesis of the protein. Detection of a protein may be accomplished by any known function, such as **enzymatic** activity or **ligand binding** activity. The presence of a protein in a cell does not insure the presence of the protein-encoding mRNA, as the protein could be present as a stable form from an earlier expression of an mRNA that is now degraded. On the other hand, a mRNA encoding a protein of interest could be present in a tissue, but remain untranslated. One technique that can be used to insure the presence of the mRNA of interest in an RNA preparation is to translate the total RNA in an *in vitro* translation reaction and then assay the total resulting protein product for the expected protein. The two high-activity *in vitro* translation systems in common use are those prepared from rabbit reticulocytes and wheat germ (14, 15).

Given that a tissue source can be identified that contains the RNA of interest, there may be a possibility of enriching for the desired mRNA. Only a small fraction of total cellular RNA is mRNA that is directed to ribosomes for translation into protein (Table 1). The majority of cellular RNAs function in other ways to aid translation, often with structural roles. Enrichment methods aim to remove the more abundant structural RNAs selectively from the mRNAs. Enrichment of polyA + mRNA by hybridization with immobilized oligo (dT), followed by stringent washing to remove the abundant, structural, poly A – RNAs, is a common method used to prepare the mRNA template for synthesis of cDNA representing protein-encoding mRNAs (16). To reduce contamination by mitochondrial poly A + RNA, the mitochondria may be removed by cell fractionation prior to total RNA extraction, although the extra time and handling of cells required could lead to some loss or degradation of RNA. Isolation of full-length mRNA of nuclear origin based on the unique m^7G cap structure might also serve as an alternative to cell fractionation to reduce those RNA messages of mitochondrial origin often present in RNA preparations (17). Translational inhibitors have been used to stabilize ribosome-bound mRNA that is degraded during translation (18), and as selective RNA degradation pathways are increasingly well characterized, there is an increasing promise of specific inhibitors of RNA degradation for use in preparing mRNA that normally has a relatively short half-life.

Table 1. Cellular Distribution of RNA in HeLa Cells

Cellular Location	% of Total	Average $t_{1/2}$
Nucleus	**10**	
hnRNA	4.0	20 min
snRNA	2.5	100 hours
pre-rRNA	3.5	15 min
Cytoplasm	**85**	
mRNA	2.0	8–10 hours
rRNA	75.0	107 hours
tRNA	8.0	80 hours
Mitochondrion	**5**	
mit-mRNA	0.5	8–10 hours
mit-rRNA	3.5	107 hours
mit-tRNA	1.0	80 hours[a]

[a] *Note*: These values are approximate ones based on experimental observations made during repeated isolation of RNA from HeLa cell cultures.

Among poly A + RNA, there are messages of low, middle, and high abundance. The process of normalizing cDNA is used to reduce the relative number of high- and middle-abundance mRNA represented in the cDNA product. In this way, relatively fewer cDNA clones need to be screened in order to isolate a low-abundance message copy from a cDNA library. Preferred removal of cDNAs representing high- or middle-copy abundance mRNA is based on the rate of strand reannealing in a denatured cDNA sample (19). The two strands of a cDNA representing a high-abundance message have a higher probability of finding each other in a mixture and anneal before those of low-abundance cDNA. When annealed or double-stranded, the cDNA is separated from unannealed or single-strand cDNA by the use of hydroxyapatite chromatography. After a short annealing time, the low-abundance cDNA will remain in the single-strand chromatography fractions. These fractions are collected and allowed to anneal fully for use as normalized cDNA. Alternatively, subtractive hybridization is a technique used for the enrichment of, eg, tissue-specific or developmental stage-specific mRNA in the preparation of subtraction cDNA libraries.

2.2. Synthesis of the cDNA First Strand

The two cDNA strands are prepared independently. In the first-strand synthesis, the use of an RNA-dependent DNA polymerase results in a mixture of cDNA–RNA hybrid molecules in which the DNA strand is complementary to the original RNA, but possibly of shorter length (Fig. 2). The reverse transcription systems in common use are based on the avian myeloblastosis reverse transcriptase (AMV-RT) prepared from purified avian myeloblastosis virus particles or on the Moloney murine leukemia virus reverse transcriptase (MMLV-RT) prepared from a recombinant *Escherichia coli* strain (20). The purified AMV-RT has a stronger endogenous RNAse H activity than the cloned MMLV-RT, thus increasing the possibility of unwanted side reactions when using AMV-RT. However, purified AMV-RT may be more stable than MMLV-RT at the elevated temperatures used to reduce premature termination caused by **secondary structure** in the RNA template. RNase H is an endoribonuclease that specifically hydrolyzes the phosphodiester bonds of RNA in a DNA–RNA hybrid to produce products with terminal groups 3′-OH and 5′-P. Both AMV-RT and MMLV-RT have a tendency to begin second-strand synthesis prematurely through a reaction in which reverse transcriptase uses DNA rather than RNA as a template by forming a hairpin structure that serves as a template-primer substrate (21). Hairpin formation may be inhibited by the addition of sodium pyrophosphate and **spermidine**, although the RNase H activity is not inhibited with these conditions. The RNase H activity present in AMV-RT may provide a better opportunity for favorable hairpin formation by leaving single-stranded regions of DNA available for self-hybridization; this side reaction is more of a problem when AMV-RT is used. Heat-stable DNA polymerase isolated from *Thermus thermophilus* is capable of reverse transcription in the presence of MnCl *2*, which is a common alternative to the use of reverse transcriptases (22). Each system of reverse transcription has some advantages, as will be discussed, and should be considered with a view of how the second-strand synthesis will be performed. In addition to reverse transcriptase, first-strand synthesis requires deoxyribonucleotide triphosphates, dATP, dGTP, dTTP, and dCTP (or 5-metyl dCTP which may be substituted for dCTP in order to protect the cDNA from 5-methyl dCTP-sensitive restriction enzymes that may be used in subsequent cloning steps). The first-strand synthesis reaction also requires primers.

Figure 2. Three separate schemes of second-strand cDNA synthesis from the DNA–mRNA hybrid. (**a**) A classic methoc makes advantage of a looped back first strand as a primer for second-strand synthesis. After second-strand synthesis, S1 nuclease digestion of the single-strand loop structure results in an available free end for vector incorporation. (**b**) Termin transferase-directed extension of the 3′ end of the first strand results in a dG stretch that provides a binding sight for an oligo dC primer to initiate second-strand synthesis. The undesired dG stretch on the first-strand oligo dT primer is remov by restriction endonuclease digestion targeted to a site present in the oligo dT primer or in the recipient vector if vector priming is used. (**c**) Added RNase H degrades the RNA in the DNA–RNA hybrid product of first-strand synthesis, result in a series of RNA primers that are extended during second-strand synthesis. Subsequent ligation may aid the recovery o full-length cDNAs.

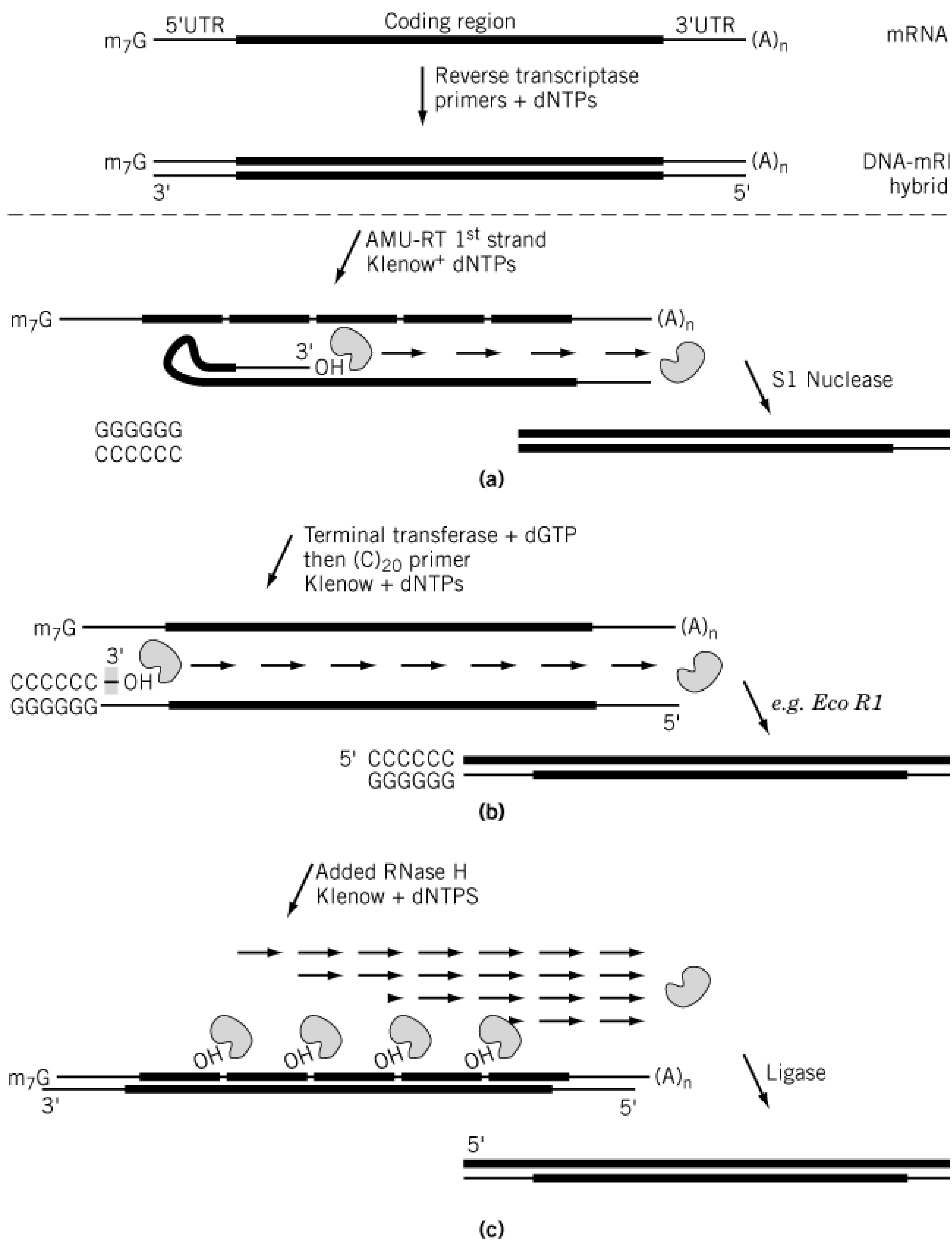

Unlike **RNA polymerases**, which bind a recognition sequence in a double-strand DNA template to initiate polymerization, replicative-type DNA polymerases require primers with a free 3′-OH group and a short double-stranded sequence. Note that a consideration of the primers to be used for the first-strand synthesis may serve to direct a more representative cDNA or cDNA better suited to the research aim. Because all mRNA, except animal histone mRNA, terminate with a 3′ poly A tract, the use of a $p(dT)_{10–15}$ oligonucleotide as a first-strand primer ensures that the synthesis begins at the 3′ end of mRNA, even when total RNA is used as a template for reverse transcription. A disadvantage of this primer is that the 5′ end of longer mRNA may be underrepresented in the cDNA product, since the chance that processive synthesis will continue to the 5′ end decreases with product length. The mRNA 3′ terminal poly A tracts with undesirable average lengths of ≈200 nucleotides can be avoided by the use of an "anchored p(dT) oligo," which has an equal concentration of dA, dC, or dG at the 3′ end of $p(dT)_{12}$ dN. Such an oligo mixture initiates first-strand synthesis at the position immediately adjacent to the beginning (5′) of the poly A tract, with an expected reduction in the length of the poly A tract captured in the cDNA. A random primer of six oligodeoxynucleotides used in place of $p(dT)_{10–15}$ may result in a more representative first-strand synthesis, since at least some of the primers should find matching hybridization sequences near the middle and 5′ end of the RNA and thus are frequently extended to the 5′ end of the template. A random primer is a better choice for use with poly A(–)RNA, which is not complementary to $p(dT)_{10–15}$. A technical consideration for random primed first-strand synthesis is the amount or ratio of primer to template that should be used, since more than one primer for each template could lead to interference between polymerase initiating on different primers hybridized to the same RNA template molecule. This will result in premature termination and a smaller average cDNA product length in the sample. Mixtures of random-primed and oligo dT-primed first-strand synthesis products should equally represent the length of RNA.

Another choice of primer to initiate first-strand synthesis is a sequence-specific primer, a primer complementary to a known sequence within the mRNA of interest. The design of a sequence-specific primer depends, of course, on some available sequence information. A very conserved sequence common to a group of possibly related mRNAs used for the preparation of a limited cDNA library is an example of the application of a sequence-specific primer. Whichever type of primer is used for the initiation of first-strand synthesis, extra sequence at the 5′ end of a primer, such as a restriction site sequence or a second primer-binding site, should not interfere with polymerase-directed extension of the 3′ primer end. Thus, the 5′ end of the primer may serve as a "sticky end" to incorporate the cDNA into a vector or as a primer target for subsequent amplification of the cDNA by PCR.

2.3. Synthesis of the Second Strand

As for first-strand synthesis, second-strand synthesis requires a polymerase, dNTPs, and a primer added to a template. In this case, the template is the product of the first-strand synthesis reaction. Since the template is DNA, a DNA-dependent DNA polymerase, most commonly *E. coli* DNA polymerase I or the **Klenow fragment** of DNA polymerase I, is used for second-strand synthesis. Additionally, reverse transcriptase added as a "chaser" reportedly facilitates second-strand synthesis through obstructions caused by secondary structure in the template (23). The product of the second-strand synthesis reaction is double-strand cDNA ready for steps leading to recombinant vector integration. The choice of primers that might serve to direct the synthesis of the second strand is limited, since the 3′ terminal sequence of the first strand varies greatly among the first-strand synthesis product population; there is no common sequence at the 3′ end of the first-strand product available for primer hybridization. Primer design for second-strand synthesis has conventionally been approached in one of three ways: (1) the classic method of hairpin-loop priming followed by S1 nuclease digestion, (2) RNAse H treatment to generate RNA primers, or (3) homopolymeric tailing, also known as vector priming (see Fig. 2). RNAse H is commonly available in a pure form for the second-strand synthesis reaction (Fig. 2**c**). Added RNAse H is used to generate short RNA primers that are extended to form the second strand (24, 25). The relative technical simplicity, high yield, and large average product length achieved with the RNAse H method have proven it to be the superior approach generally, although other methods may continue to have specific applications and certainly have had a central role in characterization of the potential side reactions that affect the yield and average size of the cDNA product.

The classic method of second-strand synthesis (26, 27) takes advantage of the tendency for the 3′ end of the first strand to fold back and form a DNA duplex with sequences located further 5′ or upstream on the same DNA strand (Fig. 2**a**). A consequence of the duplex or hairpin formation is availability of the self-primed template for second-strand synthesis. After removal of the RNA, reagents for second-strand synthesis are added, and so the second strand is generated. The product is double-strand cDNA covalently closed at the end corresponding to the 5′ end of the original mRNA. The addition of S_1 nuclease, a single-strand-specific nuclease, results in cleavage of the single-strand loop to produce free 5′ and 3′ ends, which are necessary for subsequent integration into a cloning vector. Although the use of S_1 nuclease, which has a potential of hydrolyze double-stranded DNA when used in excess, is often cited as the major disadvantage of the classical method, it is the necessary loss of sequence information that is the true technical fault in the method. Since at least some sequence is involved in the hairpin formation, the sequence of the 5′ end of the original mRNA is not represented in the cDNA product when this classical method of second-strand synthesis is used.

The method of homopolymeric tailing or vector priming relies on the use of *terminal deoxynucleotidyltransferase*, an enzyme that catalyzes the sequential addition of available nucleotide triphosphates to the free 3′ end of a DNA strand. Thus, a homopolymer tail made by extension of the free 3′ end of the cDNA strand resulting from the first-strand synthesis reaction serves as the primer site for second-strand synthesis (Fig. 2**b**). The application of homopolymer tailing to second-strand synthesis preserves the cDNA sequence representing the original 5′ end of the mRNA template, since priming is from sequence added by terminal transferase (28, 25). After first-strand synthesis initiated from a T-tailed vector, the 3′ end of the newly formed cDNA strand is the target for homopolymer tailing. The use of dGTP for the tailing reaction consistently results in an average of 20 G nucleotides on both the 3′ end of the cDNA first strand and on the free 3′ end of the vector. The consistent length of the tail with use of dGTP is apparently due to structural constraints, which cause decreased tailing after 20 Gs (29, 30). A restriction site in the vector is used to remove the G-tail from the vector, without affecting the G-tail on the cDNA, which as a DNA–RNA hybrid is a poor substrate for restriction endonucleolytic cleavage (31). Finally, an oligo $p(dC)_{20}$ primer is added, along with other reagents required for second-strand synthesis. The $p(dC)_{20}$ primer may be designed to have a 5′ end complementary to the overhang of the vector restricted end to aid in subsequent circularization of the recombinant DNA; otherwise, both the cDNA and vector ends may be made flush or blunt prior to circularization. Many variations of the vector priming method briefly described here have been described in detail elsewhere, but all make use of terminal transferase (32). The disadvantages of being more technically difficult and having more steps, as well as having a stretch of 20 G nucleotides at the vector-cDNA boundary (which could require special techniques for sequencing and subcloning), might be balanced by the important potential of increasing the number of full-length clones when using this method of second-strand synthesis.

Isolation of a cDNA corresponding to the intact full-length mRNA molecule often presents a challenge. Methods that increase the frequency of obtaining full-length clones in a cDNA synthesis reaction are often preferred. Losses of cDNA may occur at each step of the synthesis, from RNA isolation to vector incorporation. Losses of full-length cDNA may also occur due to incomplete replication of template by polymerase. For example, the presence of secondary structure in the RNA template may impede the progress of reverse transcriptase during first-strand synthesis, resulting in the formation of a partial cDNA beginning at the primer site and ending at the site where the secondary structure is encountered by the polymerase. Technical manuals that contain detailed protocols for cDNA synthesis often describe ways to monitor the progress of cDNA synthesis to give an indication of the reaction yields, or the incurred losses, and also the average size of the cDNA strand. A method designed to extend a partial cDNA isolated by a selection procedure called RACE (rapid amplification of cDNA ends) may be used to obtain the corresponding full-length clone (33). The actual 5′ end of an mRNA should, however, be mapped against the gene and/or correlated with the N-terminal sequence of the protein where possible. Primer Extension is frequently used to determine the precise 5′ end of an mRNA, and this method only requires enough sequence information for primer design.

3. Uses of cDNA

The final steps in cDNA synthesis are often those leading to vector integration. The use or application of cDNA is largely determined by the type of vector that is chosen to contain the cDNA. Vector integration is, therefore, the first step toward fitting the cDNA to the type of application that will be made or toward developing a selection strategy for the isolation of a cDNA of interest from a library. Recent progress in the development of cloning vectors for specialized applications and of methods of efficiently adapting the cDNA ends to fit the vector ends have resulted in a lot of flexibility in the combination of available vector features when making a choice from the long list of commercially available cloning vectors. The immediate aim of retaining all the newly synthesized cDNA through the process of vector integration and host transformation, while keeping the desired vector features, is frequently satisfied by the use of a **phagemid** (34). A phagemid vector combines features of lambda phage, filamentous phage, and plasmid vectors into one cloning vector (35, 36). The efficiency of host cell transformation through packaging of cDNA into viral particles, and subsequent viral infection as performed with the use of a l phage cloning vector, cannot be matched by even the optimal conditions for direct host-cell transformation with plasmid DNA. There is consequently less potential for cDNA loss during host cell transformation with a l phage system when compared to a plasmid system. The lower background that results from the screening of plaques rather than colonies with sequence hybridization probes or antibody probes offers another significant advantage to the use of viral vectors. Plasmid vectors offer advantages over l phage vectors for the characterization of the cDNA inserts, due to the necessarily large size of l phage vectors. Phagemid vectors contain a plasmid vector within a l phage vector and additional sequences derived from filamentous phage that contribute to the *in vivo* excision of the plasmid from the l phage vector. Thus, for characterization of individual selected cDNA clones, the original phage clones are converted to plasmid clones. Although it is technically straightforward to subclone a single cDNA clone from one vector to another, it is technically difficult to subclone an entire cDNA library from one to another vector without some loss of cDNA. Whichever type of vector is used to receive newly made cDNA, consideration of the vector features required for selection of a cDNA of interest from a library and the efficiency of the process of integration and host-cell transformation should be given prior to vector integration of cDNA as a library.

Possibly the greatest benefit of aquiring a new cDNA of interest from a cDNA library is the sequence information that can be derived from it. In addition to the encoded protein sequence, comparison of a cDNA sequence with the corresponding gene sequence reveals or confirms the location of any introns present in the gene. Analysis of a set of positives identified by rescreening of a library with the now available hybridization probe may provide some indication of the variability of the gene transcripts, eg, the presence of alternate splice sites or multicopy genes with minor sequence variations. The presence of viral RNA polymerase recognition sequences, most commonly SP6 and T7 **promoters**, in many cloning vectors are useful for the *in vitro* production of anti-sense RNA probes that may be used for the high-sensitivity detection of gene expression. Likewise, PCR primers may be designed from the sequence information to provide an alternate method of sensitive or quantitative gene expression analysis. The presence of potential post-transcriptional regulatory elements in the untranslated regions represented in the cDNA may be identified through computer-assisted sequence analysis and database comparisons. Although any number of extremely sophisticated uses for cDNA sequence information may be envisioned for a particular application, a generally useful benefit is the possibility to generate peptide antibodies to encoded peptide epitopes predicted to be on the protein surface.

Vectors are available with many combinations of features. A particularly useful vector feature for many types of applications is the inclusion of sequences that support cDNA expression. As the sequences required for correct initiation of translation differ among organisms, expression vectors, or an expression cassette within a cloning vector, are designed for use as a set with a matching host cell. The promoter sequences included to drive the transcription of the expression cassette and efficient transcriptional termination signals are likewise active in the same host. As there are no introns to be removed, expression of many encoded eukaryotic proteins is supported in strains of *E. coli*, provided that these proteins are not toxic to the *E. coli* host strain used. In order to avoid the possible toxic effects of some eukaryotic proteins, expression vectors with inducible promoters are available to postpone the cDNA expression to a point of vigorous growth so that significant protein production is accomplished before the host culture dies. The activity of eukaryotic proteins produced in prokaryotic host cells may be deficient due to the absence of factors required for proper protein folding in vivo, for post-translational modifications essential for the activity, or even for correct intracellular localization. Eukaryotic expression systems may better support the production of eukaryotic proteins with natural levels of activity and are designed for maximum protein production. Such expression systems may support continued replication of the vector containing a cDNA insert, in addition to containing an **expression cassette** with an active promoter and signals for transcription termination and translation initiation. Both prokaryotic and eukaryotic expression systems with matched vector and host are designed to produce proteins in quantities required for their structural characterization from manageable volumes of cell culture. Accurate physical measurements that require purified proteins may take advantage of "built-in" purification aids available in some expression vectors. Expression of a cDNA as a **fusion protein** aids in the isolation of protein from cell cultures. Provided a cDNA is cloned in-frame in relation to a vector sequence that encodes a polypeptide chain with a known ligand affinity, the resulting fusion protein may be purified from cell lysates by passage through an affinity chromatography column containing the immobilized ligand. The presence of a proteinase peptidase recognition sequence facilitates proteolytic removal of the vector-encoded polypeptide and elution of the cDNA-encoded protein from the affinity column.

An additional type of expression vector that is adapted to cDNA selection is one designed for use with a yeast host strain. The yeast 1, 2, and 3-hybrid systems have been designed to isolate a cDNA clone from a library based on the encoded protein's recognition or specific binding to a DNA, protein, or RNA sequence, respectively (37-39) (see Two-Hybrid Systems). In this way, cDNA selection is facilitated by its expression inside a yeast host cell that has been genetically altered for the selection. In order to perform the selection, an entire cDNA library is cloned into a shuttle vector that will support replication in *E. coli*, as well as replication and expression (as a fusion protein) in the yeast host. The library is amplified for transformation into the recipient yeast host strain, which is altered in such a way that specific binding of a target sequence or "bait sequence" results in a positive selection. The yeast hybrid systems typify advances in the use of traditional genetic strains adapted for functional cloning of cDNA from higher organisms, and yeast has consequently become a tool for functional cloning through molecular recognition, extending the use of cDNA as an aid to the selection of novel factors. Thus, a factor that binds to a DNA sequence, such as a transcription factor that binds to a gene promoter element, may be difficult to isolate by biochemical means due to its low intracellular abundance, but it might be cloned with the yeast 1-hybrid system. Likewise, a factor that binds to a protein might be cloned with the 2-hybrid system, or an RNA-binding protein with the yeast 3-hybrid system.

4. Summary

cDNA is a faithful double-stranded DNA copy of RNA and, as such, can represent those genes that are expressed as RNA in a source tissue. When integrated into an appropriate cloning vector to form recombinant DNA, cDNA may provide a continuous renewable source of genetic material for hybridization probes, designed reporters of biological activity, or pure encoded protein. The benefits of protein production and a myriad of specific research applications have made cDNA a universal tool for basic and applied cell and molecular biology research. The potential for using cDNA in molecular methods designed to select for activities that contribute detectable cellular phenotypes has provided possible alternatives or improvements to genetic and biochemical approaches.

Bibliography

1. D. Gillespie and S. Spiegleman (1965) J. Mol. Biol. **12**, 829–842.
2. H. M. Temin and S. Mizutani (1970) Nature **226**, 1211–1213.
3. D. Baltimore (1970) Nature **226**, 1209–1211.
4. M. G. Sarngadharan et al. (1972) Nature New Biol. **240**, 67–72.
5. E. M. Scolnick (1971) Develop. Biol. **26**, 175–176.
6. J. C. Barrett et al. (1979) Cancer Res. **39**, 1504–1510.
7. M. Noda (1990) Molec. Carcinogenesis **3**, 251–253.
8. C. P. Carstens et al. (1995) Gene **164**, 195–202.
9. L. Rowen et al. (1997) Science **278**, 605–607.
10. M. Boguski and G. D. Schuler (1995) Nature Genet. **10**, 36971.
11. M. D. Adams et al. (1995) Nature **377**, Suppl., 3–174.
12. S. Henikoff et al. (1997) Science **278**, 609–614.
13. R. L. Tatusov et al. (1997) Science **278**, 631–637.
14. B. E. Roberts and B. M. Paterson (1973) Proc. Natl. Acad. Sci. USA **70**, 2330.
15. C. W. Anderson et al. (1983) Methods Enzymol. **101**, 635.
16. H. Aviv and P. Leder (1972) Proc. Natl. Acad. Sci. USA **69**, 1408–1412.
17. I. Edery et al. (1995) Mol. Cell Biol. **15**, 3363–3371.
18. J. Ross (1997) Bioessays **19**, 527–529.
19. T. G. Coche (1997) Methods Mol. Biol. **67**, 359–369.
20. M. Roth et al. (1985) J. Biol. Chem. **260**, 9326–9335.
21. M. S. Krug and S. L. Berger (1987) Methods Enzymol. **152**, 318.
22. C. Rüttimann et al. (1985) Eur. J. Biochem. **149**, 41–46.
23. U. Gubler (1987) Methods Enzymol. **152**, 325.
24. H. Okayama and P. Berg (1982) Mol. Cell Biol. **2**, 161–170.
25. U. Gubler and B. J. Hoffman (1983) Gene **25**, 263–269.
26. A. Efstratiadis et al. (1976) Cell **7**, 279–288.
27. F. Rougeon and B. Mach (1976) Proc. Natl. Acad. Sci. USA **73**, 3418–3422.
28. H. Land et al. (1981) Nucl. Acids Res. **9**, 2251–2266.
29. A. Dugaiczyk et al. (1980) Biochemistry **19**, 5869–5873.
30. A. Otsuka (1981) Gene **13**, 339–346.
31. W. H. Eschenfeldt et al. (1987) Methods Enzymol. **152**, 339.
32. P. L. Deininger (1987) Methods Enzymol. **152**, 376.
33. M. A. Frohman et al. (1988) Proc. Natl. Acad. Sci. USA **85**, 8998–9002.
34. M. A. Alting-Mees et al. (1992) Methods Enzymol. **216**, 483.
35. D. Hanahan (1983) J. Mol. Biol. **166**, 557–580.
36. J. M. Short et al. (1988) Nucl. Acids Res. **16**, 7583–7600.
37. S. Fields and O. Song (1989) Nature **340**, 245–247.
38. D. J. SenGupta et al. (1996) Proc. Natl. Acad. Sci. USA **93**, 8496–8501.
39. Z. F. Wang et al. (1996) Genes Develop. **10**, 3028–3040.

Suggestions for Further Reading

40. V. B. Chanda, ed. (1997) *Current Protocols in Molecular Biology*, John Wiley & Sons, New York.
41. I. G. Cowell and C. A. Austin, eds. (1997) *Methods in Molecular Biology—cDNA Library Protocols*, Humana Press, Totowa, NJ.
42. Suppliers of the reagents used for cDNA synthesis often supply excellent technical manuals.

Complementation

The term complementation usually refers to the situation where two defective genomes in the same cell together support a normal or nearly normal **phenotype**, each supplying the function that the other lacks. Another meaning of the term, in the context of DNA manipulation, is the repair of a mutational deficiency in an organism or cell culture by artificially introducing a **gene** that supplies the missing function. This is a potent way of cloning genes selected according to function. In either sense, complementation provides a way of discriminating between gene functions and of defining genes as functional units.

1. Complementation and the definition of the functional gene

Classical genetics was based upon clear-cut heritable variants, either induced by mutagenic treatments or, in earlier days, just turning up as "sports" in wild or cultivated populations. The geneticists' favorite organisms, notably **maize** (*Zea mays*) and the fruit-fly (***Drosophila*** *melanogaster*), were **diploid**. Most mutations were recessive to **wild type**, which is what would be expected if they mostly represented losses of function that could be more or less adequately supplied if one gene out of two was normally active.

As mutants accumulated, they were attributed to the same or different genes on the basis of two criteria. First, it was supposed that mutations in the same gene were inseparable by recombination. A diploid that carries two different mutant **alleles** (ie, alternative forms) of a particular gene should never produce nonmutant or double-mutant germ cells by free reassortment or **crossing-over** at **meiosis**. According to the second criterion, mutations in the same gene should affect the organism in similar or at least related ways. Similarity or overlap of functional effects was judged by individual appearance (phenotype) and also and more rigorously by failure of the mutant chromosomes to complement each other's defects in the hybrid diploid. (In fact, the term complementation did not come into use until the late 1950s, and I use the word with hindsight.)

A classical example of using the complementation criterion, and one of the first in which it was thrown into doubt, involves the sex-linked *white* (*w*) gene of *Drosophila*, one of several genes governing eye color. A considerable number of recessive mutant *w* alleles had been identified. They diluted the normal red-brown eye pigment to various degrees when the same allele was present on both X-chromosomes (***homozygous***) in females, or on the single X in males. Females that had two different mutant *w* alleles (***heterozygous***) had dilute eye colors generally intermediate between the colors of the two homozygotes. Thus females of constitution *white/ apricot* (w/w^a) have pale apricot eyes, not wild-type red as would be expected if each mutant X-chromosome could provide the pigment-forming function lacking in the other.

In 1952, E. B. Lewis (1) found that, at very low frequency (about 1 in 10,000), w/w^a females produce eggs of recombinant types, with neither mutation or both. By the attached-X technique, which need not be described here, he showed that these recombinants arise by crossing-over between the X-chromosomes, just as if *white* and *apricot* were mutations at distinct, though very closely linked loci. Accordingly he gave them different symbols, *w* and *a*, and rewrote the constitution of the female parent wa^+/w^+a, where the + superscripts denote the respective wild-type alleles.

The remaining anomaly was what Lewis called the *cis* /*trans* position effect (Fig. 1). Two kinds of doubly heterozygous constitution could be compared, the original so-called *trans* arrangement wa^+/w^+a, that has the two mutations on opposite chromosomes, and the *cis* arrangement, $w^+ a^+/wa$. They had identical overall gene content, but the former had pale apricot eyes and the latter was fully wild type. w^+ and a^+ could act cooperatively to promote normal levels of eye pigment only when they were together on the same chromosome. Lewis called their relationship ***pseudoallelic***: allelic according to their failure to complement each other but nonallelic according to their ability to recombine. A formally identical situation at the *Drosophila lozenge* locus had already been reported by M. M. Green (2).

Figure 1. Lewis's (1) *cis-trans* comparison using two mutations in the *Drosophila melanogaster* X-linked *white* (*w*) gene. The mutations *white* (*w*) and *apricot* (w^a, shown here as *a*) are each recessive to wild type in females but do not complement one another in *trans*. By this criterion they are allelic in spite of being separable at low frequency by recombination.

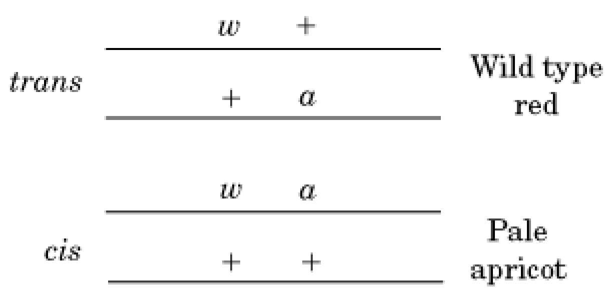

For Lewis and Green at that time, the recombination criterion for allelism took priority, and the reason for the position effect was a matter for speculation. Before long, however, high-resolution recombination analysis of series of mutants in the microbial world, first in the fungus ***Aspergillus*** *nidulans* (3) and then in the bacterial virus (**bacteriophage**) T4 (4), revealed that pseudoallelism, in Lewis's sense, was much more the rule than the exception. It was rather rare for independently occurring mutations to be “truly” allelic. Almost all pairwise combinations of noncomplementing mutants showed some low frequency of recombination when crossed together. Soon afterward, the same was shown to be true in two bacterial species, *Escherichia coli* and *Salmonella typhimurium* (5), which have no regular diploidy or meiosis but other means exist for obtaining partial diploids and tests for complementation and recombination (see Complementation Tests). In one example after another, it was shown that most mutations within functional genes are at different mutually recombinable sites which, by different methods in different organisms, could be mapped in a closely spaced linear sequence that was continuous with the much longer sequence of the whole chromosome.

Following his very extensive analysis of the *rII* series of mutants in phage T4 ((4), see Complementation Tests), S. Benzer proposed replacing the word gene with a new term, **cistron**, meaning the unit of function as defined by Lewis's *cis*/*trans* comparison. When the *cis* and *trans* phenotypes are identical (wild type, if the mutants involved were recessive), the mutations are in different cistrons, affecting different functions. If *trans* is mutant and *cis* normal (or relatively so) the mutants are in the same cistron. The concept has been universally accepted, but the term cistron has dropped out of use. Now “gene” is generally used in the same sense, and the full *cis-trans* test is rarely applied. The theoretical reason for the comparing *trans* ($m1 + / + m2$) with *cis* ($m1m2/ + +$), rather than just *trans* with the wild type, is that it controls the possibility that the cumulative effect of two heterozygous mutations in different genes could be a sub-wild phenotype, even though each is individually recessive to its wild-type allele. In practice, however, recessive alleles usually remain recessive even when several of them are present together, and so the *trans*/wild comparison, the simple complementation test, is usually deemed sufficient.

Although diploidy provides the means for complementation testing in higher plants and animals and also in budding **yeast**, alternative methods, described under Complementation tests, have to be used for habitually haploid organisms, such as bacteria, viruses, and most fungi.

1.1. Complementation and gene cloning *in yeasts*

Cloning wild-type alleles of yeast genes with metabolic functions and mutating to give **auxotrophic** phenotypes, became straightforward following the development of the Saccharomyces two-micron (2-µm) **plasmid** as a cloning vehicle (7). This plasmid also replicates in the other major experimental yeast species, the fission yeast *Schizosaccharomyces pombe*. It has been most useful as a component of a series of hybrid **shuttle vectors**, capable of replication either in yeast or in *Escherichia coli*. These usually incorporate the replicative origin of the *E. coli* plasmid ColE1 and a gene for antibiotic resistance (e.g., to **tetracycline**) that can be selected for in the bacterial host.

To select and clone a yeast gene, fragments of total yeast DNA, produced by digestion with a **restriction endonuclease** (or sometimes by sonication), are ligated into the closed-loop, double-stranded DNA of a shuttle vector and introduced en masse by one of the standard transformation procedures into mutant yeast cells, which then are plated on a medium on which they grow to form colonies only if their mutational deficiency has be repaired. (see Cloning) The first yeast genes to be cloned were selected because they conferred on auxotrophic (nutritionally exacting) mutants the ability to form colonies on a minimal (unsupplemented) growth medium. But any gene that mutates to give a conditional no-growth phenotype can be cloned in essentially the same way. Temperature sensitive mutants have been a particularly rich source of cloned genes. Almost any essential protein can be mutated to a temperature-sensitive form, functional at, say, 30°C but not at 36°C. Mutant cells grown at the permissive temperature are transformed with a gene “library” and selected for repair of function at the restrictive temperature.

The shuttle vector bearing the selected gene replicates autonomously either in yeast or after transfer to *E. coli*. The bacterial host is more efficient for mass propagation of the clone. When sufficiently amplified, the cloned gene is cut out of the vector, and its structure and function are analyzed in various ways, most obviously by DNA sequencing. The general method is outlined in Fig. 2.

Figure 2. Cloning and amplifying a yeast gene in a shuttle vector selected by its complementation of a yeast auxotrophic (leucine-requiring) mutant. Open and filled circles indicate replication origins for propagation in yeast and *E. coli*, respectively. Based on Beggs' first demonstration of the method (7).

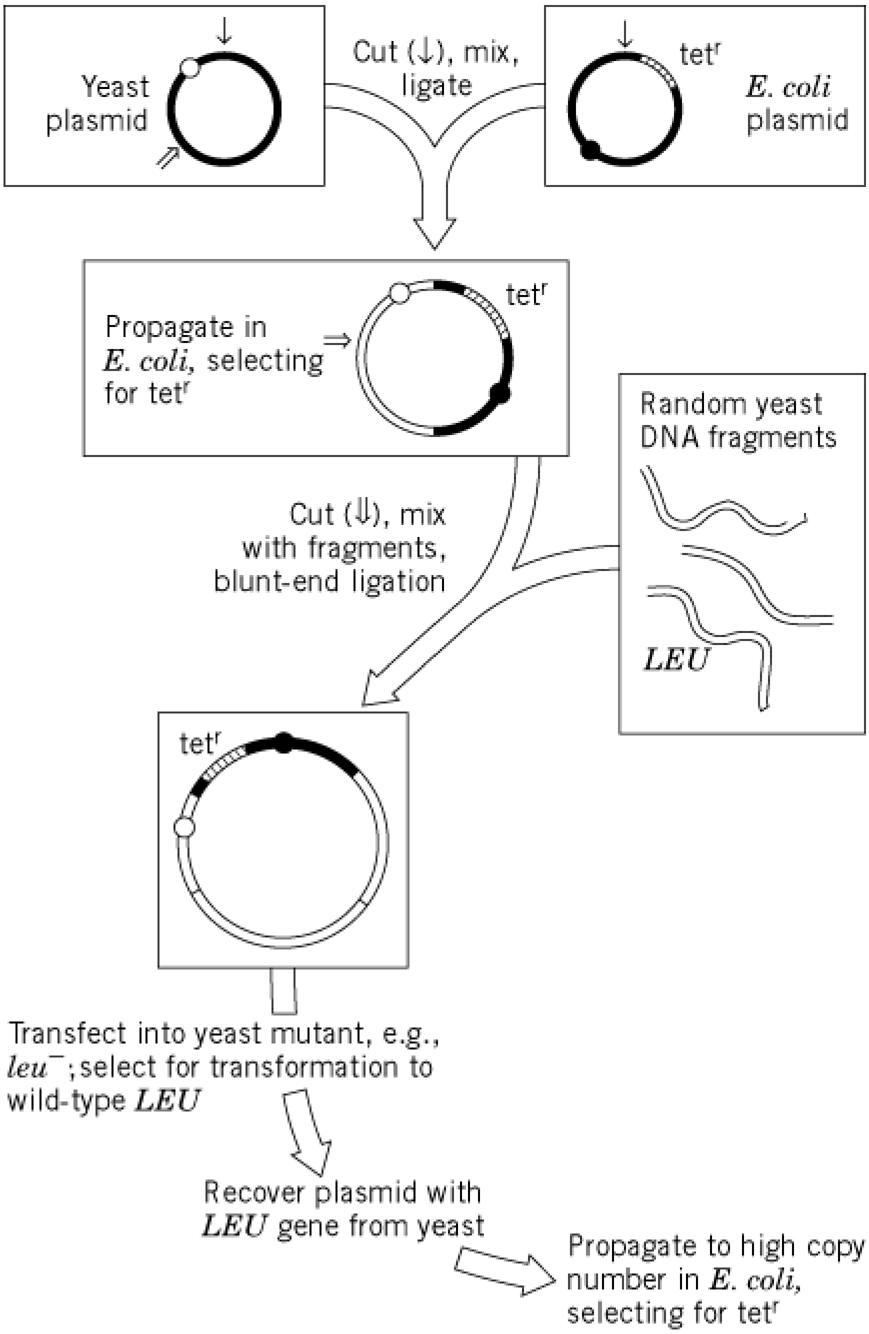

The complementation of yeast mutants is used for cloning yeast genes and also genes from such distant organisms as *Drosophila* and humans. One good example is cloning the human equivalent of the *Schizosaccharomyces pombe* (fission yeast) *CDC2* gene (8). *S. pombe* temperature-sensitive *cdc2* mutants cannot complete their cell cycle at elevated temperature (36°C) because the mutant *cdc2* gene product, a protein kinase that provides a signal essential for initiating cell division, is inactivated at this temperature. Transformation of mutant cells with a human cDNA library cloned in a replicating plasmid led to the isolation of a few colonies that harbor hybrid plasmids carrying the desired cDNA sequence. The cloning plasmid used in this instance differs from that illustrated in Fig. 2 in that its replication in fission yeast depends on a DNA sequence from the monkey **SV40 virus**, which replicates well in *S. pombe*, not on the yeast 2-mm plasmid. To clone mammalian gene sequences in yeasts, it is generally necessary to use cDNA rather than genomic DNA. Mammalian **introns** are not effectively spliced out in yeast cells and, in any case, often make the gene too long for cloning in one piece.

1.2. In Neurospora

Although yeast species that have a single-cell, colony-forming habit and are accessible to replicating plasmids are especially convenient for cloning genes, the complementation principle can also be applied to filamentous fungi and has been particularly successful in *Neurospora crassa*. This species has the disadvantage that it has no convenient plasmid that stably replicates without integration into the chromosomes. Consequently, although auxotrophic mutants are "rescued" by transformation with fragments of total *Neurospora* DNA, it is not so easy to recover the transforming sequences from the transformed cultures. This difficulty was overcome by sib selection (9).

The method is making a library of *Neurospora* DNA sequences in some suitable vector (sufficient in number so that it is probable that the great majority of genes are represented), dividing the clones into a number of pools, and testing DNA isolated from each pool for its ability to repair the mutant of interest. Then a pool that works (and there is usually at least one) is subdivided into smaller pools for further tests, and then to still smaller pools, until the hunt is narrowed down to a small number of clones that can be tested individually. Though obviously laborious, the method has been very successful. It has been used for cloning genes of metabolic function and also for the loci (actually gene complexes) that govern fungal **mating type** by complementation of mating-deficient mutants (10, 11).

1.3. In Drosophila

Many gene functions involved with basic cellular processes are common to yeast and mammals. Then it is not surprising to find that others, more to do with tissue differentiation, are common to most animals. Because the genetic control of development is better understood in *Drosophila* than in any other animal, it is of interest to ask whether some of the relatively well-characterized *Drosophila* genes have mammalian equivalents. Flies cannot be used for the kind of mass screening of gene libraries that is possible with yeast, but it is not difficult to find out whether some particular mouse gene or cDNA clone complements a *Drosophila* mutant.

It is relatively easy to get exotic DNA into the *Drosophila* genome by inserting it into the transposable P element and injecting the construct into early embryos. Thus the mouse gene M33, cloned on the basis of its sequence similarity to the *Drosophila polycomb* (*Pc*) gene, was successfully introduced into *Pc* mutant flies (12). The mutants, which usually have sex combs on all legs of the male instead of just on the front pair as in the wild type, were partially normalized by inserting one copy of M33 into their genome and were restored almost to wild type by two copies. *Pc* protein is one of a group of chromosomal proteins that act together to prevent certain developmentally important genes from being expressed in the wrong places or at the wrong times. This experiment strongly indicates that there is a mammalian gene that has a similar function.

Bibliography

1. E. B. Lewis (1952) Proc. Natl. Acad. Sci. USA **3**, 953–961.
2. M. M. Green and K. C. Green (1949) Proc. Natl. Acad. Sci. USA **35**, 586–591.
3. R. H. Pritchard (1953) Heredity **9**, 343–371.
4. S. Benzer (1955) Proc. Natl. Acad. Sci. USA **41**, 344–354.
5. P. E. Hartman, J. C. Loper, and D. Serman (1960) J. Gen. Microbiol. **22**, 323–368.
6. S. Benzer (1958) In *The Chemical Basis of Heredity* (W. D. McElroy and B. Glass, eds.), Johns Hopkins Press, Baltimore, pp. 70–93.
7. J. D. Beggs (1978) Nature **275**, 104–109.
8. M. G. Lee and P. M. Nurse (1987) Nature **327**, 31–33.
9. S. J. Vollmer and C. Yanofsky (1986) Proc. Natl. Acad. Sci. USA **83**, 4867–4873.
10. N. L. Glass, J. Grotelueschen, and R. L. Metz (1990) Proc. Natl. Acad. Sci. USA **87**, 4912–4916.
11. C. Staben and C. Yanofsky (1990) Proc. Natl. Acad. Sci. USA **87**, 4917–4921.

12. J. Muller, S. Gaunt, and P. A. Lawrence (1995) Development **121**, 2847–2852.

Complementation Tests

The **gene** is best defined as an integral unit of genetic function, in the sense that none of its parts functions normally in isolation from the others. If so, two different forms (**alleles**) of the same gene, both more or less inactivated by mutation, should not make good each other's defects when together in the same cell. They should not, in other words, show complementation. On the other hand, two genomes that have mutations in different genes should complement each other to produce a wild-type phenotype, provided that each mutant allele is recessive to its **wild-type** counterpart. This complementation criterion is of great importance because it permits assigning mutations to the same or to different genes without a detailed analysis of gene functions. When mutations are closely linked and have fairly similar phenotypic effects, it is always likely that they are in the same gene. But it is not uncommon to find close linkages of separate genes whose function is related. A complementation test provides much stronger evidence.

The interpretation of complementation tests is itself subject to certain difficulties, which are discussed separately under the heading **Allelic complementation**. Here we make the simplifying assumption that complementation between recessive mutations means that they are in different genes.

For a complementation test, it is necessary to bring two mutant genomes, or at least relevant parts of genomes, together in the same cell. In organisms including animals, higher plants and budding **yeasts**, that have a stable **diploid** phase in their life cycles, this can be simply achieved by making a sexual cross between mutant strains. In microorganisms that have no stable diploid phase, various other means have to be employed. In haploid filamentous **fungi**, heterokaryons that have two genetically different kinds of nuclei in a common cytoplasm provide a satisfactory substitute for diploidy. In **bacteria**, where neither diploidy nor heterokaryosis is usually available, there are various ways of introducing fragments of the genome from one cell to another to make partial diploids (merodiploids). This makes it possible to test for complementation of genes located within the duplicated fragment (Fig. 1). In **viruses**, especially bacterial viruses (**bacteriophages**), complementation tests can be carried out simply by mixed infections.

Figure 1. Three general ways of making complementation tests: (**a**) by diploidy (higher plants, animals and the budding yeast *Saccharomyces cerevisiae*); (**b**) by heterokaryosis (fungi, such as *Neurospora crassa* and sometimes cultured mammalian cells); (**c**) by addition of a genomic fragment to a haploid genome (bacteria, such as *Escherichia coli* and *Salmonella typhimurium*). In each diagram, 1 and 2 are different mutations, and + stands for the corresponding nonmutated sites.

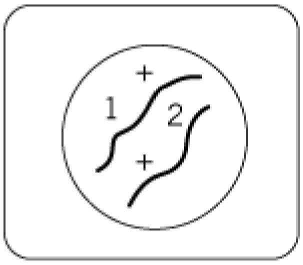

(a)

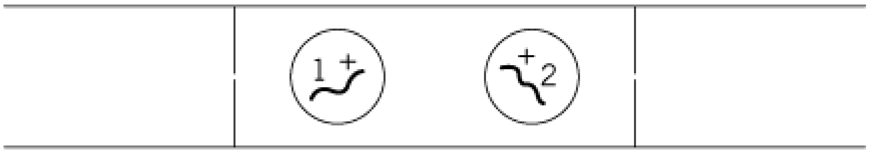

(b)

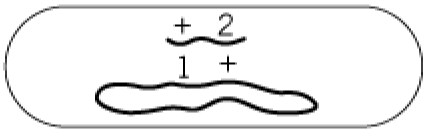

(c)

1. Complementation Tests in Diploids

The most extensive complementation testing using diploids has been carried out in the budding yeast *Saccharomyces cerevisiae* and the fruit fly ***Drosophila*** *melanogaster*. These are the diploid organisms that have most experimentally induced mutants sorted into genes.

Saccharomyces has the great advantage as an experimental organism of propagating itself equally well as a haploid or a diploid. Haploid cells are of two different mating types, called *a* and a. In wild strains, the cells are constantly interconverted by a genetic switching mechanism but are stabilized in nonswitching laboratory strains. Most yeast genetics is based on the use of **auxotrophic** mutants that grow only if given some specific nutritional supplement which they can no longer synthesize—most commonly an amino acid, a **purine** or **pyrimidine** base, or a vitamin. Such mutants can be readily obtained in haploid strains. For comprehensive complementation testing, it is necessary to isolate each mutant in both mating types from a cross to wild type. Then haploid cells of pairs of mutants of opposite mating types are mixed at marked positions on plates of unsupplemented agar growth medium. Sexual fusion to form diploid cells occurs almost immediately, and the diploids grow if the two mutations complement each other's nutritional deficiencies. The result is quite clear after overnight incubation. Auxotrophs that have different nutritional requirements always complement, but mutants that have the same requirement may or may not do so because several different genes acting in sequence are usually necessary to synthesize a single end product. The results split the mutants that have a common requirement, say, for the amino acid histidine, into clear-cut complementation groups - *his1*, *his2*, *his3*, etc. Every member of one group complements every members of any other group, but only sporadic and fairly infrequent complementation occurs within groups (see Interallelic Complementation). In general, complementation groups equate to genes, and each one is deficient in one enzyme of the biosynthetic pathway.

In the fruit-fly, *Drosophila melanogaster*, which is certainly the most intensively investigated multicellular organism, many mutants have been assigned to allelic series based on the mutant phenotypes of their heteroallelic combinations. The famous example of multiple alleles of the *w* (white-eye) gene is referred to under Complementation. Most of the allelic series have consisted of viable mutants, all within the same short chromosome segment, and obviously related phenotypes that made their allelic relationship are very likely even without complementation testing. However, nonvisible mutations, **recessive lethals**, have been much used in attempts to establish the total number of genes that have essential functions residing within a particular chromosome segment. Complementation is the only guide for classification of lethals.

A broadly applicable experimental scheme is shown in Fig. 2. The method is selecting, after heavy mutagenization, a large number of **recessive lethal** chromosomes based on their failure to complement a deletion of a short, defined chromosome segment, and maintaining them in breeding stocks combined with a "balancer" chromosome. A *Drosophila* balancer chromosome carries a dominant viable mutation to show that it is present and a recessive lethal mutation to ensure that any fly that carries it also has the chromosome against which the balancer is supposed to be balanced. The balancer chromosome also contains an inverted segment, or complex of inverted segments, to inhibit its recombination with the mutagenized chromosome, or else has genetic markers to ensure that recombination within the mutagenized region can be avoided. Crosses between flies that have different recessive lethals, each in combination with the same balancer, produce a predicted one-third of their progeny free of the balancer, if the two are in different genes and therefore complement one another, but no progeny without the balancer if they are in the same gene.

Figure 2. The isolation of recessive lethal mutations in *Drosophila* and testing them for complementation. (**a**) Male flies treated with a mutagen and mated to females carrying a balancer third chromosome that has the marker mutations *Sb* (do bristle phenotype, recessive lethal) and *e* (recessive ebony body colour). Flies in the next generation that have mutageniz chromosome 3 covered by the balancer, are crossed to flies that have a third-chromosome deletion and the *e* marker, bala against *Sb*. If the mutagenized third chromosome has a recessive lethal mutation (x) at a site within the deletion, there ar viable progeny that do not carry *Sb*. Then, the recessive lethal is present, balanced against the *Sb* chromosome in all viab progeny that are not ebony (*e*/*e*). (**b**) When *1*/*Sb* and *2*/*Sb* flies are crossed (*1* and *2* are two different lethals), one-third o viable progeny should be wild type (without *Sb*) if *1* and *2* are in different complementation groups (equivalent to genes) exhibit *Sb* if *1* and *2* are in the same complementation group. Based on Ref. 1.

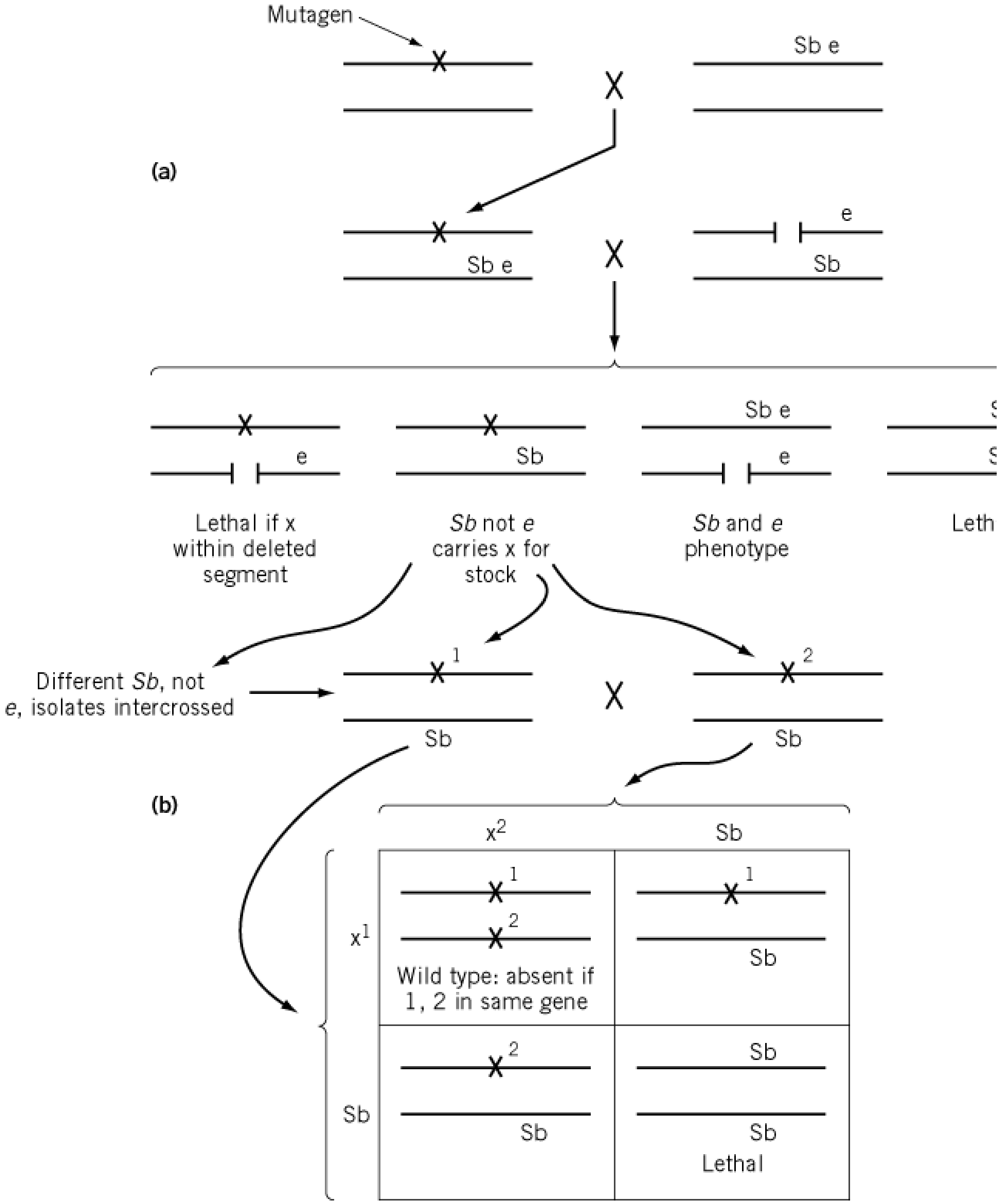

In the study on which Fig. 2 is based (1), a total of 268 recessive lethals that fall within a segment of chromosome 3 comprising 26 polytene chromosomal bands could be assigned to 25 complementation groups. The numbers were sufficiently great to make it likely that most, if not all, of the genes that have essential functions and therefore can mutate to recessive lethality had been identified. The gene number was probably underestimated because there are certainly genes that can be deleted without lethality. Nevertheless, the agreement between chromosome band number and the apparent number of essential genes (now found in several different experiments) is too close to be without significance.

2. The Use of Heterokaryons

Filamentous fungi, or at least those (eg, ***Neurospora*** *crassa*, ***Aspergillus*** *nidulans*) that have been well studied genetically, are naturally haploid except for the immediate product of sexual fusion, which immediately undergoes meiosis to provide nuclei for haploid **spores**. In *Aspergillus*, however, rare vegetative diploids are obtained by selection (2). In *Neurospora*, where this is not possible, complementation tests are easily carried out with haploid heterokaryons, mixed cultures in which the filamentous hyphae have undergone fusions to bring the two different kinds of haploid nuclei together in the same cytoplasm (3).

For heterokaryon formation, *Neurospora crassa* strains have to be of the same mating type, and identical with respect to a number of other genes governing vegetative compatibility. These requirements are automatically met if the mutants under test have all been isolated in the same wild-type strain, as is usually the case. Given vegetative compatibility, fusions occur readily as soon as mixed mutant inocula of conidia (asexual spores) begin to germinate. *Neurospora* filaments (hyphae) are coenocytic. Numerous nuclei are present together in each cytoplasmic compartment, and the nuclear ratio in a heterokaryon is quite variable but is determined at least approximately by the ratio of the two kinds of conidia in the initial mixed inoculum. The nuclear ratio is, in fact, not usually critical. If, as is usually the case, the mutants under test are auxotrophic (ie, have special nutritional requirements) and the mixed inoculation is on a minimal medium on which neither mutant grows by itself, the heterokaryon grows vigorously if the mutants complement one another.

At least in *Neurospora*, different genes can complement each other perfectly efficiently in heterocaryons even though they are separated in different nuclei. This is not at all surprising. Genes act, after all, by exporting their messenger RNA to the **cytoplasm**. Reports indicate that complementation in *Aspergillus* is more efficient in diploids than in heterokaryons, but one suspects that this is because, in this fungus, the different nuclear types are not sufficiently closely intermingled. A large number of *Neurospora* auxotrophic mutants have been efficiently classified into complementation groups, equivalent to genes, by heterokaryon testing. An example is shown in Fig. 3 (4).

Figure 3. The result of complementation tests by heterokaryon formation on 46 *Neurospora* mutants that cannot utilize acetate. Nearly all possible pairwise mixtures of mutant conidia were inoculated into a medium containing acetate as the sole carbon source. Growth occurred only if the mutants showed complementation. In the matrix shown, the mutants, designated by their original isolation numbers, are divided into seven different complementation groups. All intergroup combinations showed complementation and grew like wild type. Most or all combinations within a group did not grow. The growth shown by a few pairs of mutants within group 6 is evidence for *inter* **allelic complementation**. From Ref. 4.

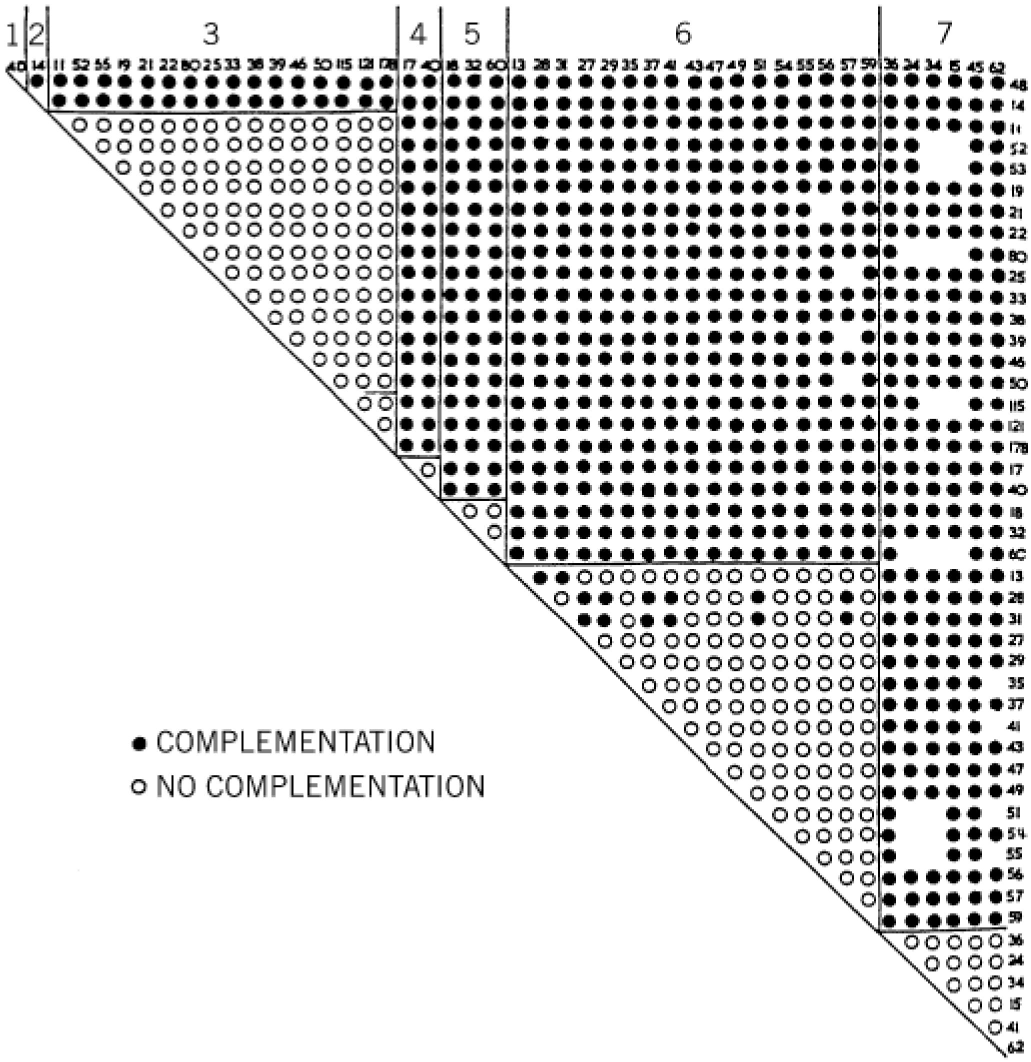

Humans, of course, are diploid, but complementation testing by controlled sexual crossing is obviously out of the question. Here again, heterokaryosis may provide an alternative, and cells in culture may serve as surrogates for people. One good example is an analysis of the human *xeroderma pigmentosum* syndrome, caused by genetic deficiency in DNA repair (5). Cultured cells isolated from different patients were induced to fuse by treating them with heat-inactivated Sendai virus. Complementation in the resulting heterokaryotic cells was assessed by their ability or inability to incorporate a radioactive precursor into their DNA following damage by UV light. The results permitted assigning the different mutations to four different complementation groups, putatively different genes (Fig. 4).

Figure 4. The use of heterokaryosis for complementation testing of cultured cells from human Xeroderma Pigmentosum (XP) patients (5). The syndrome that is excessive sensitivity to uv light is a consequence of failure to repair damaged DNA by excision followed by new synthesis. (**a**) Cultured fibroblasts from different patients were mixed and induced to undergo fusions. The resulting cells, some now heterokaryotic, were irradiated and cultured in the presence of tritiated **thymidine** to see whether they responded to the DNA damage by incorporating this radioactive DNA precursor into their nuclei. The original XP mutant cells, or noncomplemented heterokaryons, incorporated no tritium, but certain pairs of mutant cells showed complementation. (**b**) The complementation matrix with the division of 12 XP mutations into four complementation groups A-D. Here the cells are diploid and homozygous for the different mutations instead of haploid as in the *Neurospora* example (Fig. 3), but the principle is the same. +, complementation; 0, no complementation; –, test not done.

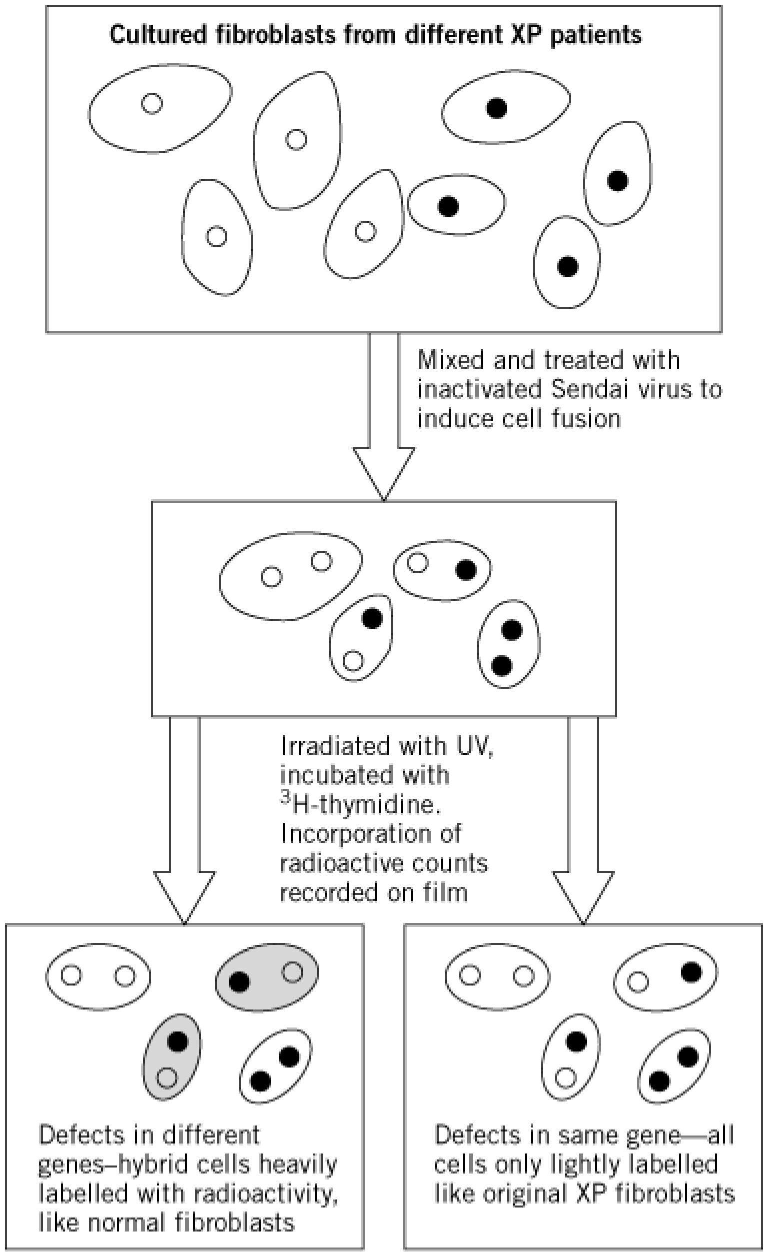

(a)

	A 1	A 2	A 3	B 1	C 1	C 2	C 3	C 4	C 5	D 1	D 2	D 3
A 1	0	0	0	+	+	+	+	−	+	+	−	+
A 2		−	0	+	+	+	−	−	−	+	−	+
A 3			0	+	+	+	+	+	+	−	+	+
B 1				0	+	+	+	+	+	+	+	+
C 1					0	0	0	0	0	+	+	+
C 2						0	0	0	0	+	−	+
C 3							0	0	0	+	−	+
C 4								−	0	−	+	−
C 5									0	+	+	+
D 1										0	0	0
D 2											−	0
D 3												0

(b)

2.1. In Viruses by Mixed Infection

S. Benzer's very extensive complementation testing of bacteriophage T4 mutants (see also Complementation) depended on infection of bacterial cells with mixtures of phage particles (6). Mixed infection is analogous to heterokaryosis because two different whole genomes are present in a somewhat indeterminate ratio, but the difference is that the simple viral genomes are not enclosed in **nuclei**. The mutants under study (class *rII*) were distinguished by growing on one *Escherichia coli* strain (B) but not on another (K). Complementation between pairs of mutants was checked by superimposing *rII* phage inocula on lawns of K cells, usually with a small admixture of B cells to allow at least some viral propagation. Three results were clearly distinguished: (1) complementation of the two mutants—total clearing of the mixedly infected patch due to lysis of all the cells in that area; (2) no complementation, but some formation of wild-type phage by recombination during mixed growth, shown by scattered spots of lysis; and (3) much less commonly, neither complementation nor recombination—no lysis at all (Fig. 5**a**). These results were interpreted to mean that (1) mutant sites are in different cistrons (ie, different functional genes); (2) mutants are at different sites in the same cistron; and (3) mutants are at the same site, or one is a deletion overlapping the other. The complementation results split the *rII* mutants cleanly into two mutually complementing groups or cistrons. Recombination analysis using a set of overlapping deletion mutants showed that these two cistrons correspond to two adjacent, nonoverlapping segments of the phage “chromosome”, which is not actually a chromosome in the cytological sense but a single molecule of **double-stranded DNA**.

Figure 5. Two examples from bacteria of complementation tests that distinguish between complementation and recombi (**a**) Testing for complementation between *rII* mutants of bacteriophage T4. These mutants grow well in *Escherichia coli* B but not at all in strain K12(l). Mixed infections on a lawn of K cells that have a minor admixture of B cells to permit s joint growth give total clearing (lysis) if mutants *rII-1* and *rII-2* are in different genes (cistrons), and lysis only in spots b of recombination, if they are at different sites in the same gene. Based on Ref. 6. (**b**) Abortive transduction as a criterion complementation in *Salmonella typhimurium*. Phage P22 grown on histidine-requiring (*his-*) mutant 1 was used to infect mutant 2. Surviving bacteria were tested for their ability to grow on a histidine-free medium. Rather numerous tiny (abo colonies showed that a nonreplicating fragment of DNA from mutant 1 complements mutant 2. The absence of such tiny colonies signifies no complementation. In either case, vigorously growing colones arise by recombination between the b chromosome and the incoming fragment, provided that 1 and 2 are at different sites. Based on Ref. 7.

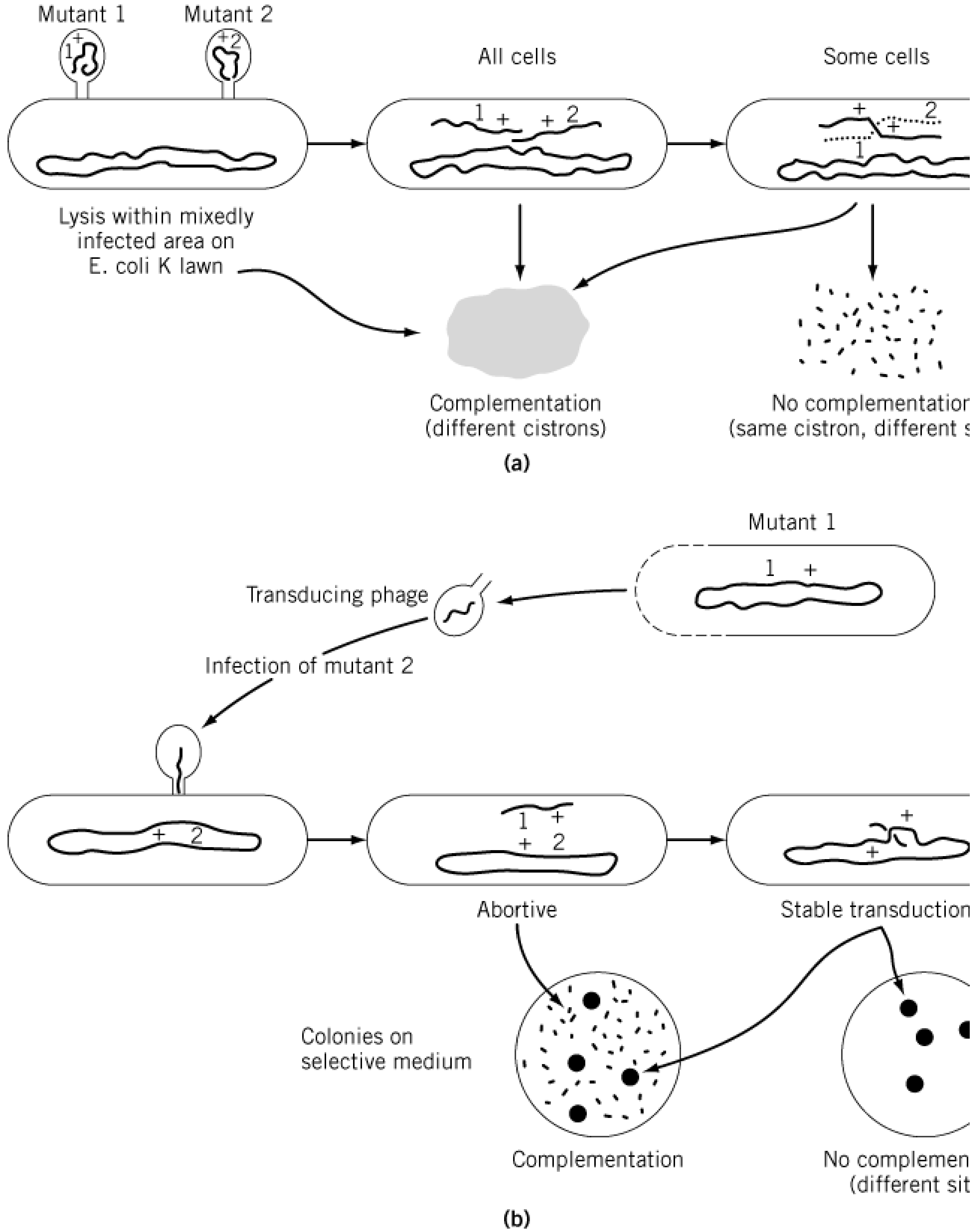

2.2. By Partial Diploids (Merodiploids) in Bacteria

It is not possible to test in bacteria for complementation between whole genomes because, at least in those species that are well-analyzed genetically, there is neither a stable diploid phase nor any sexual process that transfers a whole genome from one cell to another. However, bacteria acquire extra genomic fragments in three general ways: (1) by infection with defective bacteriophages which, “by mistake", have picked up bacterial DNA (**transduction**); (2) by joining a fragment of bacterial DNA to the DNA of a plasmid that brings about its own intracellular transfer (**conjugation**); and (3) by uptake of free DNA (transformation). The first two methods have been important in complementation analysis.

Transduction has been the principal means of classification and mapping of auxotrophic mutants of the bacterium *Salmonella typhimurium*. Bacteriophage **P22** grown on one mutant strain (the donor) is used to infect a second mutant strain, perhaps requiring supplementation with the same nutrient, such as an amino acid. Most of the infected bacteria are lysed, but some survive, are now lysogenic, and harbor the phage in latent form (see Lysogeny). Some survivors have acquired some fragment or other of the genome of the donor bacterium by infection from defective bacteriophage. The donor DNA is replicated in the recipient cell only if it recombines into the recipient chromosome and replaces the equivalent recipient segment. More commonly the donor DNA persists without replication, and its genes are expressed only in the primary recipient cell and in a few surrounding cells by diffusion of gene products. The appearance of tiny colonies of cells (abortive transductants) that grow transiently without the nutritional supplement, demonstrates complementation between the recipient genome and the donor genomic fragment. Usually a much smaller number of large strongly growing colonies results from chromosomal integration of a donor fragment and recombination between donor and recipient mutational sites to reconstitute a wild-type gene. The presence of large colonies without abortive ones shows that the mutations are at different sites within the same gene or cistron (Fig. 5**b**). Failure to form any colonies at all means (apart from possible experimental error) that the two mutations are at the same site or that one is a deletion overlapping the other (7).

The plasmid that is used to bring about partial diploidy in *E. coli* is the transmissible "sex factor" F, a closed-loop DNA molecule that replicates autonomously in the bacterial cell and is occasionally integrated by **crossing-over** into the much larger loop of the bacterial chromosome. The integrated plasmid DNA undergoes occasional excision, usually precisely, but sometimes carries with it an adjacent segment of bacterial DNA, the nature of which depends on where the plasmid happened to have been inserted. This modified F is called F′ and, like F itself, is transmitted from cell to cell. F′-*lac* plasmids that carry segments of DNA from the lac operon of the bacterial chromosome, were of great importance in elucidating the complementation relationships of *E. coli lac* mutants (a topic dealt with separately under cis-dominance).

Bibliography

1. J. Gausz, H. Gyurovics, G. Beneze et al. (1981) Genetics **98**, 775–789.
2. J. A. Roper (1952). Experientia **8**, 14–15.
3. G. W. Beadle and V. L. Coonradt (1944) Genetics **29**, 291–308.
4. R. B. Flavell and J. R. S. Fincham (1968) J. Bacteriol. **95**, 1056–1062.
5. K. H. Kraemer, H. G. Coon, R. A. Petinga et al. (1975) Proc. Natl. Acad. Sci. USA **72**, 59–63.
6. S. Benzer (1959) Proc. Natl. Acad. Sci. USA **45**, 1607–1620.
7. P. E. Hartman, Z. Hartman, and D. Serman (1960) J. Gen. Microbiol. **22**, 354–358.

Complex Loci

In classical **genetics**, the word locus referred to a position on a chromosome marked by a **gene** difference that has a **phenotypic** effect. Neither the locus nor the gene were thought to be subdivisible by recombination, and so locus and gene were treated almost as synonyms. The idea of complex loci arose from examples, especially from *Drosophila* and **maize**, of different mutations, apparently at the same chromosome locus, that give a range of different phenotypic effects, suggesting that the locus harbors some rather complex kind of gene.

With our modern knowledge, the word locus can take either of two very different meanings. It may mean just the genetically mapped site of a mutation, which, at the molecular level, is quite likely to be no more than a single base-pair change within the long DNA sequence of a gene. But, in the context of complex loci, it can mean a relatively short chromosomal segment (not frequently split up by genetic recombination) that contains a cluster of genes among which there is some functional connection. So complex loci, though of somewhat confused etymology, is a useful heading under which to review the evidence for chromosomal units of function at a level higher than that of the individual gene.

This article does not cover examples of loci that mutate to give various phenotype effects when the varied effects are due to mutations in a single gene that has multiple functions. Such genes that encode "multiheaded" enzymes (see Multifunctional Proteins) are sometimes called "cluster genes" in fungal genetics to distinguish them from the gene clusters with which they may initially be confused. Some examples are reviewed under **Allelic Complementation**. Nor are we concerned with single genes that have multiple modes of **intron** splicing, which yield alternative messenger RNAs (see examples under Gene Structure). And we obviously cannot include groups of functionally diverse genes that just happen to be very closely linked, for that would make virtually all genes parts of one complex locus or another. To qualify as a complex locus, in our present sense, a gene cluster must have some kind of unity in structure, in function, or in both.

Gene clusters that fulfil this criterion have been found in **fungi**, flowering **plants**, *Drosophila* and mammals, and this article reviews examples from each of these kinds of organisms. We do not deal here with **bacteria**. Operons, which might be viewed as complex loci but are not usually so termed, are dealt with under their own heading. Also excluded from this article are highly repetitious tandemly arrayed genes required by the cell in very high dosage. The preeminent example is **ribosomal** RNA genes in the **nucleolus organizer** chromosomal regions of eukaryotes. Histone genes are also highly repetitive and are concentrated in clusters in some organisms, including *Saccharomyces* yeast. This is arguably more repetition than complexity.

1. Fungi

In fungi, the self-incompatibility and cross-compatibility in sexual mating in many species is determined by **mating-type** loci, which virtually always consist of more than one gene. A relatively simple example is the maize smut fungus, *Ustilago maydis*, whose two loci, *a* and *b*, control the specificity of sexual fusion and the formation of an invasive dikaryotic mycelium after fusion, respectively. The *a* locus has two "**alleles**," *a1* and *a2*, each of which consists of two genes, one that encodes a polypeptide pheromone and the other a pheromone **receptor**. The *a1* pheromone is recognized by the *a2* receptor and the *a*2 pheromone by the *a*1 receptor. There is no close homology between *a1* and *a2*, and they do not recombine with each other. The *b* locus exists in numerous alternative forms. Each consists of two closely spaced, divergently transcribed genes called *bE* and *bW* that encode the two components of a dimeric transcriptional activator. But dimerization occurs only between *bE* and *bW* products of different mating types (1).

The ink-cap mushroom fungus, *Coprinus cinereus* (like *Ustilago*, a member of the Basidiomycete class), also has two mating-type loci, *A* and *B*. The *A* locus, which controls the ability to form a fruiting dikaryon, is the most thoroughly investigated. Here the situation resembles that at the *Ustilago b* locus, except that genes that encode dimerizing monomers, thought to be transcriptional activators on the basis of their **homeobox**-like sequence motifs, are distributed in multiple copies between two subloci, *A*a and Ab, between which rare recombination occurs (2) (Fig. 1). Again, dimerization occurs only between the products of different mating types.

Figure 1. The structures of mating type loci in Basidiomycete fungi. (**a**) The *b* locus of *Ustilago maydis*. The *bW* and *bE* gene products form W-E protein dimers to activate transcription of genes necessary for sexual development. Each exists in multiple allelic forms. Effective dimers are not formed by W-E combinations from the same strain. Gene segments that encode homeodomain-like protein sequences are filled. (**b**) The archetypal *A* mating type locus of *Coprinus cinereus*. The system works in principle as in the *Ustilago b* locus, except that here there are four pairs of genes, *a*, *b*, *c*, and *d*, any one of which can function in promoting fertility. The archetype is a composite of known mating-types, all of which are missing one or another part of it. From Refs. 1 and 2 by permission.

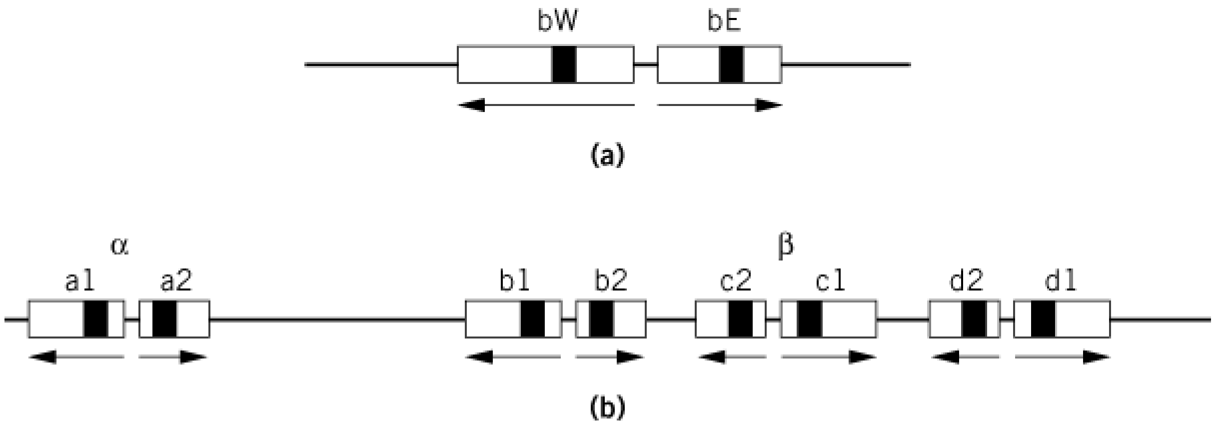

Ascomycete fungi, such as *Neurospora crassa* and *Saccharomyces cerevisiae*, simpler than Basidiomycetes, have only two mating types (*A* and *a* in *Neurospora, a* and a in *Saccharomyces*), but the genetic loci that determine them are still complex. *Neurospora A* contains three genes (Fig. 2) and *Saccharomyces* a contains two, though each of the *a* mating-type loci has only a single gene. The two alternative mating-type loci in both organisms are completely nonhomologous, and the same is true for the *Ustilago a* locus. It has been customary to call the alternative occupants of these mating-type loci "alleles," but in the light of present knowledge this terminology is inappropriate because it implies different forms of a single gene. The new word idiomorphic has been suggested for the relationship between quite different genes or gene clusters that are alternative occupants of the same locus (3). Much the same applies to the yeast mating-type system that has the additional complication of mating-type switching.

Figure 2. The mating type loci of the Ascomycete fungus *Neurospora crassa*. *A1* and *a1*, quite unrelated in sequence, act in a complementary way to permit sexual reproduction. *A2* and *A3* function in postfertilization fruiting-body development. From Ref. 3 by permission.

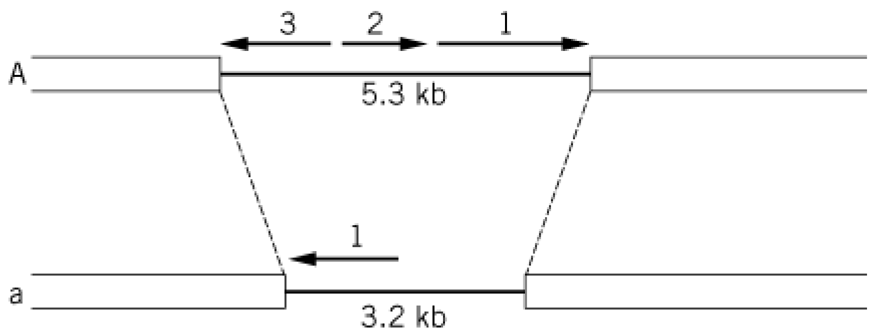

Fungi also provide examples of another kind of locus complexity, the tight clustering of separate genes that co-operate in a particular area of metabolism. The *Neurospora crassa Qa* cluster is a particularly good example (Fig. 3). Here a DNA segment of only 18 kbp harbors seven different genes, the transcription of which is increased 50- to 1000-fold when the fungus is forced to grow using quinate as a sole carbon source. Three of these genes encode the three enzymes that, acting in sequence, oxidize quinic acid to protocatechuic acid. Two genes encode regulatory proteins that control the transcription of the whole cluster. One gene is a transcriptional activator and the other a repressor that cancels the function of the activator but whose own effect is nullified by binding to quinate. The remaining two genes have no identified function and are recognized solely as **open reading frames** (4). The significance of the gene clustering is not fully understood, but it seems plausible to suggest that derepression of transcription is facilitated by an induced unfolding of **nucleosomal** structure that extends across the entire complex.

Figure 3. The *Qa* (quinate-utilization) gene cluster of *Neurospora crassa*. The genes *qa-3, qa-2*, and *qa-4*, respectively, encode quinate dehydrogenase, catabolic dehydroquinase, and dehydroshikimate dehydratase, which act sequentially to degrade quinate. *qa-1S* and *qa-1F* encode regulatory proteins, that respectively repress and activate transcription of the whole cluster. *qa-Y*, it is thought, encodes a quinate transporter protein, and *qa-X* has no known function (4).

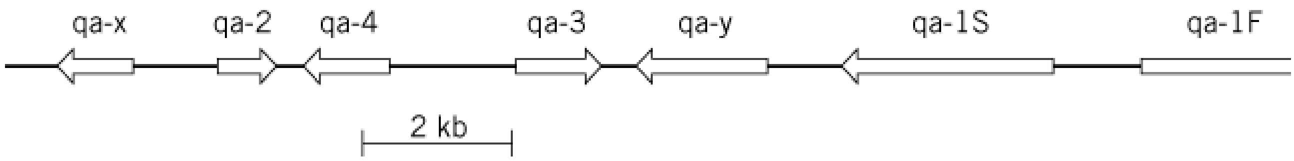

2. Flowering plants

A long-standing example from what used to be, pre-*Arabidopsis*, the geneticists' favorite plant, is the *R* locus of *Zea mays* that is necessary for pigmentation and encodes transcriptional activators for genes that encode pigment-synthesizing enzymes. It was an early example of locus complexity because it has two independent functions. Some recessive loss-of-pigment alleles affect only the red color in the plant whereas others affected only the seed. Analysis at the DNA level has revealed the situation shown in Fig. 4 (5). The *R* locus contains three genes. One gene (*P*) is specific for plant pigment, and the other two (*S1*, *S2*) apparently duplicate the function in seeds. Presumably their distinct tissue specificities are due to different promoter/**enhancer** sequences. There is also a partial and presumably functionless duplication of *P*. An origin by **duplication** and subsequent partial **divergence** of function is the most obvious explanation for the clustering of these functionally related genes, although the opposite orientations of *S1* and *S2* are a puzzle.

Figure 4. The complex *R* locus of *Zea mays*. *P* controls red pigment synthesis in the plant generally and the duplicate *S* genes in the seed. *S1* and *S2*, transcribed divergently, are each similar to *P* except that they lack the segment shown hatched. This segment is present as a tandemly duplicated fragment, presumably nonfunctional. Sequence information suggests that this scrambled arrangement is due to the activity of a transposable element (5). “Alleles” of *R*, R^g (red seed, green plant), and r^r (colorless seed, red plant) are, respectively, due to loss of *P* and *S* function. The *P* and *S* components can be separated by meiotic crossing over at frequencies on the order of 10^{-4} to 10^{-3}.

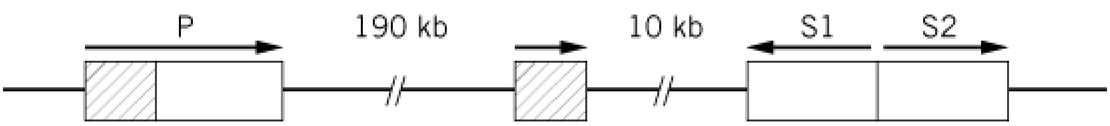

A long-standing problem in plant biology has been the various systems of self-incompatibility, often controlled by what are multiple alleles at a single locus, usually called *S*. The general principle is that pollination is prohibited if the pollen grain and stigma (or, in the *Brassica* family, the pollen mother cell and stigma) have an allele in common. The *Brassica S* locus, one of the best analyzed, contains two genes, each present in the population in multiple allelic forms, that control the incompatibility response of the stigma. A third S locus gene, expressed in the pollen and determining pollen specifity, has also been identified (6). Here, as in the analogous self-incompatibility in fungi, the functional reason for the multiple genes all in the same locus is obvious. For the system to work, the different specificities have to be mutually exclusive in the haploid genome.

3. Drosophila

In the fruit fly, *Drosophila melanogaster*, a classical example of locus complexity, perhaps originally generated by tandem duplications, is provided by the scute (*sc*) and achaete (*ac*) families of mutations (7, 8). These affect the bristles in the wings and mid-thorax of the fly, really parts of the fly's neural system, the origin of which can be traced back to the transcription of scute and achaete, usually both together but sometimes one more than the other, in rather precisely positioned bristle mother cells in the wing imaginal disc of the larva. It seems that *sc* and *ac* largely duplicate each other's functions and, before molecular analysis, the basis for recognizing two different genes was not clear. Different mutations in the *sc/ac* locus eliminate different bristles or different combinations of bristles, and, to the extent that their effects are nonoverlapping, complement one another in *trans*. Now that the *sc/ac* locus has been analyzed at the DNA level, it is seen that there are six genes within the approximately 100 kbp that comprise the *sc/ac* complex (7, 8) (Fig. 5), of which at least four are involved with the neural/bristle system. *sc* and *ac* apparently have the major roles. Most of the mutations that affect the positioning of bristles actually fall between the genes. Several are chromosomal rearrangements that have breakpoints within the *ac/sc* complex, and it is thought they exert their effects by separating *ac* and/or *sc* from enhancer sequences, several of which have been identified in the *sc/ac* region. The patterns of transcriptional activation of *sc* and *ac* and hence the positioning of bristles, it is thought, reflect the distribution of a number of enhancer-binding proteins, the identity of which remain to be established. The genes and the enhancers together may be seen as an integrated system for responding to a pattern of positional information set by the products of other genes.

Figure 5. The *scute-achaete* (*sc/ac*) complex at the tip of the *Drosophila melanogaster* X-chromosome. Genes that have functions in neural/bristle development are shown as filled arrows, and other genes, apparently unrelated in function, as (arrows (*y* = *yellow*). Thin vertical arrows indicate the breakpoints of segmental rearrangements that affect the bristle phe (*sc*^{6} is a deletion). Regions that include enhancer sequences are shown hatched. The different bristle phenotypes are beli be due to separation of *sc* and/or *ac* from enhancers. Redrawn and simplified from Ref. 8 by permission.

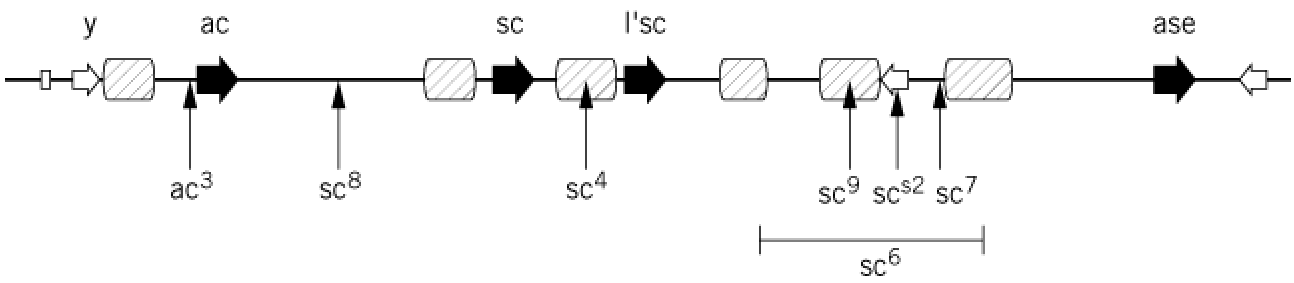

4. Mammals

Many clusters of related genes have originated through tandem duplication and subsequent functional divergence. Obvious examples are the globin gene clusters in animals and humans (see under Globins, Gene Structure). The b-globin gene cluster has a common ancestral origin and is also functionally integrated through the locus control region.

The clustered **HOX genes**, which are of profound importance in animal development and encode homeobox-containing proteins, were discovered in mammals and now in other animal groups through their significant similarities to the genes of the linked *bithorax* and *Antennapedia* complexes of *Drosophila*. Five unlinked clusters of HOX genes in mouse and humans each consist of up to 13 tandemly arranged genes within a region on the order of 100 kbp of DNA. Through their homeobox-encoding segments, the genes of one cluster have only a very limited degree of sequence similarity to each other but have a greater resemblance to genes in corresponding positions in other clusters in the same species or even in different species. Because they were not identified through the classical genetic route of mutation mapping, the HOX clusters of mammals are not usually called loci though, confined as they are within chromosomal segments that correspond to a small fraction of a **centimorgan**, they are sufficiently tightly linked to qualify for that title, and they also fulfil the criterion of functional integration. The almost uncanny correspondence between the linear sequence of genes within each cluster and the anterior-posterior order of the body segments that the genes affect clearly indicates some function for the clustering and ordering of the genes, though this is still mysterious.

The mammalian major histocompatibility complex (MHC), intensively investigated in mouse, and its human equivalent the human leucocyte antigen (HLA) complex, is encoded by genes spread over rather too large a section of chromosome to be called a locus. Indeed, the positions of individual antigen-encoding genes within it are themselves often called loci. In humans it encompasses about four megabases of DNA and 3 to 4 centimorgans. But it may be regarded as at the upper end of the size range of clusters of functionally related genes, and so it is relevant to mention it here. A diagram showing of the structure of the complex, and its scale in relative to the whole chromosome is shown in Fig. 6. Because there is significant homology among the different genes, at least within each of the two main subclusters, the close linkage is likely to be due to duplication by short-range transposition and subsequent diversification. But it may also have been maintained by natural selection, because their continued coupling is advantageous if certain combinations of alleles of different genes confer disease resistance (10).

Figure 6. The arrangement and spacing of genes within the major histocompatibility complex (MHC) of mouse. Class I genes encode transplantation antigens mediating graft rejection (K, D, L), or other cell-surface antigens (Qa, Ti). Class II genes encode antigens involved in the immune response. Class III genes encode components of the complement system. Meiotic recombination within the complex is infrequent but not very rare (genetic map distances are shown in centimorgans, cM). After Ref. 9 by permission.

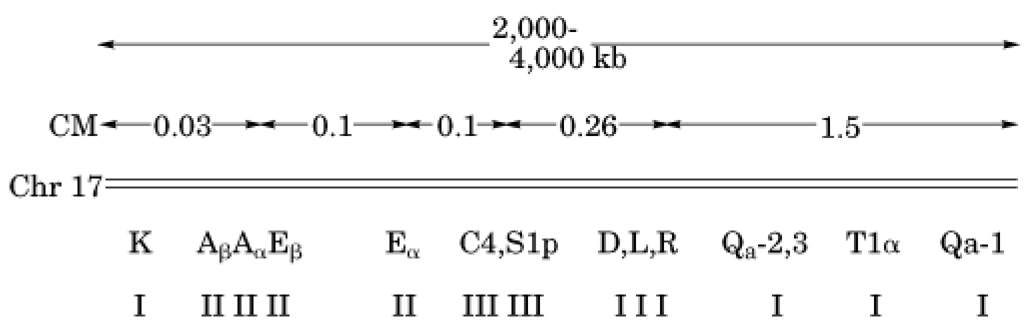

An entirely different kind of complex locus is involved in determining hypervariable proteins of the mammalian immune system, immunoglobulins and T-cell receptor proteins. These are not really gene clusters but rather banks of gene components that are assembled by DNA splicing reactions in a large number of different ways to provide coding sequences for proteins of almost any required specificity. In mammals, as exemplified by mouse, there are six known rearranging complexes of the mouse immune system, three (heavy-chain and two light-chain) for immunoglobulin components and three (a, b and g polypeptides) for T-cell receptor components. A diagram to scale of the completely sequenced human b-chain locus that extends over 600 kb is shown in Fig. 7 (11). Here the functional reason for clustering is obvious. It is only surprising that the sequences destined to be spliced together are as widely separated as they are. Presumably they are brought close during the splicing process by the formation of some very extensive DNA loops.

Figure 7. The arrangement and spacing of the part-genes which, when appropriately spliced together, encode b-chains of the human T-cell receptor. Splicing of DNA during T-cell differentiation brings together one C “constant”, one J (“junction”), one D (“diversity”), and one V (“variable”) sequence to encode a large number of alternative b-chains. J on the map stands in each case for six or seven short alternatively used junction sequences. The other marked elements are all single units. All are transcribed/translated from left to right, except for the rightmost V which is inverted and doubtfully functional. The splicing occurs in stages, first D to J, then DJ to V, and finally VDJ to C. The diagram has been simplified by omitting the pseudogenes and incomplete V sequences, which approximately equal the functional genes in number and are interspersed among them. T = trypsinogen gene, the presence of which, in multiple copies, within the b-chain complex, has uncertain functional significance. After Ref. 11 by permission.

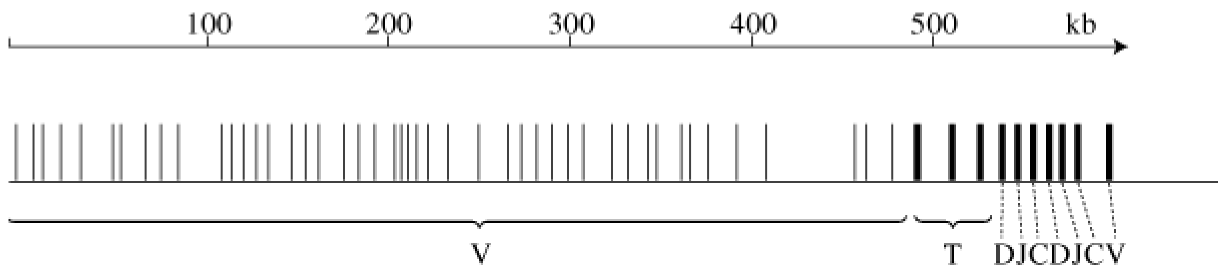

Bibliography

1. F. Banuett (1992) Trends in Genetics **8**, 174–180.
2. E. H. Pardoe, S. F. O"Shea, and L. S. Casselton (1996) Genetics **144**, 87–94.
3. N. L. Glass and M. A. Nelson (1994) In *The Mycota I.* (J. G. H. Wessels and F. Meinhardt, eds.), Springer-Verlag, Berlin, pp. 295–306.
4. R. F. Geever, L. Huiet, J. A. Baum, B. M. Tyler, V. B. Patel, B. J. Rutledge, M. E. Case, and N. H. Giles (1989) J. Mol. Biol. **207**, 15–34.
5. E. L. Walker, T. P. Robbins, T. E. Bureau, J. Kermicle, and S. L. Dellaporte (1995) EMBO J. **14**, 2350–2363.
6. C. R. Schopfer, M. E. Nasrallah, and J. B. Nasrallah (1999) Science **286**, 1697–1700.
7. S. Campuzano and J. Mondolell (1992) Trends in Genetics **8**, 202–207.
8. J. L. Gomez-Skarmeta, I. Rodriguez, C. Martinez, J. Culi, D. Ferres-Marco, D. Beamonte, and J. Mondolell (1995) Genes Dev. **9**, 1869–1882.
9. L. Hood, M. Steinmetz, and B. Malissen (1983) Annu. Rev. Immunol. **1**, 529–568.
10. I. P. M. Tomlinson and W. F. Bodmer (1995) Trends Genet. **11**, 493–498.
11. L. Rowen, B. F. Koop, and L. Hood (1996) Science, **272**, 1755–1762.

Compressibility

Compressibility is an important measure of the atomic packing and flexibility of protein molecules. Measurement of this quantity is possible, in principle, only for proteins in solution. The partial specific compressibility of a protein in solution b is defined as the change in the partial specific volume v_2^0 with increasing pressure. Since the atomic van der Waals volume, v_c, may be assumed to be incompressible, the experimentally determined b of a protein can be mainly attributed to its cavities v_{cav}, and to changes in hydration Dv_{sol}:

$$\bar{\beta} - (1/\bar{v}_2^0)(\partial \bar{v}_2^0/\partial P) = -(1/\bar{v}_2^0[(\partial v_{cav}/\partial P) + (\partial \Delta v_{sol}/\partial P)] \qquad (1)$$

(see Partial Specific (Or Molar) Volume). The first term on the right-hand side contributes positively, and the second term negatively, to b. Thus, a positive b value can be ascribed to a large cavity effect overcoming the hydration effect. There exist two types of compressibilities, depending on the experimental conditions: adiabatic and isothermal. Most compressibility studies of proteins have been of adiabatic compressibility because of its accuracy and technical convenience.

1. Adiabatic Compressibility

The partial specific adiabatic compressibility b_s is calculated with the Laplace equation, $b_s = 1/u^2d$, where u is the sound velocity and d the density of the protein solution. The sound velocity is usually measured with an accuracy of 1 cm sec^{-1} by using a resonance or sing-around pulse method at 3 to 6 MHz. All amino acids show large negative b_s, with values between -62.5×10^{-12} cm^2 dyn^{-1} (for glycine) and -21×10^{-12} cm^2 dyn^{-1} (for tryptophan) at 25°C, because they have a negligibly small amount of cavity. Data for b_s have been reported for about 40 different proteins; some values in water (or in dilute buffer at neutral pH) are listed in Table 1. Fibrous proteins show negative b_s, indicating the dominant effects of the surface on hydration relative to internal cavity volume. On the contrary, most globular proteins have positive b_s, due to the large contribution of the internal cavities overcoming the hydration effect. This is consistent with the fact that more than 50% of the total surface area is buried in the interior of a folded protein molecule.

Table 1. Partial specific volume (v_2^0), compressibility (b_s and b_T), and volume fluctuation (dV_{rms}) of proteins in water at 25°C (1, 4)

Protein	**v_2^0 (cm^3 g^{-1})**	**b_s (10^{-12} cm^2 dyn^{-1})**	**b_T[a] (10^{-12} cm^2 dyn^{-1})**	**dV_{rms}[b] (cm^3 mol^{-1})**
		Globular proteins		
Cytochrome c	0.725	0.07	4.27	30.8 (0.34)
Soybean trypsin inhibitor	0.713	0.17	4.44	41.1 (0.20)
Trypsin	0.717	0.92	5.16	46.0 (0.28)
Ribonuclease A	0.704	1.12	5.48 (5)	36.2 (0.38)

Peroxidase	0.702	2.36	6.70	68.3 (0.24)
a-Chymotrypsin	0.717	4.15	8.32	62.2 (0.33)
Lysozyme	0.712	4.67	7.73 (12.3)	44.2 (0.43)
Carbonic anhydrase	0.742	6.37	10.5	76.0 (0.34)
a-Lactalbumin	0.736	8.27	12.4	56.9 (0.54)
b-Lactoglobulin	0.751	8.45	11.8	63.6 (0.46)
Myoglobin	0.742	8.98	13.1	64.1 (0.51)
Ovalbumin	0.746	9.18	12.1	101 (0.30)
BSA	0.735	10.5	14.6 (13.4)	135 (0.27)
		Fibrous proteins		
Gelatin	0.689	–2.5		
F-actin	0.720	–6.3 (20°C)		
Myosin	0.724	–18 (20°C)		
Tropomyosin	0.733	–41 (20°C)		

[a] The values in parentheses represent the experimental data; the other values were calculated with Equation 2 of the text.

[b] The values in parentheses represent the ratio (%) of dV_{rms} to the total protein volume.

Some assumptions are necessary for estimating separately the contributions of cavities and hydration to b_s. A rough estimation suggests that the intrinsic compressibility of globular proteins free from hydration is of the order of (10 to 20) × 10^{-12} cm^2 dyn^{-1}. This value is comparable to the adiabatic compressibility of normal ice, suggesting that an internal protein structure is as rigid as ice.

As can be seen in Table 1, the value of b_s varies over a wide range and is sensitive to the structural characteristics of individual proteins. For example, lysozyme has a considerably smaller b_s than does a-lactalbumin, in spite of their great similarities in primary and tertiary structures. However, the compressibility-structure relationships of proteins have been scarcely discussed on a molecular level, because of the complicated contribution of hydration. The contributions of some structural factors have been deduced by the statistical analyses of b_s data on globular proteins (Ref. 1). From the ratio of accessible surface area to volume, b_s would be expected to increase with increasing molecular weight, but there appears no definite correlation between b_s and molecular weight. Instead, a positive correlation is found between b_s and the partial specific volume. Hydrophobic proteins show large positive b_s, probably due to an enhanced imperfect packing of nonpolar residues localized in the interior of the molecule. Typical a-helical proteins, such as myoglobin and bovine serum albumin have very large b_s, even though the a-helix itself is rigid, predominantly nonhelical proteins, such as **trypsin** and soybean trypsin inhibitor, have small b_s. These results suggest that the a-helix could be a dynamic domain for the thermal fluctuation of proteins. Four amino acids (Leu, Glu, Phe, and His) show statistically a strong ability to increase b_s, whereas another four (Asn, Gly, Ser, and Thr) decrease it, although the meaning of this is obscure. A single amino acid substitution can bring about a noticeable change in b_s, probably due to modified atomic packing, even though it is rare to observe any visible changes in the tertiary structures of mutants by X-ray crystallography.

Adiabatic compressibility data for nonnative conformations and for unfolding processes, in combination with partial specific volume, also present useful information on the principles of protein structure that cannot be obtained by spectroscopic techniques. Unfolding of a protein with strong denaturants such as **guanidinium** chloride decreases the compressibility and specific volume, but it is known that the compressibility increases and the partial specific volume decreases on thermal and pressure denaturation.

2. Isothermal Compressibility

The volume fluctuations and the pressure-dependent properties of proteins are theoretically related to the partial specific isothermal compressibility b_T, rather than the adiabatic one b_s. To determine b_T, the solution density or partial specific volume must be measured as a function of pressure, under hydrostatic pressure or centrifugal force. Such an experiment is very difficult, however, and few b_T data are available for proteins, because high pressure may cause protein denaturation and modify preferential solvent interactions. Approximate values of b_T may be estimated from b_s by utilizing the relationship

$$\beta_T = \beta_s + \alpha^2 T / C_p d \tag{2}$$

if the thermal expansion coefficient a and the **heat capacity** at constant pressure C_p, are known or can be reasonably inferred. Such assumed b_T values are listed in Table 1, along with some experimental data. Despite many assumptions, the calculated values of b_T are not so very different from the experimentally observed ones. The value of b_T is greater than b_s by (3 to 4) $\times 10^{-12}$ $cm^2\ dyn^{-1}$; these differences are comparable to those found for the amino acids.

There are some other methods to evaluate the isothermal compressibility of proteins, although the value obtained is not a partial quantity in solution. Kundrot and Richard (2) reported 4.7×10^{-12} $cm^2\ dyn^{-1}$ for b_T of lysozyme by comparing its X-ray crystallographic volume at atmospheric pressure and 1000 atmospheres. Contraction of the molecule was distributed nonuniformly; one domain was essentially incompressible, but another had a large compressibility. Computer simulations, such as molecular dynamics, **Monte Carlo**, and normal mode analyses, are also available. Normal mode analysis of myoglobin yielded $b_T = 9.37 \times 10^{-12}$ $cm^2\ dyn^{-1}$.

According to statistical thermodynamics, the volume fluctuation dV_p of a protein with volume V_p is related to its isothermal compressibility b_T (Ref. 3):

$$\overline{\partial V_p^2} = kTV_p\beta_T \tag{3}$$

where k is the Boltzmann constant and T the absolute temperature. The root-mean-square fluctuation of the partial molar volume dV_{rms}, which was estimated by using b_T instead of b_T, is listed in the last column of Table 1. The volume fluctuation is only about 0.3% of the overall dimensions of protein, but the dV_{rms} values estimated by this method are the lower limit of the probable fluctuations, since the solvation factor is still included in the value of b_T that was used. If the intrinsic isothermal compressibility of a protein itself, which is not easy to determine, is used instead of b_T, a greater volume fluctuation (up to 50% greater) might be expected for a protein without hydration. Although many assumptions are used in estimating b_T and the fluctuation of volume, the values obtained are considered to be reasonable; if concentrated in one area at one particular moment, the fluctuation in volume could produce sufficient cavities or channels to allow the entry of solvent or probe molecules to account for phenomena such as hydrogen exchange and fluorescence quenching observed with folded proteins.

Bibliography

1. K. Gekko and Y. Hasegawa (1986) Biochemistry **25**, 6563–6571.
2. E. Kundrot and F. M. Richards (1987) J. Mol. Biol. **193**, 157–170.
3. A. Cooper (1976) Proc. Natl. Acad. Sci. U.S.A. **73**, 2740–2741.
4. K. Gekko (1991) In *Water Relationship in Food* (H. Levine and L. Slade, eds.), Plenum Press, New York, pp. 753–771.

Suggestions for Further Reading

5. A. P. Sarvazyan (1991) Ultrasonic velocity of biological compounds. Annu. Rev. Biophys. Chem. **20**, 321–342.
6. K. Gekko (1996) Hard proteins and soft proteins: Structural flexibility as revealed by compressibility. Protein, Nucleic Acid and Enzyme (*Tanpakusitu, Kakusan, Koso*, in Japanese) **41**, 2025–2036.

Computer Simulation of Biological Molecules

Biological molecules are systems of enormous complexity. This makes it exceedingly difficult to elucidate the details of biological activities using only experimental techniques. Despite enormous progress in structural studies of proteins, it is hard to determine uniquely how the particular function is determined by the given structure. A mathematical description of the energy of a macromolecule in terms of its atomic coordinates is, in principle, sufficient to predict relevant biological properties. However, such a description can only be handled by powerful computers. Having the proper model of a macromolecule should allow one to simulate its properties as if one is dealing with the actual molecule. Such an approach, called *computer simulation*, offers what is probably the best way of describing the function of macromolecules.

The relationship between the energy of molecules and the position of its atoms is called a potential function or a *force field*. A reasonable potential function provides the first step for modeling a molecule. In principle, one can obtain potential functions by using quantum mechanical methods that describe the entire molecule as a supermolecule. However, such methods are not yet practical for describing macromolecules. Some progress can be made using **hybrid QM/MM approaches**, but, in general, it is essential to use approximated potential functions whose parameters are based on empirical information (1-5).

Potential functions can be based on **all-atom molecular models** that describe the interactions between all the atoms of the given molecule or on **simplified models** where the forces due to several atoms are described by a single interaction center. Examination of molecular properties using the corresponding potential functions is known as molecular mechanics. This term is usually reserved for the use of **energy minimization** and **normal mode analysis** methods. The use of potential functions to solve the equation of motion of atoms is known as molecular dynamics (MD). This method gives the atomic position as a function of time and provides a powerful way of obtaining dynamical and time average properties. In some cases one can obtain useful insight by using **Brownian dynamics**. Frequently it is sufficient to know the properties of macromolecules at their minima. Generating starting configurations in the search for such minima can be done by **Monte**

Carlo methods Monte Carlo calculations and other sampling approaches. Apparently, the most important biological properties are reflected in most cases by thermodynamic properties and not dynamical properties. In particular the **Free Energy** provides the most important connection between structure and function, while the knowledge of the individual contributions to free energy from **enthalpy** and **entropy** is less critical for reproducing functional properties of macromolecules. The free energy of macromolecules can be evaluated by several approaches and, in particular, by the free energy perturbation (FEP) and linear response approximation (LRA) methods. Free energy calculations are frequently based on the use of **thermodynamic cycles** (3, 4, 6).

The potential functions that describe the energetics of macromolecules reflect different types of interactions. This includes **bonding** and van der Waals interactions that determine the steric properties of the given molecule and electrostatic interactions (that include hydrogen bonding and other **dipolar** and **ionic interactions**). The free energy of macromolecules is largely dependent on electrostatic energies, which reflect the effect of polar and ionized groups and its compensation by the polarization of the solvent around the protein (6, 7). These energies involve **long-range interactions,** whose accurate evaluation present a major challenge. Electrostatic energies can be modeled by using **implicit models** where the solvent molecules (and sometimes the protein dipoles) are represented implicitly. The use of a **dielectric constant** in an electrostatic model is a form of implicit model, and, in fact, the dielectric constant in many electrostatic models is not related at all to the true protein dielectric constant but to the properties that are not simulated explicitly (6, 8). *Computer simulations of biological molecules has been particularly effective in studies of the following subjects.*

1. Energetics (Thermodynamics and Equilibrium Properties)

Simulation of the free energies of different biological processes provide the “missing link” between the corresponding structures and functions. This is particularly true with regard to electrostatic free energies. However, obtaining reliable free energies by computer simulations is very challenging and requires validation by discriminative benchmarks. One of the most effective test in of calculations of free energies in proteins in general and electrostatic models in particular is provided by calculations of absolute **pK_as of ionizable groups** in proteins (8). The basis for calculating this quantity is the relationship (6)

$$2.3RT(pK_a^p - pK_a^w) = \Delta\Delta G_{sol}^p(AH \rightarrow A^-) - \Delta\Delta G_{sol}^w(AH \rightarrow A^-) \qquad (1)$$

where the superscripts *p* and *w* denote protein and water, respectively, and $DDG_{sol}(AH \rightarrow A^-)$ is the difference in solvation energy between the protonated and deprotonated states of the acid. Although early models only considered the change of pK_as due to the effect of protein ionized groups (9), it is now recognized that the most important factor is the self-energy (6) (or “solvation energy”), which is the energy of forming the charge in its protein environment when the other charges are turned off. The modulation of this effect is largely determined by the protein permanent dipoles (6). Obtaining reliable estimates of the self-energy by Free Energy Perturbation is very challenging, but significant progress has been made (3, 10). Apparently, it is essential to treat long-range effects in a consistent way in order to obtain meaningful results in pK_a calculations (10). It is frequently simpler to obtain better results by simplified solvent models (6) and by models that treat the solvent as a dielectric continuum (11). However, one must bear in mind that models that treat the protein in a uniform dielectric without considering the microscopic nature of the protein permanent dipoles cannot reproduce the correct physics of ionized groups in proteins (6, 8).

Redox energies of biological cofactors play a major role in **electron transfer** processes. Such energies can be evaluated by simulation methods using a similar approach to that used in equation 1 and evaluating the change in solvation energy upon moving the charge from water to the protein. FEP calculations of redox energies were reported by several workers, and related studies in photosynthetic reaction centers were also presented. Here the proper treatment of the solvent around the protein is quite crucial (12). As in the case of pK_a calculations, one finds that simplified models (13) and continuum models (14, 15) are quite effective.

Reliable calculations of free energies of **ligand binding** are crucial for quantitative progress in rational drug design. FEP has been used extensively in studies of binding free energies (3). Most early studies involve simple cases of small changes in the ligand (16). Calculations of absolute binding free energies are much more challenging (3, 17) and involve major convergence problems. Here the use of the LRA has been found to be quite effective (17-19). Extensive progress has also been made with simplified models (17, 19, 20) and with more phenomenological approaches (21, 22).

The permeation of ions through membrane channels plays a major role in biophysics. Here, the challenge is in evaluating the energy of an ion in the channel relative to its energy in solution and using the energetics in determining the conductance of the channel. Reliable simulation of such systems requires one to properly represent the channel and its surrounding membrane and water environment. The energy contribution of the membrane-induced dipoles must be included in consistent calculations. Consistent FEP studies of the energetics of moving an Na^+ ion to the center of the **gramicidin A** channel have been reported with a reasonable result (23). Incomplete modeling of the boundaries of the simulated system and long-range interactions can lead to significant overestimates of the penetration barrier (eg, the results of ref. 24). Semimacroscopic studies of ion channels are quite useful and much less challenging than full microscopic calculations (10, 25, 26). The recent emergence of the structure of a bacterial **potassium channel** (27) have highlighted the need for reliable FEP calculations, and some progress has been already made (28).

2. Structural Properties

Molecular simulations can be used to refine, and sometimes predict, structural properties. Energy minimization approaches were the first to be used successfully in relaxing bad steric contacts in X-ray crystallography (29). Such approaches were also used in more systematic refinements of protein structures (30). The emergence of powerful computers allows one to use more rigorous statistical mechanical approaches coupled with MD simulations in exploring structural properties (31).

Simulations are also very useful in evaluating and analyzing temperature factors and interpreting the meaning of the corresponding experimental results.

All-atom simulation approaches are still quite ineffective in predicting protein-structures, and one has to resort to simplified models. Even when one starts from the X-ray structure, it is not trivial to have the simulated structure identical to the observed one. The problems involved include the need for reliable potential function and, perhaps more importantly, the need to have a realistic description of the solvent (32) and proper treatment of long-range forces.

3. Dielectric Properties

Although proteins cannot and should not be described as a medium of a uniform dielectric constant, it is important to understand the dielectric properties of proteins. Experimental attempts to determine local dielectric constants are far from being unique, and simulation studies can provide great insight. In relating the simulated dielectric constant to experimental observations, one should take into account the effect of the solvent around the protein, which is also referred to as the *reaction field* (33). Consistent simulations of the overall dielectric constant of solvated proteins have been reported by several workers (34-36). It has been found that the local dielectric at protein active sites is quite large and quite different than the low value usually deduced from dielectric measurements (37). Simulations are also very effective in analyzing the fast time components of dielectric **relaxation times** (34, 36).

4. Dynamical Properties

MD simulations and related approaches provide powerful ways of evaluating dynamical properties. Many of these properties can be casted in terms of the **corresponding time correlation function** (38).

$$C_A(t) = \frac{1}{\tau}\int_0^{\tau} A(t')A(t+t')dt' \tag{2}$$

where A is the property of interest and t is a sufficiently long simulation time. For example, the diffusion constant, D, can be obtained from the velocity autocorrelation, $C_v(t)$, by

$$D = \frac{1}{3}\int_0^{\infty} C_v(t)dt \tag{3}$$

This relationship can be used in comparing simulations to experiments and in analyzing the microscopic meaning of experimentally deduced parameters. The dynamical range accessible to simulation studies can be probed by several approaches, and significant progress has been made in comparing simulations to the results of inelastic **neutron scattering** (39).

Molecular fluctuations are characterized by correlation times, which are closely related to the underlined relaxation processes. Relevant relaxation times can be evaluated by simulation studies using:

$$\tau_A^{-1} = C_A(0)^{-1}\int C_A(t)dt \tag{4}$$

The fluctuations of the macroenvironments of proteins can play an important role in fast reactions. This is true in particular with regard to the effect of electrostatic fluctuations on charge transfer processes such as electron transfer reactions. The rate of such reactions is determined by the effect of the protein fluctuation on the difference between the energies of the reactant and product state. Such an approach has been used in studies of the dynamics of the primary event in photosynthesis 26, 40-42. The same approach can be used in studies of photoisomerization processes, although in such cases one needs to account for a large coupling between the electronic states. As much as rate constants of regular chemical reactions are concerned, the most important factors are activation energies (see below) and not dynamical effects. Nevertheless, the chance that a trajectory that reaches the transition state will lead to reaction of the transmission factor is a dynamical effect. This factor can be evaluated using MD simulation by running trajectories downhill from the transition state (43) (Fig. 1). However, the transition factor is usually close to unity in reactions with significant activation barrier (4, 26) (Fig. 1).

Figure 1. A downhill trajectory for the proton transfer step in the catalytic reaction of trypsin. The trajectory moves on the actual ground state potential, from the top of the barrier to the relaxed enzyme–substrate complex. 1, 2, and 3 designate different points along the trajectory, whose respective configurations are depicted in the upper part of the figure. The time reversal of this trajectory corresponds to a very rare fluctuation that leads to a proton transfer from Ser 195 to His 57. (adapted from ref. 4).

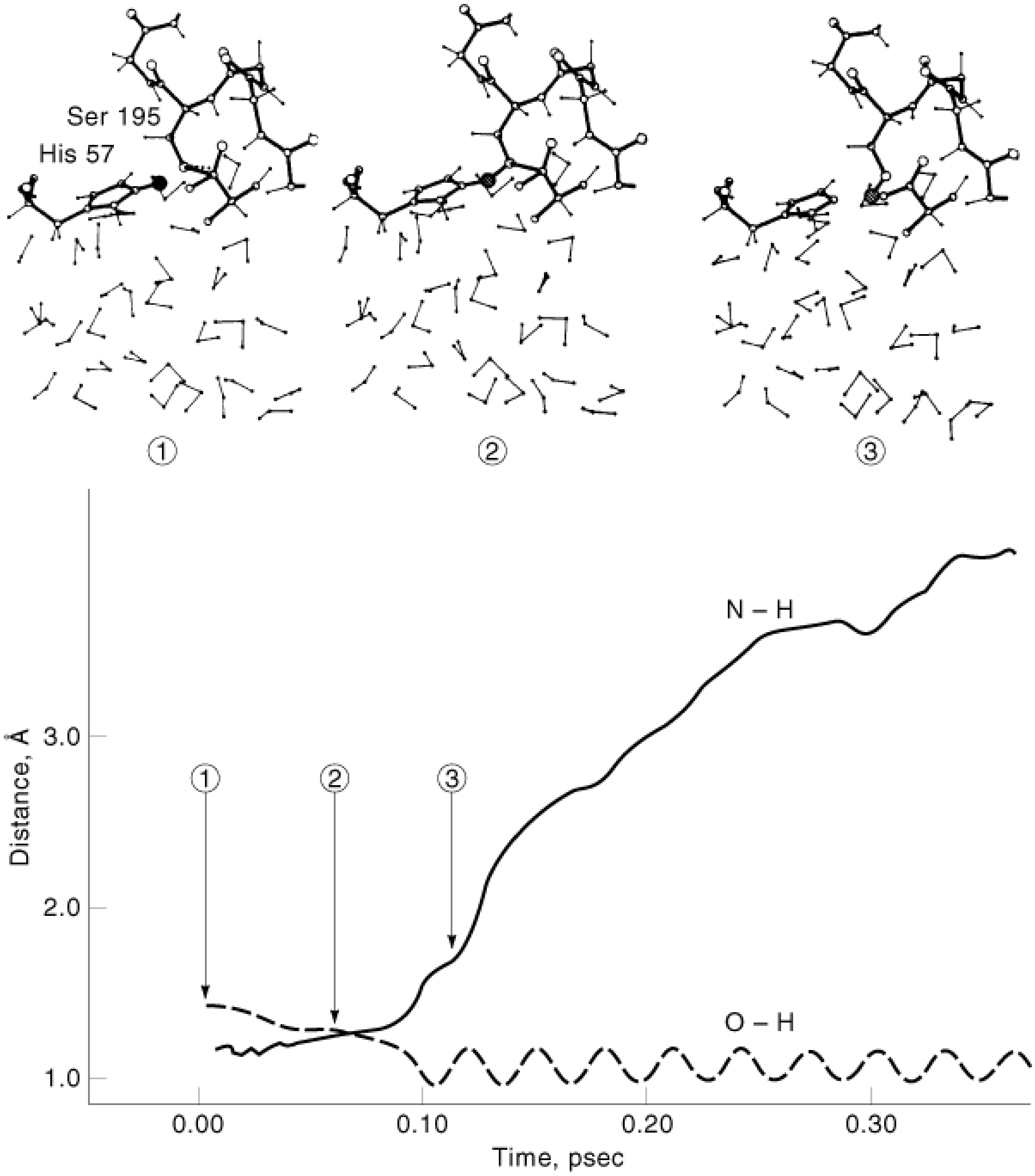

5. Rate of Biological Processes

The rate constant of processes in condensed phases can be expressed as:

$$k = F(k_B T/h) \exp\{-\Delta g^{\neq}/k_B T\} \quad (5)$$

where k_B is the Boltzmann constant, T is the absolute temperature, h is the Planck constant, F is the **transmission factor** of section 3, and $Dg^{\ddagger}$ is the activation-free energy. For most reactions with large $Dg^{\ddagger}$, one finds that F is close to unity and, thus, the most important factor is $Dg^{\ddagger}$. Enzymes catalyze their reactions by reducing activation-free energies (44), and one of the most important questions in structure function correlation is how this reduction of $Dg^{\ddagger}$ is accomplished (4).

Molecular simulations should allow one to evaluate activation free energies and transmission factors and to probe the molecular origin of enzymatic reactions. However, such reactions involve bond making and bond making processes that cannot be described by simple force fields. It is also impractical to describe the complete enzyme/substrate complex by high level quantum mechanical approaches. A possible alternative is provided by **hybrid Quantum mechanics/molecular mechanics (hybrid QM/MM)** methods 4, 45-49. Such methods describe only parts of the reacting system quantum mechanically, while treating the rest of the protein classically. QM/MM approaches are very promising, but the corresponding results are not yet quantitative (26). An alternative, which is, at present, the most reliable way of simulating enzymatic reaction, is provided by the Empirical Valence Bond (EVB) approach (4, 26, 50, 51). The EVB method describes the reaction potential surface by a valence bond method that considers the different resonance structures of the reactant and product fragments and their interaction with the surrounding protein and solvent. This method is calibrated by considering the reference reaction in water so that it focuses on the difference between the reaction in protein and solution, which is much easier to obtain than to predict the reaction potential surface in the protein by a first principle approach.

The EVB approach can be used to calculate conveniently and efficiently activation-free energies of enzymatic reactions using a combination of FEP and umbrella sampling approaches (4, 50). The activation energies can be converted to rate constants of enzymatic reactions using equation 5.

6. Protein Folding

Models that use **simplified representation** of the protein amino acids (52) have provided a powerful understanding of the protein folding process (53-56). Such models are sometimes classified as *on-lattice* and *off-lattice* models. On-lattice models consider the simplified representation along a regular cubic lattice (thus allowing exact enumeration at the expense of somewhat unrealistic structure), while the off-lattice models try to provide more realistic representation (52). Simplified models are used extensively in understanding the relationship between sequence to folding probability and to the specific folded structure (52-56) and in deducing the sequence of events in the folding process (53). The gradual increase in computer power makes it tempting to use all-atom simulations in studies of folding processes. Some advances have been made (57-59), and more will follow. A promising effective approach is the use of the simplified representation as a reference potential for all-atom calculations (60).

Bibliography

1. S. Lifson and A. Warshel (1968) J. Chem. Phys. **49**, 5116.
2. U. Burkert and N. L. Allinger (1982) *Molecular Mechanics*, American Chemical Society, Washington, DC.
3. P. Kollman (1993) Chem. Rev. **93**, 2395–2417.
4. A. Warshel (1991) *Computer Modeling of Chemical Reactions in Enzymes and Solutions* John Wiley & Sons, New York.
5. A. T. Hagler, E. Huler, and S. Lifson (1977) J. Am. Chem. Soc. **96**, 5319.
6. A. Warshel and J. Åqvist (1991) Ann. Rev. Biophys. Chem. **20**, 267–298.
7. P. E. Smith and B. M. Pettitt (1994) J. Phys. Chem. **98**, 9700–9711.
8. C. N. Schutz and A. Warshel (2001) Proteins: Struc., Func., and Gen. **44**, 400–417.
9. C. Tanford and J. G. Kirkwood (1957) J. Am. Chem. Soc. **79**, 5333.
10. F. S. Lee, Z. T. Chu, and A. Warshel (1993) J. Comp. Chem. **14**, 161–185.
11. B. Honig, K. Sharp, R. Sampogna, M. R. Gunner, and A. S. Yang (1993) Proteins: Struc., Func., and Gen. **15**, 252–265.
12. R. G. Alden, W. W. Parson, Z. T. Chu, and A. J. Warshel (1995) J. Am. Chem. Soc. **117**, 12284–12298.
13. P. J. Stephens, D. R. Jollie, and A. Warshel (1996) Chem. Rev. **96**, 2491.

14. M. R. Gunner and B. Honig (1991) Proc. Natl. Acad. Sci. U.S.A. **88**, 9151–9155.
15. H-; X. Zhou (1994) J. Am. Chem. Soc. **116**, 10362–10375.
16. T. P. Straatsma and J. A. McCammon (1992) Ann. Rev. Phys. Chem. **43**, 407–435.
17. F. S. Lee, Z. T. Chu, M. B. Bolger, and A. Warshel (1992) Prot. Eng. **5**, 215–228.
18. J. Åqvist, C. Medina, and J.–E Samuelsson. (1994) Prot. Eng. **7**, 385–391.
19. Y. Y. Sham, Z. T. Chu, H. Tao, and A. Warshel (2000) Proteins: Struct. Funct. Genet. **39**, 393–407.
20. N. Froloff, A. Windemuth, and B. Honig (1997) Protein Sci. **6**, 1293–1301.
21. G. Verkhivker, K. Appelt, S. T. Freer, and J. E. Villarfranca (1995) Prot. Eng. **8**, 677–691.
22. I. Muegge and Y. C. Martin (1999) J. Med. Chem. **42**, 791–804.
23. J. Åqvist and A. Warshel (1989) Comments Mol. Cell Biophys. **6**, 91.
24. B. Roux and M. J. Karplus (1993) Am. Chem. Soc. **115**, 3250–3260.
25. V. Dorman, M. B. Partenskii, and P. C. Jordan (1996) Biophys. J. **70**, 121–134.
26. A. Warshel and W. W. Parson *Quart. Rev. Biophys*. In Press.
27. D. A. Doyle, J. M. Cabral, R. A. Pfuetzner, A. L. Kuo, J. M. Gulbis, S. L. Cohen, B. T. Chait, and R. MacKinnon (1998) Science **280**, 69–77.
28. V. Luzhkov and J. Aqvist (2001) Biochimica et Biophysica Acta **36446**, 1–9.
29. M. Levitt and S. J. Lifson (1969) J. Mol. Biol. **46**, 269–279.
30. A. Jack and M. Levitt (1978) Acta Cryst. A **34**, 931.
31. A. T. Brunger (1988) *XPLORE Manual*, 1.5 ed., Yale University, New Haven, CT.
32. M. Levitt and R. Sharon (1988) Proc. Natl. Acad. Sci. U.S.A. **85**, 7557–7561.
33. L. J. Onsager (1936) Am. Chem. Soc. **58**, 1486.
34. G. King, F. S. Lee, and A. J. Warshel (1991) Chem. Phys. **95**, 4366–4377.
35. T. Simonson and D. J. Perahia (1995) Am. Chem. Soc. **117**, 7987.
36. W. F. vanGunsteren and A. E. Mark (1992) Eur. J. Biochem. **204**, 947.
37. A. Warshel and A. Papazyan (1998) Curr. Opin. Struct. Biol. **8**, 211–217.
38. D. A. McQuarrie (1976) *Statistical Mechanics*, Harper and Row, New York.
39. S. Cusack (1989) Chemica Scripta **29A**, 103–107.
40. A. Warshel and W. W. Parson (1991) Annu. Rev. Phys. Chem. **42**, 279–309.
41. S. Creighton, J.–K. Hwang, A. Warshel, W. W. Parson, and J. Norris (1988) Biochemistry **27**, 774–781.
42. K. Schulten and M. Tesch (1991) Chem. Phys. **158**, 421–446.
43. C. H. Bennet (1997) *Algorithms for Chemical Computations*, ACS, Washington, DC.
44. L. Pauling (1946) Chem. Eng. News **263**, 294.
45. A. Warshel and M. Levitt (1976) J. Mol. Biol . **103**, 227–249.
46. V. Théry, D. Rinaldi, J.-L. Rivail, B. Maigret, and G. G. Ferenczy (1994) J. Comp. Chem. **15**, 269–282.
47. J. Gao (1995) *Reviews in Computational Chemistry*, Vol. **7**, VCH, New York.
48. A. J. Mulholland, G. H. Grant, and W. G. Richards (1994) Prot. Eng. **6**, 133–147.
49. R. B. Murphy, D. M. Philipp, and R. Friesner (2000) J. Comput. Chem. **21**, 1442–1457.
50. J. Åqvist and A. Warshel (1993) A. Chem. Rev. **93**, 2523–2544.
51. J. Lobaugh and G. A. Voth (1996) J. Chem. Phys. **104**, 2056–2069.
52. M. Levitt and A. Warshel (1975) Nature **253**, 694.
53. J. N. Onuchic, P. G. Wolynes, Z. Luthey-Schulten, and N.D. Socci (1995) Proc. Natl. Acad. Sci. U.S.A. **92**, 3626–3630.

54. A. Godzik, A. Kolinski, and J. J. Skolnick (1993) Comp.-Aided Mol. Des. **7**, 397–438.
55. K. Yue and K. A. Dill (1992) Proc. Natl. Acad. Sci. U.S.A. **89**, 4163–4167.
56. E. Shakhnovich, G. Farztdinov, A. M. Gutin, and M. Karplus (1991) Phys. Rev. Lett. **67**, 1665–1668.
57. E. M. Boczko and C. L. Brooks, III (1995) Science **269**, 393–396.
58. V. Daggett and M. J. Levitt (1993) Mol. Biol. **232**, 600–619.
59. T. Lazaridis and M. Karplus (1997) Science **278**, 1928–1931.
60. Z. Z. Fan, J. K. Hwang, and A. Warshel (1999) Theor. Chem. Accounts **103**, 77–80.

Suggestions for Further Reading

61. M. P. Allen and D. J. Tildesley (1987) *Computer Simulation of Liquids*, Oxford University Press, Oxford.
62. A. Warshel (1991) *Computer Modeling of Chemical Reactions in Enzymes and Solutions*, John Wiley & Sons, New York.

Concatemers

A concatemer is a multimeric molecule of **DNA** formed by identical monomers arranged linearly in the same head-to-tail orientation. Closure of a **bacteriophage** DNA molecule upon entry into the bacterial host cell is a relatively simple process. The complementary single-stranded ends anneal in a reaction that is thermodynamically favored and by conditions that restrict diffusion and keep the ends close to each other. **Annealing** is followed by covalent joining, catalyzed by the host DNA Ligase, which forms phosphodiester bonds. Opening of the circular DNA molecule, coupled to its encapsidation to form mature phage particles, however, is rather complex.

Capsid precursors interact with the newly replicated DNA molecules in the form of concatemers (1, 2), which are the product of DNA replication proceeding in two stages. First, the DNA injected into the host is circularized and covalently closed, as previously described. In the case of the lambda phage, the DNA undergoes several stages of DNA replication in which the circular DNA rings generate daughter rings. Then, during phage vegetative growth, **rolling-circle** replication gives rise to *linear* concatemers of l DNA. These concatemers, which in the absence of packaging may be up to 10 chromosomal units long, are the normal substrates for packaging.

RNA primers for DNA synthesis are excised during the process. This raises the question of how the extreme ends of linear DNA can be completed. Not only must a small RNA fragment initiate at the 3′ terminal nucleotide of the template strand, but the sequence must be filled in after ribonucleotide removal. This dilemma was resolved using phage T7 DNA, which has the property of having redundant ends. The sequence of about 160 bp found at the left end is repeated exactly at the right end of the molecule. When the linear T7 molecules replicate, they do not generate unit-length progeny molecules, but very long concatemers (units linked end to end) containing the complete genome sequence repeated over and over.

Bibliography

1. D. Kaiser and T. Masuda (1973) Proc. Natl. Acad. Sci. USA **70**, 260–264.
2. D. Kaiser, M. Syvanen, and T. Masuda (1974) J. Supramol. Struct. **2**, 318–328.

Conditional Lethal Mutations

Mutations that cause lethality under one condition (the restrictive or nonpermissive condition) but not another (the permissive condition) are called conditional lethal mutations, or loosely, conditional lethals. Conditional lethal mutations have an honored position in molecular biology. The recognition that a **gene** is not indivisible, the determination of the triplet nature of the genetic code, and the discovery of **nonsense codons**, all resulted from studies of a particular class of conditional lethal mutants of **bacteriophage** T4. T4 *rII* mutants grow on *Escherichia coli* strain B (the permissive host) but not on *E. coli* strain K-12 when it is **lysogenic** for bacteriophage **lambda** (the nonpermissive host). Interestingly, the function of the proteins encoded by the two *rII* genes remains unknown. The conditional lethality of the *rII* mutants allowed geneticists to grow the phage, to perform genetic crosses on the permissive host, and then to analyze the results on the nonpermissive host.

Conditional lethal mutations are the only genetic way to identify essential genes in haploid organisms or cells. By definition, a mutant with a null mutation in an essential gene cannot be isolated in the haploid state (in **diploid** organisms, recessive lethal mutations on autosomes are **complemented** by the other functional **allele**). Conditional lethal mutations are usually identified by screening mutant clones for growth under permissive conditions but not under restrictive conditions. Lethal in this case does not always mean conveying death. For example, auxotrophies are considered a class of conditional lethals because the auxotrophic cells grow only in the presence of the required growth factor, although they do not necessarily die in its absence. The more typical classes of conditional lethals are host-range mutants (described above), **temperature-sensitive mutants**, and cold-sensitive mutants. Nonsense mutations are considered conditionally lethal because the mutation is suppressed when a suppressor transfer RNA is present.

Conditional lethal mutations are a powerful way to identify protein–protein interactions. A mutation that renders a protein inactive at high or low temperature, for example, may be suppressed by a compensating mutation in the gene encoding a protein that interacts with it. To conclude that the two proteins interact, the suppression must be allele-specific, ie, not caused by general suppression (as in the case of tRNA nonsense suppressors). In addition, other events, such as gene duplication, suppress conditional lethals. Interacting proteins are also identified by synthetic lethal mutations, which are mutations in each of two genes, neither of which is lethal alone but which are lethal when together in the same cell.

Suggestions for Further Reading

A. Adams, D. E. Gottschling, C. Kaiser, and T. Sterns (1998) *Methods in Yeast Genetics: A Laboratory Course Manual*, Cold Spring Harbor Laboratory Press, Cold Spring Harbor, NY.

E. M. Phizicky and S. Fields (1995) Protein-protein interactions: methods for detection and analysis, Microbiol. Rev. **59**, 94–123.

A. Griffiths, J. H. Miller, D. Suzuki, R. Lewontin, and W. Gelbart (1996) *An Introduction to Genetic Analysis*, 6th ed., W. H. Freeman, New York.

J. Beckwith and T. Silhavy (1992) *The Power of Bacterial Genetics: A Literature-Based Course*, Cold Spring Harbor Laboratory Press, Cold Spring Harbor, NY.

T. D. Brock (1990) *The Emergence of Bacterial Genetics*, Cold Spring Harbor Laboratory Press, Cold Spring Harbor, NY.

Configuration

Although configuration and conformation are listed as synonyms in the *Oxford English Dictionary* (1), in chemistry and biochemistry they have specific and separate meanings differentiated by time or energy. Both terms refer to the organization of atoms in space, but configuration refers to the element that remains invariant in time in the absence of any covalent bonds being altered, whereas conformation refers to the relative orientation in space of atoms that can vary by rotation about single bonds and consequently varies in real time for biological molecules. The absolute configuration identifies the arrangement of atoms that generates **chirality** in a molecule. Following Pasteurs identification of the two chiral forms of tartaric acid, it was only known that they differed by being nonsuperimposable mirror images. This ambiguity was resolved when the crystal structure of (+) tartaric acid was determined by Bijvoet and co-workers (2). By this means, the absolute configuration of many related molecules became identifiable.

The designation of the configuration of a chiral center was problematic for nearly a century. Fischer introduced a general procedure that identified enantiomers as either D- or L- (3) based on whether the nonhydrogen substituent was on the right or left when the molecule was drawn as a “Fischer projection” (Fig. 1). This nomenclature permeates biochemistry through the now colloquial names of amino acids, carbohydrates, and lipids.

Figure 1. A Fischer projection. By convention, it has the vertical bonds directed away from the viewer and horizontal bonds directed out toward the viewer. The configuration of each chiral carbon in D-ribose is D because the nonhydrogen substituent is drawn to the right. For sugars, the enantiomer is defined by the bottom chiral carbon when the carbon chain is oriented vertically with the carbonyl carbon at the top; thus, D-ribose is pictured.

D-ribose

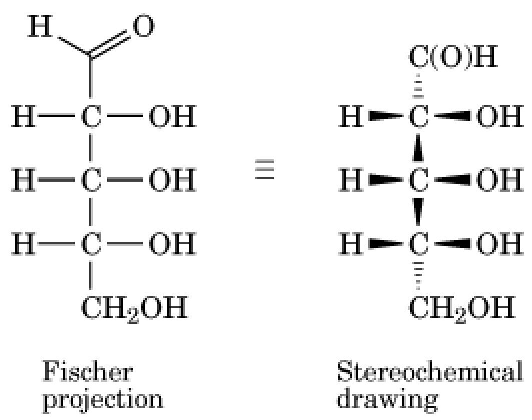

The Fischer nomenclature leads to ambiguities (4). A rigorous and unambiguous method of identifying configuration proposed by Cahn et al. has been adopted for specifying absolute configuration as either (*R*) or (*S*) for chiral tetrahedral centers (5). The procedure requires the assignment of priority to the four substituents that generate a chiral center, followed by a procedure to identify the arrangement as either (*R*) or (*S*). The four rules for assigning priority are:

1. Substituents are assigned their priority in order of decreasing atomic number of the atom directly bonded to the chiral center.
2. If two or more atoms receive the same priority in step 1, the atoms bonded to each of the equal priority atoms are examined one at a time. If the two groups are not differentiated by the atom of greatest priority, the second and third atoms are compared successively.
3. Heavier isotopes take precedence over lighter isotopes, eg, ^{2}H over ^{1}H and ^{14}C over ^{12}C.
4. Double bonds are counted as two bonds to the same atom.

Once the relative priorities of the four substituents are assigned, the bond to the lowest priority group is oriented directly away from the observer, and the remaining three groups are viewed in a plane. If the arc connecting the three groups in order of highest to lowest priority is clockwise, the chiral center is assigned the (*R*) configuration (from the Latin rectus), whereas if the arc is counterclockwise, the center is assigned the (*S*) configuration (from the Latin sinister). These assignments are shown in Figure 2.

Figure 2. Assignment of the relative priorities of the four substituents on the chiral a-carbon of serine. The carboxylate carbon takes precedence over the hydroxymethyl carbon because it has three bonds to oxygen. The assignment of the (*S*) configuration results from the counterclockwise arc that connects the substituents in order of precedence.

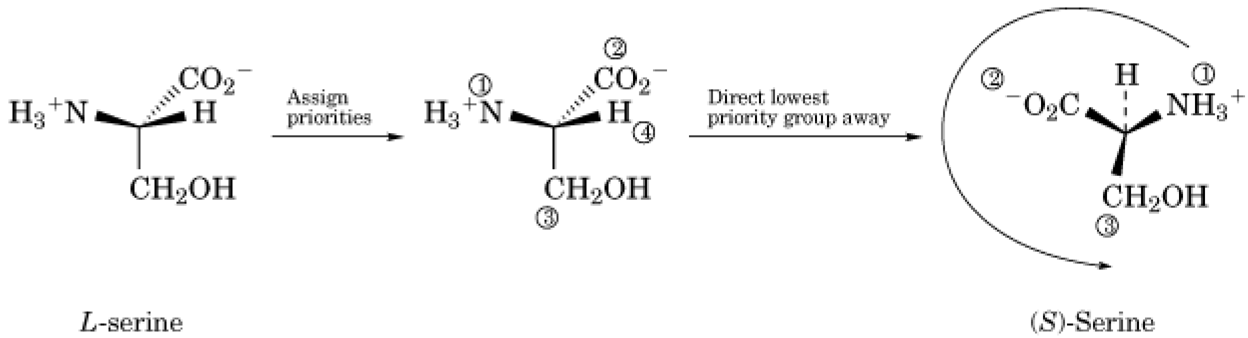

. Assignment of the relative priorities of the four substituents on the chiral a-carbon of serine. The carboxylate carbon takes precedence over the hydroxymethyl carbon because it has three bonds to oxygen. The assignment of the (*S*) configuration results from the counterclockwise arc that connects the substituents in order of precedence. [Full View]

Bibliography

1. *Oxford English Dictionary*, 2nd ed. (1989) Clarendon Press, Oxford.
2. J. M. Bijvoet, A. F. Peerdeman, and A. J. van Bommel (1951) Nature **168**, 271.
3. E. Fischer (1891) Ber. Dtsch. Chem. Ges. **24**, 2683.
4. E. L. Eliel (1962) *Stereochemistry of Carbon Compounds*, McGraw-Hill, New York, Chap. "5".
5. R. S. Cahn, C. K. Ingold, and V. Prelog (1966) Angew. Chem. Int. Ed. **5**, 385–415.

Suggestions for Further Reading

6. J. March (1985) *Advanced Organic Chemistry*, Wiley-Interscience, New York, pp. 93–99.
7. K. Mislow (1966) *Introduction to Stereochemistry*, W. A. Benjamin, New York, pp. 86–97.

Confocal Microscopy

Confocal microscopy is now a well-established tool for the examination of subcellular structure and function and complements light and electron microscopy. Because of its high temporal resolution, confocal microscopy allows for the visualization of living as well as fixed tissues and cells, and therefore dynamic processes can be examined and analyzed quantitatively as they actually occur. Confocal microscopy offers several advantages over conventional light microscopy, among which are an increase in contrast, resolution, and clarity (1). Conventional light microscopy provides a two-dimensional (2-D) image of the specimen in the focal plane of the objective lens, but this image is contaminated by out-of-focus images of the specimen above and below the focal plane. Confocal microscopy provides a 2-D image in the focal plane without the out-of-focus information. Furthermore, the resolution of images from a confocal microscope is improved by a factor of 1.4–1.75 (2). Through computer control of the focus and acquisition of images, modern confocal light microscopes can collect a series of 2-D images (or "optical sections") through the specimen producing a three-dimensional (3-D) image. Four-dimensional imaging (4-D), defined as 3-D imaging over time, is a recently developed extension in which 3-D images are recorded at periodic time intervals (3).

The basic principle of the confocal microscope is to eliminate the scattered, reflected, or fluorescent light from out-of-focus planes by making the illumination, specimen, and detector all have the same focus, ie, they are confocal. In effect, this microscope will image only the very thin optical section on which the beam is focused. Matched pinholes are used, one at the light source which is imaged onto the specimen to function as a probe that is scanned over the specimen, and one at the detector to capture only a narrow plane of focus. Thus, the out-of-focus blur from areas above and below the focal plane are eliminated. The matched pinhole apertures improve the lateral resolution over conventional light microscopes by a factor of 1.4 with the use of circular apertures and 1.75 with annular apertures (2). Confocal microscopes are often designed to scan in a raster pattern over the sample in which the microscope illuminates one spot at a time, scanning the spot along parallel lines in the focal plane. Lasers are an ideal illumination source for raster scanning because they provide an intense beam of monochromatic radiation that can be condensed onto a small spot. Hence many confocal microscopes are laser scanning (LSCM).

Applications of LSCM include (i) determining the location of proteins, lipids and nucleic acids, cytoskeletal structures and organelles within cells (4, 5), using fluorescent dyes, antibodies, phalloidin, and lectins, (ii) observing ionic fluctuations, such as calcium, magnesium, and pH, in cells and organelles (6), and, (iii) measuring membrane potential using fluorescent dyes (7). The power of 4-D imaging in molecular biology was illustrated by the noninvasive monitoring by LSCM of mitotic events, and cleavage and migration patterns of fertilized sea urchin eggs labeled with $DiOC_6$ (8). Macromolecules and subunits can be characterized by immunocytochemical fluorescence probes, which involves the use of antibodies labeled with fluorophores (9). When more than one fluorophore is used, 3-D multilabel (multicolor) imaging can be used to map the 3-D relationship of the labeled structures. For example, z-series collected from two different channels, fluorescein and rhodamine, can be merged into a single reconstruction. By rotating the rendered volume, particular nuances of the structural relationships highlighted by the bound fluorophores may be revealed (10, 11). It is not only important to know that a particular compound is present in a specific cell type or subcellular component, but it is also important to detect and quantify changes in local concentrations of such compounds. Quantitative immunocytochemistry utilizes the principles of stereology and statistical analyses (12) and can be coupled to LSCM to detect differences in immunoreactivity. This method has been used to measure the distribution of integral membrane proteins in the vertebrate retina and to determine the distribution of transport vesicles (13).

Many of the advantages of a confocal light microscope can be achieved with a standard light microscope equipped with a digital camera interfaced to a computer, which controls the microscope stage and focus control as well as run rapid deconvolution algorithms (14). With knowledge of the 3-D point spread function of the microscope, the deconvolution algorithms remove out-of-focus signal to produce images comparable in quality to LSCM images. The advantages of the deconvolution confocal microscope are that (i) the system expense is a fraction of the cost for a LSCM system, and (ii) lower illumination levels can be used, since all of the light emitted from the specimen is used in forming the 3-D image. Lower illumination minimizes the problem of photobleaching of fluorophores used to label the specimen. A disadvantage of this approach is that the full 3-D deconvolution process can take significantly more time to produce a 3-D image than does a confocal microscope.

Bibliography

1. A. Boyde (1990) "Confocal optical microscopy",In *Modern Microscopies* (P. J. Duke and A. G. Michette, eds.), Plenum Press, New York, pp. 185–204.
2. E. M. Slayter and H. S. Slayter (1992) *Light and Electron Microscopy*, Cambridge University Press, Cambridge, UK.
3. S. A. Stricker, S. Paddock, and G. Schatten (1990) J. Cell Biol. **111**, 113a.
4. A. H. Cornell-Bell et al. (1993) "Membrane glycolipid trafficking in living polarized pancreatic acinar cells: Assessment by confocal microscopy", In *Methods in Cell Biology*, Vol. **38**: *Cell Biological Applications of Confocal Microscopy* (B. Matsumoto, ed.), Academic Press, San Diego, pp. 222–241.
5. I. L. Hale and B. Matsumoto (1993) "Resolution of subcellular detail in thick tissue sections: Immunohistochemical preparation and fluorescence confocal microscopy", In *Methods in Cell Biology*, Vol. **38**: *Cell Biological Applications of Confocal Microscopy* (B. Matsumoto, ed.), Academic Press, San Diego, pp. 290–325.
6. A. Boyde (1995) "Confocal optical microscopy", In *Image Analysis in Histology: Conventional and Confocal Microscopy* (R. Wootton et al., eds.), Cambridge University Press, Cambridge, UK, pp. 151–196.
7. L. M. Loew (1993) "Confocal microscopy of potentiometric fluorescent dyes", In *Methods in Cell Biology*, Vol. **38**: *Cell Biological Applications of Confocal Microscopy* (B. Matsumoto, ed.), Academic Press, San Diego, pp. 195–210.
8. S. A. Stricker et al. (1992) Dev. Biol. **149**, 370–380.
9. T. C. Brelje, M. W. Wessendorf, and R. L. Sorenson (1993) "multicolor laser scanning confocal immunofluorescence microscopy: Practical application and limitations", In *Methods in Cell Biology*, Vol. **38**: *Cell Biological Applications of Confocal Microscopy* (B. Matsumoto, ed.), Academic Press, San Diego, pp. 98–182.
10. W. Galbraith et al. (1989) Soc. Photo-Opt. Instrum. Eng. **1063**, 19–20.
11. M. W. Wessendorf (1990) In *Handbook of Chemical Neuroanatomy*, Vol. **8** (A. Bjorklund et al., eds.), Elsevier, Amsterdam, pp. 1–45.
12. J. T. McBride (1995) "Quantitative immunocytochemistry", In *Image Analysis in Histology: Conventional and Confocal Miscroscopy* (R. Wootton et al., eds.), Cambridge University Press, Cambridge, UK, pp. 339–354.
13. B. Matsumoto and I. L. Hale (1993) In *Methods in Neuroscience*, Vol. **15** (P. C. Hargrave, ed.), Academic Press, San Diego, pp. 54–71.
14. D. Agard (1984) Ann. Rev. Biophys. Bioeng. **13**, 191–219.

Conformation

Nonidentical spatial arrangements of the atoms of a molecule achieved by rotation about single bonds are referred to as different conformations (1). Two molecules differing in their conformation may be referred to as conformers . Because rotations about single bonds are usually rapid, conformers are rapidly interconverted, making it difficult to separate individual conformers. Note one exception to this rule is rotation about the C–N single bond of the peptide bond of polypeptides, which has partial double-bond character, so it is planar and the *cis* and *trans* conformations are only slowly interconverted (see Cis/Trans Isomerization). The conformation of a molecule may then be largely specified by characterizing the rotations about its single bonds. These rotations are quantified by determining the torsion angle or dihedral angle. Individual torsion angles may be qualitatively described as eclipsed, **gauche**, or **anti** (Fig. 1), or more formally named *syn* periplanar, clinal, and *anti* periplanar; they are quantified, as described in Torsion angle.

Figure 1. The common description of a conformation, illustrated by ethylene glycol. When the substituents are superimposed, the conformation is described as *eclipsed*; when they are staggered, the conformation is *gauche* if the large substituents are roughly separated by 60° and *trans* or *anti* if they are opposite.

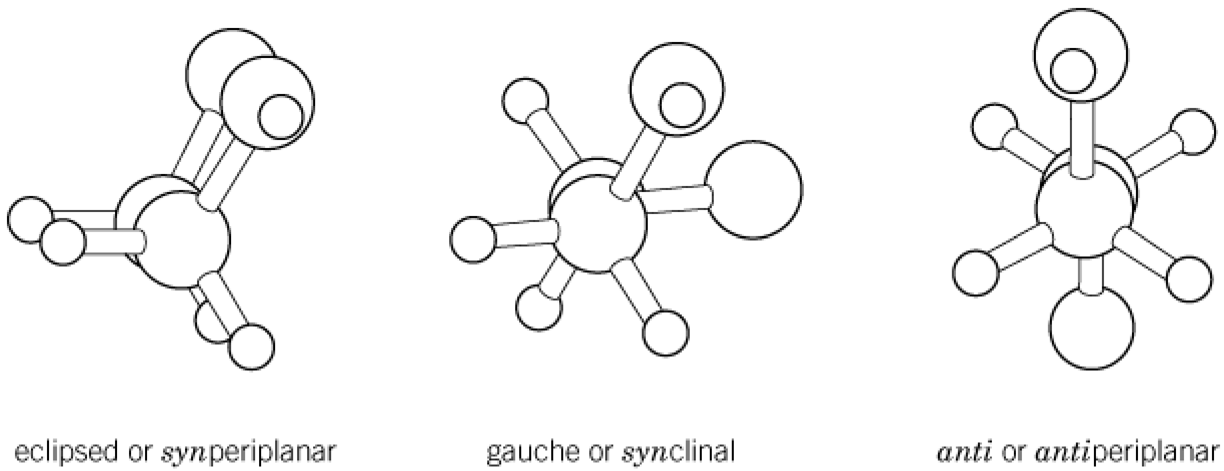

Other common combinations of torsion angles lead to descriptive names for common groups of atoms, eg, the 2′-endo conformation of **ribose** describes all five of the torsion angles of the furanose ring. This practice extends to larger biomacromolecules. The conformation of a small repeating segment of a biomacromolecule is characterized by its torsion angles along the backbone. Thus specification of the phi (f) and psi (y) angles for an oligopeptide (see Ramachandran Plot) describes its conformation as alpha-**helical** or beta-**sheet** (2). The specification of the torsion angles along the phosphodiester backbone of a polynucleotide also will determine whether the conformation is of the A, B, or Z type (3) (see DNA Structure).

A stable three-dimensional structure of a biological macromolecule is referred to as its conformation. Because rotation about single bonds is energetically easy, a unique conformation does not exist, as at least one single bond will be changing rapidly. A cooperative change of several torsion angles, such as occurs in the protein unfolding or melting of double-stranded DNA, may have a significant energetic barrier. The interconversion of the two conformations is then identified as a *conformational change* , where the implication is that the macromolecule has been converted from one family of conformations to an experimentally distinguishable family of conformations.

Bibliography

1. E. L. Eliel et al. (1967) *Conformational Analysis*, Wiley-Interscience, New York.
2. G. E. Schulz and R. H. Schirmer (1979) "Principles of Protein Structure", *Springer Advanced Texts in Chemistry* (C. R. ed.), Springer-Verlag, New York.
3. W. Saenger (1984) *Principles of Nucleic Acid Structure*, Springer Advanced Texts in Chemistry (C. R. Cantor, ed.), Springer-Verlag, New York.

Suggestions for Further Reading

4. C. R. Cantor and P. R. Schimmel (1980) *Biophysical Chemistry, Part I: The Conformation of Biological Macromolecules*, W. H. Freeman, San Francisco, CA.
5. E. L. Eliel (1962) *Stereochemistry of Carbon Compounds*, McGraw-Hill, New York, pp. 124–137.

Conotoxins

Perhaps the largest array of **channel**-binding toxins is produced by marine gastropods of the genus *Conus*, which includes more than 500 species (1, 2). These animals appear to have developed the ability of generating a very large number of toxin variants starting from a basic peptide structure consisting of relatively few residues (Fig. 1). In such a way, they produce venoms containing complex mixtures of toxins, capable of binding and blocking the activity of several ion channels. Moreover, some conotoxins are capable of binding differentially to the various **isoforms** of an ion-specific channel, thus providing precious tools to pharmacologists and neuroscientists (1).

Figure 1. Peptide toxins contained in *Conus* venoms. *Conus* spp. produce a highly complex mixture of toxins. Shown here are the consensus sequences and disulfide connections of toxins specific for the acetylcholine receptor (a-conotoxins), sodium channels (m- and d-contoxins), calcium channels (w-conotoxins), and the NMDA glutamate channel (conantokins). O indicates *trans*-4-hydroxyproline, plus a positively charged residue, g a g-carboxyglutamate, and a an amidated a-carboxyl. The disulfide connectivity of d-conotoxins is not established.

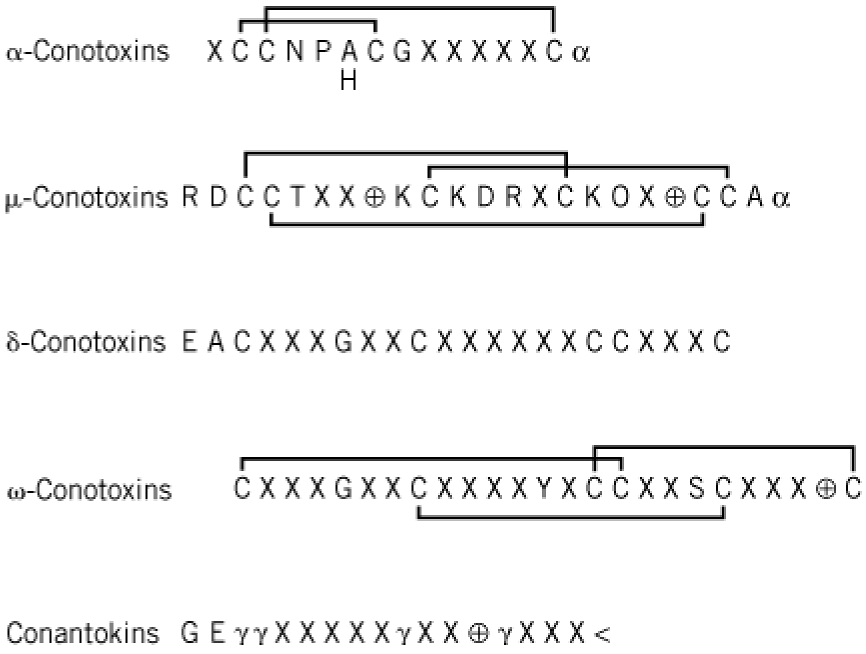

The m-conotoxins are 22 residue-long basic peptides and include three hydroxyproline residues and six cysteines that form three disulfide bonds (Fig. 1). These conotoxins have an ellipsoid shape with the basic residues, which are essential for the binding activity, clustered on one side of the molecule (2, 3). m-conotoxins bind to the tetrodotoxin binding site of the **sodium channel**, thereby inhibiting the propagation of the action potential and causing flaccid paralysis. Another family of conotoxins specific for sodium channels is that of the d-conotoxins, whose binding causes an increased conductance of such voltage-gated channels (4).

w-conotoxins act on voltage-gated **calcium channels** and inhibit calcium entry through the presynaptic membrane, thus preventing the release of neurotransmitters. Their peptide chain consists of 24 to 30 residues and three disulfide bonds (Fig. 1). A frequently used w-conotoxin is G_{VIA}, a 27 residue-long peptide that is very specific for calcium channels containing the a1B subunit, such as the N-type calcium channel present at the neuromuscular junction of vertebrates. The specificity of different w-conotoxins for different vertebrates is exploited in studying the function and anatomical distribution of calcium channels (1).

The largest family of conotoxins is that of the a-conotoxins, 13 to 18 residue-long peptides, whose folding is dominated by two disulfide bonds (Fig. 1). These paralytic neurotoxins bind specifically to the nicotinic acetylcholine receptor and different a-conotoxins are able to distinguish between different neuronal isoforms of the receptor. *Conantokins* are *Conus* peptides with yet another channel specificity: They bind to the NMDA-sensitive glutamate channels. They are peptides of 17 to 21 residues with no cysteine but four **gamma-carboxyglutamate** residues (1) (Fig. 1). Very short *Conus* peptides are conopressins, which consist of nine amino acid residues with a single disulfide bond and are specific for the vasopressin receptor.

Bibliography

1. R. Rappuoli and C. Montecucco (1997) *Guidebook to Protein Toxins and Their Use in Cell Biology*, Sambrook and Tooze, Oxford University Press, Oxford, UK.
2. B. M. Olivera, G. Miljanich, J. Ramachandran, and M. E. Adams (1994) Ann. Rev. Biochem. **63**, 823–867.
3. J.-M. Lancelin et al. (1991) Biochemistry **30**, 6908–6916.
4. K. Shon (1995) Biochemistry **34**, 4913.

Conservative Substitutions

Missense mutations cause the substitution of one amino acid for another in the protein encoded by the mutant **gene**. The effect of such a change on the protein's function will often depend on how similar the new amino acid is to the original one. Amino acids are classified by their acidity, polarity, hydrophobicity, and structure. Substitutions are considered conservative if the change is between amino acids of the same class. However, a better criterion is whether the substitution has occurred during the evolution of related proteins. The mutations that give rise to conservative amino acid substitutions are considered evolutionarily neutral mutations, or nearly so. Lists of likely conservative substitutions are found in many laboratory manuals, for example (1).

Bibliography

1. A. Ellington and J. M. Cherry (1991) In *Current Protocols in Molecular Biology* (F. M. Ausubel, R. Brent, R. E. Kingston, D. D. Moore, J. G. Seidman, J. A. Smith, and K. Struhl, eds.), Wiley, New York, pp. A.1C.1–A.1C.10.

Constant (C) Region

The heavy and light chains of immunoglobulins contain (a) **variable (V) regions** of approximately equal size (ie, about 110 amino acid residues), and (b) constant (C) regions that contain a multiple of 110 residues, one for the L chain and three or four for the H chains, depending upon the isotype. Whereas the V regions are involved in antigen recognition, C regions are devoted to effector functions, such as **complement** fixation, transplacental passage, or attachment to various cell types. C regions are organized on a basic **domain** structure, corresponding to the 110-residue subunit of Ig with an autonomous three-dimensional protein structure, as shown by X-ray crystallography (see Immunoglobulin Structure). This structure, known as the immunoglobulin constant domain fold, provides the basis for the general organization of a large number of proteins, known as the Ig superfamily.

The existence of different C regions was first shown by immunochemistry, because specific antisera could distinguish two types of light chains, known as l) light chains, and five discrete isotypes of H chains, which dictate the organization into the five classes of immunoglobulins (IgA, IgD, IgE, IgG, IgM). Definitive understanding of the basis of isotype structure was obtained by protein sequencing and finally by DNA sequencing. Within each Ig class, one may distinguish subclasses, as in the case of the g chain or the a chains in humans.

Most of the effector functions of immunoglobulins are supported by the last two or three COOH-terminal domains of the heavy chains, depending upon the class. The most interesting feature of constant regions is their ability to bind to a receptor family, termed **Fc receptors** (FcRs), because binding involves the Fc region of Ig. FcRs represent adaptors that can confer on a variety of cell types any antibody specificity, depending on which Ig will bind to the receptor. There is an FcR specific of each soluble isotype, IgG, IgA, and IgE. One distinguishes FcRs of high affinity (FcR type I) that fix Ig monomers and FcRs of low affinity (FcR type II) that bind Ig only when aggregated or as multivalent complexes. Depending on which cell type FcR is anchored, they express an cytoplasmic tail of variable size, which may result from alternative splicing and that contains various signaling motifs such as an immunoreceptor tyrosine-based activation motif and an immunoreceptor tyrosine-based inhibition motif. $Fc\epsilon RI$, present on mast cells, basophils, and eosinophils, plays a major role in anaphylaxis, because it will fix monomeric IgE. Upon cross-linking by antigen, this FcR is triggered, leading to the cascade of events that are responsible for degranulation of the corresponding cells and thus to the liberation of pharmacologically active molecules that account for immediate hypersensitivity. $Fc\epsilon RII$ (CD23) binds aggregated IgE, or IgE already cross-linked by antigen. It is present at the surface of many cell types, including B cells. It may also be cleaved and release several soluble products that have a **cytokine**-like activity. FcgRI is found on monocytes, eosinophils, and neutrophils and binds to monomeric IgG, whereas FcRaI is present on macrophages, neutrophils, and T and B cells.

This demonstrates the extraordinary plasticity and amplification of molecules of the immune system and illustrates the huge diversity of functions that are linked to the constant regions of immunoglobulins.

See also entries Antibody, Immunoglobulin, and Isotype.

Suggestions for Further Reading

F. Shakib (1986) *Basic and Clinical Aspects of IgG Subclasses, Monographs in Allergy*, Vol. **19**, Karger, Basel.

J. V. Ravetch and J. Kinet (1993) Fc receptors. Annu. Rev. Immunol. **9**, 457–492.

Contact Inhibition

Cultured cells, particularly when grown as a monolayer attached to a substrate, will go through a reproducible growth cycle following subculture (1) (see Cell Line). The phases normally defined are (1) the lag phase, before the culture starts to proliferate; (2) the exponential , or log , phase, when the cells are dividing rapidly and the population doubles over a fixed time; and (3) the plateau phase, when the cell number remains stable with further time in culture. As a culture reaches the end of the exponential phase and enters plateau, it responds to cell contact, reduced substrate availability, a reduction in nutrients, and a number of other stimuli that inhibit a further increase in cell numbers. These have been divided into two major components: contact inhibition and density limitation of cell proliferation . Contact inhibition is the cessation of cell motility that occurs when a cell culture reaches confluence. It was first described from observations of randomly migrating fibroblasts made in time-lapse cinemicrography (2). Normal fibroblasts cultured at low cell density show a spindle-shaped morphology, with a reversible polarity along their long axis, which is also the direction of cell migration. When the cell encounters another similar cell, contact induces a reversal of the polarity; the ruffling in the leading tip of the cell ceases and transfers to the opposite tip, which then becomes the anterior end, and migration resumes in the opposite direction. When contact is made with another cell, the process of reversal of polarity is repeated, unless the cell is surrounded by other cells, when membrane ruffling ceases and cell migration is inhibited. In the cases of normal human or chick diploid fibroblasts, the cell assumes a parallel array that gives the appearance of whorls in the cell monolayer under low power microscopy or naked eye observation.

At the time that motility ceases, the cells are still capable of proliferation, but the culture becomes crowded following one or two population doublings, the cells assume a narrower spindle shape, and cell spreading is reduced beyond the point where the cell is able to re-enter the cell cycle (3). At this point, proliferation ceases in a normal cell culture, and the culture remains as a monolayer. Further growth is inhibited by density limitation of cell proliferation , and the culture enters the plateau phase of the growth cycle (see Cell Line). Density limitation of cell proliferation is distinct from contact inhibition, which affects primarily membrane ruffling, polarity, and cell migration. The mechanisms are, however, similar, although the detail remains obscure. Subconfluent cells have many more adhesions to the substrate than to other cells, favoring motility and proliferation. When the culture becomes confluent, the number of cell–cell adhesions (cadherins) increases, but they are still exceeded by cell–substrate adhesions (integrins), which inhibit cell motility but not proliferation. When the culture becomes crowded, the number of cell–cell adhesions increases, and cell–substrate adhesions are reduced, maintaining inhibition of motility but now inhibiting re-entry into the cell cycle. As contact with adjacent cells and contact with the substrate are mediated via different classes of **receptors** (4), the signaling that results from activation of these receptors is potentially different, although exactly how remains unclear.

In addition to alterations in cell spreading, adhesion receptors, and the actin cytoskeleton when cells reach a high density, the cells are also exposed to reduced nutrient levels, due to a higher rate of utilization, and increased levels of catabolites, both of which will tend to inhibit proliferation. In a static culture, this may generate a depleted layer above the cells, across which nutrients and growth factors must diffuse to reach the cells. The diffusion rate will be significantly slower with higher molecular weight components of the medium, including growth factors and peptide hormones such as insulin. Support for this diffusion boundary layer hypothesis was provided by experiments where local irrigation was increased, by means of a micropump, and resulted in a localized increase in the frequency of labeling with [^{3}H]-thymidine (5). As the range of the diffusion boundary was short, it was proposed that the limitation was principally in growth factors, depleted by binding to cell-surface receptors and endocytosis, which was confirmed by the observation that addition of growth factors or serum to the medium will induce further proliferation (6).

On the other hand, one of the main observations that confirms that contact inhibition and density limitation of cell proliferation are not simply evidence of environmental deterioration is the result of the so-called “wounded monolayer” experiment (7). If a confluent, growth-arrested monolayer is scored with a sharp instrument, creating a bare patch devoid of cells, the surrounding cells respond as follows. The edge cells start to show ruffling of the cell membrane bordering the wound, spread out, and migrate into the space. When they have spread beyond a critical point, they enter the cell cycle and divide, and they continue to do so until the space of the wound is filled. They then stop migrating, but continue to proliferate until the cell density in the wound matches the crowded state of the rest of the monolayer; at this point they stop dividing. Meanwhile, no other cells distant from the wound show any sign of entering the cell cycle. This confirms that a major component of density limitation of cell proliferation is due to geometry and cell shape, rather than simply nutritional or growth factor limitation.

If a culture of normal fibroblasts that is growth arrested at high density is fed with medium containing serum or growth factors, many of the cells will reenter the cell cycle, resulting in the formation of a second cell layer over the first; if this is repeated, multilayered cultures can be produced. It has been proposed that the first layer of cells secretes a collagen overlay (which may produce a further diffusion barrier) and the second cell layer grows on top of this, technically not disobeying the rules of contact inhibition and density limitation of cell proliferation. This second layer, however, is still limited by contact and density, and when it reaches confluence, it will form a second layer of parallel arrays of cells, not colinear with the first. If perfused, these cultures may continue to increase up to 20 or 30 cell layers deep (8).

When cultures of normal epithelium reach confluence, they also become contact-inhibited. In less dense cultures, however, they do not show the random migration seen in cultures of fibroblasts, but tend to grow in patches with ruffling of the membrane, cell spreading, and proliferation restricted to the outer edge of the patch (9). Their motility is limited, but when it occurs, it tends to involve the whole patch, which moves as a unit. Multilayering in normal epithelial cultures also occurs, but tends to imply maturation perpendicular to the substrate, rather than overgrowth. Epidermal cells, for example, will become stratified, with the upper layers of cells becoming progressively more keratinized. This is accentuated if the cells are grown on collagen, particularly in the presence of dermal fibroblasts and due to integrin down-regulation. Epithelial cells, which are derived from simple epithelium that is only one cell thick *in vivo*, tend to be obligate monolayers in culture. Likewise, normal endothelium from the lining of blood vessels will not pile up in culture, although after some time at high density it will tend to curl up and form secondary structures resembling capillaries (10), particularly if grown on an extracellular matrix, such as Matrigel.

Transformation allows cells to escape from the restrictions of contact inhibition and density limitation of cell proliferation (see definition of transformation in Immortalization). On one hand, they often lack, or have modified, the appropriate receptors or cell-adhesion molecules to recognize each other on contact; on the other hand, they are no longer dependent on cell spreading to allow entry into the cell cycle. Many transformed cell lines will propagate in suspension, without any substrate attachment. In addition, transformed cells often produce autocrine growth factors or have permanently active steps in the signal transduction cascades that promote cell proliferation (11-13). Hence, transformed cells will grow to a higher density and form multilayered cultures quite readily. The limitations imposed by density now tend to be diffusion-related, principally nutrient, catabolite, and gaseous (dissolved O_2 in and CO_2 out). One major limitation is the release of lactic acid by the cells, as they are generally more anaerobic in their metabolism than normal cells, and this depresses the pH, initially inhibiting proliferation and ultimately killing the cells. Although transformed cell cultures enter a plateau phase of culture when they reach a high density, the growth fraction in transformed cultures in plateau can be quite high (10–20%), unlike the plateau in normal cell cultures, where the growth fraction is very low (<5%). A steady state is reached when cell proliferation is matched by cell necrosis or apoptosis, and the cells deteriorate rapidly and irreversibly if the medium is not replenished.

The differences in response to high cell density between normal and transformed cells has been exploited in the isolation of transformed foci. If a monolayer of 3T3 cells is **transfected** with an **oncogene**, especially in the exponential phase of growth, when transfection is more efficient, it will show foci of transformed cells when the culture reaches confluence, because of the lack of contact inhibition of cell motility and density limitation of cell proliferation in successfully transformed cells (14). Likewise, transformed cells plated on a confluent monolayer will continue to grow and may form foci, or they may infiltrate the monolayer. Normal cells plated on a confluent monolayer will give a varying response, depending on the cell lineage of the confluent monolayer. If the plated normal cells are of the same lineage as the confluent monolayer, they will not grow; for instance, fibroblasts will not grow on a confluent monolayer of fibroblasts, and normal glial cells will not grow on a confluent monolayer of normal glial cells (15), whereas their transformed counterparts will. On the other hand, normal glial cells will grow on a confluent monolayer of fibroblasts, and normal keratinocytes will grow on a monolayer of normal 3T3 cells (16).

Cultures that are propagated in suspension will, of course, not encounter contact inhibition. Nevertheless, they are subject to density limitation of cell proliferation. Part of this is undoubtedly due to nutrient depletion, catabolite buildup, and pH depression, but even if limiting nutrients are replaced and the pH is stabilized, high density suspension cultures do not increase significantly above $1–2 \times 10^6$ cells/ml. Quite often suspension cultures, such as hybridomas, will remain in the plateau phase for only a short time and then deteriorate rapidly, leaving few viable cells in the culture. The reason for this appears to be that the cells tend to enter apoptosis when they reach a high density. Some moderate success has been achieved overexpressing *bcl* in these cells to inhibit apoptosis (17).

Bibliography

1. R. I. Freshney (1994) *Culture of Animal Cells, a Manual of Basic Technique*, Wiley-Liss, New York, pp. 153–157.
2. M. Abercrombie and J. E. M. Heaysman (1954) Exp. Cell Res. **6**, 293–306.
3. I. Folkman and A. Moscona, (1978) Nature **273**, 345–349.
4. S. Levenberg, B.-Z. Katz, K. M. Yamada, and B. Geiger (1998) J. Cell Sci. **111** 347–357.
5. M. G. P. Stoker (1973) Nature **246**, 200–203.
6. G. A. Dunn and G. W. Ireland (1984) Nature **312**, 63–65.
7. B. Alberts, D. Bray, J. Lewis, M. Raff, K. Roberts, and J. D. Watson (1989) *Molecular Biology of the Cell*, 3rd ed., Garland Publishing, New York, p. 898.
8. P. F. Kruse Jr. and E. Miedema (1965) J. Cell Biol. **27**, 273.
9. I. McKay and J. Taylor-Papadimitriou (1981) Exp. Cell Res. **134**, 465–470.
10. J. Folkman and C. Haudenschild (1980) Nature **288**, 551–556.
11. P. Kahn and T. Graf (1986) *Oncogenes and Growth Control*, Springer, Berlin.
12. K. Siegfried, Y. H. Han, M. A. A. DeMichele, J. D. Hunt, A. L. Gaither, and F. Cuttitta (1994) J. Biol. Chem. **269**, 8596–8603.
13. A. Balmain and K. Brown (1988) Adv. Cancer Res. **51**, 147–182.
14. R. I. Freshney (1994) *Culture of Animal Cells, a Manual of Basic Technique*, Wiley-Liss, New York, p. 233.
15. C. M. MacDonald, R. I. Freshney, E. Hart, and D. I. Graham (1985) Exp. Cell Biol. **53**, 130–137.
16. J. G. Rheinwald and H. Green (1975) Cell **6**, 331–344.
17. S. Terada, Y. Itoh, H. Ueda, and E. Suzuki (1997) Cytotechnology **24**, 135–141.

Contact Maps

Contact maps are two-dimensional representations of three-dimensional protein structures. A three-dimensional description of a protein structure composed of N structural units could be expressed as an $N \times N$ array of the pairwise distances (see Distance Geometry). This could be done for all pairs of atoms, for selected types of atoms (eg, Ca atoms), for groups of atoms (eg, side-chain centers of mass), or for entire amino-acid residues. Contact maps are generated from such matrices by taking a certain cutoff value for the pairwise distances. For example, the $N \times N$ matrix of the distances between protein Ca atoms (1, 2) can be transformed into a Ca-based contact map (3). Those Ca atoms that are closer to each other in the protein structure than the chosen cutoff distance are considered to be “in contact.” This produces a binary $N \times N$ matrix—a so-called black and white contact map. Alternatively, one may assume a set of several critical values for the distances between Ca atoms (or for other atoms or groups of atoms) and generate an integer matrix—the equivalent of a contact map with a colored or gray scale. A map of main-chain hydrogen bonds could also be considered as a variant of a protein contact map. The choice of structural units being mapped and the choice of cutoff distances determine the quality and range of structural information being stored in a contact map (see Fig. 1).

Figure 1. Schematic drawing of the structure of the B domain of protein G and its contact maps. (a) Three-dimensional structure of the B domain. (b) Ca-based contact maps: above the diagonal, the black and white map with a cutoff distance of 8 Å; below the diagonal is the gray-scale map where various shades of gray correspond to three values of the cutoff

distance, 8 (darkest), 10, and 12 Å. (c) Side-chain-based contact map. Above the diagonal, the dark squares correspond to the pairs of side chains for which the distance between at least one pair of heavy atoms is less than 5 Å. Below the diagonal, a 6.25-Å cutoff criterion has been applied to the centers of mass of the side chains. (d) The main chain hydrogen bond map for the same structure. The amino acid sequence of the protein is given along each axis in one-letter code, and the secondary structure is indicated as follows: E is extended b-strand, H is helix, and S and T are two types of turns.

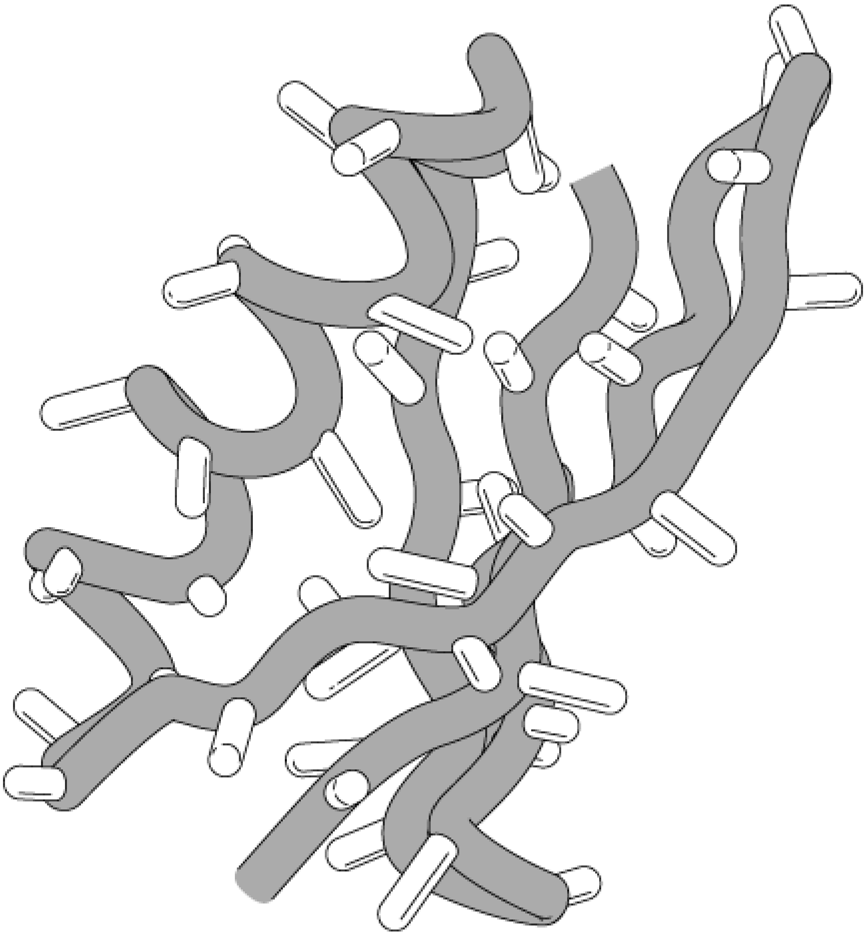

Figure 1. (*continued*) Schematic drawing of the structure of the B domain of protein G and its contact maps. (a) Three-dimensional structure of the B domain. (b) Ca-based contact maps: above the diagonal, the black and white map with a cutoff distance of 8 Å; below the diagonal is the gray-scale map where various shades of gray correspond to three values of the cutoff distance, 8 (darkest), 10, and 12 Å. (c) Side-chain-based contact map. Above the diagonal, the dark squares correspond to the pairs of side chains for which the distance between at least one pair of heavy atoms is less than 5 Å. Below the diagonal, a 6.25-Å cutoff criterion has been applied to the centers of mass of the side chains. (d) The main chain hydrogen bond map for the same structure. The amino acid sequence of the protein is given along each axis in one-letter code, and the secondary structure is indicated as follows: E is extended b-strand, H is helix, and S and T are two types of turns.

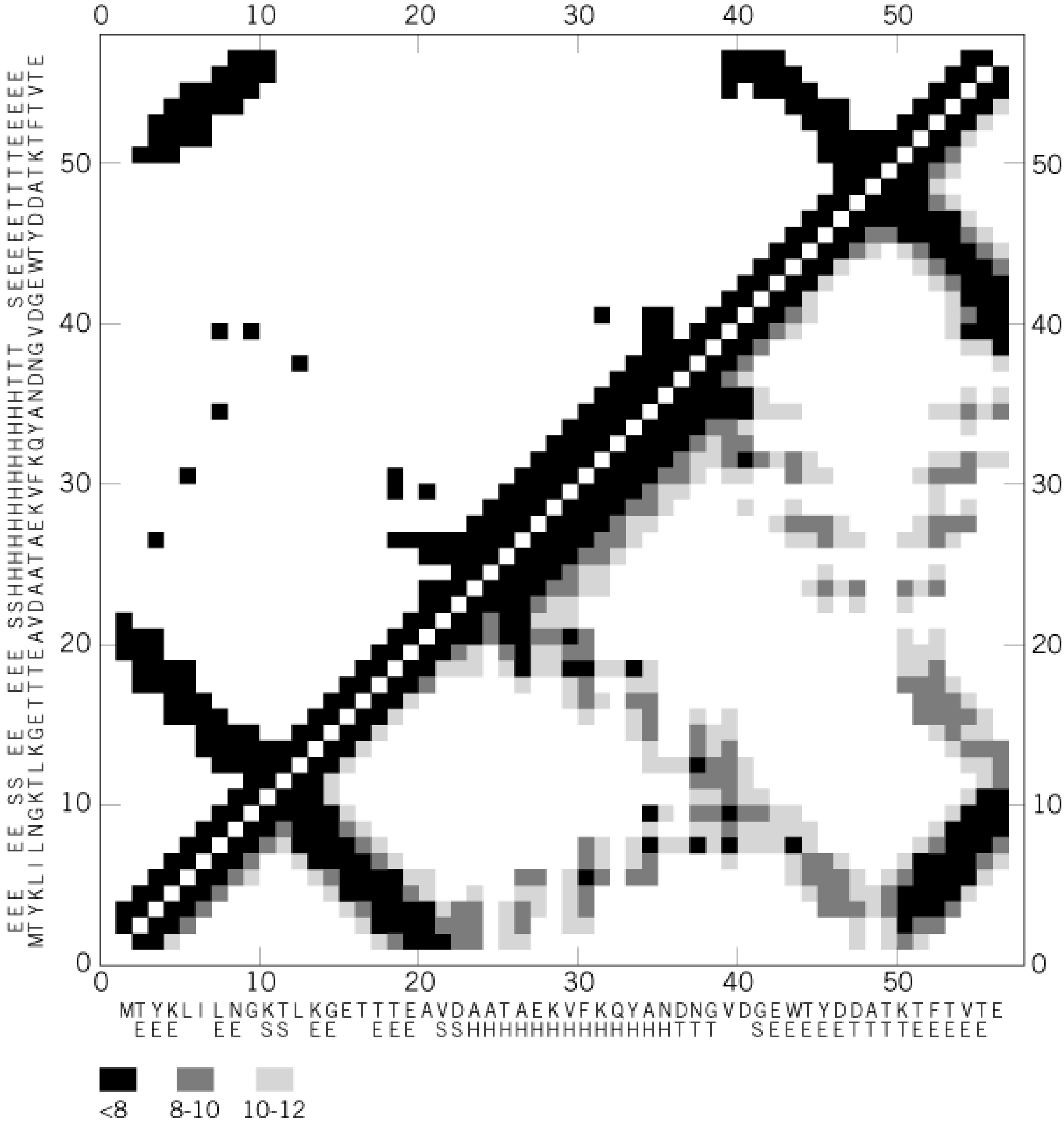

Figure 1. (*continued*) Schematic drawing of the structure of the B domain of protein G and its contact maps. (a) Three-dimensional structure of the B domain. (b) Ca-based contact maps: above the diagonal, the black and white map with a cutoff distance of 8 Å; below the diagonal is the gray-scale map where various shades of gray correspond to three values of the cutoff distance, 8 (darkest), 10, and 12 Å. (c) Side-chain-based contact map. Above the diagonal, the dark squares correspond to the pairs of side chains for which the distance between at least one pair of heavy atoms is less than 5 Å. Below the diagonal, a 6.25-Å cutoff criterion has been applied to the centers of mass of the side chains. (d) The main chain hydrogen bond map for the same structure. The amino acid sequence of the protein is given along each axis in one-letter code, and the secondary structure is indicated as follows: E is extended b-strand, H is helix, and S and T are two types of turns.

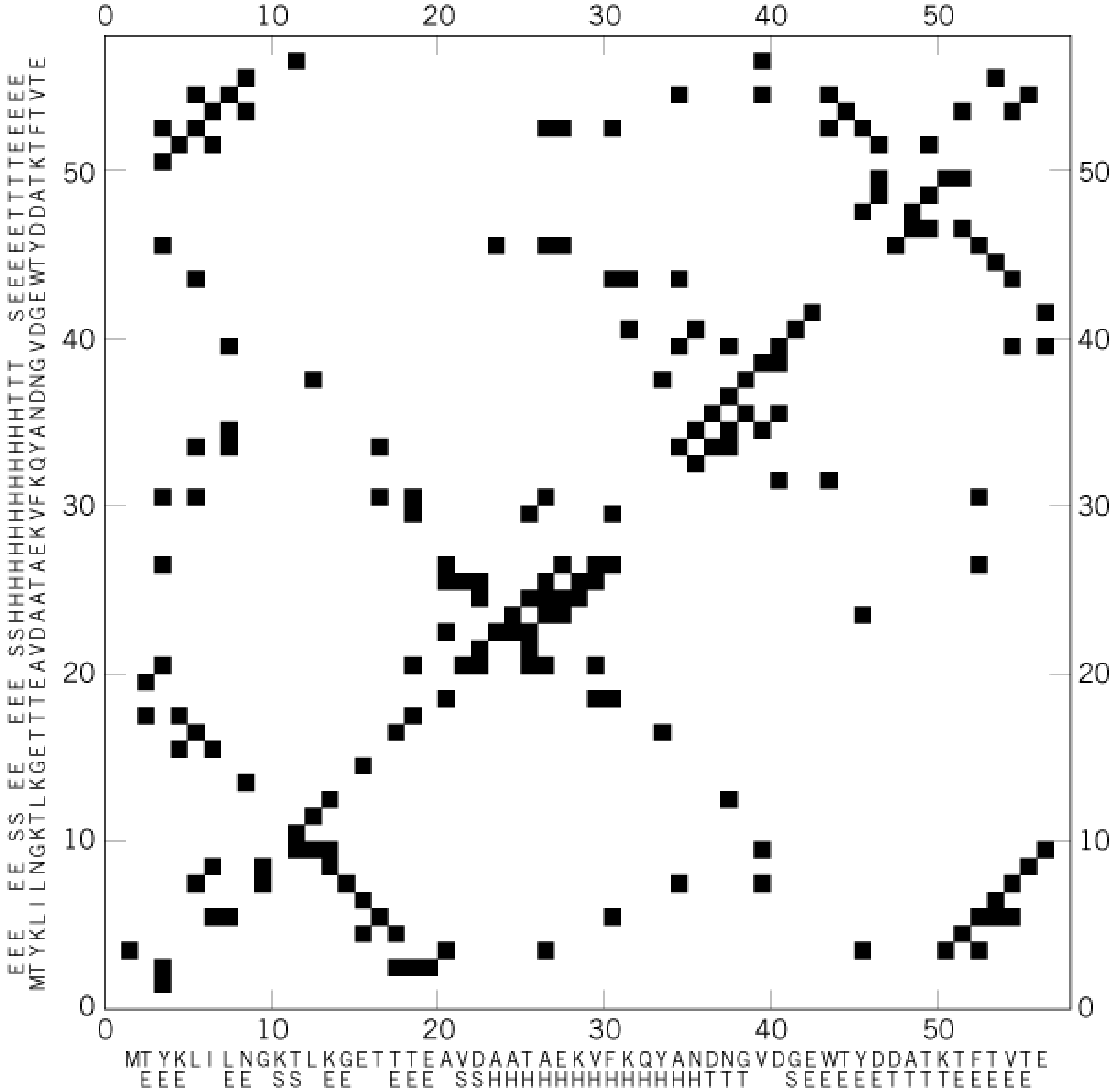

Figure 1. (*continued*) Schematic drawing of the structure of the B domain of protein G and its contact maps. (a) Three-dimensional structure of the B domain. (b) Ca-based contact maps: above the diagonal, the black and white map with a cutoff distance of 8 Å; below the diagonal is the gray-scale map where various shades of gray correspond to three values of the cutoff distance, 8 (darkest), 10, and 12 Å. (c) Side-chain-based contact map. Above the diagonal, the dark squares correspond to the pairs of side chains for which the distance between at least one pair of heavy atoms is less than 5 Å. Below the diagonal, a 6.25-Å cutoff criterion has been applied to the centers of mass of the side chains. (d) The main chain hydrogen bond map for the same structure. The amino acid sequence of the protein is given along each axis in one-letter code, and the secondary structure is indicated as follows: E is extended b-strand, H is helix, and S and T are two types of turns.

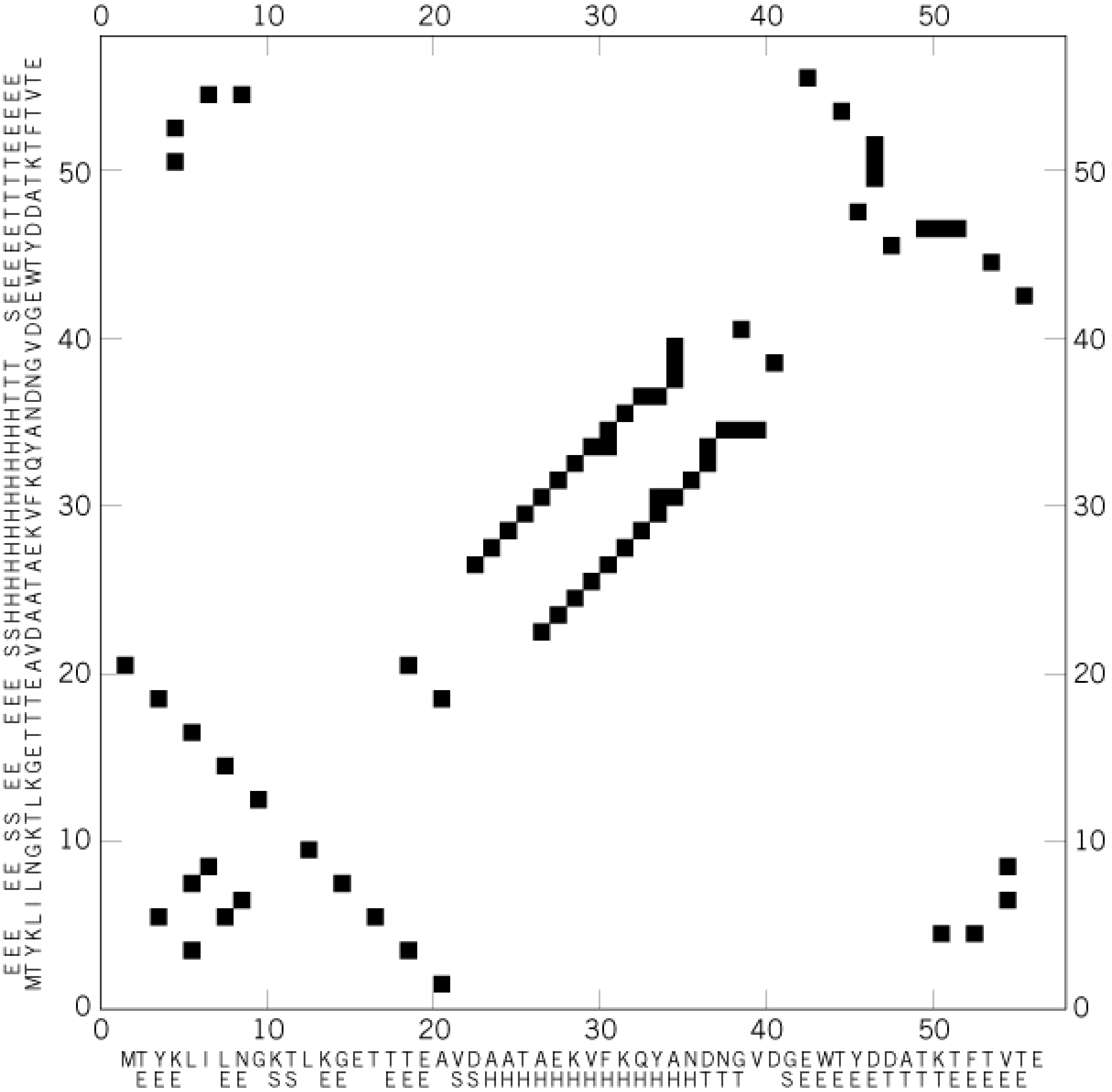

1. Contact Maps as a Fingerprint of Protein Three-Dimensional Structure

A contact map constitutes a structural “fingerprint” of a protein (4). Each protein can be identified based on its contact map. The **secondary structure**, fold topology, and side-chain packing patterns (for side-chain contact maps) can be visualized conveniently and read from the contact map. Furthermore, structural similarity between a pair of proteins is immediately apparent by a very pronounced similarity of their contact maps; in comparing two protein structures, there is no need to search all their possible relative orientations. The reconstruction of a protein structure from its contact map is more complex, although low-to-moderate resolution three-dimensional models can be easily built, even from a fragmentary contact map (5). The accuracy of the model depends on the type of contact map and the computational tools employed. A combination of protein nuclear magnetic resonance NMR spectra (see NOESY Spectrum; COSY Spectrum) constitutes a hybrid contact map of a protein, and model building from these data is an example of a map-to-structure modeling procedure (6, 7).

2. Ca-Based Contact Maps

Ca-based contact maps and distance matrices were perhaps the first commonly used maps for visualization of protein structures (3, 8, 9). An example is given in Figure 1b. These contact maps reflect well the overall topology of the protein fold, but only rather coarse structural details can be read from them. This is due to the fact that the Ca–Ca distance distributions extracted from protein structures have several convoluted peaks. These peaks correspond to various distances between pairs of various secondary structure elements (a-helices, beta-strands, etc.). Thus, a single cutoff distance is always inadequate: Too small a value would miss some helix-to-helix contacts, while too large a value may create some problems with identification of the secondary structure patterns. Gray scale maps (several cutoff ranges) communicate much more detailed structural information.

3. Side-Chain Contact Maps

Side-chain contact maps contain much richer information, not only about the topology of a protein fold and its secondary structure, but also many fine details about the packing patterns of the protein side-chains. Various conventions can be used to build side-chain contact maps; two are illustrated in Figure 1. In one case, two residues are assumed to be in contact when any two heavy atoms (ie, all except hydrogen) are a shorter distance from each other than some assumed cutoff. Due to the comparable size of all the united atom types constituting the side chains (eg, CH_2, CH, NH_2, etc.), a good choice of cutoff distance is between 4.5 and 5.0 Å (4, 10). In this range, the number of detected contacts is not sensitive to the particular choice of cutoff, and the packing pattern of the side chains is always described with high fidelity. Characteristic patterns of contacts between elements of secondary structure are an important and useful feature of these contact maps (11). Alternatively, one may build a side-chain contact map using the side-chain centers of mass as a reference. In this case, a larger value of the cutoff distance needs to be used. These cutoff values for the distance between side-chain centers of mass could be made specific for certain amino acid pairs, on the basis of the different sizes of the side chains, which produce different average contact distances for various pairs. As seen in Figure 1, the two approaches (atom based and center of mass based) lead to very similar protein representations. The patterns of the atom-based contact maps are slightly better defined.

4. Regularities of the Contact Maps Reflect Regularities of Protein Structures

Different types of contact maps reflect different aspects of the regularities seen in protein structures. The side-chain-based contact maps are a very good example (10). Near the diagonal of the map, the distinct features of the protein secondary structure can be easily read. Indeed, for extended fragments of the polypeptide chain, only residues i and i + 2 can be in contact. For a-helices, the i, i + 3 and i, i + 4 patterns of contacts are well pronounced. Furthermore, characteristic clusters of contacts further away from the diagonal reflect the packing between particular pairs of b-strands within the b-sheets. Parallel and antiparallel structures have very different features on the contact patterns. Very characteristic patterns could also be observed for other pairs of secondary-structure elements. It is even very easy to distinguish between the patterns for two helices in a helical or a/b protein and in the coiled-coil structural motifs. Figure 2 shows some typical side-chain contact map patterns.

Figure 2. Representative patterns of side-chain contact maps describing interactions between a-helices (top) and between b-strands in parallel and antiparallel beta-sheets (bottom).

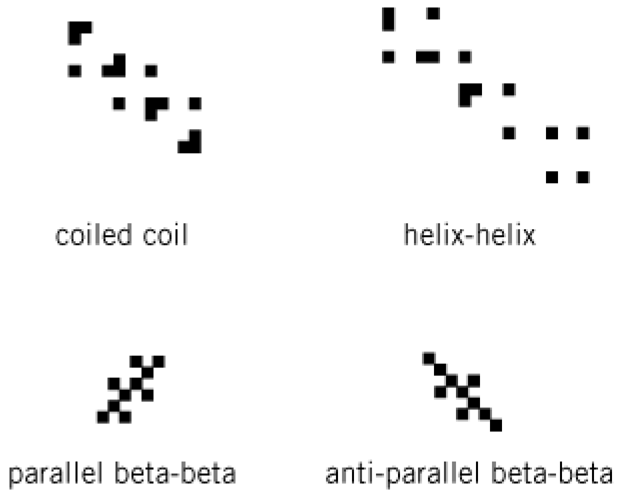

5. Application of Contact Maps in Modeling Protein Structure

Contact maps provide a very convenient way of identifying pairwise interactions within protein structures. This has been applied in various algorithms for threading protein sequences, where contact maps are actually used as ersatz template structures (4). In computer simulations of biological molecules, contact maps provide a convenient way of displaying structural changes. Also, regularities of the patterns seen in all classes of proteins can provide a guideline for designing knowledge-based multibody potentials (12, 13) and for protein modeling in a reduced (and perhaps also in all-atom) representation (13, 14). Such potentials may be necessary to reproduce the all-or-none character of protein folding transitions in model simulations (15).

One can easily recognize the distinct features of well-defined contact maps, with their characteristic patterns, after inspecting several maps of various proteins. This is an excellent example of a pattern recognition problem that could be learned by **neural network calculations**. Then such a trained network can be used for the automated recognition of good versus poor models of protein structure (16).

Bibliography

1. I. D. Kuntz (1975) J. Am. Chem. Soc. **97**, 4362–4366.
2. F. M. Richards and C. E. Kundrot (1988) Proteins **3**, 71–84.
3. M. Levitt (1976) J. Mol. Biol. **104**, 59–107.
4. A. Godzik, J. Skolnick, and A. Kolinski (1992) J. Mol. Biol. **227**, 227–238.
5. J. Skolnick, A. Kolinski, and A. R. Ortiz (1997) J. Mol. Biol. **265**, 217–241.
6. W. Braun and N. Go (1985) J. Mol. Biol. **186**, 611–626.
7. R. Kaptein, R. Boelens, R. M. Scheek, and W. F. van Gunsteren (1988) Biochemistry **27**, 5389–5395.
8. M. N. Liebman, C. A. Venanzi, and H. Weinstein (1985) Biopolymers **24**, 1722–1758.
9. D. C. Philips (1970) Biochem. Soc. Symp. **30**, 11–28.
10. A. Godzik and C. Sander (1989) Protein Eng. **2**, 589–596.
11. A. Godzik, J. Skolnick, and A. Kolinski (1993) Protein Eng. **6**, 801–810.
12. A. Kolinski, A. Godzik, and J. Skolnick (1993) J. Chem. Phys. **98**, 7420–7433.
13. A. Kolinski and J. Skolnick (1996) *Lattice Models of Protein Folding, Dynamics and Thermodynamics*, R. G. Landes, Austin, TX.
14. K. A. Olszewski, A. Kolinski, and J. Skolnick (1996) Proteins **25**, 286–299.
15. A. Kolinski, W. Galazka, and J. Skolnick (1996) Proteins **26**, 271–287.
16. M. Milik, A. Kolinski, and J. Skolnick (1995) Protein Eng. **8**, 225–236.

Contiguous Genes

The order of genes on a chromosome and the existence of directly contiguous genes can be useful in understanding their individual functions and in mapping the genome to understand the function of chromosomal **domains**. In **prokaryotes** there is often a close linkage of genes involved in a common metabolic pathway. This type of linkage is uncommon in **eukaryotes**, although examples exist, including five genes in *Neurospora crassa* involved in synthesis of chorismic acid (1) and two genes in *Drosophila* melanogaster involved in purine metabolism (2).

There are several families of closely linked genes in humans. These include genes for alcohol dehydrogenase, a-amylase, the major histocompatibility complex, a-globins, b-globins, chorionic gonadotropin, luteinizing hormone, and growth hormone. Every chromosome has at least one family cluster of undispersed genes. These clusters vary in size from several thousand base pairs to millions of base pairs with a large cluster like the major histocompatibility complex. The members of a single **gene family** are derived from the gene duplication of single ancestral genes. Whereas gene families are rare in prokaryotes, the more complex differentiative states in eukaryotes require similar gene products with subtle differences in function. An example of a well-studied locus, where genes with closely related functions are linked together, occurs at the a- and b-globin loci. At these chromosomal sites, globin genes specific for embryos, neonatal and adult animals are linked together and expressed in a sequential fashion during development (Fig. 1). The globin loci also present interesting examples of where gene linkage helps understanding the chromosomal function. All of the globin genes depend on a super enhancer known as a **locus control region** (LCR), which functions over an entire chromosomal **domain**.

Figure 1. The b-globin gene cluster, which is on the short arm of chromosome 11 in humans and includes five genes tha are sequentially expressed during development. Its locus control region (LCR) consists of five short stretches of DNA extending over a span of 12 bp. Similarly, there are three a-globin genes on the short arm of chromosome 16, but that LC comprises only one DNA sequence far upstream.

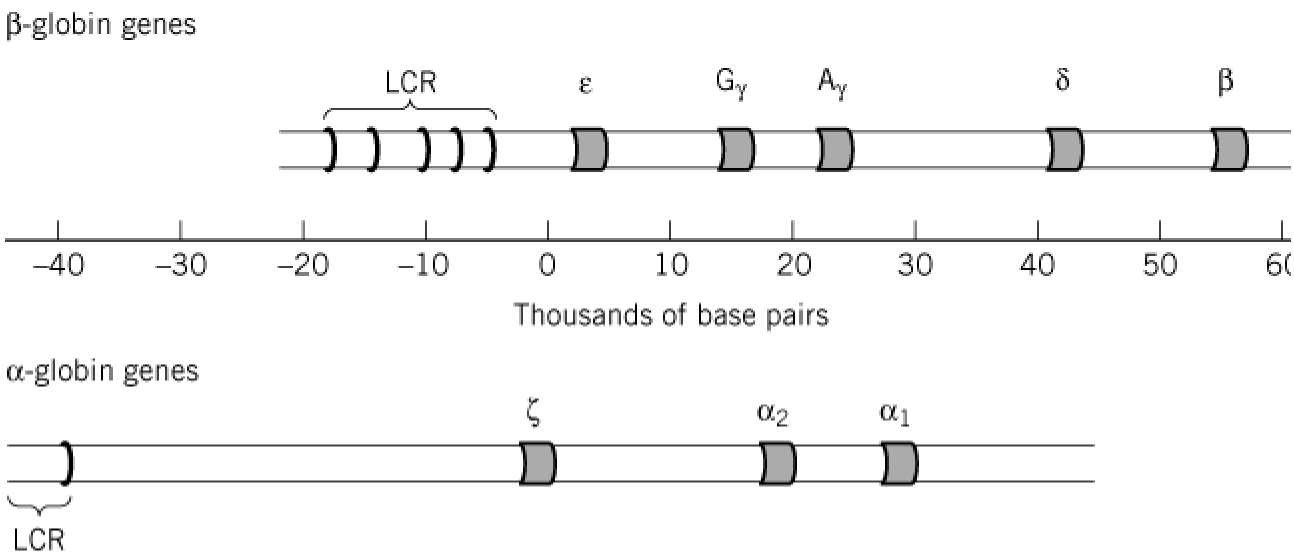

The relative order of genes is often conserved within a chromosome.This is termed linkage conservation. Linkage conservation often occurs in chromosomes isolated from distinct species. For example, in the X-chromosome there are many genes that have the same order along the chromosome in both mouse and humans. This is a useful aid in mapping new genes. There are several potential evolutionary advantages to linking certain genes together, which include common regulatory mechanisms, at the level of establishing a functional chromosomal domain, as described for the globin genes (3), or in terms of coordinate expression, as described for two genes involved in a particular metabolic pathway. There may also be regulatory mechanisms where genes compete with each other for a common regulatory element, as occurs in the globin genes at certain times in development (4).

Bibliography
1. F. H. Gaertner and K. W. Cole (1977) Biochem. Biophys. Res. Comm. **75**, 259–270.
2. M. E. Johnstone (1985) Biochem. Genet. **23**, 539–546.
3. F. Grosveld, G. B. van Assendelft, D. R. Greaves, and G. Kollias (1987) Cell **51**, 975–985.
4. M. Wijgerde, F. Grosveld, and P. Fraser (1995) Nature **377**, 209–213.

Contrast Variation

"Contrast" in scattering and diffraction experiments is defined as the difference between the mean scattering density of a component and its background, which can be a solvent or other components of an assembly of biological molecules. The greater the contrast, the more readily a component can be distinguished from its surroundings. "Contrast variation" involves the manipulation of the contrasts of specific components in a system in order to extract structural information on individual components. Contrast variation used in combination with small-angle scattering is a powerful method for examining the shapes and interactions of biological molecules in solution. If one has ordered samples, then contrast variation used in combination with **neutron diffraction** experiments can give important information on the location of disordered components that cannot be seen in X-ray diffraction experiments.

1. Contrast Variation with Neutrons

Either contrast variation experiments take advantage of inherent differences in scattering density between components of a complex or assembly, or the experimenter introduces contrast into the system by manipulating the scattering density of a specific component. Scattering densities are calculated by summing the scattering amplitudes of each atom within a volume and dividing by that volume. Because X-rays are scattered by electrons and the X-ray scattering amplitudes of atoms increase monotonically with the number of electrons, it is difficult to change the scattering density of a biological molecule in a benign way. On the other hand, neutrons provide extremely elegant and practical means for contrast variation. Neutrons are scattered by atomic nuclei in a sample. Hence neutron scattering amplitudes depend upon the complex properties of the neutron–nucleus interaction, and they show no systematic dependence on atomic number. Furthermore, isotopes of the same element can have very different neutron scattering properties. For neutrons, one of the largest differences in neutron scattering amplitude is between the isotopes of hydrogen (^1H and ^2H). Table 1 lists the coherent, elastic neutron scattering amplitudes for the atoms commonly found in biological systems. Note that the scattering amplitudes for most nuclei are positive and approximately equal. The exception is the scattering amplitude for ^{1}H which is negative, resulting from a 180° phase shift between neutrons scattered by ^{1}H compared to the other nuclei. As a consequence, the neutron scattering density of a particle depends strongly on its mean hydrogen content. The basic biological constituents, proteins, polynucleotides, and lipids, each have quite different mean neutron scattering densities (Fig. 1). Furthermore, the scattering densities for pure $^{1}H_2O$ and $^{2}H_2O$ bracket the values for biological constituents. Thus by simply varying the $^{2}H_2O$:$^{1}H_2O$ ratio in the solvent, one can do a contrast variation experiment on a protein–DNA complex, or a membrane protein in a bilayer. For a complex of proteins, selective deuteration of individual proteins provides a way of altering their mean neutron scattering densities for contrast variation studies. Recently, it has been demonstrated that one can obtain dramatically increased contrast effects using a novel method of "spin contrast variation." This method uses polarized neutron scattering from samples labeled with dynamically polarized nuclei and has been demonstrated to be effective for studying biological systems by locating RNA (1) and proteins (2, 3) in ribosomes.

Table 1. Coherent Neutron Scattering Lengths, b_{coh}, and Corresponding X-Ray Scattering Factors, $f_{X\text{-ray}}$, for Biologically Relevant Nuclei

Atom	Nucleus	(10^{-12} cm)	f_X for q = 0(10^{-12} cm)[a]
Hydrogen	^{1}H	–0.3742	0.28
Deuterium	^{2}H	0.6671	0.28
Carbon	^{12}C	0.6651	1.69
Nitrogen	^{14}N	0.940	1.97
Oxygen	^{16}O	0.5804	2.25
Phosphorous	^{31}P	0.517	4.23
Sulfur	mostly ^{32}S	0.2847	4.5

[a] X-ray scattering amplitudes are normally given in units of electrons, but have been converted to cm here for comparison with neutron scattering amplitudes. At very short wavelengths and low-Q, the X-ray coherent scattering cross-section of an atom with Z electrons is $4p(Zr_0)^2$, where $r_0 = e^2/m_e c^2 = 0.28 \times 10^{-12}$ cm.

Figure 1. Average scattering length densities for biological molecules as a function of the fraction of D_2O in the solvent. The slope of the lines arises from the exchange of labile hydrogens.

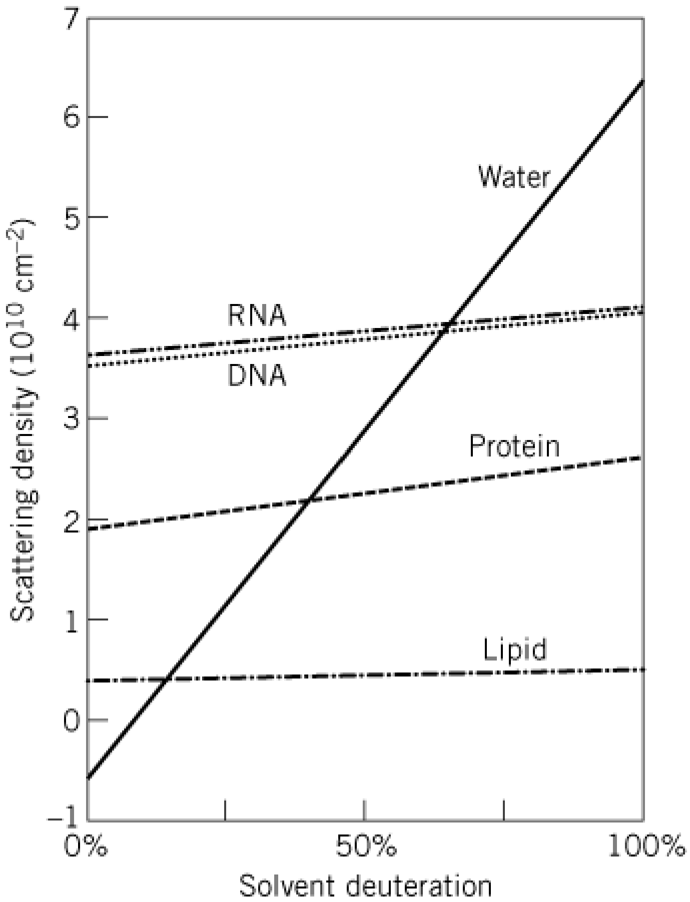

2. Small-Angle Scattering with Contrast Variation

The scattering intensity distribution from a homogeneous solution of monodisperse particles in a solution can then be expressed as

$$I(Q) = \int\int \Delta\rho(\mathbf{r}_1)\Delta\rho(\mathbf{r}_2)\frac{\sin Q|\mathbf{r}-1-\mathbf{r}_2|}{Q|\mathbf{r}_1-\mathbf{r}_2|}d\mathbf{r}_1 d\mathbf{r}_2 \qquad (1)$$

The integration is taken over the volume of the particle. Q is the momentum transfer or scattering vector amplitude and is equal to 4p(sin q)/l, where q is half the scattering angle, and l is the wavelength of the incident neutron radiation. Dr(**r**) = r(**r**) – r_s is the "contrast," or neutron scattering density difference between the particle and the solvent. For uniform scattering density particles, if one can "match," or make equal, the scattering density of a particle and its solvent, then the small-angle scattering from that particle will be zero; that is, the particle will become "invisible" in the scattering experiment. For a multicomponent assembly, one can use this technique to study the shape of an individual component within the assembly. Rigorous solvent matching can be difficult, however, and is made more difficult when there are significant internal density fluctuations within the component being matched.

For a two-component complex in solution, one can conduct a series of measurements at different contrast points ("contrast series") to extract the basic scattering functions of individual components. Ignoring internal scattering density fluctuations, the scattering from a two-component complex in solution can be written as

$$I(Q,\Delta\rho_1,\Delta\rho_2) = \Delta\rho_1^2 I_1(Q) + \Delta\rho_1\Delta\rho_2 I_{12}(Q) + \Delta\rho_2^2 I_2(Q) \qquad (2)$$

The subscripts 1 and 2 refer to each component; and $Dr_{1(2)} = r_{1(2)} - r_s$, where $r_{1(2)}$ is that mean scattering density for component 1 (or 2). $I_1(Q)$ and $I_2(Q)$ represent the scattering of components 1 and 2, respectively, while $I_{12}(Q)$ is the cross term. A set of scattering measurements with different solvent scattering densities, or contrasts, gives a set of equations in the form of equation 2, which can be solved by linear least-squares regression to give the three basic scattering functions $I_1(Q)$, $I_2(Q)$, and $I_{12}(Q)$. Using these functions, the individual structural parameters for each component such as molecular weight, radius of gyration, R_g, and the pair distribution function, $P(r)$, can be calculated, as well as information on the relative dispositions of the individual components (see Small-Angle Scattering and Radius Of Gyration for details). $P(r)$ is the probable frequency distribution of all vector lengths between pairs of volume elements within the scattering component, weighted by the product of the scattering densities of each pair of volume elements. $P(r)$ is calculated as the indirect Fourier transform of the basic scattering function for each component, and its second moment gives R_g for that component. The indirect Fourier transform of the cross term $I_{12}(Q)$ gives the pair distribution function containing intercomponent vector lengths, which can give information on the distance between the two components.

Ibel and Stuhrmann (4) proposed an alternative approach to determining the relative dispositions of components in a complex. They showed that the $R_g^{\,2}$ dependence on the scattering contrast can be written as

$$R_g^2 = R_m^2 + \frac{\alpha}{\Delta\rho} - \frac{\beta}{\Delta\rho^2} \qquad (3)$$

where R_m is R_g at infinite contrast; and $Dr = r - r_s$, where r is the mean scattering density for the complex and r_s is the scattering density of the solvent. The coefficient a is related to the second moment of the scattering density fluctuations about the mean value for the complex, while b is related to the square of the first moment of the density fluctuations about the mean. If the sign of a is positive, the lower scattering density component is more toward the inside of the complex than the higher scattering density component. A negative a indicates the reverse. b is proportional to the square of the separation of the centers of mass of the two components. If b is zero, then the centers of mass are coincident.

3. Deuteration of Biological Molecules

Neutron scattering and/or diffraction experiments using contrast variation frequently depend upon the ability to reconstitute complexes with specific components labeled uniformly with deuterium. Deuteration of biological molecules is achieved by growing microorganisms on deuterated media. Relatively high average levels of deuteration (50% for nucleic acids, 70 to 80% for proteins) can be achieved by growing organisms on ^2H_2O with normal protiated carbon sources (5). Typically, however, the aromatic groups are not highly deuterated using this approach. Higher levels of enrichment (> 99%) are achieved using deuterated nutrients and ^2H_2O (5). Deuterated algal hydrolysate provides an excellent rich growth medium for *E. coli* containing an expression system with a specific protein of interest. If the expression is sufficiently robust, deuteration can be achieved in minimal growth media with deuterated glucose, glycerol, or succinate in ^2H_2O. Intermediate levels of uniform deuterium labeling can be achieved by diluting ^2H with ^1H in the growth medium.

4. Examples of the Application of Contrast Variation

4.1. Small-Angle Scattering and Contrast Variation

Examples of significant advances based on small-angle neutron scattering with contrast variation include: the solution structure of the nucleosome core particle showing the DNA winding around the outside of the histone core (6, 7); mapping the radial distribution of protein and nucleic acid components in the influenza virus (8); determining the subunit structure of DNA-dependent **RNA polymerase** (9) and its relationship to a 130-bp DNA fragment (10); the subunit structure of a ribosome particle, showing the dispositions its components (11, 12) (see Neutron Diffraction And Scattering); and the determination of the conformations and dispositions calmodulin complexed with its target enzymes (13) and of the evolutionarily related muscle protein troponin C (TnC) complexed with its regulatory target troponin I (TnI) (13) which acts as a calcium-sensitive “switch” to regulate the contractile apparatus. Figure 2 illustrates this latter experiment, showing the model derived from a neutron contrast series on complexes of TnI with deuterated TnC in its calcium-saturated form (14). The neutron data show TnC in the complex has the unusual dumbbell shape evident in the TnC crystal structure (15, 16), while TnI forms a spiral structure that passes through two hydrophobic clefts in each globular domain of TnC. The diameter of the TnI central spiral is close to that expected for an a-helix. The model suggests a mechanism for the action of the calcium-sensitive TnC/TnI molecular switch. The hydrophobic cleft of the *N*-terminal regulatory domain of TnC alternately opens and closes (in response to calcium binding and release) and thus binds and releases TnI, which in turn switches “off” and “on” TnI's inhibition of the interactions between the muscle fibers required for contraction.

Figure 2. Model structure for the muscle protein complex troponin C/troponin I derived from small-angle neutron scattering and contrast variation (14). Troponin C is represented as a space filling model based on its crystal structure, and the green crosses represent the volume occupied by the troponin I. This figure is based on work done at Los Alamos National Laboratory. See color insert.

4.2. Diffraction Experiments with Contrast Variation

In crystals of large biomolecular complexes, there are frequently disordered regions, even when the diffraction data extend to relatively high resolution. The scattering from the disordered components is seen predominantly at low-*Q*—that is, in the "small-angle" region where the contrast effects can be strong. Deuteration strategies similar to those used in small-angle neutron scattering allow for contrast manipulation. Phase information can be derived for the low-*Q* data using contrast-variation procedures (17), beginning with starting phases from a X-ray crystallography or a model structure and using the contrast-variation relationships to produce the best scattering-density maps (18). Examples of experiments using contrast variation and low-resolution neutron crystallography include the determination of the location of 25% of the protein and the RNA in crystals of the Tomato Bushy Stunt Virus (19) that were "missing" in the 2.8 Å resolution X-ray structure. The most important conclusion of this study is that at the virus radius where the protein and RNA interact, the quasi-equivalence of the 180-protein subunits breaks down, and the RNA interacts preferentially with 60 of the subunits. This observation favors a model for self-assembly in which the RNA interacts with trimers of protein to form an icosahedral scaffolding in which the gaps are filled by the other 120 subunits which have nonspecific contacts with the RNA (see Capsids, Viral). Another example of the application of low-resolution neutron diffraction and contrast variation is in membrane protein crystallography, where it has been used to locate and orient detergent molecules with respect to the protein (20, 21). These experiments take advantage of the inherent high contrast between detergent and ^2H_2O; and they provide information on the role of detergent in membrane protein crystallization, as well as the potential lipid–protein interactions.

Bibliography

1. J. Wadzack et al. (1997) J. Mol. Biol. **266**, 343–356.
2. R. Willumeit et al. (1996) J. Mol. Struct. **383**, 201–211.
3. J. Zhao and H. B. Stuhrmann (1993) J. Phys. IV **3**, 233–236.
4. K. Ibel and H. B. Stuhrmann (1975) J. Mol. Biol. **93**, 255–265.
5. H. L. Crespi (1977) *Stable Isot. Life. Sci., Proc. Tech. Comm. Meet. Mod. Trends Biol. Appl. Stable Isot.*, IAEA, Vienna, pp. 111–121.
6. J. F. Pardon et al. (1975) Nucleic Acids Res. **2**, 2163–2176.
7. P. Suau et al. (1977) Nucleic Acids Res. **4**, 3769–3786.
8. S. Cusack, R. W. H. Ruigrok, P. C. J. Krygsman, and J. E. Mellema (1985) J. Mol. Biol. **186**, 565–582.
9. P. Stöckel et al. (1980) Eur. J. Biochem. **112**, 411–417 and 419–423.
10. H. Lederer, K. Mortensen, R. P. May, G. Baer, H. L. Crespi, and H. Heumann (1991) J. Mol. Biol. **219**, 747–755.
11. M. S. Capel, D. M. Engelman, B. R. Freeborn, M. Kjeldgaard, J. A. Langer, V. Ramakrishnan, D. G. Schindler, D. K. Scheider, B. P. Schoenborn, I. Y. Sillers, S. Yabuki, and P. B. Moore (1987) Science **238**, 1403–1406.
12. R. P. May, V. Nowotny, P. Nowotny, H. Voß, and K. H. Nierhaus (1992) EMBO J. **11**, 373–378.
13. J. K. Krueger, G. Zhi, J. T. Stull, and J. Trewhella (1998) Biochemistry **37**, 13997–14004.
14. G. A. Olah and J. Trewhella (1994) Biochemistry **33**, 12800–12806.
15. O. Herzberg and M. N. G. James (1985) Nature (London) **313**, 653–659.
16. M. Sundaralingham et al. (1985) Science **227**, 945–948.
17. M. Roth, A. Lewitt-Bentley, and G. A. Bentley (1984) J. Appl. Crystallogr. **17**, 77–84.
18. M. Roth (1991) In *Int. Union Crystallogr., Crystallogr. Symp.* **5** (Crystallogr. Comput. **5**) (D. M. Moras, and A. D. Podjarny, eds.), Oxford University Press, Oxford, U.K., pp. 229–248.
19. P. Timmins, D. Wild, and J. Witz (1994) Structure **2**, 1191.
20. M. Roth et al. (1989) Nature **340**, 659–662.
21. P. Timmins, E. Pebay-Peyroula, and W. Welte (1994) Biophys. Chem. **53**, 27–36.

Suggestions for Further Reading

22. L. A. Feigen and D. I. Svergun (1987) *Structure Analysis by Small-Angle X-Ray and Neutron Scattering*, Plenum Press, New York.
23. B. Jacrot (1976) Rep. Prog. Phys. **39**, 911–953.
24. P. B. Moore (1982) "Small-Angle Scattering Techniques for the Study of Biological Macromolecules and Macromolecular Aggregates", In *Methods of Experimental Physics*, Vol. **20** (G. Ehrenstein and H. Lecar, eds.), Academic Press, New York, pp. 337–390.
25. B. P. Schoenborn and R. B. Knott (eds.) (1996) *Basic Life Sciences*, Vol. **64**: Neutrons in Biology, Plenum Press, New York.
26. H. B. Stuhrmann (1987) "Molecular Biology". In *Methods of Experimental Physics*, 23, Part C, Academic Press, New York.

Controlling Element

Controlling element is the term used by Barbara McClintock (1) to describe the new genetic elements she found in the late 1940s that "can modify and control the action of the genes themselves" and "may move from location to location within the chromosome complement without losing its identity." We now know such elements as transposable elements—that is, discrete pieces of DNA that can move from place to place within a genome. Such elements are extremely widespread and have been found in virtually all organisms that have been examined. It is interesting that she discovered these elements that we now know to be mobile DNA before the structure of DNA was established in the early 1950s. The first molecular characterization of transposable elements came nearly 20 years later, after their discovery in bacteria, where DNAs containing them could be isolated and characterized (2).

McClintock was a maize geneticist and cytogeneticist. Her discovery of controlling elements resulted from the study of irregular patterns of pigment in maize kernels (ie, variegations of pigment patterns) that arose in some ears. Such variegation results in changes in pigment gene expression during kernel development. We now know that such variegation reflects the insertion of a transposable element to inactivate a gene and the subsequent excision of the element at a later time, restoring gene function. Having earlier studied chromosome breaks that resulted from unusual chromosome fusions, she was also quick to appreciate that some variegation resulted from chromosomal breakage at a particular site. She proposed that there was an element *dissociation* (Ds) at the breakage site and suggested that variegation results from the loss of genes downstream of this site following chromosome breakage.

Identification of an element that could cause chromosome breaks was novel, but even more dramatic was her finding that the element could move to another chromosomal site and again cause instability via chromosome breakage. McClintock realized that another element in addition to Ds was required to cause breaks at Ds and also to promote the translocation of Ds to another chromosomal position—that is, that another element encodes a product that promotes the movement of Ds. She named this other element *activator* (Ac) and also established that Ac could move from place to place.

We now know that Ac is an intact (autonomous) element (about 2.9 kbp) encoding a recombinase, a transposase, that acts on special sequences at the tips of the element to promote its translocation; Ds is a deleted version of Ac that lacks the transposase but still has the special terminal recombination sequences, so that Ac transposase can promote movement of Ds. Ds is called a **nonautonomous element** because it requires the presence of transposase provided by another element.

Bibliography

1. B. McClintock (1956) Cold Spring Harbor Symp. Quant. Biol. **21**, 197–216.
2. P. Starlinger (1977) In *DNA Insertion Elements, Plasmids, and Episomes* (A. I. Bukhari, J. A. Shapiro, and S. L. Adhya, eds.), Cold Spring Harbor Laboratory, Cold Spring Harbor, NY, pp. 25–30.

Convergent Evolution

Convergence is defined as an evolutionary event in which two morphological or molecular traits become similar during evolution due to a similarity in environment or selection pressure, even though these traits have independent ancestors or origins. In the case of amino acid or **nucleotide sequences**, there is little known evidence for convergence; the probability of two sequences becoming similar by convergence seems vanishingly small, and any similarities in sequence are attributed to divergent evolution. Yet even the absence of sequence similarity cannot be taken as evidence of convergence, as this will also result from extensive divergence between two sequences that originated from a common ancestor. In many such cases where proteins related functionally have no detectable sequence homology, their three-dimensional protein structures are very similar; protein structure appears to change more slowly than does the primary structure, and such cases seem to be further examples of divergent evolution.

There are, however, some examples of convergence that are apparent in the protein structure and the active sites of enzymes. For example, there are several kinds of serine proteinases. One family of these proteinases, represented by **chymotrypsin**, has very similar tertiary structures and active sites, containing a catalytic triad of serine, histidine, and aspartic acid residues. The serine proteinase subtilisin also contains an extremely similar triad structure, even though the rest of its tertiary structure and sequence is unrelated to the chymotrypsin family (Fig. 1) (1). Moreover, the three residues constituting the catalytic triad occur in different orders in the primary structures, making it virtually inconceivable that the two families of proteins arose from a common ancestor. Furthermore, serine carboxypeptidase II also contains a catalytic triad at its active site, even though its catalytic mechanism is entirely different. It is considered that the very similar triad structures of these different protein families emerged from their respective and independent ancestors by positive natural selection. This is one of the best characterized examples of convergent evolution.

Figure 1. Convergent evolution of the active site residues in subtilisin, chymotrypsin, and serine carboxypeptidase II. Al relative positions of active-site residues differ in the amino acid sequences among subtilisin, chymotrypsin, and serine carboxypeptidase II, they have a common catalytic triad consisting of Ser 221, His 64, and Asp 32 in subtilisin; of Ser 1 and Asp102 in chymotrypsin; and of Ser 146, His 397, and Asp 338 in serine carboxypeptidase II. Thus, they are conside examples of convergence or convergent evolution (2).

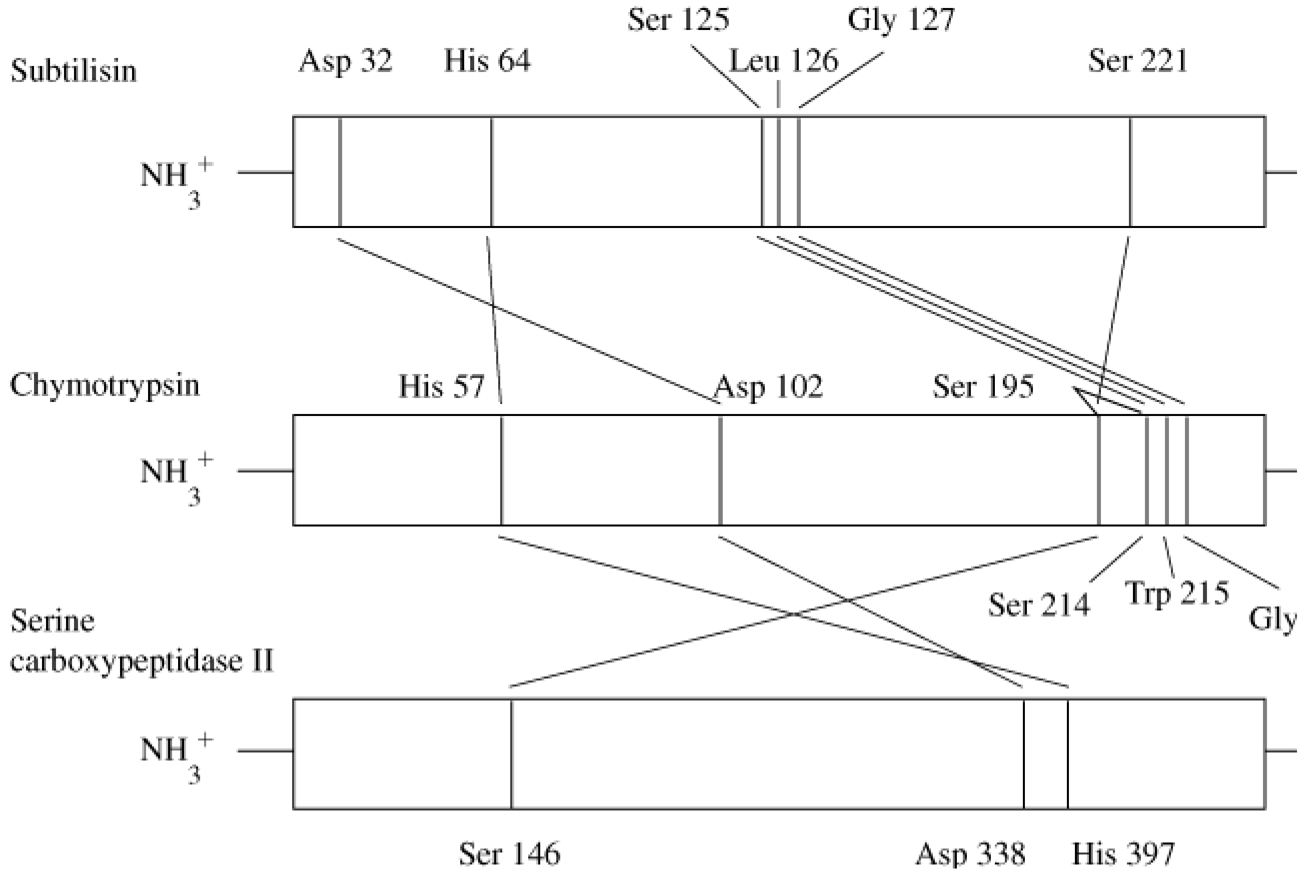

There are other examples of enzymes with the same functions but sufficient differences to make it clear that they have not arisen from the same ancestor, but that the same function has arisen independently by a type of convergent evolution (Table 1) (2).

Table 1. Some Enzymes that Have Evolved Independently on More Than One Occasion, by Convergent Evolution

Superoxide dismutases
Adolases
Sugar kinases
Serine proteinases
Alcohol dehydrogenases
Aminoacyl tRNA synthetases
Ribonucleotide reductases
Topoisomerases
Phosphoenoylpyruvate carboxykinases
Malate dehydrogenases

Bibliography
1. D. Voet and J. G. Voet (1995) *Biochemistry*, 2nd ed., Wiley, New York.
2. A. Doolittle (1994) Trends. Biochem. Sci. **19**, 15–18.

Coomassie Brilliant Blue

Proteins are most frequently detected after gel electrophoresis by fixing them in the gel, so that they do not diffuse further, and then staining them to produce a colored zone. The most sensitive stain is silver stain, but the stain used most frequently is Coomassie Brilliant Blue. It has two frequently encountered forms, R250 and G250, whose structures are depicted in Figure 1. Although the two dyes are structurally very similar, they require different physical and staining procedures and are not interchangeable in any particular protocol. These two dyes do not react chemically with proteins but merely form noncovalent complexes. The interaction with proteins is believed to be primarily ionic and involves the acidic sulfonate groups on the dye and basic groups on the protein, but nonpolar **van der Waals** forces are probably also involved. Consequently, the dyes do not bind equally to all proteins, so two electrophoretic bands with the same blue color need not contain the same amount of protein (1).

Figure 1. The chemical structures of the R250 and G250 forms of Coomassie Brilliant Blue. They differ only in the nature of the group R.

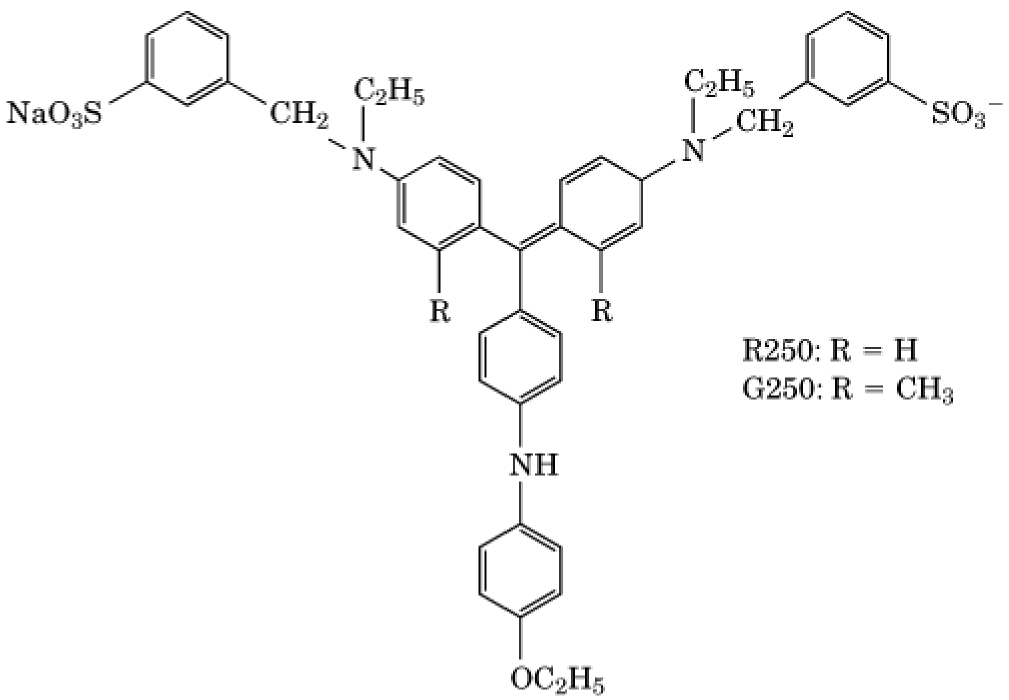

Electrophoresis gels are readily stained by placing the gel in a liquid containing the Coomassie dye plus an agent to fix the protein bands, usually acetic acid plus methanol; a solution of 10% (w/v)

trichloroacetic acid plus 10%(w/v) sulfosalicylic acid is very effective for fixing and staining. Fixed and insoluble proteins bind the dye tightly. It is usually necessary to remove the excess dye from the staining mixture before the bands on the gel can be seen. This is usually accomplished simply by washing the gel in the fixative solution, but it can also be accomplished by adding an agent, such as polyurethane foam, that binds the excess dye tightly. It is important not to remove all of the excess dye from the solution because then the dye bound to the protein bands dissociates and the gel becomes bleached. The procedure is simplified if the Coomassie dye is only slightly soluble in the original staining mixture; the protein takes up the dye from the solution, but the background color remains weak.

A number of other dyes, such as Ponceau S and Amido black, can be used in the same way, but they are not as sensitive as the Coomassie dyes. Coomassie Brilliant Blue detects approximately 0.1 µg of protein in a band on a polyacrylamide gel.

Coomassie Brilliant Blue, particularly G250, is also used to quantify the amount of protein in solution, which is known as the Bradford assay (2). The dye complexed to protein has an altered **absorbance** spectrum. Under certain acidic conditions, the absorbance maximum shifts from 465 to 595 nm upon binding to a protein. Even though different proteins give somewhat different responses in this assay, its simplicity makes it widely used.

Bibliography

1. M. Tal, A. Silberstein, and E. Nusser (1980) J. Biol. Chem. **260**, 9976–9980.
2. M. M. Bradford (1976) Anal. Biochem. **72**, 248–254.

Cordycepin

Cordycepin is 3′-deoxyadenosine, but is normally used in molecular biology as the triphosphate form. 3′-Deoxyadenosine triphosphate is a chain-terminating nucleotide analogue of ATP that can be incorporated into an **RNA** by polyadenylate polymerase. This inhibits further elongation of the poly A tail due to the absence of the 3′-hydroxyl group. The cordycepin triphosphate has been used primarily to study the polyadenylation reaction *in vitro*, where it has allowed this reaction to be resolved into two distinct steps: cleavage of the messenger RNA precursor and the addition of the poly A tail (see Polyadenylation) (1, 2).

Bibliography

1. M. Sheets, P. Stephenson, and M. Wickens (1987) Mol. Cell Biol. **7**, 1518–1529.
2. C. Moore, H. Skolnik-David, and P. Sharp (1986) EMBO J. **5**, 1929–1938.

Suggestion for Further Reading

3. W. Keller and L. Minvielle-Sebastia (1997) A comparison of mammalian and yeast pre-mRNA 3¢-end processing, Curr. Opin. Cell Biol., **9**, 329–336.

Corepressor

A corepressor is a molecule that binds to a sequence-specific DNA binding protein and enables that protein to direct transcriptional repression. The term is used to apply to two types of mechanism. In the first case, a small molecule binds to and effects a conformational change in a DNA-binding protein, thus, enabling binding to a specific DNA sequence. One example of this mode of action is the binding of tryptophan to the tryptophan repressor. The second type of corepressor is a protein that forms a specific complex with a sequence-specific DNA binding protein and then itself inhibits transcription either directly or indirectly. One example of such an activity is the complex formed in eukaryotes between histone deacetylases and DNA-targeted regulators via an adaptor protein.

COS Cells

COS cells are monkey kidney fibroblasts (Fig. 1); they have become popular in recent years because they support certain strains of replication-deficient animal **viruses** (1, 2) and can be **transfected** easily (3, 4). Two lines are in common use, COS-7 (ATCC CRL-1651) and COS-1 (ATCC CRL-1650).

Figure 1. Confluent culture of COS-7 cells. Phase contrast, Olympus CK microscope, 20× objective.

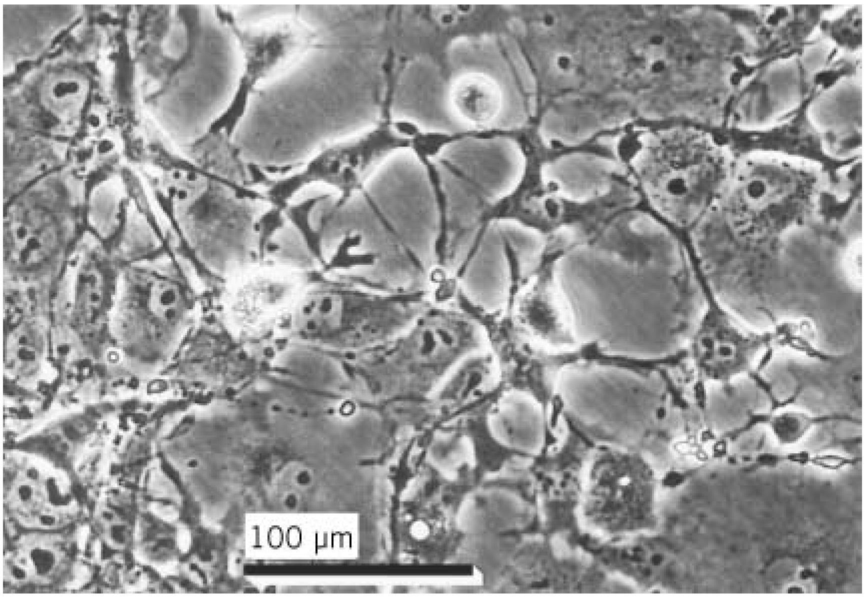

1. Origin

Both cell lines were derived from CV-1 cells (ATCC CCL-70), an established cell line of simian fibroblasts, by transformation with an origin-defective mutant of **SV40 virus** (1). Both are **T-antigen**-positive, permit lytic growth of SV40, and support the replication of temperature-sensitive mutant SV40 tsA209 and of SV40 mutants with deletions in the early region. COS-1 cells contain a single integrated copy of the complete early region of the SV40 genome.

2. Properties

COS cells are propagated as a monolayer in the alpha modification of Eagle's minimal essential medium (a-MEM) supplemented with 10% fetal bovine serum (see Serum Dependence) or in Dulbecco's modification of Eagle's medium. They grow rapidly, with an approximate population doubling time of 18 h.

3. Usage

COS cells have been used extensively in DNA transfer studies (5-7) and have been transfected by a number of different methods, including calcium phosphate (8), DEAE (4), and lipid transfection (9).

Bibliography

1. Y. Gluzman (1981) SV40-transformed simian cells support the replication of early SV40 mutants. Cell **23**, 175–182.
2. F. Unckell, R. E. Streeck, and M. Sapp (1997) J. Virol. **71**, 2934–2939.
3. Y. Cao, D. M. Stafforini, G. A. Zimmerman, T. M. McIntyre, and S. M. Prescott (1997) J. Biol. Chem. **273**, 4012–4020.
4. J. J. Schwartz and R. Rosenberg (1998) in *DNA Transfer to Cultured Cells*, K. Ravid and R. I. Freshney, eds., Wiley-Liss, New York, pp. 179–192.
5. V. Misra, H. J. Klamut, and A. M. Rauth (1998) Transfection of COS-1 cells with DT-diaphorase cDNA: Role of base change at position 609. Br. J. Cancer **77**, 1236–1240.
6. S. G. Plonk, S. K. Park, and J. H. Exton (1998) J. Biol. Chem. **273**, 4823–4826.
7. B. Corsi, F. Perrone, M. Bourgeois, C. Beaumont, M. C. Panzeri, A. Cozzi, R. Sangregorio, P. Santambrogio, A. Albertini, P. Arosio, and S. Levi (1998) Biochem. J. **330**, 315–320.
8. J. V. O"Mahoney and T. E. Adams (1998) in *DNA Transfer to Cultured Cells*, K. Ravid and R. I. Freshney, eds., Wiley-Liss, New York, pp. 125–145.
9. V. V. Bickko (1998) In *DNA Transfer to Cultured Cells* (K. Ravid and R. I. Freshney, eds., Wiley-Liss, New York, pp. 193–212.

COSY Spectrum

Correlation spectroscopy (COSY) was among the first two-dimensional (2D) nuclear magnetic resonance (NMR) experiments to be developed. In COSY–type experiments, cross peaks arise in a 2D map at the intersections of two chemical shifts if a resolved spin-coupling interaction exists between the nuclei characterized by the two shifts. The cross peaks have considerable fine structure, consisting of positive and negative signals if the lines of the spectrum are sufficiently narrow.

The appearance of the cross peaks in a COSY–type experiment relates to a quantum-mechanical phenomenon known as coherence transfer. In NMR, a coherence is characterized by a specific Larmor precessional frequency that is essentially defined by the magnetic field of the spectrometer and the chemical shifts of the spins involved in the creation of the coherence. A cross peak in COSY–type experiments develops because magnetization that was initially characterized by one precessional frequency is converted at some point to a coherence that precesses at a different frequency, defined by another chemical shift. The COSY 2D experiment in effect measures the precessional frequency of the coherence during both parts of the experiment. Coherence transfer occurs only if spins are J-coupled to each other. In peptide and protein systems, the appearance of a cross peak in proton-proton COSY experiments generally identifies sets of protons that are adjacent to each other in the covalent structure. With sufficiently narrow lines, it is possible to analyze the structure of COSY cross peaks to obtain values for the spin-spin coupling constant involved in the coupling interaction signaled by the cross peak.

Many variations on the basic ideas of the COSY experiment are now available, including DQFCOSY (double quantum filtered COSY). The advantages of the DQFCOSY experiment include a much narrower set of diagonal peaks (so that cross peaks close to the diagonal can be detected more readily) and drastic reduction of the intensities of singlets. Such singlets tend to be very intense and can cause noise and various artifacts in a 2D spectrum.

Note the requirement that a resolved spin-coupling interaction be present for optimum detection of a COSY–type cross peak. With greater molecular weights of samples, proton NMR spectral lines increase in width. Under these conditions, the positive and negative components of COSY cross peaks can begin to cancel one another, with the detection of the cross peak relative to noise becoming more difficult. Thus, although the presence of a cross peak in a COSY–type spectrum indicates mutual spin coupling between (probably) adjacent groups of protons, the absence of a cross peak in a COSY–type spectrum cannot be taken as evidence that two nuclei are not coupled to each other.

Suggestions for Further Reading

R. J. Abraham, J. Fisher and P. Loftus (1988) *Introduction to NMR Spectroscopy*, Wiley, New York.

Two-dimensional NMR Spectroscopy: applications for chemists and biochemists, 2nd ed. (1994) (W. R. Croasmun and R. M. K. Carlson, eds.), V.C.H., New York.

A. E. Derome (1987) *Modern NMR Techniques for Chemistry Research*, Pergamon, Oxford

S. W. Homans (1992) *A Dictionary of Concepts in NMR*, Clarendon, Oxford.

R. S. Macomber (1998) *A Complete Introduction to Modern NMR Spectroscopy*, Wiley, New York.

D. L. Turner (1985) Prog. NMR Spectrosc. **17**, 281–358.

D. E. Wemmer (1988) In *Recent Advances in Organic NMR Spectroscopy* (J. B. Lambert and R. Rittner, eds.), Norell Press, Landisville, New Jersey.

Counting Residues

Natural proteins have integral numbers of each of the twenty amino acids in a polypeptide chain, but most currently accepted methods of determining this number by amino acid analysis yield only a nonintegral ratio of moles of amino acid per mole of protein. This value is rarely close to an integer because of experimental error and uncertainty about the **molecular weight** of the protein. The method described here determines the integral number of residues of certain amino acids, independently of any other property of the polypeptide chain, including its molecular weight. Then this information is combined with amino acid analysis to determine a more accurate value for the molecular weight and the number of other amino acids. The method also provides information about the net charge on a protein.

The general procedure is to modify the *N* residues of a given amino acid gradually and specifically, so as to generate a complete spectrum of molecules with 0, 1, 2, 3, ¼, *N* of the groups modified. A single modification reaction can be used, varying the average extent of the reaction. Alternatively, one uses the competition with a related, but distinguishable reagent and carry out the modification to completion. Then the modified species generated are counted after separating them by a technique sensitive only to the number of groups modified by the particular reagent. The most useful modifications are those that alter the electric charge of a residue. Then the number of modifications introduced is determined by separating the various species by electrophoresis, isoelectric focusing, or ion exchange chromatography. The separation must be sensitive only to the number of groups modified in charge, not which particular ones in the polypeptide chain. This is usually accomplished by carrying out the modification and the separation on unfolded molecules, where differences between the *N* residues are minimized. There should be (*N* + 1) species present.

The thiol groups of cysteine residues are reacted with a reagent like **iodoacetic acid**, which introduces an acidic group. This reaction competes with that with the closely related iodoacetamide, which is neutral and does not introduce a charged group. The reaction of the thiol groups is taken to completion, and the number of acidic groups introduced is varied by varying the ratio of iodoacetic acid to iodoacetamide (Fig. 1). The number of acidic groups introduced is determined by electrophoresis under denaturing conditions. In addition to the number of total cysteine residues or thiol groups, the number of disulfide bonds can be determined by counting the thiol groups present before and after reduction of the disulfide bonds.

Figure 1. Counting the six cysteine residues of reduced BPTI. The reduced protein was reacted with the neutral iodoacetamide (1st lane), acidic iodoacetic acid (5th lane), and mixtures of the two in the ratios 1:1, 1:3, and 1:9 in lanes 2, 3, and 4, respectively. Lane 6 contains a mixture of equal portions of the samples applied to lanes 1 to 5. Electrophoresis of the basic protein was in 8 *M* urea from top to bottom. The electrophoretic mobility is decreased in proportion to the number of acidic carboxymethyl groups on each molecule; the number for each of the electrophoretic bands is indicated at the right. The competition between the two reagents indicates that iodoacetamide reacts three times more rapidly than iodoacetic acid under the conditions used here. From Ref. 1.

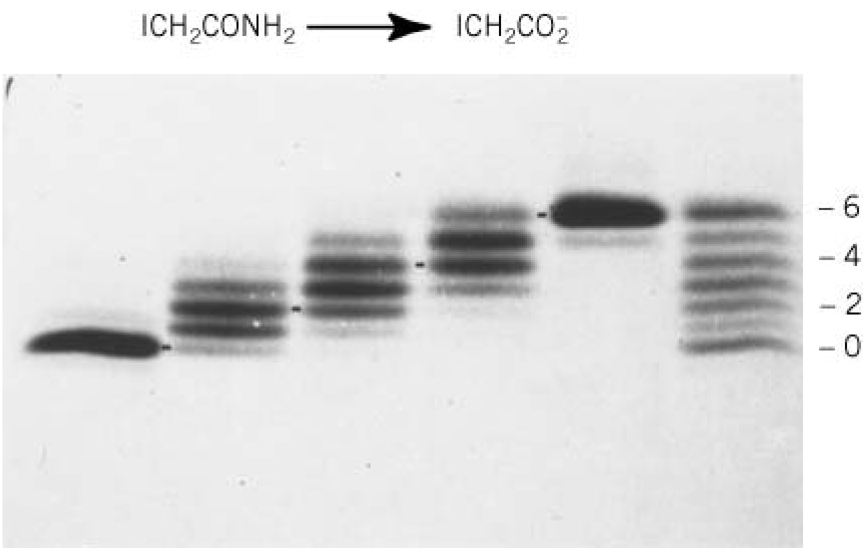

The amino groups of **lysine residues** and at the N-terminus can be modified specifically by reacting them with a reagent like succinic anhydride, which replaces a basic amino group with an acidic group. Consequently, the net charge of the protein can change by up two units for each amino group reacted. The reaction is varied in its extent by varying the amount of reagent added to the unfolded protein (Fig. 2).

Figure 2. Counting amino groups of bovine **ribonuclease A** (**a**) and horse ferri**cytochrome c** (**b**) by electrophoretically separating the mixtures produced by progressive succinylation. The original unmodified protein is on the left, and the degree of succinylation increases to the right. Electrophoresis was in 8 M urea at pH 3.6 from top to bottom. The separate lane on the far right is of a mixture obtained by combining all of the individual samples. In this case, electrophoresis was at the slightly lower pH of 3.45. Alternating bands are marked by arrows, and the number of succinyl groups is indicated for a few of the bands. The results confirm the presence of 11 and 19 amino groups in ribonuclease A and cytochrome *c*, respectively. From Ref. 2.

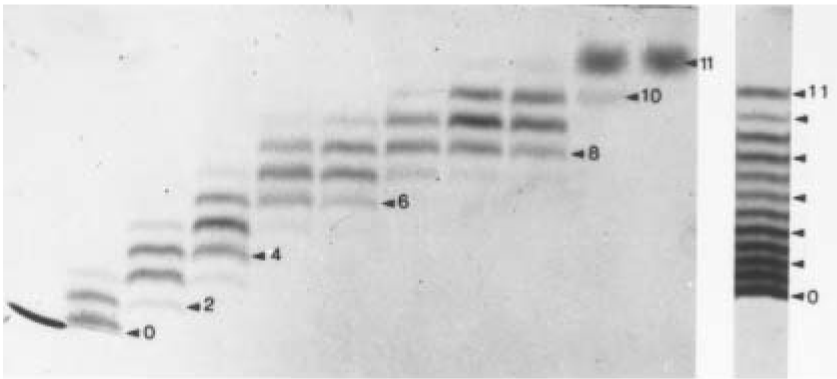

(a)

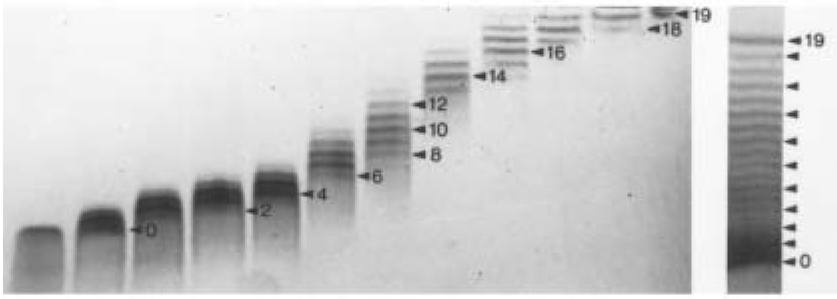

(b)

Other amino acids for which specific modifications are possible may be counted in the same way, in theory, but the specific techniques have not yet been developed.

In each of the previous procedures, the number of groups modified is counted by the number of new bands apparent by electrophoresis. Electrophoretic mobility is proportional to the net charge of the protein molecule, which is changed gradually by modifiying specific residues. Therefore, the net charge on the original protein molecule can be determined by measuring the degree of modification necessary to give the protein zero electrophoretic mobility or by using stepwise modification to establish a scale for electrophoretic mobility as a function of changes in net charge.

Bibliography

1. T. E. Creighton (1980) Nature **284**, 487–489.
2. M. Hollecker and T. E. Creighton (1980) FEBS Lett. **119**, 187–189.

Suggestion for Further Reading

3. M. Hollecker (1997) In *Protein Structure: A Practical Approach*, 2nd ed. (T. E. Creighton, ed.) IRL Press, Oxford, pp. 151–164.

Covalent Catalysis

Covalent catalysis by an enzyme involves the formation, along the reaction pathway, of a covalent enzyme intermediate that can be formed and broken down at a rapid rate. Covalent bonds are formed most commonly as a result of the attack by an enzyme nucleophilic (electron-rich) group on an electrophilic (electron-deficient) moiety of the substrate that is bound at the active site. The nucleophilic groups that are present on the side-chains of amino acid residues are $RCOO^-$, RNH_2, R–OH, and the nitrogen atoms of the imidazole ring of histidine residues. The electrophilic moieties of substrates may be acyl, phosphoryl, or glycosyl groups, so the covalent intermediates would be acyl-, phosphoryl-, and glycosyl-enzyme complexes, respectively. The reactions involved in the formation of an acyl-enzyme are

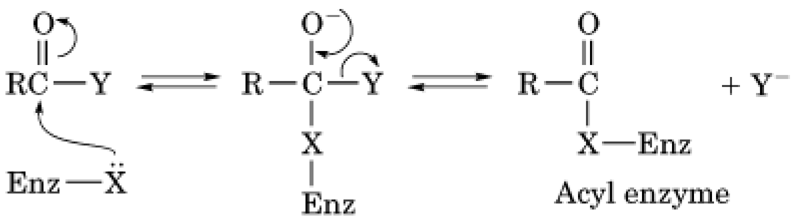

The second step in covalent catalysis is the attack by a low-molecular-weight nucleophile on the covalent intermediate to release the second reaction product. If the attacking nucleophile is water, the enzyme would catalyze a hydrolytic reaction that conforms to a **kinetic mechanism** with the ordered release of products. If the attacking nucleophile were a second substrate, the reaction would have a ping-pong kinetic mechanism.

Enzyme molecules are poor in electrophilic groups. But electrophilic catalysis does occur with those enzymes that contain metals (see Metal-Requiring Enzymes) or prosthetic groups (see Coenzyme, Cofactor) that act as electron sinks during catalysis.

As a large number of enzymes catalyze reactions through the formation of covalent intermediates, it appears that the this type of catalysis offers some general advantages (1). It has been considered that the immobilization of a covalent intermediate should provide a significant **entropic** driving force and catalytic efficiency is increased by having multiple bond-making and bond-breaking steps occurring within a single active site.

Bibliography

1. C. Walsh (1979) *Enzymatic Reaction Mechanisms*, W. H. Freeman and Company, San Francisco, Calif., pp. 39–41.

CpG Islands

In some animals, cytosine bases occurring in the sequence CG are frequently methylated to 5-methylcytosine (see Methylation, DNA). Yet even in species where most such residues are methylated, there are genome segments, known as *CpG islands*, which are conspicuously not methylated. These are short, dispersed regions of DNA with a high frequency of CpG dinucleotides relative to the bulk genome, but they are not methylated. In the haploid human genome, it is estimated that there are some 30 to 45 × 10^3 CpG islands. Such regions of DNA are at least 200 bp in length and have a $G + C$ content greater than 50%. Outside these islands, the frequency of CpG sequences is depleted to about only 20% of that expected on a random basis. This bias against CpG sequences that would be methylated is believed to be caused by methylcytosine bases that deaminate spontaneously 10 to 20 times more readily than normal cytosine bases. Furthermore, the product of deamination of 5-methylcytosine is thymine, a normal base, so this mutagenic event is more difficult to repair than usual (see DNA Repair).

CpG islands are associated with the 5′ ends of **housekeeping genes** and of a few tissue-specific genes (highly tissue-specific genes usually lack islands). They have an open chromatin structure, and it has been postulated that they are sites of interaction between transcription factors and **promoters**. All known widely expressed genes are associated with more than one CpG island, which usually includes the transcription start site, and a few of these genes have an additional island in the 3′ direction. The average length of CpG islands is about 240 bp in widely expressed genes, but there is no typical size. Most are between 200 and 1400 bp, and a majority of islands are 200 to 400 bp. The average size of islands associated with genes with limited expression is slightly smaller.

Less than half of tissue-specific expressed genes and of those with limited expression are associated with CpG islands that occur in one or more exons. This implies that CpG islands may be used to identify transcripts, since they occur in exons. Furthermore, CpG islands cover the whole or part of the promoter regions containing canonical TATA box and CAAT box, and they include GC-rich promoters lacking a typical TATA box. Such promoters are considered typical of housekeeping genes.

Suggestion for Further Reading

S. H. Cross and A. P. Bird (1995) CpG islands and genes, Curr. Opin. Genet. Dev. **5**, 309–314.

Cristae

Electron microscopy of mitochondria demonstrates that the inner mitochondrial membrane (IM) folds towards the inner part of the mitochondrion and then folds back (Figure 1), thereby forming structures that are called cristae (see Mitochondria). The same morphological evidence has shown that a relationship exists between the development of cristae and the functional activity of mitochondria, which is, in turn, related to the energy requirement of the cell. In fact, folding of the inner mitochondrial membrane is a prerequisite for the structural organization of respiratory enzyme complexes (see ATP Synthase). The IM defines the intermembrane space (IS) and the mitochondrial matrix (M), where most soluble enzymes and the **protein biosynthesis** apparatus are localized, while the respiratory enzyme complexes are localized in the IM. Recently, detailed analysis of mitochondrial inner and outer membranes (OM), of their contacts, and of the localization of proteins in the two membranes, in the intermembrane space, and in the matrix, has led to very important developments in our understanding of the essential aspects of mitochondrial transport. Since the IM and OM separate two distinct spaces in mitochondria, proteins encoded by the cell nucleus and targeted to the mitochondria can be destined to either one of these spaces, or to be integral components of the IM or OM.

Figure 1. Morphology of a mitochondrion derived from electron microscopy (OM = outer membrane; IM = inner membrane; IS = intermembrane space, M = matrix).

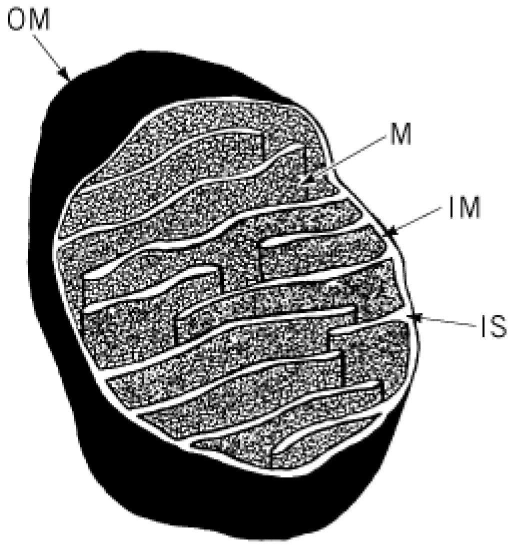

Sorting of proteins to mitochondria is generally mediated by presequences, which are by signals composed of 15–35 amino acid residues at the amino terminus (see Signal Peptide). Most proteins to be targeted to the mitochondrion are therefore synthesized on cytoplasmic ribosomes as precursors and then transferred to **receptor** proteins on the mitochondrial surface. The pre-sequences are then inserted across both membranes at contact points, through distinct outer and inner protein-conducting channels. Many components of this complex machinery for importing proteins have recently been identified (1).

Transport requires unfolding and refolding of proteins by chaperonins and is followed by removal of the presequence by a proteinase in the mitochondrial matrix. Signal peptides are needed not only for routing proteins to mitochondria but also to reach the correct mitochondrial location. Proteins may actually remain in the matrix, assemble with other proteins in the IM, or be transported to the IS through the IM. An inner membrane–associated proteinase is then used to cleave a second signal peptide from these proteins. However, this very interesting scheme is not general, since some proteins lacking a signal peptide can also be imported into mitochondria.

Bibliography

1. T. Lithgow, B. S. Glick, and G. Schatz (1995) Trends Biochem. Sci. **20**, 98–101.

Critical Micelle Concentration

Many properties of a detergent in aqueous solution depend on its critical micelle concentration (cmc), which in turn is determined by the chemical structure of the detergent. In aqueous solution, detergents remain either in aggregated (micellar) or monomeric states, and the cmc is the maximum concentration at which the detergent molecules remain as monomers. An increase in detergent concentration above the cmc leads to the formation of micelles or mixed micelles with the solubilized lipid and protein molecules (see Detergents). Although the formation of mixed micelles of detergents with lipid and protein molecules is an important requirement in detergent solubilization of plasma membrane proteins and lipids, a low cmc may not be essential for efficient membrane solubilization because the cmc value alone does not always reflect a detergent's ability to dissociate membranes. For example, sodium dodecyl sulfate (SDS) is strongly ionic and has a cmc of ~0.23% at 25°C, whereas MEGA-10 is polar but nonionic and has virtually the same cmc of ~0.22%. Yet SDS is probably the strongest **denaturing** detergent known, whereas MEGA-10, just like MEGA-8, is much less disruptive to biomembranes (1, 2). A very similar picture emerges from comparing sodium cholate, which is strongly ionic and denaturing, with CHAPS, which is moderately zwitterionic and much less denaturing, even though both have a cmc of ~0.5% (2). Because the cmc values are also the result of certain more fundamental factors, such as structural features and ionic properties of the detergents (ie, nonionic, moderately ionic, or strongly ionic, and the membrane-dissociating property of a detergent is directly related to such factors), one effective way of classifying detergents is based on their structure and ionizability, rather than their cmc values (see Detergents).

Bibliography

1. M. Hanatani, K. Nishifuji, M. Futai, and T. Tsuchiya (1984) J. Biochem. **95**, 1349–1353.
2. A. C. Newby, A. Chrambach, and E. M. Bailyes (1982) *Techniques in Lipid and Membrane Biochemistry*, B409, Elsevier/North-Holland, pp. 1–22.

Crosslinking

Crosslinking refers to linking separate chemical functionalities covalently. Crosslinking is usually achieved through use of a bifunctional crosslinking reagent, specifically, a compound having two reactive groups that react chemically with the two functional groups that become crosslinked. In this case, only two functional groups are usually crosslinked, but, with other types of reagents, higher order crosslinking is possible. Crosslinking can be either intramolecular (between separate functional groups on the same molecule) or intermolecular (between functional groups located on separate molecules). In the latter case, it is usually between two macromolecules or between a macromolecule and a relatively small molecule. Crosslinking is usually used to detect groups that are in much greater proximity than would be expected from just their bulk concentrations, due to the structures and associations of the molecules of which they are part. In biochemical applications, the chemical functions that can be crosslinked may be components of all classes of macromolecules (proteins, **nucleic acids**, carbohydrates, and lipids). For simplicity, this article focuses on crosslinking involving the functional groups of proteins, predominantly **amino**, **thiol**, imidazole and carboxyl groups (ie, the nucleophilic side chains of certain amino acids); however, the concepts are the same for the other classes of macromolecules. It should be noted that crosslinking also occurs naturally, resulting from oxidation, radiation, or the action of certain enzymes.

A distinction is sometimes made between the terms *crosslinking* and *conjugation* (or bioconjugation). In this case, crosslinking is used to denote the covalent linkage of only molecules that are associated naturally, such as the subunits of an oligomeric protein or a hormone and its **receptor**. Conjugation, in contrast, refers to the covalent linkage of molecules that lack affinity for one another. The resulting covalent complexes, referred to as conjugates, have a multitude of uses, especially in biotechnology (see Enzyme Immobilization And Conjugation). The distinction between crosslinking and conjugation is maintained in this article.

1. Uses of crosslinking

On the basis of the variety of the crosslinking reagents that are available and of the molecules that can be crosslinked, plus the types of experimental questions that can be answered, crosslinking is among the most versatile of biochemical techniques. In the case of proteins, for example, some information about their three-dimensional structure can be gained through identifying specific amino acid residues that are readily crosslinked intramolecularly (1). Crosslinking can also be used as a general conformational probe to detect structural changes in a protein, such as might be induced by **ligand binding** (2). Inasmuch as crosslinking can hinder conformational transitions and the dissociation of oligomers, it can also be used to stabilize the **tertiary** or quaternary structures of proteins. Thus, it can "lock" a protein into a particular functional state (3) or stabilize an oligomeric protein for subsequent physical studies, such as electron microscopy. A careful analysis of the mass and composition of crosslinked complexes allows a minimal subunit stoichiometry to be determined; this is especially useful for insoluble oligomers, such as those found in membranes (4). Information concerning the symmetry of oligomeric proteins can also be obtained from crosslinking (5, 6). One of the most common uses of crosslinking is to identify neighboring proteins in a complex (7), and this can be extended to include determination of the specific regions of each that are crosslinked (8). By varying the length of the crosslinker, one can also obtain a limit for the maximum distance that can separate neighboring proteins (6). In addition to giving both relative and absolute structural information, crosslinking can be used for general screening. For example, one can identify the receptor for a particular ligand, such as a hormone (9).

It must be emphasized that for all the above applications, interpretations can be made only for those crosslinked complexes that are generated. The absence of crosslinking does not mean that two molecules do not interact, only that they are not crosslinked under the specific set of experimental conditions chosen, which includes the crosslinking reagent used. Because crosslinking requires the proper positioning of those functional groups having the appropriate chemical reactivities, one cannot expect all interacting molecules to be crosslinked by any given reagent.

2. Crosslinking Procedures

Crosslinking, like chemical modification of proteins, is an empirical procedure, and both processes are influenced by the same variables, namely temperature, pH, concentrations of reactants, and time. In crosslinking, however, the influence of the latter two variables is more complex. Because nucleophilic side chains of amino acids are considerably more reactive when deprotonated, the pH of the reaction is important in controlling the extent of crosslinking and the selectivity for particular side chains. Regarding concentrations, the amounts of both the crosslinker and the proteins can influence crosslinking, with low concentrations of protein and crosslinker generally favoring intramolecular crosslinking. Adding the crosslinker over time, instead of as a single addition, favors a greater extent of crosslinking. Differences in selectivity of the reactive groups of bifunctional reagents, especially heterobifunctional crosslinkers, for protein functional groups can be maximized using a two-step reaction. In this procedure, one protein is first derivatized with the crosslinking reagent and then purified to remove excess free reagent before being exposed to the second protein. This two-step procedure, which allows for each of the two reactions to be performed under different conditions, is particularly useful for enzyme immobilization and conjugation, when the two molecules do not normally associate with each other.

Following crosslinking, the covalent complexes formed are commonly identified as new electrophoresis bands in sodium dodecyl sulfate–polyacrylamide gel electrophoresis (SDS-PAGE), with altered molecular weights, although care must be taken, because intramolecular crosslinking can alter the migration of individual polypeptides with this technique. Alternatively, in simple systems, covalently linked complexes can be identified as components with increased **Stokes radii** in size exclusion chromatography. If either the crosslinker or the crosslinked protein has identifiable physical or chemical characteristics, these can aid in the identification of complexes. Once crosslinked complexes have been identified, complete analysis of their composition and stoichiometry can still be challenging, especially when multiple proteins are present. One useful method for identifying the proteins composing a complex is to use a cleavable crosslinker so that the original components can be regenerated from the fractionated complex (7). Another useful method is to perform Western blots on the fractionated complex using antibodies against potential components (2). Once the components have been identified, their stoichiometry in the complex is deduced from its overall mass. The ultimate step in analysis is to determine directly the actual amino acid residues that are crosslinked. Using conventional protein sequencing by Edman Degradation, the sequences of the two crosslinked peptides are obtained simultaneously, with the crosslinked residues represented by gaps in the sequences; however, identification of crosslinked peptides by mass spectrometry is becoming increasingly common.

Bibliography

1. F. C. Hartman and F. Wold (1967) Biochemistry **6**, 2439–2448.
2. O. W. Nadeau, D. B. Sacks, and G. M. Carlson (1997) J. Biol. Chem. **272**, 26296–26201.
3. R. E. Benesch and S. Kwong (1991) J. Prot. Chem. **10**, 503–510.
4. E. Heymann and R. Montlein (1980) Biochem. Biophys. Res. Commun. **95**, 577–582.
5. F. Hucho, H. Mullner, and H. Sund (1975) Eur. J. Biochem. **59**, 79–87.
6. J. Hajdu, S. R. Wyss, and H. Aebi (1977) Eur. J. Biochem. **80**, 199–207.
7. D. Dey, D. E. Bochkariov, G. G. Jokhadze, and R. R. Traut (1998) J. Biol. Chem. **273**, 1670–1676.
8. V. Rossi, C. Gaboriaud, M. Lacroix, J. Ulrich, J. C. Fontecilla-Camps, J. Gagnon, and G. J. Arlaud (1995) Biochemistry **34**, 7311–7321.
9. T. H. Ji (1977) J. Biol. Chem. **252**, 1566–1570.

Suggestions for Further Reading

10. G. Mattson, E. Conklin, S. Desai, G. Nielander, M. D. Savage, and S. Morgenson (1993) A practical approach to crosslinking, Mol. Biol. Rep. **17**, 167–183.
11. S. S. Wong (1993) *Chemistry of Protein Conjugation and Cross-Linking*, CRC Press, Boca Raton, FL. (An outstanding book describing all aspects of the chemistry and uses of bifunctional reagents in crosslinking and conjugation, with an extensive bibliography for each chapter.)

Cruciform (Holliday Junction)

A key intermediate in DNA recombination is the **Holliday junction** that involves the joining of four homologous DNA strands into a cruciform arrangement, as visualized by electron microscopy some years ago. **Supercoiling** also can induce the formation of the cruciform for inverted repeat sequences. Detailed structural analysis of the cruciform DNA structure became possible when specific sequences were designed to form a so-called immobile junction. Studies on those molecules using gel electrophoresis and **fluorescence** indicated that the structure has a stacked X shape (ie, not tetrahedral) in the presence of metal ions (eg, Mg^{+} or $Co(NH_3)_6^{3+}$). Models of the detailed structure at the junctions have been proposed. One such model involves a right-handed, antiparallel X structure, with two stacked helices crossing over each other with a crossover angle of ~ 60° (or 120°). Within each helix of the X structure, the two arms are collinear and the junction site is folded. A number of B-DNA structures determined by X-ray crystallography showed helix–helix packing contacts in the crystal lattice that are remarkably similar to the X structure. Recently the crystal structures of two proteins that are involved in the recombination process have been solved in the presence of their DNA substrate. The crystal structure at 2.4 Å resolution of Cre recombinase bound to a loxP DNA substrate showed that four recombinases and two loxP sites form a synapsed structure in which the bound DNA adopts a conformation similar to the four-way Holliday junction (1). The synapse assembly has a pseudofourfold symmetry, and the junction core is less compact than that proposed for the "free" Holliday junction.

Bibliography

1. F. Guo, D. N. Gopaul, and G. D. Van Duyyne (1997) Nature **389**, 40–46.

Cryoelectron Microscopy

Cryoelectron microscopy can be divided into two classes, depending on whether the specimen is *hydrated* or *dry*. Table 1 provides a brief description of the possible methods of specimen preparation. In each method, the specimen is initially frozen and can subsequently be observed in a cryoelectron microscope, or can be further preserved by drying or making a replica for observation in a conventional electron microscope.

Table 1. Methods of Specimen Preparation in Cryoelectron Microscopy

Frozen Hydrated Specimens	**Dry Specimen Previously Frozen**
1. *Vitrified film of ice* A thin layer of macromolecules in aqueous suspension is rapidly frozen by plunging in a cryogen, eg, ethane, and transferred to a cryoelectron microscope.	1. *Freeze drying* Cells or tissues are frozen, then lyophilized. The remaining material is dried and stabilized for transfer to a conventional electron microscope. Alternatively, a replica is made.
2. *Frozen section* Cells or tissues are rapidly frozen by contact with a cold metal block, sometimes under high pressure, then sliced into thin sections at ~< –160 C°.	2. *Freeze fracture* Cells or tissues are frozen, then fractured. A replica of the fractured surface is made.
Subsequently, sections are transferred to a cryoelectron	3. *Freeze etching*

microscope.

Freeze fracture followed by freeze drying.

4. *Freeze substitution*

Tissues are frozen, then the ice is replaced at low temperature by an organic solvent. Conventional plastic embedment follows.

5. *Cryoimmunohistochemistry*

Tissues are first chemically fixed, then suffused with a cryoprotectant and frozen for sectioning. Immunolabelling of the thawed sections follows.

The development of techniques for visualizing frozen hydrated tissues and macromolecules has been a boon for studying structures in a state that closely approximates their native condition (1). Because freezing takes place very rapidly, these techniques offer the ability to examine dynamic events with high time resolution. For example, the structure of the open-channel form of the acetylcholine receptor was elucidated from membrane crystals that were briefly activated (< 5 ms) with droplets containing acetylcholine (2). Small conformational changes triggered by acetylcholine were detected in the frozen hydrated crystals. The spatial resolution of periodic structures, eg, protein crystals, can also be high, extending to 3.3 Å (3; Perkins, unpublished results). Moreover, these structures can be examined unstained by utilizing the intrinsic contrast difference between the biological specimen and vitreous ice. Thus, the effects of solvent composition on the structure and aspects of interacting components can be examined (2).

Fundamental to examining frozen hydrated specimens is the preservation of the environment by rapid freezing (4). Rapid freezing causes the water of the specimen and its environment to be trapped in a vitreous (amorphous or glass-like) state. This vitreous state prevents damage to the specimen caused by the formation of ice crystals when the specimen is frozen more slowly. The specimens preserved in thin films of vitreous ice generally retain a high degree of structural integrity. However, it is crucial to maintain the specimen at below ~ –140° C because vitreous ice tends to crystallize above this temperature (4).

A wide range of frozen hydrated specimens has been examined in cryoelectron microscopes. Most studies have concentrated on macromolecules and their assemblies hydrated and frozen in thin films. To a lesser extent cryosections of biological tissues have also been studied (5-9), but the difficulty of freezing of bulk material without formation of ice crystals has hampered progress. The first published results obtained of macromolecules were from viruses, fairly robust particles (10). Early work produced 3-D reconstructions at relatively low resolution, ~ 2–3 nm (10-13), although certain viruses produced data to ~ 1 nm resolution (14). Important new information about viral structures was obtained even at lower resolution. Recent work has extended the resolution of complex viruses beyond 1 nm (15, 16). By combining cryoelectron microscopy with X-ray crystallography, near atomic resolution detail of the overall architecture of large complexes and of the interactions between the components can be obtained. An instructive example is the 3-D structure of rhinovirus 14 complexed with Fab fragments determined at 0.4 nm resolution (17).

Although the contrast in frozen hydrated specimens is low compared to negatively stained specimens, the signal can be significantly boosted by averaging many identical particles together using Fourier averaging for crystals (2, 17) and correlational averaging for single particles as discussed below (15, 16, 18). Vitreous ice embedment is particularly useful for visualizing the specimen interior compared to negative stain, which accumulates around areas accessible to the aqueous phase, thus usually showing only the molecular envelope. Hence, in general only those portions of integral membrane proteins extending beyond the lipid bilayer are observed in negative stain. However, exceptions to this limitation of negatively stained membrane proteins have been found (19-22). In certain instances, frozen hydrated crystals of membrane proteins do not provide resolution as high as the same crystals in negative stain (23). Vitreous ice embedment of delicate specimens, such as chromosomes or DNA fragments (9, 24, 25) has provided impressive results, since this type of specimen is commonly poorly preserved in other embedment media. Another example is the direct visualization by cryoelectron microscopy of A-, P-, and E-site transfer RNAs in the *E. coli* ribosome (26).

Cryofixation of tissues is an alternative to conventional chemical fixation of subcellular ultrastructure. Vitrification of ice can frequently be achieved to a depth of 10–20 µm when tissues are frozen by slamming them against a polished copper block cooled to the temperature of liquid nitrogen or liquid helium (27). High-pressure freezing can freeze samples in vitreous ice to depths as great as 100 µm, since the increase in volume going from water to ice is impaired by a high-pressure environment inhibiting the growth of ice crystals. Cryofixation is usually the choice for immunocytochemistry because it retains the antigenic properties of the specimen better than chemical fixation. With good vitrification, freeze-etching or freeze-substitution (Table 1) can provide information about structures stabilized with a mechanism different from chemical fixation.

Bibliography

1. J. Jaffe and R. M. Glaeser (1984) Ultramicroscopy **13**, 373–378.
2. P. N. T. Unwin (1995) Nature **373**, 37–43.
3. J. Brink, W. Chiu, and M. Dougherty (1992) Ultramicroscopy **46**, 229–240.
4. J. Dubochet et al. (1982) J. Microscopy **128**, 219–237.
5. J.-J. Chang et al. (1983) J. Microscopy **132**, 109–123.
6. J. Dubochet et al. (1983) J. Bacteriol. **155**, 381–390.
7. A. W. McDowall et al. (1983) J. Microscopy **131**, 1–9.
8. A. W. McDowall et al. (1984) J. Mol. Biol. **178**, 105–11.
9. A. W. McDowall, J. M. Smith, and J. Dubochet (1986) EMBO J. **5**, 1395–1402.
10. J. Adrian et al. (1984) Nature **308**, 32–36.
11. J. Lepault and K. Leonard (1985) J. Mol. Biol. **182**, 431–441.
12. F. P. Booy et al. (1985) J. Mol. Biol. **184**, 667–676.
13. R. H. Vogel et al. (1986) Nature **320**, 533–535.
14. J. Lepault (1985) J. Microscopy **140**, 73–80.
15. B. Bottcher, S. A. Wynne, and R. A. Crowther (1997) Nature **386**, 88–91.
16. J. F. Conway et al. (1997) Nature **386**, 91–94.
17. T. J. Smith (1996) Nature **383**, 350–354.
18. M. van Heel, G. Harauz, and E. V. Orlova (1992) J. Struct. Biol. **116**, 17–24.
19. B. Karlsson et al. (1983) J. Mol. Biol. **165**, 287–302.
20. B. Bottcher, P. Graber, and E. J. Boekema (1992) Biochem. Biophys. Acta **1100**, 125–136.
21. S. Karrasch et al. (1996) J. Mol. Biol. **262**, 336–348.
22. G. A. Perkins et al. (1997) Biophys. J. **72**, 533–544.
23. J. M. Valpuesta, R. Henderson, and T. G. Frey (1990) J. Mol. Biol. **214**, 237–251.
24. J. Dubochet et al. (1994) Nature Struct. Biol. **1**, 361–363.
25. J. Bednar et al. (1995) J. Mol. Biol. **254**, 579–594.
26. R. K. Agrawal et al. (1996) Science **271**, 1000–1002.
27. J. Dubochet (1995) Trends Cell Biol. **5**, 366–369.

Crystallization

The determination of the three-dimensional structures of proteins by X-ray crystallography requires the availability of large, well-ordered crystals. These are difficult to obtain. The crystallization of any given protein requires long painstaking work, including much trial and error in the choice of environmental conditions (pH, temperature) and crystallizing agents.

The basic requirement is the availability of the protein in *very* pure form, free of all other molecules, such as traces of nucleic acids, in a single form (absence of **isoforms**), in a solution that is free of any dust particles. If liganded to any **coenzymes**, cofactors, or effectors, all molecules must be equally liganded; all molecules must be in the native state, and there must be no partial oligomer formation.

The basic approach is to prepare a protein solution at high concentration (10 to 100 mg/ml) in a crystallizing solvent at conditions at which the solution is close to saturation. Then the solution is gradually brought to supersaturation by, eg, slow variation in pH or temperature. All changes must be brought about slowly and the solution not subjected to shocks, such as mixing. This allows the formation of crystal nuclei. Amorphous aggregates must be totally avoided. Once nuclei are formed, the system is induced to crystallize further by the addition of protein to these nuclei, avoiding the formation of new ones, since the aim is to form large crystals. See the specialized literature for further details.

Typical crystallizing agents are (1) salts $(NH_4)_2SO_4$, Na_2SO_4, Na citrate, $MgSO_4$; (2) organic molecules [2-methyl-2,4-pentanediol (MPD), ethanol, isoproponal, acetone, dioxane, 1,3-propanediol]; (3) polyethylene glycols (molecular weight between 2,000 and 20,000). See also Vapor Phase Crystallization.

Suggestions for Further Reading

T. L. Blundell and L. N. Johnson (1976) *Protein Crystallography*, Academic Press, New York.

H. W. Wyckoff, C. H. W. Hirs, and S. N. Timasheff, eds., (1985) *Methods in Enzymology*, Chaps. "2"–"15", Academic Press, New York.

Crystallography

Crystals are very important for molecular biology because they are required for detailed structure determination of macromolecules using X-ray crystallography. The scientific study of crystals is very old. Its origin can be traced back to 1669 when Nicolaus Steno noticed that the angles between the faces in growing crystals remain constant. Individual crystals may differ in shape appreciably, but the angles between corresponding faces are always the same. A century later, René Just Hauy proposed that crystals are built from small units whose shape is a parallelepiped. An extensive review of the history of crystallography is given in Ref. 1. The physical properties of crystals are, generally not equal in all directions. Their optical, magnetic, and electric properties vary with crystal direction, and this is the reason that crystals are widely used for physical measurements and in industrial processes, for instance, a quartz crystal in a clock or watch. The wealth of variable characteristics is a consequence of the regular packing of the ions, atoms, or molecules in the crystal. This internal regularity had been suggested since Hauy, but it could only be proven with the introduction of X-ray crystallography. In this technique, the crystal acts as a grating and diffracts X-rays in directions specific for the repeating distances in the crystal. In addition, it became possible to elucidate the internal structure of crystals, that is, the arrangement and structure of the molecular composition.

In the regular packing inside the crystal, three repeating vectors can be recognized: **a**, **b**, and **c**, with angles a, b, and g between them. These three vectors define a unit cell in the crystal lattice. From morphological crystal symmetry considerations, that is, the rotational axes, mirror planes, and centers of symmetry observed in the shape of crystals, 32 combinations of these symmetry elements (point groups) are possible. They can be assigned to seven, and not more than seven, crystal systems (2): triclinic, monoclinic, orthorhombic, tetragonal, trigonal, hexagonal, and cubic. Internally, a crystal has more symmetry operators. Translational symmetry is added to the symmetry axes and the mirror planes. These operators can be combined in 230 different ways, leading to 230 space groups, introduced by Schoenflies and Fedorow at the end of the nineteenth century (Ref. 1, p. 114; 2).

Because biological macromolecules have an asymmetrical structure, they can only form crystals without mirror planes or centers of symmetry. This restricts the number of space groups appreciably for these molecules.

Bibliography

1. P. Groth (1926) *Entwickelungsgeschichte der Mineralogischen Wissenschaften*, Julius Springer, Berlin.
2. International Union of Crystallography (1992) *International Tables for Crystallography*, Vol. **A** (T. Hahn, ed.) Kluwer Academic Dordrecht, Boston, London.

Suggestion for Further Reading

3. J. P. Glusker, M. Lewis, and M. Rossi (1994) *Crystal Structure Analysis for Chemists and Biologists*, VCH, New York, Weinheim, Cambridge.

C_0t Curve

A C_0t curve describes the sequential complexity of a DNA sample. It describes the kinetics of reassociation and re**annealing** of a sample of double-stranded DNA that has been (*1*) fragmented to small pieces, approximately 400 nucleotides, (*2*) denatured to single strands, and (*3*) then permitted to reanneal. The extent to which two complementary DNA strands reassociate is proportional to C_0t. C_0 is the original molar concentration of the complementary strands of DNA, and *t* is the incubation time. $C_0t_{1/2}$ is the value of C_0t required for completing half of the reannealing reaction. If the sequences of all initial DNA fragments were identical, complementary fragments encounter each other readily and the mixture reanneals readily at a low value of C_0t. At the other extreme, reannealing is very slow and occurs only at high C_0t values if the original DNA contains many different sequences, so that the concentrations of complementary strands are very low and they encounter each other only infrequently. The value of $C_0t_{1/2}$ is a measure of the sequential complexity of the original DNA.

Such studies on genomic DNA were one of the first indications that genomes often contain repetitive DNA. Such DNA segments are present in higher concentrations than those segments present in only one copy per genome, and this fraction of the DNA reanneals at a correspondingly lower C_0t value. The results indicate that different sequences are present in widely varying frequencies throughout the genome, and only a fraction occurs only once per genome.

Cubitus Interruptus **Genes**

In Drosophila development, the **phenotype** associated with a gain-of-function mutation of the *cubitus interruptus* (*ci*) gene was first described in 1971 by Hochman (1). Later, this gene was categorized as a segment polarity gene because the loss of *ci* function results in the loss of naked regions in the segments of larval cuticle (2). The *ci* gene encodes a **zinc-finger** protein, CI, that stimulates transcription in response to the ***hedgehog*** (*hh*) signal transduction cascade, which helps to establish the anterior-posterior positional information in the embryonic segments and imaginal discs. The morphogen in vertebrates, Sonic hedgehog (*Shh*), induces and patterns many developmental processes, at least in part through regulating the expression of the vertebrate *ci* **homologues** *Gli1*, *Gli2*, and *Gli3*, which then transcribe a second level of *Shh* target genes. The importance of these genes in growth and development is illustrated by the fact that the Gli1 protein is amplified in glioblastoma cells.

1. Protein Structure of CI and Gli

Both the *ci* and *Gli* genes encode proteins with five highly homologous, tandemly repeated zinc fingers that act as **DNA-binding** domains and are distinguishable from other zinc-finger domains (3-6). The protein products of these genes are required for the transcription of *hh* target genes during development. Because the *Gli* and *ci* genes respond to the same signaling pathway and share a common DNA-binding domain, they are considered to be homologues, even though there is very little conservation on the amino acid sequence level between CI and Gli proteins outside of the zinc-finger region. Three members of the *Gli* gene family (*Gli1*, *Gli2*, and *Gli3*) have been identified in mouse, chicken, and zebrafish (7, 8). Two *Gli* genes have been identified in ***Caenorhabditis elegans*** (9), four in Xenopus (10). They share various degrees of similarity with the zinc finger region, which represents the greatest degree of homology among the family. The zinc fingers are responsible for the DNA-binding activity of both CI and Gli proteins as demonstrated by both in vitro binding assays and in vivo experiments, in which expression of a transgene is driven by Gli binding sites (4, 5, 11, 12). The consensus DNA-binding site for CI and Gli proteins has also been characterized by isolating and comparing **genomic** DNA fragments that can bind to Gli1. The core sequences were further confirmed by DNase footprinting (13). The X-ray crystallography structure of the Gli1 zinc fingers bound to the DNA binding site has been solved (14). Zinc finger 1 does not contact the DNA, whereas the rest of the four fingers wrap around the DNA, with fingers 4 and 5 making most of the base contacts with the DNA. This structure might explain the higher homology shared by zinc fingers 3–5 among the members of the *Gli* gene family. **Bandshift assays** demonstrate that full-length Gli1, full-length Gli3, or a GST protein fused to the CI zinc finger domain translated in vitro can bind to the Gli DNA binding site **consensus sequence** (5, 11, 13). When the CI zinc-finger **domain** is fused to a heterologous activation domain, it functions as a transcriptional activator in fly imaginal discs and embryos (15). Furthermore, CI can transactivate a reporter gene driven by Gli binding sites in yeast (12) and in fly cell lines (16). All of these experiments suggest that *ci* functions as a transcription factor that binds DNA through its zinc-finger domain. The amino acid residues of CI that are N-terminal to the zinc-finger domain are rich in alanine residues, a characteristic of transcriptional repressor domains (17). When a CI protein that is truncated C-terminal to the zinc-finger region is expressed in the anterior compartment of the fly embryonic segments, it causes downregulation of *ci* target genes (15). This result supports the idea that the N-terminus of CI has a repressor function. The C-terminus of the CI protein is highly acidic, a characteristic of transcriptional activators (18). When introduced into Drosophila embryos, a CI protein in which the N-terminus is deleted can function as a transcriptional activator to enhance *ci* target gene expression, indicating that the activation domain resides in the C-terminus (15).

2. Expression and Function of *ci*

The repeating segments of the fly embryo are established during blastoderm stage through a series of hierarchical interactions among the maternal gap and pair-rule genes. The segment polarity genes specify the anterior-posterior polarity of each segment during gastrulation. Consequently, it is no surprise that most of the segment polarity genes describe interdependent signal transduction cascades. *Ci* is a member of the *hh* signal transduction pathway and encodes a zygotic gene that is not detected until early cellular blastoderm stage (stage 5). Before stage 11, expression of CI protein closely follows the pattern of *ci* transcripts. Both protein and message are detected initially on the dorsal surface of the embryo. As development progresses, the domain of *ci* transcription and protein expression extends ventrally and, by stage 10, encompasses the entire embryo. Coincident with the onset of ectodermal segmentation, both the message and the protein are restricted to the anterior compartment of each segment by the ***engrailed*** (*en*) gene, resulting in 15 broad, metamerically repeating stripes. At stage 11, the protein expression pattern no longer coincides with the transcript pattern. Although transcripts are still uniformly distributed throughout the anterior compartment of each segment, the protein stripe within each segment is graded so that higher levels of protein are detected in the rows of cells that define the posterior edge of the anterior-posterior (A/P) boundary and lower levels are seen in the middle of the CI-expressing stripe. This pattern of expression also exists in imaginal discs, where *ci* is uniformly transcribed in the entire anterior compartment and higher levels of CI are detected along the A/P boundary (3, 19). It should be noted that the protein staining patterns were obtained with antibody made against the C-terminus of CI and detected only the full-length protein. The discrepancy found between transcript and protein levels in the segments and discs indicates that CI is subject to post-transcriptional regulation.

The *ci* transcription pattern is regulated by various unidentified factors and is mediated through the regulatory sequences in the *ci* promoter. Using transgenic flies that carry the *LacZ* reporter gene under the control of different *ci* regulatory sequences, it has been shown that various elements in the *ci* promoter differentiate embryonic from disc expression (20). Although the sequences required for the repression of *ci* transcription in the posterior compartment of the embryonic segments and imaginal discs are different, they both contain binding sites for the *engrailed* protein, EN, consistent with the genetic data showing that *en* inhibits *ci* transcription in the posterior compartment. EN protein expressed in bacteria protects specific DNA sequences in the *ci* regulatory region that have been shown to mediate *ci* repression in the posterior compartment (20). In addition, EN binds the *ci* gene in polytene chromosomes, and misexpression of *en* by the **heat-shock** promoter greatly reduces *ci* mRNA levels (20). Furthermore, Eaton and Kornberg (21) have shown that *ci* transcripts expand into the posterior compartment of both embryonic segments and imaginal discs in *en* mutant flies (21).

Genetic epistasis experiments place *ci* within the *hh* signaling cascade. It acts downstream from the *hh* receptor *patched* (*ptc*) and *smoothened* (*smo*), a transmembrane protein that is coupled to *ptc* and transduces the *hh* signal. *Ci* also acts upstream of the *hh* target genes (see Hedgehog Signaling). CI is an activator of transcription in the cells that receive an *hh* signal. These cells abut the posterior edge of the A/P boundary where high levels of CI are expressed. The cells expressing lower levels of CI are outside the range of *hh* activity and, in these cells, CI is a repressor of the *hh* target genes (19, 22). Recently, great progress has been made toward understanding the cellular mechanism involved in determining whether *ci* is an activator or a repressor. The first insight comes from the observation that CI exists in two forms: the 155-kDa full-length activator form and a 75-kDa proteolytic fragment (22). In the absence of an *hh* signal, a proteolytic event generates the 75-kDa form by cleaving the sequences C-terminal to the zinc-finger domain from the full-length protein. Because the resulting 75-kDa proteolytic product has both the zinc-finger DNA-binding domain and the N-terminal repressor domain, it functions as a repressor, preventing the activation of *ci* target genes. Antibodies made against the N-terminus of CI (AbN), which detect both full-length CI and the proteolytic fragment, stain the entire anterior compartment of the embryonic segments and imaginal discs. On the cellular level, the antibody staining is distributed evenly in both the nucleus and the cytoplasm (15, 22). On the other hand, full-length CI resides primarily in the cytoplasm. The levels are very low in the cells of the anterior compartment that do not receive an *hh* signal and are very high along the A/P boundary that contacts the *hh*-producing cells (19). This expression profile suggests that *hh* signaling regulates full-length CI levels post-transcriptionally. Genetic and cell culture experiments support this hypothesis. The hh^{Mrt} mutation results in a dominant misexpression of *hh* in the wing disc. In these animals, high levels of CI protein are detected along the anterior wing margin, where ectopic *hh* is expressed (23). Suppression of *hh* expression by shifting a temperature-sensitive *hh* mutant (hh^{9k94}) to nonpermissive temperatures causes decreased levels of CI along the A/P boundary in imaginal discs (15). The transmembrane protein PTC, the product of the *patched* gene, is the receptor for HH and, in the absence of HH binding, inhibits the *hh* signaling pathway. The binding of HH to PTC relieves the inhibition of *ptc* on *smo*, the positive transducer of *hh* signaling (see Hedgehog Signaling). In *ptc* mutants, *smo* is constitutively active, and *hh* target gene expression becomes independent of a *hh* signal (24-28). As expected, high levels of full-length CI are distributed uniformly in the anterior compartment of *ptc* mutants (15). Overexpression of *ptc* in wing discs results in the downregulation of full length CI along the A/P boundary without changing the *ci* messenger RNA levels, providing further evidence that *hh* regulates CI protein levels post-transcriptionally (23).

The mechanism involved in the *hh* regulation of full-length CI levels is currently under intense investigation. It has been shown that a domain C-terminal to the zinc-finger domain and N-terminal to the sites **phosphorylated** by protein kinase A is responsible for the retention of the 155-kDa full-length CI in the cytoplasm (22). Because the 75-kDa repressor form of CI does not contain this domain, its nuclear localization is not regulated. The 155-kDa CI protein forms a complex with *costal2* (*cos2*), a protein related to kinesin, *fused* (*fu*), a **serine/threonine protein kinase**, *suppressor of fused* (*su*(*fu*)), and other unidentified proteins. This complex is tethered to microtubules, thus anchoring CI in the cytoplasm. When cells receive an *hh* signal, the complex dissociates from microtubules, releasing the full-length CI from the cytoskeletal structure and presumably making it more accessible to nuclear translocation. *Hh* signaling also inhibits CI proteolysis, which accounts for the increased levels of full-length CI detected along the A/P boundary (22, 29, 30).

Protein kinase A (PKA) antagonizes *hh* and negatively regulates *ci* activity (see Hedgehog Signaling). Recent studies have helped to elucidate the mechanism involved in this regulation. Loss of PKA function or inhibition of PKA activity increases the levels of full-length CI in both embryos and discs (23). Cell culture experiments have provided details about the mechanism involved in the PKA regulation of CI (31). CI has consensus PKA phosphorylation sites at four serine residues in its C-terminus. Substitution of the serine residue with alanine in any of the first three PKA sites inhibits CI proteolysis, thus increasing the levels of full-length CI and stimulating CI-mediated transcription, suggesting that CI is the direct target of PKA regulation. Recently an F-box/WD40-repeat protein encoded by *slimb* has been identified in flies (32). Loss of *slimb* function causes the formation of supernumerary limbs and the accumulation of high levels of full-length CI. Because *slimb* is related to a yeast protein, cdc4p, that is involved in targeting cell-cycle regulators to the **ubiquitin**-mediated **protein degradation** pathway, *slimb* has been hypothesized to mediate CI proteolysis.

Evidence obtained both *in vitro* and *in vivo* suggests that *ci* directly mediates transcription of the *hh* target genes. Consensus CI binding sites have been identified in the promoter regions of *ptc* and *wg*, and CI has been shown to bind to these sites both in vitro and in vivo (11, 12, 22). In cell culture, CI transactivates a reporter gene driven by the *wg* (***wingless***) promoter region that contains the CI binding sites (11). Both endogenous and ectopic *hh* signals transactivate a *lacZ* gene driven by the 758-bp minimal *ptc* promoter in a CI binding site-dependent manner in transgenic flies (12). These experiments support the idea that CI is a transcription factor that mediates the *hh* signal in the nucleus. *Ci* also functions as a suppressor of *hh* gene expression. *Ci* mutant clones generated in the anterior compartment of the imaginal discs ectopically express HH and induce the ectopic expression of *ci* and *hh* target genes in the surrounding wild type cells, presumably through the inductive function of the ectopic *hh* (33).

3. Gli Expression and Function in Vertebrates

A number of different *hh* homologues exist in vertebrates, and they also play important roles in the specification of cell fate. The transcription factors that respond to these vertebrate signaling cascades are considered homologues of *ci* because the zinc-finger motif that defines their DNA binding domains is more similar to that of CI than any other zinc-finger proteins. To date, three *ci* homologues, *Gli1*, *Gli2* and *Gli3*, have been studied in detail.

In mouse, all three *Gli* genes are detected initially during gastrulation at 7.5 days postcoitum (dpc) in broad domains in both ectoderm and mesoderm. As development progresses, the expression patterns of the three genes become more restricted and, by the completion of organogenesis, their expression is no longer detected. *Gli1* expression overlaps with *Sonic hedgehog*(*Shh*) expression initially in the ventral midline; however, by 9.5 dpc *Gli1* is excluded from *Shh*-expressing cells and is restricted to a narrow stripe of cells that lies along the caudal-rostral axis of the ventral neural tube and lateral to the *Shh*-expressing floor plate cells. The *Gli2* and *Gli3* expression patterns are widespread within the dorsal neural tube in domains that do not overlap with regions of *Gli1* expression. While *Gli2* expression is relatively homogenous and broad, *Gli3* is expressed as a gradient, with highest concentrations found in the dorso-lateral cells of the neural tube. This dorsal-ventral pattern of expression is maintained throughout the development of the brain and spinal cord (7, 34, 35). In the somites, all three *Gli* genes are expressed in the dorsal-lateral mesochymal cells (dermomyotome), suggesting that the *Gli* genes are involved in myogenesis. The *Gli1* message is also detected in the ventral medial somite (sclerotome), whose development is patterned by *Shh*. *Gli3* is expressed throughout the newly formed somite, and its expression becomes restricted to the dorsal medial myotomal cells as development progresses (7, 36). As in the developing neural tube, the initial *Gli1* expression pattern in the limb bud overlaps that of *Shh* in the posterior mesochyme and then becomes restricted to the posterior cells immediately adjacent to the ZPA (zone of polarization activity) that expresses *Shh*. Except in the posterior margin, *Gli2* and *Gli3* are expressed throughout the limb bud, with higher levels of *Gli3* expression detected in the autopod. During bone formation, *Gli1* is expressed strongly in the perichondrium surrounding the cartilage elements where *Indian hedgehog* (*Ihh*) is expressed, and *Gli2* and *Gli3* are expressed in the tissues surrounding the perichondrium (37). *Gli1* transcripts are also detected in developing lung, gut, gonad, and eye (7, 38).

That *Gli1* is expressed in cells adjacent to those that express *Shh* or *Ihh* is reminiscent of the relationship between *hh* and *ci* and suggests that *Gli1* is one of the *hh* target genes and may transduce the *hh* inductive pathways. Transgenic or Strong's luxoid mutant mice that misexpress *Shh* induce ectopic *Gli1* expression in the neighboring cells (37, 38). Removal of the notochord from wild-type quail embryos abolishes *Gli1* expression, and supplementing the same embryos with SHH restores *Gli1* expression (36), supporting the notion that *Gli1* is a target of *Shh*. Ectopic expression of *Gli1* induces ectopic expression of the ventral neural tube markers *HNF-3b* (hepatocyte nuclear factor-3b), *patched* (*ptch*), and *Shh*. In addition, ectopic *Gli1* expression in mouse and Xenopus suppresses the expression of the dorsal neural tube marker *Pax-3*. This phenotype is reminiscent of the ectopic floor plate differentiation obtained with a gain of *Shh* function. *Gli1* also induces ectopic ventral neuronal differentiation, as shown by its ability to induce the expression of the ventral neuron markers, serotonin and dopamine. This inductive activity may be a secondary effect of *Shh*, because *Gli1* also induces *Shh* expression (34, 35, 39). The promoter region of *HNF-3b* contains Gli binding sites that can bind to *Gli1 in vitro*. Tissue culture experiments demonstrate that *Shh* can transactivate a reporter gene that is controlled by the Gli binding sites found in the *HNF-3b* promoter. Mutating the Gli consensus binding site in the *HNF-3b* promoter abrogates the *Shh* response, showing that this site is required for *Shh*-dependent transactivation (40). The best evidence that *Gli1* is a mediator of *Shh* signaling comes from experiments in transgenic mice that express a *LacZ* reporter gene driven by the *HNF-3b* minimal promoter. In these animals, b-galactosidase expression is detected in the floor plate, and this expression depends on the presence of an intact Gli binding site (40). Taken together, these studies imply that the transcription of the *Gli1* gene is induced by *Shh*, whereupon the *Gli1* protein activates an array of genes needed to differentiate the floor plate and the ventral neurons. This pattern of regulation also exists in limb development. Marigo et al (8) have shown that misexpression of *Shh* in the anterior limb bud causes ectopic *Gli1* expression, and expression of a Gli-VP16 fusion protein activates the *Shh* target gene *ptch*. *Gli* is also a target for *Ihh* and mediates *Ihh* function in bone morphogenesis. In a developing bone, the prehypertrophic cells of cartilage express *Ihh* and the receptor for parathyroid/parathyroid related protein (PTH/PTHrP). On secretion, *Ihh* stimulates *Gli1* expression in the perichondrial cells, leading to the synthesis of PTHrP, which is then secreted and binds to its receptor on the *Ihh*-producing cells. Stimulation of the PTHrP signaling pathway ensures the proliferative state of the prehypertrophic cells and prevents their premature ossification (41, 42).

Our understanding of *Gli2* function comes mainly from experiments with *Gli2* knock-out mice. *Gli2* loss-of-function mutations result in the absence of floor plate differentiation, severe axial skeletal abnormalities, and downregulation of the *Shh* target genes, such as *ptch* and *Gli1*. These results suggest that *Gli2* functions as a transcriptional activator of *Shh* target gene expression in certain structures during development (43). Injecting frog embryos with *Shh* or *Gli1* causes ectopic expression of *Gli2*, implying that *Gli2* transcription is activated by *Gli1* in response to *Shh* signaling (35).

Gli3 has been proposed for several reasons to function as a repressor of *Shh*. First, the expression patterns of *Gli3* and *Shh* are mutually exclusive (8, 34, 35, 44). Second, *Gli3* can suppress the activation of the *HNF-3b* promoter by *Gli1* in cotransfection assays (40). Third, *Gli3* knock-out mice (*Xt*) misexpress *Shh* in the anterior limb bud and dorsal neural tube, domains that normally express *Gli3* (35). Genes that are involved in limb outgrowth and patterning, such as *ptch* and *Hox*, and those for fibroblast growth factors (FGFs) and bone morphogenic proteins (*Bmp*) are also ectopically expressed in *Gli3* mutant mice due to the misexpression of *Shh* (45). This cascade of misexpression might explain the extra autopods associated with the heterozygous *Xt* mouse. Whereas *Gli3* is a repressor of *Shh*, *Shh* acts to repress *Gli3*. The misexpression of *Shh* by viral infection downregulates *Gli3* in the chick limb, and the ectopic expression of *Gli1* in the dorsal tube of transgenic mice suppresses the normal dorsal *Gli3* expression (8, 39). These results support the notion that CI function is accomplished by two Gli proteins in vertebrates, with *Gli1* acting as an activator and *Gli3* as a repressor, respectively, of *Shh* target gene expression.

Although Gli proteins have distinct expression patterns and cause different phenotypes when disrupted individually, they share some functional redundancies. Both *Gli1* and *Gli2* can induce motor neuron differentiation, and this redundancy may explain the fact that motor neuron induction is unaffected in homozygous *Gli2* mutant mice (43).

From an evolutionary perspective, many interesting parallels exist between the Drosophila and vertebrate *hh* signaling pathways. In Drosophila, *hh* suppresses the activity of the CI repressor by inhibiting the proteolysis of the 155-kDa CI protein. *Shh* signaling suppresses the activity of the *Gli3* repressor by inhibiting its transcription. CI suppresses *hh* expression, and *Gli3* suppresses the transcription of *Shh* in the cells where CI or Gli is active. In the presence of an *hh* signal, the 155-kDa CI protein is an activator of *hh* target genes, and this activity has evolved in vertebrates into the functions of *Gli1* and *Gli2*. Clearly, continued studies of CI and the Gli family members will elucidate the evolution of the signaling systems that drive the developmental process.

Bibliography

1. B. Hochman (1971) Genetics **67**, 235–252.
2. C. Nusslein-Volhard and E. Wieschaus (1980) Nature **287**, 795–801.
3. T. V. Orenic, D. C. Slusarski, K. L. Kroll, and R. A. Holmgren (1990) Genes Dev. **4**, 1053–1067.
4. K. W. Kinzler, J. M. Ruppert, S. H. Bigner, and B. Vogelstein (1988) Nature **332**, 371–374.
5. J. M. Ruppert, B. Vogelstein, K. Arheden, and K. W. Kinzler (1990) Mol. Cell. Biol. **10**, 5408–5415.
6. D. C. Hughes, J. Allen, G. Morley, K. Sutherland, W. Ahmed, J. Prosser, l. Lettice, G. Allan, M.-G. Mattei, M. Farrall, and R. E. Hill (1997) Genomics **39**, 205–215.
7. C.-C. Hui, D. Slusarski, K. A. Platt, R. Holmgren, and A. L. Joyner (1994) Dev. Biol. **162**, 402–413.
8. V. Marigo, R. L. Johnson, A. Vortkamp, and C. J. Tabin (1996) Dev. Biol. **180**, 273–283.
9. D. Zarkower and J. Hodgkin (1992) Cell **70**, 237–249.
10. J.-C. Marine, E. J. Bellefroid, H. Pendeville, J. A. Martial, and T. Pieler (1997) Mech. Dev. **63**, 211–225.
11. T. v. Ohlen, D. Lessing, R. Nusse, and J. E. Hooper (1997) Proc. Natl. Acad. Sci. USA **94**, 2404–2409.
12. C. Alexandre, A. Jacinto, and P. W. Ingham (1996) Genes Dev. **10**, 2003–2013.
13. K. W. Kinzler and B. Vogelstein (1990) Mol. Cell. Biol. **10**(2), 634–642.
14. N. P. Pavletich and C. O. Pabo (1993) Science **261**, 1701–1707.
15. J. Hepker, Q.-T. Wang, C. K. Motzny, R. Holmgren, and T. v. Orenic (1997) Development **124**, 549–558.
16. H. Akimaru, Y. Chen, P. Dai, D.-X. Hou, M. Nonaka, S. M. Smolik, S. Armstrong, R. H. Goodman, and S. Ishii (1997) Nature **386**, 735–738.
17. K. Han and J. L. Manley (1993) EMBO J. **12**, 2723–2733.
18. P. J. Mitchell and R. Tjian (1989) Science **245**, 371–378.
19. C. K. Motzny and R. Holmgren (1995) Mech. Dev. **52**, 137–150.
20. C. Schwartz, J. Locke, C. Nishida, and T. B. Kornberg (1995) Development **121**, 1625–1635.
21. S. Eaton and T. B. Kornberg (1990) Genes Dev. **4**, 1068–1077.
22. P. Aza-Blanc, F.-A. Ramirez-Weber, and T. B. Kornberg (1997) Cell **89**, 1043–1053.
23. R. L. Johnson, J. K. Grenier, and M. P. Scott (1995) Development **121**, 4161–4170.
24. A. Martinez-Arias, N. E. Baker, and P. W. Ingham (1988) Development **103**, 157–170.
25. T. Tabata and T. B. Kornberg (1994) Cell **76**, 89–102.
26. J. Capdevila, M. P. Estrada, E. Sanchez-Herrero, and I. Guerrero (1994) EMBO J. **13**, 71–82.
27. J. Capdevila and I. Guerrero (1994) EMBO J. **13**, 4459–4468.
28. W. Li, J. T. Ohlmeyer, M. E. Lane, and D. Kalderon (1995) Cell **80**, 553–562.
29. D. J. Robbins, K. E. Nybakken, R. Kobayashi, J. C. Sisson, J. M. Bishop, and P. P. Therond (1997) Cell **90**, 225–234.
30. J. C. Sisson, K. S. Ho, K. Suyama, and M. P. Scott (1997) Cell **90**, 235–245.
31. Y. Chen, N. Gallaher, R. H. Goodman, and S. M. Smolik (1998) Proc. Natl. Acad. Sci. USA **95**, 2349–2354.
32. J. Jiang and G. Struhl (1998) Nature **391**, 493–496.
33. M. Dominguez, M. Brunner, E. Hafen, and K. Basler (1996) Science **272**, 1621–1625.
34. J. Lee, K. A. Platt, P. Censullo, and A. R. i. Altaba (1997) Development **124**, 2537–2552.

35. A. R. i. Altaba (1998) Development **125**, 2203–2212.
36. A.-G. Borycki, L. Mendham, and C. P. Emerson Jr. (1998) Development **125**, 777–790.
37. K. A. Platt, J. Michaud, and A. L. Joyner (1997) Mech. Dev. **62**, 121–135.
38. J. C. Grindley, S. Bellusci, D. Perkins, and B. L. M. Hogan (1997) Dev. Biol. **188**, 337–348.
39. M. Hynes, D. M. Stone, M. Dowd, S. Pitts-Meek, A. Goddard, A. Gurney, and A. Rosenthal (1997) Neuron **19**, 15–26.
40. H. Sasaki, C.-c. Hui, M. Nakafuku, and H. Kondoh (1997) Development **124**, 1313–1322.
41. A. Vortkamp, K. Lee, B. Lanske, G. V. Segre, H. M. Kronenberg, and C. J. Tabin (1996) Science **273**, 613–621.
42. B. Lanske, A. C. Karaplis, K. Lee, A. Luz, A. Vortkamp, A. Pirro, M. Karperien, L. H. K. Defize, C. Ho, R. C. Mulligan, A.-B. Abou-Samra, H. Juppner, G. V. Segre, and H. M. Kronenberg (1996) Science **273**, 663–666.
43. Q. Ding, J. Motoyama, S. Gasca, R. Mo, H. Sasaki, J. Rossant, and C.-c. Hui (1998) Development **125**, 2533–2543.
44. R. Burke and K. Basler (1997) Curr. Opinion Neurobiol. **7**, 55–61.
45. D. Buscher, B. Bosse, J. Heymer, and U. Ruther (1997) Mech. Dev. **62**, 175–182.

Suggestions for Further Reading

46. A. R. Altaba (1997) Catching a Gli-mpse of hedgehog. Cell **90**, 193–196.
47. L. G. Biesecker (1997) Strike three for *GLI3*. Nature Genet. **17**, 259–260.
48. U. Radhakrishna, A. Wild, K.-H. Grzeschik, and S. E. Antonarakis (1997) Mutation in *Gli3* in postaxial polydactyly type A. Nature Genet. **17**, 269–271.

Cyclic AMP (3′,5′-cyclic AMP, cAMP)

Nucleotides play a universal role in life, as components of nucleic acids, as forms in which chemical free energy is stored, and as regulators of gene expression or enzyme activity. Cyclic adenosine 3′,5′-monophosphate (cAMP) plays a universal role in the control of gene expression as well as in the integration of metabolic functions. It is present both in eucaryotes and in procaryotes (see 1 for early recognition of cAMP presence in bacterial genera). cAMP seems to be absent only from archaebacteria (but see Adenylate Cyclases). Its presence was controversial in plants, but a work from the J. Schell laboratory investigating opine catabolism in plants resulted in the cloning of a gene that appeared to specify cAMP synthesis in plants. It was, however, later reported that this work was a fake, so that it is now admitted that plants do not make cAMP (2). Cyclic AMP has been reported to exist in cyanobacteria and in algae. This ubiquity explains the major interest displayed in its mode of synthesis, and the vast amount of literature devoted to the enzymes that produce cAMP from ATP, the adenylate cyclases (E. C. 4.6.1.1). Because cAMP is a regulatory molecule, it must be either excreted in the environment or inactivated in order not to accumulate. This is performed by 3′,5′-cyclic-nucleotide phosphodiesterases (E. C. 3.1.4.17). These enzymes are generally specific for cyclic nucleotides (namely cAMP and cGMP) and sometimes specific for cAMP or cGMP alone. A variety of natural inhibitors modulate their activity (nucleoside triphosphates, pyrophosphate, and especially methylated xanthines, such as theophylline) by a variety of processes involving protein phosphorylation or calcium. Adenylate cyclases (see entry) form four independent classes of enzymes, and this raises the question of the origin of cyclic nucleotides as regulatory molecules, as well as their universal implication in regulatory networks. Because it is very polar and negatively charged, cAMP does not permeate easily into cells (unless through specific transporters, generally unknown at present). More lipophilic analogs such as N6,O2′-dibutyryladenosine-3′,5′ monophosphate are, therefore, used to modulate its concentration and mimic its effect in cell cultures *ex vivo,* but *in vivo* inhibitors of phosphodiesterase or specific mediators (neuromediators in particular) are used for therapeutic purposes where cAMP concentration must be altered.

Cyclic AMP was discovered in 1958 by E. Sutherland, who obtained a Nobel prize in 1971 for this and other discoveries on hormone action. As he has himself written, it is within the scope of molecular biology that cAMP was discovered: *"When I first entered the study of hormone action, some 25 years ago, there was a widespread feeling among biologists that hormone action could not be studied meaningfully in the absence of organized cell structure. However, as I reflected upon the history of biochemistry, it seemed to me there was a real possibility that hormones might act at the molecular level".* Sutherland built up a cell-free system where well-known hormones could control glycolysis *in vitro.* Using this system he isolated a small thermostable molecule that was able to activate glycogen phosphorylase. Chemical analysis of the molecule permitted its identification as adenosine 3′-5′ cyclic monophosphate. Synthesis of cAMP was shown to be the result of the action of an enzyme, adenylate cyclase, that generated cAMP and PPi from ATP, when activated by adrenaline (3). Since this pioneering work, the study of cAMP-mediated effects required the identification of the structure, function, and regulation of adenylate cyclases, the cAMP synthesizing enzymes. And, contrary to expectation, this did not yield a unifying picture of the role of cAMP, but, rather, demonstrated that this molecule has been used over and over again by living organisms for very different functions.

At the time of cAMP discovery, the aphorism of Jacques Monod, *"what is true for Escherichia coli is true for the elephant,"* induced biochemists to try bacterial systems to unravel cAMP function. After the discovery of cAMP by Sutherland in 1958, Mackman and Sutherland (4) demonstrated that glucose-starved *E. coli* cells accumulated cAMP. Ullmann and Monod (5) later established that part of the catabolite repression phenomenon (see entry) was controlled by cAMP. This discovery raised hopes that the study of this mediator in bacteria would help to understand what happens in eucaryotes (even perhaps in higher eucaryotes). However, it soon became clear that cAMP in eucaryotes was generally, as found by Sutherland, a "second messenger" that was used as an intracellular relay molecule to the action of extracellular hormones, while it acted directly on transcription via its receptor, the Catabolite Activator Protein (see entry) in *E. coli* (6). Study of the slime mold *Dictyostelium discoïdeum* revealed another function of cAMP, phylogenetically linked to is hormone-mediated action in higher eucaryotes, namely a pulsatile synthesis and degradation used by bacteria as a signal to control their aggregation properties as a differentiating multicellular organism (7).

The universal role of cAMP in controlling such diverse metabolic processes is puzzling because the enzymes needed for its synthesis, adenylate cyclases, are extremely varied and submitted to a wide variety of regulations (see entry). Why does this result in the synthesis of the same molecular species, cAMP? Is not all the regulatory process lost in this way? How can the cAMP signal generated by one enzyme type be distinguished from another? Compartmentalization is often invoked in this process, but, while this is relatively easily accounted for in the case of macromolecules, this is difficult to see in the case of small molecules such as cAMP. Another usual answer is to say that it is the combination of hormonal receptors of differing types and cAMP—and not cAMP alone—that is required for specificity. But would not cAMP synthesized from different sources also be recognized? Another answer is to remark that cAMP is known to be only one among many second messengers: cGMP has been added to the list as well as inositol phosphates, phosphatidyldiglycerides, calcium, etc (see corresponding entries). This certainly permits generation of a combinatorial control of activities, but would be very sensitive to accidental synthesis of cAMP. Cyclic AMP is not synthesized in a steady state way (even in bacteria). It is, therefore, important not to consider cAMP as such, with some average concentration, but to consider the shape of its time-dependent variation in concentration. In fact, observations are accumulating that strongly suggest that cAMP does not have the same effect when it is delivered in a steady state fashion, rather than in a pulse (or a series of pulses) (7).

The motile and aggregating amoeba *D. discoïdeum* has been used as a paradigm for cell differentiation because undifferentiated cells start to differentiate into specific tissues some time after starvation. Secreted in the external medium, cAMP is necessary for aggregation. The genetics, biochemistry, cellular biology, and physiology of phenomena involving cAMP have been investigated in detail in this organism, where it controls, as in higher eucaryotes, a protein phosphorylation cascade, initiated after a regulatory cAMP-binding subunit of a protein kinase detaches from its target enzyme. This cascade is necessary not only for chemotaxis and aggregation but also for the triggering of genes involved in differentiation. The regulation of cAMP pulsatile concentration is mediated by two sets of enzymes adenylate cyclases and phosphodiesterases. In contrast with the situation with higher eucaryotes, however, cAMP and phosphodiesterase control operates not from the interior of the cell but from the external medium. This requires specific membrane receptors for cAMP and a process of signal transduction (see entry). In *D. discoïdeum* the pulses are generated by an appropriate coupling between adenylate cyclase activity, phosphodiesterase activity, and diffusion. The main observation is that variation in the cAMP pulse frequency changes the response of the cell. Many biochemical models can account for such cAMP pulses. These models require simple enzyme properties (in particular standard nonlinear features, such as self-activation and desensitization after saturating activity). They do not require the existence of many gene products, but only a specific behavior of enzymes (appropriate Vm and Km of biosynthetic and degradative enzymes). Assuming that cAMP concentration modulation in time is the control event is, therefore, not a biochemical paradox.

In bacteria, Utsumi et al (8) have investigated cyclic AMP synthesis during the cell cycle of *E. coli* on synchronized cells, and they have given an unambiguous demonstration that there was a strong correlation of cAMP synthesis and replication or cell division, suggesting that the molecule may play some role in the cell cycle. This is also correlated with the position of the adenylate cyclase gene near the chromosome's origin of replication and with its very low level of expression, suggesting that expression is strongly coupled to DNA replication. This observation has long been overlooked because cells deficient for adenylate cyclase or CAP are viable, suggesting that cAMP is dispensible. Specific time-dependent variation of the concentration of cAMP for fine coordination of replication and division in *E. coli* is achieved by excretion of the nucleotide, rather than coupling to the activity of a phosphodiesterase (6). In this respect it is interesting that high concentrations of cAMP produced by foreign genes in *E. coli* are not toxic until they reach a very high level (at least 10-fold the normal concentration), whereas much lower concentration of cAMP produced by the endogeneous adenylate cyclase are toxic (9). Cyclic AMP has been formally linked to catabolite repression, but there are many catabolite sensitive operons that do not respond to cAMP. In addition cAMP synthesis is very strong in *E. coli* when cells enter the stationary phase of growth, suggesting that it could be a cell-to-cell signal as it is in *D. discoïdeum.* This may be one of its function in other bacteria (such as Rhizobium species), where it is clearly not linked to catabolite repression.

In the same way, intracellular and extracellular levels of cAMP vary during the cell cycle of *Saccharomyces cerevisiae.* Using centrifugal elutriation, Smith et al (10) showed that the intracellular cAMP concentration followed the stages of the cell cycle, being highest during the division cycle and lowest immediately before or just after cell separation; at the same time the external cAMP concentration did not vary. Therefore, in yeast, as in *E. coli,* it appears that the role of the external medium is to behave as a sink. These observations substantiate the demonstration that, under normal conditions, appropriate enzyme systems can generate a specific time-dependent pattern of cAMP concentration. As in the case of *E. coli,* it is known that in *S. cerevisiae* adenylate cyclase is dispensible in mutants of the cAMP receptor, and in *S. pombe* adenylate cyclase is dispensible during vegetative growth (11). But, as in this former case, cells that carry the mutation and are deficient in adenylate cyclase have several growth defects. In this respect, the function of the time-dependent cAMP pattern could be optimization of transient processes, in particular cell division and chromosome segregation.

In all these cases cAMP is recognized on the cell surface by a specific receptor. It is, therefore, interesting to identify cases where membrane targets of cAMP have been demonstrated (*D. discoïdeum* aside). Nerve cells typically generate and are sensitive to transient signals; they also have very involved patterns of adenylate and guanulate cyclase regulation (see entries). In this respect it is important to observe that cGMP (but also cAMP) has been shown to be involved as a central molecule in vision, taste, and olfaction. In particular, in addition to their role as second messengers in protein phosphorylation cascades, cyclic nucleotides are involved at the membrane surface, but intracellularly, in gating ion channels in olfactory and taste neurons. This certainly permits generation of a variety of time-dependent patterns for cAMP regulation, as a function of environmental inputs as well as of the fine molecular structure of the enzyme or its subunits (12, 13). Because ion channels are involved in the main functions of neurons (firing patterns), this makes cyclic nucleotides important in learning processes.

Indeed, many experiments have demonstrated that cAMP is involved as a mediator of learning and memory in invertebrates [*Aplysia* (14) and *Drosophila melanogaster* (15)], as well as vertebrates (16, 17). The study of mutants of *D. melanogaster* that are defective in learning or memory has been of major importance in our understanding of the physiology, biochemistry, and anatomy underlying conditioned behaviors. *D. melanogaster* learning mutants have been separated into two general classes: those with structural defects in the brain and those without obvious brain alterations. From studies of mutants affected in the brain structure, two areas have been found to be involved in conditioned behavior: the mushroom bodies and the central complex. Analysis of the mutants has shown that many types of molecules are involved in learning, but the cAMP-mediated phosphorylation cascade has emerged as especially important. During learning, time-dependent processes are involved in the stabilization of synapses, a general view being that they are created during growth as transient entities that can either regress or be stabilized. In this process, the evolution of the synaptic pattern is dependent on the pattern of neurotransmitter delivery. Analysis of the minimal requirements for synapses stabilization suggests that neurotransmitter release must be coupled to some other transient metabolic process in a retrograde manner in order to yield a stable geometry (18). In the cases where cAMP is involved, one can, therefore, speculate that the role of this mediator is to trigger an appropriate biochemical process when the proper time-dependent control of its synthesis is at work (19). Accordingly, once again, it is not the cAMP concentration that is important, but, rather, the time-variation of its concentration. In the process of learning, the regulation of adenylate cyclase activity would, therefore, be exquisitely tuned to permit delivery of the molecule in the proper time-dependent manner.

In *D. melanogaster,* five different genes have proven important for normal learning: *dunce* (a cAMP phosophodiesterase), rutabaga (an adenylyl cyclase), amnesiac (a product similar to adenylate cyclase activating peptides), *DCO* (protein kinase A), and *dCREB2* (a cAMP-response element binding protein). The products of many of these learning mutants are enriched in mushroom bodies. A process involving control of transcription by the cAMP response element binding protein (CREB)-responsive plays a central role in the formation of long-term memory in *D. melanogaster, Aplysia* and mammals. This is one of the examples where cAMP is involved in the control of transcription in eucaryotes, as it is in eubacteria, although through a different chain of events. Agents that prevent CREB activity interfere with the formation of long-term memory, whereas agents that increase the amount or activity of the transcription factor accelerate the process, thus indicating that CREB is essential for the switch from short-term memory to long-term memory (protein synthesis dependent) (20). Further work involving inbred mice strains as well as knock-out mutants affecting the hippocampal region demonstrated that both the genetic background and the temporal pattern of synaptic activity affects the cAMP-dependent synaptic plasticity (21).

Bibliography

1. M. Ide (1971) Arch. Bioch. Biophys. **144**, 262–268.
2. T. Ichikawa, Y. Suzuki, I. Czaja, C. Schommer, A. Lessnick, J. Schell, and R. Walden (1998)

Nature 390–396.
3. E. W. Sutherland (1972) Science **177**, 401–408.
4. R. S. Mackman and E. W. Sutherland (1963) Fed. Proc. **22**, 470.
5. A. Ullmann and J. Monod (1968) FEBS Lett. **2**, 714–717.
6. A. Ullmann and A. Danchin (1983) Adv. Cyclic Nucl. Res. **15**, 1–52.
7. J. Dallon and H. Othmer (1997) Philos. Trans. R. Soc. Lond. B Biol. Sci. **352**, 391–417.
8. R. Utsumi, M. Kawamukai, H. Aiba, M. Himeno, and T. Komano (1986) J. Bacteriol. **168**, 1408–1414.
9. A. Danchin (1993) **27**, 109–162.
10. M. E. Smith, J. R. Dickinson, and A. E. Wheals (1990) Yeast **6**, 53–60.
11. T. Maeda, N. Mochizuki, and M. Yamamoto (1990) Proc. Natl. Acad. Sci. U.S.A. **87**, 7814–7818.
12. T. Leinders-Zufall, M. Rand, G. Shepherd, C. Greer, and F. Zufall (1997) J. Neurosci. **17**, 4136–4148.
13. W. Zagotta and S. Siegelbaum (1996) Annu. Rev. Neurosci. **19**, 235–263.
14. C. Bailey, C. Alberini, M. Ghirardi, and E. Kandel (1994) Adv. Second Messenger Phosphoprotein Res. **29**, 529–544.
15. R. Davis (1996) Physiol. Rev. **76**, 299–317.
16. R. Bourtchuladze, B. Frenguelli, J. Blendy, D. Cioffi, G. Schutz, and A. Silva (1994) Cell **79**, 59–68.
17. Z. Xia and D. Storm (1997) Curr. Opin. Neurobiol. **7**, 391–396.
18. J. P. Changeux and A. Danchin (1976) Nature **264**, 705–712.
19. Y. Zhong and C. F. Wu (1991) Science, **251**, 198–201.
20. J. Yin and T. Tully (1996) Curr. Opin. Neurobiol. **6**, 264–268.
21. P. V. Nguyen, S. N. Duffy, and J. Z. Young (2000) J. Neurophysiol. **84**, 2484–2493.

Cyclic Amp Receptor Protein (CRP)/Catabolite Gene Activator Protein (CAP)

The cyclic AMP receptor protein (CRP), or catabolite gene activator protein (CAP), of *Escherichia coli* is one of the best characterized transcription factors. It was discovered more than 25 years ago as a protein that binds **cyclic AMP** (cAMP) and stimulates **gene expression** of the lac operon (1, 2). Since then, CRP has attracted attention as the paradigm of gene activator proteins. It is now known that CRP, in conjunction with cAMP, participates as a global transcription factor in a wide regulatory network, both activating and repressing a large set of operons. One mechanism of catabolite repression is due to the reduction in the intracellular concentrations of both cAMP and CRP.

The CRP protein is composed of two identical subunits of 209 amino acid residues each. It is active when complexed with cAMP, which behaves as an **allosteric** effector. It is a prototype of sequence-specific DNA-binding proteins containing a helix–turn–helix motif. The cAMP–CRP complex binds to specific DNA sites in various operons. On binding DNA, it bends the DNA and interacts with **RNA polymerase** and/or other regulatory proteins to regulate transcription of the target operons.

Following early studies on the properties of purified CRP, the *crp* gene was **cloned** and sequenced in

1982 (3, 4). The X-ray crystallography structure of CRP complexed with cAMP was solved in 1981 (5). This confirmed the dimeric nature and **domain** structure of CRP deduced from biochemical studies. The subunit has two domains (Fig. 1**a**). The larger *N*-terminal domain is responsible for cAMP binding and for dimerization. The smaller *C*-terminal domain contains a helix–turn–helix DNA-binding motif. CRP is one of the first regulatory proteins where the helix–turn–helix motif was identified. CRP alone is able to bind to DNA nonspecifically. The binding of cAMP induces a conformational state that binds to specific sequences with a dyad symmetry. The detailed nature of the structural changes in CRP caused by cAMP remains unknown.

Figure 1. Structures of the CRP monomer and the CRP-DNA complex. The crystallographic coordinates were obtained from the Brookhaven Protein databank (accession code 1CGP). The images were generated by Protein Adviser (FQS). (**a**) The two domains of a CRP monomer. The larger *N*-terminal domain is responsible for cAMP binding and for dimerization. The smaller *C*-terminal domain contains a helix–turn–helix motif that is involved in DNA binding. (**b**) The CRP dimer bound to a consensus DNA site. The positions that are responsible for transcription activation (activating regions) are highlighted by space-filling models. Activating region 1 contacts the *C*-terminal domain of a subunit of RNA polymerase (8), while activating region 2 contacts the *N*-terminal domain of a subunit of RNA polymerase (9).

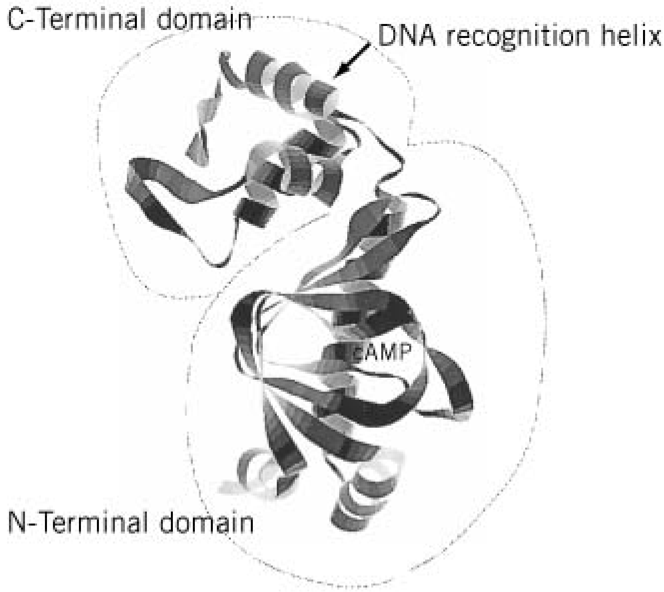

(a)

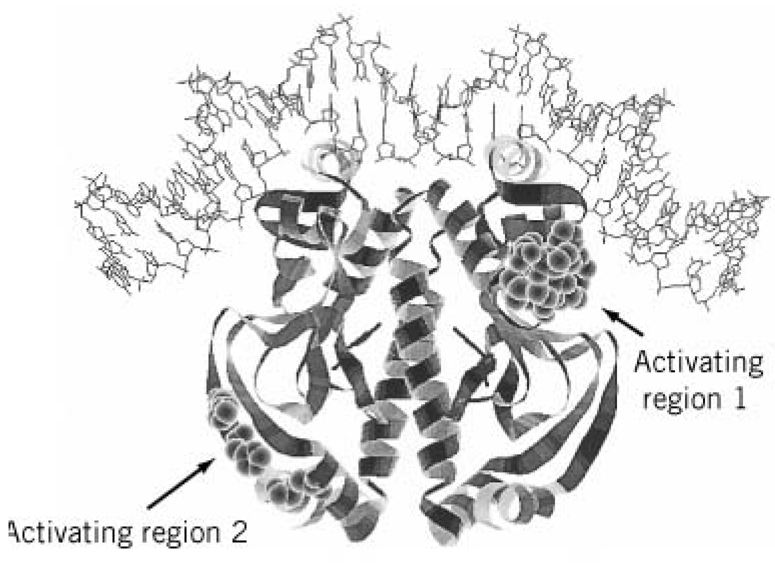

(b)

The DNA sequences of many CRP binding sites, and a resulting **consensus sequence**, have been determined. They include variations of the 22-bp palindromic sequence, 5′-AAATGTGATCTAGATCACATTT-3′, in which the two TGTGA motifs are relatively well conserved in different promoters. The binding of cAMP–CRP to target DNA induces bending of the DNA (6). The structure of cocrystals of cAMP-CRP bound to a 30-bp DNA target was determined in 1991 (7). It shows the helix-turn-helix motifs of the two subunits inserted into successive major groves of a DNA that is bent by 90°C (Fig. 1**b**).

In promoters where CRP alone is sufficient to activate transcription, the role of the cAMP–CRP complex is to enhance functional binding of RNA polymerase (8, 9). Binding of cAMP–CRP or RNA polymerase to these promoters stimulates the other's binding. An example is the *lac* promoter, where the CRP-binding site is centered on base pair –61, which is one of the preferable positions for CRP action. Another position where CRP activates transcription efficiently is –41, as in the *gal* promoter (see Gal Operon). Changing these two standard distances reduces or eliminates CRP action. Only when this change is by an integral number of turns of DNA double helix is the ability of CRP to activate transcription retained to some extent, suggesting that both CRP and RNA polymerase must bind to the same face of the DNA (10, 11). Genetic and biochemical analysis revealed that cAMP–CRP activates transcription by directly contacting RNA polymerase at these simple promoters. A surface-exposed loop in the *C*-terminal domain of CRP and the *C*-terminal part of the a subunit of RNA polymerase are primarily responsible for the contact between two proteins (8). An additional contact between the *N*-terminal domain of CRP and the *N*-terminal domain of a subunit is also involved in transcription activation at the promoters where the CRP site lies at –41 (9). The interaction between CRP and RNA polymerase is needed transiently to stimulate events leading to the formation of an open complex in these simple promoters (12). The contribution of CRP-induced DNA bending to transcription activation is still unclear. The CRP-binding site lies well upstream in several CRP-dependent promoters. In these cases, CRP acts as a coactivator of a second activator that is presumed to be responsible for the direct interaction with RNA polymerase. In the example of the *araBAD* promoter, CRP binds around –94 and the second activator AraC binds in the region between the CRP and RNA polymerase sites (13) (see ara Operon).

CRP also acts as a repressor or a corepressor in several operons. A simple example is the *cya* promoter, where cAMP–CRP inhibits the action of RNA polymerase by binding a target site located within the promoter (14). A more complex mechanism of repression is found in the operons that are coordinately regulated by CRP and CytR. Most of these promoters possess tandem CRP-binding sites that flank the CytR operator. An example is the *deo* promoter, where the CRP-binding sites are located at –41 and –94. The binding of cAMP-CRP to these sites dramatically enhances the binding of CytR to its operator, resulting in the formation of a repression complex containing both cAMP–CRP and CytR (15).

Although many studies have been identifying the regions of both transcription factors and RNA polymerase that are responsible for protein–protein and protein–DNA interactions, how these interactions lead to transcription activation is largely unknown. CRP, along with its target promoters, will continue to be a useful system for further understanding of molecular mechanisms of transcriptional regulation, including this fundamental question.

Bibliography

1. G. Zubay, D. Schwartz, and J. R. Beckwith (1970) Proc. Natl. Acad. Sci. USA **66**, 104–110.
2. M. Emmer, B. deCrombrugghe, I. Pastan, and R. L. Perlman (1970) Proc. Natl. Acad. Sci. USA **66**, 480–487.
3. H. Aiba, S. Fujimoto, and N. Ozaki (1982) Nucleic Acids Res. **10**, 1345–1361.
4. P. Cossart and B. Gicquel-Sanzey (1982) Nucleic Acids Res. **10**, 1363–1378.
5. D. B. McKay and T. A. Steitz (1981) Nature **290**, 744–749.
6. H.-M. Wu and D. M. Crothers (1984) Nature **308**, 509–513.
7. S. C. Schultz, G. C. Shields, and T. A. Steitz (1991) Science **253**, 1001–1007.
8. S. Busby and R. H. Ebright (1994) Cell **79**, 743–746.
9. S. Busby and R. H. Ebright (1997) Mol. Microbiol. **23**, 853–859.
10. K. Gaston, A. Bell, A. Kolb, H. Buc, and S. Busby (1990) Cell **62**, 733–743.
11. C. Ushida and H. Aiba (1990) Nucleic Acids Res. **18**, 6325–6330.
12. H. Tagami and H. Aiba (1998) EMBO J **17**, 1759–1767.
13. R. B. Lobell and R. F. Schleif (1991) J. Mol. Biol. **218**, 45–54.
14. H. Aiba (1985) J. Biol. Chem. **260**, 3063–3070.
15. L. Søgaard-Anderson and P. Valentin-Hansen (1993) Cell **75**, 557–566.

Suggestions for Further Reading

16. G. Zubay (1980) The isolation and properties of CAP, the catabolite gene activator. Methods Enzymol. **65**, 856–877.
17. J. L. Botsford and J. G. Harman (1992) Cyclic AMP in prokaryotes, Microbiol. Rev. **56**, 100–122.
18. D. M. Crothers and T. A. Steitz (1992) "Transcriptional activation by *Escherichia coli* CAP protein", in *Transcriptional Regulation*, S. L. McKnight and K. R. Yamamoto, eds., Cold Spring Harbor Press, Cold Spring Harbor, New York, Vol. **1**, pp. 501–534.
19. A. Kolb, S. Busby, H. Buc, S. Garges, and S. Adhya (1993) Transcriptional regulation by cAMP and its receptor protein. Annu. Rev. Biochem. **62**, 749–795.

Cyclic GMP (Cyclic Guanosine 3′,5′-Monophosphate, cGMP)

Cyclic GMP, a structural analog of **cyclic AMP**, occurs at similarly low concentrations (*i.e.*, in the micromolar range) in many animal tissues. It is synthesized by guanylate cyclases, which correspond to the adenylate cyclases that synthesize cyclic AMP, and is destroyed by specific **phosphodiesterases**.

A functional role for cyclic GMP in **bacteria** is controversial. It is present in *Escherichia coli* but at such a low intracellular concentration (nanomolar, corresponding to about one molecule per cell) that hardly makes it a significant molecule. In addition, the sequence of the *E. coli* genome does not reveal any gene product that could code for a guanylate cyclase. There are many reports suggesting the presence of cGMP in bacteria (1), but its presence is perhaps most likely in myxobacteria, where it could be involved in cell aggregation and differentiation.

In contrast, cGMP is universally in **eukaryotes** (except in **plants**). It is generally involved in processes leading to activation of specific regulation cascades, which are differentially controlled by appropriate mediators, or leading to control specific processes for neuronal activation of sense organs, such as the sensitivity to light of retina receptor cells and the triggering of olfaction and taste (2-4). The organization of guanylate cyclase and the control elements is sometimes similar to but distinct from the organization of hormonally regulated adenylate cyclase. In particular, **G-protein**-mediated regulation of vision operates on the phosphodiesterase rather than on the cyclase.

Phototransduction systems in vertebrates and invertebrates share a great deal of overall strategic similarity but differ significantly in the underlying molecular machinery. In the dark, vertebrate retinal rod cells synthesize a high level of cGMP that keeps gated **sodium channels** open in the plasma membrane of the outer segment (5). Light closes these channels by activating an enzymatic cascade that leads to rapid hydrolysis of cGMP by cGMP-specific phosphodiesterase (6). This hyperpolarizes the cell and modulates transmitter release at the synaptic buttons. Photoexcited rhodopsin triggers a transducer protein (transducin), which is related to G-proteins by catalyzing the exchange of GTP for bound GDP. Subsequently, the activated GTP-form of transducin switches on the phosphodiesterase. The cascade that has an overall gain of 10^5, is turned off by the GTPase activity of transducin and by the action of two proteins, rhodopsin kinase and arrestin . The kinetics of the reactions in the cGMP cascade limit the temporal resolution of the visual system, and statistical fluctuations in the reactions limit the reliability of detecting dim light. Together with **calcium** ions and **inositol phosphates**, cGMP controls visual excitation and adaptation. A light-induced fall in the internal free Ca^{2+} concentration subsequently stimulates resynthesis of cGMP, antagonizes the catalytic activity of rhodopsin, and restores the high affinity of the light-regulated sodium channel for cGMP, allowing the cell to adapt to background light (7).

The initial events in mollusks and arthropods are probably similar to those of vertebrates. However, whereas light activation of vertebrate photoreceptors leads to activation of cGMP-phosphodiesterase and generation of a hyperpolarizing response, activation of photoreceptors of invertebrates like Drosophila leads to stimulation of phospholipase C and generation of a depolarizing response (8). Cyclic GMP has also been implicated in modulating behavior in insects (9).

Cyclic GMP is also a second messenger in regulation mediated by natriuretic peptide hormones, but it is probably in the recently discovered nitric oxide (NO) regulation cascade that cGMP has the most unexpected role. Nitric oxide and atrial natriuretic peptide hormones play key roles in a number of neuronal functions, including learning, memory, and in blood circulation. Most experiments suggest that they exert converging actions by elevating of intracellular cGMP levels by activating soluble and membrane-bound guanylate cyclases. Cyclic GMP is the starting point for multiple signal transduction cascades, which are now beginning to be unraveled (10). In more than a quarter of a century since the discoveries of atrial granules and volume receptors in the heart atria, the search for natriuretic hormones has led to the isolation and identification of many atrial natriuretic factors (ANF) [(11), as a specific example see (12)]. In the heart, for example, ANF peptides are synthesized and stored in the Golgi apparatus of cardiac myocytes and are released in response to atrial wall stretch following acute plasma volume expansion and increased central blood volume. The mechanisms of the renal action of these potent natriuretic hormones are not yet completely unraveled. The renal hemodynamic, tubular, and adrenal, and systemic vascular effects are related to enhanced cGMP synthesis in specific medium-sized arteria, in the glomeruli and specific tubular segments, and in adrenal tissue. Specific ANF-binding sites have been detected in these target organs. A primary action of elevated cGMP levels is stimulating cGMP-dependent protein kinase (PKG), the major intracellular receptor protein for cGMP, which phosphorylates substrate proteins to trigger a regulation cascade (10).

Cyclic GMP-dependent protein kinases (PKG) also mediate some of the neuronal effects of cGMP (13), but unfortunately few PKG substrates are known in the brain. In striatonigral nerve terminals, for example, NO mediates phosphorylation of the protein phosphatase regulator, dopamine- and cyclic AMP-regulated phosphoprotein by PKG. PKG substrates are critically placed in the protein phosphorylation network and regulate protein phosphatases, intracellular calcium levels, and the function of many ion channels and neurotransmitter receptors. Nitric oxide is a signaling molecule in the nervous system of both mammals and insects. In contrast to classical transmitters, NO permeates membranes and acts on neighboring targets normally limited by diffusion barriers. This diffuse signaling is evolutionarily highly conserved. The NO forming enzyme, NO synthase, is present mostly in the nervous system, especially the brain. A soluble form of guanylate cyclase is the major target of NO action. Usually there is cellular separation of the release site and target site of NO, although exceptions to this rule exist.

As with cAMP, cGMP is important for memory in insects. In the honeybee, for example, the NO/cGMP system in the antennal lobes is implicated in the processing of adaptive mechanisms during chemosensory processing, and experimental data support a specific role of the NO system in memory formation (14).

Signal transduction in gastric and intestinal smooth muscle is mediated by receptors coupled via distinct G-proteins to various effector enzymes. Calcium is implicated in signal transduction in different ways according to the cell type (e.g., circular and longitudinal muscle cells). The initial steps involve Ca^{2+}/calmodulin-dependent activation of myosin light-chain kinase and the interaction of actin and **myosin**. Relaxation is mediated by cAMP-and/or cGMP-dependent protein kinases. A specific cascade involves G-protein-dependent stimulation of Ca^{2+} influx, leading to Ca^{2+}/calmodulin-dependent activation of a constitutive NO synthase in muscle cells that activates soluble guanylyl cyclase. The resulting activation of protein kinase A and PKG is jointly responsible for muscle relaxation (15).

Therefore, cyclic GMP is a secondary messenger that acts on targets that are sometimes similar to those of cAMP but proceed through a completely different cascade, in which the diffusible NO (and sometimes carbon monoxide) play a major role.

Bibliography

1. N. B. Bhatnagar, R. Bhatnagar, and T. A. Venkitasubramanian (1984) Biochem. Biophys. Res. Commun., **121**, 634–640.
2. L. Stryer (1986) Ann. Rev. Neurosci. **9**, 87–119.
3. T. Misaka, Y. Kusakabe, Y. Emori, T. Gonoi, S. Arai, and K. Abe (1997) J. Biol. Chem. **272**, 22623–22629.
4. T. Nakamura and G. H. Gold (1987) Nature **325**, 442–444.
5. J. T. Finn, M. E. Grunwald, and K. W. Yau (1996) Ann. Rev. Physiol. **58**, 395–426.
6. M. Chabre, J. Bigay, F. Bruckert, F. Bornancin, P. Deterre, C. Pfister, T. Vuong, and D. Baylor (1988) Cold Spring Harbor Symp. Quant. Biol. **53** (*Pt 1*), 313–324.
7. D. Baylor (1996) Proc. Natl. Acad. Sci. USA **93**, 560–565.
8. C. Zuker (1996) Proc. Natl. Acad. Sci. USA **93**, 571–576.
9. K. Osborne, A. Robichon, E. Burgess, S. Butland, R. Shaw, A. Coulthard, H. Pereira, G. RJ, and M. Sokolowski (1997) Science **277**, 834–836.
10. S. M. Lohmann, A. B. Vaandrager, A. Smolenski, U. Walter, and H. R. DeJonge (1997) Trends Biochem. Sci., **22**, 307–312.
11. H. J. Kramer and B. Lichardus (1986) Klinische Wochenschrift **64**, 719–731.
12. L. R. Forte, X. Fan, and F. K. Hamra (1996) Am. J. Kidney Dis. **28**, 296–304.
13. X. Wang and P. J. Robinson (1997) J. Neurochem. **68**, 443–456.
14. U. Muller (1997) Prog. Neurobiol. **51**, 363–381.
15. G. Makhlouf and K. Murthy (1997) Cell Signal **9**, 269–276.

Cyclins

From a simple start as a family of proteins with interesting patterns of accumulation during the cell cycle, the cyclins have grown to become key regulators of diverse cellular processes, in particular the cell cycle. Most cyclins, whether they are present only at specific times during the cell cycle or constitutively, exert their functions through their associated cyclin-dependent kinase (Cdk) binding partners. Binding to cyclins is one of the required steps in the activation of Cdks. The degradation of many cyclins by the ubiquitin system provides a means of inactivating the associated Cdk following completion of its function. A large number of cyclins have been identified including some, like the original cyclins, that have roles in cell cycle progression, and others that don't cycle and that activate Cdks involved in very different activities, such as transcription.

The first cyclins were found during studies of translational control before and after fertilization of sea urchin eggs conducted as part of the Physiology course at the Marine Biological Laboratory in Woods Hole (1). These proteins were synthesized continuously, and accumulated until their abrupt degradation during mitosis. This sawtooth pattern of accumulation hinted that cyclins might play an important role during the cell cycle, either as inducers of cell cycle transitions or, perhaps less interestingly, as proteins that responded to cell cycle states to perform functions important for that stage. Later work showed that the injection of cyclin mRNA caused frog oocytes to mature into eggs (2), that is, to progress through meiosis and to arrest in second meiotic metaphase, ready for fertilization. This result suggested that cyclins were actually inducers of the transitions into meiosis and mitosis. Subsequent work revealed that the mitotic cyclins are the regulatory subunits of maturation promoting factor (MPF) (3, 4). MPF had been characterized as a proteinaceous activity that, when withdrawn from the cytoplasm of an egg and injected into an oocyte, caused that oocyte to mature into an egg. The catalytic subunit of Xenopus MPF had recently been determined to be Cdc2, a protein kinase first identified by genetic studies in the fission yeast *Schizosaccharomyces pombe* as the key regulator of the G2-M phase transition. The following years rapidly revealed large families of proteins showing sequence similarity to the original, mitotic cyclins, and to Cdc2. The cyclins are referred to by letter (cyclin A, cyclin B, ¼) and the kinase partners have been called cyclin-dependent kinases (Cdk2, Cdk3¼). (For further discussion of these and other aspects of cyclin function, see Cell Cycle.)

One of the irreversible ratchet steps in the cell cycle is the degradation of cyclins by the ubiquitin system (5). Ubiquitin is a 76-aa protein whose covalent attachment to proteins can target them for proteolysis by the proteasome, a huge multiprotease unwinding and degrading machine. Ubiquitin is activated by its ATP-dependent covalent attachment to a cysteine side chain on an enzyme called E1. E1 then transfers ubiquitin to a cysteine of one of many E2 enzymes. The E2s can ubiquitinate substrates, often with the help of an E3. The E3s may be the most diverse and interesting components of this system. Some E3s receive the covalently bound ubiquitin; others serve as matchmakers that bring together a substrate and the appropriate E2. For the mitotic cyclins, the E3 was first termed the cyclosome, though it is now generally termed the anaphase promoting complex (APC), which consists of 8 to 12 subunits. The APC is the regulated component of the ubiquitin system for the degradation of the mitotic cyclins and serves as the target for checkpoint signals that can block cyclin degradation. Proteolysis of cyclins that act earlier in the cell cycle has been best studied in the budding yeast *S. cerevisiae* and, though mediated by the ubiquitin system, uses an “SCF complex” as the E3 component, rather than the APC.

The cyclins now comprise a large family of proteins with diverse functions, each bound to a cyclin-dependent kinase (Cdt) catalytic partner. All cyclins resemble the first mitotic cyclins (cyclin A and B) in sequence, but not all cycle during the cell cycle. Cyclins A, B, D, and E play major roles in regulating cell cycle transitions. The cell cycle stage at which each kinase functions is largely determined by when each cyclin partner accumulates during the cell cycle. Quite a few cyclins (and their associated Cdks) function in transcription. For instance, cyclin H is one of the subunits of TFIIH, a general transcription factor for RNA polymerase II involved in the phosphorylation of the C-terminal domain (CTD) of the large subunit of the polymerase. Cyclin C is a subunit of the RNA polymerase II holoenzyme, which can also phosphorylate the CTD. As more cyclins are discovered (and the alphabet is exhausted!) the majority of all cyclins will probably be noncycling regulatory subunits of protein kinases functioning in processes other than the cell cycle. The observation that the first cyclins had cyclic patterns of accumulation and were involved in cell cycle control may represent more a historical footnote owing to their relative ease of discovery than a reflection of fundamental properties of this family of proteins.

Direct roles of cellular cyclins in diseases are extremely rare. For instance, some tumor cells contain cyclin gene amplifications. Many tumors overexpress cyclin messenger RNAs, presumably a secondary consequence of increased rates of cell proliferation. Much more important, however, is the general circumvention of normal cell cycle controls that is a hallmark of cancers. This topic is discussed in Cell Cycle. Interestingly, some viruses have co-opted cyclins to subvert normal cell cycle controls (6). For instance, the Kaposi Sarcoma Associated Herpesvirus encodes a D-type cyclin. Following infection, this cyclin associates with Cdk6, which is involved in progression through the G1 phase of the cell cycle, and activates it in a manner that makes it resistant to Cdk inhibitor proteins that normally restrain G1 progression. The infected cell is thereby pushed into S phase, allowing the virus to replicate and to produce progeny virus. This situation provides yet another example of how viruses have adapted normal cellular proteins for their own ends.

Bibliography

1. T. Evans, E. T. Rosenthal, J. Youngblom, D. Distel, and T. Hunt (1983) Cell **33**, 389–396.
2. K. I. Swenson, K. M. Farrell, and J. V. Ruderman (1986) Cell **47**, 861–870.
3. J. C. Labbé, J. P. Capony, D. Caput, J. C. Cavadore, J. Derancourt, M. Kaghad, J. M. Lelias, A. Picard, and M. Dorée (1989) EMBO J. **8**, 3053–3058.
4. J. Gautier, J. Minshull, M. Lohka, M. Glotzer, T. Hunt, and J. L. Maller (1990) Cell **60**, 487–494.
5. A. M. Page and P. Hieter (1999) Annu. Rev. Biochem. **68** 583–609.
6. H. Laman, D. J. Mann, and N. C. Jones (2000) Curr. Opin. Genet. Dev. **10**, 70–74.

Suggestions for Further Reading

7. D. O. Morgan (1997) Cyclin-dependent kinases: engines, clocks, and microprocessors. Annu. Rev. Cell Dev. Biol. **13**, 261–291.
8. A. Murray and T. Hunt (1993) *The Cell Cycle*, W.H. Freeman and Company, New York.

Cyclodextrins

Cyclodextrins are cyclic oligosaccharides with a truncated cone shape and an axial void cavity (Fig. 1). The diameter and the volume of the cavity vary with the number of glucose units in the cyclodextrin ring (1). The most commonly used cyclodextrin is b-cyclodextrin, which has seven glucose units and a cavity with a diameter of 0.78 nm and a volume of approximately 35 nm^3. Other natural cyclodextrins, such as a- and g-cyclodextrin, with six and eight glucose units and 0.57- and 0.95-nm cavity diameters, respectively, are also frequently used. The outer surface of the cyclodextrin molecule is hydrophilic, because the majority of the hydroxyl groups project outward, resulting in good water solubility. The internal cavity is relatively nonpolar, and it can encapsulate nonpolar solutes of appropriate dimensions, with binding occurring through various nonpolar interactions. Such binding is known as *inclusion complexation*.

Figure 1. Cyclodextrin structure.

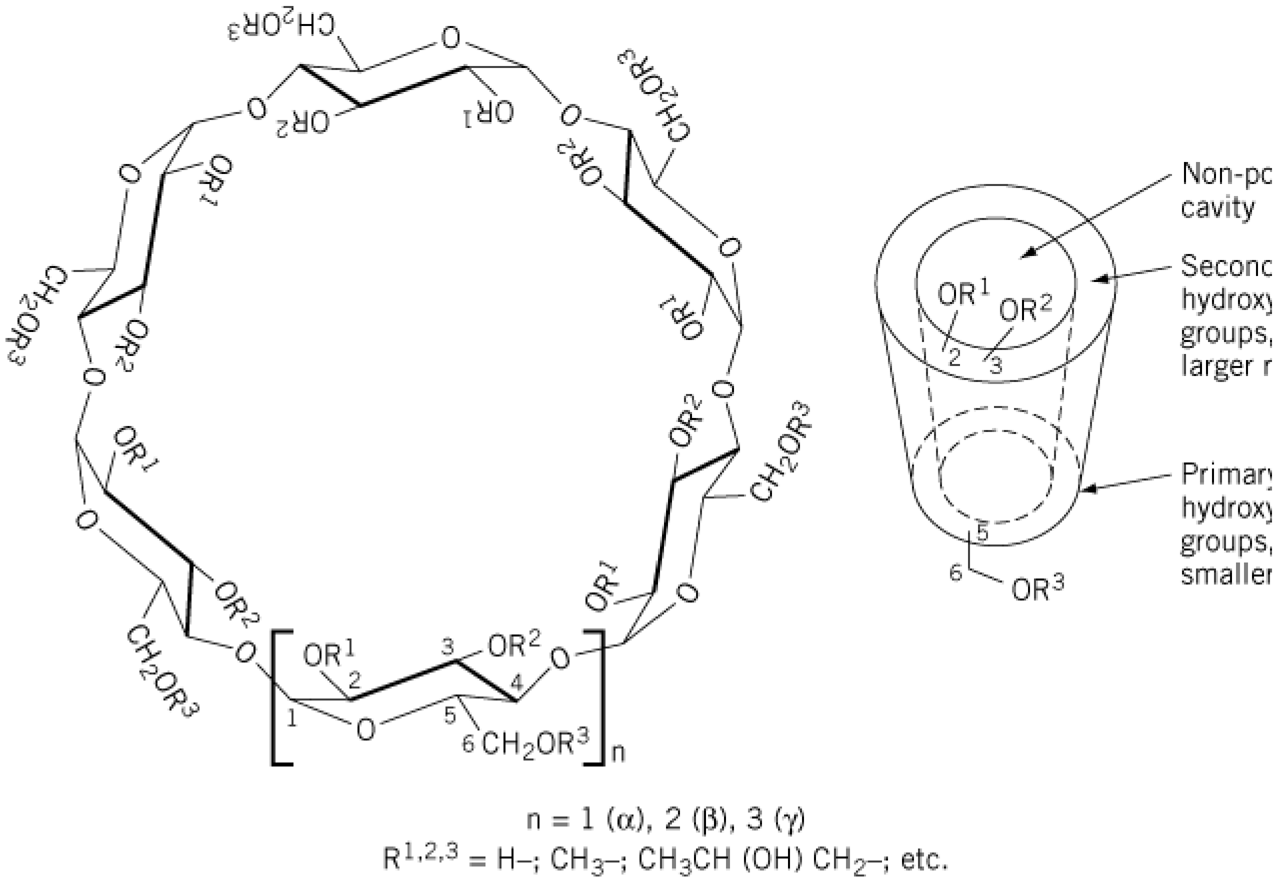

The conformation of cyclodextrins in aqueous solution is believed to be that of the truncated cone of Figure 1. Molecules of **hydrophobic** compounds of appropriate size and shape penetrate into the cavity and are bound mainly through hydrophobic interactions, whose strengths depend on the efficiency of the contact. The edge of the torus of the larger circumference consists of secondary hydroxyl groups that are attached to **chiral** carbons (C2 and C3 of the glucose units). This structure results in variable binding affinities for different enantiomers, probably due to interactions of the chiral solute with the chiral entrance to the cavity (2). The primary hydroxyl groups of the glucose monomers make up the smaller edge of the cone. Chemical derivatization of natural cyclodextrins via modification of their hydroxyl groups is currently an area of very active research (3-6). Such modifications are yielding materials of varying complexation selectivities and physicochemical properties, such as improved solubility (7).

Hoffmann and Bock (8) have examined complex formation between different cyclodextrins and **nucleotides**. They found that adenosine, cytidine, guanosine, uridine, inositol, and deoxythymidine monophosphates (AMP, CMP, GMP, UMP, IMP, and dTMP) did not form a complex with a-cyclodextrin, but b-cyclodextrin readily bound AMP and IMP. It was concluded that that these six nucleotides are too bulky to fit into the cavity of a-cyclodextrin. When a complex is formed with b-cyclodextrin, the ribose and phosphate groups of the nucleotides exert a stabilizing effect by establishing hydrogen bonds with the outer rim of the cyclodextrin molecules. The position of the phosphate group is not important; increasing distance of the phosphate group from the base increased the stability of the complex. Larger oligonucleotides exhibited decreasing tendencies for complex formation, but the extent of complexation depended significantly on their base composition. Interestingly, polynucleotides with double- or triple-helical structures did not show any complexation with b-cyclodextrin (9). Transfer RNA, which comprises both helical and nonhelical structures, can interact with cyclodextrins, and these complexes have been used extensively for tRNA studies.

Cyclodextrins have also been used in labeling nucleic acid molecules in various biochemical analysis applications, especially in DNA sequencing. Cyclodextrin labels provide potentially high signal efficiency and versatility in label colors, while maintaining uniform chemical and physical properties. Cyclodextrin tracers are prepared by coupling the cyclodextrin to specific binding substances, such as nucleic acids, and forming inclusion complexes with the fluorophores. Then the DNA molecules are sequenced using cyclodextrin-labeled chain terminators. This method allows DNA sequencing with high sensitivity and high throughput (10).

Ikeda et al. (11) reported the use of anthryl(alkylamino)–cyclodextrin complexes as chemically switched DNA intercalators that were allosteric. On adding a ligand that is tightly bound in the cyclodextrin cavity, such as 1-adamantol, the host molecule releases the anthryl unit, which then leads to strong intercalation with the double-stranded DNA molecule. This principle could be extremely useful in nucleic acid reactions of medicinal and biotechnological importance, particularly in view of the established methods to modify cyclodextrins for specific interactions with a wide range of substances, for new drug delivery systems.

Cyclodextrins and their analogs can also be used as carriers to increase cellular uptake of phosphorothioate antisense oligonucleotides. Cellular uptake of phosphorothioate oligodeoxynucleotides in the presence of various cyclodextrin analogs was found to depend on the concentration and the time. In particular, 2-hydroxypropyl-b-cyclodextrin (HPbCD), 2-hydroxyethyl-b-cyclodextrin (HEbCD), and a mixture of various HPbCDs having different degree of substitution were observed to increase the uptake of phosphorothioate oligodeoxynucleotides two- to threefold in 48 h (12).

Cyclodextrins and derivatives are used to enhance the bioavailability of many water-insoluble pharmaceuticals (13). The solubilization results in fast and quantitative *in vivo* delivery for intravenous and intramuscular dosing. A decrease in irritation at the administered site can be observed (14). The solubility of hormones such as hydrocortisone was enhanced 72-fold using randomly methylated b-cyclodextrin (15). Sublingual administration of g-cyclodextrin complex of testosterone avoided rapid first-pass loss of the hormone and directed it effectively into the circulation; administration of the complex into the stomach resulted in much lower circulatory hormone levels (16).

The relatively good water solubility of the cyclodextrins makes these materials useful in chromatography and electrophoresis separation methods, such as in HPLC (high-performance liquid chromatography) and capillary zone electrophoresis (CZE) (17, 18). Buffer systems, even with organic modifiers, can be used to control the pH or modify other secondary equilibrium. Temperature also has a significant effect on selectivity in cyclodextrin-mediated separation systems.

1. Acknowledgment

The authors gratefully acknowledge Professor József Szejtli for his stimulating discussions.

Bibliography

1. J. Szejtli (1988) In *Cyclodextrins and Their Inclusion Complexes*, Cyclodextrin Technology, Kluywer, Dordrecht, The Netherlands.
2. A. Guttman et al. (1988) J. Chromatogr. **488**, 41–53.
3. B. Sébille (1987) In *Cyclodextrin Derivatives, Cyclodextrins and their Industrial Uses*, D. Duchêne, ed., Editions de Santé, Paris, pp. 353–385.
4. K. Uekama (1985) Pharm. Intl. **6**, 61–65.
5. J. Pitha et al. (1986) Intl. J. Pharm. **29**, 73–82.
6. B. W. Müller and U. Brauns (1985) Intl. J. Pharm. **26**, 77–88.

7. Y. Y. Rawjee, D. E. Stark, and Gy. Vigh (1993) J. Chromatogr. **635**, 291–306.
8. L. Hoffmann and R. M. Bock (1970) Biochemistry **9**, 3542–3550.
9. J. Szejtli, ed. (1982) *Proceedings of the 1st International Symposium on Cyclodextrins*, Reidel, Dordrecht, The Netherlands.
10. K. M. Kosak, PCT Intl. Appl. (WO 9102040, 2/21/1991), 69pp.
11. T. Ikeda, K. Yoshida, and H. J. Schneider (1995) J. Am. Chem. Soc. **117**, 1453–1454.
12. Q. Zhao, J. Temsamani, and S. Agrawal (1995) Antisense Res. Devel. **5**, 185–192.
13. R. A. Rajewski and V. Stella (1996) J. Pharm. Sci. **85**, 1142–1169.
14. T. Loftsson and M. E. Brewster (1996) J. Pharm. Sci. **85**, 1017–1025.
15. J. Szejtli (1994) Med. Res. Rev. **14**, 353–386.
16. J. Pitha, E. J. Anaissie, and K. Uekama (1987) J. Pharm. Sci. **76**, 788–790.
17. S. Ahuja (1991) In *Chiral Separations by Liquid Chromatography*, American Chemical Society, Washington, DC.
18. A. Guttman (1996) In *Handbook of Capillary Electrophoresis*, 2nd ed., J. P. Landers, ed., CRC Press, Boca Raton, pp. 75–100.

Cycloheximide

$C_{15}H_{23}NO_4$ (Fig. 1; molecular mass, 281.35). Cycloheximide is an antibiotic produced by *Streptomyces griseus*, and it inhibits protein biosynthesis in eukaryotes. Cycloheximide does not affect protein synthesis in prokaryotes or in mitochondria. It binds to the 60S subunit of eukaryotic ribosomes and inhibits the peptidyl transferase activity. The inhibition of peptidyl transfer causes a stack of ribosomes on the messenger RNA, generating polysome accumulation in cells. Cycloheximide is frequently used for the study of gene expression in eukaryotes as an inhibitor of protein synthesis *in vivo*, as well as *in vitro*.

Figure 1. Cycloheximide.

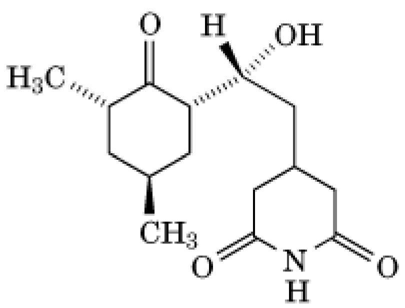

Cyclophilin

Historically, an 18-kDa cytosolic protein from pig kidney was the first peptidyl prolyl cis/trans isomerase (abbreviated PPIase) discovered and characterized enzymatically (1). These enzymes catalyze the rotation of a peptidyl prolyl moiety in peptides and proteins. In 1989 it was found that this protein is nearly identical in its primary structure to the already known cytosolic receptor of the immunosuppressive undecapeptide cyclosporin A in human T lymphocytes, previously named cyclophilin [Cyp18; for nomenclature see (2)] (3-5). This enzyme represents the archetype of cyclophilins in that it constitutes the catalytic **domain** of larger cyclophilin-like proteins. Now two additional families of such isomerases are known, those that bind FK506 (FKBP) and the parvulin family.

Alignment of amino acid sequences of the cyclophilin family defines residues that are highly conserved among vertebrates, plants, fungi, and bacteria. Nearly perfect conservation is located primarily in the central segment of the protein, including the sequences -Phe-His-Arg-Ile/Val-Ile-$(Xaa)_5$-Gln-Gly-Gly- at positions 53 to 65 and -Met-Ala-$(Xaa)_{9–10}$-Gln-Phe-Phe/Tyr-Ile/Val- at positions 100 to 114, where Xaa is any amino acid and / separates alternatives. These sequences are used as typical **motifs** to search for other cyclophilins. The three-dimensional structure of the archetypal cyclophilin consists of an eight-stranded antiparallel b-sheet barrel capped by a-**helices** (6, 7).

The characterization of 11 distinct cyclophilin genes in the genome of the nematode *Caenorhabditis elegans* demonstrates that organisms use numerous cyclophilins (8). As many as 12 human homologues have been identified thus far from the initial assessment of gene diversity by expressed sequence tag analysis. The C-terminal and/or N-terminal amino acid extensions of larger cyclophilins consist of additional **domains**, directing the proteins into specific cellular compartments, mediating protein/protein and DNA/protein interactions, or generating other biochemical functions.

The cytosolic Cyp18 often represents the major cyclophilin of cells. Kidney tubules and endothelial cells, for example, contain 10 µg of Cyp18 per mg total protein (9). Despite the numerous studies reporting the three-dimensional structures of Cyp18-bound oligopeptide substrates and inhibitors (10-12), a definite catalytic mechanism for cyclophilins and other PPIases is still lacking. It is currently believed that catalysis arises from a combination of desolvation of the substrate and substrate-assisted catalysis. Electrophilic assistance, for example, by the Arg55 residue of Cyp18, can also be envisaged to account for the more effective catalysis found for cyclophilins, compared to FKBPs. The positively charged side-chain of this amino acid residue is located within **hydrogen-bonding** distance and perpendicular to the plane of the substrate proline ring in Cyp18/substrate complexes. This environment may cause additional weakening of the reactive C–N linkage by immobilizing the lone pair of electrons of the nitrogen atom. Indeed, a Cyp18 variant in which Arg55 has been replaced retains only 0.1% of the wild-type enzymatic activity (13).

Because of the putative functional redundancy and overlapping of the many PPIases present in most organisms, gene deletion experiments often do not lead to a recognizable **phenotype** under normal growth conditions. Among the seven cyclophilins found in *S. cerevisiae*, deletions of only two are associated with any phenotype. Disruption of *Cpr3*, the gene encoding the **mitochondrial** isoform of yeast cyclophilin, affects growth on L-lactate medium (14), whereas *cpr7*D cells are defective in normal cell growth (15). The expression of many PPIase genes seems to be sensitive to **heat shock** and to the chemical **stress response**.

Recently, it was shown that host cell cytosolic Cyp18 is required for **HIV**-1 infection before **reverse transcription** but subsequent to receptor binding and membrane fusion in T cells (16). A proline-rich segment of the capsid domain of $Pr55^{gag}$ mediates incorporation of Cyp18 into HIV-1 virions

(17). This conserved segment that contains four proline residues occurs in the sequence -Pro-$(Xaa)_4$-Pro222-$(Xaa)_2$-Pro-$(Xaa)_5$-Pro-. Mutant proteins of HIV-1_{HXB2} that have **site-directed mutations** in which Pro222 is replaced by Ala or Gly221 by Ala, fail to bind to the **fusion protein** glutathione-S-transferase/Cyp18. Virions that contain these altered proteins cannot sequester Cyp18 into the released virions, emphasizing the importance of the Gly-Pro^{222} bond for $Pr55^{gag}$ /Cyp18 complex formation. The ability of many cyclosporin derivatives to dissociate the $Pr55^{gag}$/Cyp18 complex reveals a quantitative relationship between Cyp18 inhibition and complex decomposition. Obviously, the antiviral effect of cyclosporin A must be caused by a pathway distinctive from immunosuppression because cyclosporin A derivatives with negligible immunosuppressive activity, but high affinities for the active site of Cyp18, retain potent anti-HIV activity (18-20).

A genetic **cDNA** screen was used to identify the bovine homologue of the retina-specific cyclophilin NinaA of *Drosophila*. The membrane-localized PPIase of the secretory pathway of the fly is required for proper folding and trafficking of Rh1-6 opsin in photoreceptor cells (21). The bovine RanBP2 cyclophilin has a domain that binds to the GTPase Ran, as well as to red/green opsin. A still unknown modification of opsin, possibly a prolyl bond isomerization catalyzed by the Cyp-domain of RanBP2, augments and stabilizes the interaction between the Ran-binding domain and opsin. This modification is important in membrane trafficking of long-wavelength opsin in photoreceptors (22).

Bibliography

1. G. Fischer, H. Bang, and C. Mech (1984) Biomed. Biochim. Acta **43**, 1101–1111.
2. G. Fischer (1994) Angew. Chem., Int. Ed. Engl. **33**, 1415–1436.
3. R.E. Handschumacher et al. (1984) Science **226**, 544–547.
4. G. Fischer et al. (1989) Nature **337**, 476–478.
5. N. Takahashi, T. Hayano, and M. Suzuki (1989) Nature **337**, 473–475.
6. R.T. Clubb, S.B. Ferguson, C.T. Walsh, and G. Wagner (1994) Biochemistry **33**, 2761–2772.
7. H. Ke (1992) J. Mol. Biol. **228**, 539–550.
8. A.P. Page, K. Macniven, and M.O. Hengartner (1996) Biochem. J. **317**, 179–185.
9. B. Ryffel et al. (1991) Immunology **72**, 399–404.
10. G. Pflügl et al. (1993) Nature **361**, 91–94.
11. H.M. Ke et al. (1994) Structure **2**, 33–44.
12. Y.D. Zhao and H.M. Ke (1996) Biochemistry **35**, 7362–7368.
13. L.D. Zydowsky et al. (1992) Protein Sci. **1**, 1092–1099.
14. E.S. Davis et al. (1992) Proc. Natl Acad. Sci. U.S.A. **89**, 11169–11173.
15. A.A. Duina, J.A. Marsh, and R.F. Gaber (1996) Yeast **12**, 943–952.
16. D. Braaten, E.A. Franke, and J. Luban, (1996) J. Virol. **70**, 3551–3560.
17. E.T. Franke, H.E.H. Yuan, and J. Luban (1994) Nature **372**, 359–362.
18. B. Rosenwirth et al. (1994) Antimicrob. Agents Chemother. **38**, 1763–1772.
19. S.R. Bartz et al. (1995) Proc. Natl Acad. Sci. USA **92**, 5381–5385.
20. C. Aberham, S. Weber, and W. Phares (1996) J. Virol. **70**, 3536–3544.
21. E.K. Baker, N.J. Colley, and C.S. Zuker (1994) EMBO J. **13**, 4886–4895.
22. P.A. Ferreira, T.A. Nakayama, W.L. Pak, and G.H. Travis (1996) Nature **383**, 637–640.

Suggestions for Further Reading

23. A. Galat and S.M Metcalfe (1995) Peptidylproline *cis/trans*isomerases, Prog. Biophys. Molec. Biol. **63**, 67–118; contains an exhaustive bibliography of many aspects of PPIases.
24. C.C. Trandinh, G.M. Pao, and M.H. Saier (1992) Structural and evolutionary relationships among the immunophilins—two ubiquitous families of peptidyl-prolyl *cis/trans* isomerases,

FASEB J. **6**, 3410–3420; contains a detailed analysis of the amino acid sequences of PPIases.
25. G. Wiederrecht and F. Etzkorn (1994) The immunophilins, Persp. Drug Disc. Design **2**, 57–84.
26. D.M. Armistead and M.W. Harding, (1993) Immunophilins and immunosuppressive drug action, Ann. Rep. Medicinal Chem. **28**, 207–213.

Cyclosporin

The cyclosporin family of secondary metabolites from the **fungus** imperfectus *Beauveria nivea* are cyclic undecapeptides characterized by an enormous spectrum of biological effects. The most widely used derivative, cyclosporin A (CsA), is immunosuppressive, antiinflammatory, and antichemotactic, and combats multidrug-resistance and viral, fungal, and parasitic infections, without being cytotoxic to mammalian cells (1, 2). Among a number of other *N*-methyl amino acids, CsA contains an uncommon amino acid at position 1, the (4*R*)-4([(*E*)-2-butenyl]-4-*N*-dimethyl-L-threonine (Fig. 1). Several minor congeners of CsA, designated CsB, CsC ¼ CsZ, have been found as by-products of the fermentation process. The [D-MeVal^{11}]-CsA derivative (CsH) is devoid of most biological effects, thereby serving as a control for nonspecific interactions. Other derivatives have been developed that exhibit a more restricted spectrum of biological activities compared to CsA. For example, [L-MeLeu(3-OH)^{1},MeAla^{4,6}]-CsA is nonimmunosuppressive but has enhanced antiviral efficacy (3). In the fungus, non-ribosomal synthesis of cyclosporins occurs on a huge, single-chain enzyme with a molecular mass of 1,689 kDa, termed cyclosporin synthetase . It utilizes unmethylated natural amino acids, ATP/Mg^{2+} and S-adenosyl-L-methionine as starting materials in biosynthesis (4). Beside its use as a powerful tool for unraveling the molecular basis of the cellular immune response, the therapeutic application of CsA has revolutionized the likelihood of success for organ transplantation since its introduction in 1983 (5). Other disorders with immune components, like psoriasis and juvenile diabetes, are relieved with the aid of cyclosporins.

Figure 1. Structure of cyclosporin A.

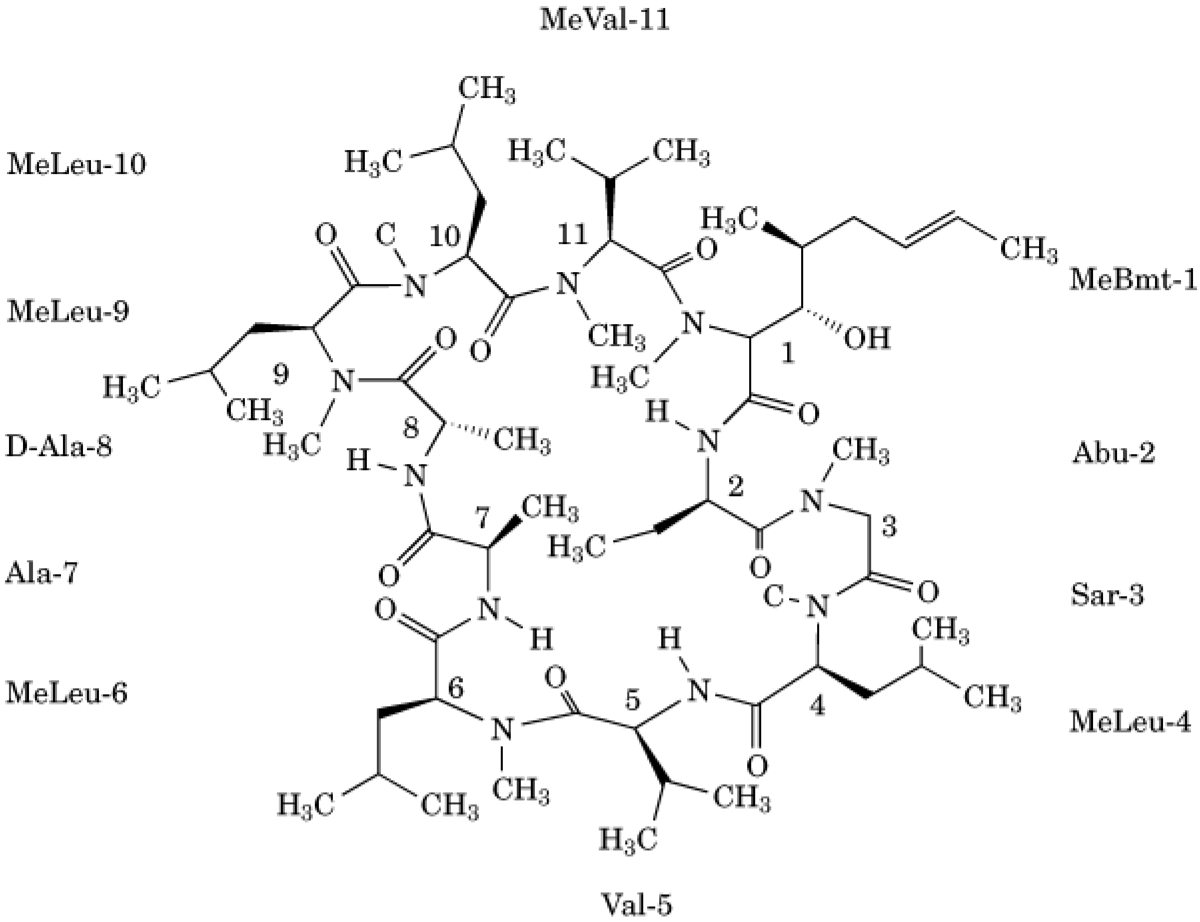

The dramatic effects of CsA on the cellular immune response, in which the T cells remain in a nonproliferative state, results primarily from the impaired expression of a number of lymphokine genes. This could include a variety of interleukins (IL-2, IL-3, IL-4), factors, such as granulocyte macrophage colony stimulating factor (GM-CSF), tumor necrosis factor a (TNF-a) and **g-interferon**, and the **oncogene** c-myc, all synthesized subsequent to antigen stimulation of T cells. Initial investigations identified cytosolic cyclophilin Cyp18 as the specific receptor for CsA in T cells, but minor **isoenzymes** cannot be completely ruled out yet.

The three-dimensional structure of the inhibitory CsA/Cyp18 complex was determined by X-ray crystallographic and NMR methods (6-8). The structure of Cyp18 is hardly affected by complex formation, whereas that of CsA bound to Cyp18 is dramatically different when in nonpolar organic solvents or in the solid state. In response to the altered conformation of CsA in the complex, the inhibition of the PPIase activity of Cyp18 by CsA is time-dependent, including a ***cis/trans* isomerization** of the peptide bond between MeLeu^{9}-MeLeu^{10}. Site-directed mutagenesis of Cyp18 indicates the involvement of a **hydrophobic** pocket of side-chains, with Trp121 as a major determinant, in the tight binding of CsA to Cyp18, with an inhibition constant, K_i of 2.3 nM. Comparison of Cyp18/substrate complexes with Cyp18/CsA indicates that the peptide chain of CsA runs in the opposite direction. The MeVal11 side-chain of the inhibitor occupies the place of the substrate proline ring.

In some cases, binding of cyclosporins to the targeted cyclophilin and inhibition of its PPIase activity may explain the biological effect of cyclosporins. In contrast, binding of CsA to Cyp18 is necessary, but not sufficient, to arrest signals for the cellular immune response. For example, [MeAla^{6}]-CsA is an excellent inhibitor of the PPIase activity of Cyp18 but has only 1% of the immunosuppressive effect of CsA, whereas the weak inhibitor [$MeBm_2t^1$]-CsA (K_i > 1 μM) still shows a considerable fraction of the CsA effect (9).

Thus, for immunosuppression CsA (like FK506 and rapamycin) is best viewed as a pro-drug that is activated functionally when bound to Cyp18 (10). Once formed from the components, the complexes CsA/Cyp18 or FK506/FKBP12 bind to and inactivate reversibly, in a noncompetitive mechanism, the Ca^{2+}- and calmodulin-dependent, heterodimeric protein **phosphatase** 2B (calcineurin). This enzyme catalyzes the dephosphorylation of Ser/Thr residues in phosphorylated proteins (11, 12). As a result of dephosphorylation, this enzyme induces the phosphorylated cytoplasmic subunit of NF-AT to translocate into the nucleus for association with the newly synthesized nuclear subunit of NF-AT to form a functional transcription factor (13).

Bibliography

1. J. F. Borel, C. Feurer, H. Gubler, and H. Stahelin (1976) Agents Actions **6**, 468–475.
2. J. F. Borel (1989) Pharmacol. Rev. **41**, 259–371.
3. S. R. Bartz et al. (1995) Proc. Natl Acad. Sci. U.S.A. **92**, 5381–5385.
4. A. Lawen and R. Zocher (1990) J. Biol. Chem. **265**, 11355–11360.
5. C. R. Stiller (1996) Transplant. Proc. **28**, 2005–2012.
6. J. Kallen et al. (1991) Nature **353**, 276–279.
7. H. M. Ke et al. (1994) Structure **2**, 33–44.
8. S. W. Fesik et al. (1991) Biochemistry **30**, 6574–6583.
9. N. H. Sigal et al. (1991) J. Exp. Med. **173**, 619–628.
10. S. L. Schreiber (1991) Science **251**, 283–287.
11. J. Liu et al. (1991) Cell **66**, 807–815.
12. J. Liu et al. (1992) Biochemistry **31**, 3896–3901.
13. N. A. Clipstone, D. F. Fiorentino, and G. R. Crabtree (1994) J. Biol. Chem. **269**, 26431–26437.

Suggestions for Further Reading

14. A. Lawen (1996) Biosynthesis and mechanism of action of cyclosporins, Prog. Med. Chem. **33**, 53–97. This nice review about cyclosporin A-mediated immunosuppression includes a summary of the biosynthesis of cyclosporin derivatives.
15. P. F. Halloran and J. Madrenas (1991) The mechanism of action of cyclosporine—a perspective for the 90s, Clin. Biochem. **24**, 3–7.
16. M. Thali (1995) Cyclosporins: Immunosuppressive drugs with anti-HIV-1 activity, Mol. Med. Today, **6**, 287–291.
17. J. Clardy (1995) The chemistry of signal transduction, Proc. Natl Acad. Sci. U.S.A. **92**, 56–61.
18. H. Fliri, G. Baumann, A. Enz, J. Kallen, M. Luyten, V. Mikol, R. Movva, V. Quesniaux, M. Schreier, M. Walkinshaw, R. Wenger, G. Zenke, and M. Zurini (1993) Cyclosporins—structure-activity relationships, Immunosuppressive Antiinflammatory Drugs **696**, 47–53.
19. G. Fischer (1994) Peptidyl-prolyl cis/trans isomerases and their effectors, Angew. Chem., Int. Ed. Engl. **33**, 1415–1436.

Cystatin

Cystatin is a protein inhibitor of cysteine proteinases from chicken egg white that gave its name to a family and superfamily of such inhibitors [see Cysteine (Cys, C); Proteinase Inhibitors, Protein].

Cysteine (Cys, C)

The amino acid cysteine is incorporated into the nascent polypeptide chain during **protein biosynthesis** in response to two **codons**—UGU and UGC—and represents only 1.7% of the residues of the proteins that have been characterized. The cysteinyl residue incorporated has a mass of 103.15 Da, a **van der Waals volume** of 86 Å^3, and an accessible surface area of 140 Å^2. Cys residues are one of the most conserved type of residue during divergent evolution; they are interchanged in **homologous** proteins most frequently with serine residues.

The thiol group of the Cys side-chain

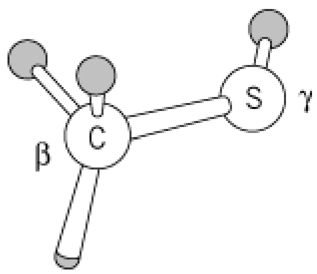

is the most reactive of any of the normal amino acids. It undergoes numerous chemical reactions with a variety of reagents (see Thiol Groups). These reactions provide means for counting and measuring the number of Cys residues present in a protein (see Counting Residues and -Dithiobis-(2-Nitrobenzoic Acid), DTNB). It is the ionized thiolate anion that is reactive, and only it has **absorbance** in the UV region; the pK_a value of a typical exposed Cys thiol group is 8.7, but deviations as low as 3.5 and greater than 11 are known, depending on the environment (1).

In the nonionized form, the thiol group is not very polar or reactive, and thiol groups may be buried in folded proteins without the need for any hydrogen bonding. Approximately 40–50% of Cys residues are fully buried in folded protein structures. They occur predominantly in beta-sheet type of **secondary structure**. Cys residues can serve as efficient "capping" residues at the *N*-termini of a-helices in which their thiol group interacts with the hydrogen bonding groups of the backbone; the pK_a can then be decreased and the thiol groups made more reactive; probably for that reason, Cys residues occur at such positions in folded proteins only when important for function (2).

A notable tendency is for two Cys residues of the same or different polypeptide chains to form disulfide bonds. This occurs only if the protein conformation permits, and disulfide formation is a useful probe of **protein folding** *in vitro*. *In vivo*, disulfide bonds are usually inserted primarily into proteins to be secreted by the catalyst protein disulfide isomerase.

If a protein is hydrolyzed to amino acids under conditions in which the disulfide bond persists, two cysteine amino acids linked by a disulfide bond result, which historically was known as the amino acid cystine. Peptide bonds preceding Cys residues can be cleaved by cyanylation with 2-nitro-5-thiocyanobenzoic acid, followed by incubation at alkaline pH (3). The reaction is specific for Cys residues but has the disadvantage that the new *N*-terminus generated is blocked and not amenable to further **sequencing** by the Edman Degradation.

Thiol groups have intrinsic affinities for many metal ions, and they are used in proteins to ligate ions of zinc, iron, and copper. In an extreme example, metallothioneins about a third of the residues are Cys. The thiol groups of Cys residues are also used as nucleophiles in catalysis in the thiol proteinases.

Cys residues are the sites of several types of post-translational modifications, in addition to disulfide formation. **Farnesyl groups** and geranylgeranyl groups can be added to Cys residues at the *C*-termini of certain proteins, after removal of a few *C*-terminal residues. **Palmitoyl groups** can be attached in thioester linkages to the side chains of Cys residues.

Bibliography

1. J. W. Nelson and T. E. Creighton (1994) Biochemistry **33**, 5974–5983.
2. T. Kortemme and T. E. Creighton (1995) J. Mol. Biol. **253**, 799–812.
3. G. R. Stark (1977) Meth. Enzymol. **47**, 129–132.

Cysteine Proteinase Inhibitors

Cysteine proteinase inhibitors attracted wide attention and, after serine proteinase inhibitors [see Serine Proteinase Inhibitors, Protein], have the most frequently described members. Most but not all of these belong to the cystatin superfamily, which is frequently divided into three families: the stefin, the cystatin, and the kininogen families. The stefins are low molecular weight (about 100 residues) molecules without attached carbohydrate and without any intramolecular disulfide bridges. They are extremely stable intracellular proteins. The word *stefin* comes from the name of the J. Stefin Institute in Ljubljana (Slovenia), where the first stefin was discovered. Cystatins proper are only slightly bigger than stefins (120–130 residues). They contain two disulfide bridges near their COOH terminals and typically are secretory proteins. The family and superfamily are named after chicken egg white cystatin, which was discovered long before the other cystatins became popular. The third family of cystatins is the kininogen family. Proteins are assigned to it on the basis of the high molecular weights of its members, predominantly HMW (high molecular weight) (120 kD) and LMW (low molecular weight) (68 kD) kininogens. Kininogens are glycosylated and contain numerous disulfide bridges. Each contains three cystatin like repeats.

All cystatin family members inhibit only cysteine proteinases and only those related to papain but, within this broad group, they exhibit little discrimination between individual enzymes. In strong contrast to serine proteinase inhibitors, cystatins react with enzymes whose catalytic sulfhydryl group is significantly blocked. The mode of association was elucidated in detail from the three-dimensional structure of a complex of stefin A with papain.

In avian and mammalian cells, there are present cysteine proteinases called calcium-activated neutral proteinases (CANP), or calpains. These complicated multidomain enzymes are of great importance in the metabolism of muscles. They are controlled by a closely related family of molecularly complex endogenous protein inhibitors—calpastatins.

Suggestions for Further Reading

A. J. Barrett (1981) Cystatin, the egg white inhibitor of cysteine proteases. Methods Enymol. **80**,

771–778.

W. M. Brown and K. M. Dziegielewska (1997) Friends and relations of the cystatin superfamily—new members and their evolution. Protein Sci. **6**, 5–12.

H.-H. Otto and T. Schimeister (1997) Cysteine proteases and their inhibitors. Chem. Rev. **97**, 133–171.

Cystine Knot

The cystine knot is a common protein motif that occurs in some protein structures. It incorporates an antiparallel b-sheet and three disulfide bonds, one of which passes through a ring formed by the other two disulfides (Fig. 1). Two families of cystine knot motifs have been identified. One is the growth factor cystine knot family (1, 2) that includes **nerve growth factor**, **transforming growth factor b2**, platelet derived growth factor, and human chorionic gonadotrophin. In this topology, the six cysteine residues (designated CI through CVI) form three disulfide bridges (CI-IV, CII-V, CIII-VI), with CI-IV passing through the ring formed by the disulfides of CII-V and CIII-VI. The size of the ring varies from 8 to 14 residues. The b-sheet is formed from four antiparallel b-strands. These cystine knot growth factors are all dimeric, but their dimer interfaces differ.

Figure 1. Schematic representation of the backbone structure of the growth factor cystine knot protein, nerve growth factor (4). b-Strands are shown as arrows, and the three disulfide bonds of the cystine knot are shown in gray, with the sulfur atoms depicted as gray spheres. The *N*- and *C*-termini are labeled. This figure was generated using Molscript (5) and Raster3D (6, 7).

The second group is the inhibitor cystine knot family (3) and includes the neurotoxin w-conotoxin GVIA and the uterotonic peptide kalata B1. The inhibitor cystine knot motif has the same disulfide bond pattern as the growth factor cystine knot, but in this case the knot is formed by CIII-VI passing through the ring formed by disulfides CI-IV and CII-V. The ring of the inhibitor cystine knot varies from 8 to 12 atoms, and the b-sheet is triple stranded and antiparallel.

[See also Disulfide Bonds and Beta-Sheet.]

Bibliography

1. N. Q. McDonald and W. A. Hendrickson (1993) Cell **73**, 421–424.
2. N. W. Isaacs (1995) Curr. Opin. Struct. Biol. **5**, 391–395.
3. P. K. Pallaghy, K. J. Nielsen, D. J. Craik, and R. S. Norton (1994) Protein Sci. **3**, 1833–1839.
4. N. Q. McDonald et al. (1991) Nature **354**, 411–414.
5. P. J. Kraulis (1991) J. Appl. Crystallogr. **24**, 946–950.
6. E. A. Merritt and M. E. P. Murphy (1994) Acta Crystallogr. **D50**, 869–873.
7. D. J. Bacon and W. F. Anderson (1988) J. Mol. Graphics **6**, 219–222.

Cytochalasin

Cytochalasins are a group of fungal metabolites that can permeate cell membranes and exert very strong effects on the cytoskeleton: ruffling and translocation are stopped, and cells round up (1, 2). In addition, cytochalasins A and B also inhibit glucose transport across the plasma membrane. Although it was originally believed that the main action of the cytochalsins on the cytoskeleton was binding with high affinity to the barbed, or fast-growing end of the actin filament, and inhibiting subunit addition and loss, it has become clear that the effects are more complex. The concentrations of cytochalasins used in cell biological experiments will have strong effects on actin monomers and may convert much of a cell's monomeric G-ATP actin to G-ADP actin (3). In addition, even at saturating concentrations cytochalasins do not completely block the fast-growing ends with respect to subunit addition or loss (3). Thus, the action of cytochalsin on a living cell is likely to be complicated and may affect the interactions of actin with many actin-binding proteins. Nevertheless, as a result of the large effect cytochalsins have on actin, they have been widely used to study the role of the actin cytoskeleton in cellular processes.

Bibliography

1. I. Yahara, F. Harada, S. Sekita, K. Yoshihira, and S. Natori (1982) J. Cell Biol. **92**, 69–78.
2. M. Schliwa (1982) J. Cell Biol. **92**, 79–91.
3. P. Sampath and T. D. Pollard (1991) Biochemistry **30**, 1973–1980.

Cytochrome P450

Cytochromes P450 (designated here as P450) arise from a superfamily of **genes** that encode hemoproteins with molecular weights of 40 to 55 kDa and extraordinarily diverse properties and functions. P450 is nearly ubiquitous in the biotic world, with over 500 genes characterized in **plants**, animals, **fungi**, and **bacteria**, although it is not present in all organisms. Of the substrates of P450, 1000 are known, and there are perhaps as many as 10^6 in total; more than 40 different reactions are catalyzed (1). These enzymes play a critical role in:

1. Detoxification of bioactive molecules in vertebrates, insects, and plants
2. Metabolic activation of compounds that are both beneficial (drug precursors, hormones) and detrimental (carcinogens)
3. Biogenesis and catabolism of many endogenous compounds, including steroid hormones, vitamin D, biological insecticides, fatty acids, insect pheromones, and plant lignins and pigments

The P450 that metabolize xenobiotics appear to have no critical physiological functions, since mice with disrupted genes for these proteins had no obvious phenotypic abnormalities (2, 3). Most P450 proteins are membrane-bound in the endoplasmic reticulum (microsomes) or mitochondria, but soluble forms are present in bacteria. In mammals, the greatest concentrations of P450, particularly the detoxification forms, are present in the liver, but they are probably present in most tissues of the body, with relatively high concentrations in the intestines, lungs, nasal epithelia, and steroidogenic tissues. The genes for these enzymes differ in size, **intron** number, and **chromosomal** location. **Gene expression** of subsets of the P450 is regulated by a variety of substances, including xenobiotics such as aromatic hydrocarbons, barbiturates, and **peroxisomal** proliferators, and by endogenous steroid and polypeptide hormones.

The name cytochrome P450 is based on the characteristic increase in the absorbance of the protein heme group at 450 nm upon binding of CO and reduction of its iron atom. P450 differ structurally from most cytochromes because the fifth coordination group of the iron atom of the heme is occupied by a thiolate group from a cysteine residue and the sixth is occupied by water. They differ functionally because P450 are monooxygenases and not simply electron carriers (see Cytochromes).

1. Classification

On the basis of amino acid sequence similarity, the P450 are divided into more than 100 families and subfamilies (4). The various P450 within a gene family generally have >40% sequence identity, and members within a subfamily have identities >55% within mammalian species and >46% overall. P450 with >97% identity are arbitrarily considered **allelic** variants unless there is independent evidence for separate gene loci. Genes from animals, fungi, plants, or bacteria are assigned family numbers 1–49, 51–69, 71–99, and 101 and above, respectively. Family 51 is represented in plants and mammals, as well as fungi.

The recommended nomenclature for P450 genes is an italicized *CYP* (*Cyp* for mouse and *Drosophila*) followed by an Arabic number designating the family, a letter for the subfamily, and a second number for the member of the subfamily, eg, *CYP1A1* (4). Identical terminology is used for gene products, except that the name is not italicized. Trivial names of P450 and other designations of the proteins, such as cytochrome P450 1A1, P450 1A1 or 1A1, are also considered acceptable in publications so long as the official name is specified.

2. Catalytic Activity

The overall reaction catalyzed by P450 is

$$\mathrm{RH} + \mathrm{O_2} + \mathrm{NADPH} + \mathrm{H^+} \longrightarrow \mathrm{ROH} + \mathrm{H_2O} + \mathrm{NADP^+}$$

where R is an organic substrate. One oxygen atom of the O_2 is incorporated into the substrate and the other is reduced to water, so P450 is both a monooxygenase and mixed-function oxidase. Further reactions and rearrangements lead to more than 40 different types of chemical reactions, including aliphatic and aromatic oxidations, N-, S-, and O-dealkylations, oxidative deamination, and peroxidation.

The P450 reaction cycle starts with the binding of the substrate to the ferric form of P450, which is followed by reduction of the heme iron atom by acceptance of an electron, binding of O_2, activation of the oxygen by acceptance of a second electron, and scission of the oxygen molecule, followed by formation of water, a hydroxylated product, and ferric P450. The two electrons from NADPH are donated either to microsomal P450, through a flavoprotein, P450 reductase, or to mitochondrial and bacterial P450, sequentially through a flavoprotein (a ferredoxin reductase) and an iron-sulfur ferredoxin. In rare cases, the P450 and P450 reductase are fused into a single protein (5). Cytochrome b_5 increases the activity of some P450 *in vitro*, either as a source of the second electron or **allosterically** (6).

3. Structure

The catalytic domain of membrane-bound P450 is oriented toward the cytoplasm for the microsomal forms and toward the matrix for the mitochondrial forms. The microsomal P450 are inserted into the membrane in a cotranslational, signal recognition particle-dependent manner (7). The N-terminal 20 to 25 amino acid residues function as a membrane-insertion and halt-transfer signal and are not cleaved, so they anchor the protein to the membrane. The mitochondrial P450 contain standard cleavable mitochondrial targeting signals at their N-terminus, but the mode of insertion into the inner membrane of the mitochondria is not known.

The three-dimensional structures of soluble bacterial P450, but not any membrane-bound P450, have been determined. Although the primary sequence is dissimilar among these bacterial proteins, a common "P450 fold" is present in each (see Protein Structure), which suggests that a similar core structure will also be present in eukaryotic membrane-bound P450 (8). The P450 structure contains an **alpha-helical** region and a beta-sheet region, which constitute about 70 and 20%, respectively, of the polypeptide chain. The sequence FXXGXXXCXG, which includes the heme-binding cysteine residue, is conserved in nearly all P450. Structures of eukaryotic P450 have been predicted from amino acid sequence alignments and homology molecular modeling with bacteria P450 (see Protein Structure Prediction), and predictions of residues that interact with substrates have been generally consistent with the observed effects of mutations (9, 10).

4. Gene Structure

The sizes of the eukaryotic P450 genes, from the transcription initiation site to the polyadenylation site, vary dramatically, from about 3 kb for the *CYP21* genes to >70 kb for *CYP19* genes (11). In higher eukaryotes, the number of **introns** varies from 6 to 13, and the sites of insertion of introns are almost always conserved within a family, but only rarely between families. **Polymorphism** is common in P450 genes and underlies genetic differences in drug metabolism and congenital diseases in humans. The families of P450 genes are dispersed among at least nine chromosomes in humans and mice, but occasionally families cluster together, such as families 1, 11, and 19. Subfamilies within a family also may be dispersed to separate chromosomes or may cluster together, and members of the *CYP2A*, *CYP2B*, and *CYP2F* subfamilies are intermingled (4, 12). The gene duplication leading to the *CYP21A* locus included the C4 histocompatibility gene, so the two P450 genes alternate with the C4 gene. In spite of the diversity of P450 genes, their similarity in primary structures, the common three-dimensional fold, and some conserved intron sites among P450 genes support the idea that the P450 superfamily evolved by **divergence** from a common ancestral gene.

5. Gene Expression

P450 genes are expressed in tissue-, developmental-, and sex-specific patterns. The mechanisms regulating these patterns of expression are best understood in the liver and adrenal gland. An **orphan receptor** containing a **zinc finger**, termed Ad4BP or steroid factor-1 (SF-1), has been shown to be critical for the developmental and tissue-specific expression of P450 genes that are required for the biogenesis of adrenal and sex steroid hormones (13). The SF-1 gene has been disrupted in mice, with major effects on differentiation of the adrenal gland and gonads, pituitary gonadotropin function, and the ventral medial hypothalamus (14), so this gene has important developmental functions as well as effects on the expression of P450 genes. *CYP19*, aromatase, contains SF-1 sites, but its tissue-specific expression is also dependent on alternate **promoters** and transcription initiation sites (15).

All the known liver-enriched regulatory factors have been implicated in the expression of one or more P450 genes. Examples in which functional binding sites for liver-enriched factors have been demonstrated include HNF-1a for *CYP2E1*, HNF-4 for *CYP2C1/2/3*, DBP for *CYP2C6* and *CYP7*, HNF-3 for *CYP2C6*, C/EBPb for *CYP2D5*, and C/EBPa and C/EBPb for *CYP2B1/2* (16, 17). A variety of ubiquitously expressed factors also contribute to basal expression of the *CYP* genes. The developmental expression of *CYP2C6* correlates with the developmental activation of DBP (16), and the diurnal expression of DBP underlies the diurnal regulation of *CYP7* (18). Activation of *CYP2D5* by C/EBPb also requires the constitutive factor Sp1, which has a binding site near that of C/EBPb (16).

5.1. Sex-dependent Expression

The sex-dependent expression of several P450 genes in rodents may be mediated by more than one mechanism. In rats, the sex-specific expression of *CYP* genes is dependent on different patterns of growth hormone secretion in the two sexes. STAT transcription factors (19) and phospholipase$_{\mathbf{A2}}$ (20) may be involved in the growth hormone-regulated male-specific expression of specific *CYP* genes, but additional studies are required to establish the exact mechanism. In mice, a sex difference information (SDI) element is present in male-specific *Cpy2d9* and female-specific *Cyp2a4* (21). The SDI contains a CpG sequence that is **methylated** in a sex-dependent way, and a factor has been identified that binds in a methylation-dependent manner (22). The exact role of this factor is not yet resolved, as its tissue and developmental expression differs from that of the *CYP* genes.

5.2. Aromatic Hydrocarbons
The expression of subsets of the xenobiotic-metabolizing P450 genes is regulated by aromatic hydrocarbons, peroxisomal proliferators, and barbiturates. The induction of *CYP1A1* by aromatic hydrocarbons, including the halogenated aromatic hydrocarbon 2,3,7,8-tetrachlorodibenzo-*p*-dioxin, is best understood. Genetic differences in the induction of *Cyp1a1* in mice and in variants of cultured mouse hepatoma Hepa 1 cells contributed critically to the identification of a regulatory locus *AhR*, which encodes the aromatic hydrocarbon receptor, and a second gene, the Ah receptor nuclear translocator *Arnt*, which encodes a protein required for the **nuclear import** of AhR (23, 24). The AhR is complexed with the **molecular chaperone** hsp90 in the cytoplasm in uninduced cells, which is essential to maintain a functional AhR. Binding of the ligand results in the dissociation of hsp90 and localization of AhR in the nucleus. Arnt is a nuclear protein that binds to liganded AhR and is required for the binding of AhR to the DNA binding site (25). AhR/Arnt bind to multiple sites within an enhancer about 1 kb from the start site of transcription and disrupt the **nucleosomal** structure of the enhancer (23). In turn, the nucleosomal structure of the promoter region is also disrupted in a manner dependent on the **transactivation** domain of AhR, which then allows the binding of regulatory proteins to the proximal promoter. The core sequence of the binding sites, which have been designated xenobiotic-, dioxin-, or Ah-**response elements** by different investigators, is 5′-TNGCGTG-3′. Arnt binds to the core sequence, and AhR binds to the flanking sequence. Both AhR and Arnt contain (1) basic loop-helix-loop (bLHL) motifs near their N-termini; (2) PAS **domains**, which exhibit homology with the *Drosophila* proteins, Per and Sim; and (3) glutamine-rich, putative transcriptional activation domains in the C-terminal region (24). The ligand and hsp90 interact with sequences near the PAS domain of AhR, and the binding of AhR to Arnt involves the bHLH and PAS domains of each protein. Arnt is capable of transactivation independently, but AhR transactivation requires the association of AhR with Arnt.

5.3. Peroxisomal Proliferators
Induction of expression of the *CYP4A* genes by peroxisomal proliferators and fatty acids requires peroxisomal proliferator-activated receptor-a (PPARa), a member of the steroid hormone receptor family (26). CYP4A P450 catalyze the w-hydroxylation of fatty acids, including arachidonic acid, which may ultimately result in the degradation of the fatty acids by peroxisomes. The induction of *CYP4A* genes is defective in mice with disrupted PPARa genes (27). PPARa forms a heterodimer with retinoid-X-receptor (RXR) to activate the gene. The predominant sequence in *Cyp4A6* that confers the response to peroxisomal proliferators contains an imperfect repeat of the sequence AGGTCA, with a single base pair between the repeats and additional sequence to the 5′ side of the repeat. The 5′ sequence appears to be important for the specificity of binding of PPARa/RXRa to the nonconsensus, imperfect repeat of the peroxisomal proliferator response element present in *CYP4A6* (26).

5.4. Barbiturates
Induction of P450 genes by barbiturates is not well understood. Neither a barbiturate receptor nor specific barbiturate response elements in mammalian genes have been defined, and different mechanisms may be involved for different P450 (28). The system best understood is the induction by barbiturates of Bm-1, Bm-2, and Bm-3 P450 in ***Bacillus*** *megaterium* (29). In untreated cells, a repressor, Bm3R1, binds to a palindromic 20-bp sequence upstream of a promoter that drives the expression of both the repressor and Bm-3. In the presence of barbiturate, the binding is reversed,

which may result from direct effects on the repressor, but positively acting factors are also induced that compete for the binding of the repressor at the palindromic site and at sites termed "barbie boxes" present in the 5′ regions of the Bm-3 and Bm-1 genes. In the mammalian *CYP2B1/2* genes, evidence has been presented for phenobarbital responsive sequences in both the proximal promoter region, including barbie-box-like sequences (30), and in distal phenobarbital-responsive enhancers (31, 32). Identification of specific responsive elements and characterization of the cognate binding proteins will be required to establish the role of these regions in phenobarbital induction.

5.5. Glucocorticoids

A number of *CYP* genes are also modulated by glucocorticoids. In some cases, the effect is mediated through the classical glucocorticoid receptors, such as modulation by glucocorticoids of aromatic hydrocarbon induction of *CYP1A1* and phenobarbital induction of *CYP2B* genes (33). In other cases, such as *CYP3A* genes, the response to glucocorticoids occurs by nonclassical mechanisms that remain to be elucidated (34).

5.6. Cyclic AMP

Genes for P450 involved in steroid metabolism are induced by polypeptide hormones via **cyclic AMP**-mediated (cAMP) mechanisms (35). In the adrenal gland, *CYP11A*, *CYP11B*, *CYP17*, and *CYP21* are regulated in this way. Interestingly, even though each of these genes probably evolved from a common ancestor, different regulatory elements in the promoter of each gene mediate the cAMP response. A classical CREB binding site is present in *CYP11B*, but binding sites for proteins other than CREB are present in other genes, and different sites are present in ***orthologous** genes* in different species. In bovine *CYP11A*, a binding site for Sp1, a constitutive factor, mediates the cAMP response (36), and members of the **homeodomain** PBX family of helix-turn-helix motif proteins bind to the cAMP-responsive element in *CYP17* (37). Multiple proteins bind to many of these elements, and those that predominate *in vivo* remain to be identified.

Bibliography

1. M. J. Coon, A. D. N. Vaz, and L. L. Bestervelt (1996) FASEB J. **10**, 428–434.
2. H. C. L. Liang et al. (1996) Proc. Natl. Acad. Sci. USA **93**, 1671–1676.
3. S. S. T. Lee, J. T. M. Buters, T. Pineau, P. Fernandez-Salguero, and F. J. Gonzalez (1996) J. Biol. Chem. **271**, 12063–12067.
4. D. R. Nelson et al. (1996) Pharmacogenetics **6**, 1–42.
5. L. O. Narhi and A. J. Fulco (1987) J. Biol. Chem. **262**, 6683–6690.
6. H. Yamazaki, W. W. Johnson, Y.-F. Ueng, T. Shimada, and F. P. Guengerich (1996) J. Biol. Chem. **271**, 27438–27445.
7. B. Kemper and E. Szczesna-Skorupa (1989) Drug Metabol. Rev. **20**, 811–820.
8. C. A. Hasemann, R. G. Kurumbail, S. S. Boddupalli, J. A. Peterson, and J. Deisenhofer (1995) Structure **2**, 41–62.
9. O. Gotoh (1992) J. Biol. Chem. **267**, 83–90.
10. C. von Wachenfeldt and E. F. Johnson (1995) In *Cytochrome P450—Structure, Mechanism, and Biochemistry* (P. Ortiz de Montellano, ed.), Plenum Press, New York, pp. 183–223.
11. B. Kemper (1993) In *Frontiers in Biotransformation* (K. Ruckpaul and H. Rein, eds.), Vol. **8**, Akkademie Verlag, Berlin, pp. 1–58.
12. S. M. G. Hoffman, P. Fernandez-Salguero, F. J. Gonzalez, and H. W. Mohrenweiser (1995) J. Mol. Evol. **41**, 894–900.
13. D. S. Lala, D. A. Rice, and K. L. Parker (1992) Mol. Endocrinol. **6**, 1249–1258.
14. K. L. Parker and B. P. Schimmer (1996) Trends Endo. Metab. **7**, 203–207.
15. M. S. Mahendroo, C. R. Mendelson, and E. R. Simpson (1993) J. Biol. Chem. **268**, 19463–19471.
16. F. J. Gonzalez and Y.-H. Lee (1996) FASEB J. **10**, 1112–1118.

17. Y. Park and B. Kemper (1996) DNA Cell Biol. **15**, 693–701.
18. D. J. Lavery and U. Schibler (1993) Genes Develop. **7**, 1871–1884.
19. D. J. Waxman, P. A. Ram, S. H. Park, and H. K. Choi (1995) J. Biol. Chem. **270**, 13262–13270.
20. P. Tollet, M. Hamberg, J. Å. Gustafsson, and A. Mode (1995) J. Biol. Chem. **270**, 12569–12577.
21. H. Yoshioka, M. Lang, G. Wong, and M. Negishi (1990) J. Biol. Chem. **265**, 14612–14617.
22. N. Yokomori, R. Kobayashi, R. Moore, T. Sueyoshi, and M. Negishi (1995) Mol. Cell Biol. **15**, 5355–5362.
23. J. P. Whitlock Jr. et al. (1996) FASEB J. **10**, 809–818.
24. O. Hankinson (1995) Ann. Rev. Pharmacol. Toxicol. **35**, 307–340.
25. R. S. Pollenz, C. A. Sattler, and A. Poland (1993) Mol. Pharmacol. **45**, 428–438.
26. E. F. Johnson, C. N. A. Palmer, K. J. Griffin, and M.-H. Hsu (1996) FASEB J. **10**, 1241–1249.
27. S. S.-T. Lee et al. (1995) Mol. Cell Biol. **15**, 3012–3022.
28. D. J. Waxman and L. Azaroff (1992) Biochem. J. **281**, 577–592.
29. Q. Liang and A. J. Fulco (1995) J. Biol. Chem. **270**, 18606–18615.
30. L. Prabhu et al. (1995) Proc. Natl. Acad. Sci. USA **92**, 9628–9632.
31. E. Trottier, A. Belzil, C. Stoltz, and A. Anderson (1995) Gene **158**, 263–268.
32. Y. Park, H. Li, and B. Kemper (1996) J. Biol. Chem. **271**, 23725–23728.
33. R. A. Prough, M. W. Linder, J. A. Pinaire, G.-H. Xiao, and K. C. Falkner (1996) FASEB J. **10**, 1369–1377.
34. L. C. Quattrochi, A. S. Mills, J. L. Barwick, C. B. Yockey, and P. S. Guzelian (1995) J. Biol. Chem. **270**, 28917–28924.
35. M. Waterman (1994) J. Biol. Chem. **269**, 27783–27786.
36. P. Venepally and M. Waterman (1995) J. Biol. Chem. **270**, 25402–25411.
37. N. Kagawa, A. Ogo, Y. Takahashi, A. Iwamatsu, and M. R. Waterman (1994) J. Biol. Chem. **269**, 18716–18719.

Suggestions for Further Reading

38. FASEB Journal series of 12 reviews, *"The cytochrome P450: structure, function, regulation, and genetics"* (1996/97) Initial review in FASEB J. (1996) **10**, 205. This series presents four reviews each on the structures of P450, regulation of xenobiotic-metabolizing P450, and regulation of P450 that metabolize endogenous compounds.
39. C. Ioannides, ed. (1996) *Cytochromes P450—Metabolic and Toxicological Aspects*, CRC Press, New York. Comprehensive reviews of the drug metabolizing P450, primarily families 1–4.
40. T. Omura, Y. Ishimura, and Y. Fujii-Kuriyama, eds. (1993) *Cytochrome P450*, VCH, New York. A concise introduction to P450.
41. P. R. Ortiz de Mantellano, ed. (1995) *Cytochrome P450—Structure Mechanism, and Biochemistry*, 2nd ed., Plenum Press, New York. Excellent comprehensive reviews of P450, including chapters on the regulation of gene expression by xenobiotics, hormones, and cAMP-mediated mechanisms.
42. M. A. Schuler (1996) Plant cytochrome P450 monooxygenases. Crit. Rev. Plant Sci. **15**, 235–284. A comprehensive review of plant P450.

Cytochromes

Cytochromes are iron-containing proteins that facilitate the movement of electrons in a wide variety of metabolic processes (see Electron Transfer Proteins). Cytochromes are widely distributed throughout nature. They are found in all **eukaryotes** and in most, but not all, **prokaryotes**. The prosthetic group or chromophore of cytochromes is heme, an iron-containing porphyrin. The prototypic form of heme in cytochromes is protoheme IX, which consists of iron, two vinyl side chains, four methyl groups and two propionic acid side chains on a conjugated tetrapyrole ring (Fig. 1). Protoheme IX is the prosthetic group of *b*-type cytochromes and the family of proteins known as cytochrome P450. The *c*-type cytochromes have heme *c* as the prosthetic group, in which protoheme IX is covalently bound to the protein through one or, more commonly, two thioether bonds to cysteine side-chains. Heme *a*, found in *a*-type cytochromes, has a long isoprenoid tail substituted on one of the vinyl groups and a formyl group replacing a methyl. Further variations in heme structure are found in isolated cases, for example, cytochrome *d* and cytochrome *o* (1) but will not be discussed here. Cytochrome P450 and **cytochrome *c*** are discussed elsewhere in this volume.

Figure 1. The structures of (**a**) protoheme IX, (**b**) heme *c*, and (**c**) heme *a*.

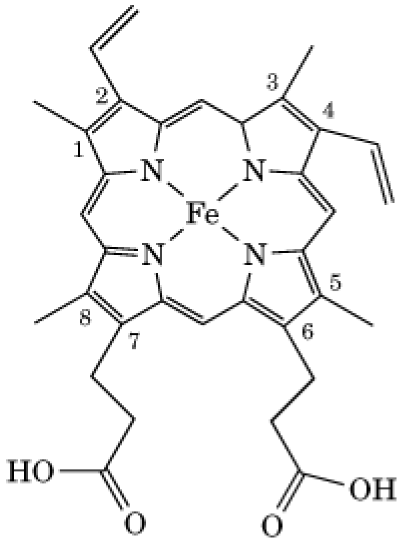

(a)

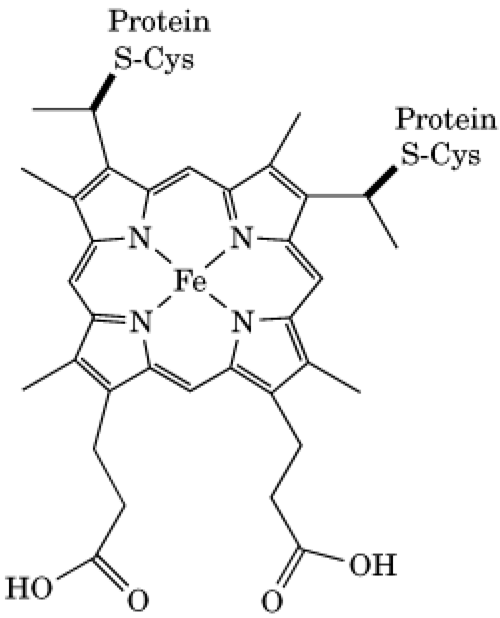

(b)

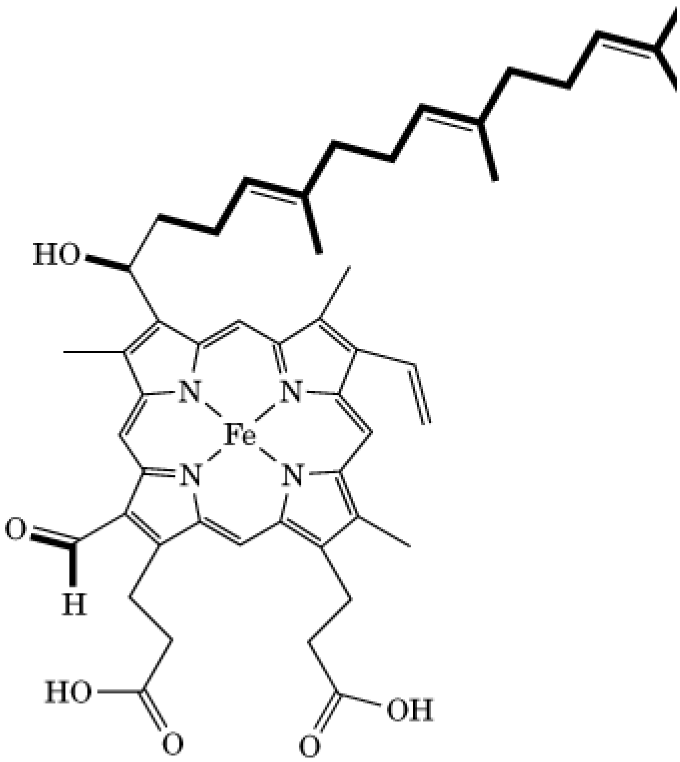

(c)

The iron in cytochromes, is either penta- or hexa-coordinate. Porphyrin nitrogen atoms fill four coordination positions (in-plane coordination, see Fig. 1) and appropriate ligands are positioned below the heme plane (5-coordinate) and, in most cases also above the heme plane (6-coordinate). The out-of-plane ligands in typical *c*-type cytochromes, are the N_3 atoms of histidine residues and the sulfur atom of methionine (Fig. 2). Ligation in the *b*-type cytochromes is generally by two His residues (Fig. 2) and by one or two His in the cytochromes *a*. Variations exist, however. For example, the out-of-plane ligation is by two His residues in cytochrome c_3, and by one His and an open position in cytochrome c'. Cytochromes are associated with the inner membrane of mitochondria, that of **microsomes**, the **thylakoid** membrane in chloroplasts, and the plasma membrane in **bacteria** (see Membranes). However, soluble forms (typically *c*-type cytochromes) are found in the space between the inner and outer mitochondrial membranes and in the **periplasmic** space in bacteria.

Figure 2. Stereo representations of the structure of tuna cytochrome *c* (upper stereo pair) and microsomal cytochrome b_5 (lower stereo pair). In cytochrome *c*, the N-terminal a-helix is at the *top*, the Met80 ligand is on the *left*, and the His18 ligand on the *right*. In cytochrome b_5, the N-terminus is at the lower *right* the His61 ligand is on the *left*, and the His37 ligand is on the right. The heme propionates are oriented toward the solvent.

The physiological activity in all cytochromes is the reversible oxidation and reduction of the iron atom, which cycles between the ferric (Fe^{3+}) and ferrous (Fe^{2+}) states. From a physiological standpoint, an important property of cytochromes is their oxidation-reduction **(redox)** potential, which is E_o' at pH 7. The redox potential measures the relative stabilities of the oxidized (ferric) and reduced (ferrous) forms and therefore their tendencies to donate and accept electrons, respectively. At pH 7 in aqueous solution, the redox potential of H_2 is –414 mV and that of O_2 is +816 mV. With relatively minor exceptions, these define the biological range. Cytochromes have redox potentials somewhere between these limits. In biological electron transfer, the direction of electron flow is from lower to higher potentials in the limit from hydrogen to oxygen. Thus the redox potential of a particular cytochrome determines, to a first approximation, where it is positioned relative to other redox compounds in electron transfer pathways (see Electron Transfer Proteins). The *c*-type cytochromes have redox potentials ranging from –400 to +450 mV, depending on the structural family and species, although they typically vary between only +200 and +300 mV in eukaryotic *c*-type cytochromes. The *b*-type cytochromes have redox potentials that range from –200 to +150 mV, and the *a*-type cytochromes have potentials in the +220 to +400 mV range.

The role of the protein moiety in cytochromes is threefold. First, the protein provides the out-of-plane ligands and, in the case of *c*-type cytochromes, the covalent attachment sites for the heme. Secondly, the protein provides the proximal environment for the heme, a nonpolar molecule that is not water-soluble, controls the exposure of the heme to the solvent, and interacts with the heme to modulate the redox potential. Thirdly, the protein surface provides the sites for the interaction with electron donors and acceptors because in all known cases the heme iron is buried in the protein's interior. Thus, the redox potential is modulated by a combination of the nature of the out-of-plane ligands, the immediate protein environment, and the solvent exposure of the heme.

The redox potentials dictate the direction of electron flow. For example, mitochondrial cytochrome *c* $(E'_o = +260\ \mathrm{mV})$ cannot significantly reduce oxidized pyridine nucleotide (NAD^+, $E'_o = -320\ \mathrm{mV}$). They do not, however, explain the specificity and efficiency of biological electron transfer. Within a biological milieu, a large number of redox compounds exist close to each other. These include small organic compounds, such as flavins and pyridine nucleotides (for example, NAD^+); oxygen (in aerobes); inorganics, such as nitrates, nitrites, sulfates, and sulfhydryls; and a variety of redox proteins, including non-heme-iron sulfur proteins, flavoproteins, cytochromes, and copper proteins (see Electron Transfer Proteins). Thus, from an energetic standpoint, substantial opportunities exist for electrons to flow in a great variety of directions. This does not happen, and electron flow occurs with very high efficiency (approaching 100%) only within specific pathways (for example, in respiration or photosynthesis). This incredible efficiency, the essence of life, is mediated by the surface of the protein, which provides recognition sites that determine which redox compounds interact on a physiological timescale, that is, it determines how fast electrons are transferred, and the direction of electron flow (2, 3). This kinetic control means that energetically equivalent reactions can take place on timescales that differ by many orders of magnitude. For example, reduced pyridine nucleotide reduces mitochondrial cytochrome *c* slowly (in seconds), whereas cytochrome c_1 $(E'_o = +220\ \mathrm{mV})$ reduces the same cytochrome in milliseconds, even though reduction by pyridine nucleotide is more strongly favored energetically in the first case (65.7 kJ/mol versus 3.8 kJ/mol).

The interactive domains of the cytochromes are defined by the amino acid side chains positioned on their molecular surface that dictate their sites of interaction. The structure of the complex between two electron transfer proteins determines the proximity and orientation of the relevant prosthetic groups (the two hemes in the case of electron transfer between two cytochromes). Three factors play a role in defining the interactive domains. First, the positioning of charged amino acid side chains on the surface of interacting molecules result in electrostatic interactions, either attractive or repulsive, that define the interaction domain (4). Secondly, the distance between redox centers (heme irons in the case of cytochromes) influences the rate of electron transfer. This distance is controlled by the size and nature of the amino acid side chains in the interactive domain (2). Third, two interactive domains that interact must be complementary physically and structurally, even if defined by nonpolar van der Waals interactions (2, 3). Apparently, during the course of evolution, mutations have occurred that optimize the rate of electron flow through relevant metabolic pathways by modulating the amino acid side chains defining the interactive domains, thus allowing competing redox reactions to occur in close proximity and channeling the flow of electrons through the appropriate pathway.

From the standpoint of solubility, cytochromes exist in three types of environments. Soluble forms are typically *c*-type cytochromes that are free to diffuse between electron donors and acceptors. Integral membrane proteins, that is, transmembrane proteins, have only part of the molecule exposed to solvent. The majority of the molecule is integrated into the membrane. Examples are *a*-type cytochromes and some *b*-type cytochromes. Peripheral membrane proteins are strongly associated with a membrane or with integral membrane proteins and have a substantial portion of the molecule in solution. Examples are cytochrome b_5 and cytochromes c_1 and *f*.

1. *A*-type Cytochromes

Cytochromes *a* and a_3 are components of cytochrome oxidase, or complex IV, of the mitochondrial electron transfer chain and are found in all eukaryotic organisms and many aerobic prokaryotes. Cytochrome oxidase catalyzes the four-electron reduction of O_2 to H_2O, utilizing cytochrome *c* as the electron donor. Cytochrome *a*, which is hexa-coordinate, mediates the transfer of electrons from cytochrome *c* to the penta-coordinate cytochrome a_3 (with the intermediate participation of a copper atom;), which provides the site for oxygen reduction. Variants of cytochrome oxidase are found in some aerobic bacteria that do not contain hemes other than heme *a*. Examples are cytochrome *bo*, which uses quinols as the electron donor in *Escherichia coli* and cytochrome cbb_3 in *Rhodobacter sphaeroides*, which has cytochrome *c* as an electron donor (1). Thus, the heme type can vary, although the function, the reduction of molecular oxygen to water, remains constant. Cytochrome oxidase is an integral membrane protein and couples the transfer of electrons and the corresponding redox energy with the movement of protons across the inner mitochondrial or periplasmic membrane, driving the synthesis of ATP (see Proton Motive Force). From an evolutionary standpoint, there is structural and amino acid sequence homology between eukaryotic and bacterial cytochrome oxidase (1). In addition, a variety of other enzymes exist that are structurally related to cytochrome oxidase and generally use cytochrome *c* or an electron donor, such as nitrous oxide reductase, which reduces N_2O to N_2 and utilizes copper as the prosthetic group, but has sequence homology with cytochrome oxidase and utilizes cytochrome *c* as its electron donor (1). Another example is nitric oxide reductase, which catalyzes the reduction of nitric oxide to nitrous oxide. Although it is a cytochrome *bc* complex, it has a transmembrane component and homology to portions of cytochrome oxidase (1).

2. *B*-type Cytochromes

The *b*-type cytochromes fall into two broad categories: (1) a family of relatively large cytochromes containing protoheme IX that are part of integral membrane protein complexes like cytochrome bc_1 and cytochrome b_6f; (2) a family of cytochrome b_5-like proteins that are peripheral proteins, typically anchored to a membrane, or are components of protein complexes like flavocytochrome b_2 and sulfite oxidase. The cytochrome bc_1 complex and its homologue in plants, cytochrome b_6f, catalyze the transfer of electrons from quinones to cytochrome *c* (in animals) or to plastocyanin (in plants) coupled with the movement of protons across the inner mitochondrial or the thylakoid membranes, which drives the synthesis of ATP (see ATP Synthase). The mitochondrial cytochrome bc_1 complex, also known as complex III, has the cytochrome *b* component integrated into the membrane through a number of transmembrane a-**helices** (5). The cytochrome c_1 component is anchored to the membrane and is the electron donor to cytochrome *c*. Cytochrome *b* is also a component of succinate dehydrogenase (also known as complex II), a complex integral membrane protein that participates in the mitochondrial electron transfer pathway (6). Succinate dehydrogenase oxidizes succinate to fumarate. The electrons reduce quinone and feed into the mitochondrial electron transfer chain.

Because of their large size and strong association with membranes, cytochromes *b* are not as well understood as the generally small and water-soluble *c*-type cytochromes (cytochromes c_1 and *f* are exceptions in terms of size and solubility). Thus the extent of structural and functional diversity among the cytochromes *b*, particularly in prokaryotes, remains an open question.

Proteins of the cytochrome b_5 family contain a cytochrome b_5 domain (Fig. 2) and, in the case of the mitochondrial and microsomal members, a hydrophobic tail or anchor that associates the cytochrome with the relevant membrane (7). The structure of cytochrome b_5 is shown in Fig. 2. In nitrate reductase, sulfite oxidase, and flavocytochromes b_2, the cytochrome b_5 domain is tightly associated with a flavoprotein that specifies the particular enzymatic activity. The cytochromes b_5 domain acts as an electron acceptor from the molybdenum (Mo)-pterin cofactor in sulfite oxidase or from protein-bound flavin in cytochrome b_5 reductase, nitrate reductase, P450 reductase, and flavocytochrome b_2. The cytochrome b_5 electron acceptor is cytochrome *c* in the flavocytochrome b_2 and sulfite oxidase systems, and a Mo-pterin cofactor in nitrate reductase. In microsomal systems, cytochrome P450 and a variety of acyl-CoA desaturases are the electron acceptors. In red blood cells, cytochrome b_5 reduces methemoglobin (see Hemoglobin). Thus, cytochrome b_5 has evolved the ability to function in a diverse group of electron transfer pathways and with a variety of electron donors and acceptors (7).

3. *C*-type Cytochromes

These cytochromes are discussed in more detail elsewhere in this encyclopedia, but it is important to note that this is a diverse group of cytochromes consisting of a variety of structural motifs and functions (8). Although restricted to mitochondrial cytochrome *c* and cytochrome c_1 (discussed previously) in eukaryotes and key components in the respiratory electron transfer chain, a variety of bacterial *c*-type cytochromes have evolved into a diverse and complex array of structures and function. In terms of structural families, the cytochromes *c* include the mitochondrial cytochrome *c* family and their bacterial homologies, cytochrome c_1 and *f*, and the cytochromes c_3, cytochromes c', flavocytochromes *c*, cytochrome c_4, and cytochromes c_5. Now, only cytochrome c_3 and *c*-type cytochromes that are related to mitochondrial cytochrome *c* are well understood in both structure and function.

The basic structural motif of the mitochondrial cytochrome *c* family has been maintained throughout evolution. Figure 2 presents the structure of tuna cytochrome *c*. In contrast to cytochrome b_5, the heme propionates are buried and not solvent accessible. Cytochromes utilizing the cytochrome *c* structural motif are found in almost all bacteria but differ primarily in their redox potentials, which vary from approximately +50 to +450 mV, and in the type and distribution of amino acid side chains on their molecular surfaces.

4. Summary

Cytochromes evolved early in the development of life on this planet, and they have retained the basic functional group protoheme IX (with relatively minor variations) throughout evolution. A number of basic structural motifs have evolved that are found in both prokaryotes and eukaryotes, including the mitochondrial cytochromes *c* and their bacterial precursors, the cytochrome b_5 family, the cytochrome oxidases, the membrane-spanning cytochromes *b*, and the cytochrome c_1/b_6 family. It is striking that a relatively small number of structural families have evolved to take advantage of diverse metabolic opportunities, capturing redox energy to produce ATP and adapting to available ecological niches.

Bibliography

1. M. Saraste, J. Castresana, D. Higgins, M. Lübben, and M. Wilmanns (1996) In *Origin and Evolution of Biological Energy Conversion* (H. Baltscheffsky, ed.) VCH, New York, pp. 255–289.
2. G. Tollin, T. E. Meyer, and M. A. Cusanovich (1986) Biochim. Biophys. Acta **853**, 29–41.

3. T. E. Meyer, G. Tollin, and M. A. Cusanovich (1994) Biochimie **76**, 480–488.
4. J. A. Watkins, T. E. Meyer, G. Tollin, and M. A. Cusanovich (1994) Protein Sci. **3**, 2104–2114.
5. P. N. Furbacker, G.-S. Tae, and W. A. Cramer (1996) In *Origin and Evolution of Biological Energy Conversion* (H. Baltscheffsky, ed.), VCH, New York, pp. 221–253.
6. B. A. C. Ackrell, M. K. Johnson, R. P. Gunsalus, and G. Cecchini (1992) In *Chemistry and Biochemistry of Flavoenzymes*, Vol. **III** (F. Müller, ed.), CRC Press, Boca Raton, pp. 229–297.
7. F. Lederer (1994) Biochimie **76**, 674–692.
8. T. E. Meyer, J. J. van Beeumen, R. P. Ambler, and M. A. Cusanovich (1996) In *Origin and Evolution of Biological Energy Conversion* (H. Baltscheffsky, ed.), VCH, New York, pp. 71–108.

Suggestions for Further Reading

9. T. E. Meyer and M. A. Cusanovich (1989) Structure, function and distribution of soluble bacterial redox proteins, Biochim. Biophys. Acta **975**, 1–28.
10. R. H. Scott and A. G. Mauk, eds. (1996) *Cytochrome c. A. Multidisciplinary Approach*, University Science Books, Mill Valley.
11. G. R. Moore and G. W. Pettigrew (1990) *Cytochromes c*, Springer-Verlag, New York.

Cytogenetics

Cytogenetics is the study of **genetics** by visualization of chromosomes and chromosomal aberrations, usually through light microscopy. There is a distinguished history of chromosomal visualization for analytical purposes. Longley defined the morphology of **maize** chromosomes (reviewed in Ref. 1), which opened the door for subsequent work on maize cytogenetics by McClintock (2). Staining of **prophase** and early **metaphase** maize chromosomes with acetocarmine allowed McClintock to identify 10 distinct linkage groups. In turn this laid the foundation for other maize cytogeneticists to identify chromosomal translocations and **inversions** visually. For example, it was possible to demonstrate that there is a correspondence between marker genes and cytologically defined chromosomal domains in crosses between heterozygous strains (3). Cytogenetics in *Drosophila melanogaster* received an enormous stimulus from the systematic study of the polytene chromosomes in salivary glands (4). These chromosomes have visibly distinct banding patterns under a phase microscope and after staining. Each of the four *Drosophila melanogaster* chromosomes have easily differentiated band patterns. The thousands of bands served as markers that allowed cytogeneticists to discern small deletions, duplications, translocations, and transpositions. Cytological experiments in *Drosophila* also allowed the discovery of the position effect, the phenomenon in which the position of a gene relative to heterochromatin influences the efficiency with which it is expressed (5).

Improvements in cytogenetics eventually allowed visualizing metaphase chromosomes in somatic cells in culture. Only in 1956 was it established by these methodologies that human cells contain 46 chromosomes (6). Likewise cytogenetic approaches allowed the discovery that children with Down's syndrome are **trisomic** for chromosome 21 (see Autosome). Medical cytogenetics has since been advanced by chromosome stains, such as Giemsa, that enable separating individual chromosomes in sufficient numbers for highly focused analysis of their biochemistry and genetics (see G Banding).

Bibliography

1. A. E. Longley (1952) Bot. Rev. **18**, 399–412.
2. B. McClintock (1929) Science **69**, 629–632.
3. H. B. Creighton and B. McClintock (1931) Proc. Natl. Acad. Sci. USA **17**, 485–491.
4. E. Heitz and H. Bauer (1933) Z. Zellforsch Mikrosc. Anat. **17**, 67–81.
5. A. H. Sturtevant (1925) Genetics **10**, 117–147.
6. J. H. Tijo and A. Lean (1956) Hereditas **42**, 1–6.

Cytokeratins

Cytokeratins form long filaments (they are one of the family of intermediate filament proteins; see also Keratins) that extend in a sinuous manner between the cytoplasmic surface of the cell nucleus and the plasma membrane of epithelial cells. The cytokeratin filaments appear to attach to the cytoplasmic side of the nuclear envelope, often close to the nuclear pore complexes. From there they radiate outward and link to or loop through the portions of the **desmosomes** or adhesion plaques that lie on the inner side of the cell membrane.

Cytokeratin chains can be divided into two groups: "acidic" Type I and "neutral-basic" Type II. In general, the Type II chains have higher isoelectric points and higher molecular weights than their Type I counterparts. Each chain comprises nonhelical end **domains** separated by a flexible rodlike structure. The *N*- and *C*-terminal domains in the epidermal keratins (or cytokeratins) have a characteristic substructure arranged about the rod domain with bilateral symmetry: E1, V1, H1 in the *N*-terminal domain and H2, V2, E2 in the *C*-terminal domain (1). The H1 and H2 subdomains, located respectively immediately *N*- and *C*-terminal to the rod domain, have sequences that are highly **homologous** regions within each chain type. The V1 and V2 subdomains are variable in length and sequence but always have a high content of glycine and serine residues. The E1 and E2 subdomains lie at the extreme ends of the molecule and are short, generally basic regions.

Between the terminal domains, the amino acid sequence has a heptad repeat substructure characteristic of a coiled-coil conformation (2). The latter thus consists essentially of coiled-coil rod domains (segments 1A, 1B, 2A, and 2B), joined by short linking domains (L1, L12, and L2), and results in a rod of total length 46.2 nm (Fig. 1). Each molecule contains a pair of different chains (Type I and Type II) aligned parallel to one another and in axial register (3-5). Segments 1B and 2 (= 2 A + L2 + 2B) each contain highly regular distributions of both acidic and basic residues (2). Thus each rod segment can be modeled as alternating bands of positive and negative charge, with a period of about 1.4 to 1.5 nm. Pairs of molecules aggregate through their rod domains in three antiparallel modes: (i) with their 1B segments largely overlapped, (ii) with their 2B segments largely overlapped, and (iii) with their entire lengths largely overlapped. In cytokeratins there is also a short head-to-tail overlap of about eight residues between parallel molecules (6). The antiparallel interactions originate in large part by the maximization of electrostatic interactions, which are possible as a consequence of the regular charge distribution in neighboring rod domains. They are also both specified and stabilized by interactions between the H1 (and presumably H2) subdomains, the head-to-tail overlap region, and the link L2. Cross-links formed between lysine residues in cytokeratins have been characterized (Fig. 2), thus confirming the modes of aggregation originally proposed on theoretical grounds (see earlier). This work also allowed the projected (axial) lengths of the links L1, L12, and L2 to be determined, together with the relative axial staggers between various coiled-coil rod segments (6, 7). These data allow a surface lattice structure to be constructed that predicts a near-axial period in the cytokeratin of 22.6 nm (the experimentally observed value is

22.7 nm). **Scanning transmission electron microscope** (STEM) data indicate that *in vitro* assemblies may contain about 16, 24, 32, or 40 chains, but it seems that only the 32-chain variant is present *in vivo*. The STEM data, nonetheless, would indicate that the cytokeratin may have a substructure in which an eight-chain entity, a protofibril, is present. *In vitro* two, three, four, or five of these protofibrils may aggregate in a nonspecific manner.

Figure 1. Schematic cytokeratin intermediate filament molecule. The rod domain is of approximate length 46 nm, with coiled-coil segments 1A, 1B, 2A, and 2B and non-coiled-coil links L1, L12, and L2. A break in the phasing of the heptad repeat, known as a stutter, occurs at the center of segment 2B. The *N*- and *C*-terminal domains contain E (end), V (variable but rich in glycine and serine residues), and H (homologous) subdomains arranged about the rod domain with bilateral symmetry. (From Ref. 8, with permission.)

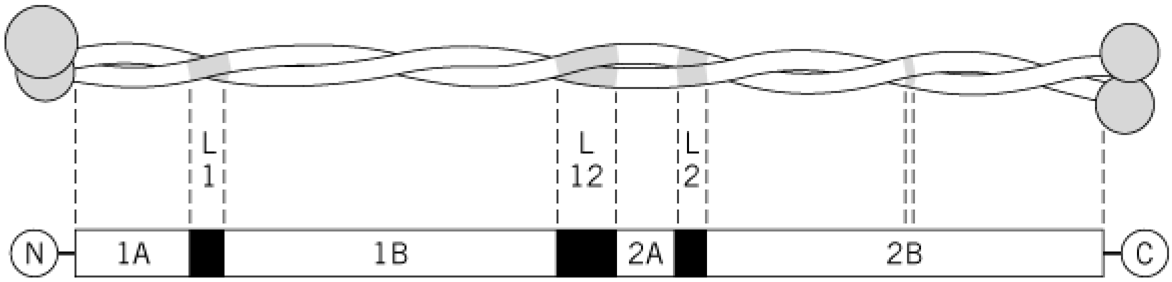

Figure 2. The cross-links induced chemically between lysine residues are shown for human K5/K14 epidermal keratin IF. The cross-links between the two polypeptide chains within a molecule (*left*) show that the chains are parallel and in axial register. Cross-links between molecules indicate that the molecules aggregate antiparallel through one of three modes, with (i) their 2B segments largely overlapped (A_{22}), (ii) the entire molecules largely overlapped (A_{12}), and/or (iii) their 1B segments largely overlapped (A_{11}). Combination of A_{22} and A_{11} results in a small head-to-tail overlap of about 1 nm between parallel molecules. (From Ref. 7, with permission.)

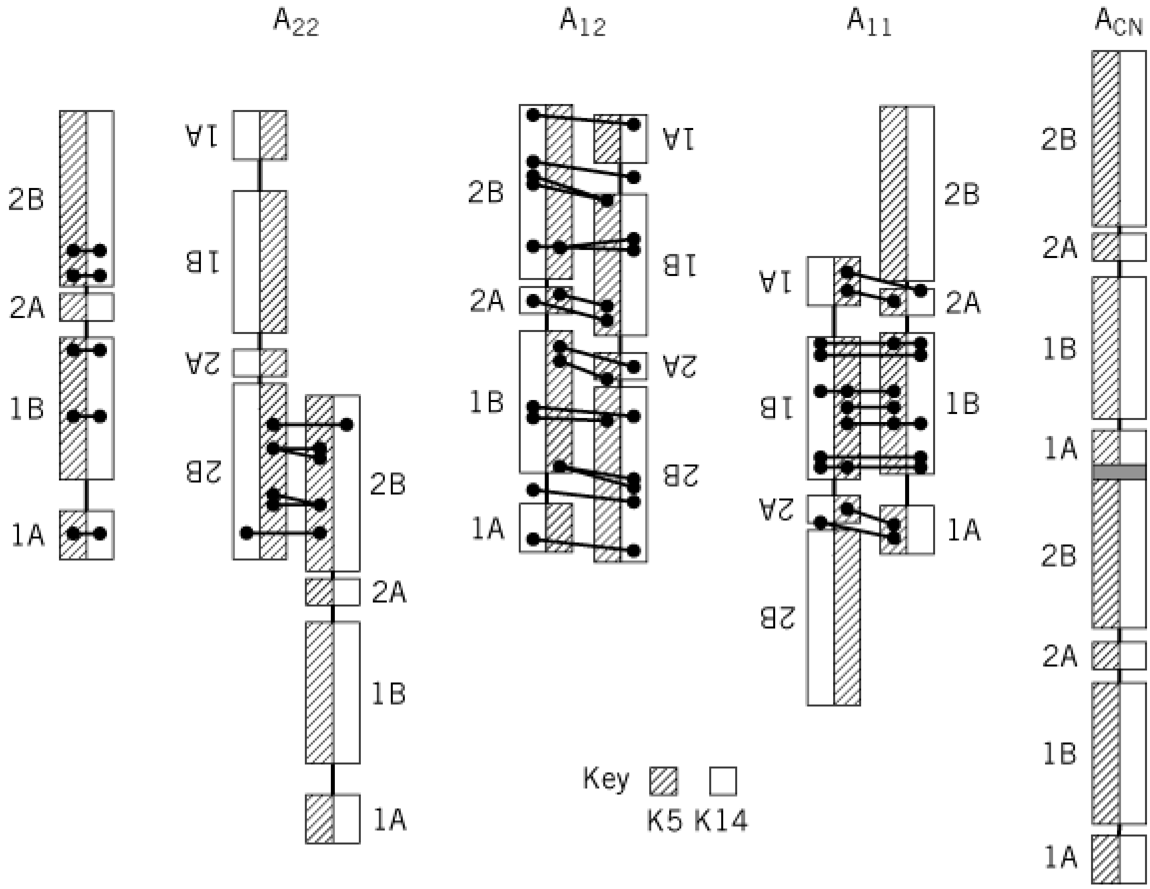

Characterization of a large number of gene mutations leading to keratinopathies has been achieved in recent years. The resulting sequence changes lie very largely in or close to the head-to-tail overlap region comprising the conserved sequences at the *N*-terminal end of segment 1A and the *C*-terminal end of segment 2B. A reasonable conclusion is that this interaction is subtly modified by the mutated residue and becomes less able to stabilize the cytokeratin *in vivo*.

Bibliography

1. P. M. Steinert, D. A. D. Parry, W. W. Idler, L. D. Johnson, A. C. Steven, and D. R. Roop (1985) Amino acid sequences of mouse and human epidermal type II keratins of M_r 67000 provide a systematic basis for the structural and functional diversity of the end domains of keratin intermediate filament subunits. J. Biol. Chem. **260**, 7142–7149.
2. W. G. Crewther, L. M. Dowling, P. M. Steinert, and D. A. D. Parry (1983) Structure of intermediate filaments. Int. J. Biol. Macromol. **5**, 267–274.
3. P. M. Steinert (1990) The two-chain coiled-coil molecule of native epidermal keratin intermediate filaments is a type I–type II heterodimer. J. Biol. Chem. **265**, 8766–8774.
4. M. Hatzfeld and K. Weber (1990) The coiled-coil of *in vitro* assembled keratin filaments is a heterodimer of type I and type II keratin: use of site-specific mutagenesis and recombinant protein expression. J. Cell Biol. **110**, 1199–1210.
5. P. A. Coulombe and E. Fuchs (1990) Elucidating the early stages of keratin filament assembly. J. Cell Biol. **111**, 153–169.
6. P. M. Steinert, L. N. Marekov, R. D. B. Fraser, and D. A. D. Parry (1993) Keratin intermediate filament structure: crosslinking studies yield quantitative information on molecular dimensions and mechanism of assembly. J. Mol. Biol. **230**, 436–452.
7. P. M. Steinert, L. N. Marekov, and D. A. D. Parry (1993) Conservation of the structure of

keratin intermediate filaments: molecular mechanism by which different keratin molecules integrate into pre-existing keratin intermediate filaments during differentiation. Biochemistry **32**, 10046–10056.

8. D. A. D. Parry and R. D. B. Fraser (1985) Intermediate filament structure: 1, Analysis of IF protein sequence data. Int. J. Biol. Macromol. **7**, 203–213.

Suggestions for Further Reading

9. D. A. D. Parry and P. M. Steinert (1995) *Intermediate Filament Structure*, Springer-Verlag, Heidelberg.
10. R. D. Goldman and P. M. Steinert (1990) *Cellular and Molecular Biology of Intermediate Filaments* (eds.), Plenum Press, New York.
11. E. Fuchs and K. Weber (1994) Intermediate filaments: structure, dynamics, function and diseases. Annu. Rev. Biochem. **63**, 345–382.

Cytokinins

1. History

The first discovery that plants make compounds that stimulate cell division dates back to 1913, when Haberlandt (1) demonstrated that an unknown substance present in vascular tissues of various plants caused cork cambium formation and wound healing in cut potato tubers. These molecules were later called *cytokinins*, from the Greek "cytokinesis" (cell division). In the 1940s, van Overbeek et al. (2) showed that similar compounds were also present in the milky endosperm of immature coconuts. In 1954, Miller et al. (3) isolated a substance, formed by partial breakdown of herring sperm **DNA**, that, in synergy with auxin, stimulated cell division in tobacco pith cells very actively. The molecule was called *kinetin* (6-furfurylamino purine). *Trans*-zeatin (6-(4-hydroxy-3-methylbut-*trans*-2-enylamino) purine) was the first cytokinin to be identified from maize endosperm (4) (Fig. 1).

Figure 1. Structural formula of *trans*-zeatin.

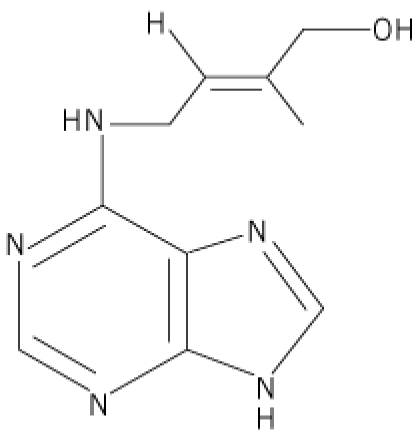

2. Biosynthesis and Metabolism

Natural cytokinins (CKs) are primarily purine derivatives with an N^6-substituted isopentenylated side chain (iP-type CKs) (5). However, a series of CKs with an aromatic side chain (eg, benzyl-adenine) have been demonstrated in certain species (6, 7). The most abundant naturally occurring CKs are CK nucleosides and CK nucleotides (5). Certain phenolic compounds also possess cell-division-promoting activity, but are not classified as true cytokinins (8).

The origin of CKs in plants remains a subject of debate. Roots are the primary sites of cytokinin biosynthesis, although limited synthesis in the shoot has also been demonstrated (9, 10). CKs have been proposed to be transported from root to shoot by the transpiration stream in xylem tissues, but conclusive evidence is lacking (11). Even though present throughout the plant, CKs have never been proven to be synthesized by endogenous, plant-borne enzymes. Because many root-associated bacteria are cytokinin producers, it has been hypothesized that CKs are made exclusively by these microbial symbionts (12).

Cytokinins can be synthesized via a direct (*de novo*) or an indirect (transfer RNA) pathway. The main source of free CKs is the *de novo* pathway. The key step is the formation of N^6-(D^2-isopentenyl) adenosine-5′-monophosphate from D^2-isopentenyl pyrophosphate and AMP catalyzed by isopentenyltransferase. The isopentenyl side chain originates from mevalonate, which also serves as a precursor to abscisic acid, gibberellins, and brassinosteroids. Isopentenyltransferase was first characterized from bacteria and slime molds (5, 7). Different constructs using the Agrobacterium isopentenyltransferase *IPT* (*tmr*) **gene** were used to generate constitutive or controlled cytokinin overproduction in **transgenic** plants (13-15). These studies mainly confirmed the classical view of cytokinin action in plants. Specific manipulation of senescence was achieved by placing the *IPT* gene under the control of a senescence-specific **promoter** (16). Recently, isopentenyltransferase activity was also demonstrated in plants (17), but the enzyme was never purified to homogeneity, nor have plant genes encoding isopentenyltransferase been **cloned**. This is the major reason why CK production by the plant itself is still questioned. An Arabidopsis mutant with sixfold elevated CK levels was isolated from a screen for seedlings with multiple cotyledons (18, 19). The **phenotype** of this *amp1* (*altered meristem program1*) mutant is reminiscent of several CK effects, including enhanced lateral branching, elevated rate of leaf formation, induction of flowering and floral morphological abnormalities, and delayed senescence. In addition, *amp1* displays a de-etiolated phenotype in the dark and is an **allele** of *cop2* (*constitutive photomorphogenic 2*). It was proposed that CK induces light-regulated genes in a light-independent fashion (19). The *AMP1* gene product may be required for CK degradation, or it could be a negative regulator of CK biosynthesis. A second mutant *cri* (*cristal*) that accumulates sixfold more CK than the wild type was recently identified (20). *Cri1* mutants are phenotypically different from *amp1* and show symptoms of vitrification.

The second biosynthetic route for CKs is via tRNA. Modified bases in tRNA, including isopentenylated bases, have been found in virtually all organisms investigated (21). CK modification in tRNA is always at the adenosine residue immediately 3′ to the anticodon of tRNAs that read codons starting with U (5). These CK residues in tRNA may serve as a direct, albeit not major, precursor of free CK, as a result of tRNA turnover. The rate of CK release in this way is dependent on the metabolic activity of the cell. The major CK in tRNA is *cis*-zeatin, with very low CK activity, but it can be converted to the biologically active *trans* isomer (Fig. 1) by a *cis–trans* isomerase (22) (see Cis/Trans Isomerization).

Several modifications can occur to the N^6-substituted side chain and purine ring. Formation of zeatin and its nucleoside and nucleotide derivatives, most probably by hydroxylation of the isopentenyl adenine moiety, is common in most plant tissues. The hydroxylase that mediates this conversion was isolated from cauliflower (23). O-Glycosylation of hydroxylated CKs is often observed, but leads to a considerable decrease in activity (5). CK-*O*-glucosides can be converted to free active CK by the action of b-glucosidases. In contrast, modification of the purine ring by *N*-glucosylation of the 3, 7, or 9 position yields inactive, stable derivatives that cannot generate free CKs. *N*-Glucosylation is thus expected to play an important role in regulating the levels of active CKs. An additional control is exerted by CK oxidase (24, 25). This enzyme catalyzes degradation of the N^6-(D^2-isopentenyl) side chain and irreversibly leads to loss of CK activity. CK nucleotides are not accepted as a substrate. A general role for CK oxidase is to contribute to CK homeostasis in plants (26).

3. Signal Perception and Transduction

A number of CK-binding proteins have been described, one of which is a potential CK **receptor** (27, 28). The latter is a cytosolic protein that reversibly binds zeatin and is involved in transcriptional activation in the presence of zeatin, but not in its absence. Only the *trans* isomer elicited the observed effect.

Two candidate plasma membrane CK receptors were identified by mutational analysis (29, 30). Mutants of *Arabidopsis* that exhibit shoot formation in tissue culture in the absence of CK were obtained by an activation-tagging approach. The *CKI1* (*cytokinin-independent 1*) gene was isolated and encodes a protein similar to two-component regulators of bacteria (29). As in the case of the ethylene receptor ETR1 (see Ethylene), CKI1 is a hybrid kinase with fused sensor and receiver domains. Based on this analogy and on the fact that constitutive overexpression of *CKI1* results in typical effects of CK action, CKI1 is hypothesized to encode a CK receptor. Overexpression would enable cells to sense endogenous concentrations below the threshold, which normally leads to CK response. Intriguingly, phytochromes also display similarities with two-component systems. It has been speculated that they might regulate other two-component systems, thus enabling cross-talk between the ethylene and CK pathways (31). A second candidate CK receptor is a seven-transmembrane domain receptor (7TM), characteristic in **G-protein** signaling and involved in transduction of extracellular signals (30). The *Arabidopsis GCR1* (*G-coupled receptor 1*) gene was isolated by polymerase chain reaction (**PCR**), and **antisense** mutagenesis with a 35S a*GCR1* construct resulted in reduced cotyledon and leaf expansion and a single flowering stem, a phenotype reminiscent of the *cyr1* (*cytokinin resistant 1*) mutant (see text below). However, *GCR1* and *CYR1* do not represent the same gene (30).

The above findings confirm the involvement of both phosphorylation and G proteins in CK signaling (32). Sense and antisense expression in tobacco of a gene encoding a small GTP-binding protein from rice resulted in a dwarf phenotype and abnormal flower development, correlating with a sixfold elevation of CK levels compared to wild type (33). **Phosphorylation** plays an important role in cell cycle control by CK (32). In addition, evidence was given for involvement of intracellular Ca^+ in CK signaling (see Calcium Signaling) mostly from studies in mosses (32). Finally, the similarity of a CK-binding protein to *S*-adenosyl-homocysteine hydrolase raised the possibility that some CK effects might be mediated through control of **methylation** of DNA and/or proteins (34).

Further progress in understanding CK Signal Transduction is expected from mutant studies. Several CK-resistant mutants have been identified, mainly in *Arabidopsis* (35). Five loci have been studied in detail. The majority were isolated using a root elongation response in the presence of CK. In certain cases, resistance to other hormones was found. For instance, the *ckr1* (*cytokinin resistant 1*) mutant is allelic to *ein2* (*ethylene-insensitive 2*), indicating cross-talk with the ethylene pathway. It was demonstrated that the inhibition of root elongation by CK results from an induction of ethylene biosynthesis (36). This was exploited by screening for the absence of triple response in the dark, in the presence of kinetin (37). The *cin5* (*cytokinin-insensitive 5*) mutant affects the 1-aminocyclopropane-1-carboxylate synthase gene *5* in *Arabidopsis*. Disruption of the carboxyl terminus of the same isoform leads to ethylene overproduction, previously identified as an *ethylene overproducer* (*eto2*) mutant. A third class of CK–resistant mutants is *cyr1* (38). In contrast to *ckr1* and *cin5*, *cyr1* displays an abnormal shoot phenotype: cotyledons and leaves fail to expand, a limited number of leaves are formed, and a single infertile flower is made. No resistance to other hormones was observed; however, *cyr1* is hypersensitive to abscisic acid (38). *Cyr1* is probably allelic to *emf2* (*embryonic flower 2*). *EMF* gene products might function in the maintenance of vegetative growth (39). The *stp1* (*stunted plant 1*) mutant has a reduced sensitivity to CKs, both in assays for elongation and radial swelling of the root (40). The general morphology was not affected, but a reduction in growth rate was observed. The function of the *STP1* gene product remains to be elucidated. Finally, a recent study describes identification of three loci involved in control of cell division and plant development (41). The corresponding mutants were called *pasticcino* (*pas*) and showed hypertrophy of their apical parts when grown on CK-containing medium, a phenotype reminiscent of abnormal shoots regenerated on media with unbalanced auxin/CK ratio and strikingly similar to the fasciation disease caused by *Rhodococcus fascians* (41). The altered embryo, root, and leaf development result from uncoordinated cell divisions. *PAS* genes are hypothesized to play a role in CK signaling, because no differences in CK levels were found compared to wild type.

4. Downstream Targets

Primary CK response genes have not yet been isolated, nor have CK responsive cis-acting elements or trans-acting factors been identified (42). A large number of genes that are either induced or repressed upon CK treatment have been described. Controls are exerted at a transcriptional or post-transcriptional level. Changes in gene expression were observed between 2 h and 48 h after treatment. Many of these secondary CK response genes are involved in light regulation and nutrition (32, 42).

5. Effects

Depending on temporal and spatial factors, a particular subset of downstream target genes is activated by CK treatment and results in one of many described effects. Cytokinins regulate many aspects of plant growth and development, including cell division, enlargement, and differentiation, as well as chloroplast development, release of apical dominance, nutrient mobilization, flowering, and delay of senescence (43, 44).

Bibliography

1. G. Haberlandt (1913) Sitzungsber. K. Preuss. Akad. Wissensch., 318–345.
2. J. van Overbeek, M. E. Conklin, and A. F. Blakeslee (1941) Science **94**, 350–351.
3. C. O. Miller, F. Skoog, M. H. Von Saltza, and F. Strong (1955) J. Am. Chem. Soc. **77**, 1392–1393.
4. D. S. Letham (1963) Life Sci. **8**, 569–573.
5. C.-m. Chen (1997) Physiol. Plant. **101**, 665–673.
6. M. Strnad, W. Peters, E. Beck, and M. Kamínek (1992) Plant Physiol. **99**, 74–80.
7. E. Prinsen, M. Kamínek, and H. Van Onckelen (1997) Plant Growth Regul. **23**, 3–15.
8. R. A. Teutonico, M. W. Dudley, J. D. Orr, D. G. Lynn, and A. N. Binns (1991) Plant Physiol. **97**, 288–297.
9. A. Carmi, and J. Van Staden (1983) Plant Physiol. **73**, 76–78.
10. C.-M. Chen, J. R. Ertl, S. M. Leisner, and C.-C. Chang (1985) Plant Physiol. **78**, 510–513.
11. P. D. Hare, W. A. Cress, and J. van Staden (1997) Plant Growth Regul. **23**, 79–103.
12. M. A. Holland (1997) Plant Physiol. **115**, 865–868.
13. J. I. Medford, R. Horgan, Z. El-Sawi, and H. J. Klee (1989) Plant Cell **1**, 403–413.
14. T. Schmülling, S. Beinsberger, J. De Greef, J. Schell, H. A. Van Onckelen, and A. Spena (1989) FEBS Lett. **249**, 401–406.
15. J. J. Estruch, E. Prinsen, H. Van Onckelen, J. Schell, and A. Spena (1991) Science **254**, 1364–1367.
16. S. Gan and R. M. Amasino (1997) Plant Physiol. **113**, 313–319.
17. J. R. Blackwell and R. Horgan (1994) Phytochemistry **35**, 339–342.

18. A. M. Chaudhury, S. Letham, S. Craig, and E. S. Dennis (1993) Plant J. **4**, 907–916.
19. A. N. Chin-Atkins, S. Craig, C. H. Hocart, E. S. Dennis, and A. M. Chaudhury (1996) Planta **198**, 549–556.
20. V. Santoni, M. Delarue, M. Caboche, and C. Bellini (1997) Planta **202**, 62–69.
21. N. Murai (1981) In *Cytokinins: Chemistry, Activity and Function* (D. W. S. Mok and M. C. Mok, eds.), CRC Press, Boca Raton, FL, pp. 87–99.
22. N. V. Bassil, D. W. S. Mok, and M. C. Mok (1993) Plant Physiol. **102**, 867–872.
23. C.-m. Chen and S. M. Leisner (1984) Plant Physiol. **75**, 442–446.
24. D. J. Armstrong (1994) In *Cytokinins: Chemistry, Activity, and Function* (D. W. S. Mok and M. C. Mok, eds.), CRC Press, Boca Raton, FL, pp. 139–154.
25. R. J. Jones and B. M. N. Schreiber (1997) Plant Growth Regul. **23**, 123–134.
26. S. Eklöf, C. Astot, T. Moritz, J. Blackwell, O. Olsson, and G. Sandberg (1996) Physiol. Plant. **98**, 333–344.
27. C. Brinegar (1994) In *Cytokinins: Chemistry, Activity, and Function* (D. W. S. Mok and M. C. Mok, eds.), CRC Press, Boca Raton, FL, pp. 217–232.
28. O. N. Kulaeva, N. N. Karavaiko, S. Y. Selivankina, Y. V. Zemlyachenko, and S. V. Shipilova (1995) FEBS Lett. **366**, 26–28.
29. T. Kakimoto (1996) Science **274**, 982–985.
30. S. Plakidou-Dymock, D. Dymock, and R. Hooley (1998) Curr. Biol. **8**, 315–324.
31. J. W. Reed (1998) Trends Plant Sci. **3**, 43–44.
32. P. D. Hare, and J. van Staden (1997) Plant Growth Regul. **23**, 41–78.
33. H. Sano, S. Deo, E. Orudgev, S. Youssefian, K. Isizuka, and Y. Ohashi (1994) Proc. Natl. Acad. Sci. USA **91**, 10556–10560.
34. S. Mitsui, T. Wakasugi, and M. Sugiura (1996) Plant Growth Regul. **18**, 39–43.
35. J. Deikman (1997) Plant Growth Regul. **23**, 33–40.
36. A. J. Cary, W. Liu, and S. H. Howell (1995) Plant Physiol. **107**, 1075–1082.
37. J. P. Vogel, K. E. Woeste, A. Theologis, and J. J. Kieber (1998) Proc. Natl. Acad. Sci. USA **95**, 4766–4771.
38. J. Deikman and M. Ulrich (1995) Planta **195**, 440–449.
39. C.-H. Yang, L.-J. Chen, and Z. R. Sung (1995) Dev. Biol. **169**, 421–435.
40. T. I. Baskin, A. Cork, R. E. Williamson, and J. R. Gorst (1995) Plant Physiol. **107**, 233–242.
41. J.-D. Faure, P. Vittorioso, V. Santoni, V. Fraisier, E. Prinsen, I. Barlier, H. Van Onckelen, M. Caboche, and C. Bellini (1998) Development **125**, 909–918.
42. T. Schmülling, S. Schäfer, and G. Romanov (1997) Physiol. Plant. **100**, 505–519.
43. A. N. Binns (1994) Annu. Rev. Plant Physiol. Plant Mol. Biol. **45**, 173–196.
44. P. J. Davies (1995) *Plant Hormones: Physiology, Biochemistry and Molecular Biology*, Kluwer, Dordrecht, The Netherlands.

Cytomegalovirus

Cytomegaloviruses (CMVs) are a distinct subgroup of herpesvirus and are classified as subfamily *Betaherpesvirinae* in the *Herpesviridae* family. CMV forms a characteristic nuclear inclusion, which gives an “owl's eye” appearance to infected cells. Many animal species have their own species-specific CMV.

Human CMV maintains a collinear genomic organization, but no significant nucleotide sequence homology with other animal CMVs. Human CMV is also designated as human herpes virus 5 (HHV-5). A great majority of the human population are infected with CMV, without any symptoms by adulthood. CMV is excreted in the urine of infants and intermittently in saliva of healthy seropositive adults. Human CMV may cause diseases such as congenital cytomegalic inclusion disease and infectious mononucleosis. The importance of human CMV as a pathogen has been increasingly correlated with the rising number of immunodeficient patients due to immunosuppressive therapy after transplantation, acquired immune deficiency syndrome (AIDS), and so on.

Mature virions of CMV are 150 to 200 nm in diameter and have an envelope composed of a lipid bilayer and viral glycoproteins. Inside the envelope, a tegment or matrix surrounds an icosahedral capsid, which contains a double-stranded, linear DNA genome. Two types of noninfectious particles, in addition to infectious virions, are produced in cells infected with human CMV. Dense bodies do not contain nucleocapsid or viral DNA and are essentially enveloped tegment protein. Noninfectious enveloped particles have a capsid but no electron-dense DNA core.

Equine CMV has a genome of 180 kbp, while the genomes of human, simian, and murine CMVs are 230 to 240 kbp. Human CMV is unique among animal CMVs in that it has a genome structure similar to herpes simplex virus 1 (HSV-1, class E structure). Two unique sequences (UL and US) are flanked by inverted repeats. Inversion of the UL and US segments mediated by inverted repeats can give rise to four different genomes. Other animal CMVs are less complicated in genome structure, and genome inversion is not known for them.

The genome of the AD169 strain of human CMV has been sequenced. Two hundred and eight open reading frames (ORFs) with a coding capacity of at least 100 amino acid residues were identified in the genome. Although only a few of these ORFs have been actually shown to encode proteins, at least 40 have been shown to be dispensable for replication. ORFs have been designated by their location with regard to the unique and repeated sequences (TRL, UL, IRL, IRS, and US) and sequential numbers. By analogy to HSV-1, roughly one-quarter of these ORFs are predicted to encode proteins required for DNA replication and metabolism functions, and three-quarters for virion maturation and virion structure.

Human CMV shows a highly restricted host range and takes 48 to 72 h to yield detectable amounts of progeny virions. Primary human differentiated cells, such as skin or lung fibroblasts, as well as chimpanzee cells, support human CMV replication, but undifferentiated, transformed, or **aneuploid** cells are usually nonpermissive for CMV replication. The genes of CMV have been classified into three sequential, kinetic classes: a(immediate early), b(delayed early) and g(late) genes. Expression of the latter two relies on the a gene products. The b gene products mainly serve DNA replication and metabolism, while g gene products encode structural proteins.

Suggestion for Further Reading

E. S. Mocarski Jr. (1996) "Cytomegaloviruses and Their Replication". In *Fields Virology*, 3rd ed. (B. N. Fields et al., eds.), Lippincott-Raven, Philadelphia, pp. 2447–2492.

Cytoplasmic Inheritance

Most of the genetic information of a eukaryotic cell resides in its nucleus, and some is found in the cytoplasm. Each **mitochondrion** and chloroplast contains several copies of specific DNA molecules that carry some of the genetic information for the organelle; the rest is encoded in nuclear **genes**. Organelle genes are **transcribed** and **translated** in the organelles themselves through a genetic code that diverges in many cases from the standard one, while the proteins encoded in nuclear genes are imported into the organelle after their **protein biosynthesis** on cytoplasmic ribosomes. As a consequence of this shared genetic determination, there are many cases of nuclear and organelle mutants that exhibit similar phenotypes.

Most organelle genomes consist of circular double-stranded DNA molecules (Table 1). After considerable controversy, it seems clear that many mitochondrial DNA molecules are linear rather than circular.

Table 1. Some Genomes from Mitochondria and Chloroplasts, with Indication of Their Size, Number of Confirmed or Putative Translatable Genes (Open Reading Frames, ORFs), and number of genes for transfer RNA and ribosomal RNA[a]

Species	Number	Size (kb)	ORF	tRNA	rRNA
Mitochondrial Genomes					
Saccharomyces cerevisiae	L36885	78	13	24	4
Schizosaccharomyces pombe	X54421	19	10	25	2
Drosophila melanogaster	U37541	20	13	22	2
Caenorhabditis elegans	X54252	14	12	22	2
Homo sapiens	X93334	17	13	22	2
Chlamydomonas reinhardtii	U03843	16	8	3	14
Arabidopsis thaliana	Y08501, Y08502	367	81	19	3
Chloroplast Genomes					
Euglena gracilis	X70810	143	66	41	11
Nicotiana tabacum	Z00044	156	107	37	8
Oryza sativa	X15901	135	113	46	8

[a] Data taken from the indicated EMBL sequence accession numbers.

Organelles may contain molecules of DNA other than their own chromosomes. Examples are the two linear plasmids of the mitochondria of *Zea mays* that result in the absence of functional pollen (androsterility); they are very useful for the commercial production of hybrid seed (see Heterosis). Another example is *kalilo*, a linear plasmid of *Neurospora crassa* that blocks mitochondrial functions when it integrates into the mitochondrial DNA; the result is senescence, the inability for indefinite vegetative growth.

Other cytoplasmic bodies with their own genetic information range from various self-replicating particles to **viruses** and complete endosymbiotic cells. Their genomes may consist of DNA or RNA. First to be discovered were the *kappa* particles of *Paramecium aurelia* (1), but many others are known, such as the *killer* particles in *Saccharomyces cerevisiae* and the s particles that render

Drosophila melanogaster specially sensitive to carbon dioxide.

1. Heteroplasmons and Mosaicism

A cell contains numerous copies of organelle DNA molecules, up to several thousand, and these need not be identical (heteroplasmon). Organelle genomes are notoriously unstable and suffer frequent point mutations and large rearrangements. Heteroplasmons can be produced by these spontaneous changes or by cell fusion. Contrary to the usual behavior of **heterozygotes**, the relative proportion of two variants in a heteroplasmon is not fixed, giving rise to mosaicism in cell clones.

In some cases, one of the variants imposes itself because of its faster reproduction. Thus, most *petite* mutants of the yeast *Saccharomyces cerevisiae*, lacking aerobic metabolism, carry changes in their mitochondrial DNA. Some of these are called *suppressive*, because mutant mitochondria displace wild-type mitochondria in heteroplasmons. Wild-type mitochondria, on the other hand, impose their phenotype when mixed with mitochondria that carry petite mutations called *neutral*.

In other cases, the two variants may be found in various relative proportions, or even pure, in different cells, as would be expected from random genetic drift. Many variegated ornamental plants exhibit patches or streaks of different colors in their stalks and leaves, ranging from normal green to whitish. This phenotype may have many causes; in the plant *Mirabilis jalapa*, the colors depend on the presence of mutant chloroplasts, mixed with the normal ones in various proportions.

Recombination can occur between the various forms of chloroplast DNA or mitochondrial DNA in heteroplasmons, as shown for example for chloroplast markers of *Chlamydomonas reinhardtii* and mitochondrial markers in *Saccharomyces cerevisiae*.

2. Heterokaryon Test

The fusion of two cells that differ in both nuclear and cytoplasmic markers results in cells that are at the same time heterokaryons and heteroplasmons. Vegetative multiplication of the heterokaryon produces three kinds of cells: heterokaryons and two homokaryons, one for each of the kinds of nuclei. Cytoplasmic traits may segregate in various ways, all independent of the segregation of the nuclei. Homokaryotic segregants may show new combinations of cytoplasmic and nuclear markers. This test requires that the nuclei in the heterokaryon do not fuse, but remain separate, so that they can segregate to different daughter cells. The test has been extended to the yeast *Saccharomyces* by the use of dominant *kar* mutations that block nuclear fusion after mating, thus giving rise to heterokaryons.

3. Reciprocal Crosses

The results of reciprocal crosses offer a test for cytoplasmic inheritance when the two parents do not contribute equally to the cytoplasm of the zygote. The most frequent case in animals and plants is *matrilinear inheritance*, in which all individuals inherit from their mothers only, because of the larger size and contribution of female gametes. Examples are the variegation in *Mirabilis*, the first report of this heredity pattern (2), androsterility in *Zea*, and several human diseases due to mitochondrial mutations, such as Leber's hereditary optic neuropathy.

The matrilinear rule is not absolute. The s particles of *Drosophila* are transmitted most often by the ova (egg), but sometimes by sperm. Chloroplasts may be provided by the male, as in the conifers, or by both parents, as in *Oenothera*. Mammals have powerful mechanisms to exclude the mitochondrial DNA of the sperm from the embryo, and the failure of these mechanisms might produce exceptions to the matrilinear rule.

Uniparental inheritance is observed with the *poky* mitochondrial mutants and the *kalilo* plasmid in the fungus *Neurospora crassa*. When two haploid strains of different **mating type**, *A* or *a*, are crossed, either can provide the large protoperithecia or the small conidia that fuse to produce the zygote. All offspring inherit the cytoplasmic markers from the protoperithecia donor, irrespective of its mating type.

Uniparental inheritance can occur even when the gametes are similar in size, as in *Chlamydomonas reinhardtii*. The zygote is formed by the fusion of seeming identical cells of the two mating types, called mt^+ and mt^-. Almost all the offspring inherit the chloroplast markers of the mt^+ parent only, because the DNA of the mt^- parent is usually destroyed (3).

There are cases of maternal inheritance that are not due to cytoplasmic genes.

Bibliography

1. T. M. Sonneborn (1938) Science **88**, 503.
2. C. Correns (1909) Z. Indukt. Abst. Vererbungsl. **1**, 291–329.
3. R. Sanger (1954) Proc. Natl. Acad. Sci. USA **40**, 356–363.

Suggestions for Further Reading

4. G. J. Hermann and J. M. Shaw (1998) Mitochondrial dynamics in yeast. Annu. Rev. Cell Dev. Biol. **14**, 265–303.
5. R. N. Lightowlers, P. F. Chinnery, D. M. Turnbull, and N. Howell (1997) Mammalian mitochondrial genetics: heredity, heteroplasmy and disease. Trends Genet. **13**, 450–455.
6. N. G. Larsson and D. A. Clayton (1995) Molecular genetic aspects of human mitochondrial disorders. Annu. Rev. Genet. **29**, 151–178.
7. J. Nosek, L. Tomaska, H. Fukuhara, Y. Suyama, and L. Kovac (1998) Linear mitochondrial genomes: 30 years down the line. Trends Genet. **14**, 184–188.
8. M. Sugiura (1995) The chloroplast genome. Essays Biochem. **30**, 49–57.

Cytoskeleton

The cytoskeleton consists primarily of three types of filament: microtubules (about 25 nm in diameter), **actin**-containing microfilaments (initially thought to be 5 to 7 nm in diameter but now known to be about 10 nm in diameter), and intermediate filaments (about 10 nm in diameter). The latter were so named because they were intermediate in size between the long-established and well-characterized microtubules and microfilaments. Microtubules are filamentous structures often many microns in length that occur in the cytoplasm of eukaryotic cells. The actins are a highly conserved family of eukaryotic proteins, and actin filaments are perhaps best known for the highly specific interactions they make with **myosin** thick filaments that results in **muscle** contraction. Many actin-binding proteins play important roles in establishing the cytoskeleton *in vivo* and in allowing it to function appropriately. For example, fimbrin and a-**actinin** aggregate and cross-link microfilaments into bundles, severin severs actin filaments, b-actinin acts as an actin filament-capping protein, and ponticulin (a **transmembrane protein**) binds actin filaments and spectrin binds and links the microfilaments to the cell membrane. See Actin, Microfilament, Microtubules, Intermediate Filaments, Cytokeratins, and Keratins for further information on various components of the cytoskeleton.

Cytotoxic T Lymphocytes

The main interest to molecular biology of cytotoxic T lymphocytes is probably mechanistic. These cells are able to destroy other cells. How do they achieve this? The 40-odd year-old history of this field started with immunology and defense, and the cellular phenomenology that was possible at the time. It now culminates with the realization that the long-sought mechanisms of cytotoxicity convey in fact molecular signals of cell death. Thus, fundamental research on cytotoxic T cells now goes beyond immunology, becoming part of the booming research effort on programmed cell death.

It was shown in 1960 that white peripheral blood cells from alloimmune dogs were able to lyse *in vitro* target cells bearing the corresponding **alloantigens** (1). We now know that many different cell types have this ability to destroy other cells, in particular lymphoid cells, and among these T (i.e., *thymus-derived*) lymphocytes. There are two varieties: CD4+ and CD8+ lymphocytes. When activated, both varieties can be cytotoxic through a Fas-based mechanism, and in addition CD8+ cells can be cytotoxic via a perforin-granzyme-based mechanism. These two mechanisms will be considered in more detail below. A main role of cytotoxic T cells is to lyse syngeneic cells presenting surface determinants originating from **viruses** or other intracellular microorganisms. These, when within cells, are out of reach of other immune system effectors. Destruction of infected cells destroys the microorganism or exposes it to other effector mechanisms. Cytotoxic T cells thus fight intracellular pathogens. Interestingly, cytotoxic T cells can also destroy normal, uninfected cells, such as Fas-bearing activated lymphocytes, thus in part ensuring down-regulation of immune responses. Neither the perforin- nor the Fas-based mechanisms in isolation, nor both together, seem to account fully for graft rejection.

When an effector cell approaches a target cell, it “recognizes” it through an array of diverse molecules at the surface of the effector cell (TCR/CD3/peptide, CD4 or CD8, LFA-1, etc.) and of the target cell (Class I or Class II MHC, ICAM-1, etc.). How, then, does the cytotoxic cell destroy the target cell? First indications were obtained at a phenomenological level. Engagement of the above-mentioned molecules leads to effector cell activation, including an increase in the concentration of free cytoplasmic calcium (2) within a matter of minutes, immediately followed by reorientation within the effector cell of the secretory apparatus towards an area facing the target cell (3). This suggested the possible participation of secretory phenomena in at least one mechanism of cytotoxicity. Many cytotoxic T cells indeed contain peculiar cytoplasmic granules. Their content can be released by degranulation in the extracellular fluid on target cell recognition (see Protein Secretion).

Among the phenomena then observed in the target cell is the early disintegration of nuclear DNA (4, 5) into fragments of around 180 bp, and multiples thereof, corresponding to the size of **nucleosome**-shielded DNA, which is due to the action of one or several **endonucleases** activated early in the sequence of events leading to target cell death. Other events in this sequence include an influx of calcium, condensation of the cytoplasm, fragmentation of the cytoplasm and nucleus, and only very late secondary membrane disruption. This phenomenology of cell death is very similar, if not identical, for example in developmental circumstances. In all cases, the same program seems to govern the course of events in a cell that dies, including, as we now know, a similar cascade of molecular events and the same “apoptotic” morphological traits (6). What may be different is merely the signaling of this death program. The nature of the signals produced by cytotoxic cells has been largely unraveled by studies at the molecular level.

1. The Perforin/Granzyme B Mechanism of Cytotoxicity

A first approach to identify molecules involved in cytotoxicity has been to look for effector cell molecules themselves endowed with cytotoxic activity. This approach led to the detection (7, 8), characterization, and cloning of *perforin*, a 60-kDa protein present in granules in the cytoplasm of many cytotoxic T and NK (natural killer) cells. At high concentrations, it can act on membranes as a calcium-dependent channel-former; most interestingly, it shows significant homology to the terminal components of the complement system cascade. A formal demonstration that perforin was involved in a mechanism of cytotoxicity was provided by several groups (9), all showing that cytotoxicity mediated by T cells was greatly impaired in mice made perforin-deficient through gene targeting.

Other molecules present in granules of cytotoxic T cells were identified by subtractive cloning. Prominent among molecules isolated this way were a number of serine proteinases, such as CTLA-1/CCP1/Granzyme B (10-12) and H Factor/CTLA-3/Granzyme A (10, 12, 13). Granzyme B was demonstrated through gene targeting to be required in a mechanism of cytotoxicity (14).

A current view on the cooperation between perforin and Granzyme B within the same mechanism of cytotoxicity is as follows. On recognition of the target cell, perforin- and granzyme B–containing granules in the effector cell reorient towards the target cell and are triggered to **exocytose**. Granzyme B may somehow enter the target cell and migrate into a target cell compartment where it would be innocuous, but from which it can be released by perforin at sublytic concentrations (15-17). Intracellularly released Granzyme B would then activate the standard programmed cell death cascade, through direct cleavage and therefore activation (18) of some of the ICE-family cysteine proteases called caspases. However, while target cell death mediated by Granzyme B (or at least by purified granules) may involve caspase activation for phenomena such as DNA fragmentation, it may, interestingly, use a noncaspase pathway for cell membrane disruption (19).

2. The Fas-Based Mechanism of Cytotoxicity

Through a **somatic cell** genetic approach it was found (20) that another mechanism of T cell–mediated cytotoxicity required a protein called Fas/APO-1/CD95 (21, 22) at the target cell surface. This in turn led to the cloning of the Fas ligand that is expressed at the effector cell surface (23). Fas belongs to a family of **receptors** (including Fas, TNF-R1, DR3, DR4, DR5), most or all of which are very efficient at transducing a signal interpreted as a cell death signal, while Fas ligand belongs to a family of corresponding ligands (including the Fas ligand, the TNFs, TRAIL, etc.). Involvement of Fas in cytotoxicity may be a reflection *in vitro* of the main roles of the Fas system *in vivo*, such as down-regulation of the immune response (24), protection against the immune system (25, 26), or potential major physiopathological effects (27).

Target cell Fas and effector cell Fas ligand define molecularly the Fas-based mechanism of cytotoxicity. In this mechanism, when an effector cell encounters a target cell, engagement of the T cell receptor of the effector cell by target cell major histocompatibility complex (MHC) leads to expression of the Fas ligand at the effector cell surface. Fas-ligand expression can be induced on CD8+ and on Th0 and Th1 CD4+ T cells (28-30) following specific recognition of antigen through the T cell receptor. This induction seems to involve the activation of **tyrosine kinases**, requires RNA and protein synthesis and the presence of calcium, and is inhibited by cyclosporin A (31-34). Other molecules may be involved, such as Myc and Max, 9-*cis*-**retinoic acid**, and its receptors, the **orphan receptor** for steroids, Nur77, and ALG-3.

Once expressed, effector cell Fas ligand engages target cell Fas, which leads to target cell death. In more detail, engagement of Fas leads in a matter of seconds to protein recruitment via the Fas "death domain," the cytoplasmic segment of Fas that is necessary and sufficient to transduce a death signal (35, 36). First, FADD/MORT-1 (37, 38) directly binds the death domain of Fas via its own *C*-terminal death domain. FADD/MORT-1 also includes an *N*-terminal death effector domain through which it associates with another molecule, FLICE/MACH (39, 40). FLICE/MACH includes two death effector domains at its *N* terminus and, strikingly, a caspase-homology domain at its *C* terminus (39, 40). Thus, the Fas-FADD-FLICE complex provides a remarkably direct link from a membrane signal to caspase activation, which is required for programmed cell death.

3. Concluding Remarks

The perforin-based and the Fas-based pathways account for most, and perhaps all, of T cell–mediated cytotoxicity (41-44), at least as assessed in a 4-hr assay *in vitro.* Other molecules, such as TNF-R1 or the TRAIL receptors, may play a role in longer assays. The Fas pathway is used by both $CD4^+$ (mostly Th1) and $CD8^+$ effector cells, while the latter also use the perforin/granzyme pathway. Thus, in $CD8^+$ T cells, two signals may stem from the T cell receptor/CD3 complex on antigen-specific recognition, one of them leading to granule exocytosis and the other one leading to transcription of the Fas ligand gene. Neither the exact nature of these distinct signals (45), nor whether they can be triggered simultaneously in a given cytotoxic cell is known as yet.

More generally, both mechanisms of T cell–mediated cytotoxicity seem to act by signaling the caspase activation step of the evolutionarily conserved programmed cell death cascade within the target cell. In this sense, the emergence in evolution of T cell–mediated cytotoxicity has not required the invention of new mechanisms of killing, but merely of new ways of signaling a preexisting programmed cell death cascade.

Bibliography

1. A. Govaerts (1960) J. Immunol. **85**, 516–522.
2. M. Poenie, R. Y. Tsien, and A.-M. Schmitt-Verhulst (1987) EMBO J. **6**, 2223–2232.
3. A. Kupfer, G. Dennert, and S. J. Singer (1985) J. Mol. Cell. Immunol. **2**, 37–49.
4. J. H. Russell, V. Masakovski, T. Rucinsky, and G. Phillips (1982) J. Immunol. **128**, 2087–2094.
5. J. J. Cohen et al. (1985) Adv. Exp. Med. Biol. **184**, 493–508.
6. J. F. R. Kerr, A. H. Wyllie, and A. R. Currie (1972) Br. J. Cancer **26**, 239–257.
7. P. A. Henkart (1985) Annu. Rev. Immunol. **3**, 31–58.
8. E. R. Podack (1985) Immunol. Today **6**, 21–27.
9. D. Kägi et al. (1994) Nature **369**, 31–37.
10. J.-F. Brunet et al. (1986) Nature **322**, 268–271.
11. C. G. Lobe et al. (1986) Science **232**, 858–861.
12. D. Masson and J. Tschopp (1987) Cell **49**, 679–685.
13. H. K. Gershenfeld and I. L. Weissman (1986) Science **232**, 854–858.
14. J. W. Heusel et al. (1994) Cell **76**, 977–987.
15. C. J. Froelich et al. (1996) J. Biol. Chem. **271**, 29073–29079.
16. D. A. Jans et al. (1996) J. Biol. Chem. **271**, 30781–30789.
17. L. Shi et al. (1997) J Exp. Med. **185**, 855–866.
18. A. J. Darmon, D. W. Nicholson, and R. C. Bleackley (1995) Nature **377**, 446–448.
19. A. Sarin et al. (1997) Immunity **6**, 209–215.
20. E. Rouvier, M.-F. Luciani, and P. Golstein (1993) J. exp. Med. **177**, 195–200.
21. S. Yonehara, A. Ishii, and M. Yonehara (1989) J. Exp. Med. **169**, 1747–1756.
22. B. C. Trauth et al. (1989) Science **245**, 301–305.
23. T. Suda, T. Takahashi, P. Golstein, and S. Nagata (1993) Cell **75**, 1169–1178.
24. J. H. Russell, B. Rush, C. Weaver, and R. Wang (1993) Proc. Nat. Acad. Sci. USA **90**, 4409–4413.
25. D. Bellgrau et al. (1995) Nature **377**, 630–632.
26. T. S. Griffith et al. (1995) Science **270**, 1189–1192.
27. L. E. French and J. Tschopp (1997) Nat. Med. **3**, 387–388.
28. T. Suda et al. (1995) J. Immunol. **154**, 3806–3813.

29. F. Ramsdell et al. (1994) Internat. Immunol. **6**, 1545–1553.
30. L. L. Carter and R. W. Dutton (1995) J. Immunol. **155**, 1028–1031.
31. A. Anel et al. (1994) Eur. J. Immunol. **24**, 2469–2476.
32. A. Anel et al. (1995) Eur. J. Immunol. **25**, 3381–3387.
33. F. Vignaux et al. (1995) J. Exp. Med. **181**, 781–786.
34. M.-F. Luciani and P. Golstein (1994) Roy. Soc. Phil. Trans. B **345**, 303–309.
35. N. Itoh and S. Nagata (1993) J. Biol. Chem. **268**, 10932–10937.
36. M. P. Boldin et al. (1995) J. Biol. Chem. **270**, 387–391.
37. M. P. Boldin et al. (1995) J. Biol. Chem. **270**, 7795–7798.
38. A. M. Chinnaiyan, K. O''Rourke, M. Tewari, and V. M. Dixit (1995) Cell **81**, 505–512.
39. M. P. Boldin, T. M. Goncharov, Y. V. Goltsev, and D. Wallach (1996) Cell **85**, 803–815.
40. M. Muzio et al. (1996) Cell **85**, 817–827.
41. D. Kägi et al. (1994) Science **265**, 528–530.
42. B. Lowin, M. Hahne, C. Mattmann, and J. Tschopp (1994) Nature **370**, 650–652.
43. H. Kojima et al. (1994) Immunity **1**, 357–364.
44. C. M. Walsh et al. (1994) Proc. Natl. Acad. Sci. USA **91**, 10854–10858.
45. M. T. Esser, B. Krishnamurthy, and V. L. Braciale (1996) J. Exp. Med. **183**, 1697–1706.

Suggestions for Further Reading

46. G. Berke (1994). The binding and lysis of target cells by cytotoxic lymphocytes: Molecular and cellular aspects. Annu. Rev. Immunol. **12**, 735–773.
47. P. A. Henkart (1994). Lymphocyte-mediated cytotoxicity: two pathways and multiple effector molecules. Immunity **1**, 343–346.
48. S. Nagata and P. Golstein (1995). The Fas death factor. Science **267**, 1449–1456.
49. M. E. Peter, F. C. Kischkel, S. Hellbardt, A. M. Chinnaiyan, P. H. Krammer, and V. M. Dixit (1996). CD95(APO-1/Fas)-associating signalling proteins. Cell Death Differ. **3**, 161–170.

D Gene Segment

The existence of D genes encoding a short region of the third complementarity determining region (CDR3) of immunoglobulin heavy chains was first postulated when it was apparent that expressed H chains between the sequences encoded by the **variable** (V) and **J (joining)** genes contained a segment variable in length that had no counterpart in either gene. It turned out that variability of this region resulted from 2 causes: One was the existence of a set of D genes (D for Diversity); the second was due to the presence of nucleotides that were not germline encoded but added enzymatically at both the VD and the DJ junctions by terminal-deoxynucleotidyl-transferase, which is specifically expressed in lymphocytes. As the result of these combined events, heavy-chain CDR3 appeared as the most hypervariable region of Ig molecules, and therefore of prime importance as a basis for antibody specificity.

D gene segments appear to be present in all heavy-chain gene loci, from the lowest vertebrate species. In humans, about 30 D gene segments have been identified, clustered between the IgVH locus and the JH genes. The various D genes differ in length, but are always limited to a small number of potential **codons**. They are flanked on both their 5′ and 3′ ends by the conventional recombination signal sequences recognized by the RAG1 and RAG2 recombinases. The spacers are of different length on each side, so they meet with the 12/23 alternate size rule, to recombine with VH and JH gene segments. D genes make a major contribution to heavy-chain variability of CDR3, not only because of their number and sequence diversity, but also because they are used in many alternate possibilities: (a) They may be inserted in either orientation; (b) any reading frame may be used (in humans, not in the mouse; see text below), although one is more frequently encountered; (c) they may join to each other, so that examples of as many as four fused D genes have been described, thus providing a CDR3 of unusual length; and (d) they may be partially deleted at both ends before being inserted between the V and J genes. All of this clearly can generate a huge diversity potential.

In the mouse, minor differences from the above situation in D gene use and function have been reported, due to the fact that there is essentially only one reading frame used by murine D genes. There are two reasons for this. One gene rearrangement introduces a stop codon in the 3′ JC sequence. The second reason is more complicated. Some mouse D genes have a **promoter**-like region that can be activated after the first gene rearrangement making the DJ joint has been performed. In that case, a D-J-Cm protein is synthesized, which becomes exposed at the surface of the preB cell and blocks any further gene rearrangement (see B Cell), but is unable to contribute a functional immunoglobulin.

The genes for T-cell receptors (TCRs) have also D genes on the b and d chains. There are only a number of D genes, which are used in either orientation and reading frame. They have 12-bp spacers of identical length on both 5′ and 3′ flanking recombination signal sequences, corresponding to the 23-bp spacers of the V and J genes. TCR D genes also contribute to CDR3, a region that is most variable, as for immunoglobulins.

See also entries Gene Rearrangement and Recombinase.

Suggestions for Further Reading

F. Matsuda and T. Honjo (1994) Organization of the human immunoglobulin heavy-chain locus. Adv. Immunol. **62**, 1–29.

H. Sakano, Y. Kurosawa, M. Weigert, and S. Tonegawa (1982) Identification and nucleotide sequence of a diversity DNA segment (D) of immunoglobulin heavy chain genes. Nature **290**, 562–565.

H. Gu, D. Kitamura, and K. Rajewsky (1991) B-cell development regulated by gene rearrangement—arrest of maturation of membrane bound Dm protein and selection of DH element reading frames. Cell, **65**, 47–54.

Dansyl Chloride

The repetitive nature of the Edman Degradation reaction opened the way to protein sequencing and to automation in the form of protein sequencers, but manual Edman degradations also became popular during much of the 1960s and 1970s.

One major manual method used dansyl (1-dimethylaminonaphthalene-5-sulphonyl) chloride (Fig. 1, see top of next page) to detect the new N-terminus after each Edman cycle (1). Combined with purification of peptides on paper by high-voltage electrophoresis and chromatography (see Peptide

Mapping), it made protein sequence analysis accessible to many laboratories without the need for large equipment. It also avoided the difficulties in identification of the phenylthiohydantoin (PTH)-amino acids that existed early, and replaced PTH-identification with dansyl-amino acid identification. The latter became rapid and reliable by **thin-layer chromatography** (2). Hence, many of the original protein primary structures determined used this methodology, originating from the MRC Laboratory of Molecular Biology, Cambridge, England. Together with the Sanger method of DNA sequencing later developed there, the "dansyl-Edman/paper purification" technique made this laboratory the leader in sequencing technology for a long time in the 1960s and 1970s.

Figure 1. Principle of the "dansyl-Edman" modification of the Edman degradation reaction, with N-terminal analysis of separate samples. PITC, phenylisothiocyanate; ATZ, anilinothiazolinone; PTH, phenylthiohydantoin; Dansyl, 1-dimethylaminonaphthalene-5-sulphonyl.

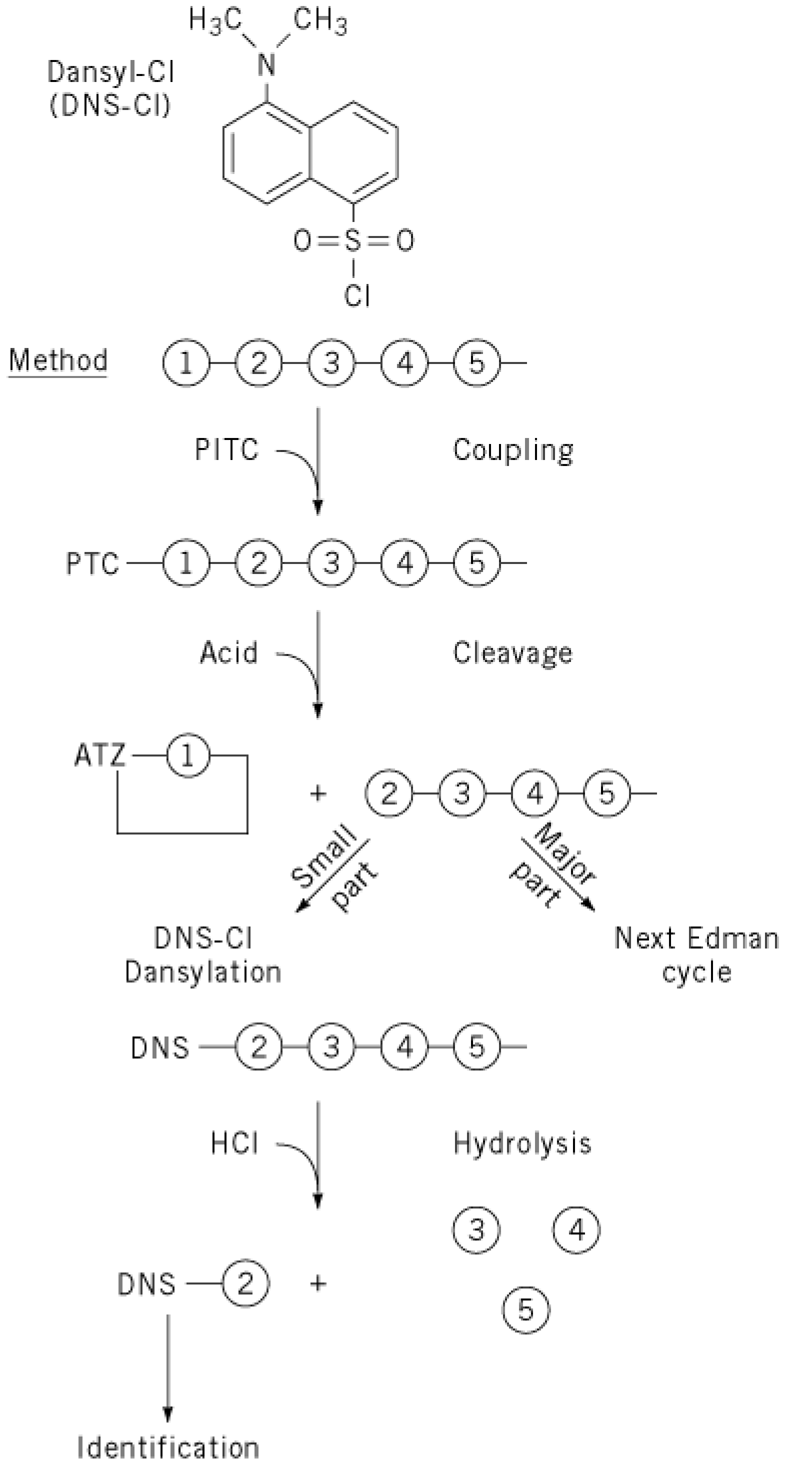

Dansyl chloride reacts with protein N-termini much like the original Sanger reagent, fluorodinitrobenzene (FDNB) (3), but it is easier to use, more sensitive, and fluorescent, making it easily detectable. Dansyl chloride is still used for protein labeling in many cases where fluorescence is desirable.

Bibliography

1. W. R. Gray (1967) Methods Enzymol. **11**, 469–475 and (1972) **25**, 121–138.
2. K. R. Woods and K.-T. Wang (1967) Biochim. Biophys. Acta **133**, 369–370.
3. F. Sanger (1945) Biochem. J. **39**, 507–515.

Databases

Molecular biology is an empirical discipline that requires observing and understanding different types of data. For example, a **gene** may imply a physical location on the chromosome, a **nucleotide sequence**, an amino acid sequence, a three-dimensional protein structure, a molecular component of cellular function, a regulatory mechanism of **gene expression**, or even a **phenotypic** difference caused by mutation. In addition to this variability, the quantity of molecular biology data is increasing rapidly, especially for gene and protein sequences and 3-D structures, due to advances in experimental technologies. Molecular biology databases are a number of resources available over the Internet that comprise a bioinformatics infrastructure for biomedical sciences. Each database contains a specific type of data that has cross-references to other databases, which can be used for integrated information retrieval. This is possible because a database is generally organized as a collection of entries, and connections can be made at the level of entries without standardizing how data items should be organized within an entry. The advent of the World Wide Web (WWW) in the early 1990s was a boon to molecular biology databases because the concept of hyperlinks is fully compatible with the practice of cross-references. The WWW also dramatically increased the accessibility of computers to biologists. The primary resources of molecular biology databases are bibliographic databases, sequence databases, and structure databases.

Although bibliographic, sequence, and structural aspects of molecular biology are relatively easy to computerize, the next step is to organize their functional aspects. There are resources in that direction, such as motif libraries that contain higher level knowledge abstracted from sets of functionally related sequences and pathway databases that contain computerized knowledge of molecular interactions and biochemical pathways. Representative examples of these resources are shown in Table 1.

Table 1. Selected List of Molecular Biology Databases

Data Type	Database	Organization
Biomedical literature	Medline	National Center for Biotechnology Information (NCBI)
Nucleotide sequence	GenBank	
	EMBL	European Bioinformatics Institute (EBI)
	DDBJ	National Institute of Genetics, Japan
Amino acid sequence	PIR	National Biomedical Research Foundation
	SWISS-PROT	Swiss Institute of Bioinformatics (SIB)
Sequence motif	PROSITE	
3-D structure	PDB	Brookhaven National Laboratory

Biochemical pathway	KEGG	Kyoto University

Abstraction of a real problem is made through a data model. For example, data are organized in two-dimensional tables in the relational data model. The relational database based on the relational model has been widely used in a number of applications, including some of the sequence databases. Although in principle all different types of molecular biology data can be stored in a single, unified, relational database, this is impossible in practice because of the varying views of how data items should be organized and related. In the current web of molecular biology databases, different types of data are integrated by a loose coupling based on links (cross-references), rather than a tight coupling based on unified schema. This approach is extended to include other types of links, especially similarity links computed by similarity search algorithms and biological links representing molecular interactions, which can also be integrated for biological reasoning (1). The major bioinformatics servers shown in Table 2 provide link-based database retrieval systems, such as Entrez at NCBI, SRS at EBI, and DBGET/LinkDB at GenomeNet in Kyoto.

Table 2. WWW Addresses for the Major Bioinformatics Servers

Server	Address
NCBI	www.ncbi.nlm.nih.gov
EBI	www.ebi.ac.uk
ExPASy	(site currently unavailable)
GenomeNet	www.genome.ad.jp

In scientific disciplines, the merit of storing and managing information in a computer was first realized in bibliographic databases, which were designed for humans to read and understand. In the next step, factual data reported in the literature were computerized in factual databases, such as in sequence databases, which made more sophisticated retrieval available, for example, sequence similarity searches. Even in this case, however, the database is still a static resource to be retrieved, and it is up to humans to make sense out of the retrieved data. In contrast, the knowledge of links or relationships is more dynamic in nature. For example, ancestors in a family can be retrieved from a "deductive" database that contains parent–child relationships and the rules for combining them. Thus, knowledge is different from data or information, in that new knowledge can be generated dynamically from existing knowledge by logical reasoning. In the era of mass data production, molecular biology requires logical computation based on empirical knowledge rather than numerical computation based on first principles (see Bioinformatics). The web of molecular biology databases also requires a new generation of knowledge bases.

Bibliography

1. M. Kanehisa (1997) Trends Biochem. Sci. **22**, 442–444.

Daunomycin

Daunomycin (synonym: daunorubicin) is the prototype of the clinically important anthracycline antibiotics that are widely used in cancer chemotherapy. Daunomycin and its close relative adriamycin are natural products isolated from various *Streptomyces* species. These two anthracyclines are probably the most widely used antitumor agents worldwide (1, 2). Daunomycin is primarily used in the treatment of acute leukemias. The structure of daunomycin is shown in Figure 1; it is composed of two major parts: an anthraquinone ring system and the pendant daunosamine, an amino sugar.

Figure 1. The chemical structure (**a**) and molecular model (**b**) of the anthracycline antibiotic daunomycin.

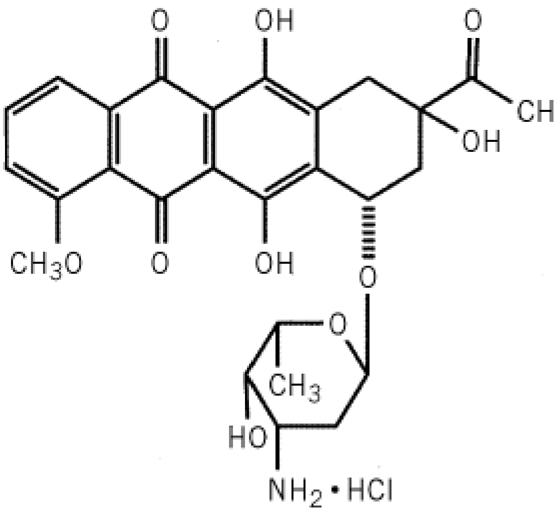

(a)

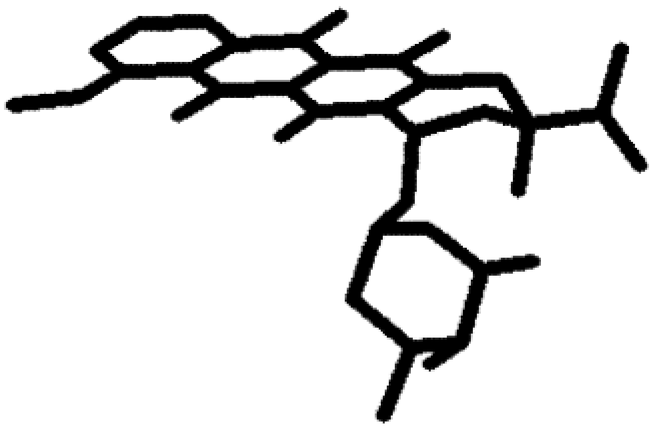

(b)

Daunomycin rapidly permeates into cells, passing through the membrane into the cytoplasm, and then accumulates in the nucleus, where it binds avidly to **DNA**. It binds to DNA by the process of intercalation, in which the anthraquinone ring inserts between adjacent DNA base pairs. The daunosamine moiety provides additional interactions that stabilize the complex by fitting into the minor groove of the DNA double helix, where it participates in van der Waals interactions. These additional interactions in the minor groove distinguish daunomycin from simple intercalators like ethidium bromide, which are stabilized only by the interactions within the intercalation site. Figure 2 shows the structure of a daunomycin–DNA complex determined by X-ray crystallography (3). Intercalation simultaneously lengthens and unwinds the DNA duplex, and it stabilizes DNA against thermal denaturation, increasing its **Tm (melting temperature)**.

Figure 2. Structure of a daunomycin–DNA complex. The anthraquinone portion of daunomycin (shown in a space-filling representation) is intercalated between the CpG step in a DNA oligonucleotide (shown in a stick representation). The daunosamine portion of daunomycin lies in the DNA minor groove. This figure was prepared from coordinates (file DDF01) deposited in the Nucleic Acid Database (Rutgers University), http://ndbserver.rutgers.edu.

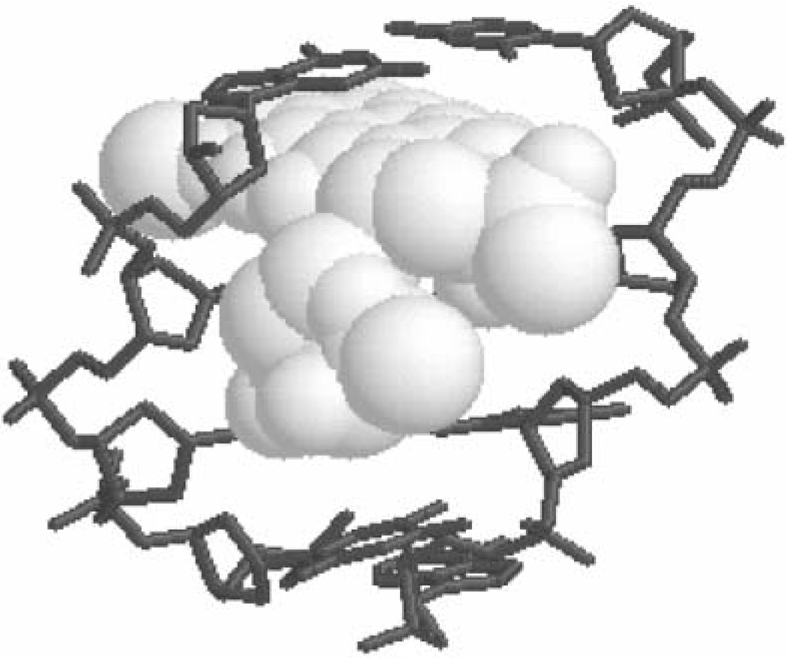

Daunomycin, despite its small size (527.5 MW), exhibits several levels of **molecular recognition** (4). It is structurally specific and strongly prefers to bind to right-handed, B-form DNA over alternate helical forms. Daunomycin will **allosterically** convert left-handed Z DNA to an intercalated, righted-handed form (5). There is pronounced sequence selectivity in the binding of daunomcyin to DNA, which is revealed by DNase I footprinting experiments. Daunomycin binds preferentially to the triplet sequences 5′(A/T)GC and 5′(A/T)CG, where the notation (A/T) indicates that either A or T may occupy the sequence position (6, 7).

The mechanism by which daunomycin acts to kill cancer cells remains incompletely defined, and it may involve inhibition of several different cellular functions. Daunomycin, like most intercalators, is an effective inhibitor of DNA replication and of transcription, both *in vitro* and *in vivo*. The most likely intracellular target for daunomycin, according to recent evidence, is the enzyme topoisomerase II (see DNA Topology). Daunomycin poisons this key enzyme, by trapping an intermediate enzymatic species in which cleaved DNA strands are covalently attached to topoisomerase II, by preventing the normal resealing of the duplex DNA after strand passage (8). A comprehensive study of several anthracycline derivatives, including daunomycin, showed that intercalation is necessary, but not sufficient, for inhibition of topoisomerase II (9).

The anthraquinone moiety of daunomycin readily undergoes a number of oxidation–reduction reactions, with the production of oxygen free radicals. These free radicals can damage cells, and they may represent another important mechanism in the cytotoxicity of daunomycin. A serious, complicating side effect in the clinical use of daunomycin in cancer chemotherapy is its cardiotoxicity (1, 2). Free-radical production has been implicated as the primary cause of such cardiotoxicity.

Daunomycin was one of the first effective cancer chemotherapeutic agents identified, and it remains clinically important after over 30 years of use. It is one of the best characterized and understood intercalators and serves as an important model for understanding how small molecules bind to DNA.

Bibliography

1. R. B. Weiss (1992) Semin. Oncol. **19**, 670–686.
2. G. N. Hortobagyi (1997) Drugs **54**, 1–7.
3. A. H.-J. Wang (1992) Curr. Opin. Struct. Biol. **2**, 361–368.
4. J. B. Chaires (1996) in *Advances in DNA Sequence Specific Agents*, Vol. **2** (L. H. Hurley and J. B. Chaires, eds.), JAI Press, Greenwich, CT, pp. 141–167.
5. J. B. Chaires (1986) J. Biol. Chem. **261**, 8899–8907.
6. B. Pullman (1990) Anti-cancer Drug Design **7**, 96–105.
7. J. B. Chaires, J. E. Herrera, and M. J. Waring (1990) Biochemistry **29**, 6145–6153.
8. F. Zunnino and G. Capranico (1990) Anti-cancer Drug Design **5**, 307–317.
9. A. Bodley et al. (1989) Cancer Res. **49**, 5969–5978.

Suggestions for Further Reading

10. F. Arcamone (1981) *Doxorubicin*, Academic Press, New York.
11. J. W. Lown, ed. (1988) *Anthraacycline and Antrhacenedione Based Anticancer Agents*, Elsevier, Amsterdam.
12. W. Priebe, ed. (1995) *Anthracycline Antibiotics: New Analogues, Methods of Delivery, and Mechanism of Action*, ACS Symposium Series 574, American Chemical Society, Washington, DC.

DEAD and DEAH Domains

DEAD and DEAH domains contain a characteristic Asp-Glu-Ala-Asp/His sequence that is usually abbreviated DEAD or DEAH, using the amino-acid one-letter code. The **domains** belong to a large superfamily of enzymes involved in nucleic acid metabolism. Both DEAD and DEAH domains alter nucleic acid secondary structure in a nucleoside triphosphate (NTP)-dependent manner. Many function as either DNA helicases or RNA Helicases, which unwind DNA and RNA duplexes, respectively.

The general properties of DEAD/DEAH domains are summarized, and the functions of several well-characterized DEAD and DEAH domains are reviewed. Included are the DEAD domain of eukaryotic initiation factor 4a, eIF-4A, and the precursor RNA processing (PRP) DEAH domains found in the spliceosome, a multiprotein complex responsible for processing pre-messenger RNA into mRNA (see RNA Splicing). Finally, the structural basis for sequence conservation will be discussed using the **X-ray crystallographic** structures of the DExx DNA helicases from *Bacillus stearothermophilus* and *Escherichia coli* and the DExH RNA helicase from the hepatitis C virus (HCV).

1. Identification and Classification of DEAD and DEAH Domains

Helicases are enzymes that remove double-stranded regions of nucleic acid when single-stranded RNA and DNA are required. Regulated production of single-stranded nucleic acids occurs during many cellular processes, including replication, recombination, and transcription. The energy required for unwinding is derived from the hydrolysis of NTPs such as ATP.

Amino acid sequences can be used to identify and classify helicases. Helicase sequences contain seven regions or motifs of conserved residues (1). On the basis of the sequences of the individual motifs, helicases have been broadly grouped into two major superfamilies, SFI and SFII, and several smaller families [(2), Fig. 1). With the increased availability of genome information, helicases are frequently identified from their sequences alone, prior to the demonstration of helicase activity *in vitro*.

Figure 1. Representative examples of conserved sequence motifs. The seven common sequence motifs of DEAD and DI
one-letter code. Helicases from both superfamilies I and II are given. The NTP-binding sequences within motifs I and II
of the structures of the *E. coli* Rep DNA and HCV RNA helicases revealed similar spatial arrangements of all motifs exc
the following abbreviations: Rep, *E. coli* Rep DNA helicase; PcrA, *B. stearothermophilus* PcrA DNA helicase; eIF-4A, e
helicase; HCV, RNA helicase domain of HCV NS3 protein, and PRP22, *S. cerevisiae* precursor RNA processing protein

	Motif					
	I	Ia	II	III	IV	V
Protein						
SFI						
Rep	AGAGSGKT	FTNKAA	DEYQ	VGDDDQS	IKLEQNYRS	QLMT
PCRA	AGAGSGKT	FTNKAA	DEYQ	VGDADQS	ILLEQNYRS	MLMT
SF2						
eIf-4A	AQSGTGKT	PTRELA	DEAD	LSATMP		LITT
HCV	APTGSGKS	PSVAAT	DECH	ATATPP	LIFCHSKKK	VVST
PRP22	GETGSGKT	PRRVAA	DEAH	VTSATL		DGIY

The energy for helicase-mediated unwinding of nucleic acid duplexes is derived from the hydrolysis of NTPs. Consequently, amino acid residues known to bind NTPs in other proteins are among the most conserved across the helicase families. By analogy with structures of ATP:protein complexes, the conserved lysine residue embedded in the Ala-x-x-Gly-x-Gly-Lys-Thr sequence of motif I probably interacts with the b and g phosphates of NTP (Fig. 2). Similarly, NTPases share an aspartic acid residue in motif II that ligates the magnesium of the NTP: Mg^{+2} complex (Fig. 2). In the DEAD and DEAH domains, this conserved aspartic acid occurs within the title sequences Asp-Glu-Ala-Asp/His. In 1982, Walker et al. (3) identified the functional significance of these motifs through sequence comparisons of ATP-utilizing enzymes. For this reason, motifs I and II are also referred to as Walker motifs A and B. In the literature, DEAD domains are occasionally referred to as DEAD-box proteins.

Figure 2. Stereoscopic views of an enzyme:ATP complex. Interactions made by the conserved lysine and aspartic acid residues of the protein with the ATP phosphates and Mg^{2+}, respectively, are highlighted. The protein backbone is shown as ribbons and the bound ATP in the ball-and-stick representation. Phosphate atoms are shown as solid spheres. The Mg^{2+} ion is situated between the phosphate oxygen and aspartic acid. For clarity, the complete coordination of the Mg^{2+} is not shown. Coordinates were taken from the crystal structure of the human cyclin-dependent kinase 2:ATP complex [(28), PDB entry 1HCK].

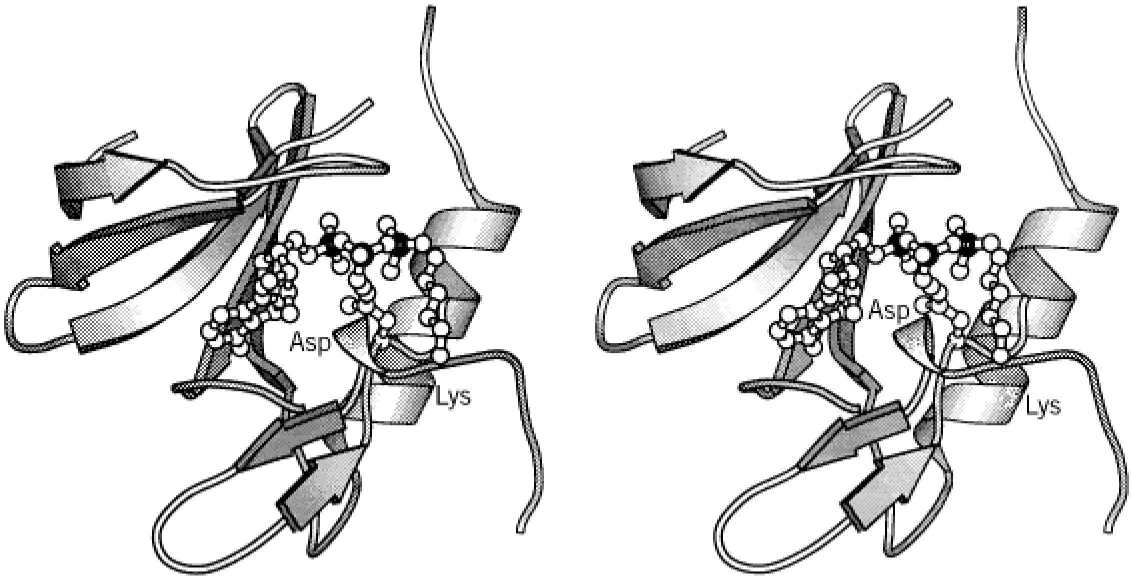

Initially, the classification of helicases by residues within motif II grouped functionally related proteins. However, as more helicase sequences became known, many exceptions to the strict conservation of motif II residues within functional families have been found. Indeed, a new DExH domain family containing helicases from positive-strand viruses has been proposed (4). For these enzymes, a variety of residues can be accommodated at the third position. Overall, amino acid sequence comparisons suggest that the DEAD and DEAH domains belong to a larger family of DExx domains, where x indicates sequence variability at the third and fourth positions of the DEAD/DEAH motif.

2. General Properties of DEAD and DEAH Domains

Isolated DEAD and DEAH domains typically exhibit NTPase activity that can be stimulated by the addition of nucleic acid polymers. The domains bind NTPs with **dissociation constants** in the micromolar range. K_m values for ATP of 80, 260, and 250 µM were measured for eIF-4A (5), PRP16 (6) and HCV helicases (7), respectively. Unlike eIF-4A, which is an obligate ATPase (8), little specificity for NTP is observed for some DEAD and DEAH domains. K_m values for ATP, CTP, GTP, and UTP ranged from 260 to 580 µM for the PRP16 DEAH domain (6) and from 250 to 1300 µM for the HCV DExH helicase (7). For the HCV helicase, the addition of poly U increases its ATPase activity approximately 10-fold (9). In the case of eIF-4A, the addition of poly U increases the ATPase activity approximately 8-fold (8).

The mechanism by which NTP hydrolysis is coupled to the modification of a nucleic acid secondary structure remains one of the most interesting questions regarding the function of DEAD and DEAH domains. As outlined below, several lines of evidence support the hypothesis that the hydrolysis reaction produces conformational changes in the domain. The changes alter the stability of the bound nucleic acid to favor the single-stranded form.

DEAD and DEAH domains typically contain ~300 residues and frequently reside within a longer sequence, or as subunits of a larger protein complex. For example, each of the seven *Saccharomyces cerevisiae* PRP splicing factors contains a DEAD/H domain. One of the larger splicing factors, PRP22, also contains an amino-terminal RNA-binding domain (6). The human DNA helicase II has two double-stranded **RNA-binding** domains, a DExH domain, and a glycine-rich domain (10). The HCV nonstructural protein 3 (NS3) is a bifunctional enzyme with an amino-terminal serine proteinase activity and a helicase activity in the carboxy-terminal DExH domain (11).

3. DEAD Domains

One of the most well-characterized DEAD domains is eukaryotic initiation factor 4A, eIF-4A. eIF-4A is one of three initiation factors required for binding of the 40S ribosomal subunit to mRNA during the initiation of translation. The ribosome-binding reaction requires ATP hydrolysis. During initiation of translation, eIF-4A may use the energy of ATP hydrolysis to disentangle structured regions in the 5′-untranslated regions of messenger RNA. When complexed with eIF-4B *in vitro*, eIF-4A unwinds duplex RNA in an ATP-dependent manner.

The biochemical characterization of eIF-4A provided the first detailed views of RNA helicase activity, which serve as a framework for comparison of newly discovered helicases. Studies of eIF-4A are reviewed in (12) and (13).

Mutational studies on eIF-4A demonstrated the functional importance of residues in motifs I and II. For example, the conversion of residues within the DEAD sequence to either NEAD or DQAD (substitution of the first conserved aspartic acid with asparagine, or the second residue with glutamine) abolished ATPase activity (12). The same result was observed when the conserved lysine residue in motif I was changed to asparagine. Similar experiments with other DExH domains have confirmed that these amino acid residues are essential.

Studies of the eIF-4A mechanism support the hypothesis that alterations in RNA structure are induced by conformational changes in the DEAD domain. By monitoring the domain's susceptibility to **proteolysis**, ADP was found to cause conformational changes in both the free eIF-4A and eIF-4A:RNA complex (14). Conformational changes were also observed on the binding of an ATP analog to the eIF-4A:RNA complex. Similarly, the observed nucleic acid-dependent differences in eIF-4A affinity for either ADP.Mg^{+2} or ATP.Mg^{+2} were also thought to reflect structural changes in eIF-4A.

4. DEAH Domains

The DEAH domains are involved in RNA processing and display many features common among helicases. Originally classified as DEAH domains, new sequence information has expanded the classification to DEAD/H domains. DEAD/H helicases are associated with the large ribonucleoprotein (RNP) complex called the spliceosome. The spliceosome processes pre-messenger RNA to remove intervening untranslated sequences called **introns**, so the resultant messenger RNA contains only expressed sequences, or exons.

A number of precursor RNA processing (PRP) proteins associate with the spliceosome. The proteins contain either DEAD or DEAH domains and are also called splicing factors. Similar to many helicases, the isolated DEAH domain protein, PRP22, exhibits ATPase activity that is stimulated by the addition of poly(U) RNA (15). Mutagenesis studies of PRP22 variants demonstrated that the ATPase activity requires the conserved lysine residue of motif I. Although helicase activity has been demonstrated for the DEAH splicing factor PRP16 *in vitro*, the functional significance of these data is unclear (6). Most evidence suggests that the PRP splicing factors interact directly with the RNA in the spliceosome, to modulate RNA structure for efficient processing (15-17).

5. Structures of DExx and DExH Domains

X-ray crystallographic structures of several helicases have been reported. The structures include two DExx DNA helicases belonging to SFI, *Bacillus stearothermophilus* PcrA helicase (18), and *E. coli* Rep helicase (19), and the HCV RNA DExH domain of SFII (20, 21).

The helicases are multidomain structures (Fig. 3). The DNA helicases fold into structurally similar halves, with two domains each. Each half is composed of a bab domain and an **alpha-helical** domain. A deep groove separates the two major helicase domains. The HCV RNA helicase domain contains three folded units: two bab domains and one a-helical domain. Comparison of the helicase structures revealed that the bab domains are structurally similar in both overall fold and their relative spatial orientation (22).

Figure 3. Structural features of DExx and DExH domains. The ribbons trace the polypeptide backbones of the HCV RN (left drawing, part **a**) and *E. coli* Rep DNA helicase (right drawing, part **a**). The upper left domain in each structure is the domain (shown in the lightest ribbon). The NTP-binding domain and second domain (shown in the darkest ribbon) share bab fold. Many of the conserved sequence motifs are located near the deep groove that separates the bab domains. A det motif II, III, and VI residues of the HCV RNA helicase is shown in stereoscopic representation (part **b**). Figures prepare Molscript (29).

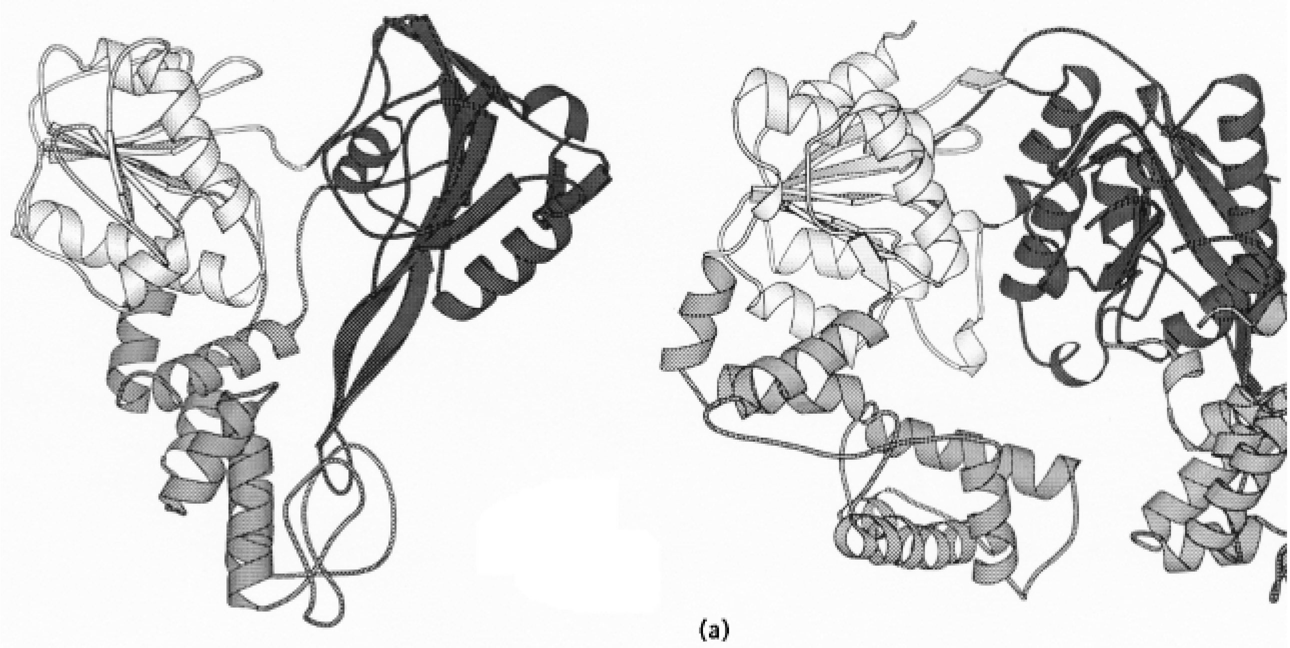

(a)

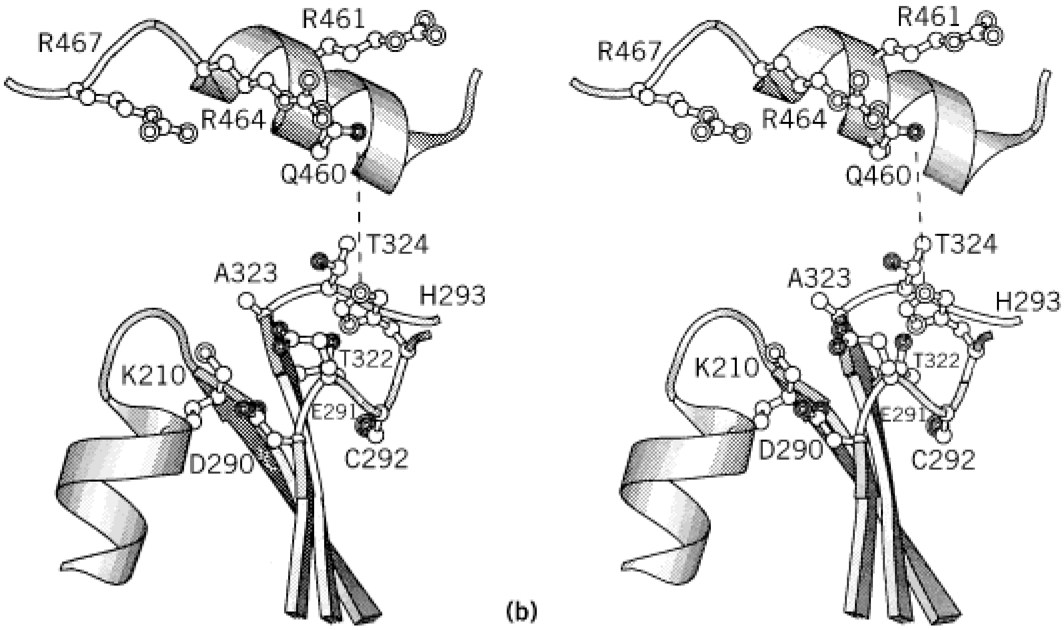

(b)

Both helicase motifs I and II are located within one of the bab domains. The overall fold of the bab domain and spatial arrangement of residues in motifs I and II are similar to conserved features present in other NTP-utilizing enzymes. The crystallographic structure of the PcrA:ADP complex also showed nucleotide binding to this domain (18). The structural studies taken together, including comparison of the superfamily I and II proteins, have identified the NTP-binding domain.

The structural studies also revealed conformational flexibility that is potentially important in helicase function. Comparison of the independent molecules in the HCV RNA helicase crystals revealed that one of the bab domains could rotate relative to the remainder of the molecule (21). When the helicase structures are compared to those of NTP-binding proteins known to function as molecular switches, the observed structural changes in the helicase were found to involve residues at the end of a beta-strand previously shown to constitute part of the energy transducing mechanism (18, 21). These residues in the DExH domain map to motif III, which mutagenesis studies have shown is required for coupling NTP hydrolysis to unwinding (12, 23). Some indication of the extent of possible structural changes is found in the structure of the Rep DNA helicase complexed with a short oligonucleotide, where two orientations differing by a 130-deg rotation about a hinge region of the protein were observed for one of the helical subdomains (19).

6. Roles of DEAD and DEAH Residues

The mechanistic roles of the first and last residues of the DEAD and DEAH have been largely deciphered. Structural studies on the free and ADP-bound forms of DExx and DExH domains support the participation of the conserved aspartic acid in binding the NTP phosphate groups. Comparison of the structures of ATP:protein complexes suggests that the aspartic acid probably coordinates either the Mg^{+2} of the $NTP.Mg^{+2}$ complex, or it interacts with the phosphate groups via an intervening water molecule. However, the exact nature of the interaction has yet to be defined.

The last residue of the motif II tetrapeptide is involved in coupling the energy generated by NTP hydrolysis to duplex unwinding. Researchers working with eIF-4A generated a molecule in which the wild-type DEAD sequence was changed to DEAH (12). The ATPase activity of the modified eIF-4A was slightly enhanced, but the helicase activity was decreased 90% relative to the wild-type molecule. In a similar set of experiments, the DExA mutants of the DExH vaccinia virus nucleoside triphosphate phosphohydrolase II (NP-II) (5) and HCV RNA helicase exhibited NTPase activity and RNA binding comparable to the wild-type protein (24). In contrast, the RNA unwinding activity of these proteins was essentially undetectable.

Crystal structures of the DExH domains show that the histidine side chain is oriented toward the deep groove separating the two bab domains. Although a detailed structural description of the precise role played by the last residue of motif II in the helicase reaction has not been determined, the structures show that the histidine residue is close to conserved residues in motif VI. Mutagenesis experiments on eIF-4A (25) and vaccinia virus NP-II (26) demonstrated that residues in motif VI are required for helicase activity. Altered proteins exhibit decreased ATPase and helicase activities, without compromised RNA binding (27). The structural proximity of the DExH histidine and residues of motif IV offers the possibility that the residues interact directly during the helicase catalytic cycle (Fig. 3).

7. Conclusion

The well-characterized DEAD and DEAH domains play essential roles in nucleic acid metabolism. Structural and mutagenesis studies, and amino acid sequence comparisons, have revealed the functions of the first D residue and the terminal D and H residues, although the mechanistic details of their interactions have not been determined. The DEAD and DEAH sequences are required for nucleoside triphosphate hydrolysis and, along with residues of motifs Ia, III, and VI, are required for coupling hydrolysis to mechanical action.

DEAD and DEAH domains occur widely in nature and exhibit a variety of biological functions. The functional diversity of these domains constitutes a challenge for classification by sequence-based approaches. Overall, the DEAD, DEAH, and DExH domains appear to be required in processes involving large-scale conformational changes of domain and substrate. Thus, their utilization as molecular motors is emerging as a unifying theme (14).

Bibliography

1. S. Schmid and P. Linder (1992) D-E-A-D protein family of putative RNA helicases. Mol. Microbiol. **6**, 283–291.
2. A. Gorbalenya and E. Koonin (1993) Helicase: Amino acid sequence comparisons and structure-function relationships. Curr. Opin. Struct. Biol. **3**, 419–429.
3. J. Walker, M. Saraste, M. Runswick, and N. Gay (1982) Distantly related sequences in the alpha- and beta-subunits of ATP synthase, myosin, kinases and other ATP-requiring enzymes

and a common nucleotide binding fold. EMBO J. **1**, 945–951.

4. E. Koonin (1991) Similarities in RNA helicases. Nature **352**, 290.
5. J. Lorsch and D. Herschlag (1998) The DEAD box protein eIF4A. 1. A minimal kinetic and thermodynamic framework reveals coupled binding of RNA and nucleotide. Biochemistry **37**, 2180–2193.
6. Y. Wang, J. Wagner, and C. Guthrie (1998) The DEAH-box splicing factor Prp16 unwinds RNA duplexes in vitro. Curr. Biol. **8**, 441–451.
7. K. Morgenstern, J. Landro, K. Hsiao, C. Lin, Y. Gu, M. Su, and J. Thomson (1997) Polynucleotide modulation of the protease, nucleoside triphosphatase, and helicase activities of a hepatitis C virus NS3-NS4A complex isolated from transfected COS cells. J. Virol. **71**, 3767–3775.
8. F. Rozen, I. Edery, K. Meerovitch, T. Dever, W. Merrick, and N. Sonenberg (1990) Bidirectional RNA helicase activity of eucaryotic translation initiation factors 4A and 4F. Mol. Cell Biol. **10**, 1134–1144.
9. F. Preugschat, D. Averett, B. Clarke, and D. Porter (1996) A steady-state and pre-steady-state kinetic analysis of the NTPase activity associated with the hepatitis C virus NS3 helicase domain. J. Biol. Chem. **271**, 24449–24457.
10. S. Zhang and F. Grosse (1997) Domain structure of human nuclear DNA helicase II (RNA helicase A). J. Biol. Chem. **272**, 11487–11494.
11. L. Jin and D. L. Peterson (1995) Expression, isolation, and characterization of the hepatitis C Virus APTase/RNA helicase. Archives Biochem. and Biophys. **323**, 47–53.
12. A. Pause and N. Sonenberg (1992) Mutational analysis of a DEAD box RNA helicase: The mammalian translation initiation factor eIF-4A. EMBO J. **11**, 2643–2654.
13. D. Wassarman and J. Steitz (1991) RNA splicing. Alive with DEAD proteins. Nature **349**, 463–464.
14. J. Lorsch and D. Herschlag (1998) The DEAD box protein eIF4A. 2. A cycle of nucleotide and RNA-dependent conformational changes. Biochemistry **37**, 2194–2206.
15. J. Wagner, E. Jankowsky, M. Company, A. Pyle, and J. Abelson (1998) The DEAH-box protein PRP22 is an ATPase that mediates ATP-dependent mRNA release from the spliceosome and unwinds RNA duplexes. EMBO J. **17**, 2926–2937.
16. S. Teigelkamp, M. McGarvey, M. Plumpton, and J. Beggs (1994) The splicing factor PRP2, a putative RNA helicase, interacts directly with pre-mRNA. EMBO J. **13**, 888–897.)
17. S. Kim and R. Lin (1996) Spliceosome activation by PRP2 ATPase prior to the first transesterification reaction of pre-mRNA splicing. Mol. Cell Biol. **16**, 6810–6819.
18. H. Subramanya, L. Bird, J. Brannigan, and D. Wigley (1996) Crystal structure of a DExx box DNA helicase. Nature **384**, 379–383.
19. S. Korolev, J. Hsieh, G. Gauss, T. Lohman, and G. Waksman (1997) Major domain swiveling revealed by the crystal structures of complexes of E. coli Rep helicase bound to single-stranded DNA and ADP. Cell **90**, 635–647.
20. H. Cho, H., N. Ha, L. Kang, K. Chung, S. Back, S. Jang, and B. Oh (1998) Crystal structure of RNA helicase from genotype 1b hepatitis C virus. A feasible mechanism of unwinding duplex RNA. J. Biol. Chem. **273**, 15045–15052.
21. N. Yao, T. Hesson, M. Cable, Z. Hong, A. Kwong, H. V. Le, and P. C. Weber (1997) Structure of the hepatitis C virus RNA helicase domain. Nature Struct. Biol. **4**, 463–467.
22. S. Korolev, N. Yao, T. Lohman, P. C. Weber, and G. Waksman (1998) Comparisons between the structures of HCV and Rep helicases reveal structural similarities between SF1 and SF2 super-families of helicases. Prot. Sci. **7**, 605–610.
23. D. Kim, J. Kim, Y. Gwack, J. Han, and J. Choe (1997) Mutational analysis of the hepatitis C virus RNA helicase. J. Virol. **71**, 9400–9409.
24. G. Heilek and M. Peterson (1997) A point mutation abolishes the helicase but not the nucleoside

triphosphatase activity of hepatitis C virus NS3 protein. J. Virol. **71**, 6264–6266.
25. A. Pause, N. M"ethot, and N. Sonenberg (1993) The HRIGRXXR region of the DEAD box RNA helicase eukaryotic translation initiation factor 4A is required for RNA binding and ATP hydrolysis. Mol. Cell Biol. **13**, 6789–6798.
26. C. Gross and S. Shuman (1996) The QRxGRxGRxxxG motif of the vaccinia virus DExH box RNA helicase NPH-II is required for ATP hydrolysis and RNA unwinding but not for RNA binding. J. Virol. **70**, 1706–1713.
27. C. Gross and S. Shuman (1995) Mutational analysis of vaccinia virus nucleoside triphosphate phosphohydrolase II, a DExH box RNA helicase. J. Virol. **69**, 4727–4736.
28. U. Schulze-Gahmen, H. L. De Bondt, and S.-H. Kim (1996) High-resolution crystal structures of human cyclin-dependent kinase 2 with and without ATP: Bound waters and natural ligand as guides for inhibitor design. J. Med. Chem. **39**, 4540–4546.
29. P. J. Kraulis (1991) Molscript: A program to produce both detailed and schematic plots of protein structures. J. Appl. Cryst. **24**, 946–950.

Suggestions for Further Reading

30. L. Bird, H. Subramanya, and D. Wigley (1998) Helicases: A unifying structural theme? Curr. Opin. Struct. Biol. **8**, 14–18.
31. C. Guthrie (1996) "The spliceosome is a dynamic ribonucleoprotein machine". The Harvey Lecture Series, Wiley-Liss, New York, Vol. **90**, pp. 59–80.
32. K. Holmes, C. Sander, and A. Valencia (1993) A new ATP-binding fold in actin, hexokinase and Hsc70. Trends in Cell Biol. **3**, 53–59.
33. G. Kadaré and A. Haenni (1997) Virus-encoded RNA helicases. J. Virol. **71**, 2583–2590.
34. T. Lohman (1992) Escherichia coli DNA helicases: mechanisms of DNA unwinding. Mol. Microbiol. **6**, 5–14.

Dead-End Inhibition

Dead-end inhibition of an enzyme occurs when a compound, usually a structural analogue of a substrate, combines at the active site of the enzyme, but does not undergo reaction. The resulting complex can only dissociate back to the components from which it was formed. Dead-end inhibitors are useful for determining kinetic reaction mechanisms because dead-end inhibition patterns can be characteristic of a particular mechanism. Rules have been formulated for the qualitative prediction of such inhibition patterns (1) and these rules can be summarized as follows:

1. A dead-end inhibitor affects the *slope* of a double-reciprocal plot (see Lineweaver–Burk Plot) when
   - the inhibitor and the variable substrate combine with the same enzyme form or
   - a reversible connection exists between the points of addition of the inhibitor and the variable substrate. Such a reversible connection exists only when the variable substrate adds after the inhibitor.
2. A dead-end inhibitor affects the *intercept* of a double-reciprocal plot when the inhibitor and variable substrate combine with different forms of enzyme and saturation with the variable substrate does not overcome the inhibition. Intercept effects will always be observed unless steps between the points of addition of the variable substrate and the inhibitor are at thermodynamic equilibrium.

The results of the application of the rules to kinetic mechanisms for Bi–Bi reaction mechanisms are given in Table 1. Further examples are given in Competitive inhibition, Noncompetitive Inhibition, Product Inhibition, Substrate Inhibition, and Uncompetitive inhibition.

Table 1. Dead-end Inhibition Patterns for Bi–Bi Reaction Mechanisms[a]

Mechanism	Inhibitor Combines with	Variable Substrate	
		A	*B*
Ordered	E	C	NC
	EA	UC	C
	EQ	UC	UC
	EA + EQ	UC	NC
Equilibrium-ordered	E	C	C
	EA	UC	C
Rapid equilibrium,	E + EB	C	NC
random	E + EA	NC	C
Ping-pong	E	C	UC
	F	UC	C
	E + F	NC	NC

[a] The mechanisms are illustrated under **Kinetic mechanisms**. C = linear competitive inhibition. NC = linear noncompetitive inhibition. UC = linear uncompetitive inhibition.

Bibliography

1. W. W. Cleland (1963) Biochim. Biophys. Acta **67**, 188–196.

Deamidation

Deamidation is the reverse reaction of amidation (see Carboxyl Groups) and involves release of an amine from an amide. Deamidation occurs spontaneously in proteins at asparagine and glutamine residues, which causes heterogeneity, instability, and sometimes defects in the function of the proteins.

Deamidation in proteins occurs enzymatically or chemically. Enzymes that participate in deamidating of proteins are transglutaminase and peptidoglutaminase. An amide bond in an asparagine or glutamine residue is relatively labile, especially in acidic media, and is easily hydrolyzed chemically. The rate of deamidation is sensitive to the environment of the amide. Exposed amides are more readily deamidated than those buried in the interior of a protein. Thus, denatured proteins often have high potential for deamidation.

The Asn-Gly sequence is especially notorious for rapid deamidation. The reaction shown below proceeds readily in this sequence. Additional reactions such as **racemization**, transpeptidation, and cleavage of peptide bonds take place during this reaction. These reactions also occur with the Asp-Gly sequence and pivotal components of protein deterioration.

The rates of deamidation vary with different peptides. The **half-times** for deamidation of various asparagine residues under the same conditions range from 3.3 to 277 days. Deamidation causes conformational destabilization of proteins and accelerates their degradation. Thus the deamidation of Asn or Gln residues has been regarded as a timer of protein turnover (1).

Asparaginase hydrolyzes asparagine to aspartic acid (deamidation). Because asparagine in the blood is an essential nutrient for the growth of malignant white cells, the intravenous administration of asparaginase suppresses the growth of some types of animal and human leukemias.

Bibliography

1. A.B. Robinson, J.H. McKerrow, and P. Cary (1970) Proc. Natl. Acad. Sci. USA **665**, 753–757.

Suggestion for Further Reading

2. H.T. Wright (1991) Nonenzymatic deamidation of asparagine and glutamine residues in proteins. Crit. Rev. Biochem. Mol. Biol. **26**, 1–52.

Decapentaplegic

The *decapentaplegic* (*dpp*) gene plays a key role in patterning both embryonic and adult structures in the fruitfly *Drosophila*. The name of the **locus** underscores the multiple requirements for *dpp* activity during development and refers to the wide range of defects caused by mutations in the **gene** (*decapentaplegic* = 15 defects) (1). *dpp* is one of the few haplo-insufficient loci in *Drosophila*; consequently, even a 50% reduction in *dpp* activity leads to embryonic lethality. Less severe alleles of *dpp* are viable but result in adults that have defects in structures derived from one or more imaginal discs. The *dpp* gene encodes a protein that is **homologous** to secreted growth factors of the **transforming growth factor**-b (TGF-b) superfamily. Ligands that belong to this group of signaling molecules have been identified in animals across the phylogenetic spectrum and are involved in cellular and developmental processes ranging from regulation of the cell cycle and the extracellular matrix, to establishment of embryonic pattern and aging. Genetic and molecular studies of *dpp* and the genes involved in *dpp* signal transduction have proven to be of broad general interest, because the basic mechanisms involved in generating and receiving TGF-b signals are evolutionarily conserved.

1. Molecular Features

The *dpp* gene spans ~55 kb of DNA, the bulk of which consists of a large array of *cis*-regulatory elements (2). *dpp* messenger RNA is expressed in a complex spatial and temporal pattern that reflects the multiple roles the ligand plays during development. Three major cis-acting domains regulate transcription of the gene: an upstream *dpp*-shv region required for expression in the embryonic gut and pupal wing, a central *dpp*-Hin region that directs embryonic expression, and a downstream *dpp*-disk region that regulates transcription in imaginal discs (2). These dispersed regulatory elements contribute to the genetic complexity of the locus and mediate *dpp* transcription in response to inputs from a variety of signaling pathways. For example, *dpp* expression in the blastoderm stage embryo is regulated by **Dorsal**, a transcription factor homologous to mammalian NFkB. Later in embryogenesis, *dpp* transcription in the dorsal-most cells of the germband is controlled by genes acting in the Jun kinase signaling pathway, while expression of *dpp* in the midgut is dependent on multiple factors, including **homeobox** DNA-binding proteins, the growth factor Wingless, and Dpp itself. During imaginal disc development, localized expression of *dpp* in the wing and leg discs is regulated by the ***hedgehog*** and ***wingless*** genes.

The *dpp* locus gives rise to three major and two minor transcripts through the use of alternative **promoters** that are utilized at different stages of development (2). While the mRNAs have unique 5′-untranslated sequences, they share common second and third exons that contain an open reading frame coding for a single 588-amino-acid-residue protein (see Cell Cycle and Extracellular Matrix). Dpp is most closely related to the vertebrate bone morphogenetic proteins BMP-2 and BMP-4, and it shares ~75% identity with these proteins in the carboxy-terminal region that constitutes the mature ligand **domain**. While the vertebrate BMPs were first identified by their ability to induce ectopic bone, they are now known to have important roles in embryonic development in a number of organisms, including frogs, mice, and humans. Dpp and BMP-4 can substitute for one another functionally, because a human BMP-4 transgene can rescue patterning defects in a *Drosophila* embryo lacking Dpp (3). Conversely, the fly protein can induce the formation of ectopic bone when injected subcutaneously into rats. Like other ligands belonging to the TGF-b superfamily, Dpp is processed and secreted as a **disulfide**-linked dimer of ~30kDa.

2. Dpp Signal Transduction

Dpp acts as a secreted ligand to influence the developmental fate of cells that receive the signal. Genes involved in Dpp signal transduction have been primarily identified using two strategies. Some genes have been recovered in genetic screens to isolate enhancers of weak *dpp* **alleles**, while others have been isolated in low stringency **hybridization** screens, based on their homology to TGF-b signaling components identified in other organisms.

According to the current paradigm for BMP signaling, the ligand binds a heteromeric complex of two structurally related transmembrane **serine-threonine kinases**, called the type I and type II receptors (4, 5). Formation of the ligand–receptor complex allows the type II kinase to **phosphorylate** and activate the type I receptor. A type II receptor, Punt, as well as two type I receptors, Thick veins (Tkv) and Saxophone (Sax), have been implicated in Dpp signaling. Although the role of Punt and Tkv as receptors for Dpp is well established, it appears that Sax may primarily mediate the response to other BMP-related ligands in Drosophila. Activation of Tkv results in the direct phosphorylation of a cytoplasmic protein encoded by *mothers against dpp* (*mad*). This modification triggers **Mad** to form a complex with Medea (a structurally related protein), and it enables their translocation from the cytoplasm into the nucleus. Mad and Medea contain DNA-binding domains and are thought to regulate the expression of downstream target genes in association with other transcription factors (4, 6). The Mad family of proteins is evolutionarily conserved. The human homologue of Medea (DPC4) has been identified as a **tumor- suppressor** gene, a result that appears logical in light of the known antiproliferative effects of TGF-b.

3. Biological Role of Dpp

Dpp plays an important role in the specification of cell fate and morphogenesis in a number of tissues (1). Mutations in *dpp* that interfere with production of an active ligand affect all developmental events regulated by the gene, while mutations that disrupt specific enhancer elements affect *dpp* function in a tissue- or stage-specific manner. Among the processes that require *dpp* signaling are: oogenesis; establishment of dorsal–ventral pattern during embryogenesis;

morphogenetic movements of dorsal closure; subdivision of the mesoderm along the dorsal–ventral axis; specification of the visceral mesoderm and endoderm in the embryonic gut; development of the heart, gastric cecae, salivary glands, and the trachea; and growth and patterning of imaginal discs.

The ability of Dpp to trigger distinct responses in a single field of cells has generated a great deal of interest in understanding the mechanisms underlying *dpp* function. Dpp has been shown to specify cell fate in a concentration-dependent manner; that is cells respond to different thresholds of Dpp by following distinct pathways of differentiation. A critical issue that arises is how gradients of *dpp* activity are established, and how such gradients are interpreted. Based on recent studies, two alternative mechanisms have evolved: one is based on diffusion of Dpp from its site of synthesis to generate a protein concentration gradient, and the second involves an inhibitor that diffuses into the domain where *dpp* is expressed and interferes with Dpp signaling in a graded manner. This results in a gradient of ligand activity, rather than concentration. Both types of gradients are discussed further below.

Adult structures in the fruitfly arise from imaginal discs, small groups of epithelial cells that are set aside during embryogenesis. These discs grow and are patterned during the larval and pupal stages in response to different signals. In the wing imaginal disc, Dpp acts as a long-range morphogen to specify cell fate along the anterior–posterior axis. *dpp* is expressed in a narrow domain of cells at the anterior–posterior compartment boundary, from where it diffuses to generate a gradient of protein in the surrounding tissue. Cells up to 20 cell diameters away respond to different threshold concentrations of Dpp by activating the transcription of target genes like *spalt* and *optomotor blind* (7, 8). Expression of *spalt* occurs close to the source of *dpp* protein, while *optomotor blind* expression overlaps with, and extends further than, *spalt* expression. The nested domains of Dpp target gene expression further subdivide the wing disc into distinct regions that are specified by the combination of genes expressed.

During early development, a gradient of Dpp signaling is required to establish cell fates within the dorsal half of the embryo. Peak levels of Dpp signaling specify the dorsal-most amnioserosa tissue, while lower levels are required to specify the dorsal ectoderm (9, 10). Reduction in the level of Dpp signaling results in progressive loss of dorsal structures, while increasing concentrations of Dpp can induce dorsal cell fates. Since *dpp* mRNA is expressed uniformly in all dorsal cells, it is generally believed that Dpp activity, rather than its concentration, is graded. A number of extracellular proteins are involved in generating a gradient of Dpp signaling in the embryo. A second BMP ligand, Screw, acts synergistically with Dpp to enhance signaling in the dorsal-most cells. The activity of these ligands is antagonized by a secreted factor, Short gastrulation (Sog), that can prevent ligand binding to the receptor. The inhibitor Sog is expressed in ventral cells and diffuses dorsally to generate a ligand gradient of the opposite polarity. In addition, a metalloproteinase, Tolloid (Tld), promotes signaling in dorsal cells by cleaving Sog and releasing the ligand. Thus modulation of ligand activity at multiple levels contributes to establishment of a gradient of BMP signaling in the embryo (11-14).

Similar antagonistic interactions involving homologous proteins are involved in patterning the dorsal–ventral axis in vertebrate embryos. In *Xenopus*, BMP-4 promotes ventral development, while a homologue of Sog (Chordin) promotes dorsal cell fates. Recently an amphibian homologue of Tld (Xolloid) has been shown to cleave Chordin (12). These and other studies suggest that the dorsal–ventral axes in *Drosophila* and vertebrates are specified by a similar mechanism, although they are inverted relative to one another. The extensive parallels between TGF-b/BMP signaling in vertebrates and invertebrates allow one to extend the insights gained from studying Dpp signaling in *Drosophila* to other organisms, including humans.

Bibliography

1. F. A. Spencer, F. M. Hoffman, and W. M. Gelbart (1982) Decapentaplegic: a gene complex affecting morphogenesis in *Drosophila melanogaster*. Cell **28**, 451–461.
2. R. D. St. Johnston, F. M. Hoffman, R. K. Blackman, D. Segal, R. Grimaila, R. W. Padgett, H.

A. Irick, and W. M. Gelbart (1990) The molecular organization of the *decapentaplegic* gene in *Drosophila melanogaster*. Genes Dev. **4**, 1114–1127.

3. R. W. Padgett, J. M. Wozney, and W. M. Gelbart (1993) Human BMP sequences can confer normal dorsal–ventral patterning in the *Drosophila* embryo. Proc. Natl. Acad. Sci. USA **90**, 2905–2909.
4. C.-H. Heldin, K. Miyazono, and P. ten Dijke (1997) TGF- signalling from cell membrane to nucleus through SMAD proteins. Nature **390**, 465–471.
5. J. Massague (1996) TGF- signaling: receptors, transducers, and Mad proteins. Cell **85**, 947–950.
6. K. Arora, H. Dai, S. G. Kazuko, J. Jamal, M. B. O"Connor, A. Letsou, and R. Warrior (1995) The *Drosophila schnurri* gene acts in the Dpp/TGF- signaling pathway and encodes a transcription factor homologous to the human MBP family. Cell **81**, 781–790.
7. T. Lecuit, W. J. Brook, M. Ng, M. Calleja, H. Sun, and S. M. Cohen (1996) Two distinct mechanisms for long-range patterning by Decapentaplegic in the *Drosophila* wing. Nature **381**, 1387–1393.
8. D. Nellen, R. Burke, G. Struhl, and K. Basler (1996) Direct and long-range action of a DPP morphogen gradient. Cell **85**, 357–368.
9. E. L. Ferguson and K. V. Anderson (1992) Decapentaplegic acts as a morphogen to organize dorsal–ventral pattern in the *Drosophila* embryo. Cell **71**, 451–461.
10. K. A. Wharton, R. P. Ray, and W. M. Gelbart (1993) An activity gradient of *decapentaplegic* is necessary for the specification of dorsal pattern elements in the *Drosophila* embryo. Development **117**, 807–22.
11. G. Marqués, M. Musacchio, M. J. Shimell, K. Wunnenberg-Stapleton, K. W. Cho, and M. B. O"Connor (1997) Production of a DPP activity gradient in the early *Drosophila* embryo through the opposing actions of the SOG and TLD proteins. Cell **91**, 417–426.
12. S. Piccolo, E. Agius, B. Lu, S. Goodman, L. Dale, and E. M. De Robertis (1997) Cleavage of Chordin by Xolloid metalloprotease suggests a role for proteolytic processing in the regulation of Spemann organizer activity. Cell **91**, 407–416.
13. J. L. Neul and E. L. Ferguson (1998) Spatially restricted activation of the SAX receptor by SCW modulates DPP/TKV signaling in Drosophila dorsal-ventral patterning. Cell **95**, 483–494.
14. M. Nguyen, S. Park, G. Marqués, and K. Arora (1998) Interpretation of a BMP activity gradient in *Drosophila* embryos depends on synergistic signaling by two type I receptors, SAX and TKV. Cell **95**, 495–506.

Suggestions for Further Reading

15. FlybaseConsortium (1998) FlyBase: a Drosophila database. Nucleic Acids Res. **26**, 85–88. (http://flybase.bio.indiana.edu/)
16. W. M. Gelbart (1989) The decapentaplegic gene: a TGF- homolog controlling pattern formation in Drosophila. Development **107**, 65–74.
17. P. A. Lawrence and G. Struhl (1996) Morphogens, compartments, and pattern: lessons from Drosophila? Cell **85**, 951–961.

Degeneracy of the Genetic Code

The genetic code for translation of the gene sequence in **protein biosynthesis** is degenerate—there is more than one triplet **codon** for most amino acids. For example, tyrosine is encoded by UAU and

UAC, and arginine is encoded by CGU, CGC, CGA, CGG, AGA, and AGG. Two codons that share the same first two nucleotides encode the same amino acid if the third nucleotide is either C or U, and they often do if the third nucleotide is A or G. Alternate synonymous codons are not used randomly. The GC content of the DNA, especially of bacteria, varies widely in different species, and there is a corresponding difference in **codon usage**. In bacteria and the **yeast** *Saccharomyces cerevisiae*, and even to some extent in *Drosophila* (except for the histone genes), the most frequently used codons are those that are decoded by abundant transfer RNA, and they are strongly preferred in genes expressed at high levels. In genes expressed at low levels, codon usage is more uniform (1-3). In bacteria with extreme DNA base composition biases (for example, the *Mycoplasma capricolum* genome is 25% G + C, whereas that of *Micrococcus luteus* is 74% G + C), not surprisingly, all genes have similar codon usage using those codons with the corresponding G + C content (4). Codon usage also varies among genes from the same genome. This is true of mammalian genomes but also, to some extent, in *S. cerevisiae*. Regions of differing G + C content were initially recognized in mammalian chromosomes and termed isochores. Overlying differences in codon usage between individual genes is the apparent higher density of genes in GC-rich isochores, and this may influence codon usage. As genome sequencing projects proceed, this relationship is expected to be clarified.

Bibliography
1. T. Ikemura (1981) J. Mol. Biol. **151**, 389–409.
2. M. Gouy and C. Gautier (1982) Nucl. Acids Res. **10**, 7055–7074.
3. H. Dong, L. Nilsson, and C. G. Kurland (1996) J. Mol. Biol. **260**, 649–663.
4. T. Ohama, A. Muto, and S. Osawa (1990) Nucl. Acids Res. **18**, 1565–1569.

Suggestion for Further Reading
5. P. M. Sharp and G. Matassi (1994) Codon usage and genome evolution. Curr. Opinion Genet. Develop. **4**, 851–860.

Dehydrogenases

Pyridine nucleotide-linked dehydrogenases are enzymes that catalyze oxidation–reduction reactions involving a pyridine nucleotide and the transfer of a hydride (one proton and two electrons) from or to a second substrate molecule. Most dehydrogenase reactions are readily reversible, but some are not, and the enzymes responsible for essentially irreversible reactions are referred to as *reductases*; there are exceptions, however, such as *formate dehydrogenase* . The oxidized forms of the pyridine nucleotides are **NAD** (nicotinamide adenine dinucleotide) and **NADP**. The latter nucleotide has an additional phosphoryl group attached at the 2′-position of the ribose that is part of the adenosyl moiety (Fig. 1). The general form of a dehydrogenase reaction can be illustrated by reference to the reaction catalyzed by lactate dehydrogenase (Eq. 1):

$$\text{Lactate} + NAD \rightleftharpoons \text{pyruvate} + \text{NADH} + H^+ \qquad (1)$$

Not all dehydrogenase reactions are as simple as that described by Equation 1. The oxidation reactions catalyzed by *isocitrate* and *glutamate* dehydrogenases give rise to the release of CO_2 and NH_3, respectively. NAD and NADP are written frequently as NAD^+ and $NADP^+$ even though the overall charge on the molecule is negative in the neutral pH region; the plus refers to the charge on the nitrogen atom of the nicotinamide moiety of the oxidized forms of the pyridine nucleotides.

Dehydrogenases usually show a distinct preference for one or the other of the two pyridine nucleotides; examples are given in Table 1, and a more extensive list is available (1). The binding to the enzyme of the nonpreferred nucleotide is generally weaker, and the maximum velocity is usually lower.

Figure 1. Structure of NADH / NADPH, showing the two prochiral hydrogen atoms at the 4-position of the nicotinamide moiety. R at the 2′-position of the ribose moiety represents either a hydrogen atom (NADH) or phosphoryl group (NADPH).

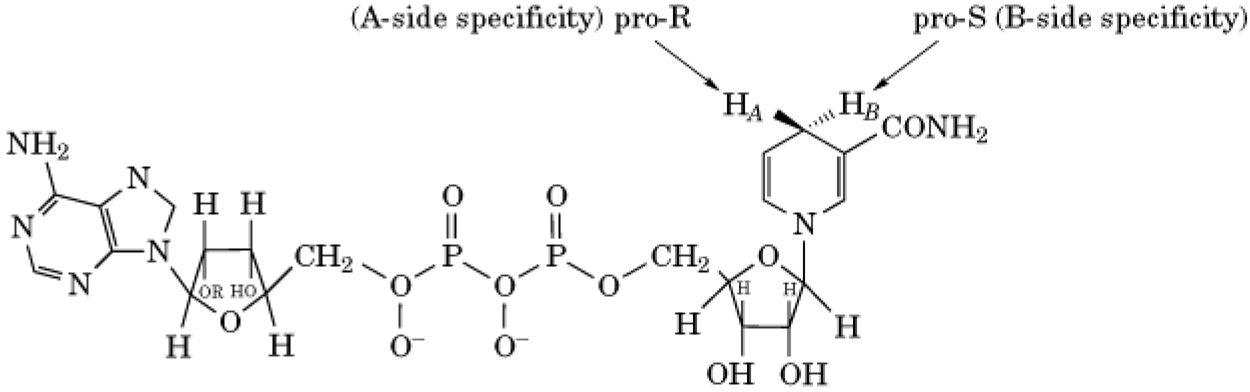

Table 1. Pyridine Nucleotide Specificity of Some Dehydrogenases

Dehydrogenase/Reductase	Pyridine Nucleotide	Stereospecificity
Alcohol	NAD	A
Glyceraldehyde-3-phosphate	NAD	B
3-Phosphoglycerate	NAD	B
Lactate	NAD	A
Glutamate	NAD/NADP	B
Glutathione	NAD/NADP	B
Dihydrofolate	NADP	A
Glucose-6-phosphate	NADP	B
Isocitrate	NADP	A

In dehydrogenase reactions (Eq. 1), the hydride is transferred to the 4-position of the nicotinamide ring of NAD or NADP (Fig. 1). The two hydrogen atoms at this position in NADH and NADPH are chemically equivalent, and the tetrahedral carbon atom is not **chiral**. However, the two hydrogen atoms at the 4-position are prochiral. The binding of reduced pyridine nucleotides to dehydrogenases is such that hydride transfer involves only one of the two hydrogen atoms. Thus, the enzymes exhibit regiospecificity, and hydride transfer occurs either from the pro-R hydrogen (A-side specificity) or from the pro-S hydrogen (B-side specificity). Examples of dehydrogenases that fall into each of these two classes are given in Table 1. Attempts have been made to explain why some dehydrogenases are A-side and others are B-side, but no convincing explanation has been forthcoming (2).

The side-specificity of dehydrogenases allows the preparation of reduced pyridine nucleotides with a deuterium (D) or tritium (T) atom replacing a hydrogen atom in either the pro-R or pro-S positions (see Hydrogen Isotopes). Extensive use has been made of deutero- and tritio-pyridine nucleotides to gain information about enzymic catalysis (3). The cleavage of a bond can be expected to be two to eight times slower than with a bond. With chemical reactions, the full isotope effect difference in rates is usually observed, because the bond-breaking step is rate-limiting. But with enzyme-catalyzed reactions, steps other than the catalytic one can be at least partly rate-limiting. This results in the observed isotope effect, with NADD or NADPD being smaller than the absolute value for the bond-breaking step. Indications as to where the rate-limiting steps lie for a particular dehydrogenase reaction come from the use of initial velocity studies to determine the apparent first-order rate constants k and the maximum velocities V with the protio- and deutero-substrates. The observed isotope effects are then calculated from the ratio of the values for $(V/K)_H$ and $(V/K)_D$, expressed as $^D(V/K)$ and the ratio of the values for V_H and V_D, expressed as ^DV. The values for these ratios usually range from 1.0 to 3.5. Low values for $^D(V/K)$ can result from the stickiness of substrates. Values for ^DV will be low whenever product release is rate-limiting (3). The tritiated forms, NADT and NADPT, can be used for determinations of $^T(V/K)$, but not from initial velocity studies, as the tritium is only a trace label. For this same reason, it is not possible to obtain values for ^TV. The value for $^T(V/K)$ will be higher than that for $^D(V/K)$ as the bond is stiffer than the bond. As $^Tk = (^Dk)^{1.442}$, the general function $[^Dk - 1]/[^Dk^{1.442} - 1]$ can be used to determine the intrinsic isotope effect for a dehydrogenase reaction (4). It is this value that gives insights into the chemical mechanism of the reaction and the nature of the transition state.

The pyridine nucleotides that function as effective substrates for most dehydrogenases have a nicotinamide–ribose linkage (Fig. 1) with a b-anomeric configuration and are referred to, for example, as b-NAD. These pyridine nucleotides also occur with an a-anomeric configuration and are found in tissue extracts, as well as commercial preparations. Both a-NADH and b-NADH undergo thermal **epimerization** reactions to produce an equilibrium mixture with 10% of the a form (5). There are no examples of a dehydrogenase that specifically uses a-NADH or a-NADPH, although alcohol dehydrogenase and lactate dehydrogenases utilize a-NADH with maximum velocities some three to four orders of magnitude lower than with b-NADH. The same side-specificity is observed with both anomers of NADH (5). By contrast, a-NADPH is a relatively good substrate for the dihydrofolate reductase that is encoded by an R-plasmid (6). The K_m value of 17 µM is comparable to the value of 4 µM for b-NADPH. The maximum velocity of the reaction with a-NADPH is 70% of that with b-NADPH. It has been proposed that those dehydrogenases which show activity with both the a- and b-anomers must have sufficient conformational freedom to permit specific orientation of the dihydronicotinamide ring for the reduction of other substrates.

Bibliography

1. G. Popjak (1970) The Enzymes **2**, 115–215.
2. N. J. Oppenheimer (1984) J. Am. Chem. Soc. **106**, 3032–3033.
3. W. W. Cleland (1982) CRC Crit. Rev. Biochem. **13**, 385–428.
4. D. B. Northrop (1975) Biochemistry **14**, 2644–2651.
5. N. J. Oppenheimer and N. O. Kaplan (1975) Arch. Biochem. Biophys. **166**, 526–535.
6. S. L. Smith and J. J. Burchall (1983) Proc. Natl. Acad. Sci. **80**, 4619–4623.

Denaturants Stabilizers

The structures of globular proteins (and other biological macromolecules) are not very stable (see Protein Stability). Therefore, it is often necessary to increase the stability by addition of inert compounds in order to maintain a biochemical activity or to preserve an assembled structure, such as various **organelles** or multisubunit enzymes. The stabilizing compounds must characteristically be added at high concentration (>1 M), since their interactions with proteins are weak (see Stabilization And Destabilization By Co-Solvents). Strongly interacting molecules, although effective in particular cases, generally tend to alter some properties of the protein molecules (see Binding).

The most frequently used stabilizing agents are 1 *M* sucrose, other sugars (trehalose, glucose), 3 to 4 *M* glycerol, neutral amino acids at 1 *M* levels (glycine, proline, alanine), methyl amines (betaine, sarcosine, trimethyl amine N oxide), polyols (sorbitol, inositol, mannitol), some salts [Na_2SO_4, $(NH_4)_2SO_4$] (see Sulfate Salts) (1). All have the property of being preferentially excluded from proteins, which imparts stabilization and precludes excessive surface contacts that could alter the local protein structure (see Preferential Hydration). Most stabilizers used in the laboratory are also cryoprotectants and osmolytes, in that they are chosen by nature to maintain high osmotic pressure in, eg, amphibians, and to protect against freezing (2).

Conversely, a number of compounds are used to denature proteins when so desired. These again act at high concentration and are characterized by their preferential binding to proteins. The most common denaturants are urea, **guanidinium** chloride, sodium dodecyl sulfate (**SDS**), trichloroacetic acid, $CaCl_2$, LiBr, and other salts on the denaturant side of the Hofmeister series (3). (See Guanidinium Salts, Hofmeister Series.)

Bibliography

1. S. N. Timasheff (1992) In *Stability of Protein Pharmaceuticals* (T. J. Ahern and M. C. Manning, eds.), Plenum, New York, pp. 265, 286.
2. P. H. Yancey, M. E. Clark, S. C. Hand, R. D. Bowlus, and G. N. Somero (1982) Science **217**, 1214–1222.
3. P. H. von Hippel and T. Schleich (1969) In *Structure and Stability of Biological Macromolecules* (S. N. Timasheff and G. D. Fasman, eds.), Marcel Dekker, New York, Chap. "6".

Denaturation Mapping

Denaturation of the **double-helical** structure of **DNA** is an essential first step in many of the most common methods for investigating **chromosomal** structure. The method relies on the unique order of bases in DNA and the capacity of two separate complementary strands to recognize each other through the process of **hybridization**. Denaturation mapping can be done using either sections of tissue or chromosomal preparations. The sample slide to be analyzed is heated to denature the double helix into two separate DNA strands. Rapid cooling of the preparation in the presence of formaldehyde keeps the DNA strands separated. The cloned gene or sequence of interest is prepared as a DNA probe in single-stranded form with a label attached. This label could be either a source of radioactivity, or an epitope recognized by an antibody (often using streptavidin as an antigen). A change in salt concentration and temperature facilitates hybridization between complementary DNA strands. The probe and chromosomal sequences compete with each other, but a sufficient excess of probe can be added so that some of the probe hybridizes to the specific site on a chromosome.

When initially developed by Pardue and Gall in 1970, the probe was labeled with the radioactive hydrogen isotope tritium (1). More recently the use of antibodies has become popular (2, 3). The antibodies are usually linked to an enzyme that acts on an appropriate substrate to generate a visible signal. This could either be a colored precipitate on the chromosome, that is detectable under a light microscope, or the antibody could be linked to a fluorochrome that is visualized by a **fluorescence** microscope. This latter technique is known as fluorescent in situ hybridization (FISH). Now modifications of this technique allow analysis under the electron microscope for increased resolution or in the **confocal microscope** that builds up three-dimensional images by optical sectioning.

A number of specialized methods have acquired their own acronyms. These include fluorescence in situ hybridization (FISH) as described; genomic in situ hybridization (GISH); whole chromosome painting (WCP); and primed in situ labeling (PRINS). GISH is a method for detecting species–specific chromosomes when the entire genomic DNA is labeled and hybridized to whole chromosomal spreads. It is useful in analyzing of cell fusion hybrids and in evolutionary studies. In WCP, DNA from a single chromosome is labeled and prehybridized with repetitive DNA to stop cross-reaction with other chromosomes from the same organism. WCP probes are available commercially for all 22 autosomes and the sex chromosomes in humans. In PRINS, the polymerase chain reaction (**PCR**) is used to label sequences on the actual chromosome or tissue. There are many other adaptations of these important methodologies.

Bibliography

1. M. L. Pardue and J. Gall (1970) Science **168**, 1356–1358.
2. J. Leary, D. Brigati, and D. C. Ward (1983) Proc. Natl. Acad. Sci. USA **80**, 4045–4049.
3. P. Lichter et al. (1990) Science **247**, 64–68.

Denaturation, Nucleic Acids

Disruption of the secondary and tertiary structures of nucleic acid polymers is promoted by exposure to extreme conditions. Most commonly, nucleic acid denaturation refers to the formation of two free single-stranded nucleic acids from a duplex. Denaturation (loss of native structure) of the polymer duplex can be promoted by a variety of conditions or agents, including heat, chemical denaturants, and extremes of pH. The stability of the duplex varies by region, and the base pair composition (% GC) determines the stability of a given region (Fig. 1). Under most conditions, regions of the duplex that are composed predominantly of AT (for DNA) or AU (for RNA) base pairs are less stable than GC-rich regions. As the conditions shift toward those favoring single-stranded polymers, the path from fully base-paired duplex to fully denatured single strands passes through intermediate states, where first the AT/AU rich regions "melt," forming internal loops, then mixed sequence regions, then finally the GC-rich regions. As the last GC-rich regions "melt," the strands separate.

Figure 1. Mechanism of melting of polymeric DNA.

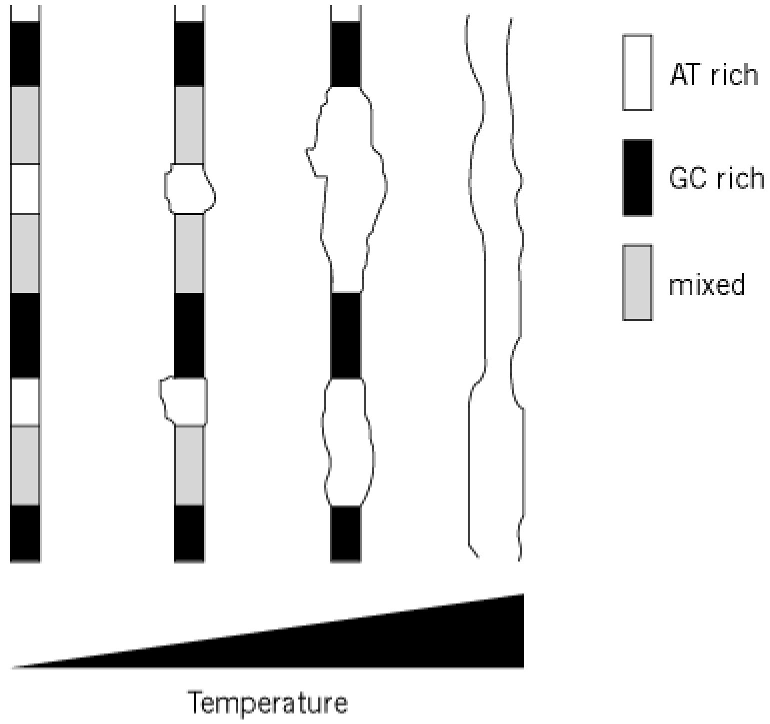

1. Thermal Denaturation

Because it is easy to manipulate, heat is frequently employed to denature nucleic acids. The temperature can be changed rapidly and reversibly in the small volumes typically employed in nucleic acid studies. Heating to temperatures above the T_m and rapid cooling can trap the strands of a duplex in the separated state. The melting transitions of mixed-sequence nucleic acid polymer duplexes are quite broad. To ensure strand separation, the duplex must be exposed to temperatures significantly above T_m. Failure to separate the strands results in a prenucleated duplex that can readily reanneal. This method does not work for oligonucleotide duplexes for which thermal denaturation is readily reversible.

Equilibrium thermal denaturation curves are used to study duplex (or other structure) thermodynamic properties. The extent of the thermally induced denaturation transition as a function of temperature is monitored either by some optical property, usually ultraviolet absorbance, or via heat capacity, as in differential scanning calorimetry. “Melting curves,” where the observed parameter is plotted as a function of temperature, contain quantitative information about the stability of the duplex and the thermodynamic origins of that stability (1). Optically monitored thermal denaturation curves are analyzed using the van't Hoff model and can readily provide thermodynamic (DH°, DS°, and DG°) and extrathermodynamic data (T_m). Not all melting transitions are consistent with the assumptions underlying the models used to extract thermodynamic data from equilibrium melting curves. Differential scanning calorimetry provides a direct model-independent means of generating thermodynamic data on thermally induced denaturation.

2. Chemical Denaturation

Chemical denaturants reduce the thermal stability of nucleic acid duplexes. Some denaturants, such as formaldehyde, form covalent bonds to the bases. Others act by altering the noncovalent interactions of the solvent with the nucleotide bases. A wide variety of reagents can induce denaturation of DNA (2). The isolated bases that, when attached to the backbone, comprise a nucleic acid are rather insoluble in aqueous solution. The **hydrophobic** character of the bases, coupled with the hydrophilic character of the sugar–phosphate backbone, push the single-strand–duplex equilibrium toward duplex formation. The stacked configuration of the bases in a duplex is favored over the unstacked bases of the single strand (see Base Pairs). There are conditions under which the bases in a single strand will stack, but the duplex also competes successfully against these structures. Inclusion of a **denaturant** solubilizes the bases, thereby reducing the energetic cost of losing the stacking interactions of the duplex. As a consequence, the thermal stability of the duplex is reduced.

3. pH-Dependent Denaturation

The stability of nucleic acid duplexes is rather insensitive to changes in hydrogen ion concentration in the vicinity of neutral pH. This is because none of the functional groups present in typical nucleic acids titrate in this region. If the pH is decreased to a value below 5 or increased to a value above 9, significant destabilization of the nucleic acid duplex is observed. Because pH is simple to manipulate, high pH frequently is used to denature nucleic acid duplexes. Care must be taken to avoid degradation of the polymers under high pH conditions, which can promote depurination and strand breakage, particularly at high temperature. The presence of mismatches or modified bases may alter the pH sensitivity of the duplex because often these anomalous structures exhibit protonation equilibria in the vicinity of neutral pH. Certain nonnatural backbone structures alter radically the pH dependence of duplex stability. Low pH stabilizes cytosine-containing pyrimidine-purine-pyrimidine triple helices. Therefore, when sequence requirements for **triple helix** formation are met, care must be taken to adjust pH so as to avoid unintended triple helix formation.

Bibliography

1. L. A. Marky and K. J. Breslauer (1987) Biopolymers **26**, 1601.
2. L. Levine, J. A. Gordon, and W. P. Jenks (1963) Biochemistry **2**, 168.

Suggestion for Further Reading

3. V. A. Bloomfield, D. M. Crothers, and I. Tinoco (1974) *Physical Chemistry of Nucleic Acids*, Harper & Row, New York.

Denaturation, Protein

The term protein denaturation usually refers to the process during which the specific properties of a native, functionally active protein disappear under some nonphysiological conditions without chemical modification of the molecule. Because the functional properties of a protein are provided by the unique disposition of all of its functional groups, the unique, native, three-dimensional protein structure, denaturation of a protein assumes that the native structure is disrupted, and the polypeptide chain partially or completely unfolds, but without any change of the covalent bonds.

The native protein structure is maintained by a delicate balance of various types of interactions between the various protein groups and the surrounding media, which depend on the environmental conditions (see Protein Stability). *In vitro* this balance is usually optimal under conditions close to physiological. Departure from them can result in protein denaturation. Correspondingly, denaturation is usually classified in accordance with the external condition inducing it, for example, by heating (see Thermal denaturation , below), by cooling (Cold denaturation), by pressure (Pressure denaturation), by acids or alkali (pH denaturation), or by **denaturants** such as urea or guanidinium salts, for example, guanidinium chloride (GdmCl) (Denaturant denaturation).

Denaturation can be characterized (1) by the extent to which the native protein structure is disrupted, the completeness of polypeptide chain unfolding (see: Unfolded Proteins); (2) by its reversibility upon restoring conditions optimal for the native state (see Reversibility, below); and (3) by its **cooperativity**. The completeness of disruption of the protein structure depends on the environmental conditions and also on the ability of the given protein to withstand the denaturing action of the environment (see Protein Stability). Studying all these aspects of protein denaturation is important for understanding the mechanism of **protein folding** and stabilization of the native protein structure, in other words, understanding the forces maintaining this structure. It is also important for the practical purpose of designing new proteins and modifying of natural proteins (see Protein Engineering). Correspondingly, this process has been extensively studied for many years using various proteins and their mutant forms, fragments and synthetic models in various solvents and by various experimental techniques. The results of these studies are summarized in numerous reviews (see bibSect). The following discussion assumes that the protein being studied is pure and no covalently modified variants are present in substantial quantity.

1. Reversibility of Denaturation

Under the appropriate conditions, the native state of a protein is usually restored when the denaturing conditions are removed. Thus the change of conformation of a protein upon denaturation, even complete unfolding of the polypeptide chain, in principle, is a reversible process determined by the environmental conditions. The folding of a polypeptide chain into a native conformation is a **thermodynamically** driven process in accordance with the genetic information included in the sequence of amino acid residues of the polypeptide chain (see Self-Assembly. This was realized first by Anson and Mirsky (1, 2), followed by Eisenberg and Schwert (3), and formulated as one of the most fundamental principles of protein science by Anfinsen (4, 5). That is why denaturation is usually reversible, so long as the newly synthesized protein has not been chemically modified *in vivo* (processed) after it has folded (see Post-Translational Modifications). However, some of the groups of proteins that are exposed by denaturation (unfolding), such as thiol groups, are highly reactive and they become covalently modified. Others interact chaotically with each other and with the groups of other molecules to form aggregates. Furthermore, exposure of nonpolar groups upon unfolding decreases the solubility of proteins, thereby enhancing their aggregation. Consequently, the observation of complete reversibility of protein denaturation is not always straightforward, especially for large proteins that have high effective molarities of reactive and nonpolar groups in the unfolded state. Observation of reversibility often requires special conditions: (1) low concentrations of protein to decrease the probability of contacts between the protein molecules; (2) increase of electrostatic repulsions between the protein molecules by the appropriate pH and ionic strength of the solution; (3) exclusion from the solution of all other reactive molecules that might react irreversibly with protein groups (eg, oxygen, compounds containing thiol groups and disulfide bonds, etc.); and (4) the use of co-solutes that increase the solubility of the unfolded proteins (eg, urea or GdmCl). The reversibility of unfolding diminishes at higher temperatures, especially above 70°C, and with prolonged incubation because of secondary temperature-induced chemical changes of protein groups, for example, reshuffling of disulfide bonds and deamidation of Asn and Gln residues (6). Renaturation (refolding) is also delayed by cis-trans isomerization of proline peptide bonds in the unfolded state (7, 8). This is especially pronounced if there are many proline residues and if in the folded state they are in the intrinsically unfavorable *cis* conformation (9). Searching for conditions under which a protein denatures reversibly is important for studying the thermodynamics of formation of protein structure, its energetic basis (see Protein Stability).

2. Cooperativity of Unfolding

The various properties of a protein molecule, observed by different methods upon varying the external conditions, change simultaneously in some cases, but not in others. Changes of different properties of a protein reflect different changes in its structure, so denaturation of protein structure can be either a single- or multistage process. Under denaturing conditions, the protein structure can change either as a whole or in several stages. Various parts of the molecule can be disrupted by different denaturing conditions.

For small globular proteins, whose a molecular mass is less than about 20 kDa, all parameters that are sensitive to structural change usually change almost simultaneously with an increase of denaturing action (Figs. 1 and 2). Therefore, denaturation of these proteins is a single-step process in which the protein undergoes a single transition from the unique native state to the denatured state. Partly folded intermediate states probably occur during unfolding/folding, but they are highly unstable and would be present at equilibrium at only very low levels. Denaturation of such proteins is approximated rather well by a two-state transition that ignores all possible intermediate states. It is assumed that their native structure breaks down and refolds in an all-or-none manner (12, 13). Because proteins consist of many structural elements connected by covalent bonds into a polypeptide chain, this assumes that all the groups (amino acid residues) of small globular proteins change their states simultaneously, that is, cooperatively.

Figure 1. Thermal denaturation of ribonuclease A at pH 2.19 according to Ref. 10; (*f*) intrinsic viscosity, (○) optical rotation at 365 nm, and (△) absorption spectroscopy.

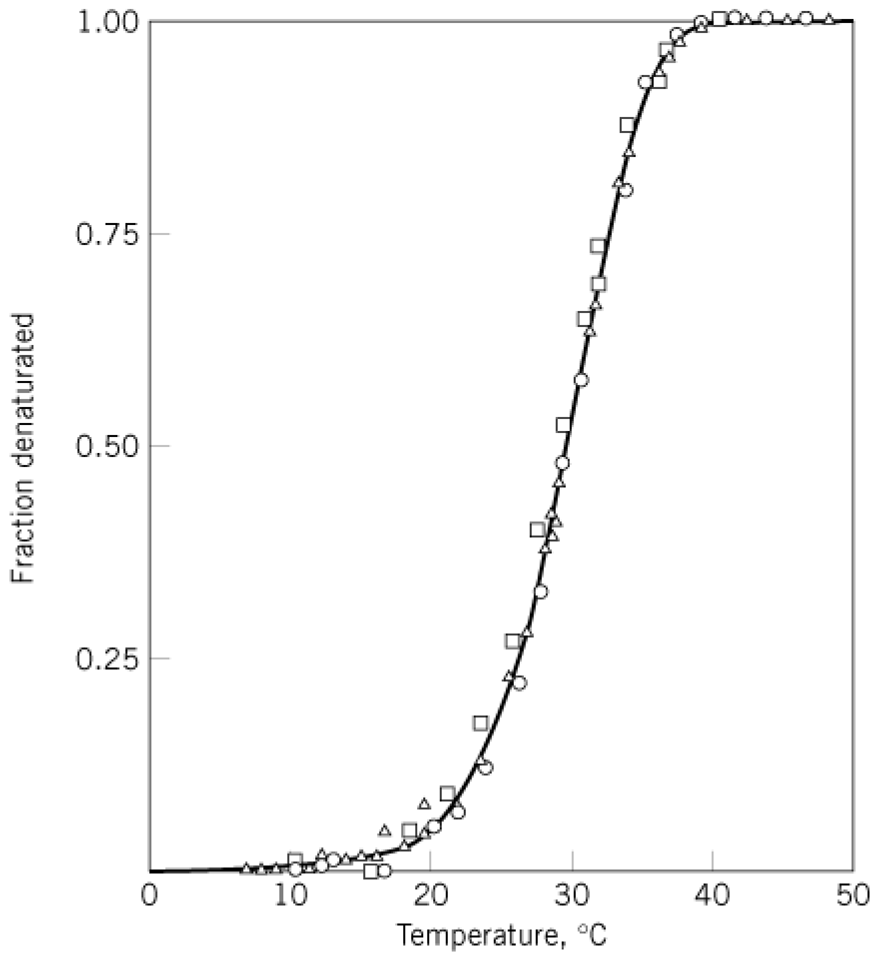

Figure 2. Urea denaturation of **ribonuclease** $\mathbf{T_1}$ according to Thomson et al. (11). (△) circular dichroism ellipticity (CD) at 238 nm; (▽) UV absorbance at 287 nm; (○) optical rotatory dispersion (ORD) at 295 nm; and (*f*) fluorescence at 320 nm.

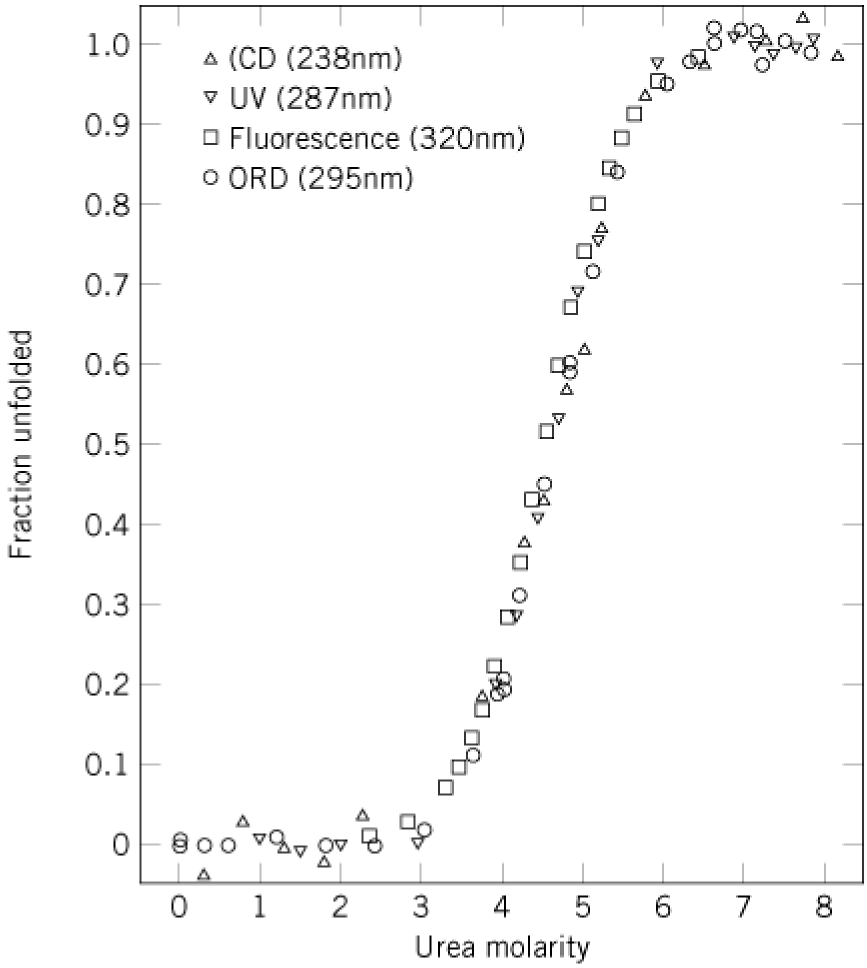

In contrast, multistage denaturation is normal for large proteins. Some smaller fragments of large proteins that separately preserve their native-like structure also denature reversibly and highly cooperatively (14-16). These observations have shown that the structures of large proteins are subdivided into cooperative units, called structural **domains**, which fold and unfold more or less independently ((17-19); for a review see Ref. 20). The stabilities of the different protein domains usually differ. So they unfold under different denaturing conditions, and the denaturation profile of such multidomain proteins is usually very complex (Fig. 3). Conversely, a complex denaturation profile usually means that the protein has a multidomain structure. It follows that the thermodynamic analysis of protein denaturation can provide information on the domain organization of large protein molecules (20-22).

Figure 3. Calorimetric characterization of the thermal unfolding of plasminogen and its proteolytically liberated domains, according to Ref. 16. The thin lines show the deconvolution of the excess heat absorption profiles into individual two-state transitions for the various domains of each of the molecules. The inserts show schematically the domain structures of the protein molecule used; complete plasminogen is at the top.

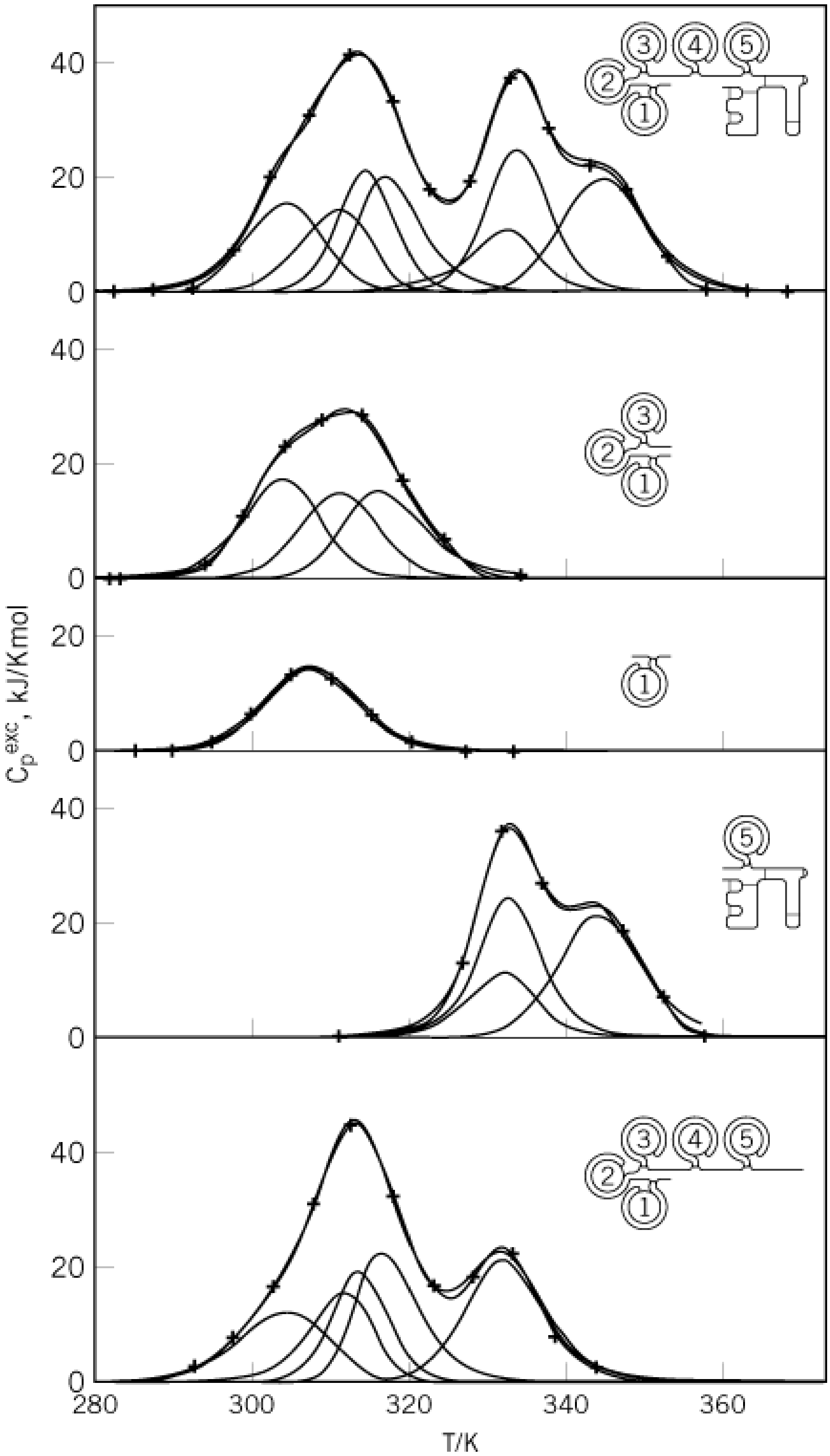

Simultaneity in changes of all properties of a protein upon denaturation is one of the tests for cooperativity of this process and, correspondingly, for the cooperativity of the protein structure. However, if the domains of the protein are similar, they denature under the same denaturing conditions, and all parameters that specify the state of the protein change simultaneously, giving the impression that the protein denatures in a single cooperative process. If such a transition is analyzed assuming that it is a two-state transition, fictitious thermodynamic parameters result that have no real meaning.

A stronger test of the cooperativity of the denaturation process consists of comparing the effective thermodynamic parameters derived from the equilibrium analysis whose real values are measured by direct experimental methods. In thermodynamic analysis of the equilibrium between two states, the effective equilibrium constant K^{eff} can be expressed as:

$$K_{eff} = \frac{Y_x - Y_n}{Y_d - Y_n} = \exp\left(-\frac{\Delta G^{eff}}{RT}\right) \tag{1}$$

where $\boldsymbol{Y}_n$ and $\boldsymbol{Y}_d$ are values of any observed parameters that characterize the pure native and the pure denatured states, respectively, $\boldsymbol{Y}_x$ represents the value of the index under the given conditions, and DG_{eff} is the effective Gibbs **free energy** difference between the two states. By following the dependence of the equilibrium constant on various fundamental intensive external parameters, such as temperature (T), pressure (P), or the activity of given ligand I (a_i), one can find the effective extensive thermodynamic parameters that specify the process, the changes in **enthalpy** DH^{eff}, **volume** DV^{eff}, and the number of bound **ligands** DN^{eff}:

$$\Delta H^{eff} = RT^2 \frac{\partial \ln K^{eff}}{\partial T} \tag{2}$$

$$\Delta V^{eff} = -RT \frac{\partial \ln K^{eff}}{\partial P} \tag{3}$$

$$\Delta N_i^{eff} = \frac{\partial \ln K^{eff}}{\partial a_i} \tag{4}$$

These effective parameters are derived assuming that the observed process represents a two-state transition, so if they correspond to the real values measured by direct experimental methods, this is a strong indication that the observed process indeed represents a two-state transition. The most efficient approach for this type of analysis is temperature-induced changes, particularly when they are observed by the associated heat effects measured by supersensitive scanning micro **calorimetry** (13). Comparing the calorimetrically measured enthalpy of the temperature-induced unfolding of a protein with the effective or van't Hoff enthalpy calculated from the sharpness of transition indicates how close the observed process is to a two-state transition.

More elaborate methods of analyzing of cooperativity, which reveal intermediate stages in the temperature-induced denaturation process consist of computer deconvolution of the calorimetrically measured excess **heat capacity** function of temperature (21, 22) or simulation of this function based on statistical mechanical modeling of the process (23, 24). Using these methods for thermodynamic analysis of the calorimetrically measured heat capacity function of a protein and of its proteolytic fragments corresponding to various domains under different solvent conditions yields quite detailed information about the domain organization of a protein. This is especially valuable for large proteins, the structures of which often cannot be studied by NMR because their large size or by X-ray crystallography methods because to their reluctance to crystallize (for a review, see Ref. 20). This approach has permitted investigating the domain organization of such large proteins as fibrinogen (15), plasminogen (16), fibronectin (25), plasminogen activator (26), recombinant factor XIII (27), and protein C (28) (see Blood Clotting).

NMR is a powerful method for analyzing the cooperativity of unfolding of small proteins and identifying any domains. Using the chemical shifts of individual proton resonances, one can follow the state of individual amino acid residues of a protein and their rate of hydrogen exchange as a function of the environmental conditions. Such analysis showed that small proteins unfold cooperatively (29), but that some of the proteins reveal indications of subdomain organization under some conditions (30-32).

The mechanism of the extreme cooperativity of unfolding/folding of single-domain proteins is still a subject of discussion. Perhaps the most important conclusion, which is most commonly accepted, is that extreme cooperativity is a specific property of heterogeneous polypeptide chains that can fold into a unique compact structure in which all groups are tightly packed that is, it represents a lock and key system. For the theoretical models of cooperativity, see (23, 33-35).

2.1. Denaturant Denaturation

Denaturants are various agents (cosolutes) that lead to denaturation of proteins when they are added to aqueous solutions (Fig. 2). The most commonly used denaturants are urea and **guanidinium** chloride (GdmCl). Most proteins denature in concentrated solutions (eg, 5 to 8 M) of these compounds. Studies of the dependence of protein conformation on the concentration of these denaturants is the simplest and therefore the most popular method for quantitatively evaluating protein stability, the more so because denaturation by denaturants is also the most reversible of the various types of denaturation. Furthermore, the very significant changes in the hydrodynamic and optical properties of proteins in concentrated solutions of these denaturants led to the conclusion that they induce the most complete unfolding of polypeptide chains (see Unfolded Proteins). The denaturant-induced denaturation of small single-domain proteins usually occurs very sharply over a small change in denaturant concentration (Fig. 2), and it usually is regarded as a cooperative, two-state transition. If so, the equilibrium studies of the influence of denaturants on a protein can provide information on the energetics of protein unfolding/folding, that is, the stability of the native protein structure. Using any parameter *Y* sensitive to the protein conformation, the equilibrium constant and the Gibbs free energy of the transition can be estimated by, Eq. (1). Usually, the value of D*G* varies linearly with denaturant concentration [D]:

$$\Delta G = \Delta G^{\circ} - m[D] \qquad (5)$$

and determines the value of D*G* at zero concentration D*G*° of denaturant (36). The parameter *m* is a measure of the dependence of D*G* on the denaturant concentration. It is believed that the value of *m* correlates very strongly with the amount of protein surface exposed to solvent upon unfolding (37).

The main difference between the effects of urea and GdmCl on protein stability is that, although urea is likely to be only a destabilizing agent, GdmCl has a dual role. At high concentrations GdmCl destabilizes the protein native state, but at low concentrations it stabilizes it (38, 39) because, in contrast to urea, GdmCl is a salt. An increase in its concentration increases its activity as a denaturant and also the ionic strength of the solution, which reduces destabilizing electrostatic interactions within proteins. If the GdmCl concentration varies and the ionic strength of the solution is kept constant by adding of neutral salts, the stability of the protein is directly proportional to the concentration of GdmCl over an extended concentration range (40). Then, the stability of the protein can be determined from Eq. (5), and it corresponds well with the estimates of D*G*° determined from calorimetric data (see Protein Stability). This equation is valid, however, only if the denaturant-induced unfolding of the protein is truly a two-state transition. Because this is not evident *a priori*, it needs to be verified.

Notwithstanding the extensive experimental data on the influence of denaturants on the state of proteins, the mechanism of this influence is yet to be understood. It is generally believed that one or both of two mechanisms are responsible for the ability of these compounds to destabilize the native state of proteins. In the first model, these solutes increase the solubility of the nonpolar side chains that form the compact cores of globular proteins (41-43). A sound argument for this hypothesis is the observation that denaturants increase the aqueous solubility of small nonpolar molecules. According to the other model, highly polar denaturants form hydrogen bonds with polar groups of proteins, particularly the peptide groups, and increase the probability of their exposure. These hydrogen bonds would have to be stronger than those formed by water (44). A strong interaction of urea with the polar groups of proteins has been concluded by studies of the influence of these cosolutes on the solubility of model compounds (45). According to calorimetric studies, urea and GdmCl interact with proteins in both the folded and unfolded states and cause a strong heat effect that is proportional to the exposed surface area and depends strongly on temperature (46, 47). It became evident that the denaturing action of urea and GdmCl is caused mainly by the enthalpic binding of these compounds. With increased temperature, the bound denaturants dissociate gradually absorbing heat that results in an apparent heat capacity increase of the protein in the presence of urea and GdmCl. This explains the observed decrease of the intrinsic **viscosity** of the unfolded polypeptide chain with increasing temperature (48). Analyzing calorimetric data by the standard model for multisite **ligand binding** was determined the number of denaturant binding sites and the binding constant (47). Timasheff (49) examined these calorimetric data in terms of preferential binding. He concluded that the weak overall thermodynamic interaction of the denaturants with proteins results from the strong favorable interactions of proteins with denaturants at the exchangeable sites that are compensated for by unfavorable interactions, almost as strong, at loci on the protein surface at which the denaturants cannot displace water. Schellman &Gassner (50) have analyzed calorimetric data for the interactions of urea and GdmCl with proteins based on the solvent-exchange model . According to this model, the free energy and preferential interactions for very weak binding and high concentrations of cosolvent do not depend on the high concentrations of cosolvent, but on its excess occupation over that of the bulk solution. The binding constant *k* and the number of binding sites *n* derived by using this model differ considerably from those derived using the standard binding model, but the values of the binding enthalpy D*H*, and of *nkDH* are rather close.

The specific interaction of urea with polar groups of proteins has been shown by X-ray crystallography using crystals of diketopiperazines (51) and proteins (52). The number of binding sites for urea and GdmCl were determined crystallographically for **ribonuclease A** and dihydrofolate reductase, and they closely correspond with the numbers estimated from calorimetric data by the standard binding model. Furthermore, binding of the denaturant significantly decreases the crystallographic B temperature factor of the protein, that is, the mobility of its native state (53). Each molecule of urea or GdmCl must interact simultaneously with several groups of the protein by forming multiple hydrogen bonds (54). If so, one might expect these denaturants to form even more extensive networks of hydrogen bonds with the groups of the unfolded polypeptide chain, increasing its rigidity and consequently its intrinsic viscosity. Then, the conformation of polypeptide chains in the presence of urea or GdmCl could not be regarded as a standard random coil because it would be a stretched random coil, at least at room temperature.

2.2. pH Denaturation

The pH of the solution is one of the most important factors that determines the state of a protein. The changes of protein structure with variation of pH are frequently complex. For of small, single-domain proteins, the intensive, denaturational changes in all parameters that characterize protein conformation usually occur over a narrow range of pH and are clearly distinguishable above a smooth background of gradual changes. In accordance with the Le Chatelier principle, pH-induced denaturation is associated with the release or uptake of protons (Fig. 4). Potentiometric titration of proteins revealed that smooth changes result from titrating of protein groups that have pK_a values not very different from those of the corresponding free amino acids, whereas the gross conformational changes associated with pH denaturation are accompanied primarily by the unmasking of buried groups (56, 57).

Figure 4. Protonation state of hen lysozyme versus pH at different temperatures, according to Ref. 55. At 25°C the protein is native at all pH values, but at higher temperatures it unfolds with decreasing pH, unmasking and

protonating the buried groups.

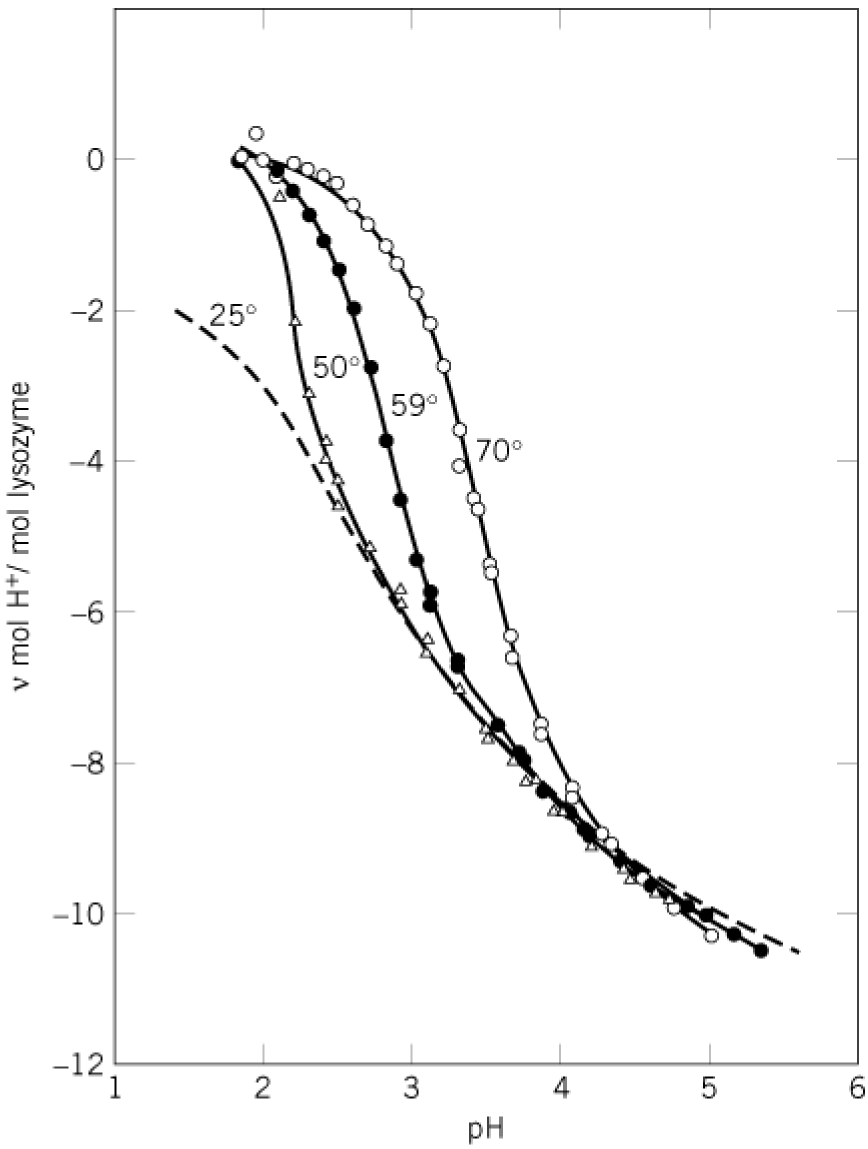

pH-induced denaturation depends on temperature and, therefore, temperature-induced denaturation depends on the pH (see Thermal denaturation). Because the temperature-induced denaturation of a small single-domain protein is a two-state transition, it was assumed that the transition induced by variation of pH at a fixed temperature is also two-state, so that the initial and the final characteristics of the protein are independent of the sequence of pH or temperature variation. Then, one can determine the Gibbs free energy difference between the native and denatured state from the potentiometrically measured pH-dependence of the protonation difference Dn(pH) between these states (55):

$$\Delta G(pH) = 2.3RT \int_{pHt}^{pH} \Delta v(pH)dpH \qquad (6)$$

where pH_t is the transition pH at which half of the molecules are in the denatured state. Comparison of Gibbs free energy values of pH- and temperature-induced denaturation showed that they indeed correspond very well, a strong argument that the pH-induced denaturation of small globular proteins can be regarded as a two-state transition (58).

Calorimetric titration studies have shown that pH denaturation of proteins creates significant heat effects that depend on temperature (Fig. 5). If corrected for the heats of protonation, the enthalpy of pH-induced protein transitions is identical to the enthalpy of the temperature-induced transition and depends similarly on temperature (55). Thus, the pH-induced denaturation of protein results in a heat capacity increase similar to that observed for temperature induced-denaturation. For the theory of acid-induced denaturation, see Refs. 56, 57, and 59 and for a review, see Ref. 44.

Figure 5. Heat of transfer of lysozyme from pH 4.8 to a given pH, at constant temperature, according to Ref. 55. At 298 K (25°C), the protein remains folded at all pH values, but it unfolds at low pH at the higher temperatures used.

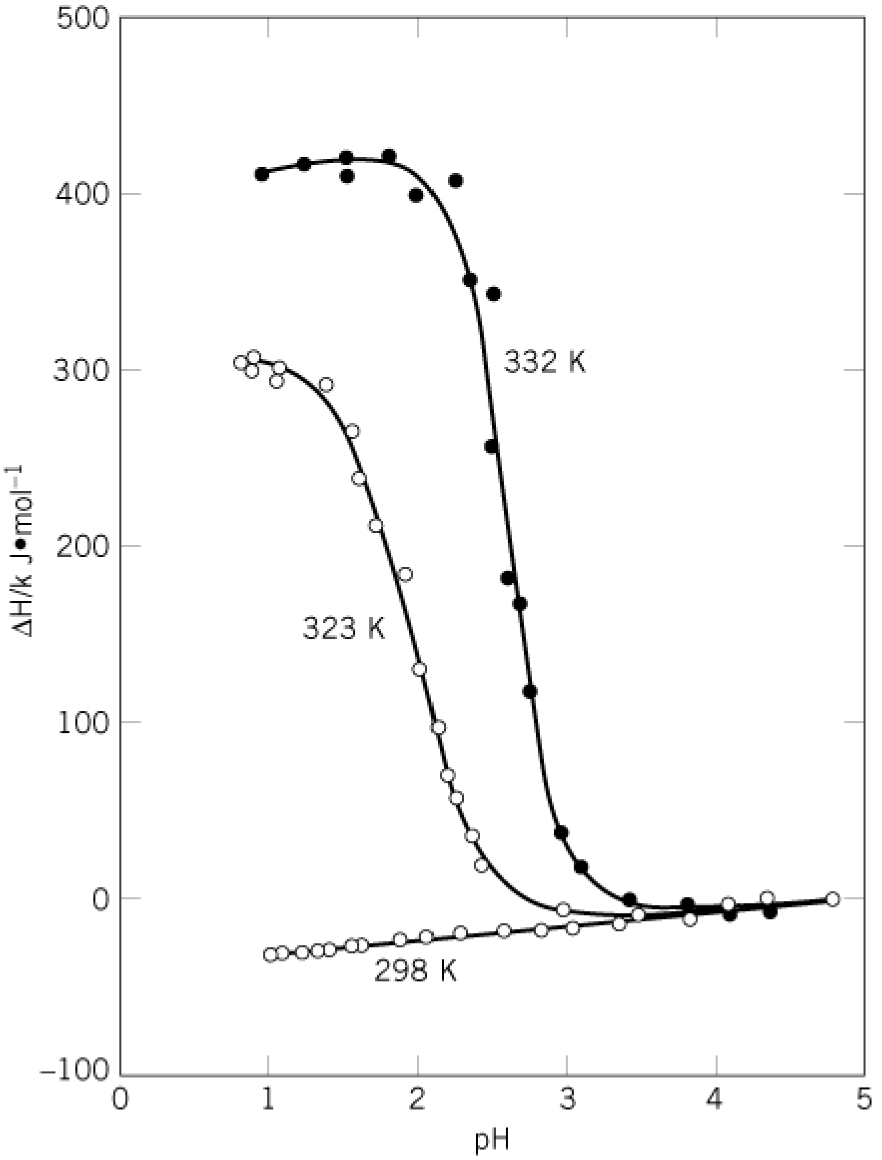

With increased temperature increasing thermal motion induces disruption of the ordered native structure of a protein. Breakdown of the native structure of small globular proteins occurs over a relatively narrow temperature range, in which all specific characteristics of the native protein change simultaneously (Fig. 1). In that temperature range the microscopic fluctuations coalesce into a global macroscopic fluctuation, that is, the macroscopic unfolding of a protein structure (60), which results in drastic changes in the rate of hydrogen exchange of the protein's amide groups (61). Therefore, the thermal denaturation of a single-domain small protein is a highly cooperative process. Because this process is induced by increased temperature, it is obvious that it should be result in an increase in the enthalpy, which is the extensive thermodynamic parameter conjugate with temperature, that is, it should proceed with heat absorption in accordance with the Le Chatelier's principle. Assuming that this process does indeed represent a two-state transition, one can estimate the enthalpy of denaturation by using Eq. (2), which is known as the van't Hoff equation .

The heat effect of denaturation can be observed directly by scanning microcalorimetery as an intensive heat absorption peak (Fig. 6). For small single-domain proteins, the calorimetrically measured enthalpy of denaturation agrees well the van't Hoff enthalpy, showing that thermal denaturation of these proteins is well approximated by a two-state transition (13). Deviation between the calorimetric and van't Hoff enthalpies does not usually exceed 5%, which means that the population of intermediate states is rather low. This was confirmed by detailed analysis of the excess heat absorption profile (63) and has been shown subsequently for many small single-domain proteins.

Figure 6. Temperature-dependence of the partial molar heat capacity of pancreatic ribonuclease A (RNase) and of sperm whale met-myoglobin (Mb) in solution at pH 4.4. The dashed lines show the heat capacities of the unfolded states, extrapolated to lower temperatures according to Eq. 9 of the text. The other line is a linear extrapolation of the heat capacity of the native state of myoglobin. Reproduced from Ref. 62.

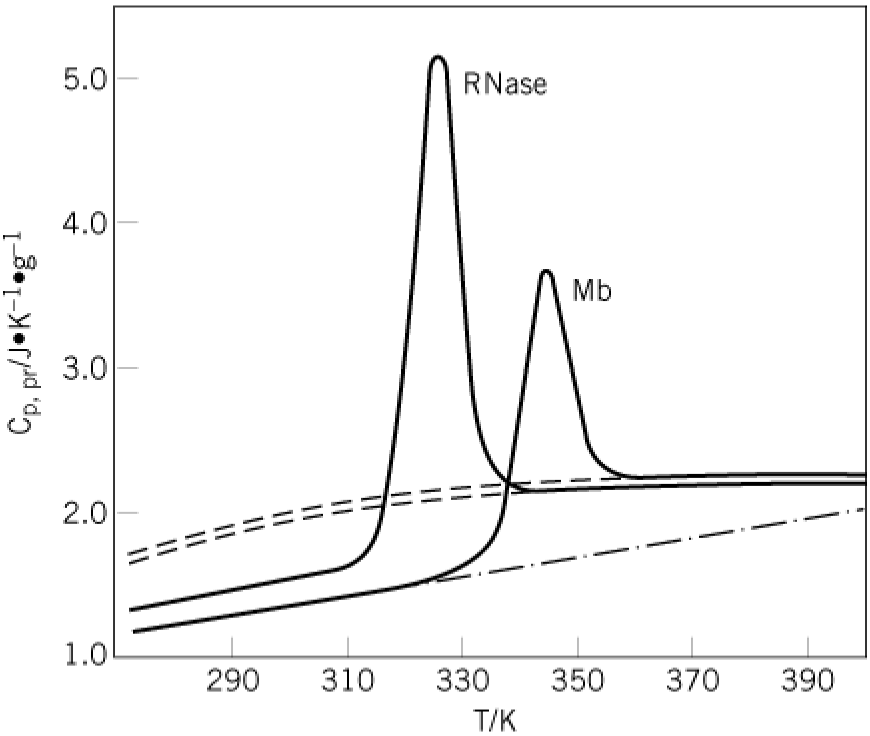

For a two-state transition at the mid-transition temperature T_t, where $K = 1$,

$$-RT_t \ln K = \Delta G(T_t) = \Delta H(T_t) - T_t \Delta S(T_t) = 0 \quad (7)$$

For the entropy of transition,

$$\Delta S(T_t) = \frac{\Delta H(Tt)}{T_t} \tag{8}$$

The most remarkable feature of the thermal denaturation of proteins is that the partial heat capacity of the denatured protein is always significantly higher by 25 to 50% than that of the native state (13, 64). The value of the denaturation heat capacity increment is specific for a given protein, depends on the temperature, and decreases at higher temperatures (65-67). Several explanations for the denaturation heat capacity increment can be suggested: (1) gradual melting of residual structure in the protein with continued increase in temperature; (2) increase of configurational freedom of the polypeptide chain upon disrupting of the rigid compact native structure of the protein molecule; or (3) hydration of the groups that are exposed to water by protein unfolding. The contribution of residual structure to the denaturation heat capacity increment is not significant because the heat capacity increment observed upon thermal denaturation is almost the same as in denaturation by denaturants, if the effects of denaturant solvation are taken into account properly (46), whereas it appears that proteins denatured by denaturants (urea or GdmCl) do not generally have residual structure. According to theoretical estimates (68), the contribution of the increased configurational freedom to the observed denaturation increment of the protein heat capacity cannot be large. Thus, the main reason for the higher partial heat capacity of the protein denatured state is that in this state more groups, particularly the nonpolar groups, are exposed to solvent, that is water. It is known that transfer of nonpolar groups into water increases the heat capacity (69-72). Exposure of the polar groups to water has the opposite effect. It decreases the heat capacity (66, 72-76). Detailed calorimetric study of the transfer of model compounds into water has also revealed that aromatic groups are not identical in hydration properties to nonpolar groups but are somewhere in between the nonpolar and polar groups (75). Thus, there are three main contributors to the heat capacity increment upon protein unfolding: exposure of the nonpolar, aromatic, and polar groups that were buried in the folded conformation. Each of them contributes in proportion to their water-accessible surface areas exposed upon unfolding (DA_{np}, DA_{arom}, and DA_{pol}, respectively). At 25°C the heat capacity increment of protein unfolding can be calculated as follows:

$$C_p^{hyd}(25°C = -(2.14\Delta A_{np} + 1.55\Delta A_{arom} - 1.27\Delta A_{pol}) \times JK^{-1}\ \mathrm{mol}^{-1} \tag{9}$$

The coefficients in this equation depend on temperature [for details, see (77)]. Ignoring this dependence and the usual identification of the aromatic groups with nonpolar groups is not justified in quantitatively analyzing thermodynamic properties of proteins (78). Upon protein unfolding, the surface area of the nonpolar plus aromatic groups exposed is greater than that of the polar groups, so unfolding of a protein results in an overall increase of the partial heat capacity (Fig. 6).

The important consequence of the denaturation heat capacity increment is that the enthalpy and entropy of denaturation are temperature-dependent functions. Indeed, because $\frac{\partial \Delta H}{\partial T} = \Delta C_p$ and $\frac{\partial \Delta S}{\partial T} = \frac{\Delta C_p}{T}$ for the enthalpy and entropy,

$$\Delta H(T)_{pH} = \Delta H(T_t)_{pH} + \int_{T_t}^{T} \Delta C_p(T)dT \tag{10}$$

and

$$\Delta S(T)_{\mathrm{pH}} = \frac{\Delta H(T_t)_{\mathrm{pH}}}{T_t} + \int_{T_t}^{T} + \frac{\Delta C_p(T)}{T} dT \quad (11)$$

Because DC_p is positive and decreases with increasing temperature, the enthalpy and entropy of protein denaturation increase asymptotically to some constant level (78, 83).

2.4. Cold Denaturation

Interest in the influence of low temperatures on the stability of native protein structure began with a paper published by Hopkins in 1930 (79). Studying the precipitation of ovalbumin upon denaturation by concentrated urea at various temperatures, he noticed that the rate of denaturation was greater at 0°C than at 23°C. Similar effects were observed later by others with other globular proteins, showing that in many cases the stability of a protein to urea or GdmCl denaturation is maximal around 30°C and decreases at lower temperatures. Meanwhile, evidence accumulated showing that many enzymes in aqueous solution, without urea or GdmCl, are inactivated at low temperature (about 0°C) but their activity was restored at room temperature (for a review, see Refs. 80 and 81). Most of these proteins are **oligomeric**, and it is likely that their cold inactivation resulted from their dissociation into subunits, as was found for several supermolecular structures, such as microtubules (82, 83). The quaternary structure of proteins is less stable than the tertiary, and its stability decreases with decreasing temperature.

The dual sensitivity of proteins to both high and low temperatures was formally explained when it was realized that protein unfolding results in a significant heat capacity increase and consequently that the enthalpy and entropy of unfolding are temperature-dependent and decrease with a decrease in temperature (Fig. 7). If so, according to the thermodynamic formalism, the Gibbs free energy difference between the unfolded and folded states of the protein should be a monotonic function of temperature but should have an extremum at the temperature at which the entropy difference between the two states decreases to zero (see Protein Stability). If the entropy and enthalpy functions continue to decrease below that point, with a change of sign in entropy, one might expect that the Gibbs free energy difference should become zero at some low temperature (Fig. 8). At this temperature, the protein should denature, that is unfold, but, in contrast to thermal denaturation at high temperature, it should proceed with a release of heat and a decrease of the enthalpy and entropy, that is, an increase in order. This paradoxical conclusion was confirmed by microcalorimetric measurements of the heat effects resulting from cooling aqueous solutions of proteins. It was shown that proteins do indeed denature upon cooling, release heat (Fig. 9), and change other properties (viscosity, circular dichroism NMR spectra) indicating that the polypeptide chain unfolds (84-86). Studies of various proteins under different conditions showed that cold denaturation is a very general property of globular proteins that depends on the environmental conditions and on their specific structure (81, 87). The temperature of cold denaturation is highest for proteins that change most in heat capacity upon unfolding and can be raised significantly by appropriate choice of solvent conditions (pH, ionic strength, buffer, presence of denaturants), which facilitate observation of this process.

Figure 7. Temperature-dependence of the enthalpy and entropy differences between the native and denatured states of ribonuclease A (RNase) and of sperm whale met-myoglobin (Mb) per mole of amino acid residues under solvent conditions that provide the maximum stabilities of these proteins. Reproduced from Ref. 62.

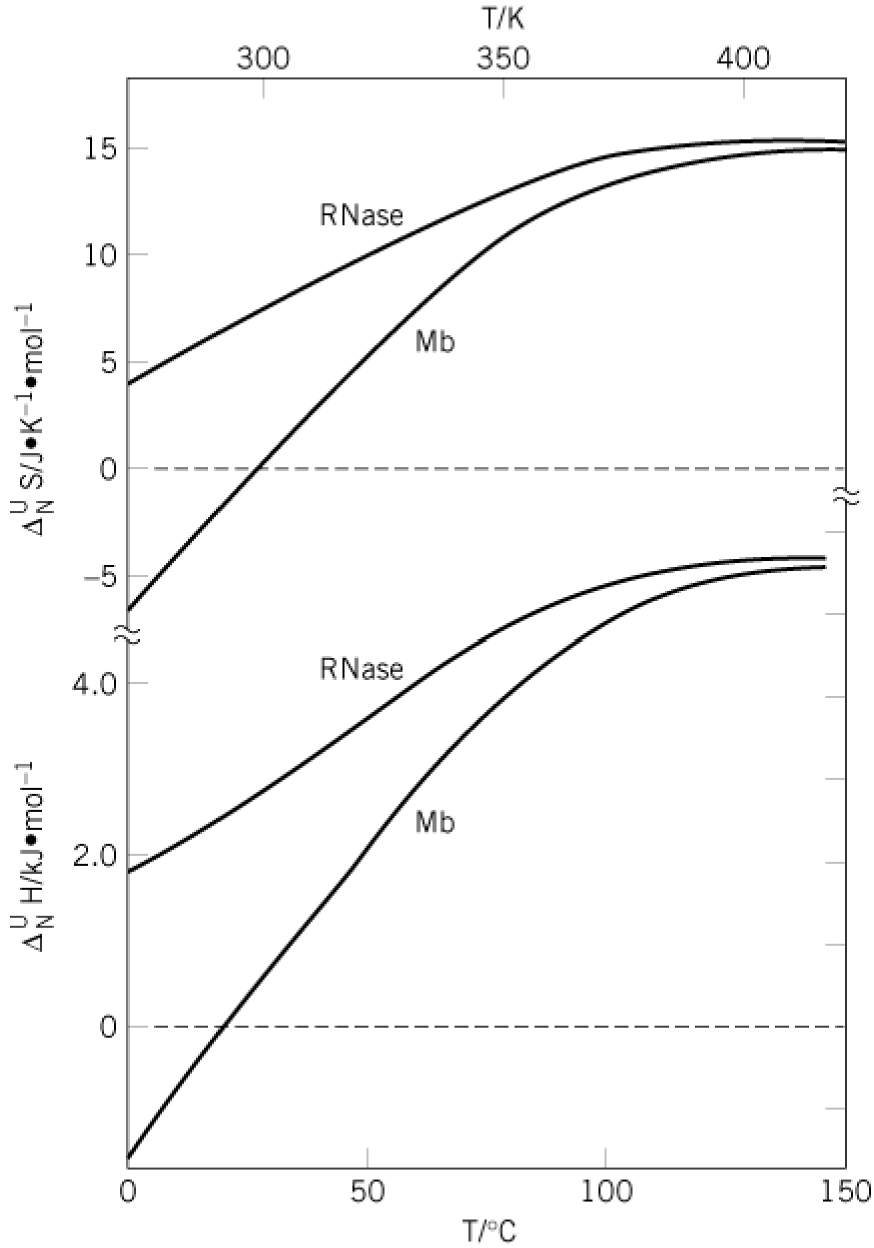

Figure 8. The Gibbs free energy difference between the denatured and native states of metmyoglobin in acetate buffer solution at the pH values indicated on the curves. Under these conditions, the protein cold denatures within the temperature range 0° to 30°C. Each curve is at a maximum when the entropy of unfolding is zero. Reproduced from Ref. 84.

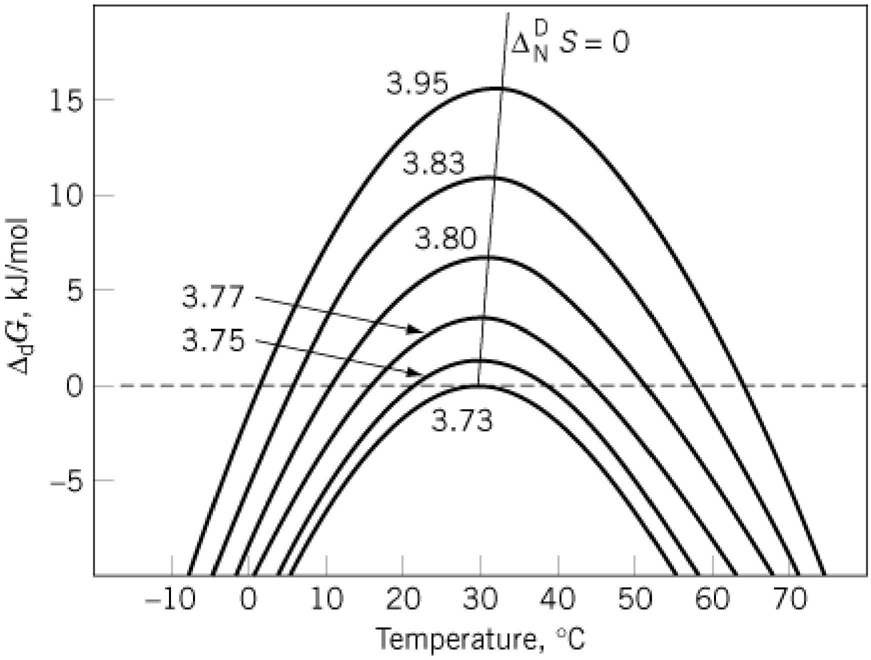

From the formal point of view, the cold denaturation of proteins is caused by the fact that the heat capacity of the unfolded protein is greater than that of the folded protein. The increased heat capacity upon protein unfolding is usually explained by the hydration of nonpolar groups (see Protein Stability), which also results in a decrease of entropy (DS^{hyd}). The latter is considered to be the main cause of the hydrophobic effect, which as an entropic force is proportional to absolute temperature (TDS^{hyd}) and should decrease upon lowering the temperature, thus destabilizing the protein. However, the real situation is not so simple. Indeed, because of the hydration heat capacity effect, the negative entropy of hydration of nonpolar groups is intrinsically temperature-dependent and increases in magnitude with decreasing temperature, thus balancing to some extent the entropic contribution of nonpolar groups to the stabilization of the folded protein's compact state. On the other hand, the unfolding of a protein results in exposing and hydrating the nonpolar groups and also polar and aromatic groups. The effects of hydrating of these groups contributes negatively to stabilizing protein structure, and the magnitude increases with decreasing temperature (77).

2.5. Pressure Denaturation
Pressure is one of the fundamental physical parameters that determine the state of any system, in particular, biological systems. Living organisms habituate at very different pressure conditions, from less than 1 bar in high mountains to thousands of bars in deep water. Therefore, it is natural that studies of pressure effects on proteins began a long time ago. In 1914, the first experiments done by Bridgmen showed that high pressure induces protein denaturation. But quantitative investigations of the effect of pressure on proteins began much later, in the middle 1960s, when it became clear that this is the only practical way to acquire information abouth the **volume** effects of protein folding (for reviews see Refs. 88-92).

Even early studies of the influence of pressure on proteins revealed that proteins are not very sensitive to pressure, and only at extremely high pressures do they exhibit changes like those observed in temperature and pH denaturation. However, according to more recent studies, particularly by high-pressure NMR spectroscopy, pressure-denatured proteins retain more residual structure than when denatured by heat, pH, or denaturants (86, 90, 93). The pressure-induced denaturation of proteins takes place over a relatively narrow pressure interval, depending on the temperature and solvent conditions, particularly the pH (Fig. 10). At the same time, the temperature and pH of denaturation also depend on pressure. Thus, these three parameters are interdependent, and variation of any one of them at fixed values of the others can lead to disruption of the native protein structure. Because denaturation of small, single domain proteins by temperature and pH is a highly cooperative process that is well approximated by a two-state transition, it was concluded that pressure-induced denaturation also represents a transition between two states, the native and denatured (94). This conclusion was confirmed by using an **electrophoretic** technique at high pressure (95), but it was challenged by later NMR studies (86, 93). In particular cases of multidomain proteins, the different domains undergo independent structural changes at specific well-defined limiting values of pressure (96). The immediate effect of pressure on oligomeric proteins is dissociation into subunits, followed by unfolding (80, 89, 90).

Figure 9. Microcalorimetric recordings of the heat effects upon cooling metmyoglobin under conditions where it cold denatures (bottom curve) and subsequent heating (top curve) that demonstrates first the refolding of the cold-denatured state and then its thermal unfolding at high temperatures. Reproduced from Ref. 84.

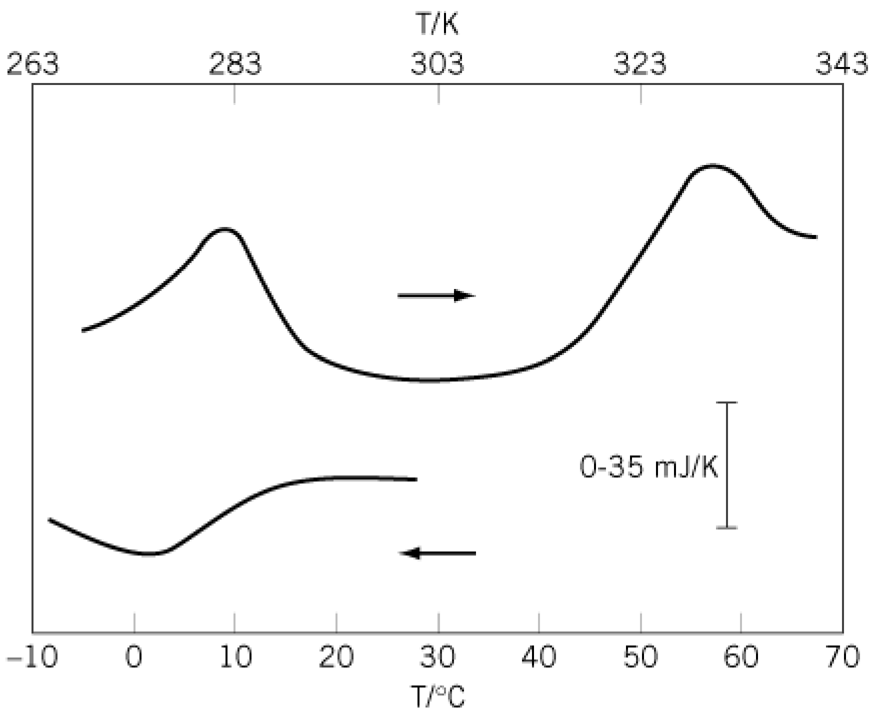

Assuming that pressure-induced denaturation represents a two-state transition, one can calculate the effective change of molecular volume upon unfolding, bearing in mind that according to the Le Chatelier principle, a pressure-induced shift in equilibrium should result in a decrease in volume that can be determined by Eq. (3). The great advantage of this approach to studying volume effects is that it does not require supersensitive volumetric techniques but can be realized by using any physical parameter (eg, **spectrophotometry**) that is sensitive to the conformational state of the protein and can indicate the pressure-induced change in equilibrium between the native and denatured states. This is important because proteins denature only at very high pressures, usually above 2 kbar.

It follows from the inefficiency of pressure in inducing protein denaturation that the volume change DV_d upon denaturation is very small, usually less than 0.5% of the total protein volume. For example, the volume decrease in denaturation of ribonuclease A is –(30 ± 10) ml/mol at an average pressure of about 1 kbar, and it decreases by –4 to –5 ml/mol when the temperature increases from 25° to 50°C (97-99). Zipp and Kauzmann (100) discussed the parallelism between the thermodynamic factors governing the process of reversible denaturation of proteins and the dissolution of hydrocarbon molecules in water. If the interior of a protein resembles a liquid or solid hydrocarbon and if significant numbers of nonpolar groups are exposed to water on unfolding, one would expect a significant volume decrease upon unfolding at low pressure. With increasing pressure, the volume reduction should become less negative and should change sign at 2kbar. However, this does not happen in protein denaturation. Therefore, the simple hydrophobic model that considers globular proteins as an oil drop or a solid hydrocarbon (101) does not work. In contrast to liquid or solid hydrocarbons, the native protein interior is densely packed, but it has some cavities and loose parts. Then, increasing hydrostatic pressure forces water molecules into the protein interior, gradually filling cavities and eventually breaking up the protein structure (90). This would explain why pressure-denatured proteins retain elements of structural organization to a much greater extent than proteins denatured by other means. But this also questions how closely pressure-induced unfolding is approximated by a two-state transition. In turn, this questions the reliability of the volume effects of protein folding that are determined by pressure denaturation.

Bibliography

1. M. L. Anson and A. F. Mirsky (1934) J. Gen Physiol. **17**, 393–398.
2. M. L. Anson (1945) Adv. Protein Chem. **2**, 361–386.
3. M. A. Eisenberg and G. W. Schwert (1951) J. Gen. Physiol . **34**, 583–606.
4. C. B. Anfinsen (1956) J. Biol. Chem. **221**, 405–412.
5. C. B. Anfinsen (1973) Science **181**, 223–230.
6. T. J. Ahern and A. M. Klibanov (1988) Methods Biochem. Anal. **33**, 91–127.
7. J. F. Brandts et al. (1975) Biochemistry **14**, 4953–4963.
8. R. L. Baldwin (1989) Trends Biochem. Sci. **14**, 291–294.
9. F. X. Schmid (1992) In *Protein Folding* (T.E. Creighton, ed.), Freeman, New York, pp. 197–241.
10. A. Ginsburg and W. R. Carroll (1965) Biochemistry **4**, 2159.
11. J. A. Thomson, B. A. Shirley, G. R. Grimsley, and C. N. Pace (1989) J. Biol. Chem. **264**, 11614–11620.
12. R. Lumry, R. Biltonen, and J. F. Brandts (1966) Biopolymers **4**, 917–944.
13. P. L. Privalov and N. N. Khechinashvili (1974) J. Mol. Biol. **86**, 665–684.
14. M. E. Goldberg (1969) J. Mol. Biol. **46**, 441–446.
15. P. L. Privalov and L. V. Medved (1982) J. Mol. Biol. **159**, 665–683.
16. V. V. Novokhatny, S. A. Kudinov, and P. L. Privalov (1984) J. Mol.Biol. **179**, 215–232.
17. D. B. Wetlaufer (1981) Adv. Protein Chem. **34**, 61–92.
18. M. G. Rossman and P. Argos (1981) Annu. Rev. Biochem. **50**, 497–532.
19. J.-R. Garel (1992) In *Protein Folding* (T. E. Creighton, ed.), Freeman New York, pp. 405–454.
20. P. L. Privalov (1982) Adv. Protein Chem. **35**, 1–104.

21. P. L. Privalov and S. A. Potekhin (1986) Methods Enzymol. **131**, 4–51.
22. E. Freire (1995) Methods Enzymol. **259**, 144–168.
23. K. P. Murphy and E. Freire (1992) Adv. Protein Chem. **41**, 313–361.
24. Y. V. Griko, E. Freire, G. P. Privalov, H. Van Dael, and P. L. Privalov (1995) J. Mol. Biol. **252**, 447–459.
25. L. V. Tatunashvili et al. (1990) J. Mol. Biol. **211**, 161–169.
26. V. V. Novokhatny, K. C. Ingham, and L. V. Medved (1991) J. Biol. Chem. **266**, 12994–13002.
27. I. V. Kurochkin et al. (1995) J. Mol. Biol. **248**, 414–430.
28. L. V. Medved (1995) J. Biol. Chem. **270**, 13652–13658.
29. C. C. McDonald, W. D. Phillips, and J. D. Glickson (1971) J. Am. Chem. Soc. **93**, 235–246.
30. F. M. Hughson, P. E. Wright, and R. L. Baldwin (1991) Science **249**, 1544–1548.
31. B. A. Schulman et al. (1995) J. Mol. Biol. **253**, 651–657.
32. S. E. Radford and C. M. Dobson (1995) Phil. Trans. R. Soc. Lond. **B 348**, 17–25.
33. K. A. Dill and D. Stigter (1995) Adv. Protein Chem. **46**, 59–104.
34. E. Freire and K. P. Murphy (1991) J. Mol. Biol. **222**, 687–698.
35. V. I. Abkevich, A. M. Gutin, and E. I. Shakhnovich (1995) J. Mol. Biol. **252**, 460–471.
36. C. N. Pace (1990) Trends Biotech. **8**, 93–98.
37. J. K. Myers, C. N. Pace, and J. M. Scholtz (1995) Protein Sci. **4**, 2138–2148.
38. L. M. Mayer and F. X. Schmid (1993) Biochemistry **32**, 7994–7998.
39. Y. Hagihara, S. Aimoto, A. Fink, and Y. Goto (1993) J. Mol. Biol. **231**, 180–184.
40. M. M. Santoro and D. W. Bolen (1992) Biochemistry **31**, 4901–4907.
41. D. B. Wetlaufewr et al. (1981) Adv. Protein Chem. **34**, 61–92.
42. M. Roseman and W. P. Jencks (1975) J. Am. Chem. Soc. **97**, 631–640.
43. R. Breslow and T. Gui (1990) Proc. Natl. Acad. Sci. USA **87**, 167–169.
44. C. Tanford (1970) Adv. Protein Chem. **24**, 1–95.
45. D. R. Robinson and W. P. Jenks (1965) J. Am. Chem. Soc. **87**, 2462–2470.
46. W. Pfeil and P. L. Privalov (1976) Biophys. Chem. **4**, 33–40.
47. G. I. Makhatadze and P. L. Privalov (1992) J. Mol. Biol. **226**, 491–505.
48. F. Ahmad and A. Salahuddin (1974) Biochemistry **13**, 245–249.
49. S. N. Timasheff (1992) Biochemistry **31**, 9857–9864.
50. J. A. Schellman and N. C. Gassner (1996) Biophys. Chem. **39**, 259–275.
51. M. M. Thayeer et al. (1992) Biophys. Chem. **46**, 165–169.
52. A. C. W. Pike and K. R. Acharia (1994) Protein Sci. **3**, 706–710.
53. J. Dunbar et al. (1997) Protein Sci. **6**, 1727–1733.
54. J. A. Gordon and W. P. Jencks (1963) Biochemistry **2**, 47–57.
55. W. Pfeil and P. L. Privalov (1976a) Biophys. Chem. **4**, 23–32.
56. J. T. Edsall and J. Wyman (1958) *Biophysical Chemistry*, Academic Press, New York.
57. J. Wyman (1964) Adv. Protein Chem. **19**, 223–286.
58. W. Pfeil and P. L. Privalov (1976c) Biophys. Chem. **4**, 41–50.

59. D. O. V. Alonso and K. A. Dill (1991) Biochemistry **30**, 5974–6985.
60. A. Ikegami (1977) Biophys. Chem. **6**, 117–130.
61. M. Nakanishi, M. Tsuboi, and A. Ikegami (1973) J. Mol. Biol. **75**, 673–682.
62. P. L. Privalov (1992) In *Protein Folding* (T. E. Creighton, ed.), Freeman and New York, pp. 83–126.
63. E. Freire and R. L. Biltonen (1978) Biopolymers **17**, 463–479.
64. J. F. Brandts (1964) J. Am. Chem. Soc. **86**, 4291–4301.
65. P. L. Privalov et al. (1989) J. Mol. Biol. **205**, 737–750.
66. P. L. Privalov and G. I. Makhatadze (1990) J. Mol. Biol. **213**, 385–391.
67. G. I. Makhatadze and P. L. Privalov (1996) In *Physical Properties of Polymers* (J. E. Mark, ed.), AIP Press, Woodbury, N.Y., pp. 91–100.
68. J. M. Sturtevant (1977) Proc. Natl. Acad. Sci. USA **74**, 2236–2240.
69. S. J. Gill, S. F. Dec, G. Olafsson, and I. Wadso (1985) J. Phys. Chem. **89**, 3758–3761.
70. O. L. Privalov and S. J. Gill (1988) Adv. Protein Chem. **39**, 191–234.
71. J. R. Livingston, R. S. Spolar, and M. T. Record (1991) Biochemistry **30**, 4237–4244.
72. G. I. Makhatadze and P. L. Privalov (1990) J. Mol. Biol. **213**, 375–384.
73. K. P. Murphy and S. J. Gill (1991) J. Mol. Biol. **222**, 699–709.
74. R. S. Spolar, J. R. Livingston, and M. T. Record (1992) Biochemistry **31**, 3947–3955.
75. P. L. Privalov and G. I. Makhatadze (1992) J. Mol. Biol. **224**, 715–723.
76. H. Gomez, V. J. Hisler, D. Xie, and E. Freire (1995) Proteins: Struct. Function Gen. **22**, 404–412.
77. G. I. Makhatadze and P. L. Privalov (1995) Adv. Protein Chem. **47**, 307–425.
78. D. R. Robertson and K. P. Murphy (1997) Chem. Rev. **97**, 1251–1267.
79. P. G. Hopkins (1930) Nature **126**, 383–386.
80. R. Jaenicke (1981) Ann. Rev. Biophys. Bioeng. **10**, 1–67.
81. P. L. Privalov (1990) CRC Crit. Rev. Biochem. Mol. Biol. **25**, 281–305.
82. S. N. Timasheff (1979) Trends Biochem. Sci. **4**, 61–65.
83. P. Dustin (1984) *Microtubules*, Springer–Verlag, Berlin.
84. P. L. Privalov, Y. V. Griko, S. Y. Venyaminov, and V. P. Kutyshenko (1986) J. Mol. Biol. **190**, 487–498.
85. Y. V. Griko, P. L. Privalov S. Y. Venyaminov, and V. P. Kutyshenko (1988) J. Mol. Biol. **202**, 127–138.
86. J. Zhang, X. Peng, A. Jonas, and J. Jonas (1995) Biochemistry **34**, 8631–8641.
87. F. Franks (1995) Adv. Protein Chem. **46**, 105–139.
88. K. Heremans (1982) Annu. Rev. Biophys. Bioeng. **11**, 1–21.
89. G. Weber and H. G. Drickamer (1983) Q. Rev. Biophys. **16**, 89–112.
90. J. L. Silva and G. Weber (1993) Annu. Rev. Phys. Chem. **44**, 89–113.
91. C. Royer (1995) Methods Enzymol. **259**, 357–377.
92. V. V. Mozhaev et al. (1996) Proteins: Struct. Function Genet. **24**, 81–91.
93. J. Jonas and A. Jonas (1994) Annu. Rev. Biophys. Biomol. Struct. **23**, 287–318.
94. J. Hermans Jr.and G. Acampora (1967) J. Am. Chem. Soc. **89**, 1547–1552.
95. S. A. Hawley and R. M. Mitchell (1975) Biochemistry **4**, 1277–1281.

96. H. G. Drickamer (1977) High Temperatures High Pressures **9**, 505–506.
97. S. J. Gill and R. L. Glogowsky (1965) J. Phys. Chem. **69**, 1515–1519.
98. D. J. F. Brandts et al. (1970) J. Am. Chem. Soc. **89**, 4826–4838.
99. S. A. Hawley (1971) Biochemistry **10**, 2436–2441.
100. A. Zipp and W. Kauzmann (1973) Biochemistry **12**, 4217–4228.
101. M. H. Klapper (1973) Prog. Bioorg. Chem. **2**, 55–132.

Suggestions for Further Reading

102. R. L. Baldwin (1991) Molten globules: Specific or nonspecific folding intermediate? Chemtracts-Biochem. Mol. Biol. **2**, 379–389.
103. T. E. Creighton, ed. (1992) *Protein Folding*, Freeman, New York.
104. T. E. Creighton (1995) An unfolding story. Curr. Biol. **5**, 353–356.
105. R. Jaenicke (1991) Protein folding: Local structures, domains, subunits, and assemblies. Biochemistry **30**, 3147–3161.
106. M. N. Jones (1979) *Biochemical Thermodynamics*, Elsevier, Amsterdam-Oxford-New York.
107. C. N. Pace (1990) Conformational stability of globular proteins. Trends Biochem. Sci **15**, 14–17.
108. P. L. Privalov (1979) Stability of proteins. Small globular proteins. Adv. Protein. Chem. **33**, 167–241.
109. P. L. Privalov (1982) Stability of proteins. Proteins which do not present a single cooperative system. Adv. Protein Chem. **35**, 1–104.
110. J. L. Silva and G. Weber (1993) Pressure stability of proteins. Annu. Rev. Phys. Chem. **44**, 89–113.
111. C. Tanford (1968) Protein denaturation. Adv. Protein Chem. **23**, 121–275; (1970) **24**, 1–95.

Dendrotoxins

The venom of the *Dendroaspsis* mamba snakes contains several toxins, termed dendrotoxins, which bind with nanomolar affinities to voltage-dependent **potassium channels** and facilitate neurotransmitter release because they prolong membrane depolarization. Their polypeptide chains consist of 57 to 60 amino acid residues, with three disulfide bonds and folding closely similar to that of **BPTI**-type inhibitors of serine proteinases. A short amino-terminal 3_{10}-helix is followed by a two-stranded b-sheet and a short COOH-terminal a-helix (1). Dendrotoxins provide yet another example of a stable protein module that has been readapted during the course of **evolution** to perform a different biological function.

Bibliography

1. J.-M. Lancelin et al. (1994) Struc. Biol. **1**, 246–250.

Density Gradient Centrifugation

Many centrifugation separations simply centrifuge an initially homogeneous sample and physically remove any heavy and large particles or molecules from the solution, leaving them as a pellet on the bottom of the centrifugation tube. In contrast, density gradient separations employ a gradient of varying, high concentrations of a small molecule, such as sucrose or cesium chloride, distributed along the axis of the centrifugally generated force. The lowest concentration is at the solution meniscus and the highest at the base. With sufficiently high concentrations of the small molecule, the density and viscosity of the solution also vary along the gradient. The density gradient is produced directly before centrifugation, or it is generated by the centrifugal force itself. A wide variety of materials is used to form gradients (Table 1), depending on which components are to be separated.

Table 1. Gradient Materials Used for Density Gradient Centrifugation[a]

Material and Typical Use	Maximum Aqueous Density (g/cm^3)
Cesium salts	
Acetate: Isopycnic separation of proteoglycans, DNA, RNA, and viruses	2.00 at 20°C
Bromide: Separation and fractionation of glycoproteins	1.72 at 20°C
Chloride: Most widely used density gradient material for isopycnic separations	1.91 at 20°C
Formate: DNA hydration	2.10 at 20°C
Oxalate: Isopycnic separation of proteoglycans, DNA, RNA	2.01 at 20°C
Ficoll: Isopycnic and rate-zonal separation of cells and subcellular fractions	1.17 at 20°C sucrose polymer
Glycerol: Rate-zonal separation of RNA, proteins and enzymes sensitive to sucrose	1.26 at 20°C
Percoll: Isopycnic separation of cells and large subcellular components	aqueous solution of polyvinylpyrrolidone-coated colloidal silica particles ~20 nm in diameter
Potassium salts	
Bromide: Isopycnic centrifugation of lipoproteins and density-labeled proteins	1.37 at 20°C
Iodide: Isopycnic centrifugation of DNA	1.72 at 24°C

and RNA	
Tartrate: Isopycnic centrifugation of viruses	1.49 at 20°C
Rubidium salts	
Chloride: Isopycnic banding of proteins	1.49 at 20°C
Trichloroacetate: Isopycnic DNA banding	1.90 at 20°C
Sodium salts	
Bromide: Rate-zonal and isopycnic separation of lipoproteins	1.53 at 20°C
Chloride: Rate zonal separation of DNA and lipoprotein fractionation	1.20 at 20°C
Iodide: Isopycnic centrifugation of DNA and RNA	1.90 at 20°C
Sucrose: Rate-zonal separation of DNA, RNA, subcellular fragments, proteins, and viruses; isopycnic banding of subcellular particlesand viruses	1.3 at 20°C

[a] Adapted from Spinpro Software from Beckman Instruments, a useful software tool. Unfortunately it still runs only under MS-DOS on Intel processor-based computer.

When a sample of molecules is subjected to centrifugation in a density gradient, they sediment toward the bottom if they have a greater buoyant density than the solution, or they will float toward the top if they have a lower density. The rates of sedimentation through the gradient of the various molecules can be measured, as in sedimentation velocity centrifugation, and depends on their buoyant densities and sedimentation coefficients **(*s*-values)**. Alternatively, the centrifugation can be continued until each molecule reaches that point in the gradient when the solution density is the same as its buoyant density. At this point the molecule neither sediments nor floats. Then different molecules are separated on the basis of differences in their buoyant densities, which can be measured in this way. The physical process of banding significantly improves the resolution of this technique.

1. Rate-Zonal Centrifugation

Separations of macromolecules or subcellular fractions with different sedimentation rates and/or sizes are accomplished by layering the sample of material as a narrow zone onto the top of a preformed gradient of the appropriate material (Table 1) and subjecting the sample to centrifugation. During centrifugation, the constituent components of the sample proceed through the gradient as individual zones, each at its specific sedimentation rate. The sedimentation process results in separating the sample components into discrete bands or zones that can be recovered from the centrifuge tube, typically by simple fraction collection (below). The shape of the gradient, that is, the change in solution density as a function of the physical length of the centrifuge tube or distance from the center of rotation, is a function of the gradient material and its concentration, the rate of centrifugation, etc. Five principal types of gradient systems used in rate-zonal separations are summarized in Table 2

Table 2. Principle Types of Gradients in Rate-Zonal Centrifugation[a]

Type	Gradient Characteristics as a Function of Distance Along Centrifuge Tube
Linear	Solution density or gradient-forming-solute concentration versus distance is linear
Isokinetic	Solution density or gradient-forming-solute concentration versus distance is usually convex but sometimes linear; all particles of the same density sediment at a constant rate at all distances from the center of rotation
Step or discontinuous	Solution densities or gradient-forming-solute concentrations versus distance form discrete zones with (relatively) large differences in density (concentration) from one to another
Shallow	Solution density or gradient-forming-solute concentration changes gradually versus distance
Sharp or steep	Solution density or gradient-forming-solute concentration changes rapidly versus distance

[a] Adapted from Spinpro Software from Beckman Instruments.

Approximate values of the sedimentation coefficients (s-values) of macromolecules and subcellular components can be obtained from rate-zonal gradient centrifugation without purifing the protein. This is accomplished in isokinetic gradients, where particles sediment at a constant rate, as in sucrose gradient centrifugation. To determine the s-value, it is necessary to include sedimentation "markers" of macromolecules with known sedimentation coefficients. It is necessary only to be able to differentiate between the various molecules, perhaps by their **spectroscopic** properties or by their biological activities.

2. Flotation in Gradient Centrifugation

This technique is a subclass or offshoot of gradient techniques. It occurs in centrifugation when the buoyant densities of the centrifuged macromolecule or subcellular components are less than that of the solution in which they are centrifuged. The rates of flotation of the individual solution components to the top of the solution are a function of their sizes, shapes and densities, just as in sedimentation to the bottom of the tube.

3. Isopycnic Gradient Centrifugation

Isopycnic procedures are used to separate macromolecules on the basis of their buoyant densities. The density gradient is chosen so as to include the densities of the species to be separated from each other. The sample to be sedimented may be prepared either by homogeneously distributing it throughout the gradient or by layering it on top of the gradient. In either case, when centrifugal force is applied to the sample, the sedimenting components move along the density gradient to where they have the same buoyant density. If they are at a lower solution density initially, they tend to sediment, whereas they tend to float when at a higher solution density. When the density gradient is maintained by the centrifugal force, and perhaps even generated by it, such as with cesium chloride (Table 1), the gradient is "self-generating." When all the molecules present are at their equilibrium positions, the centrifugal force condenses the molecules into sharp zones and maintains them. Unlike rate-zonal centrifugation, where the zones of the various molecules are constantly broadened by diffusion, but like isoelectric focusing, isopycnic density gradient centrifugation condenses the sample into a narrow zone and keeps it stable and sharp in time. This results from two opposing force fields:

diffusion, which tends to dissipate the zone, and the centrifugal field, which forces any “escaping” molecule back into its appropriate zone.

If the components to be separated have small differences in buoyant densities, the gradient used should bracket the desired density range and should also be shallow, so as to afford significant separation between components. Alternatively, if the components to be separated have large differences in buoyant densities, the gradient can be adjusted so that any undesired component either floats to the top of the gradient or sediments to the bottom, whereas the desired components are within the middle of the gradient.

4. Gradients of Viscous Materials

When viscous gradient materials, such as sucrose, Ficoll, Percoll, and glycerol, are used, the gradients are often prepared by layering steps of decreasing density in the centrifuge tube. Then the various steps are allowed to diffuse into each other (usually for 1 to 3 hours at room temperature) to form an approximately linear gradient. Alternatively, the sample is layered and centrifuged immediately through the series of discontinuous step zones; the sample often accumulates at an interface between two steps, so the steps are chosen so that different materials accumulate at different interfaces. Often a cushioning layer of high density gradient material is incorporated into the bottom of the tube to prevent the desired sample from pelleting onto the tube.

5. Salt Gradients

Cesium chloride is sufficiently heavy that it forms a substantial density gradient under the sole influence of rapid centrifugation. In this case, the starting solution can be uniform in both the cesium chloride and the sample. During centrifugation, the density gradient of cesium chloride is generated, and the molecules of the sample migrate to their isopycnic positions. The appropriate initial cesium chloride concentration must be chosen to give the desired density gradient with the centrifugal force used. It is possible to shorten the time required for attaining equilibrium by preforming the gradient, which then requires centrifugation runs of only 2 to 8 hours. Often a cushioning layer of high density gradient material is incorporated to prevent complete pelleting of the sample on the bottom of the tube.

6. Fractionating Gradients After Centrifugation

The density gradients employed aid the process of recovering the samples, minimizing the disturbance of banded zones in a centrifuge tube. Methods for recovering the banded samples depend on whether the tube in which the experiment has been performed is reusable or disposable. In the former case, the tube is held rigidly while a flat-end syringe needle of appropriate length is carefully inserted at the center of the tube down through the length of the column of gradient solution to the tube base. Then the contents are slowly pumped out. In the latter case, the bottom of the tube is punctured with a needle, and the tube contents are permitted to flow out slowly. Then they are collected in a fraction collector, perhaps after passing through a UV **absorbance**, **fluorescence**, or other detector. An alternative fractionation device for this process, a centrifuge tube slicer, is available from Beckman Instruments.

Once separated into individual fractions, the gradient samples can be analyzed for the molecules of interest, such as their enzymatic activity, spectral properties, or a **radiolabel**. The exact shape of the density gradient at the end of the centrifugation is determined by measuring the refractive index of the solution.

7. Centrifuge Rotors for Gradient Density Separations

Three types of rotor are used for density gradient centrifugation, varying in the orientation of the sample during centrifugation. In the swinging bucket rotor, the sample swings outward away from the center of rotation during centrifugation and extends at a right angle to the axis of rotation. Consequently, the force applied to the column of liquid containing the sample is always along the long axis of the liquid column, and the sedimenting sample moves along the linear axis of the applied force. Swinging bucket rotors are often used with sucrose density centrifugation. In fixed-angle rotors, the liquid column is tilted at a fixed angle relative to the axis of rotation. Thus, the centrifugal force is applied at an angle to the long axis of the tube and differentially at the cell meniscus and cell base. Fixed-angle rotors are routinely used for pelleting samples and for heavier isopycnic salt gradients, where the gradient can reorient after the centrifugation run. In vertical tube rotors, the liquid column is held parallel to the axis of rotation, and the centrifugal force is applied perpendicularly to the long axis of the tube. Because the sedimentation path is short, simply the width of the tube, these rotors permit very short run times, but with good resolution, and are useful for isopycnic separations. The advantages and disadvantages of each rotor type vary significantly with the particular application.

Suggestion for Further Reading

R. Hinton and M. Dobrota (1980) *Laboratory Techniques in Biochemistry and Molecular Biology: Density Gradient Centrifugation* (T. S. Work and E. Work, eds.), North-Holland, New York. A somewhat dated but useful compendium of techniques for preparative density gradient centrifugation.

Deoxycholate

Sodium deoxycholate, a bile acid salt, is a strongly **denaturing**, anionic detergent that is structurally close to sodium cholate. The 5-OH group of cholate is replaced with a hydrogen atom in deoxycholate (Fig. 1). This detergent has been used to solubilize many membrane-anchored proteins, such as those that are membrane-linked via a phosphatidylinositol-containing glycolipid (termed **GPI-anchored** proteins) (1, 2). Although it has rarely been shown that sodium deoxycholate solubilizes integral membrane proteins, certain insoluble, extracellular proteins, such as human lens membrane proteinase, have been efficiently solubilized by using sodium deoxycholate (3). Sodium deoxycholate has a relatively high critical micelle concentration (cmc) of ~10 mM, which makes it easy to be removed by dialysis from the solubilized proteins and lipids. Although this detergent is strongly denaturing toward integral membrane proteins, it solubilizes membrane lipids efficiently (4) and also stimultes **G-protein**-coupling to an effector, such as phospholipase C (5).

Figure 1. The structure of sodium deoxycholate.

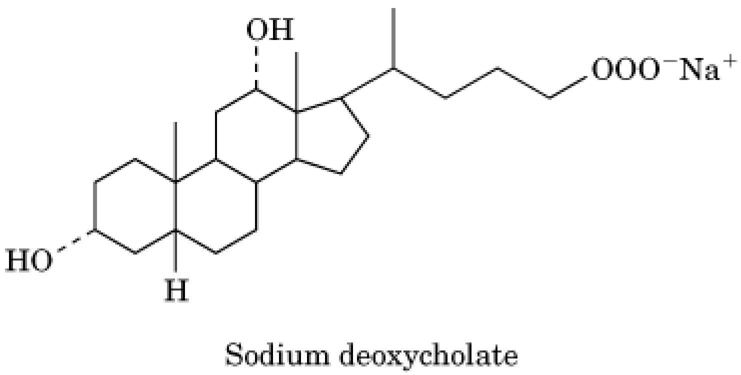

Bibliography

1. D. W. Loe, J. R. Glover, S. Head, and F. J. Sharom (1989) Biochem. Cell Biol. **67**, 214–223.
2. N. M. Hooper and A. J. Turner (1988) Biochem. J. **250**, 865–869.
3. O. P. Srivatsava and K. Srivatsava (1989) Exp. Eye Res. **48**, 161–175.
4. P. Banerjee J. B. Joo, J. T. Buse, and G. Dawson (1995) Chem. Phys. Lipids **77**, 65–78.
5. H. Nakanishi, Y. Takeyama, H. Ohyanagi, Y. Saitoh, and Y. Takai (1990) Biochem. Biophys. Res. Commun. **170**, 111–118.

Deoxycytidylate Deaminase

Deoxycytidylate deaminase (dCMP deaminase) is one of two **allosteric** enzymes in the *de novo* biosynthetic pathways to **deoxyribonucleoside triphosphates** (dNTPs); the other allosteric enzyme is ribonucleotide reductase). Inasmuch as dCMP deaminase sits at a branch point in the synthesis of pyrimidine dNTPs, the importance of this control in maintaining balanced dNTP pools can be readily appreciated.

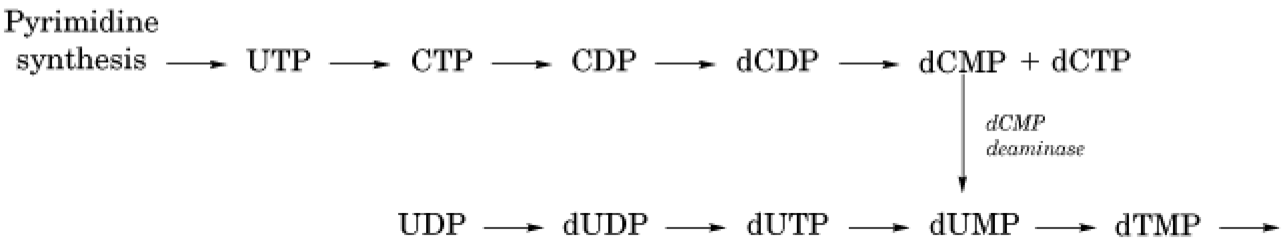

It is assumed, although not yet established with certainty, that dCMP, dCDP, and dCTP are in ready equilibrium with one another via the actions of dCMP kinase and nucleoside diphosphate kinase. Clearly, dCMP is a precursor of dCTP, and the accumulation of dCTP can be a signal to the cell to divert dCMP, *via* dCMP deaminase, to pools of thymidine nucleotides. At the same time, dTTP accumulation can signal the metabolic machinery to shut off its own synthesis, and dCMP deaminase makes an appropriate regulatory target.

Scheme 1 shows two distinct pathways to dUMP, one involving dCMP deaminase and the other involving the reduction of UDP by ribonucleotide reductase with subsequent action of nucleoside diphosphate kinase and deoxyuridine triphosphatase (dUTPase). Radioisotope labeling experiments in mammalian cells show that the deaminase-based pathway is far more significant than the second pathway as a source of dTMP residues in DNA (1).

1. Structure and Regulation of dCMP Deaminase

Deoxycytidylate deaminase was first described in the late 1950s and early 1960s in papers by the Maleys in the United States (2, 3) and by Scarano and colleagues in Italy (4). As shown above, the enzyme catalyzes the hydrolytic deamination of deoxycytidine monophosphate to deoxyuridine monophosphate, the immediate precursor to thymidine nucleotides via thymidylate synthase. As an enzyme involved in the synthesis of a specific DNA precursor, the activity of dCMP deaminase is closely correlated with the proliferative activity of the cell (2). In a series of papers in the 1960s, both the Maley and Scarano laboratories showed that vertebrate dCMP deaminase is inhibited by dTTP and activated by dCTP (3, 4). dCTP was found to be almost completely required for activity, whereas dTTP is a strong inhibitor, with inhibition constant (K_i) values in the micromolar range. Reversal of dTTP inhibition by dCTP was shown to vary with the dCTP concentration in a highly sigmoidal manner as did the variation of the enzyme velocity with the concentration of dCMP as substrate (see Allostery). Activation involved an apparent change in subunit structure of the enzyme, for the dCTP-activated enzyme from chick embryo was shown to have a sedimentation coefficient ($s_{20,w}$) of 6.78 S whereas the dTTP-inhibited enzyme had $s_{20,w}$ of only 3.63 S (3). Conformational changes were also involved, as shown in part by large circular dichroism changes resulting from dCTP binding.

In early work, the subunit structure of dCMP deaminase was more readily defined in studies with T-even bacteriophage-infected bacteria, a much more abundant source than vertebrate tissues (5, 6). The phage T2 enzyme was shown to be a homohexamer of about 120,000 molecular weight, and the phage T4 and T6 enzymes are similar. The effects of dCTP and dTTP were shown to be similar to those observed with the vertebrate enzyme. However, dCTP is not a physiological regulator in these systems. T-even phage DNA contains 5-hydroxymethyl-cytosine substituted for cytosine, and the dCTP pool in infected cells is completely replaced by 5-hydroxymethyl-dCTP. This latter nucleotide was shown to be equivalent to dCTP in its effect on phage dCMP deaminases, and it is undoubtedly the true *in vivo* positive regulator of the phage enzymes. Like other phage-coded enzymes of deoxyribonucleotide synthesis, T-even phage-coded dCMP deaminase functions as part of a multienzyme complex that evidently facilitates the biosynthesis of dNTPs and possibly their incorporation into DNA (see Thymidylate Synthase). Incidentally, the host organism for T-even phages, *Escherichia coli*, does not contain dCMP deaminase. Instead, the conversion of deoxycytidine to deoxyuridine nucleotides occurs at the triphosphate level (7) through the action of a structurally unrelated enzyme, as follows:

$$\mathrm{dCTP} + \mathrm{H_2}O \rightarrow \mathrm{dUTP} + \mathrm{NH_3} \tag{2}$$

With recombinant DNA approaches, large-scale isolation of dCMP deaminase has become possible, and structural studies are under way with the T4, **yeast**, and human enzymes (8, 9). The three dCMP deaminases show significant sequence homology at the C-terminus, but the yeast subunit is far larger than the T4 or human polypeptide chains. Both the T4 and human enzymes contain catalytically essential zinc (see Zinc-Binding Proteins). This fact, plus an apparent active-site homology with adenosine deaminase and cytidine deaminase, suggest a mechanism comparable to that of cytidine deaminase, whose structure has been determined (10; see Fig. 1). This mechanism is consistent with the potent inhibition of dCMP deaminase by tetrahydrodeoxyuridine monophosphate, a presumed transition state analogue.

Figure 1. A mechanism for the cytidine deaminase reaction, based on structural analysis of the *E. coli* enzyme. The mechanism for dCMP deaminase is probably similar or identical. Reprinted with permission from L. Betts, S. Xiang, S. A. Short, R. Wolfenden, and C. W. Carter Jr. (1994) *J. Mol. Biol*. **235**, 635–656.

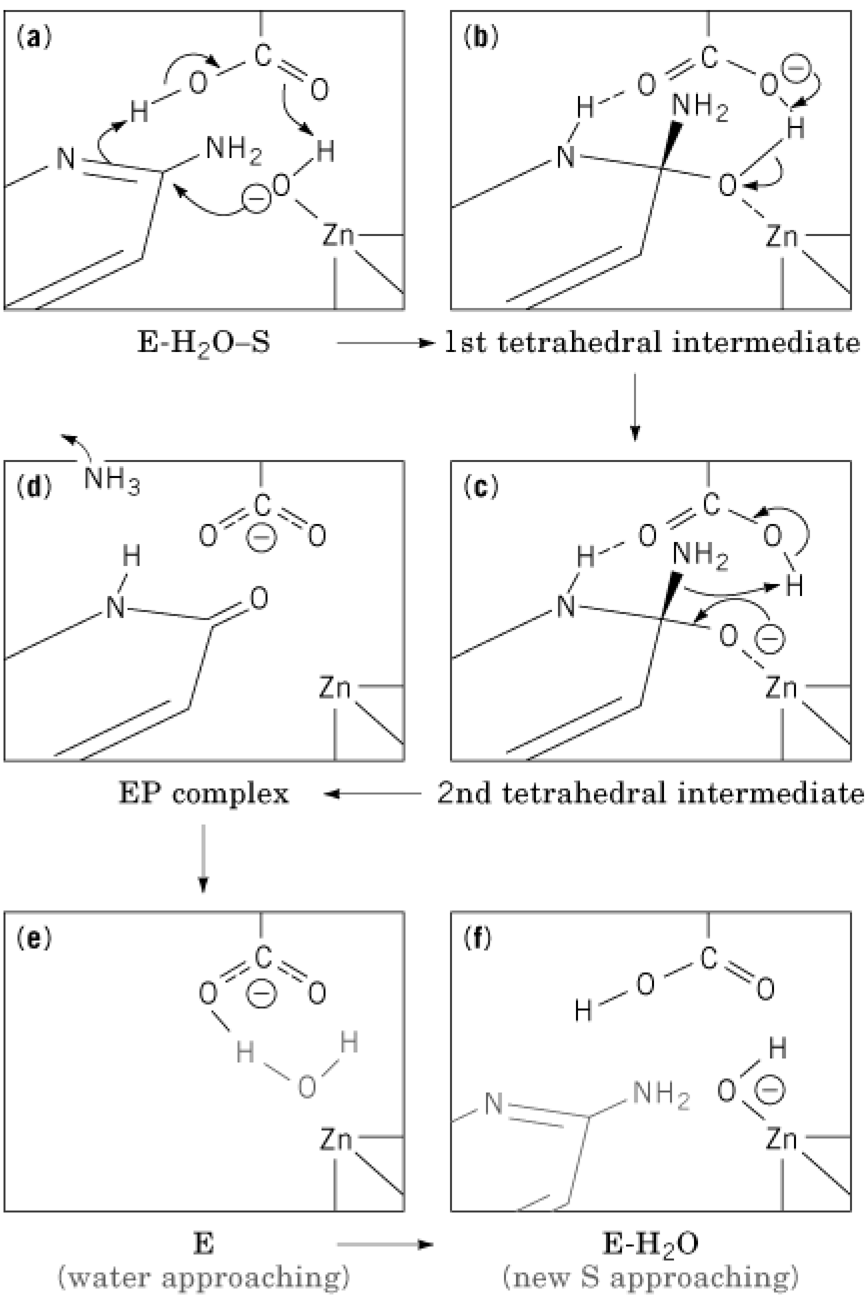

2. dCMP Deaminase is the Product of a Mutator Gene

A mutator gene is one in which the action of a mutant allele contributes toward an increase in the spontaneous mutation rate at all loci; conversely, the action of the wild-type allele contributes toward genetic stability. A classic example is the *E. coli mutH*, *mutL*, and *mutS* genes, in any of which a mutation raises the mutation rate by compromising DNA mismatch repair.

In the same sense, the gene encoding dCMP deaminase is a mutator gene, as shown first in mouse S49 cells (11), where a subline evidently deficient in dCMP deaminase activity caused accumulation of dCTP and a deficiency of dTTP consistent with the loss of a major pathway to dTTP synthesis, and an increase in spontaneous mutation rates of at least an order of magnitude. Similar results were observed in yeast (12) and in *E. coli* infected with a dCMP deaminase deletion mutant of phage T4 (13). In these latter studies, additional information was gained about the mutational events occurring as a result of the dNTP pool imbalance. Infection by the T4 deaminase deletion led to dramatic accumulations of 5-hydroxymethyl-dCTP and specific increases in mutations that occur along an AT

→ GC transition mutation pathway, as expected if mutation results from misinsertion of the abundant 5-hydroxymethyl-dCMP opposite template A. On the other hand, most of the mutations in yeast that were stimulated by dCMP deaminase deficiency were GC → CG transversion mutations, an event that does not follow in any logical fashion from the dNTP pool imbalance demonstrated in these cells.

Clearly, understanding mutagenesis induced by DNA precursor pool imbalance involves factors other than concentration-dependent competition between nucleotides that are correctly and incorrectly base-paired to a template base. Adding to the complexity is the existence of a dCMP deaminase-defective hamster V79 cell line in which a large increase in the [dCTP]/[dTTP] pool ratio has only a negligible effect on the spontaneous mutation rate (14). Based on analysis of synchronized Chinese hamster ovary cells (15), it is possible that most of the expanded dCTP pool in these cells is located outside the nucleus, where it cannot directly influence replication fidelity. In any event, it is apparent from the several systems that have been investigated that the biochemical consequences of dCMP deaminase deficiency are clear—cells or phage survive because an additional metabolic route to dTTP is present, but the [dCTP]/[dTTP] or [hydroxymethyl-dCTP]/[dTTP] ratio increases dramatically, as expected from the loss of a quantitatively major pathway. However, the genetic consequences of these events underscore the difficulty in understanding all the biochemical factors contributing to spontaneous mutagenesis.

Bibliography

1. B. R. de Saint Vincent, M. Déchamps, and G. Buttin (1980) J. Biol. Chem. **255**, 162–167.
2. F. Maley and G. F. Maley (1960) J. Biol. Chem. **235**, 2968–2970.
3. G. F. Maley and F. Maley (1968) J. Biol. Chem. **243**, 4506–4516.
4. E. Scarano, G. Geraci, and M. Rossi (1967) Biochemistry **6**, 192–201.
5. W. H. Fleming and M. J. Bessman (1967) J. Biol. Chem. **242**, 363–371.
6. G. F. Maley and F. Maley (1982) Biochemistry **21**, 3780–3785.
7. G. A. O"Donovan, G. Edlin, J. A. Fuchs, J. Neuhard, and E. Thomassen (1971) J. Bacteriol. **105**, 666–672.
8. J. T. Moore, R. E. Silversmith, G. F. Maley, and F. Maley (1993) J. Biol. Chem. **268**, 2288–2291.
9. K. X. B. Weiner, R. S. Weiner, F. Maley, and G. F. Maley (1993) J. Biol. Chem. **268**, 12983–12989.
10. L. Betts, S. Xiang, S. A. Short, R. Wolfenden, and C. W. Carter Jr. (1994) J. Mol. Biol. **235**, 635–656.
11. G. Weinberg, B. Ullman, and D. W. Martin Jr. (1981) Proc. Natl. Acad. Sci. USA **78**, 2447–2451.
12. S. E. Kohalmi, M. Glattke, E. M. McIntosh, and B. A. Kunz (1991) J. Mol. Biol. **220**, 933–946.
13. R. G. Sargent and C. K. Mathews (1987) J. Biol. Chem. **262**, 5546–5553.
14. E. Darè, L-H, Zhang, D. Janssen, and V. Bianchi (1995) J. Mol. Biol. **252**, 514–521.
15. J. M. Leeds, M. B. Slabaugh, and C. K. Mathews (1985) Mol. Cell Biol. **5**, 3443–3450.

Suggestions for Further Reading

16. P. Reichard (1988) Interactions between deoxyribonucleotide and DNA synthesis. Ann. Rev. Biochem. **57**, 349–374. This review describes the functions of dNTP biosynthetic enzmes and their roles in coordinating DNA precursor synthesis and DNA replication.
17. B. A. Kunz, S. E. Kohalmi, T. A. Kunkel, C. K. Mathews, E. M. McIntosh, and J. A. Reidy (1990) Deoxyribonucleoside triphosphate levels: a critical factor in the maintenance of genetic stability. Mutation Res. **318**, 1–64. A descriptive review of mutagenic processes resulting from DNA precursor pool imbalances.

Deoxyribonucleotide Biosynthesis And Degradation

Most cells contain five to ten times as much RNA as DNA. The deoxyribonucleotide precursors to DNA use the same pathways for synthesis of purine and pyrimidine rings as do the ribonucleotides that are used for RNA synthesis and for a host of other metabolic functions (see Purine Ribonucleotide Metabolism and Pyrimidine Ribonucleotide Metabolism). Therefore, the pathways that lead from the *de novo* purine and pyrimidine synthetic pathways toward deoxyribonucleoside triphosphates (dNTPs) are quantitatively minor. They are of obvious significance, however. Not only must they be sufficiently active to supply the cell's needs for **DNA replication, recombination**, and DNA repair but they must be activated and deactivated in coordination with the timing of DNA replication during the cell cycle because dNTPs have no known metabolic roles other than their function as DNA precursors. Moreover, the pathways must be regulated so as to provide the four DNA precursors at rates corresponding to the base composition of the genome being served. dNTP pool imbalances that develop when regulatory mechanisms are perturbed have numerous biological consequences (1)—including mutagenesis, recombination, induction of latent **viruses**, and cell death—caused by stimulation of apoptosis (2).

1. Pathways to dNTPs

1.1. Chemical Differences between RNA and DNA

It is useful to begin our survey of deoxyribonucleotide biosynthesis by considering the processes through which the chemical differences between DNA nucleotides and RNA nucleotides arise. The methyl group of thymine, which distinguishes it from uracil, arises through the transfer of a single-carbon functional group to a uracil nucleotide, catalyzed by thymidylate synthase. The presence of 2-deoxyribose as the sugar in DNA nucleotides rather than the ribose found in RNA comes about through reduction of the ribose sugar on a ribonucleotide substrate (see Ribonucleotide Reductases). Some aerobic bacteria and all anaerobic microorganisms studied carry out this reduction at the ribonucleoside triphosphate (rNTP) level. In all other organisms studied, however, the substrates for ribonucleotide reductase are the ribonucleoside 5′-diphosphates (rNDPs). Whether a particular reductase acts on rNDPs or rNTPs, a single enzyme reduces all four ribonucleotide substrates. Accordingly, the enzyme interacts with **allosteric** modifiers to ensure that the four DNA precursors are produced at rates commensurate with the base composition of the organism's genome. In this article, we will describe the predominant pathways to dNTPs that begin with reduction of rNDPs to deoxyribonucleoside diphosphates (dNDPs). These pathways are summarized in Figure 1.

Figure 1. Pathways of dNTP biosynthesis *de novo*. Although these pathways are widespread, they are not universal, as indicated in the text. Enzyme 1, ribonucleoside diphosphate reductase; 2, nucleoside diphosphate kinase; 3, dCMP kinase (probably); 4, dCMP deaminase; 5, dUTPase; 6, thymidylate synthase; 7, thymidylate kinase. CH_2 = THF is 5,10-methylenetetrahydrofolate, and DHF is dihydrofolate.

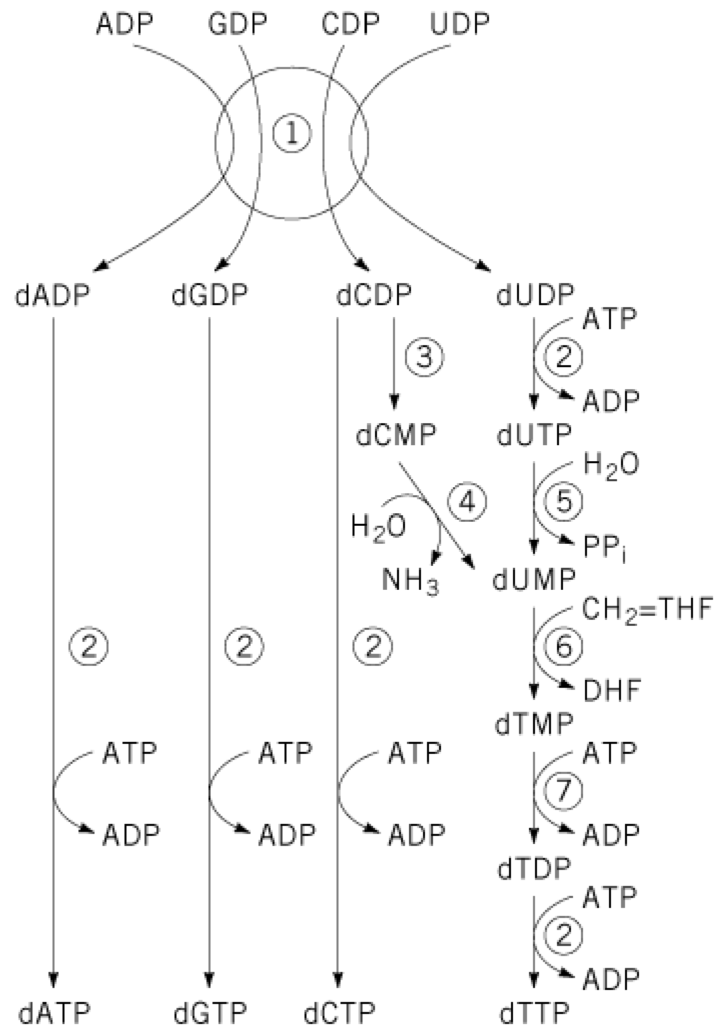

1.2. The Role of Nucleoside Diphosphate Kinase

For three of the four nucleotides—ADP, CDP, and GDP—the conversion to the dNTP involves simply a phosphorylation of the rNDP reductase product, catalyzed by nucleoside diphosphate kinase. In most cells, this enzyme is very active, and all known forms of the enzyme have very low specificity. Thus, the enzyme catalyzes the reversible transfer of the g-phosphate of any common rNTP or dNTP to the phosphate at the b-position of any common rNDP or dNDP. The equilibrium constant for each reaction catalyzed is close to unity. Thus, the direction in which a nucleoside diphosphate kinase-catalyzed reaction occurs *in vivo* depends on the concentrations of substrates and products. Because ATP is almost always the most abundant intracellular nucleoside triphosphate, most such reactions involve the ATP-dependent conversion of a ribo- or deoxyribonucleoside diphosphate to the corresponding triphosphate.

1.3. Thymine Nucleotide Biosynthesis

The biosynthesis of thymidine triphosphate is obviously more complex than that of any other dNTP given that thymine nucleotides are derived from uracil nucleotides and a methyl group must be created. In most cells, the dUDP produced by rNDP reductase action on UDP is phosphorylated to dUTP by nucleoside diphosphate kinase. dUTP is cleaved by an active pyrophosphatase, deoxyuridine triphosphatase, or dUTPase. This enzyme plays a dual role: (1) Because dUTP is a good substrate for DNA polymerase, dUTPase minimizes the steady-state pool size of dUTP and, hence, helps to exclude dUMP from DNA. (2) The dUTPase reaction is a significant biosynthetic route to dUMP, the substrate for thymidylate synthase.

Thymidylate synthase catalyzes the transfer of a single-carbon functional group from 5,10-methylenetetrahydrofolate to position 5 of the pyrimidine ring in deoxyuridine monophosphate, yielding thymidine monophosphate (Fig. 2). dTMP is phosphorylated to dTDP by , and conversion to dTTP involves nucleoside diphosphate kinase.

Figure 2. The thymidylate synthesis cycle. Enzyme 1, thymidylate synthase; 2, dihydrofolate reductase; 3, serine transhydroxymethylase. dR-P is deoxyribose 5′-phosphate; PABA is *p*-aminobenzoate; Glu_n refers to the multiple glutamate residues on naturally occurring folate coenzymes.

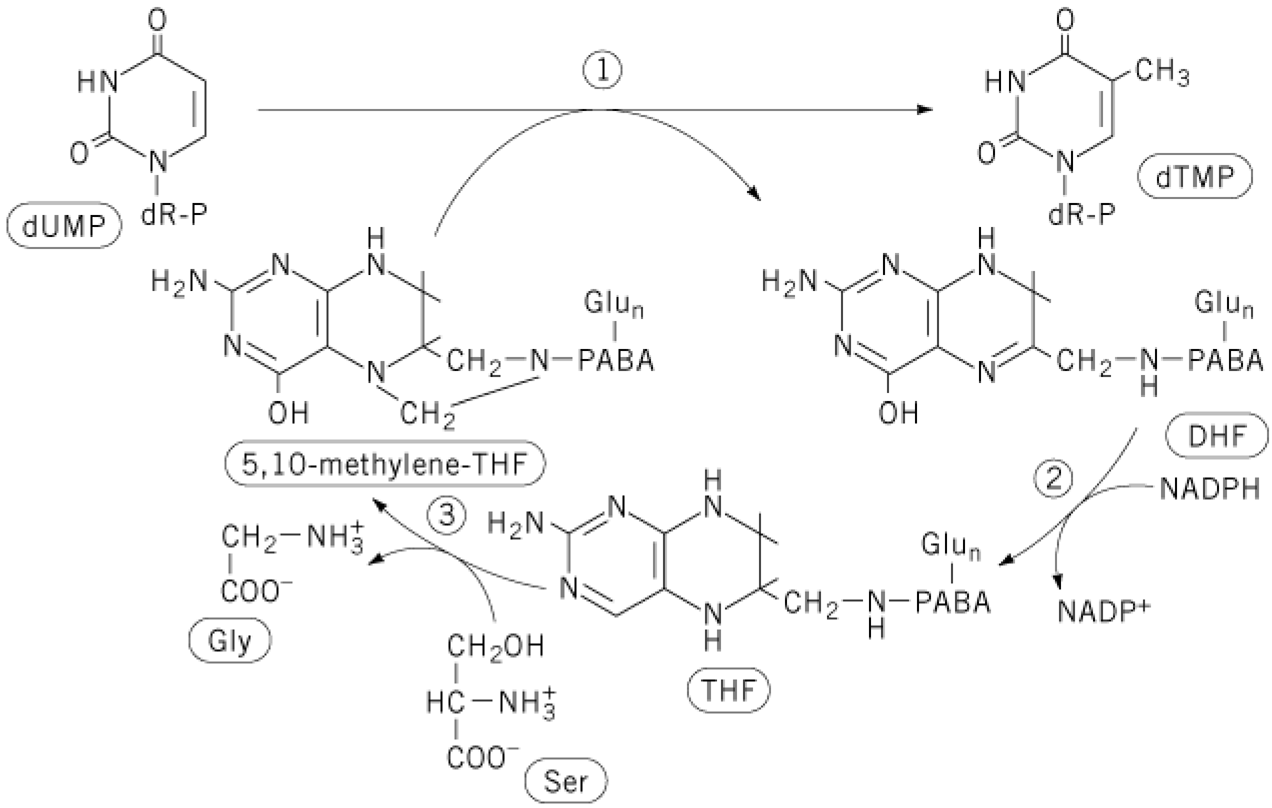

In the thymidylate synthase reaction, the transferred methylene group must be reduced to the methyl level, and the electron pair that brings this reduction about comes from the reduced pteridine ring of 5,10-methylenetetrahydrofolate. The coenzyme, therefore, loses both its methylene group and an electron pair, leading to dihydrofolate. Transformation of the coenzyme for reuse involves, first, its reduction to tetrahydrofolate by dihydrofolate reductase and, next, transfer of a single-carbon group to the pteridine ring, usually catalyzed by serine transhydroxymethylase. The stoichiometric requirement for the folate cofactor in the thymidylate synthase reaction probably explains the selective toxicity of dihydrofolate reductase inhibitors toward proliferating cells (3). Such inhibitors include Methotrexate, widely used in cancer chemotherapy, and Trimethoprim, an antibacterial agent that specifically inhibits dihydrofolate reductases of prokaryotic origin(see **Aminopterin**). Proliferating cells have a continuous requirement for dTTP synthesis, to sustain DNA replication. The greater the flux rate through thymidylate synthase *in vivo*, the more rapidly tetrahydrofolate pools will be depleted after administration of a dihydrofolate reductase inhibitor and, hence, the greater will be the sensitivity of those cells toward the growth-inhibiting or lethal effects of blockage of dihydrofolate reductase.

1.4. Biosynthetic Routes to dUMP

As noted earlier, the cleavage of deoxyuridine triphosphate to the corresponding monophosphate, catalyzed by dUTPase, provides a significant source of dUMP for the synthesis of thymine nucleotides. In most cells, however, an additional route, involving deamination of deoxycytidine nucleotides, is more important in a quantitative sense. As shown in Figure 3, the hydrolytic deamination in most organisms involves conversion of dCMP to dUMP, catalyzed by **dCMP deaminase**. In a few bacteria, including *Escherichia coli*, the deamination occurs at the triphosphate level, with conversion of dCTP to dUTP, catalyzed by dCTP deaminase. In such organisms, the conversion of CDP to dUMP occurs by the following pathway:

$$\text{CDP} \rightarrow \text{dCDP} \rightarrow \text{dCTP} \rightarrow \text{dUTP} \rightarrow \text{dUMP}$$

Figure 3. dCMP deaminase as a branch point between dCTP and dTTP synthesis. Allosteric modifiers of dCMP deaminase are shown, as is the regulation of salvage synthetic pathways. Enzyme 1, ribonucleoside diphosphate reductase; 2, nucleoside diphosphate kinase; 3, dCMP kinase (possibly); 4, dUTPase; 5, dCMP deaminase; 6, dCMP kinase; 7, thymidylate synthase; 8, thymidylate kinase; 9, deoxycytidine kinase; 10, thymidine kinase.

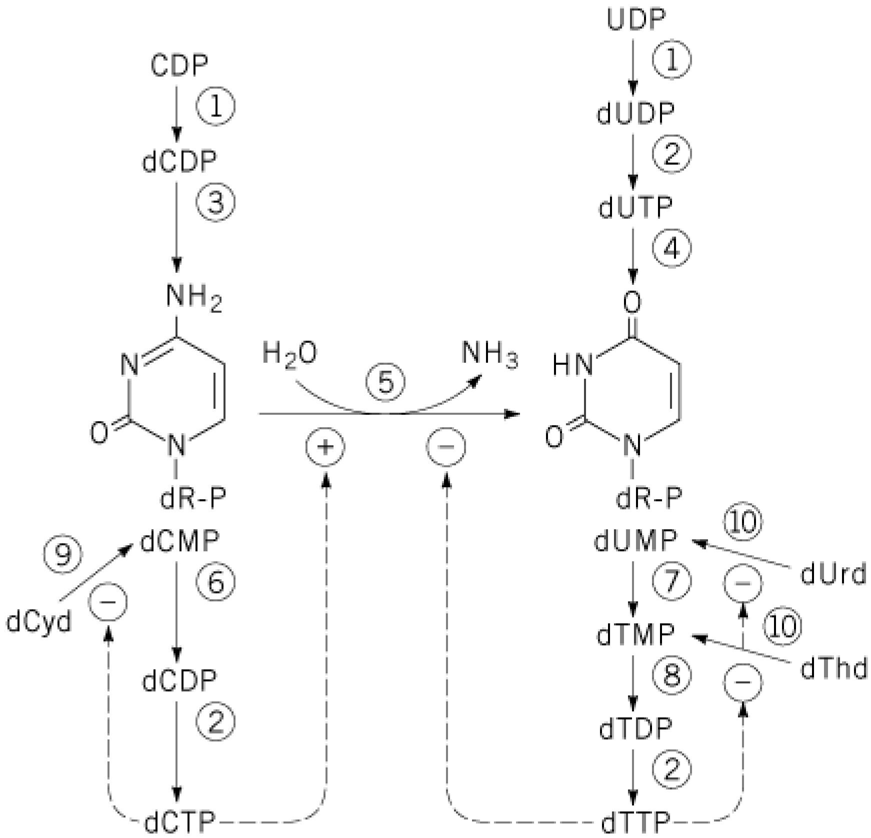

The most widespread pathway, shown in Figure 3, involves deamination at the monophosphate level. In many vertebrate cell lines, this is the predominant, often exclusive, pathway leading to dUMP (4). It is not clear why the *in vivo* flux rate from UDP to dUDP is so low, particularly when the activities of ribonucleotide reductase on CDP and UDP are regulated virtually identically as shown by assays of the purified enzyme *in vitro* (5). Whatever the reason, dCMP deaminase is an important metabolic branch point between routes to dTTP and dCTP. Allosteric regulation of this enzyme—activation by dCTP and inhibition by dTTP—ensures that these two dNTPs are produced at relative rates commensurate with their need for DNA synthesis. dCMP deaminase is not essential for cell viability, at least as determined in cell culture systems. However, mutant cells lacking dCMP deaminase have abnormally high dCTP pools (1, 6), and the resultant increase in the [dCTP]/[dTTP] pool ratio often brings about a **mutator** phenotype, in which the dCTP pool expansion stimulates its incorporation opposite template nucleotides other than dGMP (1).

2. Deoxyuridine Nucleotide Metabolism

As noted earlier, dUTPase plays a role in providing dUMP for the thymidylate synthase reaction. Of equal or greater importance is its role in minimizing the incorporation of dUMP into DNA in place of dTMP (see Deoxyuridine Triphosphatase). Cells possess two independent mechanisms to minimize the amount of dUMP in DNA: (1) dUTPase acts to deplete the dUTP pool, and hence to minimize dUMP incorporation by DNA polymerase, usually opposite dAMP in template DNA. (2) The second mechanism is a base excision repair process, starting with . This enzyme scans DNA, and when it contacts a dUMP residue, it cleaves the glycosidic bond, probably by a base-flipping mechanism (7). This reaction creates an abasic site, which initiates a repair process that results in insertion of the correct nucleotide at that site (8).

Because the base-pairing properties of uracil and thymine are essentially identical, it seems likely that the mechanisms for uracil exclusion from DNA are not designed primarily to replace dUMP with dTMP, when that dUMP is base-paired with dAMP in the template DNA. Instead, the probable target for DNA uracil exclusion is dUMP residues incorrectly paired with dGMP, but DNA-uracil *N*-glycosylase simply recognizes every dUMP residue in DNA, no matter what its partner. G · U DNA base pairs would arise most frequently by deamination of a dCMP residue paired in duplex DNA with dGMP. Cytosine undergoes spontaneous deamination at appreciable rates whether as a free nucleic acid precursor or as a residue in DNA or RNA. If C in a G · C base pair underwent deamination, the resultant G · C base pair would generate a G · C and an A · U base pair in the next round of replication and, ultimately, the deamination would lead to a G · C → A · T transition mutation. Thus, the DNA-uracil exclusion systems probably act to maintain stability of the genome.

3. Salvage Routes to dNTPs

As noted in Salvage pathways to nucleotide biosynthesis, deoxyribonucleotide salvage pathways involving uptake of extracellular precursors primarily use deoxyribonucleoside kinases. Human cells contain four such enzymes of varying specificities, two located in the cytosol and two in mitochondria, whereas other organisms, such as *E. coli*, contain thymidine kinase as the only deoxyribonucleoside kinase. Thymidine kinase has received particularly intensive study, partly because of the mechanism of its cell cycle regulation (9) but largely because the enzyme is so useful as a means for incorporating radiolabel into DNA. For reasons still not clear, thymidine competes extremely effectively with the *de novo* synthetic pathway to dTTP such that, in many animal cell systems, radiolabeled thymidine is incorporated into DNA at full specific activity, often bypassing substantial endogenous pools generated by *de novo* synthesis (10). One popular experimental organism for which this does not work is **yeast**; fungi lack thymidine kinase. Investigators have circumvented this difficulty, however, by designing yeast strains that are permeable to dTMP, strains for which exogenous dTMP can be used as a labeled DNA precursor.

For salvage of deoxyribonucleoside monophosphates released by intracellular DNA degradation, the deoxyribonucleoside monophosphate kinases play the key roles. Animal cells contain four such enzymes, each specific for one deoxyribonucleotide, ie, dAMP kinase, dCMP kinase, dGMP kinase, and dTMP kinase . The enzyme phosphorylating dAMP acts also on AMP and is the well-known adenylate kinase, or myokinase. dCMP kinase acts also on UMP, and dTMP kinase acts also on dUMP. dTMP kinase is involved also in *de novo* dTTP synthesis, as shown in Figure 1. dCMP kinase may also play a role in *de novo* dNTP synthesis. The enzyme converting dCDP (produced by ribonucleotide reductase) to dCMP, en route to dUMP and dTMP, has still not been identified. Since nucleotide kinases all have equilibrium constants close to 1, it is quite possible that the role of dCMP kinase is to carry out the synthesis of dCMP:

$$\mathrm{dCDP} + \mathrm{ADP} \rightleftharpoons \mathrm{dCMP} + \mathrm{ATP}$$

By contrast, dAMP and dGMP kinases play roles only in nucleotide salvage reactions because the *de novo* pathways lead directly from ribonucleoside diphosphate to deoxyribonucleoside diphosphate to deoxyribonucleoside triphosphate.

The action of nucleoside phosphorylases provides another route to salvage dNTP synthesis, eg, deoxyadenosine + $P_i \rightarrow$ adenine + deoxyribose-1-phosphate. Now the deoxyribose-1-phosphate can react with another base in a nucleoside phosphorylase-catalyzed reaction proceeding in the reverse direction, eg, dR-1-P + Thy $\rightarrow$ dThd + P_i. Thymidine can then become a nucleotide via the thymidine kinase reaction leading to dTMP. Although this process can significantly change relative dNTP pool sizes, it does not involve net deoxyribonucleotide synthesis; rather, it involves redistribution of the deoxyribosyl units linked to purine and pyrimidine bases.

4. Biosynthesis of Novel Nucleotides in Bacteriophage Infection

Much of what is known about pathways of dNTP synthesis in bacterial and animal cells came from investigations of the biosynthesis of unusual modified nucleotides in infection by certain bacteriophage (11). T-even bacteriophages of *E. coli* contain 5-hydroxymethylcytosine completely substituted for cytosine; many hydroxymethyldeoxycytidylate (HM-dCMP) residues in phage DNA are further modified by glycosidic links through the hydroxymethyl group to one or two glucose residues. These modifications occur through the action of phage-encoded enzymes that catalyze reactions comparable to those in cellular metabolism (Fig. 4). For example, the hydroxymethylation reaction is carried out by an enzyme, dCMP hydroxymethylase, that transfers a single-carbon group from methylenetetrahydrofolate to C-5 of dCMP, much as thymidylate synthase modifies C-5 of the pyrimidine dUMP (12); in fact, T-even phages encode a thymidylate synthase that displays significant amino acid sequence homology with dCMP hydroxymethylase. Not shown in Figure 4 is the involvement of glucosylation in the transfer of glucose to hydroxymethyl groups of HM-dCMP residues after their incorporation into DNA.

Figure 4. Metabolic pathways induced in bacteriophage infection. Solid arrows identify reactions known to be catalyzed by phage-coded enzymes; dashed arrows identify reactions catalyzed only by enzymes encoded by the host cell genome.

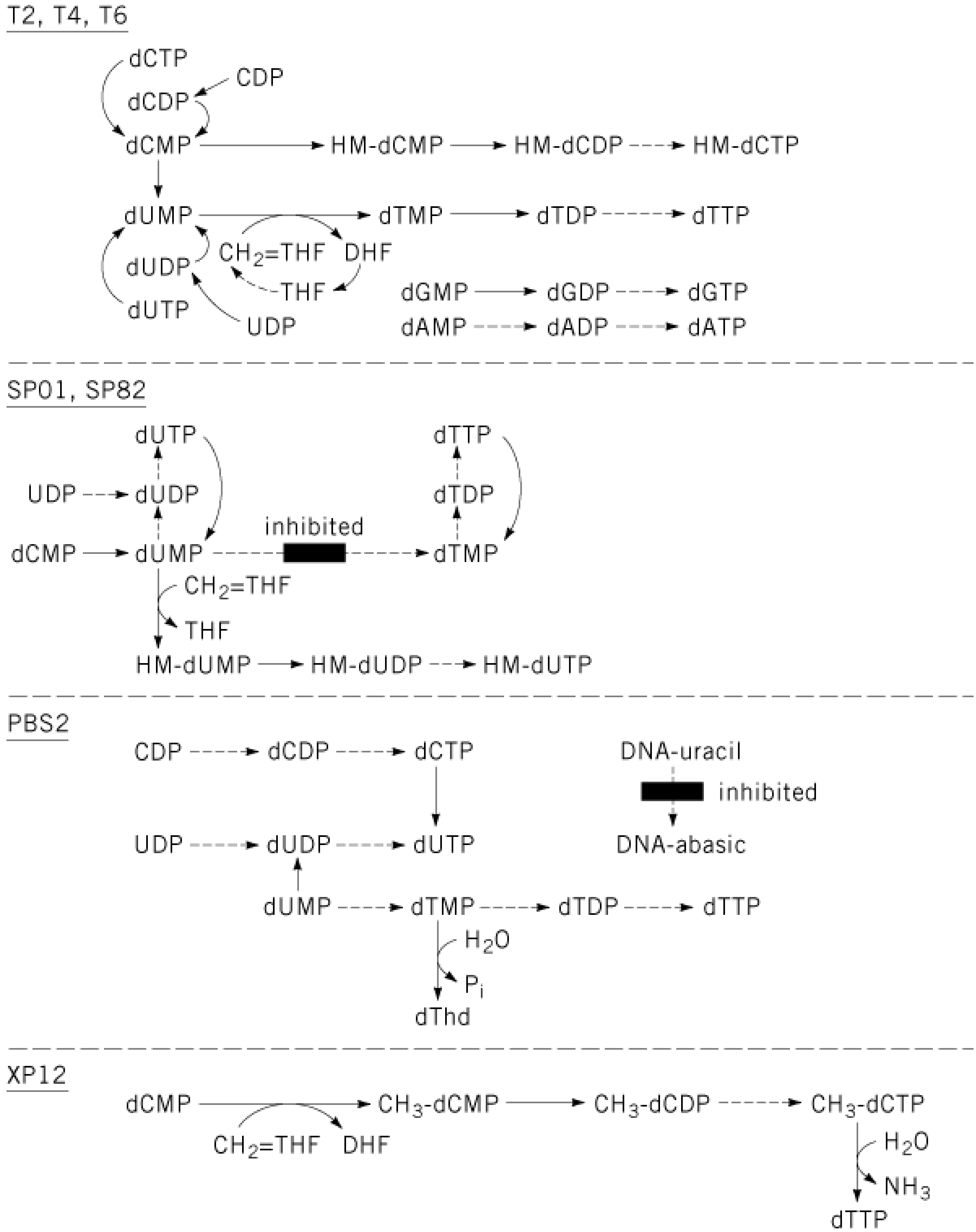

Other modifications are carried out by bacteriophage SP01 and SP82 of *Bacillus subtilis*, in which 5-hydroxymethyluracil substitutes for thymine and two other *B. subtilis* phages, PBS1 and PBS2, which replace thymine with uracil. The relevant pathways are also shown in Figure 4. Finally, the figure shows pathways induced in *Xanthomonas oryzae* by XP12, a bacteriophage in which cytosine is completely replaced by 5-methylcytosine. These base modifications help the virus to parasitize the host bacterium, overrunning pathways used by the host cell to produce its own DNA. Perhaps it should not be surprising that these are all virulent phages.

5. Deoxyribonucleoside Catabolism

5.1. Substrate Cycles and dNTP Pool Regulation

Nucleotide kinase-catalyzed reactions are readily reversible. Whereas these enzymes have long been considered to participate primarily in dNTP synthesis, there is now good evidence that nucleotide kinases function in both directions *in vivo* and that they can participate in dNTP degradation (13). For example, when DNA replication was blocked in mammalian cells with aphidicolin, intracellular dNTPs were degraded, and deoxyribonucleosides were excreted into the medium in significant amounts (13, 14), with little change in the steady-state pool size of the four dNTPs. The implication of these findings is that dNTP pool sizes are controlled not only at the level of synthesis but are also regulated by catabolism.

Under conditions that do not interfere with DNA synthesis in cultured cells, pulse-chase experiments show that the rate of utilization of a particular dNTP for DNA synthesis is equivalent to the rate at which the pool of that dNTP turns over (15, 16). These observations argue against the compartmentation of dNTP pools in animal cells; with one known exception, all the dNTP molecules in these cells are accessible to the replication machinery. The one exception is dCTP labeled by deoxycytidine (13); much of this pool is used for synthesis of the deoxycytidine counterparts to cytidine diphosphate-containing **lipid precursors**, such as CDP-choline. It is not yet clear whether these dCDP-containing “liponucleotides” play a metabolic role distinct from those of the more abundant cytidine-containing lipids.

For cells that don't excrete deoxyribonucleosides but instead degrade them further, that further degradation usually involves attack by nucleoside phosphorylases to yield deoxyribose-1-phosphate plus the free base. Further degradation of the purine and pyrimidine bases proceeds by pathways outlined in Purine ribonucleotide metabolism and Pyrimidine ribonucleotide metabolism.

5.2. Enzymatic Degradation of dGTP

A widely distributed enzyme is a dGTP pyrophosphatase , which catalyzes the hydrolytic cleavage of dGTP to dGMP and pyrophosphate. The metabolic role of this enzyme was obscure until it was found in *E. coli* that the enzyme is encoded by the *mutT* gene (17). The *mutT* gene product acts to prevent transversion mutations that proceed by G · C → T · A and A · T → C · G pathways. Mutant alleles of *mutT* cause spontaneous rates of these transversion mutations at other loci to increase by 100- to 10,000-fold. Mutations of these types are caused by oxidizing agents, such as hydrogen peroxide, which act in large part by oxidizing guanine residues in DNA to 8-oxoguanine. This oxidized purine readily base-pairs with adenine, setting in motion the events leading to mutagenesis. These realizations led to the discovery that the MutT protein is far more active in cleaving 8-oxo-dGTP than dGTP. Thus, it seems clear that the mutagenic effects of oxidizing agents include oxidation of guanine, not as a DNA residue but as a DNA precursor that is incorporated into DNA and then stimulates a transversion pathway by pairing with adenine. The MutT nucleotidase prevents this by degrading the mutagenic DNA substrate, 8-oxo-dGTP, before it has a chance to be incorporated into DNA.

E. coli contains a second dGTPase, which is distinctive in that it hydrolyzes dGTP to deoxyguanosine plus tripolyphosphate. Unlike the MutT dGTPase, which is widely distributed in organisms, this other dGTPase is found only in enteric bacteria (18). Its metabolic role is still obscure.

Bibliography

1. B. A. Kunz, S. E. Kohalmi, T. A. Kunkel, C. K. Mathews, E. M. McIntosh, and J. A. Reidy (1994) Mutation Res. **318**, 1–64.
2. F. J. Oliver, M. K. L. Collins, and A. López-Rivas (1996) Biochem. J. **316**, 421–425.
3. J. J. McCormack (1981) Med. Res. Revs. **1**, 303–331.
4. V. Bianchi, E. Pontis, and P. Reichard (1985) Mol. Cell. Biol. **7**, 4218–4224.

5. L. Thelander and P. Reichard (1979) Ann. Rev. Biochem. **48**, 133–158.
6. G. L. Weinberg, B. Ullman, and D. W. Martin Jr. (1981) Proc. Natl. Acad. Sci. USA **78**, 2447–2451.
7. R. J. Roberts (1995) Cell **82**, 9–12.
8. E. C. Friedberg, G. C. Walker, and W. Siede (1995) *DNA Repair and Mutagenesis*, ASM Press, Washington DC, pp. 147–153.
9. J. L. Sherley and T. J. Kelly (1988) J. Biol. Chem. **263**, 8350–8358.
10. C. K. Mathews (1975) Exptl. Cell Res. **92**, 47–56.
11. C. K. Mathews (1977) In *Comprehensive Virology*, Vol. **7**, (H. Fraenkel-Conrat and R. R. Wagner, eds.), Plenum Press, New York, pp. 179–294.
12. S. S. Cohen (1968) *Virus-Induced Enzymes*. Columbia Univesity Press, New York.
13. P. Reichard (1988) Ann. Rev. Biochem. **57**, 349–374.
14. B. Nicander and P. Reichard (1985) J. Biol. Chem. **260**, 9216–9222.
15. B. Nicander and P. Reichard (1983) Proc. Natl. Acad. Sci. USA **80**, 1347–1351.
16. V. Bianchi, E. Pontis, and P. Reichard (1992) Exptl. Cell Res. **199**, 120–128.
17. H. Maki and M. Sekiguchi (1992) Nature **355**, 273–275.
18. S. Quirk and M. J. Bessman (1991) J. Bacteriol. **173**, 6665–6669.

Suggestion for Further Reading

19. The best single reference in this area is Chapter "2", “"Biosynthesis of DNA Precursors",” in A. Kornberg and T. Baker (1992) *DNA Replication*, 2nd Ed., W. H. Freeman and Co., New York, pp. 53–100.

Deoxyuridine Triphosphatase

Living cells contain two enzyme systems whose primary role is evidently to assure the exclusion of uracil from DNA where thymine occurs instead. Deoxyuridine triphosphatase (dUTPase) catalyzes the hydrolysis of dUTP to deoxyuridine monophosphate and pyrophosphate, thereby removing from the nucleotide pool a precursor, dUTP, that is recognized by **DNA polymerases** as readily as is thymidine triphosphate for incorporation into DNA opposite template adenine residues. The other system involves a DNA base excision repair process that begins with the action of DNA-uracil *N*-glycosylase. This enzyme cleaves the glycosidic bond linking uracil to deoxyribose, and an oligonucleotide patch that contains the abasic site is removed and replaced.

Current interest in dUTPase focuses on its very high substrate specificity, its significance as a possible chemotherapeutic target, the evolution and functions of virus-coded forms of dUTPase, and the generation and regulation of organelle-specific isoforms in eukaryotic cells.

1. Biological Functions of dUTPase

Although dUTPase was discovered in the early 1960s (1, 2), the enzyme was not characterized as a highly purified protein until 1978 (3). Much of the interest in the 1970s related to the role of uracil metabolism in creating short DNA fragments that had been identified as intermediates in DNA replication. After Okazaki proposed that DNA replication involves the discontinuous synthesis of short DNA fragments—which became known as Okazaki Fragments—several laboratories reported that nascent DNA chains are complementary to both template DNA strands, suggesting that both daughter DNA strands grow discontinuously. However, Tye et al. (4) showed that many of the short fragments arose not as intermediates in replication but through the action of the uracil exclusion systems. Incorporation of dUMP into DNA, followed by the action of uracil *N*-glycosylase and base excision repair, caused DNA strand breakage that converted nascent high-molecular-weight DNA into small fragments. When corrections were made for this factor, it was found that **leading-strand** DNA replication occurs continuously, with short fragments of DNA arising as replication intermediates only in synthesis of the lagging strand.

Why uracil should be excluded from DNA was not immediately apparent because uracil is identical to thymine in its base pairing with adenine, and so its substitution for thymine was not expected to affect DNA function or genetic specificity significantly. Indeed, the existence of bacteriophages, such as the *Bacillus subtilis* phage PBS2, whose DNA contains uracil but no thymine (5), indicates that substituting U for T is *biologically* acceptable. However, it was recognized that uracil can arise in DNA either through incorporation of dUMP opposite dAMP or through deamination of dCMP in a G · C base pair. This latter event is potentially **mutagenic** because the resultant G · U base pair would be converted to an A · T base pair in subsequent rounds of replication. Because dUTPase has no direct involvement in these events, it was thought that dUTPase should be a dispensable function in most organisms. However, El-Hajj et al. (6) were unable to isolate a null mutant of dUTPase in *Escherichia coli*, leading them to speculate that the protein plays an additional, essential metabolic role; similar results were reported for yeast (7). In a later study, however, El-Hajj et al. (8) analyzed a **conditional lethal** dUTPase (*dut*) mutation of *E. coli* and found that it could be suppressed by a mutation in *dcd*, the structural gene for dCTP deaminase, the enzyme that synthesizes dUTP in enteric bacteria (see Deoxyribonucleotide Biosynthesis And Degradation). This finding, plus the construction of a multiple mutant bacterium that survived extensive substitution of uracil for thymine in its DNA (8), indicated that the primary role of dUTPase is indeed to keep the dUTP pool small and facilitate the exclusion of uracil from DNA. The lethality of dUTPase null mutants is ascribed, then, to excessive accumulation of dUMP in DNA, leading to double-strand breaks that result when repair of single-strand breaks occurs at nearby sites on opposite DNA strands.

2. Structure of Deoxyuridine Triphosphatase

The dUTPase molecule must be constructed to exacting design specifications in order to cleave efficiently one deoxyribonucleoside triphosphate while having little or no effect on structurally similar dNTPs needed for DNA synthesis, in particular, dUTP and dTTP. Accordingly, kinetic analysis of *E. coli* dUTPase (9) showed the ratio k_{cat}/K_m (see Enzymes) to be, remarkably, more than 10^5-fold lower for dCTP than for dUTP. The nucleotides dTTP and UTP were even poorer substrates as no action of dUTPase on these nucleotides was detectable. The effects of pH on the K_m for dUTP suggested important contributions of **hydrogen bonding** involving N3 and the carbonyl oxygen on C4 in establishing the specificity of dUTP binding to dUTPase, which is consistent with structural studies (10, 11). Crystallographic analysis of both the *E. coli* and human enzymes reveals a homotrimeric structure, with each of three substrate-binding sites made up from residues in two adjacent polypeptide chains. The bacterial enzyme was crystallized in the presence of a **competitive inhibitor**, dUDP, which identified the active site and provided a structural explanation of the kinetic observations.

3. dUTPase as a Chemotherapeutic Target

Thymidylate metabolism has long been recognized as a target for drugs that would act to inhibit DNA replication in either cancer or infectious diseases (see Thymidylate Synthase; Fluorodeoxyuridine; Dihydrofolate Reductase (DHFR)). Beginning in the early 1980s, it was recognized that a significant contributor to the lethality of inhibitors of dihydrofolate reductase or thymidylate synthase is the accumulation of dUTP and its resultant incorporation into DNA (12). Inhibition of thymidylate synthase flux either directly, by 5-fluorodeoxyuridylate, or indirectly, by inhibition of dihydrofolate reductase, was seen to cause accumulation of dUMP which, in turn, would be converted to dUTP faster than it could be cleaved by dUTPase. Hence, the resultant accumulation of dUMP in DNA was seen to cause double-strand DNA breaks by the process discussed above. The existence of a class of fluorodeoxyuridine-resistant cell mutants with elevated levels of dUTPase (13) is consistent with this interpretation. Now that X-ray crystallography structures for dUTPase are available, this enzyme has been recognized as a suitable target for structure-assisted drug design. In principle, dUTPase inhibitors could be used, either alone or in conjunction with inhibitors of dihydrofolate reductase or thymidylate synthase, to kill proliferating cells selectively by stimulating the incorporation of dUMP into their DNA.

4. dUTPase Isoforms in Eukaryotic Cells

One of the most intriguing recent developments concerning dUTPase (14) relates to the discovery of two different **isoforms** in mammalian cells, one located predominantly in the nucleus and the other localized to mitochondria (although an earlier study (15) had localized human dUTPase to the cytosol). Presumably, the mitochondrial isoform plays the same role in mitochondrial DNA synthesis as the nuclear enzyme plays for nuclear DNA replication. Of great interest is the recent finding of Ladner and Caradonna (16) that both isoforms are encoded by the same nuclear gene, with alternative splicing at the 5′ end of the dUTPase gene (Fig. 1). The use of different 5′ exons for the two isoforms (see Introns, Exons) gives a subunit size of 22 kDa for the cytosolic enzyme and 23 kDa for the mitochondrial isoform. This may be the first reported instance of alternative splicing of the same transcript to generate isoforms of the same enzyme localized in different cell compartments.

Figure 1. Alternative splicing at the 5′ end of the human dUTPase gene as a means to generate nuclear and mitochondrial isoforms of dUTPase. Exons are boxed, and open reading frames of the mitochondrial, nuclear, and common sequences are shown by different shading. Intron/exon boundaries are indicated and numbered with respect to an arbitrary start point for the 5′ end of the gene. The amino-terminal splice junction is indicated by joined lines. Reprinted with permission from R. D. Ladner and S. Caradonna (1997) *J. Biol. Chem*. **272**, 19072–19080.

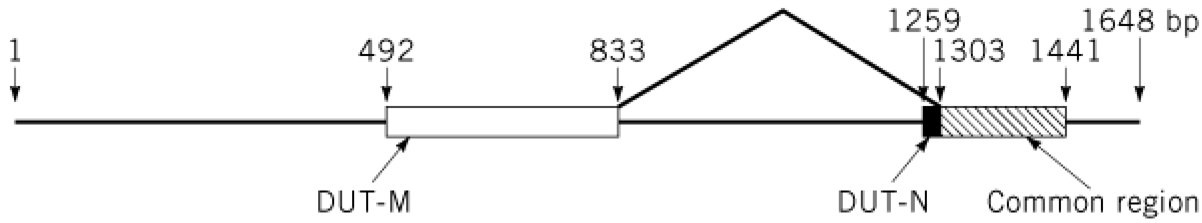

Cell-cycle analysis of protein and messenger RNA levels shows that the mitochondrial enzyme is expressed constitutively throughout the cell cycle (as is mitochondrial DNA replication), whereas the expression of the nuclear form is closely linked to nuclear DNA replication status. The nuclear isoform undergoes **protein degradation** as cells exit the cycle. Whether this differential regulation is related to **phosphorylation** of the enzyme is an intriguing unanswered question. Ladner et al. (14) showed that the cytosolic dUTPase is phosphorylated at Ser11, in a **cyclin**-dependent protein kinase phosphorylation site, whereas the same site remains unphosphorylated in the mitochondrial isoform. The functional significance of this difference has not yet been defined.

5. Virus-Encoded dUTPases

Numerous **virus**-specific forms of dUTPase have been described, including those encoded by the RNA genomes of retroviruses. The first viral dUTPase to be described (17) was shown to be an activity of dCTPase, an enzyme induced after T-even bacteriophage infection, which is responsible for exclusion of cytosine from phage DNA. This activity is essential to the observed complete replacement of cytosine by 5-hydroxymethylcytosine in the phage genome. Purification of dCTPase revealed an associated dUTPase activity (18), and both activities were shown to be intrinsic to the same protein. Also, unlike the unrelated bacterial and eukaryotic dUTPases, the phage enzyme is equally active on the respective deoxyribonucleoside diphosphates, cleaving dCDP and dUDP to dCMP and dUMP, respectively, plus inorganic phosphate. In T4, this multifunctional enzyme is encoded by gene 56. Mutants defective in this gene are lethal because they incorporate dCMP into phage DNA, and the viral genome encodes **nucleases** that specifically recognize and degrade cytosine-containing DNA.

dUTPase is encoded by the genomes of herpes viruses, pox viruses, several nonprimate lentiviruses, and type B and D retroviruses. A sequence in the *gag-pro* gene region of retrovirus genomes, originally identified as the evolutionary result of the duplication of a proteinase gene, was found, as these sequences began to accumulate in the data banks, to be homologous to dUTPase genes (19). Cloning and expression of these "pseudoproteinase" genes showed that they did indeed express functional dUTPases (20, 21). It is of particular interest that the human immunodeficiency virus (HIV) genome does not encode a dUTPase, although such a gene is expressed by the closely related feline immunodeficiency virus (FIV), which is being studied as a model for HIV infection. Lerner et al (22) infected cats with wild-type FIV and with a dUTPase-negative FIV mutant. After nine months of infection, sequence analysis of viral genomes isolated from both groups of infected animals showed a fivefold increase in mutations in the dUTPase-negative infections, most of them involving G → A transitions. These could have arisen from the formation of rG · dU base pairs during **reverse transcription** in the presence of expanded dUTP pools. Of great interest is the possibility that the extreme genetic variability of HIV is related to the lack of a dUTPase gene in the wild-type HIV genome, giving HIV the same mutator **phenotype** as observed in dUTPase-deficient FIV mutants.

Bibliography

1. L. E. Bertani, A. Häggmark, and P. Reichard (1961) J. Biol. Chem. **236**, PC67–PC68.
2. G. R. Greenberg and R. L. Somerville (1962) Proc. Natl. Acad. Sci. USA **48**, 247–257.
3. J. Shlomai and A. Kornberg (1978) J. Biol. Chem. **253**, 3305–3312.
4. B-K. Tye, P-O. Nyman, I. R. Lehman, S. Hochhauser, and B. Weiss (1977) Proc. Natl. Acad. Sci. USA **74**, 154–157.
5. A. R. Price and H. R. Warner (1975) J. Biol. Chem. **250**, 8804–8811.
6. H. H. El-Hajj, H. Zhang, and B. Weiss (1988) J. Bacteriol. **170**, 1069–1075.
7. M. H. Gadsden, E. M. McIntosh, J. C. Game, P. J. Wilson, and R. H. Haynes (1993) EMBO J. **12**, 4425–4431.
8. H. H. El-Hajj, L. Wang, and B. Weiss (1992) J. Bacteriol. **174**, 4450–4456.
9. G. Larsson, P. O. Nyman, and J-O. Kvassman (1996) J. Biol. Chem. **271**, 24010–24016.
10. G. Larsson, L. A. Svensson, and P. O. Nyman (1996) Nature Struct. Biol. **3**, 532–538.
11. C. D. Mol, J. M. Harris, E. M. McIntosh, and J. A. Tainer (1996) Structure **4**, 1077–1092.
12. M. Goulian, B. Bleile, and B. Y. Tseng (1980) J. Biol. Chem. **255**, 10630–10637.
13. C. E. Canman, T. S. Lawrence, D. S. Shewach, H. Y. Tang, and J. Maybaum (1993) Cancer Res. **53**, 5219–5224.
14. R. D. Ladner, D. E. McNulty, S. A. Carr, G. D. Roberts, and S. J. Caradonna (1996) J. Biol. Chem. **271**, 7745–7751.
15. J. A. Vilpo and H. Autio-Harmainen (1983) Scand. J. Clin. Lab. Invest. **43**, 583–590.
16. R. D. Ladner and S. Caradonna (1997) J. Biol. Chem. **272**, 19072–19080.
17. G. R. Greenberg (1966) Proc. Natl. Acad. Sci. USA **56**, 1226–1232.
18. A. R. Price and H. R. Warner (1969) Virology **39**, 882–892.

19. D. J. McGeoch (1990) Nucleic Acid Res. **18**, 4105–4110.
20. A-C. Bergman, O. Björnberg, J. Nord, P. O. Nyman, and A. M. Rosengren (1994) Virology **204**, 420–424.
21. N. A. Roseman, R. K. Evans, E. L. Mayer, M. A. Rossi, and M. B. Slabaugh (1996) J. Biol. Chem. **271**, 23506–23511.
22. D. L. Lerner, P. C. Wagaman, T. R. Phillips, O. Prospero-Garcia, S. J. Henriksen, H. S. Fox, F. E. Bloom, and J. H. Elder (1995) Proc. Natl. Acad. Sci. USA **92**, 7480–7484.

Suggestions for Further Reading

23. A. Kornberg and T. A. Baker (1991) *DNA Replication*, 2nd ed. W. H. Freeman & Co., San Francisco. This book contains a good historical account of the discovery and elucidation of the metabolic roles of dUTPase.
24. E. M. McIntosh and R. H. Haynes (1997) dUTP pyrophosphatase as a potential target for chemotherapeutic drug development. Acta Biochim. Polon. **44**, 159–171. A recent review of the prospects for developing dUTPase inhibitors as useful drugs.

Depurination

An abasic site one lacking a nucleotide base, is created at a site in DNA when the glycosidic bond connecting a **purine** base to the deoxyribose sugar is cleaved, leaving the phosphodiester backbone of the DNA intact (Fig. 1). Depurination occurs at an estimated rate of 10^4 depurinations per mammalian cell per day (1), often through spontaneous hydrolysis. Other processes in the cell that lead to depurination are enzymatic removal of altered bases by specific glycosylases or through chemical modifications of purine bases (primarily alkylation at N7) that labilize the glycosidic bond. There is good evidence that depurination plays a major role in spontaneous **mutagenic** events (2). Although apurinic sites inhibit chain elongation by **DNA polymerases**, bypass must occur because there is enhanced incorporation of nucleotides that are noncomplementary to the template bases. The rate of misincorporation varies with different polynucleotide complexes, but the frequency of misincorporation is directly proportional to the extent of depurination (2).

Figure 1. Formation of an abasic site in DNA depurination.

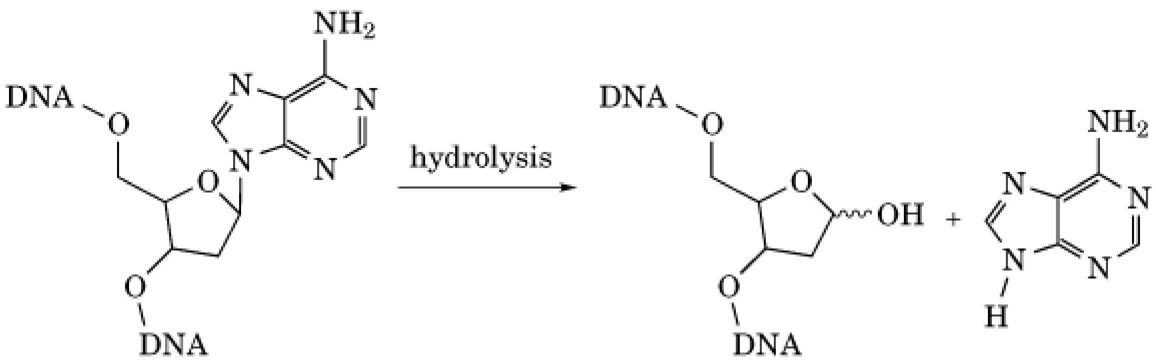

Weymouth and Loeb (3) and Kunkel et al. (4) studied the fidelity of DNA polymerases in copying natural DNA templates and the mutagenic implications of the misincorporation events. They measured revertants generated by misincorporation in *am*3 bacteriophage fX174, a mutant containing a single base-pair substitution mutation. These studies confirmed that the copying of depurinated *am*3 fX174 DNA templates by purified DNA polymerases is mutagenic, and that the frequency of revertants correlates positively with the ability of different polymerases to copy past apurinic sites. Eukaryotic DNA polymerases are error-prone and read past apurinic sites at a high frequency.

Although direct mutagenicity is readily envisaged following error-prone read through of an apurinic site, it also appears that many mutations resulting from depurination in prokaryotes are **SOS-response-dependent** (5). Miller and Low (6) examined more than 600 independent spontaneous mutations in the lacI gene of SOS-induced *E. coli*. Most were specifically G.C → T.A, and to a lesser extent A.T → T.A, transversions and occurred primarily at certain sites. These transversion mutations are thought to have arisen from the insertion of dAMP opposite purines or apurinic sites, possibly through the SOS-induction process altering the specificity of the DNA replication complex to favor misincorporation of dAMP opposite purines. Miller and Low suggested that many spontaneous mutations may result from replication past cryptic apurinic sites. There are also several lines of evidence that apurinic sites are intermediates in mutagenesis by chemicals that form bulky DNA adducts (2).

Bibliography

1. T. Lindahl and B. Nyberg (1972) Biochemistry **11**, 3610–3618.
2. L. A. Loeb (1985) Cell **40**, 483–484.
3. L. A. Weymouth and L. A. Loeb (1978) Proc. Natl. Acad. Sci. USA **75**, 1924–1928.
4. T. A. Kunkel, R. M. Schaaper, and L. A. Loeb (1983) Biochemistry **22**, 2378–2384.
5. T. A. Kunkel (1984) Proc. Natl. Acad. Sci. USA **81**, 1494–1498.
6. J. H. Miller and K. B. Low (1984) Cell **37**, 675–682.

Desmosomes, Desmocollin, Desmoglein, and Desmoplakin

Desmosomes are punctate, adhesive intercellular cell junctions that bind cells together and provide membrane anchoring points for the intermediate-filament cytoskeleton (Fig. 1). They are circular membrane domains of up to 0.5 µm in diameter. The intercellular material, or desmoglea, has a highly organized ultrastructure consisting of an electron-dense midline that is bridged to the plasma membranes of the adhering cells across a distance of ~30 nm. Close to the cytoplasmic faces of the plasma membranes are dense outer plaques, the most consistent and easily recognizable feature of these junctions, approximately 20 nm in thickness. At about 50 nm from the plasma membranes are less dense inner plaques that appear to associate with the intermediate filaments. Thus the total thickness of a desmosome from one inner plaque to the other is approximately 130 nm. The desmosomes may be thought of as the "scaffold couplings" that link the intermediate filament cytoskeleton throughout a tissue. Widely distributed, desmosomes are especially abundant in stratified epithelia, where strong intercellular adhesion is required to resist external friction. They are present in almost all epithelia, but also in cardiac muscle, the arachnoid and pia of the meninges, and the follicular dendritic cells of the lymphoid system.

Figure 1. An electron micrograph of a desmosome from mouse tongue epithelium, showing the midline (ml), the outer and inner plaques (op and ip), and the intermediate filament (if) or tonofilament.

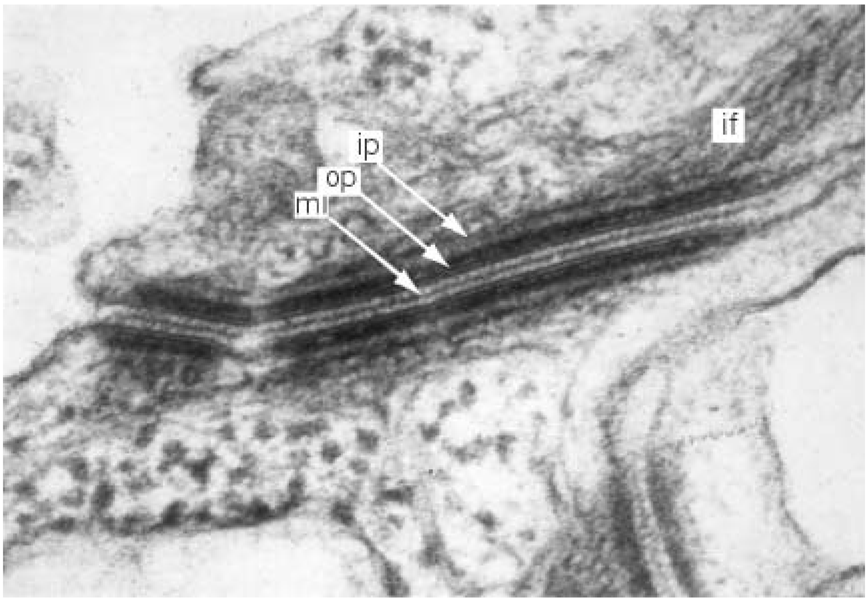

Desmosomes are macromolecular complexes consisting of at least six interacting proteins (Fig. 2). Their adhesion molecules are the desmocollins and desmogleins, members of the cadherin family of calcium-dependent cell **adhesion molecules** (1, 2). These transmembrane proteins have their extracellular domains in the desmoglea and their cytoplasmic domains in the dense outer plaques. The outer plaque contains two proteins that are members of the armadillo family named after the *Drosophila* segment polarity signaling gene. These are plakoglobin (3), also known as g-catenin and present in other intercellular junctions, and plakophilin (4). The outer and inner plaques are bridged by the plakin family member desmoplakin (5), which mediates interaction between the adhesive domain and the intermediate filaments. The most recently discovered desmosomal components are the two plakin family members, envoplakin (6) and periplakin (7), which although not exclusively epidermal, appear to be involved in cornified envelope formation.

Figure 2. Diagram showing the major principle molecular components of the desmosome and their location within its structure. The diagram shows one-half of a demosome from the midline (ml) in the intercellular space, through the plasma membrane (pm) and the outer plaque (op), to the inner plaque (ip) and the intermediate filaments. The numbers at the bottom represent distances in nanometers from the plasma membrane. The amino-terminus (n) and the carboxy-terminus (c) of each component is indicated. The positions of these have been mapped by immuno-gold labeling with domain-specific antibodies and electron microscopy (unpublished observations). The components are: DP, desmoplakin; Dsc a, desmocollin “a” form; Dsc b, desmocollin “b” form; Dsg, desmoglein; PG, plakoglobin; PP, plakophilin.

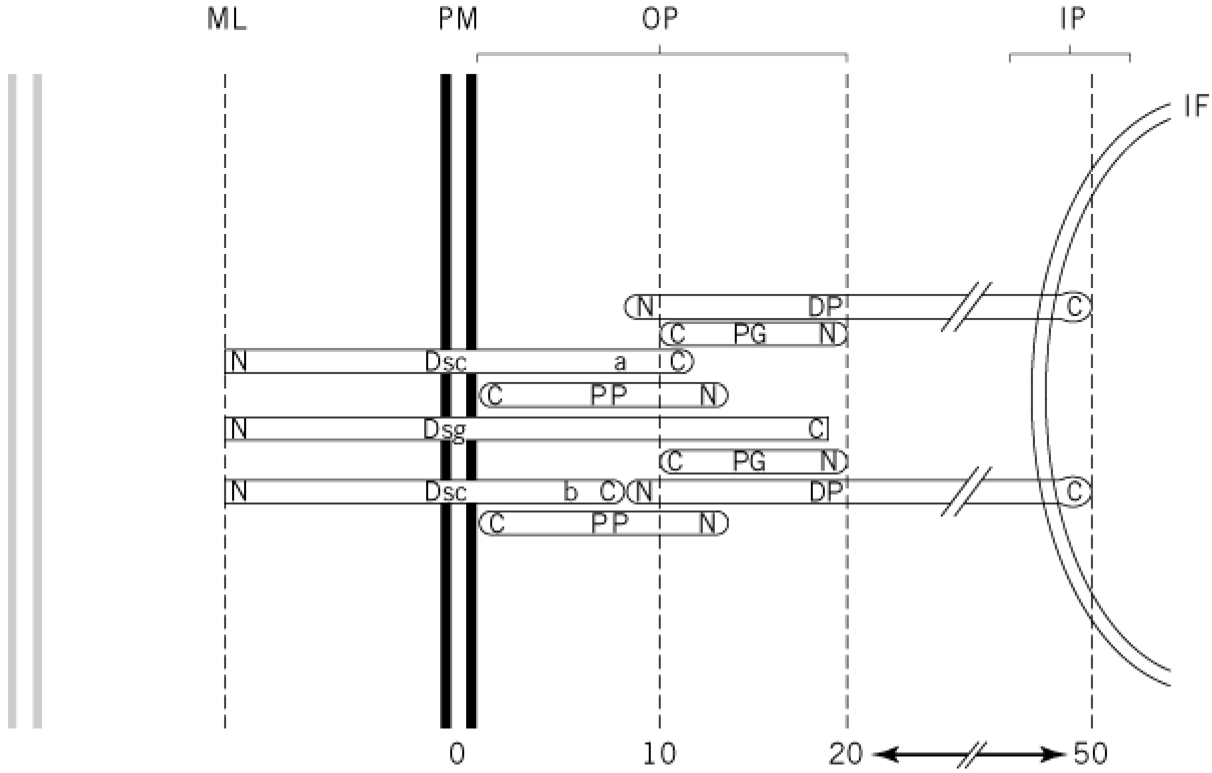

1. Desmosomal Glycoproteins

There is direct evidence that the desmocollins (Dsc) and desmogleins (Dsg) mediate desmosomal adhesion, probably by a heterophilic interaction (8). Adhesive interaction probably involves tripeptide sequences known as "cell adhesion recognition sites" near the amino termini of the glycoproteins (9). These molecules represent two subfamilies of the cadherin superfamily, each occurring as three different isoforms and the products of different genes. The molecules resemble classical cadherins in their extracellular domains, but show unique features cytoplasmically. Desmocollins have **alternatively spliced** cytoplasmic **domains** [the longer "a" form and a shorter "b" form (10)], and the desmogleins have long cytoplasmic domains containing unique 29-amino-acid-residue repeats (11). The extracellular domains of these glycoproteins form an ordered array, giving rise to the highly structured desmosomal midline region or desmoglea. Their cytoplasmic domains contribute to the structure of the cytoplasmic plaque. The precise roles of the different cytoplasmic domains are unclear. That of the desmocollin "a" form can support plaque assembly and intermediate filament attachment (12), but the functions of desmoglein and desmocollin "b" in plaque assembly have not been resolved. Both desmocollin and desmoglein have been shown to bind plakoglobin and plakophilin, and desmocollin "a" can also bind desmoplakin. Three isoforms of desmocollin and desmoglein show tissue-specific expression (13, 14). Dsc2 and Dsg2 are ubiquitous in all desmosome-bearing tissues, but Dsc1, Dsg1, Dsc3, and Dsg3 are largely restricted to stratified epithelia. Desmosomal glycoprotein genes are closely linked on chromosome 18q12, and this is of possible significance for regulation of the expression.

2. Plakoglobin

Plakoglobin is a member of the *armadillo* family of proteins. It is not exclusively desmosomal but also occurs in adherens or intermediate junctions, even in non-desmosome-bearing tissues such as endothelia. It is, like b-catenin and armadillo itself, both a junctional protein and a member of the **wingless** Wnt signaling pathway (15). In its junctional role, it combines both with desmocollin and desmoglein, or with E-cadherin, where it is mutually exclusive with that of b-catenin. Null mutations of desmoplakin in mice result in severe disruption of desmosomes in cardiac muscle and epidermis. In its signaling role, it has been shown to produce axis duplication when overexpressed in *Xenopus* embryos and combined with the adenomatous polyposis coli (APC) protein that regulates its cytoplasmic level. The cytoplasmic plakoglobin can bind to the LEF-1 transcription factor to enter the nucleus and regulate gene activity (16).

3. Plakophilin

This is an armadillo family protein that has important junctional properties and possibly a signaling function. It exists as two isoforms that show differential tissue specific expression, PP1 being predominantly expressed in stratified tissues (17) and PP2 ubiquitously (18). The first human genetic disease resulting from a desmosomal mutation was an epidermal dysplasia/skin fragility syndrome, effectively a PP1 null mutation (19). This defect resulted in loss of adhesion between epidermal keratinocytes and detachment of intermediate filaments from the cell periphery, indicating an important role for plakophilin in linking between the desmosomal adhesion molecules and the cytoskeleton. Plakophilin has been shown to bind to both desmosomal glycoproteins, desmoplakin and cytokeratin (20). Its potential signaling role is inferred from its armadillo-type structure and because it has been detected in cell nuclei.

4. Desmoplakin

This is a plakin family member, together with plectin, bullous pemphigoid antigen 1 (BAPG1), envoplakin, and periplakin (6, 7). Except for BAPG1 all have been reported to be associated with desmosomes. Desmoplakin (DP) is a ubiquitous desmosomal component. DP1 is a coiled-coil dimer with globular end **domains**. The isolated molecule has an overall length of 130 nm. DP2 lacks the central coiled rod domain and is unable to dimerize. Its length is 43 nm. Expression studies, supported by immunogold labeling and electron microscopy (see Immunoelectron Microscopy), show that the amino-terminal globular domain associates with the desmosomal plaque and the carboxy-terminal domain with the intermediate filaments (21, 22). Thus desmoplakin plays an important role in linking between the desmosomal plaque and the cytoskeleton. Although not restricted to epidermis, envoplakin and periplakin were only identified as components of the cornified envelopes of suprabasal keratinocytes (6, 7). They are essentially similar in structure to desmoplakin, and their precise role has yet to be defined. The role of plectin is more problematic, because null mutations have no apparent effect on desmosome structure and function.

Desmosomal glycoproteins are target antigens in the **autoimmune** blistering disease of pemphigus (23). Desmosomes appear at the 32- to 64-cell stage of embryonic development, where they are trophectoderm specific (24).

Bibliography

1. J. L. Holton et al. (1990) J. Cell Sci. **97**, 239–246.
2. P. J. Koch et al. (1990) Eur. J. Cell Biol. **53**, 1–12.
3. P. Cowin et al. (1986) *Cell* 1063–1073.
4. M. Hatzfeld et al. (1994) J. Cell Sci. **107**, 2259–2270.
5. H. Mueller and W. W. Franke (1983) J. Mol. Biol. **163**, 647–671.
6. C. Ruhrberg et al. (1996) J. Cell Biol. **134**, 715–729.
7. C. Ruhrberg et al. (1997) J. Cell Biol. **139**, 1835–1849.
8. N. A. Chitaev and S. M. Troyanovsky (1997) J. Cell Biol. **138**, 193–201.
9. C. Tselepis et al. (1998) Proc. Natl. Acad. Sci. USA **95**, 8064–8069.
10. J. E. Collins et al. (1991) J. Cell Biol. **113**, 381–391.
11. G. N. Wheeler et al. (1991) Proc. Natl. Acad. Sci. USA **88**, 4796–4800.
12. S. Troyanovsky et al. (1993) Cell **72**, 561–574.

13. P. K. Legan et al. (1994) J. Cell Biol. **126**, 507–518.
14. S. Schäfer, P. J. Koch, and W. W. Franke (1994) Exp. Cell Res. **211**, 391–399.
15. P. Cowin and B. Burke (1996) Curr. Opin. Cell Biol. **8**, 56–65.
16. O. Huber et al. (1996) Mech. Dev. **59**, 3–10.
17. H. W. Heid et al. (1994) Differentiation **58**, 113–131.
18. C. Mertens et al. (1996) J. Cell Biol. **135**, 1009–1025.
19. J. McGrath et al. (1997) Nature Genet. **17**, 240–244.
20. E. A. Smith and E. Fuchs (1998) J. Cell Biol. **141**, 1229–1241.
21. E. A. Bornslaeger et al. (1996) J. Cell Biol. **134**, 985–1001.
22. A. P. Kowalczyk et al. (1997) J. Cell Biol. **139**, 773–784.
23. J. R. Stanley (1995) In "Cell adhesion and human disease." Ciba Found. Symp. **189**, 107–120.
24. T. P. Fleming et al. (1991) Development **112**, 527–529.

Suggestions for Further Reading

25. D. R. Garrod et al. (1998) "Desmosomes". In *Adhesive Interactions of Cells* (D. R. Garrod, M. A. J. Chidgey, and A. J. North, eds.), JAI Press, Greenwich, CT, pp. 165–201. (A review of the latest desmosome literature and a good source of reference.)
26. K. J. Green and J. C. R. Jones (1996) FASEB. J. **10**, 871–881. (Another excellent review.)

Detergents

1. Detergents as Amphiphilic Molecules

Gene expression studies in both **eukaryotes** and **prokaryotes** eventually require detecting and enriching the expression product, usually a protein. When this gene product is a water-soluble, **cytosolic** protein, detecting and enriching it can begin by simply homogenizing the cells, followed by **centrifugally** separating the supernatant from the membrane-bound proteins that remain in the pellet. When the **gene** product is a plasma membrane protein, however, the task is complicated because the protein has to be detached from the membrane at some stage. Although some loosely attached proteins are released by treatment with salt solutions, integral membrane proteins are released only upon treatment with amphiphilic reagents, also termed detergents .

By definition, amphiphiles harbor both hydrophilic and **hydrophobic** moieties. In a water-oil or water-lipid mixture, detergent molecules accumulate at the interface. The hydrophobic arm is inserted into oil or lipid, and the hydrophilic (polar) end is introduced into water, thus justifying the adjective "*amphi*philic" used to describe this class of compounds. Depending on the degree of polarity, the hydrophilic end (the polar head group) of a detergent is either ionic or nonionic. Regardless of the difference in polar head groups, all detergents dissolve in water. The physicochemical properties of detergents dissolved in water have been the focus of vigorous biochemical research.

1.1. Physiological Importance of Detergents

Amphiphilic substances or detergents are central to our existence as living organisms. About 80% of the lipids in the alveolar lining is dipalmitoyl phosphatidylcholine that acts as a detergent to confer the crucial nonatelectic property to the lungs. This unusual proportion of a particular phospholipid is important because lower levels of this lipid in the alveolus lead to atelectasis (collapsed alveolus) in infants. Similarly, bile acids are crucial detergent molecules in the intestines. Bile acids emulsify water-insoluble fat molecules and thus help the intestinal lining to absorb them. The powerful detergents, lysophospholipids, produced in the intestine by phospholipase A_2-mediated cleavage of the C_2 fatty acid chains of phospholipids, also aid in lipid digestion. In fact both bile acids and lysophospholipids aid in lipid absorption and also help in absorbing and removing the metabolic products of fats and lipids.

2. General Strategy for Obtaining Solubilized and Reconstituted Membrane Proteins

Solubilization of a membrane protein is a procedure in which the proteins and lipids, originally cradled in the membrane, are dissociated appropriately in a buffered detergent solution. This controlled dissociation of the membrane results in the forming small protein and lipid clusters that remain dissolved in the aqueous solution. Next the solubilized material is separated from any insoluble substance (aggregated proteins and lipids that are dissociated by the detergent) by centrifugation. Then, the detergent is removed from the solubilized material because only after removing the detergent do the solubilized proteins and lipids reaggregate appropriately so that the activity of a functional protein is restored. Many of the functional membrane proteins retain their activity only when they are allowed to associate with other specific membrane proteins and lipids. Such reaggregation is inhibited in the presence of the dissociation-promoting detergent. Typical methods to remove detergents include (1) extensive dialysis of the detergent-solubilized fractions, whereby the detergent monomers are released from the dialysis bag; (2) **gel filtration**, which helps to retain the detergent monomers on the column while the high molecular weight, solubilized proteins flow through; or (3) hydrophobic chromatography, whereby the hydrophobic detergent molecules are removed by absorption into a hydrophobic matrix. The success of each procedure depends on the physicochemical properties of the detergent, which determine the formation of detergent aggregates, termed micelles (Fig. 1). Therefore, it is important to identify and define some of the factors that regulate aggregation of detergent molecules. The critical micelle concentration (cmc) is the maximum concentration at which the detergent molecules remain as monomers. Removal of detergents by dialysis or gel filtration occurs through the monomer and is difficult when the cmc is very low.

Figure 1. Structures of detergents and micelles. At the critical micelle concentration (cmc), monomeric molecules (**a**), which are stable below cmc and removable by dialysis, aggregate to form a spherical or cylindrical macromolecular micelle (**b**), which is stable above the cmc and cannot be removed by dialysis. In a micelle, the hydrophobic ends of the detergent molecules are pointed inward and away from water whereas the polar ends (head groups) are pointed outward into the aqueous phase. In the presence of a plasma membrane bilayer containing saturated and unsaturated fatty acid containing phospholipids (**c**), mixed micelles (**d**) that contain detergent molecules and plasma membrane lipids and proteins are formed.

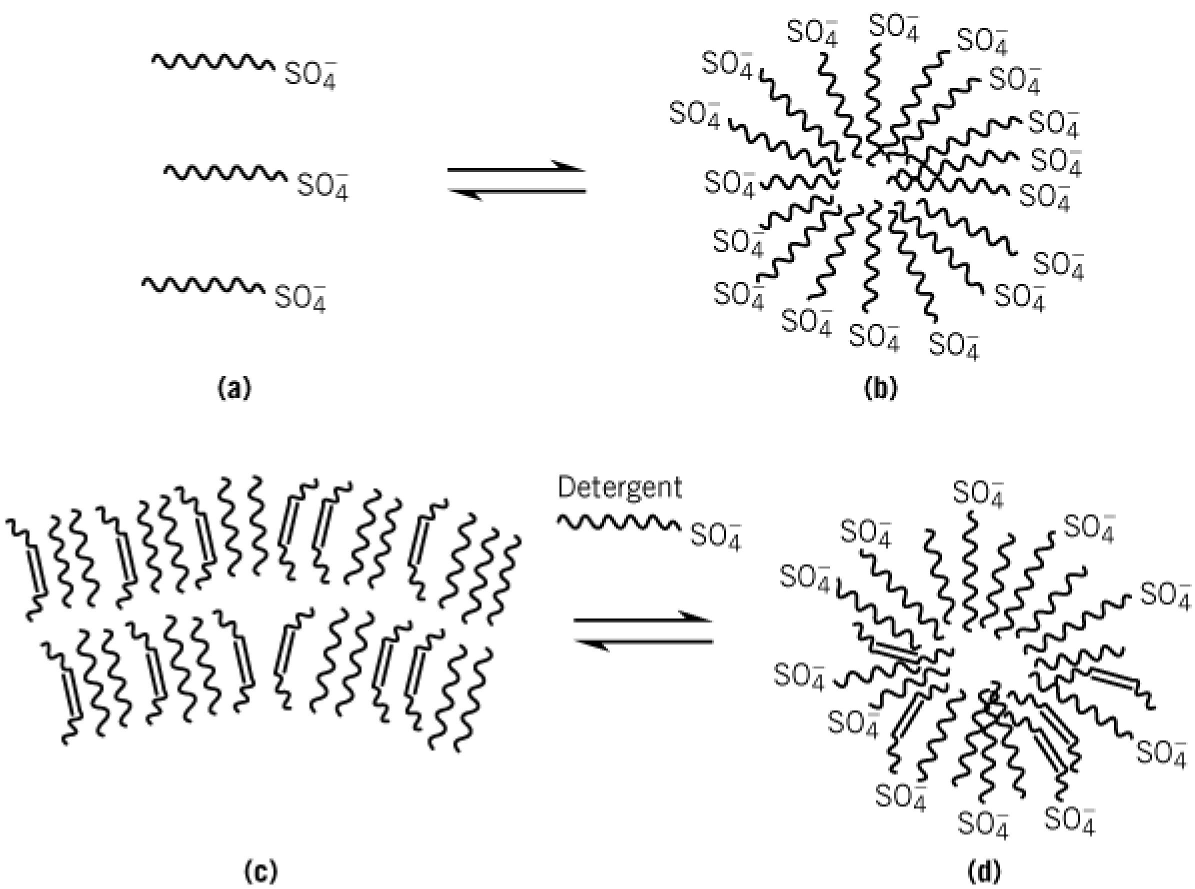

2.1. Different Classes of Detergents and Their Applicability in Solubilizing Membrane Proteins

As shown in Fig. 2, the various detergents can be structurally classified as follows:

1. Negatively charged, strongly ionic detergents: (a) a detergent with a long, flexible aliphatic chain: sodium dodecylsulfate (**SDS**) (cmc ~0.23% (*w*/*v*) or 8 mM); (b) a detergent with a rigid structure: sodium cholate (cmc ~0.43% or 10 mM). Sodium cholate (1%) has been used to solubilize the adenylate cyclase-G-protein complex (1), the dopamine D1 **receptor** (2) and many other receptors.
2. Detergents that form hydrogen bonds: (a) detergents with flexible long-chain structures: octanoyl- *N*-methylglucamide (MEGA-8) (cmc ~1.9% or 60 mM), and a long chain polyoxyether, Thesit (cmc ~0.005% or 0.09 mM), which is structurally similar to Lubrol. Although 0.5% MEGA-8 has been used to solubilize intrinsic membrane proteins (3), a Thesit concentration of 1.2% has been used with membrane proteins, such as adenylate cyclase (4). (b) more polar but non-ionic detergents with sugar rings, *n*-dodecyl-ß-maltoside (cmc ~0.009% or 0.18 mM) and n-octyl-ß-glucoside (cmc ~0.7% or 23.2 mM), which have been used to solubilize the nicotinic acetylcholine receptor [1% *n*-octyl-ß-D-glucoside, (5)], opioid receptors [0.3% *n*-octyl-ß-D-glucoside, (6)], **GABA**$_A$ receptors [1% *n*-octyl-ß-D-glucoside, (7)], photoreceptor guanylate cyclase [1% *n*-dodecyl-ß-D-maltoside, (8)], and others.
3. Hydrophobic detergents with long polyoxyether chains and aromatic rings: **Triton X-100** (cmc ~0.013% or 0.2 mM) and Triton X-114 (cmc ~0.011% or 0.21 mM), which are used to solubilize the receptors for GABA [2% Tr X-100, (9)], prostacyclin (10), prolactin [1% Tr X-100, (11)], transferrin [1% Tr X-100, (12)], insulin [2% Tr X-100, (13)] and a neuronal growth cone protein, GAP-43 [1% Tr X-114, (14)].
4. **Zwitterionic** detergents: (a) a detergent with a flexible, long-chain structure: *N*-dodecyl-*N,N*-dimethyl-3-ammonio-1-propanesulfonate (in short, propanesulfonate) (cmc ~0.12% or 3.6 mM); (b) detergents with a rigid structure: CHAPS (cmc ~0.46% or 7.4 mM) and CHAPSO (cmc

~0.5%, 8 mM), commonly used to solubilize receptors, such as those for colony-stimulating factor [0.5% CHAPS, (15)], opiates [0.6% CHAPS, (16)], neurotensin [0.6% CHAPS, (17)], **somatostatin** [0.6% CHAPS, (18)], adenosine A_1 [2.5% CHAPS, (19)] and human prostatic sex-hormone-binding globulin receptor [6.0% CHAPS, (20)].

5. Positively charged, strongly ionic detergents, for example, cetylpyridinium chloride.
6. Nonionic surfactants that form inclusion complexes, for example, cyclodextrin.
7. Specific detergents, such as digitonin, used to solubilize opioid receptors [2% digitonin, (21)], neurotensin receptors [2% digitonin, (22)], ß-adrenoreceptors (23), dihydropyridine Ca^{2+} channels [1% digitonin, (24)], and many others.

Figure 2. Classification of detergents based on structural features.

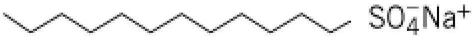

Sodium dodecyl sulfate (SDS)

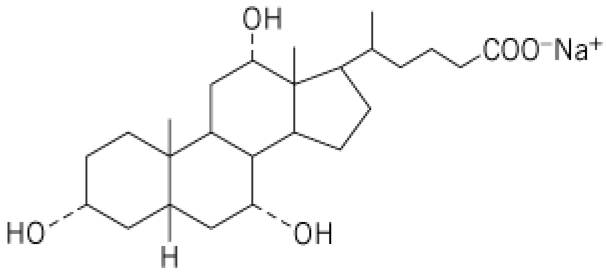

Sodium cholate (Sod. cholate)

Thesit

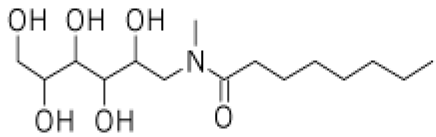

MEGA-8

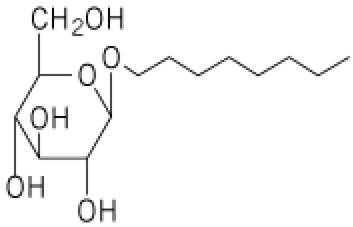

Octylglucoside (Octylglc)

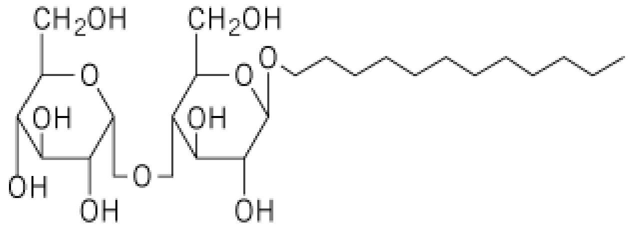

n-dodecyl-β-D-maltoside (Dodmalt)

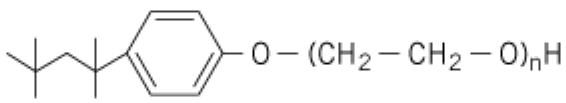

Triton X-114 (n=7) (TrX-114)
Triton X-100 (n=10) (TrX-100)

N-Dodecyl-N, N-dimethyl-3-ammonio-1-propanesulfonate (Propansulfon)

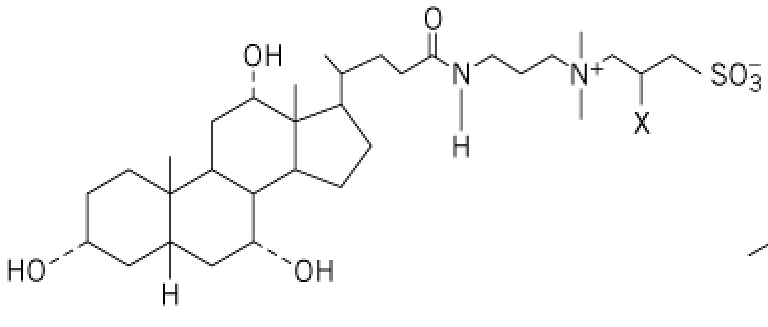

3-[(3-Cholamidopropyl)dimethylammonio]-1-propanesulfonate(CHAPS) (X=H)
3-[(3-Cholamidopropyl)dimethylammonio]-2-hydroxy-1-propanesulfonate(CHAPSO) (X=OH)

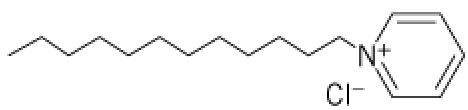

Cetylpyridiniumchloride (CPC)

Thus, the detergent concentrations used for solubilizing most biologically active receptor proteins are typically in the range of 0.5 to 2.0% (w/v), suggesting that for practical purposes the cmc is not the deciding factor for choosing detergent concentration. Instead, it is obtained empirically by optimizing protein-solubilization conditions.

The other key factor in solubilizing biologically active membrane proteins is the ratio of detergent to protein maintained during solubilization. The commonly used ratios are 1:1 (16, 19) and 2 to 3:1 (4, 7, 8). Higher ratios, such as 10:1 (20) are used less often. Optimization experiments observed that the coextracted lipids are essential for reconstituting the solubilized, sheep brain serotonin 5-HT$_{1A}$ receptor (25), and the highest yield of the active 5-HT $_{1A}$ sites was obtained with 2% CHAPS at a detergent to protein ratio of 2:1 (26). This topic is discussed in more detail later.

2.2. Other Uses of Detergents

Detergents are also used in purifying **DNA** and **RNA** molecules. For example, SDS is used to denature polynucleotide molecules during the preparation of DNA, and a structurally related detergent, sodium salt of *N*-laurylsarcosine (Sarkosyl), is used in preparing RNA (27, 28). In either case, the detergent is used to denature the biopolymers and also to inhibit certain enzymes, such as **deoxyribonucleases** and **ribonucleases**, which degrade these molecules. Thus detergents are inseparable from scientific activity whether it is to solubilize lipids and proteins or to purify DNA and RNA.

2.3. Detergent Solubilization of Membrane Lipids

A survey of the literature (1-26) indicates that there is no general agreement on the choice of detergent for a single membrane protein, and the use of five or more different classes of detergents for a given receptor solubilization, usually at a concentration 1 to 2%, irrespective of the cmc, is quite common. This could account for the variable recovery of biological activity in different preparations, but it does not explain the differential efficacy of the different detergents in solubilizing active receptor proteins.

To resolve this question, the protein- and lipid-extracting abilities of each detergent in Fig. 2 were determined. Sufficient variability was observed to explain much of the bewildering variability in the recovery of biological activity reported in the literature (26). The receptor molecule used as a marker in this study was the sheep brain serotonin 5-HT $_{1A}$ receptor, which is a member of the receptor family with seven transmembrane regions, and may couple either to adenylate cyclase or phospholipase C, depending on the type of cell in which it is expressed (26). Solubilized, high-affinity serotonin 5-HT$_{1A}$ receptor sites are reconstituted only by coextracted lipids, and adding separately isolated, pure or mixed lipids during or after solubilization is completely ineffective in reactivating an inactive preparation (25). Instead, adding lipids or lipid vesicles to already solubilized, reconstituted (in coextracted lipids) and active 5-HT$_{1A}$-R preparations inhibits the **ligand-binding** activity of the receptor. Such findings indicated that coextraction of plasma membrane lipids is important in order to maintain the functionally active conformation of lipid-sensitive membrane proteins, such as the serotonin 1A receptor. So the efficiency of many detergents in solubilizing membrane lipids was studied. Considering the total amount of lipid solubilized by each detergent, detergents with long aliphatic chains that terminate in a negative charge (SDS), a zwitterionic sequence (CHAPS or CHAPSO), or a multihydroxylic-group-containing disaccharide (*n*-dodecyl-b-D-maltoside) (DDM) clearly has greater ability to solubilize lipids, irrespective of the cmc of the detergent (Fig. 3). In contrast to detergents, such as sodium cholate or sodium deoxycholate, which are also efficient in solubilizing membrane lipids, CHAPS, CHAPSO and DDM solubilized active 5-HT$_{1A}$ receptors. These results indicate that CHAPS, CHAPSO, and DDM, which are relatively milder and nondenaturing, allow the 5-HT$_{1A}$-R-membrane lipid complex to remain undisturbed during solubilization, thus allowing recovery of the active 5-HT$_{1A}$-R following removal of these detergents (25, 26).

Figure 3. Concentration of proteins and lipids (mg/mL) in the detergent-solubilized and reconstituted vesicles, compared to the solubilization of high-affinity 5-HT_{1A} binding sites.

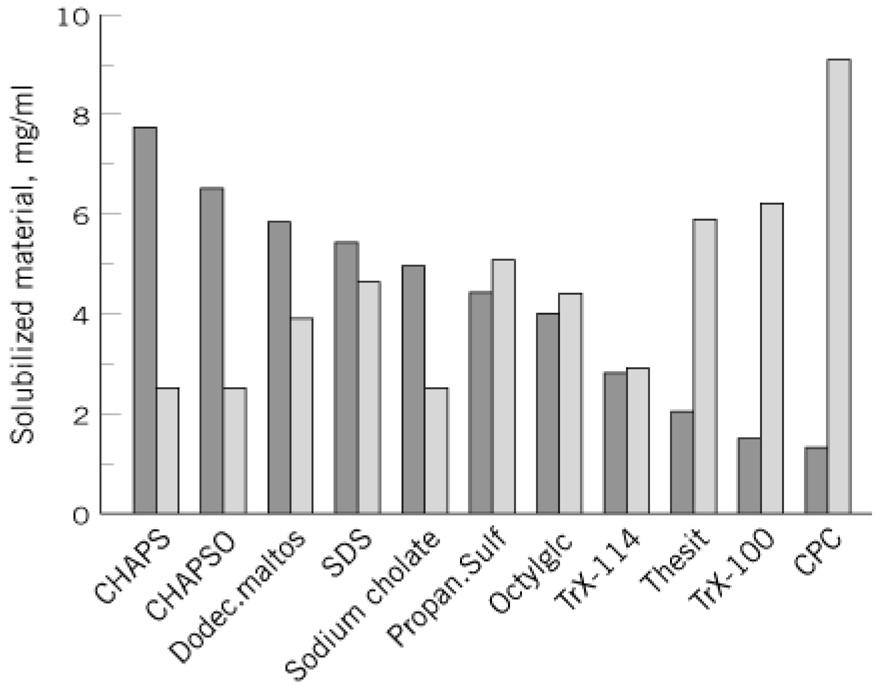

Sodium cholate has a high cmc of approximately 8 mM (or 0.5%) and is easily dialyzed like CHAPS or CHAPSO (both of which have a cmc of ~0.5%). However, although it forms vesicles (because it coextracts sufficient lipid to give a similar lipid to protein ratio of ~2:1) (Table 1 and Fig. 3), the 5-HT_{1A} receptors obtained in the reconstituted preparations are inactive. Possible explanations include nonextraction or denaturation of the protein because of the strongly ionic nature of sodium cholate. Octylglucoside presents a different picture. As a mild, nonionic, dialyzable (cmc ~0.7%) and very mildly denaturing detergent, it is often used to extract biologically active proteins (5-7). However, its inability to coextract sufficient lipid (a lipid to protein ratio of 1:1.1) probably accounts for the low amount of solubilized 5-HT_{1A} receptor activity, which contains less than 15% of the lipids in comparable DDM supernatants.

Table 1. Distribution of Lipids, Protein, and Serotonin $5HT_{1A}$ Receptor Binding Activity in the Vesicles Obtained after Detergent Removal Followed by Dialysis and Ultracentrifugation

Detergents	Lipid, mg/mL	Protein, mg/mL	PE, %	PC, %	PS, %	PI, %	SM, %	GalCers, %	C, %	$5HT_{1A}$ Receptor Binding
CHAPS	7.7	2.5	40.0	17.6	21.0	10.3	0.0	2.8	7.7	5500.0
CHAPSO	6.5	2.5	27.9	16.2	34.0	10.0	0.7	2.7	8.5	5300.0
Dodecylmaltoside	5.8	3.9	18.3	14.8	31.3	5.3	5.9	6.5	17.7	3200.0
SDS	5.4	4.6	22.0	28.7	13.0	6.8	5.0	11.2	14.0	0.0

Sodium cholate	4.9	2.5	18.2	17.0	27.9	6.0	8.5	13.4	8.5	360.0
Propanesulfonate	4.4	5.1	22.8	29.8	19.2	17.2	5.1	8.2	10.6	60.0
Octylglucoside	4.0	4.4	25.0	20.0	24.4	6.5	1.6	8.7	13.6	600.0
Triton X-114	2.8	2.9	32.5	24.2	14.3	7.6	1.5	3.8	15.9	90.0
Thesit	2.0	5.9	14.8	37.0	13.3	5.2	3.0	12.6	14.1	155.0
Triton X-100	1.5	6.2	20.5	27.7	11.6	9.8	2.7	9.8	17.9	80.0
CPC	1.3	9.1	25.0	21.0	22.6	5.7	5.7	9.6	10.7	0.0

The detergents that extract large amounts of protein but are at the lower end of the lipid extraction scale (such as Thesit, Triton X-114, Triton X-100, and CPC) cannot solubilize enough lipid to produce vesicles and do not solubilize active 5-HT_{1A} sites. Therefore, such G-protein-associated receptors require an environment containing particular lipids (enriched in PE, PS and PI) to express their biological properties fully.

The relative amounts of individual groups of lipids solubilized by the different classes of detergents are surprisingly diverse (Table 1). The inverse profiles of PC and PS are intriguing in view of earlier work showing that PC [and GalCer, sulfated GalCer (Su) and SM] are enriched in the outer membrane domain, whereas PS (and PE and PI) are enriched in the inner membrane domain (29-31). From the profile for SM it also appears that this lipid is probably localized in the PC-containing domains. This is agrees well with the idea that choline phospholipids are concentrated in the outer leaflet of the membrane bilayer. It is hard to explain this asymmetrical extraction of lipids in terms other than specific detergent binding by the protein. Thus for eight of the twelve detergents tested, it was found that the solubilization-enrichment profile of PI is similar to that of PE, indicating a similar, inner membrane localization of PE, PI, and PS. PS binds to protein kinase C on the cytosolic face of the plasma membrane and results in activating this enzyme (31). This is consistent with the idea that the PI family is the source of internally released second messengers (32). The serotonin 5-HT_{1A} receptor polypeptide has seven transmembrane **alpha-helices** and three cytosolic loops (26), which could be more strongly associated with inner membrane lipids. Differences in protein folding could explain why a strongly denaturing detergent, such as sodium cholate, is useful in solubilizing and reconstituting the dopamine D1 receptor [which can be reconstituted by adding separately isolated lipids (2)] but is ineffective in solubilizing and reconstituting the 5-HT_{1A} receptors.

3. Summary

The importance of detergents in the normal functions of a living body is irrefutable. In scientific research, detergents provide a powerful means of undertaking subcellular fractionation of macromolecules, such as proteins, RNA, and DNA. Although gene expression studies do not directly begin with protein purification, the expressed protein is finally purified or detected through biochemical methods, such as column chromatography, **Western blotting** analysis, or enzyme assays. If the expressed protein is **lysosomal** or **cytosolic**, simply homogenizing the cells in a hypotonic buffer, followed by separation of the soluble proteins by centrifugation, yields a supernatant that contains the required protein. However, if the expressed protein is, for example, a **mitochondrial** membrane protein, detergent solubilization of this protein is required before its assay. Although in earlier studies such choices of detergents were made empirically, the data presented here provide a stronger foundation for judicious analysis of the efficacy and applicability of many of the commonly used detergents. Thus, for immunoblot analysis, one might use Triton X-100 or Nonidet P-40. To solubilize proteins that do not require membrane lipids for acquiring functional activity, one might use either the Triton family of detergents, the bile acid detergents (eg, sodium cholate), or octylglucoside. On the other hand, if the protein is heavily lipid-dependent, one should test CHAPS, CHAPSO, or DDM before using other detergents. Therefore, this practical overview of the structural classification of detergents with appropriate reference to their applicability to protein and lipid solubilization and to reconstitution of functional activity could be helpful in scientific research involving expression of specific genes.

4. Acknowledgment

The author wishes to thank Dr. Michael Hogan, Neuroscience Program, for carefully reading the manuscript and for his helpful suggestions.

Bibliography

1. P. C. Sternweis and A. G. Gilman (1979) J. Biol. Chem. **254**, 3333–3340.
2. A. Sidhu (1990) J. Biol. Chem. **265**, 10065–10072.
3. J. E. K. Hildreth (1982) Biochem. J., **207**, 363–366.
4. A. K. Keenan, A. Gal, and A. Levitski (1982) Biochem. Biophys. Res. Commun. **105**, 615–623.
5. J. M. Gonzalez-Ros, A. Paraschos, M. C. Farach, and M. Martinez-Carrion (1981) Biochim. Biophys. Acta. **643**, 407–420.
6. T. Fujioka, F. Inoue, S. Sumita, and M. Kuriyama (1988) Biochem. Biophys. Res. Commun. **156**, 54–60.
7. S. M. J. Dunn, R. A. Shelman, and M. W. Agey (1989) Biochemistry **28**, 2551–2557.
8. K. W. Koch (1991) J. Biol. Chem. **266**, 8634–8637.
9. T. N. Sato and J. H. Neal (1989) J. Neurochem. **52**, 1114–1122.
10. A. K. Dutta-Roy and A. K. Sinha (1987) J. Biol. Chem. **262**, 12685–12691.
11. H. Okamura, S. Raguet, A. Bell, J. Gagnon, and P. A. Kelly (1989) J. Biol. Chem. **264**, 5904–5911.
12. A. P. Turkewitz, J. F. Amatruda, D. Borkani, S. C. Harris, and A. L. Schwartz (1987) J. Biol. Chem. **263**, 8318–8325.
13. Y. F. Yamaguchi and J. T. Harmon (1988) Biochemistry **27**, 3252–3260.
14. J. H. P. Skene and I. Virag (1989) J. Cell Biol. **108**, 613–624.
15. R. Fukunaga, E. Ishizaka-Ikeda, and S. Nagata (1990) J. Biol. Chem. **265**, 14008–14015.
16. E. A. Frey, M. E. Gosse, and T. E. Cote (1989) Eur. J. Pharmacol. **172**, 347–356.
17. J. Mazella, J. Chabry, and J. P. Vincent (1989) J. Biol. Chem. **264**, 5559–5563.
18. H. T. He, K. Johnson, K. Thermos, and T. Reisine (1989) Proc. Natl. Acad. Sci. USA **86**, 1480–1484.
19. R. Munshi and J. Linden (1989) J. Biol. Chem. **264**, 14853–14859.
20. D. J. Hryb, M. S. Khan, N. A. Romas, and W. Rosner (1989) J. Biol. Chem. **264**, 5378–5383.
21. Y. H. Wong, C. D. Demoliou-Mason, and E. A. Barnard (1989) J. Neurochem. **52**, 999–1009.
22. A. Mills, C. D. Demoliou-Mason, and E. A. Barnard (1988) J. Biol. Chem. **263**, 13–16.
23. R. A. Cerione et al. (1983) Proc. Natl. Acad. Sci. USA **80**, 4899–4903.
24. U. Kanngiesseer, P. Nalik, and O. Pongs (1988) Proc. Natl. Acad. Sci. USA **85**, 2969–2973.
25. P. Banerjee, J. T. Buse, and G. Dawson (1990) Biochim. Biophys. Acta. **1044**, 305–314.
26. P. Banerjee, J. B. Joo, J. T. Buse, and G. Dawson (1995) Chem. Phys. Lipids **77**, 65–78.
27. J. Sambrook, E. F. Fritsch, and T. Maniatis (1989) *Molecular Cloning*, 2nd ed. Cold Spring Harbor Laboratory Press, Cold Spring, NY, section 1.21.
28. P. Chomczynski and N. Sacchi (1987) Anal. Biochem. **162**, 156–159.
29. L. Freysz et al. (1982) In *Phospholipids in the Nervous System*, Vol. **1** (Metabolism) (L. Horrocks et al., eds.), Raven Press, New York pp. 37–47.
30. R. N. Fontaine, R. A. Harris, and F. Schroeder (1980) J. Neurochem, **34**, 269–277.

31. R. N. Fontaine, R. A. Harris, and F. Schroeder (1979) Life Sci. **24**, 295–400.
32. M. J. Berridge (1984) Biochem. J. **220**, 345–360.

Suggestions for Further Reading

33. J. Lasch (1995) Biochim. Biophys. Acta. **1241**, 269–292. Interaction of detergent with lipid vesicles.
34. R. J. Vonk, M. Kalivianakis, D. M. Minich, C. M. Bijleveld, and H. J. Verkade (1997) Scandinavian J. Gastroenterol.-supplement, **222**, 65–67. The metabolic importance of unabsorbed dietary lipids in the colon.
35. G. D. Henry and B. D. Sykes (1994) Methods Enzymol. **239**, 515–535. Methods to study membrane protein structure in solution.
36. A. G. DeOliveira and H. Chaimovich (1993) J. Pharm. Pharmacol. **45**, 850–861. Effect of detergents and other amphiphiles on the stability of pharmaceutical drugs.
37. A. C. Newby, A. Chrambach, and E. M. Bailyes (1982) Tech. Lipid Membrane Biochem. **B409**, 1–22. The choice of detergents for molecular characterization and purification of native intrinsic membrane proteins.

Development

Development is the process of change in an organism with time. Such change can be either morphological (such as changes in shape or structure), biochemical (such as the synthesis of specialized proteins), or both. Development usually includes all of the changes that occur during the life of an organism. These include fertilization, embryogenesis, maturation, and gametogenesis.

Embryogenesis begins with fertilization of the **gametes** to form the diploid zygote. The zygote undergoes cleavage divisions to form the blastoderm embryo. Changes in cell shape and cell movements at **gastrulation** lead to the formation of the three germ layers: the ectoderm, endoderm, and mesoderm. The process of organogenesis forms the embryonic organs.

Suggestions for Further Reading

S. F. Gilbert (1997) *Developmental Biology*, Sinauer Associates, Sunderland, MA.

L. Wolpert, R. Beddington, J. Brockes, T. Jessell, P. Lawrence, and E. Meyerowitz (1998) *Principles of Development*, Oxford University Press, Oxford, U.K.

J. M. W. Slack (1991) *From Egg to Embryo: Regional Specification in Early Development*, 2nd ed., Cambridge University Press, Cambridge, U.K.

A. S. Wilkins (1993) *Genetic Analysis of Animal Development*, 2nd edition, Wiley-Liss, New York.

Dexamethasone

Dexamethasone (9a-fluoro-16a-methylprednisolone) (Fig. 1) is a semisynthetic glucocorticoid hormone demonstrating a greater binding affinity for the glucocorticoid **receptors**, a greater potency of action, and a longer half-life, than the natural glucocorticoids. The hormone is used as a drug and in research. Its molecular mode of action is the same as that of the natural glucocorticoids—that is, by binding to the glucocorticoid receptor and activating gene transcription.

Figure 1. Structure of dexamethasone

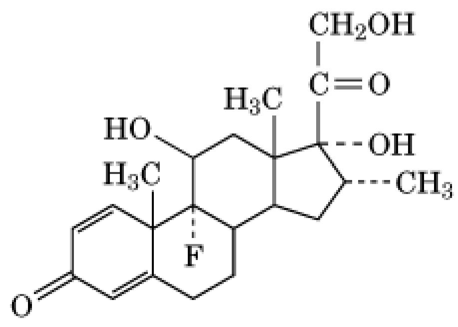

Dg-Dc Tailing

This procedure is used for cloning cDNA (complementary DNA) prepared from messenger RNA (1). Single-stranded cDNA prepared by **reverse transcriptase** is incubated with the enzyme terminal deoxyribonucleotide transferase and dCTP, which adds 5 to 10 C residues to the 3′ ends of the DNA molecules (C-tail). The second strands are synthesized with reverse transcriptase and oligo-dT as the primer, using the poly A tails of mRNA, and the double-stranded cDNA molecules are tailed with dC as before. The resulting molecules are cloned into **vector** molecules that have been tailed with poly G (about 10 bases per end) to create complementary ends to which the dC tails on the inserts hybridize. A recent modification is to use CTP instead of dCTP, which gives more uniform tails (2).

Bibliography

1. H. Land, M. Grez, H. Hauser, W. Linden Maier, and G. Scholtz (1981) Nucleic Acids Res. **9**, 2251–2266.
2. W.M. Schmidt and M.W. Mueller (1996) Nucleic Acids Res. **24**, 1789–1791.

Diafiltration

Ultrafiltration and microfiltration are able to prepare reasonably concentrated samples of macromolecules, but they permit only a limited separation of the retained solutes from the smaller or more permeable components present in the solution needing to be filtered. In order to remove such smaller components more efficiently from the retained species, the feed solution can be washed in a process known as *diafiltration*. In this process, water or an appropriate buffer solution is added to the retentate during filtration, with the membrane-permeating species being removed as the excess fluid or buffer is filtered. Such a process may be undertaken in two different modes: continuous, in which the wash fluid is added throughout filtration, or discontinuous, in which the feed solution is first concentrated by a predetermined amount using standard ultrafiltration techniques, the wash fluid is then added, and the process repeated any number of times until the final solute concentration is achieved. When using continuous diafiltration, the amount of solute remaining in the retentate may be determined from a mass balance and expressed as

$$\frac{C_R}{C_0}\exp(-N_D S) \tag{1}$$

where C_R is the concentration of the retentate, C_0 the initial concentration, N_D is the number of diavolumes, defined as the total volume of the wash fluid divided by the initial volume of the solution, and S is the solute sieving coefficient.

For discontinuous diafiltration, it is given by

$$\frac{C_R}{C_0} = \left(\frac{V}{V_0}\right) - (n+1)S \tag{2}$$

where n corresponds to the number of discontinuous diafiltration procedures.

Diagonal Methods

It is often desirable to purify selectively those peptides from a protein that contain a particular amino acid, such as all the peptides containing **cysteine residues**. This is accomplished most elegantly by so-called "diagonal" techniques (1), which rely on a change in the properties of peptides caused by the selective modification of the amino acid residues of interest. If a mixture of peptides, generated by **proteolysis** of a protein for peptide mapping, is separated in one dimension and then subjected to the same procedure a second time, but at right angles to the first, all the peptides will lie on a diagonal because they had the same mobilities in both directions. The separation can be by electrophoresis or chromatography, but it should be carried out on a two-dimensional medium, such as paper or thin-layer plates. To detect certain peptides, and to cause them to have a different mobility in the second dimension, the entire mixture of peptides is treated after the first separation so as to modify all the residues of a particular type and to change their separation properties. After the second dimension separation, the peptides containing these residues consequently lie off the diagonal of all the other peptides and are readily identified and isolated.

1. Isolating Peptides Containing Certain Amino Acids

For example, peptides containing Cys residues can be purified by blocking their thiol groups by reaction with **iodoacetic acid** (Fig. 1a) (2). A two-dimensional diagonal peptide map is prepared by electrophoresis at pH 3.5, exposing the peptides to performic acid between the two separations. This oxidizes the sulfur atom of the modified Cys residues to the sulfone:

$$-CH_2-S-CH_2-CO_2^- \xrightarrow{[O]} -CH_2-\overset{O}{\overset{\|}{\underset{\underset{O}{\|}}{S}}}-CH_2-CO_2^- \quad (1)$$

carboxymethyl-Cys

which lowers the pK_a value of the carboxyl group, so that peptides containing Cys residues are somewhat more acidic in the second dimension; they then lie to one side of the diagonal. Alternatively, the thiol groups can be reacted initially with *N*-ethylmaleimide (see Thiol Groups); the *N*-ethylsuccinimide group introduced can then be hydrolyzed to the succinamic acid by treatment with ammonia after the first separation (3).

Figure 1. Isolation and identification of cysteine residues linked by disulfide bonds or modified by reaction with iodoacetate (2). The proteins were digested with trypsin, followed by chymotrypsin, and the resulting peptides were separated by paper electrophoresis at pH 3.5 in the horizontal direction (anode at the left). After exposure to performic acid vapor, the electrophoresis was repeated in the vertical direction (anode at bottom). The peptides were visualized by staining with ninhydrin. The diagonal indicated by the dashed line is defined by peptides that were not altered by the performic acid and consequently had the same mobility in both dimensions; many of these peptides have migrated off the paper. (**a**) Reduced BPTI (bovine pancreatic trypsin inhibitor) in which the six Cys residues have been blocked by reaction with iodoacetate. The six peptides containing these residues define a second diagonal, below the first, because they were slightly more acidic in the second dimension due to their oxidation to the sulfone. These peptides are identified by the numbers of the Cys residues they contain. The amino acid residues they contain are, starting from lower left to upper right, 54 to 58 (Cys55), 27 to 33 (Cys30), 5 to 15 (Cys5 and 14), 47 to 53 (Cys51), 1 to 15 (Cys5 and 14), and 36 to 39 (Cys38). (**b**) The major one-disulfide intermediate in the BPTI disulfide folding pathway (see Protein Folding In Vitro) that had been trapped by reacting all the four free Cys thiol groups with iodoacetate. The two peptides containing Cys30 and Cys51 are absent from the second diagonal of modified Cys residues and had the same mobility in the first dimension, indicating that they were originally linked by an intramolecular disulfide bond between these two Cys residues.

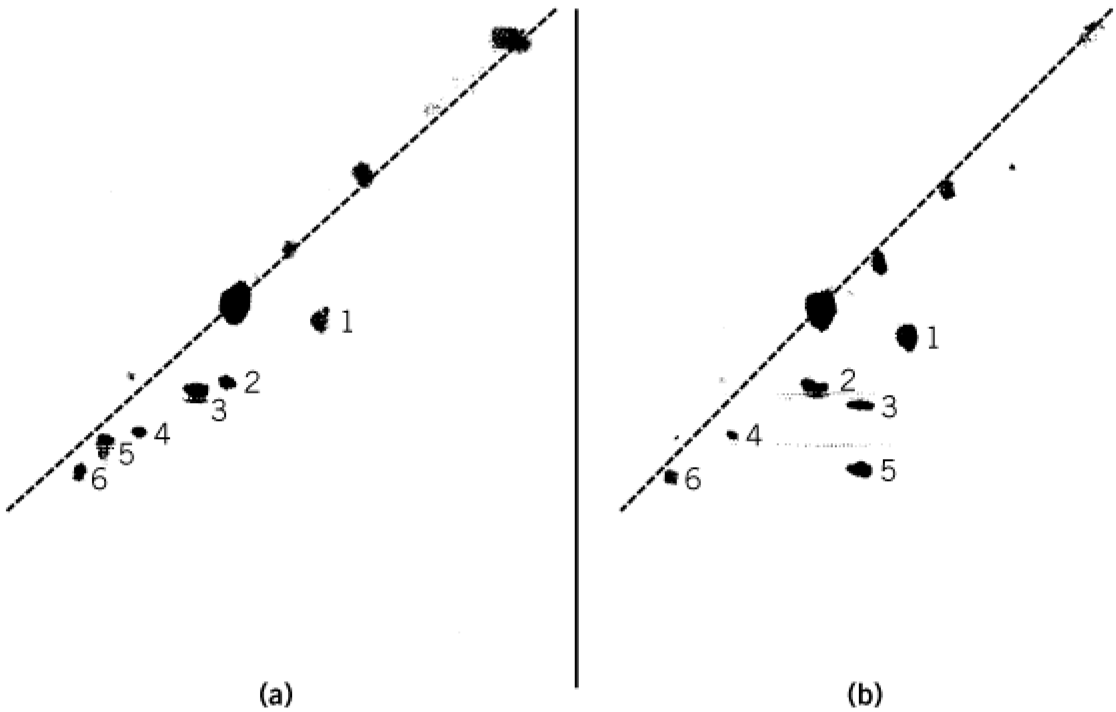

Analogous techniques have been developed for a few other residues, using appropriate chemical modifications specific for these residues. The amino groups of **Lys**-containing peptides are initially blocked with trifluroacetyl or maleyl groups, by treatment with the corresponding anhydride; these groups alter the charge and are easily removed after the first electrophoresis by acidification. **Met** residues are first alkylated with **iodoacetamide** to produce the charged sulfonium derivative. After the first electrophoresis, heating causes this derivative to cleave the polypeptide chain by a reaction analogous to that occurring in cleavage by cyanogen bromide. **His** residues are first blocked by dinitrophenylation of the side chain and then regenerated after the first electrophoresis by exposure of the peptides to a thiol-containing reagent. **Arg** residues are first blocked by reaction with cyclohexanedione and then regenerated at alkaline pH. **Trp** residues are modified by *o*-nitrophenylsulfenyl chloride after the first separation (4).

2. Characterizing Disulfide Bonds

Diagonal techniques were initially introduced by Brown and Hartley (1) for the determination of which pairs of Cys residues in a protein were linked by disulfide bonds. The protein is prepared for peptide mapping and the peptides are separated in the first dimension, under conditions where the disulfide bonds are stable and cannot rearrange or be reduced; the pairs of peptides linked by disulfide bonds consequently migrate together (Fig. 1b). The disulfide bonds are then cleaved by exposure to performic acid, which converts each such Cys residue to cysteic acid:

$$-\mathrm{Cys}-\mathrm{S}-\mathrm{S}-\mathrm{Cys}- \rightarrow 2-\mathrm{Cys}-\mathrm{SO}_3^- \tag{2}$$

The peptides originally linked by the disulfide bond are now independent and more acidic. During separation in the second dimension, they migrate differently and lie off the diagonal, but they can be related by their common mobility in the second dimension.

Diagonal techniques are best suited to two-dimensional separations, such as paper electrophoresis and chromatography, which were used extensively in the past but have now been supplanted by more modern techniques that require less material, but operate in a single dimension, such as **HPLC**. The same basic technique can be used, but the fractions from the first separation must be separated again individually.

Bibliography

1. J. R. Brown and B. S. Hartley (1966) Biochem. J. **101**, 214–228.
2. T. E. Creighton (1974) J. Mol. Biol. **87**, 603–624.
3. H. Gehring and P. Christen (1980) Anal. Biochem. **107**, 35–361.
4. T. Sasagawa et al. (1983) Anal. Biochem. **134**, 224–229.

Dialysis

Dialysis is the transport of a solute through a membrane under the influence of a difference in the concentrations (or activities) of the solute in the solutions separated by the membrane. The separation of solutes is induced by differences in their transport by diffusion through the membrane matrix. A diffusable low-molecular-weight solute can thus be separated from a solution containing nondiffusable large macromolecules. The rate of dialysis is directly proportional to the membrane area and inversely proportional to the membrane thickness. Since the 1960s, the principal clinical use of this technique has been the treatment of patients with kidney disease.

Nonclinical applications of dialysis techniques for the separation of solutes with molecular weights ranging from 100 to 100,00 Da may be on a small laboratory scale or with larger-scale commercial units for the recovery of alkai or in food processing applications. Dialysis is also important in biotechnology, as it provides a technique whereby products can be separated from fragile shear-sensitive or heat-sensitive solutions. A number of variants of the technique exist. These may be divided into batch and continuous processes. The simplest batch process is one in which a semipermeable membrane tubing made from cellulose and sealed at one or both ends contains the solution of interest. The tubing is suspended in a buffer solution or water. Small molecules contained within the solution bounded by the membrane diffuse into the surrounding buffer solution. The transfer of the substance across the membrane obeys Fick's law, if we assume that chemical equilibrium is established between the membrane and solution. If no water transfer occurs, and the mass transfer coefficient is constant along the diffusion path, the amount of substance transferred through the membrane W may be expressed as

$$W = DA\Delta C \quad (1)$$

where D is the overall dialysis coefficient of the substance, A the membrane area, and DC the logarithmic mean bulk concentration difference across the membrane based on the initial and final values.

A variation of equilibrium dialysis is *reverse dialysis*, in which the fluid contained in the semipermeable membrane tube is placed into a water-soluble polymer, such as polyethylene glycol. This causes the water to diffuse out of the membrane tube and concentrates the macromolecule within the tube.

For batch dialysis, where mass transfer is not at steady state, the transfer rate is given by

$$kt = -m \log_e \left(\frac{C_0 - C}{C_0} \right) \quad (2)$$

where k is the dialysis rate constant, t the time, m the volume of the feed ratio to diffusate, C_0 the concentration of the feed, and C the concentration of the dialysate.

Equilibration of the low-molecular-weight solutes or electrolytes by this technique can be speeded up by ensuring that the area of membrane contact is large relative to the volume of solution being dialysed. Since any molecule from the solution held within the membrane has to pass through the stagnant fluid film or boundary layer on either side of the membrane, as well as across the membrane itself, the overall dialysis rate may be enhanced by the minimization of the stagnant layers. This can be achieved by the introduction of a stirrer into the system, or by frequent changes of the dialysis fluid.

The transfer rate is also dependent on temperature. Biological materials such as proteins usually need to be dialyzed in the cold to minimize bacterial growth or protein **denaturation**. Under such conditions, the transfer of molecules will be reduced compared with that at room temperature.

If the solution requiring to be dialyzed is available in a sufficiently large quantity, continuous methods that use a *countercurrent flow* configuration to maintain a large difference in the solute concentration across the membrane may be used. For such systems, which are similar to those used in the treatment of renal failure, the amount of solute transferred across the module, if we assume that the membrane is the primary barrier to diffusion, may be expressed as

$$Q(C_{\text{in}} - C_{\text{out}}) = kA\Delta C \quad (3)$$

where Q is the flow rate of the solute undergoing dialysis, C_{in} and C_{out} are the concentrations at the inlet and outlet, k and A are as previously defined, and DC is the log mean concentration difference between the dialysis fluid and the fluid being dialyzed.

Many substances **bind** to proteins or plasma. The solute transfer referred to above relates to an unbound solute. However, a bound solute will be in equilibrium with the unbound solute, the extent of the binding being governed by the solute **association constant**. The effect of this will be that there will be an overestimate of the concentration driving force present. As free solute is removed, there will be unbinding of the solute with the effect of understating the concentration driving force.

In a single-pass situation, ie, where the dialyzing fluid flows to waste and the solute undergoing dialysis is recirculated, the solute exchange rate within the module used for dialysis is expressed in terms of dialysance D, defined as

$$D = \frac{\text{Change in concentration of the incoming solute}}{\text{Concentration driving force}} \tag{4}$$

The generalized concentration driving force will be determined by the Donnan factor a, defined as the ratio of the ionic concentrations in the dialysis fluid and in the solute undergoing dialysis at equilibrium. If the solute is noncharged, a = 1, and the measurement of the transport rates may occur by the use of a single pass flow configuration on the dialyzate side, while the fluid being dialyzed is recirculated. In such a flow configuration, provided that the volume being dialyzed V is unchanged, the concentration at time t, C_t, may be expressed in terms of the removal rate k and the initial concentration C_0 by

$$C_t = C_0 \exp - \left(\frac{kt}{V}\right) \tag{5}$$

Diastereomer

Diastereomers are stereoisomers, molecules that differ only in their spatial arrangement of atoms, that are not enantiomers (1). Diastereomers have different chemical properties. There are several common types of diastereomers. Molecules containing carbon–carbon and carbon–nitrogen double bonds will exist as two different geometric diastereomers, if both of the double-bonded atoms have two different substituents. These diastereomers are differentiated with the designation **cis** and **trans** and more formally as Z and E (from the German zusammen for together and entgegen for opposite). The Z isomer describes the orientation when the two substituents with the higher priority are on the same side of the double bond. In potentially ambiguous cases, the priority of the substituents of each double-bonded atom is determined by the Cahn, Ingold, and Prelog rules (2) (see Configuration). The other common form of diastereomers occurs when a molecule contains more than one **chiral** center. If two stereoisomers contain at least one corresponding chiral center with the same configuration and one corresponding chiral center with the opposite configuration, the molecules will be diastereomers. These two forms of diastereomers are shown in Figure 1.

Figure 1. The two common types of diastereomers are depicted, *cis*/*trans* geometric isomers and molecules containing more than a single chiral center.

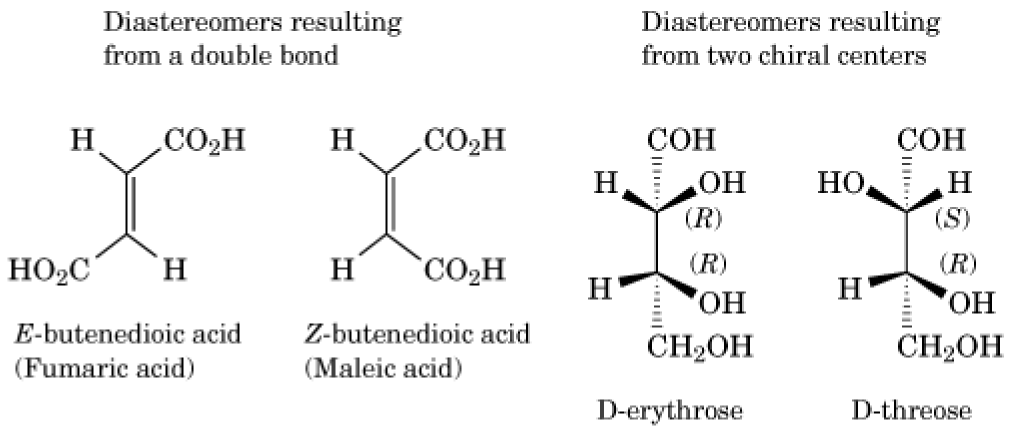

Two atoms are referred to as *diastereotopic* if, on substitution with a different isotope, they would generate different diastereomers (1, 3) (see Prochiral). Diastereotopic atoms are chemically different and, importantly, can be distinguished by NMR.

Bibliography

1. B. Testa (1982) In *Stereochemistry* (C. Tamm, ed.), Vol. **3**, Elsevier, Amsterdam, pp. 1–48.
2. R. S. Cahn, C. K. Ingold, and V. Prelog (1966) Angew. Chem. Int. Ed. **5**, 385–415.
3. D. Arigoni and E. L. Eliel (1969) In *Stereochemistry* (E. L. Eliel and N. L. Allinger, eds.), Vol. **4**, Wiley-Interscience, New York, pp. 127–243.

Suggestions for Further Reading

4. J. March (1985) *Advanced Organic Chemistry*, Wiley-Interscience, New York, pp. 104–119.
5. K. Mislow (1966) *Introduction to Stereochemistry*, W. A. Benjamin, New York, Chap. "2".
6. K. Mislow and M. Raban (1967) In *Topics in Stereochemistry* (N. L. Allinger and E. L. Eliel, eds.), Vol. **1**, Wiley-Interscience, New York, pp. 1–38.

Dicentric Chromosome

Dicentric chromosomes have two centromeres. Such chromosomes are products of chromosomal damage, breakage, and fusion. Dicentric chromosomes normally break at **anaphase**, when the centromeres have separate attachments to the spindle and are subject to forces pulling them apart.

The definition of a chromosome breakage-fusion-bridge cycle in **maize** by McClintock in 1951 was an important step in defining chromosomal dynamics (1). The origin of chromosomal breakage in this case in maize is the transposable element Dissociation (*Ds*), which causes chromosomal instability in the presence of another element called Activator (*As*). *Ds* is present at specific sites in the chromosome and transposes to a different site only in the presence of *As*. Events such as these led to the discovery of transposable elements. Two forms of this cycle have been described resulting in the appearance of either dicentric chromosomes or chromatids.

One type of cycle is shown in Figure 1. Several convenient markers are present on chromosome 9 of maize, which include colored (C1), shrunken (sh1), bronze (bz1), and waxy (wx1). Each of the two chromosomes has a *Ds* element located at the site indicated (*Ds*). When the *Ds* element is activated, chromosome breakage may occur. The acentric fragment without a centromere is lost. The ends of the two sister chromatids fuse to form a bridge, so the resulting single DNA molecule contains two centromeres. At the anaphase, the dicentric fused chromosomal arms break, so that segments of the chromosome are either duplicated or deficient in daughter cells. This cycle occurs either at **meiosis** or **mitosis**.

Figure 1. Chromosome breakage-fusion-bridge cycle in maize. (**a**) A break in maize chromosome 9 at the site of the transposable element *Ds* is indicated. (**b**) At the end of the S-phase and in G2, two sister chromatids are formed that have a break at this site (sticky ends). (**c**) The sticky ends of the two chromatids fuse to form a chromosome containing two centromeres—a dicentric chromosome. (**d**) At the anaphase, the two centromeres may be forced to move in opposite directions, leading to chromosomal breakage and forming two chromosomes, one containing a short duplication and the other a deficiency.

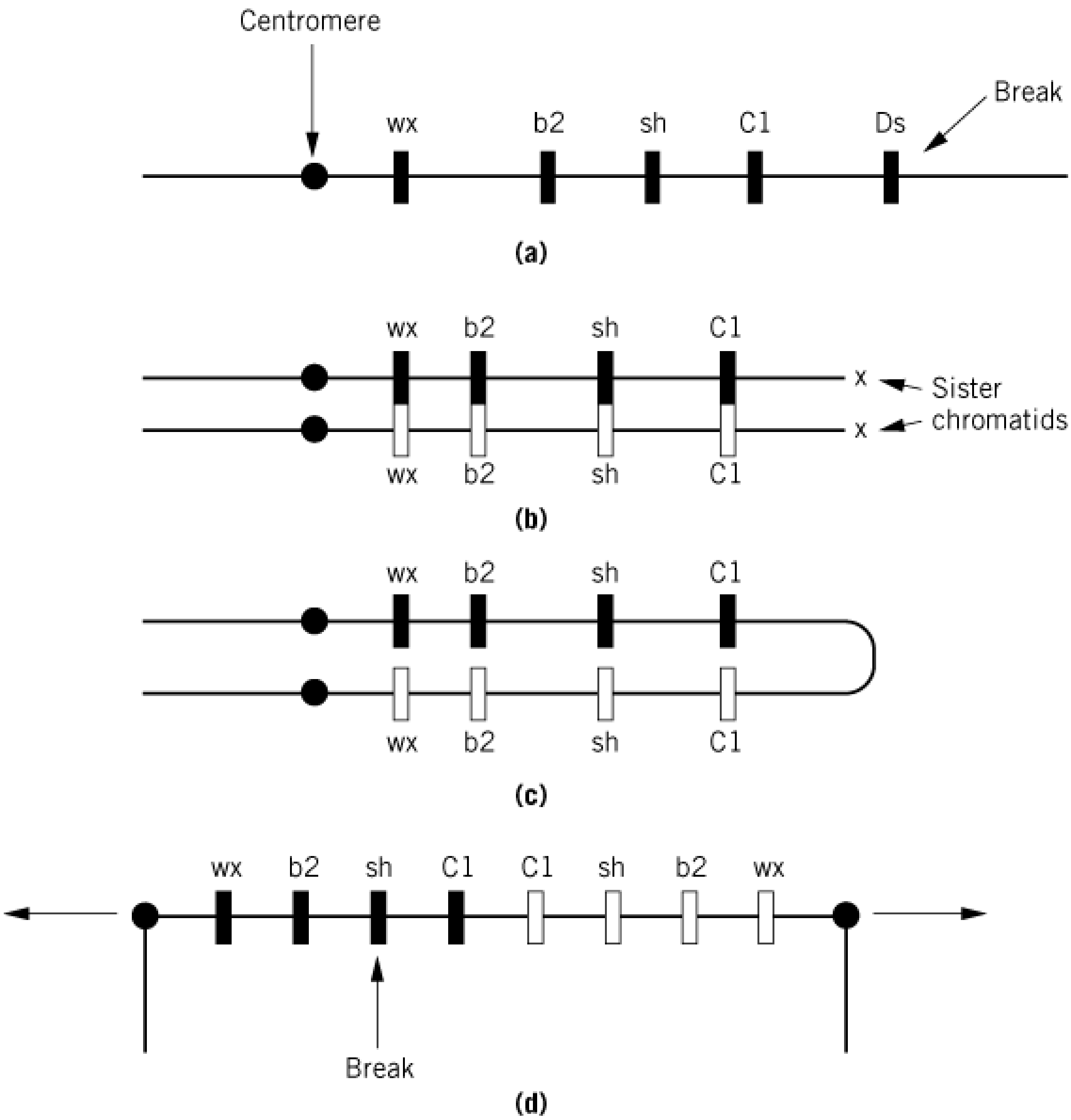

Bibliography

1. B. McClintock (1951) Cold Spring Harbor Symp. Quant. Biol. **16**, 13–47.

Dictyostelium

The cellular slime mold *Dictyostelium discoideum* has been studied in the laboratory extensively as a model eukaryotic organism. This soil amoeba has provided extraordinary opportunities for molecular biologists and biochemists to examine a wide variety of fundamental cellular functions. Developmental biologists have characterized at the molecular level *Dictyostelium's* unique **developmental** pathway. Single free-living cells can respond to a number of chemical signals, aggregate, and then differentiate into a complex multicellular organism.

A powerful library of techniques has been developed for manipulating this organism in the laboratory. Large numbers of cells can be grown, and proteins can be purified for biochemical characterization and, in some cases, structural characterization. The recent utilization of peptide proteinase inhibitors have made this increasingly easy. Genetic techniques have been developed for making mutations, and sophisticated methods have been applied for analyzing them. Genetic selection can be carried out with a variety of metabolic and drug resistance markers. **Plasmids** that either integrate into the chromosome or replicate extrachromosomally have been constructed from fragments of naturally occurring ones, and a variety of **promoters** are available for obtaining heterologous gene expression. Cell biological techniques are also well developed, yielding information on expression and localization in fixed and live cells.

A simplified schematic of the *Dictyostelium discoideum* developmental pathway is shown in Figure 1. The free-living amoebae feed on bacteria, and they can be found outside the laboratory in forest soils and detritus. In the laboratory, they can be grown in liquid media in shaking flasks or in petri plates, either in liquid media or on agar surfaces. Strains of *Dictyostelium* have been developed that can grow in synthetic and fully characterized media. On surfaces, the amoebae are motile and can use a variety of chemotaxis signals to find food and to optimize growth conditions (1).

Figure 1. A schematic diagram of the *Dictyostelium* developmental cycle.

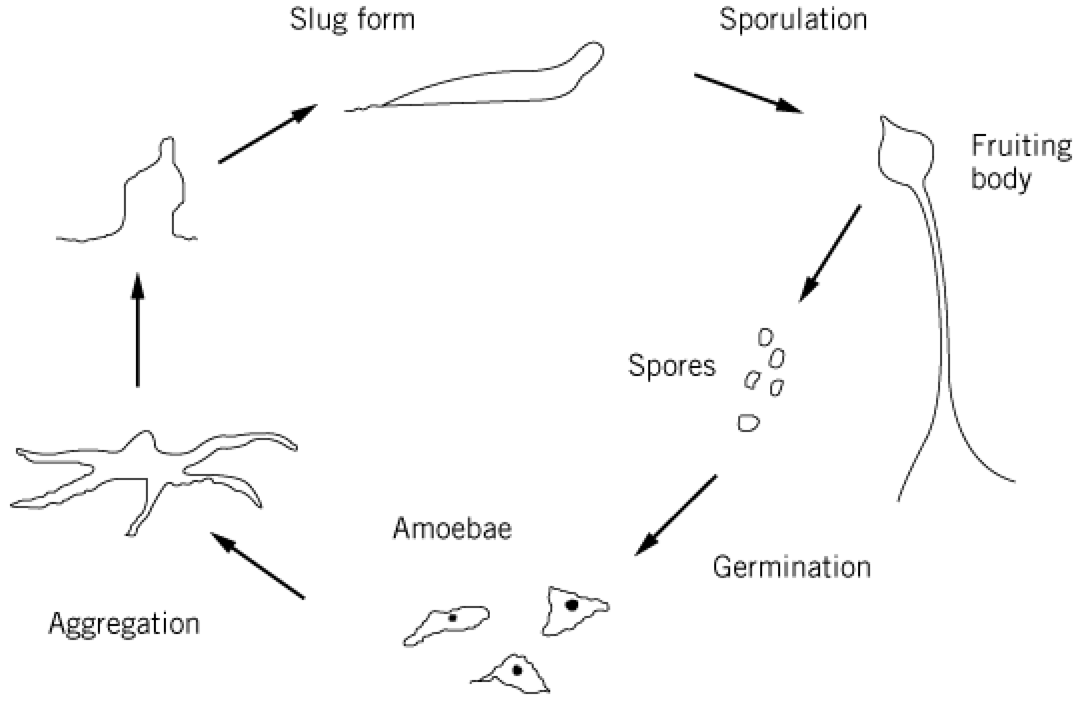

Under certain conditions, such as the onset of starvation, a population of amoebae can suspend their cell cycle and begin a highly regulated set of gene inductions, which initiates the developmental pathway. In the laboratory, this can be done synchronously. Early in this process, a series of **new enzymes** are synthesized that are responsible for the synthesis, detection, and degradation of cyclic AMP (cAMP). These enzymes are used to regulate the chemotactic response of the cells in such a way that the cells aggregate. A founder cell initiates the aggregation process by secreting pulses of cAMP. Surrounding cells, if they are competent to respond, do so in two ways. First, they migrate toward the cAMP source. Second, they secrete a cAMP pulse themselves, which serves to amplify the signal and to increase the area over which it can travel. An extracellular phosphodiesterase degrades the cAMP between the waves.

As the cells migrate, they form cell–cell contacts that serve to establish polarity signals, which are used as the aggregate forms a mound and the cells differentiate into different types and sort into different locations. The tip of the mound becomes an organizing center which, based on environmental factors, decides whether to proceed in development to a fruiting body or to search for more favorable conditions by becoming a slug. If the organism becomes a slug, the mound tips over on the surface, and the outside cells secrete an extracellular matrix, commonly known as slime, which is left behind on the surface after the organism has passed. The tip of the slug controls its migration direction chemotactically, as well as by detecting gradients of temperature and light. Migration rates can exceed 1 cm/h.

When the mound or slug is ready to proceed to form a fruiting body, the cells have differentiated, through a pattern of differential gene expression, into either of two distinct cell types: pre-stalk or pre-spore. As the pre-stalk cells migrate to the bottom of the forming structure, they differentiate terminally into a plant-like cell with a rigid cell wall. A clorinated alkyl phenone, DIF-1, is released to induce stalk cell differentiation. Pre-spore cells differentiate into small environmentally resistant spores, which are carried up by the forming stalk. The spore sac is quite sticky, which facilitates its use of insect legs as transport in the wild. When conditions are optimal, the spores can germinate and begin dividing once again as amoebae.

The haploid genome of *Dictyostelium* is about 54×10^6 base pairs in six chromosomes, and a detailed map has been assembled (2). The DNA has an unusually high content of A and T nucleotides. Complete characterization of the genome is underway. A wide variety of genetic tools have be developed for manipulation of *Dictyostelium*. Mutations can be created, and the resulting **phenotypes** can be analyzed in many ways. Naturally occurring extrachromosomal plasmids have been isolated and reconstructed into a family of vectors useful in stable or transient expression of heterologous genes. Multiple selectable markers are available, allowing the construction of strains in which complementation can be used to analyze protein–protein interactions. Homologous recombination has been shown to occur, allowing gene knockouts and gene replacements to be made.

Dictyostelium has been particularly useful in the characterization of the fundamental aspects of transmembrane signaling and cell–cell communication in the regulation of motility (3). The organism has the ability to detect and respond to a whole series of environmental factors, such as light, temperature, and moisture. It also can detect a wide variety of chemical signals, from sugars to hormones. *Dictyostelium* uses a variety of mechanisms of intracellular signaling mechanisms, including proton gradients and electrochemical gradients, as well as Ca^{2+} waves (see Calcium Signaling). Analysis of a variety of protein kinases and phosphatases and their target have illuminated a number of regulatory pathways. The dynamic cytoskeleton of *Dictyostelium* has been extensively studied, particularly actin, actin-binding proteins, and the myosins, as well as tubulin, tubulin-binding proteins, and microtubule-based motor proteins. Major rearrangements of the cytoskeleton are required during cytokinesis and cell motility. Analysis of genetic knockouts of individual genes and combinations of those for cytoskeletal proteins have been particularly useful in attempting to determine their cellular roles. Targeted gene disruptions have also been used to characterize the pathways of endocytosis and exocytosis. *Dictyostelium* feeds on bacteria using phagocytosis that is highly regulated and specific (4).

The highly regulated developmental pathway of *Dictyostelium* has been extremely valuable in terms of understanding gene induction and regulation. The appearance and disappearance of specific messenger RNAs have been mapped to specific time points during development, and many of the gene products have been characterized and their function determined. The appearance of different cell types in the aggregate, along with their sorting to yield the final fruiting body, has given insights into positional information and the cell cycle in morphogenesis.

Study of the cellular slime mold *Dictyostelium discoideum*, as a model eukaryotic organism, has produced many insights into basic cellular function. It will continue to make contributions as its many features are probed in more detail.

Bibliography

1. S. J. McRobbie (1986) Chemotaxis and cell motility in the cellular slime molds. Crit. Rev. Microbiol. **13**, 335–375.
2. W. F. Loomis, D. Welker, J. Huges, D. Meghakian, and A. Kuspa (1995) Genetics **141**, 147–157.
3. P. Devroetes (1989) *Dictyostelium discoideum*: a model system for cell–cell interactions in development. Science **245**, 1054–1058.
4. G. Vogel (1983) *Dictyostelium discoideum* as a model system to study recognition mechanisms in phagocytosis. Methods Enzymol. **98**, 431–430.

Suggestions for Further Reading

5. J. T. Bonner (1967) *The Cellular Slime Molds*, 2nd ed., Princeton University Press, Princeton, NJ.
6. K. B. Raper (1984) *The Dictyostelids*, Princeton University Press, Princeton, NJ.
7. F. Loomis, ed. (1982) *The Development of Dictyostelium discoideum*, Academic Press, New York.

8. J. A. Spudich, ed. (1987) *Dictyostelium discoideum: Molecular Approaches to Cell Biology. Methods in Cell Biology*, Vol. **28** (L. Wilson series, ed.), Academic Press, Orlando, FL.
9. R. Mutzel (1995) Experientia **51**, 1103–1196. A fine collection of multiauthor reviews.

Diethylpyrocarbonate

Diethylpyrocarbonate (DEPC) [I] is an anhydride of ethoxyformic acid and is also called ethoxyformic anhydride (EFA), diethyl dicarbonate, or diethyl oxydiformate. DEPC is a liquid (density = 1.29 g/ml) with molecular weight of 162.14. It is not stable in water and hydrolyzes to two molecules of ethanol and carbon dioxide. DEPC is a good reagent for chemical modification of histidine residues. Because DEPC inhibits **ribonuclease A**, which has histidine residues at its active site, DEPC is widely employed to protect **RNA** from enzymatic attack. DEPC is a suspected carcinogen, and therefore, it should be handled carefully.

Within the pH range 6 to 8, DEPC reacts with histidine residues to give *N*-carboethoxyhistidine [II], ethanol, and carbon dioxide (Scheme 1):

Diethylpyrocarbonate

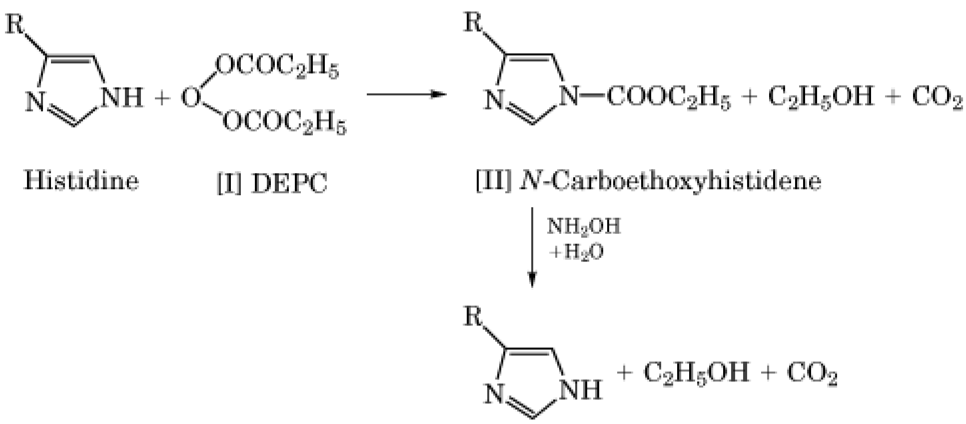

The product, *N*-carboethoxyhistidine, absorbs UV at 240 nm, and the reaction can be followed spectroscopically (De$_{240}$ = 3,200 M^{-1} cm^{-1}) (1). The product is not very stable. The **half-life** of its decay is 55 h at pH 7 and much shorter at acidic or alkaline pH values. The product is regenerated to histidine by NH_2OH (**hydroxylamine**). DEPC sometimes also reacts with amino groups and with the side chains of cysteine, tyrosine, arginine, and tryptophan residues.

To prevent the action of ribonuclease, 0.2 ml DEPC is added to 100 ml of the solution that is being treated for use with RNA. To inactivate the remaining DEPC, the solution is autoclaved (2).

Bibliography

1. E.W. Miles (1977) Methods Enzymol. **47**, 431–442.
2. M. Gilman (1995) In *Current Protocols of Molecular Biology*, Wiley, New York, pp. 4.1.4–6.

Difference Fourier

The difference Fourier is an extremely useful electron density map in protein X-ray crystallography. The location of reagents such as inhibitors or water molecules, attached to or removed from the native structure (see **Ligand binding**) is easily determined if the native crystal structure is known. It is not necessary to perform a completely new structure determination for the derivative, so long as the new crystal is isomorphous with the old one, as in isomorphous replacement. Only the intensities of the reflections in the diffraction pattern of the derivative need be collected. A normal electron density map is calculated by the equation:

$$\rho(xyz) = \frac{1}{V}\sum_h \sum_k \sum_\ell |F(hk\ell)| \times \exp[-2\pi i(hx + ky + \ell z) + i\alpha(hk\ell)]$$

If the $|F(hk\ell|$'s in this equation are replaced by D $|F(hk\ell)| = |F(hk\ell)|_{PH} - |F(hk\ell)|_P$, where P stands for the native protein and PH for the derivative, then the resulting difference electron density map shows the difference in electron density between native and the derivative. The density is positive for attachment and negative for removal of atoms (1):

$$\rho(xyz) = \frac{1}{V}\sum_h \sum_k \sum_\ell \Delta|F(hk\ell)| \times \exp[-2\pi i(hx + ky + \ell z) + i\alpha_P(hk\ell)]$$

In calculating this difference Fourier, the phase angles are those of the native protein a_P $(hk\ell)$.

Because of approximations, the heights of the peaks in a difference Fourier are only half of what they would be in a normal Fourier. Nevertheless, it is a powerful method, and the attachment or removal of a few electrons can easily be detected. It also plays a useful role in locating of heavy atoms in the isomorphous replacement method. For example, after the main heavy atom site has been found from a difference Patterson map, additional weakly occupied sites can be detected with a difference Fourier.

Bibliography
1. J. Drenth (1999) *Principles of Protein X-ray Crystallography*, Springer, New York.

Difference Spectroscopy

The absorbance of a chromophore depends on its molecular environment (see Absorption Spectroscopy). It is sensitive to changes in the solvent around an exposed chromophore (see Solvent Perturbation Spectroscopy) or in the exposure of a chromophore as a consequence of conformational transitions, such as the unfolding of a protein or the melting of double-helical DNA (see **DNA melting**). These changes in absorbance are sometimes small, so it is of advantage to measure directly the difference in absorbance between two samples in which the only difference is that the macromolecule is in different environments. This can be done in a double-beam spectrophotometer, where the two samples are placed in the sample and the reference cuvette. This is called difference spectroscopy.

For the measurement of difference spectra, it is of advantage to use an instrument with a high sensitivity, so that small differences between the two samples in the different environments can be monitored reliably and with good accuracy. The development of microprocessor-controlled instruments has greatly facilitated the measurement of difference spectra. The measured data can be stored and manipulated later, eg, by changing the wavelength and absorbance scales, smoothing the data, addition and subtraction of spectra, and the calculation of derivative spectra. Also, difference spectra can be compared with other data already in the computer memory. Changes in spectra during a reaction (kinetic difference spectra) can be measured very well by using a diode array spectrophotometer, because spectra can be recorded at a very short interval.

Suggestions for Further Reading

S. B. Brown (1980) "Ultraviolet and visible spectroscopy". In *An Introduction to Spectroscopy for Biochemists* (S. B. Brown, ed.), Academic Press, London, pp. 14–69.

J. W. Donovan (1973) Ultaviolet difference spectroscopy—new techniques and applications. Methods Enzymol. **27**, 497–525.

R. K. Poole and C. L. Bashford (1987) "Spectra". In *Spectrophotometry and Spectrofluorimetry: A Practical Approach* (D. A. Harris and C. L. Bashford, eds.), IRL Press, Oxford, UK, pp. 23–48.

F. X. Schmid (1997) "Optical spectroscopy to characterize protein conformation and conformational changes". In *Protein Structure: A Practical Approach*, 2nd ed. (T. E. Creighton, ed.), IRL Press, Oxford, UK, pp. 261–297.

Differentiation

Differentiation is the expression of specialized functions by a cell (1). Differentiation may be reversible. For example, bacteria express sets of enzymes to facilitate the use of the nutrients that they sense in their surroundings. When the bacteria sense a change in their surroundings, such as a change in the nutrients in their culture medium, they inactivate the set of enzymes appropriate for the first medium and express a different set of enzymes to facilitate use of the new nutrients. As their surroundings change, the bacteria can change back and forth between different sets of enzymes indefinitely.

In most cases, however, differentiation is not reversible. Once a cell begins expressing specialized functions, its future choices become limited. For example, human cells that begin expressing heart-specific proteins no longer have the potential to form skin. As cells become more specialized, they find their potential fates more restricted. The restriction of fates is called *determination*, and it was often shown to occur long before differentiation of any specialized functions. As our molecular tools have become more sophisticated, the distinction between determination and differentiation has become more blurred. Looking for the first detectable signs of differentiation, more sensitive techniques allow us to find molecular differences at earlier stages. When pushed to the limits, molecular techniques have increasingly shown that the basis of determination is the expression of a specialized gene product or function, that is, merely the first step in differentiation.

Bibliography

1. B. I. Balinsky (1975) *An Introduction to Embryology*, 4th ed., W. B. Saunders, Philadelphia, p. 468.

Suggestions for Further Reading

2. B. I. Balinsky (1975) *An Introduction to Embryology*, 4th ed., W. B. Saunders, Philadelphia, p. 468.
3. S. F. Gilbert (1997) *Developmental Biology*, Sinauer Associates, Sunderland, MA.
4. L. Wolpert et al. (1998) *Principles of Development*, Oxford University Press, Oxford, U.K.
5. A. S. Wilkins (1993) *Genetic Analysis of Animal Development*, 2nd ed., Wiley-Liss, New York.

Diffusion

Diffusion is the movement of molecules within a liquid driven by thermal fluctuations. It is important for most biological processes; indeed, the diffusion together of two reactants can be the limiting factor for many processes, when the reaction is said to be **diffusion-controlled**.

There are two types of diffusional motion: (*1*) *translational diffusion*, where a molecule moves its relative position within a three-dimensional system; and (*2*) *rotational diffusion*, where a molecule spins or rotates about one or more of its axes. The rates at which molecules undergo both types of diffusion are measured by their respective diffusion coefficients, D_t and D_r. The SI unit for D_t is the "Fick," or m^2/s, but for historical and other reasons, biologists tend to use the cgs (Centigrade–gram–second) system unit of cm^2/s. These measurements can give important information about the sizes, structures, and physical properties of the molecules. At room temperature and in dilute solution, a small protein of molecular weight approximately 20,000 will have D_t of about 10^{-6} cm^2/s; a large virus between 10^{-7} to 10^{-8} cm^2/s; a bacterial spore about 10^{-9} cm^2/s. Some representative values are given in Table 1.

Table 1. Translational Diffusion Coefficients and Derived Parameters of Some Molecules, Macromolecules and Biomolecular Assemblies

Substance	Molecular Weight	$10^7 \times D^{j0}_{20,w}$, cm^2/s	r_H, Å	$10^8 \times f$, g/s

Water	18	230	—	—
Sucrose	342	46.0	4.7	0.88
Ribonuclease	13,700	11.1	19.3	3.64
Ovalbumin	45,000	7.8	27.5	5.18
Fibrinogen	330,000	2.0	107	20.2
Dynein[a]	2.5×10^6	1.1*	195	36.7
Turnip yellow mosaic virus	5.7×10^6	1.4	152	28.9

[a] Although the molecular weight of dynein is smaller than that of turnip yellow mosaic virus, its diffusion coefficient is smaller because it is more asymmetric. Values of $D^{0}_{20,w}$ and molecular weight M_r for dynein are also strongly dependent on salt concentration.

1. Translational Diffusion

The translational diffusion coefficient, D_t, describes the tendency of a molecule to move (translational motion) under the influence of either (*1*) a concentration gradient or (*2*) Brownian motion.

The movement of molecules in a gradient in which their concentration varies, *dc/dx*, where *c* is the concentration (in grams per milliliter) at each point *x*, is given by Fick's first law:

$$J = -D_t(dc/dx) \tag{1}$$

where *J* is the mass of particles crossing a 1-cm^2 cross section per second.

The same D_t characterizes the Brownian diffusion of the molecule:

$$\langle x^2 \rangle = 2D_t t \tag{2}$$

where *t* is the time and $\langle x^2 \rangle$ is the average of the square of the distance the particle has moved.

The value of D_t depends not only on the intrinsic size and shape of the molecule but also on the viscosity and temperature of the medium in which it is suspended. The value of D_t must therefore be normalized to standard conditions; the standard conditions normally used are those of water at 20.0° C. The D_t corresponding to these conditions is normally designated $D_{20,w}$. It can be calculated from the value actually measured at absolute temperature T and in buffer "b," $D_{T,b}$, with the equation

$$D_{20,w} = \left(\frac{293.15}{T}\right)\left(\frac{\eta_{T,b}}{0.01}\right) D_{T,b} \tag{3}$$

where $h_{T,b}$ is the viscosity (in cgs units) of the buffer at temperature *T* and 0.01 is the viscosity of water at 20.0°C.

The value of $D_{20,w}$ can also depend on the concentration of the molecule in the solution, due to thermodynamic nonideality resulting primarily from the finite size of the molecule and its electric charge. This nonideality is represented (1) by the parameter k_d (in units of milliliters per gram) in the equation

$$D_{20,w} = D^{\circ}_{20,w}(1 + k_d c) \tag{4}$$

$D^{j0}_{20,w}$ is the value of $D_{20,w}$ at zero concentration of the molecule; its value can be estimated with equation 4 by measuring $D_{20,w}$ at several different concentrations. For diffusion measurements, the non-ideality term is often negligible and can be neglected.

The value of D_t can be measured either by following the rate of disappearance of a concentration gradient or by dynamic light scattering. The former is the traditional method of measuring D_t (2, 3). The principle is to determine how the concentration changes with time at the boundary between two solutions, one containing the molecule of interest and the other, just the buffer or dialyzate. A special diffusion cell can be used with an appropriate optical system for recording either the concentration, c, or the concentration gradient, dc/dx, as a function of distance, x, from the center of the boundary. Alternatively, the optical system of an analytical **ultracentrifuge** can be used to measure the boundary spreading in a synthetic boundary cell. A speed is chosen to be sufficiently small that sedimentation of the molecule is negligible. The Schlieren optical system is very useful, as it gives the value of dc/dx as a function of x. The value of D_t can be determined by measuring the variation in the height of the boundary, specifically, the maximum value of dc/dx, with time, t:

$$\left(\frac{A}{H}\right)^2 = 4\pi D_t t \tag{5}$$

where A is the area under the curve of dc/dx versus x. A plot of $(A/H)^2$ versus time will yield D_t from the slope; an example is given in Figure 1.

Figure 1. Measurement of the translational diffusion coefficient, D_t, for ovalbumin by the boundary spreading technique (4). As in Equation (5) of the text, the square of the ratio of area (A) to the height (H) of the boundary is plotted as a function of time.

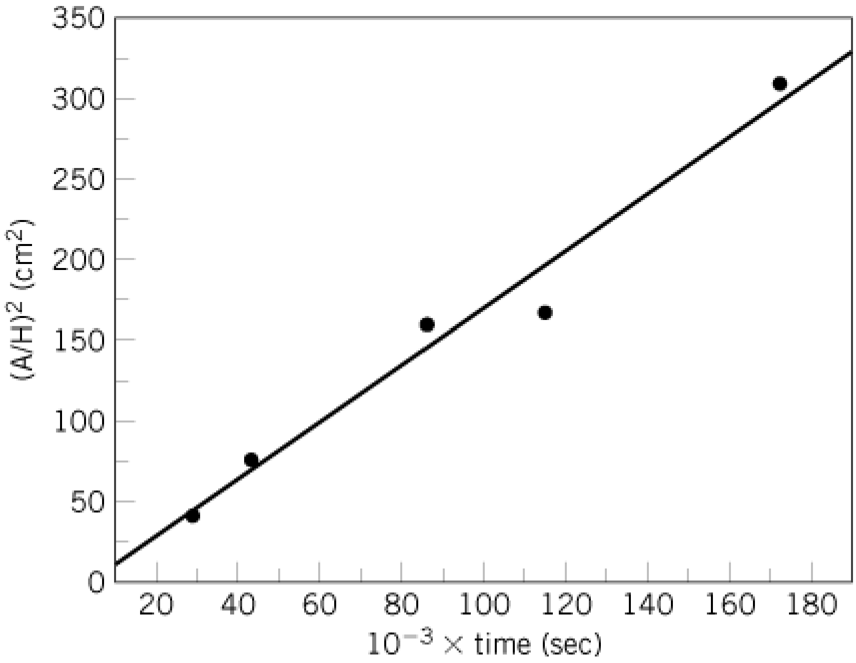

Equation 5 assumes that there is no loss of material from the boundary, that is, that the area A remains constant. This assumption is reasonable for homogeneous protein preparations but may not be valid for polydisperse materials such as mucus **glycoproteins** and polysaccharides.

These methods have also generally been superseded by dynamic light scattering. Nevertheless, the classical measurements are preferable with nonglobular macromolecules, with asymmetric shapes.

2. Interpretation of the Translational Diffusion Coefficient

The value of $D_{20,w}$ or $D^{\circ}_{20,w}$obtained by either dynamic light scattering or boundary spreading can be used to provide a number of useful characteristics about a macromolecule.

2.1. Hydrodynamic Radius

The simplest deduction that can be made from the $D^{\circ}_{20,w}$is the size of the molecule as represented by its equivalent hydrodynamic radius, r_H, which is also known as the *Stokes radius*. The r_H is the radius of the equivalent sphere that would have the same $D^{\circ}_{20,w}$. The two parameters are related by the *Stokes–Einstein equation*:

$$r_H = \frac{k_B T}{6\pi\eta_{20,w} D^{\circ}_{20,w}} \tag{6}$$

where k_B is the Boltzmann constant (1.379×10^{-16} erg/K), T is the temperature (293.15 K at 20.0°C), and $h_{20,w}$ is the viscosity of water (0.01 P at 20.0°C). If the value of D_t is not corrected to standard conditions, the appropriate values for T and h must be used. Table 1 gives the values of r_H for several macromolecules.

2.2. Frictional Coefficient, f

The **frictional coefficient** is inversely related to the diffusion coefficient, giving a measure of the resistance to movement due to both its size and shape. It can be calculated directly from $D^{\circ}_{20,w}$:

$$f = \frac{RT}{N_A D^{\circ}_{20,w}} = \frac{k_B T}{D^{\circ}_{20,w}} \tag{7}$$

where R is the gas constant (8.314×10^{-7} erg mol^{-1} K^{-1}) and N_A is Avogadro's number (6.02×10^{23}). Values of f calculated from $D^{\circ}_{20,w}$ are given in Table 1.

It is often more informative to use the **frictional ratio**, f/f_o, which is the dimensionless ratio of the observed frictional coefficient to that of an equivalent spherical molecule of the same anhydrous mass and density.

2.3. Molecular Weight (M_r)

The molecular weight of a molecule can be calculated from the combination of its diffusion coefficient and its **sedimentation coefficient**, $S^{\circ}_{20,w}$ when corrected to standard conditions. The equation analogous to (7) for the sedimentation coefficient is

$$f = \frac{M_r(1 - \bar{v}\rho_{20,w})}{N_A s^{\circ}_{20,w}} \tag{8}$$

where v is the **partial specific volume** of the macromolecule and r $_{20,w}$ is the density of the standard solvent, water at 20°C. Elimination of f between equations 7 and 8 yields the well-known Svedberg equation:

$$M_r = \frac{s^{\circ}_{20,w}}{D^{\circ}_{20,w}} \frac{RT}{(1 - \bar{v}\rho_{20,w})} \tag{9}$$

Equation 9, of course, makes it possible to calculate $D^{\circ}_{20,w}$ if both $S^{\circ}_{20,w}$ and M_r are known.

It is possible, in principle, to measure both $D^{\circ}_{20,w}$ and $S^{\circ}_{20,w}$ simultaneously from analysis of the shape of the boundary in **sedimentation velocity** analytical ultracentrifugation, although in practice this requires data of high quality and a totally homogeneous sample.

If the general shape of the macromolecule is known to a first approximation, it is possible to estimate its molecular weight from only its diffusion coefficient, just as in the case of the **sedimentation coefficient**. The power-law relation between M_r and D_t is also known as a *Mark–Houwink–Kuhn–Sakurada relation*:

$$D_t = K M_r^{-\epsilon} \tag{10}$$

where e = 0.333 for a sphere, 0.85 for a rod, and 0.5–0.6 for random coil polymers. The appropriate value of the constant K is obtained from a collection of standard molecules of known D_t and M_r (5). Of course, the shape of the macromolecule will normally be known only approximately, so any molecular weight calculated in this way must be considered only an estimate.

2.4. Shape

The translational frictional coefficient, f, or the frictional ratio, f/f_0, can be used directly to provide information about the shape of the molecule. The function defining the shape and flexibility of a macromolecule is the *Perrin translational frictional function*, P:

$$P = \frac{f}{f_0}\left(\frac{\bar{v}}{\bar{v} + (\delta/\rho_0)}\right)^{1/3} \tag{11}$$

where d is the amount of bound solvent, relative to the mass of the molecule, and r_o is the density of the bound solvent. For a molecule that is fairly rigid over a time-averaged period, the gross shape can be specified using *P* in terms of the axial ratio of the equivalent hydrodynamic ellipsoid or in terms of an arrangement of spheres, in hydrodynamic bead models (Figure 2). Computer programs are available for both types of modeling (6, 7). Especially with the latter approach, the diffusion coefficient should be used in conjunction with other hydrodynamic measurements, such as $s_{20,w}$, to obtain a unique solution to the modeling.

Figure 2. Use of diffusion measurements to represent the shapes of biomolecular assemblies using the hydrodynamic bead model approach: (**a**) from translational diffusion measurements: bead models of the slow "s" (tails out) and fast "f" (tails retracted) forms of a T-even **bacteriophage** (19); (**b**) from rotational (electric dichroism) relaxation measurements: bead models of the complex formed from a DNA fragment of 203 bp with two specific sites and two catabolite activator protein dimers (12).

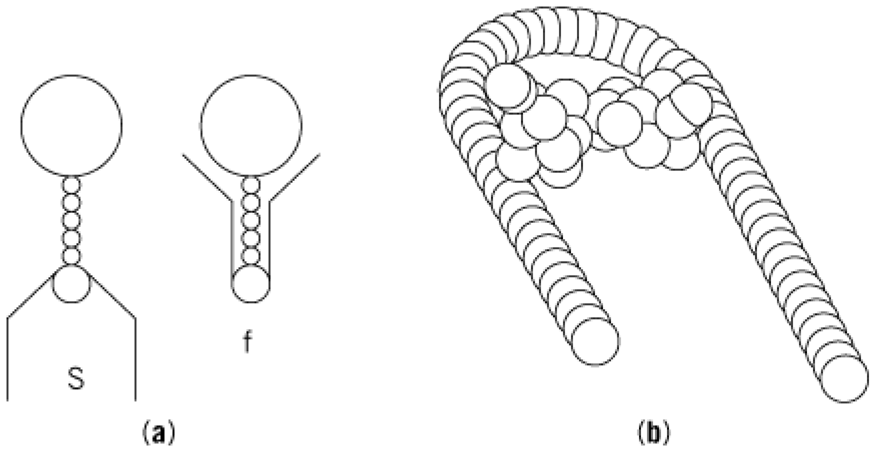

3. Rotational Diffusion

Rotational diffusion coefficients, which result from the tumbling motion of a macromolecule about an axis or axes, are very sensitive functions of the shape of the molecule and permit the inference of some parameters of the overall shape. Unfortunately, this sensitivity comes at a severe price: measurement of rotational diffusion is usually considerably more difficult than translational diffusion.

There are two principal methods for measuring rotational diffusion. One is based on fluorescence measurements and is called *fluorescence anisotropy* decay. The other is based on electrooptical measurements and is termed *electric birefringence* (or the related *electric dichroism*) decay.

3.1. Fluorescence Anisotropy Decay

Tryptophan residues provide intrinsic fluorescent chromophores in many proteins (ie, the ability to reradiate electromagnetic energy at a wavelength longer than that absorbed). If the incident monochromatic light is plane-polarized, the reradiated radiation will not only be at a longer wavelength but will also be wholly or partially depolarized depending (among other factors) on the extent of rotational Brownian motion of the macromolecule. If the macromolecule is not a protein and does not have an intrinsic fluorescent chromophore, or is a protein-containing insufficient tryptophan residues, a chromophore can be attached synthetically.

The emitted polarization is measured by two detectors, one normal to, and the other perpendicular to, the plane of polarization; the extent or "anisotropy" of polarization, $r(t)$, is recorded as a function of time, t:

$$r(t) = \frac{I_{\parallel} - I_{\perp}}{I_{\parallel} + 2I_{\perp}} \tag{12}$$

where $I_{\parallel}$ is the emitted intensity in a plane parallel to the polarization of the incident light and $I_{\perp}$ is in a plane perpendicular. In time-resolved fluorescence depolarization anisotropy, this rapid decay in anisotropy of polarization in response to a pulse of incident radiation is recorded and averaged over many pulses (in some ways, the situation is analogous to the measurement of translational diffusion using dynamic light scattering). Allowance has to be made for the decay in intensity of the chromophore itself, specifically, the decay of the intrinsic fluorescence intensity has to be deconvoluted from the anisotropy decay function. The decay in $r(t)$ with time can then be analyzed in terms of the rotational relaxation times of the molecule. There will be one relaxation time for a spherical particle, three for a particle with an axis of symmetry. For a general asymmetric molecule, there will be five relaxation times that need resolving:

$$\begin{aligned} r(t) = {} & c_1 \exp(-t/\tau_1) + c_2 \exp(-t/\tau_2) + c_3 \exp(-t/\tau_3) \\ & + c_4 \exp(-t/\tau_4) + c_5 \exp(-t/\tau_5) \end{aligned} \tag{13}$$

or, more simply $r(t) = \sum_{i=1}^{5} c_i \exp(-t/\tau_i)$where i = 15. In practice, at least two pairs of relaxation times are similar; hence the problem is one of resolving three decay constants (this will be particularly true for macromolecules with an axis of symmetry). Once resolved, these can be related to macromolecular shape and hydration (6, 7) using relations similar to Equation (11). However, extraction of decay constants from a "multiexponential decay"—of which equation (13) is an example—is what the mathematicians call "an ill-conditioned problem" and is not easy, especially if the relaxation times are relatively similar. A further problem is that the chromophore most not relative to the rest of the macromolecule.

A much simpler procedure is to measure fluorescence depolarization or anisotropy decay in the steady state, where the light source is continuous rather than pulsed (8). It can be used to obtain the harmonic mean rotational relaxation time, t_h. t_h and $1/t_{1–5}$ can all be related to the shape and hydration of the macromolecule (7, 9). A study of fibrinogen provides a good example of the application of both time-resolved and steady-state fluorescence measurements (10, 11).

3.2. Electric Birefringence Decay

Solutions of macromolecules oriented in an electric field will be *birefringent*, having different refractive indices for light polarized parallel to and perpendicular to the electric field. This is known as *electric birefringence*. A related phenomenon, for macromolecules with absorbing chromophore, is *electric dichroism*, where a solution of macromolecules oriented in an electric field exhibits different extinction coefficients parallel to and perpendicular to the electric field.

When the electric field is switched off, the birefringence (or difference in refractive indices) D*n* will decay because of rotational motions of the macromolecule:

$$\Delta n(t) = \sum_{i=1}^{5} c_i \exp(-t/\tau_i) \tag{14}$$

where i = 1–5. However, there will be just two relaxation times for molecules that can be approximated by homogeneous ellipsoidal shapes, and just one for a homogeneous ellipsoid with an axis of symmetry. An electrically homogenous spherical particle exhibits no birefringence.

Like fluorescence anisotropy decay measurements, the relaxation times t_i can be related to molecular shape and hydration (Fig. 2) (12), but there are also practical problems to be overcome. The main problem has been that of local overheating in the solution caused by the large orienting electric fields. This has meant in the past that experiments have been limited to solutions of low ionic strength. With significant advances in charge shielding in modern instrumentation, however, physiological ionic strengths are now a reality (13).

3.3. Diffusion of Small Molecules through Biomolecular Systems

Although most attention is given to diffusion phenomena in macromolecules, the importance of the diffusion through biopolymer matrices of small molecules and ions, even water molecules themselves, cannot be ignored; indeed, many physiological processes involve passive or active transport of water and other low-molecular-weight species through cellular and other matrices. As a direct comparison with macromolecular diffusion, Table 1also gives the self-diffusion coefficient at 20.0°C of water (2.3×10^{-5} cm^2/s) and a small sugar molecule, sucrose ($\sim 4.6 \times 10^{-6}$ cm^2/s); the diffusion rates are orders of magnitude greater than those for more bulky macromolecules.

Arguably the best method for measuring diffusion of water and other small molecules is *pulsed field gradient spin echo* NMR (14). Spinning charged particles, such as atomic nuclei, will have an associated magnetic dipole moment, which generates a magnetic energy when placed within a magnetic field. Quantum-mechanical considerations restrict the energies to a limited number of discrete values. Transitions between levels—whose spacing depends on the external magnetic field—correspond to radiofrequency (RF) radiation, so the nucleus will interact or "resonate" with certain radiofrequencies if the external magnetic field is varied; this is known as nuclear magnetic resonance. These frequencies, and the strength and breadth of the resonances, depend on the particular atomic nuclei that are being examined and on the environment in which they find themselves. It is therefore possible to "home in" on a particular nuclear species; for example, such nuclei could be the hydrogen atoms in a water molecule.

With the pulsed field gradient technique, an excitation pulse of RF radiation is applied across a sample—in this case a biomolecular matrix—causing alignment of spins and the generation of an NMR signal; this signal subsequently decays as a result of diffusion. If a second RF pulse is applied after an interval t, the decay processes are reversed and a refocused "echo" signal is obtained at a time 2t after application of the first pulse. This recovery process can be interrupted as follows. A pair of matched magnetic field gradient pulses that vary linearly across the sample are also applied; the first is applied between the RF pulses and the second, after the second RF pulse. The echo only has no net effect if there has been no diffusive movement of the molecules; any movement will result in an attenuation of the echo. Analysis of this attenuation can be used to determine the diffusion coefficient.

4. Acknowledgment

The author is grateful to Professor W. Derbyshire and Dr. I Farhat for their helpful comments.

Bibliography

1. S. E. Harding and P. Johnson (1985) Biochem. J. **47**, 247–250.
2. O. Lamm (1928) Z. Phys. Chem. **A138**, 313.
3. L. J. Gosting (1956) Adv. Prot. Chem. **11**, 429–554.
4. O. Lamm and A. Polson (1936) Biochem. J. **30**, 528–541.
5. P. Claes, M. Dunford, A. Kenney, and P. Vardy (1992) in *Laser Light Scattering in Biochemistry* (S. E. Harding, D. B. Sattelle, and V. A. Bloomfield, eds.), Royal Society of Chemistry, Cambridge, U.K., pp. 66–76.
6. S. E. Harding, J. C. Horton, and H. Cölfen (1996) Eur. Biophys. J. **25**, 347–359.
7. J. Garcia de la Torre, B. Carrasco, and S. E. Harding (1997) Eur. Biophys. J. **25**, 361–372.

8. G. Weber (1952) Biochem. J. **51**, 145–155.
9. J. Garcia de la Torre and V. A. Bloomfield (1977) Biopolymers **16**, 1747–1763.
10. A. U. Acuna, J. Gonzalez-Rodriguez, M. P. Lillo, and K. R. Naqvi (1987) Biophys. Chem. **26**, 55–61.
11. A. U. Acuna, J. Gonzalez-Rodriguez, M. P. Lillo, and K. R. Naqvi (1987) Biophys. Chem. **26**, 63–70
12. J. Antonsiewicz and D. Porschke (1988) J. Biomol. Struct. Dyn. **5**, 819–837.
13. D. Pörschke and A. Obst (1991) Rev. Sci. Intrum. **62**, 818–820.
14. E. O. Stekskal and J. E. Tanner (1965) J. Chem. Phys. **42**, 288–292.

Suggestions for Further Reading

15. E. Fredericq and C. Houssier (1973) *Electric Dichroism and Electric Birefringence*, Oxford Univ. Press, Oxford (classic text, although somewhat dated).
16. K. E. Van Holde (1985) *Physical Biochemistry*, Prentice-Hall, Englewood Cliffs, N. J. [Chapters 4 (general diffusion), 6 (electro-optics) and 8 (fluorescence depolarisation) give an excellent introduction.]

Diffusion-Controlled Reactions

Any catalytic or chemical process can be dissected, at least theoretically, into both physical and chemical steps. For a chemical reaction to occur, the reactants must come into physical contact in the correct proximity and orientation. Then whether they simply dissociate or undergo a reaction depends on a number of factors, especially the probability that the reaction will occur. With very facile reactions, every encounter results in a reaction, and the rate-limiting step for the overall reaction is the physical encounter of the two reactants, which is governed primarily by diffusion.

The second-order rate constant for a diffusional encounter of two molecules is $10^{10}s^{-1}$ M^{-1} for macromolecules and 10^8 to 10^9s^{-1} M^{-1} for small molecules. These numbers can, however, be altered by factors of up to 10^2 by attractive or repulsive interactions, especially electrostatic, between the reactants.

Suggestion for Further Reading

G. G. Hammes and P. S. Schimmel (1970) In *The Enzymes*, 3rd ed. (P. D. Boyer, ed.), Academic Press, New York, Vol. **2**, pp. 67–114.

DIFP (Diisopropylfluorophosphate)

Diisopropylfluorophosphate, also known as diisopropylphosphofluoridate, DIPF, and sometimes abbreviated DFP, was developed as a nerve gas during the World War II. It is an irreversible inhibitor of **acetylcholinesterase** and, more generally, an inhibitor of serine proteinases (1). In **chymotrypsin**, a typical serine proteinase, the active site Ser195 is phosphorylated by DIFP in a reaction that mimics the catalytic mechanism (Fig. 1). None of the other 27 serine residues of chymotrypsin is affected. The resultant diisopropylphosphoryl serine is stable to subsequent hydrolysis, and the phosphorylated enzyme is totally inactive. The reagent is a liquid at room temperature and is usually diluted into isopropanol before use (2). It is volatile and highly toxic: LD_{50} in mice is 3.7 mg/kg when administered orally. A more convenient reagent for inactivating serine proteinases is phenylmethane sulfonyl fluoride (PMSF) (3).

Figure 1. Reaction of the hydroxyl group of the active site serine residue of a serine proteinase with diisopropyl fluorophosphate. The product is catalytically inactive.

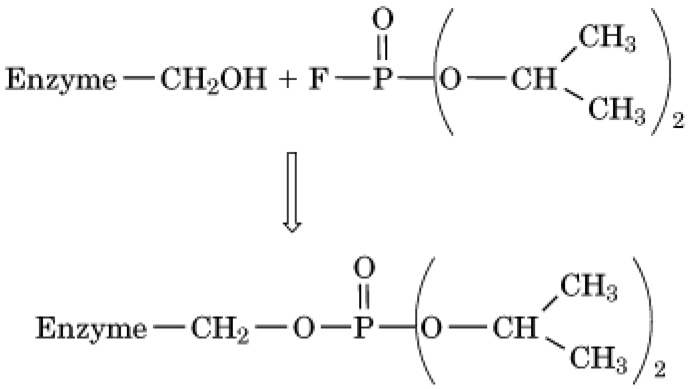

Bibliography

1. J. A. Cohen, R. A. Oosterbaan, and F. Berends (1967) Methods Enzymol. **11**, 686–702.
2. R. J. Beynon and J. S. Bond (1993) In *Proteolytic Enzymes: A Practical Approach* (R. J. Beynon and J. S. Bond, eds.), IRL Press, Oxford, U.K., p. 243.
3. B. M. Dunn (1993) In *Proteolytic Enzymes: A Practical Approach* (R. J. Beynon and J. S. Bond, eds.), IRL Press, Oxford, U.K., pp. 57–81.

Dihedral Angle

A dihedral angle is the angle between two planes (1). This is determined as the angle formed by normal lines to each plane, as shown in Figure 1. When the rotation about a single bond in a molecule is being measured, **eg**, the rotation about the peptide NCa bond, it is preferred nomenclature to use the conventions described for torsion angles . Unlike torsion angles, it is possible to determine the dihedral angle between the planes defined by any two groups of three atoms, whether they are bonded together or not. If any four atoms are specified in order: atom-1, atom-2, atom-3, atom-4, the dihedral angle is measured between the plane containing atom-1, atom-2, and atom-3 and the plane containing atom-2, atom-3, and atom-4. If the four atoms are not sequentially bonded, this dihedral angle may be referred to as an “improper dihedral” or “improper torsion” (2).

Figure 1. The dihedral angle F is the angle between the two planes defined by atoms 1, 2, and 3 and atoms 2, 3, and 4, respectively. The angle is determined as the angle between lines perpendicular to each plane.

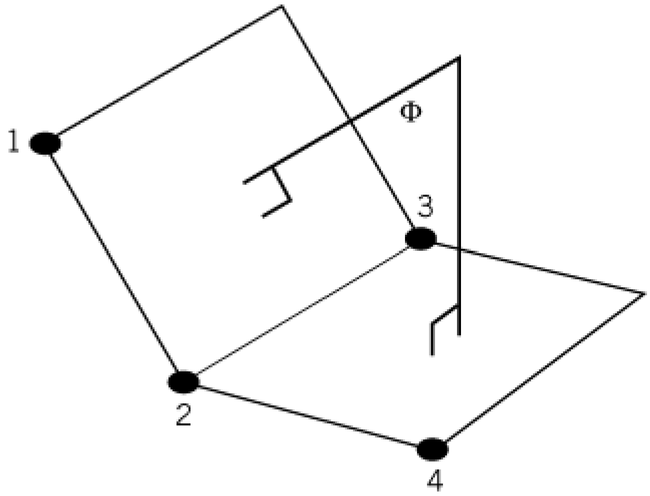

Bibliography

1. *Oxford English Dictionary*, 2nd ed. (1989) Clarendon Press, Oxford.
2. B. R. Brooks et al. (1983) J. Comp. Chem. **4**, 187–217.

Suggestion for Further Reading

3. W. Saenger (1984) *Principles of Nucleic Acid Structure*, Springer-Verlag, New York, p. 15.

Dihydrofolate Reductase (DHFR)

Dihydrofolate reductase (DHFR) catalyzes the **NADPH**-dependent reduction of 7,8-dihydrofolate to 5,6,7,8-tetrahydrofolate (E.C. 1.5.1.3). Tetrahydrofolate, in its variously modified forms, serves as a **cofactor** in the transfer of one-carbon fragments in the biosynthesis of thymidylate and **purine** nucleotides (see **Nucleosides**, **nucleotides**), as well as other metabolic functions. DHFR is universally present in every kind of living cell—**prokaryotes**, **eukaryotes** and **archaebacteria**—where it is essential for the biosynthesis of **DNA**. Thus if DHFR activity is inhibited, cellular replication cannot take place, a phenomenon that forms the basis for the action of a number of anticancer and antimicrobial pharmaceuticals (eg, **methotrexate** and **trimethoprim**) collectively known as *antifolates* . These compounds are simply inhibitors of DHFR with varying degrees of species selectivity. Though required for continuous DNA replication, the role of DHFR is a rather indirect one—that is, maintenance of the intracellular pool of tetrahydrofolate in its fully reduced state. This is necessary because during the final step of thymidylate synthesis, wherein dUMP is methylated at the 5-position to yield dTMP in a reaction catalyzed by thymidylate synthase, the reduced pteridine ring of the one-carbon donating cofactor N^5,N^{10}-methylenetetrahydrofolate is concomitantly oxidized to produce 7,8-dihydrofolate.

This article focuses solely on the molecular properties of DHFR, which, because of its biomedical importance, its conveniently small size, and its ready availability through cloning and protein engineering, has been intensively studied by essentially every enzymological and physicochemical technique available. Omitted, however, is any discussion of the several studies of **protein folding** that have been carried out with DHFR (1, 2). Nor does this article discuss what is known about how the intracellular level of DHFR is regulated during transcription (3) and translation (4) and by gene amplification (5). Also passed over without further comment is the fact that the DHFR gene has been widely employed as a selectable genetic marker (see Reporter Genes).

1. The Molecule

The polypeptide chain composing DHFR from most species is relatively short, in the range of 159 amino acids for ***Escherichia*** *coli* to 229 for *Cryptococcus neoformans* . Exceptions, however, occur in both protozoa and at least some **plants**, where the genes for DHFR and thymidylate synthase are fused and thus encode a bifunctional enzyme molecule. The degree of sequence identity among all DHFR across the biological spectrum is about 25%, with the pattern of residue conservation leaving little doubt that all are **homologous** and folded into quite similar three-dimensional structures (see Protein Structure). That structure is well established; it has been determined by X-ray crystallography for the proteins from *E. coli*, *Lactobacillus casei*, chicken, mouse, human, the protozoon *Leishmania major*, and the fungus *Pneumocystis carinii* . In all cases, these structures contain one or more bound ligands, such as the cofactor, folate, or a variety of inhibitors, so the mode of substrate binding is known in detail. A hypothetical “movie” of the *E. coli* DHFR molecule as it proceeds through its catalytic cycle has been assembled on the basis of 47 distinct crystal structures in 12 different crystal packings (6).

The molecular architecture of DHFR is typical of a basic folding plan that is seen in the case of many other enzymes, notably **NAD(P)** or **flavin** nucleotide-dependent oxidoreductases, as well as numerous enzymes that bind AMP or ATP. This kind of fold is often called an open a/b-sheet structure, because it is composed of a central twisted b-sheet flanked on both sides by a number of **a-helices**. However, this structure is quite variable in the numbers of a-helices and b-strands, their direction relative to one another, the order in which they are connected (ie, their topology), and the size and geometry of the connecting loops.

The central b-sheet of all DHFR contains eight b-strands, with the first seven strands, A–G, all parallel; the lone antiparallel strand, H, comprises the C-terminal portion of the polypeptide chain. Four a-helices flank the central b-sheet, two on each side. In vertebrate DHFR, which are slightly larger than bacterial DHFR, an extra seven-residue loop is inserted in the middle of the outermost strand G of the central b-sheet; vertebrate DHFR contain, in addition, an extra two-turn a-helix and two turns of a left-handed **polyproline**-like helix.

Both the substrate and cofactor are bound in more or less extended conformations, at approximately right angles to one another, with the pteridine ring of the substrate and the nicotinamide ring of the cofactor occupying a pocket between the carboxyl ends of strands bA and bE. They are in close contact in such a way that hydride transfer can take place between the A side (*pro-R* or *re*) of the nicotinamide ring at C4 and C6 or C7 of the pteridine ring.

2. Enzyme Kinetics

The kinetic pathway of DHFR is complicated by the participation of nine possible ligation states, each distinguished by whether the cofactor binding site and/or the substrate binding site is (i) unoccupied, (ii) occupied by the oxidized ligand, or (iii) occupied by the reduced ligand. Rate constants for the interconversion between these ligation states have been measured and assembled into complete kinetic schemes for DHFR from *E. coli* (7), *L. casei* (8), human (9), mouse (10), and *Pneumocystis carinii* (11). These schemes accurately predict **steady-state** kinetic behavior in computer simulations. Although the predominant pathways vary somewhat, in neither bacterial nor vertebrate DHFR is the chemical step (ie, proton donation to N5 and hydride transfer to C6 of dihydrofolate) **rate-limiting**. Instead, the rate-limiting steps are either substrate binding or product release. These DHFR also show evidence of a conformational isomerization prior to the chemical step, possibly involved in proton donation to N5 of dihydrofolate (12). Among the few kinetic differences between bacterial and vertebrate DHFR, most prominent is the much greater efficiency of vertebrate DHFR at catalyzing the reduction of folate.

3. Mutagenesis Studies

A plethora of mutants of DHFR (primarily from *E. coli* and human) have been engineered by site-directed mutagenesis to probe the catalytic role of evolutionarily conserved side chains. Only a handful of these mutants have been characterized both structurally and kinetically, but interpretation of the results is not straightforward for even the most thoroughly studied. For example, mutation of conserved $\mathrm{Asp27} \rightarrow \mathrm{Asn}$ of *E. coli* DHFR, or the equivalent $\mathrm{Glu30} \rightarrow \mathrm{Gln}$ in human DHFR, results in a strong pH-dependence of k_{cat}, suggesting a role for the carboxylic acid in protonation of N5 of the substrate. However, the equivalent mutation, $\mathrm{Asp26} \rightarrow \mathrm{Asn}$, in *L. casei* DHFR yields only a modest pH effect (13). Structural perturbations are minimal in these and most other such site-directed mutants, but the rate of the chemical step decreases significantly, suggesting that the entire enzyme molecule influences hydride transfer and proton donation. Further mutagenesis studies involve modification of whole a-helices (14) and loops (15) or circular permutations of the polypeptide chain (16) in an effort to understand the functional role of larger structural elements in catalysis.

4. The Transition State

At the center of the effort to understand any enzyme lies a fundamental question: How does it catalyze the reaction? In the most general terms, elementary catalysis theory dictates that the enzyme molecule must bind the transition state of the reaction many orders of magnitude more strongly than the reactants. But to progress beyond this level of understanding for any particular enzymic reaction requires that one begin with a picture of the transition state; and this is no easy matter, because the transition state is by definition an unstable, transitory molecular species. Thus one must rely on theory, and even speculation, to suggest what the transition state might look like.

In the case of DHFR, there is at least one very clear indication from the crystal structures that the enzyme molecule is indeed “designed” to bind the transition state. Certainly the transition state must involve a close approach of the two carbon atoms between which hydride ion transfer takes place, C4 of the nicotinamide and C6 of the pteridine ring. Theoretical calculations (17) predict a C4–C6 distance of 2.6 Å in the transition state, about 1 Å shorter than **van der Waals** contact distance. Happily this is just what is seen when the separate structures of the binary complexes, DHFR · folate and DHFR · NADPH, are carefully superposed on one another in the case of both the vertebrate (18) and the *E. coli* (19) enzymes. Evidence that DHFR is trying to push the C4 and C6 atoms together is seen even in ternary complexes in which both the cofactor and the pteridine are bound simultaneously; the approach distance is 0.3 to 0.5 Å shorter than the expected van der Waals distance of 3.6 Å.

Bibliography

1. B. E. Jones and C. R. Matthews (1995) Protein Sci. **4**, 167–177.
2. S. D. Hoeltzli and C. Frieden (1995) Proc. Natl. Acad. Sci. USA **92**, 9318–9322.
3. J. E. Slansky and P. J. Farnham (1996) Bioessays **18**, 55–62.
4. E. Ercikan et al. (1993) In *Chemistry and Biology of Pteridines and Folates* (J. E. Ayling et al., eds.), Plenum Press, New York, pp. 537–540.
5. J. L. Hamlin (1992) Mutat. Res. **276**, 179–187.
6. M. R. Sawaya and J. Kraut (1997) Biochemistry **36**, 586–603.
7. C. A. Fierke, K. A. Johnson, and S. J. Benkovic (1987) Biochemistry **26**, 4085–4092.

8. J. Andrews et al. (1989) Biochemistry **28**, 5743–5750.
9. J. R. Appleman et al. (1990) J. Biol. Chem. **265**, 2740–2748.
10. J. Thillet, J. A. Adams, and S. J. Benkovic (1990) Biochemistry **29**, 5195–5202.
11. S. A. Margosiak, J. R. Appleman, D. V. Santi, and R. L. Blakley (1993) Arch. Biochem. Biophys. **305**, 499–508.
12. W. A. Beard et al. (1989) J. Biol. Chem. **264**, 9391–9399.
13. J. Basran, M. G. Casarotto, I. L. Barsukov, and G. C. K. Roberts (1995) Biochemistry **34**, 2872–2882.
14. L. Li and S. J. Benkovic (1991) Biochemistry **30**, 1470–1478.
15. L. Li, C. J. Falzone, P. E. Wright, and S. J. Benkovic (1992) Biochemistry **30**, 7826–7833.
16. A. Buchwalder, H. Szadkowski, and K. Kirschner (1992) Biochemistry **31**, 1621–1630.
17. Y.-D. Wu and K. N. Houk (1987) J. Am. Chem. Soc. **109**, 2226–2227.
18. J. F. Davies et al. (1990) Biochemistry **29**, 9467–9479.
19. V. M. Reyes, M. R. Sawaya, K. A. Brown, and J. Kraut (1995) Biochemistry **34**, 2710–2723.

Suggestion for Further Reading

20. R. L. Blakley (1995) Eukaryotic dihydrofolate reductase. Adv. Enzymol. **70**, 23–102. (A thoroughly detailed review by a foremost authority.)

Dimethyl Sulfate (DMS)

This is a mutagen that is a monofunctional alkylating agent of structure CH_3–O–SO_2–O–CH_3, which reacts with nucleophilic sites primarily by an S_N2 mechanism. This mechanism involves a concerted process with the substrate, resulting in selective methylation of only the most nucleophilic sites. Thus DMS predominantly methylates nitrogen atoms on **nucleic acids**, only rarely oxygen or phosphorus. By far the most abundant lesion produced is N7-methylguanine, with minor amounts of N_1-, N_3-, and N_7-methyladenine and N_3-methyl cytosine, and trace amounts of O_6-methylguanine (1). 7-Methylguanine has base-pairing properties very similar to guanine itself, so this modification is probably not the most important cause of mutagenesis by DMS. Both 3-methyladenine and 3-methylcytosine can cause base mispairing, which may lead directly to mutagenesis by DMS (1, 2). Although probably not primarily involved in mutagenesis, methylation at the *N*7 of guanine significantly weakens the N9-glycosidic bond, leading to enhanced formation of apurinic sites (3-5). Depurination may also occur at 3-methylated adenines (6, 7), and this itself has mutagenic consequences.

DMS is both **carcinogenic** and **mutagenic** in a wide variety of organisms, producing point mutations, chromosomal aberrations, and recombinational events (reviewed by Hoffman (8)). In many mutagenesis studies, DMS is reported to be a base-pair substitution mutagen, but it also causes frameshift mutations and deletions. It has been suggested that much of the data can be explained in terms of effects of DMS on DNA **repair** processes (8, 9). Lawley and Warren (2) found that *Escherichia coli* repair processes effectively remove 3-methylguanine and 3-methyladenine, but not 7-methylguanine, residues from DNA. These authors suggested that N-3 purine alkylations may block DNA replication and stimulate enzymatic repair processes. Inaccuracies in these may lead to many of the observed mutations in bacterial systems. 7-Methylguanine is removed from the DNA of mammalian cells, although it does not interfere with DNA synthesis (10).

Bibliography

1. P. D. Lawley, D. J. Orr, and S. A. Shah (1972) Chem. Biol. Interact. **5**, 286–288.
2. P. D. Lawley and W. Warren (1976) Chem. Biol. Interact. **12**, 211–220.
3. P. D. Lawley (1966) Prog. Nucleic Acid. Res. Mol. Biol. **5**, 89–131.
4. P. D. Lawley (1974a) In *Molecular and Environmental Aspects of Mutagenesis* (L. Prakash, ed.), Thomas, Springfield, IL, pp. 17–33.
5. P. D. Lawley (1974b) Mutat. Res. **23**, 283–295.
6. P. D. Lawley and P. Brookes (1963) Biochem. J. **89**, 127–138.
7. R. H. C. San and H . F. Stich (1975) Int. J. Cancer **16**, 284–291.
8. G. R. Hoffman (1980) Mutat. Res. **75**, 63–129.
9. J. W. Drake and R. H. Baltz (1976) Annu. Rev. Biochem. **45**, 11–37.
10. D. A. Scicchitano and P. C. Hanawalt (1990) Mutat. Res. **233**, 31–38.

Diphtheria Toxin

Diphtheria was the first infectious disease shown to be caused solely by a toxin (1). Diphtheria toxin (DT) is encoded by a gene carried by temperate **bacteriophages**, such as the *o*-corynephage, that lysogenize *Corynebacterium diphtheriae* and make it toxigenic. The toxin gene is activated by the release of an iron-binding repressor protein, which binds to DNA in its holo form and in iron-depleted media is released as the apo form (1). The DT gene includes a 25-residue long amino-terminal **leader sequence** responsible for the export of DT from the cell (2, 3). After proteolytic removal of the leader sequence, DT is released by *C. diphtheriae* as a single polypeptide chain of 535 amino acid residues. This chain is rapidly cleaved *in vivo* by furin (4) and *in vitro* by different proteinases, within a loop containing three Arg residues that connects the first and second domains (Fig. 1). After such proteolytic nicking, DT is composed of two-chains: A (193 residues), responsible for the intracellular catalytic activity, and B (342 residues), responsible for binding and membrane translocation. A and B are linked by noncovalent forces and a single interchain disulfide bond. Figure 1 shows the three-domain structural organization of DT (5). The amino terminal domain (residues 1 to 193) corresponds to the A subunit, which is an **ADP-ribosyltransferase** with a cleft-shaped **NAD**-binding cavity harboring the Glu148, His21, Trp50, and Tyr65 residues that are essential for activity (5). NAD binds in such a way that its nicotinamide moiety overlaps the phenolic ring of Tyr65, and its adenine group lies over the indole ring of Trp50.

Figure 1. **Structure of diphtheria toxin**. Diphtheria toxin consists of three domains, characterized by different secondary structure elements and different biological properties. The cleft in the catalytic domain is the NAD binding site. The circled star indicates Ser-508 involved in receptor binding. The toxin is activated by selective proteolysis of a furin-sensitive loop between the A domain and T domain, which is responsible for membrane translocation.

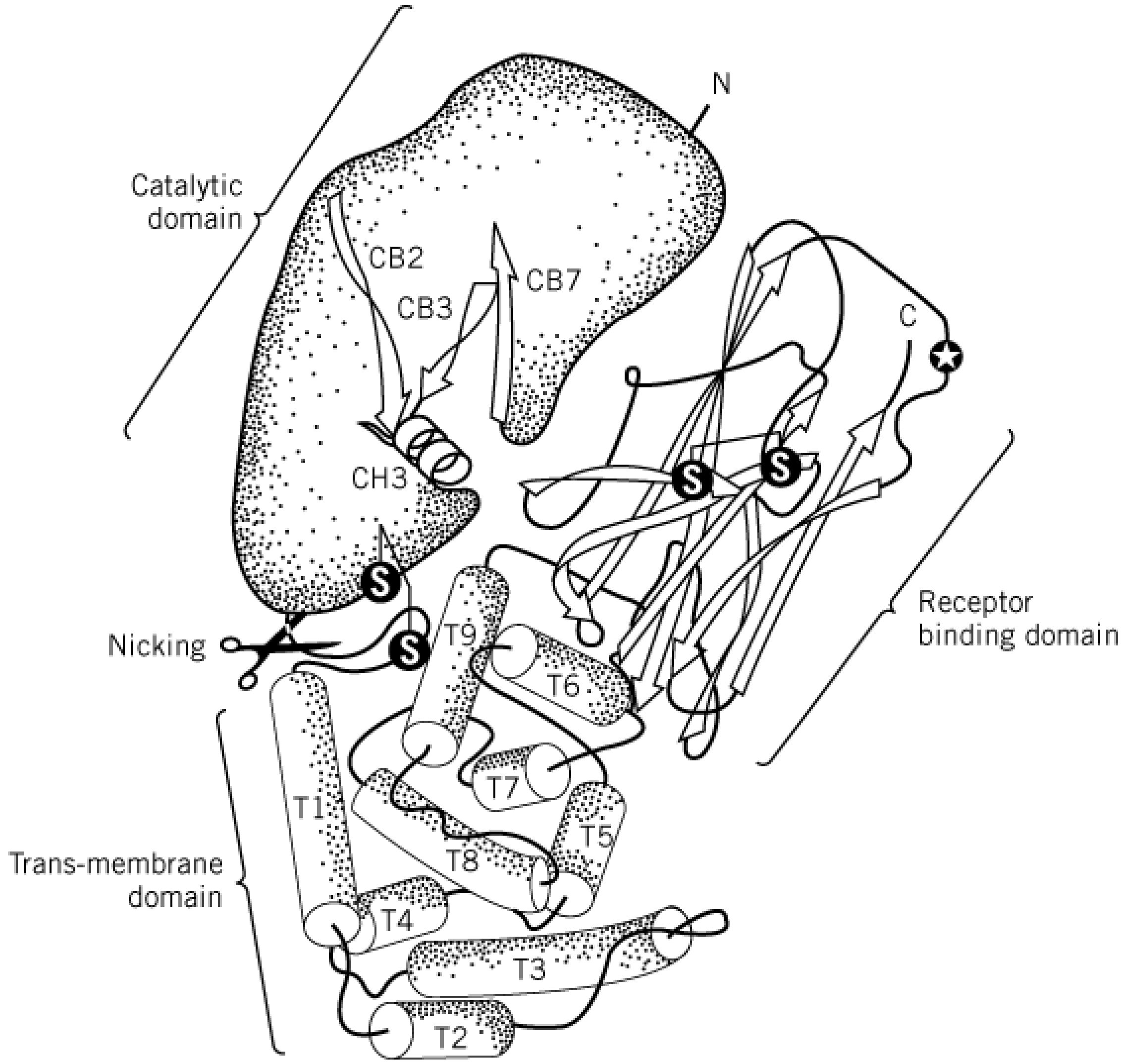

In the nicked toxin, the A domain is disulfide-linked to the T domain (residues 194 to 385), which is involved in the membrane insertion and translocation of DT. The T domain is almost entirely composed of **alpha-helices**, a type of **secondary structure** found in the membrane-embedded sector of many integral membrane proteins. The third domain R (residues 386 to 535) is a flattened ß-barrel and responsible for DT binding to its specific **receptor**, which is a protein that binds heparinlike growth factors (6). The role of this receptor in cell physiology is not known, but it was shown that CD9 enhances the sensitivity of cells to DT (7). The number of DT receptors in different cell lines correlates with their DT sensitivity. Binding is followed by internalization inside clathrin -coated **vesicles**, which uncoat and merge into early endosomes, a process that requires less than 5 min in Vero cells at 37°C (8). The acidic pH of the endosomal lumen induces a conformational change of DT, with insertion of helices of the T domain into the lipid bilayer (9, 10), to create a transmembrane channel, open laterally to lipids, that mediates the translocation of the A chain into the cytosol (11). It is not known if domain A has to unfold completely in order to pass through the B channel, but it is noteworthy that A can be boiled in **SDS** and, upon detergent removal, refolds into its active conformation. The translocation and release of A are linked to the reduction of the interchain disulfide bond, which is carried out by yet unidentified reductases. Such reduction is the rate-limiting step of the entire intoxication process (8). Only about a third of the internalized DT molecules are reduced and release their A chain into the cytosol. The remaining, unreduced two-thirds, as well as the B subunits left over on the membrane after A release, are conveyed to the **lysosomes** and degraded (8).

The A chain of DT **ADP-ribosylates**, specifically elongation factor 2 (EF-2), which becomes unable to transfer the tRNA-bound amino acid to the growing polypeptide chain, and cell **protein biosynthesis** are blocked (12). DT-A is active only on the EF-2 of **eukaryotes** and **archaebacteria** because they contain diphthamide, a **post-translationally modified** His residue, which is the unique substrate of DT and of the related exotoxin A released by *Pseudomonas aeruginosa* (12). The physiological role of diphthamide *in vivo* is unknown, particularly because cell lines mutated at this His residue, or in one of the enzymes involved in its transformation into diphthamide, appear to grow normally (12). One single molecule of DT is able to kill a cell rather rapidly (13) because it can catalyze the ADP-ribosylation of about 2000 EF-2 per hour, whereas cells in culture produce only about 1500 new EF-2 per hour, and EF-2 synthesis decreases as toxin action progresses. As a result, the lethal dose of DT in sensitive animal species (those possessing DT receptors) is below 0.1 µg DT/kg.

Bibliography

1. A. M. Pappenheimer (1982) Harvey Lect. **76**, 45–73.
2. L. Greenfield et al. (1983) Proc. Natl. Acad. Sci. USA **80**, 6853–6857.
3. G. Ratti, R. Rappuoli, and G. Giannini (1983) Nucleic Acids Res. **11**, 6589–6595.
4. J. R. Murphy (1997) In *Guidebook to Protein Toxins and Their Use in Cell Biology* (R. Rappuoli and C. Montecucco, eds.), Sambrook and Tooze, Oxford University Press, Oxford, UK.
5. S. Choe et al. (1992) Nature **367**, 216–222.
6. J. G. Naglich, J. E. Metherall, D. W. Russell, and L. Eidels (1992) Cell **69**, 1051–1061.
7. T. Mitamura et al. (1992) J. Cell Biol. **118**, 1389–1399.
8. E. Papini, R. Rappuoli, M. Murgia, and C. Montecucco (1993) J. Biol. Chem. **268**, 1567–1574.
9. K. Sandvig and S. Olsnes (1981) J. Biol. Chem. **256**, 9068–9076.
10. K. J. Oh et al. (1996) Science **273**, 810–812.
11. G. Menestrina, G. Schiavo, and C. Montecucco (1994) Mol. Aspects Med. **15**, 81–193.
12. R. J. Collier (1990) In *ADP-ribosylating Toxins and G Proteins* (J. Moss and M. Vaugham, eds.), American Society for Microbiology, Washington, DC, pp. 3–19.
13. M. Yamaizumi, E. Mekada, T. Uchida, and Y. Okada (1978) Cell **15**, 245–250.

Direct Methods

Before an electron density map can be calculated in a crystal structure determination using X-ray crystallography, the phase angles of the reflections must be found (see Phase Problem). In principle, they can be derived from the values of the amplitudes $|F(hk\ell)|$, and these are (apart from correction factors) proportional to the square root of the observed reflection intensities $I(hk\ell)$. The relationship between phases and structure factor amplitudes is due to two properties of the electron density map:

1. It is nowhere negative.
2. It is a summation of atomic electron densities.

Several types of direct methods have been derived to determine the phase angles from the structure factor amplitudes alone, and they are routinely used in structurally determining small compounds. With an increasing number of atoms, however, the power of the method becomes weaker. The maximum number of non-hydrogen atoms in the asymmetric unit is around 300. Classical direct methods are not practical for proteins unless the protein molecule is small and gives an extremely high-resolution X-ray diffraction pattern. It also helps if the protein contains one or more heavy atoms, for example, sulfur or iron (1). Although generally not practical for a complete protein structure determination, classical direct methods are suitable for locating heavy atoms from isomorphous replacement data.

A nonclassical approach to direct phase angle determination for macromolecules has been pioneered by Bricogne (2) and is still under development. It applies the maximum entropy principle. Although not yet applicable for a *de novo* structure determination, it can already be applied if combined with available information.

Bibliography

1. G. M. Sheldrick et al. (1993) Acta Crystallogr. **D49**, 18–23.
2. G. Bricogne (1993) Acta Crystallogr. **D49**, 37–60.

Suggestion for Further Reading

3. J. Drenth (1999) *Principles of Protein X-ray Crystallography*, Springer, New York.

Direct Repeats

A repeat, or repeating, **nucleotide sequence** is any of two or more identical segments of a longer sequence or identical segments of a double-stranded **DNA**. Any DNA fragment can be inserted into a long, double-stranded molecule in either of different polarities: “head on” (taking one of the ends of the duplex as a head), or “tail on.” In the long sequence, it then appears as either one strand of the fragment or the other, complementary strand. If two identical fragments are both oriented “head on,” the repeat is called a direct repeat—that is, all identical sequences encountered in a longer sequence are direct repeats. They are normally noncontiguous and separate. Contiguous direct repeats are called tandem repeats. Various types of repeats are outlined schematically in the Figure for Tandem Repeats.

One important example are the direct repeats at the ends of some transposable elements (1). Integrated retroviral genomes and retrotransposons are flanked by the long terminal repeats (LTR) of 200–500 bp. For example, the yeast transposon Ty has 330-bp LTRs at its ends. The repeats are involved in the recombination events during integration or excision of the mobile elements. The presence of the direct repeats in a sequence may actually serve as an indication of possible transposition events. When integrated in the same polarity, the transposons themselves are an example of direct repeats.

Bibliography

1. D. E. Berg and M. M. Howe, eds. (1989) *Mobile DNA* ASM, Washington, D.C.

Suggestion for Further Reading

2. B. Alberts, D. Bray, J. Lewis, M. Raff, K. Roberts, and J. D. Watson (1994) *Molecular Biology of the Cell*, 3rd ed., Garland Publishing Inc., New York.

Disc Electrophoresis

Gel electrophoresis in *discontinuous* buffer systems is known as “disc electrophoresis” (1). Its main advantage is the provision of a highly concentrated starting zone even when the sample is dilute. It employs at least two electrophoresis buffers, i.e., a buffer discontinuity. They differ in either a cation or anion, whereas the counterion is the same. One of the differing ions, known as the “trailing ion,” has an electrophoretic mobility less than the species of interest to be separated; the other, the “leading ion,” has a greater mobility. Embedded within such a system, the species of interest will, at steady-state, migrate within a moving boundary between the leading and trailing ions, at a field strength (conductance) and concentration that is fixed (“regulated”) by the mobilities and concentrations of the leading, trailing, and common buffer ions constituting the boundary. This “regulation” imposes a “regulated” mobility on all trailing species with net mobilities equal to, or greater than, the trailing ion; hence, the system is designated as “equal-mobility-electrophoretic” or isotachophoretic (see Isotachophoresis). A number of species migrating isotachophoretically in order of their net mobilities is called a “stack.” The regulation of mobilities and concentrations behind the leading ion, resulting from the requirement for electroneutrality and the conservation of mass, gives rise to an increased field strength behind the fastest migrating (leading) ion in the electric field (Fig. 1). The gradient in field strength developing behind the leading ion causes equally oriented Joule heat and pH gradients, a gradient in mobility accelerating the trailing ions until at equilibrium they have attained the net mobility of the leading ion, and a gradient of specific conductance oriented inversely to the field strength gradient (Fig. 1). The key benefit of regulation of the trailing buffer phase by the leading ion is that a macromolecular ion present in that phase will migrate within the stack at a very high concentration, estimated to be on the order of 100 mg/mL for a 100-kDa protein, independent of the degree of dilution of the macromolecule in the original sample. Therefore, very dilute samples can produce very condensed zones of sample within the gel.

Figure 1. Operation of discontinuous buffer systems. Prior to electrophoresis, a stationary boundary (dotted line) separates the trailing ion T in the cathode buffer from the leading ion L in the gel buffer. As T and L electrophorese out of the starting zone, the greater instantaneous velocity of L would tend to create behind it an “ion vacuum.” This, however, would be in violation of the laws of conservation of mass and of the maintenance of electroneutrality. Operation of these two laws gives rise to a “regulation” in the zone behind L, which leads to an increase in field strength, Joule heat, and pH, and a decrease in conductance. These, in turn, produce an increased mobility of all species migrating between T and L until they attain the net mobility of L.

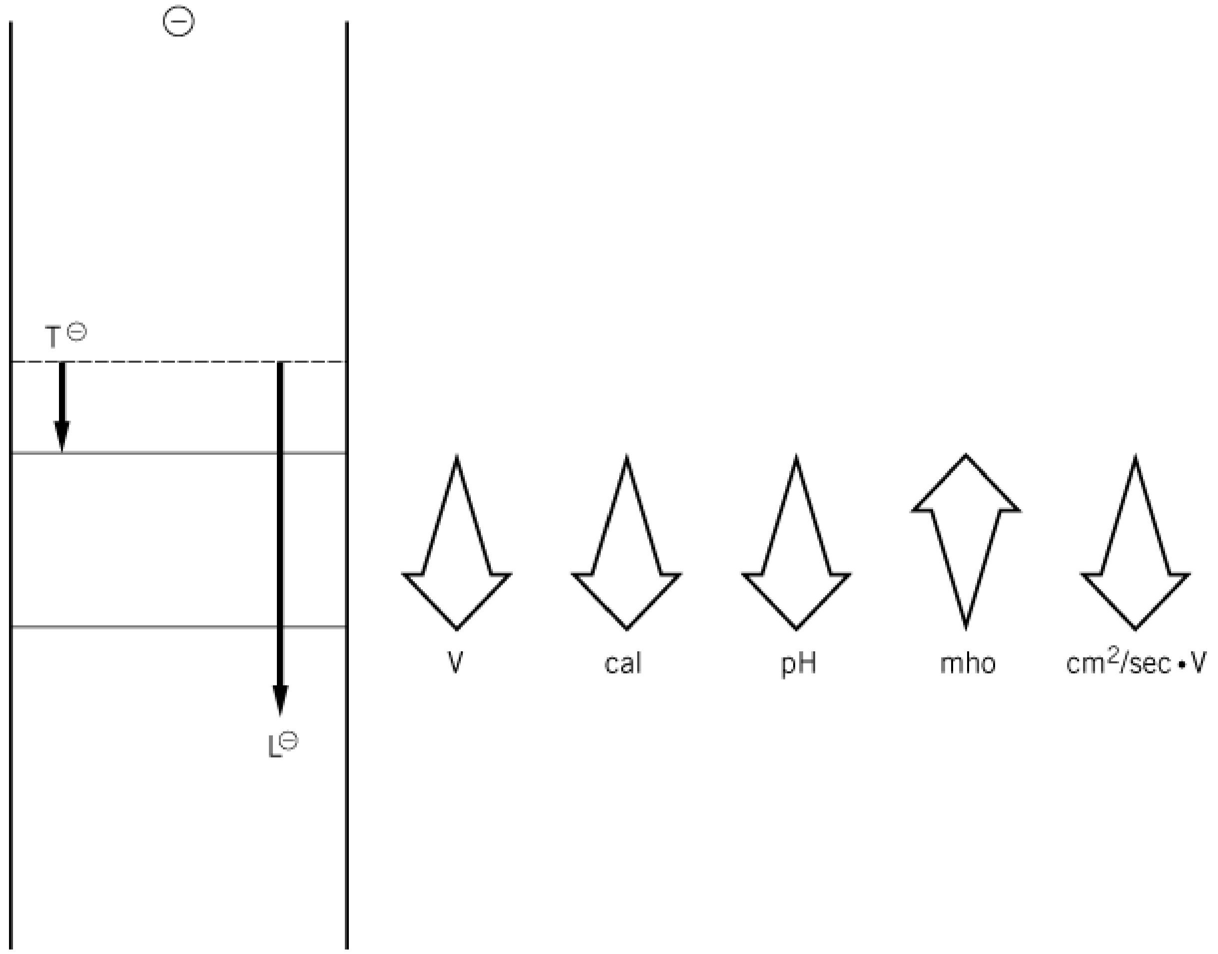

In disc electrophoresis, the concentrating (stacking) buffer phase is embedded in a gel that does not sieve but is present only to prevent convection; this gel is contiguous with a sieving gel, the "resolving gel." As the stack of moving boundaries containing the concentrated sample enters the resolving gel, the buffer boundaries are unaffected by the elevated gel concentration and changed pH, whereas macromolecules are altered in their migration by both. The retardation due to the increased gel concentration causes the macromolecules to migrate at a mobility less than that of the trailing ion. Therefore, they "unstack" and separate according to their mobilities; in contrast, the stack of buffer ions remains (Fig. 2), forming a moving boundary "front" that can be marked by an appropriate tracking dye. The ratio of macromolecular mobilities relative to the stacked tracking dye (in terms of relative mobility, R_f) characterizes an electrophoretic band and can be used, when measured at several different gel concentrations, to specify the size and net charge of the macromolecule (see Ferguson Plot).

Figure 2. Operation of gel electrophoresis in a discontinuous buffer system. (*I*) A gel electrophoresis system of four phases is set up: A cathode buffer containing the trailing ion T as a salt with any counterion X plus a tracking dye; a stacking gel of large pore size, "nonrestrictive" to the migration of macromolecular particles P and containing the leading ion L as a salt with counterion C (which is common to both stacking and resolving gels) at a pH lower than that of the resolving gel; a resolving gel at a gel concentration that lowers ("restricts") the mobility of particle P and at a pH higher than that of the stacking gel; and an anode buffer containing the common counterion C as a salt of any other ion. P is loaded on top of the stacking gel. (*II*) Upon initiating electrophoresis, a stack of L, P, and T forms by regulation (Fig. 1) in the stacking gel. (*III*) Upon arrival at the resolving gel, L and T and the tracking dye proceed as a stack at a velocity undiminished by the presence of the gel and augmented by the increased pH. In contrast, the velocity of P is lowered in the gel through "molecular sieving," so that the mobility of P now is less than that of T. That decrease in mobility is termed "unstacking" and results in the migration of all species of P in decreasing order of

their net mobility, ie, in their separation.

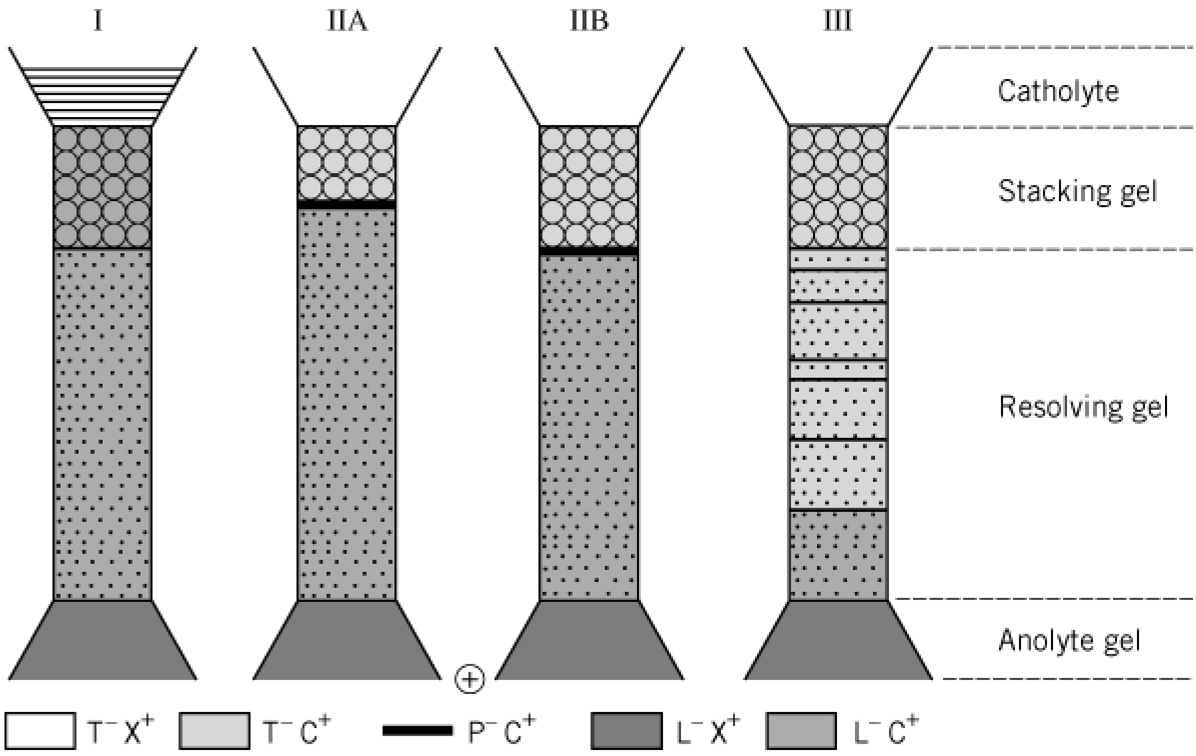

Most important, disc electrophoresis is an analytical or preparative separation method that is largely independent of the volume of the original sample; this precludes the necessity for a concentration step prior to electrophoresis. This fact is important for those applications—and they are in the majority—in which the sample is available only in dilute solution. Furthermore, the stacking gel can also assist separation by excluding from the concentrated band (the stack) species of low or high mobility relative to the displacement rate of the moving boundaries associated in the stack ("selective stacking").

Discontinuous buffer systems are available from a computer program (2) for electrophoresis across the entire pH scale, at either 0 or 25°C, and for both negatively and positively charged analytes.

Bibliography

1. L. Ornstein (1964) Ann. NY Acad. Sci. **121**, 321–349.
2. A. Chrambach (1985) In *The Practice of Quantitative Gel Electrophoresis* (V. Neuhoff and A. Maelicke, eds.), VCH, Weinheim, pp. 9–18, 85–110.

Suggestions for Further Reading

3. L. M. Hjelmeland and Chrambach (1982) The impact of L. G. Longsworth on the theory of electrophoresis. Electrophoresis **3**, 9–17.
4. T. M. Jovin (1973) Multiphasic zone electrophoresis. Biochemistry **12**, 871–890.

Discontinuous DNA Replication

Elongation of the DNA chain on the lagging strand during DNA replication is discontinuous: Short segments of DNA, called Okazaki Fragments, are repeatedly synthesized in the reverse direction of movement of the replication fork (1). This occurs because the two chains of double-helical DNA are antiparallel, and **DNA polymerase** can extend a DNA chain only in the 5′ → 3′ direction. On the leading strand, which runs 5′ → 3′ in the reverse direction to fork movement, the replicative enzyme carries out chain elongation continuously in a highly processive manner. On the other parent strand, the lagging strand, which runs 3′ → 5′ in the direction of fork movement, DNA polymerase catalyzes chain elongation only in the reverse direction of fork movement. Thus, as the replication fork proceeds, the unreplicated segment is expanded on the lagging strand. When one act of chain elongation on the lagging strand is accomplished, the next round of chain elongation must be started from a newly expanded segment on the lagging strand. To achieve completion of DNA replication on an entire region of the lagging strand, numerous enzymes cooperate at the replication fork. They are participating in primer synthesis (the initiation of Okazaki fragments), chain elongation (the extension of Okazaki fragments), and a process that connects Okazaki fragments.

In *Escherichia coli*, more than 20 different proteins participate in DNA replication (2). These were identified by screening mutants defective in DNA replication and by purifying enzymes required for *in vitro* DNA synthesis (see ***dna* genes**). From their biochemical roles at different stages of chromosomal DNA replication, it appears that at least eight proteins are involved in the discontinuous replication in *E. coli*. Those are (1) primosome proteins, including DNA helicases and primase: PriA, PriB, PriC, DnaT, DnaB, DnaC, and DnaG (primase); (2) proteins required for chain elongation: DNA polymerase III (Pol III) holoenzyme and single-stranded DNA binding protein (SSB); and (3) proteins required for connecting Okazaki fragments: DNA polymerase I (Pol I), RNaseH, and DNA Ligase. Among these proteins, the DnaB helicase, primase (DnaG), and Pol III holoenzyme are the basic components acting on the discontinuous DNA synthesis at the replication fork, probably forming a multiprotein complex called a *replisome*.

DNA polymerase cannot replicate duplex DNA without assistance. This enzyme requires single-stranded DNA as a template and an RNA or DNA primer annealed to the template. Two other enzymes enable polymerase to work on duplex DNA. One is a DNA helicase that opens up the duplex at the replication fork to provide a single-stranded template. The other is a primase that synthesizes a short RNA to prime DNA chain elongation. Several DNA helicases have been identified from *E. coli* and its phage, including DnaB, T7 gp4, and T4 gp41 (3-5). The biochemical characterization of these activities in *in vitro* DNA replication systems suggests that the primary replicative helicase binds to and moves on the lagging-strand template in the 5′ → 3′ direction, unwinding the DNA double helix as it goes. Another common property of the replicative helicases is an intimate association with a primase. The bacteriophage T7 gp4 has both primase and helicase activity within the same polypeptide chain (4). Bacteriophage T4 gp41 greatly enhances the primase activity of T4 gp61 (6). A similar functional interaction has been observed between DnaB protein and *E. coli* primase, DnaG protein (7). On most templates, DnaG exhibits a very feeble priming activity that can be greatly enhanced if DnaB first binds that DNA. This stimulation of primase activity is further increased when the DnaB helicase is activated to its processive form at the replication fork.

In *E. coli*, there are two pathways by which the DnaB helicase is loaded onto the lagging-strand template DNA: One is primosome formation directed by the PriA protein, and the other is DnaA protein-directed DnaB loading (8, 9). The former process was discovered first in the replication of bacteriophage fX174 DNA and **plasmid** ColE1 DNA, and it later appeared to be involved in the resumption of chromosomal DNA replication after replication of the *E. coli* genome has been interrupted or halted. On the other hand, the latter process was found in *oriC* plasmid DNA replication *in vitro* and is thought to form a priming complex with DnaG primase at the replication fork in *E. coli* chromosomal DNA replication.

The chain elongation of Okazaki fragments in *E. coli* is catalyzed by DNA polymerase III holoenzyme (10). This enzyme possesses a capacity to synthesize DNA with a very high processivity, sufficient for completion of about 2 kb of Okazaki fragment. In addition, the Pol III holoenzyme dissociates from the nascent Okazaki fragment and restarts the next round of Okazaki fragment synthesis from an RNA primer newly settled near the replication fork (11). Enzymes to remove primer RNA and fill the gap, such as ribonuclease H and DNA polymerase I of *E. coli*, are essential for the sealing of Okazaki fragments by DNA ligase (12). Mutants defective in either DNA polymerase I or DNA ligase show a massive accumulation of short Okazaki fragments under restrictive conditions.

Although the basic biochemical processes that occur at eukaryotic and prokaryotic replication forks are similar, there are many differences in detail (13). For example, primer synthesis in eukaryotic cells is catalyzed by DNA polymerase a, which synthesizes 2 to 12 nucleotides of RNA (initiator RNA) and further adds about 20 nucleotides of DNA to the initiator RNA. The size of Okazaki fragments (40 to 300 nucleotides) in eukaryotes is significantly shorter than those observed in prokaryotes.

Bibliography

1. R. Okazaki, T. Okazaki, S. Hirose, A. Sugino, and T. Ogawa (1976) In *DNA Synthesis and Its Regulation* (M. Goulian and P. Hanawalt, eds.), Benjamin Cummings, Menlo Park, CA, pp. 832–862.
2. K. J. Marians (1992) Ann. Rev. Biochem. **61** 673–720.
3. J. H. LeBowitz and R. McMacken (1986) J. Biol. Chem. **261**, 4738–4748.
4. J. A. Bernstein and C. C. Richardson (1989) J. Biol. Chem. **264**, 13066–13073.
5. M. Venkatesan, L. L. Silver, and N. G. Nossal (1982) J. Biol. Chem. **257**, 12426–12434.
6. D. M. Hinton and N. G. Nossal (1987) J. Biol. Chem. **263**, 10873–10878.
7. K. Arai and A. Kornberg (1979) Proc. Natl. Acad. Sci. USA **76**, 4308–4312.
8. K. Arai, R. Low, J. Kobori, J. Shlomai, and A. Kornberg (1981) J. Biol. Chem. **256**, 5273–5280.
9. T. A. Baker, B. E. Funnell, and A. Kornberg (1987) J. Biol. Chem. **262**, 6877–6885.
10. C. McHenry and A. Kornberg (1977) J. Biol. Chem. **252**, 6478–6484.
11. H. Maki, S. Maki, and A. Kornberg (1988) J. Biol. Chem. **263**, 6570–6578.
12. B. E. Funnell, T. A. Baker, and A. Kornberg (1986) J. Biol. Chem. **261**, 5616–5624.
13. J. J. Blow ed. (1996) *Eukaryotic DNA Replication*, IRL Press, Oxford.

Suggestions for Further Reading

14. M. L. DePamphilis, ed. (1996) *DNA Replication in Eukaryotic Cells*, Cold Spring Harbor Laboratory Press, New York.
15. A. Kornberg and T. A. Baker (1992) *DNA Replication*, 2nd ed., W. H. Freeman, New York.

Disease Resistance Genes, Plant

Plants are the ultimate food source for many nonphotosynthetic organisms. In natural ecosystems, plant populations are usually too fragmented for major epidemics of bacteria, fungi, **viruses**, nematodes, or other animals to threaten the survival of a plant species, although such pathogens are still likely to select for variants with enhanced resistance. In the monocultures imposed by human cultivation, disease can be severe.

Plant pathogens are classified into necrotrophs and biotrophs (1). Necrotrophs overwhelm plant defenses with toxins and hydrolytic enzymes and then feed on the dead plant material. Biotrophs need a living plant to complete their life cycle and are better thought of as parasites; they can reduce plant yields substantially, without killing their hosts. Hemibiotrophs, such as *Phytophthora infestans* which causes potato late blight, have an initial biotrophic phase that rapidly switches to necrotrophy.

The interaction between plant and pathogen is said to be compatible if disease occurs, and incompatible if it does not. Most plants are resistant to most plant pathogens; the flax rust fungus does not cause disease on wheat, and vice versa. In this example of “nonhost” resistance, incompatibility can be due to a lack of “basic compatibility”; biotrophic parasites must specialize to grow on their specific hosts.

One of the most interesting and widely studied forms of disease resistance appears to involve recognition of pathogens by plants, followed by activation of defense responses that usually culminate in the death of plant cells near where the pathogen attempts ingress. This localized cell death is often referred to as the *hypersensitive response*, or HR. It should be noted that plants, unlike mammals, lack circulating defender cells, and every plant cell must be able to mount a defense response. The HR is correlated with the production of antimicrobial proteins and reactive oxygen species (2, 3).

Soon after the rediscovery of Mendel's work, breeders noted that resistance in wheat to rusts was inherited as a single dominant Mendelian trait. In the 1940s, H. H. Flor, studying the flax/flax rust interaction, carried out genetic analysis with both the rust fungus and its plant host. **Genes** in flax for rust resistance were dominant, as in wheat. Flor also showed that virulence in the pathogen segregated as a recessive trait. From this he inferred that each pathogen must carry dominant **alleles** of genes which permitted the plant to detect that pathogen race, and he termed these *avirulence* genes. Genetic interactions such as these are often referred to as “gene-for-gene.”

Flor's work underpins the current view that resistance (*R*) genes encode receptors which recognize pathogen-derived, avirulence (*Avr*) gene-encoded ligands. Pathogens evade recognition by mutations in *Avr* genes. Why would pathogens make *Avr* gene products that permit plants which carry the corresponding *R* gene to detect them? It is believed that pathogens generate a battery of pathogenicity factors (also known as compatibility factors) which are individually dispensable. Pathogens (and plant breeders) select for variant *R* genes that can detect one of these factors. This interpretation appears to be valid for interactions of plants with bacteria, viruses, fungi, and nematodes (4).

1. Four Classes of “Gene-for-Gene” *R* Gene Products

The first gene-for-gene *R* gene to be isolated was *Pto* from tomato (5). *Pto* confers resistance to races of *Pseudomonas syringae* that carry the corresponding *AvrPto* gene, and encodes a **serine-threonine protein kinase** of the Raf family, with strongest homology to the *Drosophila* gene *Pelle*, which is involved in signal transduction between the ***Toll*** receptor and **Dorsal** transcription factor, and it may also be involved in *Drosophila* innate immunity (6, 7). Pto also carries a putative N terminal myristoylation site. It was surprising to discover that a gene putatively involved in recognition showed homology to genes involved in signal transduction rather than to known receptors. Remarkably, recent work shows that there is probably a direct interaction between the *Pto* and *AvrPto* gene products (8, 9). How could AvrPto physically interact with Pto? Many phytopathogenic *Pseudomonas* and *Xanthomonas* species encode a type III secretion pathway that actively delivers compatibility factors to the plant cell (10, 11). The same secretion pathway is involved in delivering proteins into mammalian cells attacked by *Shigella, Yersinia, Salmonella*, or pathogenic *Escherichia coli*. Mutations in the so-called *hrp* genes specifying this apparatus in *Pseudomonas* and

Xanthomonas leave the bacterium defective in both Hypersensitive Response elicitation and Pathogenicity. The *hrp* system is believed to deliver several pathogenicity factors from bacteria to plant cells, some of which (such as AvrPto) the plant evolves the capacity to recognize. The *Pto* gene is a member of a linked **gene family** of five to seven members spread over probably less than 100 kbp, one member of which, *Fen*, confers an apparent HR when treated with Fenthion insecticide. Experiments swapping **domains** between *Fen* and *Pto* have precisely localized the region involved in *AvrPto* recognition (8, 9).

The other three classes of *R* genes carry the leucine-rich repeat (LRR) motif. LRRs have been implicated in various examples of protein–protein interactions and protein–peptide interactions (12), This repeating motif creates a parallel beta-sheet that provides a recognition surface in the interaction of porcine **ribonuclease inhibitor** (PRI) with ribonuclease. Thus, the presence of LRRs is consistent with a role for *R* gene products as receptors for pathogen-specified ligands. Based on the PRI structure, a model has been proposed for the structure of various LRR proteins, including plant *R* gene products (13).

The *Cf-2*, *Cf-4*, *Cf-5* and *Cf-9* genes of tomato confer resistance to specific races of the fungal pathogen *Cladosporium fulvum* (14-16). This biotrophic fungus proliferates in the intercellular spaces of infected leaves prior to conidiation. It secretes small cysteine-rich peptides into these spaces, presumed to be compatibility factors, some of which are *Avr* gene products (17). Avr9, recognized by *Cf-9*, is a 28 amino-acid residue peptide; after secretion, Avr4 has 105 residues. The *Cf-* genes all encode **glycoproteins** that are **membrane-anchored** at the C-terminus (probably to the plasma membrane) with 25 to 38 LRRs. Binding studies showed that Avr9 binds a protein that is present even in stocks that lack *Cf-9* (18). Conceivably, this protein undergoes a conformational change upon binding Avr9, and this change is recognized by Cf-9. No evidence for direct interaction between purified Cf-9 and Avr9 has yet been obtained.

Analysis of the *Cf*-gene family has revealed interesting insights into *R* gene evolution (19). At the *Cf-9* locus, there are five homologues of *Cf-9* (including *Cf-9*). At the homologous *Cf-4* locus, there are also five members, including *Cf-4*. Comparison of these sequences has revealed a pattern of evolution by sequence exchange, presumably by either **unequal crossing over** or **gene conversion**. This is consistent with the analysis of the maize *Rp1* locus, which provides genetic evidence that novel alleles arise correlated with meiotic recombination events (20). Analysis of the ratio of synonymous to nonsynonymous codon substitutions (Ks/Ka) suggests diversifying changes in the solvent-exposed amino-acid residues of the LRR parallel beta-sheet. Consistent with this, several other members of the *Cf*-gene family confer resistance through recognition of as-yet-uncharacterized avirulence genes. A complementary study provides evidence that several of the secreted peptides of *C. fulvum* have the potential to act as *Avr* gene products (21). The picture emerging from this system reveals a battery of secreted peptides that presumably confer a pathogenicity function for *C. fulvum*, with the plant evolving the capacity to recognize and react to them through creating a recognition specificity in a *Cf*-gene homologue. How the recognition actually occurs, and what happens next, is an area of active research.

No other *R* genes have been shown to be members of this C-terminally anchored LRR class, although several Arabidopsis homologues have been identified, where in some instances they exist as linked multigene families. The nematode resistance gene $Hc1^{pro}$ is reported to be of this class (22), although the LRR sequences vary from the canonical LRR motif.

The rice *Xa21* gene confers resistance to *Xanthomonas campestris pv oryzae*, the causal agent of bacterial blight. Interestingly, it encodes a transmembrane LRR protein kinase, combining features of Pto and Cf-9 in one protein (23). This would suggest that the *AvrXa21* gene encodes a secreted bacterial protein, but thus far the *AvrXa21* gene has not been cloned, because little genetic variation has been detected within *Xanthomonas* at this locus. Again, *Xa21* is a member of a linked multigene family (24).

The largest class of *R* genes encode cytoplasmic (but probably membrane-associated) proteins that carry a canonical **nucleotide-binding** (NB) site and C-terminal stretch of LRRs. The NB carries the *kin1a* (P loop), *kin2*, and *kin3a* sites of protein kinases (25). In addition, recent comparisons have revealed a more extended homology with a domain of the *Caenorhabditis elegans Ced4* and the human *Apaf1* gene products, which led some authors (26) to christen this extended region the NB-ARC domain (standing for Nucleotide Binding, *Apaf*, R gene, and Ced4). *Apaf1* and *Ced4* encode proteins that are effectors of apoptosis. The parallel between apoptosis and the HR has been the subject of considerable interest (27, 28), and the homologies are intriguing, but no biochemical evidence is yet available to substantiate it.

These NB-LRR genes fall into two main classes:

1. *Rps2* and *Rpm1*, *Arabidopsis* genes for resistance to *Pseudomonas* strains carrying *AvrRpt2* and *AvrRpm1*, respectively, encode a putative leucine zipper (LZ) N-terminal to the NB region (29, 30). Unusually, *Rpm1* recognizes both *AvrB* and *AvrRpm1*.
2. In contrast, the tobacco *N* gene for tobacco mosaic virus (TMV) resistance, the flax *L6* gene for rust resistance, and the *Arabidopsis RPP5* gene for downy mildew resistance carry a region at the N-terminus with homology to the cytoplasmic domain of the *Toll* receptor and *interleukin* 1 receptor (31, 33). This region has recently been proposed to adopt a structure resembling the *E. coli CheY* **chemotaxis**-response element (34), and in plants it has been dubbed the TIR domain (standing for T*oll*, the interleukin 1 receptor, and resistance gene) (4). It is striking that *R* genes from different plants conferring resistance to such distinct pathogens are so similar. The *L6* gene product carries an N-terminal putative signal anchor, which could attach it to the plasma membrane.

Additional NB-LRR subclasses may exist. The tomato *I2* gene that confers *Fusarium* wilt resistance carries a putative leucine zipper between the LRRs and the NB [35]. The tomato *Prf* gene was identified by mutagenesis as required for both *Pto* and *Fen* function; it encodes an extremely long region N-terminal to the NB but is clearly of the NB-LRR class. (36).

Paradoxically, even though LRR domains are more correlated with protein-protein interactions than protein kinase domains, no direct interaction has been detected between any of these NB-LRR *R* gene products and their genetically defined candidate ligands using yeast two-hybrid systems. Nevertheless, transient expression experiments showed that *Rps2*(37) and *Rpm1* (38) must recognize *AvrRpt2* and *AvrB* within the plant cell. *AvrBs3*, recognized by the as-yet-uncharacterized *Bs3 R* gene product of pepper, is also recognized within the plant cell (39).

It is widely believed that the *R* gene products form part of a complex with other proteins to create a functional recognition and signal transduction machine. The nature of this complex is currently under vigorous investigation. Many other questions also remain unanswered. What are the bacterial *Avr* products doing in the compatible interaction? Are fungal resistance genes of the NB-LRR type recognizing fungal proteins that are delivered into the plant cell? A combination of genetic and biochemical approaches are being used to understand *R* gene product-dependent recognition and signal transduction events. *NDR1*, identified by mutagenesis as required for *Rps2* function, encodes a novel protein with two membrane-spanning domains (40). *EDS1*, required for *RPP5* function but not *Rps2* function (41), shows homology to lipases (J Parker, personal communication). Yeast two-hybrid analysis has led to the discovery of genes whose products interact with *Pto*; some are protein kinases and some are transcription factors (42, 43).

2. Resistance to Pathogen Toxins

Some pathogens produce toxins, and resistance is conferred by a dominant gene that encodes a detoxifying enzyme. The maize *Hm1* gene encodes an NADPH oxidoreductase that inactivates the

Cochliobolus carbonum HC toxin (44). *Hm1* was the first *R* gene to be isolated, but it does not conform to gene-for-gene genetics in that recessive mutations in the pathogen to overcome Hm1 have never been recovered. In the 1970s, many maize varieties carried the T cytoplasm, whose mitochondria are sensitive to T toxin from *Cochliobolus heterostrophus*, the causative agent of Southern Corn leaf blight. Resistant varieties that use a different cytoplasmic male sterility genotype were then deployed, which controlled the disease.

3. *Mlo* Recessive Resistance Genes

There are several recessive resistance genes, of which the best characterized is barley *mlo*. *Mlo* mutants have a disease lesion-mimic phenotype and enhanced resistance to all races of the powdery mildew pathogen, *Erysiphe graminis*. The *Mlo* gene encodes a protein with seven transmembrane domains that presumably regulate negatively the defense response (45). It is also the pioneer of a new family of plant genes; analysis of the *Arabidopsis* genome sequence suggests that it will contain at least 60 genes in this class, with as yet unknown biochemical function.

4. Summary

Different classes of *R* genes in plants encode either recognition and response systems, or toxin detoxification or tolerance mechanisms, or they derepress plant defense mechanisms. Many *R* genes have now been isolated; the challenge is now to find out how their gene products work.

Bibliography

1. G. N. Agrios (1988) *Plant Pathology*, Academic Press, London.
2. K. E. Hammond-Kosack and J. D. G. Jones (1996) Plant Cell **8**, 1773–1791.
3. C. Lamb and R. A. Dixon (1997) Ann. Rev. of Plant Physiol. Plant Mol. Biol. **48**, 251–275.
4. K. E. Hammond-Kosack and J. D. G. Jones (1997) Ann. Rev. Plant Physiol. Plant Mol. Biol. **48**, 575–607.
5. G. B. Martin et al. (1993) Science **262**, 1432–1436.
6. M. P. Belvin and K. V. Anderson (1996) Ann. Rev. Cell Develop. Biol . **12**, 393–416.
7. J. A. Hoffmann and J. M. Reichhart (1997) Trends Cell Biol. **7**, 309–316.
8. S. R. Scofield et al. Science **274**, 2063–2065.
9. X. Tang et al. Science **274**, 2060–2063.
10. J. R. Alfano and A. Collmer (1996) Plant Cell **8**, 1683–1698.
11. G. VandenAckerveken and U. Bonas (1997) Trends Microbiol . **5**, 394–398.
12. B. Kobe and J. Deisenhofer (1995) Curr. Opin. Struct. Biol. **5**, 409–416.
13. A. V. Kajava (1998) J. Molec. Biol. **277**, 519–527.
14. C. M. Thomas et al. (1997) Plant Cell **9**, 2209–2224.
15. D. A. Jones, C. M. Thomas, K. E. Hammond-Kosack, P. J. Balint-Kurti, and J. D. G. Jones (1994) Science (Wash.) **266**, 789–793.
16. M. S. Dixon et al. (1996) Cell **84**, 451–459.
17. P. DeWit (1997) Trends Plant Sci. **2**, 452–458.
18. M. Kooman-Gersmann, G. Honee, G. Bonnema, and P. J. G. M. De Wit (1996) Plant Cell **8**, 929–938.
19. M. Parniske et al. Cell **91**, 821–832.
20. S. H. Hulbert (1997) Ann. Rev. Phytopathol. **35**, 293–310.
21. R. Lauge, A. P. Dmitriev, M. Joosten, and P. DeWit (1998) Molec. Plant-Microbe Inter. **11**, 301–308.
22. D. G. Cai et al. Science **275**, 832–834.

23. W.-Y. Song et al. Science **270**, 1804–1806.
24. W. Y. Song, et al. (1997) Plant Cell **9**, 1279–1287.
25. T. W. Traut (1994) Europ. J. Biochem. **229**, 9–19.
26. E. A. vanderBiezen and J. D. G. Jones (1998) Curr. Biol. **8**, R226–R227.
27. J. B. Morel and J. L. Dangl (1997) Cell Death and Differ. **4**, 671–683.
28. A. M. Jones and J. L. Dangl (1996) Trends Plant Sci. **1**, 114–119.
29. A. F. Bent et al. Science **265**, 1856–1860.
30. M. R. Grant et al. Science **269**, 843–846.
31. G. J. Lawrence, E. J. Finnegan, M. A. Ayliffe, and J. G. Ellis Plant Cell **7**, 1195–1206.
32. J. E. Parker et al. (1997) Plant Cell **9**, 879–894.
33. S. Whitham et al. (1994) Cell **78**, 1011–1115.
34. F. L. Rock, G. Hardiman, J. C. Timans, R. A. Kastelein, and J. F. Bazan (1998). Proc. Natl. Acad. Sci. **95**, 588–593.
35. N. Ori et al. (1997) Plant Cell **9**, 521–532.
36. J. M. Salmeron et al. Cell **86**, 123–133.
37. R. T. Leister, F. M. Ausubel, and F. Katagiri (1996) Proc. Natl. Acad. Sci. **93**, 15497–15502.
38. S. Gopalan et al. (1996) Plant Cell **8**, 1095–1105.
39. G. VandenAckerveken, E. Marois, and U. Bonas (1996) Cell **87**, 1307–1316.
40. K. S. Century et al. (1997) Science **278**, 1963–1965.
41. J. E. Parker et al. (1996) Plant Cell **8**, 2033–2046.
42. J. M. Zhou, X. Y. Tang, and G. B. Martin (1995) EMBO J . **16**, 3207–3218.
43. J. Zhou, Y.-T. Loh, R. A. Bressan, and G. B. Martin (1995) Cell **83**, 925–935.
44. G. S. Johal and S. P. Briggs (1992) Science (Wash.) **258**, 985–987.
45. R. Buschges et al. Cell **88**, 695–705.

Distance Geometry

Many physical methods used to examine a biological macromolecule in solution produce information about the distance that separates two parts of the molecule. These methods include fluorescence **energy transfer**, chemical cross-linking**,** light scattering, and several kinds of nuclear magnetic resonance (NMR) observations. Any information about distances between different parts of a molecule limits the number of conformations that are possible for that molecule. Distance geometry is a mathematical approach that can be used to help define the conformations of a molecule that are consistent with experimental distance information (1-6).

With X-ray crystallography methods, the tertiary structure of the molecule of interest is defined by analysis of a set of diffraction data. A relation exists between every feature of the diffraction pattern exhibited by the crystal and the positions of the atoms of molecules within the crystal. When this connection is elucidated, the three-dimensional (3D) structure of the molecule is revealed. A different approach is used to find 3D structures using distance information. Consider a polymeric molecule in an extended conformation, represented by the line below.

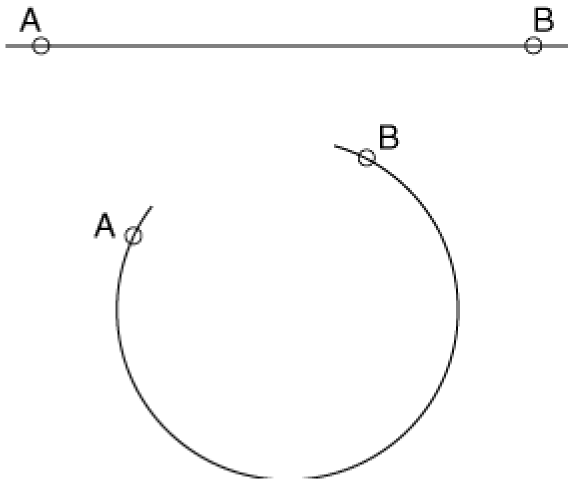

If free rotation exists about some or all of the bonds along the molecular backbone, a huge number of conformations are possible for the molecule. If, however, an experimental observation indicates, for example, that the atoms at the position labeled A must be within 0.3 nm of the atoms at the position labeled B, then the number of possible conformations for the molecule is greatly reduced—the only conformations that need further consideration are those that are consistent with the constraint that atoms at A and B must be close to each other. Other experimentally defined distances would further reduce the number of possible 3D structures. If enough such constraints exist, only one or a small family of structures is likely that is consistent with all of them. Generally, the more constraints that can be established by experiment, the better known will be the tertiary structure. NMR methods, particularly those that measure nuclear Overhauser effects (NOEs), can produce a large number of distance constraints on possible conformations of a macromolecule. An advantage in using NMR observations in this way is that the molecule of interest does not have to be in the solid (crystalline) state for successful structure determination.

An N×N matrix of distances can be defined for a molecule made up of N atoms; N (N–1)/2 unique interatomic distances exist in this matrix. If all of the distances are accurately known, mathematical methods are available to define the Cartesian coordinates of the atoms from the known distances (4). Many of the distances in the distance matrix are essentially independent of conformation and are reliably known *a priori*. Such data would include the distance between two hydrogen atoms attached to an aromatic ring. Other distances can be estimated experimentally. Information about dihedral angles and other bond angles can be used to define other distances. For some distances, however, little or no accurate distance information will be available. Thus, the distance matrix will typically be incomplete, and a unique solution for Cartesian coordinates cannot be obtained. A variety of algorithms have been developed to deal with the missing or incomplete distance information. Regardless of the approach used, distance geometry calculations typically do not produce a single conformation but an ensemble of conformations, all of which are consistent with the available distance constraints. These conformations are used as starting points for additional refinement by conformational energy minimization and simulated annealing procedures. (See also Nuclear Overhauser Effect (NOE), Simulated Annealing).

Bibliography

1. L. M. Blumethal (1970) *Theory and Applications of Distance Geometry*, Chelsea, New York.
2. G. M. Crippen and T. F. Havel (1978) Acta Crystallogr. **34**, 282–284.
3. G. M. Crippen (1981) *Distance Geometry and Conformational Calculations*, Wiley, Chichister, England.
4. W. Braun (1987) Quart. Rev. Biophys. **19**, 115–117.
5. I. D. Kuntz, J. F. Tomason, and C. M. Oshhiro (1989) Methods Enzymol. **177**, 159–204.

6. T. F. Havel (1991) Prog. Biophys. Mol. Biol. **56**, 43–78.

Suggestions for Further Reading

7. C. M. Oshiro and I. D. Kuntz (1993) Biopolymers **33**, 107–115.
8. J. W. Shriver and S. Edmondson (1994) Methods Enzymol. **240**, 415–438.
9. A. M. J. J. Bonvin and A. T. Brunger (1996) J. Biomol. NMR **7**, 72–76.
10. P. Güntert (1997) In *Protein NMR Techniques* (D. G. Reid, ed.), Humana, Totowa, New Jersey, pp. 157–194.
11. D. M. LeMaster (1997) J. Biomol. NMR **9**, 79–93.
12. J. Cavanagh, W. J. Fairbrother, A. G. Palmer III and N. J. Skelton (1995) *Protein NMR Spectroscopy*, Academic, San Diego.

Disulfide Bonds

The disulfide bond occurs in many biological molecules, most frequently in **secretory proteins**, in the form of a covalent linkage between the thiol groups of pairs of cysteine residues (Fig. 1). Formation of a disulfide bond from two thiol groups requires an oxidant as two electrons or hydrogen atoms are released:

$$2\text{–SH} \rightarrow \text{–S–S–} + 2H^{+} + 2e^{-} \qquad (1)$$

The oxidant can be oxygen, but air oxidation of thiol compounds is a complex reaction involving many steps and intermediates, being catalyzed by metal ions, and releasing by-products such as peroxides.

Figure 1. Optimal stereochemistry of a disulfide bond between two cysteine residues. The two possible CH_2—S—S—CH_2 torsion angles about the disulfide bond of +90 and –90 are equally favorable.

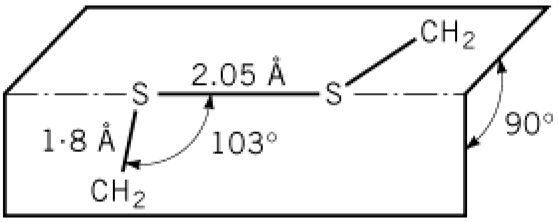

The disulfide bond is a stable covalent bond, and it would require some 60 kcal/mol (270 kJ/mol) to pull the two sulfur atoms apart. Yet this stable bond can be broken readily by a thiol group, which can react rapidly with a disulfide bond in the thiol–disulfide exchange reaction. With this reaction, disulfide bonds can be reduced by reacting them with an excess of a thiol reagent, RSH, such as b-mercaptoethanol or **dithiothreitol**:

$$P^{S}_{S} + 2RSH \leftrightarrow P^{SSR}_{SH} + RSH \leftrightarrow P^{SH}_{SH} + RSSR \qquad (2)$$

Many other reagents are available for chemically reducing disulfide bonds, such as borohydride, tributylphosphine, and tris-[2-carboxyethyl]-phosphine. The phosphines have the advantage that they function at acidic pH, where the original disulfide bond and the resulting thiol groups tend not to undergo further reactions. Furthermore, the phosphines do not react with many of the reagents that modify thiol groups, so reduction of the disulfide bond and alkylation of the thiol groups produced can be carried out simultaneously (1).

Disulfide bonds can also be cleaved by nucleophiles such as cyanide, sulfite, or hydroxide ion:

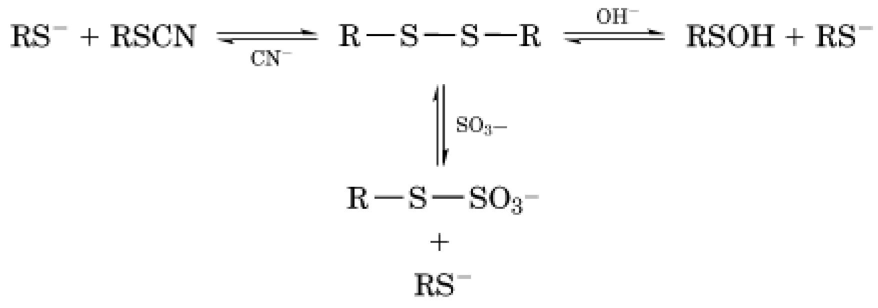

(3)

The equilibria for these reactions are such that it is difficult to drive the reactions to completion simply by adding reagent. Complete reaction can be accomplished, however, by adding a second reagent that reacts with the thiol generated. When this reagent is nitrothiosulfobenzoate (NTSB),

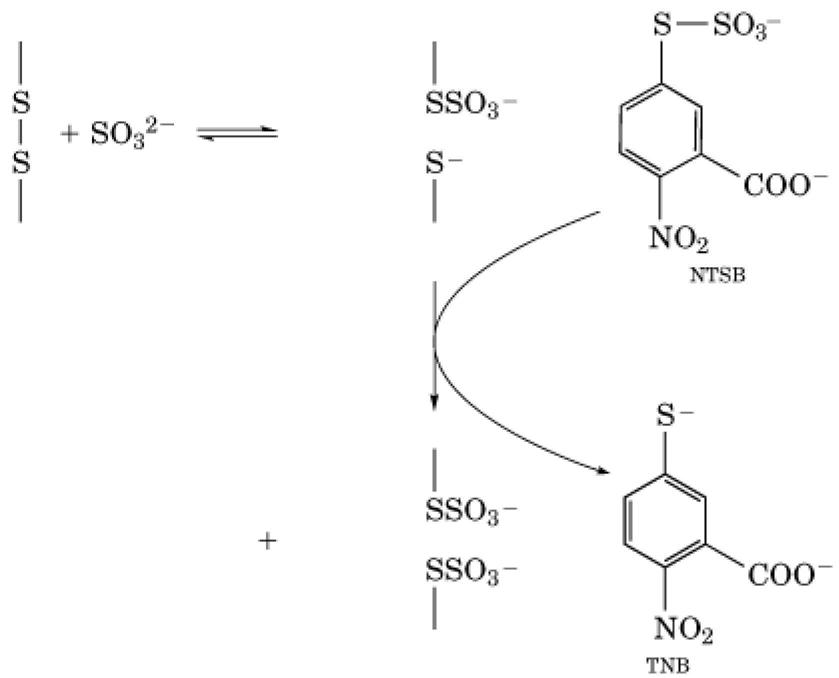

(4)

the reaction can go to completion, and one mole of the colored TNB product is generated for each mole of disulfide bond originally present. This is the most convenient assay for protein disulfide bonds so long as thiol groups are not also present.

The intrinsic free energy of a disulfide bond depends upon its angle of rotation (Fig. 1). It is most stable with a C-S-S-C torsion angle of ±90°, and an angle of 0° or 180° is believed to increase the free energy by about 28 kJ/mol. This corresponds to the free energy barrier to full rotation about the disulfide bond. Cyclic 5-membered rings, such as that of lipoic acid, have a torsion angle of only ±30° and are strained by about 15 kJ/mol. Cyclic 6-membered rings, such as that in the disulfide form of **dithiothreitol**, have torsion angles of about ±60°.

1. Disulfide Bonds in Proteins

Disulfide bonds are found most frequently in molecular biology within proteins, especially in proteins that are secreted. Most of the disulfide bonds observed in the X-ray crystallography structures of proteins have favorable stereochemistry and show little evidence of conformational strain, with close to the optimal torsion angles of ±90°. Only a few examples of hyperreactive disulfide bonds are known, such as that between the most distant cysteine residues in alpha-lactalbumin and hen lysozyme (2, 3).

As the disulfide bond is a covalent bond that is stable under appropriate conditions, which cysteine residues in a protein are paired in disulfide bonds can be determined chemically. The classical method is to fragment the protein into peptide fragments, under conditions where the disulfide bonds are kept intact. The peptide fragments are analyzed to determine which are linked by disulfide bonds. A newer technique is to reduce the disulfide bonds individually, using phosphines at acidic pH, where the disulfide bonds do not rearrange readily, and to identify the pairs of cysteine thiol groups generated (1, 4). A more elegant approach, but one not suited to modern separation techniques, is to use diagonal methods (5).

Disulfide bonds are well known to stabilize the folded conformations of proteins in which they occur, and conversely the folded conformations stabilize the disulfide bond. Many proteins that have disulfide bonds unfold when the disulfides are reduced. In considering disulfide bonds and protein stability, it is important to distinguish between the stability of the folded conformation relative to the unfolded protein, U, (i) when the disulfide bonds are kept intact:

$$\mathbf{N}_{\mathbf{S}}^{\mathbf{S}} \leftrightarrow \mathbf{U}_{\mathbf{S}}^{\mathbf{S}} \tag{5}$$

and (ii) when the disulfide bonds are reduced upon unfolding and reformed when the protein folds:

$$\mathbf{N}_{\mathbf{S}}^{\mathbf{S}} + \mathbf{2RSH} \leftrightarrow \mathbf{U}_{\mathbf{SH}}^{\mathbf{SH}} + \mathbf{RSSR} \tag{6}$$

The stability of a protein disulfide bond, relative to the reduced form of the protein, with cysteine thiol groups (Eq. 6), depends upon the degree to which the protein conformation stabilizes the disulfide bond and upon the redox potential of the environment. A protein conformation that stabilizes a disulfide bond is stabilized to the same extent by the presence of that disulfide bond (Fig. 2). The greater the stability of the protein disulfide bond, the greater its contribution to stability of the folded conformation that stabilizes it.

Figure 2. Linkage between the stability of a particular folded conformation that favors a certain disulfide bond and the stability of that disulfide bond. A protein with two cysteine residues that can form a disulfide bond (right) is illustrated in either the unfolded (top) or folded (bottom) conformations. The indicated equilibrium constants represent the stabilities of the disulfide bonds, K_{SS}, and of the folded conformation, K_F. The equilibrium constants for disulfide stability, K_{SS}, must involve another reagent, as in Eq. 7 and 8, but this is omitted for simplicity. The linkage relationship states that whatever effect the folded conformation has on the stability of the disulfide bond, the presence of the disulfide bond must have the same quantitative effect on the stability of the folded conformation. Comparable linkage relationships pertain to all interactions within the folded conformation, not just disulfide bonds.

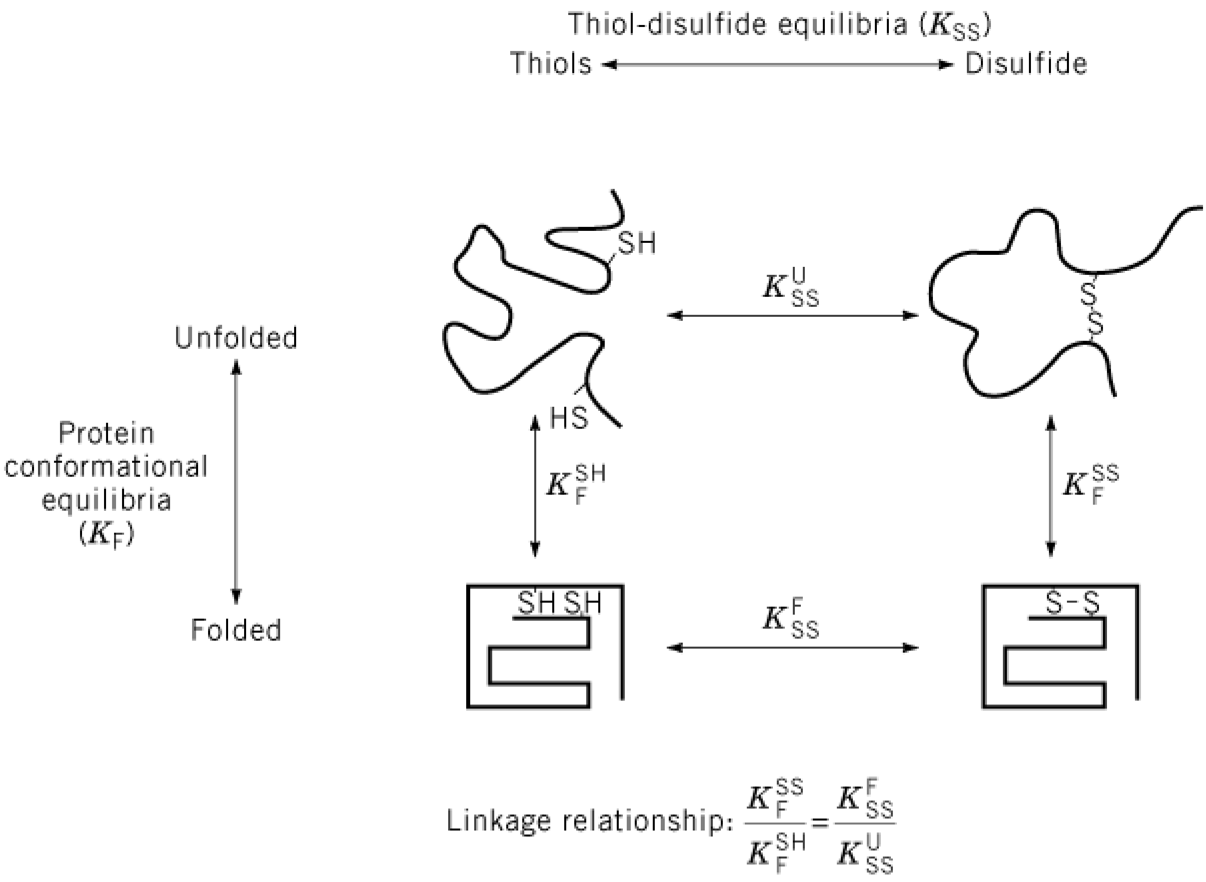

One way in which disulfide bonds stabilize the folded conformation, relative to the unfolded form with the disulfide bonds intact (Eq. 5), is by decreasing the conformational flexibility, or entropy, of the unfolded protein. The magnitude of this effect increases with increasing distance between the cysteine residues in the primary structure. It is often assumed that this is the only way that disulfide bonds stabilize the folded conformation, and equations are frequently given to predict the magnitude of the stabilization. Experimental observations indicate, however, that there are many other effects of a disulfide bond on the folded conformation, both stabilizing and destabilizing (6); the same energetically favorable disulfide bond can stabilize one folded conformation and destabilize another (7).

The redox potential determines the stability of any disulfide bond and is determined by the relative concentrations of thiol and disulfide reagents. In biological systems, this is primarily determined by the relative concentrations of the thiol and disulfide forms of glutathione, GSH and GSSG, respectively:

$$P^{SH}_{SH} + GSSG \overset{K_{eq}}{\leftrightarrow} P^{S}_{S} + 2GSH \qquad (7)$$

$$\frac{[P^{S}_{S}]}{[P^{SH}_{SH}]} = K_{eq}\frac{[GSSG]}{[GSH]^2} \qquad (8)$$

Within the cell cytosol, the concentration of GSH is generally 100-fold greater than that of GSSG, which is a moderately reducing environment, and a disulfide bond does not impart much stability. Within the endoplasmic reticulum, however, where secreted proteins fold and form disulfide bonds, the concentrations of GSH and GSSG are almost comparable (8), so any protein disulfide bond will be present about 100 times more frequently. These conditions are more oxidizing, but only stable protein disulfide bonds are generally formed and present under these conditions. Once the proteins are secreted from the cell, where the environment is usually much more oxidizing, the disulfide bonds contribute much more stability to the folded conformation.

Disulfide bonds are inserted into proteins naturally only when the protein conformation favors them. When the reduced protein, without disulfides, is unfolded, folding accompanies disulfide bond formation and can be used to determine the folding pathway (see Protein Folding In Vivo). Such pathways have demonstrated how only a slight tendency for an unfolded protein to stabilize a specific disulfide bond is consequently stabilized further by the presence of that disulfide bond, which can then lead to the formation of further disulfide bonds and the adoption of additional, and more stable, folded conformation.

Disulfide bonds are often stated to determine the folded conformations of the protein in which they occur. This cannot be the case, however, for such disulfide bonds would never be generated in a natural protein if the conformation did not favor them. In some cases, proteins have been shown to adopt exactly the same folded conformation in the absence of each of the disulfide bonds (9). Clearly, the disulfide bonds only stabilize the folded conformation and do not determine it.

Bibliography

1. J. Wu and J. T. Watson (1997) Protein Sci. **6**, 391–398.
2. K. Kuwajima, M. Ikeguchi, T. Sugawara, Y. Hiraoka, and S. Sugai (1990) Biochemistry **29**, 8240–8249.
3. J. J. Ewbank and T. E. Creighton (1993) Biochemistry **32**, 3677–3693.
4. W. R. Gray (1997) In *Protein Structure: A Practical Approach*, 2nd ed. (T. E. Creighton, ed.), IRL Press, Oxford, pp. 165–186.
5. T. E. Creighton (1989) In *Protein Structure: A Practical Approach* (T. E. Creighton, ed.), IRL Press, Oxford, pp. 155–167.
6. T. E. Creighton and D. P. Goldenberg (1984) J. Mol. Biol. **179**, 497–526.
7. A. Zapun, J. C. A. Bardwell, and T. E. Creighton (1993) Biochemistry **32**, 5083–5092.
8. C. Hwang, A. J. Sinskey, and H. F. Lodish (1992) Science **257**, 1496–1502.
9. C. P. M. van Mierlo, N. J. Darby, D. Neuhaus, and T. E. Creighton (1991) J. Mol. Biol. **222**, 353–371.

Suggestions for Further Reading

10. J. M. Thornton (1981) Disulphide bridges in globular proteins. J. Mol. Biol. **151**, 261–287.
11. T. E. Creighton (1984) Disulfide bond formation in proteins. Methods Enzymol. **107**, 305–329.
12. T. E. Creighton (1997) Protein folding coupled to disulphide bond formation. Biol. Chem. **378**, 731–744.

Dithiothreitol, Dithioerythritol

Dithiothreitol (DTT, or DTT^{SH}_{SH}) and dithioerythritol (DTE) have closely related structures, each with two thiol groups:

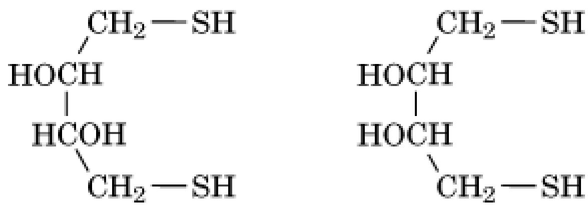

DTT^{SH}_{SH} DTE^{SH}_{SH}

(1)

They have the very useful property of forming a stable, cyclic, intramolecular disulfide bond, abbreviated here as $DTT^{S}_{S}$and DTT^{S}_{S}. Consequently, they are potent reductants of disulfide bonds, eg, RSSR:

$$DTT^{S}_{S} + RSSR \leftrightarrow DTT^{S}_{S} + 2RSH \quad (2)$$

For a typical model disulfide bond, like that of glutathione or **mercaptoethanol**, the equilibrium constant for this reaction,

$$K_{eq} = \frac{[DTT^{S}_{S}][RSH]^2}{[DTT^{SH}_{SH}][RSSR]} \quad (3)$$

has the value 200 M to 2800 M at high and low pH values, respectively (1). The dependence over the pH range of about 8 to 11 arises because of the difference in p K_a values of the thiol groups involved. The first thiol group of $DTT^{SH}_{SH}$to ionize has an apparent pK_a of about 9.2, while that of the second is about 10.2. Even with identical microscopic pK_a values, the first and second apparent pK_a values would be expected to differ by 0.6 pH units for statistical reasons, so there is little electrostatic interaction between the two thiol groups, ionization of one increasing the p K_a of the other by at most 0.4 pH units. The equilibrium constant has the unit of concentration because the disulfide bond of DTT is intramolecular, whereas that of RSSR can be considered to be intermolecular because its reduction generates two RSH molecules. The equilibrium constant can therefore be interpreted in terms of the effective molarity of the two thiol groups of DTT^{SH}_{SH}relative to each other. It has a large value of approximately 120 M because the two thiol groups are kept in reasonable proximity and are able to form a disulfide bond in a favorable 6-membered ring structure (2), even though the disulfide bond of DTT^{S}_{S}appears to be somewhat strained; it has a CSSC dihedral angle of only about 60°, rather than the most favorable 90° (3). Nevertheless, there is only a small change in enthalpy of 0.5 kcal/mol when DTT^{SH}_{SH}reduces model linear disulfide bonds, as in Eq. 2 (4). The thiol and disulfide forms may be distinguished readily by the UV **absorbance** of the disulfide form at 280 nm (5).

These reagents were introduced by Cleland (5) to overcome the limited potency of thiol reagents such as mercaptoethanol, and they are often called "Cleland's reagent." Although he appears to have overestimated their efficacy, measuring an equilibrium constant for Eq. 3 of 10^4 M, they are still some of the most effective disulfide reductants readily available.

Bibliography

1. M.-H. Chau and J. W. Nelson (1991) FEBS Letters **291**, 296–298.
2. N. J. Darby and T. E. Creighton (1993) J. Mol. Biol. **232**, 873–896.
3. S. Capasso and Z. Zagari (1981) Acta Crystallogr. **B37**, 1437–1439.
4. S. Lapanje and J. A. Rupley (1973) Biochemistry **12**, 2370–2372.
5. W. W. Cleland (1964) Biochem. **3**, 480–482.

Divergent Evolution

Divergence is defined as an evolutionary event in which two morphological or molecular traits arose from a common ancestor, and were initially identical, but became dissimilar during evolution. Divergence is, of course, extremely common and the basis for most evolution; without divergence, all lineages would remain the same.

Divergent evolution is usually apparent at the molecular level from significant similarities between the amino acid sequences of proteins and the **nucleotide sequences** of DNA or RNA. There are so many such sequences possible that it seems most improbable that two sequences could become similar by chance. Similar sequences are said to be **homologous**, and the differences between them are assumed to be related to the time since they diverged from their last common ancestor. The molecular mechanisms of evolutionary divergence of the genetic material include nucleotide substitution and deletion/insertion; chromosomal recombination, transposition, and **inversion;** gene duplication, and **gene conversion;** exon shuffling, and **domain** shuffling; and horizontal gene transfer. The number of nucleotide substitutions is a simple and useful measure of the degree of divergence between two sequences. In fact, there are a dozen methods available for estimating the number of nucleotide substitutions, using one to six parameters (1-5). Once the number of nucleotide substitutions has been estimated, a phylogenetic tree can be constructed by using those numbers, to display the pathway that the divergence has followed during evolution (6).

Divergence is contrasted with convergent evolution, which is much more rare. Convergence is an evolutionary event in which two morphological or molecular traits become similar during evolution, even though the ancestor is totally different. In the case of divergence, there must be a certain degree of similarity between two traits to suggest that they had a common ancestor. For convergence, on the other hand, a certain degree of dissimilarity must exist if the two traits originated from independent ancestors. Therefore, the distinction between divergence and convergence can be difficult to judge unless additional evolutionary information is available to indicate whether the similarities or the differences are the more significant. In the case of nucleotide or amino acid sequences, any similarities greater than expected from random are usually taken to indicate divergence. For example, the divergence of nucleotide sequences between human and chicken is shown in Figure 1, where the asterisk (*) indicates a site where nucleotide differences exist, and where 20 nucleotide sites are different and the remaining sites are the same. The probability that this similarity occurred by mere chance is extremely small. Therefore, it can be reasonably concluded that the difference in nucleotide sequences between these two species is due to divergence. Thus, it follows that divergence from the common ancestor has taken place as a result of the accumulation of nucleotide substitutions.

Figure 1. Divergence of nucleotide sequences between humans and chickens.

Human	Gly	Ile	Val	Glu	Gln	Cys	Cys	Thr	Ser	Ile	Cys	Ser	Leu	Tyr	Gln
	GGC	ATT	GTG	GAA	CAA	TGC	TGT	ACC	AGC	ATC	TGC	TCC	CTC	TAC	CAG
	*		*	*			*	***	*	**	*				*
Chicken	GGG	ATT	GTT	GAG	CAA	TGC	TGC	CAT	AAC	ACG	TGT	TCC	CTC	TAC	CAA
	Gly	Ile	Val	Glu	Gln	Cys	Cys	His	Asn	Thr	Cys	Ser	Leu	Tyr	Gln

Human	Leu	Glu	Asn	Tyr	Cys	Asn
	CTG	GAG	AAC	TAC	TGC	AAC
Chicken	CTG	GAG	ACC	TAC	TGC	AAC
	Leu	Glu	Asn	Tyr	Cys	Asn

During the process of molecular evolution, the number of nucleotide differences increases but probably never decreases. Therefore, in most cases, the evolutionary event can be explained by divergence only. Considering the tertiary structures of proteins, however, in some cases the structures are quite similar, even though their amino acid sequences, as well as their biological function, are very different. For these cases, convergence is a possibility, although it could also be simply a case of extreme divergence masking their original sequence and functional identity.

Bibliography

1. T. H. Jukes and C. R. Cantor (1969) in *Mammalian Protein Metabolism*, H. N. Munro, ed., Academic Press, New York, pp. 21–132.
2. M. Kimura and T. Ohta (1972) J. Mol. Evol. **2**, 87–90.
3. M. Kimura (1980) J. Mol. Evol. **16**, 111–120.
4. N. Takahata and M. Kimura (1981) Genetics **98**, 641–657.
5. T. Gojobori, K. Ishii, and M. Nei (1982) J. Mol. Evol. **18**, 414–423.
6. M. Nei (1987) *Molecular Evolutionary Genetics*, Columbia Univ. Press, New York.

DNA Chips

The start of the Human Genome Project in the late 1980s refocused scientists' attention on new, high-throughput technologies for handling and analyzing DNA. Several technologies developed by physicists were evaluated for their potential use in the study of biomolecules. For example, mass spectrometry techniques and the scanning tunneling microscope are now used for analyzing and sequencing DNA. Another technology developed by physicists and applied to biology is the microchip. The semiconductor industry manufactured silicon chips with smaller and smaller features, which allows for greater numbers of operations with a chip of a standardized size. This benefit of miniaturization was applied to the biological sciences in the form of multiparallel arrays of DNA fragments on a small chip. Arraying of DNA or RNA samples onto nitrocellulose or nylon membranes for hybridization studies is a very common analytical procedure in a molecular biology lab (1) (see Blotting). DNA chips or microarrays are, in principle, miniaturized versions of these standard dot-blot techniques. With great precision, thousands of DNA fragments, often amplified by **PCR**, or DNA oligonucleotides are spotted/printed onto glass microscope slides. In the case of oligonucleotides, they can also be synthesized directly on coated silicon chips (see DNA Synthesis). These DNA chips are then used to probe fluorescent-labeled DNA or RNA samples for the presence of specific complementary sequences. DNA chip technology is currently being applied in the areas of monitoring gene expression, polymorphism analysis, gene mutation analysis, and DNA sequencing.

1. Putting Genes on a Chip

The fabrication of high-density arrays on chips for parallel analysis of up to several thousand cDNA clones or PCR fragments on a surface area of approximately 1 cm^2 can be achieved by two techniques: microprinting or piezojet dispensing. The high-density arrays are deposited on the flat solid support, usually a glass slide. The key function of the printing or dispensing process is the extraction of a small volume of sample from a reservoir (eg, a microtiter plate) and the deposition of the same amount of sample fluid in each spot, at equivalent locations on each chip. The center-to-center separation of individual spots in high-density arrays is typically 150 to 500 µm. The deposited sample volume ranges form 50 to 400 pl per spot.

Microprinting devices use an array of pins with either hollow steel capillaries or flat tips. The amount of sample deposited at each spot is defined by the capillary forces acting on the droplet, which adheres to the pin after immersion into the sample reservoir. The droplets at the tips are then transferred to the spots in the array by moving the pins close to the chip surface. After each sample, the tip is cleaned by rinsing. The amount of liquid deposited depends on the size of the tip.

The piezojet is a contactless dispensing technique for subnanoliter droplets. It is based on a cylindrical piezo ceramic that compresses a glass capillary with an inner diameter of ~1 mm on application of an electric pulse. A small droplet is then expelled through the funnel-shaped orifice of the capillary. The outlet diameter of the orifice is ~50 µm. Very uniform droplets can be prepared by this method (see Fig. 1).

Figure 1. The principle of preparing and applying plasmid chip arrays (PCA), as developed by U. Certa and R. Hochstra Hoffmann–La Roche Ltd, Basel, Switzerland).

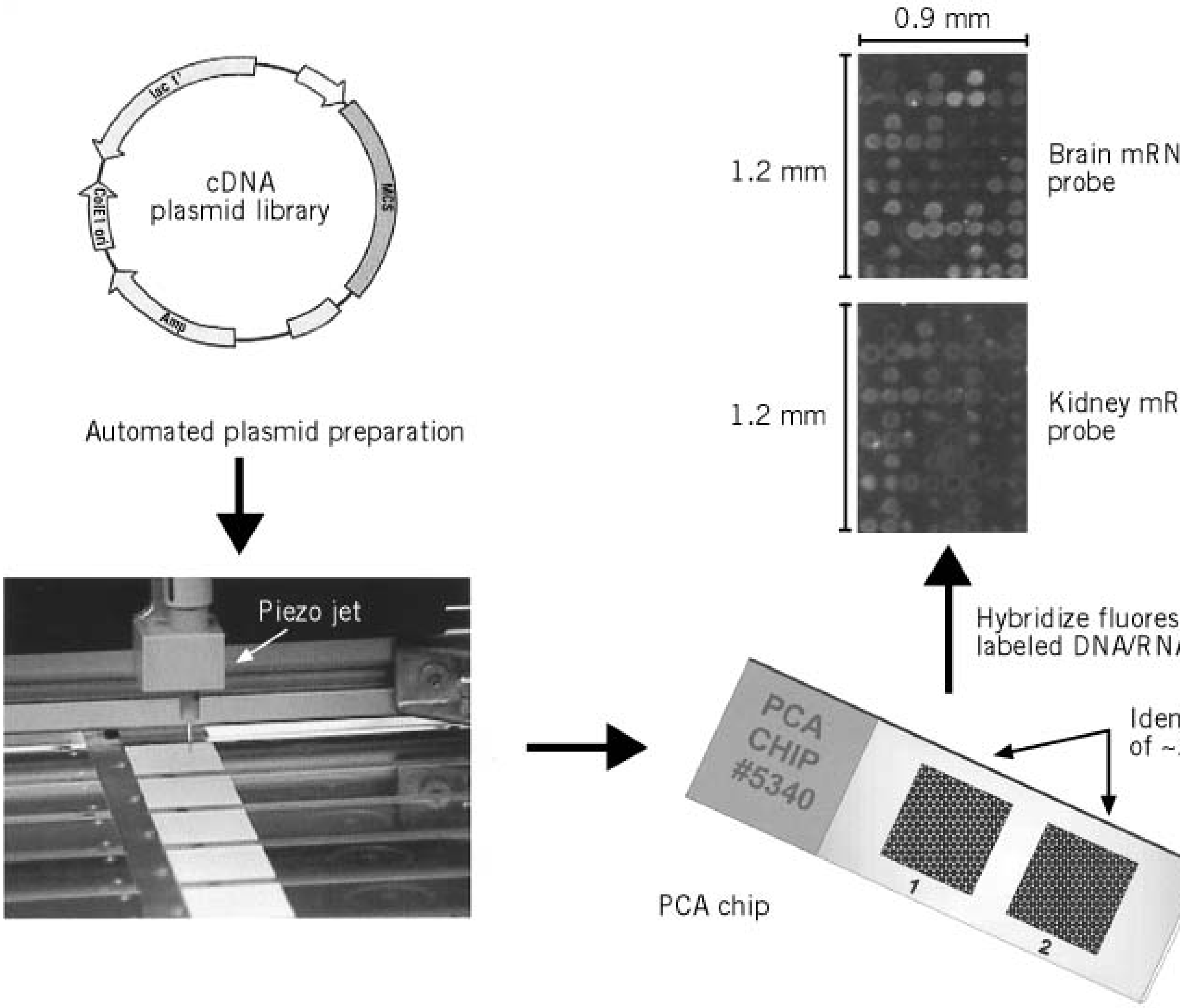

The piezojet-dispensing process consists of three steps: (1) Aspiration of an aliquot of sample through the capillary, (2) dispensing of one subnanoliter droplet of sample to equivalent spots on each chip, and (3) discharge of remaining sample volume and cleaning of the piezojet. In order to use the sample material effectively, the aspiration volume of the piezojet should be in the microliter range.

The deposited DNA has to be immobilized on the surface in order to enable the subsequent processing steps. The most commonly used attachment method is to coat the glass slides with polylysine, which holds the negatively charged DNA backbone by electrostatic interactions. Alternative methods, like **streptavidin**-coated slides to bind **biotin**-labeled DNA, and various chemical approaches to bind DNA covalently to pretreated glass, are under development.

The most elegant way to attach DNA fragments covalently onto the glass chips has been developed by Fodor and colleagues at Affymetrix (2-4). This method allows light-directed synthesis of thousands of DNA fragments (oligonucleotides) in precise locations on the microchip. To begin the process, linkers modified with a photochemically removable protecting group are attached to the solid substrate. Light is directed through a photolithographic mask, illuminating specific grid squares on the chip and causing photodeprotection, or the removal of the blocking group, in those squares. The chip is then incubated with a nucleotide harboring a photolabile protecting group at the 5′ end. The cycle continues: the chip is exposed to light through the next mask, which activates new grid sites for reaction with the subsequent photoprotected nucleotide. Using the proper set of masks and chemical steps, it is possible to construct a defined collection of oligonucleotides, generally 20 to 25 bases long, each in a predefined position on the array. A standard 1.28-cm^2 chip can currently be packaged with about 400,000 individual, well-defined oligonucleotides representing many thousand genes.

2. Monitoring Gene Expression

A bacterial genome, such as that of *Escherichia coli*, encodes 4288 different genes, the yeast *Saccharomyces cerevisiae* genome about 6000 genes; *Caenorhabditis elegans* has about two times more genes, and the human genome may contain approximately 100,000 unique genes. At least partial sequence information for all these genes will be available soon. Sequence information alone, however, is insufficient for a full understanding of gene function and the control of gene expression. Only a subset of all encoded genes is expressed in any given cell; in higher eukaryotes, this subset is smaller than in bacteria or yeast cells. The levels and the timing of gene expression determine the fate of the cells, their reproduction, differentiation, function, communication, and physiology. Methods such as **Northern blots**, nuclease protection, and RT (reverse transcriptase)- **PCR** are frequently used to measure gene transcripts, but they have the inherent disadvantage of being serial, analyzing a single messenger RNA at a time. Most comparative techniques, like subtractive hybridization, differential display (5) of amplified mRNA's on gels, and the SAGE (serial analysis of gene expression) method of Velculescu et al. (6), are laborious, often nonreproducible, and not particularly sensitive. Arrays of several thousand genes, the DNA chips, for the first time make it possible to obtain gene expression information on complete genomes (7) quickly, accurately, and efficiently. These gene arrays are in principle reverse Northern blots, where the DNA probes have been immobilized to identify and measure large numbers of mRNA species in parallel. Two prototype DNA microarrays for gene expression monitoring can be described:

2.1. cDNA Microarrays

Brown and his colleagues developed a high-capacity system to monitor the expression of many genes in parallel (8, 9). In short, the complementary DNA of expressed mRNAs from cells is collected, and individual cDNA molecules are isolated and amplified. A microsample of each cDNA from the library is then deposited by high-speed robotic printing on a polylysine-coated glass surface in an array format. Each gene has a unique location in the microarray, which may represent several thousands of genes on a few square centimeter. To compare expression of these genes between two tissues or two cell types, the $poly(A)^+$–mRNA in the two samples is copied into cDNA and labeled with two differently colored fluorescent molecules. Both probe samples are applied to a single microarray and allowed to react with the DNA on the microarray. After the appropriate washing steps, each element of the microarray is scanned for fluorescence intensity from the two colors by a laser fluorescence scanner. The observed fluorescence intensity at each array element is proportional to the number of fluorescent cDNA molecules bound to it, and the ratio of the two colors is an accurate measurement of the relative expression level of the genes in the two tissue or cell samples. Twofold changes in expression can be detected (10). As an illustration, Figure 1 shows a similar DNA microarray, the plasmid chip array (PCA), made by piezojet dispensing in the labs of R. Hochstrasser and U. Certa (F. Hoffmann-La Roche Ltd., Basel, Switzerland).

2.2. Oligonucleotide Microarrays

High-density arrays of oligonucleotide probes represent the other prototype method for mRNA expression monitoring. Sequence information about the expressed genes is used directly to select oligonucleotides and to design the photolithographic masks for combinatorial synthesis of the probes directly on derivatized glass, as described previously. The arrays are intentionally redundant, as they contain collections of pairs of probes for each of the RNAs being monitored. Each probe pair consists of a 20- to 25-mer oligonucleotide that is perfectly complementary to a subsequence of a particular message and a mismatch oligo that is identical except for a single base difference in a central position, which serves as an internal control for hybridization specificity. For array hybridization experiments, target RNA is prepared from cellular mRNA by incorporating labeled ribonucleotides in an *in vitro* transcription reaction (11), or by direct chemical attachment (12). After hybridization and washing, fluorescence imaging of the arrays is accomplished with a scanning **confocal microscope**. Because oligonucleotide probes for each gene are specifically chosen and synthesized in known locations on the arrays, the hybridization patterns and intensities can be interpreted in terms of gene identity and the relative amount of each transcript. This technology has been successfully applied for monitoring gene expression in mammalian cells (11), yeast (7), and bacteria (12), measuring expression levels of less than one copy of mRNA to several hundred copies per cell in one hybridization experiment.

3. Accessing Genetic Diversity

High-density oligonucleotide probe arrays (Fig. 2) can also be applied to a broad range of nucleic acid sequence analysis problems, including pathogen identification, polymorphism detection and sequence checking. The significant instability of internal probe–target mismatches relative to perfect matches (4, 13) is used to design arrays of probes capable of detecting differences between nucleic acid targets. To interrogate the identity of a nucleotide as position X of a known DNA sequence, four oligonucleotides can be offered with the four different choices A, G, T, C in the middle of 15 or so flanking nucleotides that perfectly match the reference sequence. The probe with the highest intensity after hybridization would indicate the identity of the unknown base. This concept can be extended to detect polymorphisms/mutations relative to a characterized **consensus sequence**. Thus, to screen 1000 nucleotides for polymorphisms/mutations would require 4000 probes. Current applications of this technique include the survey of drug-resistance mutations in **HIV**-1 reverse transcriptase and proteinase genes, a p53 mutations screen, and a cytochrome P450 allelic variants screen.

Figure 2. The basic principle of oligonucleotide microarrays (courtesy of Affymetrix, Santa Clara, CA).

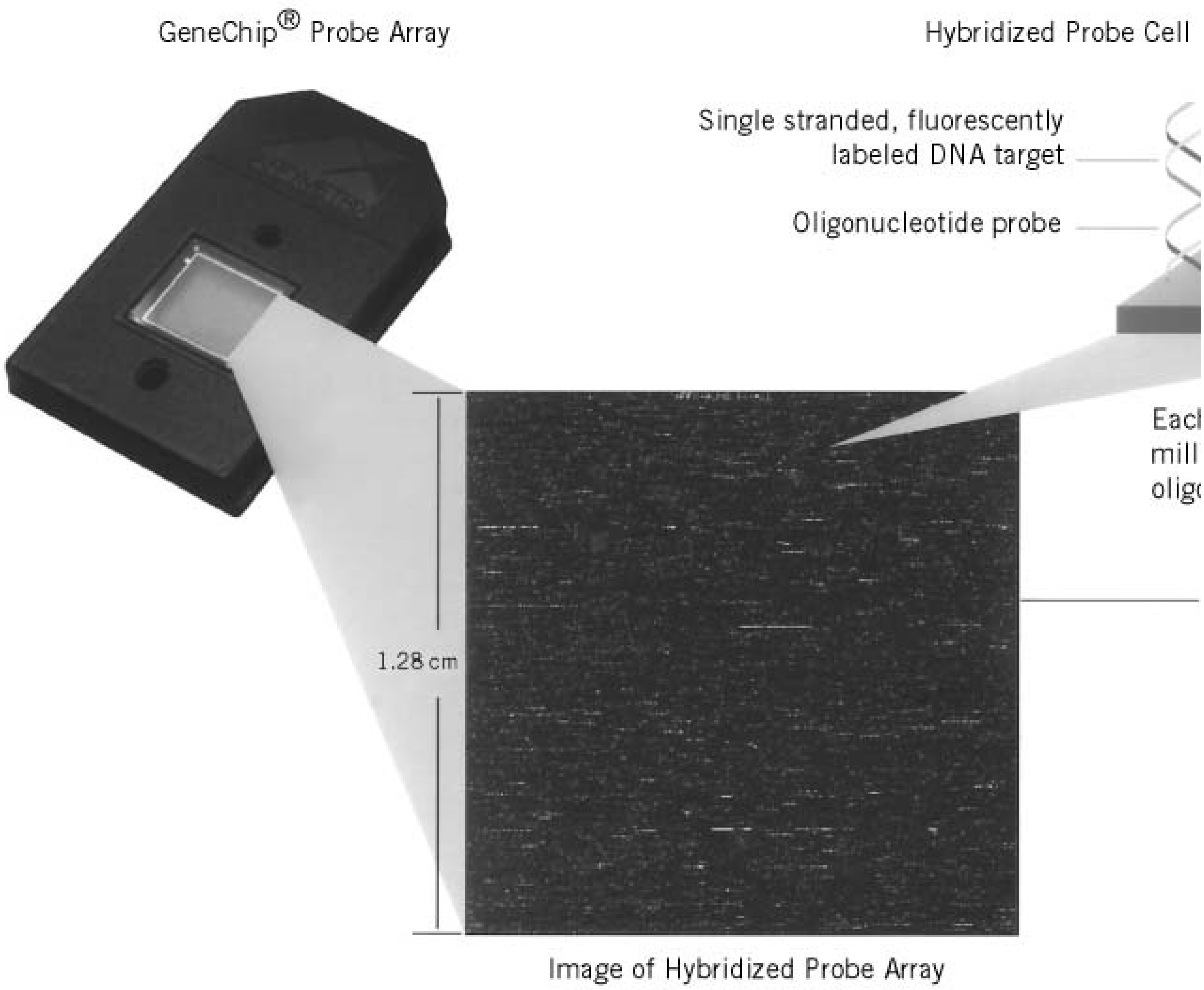

4. Sequencing by Hybridization

Hybridization can also be used to determine the sequence of unknown DNA, ie, *de novo* DNA sequencing. Sequencing by hybridization is based on the use of oligonucleotide hybridization to determine the set of constituent subsequences in a DNA fragment. This concept which was spearheaded by Crkvenjakov (14, 15) uses a microarray of all possible *n*-nucleotide oligomers, eg, 65,635 possible octamers, to identify all the *n*-mers present in an unknown DNA sequence. Powerful computational approaches are then used to assemble the complete sequence from the measured hybridization patterns. High-density oligonucleotide probe array technology shows significant promise in enabling *de novo* sequencing in a fast and reliable manner.

Bibliography

1. G. G. Lennon and H. Lehrach (1991) Trends Genet. **7**, 314–317.
2. S. P. A. Fodor, J. L. Read, M. C. Pirrung, L. Stryer, A. T. Lu, and D. Solas (1991) Science **251**, 767–773.
3. S. P. A. Fodor, R. P. Rava, X. C. Huang, A. C. Pease, C. P. Holmes, and C. L. Adams (1993) Nature **364**, 555–556.
4. A. C. Pease, D. Solas, E. J. Sullivan, M. T. Cronin, C. P. Holmes, and S. P. A. Fodor (1994) Proc. Natl. Acad. Sci. USA **91**, 5022–5026.

5. P. Liang and A. B. Pardee (1992) Science **257**, 967–971.
6. V. E. Velculescu, L. Zhang, B. Vogelstein, and K. W. Kinzler (1995) Science **270**, 484–487.
7. L. Wodicka, H. Dong, M. Mittmann, M. H. Ho, and D. J. Lockhart (1997) Nature Biotech. **15**, 1359–1367.
8. M. Schena, D. Shalon, R. W. Davis, and P. O. Brown (1995) Science **270**, 467–470.
9. D. Shalon, S. J. Smith, and P. O. Brown (1996) Genome Res. **6**, 639–645.
10. M. Schena, D. Shalon, R. Heller, A. Chai, P. O. Brown, and R. W. Davis (1996) Proc. Natl. Acad. Sci. USA **93**, 10614–10619.
11. D. J. Lockhart, H. Dong, M. C. Byrne, M. T. Follettie, M. V. Gallo, M. S. Chee, M. Mittmann, C. Wang, M. Kobayashi, H. Horton, and E. L. Brown (1996) Nature Biotech. **14**, 1675–1680.
12. A. de Saizieu, U. Certa, J. Warrington, C. Gray, W. Keck, and J. Mous (1998) Nature Biotech. **16**, 45–48.
13. R. J. Lipshutz, D. Morris, M. Chee, E. Hubbell, N. S. Kozal, N. Shen, R. Young, and S. P. A. Fodor (1995) BioTechniques **19**, 442–447.
14. R. Drmanac, I. Labat, I. Brukner, and R. Crkvenjakov (1989) Genomics **4**, 114–128.
15. R. Drmanac, S. Drmanac, Z. Strezoska, T. Paunesku, I. Labat, M. Zeremski, J. Snoddy, W. K. Funkhouser, B. Koop, L. Hood, and R. Crkvenjakov (1993) Science **260**, 1649–1652.

DNA Damage, Inducible Responses To

Agents that damage **DNA**, like other external stimuli, elicit a complex series of cellular responses in both prokaryotes and eukaryotes. The molecular mechanisms and the consequences of induction of these genotoxic responses in prokaryotes are well-understood. In eukaryotes, in contrast, the mechanisms and the effects of the multiple response reactions remain ill-defined. In *Escherichia coli* there are genotoxic response reactions that are induced mainly, but not exclusively, by bulky DNA lesions (SOS response), by alkylating agents (adaptation), and by oxidative stress (adaptive response to oxidative stress). These response reactions result in **transcriptional** activation of genes that inactivate the noxious agent, repair the damage caused by the agent (see DNA Repair), or help the cell survive the DNA damage.

1. SOS Response

The SOS response is a coordinated cellular response in *E. coli* and aids in the survival of the organism by affecting the expression of proteins that are involved in cellular division, **replication**, recombination, and excision repair (1) (see SOS Response). About 30 genes are involved. The basic mechanism of regulation is relatively simple (2, 3). Under normal conditions, the LexA repressor binds to the SOS box, with the sequence 5′-CTG-N $_{10}$-CAG-3′, to maintain repression of the SOS regulon. Directly or indirectly, DNA damage or other replication blocks generate single-stranded regions that lead to the formation of single-stranded DNA, on which the RecA protein polymerizes (4, 5). The RecA-single-stranded DNA filament binds to LexA and stimulates its autoproteolysis activity (6). Cleavage of LexA inactivates its repressor activity (2-5), allowing transcription of the SOS genes, including *lexA* and *recA* themselves. Cell division stops, excision (7, 8) and recombination (2, 3) activities increase, and the capacity of replicase to bypass the damage increases (9, 10). All of these enable the cell either to eliminate the DNA damage or to survive with damaged DNA. Upon recovery, the inducing signal disappears, and LexA accumulates and represses the cognate genes. The excision repair genes *uvrA*, *uvrB*, and *uvr*D (7, 8) are under the control of the

LexA protein; consequently, the cellular excision repair activity increases transiently as part of the SOS response reaction and then drops down to preinduction levels after repair.

2. Adaptive Response

The adaptive response is the phenomenon of increased resistance of cells to killing and mutation by alkylating agents that results from prior exposure to lower doses of the same agent (11). The phenomenon was originally discovered in *E. coli* and was later found in other prokaryotes. There is no evidence for an adaptive response in eukaryotes or archaebacteria, although alkylating agents elicit a general stress response reaction in eukaryotes.

The molecular mechanism of the adaptive response in *E. coli* is relatively simple and known in considerable detail (12, 13) (Fig. 1). Treatment of cells with alkylating agents such as *N*-methyl-*N*′-nitro- *N*-nitrosoguanidine (MNNG) methylates multiple sites on DNA, including the backbone phosphate groups. The methylphosphotriesters that are formed by such treatments are mostly nonmutagenic and nonlethal. In contrast, the product O^6-methylguanine is a miscoding base that induces G to A transition mutations, and 3-methyladenine is a lethal lesion. However, it is the methylphosphotriesters that constitute the signal substrate for the repair of the mutagenic and lethal alkylation products.

Figure 1. Adaptive response in *E. coli*. The Ada protein transfers the methyl group from methylphosphotriesters to Cys69 of the protein. This covalent modification activates Ada as a transcription factor, which induces its own gene for repair of O^6-methylguanine, *alkA* for repair of 3-methyladenine, and *aidB* and *alkB* for protecting DNA.

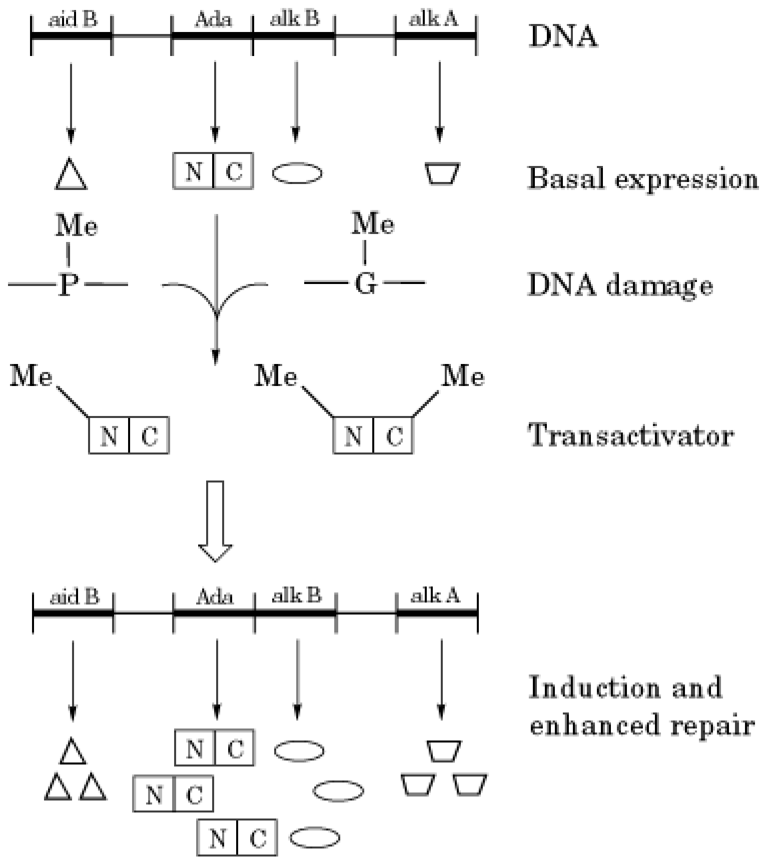

The adaptive response is a positive regulatory response reaction. The central regulator in this response reaction is the 39-kDa Ada protein (O6-methylguanine DNA methyltransferase). The structure of the Ada B protein in *E. coli* exhibits a **helix–turn–helix** variant **DNA-binding** motif, but this motif is separate from its active site (14). Ada acts both as a transcription factor and as a methyltransferase. Upon formation of methylphosphotriesters, the Ada protein transfers the methyl group from the phosphate to a cysteine residue (Cys69) in the amino-terminal domain of the molecule. This reaction induces a conformational change in the protein, which increases its affinity for the Ada box, with the sequence A_3 –N_3–A $_3$–GCGCA (12, 13), upstream of cognate **promoters**. Binding of Ada to these promoters activates transcription of target genes that are involved in preventing and repairing the damage caused by alkylating agents. The following genes are induced by Ada: the *ada* gene itself, *alkA*, *alkB* and *aidB*. The roles of these genes in cellular defense against alkylation killing and mutagenesis are summarized below.

2.1. Ada

The Ada protein performs three functions. It transfers the methyl group from O^6-methyl-guanine (or O^4-methylthymine) to Cys321 of Ada (15), it transfers the methyl group from the methylphosphotriester to Cys69, and it binds upstream of the promoters of cognate genes and acts as a positive transcriptional regulator. The order of the methyl transfer reactions is random, and they are independent of one another. In contrast, binding of Ada to promoter regions is strongly influenced by methylation of residue Cys69. Even though unmethylated Ada binds to certain promoters (such as the *ada* promoter) with low affinity, the binding is strongly stimulated by methylation of Cys69, and the binding to other promoters is completely dependent on the methylation of Cys-69. The methylation status of Cys321 has no effect on the regulatory activity of the protein. In addition to Ada, *E. coli* and some other prokaryotes contain a second alkyl transferase with no regulatory function (16).

2.2. AlkA

The AlkA protein removes 3-methyladenine and other alkylated purines by a DNA glycosylase activity. There are two 3-methyladenine DNA glycosylases (Tag). One is encoded by the *tag* gene (TagI), which is not regulated by Ada and has narrow substrate specificity. The other, which is regulated by Ada and encoded by *alkA* (TagII), removes 3-methyladenine and other methylated purines, as well as O^4-methyl thymine, and thus has a wide substrate range.

2.3. AlkB

The AlkB protein is a 27-kDa monomer that enables cells to survive DNA damage induced by SN2 alkylating agents, but not by SN1. Although it is known that the protein acts at the level of DNA, the precise mechanism of the repair reaction is not known.

2.4. AidB

The AidB protein is a 60-kDa monomer with a high degree of homology to several mammalian acetyl coenzyme A dehydrogenases, and it exhibits isovaleryl coenzyme A dehydrogenase activity. Metabolic activation by glutathione or other nonprotein thiol groups is necessary for the toxic effect of MNNG. It is possible that AidB confers resistance by affecting the intracellular thiol pool, or by acting directly on MNNG and detoxifying it. The situation is somewhat similar to the induction of *zwf* as part of the oxidative stress response reaction. This gene encodes glucose-6-phosphate dehydrogenase; upon induction of the SoxRS regulon by superoxides, the level of the dehydrogenase increases, and the enzyme in turn increases the cellular NADPH pool, which detoxifies reactive oxygen species.

2.5. Mechanism of the Adaptive Response

The homeostasis of the adaptive response is maintained as follows. Upon DNA damage by MNNG, the Ada protein, which is present at about 100 copies per cell, reacts with methylphosphotriesters and transfers the methyl group to Cys69. As a result, Ada becomes a potent transcription factor, binds upstream of the *ada-alkB*, *aidB* and *alkA* operons, and turns on these genes. Upon completion of DNA repair and elimination of the alkylating agent, the methylphosphotriester inducing signal disappears. The accumulated Ada is no longer methylated; because of its high concentration, it binds to but cannot induce the cognate genes, interfering with binding of alkylated Ada. Eventually, the alkylated Ada is degraded or diluted out by cell growth and division, and the adaptation reaction is turned off.

Human O^6-methylguanine DNA methyltransferase has been characterized in some detail (17). It has no regulatory function, but it has an unusual relation to cellular transformation. Resistance to alkylating agents has been observed in some tumor cell lines that lack O^6-methyltransferase. The resistance appears to be due to simultaneous defects in O^6-methyltransferase and in mismatch repair. An accumulation of unrepaired O^6-methylguanine lesions should lead to cell death, because of a phenomenon called futile cycling, where mismatch repair systems attempt, but fail, to repair the lesion, halting replication and finally inducing apoptosis. Therefore, in tumor cell lines that already lack O^6-methyltransferase, an additional defect in mismatch repair results in the loss of futile cycling and allows the cells to survive treatment with alkylating agents.

3. Adaptive Response to Oxidative Damage

Oxidative stress in the form of reactive oxygen species (ROS: OH, H_2O_2, $O_2^{-\cdot}$) induces the transcription of a variety of genes in both prokaryotes and eukaryotes. The molecular mechanisms of induction and the significance of the induction reaction for cellular survival have been elucidated in *E. coli*. In this organism there are two regulatory pathways. One is induced by H_2O_2 and is referred to as the OxyR regulon. The other is induced by superoxides and is referred to as the SoxRS regulon.

3.1. OxyR Regulon

The OxyR system belongs to the LysR family of single-component bacterial regulators, in which the same protein functions both as a sensor and as a signal transducer-regulator (18-20). The OxyR protein acts as both a sensor and transducer of the oxidative stress signal (Fig. 2). The activity of OxyR is regulated by the oxidation status of two cysteine residues, Cys199 and Cys208. Peroxides lead to formation of a disulfide bridge between the two cysteine residues (21). Both disulfide and dithiol forms of OxyR bind to the *oxyR* promoter, but only the disulfide form binds to the *katG* (hydroperoxidase) and *ahpC* (hydroperoxide reductase) promoters. Binding of reduced OxyR to its own promoter represses its gene, whereas the disulfide form turns on this gene, as it does to the *katG*, *ahpC*, *gorA*, and *grx1* genes. The members of this regulon are involved solely in antioxidant defense and not DNA repair.

Figure 2. Adaptive response to peroxides. Peroxides convert two cysteine thiol groups on OxyR to a disulfide bond. This activates OxyR as a transcription factor, which turns on genes whose products combat peroxides. In the absence of peroxides, glutaredoxin reduces OxyR and converts it to the inactive form.

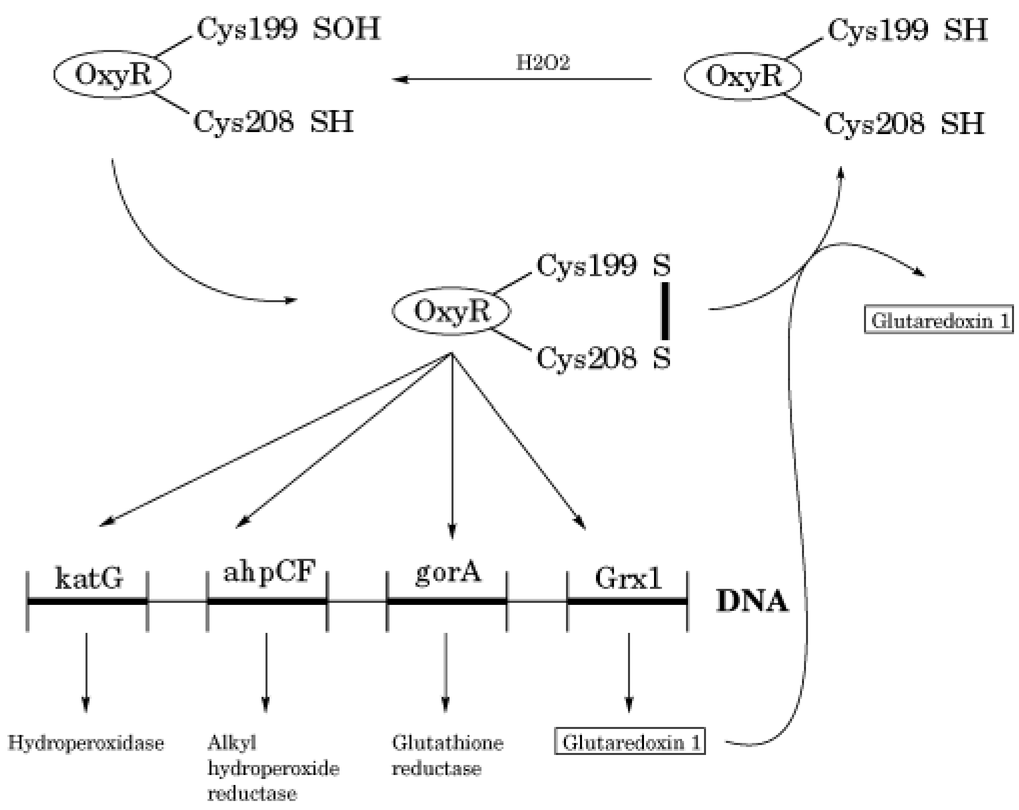

An extremely important fact regarding OxyR-mediated antioxidant response is the finding in *Mycobacterium tuberculosis* that the *oxyR* gene contains deletions and point mutations, resulting in frameshifts that make OxyR nonfunctional (22). This explains the unusual sensitivity of *M. tuberculosis* to the antituberculosis drug isoniazide. As a result of this mutation, alkylhydroperoxide reductase (encoded by *ahpC*) is not induced upon oxidative stress. Isoniazide is activated by KatG catalase-peroxidase; the reactive oxygen species that are side products of this reaction attack DNA and membrane lipids, leading to cell death. These reactive oxygen species are inactivated by alkylhydroperoxide reductase—hence the inability of *M. tuberculosis* to turn on *ahpC* in response to the oxidative burst caused by metabolizing isoniazide leads to its death by oxidative stress (22).

3.2. SoxRS Regulon

The SoxRS regulon is a two-component regulatory system that responds to superoxide stress (Fig. 3). SoxR is an iron–sulfur protein that is sensitive to superoxides, and when oxidized it becomes a transcriptional activator for SoxS. SoxS is a positive regulator of genes encoding superoxide-detoxifying and DNA–repair enzymes. The ferredoxin-like protein SoxR is a 34-kDa homodimer containing one essential [2Fe–2 S] cluster per polypeptide chain (23, 24). Both the reduced and oxidized forms of SoxR bind to the SoxS promoter, with comparable affinities, although binding of the reduced form does not induce transcription. Increased superoxides in the cell convert OxyR to the oxidized form and activate it as a transcription factor. Thus, the activation occurs not by increasing the affinity of SoxR for DNA, but by causing a conformational change in the protein that facilitates the binding of RNA polymerase to the *soxS* promoter and initiation of *soxS* transcription. While the *soxS* promoter is bound by the reduced form of SoxR, the distance between the two signature sequences is shorter than optimal for **RNA polymerase** binding. The conformational change induced in SoxR by oxidation results in overwinding of the promoter, which aligns the –35 and –10 sequences in register for optimal binding by RNA polymerase. The net result is about a 50-fold increase of *soxS* transcription. The SoxS protein then activates transcription of other genes that detoxify superoxides or repair DNA damage caused by superoxides. The following enzymes/proteins are up-regulated by SoxS: SodA Mn^{2+}-superoxide dismutase), Nfo (endonuclease IV, which is a type-II AP endonuclease), MicI (which inhibits the synthesis of a porin, thereby blocking the uptake of $O_2^{-\cdot}$) generators), aconitase, O_2-insensitive fumarase (which replaces $O_2^{-\cdot}$) damaged enzymes), flavodoxin, $NADP^+$ oxidoreductase (Fpr, which reactivates damaged Fe-S centers), and Zwf (glucose-6-phosphate dehydrogenase) which generates the NADPH that is used by Fpr and also perhaps directly reacts with superoxides and eliminates the offending agents).

Figure 3. Adaptive response to superoxides. The SoxR protein has a [2Fe–2 S] active center. The protein binds to the *soxS* promoter in reduced form, but does not turn it on. Upon oxidation by superoxides, it overwinds the promoter of *soxS*, making it a high-affinity site for RNA polymerase. Increased transcription of *soxS* leads to increased SoxS protein, which is a transcriptional activator that turns on genes involved in inactivating superoxides (*zwf*, *sodA*) or repairing DNA (*nfo*).

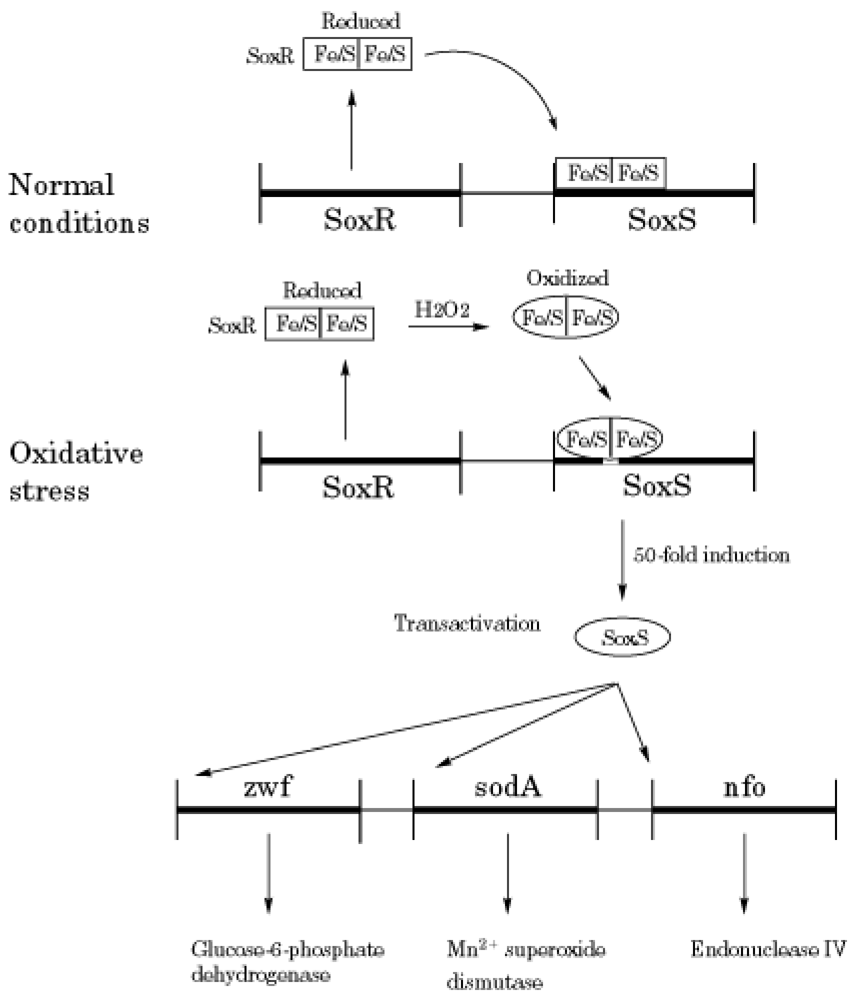

Induction of the members of this regulon enables the cell to reduce the uptake of superoxide generators, inactivates the superoxides, and repairs the DNA damage caused by oxidative stress. Upon disappearance of the inducing signal, the reduced state of the intracellular milieu is restored, which leads to conversion of the Sox from the oxidized to the reduced forms and the turning off of the oxidant stress response reaction.

In mammalian cells, oxidative stress induces many genes and regulates several transcription factors, including AP1 (25) and p53 (26, 27). However, the physiological relevance of these effects is not clear at present.

Bibliography

1. C. J. Kenyon and G. C. Walker (1980) Proc. Natl. Acad. Sci. USA **77**, 2819–2823.
2. J. W. Little, S. H. Edmiston, Z. Pacelli, and D. W. Mount (1980) Proc. Natl. Acad. Sci. USA **77**, 3225–3229.
3. R. Brent and M. Ptashne (1981) Proc. Natl. Acad. Sci. USA **78**, 4204–4208.
4. A. J. Clark and A. D. Margulies (1965) Proc. Natl. Acad. Sci. USA **53**, 451–459.
5. N. L. Craig and J. W. Roberts (1980) Nature **283**, 26–30.
6. J. W. Little (1984) Proc. Natl. Acad. Sci. USA **81**, 1375–1379.
7. A. Sancar, G. B. Sancar, W. D. Rupp, J. W. Little, and D. W. Mount (1982) Nature **298**, 96–98.
8. G. B. Sancar, A. Sancar, J. W. Little, and W. D. Rupp (1982) Cell **28**, 523–530.
9. S. J. Elledge and G. C. Walker (1983) J. Mol. Biol. **164**, 175–192.
10. M. Rajagopalan, C. Lu, R. Woodgate, M. O"Donnell, M. F. Goodman, and H. Echols (1992) Proc. Natl. Acad. Sci. USA **89**, 10777–10781.
11. L. Samson and J. Cairns (1977) Nature **267**, 281–283.
12. Y. Nakabeppu and M. Sekiguchi (1986) Proc. Natl. Acad. Sci. USA **83**, 6297–6301.
13. I. Teo, B. Sedgwick, M. W. Kilpatrick, T. V. McCarthy, and T. Lindahl (1986) Cell **45**, 315–324.
14. M. H. Moore, J. M. Gulbis, E. J. Dodson, B. Demple, and P. C. E. Moody (1994) EMBO J. **13**, 1495–1501.
15. P. Karran, T. Lindahl, and B. Griffin (1979) Nature **280**, 76–77.
16. P. M. Potter, M. C. Wilkinson, J. Fitton, F. J. Carr, J. Brennand, and D. P. Cooper (1987) Nucleic Acids Res. **15**, 9177–9193.
17. K. Tano, S. Shiota, J. Collier, R. S. Foote, and S. Mitra (1990) Proc. Natl. Acad. Sci. USA **87**, 686–690.
18. M. F. Christman, R. W. Morgan, F. S. Jacobson, and B. N. Ames (1985) Cell **41**, 753–762.
19. G. Storz, L. A. Tartaglia, and B. N. Ames (1990) Science **248**, 189–194.
20. M. B. Toledano, I. Kullik, F. Trinh, P. T. Baird, T. D. Schneider, and G. Storz (1994) Cell **78**, 897–909.
21. M. Zheng, F. Aslund, and G. Storz (1998) Science **279**, 1718–1721.
22. V. Deretic, E. Pagan-Ramos, Y. Zhang, S. Dhandayuthapani, and L. E. Via (1996) Nature Biotech. **14**, 1557–1561.
23. P. Gaudu and B. Weiss (1996) Proc. Natl. Acad. Sci. USA **93**, 10094–10098.
24. H. Ding, E. Hidalgo, and B. Demple (1996) J. Biol. Chem . **271**, 33173–33175.
25. S. Xanthoudakis, G. Miao, F. Wang, Y. C. E. Pan, and T. Curran (1992) EMBO J. **11**, 3323–3335.
26. D. Parks, R. Bolinger, and K. Mann (1997) Nucleic Acids Res. **25**, 1289–1295.
27. L. Jayaraman, K. G. K. Murthy, C. Zhu, T. Curran, S. Xanthoudakis, and C. Prives (1997) Genes and Dev. **11**, 558–570.

Suggestions for Further Reading

28. E. M. Witkin (1976) Ultraviolet mutagenesis and inducible DNA repair in Escherichia coli. Bacteriol. Rev. **40**, 869–907.
29. J. W. Little and D. W. Mount (1982) The SOS regulatory system of Escherichia coli. Cell **29**, 11–22.
30. G. C. Walker (1984) Mutagenesis and inducible responses to DNA damage in Escherichia coli. Microbiol. Rev. **48**, 60–93.
31. B. Demple (1991) Regulation of bacterial oxidative stress genes. Annu. Rev. Genet. **25**, 315–

337.
32. T. Lindahl, B. Sedgwick, M. Sekiguchi, and Y. Nakabeppu (1988) Regulation and expression of the adaptive response to alkylating agents. Annu. Rev. Biochem. **57**, 133–157.
33. S. Mitra and B. Kaina (1993) Regulation of repair of alkylation damage in mammalian genomes. Progr. Nucleic Acids Res. Mol. Biol. **44**, 109–142.

DNA Degradation *In Vivo*

Low levels of DNA degradation occur continuously in all cells, from bacteria to humans, in conjunction with various DNA repair processes. Probably 90% of this degradation can be attributed to excision repair, during which only a few **nucleotides** are released from each damaged site by the actions of repair **endo** and **exonucleases** and recycled in the overall process. Within a population of cells, high levels of DNA degradation occur in individual cells that need elimination from the population. This need occurs either because their DNA has become too heavily damaged to be successfully repaired, because the cells have been infected with bacteriophages or **viruses** or, during development and tissue remodeling in multicellular organisms, because these cells have received signals instructing them to commit suicide. In higher **eukaryotes**, this cell suicide is known as apoptosis. In this case, the chromatinDNA is fragmented and packaged with other cellular materials into apoptotic bodies that are engulfed by adjacent healthy cells in the tissue and digested in their **lysosomes**. The digestion products are recycled in these cells.

Most chromatin DNA fragmentation in eukaryotic cells follows an ordered path that yields first 300-kbp double-strand (ds) fragments, then 50-kbp ds fragments and lastly a range of small ds fragments that are multiples of nucleosome -sized DNA, 180–200 bp (1). This fragmentation pattern reflects the different levels of packing of the DNA in the chromatin. Six 50-kbp loops form 300-kbp rosettes that are stacked together. Cleavage between rosettes releases the 300-kbp fragments, and cleavage at the bases of the loops releases 50-kbp linear ds DNA that is readily cleaved between nucleosomes to small fragments that have 3′-OH and 5′-P termini. When separated by gel electrophoresis in agarose, the latter appear as a characteristic “ladder” of DNA. All stages of the fragmentation are Mg^{2+}-dependent, but the subsequent cleavage to small fragments is also activated by Ca^{2+}. This may indicate that there is more than one **nuclease** involved in chromatin DNA cleavage. In a few cases, the earlier stages of fragmentation are sufficient for apoptosis to proceed to completion. Random DNA degradation occurs during cell necrosis as a result of very heavy damage to the cell or tissue injury and is accompanied by lysosome disruption and cytolysis.

Except for a small body of work on *Escherichia coli*, little is known about cell suicide in bacteria. When DNA bacteriophages that have not adapted to growth in *E. coli* are cleaved by host restriction enzyme nucleases, the resulting ds DNA fragments are degraded to small oligonucleotides by a nuclease with Mg^{2+}- and ATP-dependent endo- and exonuclease activities encoded by the recB, recC, and recD genes, the recBCD nuclease. This nuclease normally acts in recombination and in recombinational ds break repair, a minor DNA repair pathway. Some bacteriophages that have adapted to *E. coli* contain genes that encode specific inhibitors of the recBCD nuclease. This nuclease is also responsible for degrading genomic DNA damaged beyond repair by UV light or ionizing radiation (2), but the details of the process are not known. The enzyme has **homologues** in many other species of bacteria.

The identity of the nucleases that are responsible for chromatin DNA degradation during apoptosis in higher eukaryotes remains uncertain. Two difficulties encountered are that **nuclei** contain very low levels of active nucleases and that they are readily contaminated during isolation by nucleases from other **organelles** . The potent **mitochondrial** nuclease has been shown to contaminate nuclei isolated from calf thymus (3), a tissue that exhibits a high rate of apoptosis, although this nuclease is not known to act in chromatin DNA degradation. DNase II, an acid **deoxyribonuclease** (DNase) normally found in the lysosomes, generates a ladder of ds DNA fragments when incubated with isolated nuclei at acidic pH. A small decrease in intracellular pH (0.3 pH units) occurs during apoptosis (4), but this would not be enough to result in appreciable activation of DNase II, even if it had a bona fide nuclear location. DNase II is not metal ion–dependent and makes ds breaks with 3′-P and 5′-OH groups, termini not found on the apoptotic ds DNA fragments. However, the corresponding acid DNase of the flatworm, Caenorhabditis *elegans*, does play a role in apoptosis, namely, in digesting the apoptotic bodies when engulfed by healthy cells. A loss of function of the nuclease caused by mutation of the *nuc1* gene led to accumulation of the apoptotic bodies in the lysosomes (5).

Considerable attention has been paid to **DNase I** as a possible candidate for chromatin DNA fragmentation (6). It is Mg^{2+}-dependent and Ca^{2+}-activated and makes the appropriate ds breaks in DNA. Where expressed, DNase I occurs in an inactive complex with actinthat is activated *in vitro* by proteolysis. However, the activity is not expressed in many cell types that undergo apoptosis and, when DNase I is added to isolated nuclei, a smear of randomly cleaved DNA results, rather than a ladder of DNA fragments. Overexpression of the bovine DNase I gene in monkey COS cells induced chromatin DNA ladder formation. However, expression of any nuclease activity in the nuclei may “damage” (nick or cleave) DNA sufficiently to trigger activation of the endogenous apoptotic program.

A bewildering array of other Ca^{2+}, Mg^{2+}-endonucleases, which vary in size from 18 to 97 kDa and generate ladders of DNA in isolated nuclei, have also been proposed to act in chromatin DNA degradation (7). These have been isolated from nuclei of apoptotic cells, but none have been fully characterized, no inactive forms have been reported, and little is known about their possible relationships. The smallest of these is NUC-18 (18 kDa), which has been identified as a cyclophilin (8). Cyclophilins have peptidyl prolyl cis–trans isomerase activity and play a role in **protein folding**. Since the specific nuclease activity associated with purified cyclophilins is very low, this activity may be associated with a contaminant. The largest (97 kDa) species cross-reacts with antibody raised against purified endo-exonuclease from *Neurospora crassa* (7), a Mg^{2+}-dependent enzyme with homologues in other **fungi**and **yeast** that has been shown to act in recombination and in recombinational ds break repair (3). It may be the eukaryotic counterpart of the bacterial recBCD nuclease. It occurs in both active and inactive forms and has endonuclease activity with both DNA and RNA and exonuclease activity with DNA. A mammalian endo-exonuclease, synergistically activated by Ca^{2+}, has been isolated from monkey CV-1 cells (9). It is the major degradative nuclease in nuclei of human leukemia cells, present entirely in inactive form. Proteolysis of endo-exonuclease has been detected by immunoblotting in response to different apoptotic agents and yielded polypeptides identical in sizes to the various Ca^{2+}, Mg^{2+}-endonucleases isolated from apoptotic cells by others. Proteolysis, an essential feature of apoptosis, may result in the activation and turnover of endo-exonuclease. Direct activation of endo-exonuclease, circumventing the apoptotic signaling pathways, could lead to new therapies in eliminating unwanted cells.

Bibliography

1. P. R. Walker, S. Pandey, and M. Sikorska (1995) Cell Death Differ. **2**, 93–100.
2. G. R. Smith (1988) Microbiol. Rev. **52**, 1–28.
3. M. J. Fraser and R. L. Low (1993) "Fungal and mitochondrial nucleases", in *Nucleases*, 2nd ed. R. J. Roberts, S. M. Linn, and S. Lloyd, eds., Cold Spring Harbor Laboratory Press, Cold Spring Harbor, New York, pp. 171–207.

4. M. A. Barry and A. Eastman (1993) Arch. Biochem. Biophys. **300**, 440–450.
5. J. Hevelone and P. S. Hartman (1988) Biochem. Genet. **26**, 447–460.
6. B. Polzar et al. (1993) Eur. J. Cell Biol. **62**, 397–405.
7. M. J. Fraser et al. (1996) J. Cell Sci. **109**, 2343–2360.
8. J. W. Montague, M. L. Gaido, C. Frye, and J. A. Cidlowski (1994) J. Biol. Chem. **269**, 18877–18880.
9. C. Couture and T. Y.-K. Chow (1992) Nucl. Acids Res. **20**, 1379–1385.

Suggestion for Further Reading

10. M. J. Fraser (1996) *Endo-exonucleases: Actions in the Life and Death of Cells*, Bioscience Report, R. G. Landes Co., Austin, Texas, pp. 1–73.

DNA Dynamics

DNA possesses many properties associated with a linear polymer, including various mechanical (rigidity) and motional properties. The normal B-DNA is considerably more flexible than both A-DNA and Z-DNA. DNA structure in solution has two classes of motional properties: large-scale and local motions. The large scale tumbling motion of a DNA duplex of the size in the range of 10–100 base pairs has a correlation time of nanoseconds to microseconds. It is related to rigidity of the duplex (of varying composition and sequence) as measured by the persistence length. This global flexibility of DNA can be used to understand the behavior of DNA in solution and in gels. There are also local motions that are important in the biological functions of DNA. The dynamic properties of DNA allow it to stretch, bend, twist, and so on. The binding of many intercalators to DNA requires that adjacent DNA base pairs be separated to 6.8 Å in order to accommodate the aromatic intercalator. This is a large conformational change (including sugar pucker rearrangements), involving many torsion angles. Since the binding of intercalators is a reversible process, DNA must be in constant motions, so that the on-off binding process can happen at any time. Figure 1 shows the high resolution structure of the complex between the anticancer drug daunorubicin and CGCGCG **crosslinked** by formaldehyde (1). Finally, the motion of DNA or drug–DNA complexes may be analyzed by high resolution X-ray crystallography structure refinement that incorporates refinement of anisotropic temperature factors. This demonstrates that various parts of the complex have different motional properties, as is evident in their thermal ellipsoids.

Figure 1. The three-dimensional structure of the daunorubicin–CGCGCG complex (Protein Database DDF023).

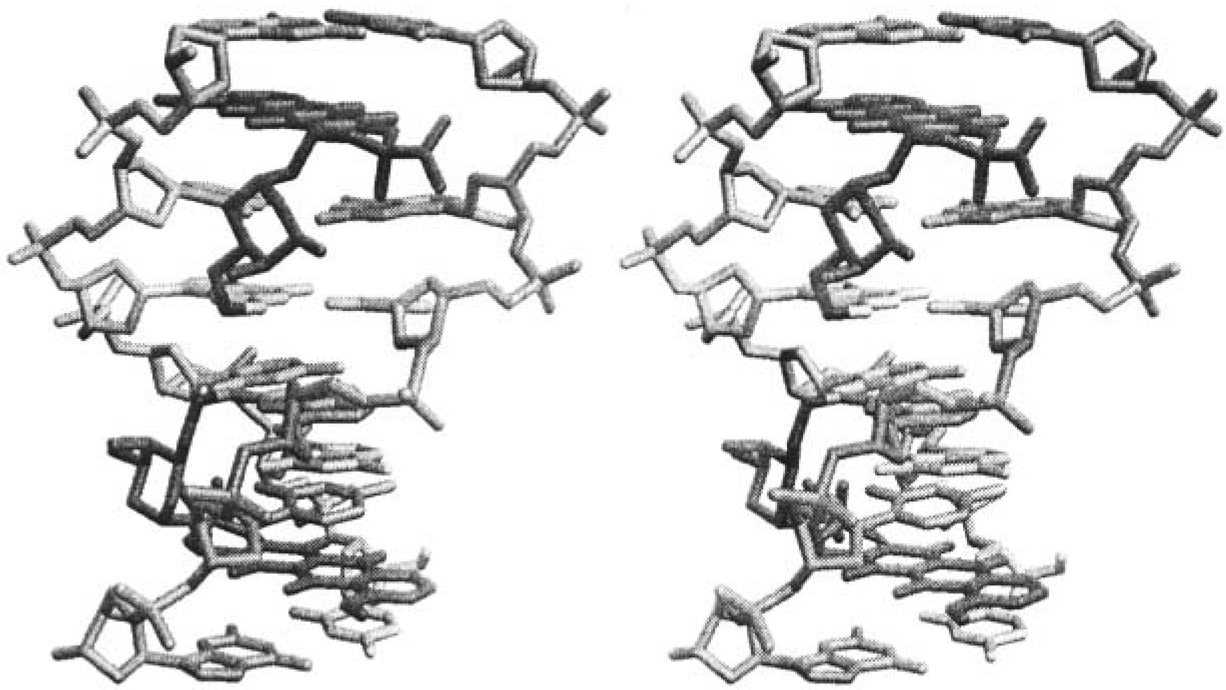

Some dinucleotide steps, such as CpG, TpA, or TpG (= CpA), appear to be more flexible (see Base Pairs). In fact, those steps are the preferred binding sites for intercalator binding. They are also the preferred kinked sites induced by binding of proteins. The local dynamic property associated with the CpG site (and other sites) has been probed by high resolution and solid-state nuclear magnetic resonance (NMR) spectroscopy (2). The line shape analysis of the ^{2}H-NMR spectra of the dodecamer CGCGAATTCGCG, with the ^{2}H probe incorporated at different sites of the DNA, suggested that the deoxyribose of the C9 residue has a greater motional amplitude than do the other nucleotides. The atypical motional property of the CpG step has been attributed to be correlated with the cleavage at this site by the restriction enzyme EcoRI. Therefore, the local dynamics of DNA clearly play important roles in DNA bending induced by proteins, in binding of intercalators, in restriction enzyme action, and undoubtedly in other biological functions.

Bibliography

1. A. H.-J. Wang, Y.-G. Gao, Y.-C. Liaw, and Y.-K. Li (1991) Biochemistry **30**, 3812–3815.
2. B. H. Robinson, C. Mailer, and G. Drobny (1997) Annu. Rev. Biophys. Biomol. Struct. **26**, 629–638.

Dna Genes

Mutations in certain **genes** can adversely affect DNA replication and, as such, these genes have been designated as "*dna* genes." Each *dna* gene falls within one of two groups distinguished by how the kinetics of DNA synthesis are influenced when cells harboring a conditional mutation in that gene are shifted from permissive to nonpermissive conditions: (*1*) Mutations of genes whose products are involved in initiation of replication exhibit a slow-stop **phenotype**; DNA synthesis is sustained until ongoing rounds of replication are completed. Proteins encoded by these genes include initiator proteins, **heat-shock** proteins, and a protein involved in **primosome** assembly. (*2*) Mutations of genes whose products participate in DNA elongation exhibit an immediate or fast-stop phenotype. Genes encoding **helicases**, primases, and subunits of **DNA polymerases** fall within this category.

1. Initiation Genes

Among the first temperature-sensitive DNA replication mutants to be isolated from *Escherichia coli* were those mutated in the *dnaA* gene. These mutants exhibited a slow-stop phenotype, implicating the gene product in initiation of replication (1). It is now known that the 52.5-kDa DnaA protein initiates replication by recognizing the **origin of replication**, melting the double-stranded DNA, and recruiting replication machinery to this site. The *dnaA* gene, found at 83.6 minutes on the *E. coli* chromosomal map (2), is one of the mostly highly conserved of the *dna* genes in **prokaryotes** . **Homologues** have been identified in at least 16 species of evolutionarily distinct **gram-negative** and gram-positive bacteria (3). Two regions within the gene are conserved: a short amino terminal and a long *C*-terminal encoding segment are highly homologous among species (3).

In *E. coli*, the *dnaA* gene is the first gene in an **operon** also containing *dnaN* (a gene encoding the b subunit of DNA polymerase III holoenzyme) and *recF* (involved in recombination). The gene *gyrB* follows these three genes but probably is not part of the transcription unit (4). Regulation of the *dnaA* gene occurs via two **promoters** found 240 and 160 nucleotides upstream of the start site, denoted dnaA1p and dnaA2p,and a DnaA binding site, called a “DnaA box,” that is found between these two promoters. In *E.coli* and *Bacillus subtilis*, DnaA protein regulates its own expression by binding to the DnaA box and inhibiting transcription of the gene (4). Other mechanisms of regulation include sequestration of the hemimethylated form of the gene and ppGpp signaling (4).

The arrangement of the operon in which dnaA is found is highly conserved, with the *dnaA* gene linked to the *dnaN* gene in most bacterial species. The gene arrangement, *dnaA-dnaN-recF-gyrB*, has been identified in numerous bacterial species, including *E. coli* (3), *Caulobacter crescentus* (5), *Proteus mirabilis* (6), *Staphylococcus aureus* (7), and *Mycobacterium tuberculosis* (8). *Borrelia burgdorferi* has a unique gene arrangement, *rpmH-dnaN-dnaA-gyrB*, which is most likely the result of a genetic rearrangement during evolution (9). In addition to its proximity to the *dnaN* gene, *dnaA* is found closely linked to oriC in most bacterial species. An exception is *E. coli*, where the *dnaA* gene is found almost 42 kbp counterclockwise of oriC (4).

Numerous extragenic **suppressors** of *dnaA* mutations in *E. coli* suggest that there is a complicated interaction of DnaA with numerous other proteins. For example, specific mutations in the genes encoding the b subunit of RNA polymerase (*rpoB*), topoisomerase I (*topA*), thioredoxin (*trx*), and the chaperonins GroES (*groES*) and GroEL (*groEL*) are able to suppress temperature-sensitive *dnaA* mutants (3).

In addition to mutations of the *dnaA* gene, mutant forms of the *E. coli dnaC* gene (99 minutes) (2) hinder initiation of replication. The 27.9-kDa DnaC protein delivers DnaB helicase to the DnaA protein–oriC complex. *E. coli dnaC* is found within an operon that also contains *dnaT* (involved in primosome assembly) and an unknown gene, *p18*. These genes are cotranscribed from a promoter located approximately 104 base pairs upstream of *dnaT* (10). Conservation of the *dnaC* gene among bacterial species is not well documented, but DnaC from *Salmonella typhimurium* can substitute for *E. coli* DnaC in an *in vitro* replication assay (11). While most temperature-sensitive *dnaC* mutants exhibit a slow-stop phenotype, two temperature-sensitive *dnaC* mutants, *dnaC1* and *dnaC7*, cause a fast stop in DNA synthesis, suggesting that DnaC protein also plays a role in elongation (12). In *B. subtilis*, mutations in the *dnaB*, *dnaC*, and *dnaD* genes render cells defective for initiation. The *dnaB* gene is found at 250 degrees on the chromosomal map (13), encodes a 472-residue protein, and bears no homology to any known *dna* genes (14). The *dnaB* gene product is required for the binding of the chromosomal origin to the membrane and is necessary for the initiation of replication (15). *DnaB* is cotranscribed with the *dnaI* gene, whose product is required for an unknown step of chromosomal replication (16). The *dnaC* gene product of *B. subtilis* has been suggested to be a DNA helicase and has been shown to bear 42% homology to the *E.coli* helicase, DnaB (17). *B. subtilis dnaD* mutants are also defective in initiation, as a result of an unknown mechanism. This gene has been mapped to 200 degrees on the *B. subtilis* chromosome and encodes a 232-residue protein with no known homologue in *E. coli* (18).

Temperature-sensitive mutants of the *dnaR* gene of *E.coli* are also defective in initiation of chromosomal replication. This gene is found at 26.3 minutes on the chromosomal map (19) and encodes phosphoribosyl pyrophosphate (PRPP) synthetase; PRPP is a precursor for the synthesis of nucleotides and the amino acids histidine and tryptophan (20). Mutants are capable of producing enough PRPP for replication, implicating another role for PRPP in replication besides as a nucleotide precursor. Interestingly, wild-type *dnaR* is required for DnaA-dependent, but not for DnaA-independent, chromosomal replication (21). In addition, functional DnaA protein is required for mutations in the gene encoding ribulosephosphate epimerase (rpe) to suppress the temperature sensitivity of *dnaR* mutants. Some *dnaR* mutations are also suppressed by mutations in the gene for **RNA polymerase**, *rpoB*. It is hypothesized that the dnaR gene product interacts with the products of the *dnaA* and *rpe* genes during initiation of DNA replication, possibly in a transcriptional event (22).

2. Heat Shock Genes

The products of the *dnaJ* and *dnaK* genes are involved primarily in the heat shock response, where their expression is induced by increased temperatures or other environmental stresses. These proteins act as **molecular chaperones** that use nucleoside triphosphate hydrolysis to disrupt **hydrophobic** interactions and thus facilitate proper folding of proteins (12, 23) (see Protein Folding In Vitro). In addition to their role in the heat shock response, the *E. coli* proteins encoded by *dnaJ* and *dnaK* are required for initiation of replication at the lambda phage origin (24), which led to their designation as *dna* genes. For the most part, mutations in these genes do not affect *E. coli* chromosomal replication, but instead affect processes such as chromosome segregation, **plasmid** maintenance, and normal cell growth, division, and survival (12, 25). An exception is the *dnaK*111 mutant, which is defective for initiating DNA replication at nonpermissive temperatures (26).

The *dnaJ* and *dnaK* genes are the most highly conserved of all the *dna* genes. Homologues of *E. coli dnaJ*, a member of the Hsp40 protein family, have been identified in bacterial species such as *Mycobacterium tuberculosis* (27), *B. subtilis* (27), *Clostridium acetobutylicum* (27), *B. burgdorferi* (28), *C. crescentus* (29), *S. aureus* (30), and *Lactococcus lactis* (27); in the **archaeon** *Methanosarcina mazei* (31); and in **eukaryotes** such as *Saccharomyces cerevisiae* (32), *Schizosaccharomyces pombe* (33), and *Homo sapien* (34). Homologues of *E. coli dnaK*, a member of the Hsp70 protein family, have been identified in bacterial species such as *B. subtilis* (28), *B. burgdorferi* (28), *C. crescentus* (35), *Zymomonas mobilis* (36), *Clostridium acetobutylicum* (31), *Chlamydia trachomatis* (37); in the archaeon *M. mazei* (31); as well as in eukaryotes such as *S. cerevisiae* (38), *Drosophila melanogaster* (38), and *H. sapien* (12). In *E. coli*, a single operon (39) of *dnaK-dnaJ* is found at 0.3 minutes (2). The gene arrangement *grpE-dnaK-dnaJ* has been identified in *E. coli* (28), *B. burgdorferi* (28), *B. subtilis* (40), *Chlamydia acetobutylicum* (28), *Clostridium acetobutylicum* (41), *Bacillus stearothermophilus* (42), and *S. aureus* (30). In contrast, the *dnaK* operons of *C. trachomatis* and *Lactococcus lactis subsp. lactis* are unique in that the *dnaJ* gene is absent from this region (43). In *E. coli*, *dnaJ* and *dnaK* are transcribed from a promoter located at the head of the *dnaK* cistron (44). *In B. subtilis*, two primary transcripts are synthesized by the *dnaK* operon. One is the entire *dnaK* operon, resulting in both *dnaK* and *dnaJ* transcripts, and the other is the result of transcription starting from an internal vegetative promoter immediately upstream of *dnaJ*. This promoter sequence is found in numerous gram-positive organisms (27, 42). Another common feature of organisms containing the *dnaK* operon is a nine-base-pair inverted repeat upstream of the promoter region. This region, called CIRCE (controlling inverted repeat of chaperone expression), acts as a negative *cis* element of the *dnaK* operon (45) and has been found in at least 27 eubacterial species (37). The *dnaK* operon in *C. crescentus* is regulated by two promoters; P1 is heat shock inducible, while P2, a sigma 70-like promoter, is under temporal control (29).

3. Primosome Assembly Genes

The *dnaT* gene of *E. coli* has been mapped to 99 minutes on the chromosome (2). The 19.5-kDa DnaT protein (formerly protein i) is required for bacteriophage FX174-type primosome assembly (12) and functions in transferring DnaB from the DnaB–DnaC complex to the PriA–PriB–DNA complex (46). This gene is found immediately upstream of *dnaC*, where it is transcribed along with dnaC and an unknown gene, *p18*, from a promoter located approximately 100 base pairs upstream of *dnaT* (10).

4. Helicase Genes

The *dnaB* gene of *E. coli* encodes a DNA helicase, DnaB, required to unwind double-stranded DNA at the replication fork (47). The *dnaB* gene consists of 1413 base pairs (48) and is found at 92 minutes on the chromosomal map (2). This gene lacks a typical Shine-Dalgarno sequence, while a potential promoter sequence at nucleotides –32 to –37 has been identified (48). The *dnaB* genes of *S. typhimurium* and *E. coli* are identical in length (49), are 93% identical in their corresponding amino acid residues (49), and are functionally interchangeable (50). DnaB-like proteins include gene 4 helicase of coliphage T7 (49), gene 12 protein of *Salmonella* phage P22 (49), and ban (b analog) of P1 phage (12). The *dnaC* gene of *B. subtilis* is 42% identical to *E. coli dnaB* (17), but the *dnaC* gene product's potential role as a helicase has not been demonstrated.

5. Primase Genes

The 1740 base pair (51) *dnaG* gene of *E. coli* has been mapped to 67 minutes on the chromosome (2) and encodes DNA primase, a 65.6-kDa enzyme responsible for the synthesis of small RNA that serve as primers for initiation of replication (46). Homologues of *dnaG* have been found in *S. typhimurium* (52), *B. subtilis* (formerly called *dnaE*) (12), and *Rickettsia prowazekii* (53). The *dnaG* gene is part of a macromolecular synthesis operon, which contains genes for multiple processes such as translation, replication, and transcription (54). In *E. coli*, *dnaG* is the second gene in this operon, which also contains *rpsU* (encodes S21 protein) and *rpoD* (encodes the sigma 70 subunit of RNA polymerase). The key regulatory features of this operon include tandem promoters found upstream of *rpsU*, a termination codon between *rpsU* and *dnaG*, and an RNA processing site separating *dnaG* and *rpoD* (55). In addition, a poor ribosome binding site and the use of rare codons keeps primase levels relatively low compared to those of S21 and the sigma subunit (55). The gene order *rpsU-dnaG-rpoD* is found in at least 11 gram-negative species (54), including *S. typhimurium* (56) and *Pseudomonas putida* (57). The regulatory sequences within this operon are also somewhat conserved (54).

The macromolecular synthesis operons of *B. subtilis* and *Listeria monocytogenes* also contain the *dnaG* gene upstream of *rpoD*. However, unlike the *E. coli* operon, upstream of *dnaG* these operons contain **open reading frames**, *orf23* and *orf17*, respectively, whose products are homologous with each other, but not with *E. coli* S21 (58, 59). Like the *E. coli* operon, that of *B. subtilis* is regulated by multiple promoters. The use of rare codons in the *orf23* and primase genes keeps their expression at somewhat lower levels than that of *rpoD* (58).

6. DNA Polymerase Subunit Genes

In *E. coli*, DNA polymerase III is the replicative polymerase, and many of its subunits are encoded by *dna* genes. The core polymerase a-subunit is encoded by the *dnaE* gene (60), which is 4600 base pairs long (61), is found at 4 minutes on the chromosomal map (2), and is in a proposed operon containing at least seven genes (62). The *dnaE* gene of *S. typhimurium* also encodes the a-subunit. The product of this gene is similar in size and 97% identical to the corresponding *E. coli* protein (62). In *B. subtilis*, the a-subunit is encoded by the *dnaF* gene. Mutations of this gene can result in either a slow- or fast-stop in DNA synthesis (12). Inherent in the *dnaF* gene product is a 3′ to 5′ exonuclease activity that is encoded by a separate gene in *E. coli*, *dnaQ*. As such, the amino-terminal domain of the *B. subtilis dnaF* gene product has 26% homology to the ε-subunit encoded by *E. coli dnaQ* (63). Given that the exonuclease activity is inherent in the core polymerase product of the *dnaF* gene in *B. subtilis*, it has been suggested that the *dnaQ* gene of gram-negative bacteria may have evolved from the *dnaF* gene of gram-positive bacteria (64).

The b-subunit (**sliding clamp**) of *E. coli* DNA polymerase III is encoded by the *dnaN* gene (65), which maps to 83 minutes on the chromosome (2). This subunit is responsible for the great processivity and high rates of association and dissociation of the holoenzyme from one template to another. Homologues of this gene have been identified in *B. subtilis* (formerly called *dnaG*) (12), *C. crescentus* (5), *M. luteus* (66), *M. capricolum* (67), and *B. burgdorferi* (9). In most organisms, the *dnaN* gene is found in an operon between *dnaA* and *recF* (68). In *E. coli*, the expression of the *dnaN* gene is dependent on three promoters within the translated region of *dnaA*. Although *dnaA* and *dnaN* are part of the same operon, transcription from these promoters can occur independently of transcription of *dnaA*, thus uncoupling the regulated expression of *dnaN* and *dnaA* . In addition, *dnaN* can be cotranscribed with *dnaA* from the two *dnaA* promoters, *dnaA*1p and *dnaA*2p (69).

The *dnaQ* (also called *mutD*) gene of *E. coli* encodes the 27.5-kDa ε-subunit that functions as a 3′ to 5′ exonuclease (70). The *dnaQ* gene is the only *dna* gene that does not exhibit either a slow- or a fast-stop phenotype. Instead, mutants of this gene display a **mutator** phenotype in which there is an increased rate of spontaneous mutations (46). The *dnaQ* gene is adjacent to the gene encoding ribonuclease H, *rnhA*. The two genes are transcribed in opposite directions from promoters located in an intervening 64 base pair region (71). In *S. typhimurium*, *dnaQ* also encodes the ε-subunit (72).

The t- and g-subunits of *E. coli* polymerase III are both encoded by the *dnaX* gene (12) located at 11 minutes on the chromosome (2). The 71-kDa t-subunit, the full-length product of the *dnaX* gene, functions in dimerization of the core polymerase to coordinate leading and lagging strand synthesis (73). The 47-kDa g-subunit is encoded by only a portion of the *dnaX* gene. The g-subunit is a component of the g-complex, which functions in the loading of the b sliding clamp onto primed DNA (74). The g-subunit was originally identified as a product of the *dnaZ* gene, which was later mapped within *dnaX*. Synthesis of the smaller g-subunit occurs via an interesting mechanism during translation of the *dnaX* message; a –1 translational **frameshift** at a stretch of six adenines preceding a stable hairpin results in a UGA stop codon that terminates translation and thus produces the smaller g-subunit (12). *DnaX* homologues encoding t and g-subunits, as well as the frameshift signal, have been identified in *Thermus thermophilus* (75), *S. typhimurium* (76), and several other organisms. *C. crescentus* also contains a *dnaX* homologue whose expression, as for many of the replication genes of this organism, is under cell cycle control (77).

7. Other Bacterial *Dna* Genes

Mutations in the *dnaC* gene of *C. crescentus* (78) and the *dnaH* gene of *B. subtilis* (12) result in an immediate stop in replication. However, the exact roles of the gene products are unknown, and these genes do not appear to be homologous to any *E. coli* genes. In *E. coli* the *dnaY* gene encodes an arginine transfer RNA for a rare **codon**, and mutations in *dnaY* induce a fast-stop phenotype (12). Mutants of *B. subtilis dnaI* are inhibited for chromosomal replication at an unknown step, possibly primosome assembly. This gene, which has no known *E. coli* homologue, maps to 250 degrees on the chromosome and is cotranscribed with the *dnaB* gene (16).

8. Yeast *Dna* Genes

Yeast mutants defective in **mitotic** DNA replication have led to the identification and designation of numerous *dna* genes (79). Many of these have since been shown to be identical to genes known to be involved in progression through the cell cycle. For example, *DNA1, DNA6, DNA19, DNA33, DNA39*, and *DNA43* are identical to *CDC22, CDC34, CDC36, CDC65, DBF3*, and *MCM10*, respectively (80-82).

The essential *DNA2* gene of *S. cerevisiae* encodes a structurally unique 172-kDa 3′ to 5′ helicase. Biochemical and genetic evidence suggest that the *DNA2* helicase is involved in the resolution of Okazaki Fragments (83-85).

Bibliography

1. M. Kohiyama (1968) Cold Spring Harb. Symp. Quant. Biol. **33**, 317–324.
2. M. K. B. Berlyn, K. B. Low, and K. E. Rudd (1996) In *Escherichia Coli and Salmonella: Cellular Molecular Biology* (F. C. Neidhart et al., eds.), American Society for Molecular Biology, Washington, DC, pp. 1719–1902.
3. K. Skarstad and E. Boye (1994) Biochim. Biophys. Acta **1217**, 111–130.
4. W. Messer and C. Weigel (1996) In *Escherichia Coli and Salmonella: Cellular and Molecular Biology* (F. C. Neidhardt et al., eds.), American Society for Molecular Biology, Washington, DC, pp. 1579–1601.
5. R. C. Roberts and L. Shapiro (1997) J. Bacteriol. **179**, 2319–2330.
6. O. Skovgaard (1990) Gene **93**, 27–34.
7. J. C. Alonso and L. M. Fisher (1995) Mol. Gen. Genet. **246**, 680–686.
8. L. Salazar, H. Fsihi, E. de Rossi, G. Riccardi, C. Rios, S. T. Cole, and H. E. Takiff (1996) Mol. Microbiol. **20**, 283–293.
9. I. G. Old, D. Margarita, and I. Saint Girons (1993) Nucleic Acids Res. **21**, 3323.
10. H. Masai and K. Arai (1988) J. Biol. Chem. **263**, 15083–15093.
11. J. A. Kobori and A. Kornberg (1982) J. Biol. Chem. **257**, 13757–13762.
12. A. Kornberg and T. Baker (1992) *DNA Replication*, 2nd ed., W. H. Freeman, New York.
13. N. Ogasawara, S. Moriya, P. G. Mazza, and H. Yoshikawa (1986) Nucleic Acids Res. **14**, 9989–9999.
14. T. Hoshino, T. McKenzie, S. Schmidt, T. Tanaka, and N. Sueoka (1987) Proc. Natl. Acad. Sci. USA **84**, 653–657.
15. S. Winston and N. Sueoka (1980) Proc. Natl. Acad. Sci. USA **77**, 2834–2838.
16. C. Bruand and S. D. Ehrlich (1995) Microbiology **141**, 1199–1200.
17. Y. Sakamoto, S. Nakai, S. Moriya, H. Yoshikawa, and N. Ogasawara (1995) Microbiology **141**, 641–644.
18. C. Bruand, A. Sorokin, P. Serror, and S. D. Ehrlich (1995) Microbiology **141**, 321–322.
19. Y. Sakakibara (1992) J. Mol. Biol. **226**, 979–987.
20. Y. Sakakibara (1992) J. Mol. Biol. **226**, 989–996.
21. Y. Sakakibara (1993) J. Bacteriol. **175**, 5559–5565.
22. Y. Sakakibara (1997) Mol. Microbiol. **24**, 793–801.
23. C. Gross (1996) In *Escherichia Coli and Salmonella: Cellular and Molecular Biology* (F. C. Neidhardt et al., eds.), American Society for Molecular Biology, Washington, DC, pp. 1382–1399.
24. K. Liberek, C. Georgopoulos, and M. Zylicz (1988) Proc. Natl. Acad. Sci. USA **85**, 6632–6636.
25. B. Bukau and G. C. Walker (1989) J. Bacteriol. **171**, 2337–2346.
26. Y. Sakakibara (1988) J. Bacteriol. **170**, 972–979.
27. M. van Asseldonk, A. Simons, H. Visser, W. M. de Vos, and G. Simons (1993) J. Bacteriol. **175**, 1637–1644.
28. K. Tilly, R. Hauser, J. Campbell, and G. J. Ostheimer (1993) Mol. Microbiol. **7**, 359–369.
29. M. Avedissian, D. Lessing, J. W. Gober, L. Shapiro, and S. L. Gomes (1995) J. Bacteriol. **177**, 3479–3484.
30. T. Ohta, K. Saito, M. Kuroda, K. Honda, H. Hirata, and H. Hayashi (1994) J. Bacteriol. **176**,

4779–4783.
31. E. Conway de Macario, C. B. Dugan, and A. J. Macario (1994) J. Mol. Biol. **240**, 95–101.
32. A. J. Caplan and M. G. Douglas (1991) J. Cell Biol. **114**, 609–621.
33. S. K. Park, S. K. Chon, and H. S. Yoo (1995) Biochim. Biophys. Acta **1262**, 87–90.
34. T. Raabe and J. L. Manley (1991) Nucleic Acids Res. **19**, 6645.
35. S. L. Gomes, J. W. Gober, and L. Shapiro (1990) J. Bacteriol . **172**, 3051–3059.
36. G. P. Michel (1993) J. Bacteriol. **175**, 3228–3231.
37. M. Tan, B. Wong, and J. N. Engel (1996) J. Bacteriol. **178**, 6983–6990.
38. J. C. Bardwell and E. A. Craig (1984) Proc. Natl. Acad. Sci. USA **81**, 848–852.
39. M. Ohki, F. Tamura, S. Nishimura, and H. Uchida (1986) J. Biol. Chem. **261**, 1778–1781.
40. M. Wetzstein, U. Volker, J. Dedio, S. Lobau, U. Zuber, M. Schiesswohl, C. Herget, M. Hecker, and W. Schumann (1992) J. Bacteriol. **174**, 3300–3310.
41. F. Narberhaus, K. Giebeler, and H. Bahl (1992) J. Bacteriol . **174**, 3290–3299.
42. G. Homuth, S. Masuda, A. Mogk, Y. Kobayashi, and W. Schumann (1997) J. Bacteriol. **179**, 1153–1164.
43. T. Eaton, C. Shearman, and M. Gasson (1993) J. Gen. Microbiol. **139**, 3253–3264.
44. H. Saito and H. Uchida (1978) Mol. Gen. Genet. **164**, 1–8.
45. U. Zuber and W. Schumann (1994) J. Bacteriol. **176**, 1359–1363.
46. K. J. Marians (1996) In *Escherichia Coli and Salmonella: Cellular and Molecular Biology* (F. C. Neidhardt et al., eds.), American Society for Molecular Biology, Washington, DC, pp. 749–763.
47. J. H. LeBowitz and R. McMacken (1986) J. Biol. Chem. **261**, 4738–4748.
48. N. Nakayama, N. Arai, M. W. Bond, Y. Kaziro, and K. Arai (1984) J. Biol. Chem. **259**, 97–101.
49. A. Wong, L. Kean, and R. Maurer (1988) J. Bacteriol. **170**, 2668–2675.
50. R. Maurer and A. Wong (1988) J. Bacteriol. **170**, 3682–3688.
51. B. L. Smiley, J. R. Lupski, P. S. Svec, R. McMacken, and G. N. Godson (1982) Proc. Natl. Acad. Sci. USA **79**, 4550–4554.
52. L. Rowen, J. A. Kobori, and S. Scherer (1982) Mol. Gen. Genet. **187**, 501–509.
53. G. L. Marks and D. O. Wood (1993) Gene **123**, 121–125.
54. J. Versalovic, T. Koeuth, R. Britton, K. Geszvain, and J. Lupski (1993) Mol. Microbiol. **8**, 343–355.
55. Z. F. Burton, C. A. Gross, K. K. Watanabe, and R. R. Burgess (1983) Cell **32**, 335–349.
56. J. G. Scaife, J. S. Heilig, L. Rowen, and R. Calendar (1979) Proc. Natl. Acad. Sci. USA **76**, 6510–6514.
57. P. Szafranski, C. L. Smith, and C. R. Cantor (1997) Biochim. Biophys. Acta **1352**, 243–248.
58. L. F. Wang and R. H. Doi (1986) Nucleic Acids Res. **14**, 4293–4307.
59. R. Metzger, D. P. Brown, P. Grealish, M. J. Staver, J. Versalovic, J. R. Lupski, and L. Katz (1994) Gene **151**, 161–166.
60. M. M. Welch and C. S. McHenry (1982) J. Bacteriol. **152**, 351–356.
61. D. Shepard, R. W. Oberfelder, M. M. Welch, and C. S. McHenry (1984) J. Bacteriol. **158**, 455–459.
62. E. D. Lancy, M. R. Lifsics, P. Munson, and R. Maurer (1989) J. Bacteriol. **171**, 5581–5586.
63. B. Sanjanwala and A. T. Ganesan (1989) Proc. Natl. Acad. Sci. USA **86**, 4421–4424.
64. Y. Huang, D. K. Braithwaite, and J. Ito (1997) FEBS Lett. **400**, 94–98.
65. P. M. Burgers, A. Kornberg, and Y. Sakakibara (1981) Proc. Natl. Acad. Sci. USA **78**, 5391–5395.

66. M. Q. Fujita, H. Yoshikawa, and N. Ogasawara (1990) Gene **93**, 73–78.
67. M. Q. Fujita, H. Yoshikawa, and N. Ogasawara (1992) Gene **110**, 17–23.
68. M. E. Armengod, M. Garcia-Sogo, and E. Lambies (1988) J. Biol. Chem. **263**, 12109–12114.
69. A. Quinones and W. Messer (1988) Mol. Gen. Genet. **213**, 118–124.
70. R. Scheuermann, S. Tam, P. M. Burgers, C. Lu, and H. Echols (1983) Proc. Natl. Acad. Sci. USA **80**, 7085–7089.
71. H. Maki, T. Horiuchi, and M. Sekiguchi (1983) Proc. Natl. Acad. Sci. USA **80**, 7137–7141.
72. M. R. Lifsics, E. D. Lancy Jr., and R. Maurer (1992) J. Bacteriol. **174**, 6965–6973.
73. S. Kim, H. G. Dallmann, C. S. McHenry, and K. J. Marians (1996) J. Biol. Chem . **271**, 21406–21412.
74. H. Xiao, V. Naktinis, and M. O"Donnell (1995) J. Biol. Chem. **270**, 13378–13383.
75. O. Yurieva, M. Skangalis, J. Kuriyan, and M. O"Donnell (1997) J. Biol. Chem. **272**, 27131–27139.
76. A. Blinkova, M. F. Burkart, T. D. Owens, and J. R. Walker (1997) J. Bacteriol. **179**, 4438–4442.
77. E. Winzeler and L. Shapiro (1996) J. Mol. Biol. **264**, 412–425.
78. N. Ohta, M. Masurekar, and A. Newton (1990) J. Bacteriol . **172**, 7027–7034.
79. L. B. Dumas, J. P. Lussky, E. J. McFarland, and J. Shampay (1982) Mol. Gen. Genet. **187**, 42–46.
80. J. A. Prendergast, L. E. Murray, A. Rowley, D. R. Carruthers, R. A. Singer, and G. C. Johnston (1990) Genetics **124**, 81–90.
81. D. R. Evans, R. A. Singer, G. C. Johnston, and A. E. Wheals (1994) FEMS Microbiol. Lett **116**, 147–153.
82. A. M. Merchant, Y. Kawasaki, Y. Chen, M. Lei, and B. K. Tye (1997) Mol. Cell. Biol. **17**, 3261–3271.
83. M. E. Budd, W. C. Choe, and J. L. Campbell (1995) J. Biol. Chem. **270**, 26766–26769.
84. M. E. Budd and J. L. Campbell (1997) Mol. Cell. Biol. **17**, 2136–2142.
85. D. F. Fiorentino and G. R. Crabtree (1997) Mol. Biol. Cell. **8**, 2519–2537.

Suggestion for Further Reading

86. A. Kornberg and T. Baker (1992) *DNA Replication*, 2nd ed., W. H. Freeman, New York.

DNA Glycosylases

Base excision repair is the system for repairing abnormal bases in DNA. The abnormal bases and simple base lesions are removed from DNA by the combined actions of DNA glycosylases (1-3) and AP (apurinic/apyrimidinic) endonucleases. The basic reaction carried out by glycosylases is the cleavage of the glycosylic bond joining the base to deoxyribose. Some of the glycosylases cleave both the glycosylic bond and the phosphodiester bond 3′ to the resulting AP site in a more or less concerted reaction. Hence, these DNA glycosylases have been classified as either “pure” glycosylases or as glycosylase/AP lyases.

1. Uracil DNA Glycosylases

Uracil in DNA arises from two sources: (i) direct misincorporation into DNA in place of thymine by **DNA polymerases** and (ii) deamination of cytosine. Most DNA polymerases cannot discriminate between dTTP and dUTP; hence the rates of incorporation of thymine and uracil into DNA are proportional to the concentrations of the corresponding dNTPs in the nucleotide pool. The dTTP:dUTP ratio is about 1000:1, so about one uracil is incorporated into each Okazaki fragment during DNA replication. The second source of uracil in DNA is that produced by deamination of cytosine. Cytosine deaminates at normal pH and temperature at a rate of $10^{-16}s^{-1}$ for double-stranded DNA and at a rate of $10^{-10}s^{-1}$ for single-stranded DNA. The deamination rate is greatly accelerated by low pH, high temperature, and oxidants. Uracil in DNA is removed by uracil glycosylases. Two have been identified in *Escherichia coli* and in humans (4): (i) uracil glycosylase and (ii) the double-strand-specific thymine glycosylase, which has also been shown to act on uracil residues in double-stranded DNA.

1.1. Uracil DNA Glycosylase (UDG)

The classic UDG is a 25- to 30-kDa monomeric protein with no cofactor or metal ion requirement. The enzyme is highly conserved between prokaryotes and eukaryotes, and it is the major uracil glycosylase in most organisms examined. The enzyme acts on single- and double-stranded DNA with equal efficiency. UDG is one of the several known DNA modification/repair enzymes that during catalysis flip out the base from inside the helix into a cavity within the enzyme (5-7). After cleaving off the base, the enzyme dissociates from DNA. This UDG has no detectable AP lyase activity.

1.2. Thymine–DNA Glycosylase (TDG)

In humans, this enzyme specifically removes thymines from T-G mismatches and uracils from U-G mismatches within double-stranded DNA (4-6). It is thought that the major source of mismatched thymines in mammalian cells is deamination of 5-methylcytosine bases, which creates a T-G mismatch. Because about 20% of cytosine bases are methylated in mammalian cells, even low-frequency deamination of MeCyt generates high levels of T-G mismatches. Hence it is likely that TDG plays an important role in preventing mutations and maintaining genomic stability.

Even though DNA glycosylases in general, and UDG in particular, are considered to be highly specific enzymes, recent work has shown that UDG removes from double-stranded DNA many oxidized pyrimidines generated by ionizing radiation, and even normal pyrimidines (7). The $\boldsymbol{K_m}$ and k_{cat} catalytic parameters for removal of these lesions were found to be within the physiologically relevant range, so it is possible that UDG and TDG also perform auxiliary functions in repairing DNA damage caused by oxidative stress, in addition to their primary roles.

2. Thymine Glycol DNA Glycosylase

The prototype of thymine glycol DNA glycosylases is *E. coli* endonuclease III (8). It is a 40-kDa polypeptide chain with a [4Fe–4S] cluster (9) (see Iron–Sulfur Proteins). This enzyme has been detected in various organisms by one of its multiple activities and, accordingly, was given various names: endonuclease III, UV endonuclease, redoxendonuclease, and others. The enzyme has been highly conserved during evolution. Enzymes with sequence and functional homology to *E. coli* endonuclease III exist in yeast and humans (10). These enzymes have a relatively wide substrate spectrum and act on ring-saturated, ring-contracted, and ring-rearranged pyrimidines. The crystal structure of *E. coli* endonuclease III has been determined (11). The enzyme flips out of damaged base into the active site and cleaves the glycosylic bond and the 3′ phosphodiester bond of the resulting AP site, before dissociating from DNA. The iron–sulfur center within the protein has no catalytic role. Catalysis does not involve **redox** chemistry, but it occurs by a simple lyase reaction involving the ϵ-amino group of a lysine residue.

3. Methylpurine DNA Glycosylase (MPG)

The MPG enzyme was originally identified as “3-methyladenine DNA glycosylase”; hence it is also referred to by that name (12, 13). There are two enzymes in *E. coli* with MPG activity, one that has a narrow substrate spectrum called TagI, and a second, TagII, with a much greater substrate range (14). The eukaryotic enzymes, including that in humans, are more similar to TagII with respect to their substrate preference than to TagI of *E. coli*. MPGs act on 3-methyladenine, 7-methyladenine, and O^4-methylthymine. They clearly also repair alkylated bases other than methyl purines, and hence “alkylated purine DNA glycosylase” would perhaps be a more appropriate name for this group of enzymes. They have no overt AP lyase activity.

4. 8-Oxoguanine Glycosylase

This enzyme was first identified as “formamidinopyrimidine DNA glycosylase” for the name of the substrate (FAPy) that is generated from guanine by ionizing radiation (15). Subsequently, it was found that the enzyme is very active on 8-oxoguanine, which is generated in vast quantities in the DNA by ionizing radiation and by oxidative stress. The enzyme is a 20-kDa monomer with no requirement for cofactors or divalent cations. The enzyme is widespread in the biological world, having been found in *E. coli*, yeast, and humans. It is a glycosylase and an AP lyase. In addition to cleaving the 3′ phosphodiester bond by b-elimination, it also cleaves the 5′ phosphodiester bond by d-elimination. Thus, this is a unique glycosylase that performs glycosylase/b-d-elimination by a concerted mechanism; in doing so, it generates a one-nucleotide gap.

5. Pyrimidine Dimer Glycosylase

This enzyme has been found in two sources thus far: **T4 phage** and *Micrococcus luteus*. The enzymes from the two sources share sequence homology and are presumed to act by the same mechanism. Both are 18-kDa monomers, with no cofactor and no requirement for divalent cations. The enzyme cleaves the glycosylic bond of the 5′ base of cyclobutane dimer and the intradimer phosphodiester bond by b-elimination. Thus, the cleavage generates a 3′-OH end and a 5′ terminus with a dangling pyrimidine dimer (16). The 5′ end must be further processed by a 5′- to 3′-exonuclease before DNA polymerase can produce a ligatable product. The structure of T4 endonuclease V complexed with substrate indicates that the enzyme flips out one of the adenine bases opposite the pyrimidine dimer (17). This binding mechanism explains the high specificity for pyrimidine dimers in double-stranded DNA.

6. A-G Mismatch DNA Glycosylase

The 8-oxoguanine lesion is a frequent product of ionizing radiation and oxidative damage to DNA. Most often, 8-oxoguanine mispairs with adenine during replication. The resulting adenine-8-oxoguanine mispair is the substrate for A-G mismatch DNA glycosylase (18). This 30-kDa enzyme has limited sequence similarity to endonuclease III (thymine glycol endonuclease) and also has a [4Fe–4S] center. The protein in *E. coli* is encoded by the *mutY* gene; hence the enzyme is also referred to as MutY glycosylase. The enzyme also cleaves A residues in A-G mismatches, albeit at a lower efficiency than A-8-oxoG mismatches. In addition to glycosylase activity, it also possesses AP lyase activity and thus cleaves the 3′ glycosylic bond 3′ to an AP site, either as part of glycosylase/AP lyase concerted reaction or as an independent AP lyase acting on an isolated AP site.

Bibliography

1. T. Lindahl (1974) Proc. Natl. Acad. Sci. USA **71**, 3649–3653.
2. T. Lindahl (1976) Nature **259**, 64–66.
3. J. Laval (1977) Nature **269**, 828–832.
4. P. Gallinari and J. Jiricny (1996) Nature **383**, 735–738.
5. S. Klimasauskas, S. Kumar, R. J. Roberts, and X. Cheng (1994) Cell **76**, 357–369.

6. T. E. Barrett, R. Savva, G. Panayotou, T. Barlow, T. Brown, J. Jiricny, and L. H. Pearl (1998) Cell **92**, 117–129.
7. K. G. Berdal, R. F. Johansen, and E. Seeberg (1998) EMBO J. **17**, 363–367.
8. B. Demple and S. Linn (1980) Nature **287**, 203–208.
9. R. P. Cunningham, H. Asahara, J. F. Bank, C. P. Scholes, J. C. Salerno, K. Surerus, E. Munck, J. McCracken, J. Peisach, and M. H. Emptage (1988) Biochemistry **28**, 4450–4455.
10. T. P. Hilbert, W. Chaung, R. J. Boorstein, R. P. Cunningham, and G. W. Teebor (1997) J. Biol. Chem. **272**, 6733–6740.
11. C. Kuo, D. E. McRee, C. L. Fisher, S. F. O''Handley, R. P. Cunningham, and J. A. Tainer (1992) Science **258**, 434–440.
12. Y. Nakabeppu, H. Kondo, and M. Sekiguchi (1984) J. Biol. Chem. **259**, 13723–13729.
13. G. Evensen and E. Seeberg (1982) Nature **296**, 773–775.
14. J. Labahn, O. D. Scharer, A. Long, K. Ezaz-Nikapy, G. L. Verdine, and T. E. Ellenberger (1996) Cell **86**, 321–329.
15. S. Boiteux, T. R. O''Connor, and J. Laval (1987) EMBO J. **6**, 3177–3183.
16. W. A. Haseltine, L. K. Gordon, C. P. Lindan, R. H. Grafstrom, N. L. Shaper, and L. Grossman (1980) Nature **285**, 634–641.
17. D. G. Vassylyev, T. Kashiwagi, Y. Mikami, M. Ariyoshi, S. Iwai, E. Ohtsuka, and K. Morikawa (1995) Cell **83**, 773–782.
18. K. G. Au, S. Clark, J. H. Miller, and P. Modrich (1989) Proc. Natl. Acad. Sci. USA **86**, 8871–8881.

Suggestions for Further Reading

19. K. Sakumi and M. Sekiguchi (1990) Structure and function of DNA glycosylases. Mutat. Res. **236**, 161–172.
20. E. Seeberg, L. Eide, and M. Bjoras (1995) The base excision repair pathway. Trends Biochem. Sci. **20**, 391–397.
21. R. J. Roberts (1995) On base flipping. Cell **82**, 9–12.

DNA Helicase

Transient production of single-stranded **DNA** from the double helix is necessary prior to several DNA metabolic reactions, such as DNA replication, DNA repair, recombination, and transcription. DNA helicases unwind duplex DNA into two single DNA strands, ie, they disrupt the hydrogen bonds of double helical DNA by successively translocating along DNA, using the energy from hydrolysis of nucleoside triphosphates (NTP, usually ATP). Since the NTP hydrolysis is coupled to DNA binding, all helicases have DNA-dependent NTPase activity (see ATPase). Due to the involvement of helicases in various cell functions, most organisms have more than 10 helicases, and indeed, at least 12 helicases have been identified in *Escherichia coli* since the discovery of helicase I in 1976 (1). During DNA replication, a specific class of helicase unwinds duplex DNA ahead of the **replication fork**, which is the so-called "replicative helicase" and indispensable for cell proliferation. In addition to multiple helicases in cells, **bacteriophages** and eukaryotic **viruses** have their own helicases, which function in their specific propagation processes.

Unwinding of a DNA duplex by helicases is assayed independently of their particular DNA metabolic function, using partial duplex DNA that carries a short DNA annealed to a longer single-stranded DNA. The unwinding activity is manifested by the release of the short DNA from the duplex, which is detected as a faster-migrating DNA band in gel electrophoresis. The unwinding reaction proceeds in a unique direction defined as either a 5′-3′ or 3′-5′polarity with respect to the strand of DNA on which the helicase is bound. The polarity used to classify the enzyme (Table 1) is determined by similar unwinding assays using two duplex DNA carrying either 5′ or 3′ extensions of single-stranded DNA (Fig. 1).

Figure 1. Helicase assay and determination of the polarity by electrophoresis.

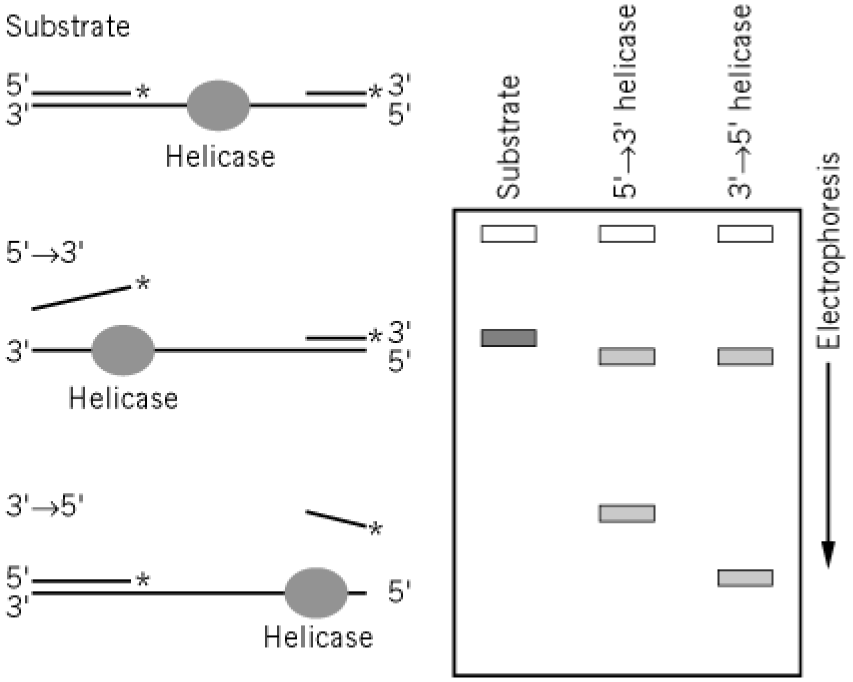

Table 1. DNA Helicases and Their Properties

Function	Helicase	Assembly State[a]	Polarity[a]	Source
Replication	DnaB	Heaxmer	$5' \rightarrow 3'$	*E. coli*
	T4 gene 41	Haxamer	$5' \rightarrow 3'$	T4 phage
	T7 gene 41	Hexamer	$5' \rightarrow 3'$	T7 phage
	SV40 T antigen	Hexamer	$3' \rightarrow 5'$	SV40 virus
	DNA2	Nd	$3' \rightarrow 5'$	Yeast
	Rep	Dimer	$3' \rightarrow 5'$	*E. coli*
Repair	RuvB	Hexamer	$5' \rightarrow 3'$	*E. coli*
	RecBCD	Trimer (hexamer)	Nd	*E. coli*
	RAD26	Nd	Nd	Yeast

	(CSB/ERCC6)			(human)
Repair and transcription	RAD25 (XPB/ERCC3)	Nd	$3' \rightarrow 5'$	Yeast (human)
	RAD3 (XPD)	Nd	$5' \rightarrow 3'$	Yeast (human)
Transcription termination	Rho	Hexamer	$5' \rightarrow 3'$	*E. coli*
Conjugation	Helicase I/Tra I	Oligomer	$5' \rightarrow 3'$	F plasmid
Unknown	Helicase III	Oligomer	$5' \rightarrow 3'$	*E. coli*
	ATPase B	Nd	$5' \rightarrow 3'$	Mouse

[a] Nd = not determined.

Comparison of the primary structures of helicases revealed the presence of conserved motifs, which define several classes of the helicase family (2). A subfamily of helicases carry seven conserved motifs, but other subfamilies, which include most hexameric helicases (see below), retain only subsets of the motifs. Among the motifs, two called “A” and “B” are commonly detected in all helicases and function as a **nucleotide-binding** site. These two motifs are necessary but not sufficient for helicase functions, since the B motif corresponds to the so-called **DEAD** or DExH box, which is also observed in several RNA-binding proteins. Therefore, many putative DNA or RNA helicases are proposed on the basis of just their predicted primary structures, without the identification of actual biochemical activities.

Although the precise mechanisms of their unwinding action are not understood, their characteristic oligomeric states, mainly as dimer or hexamer, propose simple explanations for their biochemical reactions. The dimeric form, such as the *E. coli* Rep helicase, provides an unwinding mechanism promoted by a rolling or inchworm movement, using two DNA-protein contacts. In this case, two DNA-binding sites alternate binding of single-stranded and duplex DNA, catalyzing unwinding. In the case of hexameric helicases, such as DnaB, T7 phage gene4 protein, and SV40 virus large T Antigen, they have a common ring structure, with a central hole through which DNA passes, as analyzed by electron microscopy. It is still unclear how DNA passes through the hexamer and how the unwinding reaction occurs within the molecule. Interestingly, these hexameric helicases are often members of large functional protein complexes, as in the case of typical replicative helicases, and are expected to have roles as motor molecules that may simultaneously unwind the DNA and transfer the protein complexes along DNA.

Replicative helicases have been identified only from bacteria, bacteriophage, and viruses, not from eukaryotic cells. This is mainly because there has not been any reliable *in vitro* replication system in eukaryotes to confirm whether a helicase of interest is functional in replication or not. A yeast essential gene, *dna2*, has been identified as a DNA replication mutant by screening using a permeabilized cell replication assay (3). Since this gene product has five conserved helicase motifs and actually exhibits helicase activity, it is a candidate for the yeast replicative helicase, although there is insufficient direct evidence. The known replicative helicases often have close connections with other replication activities and sometimes possess additional characteristics; eg, primase activity in T7 gene4 helicase and replication origin binding in SV40 T antigen. T antigen also interacts physically with several replication proteins and cooperatively promotes the initiation of viral DNA replication. The *E. coli* replicative helicase, DnaB, exhibits the closer physical and functional link with the replication fork components, and the rate of helicase movement is coordinately stimulated by interaction with the DNA polymerase (4).

Recent improvements in identifying the causative genes of many human heritable diseases revealed that the defects of certain helicase functions cause several human diseases, including Xeroderma pigmentosum, Cockayne's syndrome, Bloom's syndrome Werner's syndrome, and ATR-X syndrome (5). These diseases are apparently related to the defects of genes whose functions are involved in nucleotide excision repair, recombination, replication fidelity, and chromosome transmission, and they exhibit cancer-prone **phenotypes** because of the difficulty in maintaining genome integrity. Such human disease-related helicases are conserved among eukaryotes, and their counterparts are often identified as RAD genes in yeast (Table 1).

Bibliography

1. M. Abdel-Monem et al. (1976) Eur. J. Biochem. **65**, 441–449.
2. A. E. Gorbalenya and E. V. Koonin (1993) Curr. Opin. Struct. Biol. **3**, 419–429.
3. M. E. Budd and J. L. Campbell (1995) Proc. Natl. Acad. Sci USA **92**, 7642–7646.
4. S. Kim et al. (1996) Cell **84** 643–650.
5. T. M. Lohman and K. P. Bjornson (1996) Ann. Rev. Biochem. **65**, 169–214.

DNA Libraries

Recombinant DNA technologies developed in the early 1970s (1-6) form the core of all DNA-based molecular combinatorial libraries. Genetic sequences of interest are recombined with a replication-competent DNA vector, such as a plasmid or bacteriophage. Each individual genetic sequence fragment is enzymatically ligated into a receptive vector, to form a unique recombinant clone. The population of individual recombinants is then reintroduced into an appropriate host cell in order to constitute a functional library. Modern cloning technologies allow the preparation of up to 10^9 recombinants in a single library, with greater numbers requiring a substantial scale-up that is beyond the resources of most researchers.

A different type of recombinant design is seen in some oligonucleotide-based libraries that require no vector for their survival (7-9). The replication elements in these oligonucleotides are built into their sequences in the form of primer binding sites. These libraries can be amplified *in vitro* by the polymerase chain reaction (PCR) using additional oligonucleotides capable of annealing to the termini of the library molecules (10). Other amplification technologies can be used to replicate oligonucleotide libraries, including the ligase chain reaction (11), self-sustained sequence replication (12), and strand displacement amplification (13). Because oligonucleotide-based libraries are prepared chemically and require no cloning steps, they can achieve very high sequence complexities on the order of 1×10^{15} different species or more.

Recent technological advances have introduced a novel type of oligonucleotide-based DNA library in which defined sets of sequences are synthesized chemically and displayed in a two-dimensional array. A highly publicized approach developed by Affymetrix employs photolithographic masking procedures to construct very high-density oligonucleotide arrays on silicon chips. One such product developed by Affymetrix is the p53 chip, which displays a large number of common disease-related p53 gene mutations represented as oligonucleotide sequences. Any clinical specimen can be rapidly assayed over this chip by hybridization of nucleic acids in order to determine the genotype of p53 genes expressed by the specimen tissue. The development of further disease-related gene chips has enormous potential to carry clinical diagnosis to the molecular level where appropriate highly individualized therapies may be ascertained (eg, pharmacogenomics (14)) (see DNA Chips).

The intended use of recombinant libraries determines numerous aspects of library design and construction. The vector provides essential functions, such as an **origin of replication**, that enable replication and survival of the recombinant clone within the host cell. A selectable marker such as an antibiotic-resistance gene provided by the vector provides a means to eliminate any cells that have not taken up a recombinant clone. Unique restriction enzyme sites in the vector allow efficient insertion of foreign DNA fragments into defined contexts. Various expression control elements engineered into the vector permit selective expression of RNA or protein encoded by the cloned DNA fragment. Vectors that contain certain viral signal sequences can be packaged into viral particles in infected cells, thereby enabling highly efficient viral-mediated gene transfer into noninfected cells. In addition, cloning vectors often provide genetic markers that confer desirable properties upon the expression products. For example, DNA encoding an open reading frame may be fused in frame to the *C*-terminus of glutathione-S--transferase (GST) (15). The resulting GST-fusion protein can then be easily purified by affinity chromatography over **glutathione**-agarose resin. Finally, “shuttle” vectors contain multiple origins of replication, supporting growth of the recombinant clone in bacteria as well as in relevant experimental systems, such as yeast and mammalian cells.

Plasmid vectors are by far the most commonly used cloning vectors for relatively short DNA fragments ranging from several hundred to several thousand nucleotides. This size range is sufficient to carry the coding sequence portions of most genes. However, because genes from many organisms contain varying amounts of nonexpressed intervening sequences (**introns**), cloning of complete genes or gene clusters often requires the use of vectors that can accommodate DNA inserts exceeding 10 kilobase pairs (kbp) or more. The lambda phage particle can package approximately 50 kbp of DNA, but the lambda phage itself requires at least 30 kbp of essential phage genes for viability, limiting its insert carrying capacity to no more than 20 kbp. Some improvement is seen with “cosmid” vectors, which are composite vectors containing both plasmid replication elements and the lambda phage cos packaging signal. One type of cosmid vector can package up to 40 kbp of foreign DNA into lambda phage capsids (16). Gene mapping studies and investigations into chromosome structure require cloning vectors with even larger capacity, called *artificial chromosomes* (ACs). Thus, YACs are yeast artificial chromosomes that contain yeast centromere, telomere, and **autonomous replication sequence** (ARS) elements, as well as appropriate yeast selection markers (17, 18). YACs allow the cloning and maintenance of fragments of genomic DNA up to several hundred kilobase pairs in length. Similarly, ACs have been constructed that allow introduction of large foreign sequences into bacteria (called BACs) and mammalian cells (called MACs) (19).

DNA libraries may be categorized according to the source and the context of foreign DNA within the library. Genomic libraries often contain relatively large DNA inserts in phage or AC vectors. These inserts are typically not expressed, although there are exceptions. **cDNA library** inserts are derived from DNA copies of messenger RNA that are generated by the enzyme **reverse transcriptase**. mRNA is a useful source for protein-coding DNA sequences, as the nonexpressed intervening sequences have been removed through the process of pre-mRNA processing. Thus, protein-coding sequences that are interspersed throughout a gene are arranged contiguously within a cDNA, whereupon it becomes trivial to infer the encoded protein sequence using the genetic code. cDNA libraries usually provide some means to express open reading frames encoded within the DNA insert, both as RNA transcripts and protein translation products. Expression libraries may, however, also be based on genomic DNA and oligonucleotides, either cloned into a vector or as linear molecules that can be amplified *in vitro*.

“Virtual libraries” are a relatively new concept in DNA libraries. Sequence information emerging from large-scale sequencing projects is incorporated into ever-expanding computer databases, where cross-references can be established between any sequence and its associated functional information. Thus, a database can serve as a virtual library that can greatly expedite the identification and recovery of molecules with desired properties. Examples of public sequence databases include

GenBank and the Cancer Genome Anatomy Project (CGAP). Such virtual libraries enable tasks that once required working with actual molecules *in vitro* to be accomplished much more rapidly *in silico* using only the information contained within those molecules. For example, a scientist that identifies a sequence fragment of a protein associated with a particular disease can, through the genome databases, identify a full-length DNA sequence associated with that protein. The DNA sequence in turn provides a great deal of useful information, including the likely sequence and structure of the protein, as well as a set of primer sequences that can be used to clone the full-length gene representing that protein. Many modern database resources also maintain banks of cosmid or AC clones that are (or will be) correlated with every sequence in the database. Such resources make it possible to move from an unknown protein band obtained through gel electrophoresis to a cloned and expressed gene for that protein in a matter of days—a task that often required several years to accomplish only a decade ago.

See also Combinatorial Libraries, Libraries, Combinatorial Synthesis, Affinity Selection, Genomic Libraries, cDNA Libraries, Expression Libraries, Peptide Libraries, and Phage Display Libraries.

Bibliography

1. R. M. Lawn, E. F. Fritsch, R. C. Parker, G. Blake, and T. Maniatis (1978) Cell **15**, 1157–1174.
2. S. N. Cohen, A. C. Chang, H. W. Boyer, and R. B. Helling (1973) Proc. Natl. Acad. Sci. USA **70**, 3240–3244.
3. N. E. Murray and K. Murray (1974) Nature **251**, 476–481.
4. M. Thomas, J. R. Cameron, and R. W. Davis (1974) Proc. Natl. Acad. Sci. USA **71**, 4579–4583.
5. T. Maniatis, R. C. Hardison, E. Lacy, J. Lauer, C. O"Connell, D. Quon, G. K. Sim, and A. Efstratiadis (1978) Cell **15**, 687–701.
6. G. K. Sim, F. C. Kafatos, C. W. Jones, M. D. Koehler, A. Efstratiadis, and T. Maniatis (1979) Cell **18**, 1303–1316.
7. C. Tuerk and L. Gold (1990) Science **249**, 505–510.
8. A. D. Ellington and J. W. Szostak (1990) Nature **346**, 818–822.
9. D. E. Tsai, D. S. Harper, and J. D. Keene (1991) Nucleic Acids Res. **19**, 4931–4936.
10. K. Mullis, F. Faloona, S. Scharf, R. Saiki, G. Horn, and H. Erlich (1986) Cold Spring Harb. Symp. Quant. Biol. **51**, 263–273.
11. F. Barany (1991) Proc. Natl. Acad. Sci USA **88**, 189–193.
12. R. R. Breaker and G. F. Joyce (1994) Proc. Natl. Acad. Sci. USA **91**, 6093–6097.
13. G. T. Walker, M. S. Fraiser, J. L. Schram, M. C. Little, J. G. Nadeau, and D. P. Malinowski (1992) Nucleic Acids Res. **20**, 1691–1696.
14. A. Persidis (1998) Nat. Biotechnol. **16**, 209–10.
15. D. B. Smith and K. S. Johnson (1988) Gene **67**, 31–40.
16. B. Hohn and J. Collins (1980) Gene **11**, 291–298.
17. P. Guzman and J. R. Ecker (1988) Nucleic Acids Res. **16**, 11091–11105.
18. A. Coulson, R. Waterston, J. Kiff, J. Sulston, and Y. Kohara (1988) Nature **335**, 184–186.
19. M. Ikeno, B. Grimes, T. Okazaki, M. Nakano, K. Saitoh, H. Hoshino, N. I. McGill, H. Cooke, and H. Masumoto (1998) Nat. Biotechnol. **16**, 431–439.

DNA Ligase

1. Physiological Functions

Several fundamental biological processes involve one or more steps in which an enzyme, DNA ligase, catalyzes the covalent joining of one piece of **DNA** to another (1-3). For example, DNA altered spontaneously or by environmental causes is restored to its original base sequence by DNA repair. DNA is duplicated by DNA replication and rearranged by homologous recombination. All these processes require DNA ligase activity to link preformed pieces of DNA to one another.

During one form of DNA repair, damaged nucleotides are removed by enzymes to leave ultimately a gap in one strand of the duplex DNA, which is then filled by a **DNA polymerase** to form a product with a discontinuity (nick) between two adjacent nucleotides in the phosphodiester backbone. Likewise, semidiscontinuous DNA replication leads to the formation of Okazaki Fragments that abut one another on the complementary parental DNA template strand so that a nick exists between their termini. Finally, pieces of DNA from two different chromosomes become associated during recombination so that similar nicked duplexes are formed in each chromosome. DNA ligase catalyzes the covalent joining of the DNA strands to seal the nicks and form intact, recombined duplexes. The enzyme is involved in other functions as well; whenever two pieces of DNA must be covalently joined or a DNA molecule circularized, DNA ligase probably catalyzes the reaction.

DNA fragments with appropriate termini that are aligned on a complementary strand so that their ends are juxtaposed can be joined by DNA ligase to form a phosphodiester bond (Fig. 1). For effective joining, the two strands (A and B) must be directly abutted without a gap (no missing base pairs) and must also have a 3′-OH on strand A and a 5′-PO_4 on strand B. The 3′-hydroxyl (-OH) of fragment A is ligated to the 5′-PO_4 of B to form a 3′ → 5′ phosphodiester bond. These two strands are abutted by base pairing with a complementary, intact strand (C). Since the formation of a phosphodiester bond is endergonic, ATP or NAD^+, depending on the source of the enzyme, acts as a cofactor to supply the energy.

Figure 1. The overall DNA ligase reaction. A nick with a 3′-hydroxyl (━OH) on strand (A) adjacent to a 5′-phosphate (P━) terminated strand (B) on a complementary strand (C) is converted to an intact phosphodiester bond (━P━). ATP or NAD^+ supply the energy for bond formation (see text), and PP_i or NMN, respectively, is the other product of the reaction. Long horizontal lines represent DNA strands with the polarity indicated; vertical lines represent base pairs.

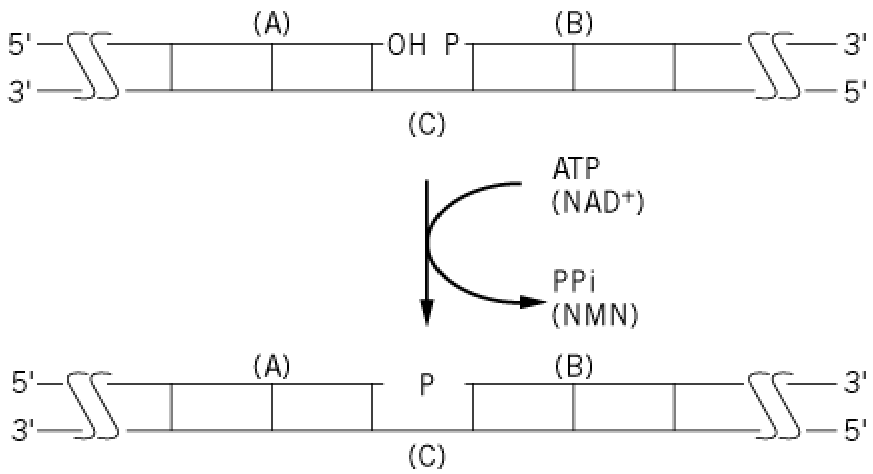

2. Distribution

All free-living organisms are believed to produce one or more DNA ligases. Until recently, **bacteria** were thought to contain a single DNA ligase that performed all their DNA joining reactions (see text below). **Yeast** appears to have two DNA ligases. Some **bacteriophage** and animal **viruses** also encode DNA ligases. Higher **eukaryotes** probably contain four different DNA ligases that are specialized to perform particular tasks. The DNA ligases from animal and **plant** cells, **archaebacteria**, bacteriophage, and animal viruses use ATP as the energy-supplying cofactor for the ligation reaction. **Eubacteria**, with a single reported exception, use NAD^+ for this purpose. Cheng and Shuman (4) have shown that *Haemophilus influenzae* contains an ATP-dependent ligase, in addition to the expected NAD^+-dependent enzyme. Whether this finding represents an anomaly in the general cofactor-utilization classification scheme awaits the demonstration of additional ATP-dependent activities in other eubacteria. Searches of the sequences of the genomes of several other eubacteria reveal potential open reading frames that share homologies with both the expected NAD^+-dependent enzymes and with ATP-dependent DNA ligases. It will be important to determine whether any of these organisms also produce ATP-dependent DNA ligases and, if so, how they relate functionally to the NAD^+-dependent enzymes.

DNA ligase is essential because of its role in the crucial DNA transactions of the cell. Cells containing **conditional** mutants of the enzyme in *Escherichia coli* are lethal when the ligase activity is severely inactivated. They display abnormal replication, repair, and recombination **phenotypes**. Because *E. coli* cells normally contain many copies of the enzyme, small amounts of residual activity can maintain viability. The enzymes in bacteria seem to act independently in their multiple roles, that is, not in specific association with other proteins. For example, the NAD^+-dependent enzyme of *E. coli* can substitute for the inactivated bacteriophage ATP-dependent DNA ligase of an infecting bacteriophage. In eukaryotes, specific proteins may associate with DNA ligases to form complexes involved in particular functions.

3. Properties

The DNA ligases comprise single polypeptide chains with molecular weights ranging from approximately 40 kDa to greater than 100 kDa, and they probably act as monomers. The **genes** of many DNA ligases have been sequenced, and several have been overexpressed and the enzymes isolated, purified, and characterized in detail. Several bacterial and bacteriophage DNA ligases are commercially available. Analyses of the sequences of genes encoding DNA ligases reveals conserved amino-acid sequence motifs among the ATP-dependent enzymes and other conserved regions among the NAD^+-dependent group. Sequence comparisons also reveal that the ATP-dependent DNA ligases are part of a superfamily that includes RNA ligases and **RNA capping** enzymes (5). The structure of only the bacteriophage T7 DNA ligase, a small, ATP-dependent enzyme, has been determined (6). It forms a bilobal structure that is reminiscent of the structures of the methyltransferases used for DNA modification.

4. Mechanism

Phosphodiester bond formation between template-aligned, abutted 3′-OH and 5-PO_4 termini proceeds in three steps, with the formation of two covalent intermediates (Fig. 2). One of these intermediates involves the enzyme, the other the DNA. In the first step of the reaction, which can occur in the absence of DNA, the enzyme reacts with ATP (or NAD^+) to form a covalent enzyme–AMP complex. The adenylyl group is joined to the ε-amino group of a lysine residue at the active site by a phosphorus–nitrogen (phosphoamide) linkage that has a large **free energy** of hydrolysis (Fig. 2a). If ATP is the cofactor, PP_i is released; if NAD^+ serves as the cofactor, nicotinamide mononucleotide (NMN) is released in this step. The free energy of hydrolysis of a phosphoanhyride bond in the ATP or NAD^+ is used to form the enzyme-bound, activated adenylyl group.

Figure 2. The DNA ligase reaction mechanism. (**a**) The enzyme [E–NH_2] is adenylylated on a specific lysine residue [E–PA] by reaction with ATP (or NAD^+) with the release of PP_i (or NMN). (**b**) The DNA is adenylylated [AP━P━] by transfer of the adenylyl group from the enzyme to the 5′-PO_4 at the nick. (**c**) The enzyme catalyzes an attack of the 3′-OH at the nick on the activated phosphate, to form the 3′ → 5′ phosphodiester bond and release the enzyme. Long horizontal lines represent DNA strands with the polarity indicated; vertical lines represent base pairs.

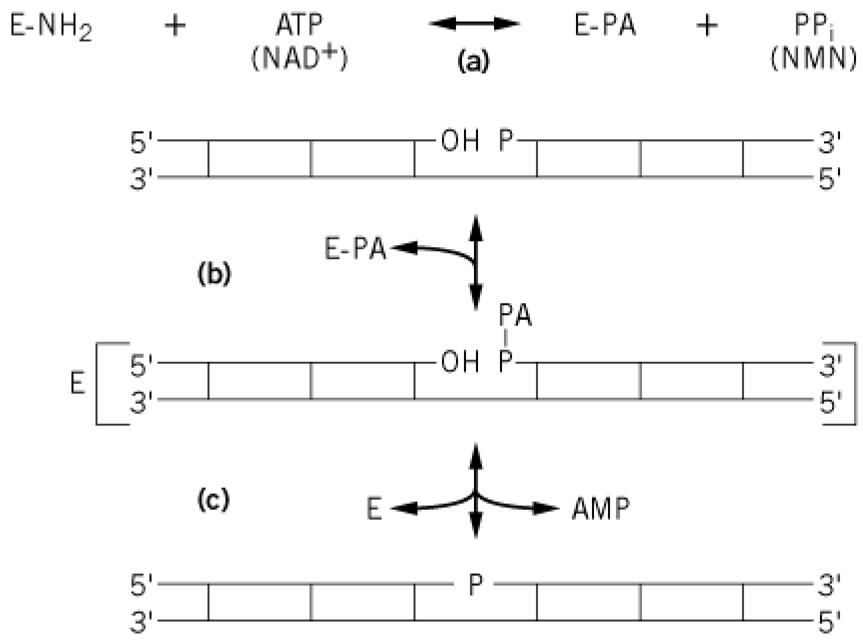

In the next step, the second covalent intermediate is formed when the adenylyl group is transferred from the enzyme to the terminal 5′-PO_4 at the DNA nick, to form an AMP (5′ → 5′) DNA phosphoanhydride linkage (Fig. 2b). In the final step of the reaction, which requires the free (unadenylylated) form of the enzyme, the AMP is displaced from the DNA by a nucleophilic attack of the 3′-OH of the adjacent DNA fragment to form the phosphodiester bond and to release the AMP from the DNA Fig. 2c).

Both covalent intermediates in the reaction have been isolated and are kinetically competent in the reaction. The reaction requires a divalent metal cation, most likely Mg^{2+} in the cell. Steady-state kinetic analysis of the *E. coli* enzyme shows that it follows ping-pong kinetics—consistent with the described mechanism (see Kinetic Mechanisms, Enzyme). The overall reaction is reversible. The first step is readily reversed, as indicated by the facile ATP–PP_i or NAD^+ NMN **isotope exchange reactions** catalyzed. The enzyme also catalyzes an AMP-dependent nicking–closing (topoisomerase) activity that will relax positively or negatively supercoiled DNA (see DNA Topology), indicating that the second step is also reversible.

The nature of the ends of DNA fragments affects the ability of DNA ligase to join them together. For example, duplex substrates with so called cohesive, “sticky” ends are readily joined by all DNA ligases (Fig. 3**a**). These substrates are formed from DNA fragments that contain short, complementary single-stranded extensions at their termini; two or more such nucleotides are required for efficient joining. These extensions can be of either strand, so long as they allow the two duplexes to anneal to one another and provide the requisite abutted 3′-OH and 5′-PO_4 termini. The ends of these duplex fragments hybridize to form a substrate in which there is a ligatable discontinuity in each strand. In essence, the complementary strands serve to convert the intermolecular joining of the two DNA pieces into an intramolecular reaction by bringing them together. Another class of duplex substrates, specifically, those with **blunt ends** (Fig. 3**b**), which have no single-stranded extensions, are much less efficiently ligated, because the fragments to be joined are not brought into proximity by a template strand. The efficiency of this intermolecular blunt-end joining reaction depends greatly on the particular ligase. Bacteriophage T4 ligase performs the reaction best and has been extensively used for this purpose, whereas the enzyme from *E. coli* will join blunt-end duplexes only in the presence of excluded-volume agents, such as **polyethylene glycol**. Other DNA structures, such as those with noncomplementary, protruding ends or nonabutted fragments creating a gap on a template strand, can be ligated, but inefficiently. T4 DNA ligase is again more tolerant of these unusual structures than is the bacterial enzyme.

Figure 3. Common DNA ends joined by DNA ligase. (**a**) Fragments with a 5′ extension (shown here) or with a 3′ extens and complementary bases (sticky ends) form a ligatable structure. (**b**) Ligation of blunt ends. Long horizontal lines repre DNA strands with the polarity indicated; vertical lines represent base pairs.

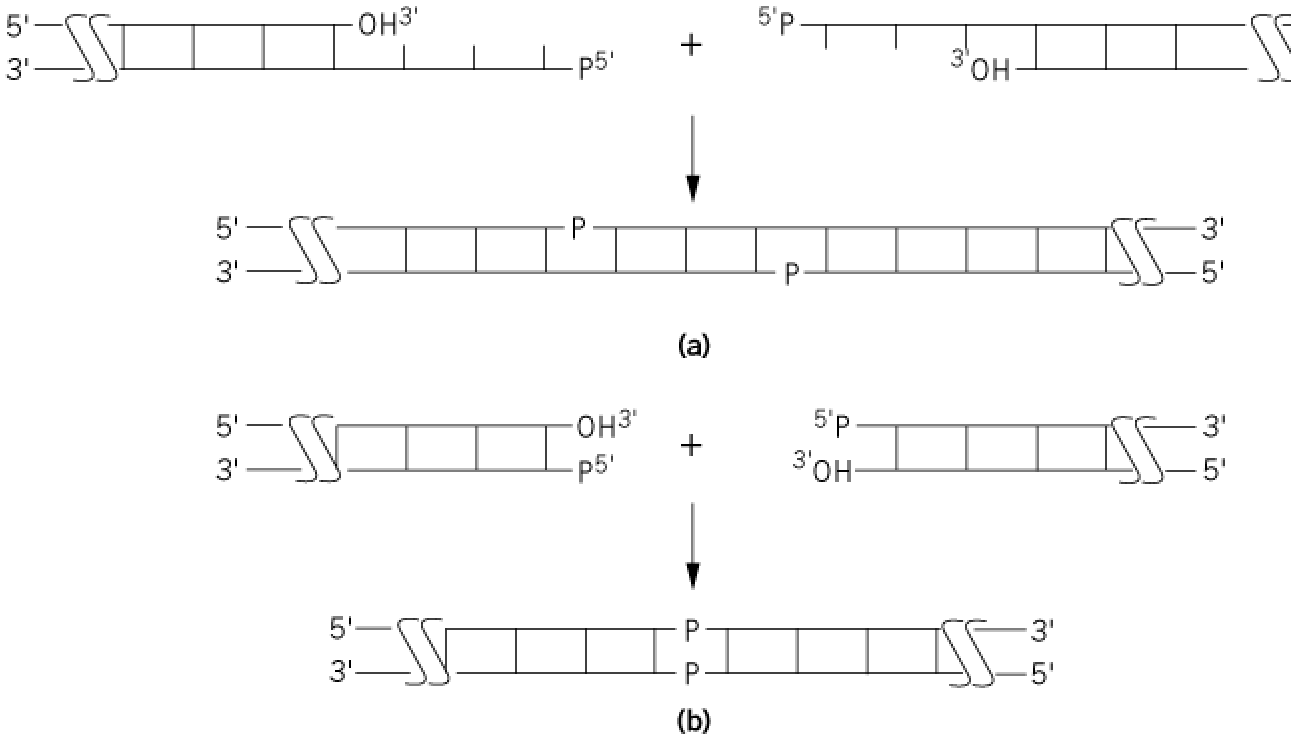

5. Polynucleotide Substrates

The physiological polynucleotide substrates for DNA ligase are predominantly DNA chains brought into proximity by a third, complementary DNA template strand as shown in Figure 1. Studies of various combinations of RNA and DNA substrates reveal that DNA ligases will also sometimes use RNA *in vitro*. RNA can be joined to RNA on either a DNA or RNA template. RNA with a 3′-OH can also be joined to DNA with a 5′-PO_4 on a DNA template. Likewise, DNA with a 3′-OH can be joined to RNA with a 5′-PO_4 on a DNA template. The exact combinations of oligonucleotide types and the efficiencies of the joinings again depend on the particular enzyme used and the reaction conditions employed. T4 DNA ligase is again often more permissive in these “unnatural” ligations than is the *E. coli* enzyme. On binding to the DNA, the ATP-dependent enzymes may specifically recognize a nick in the duplex that contains the requisite 3′-OH and 5′-PO_4 termini (7). Vaccinia virus DNA ligase appears to require a B-DNA helix to the 5′ side of the nick, suggesting that substrate conformation is another parameter that can influence recognition (8). It should be noted that some studies of substrate requirements were carried out with homopolymeric substrates and that the results might be quantitatively different for substrates containing heterogeneous sequences.

6. Assays

Several assays have been used to quantify DNA ligase activity. [^{3}H]poly d(A-T) folds on itself to form base pairs that create a dumbbell-like structure with a nick that can be sealed by DNA ligase to form a covalently closed, single-stranded circle. This product of the ligase reaction is resistant to **exonuclease** III, whereas the unsealed substrate is hydrolyzed to deoxyribonucleotides by the exonuclease. The rejoining, as determined by gel electrophoresis, of a mixture of fragments formed by a restriction enzyme digestion of a **plasmid** is a common, qualitative assay. Synthetic oligodeoxyribonucleotides allow the scheme outlined in Figure 1 to serve as an assay. If strand A is labeled at its 5′ end with ^{32}P, DNA ligase will convert the radiolabeled 5′-phosphate into a product with a phosphomonoester-resistant bond that can be quantified directly; alternatively, the longer product can be detected by gel electrophoresis. Analogously, [5′-^{32}P]d(pT)$_n$ oligonucleotides aligned on a long poly d(A) template serve as substrates for a similar assay in which the products can be quantified. The restoration of transforming activity to DNA that has been partially inactivated by **deoxyribonuclease** treatment has also served as an assay. Finally, the adenylylated enzyme formed in the first step of the reaction can be assayed by using an appropriately **radiolabeled** ATP or NAD^+ and determining the acid-precipitable, protein-bound label, or by observing the difference in migration of the free and adenylylated enzyme during polyacrylamide electrophoresis. The first step of the reaction can also be assayed by measuring an ATP–PP_i or NAD^+-NMN exchange reaction.

7. Applications

DNA ligase is extensively used in recombinant DNA technology. The most frequently used enzymes are produced from the cloned genes of *E. coli, Thermus aquaticus*, and bacteriophage T4. Whenever one wishes to join two DNA fragments together, DNA ligase can be employed. For example, it is widely used in **vector** constructions to link DNA fragments to form chimeric molecules. DNA ligase is also used to attach duplex oligodeoxyribonucleotide linkers or adapters to a longer DNA to facilitate its further manipulation. A number of site-directed mutagenesis protocols depend on DNA ligase, in conjunction with a DNA polymerase, to form an intact, sequence-altered strand of DNA on an unaltered, circular template strand. Upon transfection and replication, progeny duplex molecules containing the mutation are produced. DNA ligase has often been used to join chemically synthesized, appropriately hybridized oligodeoxyribonucleotides for *de novo* gene synthesis. Because of the strict requirements for the structure and nature of its DNA substrate, the enzyme can also be used to determine whether a 3′-OH or 5′-PO_4 exists at a DNA nick or if a gap is present in one strand of a DNA duplex. It can be used to quantify the number of nicks in a DNA molecule by using a radiolabeled adenylylated enzyme and measuring the amount of radioactive AMP released. When used to circularize short fragments, the enzyme has been used to study the stiffness, twisting, bending, and helical repeat of DNA. For example, because the ends of a fragment must be brought into proper alignment for effective ligation, one can learn about the number of base pairs per turn of the DNA. Similarly, DNA ligase can be used to study the ability of another protein to bend DNA on binding, because the bending can facilitate the ligation by bringing the ends of the duplex fragment into proximity. The enzyme has also proved useful for the synthesis of defined-sequence RNA by efficiently joining RNA strands on a DNA template (9). The ligase chain reaction, which depends on two pairs of oligodeoxyribonucleotides annealing to the top and bottom strands of a denatured target duplex at a given locus to form ligatable complexes, serves as an efficient DNA amplification method (10). The amplification is based on the principle that the products of the ligations on each strand can themselves serve as templates for further ligations of the excess starting oligonucleotides, leading to an exponential increase in product on sequential heat denaturations and ligations. Use of a thermostable DNA ligase allows repeated denaturations of the nucleic acids without the need for addition of further enzyme. Because conditions can be chosen so that ligase strictly requires fully base-paired nucleotides at the nick, the ligase chain reaction can be used to detect mutations through the use of appropriately designed oligonucleotides (11). Oligonucleotides that hybridize to the target so that the nick is fully base-paired are amplified, whereas those that do not are unreactive. DNA ligase has also been used to enhance DNA sequencing by hybridization on microchips by joining fully base-paired oligonucleotides to form longer, detectable products (12). Although alternative schemes that do not require DNA ligase have been devised for accomplishing some of these functions, the enzyme remains a staple for nucleic acid manipulations.

Bibliography

1. I. R. Lehman (1974) Science **186**, 790–797.
2. A. E. Tomkinson and D. S. Levin (1997) BioEssays **19**, 893–901.
3. M. J. Engler and C. C. Richardson (1992) in *The Enzymes*, Vol. **XV**, pp. 3–29.
4. C. Cheng and S Shuman (1997) Nucleic Acids Res. **25**, 1369–1374.
5. S. Shuman and B. Schwer (1995) Mol. Microbiol. **17**, 405–410.
6. H. S. Subramanya, A. J. Doherty, S. R. Ashford, and D. Wigley (1996) Cell **85**, 607–615.
7. V. Sriskanda and S. Shuman (1998) Nucleic Acids Res. **26**, 525–531.
8. J. Sekiguchi and S. Shuman (1997) Biochemistry **36**, 9073–9079.
9. M. J. Moore and P. A. Sharp (1992) Science **256**, 992–997.
10. M. Wiedmann, W. J. Wilson, J. Czajka, J Luo, F. Barany, and C. A. Batt (1994) PCR Applications **3**, S51–S64.
11. K. Abravaya, J. J. Carrino, S. Muldoon, and H. H. Lee (1995) Nucleic Acids Res. **23**, 675–682.
12. S. Dubiley, E. Kirillov, Y. Lysov, and A. Mirzabekov (1997) Nucleic Acids Res. **25**, 2259–2265.

Suggestions for Further Reading

13. S. Shuman (1996) Closing the gap on DNA ligase, Structure **4**, 653–656. (A minireview that correlates the T7 DNA ligase structure with the sequences of the superfamily of nucleotidyl transferases to examine the mechanisms of the reactions.)
14. H.-M. Eun (1996) *Enzymology Primer for Recombinant DNA Technology*, Academic Press, San Diego, pp. 109–132. (A review of the properties, assay conditions, and applications of *E. coli* and bacteriophage T4 DNA ligases.)

DNA Polymerase I and Klenow Fragment

Escherichia coli DNA polymerase I (pol I) has served for several decades as the prototype **DNA-dependent DNA polymerase**. Pol I, one of three such polymerases found in *E. coli*, has important roles during DNA replication, genetic recombination, and DNA repair. Pol I, the first polymerase discovered in bacteria, is required for rapid, efficient growth in rich media. This enzyme contains three activities: 5′-3′ polymerase, 3′-5′ exonuclease (for proofreading), and 5′-3′ exonuclease (for **nick translation**, excision repair, and hydrolysis of the RNA primers during DNA replication). Mild proteolytic digestion of *E. coli* DNA polymerase I (103 kDa) results in forming of two products: (1) the large Klenow fragment (68 kDa) that contains both the DNA polymerase and 3′-5′ exonuclease (proofreading) activities and (2) a smaller fragment (35 kDa) that contains the 5′-3′ exonuclease activity. Pol I is the most abundant polymerase in *E. coli* (400 molecules per cell), and it functions primarily to fill DNA gaps during repair and replication. The early cloning and overexpression of the Klenow fragment (1) and the determination of its three-dimensional structure (2) have allowed better understanding of polymerization mechanisms, molecular mechanisms of 3′-5′ exonuclease activity, and structure-function relationships of polymerases.

1. Subunits of Pol I and Their Properties

DNA polymerase I, a product of the *PolA* gene which maps at minute 86 of the *E. coli* K12 chromosome (3), is a single-subunit enzyme that functions autonomously of other replicative factors. Pol I is cleaved into two subunits by mild **proteolysis** with **trypsin**. The N-terminal 5′-3′ exonuclease **domain** contains 323 amino acid residues, and the C-terminal fragment contains 605 residues (4, 5), which is frequently called the Klenow fragment.

Much of the biochemical understanding of the polymerase and 3′-5 exonuclease functions stems from studies of the Klenow fragment. The Klenow fragment incorporates individual deoxyribonucleotides at a relatively modest rate of 50 nucleotides/s (6), and is moderately processive (on average, it synthesizes 50 nucleotides after binding and before dissociation). The Klenow fragment also acts as a **reverse transcriptase** by copying RNA templates (7), albeit distributively (i.e., incorporating one to two nucleotides per binding event), but the biological relevance of this activity is not known. The fidelity of Klenow polymerase during DNA-templated DNA polymerization is approximately 1/50,000 (i.e., one misincorporation per 50,000 nucleotides), and this fidelity is derived in part from its 3-5′ editing activity. Mutant Klenow fragments that have nonfunctional proofreading activity have an approximate fidelity of 10^{-3} (8). Both the fidelity and processivity of the Klenow fragment are influenced by reaction conditions. Both parameters are enhanced when the pH is decreased from 9.8 to 6.2 (9).

The smaller 35-kDa domain that has 5′-3′ exonuclease activities functions in pol I to degrade DNA and RNA to monomers and small oligomers. The polymerase and 5′-3′exonuclease domains act in concert during nick translation to remove Okazaki Fragments by using the 5′-3′ exonuclease activity and to fill in the resulting gap. The entire *polA* gene can be deleted without effecting the viability of *E. coli* during growth in a minimal medium.

2. *In Vivo* Functions

Much of the understanding about the *in vivo* roles of Pol I has resulted from studying *PolA* mutants. These studies show that the entire *polA* gene can be deleted without affecting cell growth and viability during slow growth in minimal media. However, either the large 68-kDA fragment or the small 35-kDA fragment is necessary for growth in rich media (10). In the absence of sufficient pol I activity, either Pol III or Pol II (which lacks 5′-3′ exonuclease activity) and ribonuclease H (the enzyme that removes RNA from RNA/DNA hybrids) potentially substitute for Pol I. The mutant strains lacking the *polA* gene are susceptible to UV light and DNA damage resulting from the alkylating agent methylmethane sulfonate. The *polA*-deficient strains also remove Okazaki fragments 10-fold slower that the wild type. A *polA* mutant that contains an amber mutation (i.e., a stop codon that produces a truncated protein), resulting in diminished (10^{-2}) polymerase activity but nearly normal exonuclease activity, is sensitive to UV and DNA alkylation damage, suggesting pol I has an essential role during DNA repair (11). Further genetic studies with *polA-lacZ* gene fusion showed that exposure to DNA-damaging agents, including 4-nitroquinoline- *N*-oxide, UV light, mitomycin C, and methyl methanesulfonate, augments Pol I expression (12).

The importance of Pol I's role in nucleotide excision repair is well accepted. Nucleotide excision repair functions to remove bulky DNA adducts and pyrimidine dimers that occur after UV exposure.

During removal of pyrimidine dimers, the UvrABC protein complex binds to the lesion and forms nicks about 11 nucleotides apart that flanking the damaged residue. Next, the **helicase** UvrD displaces the DNA between the nicks, thus removing the damaged portion. Lastly, Pol I fills the resulting 11-nucleotide gap. Pol I uses its essential 5′-3′ exonuclease activity to cleave the 5′ nucleotides of the gap. The balance of polymerase activity and simultaneous 5-3′ exonuclease activity ensures proper closure of the gap, leaving behind a nick. The last step in this repair process is ligation of the nick by a DNA Ligase. DNA pol I also uses this nick translation activity to polymerize DNA and remove Okazaki fragments simultaneously during replication.

3. Structure of Klenow Fragment

The Klenow fragment was the first polymerase whose three-dimensional structure was solved (2). The **X-ray crystallographic** structure of the Klenow fragment morphologically resembles the human right hand, complete with finger, palm, and thumb domains (Fig. 1). The structure illustrates that the N-terminal 3′-5′ exonuclease domain and the C-terminal polymerase domain are separated by about 30 Å. The structure of the Klenow fragment complexed with double-stranded DNA in an "editing mode" shows that about 5 to 8 bp of DNA are housed by the Klenow fragment in a large positively charged cleft, and about 4 nucleotides of the primer from the 3′ end need to be melted from the template and then shifted to the exonuclease site during exonuclease degradation of the primer strand (13). If the DNA were housed in the polymerase active site, it is predicted that there would be a 90° bend, similar to that in the HIV-1 **reverse transcriptase** /DNA structure (14, 15).

Figure 1. Ribbon diagram of the Klenow fragment in the absence and presence of DNA. The Klenow fragment morphol
contains fingers, thumb, palm, and 3′-5′ exonuclease subdomains. The primer strand of the DNA is bound in the 3′-5′ ex
polymerase is in its editing mode. A conformational change to the polymerizing mode allows continuation of DNA syntl
conformational change involves transferring the primer terminus across 30 Å, complete hybridization of the primer-temp
subdomain.

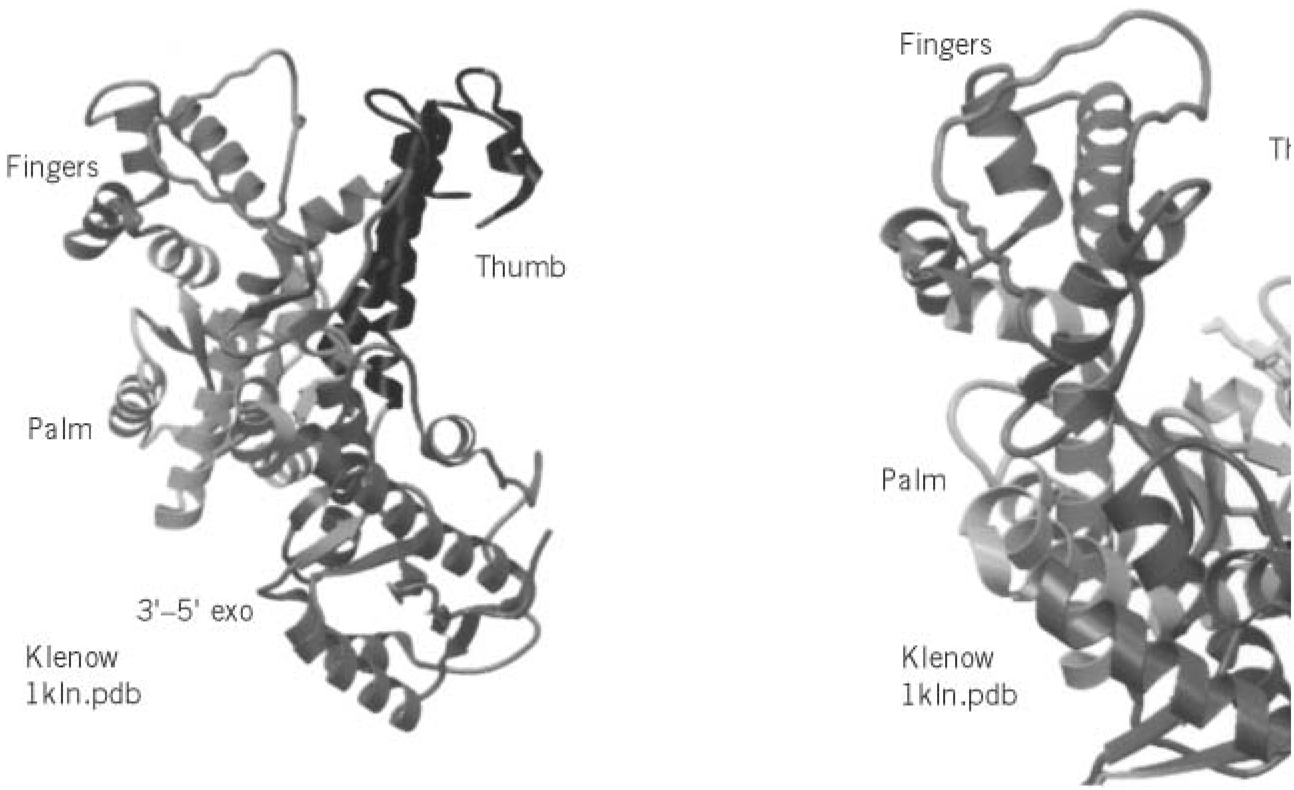

The polymerase active site, where dNTP binding and the chemical catalytic steps occur is located in the palm subdomain. It is thought from numerous biochemical and sequence alignment studies that the triphosphate of the incoming dNTP/divalent metal complex binds at the conserved Asp882, Glu883, and Asp705, whereas the base of the incoming nucleotide and its base pairing with the template is sensed by Tyr766 located in the conserved **a-helix** O. There is currently some confusion about the roles of Arg754 and Lys758, the two other conserved residues of helix O. Some believe that these residues bind the phosphates of the incoming dNTP. However, it is more likely that these residues are involved in template binding or perhaps pyrophosphate exchange (16).

The Klenow/double stranded DNA complex locked in an “editing mode” has given us numerous insights into the mechanism of the 3′-5′ exonuclease activity. In the structure, the exonuclease domain binds four bases of partially melted single-stranded DNA. The catalytic triad of Glu357, Asp355, and Asp501 bind two divalent cations, which facilitate a nucleophilic attack on the 3′ primer residue. The current model for the nucleophilic attack mechanism is that one of the metals deprotonates a water molecule, thus creating a nucleophile that, in turn, attacks the phosphate group of the 3′ primer residue. The two metals are in position to stabilize the resulting pentavalent phosphorous intermediate created by the nucleophilic attack, thus reducing the activation energy of the reaction (17). A similar two-metal phosphoryl-transfer mechanism has been proposed at the polymerase active site for the Klenow fragment (18), HIV-1 reverse transcriptase (19), and DNA polymerase b (20).

4. Kinetic Scheme of DNA Polymerization

A detailed kinetic mechanism has been presented using the Klenow fragment (21). The general mechanism involves these sequential steps: (1) binding of the polymerase to its template-primer, (2) binding of the appropriate dNTP to the pol-DNA complex; (3) a protein conformational change that positions the a phosphate of the incoming nucleotide near the 3′-OH group of the primer, (4) nucleophilic attack, resulting in phosphodiester bond formation (5) release of the pyrophosphate; and (6) translocation toward the new 3′-OH of the primer. Of these six steps, the protein conformational change is the slowest or rate-limiting step. The conformational change and nucleophilic attack step function together to sense proper **Watson–Crick base pairing** and thus contribute to the fidelity of this enzyme. If an improperly paired base is inserted, incorporation of the next base is very slow. This allows time for partitioning of the primer to the exonuclease site and the subsequent cleavage of the incorrect nucleoside. The presence of this proofreading 3′-5′ exonuclease activity aids in promoting the fidelity of the enzyme four- to seven-fold.

5. Uses in Molecular Biology

The Klenow fragment has been cloned, overexpressed, and purified, and it is widely used in laboratories. Among its uses today include incorporating radiolabeled nucleotides onto 3′ DNA ends, conducting fill-in reactions of gaps in double-stranded DNA, and synthesizing blunt DNA ends after restriction digestion.

Bibliography

1. C. M. Joyce and N. D. Grindley (1983) Proc. Natl. Acad. Sci. USA **80**, 1830–1834.
2. D. L. Ollis, P. Brick, R. Hamlin, N. G. Xuong, and T. A. Steitz (1985) Nature **313**, 762–766.
3. B. J. Backmann (1983) Microbiol. Rev. **47**, 180–230.
4. D. Brutlag, M. R. Atkinson, P. Setlow, and A. Kornberg (1969) Biochem. Biophys. Res. Commun. **37**, 982–989.
5. H. Klenow and I. Henningsen (1970) Proc. Natl. Acad. Sci. USA **65**, 168–175.
6. R. D. Kuchta, P. Benkovic, and S. J. Benkovic (1988) Biochemistry **27**, 6716–6725.
7. L. A. Loeb, K. D. Tartof, and E. C. Travaglini (1972) Nat. New Biol. **242**, 66–69.

8. K. Bebenek, C. M. Joyce, M. P. Fitzgerald, and T. A. Kunkel (1990) J. Biol. Chem. **265**, 13878–13887.
9. K. A. Eckert and T. A. Kunkel (1993) J. Biol. Chem. **268**, 13462–13471.
10. C. M. Joyce and N. D. Grindley (1984) J. Bacteriol. **158**, 636–643.
11. W. S. Kelley and C. M. Joyce (1983) J. Mol. Biol. **164**, 529–560.
12. G. Wandt, S. Kubis, and A. Quinones (1997) Mol. Gen. Genet. **254**, 98–103.
13. L. S. Beese, V. Derbyshire, and T. A. Steitz (1993) Science **260**, 352–355.
14. C. M. Joyce and T. A. Steitz (1994) Annu. Rev. Biochem. **63**, 777–822.
15. A. Jacobo-Molina, J. Ding, R. G. Nanni, A. D. Clark Jr., X. Lu, C. Tantillo, R. L. Williams, G. Kamer, A. L. Ferris, P. Clark, A. Hizi, S. H. Hughes, and E. Arnold (1993) Proc. Natl. Acad. Sci. USA **90**, 6320–6324.
16. M. Suzuki, A. K. Avicola, L. Hood, and L. A. Loeb (1997) J. Biol. Chem. **272**, 11228–11235.
17. L. S. Beese and T. A. Steitz (1991) EMBO J. **10**, 25–33.
18. T. A. Steitz and J. A. Steitz (1993) Proc. Natl. Acad. Sci. USA **90**, 6498–6502.
19. P. H. Patel, A. Jacobo-Molina, J. Ding, C. Tantillo, A. D. Clark Jr., R. Raag, R. G. Nanni, S. H. Hughes, and E. Arnold (1995) Biochemistry **34**, 5351–5363.
20. H. Pelletier, M. R. Sawaya, A. Kumar, S. H. Wilson, and J. Kraut (1994) Science **264**, 1891–1903.
21. R. D. Kuchta, V. Mizrahi, P. A. Benkovic, K. A. Johnson, and S. J. Benkovic (1987) Biochemistry **26**, 8410–8417.

Suggestions for Further Reading

22. A. Kornberg and T. A. Baker (1992) *DNA Replication*, Freeman, New York.
23. E. Arnold, J. Ding, S. H. Hughes, and Z. Hostomsky (1995) Structures of DNA and RNA polymerases and their interactions with nucleic acid substrates, Curr. Opinion Struct. Biol. **5**, 27–38

DNA Repair

DNA repair is the set of enzymatic reactions that correct two types of structural anomalies in **DNA** (1). The first class of anomalies involves normal bases in an abnormal sequence context and includes mismatches, loops (extra nucleotides in one strand relative to the complementary strand), and bulges (a stretch of >1 noncomplementary base within the duplex). The second class, which is referred to as **DNA damage** or DNA lesions, encompasses abnormal nucleotides (modified, fragmented, cross-linked) within a normal or noncomplementary sequence context.

1. Mismatch Repair

Mismatches and related anomalous structures arise from errors in DNA replication and from recombination between partially **homologous** (homeologous) sequences. In addition, deamination of methylcytosine spontaneously or by acidic pH is a major cause of converting a G-C base pair to a G · T mismatch (2). The other source of simple mismatches is incorporation errors by **DNA polymerases** and the presence of a small fraction of bases in the template or in the nucleotide pool in **tautomeric** forms that lead to abnormal, yet complementary, **hydrogen bonding** and misincorporation. Loops often result from slippage/dislocation of template or nascent strand at monotonous sequences, such as oligo dA · dT tracts or microsatellite DNA consisting of di- or trinucleotide repeats. Bulges are often caused by recombination between two related sequences with a noncomplementary sequence surrounded by homologous sequences.

Mismatches are repaired by two general mechanisms: **base-excision repair** and the general mismatch repair system (3). In the base-excision repair pathway, the mismatched base (eg, the T in the G · T mismatch) is released by a glycosylase enzyme, and the resulting abasic sugar is removed by the combined actions of *AP lyase*, which cuts the polynucleotide chain 3′ to the apurinic/apyrimidinic (AP) site, and *AP endonuclease*, which cuts 5′ to the AP site. The resulting one-nucleotide gap is filled in by a **DNA polymerase** and sealed by a ligase (see Base Excision Repair). In the general mismatch repair system, an endonuclease incises the newly synthesized strand anywhere from 100 to 1000 nucleotides away and either 5′ or 3′ to the mismatch. The intervening region is removed past the mismatch by exonucleases, and the resulting gap is filled in by DNA polymerase and is ligated to restore the normal duplex (see Mismatch Repair).

Defects in the general mismatch repair system (nucleotide excision/long-patch repair) cause hereditary nonpolyposis colorectal cancer (HNPCC) in humans. In addition, mismatch repair defects have been found in several sporadic cancers (3).

2. Damage Repair

DNA damage in the form of base modification, base adduction, base fragmentation, and phosphodiester bond cleavage is caused by many agents including radiation in the form of X-rays (4), ultraviolet (5, 6), and microwave; and chemicals (7) ranging in reactivity from the relatively inert water to highly reactive oxygen radicals and activated polyaromatic hydrocarbons (Table 1). The most common lesions induced in DNA by ionizing radiation and active oxygen species are oxidized and fragmented purines, pyrimidine hydrates and glycols, abasic sites, and single- and double-strand breaks (8, 9). The major lesions induced by ultraviolet light are cyclobutane pyrimidine dimers and [6–4] dipyrimidine photoproducts. There is a virtually infinite variety of lesions produced in DNA by chemical agents. Among those, benzo[*a*]pyrene-, aflatoxin-, and acetylaminofluorene–guanine adducts are carcinogenic DNA lesions produced by natural and synthetic compounds. Similarly, some anticancer drugs cause DNA damage. Mitomycin C, cisplatin, and cyclophosphamide form monoadducts with guanine bases or cause interstrand cross-links between guanines in each of the two strands of the duplex. Psoralen makes intrastrand thymine monoadducts or interstrand thymine–psoralen–thymine cross-links. Alkylating agents such as methyl methane sulfonate, nitrosoguanidine, and nitrogen– and sulfur–mustard attack essentially all nucleophilic groups in DNA, producing at least 12 different base alkylation adducts and phosphorothioesters (7).

Table 1. Causes and Types of DNA Lesions and Mechanisms of DNA Repair

Type of DNA lesion	Cause	Repair Mechanism
A. Base mismatches, loops and bubble structures	Replication errors	1. Base excision
	Recombination	2. General mismatch repair
	Spontaneous deamination	
B. DNA lesion/base lesions		

1. Deamination and depurination	Heat	1. Base/nucleotide excision
2. Alkylation/aryl adducts	Natural and synthetic alkylators	2. Base/nucleotide excision
3. Intrastrand cross-links	Ultraviolet light, cisplatin	3. Nucleotide excision
4. Interstrand cross-links	Psoralen, melphalen, cisplatin	4. Nucleotide excision/recombination
C. Strand discontinuities		
1. Single-strand break	Ionizing radiation, oxidative stress	1. Ligation
2. Double-strand break	Ionizing radiation	2. Ligation/recombination

DNA lesions in the form of modified or adducted bases, interstrand cross-links, or discontinuity in one (nick) or both (break) strands interfere with replication, transcription and recombination of DNA; they also cause mutations or cell death, due to the inability to replicate or to a mutation in an essential gene. Furthermore, because many of the agents that cause damage are present in the cell's normal habitat, DNA damage is a frequent occurrence that the cell must deal with on a continuous basis in order to maintain its integrity and survival (9). Hence, cells possess many biochemical reaction pathways (DNA repair mechanisms) to eliminate damage from their chromosomes. These pathways fall into three main categories (1, 10): (i) base excision, (ii) nucleotide excision (or simply excision), and (iii) direct repair mechanisms. As should be apparent from this enumeration, there are extensive functional similarities between the mismatch and damage repair systems. This is not surprising, because the double-helical nature of DNA dictates the types of operations that can be applied to it to remove a mismatched or a damaged base: The mismatch or damage may be removed in the form of a base (11, 12) or a (oligo)nucleotide (10), which creates a single-stranded gap that can be filled using the intact (correct) strand as a template. However, damage repair includes additional mechanisms in its repertoire. One of these is direct repair (1). In this type of repair the chemical bonds that comprise the lesion are broken to restore the normal bases. An example of this type of repair includes photoreactivation by **photolyase**, which breaks the two sigma bonds between adjacent thymines to restore the dimer to a thymine dinucleotide (13) (see Photolyase/Photoreactivation), and O^6-methylguanine DNA methyltransferase, which breaks the single bond between the O6 of guanine and the alkyl group and thus restores the normal base (14) [see O6-Methylguanine-DNA Methyltransferase (MGMT)]. Ligation of a single-strand or double-strand break that is not accompanied by base loss may also be considered an example of direct repair. Finally, recombinational repair is also a repair mechanism unique to damaged DNA. This repair mechanism is employed by the cell when both strands of the duplex are damaged so that the duplex cannot be fixed by direct repair or by base and nucleotide excision repair systems, because these systems rely on an intact strand in the duplex (1). In this rather elaborate repair mechanism, the damaged region of the duplex is replaced by using a homologous duplex to retrieve genetic material and/or information. This repair system uses the enzymes of both nucleotide excision repair and genetic recombination systems (see Recombinational Repair).

Bibliography

1. A. Sancar and G. B. Sancar (1988) DNA repair enzymes. Annu. Rev. Biochem. **57**, 29–67.
2. T. A. Kunkel (1992) DNA replication fidelity. J. Biol. Chem. **267**, 18251–18254.
3. P. Modrich and R. Lahue (1996) Mismatch repair in replication fidelity, genetic recombination, and cancer biology. Annu. Rev. Biochem. **65**, 101–133.

4. M. Dizdaroglu (1992) Measurement of radiation induced damage to DNA at the molecular level. Int. J. Radiat. Biol. **61**, 175–183.
5. D. E. Brash (1988) UV mutagenic photoproducts in *E. coli* and human cells: a molecular genetics perspective on human skin cancer. Photochem. Photobiol. **48**, 59–66.
6. S. Tornaletti and G. P. Pfeiffer (1996) UV damage and repair mechanisms in mammalian cells. Bioessays **18**, 221–228.
7. B. Singer and J. T. Kusmierek (1982) Chemical mutagenesis. Annu. Rev. Biochem. **51**, 655–693.
8. E. S. Henle and S. Linn (1997) Formation, prevention and repair of DNA damage by iron/hydrogen peroxide. J. Biol. Chem. **272**, 19095–19098.
9. K. B. Beckman and B. A. Ames (1997) Oxidative decay of DNA. J. Biol. Chem. **272**, 19633–19636.
10. A. Sancar (1994) Mechanisms of DNA excision repair. Science **266**, 1954–1956.
11. E. Seeberg, L. Eide, and M. Bjoras (1995) The base ecision repair pathway. Trends Biochem. Sci. **20**, 391–397.
12. M. L. Dodson, M. L. Michaels, and R. S. Lloyd (1994) Unified catlytic mechanism for DNA glycosylases. J. Biol. Chem. **269**, 32709–32712.
13. A. Sancar (1996) No "End of History" for photolyases. Science **272**, 48–49.
14. L. Samson (1992) The suicidal DNA repair methyltransferases of microbes. Mol. Microbiol. **6**, 825–831.

DNA Replication

DNA replication in a chemical sense is the process by which an exact copy of a **DNA** molecule having a specific base sequence is synthesized. Exact copies of a linear DNA molecule can be replicated *in vitro* using purified **DNA polymerases** and proper primers. A recent advance in the long **PCR** method has made it possible to amplify DNA molecules as long as several tens of kilobases. In biology, however, DNA replication is defined as the duplication of the entire genome DNA in the cell. Basic mechanisms of replication of **plasmids**, **bacteriophages**, animal **viruses**, and bacterial chromosomes have been elucidated at the molecular level. On the other hand, knowledge of the replication of **eukaryotic** genomes is still limited, although increasing rapidly. A variety of structures and types of replication are known among plasmids, bacteriophages, plant and animal viruses. Mitochondria genomes are known to have a unique mode of replication. Here, replication of the genomes (conventionally called chromosomes) of **prokaryotes** (bacteria) and eukaryotes will be described, since the replication of genome DNA is a process essential for basic cellular functions, cell cycle, cell division, and cell differentiation.

1. Prokaryotic Genomes (Chromosomes)

Bacterial genomes usually consist of circular DNA of one to eight megabases and comprise a single replication unit, a replicon. The general aspects of genome replication have been elucidated in *Bacillus subtilis* and *Escherichia coli*, representatives of **Gram positive** and Gram negative bacteria, respectively. In both genomes, replication is initiated from a genetically defined site, oriC (see Replication Origin), proceeds bidirectionally and symmetrically at about the same elongation rate, and terminates at the defined region, terC, of the genome (Fig. 1) (see Termination Of DNA Replication). Isolation of *dna* temperature-sensitive mutants has revealed that the three processes, initiation, elongation, and termination of replication, are regulated independently by multiple gene products. Genetic and biochemical studies subsequently revealed multiple protein complexes, the *primosome* and *replisome*, for the initiation and replication machinery, respectively (see DNA Replication Proteins). In contrast, termination is achieved by a single protein, Rtp.

Figure 1. Replication of circular prokaryotic chromosome. Replication of a circular chromosome is schematically shown. Replication is initiated by unwinding of a specific site of the chromosome, the origin of replication (oriC), followed by the synthesis of two leading strands and lagging strands in opposite directions. Elongation proceeds bidirectionally, with the same rate of synthesis at the two replication forks. Elongation terminates at a specific site, the terminus of replication.

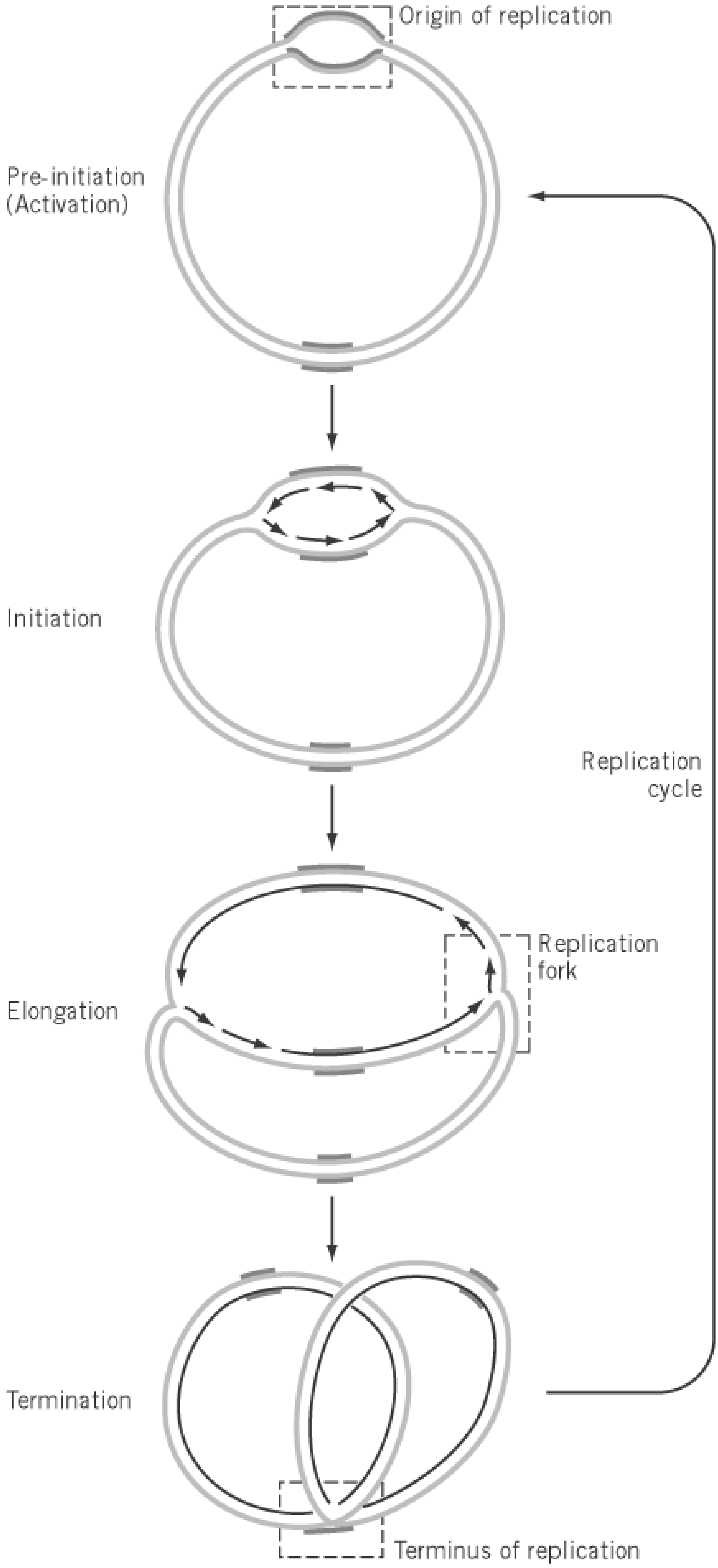
Origin of replication
Pre-initiation
(Activation)
Initiation
Replication
cycle
Elongation
Replication
fork
Termination
Terminus of replication

Regulatory DNA elements required for initiation, oriC, were identified by cloning of sequences that confer upon circular DNA the ability of autonomous replication as extra chromosomal elements in the cell (1). The oriC was first identified in *E. coli*, and it was then found that one of the *E. coli* Dna proteins, DnaA, functioned as an initiator of replication by binding to a sequence-specific element, the DnaA-box, to activate oriC and to unwind the AT-rich region within oriC (2). The combination of the DnaA-box and the DnaA protein functioning as *cis* and *trans* regulatory elements in the initiation of replication was subsequently found to exist commonly in many **eubacteria** (3). A replicon mechanism consisting of two regulatory elements, the replicator in *cis* and initiator in *trans*, that was proposed as early as 1963 (4) has been confirmed in prokaryotes (see Replicon).

The elongation of replication is much more complicated than it was thought in the late 1950s when semi-conservative DNA replication was demonstrated and Kornberg discovered DNA polymerase I, which apparently copied double-stranded DNA *in vitro*. This complexity is due to the fact that the two strands of DNA are oriented in opposite directions in terms of the phosphodiester bonds and DNA polymerases can function in only one, the 5′ to 3′ direction. Extensive analysis of growing replication forks in *E. coli* led to the discovery of asymmetric discontinuous DNA replication in which synthesis of the 5′ to 3′ strand proceeds sequentially (the **leading strand**), whereas the opposite strand (lagging strand) is synthesized in short pieces, using an RNA primer, and subsequently joined together. The small RNA–DNA fragments of some 500 to 1000 bases synthesized during the discontinuous replication were named Okazaki Fragments after the researcher who discovered this mechanism (5). At least five enzymes, DNA helicase, primase, DNA polymerase I and III, and DNA Ligase, are involved in this process (Fig. 2) (see DNA Replication Proteins). These proteins are assumed to form a supramolecular complex, the replisome, and may be attached to the cell membrane. The initiation of replication is the synthesis of the first primer RNA–DNA molecule on both strands of DNA at the unwound region of oriC, which eventually become leading strands extended in both directions. The formation of the replisome at oriC requires the activation of oriC by DnaA and subsequent formation of the primosome complex, which includes the DNA helicase, DnaB in *E. coli*. The synthesis of lagging strands may be initiated after the formation of a considerable size of single-stranded region by elongation of the leading strand, but the detailed mechanism of synthesis of neither the first primer RNA nor the first lagging strands is known (Fig. 3).

Figure 2. Semiconservative and RNA-primed discontinuous replication. The mode of synthesis of leading strand and lagging strand at the replication fork is shown schematically. (**1**) Unwinding of double strand by helicase, (**2**) stabilizatio of single-stranded regions by single-strand DNA binding proteins (SSB) in prokaryotes (= p) or RPA in eukaryotes (= e) (**3**) primer RNA synthesis by primase (in p) or polymerase a-primase complex (in **e**), (**4**) lagging strand synthesis by DN polymerase III (in p) or polymerase d/e (in **e**), (**5**) degradation of primer RNA by polymerase I (in p) or ribonuclease H (**e**), and (**6**) leading strand synthesis by polymerase III (in p) or polymerase d/e (in **e**).

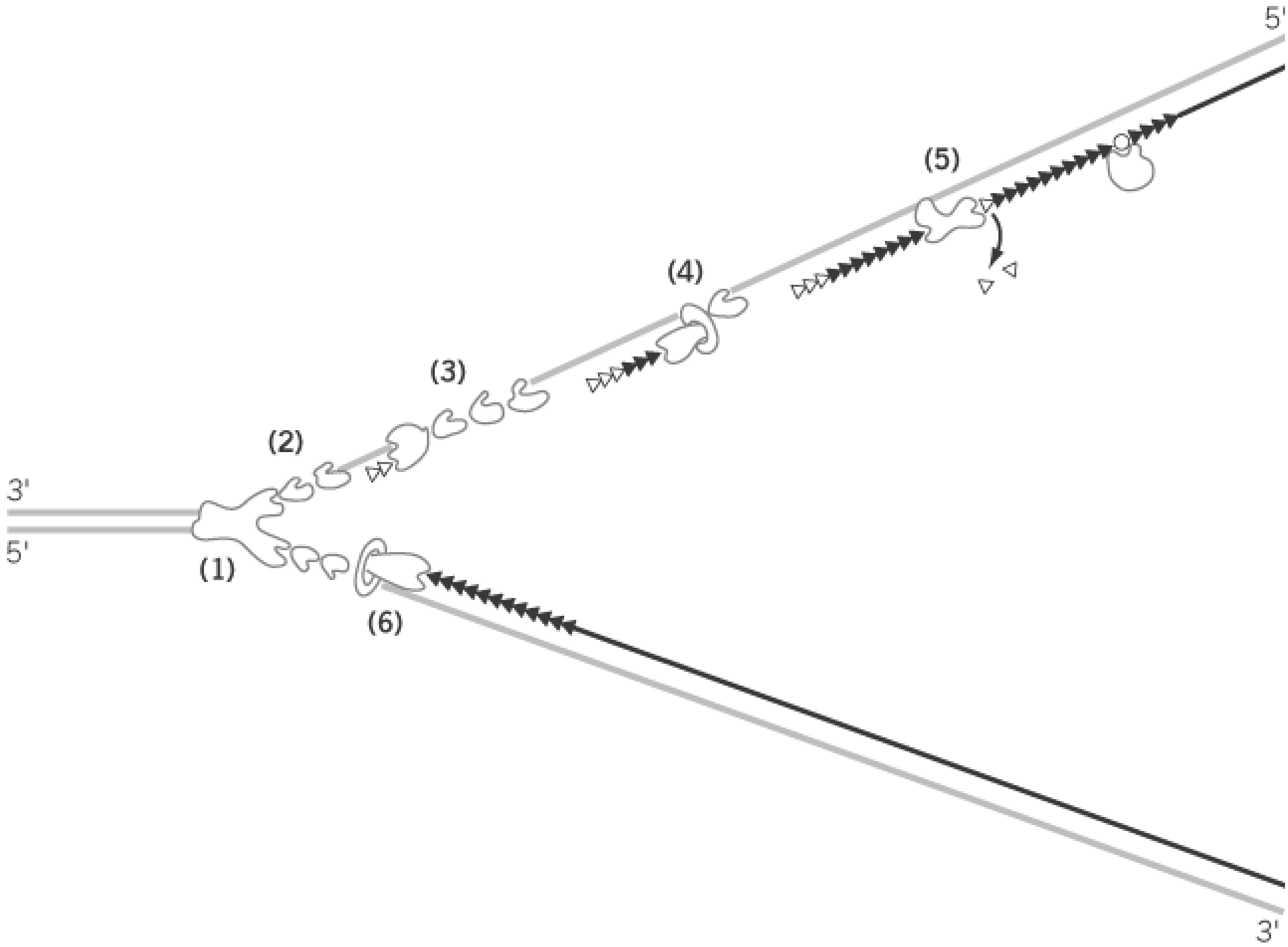

Figure 3. Mechanism of initiation of replication of prokaryotic chromosomes. The OriC of *E. coli* and initiation from the oriC by the function of DnaA protein followed by DNA helicase and finally by assembly of the replication machinery is shown schematically. The DnaA box is a 9-mer sequence (consensus sequence is TTATCCACA) and DnaA protein is conserved in many eubacteria. The DnaB helicase is also conserved in at least *E. coli* and *B. subtilis*.

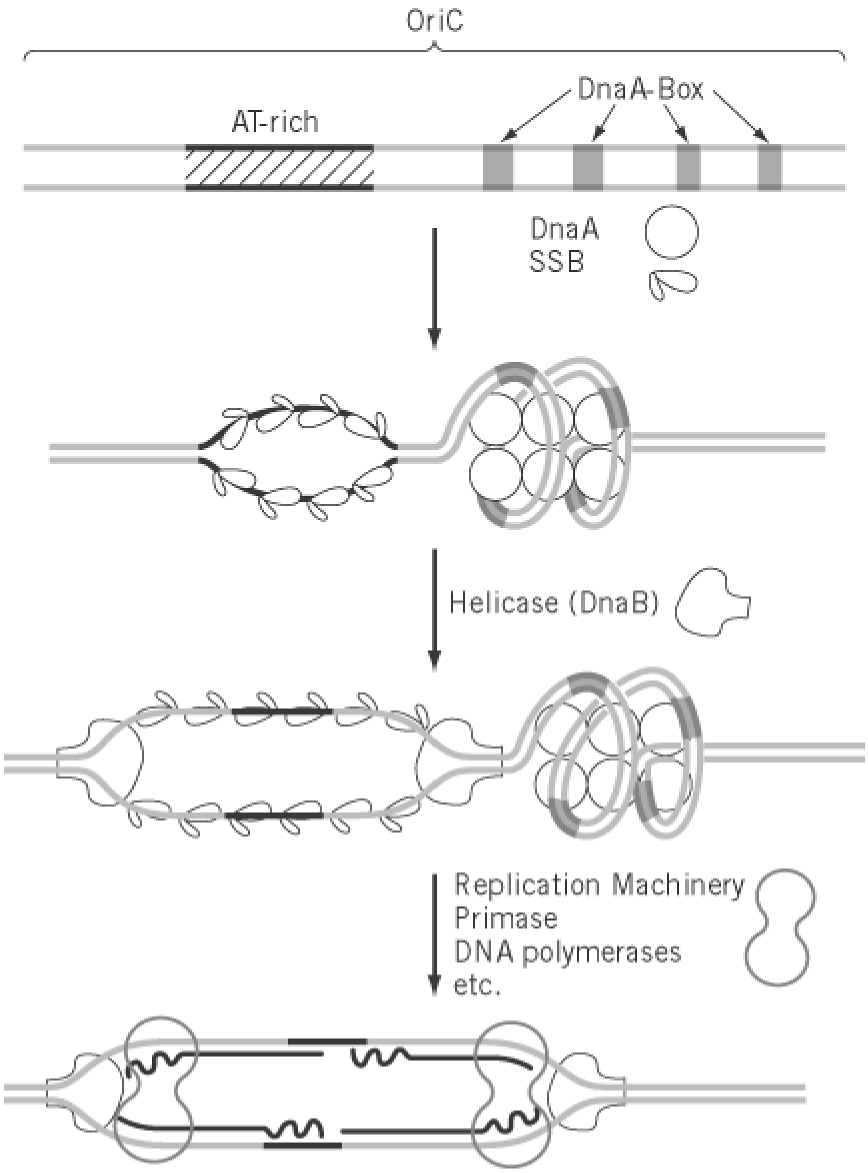

Elongation at the macroscopic scale proceeds bidirectionally along the circular genome at about the same rate, 50 kilobases/min, and completes at the fixed region, the terminus where two forks meet (s Termination Of DNA Replication). Two sets of three (a total of six) termination signals, oriented in opposite directions, are found in both E. coli (6) and B. subtilis (3) chromosomes at about 180o from oriC, to which a protein known as replication termination proteinein, Rtp, binds and inhibits the elongation in one direction. The distance between the nearest two signal sets is 270 kb in *E. coli* and 59 kb in *B. subtilis*. Although the mechanism of termination is basically the same in *E. coli* and *B. subtilis*, there is no homology in these terC sequences nor in the primary structures of Rtp. This is in sharp contrast to the extensive conservation of the DnaA protein and the DnaA-box sequence among eubacteria. The tertiary structure of *B. subtilis* Rtp protein reveals the mechanism of inhibition of DN replication at the molecular level (7). Termination of replication results in the two daughter chromosomes entwined about one another. Resolution of such a structure into two separate chromosomes can be achieved by the action of DNA gyrase (8) (see DNA Topology). In addition to the termination site, pausing sites where DNA replication slows down significantly are found near th termination sites of the *E. coli* chromosome, and their possible involvement in recombination has be discussed (9).

2. Eukaryotic Chromosomes

Studies on the replication of a viral genome, SV40, have provided the basic knowledge about DNA replication in eukaryotic cells, because it replicates using host proteins, except for a single viral protein, T Antigen. T antigen was first identified as a protein responsible for tumor transformation o mammalian cells by the tumor virus and hence was named as Tumor antigen. Subsequently, it was found that the T antigen is an initiator protein and a helicase that acts on the origin of the 3-kb circul SV40 genome (10). Success in reconstitution of an *in vitro* replication of the entire SV40 genome le to the identification and purification of enzymes and protein factors involved in the initiation and elongation of replication and separation of replicated molecules (see DNA Replication Proteins). Th basic mechanism of synthesis of leading strand by DNA polymerase d/e and of lagging strand by the combination of the DNA polymerase a-primase complex and polymerase d/e has been elucidated (11 (Fig. 2). In addition, various factors, such as RPA, RFC, and proliferating cell nuclear antigen (**PCNA**), were identified to facilitate the efficient and progressive replication of the viral genome (1 A topoisomerase, topoisomerase II, was found essential for resolving the concatenated structure formed at the end of replication of the circular genome. Since no *in vitro* replication system is availa using cellular genome DNA as template, the molecular mechanism of replication established by the study of SV40 genome is still the sole model of eukaryotic DNA replication and serves as a unique system to identify factors involved in DNA replication and its regulation (see Replication Fork (Y-Fork Intermediate)) (13).

The mechanism of initiation of replication of the SV40 genome is similar to, and rather simpler than that of bacterial genome, because T antigen acts as helicase as well as the initiator. However, it did n provide a model for the initiation of replication of cellular chromosomes composed of multiple replicons, which was first demonstrated by the autoradiography of replicating chromosomes in 1968 Huberman and Riggs (14). In general, the genomes of eukaryotic cells are estimated to contain abou one origin every 10 to 330 kbp (15). Extensive searches for chromosomal replication origins through the cloning of autonomously replicating sequences (**ARS**) have mostly failed, except for **yeast** chromosomes of *Saccharomyces cerevisiae* and *Schizosaccharomyces pombe*. A number of ARS ha been isolated from the 16 chromosomes of *S. cerevisiae*. In particular, 14 ARS in a 200-kbp portion chromosome III (16) and 10 ARS in the 300-kbp entire chromosome VI (17) were identified. All AR contain a common sequence of 11 bp ARS consensus sequence (ACS) that is essential for autonomo replication, plus additional nonspecific AT-rich sequences whose deletion causes a significant reduction in ARS activity. In some cases, a binding site for a **transcriptional factor** is located near t ACS and enhances its ARS activity. The ARS from *S. cerevisiae* is unique, and no **homologous** sequence of the approximately 100-bp ACS was found in other eukaryotes. ARS cloned from the ot yeast *S. pombe* require a region of about 1 kbp containing several AT-rich clusters, with no single specific sequences like ACS essential for ARS activity. The two-dimensional gel electrophoresis of chromosomal fragments developed by Brewer and Fangman (18) has successfully detected the eye-form intermediates of replicating intermediates clearly separated from Y-form intermediates (see Replication Fork (Y-Fork Intermediate)). Using this method, some ARS are found to function as efficient origins of chromosomal replication in *S. cerevisiae*. However, some of the active ARS in plasmids were found to be very inefficient or silent on the chromosome, suggesting a role of chroma structure in origin activity. Not all origins are fired at the same time in **S phase**, but they are initiate sequentially in a fixed order (19). A regulatory factor determining the efficiency and timing of initiation of late replicating origins have been identified (24).

Origins from genomes of higher organisms are ambiguous. Attempts to isolate ARS from mammalia chromosomes are difficult to reproduce and therefore controversial. The best-studied origin, near the dihydrofolate reductase (DHFR) gene in the Chinese hamster genome, showed variation in size from 0.5 to 55 kbp, depending on the methods used to detect origin activity (20). Systematic studies on la chromosomal segments have revealed that most fragments longer than 10 kbp can provide some AR activity in mammalian cells, suggesting that DNA length is more critical than DNA sequence. In ma cases, initiation occurs randomly within several kilobases, which is called the initiation *zone* rather than the origin. The concept of a replicator that is proposed in the original replicon hypothesis shoul be reexamined in these complex origins, in terms of the recognition site of initiators and the actual si of initiation of replication (see Replicon).

As for *trans* factors for initiation, no single initiator protein like bacterial DnaA or SV40 T antigen h been found in eukaryotic cells. Instead, a complex consisting of six proteins was found to recognize yeast ARS through binding to the ACS and named accordingly as the origin recognition complex (ORC) (21). The ORC was subsequently found to be well conserved from yeast to humans. Howeve the mechanism of how ORC recognizes seemingly nonspecific origin sequences on chromosomes other than *S. cerevisiae* is not clear. An *in vitro* DNA synthesis system using a Xenopus egg extract and sperm chromosomes provided a unique system for studying the biochemistry of initiation of chromosomal replication, and it led to the discovery of the licensing factor that permits replication o multiple replicons of the chromosome once in the cell cycle (22, 23). Genes homologous to the Xenopus licensing factor were identified among MCM genes of *S. cerevisiae*, and a MCM complex composed of six proteins that binds to ARS through interaction with ORC was subsequently discovered. Genetic studies with *S. cerevisiae* show that the formation of the MCM–ORC–ARS complex is not sufficient to activate the origin of the chromosome, and additional factors, protein kinases that interact with MCM or ORC directly or indirectly, were being discovered. Extensive studies on the regulatory network of the replication complex are expected to elucidate the molecular mechanism of signal transduction from the cell cycle engine, cdk/cyclin kinase, to the chromosomal origin of replication. The MCM complex, as well as the factors interacting with MCM and ORC, are conserved widely in eukaryotes, suggesting that the molecular mechanism elucidated in the yeast an frog provides principles that guide the studies on more complicated chromosomes including human chromosome (Fig. 4).

Figure 4. Mechanism of initiation of replication of a *Saccharomyces cerevisiae* chromosome. Minimal structure of the ARS contains a 11-bp sequence-specific region (ACS) that is essential for the origin, and surrounding stimulative regio that are rich in AT and called DNA unwinding elements (DUE). The ORC binds to ACS throughout cell cycle. MCM (licensing factor) complex binds to ORC at the G2-M phase of the cell cycle, and the double complex may be activated by several protein kinases, including CDC6 and DBF4/CDC7, to produce a single-stranded region that serves as the ent site for helicase and eventually for the replication machinery. The mechanism is hypothetical, as the last two steps have not been proven experimentally.

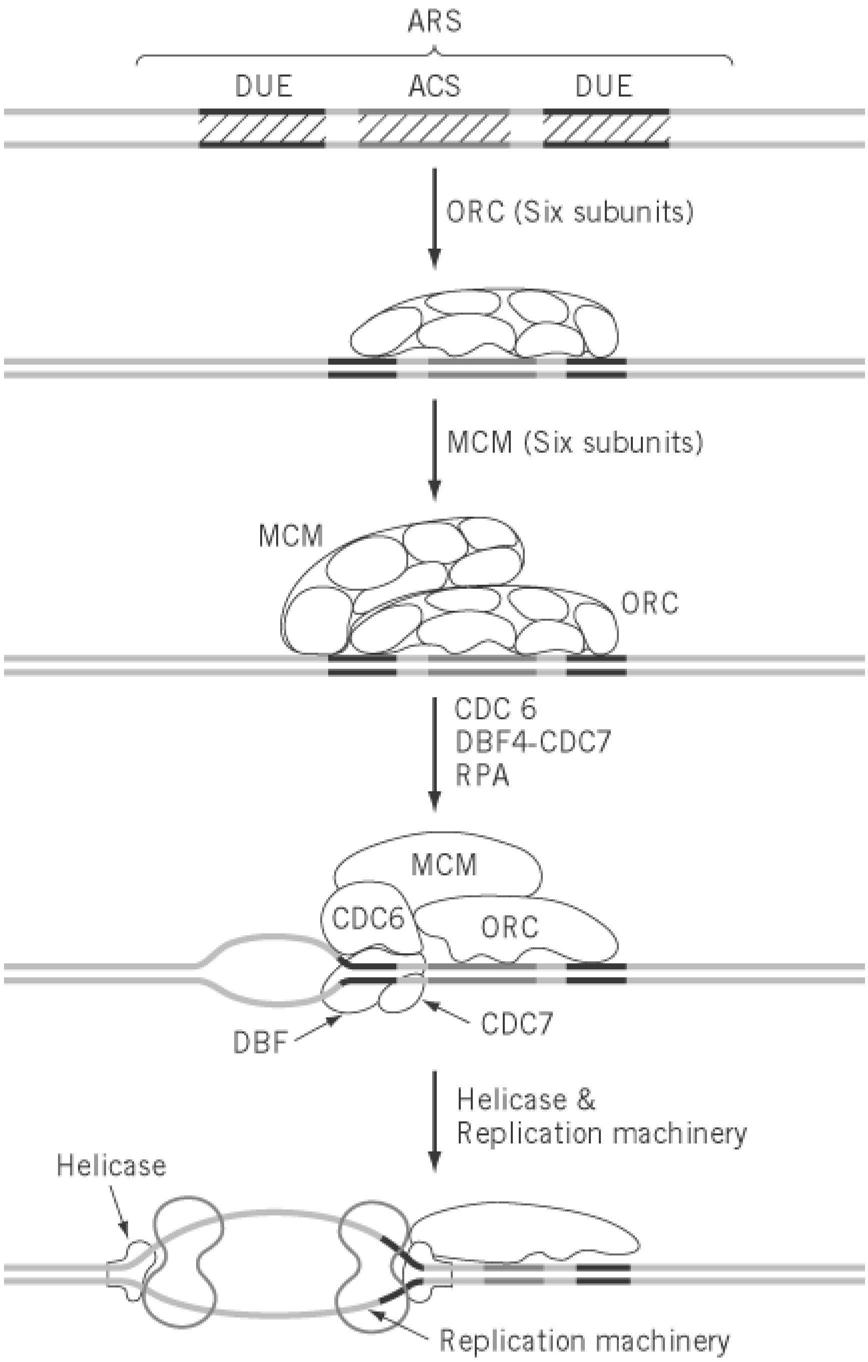

Termination of replication of adjacent replicons occurs when two forks moving in opposite direction meet. Although specific termination sites between the two adjacent replicons have not been identifie the structure of replicated replicons at the termination sites must be similar to the ends of the circulaı chromosomes of bacterial and viral genomes and require topoisomerases to resolve the structure to separate two sister strands. Termination of the ends of linear chromosomes requires a more specific structure, the telomere, to prevent shortening of the chromosome due to the discontinuous replicatioı mechanism.

Bibliography

1. Y. Hirota, S. Yasuda, M. Yamada, A. Nishimura, K. Sugimoto, H. Sugisaki, A. Oka, and M. Takanami (l978) Cold Spring Harbor Symp. Quant. Biol. **4**, 129–138.
2. D. Bramhill and A. Kornberg (1988) Cell **54**, 915–918.

3. H. Yoshikawa and R. G. Wake (1993) In *Bacillus subtilis and other Gram Positive Bacteria* (A. Sonenshein, J. A. Hoch, and R. Losick, eds.), American Society of Microbiologists, Washington DC, pp. 507–528.
4. F. Jacob, S. Brenner, and F. Cuzin (1963) Cold Spring Harbor Symp. Quat. Biol. **28**, 329–348.
5. R. Okazaki et al. (1975) In *DNA Synthesis and Its Regulation* (M. Goulian, P. Hanawalt, and F. Fox, eds.), Benjamin Cummings, Menlo Park, CA, pp. 832–862.
6. M. Hidaka, M. Akiyama, and T. Horiuchi (1988) Cell **55**, 467–475.
7. D. E. Bussiere, D. Bastia, and S. White (1995) Cell **80**, 651–660.
8. T. Horiuchi and Y. Fujiyama (1995) J. Bacteriol. **177**, 783–791.
9. T. R. Steek and K. Drlica (1984) Cell **36**, 1081–1088.
10. H. Stahl, P. Droge, and R. Kippers (1986) EMBO J. **5**, 1939–1944.
11. T. Tsurimoto, T. Melendy, and B. Stillman (1990) Nature **346**, 534–539.
12. T. Tsurimoto and B. Stillman (1990) Proc. Natl. Acad. Sci. USA **87**, 1023–1027.
13. B. Stillman (1994) Cell **78**, 725–728.
14. J. A. Huberman and A. D. Riggs (1968) J. Mol. Biol. **32**, 327–341.
15. R. Hand (1978) Cell **15**, 317–325.
16. S. A. Greenfeder and C. S. Newlon (1992) Mol. Biol. Cell **3**, 999–1013.
17. K. Shirahige, T. Iwasaki, M. B. Rashid, N. Ogasawara, and H. Yoshikawa (1993) Mol. Cell. Biol. **13**, 5043–5056.
18. B. J. Brewer and W. L. Fangman (1987) Cell **51**, 463–471.
19. W. L. Fangman, R. H. Hice, and E. Chlebowicz-Sledziewska (1983) Cell **32**, 831–838.
20. D. M. Gilbert, H. Miyazawa, F. S. Nallaseth, J. M. Ortega, J. J. Blow, and M. L. DePamphilis (1993) Cold Spring Harbor Symp. Quant. Biol. **58**, 475–485.
21. S. P. Bell and B. Stillman (1992) Nature **357**, 128–134.
22. J. J. Blow and R. A. Laskey (1988) Nature **332**, 546–548.
23. H. Kubota and H. Takizawa (1993) J. Cell Biol. **123**, 1321–1331.
24. K. Shirahige, Y. Hori, K. Shiraishi, M. Yamashita, K. Takahashi, C. Oluse, T. Tsurimoto, and H Yoshikawa (1998) Nature **395**, 618–621.

Suggestions for Further Reading

25. M. L. DePamphilis, ed. (1966) *DNA Replication in Eukaryotic Cells*, Cold Spring Harbor Laboratory Press, New York.
26. A. Kornberg and T. A. Baker (1992) *DNA Replication*, 2nd ed., W. H. Freeman, New York.

DNA Replication Proteins

Various DNA replication systems from bacteria, **plasmids**, **bacteriophage**, **viruses**, and **eukaryotic** cells have been studied to elucidate the mechanism of DNA replication. It emerged that most of them can complete the reaction with a limited number of enzymes called *replication proteins* (or factors) (Table 1). The primary experiments were identification, as **conditional mutants** for bacterial growth and DNA synthesis, of the ***dna* genes** from *Escherichia coli* that encode replication proteins (1, 2).

About a dozen *dna* genes were identified and grouped as quick- or slow-stop mutants, which indicate whether the gene products are involved in the elongation or initiation stages, respectively. Development of *in vitro* DNA replication systems with *E. coli* crude lysates for single-stranded DNA phage and the *E. coli* chromosomal origin made it possible to identify and purify replication proteins by complementation of the missing activity caused by these mutations. In addition, some replication proteins were identified as proteins harboring known enzymatic activities required for replication, such as DNA Ligase, single-stranded DNA binding protein, ribonuclease H, topoisomerase I, and DNA gyrase (see DNA Topology). DNA gyrase subunits were also identified as drug-sensitivity gene products.

Table 1. Essential Replication Proteins from Prokaryotes and Eukaryotes

Stage	Function	*E. coli*	l phage	T4 phage	Mammalian (SV40)	*S. cerevisiae*
Pre-initiation		DnaA	O protein			
	Initiator			?	ORC? (Tag)	ORC (1 ~ 6)
		DnaC	P protein			
					MCM?	MCM (2 ~ 7)
	Activator	RNA polymerase			CDK/cyclin?	CDK/cyclin?
					CDC6?	DCD6?
					CDC7/DBF4?	CDC7/DBF4?
Initiation	Replication	DnaB		Gene 41	MCM? (Tag)	DNA2?
	DNA helicase					
	ssDNA binding protein	ssb		Gene 32	RPA (replication protein A)	yRPA (RFA1, 2, 3)
	Primase	DnaG		Gene 61	DNA polymerase a/primase	primase (PRI1, PRI2)
Elongation	DNA polymerase	DNA polymerase III		Gene 43	DNA polymerase a/primase	DNA polymerase I (pola: POL1 = CDC17)

				DNA polymerase s	DNA polymerase II (pol e: POL2)
				DNA polymerase e	DNA polymerase III (pol d: POL3 = CDC2)
	DNA polymerase	bsubunit	Gene 45	PCNA (proliferating cell nuclear antigen)	yPCNA (POL30)
	Accessory proteins				
		g complex	Gene 44/62	RFC (replication factor C)	yRFC (CDC44 = RFC1, RFC2, RFC3, RFC4, RFC5)
	Swivel	Gyrase	T4 Topo	Topoisomerase I	TOP 1
		TopA		Topoisomerase II	TOP 2
Maturation	Decatenation	Gyrase		Topoisomerase II	TOP 2

Some proteins that have roles in other cellular processes function as replication proteins at specific stages in DNA replication; eg, **RNA polymerase** is necessary to activate several replication origins or to synthesize primer RNA; a **heat-shock** protein, grpE, is required to initiate lambda phage DNA replication, and thioredoxin is involved in T7 phage DNA polymerase.

Replication of T4 phage DNA is dependent primarily on its own encoded proteins, and a search for its replication proteins was carried out by the **conditional mutant** technique. As a result, seven replication proteins essential for the DNA synthesis, and many proteins with related functions, were identified.

Reconstitution of these replication reactions revealed that the replication factors do not react with a template DNA individually, but as a multimeric protein complex. Furthermore, the configurations and functions of the complex alter successively, from pre-initiation to elongation stages. For example, an assembly of DNA helicase and primase (and the assembly factors in some cases), called the *primosome*, is formed at the replication origins (or the assembly sites); subsequently, the addition of two DNA polymerase subunits and their accessory proteins in this complex generates a *replisome*, a super-protein complex that synthesizes **leading and lagging** DNA strands coordinately at a replication fork (2).

Due to the difficulty of applying **genetics** to most eukaryotes, the identification of eukaryotic replication proteins was started by a search of activities known to be involved in replication, such as DNA polymerases, topoisomerases, and DNA ligases. In contrast, a unicellular eukaryote, the **yeast** *Saccharomyces cerevisiae*, is exceptionally adaptable for genetic analysis, and many genes necessary for the cell cycle to progress have been identified. However, it was difficult to identify their biochemical activities and distinguish their requirement in DNA replication, due to the absence of any *in vitro* replication systems. The first breakthrough in studies of eukaryotic replication proteins occurred with the development the SV40 virus *in vitro* DNA replication system using human cell lysates (for a review, see (3)). Replication of this virus largely relies on the replication functions of the cell, so fractionation could identify the required proteins; this has isolated several replication proteins also involved in cellular chromosomal DNA replication. Furthermore, because these replication proteins are highly conserved throughout eukaryotes, several yeast replication genes were identified by homology searches (Table 1). Using previously and newly identified replication proteins, the process of SV40 DNA replication was totally reconstituted, and the functions of the proteins in DNA replication have been well elucidated (4). The replication reaction can be roughly divided into four stages: pre-initiation, initiation, elongation, and segregation (maturation), and specific sets of replication proteins are required to process these stages. The SV40 replication system primarily reproduced the cellular replication reaction from elongation to maturation but, in contrast, insufficient information about cellular initiation proteins was obtained from this viral system. One characteristic feature of eukaryotic DNA elongation obtained from the analysis is the involvement of multiple DNA polymerases in one replication fork.

Another breakthrough was the discovery of the origin recognition complex (ORC) from yeast (5) and licensing factor (MCM) from Xenopus (6). ORC specifically binds to the yeast replication origin sequence in an ATP-dependent manner and is a strong candidate for the initiator protein. MCM is a key player in the licensing reaction, and yeast MCM forms a pre-replicative complex at the origin, together with ORC. Through studies on their functions, the understanding of yeast chromosomal DNA replication has progressed drastically. Furthermore, these proteins are also highly conserved among eukaryotes, implying the existence of a common mechanism to initiate eukaryotic chromosomal DNA replication.

Another specific feature of eukaryotic replication proteins is that the replication process is tightly linked with several eukaryote-specific processes, such as cell-cycle control and chromatin assembly, so the boundary between replication and these processes is ambiguous. Therefore, **cyclin**-dependent kinases, licensing factors, and chromatin assembly factors are part of replication factors in eukaryotes and, indeed, some of them form assemblies with major replication proteins at replication foci during **S phase**.

Bibliography

1. T. A. Baker and A. Kornberg (1992) *DNA Replication*, 2nd ed., W. H. Freeman, New York, pp. 478–483.
2. K. J. Marians (1992) Ann. Rev. Biochem. **61**, 673–719.
3. B. Stillman (1989) Ann. Rev. Cell Biol. **5**, 197–245.
4. S. Waga and B. Stillman (1994) Nature **359**, 207–212.
5. S. P. Bell and B. Stillman (1992) Nature **357**, 128–134.
6. Y. Kubota et al. (1995) Cell **81**, 601–609.

DNA Sequencing

One of the fundamental methods of molecular biology is determining the sequences of bases in specific segments of DNA. The sequence information can be used to help deduce the function of the DNA segment, map its chromosomal location, determine how it might be involved in regulating gene expression or replication, or elucidate how it interacts with proteins. For example, the sequence of an unknown complementary DNA (cDNA) can be used to deduce the sequence of the protein encoded by its parent messenger RNA. In turn, this protein sequence can be compared with the sequences of all known proteins, giving clues to function and evolutionary origin (see Sequence Analysis).

1. Chain Termination, Sanger Method

The chain-termination method of DNA sequencing was first described by Sanger in 1977. This method involves synthesizing a DNA strand by a **DNA polymerase** *in vitro*. Synthesis is initiated at only one site, where a primer anneals to the template. The growing chain is terminated by incorporating a 2′,3′-dideoxynucleoside triphosphate (ddNTP) that does not support continued DNA synthesis (hence the name chain termination).

DNA polymerases initiate synthesis only at the 3′-end of a primer annealed to a DNA template. For most sequencing applications, the primer is a short synthetic oligonucleotide (18 to 35 nucleotides long) that is complementary in sequence to the template at a unique position adjacent to the region to be sequenced. The primer is hybridized to the template at the appropriate temperature (Fig. 1). Once this duplex is formed, the primer is extended by the DNA polymerase in the presence of the four deoxynucleoside triphosphates (dGTP, dATP, dTTP, and dCTP; dNTP corresponds to any one of the four).

Figure 1. Annealing of primer to template DNA.

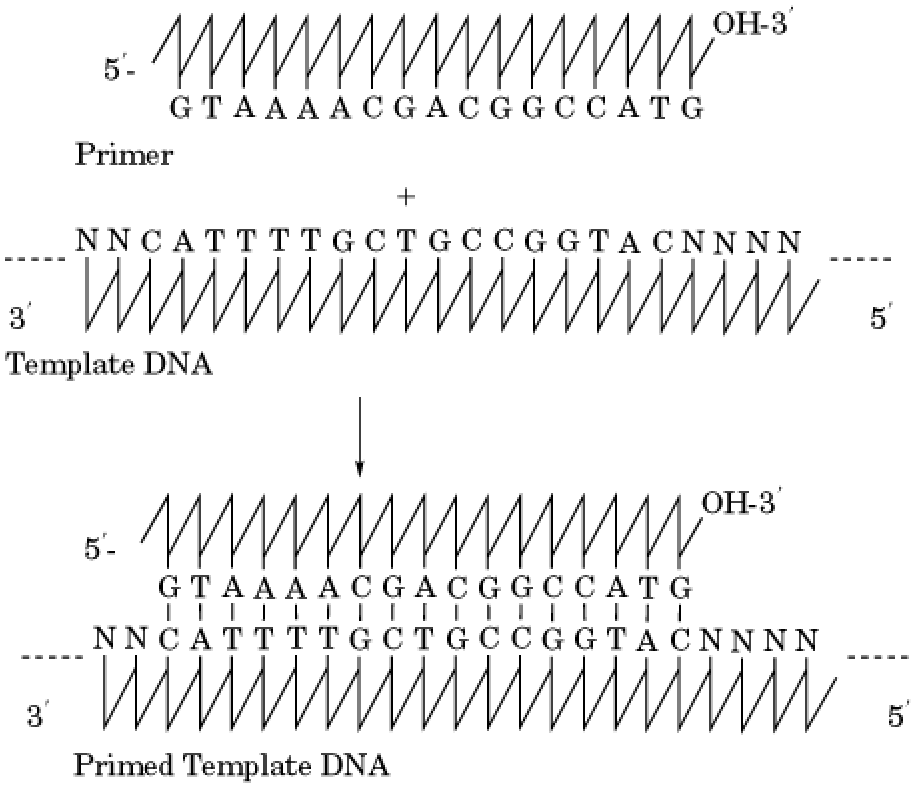

Polymerization of the new strand requires a free 3′-hydroxyl group (Fig. 2). As long as dNTPs are incorporated, there is a 3′ hydroxyl group available for continued polymerization of the growing chain (Fig. 3). However, dideoxynucleoside triphosphates (ddNTPs) lack a 3′-hydroxyl group and terminate chain elongation when incorporated into the DNA. Consequently, synthesis, directed by a sample of template DNA that has a unique primer, in the presence of all four deoxy- and one dideoxynucleoside triphosphate yields a population of molecules that have a common 5′-end, plus 3′-ends all of which have the same terminal dideoxynucleotide base, but have a distribution of sizes depending on the site at which the ddNTP is incorporated (Fig. 4). Thus, the size of each fragment is determined by the sequence of the template. Typically, four separate reactions are performed, each with a different ddNTP. The products of the four reactions are analyzed by electrophoresis using a denaturing polyacrylamide gel, which accurately separates the products by size. Because the size of each fragment is determined by the template sequence, this sequence can be determined from the order of the bands on the gel.

Figure 2. Biochemistry of chain elongation. In the presence of dNTPs, DNA polymerase catalyzes the condensation of deoxynucleoside triphosphate at the 3′-end of a primed template, releasing pyrophosphate.

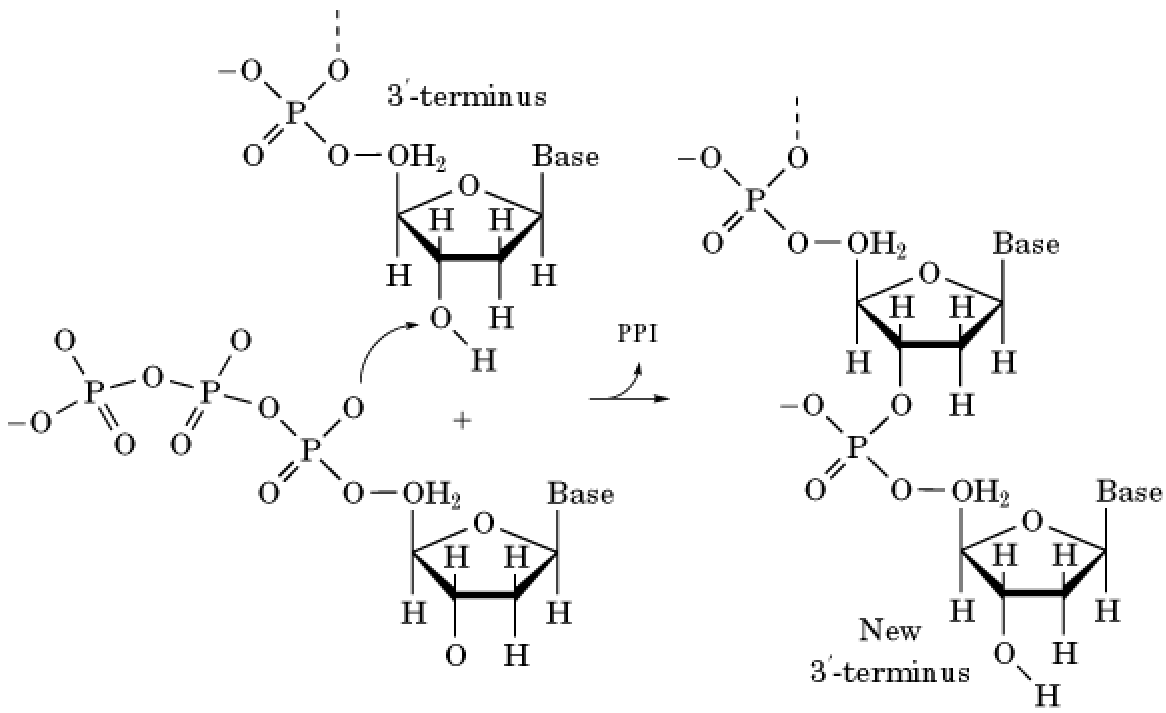

Figure 3. Chain elongation by DNA polymerase. As long as dNTPs are incorporated, there is a free 3′-hydroxyl group available for continued polymerization of the growing chain.

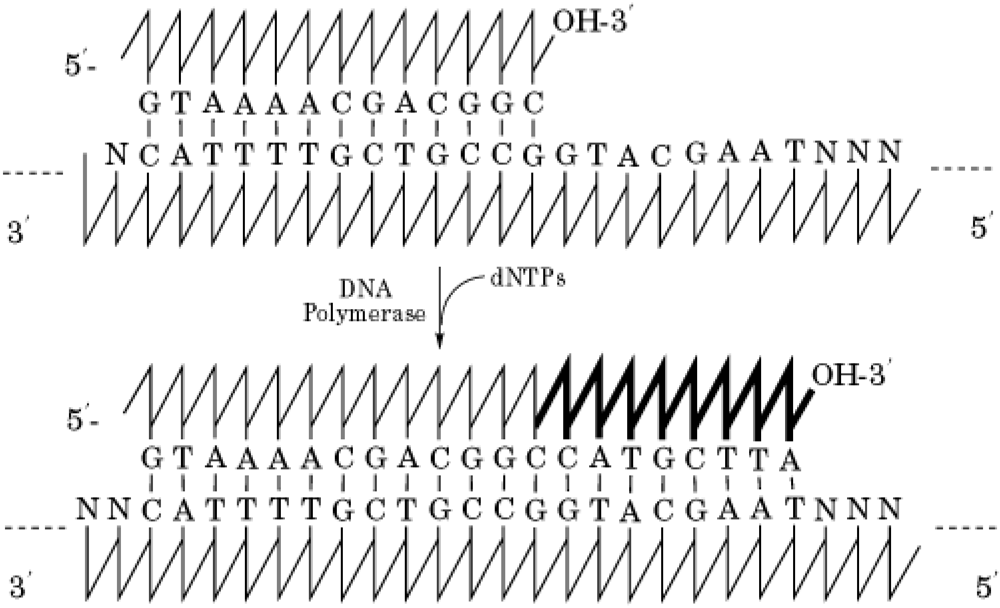

Figure 4. Chain termination. Synthesis from a unique primer in the presence of all four deoxy- and one dideoxynucleoside triphosphate yields a population of molecules with common 5′ ends, but different 3′-ends, depending on the site at which a ddNTP is incorporated.

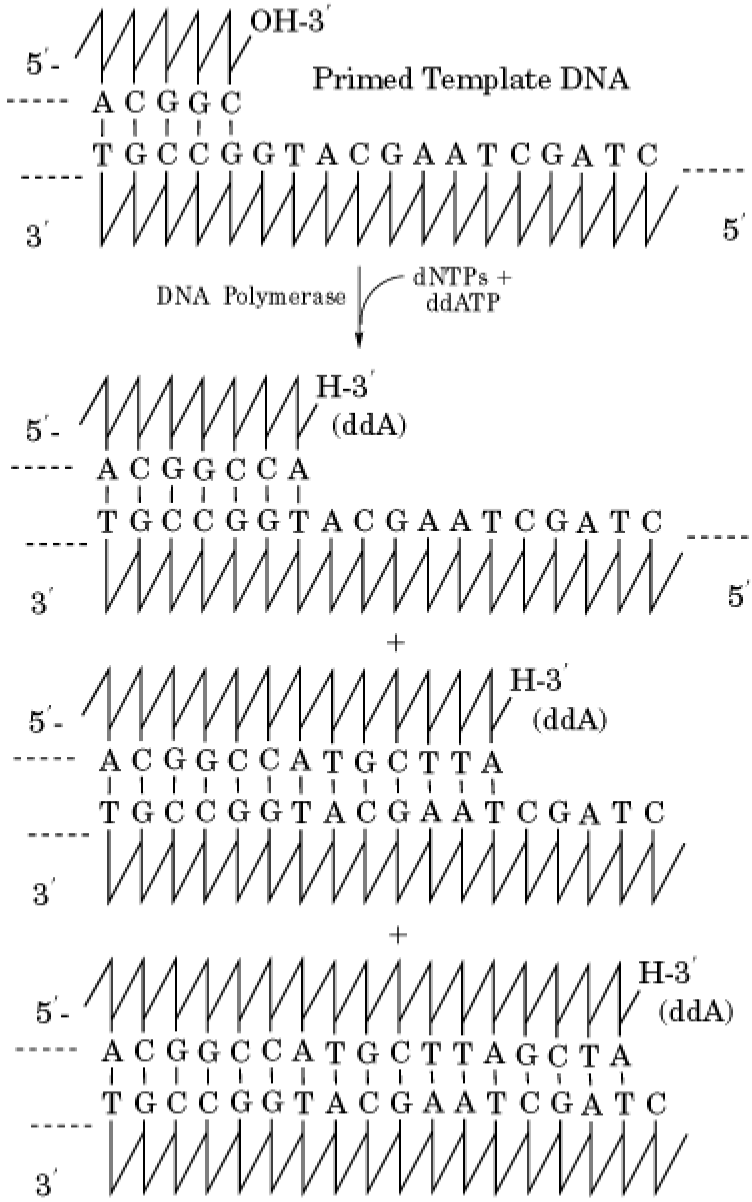

2. Chain Cleavage, Maxam–Gilbert Method

Another general sequencing method, known as the chain-cleavage or Maxam–Gilbert method, has also been used extensively. This method works by a similar method of mapping DNA sequence to DNA size, but does so by degrading existing DNA chains, rather than synthesizing new ones. A sample of purified DNA to be sequenced is first labeled at one end. Then the DNA is subjected to a chemical treatment that breaks each DNA molecule at random, but only at places where one (or a defined subset) of the bases occurs. The result is a population of labeled molecules whose sizes are determined by the sequence. Determination of the sizes on samples cleaved with several sequence-specific cleavage treatments yields complete sequence information. Unfortunately, it is difficult to find chemical cleavage conditions that consistently give unambiguous, clean cleavage products, and few labeling methods can be used that provide labels stable enough for these treatments. For these and other technical reasons, chain-cleavage methods are rarely used today.

Suggestions for Further Reading

F. Sanger, S. Nicklen, and A. R. Coulson (1977) DNA sequencing with chain-terminating inhibitors, Proc. Natl. Acad. Sci. USA. **74**(12), 5463–5467.

A. M. Maxam and W. Gilbert (1977) A new method for sequencing DNA, Proc. Natl. Acad. Sci. USA **74**(2), 560–564.

A. M. Maxam and W. Gilbert (1980) Sequencing end-labeled DNA routinely with base-specific chemical cleavages, Methods Enzymol. **65**, 499–560.

DNA Structure

The central roles of deoxyribonucleic acid (DNA) in life, especially those associated with the storage and transfer of genetic information, are now well established. The discovery of the structure of DNA double helix by Watson and Crick nearly half a century ago ushered the modern biology into a new era and forever changed the landscape of biology. It became clear that the three-dimensional structure of DNA is intimately associated with its function. Recently, the rapid advances in the ability to determine the structures of biological macromolecules has produced a great wealth of information. In the field related to DNA structure, we begin not only to understand the subtle, yet important, sequence-dependent conformation associated with the canonical Watson–Crick DNA double helix, but also to discover new structural forms of DNA and to visualize how DNA interacts with important biomolecules, such as proteins and drugs. A better understanding of the structural basis for the function of DNA will facilitate the rational design of compounds that contribute to improve the quality of life. The out-pouring of the DNA sequence information through various genome projects has made the effort of getting structural information associated with DNA an urgent one.

1. Chemical Structure

DNA is a biological polymer made of the deoxynucleotide building blocks (Fig. 1). Nucleotides, nucleosides, and nucleobases are discussed in that entry. The polynucleotide chain has a directionality due to the specific internucleotide phosphodiester linkage between the O3′ and O5′ atoms from two neighboring deoxyriboses. By convention, a polynucleotide chain is described as going from the 5′ to the 3′ direction. DNA oligonucleotides can now be synthesized routinely for a wide range of applications, including structural studies (see DNA Synthesis). For convenience, DNA oligonucleotides are denoted with their sequence in a form such as d(CGCGAATTCGCG).

Figure 1. The torsion angles (a, b, g, d, ε, z) of a polynucleotide sugar-phosphate backbone and the glycosyl torsion angle c are shown. The diagram show a fragment of B-DNA; therefore the deoxyribose conformation is C2′-*endo*, the glycosyl angle c is *anti*, and the a/z combination is gauche⁻/gauche⁻.

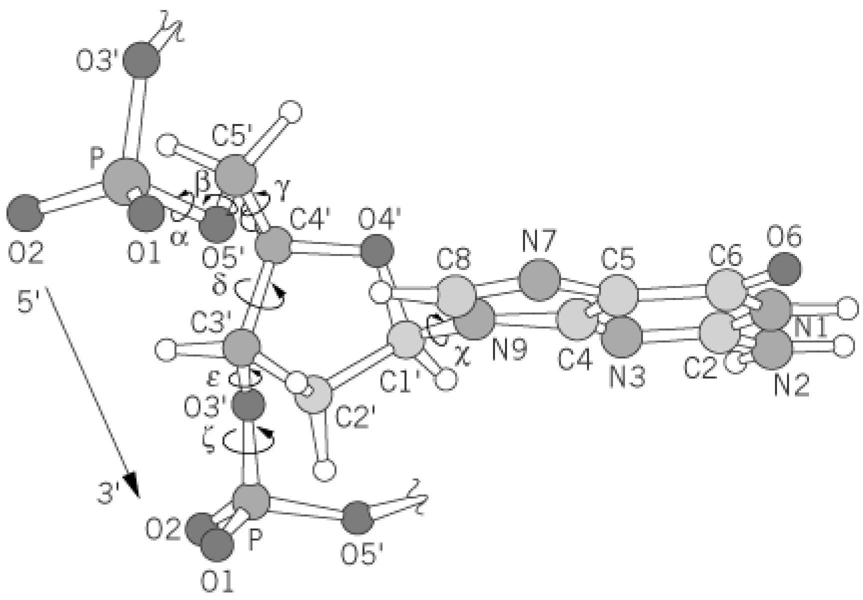

DNA is a polyelectrolyte because of the negative charges associated with the phosphate groups. The negatively charged DNA is neutralized by the positive charges of metal ions, polyamines, or proteins. Metal ions, such as sodium, potassium, or magnesium ions, are used in the screening of the DNA negative charges by interactions with the phosphate oxygen atoms, in enzyme reactions (eg, Mg^{2+} in **DNA polymerase's** function), or in the folding of more complex structures, such the guanine quartet structure.

The sugar–phosphate polynucleotide chain consists of many single bonds around which the attached atoms may rotate. The definition of the torsion angles of the DNA backbone is shown in Figure 1. The deoxyribose ring is nonplanar, and adopts two preferred "puckers," namely, C2′- *endo* and C3′-*endo* conformations. Two parameters, the sugar pseudorotation phase angle and its maximum torsion angle (ie, pseudorotation amplitude), are normally used to describe the puckering modes available in terms of the sugar torsion angles. Two preferred orientations (*anti* or *syn*) of the base with respect to the sugar (as defined by the torsion angle about the C1′━N glycosyl bond c) are found.

DNA predominantly exists as an antiparallel double-stranded helix. The two strands are helically coiled, which maximizes the exposure of the negatively charged sugar–phosphate backbone to water and shields the **hydrophobic** aromatic bases in the middle from water. In the Watson–Crick base pairs of guanine with cytosine (G:C) and adenine with thymine (A:T), the specificity of base pairing is provided by hydrogen bonds. It should be noted that other types of base pairs are also known to exist, and they often are involved in unusual DNA structures.

2. DNA Double Helices

The polymorphism of DNA associated with different helical forms, under the influence of different environmental conditions, has begun to emerge in recent years. Much of the detailed structural information of DNA has been obtained through the high resolution X-ray crystallography analysis and nuclear magnetic resonance (NMR) spectroscopic analysis of DNA oligonucleotides with defined sequences. A survey of the Nucleic Acids Database (site currently unavailable) and their complexes with proteins and drugs indicates that hundreds of crystal structures are available. Additional structures solved by NMR can also be found in the Brookhaven Protein Database (`http://www.pdb.bnl.gov/`). The structural features of the three common types of DNA helices—namely, the B-DNA, A-DNA, and Z-DNA—are illustrated in Figure 2, detailed in Table 1, and described in more detail in the individual entries.

Figure 2. End view and side view of the B-DNA, A-DNA, and Z-DNA helices. Note the decrease in diameter, as well as the relative positions of the base pairs and backbone to the helix axis. See color insert.

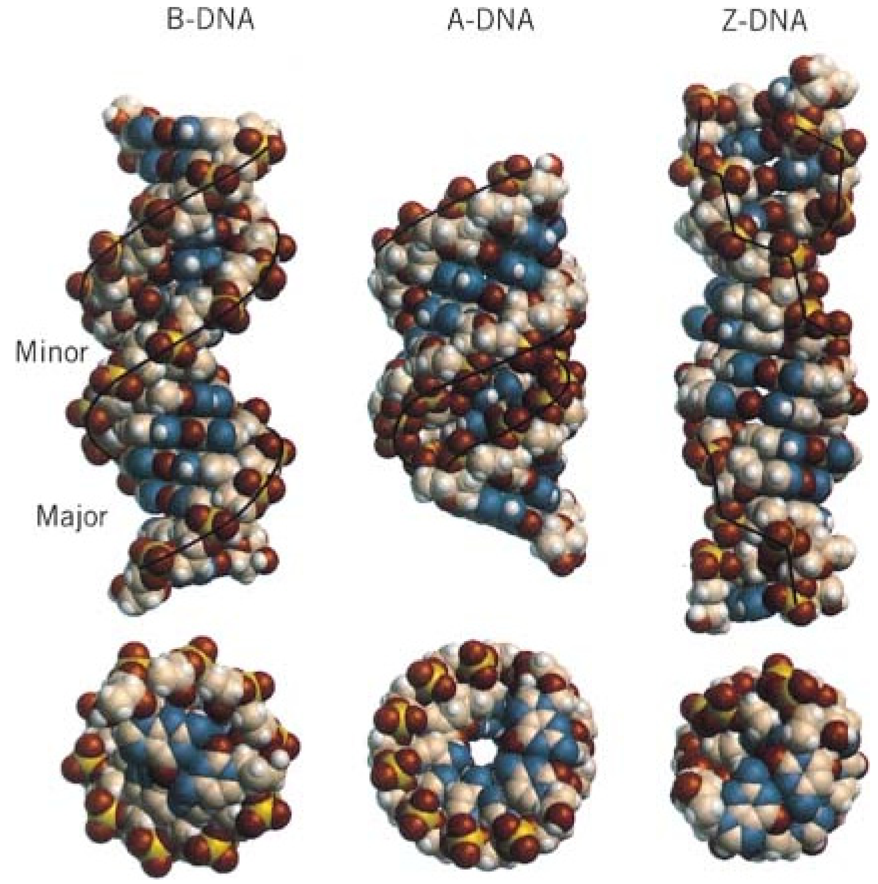

Table 1. Structural parameters of B-DNA, A-DNA, and Z-DNA

Structural Parameter Helical Sense	B-DNA Right-handed	A-DNA Right-handed	Z-DNA Left-handed
Repeat unit (bp)	1	1	2
Base pair/turn (degrees)	10.4	11	12
Tilt (degrees)	~ 0	19	–9
Rise per base pair (Å)	3.3	2.3	3.7
Helical pitch (Å)	34	25.4	45
Glycosyl angle	*anti*	*anti*	*anti* at C/*syn* at G
Sugar pucker	C2′-*endo*	C3′-*endo*	C2′-*endo* at C C3′-*endo* atG
Phosphate conformation (a/z)	–40/–98°	–88° /–44°	–146° /80° at C

			60° /–58° at G
Helical diameter (Å)[a]	~ 20	~ 25	~ 18
Major groove	Wide and deep	Narrow and deep	Flattened
Minor groove	Narrow and deep	Wide and shallow	Narrow and deep

[a] Conversion factor for angstroms to meters is 1.0 × 10⁻.

3. Hydration

The hydration environment around a DNA double helix plays an important role in determining the type of conformation adopted and in determining other properties. Recent structural work suggested that some proteins, such as the Trp repressor (see TRP Operon) and the EcoRI restriction enzyme, recognize DNA sequences through direct hydrogen bonds, nonpolar contacts, indirect structural effects, and, surprisingly, water-mediated interactions. Thus specific water molecules play critical roles in the sequence-specific recognition by proteins. More recently, it was found that water molecules play a different role in that they modulate the binding of sequence-nonspecific DNA-binding proteins (eg, Sac7d) to DNA of random sequence (1). Thus it is now generally accepted that the hydration shell surrounding the DNA molecule plays an important role in DNA recognition by proteins and other ligands, such as DNA-binding anticancer drugs.

4. Novel DNA Structures

Certain sequences of DNA form three-dimensional structures that are not the common A-, B- or Z-DNA double helices. Those sequences form higher order structures such as a hairpin loop, **triple-stranded** structures, tetrastranded structures, and cruciform. They often involve nonstandard base pairs. For example, the self-pairing of guanine bases are found in the tetrastranded guanine-quartet structure. Specific functions have already been identified for some of these higher order structures. The known multistranded structures include the Guanine Quartet, the I-Motif, the triple helix, and the Cruciform (Holliday Junction), which are described in the individual entries. Some of the novel double-stranded structures are discussed here.

4.1. Bend DNA

Certain DNA sequences have abnormal mobilities in gel electrophoresis. For example, DNA fragments having repeats of $(A)_n$ nucleotides (with $n \geq 4$), separated by another four to five nucleotides and phased with the helical repeat, migrate in the gel significantly more slowly than do those having mixed sequences. It was discovered that the 5′-AAAAA sequence has an intrinsic bending property that can be demonstrated by the increased efficiency of cyclization of those bend DNA fragments. The molecular basis of the intrinsic bendability of the $(A)_n$ sequence has been investigated. The high propeller twist associated with the A-T base pair in the $(A)_n$:$(T)_n$ sequence may play an important role in this property. The bend in those sequences is relatively smooth, resulting in a curved DNA structure. The opening (roll) of the bend is toward the minor groove. Many proteins induce such a smooth bending, by having many small single-step bends, which has been observed in the crystal structures of a number of protein–DNA complexes, exemplified by the structure of the 434 repressor–DNA complex (Protein Database accession number PDR015) shown in Figure 3**a**.

Figure 3. Two types of DNA bending modes. (**a**) Smooth bending found in the 434 repressor–DNA complex (Protein Database PDR015). (**b**) Sharp kink found in the Sac7d–DNA complex (Protein Database 1AZP).

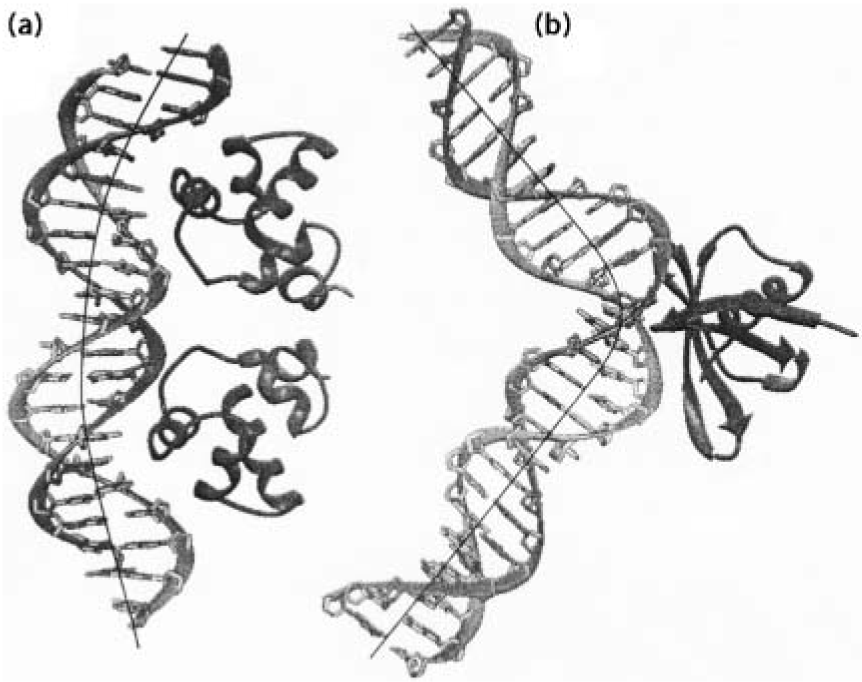

Another type of bend DNA is found to have a sharp kink at a localized site, usually caused and stabilized by DNA-binding proteins bound to DNA. A relevant example is found in a recent structure of the complex between a chromosomal 7-kDa protein Sac7d from the hyperthermophilic archaeabacterium *Sulfolobus acidocaldarius* and DNA oligonucleotides (1). The DNA is kinked sharply at the C_2pG_3 step in the Sac7d-GCGATCGC complex (Figure 3 **b**). The sharp kink is caused by the intercalation of the side chains of amino acid residues Val26 and Met29 of the Sac7d protein into DNA base pairs from the minor groove direction, widening the minor groove at this step.

This type of sharp DNA kink has been observed in the complexes of TATA-box binding protein (TBP), and two **HMG**-box containing proteins, LEF-1 and SRY, with their cognate-specific DNA sequences. Remarkably, both Sac7d and TBP use amino acids on a beta-sheet for the intercalation, whereas in LEF-1 and SRY use the amino acids located at the corner of the **alpha-helical** L-shaped HMG box for the intercalation. A more thorough discussion of the structural basis of the various types of DNA bending has appeared recently (2).

4.2. Triplet-Repeat Sequences

Recently a number of human genetic diseases have been correlated with expansions of triplet repeats of the DNA sequence $(CNG)_n$. The $(CGG)_n$ repeat in the X-chromosome is responsible for fragile-X syndrome, the $(CAG)_n$ repeat is associated with Huntington's disease and spinobulbar muscular atrophy, and finally the $(CTG)_n$ repeat is associated with myotonic dystrophy. How these unusual repetitive sequences correlate with the etiology of these diseases, and the mechanism by which those repeats are expanded during DNA replication, are under intense scrutiny. Some have proposed that a “slippage” process occurs because of the ease of the formation of hairpin structures for these repeating sequences. Certain triplet repeats, such as $(CAG)_n$ and $(CTG)_n$, but not $(CGA)_n$, have a strong propensity to form hairpin structures. Therefore, a DNA duplex encoding the $(CAG)_n$:$(CTG)_n$ repeats may easily exchange between duplex and cruciform, especially under negative **supercoiling** strain. If there are proteins or other ligands (eg, drugs) that can stabilize the stem of the cruciform, this process would be inhibited. The three-dimensional structures of several DNA oligonucleotides associated with those novel triplet repeats have been studied, primarily by NMR. The $(CAG)_n$ repeat can form a stable duplex structure incorporating "sheared" G-A mismatched base pairs. The duplex structure associated with the $(CCG)_n$ repeat appears to have the C nucleotides extruded from the helix. The structural and functional studies of those unusual repeats remain very active (3). (See also Trinucleotide Repeats.)

4.3. Parallel-Stranded DNA Duplex

A new addition to non-canonical DNA structures is the parallel-stranded (PS) DNA structures. The question of whether a stable DNA duplex can be parallel has been addressed previously (4). A series of A,T-containing DNA sequences was designed to form parallel duplexes using reversed Watson–Crick base pairs. The stability of those PS duplexes is modest; for example, the T_m **(melting temperature)** of a 21-mer PS-duplex is 15°C lower than that of the corresponding antiparallel duplex. A different motif was the non-Watson–Crick homo base-paired parallel-stranded DNA, called P-DNA. It was demonstrated that the d(CGA) sequence has a strong propensity to form the P-DNA structure (5).

An important requirement for a hetero base-paired parallel duplex is that the two glycosyl bonds within a base pair have to come from opposite directions, because of the identical chain polarity. For the normal nucleic acid bases, this can be accomplished using the reverse Watson–Crick base-pair conformation. However, A-T and G-C base pairs in a reverse Watson–Crick conformation are not isostructural, due to their hydrogen-bonding restrictions. Therefore, it has not been easy to design a stable PS duplex in which all four bases can be incorporated in random order.

This difficulty has been overcome by using alternative nucleosides, 2′-deoxyisoguanosine (iG) and 2′-deoxy-5-methyl-isocytosine (iC), which can form stable reverse Watson–Crick base pairs with the normal 2′-deoxycytosine (C) and 2′-deoxyguanosine (G), respectively. Indeed, oligodeoxynucleotides containing iG and iC can form remarkably stable parallel-stranded duplexes with the complementary (G,C)-containing DNA or RNA strands (6). The ability of (iG,iC)-containing DNA oligomers to form specific stable parallel-stranded duplexes may offer new opportunities for designing useful probes for applications such as antisense or aptamer molecules.

5. Summary

In conclusion, the importance of DNA structure and dynamics in biology is very clear. The rapid advancement in genomics, molecular biology and structural biology (including synchrotron) offers an exciting future in the investigation of the protein and nucleic acid structures associated with new and significant biological functions. One can now attack problems that were unthinkable just a few years ago. The structure of the nucleosome has been determined at 2.8 Å resolution and the detailed DNA conformation has been presented (7). The structure of the ribosome particle is on its way to be elucidated at a resolution high enough to visualize individual proteins and RNA. It can be certain that many structures of novel DNA sequences and important protein–DNA complexes will be forthcoming at a rapid pace in the next few years.

Bibliography

1. H. Robinson, Y.-G. Gao, B. S. McCrary, S. P. Edmondson, J. W. Shriver, and A. H.-J. Wang (1998) Nature **392**, 202–205.
2. R. E. Dickerson (1998) Nucleic Acids Res. **26**, 1906–1926, and references cited therein.
3. A. M. Gacy and C. T. McMurray (1998) Biochemistry **37**, 9426–9434, and references cited therein.
4. J. H. van de Sande et al. (1988) Science **241**, 551–557.
5. H. Robinson and A. H.-J. Wang (1993) Proc. Natl. Acad. Sci. USA **90**, 5224–5228.

6. X.-L. Yang, H. Sugiyama, S. Ikeda, I. Saito, and A. H.-J. Wang (in press) Biophys. J.
7. K. Luger, A. W. Mader, R. K. Richmond, D. F. Sargent, and T. J. Richmond (1997) Nature **389**, 251–260.

Suggestions for Further Reading

8. W. Saenger (1984) *Principles of Nucleic Acid Structure*, Springer-Verlag, New York.
9. C. R. Calladine and H. R. Drew (1992) *Understanding DNA*. Academic Press, San Diego.
10. R. R. Sinden (1994) *DNA Structure and Function*, Academic Press, San Diego.
11. G. M. Blackburn and M. J. Gait, eds. (1996) *Nucleic Acids in Chemistry and Biology*, Oxford Univ. Press, New York.
12. S. M. Hecht, ed. (1996) *Bioorganic Chemistry: Nucleic Acids*, Oxford Univ. Press, New York.

DNA Synthesis

The introduction of methods for the chemical synthesis of oligo- and poly- deoxyribonucleotides (DNA sequences) has had a very considerable effect on the development of molecular biology. This is clearly apparent from other sections of the Encyclopedia. The three most important factors to be taken into account in the chemical synthesis of DNA sequences are:(1) the choice of suitable protecting groups for the 2’-deoxyribonucleoside building blocks [**1**], (2) the development of phosphorylation procedures that are suitable for the introduction of the internucleotide linkages, and (3) the purification of the synthetic DNA sequences themselves. The choice of protecting groups is of crucial importance. The protecting groups selected should be easy to introduce; they should also remain completely intact throughout the assembly of the DNA sequences and be easily removable under conditions where the synthetic DNA is completely stable.

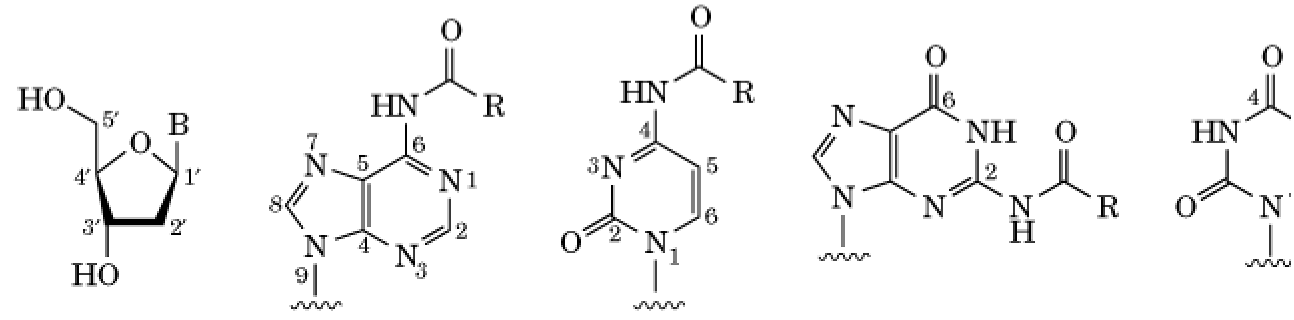

1 **2a**; R = Ph **3a**; R = Ph **4a**; R = Me_2CH **5**

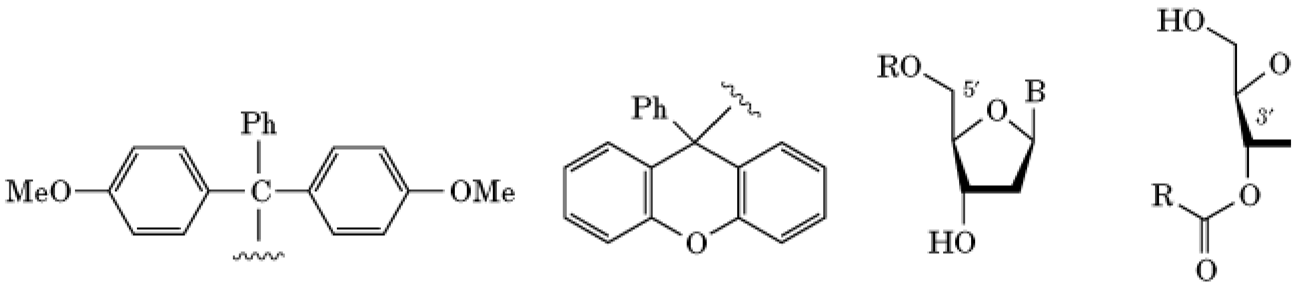

(DMTr) **6** (Px) **7** **8a**; R = **6** **b**; R = **7** **9a**; R = CH_2C

Structure 1. DNA synthesis.

1. Protecting Groups for 2'-Deoxynucleosides

In order to avoid side reactions during phosphorylation, the adenine, cytosine, and guanine base residues are generally protected with acyl groups [e.g. as in **2a, 3a**, and **4a**, respectively], but thymine residues [**5**] are usually left unprotected (1). It may sometimes be desirable (2) to protect thymine residues [**5**] on *O*-4 and *N*-2-acylguanine residues [**4**] also on *O*-6, but this depends on the phosphorylation procedure used. An important feature of DNA chemistry is that the glycosidic linkages, and especially those of purine deoxyribosides, are very sensitive to acid. Thus, the (di-*p*-anisyl)phenylmethyl (DMTr, [**6**]) and the 9-phenylxanthen-9-yl (Px, [**7**] groups, which are removable under relatively mild acidic conditions, are particularly useful for the protection of the 5'-hydroxy functions of 2'-deoxynucleosides [as in **8a** and **8b**, respectively]. 5'-O-Acyl-protected deoxynucleosides ([**8**] R = acyl) have also been used as starting materials, particularly in the solution phase synthesis (see below) of DNA sequences. Acyl groups are also used to protect the 3'-hydroxy functions of deoxynucleosides [e.g. as in **9a**]. Both *N*-acyl and *O*-acyl protecting groups are usually removed at the end of the synthesis by ammonolysis under conditions where DNA is completely stable.

2. Phosphorylation Methods

There are essentially three phosphorylation methods (Fig. 1) that have been used successfully in the chemical synthesis of relatively high molecular weight DNA sequences.

Figure 1. Phosophorylation methods.

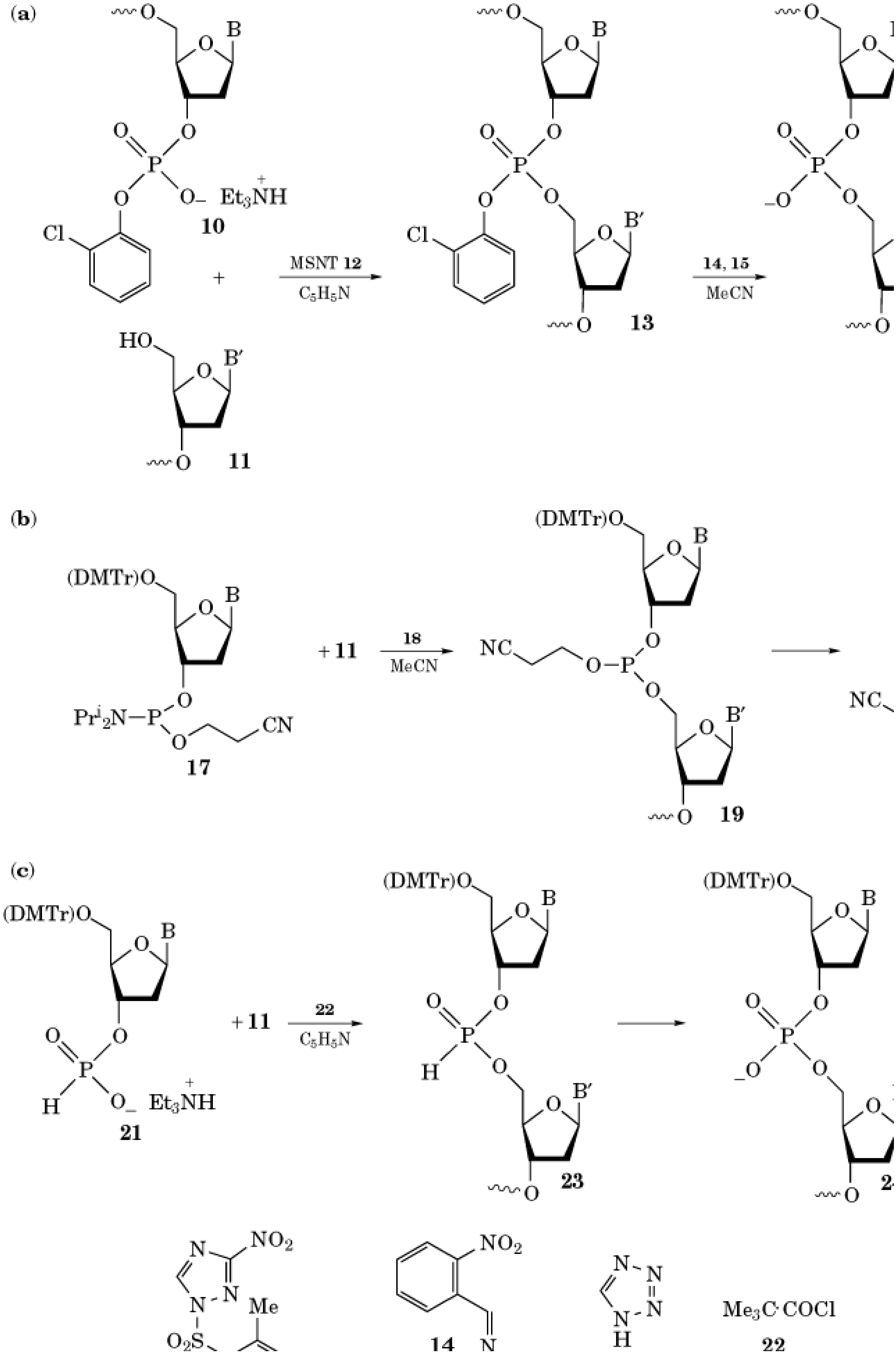
(a)
10
11
MSNT 12
C5H5N
13
14, 15
MeCN
(b)
17
+ 11
18
MeCN
19
(c)
21
+ 11
22
C5H5N
23
14
Me3C·COCl
22

2.1. Phosphotriester Approach

The first method, which involves coupling a protected nucleoside or oligonucleotide 3'-(2-chlorophenyl) phosphate [**10**] with a protected nucleoside or oligonucleotide component with a free 5'-hydroxy function [**11**] (Fig. 1a), is usually referred to as the *phosphotriester approach* (3) as all of the internucleotide linkages are protected as phosphotriesters throughout the assembly of the target DNA sequences. In a now obsolete method known as the *phosphodiester approach*, the internucleotide linkages were left unprotected throughout the assembly of the DNA sequences. Coupling between the two components [**10**] and [**11**] is usually effected by a condensing agent such as 1-(mesitylene-2-sulfonyl)-3-nitro-1,2,4-(1*H*)-triazole (MSNT) [**12**] in anhydrous pyridine solution (4). The 3'-(2-chlorophenyl) phosphate component [**10**] is usually used in slight (*ca.* 20% to 25%) excess, and the condensing agent (e.g., MSNT), which also acts as a dehydrating agent, is used in greater excess. A very important feature of the phosphotriester approach is that the first unblocking step of the fully-assembled DNA sequence is effected by treatment (4) with an excess each of an appropriate oxime (such as (*E*)-2-nitrobenzaldoxime [**14**]) and N^1,N^1,N^3,N^3-tetramethylguanidine [**15**]. Such oximate treatment leads to complete removal of the 2-chlorophenyl protecting groups without any concomitant cleavage of the internucleotide linkages. *N*- and *O*-Acyl protecting groups [as in **2, 3, 4** and **9**] are subsequently removed by treatment with concentrated aqueous ammonia, and the 5'-terminal acid-labile protecting group [as in **8a** and **8b**] is removed under mild conditions to leave the fully unprotected DNA sequence. The phosphorotriester approach is an extremely versatile method for the synthesis of DNA sequences; it can be used both in solution phase (by the stepwise addition of mononucleotides or by the addition of oligonucleotide blocks) (4) and in **solid phase synthesis** (5).

2.2. H-Phosphoroamidite Approach

The second phosphorylation method is generally based on protected nucleoside 3'-(2-cyanoethyl) *N,N*-di-isopropylphosphoramidites [**17**] and may be referred to as the *phosphoramidite approach* (6). In the presence of relatively weak acids (e.g., 1*H*-tetrazole [**18**]), such phosphoramidites [**17**] become powerful phosphitylating agents and react with protected nucleoside or oligonucleotide components with free 5'-hydroxy functions [**11**] (Fig. 1b) to give protected phosphite triesters [**19**]. These phosphite triesters triesters are sensitive intermediates and are usually immediately oxidized (e.g., by treatment with iodine and 2,6-lutidine in aqueous tetrahydrofuran) to give the corresponding phosphotriesters [**20**]. The 2-cyanoethyl protecting groups are removed from the fully-assembled DNA sequences, together with the *N*- and *O*-acyl protecting groups, by treatment with concentrated aqueous ammonia. A crucial aspect of the phosphoramidite approach is that activated derivatives of *phosphorous* acid are much more reactive than corresponding activated derivatives of *phosphoric* acid. Therefore, in the phosphoramidite approach, coupling yields tend to be somewhat higher, and the coupling recations are faster than they are in the phosphotriester approach. Largely for these reasons, the phosphoramidite approach has become the method of choice for the automated solid phase synthesis of DNA sequences (see text below); it has, therefore, been very widely used in the chemical synthesis of the relatively small quantities of the DNA sequences that are required in most molecular biological studies.

2.3. H-Phosphonate Approach

The third phosphorylation method is based on protected nucleoside 3'-(H-phosphonate) monoesters [**21**] as building blocks and is generally referred to as the *H-phosphonate approach* (78). Both H-phosphonate building blocks [**21**] and 2-chlorophenyl phosphates [e.g., **10**] are very easy to prepare; they are also more stable and easier to handle than phosphoramidite building blocks [**17**]. However, partly perhaps because they are less bulky, H-phosphonates [**21**] undergo coupling reactions more rapidly than the corresponding 2-chlorophenyl phosphates. Thus, coupling between a nucleoside 3'-(H-phosphonate) building block [**21**] and a protected nucleoside or oligonucleotide with a free 5'-hydroxy function [**11**] (Fig. 1c) occurs very rapidly in the presence of a condensing agent such as pivaloyl chloride [**22**] (8) in pyridine solution to give the corresponding H-phosphonate diester [**23**]. Such H-phosphonate diesters [**23**] are particularly sensitive to base-catalyzed hydrolysis, and for this reason almost all synthetic studies involving the H-phosphonate approach have been carried out in the solid phase (see text below). When a particular DNA sequence has been fully assembled, the H-phosphonate diester groups [as in **23**] are oxidized (e.g., with iodine in the presence of a base in aqueous tetrahydrofuran) to give unprotected phosphodiester internucleotide linkages [as in **24**] before the *N*- and *O*-acyl protecting groups are removed by treatment with concentrated aqueous ammonia. Despite its merits and its potential as an important synthetic method, the H-phosphonate has not been as widely used as the phosphoramidite approach in solid-phase synthesis. However, recent studies suggest that a modified H-phosphonate approach (see text below) may well become the method of choice in the solution-phase synthesis of DNA sequences. Indeed, there is no obvious reason why such a modified H-phosphonate approach could not also be applied successfully to solid-phase synthesis.

3. Solid-Phase DNA Synthesis

Relatively high molecular weight DNA sequences have been prepared successfully by the phosphotriester approach in solution by following essentially the procedure indicated in outline in Figure 1a. However, solution-phase synthesis is relatively laborious in that **chromatographic** purification steps are usually necessary after each coupling step. Nevertheless, if a very large quantity of a specific sequence is required (see text below), solution-phase synthesis may very well prove to be the method of choice. If, on the other hand, relatively small (i.e., milligram to gram) quantities of material are required for biological or biophysical studies, there is little doubt that solid-phase synthesis is to be preferred. While all three of the above phosphorylation methods (Fig. 1) have been used in solid-phase synthesis, the phosphoramidite approach (9) has emerged as the method of choice. This is mainly because its use leads to high coupling efficiencies and no significant side reactions. Furthermore, most commercial automatic synthesizers have been designed specifically to accommodate phosphoramidite chemistry. The main advantages of solid-phase synthesis, particularly by the phosphoramidite approach, are: (1) that it is very rapid and a DNA sequence containing, say, 50 nucleotide residues can easily be assembled and unblocked within one day; (2) only one purification step is required at the end of a synthesis as the growing DNA sequence is attached to a solid support (such as controlled pore glass [CPG] or polystyrene), and the excesses of all reagents are washed away; (3) all chemical reactions can be made to proceed in very high yield by using large excesses of reagents; and (4) the whole process may be fully automated in a DNA synthesizer. Solid-phase DNA synthesis has been developed to such an extent that the whole process can be carried out by a competent technician with no specialist knowledge of nucleotide chemistry. Automatic synthesizers, some of which are capable of assembling several different specific DNA sequences simultaneously, are readily available, and all the necessary building blocks [particularly phosphoramidites **17**] and other reagents and solvents may be purchased in containers that are designed to be attached directly to the synthesizer.

The main steps in a synthetic cycle (i.e., the addition of one nucleotide residue) in solid-phase DNA synthesis by the phosphoramidite approach (10) are illustrated in outline in Figure 2a. Bottles containing solutions of each of the four main phosphoramidites [e.g. **17**, B = **2a,3a,4a** and **5**] in acetonitrile and other reagents and solvents are attached to the appropriate ports on the synthesizer. The desired 3'-terminal nucleoside residue is generally attached to the solid support (P; usually CPG or polystyrene) through a succinoyl linker [as in **25**], and this material is contained in a small column that is inserted in the synthesizer. The first step (Fig. 2**a**, step i) in the synthetic cycle involves treatment with acid to remove the 5'-*O*-DMTr protecting group [**6**] from the solid-supported 3'-terminal nucleoside residue [**25**]. The next step (step ii, the coupling step) is the *1H*-tetrazole-catalyzed reaction between a phosphoramidite [**17**] and the released 5'-hydroxy function [as in **26**] to give a phosphite triester [**27**]. A large excess each of the appropriate phosphoramidite [**17**] and 1*H*-tetrazole [**18**] are delivered automatically, leading to an anticipated coupling efficiency of *ca.* 98.5%. It is then important to "cap" any remaining 5'-hydroxy functions. This is effected by reaction with a very large excess of acetic anhydride in the presence of 1-methylimidazole and 2,6-lutidine in tetrahydrofuran solution (step iii). "Capping" in each synthetic cycle ensures that, at the end of the synthesis, most of the truncated sequences will be of significantly lower molecular weight than the target DNA sequence, thereby facilitating its purification. The phosphite triester group [as in **27**] is then oxidized (step iv) to a phosphotriester group. The first synthetic cycle is now complete. A number of washing steps are involved in addition to steps i to iv, and the whole cycle usually requires less than 8 min. The removal of the 5'-*O*-DMTr protecting group [**6**] [to give **28**] is the first step of the second synthetic cycle, and this is followed by another coupling reaction involving the appropriate phosphoramidite building block [**17**]. It is essential that the acetonitrile solutions containing the phophoramidites [**17**] and 1*H*-tetrazole [**18**] should be as dry as possible. The efficiency of the coupling steps may be estimated spectrophotometrically by measuring the quantities of the colored (di-*p*-anisyl)phenylmethyl ($DMTr^+$) cations released at the beginning of each synthetic cycle. It is essential that the "detritylation" and coupling steps (steps i and ii, respectively) should proceed as nearly quantitatively as possible, and that "capping" (step iii) should be as efficient as possible. Clearly, oxidation (step iv) of the phosphite triester to the phosphotriester group should also go to completion in each cycle. If the average coupling efficiency is 98.5%, it should be possible to prepare DNA sequences containing 50 and 100 nucleotide residues in *ca.* 47% and 22% overall yields, respectively. However, if the average coupling efficiency is only 97.5%, then the overall yields of a 50-mer and a 100-mer would fall to *ca.* 29% and 8%, respectively. Therefore, if reasonable care is taken, it should be possible to prepare DNA sequences containing up to *ca.* 100 nucleotide residues by solid-phase phosphoramidite synthesis.

Figure 2. *Reagents*: i, 3% $Cl_3C{\cdot}CO_2H,CH_2Cl_2$; ii, *1H*-tetrazole **18**, MeCN; iii, Ac_2O, 2,6-lutidine, 1-methylimidazole, T
H_2O-pyridine-THF; v, conc. aq. NH_3,55°C; vi, H^+,H_2O. Ⓟ: solid support, eg, CPG.

(**a**)

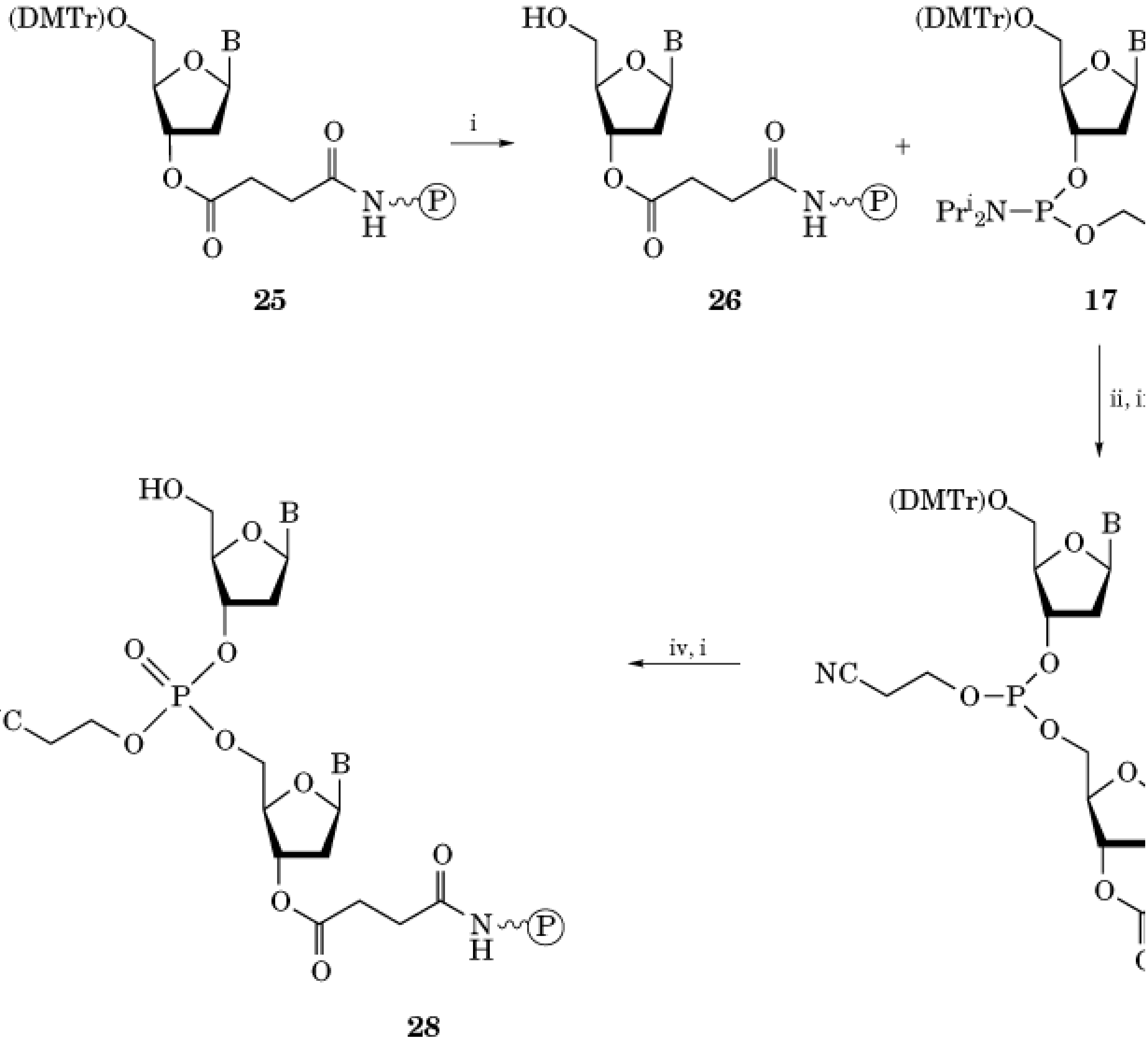
(DMTr)O
B
O
N
H
P
25
i
HO
26
+
17
Pr$^{i}_{2}$N
ii, i
NC
iv, i
28

(**b**)

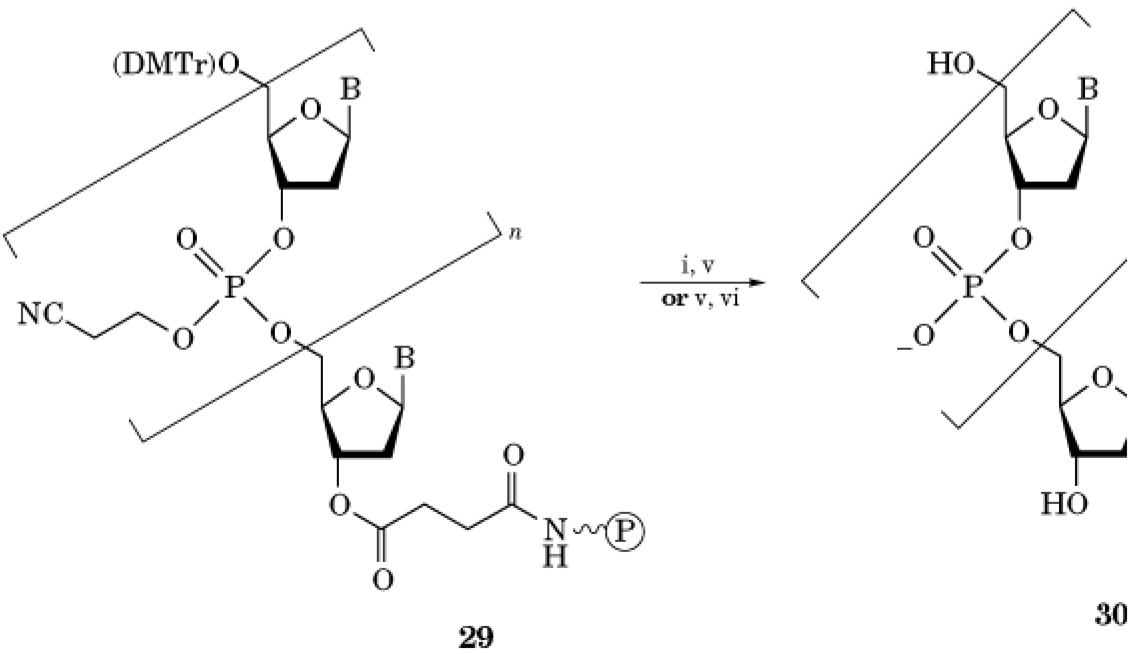
(DMTr)O
B
O
P
NC
n
N
H
P
29
i, v
or v, vi
HO
30

The target DNA sequence [**29**] is fully assembled after *n* complete synthetic cycles. The products must then be released from the solid support, and all the protecting groups need to be removed. Two alternative unblocking procedures are indicated in Fig. 2b. First, the 5'-terminal DMTr protecting group [**6**] is removed in what would be step i of the (*n*+1)th synthetic cycle. The loaded solid support is then treated with concentrated aqueous ammonia, usually at *ca.* 55°C (step v). This leads to the detachment of the synthetic DNA sequence from the solid support, the removal of all of the 2-cyanoethyl protecting groups from the internucleotide linkages and all of the *N*-acyl protecting groups from the base residues. The crude products obtained contain the target DNA sequence [**30**], contaminated with "capped" truncated sequences; this material is usually purified by high-performance liquid chromatography (HPLC) or by polyacrylamide gel electrophoresis (PAGE). In an alternative procedure (Fig. 2b, steps v and vi), the ammonolysis step is carried out before the removal of the 5'-terminal DMTr protecting group. The latter procedure is advantageous if purification of the crude products is to be carried out by **reversed-phase** HPLC as the difference between the retention times of the "capped" truncated sequences and the DNA target sequence, which is still protected with a 5'-*O*-DMTr group, is thereby increased. The DMTr protecting group is then removed by acidic hydrolysis under very mild conditions (step vi).

Automated solid-phase synthesis by the phosphoramidite approach has also been used successfully (11) in the preparation of DNA sequences in which the base residues, sugar residues, and internucleotide linkages are modified. DNA sequences with attached **fluorescent** and other **reporter** groups have also been prepared by solid-phase synthesis. Such modified DNA sequences have found numerous important applications in molecular biology.

4. Solution-Phase DNA Synthesis

Of the three phosphorylation methods described above, only the phosphotriester approach (Fig. 1a) is really suitable for the synthesis of DNA sequences in solution. This method, which was developed largely in the 1970s, is very versatile and is particularly suitable for the coupling of oligonucleotide blocks (i.e., the addition of two or more nucleotide residues at a time) as well as for stepwise synthesis. Phosphotriester block coupling was a key feature of the original synthesis of the human insulin gene (12). Although the methodology has been refined (13) since then, the development of automated solid-phase synthesis (see above) in the 1980s provided a much faster and less labor-intensive method for the preparation of the very small (usually milligram or even smaller) quantities of synthetic DNA sequences that are generally required in molecular biology. Solution-phase synthesis is much more laborious in that it is normally advisable to purify the products by chromatography after each coupling step. Although such purification processes need not necessarily amount to much more than filtration through a bed of silica gel, they are time consuming. Furthermore, solution-phase synthesis has not yet been automated. It is, nevertheless, not at all unlikely that solution-phase synthesis will become the method of choice if really large (i.e., multikilogram to tonne) quantities of moderately sized (containing *ca.* 20 nucleotide residues) DNA sequences or their analogs are required in **anti-sense** or antigene chemotherapy. Automated solid-phase synthesis has recently been scaled-up to the multigram level (14) in order to provide sufficient material for clinical trials. However, if such clinical trials are successful and very much larger quantities of pure DNA sequences and their analogs are required for drug purposes, further substantial scaling-up of solid-phase synthesis may not prove to be a practical proposition. It is quite likely that the solution-phase synthesis or perhaps a combination of solution-phase and solid-phase synthesis might lend itself much more readily to scaling-up. The phosphotriester approach has the further advantage that the fully-protected intermediates obtained are soluble in organic solvents and may, therefore, be purified by conventional chromatographic techniques, and, after all of the protecting groups have been removed, the unprotected DNA sequences obtained may, if necessary, be further purified in the same way as material that has been prepared on a solid support.

It is anticipated that success in the design of oligonucleotide drugs will stimulate further research and consequent improvements in solution-phase synthesis. Indeed, a modified phosphotriester approach involving low temperature H-phosphonate coupling (Fig. 3, step i) has recently been proposed (15).

This method appears to be more efficient than the conventional phosphotriester approach (Fig. 1a) in that virtually quantitative coupling yields are obtained, and no significant side-reactions are observed. The sensitive H-phosphonate diesters [corresponding to **23**] (Fig. 1c) are not isolated but are immediately converted at a low temperature into much more stable *S*-(4-chlorophenyl) phosphorothioates [**34**] by treatment with the phthalimide derivative [**33**] (Fig. 3, step ii). After the desired DNA sequence has been assembled, the *S*-(4-chlorophenyl) phosphorothioate groups [as in **34**] are quantitatively converted into phosphodiesters [as in **16**] by standard oximate treatment (Fig. 1a).

Figure 3. *Reagents*: i, **32**, C_5H_5N,CH_2Cl_2, –40°C, ii, a, **33**, C_5H_5N,CH_2Cl_2,–40°C, b, $C_5H_5N–H_2O$ (1 : 1 v/v), –40°C to room temp.; iii, **14, 15** (Fig. 1), MeCN, room temp.; iv, conc. aq. NH_3,55°C.

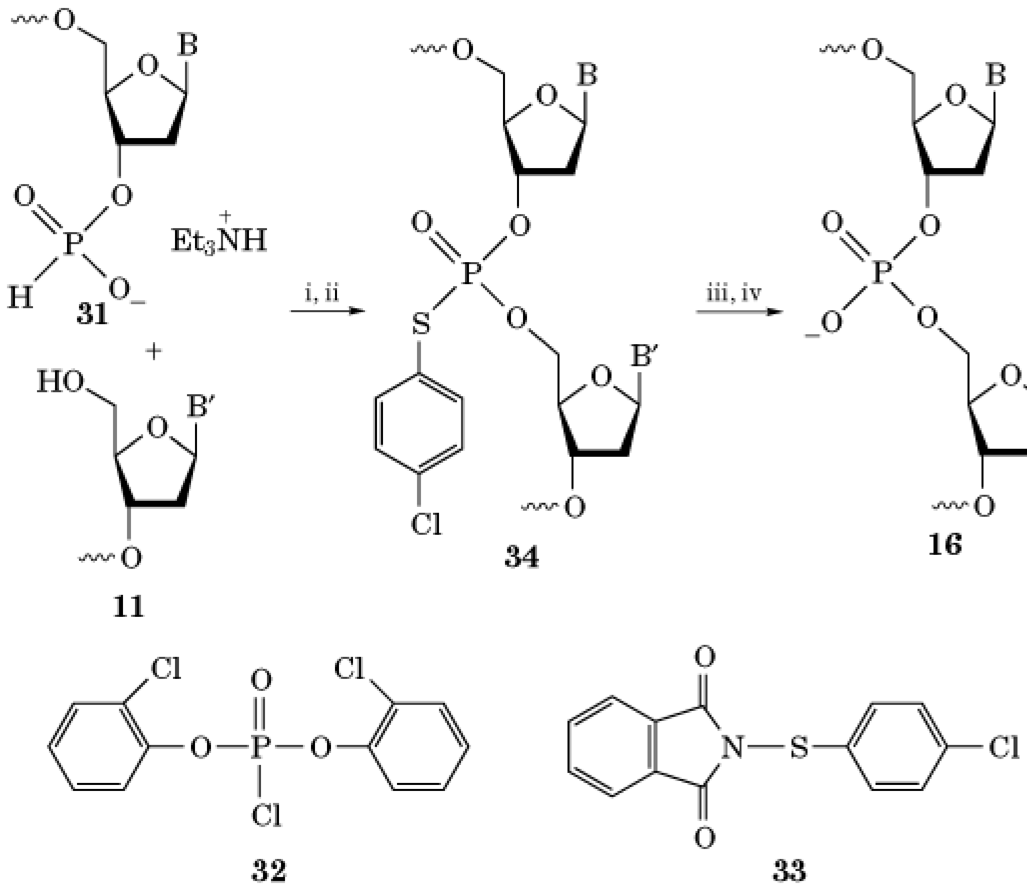

Bibliography

1. H. G. Khorana (1968) Pure Appl. Chem. **17**, 349–381.
2. C. B. Reese and P. A. Skone (1984) J. Chem. Soc., Perkin Trans. **1**, 1263–1271.
3. C. B. Reese (1978) Tetrahedron **34**, 3143–3179.
4. J. B. Chattopadhyaya and C. B. Reese (1980) Nucleic Acids Res. **8**, 2039–2053.
5. C. Christodoulou (1993) In *Methods in Molecular Biology*, Vol. **20**: Protocols for Oligonucleotides and Analogs, (S. Agrawal, ed.), Humana Press, Totowa, pp. 19–31.
6. S. L. Beaucage and M. H. Caruthers (1981) Tetrahedron Lett. **22**, 1859–1862.
7. P. J. Garegg, T. Regberg, J. Stawinski, and R. Strömberg (1985) Chemica Scripta **25**, 280–282.
8. B. C. Froehler and M. D. Matteucci (1986) Tetrahedron Lett. **27**, 469–472.

9. S. L. Beaucage and R. P. Iyer (1992) Tetrahedron **48**, 2223–2311.
10. T. Brown and D. J. S. Brown (1991) in *Oligonucleotides and Analogues: A practical Approach*, (F. Eckstein, ed.), IRL Press, Oxford, pp. 1–24.
11. S. Agrawal, ed. (1994) *Methods in Molecular Biology*, Vol. **26**: Protocols for Oligonucleotide Conjugates, Humana Press, Totowa.
12. R. Crea, A. Kraszewski, T. Hirose, and K. Itakura (1978) Proc. Natl. Acad. Sci. USA, **75**, 5765–5769.
13. C. B. Reese and Zhang Pei-Zhuo (1993) J. Chem. Soc., Perkin Trans. **1**, 2291–2301.
14. M. Andrade, A. S. Scozzari, D. L. Cole, and V. T. Ravikumar (1997) Nucleosides & Nucleotides **16**, 1617–1620.
15. C. B. Reese and Q. Song (1999) J. Chem. Soc., Perkin Trans. **1**, 1477–1486.

Suggestions for Further Reading

16. S. A. Narang, ed. (1987) *Synthesis and Applications of DNA and RNA*, Academic Press, Orlando.
17. F. Eckstein, ed. (1991) *Oligonucleotides and Analogues: A Practical Approach*, IRL Press, Oxford.
18. S. Agrawal, ed. (1993) *Methods in Molecular Biology*, Vol. **20**: Protocols for Oligonucleotides and Analogs, Humana Press, Totowa.
19. S. Agrawal, ed. (1993) *Methods in Molecular Biology*, Vol. **26**: Protocols for Oligonucleotide Conjugates, Humana Press, Totowa.
20. S. L. Beaucage and M. H. Caruthers (1996) In *Bioorganic Chemistry: Nucleic Acids*, (S. M. Hecht, ed.), Oxford University Press, New York, pp. 36–74.
21. S. L. Beaucage, D. E. Bergstrom, G. D. Glick, and R. A. Jones, eds. (2000) *Current Protocols in Nucleic Acid Chemistry*, Wiley, New York, pp. 3.1.1–3.4.11

DNA Topology

Double-stranded acquire DNA structures topological properties if organized into a topological domain, which is a closed region in which the two strands are linked. The known types of elementary topological domains are closed circular duplex DNA (cdDNA), in which the two strands are separately covalently continuous; and **protein**-sealed closed DNA loops (Fig. 1) (1). The vast majority of experimental and theoretical work on DNA topological domains has been done with purified closed circular DNA. An elementary topological domain, in which the DNA is topologically monomeric, is one in which the axis of the DNA is not itself linked to that of any other DNA. DNAs of this type are widespread in nature, including bacterial plasmids and episomes, the virion and replicative forms of both eucaryotic and procaryotic viruses, mitochondrial DNA, and many others (2). The nomenclature used to describe these molecules derives in part from protein chemistry and is imprecise when applied to closed circular DNA. Among the terms commonly used are *superhelical DNA* and *supercoiled DNA*. These are not meant to indicate different structural types, but are used as synonyms to indicate that the DNA in question is more compact than either its relaxed closed circular or nicked circular counterpart. They are used interchangeably with the more generic *closed circular DNA* or, alternatively, *closed duplex DNA* (*cdDNA*).

Figure 1. Depiction of the two kinds of elementary topological domains. (**a**) The structure of a closed duplex DNA (cdDNA), shown here as a relaxed duplex (rdDNA). Both strands in this DNA are covalently continuous, and the linking number is an integer. There are eight nodes in the projection shown here, and $Lk = +4$. (**b**) The structure of a DNA loop. The topological domain is maintained by tight binding to a dimeric protein. In the example shown, $Lk \approx 6$. The exact value of Lk depends on the precise location at which the two strands are fixed together by the protein sealant, and Lk can consequently be a fractional number. (Reproduced with permission from Ref. 1; copyright 1986, Macmillan Publishing Co.)

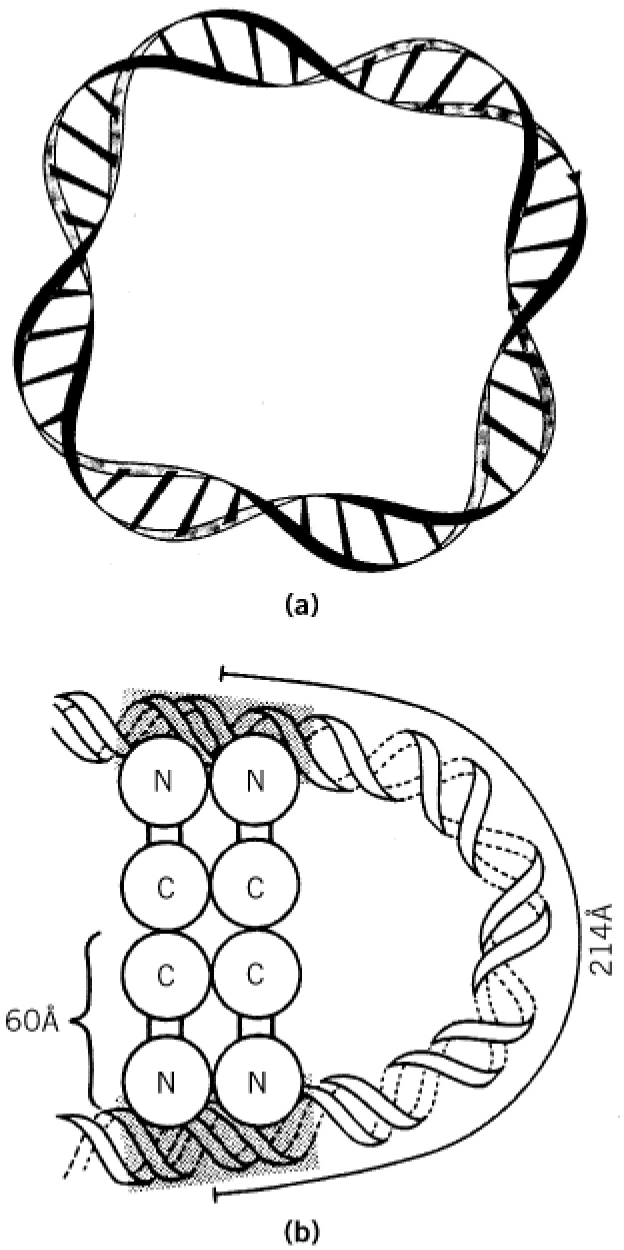

Protein-sealed DNA loops can occur locally in parts of DNA molecules that are not necessarily closed circular. Examples of these are the genome of *Escherichia coli*, which is organized into separate topological domains by bound proteins (3, 4), the **lambda repressor** (5, 6), several prokaryotic transcription regulation systems (7), site-specific recombination and transposition (8), and the binding of the *Sfi*I restriction enzyme (9). It should be noted that protein-sealed DNA loops, in contrast to cdDNAs, are held together by noncovalent bonds. The integrity of this type of topological domain is therefore relatively less certain. Systematic determinations of the stability of DNA loops as a function of linking number have not yet been reported.

DNA can also be organized into higher order (nonelementary) topological domains, in which the duplex DNA axes of one or more circular DNAs are themselves linked. Knotted DNA, one of the possible outcomes of site-specific recombination, represents a class in which the duplex axis of a single DNA forms a knot. Catenated DNA, in which the axes of two or more DNA submolecules are linked, contains one or more higher order topological domains. The submolecules themselves may or may not contain individual elementary topological domains. Schematic depictions of DNA knots and catenanes for some simple cases are shown in Figure 2 (10).

Figure 2. Two kinds of higher order topological domains. (**a**) Two closed circular, but not supercoiled, DNAs are linked once to form a catenane. Here the higher order linking number (called the *catenation* number in this case) is 1, since the axes of the two DNAs are linked once. (**b**) The axis of a single DNA molecule is knotted into a trefoil. (Reproduced with permission from Ref. 10; copyright 1986, Academic Press.)

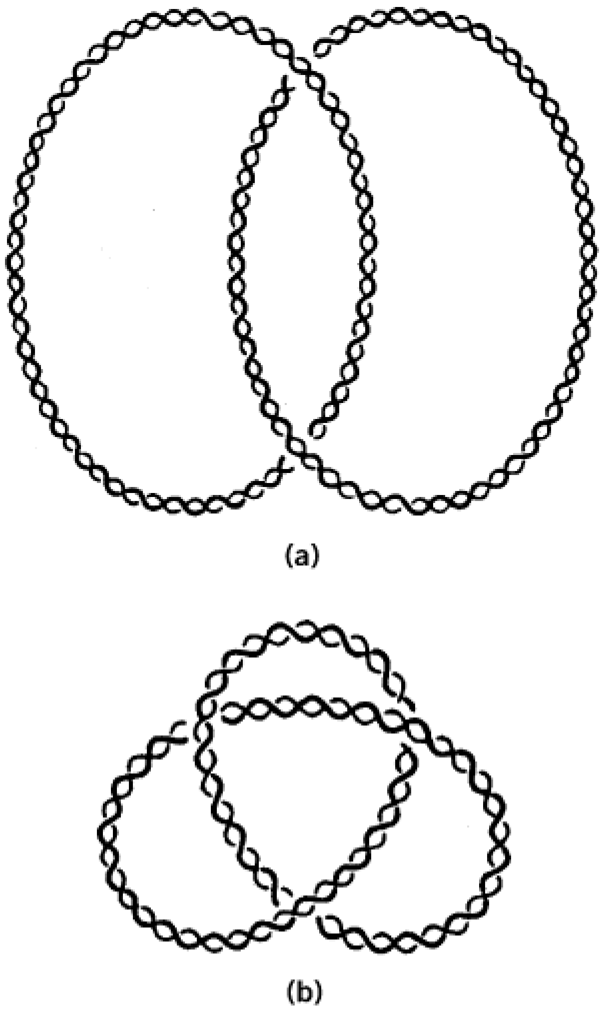

The formation of an elementary topological domain has a major influence on many DNA properties and, in addition, creates some properties that are entirely new. The properties modified may be roughly divided into two classes: structure (see Supercoiling of DNA) and energetics (see Superhelical DNA Energetics). The principal features of DNA structure affected are the duplex **twist** and the disposition in space of the DNA axis. Neat closed circular DNAs tend to form fairly regular, often branched superhelices in solution. A topological domain has a specific free energy, called either the *topological domain free energy* or the *free energy of superhelix formation*. This quantity generally increases with the extent of supercoiling of either chirality. The equilibria of all binding reactions that involve changes in either the DNA twist or in the writhe are shifted by the inclusion of this free-energy term. Examples are the binding of intercalative drugs, such as ethidium bromide, and of proteins, such as **RNA polymerase**.

The new property created by the formation of a closed circular DNA is the linking number, *Lk*, which is a measure of how many times the two duplex strands are interwound. It is constant for a given topological domain and can be changed only by one or more chain scissions. This makes possible the formation of DNA topoisomers , which are closed circular DNAs that differ only in *Lk*. Topoisomers can be reversibly interconverted with enzymes known as **topoisomerases**. The properties of individual topoisomers depend strongly on the magnitude of the associated linking number. Topoisomers can, under appropriate conditions, be physically separated by means of gel electrophoresis. Figure 3 (11) shows such a fractionation for a representative closed circular DNA.

Figure 3. An example of the separation of DNA topoisomers by electrophoresis in an agarose gel. The three strips show the stepwise relaxation of closed circular SV40 DNA at 0° by incubation with a topoisomerase. Lane 1 shows the original mixture of superhelical (fastest band, labeled “Native cdDNA”) and nicked circular (slowest band, labeled “ndDNA”) species. Lanes 2 and 3 show the formation of topoisomers following 5 min and 30 min of incubation. The lowest energy product DNA is labeled “rdDNA,” and the starting superhelical DNA had D*Lk* = –23. The individual bands contain topoisomers that differ by unity in linking number. (Because of limited gel resolution at higher D*Lk*, not all of the higher topoisomers can be seen in this gel.) (Reproduced with permission from Ref. 11; copyright 1975, National Academy of Sciences.)

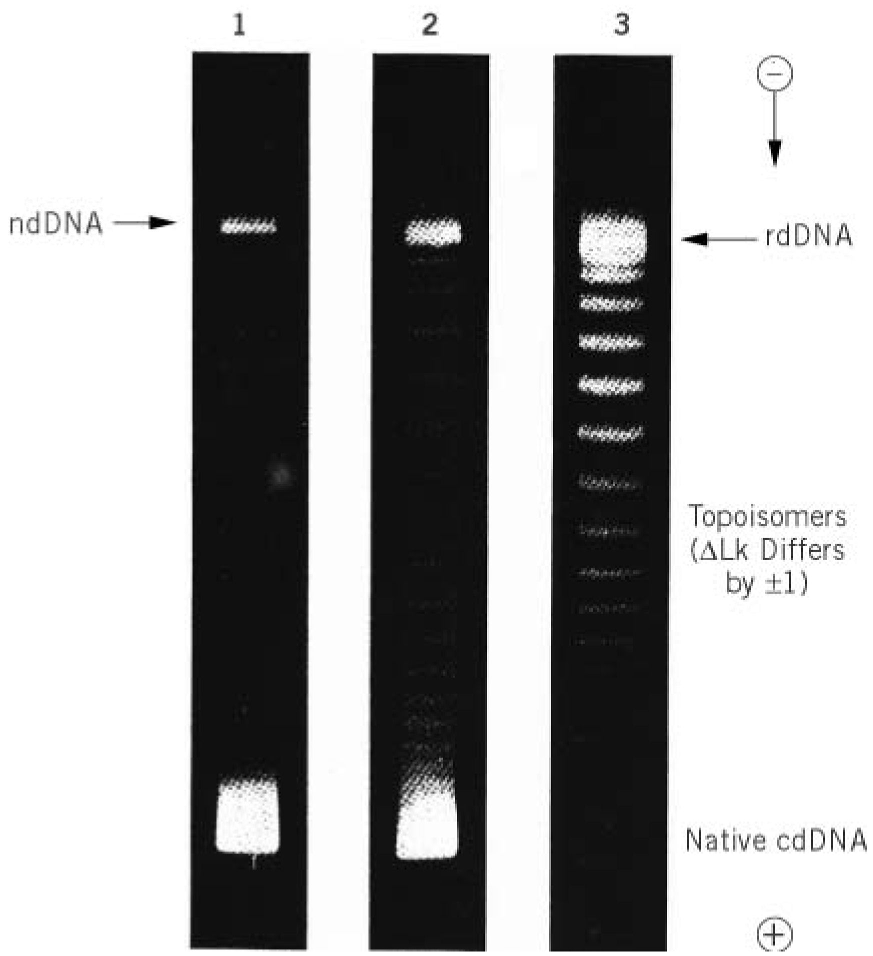

Finally, the two DNA backbone strands whose interwinding defines a topological domain contain no chemical bonds in common (except for a possible indirect connection *via* a protein sealant).

Nonetheless, the two strands can be separated only by the breakage of a covalent bond. This type of connection is sometimes termed a *topological bond*.

Bibliography

1. M. Ptashne (1986) Nature **322**, 697–701.
2. W. R. Bauer (1978) Ann. Rev. Biophys. Bioeng. **7**, 287–313.
3. A. Worcel and E. Burgi (1972) J. Mol. Biol. **71**, 127–147.
4. P. Sloof, A. Maagdelijn, and E. Boswinkel (1983) J. Mol. Biol. **163**, 277–297.
5. J. Griffith, A. Hochschild, and M. Ptashne (1986) Nature **322**, 750–752.
6. A. Hochschild and M. Ptashne (1986) Cell **44**, 681–687.
7. A. Hochschild (1990) In *DNA Topology and its Biological Effects* (N. R. Cozzarelli and J. C. Wang, eds.), Cold Spring Harbor Laboratory Press, Cold Spring Harbor, NY, pp. 107–138.
8. G. Chaconas, B. D. Lavoie, and M. A. Watson (1996) Curr. Biol. **6**, 817–820.
9. L. M. Wentzell and S. E. Halford (1998) J. Mol. Biol. **281**, 433–444.
10. A. Maxwell and M. Gellert (1986) Adv. Protein Chem. **38**, 69–107.
11. W. Keller and I. Wendel (1975) Cold Spring Harb. Symp. Quant. Biol. **39** (Pt. 1), 199–208.

Suggestions for Further Reading

12. W. R. Bauer, F. H. C. Crick, and J. H. White (1980) Supercoiled DNA, Sci. Am. **243**, 118–122. (This article contains many useful illustrations of the major features of DNA topological domains.)
13. D. R. Bates and A. Maxwell (1993) *DNA Topology*, Oxford Univ. Press, London. (This is an excellent monograph that covers most aspects of DNA topology in considerable detail.)
14. N. R. Cozzarelli and J. C. Wang (1990) *DNA Topology and Its Biological Effects*, Cold Spring Harbor Press, Cold Spring Harbor, NY. (This is a more general collection of articles including the influence of DNA topology on DNA–protein interactions, superhelical structure, and DNA enzymology.)

DNA-Binding Proteins

DNA binding proteins serve two principal functions: to organize and compact the chromosomal DNA and to regulate and effect the processes of transcription, DNA replication, and DNA recombination. The organization of chromosomal DNA is accomplished by abundant proteins which can bind to many sites and lack sequence specificity. In *Enterobacteria* this function is performed by FIS, H-NS, and HU proteins and in eukaryotic nuclei by the histone octamer and the linker histones, H1 and H5. By contrast, regulation of the enzymatic processes that manipulate DNA requires precise targeting to particular DNA sequences. This involves the specific recognition of the base sequence by a protein or proteins. Such proteins act genetically as repressors or activators either by themselves or in combination with corepressors or coactivators.

DNA binding is specified by a large number of disparate protein motifs. Within any particular class of motif the degree of sequence selectivity is highly variable, eg, among proteins with the helix-turn-helix-motif the *lac* repressor shows a high degree of sequence specificity whereas the FIS protein possesses little. The most commonly encountered types of motif are listed in Table 1.

Table 1. Commonly Encountered Types of Motif

Motif	Target	Sequence Specificity	Examples
Histone fold	Backbone	None	Core histones, TAFs
Helix-turn-helix	Major groove	Highly variable	FIS, C_I repressor, CAP
Homeodomain			
POU domain			
Winged helix			HNF3, histone H5
ETS domain			
Zinc-containing motifs			
Zinc finger	Major groove	Generally high	TFIIIA, Tramtrack
Receptor DBD	Major groove		Glucocorticoid receptor
Gal4 DBD	Major groove		GAL4
GATA	Major+minor grooves		GATA-1
bZip	Major groove	High	GCN4, Fos-Jun
Helix-loop-helix	Major groove	High	Myc, Achaete
HMG domain	Minor groove	Variable, but low	HMG1, SRY, TCF-1, UBF
HU class	Minor groove	Variable, but low	HU, IHF, TF1
TBP domain	Minor groove	High	TBP
GRP motif	Minor groove	Low, preference	Hin recombinase, HMG14/17

Frequently more than one type of binding motif is found in a particular protein. In both the l C_I repressor and the Hin recombinase DNA binding by a helix-turn-helix motif is stabilized by additional interactions mediated by an extended strand tracking along the minor groove. Similarly binding in other proteins may be stabilized by contacts between extended peptide loops and the sugar-phosphate backbone. Bivalence, or the ability to bind to two distinct double-helical surfaces, is a characteristic of some proteins, notably the globular domain of histone H5, which can bind two adjacent duplexes, and the l Int protein, which can define a DNA loop.

DNA-Dependent DNA Polymerases

DNA-dependent DNA polymerases synthesize deoxyribonucleic acid (**DNA**), a role that is central to accurately transmitting **genetic** material from generation to generation. This family of polymerases functions in a **template**-dependent manner to insert incoming nucleotides that are encoded by the template onto a growing primer. Polymerases are highly proficient at inserting nucleotides with proper **Watson–Crick base pairing**. DNA-dependent DNA polymerase exhibits unique roles during DNA replication and DNA repair. This article focuses on the characteristics of **prokaryotic** and **eukaryotic** DNA polymerases and the roles of each.

1. Primary Sequence, Structure, and Evolution

Sequence analysis studies (1) have divided the DNA-dependent DNA polymerase family into three subfamilies: (1) pol I type (which includes **Taq polymerase** and those from **bacteriophage** T5 and T7); (2) pol a type (which includes phage T4 polymerase and those from **vaccinia**, adenovirus, and herpes viruses); and (3) pol b type (which includes **terminal deoxynucleotidyl transferase**).

The presence of **homologous** regions in these diverse polymerases suggests that these enzymes evolved from a common ancestor (See Polymerases for a table of common motifs). All three subfamilies share two common motifs (A and C), whereas only pol I and pol a types also share a third (B). The **X-ray crystallographic** structure of the Klenow fragment of pol I suggests that motif A is involved in binding the divalent metal cofactor and deoxynucleoside triphosphates (dNTP), motif B is involved in binding the template and bases of the incoming dNTP, and motif C is involved in binding the metal cofactor. The structure of pol b shows DNA bound in an orientation 180° opposite to that observed in the complexes of DNA with **HIV**-1 **reverse transcriptase** and with the Klenow fragment (2). Thus, it is thought the pol b and terminal deoxynucleotidyl transferase are evolutionarily distinct from the other DNA-dependent DNA polymerases (3).

2. Prokaryotic DNA Polymerases

Escherichia coli contains three polymerases, designated DNA pol I, II, and III.

2.1. Pol III

The **holoenzyme** of DNA pol III (Fig. 1) is composed of 10 polypeptide subunits and is present in approximately 15 copies per bacterial cell. It is the principle polymerase responsible for replicating the genome. Pol III is purified either intact or as a core enzyme separate from its accessory factors. The Pol III core consists of the polymerase subunit *a* (140 kDa; expressed from the *DnaE* gene; Ref. 4), a proofreading subunit ε (28 kDa; from *dnaQ* or *mut D* gene; Ref. 5), and subunit q (10 kDa; *holE*). The processivity (i.e., the number of nucleotides synthesized per binding event) of the core enzyme is about 10 (6). This processivity is enhanced to several thousand nucleotides by the addition of subunit b (40 kDa), which functions as a dimer resembling a hexagonal **sliding clamp** (7). The q subunit (71 kDa) dimerizes readily, which, it is thought, facilitates the interaction of two polymerase core molecules. Evidence suggests that two polymerase core molecules act in concert but in opposite directions to synthesize the leading and lagging strands simultaneously (Fig. 1). The final component of the pol III holoenzyme is the g complex, which is composed of two subunits each of d, d′, g, c, and j. The g complex is a DNA-dependent ATPase that functions as a **clamp loader** (8). The hydrolysis of ATP facilitates loading of subunit b onto double-stranded DNA.

Figure 1. Model of the pol III replication complex during leading and lagging strand synthesis. Dimerization of the t domain facilitates the interaction of two core pol III molecules. This dimerization potentially allows concerted synthesis of both leading and lagging strands by one large polymerase complex. Other proteins that assist during repication in *E. coli* include DNA B helicase, primase, and single-stranded binding protein (SSB). Arrows show the 5′-3′ direction of polymerization.

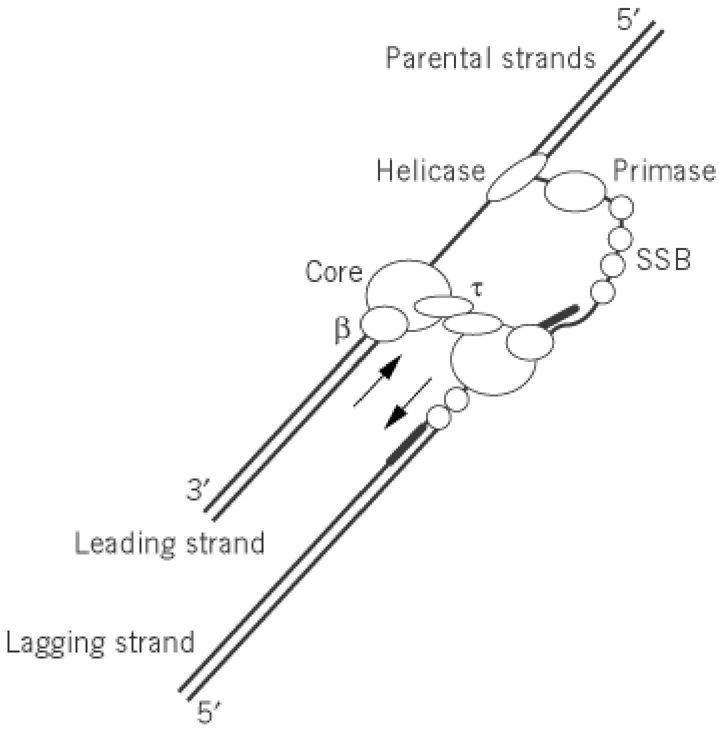

2.2. Pol I

DNA polymerase I (pol I; expressed from the *polA* gene), is a single polypeptide chain that encodes at least three separate catalytic activities. It is present at approximately 400 copies per cell, functions during DNA repair in *E. coli*, and also exhibits a minor role in DNA replication. The three catalytic activities of pol I are: (1) 5′-3′ polymerization, (2) 3′-5′ exonuclease (proofreading); and (3) 5′-3′ exonuclease (involved in **nick translation**). Mild proteolysis of pol I yields an amino-terminal 5′-3′ exonuclease domain and the COOH-terminal Klenow fragment, which contains polymerization and 3′-5′ proofreading activities (9). For details on pol I functions see DNA Polymerase I and Klenow Fragment.

2.3. Pol II

DNA polymerase II (a product of the *polB* gene) contains a 3-5′ exonuclease activity, but lacks a 5′-3′ exonuclease. The amount of Pol II activity is comparable to that of pol III in crude extracts from *PolA- E. coli*, and its nucleotide sequence resembles pol a-type polymerases. However, the precise roles of pol II in DNA metabolism remain to be established. Mutational studies with *E. coli* show that the *pol B* gene is not required for growth or for repair after UV damage.

3. Eukaryotic Polymerases

The six known polymerases in eukaryotes are pol a, b, g, d, ε, and z (see Table 1). Much of our understanding of the proteins and their roles in eukaryotic replication fork has stemmed from studying the SV40 virus replication system *in vitro* (10).

Table 1. Eukaryotic Polymerases

	a	b	g	d	ε	z

Mass of core (kDa)	165	39	140	124	255	173
Mass of other subunits (kDa)	70,58,49			51	55	29
Chromosome map (core)	Xp21.3-p22.1	8p11-p12	15q24	19q13.3-q13.4	12	?
Function	Extends primers	Repair	Replication	Replication	Replication	Bypass
Location	Nucleus	Nucleus	Mitochondria	Nucleus	Nucleus	(Nucleus)
3′-5′ Exonucleus	No	No	Yes	Yes	Yes	No
Fidelity	10^{-6}	10^{-5}	?	10^{-6}	10^{-6}	?
Processivity (nt)	10	5	100	10	1000	?
Core subunit cloned	Yes	Yes	Yes	Yes	Yes	No

3.1. DNA Polymerase a

This polymerase is composed of four subunits: (1) a 165- to 180-kDa phosphorylated **glycoprotein** that exhibits polymerase activity (its gene is located on human chromosome Xp21.3-p22.1.); (2) a 70-kDa phosphoprotein with unknown function; and (3 and 4) 49- and 58-kDa subunits that have primase activity (11). An early study in which monoclonal antibody against human DNA polymerase a was **microinjected** into mammalian cells showed that DNA replication is inhibited (12). Subsequent studies showed that this inhibition results from decreased extension of Okazaki Fragments. It was originally thought the primary function of pol a is to synthesize the lagging strand, but pol a's lack of an exonuclease domain and its poor processivity (about 10 nucleotides) cast some doubts. More recent studies of the SV40 replication system suggest that pol a functions to synthesize the RNA primer for both the leading and the lagging strands *via* its primase subdomain and to extend the RNA primer by several nucleotides on both strands via its polymerase domain (13). The majority of leading and lagging strand synthesis can potentially be carried out by polymerases d and ϵ. Mutational analysis in **yeast** of active polymerase a, d, and ϵ subunits show that each is essential for growth.

3.2. Polymerase b

This is a 39- to 45-kDa monomeric protein in vertebrates that is constitutively expressed (its gene is located on human chromosome 8p11-12) and considered the principle enzyme involved in filling in small DNA gaps resulting from excising damaged bases (14). Although expressed as a single polypeptide chain, pol b contains an N-terminal 8-kDa domain, which has apurinic lyase activity responsible for cleaving the 5′ phosphate-ribose residue during base excision repair, and a 31-kDa C-terminal domain that contains the polymerase active site. Pol b misincorporates noncomplementary nucleotides at a relatively high frequency, one per 5000 nucleotides polymerized (15) and lacks a 3′-5′ exonuclease (proofreading) activity. Thus, DNA repair by pol b may be highly error-prone. Pol b repairs gaps of six nucleotides or less highly processively but exhibits distributive synthesis in longer gaps. Of the three types of DNA repair, base excision repair (which leaves gaps of either one nucleotide or up to 10 nucleotides *via* unique mechanisms), nucleotide excision repair (which leaves gaps of about 30 nucleotides), and mismatch repair (which leaves gaps of hundreds of nucleotides), it is thought that pol b is involved primarily during base excision repair. A **knockout strain** of the pol b gene is embryonically lethal in mice, indicating that pol b is essential for normal development

(16). However, the pol b-like gene of ***Saccharomyces cerevisiae*** (*Pol4*) may be disrupted without affecting yeast viability and only marginally affecting sensitivity to methylmethanesulfonate, a DNA alkylating agent (see Mutagenesis). Apparently, either pol d or ε can substitute for pol b during base excision repair in *S. cerevisiae* (17). It has also been shown that the pol b localizes to synaptic foci during the **prophase** of **meiosis** I, suggesting that pol b activity is required to fill gaps during meiotic recombination in cells (18).

3.3. Polymerase g

This is a monomeric, 140-kDa enzyme that contains both polymerase and 3′-5′, exonuclease activities. Although encoded in the nucleus, pol g is primarily responsible for replicating and repairing the **mitochondrial** genome. The gene that encodes human pol g (located on chromosome 15q24) has just recently been cloned. The amino acid sequence of human pol g is 40 to 50% identical to pol g from yeast and Drosophila, pol g is also highly homologous to *E. coli* DNA pol I (19).

3.4. Polymerase d

This polymerase consists of a large catalytic polypeptide chain of 124 kDa from a gene located on chromosome 19q13.3q13.4, and a small polypeptide chain of 51 kDa from a gene located on chromosome 7. Mammalian pol d was first discovered in and purified from rabbit bone marrow, the catalytic subunit of human DNA pol d has been cloned and expressed in **Baculovirus**-infected cells (20). It is one of two nuclear mammalian DNA polymerases that has 3′-5′ exonuclease (proofreading) activity (21). The processivity of pol d is approximately 10 nucleotides, but this increases to well over 1000 nucleotides after the enzyme associates with a homotrimer of 36-kDa subunits of proliferating cellular nuclear antigen (PCNA), which forms a **sliding clamp** (22). In the SV40 replication system, pol d conducts most of both leading and lagging strand synthesis, complete replication in this system requires PCNA. Other proteins required for efficient pol d function include replication factor C (a phosphatase that loads PCNA onto the Pol d-DNA complex via an ATP-dependent reaction) and replication protein A (a **single-stranded binding protein** involved in reducing secondary structures of the template strand). Because of its high processivity, the Pol d–PCNA complex may also have important roles in filling DNA gaps during mismatch repair, nucleotide excision repair, and long-patch base excision repair (17).

3.5. Polymerase ε

This polymerase has a large catalytic subunit of 170 kDa, whose gene is located on chromosome 12q24.3. It shares many properties with pol d, including the presence of 3′-5′ exonuclease activity and very high processivity. Like pol d, pol ε was also first discovered in rabbit bone marrow. Human pol ε has been purified from HeLa cells and from placenta. The precise size of pol ε remains controversial, as its various subunits continue to be identified. Interestingly, with multisubunit DNA polymerases like pol d and pol ε the large subunit is invariably responsible for DNA polymerization. Unlike pol d, pol ε is thought to be highly processive and synthesizes approximately 1000 nucleotides per binding event even when not associated with PCNA. Pol ε interacts with PCNA at physiological ionic concentrations, thus further augmenting the enzyme's processivity and activity. The *in vivo* roles of pol d and ε have not been adequately distinguished, but it is thought that both have roles in leading and lagging strand synthesis and in mismatch, nucleotide excision, and long-patch base excision repair.

3.6. Polymerase z

This sixth DNA polymerase has been described in *S. cerevisiae*. Pol z is composed of two subunits of 173 kDa (product of the yeast REV3 gene) and 29 kDa (REV7 gene). The Rev3–Rev7 complex incorporates nucleotides across damaged DNA templates (23). DNA lesions including **thymine dimers**, abasic sites, and DNA adducts are potent at arresting DNA synthesis. The translesion bypass function ascribed to pol z could be important when efficient and rapid DNA synthesis across damaged DNA is needed during replication.

Bibliography

1. M. Delarue, O. Poch, N. Tordo, D. Moras, and P. Argos (1990) Protein Eng. **3**, 461–467.
2. H. Pelletier, M. R. Sawaya, A. Kumar, S. H. Wilson, and J. Kraut (1994) Science **264**, 1891–1903.
3. P. H. Patel, A. Jacobo-Molina, J. Ding, C. Tantillo, A. D. Clark Jr., R. Raag, R. G. Nanni, S. H. Hughes, and E. Arnold (1995) Biochemistry **34**, 5351–5363.
4. H. Maki and A. Kornberg (1985) J. Biol. Chem. **260**, 12987–12982.
5. R. H. Scheuermann and H. Echols (1984) Proc. Natl. Acad. Sci. USA **81**, 7747–7751.
6. P. J. Fay, K. O. Johanson, C. S. McHenry, and R. A. Bambera (1982) J. Biol. Chem. **257**, 5692–5699.
7. P. T. Stukenberg, P. S. Studwell-Waughan, and M. O"Donnell (1991) J. Biol. Chem. **266**, 11328–11334.
8. R. Onrust, P. T. Stukenberg, and M. O"Donnell (1991) J. Biol. Chem. **266**, 21681–21686.
9. D. Brutlag and A. Kornberg (1972) J. Biol. Chem. **247**, 241–248.
10. J. Li and T. J. Kelly (1984) Proc. Natl. Acad. Sci. USA **81**, 6973–6977.
11. D. A. Adler, B. Y. Tseng, T. S. Wang, and C. M. Disteche (1991) Genomics **9**, 642–646.
12. L. Kaczmarek, M. R. Miller, R. A. Hammond, and W. E. Mercer (1986) J. Biol. Chem. **261**, 10802–10807.
13. R. J. Hickey and L. H. Malkas (1997) Crit. Rev. Eukaryotic. Gene Expression **7**, 125–157.
14. J. Abbotts, D. N. SenGupta, B. Zmudzka, S. G. Widen, V. Notario, and S. H. Wilson (1988) Biochemistry **27**, 901–909.
15. T. A. Kunkel and L. A. Loeb (1981) Science **213**, 765–767.
16. H. Gu, J. D. Marth, P. C. Orban, H. Mossmann, and K. Rajewsky (1994) Science **265**, 26–28.
17. A. Blank, B. Kim, and L. A. Loeb (1994) Proc. Natl. Acad. Sci. USA **91**, 9067–9051.
18. A. W. Plug, C. A. Clairmont, E. Sapi, T. Ashley, and J. B. Sweasy (1997) Proc. Natl. Acad. Sci. USA **94**, 1327–1331.
19. P. A. Ropp and W. C. Copeland (1996) Genomics **36**, 449–458.
20. J. Q. Zhou, C. K. Tan, A. G. So, and K. M. Downey (1996) J. Biol. Chem. **271**, 29740–29745.
21. J. J. Byrnes, K. M. Downey, B. G. Que, M. Y. Lee, V. L. Black, and A. G. So (1977) Biochemistry **16**, 3740–3746.
22. T. S. Krishna, X. P. Kong, S. Gary, P. M. Burgers, and J. Kuriyan (1994) Cell **79**, 1233–1243.
23. J. R. Nelson, C. W. Lawrence, and D. C. Hinkle (1996) Science **272**, 1646–1649.

Suggestion for Further Reading

24. A. Kornberg and T. A. Baker (1992) *DNA Replication*, Freeman, New York.

DNA:Protein Binding Specificity

DNA-binding proteins that bind to DNA in a sequence-specific manner have evolved to deal with a problem not normally encountered by enzymes, namely that the substrate, a specific segment of DNA, is immersed in a sea of other DNA sequences on the same molecule that are chemically and structurally very similar to the specific substrate. This is a problem that is fundamentally different from the problem of the discrimination of various small molecular substrates by enzymes, which can be based at least in part on the size and shape of the substrates. More than 20 years ago, it was pointed out that the nonspecific DNA-binding sites might be poor substrates when compared to the specific site, but they nevertheless significantly reduce the concentration of the free protein, simply because they are present in huge molar excess (1, 2). All known site-specific DNA-binding proteins also have a finite affinity for the nonspecific sites (3, 4). In this context, nonspecific DNA-binding is defined as binding that is equiprobable at any particular point along the DNA. In practice, specific and nonspecific binding constants are often determined by measuring the apparent dissociation constants of the complex of a protein with DNA containing either a specific DNA site (S) or a sequence that is completely heterologous (NS):

$$\begin{aligned} \mathrm{P} + \mathrm{S} &\rightarrow \mathrm{PS}\, K_{\mathrm{D}}(\mathrm{S}) = [\mathrm{P}][\mathrm{S}]/[\mathrm{PS}] \\ \mathrm{P} + \mathrm{NS} &\rightarrow \mathrm{PNS}\, K_{\mathrm{D}}(\mathrm{NS}) = [\mathrm{P}][\mathrm{NS}]/[\mathrm{PNS}] \end{aligned} \tag{1}$$

Table 1 compares the **dissociation constants** for specific and nonspecific binding for a number of different types of DNA-binding proteins. When referring to Table 1, it must be kept in mind that the apparent dissociation constants depend significantly on the conditions of the measurement, such as the temperature (5-15), pH (15-20), and concentration and type of cations and anions (13, 14, 16, 20, 22). A second complication stems from the fact that the stability of the specific complex is in some cases dependent on the DNA sequences flanking the specific binding site. A 17-fold difference in the dissociation constants is seen for the complexes of the restriction enzyme EcoRV and DNA sequences containing a cognate binding site with different flanking sequences (20). In addition, the apparent dissociation constants of the protein complexes with nonspecific DNA depend on the length of the DNA probe. All values for K_D(NS) in Table 1 were corrected for the length of the DNA probe by dividing the measured K_D(NS) by the twofold difference between the length of the probe and the length of the DNA-binding site of the specific complex.

Table 1. Specificities of Prokaryotic and Eukaryotic DNA-Binding Proteins

Protein	Specific Site	K_D(S) (M)	K_D(NS) (M)	K_D (NS)/K_D (S)	- DD*G* (kcal/mol)	Reference
Repressors						
lac	O^{sym}	8.3×10^{-12}	2.4×10^{-4}	2.9×10^{7}	10.1	27
l cI	O_R1	1.2×10^{-10}	4.0×10^{-4}	3.3×10^{6}	8.7	28
	O_R2	6.7×10^{-10}		6.0×10^{5}	7.7	
	O_R3	6.3×10^{-9}		6.3×10^{4}	6.4	
l Cro	O_R1	8.3×10^{-12}	1.5×10^{-6}	1.8×10^{5}	6.6	29
	O_R2	$1.2\times10^{-}$		1.3×10^{4}	5.1	

		10				
	O_R3	2.0×10^{-12}		7.5×10^{5}	7.3	
trp	Wild-type op.	2.2×10^{-9}	4.2×10^{-5}	1.9×10^{4}	5.8	8
P22 Arc	Left half-site	2.7×10^{-11}	4.7×10^{-8}	1.7×10^{3}	4.3	30
MetJ	MetBox	1.6×10^{-6}	5.0×10^{-4}	3.1×10^{2}	3.4	9
Restriction Endonucleases						
EcoRI	GAATTC	5.9×10^{-12}	2.8×10^{-4}	4.7×10^{7}	10.3	23
EcoRV	GATATC	3.8×10^{-10}	1.0×10^{-5}	2.6×10^{4}	6.0	20
Transcription Factors						
CAP	lac Promoter	1.2×10^{-11}	1.4×10^{-6}	1.2×10^{5}	6.8	31
IHF	l attP H′	1.6×10^{-9}	2.9×10^{-6}	1.8×10^{3}	4.4	32
TBP	TATAAAAG	3.7×10^{-9}	$> 1.0\times10^{-5}$	$> 2.7\times10^{3}$	>4.6	33
MEF-2C	TATAAATA	1.1×10^{-7}	$> 1.2\times10^{-5}$	$> 1.1\times10^{2}$	>2.7	34, 35
GCN4	ATGACTCAT	3.5×10^{-8}	1.1×10^{-6}	3.1×10^{1}	2.0	13
	ATGACGTCAT	2.7×10^{-8}		4.1×10^{1}	2.2	
MASH-1	CAGGTG	5.9×10^{-9}	1.9×10^{-8}	3.2	0.7	15, 36
E12	CAGGTG	1.4×10^{-8}	1.9×10^{-7}	1.4×10^{1}	1.5	36
MyoD/E12	CAGGTG	7.5×10^{-9}	7.9×10^{-8}	1.1×10^{1}	1.4	37

Table 1 shows that the dissociation constants of the specific complexes span a range of approximately six orders of magnitude. The tightest complexes have K_D(S) values that lie in the picomolar concentration range. Interestingly, the specific DNA complexes of bacterial proteins are generally more stable than the complexes of eukaryotic DNA-binding proteins, most probably due to the longer DNA-binding sites in the prokaryotic complexes.

The dissociation constants of the nonspecific complexes listed in Table 1, on the other hand, span only approximately four orders of magnitude. For the nonspecific complexes, the eukaryotic proteins bind to DNA more tightly than the prokaryotic ones. Therefore, the DNA-binding specificity (defined as K_D(NS)/K_D(S)) of prokaryotic DNA-binding proteins is, in most cases, significantly greater than that of eukaryotic transcription factors.

It is interesting to consider these observations in the context of the size of both the bacterial and the mammalian genomes. The *E. coli* genome consists of 4×10^6 bp. Of the proteins listed in Table 1, the restriction enzyme EcoRI displays the highest DNA-binding specificity (K_D(NS)/K_D(S) = 4.7×10^7) (23). The specific DNA-binding site of EcoRI has the sequence GAATTC. Such a hexamer sequence would occur statistically approximately 1000 times in the *E. coli* genome. As a consequence, approximately 1.1×10^4 times more protein is bound to the specific DNA site than to the nonspecific sites:

$$[\mathrm{PS}]/[\mathrm{PNS}] = K_D(\mathrm{NS}) \cdot [\mathrm{S}]/K_D(\mathrm{S}) \cdot [\mathrm{NS}] \qquad (2)$$

On the other hand, to bind 50% of the time to a unique binding site of the mammalian chromosome would require that the specificity of a transcription factor be > 3×10^9 (the size of the mammalian chromosome). Statistically, a minimal length of 16 bp is required to ensure that a given binding site is unique on the mammalian chromosome. Most transcription factors bind, however, to DNA sites that are too short to be unique on the mammalian chromosome. Proteins containing the basic **helix–loop–helix motif** (BHLH), for example, bind to the sequence CAGGTG, which occurs approximately 7×10^5 times on a mammalian chromosome. The expression of MyoD, which recognizes DNA through a BHLH domain, can activate myogenesis in a wide variety of cell types including myoblasts and fibroblasts (24, 25), while the BHLH-protein MASH-1 promotes the differentiation of committed neuronal precursor cells (26). BHLH proteins need to bind to DNA with a specificity of approximately 4×10^3 in order to bind with equal probability to a nonspecific site and to one of the approximately 700,000 specific sites on the mammalian chromosome. But even then, MASH-1 would still activate transcription from MyoD target promoters and vice versa. Such arguments may be part of the explanation why transcriptional regulation in higher organisms relies on multiprotein complexes with the potential for combinatorial interactions.

Bibliography

1. P. H. von Hippel and J. D. McGhee (1972) Annu. Rev. Biochem. **41**, 231–300.
2. S.-y. Lin and A. D. Riggs (1975) Cell **4**, 107–111.
3. M. T. Record Jr. and R. S. Spolar (1990) In *The Biology of Nonspecific DNA–Protein Interactions* (A. Revzin, ed.), CRC Press, Boca Raton, FL, pp. 33–69.
4. P. H. von Hippel (1994) Science **263**, 769–770.
5. J.-H. Ha, R. S. Spolar, and M. T. Record (1989) J. Mol. Biol. **209**, 801–816.
6. Y. Takeda, P. D. Ross, and C. P. Mudd (1992) Proc. Natl. Acad. Sci. USA **89**, 8180–8184.
7. L. Jin, J. Yang, and J. Carey (1993) Biochemistry **32**, 7302–7309.
8. J. E. Ladbury, J. G. Wright, J. M. Strutevant, and P. B. Sigler (1994) J. Mol. Biol. **238**, 669–681.
9. D. E. Hyre and L. D. Spicer (1995) Biochemistry **34**, 3212–3221.
10. P. E. Merabet and Ackers (1995) Biochemistry **34**, 8554–8563.
11. V. Petri, M. Hsieh, and M. Brenowitz (1995) Biochemistry **34**, 9977–9984.
12. T. Lundbäck, C. Cairns, J.-Å. Gustafsson, J. Carlstedt-Duke, and T. Härd (1993) Biochemistry **32**, 5074–5082.
13. T. Lundbäck and T. Härd (1996) Proc. Natl. Acad. Sci. USA **93**, 4754–4759.
14. C. Berger, I. Jelesarov, and H. R. Bosshard (1996) Biochemistry **35**, 14984–14991.
15. J. H. Carra and P. L. Privalov (1997) Biochemistry **36**, 526–535.
16. A. G. E. Künne, M. Sieber, D. Meierhans, and R. K. Allemann (1998) Biochemistry **37**, 4217–4223.
17. M. T. Record Jr., J.-H. Ha, and M. A. Fisher (1991) Methods Enzymol. **208**, 291–343.
18. D. F. Senear and G. K. Ackers (1990) Biochemistry **29**, 6568–6577.

19. J. D. Taylor, I. G. Badcoe, A. R. Clarke, and S. E. Halford (1991) Biochemistry **30**, 8743–8753.
20. L. Li, D. von Kessler, P. A. Beachy, and K. S. Matthews (1996) Biochemistry **35**, 9832–9839.
21. L. E. Engler, K. K. Welch, and L. Jen-Jacobsen (1997) J. Mol Biol. **269**, 82–101.
22. M. T. Record Jr., T. M. Lohman, and P. de Haseth (1976) J. Mol. Biol. **107**, 145–158.
23. M. T. Record Jr., P. L. deHaseth, and T. M. Lohman (1977) Biochemistry **16**, 4791–4796.
24. L. Jen-Jacobsen (1997) Biopolymers **44**, 153–180.
25. C. P. Emerson (1993) Curr. Opin. Genet. Dev. **3**, 265–274.
26. A. B. Lassar and A. Munsterberg (1994) Curr. Opin. Cell. Biol. **6**, 432–442.
27. L. Sommer, N. Shah, M. Rao, and D. J. Anderson (1995) Neuron **15**, 1245–1258.
28. D. E. Frank, R. M. Saecker, J. P. Bond, M. W. Capp, O. V. Todikov, S. E. Melcher, M. M. Levandovski, and M. T. Record Jr. (1997) J. Mol. Biol. **267**, 1186–1206.
29. D. F. Senear and R. Batey (1991) Biochemistry **30**, 6677–6688.
30. Y. Takeda, A. Sarai, and V. M. Rivera (1989) Proc. Natl. Acad. Sci. USA **86**, 439–443.
31. B. M. Brown and R. T. Sauer (1993) Biochemistry **32**, 1354–1363.
32. M. G. Fried and D. M. Crothers (1984) J. Mol. Biol. **172**, 241–262.
33. S.-W. Yang and H. A. Nash (1995) EMBO J. **14**, 6292–6300.
34. S. Hahn, S. Buratowski, P. A. Sharp, and L. Guarente (1989) Proc. Natl. Acad. Sci. USA **86**, 5718–5722.
35. D. Meierhans, M. Sieber, and R. K. Allemann (1997) Nucleic Acids Res. **25**, 4537–4544.
36. D. Meierhans and R. K. Allemann (1998) J. Biol. Chem. **273**, 26052–26060.
37. D. Meierhans, C. el Ariss, M. Neuenschwander, M. Sieber, J. F. Stackhouse, and R. K. Allemann (1995) Biochemistry **34**, 11026–11036.
38. A. G. E. Künne, D. Meierhans, and R. K. Allemann (1996) FEBS Lett. **391**, 79–83.

DNA:Protein Interaction Thermodynamics

1. Specific Interactions

The precise recognition of a defined DNA sequence by a DNA-binding protein requires an optimal shape complementarity between the interacting species. As a result, a large number of noncovalent interactions form at the interface between the DNA and the protein. Individual interactions often contribute only a small amount to the overall stability of the complex. Nevertheless, all of these interactions are important for the preferred binding of the protein to the specific DNA site (or the discrimination of the nonspecific site).

Early concepts about the determination of specificity in DNA protein complexes relied on "direct-readout," which is based on the interaction between the functional groups of the proteins and the DNA bases (1, 2). Structural studies of DNA–protein complexes showed that specific interactions are mediated by hydrogen bonds, electrostatic interactions between charged groups, **and** van der Waals interactions. Constrained hydrogen bonding interactions can be made between the polypeptide backbone or short side chains and the nucleobases. Longer side chains make more flexible contacts with the DNA. They are, however, often orientated in space by other amino acid side chains or by making two contacts to the same base, to adjacent bases, or to a base and a phosphodiester group. In these cases, the **enthalpic** gain of the interaction is often reduced by a negative **entropic** contribution stemming from the reduction of conformational flexibility of the amino acid side chain. The X-ray crystallography structures of the DNA complex of the basic **helix–loop–helix** (BHLH) proteins MyoD (3) and E47 (4) provide examples of bidentate and bridging interactions. Arg(111) of MyoD, which contacts both N(7) of guanine and an oxygen of the adjacent phosphodiester, provides an example of a bridging interaction (Fig. 1). A hydrogen bond between N(e) of Arg(111) and the hydroxyl group of a threonine residue further restricts the mobility of Arg(111). Arg(111) also forms a bidentate interaction with guanine through hydrogen bonds with N7 and O4, the latter being mediated by a water molecule. Another example is provided by the carboxyl group of a Glu(47), which makes hydrogen bonds to N7 of an adenine and to N4 of the adjacent thymine, thereby specifying the first two bases of the Glu(47) binding site (Fig. 2). A neighboring arginine residue orientates the glutamate in space through the formation of a “clamp” between the phosphate backbone and the peptide. An important consequence of the formation of such hydrogen bonding networks that severely restrict the conformational flexibility is that the specificity is achieved, at least in part, through selection of the smallest number of destabilizing interactions (5). The restriction enzymes EcoRI, EcoRV, and BamHI rely for specificity to a large extent on discrimination against noncognate sites (Ref. 6 and references therein).

Figure 1. Diagram showing the structure of the BHLH domain of MyoD from amino acid Asp(109) to Thr(115) and the key contacts of Arg(111) with guanine and the adjacent phosphodiester of the E-box sequence CANNTG (60). Note that the contact of Arg(111) to O6 of guanine is mediated by a water molecule and the stabilization of the arginine side chain through an hydrogen bond with the hydroxyl group of Thr(115). This display was created from the coordinates of the DNA complex of MyoD (3).

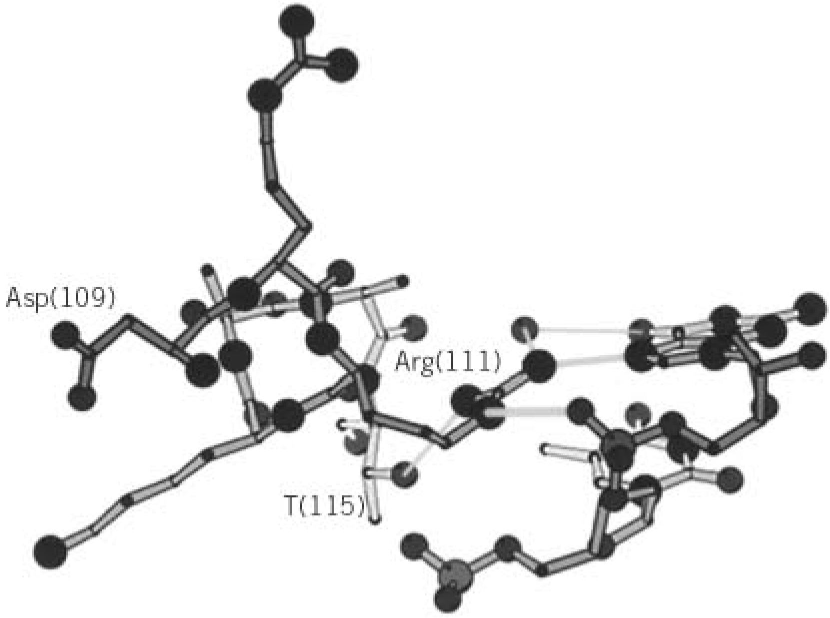

Figure 2. Networked hydrogen-bonding interactions between glutamate(345) and arginine(348) of E47 and the CpA dinucleotide of the E-box DNA sequence (5). E(345) is hydrogen-bonded to N4 of cytosine and to N6 of adenine. Note the “clamp” function of R(348) which connects the phosphate backbone to E(345), thereby locking the conformation of the side chain of E(345). The b and g-CH_2 groups of E(345) make van der Waals contacts to the methyl group of thymine. The program MacMoMo (183) was used to create this display from the coordinates of the DNA complex of E47 (4).

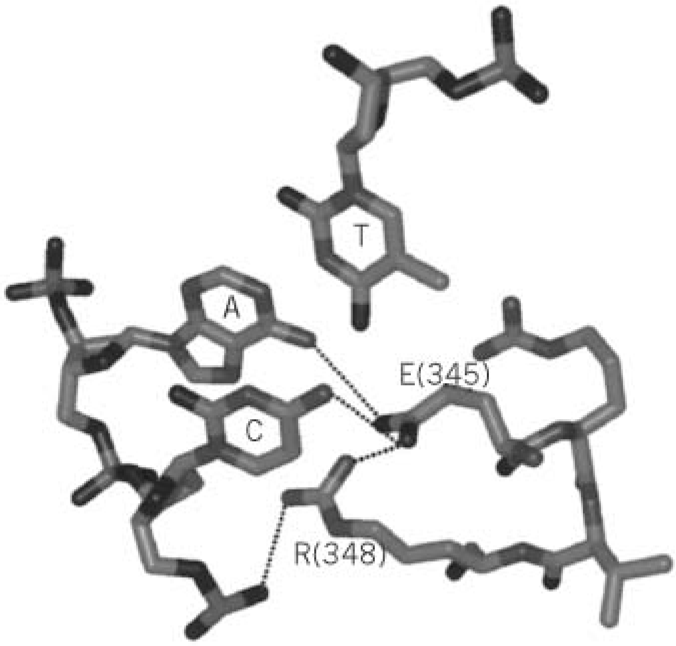

To the best of our knowledge, there is no site-specific DNA-binding protein for which a complete thermodynamic description of the association reaction with DNA is available, and only relatively few data are available for eukaryotic proteins. However, thermodynamic studies with the prokaryotic **Lac**, Mnt, trp, l **Cro**, Arc, and l cI repressors (7-16), the restriction endonucleases EcoRI (17-22), EcoRV (6, 23), BamHI (6), and RsrI (20), the cyclic AMP receptor protein (CRP)/catabolite activating protein (CAP) (24), the DNA-binding domain of glucocorticoid receptor (25), and the consequences of altered interactions between amino acid side chains and bases have been addressed through **site-directed mutation** of either the protein or the DNA. The results from these experiments are difficult to interpret, because of a multitude of subtle energetic changes resulting from the altered bond, perturbation of the local structure of the DNA and/or the protein, and changes in solvation. Nevertheless, a study by the group of Jen-Jacobsen of the interaction of EcoRI with a series of base-analogues in the absence of Mg^{2+} indicated that each hydrogen bond between the protein and the DNA stabilizes the complex by approximately 1.4 kcal/mol (19, 21). For the DNA complex of Trp repressor, the replacement of N7 of individual purines with carbon led to an increase in the **free energy** of binding of approximately 1 kcal/mol when the particular nitrogen atom formed a hydrogen bond to the repressor in the wild-type complex (26). Several other studies confirmed a value of 1 to 1.5 kcal/mol of stabilization for every hydrogen bond formed (23, 27). On the other hand, replacing an adenine, the N6 of which forms a hydrogen bond with a glutamate of the basic helix–loop–helix (BHLH) protein E12 (Fig. 2), with a purine led to a reduction of only approximately 0.8 kcal/mol of the stability of the E12 DNA complex in electrophoretic **mobility shift assay** experiments (5).

Van der Waals interactions between the protein and the methyl group of thymine that projects into the major groove in B-DNA provide another possibility for the formation of specific interactions. A careful thermodynamic study of the interaction between the methyl group of thymine –5 of the O_R3 operator and a methylene group of Lys32 of the Cro repressor from phage l indicated that the van der Waals interaction stabilizes the complex by 1.6 kcal/mol (7). When this methyl group was removed by replacing thymine with uracil, the binding enthalpy was reduced, with no observable change in the binding entropy, as would be expected for such an interaction, especially because the conformation of Lys33 in Cro is stabilized by a bidentate interaction with N7 and O6 of guanine (–4) of O_R3. However, the creation of a cavity by the removal of the methyl group could potentially lead to the trapping of a water molecule. Such a case has been observed for the DNA complex of the DNA-binding domain of the glucocorticoid receptor, where a favorable enthalpic contribution compensated for the unfavorable entropic effect of approximately 1 kcal/mol when a methyl group was removed from a thymine (28) that did not make specific contacts to the protein (29). Other studies confirmed that van der Waals interactions between a protein and a thymine methyl group stabilize the complex by between 0.5 and 2 kcal/mol (7, 19, 23, 24, 27, 30-33).

DNA-binding proteins make extensive contacts to the phosphodiester groups of the DNA backbone through charged and uncharged side chains. It is not easy to estimate the contribution from these interactions to the overall stability of the complex. One approach is to determine the contribution of the polyelectrolyte effect from the dependence of the reaction free energy on the concentration of univalent salts and to add a contribution for the interactions between the DNA phosphates and uncharged amino acid residues. It is important to keep in mind that the polyelectrolyte effect is a consequence of the fact that DNA is a polyanion of high axial charge density (reviewed in Refs. 11, 34, and 35). The association reaction is therefore driven by the release of monovalent cations (at least at low salt concentrations) (36-38). The salt-dependence of binding to various specific and nonspecific DNA sequences is often different, indicating that protein-phosphate contacts are involved in determining the specificity of DNA binding (39-44).

Anions bind to proteins with relatively small binding constants (45), and their effects are most likely not of electrostatic nature (see Hofmeister Series and Salting In, Salting Out). Anions seem to affect the dissociation constants of DNA–protein complexes, especially at high anion concentrations (46, 47). The nature of the anion is important, and replacing chloride with glutamate can increase the sequence-specific DNA-binding affinity by as much as 80-fold (43). At 25°C in a low salt buffer, the leucine zipper protein GCN4 binds to an ATF/CREB site (ATGACGTCAT) and to an AP-1 site (ATGACTCAT) with the same affinity. In a buffer containing 250 mM potassium glutamate, however, the dissociation constant of the AP-1 complex was approximately one order of magnitude smaller than for the ATF/CREB complex (48).

In order to understand fully the DNA-binding specificities displayed by proteins, it is necessary to define the energetic differences between the interactions in specific and nonspecific complexes (see DNA:Protein Binding Specificity). Model studies of the DNA-binding reactions of oligopeptides suggest that the nonspecific complex is a loose association held together by Coulombic interactions between positively charged residues of the protein and the negatively charged phosphate backbone of the DNA (49, 50). In these studies, the number of DNA phosphates contacted, as well as the number of monovalent cations thermodynamically released on binding, was found to be approximately equal to the number of positively charged side chains in the peptides (49-56). Thermodynamic studies indicate that the number of phosphate contacts is often greater in the nonspecific complexes than in the specific ones (6, 11, 57).

Only two structures of nonspecific complexes are currently known, namely those involving the restriction endonuclease EcoRV (58, 59) and the DNA-binding domain of glucocorticoid receptor (29). Glucocorticoid receptor binds to DNA sequences containing inverted repeats separated by three base pairs. In the X-ray crystallography structure analysis of the DNA complex of glucocorticoid receptor, an oligonucleotide was used where the spacing had been increased to four base pairs. Therefore, while one protein subunit bound specifically to the one inverted repeat, the other faced a nonspecific binding site. Both subunits introduced an a-helix into the major groove of the oligonucleotide, which was opened up by approximately 2 Aring; on the specific side. This distortion is most likely achieved through the higher number of interactions in the specific complex. Comparison of the specific and the nonspecific complexes of EcoRV revealed that a loop that penetrates the major groove is partially disordered in the nonspecific case and not well-buried in the groove. The buried surface area (*vide infra*) is more than 1570 Aring;^{2} larger in the specific complex than in the nonspecific one (58).

An interesting case is provided by the BHLH protein MASH-1. The DNA-binding specificity of MASH-1 was found to be very low for all conditions studied (39, 60). While no three-dimensional structure for a "nonspecific" complex of MASH-1 or any other BHLH protein has been determined, the available data suggest that the specific and "nonspecific" complexes are very similar (5, 39, 60, 61), and it appears that BHLH proteins might have only one binding mode. This is most probably a consequence of the exposed recognition a-helix that adopts its helical conformation only on DNA binding (39, 60). In many other proteins that rely on an a-helix for DNA recognition, the conformation of the recognition helix is stabilized through interactions with other parts of the DNA-binding domain.

2. Water-Mediated Contacts

Specific interactions between a protein and DNA are often mediated by bound water molecules. General thermodynamic arguments show that the entropic cost of transferring a water molecule from bulk water to a specific site within a protein or at the interface between the protein and DNA is in the range of 0 to 7 cal $mol^{-1}K^{-1}$, corresponding to a free energy change of between 0 and 2 kcal mol^{-1} at ambient temperature (62). The free energy cost varies thereby with the polarity of the environment of the bound water.

An example of a specific contact that is mediated by a water molecule is shown in Figure 1. The interaction between N(h) of Arg(111) of MyoD and the O6 of guanine is mediated by a well-ordered water molecule (3). Other examples of specific interactions that are mediated by well-resolved water molecules have been found in the DNA complexes of cI repressor (63), Hin recombinase (64), the restriction endonuclease BamHI (65), the DNA-binding domains of estrogen receptor (66), papillomavirus-1 E2 (67), and the **antennapedia**(C39 S) homeodomain (68). The DNA complex of the transcription factor GATA-1 is devoid of water molecules that mediate contacts between the protein and the nucleobases, but several water molecules were found between the protein and the phosphate backbone (69).

The 1.9 Aring; resolution crystal structure of the complex between the Trp repressor and its operator revealed that water-mediated contacts are the principal means for site-specific recognition (70, 71). Of the 90 water molecules that are intrinsic to the chemistry of the complex, 26 are located within the protein–DNA interface (13 in each half-site). Three of these 13 mediate four contacts between the nucleobases and the protein. Interestingly, these three hydration sites are already fully occupied in the free DNA (72). The water molecules should therefore be considered as intrinsic parts of the DNA structure and as noncovalent extensions of the DNA molecule that can be used for the stereospecific recognition of the *trp* operator (see TRP Operon). Similarly, the water molecule that mediates the contact between the backbone NH of Asn(79) and the N7 of guanine is present in all of the refined crystal structures of the uncomplexed repressor, and the water between Asn(80) and the DNA is seen in most of the refined structures of the free protein (73). These water molecules can therefore be considered functional extensions of the protein surface.

While water molecules are clearly important for both affinity and specificity in many DNA complexes of transcription factors, it must be stressed that some DNA–protein interfaces are completely devoid of water. For example, the 3100 Aring;^{2} interface between TBP and TATA-box containing DNA sequences is characterized by a perfect complementarity and complete exclusion of water (74-77).

3. Dehydration Effects

Thermodynamic studies demonstrated that site-specific DNA-binding reactions are characterized by negative and relatively large changes in the **heat capacity**. As a consequence, the enthalpic (D *H*) and the entropic (*T*D *S*) contributions to the free energy change (D *G*) of the binding reactions vary with temperature in an almost parallel manner, making D*G* nearly independent of temperature. Again, there are much more data available for prokaryotic DNA-binding proteins. Only recently have good thermodynamic data for the interaction between eukaryotic transcription factors and DNA become available. The reactions studied include the association reactions between histones and DNA (78), **RNA polymerase** Es^{70} and the P_R **promoter** of lambda phage (79), Lac repressor and the *lac* O^+ operator (80), the mnt repressor and the mnt operator site O_{mnt} (81), the headpiece of Lac repressor and the *lac* operator (82), the restriction endonuclease EcoRI and its cognate binding site (82), Cro repressor and the O_R3 operator site (7), the DNA-binding domain of glucocorticoid repressor and a glucocorticoid response element (25, 28), Trp repressor and operator (8, 9), l cI repressor with various combinations of the three operator sites $O_R(1)$, $O_R(2)$, and $O_R(3)$ (10), the transcriptional activator **cyclic AMP response protein** (CRP) complexed with two molecules of cAMP and its consensus binding site (83, 84), the transcription factor GCN4 and both an ATF/CREB and an AP-1 binding site (48), and the DNA-binding domain of the basic **helix–loop–helix** (BHLH) protein MASH-1 and E-box containing and heterologous DNA sequences (39).

It is now generally accepted that large negative values of the heat capacity change, Dc_p, are the hallmark of biological reactions that form large highly complementary interfaces, irrespective of the overall stability of the complexes formed (9, 82). The areas buried in specific protein DNA complexes range from ~ 1000 to ~ 5500 *Aring*;[2] (29, 39, 48, 75, 84, 85), and the heat capacity changes are caused by the removal of large amounts of nonpolar surface area from water on complex formation, accompanied by release of water. Although the change in water-accessible nonpolar surface area makes the dominant contribution to $D\,c_p$, the changes in water accessibility of the polar surface areas (mainly due to the burial of the peptide backbone) also make a smaller contribution of opposite sign (86) (see Hydration).

Because the observed values of Dc_p for the DNA-binding reactions of some proteins are too large to be accounted for solely by the amount of buried surface area in a "rigid body" association, conformational changes of both the protein and the DNA appear to occur (see below) (84, 87, 88).

Binding of proteins to DNA in a nonspecific fashion involves almost no changes in heat capacity (7, 9, 48), indicating that the formation of nonspecific complexes does not involve major dehydration. An interesting exception is provided by the DNA-binding domain of the transcription factor MASH-1. The association reaction between MASH-1 and an E-box-containing oligonucleotide, the natural target of MASH-1, is characterized by a heat capacity change of –733(±99)cal mol^{-1} K^{-1}, while the formation of a complex with heterologous DNA results in a Dc_p of –575cal mol^{-1} K^{-1} (39). X-ray crystallography studies of the specific complexes of BHLH proteins showed that the DNA is contacted by an a-helix that fits snugly into the major groove (3, 4). Circular dichroism spectroscopy suggested that the protein conformation of MASH-1 was rather similar in the "specific" and the "nonspecific" complexes (39, 60). Unlike other DNA-binding proteins, all DNA complexes of MASH-1 appear to show the thermodynamic characteristics of specific complexes, irrespective of the particular DNA sequence.

The number of water molecules released on formation of a complex between a protein and DNA can be estimated by measuring the dissociation constant as a function of the osmotic strength altered through the addition of neutral salts (89-91). Such osmotic-stress methods have so far been applied to only a few DNA-binding reactions, namely the restriction endonucleases EcoRI (92, 93), EcoRV and PvuII (94), the gal repressor (95), Hin recombinase (96), the cyclic AMP receptor from *E. coli* (97), and the homeodomain containing the transcriptional activators **ultrabithorax** and deformed (98).

Formation of the complex between CRP and the C1 site in the *lac* promoter is accompanied by the release of 79 (±11) water molecules, while 56 (±10) water molecules are taken up when CRP is transferred from the C1 site to a nonspecific site (97). Depending on the neutral salt used, between 100 and 180 water molecules are released when gal repressor binds to the O_I operator site (95). An additional 6 (±3) waters are released when the repressor is transferred from O_I to O_E, to which it binds with enhanced affinity. Interestingly, despite the close sequence similarity in their homeodomains, water activity affects differentially the DNA binding of Ultrabithorax and Deformed (98). Between 22 and 27 water molecules were released for DNA binding by Ultrabithorax, while only 5 water molecules were released when Deformed bound to its optimal sequence. On the other hand, the DNA sequence did not exert a strong effect on the magnitude of the water release associated with DNA binding by Ultrabithorax.

The osmotic-stress methods yield a value for the number of water molecules released, which is the difference between the water molecules released and those taken up, for example as a consequence of the exposure of additional surface area due to unfolding.

4. Conformational Changes of the Protein on DNA Binding

Even though in some specific complexes the tightly packed interfaces between the protein and the DNA result from the docking of well-ordered, preexisting surfaces, in an increasing number of cases the conformations of both the protein and the DNA are found to change markedly in the complex. The DNA-binding reaction of the BHLH protein MASH-1, for instance, is characterized by a transition of the peptide from a largely unfolded to a mainly a-helical conformation (60). Even at concentrations well above the dimerization constant for the MASH-BHLH domain, where the HLH domain is stably folded, the basic region adopts an ordered conformation only upon binding DNA (39). A similar transition was observed with the DNA-binding domains of GCN4, Fos, and Jun, where the basic region undergoes a transition to an a-helical structure upon binding to DNA (99-101). In these cases, the association does not result from a simple alignment of rigid, complementary surfaces, but rather follows what is generally known as an "induced fit" mechanism (102).

Because of a reduction in water-accessible surface area, folding transitions that occur on DNA binding result in a negative heat capacity change Dc_p (see text above). Because experimental values for D c_p are often too large to be accounted for simply by the reduction in water-accessible surface area in a rigid body association, Spolar and Record (84) have suggested how to dissect the various contributions to the entropy change. Consider as an example the DNA-binding reaction of the BHLH domain of MASH-1. This reaction shows a strong temperature dependence for both the measured DH and TD S, which compensate to make DG almost insensitive to temperature. A notable consequence is the existence of a temperature T_S, for which TDS changes sign. Therefore, the following equation holds at T_S:

$$-\Delta S_{\text{other}} = \Delta S_{\text{HE}}(T_{\text{S}}) + \Delta S_{\text{RT}} + \Delta S_{\text{PE}}$$

The total change in entropy consists of a contribution DS_{HE} from the hydrophobic effect, the unfavorable entropic term D S_{RT}, due to the reduction in rotational and translational degrees of freedom on association, the contribution from the polyelectrolyte effect DS_{PE}, and DS_{other}, which results primarily from conformational changes in the protein and/or the DNA (84). DS_{HE} (T_S) can be calculated from measured thermodynamic data according to the equation

$$\Delta S_{\text{HE}}(T_{\text{S}}) = 1.35\Delta c_{\text{p}} \ln(T_{\text{s}}/386)$$

For MASH-1, T_S was determined as 271 K and a value of –357 cal mol^{-1} K^{-1} was calculated for DS_{HE} (T_S) (39). The polyelectrolyte effect could be estimated from the salt dependence as 50 cal mol^{-1} K^{-1} ((39); Meierhans, unpublished results), while DS_{RT} for a bimolecular reaction was taken to be –50 cal mol^{-1} K^{-1} (103, 104). The change in entropy resulting from local folding transitions coupled to DNA could therefore be calculated as 357 cal mol^{-1} K^{-1}. This was interpreted to indicate that approximately 54 amino acid residues of the basic region are involved in the folding reaction, or 27 residues per BHLH subunit; this interpretation is supported by CD studies of the DNA-binding reaction of MASH-BHLH and nuclear magnetic resonance (NMR) studies of the BHLH protein E47 (39, 105).

Comparison of the experimentally determined and the calculated Dc_p for the association reaction of the transcription factor GCN4 and DNA suggested that approximately 7 amino acid residues of the basic region of this basic-zipper protein underwent a transition from a random to an a-helical conformation (48). The high-resolution structures of uncomplexed Trp repressor and its specific DNA complex indicate that 16 residues of helix D are disordered in the free repressor and a-helical in the DNA complex (106-109) [it should be pointed out that this interpretation of the structural data has been challenged (35)]. The same value for the number of residues that change conformation upon DNA binding was obtained from thermodynamic data, where D S_{other} was determined as –94 cal mol^{-1} K^{-1} (8).

Structural data suggest that conformational changes also occur for the DNA-binding reaction of the DNA-binding domain of glucocorticoid receptor (110-113). These results are in good agreement with thermodynamic measurements and indicate a folding transition in approximately 18 residues per protein subunit (25). Another example of a conformational change is provided by the Antennapedia homeodomain. An *N*-terminal extension that is flexible in the free protein becomes ordered on DNA binding and contacts the minor groove of the DNA (114-116). Unfortunately, there are no thermodynamic data available for this system.

Thermodynamic studies suggest conformational changes for the DNA-binding reactions of the following proteins: the lac (117), Gal (118), and Mnt (84) repressors binding to their operator sequences, and **RNA polymerase** binding to the l P_R promoter.

For a number of DNA-binding proteins, complex formation is accompanied by changes in the **tertiary** or quaternary structure. For example, thermodynamic analysis of the DNA-binding reaction of the l Cro protein, under conditions where it exists as a stably folded dimer in solution, indicated a relatively small D S_{other} of 18 cal mol^{-1} K^{-1} (7). Information from the crystal structures of both free and complexed Cro suggests that this entropy change may reflect changes in quaternary structure of the Cro dimer on DNA binding (119, 120).

Other proteins for which structural evidence exists for coupled structural changes on binding to DNA include the endonuclease EcoRV and the transcriptional activator CRP. The DNA-binding pocket of EcoRV is not accessible in the free protein, and the cleft between the two protein subunits is too narrow to accommodate the DNA. Consequently, the pocket must be opened up through a combination of tertiary and quaternary structural transitions (58). For CRP, the relative orientations of the amino- and the carboxy-terminal domains change significantly on DNA binding. However, the structures of the DNA complexes of CRP and EcoRV revealed that optimal shape complementarity between these proteins and DNA is achieved not only through conformational adaptations of the protein, but also through changes in the structure of the DNA.

5. Conformational Changes of the DNA upon Protein Binding

While many proteins recognize regular B-DNA through the formation of a number of hydrogen bonds and van der Waals interactions between amino acid side chains and functional groups of the bases, it has long been recognized in many cases that DNA can adopt a bent conformation when bound to a protein (121). A dramatic example of protein-induced DNA bending is provided by the structure of integration host factor (IHF) bound to the H′-site of phage l, in which the 34-bp piece of

DNA is literally wrapped around the protein, creating a buried protein–DNA interface of 4600 $Å^2$ (Fig. 3) (122, 123). The DNA is bent by more than 160°, thereby almost completely reversing the direction of the DNA within a short distance.

Figure 3. Van der Waals representation of the IHF–DNA complex (122). The drawing illustrates both the massive DNA bend induced by the protein and the large contact surface of ~ 4600 $Å^2$ between protein and DNA. The DNA sequence is indicated.

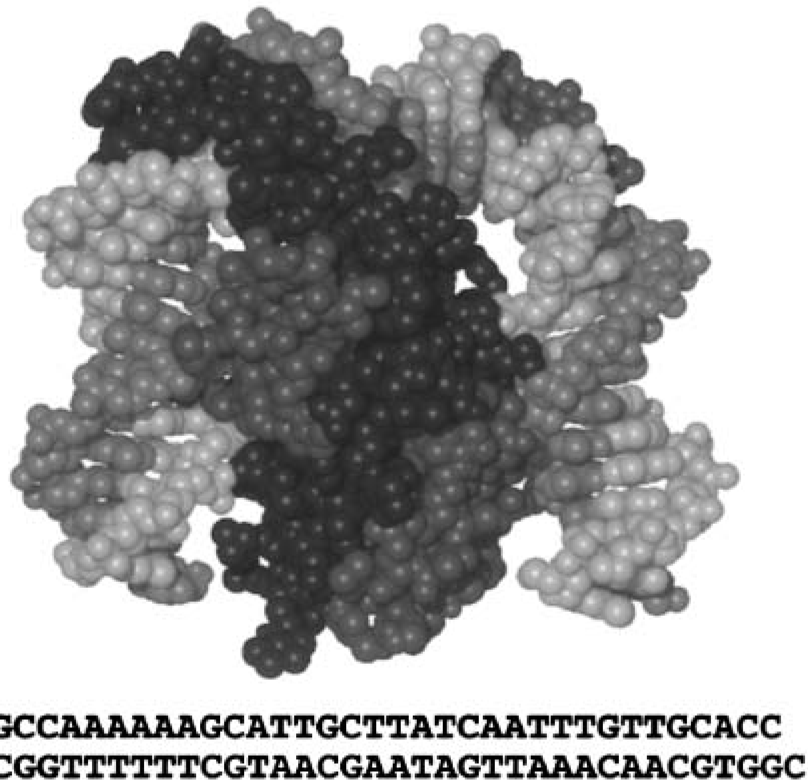

Other examples of strong protein-induced bends are provided by the structures of the DNA complexes of the purine repressor PurR (124), the sex-determining protein SRY (125), the pre-B- and T-lymphocyte-specific factor LEF-1 (126), and the human **oncogene** product ETS1 (127). In none of the above cases would it have been possible to predict the dramatic bends observed in the complexes from simple inspection of the DNA sequence.

Conversely, studies with 434 repressor indicated that its DNA-binding affinity was modulated by the flexibility of the noncontacted nucleobases at the center of the binding site (128, 129). A linear relationship was found between the free energy of the association reaction between 434 repressor and operator mutants and the flexibility of their central sequences (130). Similar results had been obtained for the Cro repressor from bacteriophage l (131). These studies indicated for the first time that intrinsic sequence-dependent properties are important for the formation of DNA–protein complexes.

Sequence-dependent bending of double-stranded DNA often occurs at the junctions between regions of G–C and A–T base pairs. DNA bending of 10° to 20° has been observed in the crystal structures of oligonucleotides containing an AT-core (132). While such sequences can be bent, however, they are not necessarily bent. The transition from G–C to A–T base pairs renders this region of the DNA flexible and capable of potentially undergoing a bend. Such facultative bending is illustrated by the

X-ray structure of the dodecamer d(CGCGAATTCGCG) (Fig. 4), in which a bend of 18° occurs at the GC/AT junction at one end of the helix, while the helix remains unbent at the chemically equivalent junction at the other end of the helix (133, 134). The molecular mechanism of such facultative bending has been reviewed in detail elsewhere (135).

Figure 4. Facultative bending into the major groove at one end of the dodecamer duplex $[d(CGCGAATTCGCG)]_2$ (134). Note the positive roll at the CpG and GpA steps and the negative propeller twisting in the central four base pairs. Overall and local helical axes are shown.

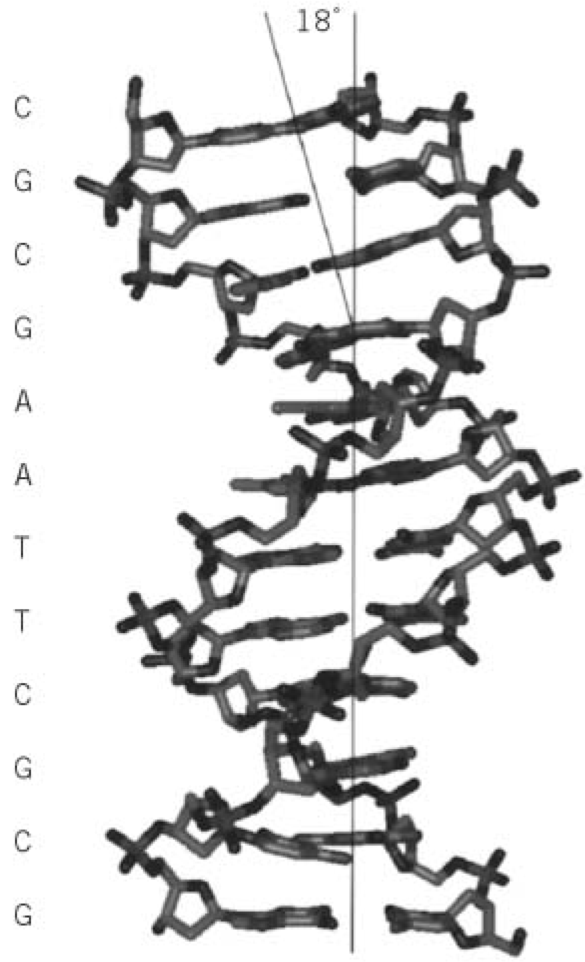

The recognition sequences of **serum response factor** (SRF) (136) (see MADS-Box Proteins), TATA-binding protein (TBP) (74-77), the restriction endonucleases EcoRI and EcoRV (58, 137), and EcoRI DNA methyltransferase (138) all have AT-rich core sequences, characterized by increased bendability. The crystal structure analyses of DNA complexes of these proteins revealed that they take advantage of the inherent bendability of their DNA targets. The DNAs adopt significantly bent conformations in all of these complexes.

Myocyte enhancer factor-2C (MEF-2C) interacts with DNA in a similar fashion to SRF (139, 140), and its consensus DNA-binding site was determined in polymerase chain reaction (**PCR**)-mediated binding site selection assays as $CTA(A/T)_4TAG$ (141). A detailed analysis of the affinities of MEF-2C for DNA of varying sequence revealed that mutations within the central four base pairs are tolerated so long as adenine is replaced with thymine or vice versa (139, 142). However, the replacement of the central bases with guanine and cytosine significantly diminished the affinity for MEF-2C (Table 1).

Table 1. DNA Binding Parameters for MEF-2C (2–117) and GG-MEF-2C(1–117)

	$[P_{1/2}]$ (nM)[a]	
DNA Sequence	**MEF-2C(2–117)**[b]	**GG-MEF-2C(1–117)**[c]
TGCTGC **TATAAATA** GAGTGA	**110** (±**20**)	**103** (±**9**)
TGCTGC **TATATATA** GAGTGA	**130** (±**25**)	**82** (±**5**)
TGCTGC **TTTAAATA** GAGTGA	**118** (±**11**)	**112** (±**28**)
TGCTGC **TATTAATA** GAGTGA	**117** (±**23**)	**203** (±**14**)
TGCTGC **TAATAATA** GAGTGA	**108** (±**20**)	**227** (±**22**)
TGCTGC **AAAAAAAA** GAGTGA	**742** (±**163**)	**1004** (±**195**)
TGCTGC **TATGCATA** GAGTGA	**1072** (±**200**)	**1780** (±**370**)
CTGCTGC **TATA-ATA** GAGTGA	**129** (±**26**)	**207** (±**32**)
CTGCTGC **TATAAAT-** GAGTGA	**109** (±**11**)	**135** (±**12**)
CTGCTGC **-ATAAAT-** GAGTGAC	**339** (±**73**)	**1896** (±**417**)
CTGCTGC **TAT—ATA**GAGTGAC	**126** (±**21**)	**115** (±**12**)

[a] Protein concentration for which 50% of the DNA binding sites are filled.

[b] Ref. 139.

[c] Ref. 142.

A correlation was observed between the affinity of MEF-2C for a mutant site and the intrinsic bendability of the site. MEF-2C binds to a DNA site with an alternating run of eight thymines and adenines with maximal affinity, while the affinity for an inherently rigid A-tract sequence is reduced by more than one order of magnitude (Table 1). Because of its poor stacking (Fig. 5), the deformability of a TA step is inherently much greater than that of an AT or an AA step (74, 121, 135, 143-152). A simple mechanical model to explain this observation has been provided by Finch and co-workers (135, 153). The proximity of the methyl groups of two successive thymines and the methyl groups and the phosphate backbone make the helix rather rigid (Fig. 5). In an AT step, the stacking of the methyl group with the adjacent adenine and the intervening sugar phosphate backbone again prevents bending by a roll mechanism. However, in a TA step the methyl group projects into the major groove without any significant stacking interactions with either the adjacent adenine or the phosphate backbone, and this step therefore displays a higher deformability than the AA and AT steps.

Figure 5. Schematic representations of the ApT-, TpT-, and TpA-dinucleotide steps indicating the sequence specific conformational differences between these steps. The DNA is viewed from the major groove indicated by Ma. The thymine methyl groups are indicated by small spheres. The methyl groups belonging to the right strand are shaded. The twist, slide, and roll movements that could create sterically unfavorable interactions are marked with ×. The regions of

the DNA which clash due to these movements are indicated. This part of the figure was adapted from Suzuki et al. (153). The differences in the nearest-neighbor stacking energies are given on the right, indicating that the most favorable stacking interaction is observed for Pu–Py dinucleotide steps (143, 147).

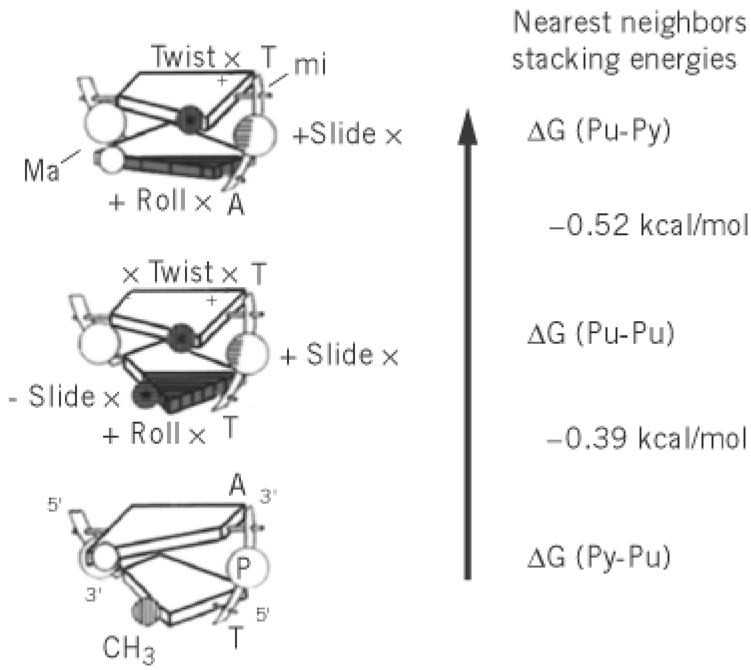

Reducing the length of the AT run from eight to six nucleosides by removing the first and the eighth base of the run (which generates a consensus site for SRF) reduced the stability of the MEF-2C complex almost 20-fold (Table 1). When the six AT bases consisted of alternating thymines and adenines, however, MEF-2C bound to the corresponding oligonucleotide again with almost the same affinity as to a MEF-2C site of length eight. This observation strongly supports the proposal that the inherent bendability of the DNA-binding site is a principal determinant of the DNA-binding specificity of MEF-2C (139, 140, 142). The affinities of the various AT-rich sequences for MEF-2C might be a measure of the relative bendability of the unbound DNA.

Similarly, a comparison of the DNA structure of the free uncomplexed Trp operator with that observed in the trp repressor–operator complex provided evidence that particular DNA sequences might be predisposed to adopt a non-B-form conformation in protein complexes (72).

Circular dichroism spectroscopy and bending analysis by circular permutation assays revealed that MEF-2C potentiates the natural tendency of its DNA target to adopt a bent conformation (142). DNA binding by MEF-2C is accompanied by DNA bending of approximately 70°, irrespective of the particular DNA sequence. This observation depends on the presence of the *N*-terminal methionine residue. In its absence, DNA containing a high-affinity binding site is bent by only 49°, while heterologous sequences remain unbent (139, 142). The differences in DNA-binding affinity are much less pronounced in the absence of the *N*-terminal methionine (Table 1). The *N*-terminal methionine appears to anchor MEF-2C to the ends of the AT run, thereby orientating the protein properly on the DNA. In the minor groove, A–T base pairs can be distinguished from G–C base pairs by the lack of a heterocyclic atom at C2 of adenine. Based on the SRF structure (see MADS-Box Proteins), it had been suggested that the *N*-terminal methionine of MEF-2C is located over A4 and could specify the adenine by means of hydrophobic interaction with C2 of adenine (136). However, the observation that MEF-2C can bind with high affinity to a run of three alternating TA steps indicated that the *N*-terminal methionine does not interact with C2 of adenine (154) of the MEF site. With the short TA run, the steric clash between the side chain of methionine and the amino group on C2 of guanine (154) would reduce the stability of the complex significantly (142). It is therefore more likely that the side chain of the *N*-terminal methionine packs against the sugar ring of the nucleotide (154).

When a protein binds to a more rigid DNA sequence, it often does not bend DNA, or a substantial amount of the binding free energy must be used to bend the DNA target. Even in these cases, however, proteins often target the most deformable base step within their target sequence. The purine repressor, PurR, which is involved in the biosynthesis of purines and pyrimidines, binds to runs of four consecutive adenines and thymines, interrupted by the dinucleotide CG (155). PurR bends the DNA into the major groove by 45° through the insertion of a hinge into the minor groove and intercalation of the side chains of two leucine residues into the CG step (124). **Calorimetric** analysis suggested that purine–pyrimidine steps stack more stably than do purine–purine or pyrimidine–pyrimidine steps by approximately 0.52 kcal/mol, while the stacking energy of pyrimidine–purine steps is reduced by another 0.39 kcal/mol (Fig. 5) (143, 147). Therefore, CpG is the step that can be unstacked most easily within the pur operator. Similarly, the bending of 22° of the PRDI site within the **interferon**-b promoter in the complex with interferon regulatory factor (IRF) occurs at the CpA step which is the most easily unstacked dinucleotide in the PRDI sequence, ACTTTCACTTCTC (156). The cocrystal structure of the DNA complex of the chromosomal protein Sac7d from the hyperthermophile *Sulfolobus acidocaldarius* revealed that the DNA is kinked by 61° through the intercalation of two amino acid side chains, namely Val26 and Met29 between the bases of the dinucleotide C(2)G(3) (157). This is the base step that is most easily unstacked in the DNA sequence GCGATCGC. All these examples demonstrate that proteins recognize DNA not only through specific contacts with the nucleobases, but also through inherent, sequence-dependent properties of the DNA. Therefore, considering the properties of both the protein and the DNA makes possible an understanding of the sequence specificity and the observed DNA bend in DNA–protein complexes (135, 158).

The binding specificity of a protein is determined by the difference in binding affinities of the protein for the specific and the nonspecific sites. DNA bending is an energy costly process, even for sequences of enhanced bendability (Fig. 6). Some of the binding free energy must be used to bend a DNA molecule which, in the absence of protein, adopts either an unbent or an only slightly bent conformation. Therefore, protein-induced DNA bending can contribute to the overall specificity of a DNA-binding protein (142, 159-161). MEF-2C, for example, must use some of the binding free energy from specific interactions to induce bending at the specific site. In the case of a MEF-2C mutant lacking the *N*-terminal methionine, however, no binding free energy appears to be used for the bending of the nonspecific complex (139, 142). Consequently, the difference between the free energies of the specific and the nonspecific complexes is reduced because of the unfavorable contribution from bending the specific DNA. On the other hand, MEF-2C(1–117), which contains the *N*-terminal methionine, bends both specific and nonspecific DNA, thereby increasing the difference in the free energy between the specific and the nonspecific complexes. The increased DNA-binding specificity of MEF-2C(1–117) over that of MEF-2C(2–117) relies therefore in part on the fact that MEF-2C(1–117) bends DNA irrespective of the particular sequence. MEF-2C(1–117) appears to select DNA-binding sites that are characterized by increased bendability, because for these DNA sequences less binding free energy must be expedited to force them into the bent conformation necessary for the optimal shape complementarity observed in the complexes. Interestingly, the CD spectra of the DNA complexes of MEF-2C(1–117) indicated that the conformation of the DNA was independent of its sequence, at least within the resolution of CD spectroscopy (142), while the CD spectra of the DNA in the MEF-2C(2–117) complexes varied strongly with the DNA sequence (139, 142). Scanning tunneling microscopy has indicated that the specific and nonspecific DNA complexes of l Cro are characterized by similar bend angles. The bend angle induced by binding of a Cro dimer to DNA was determined as 69° ± 11° and 62° ± 23° for specific and non-specific DNA, respectively (159).

Figure 6. Free energy diagram illustrating the effect of DNA bending on the stabilities of the complexes of protein P

with DNA D. The DNA-binding specificity DD*G* is defined as the difference of the binding free energies for the formation of the specific and nonspecific complexes: DDG = DG_{SP} – DG_{NS}. The total free energy for the formation of the specific and the nonspecific complexes can be partitioned into the contributions from the (favorable) interactions between the DNA and the protein, D *G*(Int), and the (unfavorable) free energy change required to bend the DNA, D*G* (Bend).

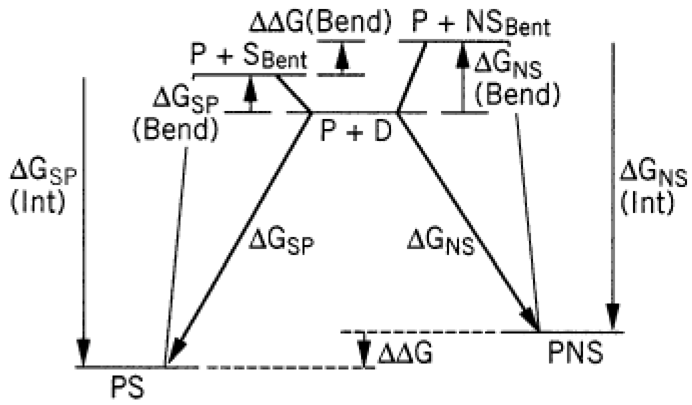

$$\Delta\Delta G = \Delta G_{SP} - \Delta G_{NS}$$
$$= \Delta G_{SP}(\mathrm{Int}) + \Delta G_{SP}(\mathrm{Bend} - \Delta G_{NS}(\mathrm{Int}) - \Delta G_{NS}(\mathrm{bend})$$
$$= \Delta\Delta G(\mathrm{Bend}) + \Delta\Delta G(\mathrm{Int})$$

In order to bend DNA, proteins use primarily two mechanisms. In the first, kinks are introduced through the intercalation of amino acid side chains between adjacent base pairs. In the IHF–DNA complex, two intercalating proline residues projecting from the tip of each b-hairpin arm introduce large kinks at symmetrically displaced ApA steps. SRY (125) and LEF-1 (126), which are structurally similar proteins, use nonaromatic, hydrophobic amino acids to intercalate into base steps from the minor grove side of the double helix, creating a widened minor grove and a dramatically bent DNA. TATA box-binding protein induces strong bends of approximately 45° at either end of the TATA box through the intercalation of two phenylalanine rings between two adjacent base pairs (74-77), while the hyperthermophile chromosomal proteins Sac7d bends DNA by 72°, primarily through the intercalation of Val(26) and Met(29) at a single CpA base step (157).

The second mechanism for the introduction of bends into DNA was originally proposed by Rich (162). Asymmetric neutralization of the negative charges of the phosphodiesters by cationic amino acid residues could result in unbalanced Coulombic repulsions between the negative charges on DNA, causing DNA to collapse toward the bound protein (162-164). For example, the X-ray structure of **serum response factor** bound to its target DNA sequence indicated that asymmetric charge neutralization is at least partly responsible for the DNA bend angle of 72° (136). Several positively charged amino acid residues of SRF bind the phosphate groups on only one side of the SRF-site (Fig. 7). The three positively charged amino acids that interact with the distal ends of the DNA provide the hands through which SRF pulls up the far ends of the DNA. In addition, Arg143 lies in an extended conformation along the floor of the minor grove and stabilizes the relatively large propeller twists at the central base steps, which are characteristic of AT-rich regions. These interactions also facilitate the bending of DNA. The members of the MEF-2 family of proteins most probably follow a similar mechanism to induce bends into DNA (142). However, the bending of the AT-rich target sequences of SRF and of the MEF-2 proteins is helped by the intrinsically high bendability of these DNA sequences (135). The X-ray structure of the complex between the bZ protein GCN4 and an ATF-site-containing DNA revealed that the DNA was unbent (165). On the other hand, the heterodimer of the bZ proteins Jun and Fos appears to induce DNA bending when bound to an AP-1 site (166-168), although some controversy exists on this point (169-173). The identity of the amino acids just *N*-terminal to the basic region appears to be important for DNA bending, in that cationic amino acids in these positions contact the negatively charged phosphate diesters on only one face of the DNA, thereby inducing the DNA to bend away from the leucine zipper (174-178). The corresponding amino acids in GCN4 are the uncharged Pro–Ala–

Ala, consistent with the observation that GCN4 does not bend AP1-site-containing DNA. Analysis of the bending properties of GCN4 mutants revealed that cationic amino acids in these positions induce DNA bending toward the neutralized surface, while anionic amino acids induce bending in the opposite direction (179).

Figure 7. Interactions between positively charged amino acid side chains and DNA phosphates in the SRF–DNA complex (136). Note that these contacts occur only on one side of the duplex, causing the DNA to bend towards the protein. The histidines and lysines on either end of the duplex serve as handles to further bend the DNA (the DNA used is too short to allow formation of the His-phosphate contact on the left-hand side).

While DNA bending is the most dramatic change observed upon DNA binding, many other more subtle conformational rearrangements of the DNA have been observed. While a slight bending of the DNA of approximately 25° has been observed in the crystal structure of the 434 repressor–DNA complex (180, 181), the major characteristic is the significantly overwound DNA in the region of the central four base pairs of the binding site. Relative to canonical B-DNA, the net overtwisting is approximately 20°. Although these four base pairs are not in direct contact with the repressor, operators with A–T or T–A base pairs at these positions are bound more strongly than those bearing C-G or G-C (182). A relationship between the intrinsic twist of an operator, as determined by the sequence of its central bases, and its affinity was observed: Operators with lower affinity are undertwisted relative to operators with higher affinity (128).

Bibliography

1. N. C. Seeman, J. M. Rosenberg, and A. Rich (1976) Proc. Natl. Acad. Sci. USA **73**, 804–808.
2. J. M. Rosenberg and P. Greene (1982) DNA **1**, 117–124.
3. P. C. Ma, M. A. Rould, H. Weintraub, and C. O. Pabo (1994) Cell **77**, 451–459.
4. T. Ellenberger, D. Fass, M. Arnaud, and S. C. Harrison (1994) Genes Dev. **8**, 970–980.
5. M. Sieber and R. K. Allemann (1998) Biol. Chem. **379**, 731–735.

6. L. E. Engler, K. K. Welch, and L. Jen-Jacobsen (1997) J. Mol Biol. **269**, 82–101.
7. Y. Takeda, P. D. Ross, and C. P. Mudd (1992) Proc. Natl. Acad. Sci. USA **89**, 8180–8184.
8. L. Jin, J. Yang, and J. Carey (1993) Biochemistry **32**, 7302–7309.
9. J. E. Ladbury, J. G. Wright, J. M. Strutevant, and P. B. Sigler (1994) J. Mol. Biol. **238**, 669–681.
10. P. E. Merabet and Ackers (1995) Biochemistry **34**, 8554–8563.
11. M. T. Record Jr., J.-H. Ha, and M. A. Fisher (1991) Methods Enzymol. **208**, 291–343.
12. D. F. Senear and G. K. Ackers (1990) Biochemistry **29**, 6568–6577.
13. C. D. Waldburger and R. T. Sauer (1995) Biochemistry **34**, 13109–13116.
14. D. E. Frank, R. M. Saecker, J. P. Bond, M. W. Capp, O. V. Todikov, S. E. Melcher, M. M. Levandovski, and M. T. Record Jr. (1997) J. Mol. Biol. **267**, 1186–1206.
15. B. M. Brown and R. T. Sauer (1993) Biochemistry **32**, 1354–1363.
16. T. L. Smith and R. T. Sauer (1995) J. Mol. Biol. **249**, 729–742.
17. L. Jen-Jacobsen, M. Kurpiewski, D. Lesser, J. Grable, H. W. Boyer, J. M. Rosenberg, and P. J. Greene (1983) J. Biol. Chem. **258**, 14638–14646.
18. L. Jen-Jacobsen, D. Lesser, and M. Kurpiewski (1986) Cell **45**, 619–629.
19. D. R. Lesser, M. R. Kurpiewski, and L. Jen-Jacobsen (1990) Science **250**, 776–786.
20. C. R. Aiken, L. W. McLaughlin, and R. I. Gumport (1991) J. Biol. Chem. **266**, 19070–19078.
21. D. R. Lesser, M. R. Kurpiewski, T. Waters, B. A. Connolly, and L. Jen-Jacobsen (1993) Proc. Natl. Acad. Sci. USA **90**, 7548–7552.
22. L. Jen-Jacobsen (1995) Methods Enzymol. **259**, 305–344.
23. P. C. Newman, V. U. Nwosu, D. M. Williams, R. Cosstick, F. Seela, and B. A. Connolly (1990) Biochemistry **29**, 9891–9901.
24. A. Gunasekera, Y. W. Ebright, and R. H. Ebright (1992) J. Biol. Chem. **267**, 14713–14720.
25. T. Lundbäck, C. Cairns, J.-Å, Gustafsson, J. Carlstedt-Duke, and T. Härd (1993) Biochemistry **32**, 5074–5082.
26. S. A. Smith, S. B. Rajur, and L. W. McLaughlin (1994) Nat. Struct. Biol. (1994) **1**, 18–22.
27. J. M. Mazarelli, S. B. Rajur, P. L. Iadarola, and L. W. McLaughlin (1992) Biochemistry **31**, 5925–5936.
28. T. Lundbäck and T. Härd (1996) Proc. Natl. Acad. Sci. USA **93**, 4754–4759.
29. B. F. Luisi, W. Xu, Z. Otwinowski, L. P. Freedman, and K. R. Yamamoto (1991) Nature **352**, 497–505.
30. D. V. Goeddel, D. G. Yansura, M. H. Caruthers (1977) Nucleic Acids Res. **4**, 3039–3052.
31. D. V. Goeddel, D. G. Yansura, and M. H. Caruthers (1978) Proc. Natl. Acad. Sci. USA **75**, 3578–3582.
32. E. F. Fisher and M. H. Caruthers (1979) Nucleic Acids Res. **7**, 401–416.
33. Y. Takeda, A. Sarai, and V. M. Rivera (1989) Proc. Natl. Acad. Sci. USA **86**, 439–443.
34. C. F. Anderson and M. T. Record Jr. (1995) Annu. Rev. Phys. Chem. **46**, 657–700.
35. T. M. Härd and T. Lundbäck (1996) Biophys. Chem. **62**, 121–139.
36. T. M. Lohman, P. L. deHaseth, and M. T. Record Jr. (1980) Biochemistry **19**, 3522–3530.
37. G. S. Manning (1978) Q. Rev. Biophys. **11**, 179–246.
38. D. P. Mascotti and T. M. Lohman (1990) Proc. Natl. Acad. Sci. USA **87**, 3142–3146.
39. A. G. E. Künne, M. Sieber, D. Meierhans, and R. K. Allemann (1998) Biochemistry **37**, 4217–4223.

40. M. T. Record Jr., P. L. deHaseth, and T. M. Lohman (1977) Biochemistry **16**, 4791–4796.
41. T. M. Lohman, C. G. Wensley, J. Cina, R. R. Burgess, M. T. Record Jr. (1980) Biochemistry **19**, 3516–3522.
42. M. C. Mossing and M. T. Record Jr. (1985) J. Mol. Biol. **186**, 295–305.
43. J.-H. Ha, M. W. Capp, M. D. Hohenwalter, M. Baskerville, and M. T. Record Jr. (1992) J. Mol. Biol. **228**, 252–264.
44. D. F. Senear and R. Batey (1991) Biochemistry **30**, 6677–6688.
45. M. T. Record Jr., C. F. Anderson, and T. M. Lohman (1978) Q. Rev. Biophys. **11**, 103–178.
46. S. Leirmo and M. T. Record Jr. (1990) In *Nucleic Acids and Molecular Biology*, Vol. **4** (D. M. J. Lilley and F. Eckstein, eds.), Springer, Berlin, p. 123.
47. P. H. von Hippel and T. Schleich (1969) Acc. Chem. Res. **2**, 257–265.
48. C. Berger, I. Jelesarov, and H. R. Bosshard (1996) Biochemistry **35**, 14984–14991.
49. W. Zhang, J. P. Bond, C. F. Anderson, T. M. Lohman, and M. T. Record Jr. (1996) Proc. Natl. Acad. Sci. USA **93**, 2511–2516.
50. S. Padmanabhan, W. Zhang, M. W. Capp, C. F. Anderson, and M. T. Record Jr. (1997) Biochemistry **36**, 5193–5206.
51. M. T. Record Jr., T. M. Lohman, and P. de Haseth (1976) J. Mol. Biol. **107**, 145–158.
52. J. D. McGhee and P. H. von Hippel (1974) J. Mol. Biol. **86**, 469–489.
53. W. H. Braunlin, C. F. Anderson, and M. T. Record Jr. (1987) Biochemistry **26**, 7724–7731.
54. G. E. Plum and V. A. Bloomfield (1988) Biopolymers **27**, 1045–1051.
55. D. P. Mascotti and T. M. Lohman (1992) Biochemistry **31**, 8932–8946.
56. D. P. Mascotti and T. M. Lohman (1993) Biochemistry **32**, 10568–10579.
57. M. Takahashi, B. Blazy, A. Baudras, and W. Hillen (1983) J. Mol. Biol. **167**, 895–899.
58. F. K. Winkler, D. W. Banner, C. Oefner, D. Tsernoglou, R. S. Brown, S. P. Heathman, R. K. Bryan, P. D. Martin, K. Petratos, and K. S. Wilson (1993) EMBO J. **12**, 1781–1795.
59. D. Kostrewa and F. K. Winkler (1995) Biochemistry **34**, 683–696.
60. D. Meierhans, C. el Ariss, M. Neuenschwander, M. Sieber, J. F. Stackhouse, and R. K. Allemann (1995) Biochemistry **34**, 11026–11036.
61. A. G. E. Künne, D. Meierhans, and R. K. Allemann (1996) FEBS Lett. **391**, 79–83.
62. J. D. Dunitz (1994) Science **264**, 670.
63. L. J. Beamer and C. O. Pabo (1992) J. Mol. Biol. **227**, 177–196.
64. J.-A. Feng, R. C. Johnson, and R. E. Dickerson (1994) Science **263**, 348–355.
65. M. Newman, T. Strzelecka, L. F. Dorner, I. Schildkraut, and A. K. Aggarwal (1995) Science **269**, 656–663.
66. J. W. R. Schwabe, L. Chapman, J. T. Finch, and D. Rhodes (1993) Cell **75**, 567–578.
67. R. S. Hedge, S. R. Grossman, L. A. Laimins, and P. B. Sigler (1992) Nature **359**, 505–512.
68. M. Billeter, P. Güntert, P. Luginbühl, and K. Wüthrich (1996) Cell **85**, 1057–1065.
69. G. M. Clore, A. Bax, J. G. Omichinski, and A. M. Gronenborn (1994) Structure **2**, 89–94.
70. P. B. Sigler (1992) In *Transcriptional Regulation*, Vol. **1** (S. L. McKnight and K. R. Yamamoto, eds.), Cold Spring Harbor Laboratory Press, Cold Spring Harbor, NY, pp. 475–499.
71. P. B. Sigler (1993) *Proceedings of the Robert A. Welch Foundation, 37th Conference*, pp. 63–76.
72. Z. Shakked, G. Guzikevich-Guerstein, F. Frolow, D. Rabiovich, A. Joachimiak, and P. B. Sigler (1994) Nature **368**, 469–473.

73. C. L. Lawson, R.-G. Zhang, R. W. Schevitz, Z. Otwinowski, A. Joachimiak, and P. B. Sigler (1988) Proteins **3**, 18–31.
74. Z. S. Juo, T. K. Chiu, P. M. Leiberman, I. Baikalov, A. J. Berk, and R. E. Dickerson (1996) J. Mol. Biol. **261**, 239–254.
75. Y. Kim, J. H. Geiger, S. Hahn, and P. B. Sigler (1993) Nature **365**, 512–529.
76. J. L. Kim, D. B. Nikolov, and S. K. Burley (1993) Nature **365**, 520–527.
77. J. L. Kim and S. K. Burley (1994) Nat. Struct. Biol. **1**, 638–653.
78. M. C. Polyakow, M. H. Champagne, and M. P. Daune (1972) Eur. J. Biochem. **26**, 212–219.
79. J. H. Roe, R. R. Burgess, and M. T. Record (1985) J. Mol. Biol. **184**, 441–453.
80. P. A. Whitson, J. S. Olson, and K. S. Matthews (1986) Biochemistry **25**, 3852–3858.
81. A. K. Vershon, S.-M. Liao, W. R. McClure, and R. T. Sauer (1987) J. Mol. Biol. **195**, 311–322.
82. J.-H. Ha, R. S. Spolar, and M. T. Record (1989) J. Mol. Biol. **209**, 801–816.
83. R. H. Ebright, Y. W. Ebright, and A. Gunasekra (1989) Nucleic Acids Res. **17**, 10295–10304.
84. R. S. Spolar and M. T. Record Jr. (1994) Science **263**, 777–784.
85. J. Janin and C. Chothia (1990) J. Biol. Chem. **265**, 16027–16030.
86. R. S. Spolar, J. R. Livingstone, and M. T. Record Jr. (1992) Biochemistry **31**, 3947–3955.
87. P. H. von Hippel (1994) Science **263**, 769–770.
88. S. K. Burley (1994) Nat. Struct. Biol. **1**, 207–208.
89. V. A. Parsegian, R. P. Rand, N. L. Fuller, and D. C. Rau (1986) Methods Enzymol. **127**, 400–416.
90. V. A. Parsegian, R. P. Rand, and D. C. Rau (1995) Methods Enzymol. **259**, 43–94.
91. R. P. Rand (1992) Science **256**, 618.
92. C. R. Robinson and S. G. Sligar (1993) J. Mol. Biol. **234**, 302–306.
93. C. R. Robinson and S. G. Sligar (1994) Biochemistry **33**, 3787–3793.
94. C. R. Robinson and S. G. Sligar (1995) Proc. Natl. Acad. Sci. USA **92**, 3444–3448.
95. M. M. Garner and D. C. Rau (1995) EMBO J. **14**, 1257–1263.
96. C. R. Robinson and S. G. Sligar (1996) Protein Sci. **5**, 2119–2124.
97. K. M. Vossen, W. R. Daugherty, and M. G. Fried (1997) Biochemistry **36**, 11640–11647.
98. L. Li and K. S. Matthews (1997) Biochemistry **36**, 7003–7011.
99. L. Patel, C. Abate, and T. Curran (1990) Nature **347**, 572–575.
100. M. A. Weiss, T. Ellenberger, C. R. Wobbe, J. P. Lee, S. C. Harrison, and K. Struhl (1990) Nature **347**, 575–578.
101. K. T. O"Neil, R. K. Hoess, and W. F. DeGrado (1990) Science **249**, 774–778.
102. D. E. Koshland Jr. (1958) Proc. Natl. Acad. Sci. USA **44**, 98–104.
103. A. V. Finkelstein and J. Janin (1989) Protein Eng. **3**, 1–3.
104. J. Janin and C. Chothia (1978) Biochemistry **17**, 2943–2948.
105. R. Fairman, R. K. Beran-Steed, and T. M. Handel (1997) Protein Sci. **6**, 175–184.
106. Z. Otwinowski, R. W. Schevitz, R.-G. Zhang, C. L. Lawson, A. Joachimiak, R. Q. Marmorstein, B. F. Luisi, and P. B. Sigler (1988) Nature **335**, 321–329.
107. M. R. Gryk, M. D. Finucane, Z. Zheng, and O. Jardetzky (1995) J. Mol. Biol. **246**, 618–627.
108. D. Zhao, C. H. Arrowsmith, X. Jia, and O. Jardetzky (1993) J. Mol. Biol. **229**, 735–746.

109. C. H. Arrowsmith, J. Czaplicki, S. B. Iyer, and O. Jardetzky (1991) J. Am. Chem. Soc. **113**, 4020–4022.
110. H. Baumann, K. Paulsen, H. Kovåcs, H. Berglund, A. P. H. Wright, J.-A. Gustafsson, and T. Härd (1993) Biochemistry **32**, 13463–13471.
111. T. Härd, E. Kellenbach, R. Boelens, R. Kaptein, K. Dahlman, J. Carlstedt-Duke, L. P. Freedman, B. A. Maler, E. I. Hyde, J. A. Gustafsson, and K. R. Yamamoto (1990) Biochemistry **29**, 9015–9023.
112. H. Berglund, H. Kovåcs, K. Dahlman-Wright, J.-Å Gustafsson, and T. Härd (1992) Biochemistry **31**, 12001–12011.
113. M. A. L. Erikkson, H. Berglund, T. Härd, and L. Nilsson (1993) Proteins **17**, 375–390.
114. Y. Q. Qian, M. Billeter, G. Otting, M. Müller, W. J. Gehring, K. Wüthrich (1989) Cell **59**, 573–580.
115. G. Otting, Y. Q. Qian, M. Billeter, M. Müller, M. Affolter, W. J. Gehring, and K. Wüthrich (1990) EMBO J. **9**, 3085–3092.
116. M. Billeter, Y. Q. Qian, G. Otting, M. Müller, W. Gehring, and K. Wüthrich (1993) J. Mol. Biol. **234**, 1084–1097.
117. M. Lewis, G. Chang, N. C. Horton, M. A. Kercher, H. C. Pace, M. A. Schumacher, R. G. Brennan, and P. Lu (1996) Science **271**, 1247–1254.
118. M. Brenowitz, E. Jamison A. Majumdar, and S. Adhya (1990) Biochemistry **29**, 3374–3383.
119. R. G. Brennan, S. L. Roderick, Y. Takeda, and B. W. Matthews (1990) Proc. Natl. Acad. Sci. USA **87**, 8165–8169.
120. R. G. Brennan (1991) Curr. Opin. Struct. Biol. **1**, 80–88.
121. A. Klug, A. Jack, M. A. Viswamitra, O. Kennard, Z. Shakked, and T. A. Steitz (1979) J. Mol. Biol. **131**, 669–680.
122. P. A. Rice, S.-W. Yang, K. Mizuuchi, and H. A. Nash (1996) Cell **87**, 1295–1306.
123. S.-W. Yang, and H. A. Nash (1995) EMBO J. **14**, 6292–6300.
124. M. A. Schumacher, K. Y. Choi, H. Zalkin, and R. G. Brennan (1994) Science **266**, 763–770.
125. M. H. Werner, J. R. Huth, A. M. Gronenborn, and G. M. Clore (1995) Cell **81**, 705–714.
126. J. J. Love, X. Li, D. A. Case, K. Giese, R. Grosschedel, and P. E. Wright (1995) Nature **376**, 791–795.
127. M. H. Werner, G. M. Clore, C. L. Fisher, R. J. Fisher, L. Trinh, J. Shiloach, and A. M. Gronenborn (1995) Cell **83**, 761–771.
128. G. B. Koudelka and P. Carlson (1992) Nature **355**, 89–91.
129. D. W. Rodgers and S. C. Harrison (1993) Structure **1**, 227–240.
130. H. R. Drew, M. J. McCall, and C. R. Calladine (1988) Annu. Rev. Cell Biol. **4**, 1–20.
131. A. Mondragon and S. C. Harrison (1991) J. Mol. Biol. **219**, 321–334.
132. R. E. Dickerson, D. Goodsell, and M. L. Kopka (1996) J. Mol. Biol. **256**, 108–125.
133. R. Wing, H. Drew, T. Takano, C. Broka, S. Tanaka, K. Itakura, and R. E. Dickerson (1980) Nature **287**, 755–758.
134. H. R. Drew, R. M. Wing, T. Takano, C. Broka, S. Tanaka, K. Itakura, and R. E. Dickerson (1981) Proc. Natl. Acad. Sci. USA **78**, 2179–2183.
135. R. K. Allemann and M. Egli (1997) Chem. Biol. **4**, 643–650.
136. L. Pellegrini, S. Tan, and T. J. Richmond (1995) Nature **376**, 490–498.
137. Y. Kim, J. C. Grable, R. Love, P. J. Greene, and J. M. Rosenberg (1990) Science **249**, 1307–1309.

138. B. W. Allan and N. O. Reich (1996) Biochemistry **35**, 14757–14762.
139. D. Meierhans, M. Sieber, and R. K. Allemann (1997) Nucleic Acids Res. **25**, 4537–4544.
140. D. Meierhans and R. K. Allemann (1997) Protein Expr. and Purif. **11**, 297–303.
141. L. A. Gosset, D. J. Kelvin, E. A. Sternberg, and E. N. Olson (1989) Mol. Cell. Biol. **9**, 5022–5033.
142. D. Meierhans and R. K. Allemann (1998) J. Biol. Chem. **273**, 26052–26060.
143. O. Gotoh and Y. Tagashira (1981) Biopolymers **20**, 1033–1042.
144. C. R. Calladine (1982) J. Mol. Biol. **161**, 343–352.
145. R. E. Dickerson (1983) J. Mol. Biol. **166**, 419–441.
146. A. A. Travers and A. Klug (1990) In *DNA Topology and its Biological Effects* (N. R. Cozzarelli and J. C. Wang, eds.), Cold Spring Harbor Laboratory Press, Cold Spring Harbor, NY, pp. 57–106.
147. S. G. Delcourt and R. D. Blake (1991) J. Biol. Chem. **266**, 15160–15169.
148. J. R. Quintana, K. Grzeskowiak, K. Yanagi, and R. E. Dickerson (1992) J. Mol. Biol. **225**, 379–395.
149. A. Klug (1993) Nature **365**, 486–487.
150. A. A. Travers and J. W. R. Schwabe (1993) Curr. Biol. **3**, 898–900.
151. D. M. Goodsell, M. L. Kopka, D. Cascio, and R. E. Dickerson (1993) Proc. Natl. Acad. Sci. USA **90**, 2930–2934.
152. M. Suzuki and N. Yagi (1995) Nucleic Acids Res. **23**, 2083–2091.
153. M. Suzuki, N. Yagi, and J. T. Finch (1996) FEBS Lett. **379**, 148–152.
154. A. Ishihama (1988) Trends Genet. **4**, 282–286.
155. H. Zalkin and J. E. Dixon (1992) Prog. Nucleic Acids Res. Mol. Biol. **42**, 259–287.
156. C. R. Escalante, J. Yie, D. Thanos, and A. K. Aggarwal (1998) Nature **391**, 103–106.
157. H. Robinson, Y.-G. Gao, B. S. McCrary, S. P. Edmondson, J. W. Shriver, and A. H.-J. Wang (1998) Nature **392**, 202–205.
158. R. E. Dickerson (1998) Nucleic Acids Res. **26**, 1906–1926.
159. D. A. Erie, G. Yang, H. C. Schultz, and C. Bustamante (1994) Science **266**, 1562–1565.
160. A. Shepartz (1995) Science **269**, 989.
161. D. A. Erie and C. Bustamante (1995) Science **269**, 989–990.
162. A. Rich (1978) Fed. Eur. Biochem. Soc. **51**, 71–81.
163. J. K. Strauss and L. J. Maher III (1994) Science **266**, 1829–1834.
164. A. Sivolob and S. N. Khrapunov (1997) Biophys. Chem. **67**, 85–96.
165. W. Keller, P. König, and T. J. Richmond (1995) J. Mol. Biol. **254**, 657–667.
166. T. K. Kerppola and T. Curran (1991) Cell **66**, 317–326.
167. T. K. Kerppola and T. Curran (1991) Science **254**, 1210–1214.
168. T. K. Kerppola (1997) Biochemistry **36**, 10872–10884.
169. P. J. Hagerman (1996) Proc. Natl. Acad. Sci. USA **93**, 9993–9996.
170. T. K. Kerppola (1996) Proc. Natl. Acad. Sci. USA **93**, 10117–10122.
171. R. J. McCormick, T. Badalian, and D. E. Fisher (1996) Proc. Natl. Acad. Sci. USA **93**, 14434–14439.
172. A. Sitlani and D. M. Crothers (1996) Proc. Natl. Acad. Sci. USA **93**, 3248–3252.
173. G. McGill and D. E. Fisher (1998) Chem. Biol. **5**, R29–R38.
174. T. K. Kerppola and T. Curran (1993) Mol. Cell. Biol. **13**, 5479–5489.
175. D. N. Paolella, C. R. Palmer, and A. Schepartz (1994) Science **264**, 1130–1133.

176. D. A. Leonard, N. Rajaram, and T. K. Kerppola (1997) Proc. Natl. Acad. Sci. USA **94**, 4913–4918.
177. D. N. Paolella, Y. Liu, M. A. Fabian, and A. Schepartz (1997) Biochemistry **36**, 10033–10038.
178. J. K. Strauss-Soukup and L. J. Maher III (1997) Biochemistry **36**, 10026–10032.
179. J. K. Strauss-Soukup and L. J. Maher III (1998) Biochemistry **37**, 1060–1066.
180. J. E. Anderson, M. Ptashne, and S. C. Harrison (1987) Nature **326**, 846–852.
181. A. K. Aggarwal, D. W. Rodgers, M. Drottar, M. Ptashne, and S. C. Harrison (1988) Science **242**, 899–907.
182. G. P. Koudelka, S. C. Harrison, and M. Ptashne (1987) Nature **326**, 886–888.
183. M. Dobler (1992) MoMo (color version 1.4) ETH-Zurich.

DnaK/DnaJ Proteins

These proteins were originally discovered because mutations in their encoding genes block the replication of lambda phage in *Escherichia coli* (1). Mutations in these genes were later shown to exert pleiotropic effects on bacterial metabolism, including defects in DNA and RNA synthesis, **proteolysis**, **cell division**, **temperature-sensitive** growth, and the overproduction of **heat shock** proteins. All these effects are believed to result from changes in protein–protein interactions mediated by complexes of DnaK protein with DnaJ protein and a third protein encoded by the *grpE* gene that acts as a nucleotide-exchange factor (2-5). The DnaK and DnaJ proteins act as **molecular chaperones** in the folding (6), export (7), and degradation (8, 9) of both newly synthesized and stress-denatured polypeptide chains, and in the dissociation of oligomeric complexes essential for the initiation of phage and **plasmid DNA** replication (10). This multifaceted property stems from the ability of both DnaK and DnaJ proteins to bind and release **hydrophobic** segments of an unfolded polypeptide chain in an ATP-driven reaction cycle.

Unlike the chaperonins, the DnaK and DnaJ proteins release their polypeptide substrates in unfolded states, and thus their binding serves only to shield such unfolded polypeptides transiently from premature folding during translation and from aggregation under conditions producing a **stress response**. Both the DnaK and the DnaJ proteins also have the unusual property of altering the conformations of proteins that are native, and thus seemingly fully folded; such proteins may expose chaperone recognition elements that are shielded in other proteins. The ability of both DnaK and DnaJ proteins to bind to the **heat shock** transcription factor **sigma** 32 is believed to be part of the autoregulation of stress gene expression in *E. coli* (3, 11).

The DnaK protein is a weak ATPase and is about 50% identical in primary structure to the eukaryotic family of hsp70 proteins (see BiP (Hsp70)), while the DnaJ protein has homologues called hsp40 proteins in the cytosol, mitochondria, chloroplasts, and endoplasmic reticulum of eukaryotic cells (6). Genes for homologues of both DnaK and DnaJ proteins have been identified in *E. coli* (12, 13); the expression of these genes is induced by exposure to low, rather than high, temperatures (14).

Like all the hsp70 proteins, DnaK possesses an N-terminal ATPase **domain** and a *C*-terminal peptide-binding domain; the crystal structure of the latter is known (15), as is that of the ATPase domain of a **homologous** mammalian hsc70 protein (16). Polypeptides bind in extended conformations to a compact b-sandwich containing two four-stranded antiparallel b-strands. Optimal binding is produced by runs of seven hydrophobic residues; the most important determinant of peptide binding is the central binding pocket for a leucine residue. The ATPase domain transmits ATP-dependent conformational changes to the peptide-binding domain. All the DnaJ proteins possess a conserved *J* domain of 70 residues, which interacts with hsp70 proteins. The NMR structure of this *J* domain reveals a scaffolding of four a-helices bearing at its exposed end a conserved tripeptide in a loop region (17); amino acid substitution in this tripeptide prevents binding to DnaK (18). The *J* domain is followed by a glycine-phenylalanine-rich region, and then a cysteine-rich domain resembling a **zinc finger** that is involved in binding to unfolded polypeptides (19). Thus the binding of DnaJ to DnaK combines the functions of two chaperones that have rather different specificities for binding to hydrophobic amino acid residues.

Bibliography

1. D. E. Friedman, E. R. Olson, C. Georgopoulos, K. Tilly, I. Herskowitz, and F. Banuett (1984) Microbiol. Rev. **48**, 299–325.
2. C. Georgopoulos, K. Liberek, M. Zylicz, and D. Ang (1994) In *The Biology of Heat Shock Proteins and Molecular Chaperones* (R. I. Morimoto, A. Tissieres, and C. Geogopoulos, eds.), Cold Spring Harbor Press, New York, pp. 209–249.
3. B. Bukau (1993) Mol. Microbiol. **9**, 671–680.
4. J. Rassow, O. von Ahsen, U. Borner, and N. Pfanner (1997) Trends Cell Biol. **7**, 129–133.
5. D. M. Cyr, T. Langer, and M. G. Douglas (1994) Trends Biochem. Sci. **19**, 176–181.
6. F. U. Hartl (1996) Nature **381**, 571–580.
7. J. Wild, E. Altman, T. Yura, and C. A. Gross (1992) Genes Develop. 1165–1172.
8. S. A. Hayes and J. F. Dice (1996) J. Cell Biol. **132**, 255–258.
9. D. B. Straus, W. A. Walter, and C. A. Gross (1988) Genes Develop. **2**, 1851–1858.
10. M. Zylicz (1993) Phil. Trans. Roy. Soc. B **339**, 255–373.
11. J. Gamer, H. Bujard, and B. Bukau (1992) Cell **69**, 833–842.
12. T. H. Kawula and M. J. Levivelt (1994) J. Bacteriol. **176**, 610–619.
13. B. L. Seaton and L. E. Vickery (1994) Proc. Natl. Acad. Sci. USA **91**, 2066–2070.
14. M. J. Lelivelt and T. H. Kawula (1995) J. Bacteriol. **177**, 4900–4907.
15. X. Zhu, X. Zhao, W. F. Burkholder, A. Gragerov, C. M. Ogata, M. E. Gottesman, and W. A. Hendrickson (1996) Science **272**, 1606–1614.
16. K. M. Flaherty, C. Deluca-Flaherty, and D. B. McKay (1990) Nature **346**, 623–628.
17. R. B. Hill, J. M. Flanagan, and J. H. Prestegard (1995) Biochemistry **34**, 5587–5596.
18. D. Wall, M. Zylicz, and C. Georgopoulos (1994) J. Biol. Chem. **269**, 5446–5451.
19. A. Szabo, R. Korszun, F. U. Hartl, and J. Flanagan (1996) EMBO J. **15**, 408–417.

DNase 1 Sensitivity

DNase 1 (deoxyribonuclease 1) is an enzyme that cuts **DNA** with relatively little specificity. The enzyme is reasonably large (>30,000 Da), so that assembing DNA into nucleosomes and chromatin impedes its enzymatic activity by limiting access to the DNA double helix. Sensitivity to DNase I is commonly believed to reflect the degree to which DNA is compacted in the chromosome. However other variables, such as proteins that like to bind DNase I and the actual structure of the DNA, might also influence enzymatic activity. DNase I likes to bind to DNA across the **minor groove** of the **double helix**.

Early experiments demonstrated the selective association of nonspecific DNA-binding proteins (prokaryotic **RNA polymerases**) with **transcriptionally** active chromatin. Following these advances, Weintraub, Felsenfeld, and colleagues showed that a comparable general accessibility to **nucleases** is associated with transcriptional activity (1, 2). This general sensitivity to nucleases includes the coding region of a gene and may extend several kilobases to either side of it, potentially defining a chromosomal **domain** . DNase I normally introduces double-strand breaks into transcriptionally active chromatin more than 10 times more frequently than into inactive chromatin. However, the exact structural basis of this generalized sensitivity is unknown. Careful analysis reveals that the untranscribed regions are just as sensitive to DNase I digestion as the transcribed regions, provided the last-cut approach to the measurement of DNase I sensitivity is used. This is defined as digestion by DNase I to fragments so small (smaller than 50 bp) that the DNA no longer hybridizes efficiently to complementary strands after **denaturation** (3). A certain length of DNA is necessary to allow specific recognition (**hybridization**) of two separated single-stranded regions. An important question not yet completely resolved is whether transcription is required to generate generalized nuclease sensitivity in certain instances or whether sensitivity always precedes transcription.

A useful example of the regulated appearance of DNase I sensitivity of a gene is provided by experiments on the action of **mitogens** on quiescent cells. In response to mitogens, a subset of genes, called the immediate-early genes , is rapidly induced (4). The most studied examples of such genes are *c-myc* and *c-fos*. These two **proto-oncogenes** are transcriptionally activated within minutes. Coincident with transcription, the chromatin structure of the proto-oncogenes becomes more accessible to nucleases. Once proto-oncogene transcription ceases, preferential nuclease accessibility is lost (5). Possible conformational changes in nucleosome structure might account for such effects. It has been proposed that histone H3 cysteine residues might become accessible in nuclease-sensitive chromatin, reflecting conformational changes within the nucleosome. However, the recruitment of **RNA polymerase** or other components of the transcriptional machinery may also provide the thiol groups that bind to the columns retaining active chromatin (6). Nevertheless, the rapidity of the changes in nuclease sensitivity (<90 s) and their propagation in both directions 5′ and 3′ to the **promoter** means that transcription and hence RNA polymerase or **HMG proteins** cannot account for all of the observed changes. This is consistent with some retention due to histone H3 in higher eukaryotes. In fact, the speed of the response suggests that changes in nuclease sensitivity precede transcription, and they may play a role in regulating *c-fos* expression.

It is interesting that one of the earliest mitogen-induced nuclear signaling events coincident with proto-oncogene induction is the rapid **phosphorylation** of histone H3 on serine residues within its highly charged, basic, amino-terminal **domain**. **Acetylation** of the amino-terminal domains of the core histones is also likely to be a component of transcriptional activation. Whether these changes are localized to chromatin regions containing either *c-fos*, *c-myc* or the other immediate-early genes has not yet been determined (7). An additional component contributing to the prior sensitization of the proto-oncogenes to nucleases may come from the existence of trans-acting factors already associated with the promoter (8). Such interactions are responsible for the second landmark in chromatin: DNase I hypersensitive sites. These sites are the first places where DNase I introduces a double-strand break in chromatin. They usually involve small segments of DNA sequences (100 to 200 bp) and are two or more orders of magnitude more accessible to cleavage than in inactive chromatin. As the most accessible regions of chromatin to non-histone DNA-binding proteins, DNase I hypersensitive sites generally denote DNA sequences with important functions in the nucleus. Cleavage at these sites might, however, preferentially solubilize chromatin, leading to an increase in the general accessibility of a chromatin domain to DNase I. The results emphasize the utility of DNase I as a probe for both actively transcribed genes and for detecting of regulatory DNA in the chromosome.

Bibliography

1. H. Weintraub and M. Groudine (1976) Science **193**, 848–856.
2. W. I. Wood and G. Felsenfeld (1982) J. Biol. Chem. **257**, 7730–7736.
3. K. Jantzen, H. P. Fritton, and T. Igo-Kemenes (1986) Nucleic Acids Res. **14**, 6085–6099.
4. L. F. Lau and D. Nathans (1987) Proc. Natl. Acad. Sci. USA **84**, 1182–1189.
5. J. Feng and B. Villeponteau (1990) Mol. Cell. Biol. **10**, 1126–1132.
6. J. Walker et al. (1990) J. Biol. Chem. **265**, 5736–5746.
7. L. C. Mahadevan, A. C. Willis, and M. J. Barrah (1991) Cell **65**, 775–783.
8. R. E. Herrara, P. E. Shaw, and A. Nordheim (1989) Nature **304**, 68–70.

Domain, Chromosomal

A chromosomal domain can be defined at either a structural level or a functional level. At this time, there is frustratingly little information concerning the relationship between these two organizational levels. Our most thorough understanding of chromosomal organization is for the most condensed, and hence most visible, of chromosomes, those at **metaphase** . Although folding of **DNA** into nucleosomes leads to a sevenfold compaction in length, and the subsequent folding of arrays of nucleosomes into the chromatin fiber to a further sevenfold compaction, a massive 250-fold compaction of DNA follows the organization of the chromatin fiber into a metaphase chromosome. One model proposed to account for this compaction suggests an organization of the fiber into loops that are radially arranged along the axis of the chromosome (1). It has also been suggested that such loops represent functional chromosomal domains.

The evidence for the organization of the chromatin fiber into loops attached to a central axis in normal cells comes from several experimental approaches. Long-standing observations on the morphology of lampbrush chromosomes in amphibian oocytes show a succession of loops emerging from a single chromosomal axis. Worcel developed a model for the *E. coli* chromosome that predicted its organization into independent domains or loops. Then these studies were extended to **interphase** chromosomes from *Drosophila* cells. Intact chromosomes were subjected to very mild digestion with **DNase I** to produce single-strand nicks. Then the resulting chromosomal fragments were examined in sedimentation velocity centrifugation experiments to determine their size. It was found that the length of the fragments decreases gradually until a plateau value of approximately 85,000 bp of DNA is reached (2). This suggests that the chromatin fiber is organized into fairly uniform domains containing about 100 kbp of DNA complexed with protein. A second approach to determinating the size of structural domains in the chromosome involves **electron microscopic** examination of nuclei extracted from histones by exposure to high-salt solution. It is possible to measure the length of DNA directly on the microscope grid from where it exits a residual nuclear structure (the nuclear matrix or scaffold) to where it reenters this structure. Estimated loop sizes between 40 and 90 kbp were obtained using this technique, which were consistent with biochemical measurements (3).

The development of pulsed-field gel electrophoresis allowed more systematic analysis of the separation of cleavage sites following mild nuclease digestion of nuclei (4). This technique allows resolving very large DNA molecules by agarose electrophoresis. Nuclei of **eukaryotic** cells contain an **endonuclease** (which was first responsible for the discovery of the nucleosomal repeat) that can be activated under controlled conditions (by the addition of exogenous Ca^{2+}/Mg^{2+} to nuclei) and which is believed to have little sequence specificity. It might be expected that cleavage of DNA by this enzyme would be inhibited by folding of DNA into the chromatin fiber, but that structural discontinuities, perhaps where the loop is attached to the chromosomal axis, might allow cleavage if the enzyme were activated. Activation of this enzyme followed by resolving the resultant DNA fragments on pulsed-field gels would potentially allow determining loop sizes. A related approach to this problem uses the observation that topoisomerase II is a major component of chromosomes and, potentially, of the nuclear matrix or scaffold. The enzymatic action of topoisomerase II introduces a double-strand break into DNA, which is then resealed. These double-strand breaks can be stabilized by the use of specific drugs (e.g., epipodophyllotoxins) that inhibit the enzyme (5). Preferential cleavage sites in nuclei spaced 50 to 300 kbp apart were detected using both the endogenous nuclease or topoisomerase II in the presence of the specific inhibitors of the rejoining of the double helix. Closer analysis revealed a hierarchy of digestion, where the 300-kbp cleavage products appeared before those of 50 kbp. It has been suggested that the 50-kbp intermediate in digestion represents the first level of organization of the chromatin fiber into loops, whereas the 300-kbp kinetic intermediate represents the next level of organization. Taken together, these observations establish a strong case that large independent loops (50 to 100 kb) of the chromatin fiber represent a unit of chromosomal structure.

Many studies have focused on the non-histone proteins in the nucleus that might represent sites of attachment of chromatin at the base of loops and the DNA sequences associated with them. The biochemical nature of the nuclear skeleton, the nuclear scaffold, and the nuclear matrix that might organize DNA in the nucleus has been the subject of much debate. Initially, the metaphase scaffold of a chromosome had a morphological definition as the complex structure at the axis of a mitotic chromosome, visualized after swelling and extraction of the histones. Biochemical extraction with high-salt (2 M NaCl) or with the detergentlike lithium diiodosalicylate (LIS) was used to define the residual nucleoprotein complex at which DNA was attached to the chromosome during interphase. Now this nuclear “matrix” (after high-salt extraction) or “scaffold” (after LIS extraction) is known to contain a substantially more complex group of proteins than the metaphase scaffold itself (6). The use of these nonphysiological extraction procedures was criticized because they cause rearrangements of protein–DNA interactions and nonspecific aggregation. An alternate strategy to study nuclear infrastructure is to encapsulate cells in agarose, to extract most of the chromatin, and to leave the nucleoprotein complexes essential for nuclear integrity under physiological conditions. This last methodology generates a nuclear “skeleton” that can transcribe and replicate DNA,which indicates that functionally relevant enzymatic complexes are retained. Recent comparative experiments confirm that the nuclear matrix or scaffold interacts with gene-poor regions of the genome, whereas the nuclear skeleton interacts with gene-rich regions (7). It is now clear that the function and composition of the nuclear skeleton is very different from that of the nuclear matrix or scaffold. All define chromosomal domains, yet the reasons for generating attachments to the chromatin fiber differ.

The nuclear “scaffold” is the best-defined entity with respect to both biochemistry and genetics. A major set of proteins found in the scaffold fraction includes Sc (scaffold proteins) I, II, and III (8). The function of Sc III is unknown. Sc I (170 kDa), however, is now known to be topoisomerase II, and Sc II is known to be a heterodimeric coiled-coil protein. The enzymatic activity of topoisomerase II passes DNA strands through one another. It can cause a double strand break in DNA and rejoin it. Antibodies to topoisomerase II allowed demonstrating that the protein is an integral component of mitotic chromosomes (9). Moreover, the efficiency of recovery of total cellular topoisomerase II in the scaffold fraction (>70%) makes it unlikely that the association with the scaffold fraction is accidental. Consistent with the current view that the chromatin fiber folds further into the chromosome, immunolocalization data show that topoisomerase II is found in a large number of discrete foci scattered throughout the axial region of chromosomes. These foci are very uniform in size, suggesting that they represent discrete structural complexes. Each is believed to be an anchoring complex to which chromatin loops are attached. The presence of topoisomerase II in these complexes can be rationalized by the necessity of unraveling DNA knots and tangles that are inevitably generated during processive enzymatic processes, such as DNA replication and transcription . In fact, if topoisomerase II is inactivated *in vivo* by mutation, the mutant cells die because they cannot separate their chromosomes at the end of mitosis (10).

The Sc II protein has a much more active role in directing mitotic chromosomal condensation than topo II. Now ScII is recognized as a member of the stability and maintenance of chromosomes (SMC) family of proteins. The function of this family of proteins was first characterized in the **yeast**, *Saccharomyces cerevisiae* (11). SMC proteins are conserved in structure from **fungi** to vertebrates. Each consists of five major regions: a **nucleotide-binding region**, a region of the alpha-helix with the potential to form a coiled-coil protein–protein interaction domain, a hinge region, a second coiled-coil domain, and a carboxy-terminal region. Mutational analysis indicates that all of these domains are required for SMC protein function. SMC proteins assemble into **oligomeric** structures. There are at least four different SMC proteins in *S. cerevisiae*, and all are essential for viability, which suggests that they have essential nonoverlapping functions. The phenotypes of SMC mutant cells in yeast fail to undergo **mitosis**, and the undivided nucleus splits partially. This **phenotype** is very similar to that of topoisomerase II mutants in yeast. Closer investigation reveals that SMC mutant cells fail to condense and segregate their chromosomes (11). In spite of this clear genetic evidence that topoisomerase II and the Sc II proteins have essential roles in chromosomal organization, evidence that they have a specific association with DNA is lacking thus far. Thus the nucleic acid contribution to the assembly and function of chromatin loops or structural domain remains unclear.

It has been suggested that the nuclear matrix or scaffold contains specific DNA sequences known as scaffold or matrix attachment regions (SARs and MARs). Evidence that the sequences function in chromosomal dynamics comes from the synthesis of an artificial protein that preferentially binds to these AT-rich sequences (12). This protein interfered with the chromosomal dynamics normally observed during nuclear decondensation or chromosomal condensation in *Xenopus* egg extracts. In the absence of the identification of *bona fide* scaffold attachment sequence-binding proteins *in vivo* and examination of their function, however, whether scaffold or matrix attachments have an active role in chromosomal function remains speculative. Such attachments might promote transcriptional activity *in vivo* (13). In **plants** there is compelling evidence that AT-rich segments of the genome that have been biochemically defined as scaffold attachment regions promote the activity of genes in *cis* . Histone H1 binds preferentially to these AT-rich DNA sequences. It has been suggested that proteins, such as high mobility group (**HMG** I/Y) might displace histone H1 selectively from scaffold attachment regions that contribute to the local control of transcriptional activity (14). It must be proven that this type of selective association of proteins with scaffold attachment regions occurs *in vivo* . It has long been known that lysine-rich proteins like histone H1 interact with AT-rich DNA. Hence the significance of *in vitro* binding experiments that enrich lysine-rich proteins bound to AT-rich scaffold attachment regions remains questionable. A subfamily of sites determined by such procedures as matrix attachment sites (A elements) can be found at the boundaries of a 24-kbp region of **DNase I-sensitive** chromatin containing the chicken lysozyme gene. Sippel and colleagues demonstrated that the A elements insulate a gene from chromosomal effects in stable transformants, but they are not required in transient assays for high levels of gene activity. These A elements also give high-level position-independent, copy-number dependent expression of a *trans* gene in **transgenic** mice (15).

Evidence for the functional specialization of chromosomal domains came initially from cytological analysis of polytene chromosomes. Immunologic staining has revealed the specific distribution of several non-histone proteins, including RNA polymerase II and proteins apparently responsible for generating inactive heterochromatin (HP1, see Chromocenter). Grossbach and colleagues used antibodies against variants of histone H1 to demonstrate that the localization of particular linker histones is highly specific for individual chromosomal domains within polytene chromosomes (16). In contrast, a similar approach with antibodies raised against HMG14-related proteins led to the general **immunofluorescent** staining of transcriptionally active domains. Turner found that individual chromosomal domains within polytene chromosomes can be significantly enriched with forms of histone H4 that have particular states of posttranslational modification (17). This is where a covalent modification such as acetylation of lysine residues is added by an enzyme after the protein has been synthesized. These experiments indicate that specific proteins and modifications can be targeted to particular chromosomal regions.

Additional support for the division of the chromosome into individual functional domains came from the discovery of **locus control regions** (**LCR**). DNase I hypersensitive sites are useful in defining important DNA sequences. DNase I cleavage of the human b-globin locus revealed the existence of four strongly nuclease-sensitive sites located 10 to 20 kbp upstream of the cluster of human b-globin genes (18) (see Contiguous Genes). These sites, known as locus control regions (LCRs), represent cis-acting elements that allow genes integrated into a chromosome to be expressed independently of chromosomal position, i.e., position effects are abolished. Consequently, LCRs allow each copy of a gene integrated in multiple copies to be expressed equivalently within a particular chromosomal domain, so that gene expression is copy-number dependent. When all four DNase I hypersensitive sites comprising the LCR are placed adjacent to reporter genes, they function like enhancers. However, three of the four sites do not function as enhancers in transient expression sites but only do so after incorporation into the chromosome. This suggests that the LCRs may play a special role in stabilizing an accessible chromatin structure distinct from the function of a normal enhancer element (19) (Fig. 1). Several models have been proposed for LCR function, including unraveling of the chromatin fiber, functions similar to normal enhancers, and stabilization of specific nucleoprotein complexes that are functional for transcription only in the presence of the LCR. Evidence consistent with the propagation of an altered chromatin structure comes from transgenic experiments in which LCRs confer hypersensitive sites and general DNase I sensitivity, whereas promoter elements do not. This suggests that LCRs may be able to overcome the inhibitory influences of localized regions of heterochromatin. It has been suggested that LCRs or regions adjacent to them might define the boundaries of an active chromatin domain through attachment to a nuclear matrix or scaffold. At this time there is no positive evidence to suggest that this is the case *in vivo*.

Figure 1. A model for locus control region (LCR) function where the LCR defines a functional chromosomal domain. We propose that the LCR recruits histone acetyltransferases that acetylate histones in the functional domain and lead to an expanded and destabilized chromatin fiber. Within this domain are promoter and enhancer sequences that themselves function more effectively when chromatin higher order structure is destabilized. In this model nuclear matrix attachment sites are boundaries to separate the LCR-controlled chromosome domain from condensed chromatin containing hypoacetylated histones.

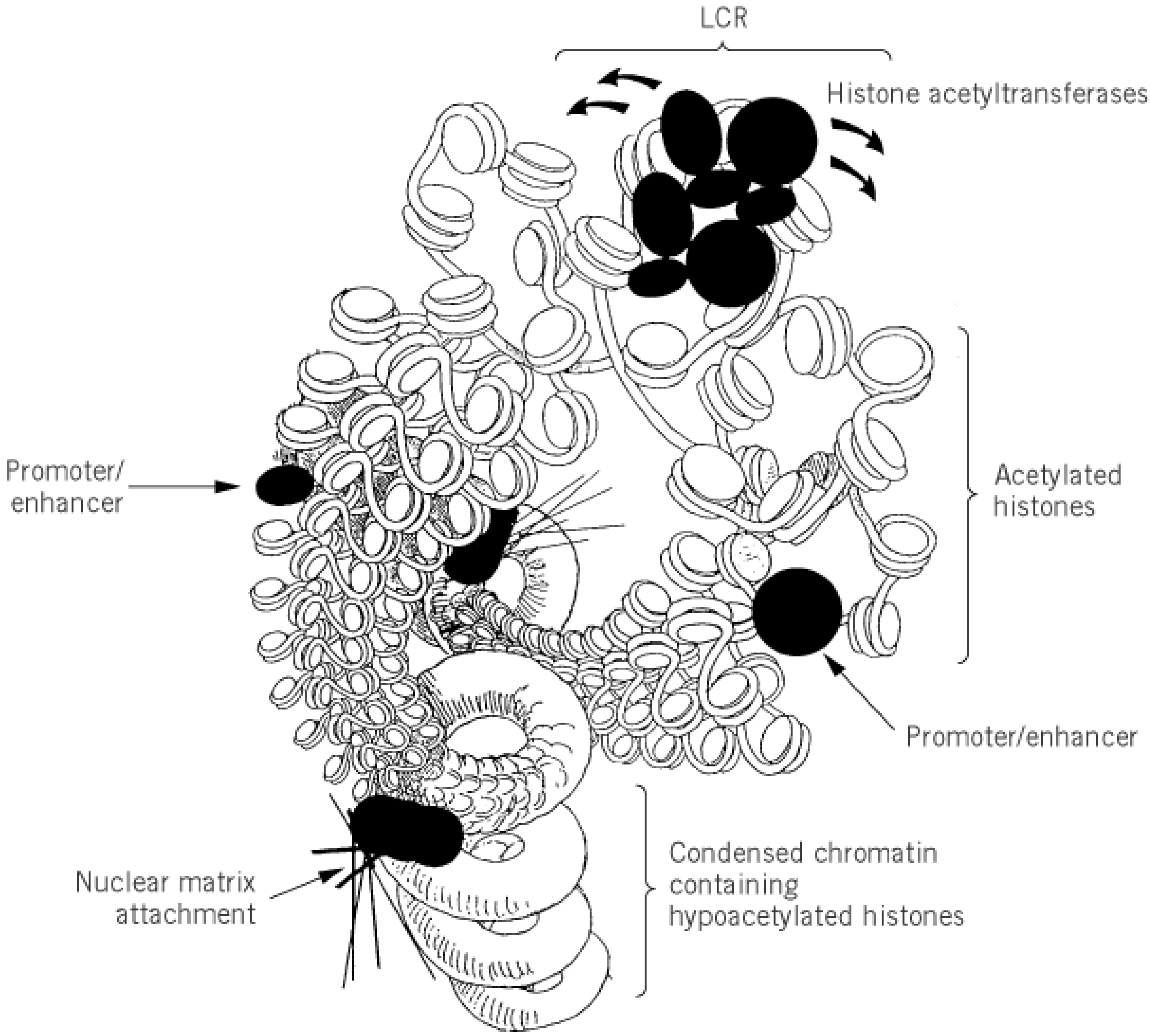

Schedl and colleagues have used transposable elements (P-elements) that can introduce stable transformants into the germ line of *Drosophila melanogaster* to define a distinct "insulator" element that might help delimit functional chromosomal domains. Using the *hsp70* gene, these investigators defined DNA sequence elements that contain DNase I hypersensitive sites to either side of the *hsp70* genes. These specialized chromatin structural (scs) elements conferred position-independent, **copy-number**-dependent transcription from the white **promoter**, with the exception of one insertion into heterochromatin within the *Drosophila* X-chromosome. Importantly, the scs elements do not behave as scaffold attachment regions that establish a functional separation between the two sequences (20). It has been recognized that the *Drosophila* **suppressor** of hairy-wing protein and the complex that it assembles with the gypsy transposable element have comparable "insulating" properties.

It is important to observe that scs, gypsy, or A elements block enhancer function if the element is between the enhancer and the promoter. This capacity to block activation or silencing effects has led to the current definition of these elements as insulators. Enhancers normally act over very long distances (many kilobases). It is hard to imagine how a short DNA sequence (100 to 200 bp) could inhibit DNA looping, which suggests that enhancers in this case function by an alternate mechanism, perhaps related to chromatin folding or nuclear compartmentalization (see Figure 1). Additional insight comes from experiments suggesting that gene regulation occurs by progressively altering the structure of chromatin domains that are continuous in the chromosome. In the bithorax complex, three genes (*Ubx*, *abd-A* and *Abd-B*), are aligned 5′ to 3′ in the order in which they are expressed during development and, remarkably, in the structures whose origin they control in an anterior to posterior direction in the fly. It has been suggested that each of these three large (> 20 kbp) segments of DNA are activated in succession. Several mutations in the bithorax complex are consistent with this hypothesis because by removing a boundary between two domains of chromatin, the anterior-posterior boundary between different structures is also removed. In this model, boundary elements prevent the propagation of a particular chromatin modification by functioning as a barrier. Once again, this type of genetic analysis provides strong evidence for the existence of chromosomal domain boundaries.

Bibliography

1. J. R. Paulson and U. K. Laemmli (1977) Cell **12**, 817–828.
2. C. Benyajati and A. Worcel (1976) Cell **9**, 393–407.
3. P. R. Cook and I. A. Brazell (1975) J. Cell Sci. **19**, 261–279.
4. J. Filipski et al. (1990) EMBO J. **9**, 1319–1327.
5. G. L. Chen et al. (1984) J. Biol. Chem. **259**, 13560–13566.
6. S. M. Gasser, B. B. Amati, M. E. Cardenas, and J. F. Hofmann (1989) Int. Rev. Cytol. **119**, 57–96.
7. J. M. Craig, S. Boyle, P. Perry, and W. A. Bickmore (1977) J. Cell Sci.
8. C. D. Lewis and U. K. Laemmli (1982) *Cell* 29, 171–181.
9. W. C. Earnshaw and M. M. S. Heck (1985) J. Cell Biol. **100**, 1716–1725.
10. S. DiNardo, K. Voelkel, and R. Sternglanz (1984) Proc. Natl. Acad. Sci. USA **81**, 2616–2620.
11. D. Koshland and A. Strunnikov (1996) Ann. Rev. Cell Dev. Biol. **12**, 305–333.
12. R. Strick and U. K. Laemmli (1995) Cell **83**, 1137–1148.
13. L. G. Poljak, C. Seum, T. Mattioni, and U. K. Laemmli (1994) Nucleic Acids Res. **22**, 4386–4394.
14. K. Zhao, E. Kas, E. Gonzalez, and U. K. Laemmli (1993) EMBO J. **12**, 3237–3247.
15. A. Stief, D. M. Winter, W. E. H. Stratling, and A. E. Sippel (1989) Nature **341**, 343–345.
16. E. Mohr, L. Trieschmann, and U. Grossbach (1989) Proc. Natl. Acad. Sci. USA **86**, 9308–9312.
17. B. M. Turner, L. Franchi, and H. Wallace (1990) J. Cell Sci. **96**, 335–346.
18. F. Grosveld, G. B. von Assendelft, D. R. Greaves, and G. Kollias (1987) Cell **51**, 975–985.
19. T. Jenuwein, W. C. Forrester, R. G. Qui, and R. Grosschedl (1993) Genes Dev. **7**, 2016–2032.
20. R. Kellum and P. Schedl (1991) Cell **64**, 941–950.
21. V. Orlando and R. Paro (1993) Cell **75**, 1187–1198.

Suggestion for Further Reading

22. A. P. Wolffe (1998) *Chromatin: Structure and Function*, 3rd ed., Academic Press, London.

Domain, Protein

Protein domains, sometimes referred to as protein folds or modules, are thought to be the building blocks of protein structure, function, and evolution. A domain is generally defined as that part of a protein's structure that can fold independently of the remainder of the protein. The tertiary structure of a protein's polypeptide chain is assembled into one or more protein domains, each domain usually incorporating between 50 and 150 amino acid residues. Proteins having fewer than 100 residues in their polypeptide chains are usually single-domain proteins. Multidomain proteins incorporate more than one domain in their structure and have long polypeptide chains. Generally, the individual domains of a multidomain protein are formed from consecutive stretches of sequence that are connected by a single short length of linking polypeptide chain. These linking regions may be the source of conformational flexibility in the tertiary structure of the protein, and the links can be susceptible to cleavage by proteinases (thereby producing stable protein domain fragments).

Individual domains within a protein structure often have distinct roles, including catalytic, regulatory, binding, recognition, or oligomerization functions. Protein domains are categorized into different structural classes (1, 2) based on their **secondary structure**, including (a) those containing mostly a-helix (all-a), (b) those containing mostly b-strands arranged in antiparallel beta-sheet (all-b), (c) those containing mostly alternating a-helix and b-strand elements (a/b), and (d) those containing a-helix and b-strand elements that are separated rather than alternating in the polypeptide chain (a + b). Some also classify small proteins (<10 kDa) that are stabilized by disulfide bonds or metal ion interactions as a separate class. Recently a new class of protein domain, called the parallel b-helix, that contains only parallel b-strands has been identified (3). Classification of domain structure beyond this level is complex, but databases that define different structural types of protein domains have been developed (4-7) (see Structure Databases).

[See also Protein Structure.]

Bibliography

1. J. S. Richardson (1981) Adv. Protein Chem. **34**, 167–339.
2. M. Levitt and C. Chothia (1976) Nature **261**, 552–558.
3. M. D. Yoder, N. T. Kneen, and F. Jurnak (1993) Science **260**, 1503–1507.
4. A. G. Murzin, S. E. Brenner, T. Hubbard, and C. Chothia (1995) J. Mol. Biol. **247**, 536–540 and `http://scop.mrc-lmb.cam.ac.uk/scop`
5. C. A. Orengo et al. (1997) Structure **5**, 1093–1108 and `http://www.biochem.ucl.ac.uk/bsm/cath`
6. A. S. Siddiqui and G. J. Barton (1995) Protein Sci. **4**, 872–884 and (site currently unavailable)
7. R. Sowdhamini, S. D. Rufino, and T. L. Blundell (1996) Folding Des. **1**, 209–220 and `http://www-cryst.bioc.cam.ac.uk/~ddbase`

Suggestions for Further Reading

8. C. Branden and J. Tooze (1991) *Introduction to Protein Structure*, Garland, New York.
9. T. E. Creighton (1993) *Proteins: Structures and Molecular Properties*, W. H. Freeman, New York.
10. D. G. Hardie and J. R. Coggins (1986) *Multidomain Proteins—Structure and Evolution*, Elsevier, Amsterdam.

Domain Shuffling

Proteins are often composed of one or more functional **domains**. In particular, when a certain protein possesses more than one domain, it is called a mosaic protein. Domain shuffling is a phenomenon where the **gene** segments coding for functional domains are shuffled between different genes during evolution. The boundaries between different domains may or may not correspond to the intron–exon boundaries of the encoding gene. In fact, in certain cases a single domain is encoded by more than one exon, whereas an exon contains a number of functional domains. Therefore, the "exon shuffling" theory is not necessarily the same as the "domain shuffling" theory. Although there are many cases where domain shuffling must have taken place, it is not known what molecular event causes this, and this is important to determine. For more details, see Exon Shuffling.

Dorsal/Cactus Complex

In the *Drosophila melanogaster* embryo, dorsoventral polarity is determined by a concentration gradient of the transcription factor Dorsal in the nucleus (1-3). Prior to axis formation, Dorsal is held in the cytoplasm by an inhibitor, Cactus (4-6). During early embryonic development, **proteolysis** of Cactus in response to a signal transduced on the ventral side of the syncytial embryo releases Dorsal (7-9). Free Dorsal translocates into ventral nuclei, where it directs expression of ventral-specific **genes** and represses expression of dorsal-specific genes (10). In this manner, the spatially graded disruption of the Dorsal/Cactus complex establishes the dorsoventral body axis (11).

Dorsal and Cactus are **translated** from messenger RNAs synthesized in the ovary and form a complex distributed uniformly in the unfertilized egg. Following fertilization, 14 rounds of replication and nuclear division occur prior to cellularization, so that axis formation occurs in the context of a syncytium containing hundreds, and eventually thousands, of nuclei. Within this syncytium, spatially regulated **protein degradation** of Cactus leads to a gradient of Dorsal nuclear localization, with the highest levels of nuclear Dorsal along the ventral midline and lowest levels in the dorsal half of the embryo.

Dorsal and Cactus were identified on the basis of **maternal-effect** mutations that disrupt embryonic pattern formation (12). Embryos generated by females lacking Dorsal have a dorsalized phenotype; there is no nuclear Dorsal and hence only dorsal-specific tissues are formed. Females homozygous for a mutation that inactivates Cactus generate embryos with an opposite, ventralized phenotype, in which Dorsal enters nuclei on both the ventral and dorsal sides of the embryo (4). Ten additional genes mutate to a dorsalized phenotype; these loci encode components of the signaling pathway that regulates release of Dorsal from the Dorsal/Cactus complex.

The signal transduction pathway that directs the asymmetric nuclear translocation of Dorsal is initiated by Pipe, Nudel, and Windbeutel, the products of three genes expressed in the somatic cells of the ovary (13). A ventrally localized signal is then amplified by an extraembryonic serine proteinase cascade involving the Gastrulation Defective, Snake, and Easter proteins (14-16). The result is a proteolytically activated form of Spätzle, the activating ligand for the transmembrane receptor **Toll** (17). Transduction of a signal from activated Toll to the Dorsal/Cactus complex requires a scaffolding protein, Tube, and a protein kinase, Pelle (18, 19). Dorsal binds specifically to both Tube and Pelle, which also bind to one another (20, 21). Both Dorsal and Cactus appear to undergo **phosphorylation** in response to Toll activation (8, 22, 23). Phosphorylation of Cactus is critical for signal transduction; the role of Dorsal phosphorylation in signaling is not yet clear.

Once within ventral nuclei, Dorsal serves to activate expression of ventral-specific genes (eg, *twist*) and repress expression of dorsal-specific genes, e.g., *zen* (24). By themselves, Dorsal dimers activate transcription; repression requires binding to a corepressor, the Groucho protein (25). Dorsal function is not uniform across the ventral half of the embryo. Instead, the gradient of nuclear localization is translated as a series of threshold responses into stripes of gene activation and cell fate determination

(26).

Whereas maternally expressed Dorsal, Cactus, Toll, Tube, and Pelle function in embryonic patterning, zygotically expressed forms of these proteins mediate an immune response in the fat body, the *Drosophila* organ most similar to the mammalian liver (27). The immune response, which directs expression of **peptide antibiotics** upon infection, also involves at least two other proteins closely related in sequence to Dorsal. These proteins, DIF (Drosophila immunity factor) and Relish, appear to be regulated in a manner similar to that observed for Dorsal (28, 29).

The immune function of the Dorsal/Cactus complex has been broadly conserved during evolution; NF-kB and IkB, homologues of Dorsal and Cactus, play a critical role in the mammalian acute phase response, as do counterparts of Toll and Pelle (30-32). Activation of NF-kB in response to stimulation of cells with **cytokines**, such as **tumor necrosis factor**-a and **interleukin**-1, leads to activation of genes that regulate both the inflammatory and immune responses. Recent data suggest that the NF-kB/IkB complex, like the Dorsal/Cactus complex, may also function in pattern formation (33, 34).

The central feature of the Dorsal protein is a multifunctional region termed the Rel homology **domain**. This region mediates the binding of Dorsal to itself, to Cactus, to other specific protein pairing partners, and to DNA (6, 20, 35, 36). The Rel homology domain also contains a nuclear localization signal (NLS) that drives translocation of free Dorsal into the nuclei of the syncytial blastoderm (see Nuclear Import, Export). It is thought that Cactus retains Dorsal outside nuclei, not by actively tethering Dorsal in the cytoplasm, but rather by occluding this NLS and thereby blocking nuclear translocation (36).

The Dorsal/Cactus complex consists of a dimer of the *Drosophila* transcription factor Dorsal bound to a monomer of its cytoplasmic inhibitor, Cactus (37). Complex formation requires an interaction between the Dorsal Rel domain and a set of six tandemly arrayed motifs in Cactus. These motifs, termed ankyrin repeats, are found among proteins of widely varying function and have been shown to serve as sites of protein–protein interaction. Interaction with Dorsal requires all of the ankyrin repeats in Cactus (5, 6). Carboxy-terminal to the ankyrin repeats is a **PEST domain** . PEST domains, rich in the amino acid residues proline, glutamine, serine, and threonine, are found in many proteins whose activity is regulated by proteolysis.

Two regions of Cactus govern its susceptibility to degradation (7-9). The PEST domain influences the overall stability of Cactus, whereas a motif amino-terminal to the ankyrin repeats is specifically required for degradation in response to Toll-mediated signaling. The activities of both sites appear to be regulated by phosphorylation (8, 9, 38). Similar sites govern the proteolysis of the IkB proteins, for which it has been directly demonstrated that phosphorylation of serine residues in the amino-terminal motif triggers a rapid and efficient degradation mediated by the proteasome (39-42).

Bibliography

1. S. Roth, D. Stein, and C. Nüsslein-Volhard (1989) Cell **59**, 1189–1202.
2. C. A. Rushlow, K. Han, J. L. Manley, and M. Levine (1989) Cell **59**, 1165–1177.
3. R. Steward (1989) Cell **59**, 1179–1188.
4. S. Roth, Y. Hiromi, D. Godt, and C. Nüsslein-Volhard (1991) Development **112**, 371–388.
5. R. Geisler, A. Bergmann, Y. Hiromi, and C. Nüsslein-Volhard (1992) Cell **71**, 613–621.
6. S. Kidd (1992) Cell **71**, 623–635.
7. M. P. Belvin, Y. Jin, and K. V. Anderson (1995) Genes & Development **9**, 783–793.
8. M. Reach, R. L. Galindo, P. Towb, J. L. Allen, M. Karin, and S. A. Wasserman (1996) Dev. Biol. **180**, 353–364.
9. A. Bergmann, D. Stein, R. Geisler, S. Hagenmaier, B. Schmid, N. Fernandez, B. Schnell, and C. Nüsslein-Volhard (1996) Mech. Dev. **60**, 109–123.

10. J. Rusch and M. Levine (1996) Curr. Opin. Genet. Dev. **6**, 416–423.
11. D. Morisato and K. V. Anderson (1995) Annu. Rev. Genet. **29**, 371–399.
12. K. V. Anderson and V. C. Nusslein (1984) Nature **311**, 223–227.
13. D. Stein, S. Roth, E. Vogelsang, and C. Nüsslein-Volhard (1991) Cell **65**, 725–735.
14. K. D. Konrad, T. J. Goralski, and A. P. Mahowald (1988) Dev. Biol. **127**, 133–142.
15. Y. S. Jin and K. V. Anderson (1990) Cell **60**, 873–881.
16. C. L. Smith and R. DeLotto (1994) Nature **368**, 548–551.
17. D. S. Schneider, Y. Jin, D. Morisato, and K. V. Anderson (1994) Development **120**, 1243–1250.
18. A. Letsou, S. Alexander, K. Orth, and S. A. Wasserman (1991) Proc. Natl. Acad. Sci. USA **88**, 810–814.
19. C. A. Shelton and S. A. Wasserman (1993) Cell **72**, 515–525.
20. D. N. Edwards, P. Towb, and S. A. Wasserman (1997) Development **124**, 3855–3864.
21. E. A. Drier and R. Steward (1997) Semin. Cancer Biol. **8**, 83–92.
22. A. M. Whalen and R. Steward (1993) J. Cell Biol. **123**, 523–534.
23. S. K. Gillespie and S. A. Wasserman (1994) Mol. Cell. Biol. **14**, 3559–3568.
24. J. Jiang, C. A. Rushlow, Q. Zhou, S. Small, and M. Levine (1992) EMBO J. **11**, 3147–3154.
25. T. Dubnicoff, S. Valentine, G. Chen, T. Shi, J. A. Lengyel, Z. Paroush, and A. J. Courey (1997) Genes Dev. **22**, 2952–2957.
26. J. Jiang and M. Levine (1993) Cell **72**, 741–752.
27. B. Lemaitre, N. Emmanuelle, L. Michaut, J.-M. Reichhart, and J. A. Hoffmann (1996) Cell **86**, 973–983.
28. Y. T. Ip, M. Reach, Y. Engstrom, L. Kadalayil, H. Cai, S. Gonzalez-Crespo, K. Tatei, and M. Levine (1993) Cell **75**, 753–763.
29. M. S. Dushay, B. Asling, and D. Hultmark (1996) Proc. Natl. Acad. Sci. USA **93**, 10343–10347.
30. I. M. Verma, J. K. Stevenson, E. M. Schwarz, D. Van Antwerp, and S. Miyamoto (1995) Genes Dev. **9**, 2723–2735.
31. Z. Cao, W. J. Henzel, and X. Gao (1996) Science **271**, 1128–1131.
32. R. Medzhitov, P. Preston-Hurlburt, and C. A. Janeway Jr. (1997) Nature **388**, 394–397.
33. P. B. Bushdid, D. M. Brantley, F. E. Yull, G. L. Blaeuer, L. H. Hoffman, L. Niswander, and L. D. Kerr (1998) Nature **392**, 615–618.
34. Y. Kanegae, A. T. Tavares, J. C. Izpisúa Belmonte, and I. M. Verma (1998) Nature **392**, 611–614.
35. K. Tatei and M. Levine (1995) Mol. Cell. Biol. **15**, 3627–3634.
36. S. Govind, E. Drier, L. H. Huang, and R. Steward (1996) Molecular & Cellular Biology **16**, 1103–14.
37. K. Isoda and C. Nüsslein-Volhard (1994) Proc. Natl. Acad. Sci. USA **91**, 5350–5354.
38. Z.-P. Liu, R. L. Galindo, and S. A. Wasserman (1997) Genes Dev. **11**, 3413–3422.
39. K. Brown, S. Gerstberger, L. Carlson, G. Franzoso, and U. Siebenlist (1995) Science **267**, 1485–1488.
40. J. DiDonato, F. Mercurio, C. Rosette, J. Wu-Li, H. Suyang, S. Ghosh, and M. Karin (1996) Mol. Cell. Biol. **16**, 1295–1304.
41. Z. Chen, J. Hagler, V. J. Palombella, F. Melandri, D. Scherer, D. Ballard, and T. Maniatis (1995) Genes Dev. **9**, 1586–1597.
42. E. B. Traenckner, H. L. Pahl, T. Henkel, K. N. Schmidt, S. Wilk, and P. A. Baeuerle (1995) EMBO J. **14**, 2876–2883.

Suggestions for Further Reading

43. D. Stein, S. Roth, E. Vogelsang, and C. Nüsslein-Volhard (1991) Cell **65**, 725–735.
44. M. P. Belvin, Y. Jin, and K. V. Anderson (1995) Genes Dev. **9**, 783–793.
45. B. Lemaitre, N. Emmanuelle, L. Michaut, J.-M. Reichhart, and J. A. Hoffmann (1996) Cell **86**, 973–983.
46. J. Rusch and M. Levine (1996) Curr. Opin. Genet. Dev. **6**, 416–423.
47. D. N. Edwards, P. Towb, and S. A. Wasserman (1997) Development **124**, 3855–3864.

Dorsoventral Polarity

The establishment of dorsoventral polarity in the *Drosophila* embryo has been the subject of extensive genetic, developmental, and biochemical analyses. At least three different signaling pathways are required for proper dorsoventral polarity, two that are under **maternal control** and a third pathway that requires expression of the genes in the embryo itself. All of these signaling pathways must operate correctly for normal dorsoventral patterning of the embryo.

During oogenesis, the oocyte is surrounded by specialized somatic cells called follicle cells. The follicle cells secrete the various layers of the chorion, or egg shell, during oogenesis. The chorion differs in structure along the dorsoventral axis, showing that the follicle cells have dorsoventral positional information. In addition, the oocyte itself, as well as the resulting embryo, has a dorsoventral polarity. The coordination of dorsoventral polarity between the follicle cells and the growing oocyte involves a signaling pathway of at least 13 different genes and appears to involve signaling from the oocyte to the follicle cells, and then signaling back from the follicle cells to the oocyte (1). That the oocyte sends a dorsalizing signal to the follicle cells is shown by mutations in several genes, including the gurken gene. The *gurken* gene encodes a transforming growth factor a (TGFa)-like protein that must be expressed in the oocyte in order for the follicle cells to make dorsal chorion structures (2). Loss of *gurken* function in the oocyte leads to ventralization of the follicle cells. That the follicle cells in turn send a dorsalizing signal is shown by mutations in the *torpedo* gene. Loss of *torpedo* function in the follicle cells causes the oocyte (and embryo) to be ventralized (3). The *torpedo* gene encodes an **EGF receptor**. Human TGFa has been shown to bind and activate an ectodermal growth factor (EGF) receptor (4), which suggests that *torpedo* proteins in the follicle cell membranes are receptors for *gurken* proteins secreted by the oocyte.

Signaling back from the follicle cells to the oocyte involves another pathway that is conserved in the human immune system. This pathway is the ***dorsal*** pathway in *Drosophila*, and it includes at least 12 maternally acting genes (5). Mutations in 11 of these genes cause the oocyte and resulting embryo to be dorsalized. These are the dorsal group of mutations, because they all seem to function to activate the *dorsal* protein in the embryo (6). The *dorsal* protein is homologous to the NF-kB/rel proteins required for signaling in the human immune system (7). Mutations in the *cactus* gene cause the oocyte and embryo to be ventralized. *Cactus* encodes a homologue of the IkB protein (8), which binds and inhibits NF-kB/rel. *Cactus* appears to bind and inhibit *dorsal* in *Drosophila* (9). The nuclear localization of *dorsal* protein in the embryo initiates the third signaling pathway in dorsoventral patterning in the *Drosophila* embryo.

The third signaling pathway required for dorsoventral patterning in the *Drosophila* embryo is encoded by zygotically active genes, in contrast to the maternal requirements for the first two signaling pathways. This zygotic signaling pathway appears to use the TGFb homologue decapentaplegic (*dpp*) as the dorsal signal. Loss of *dpp* activity in the embryo causes ventralization (10). Another TGFb homologue, *screw*, also appears to be required zygotically for dorsalization of the embryo (11). *Dpp* and *screw* may act synergistically in dorsalizing the embryo, because injection of *dpp* messenger RNA can partially suppress the phenotype of *screw* mutants, and antimorphic *screw* mutations enhance loss of *dpp* activity (11). Three other genes required for dorsalizing the embryo encode homologues of subunits of vertebrate TGFb receptors. These are the genes *punt, thick veins*, and *saxophone* (1). Activation of these receptors by the *dpp* and *screw* proteins appears to activate transcription of the *zerknüllt* (*zen*) gene. *Zen* is a **homeobox**-containing transcription factor that is required for dorsalization of the embryo (12). Thus, dorsoventral polarity in the *Drosophila* embryo begins with a signal from the developing oocyte to the follicle cells, a return signal from the follicle cells to the oocyte confirming dorsoventral polarity, and the final activation of at least one transcription factor in dorsal cells of the embryo.

Bibliography

1. D. Morisato and K. V. Anderson (1995) Annu. Rev. Genet. **29**, 371–399.
2. F. S. Neuman-Silberberg and T. Schüpbach (1993) Cell **75**, 165–174.
3. J. V. Price, R. J. Clifford, and T. Schüpbach (1989) Cell **56**, 1085–1092.
4. R. Derynck, A. B. Roberts, M. E. Winkler, E. Y. Chen, and D. V. Goeddel (1984) Cell **38**, 287–297.
5. Reference 1, p. 379.
6. S. Roth, D. Stein, and C. Nüsslein-Volhard (1989) Cell **59**, 1189–1202.
7. R. Steward (1987) Science **238**, 692–694.
8. R. Geisler, A. Bergmann, Y. Hiromi, and C. Nüsslein-Volhard (1992) Cell **71**, 613–621.
9. S. Kidd (1992) Cell **71**, 623–635.
10. V. Irish and W. M. Gelbart (1987) Genes Dev. **1**, 868–879.
11. K. Arora, M. S. Levine, and M. B. O"Connor (1994) Genes Dev. **8**, 2588–2601.
12. C. Rushlow, H. Doyle, T. Hoey, and M. Levine (1987) Genes Dev. **1**, 1268–1279.

Suggestions for Further Reading

13. D. Morisato and K. V. Anderson (1995) Signaling pathways that establish the dorsal–ventral pattern of the Drosophila embryo. Annu. Rev. Genet. **29**, 371–399.
14. A. González-Reyes, H. Elliott, and D. St. Johnston (1995) Polarization of both major body axes in Drosophila by gurken–torpedo signaling. Nature **375**, 654–658.
15. R. P. Ray and T. Schüpbach (1996) Intercellular signaling and the polarization of body axes during Drosophila oogenesis. Genes Dev. **10**, 1711–1723.
16. S. A. Holley and E. L. Ferguson (1997) Fish are like flies are like frogs: conservation of dorsal-ventral patterning mechanisms. Bioessays **19**, 281–284.

Dosage Compensation Effect

Dosage compensation is a mechanism by which the activity of X-linked **genes** is made equal in the two sexes of the type XX and XY, in which one sex has two X-chromosomes and the other only one. In placental mammals, marsupials, and some monotremes, compensation is achieved by the inactivation of one X-chromosome in **somatic cells** of females (1). During embryonic development of the mouse, both X-chromosomes are active, and differentiation between the active form Xa and the inactive form Xi occurs in the primitive **ectoderm**. Once inactivation has been initiated at this stage, the same X-chromosome remains inactive in the descendants of each cell after **mitosis** throughout the life of the mouse. Reactivation of chromosome Xi in females occurs at the time of **meiosis**, so that both X-chromosomes are active in oocytes. In male **germ cells**, the single X-chromosome becomes inactive at the late spermatogonial stage.

The chromatin of chromosome Xi is in the condensed state, and its DNA replication begins later than in Xa or in autosomes. The cytosine bases of CpG Islands near the 5′ **promoter** regions of genes are heavily methylated on chromosome Xi, but not on Xa (2) (see Methylation, DNA). Differential hypersensitivity to digestion by **deoxyribonuclease** indicates altered binding of proteins to the DNA and different packaging of nucleosomes in the two X-chromosomes (3).

During studies of translocations between the X- and autosome chromosomes in mice, it was observed that only one of the two X-chromosomes undergoes inactivation which spreads from the inactive segment into the attached autosomal material. It appears as if an inactivation center existed on the X-chromosome, which becomes blocked on one X-chromosome (which becomes Xa) only at the time inactivation is initiated. The location of the inactivation center has been accurately mapped in human and mouse from studies of chromosomal translocations and deletions. A gene, called *XIST* in humans and *Xist* in the mouse, maps in the region of the inactivation center and is expressed by Xi but not by Xa (4). In the male, *Xist* is expressed only in the testis, suggesting a role in inactivation of the single X-chromosome in male germ cells. No protein product of *Xist* or *XIST* has yet been identified.

In **Drosophila** *melanogaster*, where X-chromosome is not inactivated, both X-chromosomes are transcribed in females. Compensation occurs by up-regulation and a doubled rate of transcription of the single X-chromosome in males. As a result, the level of transcription of the genes carried by the X-chromosome is the same in both sexes. The increase in the rate of transcription in males is caused by binding of transcription factors, called *msl-1*, *msl-2*, and *msl-3*, to *enhancer* elements on the X-chromosome. These transcription factors appear to act at the level of the chromatin structure and have been extensively studied in the polytene salivary gland chromosomes, where they bind codependently to the same set of sites along the male X-chromosome. Molecular characterization of the protein coded by *msl-2* has to a great extent solved the question of how *msl*-mediated dosage compensation is restricted to males. Cloning and molecular analyses of the *msl* genes have substantiated the proposal that the MSL proteins function as a multimeric complex to mediate dosage compensation (5), (6).

In the nematode **Caenorhabditis elegans**, equalization of transcription seems to occur by down-regulation in XX animals.

Bibliography

1. S. M. Gartler and A. D. Riggs (1983) Ann. Rev. Genet. **17**, 155–190.
2. A. D. Riggs (1990) Phil. Trans. R. Soc. London **B326**, 285–297.
3. G. P. Pfeifer and A. D. Riggs (1991) Genes Dev. **5**, 1102–1111.
4. M. F. Lyon (1991) Trends Genet. **7**, 69–70.
5. S. Zhou et al. (1995) EMBO. J. **14**, 2884–2895.
6. G. J. Bashaw and B. S. Baker (1996) Curr. Opin. Genet. Dev. **6**, 496–501.

Dot Plot

The dot plot, introduced by Gibbs and McIntyre (1), is a two-dimensional visual comparison method, useful for revealing regions of similarity between pairs of sequences or structures (2). Typically, the *X* axis represents one sequence and the *Y* axis represents the other. Every point in the plot is then scored for the similarity of the residue in sequence X with the similarity of the residue in sequence Y, and the point is plotted if the residues are scored as similar in a residue substitution matrix. Diagonal lines in the plots then indicate regions where consecutive residues are scored as similar. Insertions and deletions (Indels) are revealed by termination of a diagonal segment, followed by initiation of a new but offset diagonal. To improve the signal-to-noise ratio, it is usual to sum the scores in short windows spanning each residue: overall, fewer points are plotted, but divergent matches with rather few identities can be revealed. Cutoffs determining which points are plotted may be set using a variety of heuristic or probabilistic measures. The "double matching probability," introduced by McLachlan (3), is an estimate of the likelihood that the given score would arise by chance in two infinitely long sequences and is widely used to provide the scale for plotting points. The user can then choose the significance level cutoff to determine which points to plot.

Dot plots can reveal recurring similarities within a sequence by self-comparison. In this case, repeated sequences appear as a series of off-center partial diagonals. Tandem Repeatsresult in a regular set of diagonals, consecutively decreasing in size by one repeat, moving away from the central diagonal (Fig. 1). Dispersed repeats also provide dispersed diagonals, one between each repeat element.

Figure 1. Dot plot showing 15 tandemly repeated KH domains in the chicken vigilin sequence. The larger the dots, the higher the matching segment score. A break in the diagonals spanning position 940 indicates a ~ 40-residue insertion in one of the domains.

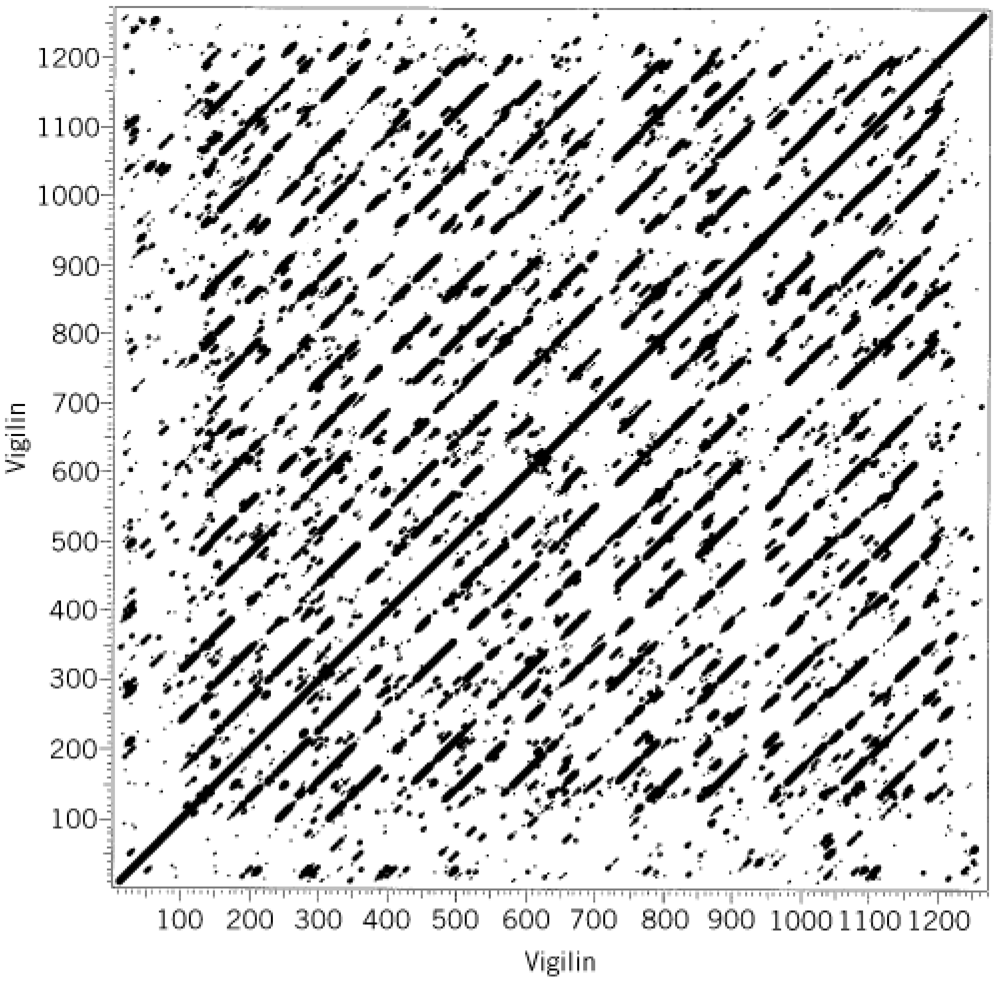

Dot-plot self-comparisons can be used to reveal elements of double-stranded secondary structure in folded RNAs. In the simplest case, points are plotted whenever a pair of residues are able to **base pair**. More sensitive dot-plot algorithms use energy rules based on base pairing, base stacking, bulging, and looping, allied to dynamic programming algorithms (4). Therefore diagonals indicate runs of complementary residues able to form double helices . Looped out *bases*, which often occur in *RNA secondary structure*, are indicated by short offsets in consecutive diagonals.

Another variety of dot plot (5) may be used to compare two protein tertiary structures for regions of similarity, although interpretation is more complex. In this case, the plotted points typically represent distances between Ca carbons, so the plots are also known as distance plots or contact maps. Characteristic recurring patterns indicate **secondary structure** elements such as a-helices and b-strands. Long-range contacts are distributed irregularly in the plot. A useful automatic method to detect structural similarities by analyzing and superposing sets of self-contact plots has been implemented in the program Dali available on the WWW (6).

Dot plots are sometimes used in other ways for presenting sequence or structure information. For example, contact plots are a convenient way to summarize the residue contacts revealed in a structural investigation by nuclear magnetic resonance (NMR).

Bibliography

1. A. J. Gibbs and G. A. McIntyre (1970) Eur. J. Biochem. **16**, 1–11.
2. R. Staden (1982) Nucleic Acids Res. **10**, 2951–2961.
3. A. D. McLachlan (1971) J. Mol. Biol. **185**, 39–49.

4. J. A. Jaeger, D. H. Turner, and M. Zucker (1990) Methods Enzymol. **183**, 281–306.
5. D. C. Phillips (1970) Biochem. Soc. Symp. **31**, 11–28.
6. L. Holm and C. Sander (1993) J. Mol. Biol. **233**, 123–138.

Suggestion for Further Reading

7. D. Sankoff and J. B. Kruskal (1984) *Time Warps, String Edits and Macromolecules: The Theory and Practice of Sequence Comparison*, Addison-Wesley, Reading, MA.

Double Minute Chromosome

Double minute chromosomes (DMs) are generated as a consequence of DNA **amplification**, which is a large increase in the numbers of a specific gene and its adjacent DNA on either side, because of their selective replication. Some types of amplification result from specific developmental requirements, such as the synthesis of multiple copies of the large ribosomal RNA genes in *Xenopus laevis* **oocytes** (1). This amplification of ribosomal RNA genes meets the enormous needs for ribosomal synthesis during *Xenopus* oogenesis. More typically, DNA amplification of the type that leads to the appearance of DMs occurs as part of an environmental **stress response** in cells in culture.

Tissue culture cells exposed to a toxic substance, such as those used in cancer chemotherapy, often eventually become resistant to the substance. One way of achieving a resistant state is to amplify a gene whose product metabolizes the toxic substance into a safer nontoxic form. A typical example is the amplification of the gene encoding dihydrofolate reductase (DHFR), an enzyme involved in thymidine synthesis, in response to methotrexate, which is an inhibitor of DHFR synthesis (see Aminopterin, Methotrexate, Trimethoprim, and Folic Acid). Amplification of the DHFR gene can also be stimulated in response to other environmental conditions, such as UV light and hydroxyurea (2).

Two visible manifestations of the amplification process occur at the chromosomal level. One is the appearance of extended regions in the chromosome known as homogeneously staining regions (HSRs), whose staining characteristics differ from those of normal chromosomal. These HSRs are the sites of DNA amplification (3). The second visible change in chromosomal material is the appearance of DMs that contain the same amplified DNA, but have become extrachromosomal. The relationship between DMs and HSRs is not completely clear, but it is likely that DMs are unstable precursors of HSRs. Human primary tumors contain DMs 90% of the time, 7% contain HSRs, and 3% contain both DMs and HSRs. When cell lines are grown for extended periods of time under drug-resistant conditions, greater numbers of HSRs appear and fewer DMs are found.

DMs are basically **acentric** extrachromosomal elements that are small fragments of chromosomes. Each DM contains between 1 to 2 megabase pairs of DNA and can replicate itself. Therefore DMs function as minichromosomes . The physical organization of the DNA is that of a **supercoiled** circle (4). Because DMs are acentric they are progressively lost during **cell division**, unless they replicate multiple times in any cell cycle. In general they segregate randomly between daughter cells at **mitosis**, leading to unequal numbers in daughter cells. As many as 20 DMs containing DHFR DNA are found in some methotrexate-resistant **cell lines**. **Oncogenes** might also be present in the amplified DNA of DMs and HSRs. For example, the *c-Ki-ras* oncogene is amplified more than 30-fold in DMs and HSRs in certain adrenocortical tumor cell lines (5). Double minute chromosomes are important indicators of abnormal cellular behavior, and they may well reflect an advanced stage of malignancy.

Bibliography

1. D. D. Brown and I. Dawid (1968) Science **160**, 272–280.
2. J. K. Cowell (1982) Ann. Rev. Genet. **16**, 21–45.
3. J. E. Looney and J. L. Hamlin (1987) Mol. Cell Biol. **7**, 569–579.
4. E. P. Garvey and D. V. Santi (1986) Science **233**, 535–538.
5. M. Schwab et al. (1983) Nature **303**, 497–501.

Suggestion for Further Reading

6. M. S. Clark and W. J. Wall (1996) *Chromosomes. The Complex Code*, Chapman and Hall, London.

Downstream

Nucleotide sequence elements located downstream from protein-coding sequences are defined by the direction of transcription. They are primarily involved in termination of transcription and in messenger RNA (mRNA) processing, in particular, polyadenylation. Prokaryotic terminators typically have runs of T at the termination point, preceded by complementary symmetrical sequences, which provide the potential for formation of hairpin structures at the ends of the mRNA (1). The hairpins presumably cause transcription to pause, a phenomenon known as **attenuation**, before the complete arrest.

The mechanism of transcription termination in eukaryotes is not fully understood (2, 3). There are usually many alternative locations for the termination points for the same gene, within a downstream region as large as several thousand bases. It appears that, in a manner similar to that in prokaryotic terminators, transcription elongation in eukaryotes first slows down, due to formation of secondary structure in the mRNA, and then terminates within a nearby U-rich sequence (3). At the noncoding 3′-end of newly formed eukaryotic RNA transcripts several polyadenylation signals usually exist with the **consensus sequence** AAUAAA. One of these sites (but not always the same in different rounds of transcription of the same gene) is somehow selected for the RNA cleavage, which occurs about 20 bases downstream from the site, and for subsequent polyadenylation of 3′-end of the mRNA. Polyadenylation of mRNA is also known in prokaryotes, although it is not as site specific or extensive as in eukaryotes (4).

The eukaryotic downstream sequences—in particular those located within 3′-ends of the RNA transcripts—are also involved in many external functions. For example, they can act in *trans* and control the efficiency of the, stability, and compartmentalization of an mRNA (5).

Bibliography

1. K. S. Wilson and P. von Hippel (1995) Proc. Natl. Acad. Sci. USA **92**, 8793–8797.
2. N. J. Proudfoot (1988) Trends Biochem. Genet. **14**, 105–110.
3. O. Resnekov et al. (1988) Gene **72**, 91–104.
4. N. Sarkar (1997) Ann. Rev. Biochem. **66**, 173–197.

5. C. J. Decker and R. Parker (1995) Curr. Opin. Cell Biol. **7**, 386–392.

Suggestion for Further Reading

6. B. Alberts, D. Bray, J. Lewis, M. Raff, K. Roberts, and J. D. Watson (1994) *Molecular Biology of the Cell*, 3rd ed., Garland Publishing Inc., New York.

Drosophila EGF Receptor

Processes of cell–cell interaction are the key to development of distinct cell and tissue fates in embryonic and postembryonic stages. Focusing on signaling pathways triggered by transmembrane receptors provides molecular clues to these events. In addition, genetic approaches allow the identification of signaling elements in the pathway and provide the hierarchy. For every pathway triggering morphogenesis, it is necessary to understand how signals triggering the pathway are initiated in a defined point in space and time, and how these signals spread to activate the receptor in neighboring cells. It is also crucial to know how different levels of signaling by the receptor are translated to distinct patterns of gene expression and, finally, which mechanisms are employed to restrict or terminate signaling.

The *Drosophila* epidermal growth factor (EGF) receptor is a case in point. Only a single receptor of this family has been identified in the *Drosophila* genome. This receptor carries out an extremely diverse array of functions throughout development. In all cases, a conserved signaling "cassette" is utilized. The signaling elements identified thus far constitute a robust signaling system that leads to reproducible patterning, in spite of possible variations in the levels of individual components.

1. Components

1.1. Receptor
The EGF receptor of *Drosophila* shows a high degree of sequence homology to its vertebrate counterparts, in both its intracellular **tyrosine-kinase** domain and its extracellular ligand-binding domain (1, 2). The receptor is expressed ubiquitously throughout most stages of development. Thus, local activation of the pathway must be regulated by other means.

1.2. Ligands
The singularity of the receptor in *Drosophila* is compensated by several ligands that confer different aspects of regulation. The primary activating ligand is called Spitz. It is a protein containing a **signal sequence**, a single EGF motif, a putative dibasic cleavage signal, and a **transmembrane**, and a cytoplasmic **domain** (3). This structure is reminiscent of transforming growth factor a (TGFa), an activating ligand of the vertebrate EGF receptor. Like the receptor, the precursor form of Spitz is ubiquitously expressed. However, because the precursor form is inactive, this does not lead to receptor activation. The key to receptor activation is the **proteolytic** processing of Spitz, to release the secreted form containing the EGF motif (4). Although the precise regulation of this cleavage is still unknown, components regulating it will be described below. Secreted Spitz is a very active ligand, and its misexpression leads to dramatic changes in cell fates through high levels of activated MAP kinase.

A second activating ligand is Vein, which contains a signal peptide, a single EGF motif, and an immunoglobulin domain (5). Vein is secreted constitutively and is a weaker ligand; its absence or misexpression do not induce dramatic changes in cell fates. While in some contexts Vein functions as a single ligand (6), in other cases it appears to cooperate and complement Spitz in the same tissues.

A third activating ligand is Gurken, encoding a protein with an overall structure similar to Spitz (7). There is no evidence that Gurken must be cleaved in order to be active. Gurken expression and activity are restricted to the female ovary, where it is responsible for inducing initially the posterior cell fates of the follicle cells covering the oocyte, and subsequently the dorsal cell fates. The expression of Gurken, and especially the localization of its messenger RNA in the proximity of the oocyte nucleus, is highly regulated.

Finally, a fourth ligand is Argos, encoding a secreted protein with a signal peptide and a single EGF motif (8). In contrast to the other ligands, Argos is an inhibitory ligand. Its expression abolishes the capacity of the receptor to respond to activation by Spitz (9). Transcription of Argos is induced by the activated EGF receptor pathway, thus constituting an inhibitory feedback loop (10).

1.3. Accessory Signaling Molecules

Among the mutants that displayed a phenotype similar to *spitz* were the genes *rhomboid* and *Star*, encoding novel transmembrane proteins with multiple and single transmembrane domains, respectively (11-13). A variety of observations suggest that these two proteins regulate the processing of Spitz. Ectopic expression of secreted Spitz can overcome the *rhomboid* and *Star* mutant phenotypes (4). In addition, Rhomboid and Star can function nonautonomously; namely, their expression in one set of cells will give rise to activation of the EGF receptor pathway in neighboring cells, consistent with their capacity to induce a diffusible signal (14). How Rhomboid and Star contribute to Spitz processing is an open question, as they have no **proteinase**-homology domains. Rhomboid homologues have been identified in Caenorhabditis *elegans* and humans, raising the possibility that the same molecules may be regulating ligand processing in other species.

The clue to the dynamic activation pattern of the EGF receptor pathway seems to lie in the expression pattern of Rhomboid. It is possible to follow the activation of the EGF receptor pathway, as well as that of other tyrosine kinase receptors, by an antibody directed against the activated (double **phosphorylated**) form of MAP kinase. The pattern induced by EGF receptor activation can be identified, and it disappears specifically in mutants for the EGF receptor, *spitz*, *rhomboid*, or *Star*. This pattern follows precisely the expression of *rhomboid* (15).

2. Biological Example of Single Signaling Burst: The Embryonic Ventral Ectoderm

The earliest function of the EGF receptor pathway in the embryo entails the induction of ventral ectodermal cell fates. Following gastrulation, a group of ~ 8 cells on each side of the ventral midline are designated as neuroectodermal cells. Within this region, different rows of cells assume different fates, through activation of the EGF receptor pathway. The capacity of the pathway to induce graded fates stems from the fact that the activating signal, secreted Spitz, emanates from a single row of cells, the midline glial cells, positioned at the ventral midline (14). Diffusion of the ligand to neighboring cells generates graded activation of the pathway, which can be visualized by the distribution of activated MAP kinase (15).

The ectodermal cells respond differently to the varying levels of EGF receptor activation. The cells closest to the source of the ligand, induce a dual response. On the one hand, MAP kinase phosphorylates and inactivates the **transcriptional** repressor Yan, an ETS domain protein. On the other hand, MAP kinase induces the transcription of Pointed P1, an ETS domain transcriptional activator. This leads to the transcription of Pointed P1-target genes in the cell row closest to the midline (16). The transcriptional responses of the cells lying further from the midline are not known.

A central target gene for Pointed P1 is *argos*. Thus, activation of the EGF receptor leads to the production of Argos protein, which diffuses to neighboring cells and reduces the level of signaling in these cells, maintaining the EGF receptor activation gradient. This system is very robust.

Reproducible patterning of the ventral ectoderm is obtained, regardless of the absolute levels of secreted Spitz. As long as Spitz is emanating from the midline and induces the inhibitor Argos in the cells receiving maximal signaling, the pattern will be generated correctly. EGF receptor signaling in the ventral ectoderm is illustrated schematically in Figure 1.

Figure 1. Signalling by the EGF receptor pathway in the embryonic ventral ectoderm. (**a**) Scheme of embryonic cross se
midline cells, positioned in the center of the ventral ectoderm. (**b**) (1) The fate of the midline cells is determined by the tı
The midline cells express the components necessary for Spitz processing, namely, the Spitz precursor, Rhomboid, and Sı
surrounding ventral ectoderm in a graded manner. (4) In the cells closest to the source, maximal EGF receptor activation
Yan and the transcription of Pointed P1. (5) A central target gene is *argos*. Its transcription leads to the diffusion of Argc
reduction or termination of receptor activation in the lateral cells.

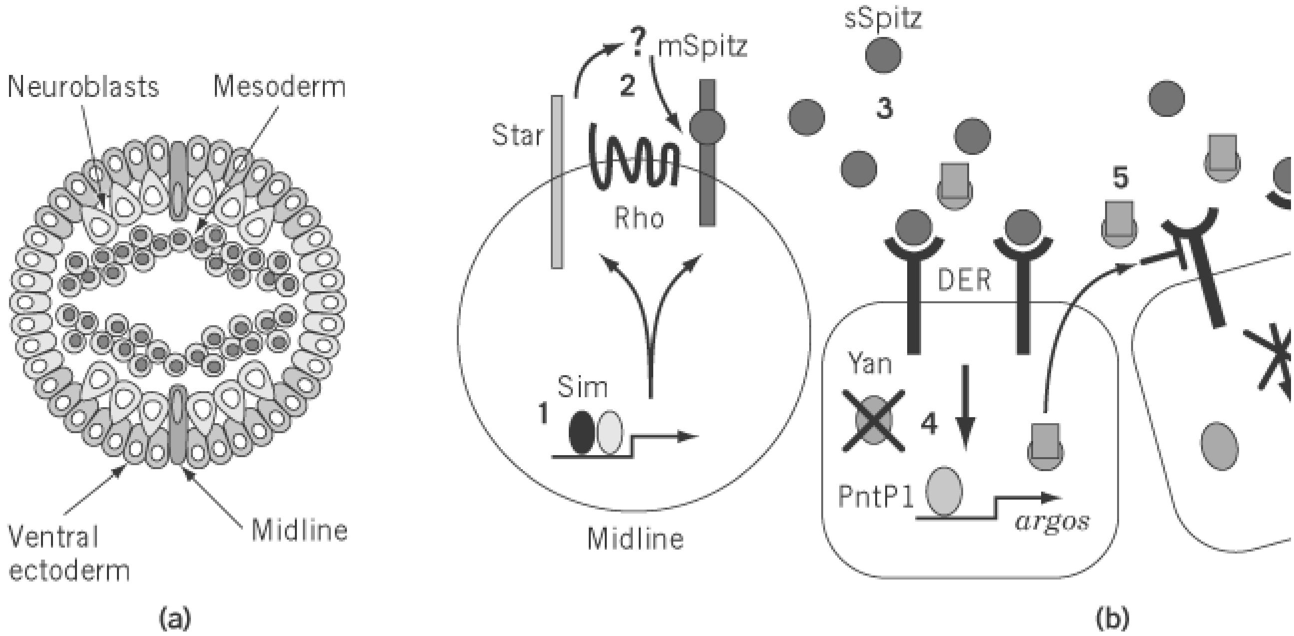

3. Multiple Bursts of Signaling: The Ovary and Eye

The above example represents a simple case, in which the pathway is only activated once. More complicated scenarios involve multiple activation cycles of the pathway in the same tissue, each time leading to different consequences. In the ovary, signaling from the oocyte to the surrounding follicle cells determines the polarity of these cells. Initially, when the egg is small and the oocyte nucleus is positioned at the posterior end, localized Gurken, a ligand for the EGF receptor, will trigger posterior cell follicle cells fates (17, 18). Subsequently, the oocyte nucleus migrates to the future dorsal anterior corner of the oocyte. Activation of the receptor by Gurken at this stage leads to the induction of dorsal follicle cell fates (19). Finally, Induction of Rhomboid expression by the EGF receptor pathway leads to a third cycle of activation by allowing processing of a ligand expressed in the follicle cells (possibly Spitz), this time patterning specific follicular structures called dorsal appendages (20). It should be noted that the final cycle of activation of the receptor was obtained by inducing Rhomboid.

This aspect becomes even more dramatic in the induction of photoreceptor cell fates in the developing eye. The first photoreceptor in each ommatidium R8 is induced independent of the EGF receptor pathway. This cell serves as a source for secreted Spitz, which will activate the receptor in neighboring cells and induce the first cohort of photoreceptors (21, 22). These newly induced cells will now also produce Argos, which prevents the signal from progressing further. It seems that the differentiating cells also express the processing machinery for Spitz, and thus induce a new round of activation. This continues for several cycles, inducing first distinct sets of photoreceptor cells and subsequently cone or pigment cells.

In conclusion, an amazingly diverse set of roles is fulfilled by the EGF receptor pathway, only a sample of which were mentioned above. They include the induction of cell fates in different contexts, as well as cell proliferation (eg, in the wing imaginal disc). In most cases, a common signaling pathway is used, both upstream and downstream of the receptor. This raises the question of specificity. It is clear that the induction of MAP kinase signaling cannot determine the final outcome. Rather, in different cell types, the same pathway induces different responses, depending on the repertoire of transcription factors that are responsive in that tissue. Differential regulation of the receptor itself appears to be directed by the multiplicity of ligands, being regulated in different ways in terms of their expression or localization, or conferring varying levels of activation.

Bibliography

1. E. Livneh, L. Glazer, D. Segal, J. Schlessinger, and B.-Z. Shilo (1985) Cell **40**, 599–607.
2. E. D. Schejter, D. Segal, L. Glazer, and B.-Z. Shilo (1986) Cell **46**, 1091–1101.
3. B. J. Rutledge, K. Zhang, E. Bier, Y. N. Jan, and N. Perrimon (1992) Genes Dev **6**, 1503–1517.
4. R. Schweitzer, M. Shaharabany, R. Seger, and B.-Z. Shilo (1995) Genes Dev. **9**, 1518–1529.
5. B. Schnepp, G. Grumbling, T. Donaldson, and A. Simcox (1996) Genes Dev. **10**, 2302–2313.
6. T. Yarnitzky, L. Min, and T. Volk (1997) Genes Dev. **11**, 2691–2700.
7. F. S. Neuman-Silberberg and T. Schüpbach (1993) Cell **75**, 165–174.
8. M. Freeman, C. Klämbt, C. S. Goodman, and G. M. Rubin (1992) Cell **69**, 963–975.
9. R. Schweitzer, R. Howes, R. Smith, B.-Z. Shilo, and M. Freeman (1995) Nature **376**, 699–702.
10. M. Golembo, R. Schweitzer, M. Freeman, and B.-Z. Shilo (1996) Development **122**, 223–230.
11. U. Mayer and C. Nüsslein-Volhard (1988) Genes Dev. **2**, 1496–1511.
12. E. Bier, L. Y. Jan, and Y. N. Jan (1990) Genes Dev. **4**, 190–203.
13. A. L. Kolodkin, A. T. Pickup, D. M. Lin, C. S. Goodman, and U. Banerjee (1994) Development **120**, 1731–1745.
14. M. Golembo, E. Raz, and B.-Z. Shilo (1996) Development **122**, 3363–3370.
15. L. Gabay, R. Seger, and B.-Z. Shilo (1997) Science **277**, 1103–1106.
16. L. Gabay, H. Scholz, M. Golembo, A. Klaes, B.-Z. Shilo, and C. Klämbt (1996) Development **122**, 3355–3362.
17. A. González-Reyes, H. Elliot, and D. St. Johnston (1995) Nature **375**, 654–658.
18. S. Roth, F. S. Neuman-Silberberg, G. Barcelo, and T. Schüpbach (1995) Cell **81**, 967–978.
19. F. S. Neuman-Silberberg and T. Schüpbach (1994) Development **120**, 2457–2463.
20. A. Sapir, R. Schweitzer, and B.-Z. Shilo (1998) Development **125**, 191–200.
21. M. Freeman (1996) Cell **87**, 651–660.
22. M. Tio and K. Moses (1997) Development **124**, 343–351.

Suggestions for Further Reading

23. R. Schweitzer and B.-Z. Shilo (1997) A thousand and one roles for the *Drosophila* EGF receptor. Trends Genet. **13**, 191–196.
24. N. Perrimon and L. Perkins (1997) There must be 50 ways to rule the signal: the case of the *Drosophila* EGF receptor. Cell **89**, 13–16.
25. J. D. Wasserman and M. Freeman (1997) Control of EGF receptor activation in *Drosophila*. Trends Cell Biol. **7**, 431–436.
26. L. A. Nilson and T. Schüpbach (1998) "EGF receptor signaling in" *Drosophila* oogenesis. In *Current Topics in Developmental Biology*, Vol. **44** (R. Pederson and G. P. Schatten eds.),

Academic Press, San Diego, pp. 203–244.

Drug Resistance

The resistance of cancer cells to cytostatic agents has been a significant impediment to the effective chemotherapy of cancer. Studies with model systems, where cancer cells grown *in vitro* were selected for resistance to specific anticancer drugs, identified two major classes of drug-resistant cells: (i) cells resistant to a single class of drugs with the same mechanism of action, and (ii) cells resistant to chemically diverse drugs with multiple mechanisms of action. The latter phenomenon was called multiple drug resistance (MDR). Some metastatic cancers are intrinsically resistant to chemotherapy, whereas others respond to treatment initially but subsequently acquire resistance, not only to the chemotherapeutic agents used against them, but to other chemically unrelated drugs as well (1). Numerous factors have been associated with MDR. These include elevated levels of protein kinase C, enhanced sodium pump activity, mutations of topoisomerase II and tubulin, and altered levels of calcium and calmodulin. It has not been possible, however, to correlate any of these clearly with the MDR **phenotype**. A large body of evidence, on the other hand, derived from studies of cells in culture, transfection experiments, histochemical studies of a wide variety of tumors graded for resistance to chemotherapy, and studies in reconstituted systems, strongly implicates energy-dependent pump systems that either exclude or extrude chemotherapeutic agents from MDR cells.

Besides human cancer cells and their rodent models, MDR pumps have been found in a wide array of organisms: bacteria, protozoa, and fungi, and mammalian cells; even plant cells have MDR pumps. These share the unique feature of excluding a fairly broad range of chemically unrelated compounds from the cell. Only some of these belong to the ATP Binding Cassette (ABC) superfamily of transporters, and they do not ubiquitously use ATP as their energy source. The majority of the bacterial pumps, for example, use the energy of the proton motive force. The ATP-dependent system that has been most extensively characterized is the *MDR*1 gene product, the multidrug transporter or P-glycoprotein (P-gp).

Many cells selected for drug resistance do not show increased levels of P-gp but nonetheless are resistant to a broad range of natural product drugs. Another member of the ABC superfamily, the MDR-associated protein (MRP1), is expressed in some of these cell lines at elevated levels. MRP1 is similar to P-gp in that it is capable of decreasing intracellular levels of drugs and is ATP-dependent. While P-gp has two membrane-spanning domains, MRP has three. The presence of a third such domain is observed in several other ABC proteins, all of which are more closely related to MRP than to any other member of this superfamily of transporters. There are now at least a dozen ABC proteins that together constitute the MRP branch of the superfamily. The most important members are (i) the human MRP, which is an anionic conjugate transporter, (ii) the multispecific organic anion transporter, MOAT or MRP-2, and (iii) SUR1, the sulfonylurea receptor. There are other significant differences between MRP and P-gp: (i) MRP1 catalyzes the efflux of anionic or neutral drugs conjugated to glutathione, glucoronate, or sulfate; (ii) some substrates of P-gp, eg, taxol, are not substrates for MRP; (iii) MDR effected by P-gp is reversed by verapamil and cyclosporin A, but not that caused by MRP. It is thus quite likely that both P-gp and MRP are drug transporters but that their detailed mechanisms of action may differ (2).

Additionally, a 110-kDa protein, the lung resistance protein, has been identified in non P-gp-resistant lung carcinoma cells. This protein is a major constituent of an intracellular ribonucleoprotein (vault) complex that consists of three other proteins of 210 kDa, 190 kDa, and 54 kDa, plus an RNA molecule. There is increasing evidence that the vault complex is involved in MDR (3).

Bibliography

1. M. M. Gottesman and I. Pastan (1993) Ann. Rev. Biochem. **62**, 385–427.
2. D. Lautier, Y. Cantrot, R. G. Deeley, and S. P. C. Cole (1996) Biochem. Pharmacol. **52**, 967–977.
3. G. L. Scheffer, P. J. Wijngaard, M. J. Flens, M. A. Izquierdo, M. L. Slovak, H. M. Pinedo, C. J. L. M. Meijer, H. C. Clevers, and R. J. Scheper (1995) Nature Medicine **1**, 578–582.

Suggestions for Further Reading

4. I. B. Roninson, ed. (1991) *Molecular and Cellular Biology of Multidrug Resistance in Tumor Cells*, Plenum Press, New York. A comprehensive reference in which numerous researchers cover almost all areas of multidrug resistance in cancer cells.
5. S. V. Ambudkar and M. M. Gottesman, eds. (1998) *Methods in Enzymology*, Vol. **292**, Academic Press, San Diego. This volume of *Methods in Enzymology* is devoted to the ABC transporters and is a very good source for methodological details covering biochemical, molecular biological, and cell biological aspects.

Duplication, Chromosomal

There are numerous types of chromosomal duplications. Each chromosome itself is duplicated during the **S-phase** of the normal cell cycle. There are also various duplications that arise from chromosome breakage and reunion cycles (see Dicentric Chromosome), which might be an important contributory factor in the evolution of genomes. There are also duplication events that encompass whole genomes. In the frog *Xenopus laevis*, different species have evolved that contain multiple sets of related chromosomes. This is called **polyploidy**. *Xenopus tropicalis* is the progenitor **diploid** species, whereas *Xenopus laevis* is pseudotetraploid (1). Although many duplicated genes are silenced, genes that remain active often show tissue or developmental differences in activity. Thus specialized gene family members may arise by both genomic duplication and by genetic duplication (see Contiguous Genes). Other examples of chromosomal duplication result from gene **amplification** (see Double Minute Chromosome).

Chromosomal duplication occurs through a variety of mechanisms, some that operate in evolutionary time, and others that occur in specialized cells during development or in response to environmental stress. The most common form of chromosomal duplication results from unequal sister chromatid exchange. This is caused by misalignment of two sister chromatids during **prophase** followed by **reciprocal recombination**, which duplicates one chromosome, whereas the other has a deficiency. Amplification of the large 18 S and 28 S ribosomal RNA genes in *Drosophila melanogaster* might occur through many reiterations of events of this type (2). It is also possible that the presence of thousands of short interspersed nuclear elements, such as **Alu** repeats or the long interspersed nuclear element (**LINE**)-1 in mammalian chromosomes, might lead to many misalignments and chromosomal duplications.

Gene amplification is another form of local chromosomal duplication. In cultured cells, treatment with methotrexate and hydroxyurea results in multiple replicative cycles of the **dihydrofolate reductase** (DHFR) gene. The molecular mechanisms controlling this overreplication of the DHFR gene are not understood, but it is assumed that the replicative process leads to the generation of free

DNA ends that then undergo homologous recombination (3). If the over-replicated DNA circularizes, double minute chromosomes are formed.

Chromosome duplication also occurs following modification of chromosomeal behavior during the cell cycle. Normally the DNA in chromosomes replicates once during **S phase**. If multiple replicative cycles occur, however, then duplicated chromosomes can coexist in the same somatic cell nucleus. If the chromosomes separate, the cell is called endopolyploid. If the chromosomes do not separate, polytene chromosomes are formed. This repeated replicative process is called endoreduplication (4). Endopolyploid cells and those containing polytene chromosomes never divide, so they represent, a somatic dead end or a state of terminal differentiation, respectively.

Bibliography

1. H. R. Kobel and L. Du Pasquier (1986) Trends Genet. **2**, 310–313.
2. S. A. Endow and K. C. Atwood (1988) Trends Genet. **4**, 348–351.
3. R. T. Schimke (1988) J. Biol. Chem. 263, 5989–5992.
4. W. Nagl (1978) *Endopolyploidy and Polyteny in Differentiation and Evolution*, Elsevier/North Holland, Amsterdam.

Dynactin

Dynactin is a large protein complex that is important for the function of cytoplasmic dynein in intracellular motility (see Motor Proteins). Dynactin was first identified as a protein complex that stimulates dynein movement of membranous organelles along microtubules (1). It has been proposed that dynactin functions to bind cytoplasmic dynein to its membranous organelle cargo. Work in diverse species from fungi to mammalian neurons suggests that an alternative function of dynactin is to link cytoplasmic dynein to the actin cortex for the movement of microtubules (2).

The backbone of the dynactin molecule is a short (~40nm) filament composed of 8 to 12 molecules of actin-related protein 1 (Arp1) (3). Arp1 shares many of the binding domains of actin, including the spectrin, myosin, and villin binding sites. Actin-capping protein is bound to one end of the dynactin filament, and a unique capping protein is located at the other end. The p150^{Glued} subunit projects from the filament. This protein is the product of the *Glued* gene of *Drosophila*, and it binds both microtubules and the intermediate-chain subunit of cytoplasmic dynein. Overexpression of another major subunit of dynactin, p50, obstructs assembly of the dynactin complex, and thus it is named *dynamitin* (4). Overexpression of p50 disrupts localization of both dynein and dynactin to membranous organelles or kinetochores. Genetic studies indicate that dynein and dynactin act in the same pathways (5).

Bibliography

1. T. A. Schroer and M. P. Sheetz (1991) J. Cell Biol. **115**, 1309–1318.
2. J. T. Carminati and T. Stearns (1997) J. Cell Biol. **138**, 629–641.
3. D. A. Schafer et al. (1994) J. Cell Biol. **126**, 403–412.
4. C. J. Echeverri et al. (1996) J. Cell Biol. **132**, 617–633.
5. T. A. Schroer (1994) J. Cell Biol. **127**, 1–4.

Suggestions for Further Reading

6. E. A. Holleran, S. Karki, and E. L. Holzbaur (1998) The role of the dynactin complex in intracellular motility, Int. Rev. Cytol. **182**, 69–109.
7. V. Allan (1994) Organelle movement. Dynactin: protrait of a dynein regulator, Curr. Biol. **4**, 1000–1002.

Dynamic Light Scattering

Dynamic light scattering (also known as photon correlation spectroscopy) from particles in solution can be used to deduce information about the size, shape, and dynamics of biological macromolecules and supramolecular assemblies. Structural analysis of individual biomolecules, conformational transitions, and intermolecular interactions can also be probed. The major use of dynamic light scattering in biology is the rapid determination of the translational diffusion constant for macromolecules in solution. The interpretation of **diffusion** constant data is frequently strengthened by combination with other information from methods, such as electron microscopy, static light scattering, and neutron or X-ray small-angle scattering. Biological systems are well-suited to study by dynamic light scattering, because they are generally large enough to be strong scatterers at low concentrations and their diffusion constants are such that they give rise to autocorrelation functions that can be readily measured. Dynamic light scattering measurements have been used for studying objects ranging in size from proteins as small as 6000 Da to intact cells as large as micrometers.

1. Theory of Dynamic Light Scattering

Dynamic light scattering measures light scattering intensity fluctuations in a small volume of a sample. For small proteins (~25kDa) these fluctuations are on the microsecond timescale, while for cells they are in milliseconds. The fluctuations are related to the Brownian motion of the particles giving rise to density fluctuations caused by variations in the number of molecules in the scattering volume and random agglomerations. This measurement in the time domain is related to the spectral density of the fluctuations in the frequency domain by a Fourier transformation. In practice, diffusion coefficients are determined using an autocorrelation function that is measured by accumulating the product of the number of photons arriving at the detector from successive time intervals. This operation is repeated thousands of times and averaged. The intensity autocorrelation function, $G_2(t)$, is obtained by storing the average products $I_{t'}I_{t+t'}$, where t is an incremented time delay, in successive channels to yield

$$G_2(t) = \langle I_{t'} \cdot I_{t+t'} \rangle \tag{1}$$

For a solution of macromolecules, assuming a Gaussian distribution of fluctuations, $G_2(t)$ is related to the scattered electric field autocorrelation function $G_1(t)$ by

$$G_2(t) = \langle I^2 \rangle + G_1(t)^2 \tag{2}$$

For translation diffusion of monodisperse particles that are small with respect to the incident wavelength, l:

$$G_2(t) = A + Be^{-2\Gamma t} \tag{3}$$

where A and B are constants that depend upon experiment geometry, and

$$D = \frac{\Gamma}{Q^2} \tag{4}$$

D is the translational diffusion coefficient, and G is the reciprocal of the characteristic decay time,

$$Q = \frac{4\pi \sin\left(\frac{\Theta}{2}\right)}{\lambda} \tag{5}$$

where O is the scattering angle. For a continuous polydisperse system, equation (4) is integrated over all sizes, and hence G values, to give

$$G_1(t) = \int G(\Gamma) e^{-\Gamma t} d\Gamma \tag{6}$$

where G(G) is a distribution function that can be evaluated.

Rotational diffusion and internal dynamics can also influence the autocorrelation functions measured in a dynamic light scattering experiments. The internal dynamics of a macromolecule in solution become important only if the amplitude of the motions is not very much smaller than the wavelength of the light. For large motions, different parts of the sample molecule will scatter out of phase, and the internal dynamics will contribute one or more relaxation times that will contribute to the decay of the autocorrelation function in a single or multiple-exponential fashion.

1.1. Examples of Dynamic Light Scattering Applications

The transcription, translation, and replication of genetic information contained in the sequences of DNA is controlled by interactions of proteins with DNA and with RNA. These interactions can be probed using dynamic light scattering. For example, the enzyme DNA gyrase (see **Topoisomerases**) catalyzes the ATP-dependent **supercoiling** of DNA. The diffusion constant for DNA gyrase measured by dynamic light scattering (1) is significantly smaller than expected based on its molecular weight, and binding of DNA to the gyrase produces no change in the diffusion constant, indicating that there is no overall conformational change. These observations, combined with parallel small-angle neutron scattering experiments to determine radius of gyration values for the gyrase and its complex with DNA, have led to the conclusion that the gyrase has grooves on its surface to accommodate the DNA in a very compact complex.

Dynamic light scattering has played a role in drug development. The pharmacological effects of drugs can depend upon their behavior in solution and the characteristics of aggregates they may form (2). Lipids can be used to “solubilize” drugs that may be insoluble in aqueous media, and hence enhance their transport and efficacy. Dynamic light scattering has been used to evaluate aggregation behavior of antidepressants (3), critical micelle concentrations, and sizes of micelles designed to encapsulate the drug Indomethecin (4), as well as to evaluate how the opiate drug loperamide alters the temperature-induced phase transition of phosphatidylcholine vesicles (5).

Dynamic light scattering has also been used to monitor the assembly of enveloped **viruses**. Lyles et al. (6) used a combination of dynamic and static light scattering with stopped flow to study matrix protein binding to nucleocapsids of vesicular stomatitis virus. Dynamic light scattering has recently become a common tool for assessing the crystallizability of macromolecules and macromolecular assemblies (7, 8). Because modern molecular biology techniques have provided sufficient amounts of pure materials, dynamic light scattering can be used automatically to “screen” large numbers of crystallization conditions to determine diffusion constants and hence evaluate possible aggregation states that inhibit crystallization.

Bibliography

1. S. Krueger et al. (1990) J. Mol Biol. **211**, 211–220.
2. D. Attwood and P. Fletcher (1986) J. Pharm. Pharmacol. **38**, 494–498.
3. A. D. Atherton and B. W. Barry (1985) J. Pharm. Pharmacol. **37**, 854–862.
4. D. Attwood, G. Ktistis, Y. McCormick, and M. J. Story (1989) J. Pharm. Pharmacol. **41**, 83–86.
5. E. Hantz, A. Cao, R. S. Phadke, and E. Taillandier (1989) Chem. Phys. Lipids **51**, 75–82.
6. D. S. Lyles, M. O. McKenzie, and R. R. Hangton (1996) Biochemistry **35**, 6508–6518.
7. A. D"Arcy (1994) Acta Crystallogr. **D50**, 469–471.
8. A. Ferre-D'Amare and S. K. Burley (1994) Structure (London) **2**, 357–359.

Suggestions for Further Reading

9. B. J. Berne and R. Pecora (1976) *Dynamic Light Scattering with Applications to Chemistry, Biology and Physics*, Wiley, New York.
10. P. A. Janmey (1993) "Application of Dynamic Light Scattering to Biological Systems. In" *Dynamic Light Scattering: The Method and Some Applications* (W. Brown ed.), Oxford University Press, Oxford, U.K.
11. R. Pecora (1985) *Dynamic Light Scattering: Applications of Photo Correlation Spectroscopy*, Plenum Press, New York.

Dynein

Dyneins are **microtubule**-based motor proteins that use the energy released by the hydrolysis of ATP to move toward the minus end of a microtubule. The dyneins are classified as either cytoplasmic or flagellar (also known as axonemal), and the flagellar dyneins are further divided into outer and inner arm dyneins. The first dyneins to be identified were the flagellar dyneins, which are the arms that project from the A microtubules of **ciliary** and flagellar axonemes. Flagellar dyneins generate the sliding force between microtubules that is the basis for the propulsive bending of flagella (and cilia) that moves cells through fluids. Cytoplasmic dyneins move membranous organelles and kinetochores along microtubules and assist in assembling the mitotic spindle. Each dynein is a large molecular complex, composed of one or more large polypeptide chains of ~500kDa, known as heavy chains, and various accessory intermediate chains (50 to 140 kDa) and light chains (8 to 45 kDa). Often the heavy chain alone is referred to as a dynein. An ~350kDa portion of each heavy chain forms a large globular head **domain**, and the rest of the heavy chain extends from the head as a thin flexible stalk. The globular head contains the motor part of the molecule, the microtubule-binding site, and the ATP hydrolysis region. Two or three dynein heavy chains are often connected by their thin stalks to a common base. The base is made up of the intermediate and light chains, which are important for binding dynein to the organelles that it transports (its cargo).

There are at least 12 different flagellar dynein heavy-chain **genes**. To date, only two uniquely cytoplasmic dynein heavy-chain genes have been identified. The major cytoplasmic dynein (Fig. 1) has a native molecular weight of 1.5×10^{6}Da and contains two identical heavy chains associated with two 74-kDa intermediate chains, four 55-kDa light intermediate chains, and light chains of 22, 14, and 8 kDa. The heavy chain of this dynein is encoded by one gene, but multiple genes have been identified for the intermediate and light intermediate chains and for the 14-kDa light chain. The heavy chain of the minor cytoplasmic dynein is encoded by a unique gene, but the intermediate or light chains, with which it is presumed to be associated, have not yet been identified. Unlike cytoplasmic dynein, flagellar outer arm dyneins have two or three different heavy chains. Inner arm dyneins are either heterodimers or monomers of heavy chains and have various accessory polypeptides.

Figure 1. Schematic representation of the overall structure of a cytoplasmic dynein.

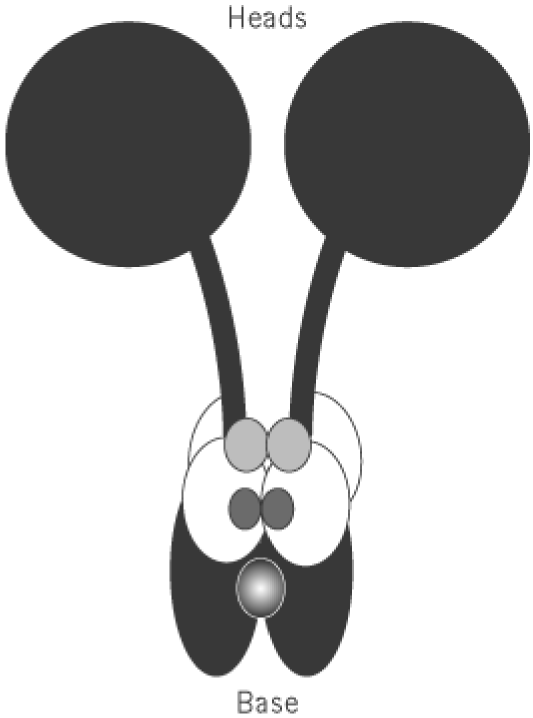

Structural analysis of the heavy-chain motor domain indicates that the head is made up of seven lobes arranged in a ring surrounding a central cavity (1). Each heavy chain has four consensus **nucleotide-binding sites** known as P loops. The first P loop, P1, is believed to be the site of ATP binding and hydrolysis for force generation (2). The role of the other P loops is unknown. In the presence of vanadate, the heavy chains are cleaved by UV photolysis into two fragments at the first P loop. The different types of dynein hydrolyze MgATP at different rates. Dyneins can be attached to glass coverslips via their bases and their heads will bind microtubules. Using computer-enhanced video microscopy, it can be observed that this bound dynein translocates microtubules across the coverslip in the presence of ATP. The velocity of cytoplasmic dynein microtubule movement *in vitro* is ~1micron/second.

Flagellar dyneins attach via their base to one of the outer doublet microtubules (the A microtubule) of the axoneme and bind directly to tubulin or to other axonemal microtubule-binding proteins. Their head domains bind to the B microtubule of the neighboring outer doublet in an ATP-sensitive manner and use the hydrolysis of ATP to push them toward the tip of the axoneme. Cytoplasmic dyneins bind to other cellular organelles. The mechanism by which dynein binds to these organelles is unknown. However, cytoplasmic dynein binds directly to artificial lipid membranes, liposomes, so dynein may bind directly to the organelle (3). There is also evidence, however, that an accessory protein complex, dynactin, is also important for cytoplasmic dynein binding to cargo (4). One dynactin subunit binds the dynein intermediate chain *in vitro*. Although they bind to different cargoes, cytoplasmic and flagellar outer arm dyneins have closely related cargo-binding subunits, the intermediate chains. The C-termini of the intermediate chains are conserved, and it is believed that they interact with the heavy chains. It is thought that the distinct intermediate-chain N-termini allow binding to different cargoes (5). Deletion of the cytoplasmic dynein heavy chain is lethal in multicellular organisms. Nonlethal mutations of cytoplasmic dynein heavy and light chains lead to axonal pathfinding defects and other pleiotropic **developmental** defects in *Drosophila* . Dyneins are regulated *in vivo*. During flagellar bending, only a subset of the flagellar dyneins function at a time. The **phosphorylation** state of an inner dynein-arm intermediate chain modulates this regulation (6). Genetic methods have also identified several proteins that make up a dynein regulatory complex, although the mechanism of the complex remains unknown. Cytoplasmic dynein heavy-chain, intermediate-chain, and light-intermediate chains are phosphorylated *in vivo*, and phosphorylation of each has been implicated in regulating dynein.

Bibliography

1. M. Samso et al. (1998) J. Mol. Biol. **276**, 927–937.
2. I. R. Gibbons (1995) Cell Motility and Cytoskeleton **32**, 136–144.
3. K. L. Ferro and C. A. Collins (1995) J. Biol. Chem. **270**, 4492–4496.
4. S. R. Gill et al. (1991) J. Cell Biol. **115**, 1639–1650.
5. C. G. Wilkerson et al. (1995) J. Cell Biol. **129**, 169–178.
6. G. Habermacher and W. S. Sale (1997) J. Cell Biol. **136**, 167–176.

Suggestions for Further Reading

7. I. R. Gibbons (1988) Dynein ATPases as microtubule motors, J. Biol. Chem. **263**, 15837–15840.
8. N. Hirokawa (1998) Kinesin and dynein superfamily proteins and the mechanism of organelle transport, Science **279**, 519–526.
9. R. B. Vallee, H. S. Shpetner, and B. M. Paschal (1989) The role of dynein in retrograde axonal transport, Trends Neurosci. **12**, 66–70.
10. R. B. Vallee and M. P. Sheetz. (1996) Targeting of motor proteins, Science **271**, 1539–1544.
11. G. B. Witman (1992) Axonemal dyneins, Curr. Opinion Cell Biol. **4**, 74–79.

Dystrophin

Dystrophin is a very large protein (molecular weight 427 kDa) located at the cytoplasmic face of the sarcolemma membrane of striated, smooth, and cardiac muscle cells and, most specifically, in the transverse tubules of the triadic structure. It represents only about 0.01% of the total skeletal muscle protein present in the tissue (1). Its absence, however, appears to be correlated with the fatal muscle-wasting disease known as *Duchenne muscular dystrophy* (incidence about 1 in 3500 of live male births). Becker muscular dystrophy, a milder form of muscular dystrophy (incidence about 1 in 35,000 of live male births), is related to defects/deletions in the dystrophin sequence. Muscular dystrophy is not related solely to the absence or mutation of dystrophin, however, because evidence has been presented to show that some membrane **glycoproteins** that normally interact with native dystrophin are **degraded** at abnormally high rates in either its absence or when it is mutated. This indicates that dystrophin may bind to and hence stabilize the structures of these dystrophin-associated proteins *in vivo*. It seems likely that dystrophin's structural role in muscle and nerve is comparable to that played by ankyrin and spectrin with membrane proteins in kidney, brain, and erythrocytes (1).

Dystrophin is a member of the spectrin superfamily of proteins and has many structural similarities with both spectrin and a-**actinin** . Each has a central rod domain, as well as globular regions located at the *N*- and *C*-termini. Like b-spectrin and a-actinin, the *N*-terminal domain of dystrophin contains a sequence that has high homology with the **actin**-binding site in a-actinin (2). *C*-terminal to the rod domain of dystrophin there is a **cysteine**-rich region about 150 residues that is somewhat akin to that in a-actinin, followed by a further 420 residues that is unique to dystrophin (1). Two putative **calcium-binding** sites occur within the *C*-terminal domain, although the sequences do differ from the consensus EF-Hand Motif, possibly significantly. Most of the defects/deletions in dystrophin that cause clinical symptoms are located within the rod domain; and very few are found in the cysteine-rich or *C*-terminal domains. These portions of the molecule *in vivo* provide the site of association with a well-characterized transmembrane protein complex. The *C*-terminal domain has been modeled as a pair of **heptad repeat**-containing regions (five and six heptads in length) separated by a proline-rich region (2). The *d* position in the heptads is largely occupied by leucine residues and is thus reminiscent of the leucine zipper structure. These regions are compatible with the formation of a two-stranded coiled-coil structure composed of parallel chains. These data suggest that dystrophin molecules may form a homodimer, or that dystrophin may form a heterodimer with *utrophin* (a dystrophin-related molecule). It is also known from electron microscopy that dystrophin molecules can assemble in a staggered manner and that these in turn may assemble further to produce end-to-end aggregates.

The rod domain in dystrophin (length estimates derived from electron microscope studies vary between 100 and 175 nm) consists of about 25 repeats, each about 109 residues long. Significant variations do occur, nonetheless; and although the repeats are homologous to those in spectrin and a-actinin, they are very much less regular, especially with regard to length. Ten of the 25 repeating motifs are largely complete (3), in contrast to the remaining 15 repeats, which lack some part(s) of the three constituent a-helices that comprise the three-a-**helix** motif (see Spectrin, where details of the conformation adopted are given). It has been proposed that dystrophin contains four **proline**-rich hinge regions within the rod domain that confer flexibility to the molecule and provide sites sensitive to **proteolysis**.

Bibliography

1. A. P. Monaco (1989) Dystrophin, the protein product of the Duchenne/Becker muscular dystrophy gene. Trends Biochem. Sci. **14**, 412–415.
2. D. J. Blake, J. M. Tinsley, K. E. Davies, A. E. Knight, S. J. Winder, and J. Kendrick-Jones (1995) Coiled-coil regions in the carboxy-terminal domains of dystrophin and related proteins: potentials for protein-protein interactions. Trends Biochem. Sci. **20**, 133–135.
3. D. A. D. Parry, T. W. Dixon, and C. Cohen (1992) Analysis of the three -helix motif in the spectrin superfamily of proteins. Biophys. J. **61**, 858–867.

Suggestion for Further Reading

4. J. M. Ervasti and K. P. Campbell (1993) Dystrophin and the Membrane Skeleton. Curr. Opin. Cell Biol. **5**, 82–87.

Eadie–Hofstee Plot

The Eadie–Hofstee plot was developed by Eadie (1) and Hofstee (2) and is one of three graphical procedures for determining values of the kinetic parameters for an enzyme-catalyzed reaction that conforms to Michaelis–Menten kinetics. It involves rearrangement of the initial velocity equation to a linear form that differs from that of the Lineweaver–Burk plot . The plot is derived from the Michaelis–Menten equation describing the dependence of the enzyme-catalyzed velocity v on the concentration of the substrate A and its Michaelis constant K_a; it is described by Equation (1):

$$v = -K_a \frac{v}{A} + V \tag{1}$$

where V is the maximum velocity of the reaction. Consequently, a plot of v against v/A yields a straight line with negative slope, equal to $-K_a$, a positive intercept on the abscissa that is equal to V/K_a, and a positive intercept on the vertical ordinate that is equal to V (Fig. 1).

Figure 1. Example of an Eadie–Hofstee plot for the determination of kinetic parameters for an enzyme-catalyzed reaction. The plot was produced by using the values of 10 and 2 (in arbitrary units) for V and K_a, respectively.

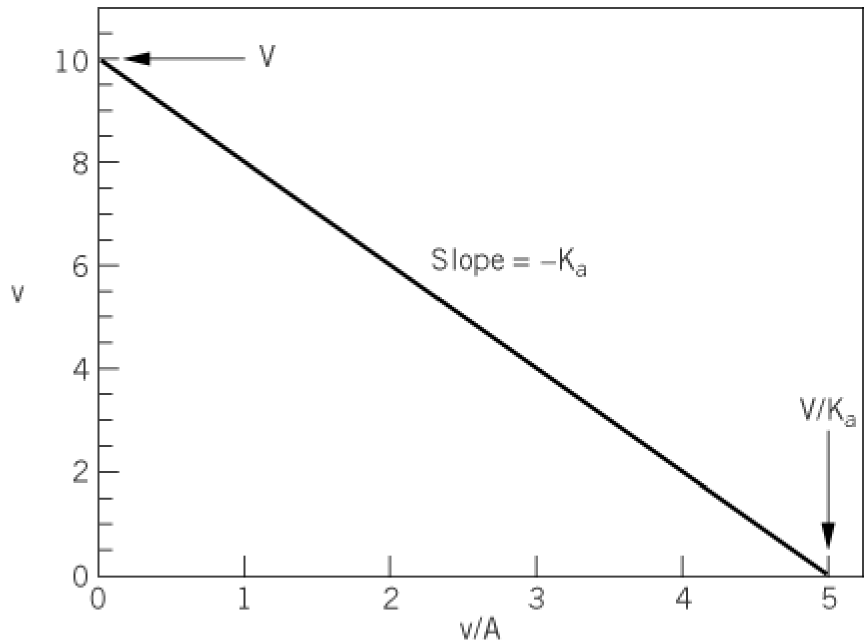

When values of V and K_a were being obtained by graphical methods, there were arguments for using this type of plot over that proposed by Lineweaver and Burk (3). But graphical procedures have now been supplanted by the use of regression analysis with computers (4).

A graphical procedure is required for the presentation of kinetic data. However, results that are presented as the variation of a dependent variable as the function of the ratio of a dependent and an independent variable, as in the Eadie–Hofstee plot, are not as readily interpreted as those presented as the variation of a dependent variable with the concentration of an independent variable. Further, the form of the kinetic equations for multisubstrate enzyme reactions becomes unnecessarily complex with the Eadie–Hofstee plot.

Bibliography

1. G. S. Eadie (1942) J. Biol. Chem. **146**, 85–93.
2. B. H. J. Hofstee (1959) Nature **184**, 1296–1298.
3. J. E. Dowd and D. S. Riggs (1965) J. Biol. Chem. **240**, 863–869.

4. W. W. Cleland (1979) Meth. Enzymol. **63**, 103–138.

Ecdysone

Pulses of the steroid hormone ecdysone coordinate postembryonic development in insects. In recent years, significant progress has been made in understanding the molecular mechanisms of ecdysone action in the fruit fly, *Drosophila melanogaster* (see ***Drosophila***). Ecdysone, bound to its **receptor** protein, directly activates primary-response genes. A subset of these genes encodes transcription factors that induce large batteries of secondary-response target genes. Dynamic changes in ecdysone titer, combined with cross-regulatory interactions among these transcription factors, determine the timing and order of regulatory **gene expression** during the onset of metamorphosis. Furthermore, connections are now being made between these genetic regulatory hierarchies and the biological responses they direct. Studies of ecdysone action in *Drosophila* have provided a foundation for understanding the molecular mechanisms of steroid hormone action during development.

1. Ecdysone Pulses During *Drosophila* Development

At specific times during development, and in response to environmental cues, neurons in the insect central nervous system release prothoracicotropic hormone (PTTH). This neuropeptide signals the adjacent ring gland to secrete the steroid hormone ecdysone into the hemolymph of the circulatory system (1). Some peripheral tissues, most notably the larval fat body, modify ecdysone into its biologically active form, 20-hydroxyecdysone. This hormone can then directly regulate gene expression through its interaction with the ecdysone receptor. Although insect endocrinologists use the term "ecdysone" to refer to the inactive form of the hormone, this word is synonymous with 20-hydroxyecdysone in the molecular biology literature.

Ecdysone pulses direct *Drosophila* through its life cycle, with peak hormone titers signaling the major postembryonic developmental transitions (Fig. 1). Larval development progresses through three **instars**, each punctuated by ecdysone-triggered molting of the cuticle. A high-titer ecdysone pulse at the end of the third instar triggers puparium formation and the onset of prepupal development. This is followed, 10–12 hours after puparium formation, by another ecdysone pulse that initiates the 3.5 days of pupal development, followed by eclosion of the adult fly (Fig. 1). Most larval tissues are destroyed during the early stages of metamorphosis and are replaced by adult tissues that develop from clusters of imaginal progenitor cells. The crawling larva thus undergoes a complete transformation, resulting in the formation of a highly motile, reproductively active adult fly. Remarkably, this transformation occurs in apparent response to a single steroid hormone, ecdysone. One focus of current research is understanding how the systemic hormonal signal is refined into the appropriate stage- and tissue-specific developmental pathways that direct this transformation.

Figure 1. The ecdysteroid titer profile during *Drosophila* development. The composite ecdysteroid titer is depicted, in 20-hydroxyecdysone equivalents from whole-body homogenates (44). Each of the developmental stages of the *Drosophila* life cycle are also shown, below a time scale in days. Reprinted with permission from Thummel (45). Copyright held by Cell Press.

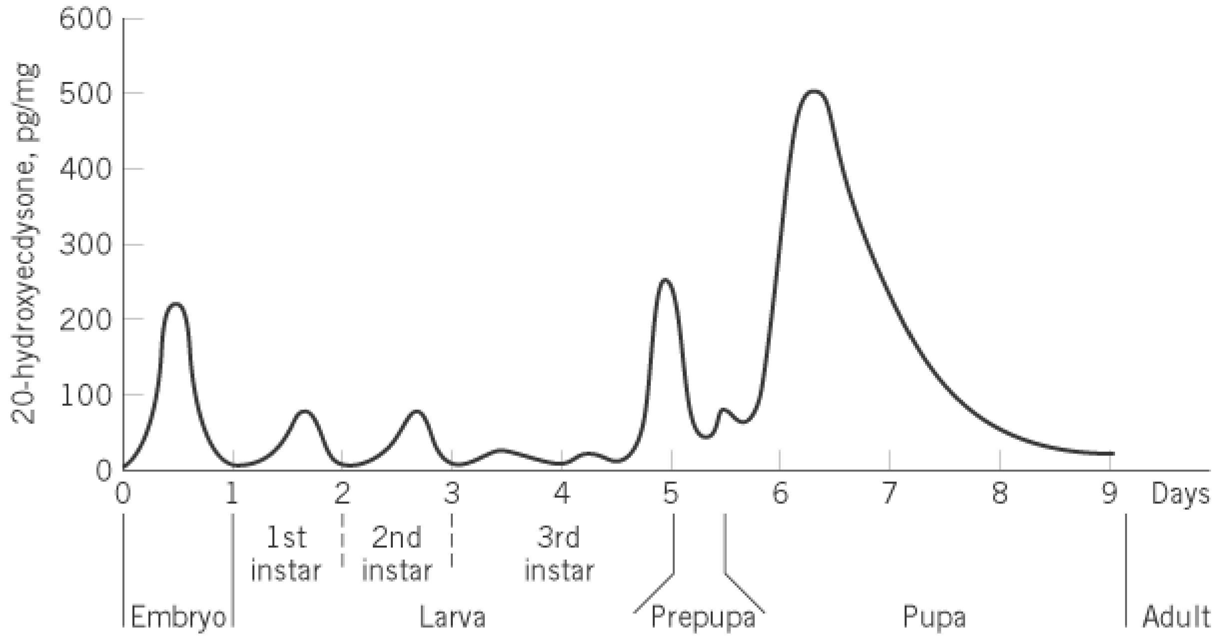

2. Ecdysone Regulation of Primary-Response Genes

Ecdysone manifests its effects on development by activating its receptor, a heterodimer of two members of the nuclear receptor superfamily: EcR and USP (see Hormone Receptors) (2, 3). Interestingly, at least two of the three protein **isoforms** encoded by the *EcR* gene are expressed in a tissue-restricted manner that can contribute to the specificity of developmental responses to ecdysone (4). EcR-B1 is expressed primarily in larval tissues that are fated to die, whereas EcR-A is expressed in developing adult structures and tissues. Both high-affinity DNA binding and ecdysone binding require EcR heterodimerization with USP, a homologue of vertebrate retinoid X receptor (see Retinoic Acids) (5, 6). The ecdysone/EcR/USP complex can then bind DNA and activate the transcription of target genes (see Hormone Response Elements). It is interesting to note that a *Drosophila* **orphan receptor**, DHR38, a homologue of the vertebrate NGFI-B receptor, can also heterodimerize with USP (7). This raises the possibility that ecdysone signaling may be modified through distinct heterodimer combinations of receptors, similar to the interactions that have been demonstrated in vertebrate organisms.

Many genes are induced directly by the ecdysone-receptor complex, presumably reflecting their immediate requirement following ecdysone pulses (8). Some of these genes, like *IMP-E1* (9) and *Fbp-1* (10), are induced by ecdysone in a restricted tissue-specific manner, whereas others, like *hsp23* (11) and *Eip28 / 29* (12), are expressed in multiple ecdysone target tissues.

A subset of primary-response genes encode transcription factors that function at the top of ecdysone-triggered genetic regulatory hierarchies. Most of these genes were defined as **puffs** that are induced directly by ecdysone in the larval salivary gland polytene chromosomes . Detailed studies by Michael Ashburner and co-workers demonstrated that these so-called early puffs appeared to encode regulatory proteins that both repress their own activity and induce large sets of secondary-response late puffs (13). The protein products of the late puffs were, in turn, thought to play a more direct role in specifying appropriate biological responses to the hormone.

Four early puff genes have been described at the molecular level. One of these, *E63-1*, encodes a calcium binding protein related to calmodulin (see Calcium Signaling), providing the possibility of cross-regulation between hormone and calcium signaling pathways (14). The remaining three genes each encode multiple transcription factor isoforms. The *Broad-Complex* (*BR-C*) encodes more than a dozen proteins, each of which carries one of four possible pairs of **zinc fingers** (15, 16). The *E74* early gene contains nested **promoters** that direct the synthesis of two related proteins, E74A and E74B, that share an identical C-terminal **ETS domain** that binds DNA (17). Similarly, the *E75* early gene contains nested promoters that direct the synthesis of three orphan members of the nuclear receptor superfamily, designated E75A, E75B, and E75C (18). Curiously, three other orphan receptor genes, *DHR3*, *E78*, and *bFTZ-F1*, correspond to ecdysone-regulated puffs in the polytene chromosomes, suggesting that this family of transcription factors may play an important role in ecdysone signaling during development (19-21).

Ecdysone dose-response studies have revealed that each early promoter is activated at a specific critical threshold hormone concentration. Combined with ecdysone titer measurements, these dose-response studies have led to a model for the timing of early gene expression during the onset of metamorphosis (22). The *EcR*, *BR-C*, and *E74B* promoters are most sensitive to ecdysone, and are induced in mid-third instar larvae in apparent response to a low-titer hormone pulse (Figs. 2 and 3). The high-titer late larval ecdysone pulse then represses some of these messenger RNAs, such as *EcR* and *E74B*, as it induces the less-sensitive promoters, including *E74A*, *E75A*, *E75B*, and *DHR3* (Figs. 2 and 3) (22, 23). The ecdysone titer drops during mid-prepupal development, allowing *bFTZ-F1* to be expressed. This gene is repressed by ecdysone and thus depends on the decrease in hormone titer for its induction (24) (Fig. 3). The rapid rise in ecdysone titer in late prepupae then recapitulates the larval pattern of early gene expression, with a burst of *EcR* and *E74B* expression preceding that of *E74A* and *E75A* (Fig. 2). In addition to these dose-dependent responses to ecdysone pulses, many early genes also cross-regulate their activity, ensuring that they will be expressed at the correct time and for the appropriate duration (see text below).

Figure 2. Temporal patterns of ecdysone-regulated gene expression during the onset of metamorphosis. A schematic representation of the ecdysone pulses is shown at the top, with the magnitude of each pulse represented by the width of the stippled bar. Developmental time proceeds from left to right, with the major ecdysone-triggered transitions marked by dotted lines. The dotted line on the left represents the second-to-third instar larval molt, and the dotted line on the right represents head eversion and the prepupal-pupal transition. Dark grey bars show the timing and duration of primary-response regulatory gene transcription, the light grey bar represents *bFTZ-F1* transcription, and the black bars represent secondary-response gene transcription. Reprinted with permission from Thummel (46).

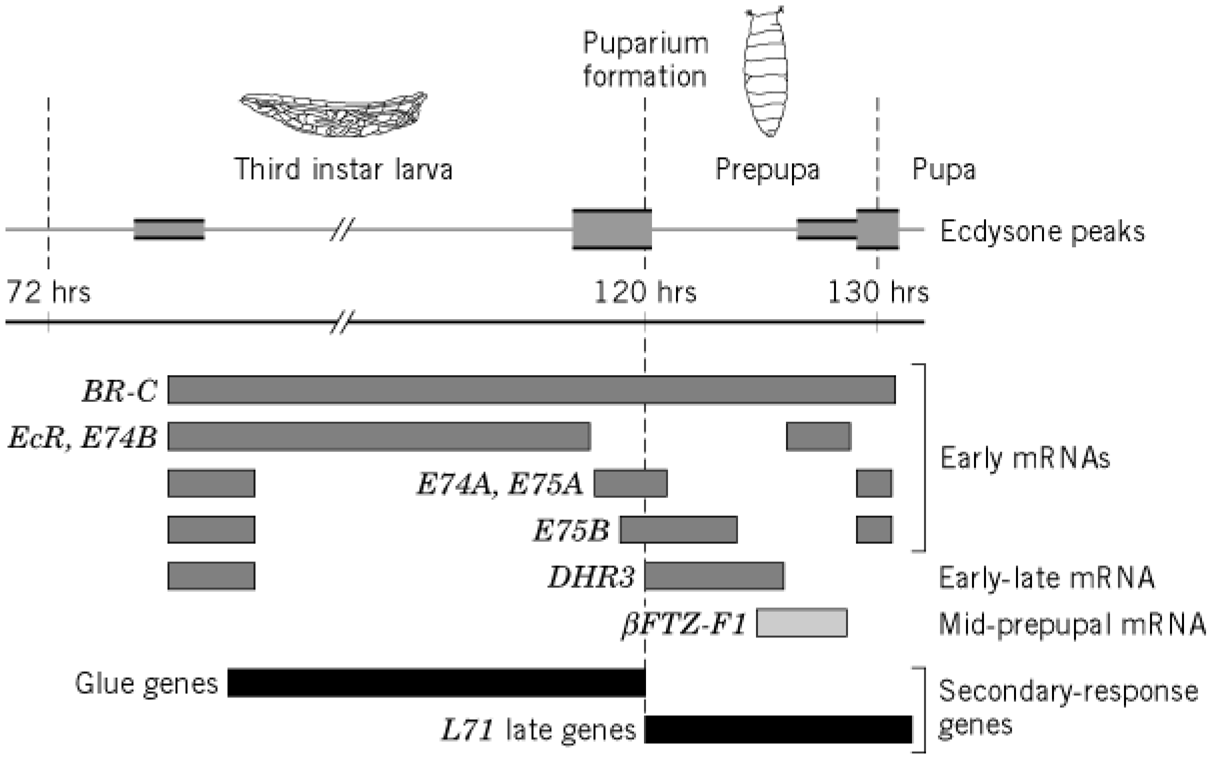

Figure 3. Multiple ecdysone-triggered regulatory hierarchies direct the onset of *Drosophila* metamorphosis. This figure summarizes regulatory interactions discussed in the text. Bars represent repressive effects, and arrows represent inductive effects. Reprinted with permission from Thummel (46).

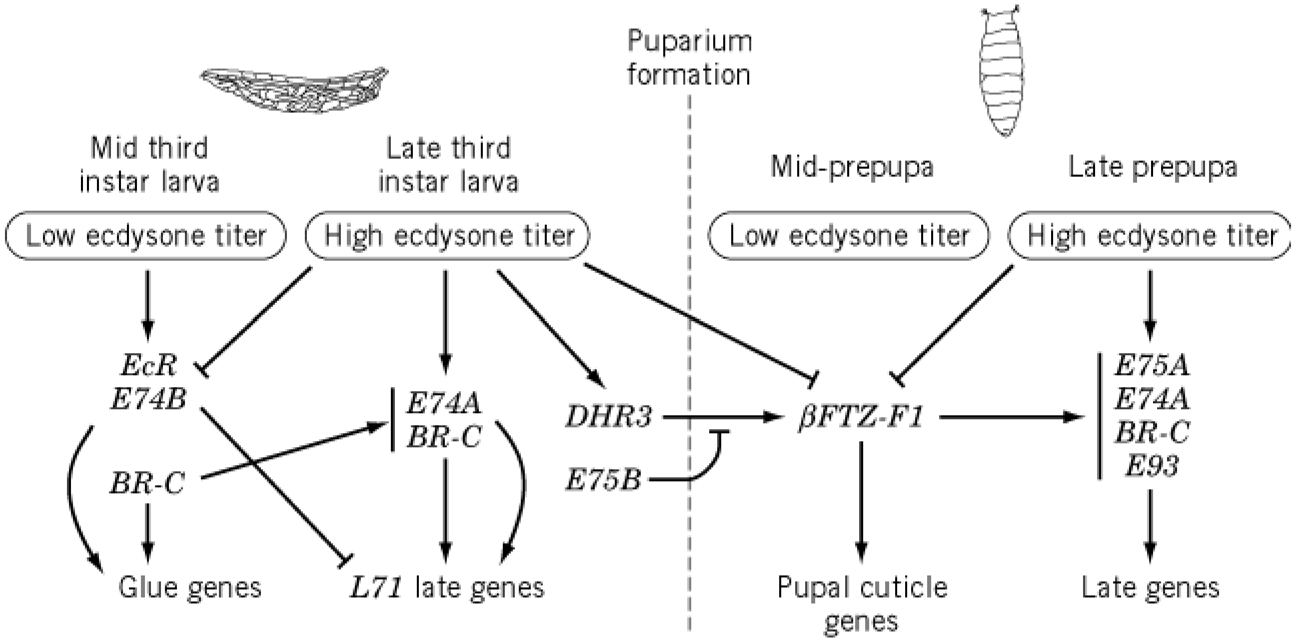

3. Regulation of Ecdysone Secondary-Response Genes

Molecular and genetic studies have demonstrated that these stage-specific patterns of primary-response regulatory gene expression are transduced into corresponding patterns of secondary-response gene activity. Two classes of secondary-response genes have been studied in the larval salivary glands: the glue genes (25, 26) and the *L71* genes from the 71E late puff (27). The glue genes are induced in mid-third instar salivary glands and encode a **polypeptide** glue that is used by the animal to affix itself to a solid surface for pupariation. In contrast, the *L71* genes are of unknown function and are induced at puparium formation, as the glue genes are repressed (Fig. 2).

Both *BR-C* and *E74B* are required for proper glue gene induction, defining a mid-third instar regulatory hierarchy in the salivary glands (Fig. 3) (28). BR-C binding sites in the glue gene enhancers are required for proper induction, indicating that this is a direct regulatory link (29). The tissue specificity of this response is directed by the Fork head **homeodomain** transcription factor that binds adjacent to the BR-C in glue gene enhancers (30, 31).

The *L71* late genes also depend on *BR-C* and *E74* for their proper induction in late third instar larval salivary glands (Fig. 3). *E74B* maintains the *L71* late genes in a repressed configuration during third instar larval development. The high-titer late larval ecdysone pulse then shuts off the E74B repressor and induces the E74A activator, which, together with the *BR-C*, directly induces *L71* transcription (Fig. 3) (32-34). These studies provide molecular support for Ashburner's proposal that early puff proteins direct the induction of late puff genes. In addition, they establish an important paradigm for understanding the mechanisms of hormone signaling in vertebrates, in which regulatory hierarchies are more difficult to define.

4. Cross-Regulation Among Ecdysone-Induced Transcription Factors

In addition to their roles in regulating ecdysone secondary-response genes, the ecdysone-induced transcription factors also regulate one another. *BR-C* is required for maximal ecdysone-induced early gene transcription in late third instar larvae (Fig. 3) (35). In this sense, *BR-C* is functioning as a competence factor that facilitates the subsequent regulatory response to ecdysone. Similarly, the early induction of *EcR* by a mid-third instar hormone pulse allows for increased levels of ecdysone receptor in preparation for the high hormone titer at the end of larval development (4).

Evidence has also been obtained for cross-regulatory interactions among the ecdysone-regulated orphan receptor genes. *DHR3*, which is induced by ecdysone in newly formed prepupae, is an inducer of *bFTZ-F1* expression in mid-prepupae (Fig. 3) (36, 37). Furthermore, this induction can be inhibited by heterodimerization of DHR3 with E75B (37). E75B protein levels normally decay during early prepupal development, thus determining the time at which DHR3 can activate *bFTZ-F1* (Fig. 2). *bFTZ-F1*, in turn, appears to be a critical competence factor for maximal reinduction of the early genes (Fig. 3) (24). Furthermore, *bFTZ-F1* is sufficient to induce the stage-specific *E93* early gene in the salivary glands of late prepupae (38). The DHR3, E75B, and bFTZ-F1 orphan receptors thus provide a regulatory link between the late larval and prepupal responses to ecdysone. Their stage-specific expression confirms that a critical developmental stage has been achieved and that the next response to the hormone should be distinct from the last response. These receptors thus provide a mechanism by which a hormonal signal can be refined into stage-specific developmental pathways.

5. From Gene Regulation to Biological Responses

Studies are currently under way that attempt to link ecdysone regulatory hierarchies with their appropriate biological responses during metamorphosis. As mentioned in the text above, most larval tissues are destroyed during prepupal and early pupal development. Recent studies have revealed that the destruction of the larval midgut and salivary gland occurs as stage-specific programmed cell death responses that display many of the hallmark features of apoptosis (39). Furthermore, the *Drosophila* death inducer genes *reaper* and *head involution defective* are coordinately induced in these tissues immediately preceding their destruction. A current focus of research is aimed at understanding how these death inducers are regulated by ecdysone at the appropriate time and place during metamorphosis. Specific neurons in the central nervous system also undergo programmed cell death in newly eclosed adults, in response to a decrease in ecdysone titer (40). Interestingly, these neurons can be distinguished by their high expression of the EcR-A isoform, suggesting that this receptor may play a key role in directing the death of these neurons.

As the larval tissues are being destroyed, the adult fly is being constructed. During prepupal development, the imaginal discs evert and elongate to form rudiments of the adult appendages. *BR-C* and *E74* both play a critical role in this process (41, 42). Studies have also shown that *bFTZ-F1* is sufficient to induce the pupal cuticle genes in mid-prepupal imaginal discs, providing a mechanism for the stage specificity of pupal cuticle deposition (Fig. 3) (43). It seems likely that future studies will provide more links between the ecdysone regulatory hierarchies and the biological responses to ecdysone during the onset of metamorphosis.

Bibliography

1. L. I. Gilbert, R. Rybczynski, and S. S. Tobe (1996) In *Metamorphosis: postembryonic reprogramming of gene expression in amphibian and insect cells* (L. I. Gilbert, J. R. Tata, and B. G. Atkinson, eds.), Academic Press, New York, pp. 59–107.
2. A. E. Oro, M. McKeown, and R. M. Evans (1990) Nature **347**, 298–301.
3. M. R. Koelle et al (1991) Cell **67**, 59–77.
4. W. S. Talbot, E. A. Swyryd, and D. S. Hogness (1993) Cell **73**, 1323–1337.
5. M. R. Koelle (1992) *Ph.D. thesis*, Stanford University.
6. T. Yao et al (1993) Nature **366**, 476–479.
7. J. D. Sutherland, T. Kozlova, G. Tzertzinis, and F. C. Kafatos (1995) Proc. Natl. Acad. Sci.

USA **92**, 7966–7970.
8. A. J. Andres and C. S. Thummel (1992) Trends Genet. **8**, 132–138.
9. J. E. Natzle, D. K. Fristrom, and J. W. Fristrom (1988) Dev. Biol. **129**, 428–438.
10. J. A. Lepesant et al. (1986) Arch. Insect. Biochem. Physiol. Supp. 1, 133–141.
11. E. B. Dubrovsky, G. Dretzen, and E. M. Berger (1996) Mol. Cell. Biol. **16**, 6542–6552.
12. A. J. Andres and P. Cherbas (1992) Development **116**, 865–876.
13. M. Ashburner, C. Chihara, P. Meltzer and G. Richards (1974) Cold Spring Harbor Symp. Quant. Biol. **38**, 655–662.
14. A. Andres and C. S. Thummel (1995) Development **121**, 2667–2679.
15. P. R. DiBello et al (1991) Genetics **129**, 385–397.
16. C. A. Bayer, B. Holley, and J. W. Fristrom (1996) Dev. Biol. **177**, 1–14.
17. K. C. Burtis et al. (1990) Cell **61**, 85–99.
18. W. A. Segraves and D. S. Hogness (1990) Genes and Dev . **4**, 204–219.
19. M. R. Koelle, W. A. Segraves, and D. S. Hogness (1992) Proc. Natl. Acad. Sci. USA **89**, 6167–6171.
20. G. Lavorgna, F. D. Karim, C. S. Thummel, and C. Wu (1993) Proc. Natl. Acad. Sci. USA **90**, 3004–3008.
21. B. L. Stone and C. S. Thummel (1993) Cell **75**, 307–320.
22. F. D. Karim and C. S. Thummel (1992) EMBO J. **11**, 4083–4093.
23. M. Horner, T. Chen, and C. S. Thummel (1995) Dev. Biol. **168**, 490–502.
24. C. T. Woodard, E. H. Baehrecke, and C. S. Thummel (1994) Cell **79**, 607–615.
25. M. A. T. Muskavitch and D. S. Hogness (1980) Proc. Natl. Acad. Sci. USA **77**, 7362–7366.
26. E. M. Meyerowitz and D. S. Hogness (1982) Cell **28**, 165–176.
27. L. G. Wright, T. Chen, C. S. Thummel, and G. M. Guild (1995) J. Mol. Biol. **255**, 387–400.
28. M. Lehmann (1996) BioEssays **18**, 47–54.
29. L. von Kalm et al. (1994) EMBO J. **13**, 3505–3516.
30. M. Lehmann and G. Korge (1996) EMBO J. **15**, 4825–4834.
31. V. Mach, K. Ohno, H. Kokubo, and Y. Suzuki (1996) Nuc. Acids Res. **24**, 2387–2394.
32. L. D. Urness and C. S. Thummel (1995) EMBO J. **14**, 6239–6246.
33. K. Crossgrove, C. A. Bayer, J. W. Fristrom, and G. M. Guild (1996) Dev. Biol. **180**, 745–758.
34. J. C. Fletcher, P. P. D"Avino, and C. S. Thummel (1997) Proc. Natl. Acad. Sci. USA **94**, 4582–4586.
35. F. D. Karim, G. M. Guild, and C. S. Thummel (1993) Development **118**, 977–988.
36. G. T. Lam, C. Jiang, and C. S. Thummel (1997) Development **124**, 1757–1769.
37. K. P. White, P. Hurban, T. Watanabe, and D. S. Hogness (1997) Science **276**, 114–117.
38. E. H. Baehrecke and C. S. Thummel (1995) Dev. Biol. **171**, 85–97.
39. C. Jiang, E. H. Baehrecke, and C. S. Thummel (1997) Development **124**, 4673–4683.
40. S. Robinow, W. S. Talbot, D. S. Hogness, and J. W. Truman (1993) Development **119**, 1251–1259.
41. I. Kiss et al (1988) Genetics **118**, 247–259.
42. J. C. Fletcher, K. B. Burtis, D. S. Hogness, and C. S. Thummel (1995) Development **121**, 1455–1465.
43. T. Murata, Y. Kageyama, S. Hirose, and H. Ueda (1996) Mol. Cell. Biol. **16**, 6509–6515.
44. L. M. Riddiford (1993) In *The Development of Drosophila melanogaster* (M. Bate and A. Martinez-Arias, eds.), Cold Spring Harbor Laboratory Press, Cold Spring Harbor, NY, pp. 899–939.

45. C. S. Thummel (1995) Cell **83**, 871–877.

46. C. S. Thummel (1996) Trends Genet. **12**, 306–310.

Suggestions for Further Reading

47. L. I. Gilbert, J. R. Tata, and B. G. Atkinson (1996) *Metamorphosis: Postembryonic Reprogramming of Gene Expression in Amphibian and Insect Cells*, Academic Press, New York.

48. J. Koolman (1989) *Ecdysone, from Chemistry to Mode of Action*, Thieme Medical Publishers, Inc., New York.

49. L. M. Riddiford (1993) In *The Development of Drosophila melanogaster* (M. Bate and A. Martinez-Arias, eds.), Cold Spring Harbor Laboratory Press, Cold Spring Harbor, NY, pp. 899–939.

50. C. S. Thummel (1996) Flies on steroids—Drosophila metamorphosis and the mechanisms of steroid hormone action. Trends Genet. **12**, 306–310.

Edman Degradation

This reaction for determining the sequences of peptides and proteins from their N-terminus was reported by Pehr Edman in the early 1950s (1-3). It now constitutes one of the oldest, if not the oldest, molecular method that is still much in use (see Protein Sequencing). It uses a three-stage reaction cycle for step-wise removal of amino acid residues from the N-terminus of a polypeptide chain. The three stages of the Edman cycle (Fig. 1) are (i) coupling, (ii) cyclization, and (iii) conversion.

Figure 1. Principles of the Edman reaction (left). Also shown is the DABITC (right) double-coupling method. Key: PIT phenylisothiocyanate; ATZ, anilinothiazolinone; PTH, phenylthiohydantoin; Dansyl (or DNS), 1-dimethylaminonaphtha sulphonyl; DABITC, 4-N,N-dimethylaminoazobenzene-4′-isothiocyanate.

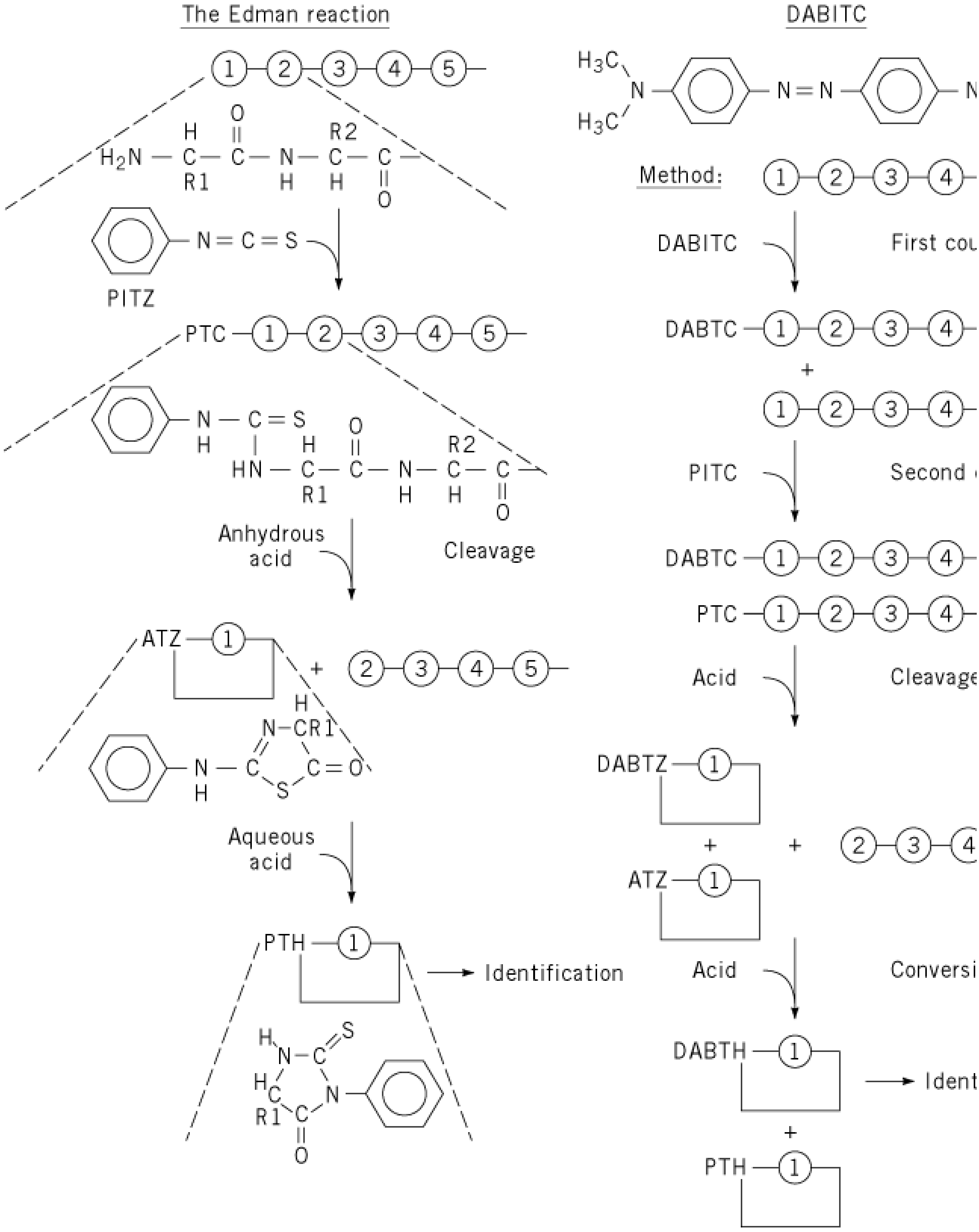

(i) *Coupling* involves a nucleophilic attack of the N-terminal a-**amino group** on the thiocyanate carbon of phenylisothiocyanate (PITC), to form the phenylthiocarbamyl-peptide derivative (PTC-peptide).

(ii) *Cyclization* constitutes the formation of the anilinothiazolinone derivative (ATZ-amino acid) in anhydrous acid, thereby liberating the N-terminal amino acid residue in a cyclic form, and leaving the remaining peptide truncated by one residue (Fig. 1).

(iii) *Conversion* involves the rearrangement of the liberated ATZ derivative to the corresponding phenylthiohydantoin derivative (PTH-amino acid) by opening of the CS bond and re-closure with the CO bond.

The reaction of protein amino groups with cyanate was known before Edman's report, but the degradative yield using cyanate was low. Edman increased the yields to useful levels by introducing thiocyanates in place of cyanates, and by determining the exact reaction conditions and pointing out the need for pure chemicals.

This reaction constitutes the start of protein chemical sequencing on a routine scale; hence it really marks the start of molecular biology as a whole. The reaction is still used in most protein laboratories worldwide, it is the basis of chemical protein sequencers, and a classical method still "modern" in molecular biology at the end of the 1990s. Essentially, the only changes that have occurred during the 50 years to this reaction are:

- use of other solvents, giving alternative and more rapid protocols,
- continued automation, miniaturization, and increase in reaction speed, now making the reaction useful for routine applications at the picomole level in 30-min cycles per residue.

It was a remarkable accomplishment of Edman to design this reaction and to directly set out all the conditions, so that it has stayed unsurpassed for 50 years of worldwide protein chemistry.

1. Protein Sequencers

After development of the Edman reaction, Edman automated the process, developing a machine to make all additions, extractions, and lyophilisations. This constituted the birth of the protein sequenator (or sequencer); the basic concept for a complete machine was published by Edman and Begg in 1967 in a now classic paper (4) in the then newly-started *European Journal of Biochemistry*.

In the first-generation sequencers, a "spinning cup" constituted the reaction center, and the sample was kept in place by centrifugal force, making extractions and reactions possible. Extraction losses were a problem in each cycle, however, soon leading Laursen and others to the idea of solid-phase attachment of the peptide to be degraded (see **Solid-phase synthesis**). Consequently, only a few years later, the solid-phase sequencer was reported (5). Although both types of sequencers were based on the same Edman chemistry (3), their different properties, including the different attachments of the samples, made them suitable for different analyses. The liquid-phase sequencer was excellent for proteins, and the solid-phase instrument was better for short peptides, because of their different sensitivities to extractive losses and to build-up of background signals.

2. Manual Edman Degradations

Once the Edman reaction and the protein sequencer existed, the really limiting factor was peptide purification on the one hand, and phenylthiohydantoin (PTH)-amino acid identification on the other. For a long time, suitable chromatographic methods did not exist, hampering both purification and identification. Peptide purification, especially the separation of large peptides, was a problem. Similarly, identification of the PTHs liberated in each Edman cycle was also a problem. The PTH derivatives were initially identified by paper chromatography, which was not fully reliable (all derivatives did not separate in one analytical step) and also required the use of several solvent systems, which wasted time and material. Subsequent developments introduced gas chromatography and **thin-layer chromatography**, both increasing the speed of identification, but still not giving a reliable one-step identification of all amino acids. These limitations contributed to the development of alternative methods, such as the dansyl and DABITC types of analysis, which did not require a major investment in equipment. One major manual method was that using dansyl (1-dimethylaminonaphthalene-5-sulphonyl) chloride to detect the new N-terminus after each Edman cycle (6) (see Dansyl Chloride). The main advantage was that it was easier to identify the residues released sequentially. Its primary importance is that it made protein sequence determination accessible to many laboratories.

A similar and later development in manual sequence analysis was the DABITC (4-N,N-dimethylaminoazobenzene-4′-isothiocyanate) method (7). In this case, protein degradation is carried out by coupling with the strongly colored DABITC, in place of PITC (Fig. 1). The DABTHs produced, which correspond to PTHs, are easily detectable by **thin-layer chromatography** (7). However, DABITC has a low coupling yield in the Edman reaction, necessitating a second coupling stage with ordinary PITC (Fig. 1, right) before the subsequent cyclization step.

At the time, both the dansyl and the DABITC methods were important, but since the 1980s these methods have gradually decreased in importance because of reliable sequencer on-line **HPLC** identification of PTH-derivatives (see below).

3. HPLC

The PTH-amino acid identification problem was finally solved with the introduction of **HPLC** in 1976 (8); subsequently, PTH amino acid identification became rapid, routine, and reliable. Although some identifications may still be difficult, PTH identification no longer constitutes the limiting factor in time or reliability.

At the same time, HPLC separations and the subsequent development of a whole battery of different chromatographic media soon also solved the problem of purification of peptide fragments from proteolytic digests.

4. Second-Generation Chemical Sequencers: Automation of All Steps

With the development of protein sequence analyzers, it became possible to determine amino acid sequences routinely, and there was an exponential increase in known protein sequences. However, analysis at this stage was still time-consuming and nonautomatic, requiring knowledge and real research. Gradually, however, a set of further inventions increased the automation and brought the actual sequence analysis more or less to the present-day automatic stage. This development essentially relied on three further inventions/improvements.

One concerned the attachment of the protein/peptide to the sequencer for analysis. This important step had several sub-steps. One was the realization that an organic cationic polymer, Polybrene (9, 10), was a suitable material capable of binding proteins and peptides to glass surfaces or other membranes. The resulting minimization of extraction losses in the washing steps of each cycle made degradations possible through to the very C-terminus of most peptides. More importantly, apart from the improvement in the lengths of degradation possible, use of Polybrene also meant that the peptide for degradation could be attached to surfaces; this therefore opened the way to the abandonment of the use of centrifugal force for attachment of the peptide for degradation. Instead, peptides could now be attached to membranes, essentially moving the degradation from the traditional "liquid phase" system to the advantageous "solid phase" (which had been started earlier by covalent attachments, cf. above) and "gas-phase" systems (11). The latter are solid phase for the attachment of the peptide to a support, and gas phase for the introduction of some reagents. These approaches are still in use and now allow rapid and sensitive analysis. Many other sub-steps in this transformation were involved. In particular, perhaps the introduction of chemical attachments of peptides to membranes (12), and the successive development of alternative, miniature column attachments for sample introductions and preparations (13), should be mentioned.

The second improvement at this stage, was the introduction of dead volume-free valve blocks, allowing use of valves with an absolute absence of cross-contamination between the reagents used in the reaction (14). In this manner, further increases in speed (because of less washing) and sensitivity (because of higher yield from lack of cross-contamination) made sequencers still more useful and rapid. Recently, this has been carried still further, and soon “chip-based blocks” may be encountered in sequencers, with all solvent delivery and removal stages in extremely small volumes of “chip-blocks” (15).

The third major advance at this stage was the introduction of automatic methods for the conversion of a thiazolinone from each cycle into the corresponding thiohydantoin. This became possible because of the introduction of a second reaction vessel (16), with separate reagents and reactions.

Once the conversion had become automated, it became possible also to link the subsequent PTH identification step to the cycle of automatic events in the sequencer, thus opening the road to on-line identification of the liberated amino acid derivative in each cycle. These on-line modes were started very early, with the introduction of HPLC, and were soon commercialized and perfected in a new set of complete sequencers, starting with the “gas-phase sequencer” that was available in the 1980s (11). Soon, the on-line approach was coupled with post-PTH-identification data treatments, allowing extensive computer interpretation at each step. All chromatograms can now be stored and compared with on-line computers and further interpreted and related to sequences in **databanks**, analyzed in modeling programs, and submitted to further computerized adjustments.

Bibliography

1. P. Edman (1950) Acta Chem. Scand. **4**, 283–293.
2. P. Edman (1953) Acta Chem. Scand. **7**, 700–701.
3. P. Edman (1956) Nature **177**, 667–668.
4. P. Edman and G. Begg (1967) Eur. J. Biochem. **1**, 80–91.
5. R. A. Laursen (1971) Eur. J. Biochem. **20**, 89–102.
6. W. R. Gray (1967) Methods Enzymol. **11**, 469–475 and (1972) **25**, 121–138.
7. J. Y. Chang, D. Brauer, and B. Wittmann-Liebold (1978) FEBS Lett. **93**, 205–214.
8. C. L. Zimmerman, E. Appella, and J. J. Pisano (1977) Anal. Biochem. **77**, 569–573.
9. G. E. Tarr, J. F. Beecher, M. Bell, and D. J. McKean (1978) Anal. Biochem. **84**, 622–627.
10. D. G. Klapper, C. E. Wilde III, and J. D. Capra (1978) Anal Biochem. **85**, 126–131.
11. R. M. Hewick, M. W. Hunkapiller, L. E. Hood, and W. J. Dreyer (1981) J. Biol. Chem. **256**, 7990–7997.
12. J. M. Coull, D. J. C. Pappin, J. Mark, R. Aebersold, and H. Köster (1991) Anal. Biochem. **194**, 110–120.
13. C. G. Miller (1994) Methods: A companion to Methods in Enzymology **6**, 315–333.
14. B. Wittmann-Liebold, A. W. Geissler, and E. Marzinzig (1975) J. Supramol. Struct. **3**, 426–447.
15. C. Wurzel and B. Wittmann-Liebold (1998) In *Microreaction Technology: Proceedings of the First International Conference on Microreaction Technology* (W. Ehrfeld, ed.), Springer Verlag, Berlin, Heidelberg, pp. 219–224.
16. W. Machleidt and H. Hofer (1980) In *Methods in Peptide and Protein Sequence Analysis* (C. Birr, ed.), Elsevier/North Holland, Amsterdam, pp. 35–47.

EDTA (Ethylenediamine-*N*,*N*,*N*′,*N*′-Tetraacetic Acid)

EDTA is a chelating agent widely used, along with EGTA, to control the concentration of divalent and trivalent cations in aqueous solutions. Its structure is given in Figure 1. It is an essential ingredient in such diverse products as laundry detergents and film developers. In the field of molecular biology, EDTA is present in many buffer solutions used for experiments where the presence of divalent and trivalent cations would interfere with the desired outcome. For example, it is used in most buffers for the initial steps of protein purification (1) from biological material, to suppress the activity of metal-dependent proteases that would otherwise degrade the desired protein.

Figure 1. Chemical structure of EDTA (ethylenediamine- *N,N,N′,N′*-tetraacetic acid).

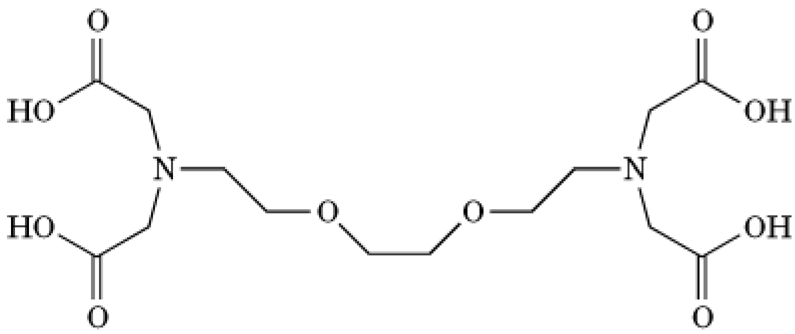

The flexibility of the molecule, and the variety of potential liganding sites within it, permit EDTA to accommodate a wide variety of cation types, preferred ligand geometries and bond lengths, thus contributing to its high affinity for most cations (Table 1) (2). In contrast to many other complexing agents, EDTA will form only a 1:1 complex with either divalent and trivalent cations, in which a single ion is chelated by all four carboxyl groups, which greatly contributes to the stability of the resulting complex. Hence, EDTA can maintain the concentration of free cations at very low levels. The high affinity of EDTA for cations is also used to removed metals from metalloproteins and to maintain them in their metal-free state. It is important to note that the binding of cations by EDTA is pH-dependent; protonation of the carboxylate moieties at low pH dramatically lowers their affinity for cations.

Table 1. Affinity of EDTA for Various Cations[a]

Metal Ion	$\log_{10} K_a$
Mg^{2+}	8.64
Ca^{2+}	11.0
Zn^{2+}	16.4
Cd^{2+}	16.4
Mn^{2+}	13.8
Cu^{2+}	18.7
Fe^{2+}	14.33

Fe^{3+}	24.23
Co^{2+}	16.3
Co^{3+}	36
Pb^{2+}	18.3

[a] The logarithm of the association constant [K_a in units of M^{-1} (reciprocal molars)] are compared at pH 7.0, 25°C, and 0.1 *M* ionic strength (2).

EDTA as the free acid is a white powder, has a molecular weight of 292.25 Da, decomposes at 240° C, and is relatively insoluble in water (0.34 g/100 mL at 25°C). The sodium and potassium salts of EDTA are also white powders and are much more readily soluble in water.

Bibliography

1. J. E. Coligan et al. (eds), *Current Protocols in Protein Science* John Wiley & Sons, Chichester, U.K. (1995).
2. A. E. Martell and R. M. Smith (1974) *Critical Stability Constants* Vol. **1**, Plenum Press, New York.

Suggestion for Further Reading

3. R. H. Crabtree (1994) "Coordination + organometallic chemistry, principles", in *Encyclopedia of Inorganic Chemistry*, Vol. **2**, R. B. King, ed., John Wiley & Sons, Chichester, U.K.

Effective Molarity

A reaction or interaction between two different molecules in dilute solution is relatively straightforward and is governed by their concentrations in that solution, plus the appropriate rate or equilibrium constant (see Kinetics). In more complex situations, however, the situation may differ from that expected from the bulk concentrations of two reactants. If they attract each other, for example by **electrostatic** or **hydrophobic interactions**, their *effective* molarities will be greater than their bulk concentrations. Similarly, a nonpolar reagent that partitions into the interiors of membranes, or any reagent that concentrates in one organelle or compartment, will react there at a much greater rate than if it were dispersed evenly throughout the system.

A special situation occurs when two reactive or interactive groups are part of the same macromolecule, such as a **protein** or **nucleic acid**. The rate constant for reaction between two such groups, or their association constant, might be known when they are individual molecules, when the observed rate or equilibrium is given by this constant times their respective concentrations, but for an intramolecular reaction or interaction, their concentration within the solution is irrelevant. Instead, it is the *effective concentration* of the two groups within the macromolecule that is important for the intramolecular interaction. The effective molarity will depend upon the structure of the macromolecule, in particular the extent to which it brings the two reactants together or keeps them apart, plus the environment in which the two groups are kept. The effective molarity for the intramolecular reaction will be essentially zero if the macromolecular structure keeps the two groups apart (of course, groups on different molecules can still react, and their bulk concentrations still govern this *intermolecular* reaction). At the other extreme, when the macromolecular structure keeps the two groups in the correct proximity and orientation for reaction, their effective molarity can be extremely large, up to 10^{10} M, concentrations that are not feasible with two independent molecules. Such values are predicted by theoretical considerations (1) and are also observed experimentally, from the ratio of the rate or equilibrium constants for the same reaction when the groups are on the same molecule and on separate molecules (2).

The large effective concentrations that are observed are believed to be due primarily to the much smaller loss of entropy that occurs when two groups on the same molecule interact. Two independent molecules that interact in solution must lose substantial translational and rotational entropy when they interact, depending upon the rigidity of the interaction. Two groups attached to the same macromolecule have already lost varying degrees of this entropy. In the ideal case, when the two reactive groups are held by the macromolecular structure in precisely the correct position for them to interact, so that there is no change in their entropy, the maximum effect and the maximum effective molarity are observed. Of course, other considerations also apply, such as if the environment of the groups is different in the macromolecule, or if they are strained and this strain is relieved upon their reaction.

Whatever the exact reason for the large effective molarities that can be measured in macromolecules, this has important consequences for understanding the stabilities of the folded structures of macromolecules. For example, the question of the role of hydrogen bonds in stabilizing protein structures has been very controversial (see Protein Stability). One might expect *a priori* that hydrogen bonds would contribute nothing to the net stability because any hydrogen bonds in the folded state would be replaced by equivalent hydrogen bonds, with the water, in the unfolded protein. But the two cases differ because the hydrogen bonds in the folded state are intramolecular, whereas those with the solvent are intermolecular. If the hydrogen bonding groups have effective molarities in the folded state greater than the solvent concentration, 55 M for water, the hydrogen bonds in the folded state will be more stable than those in the unfolded state, and they will stabilize the folded conformation. Another way of thinking about this is to consider the increased entropy of the water molecules that are liberated when the protein folds and forms intramolecular hydrogen bonds. Effective molarities of up to 10^{5} M have been measured between cysteine residues in forming disulfide bonds during **protein folding** (3). Consequently, it is not surprising that folded macromolecular structures can be stabilized by many intramolecular interactions that individually are very weak in an unfolded conformation, but occur simultaneously and cooperate to generate a folded conformation (4). The large effective molarities of reactive groups in the active sites of enzymes are also important for explaining enzymatic catalysis.

Bibliography

1. M. I. Page and W. P. Jencks (1971) Proc. Natl. Acad. Sci. USA **68**, 1678–1683.
2. A. J. Kirby (1980) Adv. Phys. Org. Chem. **17**, 183–278.
3. T. E. Creighton and D. P. Goldenberg (1984) J. Mol. Biol. **179**, 497–526.
4. T. E. Creighton (1983) Biopolymers **22**, 49–58.

Suggestion for Further Reading

5. T. E. Creighton (1993) *Proteins: Structures and Molecular Properties*, 2nd ed., W. H. Freeman, New York, "Chapters 4, 7", and "9".

EF-Hand Motif

The majority of calcium-binding proteins involved in intracellular Ca^{2+} signal transduction are characterized by a common helix–loop–helix structural protein motif in their Ca^{2+}-binding sites that is termed the EF-hand. Well over a thousand EF-hand motif sequences have been identified. An exquisite fine-tuning of the packaging of EF-hands provides these proteins with both high selectivity for Ca^{2+} and the ability to respond rapidly and efficiently to the modest (100-fold) changes in concentration associated with Ca^{2+} signals. In fact, the unique relationship between the EF-hand motif and Ca^{2+} binding extends beyond the ability to transduce Ca^{2+} signals, as other members of this protein family have critical roles in the uptake, transport and homeostasis of Ca^{2+}.

The term "EF-hand motif" was introduced by Kretsinger on examination of the three-dimensional structure of parvalbumin, the first member of the EF-hand Ca^{2+}-binding protein family whose three-dimensional structure was determined (1). A great deal of structural insight into the variability of the EF-hand motif has been obtained from subsequent X-ray crystallography and NMR solution structure analysis of EF-hand calcium-binding proteins. EF-hand motifs almost always occur in pairs packed together in a face-to-face manner, forming a stable globular domain (Fig. 1). The pairing of sites is presumed to stabilize the protein conformation, increase the Ca^{2+} affinity of each site over that of isolated sites, and provide a ready means for the **cooperativity** in the binding of Ca^{2+} that is critical to their function. The conformations of EF-hands are variable and are dependent on whether ions are bound (see Calcium-Binding Proteins).

Figure 1. Ribbon diagram of the canonical EF-hand of the *N*-terminal domain of calmodulin using the coordinates of 1CFC (3).

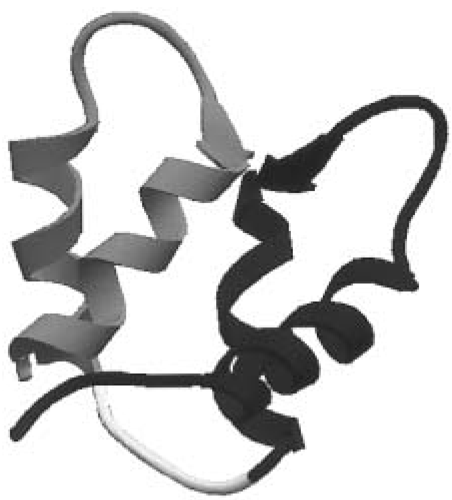

The canonical EF-hand consists of a 29-residue contiguous segment of polypeptide chain containing an a-helix designated as E in the original parvalbumin structure (residues 1–10), a loop around the calcium ion (residues 10–21), and a second a-helix designated F (residues 19–29). The consensus sequence is shown in Figure 2. Residues 10, 12, 14, 16, 18, and 21 chelate the Ca^{2+} ion. Residues 10, 12, and 14 provide monodentate oxygen ligands, and residue 21 provides a bidentate oxygen ligand, all via side-chain carboxyl groups. Residue 16 directly coordinates Ca^{2+} via its main-chain oxygen. Residue 18 ligates Ca^{2+} indirectly, through a stably bound water molecule. Other residues have been assigned specific roles in stabilizing the EF-hand motif. For example, a central

hydrophobic core is formed from the side chains of residues 2, 5, 6, and 9 of helix E; 22, 25, 26, and 29 of helix F; and 17 from the binding loop.

Figure 2. Schematic diagram of the consensus sequence for the EF-hand Ca^{2+}-binding motif. Residues marked with * have no constraints on which amino acids occur there. Residue 16, #, chelates the calcium by its backbone carbonyl oxygen atom. The residues of the E and F helices marked "n" must be nonpolar for packing of the two helices.

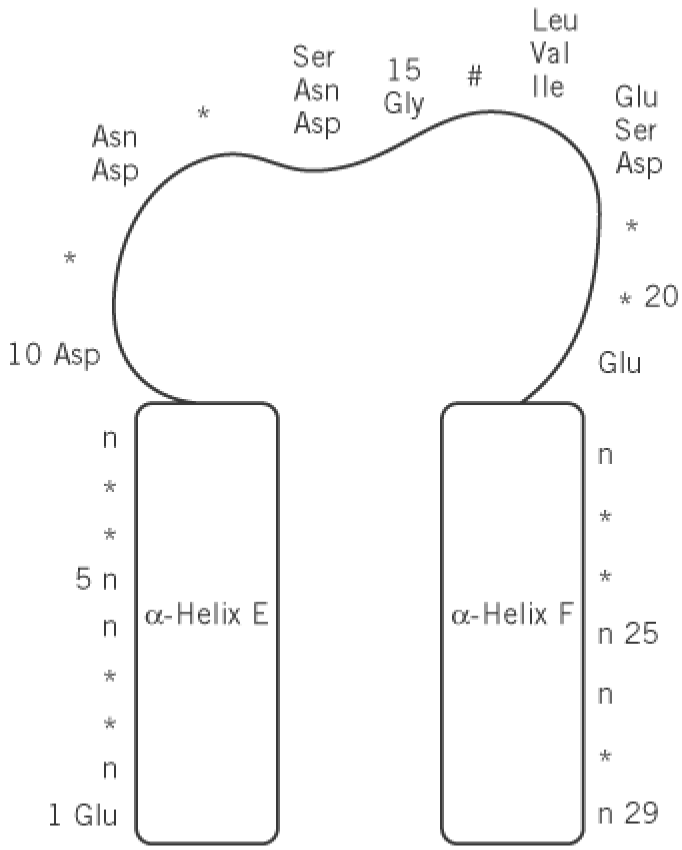

Most EF-hand proteins use this canonical motif. The S100 proteins (an important subfamily of Ca^{2+}-binding proteins), however, have a two-residue insertion and a modified coordination scheme in the first binding loop. In these pseudo-EF-hands, residues 10, 13, 15, and 18 chelate the Ca^{2+} ion via their main-chain carbonyl oxygen atoms, whereas residue 20 chelates indirectly via a water molecule, and acidic residue 23 provides bidentate ligation via its side-chain carboxylate. The role of these pseudo-EF-hands in modulating the structure or function of S100 proteins is still under investigation, although there is evidence that the packaging of a pseudo-EF-hand and a canonical EF-hand attenuates the changes in the structure and dynamics of the protein induced by the binding of calcium (2).

Bibliography

1. R. H. Kretsinger and C. E. Nockolds (1973) J. Biol. Chem. **248**, 3313–3326.
2. N. J. Skelton, J. Kördel, M. Akke, S. Forsén, and W. J. Chazin (1994) Nature Struct. Biol. **1**, 239–245.
3. H. Kuboniwa, N. Tjandra, S. Grzesiek, H. Ren, C. B. Klee, and A. Bax (1995) Nature Struct. Biol. **2**, 768–776.

Suggestion for Further Reading

4. N. C. J. Strynadka and M. N. G. James (1989) Crystal structures of the helix-loop-helix calcium-binding proteins, Annu. Rev. Biochem. **58**, 951–998.

EGF Motif

The EGF motif is a common structural **domain** found in many protein structures, especially those of proteins associated with blood clotting, fibrinolysis, neural development, and **cell adhesion**. The motif is characterized as a protein module of ~ 45 residues having six conserved cysteine residues (designated CI through CVI) that form three internal disulfide bonds with the connectivity CI-III, CII-IV and CV-VI. The motif was first found in epidermal growth factor (EGF), hence the name EGF motif or EGF-like domain. Although found as a single unit in EGF and transforming growth factor a, the EGF domain is often present as a repeating unit in much larger proteins. For example, the protein fibrillin has over 30 EGF domains. Furthermore, EGF motifs in proteins are frequently present in combination with repeating units of other modules such as the Kringle domain.

The sequence of the EGF motif is often recognizable from just the primary structure of a protein. The consensus sequence is X–X–X–X–Cys–X(2–7)–Cys–X(1–4)–(Gly/Ala)–X–Cys–X(1–13)–t–t–a–X–Cys–X–Cys–X–X–Gly–a–X(1–6)–Gly–X–X–Cys–X, where X is any amino acid (the number in brackets defining a variable number of X residues), *a* is an aromatic residue, and *t* is a **nonhydrophobic** residue (1). The tertiary structure of the EGF motif is also highly conserved and can be described as having a two-stranded antiparallel b-sheet scaffold upon which the three disulfide bonds are positioned (Fig. 1). The disulfide bonds link the *N*-terminal and *C*-terminal loop regions to the core. Binding of **calcium** ions to some classes of EGF domain further stabilizes the *N*-terminal region and is thought to cause the formation of long helical arrangements of multiple EGF motifs (2); this property may account for their proposed function of mediating protein–protein interactions.

Figure 1. Schematic representation of the backbone structure of an EGF domain (2). b-Strands are shown as arrows, and the three disulfide bonds are shown in light gray, with the sulfur atoms depicted as spheres. The *N*- and *C*-termini are labeled. This figure was generated using Molscript (3) and Raster3D (4, 5).

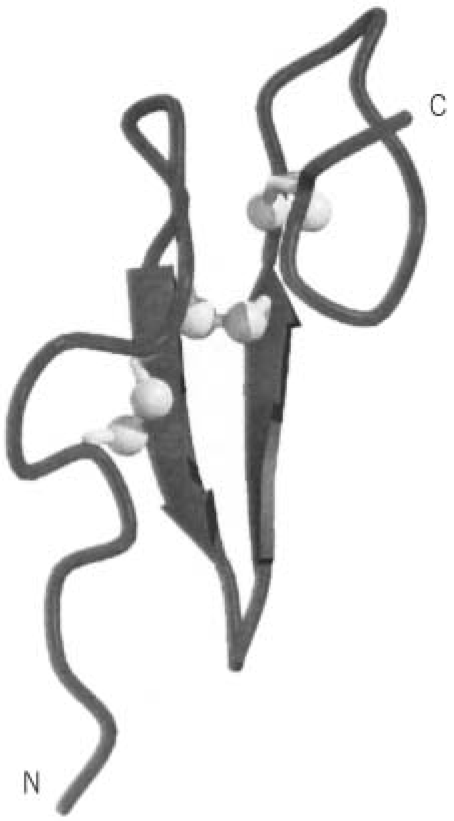

Bibliography
1. I. D. Campbell and P. Bork (1993) Curr. Opin. Struct. Biol. **3**, 385–392.
2. Z. Rao, P. Handford, M. Mayhew, V. Knott, G. G. Brownlee, and D. Stuart (1995) Cell **82**, 131–141.
3. P. J. Kraulis (1991) J. Appl. Crystallogr. **24**, 946–950.
4. E. A. Merritt and M. E. P. Murphy (1994) Acta Crystallogr. **D50**, 869–873.
5. D. J. Bacon and W. F. Anderson (1988) J. Mol. Graphics **6**, 219–222.

Suggestion for Further Reading
6. I. D. Campbell and P. Bork (1993) Epidermal growth factor-like modules. Curr. Opin. Struct. Biol. **3**, 385–392.

Egg

An *egg* is the female **gamete**, which is originally haploid and in most cases nonmotile. After fertilization by a sperm, the egg provides the basis for producing a completely new individual. Regarding this subsequent development, eggs belong to the least restricted cell types of the body, as they have the power to produce every other differentiated cell type. Eggs cannot be regarded as nonspecialized cells; instead, they prove to be very specialized cells to accomplish this task.

First, they must mediate sperm–egg interactions. This means that they must be able to induce metabolic pathways in the spermatozoon and biochemical signals from the spermatozoon must be understood, thus leading to intracellular reactions in the egg to promote fertilization. Second, after fertilization with a spermatozoon, the egg needs a machinery to promote biochemical actions that are necessary to fuse the male and female **pronuclei**. Third, the egg must be able to guide and support the very early cell divisions without, or with only minimum, nuclear control of the developing embryo. Thus, the egg must provide appropriate amounts and species of many different basic elements, such as transfer RNA, ribosomes, and many different proteins, including basic elements like transcription factors. These gene products have been **transcribed**, and in some cases **translated**, previously and are stored in the oocyte cytoplasm.

1. Morphology

Unlike other cells, eggs consists of an outer porous extracellular matrix, the *zona pellucida* (1). The zona pellucida is not primarily for mechanical protection of the egg, but its foremost task is to mediate sperm–egg interactions. It is made of long filaments consisting of three types of **glycoproteins** . In all species thus far investigated, zona pellucida glycoproteins are expressed by the ZPA, ZPB, and ZPC gene family (1). Post-translational modification of the zona pellucida glycoproteins, however, varies with the species. Most of the investigations concern the situation in the mouse. Regardless of their genetic origin, but for functional reasons, the processed glycoproteins are divided into three classes. Murine zona pellucida glycoprotein 1 (ZP1) has a molecular weight of 200 kDa and is assumed to be responsible for the structural integrity of the matrix. Zona pellucida glycoproteins 2 and 3 (ZP2, ZP3) exhibit apparent molecular weights of 99 kDa and 83 kDa, respectively; both act as sperm receptors (2). In the ZP3 receptor, an O-linked oligosaccharide of 3.9 kDa molecular weight plays a central role in recognition and binding of sperm. After induction of the cortical reaction by fertilization, both receptors are converted to their inactive forms, ZP2f and ZP3f, thereby providing a secondary block against polyspermy. In species with extracorporal fertilization, such as sea urchins, the zona pellucida is surrounded by a jelly layer. In mammals, a number of corona cells adhere to the zona pellucida at the time of fertilization.

Between the oocyte plasma membrane and zona pellucida is a region that is termed the perivitelline space. On entrance of a sperm and its fusion with the oocyte plasma membrane, calcium is released from intracellular calcium stores (see Calcium Signaling). As a consequence, the cortical granules are activated and release their proteolytic contents into the perivitelline space, which subsequently diffuse into the zona pellucida. This results in the conversion of ZP2 and ZP3 into their respective inactive forms ZP2f and ZP3f. Calcium release is necessary not only to prevent fertilization from further spermatozoa, but it is also involved in (*1*) nuclear envelope breakdown, (*2*) triggering intracellular **phosphorylation** events, and (*3*) activation of cell cycle -control proteins leading to **mitosis** after syngamy.

Figure 1. Electron microscope picture of an oocyte. The oocyte is surrounded by spermatozoa that aim to penetrate the zona pellucida. (With the friendly permission of Dr. H.-W. Michelmann.)

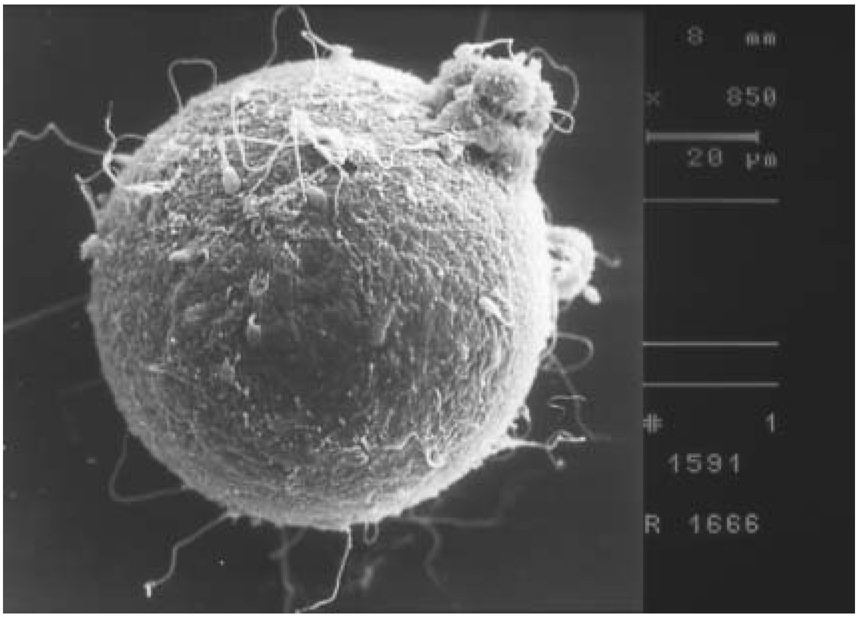

Within the oocyte plasma membrane, the egg is filled with cytoplasm that contains basic metabolites necessary for the initial divisions of the cell. Unlike the cortical granules, not all compounds of the cell cytoplasm are located uniformly. This can be seen by light microscopy and has led to a distinction of the egg's compartments. In the frog, for example, macroscopic partitioning is visible: The nucleus is located at the **animal pole**, whereas yolk is located at the vegetal pole.

Depending on the species, eggs vary considerably in their sizes and shapes. In mammals, nutrition can be provided during the very early stages of life by diffusion and then by active transport after implantation of the embryo. Therefore, there is no need for substantial nutrition in the egg and, hence, the entire egg is no larger than 0.1 mm. In species in which extracorporal development of the offspring is the rule, the situation is different. The sizes of eggs can range up to a couple of inches, due to large amounts of yolk, as is the case, for example, with birds.

Bibliography

1. J. D. Harris, D. W. Hibler, G. K. Fontenot, K. T. Hsu, E. C. Yurewicz, and A. G. Sacco (1994) DNA-Seq. **4**, 361–393.
2. P. M. Wassarman (1990) J. Reprod. Fert. Suppl., **42**, 79–87.

Eglin C

Eglin c is a widely studied, strong inhibitor of serine proteinases [see Serine Proteinase Inhibitors, Protein]. Its reactive site P_1 Leu^{45} residue endows it with specificity toward many, but not all, subtilisins, chymotrypsins, and elastases. It is an exceptionally strong inhibitor ($K_I < 10^{-13}$ M) of *Streptomyces griseus* proteinases A and B. As an efficient inhibitor of human leukocyte elastase, cathepsin G, and proteinase 3, the three human leukocyte enzymes responsible for the lung damage in emphysema and in related diseases, eglin c is of great interest to pharmaceutical companies. Eglin c consists of a single polypeptide chain of 70 amino acid residues. In spite of its lack of disulfide bridges, it is a standard-mechanism canonical inhibitor. It is a member of the potato I family, a family of inhibitors whose members either lack disulfides or contain only one. Most members of the potato I family are isolated from plants. In contrast, eglin c was isolated from the leech *Hirudo medicinalis*, where its physiological function is not known.

Suggestion for Further Reading

U. Seemüller, J. Dodt, E. Fink, and H. Fritz (1986) "Proteinase inhibitors of the leech *Hirudo medicinalis* (hirudins, bdellins, eglins)". In *Protease Inhibitors* (A. Barrett and G. Salveson, eds.), Elsevier New York, pp. 337–360.

EGTA (ethyleneglycol bis(b-aminoethyl ether)-*N,N,N′,N′*-tetraacetic acid)

EGTA is a chelating agent widely used to control the concentration of Ca^{2+} cations in biological solutions (see also -Tetraacetic Acid)). Its structure is given in Figure 1. EGTA binds Ca^{2+} 3×10^5-fold more strongly than Mg^{2+}, which makes it useful to control Ca^{2+} levels in the presence of physiological concentrations of Mg^{2+} (1-3). The binding of cations by EGTA is pH-dependent; at low pH the carboxylate moieties will be protonated, dramatically lowering the cation affinity. The high selectivity of EGTA for Ca^{2+} over Mg^{2+} is readily explained by the structure of their respective complexes (Fig. 2, see top of next page) (4, 5). While EGTA fully wraps around Ca^{2+} in a very stable octadentate complex, it cannot similarly satisfy the more stringent binding requirements of the smaller Mg^{2+}. The preference of Mg^{2+} for oxygen ligands over nitrogen ligands is so great that it binds to EGTA via the carboxylate groups only. The remaining positions in the ligand shell are filled by water. Although these complexes can be crystallized and their structure determined, they are very dynamic in solution. NMR analysis of the Ca^{2+}-EGTA complex indicates that the carboxylate moieties interchange positions rapidly on the NMR time scale, and inversion at the nitrogen atoms is observed at elevated temperatures (5), which further indicates that the complex is very dynamic. The great stability of the Ca^{2+}-EGTA complex comes from the fact that all ligands are provided by a single molecule, specifically, the stability constants have a very high entropic contribution.

Figure 1. Molecular structure of EGTA.

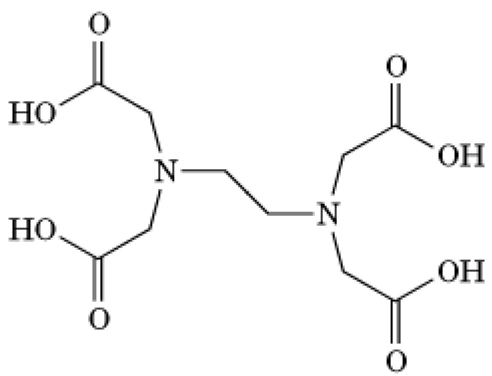

Figure 2. Three-dimensional structures of complexes of EGTA with (**a**) Ca^{2+} and (**b**) Mg^{2+}.

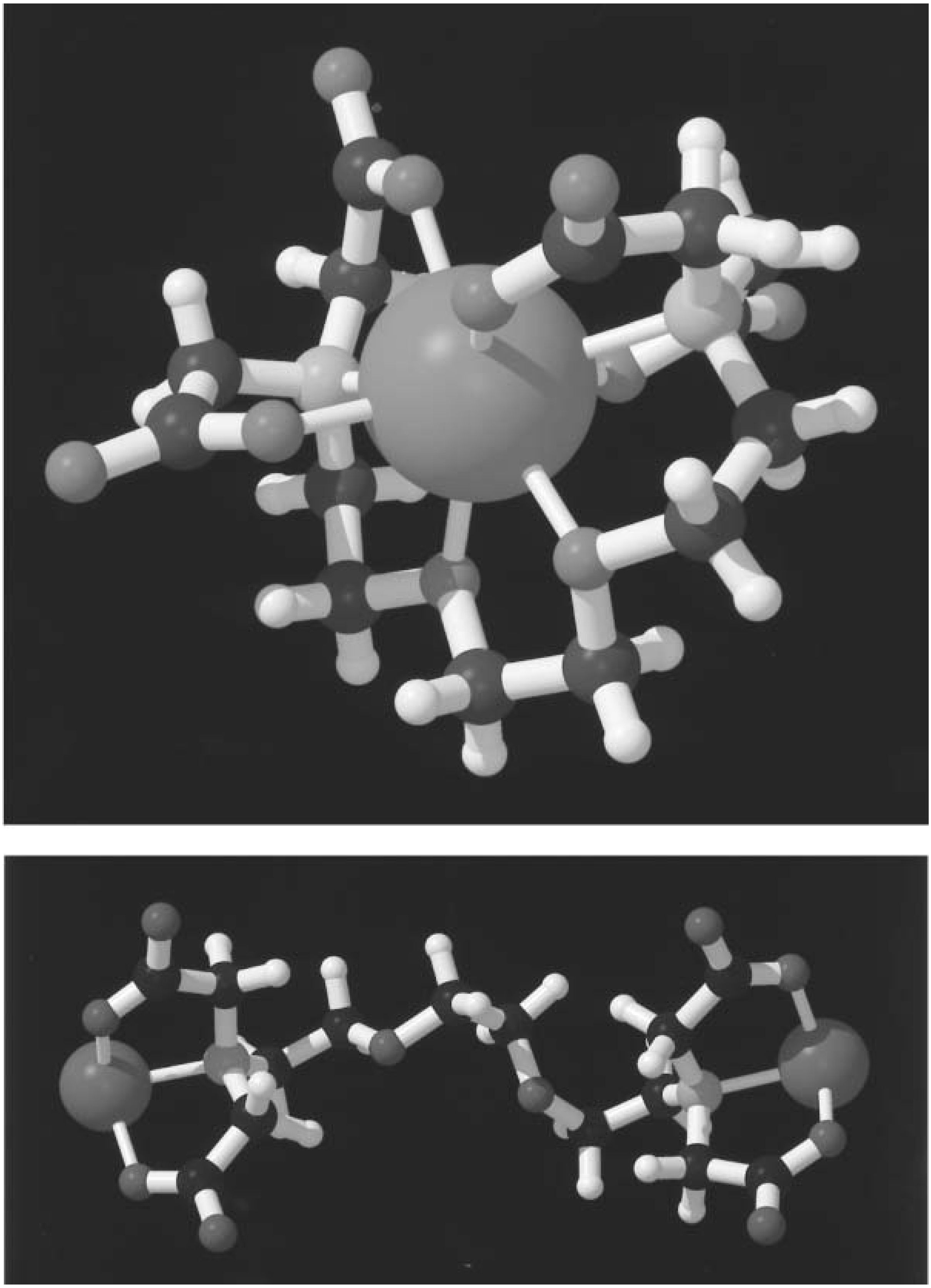

EGTA as the free acid is a white crystalline powder and has a molecular weight of 340.35 Da. The affinities of EDTA and EGTA for several cations are compared in Table 1(6).

Table 1. Comparison of Affinities of EDTA and EGTA for Various Cations[a]

Metal Ion	$\log_{10} K_{m\text{-EDTA}}$	$\log_{10} K_{m\text{-EGTA}}$
Mg^{2+}	8.64	5.3
Ca^{2+}	11.0	10.9
Zn^{2+}	16.4	12.6
Cd^{2+}	16.4	16.5

[a] The logarithms of their association constants (K_M in units of M^{-1}) are compared at pH 7.0, 25°C, and 0.1 M ionic strength (6)

Bibliography

1. A. Fabiato and F. Fabiato (1979) J. Physiol. (Paris) **75**, 463.
2. A. Fabiato (1991) In *Cellular Calcium: A Practical Approach*, J. G. McCormack and P. H. Cobbold, eds., IRL Press, Oxford, pp. 159–176.
3. M. Otto, P. M. May, K. Murray, and J. D. Thomas (1985) Anal. Chem. **57**, 1511–1517.
4. C. K. Schauer and O. P. Anderson (1987) J. Am. Chem. Soc. **109**, 3646–3656.
5. C. K. Schauer and O. P. Anderson (1988) Inorg. Chem. **27**, 3118–3130.
6. A. E. Martell and R. M. Smith (1974) *Critical Stability Constants*, Vol. **1**, Plenum Press, New York.

Ehrlich Cells

1. Origin

Ehrlich cells, more properly known as Ehrlich–Lettre ascites carcinoma, were originally established as an ascites tumor of mice (1) from Ehrlich's "Strain 7" transplantable mouse carcinoma (2), which was probably of mammary origin. Several successful attempts at tissue culture have been performed, the earliest being hanging drop preparations that were passaged for 12 years (3). Subsequently, several other laboratories have cultured Ehrlich's cells (4-9), but the cell line that has been used most frequently, and which is lodged in the American Type Culture Collection (ATCC) repository as ATCC CCL-77, is the Strain E of Ehrlich–Lettre ascites (10). These cells were established as a monolayer from a 7-day-old tumor in NCTC 109 culture medium with 10% calf serum, and subcultured by scraping. The culture lodged with ATCC has been maintained in a later modification of NCTC 109, NCTC 135 supplemented with fetal calf serum.

2. Properties

Strain E has a short population doubling time *in vitro*: 20–24 h in Strain E and 14–16 h in Strain E (4). Strain E(4) was derived from alternate *in vitro* and *in vivo* passage, adapts rapidly to culture following *in vivo* passage, and is, presumably, the strain that was submitted to ATCC. The cells tend to have a fusiform morphology *in vitro*, suggesting an undifferentiated **phenotype**, and have a hyperdiploid karyotype (modal number 44, $2C = 40$) with distinctive A chromosome, metacentric, and minute markers.

3. Usage

The Ehrlich ascites became popular because it could be expanded manyfold by *in vivo* passage, making it useful for biochemical studies involving large amounts of tissue, while it could still be maintained *in vitro* for more physiologically controlled studies. With the advent of large-scale cell culture techniques that can yield 10^9–10^{12} cells, ascites passage is less attractive, due to the contamination of the tumor with a variety of host inflammatory cells and the development of legislation limiting the use of ascites tumors.

Bibliography

1. H. Lowenthal and G. Jahn (1932) Z. Krebsforsh. **37**, 439–447.
2. P. Ehrlich and H. Apolant (1905) Berl. Klin. Wehr. **42**, 871–874.
3. A. Fisher and F. Davidsohn (1939) Nature (Lond.) **143**, 436–437.
4. G. E. Foley, B. P. Drolet, R. E. McCarthy, K. A. Goulet, J. M. Dokos, and D. A. Filler (1960) Cancer Res. **20**, 930–939.
5. M. M. Guerin and J. F. Morgan (1961) Cancer Res. **21**, 378–382.
6. J. O. Ely and J. H. Gray (1960) Cancer Res. **20**, 918–922.
7. R. Cailleau and F. Costa (1961) J. Natl. Cancer Inst. **26**, 271–282.
8. P. W. Jackson, N. Giuffre, and D. Perlman (1960) Can. J. Biochem. Physiol. **38**, 1377–1378.
9. J. A. DiPaolo (1962) Proc. Soc. Exp. Biol. Med. **109**, 616–618.
10. C. Boone, M. Sasaki, and R. W. McKee (1965) Characterization of an in vitro strain of EhrlichLettre ascites carcinoma subjected to many periodic mouse passages. J. Natl. Cancer Inst. **34**, 725–730.

Elastase

This is the designation for enzymes that degrade elastin, the elastic protein found in tissues, such as that of the lung and the aorta, that undergo repeated stretching. Elastase (E.C. 3.4.21.36) is a 25-kDa protein produced in the pancreas, in the form of an inactive precursor that is activated on secretion into the small intestine, and it helps digest dietary proteins. A different elastase found in neutrophil granulocytes (E.C. 3.4.21.37), and one of its functions may be to degrade bacterial cell walls during phagocytosis (1). The elastases are serine proteinases of the **trypsin**/chymotrypsin family, with specificity for peptide bonds involving amino acids with small side chains eg, alanine and valine).

Leukocyte elastase, a 30-kDa **glycoprotein**, degrades extracellular matrix proteins in addition to elastin, and in this regard it probably plays a role in neutrophil migration and perhaps tissue remodeling (2). It facilitates the activation of plasminogen, a protein involved in the dissolution of

blood clots (3), and it may play an important role in tumor metastasis (4). It also has an important pathological action in pulmonary emphysema (5). Under normal conditions, its activity is controlled by a1-Antitrypsin, a member of the serpin family of proteinase inhibitors. Some individuals have an inherited deficiency of this inhibitor, which leads to a proteinase/antiproteinase imbalance in lung tissue, tissue degradation, and eventually emphysema. Leukocyte elastase may also contribute to rheumatoid arthritis and inflammation.

An elastase from human alveolar macrophages has been identified as a 92-kDa enzyme that is also a *gelatinase*, that is, it degrades denatured collagen (6). This enzyme is not a serine proteinase but a zinc **metalloenzyme** and a member of the matrix metalloproteinase family. It is not yet clear whether this enzyme has a significant role in the pathogenesis of emphysema.

Bibliography

1. A. Janoff et al. (1975) In *Proteases and Biological Control* (E. Reich, D. B. Rifkin, and E. Shaw, eds.), Cold Spring Harbor Laboratory Press, Cold Spring Harbor, NY, pp. 603–620.
2. J. G. Bieth (1988) Pathol. Biol. **36**, 1108–1111.
3. R. Machovich and W. G. Owen (1990) Blood Coag. Fibrinol. **1**, 79–90.
4. M. S. O''Reilly et al. (1994) Cell **79**, 315–328.
5. W. van Steenbergen (1993) Acta Clin. Belg. **48**, 171–189.
6. S. D. Shapiro (1994) Am. J. Respir. Crit. Care Med. **150**(6 Pt 2), S160–S164.

Elastin

Elastin is the major macromolecule found in the ECM of elastic tissues such as the lung, skin, and blood vessels. The molecular properties of elastin are responsible for the elasticity. Elastin is a hydrophobic protein of about 800 amino acids that assumes a random coil configuration. Networks of elastin near the cell surface are covalently cross-linked via lysine residues, and elasticity is thought to be achieved by stretching the random coils. The protein has an abundance of proline and glycine, similar to collagen, but unlike collagen, elastin has only a small amount of hydroxyproline and lacks both hydroxylysine and carbohydrate side chains. The elastic layer is strengthened by an additional layer of microfibrils made of the protein fibrillin.

Cells may interact with elastin via an unusual 67-kDa elastin receptor. The receptor protein, unlike matrix receptors in the integrin class, is a secreted rather than transmembrane protein. It appears to mediate cell adhesion to elastin via interactions with cell surface proteins. The same receptor also binds laminin, and harbors a lectin like activity for binding sugar moieties. This protein is also found inside the cell where it may act as a chaperone to facilitate tropoelastin secretion and assembly of elastic fibers.

The functional importance of elastin is demonstrated poignantly by the recent discovery that deletions in the human elastin gene give rise to a disease known as Williams syndrome. People affected with this disease are mentally retarded (although occasionally mathematically or musically gifted), have an elfin like facial appearance and are prone to blood vessel narrowing and aneurysms.

Another disease, supravalvular aotric stenosis (SVAS), results from haploinsufficiency of elastin, and is also characterized by lumenal narrowing in blood vessels.

Additional Reading

Ramirez F., Pathophysiology of the microfibril/elastic fiber system: introduction, Matrix Biol. **19** (6), 455–456 (2000), and other reviews in the same volume.

Debelle L and Tamburro A.M., Elastin: molecular description and function, Int. J. Biochem Cell Biol. **31**(2), 261–72 (1999).

Electroelution

Molecules and particles purified by gel electrophoresis can be recovered from the gel by their electrophoresis into solution, a process termed electroelution . The procedure consists of excising the gel slices of interest, loading them onto a concentrating (stacking) gel, and electrophoresing the material contained in the slice into a recovery cup or dialysis bag attached to the bottom of the stacking gel. If the electroelution employs a single electrophoresis buffer, the sample moves directly into the recovery vessel. Electroelution of the band of interest into the stacking gel of a discontinuous buffer system of disc electrophoresis has the advantage that the material to be eluted is concentrated into a single band visualized by a tracking dye, so its collection can be visually monitored. This type of electroelution is practical with microgram amounts of sample, which can be recovered with a typical yield of 70%. Polymeric impurities in the electroeluate may be removed by gel filtration (1).

More directly, electroelution can be conducted at a right angle to the direction of migration, with instant monitoring of recovery until it is complete (2). Sequential elution of bands into a buffer chamber flushed continuously or discontinuously (designated “elution-PAGE”) is available for samples of up to milligrams, but it involves dilution of the eluate and the risk of losses in the elution chamber (3).

Bibliography

1. N. Y. Nguyen and A. Chrambach (1981) In *Gel Electrophoresis of Proteins: A Practical Approach* (B. D. Hames and D. Rickwood, eds.), IRL Press, Oxford, pp. 145–155.
2. E. Gombocz and E. Cortez (1995) Appl. Theor. Electrophoresis **4**, 197–209.
3. A. Chrambach and D. Rodbard (1981) In *Gel Electrophoresis of Proteins: A Practical Approach* (B. D. Hames and D. Rickwood, eds.), IRL Press, Oxford, pp. 93–143.

Electroendosmosis

Electroendosmosis (EEO) is the flow of solvent in the electric field during electrophoresis. EEO is caused by stationary charged groups in the gel (see Agarose) or along the inner wall of the vessel (see Capillary Zone Electrophoresis); negatively charged acidic groups in the gel or silicate groups embedded in glass surfaces bind mobile positively charged counterions electrostatically. The positively charged counterions migrate in the electric field, transporting their water of hydration and thereby giving rise to the water flow of EEO in that direction. Since the flow rate decreases with increasing distance from the glass wall, EEO is responsible for the parabolic profile of the electrophoretic band when a gel is replaced by a polymer solution (see Particle Electrophoresis). EEO can be used to enhance resolution, but more frequently it is suppressed by covering the stationary charged groupings with a neutral polymer (see Capillary Zone Electrophoresis).

EEO can be measured as the displacement in the electric field of uncharged compounds, such as cyanocobalamin in the neutral pH range or mesityl oxide. EEO decreases semilogarithmically with gel concentration, in complete analogy to electrophoretic mobility (see Ferguson Plot). Quantitative measurements of electrophoretic mobilities need to be corrected for the EEO.

Suggestions for Further Reading

H. A. Abramson, L. S. Moyer, and M. H. Gorin (1964) *Electrophoresis of Proteins and the Chemistry of Cell Surfaces*, Hafner, New York, pp. 106–108.

S. Ghosh and D. B. Moss (1974) Electroendosmosis correction for electrophoretic mobility determined in gels. Anal. Biochem. **62**, 365–370.

Electron Crystallography

Knowledge on the molecular basis of many biological processes has rapidly evolved as a result of the development of complementary techniques of molecular biology and high-resolution structural biology. Quite often the mode of action of biological macromolecules can only be understood at the atomic level. Thousands of protein structures have been solved to atomic scale resolution using X-ray crystallography, but only a handful by electron crystallography. However, electron microscopy is a technique intrinsically capable of atomic resolution. The transmission electron microscope itself can achieve resolution on the order of 0.2–0.3 nm, and the structures of small organic and inorganic molecules are routinely determined at atomic dimensions. It is now well established that the principal limitation to obtaining atomic resolution of biological specimens using electron microscopy is the specimen itself (1). Because biological molecules are sensitive to electron radiation, one must record electron micrographs of unstained specimens with very low levels of electron irradiation (this is called low-dose imaging) in order to preserve high-resolution information. Unfortunately, such low electron doses yield images with a very low signal-to-noise ratio, too low to observe any structural detail. High signal-to-noise ratio images can be obtained by averaging hundreds or thousands of low-dose images of identical structures (2). Two-dimensional crystals, thin crystals which are only one unit cell thick along one axis, currently offer the best way to average images of many molecules to build up the signal-to-noise at atomic or near-atomic resolution (3, 4). It was estimated that the average of ~5 million molecules was required to produce a 3-D density map of bacteriorhodopsin that had recognizable amino acid side chains (1, 5). Similarly, ~2.6 million molecules of light-harvesting complex II were averaged to obtain an equivalent resolution (6).

Electron crystallography encompasses the use of electron diffraction (7) and imaging of thin crystals suitable for the electron microscope. All electron images are 2-D projections of a 3-D object along the path of the electron beam. Hence, to reconstruct an object in 3-D it is necessary to collect images from different angles. The minimal number of tilted views needed to reconstruct an object at a given resolution can be calculated from geometrical considerations (8).

Once a 2-D or thin 3-D crystal is grown, the best way to evaluate its quality is to study its diffraction pattern. The quickest and easiest method is to exam electron micrographs by optical diffraction. In this technique, an electron micrograph is illuminated with laser light focused with a series of lenses to form an optical diffraction pattern showing the distribution of Fourier transform intensities in the same manner as an X-ray diffraction pattern of a 3-D crystal. The spacing and distribution of intensities in an optical diffraction pattern offers clues to the molecular packing and secondary structure (9). Optical diffraction is also an important step in judging image quality in terms of astigmatism, defocus, and drift. More information can be obtained from the computed diffraction produced by calculating the Fourier transform of the digitized image. Unlike X-ray diffraction patterns, the computed diffraction pattern will have both structure factor amplitudes and phases in the "weak phase object approximation" (thin object and sufficiently high electron energy). Hence, a reconstruction of the object can be calculated from the Fourier transform of the image using the structure factor amplitudes and phases of the crystal; this results in a reconstructed image of the average unit cell of the crystal with noise removed. Furthermore, the phase relationship of the symmetry-related spots in the computed diffraction pattern can be used to determine the crystallographic symmetry.

Diffraction patterns, similar in principle to those obtained in X-ray diffraction, are formed in the back focal plane of the objective lens in the electron microscope. By adjusting the current in the diffraction lens, the diffraction pattern can be observed on the viewing screen. The type of pattern observed depends on the arrangement of molecules in the crystal and on how well ordered they are. How the molecules are arranged within the repeating unit of a crystal (unit cell) can be determined by the symmetry of the diffraction pattern and the intensities of the diffraction spots. In addition to the molecular arrangement, diffraction patterns can reveal the degree of specimen preservation and show the distribution of ordered regions of the specimen. The further the spots extend, the higher is the resolution of the preserved detail. Diffraction patterns can be used to assess radiation damage to the specimen with increasing electron dose, as judged by fading of the higher-order diffraction spots. The size of crystals most amenable for electron diffraction of biological macromolecules is a few microns on edge and one unit cell thick, usually described as a 2-D crystal (10). However, the electron diffraction patterns of 3-D crystals can also be examined if they are less than a few hundred Angstroms thick (11); Perkins, unpublished results). Electron diffraction can also ascertain the effects of different methods of specimen preparation. If a protein has secondary structural elements aligned in parallel, as in fibers, the spacings of the diffraction spots or streaks can indicate if there is predominantly a-helix or b-sheet (12). One disadvantage of electron diffraction is that relatively large crystals (~ 100 × 100 unit cells) are needed before high-resolution spots are observed. Another disadvantage is that like X-ray diffraction, electron diffraction does not produce structure factor phases; hence the structure cannot be determined from electron diffraction alone (13).

For high-resolution structural studies, advances in imaging, computer image processing, and preservation of specimens without negative stain and fixative have been critically important. The native conformation of specimens must be preserved under high vacuum conditions, and this can be achieved using one of two types of embedment media: sugars (14-16) and vitreous ice (17), which have both been shown to preserve the protein crystal structure well enough to produce images at a resolution of 0.3 nm. In addition, the development of computer-controlled spot-scan imaging has improved the efficiency of transfer of high resolution image information (18). Improvement in the rate of data acquisition has been made using cameras employing a cooled charge-coupled device (19). Because the high-resolution signal-to-noise is low, averaging over several large (20) or many more small (4) images is necessary to restore the signal above the background. Despite several noteworthy breakthroughs, the rate of progress in determining high-resolution structures of biological macromolecules by electron microscopy has been slowed by the paucity of suitable, well-ordered crystals. Recent reviews have described crystallization methods for both water-soluble and membrane proteins (21-23). Perhaps further improvements in collecting high-resolution information from single particles will obviate the need for crystals (1).

Electron crystallography offers a viable alternative to X-ray crystallography when crystals are not large enough for X-ray diffraction or for membrane proteins (24). Integral membrane proteins have the advantage that they can be routinely reconstituted in their native environment, the lipid bilayer, and often can be forced into ordered arrays through the judicious choice of lipid/protein and detergent/protein concentrations. The first membrane protein structure revealed by electron crystallography was bacteriorhodopsin in which seven a-helices were resolved (25). Since this early work, the field of electron crystallography has advanced to the point that atomic models have been built for two membrane proteins (5, 6, 26) and good progress made toward this goal for several others (27-29). Tubulin crystals also diffract to high resolution, and electron crystallography has shown the location of the taxol-binding site (30, 31). The highest resolution structures have been generated by taking the phases from the images and the amplitudes from the electron diffraction patterns. The electron diffraction amplitudes are generally more accurate than the image amplitudes because the image amplitudes require correction for instrumental factors that affect image quality, and methods for this correction have not been fully developed (20). However, it is not always necessary for electron microscopy to be performed at high resolution to contribute to atomic resolution structures. Electron microscopy provided a critical link allowing the actin crystal structure determined by X-ray diffraction to be fit into the actin filament determined by electron microscopy (32, 33).

The structure of biological macromolecules with helical or icosahedral symmetries can be determined using the same underlying principles of electron crystallography, although the operational approaches will be different (34). Helical structures produce diffraction patterns in which the helical information is confined to regularly spaced layerlines perpendicular to the helix axis instead of discrete spots. The pattern of intensities along the layerlines usually produce X-shaped patterns. Helical symmetry provides different views of a molecule in a single image as identical molecules are arranged along a helical path, so in principle only one image is needed for a low-resolution 3-D reconstruction. As with electron crystallography, however, higher resolution requires many images in order to obtain views at many different angles and to average many images in order to improve the signal-to-noise ratio (35). The structures of helical assemblies have been solved to 0.9 nm resolution (35, 36), and higher resolution is shortly anticipated. Close to 0.7 nm resolution has been reported for a viral structure with icosahedral symmetry (37). Even with the benefits of high symmetry elements afforded by an icosahedron, more than 6000 images needed to be averaged to achieve this resolution.

Bibliography

1. R. Henderson (1995) Quarterly Rev. Biophys. **28**, 171–193.
2. R. M. Glaeser and K. H. Downing (1993) Ultramicroscopy **52**, 478–486.
3. D. Brillinger et al. (1989) J. Applied Stat. **16**, 165–175.
4. G. A. Perkins, K. H. Downing, and R. M. Glaeser (1995) Ultramicroscopy **60**, 283–294.
5. R. Henderson et al. (1990) J. Mol. Biol. **213**, 899–929.
6. W. Kuhlbrandt, D. N. Wang, and Y. Fujiyoshi (1994) Nature **367**, 614–621.
7. D. L. Misell and E. B. Brown (1987) *Electron Diffraction: An Introduction for Biologists*, Elsevier, Amsterdam, The Netherlands.
8. A. Klug (1979) Chem. Scr. **14**, 245–256.
9. F. Thon (1971) In *Electron Microscopy in Material Science* (U. Valdre, ed.), Academic Press, New York, pp. 571–625.
10. T. A. Ceska and R. Henderson (1990) J. Mol. Biol. **213**, 539–560.
11. T. W. Jeng et al. (1984) J. Mol. Biol. **175**, 93–97.
12. R. D. B. Fraser and T. P. MacRae (1973) *Conformation in Fibrous Proteins*, Academic Press, New York.
13. J. M. Baldwin and R. Henderson (1984) Ultramicroscopy **14**, 319–335.
14. P. N. T. Unwin and R. Henderson (1975) J. Mol. Biol. **94**, 425–440.
15. W. Kuhlbrandt (1988) J. Mol. Biol. **202**, 849–864.
16. G. Perkins et al. (1993) J. Microscopy **169**, 61–65.
17. J. Dubochet et al. (1988) Quarterly Rev. Biophys. **21**, 129–228.

18. K. H. Downing (1991) Science **251**, 53–59.
19. A. J. Koster et al. (1992) Ultramicroscopy **46**, 207–228.
20. J. M. Baldwin et al. (1988) J. Mol. Biol. **202**, 585–591.
21. R. Kornberg and S. A. Darst (1991) Curr. Opin. Struct. Biol. **1**, 642–646.
22. B. K. Jap et al. (1992) Ultramicroscopy **46**, 45–84.
23. W. Kuhlbrandt (1992) Quarterly Rev. Biophys. **25**, 1–49.
24. A. Engel et al. (1992) J. Struct. Biol. **109**, 219–234.
25. R. Henderson and P. N. T. Unwin (1975) Nature **257**, 28–32.
26. N. Grigorieff et al. (1996) J. Mol. Biol. **259**, 393–421.
27. A. Olofsson, V. Mallouh, and A. Brisson (1994) J. Struct. Biol. **113**, 199–205.
28. H. Hebert, I. Schmidt-Krey, and R. Morgenstern (1995) EMBO J. **14**, 3864–3869.
29. T. Walz et al. (1995) Nature Struct. Biol. **2**, 730–732.
30. E. Nogales et al. (1995) Nature **375**, 424–427.
31. S. G. Wolf et al. (1996) J. Mol. Biol. **262**, 485–501.
32. W. Kabsch et al. (1990) Nature **347**, 37–44.
33. K. C. Holmes et al. (1992) In *Mechanism of Myofilament Sliding in Muscle Contraction* (H. Sugi and G. H. Pollack, eds.), Plenum Press, New York.
34. D. G. Morgan and D. De Rosier (1992) Ultramicroscopy **46**, 263–286.
35. T. W. Jeng et al. (1989) J. Mol. Biol. **205**, 251–257.
36. D. G. Morgan et al. (1995) J. Mol. Biol. **249**, 88–110.
37. B. Bottcher, S. A. Wynne, and R. A. Crowther (1997) Nature **386**, 88–91.

Electron Imaging

Particle/wave dualism is evident in experiments with electrons. They form a beam of particles, for instance, in a synchrotron, but behave as waves in an **electron microscope**. Electrons are scattered by matter just as X-rays are (see X-Ray Crystallography). Electrons are scattered by the atomic coulombic potential distribution in the atoms. This scattering is much stronger than for X-rays and can be recorded from very tiny specimens. This is particularly valuable for obtaining information on individual regions extending over only a few unit cells of a two-dimensional crystal (see Crystallography). The imaging experiments are performed in an electron microscope at a wavelength between 0.02 and 0.04 Å, much shorter than for X-rays. Then, the Ewald sphere (see Reciprocal Space) can be regarded as a flat surface, and diffraction from a stationary crystal shows essentially the reflections in a planar section of reciprocal space. By tilting the specimen, several intersections can be obtained and combined in a more complete image of reciprocal space. The short wavelength would result in a very high image resolution if the quality of the microscope lenses were not a limiting factor. At best they allow reaching a resolution of 1.5 Å. Simple switching of lens currents changes the observation from a diffraction pattern to a real image.

Transfer of energy to the specimen and the resulting radiation damage is a limitation in applying electron scattering. This is especially serious in studying biological material. However, with very thin specimens of two-dimensional crystals and with the molecules embedded in vitreous ice or glucose, extremely interesting results have been obtained from biological specimens by short exposure times, low beam intensity, cryocooling, and a combination of diffraction data and image analysis. The phases of the structure factors of the diffracted beams are calculated from the image (see Phase Problem). They are combined with the measured amplitudes of the diffracted beams and, exactly as in X-ray diffraction, a Fourier summation gives the atomic distribution in the specimen. At the present time, the maximum resolution is 3 Å.

Suggestions for Further Reading

R. Henderson (1995) The potential and limitations of neutrons, electrons and X-rays for atomic resolution microscopy of unstained biological molecules, Q. Rev. Biophys **28**, 171–193.

International Union of Crystallography (1996) *International Tables for Crystallography*, Vol. B (U. Smueli, ed.) Kluwer Academic, Dordrecht, Boston, London, pp. 280–329.

N. Grigorieff et al. (1996) Electron-crystallographic refinement of the structure of bacteriorhodopsin, J. Mol. Biol. **259**, 393–421.

Electron Paramagnetic Resonance

1. Introduction to Electron Paramagnetic Resonance (EPR) Spectroscopy

Electron paramagnetic resonance (EPR) refers to spectroscopy of unpaired electrons, and some aspects of the technique are termed "electron spin resonance" (ESR) or "electron magnetic resonance" (EMR). Unpaired electrons in biological systems are in much lower abundance than nuclei; thus, EPR is a technique that focuses on local sites, whereas nuclear magnetic resonance **(NMR)** tends to be more global. A connection exists between EPR and NMR in the variations of EPR that are termed "electron spin echo envelope modulation" (ESEEM) and "electron nuclear double resonance" (ENDOR). In these techniques, the energies of the transitions involving electrons are modulated by nearby nuclei, and this effect provides information about the type and geometry of nuclei around the site of an unpaired electron. The term "spin" in the designations of various forms of magnetic resonance spectroscopy refers to a property of electrons (or nuclei), and it is the interaction of the spin with the magnetic field that leads to separation of energy levels between which the spectroscopic transition occurs. A magnetic field is usually required for EPR, as is a source of energy to effect transitions. In addition, a few cases exist where spin transitions can be detected in the absence of a magnetic field.

Electron transfer systems (for instance, those in **photosynthetic** membranes) provide excellent opportunities to follow the intimate details of the transfer process with EPR spectroscopy. Other naturally occurring sources of unpaired electrons that are subjects for this form of spectroscopy include complexes of a variety of molecules with nitric oxide, quinone and flavin **cofactors** in enzymes, free radical enzyme intermediates, and metal ion sites in proteins (see Metalloproteins). By definition, a free radical has a homolytically broken bond with an unpaired electron. The range of applications of EPR spectroscopy is not limited to these natural sources of unpaired electrons. The EPR probe technique of spin labeling is being applied to examine dynamics of **DNA** and proteins, to study **protein folding**, and to unravel the complex motions of membrane components.

Molecular biological approaches extend the applications of spin labeling, and these applications are generically referred to as site directed spin labeling. In addition, unpaired electrons in free radical intermediates that have a short lifetime can be studied by trapping them to give a longer-lived, secondary radical in an EPR-related technique called "spin trapping." The text below will give examples of the type of information that can be obtained by applying EPR spectroscopy to these instances of unpaired electrons in biology.

2. EPR in Photosynthesis

One of the long-standing puzzles of electron transfer in photosynthetic membranes is that the photoreaction center has pairs of molecular components arranged apparently symmetrically about a plane perpendicular to the membrane surface, yet electron transfer among the components follows a path involving primarily one-half of the dimer (see Photosynthesis and Photosynthetic Reaction Center) (1). EPR studies, especially of oriented crystals of reaction centers (2), provide precise information about small differences in symmetry of the two halves of the system. From EPR studies, it is possible to determine the orientation of orbitals involved in electron transfer between cofactors, and the positions of light atoms, such as hydrogen, on the cofactors can be determined by ENDOR with great precision (1). The various components of the electron transfer pathway—chlorophylls and quinones—can be selected for EPR by optical experiments, selective depletion of some components, and molecular biology. High-frequency EPR (1) helps to separate the spectra of different sites of unpaired electrons, much as higher frequency NMR gives better resolution of different nuclei. The manner in which electrons flow ultimately into the photosynthetic oxygen-evolving complex, which contains varied numbers of unpaired electrons associated with a cluster of four manganese atoms, is another challenge. ESEEM and ENDOR studies, together with isotope labeling (3) provide details of the structure of this site.

3. EPR of Nitric Oxide Complexes

Molecular adducts of nitric oxide give a diverse set of EPR signals that can be employed to determine the pathway of nitric oxide in tissues. Ferrous iron may or may not have unpaired spins, depending on whether it is low or high spin, but, in either case, it is, respectively, an impossible or difficult subject for EPR spectroscopy. Fortunately, the adduct of nitric oxide with ferrous iron in heme is quite suitable for EPR spectroscopy and provides a characteristic signature, shown in Figure 1. This spectrum is distinct from those of the nitric oxide adduct of either **amino**- or **thiol**- groups of protein side chains, as well as from copper adducts and adducts with other forms of iron. For further delineation of the location of nitric oxide in tissues, “spin traps” for nitric oxide are available (see section below on spin trapping). Typical spin traps for nitric oxide are ferrous ion chelated with *N*-methyl-D-glucamine dithiocarbamate or with diethylthiocarbamate.

Figure 1. The EPR spectrum of deoxymyoglobin to which nitric oxide (NO) gas was added. The spectrum was recorded at 77K and a frequency of 9.1 GHz. (Reproduced with permission from Ref. 4, Fig. 8.)

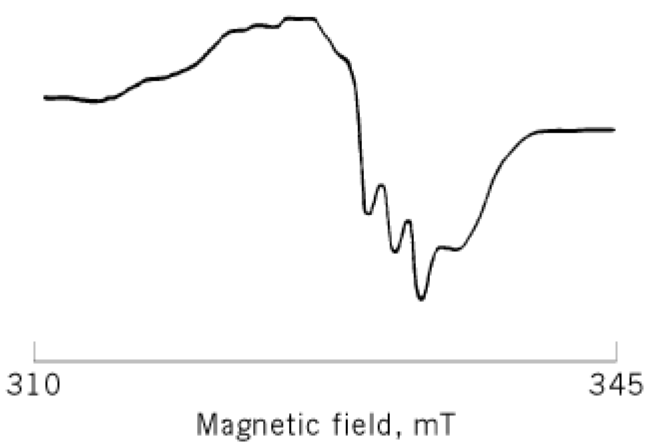

4. EPR of Free-Radical Protein Intermediates

Ribonucleotide reductases use metals and free radical chemistry to carry out reduction of ribonucleotides to deoxyribonucleotides. (56) In different sources of the enzyme, the presence of free-radical intermediates has been demonstrated to involve side chains of the amino acids tyrosine, tryptophan, cysteine and glycine. EPR spectroscopy of tyrosine radicals has been used in this system, as well as in photosynthetic membranes, to demonstrate that the unpaired electron density at the various carbon atoms of the tyrosine aromatic ring is fine tuned by hydrogen bonds to the phenolic oxygen and by the protein environment. Figure 2 gives examples of EPR of tyrosine radicals from ribonuclotide reductases of several sources. The process by which involvement of metal ions and radical side chains lead to a free radical intermediate of the ribonucleotide is thought to involve long-range electron transfer. Organic cofactors, such as flavins, also form intermediates that can be detected in EPR studies of enzyme reactions.

Figure 2. EPR spectra of tyrosine freeradicals of ribonucleotide reductase R2 subunits from different organisms. The EPR spectra were recorded at temperatures of 20 to 30K at ~9 GHz. The numbers given on the structure are the spin density distributions for the *E. coli* and *S. typhimurium* enzymes. (Reproduced with permission from Ref. 6, Fig. 3).

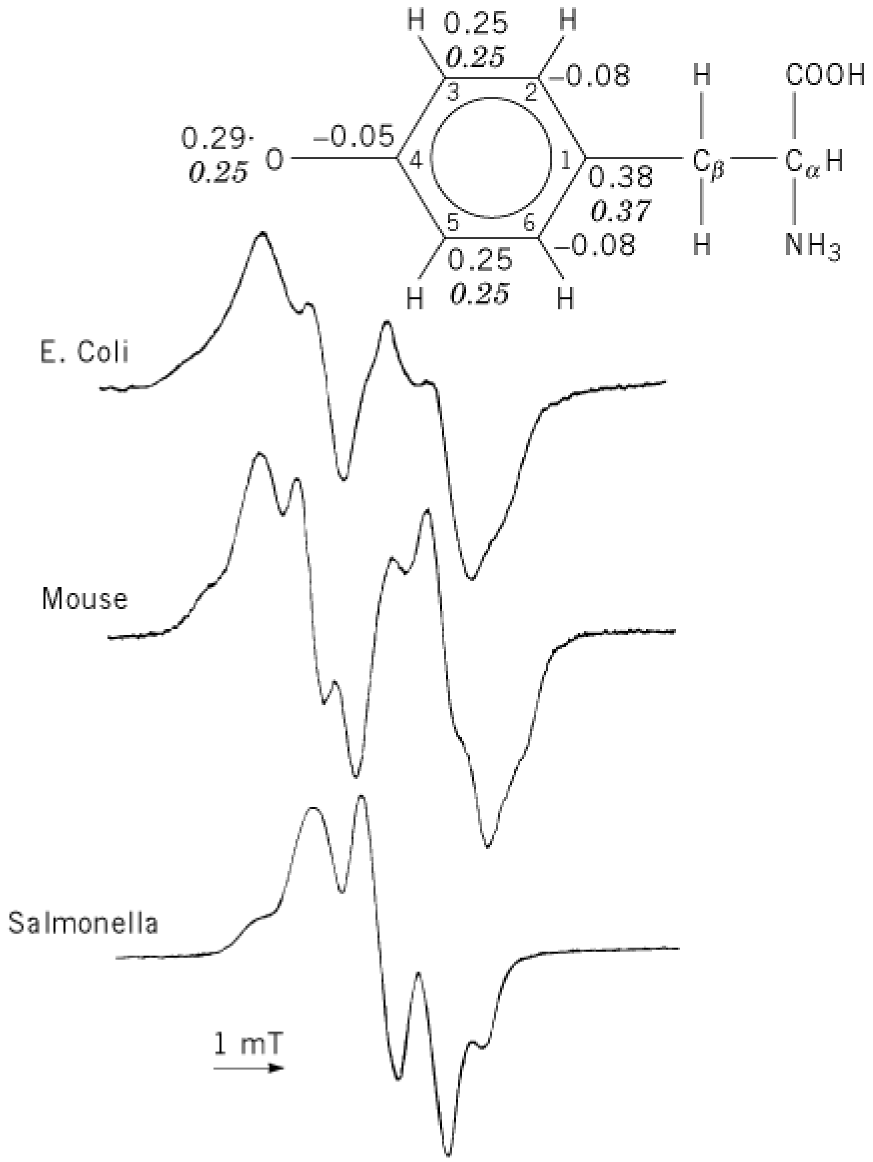

5. EPR of Metal Ions in Biology

All metals ions containing one or more unpaired electrons (paramagnetic ions) are in principle subjects for study by EPR, but the conditions for the experiments are quite varied (7). The paramagnetic ions in proteins that are commonly studied include manganese $^{2+}$, copper $^{2+}$, iron $^{3+}$, occasionally iron $^{2+}$, nickel^{3+}, and cobalt^{2+}. The conditions for the spectroscopy differ drastically, depending on which metal is the subject of study. Sometimes, mangenese ions can be detected with high sensitivity in solution at room temperature, but detection of ^{17}O ligands to the Mn^{2+} (for example from a threonine side chain in p21 ***ras***) required both low temperature and high frequency EPR (8). ENDOR and ESEEM (1) are alternative methods for detecting nuclei, such as nitrogen or hydrogen bound to, or near, metal-ion sites. Copper sites also can be detected at room temperature, but sensitivity is improved by conducting the EPR experiments at or lower than liquid nitrogen temperature. Studies of iron are almost always done at a temperature near that of liquid helium. The two primary reasons that low temperature is used in metal ion EPR are that relaxation times are too fast for temperature studies, and the signal intensity increases inversely with temperature.

Quantitative evaluation of the number of unpaired spins in different sites within a complex biochemical electron transfer system can be made by EPR and associated studies. For experiments of this type, calculations of the theoretical spectra are often needed for interpretation. Recent advances in EPR spectroscopy, particularly high-frequency EPR, provide improved resolution in samples with multiple EPR-detectable sites. Figure 3 shows a high frequency EPR spectrum of copper ion in lactoferrin, in which the copper spectrum is well separated from the signal of a manganese impurity (8, 9). At lower EPR frequencies, the manganese signal is superimposed on the central portion of the copper signal.

Figure 3. High-frequency EPR spectrum of di-cupric lactoferrin. The spectrum was recorded at 40 K and 94.1 GHz. The two regions from which significant information can be obtained are amplified in insets on the left. A feature indicated on the right is the EPR signal from an impurity of manganese ion in the sample. (Reproduced with permission from Ref. 9).

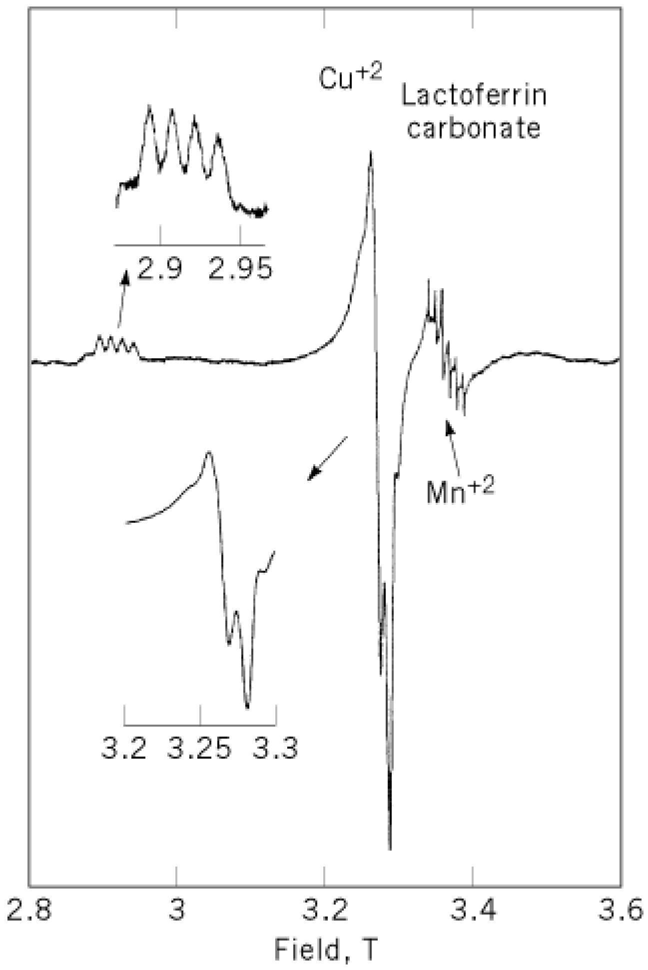

6. Spin Trapping and EPR Imaging

The EPR spectrum shown in Figure 1 was actually from a spin trapping experiment (4). In that case, the effluent from stimulated endothelial cells was passed into a solution of deoxy myoglobin, and the nitric oxide was trapped as the myoglobin heme adduct. Spin traps can also exhibit therapeutic effects in inhibition of lipoprotein oxidation (10). In a sense, EPR imaging of oxygen concentration in tissues of animals is also a spin trap experiment, but, in this case, only the magnetism of oxygen is "trapped" through its magnetic, but not chemical, interactions with a **spin label**. The degree of broadening of the EPR signal is transformed into an image (11).

Bibliography

1. H. Levanon and K. Möbius (1997) Ann. Rev. Biophys. Biomol. Struct. **26**, 495–540.
2. W. Hofbauer, A. Zouni, R. Bittl, J. Kern, P. Orth, F. Lendzian, P. Fromme, H. T. Witt, and W. Lubitz (2001) Proc. Natl. Acad. Sci. U.S.A. **98**, 6623–2228.
3. R. D. Britt, J. M. Peloquin, and K. A. Campbell (2000) Ann. Rev. Biophys. Biomol. Struct. 29, 463–495.
4. D. J. Singel and J. R. Lancaster, Jr. (1996) *Methods in Nitric Oxide Research*, M. Feelisch and J. S. Stamler, eds. John Wiley & Sons, pp. 341–356.
5. J. A. Stubbe (2001) Trends Biochem. Sci. 26, 93–99.
6. A. Gräslund and M. Sahlin (1996) Ann. Rev. Biophys. Biomol. Struct. 27, 259–286.
7. L. J. Berliner and J. Reuben, eds. (1993) In *Biological Magnetic Resonance*, Vol. **13**, EPR of paramagnetic molecules. Plenum, New York.

8. B. F. Bellew, C. J. Halkides, G. G. Gerfen, R. G. Griffin, and D. J. Singel (1996) Biochem **35**, 12186–12193.
9. B. J. Gaffney, B. C. Maguire, R. T. Weber, and G. G. Maresch (1999) Appl. Magn. Res., **16**, 207–222.
10. C. E. Thomas, D. F. Ohlweiler, and B. Kalyanaraman (1994) J. Biol. Chem. **269**, 28055–28061.
11. A. T. Yordanov, K. Yamada, M. C. Krishna, J. B. Mitchell, E. Woller, M. Cloninger, and M. W. Brechbiel (2001) Angew. Chem. Int. Ed. **40**, 2690–2691.

Suggestions for Further Reading

12. J. A. Weil, J. R. Bolton, and J. E. Wertz (1994) *Electron Paramagnetic Resonance, Elementary Theory and Practical Applications*, Wiley-Interscience, New York.
13. L. J. Berliner and J. Reuben, eds. (1998) "Biological Magnetic Resonance", Vol. **14**, *Spin labeling: The next millenium*, Plenum, New York.
14. G. R. Eaton, S. S. Eaton, and K. Ohno, eds. (1991) *EPR Imaging and In Vivo EPR*, CRC Press, Boca Raton.

Electron Microscopy

High-resolution electron microscopy presents to the molecular biologist advantages and disadvantages compared to both X-ray crystallography and NMR. The advantages are that (i) the macromolecule of interest need not necessarily be highly purified, provided that it can be unambiguously recognized, (ii) only small quantities (mg rather than mg amounts) are required, (iii) even very large macromolecules or complexes with no symmetry can be imaged easily, (iv) specimens can be imaged in their natural environment, and (v) unlike X-ray diffraction patterns, images contain both structure factor amplitudes and phases. The major disadvantages are that (i) the contrast of biological preparations in the electron microscope is inherently low, (ii) the specimen must be imaged in a high vacuum, and (iii) biological material is easily damaged by electron radiation. Electron microscopy has developed to the state where it can complement X-ray crystallography and NMR; this is especially true in the case of cryoelectron microscopy of frozen specimens with the application of computer image processing techniques. An example of how all three techniques may complement each other was the structural characterization of dihydrolipoyl transacetylase (1-3). X-ray crystallography provided the rigid core structure. NMR provided information about the flexible domains of this molecule, and electron microscopy integrated both packets of information into a detailed model.

The transmission electron microscope (TEM) is the electron counterpart to the transmission light microscope. A high-velocity, homogeneous electron beam passes through a specimen and is imaged on a phosphorescent screen or a charge-coupled device (CCD). The mechanism of image formation, however, for the TEM is by scattering, which is quite different from that of the light microscope, which is by absorption. TEMs are divided into different classes, depending on the accelerating voltages. A conventional TEM (CTEM) accelerates electrons with typical voltages between 60 and 120 kV; an intermediate-high voltage TEM (IVEM) operates between 200 and 400 kV; and a high-voltage TEM (HVEM) operates above 500 kV. The principal advantages of higher voltage TEMs are (i) the capability of imaging thicker specimens, and (ii) increased resolution of biological crystals and ice-embedded particles.

1. Thin-Section CTEM

The vast majority of biological specimens are much too thick as they occur in nature to be penetrated by the electron beam. A CTEM allows for quality imaging of specimens generally no thicker than 200 nm. Hence, the requirement for thin sections of biological material that are able to withstand both the high vacuum in the electron microscope and electron irradiation is apparent. Electron microscopy of thin sections of cells and tissues provides in situ visualization of cellular morphology and the spatial relationships of subcellular components. In order to preserve detailed structural information, the tissue must be well-fixed, dehydrated and embedded in plastic. The resolution achieved with tissue prepared this way is usually limited to 2–3 nm. Sections from the embedded tissue should be of a known and uniform thickness and free from breaks, folds, wrinkles, and chatter to produce standardized and reproducible observations (4). Because it is difficult to differentiate among the electron opacity of various cellular components, selective staining is necessary. Commonly used stains are heavy metals such as uranyl acetate and lead salts.

2. Freeze Fracturing and Etching

Thin-section techniques can be complemented by examining specimen surfaces by freeze fracturing/etching. The freeze fracture method involves the following steps: (i) cryofixation of the specimen by rapid freezing, (ii) fracturing of the specimen by cleaving it with a knife edge or breaking it, (iii) replication of the freeze-fracture plane by coating with heavy metals under high vacuum, (iv) removal of the specimen from the replica, and (v) observation of the replicas with a CTEM. The most important contribution of this technique has been the elucidation of the molecular architecture of biological membranes. During freeze fracturing, membranes are split through the hydrophobic moiety, thus exposing intramembraneous surfaces. The fracture plane often follows the contours of membranes and leaves either protrusions or depressions where it passes around organelles or vesicles (4). Smooth areas represent the lipid monolayer face, whereas particles represent integral membrane proteins.

Freeze etching is a slight modification of freeze fracturing through the process of controlled sublimation of water vapor (transition from the solid state to the gas state, bypassing the fluid state) to expose membrane surfaces or macromolecules just below the fracture plane. By etching, extracellular and intracellular structures, such as the cytoskeleton, can be visualized which would otherwise be masked. The etching can either be "normal" (< ~ 100 nm) or "deep" (up to ~ 3 µm).

Related techniques involve shadowing of macromolecules adsorbed or deposited onto a flat surface and dried by methods which minimized deformation during drying. Drying is best accomplished by sublimation as in freeze-etching and requires access to a freeze-fracture instrument; this is referred to as freeze drying and shadowing (5). A simpler method developed by Branton requires only a conventional vacuum evaporator (6). This technique involves (i) preparing the macromolecule in a high-concentration glycerol solution, (ii) spraying this solution onto mica, (iii) evaporating the solvent under vacuum, (iv) rotary shadowing with a metal such as platinum, (v) carbon coating the shadowed specimen, (vi) floating the carbon replica onto water, and (vii) picking up the replica on an electron microscope grid. Rotary shadowing is particularly useful for visualizing fibers or rod-shaped complexes such as actin/myosin. The double strands of spectrin (which forms rods ~200 nm long) were resolved using this technique with tantalum/tungsten shadowing, which produced small metal grains that increase the resolution (7).

Bibliography

1. D. DeRosier (1992) Nature **357**, 196–199.
2. A. Mattevi et al. (1992) Science **255**, 1544–1547.
3. M. A. Robin et al. (1992) Biochemistry **31**, 3463–3471.
4. M. A. Hayat (1989) *Principles and Techniques of Electron Microscopy*, CRC Press, Boca Raton, FL.

5. J. Kistler, U. Aebi, and M. Kellenberger (1977) J. Ultrastruct. Res. **59**, 76–86.
6. J. M. Tyler and D. Branton (1980) J. Ultrastruct. Res. **71**, 95–102.
7. J. R. Glenney (1987) In *Electron Microscopy in Molecular Biology* (J. Sommerville and U. Scheer, eds.), IRL Press, Oxford, pp. 167–178.

Electron Tomography

Electron tomography is defined as the generation of a 3-D reconstruction from an electron microscope tilt series (1). This powerful technique is closely related to computerized axial tomography used by CAT scanners in radiological imaging in the computational methods used to calculate a 3-D structure from many two-dimensional images or projections recorded over a wide range of tilt angles. The use of tomography has proved valuable not only for the determination of macromolecular complexes (2-4), but also for the visualization and analysis of relatively large, complex biological structures. Because of variable size, large-scale biological structures such as organelles elude crystallographic or single-particle approaches that require multiple images of identical structures. Electron tomography is especially powerful for these complex structures, but until recently, it has not enjoyed widespread application because of obstacles that are now being removed (5). Electron tomography presently is the imaging technique that provides the highest 3-D resolution (capable of 5–10 nm) of the internal features of organelle-size structures. This is accomplished by recording a series of images of a single specimen over a wide range of tilt angles with a small interval of tilt angle. Typically such a tilt series would consist of 61 images recorded at tilt angles from –60° to +60° in 2° increments. The individual images must be digitized (unless recorded directly in digital form using a CCD camera attached to the microscope), aligned to a common origin, and processed using computer algorithms, similar to those used in computerized tomography in medical imaging, to reconstruct a 3-D volume from a series of 2-D projections. Since whole cells and organelles, such as mitochondria, are relatively large, the images must be recorded from specimens embedded in semithick sections, 0.25–1 µm thick. Such thick specimens require the use of higher voltage electron microscopes, intermediate voltage electron microscopes (IVEM's) with accelerating voltages up to 400,000 volts, or high-voltage electron microscopes with accelerating voltages up to 1,200,000 volts. By comparison, typical transmission electron microscopes have accelerating voltages of approximately 100,000 volts. The higher voltage electron microscopes are relatively expensive, and most users wishing to do electron tomography of thick specimens must use instruments made available in national facilities.

Until recently, the bulk of our knowledge of the architecture of organelles and bacteria has come from untilted images of sections. The 3-D architecture is usually inferred from these images, sometimes with the aid of stereo imaging or serial-section reconstruction. Although thin-section electron microscopy provides relatively high-resolution images, an incorrect impression of the 3-D structure may be obtained because one is looking at only a very thin slice through a complex 3-D object. On the other hand, electron tomography offers an opportunity to map topology more accurately by providing improved resolution along the *z*-axis, while circumventing major deficiencies in stereo imaging and serial-section reconstructions. This technique provided the resolution necessary to observe characteristics of mitochondrial structure that differ from long-held conceptions (6,7). These newly appreciated characteristics include: (i) All observed cristae connect to the inner boundary membrane via narrow, tubular openings, termed crista junctions. (ii) Tubular cristae merge, sometimes from opposite ends of the mitochondrial periphery, to form lamellar compartments. (iii) Contact sites are not clustered about crista junctions. The full power of electron tomography is now being explored to generate 3-D distributions of specifically labeled or immunolocalized components.

Bibliography
1. J. Frank (1992) *Electron Tomography*, Plenum Press, New York.
2. R. A. Horowitz et al. (1994) J. Cell Biol. **125**, 1–10.
3. H. Mehlin, B. Daneholt, and U. Skoglund (1992) Cell **69**, 605–613.
4. M. Moritz et al. (1995) Nature **378**, 638–640.
5. J. Frank (1995) Curr. Op. Struct. Biol. **7**, 266–272.

Electron Transfer Proteins

Biological electron transfer (ET) encompasses reactions that are essential for life, such as those involved in **light harvesting, nitrogen fixation**, and **production of the high-energy metabolites**. In proteins, ET occurs between redox centers that are separated by distances much longer than a chemical bond and that in many cases are carried by different molecules. Moreover, the temperature-dependence of ET rates is often atypical (ie, non-Arrhenius type).

A general theory (1) can describe ET and thus provide a framework to guide experimentalists in their investigations on the structural control of biological ET. From these studies, it emerged, as is frequent in biology, that different solutions have evolved in different systems to solve the same general problem.

Several families of proteins involved in biological ET, with variable structures and catalytic complexity, are known in detail (see **Redox proteins**). Although a compilation is beyond the scope of this article, a brief synopsis is provided. Many of these are one-electron carrier proteins that are usually small (about 100 amino acid residues), and display no associated enzymatic function. In these proteins, the electron resides on a special cofactor, such as a heme or a metal atom, which often can donate the electron to different partners. Examples of this group are the cytochromes, cupredoxins, and ferredoxins. Other more complex proteins consist of one or more **domains** and may perform chemical reactions, such as oxidation or reduction of organic molecules. Some of them can convert the flow of charge from single electron to pairs (or more) using (i) cofactors like flavins and quinones, forming stable radical intermediates, or (ii) radicals of amino acid side chains, such as those of tyrosine or tryptophan, together with metal centers. Among others, it is worth mentioning the various respiratory complexes located in organelle and plasma membranes, the large class of detoxifying enzymes (eg, cytochrome P-450s), and photosynthetic reaction centers .

1. General Theory and Intramolecular ET

The probability of electron transfer depends on the overlap between the electron-containing orbital (wavefunction) of the donor with that of the acceptor. This overlap can be very small, because redox centers in proteins are buried and often located 10–15 Å apart; nevertheless, biological ET is usually extremely fast and specific.

In intramolecular ET, the electron must move through the protein matrix, which has been assigned a low dielectric constant (D = 2 to 4). In a classical picture, this energy barrier would be too high to be crossed by the electron; in a quantum-mechanical view, however, the electron can tunnel through the barrier with a finite probability. To relate tunneling theory and experiments, a simple description of the ET rate is given by Fermi's Golden Rule, which applies to nonadiabatic ET occurring between weakly coupled redox centers:

$$k_{et} = (\text{electronic factor})^*(\text{nuclear factor}) = (2\pi/\hbar)H^2_{AB}(\text{FC}) \qquad (1)$$

The electronic factor (H^2_{AB}), which describes the electronic coupling between donor and acceptor, can only be understood in quantum-mechanical terms and will be discussed below; $\hbar$ is the Planck constant/2p. The nuclear factor, or Franck–Condon term (FC), states that during ET the nuclei do not have time to respond, because of their large mass relative to that of the electron.

Marcus and Sutin (1) have provided a simple description of the energy terms that comprise the FC factor using potential energy curves (Fig. 1). The energy terms that determine the rate of ET are the **free energy** change (D*G*°), or driving force, and the reorganizational energy (l) (which is required to distort the equilibrium geometry of the reactant to that of the product, but without actually transferring the electron). ET will occur when the potential energies of reactants and products are equal.

Figure 1. (**a**) Potential energies of the ET donor (D) and acceptor (A), as a function of the reaction coordinate. The energies with their surrounding medium are approximated as harmonic oscillator potentials. The Franck–Condon factor can be described classically, provided that the nuclear vibration energy (w/2p) is not too high relative to the thermal energy (k_BT). (**b**) Dependence of the logarithm of the ET rate constant on –D*G*°. The ET rate is maximal at the point where –DG° = l (activationless regime).

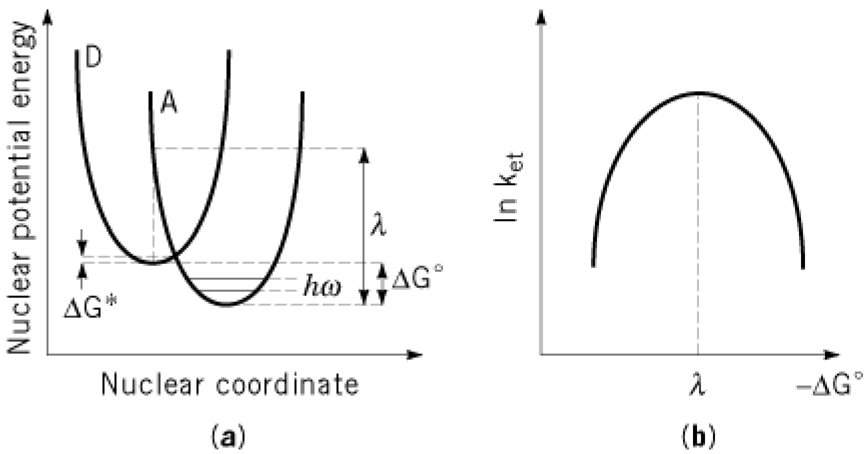

In general, the activation barrier (D*G**) is given by the expression:

$$\Delta G^* = (\Delta G^\circ + \lambda)^2/4\lambda \qquad (2)$$

Depending on the sign of (DG° + l), one can distinguish normal, activationless, and inverted regions, respectively with (DG° + l) > 0, = 0, and < 0. The ET rate goes through a maximum for DG° = –l (activationless regime), and decreases on both sides (Fig. 1), as shown in simple systems and in several redox proteins. For example, in the photosynthetic reaction center, charge recombination is prevented because the very large driving force for the initial charge separation drives the recombination reaction into the inverted region, slowing down the corresponding rate.

Using the classical approximation for the FC factor, the Fermi equation becomes

$$k_{et} = (2\pi/\hbar)H_{AB}^2(4\pi\lambda k_B T)^{-1/2}\exp[-(\Delta G^\circ + \lambda)^2/4\lambda k_B T] \quad (3)$$

where k_B is the Boltzmann constant and T is the temperature. According to Eq. (3), the main temperature-dependence comes from the exponential factor, but when the activation energy is zero ($e^0 = 1$), a weak temperature-dependence remains because of the preexponential factor, causing the rate to decrease as the temperature increases. Again this behavior has been observed for some reactions of the photosynthetic reaction centers.

The temperature-independence of some ET reactions can be explained, however, only by using a semiclassical description of the FC term, proposed by Hopfield (2), in which the term 2l$k_B T$ has been replaced by l $\hbar$w coth($\hbar$ w/2l$k_B T$). If the temperature falls below $\hbar$w/2k_B, the rate becomes nearly temperature-independent at any value of DG°.

The other term influencing the ET rate, the electronic factor (H_{AB}), represents the weak coupling of the reactant and product wavefunctions, where H stands for "Hamiltonian," the quantum-mechanical description of the system. H_{AB} yields the overlap between the orbitals A and B and is often referred to as the "electronic coupling matrix element." The degree of orbital overlap depends on the distance between the redox centers and the nature of the intervening medium, which in biological ET is the protein matrix and the solvent.

Because wavefunctions decay exponentially with distance, the electronic coupling will decrease with the distance (r–r_0) according to:

$$H_{AB}^2 = (H_{AB}^0)^2 e^{-\beta(r-r_0)} \quad (4)$$

where $H_{AB}{}^0$ represents the electronic coupling between A and B when the redox centers are in **van der Waals** contact ($r = r_0$), and its decay with distance ($r - r_0$) occurs with the coefficient b. The latter therefore describes the contribution of the intervening medium in propagating the wavefunction, and its dependence on protein structure is a matter of intense research and debate.

To obtain a correct description of the role of the intervening medium and distance on k_{et}, it is necessary to work in the activationless regime (DG° = –l) (Fig. 1). The photosynthetic reaction center proved to be an excellent test system for several reasons: (i) The three-dimensional structures of a number of reaction centers are known at atomic resolution; (ii) it contains several redox cofactors at various fixed distances; (iii) the driving force can be varied experimentally; and (iv) ET can be studied over a wide temperature range. Using experimental data obtained with proteins where the primary quinone was substituted with other compounds of different oxidation/reduction potential, Dutton and coworkers (3, 4) have shown a linear dependence of ln k_{et} on distance (over 12 orders of magnitude), with b = 1.4 Å^{-1}, r_0 = 3.6 Å, and a preexponential factor [(4p ^{2}/$\hbar$($H^2{}_{AB}$)] of 10^{13} s^{-1} (Fig. 2). These authors concluded that the ET rate in any protein follows an exponential decay of the electronic wavefunctions with distance, implying a homogeneous intervening medium.

Figure 2. Effect of distance on the intraprotein ET rate in the photosynthetic reaction center, according to Moser and Dutton (3). Following light excitation of the bacteriochlorophyll dimer ($BChl_2$), ET progresses sequentially through bacteriochlorophyll monomer (BChl), bacteriopheophytin (BPh), primary quinone, and secondary quinone (Q_A and Q_B). The resulting positively charged oxidized dimer can be re-reduced by the nearest of the four cytochromes c (cyt c). The experimentally determined rates within the reaction center fit a straight line with b = 1.4 Å^{-1}, compared to 2.8 Å^{-1}

in vacuum and to 0.7 Å^{-1} in a rigid covalent system. The line through the experimental data extrapolates to 10^{13} s^{-1} at 3 ANGSTROM, the van der Waals distance. (From Ref. 8, reproduced with permission. Copyright BIOS Scientific Publishers, 1996.)

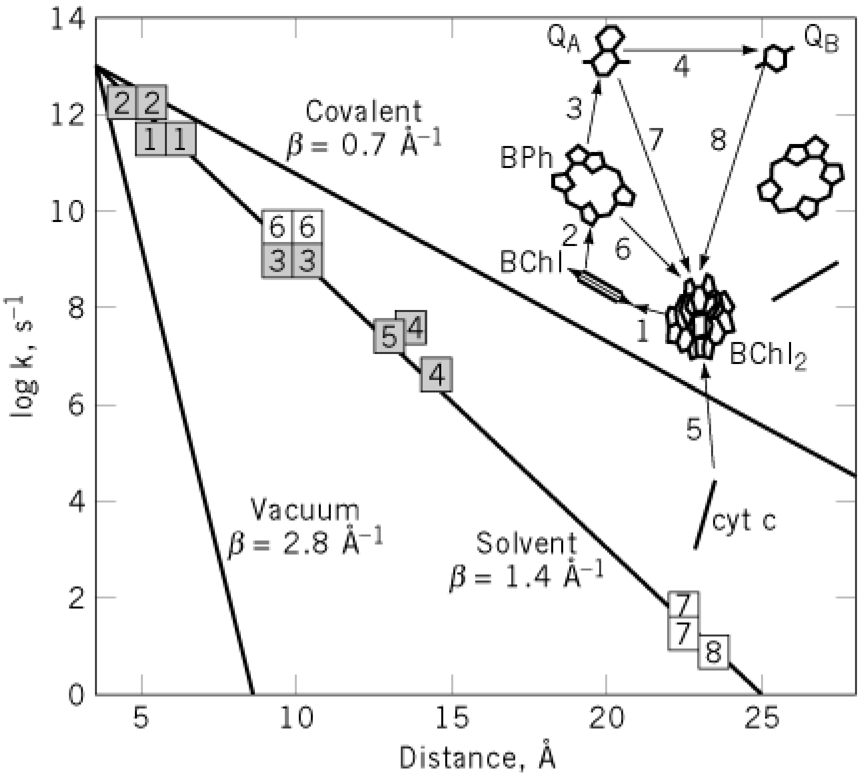

This exceptional result (Fig. 2) does not prove, however, that the tunneling barrier between the redox centers is microscopically uniform, but rather that the observed value represents an average. Gray and coworkers (5) have used proteins modified by incorporation of ruthenium (mainly myoglobins and cytochromes) as model systems to investigate the dependence of b on the structure of the intervening medium, that is, the detailed protein structure. In this and other similar studies, a plot of ln k_{et} against distance does not always yield a linear relationship, suggesting that the protein does not always provide a homogeneous energy barrier. Given the intrinsically heterogeneous packing inside a protein, and thus the variable dielectric constant, a model that takes into account the detailed structure of the intervening medium is needed. Onuchic and Beratan (6) have developed such a model, which views coupling between redox centers via pathways. In this model, the exponential decay of the electronic coupling depends not only on the distance between redox sites, but also on the detailed contacts along the ET pathway. Along a pathway, electronic decay factors (ε) through different connectivities, involving covalent (ε_C), hydrogen-bond (ε_H), and through-space (ε_S) jumps, come into play. The coupling strength decreases in the order covalent > hydrogen bond > through-space, and the total decay across the pathway is given by the sum of the individual contributions. An algorithm searching for potential ET pathways in proteins of known three-dimensional structure has been developed by these authors (Fig. 3). This model has been applied to different redox proteins in order to define the role of the intervening medium and of **secondary structure** elements on the ET rates. The model predicts that (i) hydrogen bonds provide shortcuts for the electron between otherwise unconnected protein segments, (ii) beta-sheet proteins will exhibit a greater degree of coupling than **alpha-helical** proteins, and (iii) pathways always arise in families, giving rise to the concept of “fattened” pathways and pathway tubes. The existence of multiple pathways is a challenge to protein engineering of ET proteins to enhance or inhibit ET rates by modification of residues along the most probable pathways.

Figure 3. Connectivity between redox centers according to Beratan, Onuchic, and coworkers. The figure depicts the structure of cytochrome *c*, with the heme group highlighted and the polypeptide chain sketched as a continuous line. The two histidine residues at position 33 and 39 are the sites of chemical modification with ruthenium. Dotted lines represent the calculated pathway for ET. The strongest coupling is provided by bonds at the center of a tube of pathways that connect the donor–acceptor couples within the protein. The decay factors were calculated to be: covalent bonds, $\varepsilon_c = 0.6$; hydrogen bonds, $\varepsilon_H = \varepsilon_c^2 e^{-\beta(r-r_0)}$; through-space jumps, $\varepsilon_s = 1/2\varepsilon_c e^{-\beta(r-r_0)}$), where r_0 is the reference distance for covalent bonds (1.4 Å) or hydrogen bonds (2.8 Å) and b is the decay length for through-space jumps (1.7 Å). (From Ref. 9, with permission. Copyright American Chemical Society.)

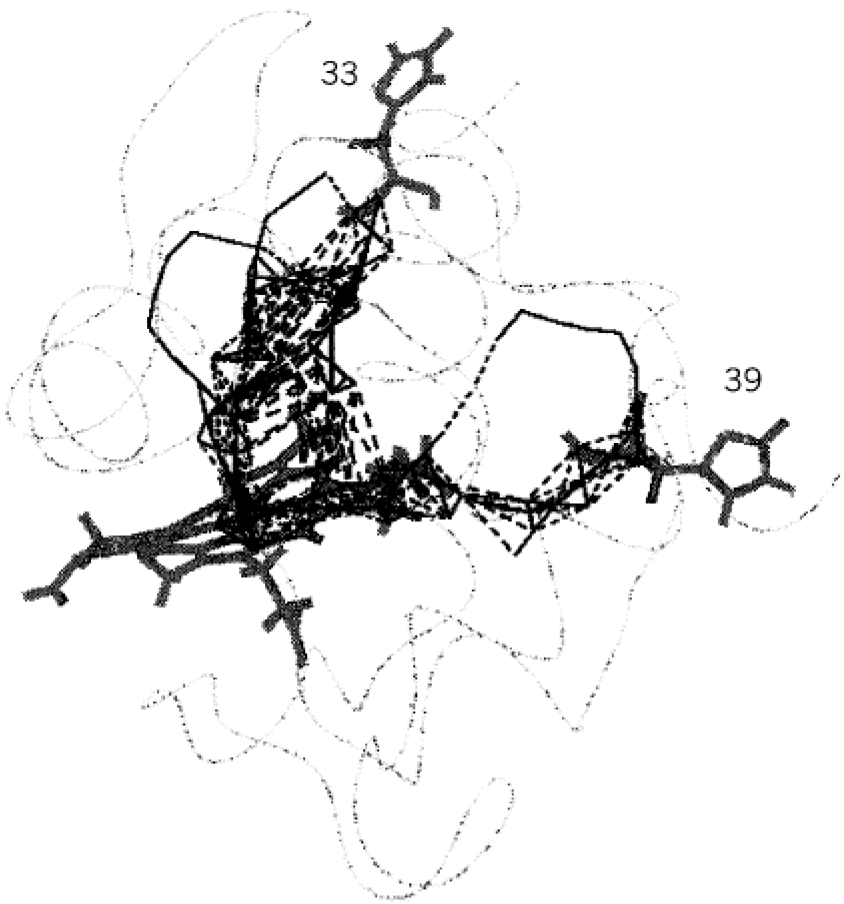

The large body of experimental data available today indicates that the two models (homogeneous and heterogeneous) are not necessarily exclusive. In some cases, the protein behaves as a homogeneous medium with “distance-dependent” exponential decay, as for photosynthetic reaction center, ruthenated azurin, and ruthenated cytochrome b_5, although different b values were reported. In other cases, the coupling decay factor was shown to be anisotropic (eg, in cytochrome *c*), giving rise to a view in which “hot” and “cold” spots for ET can be identified. Of particular importance are studies on the role of dynamic fluctuations on through-space contacts.

2. Intermolecular ET

The principles underlying ET between two proteins offer another theme for variation and control, namely, molecular recognition and protein–protein interactions as a prerequisite for ET. Some general features that have emerged from many studies will be presented in this section.

The Marcus theory ([1](#)) described above states that electron coupling between redox centers depends primarily on distance. For efficient ET, diffusible proteins must interact in such a way to maximize proximity between the redox centers within a collisional complex (AB), given that most redox active proteins are asymmetric, with their cofactor/metal generally located on one side of the macromolecule. The kinetic model that describes interprotein ET is

$$A^+ + B \underset{k_{-a}}{\overset{k_a}{\rightleftarrows}} (A^+B) \overset{k_{et}}{\rightarrow} (AB^+) \rightarrow A + B^+ \tag{5}$$

Under pseudo-first order conditions (eg, [A]≫[B]), the overall rate constant k_{12} is given by

$$k_{12} = k_a k_{et}[A]/(k_{-a} + k_{et} + k_a[A]) \tag{6}$$

Within this model, two limiting conditions can be envisaged, where either complex formation or intracomplex ET are rate-limiting.

Marcus theory allows describing the overall rate constant k_{12} as a function of the equilibrium constant K_{12}, the self-exchange rate constants of the two partners, k_{11} and k_{22}, and the work term W_{12} involved in the configurational change of reactants and products along the reaction coordinate:

$$k_{12} = (k_{11}k_{22}K_{12}f_{12})^{1/2}W_{12} \tag{7}$$

where

$$W_{12} = \exp(w_{11} + w_{22} - w_{12} - w_{21})/2RT \tag{8}$$

Equation (7) can be simplified when (a) the work terms cancel one another (ie, homonuclear and heteronuclear ET involve the same energy terms) and (b) f_{12} is close to unity, which is often the case provided that K_{12} is not too large. Under these conditions, equation (7) becomes

$$k_{12} = (k_{11}k_{22}K_{12})^{1/2} \tag{9}$$

which is frequently used and is generally referred to as the "cross-relation." For redox reactions between inorganic metal ions or complexes, Marcus theory has been experimentally verified many times, either in the general or in the "cross-relation" formulation. It has also been used to calculate reaction rates or equilibrium constants that are difficult to determine experimentally. The "cross-relation" approach has also been used to interpret protein–protein ET: Table 1reports a set of experimentally determined rate constants for some copper and heme proteins, together with the values calculated on the basis of equation (8). When comparison with known equilibrium and self-exchange rate constants was possible, the discrepancy between calculated and measured values was found to be no greater than one order of magnitude (which is considered good). In cases in which larger deviations were observed (>100 fold), efforts have been made to rationalize this discrepancy, possibly reconsidering the applicability to the system of some of the theoretical assumptions described above. The obvious assumption that may not apply is related to the anisotropy of the redox protein and thereby to the contention that ET with any partner always occurs through one and the same contact surface.

Table 1. Comparison of Experimentally Determined and Calculated (According to Marcus "Cross-Relation") Second-Order Rate Constants for Different Redox Couples

Oxidant[a] (1)	Reductant[a] (2)	K_{12}[b]	R_{11}[c] (M^{-1} s^{-1})	k_{22}[c] (M^{-1} s^{-1})	k_{12} calc. (M^{-1} s^{-1})	k_{12} exp. (M^{-1} s^{-1})
Azurin	Cyt *c*	19	8×10^5	2.5×10^2	5.5×10^4	6.4×10^4
Azurin	Cyt c_{551}	3	8×10^5	1.2×10^7	4.8×10^6	6×10^6
Cyt *c*	Cyt c_{551}	1	2.5×10^2	1.2×10^7	5.5×10^4	5×10^4
Plastocyanin	Cyt *c*	40.4	10^3	2.5×10^2	3.2×10^3	1.5×10^6
Plastocyanin	Cyt c_{551}	40.4	10^3	1.2×10^7	7×10^5	7.5×10^5
Stellacyanin	Cyt *c*	0.06	1.2×10^5	2.5×10^2	1.3×10^3	3.5×10^2
Stellacyanin	Cyt c_{551}	0.08	1.2×10^5	1.2×10^7	3.3×10^5	1.6×10^5

[a] Proteins: *Pseudomonas aeruginosa* azurin and cytochrome c_{551} (Cyt c_{551}), horse heart cytochrome *c* (Cyt *c*), and parsley plastocyanin.

[b] Equilibrium constants were calculated on the basis of midpoint redox potentials ($E_{m,7}$).

[c] Electron self-exchange rates at 20°C used in the calculation of k_{12} according to Marcus "cross-relation."

In the **diffusion**-limited case, maximal second-order rate constants for ET proteins are in the range of 10^8 to 10^9 M^{-1} s^{-1}. A negative steric factor, due to the fact that only a small fraction of the total surface of a protein is near the redox active cofactor, is partially compensated for by the solvent cage effect and long-range electrostatic interactions. The solvent cage effect increases the lifetime of the so-called encounter complex because, after collision, the two proteins are momentarily trapped by the solvent and thus experience a large number of mutual contacts by two-dimensional diffusion. Long-range electrostatic forces come into play, because many ET proteins display an anisotropy in surface charge distribution that results in a permanent dipole moment, favoring their association. This effect has been investigated through (i) the ionic-strength dependence of the second-order rate constant k_{12}, (ii) the effect of surface-charge modification by chemical modification or protein engineering, and (iii) the influence of the computed electrostatics of the redox partners in simulated docking experiments. An interesting generality related to the electrostatic makeup of ET proteins is that the docking surfaces often show a "loose" specificity, which also explains the high degree of cross-reactivity observed both *in vitro* and *in vivo* between donors and acceptors. This is shown in Figure 4 for the widely studied redox couple cytochrome *c* and cytochrome-*c*-oxidase of the respiratory chain, where the complex between the two redox partners is stabilized by multiple electrostatic interactions, and the ET pathway crucially depends on two aromatic side chains inside a patch of negative charges on the cytochrome-*c*-oxidase binding site (7).

Figure 4. Models of the three-dimensional structures of *Paracoccus denitrificans* cytochrome-*c* oxidase and horse heart cytochrome *c*, in a CPK representation. Color code: (i) On cytochrome *c*, *blue* represents positive residues (mainly lysines), *red* represents the heme, *yellow* represents phenylalanine 82, and *green* represents cysteine 17; (ii) on cytochrome-*c*-oxidase, *red* represents the negative residues (aspartates and glutamates) on subunit I (*green*), subunit II (*blue*) and subunit III (*brown*). *Yellow* represents residue tryptophan 121, and *light blue* represents tyrosine 122 forming the hydrophobic patch mediating ET (7). [Courtesy of Prof. F. Malatesta (University of Aquila, Italy) using the coordinates kindly provided by Prof. H. Michel (Frankfurt, Germany).] See color insert.

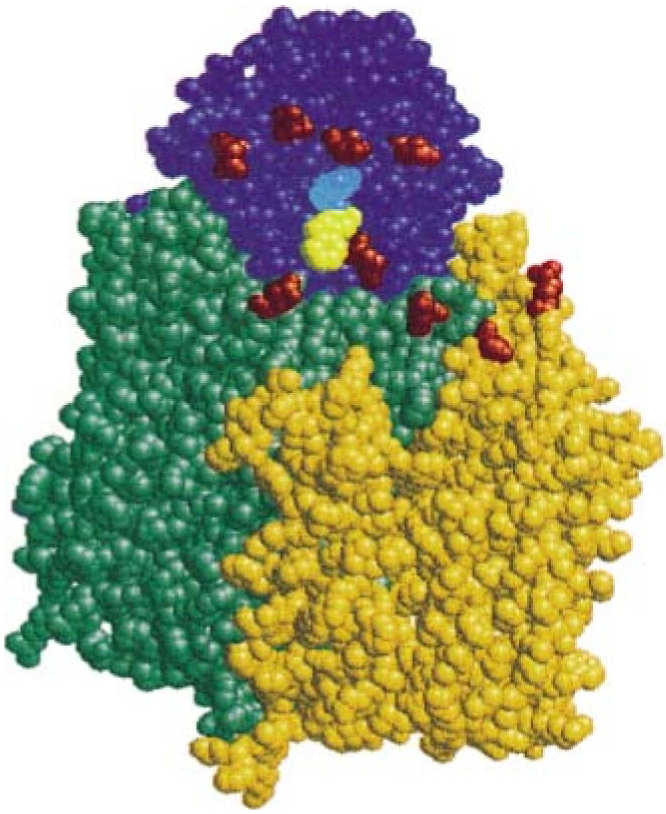

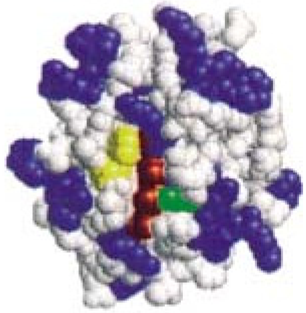

Bibliography

1. R. A. Marcus and N. Sutin (1985) Biochim. Biophys. Acta **811**, 265–322.
2. J. J. Hopfield (1974) Proc. Natl. Acad. Sci. USA **71**, 3640–3644.
3. C. C. Moser and P. L. Dutton (1992) Biochim. Biophys. Acta **1101**, 171–176.
4. C. C. Moser, J. M. Keske, K. Warncke, R. S. Farid, and P. L. Dutton (1992) Nature **355**, 796–802.
5. D. N. Beratan, J. N. Onuchic, J. R. Winkler, and H. B. Gray (1992) Science **258**, 1740–1741.
6. J. N. Onuchic and D. N. Beratan (1990) J. Chem. Phys. **92**, 722–733.
7. H. Witt, F. Malatesta, F. Nicoletti, M. Brunori, and B. Ludwig (1998) J. Biol. Chem. **273**, 5132–5136.
8. C. C. Moser and P. L. Dutton (1996) In *Protein Electron Transfer* (D. S. Bendall, ed.), BIOS Scientific Publishers, Oxford, England, pp. 1–21.
9. J. J. Regan, S. M. Risser, D. N. Beratan, and J. N. Onuchic (1993) J. Phys. Chem. **97**, 13083–13088.

Suggestions for Further Reading

10. D. S. Bendall (ed.) (1996) *Protein Electron Transfer*, BIOS Scientific Publishers, Oxford, England.
11. G. W. Canters and E. Vijgenboom (eds.) (1998), *Biological Electron Transfer Chains: Genetics, Composition and Mode of Operation*, NATO ASI Series Vol. **512** (Series C), Kluwer Academic Publishers, Dordrecht, Boston.

Electrophoresis

Electrophoresis is the movement of charged molecules or particles in an electric field. Electrophoresis may be conducted for the purposes of analytical identification or physical characterization of the various components of a sample, or for their preparative separation.

Electrophoretic migration of a molecule in any medium proceeds in the direction toward the electrode of opposite polarity to the net charge of the molecule (eg, negatively charged molecules migrate toward the positively charged electrode; cations move toward the cathode, anions toward the anode). The medium needs to be buffered at a pH that produces the appropriate direction and rate of migration. The mobilities of proteins generally increase the further the pH is from their isoelectric points (pI), increasing their net charge. However, resolution based on net charge differences improves as the net charge is reduced and is optimal when the net charge approaches zero at the pI (see Isoelectric Focusing). **Nucleic acids** and proteins complexed with the anionic detergent SDS (sodium dodecyl sulfate) exhibit high mobilities over a range of pH values above neutrality, due to their high surface negative charge densities. In addition to pH, the ionic strength, composition of the solvent, presence of detergents (see Hydrophobic Electrophoresis), and temperature govern the electrophoretic mobilities of all species in a sample, their separation, and the maintenance of their native conformations. For example, nucleic acid stability depends on the Na^+ level. Proteins aggregate at low ionic strength; high ionic strength may exceed the Joule heat dissipation capacity of the electrophoretic apparatus and "cook" the sample during electrophoresis.

Different species can often be separated on the basis of differences in their electrophoretic mobilities, which is defined as the ratio of the migration rate (cm/s) to the electric field strength (V/cm). The mobility (cm^2/s V) of a macromolecule is a function of the ratio of its surface net charge to its accessible surface area, plus the resistance to migration exerted by the medium in which the separation takes place. The resistance due to the viscosity of the medium affects species of all sizes equally and therefore does not contribute to their separation; it may, however, be augmented by the presence of polymer networks and permit separations based on differences in size and shape (see also Gel Electrophoresis; Agarose; Polyacrylamide; SDS-PAGE).

For practical reasons, samples subjected to electrophoresis need to be protected from convective mixing. This can be accomplished within a liquid sample using a density gradient when the migration of the boundary of a region of sample is observed, or in tubes of less than 0.2 mm in diameter, as in capillary zone electrophoresis. Much more commonly, electrophoresis is carried out with a gel when the sample usually migrates as a zone. In this case, the electrophoretic migration rate depends on the pore size of the gel. Alternatively, the sample may migrate within a stack of moving boundaries of buffer components, with a mobility regulated by that of the boundary (see Disc Electrophoresis; Isotachophoresis).

Separations by electrophoresis and chromatography share many of their principles of operation, but electrophoresis excels in its ability to provide simultaneous separations of many components, to exploit charge and size differences simultaneously, to be compatible with a continuum of polymer or gel concentrations that produce a "molecular sieve," and to be applicable to particle sizes ranging from simple organic acids to very large complexes and small cells (see Particle Electrophoresis).

1. Sample detection and quantification

The zone or moving boundary comprising the sample of interest can be identified and quantified by its absorbance, fluorescence, or radioactivity, by specific **antibodies** (see Protein Blots (Western Blots); Immunoelectrophoresis), by its biological activity (see Overlay Assay: Enzyme Zymography of Plasminogen Activators and Inhibitors), or by stains specific for the class of molecule. Staining with reagents specific for proteins or nucleic acids is the most common method. Before staining samples in electrophoresis gels, the sample normally must be fixed, ie, made insoluble, so that it does not diffuse during the staining process. Solvents such as acetic acid or trichloroacetic acid are often used to fix proteins; frequently, the fixing solution also contains the stain. The most general and sensitive staining method is silver stain (1). Coomassie Brilliant Blue R-250 is the most widely used protein stain, although it requires destaining by removing the excess dye, unlike the corresponding G-250 stain (2). Moreover, the commonly used acetic acid solutions are poor fixatives compared to trichloroacetic acid solutions (2, 3). Other widely used protein stains are Ponceau S and Amido black.

Rather than stain after an electrophoretic separation, the analytes can be prestained prior to electrophoresis. Prestaining is required for capillary zone electrophoresis and automated gel electrophoresis. It must be remembered, however, that the prestaining can alter the charge and shape properties of the molecules of the sample. Prestaining of proteins commonly employs derivatization by fluorescein isothiocyanate (see Gel Electrophoresis); that of nucleic acids uses the intercalating dye ethidium bromide (which is also used for poststaining without fixation), or the more recently introduced dyes DAPI (4), TOTO, or YOYO (5).

It is often possible to estimate the quantity of a particular species present in a sample by electrophoresis. Densitometry of stained gel bands has been the classical method (6). When a sample is radioactive, it may be detected and quantified by autoradiography or by counting extracted or solubilized gel slices. There are now commercial instruments for counting radioactivity in entire gel patterns (7). Fluorescence detection is especially useful with capillary zone electrophoresis or in automated gel electrophoresis apparatus (8).

Bibliography

1. C. R. Merril (1987) Adv. Electrophoresis **1**, 111–142.
2. B. An der Lan, C. Auzan, J. V. Sullivan, and A. Chrambach (1985) Electrophoresis **6**, 408–409.
3. A. Chrambach, R. A. Reisfeld, M. Wyckoff, and J. Zaccari (1967) Anal. Biochem. **20**, 150–154.
4. E. Buel and M. Schwartz (1993) Appl. Theor. Electrophoresis **3**, 253–256.
5. K. Srinivasan, S. C. Morris, J. E. Girard, M. C. Kline, and D. J. Reeder (1993) Appl. Theor. Electrophoresis **3**, 235–240.
6. M. M. Miller (1989) Adv. Electrophoresis **3**, 182–220.
7. D. M. Gersten and E. Zapolski (1991) Adv. Electrophoresis **4**, 49–79.
8. J. C. Sutherland (1993) Adv. Electrophoresis **6**, 3–43.

Suggestions for Further Reading

9. M. Bier (ed.) (1959 and 1967) Electrophoresis: Theory, Methods and Applications, Vols. **1** and **2**, Academic Press, New York.
10. Z. Deyl (ed.) (1979 and 1983) *Electrophoresis: A Survey of Techniques and Applications*, Elsevier, Amsterdam.
11. S. Hjerten (1978) "Analytical electrophoresis". In *Topics in Bioelectrochemistry and Bioenergetics*, Vol. **2** (G. Milazzo, ed.), Wiley, New York, pp. 89–128.
12. C. J. O. R. Morris and P. Morris (1976) *Separation Methods in Biochemistry*, 2nd ed., Wiley, New York, pp. 703–900.
13. V. Neuhoff, R. Stamm, I. Pardowitz, N. Arold, W. Ehrhardt, and D. Taube (1990) Essential problems in quantification of proteins following colloidal staining with Coomassie Brilliant Blue dyes in polyacrylamide gels, and their solution. Electrophoresis **11**, 101–117.
14. P. G. Righetti, C. J. Van Oss, and J. W. Vanderhoff (1979) *Electrokinetic Separation Methods*, Elsevier, Amsterdam.

Electrospray Ionization

Electrospray ionization (ESI) is a method of generating ionic forms of molecules for mass spectrometry . It generates ions directly from solution (usually an aqueous or aqueous/organic solvent system) by creating a fine spray of highly charged droplets in the presence of a strong electric field (1), as shown in Fig. 1. Subsequent vaporization of these charged droplets results in the production of multiply charged gaseous ions. The number of charges retained by an analyte can depend on such factors as the composition and pH of the electrosprayed solvent, as well as the chemical nature of the sample (2-4). For large molecules, the ESI process typically gives rise to a series of multiply charged species for a given analyte. Because mass spectrometers measure the mass-to-charge (*m*/*z*) ratio, the resultant ESI mass spectrum contains multiple peaks corresponding to the different charged states (Fig. 2).

Figure 1. The electrospray ionization process.

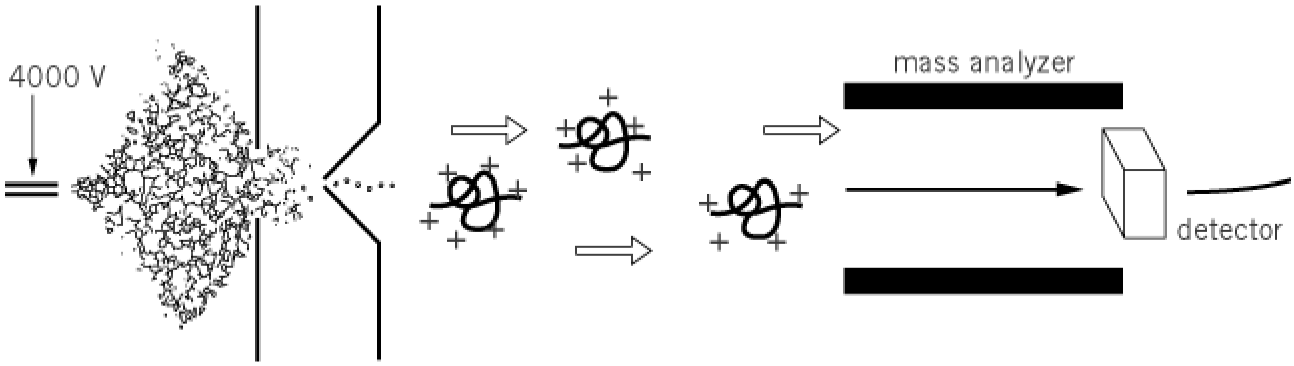

Figure 2. Examples of data generated on an ESI mass spectrometer. Proteins (left) typically produce positive multiply cl
generate negative multiply charged ions. The insets for each part show the molecular-weight spectra computer-generated

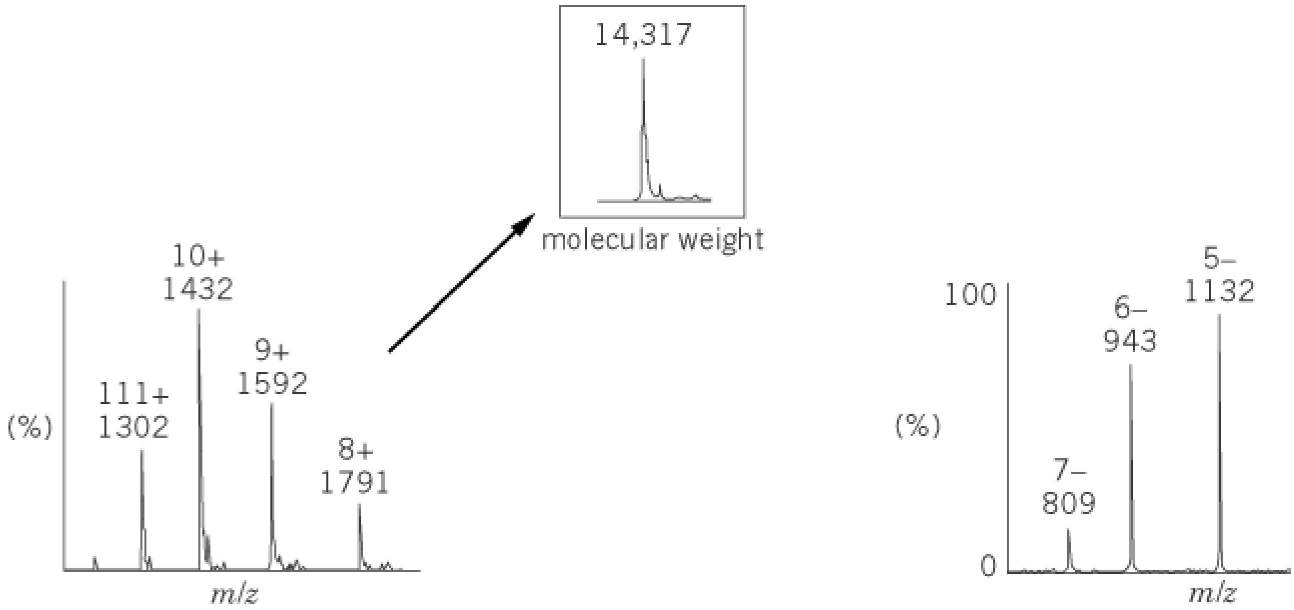

The extent of multiple charging that occurs in ESI is a unique characteristic of the technique that enables an analyte's mass to be determined with great precision, as masses can be independently calculated from several different charged states (5). The multiple charging in ESI also permits the analysis of high-molecular-weight analytes, using conventional mass analyzers that are normally limited to the detection of ions with relatively low *m/ z* ratios. For example, a 50-kDa protein will typically retain on the order of 30 to 50 charges in ESI, yielding multiply charged species with *m/z* ratios between 1000 and 2000 that are easily detected with *quadrupole mass analyzers* . Another advantage of ESI-MS is its compatibility as an interface with liquid chromatography (see Liquid Chromatography Mass Spectrometry). Electrospray ionization is compared to the other common method of ionization in Matrix-Assisted Laser Desorption/Ionization.

Bibliography

1. P. Kebarle and L. Tång (1993) Anal. Chem. **65**, A972–A986.
2. R. D. Smith, J. A. Loo, C. G. Edmonds, C. J. Barinaga, and H. R. Udseth (1990) Anal. Chem. **62**, 882–899.
3. B. T. Chait and S. B. H. Kent (1992) Science **257**, 1885–1894.
4. D. Arnott, J. Shabanowitz, and D. F. Hunt (1993) Clinical Chemistry **39**, 2005–10.
5. G. Siuzdak (1996) *Mass Spectrometry for Biotechnology*, Academic Press, San Diego.

Electrostatic Interactions

Electrostatic forces originate from the electric charges and dipoles of atoms and groups of atoms. They function inside macromolecules to maintain and to stabilize the molecular structure and to regulate the biological functions of catalysis and electron transfer. Electrostatic forces between molecules, facilitate specific molecular recognition and molecular assembly. The specific electrostatic field is determined by contributions from several factors, which originate from the intrinsic heterogeneity of biological macromolecules and from aqueous solvents.

1. Ionic Charges

In proteins, aspartic acid and glutamic acid residues have negatively ionizable side chains, and lysine, arginine, and histidine are positively ionizable. The amide and carboxyl termini of the polypeptide chain can also ionize, with, respectively, positive and negative charges. The intrinsic pK_a values of these groups in a normal aqueous environment are listed in Table 1. The actual pK_a value of a group in a folded protein can deviate from its intrinsic value, depending on the electrostatic field it experiences. The net charge of a protein is the sum of the positively and negatively ionized amino acid groups, plus any cofactor ions, and depends on the pH of the solvent. The pH at which a protein has no net charge is known as its isoelectric point. At neutral pH, most proteins are amphoteric, having both cationic and anionic groups at specific locations in the folded conformation.

Table 1. pK_a Values for Amino Acids in Peptides[a] and Bases in Nucleosides [b]

Amino Acids in Peptides	pK_a	Bases in Nucleosides	pK_a
a-NH_2	7.8	Adenine (N_1)	3.52
a-COOH	3.6	Cytosine (N_3)	4.17
Asp (C_gOOH)	4.0	Guanine (N_1)	9.42
Glu (C_dOOH)	4.5	Guanine (N_7)	3.3
His (imidazole)	6.4	Uracil (N_3)	9.38
Lys (ε-NH_2)	10.4	Thymine (N_3)	9.93
Arg (guanidine)	≈12		
Tyr (OnH)	9.7		
Cys (SgH)	9.1		

[a] Ref. 23.
[b] Ref. 24.

In **nucleic acids**, only the negative phosphate groups are charged at neutral pH, so nucleic acids do not show amphoteric properties. At very acidic or alkaline pH values, however, protonation or deprotonation of bases occurs, depending upon their pK_a values (Table 1).

2. Permanent Electric Dipoles

A molecule or a group of atoms has a permanent electric dipole if it has an unequal electron distribution. This dipole spontaneously produces its own electric field, and the molecule or group is then described as *polar*. One of the more important polar groups in macromolecules is the peptide bond, which has a large dipole moment. The polar groups interact electrostatically with other polar groups in the same or other molecules or with polar solvent molecules or ions. Permanent dipoles within most macromolecules are small and are distributed in different orientations, except for the alpha-helix. It possesses a large permanent dipole moment due to the cooperatively aligned electric dipoles of the peptide bonds of the backbone (1)

3. Polarizability and Dielectric Constant

In an external electric field **E**, an electric dipole is induced even in a neutral, nonpolar molecule or group because the outer field modifies the electrostatic balance between the electrons and the nucleus in each atom. The magnitude of this dipole is given by $m^{induced} = a_0\mathbf{E}$, where the coefficient a_0, the electronic polarizability, is proportional to the volume of the molecule or group. When the molecule or group also has additional permanent dipoles, they also reorient because of the external field. Consequently, the polarizability of a molecule is the sum of its electronic and orientational polarizabilities. The contribution from the orientational polarization of a polar group is generally much larger than that of the electronic polarization (2).

When a material is physicochemically homogeneous in a macroscopic volume, the dielectric constant of the material is related to the polarizability through the *Clausius–Mossotti* equation. Thus, the dielectric constant reflects the degree of polarizability of the material. A pure, polar liquid has a much larger dielectric constant than a nonpolar liquid. For example, the dielectric constants at 20 °C of water and cyclohexane are 80 and 2, respectively. The magnitude of the electrostatic interactions between charged groups or dipoles is relatively straightforward in such a homogeneous medium. It is inversely proportional to the distance between each pair of charges and to the dielectric constant of the medium. In contrast, proteins and nucleic acids are so heterogeneous, with polar and nonpolar groups distributed nonuniformly, that it is impossible to define an dielectric constant. Roughly speaking, however, the dielectric constant should be small in a **hydrophobic** core, perhaps 2 to 4, whereas the surface regions have larger values of 10 or larger (3).

4. Electrostatic Shielding by Polar Solvents

When a charged, polar biological macromolecule is dissolved in a polar aqueous solvent, the solvent molecules rotate in response to their interaction with the solute macromolecule in an attempt to decrease the **free energy** of the entire system. Thus, the electrostatic force produced by the solute macromolecule is significantly shielded. This free energy is called the *self-energy*, the interaction of a solute charge or electric dipole with the dielectric environment (2). In addition, the density distribution of small ions in the solvent also changes to shield the electric field originating from the solute molecule. Small metal cations are located near the negative charges, and anions are near the positive point charges, as described by the *Debye–Hückel* approximation. Double-stranded DNA or RNA has a very high negative charge density of phosphate groups of the backbone, which is almost neutralized (about 88%) by condensed counterions, which are strongly restricted along the duplex, in addition to the Debye-Hückel type interaction. The density of the condensed counterions is relatively independent of the solvent conditions, but they are released from the polymer when the double helical conformation is deformed (4).

When the response to a given electric field is monitored directly, changes in the orientation and density distribution of the solvent molecules are the major responses to an external field. Therefore, passive measurement of the individual pK_a values of the ionizable groups (5) and of the NMR chemical shift values of the nuclei (6) are good reporters of the local electrostatic field inside macromolecules. Both measurements are possible with the aid of multidimensional NMR techniques using stable isotope labeling (7). The charges and polarities of interest in proteins can be changed by site-directed mutagenesis, and the free energy difference associated with the electrostatic interaction can be evaluated (8).

5. Theoretical Approaches

Theoretical approaches to electrostatic interactions are divided between two types of theories: the macroscopic or continuum and the microscopic or molecular. In the continuum theory, the *Poisson* or *Poisson–Boltzmann* equation is solved for the solute–solvent system, assuming that the system is large enough to define its dielectric properties. Kirkwood first obtained an analytical solution for a simple spherical solute molecule embedded in a solvent with a high dielectric constant (9). With the aid of high-speed computational techniques, the exact shapes of biological macromolecules can be considered and the equations solved numerically (10). The computer program GRASP (11) is widely used to compute the electrostatic potential based on this method and to illustrate the electrostatic molecular surfaces of biological macromolecules and their assemblies, using red and blue colors for negative and positive charges, respectively. The drawbacks of the continuum theory (3) are (1) that the solute–solvent system is too heterogeneous to introduce the dielectric constant parameters and (2) that the calculations are based on static molecular conformations. Therefore, strict agreement between experiments and calculations is not expected. In the molecular theory, all of the atoms of the solute and solvent molecules are incorporated into the calculation, using the vacuum dielectric constant. Because the electric force is essentially long-range and the solvent molecules are significantly polar, reliable results are obtained only if the dynamics of the system are simulated for a sufficiently long period without simply cutting off the electrostatic forces.

6. Roles in Folded Conformations

Statistical analyses of the charge distributions on protein surfaces indicate that the charged groups are, on average, surrounded by charges of opposite sign and they tend to form ion pairs, which contribute to conformational stability (12, 13). The electrostatic contribution of ion pairs to protein stability is context-dependent, and the interaction energy of a single ion pair exposed to the solvent or even buried in the protein interior, varies experimentally from 0.5 to 5 kcal/mol. The entropic cost of forming rigid salt bridges is an opposing factor that reduces the free energy of the folded protein (14). A cooperative salt-bridge network can contribute significantly to protein stability (15), as observed frequently on the surfaces of proteins of thermophilic origins. Acidic residues occur near the positive pole of the helical dipole at the N-terminus of an a-helix (12) and basic residues near the negative pole. They represent the helix caps (16). These interactions are not context-dependent, but only the first one or two turns of an a-helix give the essential contribution to protein stability by at most about 2 kcal/mol, independent of the length of the a-helix (17).

Unfavorable electrostatic interactions destabilize the folded conformation and are important in proteins. Unpaired buried charges and isolated hydrogen bonds are energetically expensive within the hydrophobic core because of the large self-energy. Thus, **secondary structures**, such as a-helices and beta-sheets, can usually be depicted in protein cores as simply the backbone structures because they do not leave any backbone hydrogen bond donors or acceptors unpaired (18).

The condensation of counterions contributes to the conformation and the stability of double helices of DNA and RNA, which are highly charged due to the ionized phosphate groups of the backbone. The ordered double-stranded conformation depends markedly on the ionic strength, and the melting temperature of the conformation is increased as ionic strength increases. Divalent cations interact with these duplexes more strongly than monovalent cations.

7. Enzyme Catalysis

Efficient enzyme catalysis is based on the decrease in the free energy of the transition state, and it is mediated by a well-designed active site structure and the electrostatic field. Protein engineering studies employing site-directed mutagenesis have highlighted the importance of ionizable or polar residues at the active site. In the catalytic reactions of proteins, the thiol group of **cysteine residues**, the hydroxyl group of serine or the imidazole group of histidine acts as a nucleophilic catalyst at the initial stage. Ionizable side chains can act as acid and base catalysts by giving and receiving a proton, respectively. Generally, when two ionizable groups are adjacent their pK_a values deviate greatly from the intrinsic values. One value becomes higher and the other becomes lower because of the strong coupling interaction between the two ionization states. Thus, even at a neutral pH, two such ionizable side chains can form acid and/or base catalysts, which are often observed to have unusual pK_a values at the active sites of enzymes. In addition, ligated metal ions play important roles in many examples of catalysis by correctly positioning the substrate molecules, by stabilizing the transition-state conformation, or by activating water molecules to form hydroxide ions.

The **electron transfer** reaction is an essential event in energy acquisition during respiration and photosynthesis. Several prosthetic groups in proteins, such as hemes, iron–sulfur clusters, and some transition metals, such as Cu, directly govern the reaction. The electron transfer reaction is finely controlled by the surrounding peptide chains of proteins through electrostatic interactions (19). In addition, because the prosthetic groups are often buried deeply in the protein, electrons are considered to transfer from the protein surface through certain, but not unique, paths in the protein molecule (20). Electrostatic interactions often trigger large-scale structural changes, especially when coupled to ATP and GTP hydrolysis. The ionic and polar interactions of proteins with the phosphate groups of ATP and GTP become reordered after their hydrolysis. This local phenomenon causes domain movement in multidomain proteins and results in large structural changes (see ATPase and Gtpases). Likewise, several **allosteric** transitions are considered to be mediated by **salt bridges**.

8. Molecular Recognition

Molecular recognition is a major focus of modern biology and biochemistry. Specific molecular recognition of individual biological macromolecules is involved in many biological phenomena. Protein–protein interactions are critical in biological signal transduction, and they guide the assembly of multimeric proteins, generally found in cell **organelles**, **cytosol**, and cell membranes. Protein molecular surfaces are involved in the recognition of other molecules. Hydrogen bonds and salt bridges often provide specificity, which is derived from the distinctive electrostatic complementarity between the molecular surfaces. At protein–protein interfaces, on average, 0.88 hydrogen bonds are found per 100 $Å^2$ of buried accessible surface area, and from 0 to 5 intersubunit salt bridges are observed between protein dimers (21).

Protein–nucleic acid interactions are the origin of complex genetic regulation. The backbone phosphate groups interact with the basic side chains of the protein, and specific base sequences are generally recognized through hydrogen bonds and hydrophobic interactions with the protein side chains (22). In the process of association, a basic protein approaches the DNA double helix by a long-range, electrostatic attractive force. Then the protein condenses, like a group of counterions, along the DNA duplex. Some of the condensed counterions are released. Then the protein slides along the double helix by one-dimensional diffusion, scanning the sequence, until it finally becomes positioned at the specific binding site. Specific basic residues in the protein molecule form ion pairs with the exposed phosphate groups of the DNA backbone. Thus, the local DNA backbone structure, which is completely neutralized, is deformed. In fact, the DNA structures bound by proteins are often deformed from the typical B-type conformation.

Bibliography

1. A. Wada (1976) Adv. Biophys. **9**, 1–63.
2. J. N. Israelachvili (1985) *Intermolecular and Surface Forces*, Academic Press, London, Chaps. "4" and "5", pp. 36–64.
3. H. Nakamura, T. Sakamoto, and A. Wada (1988) Protein Eng. **2**, 177–183.
4. M. T. Record Jr., J. H. Ha, and M. A. Fisher (1991) Methods Enzymol. **208**, 291–343.
5. C. Tanford and R. Roxby (1972) Biochemistry **11**, 2192–2198.
6. A. C. de Dios, J. G. Pearson, and E. Oldfield (1993) Science **260**, 1491–1496.

7. Y. Oda et al. (1994) Biochemistry **33**, 5275–5284.
8. L. Serrano et al. (1990) Biochemistry **29**, 9434–9352.
9. J. G. Kirkwood (1934) J. Chem. Phys. **2**, 351–361.
10. J. Warwicker and H. C. Watson (1982) J. Mol. Biol. **157**, 671–679.
11. A. Nicholls, K. A. Sharp, and B. Honig (1991) Proteins **11**, 281–296.
12. A. Wada and H. Nakamura (1981) Nature **293**, 757–758.
13. D. J. Barlow and J. M. Thornton (1983) J. Mol. Biol. **168**, 867–885.
14. S. Dao-pin, U. Sauer, H. Nicholson, and B. W. Matthews (1991) Biochemistry **30**, 7142–7153.
15. A. Horovitz et al. (1990) J. Mol. Biol. **216**, 1031–1044.
16. J. S. Richardson and D. C. Richardson (1988) Science **240**, 1648–1652.
17. J. Åqvist, H. Luecke, F. A. Quiocho, and A. Warshel (1991) Proc. Natl. Acad. Sci. USA **88**, 2026–2030.
18. A. V. Finkelstein and O. B. Ptitsyn (1987) Prog. Biophys. Molec. Biol. **50**, 171–190.
19. T. Ichiye (1996) Structure **4**, 1009–1012.
20. A. Kuki and P. G. Wolynes (1987) Science **236**, 1647–1652.
21. S. Jones and J. M. Thornton (1995) Prog. Biophys. Molec. Biol. **63**, 31–65.
22. C. O. Pabo and R. T. Sauer (1992) Ann. Rev. Biochem. **61**, 1053–1095.
23. A. R. Fersht (1985) *Enzyme Structure and Mechanism*, 2nd ed., Freeman, New York, pp. 156, Table 5.1.
24. G. M. Blackburn (1996) in *Nucleic Acids in Chemistry and Biology: DNA and RNA structure*, 2nd ed. (G. M. Blackburn and M. J. Gait, eds.), Oxford University Press, Oxford, Chap. "2", p. 22, Table 2.2.

Suggestions for Further Reading

25. B. Honig and A. Nicholls (1995) Classical electrostatics in biology and chemistry, Science **268**, 1144–1149. Comprehensive review of the approach of the continuum theory to electrostatic interaction in proteins and DNA.
26. H. Nakamura (1996) Roles of electrostatic interaction in proteins, Quart. Rev. Biophys. **29**, 1–90. Review of theoretical and experimental analyses of electrostatic interaction in proteins. Using simple models, the electrostatic energy values revealed experimentally were physically interpreted.
27. M. F. Perutz (1978) Electrostatic effects in proteins, Science **201**, 1187–1191. Biological importance of electrostatic interaction in proteins was reviewed in several different aspects.
28. A. Warshel and S. T. Russell (1984) Calculation of electrostatic interactions in biological systems and in solutions, Quart. Rev. Biophys. **17**, 283–422. Review of the molecular theory contrasted with the empirical continuum theory.
29. W. D. Wilson (1996) "Reversible interactions of nucleic acids with small molecules". In *Nucleic acids in chemistry and biology*, 2nd ed. (G. M. Blackburn and M. J. Gait, eds.), Oxford University Press, Oxford, Chap. "8", pp. 331–374. Electrostatic features of nucleic acids were well introduced.

Ellman's Reagent, 5,5′-Dithiobis-(2-Nitrobenzoic Acid), DTNB

Barrett and Seligman (1) in 1952 used 2,2′-dihydroxy-6,6′-dinaphthyl disulfide to demonstrate thiol groups in proteins histochemically. Six years later, Ellman reported the use of bis-(*p*-nitrophenyl) disulfide for spectrophotometric measurement of thiol groups, and subsequently enhanced its water solubility by introducing carboxyl groups into the benzene rings (2). This reagent, 5,5′-dithiobis-(2-nitrobenzoic acid), DTNB, is now known as Ellman's reagent and is one of the most useful reagents for measuring thiol groups quantitatively.

The cysteine thiol groups undergo thiol–disulfide exchange with the disulfide bond of DTNB at about pH 8, to produce a mixed disulfide between them, plus 5-thio-2-nitro-benzoic acid, TNB.

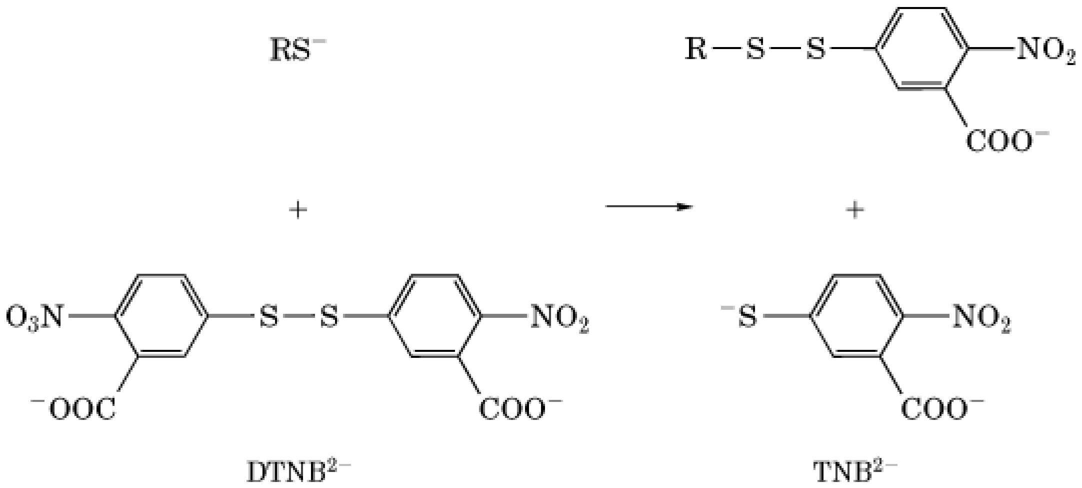

(1)

The TNB is intensely colored. Its absorption maximum is normally at 409.5 nm, but shifted to 421 nm in 6 M **guanidinium chloride** (GdmCl), which is often used to unfold proteins and make their thiol groups accessible (3). For historical reasons, however, the reaction is generally monitored at 412 nm, where the molar absorbance coefficient is 14,150 M^{-1} cm^{-1} in standard buffers and 13,700 in 6 M GdmCl. The reaction goes essentially to completion because an excess of Ellman's reagent is used, plus the pK_a of the thiol group of TNB is approximately 4.5, considerably more acidic than normal thiol groups, which have pK_a values near 9. This helps to drive the reaction to completion, as thiol–disulfide exchange favors the more acidic thiol group. Irrespective of whether the original thiol groups react only with the Ellman's reagent or also with the mixed disulfide, one mole of TNB is produced per mole of original thiol group.

The ease of use of the Ellman assay makes it widely used, and many variants of Ellman's reagent have also been devised for special purposes, such as kinetic studies at acidic pH (4).

Bibliography

1. J. R. Barrett and A. M. Seligman (1952) Science **116**, 323–327.
2. G. L. Ellman (1959) Arch. Biochem. Biophys. **82**, 70–77.
3. P. W. Riddles, R. L. Blakeley, and B. Zerner (1983) Methods Enzymol. **91**, 49–60.
4. K. Brocklehurst (1979) Int. J. Biochem. **10**, 259–274.

Elongation Factors (EFs)

Elongation of the nascent polypeptide chain during translation of protein biosynthesis requires three elongation factors (EF-Tu, EF-Ts, and EF-G) in prokaryotes and requires four factors, (EF-1 a, EF-1 b, EF-1 g and EF-2) in eukaryotes (Table 1). The basic function of these elongation factors is to recycle the delivery of aminoacyl-transfer RNA molecules to the A site of the ribosome and to **translocate** the ribosome one **codon** forward after the **peptidyl transfer** reaction. Because of this common scenario, elongation factors share high functional and structural similarities in prokaryotes and eukaryotes: EF-Tu is equivalent to EF-1 a, EF-Ts to EF-1 bg, and EF-G to EF-2 (1).

Table 1. ***Escherichia coli*** **Elongation Factors**

Factor	Molecular Mass	Number of Amino Acids	Gene	Function
EF-Tu	43,195	393	*tufA*	Bind aminoacyl-tRNA to A site; GTPase
	43,225	393	*tuf B*	Same as above
EF-Ts	30,257	282	*tsf*	GDP/GTP exchange on EF-Tu
EF-G	77,444	703	*fus*	Translocation; GTPase

The polypeptide elongation cycle can be divided into three steps: (i) delivery of aminoacyl-tRNA to the ribosome, (ii) peptidyl transfer, and (iii) translocation of the ribosome (Fig. 1). Aminoacyl-tRNA first forms a ternary complex with EF-Tu (EF-1 a) and GTP. EF-Tu is one of the most abundant proteins. In *Escherichia coli*, it comprises about 5% of the soluble protein, and the EF-Tu/ribosome ratio is up to 7:1 in rapidly growing cells. The aminoacyl-tRNA:EF-Tu:GTP ternary complex binds to the A site of the ribosome. The proper binding of EF-Tu to the ribosome and the correct base-pairing between codon and the anticodon of the tRNA trigger hydrolysis of EF-Tu-bound GTP to GDP through activation by the GTPase active center on the ribosome. Note that both EF-Tu and EF-G carry conserved G-domains for binding guanine nucleotides, but they need the common GTPase center for stimulating the hydrolysis of GTP (ribosome-dependent GTPase). Once GTP is hydrolyzed, the GDP form of EF-Tu no longer remains bound to the ribosome because of protein conformation is altered. Common to the functioning of G-proteins is that activation occurs by binding GTP, while deactivation is achieved by GTP hydrolysis. GTP and GDP act as **allosteric** effectors on their target proteins, thus altering the conformation (see GTP-Binding Proteins).

Figure 1. Elongation pathway of protein synthesis. Prokaryotic (upper) and eukaryotic (lower) elongation factors are represented in boxes.

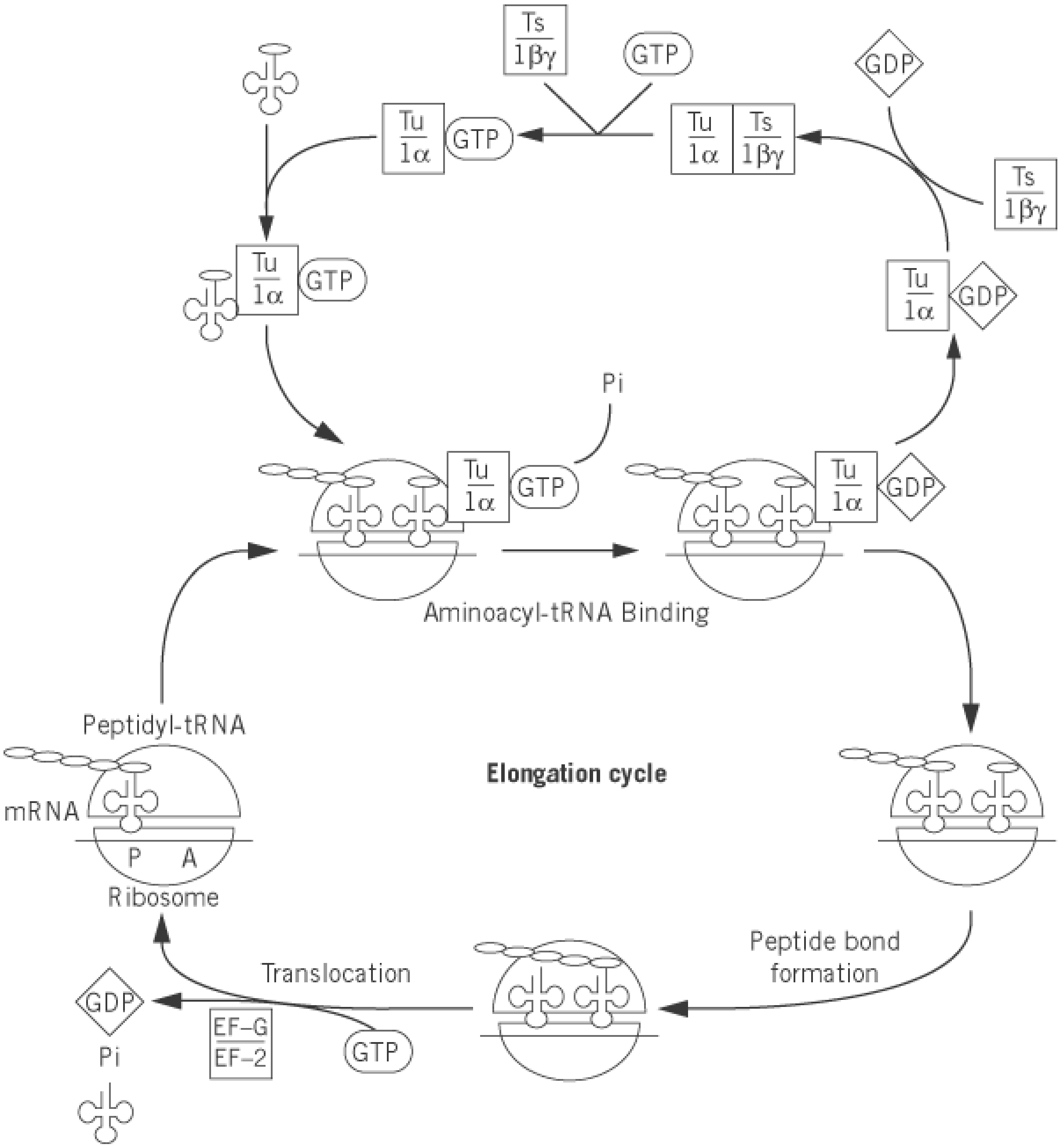

EF-Tu alone is very unstable, but is readily stabilized by GTP, GDP, or EF-Ts. EF-Ts (EF-1bg) is involved in the guanine nucleotide exchange of aEF-Tu (EF-1a). EF-Ts catalyzes conversion of the EF-Tu:GDP complex to EF-Tu:GTP, promoting the recycling EF-Tu for new ternary-complex formation.

After peptidyl transfer, the elongated peptidyl-tRNA is bound to the A site of the ribosome while the deacylated tRNA is bound to the P site. EF-G (EF-2) is a translocase protein that forwards peptidyl-tRNA from the A site to the P site on the ribosome and forwards the deacylated tRNA from the P site to the E site. The GTP form of EF-G is the active state and binds to the ribosome. Translocation of the ribosome is coordinated with the hydrolysis of GTP bound to EF-G. Presumably, GTP hydrolysis induces conformational constraints on the ribosome that lead to the movement of the ribosome. Then, the GDP form of EF-G dissociates from the ribosome.

EF-3 appears to be a unique translation factor that is found only in yeast and **fungi** (2). Together with yeast or mammalian EF-1a and EF-2, it is required for protein synthesis with ribosomes, except for mammalian ribosomes. This has prompted the suggestion that a corresponding activity in higher eukaryotes may be part of the ribosome; alternatively, EF-3 may be unique to yeast and fungi. EF-3 is known to promote the ejection of deacylated tRNA from the E site of the ribosome following translocation *in vitro*, thereby enhancing the binding of an aminoacyl-tRNA to the A site.

The three-dimensional (3D) structure of *Thermus thermophilus* EF-G comprises six subdomains, G, G′, and II–V (Fig. 2, left). The *C*-terminal part, domains III–IV, appears to mimic the shape of tRNA (3-6). The 3D structure of the ternary complex of Phe-tRNA, *Thermus aquaticus* elongation factor EF-Tu, and the nonhydrolyzable GTP analog, GDPNP, is almost completely superimposable with EF-G:GDP [Fig. 2, right (5)], showing that domains III, IV, and V appear to mimic the shapes of the acceptor stem, anticodon helix, and T stem of tRNA in the ternary complex, respectively. Domain IV of EF-G forms a protruding “rod” conformation, which is similar to the shape of the anticodon arm of tRNA. These findings strongly suggest a common requirement for the structure and function on the ribosome. This resemblance of part of EF-G and tRNA represents a novel concept of “molecular mimicry between nucleic acid and protein.”

Figure 2. The structures of elongation factor EF-G:GDP (right) and EF-Tu:GDPNP:Phe-tRNA^{Phe} (left). Domain II in EF-G and domain II in EF-Tu were placed in identical orientations, and the structures are shown side by side in a schematic representation to the same scale.(Reproduced from the diagram kindly generated by A. Ævarsson and A. Liljas.)

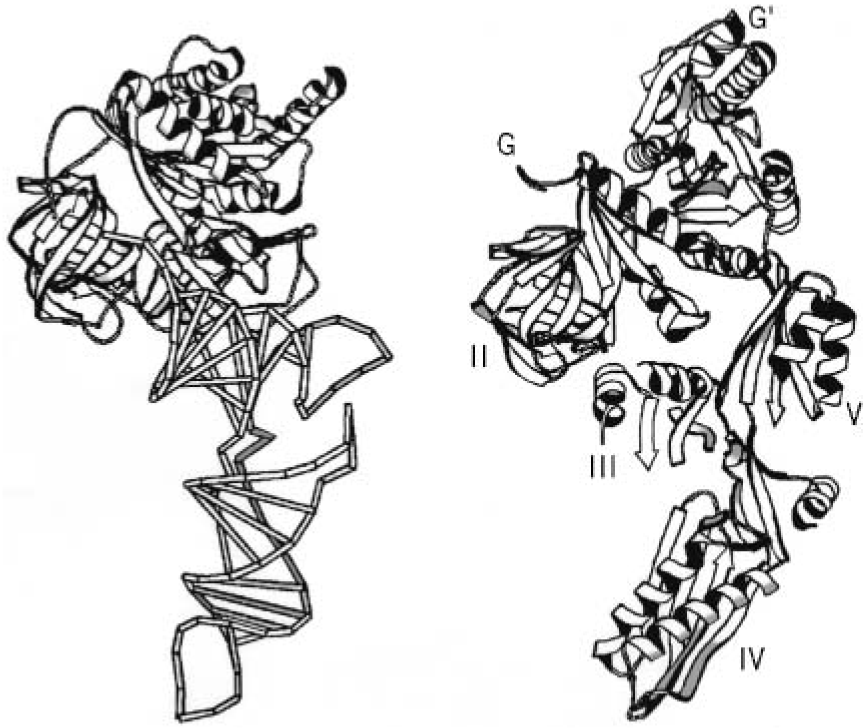

Bibliography

1. W. C. Merrick and J. W. B. Hershey (1996) In *Translational Control* (J. W. B. Hershey, M. B. Mathews, and N. Sonenberg, eds.), Cold Spring Harbor Press, Cold Spring Harbor, NY, pp. 31–69.
2. G. P. Belfield and M. F. Tuite (1993) Mol. Microbiol. **9**, 411–418.
3. A. Ævarsson et al. (1994) EMBO J. **13**, 3669–3677.
4. J. Czworkowski, J. Wang, T. A. Steitz, and P. B. Moore (1994) EMBO J. **13**, 3661–3668.

5. P. Nissen et al. (1995) Science **270**, 1464–1472.

6. K. Ito, K. Ebihara, M. Uno, and Y. Nakamura (1996) Proc. Natl. Acad. Sci. USA **93**, 5443–5448.

Suggestions for Further Reading

7. C. M. T. Spahn and K. H. Nierhaus (1998) Biol. Chem. **379**, 753–772.

8. C. G. Kurland, D. Hughes, and M. Ehrenberg (1996) In *Escherichia coli and Salmonella*, 2nd ed., (R. Curtiss III et al., eds.), American Society for Microbiology Press, Washington, D.C., pp. 979–1004.

Embryo

An embryo is the juvenile stage of an animal while it is contained within the egg membranes or the mother's body. It is formed by fertilization of the egg and undergoes morphogenesis to form differentiated organs and tissues.

Suggestions for Further Reading

B. I. Balinsky (1975) *An Introduction to Embryology*, 4th ed., W. B. Saunders, Philadelphia, p. 3.

S. Shostak (1991) *Embryology: An Introduction to Developmental Biology*, Harper Collins, New York.

J. M. W. Slack (1991) *From Egg to Embryo: Regional Specification in Early Development*, 2nd ed., Cambridge University Press, Cambridge, U.K.

Embryology

Embryology, the study of **embryos**, is the field that deals with how a single cell multiplies and changes during development to form a multicellular organism. This process by which an organism is formed is known as *embryogenesis* . Embryology can be divided into a number of smaller fields. Descriptive embryologists describe the actual events that occur during embryogenesis. Comparative embryologists study embryology in different organisms to understand how developmental mechanisms have arisen and changed during evolution. Experimental embryologists manipulate embryos in the laboratory to uncover the cellular and biochemical processes, while the more recent field of molecular embryology studies the molecules that underlie early development.

A number of species have been used extensively to study the patterns and underlying mechanisms of embryogenesis. These include the nematode *Caenorhabditis elegans*, the fruit fly *Drosophila melanogaster*, several species of marine invertebrates, such as sea urchins, starfish, and marine annelids, the African clawed toad ***Xenopus*** *laevis*, the domestic chicken, and the house mouse *Mus domesticus*.

Suggestions for Further Reading

B. I. Balinsky (1975) *An Introduction to Embryology*, 4th ed., W. B. Saunders, Philadelphia.

S. Shostak (1991) *Embryology: An Introduction to Developmental Biology*, Harper Collins, New York.

S. F. Gilbert (1997) *Developmental Biology*, Sinauer Associates, Sunderland, MA.

J. M. W. Slack (1991) *From Egg to Embryo: Regional Specification in Early Development*, 2nd ed., Cambridge University Press, Cambridge, U.K.

Enantiomer

An enantiomer is an object that has a nonsuperimposable mirror image. A right-handed helix and its mirror image are enantiomers, as shown in Figure 1. Thus, a molecule and its nonsuperimposable mirror image are both enantiomers and are both necessarily **chiral** (1). Enantiomeric molecules differ in how their solutions rotate the plane of polarized light (+ and –, for dextro and levo rotations, respectively). Enantiomers interact identically with achiral compounds, but can have different interactions with other chiral objects. The enantiomers have different **configurations**. This configuration is designated by the formally accepted rules proposed by Cahn et al., (*R*) and (*S*) (2), as described under Configuration. Because enantiomers differ in how their atoms are oriented in space, they are a special type of stereoisomer. Most enantiomers are most readily recognized by determining if each corresponding chiral center has an opposite configuration.

Figure 1. Enantiomers of a helix. The left-handed helix cannot be superimposed on its mirror image, the right-handed helix. This property makes both helices chiral and enantiomers of each other.

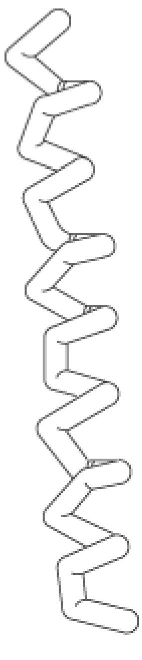

Two identical functional groups are called enantiotopic if their substitution by an isotopic label generates enantiomers (3) (see Prochiral). Thus, the protons on the amino acid glycine are enantiotopic because they are the same functional group, and alternate substitution of ^{2}H for each ^{1}H will generate the enantiomeric (*R*)- and (*S*)-[2-^{2}H]glycines.

Bibliography

1. B. Testa (1982) In *Stereochemistry* (C. Tamm, ed.), Vol. **3**, Elsevier, Amsterdam, pp. 1–48.
2. R. S. Cahn, C. K. Ingold, and V. Prelog (1966) Angew. Chem. Int. Ed. **5**, 385–415.
3. D. Arigoni, and E. L. Eliel (1969) In *Stereochemistry* (E. L. Eliel, and N. L. Allinger, eds.), Vol. **4**, Wiley-Interscience, New York, pp. 127–243.

Suggestions for Further Reading

4. E. L. Eliel (1962) *Stereochemistry of Carbon Compounds*, McGraw-Hill, New York.
5. K. Mislow (1966) *Introduction to Stereochemistry*, W. A. Benjamin, New York.
6. B. Testa (1982) In *Stereochemistry* (C. Tamm, ed.), Vol. **3**, Elsevier, Amsterdam, pp. 1–48.

Endocytosis

Endocytosis is the process whereby eukaryotic cells internalize material from their surrounding environment. Internalization is achieved by the formation of membrane-bound **vesicles** at the cell surface that arise by progressive invagination of the plasma membrane, followed by pinching off (scission), and the release of free vesicles into the cytoplasm (Fig. 1). Several different types of vesicle are generated. Each carries extracellular fluid, **macromolecules**, and particles into the cell. Extracellular materials are either free within the lumen of the vesicle or bound to its lumenal surface. Endocytosis is believed to be essential for cell viability and is required for numerous cellular functions, including (1) the provision of certain essential nutrients; (2) the removal of unwanted, nonfunctional or potentially harmful material from the extracellular medium; (3) the internalization, processing, and presentation of **antigens** by major histocompatibility complex (MHC) molecules (see Antigen Processing, Presentation); (4) the transfer of macromolecules across polarized epithelial cells; and (5) the transmission of neuronal, metabolic, and proliferative signals (see Growth Factors; Insulin). In addition, endocytosis maintains cellular homeostasis by continually monitoring the plasma membrane composition and selectively removing redundant or defective **glycoproteins**, lipids, or glycolipids for repair or degradation. Endocytosis mediates the rapid recovery of membrane components inserted into the plasma membrane during secretion and is crucial for regenerating of synaptic vesicles (see Exocytosis, Secretory Vesicles/Granules, Protein Secretion). Endocytosis is also used by a range of viral [eg, influenza virus (1)], bacterial (eg, *Legionella pneumophila*), and protozoan (eg, *Toxoplasma gondii*) pathogens, and certain protein toxins produced by plants (eg, see **Ricin**) or bacteria (eg, see Diphtheria toxin; Cholera toxin), to enter target cells (2).

Figure 1. Schematic illustration of endocytic pathways. Four different mechanisms for pinocytosis are illustrated: (1) *via* clathrin-coated pits and vesicles (CV); (2) *via* caveolae; (3) *via* noncoated pits and vesicles (NCV); and (4) *via* macropinosomes. The abbreviations used are EE, early endosome; LE, late endosome; RE, recycling endosome; ECV, endosomal carrier vesicle; and MVB, multivesicular body.

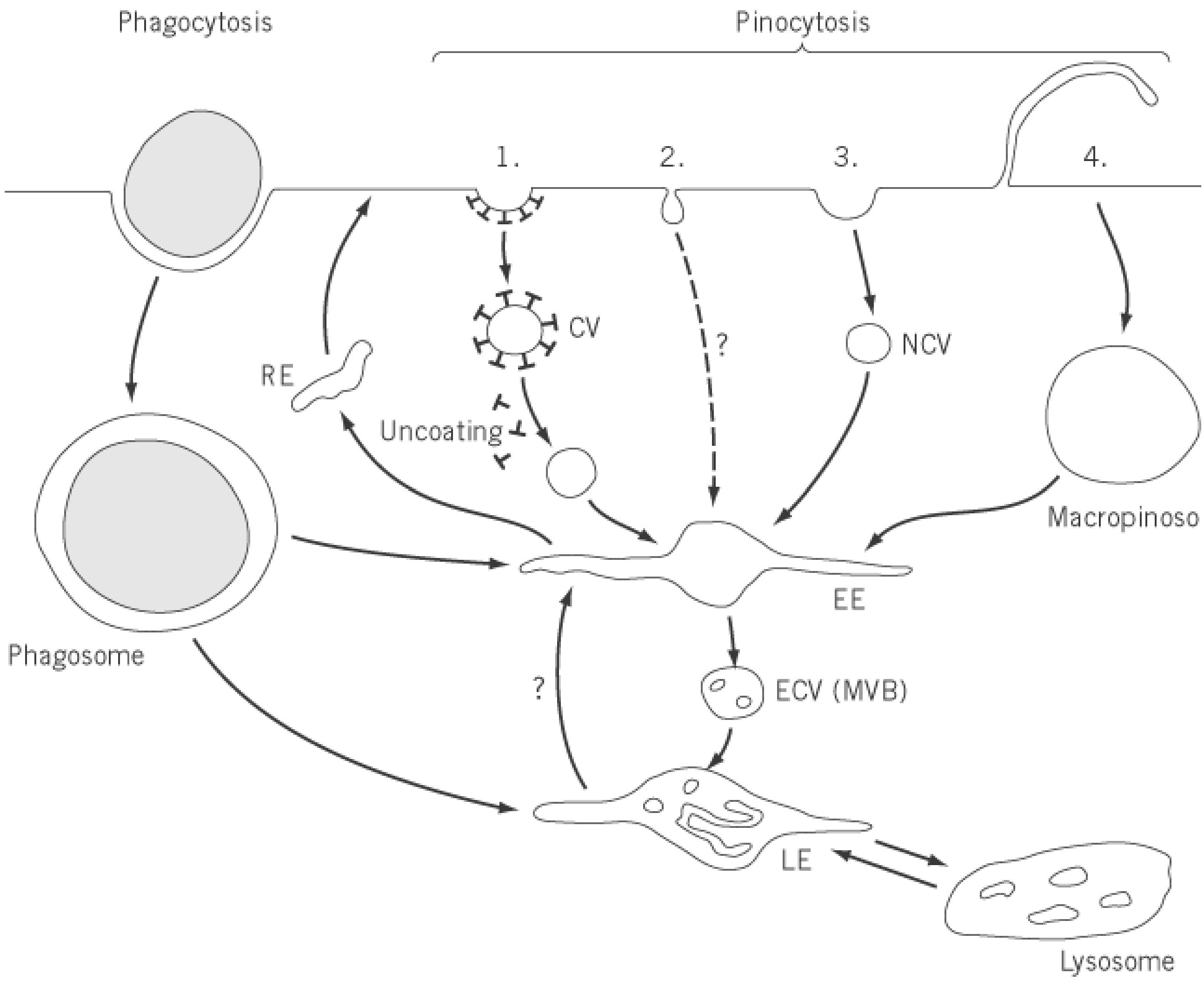

1. The Endocytic Pathway

The endocytic pathway encompasses all of the organelles in the cell that are involved in endocytosis. The pathway starts at the cell surface, which provides the membrane that forms endocytic vesicles and contains the receptors responsible for binding specific ligands internalized by these vesicles. Endocytic vesicles [phagosomes, **clathrin**-coated vesicles, caveolae, macropinosomes, and nonclathrin vesicles (see later)] derive from the plasma membrane and are directed to fuse with and deliver their membrane and content to the intracellular organelles of the endocytic pathway, the endosomes and **lysosomes**.

Lysosomes are usually regarded as the graveyard of the cell, the site where ligands internalized from the cell surface and destined for degradation are delivered and hydrolyzed. Although many receptors recycle to the cell surface, others, such as growth factor receptors, remain associated with their ligands and are delivered to lysosomes for degradation. Lysosomes are usually vesicular (~0.5 to 1 µm in diameter) and are located primarily, although not exclusively, in the perinuclear region of the cell. The pH within lysosomes can be as low as 4.8, the optimum for the many hydrolytic enzymes they contain. They derive their content from late endosomes, probably through repeated cycles of fusion with and fission from these organelles (3). In antigen-presenting cells, late endosomes and lysosomes contain large amounts of MHC II antigens and have been termed MIICs (4). In addition, lysosomes in **haematopoietic** cells are secretory organelles that undergo regulated fusion with the plasma membrane (5).

The membrane proteins, lipids, and hydrolases that make up the membrane and content of endocytic organelles are synthesized in the endoplasmic reticulum (ER) and Golgi apparatus and are subsequently transported to endosomes and lysosomes by vesicular transport. Many hydrolases carry the mannose 6-phosphate recognition marker that enables delivery *via* the mannose 6-phosphate receptors. By contrast, the membrane proteins of endosomes and lysosomes carry sorting signals (see later) that facilitate their delivery.

The endocytic pathway is extremely dynamic. In some tissue culture cells, approximately 1500 coated vesicles internalize from the cell surface every minute. This is equivalent to internalizing the membrane of the entire cell surface every 30 to 60 min (6). The surface area of early endosomes is approximately one-fifth that of the cell surface, and the entire surface area of these organelles turns over approximately every 12 min (7). Receptors, such as the **low-density lipoprotein** (LDL) receptor, are internalized very rapidly at rates of 10 to 30% of the cell surface pool per min and are recycled in 10 to 15 min back to the cell surface. Each individual receptor may mediate many rounds of internalization and recycling in its life time (8). The organization of endocytic organelles within the cell is regulated by interaction with **cytoskeletal** elements. **Actin**-based systems have been implicated in the formation of endocytic vesicles from the plasma membrane (see later), and actin/myosin and the microtubule system have been implicated in moving and positioning endocytic organelles within the cell.

2. Endocytic Mechanisms

Classically, endocytosis has been divided into phagocytosis ("cellular eating") and pinocytosis ("cellular drinking") (Fig. 1). Phagocytosis describes the internalization of large particles (>0.2 µM in diameter) following particle binding to specific plasma membrane receptors. Therefore, phagocytosis is receptor-mediated and depends on the presence of appropriate ligands. Pinocytosis is the formation of generally smaller vesicles (50 to 150 nm diameter) that transport extracellular fluid (fluid-phase endocytosis) and macromolecules specifically (receptor-mediated endocytosis) or nonspecifically (adsorptive endocytosis) bound to the plasma membrane. These vesicles are often formed constitutively from **clathrin**-coated pits independently of the presence of specific ligands, but there are alternatives to clathrin-mediated uptake (see later). The different endocytic mechanisms, more than one of which coexist and function in a single cell, are classified as phagocytosis, pinocytosis, **macropinocytosis**, and noncoated vesicles.

2.1. Noncoated vesicles

Endocytosis still occurs when clathrin-mediated uptake is blocked, as evidenced by the internalization of **ricin**, **interleukin**-2, and fluid-phase markers. Morphologically, the vesicles thought to mediate this uptake noncoated, ~80 nm in diameter, and distinct from caveolae and macropinosomes. At present, nothing is known about the molecular mechanisms responsible for this uptake process, although the continued uptake of ricin in the presence of a dominant-negative mutant form of **dynamin** suggests that it may be dynamin-independent (9).

3. Endocytosis Signals

Receptors and other proteins that undergo efficient endocytosis from the cell surface contain endocytosis signals. The signals associated with proteins that internalize through clathrin-coated pits are those that are best characterized. Four classes of endocytosis signal have been identified and studied in some detail. First are tyrosine residues within motifs similar to Phe-X-Asn-Pro-X-Tyr or Tyr-X-X-O (where X = any amino acid and O = a large **hydrophobic** amino acid), which are the endocytosis motifs identified in the LDL receptor and transferrin receptor, respectively (10). It has been proposed that these motifs form turn structures and interact either directly with clathrin (11) or with the m2 subunit of the AP-2 complex [(10) see Pinocytosis], respectively. Generally these signals are constitutively active, and proteins that contain them undergo continuous endocytosis and recycling.

A second group of signals requires pairs of hydrophobic amino acids, frequently leucine residues, although isoleucine, methionine, or valine substitutes for one of the leucines in some circumstances [e.g., MHC class II invariant chain (12)]. These so-called dileucine signals are less well characterized. There is evidence, however, that they also bind AP-2 complexes through a site or sites distinct from those bound by the Tyr-based signals. There is also evidence that in some cases (e.g., CD4) the activity of these signals is regulated by phosphorylation of adjacent serine residues (13). The signal is active when the motif is phosphorylated and inactive when dephosphorylated.

The third class of internalization signal has been identified in members of the family of seven transmembrane-domain **heterotrimeric G protein**-coupled receptors that are internalized following ligand binding. For several of these receptors, in particular the b2-adrenergic receptor, ligand-induced phosphorylation of serine residues in the serine-rich C-terminal domain of the molecule leads to recruitment of b-arrestins that uncouple associated heterotrimeric G proteins and function as adaptor complexes to recruit the receptor into clathrin-coated pits (14). Finally, in *S. cerevisiae*, a factor-induced phosphorylation of serine residues in the Ste2p receptor protein C-terminal domain leads to **ubiquitination** of Ste2p and its subsequent internalization (15). A number of mammalian cell surface receptors, including the growth hormone receptor, are also ubiquitinated following ligand binding (16). Whether this modification is required for endocytosis of the receptor and how the modification facilitates interaction with the endocytosis machinery are unclear.

Sorting signals also operate within endosomes and other sites in the endocytic pathway to specify the routing of specific proteins. The signals themselves are not well characterized. Recycling to the plasma membrane is the default pathway and may not require specific signals. However, the Tyr-X-X-O and dileucine motifs discussed previously function to target internalized proteins from early endosomes to lysosomes (12), and receptor cross-linking by multivalent ligands or antibody complexes directs sorting from early endosomes to lysosomes (17). The low pH of endocytic compartments may also influence sorting by inducing dissociation of pH-sensitive ligand-receptor interactions. Other signals, for example, a diaromatic amino acid-containing motif in the cytoplasmic domain of the cation-dependent mannose 6-phosphate receptor, function as a lysosome-avoidance motif to prevent proteins from being transported to lysosomes. How these sorting signals are interpreted is unclear for the most part, although coat proteins and adaptors have been implicated in certain steps (19). A subset of the COP1 coatomer complex has been found associated with early endosomes (20), as have clathrin and AP adaptor complexes.

4. Medical Significance

The endocytic pathway is crucial for many cellular functions. Defects in functions associated with the endocytic pathway have been linked to a number of clinical conditions. For example, failure to internalize serum LDL is associated with atherosclerosis, and defects in producing or effectively targeting lysosomal hydrolases results in a range of inherited lysosomal storage diseases. It is believed that the problems associated with Chediak-Higashi syndrome result from defects in sorting associated with late endosomes and lysosomes. Chromosomal translocations of genes that encode proteins involved in coated vesicle formation have been found in a number of lymphomas and leukemias. In addition, many bacterial, protozoan, and viral pathogens enter cells and establish infection through the endocytic pathway. It is likely that many other conditions will be linked to endocytic functions. However, the endocytic pathway is likely to provide one of the most effective routes to target and deliver drugs, DNA, or other therapeutic agents to cells.

Bibliography

1. M. Marsh and A. Helenius (1989) Adv. Virus Res. **36**, 107–151.
2. J. M. Lord and L. M. Roberts (1998) J. Cell Biol. **140**, 733–736.
3. B. M. Mullock, N. A. Bright, C. W. Fearon, S. R. Gray, and J. P. Luzio (1998) J. Cell Biol. **140**, 591–601.
4. I. Mellman, P. Pierre, and S. Amigorena (1995) Curr. Opinion Cell Biol. **7**, 564–572.

5. G. M. Griffiths (1997) Semin. Immunol. **9**, 109–15.
6. M. Marsh and A. Helenius (1980) J. Mol. Biol. **142**, 439–454.
7. G. Griffiths, R. Back, and M. Marsh (1989) J. Cell Biol. **109**, 2703–2720.
8. J. L. Goldstein, M. S. Brown, R. G .W. Anderson, and D. W. Russell (1985) Annu. Rev. Cell Biol. **1**, 1–39.
9. C. Lamaze and S. L. Schmid, (1995) Curr. Opinion Cell Biol. **7**, 573–580.
10. T. Kirchhausen, J. S. Bonifacino, and H. Riezman (1997) Curr. Opinion Cell Biol. **9**, 488–495.
11. R. G. Kibbey, J. Rizo, L. M. Gierasch, and R. G. W. Anderson (1998) J. Cell Biol. **142**, 59–67.
12. I. Sandoval and O. Bakke (1994) Trends Cell Biol. **4**, 292–297.
13. M. Marsh and A. Pelchen-Matthews (1996) In *Current Topics in Microbiology and Immunology*, Vol. **205** (D. R. Littman, ed.), Springer pp. 107–135.
14. S. S. Ferguson, L. S. Barak, J. Zhang, and M. G. Caron (1996) Can. J. Physiol. Pharmacol. **74**, 1095–1110.
15. L. Hicke and H. Riezman (1996) Cell **84**, 277–287.
16. R. Govers, P. van Kerkhof, A. L. Schwartz, and G. J. Strous (1997) EMBO J. **16**, 4851–4858.
17. P. Ukkonen, V. Lewis, M. Marsh, A. Helenius, and I. Mellman (1986) J. Exp. Med. **163**, 952–971.
18. A. Schweizer, S. Kornfeld, and J. Rohrer (1997) Proc. Natl. Acad. Sci. USA **94**, 14471–14476.
19. E. Diaz and S. R. Pfeffer (1998) Cell **93**, 433–443.
20. F. Aniento, F. Gu, R. G. Parton, and J. Gruenberg (1996) J. Cell Biol. **133**, 29–41.

Endopeptidase

Peptidases are enzymes that catalyze the hydrolysis of the **peptide bonds** that link amino acids into linear **polypeptide chains**. The Enzyme Commission of the International Union of Biochemistry and Molecular Biology classifies them as E.C. 3.4, *peptide hydrolases*. The chemical reaction that occurs can be depicted in its most simplified form as $R - CO - NH - R' + H_2O \leftrightarrow R - CO - OH + H_2N\text{-}R'$. In a linear polymer of x amino acids (x can range from 2 to >1000), there are $x - 1$ peptide bonds. Enzymes that catalyze the hydrolysis of the first or second (or sometimes even the third) peptide bond in such a linear polymer are called *exopeptidases* and, more specifically, aminopeptidases (E.C. 3.4.11–15). This is because the amino group of the first amino acid in a linear polymer of amino acids is not part of a peptide bond, and hence this end of the chain of x amino acids is called the *amino terminus* (or N-terminus). Enzymes that catalyze the hydrolysis of the last or the penultimate peptide bond in this chain are also exopeptidases, but in this case they are carboxypeptidases (E.C. 3.4.16–19). The carboxyl group of the last amino acid in the chain is similarly not part of a peptide bond, and this end of the chain is therefore the *carboxy terminus* (or C-terminus).

Peptidases that catalyze the hydrolysis of internal peptide bonds in the polypeptide chain are called *endopeptidases* (E.C. 3.4.21–24, 99). The subclass to which they are assigned depends on the particular type of mechanism they employ to achieve catalysis (see Proteinases).

Endoplasmic Reticulum

The endoplasmic reticulum (ER) is an extensive network of membranous cisternae that extends throughout much of the cytoplasm (Fig. 1). The three main functions of this organelle are: (i) biosynthesis of proteins that are destined to be secreted, deposited on the cell surface, or reside in other organelles of the exocytosis and endocytosis pathways (see Protein Secretion). (ii) synthesis of lipids; and (iii) regulation of calcium (Ca^{2+}) storage (see Calcium Signaling). Because the ability to perform these functions is essential for growth and differentiation of all cells, the ER is ubiquitous. Yet it undergoes dynamic changes that allow it to adapt to the changing physiological demands of various cells and tissues. The unique shape and architecture of the ER reflect its functional connections to other organelles. At the cell center, the ER is contiguous with the **nuclear** envelope. At the cell periphery it becomes a long, tubular network, often enveloping mitochondria and sometimes extending to the proximity of the plasma membrane (Figs. 1–2). This reticular architecture mediates the physical connections, as well as the chemical communication, between the ER and most other cellular compartments. A recurrent theme in the sections that follow, describing individual functional aspects of the ER, is the multitude of ways through which the ER exchanges biochemical components, be they ions, lipids, or proteins, with other organelles.

Figure 1. Light microscopic image of the ER. Immunofluorescence staining of a COS-1 cell expressing an ER-retained form of immunoglobulin light chain. The ER staining fills most of the cytoplasm, with the reticular appearance most evident at the periphery (arrow). The typical staining of the nuclear envelope is visible as a prominent ring (arrowhead) around the nucleus (N). Bar, 10 µm.

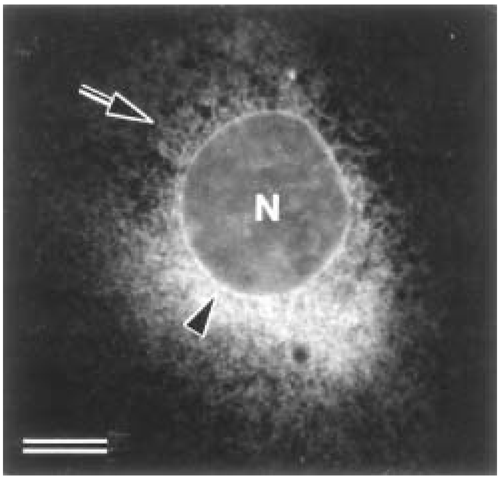

Figure 2. Electron micrograph of a plasma cell. A murine antibody-secreting cell exhibiting a typically expanded ER. Arrow, a region of the endoplasmic reticulum with stacked flattened cisternae of rough ER, each with the typical beaded appearance due to densely bound ribosomes. N, nucleus. M, mitochondrion; bar, 1 µm.

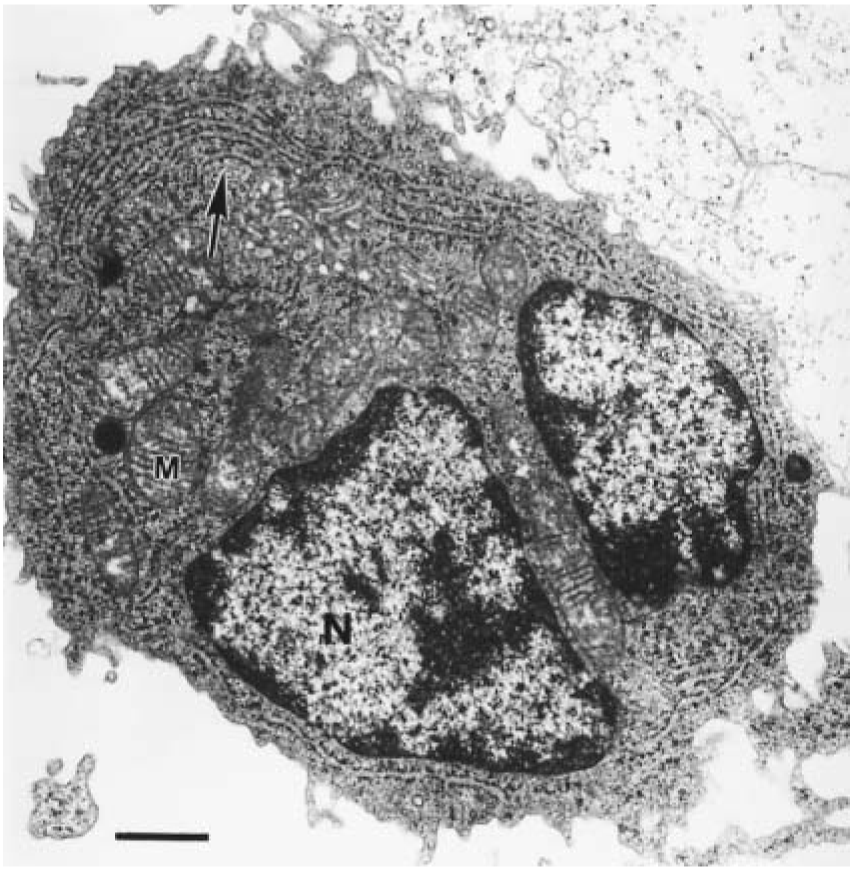

1. The Structure of the ER

The reticular architecture of the ER is maintained by numerous dynamic contacts between the ER membrane and microtubules. These connections are mediated by the molecular motor complex kinesin, which attaches to microtubules via its globular, *N*-terminal head **domain** and to the ER membrane via its *C*-terminal domain. The latter interaction is presumably mediated by kinectin, a 160-kDa integral membrane protein of the ER, which has been shown to be a kinesin receptor (1, 2). These attachments enable the ER cisternae to extend or contract along microtubules, which themselves assemble and disassemble dynamically. The dynamic nature of the ER structure is evident when cells are stressed: Drastic changes in cell shape, caused by depolymerization of microtubules, are accompanied by collapse of the reticular ER toward the cell center (3). The precise molecular regulation of the attachment to microtubules, and possibly other **cytoskeletal** elements, are yet to be elucidated. Other important unresolved issues include how the ER cisternae maintain a flattened structure, with a very high surface-to-volume ratio, and what the physiological implications are of this cisternal structure.

2. Subcompartments of the ER

In higher eukaryotes, that part of the ER to which ribosomes are attached is known as the rough ER, due to its distinctive beaded appearance in electron micrographs (4) (see Fig. 2). In "professional" secretory cells, the rough ER is the vastly predominant form, because of the demand for high throughput of **protein biosynthesis**, folding, and trafficking (see text below). The morphology of the rough ER reflects these biosynthetic roles, and underlying it is a distinct protein composition. The rough ER membrane is the site of expression of ribophorins and many other components involved in docking ribosomes and in translocating nascent proteins across the membrane (eg, see Refs. 5 and 6) (see Protein Secretion).

The remainder of the ER, devoid of attached ribosomes, is called the smooth ER. The smooth ER membrane is the site of residence of cytochrome P450 and other components of the mixed-function oxidase system. The smooth ER is also involved in synthesis of various lipids and in the assembly of lipoprotein particles. Thus, the smooth ER predominates in cells where the expression of such proteins is high (eg, hepatocytes), while it is only a small fraction of the ER in secretory cells like pancreatic acinar cells.

The ER membrane proteins are clearly segregated between the smooth and rough subcompartments, although the molecular mechanism for this segregation is unresolved. Microscopic studies following the distribution of proteins like the binding protein BiP or protein disulfide isomerase (PDI) in a variety of cells suggest that the entire lumen of the ER is contiguous, with no obvious separation between smooth ER and rough ER lumen or between the reticular ER in the cell periphery and the nuclear envelope.

In excitable cells, the ER is specialized both morphologically and biochemically and is known as the *sarcoplasmic reticulum* (SR). Smooth cisternae of the SR make frequent contacts with the membrane of muscle cells. These terminal cisternae contain complexes of proteins involved in Ca^{2+} modulation, including membrane proteins like the ryanodine receptors and specialized SR calcium-binding proteins, like calsequestrin. The segregation of proteins is clearly related to Ca^{2+} storage and release, as general lumenal proteins in the SR (like BiP) do not exhibit similar subcompartmentalization (7).

3. Protein Translocation

The rough ER is the organelle that couples protein biosynthesis to membrane translocation, allowing segregation of secretory and membrane proteins from cytosolic or nuclear proteins. Secreted and membrane proteins are marked for translocation by a **signal sequence**, which is usually cleaved early in the biosynthesis of the proteins (8). Signal sequences are generally *N*-terminal, consist of around 20 amino acid residues, and are characterized by a central string of **hydrophobic** amino acids flanked by clusters of charged residues, and a residue with a small side chain precedes the cleavage site (9). Once a signal sequence has emerged from a ribosome, that ribosome is targeted to the ER membrane, where the nascent chain is translocated across the membrane. This targeting is accomplished primarily by a cytoplasmic ribonucleoprotein complex, the signal recognition particle (SRP) (10). SRP performs three distinct activities: (i) binding to the signal sequence that is exposed on the surface of a **translating** ribosome; (ii) retarding further elongation of the nascent polypeptide; and (iii) docking onto the SRP receptor in the ER membrane. Upon completion of this sequence of events, the SRP detaches, and the signal sequence is inserted into the membrane. Due to the intrinsic hydrophobicity of signal peptides, they themselves may interact with the lipid bilayer and thus aid the translocation process at this stage. After the initial association of the nascent chain with the membrane, the ribosomes bind more avidly to the ER by protein–protein interactions with the Sec61p complex, a seven-component transmembrane complex of proteins.

Nascent polypeptides cross the lipid bilayer through a protein channel (11), known as the *translocon*. The minimal translocon has been reconstituted *in vitro* (12, 13), and the necessary components were shown to be the SRP receptor, the Sec61p complex, and a translocating chain-associated membrane protein (TRAM). Purified mammalian and yeast Sec61p complexes in detergent solution or in proteoliposomes form cylindrical oligomers of three to four heterotrimers each, with a diameter of approximately 85 Å and a central pore of approximately 20 Å. Formation of the reconstituted translocon is stimulated by association with ribosomes or with the Sec62/63p complex (14).

At early stages of translocation, prior to signal sequence cleavage, nascent chains can be shown by chemical **cross-linking** to contact the Sec61a subunit and the signal sequence receptor (p34), via both the signal peptide and the remainder of the polypeptide chain (15, 16). At later stages of translocation, which can be trapped experimentally with the use of truncated translocation intermediates, the proximity to Sec61p is markedly reduced. These data are in line with the interpretation that, at early stages of translocation, nascent chain-Sec61p interactions are in part mediated through interactions of the ribosome with components of the ER membrane, but that subsequent translocation can occur after dissociation of the ribosome (15).

Once the signal sequence enters the lumen, it is cleaved off most proteins. The enzyme responsible for this cleavage, signal peptidase, is a hetero-oligomeric membrane protein containing subunits of 12, 18, 21, 22 / 23, and 25 kDa. The 18- and 21-kDa subunits are mammalian homologues of Sec11p, a yeast protein that is necessary for signal peptide processing and cell viability. The topology of signal peptidase places the bulk of the protein in the ER lumen, including its putative **serine**-containing active site, located in the 18- and 21-kDa subunits (17).

A second route for protein entry into the ER is post-translational and independent of SRP. In this route, which is more extensively used in yeast than in higher eukaryotes, a complete polypeptide chain is made in the cytoplasm and held in an incompletely folded state by **molecular chaperones** such as cytosolic hsp70. Fully synthesized secretory precursors then engage the ER membrane by interaction with the Sec complex, which in post-translocational translocation contains further protein subunits that are required for function, in addition to those of the co-translational Sec61 complex. It is not yet known what distinguishes a polypeptide chain that uses the co-translational route from a polypeptide that is translocated post-translationally. Productive post-translational interaction with Sec61p requires displacement of hsp70 from the precursor polypeptide. This reaction is facilitated by the chaperone Ydj1p, a homologue of the *E. coli* DnaJ protein, which stimulates the inherent ATPase activity of the hsp70 chaperone. In the ER lumen, another hsp70-like chaperone, BiP, is an important part of the translocation machinery. In yeast ER, BiP is known to associate with the translocation complex via its contact with the DnaJ-homologous domain of the transmembrane protein Sec63p (18). The membrane-bound BiP can hydrolyze ATP, and the polypeptide moves through the channel formed by the Sec complex and is released at the lumenal side (19). The process of post-translational translocation is made vectorial because of the cleavage of signal sequences and because the interactions with the hsp70s on either side of the membrane are unequal; cytosolic hsp70 and BiP cannot replace each other.

In the mammalian ER, as in yeast, BiP is required for the completion of polypeptide translocation. Moreover, BiP in its ATP-bound, non-substrate-binding state also functions to seal the translocon (20). In this fashion, it sustains the permeability barrier of the ER membrane, which otherwise would be compromised by the existence of thousands of translocation channels (21).

4. Protein Post-translational Modifications

Membrane and secreted proteins can be modified by a number of post-translational modifications, the most common being glycosylation and phosphorylation. The most prevalent glycosylation is via the addition of a 14-sugar oligosaccharide onto certain Asparagine (Asn, N) residues, termed N-glycosylation. The oligosaccharide usually consists of three glucose (Glc), nine mannose (Man) and two *N*-acetylglucosamine (GlcNAc) residues and is called *high mannose*. This oligosaccharide is assembled onto a dolichol lipid carrier by a series of enzymes that reside in the ER membrane. The first seven sugars are assembled by enzymes facing the cytosol. The $Man_5GlcNAc_2$-dolichol intermediate is then translocated across the membrane, and the final assembly steps are performed on the lumenal face (22, 23).

A multisubunit enzyme, oligosaccharyltransferase (OST), is responsible for the transfer of the preassembled high-mannose oligosaccharide from the dolichol-linked donor onto Asn acceptor sites in nascent proteins on the luminal side of the ER membrane (24). These acceptor sites are within the tripeptide Asn-X-Ser/Thr (where X is any amino acid except Pro), provided that this tripeptide is accessible to OST.

Immediately upon addition to the protein, the high-mannose oligosaccharide is subjected to progressive trimming. First, the terminal Glc is removed by glucosidase I, followed by sequential removal of the next 2 Glc by glucosidase II. These steps are followed by a third trimming enzyme, a mannosidase that trims the oligosaccharide down to the Man_5–Man_8 forms (25). Additional trimming occurs after the glycoproteins traffic to the Golgi apparatus, before final remodeling to complex types of oligosaccharides.

A second type of glycosylation, O-glycosylation of serine or Threonine (Thr, T) residues by shorter and different carbohydrates, is a less frequent modification and is currently thought to take place mostly in the Golgi complex and not in the ER.

Another common protein modification is phosphorylation of Ser/Thr residues, and this modification is thought to play a regulatory role in the function of these proteins. A number of itinerant and resident ER proteins are known to be phosphorylated, on cytoplasmic domains as well as on luminal domains. The former phosphorylation can be performed by a number of known kinases in the cytosol. The phosphorylation of luminal domains has, in most cases, the hallmarks of a casein kinase II-like enzyme. However, no ER-specific kinase has yet been purified. The phosphorylation of Tyr residues, of major importance in signaling at the plasma membrane, has not yet been observed within the ER.

5. Lipids

In addition to its role in protein synthesis, the ER is a major site of lipid synthesis, and both phospholipid and sterol biosynthesis enzymes reside in this organelle. While some phospholipids are synthesized by cytosolic enzymes, much of phospholipid biosynthesis is performed by base-exchange enzymes and phospholipase D in the ER. Base-exchange enzymes alter the polar head group, allowing for interconversion of different phospholipid species. Phospholipase D hydrolyzes phospholipids to phosphatidic acid, which is used for further lipid biosynthesis.

The ER houses enzymes involved in cholesterol biosynthesis, as well as those that participate in oxidation of cholesterol to bile acids. Of them, HMG-CoA reductase is a key rate-limiting enzyme in steroidogenesis, and the intricate control of its expression is another manifestation of the communication between the ER and other organelles.

Because cholesterol and the apolipoproteins are both synthesized in the ER, much of the assembly of lipoproteins takes place in this organelle. The bulk of the very-low-density lipoprotein (VLDL) triacylglycerol and some VLDL phosphoglyceride is introduced early in the secretory pathway, soon after apolipoprotein synthesis. On the other hand, a significant fraction of VLDL phosphoglyceride associates with the resulting triacylglycerol-rich lipid–protein complexes in more distal secretory compartments, just prior to their secretion as mature VLDL.

6. Calcium

Changes in intracellular Ca^{++} concentration are a common signal transduction device linking plasma membrane receptors with the initiation of specific cellular responses, including cell growth, muscle cell contractility, and exocytosis in secretory cells. The ER and its specialized form, the SR, is a major dynamic calcium storage organelle in eukaryotic cells. Its Ca^{2+} concentration is estimated to reach 10 mM, whereas free Ca^{2+} in the cytosol is only in the nanomolar range. The ER Ca^{2+} storage capacity is provided by a multitude of luminal proteins. Among them are the ubiquitous and abundant chaperones, like GRP94, calreticulin (see Calnexin/Calreticulin), and the PDI-like proteins, or proteins whose expression is tissue-specific, like calsequestrin in the SR. Most of the Ca^{2+} binding is via multiple (as many as 50) low-affinity ($K_d = 1$ mM) binding sites per protein, but some proteins have a few high-affinity sites, including **EF-hand** domains (26). The ER membrane regulates the flow of Ca^{2+} via three types of proteins: (i) the ER/SR- Ca^{2+}-ATPase (SERCA), which is a pump that can be inhibited by the drug thapsigargin; (ii) **calcium channels**, which are either the ubiquitous inositol trisphosphate receptors or the ryanodine receptors; (iii) and Na^{+}/Ca^{2+} exchangers. Together, the membrane Ca^{2+} gates and the luminal binding proteins provide a rapid response system to mobilize Ca^{2+} as physiological conditions demand. Release of ER-stored Ca^{2+} into the cytosol affects diverse sets of proteins, such as EF-hand proteins, annexins, and the C2 region proteins (26).

The Ca^{2+} homeostasis function of the ER is most specialized in muscle cells, where Ca^{2+} mobilization is an important component of the contractile apparatus. Ca^{2+} binding proteins and Ca^{2+} channels are highly expressed in the SR, often employing muscle-specific versions of these proteins. For example, calsequestrin is an SR-specific Ca^{2+} buffer that has structural homology to calreticulin, which is expressed ubiquitously in higher eukaryotic cells. In nonexcitable cells, the need to store Ca^{2+} can be satisfied by many of the luminal proteins. For example, even though calreticulin can store Ca^{2+}, its ablation reveals that it is an essential modulator of integrin adhesive functions and integrin-initiated signaling, but is dispensable for the storage of luminal Ca^{2+} (27).

As discussed above, the structure and biochemical composition of the SR reflect its important role in mediating signals emanating from cell-surface receptors. The proximity to the plasma membrane of distal SR cisternae enriched in inositol trisphosphate and ryanodine receptors position the relevant receptors to interact with second messengers generated during signal transduction and to respond by modulating the storage or release of Ca^{2+}. Another example is the expression of phospholamban, a 52-residue protein that assembles into a pentamer in SR membranes. Phospholamban plays a role in regulating the resident Ca^{2+} ATPase through an inhibitory association that can be reversed by phosphorylation. The phosphorylation of phospholamban is initiated by b-adrenergic stimulation, identifying phospholamban as an important component in the stimulation of cardiac activity by b-agonists (28). These examples illustrate the functional connections that exist between the ER and the plasma membrane, connections that are important for efficient signal transduction.

7. Protein Folding in the ER

The lumen of the ER is the environment where all secretory polypeptide chains and those destined to reside in various cellular organelles fold. Like other **protein folding** compartments, the ER has a very high concentration of soluble proteins (estimated to be as high as 100 mg/mL), a factor that is conducive to aggregation. The ER is very different from other folding compartments in its higher oxidation/reduction potential, high Ca^{2+} concentration, and lack of energy source (ATP is imported via a special permease). These conditions necessitate the presence of a number of ER enzymes and chaperones to facilitate protein folding. Moreover, a number of mechanisms have evolved to ensure that only properly configured proteins proceed along the secretory pathway and that defective molecules are disposed of (29, 30). Indeed, most of the abundant luminal proteins are involved in protein folding.

One of the main ER chaperones is BiP/GRP78, which is the ER member of the hsp70 family of **stress-response** proteins. *In vitro*, BiP (and other hsp70 proteins) bind hydrophobic peptides, preferring peptides of 7–10 amino acids with either alternating (31) or clustered aromatic or large aliphatic residues (32). *In vivo*, BiP probably binds similar hydrophobic sequences that are exposed in the folding polypeptide chain, but inaccessible in the native structure. One important result of this activity is to minimize aggregation of the unfolded polypeptide chain. Peptide binding stimulates the slow ATPase activity of BiP, and the substrate is released after either nucleotide exchange or hydrolysis (33), allowing it another chance to bury its hydrophobic sequences as its folding progresses. In its capacity as a peptide-binding protein, BiP is often found to associate preferentially with nonsecretable or misfolded mutants, presumably because these molecules continue to expose binding sites that are buried more rapidly in wild-type molecules. In this fashion, BiP plays a role in the ER quality control system (34), either retarding the transport of proteins (35) or even targeting them for **protein degradation** (36).

As in the case of folding in the cytosol, an important rate-limiting step in folding in the ER can be the ***cis-trans*** **isomerization** of the **peptide bonds** of certain proline residues. This reaction is catalyzed by peptidyl prolylcis/trans isomerases, and it seems to be a redundant activity that several luminal proteins, including S-cyclophilin and **FK506**-binding protein 13, can perform.

A general property distinguishing cytosolic proteins from those that fold in the ER is the presence of disulfide bonds in the latter. Cysteine residues in nascent polypeptides oxidize in the lumen because of the higher redox potential, maintained by the approximately 3:1 ratio of reduced (GSH) to oxidized (GSSG) forms of glutathione (37). Because disulfide bonds form covalent folding intermediates, they are very important in the folding process (38). Thus, a number of luminal enzymes are capable of catalyzing the rearrangement of protein disulfide bonds. The most abundant of these enzymes are the 57-kDa protein disulfide isomerase and two structurally related proteins, ERp72 and ERp58. There is currently no evidence for the existence of disulfide isomerases in any other organelle of eukaryotes.

A second general property of proteins that fold in the ER is their frequent modification by Asn-linked glycosylation, as discussed above. The state of modification of these carbohydrates can be used to monitor the folding of **glycoproteins**. The terminal Glc residues on the initial high-mannose oligosaccharide are trimmed sequentially by glucosidase I, an ER membrane protein, and glucosidase II, a luminal protein. The enzyme that can reattach terminal Glc residues, UDP-Glc:glycoprotein glucosyltransferase, can distinguish between folded and unfolded polypeptides (39). Also involved in this monitoring system are the membrane-spanning calnexin and the soluble, Ca^{2+}-binding calreticulin. They are structurally related, and both can bind to monoglucosylated glycoproteins, an intermediate stage in the processing. In this way, calnexin and calreticulin bind to a partly trimmed intermediate and serve as sensors of the glycosylation state. The final Glc is then trimmed, and the glycoprotein is then either reglucosylated by the glucosyltransferase, if its state of folding is immature, or recognized as mature enough to be packaged for transport to the Golgi complex.

Although calnexin and calreticulin have similar fine specificities of binding to the trimmed oligosaccharides, they can clearly distinguish and bind different folded forms of the same protein. The basis for this difference is not clear. Nonetheless, gene ablation of calnexin and calreticulin in both *Saccharomyces cerevisiae* and mammalian cells in culture show that their roles in protein folding are redundant. An important unresolved issue is whether the **lectin**-like activity of the two chaperones is sufficient to account for their recognition of folding species, or whether the chaperones also interact with the folding polypeptides themselves.

In addition to BiP, calnexin, and calreticulin, there are several other resident ER proteins that function as molecular chaperones. Among these are GRP94 and PDI, which have been shown to associate transiently with folding intermediates. ERp72, ERp58, and the **immunophilins** are also potential chaperones or enzymes involved in folding, based on their association with other proteins and on their sequence similarity to cytosolic chaperones. GRP94 (also known as ERp99, gp96, endoplasmin, and hsp108) is a homodimeric glycoprotein that binds Ca^{2+} and ATP and makes up 5% to 10% of the total luminal protein. It is known to bind a number of peptides (40), as well as a narrow spectrum of proteins. GRP94 is a stress protein from the hsp90 family, whose synthesis is induced upon glucose starvation, Ca^{2+} depletion, or treatments with **tunicamycin** and amino acid analogues. Physiologic demands can also induce GRP94 expression: It is up-regulated during the differentiation of resting B lymphocytes into **antibody**-secreting cells (41) and within plasma cells in response to the production of nonsecretable immunoglobulins. The regulation of GRP94 under all these conditions is coordinated with other ER proteins, most notably BiP (41), and to a lesser extent

PDI and ERp72 (42). The role of GRP94 (and those of ERp72, ERp58 and immunophilins) in protein folding *in vivo* remains unclear, however, largely because its substrate specificity and detailed modes of action are still to be elucidated.

The growing list of ER chaperones raises several questions: Do they perform redundant functions or are they functionally distinct? How do they discriminate among the various proteins that fold in the ER? How do they participate in different aspects of the folding process? Regulation of the activity of molecular chaperones is another fundamental problem that is only beginning to be addressed. Phosphorylation has been shown to regulate the activity of BiP (43). GRP94, calnexin, and calreticulin are known to be phosphorylated *in vivo*, but the relation of the modification to their function is not yet understood. Thus, an intriguing emerging possibility is that ER chaperones cycle between active and inactive states that are marked by phosphorylation. The presence of so many folding factors clearly provides an environment that promotes efficient folding of proteins that are destined for export and in many cases are produced in large amounts.

8. Degradation of ER Proteins

An inevitable by-product of an active folding compartment is the presence of misfolded proteins and the need to degrade them (see DNA Degradation In Vivo). For many years it was thought that such degradation occurs within the ER itself, but this notion was challenged by the inability to demonstrate an appropriate set of ER proteinases, equivalent to those that reside in the cytosol. Recent discoveries, in both mammalian systems (44, 45) and in yeast (46, 47), have now clearly demonstrated the presence of a conserved retrograde traffic pathway, whereby misfolded secretory proteins are presented to the cytosolic proteasome machinery for degradation (48). Misfolded soluble and membrane proteins are translocated out of the ER, probably through the same Sec61 channel used for incoming nascent chains, and are guided with the aid of cytosolic hsp70 to 26S proteasome particles, many of which are in proximity to the ER membrane. Often, as in degradation of cytosolic proteins, the misfolded proteins that are translocated out of the ER are marked for degradation by covalent addition of poly-ubiquitin chains. The proteasome is apparently highly processive, because no large degradation intermediates are seen, and the products are short peptides with a narrow size distribution. For many membrane and secreted proteins, proteasome-mediated degradation is now thought to be the major route of disposal if they fail to fold properly, although the existence of a proteolytic pathway within the ER itself is still a possibility.

9. Sorting of Itinerant and Resident ER Proteins

The transport of proteins from the ER to the Golgi complex is via **vesicles**. Cargo proteins are selectively concentrated into “exit sites” marked by 10-nm-thick electron-dense cytosolic coats that are made of two distinct biochemical complexes, called COPI and COPII (49). Under the control of a fission machinery that uses small Gtpases to regulate protein–protein interactions, COP-coated vesicles bud off the ER membrane and are targeted for fusion with the next membrane in the pathway. The mechanism of membrane budding driven by COPII shows remarkable overall similarities to that of COPI budding, the coat that is also involved in intra-Golgi transport and in retrograde transport to the ER, as well as to budding of **clathrin**-containing coated vesicles, which mediate transport from the plasma membrane and from the *trans*-Golgi network. The discrimination between cargo proteins and resident ER proteins at the level of packaging into the vesicles is thought to be mediated by a family of small 24-kDa proteins (50). Vesicle budding from the ER has been reconstituted with purified membranes and three soluble proteins from yeast: Sec13 complex, Sec23 complex, and the small GTPase Sar1p (51).

Luminal residents of the ER, like the chaperones BiP and GRP94 and the enzyme PDI, use a receptor-mediated mechanism to ensure their localization within the ER lumen. Their *C*-terminus consists of the tetrapeptide Lys–Asp–Glu–Leu (KDEL), which is recognized specifically by an intracellular receptor that resides mainly throughout the Golgi complex. Similar receptors with slightly altered tetrapeptide specificities are found in lower eukaryotes. KDEL proteins that “escape” the ER are specifically retrieved by this receptor and transported back to the ER (52, 53).

Resident ER membrane proteins often have a different type of retrieval signal that distinguishes them from itinerant membrane proteins: a dibasic amino acid (either Lys–Lys or Arg–Arg) motif in their cytosolic domain near the *C*-terminus. This motif is recognized by the COPI complex, providing the basis for specifically packaging these proteins in vesicles that transport them retrogradely from the Golgi to the ER (54).

The combination of biochemical experiments reconstituting transport vesicles with the elucidation of retention mechanisms that differentiate resident ER proteins from itinerant proteins brings us closer to solving the important problem of how proteins are selectively sorted and packaged into transport vesicles, a question that is at the heart of the compartmentalization of eukaryotic cells.

10. Biogenesis of the ER

In fibroblasts, the ER accounts for 2% to 5% of the cytoplasmic volume, whereas in "professional" secreting cells, like pancreatic acinar cells or lymphoid plasma cells, the ER is considerably expanded, its cisternae are often stacked together (4), and it occupies up to 25% of the cytoplasm (Fig. 2). For example, during the development of **B cells** into plasma cells, when synthesis and secretion of immunoglobulin increase by two orders of magnitude, the ER grows, with both the volume and membrane area increasing three- to fourfold (41), and it changes from a network surrounding the nuclear envelope to one that fills the peripheral cytoplasm. There is a coordinate increase in the synthesis of the main luminal proteins, as well as of membrane proteins involved in the translocation process.

This phenomenon is probably the normal counterpart to the induction of luminal proteins observed as a result of accumulation of unfolded proteins in the ER under a variety of metabolic stresses, the so-called unfolded protein response (UPR). The accumulation of unfolded protein in the ER causes induction of the biosynthesis of ER proteins to alleviate the situation.

A second pathway of signal transduction from the ER to the nucleus regulates sterol biosynthesis. A small family of transcription factors, the sterol response element binding proteins (SREBPs), activates sterol-regulated **promoters**, such as those of the genes for the key enzyme HMG-CoA reductase or the LDL receptor, as well as other enzymes that synthesize fatty acids (55). SREBP is synthesized as an ER membrane protein; upon sterol depletion, it is processed by two proteinases, one of them probably a thiol proteinase, releasing the active DNA-binding transcription factor and enabling its translocation to the nucleus (56). In this fashion, coordinate metabolic control over two types of lipids necessary for membrane biosynthesis is maintained and is triggered by alterations in the lipid composition of the ER membrane.

HMG-CoA-reductase is also at the center of another ER biogenesis phenomenon. When it is overexpressed as a result of compactin treatment, there is a reversible proliferation of smooth ER membranes, which pack in hexagonal arrays (57). A similar elaboration of ER-derived smooth membranes is seen in various yeast strains deficient in inositol metabolism. These may represent cases where one of the feedback mechanisms that regulate the size of the ER "overreact," leading to excessive synthesis of some components, instead of coordinate synthesis of all components, as is required to maintain homeostasis of the ER.

Bibliography

1. I. Toyoshima, H. Yu, E. R. Steuer, and M. P. Sheetz (1992) J. Cell Biol. **118**, 1121–1131.
2. H. Yu, C. V. Nicchitta, J. Kumar, M. Becker, I. Toyoshima, and M. P. Sheetz (1995) Mol. Biol. Cell **6**, 171–183.
3. M. Terasaki, L. B. Chen, and K. Fujiwara (1986) J. Cell Biol. **103**, 1557–1568.
4. G. Palade (1975) Science **189**, 347–358.

5. D. I. Meyer, E. Krause, and B. Dobberstein (1982) Nature **297**, 647–650.
6. S. Tajima, L. Lauffer, V. L. Rath, and P. Walter (1986) J. Cell Biol. **103**, 1167–1178.
7. R. Sitia and J. Meldolesi (1992) Mol. Biol. Cell **3**, 1067–1072.
8. G. Blobel and B. Dobberstein (1975) J. Cell Biol. **67**, 835–851.
9. G. von Heijne (1984) J. Mol. Biol. **173**, 243–251.
10. P. Walter, I. Ibrahimi, and G. Blobel (1981) J. Cell Biol. **91**, 545–550.
11. S. M. Simon and G. Blobel (1991) Cell **65**, 371–380.
12. C. V. Nicchitta, G. Migliaccio, and G. Blobel (1991) Cell **65**, 587–598.
13. D. Gorlich and T. A. Rapoport (1993) Cell **75**, 615–630.
14. D. Hanein, K. E. Matlack, B. Jungnickel, K. Plath, K. U. Kalies, K. R. Miller, T. A. Rapoport, and C. W. Akey (1996) Cell **87**, 721–732.
15. C. V. Nicchitta, E. C. R. Murphy, R. Haynes, and G. S. Shelness (1995) J. Cell Biol. **129**, 957–970.
16. S. High, D. Gorlich, M. Wiedmann, T. A. Rapoport, and B. Dobberstein (1991) J. Cell Biol. **113**, 35–44.
17. G. S. Shelness, L. Lin, and C. V. Nicchitta (1993) J. Biol. Chem. **268**, 5201–5208.
18. S. K. Lyman and R. Schekman (1995) J. Cell Biol. **131**, 1163–1171.
19. K. E. Matlack, K. Plath, B. Misselwitz, and T. A. Rapoport (1997) Science **277**, 938–941.
20. B. D. Hamman, L. M. Hendershot, and A. E. Johnson (1998) Cell **92**, 747–758.
21. T. A. Rapoport (1992) Science **258**, 931–936.
22. R. Kornfeld and S. Kornfeld (1985) Annu. Rev. Biochem . **54**, 631–664.
23. M. D. Snider and C. B. Hirschberg (1987) Annu. Rev. Biochem. **56**, 63–88.
24. S. Silberstein and R. Gilmore (1996) FASEB J. **10**, 849–858.
25. J. Bischoff and R. Kornfeld (1983) J. Biol. Chem. **258**, 7909.
26. J. Meldolesi and T. Pozzan, (1998) Trends Biochem. Sci. **23**, 10–14.
27. M. G. Coppolino, M. J. Woodside, N. Demaurex, S. Grinstein, R. St. Arnaud, and S. Dedhar (1997) Nature **386**, 843–847.
28. I. T. Arkin, P. D. Adams, A. T. Brunger, S. O. Smith, and D. M. Engelman (1997) Annu. Rev. Biophys. Biomol. Struct. **26**, 157–179.
29. A. M. de Silva, W. E. Balch, and A. Helenius (1990) J. Cell Biol. **111**, 857–866.
30. A. Helenius, T. Marquardt, and I. Braakman (1992) Trends Cell Biol. **2**, 227–231.
31. M. J. Gething, S. Blond-Elguindi, J. Buchner, A. Fourie, G. Knarr, S. Modrow, L. Nanu, M. Segal, and J. Sambrook (1995) Cold Spring Harb. Symp. Quant. Biol. **60**, 417–428.
32. S. Rudiger, A. Buchberger, and B. Bukau (1997) Nat. Struct. Biol. **4**, 342–349.
33. G. C. Flynn, T. G. Chappell, and J. E. Rothman (1989) Science **245**, 385–390.
34. S. K. Nigam, A. L. Goldberg, S. Ho, M. F. Rohde, K. T. Bush, and M. Y. Sherman (1994) J. Biol. Chem. **269**, 1744–1749.
35. A. J. Dorner, L. C. Wasley, and R. J. Kaufman (1992) EMBO J. **11**, 1563–1571.
36. M. R. Knittler, S. Dirks, and I. G. Haas (1995) Proc. Natl. Acad. Sci. USA **92**, 1764–1768.
37. C. Hwang, A. J. Sinskey, and H. F. Lodish (1992) Science **257**, 1496–1502.
38. T. E. Creighton (1997) Biol. Chem. **378**, 731–744.
39. M. C. Sousa, M. A. Ferrero-Garcia, and A. J. Parodi (1992) Biochemistry **31**, 97–105.
40. N. E. Blachere, Z. Li, R. Y. Chandawarkar, R. Suto, N. S. Jaikaria, S. Basu, H. Udono, and P. K. Srivastava (1997) J. Exp. Med. **186**, 1315–1322.
41. D. L. Wiest, J. K. Burkhardt, S. Hester, M. Hortsch, D. I. Meyer, and Y. Argon (1990) J. Cell Biol. **110**, 1501–1511.

42. D. P. McCauliffe, Y. S. Yang, J. Wilson, R. D. Sontheimer, and J. D. Capra (1992) J. Biol. Chem. **267**, 2557–2562.
43. P. J. Freiden, J. R. Gaut, and L. M. Hendershot (1992) EMBO J. **11**, 63–70.
44. C. L. Ward, S. Omura, and R. R. Kopito (1995) Cell **83**, 121–127.
45. E. J. Wiertz, D. Tortorella, M. Bogyo, J. Yu, W. Mothes, T. R. Jones, T. A. Rapoport, and H. L. Ploegh (1996) Nature **384**, 432–438.
46. A. A. McCracken and J. L. Brodsky (1996) J. Cell Biol. **132**, 291–298.
47. M. M. Hiller, A. Finger, M. Schweiger, and D. H. Wolf (1996) Science **273**, 1725–1728.
48. E. D. Werner, J. L. Brodsky, and A. A. McCracken (1996) Proc. Natl. Acad. Sci. USA **93**, 13797–13801.
49. S. Y. Bednarek, M. Ravazzola, M. Hosobuchi, M. Amherdt, A. Perrelet, R. Schekman, and L. Orci (1995) Cell **83**, 1183–1196.
50. K. Fiedler, M. Veit, M. A. Stamnes, and J. E. Rothman (1996) Science **273**, 1396–1399.
51. M. J. Kuehn, J. M. Herrmann, and R. Schekman (1998) Nature **391**, 187–190.
52. S. Munro and H. R. Pelham (1987) Cell **48**, 899–907.
53. J. C. Semenza, K. G. Hardwick, N. Dean, and H. R. B. Pelham, (1990) Cell **61**, 1349–1357.
54. R. D. Teasdale and M. R. Jackson (1996) Annu. Rev. Cell Dev. Biol. **12**, 27–54.
55. J. B. Kim, P. Sarraf, M. Wright, K. M. Yao, E. Mueller, G. Solanes, B. B. Lowell, and B. M. Spiegelman (1998) J. Clin. Invest. **101**, 1–9.
56. M. S. Brown and J. L. Goldstein (1997) Cell **89**, 331–340.
57. R. K. Pathak, K. L. Luskey, and R. G. Anderson (1986) J. Cell Biol. **102**, 2158–2168.

Suggestions for Further Reading

58. G. Palade (1975) Intracellular aspects of the process of protein secretion. Science, **189**, 347–358.
59. R. Sitia and J. Meldolesi (1992) Endoplasmic reticulum: a dynamic patchwork of specialized subregions. Mol. Biol. Cell **3**, 1067–1072.
60. G. Blobel and B. Dobberstein (1975) Transfer of proteins across membranes. I. Presence of proteolytically processed and unprocessed nascent immunoglobulin light chains on membrane-bound ribosomes of murine myeloma? J. Cell Biol. **67**, 835–851.
61. T. A. Rapoport, B. Jungnickel, and U. Kutay (1975) Protein transport across the eukaryotic endoplasmic reticulum and bacterial inner membranes. Annu. Rev Biochem **65**, 271–303.
62. J. Meldolesi and T. Pozzan (1998) The endoplasmic reticulum Ca^{2+} store: a view from the lumen Trends Biochem. Sci. **23**, 10–14.
63. C. Hammond and A. Helenius (1995) Quality control in the secretory pathway. Curr. Opin. Cell Biol . **7**, 523–529.
64. C. Sidrauski and P. Walter (1997) The transmembrane kinase Ire 1p is a site-specific endonuclease that initiates mRNA splicing in the unfolded protein response. Cell **90**, 1031–1039.
65. M. S. Brown and J. L. Goldstein (1997) The SREBP pathway: regulation of cholesterol metabolism by proteolysis of a membrane-bound transcription factor. Cell **89**, 331–340.

Endosomes

Endosomes comprise a complex series of intracellular organelles that mediate crucial functions in the endocytosis pathway (1). Ligands internalized through **clathrin**-coated vesicles are first delivered to "early endosomes." These are tubular/vesicular organelles distributed primarily in the peripheral cytoplasm of the cell. The internal pH of these structures is mildly acidic (pH ~6.0). The low pH is established and maintained by the membrane-associated vacuolar H^+bATPaseb and regulated by the Na^+K^+ATPase. The low-pH environment is essential for certain sorting functions of endosomes. For example, it facilitates dissociation of some ligands, such as **low density lipoprotein** (LDL), from their receptors, allowing the receptor to be recycled to the cell surface and reused, whereas the ligand is retained in the cell and degraded. Disruption of the endosomal pH by weak bases, ionophores, or inhibitors of the vacuolar ATPase disrupts the sorting functions of these organelles. The acidic pH within endosomes is used by certain **viruses** (eg, influenza virus) and toxins (eg, diphtheria toxin) to facilitate membrane fusion or translocation to the cytoplasm.

Early endosomes are the primary sorting organelles in the endocytic pathway, with two principal exit routes: (1) the recycling pathway to the cell surface, and (2) the pathway to late endosomes and lysosomes (1). In addition, proteins may be sorted out of early endosomes to recycling endosomes (a subset of endosomes that have nearly neutral pH and are enriched in **transferrin receptors**), the *trans* **Golgi network** (TGN), and other locations in certain differentiated cell types (for example, the GLUT 4 glucose transporter-containing compartment in adipocytes), transcytotic vesicles in polarized cells, synaptic vesicles in neurones, and MHC class II-containing vesicles in some antigen-presenting cells (2). It is believed that transport between these compartments is mediated by carrier vesicles (although these have not been characterized in detail) that fuse with their target organelles through SNARE/NSF and Rab-dependent mechanisms (3).

Late endosomes receive internalized ligands and receptors from early endosomes and provide a second sorting compartment before lysosomes. Late endosomes are again tubular/vesicular and frequently contain many membrane vesicles or lamellae. The internal pH of late endosomes is more acid (pH ~5.5) than that of early endosomes. Transport from early endosomes to late endosomes is mediated by endosomal carrier vesicles and/or multivesicular bodies that derive from early endosomes.

The different endosomal compartments are not well-characterized biochemically or morphologically. However, analyses of the distribution of Rab family of proteins have suggested that these small Gtpasesmight provide functional markers for endosomal subcompartments (4). Thus Rab 5 is primarily associated with coated vesicles and early endosomes, Rab 7 with late endosomes, and Rab 4 with recycling endosomes (1). Because these proteins have been implicated in the specific fusion involved in vesicular transport, their restricted and unique distributions may define specific transport steps and possibly unique SNARE-dependent fusion (4).

(See also Phagocytosis; Pinocytosis; Endosome; Macropinosome.)

Bibliography

1. J. Gruenberg and F. R. Maxfield (1995) Curr. Opinion Cell Biol. **7**, 552–563.
2. I. Mellman, P. Pierre, and S. Amigorena (1995) Curr. Opinion Cell Biol. **7**, 564–72.
3. J. E. Rothman and G. Warren (1994) Curr. Biol. **4**, 220–233.
4. P. Novick and M. Zerial (1997) Curr. Opinion Cell Biol. **9**, 496–504.

Endotoxins

The majority of bacterial toxins are proteins released by **bacteria** in the medium and are termed exotoxins. However, many gram-negative bacteria, upon lysis or during division, release toxic lipid components of the outer membrane, which are therefore named endotoxins. These molecules are lipopolysaccharides (LPS) of a complex and variable nature that are capable of inducing a variety of local and systemic effects, including fever and toxic shock (1). LPS binds directly to the CD11/CD18 molecules and 95-kDa scavenger receptor of **macrophages**(3). After fixation to a plasma protein LBP, the complex LPS-LBP is capable of binding the CD14 molecule present on macrophages, neutrophils, and platelets (2). Such binding triggers a variety of effects. Platelets release prostaglandin E_2, tromboxane A $_2$, and PAF (platelet-activating factor), and these mediators induce platelet aggregation and coagulation and trombotic phenomena. Activated macrophages and neutrophils release oxygen radicals and nitric oxide, which causes the relaxation of smooth muscles. LPS are the most potent inducer of the release of **cytokines** from macrophages. It appears that such platelet and inflammatory cells responses have developed in order to respond rapidly to the presence of potentially pathogenic bacteria (3). However, such a defensive response may turn easily into harmful, even deadly, systemic effects when larger amount of LPS are released or bacteria multiply in the blood and release LPS in a tissue so rich in target cells.

Bibliography

1. J. A. Hewett and R. A. Roth (1993) Pharmacol. Rev. **45**, 381–411.
2. R. J. Ulevitch and P. S. Tobias (1995) Ann. Rev. Immunol. **13**, 437–457.
3. C. E. Mims (1995) *The Pathogenesis of Infectious Diseases*, Academic Press, London.

Engrailed Gene

In multicellular organisms, the induction and maintenance of a **differentiated** state during development depend on the expression of a large number of genes acting at multiple levels (1). Genetic and molecular studies in *Drosophila* have largely contributed to the elaboration of this concept. During the embryonic development of *Drosophila*, the anterior-posterior (A/P) organization is generated by the activity of several maternal and zygotic genes (2, 3). Many of these genes encode transcriptional regulators that sequentially subdivide the embryo into smaller domains (segments and compartments) along the A/P axis (Fig.1). The segmentation gene *engrailed* (*en*) is one of the components of this regulatory cascade that defines the A/P axis during *Drosophila* embryogenesis. The *engrailed* function is essential to specify the posterior cell identity, as well as the A/P compartment boundaries (4-7). *en* is involved not only in the establishment of the posterior cell's fate but also in its maintenance. Indeed, *en* expression remains essential throughout the fly's life, from early embryonic development to the larval and adult appendage development (8-13) (Fig.2).

Figure 1. Cascade of genes that form the anterior-posterior (A/P) axis during embryogenesis. *engrailed* is a segment pol formation of the segments. This gene directly regulates the expression of the homeotic genes involved in the identity of t expression of the *Polycomb Group* genes, in particular, *polyhomeotic* (58). It also interferes directly in morphogenesis ar structural genes, such as that for b3-tubulin (54).

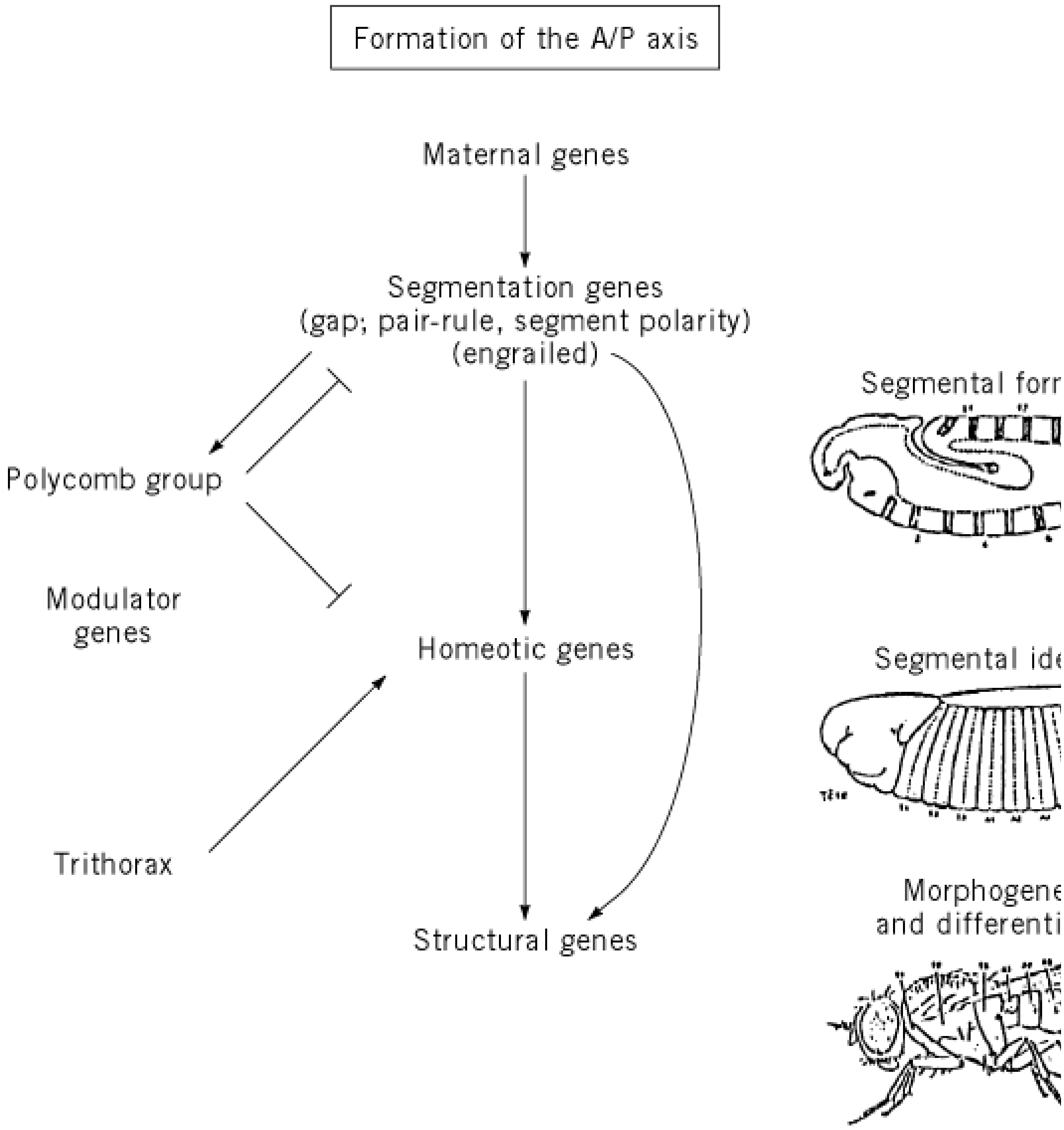

Figure 2. Expression of *engrailed* during development. In each case, the expression of *engrailed* defines the posterior cc (*en-lacZ*) producing an Engrailed–**beta-galactosidase** fusion protein has been used, and the *engrailed* gene expression f (8).

a. *engrailed* expression in a germ-band extended embryo. In this case, the transcripts were detected by ***in situ* hybridiza**

b. *engrailed* expression of third instar *en-lacZ* larval hindgut.

c. *engrailed* expression of third instar *en-lacZ* wing imaginal disk.

d. *engrailed* expression of adult *en-lacZ* wing.

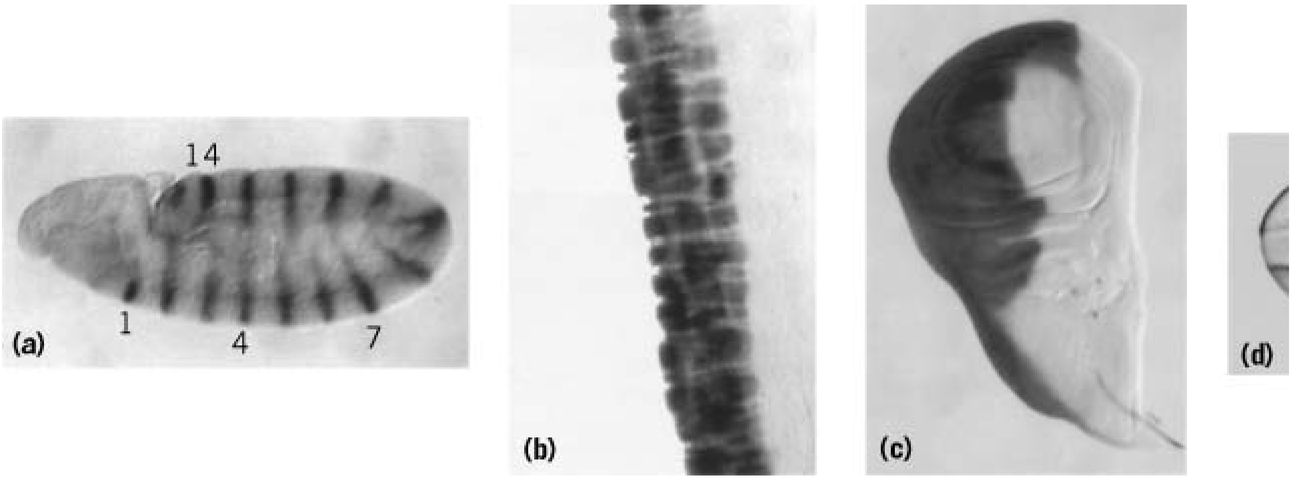

The positioning of the A/P boundaries established by the segmentation genes before gastrulation is an essential step in development because these boundaries serve as a reference for the subsequent and spatially restricted expression of the homeotic genes of the ***Bithorax*** and ***Antennapedia*** **complexes** (14). Each segment is characterized by the activity of a specific subset of homeotic genes, the other homeotic genes being repressed in that segment (14). The differential expression of the homeotic genes, which is essential to confer segmental identities, is established by the segmentation genes. The segmental identities are then maintained by the ***Polycomb*** **group** (*Pc*G) and the ***Trithorax*** **genes**, the latter being required for the maintenance of the activation of the homeotic genes (15) and of *engrailed* (16). On the contrary, *Pc*G genes are required for the maintenance of the repression of the homeotic genes (17), as well as of segmentation genes, like *engrailed* (18, 19). It has been suggested that the *Pc*G proteins form multimeric complexes that maintain repression by imprinting, limiting the accessibility of transcription factors to chromatin (17, 20, 21).

engrailed is also essential in the developing central nervous system, where it is segmentally expressed (22-24). Homologues of *engrailed* have been identified in other dipteria (25) and other organisms, such as zebrafish (26), chickens (27), mice (28, 29), and humans (30). All these organisms express *engrailed* during neurogenesis. In vertebrates, the neural tube is a segmented region, where *engrailed* expression is segmentally reiterated (31). This indicates that some of the *engrailed* functions during cell determination might be conserved during evolution. For example, the genetic network regulating the development of the brain in vertebrates involves conserved genes that control segmentation in *Drosophila* (32). In particular, the *Wnt-1/engrailed* interaction was shown to be conserved from flies to mice (33).

In the *Drosophila* epidermis, *engrailed*-expressing cells also express ***hedgehog*** (*hh*) (34), which encodes a secreted protein (Hh) that influences the pattern of cell differentiation across the embryonic segments, indicating that these *en/hh*-expressing cells have organizer properties (35). In particular, interfaces between posterior cells, which express *engrailed*, and anterior cells, which do not, were shown to be required for pattern formation (36). In the embryos, just anterior to the *en*-expressing cells, cells express ***wingless*** (*wg*), which encodes a secreted protein. During early embryogenesis, interdependent regulations between *en* and *wg* occur. Later, their expression is regulated by different mechanisms and maintained by autoregulation (35-39).

Later in development, during wing morphogenesis, *en* is also involved in the specification and the maintenance of posterior patterns, as well as in creating the compartment border. *en* activity in the posterior cells directs them to express *hh*, which is secreted anteriorly (34, 40). *en* blocks the ability of the posterior cells to respond to Hh (12), whereas its absence in the anterior cells allows them to respond to Hh. Hh acts in a stripe of anterior cells abutting the A/P boundary through the Patched (Ptc) receptor, whose expression is also activated by the Hh signal (43). These anterior cells, receiving the Hh signal, express ***decapentaplegic*** (*dpp*) (a homologue of the **transforming growth factor**-b signaling molecule) which, in turn, exerts a long-range organizing activity on the growth and patterning of both compartments (44). Hence, *en* plays a major role in the control of **imaginal disk** growth, by regulating the expression of *dpp* (44, 45). Indeed, *en* has two separable roles: a cell autonomous role in defining the posterior compartment, by repressing genes that are expressed in the anterior compartment, such as ***cubitus-interruptus*** (*ci*) (46, 11), *ptc,* and *dpp* (45), and a nonautonomous role in the anterior compartment through its regulation of *hh* (34, 47). The *en*-related gene *invected* (*inv*) encodes redundant functions, even though *inv* performs only a discrete subset of the functions ascribed to *en* (40, 42). For example, *inv* does not regulate *hh* or all the genes of the *hh* signaling pathway (41).

Engrailed (En) is a homeodomain-containing protein that performs its key role during *Drosophila* development by acting as a transcription factor (48). Despite the considerable amount of research conducted on homeodomain proteins, little is known about their mechanisms of action. One issue is understanding the specificity of their action because they all bind to DNA sequences containing the same core motif 5′-TAAT- 3′, which is essential for their DNA-binding activity; the nucleotides flanking this core provide the specificity of binding (49, 50). The N-terminal residues of the homeodomain were found to contribute to this sequence-specific association. In particular, the identity of residue 50 of Engrailed affects the base preference, both *in vitro* and *in vivo* (51-53).

Because of this remarkable conservation of binding properties among all homeodomains, the discovery of their DNA target sequences *in vivo* has been difficult. Identification of their target genes is, however, an essential step in understanding their role during development. Such a study has been performed in order to understand how *engrailed* achieves its complex regulatory role throughout development (Fig. 2).

The identification of target genes for transcription factors has been undertaken using different approaches, based on two main ideas. The first approach is functional and is based on the existence of genetic interactions between two genes. Genetic experiments have shown that En is able to repress *ci* (46), *dpp, ptc* (45), and the gene for b3-tubulin (54) and to activate the expression of several other genes, such as *en* itself (35), *hh* (34), ***Ultrabithorax*** (*Ubx*) (55, 56), and *polyhomeotic* (*ph*) (13, 54), but the direct effect of En on these genes has not always been proved.

The other approaches are based on the capacity of transcription factors to bind to specific DNA sequences. Libraries have been constructed that are enriched either in sequences that bind En *in vitro* (57) or in embryonic chromatin that binds Engrailed *in vivo* (54, 58). This latter approach has also been used successfully to identify the target genes of the homeotic protein Ubx (59, 60). In this process, DNA-protein complexes that exist in embryos are stabilized by UV crosslinking. The complexes formed with the endogenous En protein are then selected by **immunoprecipitation** with an anti-En antibody, followed by cloning.

Engrailed binding sites have also been localized directly on **polytene chromosomes** of salivary glands with an anti-Engrailed antibody. The number of En binding sites was estimated to be approximately 100 (58). Among these sites, in the 2D region, the *Pc*G gene *polyhomeotic* (*ph*) was shown to be a direct target of *engrailed*, through the combined use of these different genetic and molecular approaches. In particular, the activation of *ph* by En was shown to be required for the maintenance of the posterior cell fate and the position of the anterior-posterior boundary in the wing, a role assigned to the *en* function (13).

As already mentioned, among the known target genes of En, some are repressed, whereas others are activated by *engrailed*. Transfection experiments into cultured cells have demonstrated that En can act through a consensus En binding site, referred to as the NP site (“ATTAATTGA”), as a passive repressor, by competing with specific activators for binding sites located upstream of a basal promoter (61-63). Repression by En can also occur by competition with the general transcription factor TFIID for binding to the TATA box (64). En has also been found to function as an active repressor of transcription by binding to sites distinct from those bound by activators (65). The active transcriptional repression can also be enhanced in the presence of corepressors like Groucho (66, 67). A **domain** other than the homeodomain was found to be responsible for repression by En (65, 68). In particular, this repressor domain is able to confer the capacity to repress transcription in transfected cultured cells, as well as *in vivo* when transferred to a heterologous DNA-binding domain (65, 68, 69).

Analysis of the molecular mechanism of transcriptional activation by En showed that its binding fragment responsible for activation is different from that responsible for repression. For activation, the binding segment consists of a long stretch of "TAAT" motifs, where up to ten En proteins can bind cooperatively (70). A strong activation is, however, obtained only in the presence of a cofactor, Extradenticle (Exd), another homeodomain-containing protein. In the presence of En, Exd becomes able to bind to this segment (71, 70). When both proteins are bound to DNA, between En and Exd turn En into an activator (70). Interestingly, activation occurs even when such an activator-binding fragment is localized far away from the coding sequence, as long as an En consensus sequence, related to NP ("ATTAATTGA"), is located just upstream of the gene to be activated.

Interactions between distantly located En binding fragments could also be responsible for the *en* autoactivation that occurs at germ-band extension (35). The observation that the autoactivation of *en* depends on *exd* maternal expression suggests that Exd is involved in this phenomenon, as it is in the case of the activation of *ph* by En (72). The fragment responsible for the *en* autoactivation, which is able to bind Exd, has not yet been isolated.

Other peculiar observations have been described concerning the *engrailed* gene. Among them is the "homing" phenomenon, in which P elements containing *en* DNA sequences are preferentially inserted at the *en* locus (8). Moreover, preferential insertions of *Drosophila* transposable elements containing a particular fragment of the *engrailed* regulatory DNA have been described (73). Finally, this regulatory DNA fragment from the *engrailed* gene was also found to mediate transvection of the *white* gene (74, 75). This silencing activity results from the presence of a polycomb response element (PRE) within the fragment of *engrailed* regulatory DNA, which was shown to bind *pleiohomeotic* (76). The presence of a PRE in this fragment could also explain the homing and the preferential insertion of *engrailed* sequences in the genome, even though this has not yet been formally proved.

Bibliography

1. M. Ptashne and A. A. Gann (1990) Nature **346**, 329–331.
2. P. W. Ingham (1998) Nature **335**, 25–34.
3. M. J. Pankratz and H. Jäckle (1990) Trends Genet. **6**, 287–292.
4. T. B. Kornberg (1981) Proc. Natl. Acad. Sci. USA **78**, 1095–1099.
5. T. B. Kornberg (1981) Dev. Biol. **86**, 363–372.
6. S. J. Poole, L. M. Kauvar, B. Drees, and T. B. Kornberg (1985) Cell **40**, 37–43
7. J. P. Vincent and P. H. O"Farrell (1992) Cell **68**, 923–931.
8. C. Hama, Z. Ali, and T. B. Kornberg (1990) Genes Dev. **4**, 1079–1093.
9. L. A. Raftery, M. Sanicola, R. K. Blackman, and W. M. Gelbart (1991) Development **113**, 27–33.
10. A. Hidalgo (1994) Curr. Biol. **4**, 1087–1098.
11. I. Guillen, J. L. Mullor, J. Capdevila, E. Sanchez-Herrero, G. Morata, and I. Guerrero (1995). Development **121**, 3447–3456.
12. M. Zecca, K. Basler, and G. Struhl (1995) Development **121**, 2265–2278.
13. F. Maschat, N. Serrano, N. B. Randsholt, and G. Géraud (1998) Development **125**, 2771–2780.
14. A. Martinez-Arias and R. A. H. White (1988) Development **102**, 325–338.

15. J. A. Kennison and J. W. Tamkun (1988) Proc. Natl. Acad. Sci. USA **85**, 8136–8140.
16. T. R. Breen, V. Chinwalla, and P. J. Harte (1995) Mech. Dev. **52**, 89–98.
17. R. Paro (1990) Trends Genet. **6**, 416–421.
18. J. M. Dura and P. H. Ingham (1988) Development **103**, 733–741.
19. D. Moazed, D. O"Farrell, and P. H. O"Farrell (1992) Development **116**, 805–810.
20. J. McKeon and H. W. Brock (1991) Wilhem Roux"s Arch. Dev. Biol. **199**, 387–396.
21. H. Epstein (1992) BioEssays **14**, 411–413.
22. N. H. Patel, E. Martin-Blanco, K. G. Coleman, S. J. Poole, M. C. Ellis, T. B. Kornberg, and C. S. Goodman (1989). Cell **58**, 955–968 (1989).
23. J. A. McDonald and C. Q. Doe (1997) Development **124**, 1079–1087.
24. C. Q. Bhat and P. Schedl (1997) Development **124**, 1675–1688.
25. U. Schmidt-Ott, K. Sander, and G. M. Technau (1994) Roux"s Arch. Dev. Biol. **203**, 298–303.
26. A. Fjöse, H. G. Eiken, P. R. Njolstad, A. Molven, and I. Hordvik (1988) FEBS Lett. **231**, 355–360.
27. D. K. Darnell, T. B. Kornberg, and C. P. Ordahl (1986) J. Cell Biol. **103**, 311a.
28. A. L. Joyner and G. R. Martin (1987) Genes Dev. **1**, 29–38.
29. A. L. Joyner, K. Herrup, B. A. Auerbach, C. A. Davis, and J. Rossant (1991) Science **251**, 1239–1243.
30. S. J. Poole, M. L. Law, F. Kao, and Y. Lau (1989) Genomics **4**, 225–231.
31. M. Peifer and A. Bejsovec (1992) TIG **8**, 243–249.
32. A. L. Joyner (1996) Trends Genet. **12**, 15–20 (1996).
33. P. S. Danielan and A. P. McMahon (1996) Nature **383**, 332–334.
34. T. Tabata, S. Eaton, and T. B. Kornberg (1992) Genes Dev. **6**, 2635–2645.
35. J. Heemskerk, S. DiNardo, R. Kostriken, and P. H. O"Farrell (1991) Nature **352**, 404–352.
36. P. A. Lawrence, B. Sanson, and J. P. Vincent (1996) Development **122**, 4095–4103.
37. J. P. Vincent and P. A. Lawrence (1994) Cell **77**, 909–915.
38. J. Noordermeer, J. Klingensmith, and R. Nusse (1995) Mech. Dev. **51**, 145–155.
39. K. F. Yoffe, A. S. Manoukian, E. L. Wilder, A. H. Brand, and N. Perrimon (1995) Dev. Biol. **170**, 636–650.
40. T. Tabata, C. Schwartz, E. Gustavson, Z. Ali, and T. B. Kornberg (1995) Development **121**, 3359–3369.
41. A. J. Simmonds, W. J. Brook, S. M. Cohen, and J. B. Bell (1995) Nature **376**, 424–427.
42. E. Gustavson, A. S. Goldbourough, Z. Ali, and T. B. Kornberg (1996) Genetics **142**, 893–906.
43. V. Marigo, R. A. Davey, Y. Zuo, J. M. Cunningham, and C. J. Tabin (1996) Nature **384**, 176–179.
44. M. Sanicola, J. Sekelsky, S. Elson, and W. M. Gelbart (1995) Genetics **139**, 745–756.
45. J. Capdevila and I Guerrero (1994) EMBO J. **13**, 4459–4468.
46. S. Eaton and T. B. Kornberg (1990) Genes Dev. **4**, 1068–1077.
47. K. Basler and G. Struhl (1994) Nature **368**, 208–214.
48. C. Desplan, J. Theis, and P. H. O"Farrell (1985) Nature **318**, 630–635.
49. C. R. Kissinger, B. Liu, E. Martin-Blanco, T. B. Kornberg, and C. O. Pabo (1990) Cell **63**, 579–590.
50. A. Draganescu and T. D. Tullius (1998) J. Mol. Biol. **276**, 529–536.
51. J. Treisman, P. Gônczy, M. Vashita, E. Harris, and C. Desplan (1989) Cell **59**, 553–562.
52. S. D. Hanes and R. Brent (1991) Science **251**, 426–430.
53. S. E. Ades and R. T. Sauer (1994) Biochemistry **33**, 9187–9194.

54. N. Serrano, H. W. Brock, and F. Maschat (1997) Development **124**, 2527–2536.
55. A. Martinez-Arias, N. E. Baker, and P. N. Ingham (1988) Development **103**, 157–170.
56. R. S. Mann (1994) Development **120**, 3205–3212.
57. M. T. Saenz-Robles, F. Maschat, T. Tabata, M. P. Scott, and T. B. Kornberg (1995) Mech. Dev. **53**, 185–195.
58. N. Serrano, H. W. Brock, C. Demeret, J. M. Dura, N. B. Randsholt, T. B. Kornberg, and F. Maschat (1995) Development **121**, 1691–1703.
59. A. P. Gould, J. J. Brookman, D. I. Strutt, and R. A. H. White (1990) Nature **348**, 308–312.
60. Y. Graba, D. Aragnol, P. Laurenti, V. Garzino, D. Charmot, H. Berenger, and J. Pradel (1992) EMBO J. **11**, 3375–3384.
61. J. B. Jaynes and P. H. O"Farrell (1988) Nature **336**, 744–749.
62. K. Han, M. S. Levine, and J. L. Manley (1989) Cell **56**, 573–583.
63. J. Treisman, E. Harris, D. Wilson, and C. Desplan (1992) BioEssays **14**, 145–150.
64. Y. Ohkuma, M. Horikoshi, R. G. Roeder, and C. Desplan (1990) Proc. Natl. Acad. Sci. USA **87**, 2289–2293.
65. J. B. Jaynes and P. H. O"Farrell (1991) EMBO J. **10**, 1427–1433.
66. G. Jimenez, Z. Paroush, and D. Ish-Horowicz (1997) Genes Dev. **11**, 3072–3082.
67. E. N. Tolkunova, M. Fujioka, M. Kobayashi, D. Deka, and J. B. Jaynes (1998) Mol. Cell. Biol. **18**, 2804–2814.
68. K. Han, K. Manley, and J. L. Manley (1993) EMBO J. **12**, 2723–2733.
69. A. John, S. T. Smith, and J. B. Jaynes (1995) Development **121**, 1801–1813.
70. N. Serrano and F. Maschat (1998) EMBO J. **17**, 3704–3713.
71. M. A. van Dijk, L. T. C. Peltenburg, and C. Murre (1995) Mech. Dev. **52**, 99–108.
72. J. A. Kassis, E. Noll, E. P. VanSickle, W. F. Odenwald, and N. Perrimon (1992) Proc. Natl. Acad. Sci. USA **89**, 1919–1923.
73. J. A. Kassis (1994) Genetics **136**, 1025–1038.
74. C. Rauskolb, C. Wieschaus, and E. Wieschaus (1994) EMBO J. **13**, 3561–3569.
75. J. A. Kassis, E. P. Vansickle, and S. M. Sensabaugh (1991) Genetics **128**, 751–761.
76. J. L. Brown, D. Mucci, M. Whiteley, M. L. Dirksen, and J. A. Kassis (1998) Mol. Cell **1**, 1057–1064.

Suggestions for Further Reading:

77. P. A. Lawrence (1992) "*Engrailed*: the life history of a gene". In *The Making of a Fly: The Genetics of Animal Design*, Blackwell Scientific, London, pp. 207–210.
78. J. Treisman, E. Harris, D. Wilson, and C. Desplan (1992) The homeodomain: a new face for the helix-turn-helix? BioEssays **14**, 145–150.
79. T. B. Kornberg (1993) Understanding the homeodomain. J. Biol. Chem. **268**, 26813–26816.
80. A. Garcia-Bellido (1998) The *engrailed* story. Genetics **148**, 539–544.

Enhancer

1. Introduction/Summary

In the regulation of gene transcription, two aspects are of prime importance, namely the point of initiation and the rate of transcription. In bacteria, both of these are usually determined by short DNA sequence motifs, collectively called promoters, that are in close proximity to the initiation site. In mammals and other eukaryotes, the point of transcription initiation of protein-coding genes is determined by proximal promoter sequences, but the frequency of transcription is influenced by remote DNA sequences, termed enhancers, that can be located thousands, if not tens of thousands of basepairs from the promoter. Enhancers are typically 100–300 bp long and represent an array of binding sites for DNA-binding transcription factors. Binding of such proteins to an enhancer helps, in a collaboration between enhancer and promoter, to recruit components of the transcription apparatus. These include the **RNA polymerase** II holoenzyme and enzymes that loosen the chromatin packaging of DNA. Due to its specific DNA sequence, any given enhancer binds a subset of the many hundred transcription factors of a eukaryotic organism. Some of these proteins are present only in a given cell type, others become active only upon an external stimulus, such as a hormone. Accordingly, an enhancer can activate a linked gene only in the appropriate cell type, or in response to a specific stimulus. Many genes are controlled by several distinct enhancers, which ensures gene activation in response to different cues. Also, sequence rearrangements in enhancers may lead to the evolution of new patterns of gene expression in multicellular organisms. Due to their prominent role in rendering chromatin more accessible to DNA-interacting proteins, at least some transcriptional enhancers have additional overlapping functions in that they facilitate DNA replication, de**methylation** of cytosines at CpG sites, and site-specific DNA recombination, switch recombination and somatic hypermutation of immunoglobulin genes. Also, some enhancers act as a genetic switch between positive and negative gene regulation; under conditions where the linked gene has to remain silent, they serve as a platform for the binding of repressing factors/cofactors.

2. Discovery, Definition

In 1981, the first enhancer characterized was from the genome of simian virus 40 (=SV40) (1, 2). This enhancer sequence is naturally located between 300 und 100 bp upstream of the initiation site for early mRNAs, but could be experimentally placed at various distances from an unrelated reporter gene, which thereby was transcriptionally activated. Characterization of enhancers from SV40 and other viruses led to the following definition of a transcription enhancer: (i) a DNA sequence, typically about 200 bp in size, that strongly activates transcription of a linked transcription unit from its correct initiation site; (ii) it activates transcription independently of its orientation; and (iii) it is able to exert its function over large distances of more than 1000 bp, from a position either upstream or downstream of the initiation site (3-5).

The first cellular enhancer was discovered in the immunoglobulin (Ig) heavy chain gene (6-8). This constituted a hallmark in the understanding of gene regulation in higher organisms, because it showed that gene control by remote enhancer sequences was not a viral peculiarity. Most importantly, the Ig enhancer stimulated transcription in a cell type-specific manner, thus being the first genetic element described to have such a property. The Ig enhancer is located downstream of the initiation (5′-cap) site, within the second intron, showing that enhancers can be naturally located downstream of the site of initiation. This concept has since been widely confirmed in most eukaryotes from flies to men (Figure 1). While most of these studies were done with RNA polymerase II-transcribed genes, transcription enhancers are also associated with **ribosomal** genes that are transcribed by RNA polymerase I (9).

Figure 1. Enhancer types in different organisms. (**a-d**) Schematic representation of a mammalian gene with different
indicated (18, 3, 4). In a gene stripped of its enhancer, transcription is low or undetectable (**a**). An enhancer (array of bla
binding sites for transcription factors) can be located adjacent to the promoter, as in several viruses or metallothionein st
upstream, like in the albumin gene (**b**); or within the gene, usually as part of an intron, like in immunoglobulin (Ig) genes
also found far downstream of the transcription unit, as in T cell receptor and Ig genes (**d**). One and the same gene can als
one enhancer, to ensure activity in several cell types and in response to different stimuli (not shown here). In the baker's
(upstream activating sequences) are considered analogous to mammalian enhancer elements. They can also work in eithe

however, they are rarely, if at all, activating from positions downstream of the gene (**e**). The majority of eubacterial pron control of RNA polymerase with sigma 70 factor and cover less than 100 bp. The promoters of genes activated upon nitr driven by sigma 54 factor and show similarities to eukaryotic enhancers, in that an upstream binding site, in conjunction protein, can work from variable distances (**f**) (85-87).

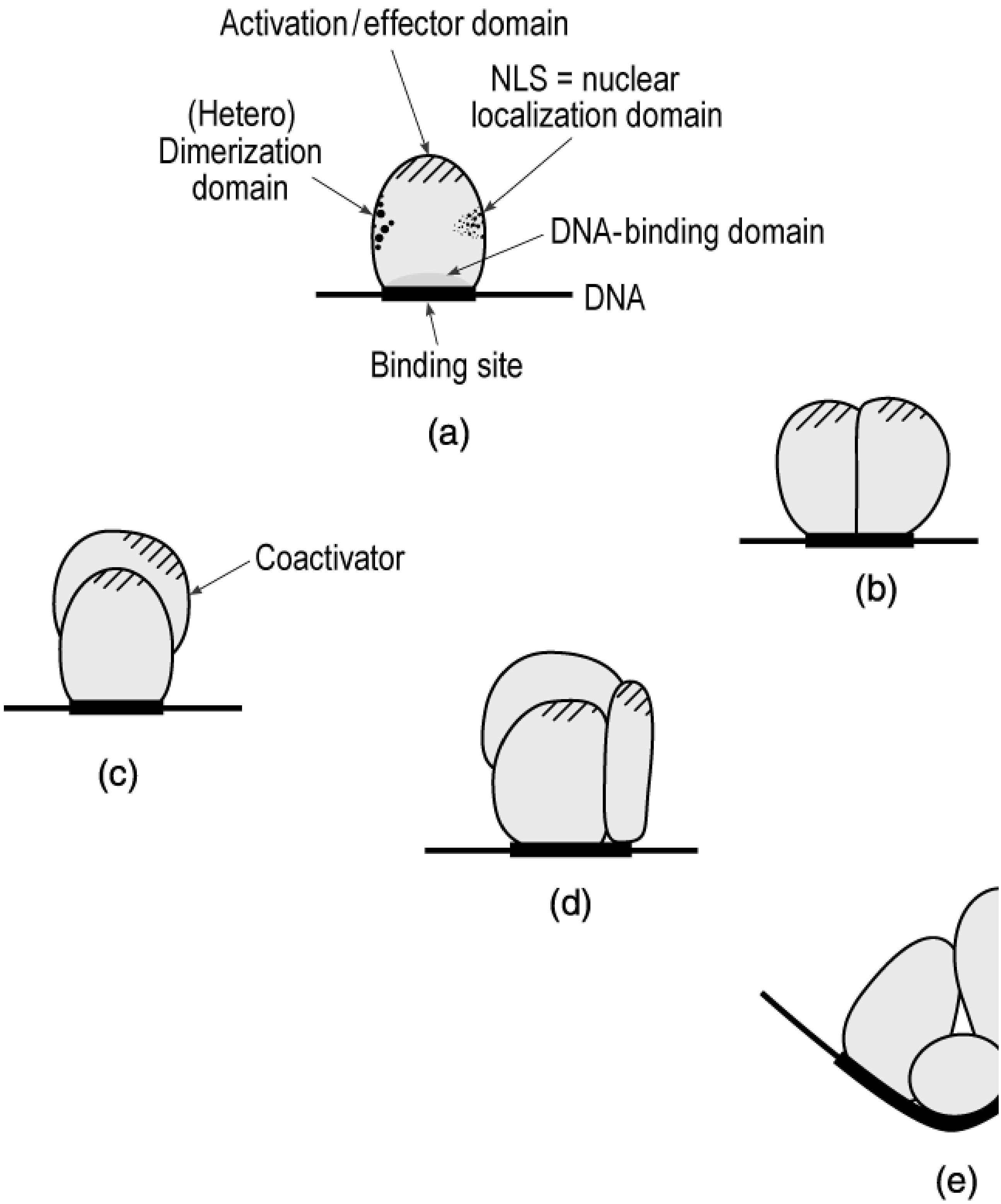

In addition to the originally discovered intronic enhancer, the immunoglobulin heavy chain locus was also found to contain a second, extended B cell-specific enhancer located far downstream of the entire **locus**, as well as additional cytokine-inducible enhancers involved in Ig class switching (10).

In many other instances, enhancers were established to play a crucial role in stage- and cell type-specific gene expression: In an interplay with the transcription factors that bind to them, enhancers ensure proper development of all multicellular organisms; see, for example, Refs. 11-13. Perhaps the most extensive studies have been done in Drosophila, where a gene for a developmental regulator protein is typically under the control of several separate enhancers. Depending on the stage and cell type, some enhancers can exert either positive or negative effects on transcription. For example, to establish a repetitive stripe pattern of even-skipped gene expression during early Drosophila embryogenesis, a single enhancer does not suffice, but one of several enhancers controls the expression of just one of these stripes (14, 15; see also 16).

3. Modular Structure of Enhancers

A typical enhancer is 100 to 300 bp long and essentially consists of an array of binding sites, each about 10 bp long, for DNA-binding transcription factors (17, 18). Every eukaryotic cell contains hundreds of different transcription factors, each with a DNA binding domain of characteristic specificity for DNA sequence recognition, plus an "activation domain". The latter establishes contacts to other components of the transcription apparatus and thus enhances the level of gene transcription. Since under some conditions, negatively acting proteins can be recruited, an activation domain was also referred to as "effector domain". The DNA sequence recognition specificity and affinity of many eukaryotic transcription factors does not match that of bacterial regulators. This seems to be compensated by a multitude of protein-protein interactions (see text below).

A given DNA site can, for example, be recognized by a monomer, by a homodimer reminiscent of bacterial regulators, or by heterodimers. It can also be recognized by heterodimers where only one partner binds DNA strongly, while the other makes only minor contacts to DNA and in turn may have a leading role in activation. More complex situations have also been documented (see Figure 2).

Figure 2. Enhancer-binding transcription factors. A typical transcription factor contains a DNA-binding domain, a nu signal for import into the nucleus, an activation/effector domain for contacts to coactivators/mediators and a (hetero)dim (**a**). Although shown here schematically, the three-dimensional structure of many transcription factors is known from X- or nuclear magnetic resonance (NMR) analysis. Binding to DNA can involve homo- or heterodimers (**b**) (e.g., see Ref. 8 transcription factor can associate with a coactivator that does not contact DNA. For example, the cell type-specific coact OcaB/OBF-1) binds to a ubiquitous factor (Oct-1) to bring about preferential activity in B lymphocytes (**c**) (89-91). A co DNA binding specificity and contribute a strong activation potential. For example, the herpes viral coactivator VP16 (= associates with the cellular Oct-1 factor and with an additional large protein termed host cell factor (HCF). By providing simplex virus recruits Oct-1 to a new DNA sequence motif present in viral promoters at the expense of proper host cell f "Architectural" proteins, that by themselves would neither activate transcription nor bind to DNA with high specificity, binding of *bona fide* transcription factors to DNA, as indicated here for the protein HMG I(Y) (center) that bends DNA b minor groove (**e**) (20); see also refs 93, 94. Superstructures composed of several such binding sites and DNA-bound fact referred to as an enhanceosome (22). DNA binding transcription factors of the enhancer and the promoter, the latter inclu binding protein (TBP) and the general transcription factor TFIIB, recruit via multiple protein-protein contacts, further ge factors, adaptor- and mediator/SRB-proteins which in turn recruit RNA polymerase II to the initiation site. Individual pr specific subset of factors for initiation; for example, the TBP-associated factors (TAFs) may be replaced by other multip shown here. Besides RNA polymerase, several enzymatic activities are associated with the initiation complex, including acetyl transferases. The latter mainly acetylate histones to ensure a loose chromatin structure permissive for transcription coordinated gene transcription is often flanked by boundary elements (= insulators) (**f**) (see text).

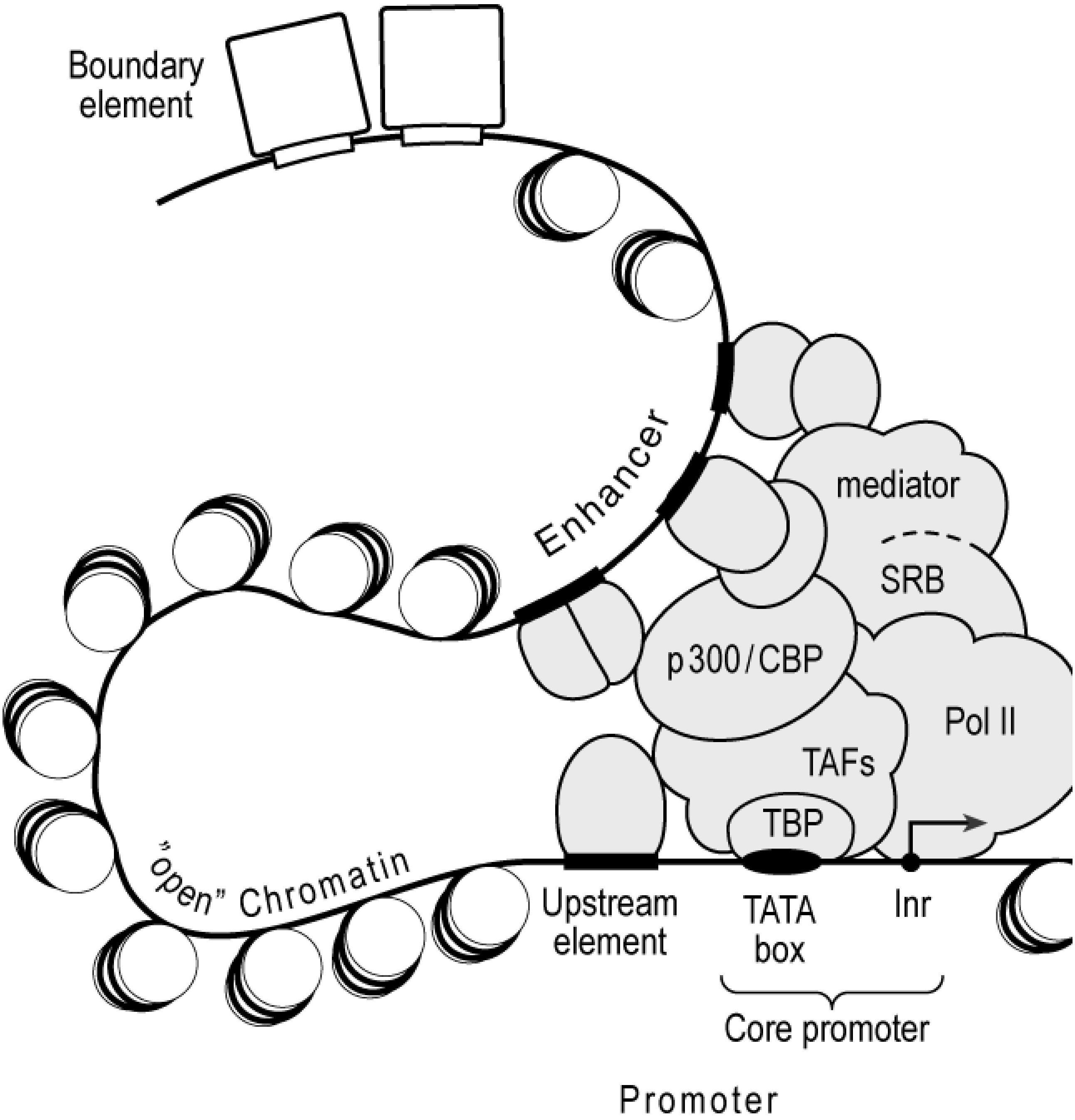

A typical enhancer has a modular structure and is composed of binding sites for several different transcription factors (17, 18), but synthetic enhancers can readily be obtained by multimerization of one and the same DNA sequence motif (19, 20). From these and other experiments, it is concluded that each binding site for a transcription factor (or factor dimer, see Figure 2) can be considered one enhancer unit that, in principle, is able to activate transcription by itself. However, single sites have poor, if any, activity, and multiple sites have to act synergistically to yield strong activation (19-21). More complex cases are also documented where a functional unit consists of some 60 bp of DNA, with several transcription factors stereospecifically aligned on it with the help of "architectural" proteins that bend the DNA, a superstructure that was termed the enhanceosome (22).

A DNA-binding transcription factor, whether bound to a distal enhancer or a proximal promoter, does not directly recruit RNA polymerase II, but instead acts via intermediary proteins to form large complexes (see below and Figure 2). Such multiprotein complexes seem to be quite forgiving towards the positioning of their DNA-binding partner, which could explain the fact that an entire enhancer, subsets of it, and in many cases even individual transcription factor binding sites in an enhancer or promoter can be inverted relative to each other without loss of activity (23, 1, 17, 24). This general property of eukaryotic regulatory DNA sequences to retain activity when inverted, was first documentend with an upstream segment of the histone H2A gene termed "modulator" (23).

4. Mechanism, Recruitment

Transcription factors may activate transcription in more than one way, but all involve some kind of recruitment process. The activation domain of a DNA-binding transcription factor binds to additional proteins (coactivators, adaptors, mediator proteins, SRB proteins), organized in multiprotein complexes that in turn establish contacts to RNA polymerase II (25, 26). The related coactivators CBP/p300, originally found to bind the mammalian DNA-binding factor CREB that is responsive to induction by cyclic AMP, contain several domains for interaction with a multitude of other transcription factors (27). Transcriptional activators are also known to contact the general transcription factor TFIIB, the TATA-box binding protein (TBP) and/or TAF proteins associated with it (28, 29).

The recruitment concept for transcriptional activation has gained credit from elegant experiments where covalent linkage of a DNA-binding transcription factor to a basal transcription factor (the TATA-binding protein TBP) rendered the *bona fide* activation domain obsolete. The same was found when a DNA-binding factor was designed to make an artificial, tight contact to the SRB complex. These findings demonstrate that linking a DNA-bound transcription factor to a component of the mediator complex is in principle sufficient to activate transcription (30-32).

The transcription factors of the enhancer are likely to bind, indirectly via cofactors, to those of the promoter to form an initiation complex, with the intervening DNA looped out. Several experiments support a looping between enhancer and promoter (eg, see Refs. 33 and 34). In spite of the compelling simplicity of the above experiments, it is unlikely that transcriptional activation is naturally brought about by a uniform mechanism. Among other evidence, this is suggested by the fact that there are different types of activation domains, when classified according to their activation properties (35, 36), and it is obvious that transcription can be controlled not only at the level of initiation but also at the level of elongation (37-39).

The coactivator and mediator protein complexes also contain several histone acetylase enzymes. Their major targets are the histones, but a number of transcription factors can also become reversibly acetylated. Acetylation of histones generally loosens chromatin structure and thus makes it more accessible to the transcription apparatus (40). Major support for this concept comes from experimental digestion of chromatin with DNaseI (41). Transcriptionally active DNA is generally DNase I sensitive, which is correlated with the presence of acetylated histones. In addition, the enhancer and promoter regions themselves are hypersensitive, due to binding of transcription factors with, at least in some cases, concomitant removal of nucleosomes (42). (Besides a genetic screen called "enhancer trap" (43, 44), the property of DNaseI hypersensitivity is the most effective method in identifying candidate enhancers from large DNA segments). Large multiprotein complexes (SRB/mediator; SWI/SNF etc.) are known to support chromatin remodelling and recruitment of the transcription apparatus (45, 25-48). Extended regions of inactive chromatin, termed heterochromatin, tend to be associated with the periphery of the nucleus (49). By fluorescence staining it was shown that a silent, peripheral gene relocalizes to a more central region upon activation of its enhancer. The general validity of this phenomen remains to be seen, and also whether such a relocalization ist the cause or the effect of transcriptional activation.

5. Evolution

In higher eukaryotes, genes regulating development are often under the control of multiple enhancers, and it was argued that enhancer shuffling was the major driving force in the evolution of new patterns of gene expression (50-53). Apart from shuffling, enhancer evolution may be facilitated by the fact that enhancer DNA sequences are more tolerant to rearrangements than protein coding sequences, which has, e.g., resulted in divergent primary enhancer sequences that nevertheless serve the same function (54). In fast-evolving viruses, a new cell type specificity is readily achieved by enhancer rearrangements, usually involving deletion-duplication of subsegments, with little alterations elsewhere in the genome (55). Duplications of enhancer subsegments, which are indicative of recent functional alterations, are also found in some cellular enhancers and in humans may even vary between ethnic groups (56). However, not every arbitrary enhancer-promoter combination can be expected to function since in any gene, promoter and enhancer(s) have co-evolved for optimal function. There are indeed documented cases of preferential, if not exclusive enhancer/promoter specificity (57-59). Nevertheless, promiscuous enhancer-promoter cooperations were found from yeast to mammals and may be the rule, rather than the exception (44, 50, 60).

6. Open Questions/Related Phenomena

Even though many aspects of eukaryotic transcription control have already been elucidated, thanks to a combination of genetics, reverse genetics and biochemistry, many questions remain. One of them concerns the mode of activation: does an enhancer allow for fine tuning of the activity of a gene within one individual cell, or can a gene only exist in two states, namely fully activated or completely switched off? In the latter case, the function of the enhancer would be to increase the probability of the gene being in the “on” state. While the first of these possibilities seems to make more sense, at least in the case of hemoglobin genes, there is evidence for the latter one (61).

Some extended enhancer regions have been referred to as LCR (locus control region). The most thorough studies were done with the hemoglobin beta chain locus, where the LCR consists of a group of at least five remote enhancers/DNase I hypersensitive regions contained within a DNA segment of 15 kb. Each LCR subdomain confers distinct activation properties in erythroid cells. The LCR, which is located some 50 kb from the most downstream beta-globin transcription unit, ensures the complete, stage-specific and cell type-specific expression pattern of the globin genes under its influence (62-64).

In spite of an ability to work over long distances, enhancer activity is confined to the same DNA molecule, i.e. to an activity in cis. In certain constellations that requires pairing of homologous chromosomes, an enhancer can also activate the promoter in the homologous locus, a phenomenon termed **transvection** (65). While well-documented in Drosophila, the relevance of transvection in mammals remains to be seen.

Perhaps due to its ability to loosen up chromatin structure, a transcription enhancer may be used for other activities besides transcriptional activation. For example, the activity of an enhancer *in cis* was also correlated with the initiation of DNA replication (66-68). Moreover, in immunoglobulin (Ig) genes, enhancers induce demethylation at CpG sites (70), site-specific gene rearrangement (VDJ joining) and also class switch recombination (71). In addition, the amazing process of localized Ig gene hypermutation in B memory cells is dependent on an active transcription enhancer (72). The Ig gene locus also harbors so-called matrix attachment regions (MARs), A+T-rich DNA segments which have little activity by themselves but in transgenic animals support long-range enhancer activity, apparently by counteracting the formation of transcriptionally inactive chromatin (73).

In a process opposite to activation, genes can be inactivated by recruitment of histone deacetylases and other proteins counteracting transcription to the promoter/enhancer region (74, 75). Non-acetylated histones tend to assume a chromatin structure that is refractory to the transcription apparatus, which is also reflected by a relative resistance to experimental DNase I digestion. A so-called silencer DNA segment can inactivate a linked gene over large distances (76-78). Again, for this purpose, DNA binding proteins recruit a number of cofactors which together block transcription (74, 75, 78, 79). Enhancers and silencers originally were described as non-overlapping DNA entities of opposite function. However, a number of enhancers, notably for developmental gene regulation in

Drosophila, also harbor binding sites for negatively acting DNA binding proteins and/or cofactors. Thus, in a cell type where the gene must not be active, an enhancer may serve a silencing purpose (80). To prevent undue spreading of an enhancer (or silencer) effect to neighboring genes, chromosomal domains of gene activity are separated from each other by so-called boundary, or insulator, sequences (81, 82)(Fig. 2).

Finally, in the process of RNA splicing, a process that bears some resemblance to transcriptional enhancement has been described. So-called splice enhancers denote RNA sequences in the primary transcript which, by means of specific protein binding, facilitate RNA processing at nearby splice sites. Unlike transcription enhancers, splice enhancers are typically located in an exon (exonic splice enhancer = ESE), consist of short sequence motifs that cannot be inverted, and act over short distances only. This process is mainly used to favor one type of splice site at the expense of another, i.e., for alternative splicing (83, 84).

Bibliography

"Enhancer" in , Vol. 2, pp. 823–828, by Walter Schaffner, Universitaet Zurich-Irchel, Zurich, Switzerland; "Enhancer" in (online), posting date: January 15, 2002, by Walter Schaffner, Universitaet Zurich-Irchel, Zurich, Switzerland.

1. J. Banerji, S. Rusconi and W. Schaffner (1981) Cell **27**, 299–308.
2. P. Moreau, R. Hen, B. Wasylyk, R. Everett, M. P. Gaub and P. Chambon (1981) Nucleic Acids Research **9**, 6047–6068.
3. M. M. Müller, T. Gerster and W. Schaffner (1988) European Journal of Biochemistry **176**, 485–495.
4. E. M. Blackwood and J. T. Kadonaga (1998) Science **281**, 60–63.
5. D. Dorsett (1999) Current Opinion in Genetics & Development **9**, 505–514.
6. J. Banerji, L. Olson and W. Schaffner (1983) Cell **33**, 729–740.
7. S. D. Gillies, S. L. Morrison, V. T. Oi and S. Tonegawa (1983) Cell **33**, 717–728.
8. M. S. Neuberger (1983) The EMBO J. **2**, 1373–1378.
9. R. H. Reeder (1990) Trends in Genetics **6**, 390–395.
10. V. Arulampalam, L. Eckhardt and S. Pettersson (1997) Immunology Today **18**, 549–554.
11. A. B. Firulli and E. N. Olson (1997) Trends in Genetics **13**, 364–369.
12. A. Gould, A. Morrison, G. Sproat, R. A. White and R. Krumlauf (1997) Genes & Development **11**, 900–913.
13. R.S. Mann (1997) Bioessays **19**, 661–664.
14. T. Goto, P. Macdonald and T. Maniatis (1989) Cell **57**, 413–422.
15. K. Harding, T. Hoey, R. Warrior and M. Levine (1989) The EMBO Journal **8**, 1205–1212.
16. J. Zhou and M. Levine (1999) Cell **99**, 567–575.
17. M. Zenke, T. Grundstrom, H. Matthes, M. Wintzerith, C. Schatz, A. Wildeman and P. Chambon (1986) The EMBO Journal **5**, 387–397.
18. E. Serfling, M. Jasin and W. Schaffner (1985) Trends in Genetics **1**, 224–230.
19. B. Ondek, A. Shepard and W. Herr (1987) The EMBO Journal **6**, 1017–1025.
20. M. D. Schatt, S. Rusconi and W. Schaffner (1990) The EMBO Journal **9**, 481–487.
21. M. Carey, Y. S. Lin, M. R. Green and M. Ptashne (1990) Nature **345**, 361–364.
22. T. Agalioti, S. Lomvardas, B. Parekh, J. Yie, T. Maniatis and D. Thanos (2000) Cell **103**, 667–678.
23. R. Grosschedl and M. L. Birnstiel (1980) Proceedings of the National Academy of Sciences of the United States of America **77**, 7102–7106.
24. L. Xu, M. Thali and W. Schaffner (1991) Nucleic Acids Research **19**, 6699–6704.
25. M. Carlson (1997) Annual Review of Cell & Developmental Biology **13**, 1–23.

26. L. C. Myers, C. M. Gustafsson, D. A. Bushnell, M. Lui, H. Erdjument-Bromage, P. Tempst and R. D. Kornberg (1998) Genes & Development **12**, 45–54.
27. R.H. Goodman and S. Smolik (2000) Genes & Development **14**, 1553–1577.
28. A. Hoffmann, T. Oelgeschlager and R. G. Roeder (1997) Proceedings of the National Academy of Sciences of the United States of America **94**, 8928–8935.
29. S.R. Albright and R. Tjian (2000) Gene **242**, 1–13.
30. A. Barberis, J. Pearlberg, N. Simkovich, S. Farrell, P. Reinagel, C. Bamdad, G. Sigal and M. Ptashne (1995) Cell **81**, 359–368.
31. S. Chatterjee and K. Struhl (1995) Nature **374**, 820–822.
32. S. Farrell, N. Simkovich, Y. Wu, A. Barberis and M. Ptashne (1996) Genes & Development **10**, 2359–2367.
33. H. P. Mueller-Storm, J. M. Sogo and W. Schaffner (1989) Cell **58**, 767–777.
34. N. Dillon and F. Grosveld (1993) Trends in Genetics **9**, 134–137.
35. K. Seipel, O. Georgiev and W. Schaffner (1992) The EMBO Journal **11**, 4961–4968.
36. J. Blau, H. Xiao, S. McCracken, O. H. P, J. Greenblatt and D. Bentley (1996) Molecular & Cellular Biology **16**, 2044–2055.
37. D. L. Bentley (1995) Current Opinion in Genetics & Development **5**, 210–216.
38. S. A. Brown, C. S. Weirich, E. M. Newton and R. E. Kingston (1998) The EMBO Journal **17**, 3146–3154.
39. T. Wada, T. Takagi, Y. Yamaguchi, D. Watanabe and H. Handa (1998) The EMBO Journal **17**, 7395–7403.
40. J.C. Rice and C.D. Allis (2001) Current Opinion in Cell Biology **13**, 263–273.
41. H. Weintraub and M. Groudine (1976) Science **193**, 848–856.
42. L. Gaudreau, A. Schmid, D. Blaschke, M. Ptashne and W. Horz (1997) Cell **89**, 55–62.
43. F. Weber, J. de Villiers and W. Schaffner (1984) Cell **36**, 983–992.
44. H. J. Bellen, O. K. CJ, C. Wilson, U. Grossniklaus, R. K. Pearson and W. J. Gehring (1989) Genes & Development **3**, 1288–1300.
45. C. J. Wilson, D. M. Chao, A. N. Imbalzano, G. R. Schnitzler, R. E. Kingston and R. A. Young (1996) Cell **84**, 235–244.
46. C. Wu (1997) Journal of Biological Chemistry **272**, 28171–28174.
47. R.D. Kornberg and Y. Lorch (1999) Current Opinion in Genetics & Development **9**, 148–151.
48. C.L. Peterson and J.L. Workman (2000) Current Opinion in Genetics & Development **10**, 187–192.
49. M. Cockell and S.M. Gasser (1999). Current Opinion in Genetics & Development **9**, 199–205.
50. M. Kermekchiev, M. Pettersson, P. Matthias and W. Schaffner (1991) Gene Expression **1**, 71–81.
51. X. Li and M. Noll (1994) Nature **367**, 83–87.
52. D. Tautz (2000) Current Opinion in Genetics & Development **10**, 575–579.
53. B.G. Magor, D.A. Ross, L. Pilström and G.W. Warr (1999) Immunology Today **20**, 13–17.
54. M.Z. Ludwig, C. Bergman, N.H. Patel and M. Kreitman (2000) Nature **403**, 564–567.
55. S. Schirm, J. Jiricny and W. Schaffner (1987) Genes and Development **1**, 65–74.
56. S. Marsh, E.S. Collie-Duguid, T. Li, X. Liu, and H.L. McLeod (1999) Genomics **15**, 310–312.
57. X. Li and M. Noll (1994) EMBO Journal **13**, 400–406.
58. G. Das, C. S. Hinkley and W. Herr (1995) Nature **374**, 657–659.
59. S. Ohtsuki, M. Levine and H. N. Cai (1998) Genes & Development **12**, 547–556.
60. G. Schaffner, S. Schirm, B. Müller, F. Weber and W. Schaffner (1988) Journal of Molecular Biology **201**, 81–90.

61. M. Wijgerde, F. Grosveld and P. Fraser (1995) Nature **377**, 209–213.
62. F. Grosveld, G.B. van Assendelft, D.R. Greaves and G. Kollias (1987) Cell **51**, 975–985.
63. M. Bulger and M. Groudine (1999) Genes & Development **13**, 2465–2477.
64. J.D. Engel and K. Tanimoto (2000) Cell **100**, 499–502.
65. V. Pirrotta (1999) Biochimica et Biophysica Acta **1424**, M1–M8.
66. J. de Villiers, W. Schaffner, C. Tyndall, S. Lupton and R. Kamen (1984) Nature **312**, 242–246.
67. M. L. DePamphilis (1993) Trends in Cell Biology **3**, 161–167.
68. P. Van der Vliet (1996) Cold Spring Harbor Laboratory Press 87–118.
69. R. Li, D. S. Yu, M. Tanaka, L. Zheng, S. L. Berger and B. Stillman (1998) Molecular and Cellular Biology **18**, 1296–1302.
70. Y. Bergman and R. Mostoslavsky (1998) Biological Chemistry **379**, 401–407.
71. E. Sakai, A. Bottaro and F.W. Alt (1999) Int. Immunology **11**, 1709–1713.
72. A. G. Betz, C. Milstein, A. Gonzalez-Fernandez, R. Pannell, T. Larson and M. S. Neuberger (1994) Cell **77**, 239–248.
73. W.C. Forrester, L.A. Fernandez and R. Grosschedl (1999) Genes & Development **13**, 3003–3014.
74. P.A. Wade (2001) Human Molecular Genetics **10**, 693–698.
75. A. El-Osta and A.P. Wolffe (2000) Gene Expression **9**, 63–75.
76. A. H. Brand, L. Breeden, J. Abraham, R. Sternglanz and K. Nasmyth (1985) Cell **41**, 41–48.
77. H. N. Cai, D. N. Arnosti and M. Levine (1996) Proceedings of the National Academy of Sciences of the United States of America **93**, 9309–9314.
78. G. Chen and A.J. Courey (2000) Gene **249**, 1–16.
79. R. E. Kingston, C. A. Bunker and A. N. Imbalzano (1996) Genes & Development **10**, 905–920.
80. S. Gray and M. Levine (1996) Current Opinion in Cell Biology **8**, 358–364.
81. R. Kellum and P. Schedl (1991) Cell **64**, 941–950.
82. A.C. Bell and G. Felsenfeld (1999) Current Opinion in Genetics & Development **9**, 191–198.
83. K. J. Hertel, K. W. Lynch and T. Maniatis (1997) Current Opinion in Cell Biology **9**, 350–357.
84. B.J. Blencowe (2000) Trends in Biochemical Sciences **25**, 106–110.
85. B. Magasanik (1988) Trends in Biochemical Sciences **13**, 475–479.
86. J. D. Gralla (1996) Current Opinion in Genetics & Development **6**, 526–530.
87. B.R. Belitsky and A.L. Sonenshein (1999) Proceedings of the National Academy of Sciences of the United States of America **96**, 10290–10295.
88. M. Beato, S. Chavez and M. Truss (1996) Steroids **61**, 240–251.
89. M. Gstaiger, L. Knoepfel, O. Georgiev, W. Schaffner and C. M. Hovens (1995) Nature **373**, 360–362.
90. Y. Luo and R. G. Roeder (1995) Molecular & Cellular Biology **15**, 4115–4124.
91. M. Strubin, J. W. Newell and P. Matthias (1995) Cell **80**, 497–506.
92. A. C. Wilson, K. LaMarco, M. G. Peterson and W. Herr (1993) Cell **74**, 115–125.
93. R. Grosschedl (1995) Current Opinion in Cell Biology **7**, 362–370.
94. C. A. Bewley, A. M. Gronenborn and G. M. Clore (1998) Annual Review of Biophysics & Biomolecular Structure **27**, 105–131.

Enkephalins

Enkephalins are pentapeptides with the sequence Tyr–Gly–Gly–Phe–X, which are the natural ligands of the opiate **receptors**. The two major enkephalins are [5-leucine] enkephalin (abbreviated [Leu] enkephalin) and [5-methionine] enkephalin (abbreviated [Met] enkephalin) (1). The peptides are derived from three precursors, pro-opiomelanocortin (POMC) and pro-enkephalins A and B (2). The prohormones are of similar size and contain multiple repeated units of enkephalins. The precursors are processed **proteolytically**, mostly in the Golgi apparatus, to the hormonally active products. The two proenkephalins show considerable sequence homology; they probably originated from a common ancestral gene by gene duplication.

The proenkephalin peptides and the enkephalins are distributed in many types of cells, especially brain, spinal cord, and gut. POMC is present in high concentrations in the corticotropic cells of the adenohypophysis and in many endocrine-related tissues (eg, adrenal medulla). Enkephalins have analgesic properties. They are also synthesized in neurons and are abundant in various regions of the hypothalamus, acting on the secretion of hormones of the hypothalamus and hypophysis (they stimulate secretion of prolactin, thyrotropin, and growth hormone and inhibit secretion of follicle-stimulating hormone/luteinizing hormone (folitropin/lutropin; FSH/LH), adrenocorticotropic hormone (ACTH), and vasopressin/oxytocin (3). The enkephalins are hydrolyzed by enkephalinases. Inhibitors of the degrading enzymes have been introduced as analgesics (4).

Bibliography

1. J. Hughes et al. (1975) Nature **258**, 577–579.
2. J. Douglass, O. Civelli, and E. Herbert (1984) Annu. Rev. Biochem. **53**, 665–715.
3. M. Ferin, D. Van Vugt, and S. Wardlaw (1984) Recent Prog. Horm. Res. **40**, 441–485.
4. J. M. Lecomte et al. (1986) In *Innovative Approaches in Drug Research* (A. F. Harms, ed.), Elsevier, Amsterdam, pp. 315–329.

Enterokinase

Enterokinase, also known as enteroprotease (E.C. 3.4.21.9), is a key enzyme in the digestion of dietary proteins in the small intestine. It catalyzes the activation of **trypsinogen** by removing six amino acids from the amino terminus of the 229-residue protein and does so with extremely high specificity. The resulting trypsin then activates all the other pancreatic proenzymes, as part of a two-step proteolytic cascade that is essential for proper digestion.

Enterokinase is a serine proteinase of the **trypsin** family and with trypsin-like specificity (1). It is synthesized in the epithelial cells of the duodenum and appears to be an intrinsic membrane protein located on the outer surface of the intestinal brush border. In fact, it is generated from a 1019-residue precursor that is proteolytically cleaved to a 235-residue light chain, which resembles trypsin and has the serine proteinase catalytic triad, plus a 784-residue heavy chain (2); the two chains are linked by a disulfide bond (3). In this regard, its properties are like those of the blood-clotting enzymes (4).

It should be noted that the term kinase is normally used to denote an enzyme that catalyzes the transfer of a phosphate group from a donor, such as ATP, to a receptor, such as glucose. In this regard, enterokinase has been misnamed. It does not catalyze phosphate transfer at all and, hence, is more appropriately called *enteropeptidase* .

Bibliography

1. A. Light and H. Janska (1989) Trends Biochem. Sci. **14**, 110–112.
2. Y. Kitamoto, R. A. Viele, H. Donis-Keller, and J. E. Sadler (1995) Biochemsitry **34**, 4562–4568.
3. A. Light and P. Fonseca (1984) J. Biol. Chem. **259**, 13195–13198.
4. L. E. Anderson, K. A. Walsh, and H. Neurath (1977) Biochemistry **16**, 3354–3360.

Enzyme Immobilization And Conjugation

Immobilization and conjugation refers to the covalent attachment of an enzyme to a solid support or to a soluble molecule through use of bifunctional crosslinking reagents (see Crosslinking). The use of immobilized enzymes in the medical, pharmaceutical, chemical, and food industries continues to increase dramatically. Future exploitation of immobilized or conjugated enzymes will undoubtedly result in the development of new biosensors and bioreactors for use in such areas as diagnostics (*in vivo* monitoring of metabolites, drugs, and proteins); environmental monitoring (detection of pathogens, toxins, and pollutants); separation sciences; the synthesis of complex, chiral organic compounds; and the detection of macromolecular interactions (reviewed in Refs. 1 and 2).

Among the most widely used bioconjugates are reporter enzymes covalently crosslinked to antibodies. These conjugates have been pivotal in the development of enzyme-linked immunosorbent assay (ELISA) systems, which allow detection of an immense variety of analytes through their specific recognition by appropriate antibodies. The two most commonly used reporter enzymes in ELISAs are alkaline phosphatase and horseradish peroxidase (HRP). The characteristics of these enzymes allow for different strategies in their conjugation to antibodies. For example, HRP contains saccharide groups that can be readily oxidized to aldehydes, which, in turn, are conjugation targets for free amino groups on the antibody. Alternatively, because HRP contains few **lysine residues**, it can be conjugated to antibodies by glutaraldehyde without significant formation of insoluble products. Several heterobifunctional crosslinking reagents, including ***N*-hydroxysuccinimide** ester/maleimide reagents, which selectively link **amino** and thiol groups, are also widely used in enzyme–antibody conjugation (3).

Enzymes can be immobilized by conjugation to a variety of different types of supports having different properties and uses. For instance, in aqueous solution polyethylene glycols have a large exclusion volume, which encompasses those molecules conjugated to them. Thus, proteinases and antibody molecules can be excluded from enzymes conjugated to these polymers, a property that can be beneficial for applications that require exposure of the conjugates to biological fluids (4). Reversible solubilization of an enzyme can be achieved through its conjugation to liposomes, using a reagent such as a **carbodiimide**; reversible precipitation and solubilization can be brought about by manipulation of the dielectric strength of the solution. Biosensor technology utilizes proteins that are immobilized by bifunctional crosslinking reagents to diverse supports (5), including carboxymethylated dextran-coated gold film, metal-coated nylon mesh, and carboxymethyl cellulose. Immobilization of enzymes on novel solid-phase matrices, such as porous zirconium, silicates, and colloidal gold, has been used in the construction of bioreactors for the industrial generation of numerous compounds. Many supports have functional groups that must be chemically activated prior to conjugation with protein; this allows activation to be carried out under harsh conditions that would otherwise be detrimental to the protein.

Bibliography

1. E. Katchalski-Katzir (1993) Trends Biotechnol. **11**, 471–478.
2. F. Svec and J. M. Frecht (1996) Science **273**, 205–211.
3. G. T. Hermanson (1996) *Bioconjugate Techniques*, Academic Press, San Diego, pp. 461–469.
4. H. C. Berger and S. V. Pizzo (1988) Blood **71**, 1641–1647.
5. G. T. Hermanson (1996) *Bioconjugate Techniques*, Academic Press, San Diego, pp. 593–629.

Suggestions for Further Reading

6. S. S. Wong (1993) *Chemistry of Protein Conjugation and Cross-Linking*, CRC Press, Boca Raton, FL. (An outstanding book describing all aspects of the chemistry and uses of bifunctional reagents in crosslinking and conjugation, with an extensive bibliography for each chapter.)
7. G. T. Hermanson (1996) *Bioconjugate Techniques*, Academic Press, San Diego. (An excellent book covering all phases of conjugation, and not limited to proteins.)
8. *Bioconjugate Chemistry* (ISSN 1043-1802), Editor-in-Chief, C. F. Meares. (A bimonthly journal published by the American Chemical Society devoted to scientific reports describing the "joining of two molecular functions by chemical or biological means.")

Enzyme-Linked Immunosorbent Assay (ELISA)

Enzyme-linked immunosorbent assay (ELISA) is a technique for quantifying a substance by use of an antibody specific for that substance that has been conjugated to an enzyme. The original ELISA was developed along the lines of a solid-phase radioimmunoassay, substituting an enzyme for a **radioactive** label (1, 2). Regardless of the experimental design used for the immunological reactions, the end result is that the antibody–enzyme conjugate is immobilized. Enzymatic activity is assayed in a subsequent reaction, and the activity is related to the quantity of analyte (antigen or antibody) present in a test sample by comparison to a set of controls of known concentration.

A key reagent for all ELISAs is the enzyme conjugate. In most cases, the enzyme is crosslinked covalently to an antibody, but experimental designs with enzyme-labeled antigen are also used. Indeed, the ELISA method is adaptable to any **ligand** and **receptor** pair. The most common enzymes used are alkaline phosphatase and horseradish peroxidase. These proteins are stable to the crosslinking procedures, and they catalyze reactions with highly chromogenic substrates, leading to very sensitive detection limits. Optical absorbance is the most common method of measuring enzyme activity, but other detection technologies are also used, such as **fluorescence** or chemiluminescence. Covalent linkage to a chromatography matrix was used to immobilize the first "immunosorbent," but use of plastic multiwell microtiter plates is now nearly universal, as these allow simultaneous monitoring of scores or hundreds of enzymic reactions in automated instruments.

The number of experimental formats used for ELISA is immense. This discussion is limited to the simplest and most useful assay designs.

1. Competitive ELISA

The first reported ELISA was a competition assay, in which adding an unlabeled competitor molecule reduced the amount of enzyme conjugate that could be immobilized (1). This remains an extremely common approach. The method begins with adsorption of antigen to the surface of a microtiter plate (Fig. 1). This non-specific adsorption occurs spontaneously, simply by allowing the antigen solution to stand in the wells of the plate. The linkage to the plate is noncovalent, but essentially irreversible, and the adsorbed antigen is seldom released during subsequent reactions and washing steps. Often a blocking step follows, in which a concentrated solution of a protein such as serum albumin is used to coat the remaining plastic surface, thereby preventing later adsorption of assay components. The plate is washed with a neutral buffer. The antibody solution of unknown concentration, and a series of controls, consisting of known quantities of the same antibody, are mixed with a fixed amount of the antibody–enzyme conjugate and added to different wells of the plate. The conjugate binds to the immobilized antigen, but so does the unconjugated antibody, and the binding of each is mutually exclusive. Thus, the higher the concentration of unconjugated antibody, the less the amount of enzyme immobilized. After allowing an interval for the antigen to be bound, the plate is again washed, and the addition of substrate initiates the enzymatic reaction. The rate of product release, or the accumulation of product after a fixed time, is determined for the unknown analyte and controls. Reactions to which no unlabeled competitor was added will have the highest absorbance, and are taken as a 100% response. Controls lacking conjugate, or lacking antigen, or to which a saturating amount of competitor was added, give the lowest absorbance. This value, reflecting background enzyme binding and the uncatalyzed chromogenic reaction, is taken as a 0% response. Data from the other controls are plotted to give a calibration curve, using a logarithmic concentration scale on the abscissa and an absorbance or percentage scale on the ordinate (Fig. 2a). The response from the unknown is compared to the calibration curve, and the corresponding concentration is read off the abscissa.

Figure 1. Competitive ELISA.

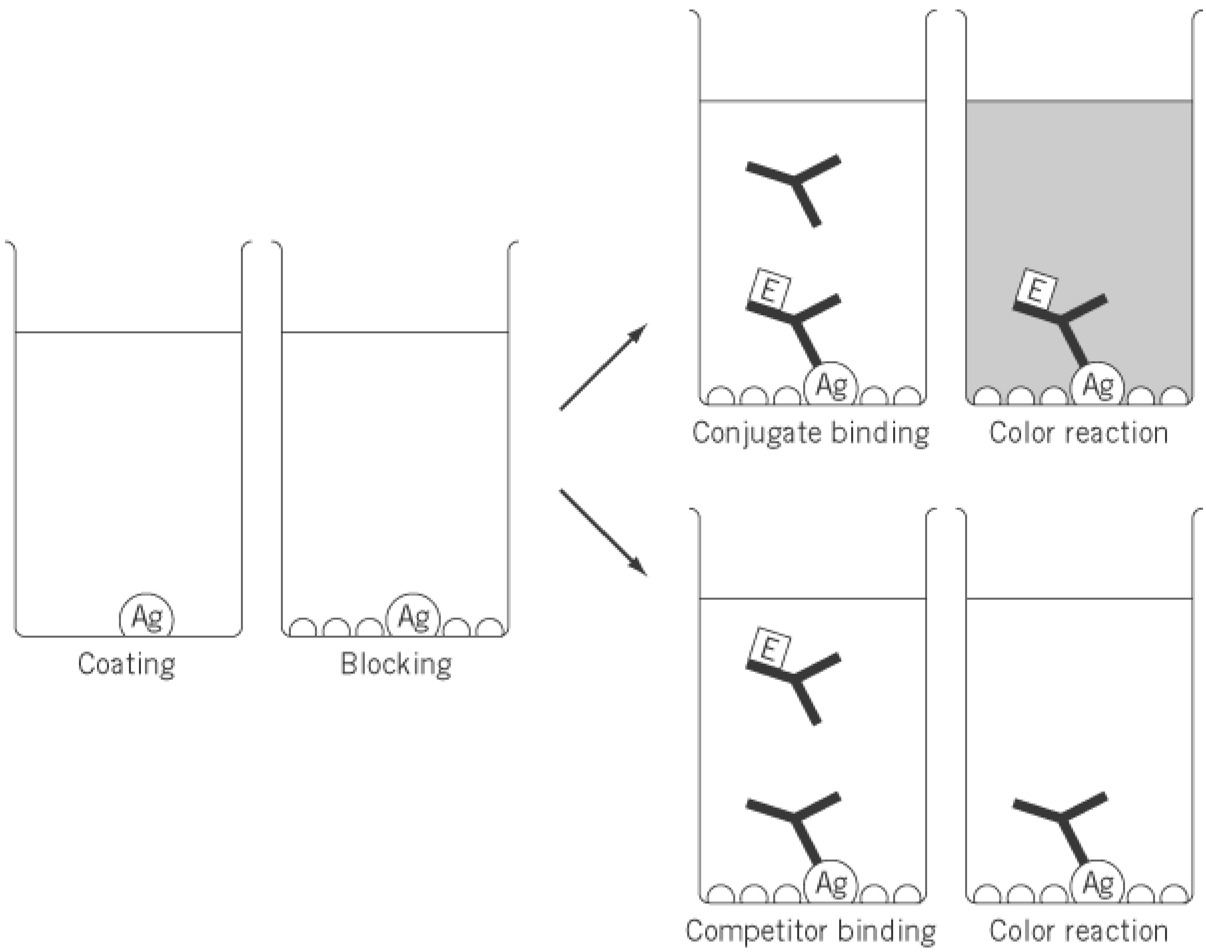

Figure 2. ELISA standard curves.

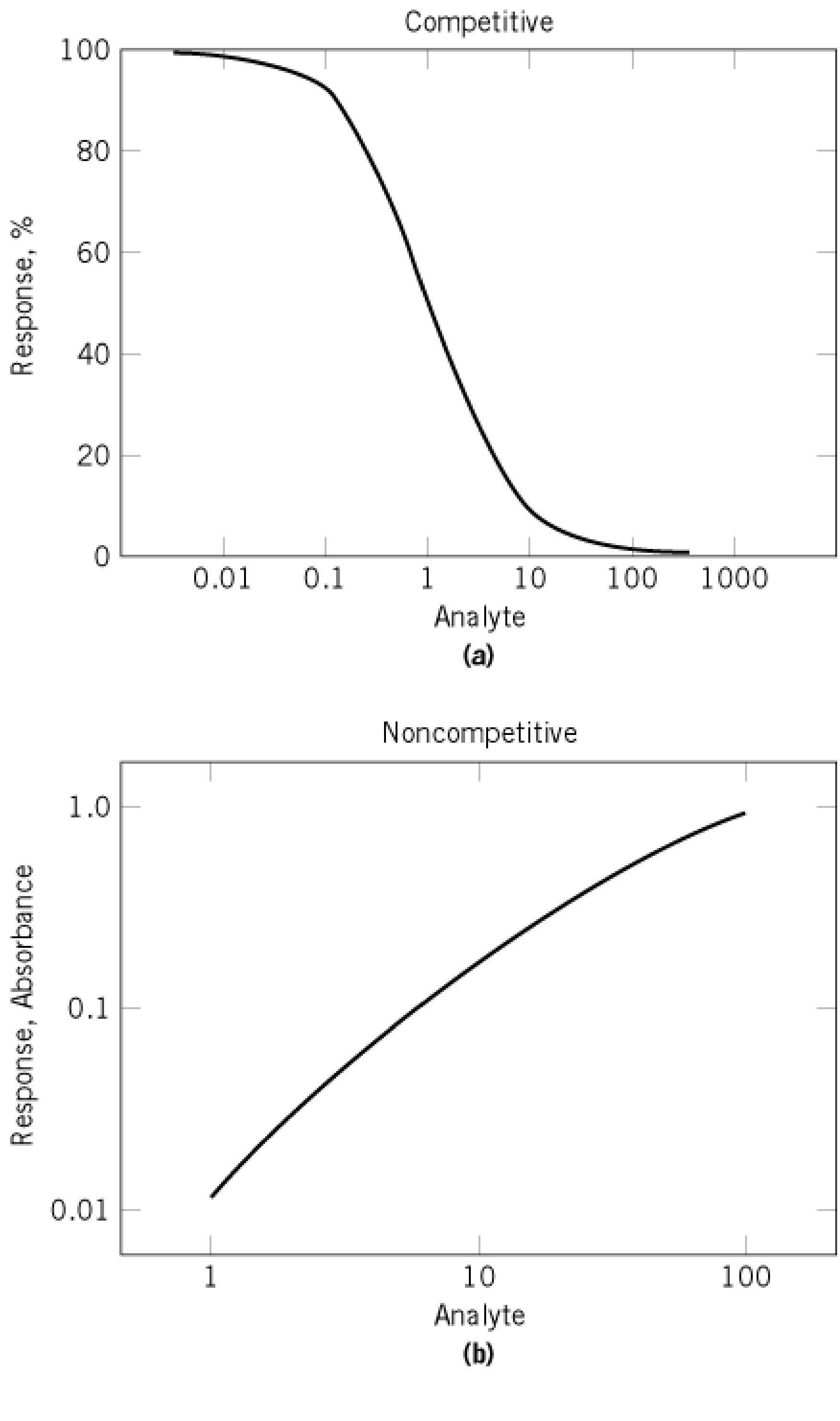

A shortcoming of this competitive design is that the response from small amounts of analyte may be almost as high as the 100% control. The change in reading due to the analyte is thus read as the difference between two large numbers. To be considered precise, the minimum readable difference must be much larger than the standard deviation of the highest point on the calibration curve, a fact that inherently limits the sensitivity of competitive ELISAs. The two noncompetitive designs that follow circumvent this limitation. The response in these assays is proportional to the analyte added; hence even a low reading may be detectable against the background level of enzymatic activity (Fig. 2b).

2. Indirect ELISA

The enzyme conjugate in an indirect ELISA (3) is an anti-antibody; the antibody that actually recognizes that the antigen is unlabeled. Quantification of the unlabeled antibody is normally the goal sought, and the indirect ELISA is most commonly used to assess the seropositivity of subjects who have potentially been exposed to pathogens. In an indirect ELISA, antigen is immobilized and the plate blocked as above (Fig. 3). The test sample is added, along with controls consisting of antibodies of the same specificity, species, and isotype as the test sample. After an interval allowed for antigen binding, the plate is washed and the conjugate added. The antibody used to make the conjugate reagent is typically a polyclonal preparation specific for constant regions of the antibody in the test sample (see Immunoglobulin Structure). Finally, enzymic activity is assayed as above. Controls are plotted on a linear or log–log scale (Fig. 2b). In this case, the response increases with increasing amount of analyte and does not necessarily reach a plateau. Reaching a plateau at high analyte concentration may indicate that the binding capacity of the unlabeled antibody in the sample exceeds the quantity of conjugate added, or more trivially, that the optical density after the color reaction is simply too great to be measured. The concentration of analyte in the test sample is interpolated from the calibration curve, as above.

Figure 3. Indirect ELISA.

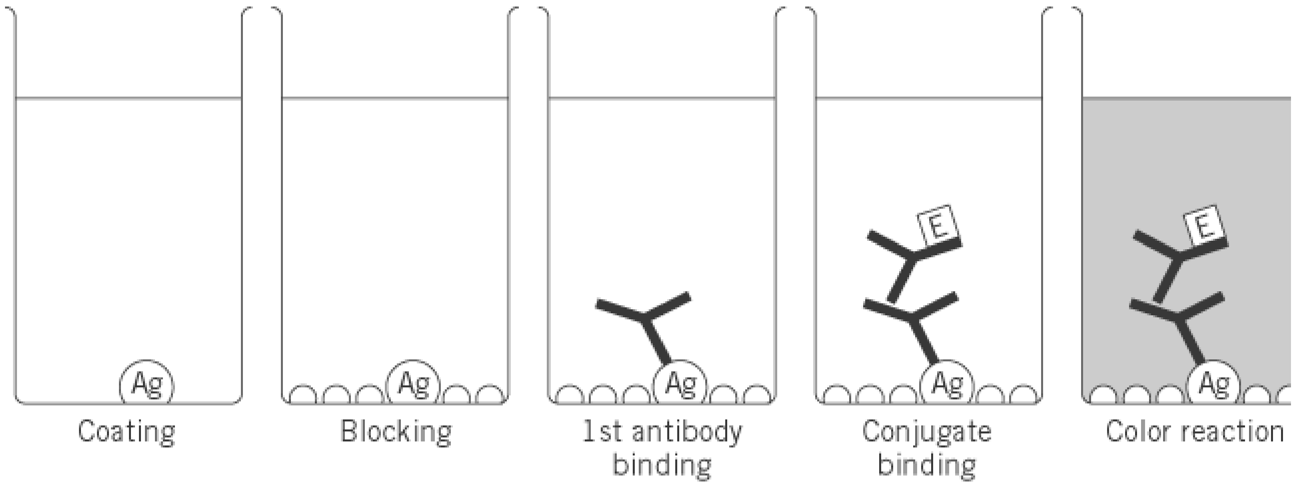

3. Sandwich ELISA for Antigen

This ELISA method (4) is conceptually similar to the indirect ELISA described above, but the analyte is usually a nonimmunoglobulin antigen that becomes “sandwiched” between an unlabeled immobilizing antibody and an antibody–enzyme conjugate (Fig. 4). The procedure begins with adsorption of a specific antibody to the surface of the assay plate. The plate is washed, and the test sample is added, along with controls consisting of known quantities of the same antigen. The plate is again washed, and the antibody–enzyme conjugate is added. This reagent binds to the immobilized antigen and hence becomes immobilized itself. A crucial aspect of the design of a sandwich assay is selection of an immobilizing antibody and a conjugate antibody that together will actually allow a “sandwich” to form. Obviously, two monoclonal antibodies that recognize the same epitope will exclude each other's binding. Use of a monoclonal immobilizing antibody is advantageous, however, since it occludes only a single epitope, leaving the remaining surface of the antigen available for deposition of the antibody–enzyme conjugate. After the conjugate is allowed to bind, the tray is washed a final time, and substrate is added to initiate the color reaction. A rising calibration curve again results, from which sample concentration is interpolated as above.

Figure 4. Sandwich ELISA.

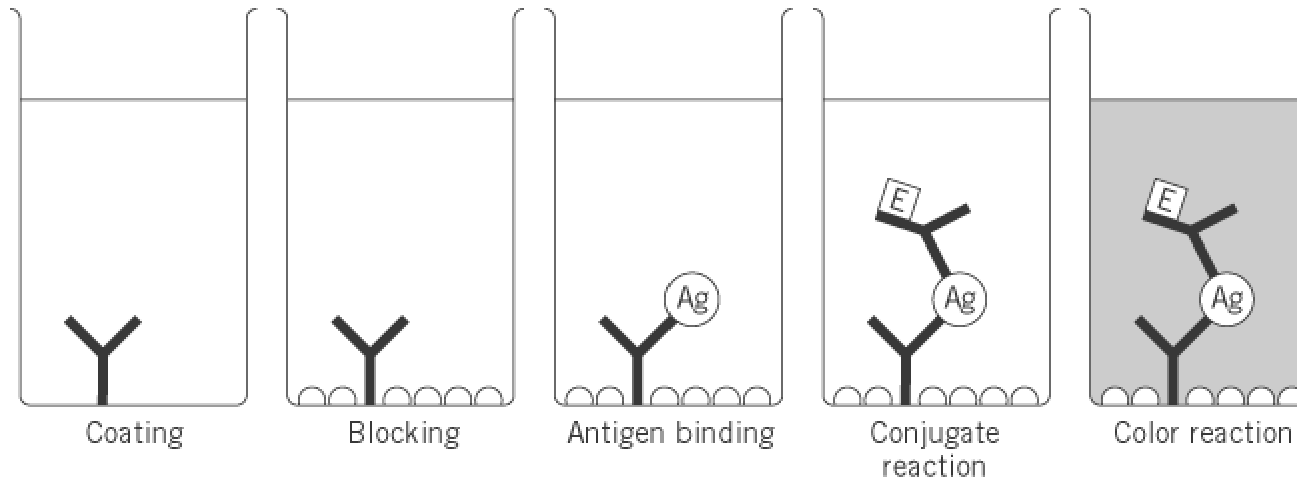

4. Affinity Determination

Many authors have equated the analyte concentration at the 50% response point in the competitive ELISA with the equilibrium **dissociation constant** for an antibody–antigen interaction. This approximation is invalid. However, ELISA can be used to measure the equilibrium constant if the indirect ELISA method is applied after equilibrium is reached (5). The antibody and antigen in question are mixed in a series of different ratios, and the solutions are allowed to come to equilibrium. The equilibrium mixtures are then transferred to an ELISA plate that has been coated with the antigen. Standards with known amounts of free antibody are run in parallel. Free antibody will bind to the immobilized antigen. It is essential that only a small fraction of the total available amount of free antibody become bound to the plate, so that the assay does not lead to an apparent shifting of the equilibrium point (6). The plate is washed, and an antibody–enzyme conjugate that binds to the immobilized antibody is added. The plate is washed again, substrate solution added, and the amount of enzyme activity determined. The color response from the reactions with the equilibrium mixtures is compared to that from the controls, and the relative response is equated to the concentration of free antibody at equilibrium. A correction can be applied to allow for the multivalency of the antibody (7). Using the measurements of free antibody and knowledge of the total antibody and antigen present, one can infer the concentrations of free and bound antigen and antibody. These data can then be graphed on a Scatchard Plot, or numerical analysis can be used to determine the association equilibrium constant for the antibody–antigen interaction.

Bibliography

1. E. Engvall and P. Perlman (1971) Immunochemistry **8**, 871–874.
2. B. K. van Weemen and A. H. W. M. Schnuurs (1971) FEBS Lett. **15**, 232–237.
3. E. Engvall and P. Perlmann (1972) J. Immunol. **109**, 129–135.
4. L. Belanger, C. Sylvestre, and D. Dufour (1973) Clin. Chim. Acta **48**, 15–18.
5. B. Friguet, A. F. Chaffotte, L. Djavadi-Ohaniance, and M. E. Goldberg (1985) J. Immunol. Meth. **77**, 305–319.
6. S. Hetherington (1990) J. Immunol. Meth. **131**, 195–202.
7. F. S. Stevens (1987) Mol. Immunol. **24**, 1055–1060.

Suggestion for Further Reading

8. D. M. Kemeny and S. J. Challacombe, eds. (1988) *ELISA and Other Solid Phase Immunoassays: Theoretical and Practical Aspects* Wiley, New York.

Enzymes

Enzymes are proteins that act as biological **catalysts**. They are produced by living cells, but are independent of those cells for their catalytic activity. Like all catalysts, they speed up the rates of chemical reactions, but their special importance lies in the fact that they can do this at neutral pH and relatively low temperatures, and do so specifically, essentially for only one chemical reaction (see Induced Fit). The rate increase, which is due to the lowering of the activation energy barrier by binding and stabilizing the transition state (see Transition State Analogue), can be as much as 10^{12}-fold (1). Under these circumstances, the uncatalyzed reaction would be barely detectable. As catalysts and under *in vitro* conditions, enzymes function at concentrations very much lower than those of the substrates on which they act. However, in the cell, the enzyme level often exceeds the substrate concentration. Enzymes increase the rate of a reaction in both the forward and reverse directions and, therefore, have no effect on the equilibrium constant K_{eq} of the reaction (see Haldane Relationship). In theory, enzymes as catalysts remain unchanged at the end of a reaction, but as enzymes are proteins, they are subject to **denaturation**, which can lead to loss of activity over the course of a reaction. Enzymes may show either absolute or broad specificity. For example, catalase acts only on hydrogen peroxide, whereas alcohol dehydrogenase oxidizes a number of aliphatic and aromatic alcohols.

Enzymes have the same general structure as all proteins (see Protein Structure). The basic structure consists of a polypeptide chain that is made up of 20 amino acid residues joined in a linear sequence by peptide bonds. The folding of the polypeptide chain gives rise to the final enzyme structure, which contains an active site at which the substrates bind to undergo reaction. It is this folding to form the active site that is responsible for the catalytic power and specificity of enzymes. The active form of an enzyme may consist of single or multiple subunits (see Oligomeric Proteins), with molecular weights ranging from about 14,000 to 4,000,000 (Table 1).

Table 1. Molecular Weights and Subunit Composition of Selected Enzymes

Enzyme	Molecular Weight	Number of Subunits
RibonucleaseA	13,700	1
Lysozyme, hen	13,900	1
Carbonic anhydrase	30,000	1
a-Amylase	50,000	2
Hexokinase	102,000	2
Alcohol dehydrogenase	150,000	4
Aspartate transcarbamoylase	310,000	12
Urease	480,000	2

Glutamine synthetase	600,000	12
Pyruvate dehydrogenase	4,000,000	1 (960,000)
		24 (90,000)
		12 (112,000)

Some enzymes bring about **energy transductions** that include the conversion of light energy to chemical bond energy in photosynthesis, as well as the conversion of chemical bond energy to mechanical energy in muscle contraction and to pumping energy for the **membrane transport** of ions against an unfavorable gradient.

The activities of enzymes are usually subject to control, not only through changes to intracellular substrate levels, but also by activation, inhibition, and covalent modification. The activity of enzymes is influenced by pH because of the presence of ionizing amino acid residues at the active site. Some enzymes require **prosthetic groups** or metal ions (see Coenzyme, Cofactor), whereas others must undergo irreversible (see Proenzyme) or reversible activation. Reversible activation is often achieved by means of **phosphorylation** or adenylylation. Glycogen phosphorylase is activated by the transfer of a phosphoryl group from ATP to a single serine residue and inactivated by a **phosphatase** that removes the phosphoryl group. By contrast, *glycogen synthase* is inactivated by the phosphorylation of a serine residue and activated through phosphatase action. The protein kinases responsible for the phosphorylation of phosphorylase and glycogen synthase are activated by 3′, 5′-cyclic AMP. The interaction of this nucleotide with the regulatory subunits on the inactive kinases causes release of the active forms of the enzymes. The reversible activation of *glutamine synthetase* involves the transfer of the AMP moiety of ATP to and from the hydroxyl group of a **tyrosine** residue. Both reactions are catalyzed by the same enzyme, *adenyl transferase* . Enzymes can be inactivated by small molecules that covalently interact with amino acid residues at the active site (see Active Site-Directed Irreversible Inhibitors) or inhibited by substrate analogues, which can behave as drugs or pesticides (see Dead-End Inhibition).

A group of enzymes that are subject to special control are the **allosteric** enzymes. The activities of these enzymes are not only more sensitive to changes in intracellular substrate concentrations, but they are also activated and/or inhibited reversibly by modifiers that are small molecules which combine at either a specific binding site on a catalytic subunit or on a special regulatory subunit. Modifiers are frequently the end-product of a metabolic pathway and have structures that differ from those of the substrates for the allosteric enzymes (see **Feedback inhibition**). The control of enzyme activity can also be achieved through their interaction with low-molecular-weight proteins, such as calmodulin.

It has been demonstrated recently that it is possible to produce monoclonal antibodies which show catalytic activity (2). The generation of catalytic antibodies, or abzymes, has occurred through the use of an antigen that resembles the transition state or an intermediate state of the reaction (see Transition State Analogue). The idea was to produce an antibody that would bind tightly to, and stabilize, the transition state complex so as to enhance the reaction rate. The rate enhancement and small number of antibodies produced with a particular antigen suggest that the analogues are not good mimics of the actual transition state, or that good catalytic activity requires more than simply the stabilization of a transition state complex. Catalytic activity is not restricted to proteins, for RNA molecules have been shown to function as enzymes. These relatively small molecules, which are generally found in viruses, have catalytic features in common with those of enzymes (3).

1. Enzyme Nomenclature

In 1956, the International Union of Biochemistry established an International Commission on Enzymes. There were several reasons why. The number of known enzymes was increasing rapidly and their naming by individual researchers was not satisfactory. Further, the names did not always convey the nature of the reaction being catalyzed and similar names were given to enzymes of different types. The first report on enzyme nomenclature was produced in 1961 and contained references to 712 enzymes. The sixth report was published in 1984 by Academic Press and contains classifications for 2,477 enzymes. The publication lists classes of enzymes as well as information about the reference number, recommended name, reaction catalyzed and other names for particular enzymes. Enzymes in this volume are categorized as Dehydrogenases, Hydrogenases, Hydrolases, Isomerases, Synthetases/Ligases, Synthases/Lyases, Oxidoreductases, Phosphotransferases, and Transferases .

Bibliography

1. L. Frick, J. P. MacNeela, and R. Wolfenden (1987) Bioorg. Chem. **15**, 100–108.
2. S. J. Benkovic (1992) Ann. Rev. Biochem. (1992) **61**, 29–54.
3. W. G. Scott and A. Klug (1996) Trends Biochem. Sci. **21**, 220–224.

Epidermal Growth Factor

The epidermal growth factor (EGF) family of proteins is defined by their sequence homology and capacity to bind and activate the EGF receptor. Also described is the ErbB receptor family, which includes the EGF receptor, which is also known as ErbB-1 and HER-1, and three sequence-related receptors. Brief mention is made of the heregulin/neuregulin growth factors, which are structurally related to EGF but do not bind to the EGF receptor, although they do bind and activate other ErbB receptors.

1. EGF Ligands

There are six known mammalian gene products that share primary sequence homology, are recognized by the EGF receptor with high affinity (**dissociation constant** in the nanomolar range), and activate intracellular signaling pathways leading to increased cell proliferation. These ligands are known as EGF, transforming growth factor alpha (TGFa), heparin-binding EGF (HB-EGF), amphiregulin, betacellulin, and epiregulin (1, 2). As noted below, two of these ligands, betacellulin and epiregulin, are able to bind not only to the EGF receptor, but also to ErbB-4, a separate member of the EGF receptor family. In addition to these ligands encoded by genes in mammalian cells, EGF growth factors are encoded by genes in the fruit fly *Drosophila* (*sptiz, gurken, vein*) (3), the nematode *Caenorhabditis elegans* (*lin*3) (4), and certain Pox-family viruses (5). The *Drosophila* gene *argos* apparently encodes an antagonist growth factor for the fly EGF receptor (3). To date, however, EGF receptor antagonists have not been found in other biological systems or created through synthetic chemistry.

Structurally, the EGF receptor ligands are small monomeric proteins of 6–10 kDa that are characterized by conserved sequence features—most notably six **cysteine** residues that, in the mature ligands, form three characteristically spaced disulfide bonds producing three loop structures within the molecule (5). Nuclear magnetic resonance (NMR) has been employed to determine the high-resolution protein structures of EGF and TGFa (see EGF Motif), while site-directed mutagenesis has revealed which amino acid residues are essential for growth factor function (6). The structures of EGF and TGFa are highly superimposable, and each is dominated by beta-sheet structure. Growth factor mutagenesis (5, 6) and an NMR study of a TGFa:EGF receptor ectodomain complex (7) implicate residues in both the amino- and carboxy-terminal domains, which are not closely packed together in the high-resolution structure. Therefore, the growth factor may use more than one surface or domain to contact the receptor binding site. This multidomain view of growth factor binding to its receptor has also provoked models in which the ligand is bivalent and capable of associating with two receptor molecules (8).

The mature proteins, especially EGF, are chemically and biologically very stable to extreme physical conditions, such as acid and heat. All the growth factors have been produced as recombinant proteins, and many are commercially available. EGF is easily derivatized with covalent probes, including ^{125}I, fluorescein, biotin, and various toxins (5). These modifications have been employed to quantify and/or visualize growth-factor interactions with receptors or, in the case of toxin conjugates, to kill cells having EGF receptors, particularly certain tumors that overexpress this receptor (9).

The mature EGF and EGF-like ligands are found in the extracellular space as freely diffusible proteins, but they are not products of the secretory pathway. The extracellular ligands are derived from the ectodomain of transmembrane precursor proteins present on the surface of cells (5). In these precursors, the EGF or EGF-like sequence is liberated into the extracellular environment as a diffusible growth factor following a series of **proteolytic** processing steps (5, 10). This means that the presence or concentration of extracellular mature growth factor is determined not only at the level of gene expression, but also by control of the extent of precursor proteolytic processing. Yet relatively little is known regarding the identity or biological control of the activity of the proteinases involved, although metalloproteinase activity is frequently implicated on the basis of inhibitor studies for the precursor processing of TGFa (11), EGF (12), HB-EGF (13), and amphiregulin (14). The existence of transmembrane precursors has raised the question of whether the precursor form of the growth factor can activate EGF receptors on adjacent cells, without the necessity for proteolytic processing. While this is not trivial to test experimentally, the available data indicate that such communication is possible (10). Whether this is biologically significant in mammals is unclear; in developmental circumstances, however, where neighboring cells obviously must communicate, such juxtacrine communication is possibly significant.

EGF and other EGF-like ligands are present in most bodily fluids (urine, milk, saliva), but they are difficult to detect in blood or serum (5). The production of these growth factors is not confined to one or two organs within the body, but it seems to occur within many tissues. Hence, the circulatory system is not essential for delivery of the growth factor to target cells. It seems likely that growth factors like the EGF ligands are examples of paracrine hormones in which the production and utilization of the ligand occurs in different cells within the same local environment of a tissue. Each EGF-like growth factor has a distinctive pattern of expression in tissues, although in certain tissues there is usually some degree of overlap with the expression of other members of this growth factor family. In the case of tumor cells, it is a frequent observation that the same cell constitutively produces and is activated by a growth factor. This is a process termed autocrine regulation and may be particularly important for TGFa, amphiregulin, and epiregulin, which are frequently expressed in tumor cells (15).

EGF is known to stimulate the proliferation of a great many cell types in cell culture, as its receptor is expressed in almost all nonhematopoietic cells (5). In the intact animal, however, enhanced proliferation of epithelial tissues is the most commonly observed response to the administration of exogenous EGF (5). Proliferation of skin and isolated epidermis have been the model system for an EGF-responsive tissue, but published data also show enhanced proliferation *in vivo* of internal epithelial tissues, such as trachea and gastrointestinal tissue. In the adult, it seems likely that the EGF family of growth factors participates in control of the relatively high level of homeostatic proliferation necessary to support epithelial tissues. Administration of EGF to fetal or newborn animals often hastens certain developmental processes, such as lung maturation and eyelid opening, respectively (5). TGFa and amphiregulin are particularly recognized as EGF family members that are expressed during gestation (16). At least one nonmitogenic biological response has been described following EGF administration to animals: the inhibition of parietal-cell acid secretion (5). It is unclear, however, whether EGF ligands normally participate in pH control within the gastric system.

In humans, the genes for EGF, TGFa, amphiregulin, and HB-EGF are localized, respectively, to chromosomes 4q25 $\rightarrow$ q29, 2p11 $\rightarrow$ p13, 4q13 $\rightarrow$ q21, and 5 (17). The genes range in size from 120 kbp and 24 exons (for EGF) to 18, 14, and 10 kb and 6 exons each for TGFa, HB-EGF, and amphiregulin, respectively. The expression of genes in this family has been demonstrated in both nontransformed and transformed cells to involve autoinduction by the homologous growth factor, or by a different member of this growth factor family (18). The autoinduction mechanism could be a significant amplification factor in autocrine tumor growth and in Poxvirus infection.

In contrast to the severe phenotype exhibited following targeted disruption of the EGF receptor gene in mice (see text below), " **knockout**" of the TGFa gene in mice produces only a mild disturbance in the function of the hair follicle and a consequent "wavy" hair **phenotype** (19, 20). While knockouts of other family members have yet to be reported, preliminary data for some also suggest mild changes in phenotype. Hence, while receptor function is indispensable in the animals, there does seem to be considerable functional redundancy within the EGF family of ligands.

2. EGF Receptors

Based primarily on sequence similarity, four members have been identified in the ErbB family of EGF receptor-related molecules (1, 2): the EGF receptor (also known as HER-1 and ErbB-1); ErbB-2 (Neu, HER-2); ErbB-3 (HER-3); and ErbB-4 (HER-4). EGF, EGF-like ligands, and heregulin (neuregulin) activate these receptors, but in distinctive and complex ways (1, 2). EGF and the EGF-like ligands (HB-EGF, TGFa, amphiregulin, betacellulin, epiregulin) recognize ErbB-1, while the heregulin growth factors bind to ErbB-3 and ErbB-4. However, some EGF family molecules can bind to the EGF receptor and another ErbB receptor. For example, betacellulin, HB-EGF, and epiregulin, but not EGF or TGFa, activate ErbB-4 as well as the EGF receptor. The heregulin isoforms bind to ErbB-3 and ErbB-4, but not to the EGF receptor. There is no known ligand for ErbB-2, which seems to function as a co-receptor with each of the other ErbB family members (21, 22).

The mature forms of these receptors contain approximately 130 kDa of protein complexed with N-linked carbohydrate (see *N*-Glycosylation) to give a molecular mass of approximately 175–185 kDa (5). Based on cloning and **sequencing** of complementary DNA for the EGF receptor prototype for this receptor family (23), the transmembrane orientation of the ErbB receptors is believed to consist of three regions, as shown in Figure 1. These are (i) an extracellular **ligand-binding** region, (ii) a cytoplasmic region, and (iii) a single **hydrophobic** transmembrane domain of approximately 24 amino acid residues. Among these ErbB family receptors, the cytoplasmic carboxy-terminal domains show similarity in size, but are the most heterogeneous domains in terms of sequence similarity. The EGF receptor is the most widely-studied and best-characterized molecule among the members of ErbB receptor family. The remaining portion of this article is, therefore, focused on the structure–function, activation, regulation, and genetic alterations of the EGF receptor.

Figure 1. Schematic representation of the EGF receptor. Based on its amino acid sequence, obtained by cDNA sequencing (23), the protein structure of the EGF receptor is subdivided into extracellular, transmembrane, and intracellular regions and into eight domains. The phosphotyrosyl residues in the carboxy-terminal domain are indicated by (P)Y.

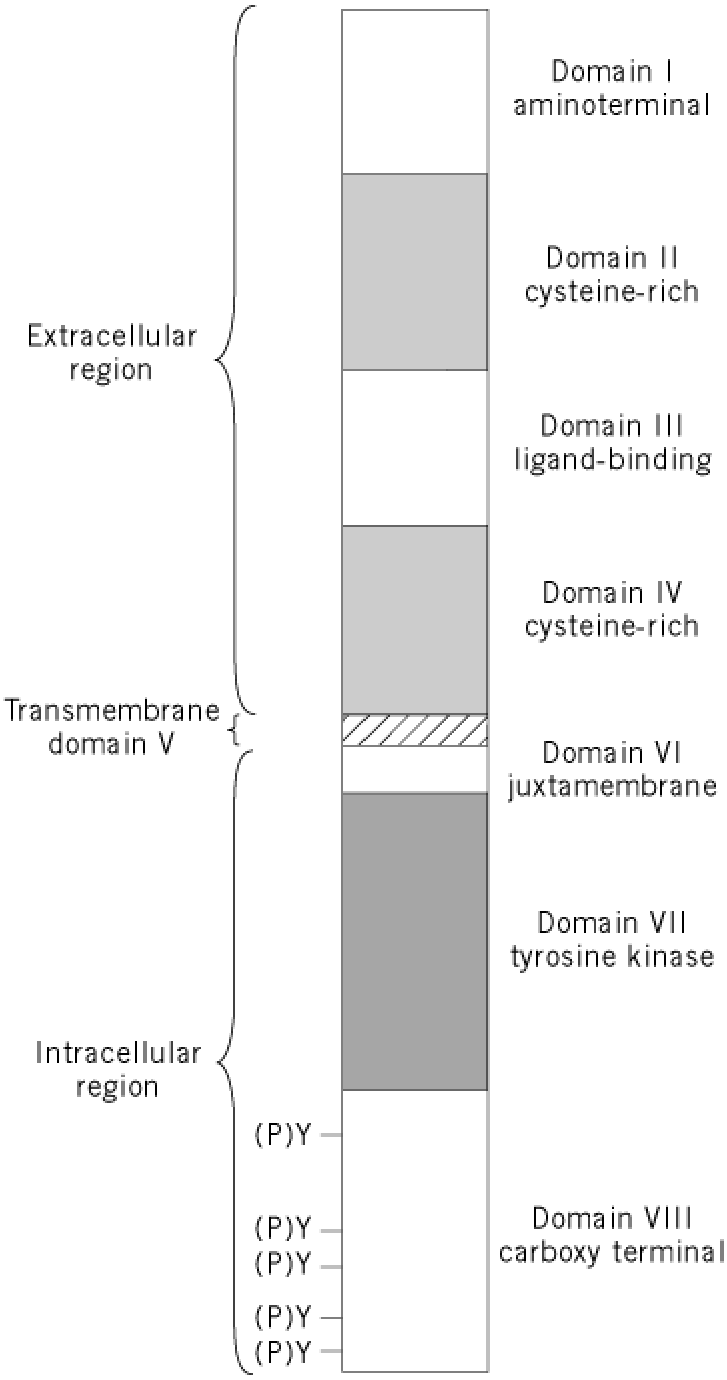

As depicted in Figure 1, the extracellular region of the EGF receptor can be divided into four **domains** based on the presence of two cysteine-rich regions (Domains II and IV). The functions of the cysteine-rich domains are not clearly understood, although they probably provide significant structural stability, because 25 disulfide bonds are found in these two domains (24). Domain III, localized between these two cysteine-rich domains, is thought to mediate ligand binding (5). There are implications that residues in Domain I may also contribute to ligand binding (25), but there are no high-resolution data to define the receptor/ligand binding site. The ectodomain of the receptor is heavily glycosylated with 10–11 N-linked oligosaccharide chains (5). Among these carbohydrates, at least three are of the high-mannose type, while the others are complex-type oligosaccharide chains. While oligosaccharide addition is necessary for correct EGF receptor folding and processing to the cell surface, there is no evidence that carbohydrate is a determinant of ligand binding or other receptor functions at the plasma membrane.

The intracellular or cytoplasmic region of the EGF receptor is composed of three domains: the juxtamembrane domain, a **tyrosine kinase** domain, and a carboxy-terminal domain (Fig. 1). The receptor is actually an enzyme (tyrosine kinase), and the kinase activity is dependent on ligand binding to the receptor ectodomain (5). Clearly, the tyrosine kinase domain is critical to the receptor's capacity to elicit biological responses, namely mitogenesis, following ligand binding. Inactivation of the kinase domain by site-directed mutagenesis abrogates EGF responses. Five tyrosine autophosphorylation sites have been identified in the carboxy-terminal domain at Tyr992, 1068, 1086, 1148, and 1173, while modification by **phosphorylation** of **serine** or **threonine** residues by **serine–threonine kinases** has been localized to both the carboxy-terminal and juxtamembrane domains. One of these, Thr654 in the juxtamembrane region, is a substrate for protein kinase C, and its phosphorylation results in attenuation of receptor tyrosine kinase activity. Phosphorylation of the tyrosine residues of the carboxy-terminal domain results in formation of "docking sites" for many of the substrates of the receptor tyrosine kinase (26).

The EGF receptor is activated by a two-step mechanism (26). First, binding of a cognate ligand to the monomeric receptor induces the formation of noncovalent receptor dimers. Although the mechanism of dimerization is not clear, it may be due to a conformational change in the receptor external domain or to bivalent binding of EGF to the receptor. Interestingly, the EGF receptor can, in response to ligand binding, also form heterodimers with other ErbB family receptors, particularly ErbB-2 and ErbB-3 (1, 2). The second step in receptor activation occurs when dimerization of the receptors leads to juxtapositioning of the cytoplasmic domains and transphosphorylation of the two receptors present in the dimer (26). Hence, autophosphorylation is probably a mixture of inter- and intramolecular phosphorylations. At present it is unclear how autophosphorylation sites may relate to the control of tyrosine kinase activity. Unlike many other tyrosine kinase receptors, none of the EGF receptor autophosphorylation sites is within the kinase domain, where it might directly regulate the kinase active site.

Based on the studies with "dominant-negative" kinase-inactive EGF receptor mutants, it has been concluded that transphosphorylation within dimers is essential for substrate phosphorylation and concomitant EGF-mediated signal transduction (26). When a kinase-inactive EGF receptor mutant is coexpressed in the same cell with wild-type receptor, heterodimers of the two receptors (wild-type and mutant) are produced in response to EGF. Kinase activation and signaling are suppressed in proportion to the relative overexpression level of the mutant receptors. The reason for attenuation of the wild-type receptor function is that kinase-inactive receptors do form dimers with the wild-type receptors, but transphosphorylation does not occur.

The cytoplasmic substrates that are phosphorylated by the EGF receptor include: (i) enzymes, such as **phospholipase C**-g1; **Src**, a cytoplasmic tyrosine kinase; the **ras** GTPase-activating protein; and the phosphotyrosine phosphatase SHP-2; (ii) the transcription factor STAT; and (iii) the nonenzymatic adapter molecules GRB-2, the p85 subunit of phosphatidylinositol 3-kinase, eps8, eps15, Nck, and Shc (1). Also, heterodimerization leads to EGF-dependent phosphorylation of ErbB-2 and ErbB-3 (1, 2). Many, but not all, of these receptor-proximal proteins have in common the presence of a noncatalytic domain of approximately 100 residues termed a *src* homology, or **SH2**, domain (27). SH2 domains recognize phosphotyrosine-containing sequences and thereby mediate association of these molecules with activated receptors. This mechanism to promote receptor association serves two purposes. First, it facilitates subsequent tyrosine phosphorylation of the SH2-containing protein by the receptor tyrosine kinase domain. Second, it relocalizes cytoplasmic SH2 molecules to the receptor carboxy-terminus and hence close to the cytoplasmic face of the plasma membrane. Relocalization may be a significant factor for those molecules that function by modifying plasma membrane phospholipids (eg, phospholipase C-g1) or those (GRB-2 and Shc) that interact with membrane-localized signal transduction target proteins, such as Ras. Actually, the GRB-2 adaptor associates with the EGF receptor, but it is not detectably phosphorylated. Therefore, relocation of GRB-2 seems to be the only function of its receptor association.

Desensitization of the activated EGF receptor is achieved by two mechanisms. The first and best understood is endocytosis of the activated receptor, followed by its degradation in **lysosomes** (28). This provides a relatively slow rate of receptor inactivation and results in the down-regulation of the cellular level of receptor protein, when receptor degradation exceeds receptor biosynthesis. To initiate this process, ligand binding to the EGF receptor induces receptor clustering in **clathrin**-coated pits and rapid internalization. Following this internalization step, ligand:receptor complexes in endosomes are targeted to the lysosome, where both the receptor and its ligand are degraded. It should be noted that during a substantial portion of this endocytosis process, EGF remains bound to the receptor and phosphotyrosine remains detectable on the receptor. Hence, the internalized receptor remains potentially functional for some period of time. Curiously, the heregulin receptors (ErbB-3 and ErbB-4) are not subject to rapid internalization following ligand binding (29).

A second means by which activated receptors are desensitized involves the phosphorylation of serine/threonine residues within the cytoplasmic domain (30). This mechanism is not, however, well understood.

Overexpression or mutation of the EGF receptor has been reported to be associated with certain malignancies (31). For example, there is frequently detected in glioblastomas a small genomic deletion of exons encoding a small region of the EGF receptor ectodomain. This mutation inhibits ligand binding but produces a constitutively active receptor. In a sizable fraction of breast cancers, the EGF receptor is overexpressed but not mutated (31, 32). Also, the EGF co-receptor ErbB-2 is even more frequently overexpressed in breast cancer. Antibodies to the EGF receptor and ErbB-2 are being evaluated for therapeutic efficacy in breast cancer clinical trials (33).

In humans, the gene encoding the EGF receptor is localized to the p13 → q22 region of chromosome 7 (17). Expression of the EGF receptor gene produces two major species of messenger RNA: 10.5 and 5.8 kb. The 5.8-kb mRNA represents a full-length cDNA that includes 5′- and 3′-untranslated sequences (23, 34). The genesis and significance of the 10.5-kb mRNA is not clearly understood, but it probably contains a longer 3′-untranslated sequence. In certain cells, a smaller mRNA (2.0 kb) is also detected. This mRNA is formed by RNA splicing and encodes the EGF receptor ectodomain. In cells expressing this mRNA, the ectodomain fragment is fully glycosylated and secreted (35). The **promoter** sequence of the EGF receptor represents a typical "**housekeeping gene**" with extremely GC-rich sequences and the absence of TATA and CAAT boxes (36).

Targeted disruption of the EGF receptor gene in mice produces multiorgan failure and embryonic lethality in most, but not all, mouse strains (37-39). In some mouse strains, it has been reported that "knockouts" of the EGF receptor live up to 8 days after birth and suffer from impaired epithelial development in skin, liver, and gastrointestinal tract. However, neurodegeneration is the most common and strain-independent phenotype of postnatal mice that lack EGF receptors (40). Gene "knockouts" of ErbB-2 (41, 42) and ErbB-4 (43) both produce deficiencies in neurodevelopment and development of the embryonic heart, leading to lethality at 10 days' gestation. Homozygous disruption of the ErbB-3 gene in mice produces severe defects in neurogenesis, specifically in Schwann cell development and the maturation of neurons, plus abnormalities in cardiac development (42, 44). In fact, defects in neural development have been noted in all ErbB knockouts, including the EGF receptor. EGF receptor-null mice, however, have not been reported to be abnormal in heart development.

3. Acknowledgment

Our work was supported by NIH grants CA24071 and CA75195.

Bibliography

1. I. Alroy and Y. Yarden (1997) FEBS Lett. **410**, 83–86.
2. D. J. Riess II and D. F. Stern (1998) Bioessays **20**, 41–48.

3. J. D. Wasserman and M. Freeman (1997) Trends Cell Biol. **7**, 431–436.
4. M. Sundaram and M. Han (1996) Bioessays **18**, 473–480.
5. G. Carpenter and M. I. Wahl (1990) In *Handbook of Experimental Pharmacology*, **95/I** (M. B. Sporn and A. B. Roberts, eds.) Springer-Verlag, Berlin, pp. 69–171.
6. L. C. Groenen, E. C. Nice, and A. W. Burgess (1994) Growth Factors **11**, 235–257.
7. C. McInnes, D. W. Hoyt, R. N. Harkins, R. N. Pagila, M. T. Debanne, M. O"Connor-McCourt, and B. D. Sykes (1996) J. Biol. Chem. **271**, 32203–32211.
8. M. A. Lemmon, Z. Bu, J. E. Ladbury, M. Zhou, D. Pinchasi, I. Lax, D. E. Engelman, and J. Schlessinger (1997) EMBO J. **16**, 281–294.
9. I. Pastan and D. FitzGerald (1991) Science **254**, 1173–1177.
10. J. Massagué (1990) J. Biol. Chem. **265**, 21393–21396.
11. J. Arribas, L. Coodly, P. Vollmer, T. K. Kishimoto, S. Rose-John, and J. Massagué (1996) J. Biol. Chem. **271**, 11376–11382.
12. P. J. Dempsey, K. S. Meise, Y. Yoshitake, K. Nishikawa, and R. J. Coffey (1997) J. Cell Biol. **138**, 747–758.
13. M. Suzuki, G. Raab, M. A. Moses, C. A. Fernandez, and M. Klagsbrun (1997) J. Biol. Chem. **272**, 31730–31737.
14. C. L. Brown, K. S. Meise, G. D. Plowman, R. J. Coffey, and P. J. Dempsey (1998) J. Biol. Chem. **273**, 17258–17268.
15. A. W. Burgess and C. M. Thumwood (1994) Pathology **26**, 453–463.
16. E. D. Adamson and L. M. Wiley (1997) In *Current Topics in Developmental Biology*, Vol. **35**, Academic Press, New York, pp. 71–120.
17. C. Soler and G. Carpenter (1995) In *Guidebook to Cytokines and Their Receptors* (N. A. Nicola, ed.), Oxford University Press, Oxford, pp. 194–197.
18. J. A. Barnard, R. Graves-deal, M. R. Pittelkow, R. DuBois, P. Cook, G. W. Ramsey, P. R. Bishop, L. Damstrup, and R. J. Coffey (1994) J. Biol. Chem. **269**, 22817–22822.
19. G. B. Mann, K. J. Fowler, A. Gabriel, E. C. Nice, R. L. Williams, and A. R. Dunn (1993) Cell **73**, 249–261.
20. N. C. Leutteke, T. H. Qiu, R. L. Peiffer, P. Oliver, O. Smithies, and D. C. Lee (1993) Cell **73**, 263–278.
21. D. Karunagaran, E. Tzahar, R. R. Beerli, X. Chen, D. Graus-Porta, B. J. Ratzkin, R. Seger, N. E. Hynes, and Y. Yarden (1996) EMBO J. **15**, 254–264.
22. D. Graus-Porta, R. R. Beerli, J. M. Daly, and N. E. Hynes (1997) EMBO J. **16**, 1647–1655.
23. A. Ullrich, L. Coussens, J. S. Hayflick, T. J. Dull, A. Gray, A. W. Tam, J. Lee, Y. Yarden, T. A. Libermann, J. Schlessinger, J. Downward, E. L. V. Mayes, N. Whittle, M. D. Waterfield, and P. H. Seeburg (1984) Nature **309**, 418–424.
24. Y. Abe, M. Odaka, F. Inagaki, I. Lax, J. Schlessinger, and D. Kohda (1998) J. Biol. Chem. **273**, 11150–11157.
25. A. E. Summerfield, A. K. Hudnall, T. J. Lukas, C. A. Guyer, and J. V. Staros (1996) J. Biol. Chem. **271**, 19656–19659.
26. J. Schlessinger and A. Ullrich (1992) Neuron **9**, 383–391.
27. C. A. Koch, D. Anderson, M. F. Moran, C. Ellis, and T. Pawson (1991) Science **252**, 668–674.
28. A. Sorkin and C. M. Waters (1993) Bioessays **15**, 375–382.
29. J. Baulida, M. H. Kraus, M. Alimandi, P. P. Di Fiore, and G. Carpenter (1996) J. Biol. Chem. **271**, 5251–5257.
30. S. J. Therous, D. A. Latour, K. Stanley, D. L. Raden, and R. J. Davis (1992) J. Biol. Chem. **267**, 16620–16626.
31. H. Modjtahedi and C. Dean (1994) Int. J. Oncol. **4**, 277–296.

32. S. B. Fox and A. L. Harris (1997) J. Mamm. Gland Biol. Neopl. **2**, 131–141.
33. J. Baselga and J. Mendelsohn (1997) J. Mamm. Gland Biol. Neopl. **2**, 165–174.
34. C. R. Lin, W. S. Chen, W. Kruiger, L. S. Stolarsky, W. Weber, R. M. Evans, I. M. Verma, G. N. Gill, and M. G. Rosenfeld. (1984) Science **224**, 843–848.
35. W. Weber, G. N. Gill, and J. Spiess (1984) Science **224**, 294–297.
36. N. P. Bates and H. C. Hurst (1997) J. Mamm. Gland. Biol. Neopl. **2**, 153–163.
37. D. W. Threadgill, A. A. Dlugosz, L. A. Hansen, T. Tennenbaum, U. Lichti, D. Yee, C. LaMantia, T. Mourton, K. Herrup, R. C. Harris, J. A. Barnard, S. H. Yuspa, R. J. Coffey, and T. Magnuson (1995) Science **269**, 230–234.
38. M. Sibilia and E. F. Wagner (1995) Science **269**, 234–238.
39. P. J. Miettinen, J. E. Berger, J. Meneses, Y. Phung, R. A. Pedersen, Z. Werb, and R. Derynck (1995) Nature **376**, 337–341.
40. M. Sibilia, J. P. Steinbach, L. Stingl, A. Aguzzi, and E. F. Wagner (1998) EMBO J **17**, 719–731.
41. K.-F. Lee, H. Simon, H. Chen, B. Bates, M.-C. Hung, and C. Hauser (1995) Nature **378**, 394–398.
42. S. L. Erickson, K. S. O"Shea, N. Ghaboosi, L. Loverro, G. Frantz, M. Bauer, L. H. Lu, and M. W. Moore (1997) Development **124**, 4999–5011.
43. M. Grassmann, F. Casagranda, D. Orioli, H. Simon, C. Lai, R. Klein, and G. Lemke (1995) Nature **378**, 390–386.
44. D. Riethmacher, E. Sonnenberg-Riethmacher, V. Brinkmann, T. Yamaai, G. R. Lewin, and C. Birchmeier (1997) Nature **389**, 725–730.

Suggestions for Further Reading

45. Listed below are key review articles arranged to reflect the chronological development of EGF research.
46. G. Carpenter and S. Cohen (1979) Epidermal growth factor, Annu. Rev. Biochem. **48**, 193–216.
47. G. Carpenter and M. I. Wahl (1990) "The epidermal growth factor family", In Handbook of Experimental Pharmacology, Vol **95/I**, Springer-Verlag, Berlin, pp. 69–171.
48. J. Schlessinger and A. Ullrich (1992) Growth factor signaling by receptor tyrosine kinases, Neuron **9**, 383–391.
49. I. Alroy and Y. Yarden (1997) The ErbB signaling network in embryogenesis and oncogenesis: Signal diversification through combinatorial ligand–receptor interactions, FEBS Lett. **410**, 83–86.
50. J. B. Duffy and N. Perrimon (1996) Recent advances in understanding signal transduction pathways in worms and flies, Curr. Opin. Cell Biol. **8**, 231–238.

Epigenetics

Epigenetics is derived from the Greek word epigenesis, which describes the Aristotelian concept that an organism develops progressively through a series of causal interactions of various parts. During the 16th and 17th centuries, the epigenetic mode of development was held in contrast to the preformation theory, which maintained that development occurred by simple enlargement of a preformed homunculus in the germ cell (for the early history of its usage, see ref. 1). More modern definitions include the concept that, during development, cells progress through microenvironments that induce a stepwise restriction of their developmental potentialities into specialized ones via changes in gene expression (2). Based on this view of development, Holliday has defined epigenetics as the study of the mechanisms "that impart temporal and spatial control on the activity of all those genes required for the development of a complex organism from the zygote to the fully formed adult" (3). More recent usage, however, has tended to emphasize the "epi" or "beyond" aspect of the term. Strohman points out that "epigenesis is the historical alternative to genetic determinism and that it establishes the basis for a level of organizational control above the genome" (4). Accordingly, molecular geneticists use the term epigenetics for a process by which the state of gene expression is modified at a given time of development and becomes heritable at the cellular or organismal level. Molecular mechanisms underlying epigenetic phenomena are known only in a few cases. The known mechanisms include modifications of **DNA** and changes in the chromatin structure, which are thought to be propagated through templating (5).

There exist a broad variety of epigenetic phenomena in many organisms. Perhaps one of the best-studied epigenetic phenomena is **mating-type** silencing in the yeast *Saccharomyces cerevisiae* (6, 7). Yeast cells possess one of two mating types, a or a, determined by which of the alternate mating-type **alleles** is present at the mating-type locus (MAT). In addition, cells harbor two other copies of mating-type genes at the loci called HML and HMR. Despite their identical sequences, the mating-type gene located at the MAT locus is active in transcription; those at HML and HMR are silent. The molecular basis of mating-type silencing appears to lie in the specific type of chromatin structure at the HML and HMR loci.

In the fruit fly, *Drosophila melanogaster*, several phenomena have been described as epigenetic. The first example, known as position effect variegation (PEV), is observed when a chromosomal segment of euchromatin is translocated adjacent to a heterochromatic region (8). Such a translocation results in variegated spreading of repression from the heterochromatic region into the euchromatic segment, causing a metastable state of expression of the translocated genes. Because the variable spreading of gene inactivation is inherited clonally, the PEV phenomenon is considered epigenetic. The second example includes the **silencing** of homeotic genes during development (9). Homeotic genes are expressed in specific domains of the body and silenced in others. This spatially regulated silencing is established in early embryogenesis and is maintained throughout development by a group of chromatin-associated proteins known as the Polycomb group proteins.

In mammals, genomic imprinting and X-Chromosome Inactivation in females are both examples of epigenetic effects. Genomic imprinting has been observed for some 20 genes whose expression in an early embryo depends on whether the allele is derived maternally or paternally (10). Some genes are inactive when derived from maternal gametes; in other genes those derived paternally are inactive. The molecular basis of imprinting is known to be methylation of the DNA. The state of inactivity is inherited clonally through subsequent cell divisions by templating of the methylated state. Particular CpG sequences in imprinted genes are methylated in gametes of one sex but not the other (see CpG Islands). The zygote therefore becomes heterozygous at imprinted genes, carrying a methylated allele and a nonmethylated allele. During development, methylated alleles are not expressed, while **homologous** copies that are nonmethylated are expressed and provide the necessary functions. In primordial germ cells (the precursors of eggs and sperms), imprinting is erased by demethylation of appropriate residues in the imprinted genes. These residues are remethylated *de novo* in gametes in either the maternal or paternal mode.

In female mammals, one of two **X chromosomes** is inactivated, appearing cytologically as a Barr body. The X chromosome is inactivated by coating with the so-called Xist RNA (11). The Xist gene on the active chromosome is turned off by methylation of its **promoter**, while the Xist gene on the chromosome to be inactivated produces Xist RNA that coats its own chromosome. Once an X chromosome is inactivated, its inactive state is clonally inherited in its descendant cells, without the need of Xist RNA. Thus, Xist RNA appears to initiate an epigenetic state that is perpetuated, without playing a further role.

Lesser known, but equally fascinating, epigenetic phenomena are found in fungi and plants. *Neurospora crassa* and *Ascobolus immersus* seem to protect their genomes from assaults by transposable elements through mechanisms known as repeat induced-point mutation (RIP) and methylation-induced premeiotically (MIP), respectively (12, 13). Transposable elements, often present in multiple copies, trigger their mutual silencing in a process known as quelling by methylation or C to T transition mutations of repeated sequences. A paramutation, found in higher plants such as maize, tomato, or tobacco, is a mitotically and meiotically heritable change in gene expression that does not involve alterations in DNA sequences (14). At paramutable loci, some alleles, called paramutable alleles, are susceptible to paramutation, others, known as paramutagenic alleles, induce paramutation in the homologous copy of the same gene.

Bibliography

1. R. J. Richards (1992) *The Meaning of Evolution*, The University of Chicago Press, Chicago, pp. 5–16.
2. C. H. Waddington (1956) *Principles of Embryology*, Allen and Unwin, London, p. 350.
3. R. Holliday (1990) Phil. Trans. Royal Soc. Lond. **B326**, 329–338.
4. R. C. Strohman (1997) Nature Biotechnol., **15**, 194–200.
5. V. E. A. Russo, R. A. Martienssen, and A. D. Riggs, eds. (1996) *Epigenetic Mechanisms of Gene Regulation*, Cold Spring Harbor Laboratory Press, Cold Spring Harbor.
6. S. Loo and J. Rine (1995) Annu. Rev. Cell Dev. Biol. **11**, 519–548.
7. S. G. Holmes, M. Braunstein, and J. R. Broach (1996) in *Epigenetic Mechanisms of Gene Regulation*, Cold Spring Harbor Laboratory Press, pp. 467–487.
8. B. T. Wakimoto (1998) Cell **93**, 321–324.
9. V. Pirrotta (1998) Cell **93**, 333–336.
10. M. A. Surani (1998) Cell **93**, 309–312.
11. B. Panning and R. Jaenisch (1998) Cell **93**, 305–308.
12. M. J. Singer and E. U. Selker (1995) In P. Meyer, ed., *Gene Silencing in Higher Plants and Related Phenomena in Other Eukaryotes*, pp. 165–177.
13. C. Goyon et al. (1994) J. Mol. Biol. **240**, 42–51.
14. V. L. Chandler et al. (1996) In *Epigenetic Mechanisms of Gene Regulation* (V. E. A. Russo, R. A. Martienssen, and A. D. Riggs, eds.), Cold Spring Harbor Laboratory Press, Cold Spring Harbor, pp. 289–304.

Suggestions for Further Reading

15. S. C. R. Elgin (1995) *Chromatin Structure and Gene Expression*, IRL Press, Oxford.
16. Cell **93**, 301–348 (1998) (includes several reviews on epigenetics).
17. Trends in Genetics, **13**, 293–341 (1997) (a special issue on epigenetics).
18. E. Jablonka and M. J. Lamb (1995) *Epigenetic Inheritance and Evolution*, Oxford University Press, Oxford.

Epigenic Patterning

In the animal kingdom, the first developmental determination of the **germ cells** is the presence of a *polarity* . This is necessary to determine early coordinates for further development and organogenesis. In other words, there are one or more mechanisms to determine which part of the cell is supposed to form the posterior, anterior, dorsal, and ventral poles. The morphological appearance of the egg before fertilization, and also shortly after, fertilization is not uniform but shows a more or less distinct polarity, which is termed the animal–vegetal polarity. In certain species, sperm can only enter at the animal pole, indicating that there must be differences in molecular composition of the opposite poles.

There are various reasons for the development of the animal–vegetal polarity. In many cases, the feeder cells of oocytes are not uniformly located around the oocytes. Thus, they are fed from one side, which results in an asymmetrical concentration of certain molecules within the oocyte plasma. Another influence to produce polarity is probably light and gravity. However, after fertilization in space or in a fast rotating clinostate, Xenopus exhibited normal embryonic development and normal axis formation (1). In eggs containing a considerable amount of yolk, gravity forces the yolk to settle down. This event takes place in amphibia after sperm entry, which enables a free rotation of the egg **cytoplasm**. This causes the formation of the vegetal and animal polarity, in which the vegetal pole contains larger amounts of yolk than the animal pole.

The other polarity of the cell is not as easily determined in the unfertilized egg. In many cases, the posterior-anterior axis is determined by the site of sperm entry. On egg activation, a number of cytoplasmic reorganizations take place. In some species a region becomes visible, the *gray crescent*, which is located opposite to the site of the sperm entry. This is the prospective area in which **gastrulation** will take place. In amphibia, this region marks the prospective backside and distal side of the embryo. In birds, the dorsal-ventral polarity is determined by the structure of the egg, and the caudal distal polarity is assumed to be based on the influence of gravity. In mammals, there are contrary observations regarding where the inner cell mass settles. This embryonic event determines at least the dorsal side, whereas the mechanism that determines the prospective axis of the head and tail is still the subject of investigation.

Nüsslein-Volhard and others have provided more information about the situation in ***Drosophila***. In this species, the presence of a genetically determined polarity of the anterior and posterior regions of the egg was demonstrated. In the anterior region, a product of the gene ***bicoid*** was found to determine the development of the head and thorax (2, 3). In *Drosophila* bcd – / – mothers, which could not produce the bicoid gene product, larvae with no heads appeared. The product of the gene *nanos* is responsible for the formation of an abdomen and germline development (4), and its highest concentration occurs in the posterior end of the egg (5). In mothers homozygous negative for the nanos gene, no abdomen is formed. Compensation of the missing gene products by injection of *bicoid* messenger RNA or *nanos* mRNA leads in each negative variant to the development of a normal phenotype. Nanos and bicoid form concentration gradients from the anterior to the posterior and activate in a concentration-dependent manner a number of zygotic segmentation genes (6, 7). Bicoid controls transcription of the *hunchback* gene (6). In this cascade, the gene *staufen* is important for the localization of maternal mRNA to the posterior pole and for bicoid mRNA to the anterior pole in the *Drosophila* egg (8). In contrast, the nanos protein suppresses translation of *hunchback* mRNA. *Hunchback* is a gene responsible for the formation of anterior structures; on inhibition of these anterior structures, posterior ones are formed. The hunchback gradient controls *caudal* , which is concluded to be a region-specific activator of abdominal segmentation genes (9). Furthermore, injection of *nanos* mRNA into the anterior end induced the development of larvae with two abdomen and no head. Two heads and no abdomen develop in larvae on injection of *bicoid* mRNA into the posterior end of the egg.

In *Drosophila*, axis formation involves a series of interactions between the oocyte and the surrounding somatic follicle cells. The dorsal and ventral sides is determined by the localization of the oocyte nucleus and *gurken* mRNA to the dorsal-anterior corner of the oocyte. Gurken protein is believed to act as a ligand for the *Drosophila* epidermal growth factor (EGF) **receptor** (10).

It must be admitted that the naming of the above genes is somewhat peculiar. Many of the genes are not named according to their function, but instead according to the **phenotype** produced when the gene is defective. In this respect, this means that the gene *dorsal* determines the development of ventral structures, not dorsal. The dorsal protein migrates into the nuclei of the ventral side and acts, similar to nanos or bicoid, as a **transcription factor**.

Bibliography

1. G. A. Ubbels (1997) Cell Mol. Life Sci. **53**, 382–409.
2. W. Driever and C. Nüsslein-Volhard (1988) Cell **54**, 83–93.
3. X. Ma, D. Yuan, K. Diepold, T. Scarborough, and J. Ma (1996) Development **122**, 1195–1206.
4. S. Kobayashi, M. Yamada, M. Asaoka, and T. Kitamura (1996) Nature **380**, 708–711.
5. E. R. Gavis, and R. Lehmann (1994) Nature **369**, 315–318.
6. W. Driever and C. Nüsslein-Volhard (1989) Nature **337**, 138–143.
7. R. Rivera-Pomar, D. Niessing, U. Schmidt-Ott, W. J. Gehring, and H. Jäckle (1996) Nature **379**, 746–749.
8. D. St. Johnston, D. Beuchle, and C. Nüsslein-Volhard (1991) Cell **66**, 51–63.
9. C. Schulz and D. Tautz (1995) Development **121**, 1023–1028.
10. S. Roth, F. S. Neuman-Silberberg, G. Barcelo, and T. Schupbach (1995) Cell **81**, 967–978.

Epimers and Epimerization

Epimers are diastereomers that are related by the inversion of configuration at a single **chiral** center (1). This definition extends the original meaning of epimer, which was used to identify sugars that differed in configuration at C2 (2). This definition intentionally excludes enantiomers, such as D- and L-alanine, since they are not diastereomers. It also excludes diastereomers that are related by the inversion of more than a single chiral center. Thus, D-glucose and D-mannose are epimers, as are D-glucose and D-galactose. D-mannose and D-galactose are not epimers, however, because they are related by inversion at two chiral centers, C2 and C4 (Fig. 1)

Figure 1. Stereochemical drawings of glucose, mannose, and galactose, with their four chiral carbons. The configurations at C2 and C4 are labeled and distinguish these three sugars. Glucose is an epimer of both mannose and galactose because they differ by the configuration of a single chiral center. Mannose and galactose have different configurations at both C2 and C4 and are not epimers.

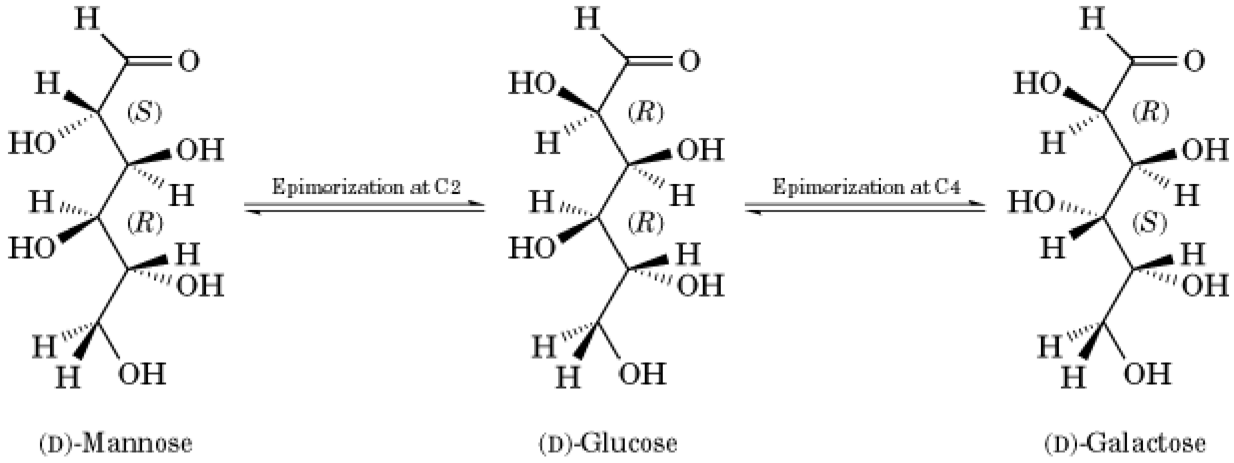

The chemical conversion of one epimer to another is called epimerization. If this interconversion is catalyzed by an enzyme, the enzyme is an epimerase. As an example, UDP-glucose-4-epimerase catalyzes the epimerization of the C4 carbon of glucose. In the reaction, UDP-glucose is epimerized to UDP-galactose. When the inversion of configuration occurs to interconvert enantiomers instead of diastereomers, the reaction is a **racemization**.

Bibliography

1. E. L. Eliel (1962) *Stereochemistry of Carbon Compounds*, McGraw-Hill, New York p. 40.
2. (1911) Chem. Abstr. **V**, 1606.

Suggestion for Further Reading

3. B. Testa (1982) "The geometry of molecules: Basic principles and nomenclatures". In *Stereochemistry* (C. Tamm, ed.), *New Comprehensive Biochemistry*, Vol. **3**, Elsevier, Amsterdam, pp. 22–24.

Epistasis

In Mendelian genetics, epistasis refers to the situation in which the phenotype caused by a mutation in one gene (A) masks the phenotype resulting from a mutation in another, nonallelic gene (B). Thus the individual carrying mutations in both genes A and B exhibits the same phenotype as the individual carrying a mutation in gene A alone. In this case, gene A is said to be epistatic over gene B, and gene B hypostatic to gene A. A classic example of epistasis is found among genes that determine mouse coat color. In the presence of albino mutant alleles, the mutant phenotypes of other coat-color determinants are not revealed, due to lack of pigment. Albino mutations, therefore, are epistatic over all other mutations that affect coat-color (1).

An epistatic relationship between two gene functions is often used to infer their relative order within a genetic pathway. Interpretation of such analysis depends on the type of genetic pathways. In biosynthetic pathways in which a series of genes modify a common intermediate substrate, epistatic genes are placed upstream of hypostatic ones. An example of such pathways is the morphogenetic pathway of **T4 phage** for head, tail, and tail-fiber assembly (2). In regulatory gene pathways, in contrast, where a member gene regulates the expression or activity of a downstream gene or gene product, epistatic genes are generally located downstream. A good example is found in the regulatory gene pathway that determines the dorsoventral body axis of the embryo in the fruit fly, *Drosophila melanogaster* (3). Most loss-of-function mutations that affect this pathway dorsalize the embryo. In contrast, a gain-of-function mutant allele of Toll, known as $Toll^{D}$, has been found that ventralizes the embryo. The presence of the opposite phenotypes allowed the investigators to combine a dorsalizing allele in a tester gene with the ventralizing allele of Toll and ask which of the two alleles is epistatic in double-mutant embryos. If the double mutant shows a dorsalized phenotype (ie, the tester allele is epistative over $Toll^{D}$), the tester gene is placed downstream of Toll. If the double mutant shows a ventralized phenotype, the tester gene is placed upstream. In this way, the genes in the pathway that affect the embryonic dorsoventral axis have been placed upstream or downstream relative to the Toll gene.

The logic of this type of analysis is straightforward if the pathway is a simple (ie, linear) series of genes or gene products. In such a pathway, the output depends solely on the activity of the terminal member of the pathway, and other members can be thought of as a series of on-off switches that determine the active or inactive state of the output gene. Regulatory gene pathways are not always simple, however, and there are situations in which epistatic genes act upstream. For excellent discussions of more complicated situations, as well as on assumptions and "rules" used in epistasis analysis, see Avery and Wasserman (4).

In population and quantitative genetics, epistasis refers to the genotype value for fitness contributed by gene interaction between two loci. The aggregate genotypic value of an individual (G) may deviate from the sum of the genotypic values attributable to the first locus (G_A) and the second locus (G_B). If it does, the deviation or nonadditive component (I_{AB}) is ascribed to epistasis, or interactions, between the two loci (5). Thus, $G = G_A + G_B + I_{AB}$. An example of epistasis can be seen when quantitative trait loci (QTL) from lines selected for high numbers of abdominal bristles in Drosophila are tested in pairwise combinations. In such tests, several pairs of QTLs for abdominal bristle number showed strong epistasis (interaction), resulting in abdominal bristle numbers that were beyond the additive effects of individual QTL (6).

Bibliography

1. W. K. Silvers (1979) *The coat Colors of Mice*, Springer-Verlag, New York.
2. M. Levine (1969) Annu. Rev. Genet. **3**, 323–342.
3. K. V. Anderson et al. (1985) Cell **42**, 779–789.
4. L. Avery and S. Wasserman (1992) Trends Genet. **8**, 312–316.
5. D. S. Falconer and T. F. C. Mackay (1996) *Introduction to Quantitative Genetics*, 4th ed, Longman, Essex, England.
6. A. D. Long et al. (1995) Genetics **139**, 1273–1291.

Suggestions for Further Reading

7. L. Avery and S. Wasserman (1992) Trends Genet. **8**, 312–316.
8. M. Wade (1992) In E. F. Keller and E. A. Lloyd, eds. *Keywords in Evolutionary Biology*, Harvard University Press.
9. T. F. C. Mackay (1996) BioEssays **18**, 113–121.

Epitope

Epitope designates an area of an antigen that interacts with a specific antibody. It has generally replaced the former name of antigenic determinant. By symmetry, the term *paratope* has been proposed for the antibody, instead of antibody combining site (also designated as antigen binding site), but is much less widely used. An extension of this terminology is to be found as idiotopes and allotopes that designate epitopes that define **idiotypic** and allotypic (see **Allotype, alloantigen**) specificities, respectively.

Epitopes are defined functionally by the interaction of the antigen with a particular antibody, so it does not represent a preformed antigenic structure in itself; instead, it is defined by the immune system. This means that identification of epitopes will depend upon the nature and the number of **B-cell** clones that will respond to the administration of antigen. It is therefore very likely that two individuals will have a different pattern of recognition of the same antigen, although large overlaps are the rule. A consequence of this is that the best tool to define an epitope is a monoclonal antibody, which constitutes a reliable and standardized reagent. The obvious requisite for a region of the antigen to be recognized as an epitope is its accessibility—that is, that it be in contact with the solvent, which is favored by the presence of hydrophilic and/or charged amino acids.

Defining the structural basis of an epitope on natural antigens, such as proteins, is an almost impossible task, because B cells, and hence antibodies, recognize epitopes directly as native structures of the antigen. This implies that most epitopes have a complex three-dimensional structural organization that is generally lost upon cleavage of the antigen. Limited proteolysis of a protein may retain some regions that still contain native epitopes, but it is quite obvious that isolation of a “pure” epitope is most often not feasible. Interesting attempts to isolate epitopes from natural proteins have nevertheless been made with some success. This is the case of myoglobin and lysozyme, for which a loop of 20 amino acids clamped by a disulfide bond has long been a prototype of an “isolated” epitope. Because of their repetitive structural organization, polysaccharides are somewhat better tools to derive epitopes. This was the case for dextran, a polymer of glucose that allowed Kabat to demonstrate that various oligosaccharides were competing with the binding of dextran to its antibodies and indicating that they could be considered epitopes of this antigen. In fact, because the optimal inhibition was obtained by a hexasaccharide, it was concluded that the size of the anti-dextran combining site was that required to accommodate a molecule having the size of this inhibitor. Most of our knowledge of the antigenicity of proteins has been gained thus far with synthetic polyamino acids that constitute simplified models of proteins, because they can have a rather monotonous organization; for example, three or four amino acids might be linked covalently to a backbone of poly-L-lysine, like those extensively studied by the group of Sela in Israel. These models favored, however, sequential epitopes, as opposed to the conformational ones that are commonly encountered in natural protein antigens. The use of haptens was of course only a first approach to define an antigenic determinant, and they gave information of interest regarding the exquisite specificity of antibody recognition.

Monoclonal antibodies (mAbs) have proven of great value in epitope mapping the surface of an antigen. Mapping is based on inhibition of one mAb by others. When complete and reciprocal inhibition is observed between two mAbs, it is concluded that both antibodies recognize the same epitope. Although not a definitive proof, it remains an acceptable conclusion. Partial inhibition is suggestive that the two mAbs recognize overlapping epitopes. Consequently, a sufficiently large collection of mAbs permits exhaustive mapping of the epitopes, which may cover the entire surface of the antigen. One must realize, however, two important points: (*1*) Some regions are more frequently recognized than others; these are the immunodominant epitopes; and (*2*) the number of mAbs that can bind simultaneously to a given antigen molecule is necessarily limited by the steric hindrance imposed by the surface of the antibody combining site that interacts with the epitope. Having said that, it is quite obvious that the overall number of epitopes that can be detected on one antigen molecule is directly related to its surface area.

By extension, the notion of **T-cell** epitopes has been defined. From a physiological point of view, it is somewhat more complicated in that it is linked directly to the mechanism of **antigen presentation** and thus requires the interaction of the antigenic structure with two partners, the **multiple histocompatibility complex** (MHC) molecules and the T-cell receptor (TCR) itself. Because antigen processing and presentation have been defined for only proteins thus far, such T-cell epitopes are **peptides**. In a sense, the structural basis for a T-cell epitope is simpler and more directly accessible than in the case of B cells, because these peptides are short and are recognized as a sequential determinant. Strictly speaking, however, the term *epitope* is reserved to that part of the peptide that interacts with the TCR, whereas regions that interact with the MHC molecule, which are of decisive importance, because it conditions immunogenicity, are described sometimes as the "agretope." Extensive analysis by site-directed mutagenesis has clearly demonstrated which key residues contributed the epitope or the agretope. Because of the differences in the structures of the cavity that bind the peptides in various MHC molecules, the size of the peptide is limited to 9 amino acid residues for those that bind to class I MHC molecules, whereas it may be somewhat larger for those that are presented by class II. A very large number of such small overlapping peptides may be derived from one protein antigen. The problem of recognition by the MHC molecules, which are in very limited number for any given individual (a few discrete molecules), is therefore very different from the huge repertoire expected from Ig and TCR molecules. What happens is that MHC molecules will "choose" only a very few peptides from one antigen, those that fit with the minimum requirements that drive the interaction with the agretope. This is why every individual will use a different way to respond to the same antigen. Using a simplified model of antigen, such as a monotonous synthetic polypeptide, the chance is high that the molecule will be **immunogenic** only in those individuals with the appropriate MHC molecules. This was the case of the strains of mice injected with synthetic polypeptides that did or did not respond, initiating the first approach to the understanding of the genetic control of the immune response and starting the elucidation of the physiological role of MHC molecules.

Both the B-cell and T-cell epitopes raise directly the problem of the repertoire of the immune system, a central notion that is directly related to the number of potential antibodies and TCR that a given organism can potentially make (see Repertoire).

See also entries Antigen, Hapten, Immunogen, and Repertoire.

Suggestion for Further Reading

A. C. Horsfall, F. C. Hay, A. J. Soltys, and M. G. Lones (1991) Epitope mapping. Immunol. Today **12**, 211–213.

Epstein-Barr Virus

Epstein–Barr virus (EBV) is a ubiquitous human herpesvirus that is the causative agent of infectious mononucleosis and associated with several malignancies, such as Burkitt's lymphoma (BL), nasopharyngeal carcinoma (NPC), some cases of peripheral T-cell lymphoma and gastric carcinoma, and B-cell lymphoma of acquired immune deficiency syndrome (AIDS) and transplant patients. EBV has the ability to immortalize human B-lymphocytes *in vitro*.

The EBV genome is double-stranded linear DNA with an approximate length of 175 kbp and a G+C content of 59%. Reiterated direct repeat sequences at both termini (TR) and within the genome (IR) separate the EBV genome into five unique regions. The EBV genome circularizes after entry into cells, and it is maintained stably as a **plasmid** .

Although the entire EBV genome is maintained in immortalized lymphocytes, virus replication usually does not occur in these cells. During a latent infection, six nuclear antigens (EBNA1, EBNA2, EBNA3A, EBNA3B, EBNA3C, and EBNA-LP), three membrane proteins (LMP1, LMP2A, and LMP2B), and two small nuclear RNAs (EBER1 and EBER2) are expressed. EBNA-LP, 2, 3A, and 3C and LMP1 are essential or critical for primary B-lymphocyte growth transformation. EBNA3B, LMP2A, LMP2B, and EBERs are dispensable for immortalization.

EBNA1 from a typical EBV strain B95-8 consists of 641 amino acid residues. A long hydrophilic **domain** of residues 459 to 607 has a **DNA-binding** activity that is nucleotide sequence-specific. The specific EBNA1 binding sequence is located at oriP, which is the origin of EBV plasmid replication. Replication from oriP requires both the ***cis*-acting** elements (the family of repeats and the dyad symmetry elements) and the viral protein EBNA1. EBNA1 binding to oriP is also required for efficient EBNA transcription, where oriP serves as an enhancer. EBNA2 induces expression of viral genes LMP1 and LMP2 and cellular genes CD21, CD23, and c-fgr. EBNA2 responsive elements have been defined in the upstream **promoter** regions of these genes. Interaction of EBNA2 with its response element is mediated by a cell protein Jk, which recognizes a GTGGGAA sequence present in all known EBNA2 response elements. EBNA3A, EBNA3B, and EBNA3C are encoded by three genes that are tandemly placed in the EBV genome and are likely to have been derived a common origin. EBNA-LP is encoded by the leader of each of the EBNA **messenger RNAs** and is **translated** from these mRNAs when the first and second exons are spliced, so as to create the EBNA-LP initiation codon. Deletion of the EBNA-LP gene reduces greatly the efficiency of B-lymphocyte immortalization by EBV.

LMP1 consists of an amino-terminal cytoplasmic domain, six **membrane**-spanning **hydrophobic** domains separated by short reverse turns, and a carboxy-terminal cytoplasmic domain. LMP1 has the ability to transform rodent fibroblasts, and it blocks differentiation in human keratinocytes. In transgenic mice, LMP1 expression causes epithelial hyperplasia. In BL cells, LMP1 induces villous projections, growth in tight clumps, NFkB activity, and expression of activation markers (CD23 and CD40), cell adhesion molecules (ICAM-1, LFA-1, and LFA-3), IL-10, and the Bcl-2 proto-**oncogene**. There are two NFkB-activating regions in the carboxy-terminal cytoplasmic domain. One of these regions associates with members of the tumor necrosis factor receptor-associated factor (TRAF) family of proteins. CD40 is a well-known mediator of growth of B lymphocytes. LMP1, through direct interaction with TRAFs, may constitutively activate CD40 signal transduction and promote cell growth. LMP2A is a substrate for B lymphocyte **src** family **tyrosine kinases**. LMP2A expression blocks calcium mobilization in B lymphocytes. There is no known function for LMP2B.

EBERs are RNAs that are not **polyadenylated**, and they have extensive primary sequence similarity to adenovirus VA1 and VA2 and cellular U6 small RNAs.

In contrast to the EBV gene expression in immortalized lymphocytes, more limited numbers of EBV genes are expressed in EBV-associated tumor cells. BL and gastric carcinoma cells express EBNA1, but do not express other EBNAs and LMPs. NPC and T-cell lymphoma cells express EBNA1 and LMPs, but do not express other EBNAs. It is known that EBNAs other than EBNA1 become targets of cytotoxic T lymphocytes. Therefore, it is important for tumor cells not to express these antigens so as to survive under normal immunity.

EBNA2 and LMP1 are particularly important for the immortalization of primary lymphocytes. These proteins, however, are not expressed in most EBV-associated malignancies, although there is a report suggesting that malignant phenotypes are dependent on the presence of EBV genomes. These observations may be extended to the pathogenic role of EBV in other EBV-associated malignancies.

Suggestions for Further Reading

E. Kieff (1996) "Epstein–Barr Virus and Its Replication". In *Fields Virology*, 3rd ed. (B. N. Fields et al., eds.), Lippincott-Raven, Philadelphia, pp. 2343–2396.

A. B. Rickinson and E. Kieff (1996) "Epstein–Barr Virus". In *Fields Virology*, 3rd ed. (B. N. Fields et al., eds.), Lippincott-Raven, Philadelphia, pp. 2397–2446.

Equilibrium Dialysis

Equilibrium dialysis is a technique for analyzing the binding of a low molecular weight ligand to a macromolecular **receptor** (1) (see **Ligand binding**). Information that can be obtained from an equilibrium dialysis experiment includes the stoichiometry of the complex formed and the affinities of the interacting components (2), plus more subtle properties such as **cooperativity** . In the simplest form of an equilibrium dialysis experiment, receptor and ligand solutions are placed in compartments on opposite sides of a semipermeable dialysis membrane. The pore diameter of the membrane is chosen to allow passage of the ligand and prevent passage of the receptor. The ligand thus redistributes between the two compartments, whereas the receptor stays in its own compartment. If the receptor binds the ligand, an excess of ligand begins to accumulate in the receptor compartment. When equilibrium is reached, two conditions are met, as long as there is no nonideality in the system: (*1*) the free ligand concentration is equal on both sides of the membrane and (*2*) the ligand in the receptor compartment is partitioned between free and receptor-bound form according to the equilibrium constant for the receptor–ligand interaction. The total ligand concentration on each side of the membrane is measured after equilibration, as is the receptor concentration, if necessary. The excess ligand concentration on the receptor side is attributed to its binding to the receptor. This basic experiment is repeated for a series of receptor and ligand concentrations. Pairs of bound and free ligand concentrations may then be analyzed by a graphical method, such as a Scatchard Plot, or fit by least squares to a binding equation to derive the relevant parameters of the receptor–ligand interaction (3).

The primary advantage of equilibrium dialysis over other techniques for measuring ligand-binding equilibrium constants is that equilibrium dialysis does not rely on assumptions that a measured property, for example, a spectral change, correlates linearly with receptor occupancy. Development of microdialysis cells and of dialysis membranes made from purified material with well-defined molecular weight cutoffs have eliminated many artifacts once associated with equilibrium dialysis. Persisting sources of error include aggregation of the ligand, which will retard or prevent its passage through the dialysis membrane, adsorption of ligand or receptor to the membrane, and changes in volume and concentration resulting from an osmotic imbalance at the start of the experiment.

The assumption that the free ligand concentration is equal on both sides of the membrane at equilibrium is not always valid. Most proteins and all **nucleic acids** are charged; thus these macromolecules accumulate a set of neutralizing counterions. A ligand of opposite charge can act as a neutralizing counterion, resulting in an imbalance between free ligand concentrations in the receptor and ligand compartments of an equilibrium dialysis experiment. This imbalance, known as the Donnan effect (4), does not reflect a biologically specific ligand–receptor interaction, but occurs with whatever counter-ion is available, as a consequence of maintaining the overall electrical neutrality of the solution. The practical impact of the Donnan effect is to give spurious evidence of an association between a ligand and receptor of opposite charge. Even if a ligand is uncharged, changes in ionic strength or pH due to redistribution of buffer ions may still interfere indirectly with an experiment. The magnitude of the Donnan ratio (an ion's concentration in the receptor compartment divided by its concentration in the ligand compartment) is greatest at high receptor concentration and low ionic strength. For example, 100 μ*M* receptor containing 10 charges in the presence of 1 m*M* NaCl will yield a Donnan ratio of 1.5, meaning that a monovalent ligand will appear to be 50% enriched in the receptor compartment. If the receptor concentration is lowered to 1 μ*M*, or the salt concentration raised to 100 m*M*, the Donnan ratio drops to 1.005. Although simple addition of salt essentially eliminates the Donnan effect as an interfering factor in equilibrium dialysis, the added ions may distort the experiment in a different way, by competing with the ligand for association with charged groups in the receptor binding site. An alternative to using high salt concentration is to measure the Donnan ratio directly and apply a correction factor (5).

Bibliography

1. I. M. Klotz, F. M. Walker, and R. B. Pivan (1946) J. Am. Chem. Soc. **68**, 1486–1490.
2. H. N. Eisen and F. Karush (1949) J. Am. Chem. Soc. **71**, 363–364.
3. J. E. Fletcher and A. A. Spector (1968) Comput. Biomed. Res. **2**, 164–175.
4. F. G. Donnan (1911) Z. Elektrochem. **17**, 572.
5. P. Suter and J. P. Rosenbusch (1977) Anal. Biochem. **82**, 109–114.

Suggestions for Further Reading

6. N. W. Huh, P. Berkowitz, R. G. Hiskey, and L. G. Pedersen (1991) Determination of strontium binding to macromolecules, Anal. Biochem. **198**, 391–393. (A modern example of equilibrium dialysis, illustrating methodology and some of the technical problems that can be encountered.)
7. I. M. Klotz (1953) "Protein interactions", in *The Proteins*, H. Neurath and K. Bailey, eds., Academic Press, New York, Chapter "8", pp. 727–806. (Early review of equilibrium dialysis.)
8. C. Tanford (1961) *Physical Chemistry of Macromolecules*, Wiley, New York. (Quantitative treatment of the magnitude of the Donnan effect is given on pp. 221–227.)

Equilibrium Potential

Current flows resulting from ions diffusing across a phase boundary establish an electrical potential difference across that phase boundary in opposition to the ion currents. The origin of this potential lies in the difference in mobilities of anions and cations as they diffuse across the phase boundary. The electric field slows the faster ion and speeds up the slower ion, so that no net transfer of charge occurs across the phase boundary. The magnitude of the diffusion potential will depend on the difference in chemical potentials of the electrolytes in the contiguous phases, as well as differences in ionic mobility. The *Planck–Henderson equation* provides a quantitative calculation for the diffusion potential Y_D; for a single electrolyte (eg, NaCl) we have

$$\Psi_D = -\frac{(u-v)RT}{(u+v)zF}\ln\frac{C_2}{C_1} \tag{1}$$

where *u* and *v* are the cationic and anionic mobilities, respectively, *R* is the gas constant, *T* is the absolute temperature, *z* is the valence of the electrolyte, *F* is the Faraday (96,500 C/mol), and C_i are the electrolyte concentrations in the two contiguous solutions. Two examples of the use of equation 1 are for (i) the *liquid junction potential* that arises when two electrolyte solutions with different concentrations form an interface and (ii) when a synthetic membrane with a selective permeability for one of the ions is inserted between the two solutions. For the ion-specific selectively permeable membrane, equation 1 becomes

$$\Psi_D = \frac{RT}{zF} \ln \frac{C_2}{C_1} \tag{2}$$

This is the equilibrium potential for the permeable ion (see Membrane Potentials).

Suggestions for Further Reading

D. A. MacInnes (1939) *The Principles of Electrochemistry*, Rheinhold, New York, Chapter "13". (This book presents a derivation of the Planck–Henderson diffusion equation, as well as an excellent description of the characterization of liquid junction potentials and their measurement.)

W. J. Edelman Jr.(ed.) (1971) *Biophysics and Physiology of Excitable Membranes*, Van Nostrand Reinhold, New York. (Contains a useful summary of the physical aspects of membrane potentials and their treatment by analytical methods.)

Estrogen Receptors

Estrogen, together with the other sex steroid hormones, progesterone and testosterone, provokes the development and determination of the embryonic reproductive system, masculinizes or feminizes the brain at birth, and controls reproduction and reproductive behaviour in the adult, plus the development of secondary sexual characteristics. Furthermore, both an atheroprotective effect of estrogen and a protective effect against osteoporosis are well documented. The hormone probably enters its target cells by diffusion (see Steroid Hormone Receptors) and activates estrogen receptors (ERs) that are paradigmatic transcription factors in eukaryotes. ERs are members of the steroid hormone receptor family that, in turn, is a subfamily of the nuclear receptor superfamily of proteins (see Steroid Hormone Receptors). Effects of ERs on the genome are mediated through binding of the hormone–receptor complex to short, specific DNA sequences, termed estrogen response elements (EREs), located in the vicinity of approximately 100 estrogen-regulated genes in each cell, and subsequent modulation of gene expression (see Hormone Response Elements and Glucocorticoid Response Element). The ERE functions as an enhancer and the ERs as enhancer binding factors that are equipped with domains and surfaces responsible for hormone and DNA binding, activation of transcription, and interaction with other nuclear partners.

Until recently, only one oestrogen receptor had been known, which is now called estrogen receptor a (ERa or NR3A1 according to a new nomenclature proposal (see Steroid Hormone Receptors)). In 1996 a second estrogen receptor, now known as estrogen receptor b (ERb or NR3A2), was identified (1). Therefore, older literature always refers to ERa and has often to be reinterpreted in the light of at least two receptors being present in many tissues.

Apart from their involvement in the development of the reproductive system, estrogens are also implicated in the growth of breast cancers. Already in 1896, Beatson observed the regression of metastatic breast cancer after ovariectomy (*ce, after estrogen withdrawal*). Since that time, various surgical and pharmacological endocrine therapies have been employed (see below). Today, the determination of the concentration of sex steroid receptors in breast cancers is performed routinely and is very important for prognosis in general and the therapeutic regimen in particular.

The molecular mechanisms by which ovarian hormones stimulate growth of breast cancers are unclear, but they are likely to involve an extensive crosstalk of ERs with other signalling pathways. ERa, for example, activates the **signal-transducing** Src/p21ras/Erk pathway in human breast cancer cells via an interaction with c-Src (see Cis Configuration). In addition, ERa can integrate signals from the progesterone receptor into this signalling cascade (see Steroid Hormone Receptors). ERa is also activated when it is complexed with **cyclin** D1, which has an important role in the development of breast cancer and is required for normal breast cell proliferation and differentiation associated with pregnancy. Furthermore, such growth factors like epidermal growth factor (EGF), can activate ERa through the mitogen-activated protein, MAP Kinases pathway, which probably involves receptor phosphorylation.

1. Domain Structure

The human ERa was cloned from cDNA libraries prepared from the MCF-7 breast cancer cell line in 1985. This cDNA clone was later shown to contain an artifactual point mutation that resulted in the substitution of a valine (mutant receptor called HEO) for a glycine (wild-type receptor called HEGO). The hERa gene encompasses 10 exons spread over 140 kbp and is regulated by at least three different **promoters** (see Fig. 1). The ERa cDNA encodes a 595–amino acid residue protein of 66 kDa. The oestrogen receptor is a modular protein composed of distinct regions corresponding to functional and structural units called **domains** that are labeled A–F (see Steroid Hormone Receptors, Fig. 1B). Transcription activation functions have been detected in regions A/B (AF-1, also called q-1 or enh-1) and E (AF-2, also called q-2 or enh-2). Region C is the DNA-binding domain (DBD), and region D is often considered as a flexible hinge region between the DNA- and ligand-binding domains. The very amino terminus of region D is also an integral part of the DBD. Region E is the ligand-(hormone)-binding domain (LBD), composed mainly of 12 a-helices, and contains AF-2 that forms the core of the most carboxy-terminal helix 12 (see text below). Beyond helix 12 starts region F, which is not required for hormone binding but seems to be important for the discrimination between agonistic and antagonistic ligands.

Figure 1. The 5′ region of the hERa gene. The promoter P1 in front of exon 1A generates transcript A encompassing a 5′-untranslated region (UTR, smaller cylinder) and the start of the coding region (larger cylinder). The other two promoters, P2 and P3, generate transcripts in which the noncoding exons 1C or 1B are alternatively spliced to the same acceptor splice site within a short upstream open reading frame found in the 5′-UTR of transcript A. Depending on tissue-specific promoter utilization, different hERa transcripts can be detected in different tissues that code for the same receptor protein, but have distinct 5′-UTRs. Common to all UTRs is the presence of short upstream open reading frames that are implicated in the regulation of translation efficiency.

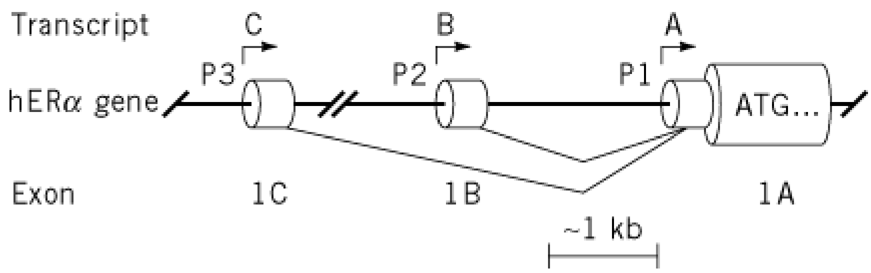

Regions C and E are not only responsible for DNA- and ligand-binding, respectively, but they encode other functions as well. At equilibrium the majority of ERa is in the nucleus, due to the presence of so called nuclear localization signals (NLS) that are believed to be required for **nuclear pore** recognition (see Nuclear Import, Export). A constitutive NLS is located at the border of region C to D, whereas a second NLS in the LBD is ligand-dependent.

ERb was found in rat prostate and later in human testis cDNA libraries using **PCR**-cloning strategies involving degenerate primers. With 8 exons spread over approximately 40 kbp, the human ERb gene is considerably smaller than the ERa gene. Several mRNA bands have been observed on RNA Blots

(Northern Blots), possibly indicating that the ERb gene is also characterized by multiple promoters, which is a general phenomenon within the steroid hormone receptor family. The human cDNA encodes a 485-residue protein that shows a high degree of homology to ERa within the DBD (96% identity) and the LBD (58%).

2. DNA Binding

All members of the steroid hormone receptor family were initially thought to bind to their cognate response elements as homodimers . Today the family also contains two oestrogen-related orphan receptors that bind to DNA as monomers (see Steroid Hormone Receptors). Moreover, the two closely related ERs, a and b, are known to bind to DNA as homodimers, but they can also form heterodimers which is an otherwise common mechanism within the nuclear receptor superfamily. Oestrogen receptor homo- or heterodimers bind to the estrogen response element (ERE) that is composed of two half-sites (AGGTCA) arranged as palindromic, inverted repeats (IRs), where the half-sites are separated by three nucleotides (IR-3). One ERE half-site is recognized by one receptor monomer. The half-site spacing of three base pairs is such that an ER homodimer binds both half sites on the same face of the DNA. The DNA-binding domain of the ERs comprises approximately 80 amino acid residues encoded by region C, plus some 14 *N*-terminal amino acids of region D. The domain contains two patterns that are reminiscent of, but clearly distinguishable from, the **zinc finger** motifs first observed in the *Xenopus laevis* transcription factor IIIA (TFIIIA; see **Zinc fingers**). The ER zinc fingers are also able to coordinate a zinc atom tetrahedrally but are of the type C_2–C_2 (see Fig. 2). Each ER monomer contains two of these particular zinc fingers, which are folded together to form a single structural domain (2). Characteristic of this fold are two highly amphipathic a-helices, one contributed by each finger, that cross at an approximately right angle at their midpoints (see Fig. 2). The **hydrophobic** surfaces of these helices form a rigid core decisive for the stability of the structure that is further strengthened by two zinc ions holding the base of a loop against the *N*-terminus of each helix. The specific interaction of an ER homodimer with DNA is determined by only a few amino acid residues located in two regions, the proximal box (P-box; see Fig. 2) and the distal box (D-box). The P-box lies at the amino terminus of the first fingers a-helix (its "knuckle"). Four amino acid residues within the P-box interact with base pairs, and only three of them are required for the discrimination between an ERE and a nonestrogen steroid hormone receptor response element. When these three residues are exchanged for the three cognate residues of the glucocorticoid receptor, ERE-specific binding is converted to glucocorticoid response element–specific binding. The five D-box residues form the weak dimerization domain within the DBD and are responsible for the recognition of the correct half-site spacing (IR-3). These dimerization forces are too weak for the DBD alone to form dimers in solution, but they make DNA-binding cooperative. The complete receptor protein exists as a homodimer in solution, due to a strong dimerisation domain within the LBD.

Figure 2. Structure of estrogen receptors. (**Top**) The functional domains (A/B to F) of hERa and b are illustrated at the primary structure level. The numbers refer to amino acid positions. Highlighted are the DNA-binding domain (DBD) in small boxes and the ligand binding domain (LBD) in larger boxes. The A/B and F domains are drawn to scale. (**Middle left**) In an exploded view of the hERa–DBD its secondary structure, characterized by two steroid hormone receptor-specific zinc fingers, is depicted. Four cysteines each tetrahedrally coordinate two zinc ions. The proximal box (P-box) responsible for specific DNA-recognition is shown on left; the distal box (D-box) mediating DBD-dimerization is shown on right. (**Bottom left**) The secondary structure explodes into a view of the crystal structure of the hERa's DBD bound to DNA. The four amino acid side chains of the P-box interacting with DNA bases are again shown in boldface. These residues are part of an a-helix responsible for specific DNA-sequence recognition that is positioned within the DNAs major groove (perpendicular to the paper plain). A second amphipathic a-helix can be seen to cross the recognition helix with the red P-box residues at a right angle. The D-box residues promoting DBD dimerization are located between the two helices. Underneath the DNA the sequence of the consensus estrogen response element (ERE) is shown. Both half-sites are organised as an inverted repeat with 3-bp spacing (IR-3). (**Middle right**) The crystal structure of the ligand-binding domain complexed with the natural ligand 17b-estradiol (E2, left) and the antihormone raloxifene (RAL, right). Decisive for a productive interaction with coactivators is the proper positioning of helix 12 (H12) over the ligand-binding pocket. (The authors thank R. Hubbard and A. Pike,

University of York, UK, for providing this part of the figure.)

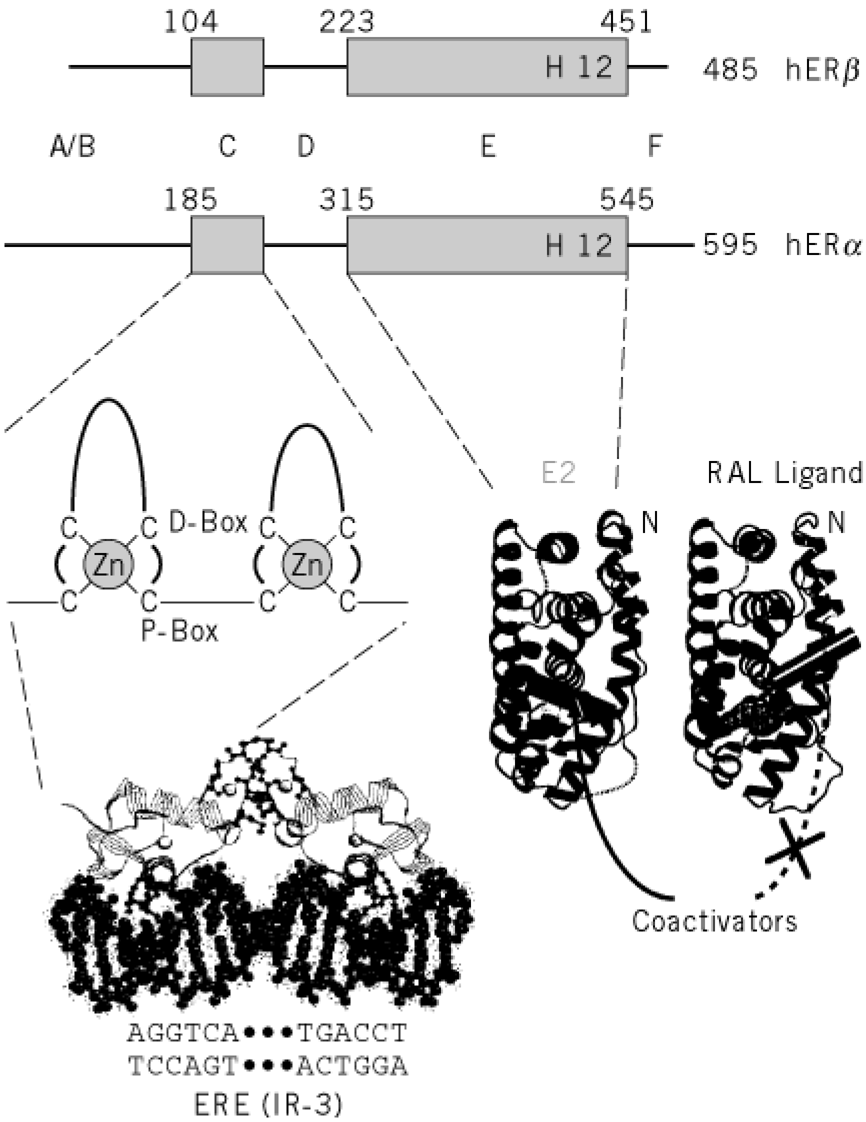

3. Ligand Binding

Estrogenic hormones, as well as synthetic antihormones, enter the target cell by simple diffusion and bind, within the cytoplasm, to a multiprotein complex of **molecular chaperones** and ER. Hormone binding induces a transformation of the ER complexes that is associated with an increase in affinity for DNA and leads to a tight association with the nuclear compartment. In addition to DNA-binding, the bound hormone confers transcriptional competence onto ERs that is exerted by two independent **transactivation** functions (see text above). The crystal structure (3) of the hERa ligand binding domain complexed with the endogenous hormone 17b-estradiol (PDB accession no. 1ERE; see Structure Databases) and the antihormone raloxifene (PDB accession no. 1ERR) have been determined (see Fig. 2). The LBD of hERa is folded into a three-layered antiparallel a-helical sandwich that creates a wedge-shaped molecular scaffold, in which the ligand-binding cavity is located at the narrower end of the domain. This cavity is completely partioned from the external environment and is closed by helix 12 operating as a "lid" after 17b-oestradiol has entered the binding pocket (see Fig. 2, left LBD structure). In "lid-on" position, AF-2 is able to interact with co-activators that in turn connect the receptors to the transcription machinery and activate transcription (for more details, see Steroid Hormone Receptors). When an antihormone-like raloxifene is bound instead, closure of the ligand binding pocket is not possible, and AF-2 cannot be placed in a transcriptionally competent position (see Fig 2, right LBD structure).

Although the precise mechanism of this ligand induced switch between active and inactive AF-2 was not known until recently, a number of proteins have been rendered functionally estrogen-dependent by fusion with the hormone-binding domain of ERa (4).

4. Hormones and Antihormones in Breast Cancer

Since Beatson's observation of regression of metastatic breast cancer after ovariectomy, in 1896, oncologists have been searching for an ideal antihormone that will prevent the proliferative effect of estrogen on breast cancer but preserves an atheroprotective effect and protects against osteoporosis without any side effects. Approximately 50% of all breast cancers contain clearly detectable amounts of hERa and are, thus, amenable to hormone therapy. Disease prognosis is better when receptors are present, probably because their presence reflects a greater degree of differentiation of the tumor, indicative of slower growth. Only approximately 50% of these receptor-positive cases also respond positively to an antihormone treatment. Several ER sequence variants were identified in human breast cancer cell lines and tumor specimens, but it is not known if these mutations are important for breast cancer progression or interfere with endocrine breast cancer therapies.

Currently, the most commonly used antihormone is tamoxifen, which is converted to 4-hydroxy-tamoxifen *in vivo*, the actual antihormone. Tamoxifen appears to antagonize estrogen action by competing with oestrogens for receptor binding. Receptor-bound tamoxifen, like raloxifene, is postulated to be unable to position helix 12 of the LBD in such a way that AF-2 is placed in a transcriptionally competent position (see discussion above). However, tamoxifen can still act as a partial estrogen agonist depending on the tissue and response examined. This is probably due to the ligand-independent and cell-specific activity of AF-1 within the receptor's A/B domain. Tamoxifen is clearly effective in receptor-positive breast cancer patients and has very few side effects. It still retains a protective effect against osteoporosis, but does not reduce the risk of cardiovascular disease. Its effectiveness was also proved in prevention trials, although a slightly increased risk for developing endometrial cancer and thromboembolic events must be taken into consideration. Other antiestrogens with a broader spectrum of positive effects than tamoxifen, such as raloxifene, are currently being tested in clinical trials.

With the discovery of a second estrogen receptor, all clinical data on antihormone therapies of receptor-positive breast cancer patients must be reevaluated. It is already known that some breast cancers express ERb but no ERa, and some express both receptors. Differing ERb/ERa ratios could explain cases that were typed receptor-negative but still responded positively toward antihormone therapy, as well as those receptor-positive cases that were refractory toward antihormone therapy. Therefore, the presence of both receptors in tumor specimens will probably be determined routinely in the near future.

5. Results from Disruption of the Mouse Estrogen Receptor a Gene

In addition to its importance for a normal postnatal sexual development, estrogen action has always been considered as a crucial factor for prenatal development. This hypothesis is generally supported by the fact that almost no ERa mutations are known. An exceptional case, however, is a 28-year-old tall man in whom a premature stop codon in position 153 of hERa could be identified (5). The patient is homozygous for this mutation, showed no response to estrogen administration, and manifested decreased bone mineral density and increased bone turnover. This homozygous human knockout already indicates that ERa is not required for prenatal development but is very important for bone maturation and mineralization in males also. Targeted disruption of the ERa gene in mice (ERKO mice (6)) showed the same result (see Gene Targeting). Homozygous ERKO mice are viable, and the external phenotypes of both sexes are normal. Internally only the females show noticeable gross differences from normal, with hypoplastic uteri as well as hemorrhagic cystic ovaries that lack corpora lutea. In addition, the mating behavior of the females is severely compromised, because they show no typical lordosis posture or receptiveness to wild-type males, even when treated with estrogen. Consequently, all homozygous ERKO females are infertile, as are the male mice. The latter show normal motivation to mount females, but they achieve less intromissions and virtually no ejaculations. Aggressive behaviors were dramatically reduced, and male-typical offensive attacks were rarely displayed by ERKO males. In addition to an altered mating behavior, spermatogenesis is disturbed, as manifested by low sperm numbers and defective sperm function. Therefore, expression of the ERa gene appears to be necessary not only for the development of the female and male reproductive systems but also for the full development of both female and male sex behavior repertoires.

With the discovery of ERb, the question of the importance of estrogen receptors for prenatal development is open again and has to await the production of ERb single- and ERa/ERb double-knockout mice.

6. Functional Differences between ERa and ERb

In light of the high homology between ERa and ERb, the question arises as to whether one receptor is a mere "backup" of the other, or whether each receptor has its own set of specific functions. ERb was shown to have DNA-binding specificity overlapping with that of ERa and activates transcription of reporter gene constructs containing EREs in transient transfections in response to estradiol. The response of both receptors to a number of estrogen agonists and antagonists has been determined in such a way, and numerous differences have been observed. Furthermore, the tissue distribution of both receptors is clearly different. Whereas some tissues contain both receptors, as does the human mammary gland, others contain only a single receptor type. One prime example are the granulosa cells of the ovaries, which contain only ERb and are devoid of ERa. Previously, the granulosa cells had been identified as a target for oestrogen action, although they were shown not to contain ERa. This puzzling finding can now be explained by the presence of ERb. Other examples are the Leydig cells of the testis, which contain ERa but no ERb, whereas the developing spermatids express ERb and ERa is absent. Therefore, with the advent of a second estrogen receptor, at least two more important parameters have to be considered when analyzing the regulation of gene expression by estrogen: the ERa/ERb- ratio and the presence of ERa/ERb-heterodimers and their distinct functions dependent on the agonist/antagonist and promoter context investigated.

Bibliography

1. G. G. Kuiper and J.Å. Gustafsson (1997) FEBS Lett. **410**, 87–90.
2. J. W. Schwabe, L. Chapman, J. T. Finch, and D. Rhodes (1993) Cell **75**, 567–578.
3. A. M. Brzozowski, A. C. W. Pike, Z. Dauter, R. E. Hubbard, T. Bonn et al. (1997) Nature **389**, 753–758.
4. T. D. Littlewood, D. C. Hancock, P. S. Danielian, M. G. Parker, and G. I. Evan (1995) Nucleic Acids Res. **23**, 1686–1690.
5. E. P. Smith, J. Boyd, G. R. Frank, H. Takahashi, R. M. Cohen et al. (1994) N. Engl. J. Med. **331**, 1056–1061.
6. D. B. Lubahn, J. S. Moyer, T. S. Golding, J. F. Couse, K. S. Korach et al. (1993) Proc. Natl. Acad. Sci. USA **90**, 11162–11166.

Suggestions for Further Reading

7. K. S. Korach (1994) Science **266**, 1524–1527.
8. M. J. Tsai and B. W. O"Malley (1994). Annu. Rev. Biochem. **63**, 451–486.
9. M. Beato, P. Herrlich, and G. Schütz (1995) Steroid hormone receptors: many actors in search of a plot, Cell **83**, 851–857.
10. H. Shibata, T. E. Spencer, S. A. Onate, G. Jenster, S. Y. Tsai et al. (1997) Recent Prog. Horm. Res . **52**, 141–164.

Estrogens

Estrogens are female sex steroid hormones derived from cholesterol. The most potent estrogen is 3,17b-estradiol (estradiol 1,3,5-estratriene-3,17b-diol). The 16a-hydroxylated derivative of estradiol, estriol, is a weak estrogen, whereas the 17b-oxidized compound, estrone, is hormonally inactive. Synthetic nonsteroid estrogens, such as diethylstilbestrol, have been introduced as therapeutic drugs in various endocrine diseases. Estrogen antagonists (eg, tamoxifen) have also found use in therapy, particularly of breast cancer.

Estradiol is synthesized in the ovary, the placenta, the adrenal cortex, and the testis. In the theca cells of the ovarian follicles, cholesterol is metabolized to progesterone and to androstendione, which in the granulosa cells is subsequently transformed to estradiol by aromatization of the A ring by the aromatase complex. This process is stimulated by FSH (folitropin).

During fetal and early postembryonic development, estrogens are responsible for inducing female characteristics and for the formation of the female genitals (oviduct, uterus, vagina). In the adult, estrogens act on the development of the secondary female sexual characteristics—for example, on the growth and differentiation of the breast glands, on the appearance of pubic and axillar hair, and on fat deposition in the skin. Estrogens affect the central nervous system and can modify sexual behavior. They also act positively on bone mass. In collaboration with progesterone, estradiol regulates the menstrual cycle. Specifically, in the first half of the cycle, estradiol stimulates proliferation of the epithelial and stromal cells of the endometrium, in preparation for ovulation.

The molecular action of estrogens, like that of the other steroid hormones, is by modulation of gene transcription (see Response Element). The hormone first binds to the estrogen receptor, a member of the superfamily of nuclear receptors, which then homodimerizes and binds to specific nucleotide sequences, the estrogen response elements. This triggers activation of gene transcription. Among the genes regulated by estrogens are **protooncogenes** of endometrium cells encoding transcription factors involved in cell replication (c-fos, c-jun, c-myc) (1-3), those encoding the progesterone receptor, growth factors, and various structural and adhesion proteins (4). In the liver, estrogens stimulate the synthesis of steroid- and thyroxine-binding proteins. The molecular effects of estradiol on the synthesis of phosphoproteins in the chick oviduct, such as ovalbumin, have been studied in detail and were instrumental in developing concepts on the mode of action of steroid hormones (5).

Bibliography

1. D. S. Loose-Mitchell, C. Chiappetta, and G. M. Stancel (1988) Mol. Endocrinol. **2**, 946–951.
2. C. Chiappetta et al. (1992) J. Steroid Biochem. Mol. Biol. **41**, 1134–123.
3. S. M. Hyder et al (1992) J. Biol. Chem. **267**, 18047–18054.
4. R. Grummer et al. (1994) Biol. Reprod. **51**, 1109–1116.
5. M. Kalimi et al. (1976) J. Biol. Chem. **251**, 516–523.

Suggestions for Further Reading

6. E. E. Baulieu and P. A. Kelly (eds) (1990) *Hormones: From Molecules to Disease*, Hermann, Paris.
7. E. Y. Adashi and P. C. K. Leung (1993) *The Ovary*, Raven Press, New York.

8. M. G. Parker (1993) *Steroid Hormone Action*, IRL Press, Oxford, U.K.

Ethidium Bromide

Ethidium bromide (phenanthridinium, 3,8-diamino-5-ethyl-6-phenyl-, bromide) is a heteroaromatic cationic dye (an aminoacridine) with the molecular formula $C_{21}H_{20}BrN_3$ and a relative molecular mass of 394.31 (Figs. 1, 2). It exists as a dark red crystalline or amorphous powder at standard temperatures and pressures. It has a melting point (and decomposition temperature) between 533 and 535 K, moderately high solubility in water (5 g/100 mL), and is essentially odorless. Ethidium bromide is a powerful mutagen, extremely toxic by inhalation, ingestion (LD_{50} 1503 mg/kg oral, rat), and skin contact, and a suspected carcinogen and reproductive toxin.

Figure 1. Ball-and-stick representation of the ethidium bromide molecule (phenanthridinium, 3,8-diamino-5-ethyl-6-phenyl-, bromide). RMM = 394.31.

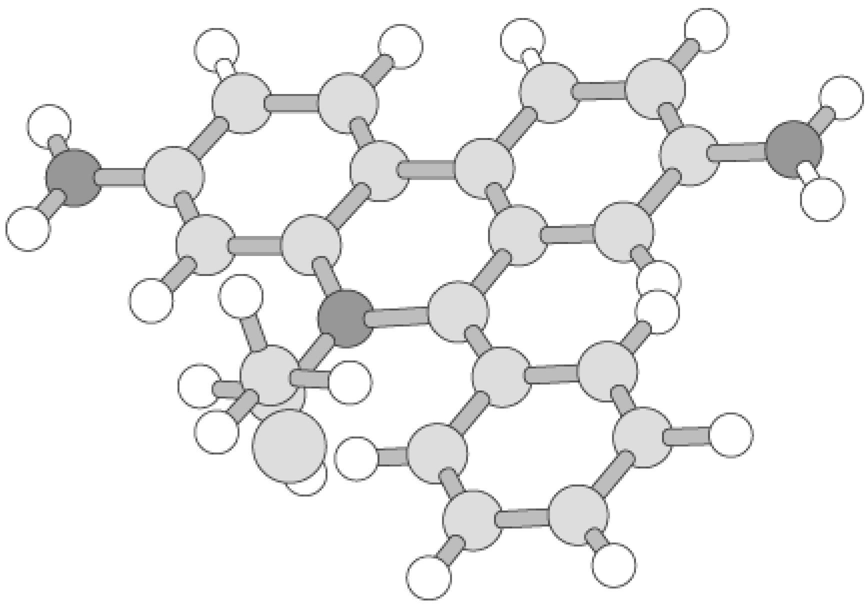

Figure 2. The intercalation of ethidium bromide into a portion of a DNA double helix. The intercalated dye increases the spacing of successive base pairs, distorts the regular phosphate backbone, and reduces the pitch of the helix.

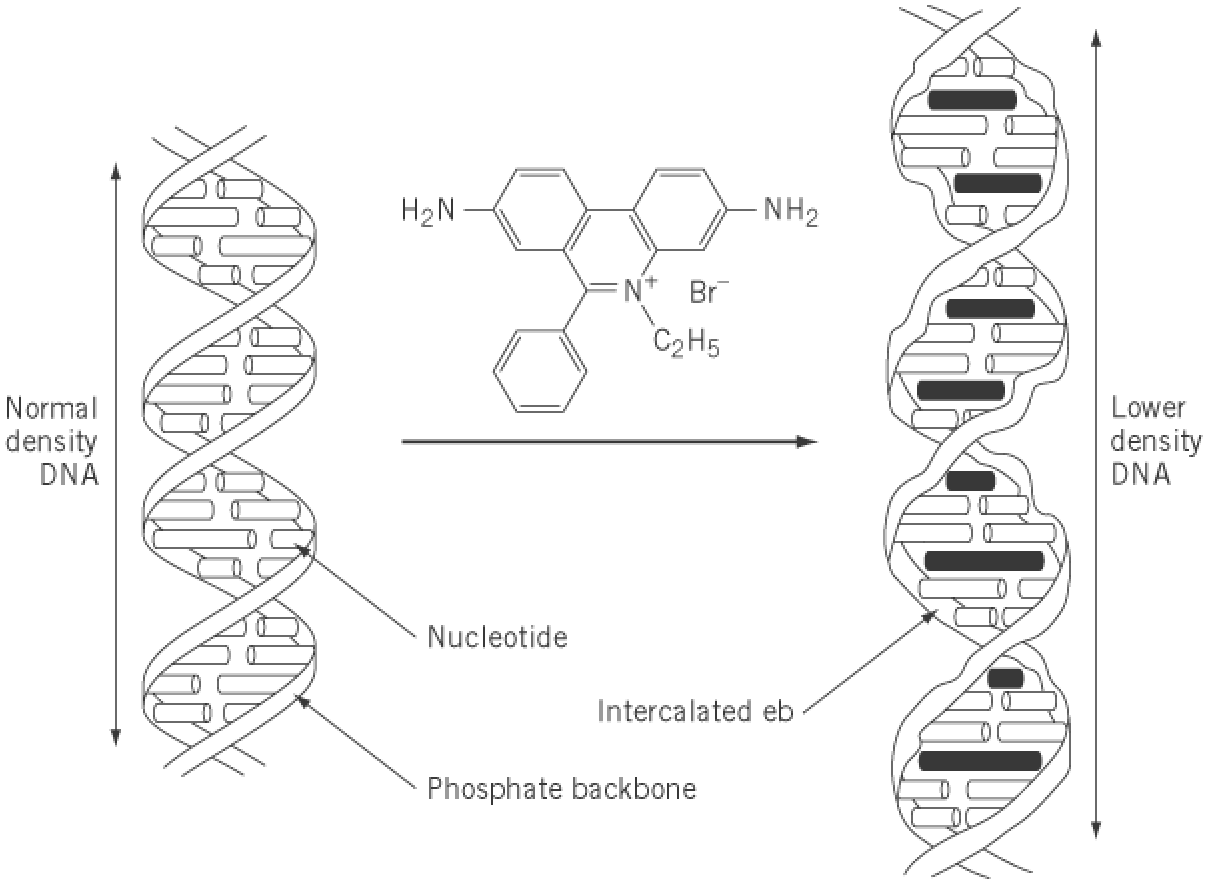

Originally, ethidium bromide (EB) found fame in the late 1940s as an antitrypanosomal, antimicrobial, antibacterial, and antiviral agent (1). It is generally agreed that these biological effects are a direct consequence of the inhibition of nucleic acid synthesis, which in turn is related to the specific binding of the drug to DNA. EB inhibits **DNA polymerase** and binds *in vitro* to both RNA and DNA. Investigation into the precise nature of the DNA-EB binding mechanism led to the discovery that the drug (and many other related molecules) binds by a mechanism termed intercalation. This process has been studied extensively during the past three decades, and the photophysical changes that accompany intercalation have been successfully applied to quantitate and structurally elucidate DNA. The nature of the DNA-EB interaction and subsequent analytical applications are the focus of this article.

1. Photophysical Characteristics of EB

EB is dark yellow in aqueous solution and possesses a broad structureless absorption spectrum (l_{max} ~ 480 nm). Increasing EB concentration leads to a red shift in the absorption maximum, accompanied by hypochromism. The existence of an isobestic point reflects a simple equilibrium between monomeric and dimeric species (2).

EB is weakly **fluorescent** in aqueous solution and possesses a broad structureless emission spectrum (l_{max} ~ 617 nm). The low fluorescent quantum yield and short fluorescent lifetime (3) in aqueous solution are attributed to efficient quenching of the excited state by the transfer of a proton to an adjacent water molecule (4, 5). Moreover, the EB dimer is not fluorescent and consequently provides an efficient mechanism for fluorescent quenching when EB is complexed in the dimeric form. Both of these phenomena prove important when EB interacts with DNA.

2. Intercalation of Dyes with DNA

Modification of DNA by binding with dyestuffs suspected to have possible chemotherapeutic effects was noted as early as the 1940s in the pioneering work of Michaelis (6). The classic intercalation mechanism for the physical interaction between drugs and DNA is discussed elsewhere in this volume, but the characteristics of dye intercalation with DNA were established primarily with reference to aminoacridones (7) and EB (1). Consequently, the fundamental attributes of classic intercalation are outlined. Very simply, intercalation describes the insertion of planar heteroaromatic molecules between adjacent nucleotide base pairs of a DNA duplex (see DNA Structure). Intercalative binding follows the neighbor exclusion principle, where every second site along the helix remains unoccupied, and thus EB intercalation occurs through interaction of the phenantridinium ring with the duplex (8). This leads to a very elegant binding model (Fig. 2). More specifically, the EB–DNA complex involves **hydrogen bonding** between the 3,8 amino substituents of the EB molecule and the phosphate groups across the two DNA strands. These hydrogen bonds maintain the orientation of the EB cation with respect to the polymer frame (9). The simplicity of this model was naturally extended to explain the interaction of other molecules with DNA. These included antitumor antibiotics whose mode of action involves interference with nucleic acid synthesis (1). The intercalation mechanism of EB with double-stranded DNA can be thought of as consisting of three fundamental features: [1] helix extension (Fig. 2); [2] local, helical unwinding during binding; and [3] insertion of EB so that the plane of the aromatic chromophore is perpendicular to the helical axis. This binding process has been confirmed by various experimental approaches including, X-ray crystallography (10), autoradiography (11), NMR spectroscopy (12), equilibrium studies (13), **viscosity** measurements (14), and calorimetry (15). Nevertheless, optical measurements have played the dominant role in the use of the EB to DNA interaction. Consequently they are discussed in detail here.

3. Intercalation of EB with DNA

The formation of a metachromatic complex between EB and DNA can be simply observed by measuring the absorption spectrum. As the DNA to EB ratio increases, the absorption spectrum shifts to longer wavelengths (3, 16, 17). The formation of such complexes causes a shift due to the stabilization of the excited state upon binding (9). The shift is observed only at high DNA to EB ratios because an excess of free dye normally masks the absorbance contribution of bound EB. Importantly, a binding constant of $2.1\times10^{6}M^{-1}$ demonstrates the high affinity of EB of DNA (18).

More relevant to the use of EB in molecular biology are the observed variations in its fluorescent characteristics on binding to polynucleotides. Broadly, both the time-integrated fluorescent intensity and the average molecular fluorescent decaytime increase dramatically on interaction with DNA (eg, the fluorescent decay time of EB in water is about 1.8 ns, compared to 23 ns in DNA) (3, 8, 19, 20). This variation can be explained by reference to Figure 2. When EB intercalates with the double helix, it sits in the **hydrophobic** pocket of the base pair system and is shielded to a large extent from solvent molecules. Consequently, the rate of excited state quenching (via proton transfer to solvent molecules) decreases, leading to an increase in both the fluorescent decay time and the fluorescent quantum yield. Because the fluorescent intensity of EB in aqueous solution is very small (due to a low fluorescent quantum yield), measuring the fluorescent signal when bound to DNA provides the most common method for DNA detection in the molecular biology laboratory (e.g., in slab gel electrophoresis and capillary zone electrophoresis) (21-23). Furthermore, the fluorescent enhancement has resulted in extensive use of EB as a probe of the topological (24, 25) and dynamic (26-29) properties of DNA.

EB is widely used as a probe in clinical DNA assays. The selective binding of EB to double-stranded DNA, combined with the exquisite sensitivity of fluorescent spectroscopy, provides an obvious route to DNA quantitation on a nanogram scale (30). With excitation at 520 nm and emission at 600 nm, EB fluorescence is enhanced approximately 30-fold in upon binding to duplexes. Moreover, the use of fluorescence detection for quantitative purposes is favorable because fluorescent enhancement is practically independent of base composition (31-33).

Nevertheless, care must be taken when using EB as a quantitative probe of DNA. Numerous studies have demonstrated a modification in the classic intercalative behavior of EB with high dye concentrations. In addition to conventional intercalation, there is also EB binds secondarily through an external site (most likely along the phosphate backbone). Binding to this secondary site occurs most readily at low ionic concentrations (<0.1 *M*), after binding at primary sites has been saturated (3, 14, 19, 21). Secondary binding is most clearly evidenced by the heterogeneous nature of fluorescent decay profiles originating from high EB to DNA ratios (3, 19). The true nature of secondary binding is still poorly understood. It must be accounted for, however, when relating time-integrated fluorescent intensities to the amounts of double-stranded DNA. In addition, variations in the fluorescent quantum yield of EB intercalated into heterogeneous natural DNA (eg, calf thymus DNA) as a function of salt concentration and temperature suggest that the detailed features of the EB to DNA complex are inextricably linked to the overall structural properties of the binding sites on the duplex chain (9).

The huge interest in the clinical use of compounds that bind strongly to DNA as antitumor agents at low concentrations has led to the study of a related class of EB compounds. Appropriately designed dimers of EB have binding affinities and fluorescent enhancements much higher than those of the monomer (18, 34, 35). Glazer and co-workers synthesized an ethidium homodimer, illustrated in Figure 3, that bisintercalates at a ratio of one dimer per four to five base pairs and is stable on electrophoresis gels. The system was used successfully to detect and quantify DNA fragments with picogram sensitivity subsequent to an electrophoretic separation (36). Current applications of bisintercalators of this kind include multiplex detection of DNA restriction fragments (37), high sensitivity detection of the products from the polymerase chain reaction (**PCR**) (36), sizing of individual double-stranded DNA fragments by flow cytometry, and the study of **DNA–protein interactions** (38). Furthermore, DNA probes that have a double-stranded region (for intercalation sites) and a single-stranded region (for recognition of specific target sequences) offer an exciting application for this generation of versatile fluorescent probes.

Figure 3. Chemical structure of an ethidium homodimer (as synthesized in Ref. 36).

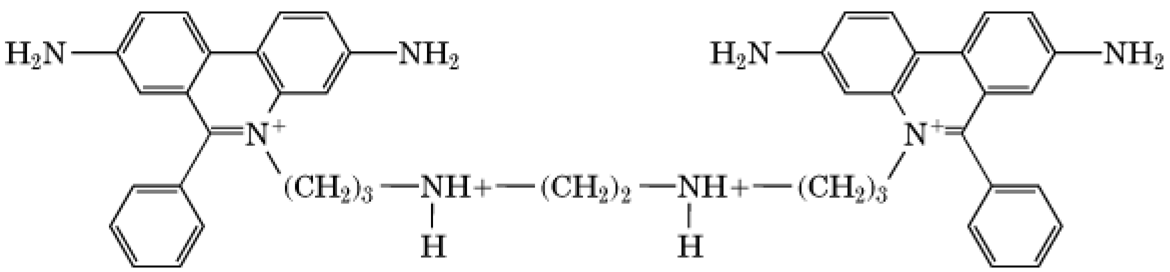

Bibliography

1. M. J. Waring (1975) *Antibiotics III. Mechanism and Action of Antimicrobial and Antitumor Agents* (J. W. Corcoran and F. E. Hahn, eds.), Berlin, Heidelberg, pp. 141–165.
2. M. Guenza and C. Cuniberti (1988) Spectrochim. Acta **44A**(12), 1359–1364.
3. C. D. Byrne and A. J. de Mello (1998) Biophys. Chem. **70**, 173–184.
4. S. J. Atherton and P. C. Beaumont (1984) Photobiochem. Photobiophys. **8**, 103–113.
5. J. Olmsted and D. R. Kearns (1977) Biochemistry **16**, 3647–3654.
6. L. Michaelis (1947) Cold Spring Harbor Symp. Quant. Biol. **12**, 131–142.
7. R. M. Acheson (1973) *Acridines* (R. M. Acheson ed.), Wiley, London, p. 878.

8. J. B. LePecq (1976) *Biochemical Fluorescence: Concepts II* (R. Chen and H. Edelhoch eds.), Dekker, New York, pp. 711–736.
9. C. Cuniberti and M. Guenza (1990) Biophys. Chem. **38**, 11–22.
10. C. C. Tsai, S. C. Jain, and H. M. Sobell (1977) J. Mol. Biol. **114**, 301–315.
11. J. Cairns (1962) Cold Spring Harbor Symp. Quant. Biol. **27**, 311–318.
12. S. Chandrasakaran, R. L. Jones, and W. D. Wilson (1985) Biopolymers **24**, 1963–1979.
13. W. D. Wilson, C. R. Krishnamoorthy, Y. Wang, and J. C. Smith (1985) Biopolymers **24**, 1941–1961.
14. J. B. Le Pecq and C. Paoletti (1967) J. Mol. Biol. **27**, 87–106.
15. F. Quadrifoglio, V. Crescenzi, and V. Giancotti (1974) Biophys. Chem. **2**, 319–324.
16. M. J. Waring (1968) Nature **219**, 1320–1322.
17. Y. S. Babayan, G. Manzini, and F. Quadrifoglio (1988) Mol. Biol. **22**(4), 714–725.
18. B. Gaugain et al. (1978) Biochemistry **17**, 5078–5088.
19. D. P. Heller and C. L. Greenstock (1994) Biophys. Chem. **50**, 305–312.
20. V. W. F. Burns (1969) Arch. Biochem. Biophys. **133**, 420–424.
21. J. Yguerabide and A. Ceballos (1995) Anal. Biochem. **228**, 208–220.
22. B. Olszanska and A. Borgul (1990) Acta Biochim. Pol. **37**(1), 59–63.
23. S. Premaratne, S. D. Swenson, M. Mandel, and H. F. Mower (1994) Biochim. Biophys. Acta **1219**, 422–424.
24. T. Ide and R. Basuga (1976) Biochemistry **15**, 600.
25. S. A. Winkle, L. S. Rosenberg, and T. R. Krug (1982) Nucleic Acids Res. **10**, 8211–8223.
26. D. P. Millar, R. J. Robbins, and A. H. Zewail (1982) J. Chem. Phys. **76**, 2080–2094.
27. D. Magde, M. Zappala, W. J. Know, and T. M. Nordlund (1983) J. Chem. Phys. **87**, 3286–3288.
28. J. C. Thomas and J. M. Schurr (1983) Biochemistry **22**, 6194–6198.
29. T. Hard and D. R. Kearns (1986) J. Phys. Chem. **90**, 3437–3444.
30. A. R. Morgan et al. (1979) Nucleic Acids Res. **7**, 547–570.
31. M. J. Waring (1965) J. Mol. Biol. **13**, 269–282.
32. E. F. Gale et al. (1981). *The Molecular Basis of Antibiotic Action*, Wiley, London.
33. F. M. Pohl, T. M. Jovin, W. Baehr, and J. J. Holbrook (1972) Proc. Natl. Acad. Sci. USA **69**, 3805–3809.
34. B. Gaugain et al. (1978) Biochemistry **17**, 5071–5078.
35. J. Markovits, B. P. Roques, and J. B. L. Pecq (1979) Anal. Biochem. **94**, 259–264.
36. A. N. Glazer, K. Peck, and R. A. Mathies (1990) Proc. Natl. Acad. Sci. USA **87**, 3851–3855.
37. H. S. Rye et al. (1992) Nucleic Acids Res. **20**, 2803–2812.
38. H. S. Rye, B. L. Drees, H. M. N. Nelson, and A. N. Glazer (1993) J. Biol. Chem. **268**, 25229–25238.

Suggestion for Further Reading

39. E. F. Gale et al. (1981). *The Molecular Basis of Antibiotic Action*, Wiley, London. This general reference book provides a complete overview of the action and use of most classes of intercalating dyes.

Ethylene

1. History

For a long time, people have recognized the ability of certain gases to stimulate fruit ripening. The ancient Chinese used to burn incense to accelerate ripening. In 1910, Cousins (1) advised the Jamaican Agricultural Department to ship oranges and bananas separately, because some emanation from the oranges (originating from fungal contamination) induced ripening of the bananas. In 1934, Gane (2) proved that ethylene is synthesized by plants and initiates fruit ripening.

The first report of effects of ethylene on vegetative growth dates from 1901, when the Russian physiologist Dimitri Neljubow (3) demonstrated that ethylene in illuminating gas causes the “triple response” in dark-grown pea seedlings: inhibited epicotyl elongation, radial swelling, and a horizontal growth habit, because of loss of geotropism (3). Deleterious effects of illuminating gas had already been observed in the previous century, when leaks in gas pipes caused precocious leaf abscission of surrounding trees.

2. Biosynthesis and Metabolism

Ethylene is a unique gaseous signaling molecule with a simple molecular structure (C_2H_4). It is active at concentrations as low as 10 nL/L of air (10 ppb). The biological precursor of ethylene in higher plants is L-methionine. By the action of S-adenosyl-L-methionine (AdoMet) synthetase, methionine and ATP are conjugated to form AdoMet (Fig. 1). Subsequently, AdoMet is converted to 1-aminocyclopropane-1-carboxylic acid (ACC) and 5′-methylthio-adenosine (MTA) by the enzyme ACC synthase. MTA is recycled to methionine. ACC is converted to ethylene, HCN, and carbon dioxide by ACC oxidase. Alternatively, ACC can be conjugated to malonyl-ACC and g-L-glutamyl-ACC (4, 5). These inactive derivatives are formed to prevent precursor accumulation and conversion to ethylene. In certain cases, however, malonyl-ACC can also serve as a source of ACC (6).

Figure 1. The ethylene biosynthesis pathway in higher plants. ACC, 1-aminocyclopropane-1-carboxylic acid; GACC, glutamyl-ACC; MACC, malonyl-ACC; MTA, 5′-methylthio-adenosine; SAM, *S*-adenosyl-L-methionine.

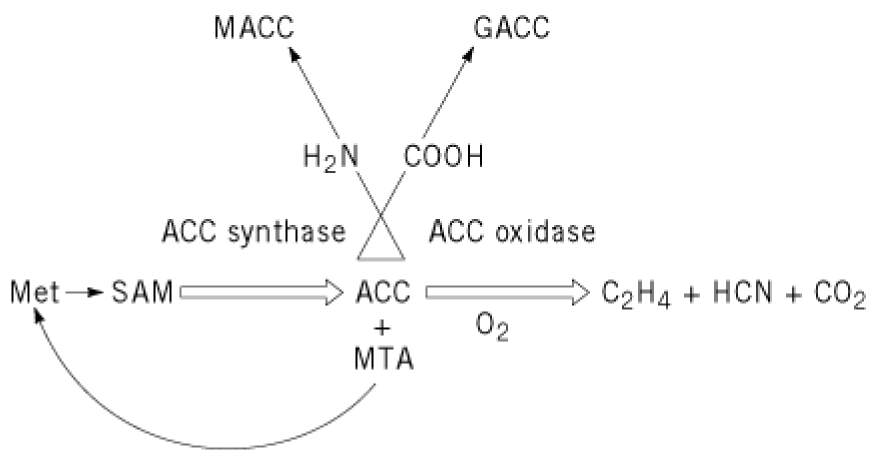

Control of ethylene biosynthesis has been observed at the level of ACC synthase and ACC oxidase activities and includes an important aspect of autoregulation (7, 8). In most cases, the ethylene levels are directly correlated with the ACC synthase activity, which is known to be highly regulated during plant development and in response to a complex array of environmental stimuli (9). Data have accumulated, however, that also indicate the importance of ACC oxidase for the regulation of ethylene synthesis (7). The synthesis of ACC does not always translate immediately into ethylene production. Interestingly, ACC is a soluble and translocatable hormone precursor, in contrast to ethylene, which, as a gas, is most probably not suited for targeted translocation processes. Translocation of ACC as a mechanism of interorgan signaling has been proposed for the regulation of plant responses to flooding stress (10, 11).

Because of its low abundance and high lability, ACC synthase proved very difficult to purify. Cloning of ACC synthase **genes** was achieved independently in several laboratories (12-14). The first nucleotide sequences of ACC synthase cDNA clones were reported by Van Der Straeten et al. (13) and Nakajima et al. (14). The former group obtained peptide sequences after 5000-fold purification of wound-induced pericarp tissue of ripening tomatoes, followed by oligonucleotide-directed screening of a cDNA library (13). Nakajima et al. (14) used an immunological approach to clone ACC synthase from a winter squash cDNA library. Sato and Theologis (12) isolated an ACC synthase clone by screening a cDNA expression library from zucchini with an antibody generated against purified ACC synthase, and the sequence was reported by Sato et al. (15). To date, clones encoding ACC synthase have been isolated from a large array of plant species. The enzyme is encoded by a highly divergent multigene family, and the expression of each gene is differentially regulated by a different subset of inducing or repressing conditions (16). Arabidopsis *thaliana* was shown to have at least five ACC synthase genes (17, 18). The *AT-ACS1* gene expression pattern was analyzed in detail using promoter-b-glucuronidase reporter gene experiments (19). It was shown that *AT-ACS1* expression was high in young and immature leaf tissues, lower in stems and in senescing tissues. The transcript levels of most ACC synthase genes are inducible by cycloheximide (16, 17), which suggests either that the messenger RNAs are labile or that transcription of ACC synthase genes is under the control of a labile repressor molecule (17). In either case, it can be concluded that ACC synthase activity is regulated predominantly at the transcriptional level. In addition, the regulation of some ACC synthase genes by various inducers may involve protein kinase activity, which in turn may be controlled through inositol-1,4,5-triphosphate (IP3)-mediated Ca^{2+} mobilization (20) (see Calcium Signaling).

A better understanding of the mechanisms involved in the transcriptional regulation of ACC synthase genes will create the possibility to control ethylene formation in a highly specific manner. To date, two strategies have been successfully applied to lower the level of ACC available for ethylene synthesis. In one experiment, the overexpression of the ACC deaminase gene of *Pseudomonas* sp. strain 6G5 in tomato plants resulted in a reduction of ethylene synthesis (21). Another approach was followed by Oeller et al. (22): expression of a tomato ripening-specific ACC synthase gene in an antisense orientation repressed ethylene synthesis almost completely. These antisense tomato fruits never get ripe until they are treated with ethylene or propylene.

Numerous attempts were made to purify the enzyme downstream of ACC synthase, namely ACC oxidase, or ethylene-forming enzyme. A clone encoding this enzyme was finally isolated in a reverse genetics approach (23). As a first step, ripening-related clones from a tomato cDNA library were isolated. For one of these clones, induction of the corresponding mRNA was tightly correlated with increased ethylene synthesis (24). **Transgenic** tomato plants expressing the cDNA in an antisense orientation were constructed, resulting in a reduction of ethylene synthesis in a gene dosage-dependent manner. In addition, these plants were delayed in fruit ripening and leaf senescence, and ethylene synthesis was also substantially reduced in wounded leaves (23, 25). Finally, the cDNA was proven to encode ACC oxidase by heterologous expression in yeast and in *Xenopus laevis* oocytes (26, 27).

With the exception of preclimacteric fruits and flowers, it was generally believed that ACC oxidase is present constitutively in plant tissues and, therefore, would not contribute to the regulation of ethylene synthesis (28). However, Grierson et al. (7) have pointed out that the rapid induction of ACC oxidase transcripts upon wounding, when assayed in dissected plant organs, may have contributed to the false belief that this enzyme is present constitutively in all tissues. To date, we know that the expression of ACC oxidase genes can be highly regulated throughout plant development (29). As for the expression of ACC synthase genes, the transcriptional regulation of ACC oxidases was also found to be controlled by **phosphorylation** and dephosphorylation events (30). Whereas ACC synthase expression was both **feedback-inhibited** and stimulated by ethylene (8), ACC oxidase was rapidly induced by ethylene treatments (31). Finally, it should be mentioned that ethylene can be metabolized to ethylene oxide (32).

3. Signal Perception and Transduction

Using the triple response for isolating ethylene mutants, and subsequent double-mutant analysis, the ethylene signal was found to be perceived through several receptors (ETR1, ERS, and maybe also EIN4 and ETR2) and was transduced via a linear pathway to the nucleus, where the expression of a set of primary ethylene-response genes is regulated (33, 34) (Fig. 2). Characterization of the *ETR1* gene suggested an explanation for the fact that different ethylene concentrations, which give different responses, can act through a common signal transduction pathway. The *ETR1* gene has significant homology with bacterial two-component regulators (35). This kind of receptor systems is known to be able to operate over a wide range of ligand concentrations, resulting in an output that is graded with stimulus intensity (36). The amino-terminal region of the protein contains **hydrophobic** stretches, each of which is predicted to span the membrane. ETR1 is a membrane-associated, **disulfide bond**-linked dimer in extracts of *Arabidopsis* and when expressed in yeast (37). Ethylene was shown to bind to the amino-terminal hydrophobic region (38), and all of the known *etr1* mutations were also located in this domain. In addition, the *etr1-1* mutation was shown to disrupt ethylene binding. These data are consistent with the chemical properties of ethylene, which is more soluble in lipids than in water and therefore will bind preferentially in a membrane environment (39). The dominant nature of *etr1* mutations, together with the redundancy of receptors, suggests that ETR1 inhibits the ethylene response in the absence of ethylene. This characteristic implies that *etr1* mutations are gain-of-function mutations, where the enzyme is locked in a catalytically active state. When ethylene binds to the receptor, this inhibitory activity is expected to be disrupted, allowing the ethylene response to occur. Accordingly, mutations preventing the binding of ethylene would then cause a constitutive inhibition of all ethylene responses.

Figure 2. Order of action of components of the ethylene response pathway in *Arabidopsis*. The pathway was established by double-mutant analysis. EIL3 is homologous to EIN3, EIL1, and EIL2; however, it has not yet been shown to be functional in ethylene signal transduction. The position of AIN1/EIN5, EIN6, and EIN7 in the pathway is unclear. AUX1, AXR1, AXR2, EIR1, and HLS1 control a subset of ethylene responses and may act in parallel to the response pathway defined by the ETR1, CTR1, and EIN2 genes.

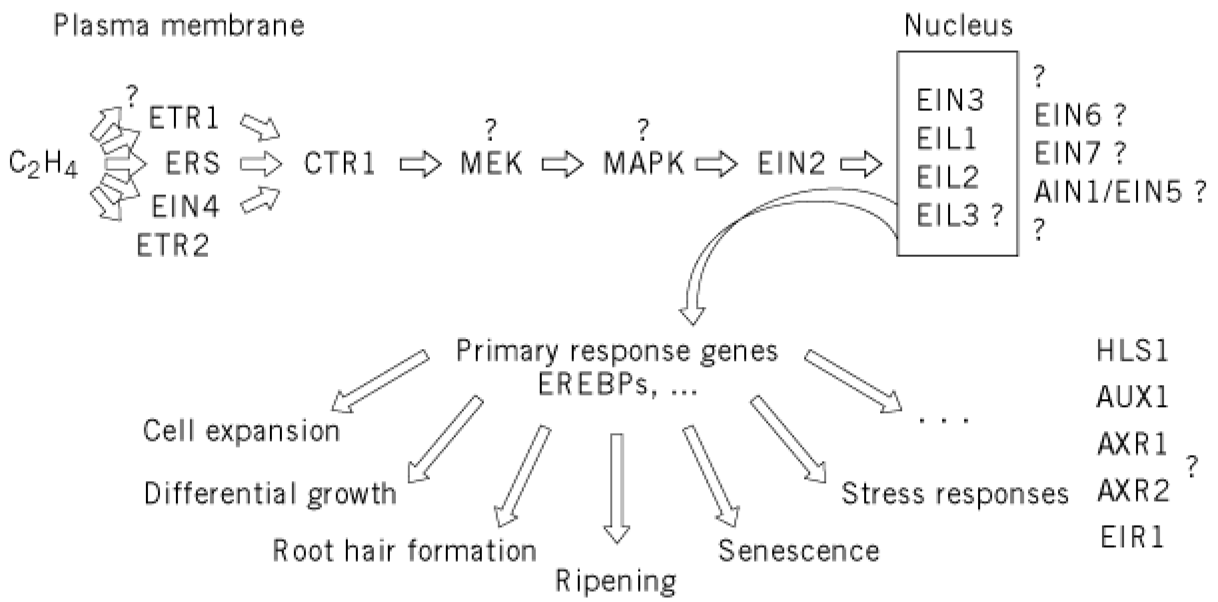

Recently, another putative *Arabidopsis* ethylene receptor, ERS (*ethylene response sensor*), was cloned (40), supporting the finding that the *Arabidopsis* genome encodes a complex family of these signal transduction proteins (35). The *EIN4* (*ethylene-insensitive 4*) gene has not yet been isolated. However, as for *etr1* mutations, *ein4* was dominant, and *ein4 ctr1* double mutants had a Ctr1 **phenotype**, indicating that EIN4 also acts upstream of CTR1 (41). Therefore, it is possible that *EIN4* belongs to the same gene family as *ETR1* and *ERS*. It should also be noted that biochemical evidence supports the existence of several ethylene-binding sites that can be classified in two types according to their rate constants for binding (42).

Downstream, the signal is transduced via CTR1, which encodes a Raf-like protein kinase (43). This observation confirms that ethylene induces a transient phosphorylation of several proteins in tobacco (44). All of the *ctr1* mutations found are predicted to disrupt the kinase activity (43). Furthermore, the homology of CTR1 to Raf-1 suggested that a MAP kinase cascade is located downstream (45). A similar combination of a “bacterial” histidine kinase and a Raf-like kinase was found for the high osmolarity glycerol pathway in yeast (46, 47). Signal transduction pathways that include Raf normally contain a MEK protein kinase, which is activated by Raf through phosphorylation (48). Subsequently, activated MEK phosphorylates a MAP kinase that, in turn, phosphorylates several downstream components. Such a MAP kinase was identified for the yeast high osmolarity glycerol pathway (49) and is also expected in the ethylene response pathway (45). To date, ethylene mutants identifying components of a putative MAP kinase cascade have not been isolated; however, screening for triple-response mutants has not yet saturated the genome (34). Given that *ctr1-1* mutations are recessive, it is expected that CTR1 is an inhibitor of the ethylene response in the absence of ethylene. If this were the case, CTR1 may be directly activated by ETR1, which in turn would be active in the absence of ethylene (34).

After CTR1, the ethylene response pathway proceeds with EIN2, followed by EIN3, EIL1, and EIL2. The order of action was based on the fact that *ein2* mutations tend to result in strong insensitivity, in contrast to *ein3* mutants, which remain more responsive to ethylene even in the case of null **alleles** (33, 41). This characteristic was confirmed by the cloning of *EIN3* and the related genes *EIL1*, *EIL2*, and *EIL3*. Overexpression of *EIN3* and *EIL1* in an *ein2* background resulted in a constitutive ethylene response phenotype (33), which can only be explained when EIN3 and EIL1 act downstream of EIN2, so that mutations in EIN2 do not inhibit the overexpression phenotype. *EIN3*, *EIL1*, and *EIL2* encode a novel class of nuclear proteins; and they seem to be regulating the same downstream components, because overexpression in each case complemented *ein3*. These proteins may be directly regulating gene transcription or may interact with transcription factors that have ethylene-regulated genes as targets (33).

A number of weakly insensitive mutants identified genes *AIN1/EIN5*, *EIN6*, and *EIN7*, which act downstream of CTR1, but their position relative to *EIN2*, *EIN3*, *EIL1*, and *EIL2* could not be determined (41, 50). In addition, certain mutations affect a specific part of the ethylene response. For example, the *HLS1* (*HOOKLESS1*) gene controls ethylene-regulated differential growth in the apical hook of etiolated seedlings (51), and the *EIR1* gene specifically regulates the ethylene sensitivity of roots (41).

The genetic analysis of ethylene signal transduction in *Arabidopsis* has been very successful and has resulted in the isolation of several components of the pathway. This research will now have to be complemented by biochemical studies and by detailed analysis of the various protein activities in relation to the existing physiological data on ethylene signaling. Additionally, progress is also expected from the use of new screening procedures to isolate novel ethylene mutants (52, 53). The analysis of light-grown populations of mutant seedlings can be complementary to the triple response screening, especially when considering the close interaction between light and ethylene during plant development (39).

4. Downstream Targets

Downstream from EIN3 and EIL1-3, the signal transduction pathway is expected to diverge into several branches that lead to specific ethylene responses. This view is corroborated by the existence of different cis-acting elements that confer ethylene inducibility in response to different inducing conditions. At least two separate mechanisms exist, one of which involves a *cis* element designated GCC box. In defense-related genes, such as chitinase (54), b-1,3-glucanase (55), and the basic pathogenesis-related (PR1) protein, a common motif was found, with the **consensus sequence** GCCGCC conserved between the *Nicotiana*, *Arabidopsis*, and *Phaseolus* GCC boxes (56). In addition, a GCC box was found in the **promoter** of the *HSL1* gene (51). Strong evidence for a key role of the GCC box in ethylene-induced transcription was given by coupling a 47-bp fragment from a tobacco b-1,3-glucanase gene containing two GCC box elements to the minimal cauliflower mosaic virus 35 S promoter and by demonstrating that it conveys ethylene responsiveness in transgenic tobacco plants (57). Four different cDNAs encoding GCC box-binding proteins were isolated by southwestern screening of a tobacco cDNA expression library with labeled GCC fragment as a probe (57). The predicted *trans* factors were named ethylene-**response element**-binding proteins (EREBPs) and defined a novel class of plant-specific transcriptional regulators. The DNA-binding domain was identified in a region of 59 amino acid residues that was fully conserved in the four EREBPs. Expression of the corresponding genes was ethylene-inducible. Several factors that play a role in development turned out to be members of the EREBP class of transcription factors, including APETALA2 (58), AINTEGUMENTA (59), and TINY (60). More recently, a DNA-binding protein involved in low-temperature expression was shown to be an additional member (61).

A mechanism independent of EREBPs appears to act during senescence of flowers and fruit ripening (62). A detailed analysis was made of the ethylene-regulated transcription of the **glutathione-*S*-transferase** gene *1* (*GST1*) during carnation petal senescence (63). A cDNA encoding a DNA-binding protein that interacts with a region of *GST1* and protects it upon footprinting using deoxyribonuclease 1 was obtained by southwestern screening (64). In tomato ripening, cooperative *cis* elements are required for ethylene regulation of *E4* gene transcription (65).

Finally, it should be noted that all the genes mentioned above are secondary response genes. Primary ethylene-responsive genes, activated within minutes after ethylene induction, remain to be identified.

5. Effects

Ethylene has been shown to participate in a diverse array of plant developmental processes, including seed germination, cell expansion, root initiation, senescence, leaf abscission, and fruit ripening in climacteric fruits (39). In addition, it controls sex determination in some monoecious species. In mango and Bromeliads, it induces flowering. Finally, ethylene is implicated in the control of biotic as well as abiotic **stress responses** (39).

Bibliography

1. H. H. Cousins (1910) III. *Agricultural Experiments* Citrus. Annual Report of the Department of Agriculture, Jamaica, 7.
2. R. Gane (1934) Nature **134**, 1008.
3. D. Neljubow (1901) Beih. Bot. Zentralbl. **10**, 128–139.
4. N. Amrhein, D. Schneebeck, H. Skorupka, and S. Tophof (1981) Naturwissenschaften **68**, 619–620.
5. M. N. Martin, J. D. Cohen, and R. A. Saftner (1995) Plant Physiol. **109**, 917–926.
6. X.-Z. Jiao, S. Philosoph-Hadas, L.-Y. Su, and S. F. Yang (1986) Plant Physiol. **81**, 637–641.

7. D. Grierson, A. J. Hamilton, M. Bouzayen, M. Köck, G. W. Lycett, and S. Barton (1992) In *Inducible Plant Proteins* (J. L. Wray, ed.), Cambridge University Press, Cambridge, U.K., pp. 155–174.
8. R. Fluhr and A. K. Mattoo (1996) Crit. Rev. Plant Sci. **15**, 479–523.
9. H. Kende (1989) Plant Physiol. **91**, 1–4.
10. K. J. Bradford and S. F. Yang (1980) Plant Physiol. **65**, 322–326.
11. M. B. Jackson (1985) Annu. Rev. Plant Physiol. **36**, 145–174.
12. T. Sato and A. Theologis (1989) Proc. Natl. Acad. Sci. USA **86**, 6621–6625.
13. D. Van Der Straeten, L. Van Wiemeersch, H. M. Goodman, and M. Van Montagu (1990) Proc. Natl. Acad. Sci. USA **87**, 4859–4863.
14. N. Nakajima, H. Mori, K. Yamazaki, and H. Imaseki (1990) Plant Cell Physiol. **31**, 1021–1029.
15. T. Sato, P. W. Oeller, and A. Theologis (1991) J. Biol. Chem. **266**, 3752–3759.
16. T. I. Zarembinski and A. Theologis (1994) Plant Mol. Biol . **26**, 1579–1597.
17. X. Liang, S. Abel, J. A. Keller, N. F. Shen, and A. Theologis (1992) Proc. Natl. Acad. Sci. USA **89**, 11046–11050.
18. D. Van Der Straeten, R. A. Rodrigues-Pousada, R. Villarroel, S. Hanley, H. M. Goodman, and M. Van Montagu (1992) Proc. Natl. Acad. Sci. USA **89**, 9969–9973.
19. R. A. Rodrigues-Pousada, R. De Rycke, A. Dedonder, W. Van Caeneghem, G. Engler, M. Van Montagu, and D. Van Der Straeten (1993) Plant Cell **5**, 897–911.
20. X. Liang, N. F. Shen, and A. Theologis (1996) Plant J. **10**, 1027–1036.
21. H. J. Klee, M. B. Hayford, K. A. Kretzmer, G. F. Barry, and G. M. Kishore (1991) Plant Cell **3**, 1187–1193.
22. P. W. Oeller, L. Min-Wong, L. P. Taylor, D. A. Pike, and A. Theologis (1991) Science **254**, 437–439.
23. A. J. Hamilton, G. W. Lycett, and D. Grierson (1990) Nature **346**, 284–287.
24. C. J. S. Smith, A. Slater, and D. Grierson (1986) Planta **168**, 94–100.
25. S. Picton, S. L. Barton, M. Bouzayen, A. J. Hamilton, and D. Grierson (1993) Plant J. **3**, 469–481.
26. A. J. Hamilton, M. Bouzayen, and D. Grierson (1991) Proc. Natl. Acad. Sci. USA **88**, 7434–7437.
27. P. Spanu, D. Reinhardt, and T. Boller (1991) EMBO J. **10**, 2007–2013.
28. S. F. Yang and N. E. Hoffman (1984) Annu. Rev. Plant Physiol. **35**, 155–189.
29. C. S. Barry, B. Blume, M. Bouzayen, W. Cooper, A. J. Hamilton, and D. Grierson (1996) Plant J. **9**, 525–535.
30. J. H. Kim, W. T. Kim, B. G. Kang, and S. F. Yang (1997) Plant J. **11**, 399–405.
31. W. T. Kim and S. F. Yang (1994) Planta **194**, 223–229.
32. I. O. Sanders, A. R. Smith, and M. A. Hall (1986) Physiol. Plant. **66**, 723–726.
33. Q. Chao, M. Rothenberg, R. Solano, G. Roman, W. Terzaghi, and J. R. Ecker (1997) Cell **89**, 1133–1144.
34. J. J. Kieber (1997) Annu. Rev. Plant Physiol. Plant Mol. Biol. **48**, 277–296.
35. C. Chang, S. F. Kwok, A. B. Bleecker, and E. M. Meyerowitz (1993) Science **262**, 539–544.
36. J. S. Parkinson (1993) Cell **73**, 857–871.
37. G. E. Schaller, A. N. Ladd, M. B. Lanahan, J. M. Spanbauer, and A. B. Bleecker (1995) J. Biol. Chem. **270**, 12526–12530.
38. G. E. Schaller and A. B. Bleecker (1995) Science **270**, 1809–1811.
39. F. B. Abeles, P. W. Morgan, and M. E. Saltveit (1992) *Ethylene in Plant Biology*, 2nd ed., Academic Press, San Diego, CA.

40. J. Hua, C. Chang, Q. Sun, and E. M. Meyerowitz (1995) Science **269**, 1712–1714.
41. G. Roman, B. Lubarsky, J. J. Kieber, M. Rothenberg, and J. R. Ecker (1995) Genetics **139**, 1393–1409.
42. N. V. J. Harpham, A. W. Berry, M. G. Holland, I. E. Moshkov, A. R. Smith, and M. A. Hall (1996) Plant Growth Regul . **18**, 71–77.
43. J. J. Kieber, M. Rothenberg, G. Roman, K. A. Feldmann, and J. R. Ecker (1993) Cell **72**, 427–441.
44. V. Raz and R. Fluhr (1993) Plant Cell **5**, 523–530.
45. J. R. Ecker (1995) Science **268**, 667–675.
46. I. M. Ota and A. Varshavsky (1993) Science **262**, 566–569.
47. T. Maeda, S. M. Wurgler-Murphy, and H. Saito (1994) Nature **369**, 242–245.
48. D. R. Alessi, Y. Saito, D. G. Campbell, P. Cohen, G. Sithanandam, U. Rapp, A. Ashworth, C. J. Marshall, and S. Cowley (1994) EMBO J. **13**, 1610–1619.
49. F. Posas, S. M. Wurgler-Murphy, T. Maeda, E. A. Witten, T. C. Thai, and H. Saito (1996) Cell **86**, 865–875.
50. D. Van Der Straeten, A. Djudzman, W. Van Caeneghem, J. Smalle, and M. Van Montagu (1993) Plant Physiol. **102**, 401–408.
51. A. Lehman, R. Black, and J. R. Ecker (1996) Cell **85**, 183–194.
52. J. Smalle and D. Van Der Straeten (1997) Physiol. Plant . **100**, 593–605.
53. J. Smalle, M. Haegman, J. Kurepa, M. Van Montagu, and D. Van Der Straeten (1997) Proc. Natl. Acad. Sci. USA **94**, 2756–2761.
54. K. E. Broglie, P. Biddle, R. Cressman, and R. Broglie (1989) *Plant Cell* **1**, 599–607.
55. G. Felix and F. Meins (1987) Planta **172**, 386–392.
56. Y. Eyal, Y. Meller, S. Lev-Yadun, and R. Fluhr (1993) Plant J. **4**, 225–234.
57. M. Ohme-Takagi and H. Shinshi (1995) Plant Cell **7**, 173–182.
58. D. Weigel (1995) Plant Cell **4**, 388–389.
59. K. M. Klucher, H. Chow, L. Reiser, and R. L. Fischer (1996) Plant Cell **8**, 137–153.
60. K. Wilson, D. Long, J. Swinburne, and G. Coupland (1996) Plant Cell **8**, 659–671.
61. E. J. Stockinger, S. J. Gilmour, and M. F. Thomashow (1997) Proc. Natl. Acad. Sci. USA **94**, 1035–1040.
62. J. Deikman (1997) Physiol. Plant. **100**, 561–566.
63. H. Itzhaki, J. M. Maxson, and W. R. Woodson (1994) Proc. Natl. Acad. Sci. USA **91**, 8925–8929.
64. J. M. Maxon and W. R. Woodson (1996) Plant Mol. Biol. **31**, 751–759.
65. R. Xu, S. Goldman, S. Coupe, and J. Deikman (1996) Plant Mol. Biol. **31**, 1117–1127.

Ethyl Methane Sulfonate (EMS)

EMS is a mutagen and a monofunctional alkylating agent of structure CH_3–CH_2–O–SO_2–CH_3, which reacts with nucleophilic sites on DNA by both S_N1 and S_N2 mechanisms. The S_N1 process involves slow generation of a very reactive intermediate that alkylates DNA with only some discrimination for nitrogen atoms. Thus treatment of DNA or whole cells with EMS leads to many

DNA products. The most significant for mutagenesis is probably O_6-ethylguanine, which base-pairs readily with thymine (1). Using bacteriophage systems, Loveless (2) showed that EMS is capable of producing high mutation frequencies, with little cell killing. The mutations produced were primarily G.C → A.T transitions, and to a lesser extent transitions containing A.T base-pairs at the mutated site, as well as frameshift mutations (3, 4). These latter events may relate to effects on DNA repair processes, while the initial events may be due to the base-pair miscoding potential of the O6-alkylguanine residues (1). EMS has often been considered the mutagen of choice for induced mutagenesis studies, being potent, easy to use, and having a well-documented mutational specificity.

Bibliography

1. P. F. Swann (1990) Mutat. Res. **233**, 81–94.
2. A. Loveless (1958) Nature **181**, 1212–1213.
3. E. Bautz and E. Freese (1960) Proc. Natl. Acad. Sci. USA **46**, 1585–1594.
4. E. Freese (1961) Proc. Natl. Acad. Sci. USA **47**, 540–545.

Ethyl-Nitrosourea

1-Ethyl-1-nitrososurea (ENU) is an ethylating and carbamoylating agent that is used as a potent mutagen in the mouse. ENU is widely used in mutagenesis of male (stem cell spermatogonia; differentiating spermatogonia; post-spermatogonial stages) and female (oocytes) mouse **germ cells**, where it introduces intragenic mutations. However, it has also been used for mutagenesis in sperm and embryonic and primordial germ cells, as well as **zygotes**. Because of its germ cell potency, ENU is the most suitable chemical mutagen for the generation of desired new mutations in the mouse. A variety of ENU-induced mouse mutants have been used as animal models for human genetic diseases. To close the **phenotype** gap in the mouse, several ENU mutagenesis programs have been initiated. The phenotype gap describes the fact that, although a great number of mouse mutants exist, there is still little known about the specific phenotypes of these mice.

ENU is a yellow-pink crystalline substance, with a melting point of 103° to 104°C and a molecular mass of 117.10. The structural formula is shown in Figure 1. ENU is not stable under physiological conditions, having a **half-life** of 34.1 min at pH 7.0 and 37°C. Because ENU is sensitive to humidity and light, it is stored below –10°C.

Figure 1. Structural formula of 1-ethyl-1-nitrosourea (ENU).

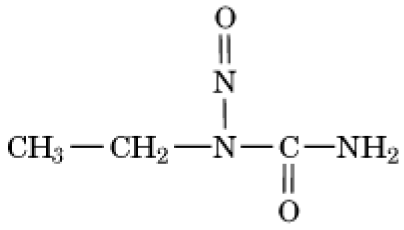

ENU produces mainly GC/AT transition mutations and, to a smaller extent, AT/GC, AT/CG, AT/TA, GC/CG, and GC/TA base substitutions. These effects are induced by ethylation of different positions within the four bases adenine, cytosine, guanine, and thymine, plus the phosphate groups of the DNA backbone. Additionally, ENU alkylates transfer RNA by the formation of 1,7-diethylguanosine. On removal of the ethyl group from O6-ethylguanine by the O6-alkylguanine-DNA alkyltransferase (AGT), S-ethylcysteine is formed. ENU also reacts with chromosomal proteins (histones) to an even greater extent than other mutagens, eg, 1-methyl-1-nitrosourea or 1-*n*-propyl-nitrosourea. Proteins are carbamoylated by the degradation product of ENU, isocyanic acid. It is likely that carbamoylation of the nuclear proteins influences DNA–histone interactions.

In mouse mutagenesis studies, ENU is the preferred mutagen in spermatogonia, with a linear relationship between the induction of mutations and doses greater than 100 mg ENU/kg. At concentrations lower than 100 mg/kg, mutation induction is nonlinear, as a result of DNA repair processes in stem cell spermatogonia. The major mutagenic lesion is the formation of O6-ethylguanine. However, analysis of mouse hemoglobin mutants Hbb and Hba induced by ENU has shown that base substitutions at A and T can also occur. This contrasts with findings in other systems and emphasizes the complexity of *in vivo* mammalian germ cell mutagenesis. ENU is considered to be a supermutagen in mouse stem cell spermatogonia, inducing recessive mutations with a very high frequency. This mutation rate is maximized by repeated intraperitoneal injections of at least 100-mg ENU/kg at weekly intervals to a total dose of 300- to 400-mg ENU/kg.

Chemical mutagens have also been used to induce mutations in arrested and maturing **oocytes** of female mice. However, the mutation rate is significantly lower than for treated male germ cells. In addition, a high proportion of mutants derived from treatment of oocytes are mosaics, resulting from lesions affecting only one strand of the DNA. Treatment of oocytes also generates approximately 30% of large (multilocus) lesions. Only treatment of post-spermatogonial stages results in a higher percentage (65%) of such large lesions. The differences in the mutagenic potential of ENU on oocytes and stem cell spermatogonia occur mainly because oocytes are nondividing cells until fertilization. Consequently, mutagenesis of zygotes by an exposure of 50-mg ENU/kg at the time when the female genome enters metaphase II results in much higher mutation rates than in stem cell spermatogonia.

Different approaches have to be taken to recover a mutant mouse **genotype**. Dominant mutations can be screened directly in offspring of mutagenized males, whereas recessive mutations can be analyzed using a three-generation breeding protocol. Gene mutations in mouse germ or somatic cells by mutagens have been detected by the specific locus test, dominant cataract method, mouse spot test, micronucleus test, or new test systems like the MutaMouse or Big Blue mouse [see Mouse].

Suggestions for Further Reading

S. D. M. Brown and J. Peters (1996) Combining mutagenesis and genomics in the mouse—closing the phenotype gap. Trends Genetics **12**, 433–435.

L. B. Russel and W. L. Russel (1992) Frequency and nature of specific-locus mutations induced in female mice by radiations and chemicals: a review. Mutation Res. **296**, 107–127.

T. Shibuya and K. Morimoto (1993) A review of the genotoxicity of 1-ethyl-1-nitrosourea. Mutation Res. **297**, 3–38.

Euchromatin

Euchromatin, which can be distinguished from heterochromatin contains the majority of transcriptionally active DNA. Euchromatin, initially identified cytologically during interphase, appears less condensed and stains less intensely with dyes than heterochromatin. Features of euchromatin may be usefully summarized by comparing the active X-chromosome with the inactive X-chromosome (see Barr Body, X-Chromosome Inactivation).

The euchromatin of the active X-chromosome contains hyperacetylated histones, which indicate potential for transcriptional activity. The active X-chromosome also contains reduced levels of methylated DNA and replicates early in S-phase. Euchromatin is also likely to be globally sensitive to digestion with nucleases such as DNase I (see DNase 1 Sensitivity).

Existence in either the euchromatic or heterochromatic states is not irreversible. This is best demonstrated by experiments in which cells containing nuclei that are predominantly heterochromatic are either transplanted into eggs or fused with other cells that are predominantly euchromatic, to generate a heterokaryon. Experimental results with heterokaryons in which two different somatic cells are fused, so that two different nuclei share a common cytoplasm, and nuclear transplantation experiments using *Xenopus* eggs have been interpreted as providing evidence for continuous regulation of a plastic differentiated state. Implicit in this model is the idea that all genes are continually regulated by *trans*-acting factors that can either activate or repress genes (1). For certain genes this is clearly true. It has also been shown, however, that considerable remodeling of chromosomal structure occurs in *Xenopus* egg and oocyte cytoplasm, during which heterochromatin is converted to euchromatin (2). A similar, albeit less impressive, remodeling of chromosomes occurs in heterokaryons. For example, the nuclei of chicken erythrocytes consist predominantly of heterochromatin containing the specialized linker histone H5. In heterokaryons formed by the fusion of chicken erythrocytes with proliferating mammalian cells, the chicken erythrocyte nuclei once again become transcriptionally active, leading to the appearance of euchromatin (3). This process is accompanied by decondensation of chromatin, enlargement of the nucleus, and the appearance of nucleoli. Transcription and replication of these nuclei are also activated.

Enlargement of the chicken erythrocyte nucleus is caused by a massive, but selective, uptake of mammalian nuclear proteins, including RNA polymerases. The specialized linker histone H5 is partially lost from the chicken erythrocyte nucleus and partially taken up by the mammalian nucleus in the heterokaryon. Histones H2A and H2B also exchange under these circumstances, but not histones H3 and H4. These results might reflect the relative affinity of the histones for DNA and their organization in the nucleosome. This reorganization is independent of DNA replication. Therefore, it is clear that chromosomal structure is quite dynamic, and some histones (H1, H2A, H2B) continually exchange with a free pool of proteins in the cytoplasm.

Several experiments suggest that at physiological ionic strength the linker histone H1 rapidly exchanges into and out of the chromatin fiber (5, 6). Histone H1 is a specific repressor for several eukaryotic genes. Presumably this dynamic property of the chromatin fiber and the nucleosome would eventually allow many *trans*-acting factors to gain access to their cognate DNA sequences. An important and unresolved question is whether this access is unlimited or whether access is restricted by chromosomal organization. It has not yet been quantitatively determined whether the level of transcriptional activity following de novo activation of a gene in a heterokaryon is identical to the transcription of the same gene in a differentiated cell. Of course, in *Xenopus* egg cytoplasm, such equivalent activation must occur for correct development to proceed through to the tadpole stage. Nuclear reprogramming, however, is more rapid here and is likely to be facilitated by DNA replication (4), although massive nucleus-wide remodeling can occur without concomitant DNA synthesis (7, 8).

Bibliography

1. H.M. Blau and D. Baltimore, J. Cell Biol. **112**, 781–783 (1991).
2. J.B. Gurdon, J. Embryol. Exp. Morph. **36**, 523–540 (1976).
3. N.R. Ringertz, U. Nyman, and M. Bergman, Chomosoma **91**, 391–396 1985).

4. S. Dimitrov and A.P. Wolffe, EMBO J. **15**, 5897–5906 (1996).
5. M.A. Lever, J.P. Th"ng,X. Sun, and M.J. Hendzel, Nature **408**, 873–876 (2000).
6. A.P. Wolffe and J.C. Hansen, Cell **104**, 631–634 (2001).
7. N. Kikyo et al., Science **289**, 2360–2362 (2000).
8. N. Kikyo and A.P. Wolffe, J. Cell Sci. **113**, 11–20 (2000).

Additional Reading

9. Wolffe A. *Chromatin: Structure and Function*, 3rd ed., Academic Press, London, U.K., 1998.

Euploid

A euploid cell is a cell that has the basic haploid number of chromosomes characteristic of that species or any exact multiple of this haploid number. Contrary situations are explained in Aneuploidy and **Polyploidy**.

Evolution

Darwin defined evolution in the *Origin of Species* as “descent with modification” (1). Although there have been various interpretations, modifications, and additions, the concepts of this definition continue to be repeated as biology develops. It seems likely that Darwin's definition will never fade away. Therefore, it is reasonable to state that evolution is the process in which the structures and functions of organisms are inherited from generation to generation, along with changes at both the morphological and molecular levels.

In his theory, Darwin treated species as populations, and he recognized several features of populations that explain the process of evolution (1). In particular, he noticed that among individuals having variation in characteristics, those having advantageous characteristics, or “fitness,” can survive by producing more offspring of their own. This is the process of natural selection. Darwin already had advanced the concept that organisms have intrinsically inherited material labeled “genetic elements” (and later found to be DNA) and the idea that the variation found among individuals in a species was random, but these were not widely accepted. De Vries proposed the mutation theory, which states that mutations appear suddenly in a population and that species will experience periods of rapid mutation (2). His mutation theory and Mendel's law on inheritance, as well as Darwin's natural selection,were synthesized to create th e synthetic or neo-Darwin theory of evolution (3). The synthetic theory of evolution views evolution in the following way. First, mutation occurs to the genetic material, namely, DNA, in a random fashion. It is a source of genetic variation. and it is heritable to the next generation by Mendelian law. Natural selection then takes place so that individuals having advantageous characteristics can survive in a population, and the offspring have the same type of mutation, which becomes spread in a population. In this way, the genetic composition changes with the time.

The study of molecular evolution is essentially based on the synthetic theory of evolution. However, the development of molecular biology has introduced more detailed and new information on molecular mechanisms for producing genetic variation, which have accelerated the advancement of evolutionary studies. The genome projects currently in progress will give insights to the evolutionary changes of genomes, structures, and functions.

Bibliography
1. C. Darwin (1859) *On the Origin of Species*, Murray, London.
2. H. De Vries (1901–1903) *Die Mutationstheorie*, Von Veit, Leipzig (1909–1910) "English translation", *The Mutation Theory*, trans. J. B. Farmer and A. D. Darbishire, Open Court, Chicago.
3. E. Mayer and W. B. Provine (1980) *The Evolutionary Synthesis*, Harvard Univ. Press, Harbridge, MA.

Evolutionary Distance

Evolutionary distance is a distance by which evolutionary closeness or remoteness can be measured quantitatively. Evolutionary distance may be separated into two distinctive levels; one morphological; the other, molecular. In the case of evolutionary distance at the molecular level, the number of nucleotide and amino acid substitutions, as well as immunological cross-reactions, are the most popular measures for evolutionary distance.

The number of nucleotide substitutions is estimated by making pairwise comparison of nucleotide sequences and correcting for multiple substitutions at the same site (see). For correction of multiple substitutions, one needs a model of nucleotide substitution; for example, the one-parameter method invented by Jukes and Cantor (1) assumed that the rates of nucleotide substitutions between all possible pairs of different nucleotides are equal to each other. In this case, the nucleotide substitution is estimated by the equation $K_n = -\frac{3}{4}\ln(1-\frac{4}{3}p)$, where p is the fraction of nucleotide differences. There are many modified and extended versions of this formula. For example, Kimura's two-parameter method was developed under the assumption that the rates of transition mutations and are different (2). In this way, four-parameter method and the six-parameter methods were also developed. The method of maximum likelihood was invented.

The number of amino acid substitutions is also used as a measure of evolutionary distance. Under the assumption that the substitution rates between any pair of amino acids are equal, the number of amino acid substitutions can be given by formula $K_a = -\ln(1-p)$, where p represents the fraction of amino acid differences. It is well known, however, that the substitution rate between a pair of similar amino acids is much higher than that between a pair of nonsimilar amino acids. Although Dayhoff (3) developed the algorithm to estimate the number of amino acid substitutions taking into account the similarity matrix of amino acids, the formula given was very complicated. To minimize this, Kimura (2) invented an empirical formula by adding one simple term, $K_a = -\ln(1-p-\frac{1}{5}p^2)$. Even though Kimura's formula was derived empirically, the substitution number estimated by this formula is very close to Dayhoff's estimate.

Immunological distances can be also used as a measure of evolutionary distance. The measurement of immunological distance uses as a measurement the intensity of immunological crossreaction between antigens and antisera that were prepared from different species (see). It has now become less popular, however, because the numbers of amino acid or nucleotide substitutions contain much more quantitative information.

Bibliography

"Evolutionary Distance" in , Vol. 2, pp. 867–868, by T. Gojobori; "Evolutionary Distance" in (online), posting date: January 15, 2002, by T. Gojobori, National Institute of Genetics, Shizuoka, Japan.

1. T. H. Jukes and C. R. Cantor (1969) *Mammalian Protein Metabolism*, Academic Press, New York.
2. M. Kimura (1983) *The Neutral Theory of Molecular Evolution*, Cambridge Univ. Press, Cambridge, UK.
3. M. O. Dayhoff (1978) Atlas of Protein Sequence and Structure, Vol. **5**, Suppl. 3, National Biomedical Research Foundation, Washington, D.C.

Evolutionary Rate

In the studies of molecular evolution, the rates of nucleotide or amino acid substitutions (per site per year) are usually used as the evolutionary rate (see Sequence Analysis). Compare two nucleotide sequences, A and B, as an example. Denote K_n as the number of nucleotide substitutions between sequences A and B. When the ancestral node, O, of the two sequences A and B is considered, it follows that nucleotide substitutions should have accumulated during the time of lineages OA and OB (Figure 1). If the divergence time between sequences A and B, which is measured by years, is denoted T, K_n is the number of substitutions that have taken place during $2T$. This is because the divergence time of OA plus OB should be equal to $2T$. Thus, the rate of nucleotide substitution (v_n) can be computed by the formula $v_n=K_n/(2T)$. The rate of amino acid substitution (v_a) can be obtained in a similar way: $v_a=K_a/(2T)$. Note that the number of nucleotide and amino acid substitutions can be estimated by a number of different methods (see Evolutionary Distance).

Figure 1. Estimating the rate of evolutionary change in nucleotide or amino acid sequences from the difference between two present-day homologous sequences. Rate of nucleotide substitution: $v_n=K_n/(2T)$; rate of amino acid substitution: $v_a=K_a/(2T)$

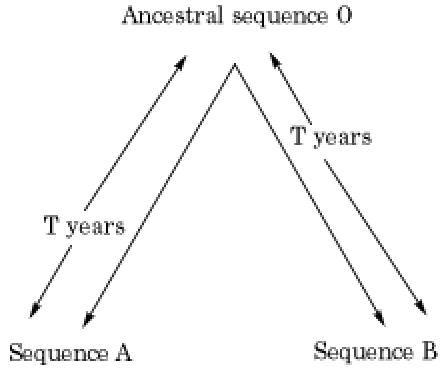

Excision Repair

Excision repair (1, 2) is a form of DNA repair involving the removal of a damaged nucleotide from DNA by dual incisions bracketing the damage (3, 4). The multisubunit enzyme system that makes the dual incision is referred to as *excision nuclease* or *excinuclease* (3). The damaged nucleotide is released in the form of an oligonucleotide, and the resulting single-stranded gap is filled in by **DNA polymerase** and sealed by a DNA Ligase. This repair mechanism, which is also referred to as "nucleotide excision repair," is a universal repair system. Excinuclease has been found in all free-living organisms, including Mycoplasma *genitalium*, which is considered a model system for "minimal cell." Although both prokaryotes and eukaryotes carry out excision repair, there are distinct differences in the mechanism in the two systems.

1. Substrate

In most organisms, excision repair is the sole mechanism for repairing bulky DNA lesions. These include the vast number of base adducts formed by polyaromatic hydrocarbons and by chemotherapeutic agents such as cisplatin, mitomycin C, and psoralen, plus the cyclobutane pyrimidine dimers and the [6–4] photoproducts induced by ultraviolet light (see Photolyase/Photoreactivation). Nucleotide excision repair is not, however, restricted to bulky adducts. Alkylated bases including O^6-methylguanine and 3-methyladenine, oxidative base lesions such as 8-oxoguanine and thymine glycols, and even apurinic/apyrimidinic sites (AP sites) are removed from DNA by excision repair (5-7). Mismatched bases are also removed with low efficiency by this enzyme system; unlike mismatch repair, however, the excinuclease cannot discriminate between the correct base and the mismatched base, and this may result in fixation of a mutation (5). The most impressive aspect of the substrate repertoire of excinuclease is that it encompasses essentially all abnormal DNA structures. It must be noted, however, that, with the exception of bulky lesions, all other lesions can be repaired by alternative repair mechanisms, including repair by O^6**-methylguanine DNA methyltransferase, DNA glycosylases, AP endonucleases**, and the mismatch repair systems. It is most likely that excision repair plays a critical backup role for these other repair systems, by repairing nonbulky DNA lesions when the normal repair enzymes are poorly expressed in a certain tissue or when a sudden burst of DNA damage exceeds the repair capacity of the specific repair mechanisms. It has been suggested that the neurological symptoms of xeroderma pigmentosum patients are caused by metabolism-induced nonbulky oxidative damage in brain cells, which overwhelms the main repair system for DNA damage caused by oxidative stress, base excision repair (7).

2. Genetics

Excision repair encompasses three basic enzymatic steps: (i) dual incisions on both sides of the damage, (ii) repair synthesis to fill in the excision gap, and (iii) ligation of the repair patch. Mutations in genes controlling any of these reactions interfere with normal functioning of excision repair. The enzymes carrying out repair synthesis and ligation are not, however, dedicated solely to repair; they also perform DNA synthesis and ligation functions during replication, recombination, and transposition. Strictly speaking, therefore, excision repair genes are the genes encoding the subunits of the excinuclease, which is the enzyme system that removes the damaged nucleotide by dual incisions bracketing the lesion. In *E. coli* and other prokaryotes, three genes—*uvrA, uvrB*, and *uvrC*—are necessary and sufficient for the excision reaction (3). In the yeast *Saccharomyces cerevisiae*, genes in the RAD3 epistasis group (RAD1, 2, 3, 4, 10, 14, 25) are required to reconstitute excinuclease (8). In humans, defects in excision repair cause xeroderma pigmentosum (XP). In this hereditary recessive disease, patients are hypersensitive to sunlight and develop skin cancers, including melanomas, at an early age. In addition, the majority of XP patients exhibit neurological signs and symptoms caused by neuronal death. There are eight XP complementation groups, XP-A through XP-G, plus the XP-variant (XP-V). Patients in complementation groups XP-A to XP-G are defective in removing pyrimidine dimers and other bulky adducts from DNA; in other words, they are defective in excision repair. In contrast, XP-V-deficient individuals exhibit normal excinuclease activity, but are defective in a process called postreplication repair. The XP complementation groups define only seven of the proteins involved in the excision reaction. In addition to these proteins, the replication protein RPA, the recombination protein ERCC1 (which makes a complex with XPF), and the transcription factor TFIIH (which includes the XPB and XPD DNA helicases and four to six additional polypeptides) are also required for dual incisions (9, 10).

There is a one-to-one correspondence between the human and yeast excinuclease genes, and similar homologous genes have been identified in all other eukaryotes tested (11). Hence, it appears that the excision repair genes and mechanism have been conserved throughout the eukaryotic kingdom. In contrast, there is no homology between the excinuclease genes of eukaryotes and prokaryotes. Certain species in the third form of life, the Archaea, appear to have XPD, XPF, and XPG homologues, and certain others have *uvrA, B, C* homologues. Hence, it appears that species in this kingdom might have either the prokaryotic or eukaryotic form of excinuclease.

3. Biochemistry

The mechanism of the excision repair reaction is quite similar in prokaryotes and eukaryotes, even though there is no structural homology between the enzyme systems: Damage is recognized by the enzyme in an ATP-independent manner, forming an unstable DNA–protein complex; then ATP hydrolysis by the proteins within the complex promotes formation of a long-lived preincision complex. Binding of a nuclease subunit triggers dual incisions, which are concerted but nonsynchronous; that is, the 33′ and 5′ incisions nearly always occur in the same DNA molecule, but the 3′ incision occurs first, followed within a fraction of a second by the 5′ incision. Following both incisions, the excinuclease proteins are replaced by replication proteins. In *E. coli*, DNA polymerase I and DNA helicase II (UvrD protein), working together, displace the excised oligomer and the subunits of the excision nuclease that remain in the postexcision complex, and they then fill in the gap (12, 13). In yeast and humans, the replication polymerase d or ε, working together with the polymerase **clamp loader** replication factor C (RF-C) and the polymerase clamp, the proliferating cell nuclear antigen (PCNA), fill in the excision gap (14). The last step is ligation of the repair patch to the parental DNA. A more detailed description of excision repair in *E. coli* and humans is given below.

3.1. Excision Repair in *E. coli* (Fig. 1)

Three subunits, UvrA, UvrB, and UvrC, are necessary and sufficient to carry out the dual incision. Their properties are summarized in Table 1. UvrA and UvrB make a heterotrimer of A_2B_1 composition that, guided by the intrinsic affinity of UvrA for damaged DNA (15, 16), recognizes subtle or gross abnormalities in the duplex structure as damage. Upon binding to the damaged DNA, ATP hydrolysis by UvrA and UvrB leads to local unwinding of the DNA and formation of a stable UvrB–DNA complex, concomitant with dissociation of UvrA from the complex (16). Here UvrA plays the role of a molecular matchmaker (17): Utilizing the energy released by ATP hydrolysis, it brings together DNA and UvrB (a protein with rather weak affinity for DNA), promotes formation of a complex between the two, and then leaves so that the complex can engage in productive reactions. Following dissociation of UvrA, the UvrC subunit binds to the UvrB–DNA complex, and the 3′ incision is made at the fourth or fifth phosphodiester bond from the damage by UvrB, perhaps with the contribution of active-site residues of UvrC (18). After the 3′ incision, the complex undergoes another conformational change that enables UvrC, perhaps aided by residues on UvrB, to make the 5′ incision at the eighth phosphodiester bond 5′ to the lesion (18). After the dual incision, UvrB, UvrC, and the “excised” dodecamer remain in a complex with the duplex. Helicase II (UvrD) binds to this complex and releases the excised oligomer and UvrC. Then, DNA polymerase I binds to the 5′ incision site and displaces UvrB, while simultaneously filling the excision gap. When the gap is filled to the 3′ end, the repaired patch is ligated to the parental DNA. There is no **nick translation** in filling in the gap and, as a consequence, the repair patch size matches precisely the size of the excision gap (13).

Figure 1. Excision repair in *E. coli*. UvrA and UvrB make up the A_2B_1 heterotrimer that, guided by the affinity of UvrA to helical distortion, recognizes DNA damage. Upon recognition, the DNA is locally unwound by the helicase action of the complex and kinked by 130°. Having performed its molecular matchmaking function, UvrA dissociates, leaving behind a stable UvrB–DNA complex that is recognized by UvrC. Upon binding of UvrC, UvrB makes the 3′ incision at the fifth phosphodiester bond and UvrC makes the 5′ incision at the eighth phosphodiester bond. Helicase II (UvrD) releases the excised dodecamer and UvrC; DNA pol I displaces UvrB and fills in the gap, which is ligated.

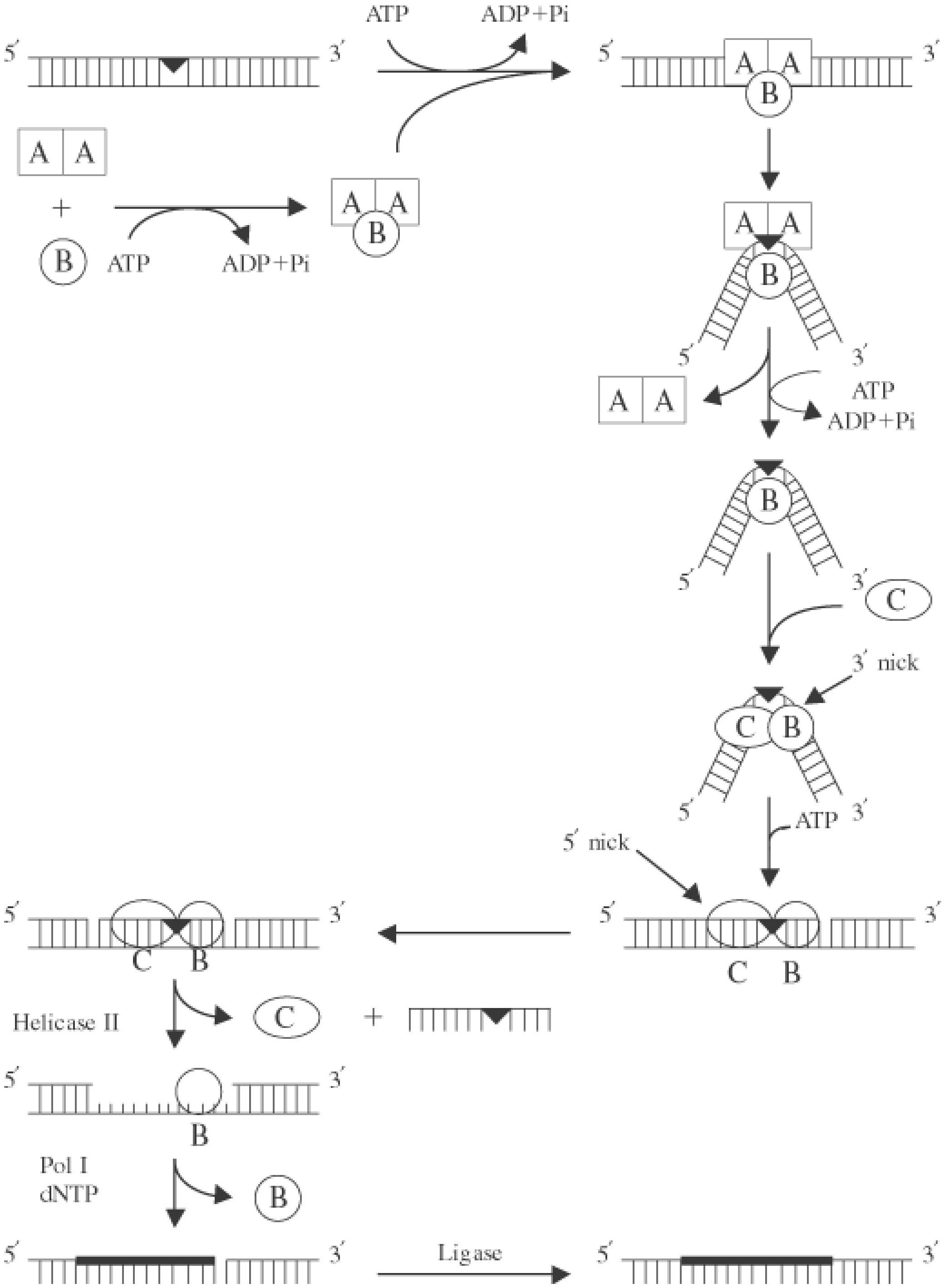

Table 1. Subunits of *E. coli* Excinuclease

Protein	M_r	Sequence Motifs	Activity	Role in Repair
Excision Nuclease Subunits				
I. UvrA	(104)	(a) Walker ATPase (2)	(a) ATPase	(a) Damage

	2			recognition (proximal)
		(b) Zinc finger (2)	(b) Damage-specific DNA binding	(b) Molecular matchmaker
		(c) Leucine zipper	(c) UvrB binding	(c) TRC
		(d) UvrA superfamily	(d) TRCF binding	
II. UvrB	78	(a) Helicase motif	(a) Latent ATPase	(a) Damage recognition (ultimate)
		(b) Homology to TRCF	(b) Latent “helicase”	(b) Unwinding duplex
			(c) Damage-specific ssDNA binding	
			(d) Binds UvrA	(c) Makes 3′ incision
			(e) Binds UvrC	
III. UvrC	69	(a) Limited homology to UvrB	(a) Nonspecific DNA binding	(a) Induces 3′ incision
		(b) Limited (40 amino acid) homology to ERCC1	(b) UvrB binding	(b) Makes 5′ incision

3.2. Excision Repair in Humans (Fig. 2)

In humans, the excinuclease activity of producing dual incisions results from the coordinated action of 16 polypeptide chains in six repair factors, listed in Table 2 (9, 10). The basic reaction carried out by human excinuclease is the incision of a phosphodiester bond that is 6 ± 3 nucleotides 3′ to the damage and 20 ± 5 nucleotides 5′, followed by release of the resulting 24- to 32-nucleotide oligomers carrying the damaged base (4, 11). The reaction proceeds as follows (19): XPA, RPA, and XPC · HHR23B (20) proteins form a transient complex at the site of the damage. This complex interacts with TFIIH, which is both a transcription factor and a repair factor (21), via XPA and XPC · HHR23B and recruits this multisubunit factor to the lesion site. TFIIH unwinds the duplex by about 5 nucleotides on the 3′ side and 10 nucleotides on the 5′ side of the damaged nucleotides (19); as a consequence, it promotes new DNA–protein interactions that lead to formation of a stable preincision complex (22). XPG has high affinity for TFIIH and enters the preincision complex, either simultaneously with TFIIH or subsequently after being recruited by TFIIH, to form a very stable DNA–protein complex in which the DNA is unwound by 15 to 20 nucleotides. Entry of XPG to the preincision complex is dependent on, and concomitant with, departure of XPC from this complex. Hence, XPC plays the role of molecular matchmaker in human excinuclease. Within this complex, the 3′ incision is made by XPG (23, 24) at the sixth ± 3 phosphodiester bond 3′ to the damage. Thus, in contrast to *E. coli*, the 3′ incision can be made in humans before binding of the subunit that makes the 5′ incision. The XPF · ERCC1 complex is recruited to the repair assembly by the strong interaction between XPA and ERCC1, which is promoted by the presence of XPG within the complex. The XPF · ERCC1 complex makes the 5′ incision at the 20th ± 5 phosphodiester bond 5′ to the damage (24). Assembly of the excision nuclease is a highly concerted reaction, so that under physiological conditions the 3′ incision is rapidly followed by the 5′ incision; therefore, uncoupled 3′ incisions do not accumulate in the cell. The dual incision generates a single-stranded DNA fragment of 24 to 32 nucleotides, which is released from the duplex (excision) (10). This is in contrast to the bacterial system, in which the “excised” oligomer remains in the postincision complex until it is released by a DNA repair auxiliary helicase (10, 12, 13). Following release of the excised oligomer, the gap is filled by DNA polymerases d and ε in a reaction that is dependent on the polymerase clamp, the proliferating cell nuclear antigen (PCNA). The size of the repair patch precisely matches the size of the excision gap, with no gap enlargement on the 5′ side or nick translation on the 3′ side of the gap (25).

Figure 2. Excision repair in humans. XPA, RPA, XPC, and TFIIH recognize damaged DNA. TFIIH unwinds the DNA by about 20 nucleotides, and a transient DNA–protein complex forms. This structure is recognized by XPG, which enters the complex concomitant with dissociation of XPC (molecular matchmaker). XPG makes the 3′ incision at the sixth phosphodiester bond and recruits the XPF · ERCC1 complex, which makes the 5′ incision at the 22nd phosphodiester bond. The excised 27-mer is released along with some of the excinuclease subunits. The excision gap is filled in by DNA Pol ε and ligated.

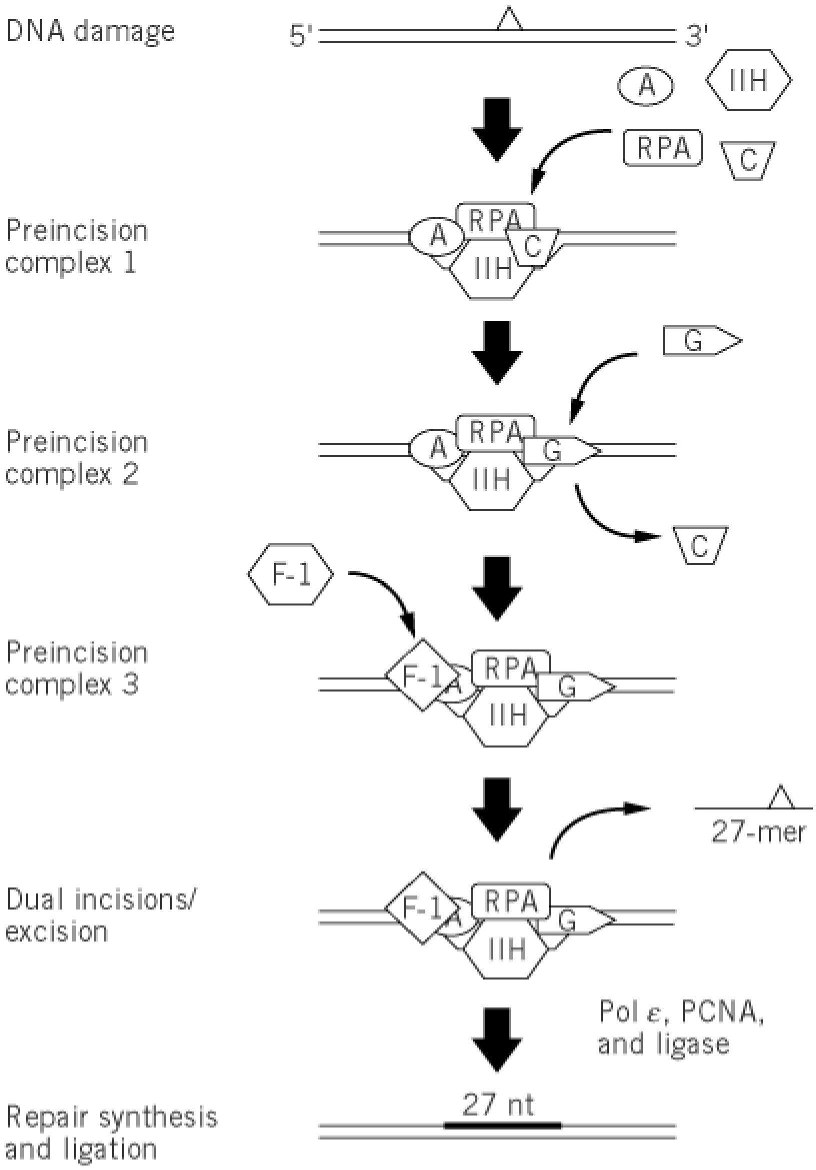

Table 2. Subunits of Human Excinuclease

Factor	Number	Proteins[a]	Sequence Motif	Activity	Role in Repair
I. XPA	1	XPA/p31	Zinc finger	DNA binding	Damage recognition
II. RPA	2	p70		DNA binding	Damage recognition
	3	p34			
	4	p11			

III. TFIIH	5	CPB/ERCC3/p89	Helicase	(a) DNA-dependent ATPase	(a) Formation of preincision complex
	6	XPD/ERCC2/p80	Helicase		
	7	p62			
	8	p44	Zinc finger	(b) “Helicase”	(b) Transcription-repair coupling
	9	Cdk7/p41	S/T kinase		
	10	CycH/p38	Cyclin	(c) GTF	
	11	p34	Zinc finger	(d) CAK	
IV. XPC	12	XPC/p125		DNA binding	(a) Stabilization of preincision complex
	13	HHR23B/p58	Ubiquitin		(b) Protection of preincision complex from degradation
V. XPF	14	XPF/ERCC4/p112		Nuclease	5′ Incision
	15	ERCC1/p33			
VI. XPG	16	XPG/ERCC5/p135		Nuclease	3′ Incision

[a] The relative molecular weights of the polypeptides are indicated, for example, by p31 for M_r = 31 kDa, and so on. GTF, general transcription factor; CAK, cyclin-dependent kinase activating kinase.

4. Transcription-Repair Coupling

Transcribed sequences are repaired more rapidly by excinuclease than are nontranscribed sequences, both in prokaryotes and in eukaryotes (26, 27). The open chromatin conformation of transcribed DNA in eukaryotes contributes to the accessibility of the DNA to repair enzymes, and hence it has a faster rate of repair compared to regions of condensed chromatin conformation. The main driving force of preferential repair of transcribed DNA, however, is the mechanistic coupling of transcription to repair. The best manifestation of this active process of coupling is the fact that, although both strands of the DNA in the gene are more accessible because of the open conformation, the transcribed strand is repaired faster than the nontranscribed (coding) DNA strand, which is repaired at essentially the same rate as the rest of the genome (28, 29). Hence it appears that the main cause of repair coupled to transcription is the recruitment of the excinuclease complex to the site of damage (30). Indeed, in both prokaryotes and eukaryotes, the damage-recognition step is the slowest step of excision repair. In the act of transcription, lesions in the template strand block the progression of **RNA polymerase**—hence the stalled complex marks the site of the lesion. In other words, RNA polymerase functions as a surrogate damage-recognition protein for lesions in the template strand. Because specific binding of repair proteins to the damage itself is very slow, due to the fact that lesions removed by excinuclease have very little in common, a stalled RNA polymerase provides a fast damage-locating mechanism and a common structural element (RNA polymerase in elongation mode) for the excision repair system. It appears both in prokaryotes and eukaryotes that a specific protein called transcription-repair coupling factor (TRCF) recognizes both the stalled RNA polymerase and a subunit of the excision nuclease and recruits the repair enzyme to the site of the lesion (30). As a result of high-specificity protein–protein interactions, rather than the low-specificity **DNA–protein interaction**, the rate of repair is accelerated. The transcription repair coupling factor is encoded by the *mfd* gene in *E. coli*, the RAD26 gene in yeast, and the *CSB* gene in humans. The molecular mechanism of transcription-repair coupling is relatively well-understood in *E. coli*, but not in eukaryotes.

4.1. Transcription-Repair Coupling in *E. coli*

The *E. coli* TRCF is a monomer of 130 kDa, and it has helicase motifs, a UvrA binding site in the NH_2-terminal half, and a RNAP-binding region in the middle (31). The protein recognizes RNA polymerase stalled at a lesion and displaces the stalled polymerase, while simultaneously recruiting the A_2B_1 complex to the damage site. The net result is the discarding of the truncated transcript and a substantial increase in the rate of damage recognition. Furthermore, because TRCF and UvrB share the same binding site on UvrA, the TRCF also helps dissociate UvrA from the A_2B_1–DNA complex and facilitates rapid formation of the UvrB–DNA complex (31), which is a prerequisite for binding of UvrC. This is followed by dual incision and the remaining steps of excision repair, which are not rate-limiting. Therefore, acceleration of the damage recognition reaction and facilitation of the dissociation of UvrA by the TRCF results in overall enhancement of the excision repair rate by nearly a factor of 10 relative to excision repair unaided by RNA polymerase and TRCF. The coupling of transcription to repair results in a decline in mutation frequency of ultraviolet-irradiated cells incubated in a medium lacking amino acids prior to plating, compared to cells plated immediately on rich medium (32). In the minimal medium, the mutagenic lesions in the transcribed genes are repaired before giving rise to mutation by DNA synthesis and replication of the lesion. Hence the gene for the *E. coli* TRCF is called *mfd* (mutation frequency decline) (32).

4.2. Transcription-Repair Coupling in Humans

The phenomenology of transcription-repair coupling in humans is similar to that in *E. coli*, although there are some important differences. Humans defective in transcription-repair coupling are afflicted with Cockayne's syndrome, a disease characterized by growth and developmental abnormalities and mild sensitivity to sunlight. Mutations in two genes, *CSA* and *CSB*, give rise to Cockayne's syndrome. Both genes have been **cloned**. The *CSB* gene is a 160-kDa monomer with helicase motifs and appears to be the functional homologue of the *mfd* gene of *E. coli*. The *CSA* protein is a 55-kDa protein with the WD sequence motif, a protein–protein interaction motif. The CSB protein is a weak ATPaseand binds to RNA polymerase II either free in solution or stalled on DNA. Significantly, in contrast to the *E. coli* TRCF, the CSB protein, even in combination with CSA protein, does not disrupt the ternary complex of RNA polymerase II stalled at a lesion (33). CSB does bind to XPA and XPG subunits of the human excinuclease, however, and may play a role similar to that of the *E. coli* Mfd protein in recruiting the repair complex to the site of damage. The mechanistic details of coupling transcription to repair are not known at present.

Both in *E. coli* and in humans, it is the nucleotide excision repair that is tightly coupled to transcription. Recently it was found, however, that transcription also stimulates removal of thymine glycols by base excision repair in a reaction that depends on the XPG protein, but not other subunits of the human excision nuclease system. The mechanistic aspects of this coupling remain to be elucidated.

5. Regulation of Excision Repair

There is a steady-state level of damage production and removal by nucleotide excision repair under physiological conditions. It would be advantageous for the cell if, upon any sudden increase of the genotoxic load, it could increase its repair capacity. Three such regulatory systems have been characterized in *E. coli*: the SOS response, the adaptive response, and the adaptive response to oxidative stress. The SOS response increases the nucleotide-excision-repair capacity of the cell by increasing the level of UvrA and UvrB subunits of excinuclease. Although DNA damage induces a dramatic stress response reaction in human cells, increased repair capacity is not part of this reaction. Human excinuclease genes are not induced at the transcriptional level by DNA damage, nor is the repair activity increased as a consequence of post-transcriptional events. In particular, DNA damage causes hyperphosphorylation of the RPA p34 subunit, but this has no effect on excision repair. Similarly, certain types of damage increase the level of p53 protein by post-transcriptional mechanisms. It has been reported that this increase stimulates repair in certain cell types, but not others. The mechanism of the p53 effect on repair is not known.

Bibliography

1. R. P. Boyce and P. Howard-Flanders (1964) Proc. Natl. Acad. Sci. USA **51**, 293–300.
2. R. B. Setlow and W. L. Carrier (1964) Proc. Natl. Acad. Sci. USA **51**, 226–231.
3. A. Sancar and W. D. Rupp (1983) Cell **33**, 249–260.
4. J. C. Huang, D. L. Svoboda, J. T. Reardon, and A. Sancar (1992) Proc. Natl. Acad. Sci. USA **89**, 3664–3668.
5. J. C. Huang, D. S. Hsu, A. Kazantsev, and A. Sancar (1994) Proc. Natl. Acad. Sci. USA **91**, 12213–12217.
6. J. C. Huang, D. B. Zamble, J. T. Reardon, S. J. Lippard, and A. Sancar (1994) Proc. Natl. Acad. Sci. USA **91**, 10394–10398.
7. J. T. Reardon, T. Bessho, H. C. Kung, P. H. Bolton, and A. Sancar (1997) Proc. Natl. Acad. Sci. USA **94**, 9436–9438.
8. S. N. Guzder, Y. Habraken, P. Sung, L. Prakash, and S. Prakash (1995) J. Biol. Chem. **270**, 12973–12976.
9. D. Mu, C. H. Park, T. Matsunaga, D. S. Hsu, J. T. Reardon, and A. Sancar (1995) J. Biol. Chem. **270**, 2415–2418.
10. D. Mu, D. S. Hsu, and A. Sancar (1996) J. Biol. Chem. **271**, 8285–8294.
11. D. L. Svoboda, J. S. Taylor, J. E. Hearst, and A. Sancar (1993) J. Biol. Chem. **268**, 1931–1936.
12. P. R. Caron, S. R. Kushner, and L. Grossman (1985) Proc. Natl. Acad. Sci. USA **82**, 4925–4929.
13. I. Husain, B. Van Houten, D. C. Thomas, M. Abdel-Monem, and A. Sancar (1985) Proc. Natl. Acad. Sci. USA **82**, 6774–6778.
14. A. F. Nichols and A. Sancar (1992) Nucleic Acids Res. **20**, 2441–2446.
15. J. T. Reardon, A. F. Nichols, S. Keeney, C. A. Smith, J. S. Taylor, S. Linn, and A. Sancar (1993) J. Biol. Chem. **268**, 21301–21308.
16. D. K. Orren and A. Sancar (1989) Proc. Natl. Acad. Sci. USA **86**, 5237–5241.
17. A. Sancar and J. E. Hearst (1993) Science **259**, 1415–1420.
18. J. J. Lin and A. Sancar (1992) J. Biol. Chem. **267**, 17688–17692.
19. M. Wakasugi and A. Sancar (1997) Proc. Natl. Acad. Sci. USA **95**, 6679–6684.
20. C. Masutani, K. Sugasawa, J. Yonagisawa, T. Sanoyama, M. Ui, T. Enomoto, K. Takio, K. Tanaka, P. J. van der Spek, D. Bootsma, J. H. J. Hoeijmakers, and F. Hanaoka (1994) EMBO J. **13**, 1831–1843.

21. R. Drapkin, J. T. Reardon, A. Ansari, J. C. Huang, L. Zawel, K. Ahn, A. Sancar, and D. Reinberg (1994) Nature **368**, 769–772.
22. M. T. Hess, U. Schwitter, M. Petretta, B. Giese, and H. Naegeli (1997) Proc. Natl. Acad. Sci. USA **94**, 6664–6669.
23. A. O''Donovan, A. A. Davis, J. A. Moggs, S. C. West, and R. D. Wood (1994) Nature **371**, 432–435.
24. T. Matsunaga, C. H. Park, T. Bessho, D. Mu, and A. Sancar (1996) J. Biol. Chem. **271**, 11047–11050.
25. J. T. Reardon, L. H. Thompson, and A. Sancar (1997) Nucleic Acids Res. **25**, 1015–1021.
26. R. C. Bockrath and J. E. Palmer (1997) Mol. Gen. Genet. **156**, 133–140.
27. V. A. Bohr, C. A. Smith, D. S. Okumoto, and P. C. Hanawalt (1985) Cell **40**, 359–369.
28. I. Mellon and P. C. Hanawalt (1989) Nature **342**, 95–98.
29. I. Mellon, G. Spirak, and P. C. Hanawalt (1987) Cell **51**, 241–249.
30. C. P. Selby and A. Sancar (1993) Science **260**, 53–58.
31. C. P. Selby and A. Sancar (1995) J. Biol. Chem. **270**, 4882–4889.
32. E. M. Witkin (1966) Science **152**, 1345–1353.
33. C. P. Selby and A. Sancar (1997) J. Biol. Chem. **272**, 1885–1890.

Suggestions for Further Reading

34. A. Sancar (1994) Mechanisms of DNA excision repair. Science **266**, 1954–1956.
35. A. Sancar (1995) Excision repair in mammalian cells. J. Biol. Chem. **270**, 15915–15918.
36. A. Sancar (1996) DNA excision repair. Annu. Rev. Biochem. **65**, 43–81.
37. S. Prakash, P. Sung, and L. Prakash (1993) DNA repair genes and proteins of Saccharomyces cerevisiae . Annu. Rev. Genet. **27**, 33–70.
38. E. C. Friedberg, G. C. Walker, and W. Siede (1995) *DNA Repair and Mutagenesis*, ASM Press.
39. R. D. Wood (1996) DNA repair in eukaryotes. Annu. Rev. Biochem. **65**, 135–167.
40. P. C. Hanawalt (1994) Transcription-coupled repair and human disease. Science **266**, 1957–1958.

Excluded Volume

No solute molecule in a solution can be present in the same space as any other molecule in the solvent. This volume of occupation is called the excluded volume V_e. The excluded volume clearly depends on the shape and conformation of the solute molecule. In a dilute solution, the centers of two identical rigid spheres cannot be placed closer to each other than a distance twice as great as their radius (Fig. 1a). Thus, any spherical molecule excludes similar molecules from a volume eight times greater than that it physically occupies. However, the excluded volume due to the interaction of any pair of particles is counted twice, so the volume excluded by all the spherical particles in the system is four times greater than their physical volumes.

Figure 1. Schematic illustration of the excluded volume of spherical molecules. (a) Each solute molecule is excluded from the space occupied by other solute molecules in solution. In very dilute solutions, each molecule of radius *R*

contributes a spherical volume of radius 2 R. (b) A cosolvent of radius R_e much greater than that of water statistically cannot be close to a protein molecule due to a steric exclusion principle, resulting in the preferential hydration of protein. [Taken from T. Arakawa and S. N. Timasheff (1).]

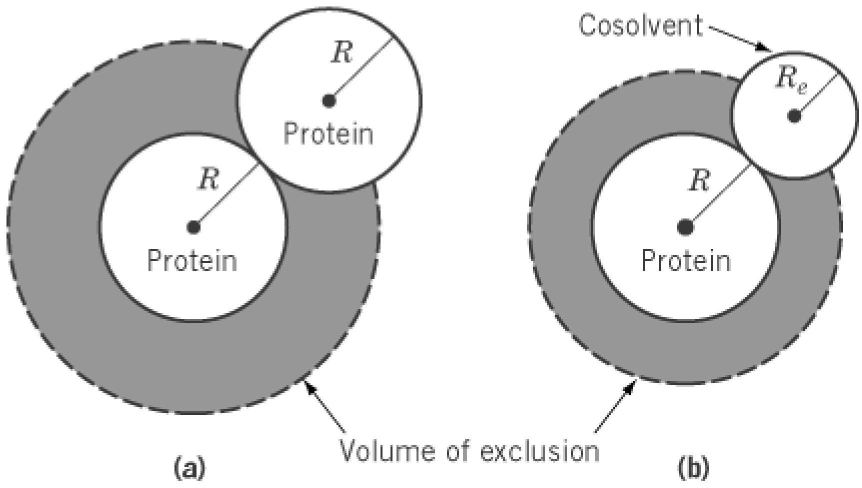

The partial specific (or molar) **volume** v_2 is usually taken as the physical volume, so $V_e = 4v_2M_2$ for a spherical solute molecule of molecular weight M_2. This should be a good approximation for globular proteins. A rigid rod-shaped solute is regarded as a cylinder, so its V_e is proportional to the length–diameter ratio of the cylinder. The excluded volume of a flexible polymer depends on its radius of gyration, which is sensitive to the polymer–solvent interaction. In a good solvent, solvent molecules are preferably accessible to a polymer, which extends the chain segment and increases the excluded volume. On the contrary, V_e is small in a poor solvent, which enhances interactions between different parts of the polymer.

Many polymer solution theories have been developed for the excluded volume of flexible polymers. It is important that the excluded volume be directly related to the second virial coefficient of polymer solutions, so this is an apt criterion for the ideality of the solutions. The excluded volume effect is more significant for nucleic acids at lower salt concentration, where the stiffness or persistence length of the chain segment is influenced by polyelectrolyte effects. The excluded volume effect is also the primary basis for the ability of water-soluble polymers, such as polyethylene glycol, to **precipitate** proteins. Preferential Hydration is partly due to steric exclusion, in that a larger cosolvent is more effectively excluded from protein surface than water (Fig. 1b).

The excluded volume effect favors any chemical reaction in which the volume decreases. This includes **ligand binding** by a protein and the association of protein subunits to form oligomers. The equilibrium constant for such a reaction is increased with the increasing concentration of macromolecules in the solution. At high concentrations, such as occur normally in the **cytosol** of cells, such effects can be very large (2).

Bibliography

1. T. Arakawa and S. N. Timasheff (1985) Biochemistry **24**, 6756–6762.
2. A. P. Minton (1981) Biopolymers **20**, 2093–2120.

Exocytosis

Exocytosis occurs in eukaryotic cells when the membrane of a cytoplasmic **vesicle** fuses with the plasma membrane, exposing the contents of the vesicle and the lumenal layer of the phospholipid bilayer to the outside world.

1. Examples of Exocytosis

Most cells can secrete proteins (see Protein Secretion). In bacteria, the proteins can be unfolded and then threaded, or translocated, across the plasma membrane. Eukaryotes translocate newly synthesized proteins into an intracellular organelle, the endoplasmic reticulum. Proteins travel from the endoplasmic reticulum by way of the **Golgi complex**, to the plasma membrane. Transport is effected by packaging the newly synthesized proteins in secretory vesicles, which must fuse their membrane with that of the plasma membrane to release their contents to the extracellular space. Thus eukaryotic cells that secrete proteins must have the molecular machinery to allow exocytosis at the cell surface. Exocytosis must be highly efficient, since few secretory vesicles are seen in most cells.

Sometimes newly synthesized proteins passing through the Golgi complex are diverted selectively into cytoplasmic storage vesicles, usually called dense core secretory granules (1). To allow cytoplasmic storage, exocytosis of such secretory granules is inhibited, causing the accumulation of granules in the cytoplasm or along the plasma membrane. Accumulation of storage or secretory granules usually gives cells a characteristic morphology; examples are the granulocytes of the **hematopoietic** system, endocrine and exocrine cells, prefertilization eggs filled with cortical granules, and protozoa such as *Paramecium* and *Tetrahymena* . A signal to the outside of such protein-storage cells can remove the inhibition to exocytosis and trigger a massive efflux of protein, a process referred to as regulated secretion.

Some endocrine cells, such as chromaffin cells or neurons, actively transport small molecules from the cytoplasm into the lumen of the dense core secretory granules, giving them high internal concentrations of both protein and the small molecules (2). The energy for the active transport comes from a proton gradient across the secretory granule membrane (3). This property is also found in bone marrow-derived cells. Mast cells, for example, package histamine to high concentrations inside their secretory granules. When cells of this type undergo exocytosis, along with the stored proteins they release massive quantities of the small molecules, which usually are identical, or are related to, neurotransmitters.

In addition to having a biosynthetic pathway for protein secretion, many eukaryotic cells have an endocytosis pathway that internalizes plasma membrane components and returns most of them to the cell surface (4). This membrane recycling pathway allows a cell to move membrane to a site where it might be more needed; for example, a region of cell growth or migration (5). The recycling pathway also allows a cell to internalize nutrients bound to receptors, to remove the nutrients, and to send the receptors back to the cell surface for more. In the final step, a membrane vesicle on the recycling pathway must fuse with the plasma membrane (that is, it must undergo exocytosis). Thus, the exocytosis machinery is essential for endocytotic recycling, as well as for protein secretion (Fig. 1).

Figure 1. Example of exocytosis in endocytosis. Exocytosis is used in other processes besides delivery of secretory proteins to the cell surface. Here, using the trafficking of low-density lipoprotein (LDL) receptor as an example, we see how exocytosis is an integral part of endocytic trafficking. (**a**) Cholesterol-containing LDLs bind to their receptors and (**b**) are internalized by endocytosis. (**c**) The endocytic vesicles fuse with an endosome (**d**) where LDL dissociates from its receptor. While LDL is eventually broken down for utilization of the cholesterol (**ef**), the LDL receptor is recycled back to the cell surface by exocytosis (**g**) so that it can be reused.

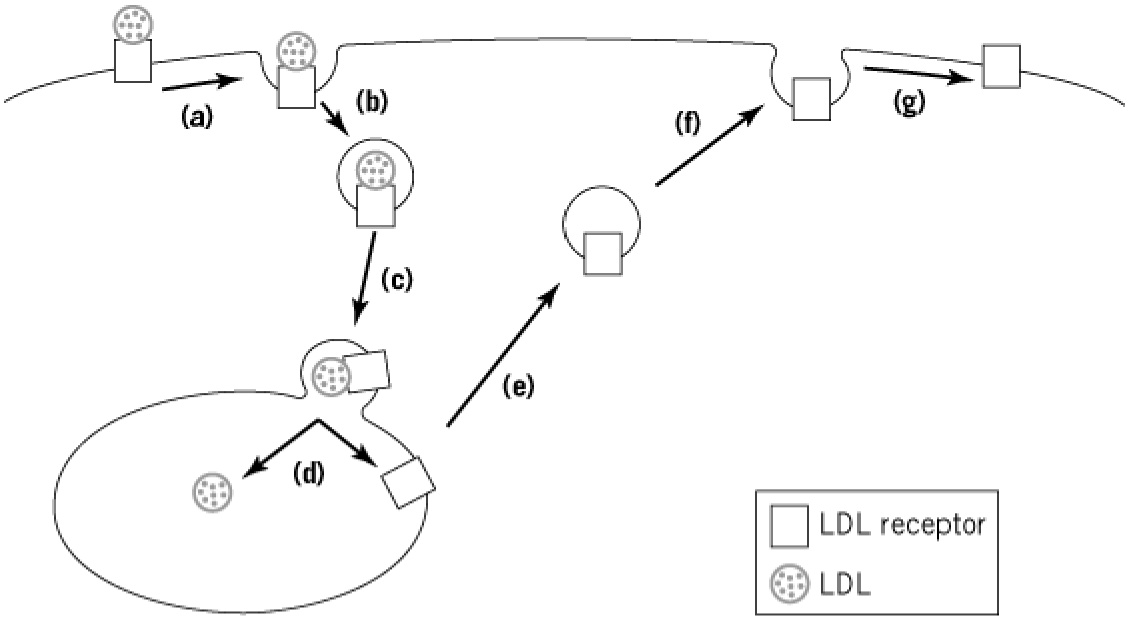

As with protein secretion, there appear to be constitutive and regulated exocytotic steps associated with membrane recycling. Membrane vesicles carrying nutrient receptors, such as the **receptors** for transferrin and low-density **lipoprotein**, fuse rapidly with the plasma membrane, independently of an external signal. In specialized cases, exocytosis is inhibited, causing an accumulation of endocytotically derived membrane vesicles (6). Two examples of such storage vesicles are synaptic vesicles and vesicles storing intracellularly a special type of glucose transporter, GLUT4 (glucose transporter 4) (7). Regulated exocytosis of the endocytotically derived vesicles can occur when the inhibition is removed, by an electrical signal in the case of the nerve cell, and by insulin in the case of GLUT4-storing fat and muscle cells.

Fortunately, similar molecular machinery seems to be used by all forms of exocytosis, regulated or constitutive, biosynthetic, or plasma-membrane recycling. Furthermore, the molecules that regulate exocytosis appear to be conserved, as are the transporters that put neurotransmitters into dense core secretory granules and into synaptic vesicles.

2. Measurements of Exocytosis

A common but crude measure of exocytosis is the appearance in the extracellular medium of the contents of a secretory vesicle that has undergone exocytosis. Thus exocytosis of synaptic vesicles (see Secretory Vesicles/Granules) at the nerve terminal causes release of neurotransmitter, and exocytosis of secretory granules from b-cells of the pancreatic islets of Langerhans releases insulin. Extracellular neurotransmitters and hormones can be measured biochemically, as can the constitutive secretion of enzymes such as invertase by yeast or proteinases by mammalian cells. Biochemical measurements are usually incapable of measuring the kinetics of exocytosis with accuracy.

The release of neurotransmitters, however, can be measured electrophysiologically with much greater precision. Most neurotransmitters activate the postsynaptic target cell by binding to closed **ion channels** and causing them to open. Measurement of current flow through the postsynaptic ion channels gives an almost instantaneous assay of the exocytosis rates in the presynaptic nerve terminal. The precision and sensitivity of electrophysiological measurements, pioneered by Dr. Bernhard Katz and his coworkers at University College, London, allowed detection of a quantum of neurotransmitter release, lasting a millisecond or so, generated by exocytosis of the contents of a single synaptic vesicle. Electrophysiology revealed that exocytosis is very rapid, occurring within 100 µs of a stimulus to the nerve terminal, and that the concentration of the neurotransmitter in the synaptic vesicle is very high, greater than 100 m*M*.

Postsynaptic currents generated by presynaptic release of neurotransmitter accurately measured the exocytosis because the receptor channels were 10 to 20 nm from the exocytosis site. Release of biogenic amines from cells such as chromaffin cells can likewise be measured rapidly and quantitatively by placing a carbon electrode close to the cell and detecting the biogenic amine by its **redox** potential (8). This technique was first applied to exocytosis by Wightman's group and is called amperometry.

Another technique widely used to study exocytosis uses the cell-surface capacitance. The electrical capacitance across the plasma membrane of a cell is proportional to its area. When exocytosis occurs, the capacitance increases because of the addition of membrane (9, 10). The sensitivity of capacitance measurements is such that it can measure the addition of the membrane of a single secretory granule. It cannot yet detect the addition of a single synaptic vesicle, since they are too small (50 nm diameter). When the capacitance signal is big enough, however, the capacitance changes give an instantaneous measurement of exocytosis.

To measure capacitance, a cell must be attached to a “patch electrode,” which allows electrical communication between the salt solution inside the electrode and the cytoplasm of the cell.

Video techniques for quantifying fluorescent markers in cells and recording changes in **fluorescence** intensity as a function of time are becoming increasingly sophisticated. Video-microscopy techniques are used to study exocytosis by loading synaptic vesicles with a membrane-impermeable fluorescent dye (11, 12). Each synaptic vesicle can contain about 30 dye molecules. When the membrane of a synaptic vesicle fuses with that of the plasma membrane, the intensity of the fluorescence decreases by a fixed amount, which can be measured using sensitive detection devices. The dye technique for studying exocytosis was pioneered by William Betz and his colleagues at the University of Colorado.

When the secretory vesicle is big enough, it is possible to observe exocytosis in the light microscope. Some protozoa, such as *Paramecium* or *Tetrahymena*, have large cytoplasmic vesicles, packed with protein, that are docked at the plasma membrane. When the light microscope is used (13), the dense contents of the secretory granules can be seen to disappear when exocytosis is triggered. The convenience of a visual assay for exocytosis has made it possible to screen for secretion mutants in organisms of this type. Exocytosis of secretory granule content can also be detected visually in sea urchin eggs and in some classes of mast cell.

3. Mechanism of Exocytosis

Exocytosis takes place in several stages. First the membrane of the vesicle recognizes the plasma membrane and forms a close association with it. Then the phospholipid bilayers are rearranged so that the membranes of the vesicle and those of the plasma membrane become continuous. Finally, the curved vesicle membrane flattens out, adopting the curvature of the plasma membrane.

Association of the cytoplasmic vesicle with the membrane is sometimes called docking . There are two types of vesicle docking, which sometimes get confused. Since exocytosis is not a random event but requires docking specifically between a vesicle and plasma membrane, the two membranes must recognize each other, presumably through protein–protein interactions. The recognition and fusion steps must be rapid processes in most cells, because few vesicles are seen adjacent to the plasma membrane or in the process of fusion. In contrast, in regulated secretory cells, such as neurons and endocrine cells, the secretory and synaptic vesicles (see Secretory Vesicles/Granules) are in a stable association with the plasma membrane. The long-lasting docking in neurons and neuroendocrine cells is presumably an adaptation that allows very rapid exocytosis in response to an extracellular signal. To avoid confusing the two forms of docking, we discuss first the generic, short-term docking, present in all eukaryotic cells.

Many of the molecular insights into exocytosis derive from mutations that affect protein secretion in yeast (see Sec Mutants/Proteins). Such mutants can have defects in all stages of the protein export pathway. Particularly relevant to exocytosis are the mutations that accumulate post-Golgi secretory vesicles in their cytoplasm. Of the three sets of gene products that affect exocytosis, the ones that are understood in most detail are the SNARE proteins (14). The name SNARE (SNAp REceptor) derives from one of the ways the proteins were discovered (discussed later) and is useful to describe their function. A v-SNARE protein on a vesicle targeted for exocytosis interacts with a t-SNARE on the target plasma membrane. The first identified member of the v-SNARE family was the synaptic vesicle protein initially called VAMP (Veside Associated Membrane Protein) (15) and later synaptobrevin (16). The characteristics of v-SNAREs on secretory vesicles include (*1*) a vestigial lumenal or extracytoplasmic domain at the **C-terminus**, which can be as small as two amino acid residues; (*2*) a single conserved transmembrane domain; (*3*) a highly conserved juxtamembrane region that has the predicted sequence of a coiled coil, and (*4*) a variable **N-terminal** domain. At the cell surface, the v-SNARE is believed to interact with two t-SNAREs. One is a member of the syntaxin family (17), which also has a small lumenal *C*-terminal **domain**, a single transmembrane domain, and a coiled-coil region. The third, a member of the SNAP (synaptosomal-associated protein)-25 family (18), is a cytoplasmic peripheral protein, also with a coiled-coil domain, and is held to the plasma membrane by covalently attached **palmitoyl groups**. The three proteins are believed to form a ternary complex via their helical domains, which facilitates fusion (19). All well-studied exocytotic events, from yeast to mammalian cells, also appear to involve close **homologues** of these three SNARE proteins (20). Even synaptic-vesicle exocytosis, where the fusing vesicle is endocytotically derived, uses SNARE proteins. This has been shown using mutations in Drosophila that affect the neuronal SNAREs VAMP/synaptobrevin or syntaxin (21, 22). The involvement of SNAREs can also be verified by use of bacterial neurotoxins. Tetanus toxin and the botulinum neurotoxins A to G are endopeptidases that specifically hydrolyze the SNARE molecules (23). Exocytosis from nerve terminals and endocrine cells is blocked by these neurotoxins, providing evidence for the involvement of the SNARE complex even in regulated exocytosis (24).

SNARE complexes form readily, even with purified components in the presence of detergents. Given their high proclivity for spontaneous interaction, it is no surprise that the SNAREs appear to be sequestered in complexes that limit their reactivity. The v-SNAREs in synaptic vesicles (VAMP/synaptobrevin) is sequestered by the synaptic-vesicle protein synaptophysin, which has four transmembrane segments (25). The corresponding t-SNARE, syntaxin, is strongly bound to a cytosolic protein, which is called the *sec*1 gene product in yeast and nsec1, for neuronal sec1, in the nervous system (26, 27). Since SNARE complexes are so energetically stable, energy must be expended to separate the SNAREs. Separation of the complex involves the ATPase NSF (*N*-ethyl maleimide sensitive factor) and two accessory proteins, called a- and b-SNAP (28). For NSF to bind, the SNAPs must bind the SNARE complexes. Thus the SNARE complexes received their name, SNAP receptors. The acronym SNAP stands for soluble NSF-acceptor protein in this case. For the t-SNARE SNAP-25, the acronym denotes synaptosomal-associated protein. The identity of the acronyms is coincidental but confusing. Currently, it is thought that NSF might act to dissociate the SNARE complex before fusion, but this is controversial (29, 30) (Fig. 2).

Figure 2. SNARE-mediated membrane fusion. (**a**) NSF and SNAP proteins bind to v-SNARE/t-SNARE complexes on membranes. (**b**) ATP hydrolysis by NSF causes dissociation of the SNARE complex so that (**c**) the v-SNARE can form a complex with a t-SNARE on a target membrane. (**d**) By an unknown mechanism complexes formed with SNAREs on opposing membranes are thought to promote membrane fusion (**e**), ending with the SNARE complex on the same membrane. NSF/SNAP must dissociate the complex again before either of the SNAREs can be reused.

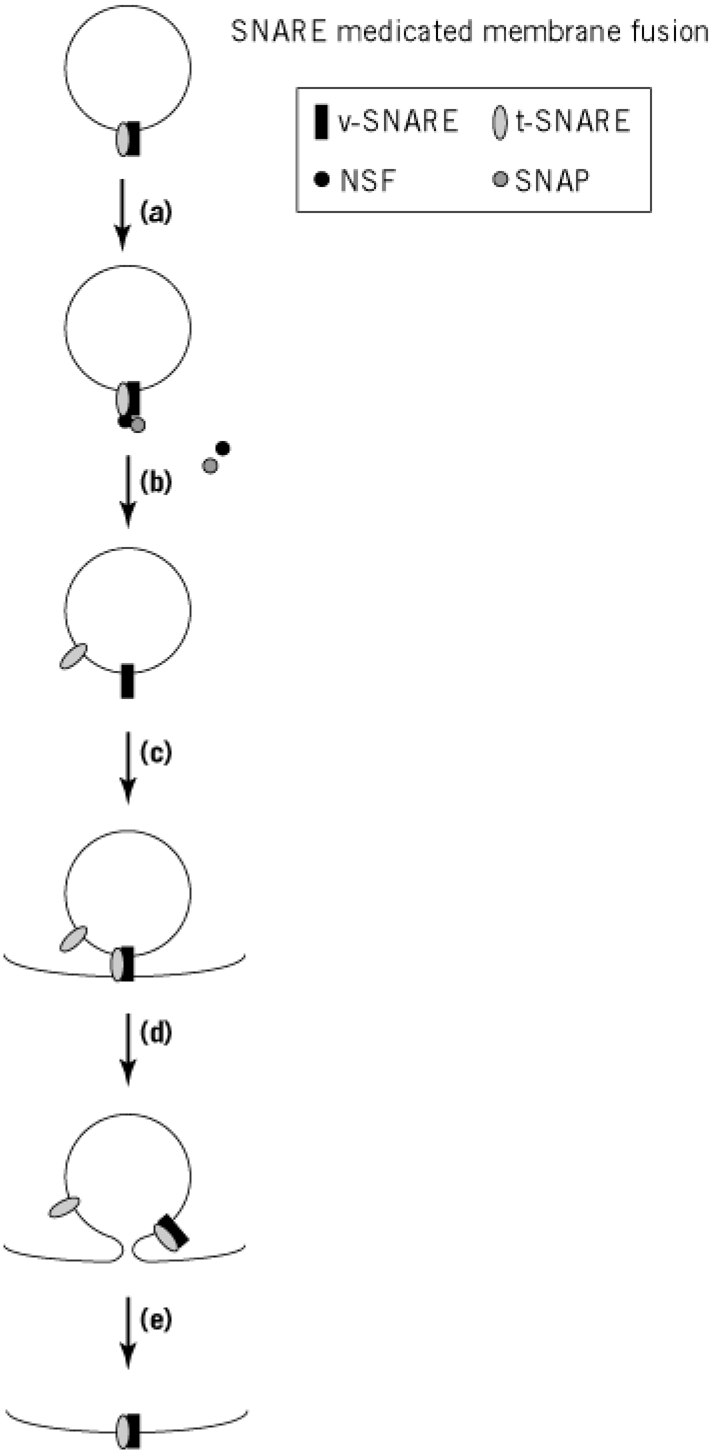

Exocytosis in yeast is also inhibited by a mutation in a small, ras-like, GTPase, the *sec*4 gene product (31). The *sec*4 protein is a member of a large class of small GTPases, the rab proteins. All secretory vesicles have a rab protein. In the case of synaptic vesicles, it is *rab*3A. Rab proteins appear to interact with a complex of proteins, of which the rabaptin complex is the prototype (32). The *rab* system seems to parallel the SNARE system in docking secretory vesicles at the plasma membrane. Thus, yeast mutations in the *rab* pathway can be rescued by overexpression of genes in the SNARE pathway (24). Another protein complex that appears to determine the site of exocytosis in yeast and mammalian cells is the exocyst (33, 34).

The final class of players in exocytosis appears to be related to actin-binding proteins, because mutations in such proteins block protein secretion (see Sec Mutants/Proteins.) The link between membrane traffic and the actin cytoskeleton is currently obscure.

4. Regulated Exocytosis

Regulated exocytosis is found in cells that have a large cytoplasmic pool of secretory vesicles. In the presence of a suitable external stimulus, the probability of exocytosis per secretory vesicle increases manyfold. In neurons and endocrine cells, the external stimulus commonly triggers in regions of the cytoplasm near **calcium channels** a rise of intracellular calcium ions from its normal low level of about 0.1 μM to levels that can range up to 100 μM and greater (35). A common conjecture is that calcium ions bind to an inhibitor of exocytosis, removing the inhibition. Good candidates for calcium sensors in neurons are members of the synaptotagmin family (36). Synaptotagmins have two **calcium-binding** domains on their cytoplasmic regions and can oligomerize. Mutations in synaptotagmin cause loss of calcium-dependent exocytosis (37). Despite the conjecture that the calcium sensor is inhibiting exocytosis, its absence in mutant organisms does not lead to high levels of exocytosis in the absence of stimulation.

Another calcium-binding protein implicated in regulated exocytosis is the CAPS protein (38). Its addition to cell-free preparations of secretory granules docked at plasma membranes restores calcium-dependent release. The CAPS protein binds to the negatively charged phospholipids, the phosphorylated forms of phosphatidyl inositol. Consistent with CAPS having a role in exocytosis is the finding that secretory granules must be primed with adenine triphosphate (ATP) in cell-free systems before exocytosis can occur (39). The ATP is required to phosphorylate the 4′ and 5′ positions on the inositol ring, catalyzed by specific phosphatidylinositol kinases. The phosphorylation state of phosphatidyl inositol is found to determine the efficiency of several membrane trafficking steps (40), but the reason is not yet clear.

The inside surface of the plasma membrane is frequently coated with a layer of cross-linked actin filaments. To allow exocytotic vesicles access to the plasma membrane, it may be necessary to remove or rearrange the subcortical actin layer. Many reports of such rearrangements have been recorded for stimulated endocrine cells. Solubilization of the actin array may be facilitated by an actin-severing protein (41).

5. The Fusion Pore

Electrophysiological measurements of exocytosis have predicted that the merging of secretory-vesicle membrane with plasma membrane is preceded by the formation of a channel, the so-called fusion pore (42). One line of evidence for such a pore comes from amperometry. When the release of a biogenic amine from a secretory granule is measured, the massive efflux of granule content is preceded by a small "step" of amine release like that predicted if the inside of the secretory granule were connected to the outside by a small channel or hole of nanometer diameter (43). A second indication of the reversible formation of a channel is "capacitance flicker." Exocytosis can be detected as a sudden increase in membrane capacitance; occasionally, however, a sudden increase is followed by a sudden decrease of exactly the same amplitude. These data are consistent with a transient and reversible fusion of secretory granule and plasma membranes. A third line of evidence supporting the idea of a fusion pore is that the current that flows through the fusion pore as the secretory-granule membrane discharges its membrane potential. From measurements of the conductance of the channel, estimates of its size can be made. When it first forms, the fusion pore seems to form a channel of about the size of a large ion channel.

The molecular nature of the fusion pore, if it exists, is unclear. Fusion between a membrane-covered virus and the plasma membrane has been studied extensively for influenza virus. The viral protein triggers fusion by undergoing a conformational change that extends a 16- to 23-amino acid residue "fusion peptide," a **hydrophobic** sequence that is essential for fusion (44). Extension of the fusion peptide requires a helical hairpin to be converted to a triple-stranded coiled-coil domain (45). The three SNARE proteins, VAMP/synaptobrevin, syntaxin, and SNAP-25, have coiled-coil domains that initiate oligomer formation. VAMP also has a small alpha-helical domain that resembles a fusion peptide. There is no experimental evidence, however, that the SNAREs form a fusion pore. Nor is it clear whether the initial hole is exclusively due to rearrangement of the lipid bilayer or to a proteinaceous channel. In influenza virus-mediated fusion, a hemifusion state is formed if the transmembrane tail of the fusion protein is replaced by a glycophosphatidylinositol anchor (46). This was interpreted to mean that the hemifusion state is an intermediate in virus-induced fusion.

Logically, membrane fusion must be initiated by the formation of one or several small holes through the membrane of both the exocytotic vesicle and the cell surface. Electrophophysiologically, the evidence for the reversible formation of such a hole is excellent. As yet, molecular knowledge lags far behind the physiology.

Bibliography

1. T. L. Burgess and R. B. Kelly (1987) Annu. Rev. Cell Biol. **3**, 243–293.
2. H. Winkler (1993) J. Anat. **183**, 237–252.
3. M. E. Finbow and M. A. Harrison (1997) Biochem. J. **324**, 697–712.
4. I. Mellman (1996) Annu. Rev. Cell Develop. Biol. **12**, 575–625.
5. C. R. Hopkins, A. Gibson, M. Shipman, D. K. Strickland, and I. S. Trowbridge (1994) J. Cell Biol. **125**, 1265–1274.
6. O. Cremona and P. De Camilli (1997) Curr. Opin. Neurobiol. **7**, 323–330.
7. S. Rea and D. E. James (1997) Diabetes **46**, 1667–1677.
8. J. M. Finnegan, K. Pihel, P. S. Cahill, L. Huang, S. E. Zerby, A. G. Ewing, R. T. Kennedy, and R. M. Wightman (1996) J. Neurochem. **66**, 1914–1923.
9. E. Neher and A. Marty (1982) Proc. Natl Acad. Sci. USA **79**, 6712–6716.
10. J. M. Fernandez, E. Neher, and B. D. Gomperts (1984) Nature **312**, 453–455.
11. W. J. Betz and G. S. Bewick (1993) J. Physiol. **460**, 287–309.
12. J. K. Angleson and W. J. Betz (1997) Trends Neurosci. **20**, 281–287.
13. J. C. Hutton (1997) Proc. Natl. Acad. Sci USA **94**, 10490–10492.
14. J. E. Rothman (1996) Protein Sci. **5**, 185–194.
15. W. S. Trimble, D. M. Cowan, and R. H. Scheller (1988) Proc. Natl. Acad. Sci. USA **85**, 4538–4542.
16. M. Baumert, P. R. Maycox, F. Navone, P. De Camilli, and R. Jahn (1989) EMBO J. **8**, 379–384.
17. M. K. Bennett, J. E. Garcia-Arraras, L. A. Elferink, K. Peterson, A. M. Fleming, C. D. Hazuka, and R. H. Scheller (1993) Cell **74**, 863–873.
18. G. A. Oyler, G. A. Higgins, R. A. Hart, E. Battenberg, M. Billingsley, F. E. Bloom, and M. C. Wilson (1989) J. Cell Biol. **109**, 3039–3052.
19. T. Sollner, M. K. Bennett, S. W. Whiteheart, R. H. Scheller, and J. E. Rothman (1993) Cell **75**, 409–418.
20. M. K. Bennett and R. H. Scheller (1993) Proc. Natl. Acad. Sci. USA **90**, 2559–2563.
21. K. L. Schulze, K. Broadie, M. S. Perin, and H. J. Bellen (1995) Cell **80**, 311–320.
22. K. Broadie, A. Prokop, H. J. Bellen, C. J. O"Kane, K. L. Schulze, and S. T. Sweeney (1995) Neuron **15**, 663–673.
23. G. Schiavo, O. Rossetto, and C. Montecucco (1994) Sem. Cell Biol. **5**, 221–229.
24. S. R. Pfeffer (1996) Annu. Rev. Cell Develop. Biol. **12**, 441–461.
25. L. Edelmann, P. I. Hanson, E. R. Chapman, and R. Jahn (1995) EMBO J. **14**, 224–231.
26. J. Pevsner, S. C. Hsu, and R. H. Scheller (1994) Proc. Natl. Acad. Sci. USA **91**, 1445–1449.
27. E. P. Garcia, E. Gatti, M. Butler, J. Burton, and P. De Camilli (1994) Proc. Natl. Acad. Sci.

USA **91**, 2003–2007.
28. J. Hay and R. H. Scheller (1997) Curr. Opin. Cell Biol . **9**, 505–512.
29. A. Banerjee, V. A. Barry, B. R. DasGupta, and T. F. J. Martin (1996) J. Biol. Chem. **271**, 20223–20226.
30. C. Ungermann, B. J. Nichols, H. R. Pelham, and W. Wickner (1998) J. Cell Biol. **140**, 61–69.
31. A. Salminen and P. J. Novick (1987) Cell **49**, 527–538.
32. H. Stenmark, G. Vitale, O. Ullrich, and M. Zerial (1995) Cell **83**, 423–432.
33. D. R. TerBush, T. Maurice, D. Roth, and P. Novick (1996) EMBO J. **15**, 6483–6494.
34. Y. Kee, J. S. Yoo, C. D. Hazuka, K. E. Peterson, S. C. Hsu, and R. H. Scheller (1997) Proc. Nat. Acad. Sci. USA **94**, 14438–14443.
35. R. Llinas, M. Sugimori, and R. B. Silver (1995) Neuropharmacology **34**, 1443–1451.
36. S. V. Popov and M. M. Poo (1993) Cell **73**, 1247–1249.
37. M. Geppert, Y. Goda, R. E. Hammer, C. Li, T. W. Rosahl, C. F. Stevens, and T. C. Sudhof (1994) Cell **79**, 717–727.
38. K. Ann, J. A. Kowalchyk, K. M. Loyet, and T. F. Martin (1997) J. Biol. Chem. **272**, 19637–19640.
39. J. C. Hay, P. L. Fisette, G. H. Jenkins, K. Fukami, T. Takenawa, R. A. Anderson, and T. F. Martin (1995) Nature **374**, 173–177.
40. P. De Camilli, S. D. Emr, P. S. McPherson, and P. Novick (1996) Science **271**, 1533–1539.
41. L. D. Hernandez, L. R. Hoffman, T. G. Wolfsberg, and J. M. White (1996) Annu. Rev. Cell Develop. Biol. **12**, 627–661.
42. S. Muallem, K. Kwiatkowska, X. Xu, and H. L. Yin (1995) J. Cell Biol. **128**, 589–598.
43. M. Lindau and W. Almers (1995) Curr. Opin. Cell Biol. **7**, 509–517.
44. A. Albillos, G. Dernick, H. Horstmann, W Almers, G. Alvarez de Toledo, and M. Lindau (1997) Nature **389**, 509–512.
45. C. M. Carr and P. S. Kim (1993) Cell **73**, 823–832.
46. G. W. Kemble, T. Danieli, and J. M. White (1994) Cell **76**, 383–391.

Exon Shuffling

When intervening sequences were discovered to split eukaryotic **genes** into segments coding for protein, the intervening sequences were named *introns* and the coding regions, exons (1) (see **Introns/exons**). Since then, heated discussion has ensued concerning the evolutionary origin and biological significance of introns in eukaryotes, because almost all of the prokaryotic genes lack introns, and the introns have no known role.

Gilbert (1) proposed a scenario in which introns simply connect neighboring exons to each other in the genome; consequently, genetic recombination would not harm the coding portions of genes if it took place within the intron regions. Such recombination within introns would facilitate the shuffling of exons, to create new exon combinations and lead to the emergence of new genes with new functions. This is the “exon shuffling” theory (see also Gene Splicing).

Exon shuffling is related to the present controversy regarding the “early” versus “late” intron theories. The early-intron theory maintains that introns existed in the ancestor genomes of prokaryotes and eukaryotes, but that all those in prokaryotes were deleted by some unknown mechanism. On the other hand, the late-intron theory contends that introns could have been inserted, similar to transposable elements, into eukaryotic genomes quite recently, at least after the **divergence** of eukaryotes and prokaryotes. This theory is based on the observation that there are many genes in which the locations of introns are not conserved among vertebrates, invertebrates, and plants (2).

If the early-intron theory is correct, exon shuffling probably had a significant role in the creation of new genes. If the late-intron theory is right, however, exon shuffling might have been significant only after the introns were inserted. The controversy remains to be resolved.

The **domain** shuffling theory is similar to the exon shuffling theory, but in sharp contrast, maintains that the unit of shuffling during evolution is a functional protein domain, not an exon. The functional domain does not necessarily correspond to the exon. Although there are some cases where it does, most functional domains consist of more than one exon or occupy only part of a large exon. For example, the Kringle domain is known to have been shuffled as a unit during evolution. The Kringle domain is a characteristic supersecondary structure frequently found in the serine proteinases involved in the blood clotting system. Even though the Kringle domain is, in most cases, split into three exons by two introns, those found in various proteins are almost always complete forms and never found as parts corresponding to the exons. At present, however, there is no known genetic mechanism for facilitating domain shuffling, and domain shuffling seems to have taken place in prokaryotes as well (3).

Bibliography

1. W. Gilbert (1978) Nature **271**, 501.
2. J. D. Palmer and J. M. Logsdin (1991) Curr. Opin. Gen. Devel. **1**, 565–570.
3. T. Gojobori and K. Ikeo (1994) Phil. Trans. Roy. Soc. Lond. B **344**, 411–415.

Expansibility

The expansion of a protein molecule with increasing temperature reflects its atomic packing and flexibility, as does its compressibility with increasing pressure. X-ray crystallography studies indicate that both the crystal lattice and protein structure expand with increasing temperature. For myoglobin, a volume expansion of 5% of the crystal lattice and 3% in the protein molecule occurred as the temperature increased from 80 to 300 K, which corresponds to a thermal expansion coefficient of 1.15×10^{-4} K^{-1} (1). **Ribonuclease A** exhibited a smaller expansion 0.9% for a temperature increase from 98 to 320 K (2). It is likely that a more compressible protein will also be more thermally expansible. It is believed that the observed expansions of proteins with temperature are due to motions of secondary structure and exposed surface loops and to a decrease in local atomic packing density (see van der Waals Surface, Volume). Thermal expansion of a protein is not uniform over the molecule, just as in the case of contraction by pressure.

It is known that the apparent and partial specific volumes (v_2) of proteins in aqueous solution are linearly dependent on temperature in the range of 4 to 45°C. Positive values for $d\,v_2/dT$ of (2.5 to 10×10^{-4} $cm^3\ g^{-1}\ K^{-1}$ have been reported, with the majority lying between (3.5 to 5) $\times 10^{-4}$ $cm^3\ g^{-1}\ K^{-1}$. These values are greater than the expansion coefficient found for the X-ray crystal structure.

If the thermal expansion of crystal structure is caused by the cavities, the positive values of dv_2/dT for folded proteins would be dominantly attributed to the hydration effect, ie, a volume increase due to dehydration of protein molecules on elevating the temperature (see Partial Specific (Or Molar) Volume). The temperature effect of v_2 is still pronounced for amino acids and small **peptides**, probably due to a large dehydration effect: dv_2/dT is 1.3×10^{-3} cm^3 g^{-1} K^{-1} for glycine and 7.3×10^{-4} cm^3 g^{-1} K^1 for triglycine. In this sense, an unfolded protein is expected to have a larger dv_2/dT value than a folded one because the accessible surface area (amount of hydration) increases on denaturation. Hawley reported that dv_2/dT increases by 0.18×10^{-4} cm^3 g^{-1} K^{-1} and 0.51×10^{-4} cm^3 g^{-1} K^{-1} on pressure denaturation of ribonuclease A (pH 2.0) and chymotrypsinogen (pH 2.07), respectively (3). However, the temperature effects on v_2 at high pressures and high concentration of denaturants, above where conformational changes or denaturation take place, are complex since the volume change of hydration Dv_{sol} may involve the contributions of changes in water structure and preferential solvent interactions.

Bibliography

1. H. Frauenfelder et al. (1987) Biochemistry **26**, 254–261.
2. R. F. Tilton Jr., J. C. Dewan, and G. A. Petsko (1992) Biochemistry **31**, 2469–2481.
3. S. A. Hawley (1971) Biochemistry **10**, 2436–2442.

Expressed Sequence Tag

An expressed sequence tag (EST) is a short stretch of **DNA** sequence that is used to identify an expressed **gene**. Although EST sequences are usually only 200 to 500 nucleotides in length, this is generally sufficient to identify the full-length **complementary DNA** (cDNA). ESTs are generated by sequencing a single segment of random **clones** from a **cDNA library**. A single sequencing reaction and automation of DNA isolation, sequencing, and analysis have allowed the rapid determination of many ESTs. Now, the majority of the sequences in sequence databases are ESTs. Although most ESTs have been isolated from humans, a large number of ESTs have been isolated from model organisms, such as *Caenorhabditis elegans* (1), *Drosophila*, rice (2), and *Arabidopsis* (3). ESTs are also being isolated from more exotic organisms, such as *Entamoeba histolytica* (4) and *Leishmania major promastigotes* (5). ESTs have numerous uses, from **genetic mapping** to analyzing gene expression, and the number of ESTs isolated from different organisms will continue to rise rapidly.

1. Generation of ESTs

The most important step in generating of ESTs is producing a cDNA library. First, messenger RNA (mRNA) is extracted from the material being studied and is used as a template by **reverse transcriptase** for cDNA synthesis. Then the DNA is **cloned** into a suitable **vector** to produce a cDNA library. Random clones are isolated from the library, and one or both ends are sequenced by single-pass sequencing.

The source of the mRNA is an organism, tissue, or cell line grown under normal conditions or treated with hormones, drugs, heat, etc. The source of the starting material depends on the type of genes to be identified and the reason for generating the ESTs. EST analysis is used to find previously undiscovered tissue-specific **genes** or to tag as many different expressed genes as possible. It is also used to examine the relative abundance of expressed genes. Libraries used for the first two types of studies are often normalized, so that highly-expressed genes and rare genes are represented more equally in the library or subtracted to reduce or eliminate the number of highly abundant clones (see Subtractive Hybridization). An alternative to normalizing or subtracting libraries is to sequence a small number of ESTs from as many different tissue types and treatments as possible because different types of genes are highly expressed under different circumstances.

It is useful if the cDNAs in the library are cloned directionally, so that ESTs are isolated specifically from either the 5′- or the 3′-end of the cDNA. 3′-ESTs often represent the 3′-untranslated region of the mRNA and are used to separate members of gene families that have similar coding sequences, whereas 5′-ESTs generally represent coding sequence and give a better idea of the type of gene being expressed.

If the starting material for mRNA isolation is limiting, cDNA minilibraries suitable for EST analysis are generated by arbitrarily primed RT-PCR (6).

2. The Multitudinous Uses of ESTs

2.1. Obtaining Full-Length cDNAs from ESTs

An EST is useful because it represents an expressed gene. Once an EST has been identified, it is usually straightforward to obtain the full sequence of the "tagged" cDNA. Some sources provide EST DNA that is used in further studies. Alternatively, the EST sequence is used to design PCR primers or hybridization probes for cloning the full-length cDNA (see Cloning). Another strategy is "virtual cloning", where computer analysis is used to array **homologous** ESTs and any other sequences from the same gene (7). Once isolated, then the full-length cDNA is used in mutagenesis, **transgenic**, and expression studies to analyze the gene function.

2.2. Genome Analysis and Mapping with ESTs

Many organisms, for example, humans, *Arabidopsis*, and *C. elegans*, will have their entire genomic DNA sequenced in the relatively near future, and certain genomes, such those of *Saccharomyces cerevisiae* and various **bacteria**, have already been entirely sequenced. In the meantime, EST analysis provides a rapid way to identify expressed genes. Now, it is not possible to predict coding sequences in genomic DNA reliably from sequence information alone. Even when complete genomic sequences are available, ESTs are useful in analyzing the genomic sequence, for example by verifying putative coding sequences and confirming **intron** and exon boundaries. They are also helpful in distinguishing pseudogenes from real genes and in identifying **alternatively spliced** transcripts, which could never be predicted from the genomic sequence alone.

ESTs are also used to provide markers for genomic mapping by converting them into "sequence tagged sites" (STS). An STS is a set of PCR primers that identifies a single gene, and STS primers are designed from the EST sequence (8). An STS can be mapped to a specific region of the genome, and if DNA contigs are available for the genome under study, the STS can specify a genomic clone. Mapping of ESTs to genomic clones will provide a map of expressed genes for each clone and, in humans, these maps can be used to identify candidate genes for inherited human diseases that have been mapped to chromosomal regions by pedigree analysis.

2.3. Gene Expression Studies Using ESTs

As mentioned previously, gene expression in different organisms, tissues, or cells, before or after different treatments, can be studied by surveying ESTs isolated from libraries created from different mRNA sources. If nonnormalized and unsubtracted libraries are used to isolate ESTs, the frequency of isolation of a particular EST indicates the relative message abundance of the tagged gene (9). It is also possible to isolate novel tissue-specific genes by merely searching EST databases (10).

2.4. Rapid Identification of New Genes and Gene Families

As of 1998, the majority of ESTs in the databases represent genes that have not been previously identified. Traditionally, gene sequences have been obtained one at a time, first by isolating a protein, by identifying a mutant and cloning the mutated gene by complementation, or by positional cloning (see Cloning). Compared with these methods, generating ESTs is a very rapid method for identifying new gene sequences.

EST database searches also provide a rapid method for finding genes similar to a gene of interest. Methods, such as PCR, using degenerate primers, or **hybridization** at low stringency also enable the identification of similar genes, but these methods are often not as successful as database searches. Databases can be searched by using either nucleic acid sequences or protein sequences. Protein comparison searches are often more fruitful because protein sequences are better conserved. Additionally, databases can be used to search for similar genes among all the represented organisms simultaneously, thus facilitating comparative studies. Once similar genes have been identified, they can be translated into protein sequences and the database searched again to find the sequences most similar to this second set of genes. Thus it is possible to identify large families of related genes rapidly by EST database analysis.

2.5. Using ESTs to Clone Specific Genes

In humans, one main goal of genomic research and EST analysis is to aid in identifying and cloning human genes related to diseases. Various groups have begun to look between species to find candidate human disease genes. One group used an EST database search to identify human cDNAs homologous to previously cloned *Drosophila* genes that have an interesting developmental mutant **phenotype** (11). Then the human sequences were mapped by several methods, and the positions of the cDNAs compared with the map positions of human disease genes. Some of the cDNAs mapped to regions containing human disease genes that cause symptoms similar to the defects in the corresponding *Drosophila* mutant genes. Thus these cDNAs are candidates for the disease genes, and further studies can be undertaken to determine whether the cDNAs and the disease genes are one and the same. Another group is systematically identifying novel human ESTs related to known genes in a variety of model organisms (12). Then the ESTs are mapped to both human and mouse maps. Again, such genes can provide candidates for human disease genes, thereby potentially speeding up their cloning and aiding in their analysis by providing a model system for further studies.

ESTs are extremely useful tools for gene analysis in organisms besides humans, although to date most effort has been spent identifying human ESTs. In any organism where a mutation has been mapped to a certain genomic region or to a genomic clone, ESTs mapping to the same region identify candidate genes. In more unusual organisms, where few genes have been previously isolated, EST analysis provides a rapidly generated survey of the types of genes expressed by the organism and is used, for example, to isolate novel genes from pathogenic organisms (4, 5). In **plants**, the weed *Arabidopsis* is often used as a model system for gene isolation. EST database searches provide a rapid means of isolating similar genes from important crop plants, in much the same way that interesting genes from model systems are used to isolate corresponding genes from humans and mice. STSs from ESTs representing important plant genes could be used as markers in selective breeding programs.

3. Some Recent Twists on EST Generation

A technique termed *serial analysis of gene expression* (SAGE) has recently been developed to perform some of the functions of EST analysis (13). Short diagnostic sequence tags (9 to 10 bp) are randomly isolated from a tissue, concatenated, cloned, and sequenced. This method allows extremely rapid identification of thousands of genes and is used either to identify new genes or to analyze relative levels of gene expression. SAGE may prove quite useful in rapid surveys of gene expression differences between tissues or between developmental and disease states. ESTs still have many advantages over this method, however. The production and concatenation of the tags are somewhat cumbersome, and the small amount of sequence information in the tags precludes many of the interesting uses that have been found for ESTs.

An ingenious method has been developed to tag promoter-proximal sequences in mouse embryonic **stem (ES) cells** . Using a gene-trap retrovirus shuttle vector (14). A large number of ES cells were selected for neomycin resistance, indicating that the retrovirus containing a promoterless neomycin-resistance gene had inserted next to the promoter of an expressed gene. These neomycin-resistant ES cells were cloned. Some cloned cells were frozen and others used to extract DNA. The DNA flanking the retrovirus was isolated and sequenced to provide a *promoter-proximal sequence tag* (PST). PSTs are ESTs derived from genomic DNA rather than cDNA, and they are used similarly to screen sequence databases and to make STSs for mapping. However, they also have an additional advantage. Each PST represents a specific ES cell line harboring a potentially disrupted gene, and mutant ES cells are used to generate mutant mouse strains (15). PSTs thus allow rapid progression from sequence analysis of a gene to analysis of its function in a mutant mouse.

4. The Future of ESTs

ESTs have already proved useful in rapidly identifying novel genes, providing markers for mapping, providing candidate disease genes, and for analyzing gene expression. Because the generation of ESTs proceeds faster than the functional identification and analysis of the genes that they represent, much future research will be directed toward determining functions for the newly identified genes and gene families. The cDNAs identified by EST analysis can be used in standard experiments designed to elucidate their cellular and developmental functions. As so many novel genes have been and are being identified, some researchers are looking for more rapid ways to analyze function or expression of large numbers of genes. A recent innovation is the use of cDNA (16) or oligonucleotide (17) microarrays that represent large numbers of genes or whole genomes. Hybridization to microarrays of labeled mRNA samples isolated from different tissues, mutant backgrounds, or developmental or growth states allows analysis of changes in gene expression for a large number of genes simultaneously. Other researchers have developed a system for monitoring the effects of gene disruption on growth in yeast for many genes simultaneously (18). The development of additional techniques for global analysis of gene expression and function will be essential for rapidly characterizing the wealth of new genes identified by EST studies.

Bibliography

1. W. R. McCombie et al. (1992) Nature Genet. **1**, 124–131.
2. K. Yamamoto and T. Sasaki (1997) Plant Mol. Biol. **35**, 135–144.
3. M. Delseny, R. Cooke, M. Raynal, and F. Grellet (1997) FEBS Lett. **405**, 129–132.
4. A. Azam, J. Paul, D. Sehgal, J. Prasad, S. Bhattacharya, and A. Bhattacharya (1996) Gene **181**, 113–116.
5. M. P. Levick, J. M. Blackwell, V. Conner, R. M. Coulson, A. Miles, H. E. Smith, K. L. Wan, and J. M. Ajioka (1996) Mol. Biochem. Parasitol. **76**, 345–348.
6. E. D. Neto, R. Harrop, R. Correa-Oliveira, R. A. Wilson, S. D. Pena, and A. J. Simpson (1997) Gene **186**, 135–142.
7. S. D. Rounsley, A. Glodek, G. Sutton, M. D. Adams, C. R. Somerville, J. C. Venter, and A. R. Kerlavage (1996) Plant Physiol. **112**, 1177–1183.
8. R. Berry et al. (1995) Nature Genet. **10**, 415–423.
9. K. Okubo, N. Hori, R. Matoba, T. Niiyama, A. Fukushima, Y. Kojima, and K. Matsubara (1992) Nature Genet. **22**, 173–179.
10. G. Vasmatzis, M. Essand, U. Brinkmann, B. Lee, and I. Pastan (1998) Proc. Natl. Acad. Sci. USA **95**, 300–304.
11. S. Banfi et al. (1996) Nature Genet. **13**, 167–174.
12. D. E. Bassett Jr., M. S. Boguski, F. Spencer, R. Reeves, S. Kim, T. Weaver, and P. Hieter (1997) Nature Genet. **15**, 339–334.
13. V. E. Velculescu, L. Zhang, B. Vogelstein, and K. W. Kinzler (1995) Science **270**, 484–487.

14. G. G. Hicks, E.-G. Shi, X.-M. Li, C.-H. Li, M. Pawlak, and H. E. Ruley (1997) Nature Genet. **16**, 338–343.
15. M. R. Capecchi (1989) Science **244**, 1288–1292.
16. M. Schena, D. Shalon, R. W. Davis, and P. O. Brown (1995) Science **270**, 467–470.
17. D. J. Lockhart, et al. (1996) Nature Biotechnol. **14**, 1675–1680.
18. V. Smith, K. N. Chou, D. Lashkari, D. Botstein, and P. O. Brown (1996) Science **274**, 2069–2074.

Suggestions for Further Reading

19. D. Gerhold and C. T. Caskey (1996) It"s the genes! EST access to human genome content, BioEssays **18**, 973–981. Excellent review of ESTs, databases and their use, and caveats.
20. E. F. Kirkness (1996) "Assessment of human gene diversity and expression patterns using expressed sequence tags. In" *Essays in Biochemistry* (D.K. Apps, ed.), Portland Press, London, U.K., pp. 1–9. Excellent clear review.
21. M. A. Marra, L. Hillier, and R.H. Waterston (1998) Expressed sequence tags-ESTablishing bridges between genomes. Trends Genet. **14**, 4–7. Good short review.

Expression Libraries

An expression library is a collection of DNA molecules that can be expressed *en masse* through enzymatic methods to yield a population of DNA, RNA, or protein products that can be screened for individuals displaying desirable properties. The DNA sequences within the library can be of natural or synthetic origin. The advantage of screening expression libraries constructed from the genome or complementary DNA (see Genomic Libraries and cDNA Libraries) is that the expression products derived are usually biologically relevant. In contrast, synthetic DNA expression libraries may yield expression products that are not found in nature. However, there are two major advantages to screening synthetic DNA expression libraries. First, the expression products that are selected for a particular purpose may perform better than natural biopolymers. Second, a great deal of information is obtained by screening synthetic libraries of known composition, because the distribution of sequences selected compared with those not selected provides structure–activity relationship (SAR) data describing molecular interactions characteristic of the target being screened.

Expression libraries contain genomic or cDNA sequences cloned into expression vectors, which are plasmids or bacteriophage genomes that have been engineered to contain regulatory elements governing expression of foreign DNA inserts. For example, vectors containing a **promoter** sequence of **T7 phage** will initiate RNA transcription at a fixed position and direction. Once transcription is initiated, the T7 **RNA polymerase** will continue making an RNA copy of the DNA coding strand, including any foreign DNA that is encountered, in progressive fashion until a T7 terminator sequence is read (by convention, the coding strand is the top strand in a 5′ to 3′, left to right, double-stranded gene depiction). The resulting polymer that is formed is thus an RNA transcript of the DNA template. Such a DNA library can only be expressed in cells that also contain the enzyme T7 RNA polymerase. Typically, the gene encoding the T7 RNA polymerase is engineered to be inducible by the addition of a soluble sugar analogue, such as **IPTG**, so that library RNA expression can be co-induced at appropriate times in the screening process. RNA expressed from DNA libraries may be the intended chemical entity to be screened, or the RNA molecules may serve as templates for the translation of protein products. If the expressed RNA molecules contain suitable prokaryotic and/or eukaryotic ribosome recognition sequences, ribosome-mediated **protein biosynthesis** will initiate at an AUG start codon. The result will be a protein molecule encoded by the original DNA template. In general, it is easiest to screen protein expression libraries when the transcription and translation occur *in vivo* using a suitable host cell. However, in certain circumstances it may be advantageous to perform the protein expression *in vitro*, using cell-free translation extracts that contain the requisite protein synthesis machinery. In either case, the population of expressed proteins can be screened for any of a range of phenotypic properties, including antibody reactivity, affinity to a target molecule, or catalysis.

The ability to engineer, at the DNA level, additional useful sequences into protein reading frames provides a powerful means of generating **fusion proteins** with desirable properties. Modern expression libraries contain many types of tags or fusion domains that facilitate **library** screening and downstream manipulation of individual clones. There are at least four types of protein fusion moieties commonly available. This list is not intended to be exhaustive but instead to illustrate the power of the technology. First, epitope tags are typically short amino acid segments fused to either the *N*- or *C*-terminus of the cloned protein. An epitope tag provides ready-made immunoreactivity to the cloned gene product through commercially available antibodies. Epitope tags are useful in both detection and purification of cloned gene products. Second, like epitope tags, affinity tags are amino acid sequences fused to either terminus of the cloned protein. The most common use of affinity tags is in affinity purification, although detection can also be performed through the tag. One commonly used affinity tag is the 6-His tag, which is simply a sequence of six **histidine** residues that bind with high affinity and specificity to nickel; therefore, 6-His fusion proteins can be purified from all other cellular proteins by affinity chromatography over nickel-agarose (1). Third, domain tags are independent units of structure and function that maintain or enhance certain activities of the proteins from which they were derived. Domain tags are useful for protein purification and detection. Common examples include **glutathione-*S*-transferase** (GST), which enables facile purification over glutathione-agarose resins (2), and **green fluorescent protein** (GFP), which is an autofluorescent protein that can be monitored in both quantitative and localization assays (3). Fourth, cleavage sequences are commonly introduced between the fusion tags and the cloned genes so that the tags can be removed following affinity purification. Cleavage elements are most commonly **proteinase** recognition sequences, although self-cleaving protein domains called inteins are becoming increasingly available (4) (see Protein Splicing).

A special type of cDNA expression library called the **two-hybrid system** (5) deserves special mention because it illustrates a powerful coupling of molecular engineering with combinatorial approaches to investigating protein function. The purpose of screening two hybrid libraries is to discover proteins that interact with a protein of interest. The system is termed “two-hybrid” because two separate plasmids have been engineered to express hybrid versions of transcriptional activators such as the yeast GAL4 protein. Normally, the GAL4 protein contains both a **DNA-binding** domain and a transcriptional activation domain. When intact GAL4 binds to its DNA recognition sequence, the transcriptional activation domain promotes transcription of adjacent gene sequences. In the two-hybrid system, the GAL4 DNA binding domain is expressed as a hybrid with the protein of interest, termed the “bait”. A second vector containing the GAL4 transcriptional activation domain is used to construct a library of cDNAs such that each cDNA is expressed as a hybrid protein fused to the GAL4 transcriptional activation domain. Neither of the hybrid GAL4 domains alone can promote transcription of a reporter gene, nor do they interact spontaneously. However, if one of the proteins expressed as a fusion with the GAL4 transcriptional activation domain happens to form a **protein-protein interaction** with the bait protein, the two GAL4 domains are brought into proximity where they can activate expression of a reporter gene. Many variations of this powerful method have since appeared, including two-hybrid systems for mammalian cells (6) and three-hybrid systems for detecting protein-nucleic acid interactions (7).

The other major type of expression library uses synthetic DNA to express DNA, RNA, or protein products for screening. Expression of RNA and protein can be mediated through cloning vectors in similar fashion to the cDNA expression libraries. Examples of cloned synthetic DNA expression libraries include **phage display** and protein engineering projects in which portions of a protein-coding sequence are randomized synthetically to derive novel proteins with altered properties. Alternatively, the synthetic DNA library may be maintained as oligonucleotides that are replicated through **PCR** or some other enzymatic amplification strategy. Expression of these types of libraries always occurs *in vitro* and usually employs a synthetic phage T7 promoter to mediate expression of RNA. Thus, RNA copies of the DNA library are produced upon incubation with purified T7 RNA polymerase and ribonucleoside triphosphate (rNTP) building blocks. The resulting single-stranded RNA can be screened for affinity to specific molecular targets (RNA aptamer libraries) or for catalytic activity (ribozyme libraries). Similarly, single-stranded DNA copies can be prepared from DNA aptamer libraries by removing one of the two DNA strands, which has been previously tagged with biotin, by **denaturation** and affinity chromatography over a streptavidin matrix. DNA aptamers are similar in many ways to RNA aptamers, but they are more resistant to chemical and enzymatic degradation. Finally, peptide aptamers can in principle be prepared by *in vitro* translation of RNA transcripts from oligonucleotide libraries, although this method is not commonly employed.

See also Combinatorial Libraries, Libraries, Combinatorial Synthesis, Affinity Selection, DNA Libraries, Genomic Libraries, cDNA Libraries, Peptide Libraries, and Phage Display Libraries.

Bibliography

1. J. Schmitt, H. Hess, and H. G. Stunnenberg (1993) Mol. Biol. Rep. **18**, 223–230.
2. D. B. Smith and K. S. Johnson (1988) Gene **67**, 31–40.
3. A. Crameri, E. A. Whitehorn, E. Tate, and W. P. C. Stemmer (1996) Nat. Biotechnol. **14**, 315–319.
4. S. Pietrokovski (1994) Protein Sci. **3**, 2340–2350.
5. C. T. Chien, P. L. Bartel, R. Sternglanz, and S. Fields (1991) Proc. Natl. Acad. Sci. USA **88**, 9578–9582.
6. Y. Luo, A. Batalao, H. Zhou, and L. Zhu (1997) Biotechniques **22**, 350–352.
7. D. J. SenGupta, B. Zhang, B. Kraemer, P. Pochart, S. Fields, and M. Wickens (1996) Proc. Natl. Acad. Sci. USA **93**, 8496–8501.

Expression Systems

Expression systems are used for the production of protein from recombinant DNA molecules (see Recombinant Proteins). They are of widespread use in industry, health care, and scientific research because of their flexibility and ability to achieve production levels exceeding those of the native source of the protein. An expression system consists of a **vector** carrying the gene encoding the protein of interest, along with the sequences necessary for transcription of the DNA into messenger RNA and translation of the mRNA into protein, plus a host providing the **enzymatic** machinery for carrying out these processes. In a homologous expression system, the gene to be expressed derives from the same species as the host whereas, in a heterologous expression system, the gene to be expressed and the host are of different origin.

1. Design of the expression vector

An expression vector not only provides the components necessary for cloning, transfer, stability, and multiplication of recombinant DNA but it also delivers the elements required for correct transcription of DNA into functional mRNA and efficient translation of mRNA into the desired protein. However, the importance of the basic elements controlling gene dosage and selection should not be ignored in the design of an expression system. A generalized **prokaryotic** expression vector is shown in Figure 1.

Figure 1. Generalized prokaryotic expression vector. The figure shows a typical prokaryotic expression vector, with a selection marker gene allowing stable maintenance of the plasmid, an **origin of replication** controlling the **copy number** of the vector, and a promoter and a ribosomal binding site positioned upstream of the gene of interest. One or more transcriptional termination sequences are positioned downstream. Furthermore, a eukaryotic expression vector would contain an extra origin of replication and an extra selectable marker to allow replication and maintenance in both *E. coli* and the eukaryotic host. The transcriptional termination signal would include a polyadenylation signal.

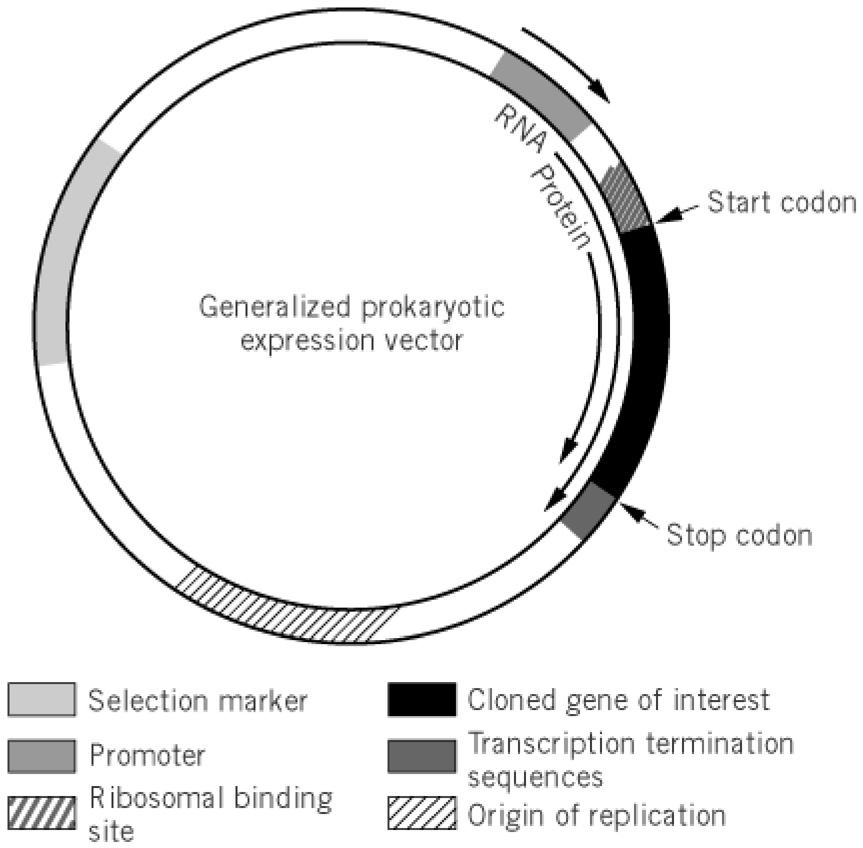

A **promoter** is a region of DNA recognized by an **RNA polymerase** and is the prerequisite for initiation of transcription. Promoters consist of characteristic sequence elements. In general, promoters from prokaryotes and **eukaryotes** differ, and a common organization pattern can be given for each. However, there can be pronounced differences between species, and more subtle variations are found within the same species, giving rise to promoters with different strengths and control mechanisms.

The strength of a promoter determines the frequency with which a gene is transcribed by controlling the rate at which the RNA polymerase and the promoter form the initiation complex. However, the strength is governed not only by the interaction with the RNA polymerase. Other proteins, so-called transcriptional activators and repressors, bind to the promoter region and regulate the process of transcriptional activation. Often, eukaryotic expression vectors provide transcriptional enhancer elements as well.

The ideal promoter for the expression of a recombinant protein not only generates the synthesis of high levels of mRNA but, even more important, it should be inducible, ie, the experimenter should be able to control its activity. However, only a few inducible promoters are tightly controlled, so that some transcription occurs even in the uninduced state. The overproduction of a protein will most often influence the cell in a negative manner and can be detrimental in the most severe cases, where the protein of interest is toxic to the host (see Poison Sequence). If this seems to be a problem, it may prove advantageous to use a weaker promoter under tighter control. Also, when overexpression seems to outstrip the host's post-translational modification, **molecular chaperone**, and proofreading systems, the use of a weaker promoter may be beneficial. For most expression systems, both constitutive and inducible promoters are available. The "on" state of the best inducible promoters can be regulated, thereby providing a means of optimization (1).

Some prokaryotic expression vectors contain antitermination elements, which stabilize the RNA polymerase on the DNA template to ensure optimal elongation of the transcript. Transcriptional terminators positioned at the 3′-end of the expressed gene restrict the size of the mRNA, minimize the sequestering of RNA polymerase, and isolate the plasmid's replication functions, thereby stabilizing the **plasmid**. Eukaryotic mRNAs are processed more extensively than prokaryotic mRNA, including such processes as **splicing** and the addition of **poly-A** tails. The signals for these steps are provided by eukaryotic expression vectors at positions downstream of the cloned gene.

The degradation of mRNA allows a biological system to adapt to changes in the environment (see RNA Degradation In Vitro). Yet the aim of the gene expression systems is to maintain a high level of mRNA for the gene of interest during its expression. The stability of mRNA can, in some cases, be increased by insertion of sequences that fold into stable **secondary structures** at the ends of the mRNA, thereby "capping" the mRNA.

The initiation of the translational process requires a **ribosomal** binding site, where the small subunit of the ribosome binds to the mRNA to form the initiation complex. The first triplet of nucleotides to be translated is the start codon, which usually has the sequence AUG. In prokaryotes, a Shine–Dalgarno sequence is positioned 4 to 13 nucleotides upstream of the start codon. This purine-rich sequence base-pairs with the 3′-end of the 16 S ribosomal RNA (rRNA) and thereby regulates the specificity of ribosomal binding. So-called specialized ribosome systems can be constructed that direct ribosomes specifically to the mRNA of interest. Site-directed mutagenesis is applied to both the Shine–Dalgarno region and the rRNA to change their sequence, while maintaining the base pairing. In eukaryotes, the formation of a translational initiation complex is directed by the **5′-cap** -structure, 7MeG(5′-5′)pppNp (N is the first nucleotide of the mRNA), at the 5′-end of the mRNA. However, several eukaryotic mRNAs have been found to be translated in a cap-independent manner (2).

Secondary structures in the 5′-untranslated region of the mRNA and around the start codon may hamper recognition of the start site. If potential secondary structures seem to be any problem, they can be eliminated by introduction of silent mutations at the third positions of the initial **codons** or by random mutagenesis in the region upstream of the start codon. Another approach to overcome the problem of secondary structures is to express the protein of interest as a **fusion protein** or to use a two- **cistron** system. In the first approach, a nucleotide sequence encoding a protein or peptide that is known to be well expressed is introduced in-frame between the start codon and the gene of interest. The resulting N-terminal fusion partner most often provides other advantages as well, such as increased stability or simplified purification (see Fusion Gene, Fusion Protein). In the second approach, a strong ribosomal binding site and the 5′-end of a well-translated gene, followed by a stop codon, is positioned immediately upstream of the gene of interest. Translation of the protein of interest will then be reinitiated immediately after the first gene.

The degeneracy of the genetic code implies that most of the 20 amino acids are encoded by two or more codons called synonymous codons. The synonymous codons are not used with equivalent frequencies by different strains or even throughout the genome of a single organism (3, 4) (see Codon Usage and Bias). Weakly expressed genes are characterized by the occurrence of infrequently used codons, which are typically recognized by rare tRNA species. It is advisable to avoid the use of rare codons when possible in systems for high-level expression.

The three stop codons UAG, UAA, and UGA differ in their efficiency in terminating translation. UAA seems to be favored in highly expressed genes and [should be used in] expression systems.

If a heterologous expression system is used, the gene of interest should preferably be devoid of **introns**, which may not be properly processed by a host of different origin than the gene. However, the presence of introns has, in some cases, been required for successful expression. In such cases, the intron can be provided by the expression vector downstream of the gene of interest.

2. Choice of host

Considerable knowledge about expression in *Escherichia coli* has accumulated over the years, and *E. coli* is often the first choice of host when a new protein has to be expressed. Furthermore, *E. coli* grows fast in inexpensive media, allowing scale-up for industrial purposes. However, proteins containing disulfide bonds are unlikely to fold correctly in the cytosol of bacteria, which is relatively reducing. Misfolding may lead to the formation of inclusion bodies, which can be both an advantage and a disadvantage. The advantages are that the protein is protected from proteolytic degradation and that the purification strategy can be simplified. However, the protein needs to be denatured and refolded, a task that can cause difficulties (see Protein Folding In Vitro). The coexpression of folding factors such as molecular chaperones, thioredoxin, or protein disulfide isomerase, which assist the folding of protein, can be beneficial in some cases. A secretion strategy may represent another solution to the problem [see Secretion Vector]. Even though *E. coli* is able to secrete proteins, the outcome of such an approach is highly unpredictable. *Bacillus* species will often be a better choice of host in such a case. Furthermore, *Bacillus* has the advantage that it does not produce endotoxins (lipopolysaccharides) and has been classified as a GRAS (which stands for *generally regarded as safe*) organism. The range of promoters available for *Bacillus* is more limited than the range for *E. coli*. Some other prokaryotic hosts, eg, *Lactococcus lactis* (5), also are gaining popularity as expression hosts.

On the other hand, bacterial systems have this limitation: they are unable to provide many of the post-translational modifications often found in eukaryotic proteins. If these modifications are needed for obtaining proper structure or activity, a eukaryotic host should be chosen.

Yeast, the simplest eukaryotic expression host, offers many advantages of both prokaryotic and eukaryotic systems. Yeasts grow rapidly in inexpensive media and are easy to manipulate genetically. Furthermore, yeasts provide an environment for carrying out secretion and providing post-translational modifications that are more similar to those found in proteins from the higher eukaryotes. The yeast strain traditionally used as a host for protein expression, *Saccharomyces cerevisiae*, is regarded as safe, given its long history of use in the production of food and beverages. More recently, the methylotrophic yeasts *Pichia pastoris* (6) and *Hansenula polymorpha* have gained popularity because of their higher production levels. However, yeast shows a tendency to hyper**glycosylate** the overexpressed protein, and the resulting high-mannose polysaccharide structures may affect the activity or folding or both, and they are potentially **immunogenic**. The filamentous **fungi**, *Aspergillus* and *Trichoderma*, are becoming increasingly popular as expression hosts, not least because of the very high amounts of protein that can be obtained with secretion systems (7).

Another eukaryotic expression system of high popularity is the baculovirus/insect cell system, which is relatively easy, cheap, and fast to use. The first generation of systems utilized the strong transcription signals for expression of the polyhedron protein of the **virus** . The baculovirus system provides more, although not all, of the features characteristic of mammalian cells, and the yields are often high. However, the high yields sometimes lead to the formation of inclusion bodies. Interestingly, the baculovirus system can be used for **phage display** of large, complex disulfide-containing proteins, thereby overcoming the limitations of the original bacterial system.

If the protein of interest is of mammalian origin and if authenticity is of utmost importance, a mammalian expression system should be chosen. It may also enable the study of an engineered protein in its natural environment; for example, a biological assay could be coupled to the expression system for the evaluation of functional effects. The basic technology is now available, but these expression systems are not very cost-efficient and are sometimes difficult to scale up. Often, it takes a long time to establish a stable system with high expression levels.

Eukaryotic expression systems can be divided into two groups: those that involve transient or stable expression of recombinant genes from transfected DNA molecules, and those that involve helper-independent viral expression vectors. Vectors used for stable expression contain a complete eukaryotic transcriptional unit inserted into a bacterial replicon. The DNA integrates at a low frequency into the host genome and usually directs the expression of the desired protein at low levels. Recombinant virus systems represent powerful tools for the expression of recombinant proteins in cultured cells, animals and man. A comparison of five different eukaryotic expression systems can be found in reference 8.

There are several factors to take into consideration before setting up an expression system. How much protein is needed? What is its application? Is authenticity important? Can the presence of heterogeneity be accepted? Are the technologies available? The choice of an expression system will depend largely on the desired use of the expressed protein; for example, even microheterogeneity can be a problem if the protein is to be used for **X-ray crystallographic** structural analysis, as these heterogeneities may hamper the crystallization process (9).

Proteolysis of heterologous proteins is another problem that should be considered in the choice of a host for expression. Bacteria and lower eukaryotes use proteolysis as a primitive immune system, which attacks and eliminates “nonself.” Different proteinase-deficient strains have been constructed to overcome this problem, but these strains grow at a lower rate, and their usefulness for solving a particular problem is often unpredictable. If proteolysis is a problem, it is advisable to test a selection of these hosts. Alternatively, a secretion strategy or a fusion protein strategy can be chosen. In the first case, the gene product is removed from the cytoplasm, where most proteinases are located. In the second case, the fusion partner can have a stabilizing effect. The method of induction of expression should also be considered when proteolysis appears to be a problem. Some induction methods (eg, heat induction) activate the **heat-shock** system of the cell, which includes a whole range of proteolytic enzymes.

In particularly difficult cases, where the protein of interest is toxic or prone to form inclusion bodies, the use of a cell-free protein biosynthesis system may be beneficial. In such a system, the enzymes needed for transcription and translation are present in a cell extract instead of a live organism. One further advantage is the possibility of introducing unnatural amino acids into the protein of interest (10, 11).

Finally, when a suitable expression system has been established, the growth and eventual induction conditions need to be optimized to obtain the maximal yield of product. It is often advisable to decrease the growth rate below the optimal by reducing the temperature, aeration, or nutrition content of the media. The risk of overloading the protein synthesizing machinery, leading to inclusion body formation or misfolded proteins, is thereby avoided. Furthermore, the expression vector is stabilized. Also, the strategy of recovering the expressed protein will influence the product yield and thus deserves optimization.

The vast number of vectors and hosts available should be able to satisfy the demands of any protein to be expressed. Yet protein expression is a somewhat empirical process, making it difficult to foresee which system should be chosen for optimal success. Advances in the understanding of how expression systems work will undoubtedly make for a higher degree of predictability than is currently the case.

Bibliography

1. R. S. Donovan, C. W. Robinson, and B. R. Glick (1996) J. Indust. Microbiol. **16**, 145–154.
2. R. J. Kaufman (1994) Curr. Opin. Biotech. **5**, 550–557.
3. S. Zhang, G. Zubay, and E. Goldman (1991) Gene **105**, 61–72.
4. K. Wada et al. (1992) Nucleic Acid Res. **20**, 2111–2118.
5. O. P. Kuipers, P. G. G. A. de Ruyter, M. Kleerebezem, and W. M. de Vos (1997) Tibtech **15**, 135–140.
6. M. Romanos (1995) Curr. Opin. Biotech. **6**, 527–533.
7. R. J. Gouka, P. J. Punt, and C. A. M. J. J. van den Hondel (1997) Appl. Microbiol. Biotechnol. **47**, 1–11.
8. S. Geisse, H. Gram, B. Kleuser, and H. P. Kocher (1996) Prot. Expr. Purif. **8**, 271–282.
9. R. Giegé and V. Mikol (1989) Trends Biotechnology **7**, 277–282.
10. D.-M. Kim, T. Kigawa, C.-Y. Choi, and S. Yokoyama (1996) Eur. J. Biochem. **239**, 881–886.
11. D. Mendel, V. W. Cornish, and P. G. Schultz (1995) Annu. Rev. Biophys. Biomol. Struct. **24**, 435–462.

Suggestions for Further Reading

12. P. Gacesa (1997) *Vectors: Expression Systems (Essential Techniques Series*), John Wiley & Sons, New York. A laboratory manual that enables the reader to make the best choice of method, conditions, and equipment for working with expression vectors. A troubleshooting guide is included.
13. D. V. Goeddel (ed.) (1990) *Methods in Enzymology*, vol. **185**, Gene Expression Technology, Academic Press, San Diego, California. The reader is provided with a basic understanding of the problems that may occur while trying to express a protein in various expression systems. Furthermore, more sophisticated solutions to the problems are provided. Strongly recommended.

Many of the books suggested under the entry "**Protein engineering**" contain several chapters about different host systems.

14. In the journal *Current Opinion in Biotechnology*, one issue per volume (usually issue 5) is dedicated to reviewing the latest advances in the field of expression systems, enabling the reader to become fully updated.

Extended X-Ray Absorption Fluorescence Spectroscopy (EXAFS)

X-ray absorption spectroscopy is particularly useful for investigating the electronic structure and local environment of the metals in metalloproteins (1). It is not limited by the physical state of the sample (e.g., gel, crystal, tissue) and, unlike X-ray crystallography, the entire structure of a crystalline molecule need not be determined to understand the local structure of the metal site. Obtaining data from light atoms, however, is very difficult. Atoms lighter than sulfur cannot be studied routinely because high vacuum is required. Most of the work reported to date has been with samples containing transition-metal ions. An intense, tunable X-ray source is required, and making measurements at a synchrotron facility must be done on a competitive basis. The ideal sample has a volume of 20 to 100 µl and a concentration of at least 1 mM. It must be maintained at low temperature while the data are being collected, so as to minimize radiation damage.

Like visible photons, X rays are absorbed by matter according to the Beer–Lambert law (see Spectroscopy) and cause changes in the energy levels of the electrons of the absorbing atom. Because the energies of X-ray photons are considerably greater than those of visible light, however, the electrons affected are those in the lower shells, principally the K- and L-shell electrons. Therefore, X rays whose energies are near those of the atomic or molecular energy levels of the metal can be used to probe the electronic structures of the metal sites. The edge region of the absorption spectrum in the top panel of Fig. 1 contains information relating to the valence state and coordination geometry of the absorbing metal atom and the chemical identities of the neighboring atoms.

Figure 1. X-ray absorption data for $\mathrm{Zn[imidazole]}_4^{2+}$ (a) Data collected as fluorescence (*F*) normalized by the initial intensity I_0. (b) EXAFS data derived from the data in (a) after subtracting a background, corresponding to the metal ion without neighbors, and multiplying by the factor k^3, where k is proportional to $E_{\mathrm{electron}} = E_{\mathrm{X-ray}} - E_{\mathrm{ionization potential}}$. (c) Fourier transformation of the EXAFS data in (b), showing the coordination shells around the Zn^{2+} ion. The first shell contains four imidazole N atoms at 2.40 Å, and the higher shells contain the other C and N atoms of the imidazole rings.

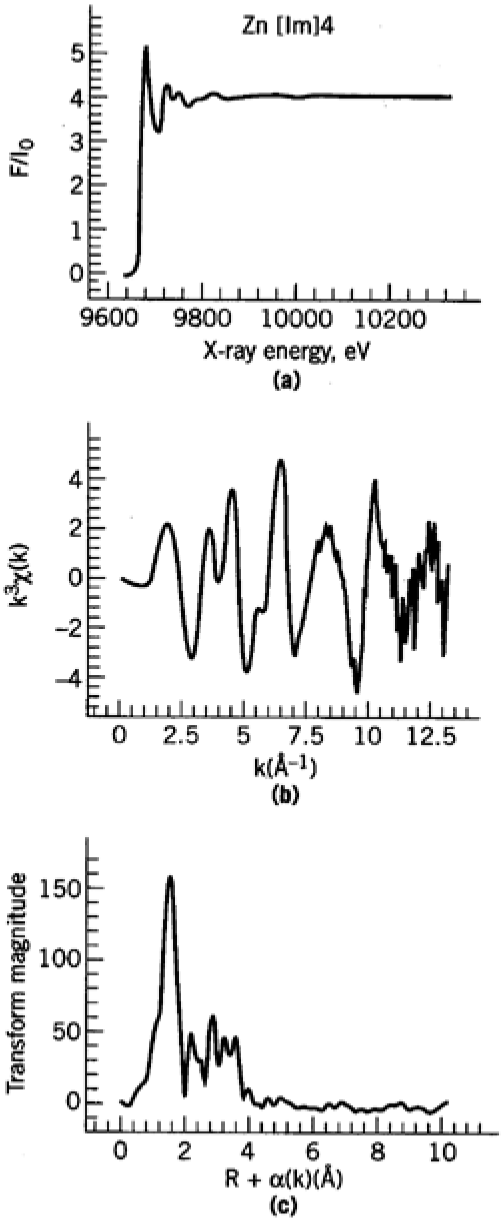

When the X-ray energy exceeds the ionization potential or threshold of the metal, which is the energy at which the inner shell electrons are promoted to the continuum, the absorption spectrum is characterized by an oscillatory structure (top panel of Fig. 1) at energies greater than the absorption edge, which is known as the extended X-ray absorption fine structure (EXAFS). This structure results from interference in the ejected photoelectron wave from the metal atom and the photoelectron wave backscattered from neighboring atoms. This interference phenomenon provides a very precise measurement of the distance to the neighboring atoms (typically ± 0.02 Å). In addition, the EXAFS oscillations contain information relating to the number of neighboring atoms of a limited range in atomic number (rows in the periodic table can generally be distinguished). Because this ejected photoelectron wave is spherical, the position in three dimensions is lost on average. In a simplified form, an equation describing these oscillations can be written as

$$k^3\chi(k) = \sum_j N_j A_j(k) \sin(2kr_j + \alpha_j(k))$$

where *k* is the wave vector, which is related to the X-ray energy, c is the oscillatory part of the X-ray absorption spectrum, N is the number of neighbors at distance r, $A(k)$ is the backscattering amplitude, which depends on the chemical identity of the neighboring atoms, and a(k) is the phase shift due to the potentials of both the absorbing metal and the neighboring atoms. The summation is over all coordination shells j, but in reality data can be collected only at distances less than about 5 Å for biological samples. The previous equation is written in this interference form to facilitate describing the data analysis necessary to determine the structural parameters.

Although X-ray absorption can be measured by observing either the transmission of X rays through the sample or the fluorescence emitted as a result of absorption, the latter is used almost exclusively for biological samples, because of its enhanced sensitivity. To obtain information about the number and average distances of the neighboring atoms, the data must be analyzed to isolate these parameters in the previous equation. Figure 1 shows the results for $Zn(imidazole)_4^{2+}$ during each step of the analysis. First, a simple linear background is subtracted from the data to normalize to zero the data below the edge region (top panel). Then, a background resembling the spectrum of the metal without neighbors (ie, a free atom) is subtracted, the energy scale is converted to wave numbers ($Å^{-1}$), and the data are multiplied by k^3. The results are displayed in the middle panel of Fig. 1. Now, the y-axis corresponds to the left side of the previous equation. Fourier transformation is used to isolate the contributions of the individual coordination shells, which converts the x-axis to r + a(k). This is similar to a radial distribution function that describes the radial electron density around the absorbing metal set at the origin. The first peak of the bottom panel of Fig. 1 is the first coordination shell, and those at greater x-axis values are further from the metal. The x-axis can be converted to r if one knows the chemical identity of the scatterers in each shell. For example, the average distance of the first shell peak is r + a(k) = 1.52 Å. It is composed of four nitrogen atoms, however, and it is known from investigating model compounds of known structure that a(k) = 0.88 Å for Zn–N coordination. This makes the average distance of those four nitrogen ligands 2.40 Å, with an estimated error of ±0.02 Å. Using model compounds, one can also determine that there are four nitrogen ligands in the first coordination shell. A more elaborate analysis, considering the higher shells of scattering atoms, would also lead to the conclusion that the ligands are imidazole. This example illustrates the need for model compound data or theoretical determination of the amplitudes and phases for each chemical type of ligand.

This example also demonstrates one limitation of EXAFS. In the absence of information about the metal-coordination environment, the data simply give an average of the number of ligands and their distances. In the best of circumstances without other biophysical or biochemical information, this method can determine only the difference between elements in the rows of the periodic table (e.g., C/N/O, S/Cl, or Se). Additional limitations occur as a result of uncertainties in the data analysis. For example, it is rarely possible to distinguish between one and two coordinated histidine residues in the presence of thiol group ligands without further information (such as knowledge of the protein primary structure). Rigorous analysis of X-ray absorption data for a complex coordination environment (e.g., metal clusters) in proteins can be impossible without methods to isolate each metal site, for example, by metal substitution.

Bibliography

1. L. S. Powers (1982) Bioch. Biophys. Acta **683**, 1–38.

Suggestions for Further Reading

2. I. Bertini, H. B. Gray, S. J. Lippard, and J. S. Valentine (eds.) (1994) *Bioinorganic Chemistry*, University Science Books, Mill Valley, CA.
3. L. Que Jr.(ed.) (1999) *Bioinorganic Spectroscopy and Magnetism*, University Science Books, Sausalito, CA.
4. G. L. Eichhorn and L. G. Marzilli (eds.) (1989) *Advances in Inorganic Biochemistry*, Elsevier, New York, Vol. **8**.

Extracellular Matrix

Extracellular matrix (ECM) is a general term for extracellular networks of fibrous glycoproteins, proteoglycans, and carbohydrates that are secreted by cells. There are a wide variety of matrix types that fulfill many important functions in developing and mature animals and plants. ECM can be categorized as strong connective tissue ECM or loose connective tissue ECM. In strong connective tissue, such as bones, teeth, antlers and horns, a meshwork of fibrous protein is strengthened by deposition of calcium phosphate. Loose connective tissue includes specialized structures such as tendons, ligaments, fascia, cartilage, cell walls, and cuticles. Also in this category are the basal laminae (or basement membranes) that underlie epithelial cell layers and surround muscle cells, fat cells, and Schwann cells, and the collagenous interstitial matrix that is secreted by fibroblasts and lies beneath the basal laminae.

ECM contributes to the structure of organisms, acting as a scaffold for building strong connective tissue, and organizing cells into specific patterns in loose connective tissue. Tendons and ligaments contain molecules that give them their unique structural features in connecting bone and muscle. ECM in the joints provides cushioning, and elastic layers around blood vessels allow control of blood flow. The basal lamina in the kidney glomerulus acts as a molecular filter, allowing smaller molecules to pass from the blood to the urine. ECM can form important barriers in tissues to coordinate cellular movements and organization of cellular layers. For example, the basal lamina underlying endothelial cells in blood vessels prevents cells from leaving the circulation, except for certain cells that have the ability to pass through. This barrier is especially important during inflammation and metastasis.

While the important structural roles played by ECM have been recognized for a long time, recent research has uncovered crucial instructive activities that direct cellular movement and regulate cellular differentiation and gene expression. Individual molecules have now been purified, and their activities have been characterized. Many ECM molecules have been shown to support adhesion of cells, and some (such as tenascin) display anti-adhesive activities that may be important in establishing tissue boundaries or pathways of migration. Early in development, neuroblasts and myoblasts contact ECM as they migrate to their final destinations. ECM is also important in axon pathfinding and synapse formation. The basal lamina surrounding muscle cells has specialized regions in the synaptic cleft at the neuromuscular junction that contains molecules important for synapse function, such as acetylcholinesterase. In addition, synaptic basal lamina contains molecules that help guide synapse formation and regeneration, such as laminins containing the b-2 subunit and agrin. *beta*-2 laminins are also important in photoreceptor development and synapse formation. ECM also acts as a reservoir of positively charged growth factors, many of which bind to negative charges in ECM molecules. Growth factors and ECM molecules act in concert to direct a wide variety of cellular traffic during tissue morphogenesis. For example, fibroblast growth factor must bind to heparan sulfate chains from proteoglycans to be stable and active. In addition, the activity of some growth factors is enhanced when cells are bound to ECM, due to a synergy of their respective intracellular signaling pathways. Finally, some ECM molecules are proteolyzed to generate smaller soluble factors. Collagen XVIII is cleaved to generate endostatin, an antiangiogenic motility factor that can prevent tumor progression in mice. It has become clear that the ECM is in part the mortar that holds cells together in tissues, but it also acts as the brick mason, guiding the development and deposition of cells within the organism.

Cells interact with and respond to specific matrix molecules via cell surface receptors such as the Integrins, which bind matrix on the outside of the cell, and send signals across the plasma membrane to regulate intracellular events. Some cells make identifiable, stable junctions with ECM via integrins. These include focal adhesions which link to the actin cytoskeleton and hemidesmosomes, which connect to intermediate filaments. Other cell interactions with ECM are more transient. Contact with the matrix can alter the polymerization dynamics of the cytoskeleton to bring about changes in cell shape important in cell adhesion, migration and polarity. Adhesion to ECM is important in cellular responses to physical/mechanical forces, such as shear stress caused by blood flow over endothelial cells. ECM can activate signaling cascades involving tyrosine kinases which control cell growth, differentiation and apoptosis (see Integrins). Other receptors may also play roles in interacting with the ECM, including proteoglycans and galactosyl transferases.

The molecular complexity of the ECM is formidable, and many components are polymerized and then interwoven by covalent and noncovalent cross-links. The specific molecular attributes of ECM components give rise to their specific functional roles. For example, collagen I, the most abundant protein in animals, forms covalently cross linked fibrils with the tensile strength of steel that are found in skin, tendon, ligament, and bone. In contrast, Collagen IV forms sheets that polymerize with heparin sulfate proteoglycans and laminin-1 to give rise to the basal lamina. The presence of negatively charged, unbranched carbohydrate polymers called glycosaminoglycans (GAGs), both as free molecules and attached to protein backbones in proteoglycans, form a cushion-like hydrated gel important in the function of joints. For example, hyaluronan, a free GAG molecule that can be as long as 20 mm if stretched from end to end, forms a viscous random coil that provides turgor pressure in spaces between cells. Aggrecan, a proteoglycan, is a key cushioning element in cartilage. The elastic properties of cross-linked elastin arrays allow lung bronchial sacs to expand and arteries to change their diameter. Many ECM proteins are composed of repeated motifs that arise from individual exons, suggesting that new proteins evolved by shuffling various exons. Electron micrographs of purified ECM molecules have revealed striking geometries, from cross-shaped structures like laminin-1, to centipede like arrays of proteoglycans in an aggrecan aggregate, to pentameric and hexameric asterisks like thrombospondin-4 and tenascin, respectively. Some ECM proteins have many different isoforms arising from both alternative splicing and multiple genes that encode homologous families of subunits. For example, there are over 20 varieties of collagens made from 38 distinct polypeptides. At least 15 types of laminin have been identified. Other ECM components such as vitronectin and fibronectin are made in one form and deposited in matrices, and a second form is an abundant component of blood plasma.

The macromolecules that make up the ECM are synthesized by cells that reside within the matrix. This includes fibroblasts in the interstitial matrix, chondroblasts in cartilage, and osteoblasts in bone. Some fibril forming ECM proteins such as collagen are made initially with N- and C-terminal extensions called propeptides that prevent polymerization until the propeptides are cleaved outside the cell. Collagen also contains posttranslationally modified hydroxyproline and hydroxy lysine, which are important for hydrogen bonds that stabilize fibrils. The enzymatic addition of the hydroxyl groups requires ascorbic acid (vitamin C), and deficiencies lead to weakened blood vessels and loose teeth characteristic of the disease Scurvy. Outside the cell, triple helical collagen monomers are cross-linked via covalent bonds to form 50 nm extracellular fibrils. Cells can assemble complex ECM arrays on their surface via the activity of integrin and dystroglycan receptors.

Once assembled, ECM is insoluble and fairly stable. For example, a collagen I molecule in bone might last 10 years before it is replaced. However, in some cases the degradation and turnover of matrix does occur, and it is carefully regulated. White blood cells must degrade the vascular basal lamina to leave blood vessels and enter inflamed tissue, and metastatic cancer cells can migrate to distant sites by violating ECM boundaries. Matrix is also degraded at certain times during development and wound healing, such as in the sprouting of new blood vessels (angiogenesis). In these cases most matrix is degraded by a family of over 20 secreted proteases called Matrix Metalloproteinases (MMPs), which require bound Zn^{2+} or Ca^{2+} for activity. MMPs are secreted as inactive precursors which are activated by proteolytic cleavage. Activity is also regulated by a family of secreted protease inhibitors called tissue inhibitors of metalloproteinases (TIMPS). The process of matrix degradation is of great importance to medical researchers interested in controlling inflammation, tumorgenesis, and metastasis.

The importance of ECM is underscored by the consequences of mutations that ablate or alter matrix components. For example, human mutations in collagen I can result in osteogenesis imperfecta (weak bones) or Ehlers-Danlos Syndrome (defective joints), or even death. Over 1,000 mutations have been identified in 22 different collagen genes, and these lead to a variety of diseases characterized by defective connective tissue. Mutations in fibrillin results in Marfan's syndrome, a disease characterized by defects in elastic tissue such as the aorta, which is subject to aneurysms. Mutations in laminin genes can lead to congenital muscular dystrophy and junctional epidermolysis bullosa, a skin blistering disease. More recently, genetic studies in model animal systems have also demonstrated the importance of ECM. For example, loss of laminin in the worm *Caenorhabditis elegans* results in defective mesodermal cell migration and axonal pathfinding under the epidermis. Mice with null (knockout) mutations in the fibronectin gene fail to develop notochord, somites, neural tube, and heart and die by embryonic day 10.

There is still a great deal to learn about the ECM. New molecular components continue to be discovered, and their functions are not yet known. Furthermore, alternatively spliced variants of known molecules, and isoforms derived from separate genes have been discovered which differ in structure and function. Proteolytic fragments of ECM molecules, such as endostatin, angiostatin, and tumstatin, are being investigated as possible anticancer treatments. The exact molecular structure of complex ECMs such as the basal lamina are not yet clear, and how cells adhere to, migrate on, and move across matrices is still not completely understood. As more genomes are sequenced, we should get a better idea of ECM complexity and evolution. Developing better treatments for important human diseases such as arthritis, cancer, and macular degeneration may be made possible by a better understanding of the ECM.

Additional Reading

Kreis T. and Vale R., eds., *Guidebook to the Extracellular Matrix, Anchor, and Adhesion Proteins*, 2nd ed., Oxford University Press, Oxford, New York, 1999.

Ruoslahti E. and Engvall E., eds., Extracellular matrix components, *Methods in Enzymology*, Academic Press, San Diego, Calif., 1994, p. 245

Hay E.D., ed., *Cell Biology of Extracellular Matrix* 2nd ed., Plenum Press, New York, 1991.

Extrachromosomal Inheritance

“Extrachromosomal inheritance” is a term to be avoided. It is used sometimes as a synonym for cytoplasmic inheritance, which usually arises from the genetic information on mitochondrial or chloroplast genomes. Using the term **chromosome** in the broad sense of any DNA or RNA molecule capable of autonomous replication, the term *extrachromosomal inheritance* has a very limited content (see **Maternal effects**).

If the term chromosome is restricted to the complex structures in the **nuclei** of the eukaryotes, then *extrachromosomal inheritance* covers both cytoplasmic inheritance and the inheritance of plasmids that replicate autonomously in the nuclei of the cells. Because their distribution patterns differ from those of the major chromosomes, their inheritance diverges from Mendelian rules (see Mendelian Inheritance).

Most nuclear plasmids are phenotypically silent and can only be detected by identification of their molecules. This is the case of the “two-micron circle,” a nuclear plasmid of *Saccharomyces cerevisiae* . Although it does not confer any phenotype to the yeast, it has been useful in the development of **vectors** for **genetic engineering**.

In bacteria, *extrachromosomal inheritance* could designate the inheritance of autonomous plasmids separate from the main chromosome (see F Plasmid).

Suggestion for Further Reading

J. R. Broach and F. C. Wolkert (1991) "Circular DNA plasmids of yeasts. In" *The Molecular and Cellular Biology of the Yeast Saccharomyces* (J. R. Broach, J. R. Pringle and E. W. Jones, eds.), Cold Spring Harbor Laboratory Press, Cold Spring Harbor, NY, pp. 297–331

Eye (Bubble)-Form Intermediate

In general, DNA replication of a **chromosome** starts from a genetically fixed site and proceeds bidirectionally. At the initial stage of replication, the replicated regions form structures like an eye (or a bubble). This form is important, as it represents the origin region of the chromosome (see Replication Origin); various methods to detect eye-form intermediates have been developed. Electron microscopy (**EM**) of the replicating DNA can detect eye-forms as large as several kilobases (1). Using a combination of digestion by appropriate restriction enzymes and electron microscopy, the origin of replications of **plasmids**, **bacteriophage**, and **virus** DNA has been identified (2). Recently, the two-dimensional gel electrophoresis method was developed to detect various forms of replication intermediates (3). Chromosomal fragments produced by digestion with restriction enzyme are separated by electrophoresis by agarose gel electrophoresis, first by size and then by shape. The distribution of intermediates on the two-dimensional (2D) gel is detected by **hybridization** with a **radiolabeled** probe of a cloned DNA fragment from or near the replication origin. Since the correlation between the size and complexity of shape of eye-forms is different from that of Y-fork intermediates (see Replication Fork (Y-Fork Intermediate)), the former can be distinguished from the latter by the shape of arcs on the 2-dimensional gel (Fig. 1). In particular, when the origin of replication is not located at the center of the fragment, the change from eye- to Y-form occurs as replication proceeds on the fragment, which results in a discontinuous distribution of arc from eye- to Y-form. This method has been used successfully to detect the chromosomal origins of **eukaryotes**, in particular of *Saccharomyces cerevisiae* (4), *Schizosaccharomyces pombe* (5), and *Drosophila* chromosomes (6). Detection of eye-forms from mammalian chromosomes is technically difficult, due to the large amount of background DNA, and this method generally produces ambiguous results as to the site of origin of replication (7).

Figure 1. Two-dimensional gel electrophoresis method to detect eye-form (bubble-form) and Y-form replication intermediates. (**a**) Examples of patterns of Y-form (left) and Eye-form (right) intermediates of the replication of *Saccharomyces cerevisiae* chromosome are shown. Intermediates were detected by hybridization with the ^{32}P-labeled probe of cloned DNA within the fragments shown in (**c**). (**b**) The photos in (**a**) are drawn schematically. Dotted lines indicate the location of linear DNA fragments of corresponding size. (**c**) The population of the intermediates detected in (**a**) and (**b**) Left panel: Replication fork moves from the left (or right) side of the fragment and proceeds to produce Y-forks of variable size. Theoretically, a Y-fork with equal branch lengths is structurally most complex and shows least mobility in the second dimension. Right panel: Replication initiates from the center of the fragment and proceeds bidirectionally, producing various sizes of bubble intermediates. The largest bubble is like a circular DNA and shows least mobility in the second dimensions. The locations of the probe used for detection in (**a**) are indicated by dotted lines. Dark spots in the photos in (**a**), and drawn schematically in (**b**), indicate that the majority of DNA detected by

the probe is nonreplicated (or completely replicated) linear molecules.

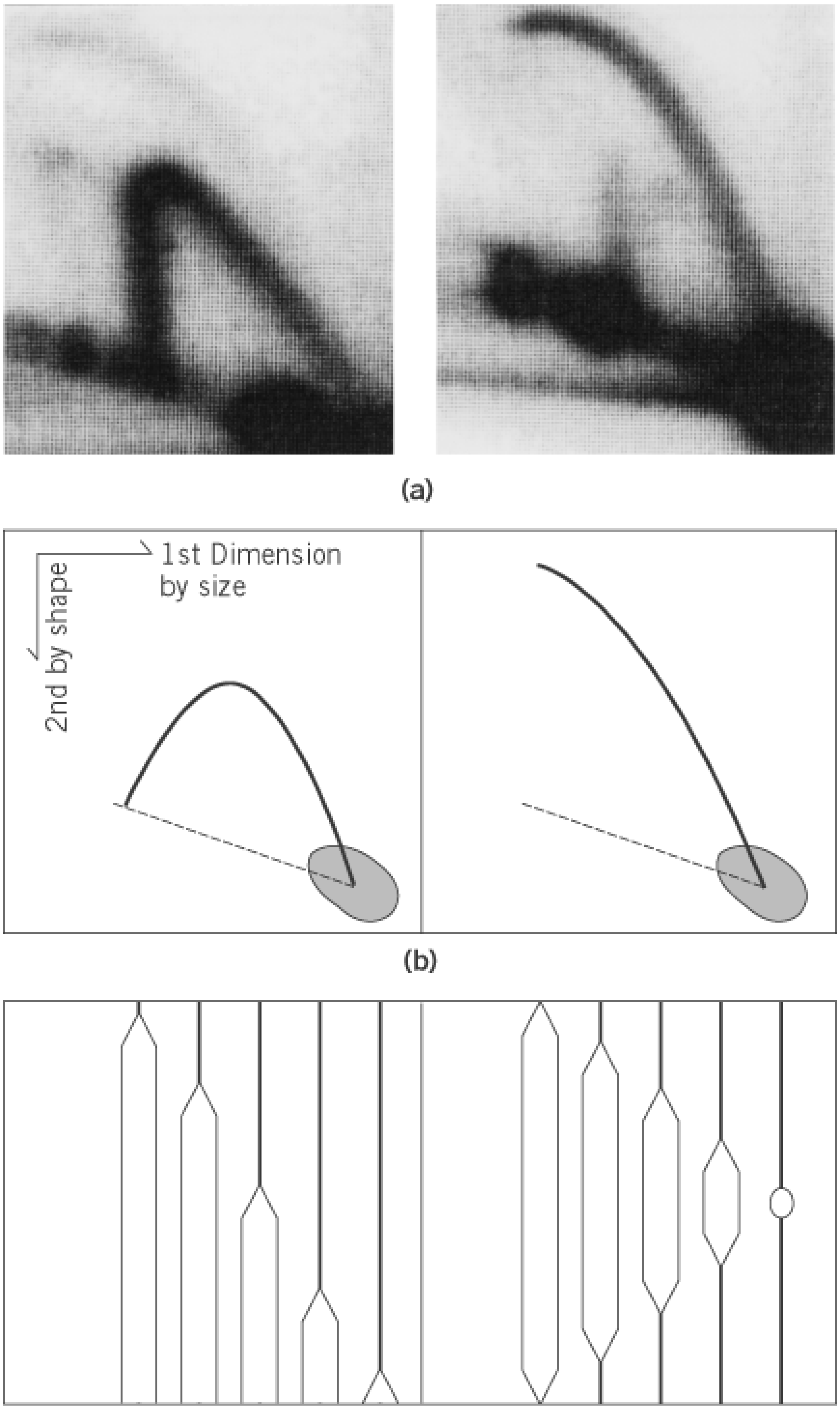

(a) (b) (c)

Bibliography

1. M. Schnos and R. B. Inman (1970) J. Mol. Biol. **51**, 61–73.
2. J. Wolfson, D. Dressler, and M. Magazin (1972) Proc. Natl. Acad. Sci. **69**, 499–504.
3. B. J. Brewer and W. L. Fangman (1987) Cell **51**, 463–471.
4. W. L. Fangman and B. J. Brewer (1991) Ann. Rev. Cell Biol. **7**, 375–402.
5. J. Zhu, D. L. Carlson, D. D. Dubey, K. Sharma, and J. A. Huberman (1994) Chromosoma **103**,

414–422.
6. T. Shinomiya and S. Ina (1991) Nucl. Acids Res. **19**, 3935–3941.
7. M. L. DePamphilis (1993) J. Biol. Chem. **268**, 1–4.

F Plasmid

In 1953 a new type of genetic element was postulated in order to account for the sexual behavior of *Escherichia coli* K-12 (1, 2). This determinant spread rapidly and independently through recipient cell populations, indicating considerable autonomy, but it was completely dispensable and conferred no **phenotype** on its host other than maleness. Nevertheless, it was stably inherited by the cells it invaded. It behaved, in essence, like a small, infectious chromosome, and it was baptized the fertility (F) or sex factor. The nature of the proposed new element was amply confirmed: F turned out to be the prototype of the circular, double-stranded DNA **plasmid**.

F was immensely important to the development of molecular genetics. By promoting transfer of chromosomal genes, it opened the way to large-scale mapping of the bacterial genome; and by acquiring and transferring small portions of the host chromosome, it could create partial **diploid** conditions that enabled analyses of bacterial **gene** function and control of **gene expression**. The nature and consequences of F-specified maleness are generally understood and are described in the entry Hfr's and F-primes. F has also been at the forefront of investigations into how low-copy number replicons are maintained stably; the mechanisms that regulate F's maintenance will be the major focus here.

Early studies of F were greatly aided by the discovery of derivatives that carry chromosomal genes (F-primes). For example, isolation of F′ lac^+ mutants (in a *lac* mutant strain) that remained Lac^+ at 30°C but segregated Lac^- at 42°C demonstrated that F carries its own replication determinants (3). The selective inhibition of F maintenance by acridine dyes (4) also pointed to the autonomy of F replication. Measurements of b-galactosidase in F^-/lac^+ and $F'lac^+/lac^+$ strains gave the first indication that the copy number of F is about the same as that of the chromosome. The strict regulation of copy number was reflected in the phenomenon of incompatibility, the inability of two F plasmids (eg F′*lac* and F′*gal*) to be coinherited. The F replication system enables integrated F to assume control of chromosome replication in strains unable to initiate it themselves, a phenomenon known as “integrative suppression” (5, 6). Beyond the initiation of replication at the origin, however, F replication becomes strictly dependent on host functions.
The term “episome” was coined to denote plasmids like F with both autonomous and passive (integrated) modes of propagation. This property turned out not to reflect a fundamental distinction from other plasmids, and the term is no longer considered useful.

1. Anatomy of F, A Mosaic

F consists of four functional blocks and a region of unknown composition (Fig. 1). The 33-kbp *tra* operon encodes the essential components of donor ability, the mating apparatus and the DNA manipulation enzymes responsible for transmitting F into recipient cells, as shown by the self-transmissibility acquired by plasmid vectors into which it, along with the origin of transfer (*oriT*), has been inserted. The ~ 13-kbp leading region that follows *oriT* is the first to enter recipient cells during transfer; only a few genes within it are known, and their involvement in transfer has not been demonstrated. The region at the other end of the *tra* operon contains a defunct replicon and appears to have acted as a trap for transposable elements; the latter contribute indirectly to mating activity, because one of them is inserted in the *finO* regulator gene, causing constitutive expression of the *tra* operon and high transfer rates, and (ii) also because homologous recombination with similar elements in the chromosome is the major route of F integration to form Hfr donors. The fourth region carries all the significant determinants of F maintenance. When isolated and joined to an antibiotic resistance gene to permit selection, it behaves as a normal plasmid (mini-F) with the same replication, partition, and stability properties as its parent F (7, 8). It is, therefore, the form most often used for studies of F maintenance.

Figure 1. Genetic map of the F plasmid. The circular F plasmid has been divided into five sectors, roughly according to function. Gene symbols are explained in the text. The **tra** arrow indicates the direction of transcription of the *tra* operon. The **oriT** arrow indicates the direction of conjugal transfer. Unshaded blocks of the circle correspond approximately to unsequenced regions. Below is the *repFIA* mini-F; note that it is shown inverted relative to F, by convention. Arrows above *ori1* and *ori2* show bi- and unidirectional replication, respectively.

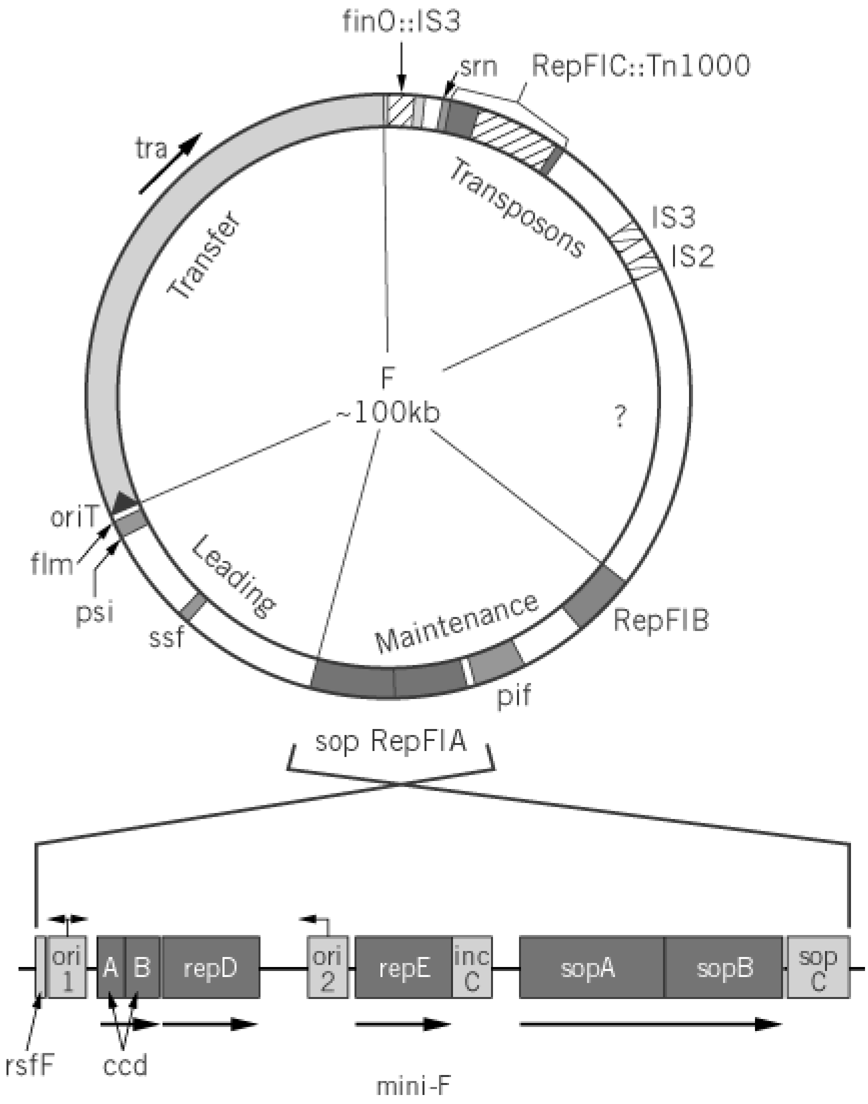

A closer view reveals F to be a mosaic of replicative determinants. Three have been identified: *repFIA*, *repFIB*, and *repFIC*. The first two can be isolated as miniplasmids, although replication of *repFIB* is partly defective, so that replication of F itself is predominantly governed by *repFIA*. The *repFIC* locus, identified as such by comparison with the *rep* sequences of other plasmids, is inactive due to insertion of Tn*1000* in a progenitor of F. Portions of F as yet unsequenced may prove to contain other replicons. The presence of multiple replicons has proved to be a common feature of large plasmids, and it suggests that many such plasmids may have arisen by the fusion and rearrangement of a limited number of ancestral plasmids (9, 10). The fact that only *repFIA* is fully functional may account for the fact that F is stably maintained in only a narrow range of hosts: *E. coli* and similar Enterobacteria.

1.1. RepFIA

The *repFIA* locus is itself an ensemble of essential and accessory maintenance functions (Fig. 1). **Electron microscopic** examination of replication intermediates showed that replication forks emanated bidirectionally from a site termed *ori1* [also called *oriV* (11)]. However, miniplasmid deletion derivatives that lack this site, but show similar replication behavior, were obtained readily (12). These replicate unidirectionally from *ori2* [*oriS* (13)], both *in vivo* and *in vitro* (14, 15). It is not known why the *ori1* site is preferred in the original mini-F. In any event, the smaller mini-F, replicating from *ori2*, has been used in most investigations.

The basic *repFIA* replicon is made up of three components. One is *ori2*. The others are the single essential replication gene, *repE*, whose product regulates all aspects of initiation, and the copy control region, *incC* (13, 16, 17). A plasmid comprising only these elements replicates normally, but is nevertheless unstable. Stable inheritance requires a mechanism to ensure that plasmid copies are directed into each of the daughter cells, and this function is provided by the adjacent *sop* locus (18). *Sop* is essentially a partition module that can act independently of the *rep* locus to which it is normally linked, to stabilize plasmid vectors in which it is inserted. Together, the *rep* and *sop* loci constitute the basic F maintenance system. This arrangement is remarkably similar to that found in the P1 prophage plasmid [a detailed level, *RepFIB* is probably a more exact analogue of the mini-P1 replicon]. Studies of mini-F and mini-P1 have been reciprocally informative.

2. F in the Cell Cycle

To ensure that F makes replicas available for both daughter cells at division, in spite of its low copy number, it would appear necessary for replication to be coordinated with the cell cycle. Viewed simply, this would imply that F replication take place at a specific time in the cycle for given growth conditions, as does the initiation of chromosome replication. However, a number of careful studies have indicated that both F and mini-F replicate in cells of all ages, without delaying cell division (eg, Refs. 19 and 20). Despite some dissenting opinion (21), it appears reasonable at present to view replication of F as more loosely coordinated with the cell cycle than that of the chromosome. How F could achieve high hereditary stability in the absence of cell cycle coordination remains unclear.

3. Replication Control

F provides the regulator of its replication, while the chromosome contributes essential components to the mechanism of initiation at *ori2*. Thus, the host DnaA initiator protein binds on one side of the origin to enhance opening of an AT-rich region (Fig. 2**a**). Initiation itself, however, requires binding of the F RepE protein to specific sites (iterons) on the other side (22), so that the duplex becomes sufficiently deformed to allow entry of **DnaB helicase** and assembly of a replication complex (23, 24) (see DNA Replication).

Figure 2. Aspects of mini-F replication. (**a**) Opening of *ori2* at initiation; **A** is DnaA protein, bound at tandem DnaA boxes (shaded DNA), **E** is RepE monomer bound to the iterons of *ori2*; together they cause melting of the AT-rich region at a 13-mer sequence similar to those that are opened at an early stage of initiation in *oriC*. (**b**) Regulation of RepE synthesis and activity. Each arm of the operator (filled arrows) contains an 8-bp subsequence of the 19-mer iteron binding sites (open arrows), suggesting that initiation, negative control, and autoregulation all depend on interaction of the same RepE binding domain with DNA. Limiting RepE synthesis by autoregulated transcription, along with limiting RepE availability through binding to *incC*, could constitute a copy-control mechanism. But how

can competitive binding be effective if an autoregulatory mechanism exists to replenish the pool of free RepE? One solution is that RepE exists in two forms: It is first synthesized as a repressor, which binds to the operator but not to the origin, and part of it is then converted to an initiator form that binds to *incC* and *ori2* . In this way, titration and autoregulation become to a large extent independent of each other (30). Indeed, the complex formed by RepE with the operator is structurally distinct from that formed with *ori2* (31). The model is further supported by the finding that most RepE is present in a dimer form with operator-binding and repressor activity. The initiator is made when the dimer is converted by the DnaK–DnaJ–GrpE chaperone machine to a monomer, which binds to the *ori2* and *incC* iterons (29). These chaperones are thus needed for normal levels of mini-F replication (32). Certain mini-F mutants that have escaped chaperone-dependence make RepE that has lost the ability to dimerize, resulting in high copy numbers (29, 33). (**c**) Principle of handcuffing and the cycle of initiation and inhibition; the interactions shown are intermolecular, but intramolecular coupling is also possible. After replication, the RepE remaining at *ori2* pairs with RepE remaining either at *incC* or at *ori2* on a second plasmid. As more RepE is made, it also pairs, inhibiting initiation by hindering access to replication proteins or impeding the structural transition needed for initiation. Failure to pair is a feature of certain copy-mutant initiator proteins of plasmids P1, RK2, and R6K (35-37). An unknown event (question mark) ruptures the coupling to allow initiation.

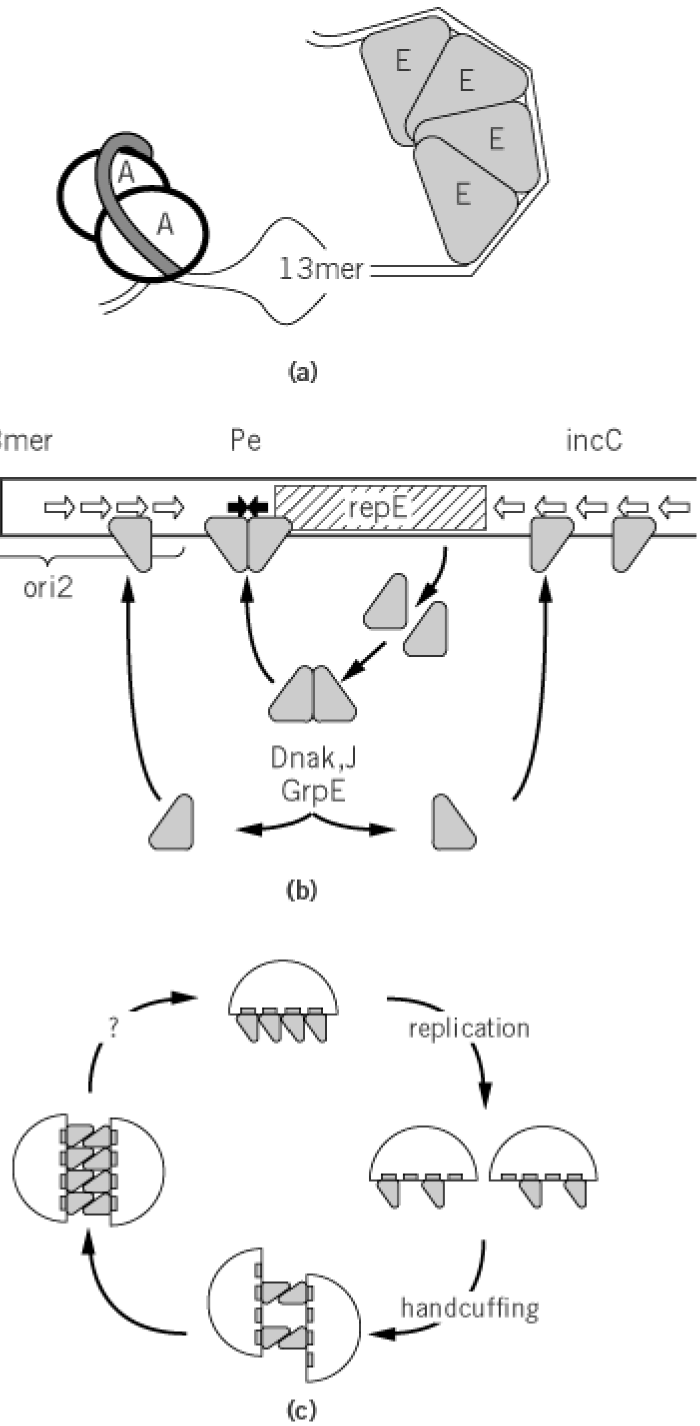

The *incC* control region acts as a brake on the formation of RepE-*ori2* initiation complexes. Additional copies of *incC* in ***trans*** inhibit replication, while deletion of *incC* causes about a fivefold increase in copy number (16, 17, 25). Because *incC* binds RepE (Fig. 2**b**), it was easy to imagine that it competes with *ori2* for RepE, controlling replication by titrating the initiator. An alternative copy-control mechanism sprang from studies of plasmids P1 and RK2 (26, 27), in which it was found that initiators bound to iteron sites can also bind to each other. The iteron regions *ori2* and *incC* could thus pair, either intra- or intermolecularly, to block initiation. This model, termed "handcuffing," would explain regulation of the frequency of initiation by a dual activity of RepE: initial reinforcement of the handcuff to prevent initiation, followed by formation of an initiation complex to start replication (Fig. 2**c**). A subtle modulation of RepE synthesis would seem necessary to allow the transition.

In fact, production of RepE initiator is finely regulated. First, RepE represses transcription of its own gene, by binding to the *repE* **promoter** (28), accounting for the limited quantities of RepE initiator. Second, newly made RepE has only this activity and is unable to initiate replication. This is because newly synthesized RepE forms dimers, which bind to the inverted repeat operator sequence in the *repE* promoter region but not to the iterons in *ori2*. To become an initiator, RepE must be converted to a monomer form (29-31). This conversion is catalyzed by the **DnaK-DnaJ** -GrpE **molecular chaperone** machine, a host function that is needed for normal levels of mini-F replication (29, 32, 33).

Despite the identification of these elements of F replication control, a satisfactory explanation of this process is still beyond us. The discovery of the essential role of the chaperone machine has served only to push the question of the key regulatory process one step further back: What determines the rate at which RepE dimer is converted to active monomer? If the handcuffing model is correct, how is the pairing broken to allow replication? Motor forces of the partition system have been proposed as keys (or boltcutters) for removing the handcuffs (34). But if handcuffed plasmids are pulled apart by the partition apparatus, how does unpairing occur in the case of partition-defective mini-F mutants, which replicate at a normal rate? The true status of *ori1* is unclear: If it is really the major origin in wild-type F, why is DnaA-assisted strand-opening over 2 kbp away essential for initiation?

4. Partition

Deletion of the *sop* region causes loss of mini-F at the rate expected for random distribution of a small number of plasmid copies to daughter cells prior to division, consistent with the disruption of an active partitioning mechanism. The *sop* region consists of three elements (Fig. 1), all essential for partition (18, 38). Two partition proteins, SopA and SopB, are encoded by the *sop* operon. SopA is the main regulator of the operon; it binds to a series of short repeated sequences in the promoter to repress transcription (39). SopB may also assist this repression, because *in vitro* it enhances the affinity of SopA for its promoter (39). The major role of SopB, however, is the formation of a partition complex with *sopC*, a series of 12 tandem repeats of 43 bp that act in ***cis*** to ensure partition, much like a eukaryotic centromere. SopB appears to bind as a dimer to an inverted repeat sequence in each 43-mer, and to wrap *sopC* DNA in positive *supercoils* to form a characteristic complex (40, 41).

How this complex acts in partition is still unknown. Current models suppose that plasmid replicas attach as paired molecules to a host structure, such as the membrane or the division septum, and that some force then splits the pairs, pulling one copy toward each pole. SopA has an ATPase activity and is presumed to have a function in partition beyond its regulatory activity. It may link the SopB-sopC complex to the host structure, where its ATPase activity could drive the separation of paired plasmid copies (42). Our ignorance of the host components with which the Sop complex interacts is presently the major barrier to understanding partition. Host mutations that influence mini-F stability have been located in the *gyrA*, *topA*, and *ugpA* genes (43-45). While the DNA topology function or membrane localization of these proteins is suggestive, there is as yet no good explanation for their roles in partition.

Recent refinements in cytochemical methods applied to bacterial cells have made possible the localization of plasmid molecules as fluorescent foci, allowing the movement of mini-F and other plasmids to be followed in individual cells and populations (20, 46). The data thus far published indicate a preferential location at mid-cell (the site of the next division septum) for mini-F (Fig. 3). After the focus doubles, presumably reflecting replication of the plasmid, the two new foci appear to move to the 1 / 4 and 3 / 4 positions, the midpoints of the emerging daughter cells, at a speed suggestive of an active, directed mechanism. Partition-defective mini-F shows a more random distribution and is often present close to the cell poles (20). These results are consistent with old observations of the paucity of sop^{+} F plasmids in anucleate cells (" minicells") created by division near the cell poles and with the contrasting abundance of *sop* mutant plasmids (47).

Figure 3. Positioning and displacement of mini-F during the cell cycle, based on microscopic examination of cells labeled with fluorescent probes (20, 46). The 1 / 4 and 3 / 4 positions in older cells become the 1 / 2 positions in new cells. Note that the smallness of the interval between the appearance of two mini-Fs and their appearance at the new cell mid-poles implies active displacement (double-headed arrow).

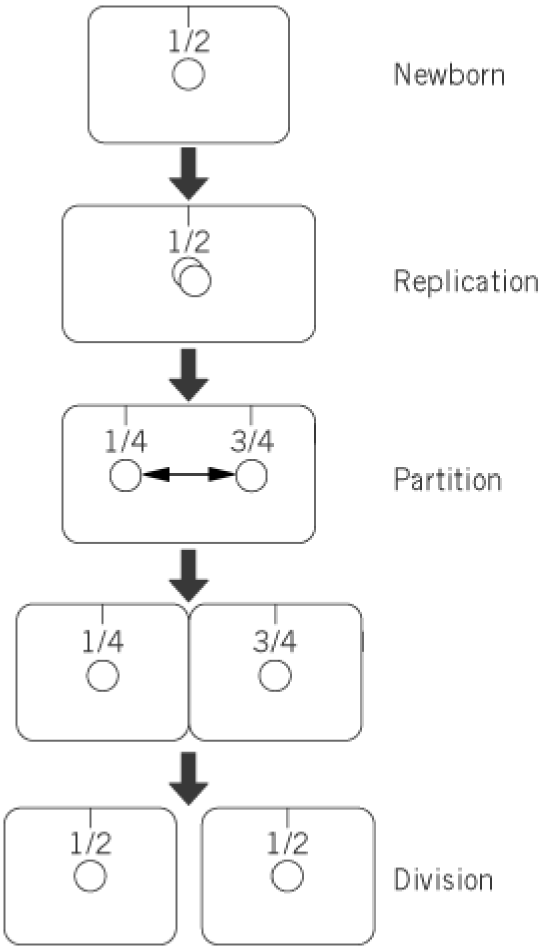

5. Resolution

The stability of DNA species that replicate as q-shaped molecules is under continual threat from the formation of dimers by homologous recombination, because this decreases the number of separate molecules available for partition and reduces initiation frequency in dimer-carrying progeny. Most such replicons have solved this problem by acquiring a site-specific recombination system that resolves dimers back to monomers. *RepFIA* is one of these. The product of the *resD* gene is necessary for the resolution, which takes place within a sequence containing an inverted repeat of 10 bp, the rfsF site (48, 49). ResD is presumed to be the **resolvase**, though *in vitro* evidence is lacking.

6. Addiction

F possesses another type of stability function that, instead of ensuring that each daughter cell inherits a plasmid copy, kills those that fail to. The host population is thus coerced into maintaining the plasmid, a situation likened to addiction (50). The *ccd* (controlled cell death) system turned out to be the first of many examples of a widespread "stable-toxin-unstable-antidote" strategy (51). The CcdB protein inhibits an essential cellular function, DNA gyrase, but in F^+ cells it is kept in check by complexing with the relatively unstable antidote protein, CcdA (52, 53). In an F^- segregant cell, the CcdA is lost by rapid **proteolysis** and cannot be replaced, and the CcdB liberated can attack gyrase and thereby kill the cell.

Two other toxin–antidote systems, *srn* and *flm*, are carried by F. SrnB promotes the degradation of **ribosomal** RNA and transfer RNA by damaging the inner membrane and allowing entry of **ribonuclease I** (54), but its synthesis is normally inhibited by an unstable **anti-sense** RNA, SrnC (55). As with the Ccd system, loss of the plasmid causes a rapid decline in the antidote SrnC, and the liberated and stabilized *srnB* messenger RNA is then translated to produce the toxin. The locus is situated next to *repFIC::*Tn*1000* and was undoubtedly once part of a viable replicon, similar to the R1 plasmid whose *hok*/ *sok* killer system it resembles. *Flm* is another *hok*/*sok* analogue. Its toxin (*flmA*) and antidote RNA (*flmB*) genes are located in the leading region (56). It is tempting to suggest that a burst of FlmA synthesis in the recipient modifies the membrane to facilitate conjugational transfer, but the actual relevance of *flm* is unknown.

Easy isolation of F^- and mini-F^- segregants suggests that these toxin–antidote systems are inefficient. This may, however, be the result of unintended laboratory selection for tolerant strains during decades of genetic experimentation. The significance of such addictive systems in the wild remains to be assessed.

7. Conjugal Aids

Two other loci in the leading region encode functions for which a role in conjugation can be envisaged. The *psiB* gene product is transiently expressed following transfer to a recipient cell, where it inhibits the SOS response, probably by preventing the activation of **RecA** protein (57). Its role might be to prevent induction of inappropriate SOS functions in the recipient. The *ssf* gene, an analogue of *E. coli ssb*, encodes a single-stranded DNA binding protein that might protect DNA entering the cell prior to its replication (58). The absence of leading region functions does not, however, impede DNA transfer or recombinant formation, at least in laboratory conditions, and their significance is thus unclear.

8. Phage Exclusion

Following infection of an F^+ cell by certain phages dubbed "female-specific", (eg, T7 and FII), expression of phage genes begins and the cell dies, but phage development is arrested. The F locus responsible is *pif* (phage inhibition by F), an operon consisting of two genes, *pifC* and *pifA*, located between the *repFIA* and *repFIB* regions. The phenotype is not understood. It appears to be due largely to interactions between PifA and the products of phage genes 1.2 and 10, but it does not seem to be related to the normal activities of these genes. These interactions somehow interrupt entry of phage DNA and cut short expression of its late genes (59). PifC represses *pif* operon transcription by binding to a short inverted repeat sequence overlapping the *pif* promoter –10 region (60). The participation of PifC in mini-F replication initiated at *ori1* has also been proposed, on the basis of the defective replication phenotypes of *pifC* **amber mutants** (61). It is also possible, however, that the phenotype is an indirect effect of PifC amber fragments binding to the *pif* promoter.

9. Perspectives

The F plasmid as a tool has largely retired from the front line of molecular genetics, to be replaced by sleeker, more powerful technologies. Nevertheless, its properties continue to be exploited, eg, its stability and low copy number make it suitable as a **vector** for cloning large fragments of eukaryotic DNA [the BAC vectors (62)]. As a biological entity, on the other hand, F has retained its mystery. We understand only dimly the control of its replication, its mechanism of partition, and the relationship of both processes to the host cell cycle, not only for F, but for all low-copy-number replicons. Finally, although whole-genome sequencing has not yet proved equal to the task of completing the sequence of F, this project is underway (R. Skurray and L. Frost, personal communications) and may well provide some surprises.

Bibliography

1. W. Hayes (1953) J. Gen. Microbiol. **8**, 72–88.
2. L. L. Cavalli, J. Lederberg, and E. M. Lederberg (1953) J. Gen. Microbiol. **8**, 89–103.
3. F. Cuzin and F. Jacob (1967) Ann. Inst. Pasteur **112**, 397–418.
4. Y. Hirota (1960) Proc. Natl. Acad. Sci. USA **46**, 57–64.
5. Y. Nishimura, L. Caro, C. M. Berg, and Y. Hirota (1971) J. Mol. Biol. **55**, 441–456.
6. K. von Meyenberg and F. G. Hansen (1980) In *Mechanistic Studies of DNA Replication and Genetic Recombination*, ICN-UCLA Symposium on Molecular and Cellular Biology (B. Alberts and C. F. Fox, eds.), Academic Press, New York, pp. 137–159.
7. K. Timmis, F. Cabello, and S. N. Cohen (1975) Proc. Natl. Acad. Sci. USA **72**, 2242–2246.
8. M. A. Lovett and D. R. Helinski (1976) J. Bacteriol. **127**, 982–989.
9. D. Lane and R. C. Gardner (1979) J. Bacteriol. **139**, 141–151.
10. P. L. Bergquist, H. E. D. Lane, L. Malcolm, and R. A. Doward (1982) J. Gen. Microbiol. **128**, 223–238.
11. R. Eichenlaub, D. Figurski, and D. R. Helinski (1977) Proc. Natl. Acad. Sci. USA **74**, 1138–1141.
12. J. J. Manis and B. C. Kline (1977) Mol. Gen. Genet. **152**, 175–182.
13. D. Figurski, R. Kolter, R. Meyer, M. Kahn, R. Eichenlaub, and D. R. Helinski (1978) In *Microbiology—1978* (D. Schlessinger, ed.), ASM, Washington, D.C., pp. 105–109.
14. T. Murotsu, H. Tsutsui, and K. Matsubara (1984) Mol. Gen. Genet. **196**, 373–378.
15. K. Muraiso, T. Tokino, T. Murotsu, and K. Matsubara (1987) Mol. Gen. Genet. **206**, 519–521.
16. P. L. Bergquist, R. A. Downard, P. A. Caughey, and H. E. D. Lane (1981) J. Bacteriol. **147**, 888–899.
17. H. Tsutsui, A. Fujiyama, T. Murotsu, and K. Matsubara (1983) J. Bacteriol. **155**, 337–344.
18. T. Ogura and S. Hiraga (1983) Cell **32**, 351–360.
19. C. E. Helmstetter, M. Thornton, P. Zhou, J. A. Bogan, A. C. Leonard, and J. E. Grimwade (1997) J. Bacteriol. **179**, 1393–1399.
20. H. Niki and S. Hiraga (1997) Cell **90**, 951–957.
21. J. D. Keasling, B. O. Palsson, and S. Cooper (1992) Res. Microbiol. **143**, 541–548.
22. T. Murotsu, K. Matsubara, H. Sugisaki, and M. Takanami (1981) Gene **15**, 257–271.
23. D. Bramhill and A. Kornberg (1988) Cell **54**, 915–918.
24. Y. Kawasaki, F. Matsunaga, Y. Kano, T. Yura, and C. Wada (1996) Mol. Gen. Genet. **253**, 42–49.

25. H. Tsutsui and K. Matsubara (1981) J. Bacteriol. **147**, 509–516.
26. S. K. Pal and D. K. Chattoraj (1988) J. Bacteriol. **170**, 3554–3560.
27. M. J. McEachern, M. A. Bott, P. A. Tooker, and D. R. Helinski. (1989) Proc. Natl. Acad. Sci. USA **86**, 7942–7946.
28. L. Sogaard-Andersen, L. A. Rokeach, and S. Molin (1984) EMBO J **3**, 257–262.
29. M. Ishiai, C. Wada, Y. Kawasaki, and T. Yura (1994) Proc. Natl. Acad. Sci. USA **91**, 3839–3843.
30. J. D. Trawick and B. C. Kline (1985) Plasmid **13**, 59–69.
31. L. Masson and D. S. Ray (1986) Nucleic Acids Res. **14**, 5693–5711.
32. Y. Kawasaki, C. Wada, and T. Yura (1990) Mol. Gen. Genet. **220**, 277–282.
33. M. Ishiai, C. Wada, Y. Kawasaki, and T. Yura (1992) J. Bacteriol. **174**, 5597–5603.
34. A. L. Abeles and S. J. Austin (1991) Proc. Natl. Acad. Sci. USA **88**, 9011–9015.
35. G. Mukhopadhyay, S. Sozhamannan, and D. K. Chattoraj (1994) EMBO J **13**, 2089–2096.
36. A. Blasina, B. L. Kittel, A. E. Toukdarian, and D. R. Helinski (1996) Proc. Natl. Acad. Sci. USA **93**, 3559–3564.
37. A. Miron, I. Patel, and D. Bastia (1994) Proc. Natl. Acad. Sci. USA **91**, 6438–6442.
38. H. Mori, A. Kondo, A. Ohshima, T. Ogura, and S. Hiraga (1986) J. Mol. Biol. **192**, 1–15.
39. H. Mori, Y. Mori, C. Ichinose, H. Niki, T. Ogura, A. Kato, and S. Hiraga (1989) J. Biol. Chem. **264**, 15535–15541.
40. D. P. Biek and J. Shi (1994) Proc. Natl. Acad. Sci. USA **91**, 8027–8031.
41. A. S. Lynch and J. C. Wang (1994) J. Mol. Biol. **236**, 679–684.
42. M. Motallebi-Veshareh, D. A. Roach, and C. M. Thomas (1990) Mol. Microbiol. **4**, 1455–1463.
43. T. Ogura, H. Niki, H. Mori, M. Morita, M. Hasegawa, C. Ichinose, and S. Hiraga (1990) J. Bacteriol. **172**, 1562–1568.
44. C. A. Miller, S. L. Beaucage, and S. N. Cohen (1990) Cell **62**, 127–133.
45. B. Ezaki, H. Mori, T. Ogura, and S. Hiraga (1990) Mol. Gen. Genet. **223**, 361–368.
46. G. S. Gordon, D. Sitnikov, C. D. Webb, A. Teleman, A. Straight, R. Losick, A. W. Murray, and A. Wright (1997) Cell **90**, 1113–1121.
47. J. E. Hogan, B. C. Kline, and S. B. Levy (1982) Plasmid **8**, 36–44.
48. D. Lane, R. de Feyter, M. Kennedy, S-H. Phua, and D. Semon (1986) Nucleic Acids Res. **14**, 9713–9728.
49. M. B. O"Connor, J. J. Kilbane, and M. H. Malamy (1986) J. Mol. Biol. **189**, 85–102.
50. H. Lehnherr, E. Maguin, S. Jafri, and M. B. Yarmolinsky (1993) J. Mol. Biol. **233**, 414–428.
51. A. Jaffé, T. Ogura, and S. Hiraga (1985) J. Bacteriol. **163**, 841–849.
52. P. Bernard and M. Couturier (1992) J. Mol. Biol. **226**, 735–745.
53. S. Maki, S. Takiguchi, T. Miki, and T. Horiuchi (1992) J. Biol. Chem. **267**, 12244–12251.
54. R. Ito and Y. Ohnishi (1983) Biochim. Biophys. Acta **20**, 27–34.
55. A. K. Nielsen, P. Thorsted, T. Thisted, E. G. Wagner, and K. Gerdes (1991) Mol. Microbiol. **15**, 1961–1973.
56. S. M. Loh, D. S. Cram, and R. A. Skurray (1988) Gene **66**, 259–268.
57. M. Bagdasarian, A. Bailone, J. F. Angulo, P. Scholz, M. Bagdasarian, and R. Devoret (1992) Mol. Microbiol. **6**, 885–893.
58. A. L. Kolodkin, M. A. Capage, E. I. Golub, and K. B. Low (1983) Proc. Natl. Acad. Sci. USA **80**, 4422–4426.
59. C. K. Schmitt and I. J. Molineux (1991) J. Bacteriol. **173**, 1536–1543.
60. J. F. Miller and M. H. Malamy (1986) Proc. Natl. Acad. Sci. USA **83**, 1433–1437.

61. R. Eichenlaub and H. Wehlmann (1980) Mol. Gen. Genet. **180**, 201–204.
62. H. Shizuya, B. Birren, U. J. Kim, V. Mancino, T. Slepak, Y. Tachiiri, and M. Simon (1992) Proc. Natl. Acad. Sci. USA **89**, 8794–8797.

Suggestions for Further Reading

63. N. Willets and R. Skurray (1987) "Structure and function of the F factor and mechanism of conjugation". In *Escherichia coli and Salmonella. Cellular and Molecular Biology*, 1st ed. (F. C. Neidhart et al., eds.), ASM Press, Washington D.C., pp. 1110–1133. The last comprehensive treatment of the F plasmid, providing all the essential information and references.
64. D. K. Chattoraj and T. D. Schneider (1997) Replication control of plasmid P1 and its host chromosome: the common ground. Prog. Nucleic Acid Res. Mol. Biol. **57**, 145–185. An up-to-date treatment of replication control that takes P1 as the reference point but generalizes the discussion to discuss fully other plasmids, such as F, with similar replicons.
65. S. Hiraga (1992) Chromosome and plasmid partition in Escherichia coli. Annu. Rev. Biochem. **61**, 283–306. A general treatment of partition in E. coli; now slightly dated, but it has all the basics.

Factor Xa

Factor X is a component of the blood clotting system. It circulates in blood plasma (8 µg/mL) as an inactive precursor of a serine proteinase (1). When the blood coagulation process is initiated, factor X is converted to factor Xa (activated factor X), which forms part of a complex that converts another serine proteinase precursor, pro-thrombin, into the active enzyme thrombin. Clotting occurs when thrombin converts fibrinogen to **fibrin**.

Factor X is synthesized in the liver as a 488-amino-acid residue precursor protein, pre-pro-X, the primary translation product of the factor X gene (2). Forty amino acids are cleaved from the amino terminus of pre-pro-X. The resultant 448-residue protein is modified by the attachment of sugars and, in a vitamin-K-dependent process, by the carboxylation of certain glutamic acid residues to form g-carboxy glutamic acid residues. It is cleaved by a specific proteinase that removes residues 140 to 142, so factor X circulates as a two-chain, **disulfide bond**-linked, enzymatically inactive protein. This heavy-chain–light-chain dimeric structure is typical of the blood coagulation proteins (3).

As might be expected, activation of blood coagulation is a carefully controlled process involving many clotting factors (see Blood Clotting). All the details of this process are not fully understood as yet, but it is known that factor X can be converted to an active enzyme by two distinct pathways, the *intrinsic* and the *extrinsic* (4). The former pathway involves activation by factor IXa, which together with factor VIIIa forms a **receptor** on the phospholipid surface of blood platelets. When factor X binds to this receptor complex, a 52-residue peptide is cleaved from the amino terminus of its heavy chain to form factor Xa. The latter pathway involves activation by factor VIIa which, in an analogous fashion, forms a platelet-bound complex with tissue factor. When factor X binds to this complex, the same peptide is cleaved from the heavy chain to give factor Xa. Calcium ions, which bind to the g-carboxy glutamic acid residues of the light chain (and also to the other clotting factors), are essential for factor X activation.

Once factor X is activated, it binds along with factor Va on the surface of platelets, where it interacts with pro-thrombin to convert this zymogen into thrombin, the end product of the so-called coagulation proteinase cascade. Factor X was first recognized as an essential part of this cascade when it was shown that it could restore coagulability to the plasma of individuals who had a specific hemorrhagic disorder. It was given the name *Stuart factor*, which was subsequently changed to factor X in an effort to systematize the nomenclature of the clotting factors.

Bibliography

1. M. Hertzberg (1994) Blood Rev. **8**, 56–62.
2. C. Miao, S. P. Leytus, D. W. Chung, and E. W. Davie (1992) J. Biol. Chem. **267**, 7395–7401.
3. E. W. Davie, K. Fujikawa, M. E. Legaz, and H. Kato (1975) In *Proteases and Biological Control* (E. Reich, D. B. Rifkin, and E. Shaw, eds.), Cold Spring Harbor Laboratory Press, Cold Spring Harbor, NY, pp. 65–77.
4. M. P. McGee and L. C. Lee (1991) J. Biol. Chem. **266**, 8079–8085.

Suggestions for Further Reading

5. U. Hedner and E. W. Davie (1989) "Introduction to hemostasis and the vitamin K-dependent coagulation factors". In *The Metabolic Basis of Inherited Disease* (C. R. Scriver, A. L. Beaudet, W. S. Sly, and D. Valle, eds.), McGraw-Hill, New York, pp. 2107–2134.
6. G. J. Broze Jr. (1995) Tissue factor pathway inhibitor and the revised theory of coagulation. Annu. Rev. Med. **46**, 103–112.

Facultative Heterochromatin

Facultative heterochromatin is the term describing regions of chromosomes that appear **heterochromatic** at certain times in the cell cycle but are not always this way. This is contrasted with constitutive heterochromatin, which is always condensed and stains strongly throughout the cell cycle (1). Facultative heterochromatin represents domains of euchromatin that are condensed and inactive in a particular cell. An excellent example of the assembly of facultative heterochromatin is found in the inactive X-chromosome (see Barr Body, X-Chromosome Inactivation). In the inactive X-chromosome, the histones are hypoacetylated, DNA is **methylated**, and the chromosome replicates late in **S-phase**. All of these traits are characteristic of inactive chromatin. Importantly, these are not irreversible modifications and can be reversed at certain points in development (see Random X-Inactivation).

The various characteristics of facultative heterochromatin effectively work together to stabilize a **transcriptionally** repressed state. The generation of antibodies against **acetylated** histones has allowed a number of general correlations concerning the possible functional roles of histone acetylation. There is also a strong correlation between histone acetylation and the transcriptional activity of chromatin. In *Saccharomyces cerevisiae* most of the genome is transcriptionally active and contains hyperacetylated core histones. Transcriptionally inactive **domains** of chromatin in **yeast**, such as the silent **mating type** cassettes and **telomeric** sequences, contain histone H4 that is hypoacetylated, except at one position, Lys12 (2). In higher eukaryotes, acetylation of histone H4 increases during the reactivation of transcription in the initially inactive chicken erythrocyte nucleus, following fusion of the erythrocyte with a transcriptionally active cultured cell, to form a heterokaryon (see Euchromatin). Histone acetylation is particularly prevalent over the specific b-**globin** genes that are actively transcribed in reticulocytes. More recent studies have demonstrated convincingly that histone hyperacetylation is actually restricted to the domain of chromatin that contains the potentially active chicken b-globin gene locus (see Domain, Chromosomal). This result indicates very specific targeting of histone acetyltransferase activity. **Immunolabeling** of polytene chromosomes in *Chironomus* and *Drosophila* also reveals a nonrandom distribution of histone H4 acetylation that correlates with transcriptional activity. Within female mammals, the transcriptionally inactive X-chromosome is distinguished by a lack of histone H4 acetylation (3). Therefore several independent experimental approaches have shown that actively transcribed and potentially active chromatin domains are selectively enriched in hyperacetylated histones, whereas transcriptionally inactive chromatin contains hypoacetylated histones.

A role for specialized chromatin structures in mediating transcriptional silencing by methylated DNA, like that found in the facultative heterochromatin of vertebrates, has been suggested by several investigators. High levels of methyl-**CpG** correlate with transcriptional inactivity and **nuclease** resistance in vertebrate chromosomes (4). Methylated DNA transfected into mammalian cells is also assembled into nuclease-resistant structures within the assembled minichromosomes, indicating the existence of unusual **nucleosomal** particles (5). These unusual nucleosomes migrate as large nucleoprotein complexes in agarose gel electrophoresis. These complexes are held together by higher order protein–DNA interactions, despite the presence of abundant **micrococcal nuclease** cleavage points within the DNA. Individual nucleosomes assembled on methylated DNA interact together more stably than on unmethylated templates.

The accessibility of chromatin to nucleases could also be affected directly by the stability with which the histones interact with DNA within the nucleosome. DNA methylation does not influence the association of core histones with the vast majority of DNA sequences in the genome. However, for certain specific sequences, such as those found in the Fragile X mental retardation gene 1 promoter, methylation of CpG dinucleotides alters the positioning of histone–DNA contacts and the affinity with which these histones bind to DNA (see Acentric Fragment). The exact chromatin structure found *in vivo* can also result from gene activity. Linker histones, such as H1, are relatively deficient in the transcribed regions of genes. So it is not surprising that transcriptionally inactive facultative heterochromatin containing methyl-CpG should show an increase in the abundance of histone H1, whereas DNA sequences lacking methyl-CpG are deficient in H1. *In vitro* studies indicate that histone H1 interacts preferentially with methylated DNA under certain conditions.

There are also features of transcriptional repression dependent on methylated DNA that can be explained by methylation-specific repressors that operate more effectively within a facultative heterochromatin environment. Transcriptional repression is strongly related to the density of DNA methylation. A non linear relationship exists between the lack of repression observed at low densities of methyl CpG and repression at higher densities. These results led to the demonstration that local domains of high methyl-CpG density confer transcriptional repression on unmethylated **promoters** in *cis*. The importance of a nucleosomal infrastructure for transcriptional repression dependent on DNA methylation is shown by the observation that immediately after injection into *Xenopus* oocyte nuclei, methylated and unmethylated templates both have equivalent activity (6). As facultative heterochromatin is assembled, however, the methylated DNA is repressed with the loss of DNase I hypersensitive sites and the loss of engaged **RNA polymerase** . The requirement that nucleosomes exert efficient transcriptional repression dependent on DNA methylation can be explained in several ways. Methylation-specific repressors might recruit a corepressor complex that directs the modification of the chromatin template into a more stable and transcriptionally inert state. One potential candidate corepressor for MeCP2 is the SIN3-histone deacetylase complex, because inhibition of histone deacetylation reverses some of the transcriptional repression conferred by DNA methylation (7). Alternatively, like histone H1, methylation-specific repressors might bind more efficiently to nucleosomal rather than to naked DNA. Any cooperative interactions between molecules could propagate their association of methylation-specific repressors along the nucleosomal array even into unmethylated DNA segments. This latter mechanism is analogous to the nucleation of heterochromatin assembly at the yeast telomeres by the DNA-binding protein RAP1, which then recruits the repressors SIR3p and SIR4p that organize chromatin into a repressive structure (8) (see Telomere). All of these potential mechanisms could individually or together contribute to assembling of a repressive facultative heterochromatin domain.

A final relevant issue is the significance of the timing of replicative initiation on facultative heterochromatin in **S-phase**. Facultative heterochromatin is normally replicated late in the S-phase. If replication disrupts both active and repressed chromatin structures, then the entire nucleus has to be remodeled after each replication. The accessibility of immature chromatin on newly replicated DNA provides a means to accomplish this remodeling. The reformation of nuclear structures, however, has other implications. If the transcription factors available in a cell are limiting, then a gene that is replicated early in the S-phase has more opportunity to assemble an active transcription complex than a gene that replicates late simply because the gene that replicates early is available for transcription factors to bind to it before all of the early replicating portion of the genome has sequestered these factors. Therefore a late-replicating gene in facultative heterochromatin experiences a relative deficiency in transcription factor availability. Transcriptionally active genes in euchromatin replicate early in the S-phase (see Euchromatin). The reason for this early replication is unknown, but possibilities include the local disruption of chromatin structure by transcription complexes, which makes that DNA more accessible to the replication machinery (9) and the observation that many transcription factors are in fact also replicative factors. An attractive variation of this model is that the type of chromatin assembled early in the S-phase is more accessible to transcription factors than chromatin assembled late in the S-phase. Early replicating chromatin may sequester histones that are more highly acetylated and consequently more accessible to the transcription factors that maintain continued transcriptional activity. The CENP-A protein that replaces histone H3 in the mammalian centromere within heterochromatin is synthesized at the very end of the S-phase, providing an example of how the cell cycle-dependent compartmentalization of **protein biosynthesis** might contribute to assembling a specialized chromatin structure (10). Although a general test of the significance of this model has not been made, it remains an attractive mechanism for explaining both the maintenance of specific patterns of gene expression in a proliferating cell type and the maintenance of domains of facultative heterochromatin.

Bibliography

1. S. W. Brown (1966) Science **151**, 417–425.
2. M. Braunstein et al. (1993) Gene Dev. **7**, 592–604.
3. P. Jeppesen and B. M. Turner (1993) Cell **74**, 281–291.
4. F. Antequera, D. Macleod, and A. Bird (1989) Cell **58**, 509–517.
5. I. Keshet, J. Lieman-Hurwitz, and H. Cedar (1986) Cell **44**, 535–543.
6. S. U. Kass, N. Landsberger, and A. P. Wolffe (1997) Curr. Biol. **7**, 157–165.
7. L. Alland et al. (1997) Nature **387**, 49–55.
8. M. Grunstein et al. (1995) J. Cell Sci. 519–536.
9. A. P. Wolffe and D. D. Brown (1988) Science **241**, 1626–1632.
10. R. D. Shelby, O. Vafa, and K. F. Sullivan (1997) J. Cell Biol. **136**, 501–513.

Suggestion for Further Reading

11. A. Wolffe (1998) *Chromatin: Structure and Function* 3d ed., Academic Press, London.

Farnesylation

Farnesylation is the process by which a cysteine residue in the C-terminal region of some eukaryotic proteins is **posttranslationally modified** with an isoprenoid lipid (the 15-carbon farnesyl group) and the exposed carboxyl group is methylated (Fig. 1). The farnesylation and carboxylmethylation increase the affinity of the protein for the membrane and have important functional consequences. The farnesyl group is one of several lipids that act as a membrane anchor for proteins. The role of the farnesyl group and other lipids in membrane anchoring is described in more detail elsewhere [see Prenylation; Membrane Anchors]

Figure 1. Modification of a C-terminal cysteine residue by a farnesyl group.

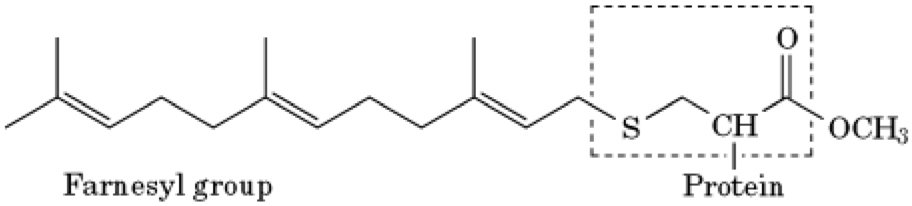

Farr Assay

The Farr assay (1, 2) is a precipitation-based immunoassay that is especially appropriate for analysis of certain antibody–antigen interactions that do not lead to an insoluble lattice of crosslinked antibody–antigen complexes (see Precipitin Reaction). Failure to crosslink is frequently encountered with haptens, small antigens, and monoclonal antibodies. The Farr assay takes advantage of a common solubility property of immunoglobulins. Ammonium **sulfate** at 50% saturation causes antibodies and immune complexes to precipitate, whereas free antigens and haptens often remain soluble. Measurement of the antigen-binding capacity of an uncharacterized antibody preparation can be achieved by mixing a fixed amount of antigen with serial dilutions of antibody, allowing the binding reaction to reach equilibrium, precipitating free and complexed antibody with ammonium sulfate, and then measuring the antigen content of the precipitate. Antigen is precipitated quantitatively until a subsaturating dilution of antibody is reached, whereupon the antigen content of the precipitates progressively decreases. Observation of a constant amount of precipitate at saturating antibody concentrations differs from the precipitin reaction, in which excess antibody actually inhibits formation of a precipitate. The Farr assay is now obsolete, but is cited frequently in older literature.

Bibliography

1. R. S. Farr (1958) J. Infect. Dis. **103**, 239–262.
2. P. Minden and R. S. Farr (1967) "The ammonium sulphate method to measure antigen binding capacity", in *Handbook of Experimental Immunology*, D. M. Weir, ed., Blackwell, Oxford, pp. 493–526.

Fate Map

1. Classical Fate Maps

A fate map is a graphic representation of the cells or regions within the embryo at one point during development that will develop into specific tissues and organs at subsequent developmental stages. The concept of the fate map may be one of the earliest abstract ideas in embryology, one that is implicit, for example, in the "homunculus" imagined by seventeenth century microscopists to be a miniature adult human that is "preformed" within the sperm. The concept of preformation was generally favored by scientists until the last half of the eighteenth century, when Caspar Friedrich Wolff, through observation of chick embryo development, postulated that embryos develop through a process he termed "**epigenesis**," whereby unpatterned tissues of the early embryo reorganize and expand to form the tissues and organs of the adult. As the cellular basis for tissue organization came to be understood by the mid-nineteenth century, it eventually became clear that embryonic development could be characterized by four cellular phases common to all vertebrate and most invertebrate embryos: (i) formation of the single-celled, diploid zygote (or fertilized egg) through union of haploid sperm and egg; (ii) **cleavage** , in which the fertilized egg undergoes mitotic division without increase in size to form the multicellular **blastula** (mammalian: blastocyst); (iii) **gastrulation**, in which blastula cells rearrange and expand to form the three **primary germ layers** (ectoderm, mesoderm, and endoderm) that are organized into the basic body plan (concepts developed in the early nineteenth century by von Baer); and (iv) **organogenesis**, in which the cells within the the three primary germ layers of the embryo form the organ and tissue primordia that develop into the tissues and organs of the *fetus* . The fetal stage of development is distinguished from the embryonic phase in that the fetus is indeed a preformed miniature of the adult that contains all of the organ and tissue rudiments (in the right places and containing differentiated cells and stem cells) that need only to expand and mature to function as adult tissues and organs. The transition from embryo to fetus occurs at about the eighth week of human development.

In the late nineteenth and early twentieth centuries, embryologists began to take an experimental approach to the study of development. Fate maps of relatively simple embryos, such as ascidians, were initially established by directly observing the fate of blastula cells during gastrulation (1). The emergence of dyes that could be applied to living tissues without damaging them ("vital dyes") permitted selective staining of parts of blastula embryos and subsequent tracing of the tissues of the embryo that developed from these stained parts. Systematic application of this procedure to trace the fate of different regions of amphibian blastulas through gastrulation led to the construction of the first detailed and comprehensive fate map of a vertebrate embryo (2, 3). Subsequent work by many individuals led to the construction of fate maps for organ rudiment primordia of a variety of chordate embryos (amphioxus, fish, amphibians, birds) (4-9). These maps continue today as the primary basis for our present day understanding of **morphogenetic** movements (2) that blastula cells undergo during gastrulation. Nevertheless, these maps are constantly being revised and refined by applying more modern techniques. For recent examples, see fish (10, 11); birds (12-15); and amphibians (16-18).

Although fate maps, such as those described previously, give a general idea how regions of the blastula give rise to the primary organ primordia of the embryo, they do not yield precise details of the way cells within those primordia give rise to the more complex tissues and organs of the fetus and adult. These events could not be adequately followed by direct observation because of the massive expansion of cells during the embryonic phase of development. Moreover, during the ensuing cell expansion and migrations, vital dyes became diluted beyond the level of detectability. The latter problem was only partially circumvented by using microscopic carbon particles to follow cell movements and rearrangements (19, 20).

In the late 1960s, however, Nicole Le Douarin developed a powerful method for embryonic fate mapping that allowed following the mapping of embryonic tissues indefinitely, even into full adulthood. Briefly, she discovered that quail cells could be distinguished from chicken cells by a nucleolus in the quail cell that developed a brilliant magenta color when stained with the Feulgen reagent (21, 22). By transplanting homologous tissues from quail embryos into chick embryos, the fate of the transplanted quail cells could be established unequivocally by histological methods. Through broad application of this method, the development of the avian embryo has been mapped in detail (see Ref. 23 for many examples) Much of this newer map supports and confirms earlier work. Nevertheless, this new method brilliantly illuminated the many limitations and previous inaccuracies of earlier methods. This is particularly true for migratory mesenchyme cells within the embryo, such as the neural crest, which, as revealed by LeDouarin and co-workers, populate a previously unknown variety of tissues and organs (24-28). In addition, the embryonic development of other mobile cell populations, such as blood cell lineages (29-34) and muscle precursor cells (35-37) and many other other tissues, were extended and clarified in ways not possible previously.

2. Mammalian Embryo Fate Maps

Fate mapping in mammalian embryos progressed much more slowly because of the relative inaccessibility of these embryos within the mother's uterus. Therefore, the fate maps in most existing textbooks are derived from the avian embryo based on assumption that mammalian development is essentially identical. Because of the recent development of methods for *in vitro* culture of early mammalian embryos, fate mapping of early mammalian development has begun. One such fate map experiment was conducted by transplanting fragments of tissue from early mouse embryos **radiolabeled** with tritiated thymidine in unlabeled embryos, followed by localizing the labeled tissues by autoradiography (38). The recent development of highly **fluorescent** dyes that can be injected into cells has greatly facilitated fate mapping of early mouse embryo tissues (39-43) To date, the most important outcome of such studies has been to establish that existing mammalian fate maps based upon the avian model are indeed valid by and large. Therefore, it is no exaggeration to state that the methods and strategies developed by Le Douarin and the resulting detailed fate maps of the avian embryo provide the most accurate and comprehensive information garnered during the twentieth century about the cellular movements underlying vertebrate embryonic development, including mammalian and human development.

3. Embryonic Fate and Developmental Potential

At the onset of development, the single-celled zygote can form all of the cell and tissue types of the adult, and this potential is apportioned during embryogenesis. The relationship between developmental potential and developmental fate is the central question that developmental biologists have been trying to understand for more than a century [the reader is directed to a recent and excellent review and discussion by Viktor Hamburger of the early experiments in this area (44)]. Wilhelm Roux first addressed this problem experimentally in 1883 by ablating one blastomere of an amphibian embryo. He found that the surviving blastomere formed an incomplete embryo, leading him to conclude that fate and potential were apportioned in concert. Although this initial conclusion was flawed, Roux's novel and experimental approach laid the foundations for what came to be known as **experimental embryology**. It was not long until it was experimentally established that developmental potential is generally more widely dispersed within the early embryo than developmental fate. Thus, a specific region of the early embryo can develop into several different tissues and organs, even though its fate represents only one of those possible outcomes. As the embryo matures, the range of potentiality of these regions becomes restricted until, ultimately, potential and fate become equal, and the tissue is deemed determined (45). The mechanism(s) that control fate and potential constitute one of the central mysteries of developmental biology. The seminal experiment that established the profound depth of this mystery was reported in 1924 by Hilda Mangold, a graduate student in the laboratory of Hans Spemann. She showed that fragments of specific regions from one amphibian gastula could induce formation of a complete second embryo when transplanted into the prospective belly region of a host gastrula (46) (an English translation of this article can be found in Ref. 47). The fact that the transplanted fragment could reprogram host tissue, fated to form abdominal structures, to form head tissues, including brain, led to the "organizer" hypothesis, in which some embryonic tissues play central roles to induce and direct the development of neighboring tissues. That discovery provided the conceptual basis for virtually all developmental biology in the twentieth century. Despite the advances in the cellular and molecular analysis of development in the last two decades of this century, the mechanistic bases for organizer function, morphogenesis, and cell determination in vertebrates remain mysteries.

4. Genetic Control of Developmental Fate

By contrast, however, research into mechanisms by which genes control embryonic development has progressed most rapidly, using the fruit fly *Drosophila*, because of the advanced state of genetic analysis in this organism. Although a fate map of the early *Drosophila* embryo was available by mid-twentieth century (48), a coherent hypothesis regarding the role of specific genes in establishing the Drosophila fate map was first proposed in 1980 (49-51) (see Ref. 52 for a broad discussion of the underlying embryological issues). This breakthrough in studying the relationship between embryonic fate maps and genetics has revolutionized the developmental biology of *Drosophila*. A large proportion of the **genes** that act developmentally in flies have vertebrate **homologues** that play key, but typically different, developmental roles. Thus, a definitive model for the genetic control of embryonic fate maps and pattern formation in vertebrates remains to be established.

5. The Difficult Relationship Between Fate Maps and Vertebrate Genetic Expression Patterns

Molecular probes for the expressed products of genes developed during the last half of the twentieth century have allowed superimposing fate maps and gene expression maps. The first use of such a technique can be traced back to at least 1957, when Holtzer and Detwiler used a fluorescent antimyosin antibody to localize the earliest appearance of differentiated muscle cells within the somite myotomes of chick embryos (53). This general approach expanded enormously in recent years and now includes in situ hybridization, which allows detecting the **RNA** products of genes. Thus the developmental expression maps of a large number of genes of both known and unknown function are now known for development of a wide range of organisms. In instances in which the patterns derived from these two types of maps coincide, it is often assumed that the molecular expression accurately reflects that of cells whose fate is known. Although this may be generally true, the assumption carries potential pitfalls of which one should be wary, at least when unaccompanied by appropriate experimental validation. Migratory cells, for example, often intermingle transiently with and are indistinguishable from nonmigratory cells. The signal from the migratory cells in such situations can be discerned if they carry an independent lineage marker, such as the quail nucleolus referred to previously, that allows distinguishing them from their nonmigratory counterparts (54). On the other hand, some gene products (particularly RNA) can appear and be degraded extremely rapidly in patterns that reflect transcriptional waves passing through specific tissues. Pourquie and co-workers discovered such transcriptional waves and distinguished them from cell migration by demonstrating discordance over time between the pattern of injected fluorescent dyes and gene expression signals (55). Finally, cells may transiently express one gene product at one period of development and then switch to expression of another. Cepko and co-workers have developed techniques in which infective retroviruses are used to follow transient expression patterns of individual cells and their progeny through complex developmental pathways (56-59). These examples serve only to illustrate that gene expression patterns can only be assumed to reflect cell lineage or fate maps until experimentally verified by independent means.

6. Transgenic Strategies for Fate Mapping

Molecular techniques are now being used to map developmental fate and potential and also to manipulate them experimentally. Retroviruses are widely used to deliver bioactive genes to influence development positively or negatively through the expression of exogenous gene products (for examples, see Refs. 60, 61). The emergence of methods for creating germ-line **transgenic** mice has led to a variety of new and imaginative approaches to analyzing of the relationship between cell fate and gene expression in mammalian development. Buckingham and co-workers have “knocked-in” a **beta-galactosidase** marker gene into a gene locus, which that controls the onset of myogenesis, to locate newly "born" muscle precursor cells in the mouse embryo (62, 63). Recently, transgenes that must undergo recombination signals to be expressed in a cell- or tissue-specific fashion have been used by Nicolas and co-workers to track cell lineage progression in early mouse development (64-66). It is important to keep in mind that, because each of these techniques depends on cell- or tissue-specific gene regulation (which is itself only beginning to be understood), each is subject to the caveats alluded to previously for the relationship between cell fate and gene expression. Nevertheless, the power of these new techniques augers well for the future analysis of mechanisms underlying the apportionment of cell fate and potential during embryonic development.

Bibliography

1. E. G. Conklin (1905) J. Acad. Nat. Sci. (Philadelphia) **2**, 13.
2. W. Vogt (1929) Roux' Arch. **120**, 385–706.
3. W. Vogt (1925) Roux' Arch. **106**, 542–610.
4. R. Wetzel (1929) Roux' Arch. **119**, 118–321.
5. E. G. Conklin (1932) J. Morphol. **54**, 69–118.
6. J. M. Oppenheimer (1936) J. Exp. Zool. **72**, 409–437.
7. J. Pasteels (1940) Biol. Rev. **15**, 59–106.
8. D. Rudnick (1943) Q. Rev. Biol. **19**, 187.
9. J. M. Oppenheimer (1947) Q. Rev. Biol. **22**, 105–118.
10. K. Woo and S. E. Fraser (1995) Development **121**, 2595–2609.
11. J. Shih and S. E. Fraser (1995) Development **121**, 2755–2765.
12. H. Eyal-Giladi and S. Kochav, (1976) Dev. Biol. **49**, 321–337.
13. M. A. J. Selleck and C. D. Stern (1991) Development **112**, 615–626.
14. Y. Hatada and C. D. Stern (1994) Development **120**, 2879–2890.
15. G. C. Schoenwolf, V. Garcia-Martinez, and M. S. Dias (1992) Developmental Dynamics **193**, 235–248.
16. S. B. Minsuk and r. R. E. Kelle (1996) Developmental Biol. **174**, 92–103.
17. T. Elul, M. A. Koehl, and R. Keller (1997) Developmental Biol. **191**, 243–258.
18. R. Harland and J. Gerhart (1997) Annu. Rev. Cell Developmental Biol. **13**, 611–667.
19. N. T. Spratt Jr. (1946) J. Exp. Zool. **103**, 259–304.
20. R. C. Fraser (1954) J. Exp. Zool. **126**, 349–399.
21. N. M. Le Douarin (1969) Bull. Biol. Fr. Belg. **103**, 435–452.
22. N. Le Douarin (1973) Exp. Cell Res. **77**, 459–468.
23. N. M. Le Douarin and M. A. Teillet, eds. (1984) *Chimeras in Developmental Biology*, Academic Press, London, San Diego.
24. N. M. Le Douarin and M. A. Teillet (1973) J. Embryol. Exp. Morphol. **30**(1), 31–48.
25. N. M. Le Douarin (1975) Birth Defects Original Article Series, **11**(7), 19–50.
26. J. Fontaine, C. Le Lievre, and N. M. Le Douarin (1977) Gen. Comp. Endocrinol. **33**(3), 394–404.
27. C. S. Le Lievre and N. M. Le Douarin (1975) J. Embryol. Exp. Morphol. **34**(1), 125–154.
28. J. M. Polak et al. (1974) Histochemistry **40**(3), 209–214.
29. E. Houssaint, M. Belo, and N. M. Le Douarin (1976) Developmental Biol. **53**(2), 250–264.
30. F. V. Jotereau, E. Houssaint, and N. M. Le Douarin (1980) Eur. J. Immunol . **10**(8), 620–627.
31. N. M. Le Douarin and F. V. Jotereau (1975) J. Exp. Med. **142**(1), 17–40.
32. N. M. Le Douarin et al. (1975) Proc. Nat. Acad. Sci. USA **72**(7), 2701–2705.
33. N. M. Le Douarin, E. Houssaint, and F. Jotereau (1977) Adv. Exp. Med. Biol. **88**, 29–37.
34. N. M. Le Douarin, F. Dieterlen-Lievre, and P. D. Oliver (1984) Am. J. Anat. **170**(3), 261–299.

35. B. Christ, H. J. Jacob, and M. Jacob (1974) Experientia **30**(12), 1446–1449.
36. B. Christ, H. J. Jacob, and M. Jacob (1977) Anat. Embryol. **150**(2), 171–186.
37. A. Chevallier, M. Kieny, and A. Mauger (1977) J. Embryol. Exp. Morphol. **41**, 245–258.
38. P. P. L. Tam and R. S. P. Beddington (1987) Development **99**, 109–126.
39. K. A. Lawson, J. J. Meneses, and R. A. Pederson (1991) Development **113**, 891–911.
40. M. Parameswaran and P. P. L. Tam (1995) Dev. Genet. **17**, 16–28.
41. P. P. L. Tam and S. X. Zhou (1996) Developmental Biol . **178**, 124–132.
42. P. P. L. Tam and R. R. Behringer (1997) Mech. Dev. **68**, 3–25.
43. P. P. L. Tam et al. (1997) Development **124**, 1631–1642.
44. V. Hamburger (1988) *The Heritage of Experimental Embryology: Hans Spemann and the Organizer*, Monographs on the History and Philosophy of Biology (R. B. R. Burian Jr., R. Lewontin, and J. M. Smith, eds.), Oxford University Press, New York and Oxford.
45. H. Spemann (1938) *Embryonic Development and Induction* Yale University Press, New Haven, CT.
46. H. Spemann and H. Mangold (1924) Roux' Archiv. **100**, 599–638.
47. B. H. Willier and J. Oppenheimer (1974) *Foundations of Experimental Embryology*, 2nd ed., Hafner, New York.
48. D. F. Poulson (1950) *Biology of Drosophila* (M. Demerec, ed.), Hafner, New York, pp. 168–270.
49. C. Nusslein-Volhard and E. Wieschaus (1980) Nature **287**, 795–801.
50. S. Roth, D. Stein, and C. Nusslein-Volhard (1989) Cell **59**, 1189–1202.
51. C. Nusslein-Volhard and S. Roth (1989) Ciba Foundation Symposium **144**, 37–55; discussion 55–64; 92–98.
52. C. Nusslein-Volhard (1979) In *Determinants of Spatial Organization* (S. S. a. I. R. Konigsberg, ed.), New York, Academic Press, pp. 185–211.
53. H. Holtzer, J. M. Marshall, and H. Finck (1957) J. Biophys. Biochem. Cytol. **3**, 705–729.
54. B. A. Williams and C. P. Ordahl (1994) Development **120**, 785–796.
55. I. Palmeirin et al. (1997) Cell **91**, 639–648.
56. D. L. Turner, E. Y. Snyder, and C. L. Cepko (1990) Neuron **4**(6), 833–845.
57. J. Price, D. Turner, and C. Cepko (1987) Proc. Natl. Acad. Sci. USA **84**(1), 156–160.
58. C. Cepko et al. (1995) Methods Enzymol. **254**, 387–419.
59. J. A. Golden, S. C. Fields-Berry, and C. L. Cepko (1995) Proc. Natl. Acad. Sci. USA **92**(12), 5704–5708.
60. C. P. Austin et al. (1995) Development **121**(11), 3637–3650.
61. D. J. Goff and C. J. Tabin (1997) Development **124**, 627–636.
62. S. Tajbakhsh et al. (1996) Developmental Dynamics **206**, 291–300.
63. S. Tajbakhsh, D. Rocancourt, and M. Buckingham (1996) Nature **384**, 266–270.
64. J. F. Nicolas, L. Mathis, and C. Bonnerot (1996) Development **122**, 2933–2946.
65. L. Mathis et al. (1997) Development **124**, 4089–4104.
66. D. L. Zinyk et al. (1998) Curr. Biol. **8**, 665–668.

Fatty Acids

The major fatty acids of plants and animals contain even numbers (14 to 26) of aliphatic carbon atoms in straight chains, with a terminal carboxylic acid group. The acids may contain up to six nonconjugated *cis*-double bonds, generally separated by two single bonds and a single methylene group. Several shorthand nomenclatures are in use to indicate the number of carbon atoms they contain and the number and position of the double bonds; for example, linoleic acid may be written either as 18:2($n-6$) or 18:2w6, where the number of carbon atoms in the chain ($n=18$) is followed by a colon and the number of double bonds (two). The position of the double bonds is set by the number of carbon atoms from the last double bond to the terminal (or w) methyl group (6); in this example, the two double bonds are between carbons 12–13 and 9–10.

Fatty acids appear as the free acids only when bound to serum albumin in blood. They occur in cell membranes primarily as the hydrophobic moiety in phospholipids and other membrane lipids as esters (see Lipids). Linoleic acid is one of a family of *essential* fatty acids (EFAs) that are required for growth and development in mammals. The EFA all contain the ($n-6$) terminal structure, which cannot be synthesized by mammalian cells because they are unable to introduce *cis*-double bonds beyond carbon 9 in fatty acids. The EFA must therefore be obtained from plants whose enzyme systems do synthesize the ($n-6$) terminal structure. Some of the more abundant fatty acids in cells are listed in Table 1.

Table 1. Some of the More Abundant Fatty Acids in Animals

Systematic Name	Common Name	Shorthand Notation
Saturated		
Dodecanoic	Lauric	12:0
Tetradecanoic	Myristic	14:0
Hexadecanoic	Palmitic	16:0
Octadecanoic	Stearic	18:0
Eicosanoic	Arachidic	20:0
Docosanoic	Behenic	22:0
Tetracosanoic	Lignoceric	24:0
Monoenic		
cis-9-Dodecenoic	Lauroleic	12:1($n-3$) 12:1w3
cis-9-Tetradecenoic	Myristoleic	14:1($n-5$) 14:1w5
cis-9-Hexadecenoic	Palmitoleic	16:1($n-7$) 16:1w7
cis-9-Octadecenoic	Oleic	18:1($n-9$) 18:1w9
cis-11-Octadecenoic	*cis*-Vaccenic	18:1($n-7$) 18:1w7
cis-9-Eicosenoic	Gadoleic	20:1($n-11$) 20:1w11
cis-13-Docosenoic	Erucic	22:1($n-9$) 22:1w9
cis-15-Tetracosanoic	Nervonic	24:1($n-9$) 24:1w9
Polyunsaturated (PUFA)		
9,12-Octadecadienoic	Linoleic	18:2($n-6$) 18:2w6
6,9,12-Octadecatrienoic	g-Linolenic	18:3($n-6$) 18:3w6
8,11,14-Eicosatrienoic	Homo-g-linolenic	20:3($n-6$) 20:3w6
5,8,11,14-Eicosatetraenoic	Arachidonic	20:4($n-6$) 20:4w6

9,12,15-Octadecatrienoic	a-Linolenic	18:3($n-3$)	18:3w3

Suggestions for Further Reading

W. W. Christie (1982) *Lipid Analysis*, 2nd ed., Pergamon Press, Oxford, U.K. (In addition to analytical methods for analysis of lipids, this book presents a useful summary of fatty acid structures and an extensive bibliography.)

J. A. Erwin (ed.) (1973) *Lipids and Biomembranes of Eukaryotic Microorganisms*, Academic Press, New York. "Chapter 2". (A concise presentation of the comparative biochemistry of fatty acids in eukaryotic microorganisms, and the diversity of fatty acid structures in nature.)

A. I. Laskin and H. A. Lechevalier (1973) *Handbook of Microbiology*, Vol. **II**, CRC Press, Cleveland. (Contains an extensive listing of fatty acids and their properties. A sourcebook for the fatty acid composition of microorganisms.)

Female

The female is one of the two possible **sexes** in nature, the other being the male. Characteristically, mature females produce **oocytes**. In species with intracorporal fertilization, the most predominant feature of a female is the limited number of **gametes** that can be produced. For example in mammals, primordial **germ cells** divide by **mitosis** in females until a certain number (200,000) of oocytes is reached. After birth, these mitotic divisions come to a standstill, and **meiosis** and further maturation of oocytes occurs after puberty at ovulation. Ovulation is not a continuous production of eggs, but involves a selection process in which certain ones are able to become dominant and cause atresia in others. These events typically occur in cycles, with a duration of 21 to 28 days. However, spontaneous or inducable ovulations can also take place, as in the cat or rabbit. Although the number of oocytes produced seems to be more than sufficient, it is apparent, for example, in humans, that the fertile period in the life span of a female is, unlike in males, restricted to a certain age and, within this age, to certain days periodically. This fact is probably the most typical feature of females with regard to **reproduction**.

Considering that each individual strives to transfer its genes to the next generation, the limited number of gametes with a chance to be fertilized causes females to take greater care of each individual gamete than males do. In females, natural selection therefore proceeded in a different way than in the male. Reproductive success in females is optimized when the offspring are actually raised and attain the ability to reproduce in the next generation. As a consequence, females not only use substantial resources in producing a single gamete, by adding nutrition (yolk) (1) and all necessary substances for initial cell divisions and growth of the cells, but, especially in higher chordates, they also provide basic nutrition for the offspring born (2). This is especially the case in mammals, where nutrition and protection is provided for a prolonged time after birth during childhood by the mammary glands, which are a typical female feature. Also, as can be seen in primates, raising of the offspring is done mostly by the female, although there are exceptions (3). Natural selection does not occur in a competition in which genes must be spread, but the most successful female is the one that is best able to protect and raise the offspring. In this respect, it is evident why females in the animal kingdom are better adapted to the environment with regard to hair or feathers, because this serves as a protection against predators. The appearance of this kind of sexual dimorphism depends on the degree of specialization among the two sexes.

In species with extracorporal fertilization, such as frogs and fishes, differences between the two sexes are smaller than in mammals. In these species, both the male and female produce a vast number of gametes to form numerous new individuals. In these species, parental care for the offspring is not the rule. As a consequence, the **phenotypically** visible differences between the sexes vanish. Nevertheless, for the sake of reproductive success, females invest more than males, because the cost of producing eggs is greater than that of producing sperm.

The common biological necessity in females of a greater investment in reproduction has evolved common characteristic features among females of different species. For example, the genitalia of the female consist of **germ-cell** conducting parts (tubes) as well as of germ-cell preserving parts (uterus). Although both male and female genital cells have the same origin in the primordial urogenital tract and in the primordial germ cells, the lack of male hormones due to the absence of the testis-determining factor allows the development of mullerian ducts (see Sex). The fate of these organs is to develop finally to an uterus and a vagina during embryogenesis. Also, the hormonal situation is different in females and males. After puberty, cyclic hormonal actions take place in the female. The expression of follicle-stimulating hormone (FSH) and luteinizing hormone (LH) are directed by FSH-releasing hormone and LH-releasing hormone, respectively. FSH and LH induce ovulation and the expression of estrogen and progesterone, which occurs in the follicle.

In the cascade of sex determination and in adults, hormones are also responsible for the expression of the female phenotype. This includes psychological behavior. Hormones in the female direct fertilization events like ovulation and behavior, eg to indicate the mating time for males.

In higher organisms, the female is the homogametic sex XX, the male the heterogametic XY. Sex determination occurs by the dependence of the presence or absence of the testis-determining factor (SRY), a gene located on the Y-Chromosome in mammals. In these species, therefore, sex determination is dependent on the sperm that successfully fertilizes the oocyte. In birds, some amphibians, and insects, the situation is reversed: The homogametic sex is male, the heterogametic sex is the female. Instead of two X-chromosomes, the chromosomes in the female are ZW, and sex determination occurs during ovulation (see Sex).

Parthenogenesis is possible only with eggs and occurs in some genera of lizards. In some species of fish, spermatozoa are necessary only for the induction of the egg, not for a genetic contribution.

Bibliography

1. T. D. Williams (1994) Biol. Rev. Camb. Phil. Soc. **69**, 35–59.
2. G. N. Wade and J. E. Schneider (1992) Neurosci. Biobehav. Rev. **16**, 235–272.
3. J. W. Makin and R. H. Porter (1984) Behav. Neural. Biol. **41**, 135–151.

Ferguson Plot

Measuring the **electrophoretic** mobility of a macromolecule at several gel (polymer) concentrations (see Gel Electrophoresis) provides information about its size and surface net charge density. In the ideal case, a plot of the logarithm of the mobility versus the gel concentration is linear and known as a Ferguson plot . The slope of such a plot gives the retardation coefficient , which is a measure of the size, shape, and conformation of the macromolecule. The intercept at zero gel concentration provides a measure of the free electrophoretic mobility, the mobility it would have in the absence of gel, which is related to the net charge on the molecular surface. In contrast, the mere inspection of one electrophoretic pattern or measurement of the mobility of one band gives no information whatsoever concerning the size or net charge of the migrating species; even a comparison with standard macromolecules is usually unreliable.

To generate a Ferguson plot, several gel (or polymer) concentrations are used simultaneously in a multitube or multichannel electrophoresis apparatus. Alternatively, a **transverse gradient** of gel concentration can be used in a single-slab gel. The slopes and intercepts of the Ferguson plot are computed and translated to parameters descriptive of the size and net charge, including their statistical limits, using relevant computer programs (1). Even without such translation, the Ferguson plot can be used to recognize qualitative relationships between the size or net charge of related bands of an electropherogram, or to test the possibility that two species are identical. Recognition of the nature of the relationships between bands helps to decide whether to use separation methods based primarily on size (see Gel Electrophoresis; Capillary Zone Electrophoresis) or charge (see Isoelectric Focusing; Isotachophoresis).

A linear Ferguson plot is expected from a simple mathematical model of a rigid ball passing through an inert random fiber network of the gel matrix (the Ogston model); it is observed experimentally with relatively rigid and spherical proteins passing through gels electrophoretically. In contrast, Ferguson plots derived with agarose gels are convex, presumably due to the progressive supercoiling of double-helical agarose with decreasing concentration. They are concave when used with DNA fragments, presumably due to the progressive stretching of the DNA molecule with increasing gel concentration.

Bibliography

1. D. Tietz (1988) Adv. Electrophoresis **2**, 109–170.

Suggestions for Further Reading

2. A. Chrambach and D. Rodbard (1971) Polyacrylamide gel electrophoresis. Science **172**, 440–451.
3. J. L. Hedrick and A. J. Smith (1968) Size and charge isomer separation and estimation of molecular weights of proteins by disc gel electrophoresis. Arch. Biochem. Biophys. **126**, 155–164.

Ferredoxins

Ferredoxins (Fds) are simple iron–sulfur proteins; that is, they do not contain other **prosthetic groups** beside one or two iron-sulfur (FeS) clusters. The first Fd to be discovered was that from *Clostridium pasteurianum* in 1962, immediately followed by the one from plant chloroplasts (1). Fds are ubiquitous, small, generally very acidic proteins, diverse in structure and function, that are involved mainly as electron carriers of low oxidation/reduction potential in fundamental metabolic processes like photosynthesis, nitrogen fixation, and assimilation of hydrogen, nitrogen, and sulfur. Recently, functions other than **electron transfer** have been discovered for some members of the very large class of FeS proteins. Indeed, it has become clear that most bacteria and plants contain not just one Fd, but a variety, distinguished by amino acid sequence, FeS cluster type, redox potential, and function. The Archaebacteria are particularly rich in Fds: *Methanococcus jannaschii* has 8 Fds and 6 polyFds, and *Archeoglobus fulgidus* has 8 Fds; as are the diazotroph bacteria (there are 8 to 9

Fds in *Azotobacter vinelandii*), followed by higher plants, from which at least six soluble Fds have been isolated. In bacteria, the number of Fds varies widely: just one Fd in *Bacillus subtilis*, but four in both *Mycobacterium tubercolosis* and *Escherichia coli*. In the first completed eukaryotic genome, that of the yeast *Saccharomyces cerevisiae*, only one Fd is present, which is similar to Fds found in mammalian mitochondria (adrenodoxin/renodoxin) that function in the hydroxylations catalyzed by cytochrome P450 for formation of steroid hormones, vitamin D metabolites, and bile acids.

Fds contain iron and sulfur atoms, organized in three different types of iron–sulfur clusters that are defined as 2Fe–2 S, 4Fe–4 S, and 3Fe–4 S (see Iron–Sulfur Proteins). These proteins absorb light in the 300- to 500-nm wavelength region: their solutions are brownish in color and become paler upon reduction. Typical **electron para-magnetic resonance** signals are shown by Fds in either the oxidized or reduced states. These proteins are sensitive to acids, oxidants, mercurials, and alkylating agents, but they show fair stability in the pH range 6 to 9 and to heat **denaturation** in the absence of oxygen. Fds are best divided into two classes: 2Fe–2 S Fds and 4Fe–4 S Fds, that may include the 3Fe–4 S clusters.

1. 2Fe–2 S Ferredoxins

These Fds are ubiquitous hydrophilic proteins of 11 to 15 kDa containing one 2Fe–2 S cluster that function as one-electron carriers. The iron-binding amino-acid sequence motif is Cys–X_4–Cys–X_2–Cys, which provides three of the four Cys ligands to the cluster; the fourth Cys ligand is distant in the primary structure. In some bacterial Fds of the hydroxylating dioxygenases (2) and in adrenodoxin, the spacing between the two first Cys residues is X_3 and X_5, respectively. The reduction potential varies in the range –400 to –100 mV (relative to the hydrogen electrode). The prototype of this class is the plant-type Fd (3), which has the role of distributing electrons received from the photoreduced photosystem I to several ferredoxin-dependent enzymes. The protein structure motif characteristic of these proteins is called "b-grasp" (a five-stranded **b-sheet** with an **a-helix** lying on top of the sheet). Adrenodoxin and putidaredoxin have additional small interaction **domains**.

2. 4Fe–4 S and 3Fe–4 S Ferredoxins

The prototype bacterial ferredoxin (4, 5) contains FeS clusters of the so-called "cubane" type, in which the four iron and four sulfide atoms are placed alternatively on the corners of a somewhat distorted cube. Coordination to the protein typically occurs through four cysteine thiolate groups to the four iron atoms. The most common bacterial ferredoxins contain two such clusters in a polypeptide chain of 50 to 60 residues. These proteins are typically found in anaerobes, where they are involved in one-electron transfer in low-potential systems, collecting reducing equivalents from a wide variety of substrates and metabolic cycles. A structural distinction has been made between the above classes of ferredoxins, which have been divided into "clostridial-type" and "photosynthetic bacterial and nif-related" ferredoxins. The former contain two Cys–X_2–Cys–X_2–Cys–X_3–Cys–Pro motifs, while the latter contain one motif of that type and the more unusual Cys–X_2–Cys–$X_{7–9}$–Cys–X_3–Cys–Pro motif. All these proteins are low-potential electron carriers, with typical reduction potential in the –390 to –450 mV range.

Some of the clostridial-type ferredoxins found in *Desulfovibrio spp* and in extreme **thermophiles** such as *Pyrococcus furiosus* contain a Cys–X_2–Asp–X_2–Cys binding motif, with a remote Cys residue as the fourth ligand and the Asp available to take the place of the missing central Cys residue of this sequence. These proteins contain a 3Fe–4 S cluster, which can be converted reversibly to a 4Fe–4 S cluster upon addition of iron and which may bind to exogenous ligands, such as thiol groups and cyanide. Cornerless cubanes containing the 3Fe–4 S clusters may be formed upon oxidation (by oxygen or ferricyanide) of regular 4Fe–4 S clusters, in a possibly reversible process.

Bibliography

1. D. I. Arnon (1988) Trends Biochem. Sci. **13**, 30–33.
2. J. R. Mason and R. Cammack (1992) Annu. Rev. Microbiol . **46**, 277–305.
3. D. B. Knaff (1996) In *Oxygenic Photosynthesis: The Light Reactions* (D. R. Ort and C. F. Yocum, eds.), Kluwer, The Netherlands, pp. 333–361.
4. M. Bruschi and F. Guerlesquin (1988) FEMS Microbiol. Rev. **54**, 155–176.
5. J. J. G. Moura, A. L. Macedo, and P. N. Palma (1994) Methods Enzymol. **243**, 165–188.

Suggestions for Further Reading

6. P. J. Stephens, D. R. Jollie, and A. Warshel (1996) Protein control of redox potentials of iron-sulfur proteins. Chem. Rev. **96**, 2491–2513.
7. H. Matsubara and K. Saeki (1992) Structural and functional diversity of ferredoxins and related proteins. Adv. Inorg. Chem. **38**, 223–280.
8. H. M. Holden et al. (1994) Structure–function studies of [2Fe–2 S] ferredoxins. Bioenerg. Biomembr. **26**, 67–87.

Ferritins

Ferritins and transferrins are nonheme iron-transport proteins that provide the crucial link between dietary iron and organismal heme-iron pools (hemoglobin, myoglobin, and hemosiderin) in maintaining iron homeostasis in mammals. Ferritin is a large protein (ca. 500 kDa) that consists of an aggregate of so-called heavy and light chains, which form a hollow shell in the apo form. Each apoferritin molecule can take up 4500 iron atoms, effectively shielding them from harmful reactions with peroxide and superoxide.

Transferrins are much smaller proteins that take up iron by binding to the transferrin receptor (TfR) at the cell surface. The complex is subsequently internalized by endocytosis, and then the iron dissociates into the cytoplasm, where it is free to be taken up by ferritin and other cellular proteins.

The messenger RNAs for transferrin receptor and for both ferritin subunits contain so-called iron-response elements (IREs), which are RNA structures containing a stem and a loop that has the consensus sequence CAGUGX (1). This regulates the translation of the mRNAs.

Bibliography

1. M. W. Hentze and L. C. Kühn (1996) Proc. Natl. Acad. Sci. USA **93**, 8175–8182.

Suggestions for Further Reading

2. H. Sigel and A. Sigel (series eds.) (1974–1998) *Metal Ions in Biological Systems*, Dekker, New York, Vols. **1–35**.
3. R. J. Cousins (1994) Metal elements and gene expression, Annu. Rev. Nutr. **14**, 449–469.

Fertilization

In the animal kingdom, fertilization is a unique event in which a male and female haploid **gamete** join and follow a cascade of highly regulated events that results in the production of a new individual (Fig. 1). During the early stages of fertilization, the two morphologically disparate gametes, the **oocyte** and the sperm, follow a very specific process of recognition and fusion. The interactions between the two gametes and with their tubal environment are mediated by highly specialized molecules located on the outer surfaces of membranes of the gametes and on the surrounding epithelia. The molecular interactions between the oocyte and spermatozoon are also unique with regard to gene function. Both gametes are haploid, and furthermore the nucleus is greatly condensed in the spermatozoa. Thus, no gene transcription takes place; consequently, all biochemical and molecular biological interactions must be done by proteins and, to some extent, by pretranscribed RNA of the oocyte. This means that regulation of the nucleus does not take place; instead, proteins and RNA involved in the fertilization process act autonomously. On the spermatozoon, the adhesion molecules are divided into primary and secondary ligands (see Acrosome). Primary ligands are involved in initial gamete binding, whereas secondary ligands, such as proacrosin, come into action after the acrosome reaction has taken place. In the oocyte, interactions with the other gamete are mediated by an extracellular matrix, the *zona pellucida* (see Egg). This organelle consists of three **glycoproteins**, ZP1, ZP2, and ZP3, of which ZP1 is responsible for structural integrity, whereas ZP2 and ZP3 have been shown to have sperm receptor activity (1). In the mouse, primary ligands interact with ZP3, whereas secondary ligands like proacrosin also bind strongly to ZP2. Only after completion of all complementary signals and responses is penetration of the spermatozoon through the zona pellucida possible, which directs the transfer of the male genetic information to the oocyte. The fertilization process has been divided into individual steps by Wassarman (1), in a widely accepted scenario:

1. **Capacitation**. In the female genital tract, ejaculated spermatozoa undergo a process called *capacitation*. This maturing process of spermatozoa is necessary to gain full fertilization capacity, but the basic mechanisms are not fully understood. Lectins from the seminal cytoplasm adhering to the surface of the acrosomal cap undergo a change in conformation and adopt structures that enable coupling of primary receptors.
2. **Attachment**. *In vitro* fertilization experiments demonstrated that the oocyte and spermatozoa initially are attached only loosely. This loose attachment is not species-specific, and the spermatozoa can be removed easily from the egg by small turbulences.
3. **Primary binding**. After the initial contact, the sperm bind tightly to the zona pellucida. This species-specific interaction is mediated by primary receptors and ligands. Now the spermatozoa cannot be removed easily from the egg by physical means.
4. **Acrosome reaction**. Triggered by the contact with the zona pellucida, spermatozoa undergo exocytosis, known as the *acrosome reaction*. This involves hyperactivation of the motile spermatozoa, multiple point fusion of sperm cytoplasm and the outer acrosomal membrane, formation of hybrid vesicles, and exposure of the inner acrosomal membrane. Enzymes (mainly proacrosin) and inner acrosomal components that are necessary for binding, local lysis, and penetration of the zona pellucida are released and come into action.
5. **Secondary binding**. After the acrosome reaction, secondary ligands and receptors maintain the affinity between the two gametes. The forces are strong enough to keep the spermatozoa tightly attached to the zona pellucida. Adhesive proteins like proacrosin play an important role in high affinity binding.
6. **Penetration**. After exposure of the inner acrosomal membrane, the predominant molecule of the acrosome, *acrosin*, has been generated from the precursor proacrosin. It acts as a binding molecule and also a proteinase; these two phenomena together enable the sperm to bind and lyse the zona pellucida locally. The spermatozoon is driven through the zona pellucida, forced by the motile sperm tail.

7. **Fusion**. The spermatozoon that first reaches the perivitelline space then fuses with the egg plasma membrane to form a zygote. On entry of the spermatozoon, the egg is activated, which leads finally to the unification of the male and female **pronuclei**.
8. **Primary block to polyspermy**. In order to prevent several spermatozoa fusing with the oocyte, a rapid depolarization of the egg plasma membrane occurs within seconds after gamete fusion.
9. **Cortical reaction and zona hardening**. The cortical granules of the egg, which can be regarded as **lysosome**-like **organelles**, release a variety of lytic enzymes on the fusion of a spermatozoon with the egg plasma membrane. The cortical granule contents are then deposited into the perivitelline space; when they enter the zona pellucida, the ZP2 and ZP3 glycoproteins are converted into ZP2f and ZP3f, the respective inactive forms of the receptor. This modification of the zona pellucida glycoproteins constitutes a permanent secondary block to polyspermy.

Figure 1. Sperm–egg interaction. Capacitated spermatozoa bind to the zona pellucida via primary ligands and receptors. This event triggers the acrosome reaction of the spermatozoa and activates secondary ligands on the sperm. (With the friendly permission of Dr. H.-W. Michelmann.)

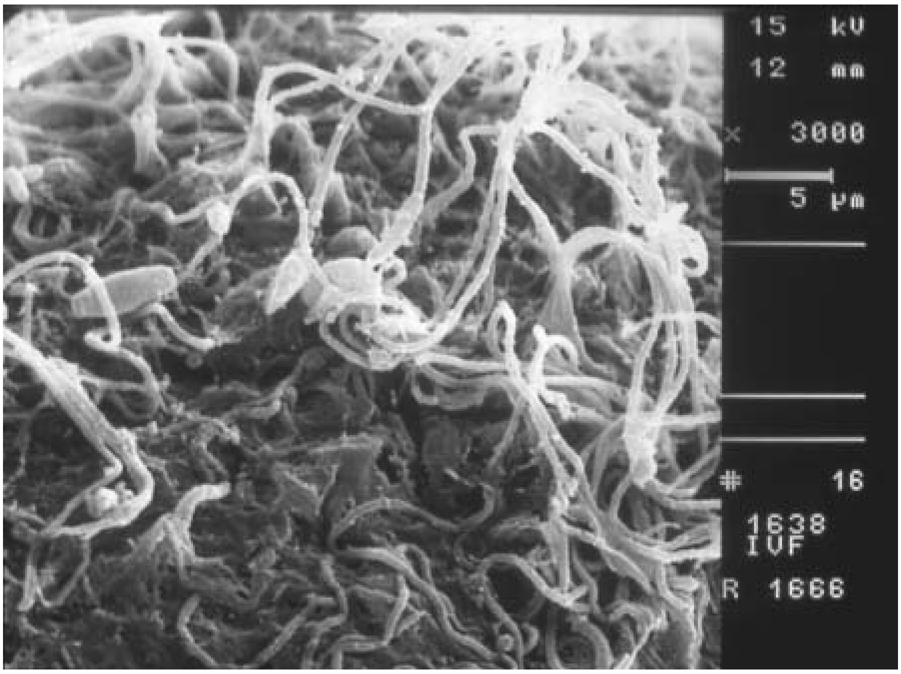

Bibliography
1. P. M. Wassarman (1990) J. Reprod. Fert. Suppl. **42**, 79–87.

Fiber Diffraction

Fiber diffraction is a method of using X-ray diffraction to obtain structural information from a fibrous preparation of the material, rather than a three-dimensional crystal (see X-Ray Crystallography). Fibers consist of elongated molecules that are aligned parallel to each other along the fiber axis. In biological fibers, such as hair, collagen and **muscle**, the molecules are naturally aligned. In others the molecules must be forced to align by drawing them from a concentrated solution or by flow through a capillary. Magnetic and electric fields also have an effect.

The relatively weak X-ray scattering from fibrous specimen means that long exposures are necessary to record the diffraction pattern, and special cameras have been developed for the purpose. A fiber X-ray diffraction pattern shows series of lines of intensity perpendicular to the fiber axis, called layer lines. If the fiber axis is vertical, the layer lines are horizontal. Their distance is related to the periodicity along the fiber axis. The middle line is called the zero layer line or equator. The meridian is an imaginary line running vertically through the center of the diffraction pattern. The quality of the pattern depends on the degree of alignment of the molecules, but an X-ray fiber diffraction pattern is rarely of sufficiently high quality to determine a structure at atomic resolution. The best results are obtained with synchrotron radiation of cryocooled specimens.

In the 1930s, Astbury used fiber diffraction to group protein fibers into three types: a-fibers, b-fibers, and collagen. For a structural determination from fiber data, chemical information about the fiber is needed to postulate a model and to refine this model, obeying any symmetry constraints, until it predicts the observed intensities reasonably well. In this way, Watson and Crick arrived at the structure of **DNA** (1) and Pauling at the model for the a-helix (2). For larger structures, this is not so easy, and then isomorphous replacement is applied, as in protein crystal structure determination.

Fibers usually consist of helical arrangements of the building units. Cochran, Crick, and Vand found that the intensity diffracted by a continuous helix on the *n*th layer line is proportional to J^2_n (2p*Rr*) (3). The intensity distribution is cylindrically symmetrical around the reciprocal axis parallel to the fiber axis. *R* is the distance in reciprocal space to this axis, and *r* is the radius of the helix. J_n is a Bessel function of order *n*. These Bessel functions are oscillating functions that fade away with the distance from the origin. Therefore, the highest values are found close to the origin, which here is the meridian in the diffraction picture. But with increasing order *n*, these maximum values are found at a greater distance from the origin and become smaller. The combination of these properties creates the X-shaped diffraction picture characteristic of a helical structure (Fig. 1).

Figure 1. Schematic depiction of the typical diffraction pattern of a continuous helix.

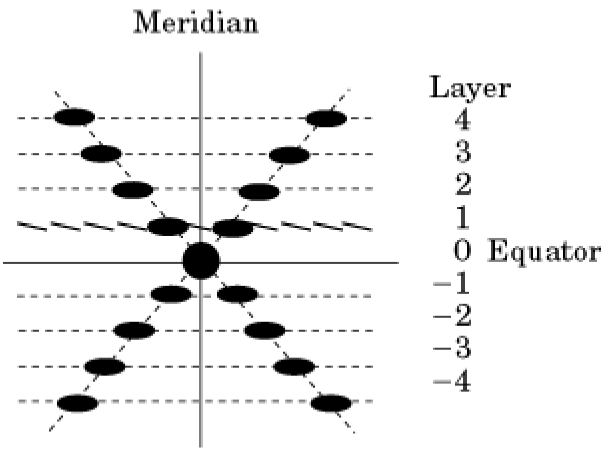

Actual helices are not continuous, and the effect is that the intensity on a layer line depends on the structural repeat. If *P* is the pitch of the helix and *p* the axial rise from building unit to building unit along the helix axis, layer line numbers ℓ obey the equation $\frac{\ell}{c} = \frac{n}{P} + \frac{m}{p}$, where *c* is the structural repeat distance along the helix axis, n is the order of a Bessel function, and m is (like n) a whole number. This is illustrated by the following example. For the a-helix, $P = 5.4$ Å, and $p = 1.5$ Å. The structure repeats itself along the helix axis over a distance $c = 27$ Å. Therefore,

$$P = \frac{c}{5} \qquad p = \frac{c}{18} \qquad \frac{\ell}{c} = \frac{n}{P} + \frac{m}{p} = \frac{5n}{c} + \frac{18m}{c}$$

For layer line $\ell = 0$, this can be reached with the following combinations:

$n =$	–36	–18	0	+18	+36
$m =$	+10	+5	0	–5	–10

and for layer line $\ell = 1$ with

$n =$	–25	–7	+11	+29	+47
$m =$	+7	+2	–3	–8	–13

The intensity on every layer line is determined by a large number of Bessel functions J_n, but they have a nonnegligible value only for small n. Therefore, strong reflections occur on the zero layer line ($\ell = 0$) in the a-helix diffraction pattern, but not on the first one ($\ell = 1$). Layer line18 also has a strong reflection.

Bibliography

1. J. D. Watson and F. H. C. Crick (1953) Nature **171**, 737–738.
2. L. Pauling, R. B. Corey, and H. R. Branson (1951) Proc. Natl. Acad. Sci. USA **37**, 205–211.
3. W. Cochran, F. H. C. Crick, and V. Vand (1952) Acta Crystallogr. **5**, 581–586.
4. A. Klug, F. H. C. Crick, and H. W. Wyckoff (1958) Acta Crystallogr. **11**, 199–213. A complete treatment of the theory of fiber diffraction.
5. D. A. Marvin and C. Nave (1982) In *Structural Molecular Biology, Methods and Applications* (D. B. Davies, W. Saenger, and S. S. Danyluk, eds.), Plenum, New York, London, pp. 3–44. A review.

Fibrinogen

Blood clots when soluble fibrinogen is cleaved by thrombin to generate fibrin monomers which polymerize spontaneously, non-covalently and rapidly to form the insoluble fibrin clot, which is further stabilized by covalent cross-linking catalyzed by the transglutaminase, factor $XIII_a$ [see Blood Clotting]. This remarkable property is dependent on the symmetrical multi-chain structure of fibrinogen, the proteolytic exposure of cryptic binding sites, and the high concentration of fibrinogen in blood plasma (2–4 mg/mL). The cessation of bleeding is further enhanced by fibrin acting as a cofactor in blood platelet aggregation. The fibrin clot further acts as a provisional matrix for the subsequent repair of the wound.

Fibrinogen is a disulfide-bonded hexameric protein, arranged as a dimer of Aa, Bb and g chains.

These are the products of three distinct, but related, genes located in close association on human chromosome 4. The mature chains are 625, 461 and 411 residues, respectively, resulting in a molecular weight of 350 kDa for the hexamer. The gross topological structures of fibrinogen and fibrin have been deduced by both biochemical and biophysical methods. The overall appearance of fibrinogen is a linear trinodular structure 475 Å in length, with each nodule separated by an intervening rod-like region (1) (Figure 1). The N-terminal regions of all six chains are contained in the highly disulfide-bonded central nodule, the N-terminal disulfide knot. The N-termini of the Aa and Bb chains protrude from the nodule, while the g chains have shorter N-terminal sequences. Triple-chained coiled coils connect the central to the distal nodules, each of which is composed of two homologous globular domains comprising the C-terminal regions of the Bb and g chains. The longer Aa chain folds back along the axis of the molecule, to end in a globular domain that interacts with the N-terminal disulfide knot.

Figure 1. Schematic model of fibrin polymerization and its subsequent dissolution.

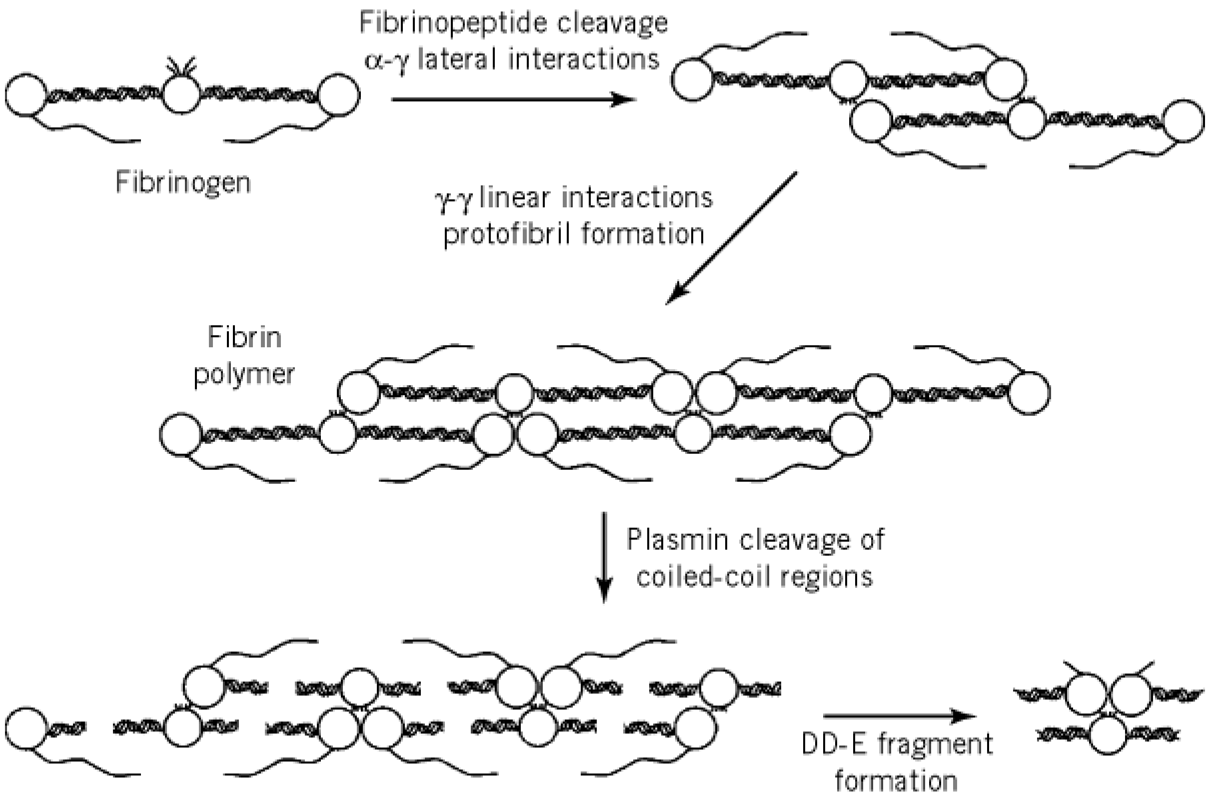

Structures have been determined by X-ray crystallography for various C-terminal proteolytic fragments of human fibrinogen (2, 3) and, although intact human fibrinogen has yet to be crystallized, the structure of native chicken fibrinogen has been resolved at a resolution of 2.7 Å (4). The triple-chained connecting regions are susceptible to proteolysis, generating two major fragments: fragment E corresponding to the central N-terminal nodule (approximately 15% of the molecule) and fragment D containing the distal globular domains (the two identical fragments accounting for approximately 50% of the molecule). Both of these fragments contain substantial portions of the cleaved coiled coil regions with the remainder of the protein accounted for by the C-terminal regions of the Aa chains.

Fibrin polymerization essentially occurs in three sequential steps. Firstly, thrombin cleaves the N-terminal regions of the Aa and Bb chains at Arg16-Gly17 and Arg14-Gly15, respectively, releasing fibrinopeptides A and B. The N-terminal sequence of the fibrin a chain (Gly17-Pro-Arg-Val) is the major determinant of fibrin polymerization which proceeds efficiently without further modification to the fibrin(ogen) structure, and synthetic peptides corresponding to this sequence can inhibit the polymerization of fibrin monomers (5). By contrast the b-chain sequence (Gly15-His-Arg-Pro), which is generated more slowly, although binding to fibrinogen and fragment D, cannot inhibit polymerization. Secondly, the new N-termini of fibrin monomer spontaneously interact with binding sites in the two homologous distal globular domains, with the g-chain site particularly implicated (3). Both sites are large cavities that bind a-chain Gly-Pro-Arg ligands, but the g-chain cavity is the more specific and does not bind b-chain Gly-His-Arg ligands. It is also the more distal of the two C-terminal domains and is able to intermolecularly associate in a specific “end-to-end” manner (2). Thus adjacent g-chain sites are closely situated for optimal binding of the dimeric a-chain N-terminal residues and the efficiency of polymerization derives from both a-g lateral and g-g linear interactions. The symmetry of fibrin(ogen) allows oligomerization to proceed in both directions, generating a two-molecule thick protofibril with a half-staggered overlap (Figure 1). Finally, the fibrin fibrils are reinforced by the transglutaminase activity of factor $XIII_a$. The g-g linear interactions are the major sites for the introduction of intermolecular g-glutamyl-ε-amino-lysine isopeptide crosslinks, subsequently the globular C-terminal domains of the a chains of adjacent laterally aligned protofibrils are also crosslinked, resulting in the mature, covalently stabilized fibrin mesh. Under physiological conditions these fibers are of the order of 1 µM in diameter and thus several hundred fibrin units wide.

The assembly of fibrin also reveals epitopes that are involved in its subsequent dissolution by plasmin. Conformational changes in the vicinity of the C-terminal globular domains are thought to reveal the binding sites for tPA that are responsible for the fibrin-specific potentiation of its activity [see Plasminogen Activators]. These sites are g312-324 in the C-terminal globular domain and Aa148-160, a region interacting with the Bb-chain C-terminal globular domain. The initial binding sites for plasminogen also reside in fragment D, but subsequent plasmin degradation of fibrin reveals C-terminal Lys residues that act as supplementary sites for plasminogen binding, thereby propagating plasminogen activation. Once generated plasmin can attack 50-60 of the 358 Lys and Arg residues present in each fibrin molecule, although only 10% are cleaved rapidly. The initial cleavages release the C- and N-termini of the a and b chains, respectively, followed by the cleavages in the extended coiled-coil regions that lead to dissolution of the organized fibrin structure (see Figure 1).

1. Fibrin Polymerization

The generation of fibrin from fibrinogen and its polymerization essentially occur in three sequential steps.

1. Thrombin cleaves the *N*-terminal regions of the Aa and Bb chains of fibrinogen at the peptide bonds Arg16–Gly17 and Arg14–Gly15, respectively, releasing fibrinopeptides A and B. No further covalent modification to the fibrin(ogen) structure is necessary for polymerization to proceed efficiently. The new N-terminal sequence of the fibrin a chain (Gly17–Pro–Arg–Val) is the major determinant of fibrin polymerization; synthetic peptides corresponding to this sequence can inhibit the polymerization of fibrin monomers (4). By contrast, the new b-chain *N*-terminal sequence (Gly15–His–Arg–Pro), which is generated more slowly, cannot inhibit polymerization, even though it binds to fibrinogen and to fragment D.

2. The new *N*-termini of the fibrin monomers spontaneously interact with binding sites in the two homologous distal globular domains, with the g-chain site particularly implicated (3). Both sites are large cavities that bind the a-chain-like peptide Gly–Pro–Arg, but the g-chain cavity is the more specific and does not bind g-chain Gly–His–Arg peptides. It is also the more distal of the two *C*-terminal domains and is able to associate intermolecularly in a specific end-to-end manner (2). Thus adjacent g-chain sites are closely positioned for optimal binding of the dimeric a-chain *N*-terminal residues. The efficiency of polymerization derives from both a–g lateral and g–g linear interactions. The symmetry of fibrin(ogen) allows oligomerization to proceed in both directions, generating a two-molecule thick protofibril with a half-staggered overlap (Fig. 1).

3. The fibrin fibrils are reinforced by the transglutaminase activity of factor $XIII_a$. The g–g linear interactions are the major sites for the introduction of intermolecular isopeptide crosslinks between g-glutamyl carboxyl and lysine-e-amino groups. Subsequently, the globular *C*-terminal domains of the a chains of adjacent laterally aligned protofibrils are also crosslinked, resulting in the mature, covalently stabilized fibrin mesh. Under physiological conditions, these fibers are of the order of 1 µm in diameter, and thus several hundred fibrin units wide.

2. Dissolution of the Fibrin Clot

The assembly of fibrin also makes accessible epitopes that are involved in its subsequent dissolution by plasmin, after its activation from plasminogen by tissue-type plasminogen activator (tPA). The activity of tPA is potentiated specifically by fibrin, and conformational changes in the vicinity of the *C*-terminal globular domains of fibrin are thought to reveal the binding sites that are responsible. These sites are residues 312–324 in the *C*-terminal globular domain of the g chain and 148–160 of Aa, a region that interacts with the Bb-chain *C*-terminal globular domain. The initial binding sites for plasminogen also reside in fragment D, but subsequent plasmin degradation of fibrin uncovers *C*-terminal lysine residues that act as supplementary sites for plasminogen binding, which thereby propagate plasminogen activation. Once generated, plasmin can attack 50–60 of the 358 Lys and Arg residues present in each fibrin molecule, although only 5 or 6 are cleaved rapidly. The initial cleavages release the *C* and *N* termini of the a and b chains, respectively, followed by the cleavages in the extended coiled-coil regions that lead to dissolution of the organized fibrin structure (see Fig. 1).

Bibliography

"Fibrinogen" in , Vol. 2, pp. 907–909, by Vincent Ellis, University of East Anglia, School of Biological Sciences, Norwich, United Kingdom, NR4 7TJ; "Fibrinogen" in (online), posting date: January 15, 2002, by Vincent Ellis, University of East Anglia, School of Biological Sciences, Norwich, United Kingdom, NR4 7TJ.

1. W.R. Fowler and H.P. Erickson (1979) J. Mol. Biol. **134**, 241–249.
2. G. Spraggon, S.J. Everse and R.F. Doolittle (1997) Nature, **389**, 455–462.
3. K.P. Pratt, H.C. Côté, D.W. Chung, R.E. Stenkamp and E.W. Davie (1997) Proc. Natl. Acad. Sci. USA, **94**, 7176–7181.
4. Z. Yang, J.M. Kollman, L. Pandi and R.F. Doolittle (2001) Biochemsitry (In Press)
5. A.P. Laudano and R.F. Doolittle (1980) Biochemistry, **19**, 1013–1019.

Suggestions for Further Reading

6. M.W. Mosesson, K.R. Siebenlist and D.A. Meh (2001) The structure and biological features of fibrinogen and fibrin. Ann. N Y Acad. Sci. **936**, 11–30.

Fibroblast Growth Factors

The fibroblast growth factors (FGFs) are a family of polypeptide growth factors that control many different biological processes *in vivo*. Their biological effects are mediated by association with specific cell-surface receptors of the intrinsic **tyrosine kinase** class (see Tyrosine Kinase Receptors). Their activity is modulated by association with cell-surface heparan sulfate containing glycosoaminoglycans and other cofactors.

1. Fibroblast Growth Factor Ligands

The FGF family in mammals currently comprises 14 different polypeptide chains that act as ligands, FGF1–FGF10 and FGF15–FGF18, and share an overall sequence identity of about 40%. The FGF family is highly conserved in animals: **homologues** have been isolated from a wide variety of species, including birds, amphibians, fish, insects, and nematodes (reviewed in Ref. 1). In addition to the defined family of FGF ligands, four related genes, FHF1–FGF4 (also known as FGF11–FGF14), have been isolated from expressed sequence tag (EST) projects that exhibit sequence similarity to canonical FGF ligands, but whose biological function is currently unknown (2). It is very possible that further FGF family members remained to be identified.

The protein structures of both FGF1 and FGF2 have been determined by X-ray crystallography (3). The two structures are remarkably similar and exhibit a novel 12-stranded b-trefoil topology (Fig. 1). This characteristic structure is shared with a biologically unrelated growth factor, **interleukin** -1 (IL1).

Figure 1. A molecular model of the interaction between FGF and the extracellular domain of FGF-R. The model was created by docking the crystal structure of FGF-2 (3) in place of the homologous IL1 in the crystal structure of the IL-1/IL1-R complex (9). The model shows only one half of the active complex, which is composed of two molecules of FGF and two receptors.

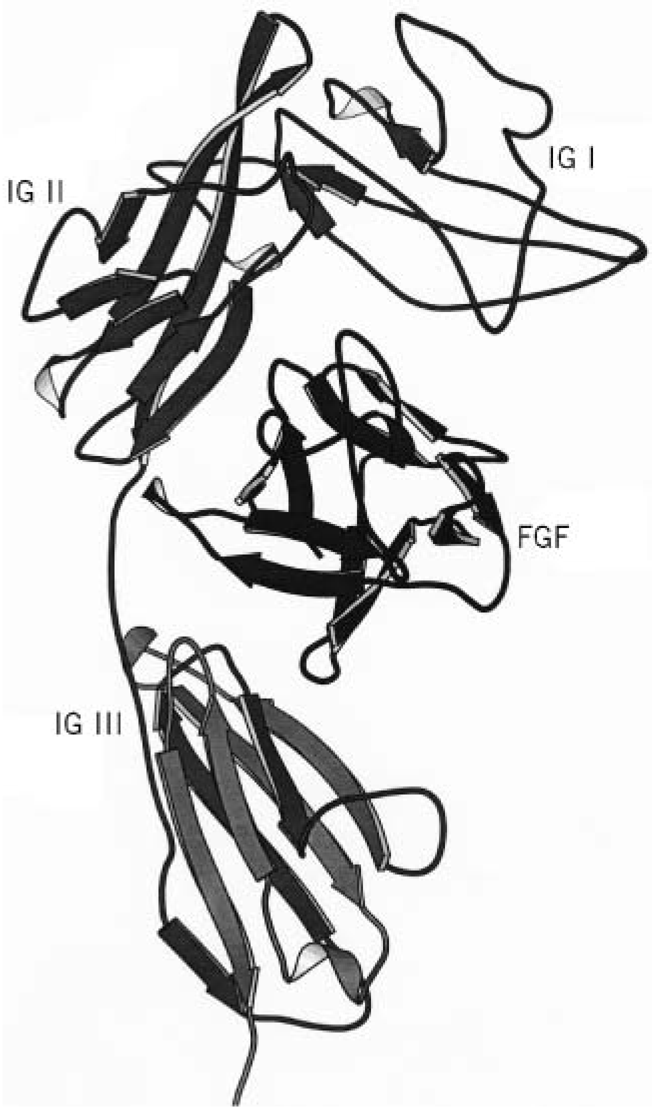

FGF family ligands exhibit distinct and characteristic patterns of tissue-specific gene expression during development and adulthood, suggesting that, despite their diversity, each may exhibit distinct biological functions *in vivo*. Although in most cases FGFs are expressed as a secreted molecules and elicit their biological effects in the extracellular milieu, an intriguing feature of two FGF family members, FGF1 and FGF2, is that they lack classic secretory signal peptides and, in most cases, appear to remain in an intracellular location (see Protein Secretion). This suggests that these FGFs may either require cell lysis to act or that they are released under certain conditions by a nonstandard protein export mechanism.

2. FGF Receptors

The biological effects of the FGF family of ligands are mediated by association with a family of related cell-surface receptors of the intrinsic tyrosine kinase class. The FGF family of receptors is encoded by four related genes, FGF-R1–FGF-R4. FGF-R genes have been isolated from mammals, birds, fish, amphibians, Drosophila. and nematodes (1). Individual FGF-R genes exhibit significant conservation between species and conserved features shared between the entire family. Individual FGF ligands exhibit defined patterns of receptor specificity (4), whereby some ligands interact with all FGF-R family members and others exhibit significantly more restricted affinities.

The extracellular region of the FGF-Rs comprises three domains, IgI, IgII and IgIII, which contain immunoglobulin motifs of the immunoglobulin superfamily (IgSF). Each Ig domain is encoded by two exons. In FGF-R1–FGF-R3, the IgIII domain is generated by alternative splicing of a common IgIIIa exon onto a variant IgIIIb or IgIIIc exon. The expression of FGF-R IgIII splice variants is subject to developmentally regulated gene-specific alternative splicing mechanisms (5). The selection of IgIII exons by alternative splicing mechanisms is of major functional significance because it dictates ligand specificity of FGF-Rs (6). The analysis of chimeric FGF-Rs containing variable regions from each splice variant has revealed that the interaction of an FGF ligand with its cognate receptor involves regions of both IgII and IgIII (7). Molecular models of the FGF-R ectodomain (Fig. 1) have been generated, on the basis of relationships to other IgSF family members and the crystal structure of the structurally related ligand IL1 (8, 9). These suggest that the active complex is composed of two molecules of ligand and two molecules of receptor. The ligand interacts with epitopes in both the second and third Ig domains of the receptor. These studies also reveal the existence of an extended linker domain between the IgII and IgIII domains of IL1-R. This leads to a general scheme for FGF/receptor engagement in which two independent epitopes in the ligand interact with cognate sites in IgII and IgIII. This interaction may involve interdomain reorientation on ligand binding, facilitated by the linker domain.

3. FGF Cofactors

The biological actions of FGF ligands may involve a variety of cofactors, apart from the transmembrane tyrosine kinase receptors. The most prominent of these is the sulfated oligosaccharide heparan sulfate (HS), which has been shown in many studies to interact with FGF ligands with high affinity. The crystal structure of FGF2 complexed with a linear hexasaccharide (10) reveals that this interaction occurs via binding of sulfated groups of HS to a cluster of basic residues exposed on one face of the FGF ligand. The biological role of HS in FGF action is still the subject of controversy. It has been shown that HS is, in some cases, required for FGF action (5). This has been argued to result from either HS-mediated ligand dimerization, or interaction of HS with both ligand and receptor. Others have proposed that the role of HS is simply to concentrate FGF ligand in the vicinity of the receptor (reviewed in Ref. 11).

A second FGF-binding protein is the cysteine-rich FGF receptor (12) that has been identified in many tissue types. This is a transmembrane protein, unrelated to FGF-Rs, which binds FGF ligands with high affinity. The cysteine-rich FGF receptor has been identified recently as a cell adhesion ligand of E-selectin, an inducible cell adhesion molecule that mediates the binding of neutrophils to endothelial cells and functions as a Ca^{2+}-dependent lectin. The signaling potential of this receptor, and the relationship between the interaction with E-selectin and FGF ligands, remain to be determined.

Several agents exist that interact directly or indirectly with FGF-Rs. Two proteins have been isolated by interaction screens in yeast that are unrelated to FGF ligands in sequence but appear to potentiate FGF-R signaling when overexpressed in Xenopus embryos (13). Genetic analysis of FGF signaling in *Drosophila* has revealed the existence of a conserved family of proteins, Sproutys, which, on genetic grounds, act to antagonize FGF receptor-mediated signaling pathways (14). Finally a variety of lines of evidence suggest that some effects of the homotypic cell adhesion molecules L1 and N-Cam may be mediated by direct, or indirect, activation of FGF-R signaling (15). Together these findings indicate that FGF signaling mediated by receptor–ligand interactions may be tightly constrained by the presence of specific cofactors *in vivo*.

4. Biological Actions of FGF Ligands

Genetic evidence, from gain-of-function or loss-of-function experiments, shows that the FGF family of ligands in higher vertebrates exhibits a diversity of biological functions at different times and places during embryonic and postnatal development. These include mesoderm induction, patterning of the nervous system, limb induction and outgrowth, and the development of various tissues and organs, such as the hair, ear, lungs, and teeth (reviewed in Ref. 16). The analysis of mice harboring null mutations of FGF receptors reveals that each FGF-R has distinct biological roles *in vivo* and, in particular, that FGF signaling is required at early stages of embryonic development. Thus genetic inactivation of FGF-R1 leads to early postimplantation lethality resulting from aberrant mesodermal patterning (17). Genetic inactivation of FGF R2 leads to preimplantation lethality (18), with a phenotype similar to that of homozygous null FGF-4 mice. Homozygous null FGF-R3 mice exhibit severe and progressive bone dysplasia with enhanced and prolonged endochondrial bone growth, indicating that signaling mediated by FGF-R3 acts as a negative regulator of endochondrial ossification (19).

The FGF/FGF-R axis also has considerable significance for clinical disorders of craniofacial and limb development. One of the commonest forms of inherited dwarfism, achondroplasia, arises from specific mutations in the transmembrane domain of FGF-R3 (20). This results in activation of FGF-R signaling and premature termination of long-bone extension. Moreover, mutations in the FGF-R1–FGF-R3 genes have been identified in dominantly inherited human craniofacial malformation syndromes (reviewed in Ref. 21) such as those of Crouzon, Pfeiffer, and Apert. These syndromes are all characterized by craniosynostosis (abnormal development and/or premature fusion of the cranial sutures) and additional phenotypic features such as syndactyly (digit fusion) in the Apert syndrome. The majority of these mutations described are clustered within a specific region of the extracellular domain of the receptor. In the case of Crouzon–Pfeiffer syndromes, mutations are predicted to disrupt the pattern of **disulfide bonding** in the extracellular domain (22), leading to activation of signaling via intermolecular disulfide bonding of mutant receptors. In Apert syndrome, all cases characterized to date involve specific amino acid substitutions of two adjacent amino acid residues, Ser252 and Pro253, predicted to lie in the linker region joining Ig domains II and III. The consequence of these mutations appears to be enhanced affinity for specific FGF ligands (23), which results in activation of FGF signaling in the developing suture.

5. Conclusions

The FGFs exemplify many generic features of growth factors. There are multiple ligands and receptors, each of which executes specific functions in development and adult physiology. Individual FGFs can also exert several different functions, which are not limited to the control of cell multiplication. In particular, FGFs seem to play important roles in patterning tissues of the developing embryo. FGF signaling is strictly local in action and modified by the concurrent activity of various cofactors. Finally, the dynamics of signaling elicited by FGF-R activation seems to play a critical role in the development of specific tissues.

Bibliography

1. F. Coulier, P. Pontarotti, R. Roubin, H. Hartung, M. Goldfarb, and D. Birnbasum (1997) Of worms and men: an evolutionarey perspective on the fibroblast growth factor (FGF) and FGF receptor families, J. Mol. Evol. **44**, 43–56.
2. P. M. Smallwood, Munoz-San Juan, P. Tong, J. P. Macke, S. H. Hendry, D. J. Gilbert, N. G. Copeland, N. A. Jenkins, and J. Nathans (1996) Fibroblast growth factor (FGF) homologous factors: new members of the FGF family implicated in nervous system development, Proc. Natl. Acad. Sci. USA **93**, 9850–9857.
3. X. Zhu, H. Komiya, A. Chirino, S. Faham, G. M. Fox, T. Arakawa, B. T. Hsu, and D. C. Rees (1991) Three-dimensional structures of acidic and basic fibroblast growth factors, Science **251**, 90–93.
4. D. M. Ornitz, X. J. , J. S. Colvin, D. G. McEwen, C. A. MacArthur, F. Coulier, G. Gao, and M. Goldfarb (1996) Receptor specificity of the fibroblast growth factor family, J. Biol. Chem. **271**, 15292–15297.
5. D. E. Johnson, P. L. Lee, J. Lu, and L. T. Williams (1990) Diverse forms of a receptor for acidic and basic fibroblast growth factors, Mol. Cell. Biol. **10**, 4728–4736.

6. D. Givol and A. Yayon (1992) Complexity of FGF receptors: genetic basis for structural diversity and functional specificity, FASEB J. **6**, 3362–3369.
7. T. E. Gray, M. Eisenstein, T. Shimon, D. Givol, and A. Yayon (1995) Molecular modeling based mutagenesis defines ligand binding and specificity determining regions of fibroblast growth factor receptors, Biochemistry **34**, 10325–10333.
8. A. Bateman and C. Chothia (1995) Outline structures for the extracellular domains of the fibroblast growth factor receptors, Nat. Struct. Biol. **2**, 1068–1074.
9. G. Vigers, L. J. Anderson, P. Caffes, and B. J. Brandhuber (1997) Crystal structure of the type-1 interleukin-1 receptor complexed with interleukin-1 beta, Nature **386**, 190–193.
10. S. Faham, R. E. Hileman, J. R. Fromm, R. J. Linhardt, and D. C. Rees (1996) Heparin structure and interactions with basic fibroblast growth factor, Science **271**, 1116–1120.
11. D. E. Johnson, J. Lu, H. Chen, S. Werner, and L. T. Williams (1991) The human fibroblast growth factor receptor genes: a common structural arrangement underlies the mechanisms for generating receptor forms that differ in their third immunoglobulin domain, Mol. Cell. Biol. **11**, 4627–34.
12. A. Yayon, M. Klagsbrun, J. D. Esko, P. Leder, and D. M. Ornitz (1991) Cell surface, heparin-like molecules are required for binding of basic fibroblast growth factor to its high affinity receptor, Cell **64**, 814–818.
13. J. Schlessinger, I. Lax, and M. Lemmon (1995) Regulation of growth factor activation by proteoglycans: What is the role of the low affinity receptors? Cell **83**, 357–360.
14. L. W. Burrus, M. E. Zuber, B. A. Lueddecke, and B. B. Olwin (1992) Identification of a cysteine-rich receptor for fibroblast growth factors. Mol. Cell. Biol. **12**, 5600–5609.
15. N. Kinoshita, J. Minshull, and M. W. Kirschner (1995) The identification of two novel ligands of the FGF receptor by a yeast screening method and their activity in Xenopus development, Cell **83**, 621–630.
16. N. Hacohen, S. Kramer, D. Sutherland, Y. Hiromi, and M. Krasnow (1998) Sprouty encodes a novel antagonist of FGF signaling that patterns apical branching of the Drosophila airways, Cell **92**, 253–263.
17. E. J. Williams, J. Furness, F. S. Walsh, and P. Doherty (1994) activation of the FGF receptor underlies neurite outgrowth stimulated by L1, N-CAM, and N-cadherin, Neuron **13**, 583–594.
18. A. O. Wilkie, G. M. Morriss-Kay, E. Y. Jones, and J. K. Heath (1995) Functions of fibroblast growth factors and their receptors, Curr. Biol. **5**, 500–507.
19. T. P. Yamaguchi, K. Harpal, M. Henkemeyer, and J. Rossant (1994) fgfr-1 is required for embryonic growth and mesodermal patterning during mouse gastrulation, Genes Dev. **8**, 3032–3044.
20. E. Arman, R. Haffner-Krausz, Y. Chen, J. K. Heath, and P. Lonai (1998) Fibroblast growth factor receptor 2 (FGFR2) is required for formation of the egg cylinder, Proc. Natl. Acad. Sci. USA **95**, 5082–5087.
21. C. Deng, A. Wynshaw-Boris, F. Zhou, A. Kuo, and P. Leder (1996) Fibroblast growth factor receptor 3 is a negative regulator of bone growth, Cell **84**, 911–21.
22. G. A. Bellus, I. McIntosh, E. A. Smith, A. S. Aylsworth, I. Kaitila, W. A. Horton, G. A. Greenhaw, J. T. Hecht, and C. A. Francomano (1995) A recurrent mutation in the tyrosine kinase domain of fibroblast growth factor receptor 3 causes hypochondroplasia, Nat. Genet. **10**, 357–359.
23. A. O. M. Wilkie (1997) Craniosynostosis: genes and Mechanism. Human Mol. Genet . **6**, 1647–1656.

Suggestions for Further Reading

24. I. J. Mason (1994) The ins and outs of fibroblast growth factors, Cell **78**, 547–552.
25. A. O. Wilkie, G. M. Morriss-Kay, E. Y. Jones, and J. K. Heath (1995) Functions of fibroblast

growth factors and their receptors, Curr. Biol. **5**, 500–507.

Fibronectin

Fibronectin is a fibrillar extracellular matrix (ECM) **glycoprotein** that binds to cells and other matrix molecules, thereby contributing to the organization of the matrix and providing important adhesive sites for cells. Fibronectin is found throughout the vertebrate body, including the brain, which lacks a recognizable ECM but expresses ECM molecules like fibronectin transiently in early development. Fibronectin is a dimer of 240-kDa monomers linked at the C-terminus by a pair of disulfide bonds. The protein is made of similar but nonidentical repeating domains (types I, II, III), most of which are derived from a single exon (see Introns, Exons). The type III repeat, about 90 amino acid residues in length, occurs 15 times in each monomer and is a structural element found in other proteins as well. While the protein is encoded by a single gene, multiple splicing variants give rise to diverse **isoforms** that differ in their cell binding sites and functions. One isoform is found as an abundant protein in blood and is thought to participate in wound healing, phagocytosis by white blood cells, and blood clotting. Other forms are incorporated into fibrils in the ECM. The regions of the protein that bind to matrix molecules and cells have been uncovered by using mild proteinase digestion and column chromatography to isolate and characterize the fragments. The fibronectin monomer has two binding sites each for heparin and **fibrin**, and a single binding site for collagen. Further analysis of small synthetic peptides has led to the identification of the sequence -Arg-Gly-Asp- (RGD), which is bound by many cells via integrin receptors alpha-5/beta-1, alpha-3/beta-b1, alpha-v/beta-1, and alpha-v/beta-3. The RGD site occurs in a type III repeat on a loop extended above the surface of the domain, which is thought to provide easy access to cells. The RGD sequence is also found in other matrix proteins recognized by integrins, such as vitronectin. An **alternatively spliced** region (type III connecting segment or V) contains a second binding motif -Leu-Asp-Val- (LDV), which is the main part of the binding site for another integrin (alpha-4/beta-1) (see Integrins).

Fibronectin is one of the best-characterized ECM glycoproteins. *In vitro*, it supports adhesion of many cell types, and it can also stimulate cell proliferation, differentiation, and migration. Cells in culture often flatten and develop prominent actin arrays in response to fibronectin. The response depends on the particular cell type and its array of fibronectin receptors. The importance of fibronectin in migration of cells has been demonstrated for neural crest cells in birds and gastrulating embryonic cells of frogs, where injected antibodies and RGD-containing peptides will block cell migration. In genetically engineered mice lacking fibronectin, death occurs early in embryogenesis in part because of a failure of mesodermal cells to develop, resulting in defects in the development of the notochord, somites, blood vessels, and heart.

Suggestions for Further Reading

1. R. O. Hynes (1989) *Fibronectins*, Springer-Verlag, New York.
2. C. Chothia and E. Y. Jones (1997) The molecular structure of cell adhesion molecules. Ann. Rev. Biochem. **66**, 823–862.

Fibrous Proteins

Although the fibrous proteins represent a diverse collection of structures, they can nonetheless be grouped conveniently into four classes: (i) the a-fibrous proteins, (ii) the b-fibrous structures, (iii) the collagen proteins, and (iv) those proteins that assemble into filamentous arrays but are individually globular in form. In general, all fibrous proteins contain strong repeating elements in their structures, often in the form of tandem sequence motifs. These motifs not only specify the **secondary structure**, but also play a recognizable and identifiable role in the assembly to higher levels of order. Fibrous proteins have often been used as model systems to provide insights into the structures of the more complex globular proteins.

1. a-Fibrous Structures

a-Fibrous proteins can exist *in vivo* either as individual elongated molecules (such as laminin in basement membranes and fibrinogen in blood plasma) or as filamentous assemblies (such as **myosin** in **muscle** thick filaments, **desmin** in Type III intermediate filaments, and fibrin molecules in **blood clots**). The protein sequences of all members of this family have a high propensity to form a-**helices**, which are stabilized by hydrogen bonds that lie approximately parallel to the helix axis. In addition, the a-fibrous proteins contain a characteristic heptad repeat (see also Coiled-Coils and Cytokeratins) in which nonpolar residues alternate three and four residues apart. The apolar stripe on the surface of the right-handed a-helix becomes internalized when several such a-helices aggregate and assemble into a left-handed ropelike structure (1). Although **hydrophobic** forces are very important in driving the assembly, interchain electrostatic interactions contribute significantly to determining the relative chain orientations and axial stagger, as well as the stability (1-3). In these filament-forming structures, the amino acid sequence contains a highly regular linear disposition of acidic and basic residues. The periods are usually 180° out of phase, which generates a simple rod structure with alternating bands of positive and negative charge. Consequently, assembly into the filamentous form is specified in large part by maximization of intermolecular ionic interactions, rather akin to an ionic zipper. Those a-fibrous proteins lacking periodicities in charged residues do not form regular filamentous assemblies, as judged by data currently available. In these cases, the molecules exist as separate entities, or assembly occurs in a less regular manner via non-helical domains elsewhere in the molecule, most typically at the *N*- and *C*-terminal ends.

2. b-Fibrous Structures

The b-fibrous structures were first observed in silk proteins. The fundamental structure is that of an extended array of b- strands held together in a b-sheet by a regular disposition of hydrogen bonds perpendicular to the axes of the chains (see Beta-Sheet). Two or more such sheets then aggregate into a b-crystallite. Relatively few sequence data on silks are available, but it is likely that many of them have repeating amino acid sequence motifs. This is based on the observation that the amino acid compositions are generally very simple, with perhaps only a small number of amino acids, such as glycine, alanine, serine, and glutamine, represented in any significant number. On this basis it is thought that many silks contain a dipeptide repeat (or possibly a multiple), although there are non-b-forming examples, such as *Nematus ribesii and Apis mellifera*, that almost certainly have three- and seven-residue repeats, because they give rise to a collagen and a-fibrous X-ray fiber diffraction pattern, respectively. Those silks with a dipeptide repeat, however, automatically give rise to a b-sheet with the two residues in the repeat spatially separated on opposite sides. This can give a sheet with an apolar face, for example, which can then readily assemble with the same face in a second sheet. It has been assumed that the b-sheets are planar in the silk structures, but this may not be the case *in vivo*. In fact, it is known that the b-sheets are twisted, probably in a right-handed manner, for both feather and scale keratins. In all fibrous proteins, the b-sheets are composed of antiparallel chains: in globular proteins both parallel and antiparallel b-sheets are found.

3. Collagen Class

The collagen class of fibrous proteins is characterized by a triplet repeat of the form (Gly–X–Y) $_n$, where X and Y are often proline and hydroxyproline (see Collagen). Type I collagen molecules, each of length 300 nm, aggregate with an axial stagger of distance D (67 nm) or a multiple to generate fibrils. Collagen types II, III, V, and XI also form D-periodic fibrils, but type VI collagen forms fibrils with a different periodicity. Other collagen types (IV, VII, VIII, IX, X, XII, XIII, and XIV) are non-fibril-forming but can be classified further as either basement membrane collagens (IV, VII), short-chain collagens (VIII, X), or fibril-associated collagens (IX, XII, XIV).

4. Filamentous Arrays

The last group of fibrous proteins comprise proteins that are globular in shape but assemble either helically or as a long string to form, respectively, a regular or semiregular filamentous structure. A good example of the former system is actin, in which G-actin (globular) assembles into F-actin filaments (fibrous). These, together with other proteins such as **tropomyosin** and **troponin**, form the thin filaments of **muscle**. **Titin**, a protein from muscle, consists of a series of globular domains strung together and is thus an example of the second type of filament-forming fibrous protein. The short arms in laminin are likewise composed of globular regions strung together in a near linear manner.

Bibliography

1. C. Cohen and D. A. D. Parry (1990) -helical coiled-coils and bundles: how to design an -helical bundle. Proteins Struct. Funct. Genet. **7**, 1–15.
2. D. Krylov, I. Mikhailenko, and C. Vinson (1994) A thermodynamic scale for leucine zipper stability and dimerization specificity: e and g interhelical interactions. EMBO J. **13**, 2849–2861.
3. O. D. Monera, C. M. Kay, and R. S. Hodges (1994) Electrostatic interactions control parallel and antiparallel orientation of -helical chains in two-stranded -helical coiled-coils. Biochemistry **33**, 3862–3871.
4. D. J. S. Hulmes, A. Miller, D. A. D. Parry, K. A. Piez, and J. Woodhead-Galloway (1973) Analysis of the primary structure of collagen for the origins of molecular packing. J. Mol. Biol. **79**, 137–148.

Suggestions for Further Reading

5. R. D. B. Fraser and T. P. MacRae (1973) *Conformation in Fibrous Proteins and Related Synthetic Polypeptides*, Academic Press, London.
6. D. J. S. Hulmes (1992) The collagen superfamily—diverse structures and assemblies. Essays Biochem. **27**, 49–67.

Fill-In Reaction

DNA fragments with 5′-overhanging ends are converted to **blunt-ended** molecules by reacting with the **Klenow fragment** of *Escherichia coli* DNA polymerase. This makes the overhanging ends double-stranded and is called the fill-in reaction. The fill-in reaction is often used to join fragments with different **cohesive ends** by converting the cohesive ends to blunt ends. This reaction is also used to introduce a frameshift mutation into a **gene**. A **plasmid** containing the gene is cut within the gene using a restriction enzyme to produce ends with a 5′-overhang. The overhang is filled in and the ends are re**ligated**. As long as the length of the overhang is not divisible by three, this procedure changes the reading frame of the gene downstream of the restriction site (see **Protein biosynthesis**).

Filter Binding Assays

The term *filter binding assay* is used to describe a variety of different techniques in biochemistry, immunology, virology and molecular biology. In molecular biology a filter binding assay is used to characterize **DNA–protein interactions**. This particular technique is also referred to as a *filter assay* or a *protein binding assay*, and it can be used to identify and characterize both DNA-binding proteins and the DNA sequences that interact with these proteins. The filter binding assay is based on the observation that proteins, but not double-stranded DNA molecules, bind to the surface of nitrocellulose membrane filters (1, 2). Therefore, if a DNA-binding protein is incubated with a specific DNA sequence before analysis in the filter binding assay, the resulting DNA–protein complex and any excess protein will bind to the membrane filter, while uncomplexed DNA will pass through. The amount of the DNA–protein complex retained on the membrane filter can be determined by using **radiolabeled** DNA to form the DNA–protein complexes and to quantify the amount of radioactivity retained on the nitrocellulose membrane by scintillation counting. The filter binding assay can be very quick if a multifilter vacuum filtration unit is used.

The filter binding assay offers a simple, rapid, sensitive, and versatile assay capable of providing information about the interactions between a DNA-binding protein and a specific DNA sequence. The use of radioactive DNA makes low concentrations of DNA and protein feasible. A typical experiment involves the titration of a constant amount of radiolabeled DNA with the DNA-binding protein of interest. The amount of radioactivity retained on the membrane increases with increasing protein concentration until all the radioactive DNA that can bind to the specific DNA-binding protein is depleted from the incubation mixture. Binding affinities can be determined by observing the level of specific complexes formed in the presence of a nonradioactive competitor DNA. The kinetics of association and dissociation of a specific DNA–protein complex can also be studied in the filter binding assay. However, filter binding assays cannot differentiate between dissimilar DNA–protein complexes, so this assay is effective only when one DNA–protein complex is formed. In addition, the DNA-binding protein must not be denatured during the purification process, because the filter binding assay is dependent on the interaction between the DNA-binding protein and a specific DNA sequence.

Because various membrane filters differ in binding specificities, the ability of nitrocellulose membranes to bind proteins and not native DNA is critical to the success of the filter binding assay. However, the molecular basis for this discrimination is not well understood. Both **electrostatic** and **hydrophobic** interactions have been suggested to be involved in the binding of macromolecules to nitrocellulose, but hydrophobic interactions are assumed to play the dominant role in the binding process (see Nitrocellulose). Although native DNA does not bind to nitrocellulose, heat-denatured DNA will (3) and should not be used in this assay. In addition, the native DNA tested in the assay must be free of contaminating proteins that could bind the DNA to the nitrocellulose membrane in the absence of the DNA-binding protein being tested.

Most proteins bind to nitrocellulose, but individual binding affinities are dependent on the surface characteristics of the particular protein. Therefore, the retention of a particular DNA–protein complex on the nitrocellulose filter will depend on the surface characteristics of the protein, the binding capacity of the nitrocellulose membrane, the time that the DNA–protein complex has to interact with the filter, and the regimen used to wash the filter. A rapid flow rate through the filter may not permit the binding of some DNA–protein complexes to the nitrocellulose membrane, and extensive washing of the filter may remove DNA–protein complexes with low affinities for nitrocellulose. The optimum conditions needed to bind a DNA–protein complex to the nitrocellulose membrane will be different for each protein and should be investigated for each filter binding assay.

Bibliography

1. O. W. Jones and P. Berg (1966) J. Mol. Biol. **22**, 199–209.
2. A. D. Riggs, H. Suzuki, and S. Bourgeois (1970) J. Mol. Biol. **48**, 67–83.
3. A. P. Nygaard and B. D. Hall (1963) Biochem. Biophys. Res. Commun. **12**, 98–104.

Suggestions for Further Reading

4. O. Papoulas (1987) "Rapid separation of Protein-Bound DNA from Free DNA Using Nitrocellulose Filters". In *Current Protocols in Molecular Biology*, Vol. **2** (F. M. Ausubel et al., eds.), Wiley, New York, pp. 12.8.1–12.8.9.
5. P. G. Stockley (1994) "Filter-Binding Assays". In *Methods in Molecular Biology*, Vol. **30** (G. G. Kneate, ed.), Humana Press, Totowa, NJ, pp. 251–262.
6. A. Revzin (1996) "Nucleic Acid–Protein Complexes". In *and Molecular Medicine*, Vol. **4** (R. A. Meyers, ed.), VCH, Weinheim, Germany, pp. 243–253.

Fingerprint, Protein

Two-dimensional peptide mapping, or protein fingerprinting, was introduced by Ingram in 1956 (1). In this approach, the protein is cleaved by **trypsin** or another proteinase to obtain complete digestion into peptides. Then, the peptides are separated on a solid support by electrophoresis in the first dimension and chromatography in the second, to produce a two-dimensional pattern or map. The position of each peptide is determined by its mobilities in the two dimensions and is sensitive to its covalent structure. The advantage of a two-dimensional separation is that many peptides are separated simultaneously, and two different mobilities of each can be examined.

Fingerprints are most useful in comparing closely related proteins because the one or a few peptides that differ are often easy to detect. They end up at altered positions, whereas the majority of the peptides are unaltered and remain at the same positions in each map. The latter serve as references in detecting spots corresponding to variant peptides. The deviating peptides are eluted from the support and characterized by amino acid analysis, by sequence determination, as with the Edman Degradation, or by mass spectrometry. This approach requires that a significant number of the peptides generated have identical sequences. Thus, two-dimensional peptide mapping is used to evaluate the extent of identity among closely homologous proteins.

A classical example of protein fingerprinting is the early work by Ingram on the **sickle cell** form of hemoglobin (1). Tryptic mapping revealed an altered position for only one pair of peptides detected after two-dimensional separation of the digests of normal and sickle cell hemoglobins. Glu6 of the normal b-chain is replaced by Val in the sickle form because of an A to T mutation in the corresponding **codon** of the b-chain gene (2).

The protein substrates for digestion are purified in solution by conventional chromatographic techniques or isolated via SDS-PAGE, followed by electroelution (3). The protein is **precipitated** with **trichloroacetic acid** (30% (w/v)) at 4°C for 4 h to desalt the preparation and to concentrate the protein in a small volume before digestion. After centrifugation, removal of the supernatant, and gently washing with acetone the "pellet" at –20°C (the pellet is not normally visible), the appropriate digestion buffer is added, followed by the proteolytic enzyme. This is efficient if the amount of protein is greater than about 1 nmol. The protein substrate may also be digested directly in the SDS/polyacrylamide gel without previous electroelution (see Cleveland Map). It is detected by brief staining with Coomassie Brilliant Blue or by visualization using 1 *M* KCl, followed by excision and treatment of the gel slice by a combination of drying and rehydration in digestion buffer that contains the proteinase (4, 5). Small, proteolytically cleaved peptides will diffuse out, while undigested or only partially digested proteins remain in the gel piece. The outer liquid that contains the peptides is concentrated by **lyophilization** to a small volume suitable for application to the first dimension of the mapping. Frequently, the amount of peptide material is insufficient for visualization of the map via standard staining (using ninhydrin). In this case **radiolabeling** of the protein or detection by **fluorescence** techniques is necessary.

Trypsin is often used for proteolysis because of its high specificity for cleavage at lysine and arginine residues, which can be taken to completion. An enzyme to substrate ratio of about 1:50 (w:w) is often used in a volatile buffer of ammonium bicarbonate, pH 8.1, at 37°C for 2 to 24 h. Even large polypeptides are completely degraded into small peptides that are separated by the combination of electrophoresis and chromatography. However, for proteins that generate a large number of peptides, radiolabeling and autoradiography are often necessary to obtain a distinct pattern without too many spots that overlap or cluster. For this purpose, one frequently employs labeling of cysteine residues by carboxymethylation with [^{14}C]-**iodoacetic acid**, of tyrosine residues by **iodination** with ^{125}I, or of proteins **phosphorylated** with ^{32}P.

Electrophoresis is the normal separation in the first dimension before ascending **thin-layer chromatography** in the second. The glass or plastic support is covered by a thin silica or cellulose layer. The electrophoresis buffers should contain volatile components. Many solvent systems have been suggested for the second dimension (6), but they have an organic solvent in common, often an alcohol, to promote the chromatographic mobility of **hydrophobic** peptides. A classical solvent is composed of butanol, acetic acid, water, and pyridine in volume ratios of 15:3:12:10 at pH 4 to 5. After drying, the fingerprint is visualized by ninhydrin, fluorescent techniques, stains for specific residues, or autoradiography.

Fingerprinting gives information on the subunits and the homogeneity of a protein. The number of total spots, or of those containing Cys, Tyr or other residues that are detected specifically, can be compared with the number of peptides expected from amino acid analysis and the molecular weight of the protein. If the sample is homogeneous and composed of a single polypeptide chain, the number of peptides generated should fit the frequency expected from the composition. If the number of spots detected is substantially lower, it probably indicates that the protein is composed of multiple, identical, polypeptide chains. If it is significantly higher, the sample has more than one individual polypeptide.

Two-dimensional peptide mapping is also efficient in analyzing structural variants of the same polypeptide, that is, protein **isozymes** (Fig. 1), or in identifying truncated forms and other types of posttranslational modification. Then, peptide maps reveal whether smaller or deviating polypeptides are related to other forms of the protein (identical peptide maps except for missing or deviating fragments) or are unrelated (no peptide similarities). Finally, two identical dimensions of peptide mapping, carried through with an intermediate step of chemical modification to alter a specific amino acid type, are used to detect all peptides containing that type of residue. This was the principle for the previously so popular "**diagonal**" methods (7) based no separations on paper or thin-layer plates. The peptides that contain the modified residue are differentiated by modifying them covalently after the first dimension. The second dimension is identical to the first, so that all of the unmodified peptides have the same mobilities in both dimensions. Only the modified peptides lie running off the diagonal formed by the unaltered peptides. Now, this approach like all original mappings, can be extended to modern situations by two identical runs of HPLC, capillary electrophoresis, or other microseparation. Again, the principle is always to detect any forms that deviate between the two separations.

Figure 1. Two-dimensional peptide map of acidic peptides of two similar isozymes (with E and S subunits, left and right, respectively) of an alcohol dehydrogenase. Resolution was by paper electrophoresis at pH 6.5 (horizontal) and at pH 3.5 (vertical). Strips of paper from the first dimension were stitched in opposite polarity so that the maps form mirror images through a vertical center line. The spots that differ in the E and S maps are marked (E1 and S3 are clear extra spots; S4 and S5 have only slightly shifted positions). From Ref. 8 with permission.

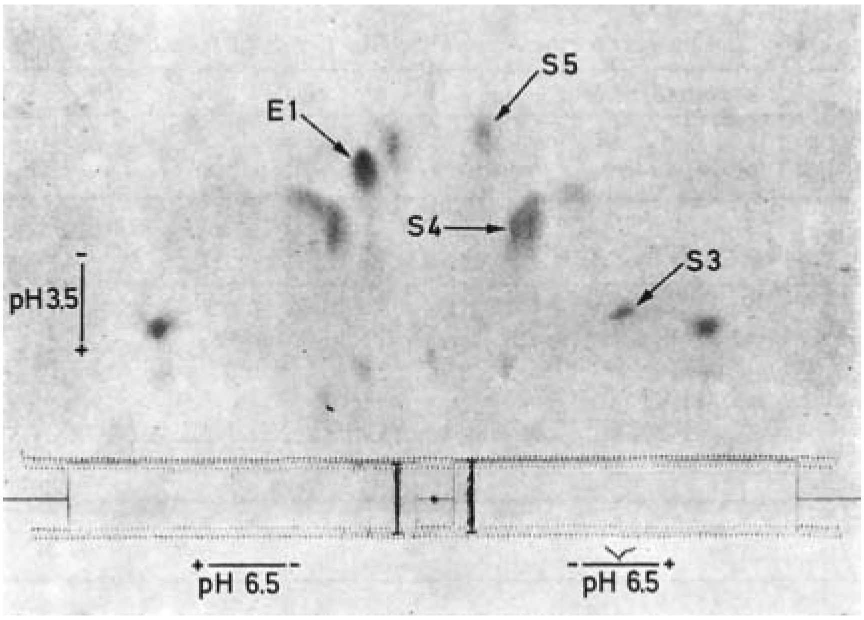

Bibliography

1. V. M. Ingram (1956) Nature **178**, 792–794.
2. V. M. Ingram (1957) Nature **180**, 326–328.
3. M. W. Hunkapiller et al. (1983) Methods in Enzymology **91**, 227–236.
4. J. Rosenfeld et al. (1992) Anal. Biochem. **203**, 173–179.
5. U. Hellman et al. (1995) Anal. Biochem. **224**, 451–455.
6. W. J. Gullick (1986) In *Practical Protein Chemistry: A Handbook* (A. Darbre, ed.), Wiley, Chichester, U.K., pp. 207–225.
7. J. R. Brown and B. S. Hartley (1966) Biochem. J. **101**, 214–218.
8. H. Jörnvall (1970) Eur. J. Biochem. **16**, 41–49.

Fingerprinting DNA

“DNA fingerprinting” refers to methods of detecting, in **eukaryotes**, unique **DNA** patterns, which allow the identification of individuals with a probability of error similar to (or lower than) that obtained by comparing fingerprints in humans. These unique, individual patterns of DNA are the result of Mendelian inheritance of polymorphic, **hypervariable loci** of repetitive DNA. The most useful loci are those consisting of tandem repeats of short (15 to 60 bp) or very short (3 to 5 bp) specific base sequences. Different **alleles** are produced by variation in the number of repeats per locus, an event that arises by **unequal crossing over**, "slippage" during DNA replication, or other means (see text below). These phenomena are favored by tandem repetition, and they are responsible for a mutation frequency several times greater than that of "traditional" point or chromosomal mutations. They can give rise to arrays of up to several hundred such repeated units.

The terms "**minisatellites**" and "**microsatellites**" are commonly used to define these loci. The names are derived from the general definition of "satellite" for repetitive DNA, because its buoyant density frequently differs from that of the bulk DNA, due to a shift in its average base composition (G and C are usually present in increased amounts). This alters the buoyant density of such DNA and causes it to separate from the bulk of fragmented DNA as a separate satellite band in CsCl buoyant density gradient centrifugation .

Historically, DNA fingerprinting was introduced in 1985 in the article "Hypervariable minisatellite regions in human DNA" by A. Jeffreys et al. (1). These authors discovered a 33-bp region repeated four times in an **intron** of the human myoglobin **gene**. The same region was found scattered randomly in other parts of the human genome, as well as in the genomes of most vertebrates. The number of repeats of this unit varies widely at different loci, but the basic 33-bp element can always be recognized, mainly from the presence of a stable 16-bp "core."

Many other loci sharing the properties of Jeffreys' first minisatellite were found to be scattered in the genomes of most higher organisms (2-4). Arrays belonging to the same "family" of minisatellites can be identified by the specific, stable core sequence present in every one of its tandemly repeated units, the polycore . The very great variability in the length of minisatellites in different locations of a single genome, and among genomes, represents a highly reliable means of individual identification. Its best use is in comparing individuals of single families or very small populations (see text below).

Technically, individual DNA patterns are produced by digesting genomic DNA with one or more restriction enzymes whose recognition sites (preferably not exceeding four bases) are not present in the repeated unit. Minisatellites will thus survive digestion, and the restriction fragments containing them can be resolved by agar gel electrophoresis according to their length (ie, molecular weight). They can then be transferred to a nylon membrane by blotting and can be identified by **hybridization** with an appropriate labeled oligonucleotide probe (see **Southern blotting**). A sensitive probe is a tandem repeat of sequences complementary to the polycore of the minisatellite under study. The labeling is either by radioactivity or by one of several enzymatic reactions leading to a visible product (see **ELISA**). The result is a ladder of DNA restriction fragment bands containing the polycore sequence, representing DNA fragments of different molecular weights, which is referred to as a "DNA profile." Different individuals normally have different DNA profiles, unless they are related genetically.

Comparison of different profiles can only be made between closely similar electrophoretic lanes; it is thus essential that individual profiles to be compared are run on the same gel. The index of similarity commonly used in comparing profiles is the "band sharing coefficient ," which gives the probability that a band of a given molecular weight will be shared within a fingerprint (5). Shared bands are those that have migrated in the gel the same distance and are therefore aligned in adjacent lanes.

Although the stretch of DNA that can be amplified by the polymerase chain reaction (**PCR**) is much shorter than the longest minisatellite variants, fingerprints have recently been produced by PCR using arbitrary primers (6, 7). This technique has proved simpler and has provided more information on types and frequencies of mutations occurring within individual minisatellites.

1. Microsatellites

Microsatellites represent a category of short tandem repeats whose length does not exceed 2 to 5 bp; they share the variability in repeat number of minisatellites, although not quite so great, and always remain within the limits of length that can be comfortably amplified by PCR. Technically, this is a great advantage; it only requires that the flanking sequences be known, to provide the primers required for PCR. Microsatellites are abundant in higher vertebrates, scattered in the genome at individual loci. In contrast with Jeffreys' multilocus minisatellites, microsatellites tend to be species- or taxon-specific; their abundance, however, frequently allows one to find some that are present in most species of a rather high taxon group. They have been mentioned here because of their structural similarity with minisatellites, but their use is different and will not be described here.

2. Multilocus and Unilocus DNA Fingerprints

The above discussion has been of multilocus fingerprinting, where the minisatellite is present at multiple loci within the genome. Some minisatellites are, however, present at only a single locus. Variability in their repeat number is still very great, however, causing heterozygosity to be the rule and a very high polymorphism in repeat number among individuals. The distinction between the two types of multilocus and unilocus minisatellites is not clear cut, however. If a family of minisatellites is hybridized with a probe at high stringency (high temperature of annealing or high salt concentration), the number of hybridizing bands in the gel will be decreased, in some cases, to a single one. This occurs when the repeats are similar, but not identical; random point mutations may cause single repeats to diverge slightly and to hybridize with the probe only under conditions of low stringency.

Hypervariable single-locus minisatellites have a number of advantages over multilocus fingerprints. The main advantage is probably their straightforward identification in different individuals and their unambiguous recognition as alleles of the same locus of any variable band identified by a specific probe. This makes single-locus fingerprinting more suitable than multilocus for population analysis.

The isolation of single-locus minisatellites is achieved by separating on the basis of size DNA fragments from a genome expected to be rich in minisatellites (G–C rich), cloning them in **cosmid vectors** made to accept inserts within a given range of sizes (charomids), and propagating them in rec-minus bacteria, to overcome the instability typical of any tandem-repeated sequence (8). Specific polycore probes will identify individual minisatellite loci in the vectors plated at low density. Those that hybridize with the probe at high stringency are potential single-locus minisatellites, which can be isolated and sequenced to construct probes that will be very specific.

3. Applications

The best use of multilocus fingerprinting is in the identification of individuals. The probability that two unrelated individuals share the same electrophoretic pattern is exceedingly low. The proportion of electrophoretic bands shared by two unrelated members of a population, a and b, is $x = ((N_{ab}/N_a)+(N_{ab}/N_b))/2$, where N_{ab} is the number of bands common to the two individuals and N_a and N_b are the total number of bands observed in the two individuals (usually up to 30). The band sharing coefficient, x, is related to the allele frequency q by the equation $x = 2q–q^2$, assuming that shared bands are identical alleles from the same locus and that all bands have the same population frequencies. If the bands are indeed independent markers, the mean probability that all N bands in an individual's profile are present in a second unrelated individual is x^N. For an individual with 30 scorable bands in a population with an average $x = 0.2$, the probability of another unrelated individual sharing the same pattern is less than 10^{20}.

These characteristics prompted the forensic use of DNA fingerprinting in criminal and civil areas (9, 10). Identification of individuals from traces of biological material is possible, given the small amount (nanograms) of DNA required for a profile and the resistance to degradation of DNA, even under the most unfavorable environmental conditions.

Multilocus fingerprinting is also the method of choice for determining close genetic relatedness ($r = 0.5$ or, at most, 0.25). The Mendelian segregation of bands ensures that a progeny inherits, on average, a random 50% of its bands from each parent. Extra bands (ie, those not present in either parent) are found with a frequency ranging from 10^2 to 10^4, as a result of the high but variable mutation rate of minisatellites of different sizes. In practice, both in the forensic field and in fields dealing with animal behavior, the most common problem easily solved by multilocus fingerprinting is the assessment of paternity. When the profiles of all partners (mother, progeny, and presumed father) are available, paternity can be affirmed or rejected with probabilities that depend on the total number of bands, on the proportion of bands shared, on the presence of new bands (mutations), and on the assumption of independence among loci. In individual cases, neither the probability of mutation nor that of loci not being independent severely affect the diagnosis. For example, the probability of not detecting incorrect paternity (ie, that the putative father will possess by chance say six of the paternal specific bands) is of the order of 5×10^5 (so long as the putative father is not related to the true one).

In the animal field, this method of paternity testing has shown how widespread is the phenomenon of "extra-pair copulation" in species classified as monogamous (11).

In population studies, multilocus fingerprinting is not the best method of analysis. The average band sharing coefficient between pairs of random, unrelated members of even a large population depends upon both inbreeding and polymorphism. Specifically, high band sharing could indicate that the population is partly inbred (ie, is not a random-mating one) or that it was subjected to a recent population bottleneck that reduced drastically the number of individuals and the range of minisatellite's sizes still represented.

Population-level comparisons may be carried out only among populations effectively so small that individual variability is drastically reduced and population-specific genotypes may emerge. One of the main problems in population analysis is the impossibility of assigning bands to a specific locus: Bands shared (co-migrating) by different individuals are not necessarily identical alleles of a single locus. This problem is overcome by using single-locus probes: If more than one is available for the same study, the total amount of information (ie, number of usable bands) will approach that of multilocus fingerprinting. Presently, microsatellites have supplanted single-locus minisatellites in population genetic analysis: The type and amount of information obtained is similar, but the method of revealing microsatellite patterns is much simpler and faster.

Single-locus minisatellites found to segregate in close association with genetic traits have been very useful in the mapping of these traits (12) and, sometimes, in the isolation of the linked gene. In human medical genetics, single-locus minisatellites have been used as markers of potentially hereditary diseases, when linkage could be shown between the two in sufficiently extended pedigrees. Also, synthetic oligonucleotides, especially if rich in G and C, have been used as probes for detecting minisatellites to be used for mapping human genetic diseases (13, 14). Again, microsatellites have now entirely supplanted minisatellites for this purpose.

Bibliography

1. A. J. Jeffreys et al. (1985) Nature **314**, 67–73.
2. T. Burke and M. W. Bruford (1987) Nature **327**, 149–152.
3. A. J. Jeffreys (1987) Anim. Genet. **18**, 1–15.
4. M. Georges et al. (1988) Cytogenet. Cell Genet. **47**, 127–131.
5. M. Lynch (1990) Mol. Biol. Evol. **7**, 478–484.
6. J. Welsh and M. McClelland (1990) Nucleic Acids Res. **18**, 7213–7218.
7. J. Welsh, N. Rampino, M. McClelland, and M. Perucho (1995) Mutat. Res. **338**, 215–229.

8. J. A. L. Armour, S. Povey, S. Jeremiah, and A. J. Jeffreys (1990) Genomics **8**, 501–512.
9. B. E. Dodd (1985) Nature **318**, 506–507.
10. A. M. Ross and H. W. J. Harding (1989) Forensic Sci. Int. **41**, 197–203.
11. T. Burke (1989) TREE **4**(5), 139–144.
12. T. G. Krontiris (1995) Science **269**, 1682–1683.
13. Y. Nakamura et al. (1987) Science **235**, 1616–1622.
14. R. Schafer et al. (1988) Electrophoresis **9**, 369–374.

Suggestions for Further Reading

15. L. T. Kirby (1990) *DNA Fingerprinting. An Introduction*, Stockton Press, New York.
16. A. J. Jeffreys et al. (1991) "Principles and recent advances in DNA fingerprinting". In *DNA Technology and Its Forensic Applications* (G. Berghaus, B. Brinkmann, G. Rittner, and M. Staak, eds.), Springer-Verlag, Berlin, pp. 3–19.
17. M. W. Bruford, O. Hanotte, J. F. Y. Brookfield, and T. Burke (1992) "Single locus and multilocus DNA fingerprinting". In *Molecular Genetic Analysis of Populations. A Practical Approach* (A. R. Hoelzel ed.), IRL Press, Oxford, U.K., pp. 225–269.
18. K. Rassmann, A. Zischler, and D. Tautz (1996) "DNA multilocus fingerprinting using simple repeat motif oligonucleotides". In *Molecular Genetic Approaches in Conservation* (T. B. Smith and R. K. Wayne, eds.), Oxford University Press, New York, pp. 238–250.

FK506

The immunosuppressive drug FK506 (also known as tacrolimus) is a 23-membered macrocyclic lactam (Fig. 1) that was first isolated from a strain of *Streptomyces tsukubaensis* in Japan in 1987 (1). In addition to blocking the T cell immune response, FK506 has neuroprotective properties (2, 3) and antiparasitic effects (4). It was first used clinically for immunosuppression in 1989. The target of FK506 for immunosuppression is thought to be the cytosolic FK506-binding protein, FKBP12, which is also a **peptidyl prolyl *cis*/ *trans*** isomerase (PPIase). Upon binding to FKBP12 within a deep **hydrophobic** pocket, the **imide** bond of FK506 adopts a *trans* conformation, concomitant with reorganizing the conformation of the pipecolinic ring and of the pyranose ring. Recently, a cell-permeable, covalently linked dimer of FK506 (FK1012) was constructed as a tool to achieve controlled cross-linking of intracellular receptor domains for gene activation (5). It utilizes the high binding affinity of FK506 for the receptor FKBP12, which is effective at less than nanomolar concentrations. A number of derivatives that bind to and inhibit FKBP have been reported, some immunosuppressive and others not (6).

Figure 1. The structure of immunosuppressant FK506.

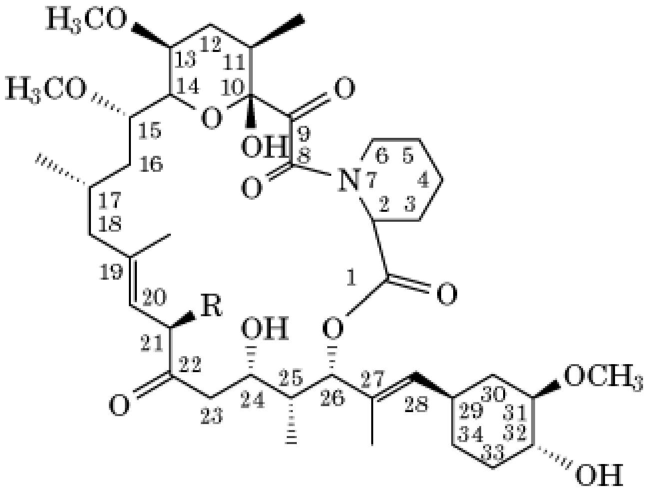

FK506 R: $CH_2CH{=}CH_2$
ascomycin R: CH_2CH_3

Despite structural similarities to rapamycin in a major part of the macrocycle, many biological effects of FK506, including the arrest of clonal T cell expansion, are reminiscent of another class of immunosuppressants, cyclosporin A (CsA), rather than rapamycin. This finding was the first evidence of a common upstream target for the two different classes of immunosuppressants, FK506 and cyclosporin A. As monitored by affinity chromatography, the FKBP12/FK506 complex binds the same protein from a calf thymus extract, the protein **phosphatase** calcineurin, as has been obtained with the complex of CsA and its target cyclophilin Cyp18. In both cases noncompetitive inhibition by the complex is observed in the nanomolar concentration range. Considering that the structures of Cyp18/CsA and FKBP12/FK506 are unrelated in amino acid sequence and spatial organization, the similar inhibition of calcineurin is striking. FK506 acts as a pro-drug, in that only the complex of the drug and its receptor is active. Two segments of FKBP12 comprising the loops in the region of residues 40 and 80 plus an effector region of FK506, the carbon chain C17 to C32, may be involved in drug activation. In the **X-ray crystallographic** structure of the human FKBP12/FK506/calcineurin complex, the FKBP12/FK506 portion contacts two distinct areas on calcineurin that do not directly obstruct both the active site and the substrate-binding cleft of the protein phosphatase. On the contrary, blocking a rather distant subsite of the phosphatase/protein phosphate recognition region is responsible for phosphatase inhibition (8).

Both CsA and FK506 block the induction of clonal T cell expansion at the early G_0 to G_1 transition of the cell cycle. They exert down-regulation of transcription of a number of similar lymphokine genes.

Bibliography

1. T. Kino et al. (1987) J. Antibiot. **40**, 1249–
2. W.E. Lyons et al. (1994) Proc. Natl. Acad. Sci. USA **91**, 3191–3195.
3. J. Sharkey and S.P. Butcher (1994) Nature **371**, 336–339.
4. A. Moro et al. (1995) EMBO J. **14**, 2483–2490.
5. D.M. Spencer, T.J. Wandless, S.L. Schreiber, and G.R. Crabtree (1993) Science **262**, 1019–1024.
6. D.M. Armistead and M.W. Harding (1993) Ann. Rep. Med. Chem. **28**, 207–215.
7. J. Liu et al. (1991) Cell **66**, 807–817.
8. C.R. Kissinger et al. (1995) Nature **378**, 641–644.

Suggestions for Further Reading

9. J.R. Luly (1991) Mechanism-based immunosuppressants, Ann. Rep. Med. Chem. **26**, 211–219.
10. T.R. Brazelton and R.E. Morris (1996) Molecular mechanisms of action of new xenobiotic immunosuppressive drugs - tacrolimus (FK506), sirolimus (rapamycin), mycophenolate (mofetil) and leflunomide, Curr. Opinion Immunol. **8**, 710–720.
11. S.H. Snyder and D.M. Sabatini (1995) Immunophilins and the nervous system, Nature Med. **1**, 32–37; summarizes immunophilins in the nervous system.
12. M.E. Cardenas, D. Zhu, and J. Heitman (1995) Molecular mechanism of immunosuppression by cyclosporine, FK506 and rapamycin, Curr. Opinion Nephrol. Hypertens. **4**, 472–477.

Flagella—Prokaryotes

Flagella are the propulsive **organelles** of a wide variety of unicellular organisms, both **prokaryotes** and **eukaryotes**. However, prokaryotic flagella differ in almost every respect from their eukaryotic counterparts (see **Flagella—eukaryotes**).

1. Motility and Behavior

Prokaryotic flagella are largely external appendages that project far from the cell surface (Fig. 1, top right); for example, a typical rod-shaped **bacterium** is about 1 or 2 µm long, but its flagellar filaments can be 10 µm long. The motor resides at the cytoplasmic membrane and is a rotary device that transmits the rotation to the external flagellar filament. The motor is not driven by ATP hydrolysis like most mechanoenzymes (see **Energy transduction**), but by a proton-motive force (or in some marine and alkaliphilic bacteria, by a sodium-motive force); protons that have been actively pumped out of the cell by the electron transport chain are allowed to flow down their electrochemical potential gradient through the flagellar motor and surrender their potential energy in return for hydrodynamic work against the resistance of the aqueous medium (see also Chemiosmotic Coupling). The filament is very thin (about 20 nm in diameter) compared to its length, with a length/diameter ratio of about 500, and has a completely regular helical or corkscrew shape. When rotated by the motor, it therefore functions as a propeller or Archimedes screw. Depending on the handedness of the helix (left-handed or right-handed) and the direction of rotation of the motor (counterclockwise or clockwise), the cell will experience a pushing or a pulling force. The flagellar motors of most bacteria are reversible, that is, they possess a switch or gear that will alternate the direction of rotation between counterclockwise and clockwise rotation. In the simplest cases, such as *Pseudomonas* spp., which have a single flagellum at one pole of the cell, this results in a shuttling motion. In the case of species such as *Escherichia coli* or *Salmonella*, which have several flagella originating more or less randomly around the cell body, the rotation direction that corresponds to pushing results in the individual flagellar filaments coalescing into a propulsive bundle to produce the motion called *running* or *swimming*, while the opposite direction causes the bundle to fly apart and produce a chaotic motion called *tumbling*. This tumbling randomly orients the cell, so that the next episode of swimming is largely uncorrelated with the previous one. The resulting trajectory is a zigzag or random walk in three-dimensional space.

Figure 1. The bacterial flagellum, showing its four major structural elements: external structure (white), basal body

(light gray), motor/switch (medium gray), and export apparatus (dark gray), along with their various substructures. The outer membrane (OM), periplasmic space (PERI), and cytoplasmic membrane (CM) of the bacterium, in which the flagellum machinery is embedded, are also shown. To drive motor rotation, protons flow through the motor down their potential gradient (toward lower H^+ concentration). External proteins, such as flagellin (black ovals), are selectively passed through the export apparatus, travel down a central channel in the nascent structure, and assemble at its distal end. Most of the flagellum is tiny, so that only the filaments are evident at the scale of the bacterial cell (**top right**).

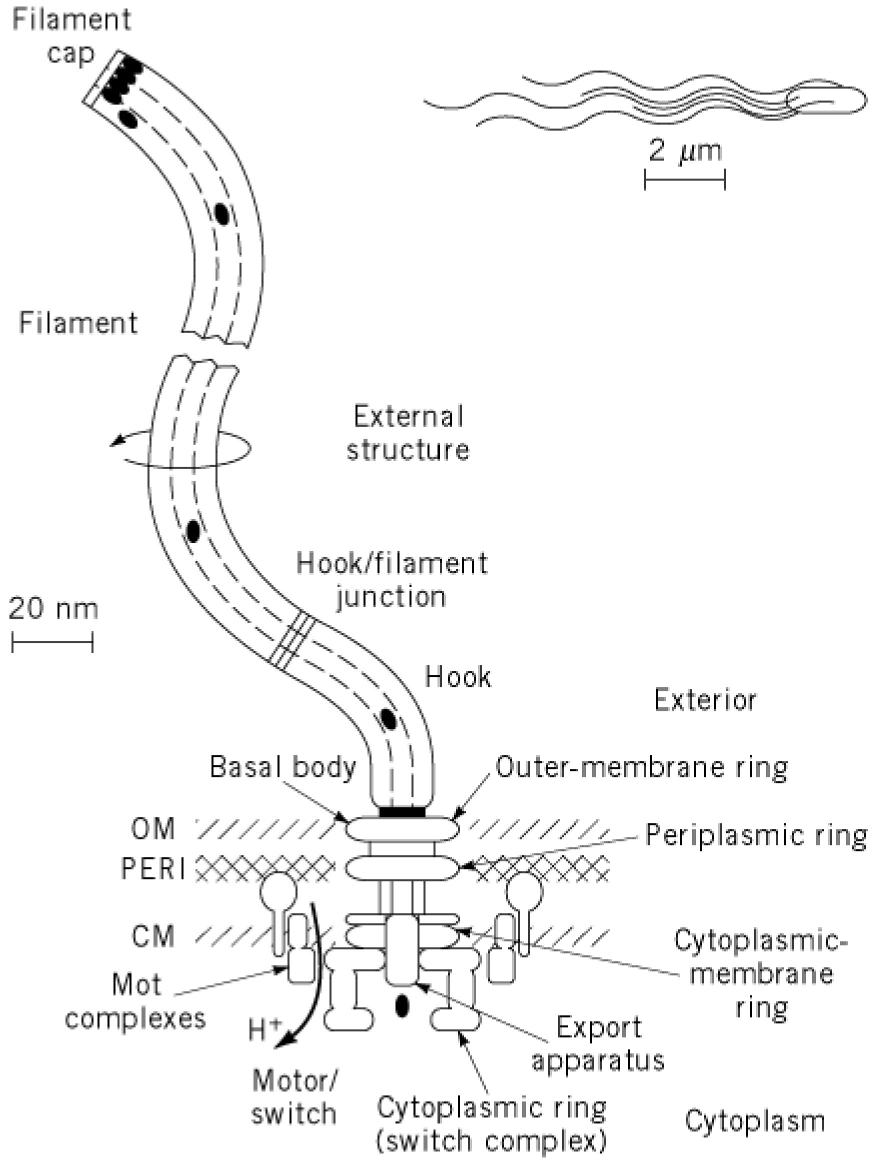

The above description applies when the cell is moving in an isotropic environment. However, if there are gradients of various chemicals (beneficial ones such as the amino acid aspartate or noxious ones such as phenol) and if the cell has **receptors** to detect these chemicals (or light, pH, temperature, etc.), it carries out an ongoing evaluation of whether its environment is improving or deteriorating. If the former is correct, it keeps going; if the latter is correct, it tumbles and then reevaluates whether its new direction is better than its old one. The net effect is a statistical drift to a better life; this behavior is called chemotaxis (or, more generally, *taxis*). The evaluation is in time, even though it is achieved by travel through space—a stationary bacterium could not make the measurement. Thus bacteria possess a rudimentary memory.

2. The Flagellar Gene System

Flagellar, motility, and chemotaxis **genes** (about 60 in all, depending on definition) are highly clustered into just four main regions of contiguous genes (Fig. 2). The organization of the genes shown in Figure 2 is for *Salmonella* (and is almost identical for *E. coli*); in other species, such as the developmental bacterium *Caulobacter crescentus* or the **Gram-positive** bacterium *Bacillus subtilis*, the genetic organization is somewhat different. The four gene clusters contain operons ranging in size from a single gene to more than 20 in some species. These operons fall into a hierarchy of expression by transcription, with gene products at one level playing a role in transcription of lower levels. In most cases, the controlling elements are of a more or less conventional sort, such as transcriptional activators and dedicated sigma factors for transcription initiation. However, there are at least two unconventional mechanisms. The first is a negative regulator, FlgM, which operationally seems like a **repressor** but is in fact an anti-sigma factor rather than a DNA-binding protein. The second is the highly unusual mechanism by which FlgM is inactivated in the last stage of the expression hierarchy; when flagellar assembly has proceeded to a fairly advanced degree, the flagellar structure itself becomes competent to export FlgM from the cell (thus inactivating it), using the same export pathway that is used for the process of flagellar export/assembly itself (see text below).

Figure 2. The four clusters of flagellar genes on the chromosome of *Salmonella*, along with their positions (Cs, centisom
the operons (open arrows) and the genes they contain. Different gene symbols (*flg*, *flh*, and *fli*) are used for the four regic
Region II, which contains flagellar genes, also contains motility (*mot*) genes (see text and Fig. 1) and chemotaxis (*che*) g

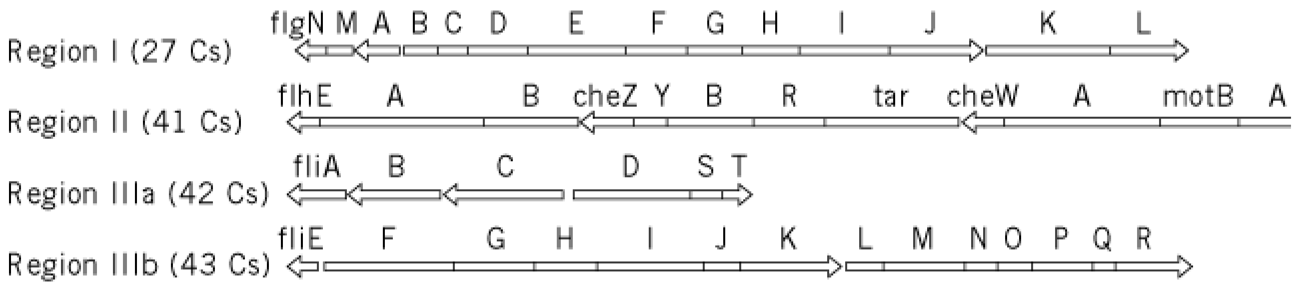

3. Flagellar Structure and Function

Flagellar structure can be divided into several categories (Fig. 1):

1. *External structure*. This is the structure that is most evident by light or electron microscopy and includes the helical filament and a hook-shaped structure that acts as a universal joint for the filament.
2. *Basal body*. This structure is embedded in the cell surface (outer membrane, **periplasmic** space, and cytoplasmic membrane) and consists of (a) a rod whose distal end is joined to the hook, (b) an outer-membrane ring and a periplasmic ring, which together act as a bushing for the rod, and (c) a cytoplasmic-membrane ring to which the proximal end of the rod is firmly attached. The external structure and the basal body are passive components; that is, they are not part of the energy transducing machinery.
3. *Motor/switch*. The motor/switch can be subdivided into two categories. The first is a set of so-called Mot complexes that surround the cytoplasmic-membrane ring; these complexes, which are stationary, are involved in the generation of torque but not in the switching of rotation direction. The second is a cylindrical switch complex or cytoplasmic ring, mounted onto the cytoplasmic-membrane ring and projecting into the cytoplasm. The switch complex is involved both in the generation of torque (together with the Mot complexes) and in the switching of rotation direction. It is the rotating element of the motor and causes the cytoplasmic-membrane ring, the rod, the hook, and the filament to rotate as a single unit.

4. *The export apparatus*. This is the least understood structure, but available evidence suggests that it is located at the center of the cytoplasmic-membrane ring and projects out into the cytoplasm. There may also be components that shuttle between the cytoplasm and the components associated with the membrane.

The protein composition and approximate subunit stoichiometry of most of the substructures of the flagellum are known:

1. filament cap (FliD), ~10 subunits;
2. filament (FliC or flagellin), ~20,000 subunits;
3. hook/filament junction (FlgK/FlgL), ~10 subunits each.
4. hook (FlgE), ~130 subunits;
5. rod (FlgB, FlgC, FlgF, FlgG, FliE), ~5 to 25 subunits each;
6. outer-membrane ring (FlgH), ~25 subunits;
7. periplasmic ring (FlgI), ~25 subunits;
8. cytoplasmic-membrane ring (FliF), ~25 subunits;
9. cytoplasmic ring or switch complex (FliG, FliM, FliN), ~30 to 40 subunits each;
10. Mot complexes (MotA, MotB), ~12 subunits each;
11. export apparatus (composition and stoichiometry not well-characterized).

Thus there is a wide range of stoichiometries, with flagellin being by far the most abundant.

4. Flagellar Morphogenesis and the Flagellar Protein Export Process

The assembly of the flagellum proceeds for the most part in a linear fashion—that is, subunit by subunit of the first substructure, then subunit by subunit of the second substructure onto the first, and so on. The first substructures to be assembled are those associated with the cytoplasmic membrane, and the last are the ones furthest away from the cell. Thus a description (oversimplified) of the order would be: cytoplasmic-membrane ring and export apparatus → switch complex and Mot complexes → basal–body rod → periplasmic and outer-membrane rings → hook → filament.

The subunits of the basal-body rod, the hook, the filament, and some other minor but essential substructures are added to the distal end of the growing structure and get there by first passing through the export apparatus (in a process that probably requires energy and certainly requires specificity of recognition) and then traveling down a central core that exists in the structure (Fig. 1).

4.1. The Flagellar Export Pathway is a Type III Secretory Pathway

It has recently become evident that the pathway for export of flagellar proteins is but one member, albeit a rather special one, of a large family of pathways that are used by pathogenic bacteria for the secretion of virulence factors directed against the host; these pathways are called type III secretory pathways (see Protein Secretion). The similarities within this family extend beyond operational ones, such as lack of signal peptide cleavage, to biochemical ones. There are at least six flagellar components (FlhA, FlhB, FliI, FliP, FliQ, FliR) that have homologues in the virulence factor secretory apparatus. FliI is an ATPase, which could be driving **active transport** of the protein substrates. Remarkably, it is homologous to a fundamentally important protein for bacteria (and for mitochondria and **chloroplasts**): the catalytic subunit of the proton-translocating F_0F_1-ATPase (see ATP Synthase).

Suggestions for Further Reading

1. R. M. Macnab (1996) "Flagella and motility". In *Escherichia coli and Salmonella: Cellular and Molecular Biology* (F. C. Neidhardt, R. Curtiss III, J. L. Ingraham, E. C. C. Lin, K. B. Low Jr, B. Magasanik, W. S. Reznikoff, M. Riley, M. Schaechter, and H. E. Umbarger, eds.), 2nd ed., ASM

Press, Washington, DC, pp. 123–145. [A comprehensive review of flagella and motility in *E. coli* and *Salmonella*, with 214 references.]

2. G. W. Ordal, L. Màrquez-Lagaña, and M. J. Chamberlin (1993) "Motility and chemotaxis". In *Bacillus subtilis and Other Gram-Positive Bacteria: Biochemistry, Physiology and Molecular Genetics* (A. L. Sonenshein, J. A. Hoch, and R. Losick, eds.) ASM Press, Washington, DC, pp. 765–784. [Comprehensive coverage of motility and chemotaxis in Gram-positive bacteria, with 153 references.]
3. J. Wu and A. Newton (1997) Regulation of the *Caulobacter* flagellar gene hierarchy; not just for motility. Mol. Microbiol. **24**, 233–239. [A microreview of the inter- related regulation of the cell cycle and regulation of expression of the flagellar gene system in *Caulobacter crescentus*, with 47 references.]
4. R. Losick and L. Shapiro (1993) Checkpoints that couple gene expression to morphogenesis. Science **262**, 1227–1228. [A concise summary of the remarkable mechanism of genetic regulation by export of the regulatory protein FlgM.]
5. F. Van Gijsegem, C. Gough, C. Zischek, E. Niqueux, M. Arlat, S. Genin, P. Barberis, S. German, P. Castello, and C. Boucher (1995) The *hrp* gene locus of *Pseudomonas solanacearum*, which controls the production of a type III secretion system, encodes eight proteins related to components of the bacterial flagellar biogenesis complex. Mol. Microbiol . **15**, 1095–1114. [A primary publication describing a typical type III virulence factor secretory system and emphasizing its relationship to flagellar protein export.]

Flow Cytometry

Flow cytometric analysis of **eukaryotic** cells, also known as fluorescence-activated cell sorting (FACS), was first developed in the late 1960s. FACS has been a tool primarily of immunologists because of its power in dissecting the complex subsets of cells derived from the blood. It has found clinical application in the classification of leukemias and lymphomas, as well as a tool for prognosis in HIV disease. Because of the relative expense of the equipment, it has been slow to progress into many other areas of biological research. However, the past decade has seen significant expansion in the techniques that are designed for FACS analysis. In particular, several developments came about that make FACS an extremely powerful tool for molecular biology analysis. These include (a) the development of FACS-based assays for reporter genes (initially, b-**galactosidase**; now including several other hydrolases) and (b) the introduction of the inherently fluorescent proteins, such as green fluorescent protein (GFP; see Luciferases And Luciferins). As the technology becomes cheaper and more widespread, these applications (and others) will become a common tool in the arsenal of molecular biology.

1. Molecular Biology by FACS: A Basic Overview

Flow cytometry is a technology that characterizes populations of cells, on a cell-by-cell basis, in terms of their fluorescence properties. Several different fluorescent signals can be monitored simultaneously and independently. On the basis of the amount of each fluorescence exhibited by each cell, the instrument can decide whether that cell should be sorted (separated from all others) or simply discarded. The sorted cells can be recovered in a viable state for further biochemical processing or culture. Most flow cytometric sorters can process as many as 5000 cells per second, with excellent purity and specific recovery of cells occurring as infrequently as one in a million.

Fluorescence is the fundamental parameter evaluated by a flow cytometer, so the most common molecular biology technique performed by FACS is quantification of reporter gene activity. Thus, either intrinsic or enzymatically generated fluorescence serves as the surrogate assay for the number of protein molecules synthesized from a particular gene construct introduced into the cell. The intensity of the fluorescence is, in general, linearly related to the expression from the gene construct, so the FACS can quantify directly, on a cell-by-cell basis, the **translation/transcription** activity of the reporter gene.

It is important to recognize that the measurement is made on each cell independently, so the analysis of a cell population can be displayed as a distribution of activities. Thus, heterogeneous gene expression within a population can be resolved; for example, the presence of a few highly expressing cells along with a majority of nonexpressing cells is easily detected. Furthermore, the sorting capabilities of the instrument can then be used to isolate either the positive or negative cell fraction.

Cells are passed through the interrogating laser beam one-by-one in a stream, so it is necessary that the sample be prepared as a suspension of individual cells. It is possible to monitor adherent cell populations after removing the cells from the substrate—for example, by treatment with a proteinase such as **trypsin** . It is not possible, however, to use the FACS on solid tissue samples without dispersing the cells. Virtually any cell type can be used; successful assays have been performed on **bacteria**, **yeast**, and **Drosophila** cells, as well as on a wide variety of mammalian cells.

2. Reporter Genes assays for FACS

The most common application of FACS in molecular biology is the quantitative measurement of reporter gene expression. A variety of reporter genes are amenable to FACS analysis, including cell surface markers, hydrolases, and GFP. Surface markers are genes coding for membrane-bound proteins that are not normally expressed by the cells of interest. These can be detected using fluorescently conjugated monoclonal antibodies and standard immunophenotyping methods. These assays are not necessarily quantitative; that is, the amount of surface expression may not always correlate with transcriptional activity. The introduction of foreign proteins on the surface of cells also prevents the introduction of such cells into a host, because of immunological rejection.

The other types of assays rely on intracellular expression of proteins that can be detected enzymatically or are inherently fluorescent, such as GFP. In 1988, Nolan et al. developed the first FACS-based assay for an enzymatic reporter gene (1-3). This assay uses the fluorogenic substrate fluorescein digalactoside (FDG). FDG is nonfluorescent until hydrolyzed; it can be easily introduced into the cytoplasm of cells. Cells that have high b-galactosidase activity (eg, that are transfected with the bacterial *lacZ* gene controlled by a promoter active in the host cells) will hydrolyze the FDG to yield fluorescent **fluorescein**. The amount of fluorescence generated is quantitatively related to the amount of cellular b-galactosidase. This assay has extreme sensitivity (it can detect cells with as few as 5 molecules of enzyme) and a large dynamic range (at least 5 orders of magnitude). More recently, assays for b-glucuronidase and b-glucosidase have also been introduced that are similar to the one for b-galactosidase (4).

The last few years has seen an explosion in the use and development of GFP as a reporter gene. A variety of mutations have been introduced into the gene to produce proteins that are more highly fluorescent and with altered fluorescence spectra. The primary advantage of the GFP assay is ease of use: the expressing cells become spontaneously fluorescent. In addition, the genes encoding the varieties of GFP are relatively small (~1.5 kb) compared to *lacZ* (~3.5 kb), giving greater flexibility in designing vectors.

3. Why Is FACS Such a Powerful Tool?

There are three principal reasons:

1. FACS analyses collect data on each individual cell, presenting the data as a distribution of activity.
2. FACS analysis is multiparametric (the ability to measure several parameters simultaneously on each cell).
3. The FACS can viably sort cells based on these measurements.

4. Analysis of a Distribution

Biological systems are rarely, if ever, homogeneous. Indeed, even the responsiveness of a **clone** is often complex. This has become even more evident since the advent of FACS analysis. Figure 1 shows two examples of such heterogeneity. These examples demonstrate how a cloned population of cells (which has a uniform, single integration of a reporter gene construct) responds in a heterogeneous way to stimulations. It is immediately apparent that such complexity is completely missed by using standard, bulk assays for reporter gene activity. Bulk assays measure the average amount of activity in a population, with no information about the distribution within that population. The figure demonstrates that the signal transduction mediated by effector molecules does not affect all cells identically; some respond rapidly, whereas others remain resting for at least a period of time.

Figure 1. Three examples of flow cytometric analysis of gene expression. (**a**) A reporter gene construct consisting of a transcriptional fusion of the *lacZ* gene to the HIV long-terminal repeat (LTR), the promoter/enhancer region for HIV typ stably transfected into 293 S cells. Basal expression is shown in the *top left* panel. After stimulation with tumor necrosis (TNF) or **phorbol ester** (phorbol myristate acetate, PMA) for 6 h, most cells have significantly elevated the expression c reporter gene. Thus, the response to these factors is not homogeneous, even within this cloned cell line. The synergistic s (TNF+PMA) results in activation of the construct in virtually all cells. (**b**) In this example, the *lacZ* gene was fused to a i promoter containing three adjacent binding sites for NF-AT, the nuclear factor of activated T cells, and transfected into t transformed Jurkat T cell line. The b-galactosidase activity corresponds to the degree of activation of the nuclear factor. After stimulation of the cells with PMA+ionomycin, there is a graded response over time. At the early time points, some responded and others haven't; note the dichotomy in the response. Those cells that have responded have fully turned on t promoter (ie, the position of the positive peak at 2 h is essentially the same as at 12 h). What increases over time is the *fr* responding cells. (*Right*) Cells stimulated with PMA+ionomycin for 2 h were stained for b-galactosidase activity and DN content. The multiparametric capability of the FACS allows the simultaneous measurement of these values. This analysi that cells progressing through the cell cycle are more likely to respond early after stimulation (nearly half of the respondi are in S+G_2M; less than one-third of nonresponding cells are in cycle). (**c**) The generation of spectral mutants of the inhe fluorescent GFP allows for simultaneous measurement of two different genetic elements in the same cell. “Vex” is viole GFP, and “Bex” is blue-excited GFP. In this example, cells were infected with retroviruses expressing one or the other C Uninfected cells, singly infected cells, and cells infected with both viruses can be easily distinguished by measuring the t fluorescence signals by FACS.

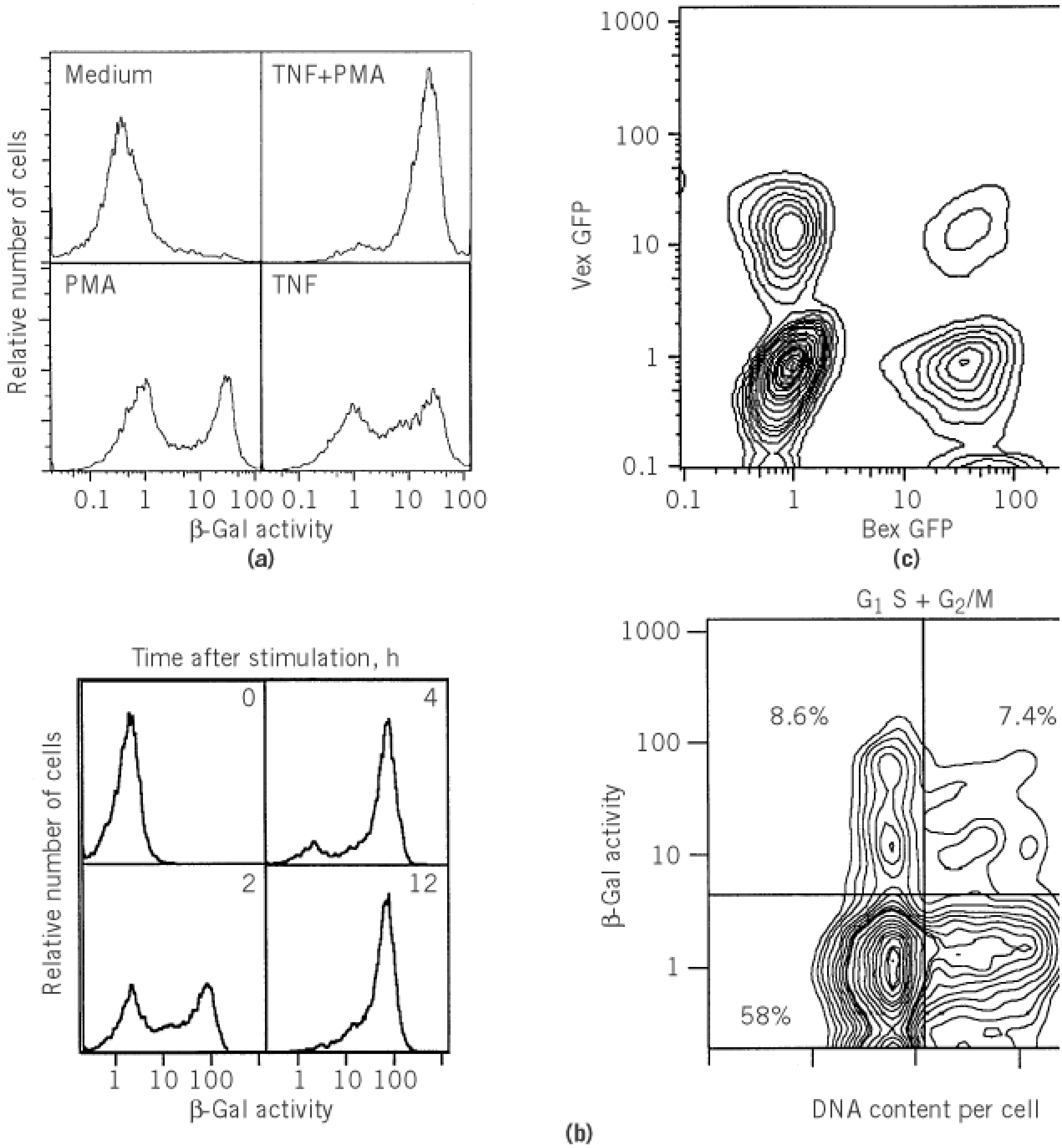

5. The Power of Multiparametric Analysis

A typical FACS experiment can measure at least three different fluorescent species, in addition to measurements related to cell size and shape. Thus, one can combine a typical reporter gene expression assay (using one fluorescent channel) together with two other assays. These might include assays to measure DNA or RNA content, cell surface **phenotype**, viability, and so on. In addition, one could choose a second, independent reporter gene assay using a second color, in order to measure simultaneously two independent genetic elements (ie, enhancers, promoters, repressors). Figure 1 c shows such an analysis, using two different versions of the inherently fluorescent protein GFP (5). Another analysis that can benefit from such simultaneous measurement is the dissection of enhancer elements. By transfecting the same cells with different reporter genes fused to different enhancer elements, one can now measure the relative activity of each enhancer element in the same cell in response to stimulations.

6. Sorting (Selection)

Perhaps one of the most underutilized capabilities of the FACS is the ability to sort cells viably based on any of the measurement parameters. Effectively, this means that any reporter gene used in the context of the FACS becomes (in addition) a selectable marker. Selection by FACS has several advantages over standard drug-based cytotoxic selectable markers. Generally, selectable marker systems rely on a combination of toxic compounds and genes that encode resistance or sensitivity to the toxic compound. These systems work by killing or halting the growth of all cells that do not (or do) produce some threshold amount of the protein encoded by the selectable marker gene.

Survival-dependent selection systems have several disadvantages. For example:

1. The selection system is inherently toxic, often even to cells expressing the resistance gene.
2. The selection generally takes many cell divisions, or a period of weeks for mammalian cells.
3. The cells below (or above) the threshold amount of the selecting protein are dead and unavailable for further study.
4. It is difficult or impossible to select for different expression levels of the marker.
5. The cells must generally be able to reproduce in culture.

On the other hand, FACS analysis of reporter genes allows the sorting capabilities of the FACS to isolate cells based on virtually any level of expression of the nontoxic reporter genes. The FACS can analyze and sort from as many as 5000 cells per second, so 1 cell in 10 million could be selected in an hour of sorting, making FACS as efficient as drug-based selectable markers.

The ability to select cells based on a particular level of expression is a big advantage over standard selection methods, for several reasons. First of all, cells expressing very low levels of the b-galactosidase enzyme (eg, 10 molecules) can be detected and sorted; such low levels might not be sufficient to confer drug resistance. Second, cells expressing virtually any level of enzyme can be selected (for instance, only those expressing more than 100,000 molecules per cell). Third, cells that rapidly change expression of the reporter gene in response to a stimulus can be selectively sorted. These capabilities give FACS assays the ability to select cells that would be impossible to select using standard drug selection methods.

Finally, the ability to sort cells based on gene expression levels allows the concomitant determination of other parameters that can only be determined by, for example, biochemical assays on lysates. For instance, by sorting cells with different expression levels and then doing messenger RNA quantification on the sorted cells, a comparison of message levels within defined subsets of a population can be done (eg, see Ref. 2).

7. Summary

Besides the analysis of reporter genes, other technologies are becoming available for FACS analysis. For instance, fluorescent *in situ* **hybridization** (FISH) for both RNA and DNA, even after *in situ* polymerase chain reaction (PCR), has been successfully performed by FACS. The FACS-based enzyme assays have also been extended to nonmammalian systems. Reporter gene analysis has been performed in **plant** cells (6), **Drosophila** cells (7), **yeast** (8), and **bacteria** (8, 9), complete with viable sorting of the cells for further analysis.

Flow cytometric analysis is an aspect of the majority of immunologically related research, as can be evidenced by perusing any immunology journal. Since the relatively recent introduction of this technology to molecular biology, it has been growing quickly as the applications become more advanced and as the technology becomes more accessible. Flow cytometry has already proven to be a unique and powerful adjunct for molecular analyses; in the years to come, it will undoubtedly become a common tool.

Bibliography

1. G. P. Nolan, S. Fiering, J. F. Nicolas, and L. A. Herzenberg (1988) Proc. Natl. Acad. Sci. USA **85**, 2603–2607.
2. S. Fiering, M. Roederer, G. P. Nolan, D. R. Micklem, D. R. Parks, and L. A. Herzenberg (1991) Cytometry **12**, 291–301.
3. M. Roederer, S. N. Fiering, and L. A. Herzenberg (1991) Methods **2**, 248–260.
4. M. Lorincz, M. Roederer, L. A. Herzenberg, and G. P. Nolan (1996) Cytometry **24**, 321–329.
5. M. T. Anderson, I. M. Tjioe, M. C. Lorincz, D. R. Parks, L. A. Herzenberg, G. P. Nolan, and L. A. Herzenberg (1996) Proc. Natl. Acad. Sci. USA **93**, 8508–8511.
6. D. W. Galbraith, G. M. Lambert, R. J. Grebenok, and J. Sheen (1995) Methods Cell Biol. **50**, 3–14.
7. M. A. Krasnow, S. Cumberledge, G. Manning, L. A. Herzenberg, and G. P. Nolan (1991) Science **251**, 81–85.
8. R. Nir, Y. Yisraeli, R. Lamed, and E. Sahar (1990) Appl. Environ. Microbiol. **56**, 3861–3866.
9. F. Russo-Marie, M. Roederer, B. Sager, L. A. Herzenberg, and D. Kaiser (1993) Proc. Natl. Acad. Sci. USA **90**, 8194–8198.

Fluctuation Test

The fluctuation test was invented by Luria and Delbrück in 1943 to determine whether bacterial **mutants** arise before any **selection** for their presence or only after the **bacteria** are subjected to selection (1). It was enormously influential because by showing that mutations arise randomly before selection, it provided strong evidence that bacteria and **viruses** are normal organisms possessing heritable genetic determinants. Thus it opened the way for the genetic analysis of bacteria and their viruses and led eventually to modern molecular biology. Luria and Delbrück measured the number of mutants resistant to **bacteriophage** T1 in a large number of replicate cultures of *Escherichia coli*. They reasoned as follows. If mutants occur after the culture is exposed to the phage (ie, in response to selection), then little variation should occur among cultures in the number of mutants. In fact, the distribution would be Poisson with the variance equal to the mean. However, if mutants arise at random during nonselective growth of cells, the probability of a mutation would be constant per generation per cell. But the consequence of that mutation would depend on when during the growth of the population the mutation occurred. In a binary dividing population, a cell that sustains a mutation gives rise to a **clone** of identical descendants, each of which is a mutant. Thus a mutation during early generations gives rise to a large clone of mutant cells, whereas a late mutation gives rise to few mutant cells. Among a large set of identical cultures of dividing cells, the few cultures in which the mutation happened in the early generations (the jackpots) have a large number of mutants, whereas the majority of the cultures have none or a few mutants. The predicted distribution, called the Luria–Delbrück distribution, has a variance much larger than the Poisson distribution. This is what Luria and Delbrück observed. Their test is known as “the fluctuation test” because it measures the degree of fluctuation in the number of mutants found in replicate cultures.

Interest in the fluctuation test has been revived recently by the controversy surrounding the phenomenon known as "directed" or "adaptive" mutation (2). By obtaining the highly variant distribution, Luria and Delbrück proved that mutations occur before selection. Because the selection they used was lethal, however, they did not prove the converse that mutations could not also arise after selection. Indeed, when the selection is not lethal, it has been found that mutations do arise in response to selection. Part, but not all, of the evidence for postselection mutation is that in a fluctuation test the distribution of the number of mutants per culture deviates from the Luria–Delbrück toward the Poisson distribution. This has inspired new models describing the distribution of mutant numbers when one or another of the underlying assumptions of the Luria–Delbrück analysis are not met (2, 3).

The fluctuation test is also useful in determining mutation rates during nonselective growth. First applied by Luria and Delbrück themselves, the computation of mutation rates has been refined since then. But all commonly applied techniques still involve assumptions and compromises. Nonetheless, the power of the fluctuation test is that a true mutation rate, ie, the number of mutational events per cell division, is obtained, not a mutant frequency that can be dramatically skewed by jackpots.

The fluctuation test consists of a large number of identical cultures inoculated with a number of cells few enough to ensure that no preexisting mutants are present. These cultures are allowed to grow, achieving at least a thousandfold increase in cell number. Then mutants are selected, usually by plating each entire culture onto a selective agar medium. After a suitable time to allow the mutant clones to grow, the resulting colonies are counted. The parameter used for calculating the mutation rate is m, the mean number of mutations (not mutants) per culture. This is, perhaps, a difficult concept to understand because it is a function of the mutation rate and also of the number of cells at risk for mutation (and thus one requirement for a proper fluctuation test is that every culture has the same number of cells). To date, however, the only solved methods to determine the mutation rate from fluctuation test results are based on the distribution of m. Then the value of m is usually divided by $2N$, twice the final number of cells in the culture, to obtain the mutation rate as mutations per cell per generation (because a culture of N cells contains a total of $2N$ cells during its entire history). Some researchers attempt to correct for asynchronous divisions by dividing m by $N/\ln 2$ instead. These calculations assume that the initial number of cells is trivial compared to the final number, that the proportion of mutants is always small, that mutants grow at the same rate as wild-type, and that reverse mutations are negligible.

The data obtained from a fluctuation test are the number of mutants x_i in each culture. From the number of mutants, there are several commonly used methods to obtain estimates of m (often called estimators), of which five are described here.

1. The P_0 method (1). If the probability of mutation is constant per cell per generation, then the number of mutations per culture has a Poisson distribution (although the number of mutants has a Luria–Delbrück distribution). The probability of no mutations (and thus no mutants) P_0, is e^{-m}, the first term of the Poisson distribution. Thus, the P_0 estimate of m is obtained from the proportion of cultures that have no mutants as $m = -\ln P_0$.
2. The method of the mean (1). Although the extreme variance of the Luria–Delbrück distribution is caused by mutations early in the growth of cultures, these are, in fact, rare events. After the critical point where the total population size (all of the cells in all of the cultures) is large enough so that the probability of a mutation approaches unity, every succeeding generation makes an equal contribution to the number of mutants (from new mutations plus the growth of preexisting mutants). Assuming that no mutations occur before the critical point, the value of m is derived as $x_{mean} = m\ln(mC)$ where x_{mean} is the mean number of mutants per culture and C is the number of cultures.
3. The graphical method (4, 5). Because each generation produces an equal number of mutants after the critical point, the accumulated distribution of the number of mutants per culture, Y_x, is

estimated as m/x, where Y_x is the number of cultures with x or more mutants. Thus a plot of log Y_x vs. log x gives a straight line with a slope of –1. The intercept at log $x = 0$ gives log m. The advantage of this method is that the straight line can be fit by eye to the intermediate values, which are not caused by jackpots.

4. The method of the median. Although the mean number of mutants fluctuates widely depending on the number of jackpots present, the median is not so influenced and is thus a more stable statistic. Lea and Coulson (6) found empirically that $(x_{median}/m) - \ln(m) = 1.24$. This equation is easily solved for m by iteration.
5. The maximum likelihood method. This method relies on solving, at least approximately, the Luria–Delbrück distribution and then generating the most likely value of m for the experimentally determined x_i values. Although this is the most accurate method of estimating m, it has been shunned in the past because of the difficulties in calculation. However, a reasonably adequate way of obtaining m is to solve Eq. (50) of Lea and Coulson (6) by iteration. In addition, Koch (7) provided exact values of m obtainable from the median and upper and lower quartiles of the distribution, which was extended to the upper quartiles by Cairns et al. (2). Simpler algorithms and sophisticated computer programs, however, make the maximum-likelihood method now computationally feasible (8).

Of these methods, the mean (2) is the least accurate because it is skewed by jackpots. The utility of the other methods depends on the value of m. If $m \leq 1$, the P_0 method (1) is reliable, so long as P_0 is determined with sufficient accuracy. When $m = 1 \text{to} 4$, the median method (4) is convenient and adequate. At values of m larger than 4, the median can still be used, but the maximum likelihood method (5) is preferable. Another advantage of the maximum likelihood method is that the standard deviation of m, and thus of the mutation rate, can be approximated (9). Further discussions and refinements can be found in Refs. 9-11.

The phenomenon of phenotypic lag, in which the expression of a new mutant phenotype is delayed, complicates determining mutation rates from fluctuation tests (3, 7, 12).

Bibliography

1. S. E. Luria and M. Delbrück (1943) Genetics **28**, 491–511.
2. J. Cairns, J. Overbaugh, and S. Miller (1988) Nature (London) **335**, 142–145.
3. F. M. Stewart, D. M. Gordon, and B. R. Levin (1990) Genetics **124**, 175–185.
4. S. E. Luria (1951) Cold Spring Harbor Symp. Quant. Biol. **16**, 463–470.
5. J. Cairns (1980) Nature (London) **286**, 176–178.
6. D. E. Lea and C. A. Coulson (1949) J. Genet. **49**, 264–285.
7. A. L. Koch (1982) Mutat. Res. **95**, 129–143.
8. S. Sarkar, W. T. Ma, and G. v. H. Sandri (1992) Genetica **85**, 173–179.
9. F. M. Stewart (1994) Genetics **137**, 1139–1146.
10. M. E. Jones, S. M. Thomas, and A. Rogers (1994) Genetics **136**, 1209–1216.
11. G. Asteris and S. Sarkar (1996) Genetics **142**, 313–326.
12. P. Armitage (1952) J. R. Stat. Soc. B **14**, 1–40.

Fluid Mosaic Model

The liquid-like properties of lipid liquid crystals are assimilated into this model for the structure of cell membranes and for the organization of its protein and lipid components. The concepts that underlie this model assume that integral membrane proteins are “a heterogeneous set of globular molecules, each arranged in an amphipathic structure, i.e. with the ionic and highly polar groups protruding from the membrane into the aqueous phase, and the nonpolar groups largely buried in the **hydrophobic** interior of the membrane” (1). In this model the membrane is perceived as a mosaic of a continuous phospholipid bilayer that is periodically interrupted by proteins randomly distributed throughout the bilayer. The phospholipid bilayer is considered a viscous solvent that allows the dissolved proteins to diffuse laterally within the plane of the membrane. (See also Membranes, and Amphipathic.)

Bibliography

1. S. J. Singer and G. L. Nicholson. (1972) Science **172**, 720–731.

Fluorescamine

Fluorescamine [I] reacts readily with primary amino groups to form highly **fluorescent** compounds [II] Scheme 1, even though fluorescamine itself is nonfluorescent. The fluorescent products have an excitation maximum at 390 nm and an emission maximum at 475 nm. These properties make fluorescamine ideal for detecting amino groups, especially in proteins, **peptides**, and amino acids. It is 10 to 100 times more sensitive in detecting primary amino groups than the ninhydrin reaction. Fluorescamine is also employed as a reporter group in protein chemistry and immunology.

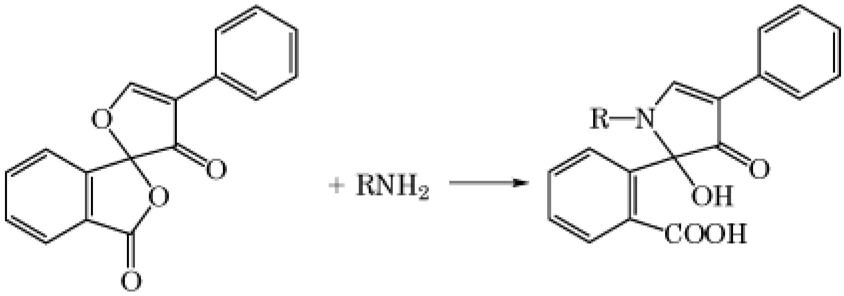

[I] Fluorescamine [II] Fluorescent compound

The formal nomenclature for fluorescamine is 4-phenylspiro[furan-2(3H),1″-(3′H)-isobenzo furan]-3,3′-dione or 4-phenylspiro[furan-2(3H),1′-phthalan]-3,3′-dione. It has a molecular weight of 278.27 and a melting point at 154 to 155°C.

Because fluorescamine has low solubility and stability in water, *o*-phthalaldehyde [III], which reacts similarly with primary amino groups and gives highly fluorescent products [IV] Scheme 2, is sometimes substituted for fluorescamine (1, 2):

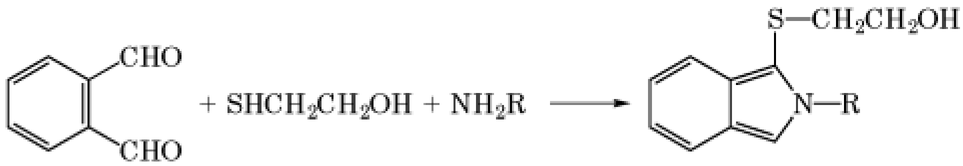

[III] o-Phthalaldehyde

[IV] Fluorescent product

To quantify proteins with fluroescamin (3), a sample solution (10 to 250 mL, containing 500 ng to 50 µg of protein) is made up to 1.5 mL with 0.05 M phosphate buffer (pH 8). Then 0.5 mL of fluorescamine solution, made by dissolving 30 mg of fluorescamine in 100 mL of dioxane, is added to it with vigorous stirring. The emission at 475 nm, upon excitation at 390 nm, is quickly determined. This method is based on the reaction with primary amino groups, so the extent of emission varies depending on the amino acid composition of the proteins, any contaminating compounds having primary amines interfere with the assay.

Fluorescamine reacts with amino acids promptly at pH 9 and yields fluorescent products. The reaction product with ammonia has low fluorescent intensity (less than 1% of the normal products with primary amines). Thus, this reaction is employed for automatic amino acid analysis with a fluorescence detector.

Fluorescamine is used to detect **electroblotted** proteins (4) by visualizing transferred proteins on the transfer membrane with UV light. This method is very sensitive, it is also applied to detect peptides on filter paper or in the eluate from column chromatography. Fluorescamine is also used to test the completeness of other reactions of primary amines (5).

Bibliography

1. G.L. Peterson (1983) Methods Enzymol. **91**, 110–119.
3. P. Bohlen et al. (1973) Arch. Biochem. Biophys. **155**, 213–220.
4. S. Best and D.W. Speicher (1995) In *Current Protocols in Protein Science* (J.E. Coligan et al., eds.), Wiley, pp. 10.8.5–7.
5. A.M. Felix and M.H. Jimmenez (1973) Anal. Biochem. **52**, 377–381.

Fluorescence Energy Transfer

In principle, the fluorescent light emitted by a fluorophore (the energy donor) can be reabsorbed by another chromophore (the energy acceptor) in the same molecule or somewhere else in the solution, provided that the absorption spectrum of the acceptor overlaps with the fluorescence emission spectrum of the donor (see Absorption Spectroscopy and Fluorescence Spectroscopy). Such an energy transfer by emission and reabsorption of light is extremely inefficient. A much more efficient energy transfer between donor and acceptor can occur in a nonradiative process, which involves the coupling of their transition dipoles. This process is called resonance energy transfer. It depends on:

1. the extent of overlap between the fluorescence band of the donor and the absorption band of the acceptor,
2. the distance between the two chromophores, and
3. the relative orientation of their transition dipoles.

Resonance energy transfer is strongly sensitive to distance and varies with the inverse sixth power of the distance R between donor and acceptor. This is very useful to measure distances in macromolecules and changes in distances as a result of conformational changes in proteins and nucleic acids. An important number in energy transfer is the characteristic transfer distance R_0. R_0 is the distance between donor and acceptor at which fluorescence emission from the donor and energy transfer to the acceptor are equally probable. Förster developed a theory to correlate the efficiency of energy transfer with R and R_0. The characteristic distance R_0 can be calculated (primarily from the spectral overlap between donor and acceptor), and consequently the distance R between donor and acceptor can be determined from the measured efficiency of fluorescence energy transfer. Values for R_0 often lie in the range between 1 and 5 nm. Thus, distances up to about 8 nm can be measured by energy transfer.

In proteins, energy is transferred primarily from **tyrosine** to **tryptophan** residues. Tryptophan residues can also transfer their energy to natural acceptors, such as **NADH**, riboflavin, or heme. For measuring distances in proteins or nucleic acids, often both donor and acceptor are introduced by site-directed labeling (see Reporter Groups). A naphthyl group is often used as the donor and a dansyl group as the acceptor in such experiments. A detailed list of useful donor/acceptor pairs is found in (1).

Bibliography

1. M. R. Eftink (1991) "Fluorescence techniques for studying protein structure". In *Methods of Biochemical Analysis* (C. H. Suelter, ed.), Vol. **35**, Wiley, New York, pp. 127–205.

Suggestions for Further Reading

2. C. S. Cantor and P. R. Schimmel (1980) *Biophysical Chemistry*, Vol. **II.**, Chap. "8", W. H. Freeman and Co., San Francisco, CA.
3. G. R. Penzer (1980) "Molecular emission spectroscopy". In *An Introduction to Spectroscopy for Biochemists* (S. B. Brown, ed.), Academic Press, London, pp. 70–114.

Fluorescence Microscopy

Fluorescence microscopy uses the contrast created by fluorescent molecules, fluorophores, that emit light of a specific wavelength when excited by incident light of a different (shorter) wavelength. By using filters, one can select an appropriate wavelength for excitation of the fluorophore and a second filter can eliminate light of wavelengths other than that emitted by the fluorophore. The second filter is very important as it removes the much more intense excitation light, so that the emitted signal is detected in the absence of the excitation light and other stray light, giving fluorescence microscopy an excellent signal-to-noise ratio. Fluorescence microscopy universally uses epi-illumination in which light from above is reflected off the surface of the specimen by light emerging from the objective lens. Epi-illumination has the advantages that (1) unabsorbed light is directed away from the observer and (2) the alignment is simplified since the objective lens acts as its own condenser. It is important to understand the capabilities and limitations of the fluorophores. Because a specimen can be stained with a finite quantity of fluorescent dye, which decays or photobleaches when illuminated, the microscope must be configured to efficiently excite and detect the limited number of emitted photons before complete bleaching has occurred. Although a large number of fluorescent dyes have been discovered, relatively few are suitable for fluorescence microscopy (1).

Immunofluorescence light microscopy is the most common technique of fluorescence microscopy and involves the use of antibodies labeled with fluorophores to visualize distributions of proteins and nucleic acids within a specimen. This technique can be performed by either *direct* or *indirect* antibody labeling. Direct immunofluorescence requires the conjugation of a primary antibody with a fluorophore, commonly rhodamine and fluorescein. Indirect immunofluorescence, on the other hand, uses a fluorophore conjugated secondary antibody which was raised against the immunoglobulin type of the primary antibody. For example, if the primary antibody is raised in a rabbit, the secondary antibody might be a goat anti-rabbit antibody. Indirect immunofluorescence is the more common of the two techniques because making a fluorophore conjugate of each primary antibody is time-consuming and can decrease the affinity or specificity for the antigen. Furthermore, the indirect technique may be more sensitive because more than one molecule of the secondary antibody may bind to a molecule of the primary antibody (2), creating an amplification of the signal. Indirect immunofluorescence has motivated the development of a large number of commercially available secondary antibodies conjugated to various fluorophores, so in order to do immunofluorescence microscopy, one need only raise and characterize the primary antibody and then purchase the secondary antibody. A key consideration in immunofluorescence microscopy is confirmation of the specificity of both fluorophore and antibodies. In order for immunofluorescence results to be validly interpreted, one must demonstrate that (i) the secondary antibody recognizes only the primary antibody, and (ii) the primary antibody recognizes only the antigen. This means that the secondary antibodies must not cross-react with intrinsic proteins and do not recognize each other. It is also necessary to establish whether autofluorescence from compounds intrinsic to the tissue can mimic the appearance of fluorophores. This test is easily done by examining an unstained specimen using the same excitation and emission filters intended for use with the fluorophore.

Fluorescence microscopy can also be used to monitor intracellular compartments through the use of fluorescent indicator dyes, which report on their local environments. Some of the fluorescent dyes useful for microscopy are membrane potential indicators such as JC-1 (3). Using this probe, it was shown that heterogeneity in mitochondrial membrane potential exists between different mitochondria in the same cell (4). Other fluorescent dyes are ion indicators, which can report the pH or concentrations of calcium, chloride, magnesium, potassium, and sodium ions either qualitatively or quantitatively (5).

With the appropriate choice of fluorescent labels and proper equipment, one can do multilabeling [sometimes called multicolor (6)] to localize two or more molecular species using fluorophores with different excitation and/or emission wavelengths. By using multicolor immunofluorescence microscopy, the neurotransmitters, serotonin and substance P, were observed in separate populations of spinal cord fibers (6) and the motor neurons and the substance P fibers, which wrap around them, could be separately visualized. Another example is the use of DiOC6 to label mitochondria and ethidium bromide to label mitochondrial DNA in *Euglena gracilis* cells (7).

Bibliography

1. R. Y. Tsien and A. Waggoner (1990) In *Handbook of Biological Confocal Microscopy*, 2nd ed. (J. Pawley, ed.), Plenum Press, New York, pp. 169–178.
2. L. A. Sternberger (1986) *Immunocytochemistry*, 3rd ed., Wiley, New York.
3. M. Reers, T. W. Smith, and L. B. Chen (1991) Biochem. **30**, 4480–4486.
4. S. T. Smiley et al. (1991) Proc. Natl. Acad. Sci. **88**, 3671–3675.
5. B. Herman and J. J. Lemasters (1993) *Optical Microscopy*, Academic Press, San Diego.
6. T. C. Brelje, M. W. Wessendorf, and R. L. Sorenson (1993) "Multicolor laser scanning confocal immunofluorescence microscopy: Practical application and limitations", In *Methods in Cell Biology*, Vol. **38**: Cell Biological Applications of Confocal Microscopy (B. Matsumoto, ed.), Academic Press, San Diego, pp. 98–182.

7. D. L. Spector, R. D. Goldman, and L. A. Leihwand (1998) *Cells: A Laboratory Manual*, Cold Spring Harbor Laboratory Press, Plainview, New York.

Fluorescence Quenching

After excitation by absorption of light (see **Absorbance spectroscopy**), a chromophore can lose the absorbed energy, and thus return from the excited state to the ground state, either by emitting a photon (observed as fluorescence) or alternatively by nonradiative processes, such as exchange of heat with the solvent. For a particular chromophore, the quantum yield of the observed fluorescence depends on the relative rates of fluorescence emission and the competing nonradiative processes. Under conditions where such nonradiative processes are very slow, one photon is emitted for every photon absorbed, and the quantum yield (the number of photons emitted per number of photons absorbed) approaches one. In practice, the observed quantum yields are often much smaller than one because nonradiative processes compete efficiently with the emission of light. Such a decrease in quantum yield is called fluorescence quenching . The collision of a chromophore with certain molecules in the solution is an effective means to quench fluorescence; such a process is called collisional quenching.

Radiationless transitions can occur by two major routes: internal conversion and intersystem crossing. In internal conversion, the first excited electronic singlet state is converted to the ground singlet state by exchange of vibrational energy (ie, heat) with the solvent. In intersystem crossing, the first excited singlet state is converted to the first excited triplet state. This triplet state is more stable than the corresponding singlet state and is very long-lived, because transitions between triplet and singlet states are nominally forbidden. They are accompanied either by heat exchange or phosphorescence (ie, emission of light with low energy).

Intersystem crossing is triggered by magnetic fluctuations in the system. It is thus greatly facilitated by collisions of the excited molecules with molecules or ions that contain unpaired electrons or loosely held electron clouds (such as acrylamide or iodide anions). The efficiency of collisional quenching depends on the frequency of the collisions, ie, on the concentration of the added quencher and exposure of the fluorophore to the solvent. The susceptibility to collisional quenching can be used to measure the degree of exposure to solvent of a fluorescing group (such as a tryptophan residue in a protein). Experimentally, the ratio of the fluorescence in the absence and in the presence of a quencher is measured as a function of the concentration of the quencher and plotted in a Stern–Volmer diagram. The Stern–Volmer quenching constant is derived from this plot. It is a measure of the exposure of the fluorophore to the quencher. Static quenchers do not obey the Stern–Volmer relationship. They form nonfluorescent complexes with the fluorophore, and the binding constant can be derived from the quenching experiments.

Suggestion for Further Reading

M. R. Eftink and C. A. Ghiron (1981) Fluorescence quenching studies with proteins. Anal. Biochem. **114**, 199–227.

Fluorescence Spectroscopy

1. Fluorescence

Fluorescence emission of light is observed when, after excitation by the absorption of a photon (see Absorption Spectroscopy), an electron returns from the first excited state back to the ground state. Absorption and emission are both virtually instantaneous processes and occur in about 10^{-15}s. The average lifetime of the excited state is about 10^{-8}s, which is a short time, but seven orders of magnitude longer than the time required for light absorption and emission. In the excited state, some energy is always lost by nonradiative processes (such as transitions between vibrational states). Therefore, the energy of the emitted light is always less than that of the absorbed light, and the fluorescence of a chromophore thus occurs always at greater wavelengths than its absorption. Fluorescence emission is much more sensitive to changes in the environment of the chromophore than light absorption. As the lifetime of the excited state is long, a broad range of interactions or perturbations can influence this state and thereby the emission spectrum. Fluorescence is thus an excellent and extremely sensitive probe to investigate the structure and function of proteins.

2. Fluorescence of Proteins

The aromatic amino acid residues phenylalanine (Phe), tyrosine (Tyr), and tryptophan (Trp) exhibit fluorescence emission when excited in the wavelength range of their absorption spectra. In proteins that contain all three aromatic amino acids, the emitted fluorescence is usually dominated by the contribution of the Trp residues, because both their absorbance at the wavelength of excitation and their quantum yield of emission are considerably greater than the corresponding values for Tyr and Phe. This is expressed by the “sensitivity” parameter (Table 1), which is 730 for Trp and 200 for Tyr. Phenylalanine fluorescence is not observed in native proteins, because its sensitivity of 4 is very low. In addition, Phe and Tyr fluorescence is also decreased by energy transfer (see Fluorescence Energy Transfer) to Trp residues.

Table 1. Absorbance and Fluorescence Properties of the Aromatic Amino Acids[a]

	Absorbance		Fluorescence		Sensitivity
Compound	**l_{max}(nm)**	**ε_{max}($M^{-1}cm^{-1}$)**	**l_{max}(nm)**	**f_F**[b]	**$\varepsilon_{max} \times f_F$**[b] **($M^{-1}cm^{-1}$)**
Tryptophan	280	5600	355	0.13	730
Tyrosine	275	1400	304	0.14	200
Phenylalanine	258	200	282	0.02	4

[a] In water at neutral pH; data are from (2).

[b] f_F, fluorescence quantum yield.

Changes in protein conformation, such as unfolding, very often lead to large changes in the wavelength and intensity of fluorescence emission. The fluorescence emission of Trp residues in native proteins can be either greater or smaller than the emission of tryptophan in aqueous solution. Consequently, the fluorescence intensity can either increase or decrease upon protein unfolding. The emission maximum is usually shifted from shorter wavelengths to about 350 nm, which corresponds to the fluorescence maximum of tryptophan in aqueous solution. The exact location of this maximum depends to some extent on the nature and concentration of the buffer. In a **hydrophobic** environment, such as in the interior of a folded protein, tryptophan emission occurs at shorter wavelengths (indole shows an emission maximum of 320 nm in hexane). As an example, the emission spectra of native and of unfolded **ribonuclease T $_1$** are shown in Figure 1. RNase T_1 contains 9 Tyr residues and only one Trp (Trp59), which is inaccessible to solvent in the native protein.

Figure 1. Fluorescence emission spectra of native (—) and of unfolded (– – –) RNase T_1. Native RNase T_1 (1.4 µM) was in 0.1 *M* sodium acetate pH 5.0; the sample of unfolded protein contained 6.0 *M* GdmCl in addition. Fluorescence was excited at (**a**) 278 nm and (**b**) 295 nm. The bandwidths were 3 nm for excitation and 5 nm for emission. Spectra were recorded at 25°C in 1 × 1 cm cells in a Hitachi F-4010 fluorimeter. From Ref. 1.

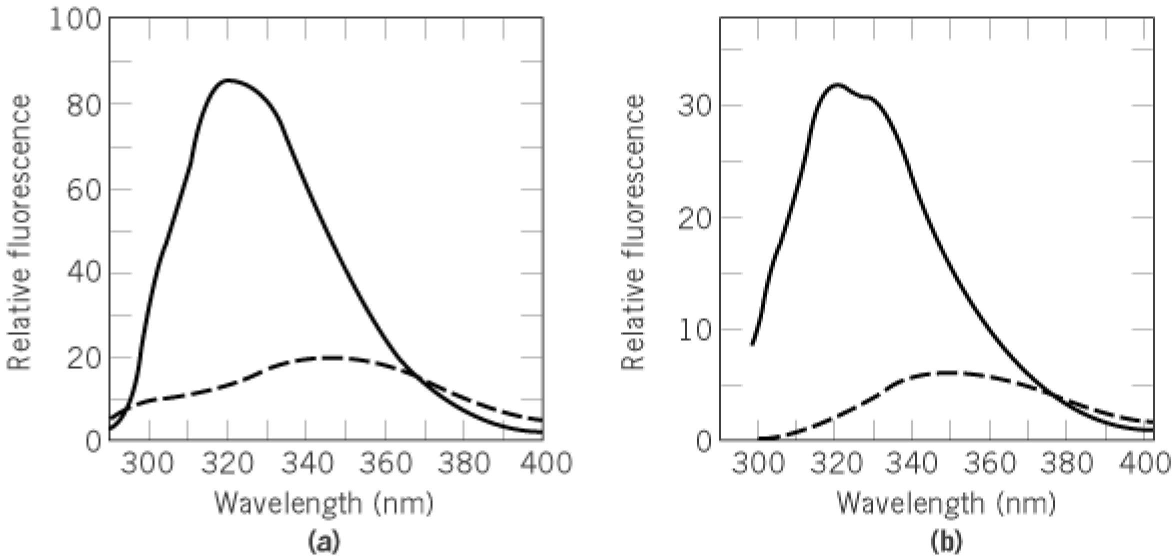

The fluorescence of the Trp residues of a protein can be investigated selectively by excitation at wavelengths greater than 295 nm. Because of the red shift and increased intensity of the absorbance spectrum of tryptophan when compared with tyrosine protein absorbance above 295 nm originates almost exclusively from Trp residues. A comparison of the emission observed after excitation at 280 and 295 nm gives information about the contribution of the Trp and Tyr residues to the observed fluorescence spectra. The data for RNase T_1 in Figure 1 show that the shapes of the fluorescence spectra observed after excitation at 278 and 295 nm are virtually identical. The measured emission originates almost completely from the single Trp59, which is inaccessible to solvent and hence displays a strongly blue-shifted emission maximum near 320 nm. Tyrosine emission is barely detectable in the spectrum of the native protein, because energy transfer to Trp residues occurs. Unfolding of RNase T_1 by **guanidinium chloride** results in a strong decrease in tryptophan fluorescence and a concomitant red shift of the maximum to about 350 nm. The distances between the Tyr residues and Trp59 increase upon unfolding, so energy transfer becomes less efficient. As a consequence, the Tyr fluorescence near 303 nm becomes visible in the spectrum of the unfolded protein when excited at 278 nm (Fig. 1*a*), but not when excited at 295 nm (Fig. 1*b*). The examples in Figure 1 indicate that, unlike absorbance, the changes in fluorescence upon folding can be very large, and the contribution of the Trp residues can be studied selectively by changing the excitation wavelength. Thus, fluorescence measurements are extremely useful to monitor conformational changes in proteins.

Multiple bands in an emission spectrum do not necessarily originate from different Trp residues of a folded protein. Figure 1 shows that even single Trp residues, such as Trp59 of RNase T_1, can give rise to several emission bands. It indicates that the protein can adopt different conformations that equilibrate more slowly than the lifetime of the excited state (about 10^{-8}s).

The fluorescence emission maximum of tyrosine remains around 303 nm, irrespective of its molecular environment. Therefore, the unfolding of proteins that contain no Trp residues is usually accompanied by changes in the intensity, but not in the wavelength of emission. As an example, the fluorescence emission spectra of the Trp59Tyr variant of RNase T_1 (which is devoid of Trp residues) in the native and unfolded states are shown in Figure 2. A decreased Tyr fluorescence in the native state (as in Fig. 2) is frequently observed. It is thought to originate in the folded state from **hydrogen bonding** of the tyrosyl hydroxyl group and/or the proximity of quenchers (see Fluorescence Quenching), such as disulfide bonds.

Figure 2. Fluorescence emission spectra of 1.5 µM of native (—) and of unfolded (– – –) Trp59Tyr-RNase T_1. This protein contains 10 Tyr residues, but no Trp residue. The native protein was in 0.1 *M* sodium acetate, pH 5.0; the unfolded sample contained 6.0 *M* GdmCl in addition. Fluorescence was excited at 278 nm, the spectra were recorded as in Figure 1. From Ref. 1.

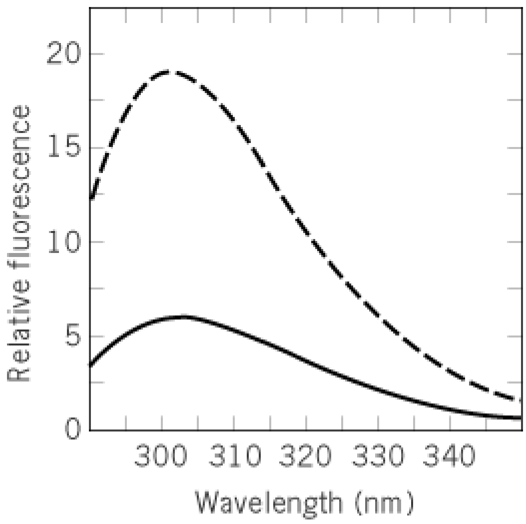

2.1. Environmental Effects on Tyrosine and Tryptophan Emission

The fluorescence intensity generally decreases with increasing temperature. This decrease is substantial, and to a first approximation, Tyr and Trp emission decrease by more than 1% per degree increase in temperature. Denaturants such as urea and guanidinium chloride also influence the fluorescence of Tyr and Trp (1).

3. Practical considerations

3.1. Fluorescence Spectrophotometers

Fluorescence spectrophotometers ("fluorimeters") are single-beam instruments. The light from an intense source (usually a Xenon lamp) passes first the excitation monochromator to select the excitation wavelength, and is then focused into the center of the cuvette. The fluorescence emission is usually monitored at a right angle relative to the exciting beam; it passes through the emission monochromator and is detected by the sample photomultiplier. Most spectrofluorimeters operate in a split-beam mode, where a small portion of the incident light is directed to a reference photomultiplier to correct the fluorescence signal for inherent instabilities of the light source. To avoid baseline drift, some instruments interrupt the light beam periodically or employ pulsed lamps. The dark periods are used to adjust the baseline during the measurement. This increases the long-term constancy of the measured fluorescence.

3.2. Cuvettes for Fluorescence Measurements

Cuvettes for measuring fluorescence have polished surfaces on all four sides. Quartz cells are required for work in the UV region. For routine work, rectangular cuvettes (0.4 × 1 cm) are convenient. Since the exciting beam illuminates only the central part of the cell, the observed fluorescence intensity does not decrease necessarily when cuvettes with reduced cross sections are used. Cuvettes and glassware are easily contaminated with fluorescing substances that may leak out of plastic containers or are present in laboratory detergents. Before measurements, the cleanliness of the cell (and the distilled water) should be checked routinely by filling the cuvette with water and recording a blank in the wavelength range of interest. There should be no emission except the Raman peak of water.

3.3. Raman Peak of Water

In water, a Raman scattering peak is observed that is separated from the incident radiation by a fixed energy difference. After excitation at 280 nm (as in fluorescence experiments with proteins) the Raman peak of water is at 315 nm, ie, it overlaps with the emission spectrum of proteins. The Raman peak must therefore be subtracted from the measured fluorescence spectra. The performance of a fluorescence spectrometer can be checked easily by recording the signal-to-noise ratio at the Raman peak of water.

Bibliography

1. F. X. Schmid (1997) In *Protein Structure: A Practical Approach*, 2nd ed. (T. E. Creighton, ed.), IRL Press, Oxford, UK, pp. 261–297.
2. M. R. Eftink (1991) In *Methods of Biochemical Analysis* (C. H. Suelter, ed.), Vol. **35**, Wiley, New York, pp. 127–205.

Suggestions for Further Reading

3. C. L. Bashford (1987) "An introduction to spectrophotometry and fluorescence spectrometry". In *Spectrophotometry and Spectrofluorimetry: A Practical Approach* (D. A. Harris and C. L. Bashford, eds.), IRL Press, Oxford, UK, pp. 1–22.
4. C. S. Cantor and P. R. Schimmel (1980) *Biophysical Chemistry*, Vol. **II**., Chap. "8", W. H. Freeman and Co., San Francisco, CA.
5. C. R. Cantor and S. N. Timasheff (1982) "Optical spectroscopy of proteins. In" *The Proteins* (H. Neurath and R. L. Hill, eds.), Academic Press, New York, pp. 145–301.
6. G. R. Penzer (1980) "Molecular emission spectroscopy". In *An Introduction to Spectroscopy for Biochemists* (S. B. Brown, ed.), Academic Press, London, pp. 70–114.

Fluorodeoxyuridine

Fluorodeoxyuridine (FUdR) is a mutagen and a potent inhibitor of thymidylate synthase (1), which leads to depletion of cellular pools of precursors to thymidine. The accuracy of both DNA replication and DNA repair is dependent upon a balanced supply of deoxyribonucleoside triphosphate (dNTP) precursors of DNA (2, 3), and perturbation of their relative levels has far-reaching effects. These include point mutation, **chromosomal** breakage, exchange or loss, as well as a stimulation of mitotic and meiotic recombination. Thus a large number of experimental systems and assays have responded positively to FUdR or its precursor 5-fluorouracil (summarized in Kunz et al. (3)), although they (unlike 5-bromo-, 5-iodo-, and 5-chlorodeoxyuridine) were not mutagenic for T4 bacteriophage in early studies (4). Unlike other nucleoside base analogues, such as 5-bromouracil or 2-aminopurine, FUdR does not directly affect base-pairing properties, but instead causes nucleotide pool imbalances through depleting dTTP and increasing dATP and dCTP pools (3).

Bibliography

1. S. S. Cohen, J. G. Flaks, H. D. Barner, M. R. Loeb, and J. Lichtenstein (1958) Proc. Natl. Acad. Sci. USA **44**, 1004–1012.
2. R. H. Haynes (1985) Basic Life Sci. **31**, 1–23.
3. B. A. Kunz, S. E. Kohalmi, T. A. Kunkel, C. K. Matthews, E. M. Mcintosh, and J. A. Reidy (1994) Mutat. Res. **318**, 1–64.
4. R. M. Litman and A. B. Pardee (1956) Nature **178**, 529–531.

Fluorography

Fluorography (or photofluorography) is the technique of photographing an image produced by light emitted from a fluorescent screen or material. Light is produced by the excitation of a fluorescent material by ionizing radiation, which is produced when charged particles (electrons or beta particles) emitted from radionuclides such as tritium (^{3}H), carbon-14 (^{14}C), phosphorus-32 (^{32}P), sulfur-35 (^{35}S), or iodine-125 (^{125}I) interact with the material. The emitted light exposes the film, and an image is recorded.

Fluorography is a common technique used in molecular biology blotting experiments to increase the sensitivity of medium-to-low energy beta-particle-emitting radioisotopes embedded in gel slices. A fluorescent screen is sometimes used to amplify the amount of light produced. A fluorescent screen is a sheet of material that is coated with fluorescent reagents (fluorophores, luminophores, or fluorochromes).

Fluorescence enhances the intensity of the image recorded in the film and makes it possible to obtain images in shorter time periods and with less radioactivity than conventional autoradiography. Fluorographic detection of blotted samples can reduce exposure times by factors of 5 to 10 and can increase sensitivity by factors of 3 to 5 over the use of dried gels (1). Fluorography works best with flashed film and exposures of film at –70°C. Film flashing helps to detect weak bands or spots. Flashing also helps to reduce the threshold of detection. Before fluorography, gels should be fixed with 30% isopropyl alcohol and 10% acetic acid to immobilize the separated proteins and to remove non-protein components that might interfere with subsequent staining.

Radiation-free fluorographic techniques for Southern blots have been developed using

chemical luminescence. Samples are placed on a chemiluminescent substrate sheet, and the blot is exposed to X-ray film for about 70 min at 37°C.

In other industrial and medical applications, fluorescent materials respond also to radiation from gamma-emitting radioisotopes, X-ray sources, electron beams, and charged particles. A fluorograph is the photograph produced by the light from fluorescent materials, and a fluoroscope is a device for viewing the light from fluorescing materials. A fluorescence digital imaging microscope is an instrument for viewing microscopic images of fluorescing substances, which are stimulated by ultraviolet light and filtered so that the observer sees only the fluorescence emission and not the stimulating light.

Fluorography is sometimes called abreuography in honor of Manuel de Abreau, a Brazilian physician who discovered the technique.

Bibliography

1. E. QuÆemÆeneur and F. Simonnet (1995) Biotechniques **18**, 100–103.

Suggestions for Further Reading

2. A. W. Rogers (1983) Practical autoradiography. Elmsford Rev. **23**, 5–39.
3. N. H. H. Heegard (1988) "Radioimmunodetection-immunovisualization by means of 14C-labeled anti-antibodies and socium salicylate fluorography on nitrocellulose". In *CRC Handbook of Immunoblotting of Proteins*, Vol. **1**, Technical Descriptions (O. J. Bjerrum and N. H. H. Heegard, eds.), CRC Press, Boca Raton, FL, pp. 189–194.
4. Amershal International, Amersham Review 23 (1984) Radioisotope detection by fluorography and intensifying screens. Amersham Res. News, pp. 1–39.

fMET (*N*-Formyl Methionine)

Protein biosynthesis usually starts with *N*-formyl methionine (Fig. 1), which is directed by the initiation codon AUG, or rarely in bacteria by GUG or UUG. The same triplet AUG is decoded as a normal methionine during elongation. These distinct types of recognition are carried out by distinct transfer RNAs, initiator $tRNA^{fMet}$ and elongator $tRNA^{Met}$. The initiator tRNA carries a methionine residue that has been formylated on its amino group (*N*-formyl-methionyl-$tRNA^{fMet}$, or fMet-$tRNA^{fMet}$). Synthesis of fMet-$tRNA^{fMet}$ proceeds in two steps: (i) aminoacylation of the initiator tRNA with methionine and (ii) formyl transfer from formyltetrahydrofolate to the methionine amino group. The latter reaction is catalyzed by a formyltransferase.

Figure 1. fMet (*N*-formyl methionine).

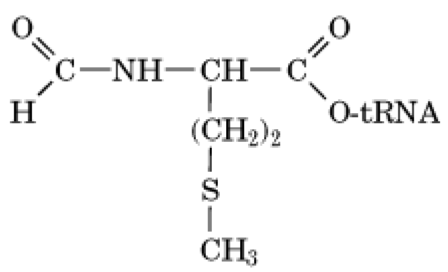

Only fMet-$tRNA^{fMet}$ is used for initiation of protein synthesis, because it enters part of the P site on the prokaryotic 30S or eukaryotic 40S ribosome subunit (see Initiation Complex and Initiation Factor (IF)). Often the *N*-terminal formyl residue is removed by a specific deformylase enzyme. Sometimes the methionine residue at the terminus is removed by an aminopeptidase. These reactions occur rather rapidly, probably when the nascent polypeptide chain reaches the length of 15 to 30 amino acids.

Focal Contact

Focal contacts, focal adhesions, or adhesion plaques are cell "junctions" by which many cell types in culture adhere to their substratum, being regions of closest approach between the lower cell surface and the substratum, a separation of approximately 10 nm. Elongated structures that may be 3 to 4 mm in length, they may be recognized as black areas by interference reflection microscopy (Fig. 1), by electron microscopy, or by staining with antibodies against one of their numerous components (1, 2) (see text below). These contacts are points at which the actin cytoskeleton associates with the cell surface, and are located at the cell-surface termini of actin **microfilament bundles**, called stress fibers. Focal contacts and stress fibers do not have clear equivalents *in vivo*, although their molecular composition resembles that of the dense bodies of smooth muscle. Nevertheless, the molecules, molecular interactions, and cellular functions that have been discovered by studying focal contacts are likely to be of great importance in regulating cell behavior *in vivo*. In tumor cells, disruption of focal contacts is associated with the transformed phenotype (3). The components of focal contacts are involved both in extracellular matrix adhesion and signal transduction.

Figure 1. (**a**, **b**) Interference reflection image (**a**) and fluorescent image showing phalloidin staining for F-actin (**b**) of a cultured fibroblast, illustrating focal contacts and stress fibers. Focal contacts are the elongated black areas in **a**. Note how the actin stress fibres terminate at focal contacts at their peripheral ends. (Photographs provided by Dr. G. Ireland.) Bar=10 μ m.

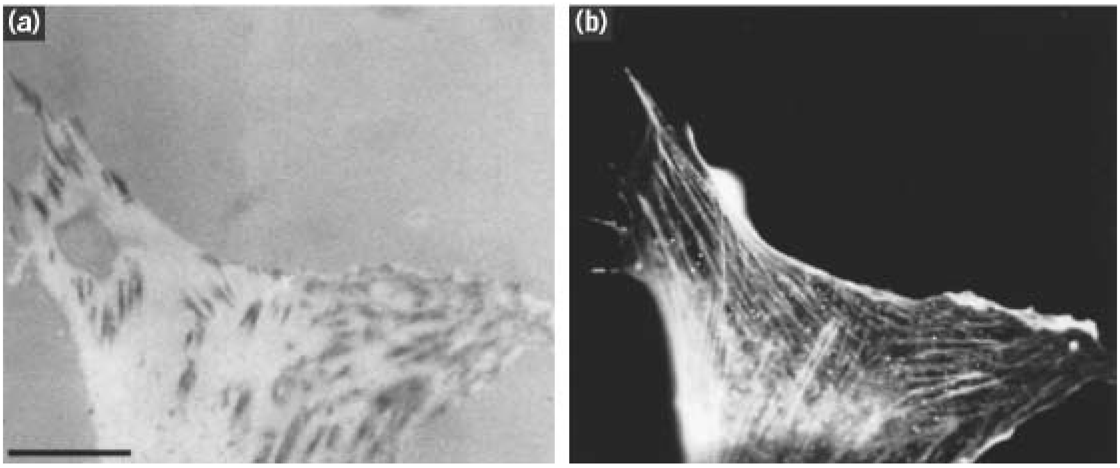

The principal adhesive components of focal contacts are integrins (4) (Fig. 2) although they also contain membrane heparan sulfate proteoglycan. These adhesion receptors bind the cell to components of the extracellular matrix, such as fibronectin and vitronectin. Several actin-binding proteins associate with the cytoplasmic side of the plasma membrane at focal contacts. These include a-actinin (2), vinculin (5), talin (6), and tensin (7), the first two of which are also found in intermediate junctions . Talin and a-actinin have been shown to bind to the cytolasmic domains of integrins, particularly the b1 subunit (6, 8). Tensin has actin filament-capping activity. The location of these proteins to focal contacts and their binding interactions are based on a variety of types of evidence, including expression of mutant proteins and *in vitro* binding between purified, recombinant, or synthetic proteins or peptide fragments. The precise manner in which these proteins interact in focal contacts is not understood. Collectively, they provide a link between the integrin adhesion receptors and the actin cytoskeleton.

Figure 2. Diagram showing some of the major components of focal contacts and their possible molecular interactions. sı
Grb 2 = growth factor receptor bound protein 2, SOS = son-of-sevenless, ILK = integrin-linked kinase, a = integrin a suk
b = integrin b subunit. Arrows indicate signaling pathways, details of which are not shown. For further details, see text.

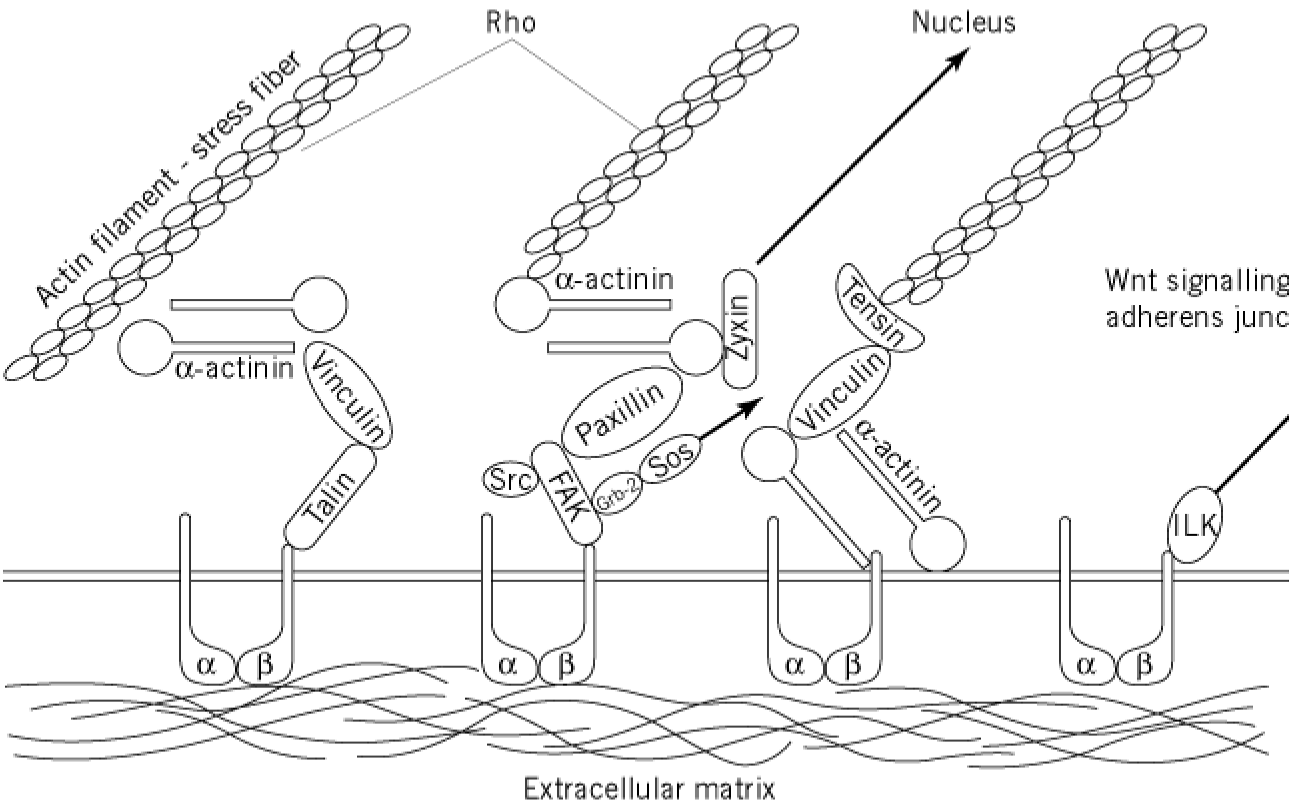

Cells must be able to break and reform focal contacts in order to move. They have been shown to contain the proteinase calpain, which is able to cleave talin and may be involved in modulating junctional adhesion (9). Alternatively, **phosphorylation** signals generated from within the cytoplasm may modulate the adhesiveness of focal adhesions through regulation of integrin function (10). The oncogenic **tyrosine kinase** pp60 ^{src} and protein kinase C, both present in focal contacts, appears to be able to modulate integrin-mediated adhesion, reducing cell-substratum adhesion (11). Such an adhesive change is likely to be important in tumorgenicity, increasing the invasive properties of cells.

An important function of focal contact components is the transduction of signals from outside the cell. Such signals may be involved in regulating a variety of cellular processes, including motility, cell division, gene expression, and apoptosis. An example of a focal adhesion signaling molecule is the focal adhesion kinase (FAK) (12). This is a tyrosine kinase that is activated by ligand binding to integrins (13). FAK has been shown to bind to the cytoplasmic domain of the b1 integrin subunit and also to the vinculin-binding protein paxillin (14). Phosphorylation of FAK in response to integrin-ligand binding increases its tyrosine kinase activity (15). It is also able to associate with a number of other signaling proteins via its various phosphotyrosine residues. Thus, it binds $pp60^{src}$ via the latter's src homology **(SH2)** domain (16) and similarly binds growth factor receptor-bound protein, or Grb2 (17). The latter interacts with the guanine nucleotide exchange factor mSOS1, which activates the **Ras** signaling pathway. FAK may also be involved in regulating focal contact turnover, because fibroblasts from FAK – /– mice show increased numbers of more persistent focal contacts (18).

Another focal contact-associated signaling molecule is the integrin-linked kinase (ILK), a **serine-threonine kinase** that can bind directly to the cytoplasmic domains of b1 and b3 integrins (19). Its kinase activity modulates cell–matrix interactions. Overexpression of ILK in epithelial cells results in reduction of tumorgenicity and loss of cell–cell adhesion and anchorage-independent growth. Furthermore, it causes down-regulation of expression of the zonula adherens adhesion molecule E-cadherin, translocation of b-catenin to the nucleus, and formation of a transcriptional regulating complex between b-catenin and the transcription factor LEF-1. Thus, ILK mediates cross-talk between cell–matrix and cell–cell adhesion, as well as regulation of the wnt signaling pathway (20).

Both paxillin and another focal-contact associated protein called zyxin possess so-called LIM domains, **zinc-finger** motifs that are also found in a number of proteins involved in the regulation of gene expression (21, 22). Paxillin becomes tyrosine-phosphorylated on matrix ligand binding, suggesting that it is involved in signal transduction (21). Zyxin binds to a-actinin, binds to other proteins that have potential signaling functions, such as the vasodilator-stimulated phosphoprotein (VASP), and has a nuclear export sequence. It has also been shown to shuttle between the focal contact and the nucleus, suggesting that it may provide a direct signaling link between matrix receptors at the cell periphery and gene regulation (23).

Regulation of focal contact formation is also regulated by the small Rho GTPase. Overexpression of Rho in quiescent cells causes focal contact formation and stress fiber assembly, whereas inhibition of Rho leads to focal contact disassembly (24). This aspect of Rho signaling is one of several integrated signaling pathways involving small Gtpases that participate in regulating cell adhesion, cell motility, and actin cytoskeleton.

Bibliography

1. J. Heath and G. A. Dunn (1978) J. Cell Sci. **29**, 197–212.
2. J. Wehland et al. (1979) J. Cell Sci. **37**, 257–273.
3. K. Burridge (1986) Cancer Rev. **8**, 18–78.
4. W. T. Chen et al. (1985) J. Cell Biol. **100**, 1103–1114.
5. B. Geiger et al. (1980) Proc. Natl. Acad. Sci. USA **77**, 4127–4131.
6. A. F. Horwitz et al. (1986) Nature **320**, 531–533.
7. A. J. Wilkins et al. (1986) J. Cell Biol. 102–103.
8. C. A. Otey et al. (1990) J. Cell Biol. **111**, 721–729.
9. M. C. Beckerle et al. (1987) Cell **51**, 569–577.
10. M. Coppolino et al. (1995) J. Biol. Chem. **270**, 23132–23138.
11. S. Kellie (1988) Bioessays **8**, 25–30.
12. M. D. Schaller et al. (1992) Proc. Natl. Acad. Sci. USA **89**, 5192–5196.
13. L. Lipfert et al. (1992) J. Cell Biol. **119**, 905–912.
14. J. D. Hildebrand et al. (1993) J. Cell Biol. **123**, 993–1005.
15. Burridge et al. (1992) J. Cell Biol. **119**, 893–903.
16. B. S. Cobb et al. (1994) Mol. Cell Biol. **14**, 147–155.
17. D. D. Schlaepfer et al. (1994) Nature **327**, 786–791.

18. D. Ilic et al. (1995) Nature **377**, 539–544.
19. G. E. Hannigan et al. (1996) Nature **379**, 91–96.
20. A. Novak et al. (1998) Proc. Natl. Acad. Sci. USA **95**, 4374–4379.
21. C. E. Turner and J. T. Miller (1994) J. Cell Sci. **107**, 1583–1591.
22. I. Sadler et al. (1992) J. Cell Biol. **119**, 1573–1588.
23. D. A. Nix and M. C. Beckerle (1997) J. Cell Biol. **138**, 1139–1147.
24. A. J. Ridley and A. Hall (1992) Cell **70**, 389–399.

Suggestions for Further Reading

25. R. O. Hynes (1992). Integrins: versatility, modulation and signalling in cell adhesion. Cell **69**, 11–25. (An excellent review of the field up to 1992.)
26. S. Dedhar and G. E. Hannigan (1996) Integrin cytoplasmic interactions and bidirectional transmembrane signalling. Curr. Opin. Cell Biol. **8**, 657–669. (An exciting review of many aspects of integrin signaling.)
27. M. C. Beckerle (1997) Zyxin: zinc fingers at sites of cell adhesion. Bioessays **19**, 949–957. (A good general consideration of focal contacts as well as an excellent zyxin review.)

Footprinting

Protein binding sites on DNA can be detected *in vivo* and *in vitro* by a technique termed “footprinting”. This depends on the principle that a bound protein molecule can protect DNA from cleavage or modification by a nuclease or a chemical reagent. The binding site is then defined by a region of reduced reactivity, which is determined by analyzing the products of the cleavage reaction on denaturing polyacrylamide gel. The footprint of the protein appears as a gap in the normal pattern of cleavage.

In vitro DNase I is commonly used for enzymatic footprinting and dimethylsulfate and hydroxyl radicals are employed for chemical footprinting. DNase I targets the minor groove of DNA and is also sensitive to the local conformation of the bound DNA such that cleavage is enhanced where the minor groove is on the outside of DNA wrapped around the protein. Dimethylsulfate under footprinting conditions methylates the N7 position of guanine in the major groove and the N2 position of adenine in the minor groove. This methylation sensitizes the sugar-phosphate backbone to mild alkaline hydrolysis, enabling the sites of reaction to be determined. For hydroxyl radical footprinting the radicals are generated by the reaction of hydrogen peroxide with an Fe^{2+} –EDTA complex (the Fenton reaction) and they react with a backbone sugar resulting in the cleavage of the backbone. This reagent targets the minor groove and lacks sequence specificity, although it is sensitive to groove width, cleaving preferentially where the minor groove is widened. A similar type of reagent, Mn-porphyrin, has the opposite conformational selectivity, cleaving DNA where the minor groove is narrow.

Footprinting Proteins

Protein footprinting is a methodology to gain information about protein conformation and interactions by probing the structure of polypeptide chain that is labeled at one end. The protein of interest is end-labeled and reacted with a probe in such a way that susceptibility of a site on the protein to the probe leads to breakage of the polypeptide backbone nearby. The sites of backbone scission are deduced from the lengths of peptides containing the end label, which can be estimated readily by SDS-PAGE. Alteration of the backbone cleavage pattern indicates that the end-labeled protein has undergone a conformational change and/or interaction with other macromolecules. The principle is the same as that for **footprinting nucleic acids**, which has been used widely. Protein footprinting has only recently become feasible with the advent of techniques to end-label proteins.

Information on scission sites or modification sites can be obtained by peptide mapping as well, but footprinting has three advantages:

1. *Facility* Peptide mapping requires purification of individual cleavage products and amino acid analysis and/or the *N*-terminal sequence of each (see Protein Sequencing). Footprinting determines the lengths of many peptides, and hence many cleavage sites, in a single operation without isolating individual fragments.
2. *Sensitivity* Determination of the *N*-terminal amino acid sequence of a peptide typically requires 10 pmol of peptide. Footprinting is generally more sensitive; for instance, **radiolabeling** has virtually no detection limit.
3. *Selectivity* In large multisubunit complexes, peptide mapping will be complicated by the plethora of peptides to be purified and analyzed. In footprinting, information is obtained only on the polypeptide chain that was end-labeled.

1. Methods to End-Label Proteins

Currently there are three ways to end-label proteins:

1. Chemical modification of the N-terminus (1, 2). The protein is first subjected to one round of Edman Degradation. All amino groups become phenylthiocarbamylated, except for the one at the very *N*-terminus, which was originally the imino group of the second amino acid residue before the Edman reaction. This unique amino group can be reacted with either a radioactive or a **fluorescent** reagent, resulting in labeling of the *N*-terminus. This method inevitably destroys the folded structure of the labeled protein prior to probing, and information can be obtained only at the level of the primary structure.
2. Specific antibody binding to either terminus (3, 4). In this method, an antibody raised against a peptide comprising the amino acid sequence of either terminus is used to detect peptides containing the terminus. A more convenient alternative is to place an epitope, against which an antibody is already available, at one end of a protein and to express the epitope-tagged protein through recombinant DNA techniques (see Protein Engineering).
3. Phosphorylation at either terminus (5, 6). This is based on the sequence specificity of protein **kinases**, such as heart muscle kinase, which is less stringent than antigen-antibody recognition. An amino acid sequence that can be phosphorylated by a kinase is attached to a protein at the gene level. The site is labeled using the kinase with [g-^{32}P] or [g-^{35}S] ATP.

2. Methods to Probe Protein Structure

As is apparent from the principle of nucleic acid footprinting, structure probing has to result in scission of the polypeptide backbone, either directly or indirectly. There are common advantages and disadvantages for each type of method. In direct probing methods, probing immediately leads to backbone scission. An advantage of direct methods is their simplicity in comparison with indirect ones, which involve additional reactions. One major drawback is that scission of the peptide backbone often renders the fragments generated more susceptible to ensuing scissions, particularly when the scission has occurred within a folded structural unit. This causes a problem, especially in quantitative analyses, when the first cleavage sites have to be identified. In indirect methods, chemical modification of a side chain is followed by scission of an adjacent peptide bond (or prevention thereof) after one or more subsequent steps. Because modification of a solvent-accessible side chain in one entire protein molecule is unlikely to perturb the folded structure extensively, or to enhance the reactivity of other residues of the same molecule, indirect methods should not suffer from the problems that direct methods do.

Hitherto, five probing methods, two direct and the other three indirect, have been devised and employed:

1. One direct method is **proteolysis** (4-6). Endoproteinases have been extensively used to delineate the **domain** structures of proteins, because well-folded structural units are more resistant to proteolysis than regions linking them. Interaction with other macromolecules may block some cleavage sites. In addition, conformational changes are often reflected in changes in susceptibility of sites cleavable by proteinases. Although proteolysis has been useful, the biophysical basis of the interaction between the probing proteinase and the probed protein molecule is not entirely understood.
2. The other direct method uses oxygen radical, typically generated by the Fenton reaction, to cleave the backbone (7). It is likely that the reactivity of the oxygen radical with the peptide backbone is more directly related to solvent accessibility than is that of proteinases. The extent of side-chain damage by the oxygen radical per backbone breakage is not known.
3. One indirect method utilizes a combination of reversible and irreversible modifications of lysine residues (8). The protein is first subjected to limited citraconylation (see Anhydrides). Removal of the citraconyl groups after irreversible **acetylation** of the remaining lysines recovers unmodified lysyl residues only at the sites where the first modification was introduced. Complete digestion of these polypeptide chains by a lysine-specific endoproteinase generates fragments that end at a first modification site.
4. A second indirect method utilizes oxidation of methionine residues, which blocks cleavage at such residues by **cyanogen bromide** (9). Oxidation of individual methionines is observed as a decrease in the amount of peptide fragments generated by cyanogen bromide. In such cases where modification prevents cleavage, the extent of cleavage must be carefully controlled to ensure that all observable peptides will not be reduced to the shortest peptide containing the end label.
5. The last method utilizes cyanylation of cysteine residues by 2-nitro-5-thiocyanobenzoic acid (10). Raising the pH induces slow cleavage of the peptide bond at the S-cyanocysteine, thus turning the modified side chain into a cleaver. Because the cyano group can transfer to a free sulfhydral, ie, an unmodified cysteine within the same peptide, during the slow cleavage, unreacted cysteine residues have to be blocked beforehand, eg, with N-ethylmaleimide.

The latter three methods were devised on the basis of side-chain modification schemes developed in the 1960s and 1970s (see Chemical Modification). More of them may be revived to create new footprinting methods.

3. Variations and Future Prospects

Various tagging technologies have been used widely in molecular and cellular biology. This indicates that use of a label is not limited to detection of peptides. For instance, some end labels can also serve to isolate terminal fragments. DNA-binding sites of a protein were delimited by immunoprecipitating peptide fragments with a terminal epitope tag, following transfer of radioactivity from DNA and partial proteolysis of the radiolabeled protein (11). Although SDS-PAGE has a fairly good resolution, other methods of determining molecular weights of proteins, such as mass spectrometry, can also be employed after peptides are separated with the use of a tag. In another example of use of a tag other than labeling, a protein kinase site was used to identify protein–protein interactions that blocked phosphorylation of the site (12).

A complex of iron and EDTA, Fe-EDTA, that generates oxygen radical can be crosslinked to specific sites on macromolecules (13). This attachment of a cleavage center onto a macromolecule rather than remaining free in solution allows mapping in the vicinity of the cleavage center (13), when combined with end labeling of its interaction partner, be it a protein molecule or a DNA molecule.

Because the principle of footprinting is the same for proteins and for nucleic acids, much parallel can be drawn from the longer experience of nucleic acids footprinting. The interference experiment scheme (14), in which macromolecules are first subjected to modification and later separated according to their remaining functionality, has yet to be applied to proteins.

Bibliography

1. D. G. Jay (1984) J. Biol. Chem. **259**, 15572–15578.
2. R. A. Jue and R. F. Doolittle (1985) Biochemistry **24**, 162–170.
3. P. Matsudaira, R. Jakes, L. Cameron, and E. Atherton (1985) Proc. Natl. Acad. Sci. USA **82**, 6788–6792.
4. J. E. Lindsley and J. C. Wang (1991) Proc. Natl. Acad. Sci. USA **88**, 10485–10489.
5. R. Hori, S. Pyo, and M. Carey (1995) Proc. Natl. Acad. Sci. USA **92**, 6047–6051.
6. V. Nktinis, J. Turner, and M. O"Donnell (1996) Cell **84**, 137–145.
7. T. Heyduk and N. Baichoo, and F. Heyduk (2001) Metal Ions Biol. Syst. **38**, 255–287.
8. R. Hanai and J. C. Wang (1994) Proc. Natl. Acad. Sci. USA **91**, 11904–11908.
9. M. V. de Arruda, H. Bazari, M. Wallet, and P. Matsudaira (1992) J. Biol. Chem. **267**, 13079–13085.
10. B. P. Tu and J. C. Wang (1999) Proc. Natl. Acad. Sci. USA **96**, 4862–4867.
11. N. F. Lue, A. Sharma, A. Mondragon, and J. C. Wang (1995) Structure **3**, 1315–1322.
12. P. T. Stukenberg, J. Turner, and M. O"Donnell (1994) Cell **78**, 877–887.
13. S. A. Datwyler and C. F. Meares, (2001) Metal Ions Biol. Syst. **38**, 213–254.
14. U. Seibenlist and R. B. Simpson, and W. Gilbert (1980) Cell **20**, 269–281.
15. T. M. Rana and C. F. Meares (1991) Proc. Natl. Acad. Sci. USA **88**, 10578–10582.
16. U. Siebenlist, R. B. Simpson, and W. Gilbert (1980) Cell **20**, 269–281.

Founder Cell

Founder cell is a term that has been used to describe an aspect in the initiation of aggregation in slime molds, especially Dictyostelium. These organisms are normally single cells, but when environmental conditions become unfavorable, they aggregate to form a composite. One cell in a population, the founder cell, will begin signaling to the others by secreting pulses of a chemoattractant. *Dictyostelium discoideum* uses the normally intracellular second-messenger molecule cyclic AMP (cAMP) as its chemoattractant. Other species use a variety of chemoattractants, such as pterin derivatives and small peptides. Cells in the immediate area of the founding cell respond in two ways. They first migrate toward the chemoattractant source, and then they secrete additional cAMP signal. An extracellular **phosphodiesterase** degrades the cAMP between the waves. The resulting temporal and spatial waves of the chemoattractant flow through the environment. As the cells respond, they move together, then pause and move again, until almost all the cells in an area are in a central aggregate. The timing of the pulses and the rate of motility, combined with the enzymatic rates of signal degradation and secretion, determine the size and shape of the aggregate (1).

Exactly what causes a single cell in a population of apparent equals to become a founder cell is unknown, but it must be tightly regulated for the aggregates to end up with an optimum number of cells. Allowing cells to divide to increase the size of the aggregate is not an option, because cell-cycle arrest occurs very early in the developmental program. Once a cell adjacent to a founder responds, that cell cannot itself become a founder. There are some data that suggest that the differentiation events that occur in the founder cell do so before neighboring cells become competent for chemotaxis. Perhaps a diffusible factor secreted from the founder is involved in that process (2).

Bibliography

1. E. Palsson et al. (1977) Proc. Natl. Acad. Sci. USA **94**, 13719–13723.
2. R. K. Raman (1976) J. Cell Sci. **20**, 497–512.

Founder Effect

When a small number of individuals from an original population immigrate to a certain place, the new population founded by those people might have much less genetic diversity compared with those of the original population (Fig. 1). This is generally the case, because a few founder people cannot have sufficient genetic variation to reflect that of the mother population. Such a drastic decrease of genetic diversity within a population is known as the founder effect. This effect most often occurs when a segment of a larger population becomes isolated as the result of colonization of a geographically isolated area, a catastrophic event, artificial isolation, and so on. These founding populations contain only a fraction of the genetic diversity of the population from which they originated.

Figure 1. Founder effect.

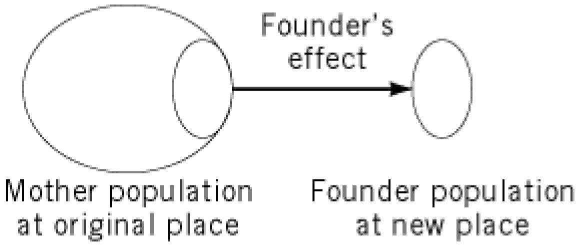

When founders are individuals sampled randomly from the mother population, the founder effect has the same influence as genetic drift, which is the stochastic change of gene frequencies due to random mating. The effect of genetic drift becomes stronger when the population size is smaller (1);

therefore, the founder effect is similar to the effect of genetic drift when the size of the initial population in a given geographical area suddenly becomes extremely small. In particular, the drastic reduction in size of a population has the same effect, which is now called the "bottleneck effect" (Figs. 2 and 3). Strictly speaking, the founder effect can be considered to be a particular form of the bottleneck effect. The difference between the founder effect and the bottleneck effect is that the former occurs in a different place, whereas the latter takes place in the same location.

Figure 2. Bottleneck effect due to a transient decrease in the population size.

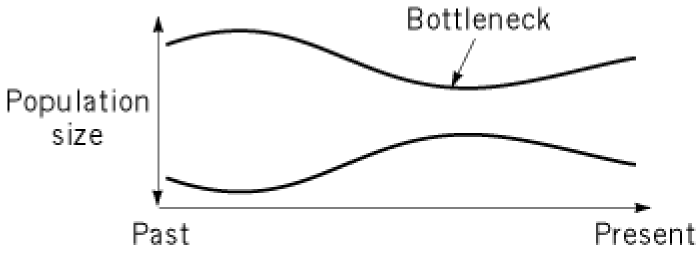

Figure 3. Decrease in the heterozygosity of individuals of a population resulting from the bottleneck effect. The bottleneck size is given by N_0. The intrinsic growth rate is given by *r*. Following the bottleneck, it is assumed that the population grows uniformly (2).

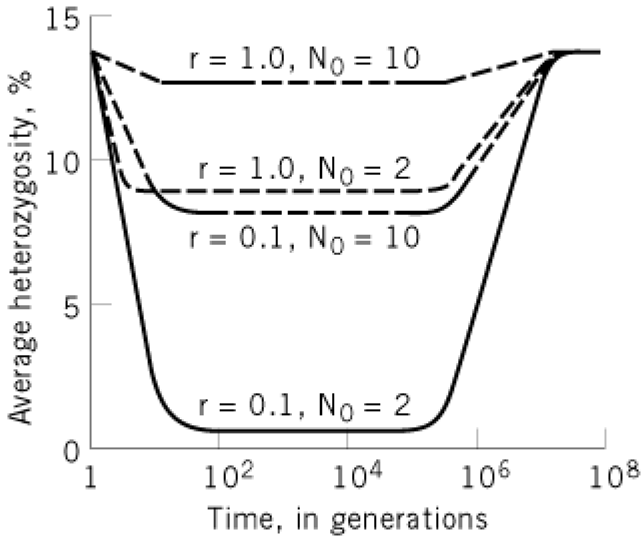

Bibliography

1. M. Nei, T. Maruyama, and R. Chakraborty (1975) Evolution **29**, 1–10
2. M. Nei (1987) *Molecular Evolutionary Genetics*, Columbia Univ. Press, New York.

Four-Helix Bundle Motif

The four-helix bundle is a common protein motif that is observed in protein structures, in which four **a-helices** pack together lengthwise, in an antiparallel manner (Fig. 1). The four a-helices that form the bundle can derive from four independent polypeptide chains or from a single polypeptide chain. This structural motif has been observed both as an isolated three-dimensional fold and as a **domain** within much larger and more complex protein structures. The helices of four-helix bundles are longer than average (~20 residues, as opposed to the usual 10) and are amphipathic, with **hydrophobic** residues buried in the core. The antiparallel packing of the helices in the bundle may be favored by interaction between the helix dipoles.

Figure 1. Schematic representation of the backbone of a four-helix bundle protein, taken from the structure of bullfrog ferritin (1). This structure has the up–down–down–up topology; the two "up" helices are shown as purple coils and the two "down" helices are shown as green coils. Note the long connecting loop between the second and third helix. Connecting loops and an additional *C*-terminal helix are shown in yellow. The *N*- and *C*-termini are labeled. This figure was generated using Molscript (2) and Raster3D (3, 4). See color insert.

The four-helix bundle is one of the simplest protein folds and is used by a wide range of proteins with diverse functions. Proteins with a four-helix bundle structure include growth hormones, **cytokines**, and ferritins. The four helices may splay apart to generate a binding pocket for **cofactors** and metal ions, or they may coil around each other to form a supercoil. In the latter case, the twist of the helices in the coiled coils alters the usual helical structure so that there are 3.5 residues per turn, rather than 3.6. This means that every seventh residue in the helix is identically placed with respect to the axis of the helix. The seven positions of this heptad repeat are denoted *a* to *g*, and residues *a* and *d* point into the core of the bundle and are usually hydrophobic.

Several classes of four-helix bundle motif have been defined. These include (a) the simple up–down–up–down topology, where consecutive helices have short connections and alternating directions, (b) the up-down-down-up topology, where there is a long loop or crossover connection between helices 2 and 3, and (c) the up–up–down–down topology that is typical of the cytokine four-helix bundles, with two long crossover connections between helices 1 and 2 and helices 3 and 4. In most cases, the helices are aligned so that each pairwise interaction is antiparallel. There are also sub-classes within each of these classifications. The simplicity of the four-helix bundle motif has made it a common target for protein design.

[See also Alpha-Helix (310-Helix and Pi-Helix) and Protein Motif]

Bibliography

1. J. Trikha, E. C. Theil, and N. M. Allewell (1995) J. Mol. Biol. **248**, 949–967.
2. P. J. Kraulis (1991) J. Appl. Crystallogr. **24**, 946–950.
3. E. A. Merritt and M. E. P. Murphy (1994) Acta Crystallogr. **D50**, 869–873.
4. D. J. Bacon and W. F. Anderson (1988) J. Mol. Graphics **6**, 219–222.

Suggestions for Further Reading

5. C. Branden and J. Tooze (1991) *Introduction to Protein Structure*, Garland, New York.
6. S. Kamtekar and M. H. Hecht (1995) The four-helix bundle: what determines a fold? FASEB J. **9**, 1013–1022.
7. N. L. Harris, S. R. Presnell, and F. E. Cohen (1994) Four-helix bundle diversity in globular proteins. J. Mol. Biol. **236**, 1356–1368. (Analyzes the diversity of four-helix bundles and gives a suggested structural taxonomy.)

Frameshift Mutation

A frameshift mutation is a type of mutation that results from the addition or deletion of ($3n \pm 1$) **nucleotides** (where n is an integer). The addition or deletion of nucleotides that are not multiples of three disrupts the triplet reading frame of the gene (see Genetic Code). Technically defined, a frameshift mutation is within the coding portion of the gene, but the term is commonly used for any insertion or deletion of a few bases. Frameshift mutations were first described by Crick *et al.* (1) who used them to decipher the triplet nature of the genetic code. Although point mutations only alter one (or no) amino acids (see Missense Mutation), frameshifts alter nearly all of the amino acids downstream of the mutation until a **nonsense codon** is encountered during translation and the polypeptide chain is terminated. Frameshift mutations are induced by a wide variety of intercalating agents, such as ethidium bromide.

Bibliography

1. F. H. C. Crick, L. Barnett, S. Brenner, and R. J. Watts-Tobin (1961) Nature (London) **192**, 1227–1232.

Frameshifting

Frameshifting is a change in reading frame during **gene** expression. Transcription errors, or a posttranscriptional process such as RNA Editing, can cause frameshifting. For example, a fraction of the b- amyloid precursor protein and ubiquitin B messenger RNAs in the lesions of Alzheimer's disease are subject to transcriptional frameshifting (1). Most of the frameshifting cases, however, occur during translation (2).

The reading frame is accurately maintained during translation. The average occurrence of frameshift errors is estimated to be 5×10^{-5} per codon or lower. Aminoacyl tRNA imbalance, due to amino acid starvation or mutations in translation factors or aminoacyl-tRNA synthetases, elevates the error rate. A class of suppressor tRNAs increases frameshifting at particular codons (3). In these cases, the effects are nonspecific. On the other hand, a minority of mRNAs have specific sites for frameshifting that is essential to synthesize the correct gene product. Such natural frameshifting is genetically programmed by specific signals on the mRNAs and, in some cases, is highly efficient (up to 50%). Almost all the known programmed frameshifting is either +1 (reading frame shifts to the 5′ direction by one nucleotide) or –1 frameshifting (to the 3′ direction by one nucleotide). An extreme exception is bypassing of 50 nucleotides within the coding region of **T4 phage** gene 60. The most crucial signal is the sequence of the frameshift site itself. Frameshift sites are often accompanied by a cis-acting sequence element (or stimulator) located either 3′ or 5′ to the frameshift site. Stem-loop or pseudoknot structures of RNA and the **Shine–Dalgarno** sequence are known to function as 3′ and 5′ stimulators, respectively (Fig. 1). In some cases, a frameshift site itself contains a rare codon or a stop codon as a shift-site stimulator. The basic function of these stimulators is to pause the elongating ribosome to trigger frameshifting. Natural frameshifting stands as a class of reprogrammed genetic decoding (or recoding).

Figure 1. –1 frameshift site motif and stimulators.

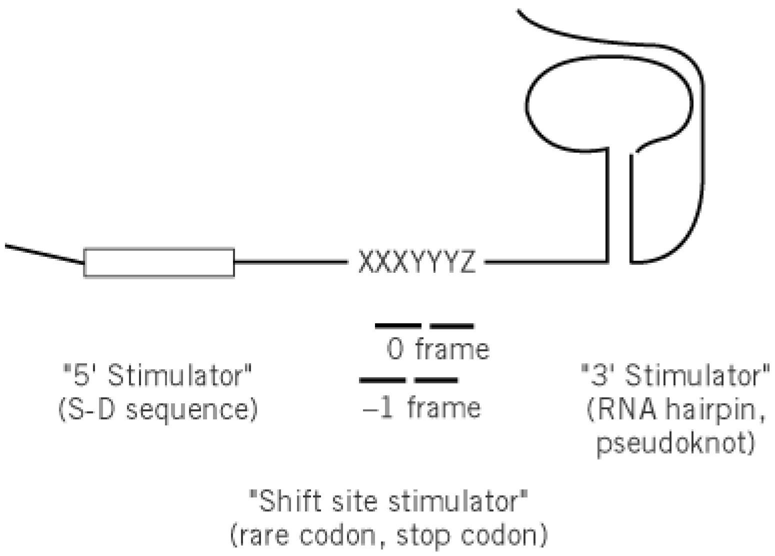

Most frameshifting has been found in *virus* genomes and mobile genetic elements. The former includes several retroviruses such as human immunodeficiency virus 1 (**HIV**-1) and plant RNA viruses, as well as bacteriophages such as MS2, **T7**, and **l**, while the latter includes yeast retrotransposons Ty1 and Ty3, and bacterial **insertion sequences** (Table 1). In many cases, frameshifting is required for the expression of polymerases (including **reverse transcriptase** and RNA-dependent RNA polymerase). Some retroviruses, such as human T-cell leukemia virus 1 (HTLV-1) or mouse mammary tumor virus (MMTV), require two frameshifting events to access the reverse transcriptase reading frame. Retroviral frameshifting appears to be a mechanism to keep the synthesis rate of the functional proteins small relative to that of the structural proteins. Although the efficiencies of these frameshifting events are different from one case to another, proper efficiencies are important for optimal viral propagation or transposition in the cases investigated. In viruses and mobile elements, –1 frameshifting is predominant, whereas some viruses and the yeast retrotransposons have +1 frameshift sites.

Table 1. Natural Frameshifting in Wild-Type Genes (2)

Designation	Sign	Double Shift	Stimulator and Features
Mammalian antizyme	+1	No	3′ pseudoknot; regulated by pathway product, polyamines (autoregulation)
Retrovirus *gag-pol*			
RSV	–1	Yes	3′ pseudoknot
HTLV-1	–1	Yes	3′ stem loop
HIV-1	–1	Yes	3′ stem loop
Coronavirus IBV	–1	Yes	3′ pseudoknot
Yeast retrotransposon Ty1	+1	No	Shift site rare arginine codon
Yeast virus L-A	–1	Yes	3′ pseudoknot
Bacterial genes			
RF-2	+1	No	5′ Shine–Dalgarno sequence; autoregulation
dnaX	–1	Yes	5′ Shine–Dalgarno sequence; 2 DNA polymerase subunits
IS insertion elements	–1	Yes	3′ stem loop or pseudoknot
Phage T7 gene *60*	+50	No	Matched take off and landing sites; 5′ polypeptide, 3′ stem loop, and stop codon

There are only a few instances of frameshifting in bona fide cellular genes. In bacteria, two chromosomal genes, *prfB* encoding release factor 2 (RF-2; see Release Factor) and *Escherichia coli dnaX* encoding the g subunit of **DNA polymerase** III, are expressed by frameshifting. The reading frame of RF-2 switches to the +1 frame, while DnaX shifts to the –1 frame. In higher eukaryotes, there is only one cellular gene known thus far to have frameshifting, the gene for antizyme that is a regulatory protein of the cellular polyamines. Both isoforms of antizyme (AZ1 and AZ2) are expressed by +1 frameshifting that is stimulated by polyamines. RF-2 and antizyme frameshifting is involved in the specific autoregulation (4, 5).

A majority of –1 frameshift sites are characteristic heptamers with a **consensus sequence** of X XXW WWY (presented as a preshift reading frame; X and Y are one of any nucleotides and W is either A or U). In addition, most of these –1 shift sites are accompanied by either pseudoknot or stem-loop structures 3′ to the frameshift site. A simultaneous shift model has been proposed for the shift mechanism, in which the ribosome and the two tRNAs in the P and A sites slip back on the mRNA by one nucleotide, forming new base paring between the tRNAs and the mRNA. Downstream RNA structures stimulate the process by, at least in part, causing ribosomal pausing at the frameshift site (Fig. 1).

Analyses of +1 frameshifting have revealed that their mechanisms are not as uniform as –1 frameshifting. The codon 3′ adjacent to the frameshift site is either a termination codon or a "hungry" codon [a codon decoded by low-abundant tRNA and thus having low efficiency (6)]. In at least two cases, tRNA slipping and pairing at the new position are not necessary.

Frameshifting can be hinted from open reading frame analysis of complementary DNA sequences or by a disagreement between the sequences of cDNA and its protein product. It is, however, sometimes difficult to prove before knowing the amino acid sequence of the protein. Frameshifting can be induced by expression of exotopic genes or artificial sequences. It is noteworthy that translational frameshifting, even with a low efficiency, can partially rescue frameshift mutations and modifies the phenotype in both experimental and naturally occurring systems, demonstrating the biological importance of frameshifting.

Bibliography

1. F. W. van Leeuwen et al. (1998) Science **279**, 242–247.
2. J. F. Atkins and R. F. Gesteland (1995) In *tRNA: Structure, Biosynthesis, and Function* (D. Söll and U. L. RajBhandary, eds.), American Society of Microbiology Press, Washington, D.C., pp. 471–490.
3. E. J. Murgola (1995) In *tRNA: Structure, Biosynthesis, and Function* (D. Söll and U. L. RajBhandary, eds.), American Society of Microbiology Press, Washington, D.C., pp. 491–509.
4. W. J. Craigen, R. G. Cook, W. P. Tate, and C. T. Caskey (1985) Proc. Natl. Acad. Sci. USA **82**, 3616–3620.
5. S. Matsufuji et al. (1995) Cell **80**, 51–60.
6. K. Kawakami et al. (1993) Genetics **135**, 309–320.

Suggestion for Further Reading

7. R. F. Gesteland and J. F. Atkins (1996) Annu. Rev. Biochem. **65**, 741–768.

Free Energy Calculations

1. Statistical Mechanical Averaging

With a given set of potential functions, one can evaluate various average properties of the system by **computer simulation**. In particular, it is useful to simulate experimentally observed macroscopic properties using microscopic models. This can be done using the theory of statistical mechanic, which tells us that the average of a given property, *A* (which is independent of the momentum of the system), is given by

(1)

$$\langle \mathbf{A} \rangle = \int \mathbf{A}(r)P(\mathbf{r})d\mathbf{r} = \int \mathbf{A}(\mathbf{r}) \exp\{-U(\mathbf{r})\beta\} d\mathbf{r}/z(U)$$

$$= \int \exp\{-U(\mathbf{r})\beta\} d\mathbf{r}$$

where b = $(1/k_B T)$ (k_B is the Boltzmann constant and T is the absolute temperature), and $d\mathbf{r}$ designates the volume element of the complete space spanned by the $3n$ vector **r** associated with the n atoms of the system (1). The evaluation of equation (1) requires us to explore all points in the entire conformation space of the given system. Such a study of a solvated macromolecule is clearly impossible with any of the available computers. However, one can hope that the average over a limited number of configurations will give similar results to those obtained from an average over the entire space. With this working hypothesis, we can try to look for an efficient way of spanning phase space. Present-day computers can be used to span a significant number of conformations by **Monte Carlo** (MC) **calculations** or by molecular dynamics (MD) methods.

Calculations of average properties may converge extremely slowly. This is the case, for example, for thermodynamic properties such as **enthalpy** and **entropy**. Fortunately, **free energies** converge faster than enthalpies or entropies, due to entropy-enthalpy compensation. This is quite useful because most biological processes depend on the relevant free energies and not on their individual components. We describe below the general methods for using simulations to obtain free energies.

2. Thermodynamic Cycles

Many biochemical processes can be described by *thermodynamic cycles* of the same type as used in chemistry (eg, the Born–Haber cycle (2, 3)). For example, the energetics associated with the deprotonation of an ionizable group in a protein can be described by the cycle as shown in Figure 1 (4). Using such a cycle allows one to replace calculation of the physical process of moving the proton from the protein to water by the much simpler comparative calculation of "mutating" the given acid from its unionized form in the protein and in water. The use of thermodynamic cycles in microscopic calculations of free energies of biological processes has been introduced in the early 1980s (4, 5), and it is now a major part of many approaches of free energy calculations of biological processes.

Figure 1. The thermodynamic cycle used to estimate the energetics of dissociation of an acidic group of a protein. The DG_i are given by $\Delta G_1 = G^w_{sol}(\mathrm{AH}) - G^p_{sol}(\mathrm{AH}), \Delta G_2 = 2.3RT(\mathrm{p}K^w_a - \mathrm{pH})$, and $\Delta G_3 = G^p_{sol}(A^-) - G^w_{sol}(A^-)$, where p and w designate protein and water, respectively.

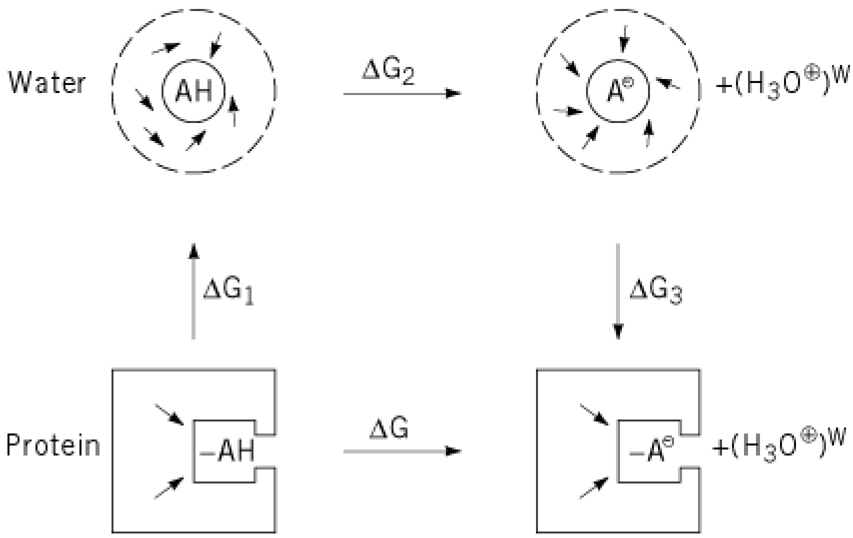

3. Free Energy Perturbation and Related Approaches

Evaluation of free energies by statistical mechanical approaches is extremely time-consuming, due to the need to sample all the relevant configurational space. Fortunately, it is possible in some cases to obtain meaningful results using perturbation approaches. Such approaches exploit the fact that many important properties depend on local changes in the macromolecules so that the effect of the overall macromolecular potential cancels out. Such calculations are usually done by the so-called **free-energy perturbation** (FEP) **method** (6, 7) [also related to the umbrella sampling method (7)]. This method evaluates the free energy associated with the change of the potential surface from U_1 to U_2 by gradually changing the potential surface using the relationship

$$U_m(\lambda_m) = U_1(1 - \lambda_m) + U_2\lambda_m \qquad (2)$$

The free-energy increment $\delta G(1 - \lambda_m \rightarrow \lambda'_m)$associated with the change of U_m to $U_{m'}$ can be obtained (7) by

$$\exp\{-\delta G(\lambda_m \rightarrow \lambda_{m'})\beta\} = \langle \exp\{-(U_{m'} - U_m)\}\beta\rangle_m \qquad (3)$$

where $\langle\ \rangle_m$ indicates that the given average is evaluated by propagating trajectories over U_m. The overall free energy change is now obtained by changing the 1_m in n equal increments and evaluating the sum of the corresponding dG:

$$\Delta G(U_1 \rightarrow U_2) = \sum_{m=0}^{n-1} \delta G(\lambda_m \rightarrow \lambda_{m-1}) \qquad (4)$$

An example of the use of Eq. (4) in calculating free energy of a biological system is given in Figure 2, which considers the solvation free energy of ionizable residues in BPTI.

Figure 2. Calculations of the free energy of charging Asp 3 and Glu 7 in BPTI. The figure describes the calculated "solvation" free energy obtained with the use of equation (4) as a function of the charge of the corresponding acid.

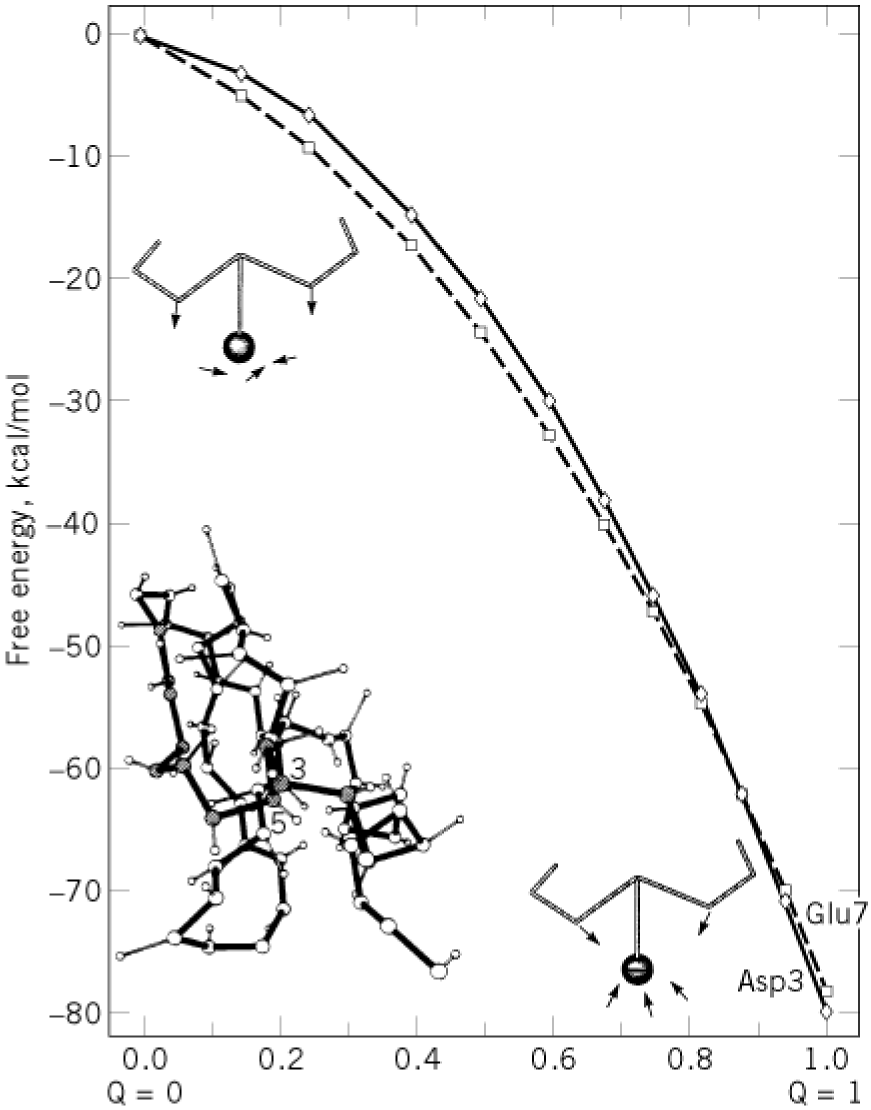

The FEP approach has been used extensively in studies of free energies of biological systems (eg, Refs. 8 and 9) and more details are given in **Computer simulation**. It must be emphasized here that the convergence of FEP approaches is quite slow and that obtaining meaningful results requires proper treatment of long-range effects.

Many times it is very useful to estimate the free energy of biological processes by the so-called *linear response approximation* (LRA) (10). This approximation assumes that the protein and solvent environment respond linearly to the forces associated with the given process. This leads (11) to the equation

$$\Delta G_{a\to b} = \frac{1}{2}(\langle U_b - U_a\rangle_a + \langle U_b - U_a\rangle_b) \tag{5}$$

Such an approximation is, for example, the basis of macroscopic electrostatic theory, where the free energy of charging a positive ion, with a charge $Q = 1$, is given by the well-known result $\Delta G = \frac{1}{2}U(Q=1)$. Although it is hard to accept that the LRA provides a reliable way of describing the energetics of macromolecules or of realistic molecular systems, it was found by simulation studies that this is a reasonable approximation in particular for processes that depend on electrostatic effects (12-14).

Bibliography

1. D. A. McQuarrie (1976) *Statistical Mechanics*, Harper and Row, New York.
2. M. Born (1919) Verh. Dtsch. phys. Ges. **21**, 13.
3. F. Haber (1919) Verh. Dtsch. phys. Ges. **21**, 750.
4. A. Warshel (1981) Biochemistry **20**, 3167.
5. C. F. Wong and J. A. McCammon (1986) J. Am. Chem. Soc. **108**, 3830.
6. R. W. Zwanzig (1954) J. Chem. Phys. **22**, 1420.
7. J. P. Valleau and G. M. Torrie (1977) *Modern Theoretical Chemistry*, Vol. **5**, Plenum Press, New York.
8. P. Kollman (1993) Chem. Rev. **93**, 2395.
9. A. Warshel and J. Åqvist (1991) Annu. Rev. Biophys. Biophys. Chem. **20**, 267.
10. R. Kubo, M. Toda, and N. Hashitsume (1985) *Statistical Physics II: Nonequilibrium Statistical Mechanics*, Springer-Verlag, Berlin.
11. F. S. Lee, Z. T. Chu, M. B. Bolger, and A. Warshel (1992) Protein Eng. **5**, 215.
12. J.-K. Hwang and A. Warshel (1987) J. Am. Chem. Soc. **109**, 715.
13. R. A. Kuharski, J. S. Bader, D. Chandler, M. Sprik, M. L. Klein, and R. W. Impey (1988) J. Chem. Phys. **89**, 3248.
14. J. Åqvist and T. Hansson (1996) J. Phys. Chem. **100**, 9512.

Free Energy Relationships

Understanding any chemical reaction requires knowledge about the transition state for the reaction, because the free energy of the transition state determines the rate at which the reaction occurs (see Kinetics). The transition state cannot be observed directly, but its properties can be inferred from the effects of changes in various parameters on its free energy, the rate of the reaction. One method of doing so is to study the chemical reaction in a series of closely related reactants and to correlate the variation in the rates of reaction with the physical parameters of the reactants. Such observations are referred to as free energy relationships.

In hydrolytic reactions, the reacting groups are generally classified as nucleophiles or electrophiles. Nucleophiles donate an electron pair, and are generally bases, whereas electrophiles have opposite properties and generally are acids. Protonation converts a nucleophile to an electrophile. For example, an $–NH^2$ group is a nucleophile, whereas its protonated $NH^+{}_3$ form is an electrophile. The strengths of their nucleophilicity and electrophilicity can be indicated by their respective tendencies to acquire or donate protons and can be measured by the pK_a value (see Buffers). The reaction of a nucleophile with a proton is similar to the reaction of the nucleophile with any other group, so that a relationship would be expected between the pK_a of a nucleophile and its reactivity in a chemical reaction. The pK_a is a measure of the relative free energy of the nucleophile, whereas the logarithm of the rate constant for a reaction is a measure of the free energy of the transition state for the reaction. Such relationships are generally evident from plots of the logarithm of the rate constant k, for a chemical reaction, versus the pK_a values of a series of related nucleophiles, known as Brønsted plots. Such plots can be made for a series of nucleophiles attacking a particular ester or amide bond, for example, or for one nucleophile attacking a series of molecules that have leaving groups with different pK_a values. Linear correlations are found frequently for a given chemical reaction and a series of related reactants, so long as the reactants are sufficiently related and no special factors, such as steric hindrance, affect their rate of reaction. The general form of the linear relationship is expressed as

$$\log k = \beta \mathrm{p}K_a + \text{constant} \quad (1)$$

When the reactant is an electrophile, the equation is the same, except that the parameter b is changed to a. The values of a are generally negative, whereas those of b are generally positive.

The slope of a linear Brønsted plot, the value of a or b, provides important information about the transition state of the reaction. Their sign and magnitude are generally interpreted as an indication of the amount of charge developed in the transition state and whether the transition state is closer to the reactants or the products in its physical properties. The values of a and b should be between 0 and 1, because complete transfer of a proton in the transition state gives a value of 1.0 and no transfer gives a value of 0. For ester hydrolysis, the values are usually 0.3 to 0.6. For example, the attack of tertiary amines on esters with poor leaving groups (e.g., alkoxides) gives values of +1.5 for the series of attacking nucleophiles and –1.5 for variation in the alcohol leaving group (1). These very large values indicate that the transition state for this reaction is close to the products. In contrast, the reaction of very basic nucleophiles with activated esters (e.g., phenolates) has relatively small values, +0.1 to 0.2 for variation of the nucleophile and –0.1 to –0.2 for variation of the leaving groups; this indicates that the transition state in this case is closer to the ester substrate.

Although free energy relationships were developed with reactions between small molecules, they are also useful in molecular biology in phenomena as diverse as **protein folding** (2).

Bibliography

1. A. Fersht (1985) *Enzyme Structure and Mechanism*, 2nd ed., W. H. Freeman, New York, pp. 147–154.
2. J. M. Matthews and A. R. Fersht (1995) Biochemistry **34**, 6805–6814.

Suggestion for Further Reading

3. S. Bernhard (1968) *The Structure and Function of Enzymes*, W. A. Benjamin, New York, pp. 175–183.

Freeze Fracture

Freeze fracture is a preparative procedure for visualizing the distribution of proteins within the lipid bilayer of membranes by transmission electron microscopy. The membrane samples are rapidly frozen to a very low temperature and then fractured with a knife blade. Fracturing occurs along planes where the intramolecular forces are weakest. In membranes, these planes occur along the center of the phospholipid bilayer, where the apposing fatty acid chains of the monolayer leaflets interact. Freeze fracturing thus exposes the nonpolar interior of the membrane. Integral membrane proteins that cross the bilayer interrupt the fracturing process and are carried along with either monolayer leaflet, leaving pits in the apposed monolayer. The fracture faces are shadowed with metal, and the proteins appear as small particles. The technique may be combined with **immunolabeling** to visualize the location of specific proteins (1).

Freeze etching utilizes freeze-drying of the fractured frozen samples to remove water, thereby exposing the components of the surfaces of the fractured samples; the surfaces are then shadowed for viewing in the electron microscope.

Bibliography

1. P. Pinto da Silva (1984) In *Immunolabeling for Electron Microscopy* (J. M. Polack and I. M. Varndell, eds.), Elsevier, Amsterdam, pp. 179–188.

Suggestions for Further Reading

2. N. J. Severs, and D. M. Shotton (1995) *Rapid Freezing, Freeze Fracture, and Deep Etching*, Wiley-Liss, New York.
3. R. L. Roberts, R. G. Kessel, and H. Tung (1991) *Freeze Fracture Images of Cells and Tissues*, Oxford University Press, New York.

Frictional Coefficient, Ratio

The translational frictional coefficient, *f*, is a measure of the resistance to movement of a molecule; this resistance is a function of both the size and the shape of the molecule. It can be measured experimentally either by its rate of diffusion or its rate of sedimentation.

As would be expected, the translational frictional coefficient is inversely proportional to the diffusion coefficient, $D°_{20,w}$, under standard conditions of water at 20.0°C and extrapolated to zero concentration:

$$f = \frac{RT}{N_A D^\circ_{20,w}} = \frac{k_B T}{D^\circ_{20,w}} \tag{1}$$

where R is the gas constant (8.314×10^7 erg mol^{-1}K^{-1}) and N_A is Avogadro's number (6.022×10^{23} mol^{-1}).

Likewise, the frictional coefficient is inversely proportional to the sedimentation coefficient, $s°_{20,\,w}$ under the same standard conditions:

$$f = \frac{M_r(1 - \bar{v}\rho_{20w})}{N_A s^\circ_{20,w}} \tag{2}$$

where v is the partial specific volume of the macromolecule and $r_{20,w}$ is the density of the standard solvent, water at 20°C.

It is usually more informative to use the **frictional ratio**, f/f_0, which is the dimensionless ratio of the observed translational frictional coefficient to that of an equivalent spherical molecule of the same anhydrous mass and density. This corrects for the size of the molecule and gives an indication of its shape. The greater the frictional ratio, the more asymmetric it is likely to be. The frictional ratio can be calculated from the diffusion coefficient by the following equation:

$$\frac{f}{f_0} = \frac{k_B T}{6\pi\eta_{20,w}} \cdot \left(\frac{4\pi N_A}{3\bar{v}M}\right)^{1/3} \frac{1}{D^{\circ}_{20,w}} \tag{3}$$

The frictional ratio depends intrinsically on the conformation, flexibility, and degree of solvation (by water, salt ions, and any other solvent molecules) of the macromolecule. This degree of water association is termed the hydration of the macromolecule, d, and is defined as the mass in grams of associated solvent per gram of anhydrous biomolecule. This associated solvent includes both chemically bound solvent and also solvent physically entrained in the interstices in the molecule. The value of d is typically between 0.2 and 0.5 g/g for proteins, although it is a notoriously difficult parameter to pin down with any accuracy.

The function defining the shape and flexibility of the biomolecule is the *Perrin translational frictional function*, *P*:

$$P = \frac{f}{f_0} \cdot \left(\frac{\bar{v}}{\bar{v} + \delta/\rho_0}\right)^{1/3} \tag{4}$$

where r_0 is the density (in grams per milliliter) of the bound solvent. For a molecule that is fairly rigid on a time-averaged basis, the gross conformation can be specified using *P* in terms of the axial ratio of the equivalent hydrodynamic ellipsoid or in terms of sophisticated arrangements of spheres called *hydrodynamic bead models* (see Diffusion).

Suggestions for Further Reading

S. E. Harding (1995) On the hydrodynamic characterisation of macromolecular conformation. Biophys. Chem. **55**, 69–93.

K. E. Van Holde (1985) *Physical Biochemistry*, Prentice-Hall, Englewood Cliffs, N. J. (Chapter 4 gives an excellent introduction).

Fungi, Filamentous

The fungi represent one of the most diverse groups of organisms encountered in the natural world; approximately 70,000 different species have been described although estimates as high as 1.5 million fungal species are likely to exist. Even though a large fraction of fungi are believed to be unculturable, their importance to the natural environment of the planet cannot be underestimated. Thus, a clear understanding of their physiology at a molecular level seems prudent if not essential. The past 10 years have seen an explosion of information in this field, due primarily to the ability to transform a wide variety of these previously intractable organisms. Yet, even with the exponential advances in recombinant techniques (especially sequencing technologies) gained over the past several years, filamentous fungi appear to be the forgotten model system; perhaps it is because the completion of the first eukaryotic genome, *Saccharomyces cerevisiae*, was a fungus, albeit a yeast, or perhaps it is because of the success of the human genome project that the perception is that we need not look at additional fungi as model organisms. However, while *Saccharomyces* provides an excellent framework for studying eukaryotic systems, it clearly lacks some critical parameters that filamentous fungi can elucidate, in particular, multicellular differentiation and pathogenicity. In addition, it should be kept in mind that a large percentage of the expressed sequence tags (ESTs) identified from filamentous fungi do not have detectable homology to sequences already present in any of the available databases, including the *Saccharomcyes* genome). Therefore, the filamentous fungi as a group provide a complex and somewhat unique perspective of the microbial world that should not be overlooked.

Two of the most well known filamentous fungi, *Aspergillus nidulans* and *Neurospora crassa*, are exceptional model organisms. They have a long genetic history and are continuing to be pursued as excellent subjects in which to study development, gene regulation, circadian rhythms, and genome structure. As the functions and interactions of proteins and intracellular molecules is elucidated from a variety of organisms, including the fungi, humans appear to have more in common with their distant eukaryotic ancestors than previously thought. It is important to keep in mind that the filamentous fungi are part of the group of organisms that include the yeasts, *Saccharomyces cerevisiae* and *Schizosaccharomyces pombe*, two of the best understood eukaryotic organisms from a genetic and molecular standpoint. In general, the molecular biology of the entire kingdom may be viewed as more similar than dissimilar; not only are there are two-component signal transduction systems, transcriptional inducers and repressors, but the conservation of protein sequence is remarkable in many areas. Wherever commonalities have been searched for they have been found, with a few exceptions that may yet prove to be due to insufficient data.

1. Why Study Fungi?

Fungi are a biochemically diverse set of organisms, producing a wide variety of acids and degradative enzymes that support their absorptive lifestyle and play an essential role in the degradative processes of our entire ecosystem. They decompose numerous substrates by secreting a wide variety of very efficient degradative enzymes, thus providing an efficient means to recycle much of the earth's biomass. In addition, their fermentative capabilities provide a means to bake bread and ferment a wide variety of fruits and vegetables. The fungi have also been exploited commercially as efficient producers of enzymes such as glucoamylase, lipase, cellulase, and pectinase. In addition, fungal secondary products have been used in the synthesis of numerous pharmaceuticals, including penicillin, cyclosporin, and mevalonin.

On the other hand, some fungi can have a devastating effect: their uncontrolled growth can irrevocably damage entire forests, crops, or agricultural feed products. Some of the most intensely studied fungi are phytopathogenic; *Magnaporthe grisea* (pathogen of rice), *Ustilago maydis* (corn), *Cryphonectria parasitica* (chestnut blight), etc. Aflatoxin, a single secondary metabolite produced by *Aspergillus flavus*, causes millions of dollar of damage to the corn industry annually. In terms of human disease, medically important species of fungi are increasing in prevalence due to a dramatic rise in the incidence of immunocompromised patients. The most significant human pathogen is *C. albicans*, a dimorphic organism that switches between a yeast-like growth phase not unlike that of its distant cousin, *S. cerevisiae*, to a hyphal growth phase that has been associated with its virulence *in vivo*. Other well-known fungal pathogens include *Aspergillus fumigatus*, *Blastomyces dermatitidis*, *Coccidioides immitis*, *Cryptococcus neoformans*, *Histoplasma capsulatum*, and *Pneumocystis carinii*. Many are associated with high mortality rates. All of these fungi are either filamentous or dimorphic in nature. A wide variety of classical genetic and modern molecular techniques are presently available to analyze these organisms, as well as the lesser well-known, but certainly not less virulent pathogens. What is important to keep in mind is the similarities between the fungi, the “big picture.” Each of the individual organisms’ details can be gleaned from further readings.

2. Physiology and Taxonomy

The taxonomy of the fungi is complex, and students interested in further classification or taxonomy of fungi are referred to Ref. 1. Over the past several decades, their special place in the taxonomy of biological organisms has been reclassified from a subdivision within the plant kingdom to part of the eukaryotic world. Within the new scheme [bacteria, archea and eukarya (2)], note that the division between plants and fungi has disappeared. Even with this new assignment, there have been many proposals for their classification based upon nutritional requirements, cytology, or morphogenesis (1, 79). Perhaps the most enlightening description of the taxonomical state of the field is described by Ainsworth, “the question of the number of kinds of fungi can be more usefully approached by first considering some of the main factors which determine their recognition. ¼ Their [fungi] recorded number and distribution is closely correlated with the number and distribution of mycologists. ¼ Some taxonomists are perhaps unduly impressed by small differences ¼ others, are lumpers ¼ recognize far fewer kinds”. By and large the fungi are regarded as having five phyla: oomycetes (water molds), zygomycetes (common molds), ascomycetes (sac fungi), basidiomycetes (club fungi) and deuteromycetes (imperfect fungi having no sexual stage). With the advent of recombinant DNA technology and new DNA sequencing paradigms, it will be possible to re-evaluate the relationships between certain fungi by their sequence **homologies**, rather than by their morphology or nutritional biochemistry. Most of the research has been centered upon a few species of the ascomycetes and basidiomyecetes although *C. albicans*, a member of the fungi imperfecti, has been the source of a great deal of research due to its critical role in medical mycology.

Like most of their taxonomy, fungal life cycles may vary from simple (as in the yeasts) to complex (as in the basidiomycetes). Fungi are typically non-photosynthetic heterotrophic organisms that absorb nutrients from their surrounding environment. As multicellular organisms, they display a wide range of morphological types from the microscopic yeasts and water molds to the multicellular mushrooms. They may exist as a multinucleate undifferentiated mass of cells during all or part of their life cycle, or form complex highly developed reproduction structures. In their vegetative state, fungal cells may be unicellular (yeast-like) or filamentous (mycelial or hyphal-like) in shape. Many are capable of switching between the two forms, which has been the source of a great deal of interest, especially with regard to the regulatory circuits involved and the effect on pathogenicity. All fungi are eukaryotic, but the cell may be uninucleate or multinucleate, haploid, diploid or dikaryotic during part of their life cycle. They typically contain a cell wall, which may explain their original classification within the kingdom of plants; however, the cell wall contains polymers of chitin and glucans rather than the more usual cellulose of plants.

3. Fungal Life Cycles and Reproduction

Fungi display a variety of reproductive choices. They may reproduce either asexually or sexually, or both. The fungal spore is specialized for reproduction, survival and, in some cases, dispersal. Not only are there heterothallic species such as *Neurospora crassa* that require different mating types in order to undergo sexual reproduction, but homothallic species (self-maters) such as *Aspergillus nidulans* and pseudohomothallic species that switch mating types (such as *Saccharomyces cerevisiae*) as well. Further, there is an assortment of fungi that do not appear to undergo sexual reproduction at all (e.g.-fungi imperfecti, including *Candida albicans*). The life cycles of *Aspergillus nidulans* and *Neurospora crassa* (Fig. 1) serve to illustrate many of the salient features found in this highly divergent group of organisms.

Figure 1. Schematic representation of the life cycles of *Aspergillus nidulans* and *Neurospora crassa*. (**a**) *Aspergillus nid* Asexual reproduction involves formation and maturation of conidiophores (described in the text) and uninucleate spores conidia. Vegetative haploids grow as monokaryotic or dikaryotic hyphae. These cells may then undergo sexual reproduc (upper portion of the cycle), initiated with the formation of specialized fruiting body called the cleistothecia. Eight binuc ascospores are formed within an unordered ascus. (**b**) *Neurospora crassa*. Asexual reproduction involves the formation c hyphae and the development of conidiophores, producing millions of multinucleate spores called macroconidia. Vegetati haploids grow as monokaryotic or dikaryotic hyphae. Cells of the opposite mating type are required for sexual reproduct Sporulation is initiated by the formation of the protoperitheicia, which is fertilized by microconidia of the opposite matir (see text). Cellular fusion is followed by a complex developmental pathway that involves synchronous nuclear division, karyogamy, and meiosis to yield hundreds of asci within the perithecium (see text for details).

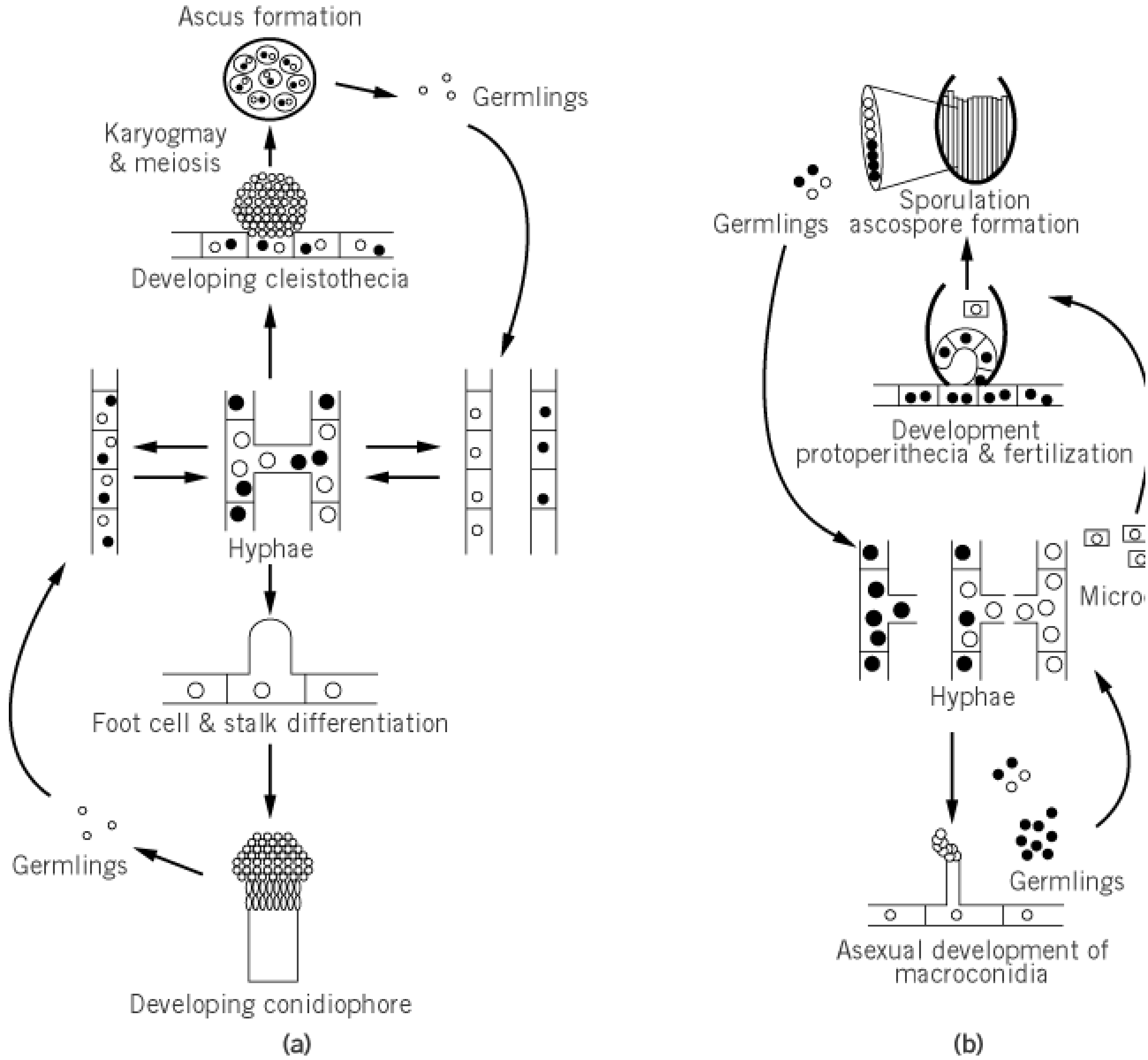

3.1. Life Cycle of *Neurospora crassa* (3, 4)
N. crassa is a haploid ascomycete found in two non-switching mating types, *A* and *a* (referred to as "big A" and "little a"). Strains of either type grow as branching, thread-like cells called hyphae. These hyphal cells are typically interconnected and multinucleated. The mycelium is homokaryotic if all the nuclei present have the same genotype, and it is heterokaryotic if they have a different genetic composition. The fusion of haploids to produce diploid nuclei is rare; thus **heterokaryons** are naturally stable.

Certain stresses (a dry environment or carbon starvation) activates the asexual developmental pathway, which is also called conidiation. Aerial hyphae grow away from the mycelial substrate and develop a spore-producing structure that contains conidiophores. Conidiophores are chains of cells that grow by budding and develop into multinucleates spores called macroconidia. These bright orange spores are an ideal means of dispersal, as they are small (5–10 mm) and abundant.

In contrast, sexual sporulation has rather exacting nutritional requirements. It begins with the formation of protoperithecia—the female reproductive apparatus of the organism. Poorly characterized metabolic and environmental signals induce protoperithecial development in the absence of strains of the opposite mating type. In fact, more is known about the conditions that inhibit development than those that activate it. For example, protoperithecia are sparsely formed on nutritionally complex media, on submerged liquid cultures, and at temperatures above 27°C. The absence of ammonium ions seems to be critical to induce their formation, as does a marginal degree of nitrogen starvation or intense carbon deprivation. In addition, blue light is known to stimulate their formation.

Development of microconidia occurs in the absence of strains of the opposite mating type. These asexual spores are small and uninucleate, grayish-brown in color. They are formed within the vegetative hyphae and rupture through the cell wall as they mature. Microconidia are thought to function primarily as male fertilizing agents for the developing protoperithecia.

Being heterothallic, *Neurospora* must mate with strains of the opposite mating type to form sexual spores or ascospores. For this, trychogynes, specialized hyphal elements that emanate from protoperithecia, are fertilized by male elements (macroconidia, microconidia, or vegetative cells) of the opposite mating type. Fusion, or plasmogamy, initiates the development of the perithecium, the multicellular sexual apparatus. After plasmogamy, the male- and the female-derived nuclei coexist in a heterokaryotic tissue and divide mitotically until they are sorted into dikaryotic tissue, in which each cell compartment contains only one nucleus of each mating type. The nuclei then pair and undergo a series of synchronous mitoses until the tip of the hyphal cell in which they reside bends to form a hook-shaped cell called a *crozier*. There, the two nuclei undergo a coordinate mitosis yielding, after septum formation, a uninucleate basal cell, a uninucleated lateral cell, and a penultimate ascus mother cell that contains one nucleus of each mating type. It is in this cell that karyogamy, meiosis, and postmeiotic mitoses take place resulting in an ascus containing eight haploid spores in an order that reflects their lineage. About 200 such asci are generated within a typical perithecium. Once mature, the ascospores are ejected from the ascus through the ostiole in the perighecial beak. Meiotic segregation and recombination can be studied in *Neurospora* by analyzing individual asci or random ejected spores.

3.2. Life Cycle of *Aspergillus nidulans* (5-7)

A. nidulans is a homothallic ascomycete that does not require different mating types for sexual reproduction. As a vegetative mycelium *A. nidulans* grows via apical extension in which genetically distinct nuclei can coexist in a single thallus as heterokaryons or separately, maintaining the homokaryotic state. Although the hyphae have what appear to be individual segments, the cross walls contain pores so that the mycelium is in fact a multinucleate structure. Within the growing mycelia mat, nuclei are also capable of fusion, producing diploid thalli. This is also a relatively rare event in naturally occurring populations, but may be accomplished in the laboratory with the use of complementing auxotrophies present in each of the donor hyphae (8).

Sexual reproduction involves the formation of specialized fruiting bodies called cleistothecia containing fertile hyphae. Since *A. nidulans* is homothallic, mating occurs within a colony of uninucleate cells, much like wild type strains of *S. cerevisiae*. Nuclear fusion (karyogamy) and meiosis occur within the cleistothecia followed by the formation of ascospores within individual asci. Further differentiation of the postmeiotic nuclei involves two mitotic divisions producing binucleate ascospore progeny.

Asexual reproduction in *A. nidulans* involves the formation of multicellular conidiophores and uninucleate conidia. In response to signals that are as yet poorly understood, a single hyphal segment from the vegetative mycelium develops into a foot cell, which differentiates a specialized stalk and metulae. Repeated divisions of the metulae give rise to uninucleate phialides cells which undergo additional rounds of division to produce conidia. Thus, conidia are uninucleate and haploid, whereas ascospores are binucleate. A great deal of research has been applied to understanding the genetic and biochemical mechanisms that govern conidial development in *A. nidulans*. See Ref. 9 for review.

Although both *Aspergillus nidulans* and *N. crassa* have long genetic systems that make them ideal for study of a wide variety of eukaryotic problems, the use of recombinant DNA techniques and transformation systems in all of the fungi has enlarged the wealth of information that can be gleaned from pursuing some of the more genetically intractable organisms.

4. Genome Structure

The **genomes** of fungi range in size from around 7-8 Mb for *Pneumocystis carinii* and *Ashbya gossypii* to near 40 Mbp for some of the basidiomycetes (see Table 1). The presence of introns may be rare, as for *C. albicans* and *A. gossypii*, or they may be widely distributed, as for *A. nidulans*. It is estimated that the filamentous fungi will contain anywhere from 4500 genes in the smallest fungi to 9,000–12,000 genes in the largest genomes (Phillipsen, personal communication) (10). Because most fungal chromosomes do not condense during mitosis, their karyotypes cannot be determined by cytological methods. A size estimate may be determined utilizing pulsed-field gel electrophoresis techniques in which whole chromosomes are resolved using alternating electrical fields. Some examples are given in Table 1.

Table 1. Genome Size and Karyotype

Organism	Size (Mb)	Number of chromosomes	References
Ashbya gossypii	8.85	7	22, 54
Aspergillus nidulans	31	8	55, 56
Candida albicans	16–17	8–9	57, 58
Coprinus cinereus	37.5	13	59
Cochliobolus heterostrophus	35	15–16	13
Histoplasma capsulatum	~31	7	60
Magneporthe grisea	40	7 + 1–4 mini chromosomes	61-63
Neurospora crassa	42.9	7	64, 65
Pneumocystis carinii	7–8	14–16	66
Saccharomyces cerevisiae	13.5	16	SGD: `http://genome-www.stanford.edu/Saccharomyces/`
Schizosaccharomyces pombe	14	3	67
Ustilago hordei	18–25	16–21	68
Ustilago maydis	22	~20	69

The genomes of fungi are known to be somewhat plastic, as evidenced by the chromosome length polymorphisms (CLPs) observed for many different species using pulsed-field electrophoretic techniques to separate whole chromosomes by size. This polymorphism can be accounted for by both mitotic and meiotic events and is observed in both sexual and asexual fungi [reviewed in (11)].

The mechanisms by which these changes are initiated are largely unknown, but the presence of repetitive elements within the genome has been suggested to play a critical role. Reciprocal translocations have been demonstrated in two isolates of *C. albicans* (12) and in *C. heterostrophus* (13), and the expansion/contraction of tandem ribosomal DNA repeats has been documented as the cause of some CLPs in *C. albicans* (14), *Coprinus cinereus* (15) and *Cladosporium fulvum* (16). Subtelomeric regions of fungi are known to contain repetitive DNA sequences that have proven useful in fingerprinting individual isolates. Until recently, fungi were thought to lack transposon elements, which have been shown to influence genome fluidity in other systems. They have been identified in a number of species; a representative few are presented in Table 2. It is interesting to note that, while transposon-mediated inactivation of essential genes would, *a priori*, have severe consequences on single-celled systems such as *S. cerevisiae*, it would be of little consequence to the coenocytic lifestyles of the small and filamentous. In fact, transposons may have had significant effects upon fungal genome evolution.

Table 2. Insertional Elements in Filamentous Fungi

Organism	Element	Size	Length of ITR (bp)	Copy no.	Reference
Nectria haematococca	Nht1	2.2 bp	–	0–100 copies	70
Fusarium oxysporum	Fot1	1.9 kbp	44	4–100	71
Botrytis cinerea	Flipper	1.8 kbp	48	0–20	72
Magnaporthe grisea	Pot2	1.9 kbp	43	~100	73
	MGR586	1.8 kbp	42	0–50	74
	MAGGY	5.6 kbp	–	0–100	75
Aspergillus niger	Tan1	2.3 kbp	44	1	76
	Vader	0.44 kbp	44	~15	76
Cochliobolus carbonum	Fcc1	1.8 kbp	64	>10	77
Neurospora crassa	Tad1-1	6.9 kbp	–	~40	78

Another source of CLPs may be dispensable or “B” chromosomes. These chromosomes are not present in all members of a species, and their absence is generally thought to offer no advantage or disadvantage to the organism. Fungi, as well as other plants and animals, have small dispensable chromosomes or portions of chromosomes that may be dispensable. Their existence has been conclusively demonstrated in *C. heterostrophus* (13), and *N. haematococca* (17).

There are a number of sequencing efforts in the fungi that will shortly answer many of the questions concerning comparative genome structure (18): *Aspergillus nidulans* (19), *Candida albicans* (20), *Neurospora crassa* (21), and *Ashbya gossypii* (22) are well on their way to completion.

5. Conclusion

The past decade has been a particularly exciting time for those working on the filamentous fungi.

With the ability to transform these organisms with homologous and heterologous fragments of DNA, it has been possible to make great strides in a number of areas. Not only has there been a much greater understanding of developmental pathways, molecular clocks, and mating type in these organisms, but topics such as incompatibility, pathogenesis and evolution have been addressed at a molecular level. Furthermore, as more genomes are squenced, bioinformatics and functional genomics will play an even greater role as scientists begin to uncover the function of each of the proteins expressed in a given organism. What was once the gold of biochemists and geneticists can now be mined by molecular biologists studying human disease since fungi allow us to peek into the world of mammalian biology. Like all reviews of this nature, this one is far from complete, space limitations prevented the inclusion of many interesting topics, however excellent reviews in the field are available (a partial list is given below): transformation systems (23, 24); mating (25-28); control of gene expression (29); protein production and secretion (30-32); development and sporulation (4, 7, 8, 25, 27, 33); DNA modification strategies (34-36); fungal chromosomes and plasmids (11, 37-41); incompatibility (42); signaling (43); virulence and pathogenesis (44-50); circadian rhythms (51, 52); evolution (53).

Precise sequence information on these genomes can be accessed at the following sites:

1. University of Georgia (*A. nidulans*): `http://fungus.genetics.uga.edu:5080/Physical_Maps.html` (as of 8/31/98)
2. Oklahoma State University cosmid and cDNA sequencing (*N. crassa* and *A. nidulans*): `http://www.genome.ou.edu/fungal.html` (as of 8/31/98)
3. University of New Mexico (*N. crassa*): (site currently unavailable) (as of 8/31/98)
4. University of Minnesota (*C. albicans*): `http://alces.med.umn.edu/Candida.html` (as of 8/31/98).

Note: There are excellent course outlines, descriptions, and lecture notes online: For plant pathogens:

1. SUNY College of Forestry and Environmental Science: `http://www.esf.edu/course/jworrall/fungi.html` (as of 8/31/98)
2. University of New Mexico: `http://taipan.nmsu.edu/EPWS310/exam-1-lectures.html` (as of 8/31/98)
3. On soil fungi by Dr. D. Jones at: (site currently unavailable)
4. And a more general outline by Dr. Bell at: (site currently unavailable)

Bibliography

1. D. L. Hawksworth, B. C. Sutton, and G. C. Ainsworth (1983) *Dictionary of the Fungi*, Commonwealth Mycological Institute, Surrey, England.
2. N. Pace (1996) ASM News **62**, 463.
3. M. A. Nelson (1996) Trends Genet. **12**, 69–74.
4. M. L. Springer (1993) BioEssays **15**, 365–374.
5. A. Clutterbuck (1974) *Aspergillus nidulans*. In *Handbook of Genetics: Bacteria, Baceteriaphages and Fungi* (R. C. King, eds.), Plenum Press, New York.
6. B. W. Bainbridge (1987) In *Genetics of Microbes* (B. W. Bainbridge, ed.), Blackie, Glasgow, London.
7. W. E. Timberlake (1990) Ann. Rev. Genet. **24**, 5–36.
8. T. H. Adams, J. K. Wieser, and J.-H. Yu (1998) Microbiol. Mol. Biol. Rev. **62**, 35–54.
9. W. E. Timberlake and A. J. Clutterbuck (1994) Prog. Indust. Microbiol. **29**, 383–427.
10. D. M. Kupfer et al. (1997) Fung. Genet. Biol. **21**, 364–372.
11. D. D. Perkins (1997) Adv. Genet. **36**, 239–398.

12. S. Iwaguchi, M. Homma, H. Chibana, and K. Tanaka (1992). J. Gen. Microbiol . **138**, 1893–1900.
13. T. Tzeng, L. K. Lyngholm, C. F. Ford, and C. R. Bronson (1992) Genetics. **130**, 81–96.
14. E. P. Rustchenko, T. M. Curran, and F. Sherman (1993) J. Bacteriol. **175**, 7189–7199.
15. P. J. Pukkila and C. Skrzynia (1993) Genetics **133**, 203–211.
16. N. J. Talbot, P. Oliver, and Coddington (1991) Mol. Gen. Genet. **229**, 267–272.
17. V. Miao, S. F. Covert, and H. D. VanEtten (1991) Science **254**, 1773–1776.
18. L. Hamer (1997) Fung. Genet. Biol. **21**, 8–10.
19. R. A. Prade et al. (1997) Proc. Natl. Acad. Sci. USA **94**, 14564–14569.
20. E. Tait et al. (1997) Fung. Genet. Biol. **21**, 308–314.
21. M. A. Nelson and D. O. Natvig (1997) Fung. Genet. Biol. **21**, 348–363.
22. S. Stenier, J. Wendland, M. C. Wright, and P. Philippsen (1995) Genetics **140**, 973–987.
23. J. Rambosek and J. Leach (1987) CRC Crit. Rev. Biotechnol. **6**, 357–393.
24. M. J. Hynes (1997) J. Genet. **75**, 297–311.
25. R. Kahmann, T. Romeis, M. Bolker, and J. Kamper (1995) Curr. Opin. Genet. Dev. **5**, 559–564.
26. J. W. Kronstad and C. W. Staben (1997) Ann Rev. Genet. **31**, 245–276.
27. E. Coppin, R. Debuchy, S. Arnaise, and M. Picard (1997) Microbiol. Mol. Biol. Rev. **61**, 411–428.
28. L. A. Casselton and N. S. Olesnicky (1998) Microbiol. Mol. Biol. Rev. **62**, 55–70.
29. M. S. Sachs (1998) Fung. Genet. Biol. **23**, 117–124.
30. D. B. Archer and P. J. F. (1997) Crit. Rev. Biotechnol. **17**, 273–306.
31. R. J. Gouka, P. J. Punt, and C. A. van den Hondel (1997) Appl. Microbiol. Biotechnol. **47**, 1–11.
32. J. P. T. W. VanDen Hombergh, L. VanDe Vondervoort, F. Tachet, and J. Visser (1997) Trends Biotechnol. **15**, 256–263.
33. D. J. Ebbole (1996) J. Genet. **75**, 361–374.
34. J. T. Irelan and E. U. Selker (1996) J. Genet. **75**, 313–324.
35. M. J. Singer and E. U. Selker (1995) Curr. Top. Microbiol. Immunol. **197**, 165–177.
36. E. U. Selker (1997) Trend. Genet. **13**, 296–301.
37. E. G. Barry and 1996 (1996) J. Genet. **75**, 255–263.
38. A. J. F. Griffiths (1995) Microbiol. Rev. **59**, 673–685.
39. D. R. Stadler (1996) J. Genet. **75**, 265–280.
40. M. Plamann (1996) J. Genet. **75**, 351–360.
41. F. Kempken and U. Kuck (1998) BioEssays **20**, 652–659.
42. J. F. Leslie and K. A. Zeller (1996) J. Genet. **75**, 415–424.
43. F. Banuett (1998) Microbiol. Mol. Biol. Rev. **62**, 249–274.
44. D. G. Panaccione (1993) Trends Microbiol **1**, 14–20.
45. R. Oliver and A. Osbourn (1995) Microbiology **141**, 1–9.
46. L. H. Hogan, B. S. Klein, and S. M. Levitz (1996) Clin. Microbiol. Rev. **9**, 469–488.
47. M. Hensel and D. W. Holden (1996) Microbiol. **142**, 1049–1058.
48. J. W. Kronstad (1997) Trends Plant Sci. **2**, 193–199.
49. D. J. Ebbole (1997) Trends Microbiol. **5**, 405–408.
50. B. E. Corner and P. T. Magee (1997) Curr. Biol. **7**, 691–694.
51. J. C. Dunlap (1996) Ann. Rev. Genet. **30**, 579–601.
52. P. Ballario and G. Macino (1997) Trends Microbiol. **5**, 458–462.

53. J. W. Taylor (1995) Arch. Med. Res. **26**, 307–314.
54. R. Altmann-Johl and P. P. (1996) Mol. Gen. Genet. **250**, 69–80.
55. H. Brody and J. Carbon (1989) Proc. Natl. Acad. Sci. USA **86**, 6260–6263.
56. D. M. Geiser and W. E. Timberlake (1996) Curr. Genet. **29**, 293–300.
57. B. B. Magee and P. T. Magee (1987) J. Gen. Microbiol. **133**, 425–430.
58. W. Chu, B. B. Magee, and P. T. Magee (1993) J. Bacteriol. **175**, 6637–6651.
59. P. J. Pukkila and L. A. Casselton, (1991) In *More Gene Manipulations in Fungi* (Bennett and Lasure, eds.) Academic Press, New York, pp. 127–150.
60. P. E. Steele, G. F. Carle, S. Kobayashi, and G. Medoff (1989) Mol. Cell. Biol. **9**, 983–987.
61. M. J. Orbach (1989) Fung. Genet. Newslett. **36**, 14.
62. D. Z. Skinner, H. L. Leung, and S. A. Leong (1990) *Genetic Map of the Blast Fungus Magnaporthe grisea* (*n* = 6). In *Genetic Maps* (S. J. O"Brien, ed.), Cold Spring Harbor Laboratory Press, Cold Spring Harbor, New York.
63. D. Z. Skinner, A. D. Budde, and S. A. Leong (1991) Theor. Appl. Genet. **87**, 545–557.
64. M. J. Orbach, D. Vollrath, R. W. Davis, and C. Yanofsky (1988) Mol. Cell. Biol. **8**, 1469–1473.
65. A. Radford and J. H. Parish (1997) Fung. Genet. Biol. **21**, 258–266.
66. M. T. Cushion, M. Kaselis, S. L. Stringer, and J. R. Stringer (1993) Infect. Immun. **61**, 4801–4813.
67. J. B. Fan et al. (1988) Nucleic Acids Res. **17**, 2801–2818.
68. K. McCLuskey and D. Mills (1990) Mol. Plant-Microb. Interact. **3**, 366–373.
69. T. G. Kinscherf and S. A. Leong (1988) Chromosoma **96**, 427–433.
70. J. Enkerli, G. Bhatt, and S. F. Covert (1997) Mol. Plant-Microb. Interact. **10**, 742–749.
71. M. J. Daboussi, T. Langin, and Y. Brygoo (1992) Mol. Gen. Genet. **232**, 12–16.
72. C. Levis, D. Fortini, and Y. Brygoo (1997) Mol. Gen. Genet . **254**, 674–680.
73. P. Kachroo, S. A. Leong, and B. B. Chatoo (1994) Mol. Gen. Genet. **245**, 339–348.
74. P. Kachroo, M. Ahuja, S. A. Leong, and B. B. Chattoo (1997) Curr. Genet. **31**, 361–369.
75. M. L. Farman, Y. Tosa, N. Nitta, and S. A. Leong (1996) Mol. Gen. Genet. **251**, 665–674.
76. E. Nyyssonen et al. (1996) Mol. Gen. Genet. **253**, 50–56.
77. D. G. Panaccione, J. W. Pitkin, J. D. Walton, and S. L. Annis (1996) Gene **176**, 103–109.
78. E. B. Cambareri, J. Helber, and J. A. Kinsey (1994) Mol. Gen. Genet. **242**, 658–665.
79. J. W. Taylor (1995) Arch. Med. Res. **26**, 304–307.

Fusion Gene, Fusion Protein

Fusion genes consist of unrelated genes, or gene fragments, that have been joined in-frame to produce a coding sequence that is **transcribed** and **translated** as a single unit. The resulting gene product is called a *fusion protein* (as well as a chimeric or hybrid protein). The fused gene elements most often encode functionally and structurally distinct protein **domains**.

In nature, several examples of fusion genes exist. Circumstantial evidence supports the hypothesis that the assembly of relatively small domains into functional proteins is an important factor in evolution (1). These natural gene fusion events result from processes such as gene duplication and exon shuffling. The possibility of deleting and adding such domains during evolution suggests that proteins are often tolerant to changes involving whole domains.

Ubiquitin, a small, highly conserved **eukaryotic** protein, is another example of a naturally occurring gene fusion, as it is expressed from gene fusions to either itself (generating polyubiquitin) or to one of two **ribosomal** proteins (2). A third example is the **genomes** of many **viruses** that consist of several genes fused together. On expression, a polyprotein is produced, which is further processed by a virus-encoded proteinase to generate single proteins (3).

Gene fusions generated by use of recombinant DNA technology have been used experimentally for a number of purposes, such as protein expression and purification, construction of reporter systems, and medical applications, as well as in systems for directed evolution of proteins. The first-mentioned application is by far the most common and, therefore, this aspect of gene fusion technology will be treated in greatest detail (see Expression Systems).

1. Gene expression and protein purification

There can be several reasons for applying the fusion gene approach in a gene expression strategy. Fusion to the desired product of an affinity chromatography or purification "handle" or "tag," with unique **ligand-binding** characteristics, allows the use of the properties of the fused handle for purification. In many cases, the handle is useful for detection purposes as well. The handle can be removed later, if necessary, to obtain the native product. The most commonly used handles seem to be protein A, which binds to immunoglobulin G; glutathione **S-transferase**, which binds to its substrate glutathione; maltose-binding protein, which binds to maltose, and poly**histidine**, which binds to metal ions (4). A combined affinity handle with more tags integrated can allow a simplified screening of various purification and detection methods (5). These general fusion systems for expression and purification ensure a reasonable expression level (when the fusion partner gene is positioned upstream of the gene of interest) and allow rapid recovery of the gene product without the need for time-consuming optimization. Other advantages of gene fusion technology with relation to protein expression and purification are summarized in Table 1.

Table 1. Alternative Purposes of Using a Fusion Strategy in Protein Expression and Purification

Problem	Solution
Low solubility, caused by misfolding	Fusion to a protein with solubilizing or chaperonelikeproperties, eg, protein A, thioredoxin, or ubiquitin (7, 8)
Proteolytic degradation	A dual-affinity approach in which the protein of interest is fused between two different affinity chromatography handles (9)
Proteolytic degradation; recovery problems	Fusion to trpE, cII, or an amphiphilic extension often results in the formation of inclusion bodies, offering protection and simplified purification; **denaturation** followed by refolding is required (10, 11)
N-terminal heterogeneity (in bacteria)	Addition of fusion partner, whose removal generates a homogeneous N-terminus
Detection	Fusion to a partner that can be readily detected by, eg, immunological methods or its enzymatic activity

Toxicity; formation of disulfide bonds (in bacteria); recovery; proteolytic degradation	The protein of interest has to be removed from the cytoplasm; fusion with a signal peptide directs the protein of interest to a specific compartment (eg, periplasm, cell wall, culture medium) [see Secretion Vector)

The removal of the affinity handle is most often the bottleneck of the purification procedure. The usefulness of chemical cleavage is limited, as these agents recognize only one amino acid and harsh conditions are often applied during the cleavage. Enzymatic methods can represent a problem if the proteinase used is not sufficiently specific. Furthermore, the cleavage efficiency can be low because of the inaccessibility of the recognition sequence by the proteinase. Finally, one or more purification steps are required to remove the proteinase again after cleavage. Now, the use of recombinant fusion proteinases equipped with a purification handle may be able to solve some of these problems. If the handle is of the same kind as that of the fusion protein to be processed, the cleavage can, in principle, be carried out directly on the column (6). Another solution to the problem of removing the fusion partner is presented in the IMPACT system (New England Biolabs), where the protein of interest is C-terminally fused to an affinity tag that binds chitin. These two fusion partners are separated by a modified protein splicing element, the intein domain. The splicing element undergoes self-cleavage at its N-terminus under reducing conditions when the fusion protein is bound on a chitin affinity column. The cleavage causes the release of the target protein while leaving the affinity tag bound to the column.

2. Potential medical applications

Many pharmaceutical protein drugs are rapidly cleared from the circulation after administration, making frequent supply of large doses of the therapeutic drug necessary. It has been demonstrated that the *in vivo* half-life of a drug can be increased by fusion to a carrier that is more stable *in vivo* (12).

Drug targeting is another interesting application of gene fusions. One portion of the fusion protein targets the drug to a specific cell type, for example, by interacting with a **receptor** molecule, whereas the other part, the drug itself, has the specific activity of interest.

Immunogenic peptides or proteins for the production of vaccines are often small and difficult to produce because high purity is necessary. A means of overcoming these difficulties is to produce the protein as a fusion protein. Normally, the native protein does not have to be released by cleavage. A particularly effective fusion partner is the serum albumin -binding region of streptococcal protein G, which seems to have inherent immunopotentiating properties, probably by providing T-cell help for antibody production (13).

The gene fusion technology has also proved valuable in gene therapy. Transcriptionally inducible systems have several critical shortcomings, such as the delay between induction and the appearance of optimal protein activity, plus the problem of activating specific genes without affecting others. **Hormone**-binding domains (HBD) of **steroid receptors** can be used to regulate heterologous proteins post-translationally. The protein to be regulated is fused to an HBD, so that it becomes inactive in the absence of hormone. The inactive state can be rapidly reversed by the addition of the cognate steroid hormone (14). Chimeric versions of the steroid hormone receptors have also been applied for the regulation of **gene expression** at the transcriptional level. The chimeric receptor is composed of an HBD, a specific DNA-binding domain, and a transcriptional activation domain, each with unique specificity. The chimeric receptor is kept in the inactive state, until an activating ligand is bound. The active chimeric receptor is now capable of binding to specific response elements associated with the target gene, thereby inducing its expression (15).

3. Research Applications

Gene fusion technology has also been used to generate powerful research tools of general interest (16). The **phage display** system is based on the fusion of the gene encoding a product of interest to one of the genes encoding a **bacteriophage** coat protein. The fusion protein will thereby be displayed on the surface of the phage, and the corresponding gene will be packaged into the phage particle, allowing its later identification by DNA sequencing. The system is used for the selection of a mutational variant of the protein of interest with specific characteristics from a pool of randomized versions of the protein.

The yeast two-hybrid system is a method developed for the detection of protein–protein interactions. The system takes advantage of the fact that many eukaryotic transcriptional activators, including the yeast GAL4, contain two discrete domains, the DNA-binding domain and the transcriptional activation domain. If the two domains are physically separated, GAL4 becomes inactive. Two different cloning vectors are used to generate separate fusions of these GAL4 domains to genes encoding proteins that potentially might interact with each other. The recombinant hybrid proteins are coexpressed in yeast. If the non-GAL4 parts of the two hybrid proteins interact with each other, the DNA-binding domain will be tethered to the transcriptional activation domain. As a result of a two-hybrid interaction, the GAL4 transcriptional activator will be functionally reconstituted and will activate transcription of reporter genes having upstream GAL4 sites. In this way, the protein–protein interaction is made **phenotypically** detectable.

Scientists have found inspiration to develop gene fusion technology by studying nature's way of evolving proteins with new functions by fusing genes encoding distinct protein domains. Gene fusion technology has now found widespread use in biotechnology and medicine and promises to be a key technology for the future.

Bibliography

1. W. Gilbert (1978) Nature **271**, 501.
2. D. Finley, B. Bartel, and A. Varshavsky (1989) Nature **338**, 394–401.
3. I. G. Maia, K. Séron, A.-L. Haenni, and F. Bernardi (1996) Plant Molec. Biol. **32**, 367–391.
4. H. M. Sassenfeld (1990) Trends Biotechnol. **8**, 88–93.
5. J. Nilsson et al. (1997) Prot. Expr. Purif. **11**, 1–16.
6. P. A. Walker et al. (1994) Biotechnology **12**, 601–605.
7. E. Samuelsson et al. (1991) Biotechnology **9**, 363–366.
8. P.-Å. Nygren, S. Ståhl, and M. Uhlén (1994) Trends Biotechnol. **12**, 184–188.
9. M. Murby et al. (1991) Biotechnol. Appl. Biochem. **14**, 336–346.
10. M. Uhlén and T. Moks (1990) Meth. Enzymol. **185**, 129–143.
11. J. G. Thomas, A. Ayling, and F. Baneyx (1997) Appl. Biochem. Biotech. **66**, 197–238.
12. S. C. Makrides et al. (1996) J. Pharmacol. Exp. Therapeut. **277**, 534–542.
13. A. Sjölander et al. (1997) J. Immunol. Methods **201**, 115–123.
14. D. Picard (1994) Curr. Opin. Biotech. **5**, 511–515.
15. V. E. Allgood and E. M. Eastman (1997) Curr. Opin. Biotech. **8**, 474–479.
16. J. B. Allen, M. W. Walberg, N. C. Edwards, and S. J. Elledge (1995) Trends Biochem. Sci. **20**, 511–516.

Suggestions for Further Reading

17. E. R. LaVallie and J. M. McCoy (1995) Gene fusion expression systems in Escherichia coli. Curr. Opin. Biotechnol. **6**, 501–506. An overview of the possibilities in the E. coli expression

system provided by gene fusion techniques. A good reference source.
18. J. Nilsson, S. Ståhl, J. Lundeberg, M. Uhlén, and P.-Å. Nygren (1997) Affinity fusion strategies for detection, purification, and immobilization of recombinant proteins. Prot. Expr. Purif. **11**, 1–16. Reviews how to benefit from a fusion strategy when working with recombinant proteins. Contains an extensive reference list.
19. M. Uhlén, G. Forsberg, T. Moks, M. Hartmanis, and B. Nilsson (1992) Fusion proteins in biotechnology. Curr. Opin. Biotechnol. **3**, 569–575. Reviews the use of fusion proteins in biotechnoloty. Provides many good references.

G Banding

G-banding is a simple technique that is usually the method of choice for identifying and studing chromosomes. The first step is to fix the chromosomes with methanol and acetic acid (Carnoy's reagent), which removes the vast majority of the histone proteins. Non-histone proteins remain behind and obviously contribute most to banding patterns. The structural basis of banding is unknown, although the G-bands are presumably where DNA is accessible to thiazine dyes. The second step in G-banding is usually to pretreat the chromosomes by enzymatic digestion using a proteinase, such as **trypsin** or a mixture of proteinases, such as pronase. Alternatively, any other treatment that damages the protein content of chromosomes, such as high pH, can be used. As enzyme digestion proceeds, the removal of structural proteins relaxes the chromosomal compaction, leading to the selective local expansion of chromosomal volume (1). The last step is to stain the chromosomal preparations with Giemsa–Leishman's stain or Wright stain. The dark G-bands alternate with light bands in **prophase** and **metaphase** chromosomes.

General features of G-bands in terms of chromatin structure include the presence of AT-rich DNA sequences, the absence of potentially active **promoter** elements (CpG Islands), and indications that chromatin is late replicating, condenses early in mitotic and meiotic prophase, and is not **DNase I sensitive**.

G-banding is most useful in the analyzing vertebrate chromosomes, where the large number of bands and hence information content has allowed accurate **phylogenetic** comparisons between species. In medical cytogenetics, banding patterns of human chromosomes achieve a resolution of up to 2000 G-bands. Chromosomes can be divided into segments dependent on the most prominent bands, which can then be further subdivided by finer analysis of visible bands. G-banding allows defining chromosomal rearrangements and breakages. For example, a chromosome break at the point Xq 27.3 (long arm, band 2, primary subband 7, subdivision 3) is associated with the form of mental retardation known as Fragile X syndrome (see Acentric Fragment).

Bibliography

1. G. D. Burkhollder and L. Duczek (1982) Chromosoma **87**, 425–435.

Suggestion for Further Reading

2. R. P. Wagner, M. P. Maguire, and R. L. Stallings (1993) *Chromosomes. A Synthesis*, Wiley-Liss, New York.

G-Protein-Coupled Receptors

Almost two thousand **genes** have been identified, on the basis of their predicted protein structure, that encode for proteins characterized as G-protein-coupled receptors (GPCRs). It is likely that there are actually several thousand. GPCRs are currently classified into 100 or so subfamilies, based on their structure, ligand specificity, and biological effects. These molecules have a characteristic sequence that predicts seven **transmembrane**-spanning segments, with a cytoplasmic tail of varying lengths. GPCRs are known to interact with a variety of hormones, neuropeptides, chemokines, biogenic amines, nucleosides, eicosanoids, phospholipids, growth factors, and aromatic compounds that act as olfactants or odorants. Some examples include thyrotropin, interleukin 8, epinephrine, and bombesin. Moreover, scores of "orphan" receptors have been identified by cDNA cloning and are still in search of ligands.

1. Receptor Structure

The wide variety of ligands for GPCRs dictate that several structural variations might allow for the variety of their regulatory features. One common feature of all of these receptors is seven stretches of 20 to 25 **hydrophobic** amino acid residues, which are thought to form a-helices that span the membrane (see a-Helix). Thus, the overall structures of these receptors resemble that of bacteriorhodopsin (1). The amino-terminal sequences lie outside the cell, and they vary in size among the family from 7 to 600 amino acid residues. In the case of some receptors, especially those for larger peptide hormones, such as thyrotropin or thrombin, the amino-terminal sequences are critically involved in ligand binding. In most cases, however, ligand binding is thought to occur primarily within key residues in the membrane-spanning regions. A series of mutational studies with the b-adrenergic receptor and other GPCRs (2) have suggested that the ligand may associate with the a-helix near the outer surface, binding in a plane parallel with the membrane. Another conserved structural feature is the loop between the fifth and sixth a-helices, the domain most critical for interactions with G proteins (see GTP-Binding Proteins). It is likely that agonist binding induces a conformational change in the receptor that permits interactions of this domain with G proteins (3). The carboxyl tail of the receptor is cytoplasmically oriented and varies in length among receptors. Mounting evidence suggests that this domain may play a crucial role in receptor cross-talk and desensitization.

Identification of the regions in GPCRs involved in ligand binding has emerged mainly from studies employing point mutations and receptor chimeras. Advances in this area have been led by studies on b-adrenergic receptors (4). Mutant forms of the receptor have been constructed and expressed in cells, to evaluate the binding of both agonists and antagonists. Studies such as these have led to models in which the ligand is thought to bind at the outer surface of the receptor, among several of the transmembrane domains. In the case of the catecholamine agonist isoproterenol, two serine residues in the fifth transmembrane helix are thought to form hydrogen bonds with the hydroxyl groups on the catechol ring (2). In addition, a phenylalanine residue in a-helix 6 participates in binding via hydrophobic interactions with the catechol ring itself. Similar types of interactions have been elucidated for nucleoside and nucleotide receptors.

Agonist binding to GPCRs is thought to induce movements among the transmembrane domains, a conformational change that is translated into G-protein interactions. Although the molecular dynamics of this process remain poorly understood, a number of models have been proposed to explain signal generation within the receptor (3). One aspect of receptor activation that may play an important role is receptor dimerization, a process that is well characterized in activation of other receptor subtypes. Recently, it has been proposed that the protonation of key transmembrane residues are required for activation. Additionally, it has been reported that intramolecular interactions within certain intracellular loops maintain the receptor in the inactive state prior to ligand binding, which is subsequently disrupted by the interaction with activating ligand.

The specificities of receptors, both for ligands and for G proteins, have been explored by construction of chimeras. Although the overall structural features of these receptors are generally conserved, there is little sequence similarity among the superfamily. Indeed, even among the three known subtypes of the b-receptor, there is only 50% identity. Thus, chimeric receptors have revealed domains of the proteins that are necessary for binding specificity and that dictate which G proteins might be coupled to each receptor (4).

2. G Proteins

The proteins that serve as tranducers for the GPCRs are known as GTP-binding proteins, or G proteins. These molecular linkers exhibit a heterotrimeric structure, consisting of a, b,and g subunits. The heterotrimeric G proteins belong to a superfamily of Gtpases, which share a common structural core. In general, the functions of G proteins are dictated by the receptors with which they interact, an interaction mediated by the asubunit. Thus far, over 30 different a subunits have been identified, along with six b and g subunits. The a subunits fall into five different classes, each with a characteristic impact on its effector.

The asubunit of G proteins interacts with guanyl nucleotides and in general controls the activity of the complex (5, 6). When no ligand is bound to the receptor, a is maintained in the GDP-bound state. In this form, a is complexed to the b and g subunits, which prevents it from interacting with effectors. b and g subunits together form a tight complex. Upon ligand binding, the receptor interacts with the asubunit, leading to the displacement of GDP and the subsequent binding of GTP. In its GTP-bound state, Ga then dissociates from the bgcomplex and is activated, interacting with effectors such as adenylate cyclase. This activation is temporal and is terminated by the intrinsic GTPase activity of Ga, which hydrolyzes the GTP, leaving GDP bound to the protein.

The GTPase activity of Gafamily members is subject to different types of regulation. The proteins can be frozen in their activated state by adding nonhydrolyzable analogues of GTP, such as GTPgS, effectively blocking the GTPase activity of the protein. Additionally, certain bacterial toxins irreversibly modify G-protein a subunits, catalyzing the covalent addition of ADP-ribose from intracellular NAD. ADP-ribosylated Ga cannot hydrolyze GTP, thus leaving the protein in a persistently active state. In the case of **cholera toxin**, this activation results in a modification of Gas, causing the persistent activation of adenylyl cyclase, and leading to massive diarrhea (5, 6). Ga proteins are also regulated by endogenous proteins called for regulators of G proteins (RGs), (7). This family of regulatory proteins now comprises over 20 members, and they seem to function as long-term regulators of G protein signaling.

Although they were originally thought to function only as inhibitors of a, bg subunits in some cases can interact directly with effectors upon their release from Ga subunits, causing either stimulation or inhibition of activity. For example, in certain neuronal systems, cells may contain different forms of adenylyl cyclase that are differentially regulated by G proteins. bg subunits can stimulate the activity of the type III form of cyclase, but have no effect, or can even inhibit, the type II form of the enzyme. Additionally, bg subunits can directly stimulate phospholipase C-b in some cells (8).

3. Effectors

In most cases, G-protein a subunits interact directly with one or more effector proteins in the plasma membrane, to induce the release of soluble second messengers that in turn amplify the hormonal signal into the cell. While the number of effectors continues to grow, four distinct types have been studied in detail: adenylate cyclases, phospholipases, **ion channels**, and **phosphodiesterases**.

Bibliography

1. J. Nathans and D. S. Hogness (1993) Cell **34**, 807–814.
2. R. J. Lefkowitz (1998) J. Biol. Chem. **273**, 18677–18680.
3. U. Gether and B. K. Kobilka (1998) J. Biol. Chem. **273**, 17979–17982.
4. T. H. Ji, M. Grossman, and I. Ji (1998) J. Bol. Chem. **273**, 17291–17302.
5. H. R. Bourne, D. A. Sanders, and F. McCormick (1990) Nature **348**, 125–132.
6. J. R. Hepler and A. G. Gilman (1992) Trends Biochem. Sci. **17**, 383–387.
7. V. Y. Arshavsky and E. N. Pugh (1998) Neuron **20**, 11–14.
8. D. E. Clapham and E. J. Neer (1993) Nature **365**, 403–406.

gal Operon

The *gal* operon of **bacteria** encodes enzymes of galactose metabolism that constitute an amphibolic pathway and is transcribed by two **promoters**. Several cis-acting DNA sequences (**control elements**) and a variety of regulatory proteins, including a **histone**-like protein, modulate the two promoters in a multitude of ways usually found in animals and not in bacteria (Table 1). The *gal* operon has revealed several new features of gene-specific transcriptional regulation that were previously unrecognized. Perhaps such multivalent control mechanisms are required to regulate the synthesis of amphibolic enzymes.

Table 1. Repression and Activation of Transcription of the *gal* Operon

Promoters	Regulatory protein and DNA elements[a]		
	GalR, HU	GalR or GalS	cAMP•CRP
	O_E, O_I	O_E	*AS*
*P*1	Repression	Repression	Activation
*P*2	Repression	Activation	Repression

[a] The regulatory effects of GalR and GalS are epistatic to the effects of cAMP•CRP.

1. Enzymes of the *gal* Operon

The galactose metabolizing enzymes (Fig. 1) are involved in (i) the catabolism of D-galactose that was either imported into the cell by **permeases** or generated intracellularly by hydrolysis of disaccharides and (ii) the synthesis of precursors (UDP galactose and UDP glucose) of complex carbohydrates (1, 2). For catabolism, only a-D-Galactose is converted to galactose-1-phosphate by galactokinase (3). b-D-galactose, generated, for example, by hydrolysis of lactose by **beta-galactosidase**, must change to the a-anomer before it can be phosphorylated. Although b-D-galactose can mutarotate spontaneously to the a-anomer at a slow rate, the enzyme aldose-1-epimerase is largely responsible for the mutarotation *in vivo* (2). Thus, aldose-1-epimerase links the enzymes of lactose and galactose metabolism into a common pathway (Fig. 1).

Figure 1. The Leloir pathway of D-galactose metabolism. As shown, D-galactose is generated intracellularly by hydrolysis of the disaccharide lactose. The parts of the pathway catalyzed by enzymes of the *gal* operon are shown in bold. They are encoded by the genes shown within the parenthesis in italics.

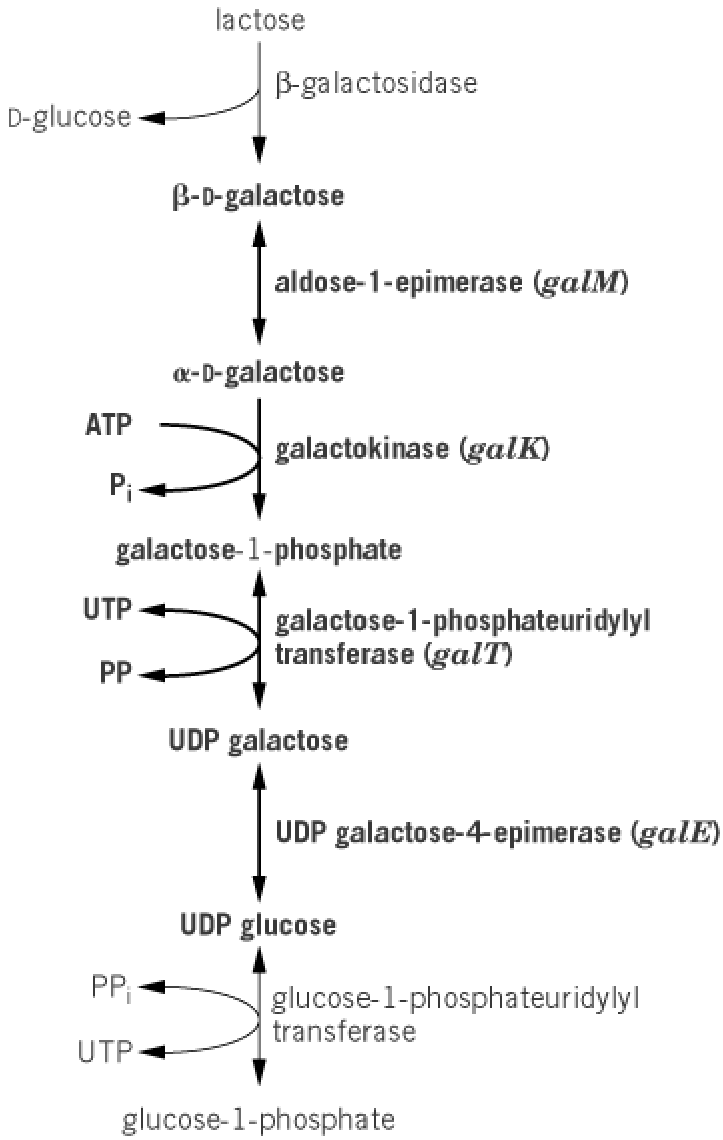

2. Regulation of Transcription

The structural genes and the associated regulatory elements of the *gal* operon are shown in Figure 2. The *gal* operon is transcribed from two promoters, *P*1 and *P*2, which are separated by 5 base pairs (bp) (4, 5). The dominant regulator of the *gal* operon is the Gal repressor (GalR) (6). GalR, together with the histone-like protein, HU, acting as a corepressor, keeps the expression from the *gal* promoters low (7, 8). The operon is induced 15-fold in the presence of D-galactose or some of its nonmetabolizable analogs, such as D-fucose (9). The inducer lifts the repression by an **allosteric** effect on GalR. It is not known whether the true inducer is the a- or the b-anomer of the sugar, or both. Besides the major negative control by GalR and HU, the two promoters are also regulated by

GalR alone (10), by a Gal isorepressor, GalS (11-13), and by a complex of cyclic AMP (cAMP) bound to cyclic AMP receptor protein (CRP), cAMP•CRP (4, 5, 14-16). As described below, *P*1 and *P*2 are regulated by these regulators in opposite directions. The *gal* promoters are also modulated by *cis*-acting DNA sequences without the participation of any regulatory proteins.

Figure 2. The structure of the *gal* operon. The regulators are shown as circles and their cognate DNA control elements as open bars. Their mode of actions are explained in the text. The adenine tracks present upstream of the promoter are not shown.

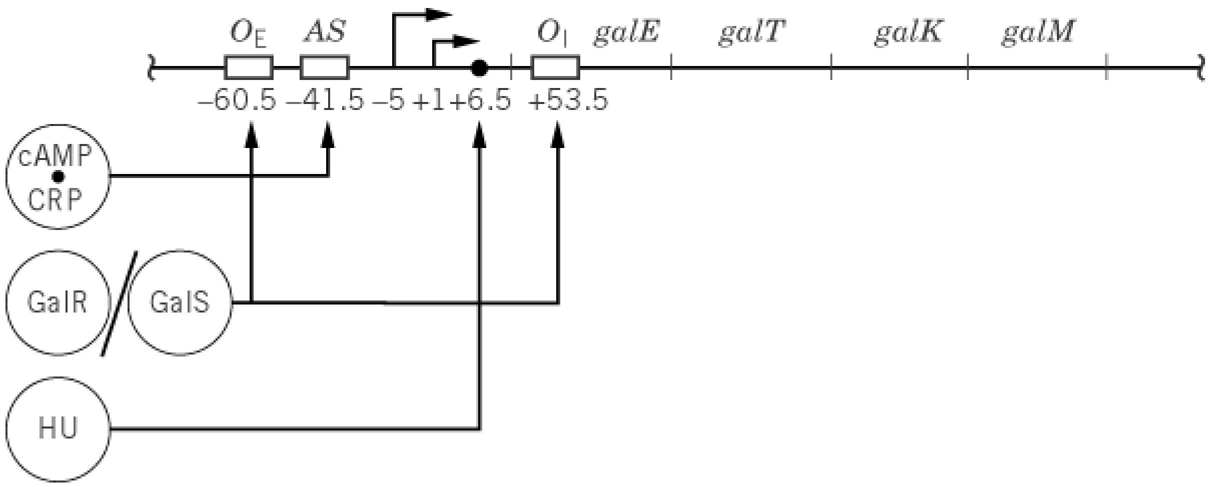

3. Regulation without Regulatory Proteins

3.1. Control of *P*1 by Adenine Tracks

The intrinsic strengths of the two promoters are comparable, and they are moderately active in the absence of any regulatory proteins, both *in vivo* and *in vitro*. *In vitro*, the intrinsic strength of *P*1 is twofold enhanced because of the periodic presence of four to six adenine residues centered at positions –84.5,–74and–63 on the DNA (17). The adenine tracks bend the DNA toward the face of *P*1 to which **RNA polymerase** binds. The DNA curvature induced by the adenine tracks may help formation of a RNA polymerase-promoter complex (caging) that is more optimal for transcription initiation at *P*1 (18).

3.2. Control of *P*2 by UTP

Transcription of the *gal* operon from the *P*2 promoter is very low when the concentration of UTP is high and *vice versa*, both *in vivo* and *in vitro* (19). UTP regulates the step of promoter clearance by RNA polymerase at the *P*2 promoter in an intriguing way. *In vitro*, RNA polymerase clears at *P*2 poorly and makes a large amount of aborted RNA oligomers, unlike at *P*1. At high concentrations of UTP, it also synthesizes pseudo-templated RNA oligomers of the composition pppAU $_n$ (n = 2to≥20) because the enzyme "stutters" while adding uridine residues present at positions 3–5 of the *P*2 RNA and not the *P*1 RNA. RNA polymerase clears the promoter more efficiently and makes template-encoded normal *gal* RNA at low UTP concentrations. The involvement of UTP in the synthesis of UDP sugars by the galactose pathway may be the reason for the control by UTP (Fig. 1) analogous to the way UTP controls its own synthesis in the pyrimidine operons (20). At high UTP concentrations, the levels of UDP galactose and UDP glucose are high and inhibit the synthesis of enzymes, specifically, galactose-1-phosphate uridyltransferase and uridine diphosphogalactose epimerase, that make them.

4. Repression by GalR and HU: DNA Looping

Transcription from the two *gal* promoters is coordinately repressed (negative control) by GalR and HU acting together (7, 8). The repression requires binding of GalR to two operators, O_E and O_I, which are similar 16-bp sequences with a dyad symmetry (Fig. 2) (21-23). O_E is located upstream of the promoters at position –60.5, whereas O_I is located within the structural gene *galE* at position +53.5. The two operator-bound GalR molecules associate with each other in the presence of the cofactor, HU (a heterodimer of two subunits, HUa and HUb), resulting in the formation of a DNA loop encompassing the promoters (8, 24) (Fig. 3). The DNA looping presumably changes the structure of the promoters, making them refractory to RNA polymerase caging (18, 25). The nucleoprotein complex that represses the *gal* promoters is called the Gal repressosome, because its formation is by binding of a histone-like component of the bacterial nucleoid as well as a repressor (26). Although GalR binds to O_E and O_I in both the absence and presence of HU, GalR binding alone does not bring about DNA looping and the associated simultaneous repression of the promoters (27). HU is absolutely necessary for the effect; it cannot be replaced by other histone-like proteins. Although HU is not a sequence-specific DNA binding protein, one molecule of HU heterodimer binds to and bends the *gal* DNA centered at an architecturally critical position (8). Genetic analysis and modeling defined the GalR surfaces interacting to form a stacked, V-shaped tetrameric structure (28, 29). Evaluation of the DNA elastic energies gave unambiguous preference to a DNA loop in which O_E and O_I adopt an antiparallel orientation causing undertwisting of DNA (29). Since HU binding depends on GalR binding to both O_E and O_I and the binding of GalR to the operators is enhanced by HU, GalR and HU bind **cooperatively** (8). GalR piggybacks HU to the critical position on the DNA through a specific GalR-HU interaction (31). The entire process facilitates the GalR-GalR interaction resulting in cooperativity. The GalR-HU contact may be transient and was not in the final repressosome structure. The dependence of HU binding on GalR renders the HU-containing nucleoprotein complex that brings about repression of *P*1 and *P*2 sensitive to inducer D-galactose for transcription derepression. Such a mechanism is an example of how DNA that is "condensed" by binding proteins and made refractory to RNA polymerase action can become available for transcription in response to specific signals.

Figure 3. The DNA looping of the *gal* promoter by binding of the GalR regulator and HU corepressor. The details of binding of the two proteins are discussed in the text.

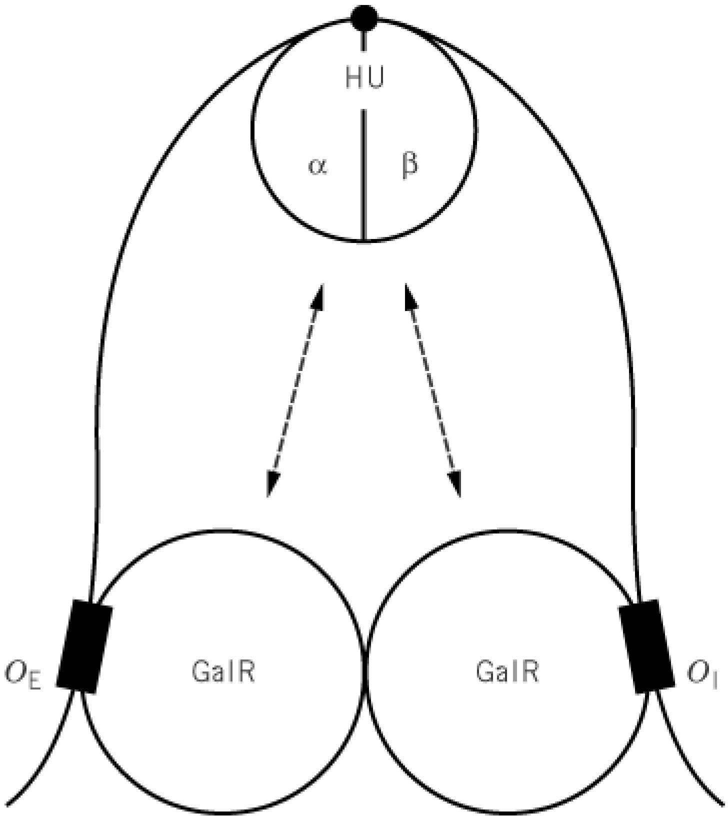

5. Regulation in the Absence of DNA Looping: Interaction between GalR and RNA Polymerase

Without DNA looping (ie, in the absence of HU), occupation of O_E alone by GalR represses *P*1 (by about four- to fivefold) and activates *P*2 (twofold) (10, 27). Binding to O_I does not affect this dual control. The activation of *P*2 and repression of *P*1 are independent of each other. GalR exerts its specific regulatory effect on one promoter even when the other is mutated. The activation of *P*2 or repression of *P*1 is not an intrinsic property of the promoter; the regulation can be reversed by switching the angular orientation of the promoters relative to O_E by inserting a 5-bp segment, that is, half of a DNA helix, between O_E and the promoters. Both activation of *P*2 and repression of *P*1 require the formation of a specific GalR-RNA polymerase-DNA complex at each promoter. RNA polymerases containing a subunits that carry specific amino acid alterations in their carboxy terminal domain (aCTD), or that are missing the aCTD, abolish the regulatory effect of GalR without affecting intrinsic transcription, suggesting that GalR activates and represses by a direct contact with the promoter-bound RNA polymerases.

5.1. Activation of *P*2

Activation of *P*2 by GalR bound to DNA at position –60.5 (–55.5 with respect to *P*2) parallels the activation of transcription of several promoters by activators that also bind around position –60 on the DNA and act by enhancing open complex formation (32). An exposed segment (not necessarily the same segment) of aCTD is contacted by the DNA-bound activator to activate transcription (33, 34). aCTD is connected to the rest of the RNA polymerase molecule by a flexible hinge (35, 36). In *P*2, as in these systems, aCTD binds at the region 40 bp upstream of *P*2 (37) (Fig. 4).

Figure 4. Repression of *P*1 promoter and activation of *P*2 promoter by a contact between DNA-bound GalR and the aCTD of RNA polymerase. The two domains aNTD and aCTD of the RNA polymerase a subunit are shown shaded.

The aCTD is connected to the rest of RNA polymerase by a flexible hinge. Note the differences in the topography of the two cases.

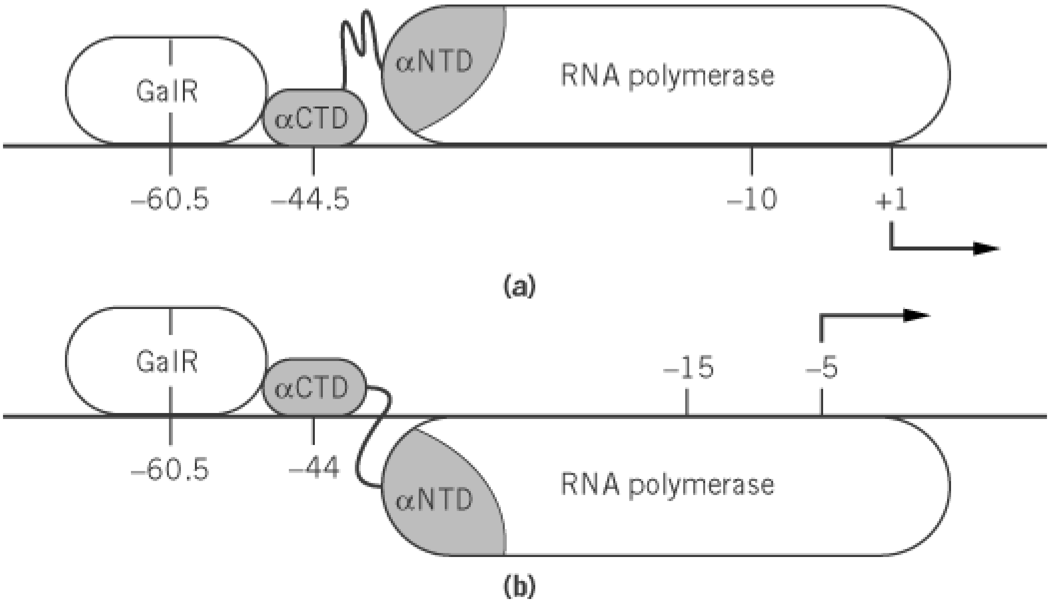

5.2. Repression of *P*1

GalR occupying DNA at position –60.5 represses *P*1, not by hindering RNA polymerase binding, but by contacting aCTD, which binds to *P*1 at position 45 bp upstream of *P*1 (10, 27, 37) (Fig. 4). GalR inhibits isomerization of RNA polymerase complex at *P*1. How contacts between the same two proteins bring about opposite effects at the two promoters remains to be determined. It is not known why and under what conditions the dual behavior of GalR toward *P*1 and *P*2 in the absence of DNA looping is triggered in cells.

6. Gal Isorepressor

The *gal* operon is also regulated by an isorepressor (GalS). Although GalS does not seem to repress the *gal* promoters by DNA looping, the isorepressor does stimulate *P*2 and repress *P*1, the same way that GalR does by binding to O_E, except that the effects are weaker. GalR and GalS modulate a few other operons, including those encoding both high- and low-affinity galactose **active transport** systems (12, 13, 38). The degree of regulation by GalR and GalS varies from operon to operon, perhaps to coordinate galactose metabolism and to transport efficiently under a wide range of galactose availability.

7. Properties of GalR and GalS

GalR and GalS are 85% similar in their amino acid sequences (12). By their homology with proteins (GalR-LacI family) whose structures are known, GalR and GalS are expected to have two-domains connected by a flexible hinge (39). A helix–turn–helix motif in the amino domain of each subunit of GalR and GalS dimers recognizes half of a dyad symmetry in O_E and O_I. The carboxy domains contain the inducer binding sites, which have been defined by isolation and characterization of inducer nonbinding (noninducible) repressor mutants, such as *galR*^{S} and by modeling (40, 41). The mechanism by which the inducer derepresses the *P*1 promoter under conditions of nonlooping by binding to the O_E-bound GalR has been studied in detail. Despite the demonstration that inducer binding can dissociate GalR from the operator, *P*1 can be derepressed under conditions when O_E is occupied by a GalR-inducer complex (42). These results show that dissociation of a repressor from an operator is not obligatory for transcription. Since the O_E-bound GalR interacts with RNA polymerase to inhibit open complex formation at *P*1 at a postbinding step, the inducer acts by allosterically neutralizing the inhibitory contact between the proteins without dissociating the repressor from DNA (10, 17).

8. Regulation by cAMP•CRP

Like GalR and GalS, the global regulator cAMP•CRP complex also has differential effects on the *gal* promoters; but unlike GalR and GalS, the complex activates transcription from *P*1 (three- to fourfold) and represses the same from *P*2 (10-fold) (14, 16). Unlike a large group of promoters, such as the *lac* promoter, in which cAMP•CRP dimer activates transcription by binding at position –61.5 on DNA and contacting RNA polymerase through the aCTD (see Lac Operon and Cyclic Amp Receptor Protein (CRP)/Catabolite Gene Activator Protein (CAP)), the regulatory complex brings about dual control in the *gal* operon by binding to DNA at position –41.5 (37, 43, 44) (Fig. 5). Whereas it is believed that cAMP•CRP represses *P*2 by sterically hindering RNA polymerase binding to the overlapping –35 element of the promoter, the molecular mechanism of activation of *P*1 is different from that in the *lac* promoter. cAMP•CRP stimulates transcription initiation at *P*1 by stimulating both RNA polymerase binding (closed-complex formation) and isomerization (45). A patch of amino acid residues (called *region 1*) of the promoter distal subunit of the cAMP•CRP dimer interacts with an a-helix (helix 1) of the aCTD and helps the latter to stretch away from the *N*-terminal domain (aNTD) to bind to the region upstream of cAMP•CRP. A different amino acid residue patch (called region 2) in the promoter proximal subunit of cAMP•CRP interacts with a different segment of the aNTD. The contact with the aCTD is responsible for increasing the RNA polymerase binding, whereas the interaction with the aNTD stimulates the isomerization step. This shows how the same regulatory protein can activate transcription initiation at two different biochemical steps by making entirely different contacts with RNA polymerase. Nevertheless, the dual roles of cAMP•CRP enable the *gal* operon to be expressed primarily from *P*1 in cAMP-proficient cells and from *P*2 in cAMP-deficient (eg, glucose grown) cells.

Figure 5. Activation of *P*1 by cAMP•CRP by two different contacts with RNA polymerase. The two domains aNTD and aCTD of the RNA polymerase a subunit are shown shaded. Details are discussed in the text.

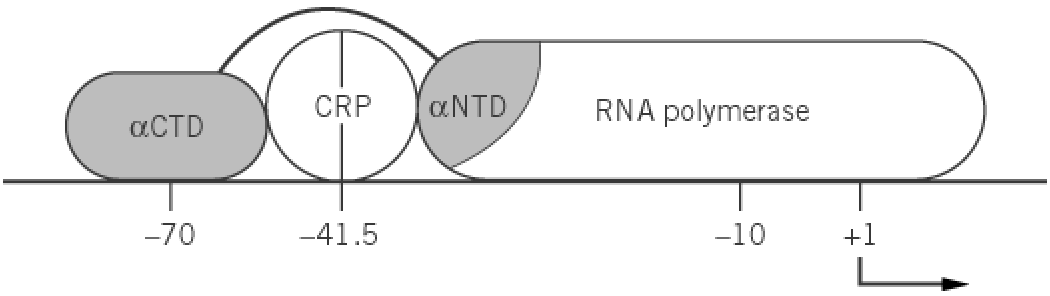

9. Summary

The study of the *gal* operon in *E. coli* has shown new ways and means of gene regulation at the level of transcription initiation: (i) how proteins bound to spatially separated sites on DNA communicate by DNA looping; (ii) how specific and nonspecific DNA binding proteins cooperate to “condense” DNA, making the latter unavailable for transcription, while remaining sensitive to an inducing signal; (iii) how the same regulator brings about opposite effects on promoters — activation and repression—by making direct contact with RNA polymerase; and (iv) how an inducer allosterically changes a repressor to neutralize the inhibitory effect of repressor still bound to DNA. Besides studying the detailed biochemical mechanisms of such controls, the two interesting questions remain: What are the physiological reasons for the multitude of controls, and how are these diverse controls coordinated in the cell?

Bibliography

"*gal* Operon" in , Vol. 2, pp. 952–956, by Sankar Adhya, National Cancer Institute, Developmental Genetics Section, Laboratory of Molecular Biology, 37 Convent Dr MSC 4264, Rm 5138, Bethesda MD 20892-4264, USA, (301)496-5138, sadhya@helix.nih.gov; "*gal* Operon" in (online), posting date: January 15, 2002, by Sankar Adhya, National Cancer Institute, Developmental Genetics Section, Laboratory of Molecular Biology, 37 Convent Dr MSC 4264, Rm 5138, Bethesda, MD 20892-4264, USA, (301)496-5138, sadhya@helix.nih.gov.

1. H. M. Kalckar (1958) Adv. Enzymol. **20**, 111–134.
2. G. Bouffard, K. Rudd, and S. Adhya (1994) J. Mol. Biol. **244**, 269–278.
3. J. R. Sherman and J. Adler (1963) J. Biol. Chem. **238**, 873–878.
4. S. Adhya and W. Miller (1979) Nature **279**, 492–494.
5. R. Musso et al. (1977) Cell **12**, 847–854.
6. G. Buttin (1963) J. Mol. Biol. **7**, 183–205.
7. T. Aki, H. E. Choy, and S. Adhya (1996) Genes to Cells **1**, 179–188.
8. T. Aki and S. Adhya (1997) EMBO J. **16**, 3666–3674.
9. G. Buttin (1963) J. Mol. Biol. **7**, 164–182.
10. H. E. Choy et al. (1995) EMBO J. **14**, 4523–4529.
11. J. P. E. Tokeson, S. Garges, and S. Adhya (1991) J. Bacteriol. **173**, 2319–2327.
12. M. J. Weickert and S. Adhya (1992) J. Mol. Biol. **226**, 69–83.
13. M. Geanacopoulos and S. Adhya (1997) J. Bacteriol. **179**, 228–234.
14. H. Aiba, S. Adhya, and B. deCrombrugghe (1981) J. Biol. Chem. **256**, 11905–11910.
15. S. Busby, H. Aiba, and B. deCrombrugghe (1982) J. Mol. Biol. **154**, 211–227.
16. H. E. Choy and S. Adhya (1993) Proc. Natl. Acad. Sci. USA **96**, 472–476.
17. M. Lavigne, H. Herbert, A. Kolb, and H. Buc (1992) J. Mol. Biol. **224**, 293–306.
18. S. Adhya et al. (1993) Gene **132**, 1–6.
19. D. J. Jin (1994) J. Biol. Chem. **269**, 17221–17227.
20. D. J. Jin, C. L. Turnbough Jr. (1994) J. Mol. Biol. **236**, 72–80.
21. R. diLauro et al. (1979) Nature (London) **279**, 494–500.
22. M. Irani, L. Orosz, and S. Adhya (1983) Cell **32**, 783–788.
23. H. J. Fritz et al. (1983) EMBO J. **2**, 2129–2135.
24. Y. Lyubchenko et al. (1997) Nucleic Acids Res. **25**, 873–876.
25. H. E. Choy et al. (1995) Proc. Natl. Acad. Sci. USA **92**, 7327–7331.
26. S. Adhya, M. Geanacopoulos, D. E. A. Lewis, S. Roy, and T. Aki (1998) Cold Spring Harbor Symp. Quant. Biol. **62**, 1–10.
27. H. E. Choy and S. Adhya (1992) Proc. Natl. Acad. Sci. USA **89**, 11264–11268.
28. M. Geanacopoulos, G. Vasmatzis, D. E. A. Lewis, S. Roy, B.-K. Lee, and S. Adhya (1999) Genes Dev. **13**, 1251–1262.
29. M. Geanacopoulos, G. Vastmatzis, V. B. Zhurkin, and S. Adhya (2001) Nature Strut. Biol. **8**, 432–436.
30. D. E. A. Lewis, M. Geanacopoulos, and S. Adhya (1999) Mol. Microbiol. **31**, 451–461.
31. S. Kar and S. Adhya (2001) Genes Dev. **15**, 2273–2281.
32. R. Ebright (1993) Mol. Microbiol. **8**, 797–802.
33. A. Ishihama (1993) J. Bacteriol. **175**, 2483–2489.

34. H. Tang et al. (1994) Genes Develop. **8**, 3058–3067.
35. E. Blatter et al. (1994) Cell **78**, 889–896.
36. Y. H. Jeon et al. (1995) Science **270**, 1495–1497.
37. T. A. Belyaeva et al. (1996) Nucleic Acids Res. **24**, 2243–2251.
38. M. J. Weickert and S. Adhya (1993) Mol. Microbiol. **10**, 245–251.
39. M. J. Weickert and S. Adhya (1992) J. Biol. Chem. **26**7, 15869–15874.
40. H. Saedler et al. (1968) Mol. Gen. Genet. **102**, 79–88.
41. Y.-N. Zhou et al. (1995) J. Mol. Biol. **253**, 414–425.
42. S. Chatterjee et al. (1997) Proc. Natl. Acad. Sci. USA **94**, 2957–2062.
43. Y. Zhou, T. J. Merkel, and R. H. Ebright (1994) J. Mol. Biol. **243**, 603–610.
44. W. Niu et al. (1996) Cell **87**, 1123–1134.
45. M. Herbert, A. Kolb, and H. Buc (1986) Proc. Natl. Acad. Sci. USA **83**, 2807–2811.

Gamma-Aminobutyric Acid (GABA)

g-Aminobutyric acid (GABA) is widely found in both vertebrates and invertebrates and in both neuronal and non-neuronal tissues. By far, its most understood and arguably most important role is as a neurotransmitter (Fig. 1). GABA is synthesised from glutamate by the enzyme glutamic acid decarboxylase (GAD). It is stored in vesicles within the synaptic terminal of neurons. When an action potential comes down the axon and reaches the synaptic terminal, calcium channels are activated, resulting in calcium influx. This leads to fusion of the neurotransmitter-containing vesicles with the cell membrane and release of the neurotransmitter, in this case GABA, into the synaptic cleft. The GABA diffuses across the synaptic gap and binds to its receptor. GABA receptors are of two types, ionotropic ($GABA_A$) or metabotropic ($GABA_B$), and their activation leads to hyperpolarization of the postsynaptic membrane and a decrease in the excitability of the cell. The response is terminated by desensitization of the receptors and by removal of the GABA from the synapse into the presynaptic terminal or surrounding glial cells. The latter is achieved through specific transporter proteins referred to as GABA transporters. Once taken up into a cell, two potential fates await it. The GABA can be taken up into mitochondria and metabolized to succinic semialdehyde (by GABA transaminase), and then to succinic acid, and enter the tricarboxylic acid pathway. This is referred to as the *GABA shunt*. Alternatively, in the presynaptic terminal, it can be recycled into synaptic vesicles and, thereby, made available for subsequent release.

Figure 1. A schematic of the vertebrate GABAergic synapse. GABA (filled circles) is generated from glutamate by glutamic acid decarboxylase (GAD). When released from presynaptic vesicles into the synaptic cleft, it diffuses across and binds to postsynaptic $GABA_A$ and $GABA_B$ receptors. It may also bind to presynaptic $GABA_B$ receptors. GABA is removed from the synaptic cleft into surrounding glial cells or the presynaptic terminal by GABA transporters. It is directly recycled into synaptic vesicles or taken up by mitochondria, converted by GABA transaminase (filled triangle) to succinic semialdehyde, and enters the tricarboxylic acid pathway.

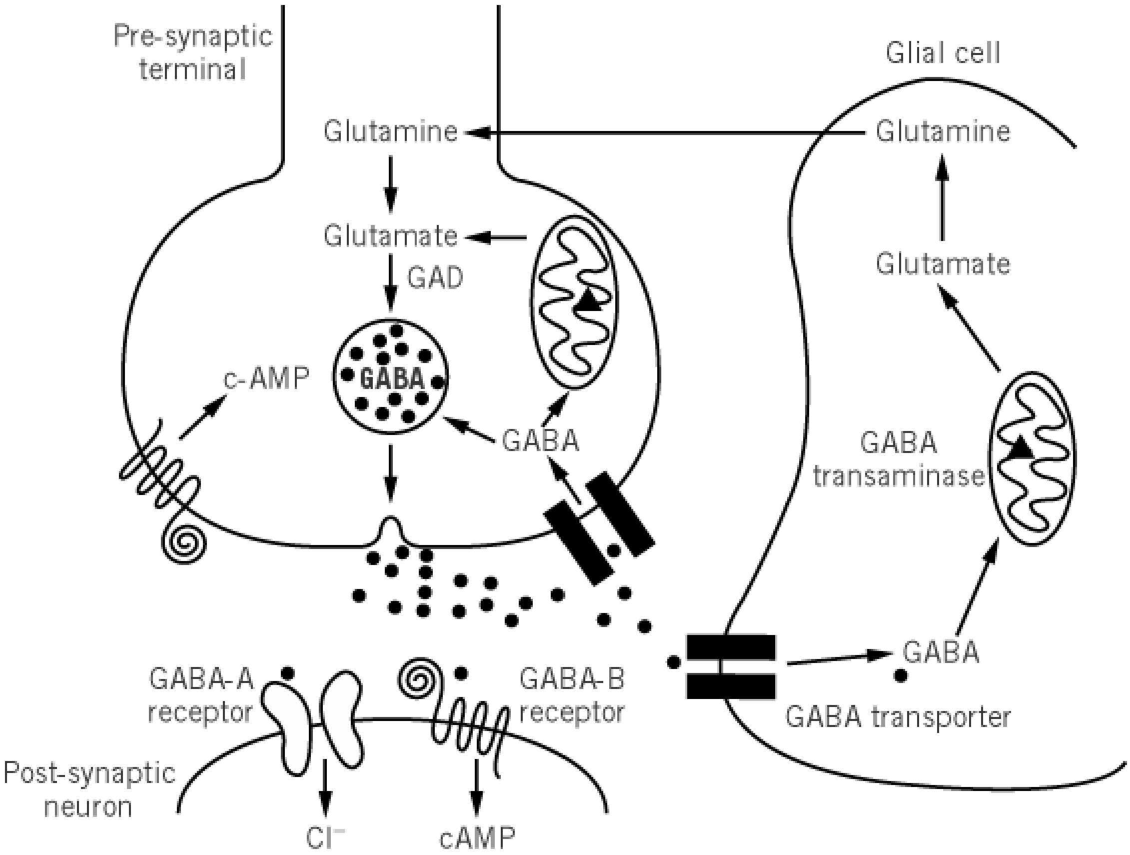

1. Glutamic Acid Decarboxylase

GAD converts glutamic acid into GABA. In mammals there are two forms, GAD65 and GAD67 (named according to their apparent molecular weights), which are the products of two different genes (1). These two forms of GAD are expressed throughout the nervous system and also in several non-neuronal tissues including the pancreas, oviduct, and the testis. Most GABAergic neurons in the brain express both forms of GAD, but their relative abundance varies (2). GAD67 is distributed widely throughout the neuron, while GAD65 tends to be concentrated at the axon terminals (3). The role of GAD in non-neuronal tissues is, in general, poorly understood. Relatively high levels of GABA and GAD are found in the islets of Langerhans beta cells of the pancreas (4). These cells are destroyed in the autoimune disease insulin-dependent diabetes mellitus, and one of the major antigens is GAD. GAD has some amino acid sequence identity with a coxackievirus polypeptide, and it has been proposed that IDDM may result from molecular mimicry between the virus and GAD (5).

2. GABA Receptors

2.1. GABA$_A$ Receptors

GABA$_A$ receptors are ligand-gated ion channels. When GABA binds to specific recognition sites on the receptor, this triggers a conformational change leading to opening of the intrinsic anion channel allowing chloride ions to flow through into the cell. This opening of the ion channel is transient (10s of milliseconds). Two molecules of GABA must bind to open the ion channel. GABA$_A$ receptors are members of a larger ligand gated ion channel family, which contains nicotinic acetylcholine receptors, strychnine-sensitive glycine receptors, and 5-HT3 receptors. To date, the mammalian GABA$_A$ receptor gene family consists of 15 subunits (a1–a6, b1–b6, g1–g3, d, e, q)(6, 7). b4 and g4 have been identified in avain brain (8). Three other subunits, r1–r3, have also been identified. They are expressed primarily in the retina and have a pharmacology that differs from $GABA_A$ receptors. As such, there are suggestions that they be classified as $GABA_C$ receptors (9). $GABA_A$ receptor subunits are 450 to 550 amino acids in length and have the structural features of the ligand-gated ion channel gene family: a putative signal peptide, a putative large extracellular domain, four putative transmembrane domains, the second of which is thought to line the pore of the channel. The subunits are classified by their relative deduced amino acid sequence homologies; within a group (eg, the a subunits), the subunits are approximately 70% homologous, whereas between groups (eg, a versus b) they are approximately 40% homologous. All the subunits have unique distributions of expression in the brain, and this expression is developmentally controlled (10). The native receptor is formed from the coassembly of the subunits in various combinations, resulting in a family of receptor subtypes. The precise subunit composition of receptor subtypes is not yet known. However, it is likely that most receptors are formed from the coassembly of a and b subunits with either a g, d, or e (or both g and q) subunit (6, 7). The receptor is a pentamer, the subunit stoichiometry of which is probably $(a)_2(b)_2(g)$ or $(a)_2(b)(g)_2$(11, 12)).

$GABA_A$ receptors are the site of action of a number of clinically important drugs including benzodiazepines (prescribed as anxiolytics, anticonvulsants, and sedatives), barbiturates, and general anaesthetics, all of which act through unique allosteric modulatory sites on the receptor, potentiating the action of GABA in opening the channel. The use of transgenic, so called “knock-in” mice has been used to delineate which $GABA_A$ receptor subtypes are responsible for the anxyiolytic properties or the sedative properties of benzodiazepines (13, 14).

$GABA_A$ receptors are also found in insects, at the neuromuscular junction and the nervous system. The subunits that have been identified (eg, *Rdl*) are homologous to vertebrate $GABA_A$ receptor subunits (15). They are the sites of action of a number of insecticides, including dieldrin. Sequencing of the *C. elegans* genome has indicated that the family of putative $GABA_A$ receptor subunits may be quite large (16).

2.2. $GABA_B$ Receptors

These are metabotropic receptors, interacting with a guanine nucleotide binding protein (G-protein) to produce its effect, which are slower than those of the ionotropic $GABA_A$ receptor (17). Activation of the $GABA_B$ receptor can lead to inhibition (or activation) of adenyl cyclase, inhibition of voltage-gated calcium channels or activation of potassium channels (18). There is evidence that $GABA_B$ receptors can be both postsynaptic and presynaptic. The postsynaptic $GABA_B$ receptors, as compared with $GABA_A$ receptors, produce a slow and long lasting inhibition. Presynaptic receptors may act as autoreceptors, acting through a feedback mechanism to reduce the release of neurotransmitter (19). The first cDNA encoding the $GABA_B$ receptor was reported in 1997 (20) and is referred to as $GABA_B1$. Subsequently, a homologous cDNA was identified ($GABA_B2$), which heterodimerizes with $GABA_B1$, and, indeed, the current consensus of opinion is that native $GABA_B$ receptors exist as such heterodimers (21). The receptor polypeptides have seven putative transmembrane domains and have significant amino acid sequence homology with metabotropic glutamate receptor gene family. There is no significant sequence homology with $GABA_A$ receptors or with other G-protein coupled receptors.

Baclofen, a $GABA_B$ receptor agonist, is used in the clinic to treat the spasticity that can result from spinal injury and also multiple sclerosis (22).

3. GABA Transporters

GABA transporters are located primarily on presynaptic terminals and surrounding glia, where they have three main functions: to regulate the concentration and duration of GABA in the synaptic cleft; to prevent the diffusion of the GABA to surrounding synapses; and to take up the GABA, thereby allowing for recycling or metabolizing. They are transmembrane proteins that use sodium and chloride ion cotransport to allow uptake of the GABA against the electrochemical gradient (23). To date, four subtypes of GABA transporter have been identified, GAT-1 (24), GAT-2 (25), GAT-3 (25), and BGT-1 (26). They are members of a larger gene family of neurotransmitter transporters including those for 5-HT, epinephrine, glycine, taurine, proline, and dopamine. The GABA transporters are approximately 600 amino acids long with 12 putative transmembrane domains and exhibit 50% to 70% amino acid sequence identity with each other. They have unique distributions in the brain, with GAT-1 being the most abundant and widespread and GAT-3 being the least abundant, with expression apparently restricted to the leptomeninges (27).

A number of compounds are known that inhibit GABA uptake by acting on GABA transporters. These include Tiagabin, which is an anti-epileptic (28).

Bibliography

1. M. G. Erlander, N. J. K. Tillakaratne, S. Feldblum, N. Patel, and A. J. Tobin (1991) Neuron **7**, 91–100.
2. S. Feldblum, M. G. Erlander, and A. J. Tobin (1993) J. Neurosci. Res. **34**, 689–706.
3. M. Esclapez, N. J. K. Tillakaratne, D. L. Kaufman and A. J. Tobin (1994) J. Neurosci. **14**, 1834–1855.
4. R. L. Sorenson, D. G. Garry, and T.C. Brelji (1991) Diabetes **40**, 1365–1374.
5. D. L. Kaufman, M. G. Erlander, M. Clare-Satzler, M. A. Atkinson, et al (1992) J. Clin. Invest. **89**, 283–292.
6. E. A. Barnard, P. Skolnick, R. W. Olsen, H. Mohler, et al (1998) Pharmacol. Rev. **50**, 291–313.
7. T. P. Bonnert, R. M. McKernan, S. Farrar, B. le Bourdelles, et al (1999) Proc. Natl. Acad. Sci. U.S.A. **96**, 9891–9896.
8. M. G. Darlison and B. E. Albrecht (1995) Semin. Neurosci. **7**, 15–126.
9. G. A. R. Johnston (1996) Trend Pharmacol. Sci. **17**, 319–323.
10. W. Wisden, D. J. Laurie, H. M. Monyer, and P. H. Seeburg (1992) J. Neurosci. **12**, 1040–1062.
11. K. H. Backus, M. Arigoni, U. Drescher, L. Scheurer, et al (1993) NeuroReport **5**, 285–288.
12. Y. Chang, R. Wang, S. Barot, and D.S. Weiss (1996) J. Neurosci. **16**, 5415–5424.
13. U. Rudolph, F. Crestani, D. Benke, B. Brunig, et al (1999) Nature **401**, 796–800.
14. R. M. McKernan, T. W. Rosahl, D. S. Reynolds, C. Sur, et al (2000) Natl. Neurosci. **3**, 587–592.
15. R. H. French-Constant, D. P. Mortlock, C. D. Shafer, R. J. MacIntyre, et al (1991) Proc. Natl. Acad. Sci. U.S.A. **88**, 7209–7213.
16. The C. elegans Sequencing Consortium (1998) Science **282**, 2012–2018.
17. N. G. Bowery (1993) Ann. Rev. Pharmacol. **33**, 109–147.
18. P. Dutar and R. A. Nicoll (1988) Nature **332**, 156–158.
19. S. Thompson, M. Capogna, and M. Scanziani (1993) Trends Neurosci. **16**, 222–226.
20. K. Kaupmann, K. Huggel, J. Heid, P. J. Flor, et al (1997) Nature **386**, 239–246.
21. F. Marshall, K. Jones, K. Kaupmann, and B. Bettler (1999) Trends Pharmacol. Sci. **20**, 396–399.
22. H. Bittiger, W. Froestl, S. Mickel, and H. R. Olpe (1993) Trends Pharmacol. Sci. **1**, 391–394.
23. S. Mager, J. Naeve, M. Quick, C. Labarca, et al (1993) Neuron **10**, 177–188.
24. J. Guastella, N. Nelson, J. J. Nelson, L. Czyzyk, et al (1990) Science **249**, 1303–1306.
25. L. A. Borden, K. E. Smith, P. R. Hartig, T. A. Branchek, and R. I. Weinshank (1992) J. Biol.

Chem. **267**, 21098–21104.
26. A. Yamauchi, S. Uchida, H. M. Kwon, A. S. Preston, et al (1992) J. Biol. Chem. **267**, 649–652.
27. M. M. Durkin, E. L. Gustafson, K. E. Smith, L. A. Borden, et al (1995) Mol. Brain Res. **3**, 7–21.
28. P. M. Crawford, M. Engelsman, S. W. Brown, T. W. Rentmeister, et al (1993) Epilepsia **34**, Suppl. 2, 182.

Suggestions for Further Reading

29. N. J. K. Tillakaratne, L. Medina-Kauwe, and K.M. Gibson (1995) Gamma-aminobutyric acid metabolism in mammalian neural and nonneural tissues. Comp. Biochem. Physiol. **112A**, 247–263.
30. L. A. Borden (1996) GABA transporter heterogeneity: pharmacology and cellular localisation. Neurochem. Int. **29**, 335–356.
31. D. L. Martin and R. W. Olsen (2001) GABA in the Central Nervous System. *Lippincott* Williams and Wilkins, Philadelphia.
32. H. Mohler (2001) *Pharmacology of GABA and Glycine Neurotransmission*. Springer, Berlin.

Gamma-Carboxyglutamic Acid

g-Carboxyglutamic acid residues are found within the highly homologous *N*-terminal domains of various vitamin K–dependent proteins (see Calcium-Binding Proteins). Such residues are generally abbreviated as “Gla”; their structure is depicted in Figure 1. Gla residues are the result of a post-translational modification of glutamic acid residues by a vitamin K-dependent carboxylase, also known as g-glutamyl carboxylase, which introduces a second carboxyl group into the side chain. The two carboxyl groups give this amino acid considerable affinity for cations, especially Ca^{2+}, as in the chelators EDTA and EGTA. This modification is required for the calcium-mediated interaction of the Gla proteins with the negatively charged phospholipid membrane and is also essential for the formation of the native protein conformation.

Figure 1. Molecular structure of a g-carboxyglutamic acid residue.

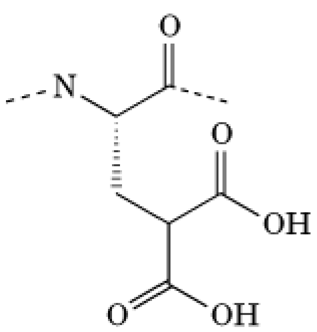

Suggestions for Further Reading

J. W. Suttie (1993) FASEB J. **7**, 445–452 (a concise review of the post-translational modification

of Glu residues to Gla in vitamin K–dependent proteins).

Gamma-Turns

A gamma-turn is a type of nonregular **secondary structure** in protein structures that causes a change in direction of the polypeptide chain. In the g-turn, a hydrogen bond is formed between the backbone carbonyl oxygen of one residue (*i*) and the backbone amide NH of the residue two positions further along the chain (*i* + 2) (Fig. 1). This (*i*) to (*i* + 2) interaction distinguishes g-turns from b-turns, which have an (*i*) to (*i* + 3) hydrogen bond. There are two types of g-turns, the classic and the inverse, which have different backbone dihedral angles for the (*i* + 1) intervening residue. The two g-turn types are, however, related by an inversion of the signs of the f and y angles (classic: 70° to 85° and –60° to –70°, respectively; inverse: –70° to –85° and 60° to 70°, respectively) (see Ramachandran Plot), so their backbone conformations are mirror images of one another. This is analogous to the difference between the type I and I′ and type II and II′ b-turns. The classic g-turn is less common than the inverse type, because of the unfavorable f and y angles, and is found almost exclusively at the ends of **hairpins** (that is, the classic g-turn usually connects two adjacent antiparallel b-strands).

Figure 1. Schematic representation of a g-turn in a protein structure. (**Left**) The g-turn is shown connecting two b-strands in a hairpin motif. (**Right**) The detailed atomic structure of the g-turn is shown. Residues are numbered 1 to 3 for (*i*) to (*i* + 2). The hydrogen bond between the backbone carbonyl oxygen of residue 1 and the backbone amide nitrogen of residue 3 is shown as a dotted line. This example is a classic g-turn, because the backbone angles for the (*i* + 1) residue are f+67° and y–48°. Oxygen atoms and nitrogen atoms are shown as dark spheres. This figure was generated by Molscript (1) and Raster3D (2, 3).

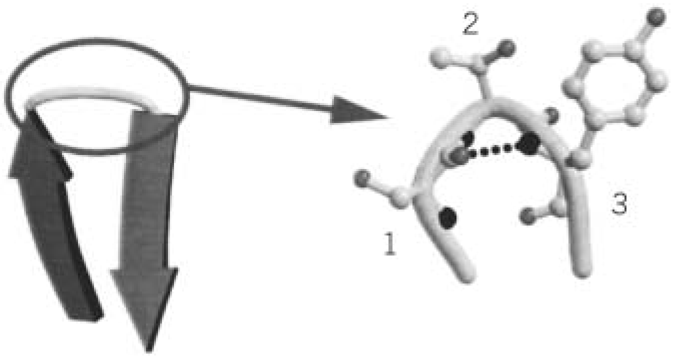

[See also Secondary Structure, Protein, Turns, Beta-Turns and Omega Loop.]

Bibliography

1. P. J. Kraulis (1991) J. Appl. Crystallogr. **24**, 946–950.
2. E. A. Merritt and M. E. P. Murphy (1994) Acta Crystallogr . **D50**, 869–873.
3. D. J. Bacon and W. F. Anderson (1988) J. Mol. Graphics **6**, 219–222.

Suggestions for Further Reading

4. G. D. Rose, L. M. Gierasch, and J. A. Smith (1985) Turns in peptides and proteins. Adv. Protein Chem . **37**, 1–109.
5. T. E. Creighton (1993) *Proteins: Structures and Molecular Properties*, 2nd ed., W. H. Freeman, New York.

Gap Junction

Gap junctions are specialized cell junctions, membrane plaques that provide hydrophilic channels for direct intercellular communication. They permit the passive diffusion of molecules of 1000 daltons or less between the cytoplasm of adjacent cells. They do not facilitate the transfer of large polymers, such as polypeptides, RNA, and DNA. Molecules that may pass through gap junctions are such as cyclic AMP, **inositol phosphates**, and **calcium** ions. They thus permit the intercellular transfer of cytoplasmic signals. Gap junctions are widespread in body tissues in both excitable and nonexcitable cells, and they are important in embryonic development.

Ultrastructurally, gap junctions appear as a pair of parallel unit plasma membranes separated by a uniform gap of 2 to 3 nm. Lanthanum infiltration reveals the presence of regularly arranged cross bridges connecting the plasma membranes (1). The junctions are composed of a regular hexagonal array of subunits, the connexons (see text below). In rat hepatocyte gap junctions, the lattice has a unit-cell dimension of 8.5 nm. The intercellular cross bridges are created by pairing of connexons between the plasma membranes of adjacent cells (2).

The connexon is the functional unit of gap junctions. This is a hexameric assembly of proteins called connexins (3) (Fig. 1). Thirteen different connexins are known from rodent tissues. The connexins range in molecular weight from 26,500 to 49,600 daltons (4). They are referred to either by a Greek nomenclature or on the basis of their molecular mass. Thus, connexin a1 is also known as Cx43, having a molecular weight of 43,000. Different connexins show greater or more specific expression in certain tissues and one, Cx38, is predominantly or exclusively expressed in the embryo. Each connexin has four helical transmembrane domains, both the amino and carboxy termini being located in the cytoplasm, and two cytoplasmic and one extracellular loops (5, 6). The third transmembrane domain is amphipathic in character, and it is believed that six of these domains from the subunits of the hexamer form the hydrophilic channel in an assembled connexon (6, 7). Two connexons in the plasma membranes of adjacent cells bind to each other by means of their extracellular loops, thus creating a hydrophilic channel between the cytoplasms of the two cells and allowing the passage of molecules of 1.5 nm or less in diameter. Formation of the gap junction intercellular channel requires a 30° rotation to interdigitate the two apposing connexons (8). Channels formed by a different connexins have differing permeability properties (9), and single-channel conductances vary from 20 to several hundred picosiemens (10). The permeability properties of gap junction channels may be modulated by **phosphorylation** and cytoplasmic calcium concentration and are voltage-dependent (10, 11). Change in the configuration of the subunits is believed to regulate the channel opening, either by blockage or by rotation, so that the channels may be either open or closed (12).

Figure 1. Gap junctions, connexons, and connexin. (**a**) The gap junction provides hydrophilic channels for intercellular communication. Connexons pair between adjacent cells, giving an intercellular gap of 2 nm with a ladder-like appearance to the intercellular space. (**b**) In cross section, each connexon appears as a hollow cylinder, the walls of which are made up of six connexin subunits. (**c**) Connexin is a molecule with four transmembrane domains: its NH_2

and COOH termini inside are the cell, and there are two extracellular and one intracellular loop. (**d**) In the junction plaque, the connexons are arranged in a hexagonal array.

The expression of several connexons in the same individual cells enables the formation of different types of channels, either homotypic channels with identical connexins paired between cells, or heterotypic channels with connexons composed of different connexins paired between cells. Alternatively, individual connexons could be heteromeric; that is, they could be composed of mixtures of connexin subunits. There is evidence that this occurs in some situations, for example, with connexins Cx32 and Cx26 (13). On the other hand, some connexins appear to be incompatible, being unable to link via their extracellular domains to form a channel—for example, connexins Cx43 and Cx40, which are expressed in the heart Purkinje fibers and the ventricular myocardium, respectively (14). This expression pattern is believed to be important in regulating the electrical conducting properties within cardiac muscle. The full functional significance of the different connexin subunits is an important area for future investigation. Connexin mutations are involved in some human diseases. Cx32 mutations are involved in the X-linked form of Charcot–Marie–Tooth syndrome (15), Cx43 in visceroatrial heterotaxia syndrome (16) and Cx26 in hereditary nonsyndromic sensorineural deafness (16). Visceroatral heterotaxia affects left- or right-sided development of the heart. The point mutations involved are believed to involve sites for connexin phosphorylation, implying that these are important for the regulation of connexin function. Null mutations of the connexin Cx43 in mice results in death shortly after birth due to swelling in and blockage of the right ventricular outflow of the heart (17). Other connexin null mutations cause equally specific defects. Thus, mice lacking Cx40 have cardiac conduction abnormalities resembling atrioventricular and bundle branch block (18), absence of Cx37 causes female infertility because failure of oocyte development (19), and mice lacking Cx46 develop cataracts because of proteolysis of lens crystallins (20). Signals transmitted through gap junctions have been implicated in cellular growth control and vice versa in tumorgenic cell lines, consistent with a tumor suppressor function for gap junctions (21). The importance of gap junctional communication in developmental signaling is demonstrated by the severe defects that result from blocking it (22).

Bibliography

1. J.-P. Revel and M. Karnovsky (1967) J. Cell Biol. **33**, 7–12.
2. D. A. Goodenough and N. B. Gilula (1974) J. Cell Biol . **61**, 575–590.
3. E. L. Hertzberg and N. B. Gilula (1979) J. Biol. Chem. **254**, 2138–2147.
4. N. M. Kumar and N. B. Gilula (1996) Cell **84**, 381–388.
5. D. L. Paul (1986) J. Cell Biol. **103**, 123–134.
6. L. C. Milks et al. (1986) EMBO J. **7**, 2967–2975.
7. D. A. Goodenough et al. (1988) J. Cell Biol. **107**, 1817–1824.
8. G. A. Perkins et al. (1998) J. Mol. Biol. **877**, 171–177.
9. J. L. Brissette et al. (1994) Proc. Natl. Acad. Sci. USA **91**, 6453–6457.
10. D. C. Spray (1994). In *Molecular Mechanisms of Epithelial Cell Junctions: From Development to Disease* (S. Citi, ed.), R. G. Landes Company, Austin, TX, pp. 195–215.
11. L. S. Musil et al. (1990) J. Cell Biol. **111**, 2077–2088.
12. P. N. T. Unwin (1987) In "Junctional complexes of epithelial cells." Ciba Found. Symp. **125**, 78–91.
13. K. A. Stauffer (1995) J. Biol. Chem. **270**, 6768–6772.
14. R. Bruzzone et al. (1993) Mol. Biol. Cell **4**, 7–20.
15. J. Bergoffen et al. (1993) Science **262**, 2039–2042.
16. S. H. Britz-Cunningham et al. (1995) N. Engl. J. Med. **332**, 1323–1329.

17. D. P. Kelsell et al. (1997) Nature **387**, 80–83.
18. A. M. Simon et al. (1998) Curr. Biol. **8**, 295–298.
19. A. M. Simon et al. (1997) Nature **385**, 525–529.
20. X. Gong et al. (1997) Cell **91**, 833–843.
21. S. W. Lee et al. (1992) J. Cell Biol. **8**, 295–298.
22. A. E. Warner et al. (1984) Nature **311**, 127–133.

Suggestions for Further Reading

23. D. A. Goodenough, J. A. Coliger, and D. L. Paul (1996) Connexins, connexons and intercellular communication. Annu. Rev. Biochem. **65**, 475–502. (An excellent review.)
24. R. Bruzzone, T. W. White, and D. A. Goodenough (1996) Bioessays **18**, 709–718. (Shorter, but also an excellent review.)

Gap Penalty

Aligned **homologous** protein and **nucleotide sequences** may include gaps inserted in one or more sequences to maximize the sequence similarity. These gaps are called indels and correspond to positions where insertion or deletion mutations have occurred. Superposition of homologous protein structures may reveal quite accurately the sites of indels. However, algorithms that **align sequences** must place the gaps at positions that maximize the score of the sequence alignment (1). Gap penalties are used to limit the number and length of gaps that can be opened in the sequences. The usual cost for inserting a gap is defined as Cost = GOP + Gaplength * GEP. Gaps scored in this way are called "affine gaps." The two parameters in the equation are GOP, the gap-opening penalty, and GEP, the gap-extension penalty. The actual values of the penalties used must be in balance with the scores for aligned sequence segments. The values depend on the sequence nature and length, the number and length of genuine gaps, and the residue exchange values in the mutation matrices that are used to score substitutions. The penalties are usually calibrated by trial and error, although it should be possible to infer a likely value from the residue exchange values (while a formal hidden Markov model (HMM) should use actual gap insertion probabilities). In certain situations, more is known about where gaps are likely to occur—for example, if a tertiary structure is known (2), or if an existing alignment is being used that already has gaps in it. In this case, gap penalties can be varied in a position-specific manner, ie, lowered at sites where gap insertion is more likely. Position-specific gap penalties are applied in alignment-based profile or HMM database searches (3, 4) and in multiple alignments—for example, by the program Clustal W (5).

A variant form of gap penalty, called a "frame penalty," is applied in some algorithms that compare a protein sequence to the three translation reading frames of a nucleic acid strand (6). As well as gap penalties for in-frame gaps, shifts in the reading frame are given an analogous cost composed of a frame-opening penalty (FOP) and a frame-extension penalty (FEP). Customization of the frame penalties can optimize alignment where errors in sequence determination result in frameshifting, or where frameshifts affecting coding sequences arise naturally due to **introns**, RNA Editing, or translational frameshifting. Introns can be crossed if the FEP is set very low. The expressed sequence tag (EST) database entries (7) have high error, and searches at the highest sensitivity require a relatively low FOP.

Optimization of gap penalties is essential for the good performance of sequence alignment algorithms, and users should take the time to conduct their own trials. Default settings cannot be optimal for all situations.

Bibliography

1. S. B. Needleman and C. D. Wunsch (1970) J. Mol. Biol. **48**, 443–453.
2. A. M. Lesk, M. Levitt, and C. Chothia Protein Engng. **1**, 77–78.
3. M. Gribskov, A. D. McLachlan, and D. Eisenberg (1987) Proc. Natl. Acad. Sci. USA, **84**, 4355–4358.
4. A. Krogh, M. Brown, S. Mian, K. Sjölander, and D. Haussler (1994) J. Mol. Biol. **235**, 1501–1531.
5. J. D. Thompson, D. G. Higgins, and T. J. Gibson (1994) Nucleic Acids Res. **22**, 4673–4680.
6. E. Birney, J. D. Thompson, and Toby J. Gibson (1996) Nucleic Acids Res. **24**, 2730–2739.
7. M. D. Adams et al. (1991) Science **252**, 1651–1656.

Gas-Liquid Chromatography

Following the suggestion by Martin and Synge (1) that the mobile phase for partition chromatography could just as easily be a gas, James and Martin (2) introduced gas-liquid chromatography in 1952. In gas-liquid chromatography, the main mechanism of retention is the partition of an analyte, which is introduced into the mobile gas phase between the gas phase and a stationary liquid phase. The latter is deposited upon the surface of small solid particles or on the walls of a capillary column (capillary gas-liquid chromatography). The theory and application of capillary columns were first expounded by Golay (3). It was found that these columns had the advantages of low resistance to gas flow and high efficiencies equivalent to thousands of plates. Analysis of lipids is the best application of (capillary) gas-liquid chromatography in molecular biology. A detailed practical description is beyond the scope of this article, so interested readers are directed to the monograph *Gas Chromatography and Lipids: A Practical Guide* by Christie (4).

Bibliography

1. A. J. P. Martin and R. L. M. Synge (1941) Biochem. J. **35**, 1358–1368.
2. A. T. James and A. J. P. Martin (1952) Biochem. J. **50**, 679–690.
3. M. J. E. Golay (1958) in *Gas Chromatography* (V. J. Coates, H. J. Noebels, and I. S. Fagerson, eds.) Academic Press, New York, pp. 1–13.
4. W. W. Christie (1989) *Gas Chromatography and Lipids: A Practical Guide*, The Oily Press, Ayr, Scotland.

Gastrula, Gastrulation

The gastrula is a stage in early embryogenesis during which the process of gastrulation occurs. After fertilization and the cleavage divisions, a single layer of cells called the **blastula** forms. The blastula may be hollow or filled with yolk. It can also consist of a large disc of cells on top of the embryo derived from large, yolky eggs [see Meroblastic Cleavage]. Regardless of the structure of the blastula, the process whereby the single cell layer gives rise to the three germ layers (endoderm, mesoderm, and ectoderm) is called gastrulation. Gastrulation usually involves changes in cell shape and cell migration. This cell migration can occur as single cells, as in sea urchin gastrulation, or the movement of sheets of cells, as in the involution of cells in fish embryos (a process called epiboly).

Suggestions for Further Reading

B. I. Balinsky (1975) *An Introduction to Embryology*, 4th ed., W. B. Saunders, Philadelphia, pp. 175–178.

S. Shostak (1991) *Embryology: An Introduction to Developmental Biology*, Harper Collins, New York.

S. F. Gilbert (1997) *Developmental Biology*, Sinauer Associates, Sunderland, MA.

L. Wolpert et al. (1998) *Principles of Development*, Oxford University Press, Oxford, U.K.

J. A. Moore (1972) *Heredity and Development*, Oxford University Press, New York.

Gauche Conformation

The mathematical term gauche means not lying in a plane. In stereochemistry, specific conformations that are related by rotation about a single covalent bond between two tetrahedral atoms have been called gauche when none of the substituent atoms lie in the same plane (see Torsion Angle). Conformers where the substituents are staggered, and the torsion angle between the largest substituents on two neighboring carbons is about 60°, are termed gauche (1). These conformers are typically *syn* or *anti* clinal in the more rigorous designation of torsional conformers (see Conformation) (2). The alternative conformations are *anti* and eclipsed. The two gauche conformers and one *anti* conformer about the C4′—C5′ ribose bond of AMP are shown in Figure 1.

Figure 1. The conformations of the three rotameric conformers of 5′—AMP. The first two are gauche because the torsion angle defined by O5′—C5′—C4′—C3′ is between 0 and ±90°. The third conformer is *anti* because this torsion angle is 180°.

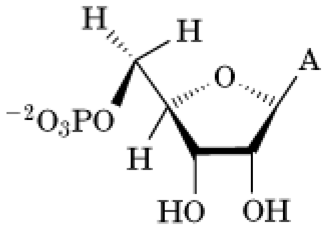

Gauche
−*syn*-Clinal

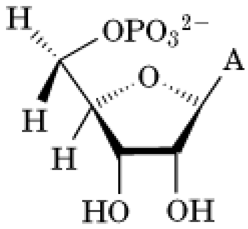

Gauche
+*syn*-Clinal

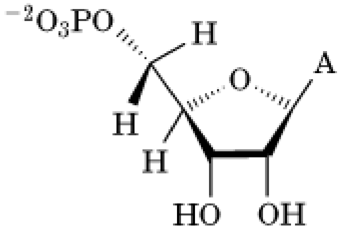

Anti
anti-Periplanar

Bibliography

1. E. L. Eliel et al. (1967) *Conformational Analysis*, Wiley-Interscience, New York, p. 10.
2. W. Klyne and V. Prelog (1960) Experientia **16**, 521.

Suggestion for Further Reading

3. W. Saenger (1984) *Principles of Nucleic Acid Structure*, Springer Advanced Texts in Chemistry (C. R. Cantor, ed.), Springer-Verlag, New York, pp. 14–17.

GC Box

A GC box is a *cis*-acting transcriptional regulatory element (see Transcription Factors, Eukaryotic promoters) that contains the sequence 5′-GGGCGG-3′ at its core and is bound by the transcription factor Sp1. GC boxes are found upstream of a number of genes transcribed by RNA polymerase II and increase the transcriptional rate of the gene above the level that could be achieved by the transcriptional core machinery in the absence of a GC box. Because Sp1 is a ubiquitous factor in eukaryotic cells, the presence of a GC box in a transcriptional regulatory region increases the level of expression of the gene. GC boxes may exist in one or multiple copies, depending on the promoter, and may be found in either orientation relative to the direction of transcription from the downstream initiation site. They are generally found upstream of the transcription initiation site and of the **TATA box**, if a TATA box is present. In some cases GC boxes, acting through the binding of Sp1, have an important role in assembling transcription complexes on promoters without an apparent TATA box.

Gel Electrophoresis

The capacity of electrophoresis to resolve macromolecules differing in size, shape, or conformation ("size separation," **molecular sieving**) is dramatically augmented when it is carried out in gels rather than simply in a buffer. This improvement in resolution arises from two causes: (1) The rate of change of electrophoretic mobility with gel concentration (the "retardation coefficient") is directly related to the size and shape of the molecule (see Ferguson Plot); and (2) the convection and dispersion of a band of macromolecules are much reduced in gels relative to solutions. Since macromolecules (proteins, nucleic acids, and carbohydrates) are the building materials of biology, gel electrophoresis has become a ubiquitous separation method in the molecular biology laboratory. Two types of polymers capable of gelation are universally used: (1) polyacrylamide and (2) agarose. The concentrations of each are selected to achieve effective molecular sieving by tailoring the pore architecture to the dimensions of the charged species to be separated.

One of the key advantages of gel electrophoresis over chromatography is the possibility of varying the gel concentration continuously so as to achieve any effective pore size within a continuum. The average pore size in a gel can range from a fraction of a nanometer (corresponding to the diameter of organic acids) to 50 to 100 nm (corresponding to the diameter of plant **viruses**) and up to nearly a micron. Another benefit of gel electrophoresis is its adaptability to gradients of pore sizes (see Pore Gradient Electrophoresis) and to the simultaneous analysis of samples containing large numbers of components: up to 30 to 50 in gels of a single dimension and up to several thousand in two-dimensional gel electrophoresis.

Gel electrophoresis of multiple samples can be carried out simultaneously on multiple channels of vertically or horizontally oriented gel slabs, using either a single gel concentration or a concentration gradient. This application of gel electrophoresis allows one to compare the mobilities of bands in the various channels of the gel. Such a comparison can give information concerning the identity or nonidentity of two macromolecules, so long as the migration distances are unaffected by differences between the channels in conductance (sample ionic strength, Joule heat dissipation, or wall adherence). When the charge densities of species are equalized, as in the case of nucleic acids or with proteins coated with an ionic detergent (see SDS-PAGE), the rate of migration may depend on primarily the particle size, due to sieving by the gel. Additional and more reliable information concerning the properties of each species in a sample can be derived from gel electrophoresis at multiple gel concentrations (see Ferguson Plot).

To be effective, gel electrophoresis needs to be conducted at an optimized gel concentration and under optimized buffer conditions (see Disc Electrophoresis). The optimal resolving gel concentration is mathematically defined for any particular pair of charged species and can be derived from the Ferguson plots of those species. For large numbers of electrophoretic separations, their automation becomes important. Two kinds of apparatus automatically record and quantify the band pattern: (1) a gel electrophoresis apparatus with an **absorbance spectroscopy** detector at the end of the migration path that records the bands as they pass sequentially, and (2) a horizontal gel slab apparatus equipped with a mobile fluorescence detector that scans the migration path at desired intervals. The latter apparatus type has preparative capacity, which allows for sequential electroelution steps, with simultaneous computation of the recovery, to ensure that it is complete. It is applicable to polymer solutions (see Particle Electrophoresis), as well as gels.

Typically, gel electrophoresis zones are detected by fixation of the band in the gel and staining with a specific dye or an enzyme activity (see Electrophoresis and Overlay Assay: Enzyme Zymography of Plasminogen Activators and Inhibitors). Fixation can be replaced by blotting, which permits additional methods of identification such as hybridization of DNA bands or the immunodetection of proteins bands by **Western blots** .

Suggestions for Further Reading

A. Chrambach (1996) Quantitative and automated electrophoresis in sieving media: Past, present and future. Electrophoresis **17**, 454–464.

D. P. Goldenberg (1997) "Analysis of protein conformation by gel electrophoresis". In *Protein Structure: A Practical Approach*, 2nd ed. (T. E. Creighton, ed.), IRL Press, Oxford, pp. 187–218.

D. Rodbard and A. Chrambach (1971) Estimation of molecular radius, free mobility and valence using polyacrylamide gel electrophoresis. Anal. Biochem. **40**, 95–134.

D. Tietz and A. Chrambach (1987) Computer simulation of the variable agarose fiber dimensions on the basis of mobility data derived from gel electrophoresis and using the Ogston theory. Anal. Biochem. **161**, 395–411.

D. Tietz and A. Chrambach (1992) Concave Ferguson plots of DNA fragments and convex Ferguson plots of bacteriophages: Evaluation of molecular and fiber properties, using desktop computers. Electrophoresis **13**, 286–294.

Gel Retardation Assay

The gel retardation assay, also known as the bandshift assay or electrophoretic mobility shift assay (EMSA), is used to detect DNA-binding proteins in crude cell extracts and to study the binding activity of purified DNA-binding proteins. It is also applicable to the study of RNA-protein interactions. The basis of the assay is that protein–DNA complexes remain intact when gently fractionated by gel electrophoresis and migrate as distinct bands more slowly than the free DNA fragment. The assay is simple and quick, and the use of radioactive binding-site DNA makes it highly sensitive. It can be used for both highly sequence-specific and nonspecific proteins, and nonspecific proteins, such as histones. Gel retardation assays can be used quantitatively to estimate dissociation constants for protein-DNA complexes. Additionally gel retardation experiments can be used to visualize protein–protein interactions between a DNA-binding protein and other non-DNA-binding proteins. The binding of a second protein to a protein-DNA complex to form a triple complex is visualized by a further retardation of mobility that is called a supershift. Supershift experiments can also be used to assay the binding of a second DNA-binding protein to the DNA or the binding of a second molecule of DNA to the protein. The assay is useful for proteins with a DNA association constant $>10^7 M^{-1}$.

A further use of the gel retardation assay is to detect DNA bending induced by a DNA binding protein. This depends on the principle that when a protein binds to a DNA fragment of moderate length (in the range of 100–250 bp) the average distance between the ends of the DNA fragment is decreased and there is a greater resistance to the passage of the complex through the pores of the gel. The extent of the resulting retardation depends on the position of the protein binding to the ends of the fragment. The greatest retardation is observed when the binding site is positioned centrally. By comparison with proteins that induce a bend of known magnitude this method can be used to obtain an estimate of the DNA bend induced by a protein.

Suggestions for Further Reading

B. F. Luisi (1995) articles on "structure of DNA-binding motifs and protein-DNA complexes", A. A. Travers, articles on "DNA bending by sequence and proteins" and M. Bianchi (1995) articles on "HMG domain proteins" in D. M. J. Lilley, ed., *DNA-Protein: Structural Interactions*, Oxford

University Press, pp. 49–75.

P. A. Rice, S. Yang, K. Mizuuchi, and H. A. Nash (1996) Crystal Structure of an IHF-DNA Complex: a Protein-Induced U-Turn, Cell, **87**, 1295–1306.

Z. Otwinowski et al. (1988) “Crystal Structure of trp Repressor/Operator Complex at Atomic Resolution,” Nature **335**, 321–329.

Z. Shakked, et al. (1994) “Determinants of Repressor/Operator Recognition from the Structure of the trp Operator Binding Site,” Nature, **368**, 469–473.

J. G. Omichinski et al. (1997) “The Solution Structure of a Specific GAGA-factor-DNA Complex Reveals a Modular Binding Mode,” Nat. Struct. Biol. **4**, 122–132.

M. Buckle and A. Travers, eds., *Methods: Protein-DNA Interactions* Oxford University Press, in press.

Gelsolin

Gelsolin is an abundant and ubiquitously expressed actin-binding protein, which confers calcium sensitivity to the regulation of the dynamics of the microfilament system (1). There are also high concentrations of a gelsolin isoform in plasma. The latter is a 755-residue protein with an N-terminal extension of 25 amino acid residues. In the presence of micromolar concentrations of Ca^{2+}, gelsolin binds alongside an actin filament, severs it at that site, and then remains bound to the (+)-end on one of the resulting fragments. Gelsolin has two actin-binding sites, and in the presence of Ca^{2+} ions it nucleates filament formation from a solution of G-actin with subsequent (–)-end growth of the polymer. From the minimal 2:1 complex of actin and gelsolin, one of the actin monomers can be released, if Ca^{2+} is removed by EGTA. The second, more tenaciously bound actin monomer can only be released by the binding of PtdIns 4,5-bisphosphate to the gelsolin. Therefore, both polyphosphoinositides and Ca^{2+} ions might be involved in the control of the effects of gelsolin on the turnover in the microfilament system. As shown by gene knockout experiments, gelsolin is not essential for survival. Only limited defects in motility processes have been detected, but overexpression of gelsolin in fibroblasts results in increased motile activity. Gelsolin has recently been shown to be a downstream effector of rac for fibroblast motility (2).

The structure of gelsolin has been studied extensively. It belongs to a family of actin-binding proteins that contain 1–6 repeats of 120–130 amino acid residues. Gelsolin has 6 such structurally related repeats (S1-S6), which may have arisen through gene triplication of a prototype gene, which subsequently went through gene duplication. First, the three-dimensional structure of a complex between actin and subfragment 1 of the cytoplasmic form of gelsolin was solved by crystallography (3), and later the 3D-structure of the entire plasma gelsolin molecule (4). Recently, electron cryomicroscopy and helical reconstruction has been used to identify gelsolin binding sites on filamentous actin (5).

The different parts of the gelsolin molecule appear to have descrete functions. Subfragment 1 binds an actin monomer in the absence of Ca^{2+} and can cap actin filaments. Subfragment S1-S6 also binds actin monomers and competes for the same binding site on actin as fragment S1, but now the binding is Ca^{2+}-sensitive. The S2 domain by itself binds to the side of actin filaments in a Ca^{2+}-independent way. Subfragment S1-S3, can sever actin filaments. Nucleation of actin polymerization can be achieved *in vitro* with S2-S6. Thus, although gelsolin can bind to the side of the actin filament in the absence of Ca^{2+}, further action to sever the actin filament requires the involvement of the Ca^{2+}-

dependent actin binding site. Polyphosphoinositides bind to the S2 domain and dissociate the actin:gelsolin complexes. Despite efforts to determine the gelsolin binding site on F-actin by cryoelectron microscopy and helical reconstructions a convincing mechanism for the severing action of gelsolin has not yet been obtained.

Bibliography

1. H. L. Yin (1987) Bioessays **7**, 176–179.
2. T. Azuma, W. Witke, T. P. Stossel, J. H. Hartwig, and D. J. Kwiatkowski (1998) EMBO J **17**, 1362–1370.
3. P. J. McLaughlin, J. T. Gooch, H.-G. Mannherz, and A. G. Weeds (1993) Nature **364**, 685–692.
4. L. D. Burtnick, E. K. Koepf, J. Grimes, E. Y. Jones, D. I. Stuart, P. J. McLaughlin, and R. C. Robinson (1997) Cell **90**, 661–670.
5. A. McGough, W. Chiu, and M. Way (1998) Biophys. J. **74**, 764–772.

Gene Amplification

A fundamental property of living cells is their orderly transmission of genetic information from generation to generation. One aspect of this property involves a mechanism that controls **genomic** replication and ensures one complete doubling of each replicon during each cell generation. Another aspect of this property is the placement of genes so that they are expressed properly and so that each daughter cell receives the genes in the appropriate configuration. Now it is appreciated that deviations from this principle occur commonly and that amplification of DNA sequences and rearrangement of sequences occur often.

Amplification of DNA sequences, the differential increase in a specific portion of the genome compared with the remainder, occurs during development and during the vegetative growth of cells. The processes of **polyploidization** and endoreduplication, where the entire chromosome complement is multiplied in one nucleus, is not discussed here. Additionally, aneuploidy (or trisomy) can also result in a differential increase in a portion of the genome, but this is distinct from DNA amplification and is not discussed further.

Developmental amplification has been documented extensively in both germ-line cells and somatic cells of many organisms. Clearly these changes in the DNA content of the nucleus of cells are carefully regulated and lead to the appearance of the extra DNA at a predetermined time and, in many cases, the dissipation of this DNA on cue.

Another type of DNA amplification (sporadic) is detected when cells are overcoming adverse environmental conditions. Amplification of this type, usually observed by selection for a desired phenotype, has been found in bacteria, yeast, insects, and vertebrates. Salient features of this amplification process are being studied in several laboratories, and several general characteristics have emerged. These include (*1*) multistep process leading to the generation of highly amplified sequences; (*2*) a karyotype characterized by chromosomal abnormalities; (*3*) a genetic instability of the resistant (amplified) phenotype which may extend into a marked clonal variation among cells; (*4*) a spontaneous rate of detection which varies but (*5*) may be increased by manipulations of the cellular growth conditions (among these, treatment with carcinogens).

Carcinogenesis has been studied since Potts' initial observation that chimney sweeps are prone to scrotal cancer. Several general characteristics of the carcinogenic process have emerged and must be accounted for in any hypothesis addressing the molecular events involved. These include (*1*) the seemingly multistep nature of the process; (*2*) the chromosomal abnormalities (in many cases non-random) that accompany most oncogenic states; (*3*) the clonal variation encountered in tumor cell populations; and (*4*) the ability of the rare (in some cases) process to be markedly increased by physical and chemical agents (known as carcinogens).

These two processes, DNA amplification and carcinogenesis, share several characteristics. Understanding of both are fundamental to our ability to understand how living organisms, single cells or complex organisms, respond to adverse environmental conditions. Several excellent reviews of both processes have appeared in the literature (1-8). This article begins by briefly reviewing programmed and sporadic amplification. The remainder addresses the measurement of sporadic DNA amplification in cells that have begun the carcinogenic process and demonstrate differing tumorigenic potential.

1. Gene Amplification and Development

1.1. In Germ-Line Cells

The earliest suggestion of developmental DNA amplification was made by King in 1908 when she described the extra “chromatin” (associated with forming nucleoli) that arose in the oocytes of the toad Bufo during pachytene (9). Later studies showed that these “masses” contain DNA, and **hybridization** studies demonstrated a great excess of sequences that code for ribosomal RNA (10). This differential synthesis of rRNA genes is correlated with the appearance of hundreds of nucleolar organizers during the pachytene stage of meiosis. Similar examples of this phenomenon are seen in other amphibians, Xenopus, *Rana*, *Eleutherodaclylus*, *Triturus* (10), and in an echuiroid worm, the surf clam (11) and many insects (12). Documentation of rDNA amplification is particularly amenable because the rDNA forms nucleoli, which are distinctive in appearance, and because most rDNA sequences have a relatively high guanosine–cytosine content, which allows separating them from bulk DNA by CsCI density gradient centrifugation. These two aspects of rDNA have been important in recognizing this and other phenomena (magnification and compensation) in which the rDNA copy number changes under various genetic conditions.

The most complete study of oogenic rRNA gene amplification has been made in *Xenopus laevis*. In this animal, the early primordial **germ cells** do not contain amplified rDNA. Amplification is initiated in both oogonia and spermatogonia of the tadpole during sexual differentiation and germ cell mitosis and results in a 10 to 40-fold increase in rDNA genes. The premeiotic amplification is lost at the onset of the meiotic prophase. This loss is permanent in male germ cells but is temporary in female germ cells. Early during the meiotic prophase, the oocyte nucleus undergoes a second burst of rDNA amplification that results in a 1000-fold increase in ribosomal genes (13). The mechanism by which the first extrachromosomal rDNA copies are produced in the premeiotic stage is unknown, although circular structures have been observed (14). Because the number and placement of ribosomal **cistrons** do not change, a mechanism involving disproportionate replication is favored. The second burst of rDNA amplification probably involves a **rolling circle** intermediate. Such structures have been observed by Hourcade et al. (15) and could account for the increase of rDNA in the oocyte during the given period (16). When the oocyte nucleoli are hypotonically disrupted, DNA rings in the shape of beaded circles are visible. Although the rDNA content is constant, the sizes and number of the rings are variable, suggesting fission and fusion of nucleoli during oogenesis (17). The sizes of the circular molecules are integral multiples of a basic unit. Using molecular techniques, it was found that this basic unit is the DNA segment that codes for one precursor rRNA molecule, plus the accompanying nontranscribed spacer region. It is interesting to note that extrachromosomal, circular molecules that contain rDNA are also found at a low frequency (0.05 to 0.15% of the total number of molecules) in *Xenopus* tissue culture cells and in *Xenopus* blood cells (18). The circles are oligomeric lengths corresponding to between one and four rDNA repeat units. The presence of interlocking circles of equal size indicates that the circles are not *in vitro* cyclization artifacts but probably represent free rRNA genes. One question this raises is whether or not free DNA circles carry other genomic sequences or if they are limited to rDNA sequences. It has been suggested that the difference in the state of rDNA between a somatic cell and an amplified germ cell may only be one of degree (14).

The cytological literature contains many other references to extrachromosomal DNA in oocytes. One of the most striking examples is found in dytiscid water beetles, such as *Rhyncosciara*. The nucleus of each oocyte contains a large chromatin mass, termed Giardina's body, in addition to the chromosomal complement. In older oocytes, this DNA is associated with multitudes of nucleoli and contains an increase in rDNA sequences (12). Hence, amplification of rDNA occurs during maturation of the oocyte. However, hybridization studies indicate that only a fraction of the extrachromosomal DNA is rDNA sequences, indicating that other DNA sequences (of unknown function) are also amplified (12).

Although the phenomenon of gene amplification in Tetrahymena, also results in a considerable increase in rDNA sequences, it is somewhat different from that in oocytes described previously. Tetrahymena contain two types of nuclei in each cell, a transcriptionally quiescent **micronucleus** that is responsible for genetic continuity and a macronucleus that is derived from the micronucleus in a developmentally regulated process whereby micronuclear sequences are eliminated, rearranged, and amplified (19-21). Considerable amplification of many micronuclear sequences occurs that results in the macronucleus containing 45 times the haploid amount of DNA. Some of this increase is accounted for by amplification of rDNA sequences, which are present as a single integrated copy in the micronucleus but in 200 copies in the macronucleus (20-22). These amplified rDNA sequences are present as linear, extrachromosomal, **palindromic** molecules (21, 23). The present data favor a model whereby excision of the single rDNA copy is followed by amplification (21).

The amplification, rearrangement, and elimination of sequences is also developmentally regulated to varying extents in the slime molds, Physarum and **Dictostelium** (Zellweger et al., 1972) and in another ciliated protozoan, *Stylonychia* (Prescott and Murti, 1973). Studies of the molecular structures of these amplified DNA sequences have been undertaken and have revealed interesting structures at the termini.

1.2. In Somatic Cells

Gene amplification during differentiation of somatic cells also occurs and again was first detected by morphological criteria. Several regions of the polytene chromosomes in the larval salivary glands of the fly *Rhynchosciara americana* showed a **puffing** response to hormone treatment that was carefully defined both temporally and spatially. These puffs contain greater amounts of DNA than surrounding regions (24). Two of these puffs, characterized at the molecular level, contain a 16-fold increase of DNA sequences that code for peptides used in the synthesis of the cocoon. Amplification and puff formation depend on the developmental stage of the cell and on the cell's position within the gland (25). Puff formation is not peculiar to the salivary gland chromosomes of *Rhynchosciara*, because it has also been observed in the cells of Malpighian tubules and intestinal cells of the same insect. In addition, puff formation has also been observed in different tissues of *Chironmidae*, *Drosophila*, *Sciara*, *Hybosciara* and other diptera (24). In some cases it is thought that it is under hormonal control (26, 27). In *Rhynchosciara* and *Sciara*, the extra DNA remains associated with the original chromosomal site until lysis at pupation (27, 28). In *Hybosciara* and *Sarcophaga*, in contrast, the extra DNA is released as micronuclei from several sites, similar to that released in the oocytes of amphibians (29). It is interesting that several of the bands that puff during the larval stage in *Rhynchosciara* are identical to those bands that are overrepresented in the differentiated chromosomes of *Sciara ocellaris*. This suggests that certain germ-line events observed in *Rhynchosciara* occur in somatic cells of other species (27).

In many cases of differentiation, somatic cells acquire adequate amounts of messenger RNA to produce abundant proteins by accumulating stable mRNA molecules over a period of days. Examples of such are the silk fibroin genes, the ovalbumin genes, and the beta-**globin** genes. It is thought that this is controlled at the transcriptional or posttranscriptional level. In other cases, however, such as during the synthesis of the insect eggshell by the ovarian follicle cells of *Drosophila*, little time is allotted to produce the specific mRNAs that are needed in large quantities. In these latter cases the rates of transcription and translation are not high enough to produce adequate amounts of protein. Spradling and Mahowald (30) found that this need is met by differential amplification of the chorion gene sequences in the ovarian follicle cells. To study the regulation of expression of the chorion gene proteins, they produced complementary DNA clones complementary to egg chamber RNA. In this way they isolated sequences that code for the major endochorion and exochorion proteins, s15, s18, s36, and s38. Using the s36 clone as a probe, they found that these sequences are more abundant in follicle cells during the terminal stages of egg chamber development than in nonovarian tissue. The sequences that code for s15, s18, and s38 were also being specifically amplified during oogenesis. Spradling (31) found that the chorion genes are located on the X-chromosome are in two clusters, s36 and s38, and are amplified 15-fold. The s15 and s18 loci are on the third chromosome and are amplified 60-fold. The genes in both clusters are amplified at the same time and both homologues are amplified equally. Sequences that flank these genes are also disproportionately replicated, but not to as great an extent. This results in a gradient of amplification that spans 90 kbp of DNA, is maximal in the center, and does not display any discrete termination sites. Amplification of the two linked chorion genes s36 and s38 (but not s15 and s18) is reduced in ocellar mutants. The ocelliless phenotype is a pleiotropic mutation characterized by homozygous females and males that totally lack ocelli (simple eyes or photosensitive organs). They also exhibit an abnormal pattern of bristles in the ocellar region of the head. Ocelliless females lack parovaria, an accessory gland of the reproducing tract, and produce abnormal chorions (which surround the egg), which leads to sterility. The ocelliless mutation has been identified as a small chromosomal inversion and has one of its break points lying near the s36 gene (32). In this inversion, the site for initiating DNA replication responsible for amplifying the chorion genes was moved near the other break point. Using cloned probes for the nonchorion genes now present near the end of the inversion, it was found that the gene copy numbers of these sequences were increased. This result suggests that clustering of the chorion genes has biological significance. Developmentally controlled activation of a single **origin of replication** can result in the amplification of several genes.

Changes in the DNA content of the nucleus of germ-line cells and somatic cells during development is common. Amplification of rRNA sequences and others that code for proteins that needed in large amounts during that particular phase of development have been extensively documented. In still other cases, the nature of the amplified DNA cannot be totally accounted for by known sequences, and it probably contains amplified sequences of unknown function. Such sequences have been implicated in the differentiation of the orchid Cynidium (33), the differentiation of peas (34), and in the flowering of the tobacco plant, Nicotiana (35). Further studies are needed to relate these instances of DNA amplification to the overall development of higher organisms.

2. Gene Amplification and Acquisition of a Selected Phenotype

Duplication and amplification of genetic material in cells has long been documented as a means for overcoming deleterious growth conditions. Unlike amplification that is specifically regulated during development, amplification as a means of survival is a more sporadic event whose frequency is often detected at levels much lower than those in developmental amplification.

2.1. Bacteria

The first well-documented example of gene duplications in bacteria that provides an adaptive advantage was seen by Novick and co-workers (36-38). Bacterial strains were grown for long periods of time in limiting concentrations of lactose in the chemostat. The bacterial strains that emerged synthesized four times the maximal normal amount of **beta-galactosidase** . The ability to produce large amounts of enzyme was unstable and could be transferred by conjugation at a time when the lac operon genes were expected to be transferred. It was concluded that the ability to overproduce beta-galactosidase was due to extra copies of the *lac* genes in these strains. The spontaneous rate of duplication was estimated at 10^{-3} and 10^{-4} in a similar system (39). Overproducers that have similar characteristics were subsequently reported for other enzymes, such as ribitol dehydrogenase, b-lactamase (40), and several others (for an excellent review, see Ref. 41). Roth and co-workers demonstrated that duplications up to a quarter of the Salmonella chromosome occur at large homologous segments, such as the rRNA genes (41, 42). Such large duplications depend on the *recA* system. On the other hand, duplications in the range of 10 to 30 kbp are independent of *recA* and do not involve very large homologous segments of DNA (42-44). Edlund and Normark (45) detected tandem duplications of 10 to 20 kbp at the *E. coli* chromosomal *ampC* locus that codes for b-lactamase and confers resistance to ampicillin . After a stepwise selection in increasing concentrations of ampicillin, 30 to 50 copies of the duplications analyzed at the restriction fragment level had different end points. The junction points of the amplified unit in one case was sequenced, and the original duplication occurred at a sequence of 12 bp that was repeated on each side of the *ampC* locus, 10 kbp apart.

Tlsty et al. (46) detected amplification as revertants of certain leaky Lac- mutants. The DNA sequences, which were amplified, contained the *lac* operon and anywhere from 7 to 32 kbp of flanking sequences. These regions were amplified 100-fold. More than 160 independent events were analyzed at the restriction fragment level, and the majority had different end points. These amplifications and as those studied by Normark are not mediated by large homologous sequences (47). Virtually all of the duplications detected and subsequently studied in bacteria have been tandem. Genetic techniques have permitted localizing the end points of these tandem duplications to two different classes of sequences, those composed of large homologous sequences of DNA (such as ribosomal genes or transfer RNA genes in *E. coli*) and those not. The former type may be visualized as occurring by a recombination system for which we have already identified the enzymes. The latter class of duplications raises the question of the lower limits of homology that may be used by such a system, or it raises the possibility that it is a different system entirely that mediates duplications whose end points lack long homologous stretches.

Several bacteriophages also amplify genetic markers. Lambda phage (45), **T4 phage** (48), and **P1 phage** (49) may use mechanisms that parallel those used by viral sequences in mammalian cells. The mechanism is yet unknown.

2.2. Yeast

Resistance to the toxic effects of copper in *Saccharomyces cerevisiae* is mediated by tandem gene amplification of the CUP1 locus (50) but differs from sporadic amplification events characterized in other organisms. The CUP1 locus of yeast codes for a small copper-binding protein. Copper-sensitive strains contain one copy of this locus and, when grown in elevated concentrations of copper, fail to produce resistant derivatives that have a higher gene copy number of CUP1 genes on one chromosome. Infrequently, copper-resistant strains isolated in the laboratory and to carry up to 10 tandem duplications of the CUP1 region, which has 2kbp. Further amplification could be achieved by growing the copper-resistant strains in elevated copper concentrations. The authors postulate that the mechanism of amplification in this instance proceeds by forming a disome for chromosome VIII (which carries the CUP1 locus). Copper-resistant mutants of the sensitive strain are disomic for chromosome VIII. Then, the amplification or tandem iteration could result primarily from subsequent unequal chromosome or sister chromatid exchanges. The formation of a disome may constitute an initial event in the process. Now the system is being used to estimate the frequency of sister chromatid exchanges, unequal crossovers, and gene conversions in this region. The break points occur in the nontranscribed spacer region (51).

A second example of gene amplification in yeast has molecular structures more similar to those described in other organisms. A yeast strain resistant to antimycin A, an alcohol dehydrogenase inhibitor, contains multiple copies of a nuclear gene, ADH4, an isoenzyme of alcohol dehydrogenase. The amplified copies are 42 kbp long, display a linear, extrachromosomal, palindromic structure, and contain **telomeric** sequences. Their structure resembles that of the amplified rDNA genes in the macronucleus of Tetrahymena and related cilliated protozoa, except that the nuclear copy remains within the chromosome. In contrast to that often observed in mammalian amplification (see later), the extrachromosomal copies of this gene are stable during mitotic growth. Amplification of the ADH4 gene is relatively rare (~10^{-10}mutations/cell/generation), and alternative mutations of antimycin A-resistance are in the majority.

2.3. Protozoans

Drug resistance in protozoan parasites is common and presents a serious problem for the chemotherapy of diseases caused by such pathogens as Trypanosoma, Leishmania, and Plasmodium (52-54). Recently, Leishmania strains resistant to the well-known chemotherapeutic agent methotrexate have been isolated and analyzed for their mechanism of resistance. Organisms that are resistant to high concentrations of methotrexate (1mM) have a 40-fold increase in dihydrofolate reductase (DHFR) which in this organism is associated with **thymidylate synthetase** (**TS**). The resistant organisms contain amplified regions of DNA that can be observed directly on **ethidium bromide**-stained gels of restriction enzyme digests. The amplified region is 56 kbp long, has a copy number about 80-fold higher than that of wild-type organisms, and codes for the DHFR-TS genes and other sequences of unknown function (56). Direct visualization of the amplified DNA fragments in this system and the amplified sequences described in the *lac* region of *E. coli* (see previous), provide a valuable advantage in identifying sequences involved in generating a desired phenotype. These sequences may be observed because of the low complexity of the genomic DNA in these organisms. The targets of most drugs used for treating pathogenic protozoans and the targets of many selection protocols in bacteria are unknown. The direct visualization of amplified DNA in these organisms provides a means for obtaining these target sequences and gaining insight into their mechanisms of action.

Recent studies have shown that *Plasmodium falciparum* contains genes analogous to the **multidrug-resistance** (mdr) genes in mammalian cells. Parasites that resist chloroquine are also resistant to other antimalarial drugs, similar to the phenomenon of multidrug resistance seen in human tumors. Wilson et al. engineered a probe using sequences that are conserved in the mammalian P-glycoprotein to identify mdr-like sequences in *P. falciparum* . Their studies showed that drug-resistant parasites contain amplified copies of these specific DNA sequences when compared to their drug-sensitive siblings.

2.4. Invertebrates

Amplification of rRNA genes in *Drosophila* during oogenesis does not occur as has been described in *Xenopus* (see previous section). However, sporadic amplification of the rRNA genes during one generation has been observed under specific genetic conditions. Amplification of the rDNA genes in this situation results in reversion to a wild-type phenotype. Each sex chromosome carries approximately 130 to 150 rRNA genes (56). The phenotype is wild type if the diploid cell carries at least one normal locus (~130genes), whereas the phenotype is altered (bobbed) if the genome carries less than 130 genes (56, 57). The intensity of the bobbed phenotype (slow development, thin chitinous cuticle, reduced body traits, and short bristles) is inversely proportional to the number of genes for rRNA. An increase in rDNA copy number is observed in the progeny of phenotypically bobbed males. It involved rapid accumulation of rDNA at either nucleolus organizer by unknown mechanisms. The rDNA that accumulates during the first generation does not have a noticeable effect on the phenotype of the fly. The phenotypic effects of the magnified rDNA become evident in the F2 progeny if the rDNA is transmitted by males and if the genotype of the F2 generation is characterized again by rDNA deficiencies. In other words, the extra copies of rDNA are eliminated if the amplified fly is crossed with a normal (bb+) female. The phenotypic inheritance of amplified rDNA requires integration and inheritance through the male germ line. Two hypotheses have been proposed to explain rDNA magnification, disproportionate replication of rDNA (58, 59) or unequal sister chromatid exchange (60). Recent experiments demonstrating the decrease of magnification frequency in organisms that carry the rDNA on a ring chromosome strongly suggest unequal crossing over as the mechanism.

Another type of amplification in *Drosophila melanogaster* differs from rDNA magnification in several characteristics. This amplification, called compensation, occurs when one nucleolus organizer of the two homologues is completely deleted (X/O or X/X-no females). In such mutants, the remaining organizer "compensates" for the deletion of the rDNA sequences by a disproportionate replication of the remaining sequences on the intact homologue. Compensation may occur only on the X chromosomal nucleolus organizer, and the extra r-DNA is not inherited in subsequent generations. DNA magnification and compensation differ in several aspects (61): (1) In contrast to rDNA magnification, which restores only wild-type levels of rDNA sequences, compensation reaches values that exceed the rDNA copy number of the nucleolus organizer in the wild-type fly. (2) Gene compensation occurs only on the X chromosomal nucleolus organizer. The Y nucleolus organizer is refractory to compensation. As discussed earlier, amplification may occur on either. (3) rDNA accumulated during compensation is not inherited in subsequent generations as is the rDNA resulting from amplification. Compensation occurs in somatic cells and is not passed along. (4) When a genotype carries only one nucleolus organizer in the diploid chromosome set and the same genotype is partially deleted for rDNA in the remaining nucleolus organizer, the conditions for both compensation and amplification are in place. Genetic studies that compare Xbb^{+}/O flies with Xbb/O flies show a much greater increase in rDNA in the Xbb/O flies, which suggests that magnification and compensation can occur simultaneously. An interaction between homologous chromosomes is a prerequisite for initiating compensation. If two complete nucleolus organizers are on one X chromosome, compensation still occurs.

Using various deficiencies for the X chromosomal heterochromatin, evidence has been presented for the existence of a genetic locus that regulates rDNA compensation (62). This locus, called the compensatory response (cr), is located outside the ribosomal cluster and in the X chromosomal heterochromatic region. The locus acts in *trans* to sense the presence or absence of its partner locus on the opposite homologue. If only one cr locus is present, it acts in *cis* by driving compensation (disproportionate replication) of adjacent rRNA genes. Not all embryos that have the proper genotype undergo compensatory amplification to emerge with an increased number of rRNA genes. Only a small fraction undergoes the putative compensatory amplification. In this respect, the amplification behaves like a mutagenic reversion to restore the functional phenotype.

Resistance to environmental agents, such as pesticides and toxic chemical waste, has been documented in laboratory stocks and natural populations of invertebrates. Selection of *Drosophila* larvae in increasing concentrations of cadmium yields strains that contain duplications of the metallothionein gene (63). The duplication is stably inherited in the absence of selection pressure and produces a corresponding increase in metallothionein messenger RNA. A survey of natural populations found that this is common (64) and may signal the early stages of the evolution of a gene family. The mosquito, *Culex quinquefasciatus*, develops resistance to various organophosphorus insecticides by overproducing the enzyme esterase B1. Molecular studies have demonstrated that the overproduction of the enzyme is the result of amplification of the esterase B1 gene some 250-fold (65). The resistant mosquito was normally developed and could reproduce. This observation raises questions of evolutionary significance for the duplication and amplification at least in invertebrates.

2.5. Plants

DNA changes in plants during response to environmental stress have been reported for flax (see Refs. 66-68). The suggestion that these changes in DNA content are induced by the environment awaits verification by further studies.

2.6. Vertebrates

DNA amplification in mammalian cells was first detected when murine tumor cell populations became resistant to chemotherapeutic drugs. Methotrexate, an often-used chemotherapeutic drug, inhibits the action of dihydrofolate reductase (DHFR), which is required for biosynthesizing thymidylate, glycine, and purines. Stepwise selection of cells in increasing concentrations of methotrexate generates highly resistant cells. Studies based on acquisition of resistance to methotrexate showed several alternative mechanisms of resistance. Cells resistant to the action of the drug had (1) altered the structure of the DHFR enzyme so that the folate analog was not efficiently bound (69-71); (2) altered their transport process so that the drug could no longer enter the cell (72); or (3) overproduced the DHFR enzyme (73, 74). Beidler and Spengler (75) detected chromosomal abnormalities in the cells that overproduce DHFR and suggested that they reflect an increase in gene dosage. Schimke and co-workers obtained a cDNA for the DHFR sequence and showed that the overproduction of DHFR results from amplification of the DHFR DNA sequence (76). Now, it is known that amplification of the DNA sequence coding for the target enzyme of a metabolic inhibitor is a common mechanism for overcoming the growth restriction (2, 77-80).

Among other examples of this phenomenon subsequently found, the best studied was amplification of the CAD gene. The CAD gene codes for a multifunctional protein that catalyzes the first three steps in the synthesis of pyrimidines. The aspartate transcarbamoylase activity is inhibited by the **bisubstrate analog**, *N* -phosphoacetyl-L-aspartate (PALA). PALA-resistant cells overproduce the aspartate transcarbamoylase and also the other two enzymes, carbamoyl synthetase and dihydroorotase (81). Wahl et al. (82) showed that overproduction of these enzymes results directly from amplification of DNA coding for these proteins.

Two other enzyme activities, orotate phosphoribosyl transferase and orotidine-5′-phosphate decarboxylase, are responsible for the final steps of pyrimidine biosynthesis and are encoded in a single polypeptide chain called UMP synthetase. Cells resistant to 6-azauridine or pyrazofurin (toxic pyrimidine analogues that inhibit the decarboxylase) demonstrate a coordinate increase in both of these enzyme activities (83). Overproduction of the two activities is due to amplification of the DNA sequences that code for the UMP synthetase (84, 85). Numerous other instances of DNA amplification have been described when the growth of cells is inhibited by metabolic inhibitors, toxic agents, or altered enzymes that have reduced efficiency. Thus a leaky mutant of hypoxanthine phosphoribosyl transferase amplifies its gene, and growth in cadmium results in amplifying metallothionein (86). Mutant mouse lymphoma cells that overproduce ornithine decarboxylase (up to 15% of total cellular protein) have been generated by selection for resistance to difluoromethylornithine (DFO), an inhibitor of the enzyme. The pseudodiploid wild-type cells become **tetraploid** when resistant to high levels of DFO (87) and amplify the ornithine decarboxylase genes. Compactin-resistant Chinese hamster ovary cells contain a 100 to 1000-fold increase in the amount of 3-hydroxy-3-methylglutaryl coenzyme A reductase, a pivotal enzyme in synthesizing cholesterol (88). Molecular analysis demonstrated that the sequences that code for this reductase are amplified 15-fold in these cells. Similarly, methionine sulfoxine-resistant cells that overproduce glutamine synthetase amplify these sequences. The discovery that multi-drug resistance in cancer chemotherapy is, in some cases, mediated by amplifying the mdr locus has been clinically important (89, 90).

As seen previously, the overproduction of an enzyme activity often indicates amplification of specific sequences. Such overproduction has been described in the resistance of cells to such diverse agents as hydroxyurea, aphidicolin, beta aspartyl hydroxymate, mycophenolic acid, tunicamycin, 5-flourodeoxyuridine (93), and several other drugs (for a comprehensive list and references, see Ref. 2). The demonstration that amplification is the basis of resistance in these cells waits cloning of the target genes in question. Although overproduction of specific enzyme activities often indicates gene amplification, exceptions exist, and each instance of overproduction must be properly analyzed before gene amplification is concluded. An example of this is seen in the studies of arginosuccinate synthetase (AS) overproduction. Canavanine is a toxic analog of arginine but is not an inhibitor of arginosuccinate synthetase. Canavanine-resistant cells overproduce arginosuccinate synthetase enzyme that is no longer subject to metabolic control by exogenous arginine (92, 93). Molecular studies show that this instance of overproduction is not due to amplification of the AS gene (92, 93) but is a regulatory mutation. A compactin-resistant regulatory mutant that overproduces HMG Co A reductase has also been found.

Selection pressure also leads to the amplifying sequences that have initially unknown functions. Baskin and co-workers (94) isolated cell mutants that are reciprocally cross-resistant to four diverse drugs; maytansine, adriamycin, Baker's antifol, and vincristine. The resistance is genetically unstable and is accompanied by the presence of double minute chromosomes (DMs) in the karyotype. These are small chromosomes that lack a centromeric sequence and therefore segregate randomly during mitosis. Genetic instability and the presence of DMs are two manifestations of gene amplification (94). Other cells that are cross-resistant to other structurally diverse and structurally unrelated drugs amplify the cell surface glycoprotein called P-glycoprotein. Resistance to agents, such as colchicine, actinomycin D, puromycin, and in some cases vinblastine, generate overproduction of a 170 kDa glycoprotein that reduces membrane permeability (89, 90).

The acquisition of a specific phenotype does not necessarily have to occur by the classic selection protocols that involve growth in cytotoxic substances. The fluorescence-activated cell sorter (FACS) allows detecting single cells that overproduce products, providing one can monitor the product (see Flow Cytometry). This instrument monitors the fluorescence of individual cells as they pass through a fluorescence detector and sorts out the rare deviant with ease. Johnston et al. (95) used this technique to detect amplification of the DHFR gene without growth in methotrexate inhibitor. Chinese hamster ovary cells were stained under nonselective conditions with fluorsceinated methotrexate, which binds quantitatively to DHFR. The cells exhibit heterogeneity in DHFR content. The cells that contain the highest DHFR content were sorted, grown in nonselective conditions, and reanalyzed. After ten successive rounds of growth and sorting, the population showed a 50-fold increase in fluorescent intensity and amplified the DHFR gene 40-fold. The population was highly resistant to methotrexate.

Using the same concept, Kavathus and Herzenberg (96) isolated mouse L-cells that amplified the human T-cell differentiation antigen, Leu-2. Mouse cells were **transfected** with the herpes simplex thymidine kinase (TK) gene and total human DNA. Transfectants that expressed Leu-2 on their surface (as detected with a fluorescent antibody) were sorted on the FACS. Although most Leu-2 transfectants had a narrow range of antigen density per cell, one showed considerable variability. The brightest cells were sorted again. Six rounds of FACS “selection” for the brightest cells produced cells with a mean fluorescence 40-fold greater than the original transfectant. The karyotype of these cells contained a multitude of DM's. A cDNA library was constructed using mRNA from the amplified Leu-2 transfectant, and the Leu-2 cDNA was identified by differential screening. The mouse line that overproduced Leu-2 antigen was confirmed as having amplified the human Leu-2 DNA sequence (96).

Thus, the FACS instrument dramatically facilitates detecting cells that contain amplified sequences, which might otherwise be overlooked in classical cytotoxic selection experiments. These cells may be detected soon after they are generated, without requiring growth into a visible colony. The FACS detects as little as a twofold increase in fluorescence. This allows identifying and isolating cells that have low or increased transient or unstable levels which be. Any fluorescent probe that quantitatively correlates with a specific molecule or metabolic process allows detecting and sorting cell populations that have successive increases (or decreases) of that tag. Using this concept, one can obtain cell variants that amplify (or delete) genes for which there is no available selective agent. The FACS provides a powerful tool for studying heterogeneity in cellular populations and specific amplification of DNA sequences.

The acquisition of a selected phenotype may often result from selection pressures that are unknown at that time. In these cases a certain phenotype may be accompanied by the manifestations of gene amplification for unknown sequences. Such an instance has been described in studying the sequences that are carried on the DMs and found in the homogeneously staining regions (HSRs) of neuroblastoma cells where these structures were first described. The sequences that are amplified in these lines are cellular “onc” genes, the N-myc oncogene (97). Now, amplification of **oncogenes** has been found in several tumor types containing DMs and HSRs (97) and is discussed later.

As a class of rearrangements, tandem duplications or amplifications cause very little loss of genetic information and are therefore probably not significantly deleterious to the cell. On the other hand, the extra copies are easily dispensed with when they are no longer necessary. This would circumvent any growth disadvantages that may be encountered under normal nutritional or environmental conditions. The only limiting factor in obtaining an amplified DNA sequence is the design of a selection system that allows detecting the sequence in question. This principle can be manipulated as a tool, that is, amplification of unknown gene sequences can be obtained to overcome defined selection conditions. For example, selection of cells that may grow in the continued presence of **DNA damaging** agents may result in some cases in amplification of DNA coding for DNA repair enzymes.

3. General Properties of Mammalian Gene Amplification

There are several characteristics of amplification that many of the systems discussed share in common. To illustrate these characteristics, I describe the general properties of methotrexate-resistant cells that result from amplifying the DHFR gene.

3.1. Multistep Selection to Obtain Highly Amplified Sequences

Classically, mammalian cells that contain amplified DHFR genes were obtained by a stepwise selection for cells that are highly resistant to methotrexate (MTX). Before the advent of cloning, the amplified phenotype was distinguished by overproduction of DHFR enzyme and the karyotypic abnormalities that accompany the overproduction. High methotrexate resistance (by virtue of amplification of the DHFR gene) cannot be obtained by a single-step selection protocol. It is a multistep process. The initial step is rate-limiting because cells that have an increased, but low copy number, are rapidly stepped up to a high level of resistance and a high copy number. When the initial increase in gene copy was examined more closely, Brown et al. (98) and Tlsty et al. (99) found that the stringency of selection is critical in obtaining cells that have amplified DHFR. Cells that amplify DHFR genes as a mechanism of resistance to methotrexate are most readily detected within a defined window of methotrexate concentration for the first step of selection. Growth of the cells above or below this range of methotrexate concentration reduces the frequency with which amplified clones were detected. Not only do incremental increases in drug concentration promote the rapid emergence of resistance, but they also specifically promote the rapid amplification of the DHFR gene (100). A shallow increment of stepwise selection allows for emergence of methotrexate-resistant amplified cells more rapidly than in a relatively large single-step selection protocol.

3.2. Karyotype Abnormalities

The second property of methotrexate resistant cells that have amplified their DHFR gene is the frequent karyotypic abnormalities in the cells. As indicated previously, abnormal chromosomal structures were associated with overproduction of the DHFR in the early studies of Biedler and Spengler (75). They described a marker chromosome in overproducing cells that have an elongated chromosomal arm. The term homogeneously staining region (HSR) was coined to describe a region of this chromosome that bands abnormally when stained with giemsa and, as was subsequently shown, is the site of the amplified DHFR sequences (76). This structure was associated with stable resistance to methotrexate. The resistant phenotype is retained even after subsequent growth in the absence of selection pressure. This is in contrast to the karyotype of cells that are unstably resistant to methotrexate. After extended growth in a nonselective medium, the resistant phenotype (amplification) diminishes rapidly and disappears. HSR structures were not found in unstably resistant cells. Close examination of the karyotype of unstably resistant cells, however, brought to light the presence of double minute chromosomes (DMs). These structures (and HSRs) were described by Balaban-Malenbaum and Gilbert (101) in cell lines obtained from human neuroblastoma. Subsequent work demonstrated that unstably resistant cells contain the amplified copies of DHFR on the double-minute chromosomes (DMs). The lack of centromeric structure in these fragments leads to their random (unequal) segregation at mitosis and a diminished number if selection pressure is no longer exerted on the cells (102).

HSRs are often found at the site corresponding to that of the amplified gene but may also be found at many other chromosomal site or sites. In several instances, multiple HSRs, each of which contain some copies of the amplified DNA sequences, are in one cell. The amplified copies of the target gene may be at the site of the resident gene or in another place or various places in the karyotype. Translocation of the amplified sequences has been observed often (103), and may provide clues about the mechanism of amplification. These translocations may be nonrandom in (see Refs. 104 and 105 for extensive review).

The mechanism leading to the generation of multiple HSRs is not known now. Typically a cell must contain a reasonable increase in gene copy number before an HSR is observed. The degree of amplification and the length of the amplified unit both play an important part in the ability to visualize an HSR. This principle is nicely illustrated by a study where only one of two cell lines, both of which have approximately 50 copies of an amplified sequence, contained a visible HSR. It is postulated that the amplified unit in the other cell line is so short that even a 50-fold reiteration does not make it visible. Similar consideration may be applied to the visualization of DMs. The chromosomal fragments are heterogeneous in size but routinely small and difficult to see. If a cell population has been selected for resistance to a high concentration of an inhibitor, amplification is extensive and DMs are more readily detected. During the initial steps of amplification, when resistance to relatively low concentrations of inhibitors is obtained, only a few DMs may be in any one cell, and visualizing them may be difficult.

The terms stable and unstable resistance are relative designations. Although cells that contain HSR's can lose the amplified gene copies when removed from selective pressure, this occurs at a much slower rate (months) than when amplified sequences reside on DMs (weeks).

What are HSRs and DMs? What is their molecular structure? Are the amplified sequences arranged in tandem configuration, in direct or inverted orientation? The first obstacle in characterizing the amplified unit derives from its large size. The DHFR gene, which is amplified to confer methotrexate resistance, is large: 31 kbp, including introns. The size of the amplified region is greater still. Gross estimates vary from 120 to 1000 kbp as the unit of DNA that is amplified. If one could analyze the end point or end points of the amplified units, information on the structure would emerge. Although the sequence of DNA that needs to be characterized is long, cloning of neighboring fragments (chromosomal walking) has been accomplished by several laboratories in both mouse and hamster models (106-108). The information derived from these endeavors has not provided the desired portrait of the amplified unit because of another obstacle. The amplified structure is continually changing at the molecular level in the chromosomal walking studies described previously. On each amplified cell studied, the amplified sequences correlate with the cloned map only up to a certain point and then diverge. Rearrangements of DNA accompany the amplification of genes, and the basic molecular DNA amplification is obscured by the dynamic aspect of the process. Karyotypic abnormalities are detected only in cells that are highly resistant to a given metabolic inhibitor (i.e., cells that have already progressed through much of the multistep process), although Hamlin and Montoya-Zavala found that the amplified DHFR gene in Chinese hamster ovary cells is uniform in size and exists in head-to-head and head-to-tail tandem repeats.

Recent studies in several laboratories have begun addressing the karyotypic abnormalities that are evident during the initial periods of selection for resistance. In contrast to classical studies on methotrexate drug resistance, where cells were grown for long periods of time in increasing concentrations of drug (stepwise selections), the recent studies are aimed at elucidating the initial molecular events of DNA amplification and have use a single-step selection with the drug. Cells resistant to these relatively low amounts of drug amplify the target sequence to a low extent, 5- to 10-fold (98, 99). DMs and HSRs that have this low copy number are difficult or impossible to detect. Small pieces of extrachromosomal DNA that are not visible with the light microscope have been reported (108-112). Several agents increase the incidence of DNA amplification. As the cells undergo the initial steps of DNA amplification within this period, other manifestations of chromosomal instability are observed, such as increases in the frequency of sister chromatid exchange, endoreduplication, and polyploidization. The production of extrachromosomal DNA has also been detected, but it is transient if selection pressure is not exerted on the cells. Pretreatment with hydroxyurea, ultraviolet light, or methotrexate itself increases the incidence of the initial amplification of the DHFR sequences (98-100). Similar observations were made using an **SV40**-transformed cell system to detect amplification of SV40 sequences (113) (see next section).

3.3. Genetic Instability

A third characteristic of methotrexate-resistant cells that have amplified the DHFR gene is the initial genetic instability of the resistant (amplified) phenotype, which is accompanied by a marked heterogeneity in the population. For example, Chinese hamster ovary cells were grown in 0.02 uM MTX and then analyzed for DHFR content by the FACS (114). The population of cells that emerged after the initial single-step selection showed a heterogeneous spectrum of DHFR content. Cloned cells from various portions of the spectrum were obtained and analyzed for homogeneity of DHFR content and stability of the elevated DHFR levels. CHO cells newly selected for methotrexate resistance are unstable with respect to DHFR levels, and the loss of the elevated DHFR levels was variable in the progeny of different cloned cells. This property of initial instability and heterogeneity is not to be confused with that described previously, in which stable and unstable resistance was associated with HSRs and DMs, respectively. The initial instability is observed in the newly selected population. When these cells are selected for a prolonged period in methotrexate, they have stable, elevated DHFR levels. During subsequent increases in the methotrexate concentration in the medium, the population becomes progressively more heterogeneous with respect to gene copy number. Once the initial increase in gene copy number has occurred, highly methotrexate-resistant populations are subsequently generated more rapidly. When the cells are grown for longer periods under fixed selection pressure (ie, at a constant methotrexate concentration) the population that emerges may contain either stable amplified genes or unstably amplified genes. The initial instability of the amplified DHFR genes in emerging, resistant CHO cells is consistent with the hypothesis that they are present as extrachromosomal pieces of DNA. Stabilization of the resistant phenotype could result from integration of these sequences into the chromosome at the site of amplification or elsewhere in the genome or could result from processes unknown now.

4. Frequency of Sporadic Amplification in Mammalian Cells

In the last few years it has become obvious that the frequency of gene amplification in different cells varies dramatically. Initially, gene amplification was measured in the models that were used to study the phenomenon, established rodent cell lines, such as S180, BHK cells, CHO cells, and 3T6 cells. The earliest type of measurement was colony formation in the presence of a given amount of cytotoxic drug, the clonogenic assay. Resistant colonies that emerged were analyzed for gene copy number. Although a critique of the various methods to measure gene amplification is beyond the scope of this review, it is important to note that the degree of stringency (concentration of the drug) is directly related to the extent of gene amplification. Therefore, incidence calculations that result from selections performed at different stringencies cannot be compared. Reported values for the rodent model systems were 10^{-6} to 10^{-4}. In 1983, Johnston et al. (95), used the flow cytometer and fluoresceinated methotrexate to analyze the emergence of cells that contain elevated DHFR enzyme content from a population that was not under selective pressure. They termed this the “spontaneous” rate of DHFR gene amplification. The emergence of individual cells that have elevated DHFR content was surprisingly high and varied considerably between clones (95). This frequency (10^{-3}) is high, especially when compared with the incidence at which methotrexate resistant colonies emerge (10^{-5}) when measured by the clonogenic assay. In a third method, (119) the entire population of cells was exposed to a stepwise selection and the populations were monitored for the appearance of subpopulations resistant to given concentrations of drug within a given time. All of these methods used rodent cell lines and concluded that amplification could occur at incidences of 10^{-6} or 10^{-4}, or rates that approached 10^{-3} events/cell/generation.

In the 1980s, studies of the frequency of gene amplification took three major directions. One approach was to study the effect of genomic position on amplification, the second was to measure amplification in different cell types and physiological states, and the third sought to identify agents that could increase the frequency of amplification.

4.1. Positional Effects

In an elegant set of experiments, Wahl et al. (116) developed a system to measure the increase in gene copy number of a specified marker placed in different locations in the genome. A CAD minigene was constructed and transfected into a Urd- hamster cell line. They found that the incidence of CAD minigene amplification varied from 10^{-3} to 10^{-3} and that the frequency was heritable. A parallel system (117) produced similar results by transfecting a DHFR minigene into a $DHFR^{-}$ cell line. Both studies concluded that the incidence of gene amplification is influenced by sequences or structures within the genome. Subsequent studies in the Wahl laboratory centered on identifying the *cis*-acting sequences that influence the frequency of gene amplification.

4.2. Nontransformed Versus Transformed Cells

In a second approach, several laboratories have begun examining the incidence of gene amplification in different cell populations. Early results, using the stepwise selection of nonturmorigenic and tumorigenic populations of CHEF cells, suggested that tumorigenic cells could amplify more rapidly than nonturmorigenic cells (115). More recently, using the clonogenic assay at defined stringencies of selection, Otto et al. (118) found a difference in the incidence of amplification between nontumorigenic and tumorigenic cell lines. In both studies, sample size was small (three and six cell lines, respectively), but extending these studies, using the clonogenic assay, to greater than 60 cell lines confirmed that generally highly tumorigenic cells amplify at a greater frequency than nontumorigenic cells. The correlation between assayed tumorigenicity and gene amplification is not strict however, and identification of the variables that help define these frequencies awaits further experimentation.

To date, most studies of gene amplification have used immortalized cell lines and biopsied tumor samples. In two studies, however, the amplification potentials of primary diploid cells, both human and rodent, were examined and compared quantitatively to the amplification potentials of their transformed counterparts. Strikingly, the difference in amplification incidence between "normal" cells and their transformed counterparts (in some cases tumorigenic) is immense (119, 120). The amplification potential was measured at two loci, the CAD gene and the DHFR gene. Quantitative data for both normal ($<2\times10^{-8}$) and transformed cell lines (10^{-4}) indicated a difference in frequency greater than four orders of magnitude (120). In one study, the generation of oubain resistance in both diploid and tumorigenic human cell lines was also measured to control for the ability to detect mutants. Although the rates of generating point mutations were identical, the generation of gene amplification at the CAD locus differed by at least four orders of magnitude. These studies suggest that there is some fundamental difference between normal cells and transformed cells that affects their ability to amplify.

In summary, these studies indicate that diploid cells lack a detectable frequency of gene amplification, whereas tumorigenic cells readily amplify DNA sequences. Present studies are designed to determine when the ability to amplify is acquired in converting a normal cell to a **neoplastic** cell and to isolate those molecular factors that regulate the process.

4.3. Enhancement of Amplification

When studies were initiated to identify agents that could increase the frequency of gene amplification, it was estimated that amplification in the rodent model systems occurs in one out of every 10^{5} cells. This is a very infrequent event if one wants to use biochemical or molecular techniques. The literature suggested that treatment of mammalian cells with carcinogenesis leads, among other things, to the production of HSRs and DMs (121). Because these two chromosomal abnormalities are linked to amplified genes, it was logical to test the possibility that treating mammalian cells with carcinogens could cause gene amplification. Studies with prototypical carcinogenic agents, such as UV light and chemical carcinogens, demonstrated that the incidence of gene amplification is increased by pretreatment with these agents (99, 122, 123). Other treatments, metabolic inhibitors, transient inhibitors of DNA synthesis, and hypoxia, could also increase the frequency of gene amplification (see Ref. 4 for a review). Most of these studies used the endogenous DHFR gene as a marker, but some also used other gene loci. In one study, MTX resistance, PALA resistance, and 5-fluorouridine resistance were cell be enhanced by treatment with ara-C, indicating that enhancement of gene amplification is not confined to the DHFR locus (124). Viral sequences also undergo amplification that is enhanced by pretreatment with carcinogenic agents. Lavi and co-workers (113, 125) observed dramatic increases in viral sequences after the cells were treated with agents, such as benzopyrene, aflatoxin, methlymethane sulfonate or a host of other carcinogens. The extent of enhanced of amplification ranged from a few fold to thousandfold. The basis for the enhanced gene amplification by carcinogen pretreatment is not yet known.

5. Considerations for Carcinogenesis

Carcinogenesis is believed to be a disruption of the homeostatic processes that control cell growth. The oncogenes identified to date contribute to this interpretation. Abnormalities in quantity or quality of growth factors, growth factor receptors, signal transducers, and proteins that control entry into the cell cycle have each been implicated in the genesis of neoplastic transformation. In addition, inactivation of those gene products that limit growth are also involved. These **tumor suppressor** activities contribute to the delicate balance that allows cells to grow when needed (tissue replacement, wound healing, etc.) and prevent cell growth when it is unneeded (terminal differentiation, senescence) (8). Mutations in each (or a combination) of these genes accumulates and results in progressive tumorigenicity. Continued accumulation of mutations allow the cells to acquire metastatic properties, such as invasiveness, angiogenesis, and drug resistance. Independent occurrences of these mutations allow tumor formation through alternate pathways (126). The process is believed to be multistep.

Gene amplification can be implicated in carcinogenesis in several different ways. Perhaps the most straightforward connection is the resulting drug resistance that occurs when detoxifying enzymes are overproduced, which is how gene amplification was discovered. The development of drug resistance remains one of the primary problems in fighting neoplasia. Obviously, elimination of drug resistance would do a great deal toward managing the disease. Experiments with tissue culture cells have shown us that a wide variety of loci may be amplified in mammalian cells. The amplification is usually manifested as an overproduction of the protein product that is targeted by the chemotherapeutic agent. Luria–Delbruck fluctuation analysis has demonstrated that amplification occurs spontaneously at a constant rate. It is the selective environment that allows them to be visualized. A study has compared the amplification rate in nontumorigenic and tumorigenic cells and found that the tumorigenic cells amplified the endogenous locus 100 times more than the nontumorigenic cell line (127). Restrictions on the loci that spontaneously amplify have not been encountered. Studies have also shown that more than one locus can be amplified at the same time (108).

The second connection between gene amplification and carcinogenesis involves the HSRs and DMs that have been observed in tumor cells for decades (121). Manifestations of gene amplification, HSRs and DMs have been widely reported in human tumor biopsy samples. Molecular studies have show that in many instances the genes amplified are oncogenes (97). It is assumed that the amplified oncogenes confer a growth advantage on the tumor cells that contain them. In some cases, amplification of specific genes correlates with the progression of some neoplasias. Seeger and Brodeur reported an increased extent and frequency of N-myc amplification in late stage neuroblastomas compared to early stage neuroblastomas. In this disease, the amplification of N-myc is used as a prognostic indicator for the severity of the disease. A similar story is emerging for the neu oncogene and its amplification in breast and ovarian cancer. A major unanswered question in the field of gene amplification is whether a nontransformed cell can ever undergo gene amplification or whether this type of genetic alteration is reserved for transformed cells alone.

The third implication of gene amplification in carcinogenesis relates to its nature. Gene amplification is a type of genetic rearrangement that (in mammals) is found only in tumor cells. Nowell (128) proposed a cellular scenario that accounts for the majority of observations made concerning neoplasia. He hypothesized that (at least in some cases) an early step in this process could be the acquisition of “genetic instability” (128). As the population of cells expands and generates a plethora of heterogeneous cells, subpopulations would emerge from the selective environment in the host and become the substrate for further change. This process could lead to the evolution of a cell population that is well suited to growth in the host tissue and can acquire the molecular characteristics that would lead to malignancy.

Nowell based his hypothesis on several pointed observations: (1) Oftimes, the karyotype of tumorigenic cells is abnormal. Rearrangements, such as deletions, aneuploidy, translocations, and homogeneously staining regions (HSRs) and double minute (DMs) chromosomes (known manifestations of gene amplification) are common. It is often easy to detect changes from the original karyotype. (2) Once a tumorigenic subpopulation emerges, further karyotypic changes are common. If Nowell's hypothesis is correct, elucidation of the molecular mechanism that underlies the continual change could provide a pivotal piece of information in our studies to understand the neoplastic process. To approach this question one could measure one or several of the types of genomic rearrangements that are detected in tumor cells. The hypothesis predicts that normal or nontransformed cells should display this abnormality at a lower frequency (or rate) than tumorigenic cells. This hypothesis has been addressed using gene amplification as the molecular marker for “genetic instability” (115, 118, 120) and, as indicated before, a vast difference in amplification ability exists. These results are consistent with the Nowell hypothesis. In two cases, deletion formation and recombination with an exogenous piece of DNA (Finn et al., 1989), the genetic rearrangement is more common in tumor cells.

6. Summary

The literature suggests that when gene amplification occurs in “normal” tissues, it is developmentally regulated. This evidence is compiled mostly from studies on *Xenopus* and *Drosophila* (see previous section). In higher organisms, the documentation of gene amplification as a developmental event is lacking. At present, we do not know if gene amplification can be developmentally programmed in mammalian cells.

Sporadic amplification occurs in unicellular organisms, such as bacteria and yeast, but it is lacking in the normal somatic tissues of higher eukaryotes. Several reports of sporadic amplification in the germ line cells of several organisms have been reported and shown to be heritable. In all of these cases, the phenotype demonstrated increased resistance to an environmental toxin (64, 65, 129). The extensive documentation of sporadic amplification in neoplastic tissues raises questions about when the neoplastic cell acquires the ability to amplify. Are the changes that initiate neoplasia the same that initiate the ability to amplify? In this regard, the stimulation of gene amplification by agents that cause cancer becomes an important observation. An insult, such as UV light, can initiate cells into the process that leads to tumor formation. Likewise, the same event can initiate and increase amplification frequency in transformed cells. Can these same agents cause gene amplification in “normal” diploid cells? These and similar questions must be answered before we can determine the extent of contributions that gene amplification holds for carcinogenesis.

Bibliography

1. J. L. Hamlin, J. D. Milbrandt, N. H. Heintz, and J. C. Azizkhan (1984) Int. Rev. Cytol. **90**, 31–82.
2. G. R. Stark and G. M. Wahl (1984) Annu. Rev. Biochem. **53**, 447–491.
3. G. R. Stark (1986) Cancer Surv. **5**, 1–23.
4. R. T. Schimke (1988) J. Biol. Chem. **263**, 5989–5992.
5. E. Farber (1984) Cancer Res. **44**, 4217–4223.
6. J. M. Bishop (1987) Science **235**, 305–311.
7. E. R. Fearon and B. Vogelstein (1990) Cell **61**, 567–579.
8. J. A. Boyd and J. C. Barrett (1990) Pharmacol. Ther **46**, 469–486.
9. H. D. King (1908) J. Morphol. **19**, 369–438.

10. J. G. Gall (1968) Proc. Natl. Acad. Sci. USA **60**, 553–560.
11. D. D. Brown and I. B. Dawid (1968) Science **160**, 272–280.
12. J. G. Gall, H. C. MacGregor, and M. E. Kidston (1969) Chromosoma **26**, 169–187.
13. M. R. Kalt and J. G. Gall (1974) J. Cell Biol. **62**, 460–472.
14. A. P. Bird (1978) Cold Spring Harbor Symp. Quant. Biol. **38**, 1179–1183.
15. D. Hourcade, D. Dressler, and J. Wolfson (1973) Cold Spring Harbor Symp. Quant. Biol. **38**, 537–550.
16. J. D. Rochaix, A. P. Bird, and A. Bakken (1974) J. Mol. Biol. **87**, 473–487.
17. C. H. Thiebaud (1979) Chromosoma **73**, 37–44.
18. J. D. Rochaix and A. P. Bird (1975) Chromosoma **52**, 317–327.
19. M. C. Yao and M. A. Gorovsky (1974) Chromosoma **48**: 1–18.
20. M. C. Yao and J. G. Gall (1974) Cell **12**, 121–132.
21. M. C. Yao, E. Blackburn, and J. G. Gall (1978) Cold Spring Harbor Symp. Quant. Biol. **38**, 1293–1296.
22. J. G. Gall and J. D. Rochaix (1974) Proc. Natl. Acad. Sci. USA **71**, 1819–1823.
23. M. C. Yao (1981) Cell **24**, 765–774.
24. M. E. Breuer and C. Pavan (1955) Chromosoma **7**, 371–386.
25. D. M. Glover et al. (1982) Proc. Natl. Acad. Sci. USA **79**, 2947–2951.
26. C. J. Bostock and A. T. Sumner (1978) *The Eukaryotic Chromosome*, North Holland, Amsterdam, pp. 256–259.
27. C. Pavan and B. da Cunha (1969) Genetics (suppl) **61**, 289–304.
28. C. Pavan (1965) Natl. Cancer Inst. Monogr. **18**, 309–323.
29. B. Da Cunha, C. Pavan, C. Morgante, and C. Garrido (1969) Genetics (suppl) **61**, 304–333.
30. A. C. Spradling and A. P. Mahowald (1980) Proc. Natl. Acad. Sci. USA **77**, 1096–1100.
31. A. C. Spradling (1981) Cell **27**, 193–201.
32. A. C. Spradling and A. P. Mahowald (1981) Cell **27**, 203–209.
33. W. Nagl, J. Hendon, and W. Rucker (1972) Cell Differentiation **1**, 229–237.
34. J. Van'T Hof and C. A. Bjerknes (1982) Mol. Cell. Biol. **2**, 339–345.
35. W. L. Wardell (1977) Plant Physiol. **60**, 885–891.
36. A. Novick and T. Horiuchi (1961) Cold Spring Harbor Symp. Quant. Biol. **21**, 239–245.
37. T. Horiuchi, S. Horiuchi, and A. Novick (1963) Genetics **48**, 157–169.
38. T. Horuichi, J. I. Tomizawa, and A. Novick (1962) Biochem. Biophys. **55**, 152–163.
39. J. Langridge (1969) Mol. Gen. Genetics **105**, 74–83.
40. S. Normark et al. (1977) J. Bacteriol. **132**, 912–922.
41. P. Anderson and J. Roth (1981) Proc. Natl. Acad. Sci. USA **78**, 3113–3117.
42. P. Anderson and J. R. Roth (1977) Annu. Rev. Microbiol **31**, 473–505.
43. S. W. Emmons and J. O. Thomas (1981) J. Mol. Biol. **91**, 147–152.
44. S. W. Emmons, V. MacCosham, and R. L. Baldwin (1975) J. Mol. Biol. **91**, 133–146.
45. T. Edlund and S. Normark (1981) Nature **292**, 269–271.
46. T. D. Tlsty, A. M. Albertini, and J. H. Miller (1984a) Cell **37**, 217–224.
47. S. K. Whoriskey et al. (1987) Genes Dev. **1**, 227–237.
48. A. Kozinski et al. (1980) Proc. Natl. Acad. Sci. USA **77**, 5064–5068.
49. J. Meyer and S. Lida (1979) Mol. Gen. Genet. **176**, 209–219.
50. S. Fogel, J. W. Welch, G. Cathala, and M. Karin (1983) Curr. Genet. **7**, 347–355.
51. M. Karin et al. (1984) Proc. Natl. Acad. Sci. USA **81**, 337–341.

52. C. H. Browning (1954) The chemotherapy of trypanosionic infections. Ann. NY Acad. Sci. **59**, 198–213.
53. W. Peters (1974) Ciba Found. Symp. **20**, 309–334.
54. E. M. Rollo (1980) *Drugs Used in the Chemotherapy of Malaria in the Pharmacological Basis of Therapeutics* (A. G. Gilman, L. S. Goodman, and A. Gilman, eds.) Macmillan, New York, 6th ed, pp. 1038–1069.
55. S. M. Beverley, J. A. Coderre, D. V. Santi, and R. T. Schimke (1984) Cell **38**, 431–443.
56. F. M. Ritossa, K. C. Atwood, and S. Spiegelman (1966) Genetics **54**, 819–834.
57. F. M. Ritossa and G. Scala (1969) Genetics **61**, 305–37.
58. F. M. Ritossa (1968) Proc. Natl. Acad. Sci. USA **60**, 509–516.
59. F. M. Ritossa, C. Boncinelli, F. Graziani, and L. Polita (1971) Proc. Natl. Acad. Sci. USA **68**, 1580–1584.
60. K. D. Tartof (1974) Science **171**, 294–297.
61. W. Kunz, C. Grimm, and G. Franz (1982) *The Cell Nucleus*, Academic Press, **Vol. XII**, pp. 155–184.
62. J. D. Procunier and K. D. Tartof (1978) Genetics **88**, 67–79.
63. E. Otto, S. McCord, and T. D. Tlsty (1989) J. Biol. Chem. **264**, 3390–3396.
64. G. Maroni, J. Wise, J. E. Young, and E. Otto (1987) Genetics **117**, 739–744.
65. C. Mouches et al. (1986) Science **233**, 778–780.
66. C. A. Cullis (1983) CRC Crit. Rev. Plant Sci. **1**, 117–131.
67. C. A. Cullis (1977) Heredity **38**, 129–154.
68. C. A. Cullis (1979) Heredity **42**, 237–246.
69. W. F. Flintoff, S. V. Davidson, and L. Siminovich (1976a) Somat. Cell. Genet. **2**, 245–261.
70. W. F. Flintoff, S. M. Spindler, and L. Siminovitch (1976b) In Vitro **12**, 749–757.
71. D. A. Haber, S. M. Beverly, M. L. Kiely, and R. T. Schimke (1981) J. Biol. Chem. **256**, 9501–9510.
72. F. M. Sirotnak, D. M. Moccio, L. E. Kelleher, and L. J. Goutas (1981) Cancer Res. **41**, 4447–4452.
73. F. W. Alt, R. E. Kellems and R. T. Schimke (1976) J. Biol. Chem. **251**, 3063–3074.
74. M. T. Hakala, S. F. Zakrzewski, and C. A. Nichol (1961) J. Biol. Chem. **236**, 952–958.
75. J. L. Biedler and B. A. Spengler (1976) Science **191**, 185–187.
76. F. W. Alt, R. E. Kellems, J. R. Bertino, and R. T. Schimke (1978) J. Biol. Chem. **253**, 1357–1361.
77. C. Tyler-Smith and C. J. Bostock (1981) J. Mol. Biol. **153**, 219–236.
78. B. J. Dolnick et al. (1979) J. Cell. Biol. **83**, 394–402.
79. W. F. Flintoff et al. (1983) Mol. Cell. Biol. **2**, 275–285.
80. P. W. Melera, J. A. Lewis, J. L. Biedler, and C. Hession (1980) J. Biol. Chem. **255**, 7024–7082.
81. T. D. Kempe, E. A. Swyryd, M. Bruist, and G. R. Stark (1976) Cell **9**, 541–550.
82. G. M. Wahl, R. A. Padgett, and G. R. Stark (1979) J. Biol. Chem. **254**, 8679–8689.
83. D. P. Suttle and G. R. Stark (1979) J. Biol. Chem. **254**, 4602–4607.
84. D. P. Suttle (1983) J. Biol. Chem. **258**, 7707–7713.
85. J. J. Kanalas and D. P. Suttle (1984) J. Biol. Chem. **259**, 1848–1853.
86. L. R. Beach and R. D. Palmiter (1981) Proc. Natl. Acad. Sci. USA **78**, 2110–2114.
87. L. McConlogue and P. Coffino (1983) J. Biol. Chem. **258**, 12083–12086.
88. D. J. Chin et al. (1982) Proc. Natl. Acad. Sci. USA **79**, 1185–1189.

89. I. B. Roninson et al. (1984) Nature **309**, 626–628.
90. I. B. Roninson et al. (1984) Proc. Natl. Acad. Sci. USA **83**, 4538–4542.
91. C. Rossana, L. G. Roa, and L. F. Johnson (1982) Mol. Cell. Biol. **2**, 1118–1125.
92. T. S. Su, H. G. O. Bock, W. E. O''Brien, and A. L. Beaudet (1981b) J. Biol. Chem. **256**, 11826–11831.
93. T. S. Su, A. L. Beaudet, and W. E. O''Brien (1981a) Biochemistry **20**, 2956–2960.
94. F. Baskin, R. N. Rosenberg, and V. Dev (1981) Proc. Natl. Acad. Sci. USA **78**, 3654–3658.
95. R. N. Johnston, S. M. Beverley, and R. T. Schimke (1983) Proc. Natl. Acad. Sci. USA **80**, 3711–3715.
96. P. Kavathus and L. Herzenberg (1983) Nature **306**, 385–387.
97. M. Schwab et al. (1983) Nature **305**, 245–248.
98. P. C. Brown, R. N. Johnson, and R. T. Schimke (1983a) Gene Struct. Regul. Dev. 197–212.
99. T. D. Tlsty, P. C. Brown, and R. T. Schimke (1984b) Mol. Cell. Biol. **4**, 1050–1056.
100. H. Rath, T. D. Tlsty, and R. T. Schimke (1984) Cancer Res. **44**, 3303–3306.
101. G. Balaban-Malenbaum and F. Gilbert (1980) Cancer Genet. Cytogenet. **2**, 339–348.
102. R. J. Kaufman and R. T. Schimke (1981) Mol. Cell. Biol. **1**, 1069–1076.
103. B. Trask and J. Hamlin (1989) Genes Dev. **3**, 1913–1925.
104. J. K. Cowell (1982) Annu. Rev. Genet. **16**, 21–59.
105. J. L. Biedler, P. W. Melera, and B. A. Spengler (1980) Cancer Genet. Cytogenet **2**, 47–60.
106. N. A. Federspiel, S. M. Beverley, J. W. Schilling, and R. T. Schimke (1984) J. Biol. Chem. **259**, 9127–9140.
107. J. Zeig et al. (1983) Mol. Cell. Biol. **3**, 2089–2098.
108. E. Giulotto, I. Saito, and G. R. Stark (1989) EMBO J. **5**, 2115–2951.
109. S. M. Carroll et al. (1987) Mol. Cell. Biol. **7**, 1740–1750.
110. B. J. Mauer et al. (1987) Nature **327**, 434–437.
111. G. M. Wahl (1989) Cancer Res. **49**, 1333–1340.
112. D. D. Von Hoff et al. (1988) Proc. Natl. Acad. Sci. USA **85**, 4804–4808.
113. S. Lavi (1981) Proc. Natl. Acad. Sci. USA **78**, 6144–6148.
114. R. J. Kaufman, P. C. Brown, and R. T. Schimke (1981) Mol. Cell. Biol. **1**, 1084–1093.
115. R. Sager, I. Gadi, L. Stephens, and C. Grabowy (1985) Proc. Natl. Acad. Sci. USA **82**, 7015–7019.
116. G. M. Wahl, R. de Saint Vincent, and M. L. DeRose (1984) Nature **307**, 516–520.
117. C. S. Gasser, C. C. Simonsen, and R. T. Schimke (1982) Proc. Natl. Acad. Sci. USA **79**, 6522–6526.
118. E. Otto, J. E. Young, and G. Maroni (1989) Proc. Natl. Acad. Sci. USA **83**, 6025–6029.
119. J. Wright et al. (1990) Proc. Natl. Acad. Sci. USA **87**, 1791–1795.
120. T. D. Tlsty (1990) Proc. Natl. Acad. Sci. USA **87**, 3132–3136.
121. P. E. Barker (1982) Cancer Genet. Cytogenet **5**, 81–94.
122. T. D. Tlsty, P. C. Brown, R. Johnston, and R. T. Schimke (1982) In *Gene Amplification* (R. T. Schimke, ed.), Cold Spring Harbor Laboratory Press, Cold Spring Harbor, New York pp. 231–238.
123. G. Rice, C. Hoy, and R. T. Schimke (1986) Proc. Natl. Acad. Sci. USA.
124. B. Goz, P. Carl, and T. D. Tlsty (1989) Mol. Pharmacol. **36**, 360–365.
125. S. Lavi and S. Etkin (1981) Carcinogenesis **2**, 417–423.
126. L. Foulds (1975) *Neoplastic Development*, Vol. **1**, Academic Press, New York.
127. T. D. Tlsty, B. Margolin, and K. Lum (1989) Proc. Natl. Acad. Sci. USA **86**, 9441–9445.

128. P. Nowell (1976) Science **194**, 23–28.
129. C. Prody et al. (1989) Proc. Natl. Acad. Sci. USA **86**, 690–694.

Gene Cluster

In many cases, functionally related **genes**, each of which codes for a separate protein, are clustered physically on a chromosome in a *gene cluster*. In **bacteria**, the **gene expression** of all members of the cluster can be under the control of a single **promoter**, and a single **operator** controls their expression. This operator and the accompanying cluster of structural genes constitute an integrated topological and functional unit, known as an operon.

In **eukaryotes**, related genes produced by gene duplication are often found clustered on a chromosome. The clusters can be rather complex, ranging from two or a few adjacent related genes, as in the case of the **apolipoprotein** A-1-III and A-IV genes on human chromosome 11, to a tandem array of several hundred identical genes. Well-studied cases of clustering include the genes for globins, the major histocompatibility complex, and **homeotic** proteins. The members of the cluster may acquire slightly different functions or are used in different stages of development, such as fetal and adult hemoglobins.

Gene Dosage

Gene dosage refers to the number of copies of a given **gene** in a cell or in a nucleus. An increase in the gene dosage may result in the production of a higher level of the product of that gene, unless the gene is subject to autonomous regulation. Where sexes differ in the number of sex chromosomes, a dosage compensation effect may keep the levels of expression similar.

Gene Duplication

Gene duplication is the creation of a copy of a **gene** within the (Fig. 1). Genes can be duplicated through several types of mechanisms. Among these are random **breakage and reunion**, **unequal crossing over** (Fig. 2), **retrotransposition** and over**replication**. Gene duplication is a major source of functional genetic diversity. This diversity is achieved through the divergence and the acquisition of new functions of the copies over time (Fig. 1).

Figure 1. Gene duplication. A duplicated copy can acquire a new function or become a pseudogene.

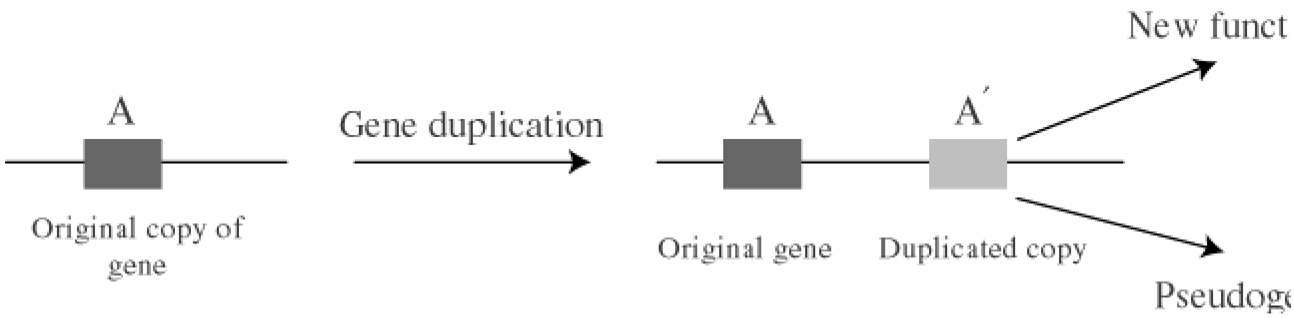

Figure 2. Creation of a gene family through gene duplication by unequal crossing-over.

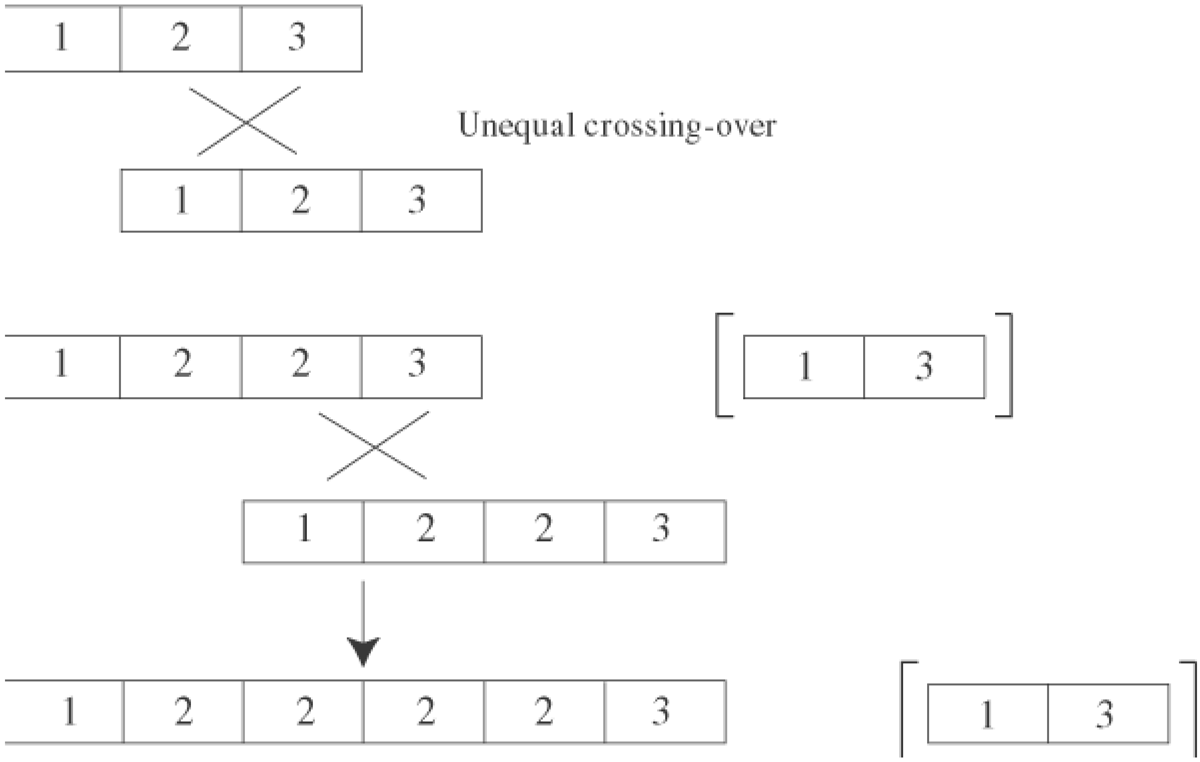

Duplication can involve either genes or , as well as entire , and be either complete or partial. Both genome duplication and gene duplication have been important in evolution. Such duplication generates a related set of genes, or , enabling an increase of genomic diversity by creating new gene functions. It is well known that the genome contains a variety of gene families in a repeated or scattered fashion. These gene families are considered to have emerged evolutionarily from their ancestral form through gene duplication (Fig. 3). Once gene duplication has taken place by unequal crossing over of one chromosome, the other chromosome may lack certain sets of genes. Therefore, it follows that the number of gene members within a particular gene family may have changed during evolution, both increasing and decreasing.

Figure 3. Concerted evolution in gene families of species A and B.

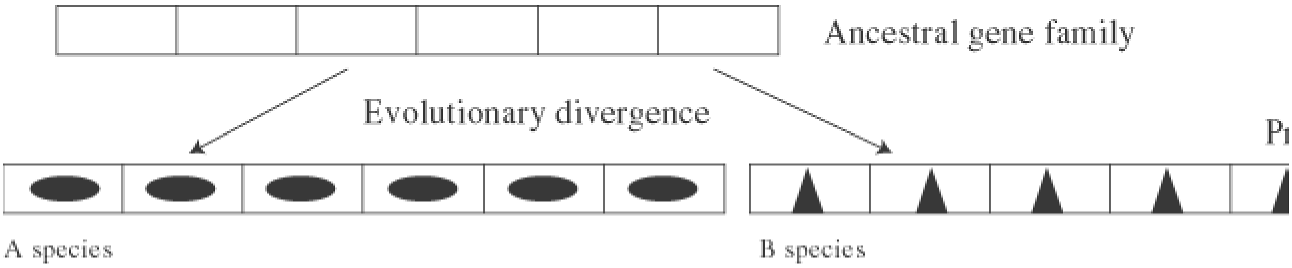

Once a particular nucleotide sustitution takes place in a given gene member, the gene member can pr within the gene family through gene duplication during evolution. When gene duplication takes plac unequal crossing over, propagation of a particular gene member within the gene family in a species i than the evolutionary divergence of the gene families between different species. In this case, the sim different gene members within a given gene family in the same species becomes greater than that be corresponding gene families in different species (Fig. 3). This type of evolution is called "concerted'

Pseudgenes are often created after gene duplication (2). Pseudogenes are dead genes in which a cop gene becomes non-functional due to a mutation-causing malfunction in the DNA sequence (Fig. 1). gene family contains a number of pseudogenes. This is also the case for the **major histocompatibili** gene family. Ohno (3) proposed that one copy of a gene duplication can enjoy the freedom to acquir that differs from the original gene. The original gene can keep its function, even if the counterpart be pseudogene. This theory implies that gene duplication can be an important source of providing new genome.

As the projects for sequencing entire genomes advance, the evolution of genome structure is starting particular attention. It is known that genome size has frequently increased as organisms have evolve increase in genome size, two major alternative hypotheses have been proposed: the genome gradual which asserts that the genome size increased due to the addition of new genes created by gene duplic "genome duplication theory," which contends that the entire genome has been duplicated, resulting i almost doubling in size. Although deletions occur in a part of the genome, the change of gene numbe taken place over an extended period of time.

Bibliography

"Gene Duplication" in , Vol. 2, pp. 977–978, by T. Gojobori; "Gene Duplication" in (online), postin 15, 2002, by T. Gojobori, National Institute of Genetics, Shizuoka, Japan.

1. T. Ohta, (1980) *Evolution and Variation of Multigene Families. Biomathematics*, Springer-Verla
2. W. H. Li, T. Gojobori, and M. Nei, (1981) Nature **292**, 237–239.
3. S. Ohno (1970) *Evolution by Gene Duplication*, Springer-Verlag, Berlin.

Gene Families

Gene families are groups of **genes** with similar sequences that have been derived from a common evolutionary ancestor. Many of the structural genes in eukaryotes are members of gene families. The number of members in a gene family can range from two to hundreds of thousands per . For example, the family has more than 500,000 copies, displaying only minor variation in their nucleotide sequences. A genome can contain hundreds of gene families, and members of a family can be either scattered over several chromosomes or clustered together on a single chromosome.

The multiple genes of a family would be expected to evolve independently. In this case, copies within a species should have the same amount of divergence as those among different species. Those within a species are usually more homogeneous, however, implying that gene family members within a species are not evolving independently and that the family members within a particular species have descended from a common ancestor after species divergence. This would suggest that there are mechanisms for maintaining homogeneity among gene family members. These mechanisms appear to be , **unequal crossing over**, and **gene conversion**. The evolution of gene families through these mechanisms is called concerted evolution. (See).

Research in the area of gene families focuses on questions such as how the copy number of members changes during evolution and how these copies move to different locations. Further research interest in this area includes investigating the effect of copy number changes on gene diversity and identifying what mechanisms preserve similarity among family members (1).

The evolutionary importance of gene families depends heavily on their specific function. In the case of **ribosomal** RNA (rRNA) gene families, for example, it is known that the gene members are highly homogeneous (Fig. 1) (2). This can be explained by the fact that of genes requires a functional ribosome. Thus, all the many gene members in this family are preserved to be highly homogeneous during evolution (3). On the other hand, the form a gene family but are known not to be homogeneous, but relatively heterogeneous. The homeotic genes are directly involved in the control of genes related to the development of organisms. In the case of mammalian homeotic gene families, a single Hox gene cluster generally contains 13 genes, and this gene cluster is repeated four times (3). The nucleotide sequences of all gene members are not homogeneous except a small portion (about 60 codons) of the gene called a **homeobox** (Fig. 2) (5). The heterogeneity among the gene members in this family is due to each gene having a specialized role in their cascade to control the development of organisms.

Figure 1. Animal genomes contain multiple tandem copies of the pre-ribosomal RNA transcription units (2). The three solid boxes of each transcription unit encode the 18 S rRNA, 5.8 S rRNA, and 28 S rRNA genes, respectively.

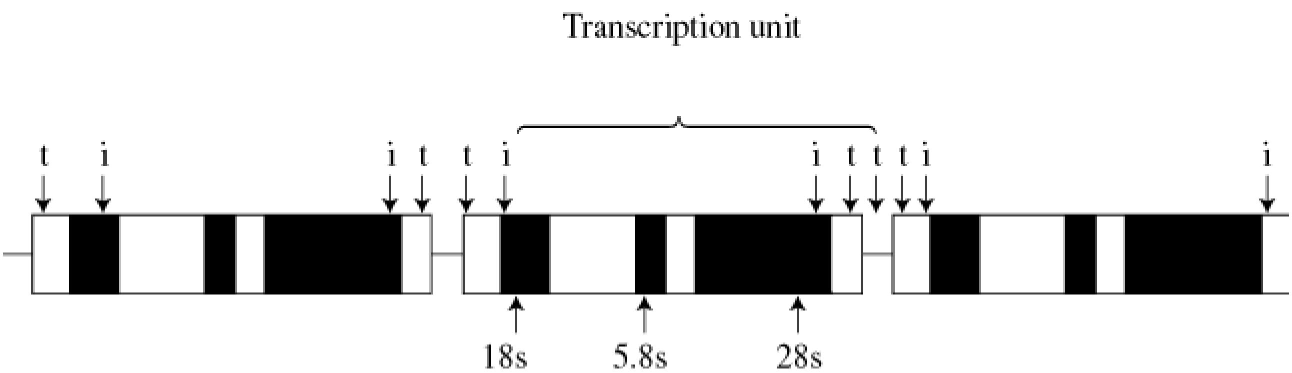

Figure 2. Genomic organization of **Antennapedia** class of **homeobox** genes of humans (5).

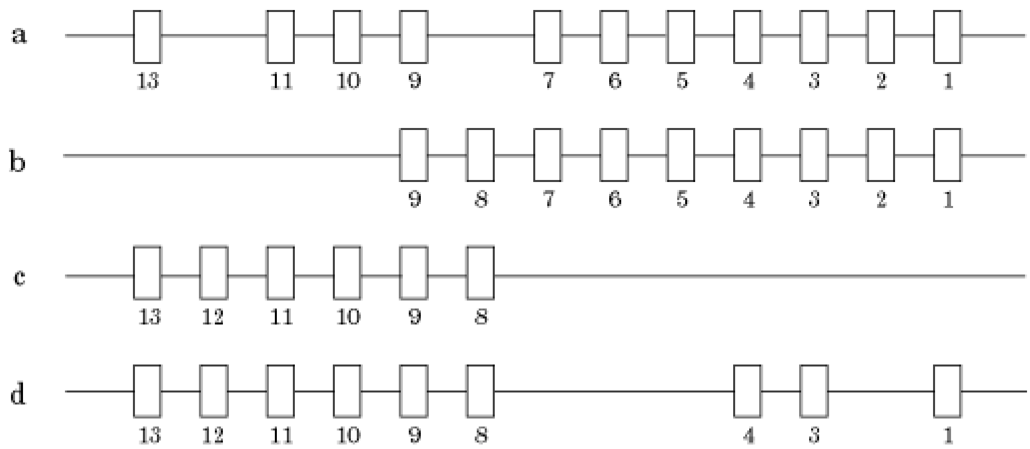

Bibliography
"Gene Families" in , Vol. 2, pp. 978–979, by T. Gojobori; "Gene Families" in (online), posting date: January 15, 2002, by T. Gojobori, National Institute of Genetics, Shizuoka, Japan.

1. T. Ohta, (1980). *Evolution and Variation of Multigene Families*, Springer-Verlag, Berlin.
2. H. Lodish, D. Baltimore, A. Berk, S. L. Zipursky, P. Matsudaira, and J. Darnell, (1995). *Molecular Cell Biology*, 3rd. ed., New York.
3. N. Arnheim, M. Krystal, R. Schmickel, G. Wilson, O. Ryder, and E. Zimmer, (1980). Proc. Natl. Acad. Sci. USA **77**; 7323–7327.
4. C. Kappan and F. H. Ruddle, (1993) Curr. Opin. Gen. Dev. **3**; 931–938.
5. W. H. Li. (1997). *Molecular Evolution*, Sinauer Associates, Sunderland, MA.

Gene Fusion

Gene fusion is a phenomenon in which two different **genes**, or parts of the genes, are fused to each other during evolution, resulting in the creation of a new gene. When two particular genes are compared between two species, they can be fused in one species and separate in the other. To say with certainty that a gene is a fused gene, the separate genes should be identified as being the ancestral form by careful examination.

Unequal crossing over may be one of the molecular mechanisms for causing gene fusion by eliminating chromosomal material between two formerly separate genes. For example, the union in fungi between A and B components of the tryptophan synthetase enzyme (see Operons), which are normally separate in bacteria, is believed to have occurred through such gene fusion events (Fig. 1) (1).

Figure 1. The gene fusion event of A and B components on tryptophan synthetase gene (1).

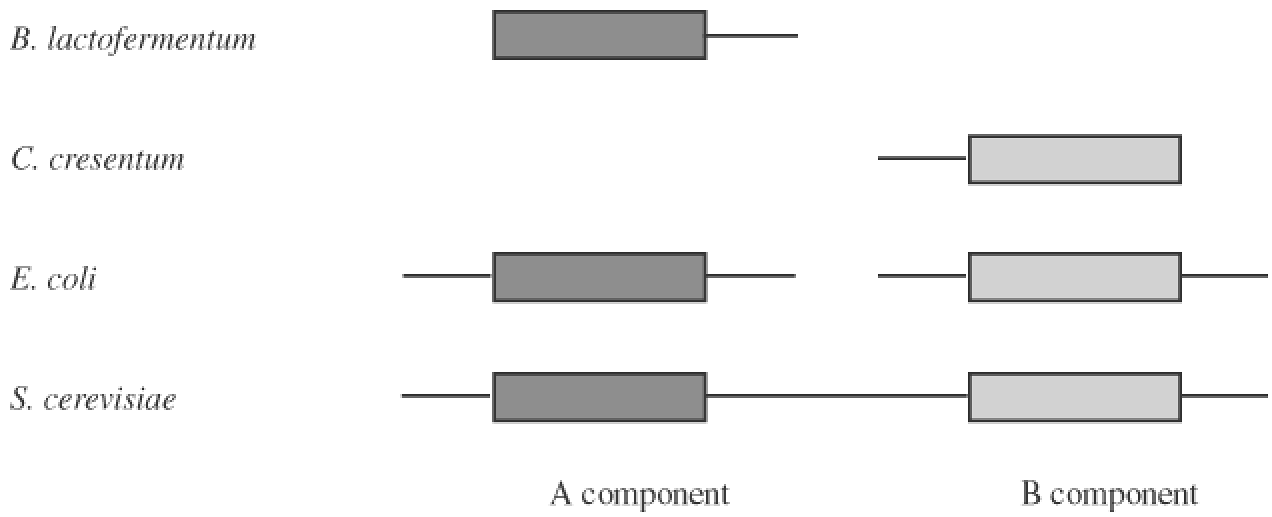

Bibliography

1. D. M. Burns, V. Horn, J. Paluh, and C. Yanofsky (1990) J. Biol. Chem. **5**, 2060–2069.

Gene Rearrangement

The unique feature of immunoglobulin gene organization is that these genes need to be rearranged before becoming functional. These rearrangements allow the immune system to generate a very large repertoire by recombination and random association of a limited number of gene segments (ie, between 200 and 300 in humans), leading to at least 10 million discrete immunoglobulins having different specificities. In the light chains, the **variable region** results from the random association of VL (Vk or Vl) and JL (Jk or Jl) genes. The heavy chains are more complex, because their diversity results from the random association of VH, D, and JH genes. Immunoglobulin genes are rearranged exclusively in the **B-cell** lineage, and these events constitute the hallmark of the B-cell differentiation in the bone marrow. Similarly, genes for the T-cell receptor (TCR) rearrange exclusively in T cells by a very similar process. Ig gene rearrangements require precise signals on the DNA, known as *recombination signal sequences* or (RSSs), that flank each of the V, D, and J gene segments and are recognized by highly specific recombinases encoded by two genes, termed RAG1 and RAG2 (for recombinase activating genes). RSSs consist of two **palindromic** sequences that are highly conserved, although not identical, between the different loci; one is a heptamer and one is a nonamer, separated by a spacer region 12 or 23 nucleotides long (Fig. 1). The two RSSs that participate to a given joint have always spacers of different lengths.

Figure 1. Recombination signal sequences of Ig and TCR genes. (**a**) The 3′ end of a Vk gene is followed by an RSS tha complementary to RSS 5′ of the Jk gene onto which Vk will be connected by the recombinase. (**b**) Schematic organizatic of the RSS in Ig and TCR genes.

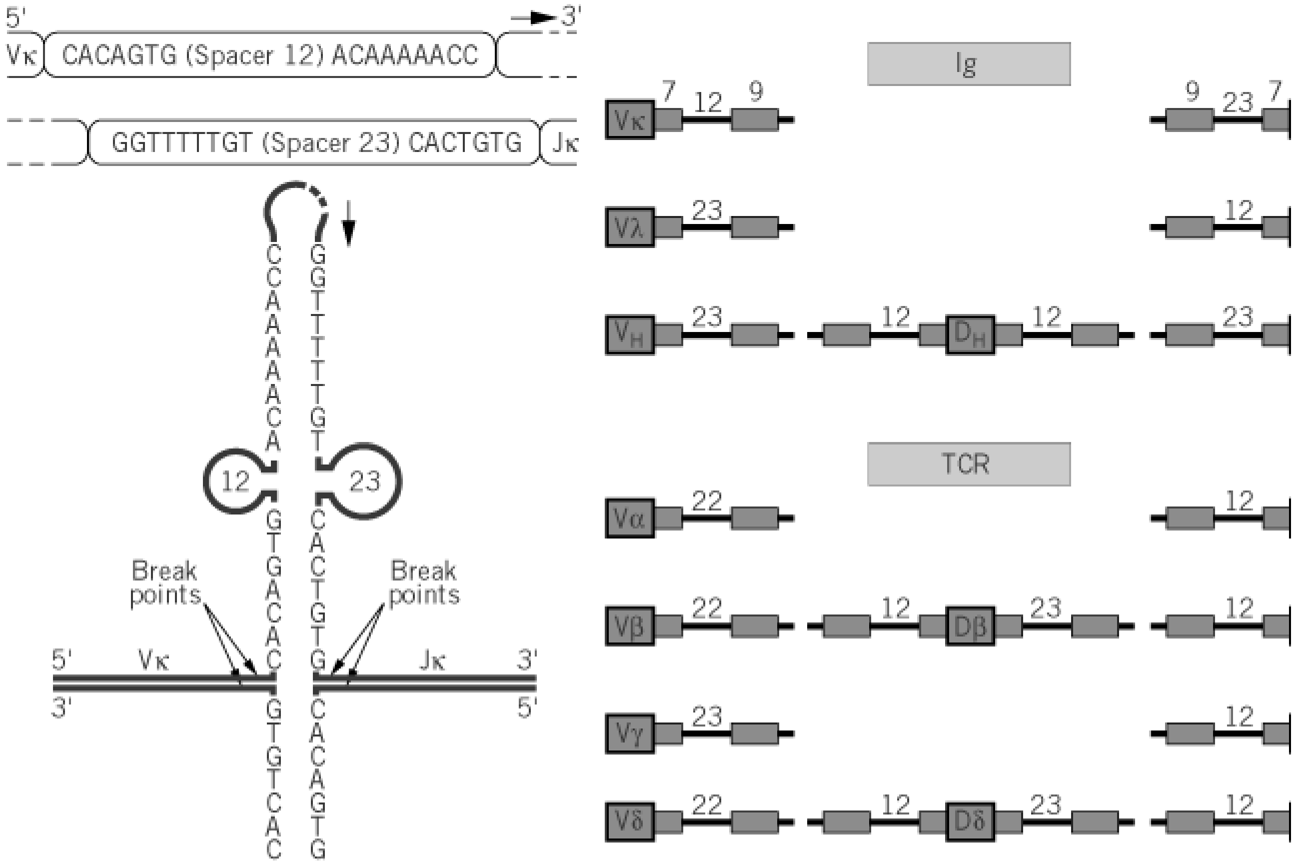

The first recombination event, DH to JH, takes place in the early proB cells and is rapidly followed by the rearrangement of one of the VH segments to D-J. Another enzyme, terminal deoxynucleotidyl-transferase, is also active in proB cells and adds nucleotides in a random fashion during the joining of D to J and of V to D-J rearrangements. Addition of these non-germline-encoded nucleotides is known as N-diversity and considerably amplifies the repertoire, because both the sequence and length of VH and VL complementarity-determining region 3 (CDR3) are modified by this mechanism. Rearrangements are strictly regulated by their end product—that is, the chain they encode once they become functional. Thus, once a m chain is synthesized, it will block the rearrangement of the second IGVH allele. This requires that the m chain be expressed as a membrane protein (mm). In a mouse rendered transgenic for a membrane VDJ-Cm chain gene, endogenous rearrangements at the IGVH locus are blocked, so that B cells will make only the transgenic m. When the same experiment is performed with a VDJ-Cm gene without the M exons (thereby encoding only the soluble form of the m chain), endogenous rearrangements are no longer blocked. The fact that m regulates rearrangement only when expressed as mm strongly suggests that it operates at the cell surface. In fact, mm is coexpressed with the so-called surrogate light chain, composed of the product of two genes, l5 and VpreB, and expressed specifically in proB and preB cells (see B Cell). l5 is highly **homologous** to l and is **disulfide-bonded** to the m chain by its penultimate cysteine residue, whereas VpreB resembles a V Ig domain. The surrogate light chain (YL) has been shown to contribute efficiently to the regulation of allelic exclusion. The negative feedback that prevents the second allele from rearranging is probably a consequence of the turning off of the terminal deoxynucleotidyl-transferase and RAG genes. The RAG genes, but not the transferase, are reactivated as the preB cells cycle and induce light-chain gene rearrangement, with the same hierarchy of control on the second allele whenever the first has rearranged. The IgK locus is activated first. If both k alleles fail to produce a functional rearrangement, the IGL enters the game, with the same type of control. Finally it should be observed that the overall process of rearrangement is not very efficient, with only about 10% final success. This is obviously the price to pay for the complexity and partial randomness of the system.

Once both H and L genes have successfully rearranged, the resulting immunoglobulin is expressed at the B-cell surface. When stimulated by an antigen, specific clones proliferate and colonize the secondary lymphoid organs (lymph nodes, tonsils, spleen, etc.), where they become organized in germinal centers, in close contact with other partners of the immune response (ie, dendritic cells and T cells). Contact with T helper (Th) cells will promote the last step of gene rearrangement, called *isotype switching*, by which the VDJ gene region will be associated with a new constant heavy-chain gene. The classical most frequent switch that occurs in immune responses is IgM → IgG. A schematic example of all the rearrangements that lead to the production of an IgG molecule is given in Figure 2.

Figure 2. Rearrangement events that lead from Ig germline genes to synthesis of IgM and IgG molecules in the mouse model. Recombination first occurs at the IGVH locus, to generate a V(D)J combination (here chosen as VHn–D3–JH4) that is transcribed with Cm and processed as a m mRNA, resulting in the expression of a m chain that will associate with k chain (here Vk1–Jk2–Ck) that results from the second wave of rearrangement targeted at the IGVK locus. IgM is first expressed as a monomer at the cell surface of immature B cell (not shown). After antigenic stimulation, the pentameric form of IgM antibody is secreted by plasma cells and is rapidly replaced by an IgG (here IgG2a), which occurs by class switching (second line from bottom). Note that the switch will not change the VDJ region, so the antibody specificity is maintained.

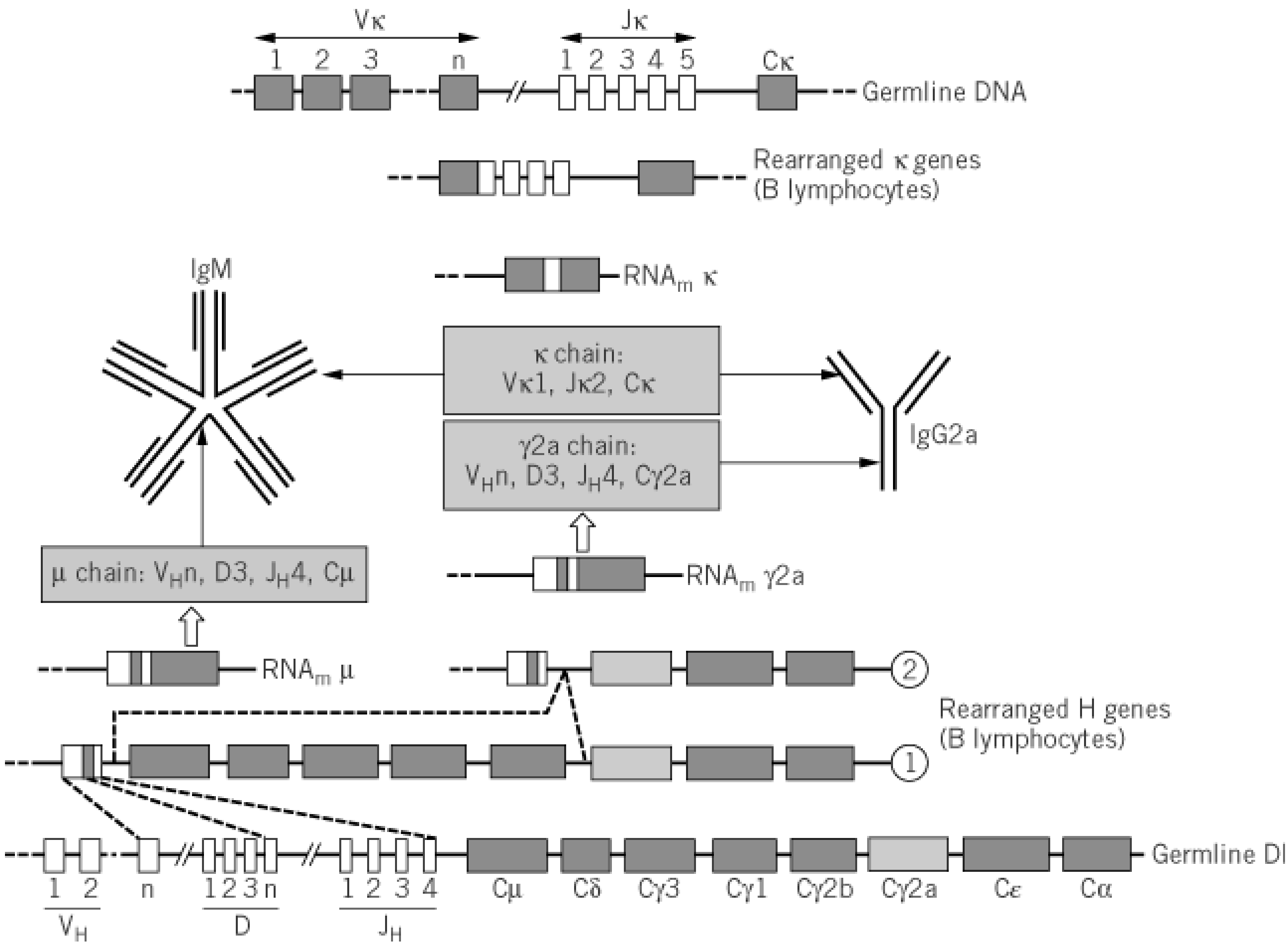

See also entries Recombinase and T-Cell Receptor (TCR).

Suggestions for Further Reading

D. G. Schatz, M. A. Oettinger, and M. S. Schlissel (1993) V(D)J recombination: molecular biology and regulation. Annu. Rev. Immunol. **10**, 359–430.

J. Chen and F. W. Alt (1993) Gene rearrangement and B cell development. Curr. Opin. Immunol. **5**, 194–200.

Gene Recruitment

Gene recruitment is a phenomenon in which a particular **gene** becomes used during evolution as a gene with a totally different function. The term “gene recruitment” was coined because a gene has evolved as if it had been recruited to exhibit a different or another function. The most remarkable example of gene recruitment occurs with the crystallin genes (Table 1). Most of the crystallin genes that are expressed in the eye were found to be expressed in other tissues as enzymes. The exact same gene is expressed and used as a structural protein in one tissue, whereas it is expressed as an enzyme in other tissues. It is now thought that the enzymatic form of this protein should be considered to be the ancestral form and that it became a crystallin by gene recruitment. It seems that change of tissue specificity of gene expression is a prerequisite for gene recruitment.

Table 1. Eye crystallins and Their Relationships to Enzymes and Stress Proteins (1)

Crystallin	Distribution	[Related] or Identical
	Ubiquitous Stress Crystallins	
		Small heat shock proteins (aB)
a	All vertebrates	
		[*Schistosoma mansoni* antigen]
		[*Myxococcus xanthus* protein S]
β γ	All vertebrates (embryonic gnot in birds)	
		[*Physarum polycephalum* spherulin 3a]
	Taxon-Specific EnzymeCrystallins	
d	Most birds, reptiles	Argininosuccinate lyase (d2)
ε	Crocodiles, some birds	Lactate dehydrogenase B
z	Guinea pig, degu rock cavy, camel, llam	NADPH:quinone oxidoreductase
h	Elephant shrews	Aldehyde dehydrogenase I
l	Rabbits, hares	[Hydroxyacyl CoA dehydrogenase]
m	Kangaroos, quoll	[Ornithine cyclodeaminase]

r	Frogs (*Rana*)	[NAPDH-dependent reductases]
t	Lamprey, turtle; moderately abundantin most vertebrates	a-Enolase
S	Cephalopods	[Glutathione *S*-transferases]
W	Octopus	[ALDH]
J	Cubomedusan jellyfish	?

Bibliography

1. G. Wistow (1993) Trends in Biochem. Sci. **18**, 301–306.

Gene Splicing

Many eukaryotic **genes** are split into a number of exons by the existence of **introns**. Gilbert coined the terms "exons" and "introns" in 1978 (1). As shown in Figure 1, (see top of next page) the human a globin gene is split into three exons by two introns. To produce the appropriate messenger RNA, introns must be removed to generate a proper collection of linked exons through gene splicing; as it occurs in the mRNA, it is commonly called RNA splicing. Therefore, in the case of eukaryotic genes, the essential information flow will be as follows; from DNA to mRNA precursor by transcription, from precursor mRNA to mature mRNA by RNA splicing, and from mature mRNA to protein by translation

Figure 1. Gene splicing steps in the production of mature eukaryotic mRNA as illustrated for the human a-hemoglobin g
Gene Splicing).

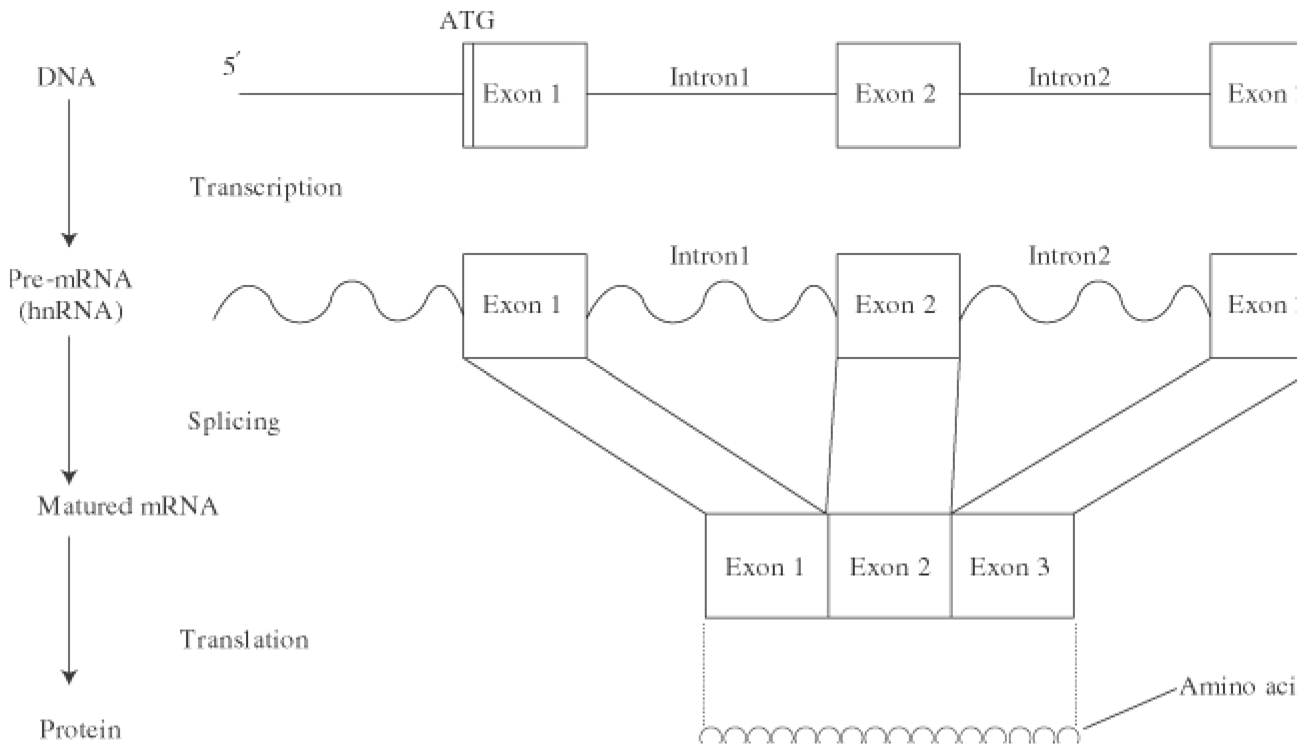

As for the evolutionary significance of the exon–intron structures of genes, the "exon shuffling" theory was proposed by Gilbert (1). He claimed that a variety of genes on the genome have been created by the shuffling and exchange of exons among different genes (1) (see Exon Shuffling). As introns do not possess any apparent function, it is considered that they are used as locations for genetic recombination. Thus, frequent shuffling of exons may have been major forces of gene evolution in eukaryotic organisms. There has, however, been some opposition to the "exon shuffling" theory. For example, the "domain shuffling" theory contends that the unit of shuffling is not an exon but a functional **domain** of a protein that may not correspond exactly to an exon (2). In fact, it is known that the Kringle domain, which is a characteristic supersecondary structure in some serine proteinases, was shuffled many times, and always as a unit, even though the Kringle domain consists of three exons (3).

With only a few exceptions, on the other hand, it is well known that prokaryotic genomes do not contain introns. If an intron is considered to have existed before the **divergence** between eukaryotes and prokaryotes, the splicing mechanism should also have existed for a long time since the early stages of evolution. This is the "early-intron" theory. On the contrary, the "late-intron" theory claims that introns have been inserted as **transposon**-like elements into various genes after the divergence of eukaryotes and prokaryotes. The evolutionary significance of gene splicing depends on which theory is correct.

Bibliography

1. W. Gilbert (1978) Nature **271**, 501.
2. R. Dolittle (1993) Sci. Am. (Oct.) 50–56.
3. T. Gojobori and K. Ikeo (1994) Phil. Trans. Roy. Soc. Lond. B **344**, 411–415.

Gene Structure

A *gene* is widely understood as the fundamental unit of genetic information, but a detailed description of a gene is not straightforward.

1. Intragenic Recombination and Colinearity with Polypeptide Chain

The first step in elucidating the structure of the *gene* was recognizing that it is subdivisible into linearly arranged, individually mutable sites. Until the 1950s it was assumed that genes are both units of function and indivisible units of genetic transmission. The functional criterion for different mutants affected in the same gene, that is **allelic**, was that, when brought together in a **heterozygote** or heterokaryon, they could not make good each other's deficiencies to produce a nonmutant **phenotype**. This criterion is still a good general guide, although, as detailed under Interallelic Complementation, there are circumstances in which it fails. The indivisibility criterion meant that two different mutant alleles of the same gene should not be able to **recombine** to yield a **wild-type** allele. This was sustainable only as long as only moderate numbers of meiotic segregants from heteroallelic **diploids** were screened.

In the fruit fly *Drosophila melanogaster*, M. M Green, working with the *lozenge* gene, and E. B. Lewis, with different genes, including *white*, demonstrated rare crossing over between mutants previously thought to be allelic and dubbed these recombining mutants *pseudoallelic* (1). Then Pontecorvo and his colleagues found that the sexually reproducing fungus *Aspergillus nidulans* produces wild-type recombinants from crosses between several pairs of alleles, with a frequency on the order of 1 in 10,000, and challenged the idea of pseudoallelism, thinking it likely that mutual recombinability is a typical feature of mutants that are allelic in the functional sense. This view was strengthened by Benzer's analysis of hundreds of mutations within the *rII* gene of **bacteriophage** T4, in which he showed that very nearly all pairwise combinations of noncomplementing mutants would yield wild-type virus at some frequency from mixed infection of bacterial cells (2). It was rare for different mutations within the same functional gene to fall at exactly the same site and, when at different sites, they would recombine with one another. It was shown that the same principle holds for the bacteria, *Escherichia coli* and *Salmonella typhimurium*, where the method of analysis was mainly **transduction**, and in fungi and *Drosophila*, where recombination within genes occurred during **meiosis**. In the **yeast** *Saccharomyces cerevisiae* the frequency of intragenic meiotic recombination is unusually high, up to several per cent of meiotic products.

When recombination between allelic mutants was discovered, it became possible to map sites of mutation within a gene in a linear sequence. There are two general ways of doing this. The first uses flanking markers, gene differences that have visible effects (markers) closely placed on each side of the gene under analysis. If intragene recombination is due to classical **crossing over**, the flanking markers occur mainly in one or other of the two "crossed-over" combinations among wild-type interallelic recombination products, depending on which way the mutational sites are placed with respect to the flanking markers. Figure 1 shows an example from the analysis of the *Drosophila rosy* gene by Chovnick *et al.* (3).

Figure 1. Recombination within the *rosy* (*ry*) gene of *Drosophila*, which encodes xanthine dehydrogenase (XDH). Larva recombinant eggs from *ry5*/*ry41* (XDH–) females were automatically selected on purine-containing food, which kills XI parents contributed only mutant *ry*. The constitutions of the eggs with respect to mutations in closely placed flanking ger further test-crosses. The *ry*+ eggs not recombined for the flanking makers are presumed to be due to conversion of one o without crossing over. The high degree of association of 5–41 recombination with one flanking marker crossover class ir *l26*. Data from Ref. 3, whose analysis includes numerous *ry* mutant sites not shown here.

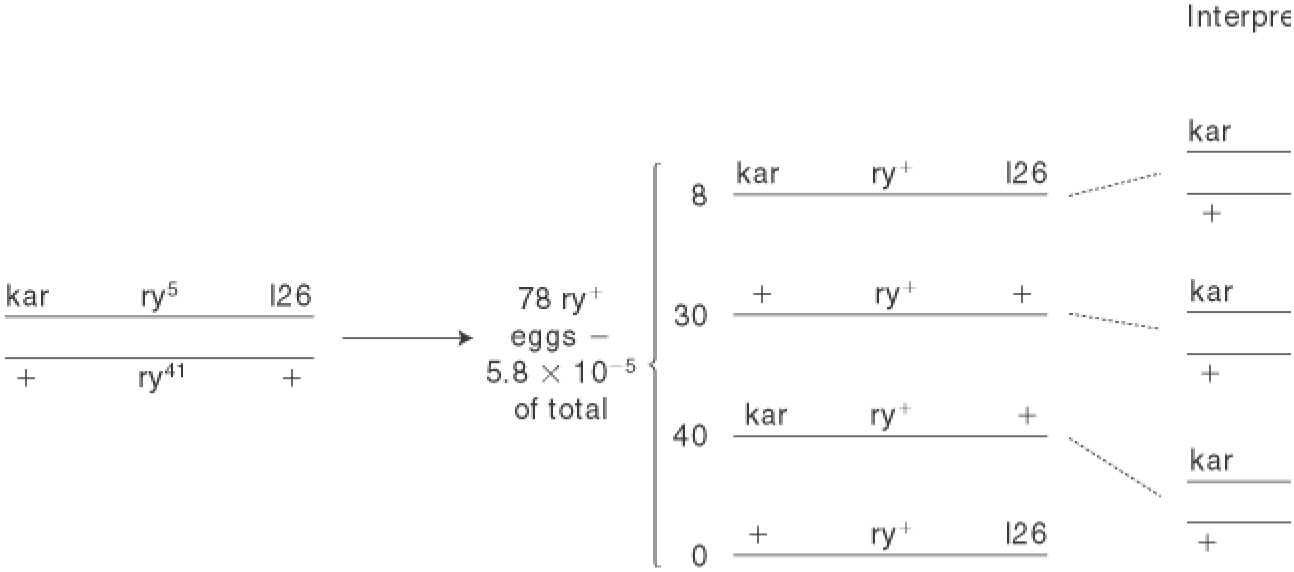

The second method, which gives clear results even when the recombination within the gene is due mainly to **gene conversion** without crossing over, relies on the principle of overlapping deletions. In any very extensive collection of allelic mutations, it is likely that some are due to deletion of segments of the gene, each of which overlaps several mutational sites and partly overlaps other deletions. No point mutation can recombine to form recombinants with a deletion that removes the corresponding nonmutant site, and neither do different deletions yield wild-type recombinants if they overlap. By crossing a suitable set of deletion mutants with each other and scoring the progeny for the presence versus absence of wild-type recombinants, one establishes the overlaps between the deletions, and then, by crossing the whole set to point mutations, localizes the mutational sites to one or other of the segments defined by the deletion overlaps. The method was first used by Benzer in his analysis of the T4 *rII* genes. An example from yeast, the *cyc-1* gene which encodes the protein of the respiratory pigment cytochrome ***c***, is explained in Fig. 2 (4).

Figure 2. Establishment of the sequence of mutant sites within the *Saccharomyces cerevisiae CYC1* gene that encodes cytochrome c. A set of overlapping deletion mutants were each tested for recombination with point mutants: + or – indicates whether or not wild-type recombinants were formed. The absence of recombinants means that the site of the point mutation falls within the segment deleted in the other parent. The deletion overlaps define the sequence of the mutant sites. The amino acid codon affected by each point mutation was determined biochemically. The sequence of codons corresponds to the sequence of mutant sites. From Ref. 4 by permission.

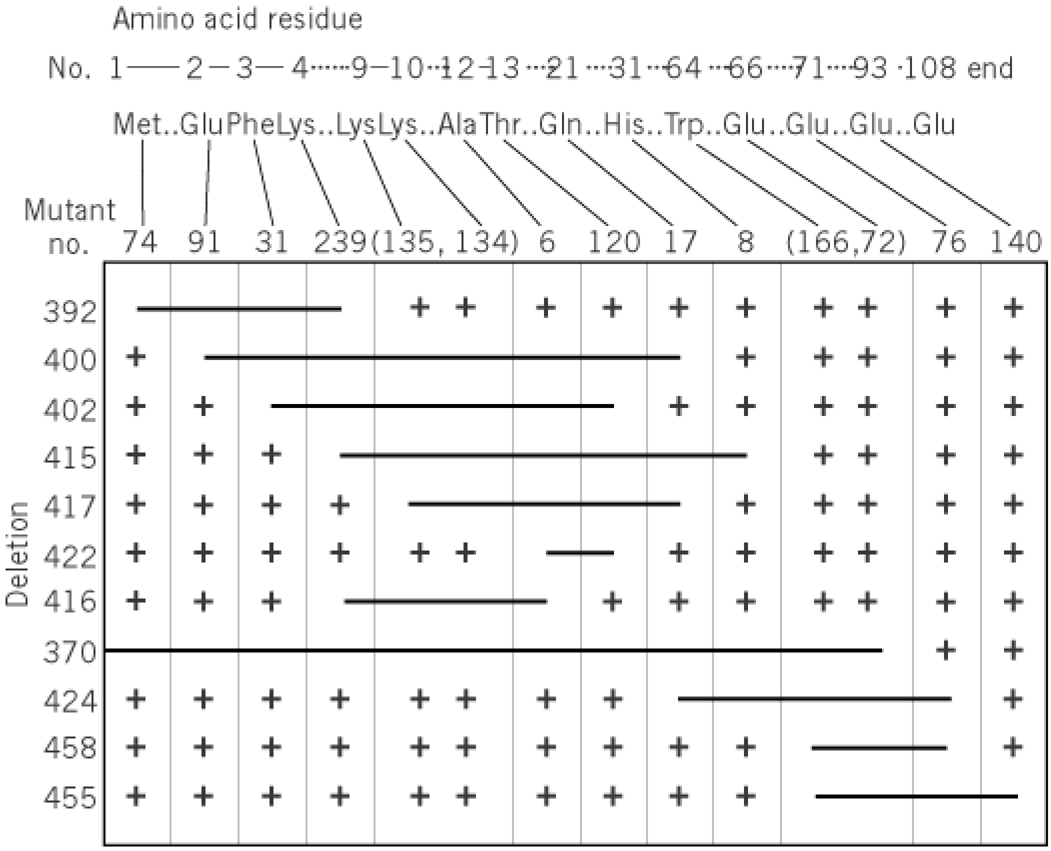

From this and many other examples, the gene emerged as a very finely subdivisible unit. Recognizing that the gene material is **DNA**, the concept, which still holds, is that every base pair of the DNA sequence is a potential site for mutation, separable from its neighboring nucleotides at some low frequency by recombination. Taken together with the idea that each gene is responsible for a single enzymic protein, which had emerged from the early *Neurospora* work, it was an obvious guess that the linear sequence of mutable and recombinable sites within the gene corresponds to the linear amino acid sequence of the polypeptide chain of the protein product.

Drosophia rosy (*ry*) and *Saccharomyces cyc-1* are particularly appropriate examples because their mutations affect well-characterized proteins, namely, the enzyme xanthine dehydrogenase in the first case and the protein of the respiratory pigment cytochrome *c* in the second. In both cases point mutations cause mostly single amino acid replacements in the polypeptide chain, and the sequence of the replacements along the polypeptide chain corresponds to the sequence of mutational sites along the gene map. The comparison is particularly extensive for yeast *cyc1* (Fig. 2). Numerous other examples could be given, and the principle, called *colinearity*, is so well established now in molecular biology that further substantiation through genetic mapping is hardly necessary. Genes, or at least those genes responsible for protein structure, are linear codes for the amino acid sequences of polypeptide chains with exceptions that are mentioned later. Parallel with examples of colinearity came the molecular identification of the gene as DNA, the demonstration of transcription of genic DNA into RNA, and the working out of the genetic **code** through which messenger RNA (mRNA) is **translated** into polypeptide sequence.

The original “one gene - one enzyme” concept was incomplete in several ways. The immediate products of genes are RNA molecules, not all of which are messengers for protein synthesis (e.g., **ribosomal, small nuclear** RNA, and transfer RNA), and not all proteins are enzymes. Among the enzymes, many are multifunctional, and one function can often be lost by mutation without eliminating other functions of the same polypeptide chain. As a result, analysis by mutation, complementation, and recombination may subdivide a gene into several functionally distinct domains, which may at first be confused with separate genes. A multifunctional, multidomain gene is sometimes called a *cluster gene*, to distinguish it from a gene cluster. Most of the known examples are in fungi, but they occur in *Drosophila* (eg, Fig. 3) and also in mammals. This sort of gene complexity is more extensively discussed under Interallelic Complementation.

Figure 3. The *Gart* gene of *Drosophila*, which exhibits several kinds of gene complexity: (1) an intron-exon structure (common to most *Drosophila* genes; introns are shown as open and exons as black segments); (2) the full-length mRNA encodes a trifunctional polypeptide that has three different enzymatic activities, abbreviated to GARS, AIRS, and GART, that catalyze successive steps in purine biosynthesis; (3) it has two polyadenylation/transcript termination sites, T1 and T2, one within the fourth intron resulting in a truncated mRNA that encodes only the functionally independent GARS domain; (4) it has a "nested" gene within its longest intron that encodes a cuticle protein and itself with an intron. From Ref. 11 by permission of the publisher, after Ref. 5.

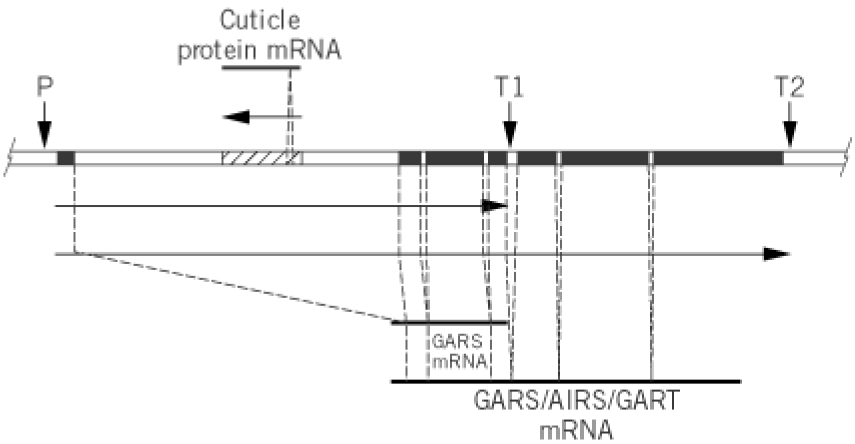

2. Transcribed and Nontranscribed DNA Strands and the Minimal Gene

In writing about gene structure, it is useful to use the terms "*upstream*" and "*downstream* " to indicate orientation with respect to the direction of transcription of DNA into RNA. Only one strand of the DNA duplex is usually transcribed, and it is important to remember that the transcribed strand of a protein-encoding gene is not the *coding strand*, in the sense that the codon sequence is as seen in the messenger RNA, but rather the opposite-polarity complement of that sequence. The transcribed strand runs upstream-to-downstream in the chemical direction 3′ to 5′, whereas the mRNA and its amino acid codons run 5′ to 3′. To deduce the amino acid sequence from the transcribed strand using the standard codon tables (see Genetic Code), one must mentally convert it into its complement: A to U, T to A, G to C, and C to G. The amino acid sequence can be read directly from the nontranscribed strand, which is therefore often called the coding strand. It is best to distinguish the strands as transcribed or nontranscribed, bearing in mind that the sequence of the latter bears the immediately recognizable codons.

Once defined as a unit of transcription into RNA, the gene may be a relatively compact structure, at least when measured against more than 10^9 DNA base pairs in a typical mammalian genome or the even greater DNA contents (C-values) of some amphibia and higher plants. We can enumerate the essential components of a protein-encoding gene as follows. There must be a **promoter** segment to which **RNA polymerase** binds to initiate transcription a little way upstream of the transcription startpoint (with the exception that RNA polymerase III works with downstream promoters), and a transcription termination and polyadenylation signal. Within the transcribed region there are sequences corresponding to the different sections of the messenger transcript: an untranslated **leader sequence** (of various lengths in different genes and sometimes important for controlling translation), a ribosome binding site and initiation codon, an **open reading frame**, and a **termination codon**. The yeast *cyc1* gene (Fig. 2) is a good example of a simple gene.

3. Expansion of the Gene Beyond the Coding Sequence

To be transcribed into mRNA for polypeptide chains or other kinds of RNA molecule, genes need be no more than a few thousand base pairs (kilobase pairs or kbp) long. How, then is one to account for the apparently huge surplus of DNA in the genomes of many higher organisms? Humans, for example, have about 30 kb of DNA per gene if the current estimate of about 100,000 genes is correct. Part of the answer lies in the host of repetitive and arguably functionless sequences that have become established. But probably equally important quantitatively are the intervening sequences (**introns**) that subdivide the coding sequences into fragments (exons) that are **spliced** together, and the introns spliced out, after the gene has been transcribed. The sizes and numbers of introns vary widely among different organisms. They are hardly present at all in bacteria in only a few genes and then seldom more than a hundred bases long in yeast, more numerous but still short in filamentous fungi, sometimes much longer in *Drosophila*, and often both very numerous and extremely long in mammals. The typical mammalian gene consists of rather short exons, each on the order of only hundreds or even tens of base pairs, separated by introns extending up to tens of kilobases long. Thus a gene, whose function is to encode a polypeptide chain of just a few hundred amino acid residues, may be spread over a tract of some 100,000 base pairs.

In addition to introns, other sequences, which may fall some distance outside the units of transcription, have some claim to be considered parts of the gene and to expand its domain. Although enhancers may occur within introns, they are probably more often outside the transcribed gene sequence, often upstream but sometimes downstream. The same applies to **silencers**. Insofar as enhancer sequences are cis-acting, which they usually are, they may be considered as falling within the gene boundaries. If so, this may somewhat complicate the idea of the gene as a discrete functional unit if the same enhancer services two or more different transcriptional units. Thus, a single **locus control region**, an approximately 20-kbp sequence, not usually called an enhancer but at least some elements of which function as such, acts on all of the genes of the human b-globin gene cluster. Genes are also functionally linked through chromatin structure, changes in which repress or release the transcription of blocks of genes (see also Epigenetics, Position Effect).

4. Programmed Gene Restructuring

Although most genes in most organisms have constant DNA sequences, the same in the cells where they are transcribed as in the germ cells through which they are transmitted, there are examples of genes in a wide range of organisms that are restructured in the process of cellular differentiation. In unicellular organisms, bacteria, yeasts, and protozoa, where any cell can found a new population, gene restructuring is always reversible within the cell. Thus the switching of **flagellar** antigen in the bacterium *Salmonella typhimurium* is brought about by the inversion of a DNA segment with the effect of “switching off” one **antigen**-encoding gene by separating it from its promoter and thereby switching on another antigen gene of which the first antigen is a repressor (7). The inversion is reversible. In *Saccharomyces* yeast, the well-known **mating type** switch is due to replacing a segment of DNA at a transcriptionally activating site with a segment copied from another locus, where it had been transcriptionally silent. The potential for both mating types is held at silent “cassette” loci at all times, but only one mating type is expressed from the segment present at the activating (or, more correctly, nonsilencing) locus. Similar mating-type switching occurs in the fission yeast, *Schizosaccharomyces pombe*. A system not dissimilar in principle but with more options that again involves the transfer of gene sequences from silent to expressed loci, operates to switch the major surface antigen of the pathogenic protozoan ***Trypanosoma*** *brucei* (8).

In all the cases just mentioned, the potential for switching back to the status quo ante is retained within the cell nucleus. The situation is very different in ciliated protozoa, such as *Paramecium*, *Tetrahymena*, and *Oxytricha*, in which two kinds of nuclei are in the binucleate cells: a virtually "silent" ***micronucleus***, which contains the basic genetic material and has the potential for differentiation in different directions (e.g., to different mating types or different surface antigens) and an active **macronucleus**, in which a selection of genes is amplified and restructured to support a particular cell type. At meiosis, which generates haploid nuclei for sexual cross-fertilization or for a kind of self-fertilization called autogamy , the macronuclei degenerate and disappear and are replaced by division and restructuring of the micronuclei, with the opportunity for switching cell type. Some of the gene rearrangement seems quite bizarre. For example, in *Oxytricha trifallax*, a gene that encodes an actin protein whose exons are labeled 1 to 10, upstream-to-downstream in the macronucleus, was reshuffled from the order 3, 4, 6, 5, 7, 9, 10, 2, 1, 8 in the micronucleus (9).

Gene restructuring in mammals is the exception rather than the rule, but is centrally important in the immune system. The functional genes for the virtually infinitely large number of different immunoglobulins and T-cell receptor proteins are pieced together in a large number of possible permutations from DNA segments that are separated by hundreds of kilobases in undifferentiated stem cells. Note that the nucleic acid splicing involved here occurs at the level of DNA, not RNA as in splicing-out of introns. This topic is dealt with in more detail under Complex Loci, Immunoglobulins, and T-cell receptor.

A different category of incomplete genes are those made functional not by rearrangement at the DNA level but by splicing their RNA transcripts to leader sequences provided by what might be called supplementary genes elsewhere in the genome. Many or most messenger RNAs in the **Trypanosomes** acquire leader sequences and cap sites in this way (10). Something similar occurs in nematodes, and such systems may be widespread in the less well explored "lower" eukaryotes.

Bibliography

1. E. B. Lewis (1952) Proc. Natl. Acad. Sci. USA **38**, 953–961.
2. S. Benzer (1959) Proc. Natl. Acad. Sci. USA **45**, 1607–1620.
3. A. Chovnick, A. Ballantyne, and D. G. Holm (1971) Genetics **69**, 179–209.
4. F. Sherman et al. (1975) Genetics **81**, 51–73.
5. S. Henikoff, M. A. Keene, K. Fechtel, and J. W. Fristrom (1986) Cell **44**, 33–42.
6. S. N. Krishnan, E. Frei, A. P. Schalet, and R. J. Wyman (1995) Proc. Natl. Acad. Sci. USA **92**, 2021–2025.
7. J. Zieg et al. (1980) Science **196**, 170–172.
8. J. H. J. Hoeijmakers et al. (1980) Nature **284**, 78–80.
9. M. Dubois and D. M. Prescott (1995) Proc. Natl. Acad. Sci. USA **92**, 3888–3892.
10. S. Lucke et al. (1996) EMBO J. **15**, 4380–4391.

Suggestion for Further Reading

11. J. R. S. Fincham (1994) *Genetic Analysis*, Blackwell Science, Oxford.

Gene Targeting

Gene targeting refers to the introduction of genetic alterations into predetermined sites within the genome via homologous recombination. A DNA vector containing genomic sequences surrounding the required genetic alteration is constructed by recombinant DNA techniques and introduced into the cell. Homologous recombination between the vector and genome results in insertion of the genetic alteration at the homologous endogenous location and production of a genetically modified cell (Fig. 1).

Figure 1. Diagrammatic representation of the generation of genetically altered mice by gene targeting. ES cell lines derived from the mouse blastocyst are cultured *in vitro* and transfected with a gene-targeting vector. Transfected cells are selected in the appropriate growth medium and homologous recombinants are identified by molecular screening methods. Correctly targeted clones are expanded and returned to recipient mouse embryos which develop to term in pseudopregnant recipient females. Chimaeric offspring which transmit the ES cell genotype through the germline are mated to generate mice heterozygous for the targeted gene. Male and female heterozygous mice are mated to generate mice homozygous for the targeted gene.

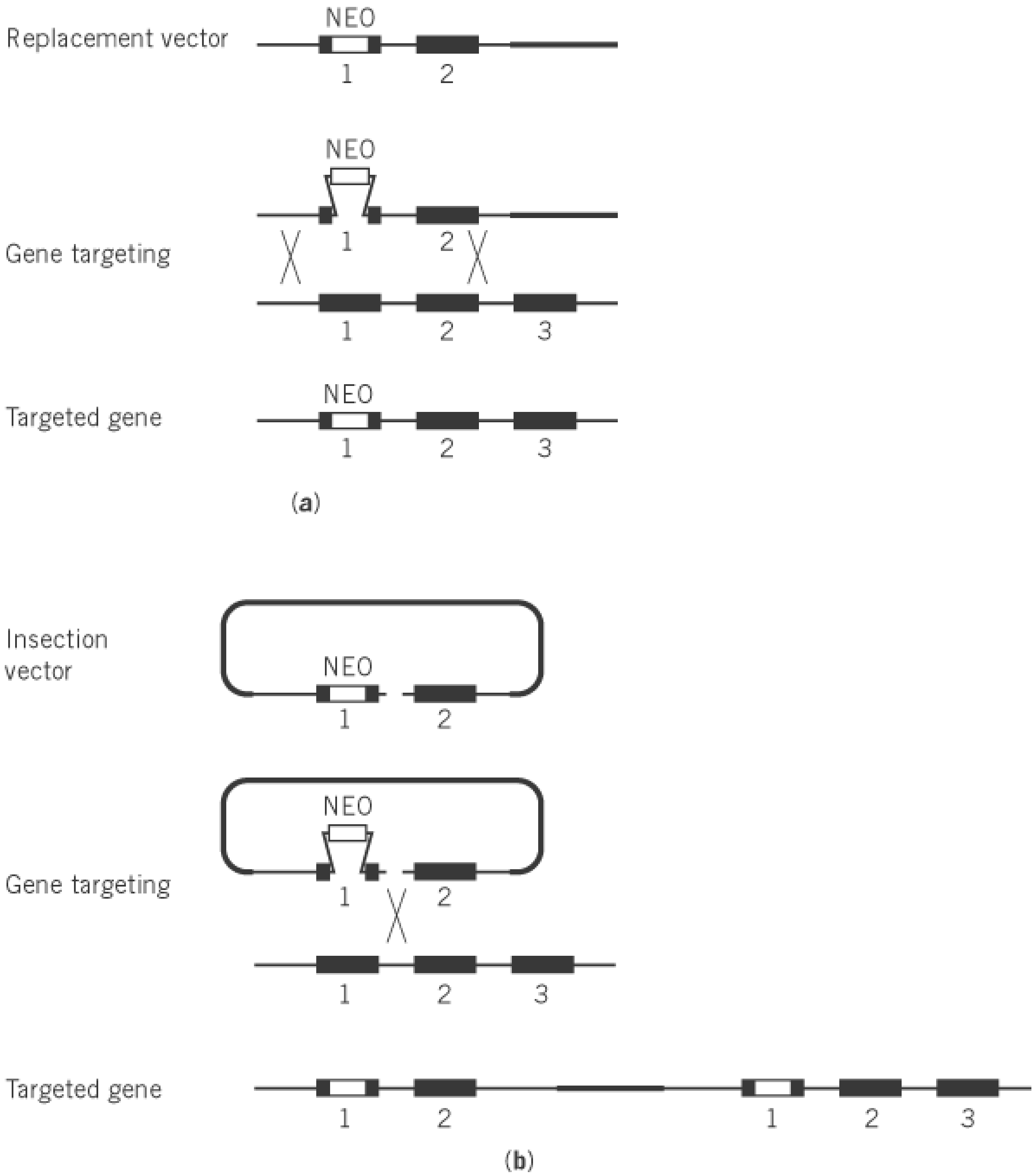

Gene targeting has been demonstrated with variable efficiencies in organisms as diverse as bacteria, yeast, and mammals, as well as in both haploid and multiploid cells. Strategies have been developed for the introduction of diverse mutations ranging from alteration of single nucleotides to incorporation of large DNA segments. Most recent interest reflects the realization that, by coupling gene targeting and reproductive technologies, genetically altered cells can be used as vectors for the creation of genetically modified multicellular organisms. This technology has been developed furthest in the mouse, and the term *gene targeting* is now most commonly applied to the generation of mutant mice. Application of gene targeting to other species has great potential for the analysis of gene function, treatment of human disease, and generation of novel agricultural products.

1. Generation of Null Mutant Mice via Gene Targeting in Embryonic Stem Cells

The early mouse embryo contains a pool of pluripotent cells that will give rise to all cell types of the embryo and adult. These cells can be isolated from preimplantation embryos and maintained in the undifferentiated state *in vitro* as embryonic stem (ES) cells. ES cells retain pluripotent differentiation capability even after long-term culture and can contribute differentiated progeny to all tissues, including the germline, following reintroduction into the mouse embryo (Fig. 2). Genetically altered ES cells can be used to transmit mutations constructed *in vitro* into the mouse germline, thereby enabling the creation of mice with predetermined mutations.

Figure 2. Diagrammatic representation of the generation of null mutations with replacement and insertion targeting vectors. (**a**) Replacement gene-targeting vector. (**b**) Insertion gene-targeting vector. Thin line, genomic DNA; thick line, plasmid DNA; numbered black boxes, exons; NEO, neomycin resistance selection cassette; X, region of homologous recombination.

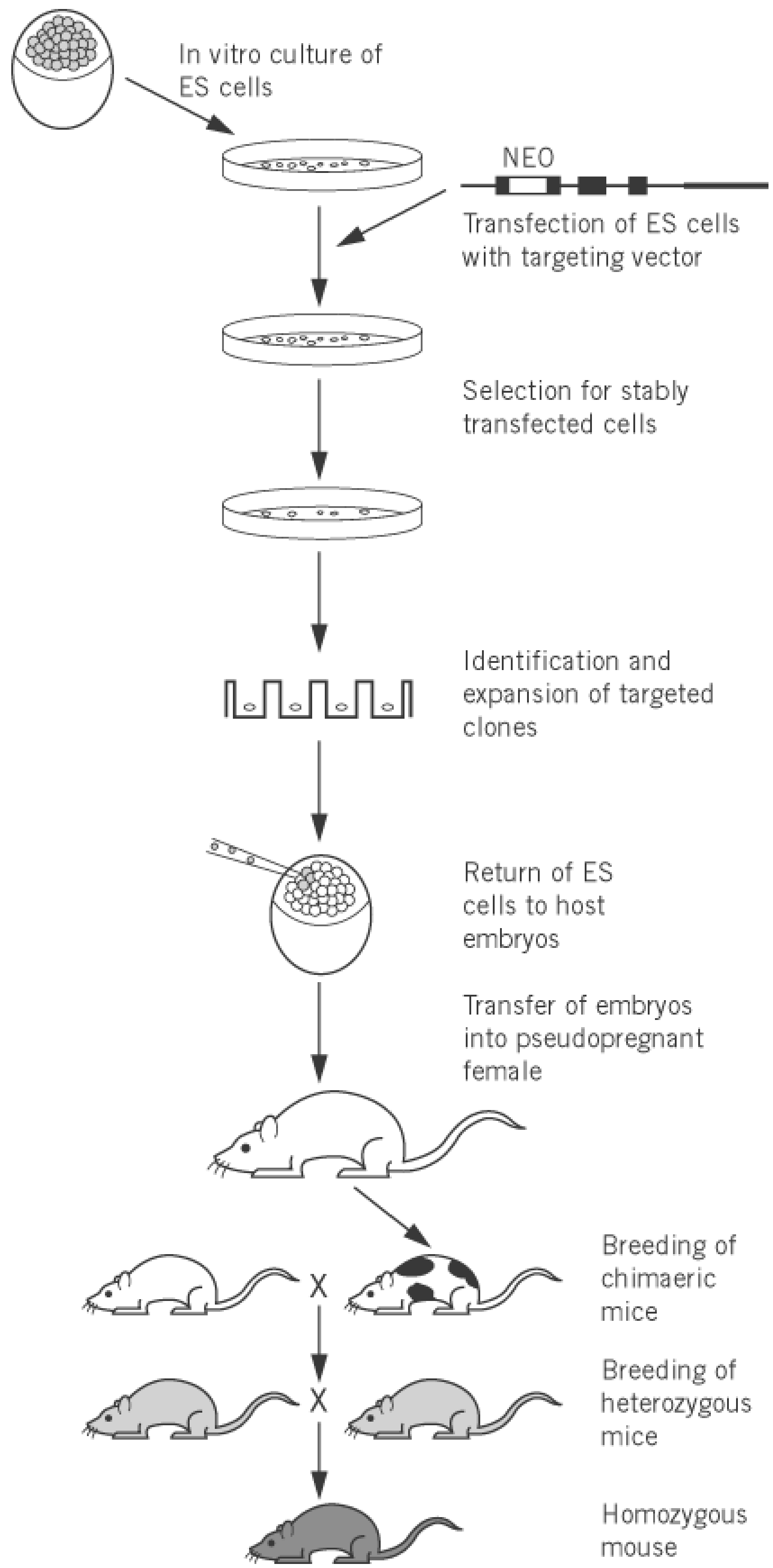

The steps involved in making a mouse that carries an inactivated gene (null mutation) are shown diagrammatically in Figure 2. Standard recombinant DNA techniques are used to isolate a genomic clone corresponding to the region to be altered and to construct a gene-targeting vector. A positive selection cassette, such as the bacterial **neomycin**-resistance gene, which provides resistance to the aminoglycoside G418, is usually positioned within the genomic clone so that it is flanked by genomic DNA sequences. The targeting vector DNA is introduced into undifferentiated ES cells grown in the presence of leukemia inhibitory factor (LIF) or a feeder cell layer. A range of standard transfection techniques allow introduction of the vector DNA into ES cells, although electroporation is most commonly used (see Transfection). In most cases the introduced DNA integrates into the genome at random sites by nonhomologous recombination, but in a few cases (in the order of 0.5% to 10%) the introduced DNA is integrated into the genome at the homologous site. Stably transfected cells are selected for expression of the selection cassette. Individual clones are expanded and screened for homologous recombination by Southern blot or polymerase chain reaction (PCR). Correctly targeted clones are expanded *in vitro* and reintroduced into host embryos by injection into the blastocoelic cavity of 3.5 days post coitum (d.p.c.) embryos, or by co-culture with 2.5 d.p.c. morulae. Embryos are returned to pseudopregnant recipient female mice and develop into **chimaeric** mice. Usually the coat colors of the host embryo and the mice from which the ES cells were obtained differ, so that chimaeric mice can be identified by their chimaeric coat coloration. Chimaeric mice in which targeted ES cells have contributed to the germline give rise to progeny that are heterozygous for the targeted gene in all cells of the body. To produce mice that are homozygous for the targeted gene, heterozygous male and female mice are mated.

The most common application of gene targeting technology in mice has been the creation of null mutants, usually by positioning the selectable marker so that it disrupts or replaces the gene of interest. Two types of vectors are used for the creation of null mutations: replacement and insertion vectors (1). Replacement vectors are linearized at the extremities or outside the homologous sequence, and the vectors remain co-linear with the target sequence (Fig. 2a). To produce null mutations, a critical section of the coding region is replaced or disrupted with the selection cassette. Insertion vectors are linearised within the region of homology, and homologous recombination of these vectors leads to duplication of the genomic sequence (Fig. 2b). To produce null mutations with insertion vectors, the coding sequence is disrupted with vector DNA that also carries a selection cassette disrupting or replacing an essential region of the coding sequence. Mice carrying specific mutations have proved extremely valuable for basic biological investigations (2-4).

2. Improvements to Gene Targeting Efficiency

2.1. Parameters

The mechanisms by which homologous recombination of replacement and insertion vectors occurs in mammalian cells are poorly understood. Genes can be targeted efficiently in ES cells regardless of whether they are expressed (5). The efficiency of homologous recombination can be increased by increasing the total amount of homology contained in a targeting vector (1, 6, 7). The relationship between the length of homology and the gene targeting efficiency is exponential between 2 and 10 kb, whereas increases in homology beyond 14 kb have little effect. The efficiency of homologous recombination can also be increased significantly by using genomic DNA for vector construction that is isogenic with the strain of mice from which the ES cells were derived (8, 9). The frequency of homologous recombination appears to be unaffected by the length of nonhomologous DNA introduced into the homologous site, at least up to 12 kb (10), and separate regions of extensive nonhomology can be introduced efficiently into the genome on a single replacement vector (11).

2.2. Vector Design

For loci that are targeted at low frequencies, identification of occasional homologous recombinants among a high background of stably transfected cells can be labor-intensive. Vector design can be modified to enrich for homologous recombinants. The positive-negative selection system (12) is based on the finding that nonhomologous regions at the extremities of replacement vectors are integrated during nonhomologous, but not homologous, recombination. A negative selection cassette, such as herpes simplex virus thymidine kinase (HSV-*tk*), which confers sensitivity to gangcyclovir or FIAU, is positioned outside the homologous sequence on a replacement vector.

Selection for vector integration, but against HSV-*tk* expression, enriches for homologous integrants (Fig. 3). When isogenic DNA vectors are used, enrichments in the range of 5- to 10-fold can be achieved. However, the findings that DNA ends can stimulate homologous recombination (13, 14), and that vector ends might initiate homologous recombination of replacement targeting vectors (11), suggest that the use of vectors containing homologous sequences at the extremities could also be advantageous. Selection cassettes that lack a **promoter** or a polyadenylation sequence (15) have also been used to improve the efficiency of gene targeting, since nonhomologous recombination of such vectors generally results in poor expression of the selection cassette. When recombined at the homologous site, the selection cassette is expressed efficiently due to appropriate positioning within the endogenous gene.

Figure 3. Diagrammatic representation of positive–negative selection gene targeting. Thin line, genomic DNA; thick line, plasmid DNA; black boxes, exons; NEO, neomycin resistance selection cassette; TK, thymidine kinase selection cassette; X, region of homologous recombination.

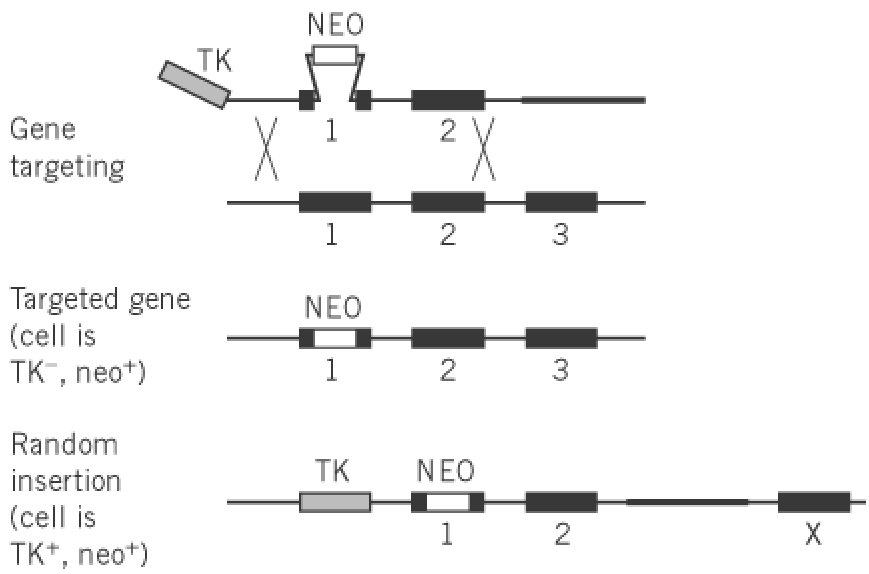

3. Applications of Gene Targeting

3.1. Mapping Gene Expression

Integration of reporter genes into the genome so that they are expressed under the transcriptional control of the endogenous gene provides a means to visualise the normal cellular sites of gene transcription *in vivo*. Expression of reporter genes such as **b-galactosidase** (*lacZ*) can be resolved at the cellular level by histochemical techniques. Chimaeric reporter/selection cassettes, such as the b-galactosidase-neomycin fusion b*geo* (16) that has the enzymatic activity of b-galactosidase and provides resistance to G418, can be used simultaneously as a reporter for gene expression and as a selection cassette for the identification of stably transfected ES cells. This eliminates potential transcriptional interference from promoters directing expression of the selection cassette in the targeting vector. Viral internal ribosome-entry site (IRES) sequences, which enable multiple coding regions to be translated from a single transcript in mammalian cells, can be used to couple expression of a reporter gene integrated into the 3′ untranslated region to expression of an unmutated open reading frame ((17), Fig. 4).

Figure 4. Diagrammatic representation of gene targeting with IRES reporter vectors to map the cellular sites of gene

expression. Thin line, genomic DNA; thick line, untranslated region, numbered black boxes, exons; IRES, internal ribosome entry site; b*geop* pA, b-galactosidase/neomycin resistance cassette with polyadenylation sequence; SA, splice acceptor; arrow, endogenous expression signals. Entry of ribosomes at the IRES in dicistronic mRNA results in translation of bgeo protein controlled by expression signals in the endogenous gene; X, region of homologous recombination.

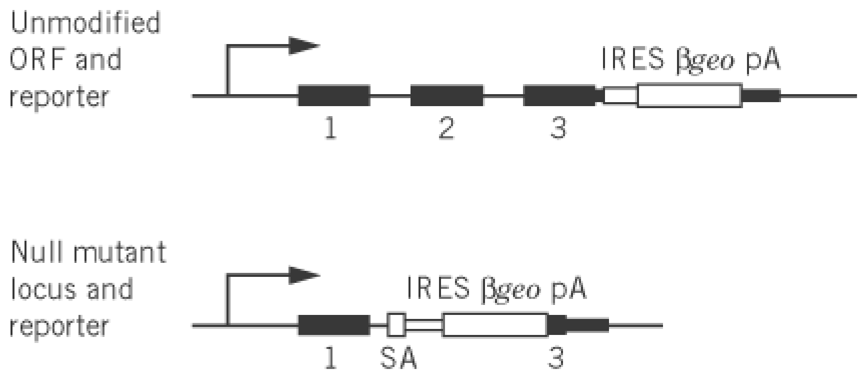

3.2. Sophisticated Genetic Alterations

Refined gene targeting systems can be used for the introduction of subtle alterations, including single nucleotide changes, into the mammalian genome. Many of these are based on positive–negative selection cassettes such as HPRT which can be selected in hypoxanthine phosphoribosyltransferase-deficient ES cells positively in HAT medium and negatively in 6-thioguanine. In the hit-and-run system, also known as the in–out system ((18, 19); Fig. 5), the endogenous locus is modified by homologous recombination with an insertion vector that carries the desired alteration and a positive–negative selection cassette. This leads to duplication of the homologous site and is positively selected. Intrachromosomal recombination results in cells that lose the duplication and selection cassettes and therefore survive negative selection. A proportion of these cells maintain the desired alteration.

Figure 5. Diagrammatic representation of the hit-and-run gene targeting approach used to generate subtle genetic modifications. Two alternate outcomes of intrachromosomal recombination are illustrated. Thin line, genomic DNA; thic line, plasmid DNA; numbered black boxes, exons; NEO, neomycin resistance selection cassette; TK, thymidine kinase selection cassette; open box, subtle mutation.

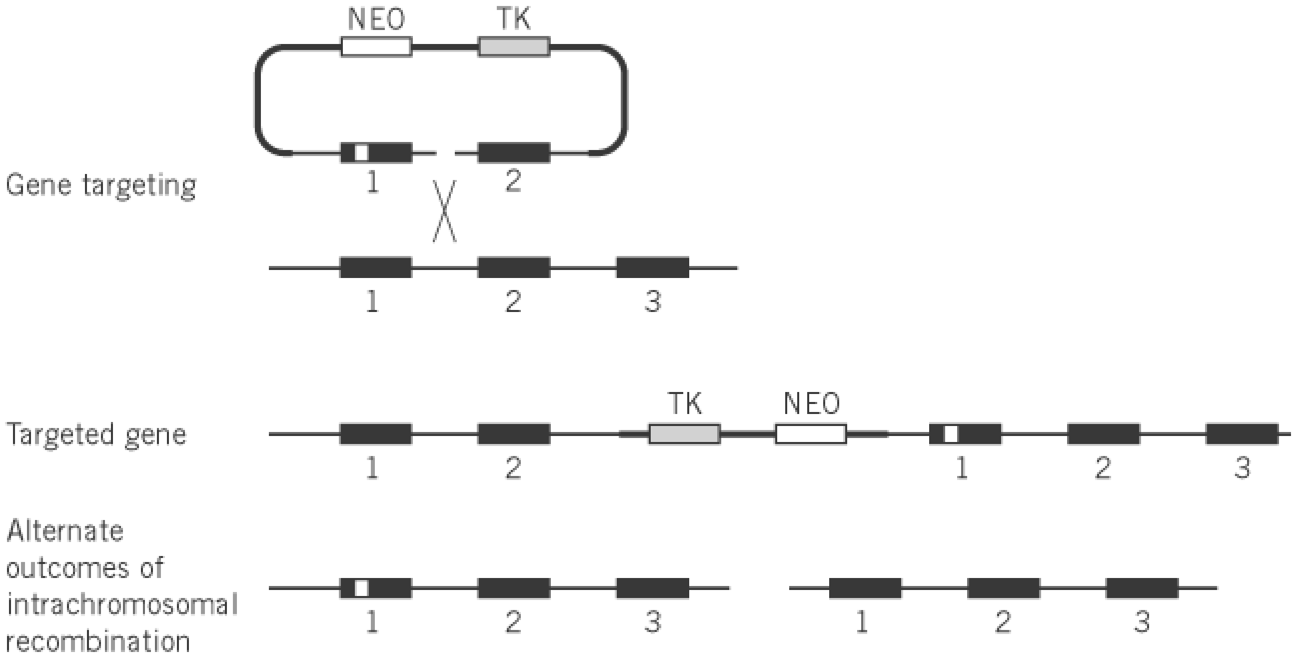

In the targeting system first suggested by Reid et al. (20), and known as double replacement (21, 22) or tag-and-exchange (23), two successive gene targeting steps are used to introduce subtle alterations into the genome (Fig. 6a). A positive–negative selection (tag) cassette is introduced into the genomic locus by gene targeting. The tag gene is replaced by the alteration of interest in a second round of gene targeting, in which direct selection for loss of the tag gene prevents survival of nonhomologous recombinants. The efficiency of second-round targeting can be compromised by a high background of resistant lines that result from physical loss of the tag cassette in the absence of homologous recombination. This most commonly results from **gene conversion** in which the tagged gene is restored to wild type by nonreciprocal transfer of genetic information from the wild-type sequence (11, 21, 22). In a modified version of tag-and-exchange targeting, termed stable tag-exchange (11), an additional positive selection cassette positioned outside the coding region is introduced on the first-round targeting vector. This cassette is not replaced during the second round of targeting and is used to select against reversion of the tagged gene to wild type. This provides a significant improvement in the efficiency of two-round gene targeting approaches. Stable tag-exchange gene targeting is therefore advantageous when investigations require the introduction of multiple, independent subtle alterations into a single locus. In cases where the presence of an exogenous selection cassette within the altered sequence may be deleterious, it can be removed by site-specific recombination using systems developed for conditional gene targeting (see text below).

Figure 6. Diagrammatic representation of two-step gene targeting approaches used to generate subtle genetic modificati
(**b**) Plug-and-socket gene targeting. Thin line, genomic DNA; numbered black boxes, HPRT, HPRT selection cassette; o
selection cassette; DSocket or SocketD, alternative nonfunctional selection cassettes; Socket, functional socket selection
recombination between DSocket and SocketD; X, region of homologous recombination.

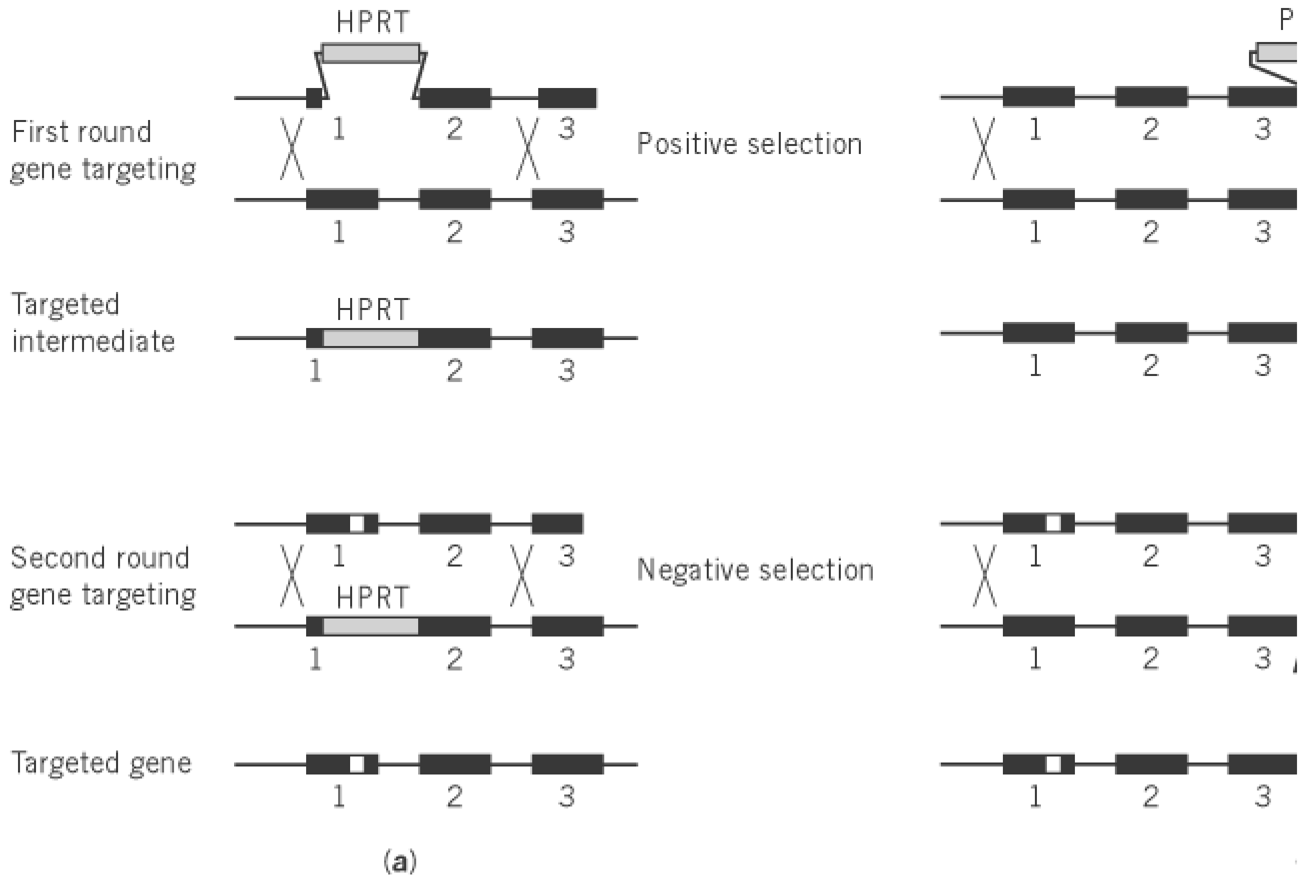

The two-step “plug and socket” system ((24); Fig. 6b) allows use of positive selection in both rounds of gene targeting. This potentially overcomes the background of cells surviving negative second-round selection due to loss of the negative-selection cassette in the absence of homologous recombination. The locus is initially targeted with a vector that contains a functional positive “plug” selection cassette and a second nonfunctional positive “socket” selection cassette positioned outside, but close to, the locus. The vector used for second-round targeting contains the desired alteration, along with an alternative nonfunctional version of the socket selection cassette. Homologous recombination creates a functional “socket” selection cassette that is selected, and it results in replacement of the plug selection cassette with the desired alteration.

3.3. Conditional Gene Targeting

Null mutations produced by conventional homologous recombination have provided valuable information about the biological significance of a large number of molecules. In cases where null mutations are lethal to the embryo, however, the role of the gene product cannot be studied at subsequent stages of development. Methods for the creation of **conditional mutations**, which allow control over the site and/or time of mutation *in vivo*, are based on site-specific recombination catalyzed by a yeast or bacteriophage DNA recombinase (Fig. 7). The bacterial Cre recombinase catalyses recombination between two specific 34-bp sequences called *loxP* sites. The locus of interest is modified by gene targeting such that *loxP* sites in the same orientation are placed on either side of the selection cassette and at the end of the gene to be mutated. The ES cells are then transfected transiently with a Cre expression cassette, resulting in recombination between *loxP* sites and deletion of the intervening sequences (see Introns, Exons). Cells in which the selection cassette alone has been deleted are identified and used to generate mice that carry a functional gene flanked by *loxP* sites. Homozygous offspring of these mice are crossed with mice that are heterozygous for the mutated gene and that also carry the Cre recombinase gene driven by a tissue-, cell-, or stage-specific promoter. Recombination and deletion/mutation of the *loxP* flanked gene is restricted to the tissues or stages of development where/when the Cre recombinase is expressed and allows direct investigation of the function of the gene at these positions or stages.

Figure 7. Diagrammatic representation of conditional gene targeting by Cre-*lox* recombination. (**a**) A targeting construct containing the gene of interest and a neomycin resistance (NEO) gene flanked by 3 *loxP* sites (black triangles) is introduced into the ES cell genome by homologous recombination. (**b**) Transient expression of Cre recombinase in the ES cells results in loss of the gene of interest, the NEO gene or both. (**c**) Cells containing the gene of interest flanked by *loxP* sites are used to generate chimaeric mice which are bred to homozygosity. (**d**) Homozygous offspring are crossed with a heterozygous mutant which carries a Cre gene driven by a cell- or stage-specific promoter, resulting in offspring in which the *loxP* flanked gene is deleted in the cells or at the stage where the Cre gene is expressed.

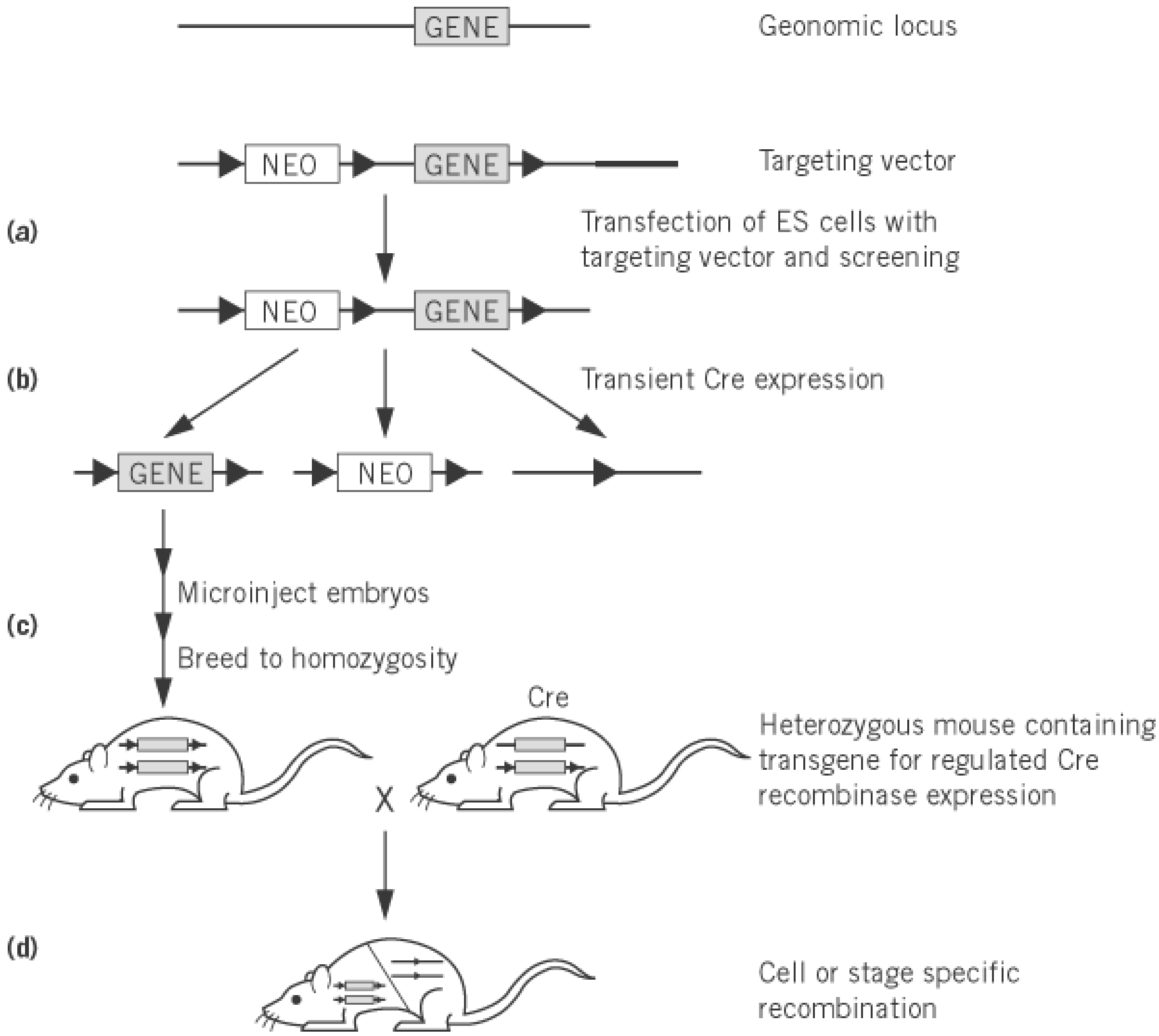

.

In addition to conditional mutations, Cre-*lox* technology can be applied to a wide variety of targeted mutation strategies, including replacement of a gene from one species with the same gene from another species (25) and insertion of a different gene into a particular genomic location (gene "knock-in"; (26)). Cre-*lox* recombination has also been used for the creation of subtle mutations (27), to enable controlled activation of gene expression by insertion of a *loxP*-flanked stop sequence between a gene and its expression signals (28), to generate complex genomic models for chromosomal rearrangements, translocations, and deletions (29), and to model diseases caused by mutations in somatic cells, such as cancers and aging.

3.4. Null Mutations *in Vitro*

Cell lines in which both **alleles** of a gene are mutated provide unique opportunities for biochemical analysis of gene function. ES cells with homozygous mutations can be isolated from homozygous mutant embryos, or constructed by genetic manipulation of heterozygous ES cell lines generated by gene targeting. This can be achieved by sequential targeting using different selection markers, or by increasing selection for expression of the neomycin-resistance gene by elevating the concentration of G418 (30), thereby selecting for rare cells in which gene conversion has replaced the wild-type allele with a second copy of the targeted allele. The developmental potential of mutated ES cells can be assessed by differentiation of the cells *in vitro*, or by examining the contribution of the cells to tissues in chimaeric mice following return to the blastocyst. This can permit analysis of cell decisions that are otherwise obscured by embryonic lethality, and in some cases it can be coupled with detailed analysis of cell differentiation by measurement of marker gene expression.

Differentiated cell lines with homozygous mutations can be isolated from mutant embryos or via *in vitro* differentiation of ES cells containing two mutated alleles. These provide a valuable resource, because the effects of mutation can be examined in established *in vitro* assays specific for differentiated cell types. The availability of a homogeneous cell population allows application of biochemical techniques, such as direct measurement of downstream effector molecules.

3.5. Disease Models

Human diseases can have as their origin a wide variety of genetic alterations, including point mutations, deletions/truncations, large chromosomal deletions, and chromosomal translocations. Animals with genomes modified to mimic these alterations can be generated by gene targeting and used to study the cellular and biochemical basis of the disease and to test potential therapies. For example, familial hypercholesterolemia caused by loss of the low-density lipoprotein receptor has been modeled by gene knockout (31), cystic fibrosis has been modeled by the creation of point mutations within the cystic fibrosis transmembrane conductance regulator gene (32), and a familial form of Alzheimer's disease has been partially modeled by replacing the mouse Ab domain in the b-amyloid precursor protein with a mutated human sequence (33). A limitation of this approach can be the failure of mice to display the mutant phenotype seen in humans. In some cases, this can be overcome by refinement of the gene targeting approach. For example, familial adenomatous polyposis coli (FAP) results in the formation of colorectal adenomas in humans due to mutation of the APC gene. Mice homozygous for an APC deletion die *in utero*, but conditional gene targeting of the mutation in the colorectal epithelium using Cre-*lox* recombination resulted in mice that develop colorectal adenomas (34).

3.6. Gene Targeting in Non-mouse Species

Theoretically, gene targeting could be used in any cell that supports homologous recombination and can undergo clonal proliferation *in vitro* following selection for recombinants. However, creation of organisms carrying the modified allele can be achieved only if an intact organism can be regenerated from the genetically modified cell. The creation of gene-targeted organisms other than mice has been restricted by the failure to isolate pluripotent ES cells from these species. A potential alternative to the use of ES cell technology is foreshadowed by the demonstration that nuclei of differentiated cells can be reprogrammed or reverted to pluripotency by insertion into enucleated oocytes. The application of this nuclear transfer technology to produce offspring that are genetically identical to the donor cells has been validated for sheep, mice, and cattle, for donor nuclei from several cell types, and for genetically modified cells (35-38). Using this technique, gene targeting would be carried out in the differentiated cells, and genetically altered organisms would be created by nuclear transfer.

Gene targeting in nonmammalian metazoans is not yet well advanced. While homologous recombination has been demonstrated in moss (39), there are not yet convincing reports of gene targeting in lower vertebrates, invertebrates, or higher plants. The latter are of particular interest, given the potential for agricultural application.

3.7. Therapeutic Gene Targeting in Humans

An important potential application of gene targeting is the precise genetic alteration of **somatic cells** for correction of disease-causing mutations by gene therapy, delivery of therapeutic compounds to the individual, or tissue reconstitution *in vitro*. Direct genetic manipulation of, for example, somatic stem cells is limited by the failure of existing technologies to support isolation, transfection, and proliferation of these cell types *in vitro*. Widespread use of genetically altered cell types for human therapy may emerge from the combination of nuclear transfer technologies, which enable reprogramming of somatic cell nuclei, and gene targeting. Somatic cell nuclei isolated from an individual could be reprogrammed to a pluripotent state by nuclear transfer, modified genetically, and differentiated *in vitro* into the cell type required for transplantation. The use of gene targeting approaches could broaden the use of genetically modified cells for human therapy. This is currently restricted by difficulties associated with controlling the location, timing, and levels of gene expression, the copy number and integration site of **transgenes**, and the host immune response to virally based vectors.

Bibliography

1. K. R. Thomas and M. R. Capecchi (1987) Cell **51**, 503–512.
2. E. P. Brandon, R. L. Idzera, and G. S. McKnight (1995) Curr. Biol. **5**, 625–634.
3. E. P. Brandon, R. L. Idzera, and G. S. McKnight (1995) Curr. Biol. **5**, 758–765.
4. E. P. Brandon, R. L. Idzera, and G. S. McKnight (1995) Curr. Biol. **5**, 873–881.
5. R. S. Johnson et al. (1989) Science **245**, 1234–1236.
6. P. Hasty, J. Rivera-Perez, and A. Bradley (1991) Mol. Cell. Biol. **11**, 5586–5591.
7. C. Deng and M. R. Capecchi (1992) Mol. Cell. Biol. **12**, 3365–3371.
8. H. te Riele, E. R. Maandag, and A. Berns (1992) Proc. Natl. Acad. Sci. USA **89**, 5128–5132.
9. J. van Deursen and B. Wieringa (1992) Nucleic Acids Res. **20**, 3815–3820.
10. S. L. Mansour, K. R. Thomas, C. Deng, and M. R. Capecchi (1990) Proc. Natl. Acad. Sci USA **87**, 7688–7692.
11. L. M. Whyatt and P. D. Rathjen (1997) Nucl. Acids Res. **25**, 2381–2388.
12. S. L. Mansour, K. R. Thomas, and M. R. Capecchi (1988) Nature **336**, 348–352.
13. K. R. Folger, E. A. Wong, G. Wahl, and M. R. Capecchi (1982) Mol. Cell. Biol. **2**, 1372–1387.
14. R. S. Kucherlapati et al. (1984) Proc. Natl. Acad. Sci. USA **81**, 3153–3157.
15. A. Bradley, P. Hasty, A. Davis, and R. Ramirez-Solis (1992) Biotechnology **10**, 534–539.
16. G. Friedrich and P. Soriano (1991) Genes Dev. **5**, 1513–1523.
17. P. Mountford and A. Smith (1995) Trends Genet. **11**, 179–184.
18. P. Hasty, R. Ramirez-Solis, R. Krumlauf, and A. Bradley (1991) Nature **350**, 243–246.
19. V. Valancius and O. Smithies (1991) Mol. Cell. Biol. **11**, 1402–1408.
20. L. H. Reid, R. G. Gregg, O. Smithies, and B. H. Koller (1990) Proc. Natl. Acad. Sci. USA **87**, 4299–4303.
21. A. Stacey et al. (1994) Mol. Cell. Biol. **14**, 1009–1016.
22. H. Wu, X. Liu, and R. Jaenisch (1994) Proc. Natl. Acad. Sci. USA **91**, 2819–2823.
23. G. R. Askew, T. Doetschman, and J. B. Lingrel (1993) Mol. Cell. Biol. **13**, 4115–4124.
24. P. J. Detloff et al. (1994) Mol. Cell. Biol. **14**, 6936–6943.
25. Y. R. Zou, W. Müller, H. Gu, and K. Rajewsky (1994) Curr. Biol. **4**, 1099–1103.
26. Y. Wang, P. N. Schnegelsberg, J. Dausman, and R. Jaenisch (1996) Nature **379**, 823–825.
27. R. M. Torres, H. Glaswinkel, M. Reth, and K. Rajewsky (1996) Science **272**, 1804–1808.
28. M. Lasko et al. (1992) Proc. Natl. Acad. Sci. USA **89**, 6232–6236.
29. R. Ramirez-Solis, P. Liu, and A. Bradley (1995) Nature **378**, 720–724.
30. R. M. Mortensen et al. (1992) Mol. Cell. Biol. **12**, 2391–2395.

31. S. Ishibashi et al. (1993) J Clin. Invest. **92**, 883–893.
32. S. J. Delaney et al. (1996) EMBO J. **15**, 955–963.
33. A. G. Reaume et al. (1996) J. Biol. Chem. **271**, 23380–23388.
34. H. Shibata et al. (1997) Science **278**, 120–123.
35. K. H. S. Campbell, J. McWhir, W. A. Ritchie, and I. Wilmut (1996) Nature **380**, 64–66.
36. I. Wilmut et al. (1997) Nature **385**, 810–813.
37. J. B. Cibelli et al. (1998) Science **280**, 1256–1258.
38. T. Wakayama et al. (1998) Nature **394**, 369–374.
39. D. G. Schaefer and J. P. Zryd (1997) Plant J. **11**, 1195–1206.

Suggestions for Further Reading

40. P. M. Wassarman and M. L. DePamphilis (eds.) (1993) In *Methods in Enzymology*, Vol. **225**: *Guide to Techniques in Mouse Development*, Academic Press, San Diego.
41. S. K. Bronson and O. Smithies (1994) J. Biol. Chem. **269**(44), 27155–27158.
42. M. R. Capecchi (1989) Trends Genet. **5**(3), 70–76.
43. P. Soriano (1995) Annu. Rev. Neurosci. **18**, 1–18.
44. L. A. Galli-Taliadoros, J. D. Sedgwick, S. A. Wood, and H. Korner (1995) J. Immunol. Methods **181**, 1–15.
45. B. Sauer (1998) Methods (a companion to Methods Enzymol.) **14**, 381–392.
46. A. Nagy and J. Rossant (1996) J. Clin. Invest. **97**, 1360–1365.

Genetic Code

1. The Universal Progenitor and Standard Code

Transfer RNA, tRNA, is the essential adapter in decoding the genetic information. The aminoacylation of specific tRNAs with particular amino acids, and productive pairing of the anticodons of these tRNAs with **cognate** codons of the messenger RNA (mRNA) are the central processes in decoding (see Aminoacyl tRNA Synthetases and Translation). Within the past 10 years, great strides have been made in discovering the intricate relationships between tRNAs and aminoacyl-tRNA synthetases that are essential for correct aminoacylation. In contrast, the identification of mRNA codons has long been established (1), and the resulting table of specifications of amino acids by codons is what is commonly called the *genetic code* (Table 1). However, the code has meaning only in terms of its readout and, since this is a dynamic process, it is necessary to consider the code and its readout together.

Table 1. The Genetic Code

	Second Position				
First Position	**U**	**C**	**A**	**G**	**Third Position**

	Phe	Ser	Tyr	Cys	**U**
U	Phe	Ser	Tyr	Cys	**C**
	Leu	Ser	Stop	Stop/Sec	**A**
	Leu	Ser	Stop	Trp	**G**
	Leu	Pro	His	Arg	**U**
C	Leu	Pro	His	Arg	**C**
	Leu	Pro	Gln	Arg	**A**
	Leu	Pro	Gln	Arg	**G**
	Ile	Thr	Asn	Ser	**U**
A	Ile	Thr	Asn	Ser	**C**
	Ile	Thr	Lys	Arg	**A**
	Met	Thr	Lys	Arg	**G**
	Val	Ala	Asp	Gly	**U**
G	Val	Ala	Asp	Gly	**C**
	Val	Ala	Glu	Gly	**A**
	Val	Ala	Glu	Gly	**G**

All organisms living on earth are derived from a common ancestor, and divergent evolution from this ancestor is the central unifying theme of biology. One of the most striking facets of derivation from a common ancestor is the presence of the universal progenitor, or standard code, in nearly all organisms. Slight deviations from this standard code have appeared in certain organisms and coding niches, such as mitochondria; these deviations are important and interesting, but they do not detract from the truth that *Escherichia coli*, elephants, and peas use the same genetic code for synthesizing nearly all their proteins.

Deciphering this standard code was triumphantly accomplished between 1961 and 1966 (1). Elegant genetic experiments showed that the code was read from a defined starting point in a nonoverlapping manner, with three bases (or formally a multiple thereof) specifying one amino acid, the next three bases the next amino acid, and so on (2). Confirmation of the triplet nature of the code came from cell-free **protein biosynthesis** experiments that showed which codons specified each amino acid. The template used in Nirenberg and Matthaei's pioneering experiment in 1961 was polyuridylate [poly (U)], which led to the synthesis of polyphenylalanine. Consequently, the first codon to be deciphered was UUU for phenylalanine; very shortly afterward, AAA and CCC were found in the same way to encode lysine and proline, respectively. The use of mixed-polymer templates revealed the composition, but not the sequence, of codons specifying certain other amino acids. However, Khorana and colleagues synthesized polynucleotides with defined repeating sequences, and this provided valuable assignments (3). The other key development was the discovery by Nirenberg and Leder in 1964 (4) that trinucleotides promote the specific binding of tRNA to ribosomes. Synthesis of all 64 trinucleotides led to assignments for about 50 codons by this method. Protein sequencing studies from mutants with combinations of **frameshift mutants** supported the conclusions. Furthermore, genetic studies by Brenner and Garen and their colleagues provided valuable insights into the termination codons.

By 1966, the various approaches together resulted in the complete deciphering of the code (1). It does not detract from this monumental achievement to point out that, if the code had not been established by these means, direct nucleic acid **sequencing** coupled with protein sequencing would have provided the answer shortly thereafter. Complete sequencing of the first gene was accomplished in 1972 by “classical” RNA sequencing of the coat protein gene of the single-stranded RNA **bacteriophage** MS2 (5). Rapid DNA sequencing was developed in 1978 and led to a massive increase in sequence information. Nucleic acid sequencing, in conjunction with protein sequencing, has repeatedly confirmed the assignments of the standard code, demonstrated its utilization in decoding the main genomes of virtually all organisms, and revealed the interesting deviations.

The standard code in which the 64 possible base triplets encode 20 amino acids is presented in Table 1. The code is redundant, in that most amino acids are encoded by more than one codon. This is due in part to wobble pairing between the tRNA and the codon. Redundancy leads to variations in **codon usage** in different organisms. Three of the 64 codons do not usually code for amino acids but are used as stop codons, to terminate translation. Certain codons, usually AUG, play a special role as start codons, initiating translation of the mRNA. The 21st amino acid, selenocysteine (Sec), is also directly encoded, but only in special cases (see “Recoding,” below).

2. Specialized Code Variants: the Mitochondrial Code

It was long considered that the genetic code could not be altered during evolution. It was thought that changes in codon meaning would have such a deleterious effect on protein products that the code was “frozen.” However, quite a number of cases of genetic code variation are now known in mitochondria, as well as in the nuclear systems, of some organisms (6-9). The known variants of the genetic code in mitochondria are shown in Table 2. The small number of products encoded by animal mitochondrial genomes has undoubtedly been important in permitting code alterations in these organelles. How these alterations might have occurred is considered in the section “Candida code and code reassignment theories.”

Table 2. Variations in Mitochondrial Genetic Code[a]

Organisms	UGA Stop	AUA Ile	AAA Lys	AGR Arg	CUN Leu	UAA Stop	Example
Vertebrates	Trp	Met	—	Stop	—	—	Human, frog
Tunicates	Trp	Met	—	Gly	—	—	*Halocynthia roretzi*
Echinoderms	Trp	—	Asn	Ser	—	—	Starfish, sea urchin
Arthropods	Trp	Met	—	Ser[b]	—	—	Drosophila spp., mosquito, honeybee
Molluscs	Trp	Met	—	Ser	—	—	Squid, *Mytilus edulis*
Nematodes	Trp	Met	—	Ser	—	—	*C. elegans, Ascaris suum*
Platyhelminthes	Trp	—	Asn	Ser	—	Tyr	*Fasciola hepatica, planaria*
Cnidarians	Trp	—	—	—	—	—	*Hydra, Metridium senile*
Yeasts Trp	Met	—	—	Thr	—		*Saccharomyces cerevisiae,Torulopsis glabrata*
Euascomycetes	Trp	—	—	—	—	—	*Aspergillus nidulans, Neurosporacrassa*
Protozoa	Trp	—	—	—	—	—	*Trypanosoma brucai, Parameciumspp.*

[a] From reference 7 with modifications.
[b] N = A, U, C, or G; R = A or G. *Only AGA (specifying Ser) is used in *Drosophila* and mosquitoes, while both AGA and AGG (each specifies Ser) are used in honeybee, locust, and brine shrimp.

An important feature of decoding in animal mitochondria is that, in many cases, one tRNA recognizes all four members of a codon family. This simplification has resulted in a greatly reduced number of tRNAs compared to cytoplasmic protein synthesis. Key to this relaxed specificity is an unmodified U at the first position of the anticodon of many tRNAs (10). The general point is that almost all the diversity in the genetic code can be explained by variations in the anticodons of tRNAs that bind to various codons.

Generally, animal mitochondrial mRNAs have a simpler structure than those of **prokaryotes** and other **eukaryotic mRNAs**. There is no 5′-leader sequence (11) and usually only a short poly A sequence in the 3′-trailer sequence (12). Metazoan mitochondrial mRNA usually start translation with an AUG or AUA codon and end with a UAA or UAG codon although, in mammalian mitochondria, AGA and AGG codons are used for termination (12, 13). Often, only the 5′ nucleotide of the UAA is directly encoded, and it is completed by addition of the poly A sequence at the 3′-end of the primary transcript of mRNAs (12).

The change of UGA from being a stop codon to specifying tryptophan (Trp) in all mitochondria, except those in plants, is due to change of the anticodon of $tRNA^{Trp}$ from CCA or CmCA (mC = 5–methyl C) to U*UA, where U* in most cases is cmnm ^{5}U (5-carboxymethyl-aminomethyl U), so that the tRNA ^{Trp} can decode both UGG and UGA codons by wobble pairing.

The $tRNA^{Met}$ capable of decoding both AUG and AUA codons in most mitochondria, except those of echinoderms and platyhelminthes, possesses at the first position of its anticodon 5-formyl C in vertebrates (14) and nematodes (15), $cmnm^{5}C$ in ascidia (16), and a modified C in addition to normal C in *Drosophila* (17). These modified nucleosides make it possible to decode A as well as G at the third codon position.

AAA codons are read as Asn, instead of the usual Lys, in starfish mitochondria; the first position of the corresponding tRNA anticodon is occupied by G (17), which may decode, at the first position, not only C and U but also A. The same is observed in Ser codons of *Drosophila* mitochondria, where AGU, AGC, and AGA codons (AGG is an unassigned codon) specify Ser. Ser is also specified by UCN codons (N = A, U,C or G). The single $tRNA^{Ser}$ responsible for decoding these codons possesses a GCU anticodon (17).

All AGN codons are read as Ser in most invertebrate mitochondria. In these cases, a modified G [7-methyl G in starfish and squid (17, 18)] or an unmodified U [in nematodes (15)] occupies the first anticodon position, so that these bases can recognize all four bases at the third codon position.

In ascidian mitochondria, the AGR codon (where R is A or G) is assigned to Gly. The anticodon of the corresponding $tRNA^{Gly}$ is $cmnm^{5}UCU$ (19).

3. Candida Code and Codon Reassignment Theories

In nine species of the asporogenic **yeast**, *Candida*, CUG encodes serine and not leucine as it does in the standard, nearly universal code (20-22) (Table 1). The tRNA translating this nonuniversal genetic code (tRNA ^{Ser} CAG) has been characterized (21) and shown to be charged with serine (21-26).

At present, there are two theories to explain the codon reassignment: the “codon capture” (26) and the “ambiguous intermediate” (27) theories. The former postulates that a codon changes to another codon via an unassigned codon and that the codon to be changed must disappear once from coding sequences to avoid insertion of an incorrect amino acid (neutral change of codon). The latter postulates that changes in the genetic code are relatively fast processes driven by natural selection and that reassignment of codons is facilitated by a translationally ambiguous intermediate, where the transitional codon is read simultaneously as either of two amino acids by two different tRNAs.

The genetic code change found in *Candida* species may be explained by either of these two theories. Santos et al (28) favor the ambiguous intermediate theory. They provided experimental evidence that expression in yeast cells of a tRNA ^{Ser} CAG with a mutation at position 33 (5′-adjacent to the anticodon) induces the **stress response** that allows cells to acquire thermotolerance. This may provide positive selection for the genetic code change by allowing yeast to adapt to sudden changes in environmental conditions.

On the other hand, Suzuki et al. (29) found what they term a “polysemous codon” in *Candida zeylanoides*, which used the CUG codon to encode both serine and, to a slight extent (3%), leucine. This is mediated by a single tRNA^{Ser} CAG capable of being charged with either amino acid. A genetic method demonstrated that the CUG codon is actually translated as either amino acid *in vivo*. Suzuki and coworkers emphasize that the dual assignment of the CUG codon is fulfilled by dual specificity of a single tRNA^{Ser} CAG, not by ambiguous translation using two different tRNA. Thus, they prefer the codon capture theory to the ambiguous intermediate theory. The existence of unassigned codons is also important evidence for the codon capture theory. Further experiments are necessary, however, to clarify unambiguously the evolutionary process of codon reassignment in *Candida* species (30).

4. Theories of the Origin of the Genetic Code

Two assumptions are commonly made in considering the origin of the genetic code.

1. First is the principle of continuity; namely, for any possible productive early scheme, there has to be some conceptual way that it could have evolved gradually to the modern genetic code without destroying all the fruits of prior evolution.
2. A second assumption is that the origin of the code was based on RNA. Since proteins are decoded from RNA templates and some RNA are catalytic, it is highly attractive to invoke a transitory “RNA world”. Perhaps no decoding was necessary if the genetic material (RNA) could mediate the catalytic functions directly.

Since discussion of the origin of the code which began in earnest in the late 1960s (31), one of the key imponderables has been whether there was originally a direct stereochemical relationship between primordial tRNAs and their cognate amino acids or whether the genetic code assignments were random, as in “the frozen accident theory” (32). Recent work (33) has shown selective binding of some amino acids by RNA, and the question of aminoacylation in the absence of proteins is being investigated, but the overall issue remains unresolved. Intertwined with this issue is the question of the relationship between the accepter and anticodon branches of tRNA. Noller has suggested that both parts were initially separate, with overlapping functions, and that they were later combined (34). Another suggestion, which is difficult to evaluate, is that they are directly related (35).

Another key imponderable in decoding is the origin of ribosomes. Several different approaches, including extensive but incomplete deproteinization experiments, have pointed to the largest rRNA (23S rRNA in *E. coli*) as the key component in peptidyl transferase (reviewed in (34)). Of course, even imagining the origin of 23S rRNA is a serious problem, although an attractive suggestion is that a protodomain originated as a spin-off of a ribozyme-catalyzed function (34). A different issue is the origin of translocation of the ribosome one codon at a time along the mRNA. Modern ribosomes have the ability of low-level synthesis of polypeptides on poly(U), (UC), or (A) in the absence of the elongation factors EF-Tu, EF-G, and GTP, suggesting that they contain the mechanism for catalyzing translocation (36) and putting the spotlight on the small subunit rRNA (16S rRNA in *E. coli*). An interesting speculation is that this originated as an RNA replicase (37). Regardless of origin, it is tempting to think that the translocation step size is determined in part by the tRNA anticodon delineating the codon size. The stability of a triplet interaction between codon and anticodon is insufficient on its own to mediate discriminatory decoding. If, for stability reasons, however, one envisages primordial tRNAs that read quintuplet codons in a primitive mRNA, it is difficult to imagine how those translation components could evolve to triplet decoding without destroying the benefits of prior evolution. Consideration of this difficulty has lead to an ingenious scheme for triplet decoding involving overlapping quintuplet pairing (38, 39), but whether such a scheme is a progenitor of modern triplet decoding is speculative. It has been proposed that in present-day decoding, the triplet codon interaction is stabilized by stacking ribosomal RNA (40). The particular regions of rRNA proposed have not been implicated in genetic studies to address this issue, but it is unclear whether this is because they are not involved or because they are essential (41).

Knowledge of the structure of the ribosome will be invaluable for efforts to understand present-day decoding which, in turn, will guide thoughts about plausible schemes for its evolutionary origin.

5. Recoding: Reprogrammed Decoding

5.1. Transient Reprogramming of Decoding

Excluding some specialized niches, the genetic information in the great majority of mRNA is readout according to the standard rules with the nearly universal code specifications (Table 1). However, a minority of mRNA that use the same translational components, or essentially so, are decoded in a different manner at one or more positions in their coding sequence. At these positions, readout is reprogrammed, and the phenomenon is termed *recoding*. In the first category, the meaning of a code word is redefined so that at least some of the protein product bears the consequence of the new meaning. In the second category, a proportion of ribosomes shift reading frame at a specific place in an mRNA and continue in the new frame, following the standard rules, to give a very different product from the ribosomes that did not shift frame (see Frameshifting). In the final category, a block of nucleotides is bypassed by the translocating ribosomes.

Recoding has been most frequently encountered in **viruses**, especially plant viruses and retroviruses, and in retrotransposons, such as yeast Ty elements and bacterial **insertion sequence** (IS) **elements**, but it is also known to be utilized in decoding several cellular genes. It probably occurs in all organisms.

5.2. Redefinition

The meaning of a sense codon can be redefined; for example, the codon GUG at internal positions specifies valine, but in the context in which it functions as an initiator, it specifies methionine or formylmethionine (see Start Codons). No cases are known in which the meaning of a sense codon at an internal position in a coding sequence is redefined. (Though mechanistically distinct from recoding, there are instances in which a sense codon gives the superficial appearance of acting as a stop codon. Consecutive rare codons, or some RNA structures, can cause the ribosome to pause and, on occasion, to drop off with a terminated polypeptide chain; see Stop Codons.)

On the other hand, stop codons in the standard code can be redefined to specify an amino acid. The most dramatic case involves the specification of the 21st encoded amino acid, selenocysteine. Until 1986 it was thought that only 20 amino acids were directly encoded (excluding the transient case of formyl methionine; see Start Codons). Then it was found—in **eubacteria**, **archae**, and mammals—that selenocysteine was directly encoded and that its codon is UGA, which in the standard code is a stop codon (42, 43). UGA specifies selenocysteine in only a very small number of species of mRNA in each cell. In nearly all other mRNA species, UGA specifies translation termination. In each mRNA in which UGA encodes selenocysteine, there is a particular mRNA structure that acts as a recoding signal to specify that UGA means "selenocysteine" in decoding this particular mRNA. In **Gram-negative** eubacteria, this structure is a particular stem-loop structure immediately following the UGA codon (44). In mammals, the equivalent specifying element, SECIS, is in the 3′ untranslated region (45). In archae, the available evidence indicates that the enabling structure can be in either the 3′ or 5′ untranslated region of the mRNA (46). Elegant studies in *E. coli* have shown that a special elongation factor, which does not form a complex with any tRNA other than selenocysteine tRNA, binds to the loop of the mRNA stem loop structure and effectively tethers the aminoacylated selenocysteine for delivery to the ribosome poised at the UGA (44). How the SECIS element in the 3′ untranslated region of mammalian mRNA that encode selenoproteins functions is a fascinating mystery. The problem is acute in human selenoprotein P mRNA, where 10 UGA codons occur within the coding region, and all probably specify selenocysteine.

The redefinition of stop to other sense codons is also well known, and there is considerable variation in the extent of recoding signals involved in the process. With retroviruses other than Spumaretroviruses, there is no independent ribosome entry to the pol gene that encodes **reverse transcriptase** and an **endonuclease**. Instead, ribosomes that initiate translation of the upstream *gag* gene synthesize some Gag-Pol fusion protein, in addition to the separate Gag product. In murine leukemia and related viruses, the *pol* gene is in the same frame as the *gag* gene and is separated from it only by a UAG "stop" codon. Approximately 10% of the ribosomes that read the *gag* gene insert glutamine at the UAG codon and synthesize a Gag-Pol fusion. This level of "readthrough" is dependent on a recoding signal in the mRNA and is 10^{3}-fold higher than the background error level in the absence of such signals. The recoding signal is a particular pseudoknot eight bases after the UAG (47). How this pseudoknot influences the oncoming ribosomes is unexplained. Redefinition of "stop" codons is common in plant virus decoding. In barley yellow dwarf virus, both local and distant signals are important for the redefinition (48) whereas, in tobacco mosaic virus, only the sequence of the six bases following the stop codon is relevant.

5.3. Programmed Ribosomal Frameshifting

At specific positions in the decoding of some genes, a high proportion of ribosomes shift frame and then resume triplet decoding to give an essential product (49) (see Frameshifting). This probably happens in all organisms, but notable examples are synthesis of the Gag-Pol polyprotein of many retroviruses, including **HIV**-1, human antizyme, barley yellow dwarf virus polymerase, *E. coli* release factor 2, and lambda phage G-T product. Some cases of programmed frameshifting serve an autoregulatory function (eg, *E. coli* release factor 2 and human antizyme); others produce different products from a single gene in a set ratio. The recoding signals range from distant sequences to a flanking 3′ pseudoknot, stem-loop structure, or rare codons, to 5′ sequences, or to a combination. The frameshifting is +1 in some cases (eg, human antizyme and *E. coli* release factor 2) and –1 in others (eg, HIV, barley yellow dwarf virus and mouse mammary tumor virus). Many cases of programmed –1 frameshifting involve the simultaneous slippage of the pairing of two tRNA anticodons with the mRNA. In contrast, in programmed +1 frameshifting, pairing of a single tRNA anticodon is often disrupted and the codon that enters the A site is either a stop codon with no cognate tRNA or a rare codon whose cognate tRNA is in short supply. Repairing of the tRNA anticodon 1 nucleotide along the mRNA has greatly reduced, or no, competition from an incoming tRNA specified by the zero frame codon.

5.4. Bypassing

Between codons 46 and 47 of phage T4 gene *60*, there are 50 nucleotides that are translationally bypassed with high efficiency (50). This remarkable instance of decoding poses many mechanistic questions, and it is not clear how widespread the phenomenon of bypassing is. However, low-level error bypassing has been encountered when overexpressing, for biotechnological purposes, a mammalian protein in *E. coli* (50).

6. Expanding the Code Experimentally

Redesigning the genetic code to allow the incorporation of amino acids that are not normally encoded by natural genes is a challenging task. The potential advantages of having unnatural amino acids at defined places in proteins are that they could be molecular beacons for structural studies and could open the potential for new structural and functional capabilities. Short proteins can be produced by solid-phase synthesis (see Peptide Synthesis), but longer proteins with unnatural amino acids are also desirable. The most ambitious approach is to create a 65th codon-anticodon pair from unnatural nucleoside bases having nonstandard hydrogen-bonding patterns (52). The more approachable, but still very difficult, task is to use the standard nucleotides to generate *in vivo* a tRNA that is competitive for reading a particular codon and aminoacylated with an unnatural amino acid, such as a keto-containing amino acid (53). Some success has been achieved *in vitro* (54-58) but, because of severe yield limitations, it is desirable to achieve the same goal *in vivo*.

A very promising start *in vivo* has recently been made (53). An essential requirement for a tRNA that delivers an unnatural amino acid is that it is not aminoacylated by the endogenous aminoacyl-tRNA synthetase. Instead, it needs to be recognized by a mutant synthetase and acylated with the unnatural amino acid. As a first step, Schultz and colleagues (53) isolated mutants of *E. coli* glutaminyl-tRNA synthetase that aminoacylate an engineered mutant of $tRNA^{Gln}$ that is not aminoacylated by the wild-type synthetase. This is a considerable feat, but major hurdles remain.

Bibliography

1. (1966) Cold Spring Harbor Symp. Quant. Biol. **31**, 1–762.
2. F. H. C. Crick, L. Barnett, S. Brenner, and R. J. Watts-Tobin (1961) Nature **192**, 1227–1232.
3. H. G. Khorana et al. (1966) Cold Spring Harbor Symp. Quant. Biol. **31**, 39–49.
4. M. Nirenberg and P. Leder (1964) Science **145**, 1399–1407.
5. W. Min Jou, G. Haegerman, M. Ysebaert, and W. Fiers (1972) Nature **237**, 82.
6. S. Osawa (1995) *Evolution of the Genetic Code*, Oxford University Press, Oxford, U.K., pp. 1–205.
7. S. Osawa, T. H. Jukes, K. Watanabe, and A. Muto (1992) Microbiol. Rev. **56**, 229–264.
8. K. Watanabe and S. Osawa (1995) in *tRNA: Structure, Biosynthesis, and Function* (D. Söll and U. L. RajBhandary, eds.), American Society for Microbiology, Washington, D.C., pp. 225–250.
9. D. R. Wolstenholme and C. M. Fauron (1995) *The Molecular Biology of Plant Mitochondria* (C. S. Levings III and I. K. Vasil, eds.), Kluver Academic Publishers, the Netherlands, pp. 1–59.
10. J. E. Heckman et al. (1980) Proc. Natl. Acad. Sci. USA **77**, 3159–3163.
11. J. Montoya, D. Ojala, and G. Attardi (1981) Nature **290**, 465–470.
12. S. Anderson et al. (1981) Nature **290**, 457–465.
13. D. R. Wolstenholme (1992) Intern. Rev. Cytology **141**, 173–216.
14. J. Moriya et al. (1994) Biochemistry **33**, 2234–2239.
15. Y. Watanabe et al. (1994) J. Biol. Chem. **269**, 22902–22906.
16. A. Kondow, S. Yokobori, T. Ueda, and K. Watanabe (1998) Nucleosides and Nucleotides, **17**, 531–539.
17. K. Watanabe et al. (1997) in *17th International tRNA Workshop*, Abstract, Chiba, Japan, p. 12-8.
18. S. Matsuyama et al. (1998) J. Biol. Chem., **273**, 3363–3368.
19. A. Kondo, S. Yokobori, T. Ueda, and K. Watanabe (1996) Nucleic Acids Symp. Ser. **35**, 279–280.
20. Y. Kawaguchi, H. Honda, J. Taniguchi-Morimura, and S. Iwasaki (1989) Nature **341**, 164–166.
21. T. Yokogawa et al. (1992) Proc. Natl. Acad. Sci. USA **89**, 7408–7411.
22. T. Ohama et al. (1993) Nucleic Acids Res. **21**, 4039–4045.

23. T. Ueda et al. (1994) Biochimie **76**, 1217–1222.
24. M. A. S. Santos and M. F. Tuite (1995) Nucleic Acids Res. **23**, 1481–1486.
25. H. Sugiyama et al. (1995) Yeast **11**, 43–52.
26. S. Osawa and T. H. Jukes (1989) J. Mol. Evol. **4**, 191–198.
27. D. W. Schultz and M. Yarus (1994) J. Mol. Biol. **235**, 1377–1380.
28. M. A. S. Santos, V. M. Perreau, and M. F. Tuite (1995) EMBO J. **15**, 5060–5068.
29. T. Suzuki, T. Ueda, and K. Watanabe (1997) EMBO J. **16**, 1122–1134.
30. T. H. Jukes, S. Osawa, M. Yarus, and D. W. Schultz (1997) J. Mol. Evol. **45**, 1–8.
31. L. E. Orgel and F. H. C. Crick (1993) FASEB J. **7**, 238–239.
32. F. H. C. Crick (1968) J. Mol. Biol. **38**, 367–379.
33. M. Yarus (1993) In *The RNA World* (R. F. Gesteland and J. F. Atkins, eds.), Cold Spring Harbor Laboratory Press, Cold Spring Harbor, New York, pp. 205–217.
34. H. F. Noller (1993) In *The RNA World* (R. F. Gesteland and J. F. Atkins, eds.), Cold Spring Harbor Laboratory Press, Cold Spring Harbor, New York, pp. 137–156.
35. S. N. Rodin and S. Ohno (1997) Proc. Natl. Acad. Sci. USA **94**, 5183–5188.
36. N. M. Rutkevitch and L. P. Gavrilova (1982) FEBS Lett. **143**, 115–118.
37. R. Weiss and J. Cherry (1993) in *The RNA World* (R. F. Gesteland and J. F. Atkins, eds.), Cold Spring Harbor Laboratory Press, Cold Spring Harbor, New York, pp. 71–89.
38. C. R. Woese (1970) Nature **226**, 817–820.
39. F. H. C. Crick, S. Brenner, A. Klug, and G. Pieczenik (1976) Origins Life **7**, 389–397.
40. H. F. Noller et al. (1986) In *Structure, Function and Genetics of Ribosomes* (B. Hardesty and G. Kramer, eds.), Springer-Verlag, New York, pp. 143–163.
41. M. O"Connor and A. E. Dahlberg (1996) Nucl. Acids Res. **24**, 2701–2705.
42. F. Zinoni, A. Birkmann, T. C. Stadtman, and A. Böck (1986) Proc. Natl. Acad. Sci. USA **83**, 4560–4564.
43. I. Chambers et al. (1986) EMBO J. **5**, 1221–1227.
44. A. Hüttenhofer, E. Westhof, and A. Böck (1996) RNA **2**, 345–366.
45. M. J. Berry, L. Banu, J. W. Harney, and P. R. Larsen (1993) EMBO J. **12**, 3315–3322.
46. R. Wilting, S. Schorling, B. C. Persson, and A. Böck (1997) J. Mol. Biol. **266**, 637–641.
47. N. M. Wills, R. F. Gesteland, and J. F. Atkins (1994) EMBO J. **13**, 4137–4144.
48. C. M. Brown, S. P. Dinesh-Kumar, and W. A. Miller (1996) J. Virol. **70**, 5884–5892.
49. J. F. Atkins, R. B. Weiss, and R. F. Gesteland (1990) Cell **62**, 413–423.
50. R. B. Weiss, W. M. Huang, and D. M. Dunn (1990) Cell **62**, 117–126.
51. J. F. Kane et al. (1992) Nucl. Acids Res. **20**, 6707–6712.
52. J. D. Bain, C. Switzer, A. R. Chamberlin, and S. A. Benner (1992) Nature **356**, 537–539.
53. D. R. Liu, T. J. Magliery, M. Pastrnak, and P. G. Schultz (1997) Proc. Natl. Acad. Sci. USA **94**, 10092–10097.
54. C. J. Noren, S. J. Anthony-Cahill, M. C. Griffith, and P. G. Schultz (1989) Science **244**, 182–188.
55. J. D. Bain et al. (1989) J. Am. Chem. Soc. **111**, 8013–8014.
56. H.-H. Chung, D. R. Benson, and P. G. Schultz (1993) Science **259**, 806–809.
57. V. W. Cornish et al. (1994) Proc. Natl. Acad. Sci. USA **91**, 2910–2914.
58. P. E. Dawson, M. C. Fitzgerald, T. W. Muir, and S. B. H. Kent (1997) J. Amer. Chem. Soc. **119**, 7917–7927.

Suggestions for Further Reading

59. S. Osawa, T. H. Jukes, K. Watanabe, and A. Muto (1992) Recent evidence for evolution of the genetic code. Microbiol. Rev. **56**, 229–264.
60. P. Schimmel (1996) Origin of the genetic code: A needle in the haystack of tRNA sequences. Proc. Natl. Acad. Sci. USA **93**, 4521–4522.
61. A. Hüttenhofer and A. Böck (1997) "RNA structures involved in selenoprotein synthesis". In *RNA, Structure and Function* (R. W. Simon and M. Grunberg-Manago, eds.), Cold Spring Harbor Laboratory Press, Cold Spring Harbor, New York, pp. 603–639.
62. S. C. Low and M. J. Berry (1996) Knowing when not to stop: selenocysteine incorporation in eukaryotes. Trends Biochem. Sci. **21**, 203–208.
63. R. F. Gesteland and J. F. Atkins (1996) Recoding: Dynamic reprogramming of translation. Ann. Rev. Biochem. **65**, 741–768.
64. J. Castresana, G. Feldmaier-Fuchs, and S. Pääbo (1998) Codon reassignment and amino acid composition in hemichordate mitochondria. Proc. Natl. Acad. Sci. USA **95**, 3703–3707.

Genetic Disease

All of the 30,000 or more human genes can mutate, and many of the mutant alleles cause or contribute to the risk of genetic disease. In some instances, pathology occurs if only one of the two alleles at a particular locus is mutant. In other instances, both alleles must be defective. There are several sources of genetic heterogeneity in disease. Different alleles at a single locus may produce different degrees of pathology or even quite different disorders. In contrast, mutations at different loci can produce the same phenotypic changes. Mutations that arise in somatic cells can also produce disease, but they cannot be transmitted to offspring.

1. Disease, Genes, and Mutations

A discussion of genetic disease should begin with a definition of disease. Most persons use the term to indicate a departure from normal function or health. This suggests that a clear distinction exists between the healthy state and disease. Although this dichotomy may be useful to insurance companies, it is not very descriptive of biological reality. Each of us is uniquely programmed genetically to cope with greater or less success with what the environment presents to us. And ultimately we are programmed not to survive. This perception was expressed by the great British physician A.E. Garrod in his 1931 monograph *The Inborn Factors in Disease*, “It is permissible to suppose that, as in the production of those wider departures from the standard of health which receive the name of diseases, both internal and external factors are at work, so also in the causation of those lesser departures, which it is difficult to name or classify, and which may be spoken of as trifling ailments, ¼”

Diseases, then, may be thought of as deviations from normality that are sufficient to interfere with function of the organism. Many such deviations are primarily associated with specific genotypes. Others are combinations of genotypic and environmental variation. Although all are of interest, our knowledge is largely limited to those diseases that are well outside the range of normal function. In the case of inherited diseases, this means that we are largely limited to considering mutations at single loci that have a large impact on the phenotype. Results from the Human Genome Project, coupled with more sophisticated statistical techniques, are making possible the detection of smaller and more complex genetic contributions to disease risk.

As of May 2001, some 9,200 loci had been identified in the human genome. Over 7,000 loci had been assigned to specific chromosomes. Many are associated with a specific inherited variation or disease. Others are defined by the existence of their protein product or messenger RNA transcript. In some instances, a gene first observed in a nonhuman species is found to have a homolog in humans. The total number of loci is estimated to be approximately 30,000. This number is derived from the complete sequence of human DNA and is much lower than earlier estimates.

All genes have the potential to mutate. It is not known, however, what portion of the total number have the potential to mutate to a form that leads to recognizable disease. This is because many genes may cause early embryonic death if mutations occur in them. For example, any mutant form of a gene that is critical in early development may be eliminated without being observed.

2. Genotypes and Disease

The ultimate role of genes is the production of proteins of the right kind and amount in the right places and times. The vast majority of genes code for protein structures, and associated with each gene are regulatory elements—stretches of DNA that interact with other proteins to determine the amount of transcription of the gene. Most of the understanding of inherited diseases is in terms of function or malfunction of specific proteins.

Whether a mutant gene causes disease depends on several factors. Insertion or deletion of a single nucleotide in the coding region causes a shift in the reading frame during translation, leading to complete absence of the gene product. Substitution of one nucleotide for another may be equally detrimental if it causes substitution of the wrong amino acid at a functional site. Or it may have no effect at all if the amino acid substitution does not modify the function of the protein. Many such variations exist in the normal human population. Some cause small differences in function that we consider normal variation. Mutations in regulatory regions of genes may change the amount of gene product—too little or too much—but not the structure of the protein.

The phenotypic effect of these changes in gene structure depend on the role of the gene. The amounts of many enzymes normally produced are in excess of the amount needed to maintain normal metabolism. These loci are described as haplosufficient, meaning that a heterozygote that has one normal and one nonfunctional allele is phenotypically normal. Many enzyme deficiencies are inherited as recessive traits because of the need for both alleles to be *non*functional for disease to occur. Haplosufficiency also characterizes other types of proteins, such as cell cycle regulators and many receptors.

Haploinsufficiency is also observed. For example, one normal copy of a b-globin gene in hemoglobin is insufficient for manufacture of adequate amounts of b-globin, and anemia results. Again, in the case of low-density lipoprotein (LDL) receptors, one normal allele is insufficient to produce the number of functional receptors required to maintain normal levels of blood cholesterol. The transmission of these traits produces pedigrees characteristic of dominant inheritance.

One group of mutations is designated dominant negative. The name derives from the fact that the mutant allele interferes with functions of the normal allele. In a typical example, the proteins form complexes either involving one type of subunit (i.e., the product of one locus) or involving multiple subunits from different loci. The product of the mutant allele may enter into the complex but interfere with function of the complex. In the simplest case of a homodimer formed from two identical subunits, only the dimer composed of two normal subunits is functional. Both the mixed dimer and the dimer composed of two mutant subunits are nonfunctional. Because heterozygotes have reduced function, the transmission pattern is that of a dominant trait.

A variation on the previous example occurs when the mutant allele produces no protein product at all. In this case, the only subunits are produced from the normal allele, and all dimers or other multimers would be functional. This is observed in some collagen disorders, where deletion of an allele causes no phenotypic effect, the normal allele being haplosufficient. Only homozygotes for the mutant allele would generate a mutant phenotype. However, if the mutation is a minor variation in the amino acid sequence, this may interfere with production of normal collagen. The trait would appear as dominant in pedigrees.

Not all mutations or inherited syndromes involve single genes. In contiguous gene syndromes, small chromosomal deletions remove multiple closely-linked genes. The person therefore has only one copy of the genes in that segment rather than the normal two. Any genes that are haploinsufficient will affect the phenotype. The WAGR syndrome involves deletion of a small region of chromosome 11 that includes genes for *W*ilms' tumor, *A*niridia, *G*enital anomalies, and *R*etardation of growth. The WAGR syndrome is therefore the sum of the single gene defects.

3. Genetic Heterogeneity

If one considers all the possible nucleotide substitutions, insertions, and deletions in a gene that is many kilobases in size, the number of potential alleles at any one locus is enormous. In practice, one would never expect to see all possible mutant alleles in a population of finite size. However, in the case of other loci that have been extensively investigated, such as the globins, phenylalanine hydroxylase, cystic fibrosis, and Duchenne muscular dystrophy (DMD), hundreds of different mutant alleles have been identified. For the most part, these are individually very rare. In the case of the *DMD* locus, mutations are quickly eliminated by natural selection, and most mutations are found on analysis to be recent and to differ from other known mutations. In the case of other loci, a particular one or two mutations will be common, reflecting an increase in the frequency through genetic drift, founder effect, or heterozygote advantage. In the case of cystic fibrosis, some 70% of the mutant alleles in persons of European ancestry involve the identical three-nucleotide deletion, one that must have occurred many thousands of years ago to be so widely distributed.

Such allelic heterogeneity often translates into phenotypic heterogeneity. This is well illustrated in mutations of the *DMD* gene. Many of the mutations are associated with a protein product (dystrophin) that has some activity. This results in a milder form of the disease (Becker muscular dystrophy). Similar variations in severity of cystic fibrosis have been associated with different allelic combinations.

Because of the very large number of alleles at some loci, the term homozygous is often a misnomer. For rare recessive traits, it means that the two alleles are defective in their function but not that they are identical. A person with two different alleles that are functionally similar is described as a compound heterozygote. Unless the genes have been analyzed at the molecular level, one cannot be certain of true homozygosity.

Locus heterogeneity also occurs. This is the situation in which mutations at any of several loci produce the same phenotype. For example, early onset familial Alzheimer disease (FAD) is transmitted as a dominant trait and can be caused by mutations of any of three loci on three different chromosomes. The primary defect is presumably different at the molecular level, but the phenotypic results are the same.

An uncommon form of genetic heterogeneity is the production of different pathological conditions depending on where mutations occur in a gene. An example is the androgen receptor gene (*AR*), located on the X chromosome. The androgen receptor, when bound to testosterone and dihydrotestosterone, acts as a transcription factor in the nucleus. A number of mutations are known that interfere with binding and prevent the androgens from acting on target organs. The resulting disorder is known as androgen resistance. Mutations at other sites in the *AR* gene cause spinobulbar muscular atrophy.

Different populations also vary in their complements of mutant alleles. The mutations that cause cystic fibrosis occur in some 2% of persons of European origin but occur at much lower frequencies in other populations. Tay-Sachs occurs at much higher frequencies among Ashkenazi Jews. These high frequencies of detrimental genes probably arose through genetic drift and founder effect, although selective advantage may account for the high frequencies in some instances, as in sickle cell anemia in Africans. Even when the overall frequencies of mutant alleles are similar in populations, the specific alleles may differ.

4. Genetic Diseases of Somatic Cells

When inherited diseases are discussed, the traditional reference is to diseases that are transmitted from one generation to the next. Many show simple dominant or recessive inheritance according to Mendelian rules. Others are more complex, being influenced by variation at multiple loci and by environment also. The variations that can be followed in pedigrees occur in the germ lines and are therefore transmissible, even though the phenotype that we observe is based on somatic cell function.

Somatic cells, of course, have the same array of genes that are in the germ line, and they are subject to mutation as well as epigenetic alterations. The great importance of somatic cell genetics became apparent from the demonstration that mutations in somatic cells are essential parts of carcinogenesis. In the simplest case of retinoblastoma, a malignant tumor occurs when both alleles of the *RB* locus become inactive through mutation in a retinoblast. The normal restraints on cell growth no longer occur, and that cell forms a clone of cells that constitutes the tumor. The genotype of the original germline has changed in the clone of somatic cells but not in the germ cells. Retinoblastoma per se cannot be transmitted to offspring.

It has long been established that the *risk* of retinoblastoma is often transmitted as a simple dominant trait. In this case, one of the two required mutant alleles is transmitted in the germ line, and only one additional mutation is required in a retinoblast in order for the tumor to arise. This pattern has been established for a number of cancers for which high risk is found in certain families.

Somatic mutation must occur frequently at many loci. In most cases, there is no way to recognize an individual cell that has mutated. It is possible in the case of cancer because of the expansion of a clonal population from the original mutant cell. There are other instances in which somatic mutations also appear to be an essential part of the disease. For example, polycystic kidney disease is a dominantly inherited condition in which many renal cysts form. Comparison of the genotypes of the cysts with those of normal cells from the same person indicates that genetic alterations have occurred in the cysts and that each is a clone. As in cancers, clonal expansion makes it possible to detect the mutation that has occurred in a single somatic cell. Apparently two mutations are necessary, and, as in retinoblastoma, one can be transmitted through the germ line to all cells of the developing embryo. The study of somatic cell genetics is likely to be an area of great future interest as analytical techniques become ever more sensitive.

Additional Reading

Scriver C.R., Beaudet A.L., Sly W.S., Valle D., eds., *The Metabolic and Molecular Bases of Inherited Disease*, 7th ed., McGraw-Hill, New York, 1995.

Strachan T. and Read A.P., *Human Molecular Genetics*, 2nd ed., Wiley-Liss, New York, 1999.

On-Line Mendelian Inheritance in Man: http://www3.ncbi.nlm.nih.gov/Omim/

Genetic Diversity

Genetic diversity is the biological diversity that is present in the genetic material or information. Genetic diversity may be represented at the DNA level, at the level, at the **chromosomal** level, at the level, and at other higher levels, such as gene interaction.

Heterozygosity is the general measure of the genetic variation per **locus** in a given population. Suppose that a population contains *n* **alleles** at a locus, designated 1, 2, 3,¼n and with respective frequencies p_1, p_2, p_3 ,¼, p_n. Designating the frequency of the i-th allele by p_i, the heterozygosity is then defined as $H = 1 - \sum p_i^2$. When we are interested in many loci, the average heterozygosity (*H*) can be computed as an unweighted average of heterozygosities over various loci. Thus, the average heterozygosity is a simple and good measure for the genetic diversity of a population (1).

For DNA sequences, the average number of nucleotide substitutions between all possible pairs of alleles sampled in the population can be measured to evaluate the genetic diversity at the DNA level. This quantity is called the “nucleotide diversity” (1). These quantities are useful for measuring the genetic diversity within a population.

Bibliography

“Genetic Diversity” in , Vol. 2, p. 1000, by T. Gojobori; “Genetic Diversity” in (online), posting date: January 15, 2002, by T. Gojobori, National Institute of Genetics, Shizuoka, Japan.

1. M. Nei (1987). "Molecular Evolutionary Genetics". Columbia University Press, New York.

Genetic Drift

For a given gene **locus**, the frequency of a particular **allele** in a **polymorphic** population provides useful information, in that it describes the genetic composition of a given population at a particular point of time during evolution (Fig. 1). In principle, the allele frequency will never remain the same; it will always change with time because of mutation, selection, and nonrandom mating. Even when random mating occurs in a population, the allele frequency will change in a random manner over time. The random change of an allele frequency over time is called “genetic drift”. In general, the effect of genetic drift is greater the smaller the population size, and the effect of selection on allele frequencies dominates the effect of genetic drift when the population size is larger.

Figure 1. Scheme demonstrating genetic drift of an allele frequency in a population by chance over time.

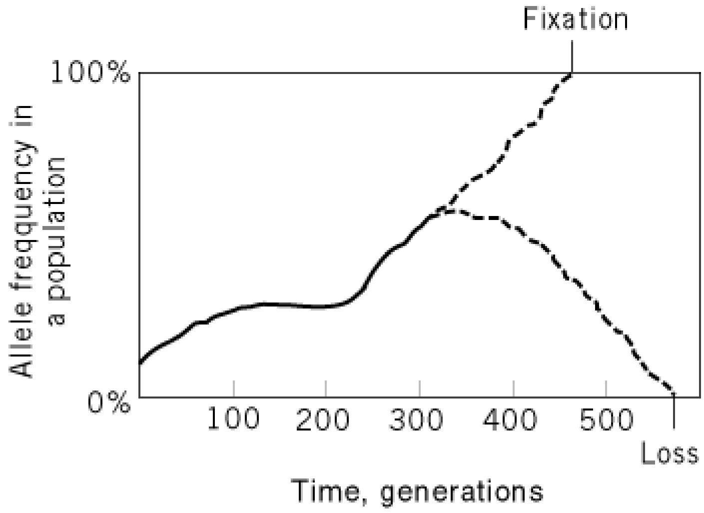

Genetic drift is an important mechanism for gene evolution because it can change the genetic composition drastically over a very short period of time, particularly when the population size is extremely small. This was initially recognized by Sewall Wright (1931) and therefore known as the Wright effect (1). The Wright effect can be seen when a small number of individuals from the mother population immigrate to a new place (the founder effect) and when the population size suddenly reduces, for reasons such as climatic change or volcanic eruption (the "bottleneck effect").

For identifying genes responsible for disease at the DNA level, it is necessary to assess linkage disequilibrium or genetic association with certain marker genes. For this practice, the effect of genetic drift should be evaluated correctly in order to discriminate between the effects of selection and of genetic drift.

Bibliography
1. S. Wright (1931). Genetics **16**, 97–159.

Genetic Marker

A genetic marker is a phenotypic variant due to a variation in the nucleotide sequence of a genome, or the phenotypic manifestation of an **allele**. The term is used frequently as a synonym of allele.

Genetic markers may affect the morphology, behavior, physiology, or chemistry of the organism, and they are defined in relation to the phenotype of the standard **wild type**. A *marker gene* is a gene whose phenotypic variants are used as genetic markers.

From a practical viewpoint we can distinguish four groups of genetic markers:

1. *Selectable* markers which enable the individuals that carry them to grow under experimental conditions that hinder similar individuals lacking the marker. Selectable markers are nearly indispensable in the genetic analysis of very large laboratory populations of **viruses**, bacteria, unicellular eukaryotes, and cultured cells. Particularly useful are the selectable markers that are also *counterselectable*; that is, certain experimental conditions allow the growth of individuals

that lack them and hinder individuals that carry them.

2. Genetic markers that are easily recognized by visual inspection of the shape, the color, and sometimes the movements of cells and organisms. They have been particularly useful in the analysis of small populations of plants and animals.
3. Genetic markers whose detection requires specific tests. Conditional lethal markers impede growth under normal conditions, but are rescued by special circumstances of the environment or the genetic background. Chemical analyses are often indispensable—for example, to detect the presence or absence of a metabolite or to distinguish the **electrophoretic** variants of a protein. Behavioral markers usually require their own specific tests. Onerous analyses can be avoided in a few cases. For example, some of the adenine auxotrophs of *Saccharomyces cerevisiae* develop a pink color under certain growth conditions; the presence of certain chemicals or certain enzymes in a cell may be revealed when they produce a colored product with certain reagents.
4. Variations in the DNA sequence that have no other phenotypic expression than the results of direct tests on the DNA (eg, restriction maps, **PCR**). Their main advantage is that they occur all over the genome, even in regions in which no other genetic markers have been located.

Genetic Suppression

Genetic suppression is the relief of a mutant phenotype by a second mutation. The second mutation gives the appearance of "suppressing" the first mutation. The suppressor mutation identifies a new site affecting the phenotype of interest, and suppression is strong evidence that the two genetic sites functionally interact. Suppressor mutations have been extremely useful for understanding genetic and biochemical phenomena. Biological systems are a tangle of interacting molecules and intersecting pathways. It should come as no surprise that mutations in one molecule are often modulated by secondary mutations in others.

Suppressor mutations can occur in the same gene as the initial mutation (intragenic suppression), or the two mutations may be in separate genes (intergenic suppression). Intragenic suppression may occur if the amino acid residues specified by the two sites must interact to give the normal function of the gene product. Intragenic suppression may also occur by the relief of a polar effect on gene expression. Intergenic suppression has been extensively used to characterize interactions between gene products. In certain cases, the suppressor mutation may establish a new pathway that supplants the pathway disrupted by the initial mutation. A special kind of suppression occurs when mutants are "rescued" by normal genes expressed from high-copy plasmids. The high concentration may facilitate an interaction between proteins that is weakened by the first mutation, or it may provide an alternative pathway to a normal phenotype. Another special kind of intergenic suppression occurs when mutations occur in transfer RNAs so that they translate stop (nonsense codons) codons as sense codons. These tRNAs (nonsense suppressors) can allow expression of genes that have suffered mutations that create stop codons within coding sequences. See "Nonsense suppression" and "tRNA suppressor" for more complete descriptions of these phenomena.

Suppressors were initially detected during studies of mutations. It was found that certain mutations express altered phenotypes only in certain genetic backgrounds. Apparently, in the non-expressing strains other genes were able to suppress these mutations. The molecular basis of these early observations has remained obscure (1), but they have been instructive for defining the principle of suppression.

In a now classic study, intragenic suppression was used to study the fundamental nature of the genetic code. Francis Crick et al. (2) showed that genes are expressed as triplets that do not overlap one another. These workers first showed that mutations that were caused by the insertion (+) or deletion (–) of nucleotides could be suppressed by a second mutation of the opposite sign, if the two mutations occurred near one another within the gene. It was concluded that genes must be read in a specific “reading frame”. Either an insertion or a deletion would shift the reading frame such that the remainder of message sequence is decoded to specify the wrong polypeptide sequence. These workers further concluded that the second mutation of the opposite sign suppresses the first mutation by restoring the initial reading frame. In between the two mutations, the gene would be translated in a wrong reading frame, but as long as the amino acid sequence of that region was not critical for protein function then the double mutant would have a wild type phenotype. Crick also used suppressor mutations to determine the size of the “codon”. It was found that although one or two insertions invariably gave a mutant phenotype, three insertions or three deletions could give a wild type phenotype. It was concluded that because the insertion or deletion of three bases did not perturb a reading frame, the genetic code is a triplet code.

Intragenic suppression can also be used to show that two amino acid within a protein molecule interact. A mutation that eliminates a critical interaction between two amino acids can sometimes be suppressed by a change in the second amino acid that restores complementarity. The first example of such an analysis is presented by Helinsky and Yanofsky (3), in which an intragenic second-site mutation restored partial function to an *Escherichia coli trpA* mutant. Such information can complement structural studies by providing confirmation of hypothetical interactions between amino acids at specific positions. Such work is greatly facilitated by site-directed mutagenesis, which allows the creation of specific mutations to test structural predictions.

Intergenic suppression is extensively used to identify and study interactions between molecules. The principle is that mutations that destroy complementary interactions between proteins may be compensated by secondary mutations that provide suitable alternative interactions. This approach has been used to identify proteins interact within biochemical, gene expression, and signal transduction pathways. This approach is also widely used to study interactions between molecules already known or suspected to interact. Examples include studies of receptor-ligand interactions and of interactions between transcription factors and promoter elements.

Another commonly used method is the identification of cloned genes that can suppress mutations when expressed at high levels. Cells are transformed with expression libraries, and suppressed isolates are selected. Suppression may occur when the overexpressed protein compensates for the defect of the initial mutation. Several molecular mechanisms are possible, and further work is usually required to elucidate the mechanism of suppression in each instance. Possible mechanisms include the restoration of a direct interaction between proteins, increasing the expression of a partially-active mutant protein, and providing a bypass of the cellular or biochemical defect of the primary mutation. A related approach, though not usually thought of as suppression, is the use of the various “two-hybrid” systems to identify interacting proteins. These are actually highly-derived examples of intergenic suppression.

Another special but widely employed kind of intergenic suppression occurs when tRNAs are mutated such that they insert a suitable amino acid at missense, nonsense and frameshift mutations. These “informational” or “translational” suppressors have been extremely useful for studying the decoding mechanisms (4). Currently, certain translational suppressors are in development as tools for protein engineering. Systems for labeling proteins with novel amino acids at specific positions would be extremely useful. Toward this end, mutant tRNAs that decode the UAG stop (classically called the “amber” codon) are being aminoacylated with nonstandard amino acids.Then these tRNAs direct the incorporation of the novel amino acid into a nascent protein if its gene has been mutated to contain an amber codon at a specific site within its coding sequence. At this time, only a few nonstandard amino acids may be incorporated in this way, but it is anticipated that it will soon be possible to label proteins with a large variety of amino acids containing affinity tags, fluors, or reactive groups (4).

Discussion of related topics can be found in “Nonsense suppression,” “Suppressor mutation,” and “Suppressor tRNA.”.

Bibliography

1. E. Kubli (1986) Trends Genet. **2**, 204–209.
2. F. H. C. Crick, L. Barnett, S. Brenner, and R. J. Watts-Tobin (1961) Nature **192**, 1227–1232.
3. D. R. Helinsky and C. Yanofsky (1963) J. Biol. Chem. **238**, 1043–1048.
4. E. J. Murgola (1994) in *tRNA: Structure, Biosynthesis, and Function* (D. Söll and U. L. RajBhandary, eds.), American Society for Microbiology Press, Washington, DC, pp. 491–509.

Genome

The *genome* is the totality of all of the **DNA** of an individual or a species. It is now taken to include all of the DNA, not just the **genes**. This definition is simple for the majority of genomes, but all of the minor DNA components must also be considered. For simple **viruses**, with a single **nucleic acid** molecule, the genome is obvious, although of course for RNA viruses it is **RNA** rather than DNA. For haploid **prokaryotes**, it is also straightforward, except for the **plasmids**, one copy of which is counted in the genome. Since prokaryotic strains and lineages differ by DNA sequence **polymorphism** and in the plasmids present, only genetic lineage genomes can be described with total accuracy. The genome of a species will be a compromise best representing all the known lineages, to make up a typical genome for the individuals of that species.

For **eukaryotes**, one haploid copy of the DNA of each of the diploid pairs of chromosomes (the autosomes) is included, plus one copy of the DNA of sex chromosomes. Thus the female and male genomes will differ if the sex chromosomes are different. One copy of the DNA from any **organelles** other than the nucleus, such as the mitochondria and chloroplasts, should be included; a complete list of such organelles is probably not yet available for any species, but many are normally unimportant. There is, of course, polymorphism of DNA sequences in a population of individuals, and the species’ genome is again a compromise to obtain a typical genome. The genome can be considered to include all of the information required to specify the species, but only for certain viruses has it actually been demonstrate that the lineage can be propagated from purified DNA. When the phrase “genome size” was first used to describe the total haploid DNA content, there were strong objections, based on the concept that there is additional information in the chromosomal proteins, and even in body structures, that is necessary to propagate the lineage. While that point of view is not common at present, the proof has not been made with eukaryotes that the DNA contains all of the information required for maintenance of the lineage or species.

The majority of the DNA of a genome is not in the genes themselves and their known associated regulatory sequence. While the phenomenon of **gene regulation** is beginning to be understood, little is known of the significance of the majority of the DNA, whether it has any functions other than acting as spacer between genes. In most species, a large fraction of the DNA is repeated sequences (see Repetitive DNA and Repeated DNA Sequence Interspersion) that cause genetic recombination and **unequal crossing over**, resulting in genomic rearrangements, but their overall significance is not understood.

Suggestions for Further Reading

T. Cavalier-Smith, ed. (1985) *The Evolution of Genome Size*, John Wiley & Sons, Chichester U.K.,

B. John and G. L. G. Miklos (1988) *The Eukaryote Genome in Development and Evolution*, Allen & Unwin, London.

Genomic Libraries

Early genomic libraries were viewed as a repository from which any genetic elements could be isolated for a given organism. Modern genomic libraries serve this function, but they also straddle the interface between genomic bioinformatics and functional biology. Thus, genomic sequences are increasingly understood in terms of their information content, comprising their RNA- and protein-coding sequences, as well as in terms of the overall organization of their embedded genetic program. Central to this information-based approach are new, highly sophisticated libraries of genomic DNA that maintain the structural context of genetic elements over several hundred kilobase pairs or more. Such libraries are essential for gene mapping projects, which will eventually produce an atlas of the genetic organization of many organisms. Detailed gene maps are required to interpret sequencing data that result from genome sequencing efforts. The genome sequencing projects themselves depend on high-quality genomic DNA libraries as a source of genetic material. The study of the genetic basis of disease makes use of sequence differences between individuals that can be ascertained through genomic libraries. These libraries also serve as a source of genetic probes that can be used for diagnosis and characterization of the relevant genotype of any individual.

Construction of genomic libraries requires particular attention during all stages of processing in order to minimize mechanical shearing of the cellular DNA. Nucleic acids become increasingly sensitive to shearing with increasing size, making it especially difficult to maintain the integrity of chromosome-sized species. Fortunately, specialized methods have been developed that enable the cloning of DNA fragments that are several hundred kilobase pairs or larger. The size of the genomic insert determines the type of vector into which the DNA is inserted. Inserts smaller than 10 kbp can be **cloned** into either plasmid or bacteriophage vectors. Cosmid vectors are required for fragments in the range of 10 to 40 kbp, while artificial chromosomes (ACs) are needed for even larger inserts.

Most genomic DNA library projects seek to represent a set of partially overlapping DNA fragments that collectively represent the entire genome of the subject organism. Such overlapping cloned inserts are ideal for chromosome “walking” approaches, in which the termini of one set of probes can be used to identify overlapping clones, which in turn can identify further overlapping clones downstream. In this manner, a set of clones can be derived that cover virtually any span of genetic sequences. Once prepared, such a repository facilitates the identification of genetic elements associated with any phenotype or disease. Three methods are employed for generating genomic DNA fragments of appropriate sizes for cloning. First, mechanical shearing can be used to produce relatively small inserts, although ligation into the vector with such fragments is typically inefficient. Because the shearing is random, this method produces a series of partially overlapping fragments. Second, and by far the most common method, is the use of restriction enzymes to prepare fragments. Digestion of DNA with restriction enzymes provides a great deal of control over the size of the resulting fragments. For example, endonucleases with a four-nucleotide recognition sequence cut on average every 256 nucleotides, while certain enzymes with large recognition sequences may cut approximately every 10^6 nucleotides. Unfortunately, complete digestion of genomic DNA with restriction enzymes eliminates any overlapping fragments; therefore, most genomic libraries employ partial digestion of genomic DNA. The degree of digestion thus influences the average fragment size, as well as the degree of fragment overlap. Another advantage of using restriction endonucleases is that the fragment termini are defined and readily clonable. The third method of preparing genomic DNA is to perform **PCR** using primers containing a region of random sequence. In the first PCR cycle, the random primer segments anneal to both strands throughout the genome and are extended in a 5′ to 3′ direction. In subsequent PCR cycles, any two oppositely oriented primers that are within sufficient proximity can generate a specific PCR product. The resulting PCR products can be prepared for cloning into an appropriate vector. Alternatively, the collection of genomic DNA fragments can be maintained and propagated as PCR products using fixed sequences, introduced during the PCR, as primer binding sites for subsequent rounds of amplification.

In general, genomic libraries are used for DNA-based studies, such as gene mapping and marker analysis; however, in certain cases they may also be useful as expression libraries. Many simpler organisms have few or no **introns**, so their genomic DNA can be directly expressed into messenger RNA and **translated** into protein. Furthermore, structural RNAs, such as **ribosomal** RNA and transfer RNA are not represented in most cDNA libraries and thus require genomic libraries to isolate appropriate DNA coding sequences. Finally, random genomic expression can be a productive means of generating RNA and peptide libraries for **epitope-** and **domain**-mapping exercises.

See also Combinatorial Libraries, Libraries, Combinatorial Synthesis, Affinity Selection, DNA Libraries, cDNA Libraries, Expression Libraries, Peptide Libraries, and Phage Display Libraries.

Germ Cell, Line

Germ cells are the cells in a multicellular organism that retain totipotency and are responsible for the propagation of succeeding generations of new individuals. Collectively, the germ cells comprise the germ line. Mature, fully differentiated germ cells in females are called eggs, or oocytes, and in males sperm, or spermatids. Undifferentiated germ cells present in animal embryos are called primordial germ cells, or PGCs. In dipterans such as *Drosophila*, PGCs are called pole cells. Flowering plants produce two types of germ cells, called microspores and megaspores. Microspores, or pollen grains, form within the stamen of the flower, and megaspores develop within the ovules of the carpels. A fundamental distinction between germ cells and other cells (somatic cells, or soma) is that, immediately prior to their final differentiation, germ cells undergo a specialized set of two cell divisions termed *meiosis*. Unlike *mitosis* , which is always coupled with DNA replication, the first meiotic division is not in organisms with sexual reproduction. Thus, meiosis reduces the ploidy of germ cells by one-half, most commonly from **diploid** to haploid. A new generation comes into being at fertilization, when the two different types of mature germ cells (for instance, egg and sperm) fuse to form a zygote . The egg and sperm nuclei also fuse to reconstitute the normal chromosome number. The zygote nucleus then divides mitotically, and it ultimately gives rise to all the cells of the organism.

1. Germ Line Specification

A common feature in animal development is that the germ line is segregated from the soma at a very early stage of embryogenesis. In many animals, germ cells develop in a region of the embryo whose cytoplasm contains specialized organelles, variously termed *P granules* , *polar granules* , or *germinal granules* (1). These organelles are assembled during oogenesis from maternally encoded gene products, and they localize asymmetrically within the egg either during oogenesis or immediately after fertilization. They are rich in RNA and protein, are not surrounded by membrane, and are associated with ribosomes and mitochondria.

Transplantation experiments in *Rana pipiens* (2), *Drosophila melanogaster* (3, 4) and Xenopus *laevis* (5), and genetic experiments in *Drosophila* (6), have demonstrated that the necessary information for germ cell determination is present in the germinal cytoplasm. In Caenorhaebditis *elegans*, P granules are distributed throughout the cytoplasm of the unfertilized egg. After fertilization, they become confined to the posterior end, such that they are found only in the posterior daughter of the first cleavage, called P_1 (7). In three subsequent mitoses, the P granules segregate to the more posterior daughter cell, called P_2, P_3, and P_4. The P_4 cell is the founder cell of the entire germ line. In *Drosophila*, pole cells arise from the pole plasm at the posterior end of the preblastoderm embryo and are the first cells to form. Pole plasm is distinguished by the presence of polar granules.

Many protein and RNA components of *Drosophila* polar granules have now been identified (reviewed in refs. 8-10), and their characterization broadly supports an early suggestion (11) that polar granules function by storing and regulating translation of maternal messenger RNAs required for germ cell determination. A protein component of polar granules in many organisms is the RNA helicase Vasa (12-17), and *vasa* activity is required in *Drosophila* for efficient translation of ***oskar*** and ***nanos***, two pole plasm-localized mRNAs (18, 19). Conversely, translation of these RNAs is repressed in *Drosophila* outside of the pole plasm (19-24). Polar granules in many species are frequently associated with mitochondria, and in *Drosophila*, mitochondrial ribosomal RNAs are associated with polar granules and may be essential for pole cell formation (25). Germ cells also possess other densely staining cytoplasmic organelles, usually termed nuage (26), which are structurally related to polar granules, and which in *Drosophila* share at least one molecular component with polar granules (12, 13, 27).

In the two-cell *Xenopus* embryo, the germ plasm is present in small aggregates near the vegetal pole (28). By the time of the second cleavage division, these aggregates have moved toward the cleavage furrows, so that each of the cells of the four-cell embryo receives a portion of the germ plasm. In subsequent cleavage divisions, however, the germ plasm is associated with one of the spindle poles and therefore is segregated to only one of the two daughter cells. At gastrulation, the germ plasm becomes perinuclear and is divided symmetrically at mitosis, so the number of PGCs increases from four to about 14 by the stage at which they exit the endoderm. In zebrafish, germ cells are not morphologically distinguishable until the 10- to 12-somite stage of development, when they are clustered on either side of the midline neighboring the third to fifth somite. However, analysis of the localization of zebrafish *vas* mRNA (17) suggests that, as in *Xenopus*, germ plasm is associated with the first two cleavage planes and condenses into four clumps, which do not further subdivide until after the 1000-cell stage. Microdissection studies in chick embryos suggest the germ line arises from the most central part of the blastodisc during the first 18 to 20 hours of development (the uterine stage), which includes cleavage and formation of the area pellucida (29).

Germ line specification in mammals may be quite different from that in other species, as mammalian oocytes lack a visible germ plasm (30). In mice, PGCs are first recognizable during gastrulation as a cluster of about 100 cells located within the midline extra-embryonic mesoderm posterior to the primitive streak (31). A key biological marker for totipotential embryonic cells is the transcription factor Oct-4 (32). Two tissue-specific enhancers have been mapped for the *Oct-4* gene, and reporter gene analysis indicates that the more distal one activates *Oct-4* expression in oocytes, morulae, and the inner cell mass of blastocyst-stage embryos, and then again in migratory and postmigratory germ cells. Trans-acting factors responsible for *Oct-4* activation have not yet been identified.

2. Germ Cell Migration

Once the germ cells have been specified, they follow an elaborate migration pathway within the interior of the embryo, culminating in an association with the gonadal mesoderm (genital ridge in vertebrates) to form the two embryonic gonads. At gastrulation, *Drosophila* pole cells are transferred within the embryo in the posterior midgut invagination. Subsequently, they actively migrate through the midgut epithelium, move dorsally, separate into two bilateral populations, and contact the overlying mesoderm (33, 34). They are then surrounded by the gonadal mesoderm and, together with that mesoderm, form the two embryonic gonads, each containing approximately 14 pole cells. Pole cells do not divide throughout the period of migration. Pole cells lacking maternal *nanos* activity migrate into the interior of the embryo, but fail to be incorporated into gonads (35). The Wunen protein, a probable phosphatidic acid phosphatase expressed on the surface of posterior midgut cells, repels germ cells and thereby limits the range of their migration on the gut (36). Later steps in germ cell migration are influenced by a large number of genes expressed in the soma, some of which, including *tinman* and *zfh-1* , have also been implicated in gonad formation (37-39).

In fish, PGCs migrate dorsally during epiboly and early gastrulation and form two groups of cells on either side of the notochord, where they remain throughout somitogenesis. The precise position of the PGCs along the anterior-posterior axis varies among different species of fish. Later in larval development, the PGCs resume cell division and coalesce into a gonad. In *Xenopus*, the PGCs become incorporated into the larval hindgut after gastrulation, then migrate through the hindgut mesentery to reach the genital ridges on either side of the dorsal aorta (40). In the chick embryo, PGCs move to the endoderm to a site where blood vessels form, and they are taken up in the bloodstream (32). They then leave the circulatory system near the position where the hindgut develops and associate with the hindgut mesentery. In the mouse embryo, PGCs disperse from extra-embryonic tissues at 8.0 days past coitum (dpc) and migrate into the hindgut epithelium (41). From 9.5 to 11.5 dpc they move out of the hindgut, along the dorsal mesentery, and ultimately reach the gonadal primordia.

3. When Does the Germ Cell Lineage become fully distinct from the Somatic Lineage?

In the *C. elegans* embryo, where the complete cell lineage is known, the germ-line or P lineage becomes distinct when the P_4 cell is formed at the 24- to 28-cell stage of embryogenesis (42). In *Drosophila*, the germ cell lineage is distinct from the soma from the time of pole cell formation; when transplanted into host embryos, labeled pole cells do not contribute to somatic tissues (43). Conversely, in vertebrate embryos, migrating PGCs are not irreversibly determined as germ line cells. Transplantation of fluorescently labeled migrating PGCs from *Xenopus* embryos into unlabeled hosts indicates that they retain the capacity to differentiate into a large variety of somatic tissues (44). In mice, 8.5-dpc and 12.5-dpc (but not 15.5-dpc) PGCs can be cultured and give rise to undifferentiated cells called EG cells (45, 46). When EG cells are injected into host blastocysts, they frequently contribute to germ line and somatic tissues. Mammalian germ cells change the **methylation** pattern of parentally **imprinted** genes upon differentiation; for at least one such gene, *Igf2*, the methylation pattern in EG cells is similar to that in germ cells and not somatic cells (46).

4. How do Germ Cells Retain Totipotency?

Few details are presently understood as to how germ cells retain the capacity to generate all the different tissues of the organism, while somatic cells become increasingly specialized. It has been observed that early PGCs in *C. elegans* and *Drosophila* transcribe essentially no mRNA (47, 48). This transcriptional silencing is correlated in both organisms with a lack of a specific phosphorylated form of RNA polymerase II in premigratory and migratory germ cells (49). Furthermore, *Drosophila* pole cells that lack *nanos* activity, and fail to colonize the gonad, activate transcription of numerous reporter genes prematurely (35). It has been suggested that the lack of gene expression in embryonic germ line cells is of fundamental importance to maintaining their totipotency.

Bibliography

1. H. W. Beams and R. G. Kessel (1974) Int. Rev. Cytol. **39**, 413–479.
2. L. D. Smith (1966) Dev. Biol. **14**, 330–347.
3. K. Illmensee and A. P. Mahowald (1974) Proc. Natl. Acad. Sci. USA **71**, 1016–1020.

4. M. Okada, I. A. Kleinman, and H. A. Schneiderman (1974) Dev. Biol. **37**, 43–54.
5. M. Wakahara (1978) J. Exp. Zool. **203**, 159–164.
6. A. Ephrussi and R. Lehmann (1992) Nature **358**, 387–392.
7. S. Strome and W. B. Wood (1983) Cell **35**, 15–25.
8. D. St Johnston (1993) in M. Bate and A. Martinez-Arias, eds. *The Development of Drosophila Melanogaster*, Cold Spring Harbor Laboratory Press, Cold Spring Harbor, New York, pp. 325–363.
9. P. F. Lasko (1994) *Molecular genetics of Drosophila oogenesis*. R. G. Landes, Austin.
10. C. Rongo and R. Lehmann (1996) Trends Genet. **12**, 102–109.
11. A. P. Mahowald (1968) J. Exp. Zool. **167**, 237–262.
12. B. Hay, L. Ackerman, S. Barbel, L. Y. Jan, and Y. N. Jan (1988) Development **103**, 625–640.
13. L. Liang, W. Diehl-Jones, and P. F. Lasko (1994) Development **120**, 1201–1211.
14. M. E. Gruidl, P. A. Smith, K. A. Kuznicki, J. S. McCrone, J. Kirchner, D. L. Roussell, S. Strome, and K. L. Bennett (1996) Proc. Natl. Acad. Sci. USA **93**, 13837–13842.
15. T. Komiya, K. Itoh, K. Ikenishi, and M. Furusawa (1994) Dev. Biol. **162**, 354–363.
16. Y. Fujiwara, T. Komiya, H. Kawabata, M. Sato, H. Fujimoto, M. Furusawa, and T. Noce (1994) Proc. Natl. Acad. Sci. USA **91**, 12258–12262.
17. C. Yoon, K. Kawakami, and N. Hopkins (1997) Development **124**, 3157–3165.
18. F.-H. Markussen, A. M. Michon, W. Breitwieser, and A. Ephrussi (1995) Development **121**, 3723–3732.
19. E. R. Gavis, L. Lunsford, S. E. Bergsten, and R. Lehmann (1996) Development **122**, 2791–2800.
20. J. Kim-Ha, K. Kerr, and P. M. Macdonald (1995) Cell **81**, 403–412.
21. P. J. Webster, L. Liang, C. A. Berg, P. Lasko, and P. M. Macdonald (1997) Genes Dev. **11**, 2510–2521.
22. A. Dahanukar and R. P. Wharton (1996) Genes Dev. **10**, 2610–2620.
23. C. A. Smibert, J. E. Wilson, K. Kerr, and P. M. Macdonald (1996) Genes Dev. **10**, 2600–2609.
24. R. P. Wharton, J. Sonoda, T. Lee, M. Patterson, and Y. Murata (1998) Mol. Cell. **1**, 863–872.
25. S. Kobayashi, R. Amikura, and M. Okada (1993) Science **260**, 1521–1523.
26. E. M. Eddy (1975) Int. Rev. Cytol. **43**, 229–280.
27. M. Wilsch-Bräuninger, H. Schwarz, and C. Nüsslein-Volhard (1997) J. Cell Biol. **139**, 817–829.
28. P. M. Whitington and K. E. Dixon (1975) J. Embryol. Exp. Morph. **33**, 57–74.
29. M. Ginsburg (1994) in J. Marsh and J. Goode, eds., *Germline Development*, Ciba Foundation Symposium 182, Wiley, Chichester: pp. 61–83.
30. E. M. Eddy, J. M. Clark, D. Gong, and B. A. Fenderson (1981) Gamete Res. **4**, 333–362.
31. M. Ginsburg, M. H. L. Snow, and A. McLaren (1990) Development **110**, 521–528.
32. Y. I. Yeom, G. Fuhrmann, C. E. Ovitt, A. Brehm, K. Ohbo, M. Gross, K. Hübner, and H. R. Schöler (1996) Development **122**, 881–894.
33. G. Callaini, M. G. Riparbelli, and R. Dallai (1995) Dev. Biol. **170**, 365–375.
34. M. K. Jaglarz and K. R. Howard (1995) Development **121**, 3495–3504.
35. S. Kobayashi, M. Yamada, M. Asaoka, and T. Kitamura (1996) Nature **380**, 708–711.
36. N. Zhang, J. Zhang, K. J. Purcell, Y. Cheng, and K. Howard (1997) Nature **385**, 64–67.
37. M. Boyle, N. Bonini, and S. DiNardo (1997) Development **124**, 971–982.
38. H. T. Broihier, L. A. Moore, M. Van Doren, S. Newman, and R. Lehmann (1998) Development **125**, 655–666.
39. L. A. Moore, H. T. Broihier, M. Van Doren, L. B. Lunsford, and R. Lehmann (1998)

Development **125**, 667–678.
40. J. Heasman and C. C. Wylie (1981) Proc. R. Soc. Lond. B Biol. Sci. **213**, 41–58.
41. M. Gomperts, C. Wylie, and J. Heasman (1994) *Germline Development*, Ciba Foundation Symposium 182, Wiley Chichester, pp. 121–139.
42. J. E. Sulston, E. Scheirenberg, J. G. White, and J. N. Thomson (1983) Dev. Biol. **100**, 64–119.
43. E. M. Underwood, J. H. Caulton, C. D. Allis, and A. P. Mahowald (1980) Dev. Biol. **77**, 303–314.
44. C. C. Wylie, J. Heasman, A. Snape, M. O"Driscoll, and S. Holwill (1985) Dev. Biol. **112**, 66–72.
45. J. L. Resnick, L. S. Bixler, L. Cheng, and P. J. Donovan (1992) Nature **359**, 550–551.
46. P. A. Labosky, D. P. Barlow, and B. L. M. Hogan (1994) Development **120**, 3197–3204.
47. M. Zalokar (1976) Dev. Biol. **49**, 425–437.
48. G. Seydoux, C. C. Mello, J. Pettitt, W. B. Wood, J. R. Priess, and A. Fire (1996) Nature **382**, 713–716.
49. G. Seydoux and M. A. Dunn (1997) Development **124**, 2191–2201.

Suggestions for Further Reading

50. H. W. Beams and R. G. Kessel (1974) "The Problem of Germ Cell Determinants," Int. Rev. Cytol. **39**, 413–479. The most complete description of the morphology of germ cell specification in a large variety of organisms.
51. J. Marsh and J. Goode, eds. (1994) *Germline Development*, Ciba Foundation Symposium, vol. 182, Wiley, Chichester, England. An excellent compendium of reviews and discussion concerning germ cell development, in many different organisms.
52. D. St Johnston (1995) "The Intracellular Localization of Messenger RNAs", Cell **81**, 161–170.
53. G. Wei and A. P. Mahowald (1994) "The Germline: Familiar and Newly Uncovered Properties," Annu. Rev. Genet. **28**, 309–324. This review includes a good discussion of genetic imprinting and culturing of mammalian germ cells. Very inclusive reference list.
54. A. Williamson and R. Lehmann (1996) "Germ Cell Development in *Drosophila*," Annu. Rev. Cell Dev. Biol. **12**, 365–391. A detailed review of the determination, formation, migration, and differentiation of germ cells in Drosophila.

Gibberellins

1. History

Gibberellins are plant hormones, tetracyclic diterpene carboxylic acids that were discovered in 1926 as a phytotoxin produced by the fungus *Gibberella fujikuroi*. The latter caused a pathological longitudinal growth in rice called "foolish seedling disease" (1). The active compound was isolated from the fungus in 1930 by Yabuta and Sumiki (2) and was called *gibberellin*. In 1958, a first gibberellin (GA_1) was purified from runner bean seeds (*Phaseolus coccineus*) by MacMillan and coworkers (3). Since this discovery, 112 gibberellins have been identified (4).

2. Biosynthesis and Metabolism

Gibberellins are isoprenoid compounds synthesized from C2 units by the mevalonic acid pathway. Geranyl geranyl diphosphate, a C20 molecule, serves as a donor for the entire carbon skeleton of gibberellins. Starting from geranyl geranyl diphosphate, biosynthesis of gibberellins can be divided into three stages according to the nature of the enzymes involved and their subcellular localization (Fig. 1). The pathway is well-characterized, owing to the existence of gibberellin-deficient mutants that are easily identified by their dwarfed stature (5, 6). Gibberellin-deficient mutants are blocked at a particular step in the pathway, and their **phenotype** can be reverted by external addition of active gibberellins.

Figure 1. Gibberellin biosynthetic pathway in higher plants. Steps involving GA1, GA2, GA4, and GA5 in *Arabidopsis* are indicated. (Adapted from Ref. 16)

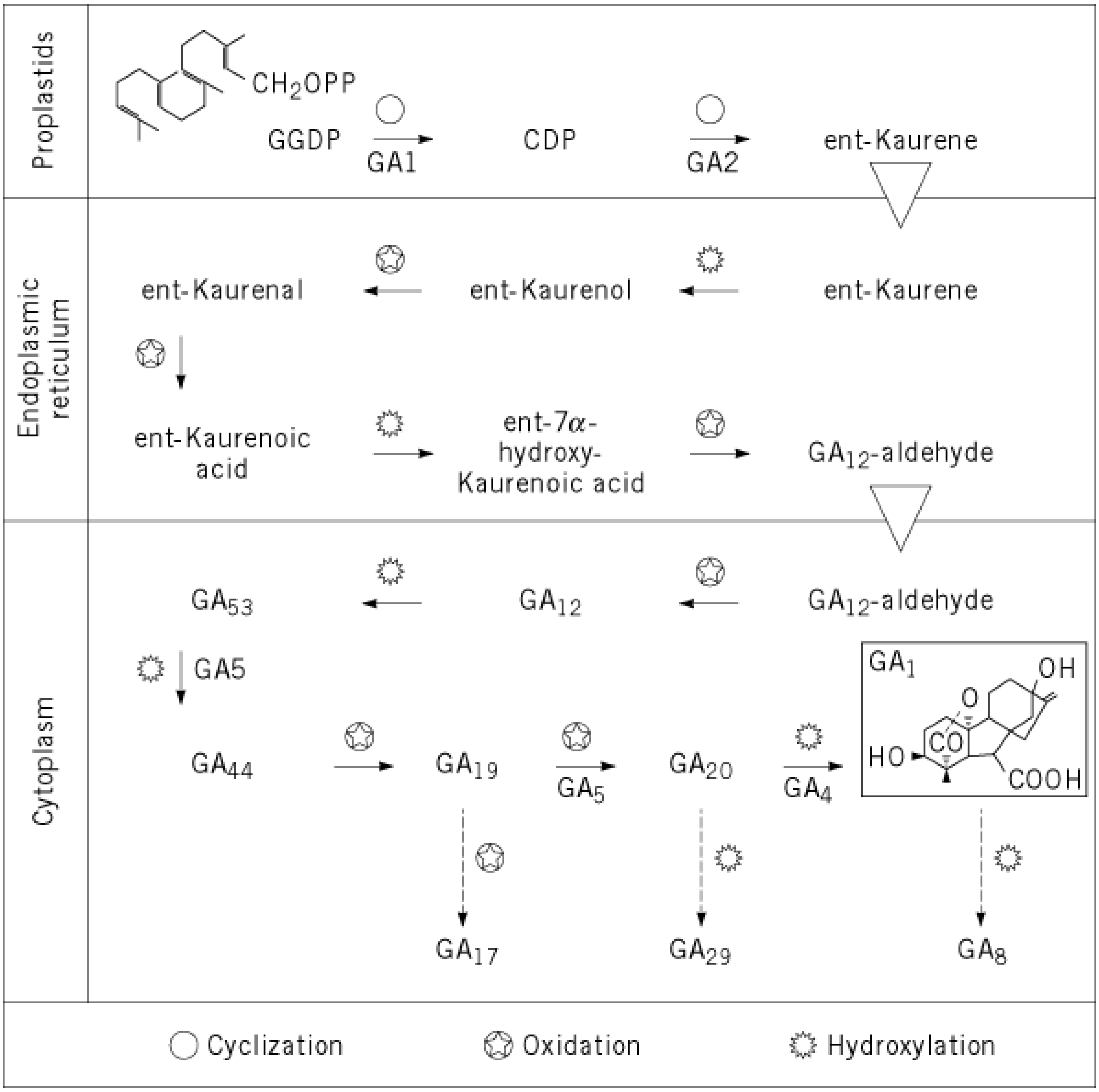

Several **genes** encoding gibberellin-biosynthetic enzymes have been characterized, and their products seem to catalyze multiple steps. First, geranyl geranyl diphosphate is converted into *ent*-kaurene by two cyclization steps. The enzymes catalyzing these reactions are *ent*-kaurene synthase A and B, also termed *ent*-copalyl diphosphate synthase (CPS) and *ent*-kaurene synthase (KS) (7). The gene encoding the CPS has been cloned from *Arabidopsis* (*GA1*) (8), maize (*Anther ear-1, An1*) (9), pea (*LS*) (10), tomato (11), and pumpkin (12), whereas that for KS was cloned from pumpkin endosperm (13) and from *Arabidopsis* (*GA2*) (14).

The KS activity is mostly associated with stroma of proplastids in rapidly dividing plant tissues (15); however, *GA1* promoter activity is also present in fully expanded leaves (16), suggesting that gibberellins are transported to responsive tissues. In Arabidopsis ***Arabidopsis***, *GA1* gene expression appears to be highly regulated during growth and development. In addition, *GA1* promoter activity was restricted to specific cell types, such as shoot apices, root tips, developing seeds and flowers, and vascular tissue of mature leaves (17).

The second stage converts *ent*-kaurene to GA_{12}-aldehyde. *Ent*-kaurene is subjected to five sequential oxidation steps, resulting in GA_{12}-aldehyde. These reactions take place in the endoplasmic reticulum and seem to be catalyzed by a single membrane-associated cytochrome P450 monooxygenase. The gene encoding this enzyme was recently cloned from maize (*Dwarf-3, D3*) (18). Its expression was observed in seedlings, developing leaves, vegetative meristems, and roots. The predicted protein carries the Fe-binding domain that is characteristic of cytochrome P450 proteins (18).

The third stage converts GA_{12}-aldehyde to various gibberellins and takes place in the cytoplasm. The first step in this process consists of the oxidation of GA_{12}-aldehyde to GA_{12}. Subsequently, GA_{12} is subjected to various reactions, depending on the organism. In the past, genes encoding one of the major enzymes involved in these reactions, GA 20-oxidase, were characterized in different species such as pumpkin (19), *Arabidopsis* (*GA5*) (20), and spinach (21). GA 20-oxidases belong to the family of 2-oxoglutarate-dependent dioxygenases. In *Arabidopsis*, GA 20-oxidases are encoded by a small multigene family. Expression of the *GA5* gene in leaves was enhanced when plants were shifted from short-day to long-day conditions, indicating photoperiod regulation. In addition, *GA5* was down-regulated by GA_4 treatment, suggesting feedback repression of the pathway (20). Finally, a 3b-hydroxylase catalyzes the formation of biologically active gibberellins. The *GA4* locus encoding a 3b-hydroxylase was recently cloned from *Arabidopsis* (22). The gene is ubiquitously expressed, but its messenger RNA is most abundant in siliques. As with *GA5, GA4* is also subjected to a feedback regulatory mechanism (23).

Relatively few gibberellins appear to be biologically active, such as GA_1, GA_3, and GA_4. The remaining ones are the precursors or the deactivated forms of active gibberellins. The latter are generally deactivated by 2b-hydroxylation. The only deactivation mutant described thus far is the slender (*sln*) genotype of *Pisum sativum* . A mutation at this locus is responsible for a large accumulation of GA_{20}, the precursor of GA_1, and gives rise to the elongated phenotype. It was suggested that *sln* encodes a regulatory protein controlling two genes involved in the degradation pathway (24). Another process in gibberellin metabolism is their conjugation to inactive derivatives, including glucosyl ethers and glucose esters, that are found mainly in seeds (25).

3. Signal Perception and Transduction

The gibberellin biosynthesis pathway is well-characterized, but much less is known about how gibberellins are perceived by the plant and how the signal is transduced to control the expression of gibberellin-regulated genes (26, 27). Biochemical studies on barley aleurone protoplasts suggested that gibberellin binds to a receptor located at the external face of the plasma membrane (28). This receptor has not yet been isolated, however, nor has any gibberellin receptor been cloned to date.

Our current knowledge of gibberellin signaling is based mainly on the characterization of four mutants of *Arabidopsis: spy* (*spindly*), *gai* (*gibberellin-insensitive*), *rga* (*repressor of ga1-3*), and *pkl* (*pickle*). None of these mutants can be entirely reverted by exogenous application of gibberellin, supporting their role in gibberellin signaling.

The *spy* mutants were screened for their ability to germinate in the presence of the gibberellin biosynthesis inhibitor paclobutrazol, which blocks the cytochrome P450 monooxygenase involved in the oxidation of *ent*-kaurene to *ent*-kaurenoic acid (29). *Spy* mutants phenocopy wild-type plants that were repeatedly treated with GA_3, presenting a constitutive gibberellin-response phenotype that is characterized by long hypocotyls, pale green foliage, increased stem elongation, early flowering, partial male sterility, and parthenocarpic fruit development. Moreover, *spy* plants remain gibberellin-responsive. *Spy* is partially epistatic to *ga1-2*. Collectively, these data indicate that SPY is a negative regulator of at least one branch in gibberellin signaling.

The *SPY* gene was recently cloned using a T-DNA tagging approach (30). The predicted SPY protein contains a tetratricopeptide repeat of 34 amino acid residues in its *N*-terminal region. This motif is also found in some other eukaryotic and prokaryotic proteins and is proposed to form an amphipathic a-helix that mediates protein–protein interactions (31). The tetratricopeptide repeat appears to be important for the normal function of SPY, because some of the mutant phenotypes result from a deletion in this motif. The *C*-terminal region of SPY shows sequence similarity to the mammalian Ser/Thr *O*-linked *N*-acetylglucosamine (*O*-GlcNAc) transferase, which plays an important role in the regulation of the activity of various nuclear and cytosolic proteins, either directly or by inhibiting their phosphorylation (32, 33). Because certain *spy* alleles are affected in the region bearing similarity to *O*-GlcNAc transferase, this activity seems to be involved in proper functioning of the *SPY* gene product.

A second player is GAI. *Gai* mutant plants present a dwarf phenotype (reduced plant height, decrease in apical dominance, and limited seed germination), comparable to gibberellin-deficient plants. The lack of response of *gai* mutants to exogenous application of gibberellin, however, suggests that the GAI protein acts in signal transduction (34, 35). *Gai* heterozygotes show an intermediate mutant phenotype, indicating that the mutation is semidominant.

The *GAI* gene was recently isolated using *Ds* transposon tagging (36). In addition, a closely related gene named *GRS* (*GAI-related sequence*) was cloned (36). Comparison of the predicted amino acid sequences of the GRS and GAI proteins with the sequence databases showed that they are members of the VHIID family of plant transcription factors defined by Di Laurenzio et al. (37). A first member of this novel class of transcription factors was called *SCARECROW* (*SCR*) and controls cell fate in *Arabidopsis* roots. The VHIID proteins are putative transcription factors that contain three main motifs: a central –Val–His–Ile–Ile–Asp–sequence, with a Leu–X–X–Leu–Leu–sequence (where X represents any amino acid residue) in its immediate vicinity, and an –Arg–Val–Glu–Arg–sequence in the *C*-terminal region (38). The Leu–X–X–Leu–Leu–motif is a signature motif in transcriptional coactivators that mediates binding to nuclear receptors (39). The GAI protein possesses a fourth sequence in its *N*-terminal region (–Asp–Glu–Leu–Leu–Ala–) that appears important for its normal function. A nearby Ser/Thr-rich stretch is a potential target of SPY action. GAI was proposed to act directly as a transcriptional repressor of target genes that promote gibberellin-mediated processes, or indirectly as a transcriptional activator that induces the expression of such a repressor (36). This hypothesis implies that gibberellin would modulate the pathway by derepression and, therefore, by inactivation of GAI. An extragenic suppressor mutant of *gai*, called *gar2* (*gai suppressor 2*), was genetically characterized (35).

A third class of gibberellin-signaling mutants is represented by *rga* (*repressor of ga1-3*) (40). *Rga* mutants were found by screening for the ability to suppress the phenotype of the *ga1-3* mutant that is impaired in the first step of the gibberellin biosynthesis pathway (41). It is important to note, however, that the *rga* mutation does not suppress the gibberellin deficiency entirely, because it has no effect on seed germination or on silique growth. All *rga* alleles are recessive, indicating that *RGA* most probably encodes a negative regulator of gibberellin signaling.

The *RGA* gene was cloned using genomic subtraction and shown to be identical to *GRS* (38). The predicted protein is a member of the VHIID family of plant transcription factors described above. Although primarily repressing the gibberellin response, RGA may also play a role in the control of gibberellin biosynthesis (38). The RGA protein contains the –Asp–Glu–Leu–Leu–Ala–sequence and the Ser/Thr-rich region, both specific to proteins controlling the gibberellin response.

A final regulator, though difficult to place in the pathway at this point, is *pickle* (*pkl*). The *pkl* mutants present a phenotype reminiscent of gibberellin-deficient or gibberellin response mutants and exhibit abnormal root development (42). The primary root meristem of these mutants retained characteristics of embryonic tissues. This phenotype was partially suppressed by addition of gibberellin. Because the *gai pkl* double mutant exhibited a strong synergistic gibberellin-deficient phenotype, it was concluded that *pkl* is defective in the gibberellin-response pathway. The gene product PKL is proposed to be a positive regulator of gibberellin signaling (43).

Figure 2 presents a model for gibberellin signal transduction based on currently available genetic and biochemical data (38, 40, 43). Gibberellin interacts with its receptor(s), thereby activating gibberellin responses as a result of inhibition of two negative regulators (branches A and B). In branch A, SPY is acting downstream of (or modulates) GAI, because the *spy* mutant is completely epistatic to the *gai* mutation. SPY presumably activates the GAI repressor function via glycosylation. The RGA protein exerts the same function as GAI and represses the transcription of genes involved in gibberellin-regulated growth and development, or it promotes the expression of such a repressor. The repressor function of RGA is activated by SPY or a putative SPY-like protein, unknown to date. This assumption is based on the fact that the *rga* and *spy* mutations have an additive effect for the common processes controlled by gibberellins, thus indicating that SPY probably does not regulate RGA. Both *O*-glycosyltransferases would repress the common gibberellin response (stem elongation, trichome initiation, apical dominance, and flower development). In addition, the "GAI/SPY" branch blocks seed germination and silique growth.

Figure 2. Gibberellin signal transduction. The active gibberellin interacts with a membrane-associated or cytosolic receptor and activates the normal gibberellin response by blocking two repressors, named GAI (branch A) and RGA (branch B). The SPY and/or SPY-like proteins regulate the GAI and RGA proteins via glycosylation. Arrows and bars denote activation and repression, respectively.(Modified from Refs. 38, 40, and 41.)

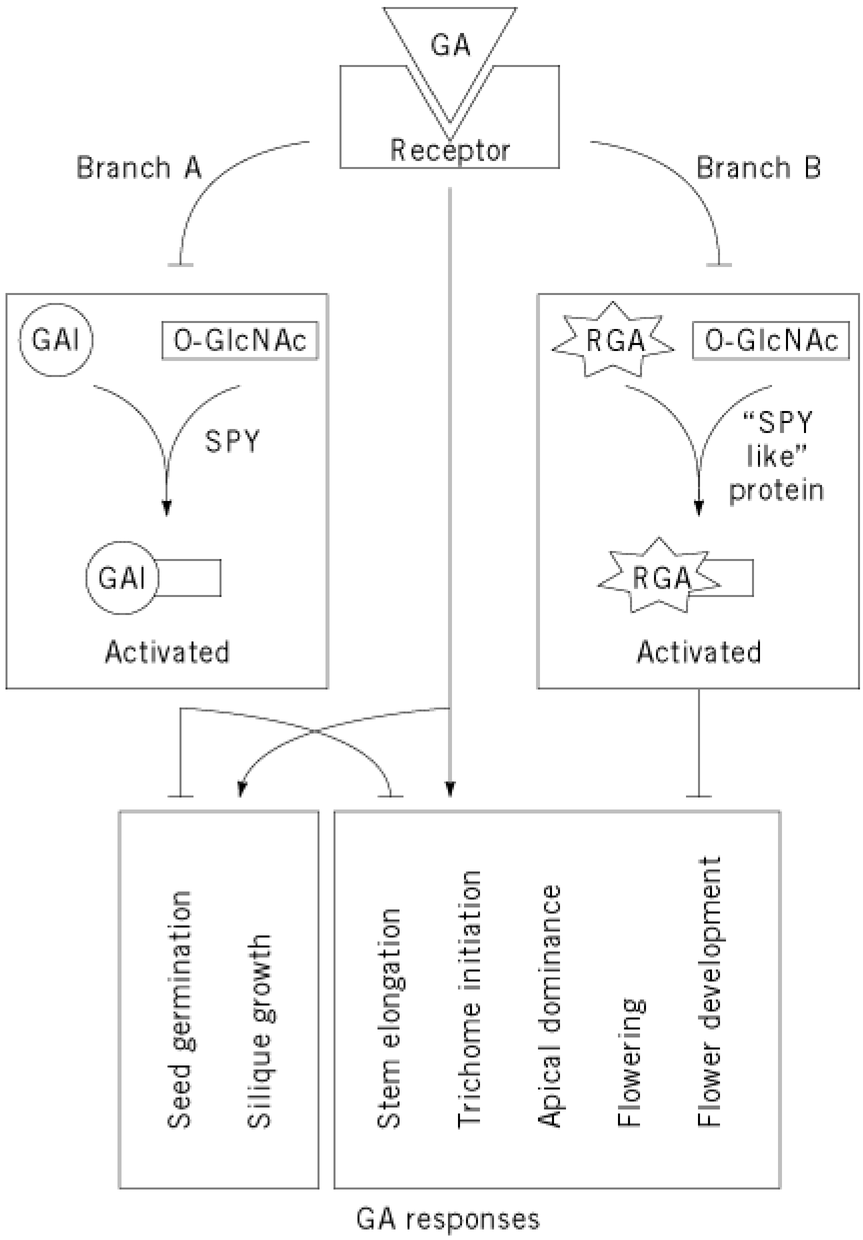

Due to their nature, SPY/RGA/GAI would act fairly late in the pathway to induce gibberellin-regulated responses. It should be mentioned that recent evidence also suggests the involvement of heterotrimeric **G proteins** and cyclic GMP in gibberellin signaling in barley aleurone cells (44, 45). The former intermediates would play a role in the early phase of signal transfer.

4. Downstream Targets

Gibberellin control of plant growth and development is achieved by modulating the expression of specific target genes. One of the best-characterized roles of gibberellins consists in the stimulation of production of hydrolytic enzymes by the aleurone cells. These hydrolytic enzymes, such as a-amylase, a-glucosidase, and a thiol proteinase, are responsible for the breakdown of starch and proteins in the endosperm (46-48). The products of these hydrolyses are absorbed by the scutellum and used by the growing embryo. *De novo* synthesis of hydrolytic enzymes induced by gibberellin is often due to the presence of a gibberellin response element (GARE) in the promoter region of the corresponding genes (49). The identification of the GARE element has led to the isolation of a myb-like *trans*-acting factor that can bind to this region, which is closely related to c-Myb and v-Myb consensus sequences (50). Furthermore, gibberellins can stimulate stem elongation by increasing the xyloglucan endotransglycosylase activity, an enzyme that cleaves the rigid structure of the cell wall and is associated with growing tissues (51, 52). In addition, gibberellins cause microtubule reorientation favoring axial elongation (53). The tonoplast–intrinsic protein g-TIP, which maintains turgor pressure, thereby favoring wall extensibility, is also induced by gibberellin application (54). In *Petunia* flower development, gibberellin induces the expression of genes such as those of chalcone synthase, chalcone isomerase, anthocyanidin synthase, and dihydroflavonol 4-reductase, which are responsible collectively for corolla pigmentation (55-59).

5. Effects

Biologically active gibberellins are involved in key processes of plant growth and development. The best-characterized roles of gibberellins consist in the control of reserve mobilization in cereals following germination and in promotion of shoot elongation through effects on both cell division and expansion. Gibberellins are also involved in the regulation of flower and fruit development and are required for germination and seedling growth in several species (60).

Bibliography

1. N. Takahashi, B. O. Phinney, and J. MacMillan (1991) *Gibberellins*, Springer-Verlag, New York.
2. T. Yabuta and Y. Sumiki (1938) J. Agric. Chem. Soc. Japan **14**, 1526.
3. J. MacMillan and P. J. Suter (1958) Naturwissenschaften **45**, 46.
4. T. Hisamatsu, M. Koshioka, S. Kubota, T. Nishijima, R. W. King, L. N. Mander, and D. J. Owen (1998) Phytochemistry **47**, 3–6.
5. R. Hooley (1994) Plant Mol. Biol. **26**, 1529–1555.
6. P. Hedden and Y. Kamiya (1997) Annu. Rev. Plant Physiol. Plant Mol. Biol. **48**, 431–460.
7. J. MacMillan (1997) Nat. Prod. Rep. **14**, 221–243.
8. T.-p. Sun, H. M. Goodman, and F. M. Ausubel (1992) Plant Cell **4**, 119–128.
9. R. J. Bensen, G. S. Johal, V. C. Crane, J. T. Tossberg, P. S. Schnable, R. B. Meeley, and S. P. Briggs (1995) Plant Cell **7**, 75–84.
10. T. Ait-Ali, S. M. Swain, J. B. Reid, T.-p. Sun, and Y. Kamiya (1997) Plant J. **11**, 443–454.
11. R. Imai, Y. Y. Yang, T. Ait-Ali, H. Kawaide, and Y. Kamaya (1996) Plant Cell Physiol. **37**

(Suppl.), S143 (#539).
12. M. W. Smith, S. Yamaguchi, T. Ait-Ali, and Y. Kamiya (1997) Plant Cell Physiol. **38** (Suppl.), S115 (#413).
13. S. Yamaguchi, T. Saito, H. Abe, H. Yamane, N. Murofushi, and Y. Kamiya (1996) Plant J. **10**, 203–213.
14. S. Yamaguchi, T.-p. Sun, H. Kawaide, and Y. Kamiya (1998) Plant Physiol. **116**, 1271–1278.
15. H. Aach, H. Bode, D. G. Robinson, and J. E. Graebe (1997) Planta **202**, 211–219.
16. T.-p. Sun and Y. Kamiya (1997) Physiol. Plant. **101**, 701–708.
17. A. L. Silverstone, C.-w. Chang, E. Krol, and T.-p. Sun (1997) Plant J. **12**, 9–19.
18. R. G. Winkler and T. Helentjaris (1995) Plant Cell **7**, 1307–1317.
19. T. Lange, P. Hedden, and J. E. Graebe (1994) Proc. Natl. Acad. Sci. USA **91**, 8552–8556.
20. Y.-L. Xu, L. Li, K. Wu, A. J. M. Peeters, D. A. Gage, and J. A. D. Zeevaart (1995) Proc. Natl. Acad. Sci. USA **92**, 6640–6644.
21. K. Wu, L. Li, D. A. Gage, and J. A. D. Zeevaart (1996) Plant Physiol. **110**, 547–554.
22. H.-H. Chiang, I. Hwang, and H. M. Goodman (1995) Plant Cell **7**, 195–201.
23. J. B. Reid, J. J. Ross, and S. M. Swain (1992) Planta **188**, 462–467.
24. J. J. Ross, J. B. Reid, S. M. Swain, O. Hasan, A. T. Poole, P. Hedden, and C. L. Willis (1995) Plant J. **7**, 513–523.
25. F. B. Salisbury and C. W. Ross (1992) In *Plant Physiology*, 4th ed. (F. B. Salisbury and C. W. Ross, eds.), Wadsworth, Belmont, CA, pp. 357–381.
26. S. M. Swain and N. E. Olszewski (1996) Plant Physiol. **112**, 11–17.
27. J. J. Ross, I. C. Murfet, and J. B. Reid (1997) Physiol. Plant. **100**, 550–560.
28. S. Gilroy and R. L. Jones (1994) Plant Physiol. **104**, 1185–1192.
29. S. E. Jacobsen and N. E. Olszewski (1993) Plant Cell **5**, 887–896.
30. S. E. Jacobsen, K. A. Binkowski, and N. E. Olszewski (1996) Proc. Natl. Acad. Sci. USA **93**, 9292–9296.
31. J. R. Lamb, S. Tugendreich, and P. Hieter (1995) Trends Biochem. Sci. **20**, 257–259.
32. L. K. Kreppel, M. A. Blomberg, and G. W. Hart (1997) J. Biol. Chem. **272**, 9308–9315.
33. W. A. Lubas, D. W. Frank, M. Krause, and J. A. Hanover (1997) J. Biol. Chem. **272**, 9316–9324.
34. M. Koornneef, A. Elgersma, C. J. Hanhart, E. P. van Loenen-Martinet, L. van Rijn, and J. A. D. Zeevaart (1985) Physiol. Plant. **65**, 33–39.
35. R. N. Wilson and C. R. Somerville (1995) Plant Physiol. **108**, 495–502.
36. J. Peng, P. Carol, D. E. Richards, K. E. King, R. J. Cowling, G. P. Murphy, and N. P. Harberd (1997) Genes Dev. **11**, 3194–3205.
37. L. Di Laurenzio, J. Wysocka-Diller, J. E. Malamy, L. Pysh, Y. Helariutta, G. Freshour, M. G. Hahn, K. A. Feldmann, and P. N. Benfey (1996) Cell **86**, 423–433.
38. A. L. Silverstone, C. N. Ciampaglio, and T.-p. Sun (1998) Plant Cell **10**, 155–169.
39. D. M. Heery, E. Kalkhoven, S. Hoare, and M. G. Parker (1997) Nature **387**, 733–736.
40. A. L. Silverstone, P. Y. A. Mak, E. C. Martínez, and T.-p. Sun (1997) Genetics **146**, 1087–1099.
41. T.-p. Sun and Y. Kamiya (1994) Plant Cell **6**, 1509–1518.
42. J. Ogas, J.-C. Cheng, Z. R. Sung, and C. Somerville (1997) Science **277**, 91–94.
43. J. Ogas (1998) Curr. Biol. **8**, R165–R167.
44. S. P. Penson, R. C. Schuurink, A. Fath, F. Gubler, J. V. Jacobsen, and R. L. Jones (1996) Plant Cell **8**, 2325–2333.
45. H. D. Jones, S. J. Smith, R. Desikan, S. Plakidou-Dymock, A. Lovegrove, and R. Hooley (1998) Plant Cell **10**, 245–253.

46. S. M. Koehler and T.-H. D. Ho (1990) Plant Cell **2**, 769–783.
47. A. K. Huttly and A. L. Phillips (1995) Physiol. Plant. **95**, 310–317.
48. B. K. Tibbot and R. W. Skadsen (1996) Plant Mol. Biol. **30**, 229–241.
49. A. K. Huttly, A. L. Phillips, and J. W. Tregear (1992) Plant Mol. Biol. **19**, 903–911.
50. F. Gubler, R. Kalla, J. K. Roberts, and J. V. Jacobsen (1995) Plant Cell **7**, 1879–1891.
51. M. C. Smith, P. R. Matthews, P. H. D. Schünmann, and P. M. Chandler (1996) J. Exp. Bot. **47**, 1395–1404.
52. P. H. D. Schünmann, R. C. Smith, V. Lång, P.R. Matthews, and P. M. Chandler (1997) Plant Cell Environ. **20**, 1439–1450.
53. H. Shibaoka (1994) Annu. Rev. Plant Physiol. Plant Mol. Biol. **45**, 527–544.
54. A. L. Phillips and A. K. Huttly (1994) Plant Mol. Biol. **24**, 603–615.
55. D. Weiss and A. H. Halevy (1989) Planta **179**, 89–96.
56. D. Weiss, A. J. van Tunen, A. H. Halevy, J. N. M. Mol, and A. G. M. Gerats (1990) Plant Physiol. **94**, 511–515.
57. D. Weiss, R. van Blokland, J. M. Kooter, J. N. M. Mol, and A. J. van Tunen (1992) Plant Physiol. **98**, 191–197.
58. D. Weiss, A. H. van der Luit, J. T. M. Kroon, J. N. M. Mol, and J. M. Kooter (1993) Plant Mol. Biol. **22**, 893–897.
59. G. Ben-Nissan and D. Weiss (1996) Plant Mol. Biol. **32**, 1067–1074.
60. S. M. Swain, J. B. Reid, and Y. Kamiya (1997) Plant J. **12**, 1329–1338.
61. H. Kende and J. A. D. Zeevaart (1997) Plant Cell **9**, 1197–1210.

Giemsa Binding

Giemsa is one of the most useful dyes for staining chromosomes in the banding patterns characteristic of different types of heterochromatin and euchromatin (see C-Banding and G Banding). It is a mixture of organic dyes including thionine, or Lauth's violet, and methylated derivatives of thionine (see Figure 1) including azure B, azure A, azure C, and methylene blue. Thionine itself stains chromosomes uniformly. The introduction of methyl groups, however, changes the properties of the molecule so that it differentially stains chromatin. The thiazine ring in the Giemsa dyes interacts with the phosphodiester backbone of **DNA** and side-stacks along the **double helix**. How this might occur in a chromatin context is not yet known. Variations in chromosomal preparations, in which the histones are removed and other chromosomal proteins digested to different extents, enhance the banding patterns obtained with Giemsa dye (see G Banding).

Figure 1. The chemical structures of thionine and methylene blue.

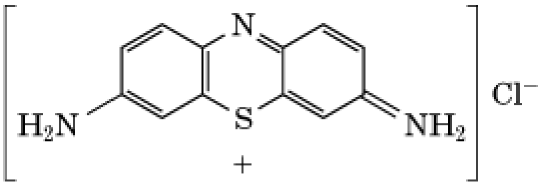

Thionine

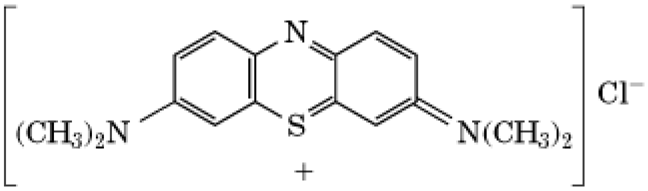

Methylene blue

Suggestion for Further Reading

1. R. P. Wagner, M. P. Maguire, and R. L. Stallings (1993) *Chromosomes*. A Synthesis, Wiley-Liss, New York.

Globins

1. Definition, structure, and properties

Globins are members of a family of oxygen-binding proteins, characterized by **homologous** amino acid sequences and a characteristic protein structure known as the “globin fold.” As illustrated in Figure 1, the globin fold is comprised of eight **alpha-helical** segments, designated A through H, which are connected by loop segments AB, BC, ¼ and GH. The nonhelical segments at the amino and carboxyl termini are designated as NA and HC, respectively. The globin fold is maintained even when the sequence identity between pairs of globins is as low as 16% (2). In most vertebrates, individual globin **polypeptide chains** consist of 141 to 153 amino acid residues. Another property of the globin fold is its ability to bind a heme group, protoporphyrin IX with a ferrous iron atom at its center. The heme group is inserted in a cleft in the protein structure between the E and F helices, known as the “heme pocket.” The iron atom is linked covalently to the imidazole N_{ε}; of the “proximal” histidine residue at position F8 (the eighth residue of the F helix). There are also many van der Waals interactions between the heme group and the amino acid side chains that line the heme pocket. Under physiological conditions, the iron atom is in the ferrous state, when it is capable of binding one molecule of O_2 on the “distal” side of the heme group. The side chain of the distal His-E7 forms a hydrogen bond with one of the oxygen atoms, stabilizing the bound oxygen (see Myoglobin). In this state, the ferrous iron is hexacoordinated with one of the oxygen atoms, N_{ε}; of His-F8, and the four pyrrole nitrogen atoms of protoporphyrin IX. When oxygen is not bound, the sixth coordination site for oxygen is left vacant, and the iron atom is only pentacoordinated.

Figure 1. The globin fold. Cylinders represent the eight a-helices. The lines correspond to the interhelical regions are

not exact and signify only the connectivity of the polypeptide chain. The bold short line indicates the side view of the heme group. From Ref. 2.

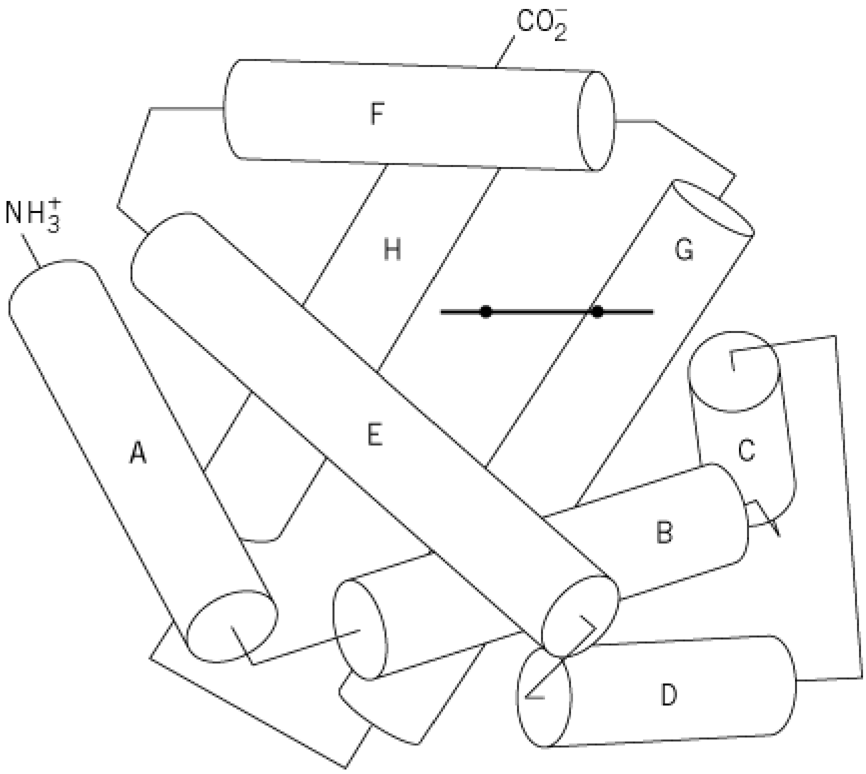

2. Distribution and Classification

Globins are found in organisms as hemoglobin (Hb) or myoglobin (Mb). Their common property is the reversible binding of oxygen. Mb is present in the muscles and stores oxygen, whereas Hb is present in the blood and transports oxygen from the lungs or gills to the peripheral tissues. Mb is usually a monomer, although sometimes a dimer, comprised of a single polypeptide chain and one heme group, whereas Hb is an oligomer or polymer composed two or more globin polypeptide chains, each with a heme group. Globin oxygen-binding proteins are even found in organisms that have no muscle or blood, including insects, **plants**, and single-celled organisms such as protozoa, **yeast**, and **bacteria**. These proteins are conventionally called hemoglobins, although some call them myoglobins because of their monomeric structures. Globin **genes** are widespread in modern plants, and plant hemoglobins are believed to have evolved from an **evolutionary** ancestor common to modern plants and animals (3).

3. Modular Structure and Evolution

The globin fold is composed of four structural units, called modules M1, M2, M3, and M4 (4) (Fig. 2). In most globins, modules M1 and M4 are encoded by two corresponding exons of the **gene** (see Introns, Exons). In contrast, modules M2 and M3, which are the structural units that hold the heme group, are encoded by a single exon. In the Hb genes of leghemoglobin (from the legume root nodule) and nematode Hb, however, this single exon is divided into two exons by the insertion of one intron. It is believed that this intron was present initially in the ancestral globin gene but lost during the molecular evolution of the other globin genes (6). Consequently, the globin fold is considered to be encoded by four exons that correspond to the four structural modules. This is one of the best indications of protein evolution by exon shuffling.

Figure 2. Schematic representation of the three-dimensional structure of the human Hb-b chain and its constituent four structural modules. (**a**) The structure of the b-chain; the heme group is bound in a pocket between helices E and F. Arrows indicate the positions of the modular joints that correspond to the positions of the introns in the b-globin gene. (**b**) The first module, at the N-terminus, encoded by Exon 1. (**c**) The joined second and third modules, encoded by Exon 2; the heme group is bound by this pair of modules. (**d**) The fourth module, encoded by Exon 3. Reproduced from Ref. 5.

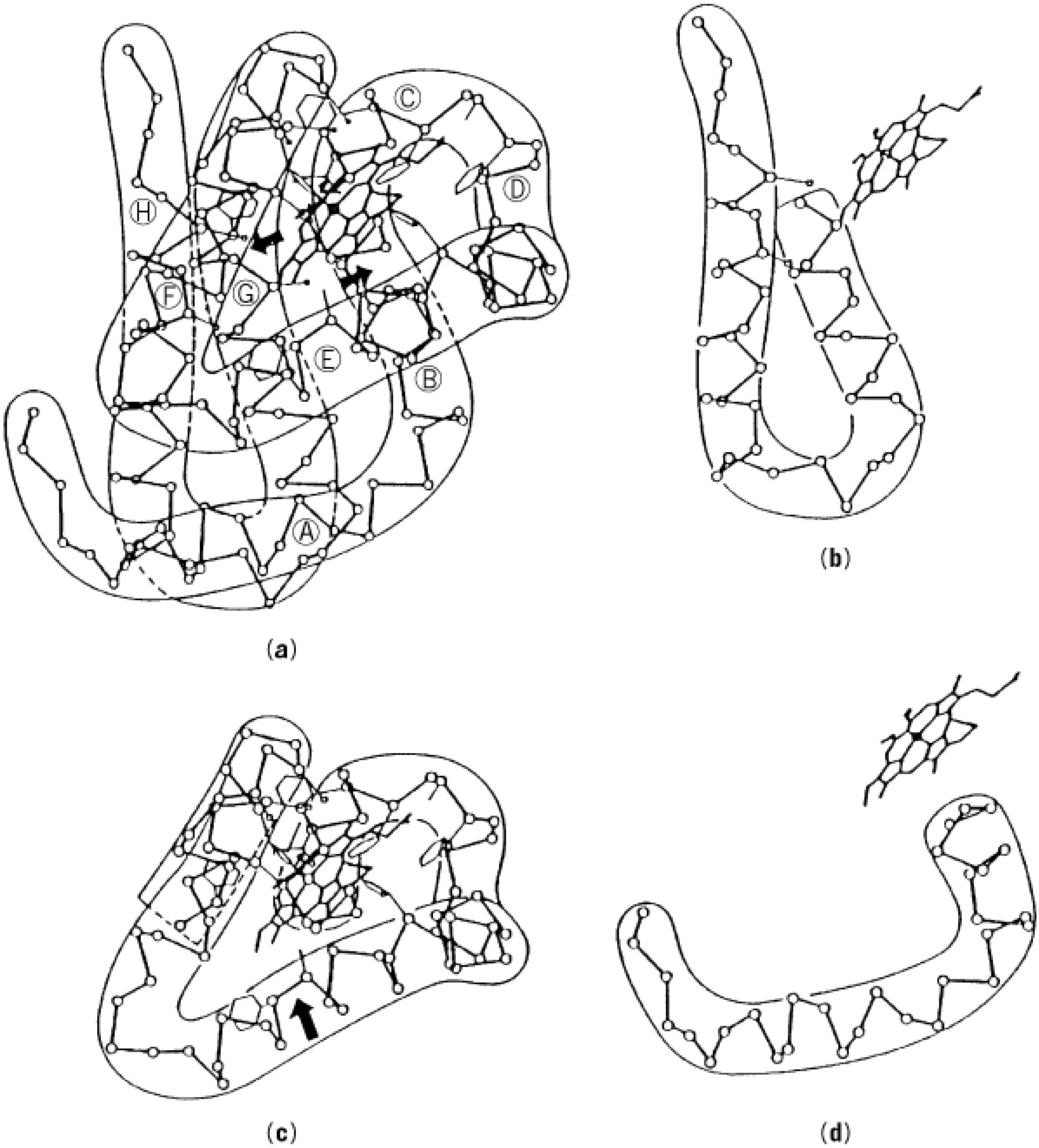

Bibliography

1. J.C. Kendrew, R.E. Dickerson, B.E. Strandberg, R.G. Hart, D.R. Davies, D.C. Phillips, and V.C. Shore (1960) Nature **185**, 422–427.
2. A.M. Lesk and C. Chothia (1980) J. Mol. Biol. **136**, 225–270.
3. J. Landsmann, E.S. Dennis, T.J.V. Higgins, C.A. Appleby, A.A. Kortt, and W.J. Peacock (1986) Nature **324**, 166–168.

4. M. Go (1981) Nature **291**, 90–92.
5. M. Go (1983) Shizen (in Japanese) **7**, 26–35.
6. M. Go (1991) In *Evolution of Life: Fossils, Molecules, and Culture* (S. Osawa and T. Honjo, eds.), Springer-Verlag, Tokyo, pp. 109–122.

Globulins

Globulins are proteins that are precipitated in both distilled water and 50% saturated ammonium sulfate. This behavior contrasts with that of albumins, which show the opposite characteristics. This operational classification was very important in protein research initially, as these two characteristics were used in purification of various proteins. It is much less important today, but the name globulin is still encountered frequently.

1. Serum a_1-Globulins

In the **electrophoretic** fractionation of serum proteins, the a-globulin fraction runs closest to serum albumin. When electrophoresis is carried out in a Veronal buffer of pH 8.6, it is subfractionated into a_1 and a_2 fractions. The former contains a1-antitrypsin (antiproteinase), a_1-acid glycoprotein, a $_1$-microglobulin, a-fetoprotein, and a-lipoprotein (HDL). The a_2 fraction contains, among others, a $_2$-microglobulin (retinol binding protein), a $_2$-macroglobulin, a_2-plasmin inhibitor, haptoglobin, and ceruloplasmin.

1.1. a_1-Microglobulin

This glycoprotein (21.76% carbohydrate by weight) is present in plasma at a concentration of 1 mg/100 ml, with a molecular weight of 33,000 and unknown biological functions. It is heterogeneous in electrophoresis, but there is no proven heterogeneity in the amino acid sequence.

1.2. a_1-Antitrypsin, Inter-a-trypsin Inhibitor

These are two proteinase inhibitors in the a-globulin fraction. They inhibit many proteinases, including **trypsin** and **chymotrypsin**, but their roles in homeostasis are not clearly established (see a1-Antitrypsin).

1.3. a-Fetoprotein

a-Fetoprotein is a protein of unknown function, but structurally related to serum albumin. Its concentration in the serum is high in the fetus but very low in the adult.

1.4. Orosomucoid

This is also called a_1-acid glycoprotein and is a glycoprotein with an unusually high content of carbohydrate, 42% by weight. It may have some evolutionary relationship to immunoglobulins.

2. Serum a_2-Globulins

2.1. a_2-Microglobulin

a_2-Microglobulin is also known as retinol binding protein (RBP) and has a molecular weight of 21,000, consisting of 181 amino acid residues, a sedimentation coefficient of 2.3 S, and no carbohydrates; its structure is known (1). It binds one molecule of retinol (vitamin A) and transports it through the circulation in association with transthyretin (formerly called prealbumin, a homotetramer of 16-kDa subunits) as a 1:1 complex of 85 kDa. Its structure consists of a two-layered **up and down b-barrel** that encloses a primarily **hydrophobic** cavity designed to bind retinol. This protein is a member of a large family of ligand transport proteins of similar structures that includes beta-lactoglobulin and a bilin-binding protein.

2.2. a_2-Plasmin Inhibitor

a_2-Plasmin inhibitor is also known as a2-antiplasmin and has a molecular weight of 67,000 and carbohydrate content of 12% by weight. It inhibits serine proteinases by forming a covalent bond with the serine residue at their active sites. This protein inhibits the degradation of fibrin clots by plasmin; in individuals who lack this protein, fibrinolysis occurs at an early stage of blood clotting, leading to a premature degradation of fibrin clot and causing serious bleeding. a_2-plasmin inhibitor obstructs the action of plasmin toward fibrin by binding to specific regions of plasmin and its precursor plasminogen.

2.3. a_2-Macroglobulin

This is a homo-tetrameric glycoprotein (7% carbohydrates) of 725,000 that inhibits almost any kind of proteinase, including those belonging to the four classes of serine, **thiol**, **metallo**, and carboxyl proteinases (2). The mechanism of inhibition is entirely different from that of other proteinase inhibitors in that, instead of binding to the active sites of the target enzymes, a_2-macroglobulin entraps medium-sized proteinases of between approximately 10,000–100,000 molecular weight within its cavity. The protein has a region in its amino acid sequence that is highly vulnerable to proteolytic attack; when one or more peptide bonds are hydrolyzed in this region, a large conformational change takes place to engulf the proteinase inside the molecular cavity and to react it with a highly reactive thiol ester bond of the macroglobulin. The active sites of the entrapped proteinases are not inhibited, and they remain active toward low-molecular-weight substrates, but are inactive toward large substrates, simply as a result of steric hindrance. The altered form of a_2-macroglobulin is rapidly cleared from the blood serum, due to its internalization after binding to the receptor molecule called LRP (standing for low-density-lipoprotein receptor-related protein) on the membrane surface of peripheral cells such as fibroblasts, macrophages, hepatocytes, and so forth (see also Macroglobulins).

2.4. Haptoglobin

This is a glycoprotein (carbohydrate content of about 19% by weight) in the serum with the capacity to bind two half-molecules of free hemoglobin in the serum, as in the case of hemolytic anemia. It is composed of a_1 and a_2 chains of 9.1- and 16,000 molecular weight, plus two identical b chains of 40 kDa. Clearance of the haptoglobin-hemoglobin complex from the blood serum has a half-life of 10 to 20 min.

2.5. Ceruloplasmin

This is a blue-colored copper-containing glycoprotein, with eight copper atoms per molecule, a carbohydrate content of about 8% by weight, and a high molecular weight of 132,000. It migrates in the a_2 region, its sedimentation coefficient is 7 S, and it is made of four heterogeneous subunits.

2.6. Antithrombins

Antithrombin III is a glycoprotein (15% carbohydrate by weight) with a molecular weight of 65,000. Its concentration in plasma is 0.2 g/l. It inhibits thrombin, activated forms of blood clotting factors IX, X, and XI, plasmin, and **trypsin**. Upon association with heparin, it inhibits blood clotting.

2.7. Cobalamin-binding Proteins

(1) IF (standing for intrinsic factor) is a 114-kDa dimeric glycoprotein. It binds two molecules of vitamin B12 (cobalamin) and helps its absorption in the intestine by binding to a specific receptor.

(2) Transcobalamin I, II, and III are vitamin B_{12}-binding and transporting proteins in the bloodstream. I is a glycoprotein (carbohydrate content of 33% by weight) and has a molecular weight of 56,000. II is a simple protein of 60 kDa. (3) A protein known as R-binder (cobalophilin) also binds cobalamin.

2.8. Thyroid Hormone-binding Proteins

The thyroid hormones, thyroxin (T4) and triiodothyronine (T3), are transported by thyroxin-binding pre-albumin, thyroxin-binding globulin, and serum albumin. Thyroxin and triiodothyronine in the blood are distributed among the three proteins in the ratios 70:10:20 and 40:30:30, respectively.

1. Thyroxin-binding pre-albumin migrates on electrophoresis to the anodic side of serum albumin, has a molecular weight of 54,980, contains 0.4% sugar, and has four subunits. The serum concentration of this protein becomes low in patients with liver disorders.
2. Thyroxin-binding globulin is an acidic glycoprotein with a molecular weight of 60,000; it is present in serum at a concentration of 15 µg/ml and strongly binds thyroxin and triiodothyronine.

2.9. Steroid Hormone-binding Proteins

These include corticosteroid-binding protein (transcortin), sex hormone-binding protein, and progesterone-binding protein. Transcortin is a glycoprotein, with a carbohydrate content of 16 to 26% by weight and molecular weight of 53,000.

3. Serum b-Globulins

3.1. Transferrin

This is an iron-binding glycoprotein in the serum with a molecular weight of 77,000. When ferric ion is bound to transferrin, it will bind to the cell-membrane transferrin receptor of erythroblasts and reticulocytes and becomes internalized as a result of receptor-linked endocytosis; apotransferrin has low affinity for the receptor. The internalized transferrin releases the bound iron as the pH inside the endosome becomes lower, and then the receptor with bound apo-transferrin reassociates with the membrane, to recycle apo-transferrin into the serum. Transferrin has two iron-binding sites per molecule, but a similar protein found in hag-fish has only one iron binding site per molecule of 44 kDa. There are several genetic variants. A protein called conalbumin in egg white and lactoferrin in milk are actually apo-transferrin, with the same amino acid sequence as the transferrin in blood serum, but with different post-translational modifications . More than 60% of the iron used by blood-producing cells for the hemoglobin biosynthesis is supplied by transferrin.

3.2. b-Lipoproteins

These include low-density and very-low-density **lipoproteins** . Serum lipoproteins are noncovalent complexes of specific proteins and lipids. They constitute a lipid transport system in the bloodstream and are classified in as chylomicrons, very-low-density lipoproteins (VLDL), low-density lipoproteins (LDL), and high-density lipoproteins (HDL). They appear in the a-globulin fraction upon electrophoresis. A further subfraction, very-high-density lipoprotein (VHDL), is often identified. Each class of lipoproteins is characterized by specific apo-proteins and immunogenicities. The density classification of lipoproteins is based on lipid content; the higher the lipid content, the lower the density. The lipid content in each class of lipoproteins is not constant but varies within a certain range of values. (More details can be found under **Lipoproteins**).

3.3. b_2-Microglobulin

This is the smaller of the two polypeptide chains that constitute the histocompatibility complex antigen, but this protein does not have specific antigenicity. The amino acid sequence has a similarity to that of the constant domains of the immunoglobulin heavy chains.

3.4. Hemopexin

This is a heme-binding protein with a molecular weight of 5700 and a carbohydrate content of 20%.

4. Serum g-Globulins

Serum g-globulins constitute the secretory immune system of vertebrates and are classified asIgA, IgD, IgE, IgG, and IgM, with Ig standing for immunoglobulin. The basic structural unit of immunoglobulins may be seen in the H_2L_2 structure of IgG, where H represents the heavy chain and L the light chain. Each light chain is disulfide-bonded to one of the heavy chains, and the two heavy chains are disulfide-bonded to form a covalently associated hetero-tetrameric subunit structure. Two antigen-binding sites are formed from the two pairs of H and L chains. The structural designs of other immunoglobulins are based on this IgG structure. More details can be found under Immunoglobulins.

5. Egg-White Globulins

5.1. Ovoglobulins

This fraction of egg white contains lysozyme and ovomacroglobulin as the major proteins in the G1 and G2 fractions, respectively. Lysozyme is a small basic protein with a molecular weight of 14,300 (129 amino acid residues), sedimentation coefficient of 1.9 S, and an isoelectric point of 11. It is an enzyme that cleaves cell-wall mucopolysaccharides at b(1–4) linkages between N-acetylmuramic acid and N-acetyl galactosamine, and thus has bactericidal activity. Chicken egg-white lysozyme is now called c-type lysozyme with a distinction from g-type lysozymes, such as that with 185 residues purified from goose eggs. Hen lysozyme constitutes about 3% of egg-white proteins and is readily crystallized. See also Lysozymes.

5.2. Ovomacroglobulin

This is a large, tetrameric glycoprotein with a molecular weight of 700,000 (4 × 170,000). It has a **proteinase**-trapping activity similar to that of serum a_2-macroglobulin. The two proteins are **homologous** in amino acid sequence and to the C3, C4, and C5 components of the blood clotting proteins. Unlike a_2-macroglobulin, ovomacroglobulin lacks the internal thiol ester bond. The presence of homologous proteins has been confirmed in the chicken, goose, crocodile, and turtle egg white (3).

6. Thyroid Globulins

Thyroglobulin is a glycoprotein (10% sugar) of molecular weight 670,000, two identical subunits, sedimentation coefficient of 19 S, and pI of 4.5. It is synthesized as an iodine-free protein in the epithelium of the thyroid gland; later it is iodinated on some of its tyrosine residues by thyroid peroxidase. Two iodotyrosine residues dimerize to form the thyroid hormones 3,3′,5,5′-tetraiodothyronine (thyroxin) and 3,3′,5-triiodothyronine. Iodination also promotes the generation of covalent dimers of thyroglobulin through disulfide bond formation. Iodination of the protein is specific to the thyroid gland of vertebrates.

7. Milk Globulins

Cow's whey contains as the principal components (50 to 60%) beta-lactoglobulin, which is peculiar to ruminant milk, and alpha-lactalbumin. b-Lactoglobulin constitutes about 50% of the whey protein; it is fractionated as an albumin fraction that does not precipitate with 50% saturation ammonium sulfate, but the purified protein shows a globulinlike solubility in water. Whey protein is fractionated into three major fractions by centrifugation, and b-lactoglobulin is the major protein in the b fraction. It is a dimeric protein of 35 kDa, sedimentation coefficient of 2.8 S, and pI of 5.2. The lactoglobulin fraction includes b-lactoglobulin and immunoglobulin derived from the mother. The three-dimensional structure of this protein is similar to that of retinol-binding proteins (4).

Bibliography

1. S. Cowan, M. E. Newcommer, and T. A. Jones (1990) Crystallographic refinement of serum retinol binding protein at 2 Å resolution, Proteins **8**, 44–61.
2. W. Borth, R. D. Feinman, S. L. Gonias, J. P. Quigley, and D. K. Strickland, eds. (1994). *Biology of Macroglobulin. Its Receptor, and Related Proteins*, Annals N. Y. Acad. Sci. **737**.
3. A. Ikai, M. Kikuchi, and M. Nishigai (1990) Internal structure of ovomacroglobulin, J. Biol. Chem . **256**, 8280–8284.
4. H. L. Monaco, G. Zonatti, P. Spadon, M. Bolognesi, L. Sawyer, and E. E. Eliopoulos (1987) Crystal structure of trigonalform of bovine -lactoglobulin and its complex with retinol at 2.5 Å resolution, J. Mol. Biol. **197**, 695–706.

Glucagon

Glucagon is a 29-residue, single-chain peptide hormone (MW 3485) (1). Its gene is located on human chromosome 2, and its primary structure is given in Figure 1. Glucagon has a regulatory function in glucose metabolism; in general, its effects are opposite those of insulin. It is synthesized by a-cells in the islets of Langerhans of the pancreas and in L-cells of the intestinal mucosa as a very much larger pre-pro-glucagon molecule of 180 amino acid residues. The signal peptide is removed proteolytically upon translocation of the nascent polypeptide chain into the endoplasmic reticulum, to generate proglucagon (160 residues); this contains within it other peptides. It is processed by the pro-hormone convertases 1/3 (PC-1/3) and PC-2 (see Peptide Hormones) differently in the two tissues (2). In the pancreas, proglucagon (PG) yields glucagon and glicentin-related peptide (GRPP). In the intestinal mucosa, glucagon-like peptides-1 (GLP-1) and -2 (GLP-2) and glicentin (a 69-residue peptide containing glucagon and GRPP) are produced (Fig. 2).

Figure 1. The primary structure of glucagon.

```
NH2-His-Ser-Gln-Gly-Thr-Phe-Thr-Ser-Asp-Tyr-Ser-Lys-
     1   2   3   4   5   6   7   8   9   10  11  12

Tyr-Leu-Asp-Ser-Arg-Arg-Ala-Gln-Asp-Phe-Val-Gln-Trp-
 13  14  15  16  17  18  19  20  21  22  23  24  25

Leu-Met-Asn-Thr-COOH
 26  27  28  29
```

Figure 2. Proteolytic processing of proglucagon (PG) in the pancreas and in the intestine. GRPP: glicentin-related peptide. GLP: glucagon-like peptide.

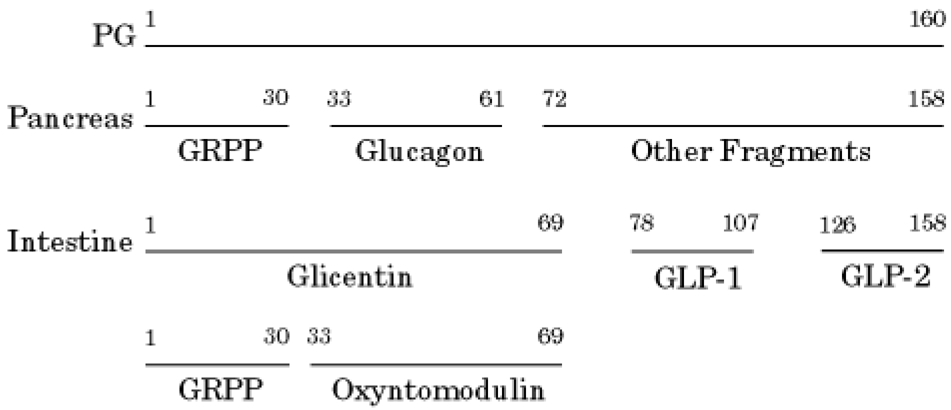

The secretory granules of the a-cells contain glucagon and discharge it by exocytosis. Active GLP-1, a potent hormone that also antagonizes insulin action, is secreted from the intestine (3-6). Consequently, differential processing of pro-glucagon gives rise to two different active peptides in the regulatory pathways. Both glucagon and GLP-1 have their own specific receptor; their genes have been **cloned** and the proteins characterized in structure-function and signal transduction studies (7, 8).

In general, glucagon and GLP-1 antagonize many actions of insulin and regulate the levels of blood glucose. Like insulin, glucagon lacks a plasma carrier, and its circulation half-life is short, approximately 3 to 6 minutes. Glucagon is removed from the circulatory system primarily by the liver and kidney. The predominant effect of glucagon is on the liver, because it is the first organ perfused by blood with the pancreatic secretions. Glucagon binds to receptors on the plasma membrane and couples through heterotrimeric G-proteins to GTP-binding proteins and adenylate cyclase. The resultant increases in cyclic AMP (cAMP) and cAMP-dependent protein kinase A (PKA) levels reverse the effects of insulin on the liver. These increases elevate the circulating glucose levels by stimulating the output of glucose from the liver by glycogenesis and promoting glycogenolysis. Glucagon secretion is inhibited by glucose. In contrast to insulin, which promotes energy storage, glucagon releases energy. It also has some effect on lipid metabolism, by reducing fatty acid synthesis and increasing fatty acid oxidation and ketogenesis. Glucagon secretion does not markedly fluctuate throughout the day, but the ratio of insulin to glucagon mediates **phosphorylation** or dephosphorylation of enzymes that regulate metabolism.

In type I diabetes, the stimulating effect of hypoglycemia on glucagon secretion is reduced. In these diabetic patients, glucose fails to inhibit glucagon secretion, but insulin injections restore the effect. On the other hand, somatostatin is an inhibitor of both glucagon and insulin secretion. A potent glucagon receptor antagonist may have therapeutic use in hypoglycemia. Consequently, the roles of glucagon and GLP-1 in glucose metabolism are presently an area of diabetes research.

Bibliography

1. P. J. Lefebvre, editor (1996) *Glucagon III–Handbook of Experimental Pharmacology*, vol. **123**, Springer, New York.
2. S. Dhanvantari, N. G. Seidah, and P. L. Brubaker (1996) Mol. Endocrinol. **10**, 342–355.
3. H. C. Fehmann, editor (1997) *The Insulinotropic Gut Hormone Glucagon-Like Peptide-1* "(Frontiers of Diabetes, vol. 13)", Karger, New York.
4. J. J. Holst (1996) Acta Physiol. Scand. **157**, 309–315.
5. M. E. Rothenberg et al. (1996) J. Biol. Chem. **270**, 10136–10146.
6. D. J. Drucker (1990) Pancreas **5**, 484–488.
7. J. Christophe (1995) Biochemica et Biophysica Acta **1241**, 45–57.

8. J. Christophe (1996) Annals New York Academy of Sci. **805**, 31–42.

Glucocorticoid Response Element

The steroid hormones are a group of substances derived from cholesterol that exert a wide a range of effects on biological processes (1) by stimulating the transcription of specific **genes** (2, 3). These effects on gene expression are mediated by specific response elements within the target genes. The relationships between the different response elements that mediate the response to each of these steroid hormones are discussed in the entry Hormone response elements. This article discusses the sequence that mediates the response to one of the classes of steroid hormones, the glucocorticoids.

The glucocorticoid response element (GRE) is found in a number of different target genes that respond to glucocorticoid. It is a short element with the sequence

5′RGRACANNNTGTYCY3′

3′YCYTGTNNNACARGR5′

where R = purine, (ie, A or G), Y = pyrimidine (ie, C or T), and N = any base. The GRE thus consists of a 6-bp palindrome in which a 6-bp sequence (RGRACA) is repeated in the opposite orientation, with a spacing between the two halves of the palindrome of 3 bp whose sequence does not matter. This palindromic sequence is bound by two molecules of the glucocorticoid **receptor** in a dimer, which mediates the response to glucocorticoid.

In cells that have not been exposed to steroid, this receptor exists in the cytoplasm complexed to a 90-kDa heat-inducible protein, hsp90. The association with hsp90 anchors the glucocorticoid receptor in the cytoplasm and prevents it activating any genes. Upon exposure to glucocorticoid, the receptor binds to the steroid, which results in the dissociation of hsp90. This leaves the receptor free to dimerize and to move to the nucleus, where the dimer binds to the palindromic GRE (Fig. 1). This binding takes place via specific regions of the receptor known as the DNA-binding **domain** and the activation domain. The bound receptor then interacts with the basal transcriptional complex of RNA polymerase and associated factors to stimulate transcription of the steroid-responsive gene. In this manner, binding the activated glucocorticoid receptor to the GRE causes the stimulation of glucocorticoid-responsive genes following exposure of the cell to steroid (4).

Figure 1. Activation of the glucocorticoid receptor GR by steroid involves dissociation of hsp90, which permits dimerization of GR and its movement to the nucleus.

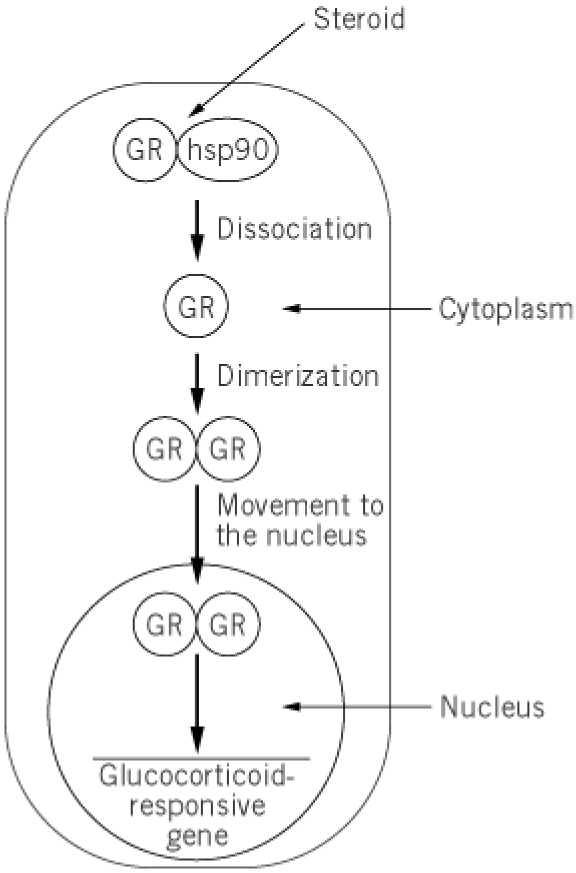

Interestingly, the glucocorticoid receptor can also inhibit the expression of specific genes, such as those encoding prolactin and pro-opiomelanocortin. This effect is achieved by the identical receptor–hormone complex that activates glucocorticoid-inducible genes. However, the DNA sequence element to which the complex binds when mediating its negative effect (nGRE) is distinct from the glucocorticoid response element (GRE) to which it binds when inducing gene expression, but the two sequences are related to one another:

GRE RGRACANNNTGTYCY

nGRE ATYACNNNNTGATCW

where N = any base, R = purine, Y = pyrimidine, and W = A or T. The similarity between the GRE and the nGRE has led to the idea that the sequence difference causes the receptor–hormone complex to bind to the nGRE in a configuration in which its activation domain cannot interact with the basal transcription complex to activate transcription in the way that occurs following binding to the positive element (5). Indeed, it has been shown that the nGRE in the pro-opiomelanocortin gene binds the glucocorticoid receptor as a trimer, rather than the dimer form that binds to the GRE and stimulates transcription (6). When bound in this manner, the GRE is likely to act simply by preventing binding of a positively acting transcription factor to this or an adjacent site, thereby preventing gene induction. In agreement with this, the nGRE in the glycoprotein hormone a subunit gene overlaps a cyclic AMP response element (CRE) and is able to inhibit gene expression only when the activating CRE is left intact (7).

Hence, the GRE and the related nGRE can bind the glucocorticoid receptor–hormone complex in distinct configurations and thereby allow glucocorticoid hormone to exert either positive or negative effects on the expression of specific target genes.

Bibliography

1. R. J. B. King and W. I. P. Mainwaring (1974) *Steroid Cell Interactions*, Butterworths, London.
2. D. S. Latchman (1998) *Eukaryotic Transcription Factors*, 3rd ed., Academic Press, London.
3. M. Beato (1989) Cell **56**, 335–344.
4. W. B. Pratt, D. J. Jolly, D. V. Pratt, S. M. Hollenberg, V. Giguere, F. M. Cadepond, G. Schweizer-Groyer, M-G. Catelli, R. M. Evans, and E-E. Bahileu (1988) J. Biol. Chem. **263**, 267–273.
5. D. D. Sakki, S. Helms, J. Carlstedt-Duke, J. A. Gustafsson, F. M. Rottman, and K. R. Yamamoto, (1988) Genes Develop. **2**, 1144–1154.
6. J. Drouin, Y. L. Sun, M. Chamberland, Y. Ganthier, A. DeLea, A. M. Nemer, and T. J. Schmidt (1993) EMBO J. **12**, 145–156.
7. I. W. Akerblum, E. P. Slater, M. Beato, J. D. Baxter, and P. L. Mellon (1988) Science **241,** 350–353.

Suggestions for Further Reading

8. H. Gronemeyer and V. Laudet (1995). Nuclear receptors. Protein Profile **2**, 1173–1308.
9. D. J. Mangelsdorf, C. Thummel, M. Beato, P. Herrlich, G. Schutz, K. Umesono, B. Blumberg, P. Castner, M. Mark, P. Shambon, and R. M. Evans (1995) The nuclear receptor super family; the second decade. Cell **83**, 835–839.
10. M. Truss and M. Beato (1993) Steroid hormone receptors: interaction with the deoxyribonucleic acid and transcription factors. Endocr. Rev. **14**, 459–479.

Glucocorticoids

Glucocorticoids (or glucocorticosteroids) are natural steroid hormones, or synthetic analogues, that regulate metabolic, developmental and immunological processes. The major natural glucocorticoids are cortisol (11 b,17,21, trihydroxy-4-pregnene-3,20-dione) (in humans) and corticosterone (11 b,21,d,hydroxypregn-4-ene-3,20-dione) (in rodents) (Fig. 1). Semisynthetic derivatives with greater hormonal activity than that of the natural steroids are dexamethasone, prednisone, and triamcinolone (Fig. 1). The synthesis of glucocorticoids in the zona fasciculata of the adrenal cortex and their release in the blood circulation is regulated by adrenocorticotropic hormone (ACTH), which is produced in the anterior lobe of the hypophysis, in response to stimuli coming either from the neuroendocrine cells of the paraventricular nuclei of the hypothalamus (corticotropin releasing hormone) or from the periphery (blood cortisol concentration). High blood cortisol levels reduce, by feedback inhibition, the production of both corticotropin-releasing hormone and ACTH. This regulatory circuit is called the hypothalamus–pituitary–adrenal axis (see Fig. 2). Glucocorticoid secretion is enhanced during stress conditions, such as anxiety, hunger, and trauma. Most effects of glucocorticoids (see Hormone Receptors) are mediated by the glucocorticoid receptors, which belong to the superfamily of nuclear receptors. There are two forms of glucocorticoid receptor, A and B, differing in their *C*-terminal regions. Upon binding the hormone, the receptor dimerizes, binds to glucocorticoid response elements (the **consensus sequence** is GGACAnnnTGTTCT), which are receptor-activated **enhancers**, and modulate gene transcription.

Figure 1. Structure of glucocorticoids.

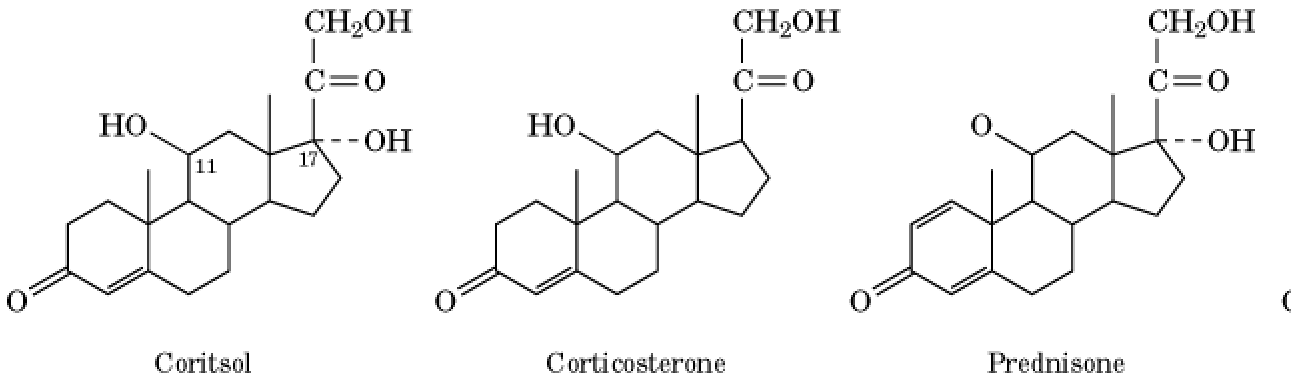

Figure 2. Regulation of cortisol production by the hypothalamus–pituitary–adrenal axis.

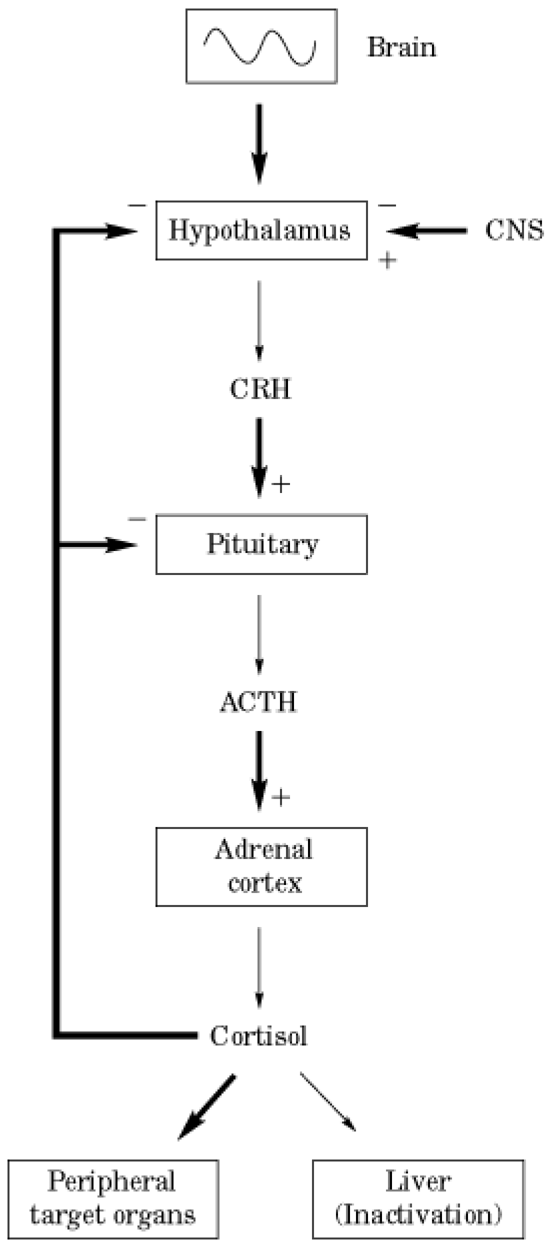

The glucocorticoids regulate the metabolism of sugars, lipids, and proteins. They stimulate glucose output from the liver, inhibit glucose utilization by tissues, and mobilize fatty acids from adipose tissue. The hormones act on muscle, bone, and lymph organs, inhibiting **protein biosynthesis** and enhancing protein degradation. Some of the amino acids released in the circulation are used for gluconeogenesis, primarily in the liver but also in kidneys. The action of glucocorticoids on gluconeogenesis represents one of the most exploited and rewarding systems for delineating the molecular mechanisms of steroid hormone action (1, 2). In gluconeogenesis, amino acids are metabolized to two-carbon precursors to be used for glucose synthesis. The biosynthesis of enzymes like tyrosine aminotransferase, alanine aminotransferase, tryptophan dioxygenase, pyruvate carboxylase, and phosphoenolpyruvate-carboxykinase, which catalyze 2C-precursor production or utilization for glucose synthesis, are induced by glucocorticoids. All steps—from binding of the glucocorticoid ligand to its receptor, to increased transcription of the genes, to translation of the messenger RNA to the respective proteins—have been studied in detail and have supported the steroid hormone gene-activation hypothesis (3). The inhibition of protein synthesis by glucocorticoids in the lymphatic system results in decreased antibody production (immunosuppression) and increased susceptibility to infection. The suppressive effects of glucocorticoids on the inflammatory response have led to new insights and a novel mechanism of action of glucocorticoids. Namely, the hormones block binding of the transcription factor NF-k B on **promoters** having NF-kB binding sites (eg, the promoter of the interleukin gene) by direct interaction between the receptor and the transcription factor, thereby inhibiting expression of the respective (eg, interleukin) gene (4).

The role of glucocorticoids in embryonic development has been investigated in transgenic mice deficient in the glucocorticoid receptor (5). These mice die within a few hours of birth because of respiratory failure due to severely atelectic lungs, probably resulting from lowered production of surfactants and from a deficiency of a glucocorticoid-inducible sodium pump. The livers of newborns have reduced capacity to activate genes for key gluconeogenic enzymes, whereas the adrenals lack a central medulla and cannot synthesize adrenaline. The hypothalamus–pituitary–adrenal axis is impaired, resulting in increased expression of corticotropin-releasing hormone and in hypertrophy of the adrenal cortex, signifying that the hypothalamus–pituitary–adrenal axis is established during fetal development, and underlining the central role of glucocorticoids in this process.

Bibliography

1. G. Schutz (1988) Biol. Chem. Hoppe Seyler **369**, 77–89.
2. S. J. Pilkis and D. K. Granner (1992) Annu. Rev. Physiol **54**, 885–909.
3. P. Karlson (1963) Perspect. Biol. Med. **6**, 203–214.
4. R. Scheinman et al (1995) Mol. Cell Biol. **15**, 943–953.
5. T. J. Cole et al. (1995) Genes Dev., **9**, 1608–1621.

Suggestions for Further Reading

6. D. N. Orth, W. J. Kovacs, and C. R. DeBold (1992) In *Williams Textbook of Endocrinology*, Vol. **9**, 8th ed. (J. D. Wilson and D. W. Foster, eds.), Saunders, London, pp. 489–620.
7. G. P. Chrousos (1992) Endocrinol. Metab. Clin. North Am. **21**, 833–858.
8. M. Truss and M. Beato (1993) Endocr. Rev. **14**, 459–479.

Glutamic Acid (Glu, E)

The **amino acid** glutamic acid is incorporated into the nascent polypeptide chain during **protein biosynthesis** in response to two **codons**—GAA and GAG—and represents approximately 6.2% of the residues of the proteins that have been characterized. The glutamyl residue incorporated has a mass of 129.12 Da, a **van der Waals volume** of 109 $Å^3$, and an accessible surface area of 183 $Å^2$. Glu residues are frequently changed during divergent evolution; they are interchanged in **homologous** proteins most frequently with **aspartic acid**, **glutamine**, **alanine**, and **histidine** residues.

The side chain of Glu residues is dominated by its **carboxyl group**:

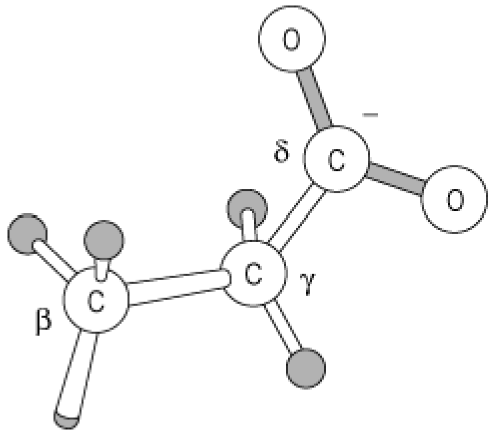

This carboxyl group is normally no more reactive than are those of corresponding organic molecules, such as acetic acid. Its intrinsic pK_a value is approximately 4.3, so Glu residues are ionized and very polar under physiological conditions; consequently, very few Glu residues are buried in folded **protein structures**, and nearly all have at least the carboxyl group on the surface. The pK_a can be shifted in folded proteins, however, and either the ionized or nonionized form can be used in the protein's function. For example, **carboxyl proteinases** have one **active-site** carboxyl group function in the ionized form, another nonionized. Asp carboxyl groups have a weak intrinsic affinity for Ca^{2+} ions and are used in many calcium-binding proteins. Certain Glu residues, particularly in proteins involved in blood clotting and bone structure, are carboxylated to yield the unusual residue g-**carboxylglutamic acid**; such residues have two adjacent carboxyl groups and bind Ca^{2+} more avidly.

Glu residues differ from Asp only in having two methylene groups, rather than one, so it might be thought that they would be very similar chemically and functionally in proteins, but this is not so. The slight difference in length of the side chains causes them to have different tendencies in their chemical interactions with the peptide backbone, so they have markedly different effects on the conformation and chemical reactivity of the peptide backbone. For example, Glu residues favor the a-**helical** conformation much more than do Asp. In folded proteins, Glu residues are most frequently found in a-helices, whereas Asp residues occur most frequently in reverse turns .

Suggestion for Further Reading

T. E. Creighton (1993) *Proteins: Structures and Molecular Properties*, 2nd ed., W. H. Freeman, New York.

Glutamine (Gln, Q)

The amino acid glutamine is incorporated into the nascent polypeptide chain during **protein biosynthesis** in response to two **codons**—CAA and CAG—and represents approximately 4.0% of the residues of the proteins that have been characterized. The glutaminyl residue incorporated has a mass of 128.14 Da, a van der Waals volume of 114 Å ^{3}, and an accessible surface area of 189 Å^{2}. Gln residues have close to average conservation during divergent evolution; they are interchanged in **homologous** proteins most frequently with Glutamic Acid (Glu, E)and Histidine (His, H) residues.

The side chain of Gln residues is the same as that of glutamic acid, except that the carboxyl group has been converted to the amide:

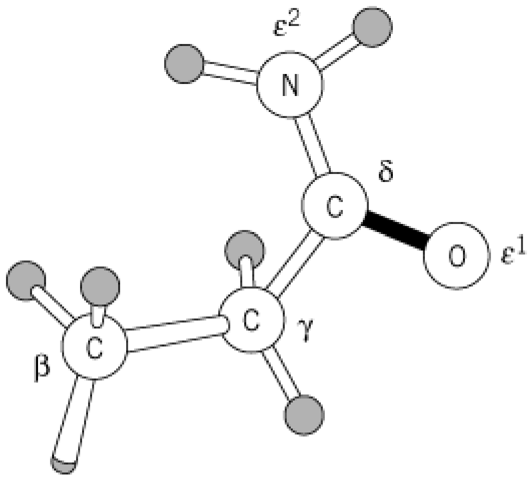

Both amino acids occur naturally and are incorporated directly into proteins during their biosynthesis. Gln residues do not arise from amidation of Glu in proteins. The amide side chain does not ionize and is not very reactive chemically. It is polar, however, as it is both a hydrogen bond donor and acceptor. The amide group is labile at extremes of pH and at high temperatures, and Gln residues can **deamidate** to Glu, although usually less rapidly than Asn residues do.

When Gln residues are at the *N*-terminus of a peptide chain, they spontaneously cyclize:

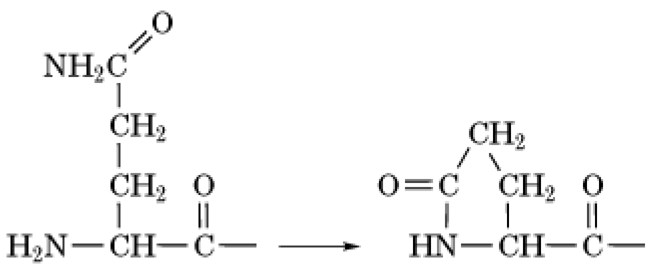

The resulting residue of pyrrolidone carboxylic acid renders the *N*-terminus unreactive in most procedures for **sequencing proteins**, such as the Edman Degradation. This residue can be removed, however, by the enzyme pyroglutamyl amino peptidase

Suggestions for Further Reading

F. Wold (1985) Reactions of the amide side-chains of glutamine and asparagine *in vivo*, Trends Biochem. Sci. **10**, 4–6.

T. E. Creighton (1993) *Proteins: Structures and Molecular Properties*, 2nd ed., W. H. Freeman,

New York.

Glutaraldehyde

The bis-homobifunctional aldehyde glutaraldehyde

$$HCO\text{–}(CH_2)_3\text{–}CHO$$

is perhaps the most frequently used chemical crosslinking agent. Because of its effectiveness as a crosslinker, glutaraldehyde has found use as a stabilizer or fixative for samples subjected to electron microscopy, for bioprosthetic materials, and in drug delivery systems (reviewed in Ref. 1). It is also routinely used to produce bioconjugates and to immobilize proteins (see Enzyme Immobilization And Conjugation).

Crosslinking by glutaraldehyde can occur through at least two distinct mechanisms (2). The first is attack by primary amino groups of the protein on the aldehydic carbons of glutaraldehyde to form Schiff bases, which can then be rendered irreversible by suitable reductants. The second mechanism is more complex and less understood, and it results in irreversible crosslinking in the absence of reductants. This alternative mechanism involves polymerization of glutaraldehyde to form heterogeneous unsaturated polymers that differ in their length and degree of unsaturation. These polymers then undergo addition at their double bonds by other nucleophilic groups of the protein. A disadvantage of glutaraldehyde is that it often brings about extensive crosslinking and formation of insoluble complexes; however, this can be minimized through use of the two-step reaction, in which one protein is reacted with glutaraldehyde, the excess reagent removed, and the second protein then added to react with the free aldehyde groups of the first (2).

Bibliography

1. A. Jayakrishnan and S. R. Jameela (1996) Biomaterials **17**, 471–484.
2. G. T. Hermanson (1996) *Bioconjugate Techniques*, Academic Press, San Diego, pp. 218–220.

Glutaredoxin

Gluta redoxin (Grx) was discovered as a small protein that contains two thiol groups and acts as a glutathione (GSH)-dependent hydrogen donor for synthesizing deoxyribonucleotides by *Escherichia coli* ribonucleotide reductase (1). Glutaredoxin in the oxidized form has a redox-active disulfide bond (Grx-S_2) and is reduced to the dithiol form (Grx-SH_2) by two molecules of GSH in a **thiol-disulfide exchange** reaction via a GSH mixed-disulfide intermediate (2, 3). Glutaredoxin is also a general GSH-disulfide oxidoreductase that reduces either disulfide bonds by a dithiol mechanism or GSH-mixed disulfides by a monothiol mechanism (2, 3). The glutaredoxin system comprises NADPH, GSH, glutathione reductase, and glutaredoxin. It catalyzes the NADPH- and GSH-dependent reduction of disulfides and keeps the inside of the cell reduced.

Glutaredoxins exist in all prokaryotic and eukaryotic cells that contain glutathione, and they are also encoded by the genes of the larger DNA **viruses**. Glutaredoxins generally have a mass of 9 to 12 kDa, and the active site has the **consensus sequence** -Cys-Pro-Tyr-Cys- (4). Glutaredoxin in mammalian cells is identical to GSH-homocystine transhydrogenase or thioltransferase. The primary structures of glutaredoxin show only limited sequence similarity to those of **thioredoxins**, but the three-dimensional structure of glutaredoxin shows that the active site dithiol/disulfide is located at the end of a beta-strand and at the beginning of an **alpha-helix**, characteristic of the thioredoxin fold. One hallmark of glutaredoxin is a binding site for GSH that is used in both the reduction of Grx-S_2 by GSH and for substrate recognition and reduction of GSH-mixed disulfides by Grx-$(SH)_2$. Glutaredoxins have numerous functions, such as acting as hydrogen donors for reductive enzymes and transmitting changes in the oxidation/reduction potential of the GSH/GSSG (glutathione disulfide) system for protein activity during thiol redox regulation and signal transduction, or in restoring oxidatively damaged proteins after oxidative stress.

1. Glutaredoxin Functions

Glutaredoxins have been isolated from *E. coli* (1, 5), yeast (6), plants (7), and mammals (8, 9) and are encoded by **T4 bacteriophage** and vaccinia virus (10-12). *E. coli* contains three different glutaredoxins: Grx1, Grx2, and Grx3 (5). Grx1 is a highly efficient hydrogen donor for ribonucleotide reductase, either in the presence of 1 mM DTT or with the more physiological system of 4 mM GSH, NADPH, and excess glutathione reductase, when the apparent Km (Michaelis constant) for Grx1 is 0.13 µM (2, 3). The apparent turnover number of glutaredoxin as a dithiol hydrogen donor for ribonucleotide reductase is tenfold higher than that of thioredoxin. Glutaredoxin was discovered in an *E. coli* mutant that lacks thioredoxin (1), and double mutants that lack thioredoxin and glutaredoxin are viable (13). This includes *E. coli* cells that lack glutathione ($gshA^-$). In combination with a thioredoxin mutation ($gshA^-$, $trxA^-$), such cells very strongly induce (up to 55-fold) Grx1 (14). Grx3 in *E. coli* has the same active site structure as Grx1, but only 6% of the V-max with ribonucleotide reductase and a 35 mV higher redox potential (E'_O) (15, 16). The function of at least Grx1 strongly depends on the GSH-concentration and the GSH:GSSG ratio, because the E'_O of the redox-active disulfide bond in glutaredoxin determines whether it is be reduced to the active dithiol (16).

Glutaredoxin functions reducing both sulfate and methionine sulfoxide in *E. coli* and yeast (17). Synthesis of Grx1 in *E. coli* is induced via the oxyR transcription factor, and Grx1 controls its activity by reducing a disulfide bond that can be formed in the protein (18). The two glutaredoxins in yeast control the defense against superoxide and hydrogen peroxide stress, respectively, in addition to their roles in deoxyribonucleotide synthesis by ribonucleotide reductase (6).

Phage T4 induces a ribonucleotide reductase upon infection of *E. coli*, and a T4 glutaredoxin (originally called thioredoxin) is also a specific hydrogen donor for the enzyme that works with GSH as a reducant (19), and a substrate for thioredoxin reductase. T4 ribonucleotide reductase uses *E. coli* Grx1 as a hydrogen donor, but not thioredoxin (19). However, T4 glutaredoxin is reduced by thioredoxin via thioredoxin reductase, favoring phage-specific DNA synthesis (20).

The transcription factor activity of nuclear factor I is regulated by glutaredoxin *in vitro*, involving formation of mixed disulfides (21). Glutaredoxin is a direct target of **oncogenic** Jun protein (22). Other roles for glutaredoxin involve reduction of dehydroascorbic acid (23) and involvement in repairing proteins that have with mixed disulfides after oxidative stress (24) or in arsenite reduction (25).

2. Amino Acid Sequences

With few exceptions [eg, see Grx2 (26)], the glutaredoxins from bacterial viruses to humans are 9- to 12-kDa proteins that have both sequence and structural homology to the members of the thioredoxin superfamily of proteins. Alignment of the amino acid sequences from diverse organisms (Fig. 1) gives a good impression of the sequence variability of these proteins. Unlike the thioredoxins, whose sequences align without gaps of more than one residue, numerous gaps of up to 5 residues are needed, in addition to the relatively long (up to 20 amino acid residues) N- and/or C-terminal extensions in some members. Several residues are strictly conserved among the glutaredoxins. The active site sequence –Cys11–Pro12–Tyr13–Cys14 (*E. coli* numbering) is the hallmark of the glutaredoxins. The tripeptide fragment that contains the proline residue with the *cis* peptide bond (Thr58–Val59–Pro60) and the residues Ile69–Gly70–Gly71–Tyr72–Thr73–Asp74 are also strictly conserved. Mammalian glutaredoxins are highly homologous to one another and, in addition to containing both N- and C-terminal extensions, contain additional non-structural cysteine residues that, analogous to the mammalian thioredoxins, might function in regulating glutaredoxin activity (9).

Figure 1. Amino acid sequence alignment of selected glutaredoxins. Sequences were taken from [a](9, 32); [b](33); [c](34); [d](acid sequences were aligned based on the three-dimensional structures of pig (29), T4 (28) and *E. coli* (Grx1) glutaredox

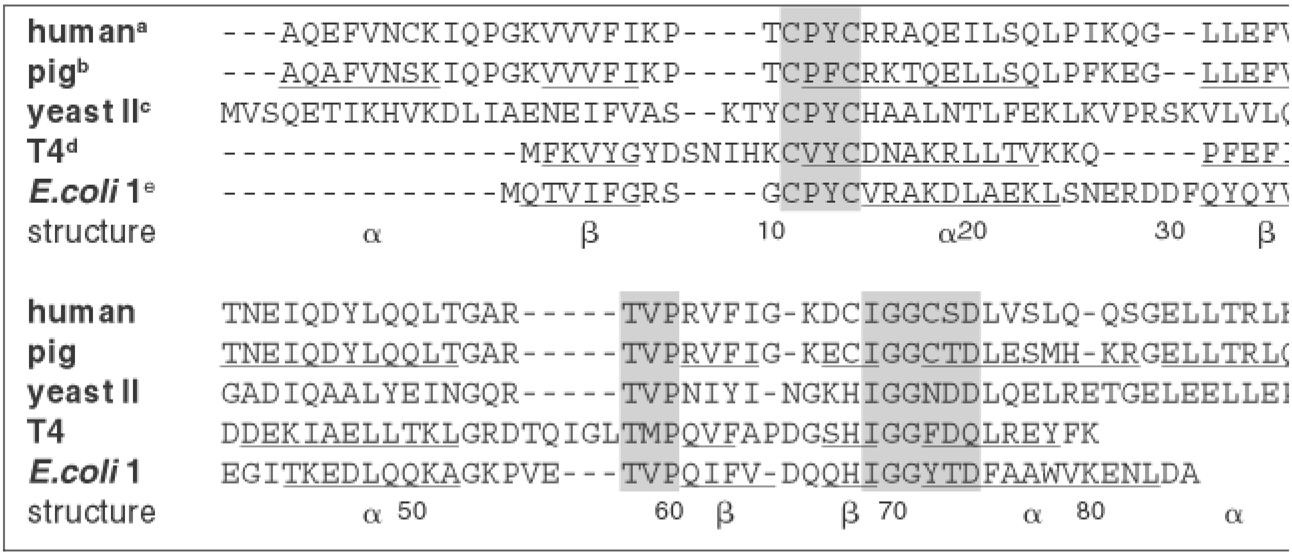

3. Mechanisms of Disulfide Reduction

As outlined in Fig. 2, glutaredoxin participates in reducing disulfide bonds in substrates by a dithiol mechanism that involves both thiol groups and a disulfide intermediate. Glutaredoxin also catalyzes monothiol reductions of GSH-mixed disulfides.

Figure 2. Mechanisms of glutaredoxin in GSH-disulfide oxidoreductions. The monothiol mechanism requires only the accessible N-terminal active-site Cys residue. The dithiol mechanism of disulfide reduction (like that in ribonucleotide reductase) requires both Cys residues (27, 35).

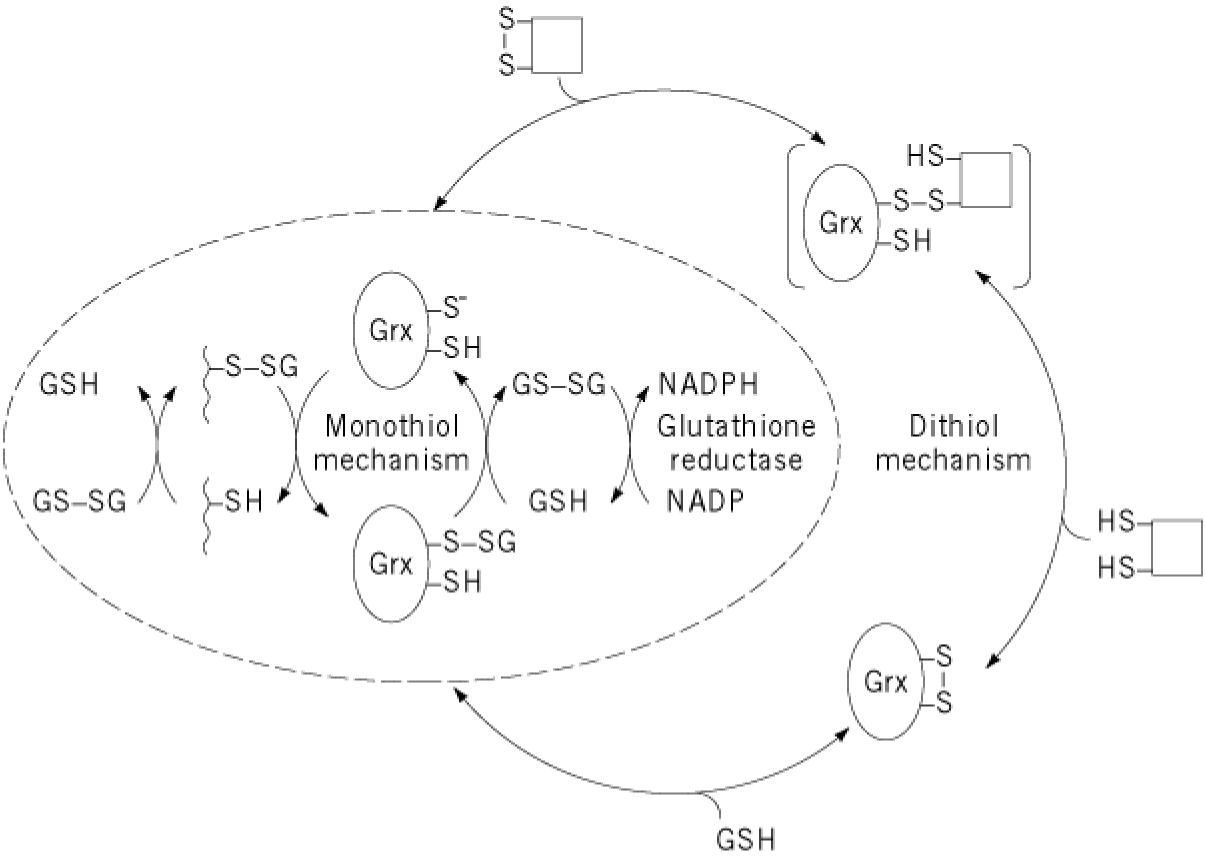

4. *E. coli* Grx Structure

Three-dimensional protein structures of oxidized and reduced *E. coli* Grx-1 (27), oxidized T4 Grx (28), and oxidized pig Grx (29) have been determined. In addition, the **secondary structures** and fold topology of reduced *E. coli* Grx-3 (15) and reduced human Grx (30) have also been reported. These studies confirm the presence of the thioredoxin fold that consists of a central four-stranded mixed b-sheet flanked by one a-helix on each face (Fig. 3). In addition to this core fold, the N- and C-terminal extensions observed in sequence comparisons contain two additional helical segments.

Figure 3. Representative NMR solution strucutre of *E. coli* Grx1 (C14 S mutant) in a mixed disulfide with GSH via Cys11 (27, 31). (**a**), Cartoon of the polypeptide backbone with the side chains of Cys11 and Ser14 displayed as sticks. The glutathione ligand is also displayed as a stick model whose bonds connect non-hydrogen atoms. (**b**) The molecular surface colored according to the electrostatic potential (dark gray: positive, medium gray: negative, and light gray: uncharged. Residues that interact with GSH are labeled at their approximate positions.

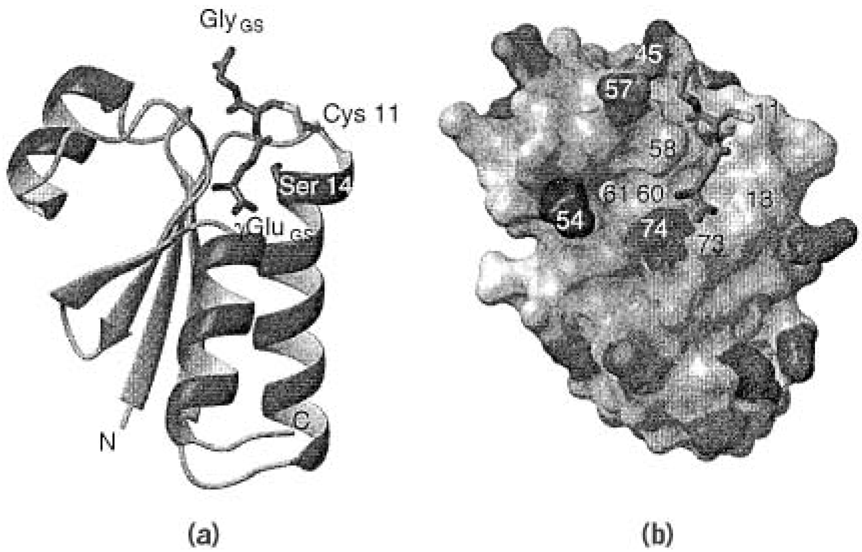

5. Glutaredoxin Mixed-Disulfide Complex with GSH

The intermolecular mixed-disulfide complex between *E. coli* Grx1 and GSH has been determined by NMR techniques (27). Mutation of the C-terminal active site Cys14 residue in *E. coli* Grx1 abolishes its activity as a dithiol reductant for ribonucleotide reductase (31), but retains its activity in the monothiol mechanism (Fig. 2). Overall, the polypeptide backbone in the complex is similar to that observed in the structures of the oxidized and reduced forms, also determined by NMR. The covalently attached glutathione is found in a largely extended conformation in a cleft formed by residues from three discontinuous regions of the polypeptide chain (Fig. 3). The intimate relationship between the Grx and glutathione is also confirmed by the fact that the ^{15}N T_{1r} relaxation rates of the amide nitrogen atoms of Cys and Gly of the glutathione are similar to those observed for the Grx backbone. The floor of the cleft is made up largely of contributions from Val 59, Pro 60, and Gly 71. The sides of the cleft are formed from Thr 58 on one side and Tyr 13 and Thr 73 on the other. Interestingly, many of these residues are in positions homologous to those residues that form the hydrophobic interaction surface in the thioredoxins. Two hydrogen bonds are present in a majority of NMR conformers: HN Val 59–CO Cys_{GS} and the HN Thr 73–aCO_2 gGlu_{GS}. Additional hydrogen bonds and salt bridges are observed in several structures, including $^{\varepsilon}NH_3$ Lys 45–aCO_2 Gly_{GS}, aNH_3 gGlu_{GS}–gCO_2 Glu 74, aCO_2 gGlu $_{GS}$–HN Tyr 72, aCO_2 gGlu $_{GS}$–HN Thr 73, and aCO_2 gGlu $_{GS}$–HO Thr 73. In addition, the aCO_2 gGlu_{GS} in a number of structures can be positioned directly over the N-terminus of the C-terminal a-helix, allowing for a favorable interaction with the dipole of the helix. Several of these interactions (salt bridge to C-terminus of GS, H-bond from CO Cys_{GS} to residue before the strictly conserved *cis* Pro, NH and OH of Ser to aCO $_2$ gGlu $_{GS}$) have homologous counterparts in the recognition of glutathione by **glutathione S-transferases** . These observations suggest that the details of the structural basis of noncovalent glutathione binding to Grx may be representative of a wider range of substrate interactions between members of the thioredoxin superfamily.

Bibliography

1. A. Holmgren (1976) Proc. Natl. Acad. Sci. USA **73**, 2275–2279.
2. A. Holmgren (1979) J. Biol. Chem. **254**, 3664–3671.
3. A. Holmgren (1979) J. Biol. Chem. **254**, 3672–3678.
4. J.-O. Höög, H. Jörnvall, A. Holmgren, M. Carlquist, and M. Persson (1983) Eur. J. Biochem.

136, 223–232.

5. F. Åslund, B. Ehn, A. Miranda-Vizuete, C. Pueyo, and A. Holmgren (1994) Proc. Natl. Acad. Sci. USA, **91**, 9813–9817.
6. S. Luikenhuis, G. Perrone, J. W. Dawies, and C. M. Grant (1998) Mol. Cell. Biol. **9**, 1081–1091.
7. K. Minakucchi, T. Yabushita, T. Masumura, K. Ichihara, and K. Tanaka (1994) FEBS Lett. **337**, 157–160.
8. M. Luthman, S. Eriksson, A. Holmgren, and L. Thelander (1979) Proc. Natl. Acad. Sci. USA **76**, 2158–2162.
9. C. A. Padilla, E. Martinez-Galisteo, J. A. Bàrcena, G. Spyrou, and A. Holmgren (1995) Eur. J. Biochem. **227**, 27–34.
10. B.-M. Sjöberg and A. Holmgren (1972) J. Biol. Chem. **247**, 8063–8068.
11. B. Y. Ahn and B. Moss (1992) Proc. Natl. Acad. Sci. USA **89**, 7060–7064.
12. B. O. Gvakharia, E. Hanson, EK. Koonin, and C. K. Mathews (1996) J. Biol. Chem. **271**, 15307–15310.
13. M. Russel and A. Holmgren (1988) Proc. Natl. Acad. Sci. USA **85**, 990–994.
14. A. Miranda-Vizuete, A. Rodrigues-Ariza, A. Holmgren, J. Lopez-Barea, and C. Pueyo (1996) J. Biol. Chem. **271**, 19099–19103.
15. F. Åslund, K. Nordstrand, K. D. Berndt, M. Nikkola, T. Bergman, H. Ponstingl, H. Jörnvall, G. Otting, and A. Holmgren (1996) J. Biol. Chem. **271**, 6736–6745.
16. F. Åslund, K. D. Berndt, and A. Holmgren (1997) J. Biol. Chem. **272**, 30780–30786.
17. M. Russel, P. Model, and A. Holmgren (1990) J. Bacteriol . **172**, 1923–1929.
18. M. Zheng, F. Åslund, and G. Storz (1998) Science, **279**, 1718–1721.
19. A. Holmgren (1978) J. Biol. Chem. **253**, 7424–7430.
20. O. Berglund and A. Holmgren (1975) J. Biol. Chem. **250**, 2778–2782.
21. S. Bandyopadhyay, D. W. Starke, J. J. Mieyal, and R. M. Gianostajski (1998) J. Biol. Chem. **273**, 392–397.
22. M. E. Goller, J. S. Jacovoni, P. K. Vogt, and U. Krause (1998) Oncogene **16**, 2945–2948.
23. W. W. Wells, D. P. Xu, Y. Yang, and P. A. Rocque (1990) J. Biol. Chem. **265**, 15361–15364.
24. C. M. Jung and J. A. Thomas (1996) Arch. Biochem. Biophys . **335**, 61–72.
25. J. Liu and B. P. Rosen (1997) J. Biol. Chem. **272**, 21084–21089.
26. A. Vlamis-Gardikas, F. Åslund, G. Spyrou, T. Bergman, and A. Holmgren (1997) J. Biol. Chem. **272**, 11236–11243.
27. J. H. Bushweller, M. Billeter, A. Holmgren, and K. Wüthrich (1994) J. Mol. Biol. **235**, 1585–1597.
28. B. O. Söderberg, B.-M. Sjöberg, U. Sonnerstam, and C.-I. Brändén (1978) Proc. Natl. Acad. Sci. USA **75**, 5827–5830.
29. S. K. Katti, A. R. Robbins, Y. Yang, and W. W. Wells (1995) Protein Sci. **4**, 1998–2005.
30. C. Sun, A. Holmgren, and J. H. Bushweller (1997) Protein Sci. **6**, 383–390.
31. J. H. Bushweller, F. Åslund, K. Wüthrich, and A. Holmgren (1992) Biochemistry **31**, 9288–9293.
32. M. R. Fernando, H. Sumimoto, H. Nanri, S. Kawabata, S. Iwanaga, S. Minakami, Y. Fukumaki, and K. Takeshige (1994). Biochim. Biophys. Acta **1218**, 229–231.
33. Y. Yang, Z. R. Gan, and W. W. Wells (1989) Gene **83**, 339–346.
34. C. P. Hollenberg, U. Kleinhans, K. Luetzenkirchen, M. R. Rad, and G. Xu (1992) *EMBL/gen bank DDBJ databanks*.
35. S. A. Gravina and J. J. Mieyal (1993) Biochemistry, **32**, 3368–3376.

Suggestions for Further Reading

36. A. Holmgren and F. Åslund (1995) Glutaredoxin, Methods Enzymol. **252**, 283–292.
37. Methods in Enzymology, Vol. **252** (1995) *Biothiols. Part B.* Glutathione and thioredoxin: Thiols in signal transduction and gene regulation.
38. J. A. Fuchs (1989) "Glutaredoxin". In *Glutathione, Chemical, Biochemical and Medical Aspects* (D. Dolphin, O. Avramovic, and R. Poulson, eds.), Part B. Wiley, New York, pp. 551–570.
39. A. Holmgren, C.-I. Brändén, H. Jörnvall and B.-M. Sjöberg (eds.) (1986) *Thioredoxin and Glutaredoxin Systems. Structure and Functions*, Raven Press, New York.

Glutathione

Glutathione was first discovered by J. de Rey-Pailhade over 100 years ago, and its structure (ie, L-g-glutamyl-L-cysteinyl-glycine, or g-Glu-Cys-Gly),

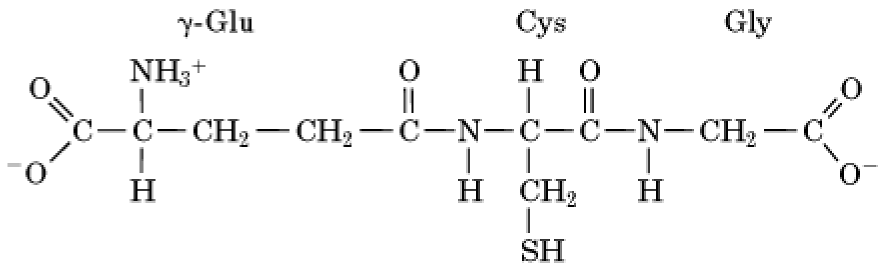

was deduced in the 1930s. It has several important functions: (i) most importantly, as a reductant; (ii) conjugation to foreign chemicals to make them more **water**-soluble, less toxic, and excretable; (iii) transport of amino acids across cell membranes; (iv) incorporation into some leukotriene structures; (v) as a **cofactor** for some enzymes; (vi) as a nontoxic storage form of cysteine; and (vii) in forming and maintaining protein disulfide bonds in the endoplasmic reticulum (ER).

Glutathione is the predominant **thiol** compound in very many cells, both prokaryotes and eukaryotes, where its total intracellular concentration is usually in the range 0.5 to 12 mM. It is present in most eukaryotes, except for those that do not have mitochondria. It is not present in many Archaebacteria, but in halobacteria it is replaced by g-Glu-Cys. Likewise, some eubacteria do not have glutathione, and it is found primarily in the bacteria of the cyanobacteria and the purple bacteria classes. It is believed that glutathione arose initially in the prokaryotic ancestors of mitochondria and chloroplasts and was acquired by eukaryotes along with these organelles.

Glutathione is synthesized from its three constituent amino acids. First, the side-chain g-**carboxyl group** of glutamic acid is joined in a peptide bond to the a-**amino group** of cysteine, by the enzyme g-glutamylcysteine synthetase. The a-carboxyl group of the resulting g-Glu-Cys is then joined in a normal peptide bond with the a-amino group of glycine, catalyzed by glutathione synthetase. Both steps are coupled to the hydrolysis of ATP. Some species of **plants** have a variant of glutathione, homoglutathione, in which the glycine residue is replaced by b-alanine, due to an **evolutionary** change in specificity of the enzyme glutathione synthetase. In **trypanosomes**, glutathione is largely replaced by the related trypanothione in which two g-Glu-Cys-Gly moieties are linked by peptide bonds through their carboxyl groups to a molecule of **spermidine**.

Glutathione is also degraded to its constituent amino acids *in vivo*, which is believed to give it an important role as a nontoxic storage form of cysteine. High levels of cysteine are toxic in some systems, in part because its amino, carboxyl, and thiol groups are well situated stereochemically to chelate metal ions, which catalyze air oxidation of its thiol group. A by-product of thiol oxidation is peroxides, which damage the cell. Glutathione is much more resistant to air oxidation and much less toxic, and it can occur safely at 10 to 100 times greater levels.

Glutathione is an essential cofactor for a number of enzymes, including formaldehyde dehydrogenase, glyoxylase, maleylacetoacetate isomerase, dehydrochlorinase, and prostaglandin endoperoxidase isomerase. The glutathione is involved transiently in the reactions they catalyze. For example, formaldehyde dehydrogenase uses NAD^+ to catalyze the oxidation of an adduct of formaldehyde and glutathione to produce *S*-formylglutathione, which is subsequently hydrolyzed by a specific lyase to yield formate and regenerate the glutathione. Glyoxylase is similar, also generating a transient intermediate adduct between its substrate, methyl glyoxal, and glutathione.

Naturally, glutathione is found in a mixture of the thiol form, GSH, and with a disulfide bond linking two glutathione moieties, GSSG. The GSH thiol group has a pK_a value of about 8.8, while the amino and carboxyl groups have normal pK_a values that are virtually the same in the disulfide form (1). There apparently are no substantial interactions between the two glutathione moieties in GSSG, and the stability of this disulfide bond is comparable to that between two other cysteine residues on unfolded peptides or proteins; the rate and equilibrium constants for thiol–disulfide exchange are close to their expected values (2).

Within the cytosol of cells, glutathione is kept primarily in the reduced GSH form, largely by reduction of GSSG by the enzyme *glutathione reductase*, at the expense of NADPH:

$$\mathrm{GSSG + NADPH + H^+ \leftrightarrow 2GSH + NADP^+} \tag{1}$$

The mechanism of this reaction is complex, as the enzyme contains a pair of cysteine residues that reversibly form a disulfide bond, plus one FAD molecule (3). As GSH and GSSG will react spontaneously with each other and with other thiol and disulfide compounds of the cell, in the thiol–disulfide exchange reaction, the ratio of GSH and GSSG reflects the general redox properties of the cell. Being present at such high concentrations, GSH is an important reductant within cells. For example, it is involved in the reduction of glutaredoxin, and it and NADPH reduce the oxidized form of vitamin C, dehydroascorbate, to the active form, ascorbate.

GSH is used for the destruction of oxidants, such as organic peroxides and H_2O_2, which would cause irreversible damage to membranes, DNA, and numerous other cellular components; this reaction is catalyzed by the enzyme *glutathione peroxidase*:

$$\mathrm{2GSH + H_2O_2 \rightarrow GSSG + 2H_2O} \tag{2}$$

This enzyme is unusual in that it has a selenocysteine residue at its active site (4).

Normally, GSH predominates over GSSG by a factor of 100 in the cytosol. This is a somewhat reducing environment that tends to keep protein cysteine residues in the thiol form (P^{SH}_{SH}) and destabilizes any disulfide bonds they may make (P^{S}_{S}),

$$\mathrm{P^{SH}_{SH} + GSSG \overset{K^{eq}}{\leftrightarrow} P^{S}_{S} + 2GSH} \tag{3}$$

although very stable disulfide bonds found in some proteins could be present under these conditions. The stability of a protein disulfide bond is determined by its intrinsic stability, K_{eq}, plus the ratio of the concentrations of GSH and GSSG:

$$\frac{[\mathrm{P}_{\mathrm{S}}^{\mathrm{S}}]}{[\mathrm{P}_{\mathrm{SH}}^{\mathrm{SH}}]} = K_{\mathrm{eq}} \frac{[\mathrm{GSSG}]}{[\mathrm{GSH}]^2} \tag{4}$$

Only very stable protein disulfide bonds, with large values of K_{eq}, could be populated in the cytosol.

In the endoplasmic reticulum (ER) of eukaryotes, in contrast, GSH and GSSG are present in nearly equal concentrations (5). With 1 mM each of GSH and GSSG, the same disulfide bond would be present in the ER to an extent 100 times greater than in the cytosol. This is sufficient to permit proteins in the ER to form disulfide bonds if their conformations stabilize them (see Disulfide Bonds); if not, the protein cysteine residues will tend to remain in the thiol form. The formation of such stable disulfide bonds in proteins in the ER is catalyzed by protein disulfide isomerase (PDI). PDI can have an unstable disulfide bond at each of its two active sites, which is readily transferred to other proteins. The PDI active-site disulfide bonds are believed to be regenerated by chemical reaction of the protein with GSSG.

Glutathione is believed to be used in some cells, such as those of the mammalian liver and kidney, for the transport of amino acids (except for proline) across the plasma membrane (Fig. 1). The extracellular amino acid is reacted with intracellular glutathione that has been shuttled to the cell surface by the integral membrane protein g-glutamyltranspeptidase. This replaces the Cys-Gly dipeptide of GSH by the amino acid and produces g-Glu-amino acid. The amino acid is liberated upon degradation of the g-Glu-amino acid by the enzyme g-glutamyl cyclotransferase, which generates 5-oxoproline instead of glutamate. The driving force for uptake of amino acids by this “group translocation” type of mechanism is the destruction of the glutathione, for the Cys-Gly moiety is also degraded, by cysteinylglycine dipeptidase; regeneration of glutamate from 5-oxoproline by 5-oxoprolinase requires hydrolysis of ATP, and resynthesis of glutathione requires another two molecules of ATP. The disulfide form of cysteine, cystine, is an especially reactive amino acid substrate of this cycle. The g-Glu-CysSSCys generated by g-glutamyltranspeptidase is rapidly reduced in the cell cytosol to g-Glu-Cys and cysteine. The g-Glu-Cys can then be converted to GSH by addition of glycine, thereby bypassing the production of 5-oxoproline. On the other hand, humans lacking g-glutamyltranspeptidase have no difficulty in transporting amino acids, and there are many other types of amino acid **transporters**. The cycle is now believed to play only a minor role in transport of amino acids, except for cysteine.

Figure 1. The g-glutamyl cycle for transporting amino acids, coupled to the degradation of glutathione (GSH; g-Glu-Cys-Gly). The amino acid (AA) on the outside of the cell (left) is coupled to glutamic acid of GSH by the membrane protein g-glutamyl transpeptidase, by replacing the dipeptide cysteinyl-glycine (Cys-Gly). The amino acid is released from the g-glutamyl residue, converting it to 5-oxoproline. The concomitant degradation of GSH is the driving force for transporting the amino acid. Resynthesizing 1 mol of GSH requires the hydrolysis of 3 moles of ATP.

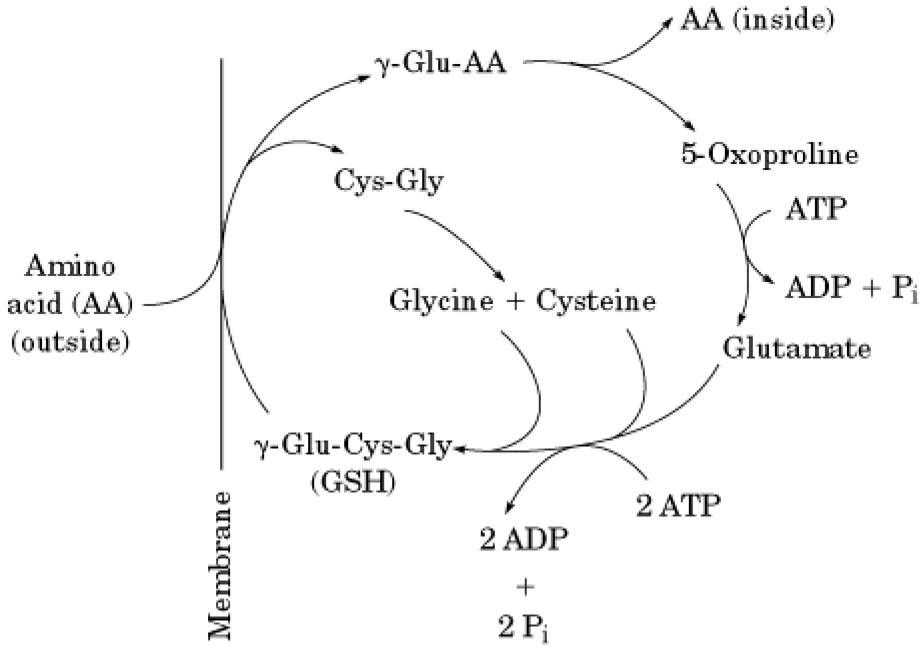

The g-glutamyl cycle is now believed to have a major role in higher organisms in the metabolism of leukotrienes, estrogens, prostaglandins, and many drugs and xenobiotics. All these molecules, often after their reaction with cytochrome P-450, are linked covalently to the thiol group of GSH by the large enzyme family of **glutathione S-transferases**. The resulting glutathione S-conjugate is then degraded to the Cys-Gly S-conjugate and then to the cysteine S-conjugate by g-glutamyltranspeptidase and cysteinylglycine dipeptidase, respectively. The cysteine S-conjugate is converted, by a specific *N*-acetyltransferase to the corresponding mercapturate, *N*-acetylcysteine S-conjugate, which is then excreted. On the other hand, this pathway can also sometimes lead to the generation of a toxic substance. For example, halogenated cysteine S-conjugates can generate highly reactive thiol-containing fragments through the action of cysteine S-conjugate b-lyases:

$$\underset{\text{cysteine S-conjugate}}{R-S-CH_2CH(NH_2)CO_2H} \rightarrow RSH + NH_3 + \underset{\text{pyruvate}}{CH_3C(O)CO_2H} \tag{5}$$

where RSH is the thiol form of the xenobiotic, which can be toxic.

The generally protective, antioxidative effects of GSH are reflected in the observations that decreased levels of GSH lead to clinical symptoms in humans and decreased resistance to viruses and other diseases.

Bibliography

1. G. Jung, E. Beitmeier, and W. Voelter (1972) Eur. J. Biochem. **24**, 438–445.
2. N. J. Darby and T. E. Creighton (1995) Biochemistry **34**, 3576–3587.
3. P. A. Karplus and G. E. Schulz (1989) J. Mol. Biol. **210**, 163–180.
4. O. Epp et al. (1983) Eur. J. Biochem. **133**, 51–69.
5. C. Hwang, A. J. Sinskey, and H. F. Lodish (1992) Science **257**, 1496–1502.

Suggestions for Further Reading

6. A. Meister and M. E. Anderson (1983) Glutathione. Ann. Rev. Biochem. **52**, 711–760.
7. N. Taniguchi, T. Higashi, Y. Sakamoto, and A. Meister, eds. (1989) *Glutathione Centennial: Molecular Perspectives and Clinical Implications*. Academic Press, San Diego.

8. R. C. Fahey and A. R. Sundquist (1991) Evolution of glutathione metabolism. Adv. Enzymol. **64**, 1–53.
9. K. D. Tew, C. B. Picket, T. J. Mantle, B. Mannervik, and J. D. Hayes, eds. (1993) *Structure and Function of Glutathione Transferases*. CRC Press, Boca Raton, Florida.
10. A. J. L. Cooper (1994) Enzymology of cysteine-S-conjugate -lyases. Adv. Pharmacol. **27**, 71–113.
11. A. J. L. Cooper and B. S. Kristal (1997) Multiple roles of glutathione in the central nervous system. Biol. Chem. **378**, 793–802.
12. N. Kaplowitz, J. C. Fernandez-Checa, R. Kannan, C. Garcia-Ruiz, M. Ookthens, and J. R. Yu (1996) GSH transporters: Molecular characterization and role in GSH homeostasis. Biol. Chem. Hoppe-Seyler **377**, 267–273.

Glutathione Transferase

Glutathione transferases (GSTs) are detoxication enzymes that occur abundantly in eukaryotic cells and also in prokaryotic organisms. The majority of the enzymes are found in the cytosol, but a significant proportion is also recovered in the **microsomes** and other subcellular membrane fractions. In mammalian liver tissue, GSTs represent several percent of the total protein content in both the **cytoplasm** and the endoplasmic reticulum, indicating they have important biological functions. All known soluble (mostly cytosolic) GSTs are dimeric proteins composed of two subunits of approximately 26-kDa molecular weight. In contrast, the microsomal GSTs, and probably the related membrane-bound enzymes, are trimers of 17-kDa subunits (Table 1). A plasmid-encoded GST that confers bacterial antibiotic resistance to fosfomycin is a structurally unrelated protein composed of two 16-kDa subunits. The cytosolic GSTs form both homodimers and heterodimers of closely related subunits, thereby increasing the multiplicity of GST **isoenzymes** .

Table 1. Structural and Catalytic Properties of Human Glutathione Transferases [a]

	Human Glutathione Transferase										
Property	A1-1	A2-2	A4-4	M1-1	M2-2	M3-3	M4-4	P1-1	T1-1	T2-2	MGST1 (activated)
Structure											
Subunit molecular mass (kDa)	26	26	26	26	26	26	26	23	27	27	17
Quaternary structure	Dimer	Dimer	Dimer	Dimer	Dimer	Dimer	Dimer	Dimer	Dimer	Dimer	trimer
Gene localization											
Chromosome (no.)	6	6	6	1	1	1	1	11	22	22	12
Substrate activity											

Aminochrome	0.04	0.03	—	0.8	150	0.14		0.08	—		
1-Chloro-2,4-dinitrobenzene	80	80	7.5	180	220	7	1.4	105	—	—	24
Cumene hydroperoxide	10	10	1	0.6				0.03	3	7	3
4-Hydroxynon-2-enal	6		190	3	4	2		2			
trans-Stilbeneoxide	0.002			5.2	0.0003	0.0004	0.003	0.002			

[a] Specific activities (mol/min per mg pure protein) are given for representative substrates. Dashes represent no measurable activity; blank spaces signify missing data. Data largely compiled from the review articles by Mannervik and Widersten (1995) and Hayes and Pulford (1995).

1. Reactions Catalyzed

GSTs catalyze reactions between glutathione (GSH) and compounds with electrophilic chemical functionalities. GSH is a tripeptide, g-L-glutamyl-L-cysteinyl-glycine, that occurs in millimolar concentrations in all types of cells and in micromolar concentrations in mammalian extracellular fluids. The reactive thiol group, –SH, of the GSH cysteine residue may serve as either a nucleophile or a reductant. In both cases, the reactions are dependent on the electron-donating properties of the sulfur atom. Its reactivity is further accentuated by ionization of the thiol group to the thiolate form. One of the catalytic functions of GSTs is to decrease the pK_a value of the GSH thiol group (9.2 in aqueous solution) to make GSH ionized under physiological conditions. The pK_a value of enzyme-bound GSH may be lowered by several pH units. Judging from the known affinities of GSTs for GSH, it would appear that most enzymes are fully loaded with GSH in its thiolate form and ready to react with the incoming second substrate.

The common denominator for essentially all GST-catalyzed reactions is nucleophilic attack by the GSH thiolate group on an electrophilic site in the second substrate. The electrophilic center of the second molecule is usually a carbon atom, but it may also be electronegative atoms, such as oxygen, nitrogen, or sulfur. The GST-catalyzed reactions involving O, N, and S as electrophilic sites often lead to unstable products, which react with a second molecule of GSH:

$$\mathrm{ROOH} + \mathrm{GSH} \rightarrow \mathrm{ROH} + \mathrm{GSOH} \quad (1)$$

$$\mathrm{GSOH} + \mathrm{GSH} \rightarrow \mathrm{GSSG} + \mathrm{H_2O} \quad (2)$$

where ROOH and ROH are, respectively, a hydroperoxide and the corresponding alcohol, and GSSG is the **disulfide** form of glutathione. In effect, such reactions accomplish reduction of organic hydroperoxides, nitrate esters, and disulfides.

The carbon-centered reactions are basically of two types: additions and substitutions. Addition reactions involve molecules such as naturally occurring a,b-unsaturated carbonyl compounds and organic isothiocyanates. The substitutions reactions involve the replacement of a chemical substituent by a glutathione group. The leaving group may be a halogenide, sulfate, or other chemical substituent with sufficient electron-withdrawing potential.

Reactions involving electrophilic carbon centers usually lead to GSH conjugates that may be excreted from the cell via ATP-dependent membrane-associated transporters, such as the multidrug resistance-associated protein (MRP) (see Drug Resistance), for subsequent disposition through the gut or the urinary tract. For urinary excretion, GSH conjugates are metabolically transformed by cleavage of the two peptide bonds of the glutathione moiety, followed by acetylation into the corresponding *N*-acetyl-cysteine derivatives, mercapturic acids. These reactions are accomplished through the action of g-glutamyl transpeptidase, a dipeptidase, and an acetyltransferase (see Glutathione).

2. Discovery

GSTs were discovered in mammalian liver as enzymes catalyzing aromatic nucleophilic substitution reactions in which GSH replaces a halogen atom in an aromatic compound, such as a chloronitrobenzene derivative (1, 2). When other classes of organic compounds, with epoxide, alkene, and other electrophilic centers, were investigated, additional enzyme-catalyzed GSH conjugations were identified (3). The introduction of improved separation techniques lead to the identification of multiple forms of GST catalyzing the same chemical reaction, i.e. **isoenzymes** in the original sense of the term (4, 5). Subsequent work with purified enzymes demonstrated that although each enzyme form has its characteristic substrate specificity profile, most GSTs catalyze reactions with a wide range of electrophiles, and the majority of the active compounds are at least to some degree substrates for several GSTs.

3. Substrates

GSTs as a family of enzymes are capable of catalyzing reactions involving literally thousands of electrophilic compounds, including many of xenobiotic origin. In this respect, the GSTs display similarities to **antibodies**, which may evolve to interact with and provide protection against an almost unlimited number of molecular structures.

The majority of the known GSTs are regarded as detoxication enzymes and are catalytically active with a large number of xenobiotics, including epoxides of potent **carcinogens**, such as benzo[a]pyrene and aflatoxin. Naturally occurring substrates include a wide variety of genotoxic compounds, such as epoxides, activated alkenes, hydroperoxides, and quinones, all products of oxidative metabolism. Organic isothiocyanates are abundant in edible plants, from which they are released in high concentrations by injuries caused by insects and microbial infections.

4. Purification

Affinity chromatography methods have been developed for the purification of GSTs. Most purification procedures involve affinity matrices based on glutathione derivatives as ligands. Immobilized *S*-hexylglutathione, first used for the purification of glyoxalase I, is linked via the a-amino group of the g-glutamyl residue of glutathione to a suitable matrix (6). This adsorbent potentially combines the affinities of the H subsite of the GST active site (see below) for the **hydrophobic** hexyl substituent and of the G subsite for the GSH moiety. Another commonly used affinity matrix makes use of GSH immobilized via its thiol group (7). Elution of bound GSTs may be effected by competition using GSH derivatives with affinity for the active site of the enzyme. Alternative elution procedures involve changing the pH of the eluent to extreme values, such as pH 10 or pH 2. When applied to crude tissue fractions, affinity chromatography based on these matrices will yield mixtures of GSTs, which can be resolved by other methods. For separation of the dimeric proteins in a functional form, chromatofocusing or ion-exchange chromatography may be used. For analytical purposes, the subunits may be resolved by **reversed-phase** high-performance liquid chromatography (HPLC).

Less specific affinity methods used for the purification of GSTs include Orange A dye chromatography and **metal chelate chromatography**. The latter methods have proved useful for the isolation of the several GSTs that do not bind to affinity matrices based on glutathione derivatives.

5. Nomenclature

The International Enzyme Commission has recommended the name RX:glutathione R-transferase (E.C. 2.5.1.18) or the trivial form glutathione transferase, which has been adopted here. Another designation commonly used is glutathione *S*-transferase, but this is inconsistent with the rational name, since the group transferred is not the sulfur of glutathione. The generally accepted abbreviation GST has probably contributed to the persistence of the *S*-prefix.

In the time period when the first GSTs were discovered, the enzymes were named in accord with the reactions used for their identification: glutathione *S*-aryltransferase, glutathione *S*-alkyltransferase, and so on. With the exception of the membrane-bound transferase catalyzing the glutathione conjugation of leukotriene A_4, named leukotriene C_4 synthase, the principle of designating GSTs by their substrates or products has been abandoned, because most enzymes have very broad substrate specificities so that accurate distinctions cannot be made.

Another nomenclature system arose from the finding that the cytosolic "Y-fraction" of rodent liver could be separated by SDS-PAGE into components that corresponded to GST subunits. These subunits were distinguished by lower indices, namely Y_a, Y_b and so on, and were further subdivided into Y_{a1}, Y_{a2}. Subunits with the same mobility but different structures were identified.

A rational nomenclature for the cytosolic or soluble GSTs is based on two principles. First, the native enzymes occur as binary combinations of GST protein subunits, so that the functional properties of the dimeric protein reflect those of its constituents subunits (8). Second, the GSTs can be divided into different classes primarily based on similarities in their amino acid sequences (9). In mammals, seven classes of soluble GSTs have been identified thus far: Alpha, Mu, Pi, Theta, Sigma, Kappa, and Zeta. Sequence identities within a class are normally >50%, but they may exceed 95%. Classification of GSTs from other biological species requires further structural studies, but designations for insect enzymes (Delta) and bacteria (Beta) have been used.

In the current nomenclature (Table 1), the soluble mammalian GSTs are denoted by a capital Roman letter indicating the class (A, M, P, T, S, K, and Z) as well as two hyphenated Arabic numerals showing their subunit composition (10). Thus, GST A4-4 is a homodimer of subunit 4 within the Alpha class, and GST A1-2 is a heterodimer composed of subunits 1 and 2 from the same class. There may also be reason to distinguish allelic variants: Human GST M1a-1b is a heterodimeric member of the Mu class composed of variants of subunit 1 in the Mu class encoded by the *GST M*A* and *GST M*B* alleles. A prefix may be used to identify the biological species from which the enzyme derives, such as "h" for the major human enzyme hGST A1-1.

The mammalian membrane-bound GST first isolated from the microsome fraction is a trimeric enzyme composed of identical subunits and cannot readily be accommodated within the nomenclature system used for the soluble GSTs. It is simply referred to as microsomal GST (MGST1). The membrane-bound GST specifically catalyzing the conjugation of leukotriene A_4 is referred to as leukotriene C_4 synthase.

6. Structure

Three distinct categories of GST protein structures are known.

6.1. Soluble GSTs

The first category includes the soluble GSTs, which are generally dimers of equal-sized subunits, each containing an active site composed of a pocket for glutathione (the G site) and a pocket for the largely **hydrophobic** electrophilic substrate (the H site) (11). Each subunit consists of two structural **domains**; (a) an *N*-terminal domain including the first one-third of the primary structure and (b) a domain formed essentially by the remaining two-thirds of the amino acid sequence (Fig. 1). The first domain is folded into a mixed **b-sheet** flanked by **a-helices** and provides the structural basis for the G site. The second one is formed by helical segments and provides the major contributions to the H site. The fold of the *N*-terminal domain is essentially the same as the fold of thioltransferase (glutaredoxin) and selenium-dependent glutathione peroxidase. Another salient feature of the dimer is a deep cleft between the subunits that may serve as a binding site in addition to the active site cavities. The fully formed dimer appears to be a structural requirement for a catalytically active GST.

Figure 1. Schematic drawings of alpha (GST A1-1), pi (GST P1-1) and mu (GST 3-3) structures with their ligands. The been chosen to show the 2 domains and C-terminal region. From Ref. (11), with permission.

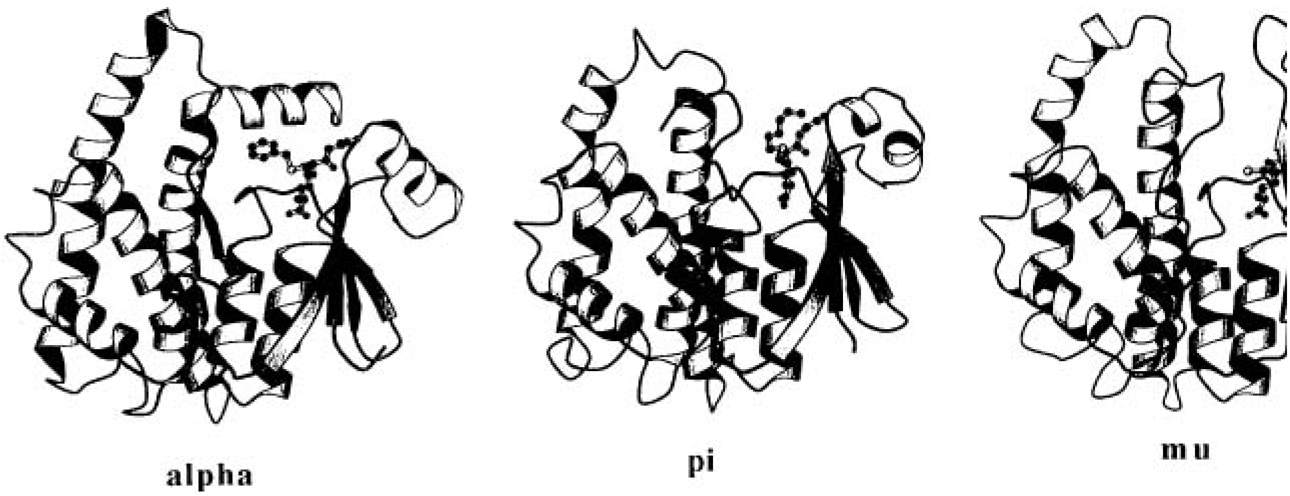

All known structures contain an *N*-capping box sequence, (Ser/Thr)–X–X–Asp, as well as a hydrophobic staple motif formed by flanking amino acid residues in the core of the folded structure. As evidenced by mutational analyses of protein folding (12), these structural signatures appear to play an important role in the nucleation and orientation of a centrally located a-helix.

6.2. Manganese-Dependent Plasmid-Encoded GST

The second category is represented by the manganese-dependent plasmid-encoded GST that is active with the antibiotic fosfomycin (13). It is a homodimer structurally related to mammalian glyoxalase I, a GSH-linked zinc protein whose structure has been determined (14). This GST is structurally unrelated to other known GSTs.

6.3. Membrane-Bound GSTs

The third category contains the microsomal MGST1 and, presumably, the additional membrane-bound GSTs. The detailed structure of MGST1 is unknown, but clearly it is not similar in structure to the soluble GSTs. The protein is a homotrimer, and the identical monomers appear to have a high content of a-helical structure.

7. Catalytic Mechanism

GSTs bind the peptide moiety of GSH in a well-defined manner so that they are specific for this thiol substrate. For all GSTs investigated, the a-carboxylate group of the g-glutamyl residue of GSH is required for the thiol group to serve as a substrate; when bound in the G subsite, the carboxylate appears to have a negative charge that is not balanced by a positively charged protein group. These observations suggest a contribution of the substrate carboxylate group to catalysis. At least for some GSTs, there is also evidence that binding of GSH induces a conformational change in the protein that promotes binding of the second substrate.

Binding of GSH to the G subsite affects the ionization of its sulfhydryl group, thereby making it more reactive. In addition, interactions with a **hydrogen-bond** donor in the active site may stabilize and orient the thiolate group for optimal interaction with the electrophilic substrate. In this manner the enzyme promotes catalysis by selecting a suitable ground-state conformation of GSH.

Binding to the H subsite also results in desolvation of the electrophilic substrate and selection of an orientation favorable for reaction with the sulfur of GSH. Some GSTs have tyrosine or other residues that afford binding specificity, as well as activation of substrates by hydrogen bonding and other electrostatic interactions.

In some, but not all, GST-catalyzed reactions, stabilization of the transition state contributes to the catalytic efficiency. Thus, the common mechanistic feature of GSTs is the activation of GSH, whereas other components of the catalytic process may differ from substrate to substrate and from enzyme to enzyme.

8. Binding Function

A ligand-binding function of GSTs of possible physiological significance was originally found in the protein fraction *Y*, of rat liver cytosol, which binds organic compounds such as certain carcinogens, dyes, and corticosteroids. The abundance of the protein (several percent of the total cytosolic protein) and its broad specificity for binding of a variety of ligands suggested a function similar to that of serum albumin in blood plasma and led to the name of "ligandin" (intracellular albumin). In the current nomenclature, ligandin corresponds to the Alpha class GST A1-1, with some contribution of the heterodimer GST A1-2. Corticosteroid binding has also been associated with GST isoenzymes of the Mu class.

The binding function of GSTs has often been ascribed to the H subsite, at which the enzyme binds the various electrophilic substrates. Some nonsubstrate compounds, especially small molecules, can bind at the H subsite with a stoichiometry of one molecule per subunit. However, X-ray crystallography studies have also shown that the deep cleft between the two GST subunits serves as an additional binding site of the dimeric structure, explaining the stoichiometry of one ligand per two subunits observed for certain ligands.

As binding proteins, GSTs have been suggested to facilitate the intracellular transport of endogenous molecules, such as heme and bilirubin, as well as other compounds of low solubility in an aqueous environment. The transport through cellular membranes of dyes, such as indocyanine green and bromosulfophthalein, which have been used in clinical liver function tests, may also be facilitated by GSTs. An auxiliary role in **active-transport** processes involving MRP and other membrane transport systems may also be suggested. However, the full significance of GSTs as binding proteins needs to be further clarified.

9. Molecular Evolution

The presence of GSH is a signature of aerobic organisms (15), as is the occurrence of GSTs. Elucidation of the details of the phylogeny of GSTs requires additional structural information. The soluble (cytosolic) GSTs are found ubiquitously, however, and all their three-dimensional structures determined, from bacteria to higher plants and mammals, have the same two-domain fold, even though sequence similarities may be undetectable. A common ancestry followed by divergent evolution is therefore indicated. The most recently discovered Kappa, Theta, and Zeta classes of

GST appear to be evolutionary precursors of the more abundant mammalian enzymes from the Alpha, Mu, and Pi classes. It has been proposed, in accordance with the symbiont theory of organelle evolution, that the Kappa class GST found in mitochondria may be a descendant from a bacterial GST. The structural similarities between the *N*-terminal domain of the soluble GSTs and other GSH-linked proteins (see text above) lends support to the hypothesis that a GSH-binding protein is a functional unit that has been combined with other functional protein units and evolved to serve diverse biological functions. The GST structure itself has evolved to fulfill alternative functions, such as that of crystallins in the eye lens of cephalopods. The various GST isoenzymes may have arisen by gene duplications, recombination of DNA segments, and random mutations .

The membrane-bound GSTs and the plasmid-encoded Mn-dependent GST seem to have undergone convergent evolution to acquire the property of catalyzing the nucleophilic attack of GSH on electrophiles. Thus, three evolutionarily unrelated superfamilies of GSTs have been recognized.

10. Differential Tissue Distribution

GSTs are found in all tissues investigated in multicellular organisms, but the expression of the multiple genes differs from tissue to tissue. Also, the enzyme distribution changes with time during the development of embryonic to adult organs. Some GSTs have a reasonably general tissue distribution, whereas others have a more restricted occurrence. Also intracellular spatiotemporal differences in GST distribution have been noted. The soluble GSTs are found mainly in the cytoplasm, but may also occur sometimes in the nucleus. The mammalian Kappa class GST is found in the mitochondrial matrix.

The differential distribution of GSTs may have toxicological consequences, since the amount and nature of a given GST will determine the capacity of a cell to resist insults from genotoxic and carcinogenic electrophiles. The presence or absence of a particular enzyme will influence the resistance **phenotype** of a tissue. In cancer cells, GSTs may contribute to drug resistance, particularly against alkylating cytostatic agents.

11. GST Genes

Mammalian cells generally appear to have more than 20 GST genes, each encoding a distinct GST subunit. In humans, as well as in rodents, the genes have been shown to be distributed on different chromosomes, and the loci for related GSTs from the same class are generally clustered on the same chromosome. In addition, pseudogenes may occur close to the active genes. This distribution supports the classification adopted for the GSTs and is in agreement with the proposal that they have diversified in evolution by gene duplication and DNA recombination.

Genetic polymorphisms are known, and the human genes for GST M1-1 and GST T1-1 are deleted in approximately 50% and 20%, respectively, of the population. The resulting enzyme deficiencies lead to increased sensitivities to gene modifications and chromosome aberrations by certain chemical agents, and they probably also lead to increased risk of contracting certain forms of cancer. On the other hand, the activity of GST T1-1 promotes the formation of mutagens from ethylene dihalogenides, and the absence of the enzyme may be advantageous under some circumstances.

12. Regulation of Gene Expression and Induction of GST Activity

The differential expression of the GSTs is governed by hormones and other factors that regulate transcription of the genes. A range of **enhancers** and other regulatory elements, shown to mediate responses in other genes, have also been shown to be functional in GST gene regulation. Particular attention has been given to the **antioxidant response element**, ARE (also called the *electrophile response element*), which has proven effective in the induction of the activity of several detoxication enzymes in mammalian systems. An extremely broad range of chemical compounds containing an electrophilic group appear to serve as inducers via ARE, suggesting that enzyme induction is a natural response to exposure to electrophiles.

13. Biological functions

GSTs serve in cellular detoxication systems and constitute the major line of defense against chemical electrophiles, many of which are genotoxic and carcinogenic. The substrates include numerous xenobiotics or their metabolically activated products—for example, epoxides of carcinogenic polyaromatic hydrocarbons. Plants produce a variety of toxic compounds as a defense against attack by insects and microorganisms, and some of them can be inactivated by GSH conjugation. For example, many edible plants produce toxic organic isothiocyanates that are substrates for human GSTs. Like their mammalian counterparts, plant GSTs are inducible enzymes that serve protective functions, one of which is to provide cellular resistance to electrophilic herbicides.

Among the biologically most important substrates are numerous oxidation products of normal cell constituents, such as lipids, nucleic acids, catechols, and other aromatic or unsaturated chemical compounds. Free-radical reactions, accompanied by chemical transformations involving reactive oxygen species, lead to a variety of electrophilic products that may cause damage to DNA and proteins. Lipid peroxidation gives rise to aldehydes and activated alkenes, and cellular oxidation of catecholamines produces ortho-quinones. These naturally occurring oxidation products, considered to be etiological factors in the development of atherosclerosis, cataract, cancer, Parkinson's, and other degenerative diseases, are all substrates of GSTs. Human GST A4-4 has particularly high activity with the lipid peroxidation product 4-hydroxynon-2-enal (Table 1), and human GST M2-2 is the most efficient enzyme with the ortho-quinone aminochrome derived from dopamine.

In addition to their catalytic functions, GSTs may serve as binding proteins (ligandin) that facilitate cellular transport of organic molecules. Some of the most abundant enzymes, such as GST A1-1, appear particularly well-suited for this purpose.

14. Biotechnology Applications

The soluble GSTs are generally stable proteins that can be produced in large quantities by heterologous expression in *Escherichia coli*. Thus, the enzymes have potential for development into useful recombinant proteins of value for biotechnical, agricultural, and medical applications. Both the catalytic and binding properties can be explored. Catalysts and binding proteins with novel specificities can be designed by a combination of mutagenesis and selection methods.

15. Glutathione Transferase as a Fusion Protein for Expression of Other Proteins

In the expression of proteins by **recombinant-DNA** methods, it is frequently found that the protein product is obtained in poor yield owing to low solubility, improper **codon usage**, **proteolytic** degradation, and so on. In many cases, these problems may be overcome by producing the desired protein product in fusion with a GST molecule. DNA encoding GST with a cleavable *C*-terminal linker to the protein to be expressed is ligated to the target DNA. GSTs are normally stable and soluble proteins that can be expressed at high levels in many cell types, and the recombinant fusion proteins usually retain these properties. The fusion protein can be purified by affinity chromatography on immobilized glutathione derivatives and, after liberation of the desired protein by proteolytic cleavage, the GST moiety can be removed by a second affinity chromatography. By this two-step purification, the desired protein may be obtained in pure form.

Bibliography

1. J. Booth, E. Boyland, and P. Sims (1961) Biochem. J. **79**, 516–524.
2. B. Combes and G. S. Stakelum (1961) J. Clin. Invest. **40**, 981–988.
3. L. F. Chasseaud (1979) Adv. Cancer Res. **29**, 175–274.
4. W. B. Jakoby (1978) Adv. Enzymol. **46**, 383–414.

5. B. Mannervik (1985) Adv. Enzymol. Relat. Areas Mol. Biol. **57**, 357–417.
6. B. Mannervik and C. Guthenberg (1981) Methods Enzymol . **77**, 231–235.
7. P. C. Simons and D. L. Vander Jagt (1981) Methods Enzymol. **77**, 235–237.
8. B. Mannervik and H. Jensson (1982) J. Biol. Chem. **257**, 9909–9912.
9. B. Mannervik, P. Ålin, C. Guthenberg, H. Jensson, M. K. Tahir, M. Warholm, and H. Jörnvall (1985) Proc. Natl. Acad. Sci. USA **82**, 7202–7206.
10. B. Mannervik, Y. C. Awasthi, P. G. Board, J. D. Hayes, C. Di Ilio, B. Ketterer, I. Listowsky, R. Morgenstern, M. Muramatsu, W. R. Pearson, C. B. Pickett, K. Sato, and M. Widersten (1992) Biochem. J. **282**, 305–306.
11. I. Sinning, G. J. Kleywegt, S. W. Cowan, P. Reinemer, H. W. Dirr, R. Huber, G. L. Gilliland, R. N. Armstrong, X. Ji, P. G. Board, B. Olin, B. Mannervik, and T. A. Jones (1993) J. Mol. Biol. **232**, 192–212.
12. B. Dragani, G. Stenberg, S. Melino, R. Petruzzelli, and B. Mannervik (1997) J. Biol. Chem. **272**, 25518–25523.
13. B. A. Bernat, L. T. Laughlin, and R. N. Armstrong (1997) Biochemistry **36**, 3050–3055.
14. A. D. Cameron, B. Olin, M. Ridderström, B. Mannervik, and T. A. Jones (1997) EMBO J. **16**, 3386–3395.
15. R. C. Fahey and A. R. Sundquist (1991) Adv. Enzymol. Relat. Areas Mol. Biol. **64**, 1–53.

Suggestions for Further Reading

16. P. D. Josephy, B. Mannervik, and P. Ortiz de Montellano (1997) *Molecular Toxicology*, Oxford University Press, New York.
17. R. N. Armstrong (1997) Structure, catalytic mechanism, and evolution of the glutathione transferases. Chem. Res. Toxicol. **10**, 2–18.
18. K. A. Marrs (1996) The functions and regulation of glutathione *S*-transferases in plants. Annu. Rev. Plant Mol. Biol. **47**, 127–158.
19. B. Ketterer (1988) Protective role of glutathione and glutathione transferases in mutagenesis and carcinogenesis. Mutat. Res. **202**, 343–361.
20. B. Mannervik and M. Widersten (1995) "Human glutathione transferases: classification, tissue distribution, structure and functional properties". In *Advances in Drug Metabolism in Man* (G. M. Pacifici and G. N. Fracchia. eds.), European Commission, Luxembourg, pp. 407–459.
21. J. D. Hayes and D. J. Pulford (1995) The glutathione *S*-transferase supergene family: regulation of GST and the contribution of the isoenzymes to cancer chemoprotection and drug resistance. CRC Crit Rev. Biochem. Mol. Biol. **30**, 445–600.

Glycine (Gly, G)

The amino acid glycine is incorporated into the nascent polypeptide chain during **protein biosynthesis** in response to four **codons**—GGU, GGC, GGA, and GGG—and represents approximately 7.2% of the residues of the proteins that have been characterized. The glycyl residue incorporated has a mass of 57.05 Da, a **van der Waals volume** of 48 Å^3, and an accessible surface area of 85 Å^2. Gly residues are changed during divergent evolution less frequently than average; when they are, they are interchanged in **homologous** proteins most frequently with alanine, serine, aspartic acid, and asparagine residues.

Gly is the simplest amino acid residue, with only a hydrogen atom for a side chain. Note that the a-carbon atom of Gly is not asymmetric, in contrast to the other amino acids incorporated into proteins, because it is bonded to two H atoms. Consequently, this amino acid does not occur as D or L isomers.

The absence of a larger side chain gives the polypeptide backbone at Gly residues much greater conformational flexibility than at other residues. For example, about 61% of the possible values of the torsion angles f and y of a Ramachandran Plot are permitted with a Gly residue, in contrast to the 30% with other residues; moreover, the Ramachandran plot of allowed torsion angles is symmetric. This extra flexibility tends to decrease the overall average dimensions of unfolded polypeptide chains, as the Gly residues permit the chain to reverse directions more readily. This is also used in native protein structures, where Gly residues occur most frequently in reverse turns. The extra flexibility of the Gly residue in an unfolded polypeptide chain is believed to destabilize all fixed conformations, and Gly residues decrease the tendency to adopt an **alpha-helical** conformation.

The precursors of some peptide hormones, such as melanocyte stimulating hormone, have a Gly residue at the *C*-terminus that becomes converted to an amide group enzymatically).

Suggestion for Further Reading

T. E. Creighton (1993) *Proteins: Structures and Molecular Properties*, 2nd ed., W. H. Freeman, New York.

Glycogen Phosphorylase

Glycogen phosphorylase (E.C. 2.4.1.1) catalyzes the first step in the intracellular degradation of glycogen to form individual molecules of glucose that are used for energy needs. Glycogen is a polymeric storage form of sugar consisting of glucose joined into long chains by the elimination of water between the first carbon of one glucose and the fourth of another, forming a-1,4 links. Every four to five glucose units, a branch is introduced by an a-1,6 link, resulting in a compact, highly branched molecule, spherical in shape, and containing as many as a million glucose units. Phosphorylase carries out a phosphorolytic cleavage of the 1,4 links, as shown below:

$$(\alpha-1,4-\mathit{glucoside})_n + \mathrm{HPO}_4^{2-} \leftrightarrow (\alpha-1,4-\mathrm{glucoside})_{n-1} + \alpha-\mathcal{D}-\mathrm{glucose}-1-\mathrm{PO}_3^{2-} \qquad (1)$$

The 1,6 branchpoint links are removed by a separate enzyme, the glycogen debranching enzyme, so that phosphorylase can then degrade virtually the entire molecule. Phosphorylase exists in two forms, *a* and *b*, differing covalently only in that Ser14 is phosphorylated in form *a*. In muscle, the nervous signal for contraction, calcium release, also activates the inactive phosphorylase *b* of resting muscle through the action of phosphorylase kinase . In liver, the inactive phosphorylase of a well-fed animal is activated by the signal of the pancreatic hormone glucagon that blood sugar levels are low, again via the mediation of phosphorylase kinase. Phosphorylase was one of the first enzymes recognized to be under hormonal control by protein **phosphorylation**, as well as subject to **allosteric** controls. It can be prepared in large amounts in pure crystalline form from muscle, and this made it the subject of intense study by a number of laboratories, culminating in the determination of its three-dimensional structure at atomic resolution by X-ray crystallography. The structures of several of its forms, plus associated biochemical experiments, have resulted in a better understanding of the function of this large and complicated enzyme.

1. Discovery and Early Developments

Carl and Gerty Cori discovered phosphorylase in 1936 when they isolated a new sugar phosphate from minced muscle mixed with water and inorganic phosphate. By characterization and synthesis, they proved that the new compound was a-D-glucose-1-phosphate and showed that it was formed from glycogen by the chemical reaction depicted in equation (1). The purified enzyme required AMP for activity, and when all attempts failed to demonstrate its participation in the catalytic mechanism, as other known coenzymes did, this became recognized as perhaps the first example of an allosteric activator. In 1941, a second form of phosphorylase was isolated and crystallized that did not require AMP for activity, although the latter decreased the $\boldsymbol{K_m}$ **(Michaelis constant)** values for the substrates; this was termed the *a* form, while the first was termed the *b* form.

During the 1950s, it was discovered that phosphorylase *a* was twice the molecular weight of phosphorylase *b* and that a new enzyme, now known as a **protein phosphatase**, converted form *a* to *b*. Chemical modification of the thiol groups inactivated the enzyme, accompanied by dissociation of the *a* form into four identical subunits and dissociation of the *b* form into two identical subunits. The number of moles of AMP binding to the enzyme equaled the subunit composition of the two forms. However, under *in vivo* conditions and bound to glycogen, phosphorylase *a* is dimeric. This was the first demonstration that enzymes contain subunits (see Quaternary Structure); the only proteins known earlier to have subunits were hemoglobin and insulin. The conversion of phosphorylase *b* to *a* was shown to involve the phosphorylation of residue Ser14 of each subunit by the specific phosphorylase kinase. A second organic phosphate moiety present was discovered to be pyridoxal phosphate (PLP), a derivative of vitamin B6. The **kinetic mechanism** was proven to be rapid equilibrium random Bi–Bi, meaning that either substrate can bind first, that kinetic constants approximate binding constants, and that the rate-limiting steps are to be found in the interconversion of the ternary complexes. Graves and Wang (1) have published a comprehensive review of the literature up to 1972, a convenient date because it occurs just before the crystallographic studies provided detailed structures and insights into function and regulation.

2. Structure–Function Relationships

In 1970, a new tetragonal crystal form of phosphorylase *b* was discovered in the Oxford laboratory of L. N. Johnson and her colleagues. These macrocrystals belonged to space group $P4_32_12$; and the asymmetric unit was one monomer, with the protein dimer formed by the crystallographic twofold axis, making the crystals suitable for X-ray crystallography. The crystals were grown at low salt concentrations in the presence of IMP. Isomorphous crystals of phosphorylase *a* were later grown in Edmonton, Canada, by using 50 mM glucose to force dimers. The structure of phosphorylase *b* was determined in Oxford by Johnson et al., while that of the *a* form was determined by Fletterick et al. in Edmonton, initially using phases from Oxford to locate the heavy atoms used in isomorphous replacement. The structural studies to 1979 have been summarized in a review (2).

The complete amino acid sequence of phosphorylase was determined in the Seattle laboratories of Fischer, Neurath, Titani, and Walsh by adroit use of all conventional **sequencing** technologies, just in time for use in the three-dimensional structure determination. Each subunit of phosphorylase *a* consists of a single polypeptide chain of 842 amino acids. The *N*-terminal serine is acetylated and Ser14 is phosphorylated, while pyridoxal phosphate is bound to Lys680 via a Schiff Base. Counting the three nonprotein moieties, the molecular weight of phosphorylase *a* is 97,512, while that for the *b* form subunit, often used as a molecular weight standard, is 97,434.

The tetragonal crystals of phosphorylases *a* and *b* have unit cell dimensions of $a = b = 128.4$ Å and $c = 116.4$ Å. The topology and packing are typical of a/b-type proteins, with 50% content of **a-helix** content and 30% **b-sheet** (see Protein Structure). The dimeric structures of the two forms *a* and *b* are very similar, except that in the absence of the phosphate group on Ser14, the *N*-terminal 16 residues are disordered in phosphorylase *b*. When Ser14 is phosphorylated, these residues fold into a distorted helix that is bound to the rest of the protein. Two large **domains** compose the monomer, with the *N*-terminal domain consisting of 490 residues. The latter has a core of b-sheet consisting of nine b-strands describing a 180° right-handed twist flanked by helical segments, loops, and some additional b-strands. This domain contains the AMP binding site near Tyr75 and only 10 Å from the Ser14-phosphate group. The allosteric inhibitors ATP and glucose-6-phosphate also bind here. In a helical part of the domain, some 30 Å from either the activator site that binds AMP or the catalytic site, is found the glycogen storage site, which binds oligosaccharides in a helical form slightly distorted from that of amylose. Because binding here is some 20-fold tighter than at the active site, it is suggested that phosphorylase is anchored by these sites to a glycogen particle, whether or not it is acting on other glycogen end-chains at the active site. Components of the active site and the inhibitor site for caffeine (Phe285) are found at the interface with the C-terminal domain. The latter domain contains a core of six parallel b-strands, with a twist and connectivity to surrounding a-helices that is topologically similar to the nucleotide-binding motif of the dehydrogenases, although more buried by additional helices and loops. The deep cleft between the two domains contains (a) the active site, which is buried deeply, next to the phosphate group of PLP, and (b) the entrance between Phe285 and Tyr613, which is "locked" when caffeine binds in between. The two subunits undertake many interactions when they associate to form the dimer, including shared binding sites for AMP and for the phosphate of Ser14 and long paired loops/helices (the "towers") that extend reciprocally toward the symmetry-related active sites. The dimer possesses a concave catalytic face containing the active sites and glycogen storage sites, by which it may bind to glycogen while exposing the convex control face to the action of phosphorylase kinase or phosphatase. A computer drawn space-filling model of the control face is shown in Fig. 1.

Figure 1. Space-filling model of the control face of the phosphorylase *a* dimer viewed down the twofold axis. Positively charged residues are blue, negatively charged residues are red, and the phosphate groups of the two Ser14 residues are magenta, while noncharged residues of the *N*-terminal a-helices are yellow. The *N*-terminal segments, identified by the phosphates and yellow residues, lie across the subunit interface. This T-state structure, with the phosphates fully exposed and surrounded by positive charges, represents the favored substrate for protein phosphatase. (Courtesy of Drs. R. Read and A. Muir, Department of Biochemistry, University of Alberta.) See color insert.

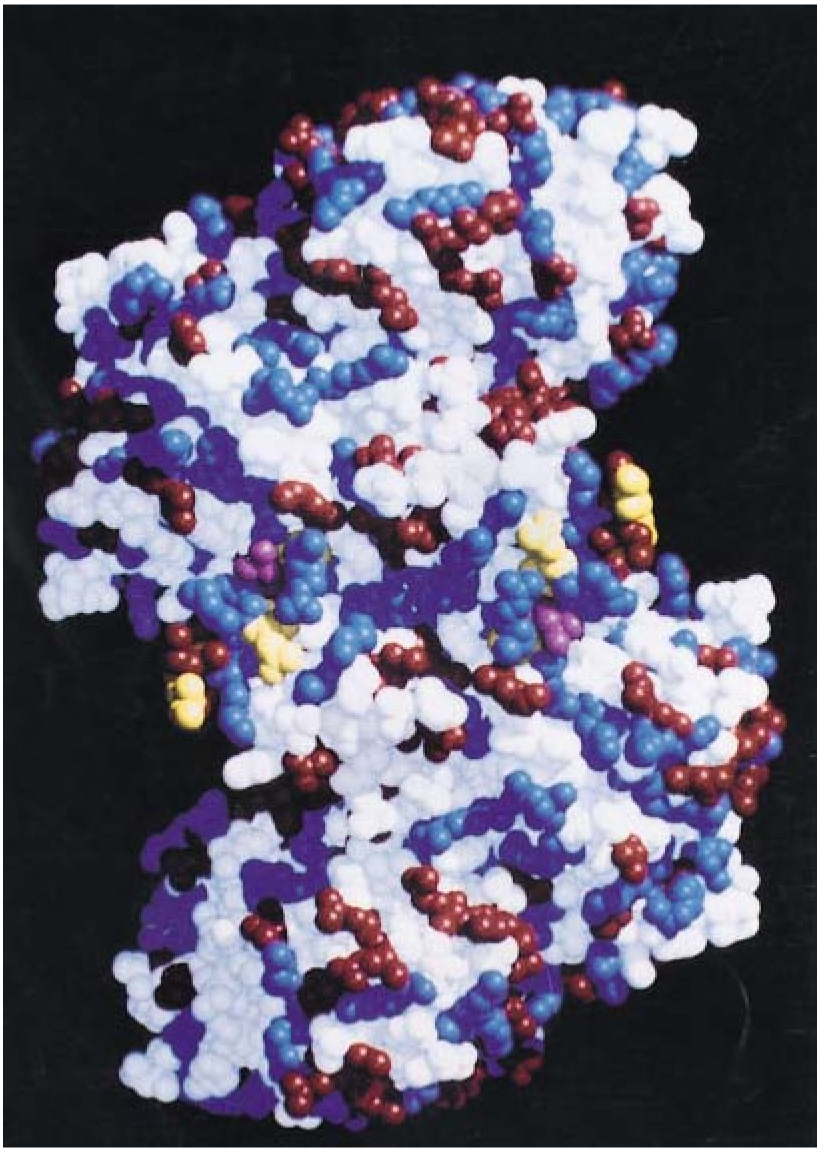

Studies on the catalytic mechanism of phosphorylase have been reviewed up to 1985 (3) and centered around the role of pyridoxal 5′-phosphate. The coenzyme, sandwiched between the two domains, plays an unusual structural role because its removal leads to an inactive monomer. Extensive analog studies have eliminated all parts of the coenzyme from participating in catalysis except the phosphate, which must be capable of forming a dianion. In 1977, Graves et al. found that phosphorylase *b* reconstituted with pyridoxal, and hence inactive, regained appreciable activity in the presence of inorganic phosphate (P_i), phosphite, or fluorophosphate. Furthermore, pyrophosphate showed competitive inhibition with both glucose-1-P and the activating phosphite, while binding only one mole per monomer. That same year, crystallographic studies placed only the phosphate of the coenzyme near the substrate, 7.0 Å from the latter's phosphate in these crystals, which are in the allosteric T state. These results led to the interacting phosphates hypothesis that was strengthened by a number of experiments, including the reconstitution of the enzyme with pyridoxal pyrophosphate glucose. This compound contains both substrate and coenzyme covalently linked, and the enzyme could transfer the glucose to an added oligosaccharide. This suggested that the coenzyme phosphate might act as an electrophile (Lewis acid). However, the alternative hypothesis that the coenzyme phosphate acts as a proton donor (Brønsted acid) now appears more likely, especially considering the crystallographic studies of time-resolved catalysis in the crystalline state (4). Phosphorylase catalyzes the phosphorylation of heptenitol to heptulose 2-phosphate, and the latter, a potent inhibitor, is found in the crystal structure with a hydrogen bond between its phosphate and that of the coenzyme. This suggests that in the normal phosphorolysis of glycogen, the proton of P_i attacks the glycosidic bond, cleaving it, while the substrate P_i immediately gains a proton from the PLP phosphate. The phosphate anion stabilizes the glucosyl carbonium ion, necessary to maintain the alpha anomeric configuration. The reaction is completed by a nucleophilic attack of the phosphate on the carbonium ion to form glucose 1-phosphate.

3. Regulation

The two forms of the enzyme differ markedly in their allosteric regulatory properties. The *b* form is activated by AMP or IMP and is inhibited by ATP, ADP, glucose, and glucose-6-phosphate; the *a* form is not subject to these controls, but is still inhibited by glucose. Glucose binds at the active site of phosphorylase and is a competitive inhibitor of glucose-1-P, a primitive end-product **feedback inhibition** control. The crystals of phosphorylase *a* grown with glucose are in the allosterically inhibited T state, while those of phosphorylase *b* grown with IMP are also in the T state, permitting a direct comparison of the effect of phosphorylating Ser14 on the structure (5, 6). The *b* form requires AMP for activity, but full conversion to the active R state requires substrate, while ATP and glucose-6-phosphate compete for the AMP site and represent energy and end-product allosteric controls, respectively. While the allosteric ratio of T to R for unliganded *b* is of the order of 3,000, that for the *a* form is only 10, allowing full activity of the latter with substrates alone, while only the slight activation of the *a* form by AMP is inhibited by ATP. Phosphorylase *a* may be said to have "escaped allosteric control," the latter form of regulation having been superseded by covalent modification, under extracellular hormonal and neural regulation. Because AMP binds 200 times more tightly to the *a* than the *b* form, it is obvious that a large portion of its binding energy to the *b* form is utilized in the allosteric conformational change and that the interactions of the Ser14 phosphate group must be responsible. Comparison of the two T-state tetragonal crystal structures reveal that the disordered *N*-terminal segment, residues 5–16, of the *b* form becomes an ordered helix which lies across the dimer interface in the *a* form, with eight new intersubunit hydrogen bonds between polar groups, plus additional **hydrophobic** interactions. In addition, the AMP binding site is more fully formed and capable of greater interaction with the ligand. The tighter subunit associations of the dimer in the *a* form account for it obeying the allosteric **concerted model** of Monod et al., whereas phosphorylase *b* follows the **sequential model** of Koshland et al. (with intermediate forms occurring). Thus the structural studies of phosphorylases *a* and *b* have resolved an old controversy within a single enzyme.

Bibliography

1. D. J. Graves and J. H. Wang (1972) " -Glucan Phosphorylases", In *The Enzymes*, Vol. **7**, 3rd. ed., Academic Press, New York, pp. 435–482.
2. R. J. Fletterick and N. B. Madsen (1980) Annu. Rev. Biochem. **49**, 31–61.
3. N. B. Madsen and S. G. Withers (1986) In *Vitamin B_6 Pyridoxal Phosphate*, Part B, John Wiley & Sons, New York, pp. 355–389.
4. L. N. Johnson (1989) Carlsberg Res. Commun. **54**, 203–229.
5. S. R. Sprang et al. (1988) Nature **336**, 215–221.
6. M. F. Perutz (1988) Nature **336**, 202–203.

Suggestions for Further Reading

7. N. B. Madsen (1997) "Glycogen". In *Encyclopedia of Human Biology*, Vol. **4**, 2nd ed., Academic Press, San Diego, pp. 341–351. [A summary of glycogen metabolism.]
8. N. B. Madsen (1986) "Glycogen Phosphorylase", In *The Enzymes*, Vol. **17**, 3rd ed., pp. 365–394. [Updates the previous review, with emphasis on phosphorylation of Ser14 and its consequences.]

N-Glycosylation

Glycoproteins are characterized by the presence of carbohydrates covalently linked to amino acid residues. More than a dozen different protein–carbohydrate linkages have been identified in glycoproteins, and they are often categorized as either *O*-glycosidic (*O*-glycans or *O*-linked oligosaccharides), in which carbohydrate is covalently attached to protein via a hydroxyl group in the side chains of several amino acids, or *N*-glycosidic (*N*-glycans or *N*-linked oligosaccharides), in which sugar is covalently attached to protein through the amide nitrogen of asparagine residues. Protein glycosylation is the most diverse type of post-translational modification of proteins. The biochemical processes through which these linkages are generated are commonly called O-glycosylation and *N* -glycosylation pathways, and each pathway involves dozens of different enzymes. There are dramatic differences between these pathways in terms of their subcellular localization, the enzymes involved, the structures of the oligosaccharides synthesized, and the biological functions the glycans. *N*-Glycosylation is best characterized in animal and plant cells, but *N*-linked sugars have also been observed in bacterial glycoproteins. As we shall see, *N*-glycosylation of proteins is an exceedingly complex pathway, involving the building, trimming, and elongation of relatively large oligosaccharides as they pass through the various secretory organelles.

1. Different Types of *N*-Glycans

Examples of different types of *N*-glycan in animal cells are shown in Figure 1a. *N*-glycans contain a common pentasaccharide core composed of two *N*-acetylglucosamine (GlcNAc) residues and three mannose (Man) residues. N-Glycans are classified in three broad groups on the basis of their overall composition. *N*-Glycans that contain primarily Man residues in terminal, nonreducing positions are termed high mannose- or polymannose-type. In contrast, *N*-glycans that contain sugars other than Man in terminal nonreducing positions, such as sialic acid (NcuAc) or galactose (Gal), are classified as complex-type. A relatively simple example of a biantennary complex-type *N*-glycan (Fig. 1a) is compared to an example of a more highly branched version, known as a tetraantennary complex-type *N*-glycan. Those *N*-glycans that have features shared by both high mannose and complex-type are classified as hybrid-type. Thousands of structurally different *N*-glycans have been identified, and they may contain many additional sugars to those shown in Figure 1a. It should be noted that glycoconjugates are highly unusual in their structural motifs when compared to other classes of macromolecules . For example, most glycoconjugates, in contrast to nucleic acids and proteins, are generally branched rather than linear. The branched nature allows the generation of highly compacted and diverse structures. In contrast to nucleic acids and proteins, which are synthesized on templates, glycoconjugates are synthesized without a template, and their assembly requires the stepwise addition of monosaccharides from activated sugar precursors by individual enzymes termed glycosyltransferases. The diversity of *N*-glycan structures is generated by the inherent branching potential, the types and activity levels of the glycosyltransferases expressed in cells, the glycoprotein species, and a host of other factors (1).

Figure 1. Structure and biosynthesis of *N*-glycans: (**a**) examples of different types of *N*-glycans; (**b**) steps in assembly of $Glc_3Man_9GlcNAc_2$-P-P-dolichol in RER membrane; (**c**) reaction catalyzed by the oligosaccharyltransferase (OST); (**d**) early-stage trimming reactions of high mannose-type *N*-glycans in the RER and Golgi apparatus; (**e**) late-stage processing of high mannose-type *N*-glycans and their conversion to hybrid- and complex-type chains; (**f**) branching of complex-type *N*-glycans by *N*-acetylglucosaminyltransferases in the Golgi apparatus; (**g**) different types of terminal glycosylation observed in complex-type *N*-glycans; (**h**) biosynthesis of phosphorylated high mannose-type *N*-glycans in lysosomal enzymes.

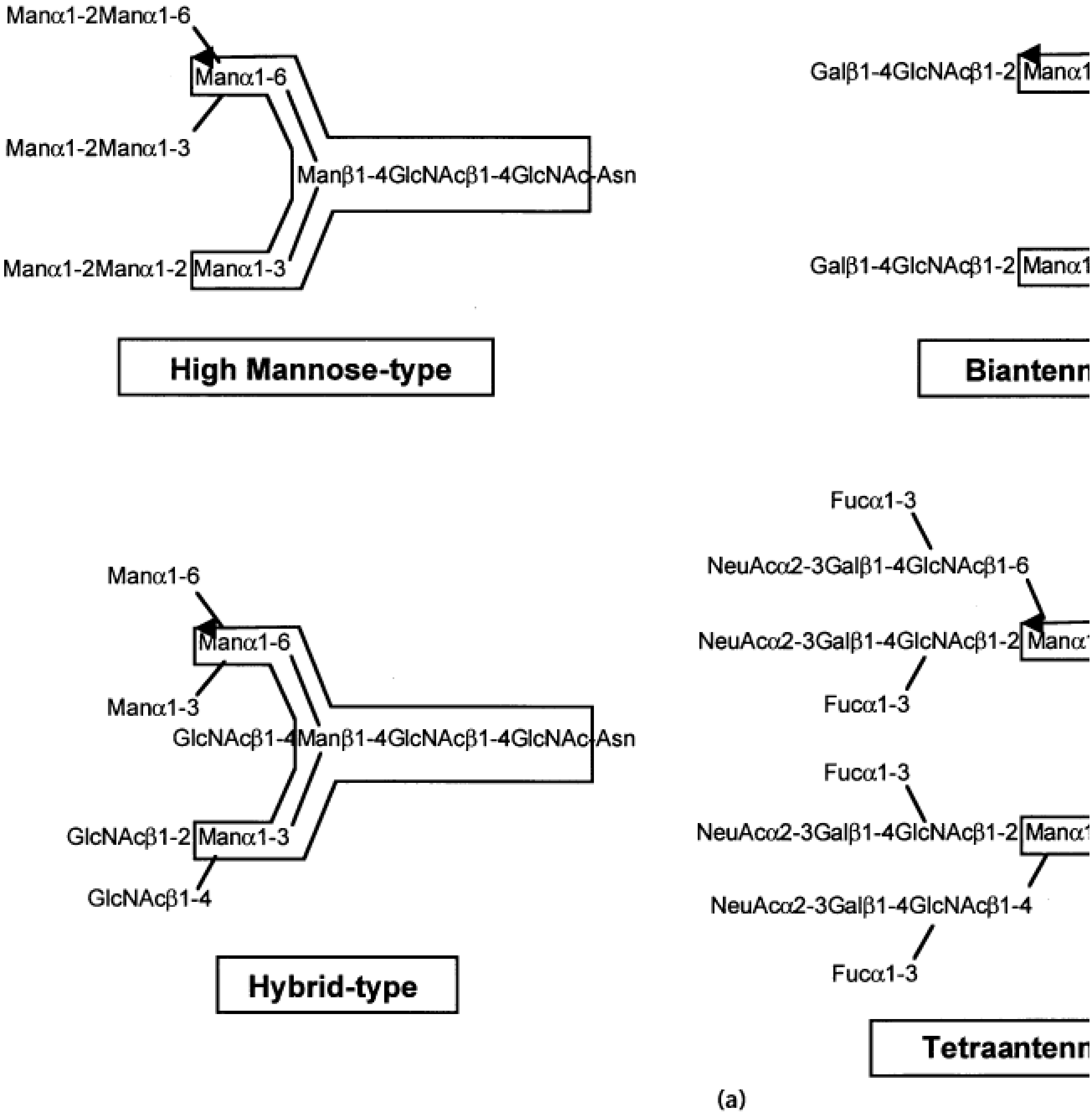

Figure 1. (*continued*) Structure and biosynthesis of *N*-glycans: (**a**) examples of different types of *N*-glycans; (**b**) steps in assembly of $Glc_3Man_9GlcNAc_2$-P-P-dolichol in RER membrane; (**c**) reaction catalyzed by the oligosaccharyltransferase (OST); (**d**) early-stage trimming reactions of high mannose-type *N*-glycans in the RER and Golgi apparatus; (**e**) late-stage processing of high mannose-type *N*-glycans and their conversion to hybrid- and complex-type chains; (**f**) branching of complex-type *N*-glycans by *N*-acetylglucosaminyltransferases in the Golgi apparatus; (**g**) different types of terminal glycosylation observed in complex-type *N*-glycans; (**h**) biosynthesis of phosphorylated high mannose-type *N*-glycans in lysosomal enzymes.

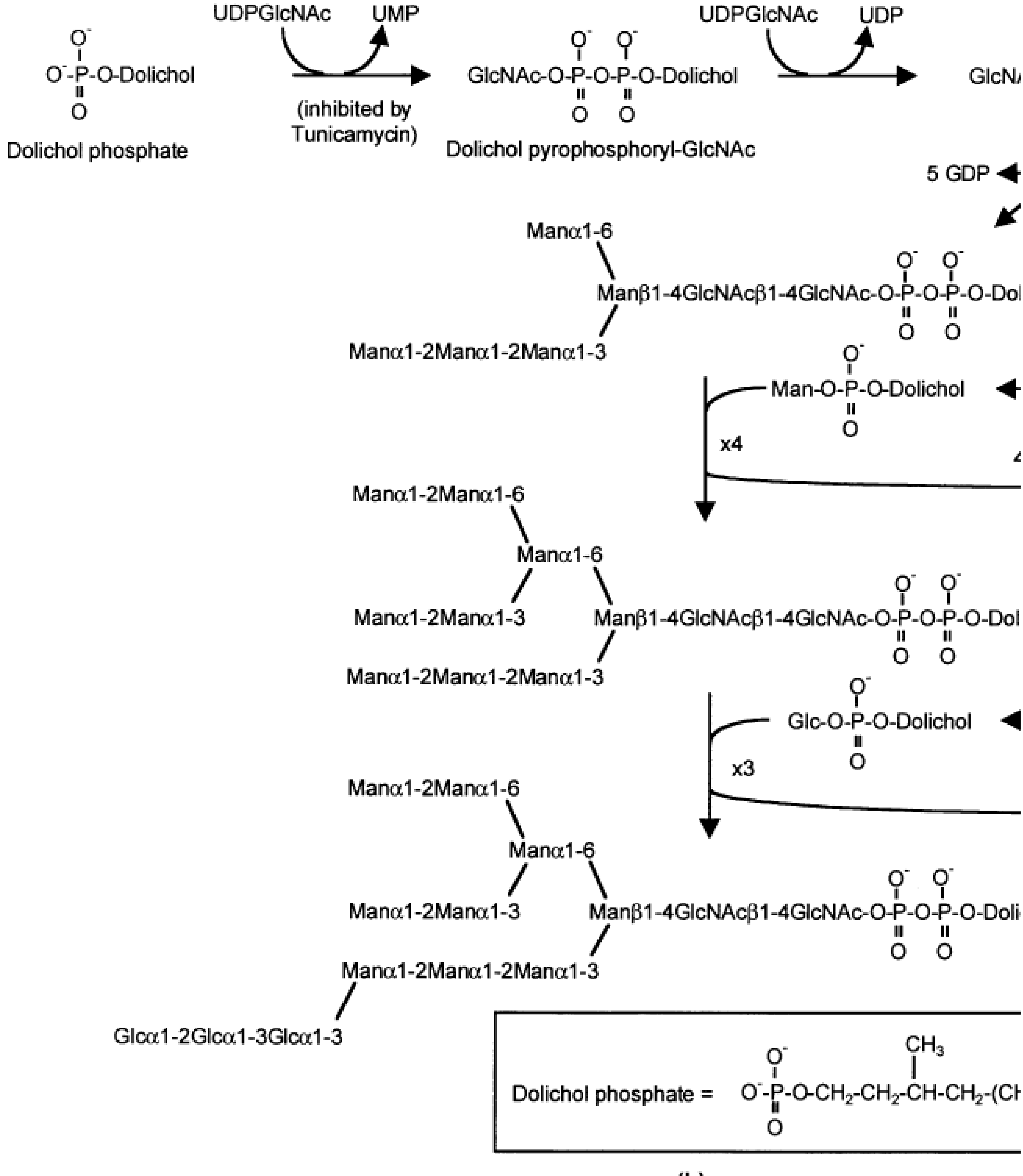

Figure 1. (*continued*) Structure and biosynthesis of *N*-glycans: (**a**) examples of different types of *N*-glycans; (**b**) steps in assembly of $Glc_3Man_9GlcNAc_2$-P-P-dolichol in RER membrane; (**c**) reaction catalyzed by the oligosaccharyltransferase (OST); (**d**) early-stage trimming reactions of high mannose-type *N*-glycans in the RER and Golgi apparatus; (**e**) late-stage processing of high mannose-type *N*-glycans and their conversion to hybrid- and complex-type chains; (**f**) branching of complex-type *N*-glycans by *N*-acetylglucosaminyltransferases in the Golgi apparatus; (**g**) different types of terminal glycosylation observed in complex-type *N*-glycans; (**h**) biosynthesis of phosphorylated high mannose-type *N*-glycans in lysosomal enzymes.

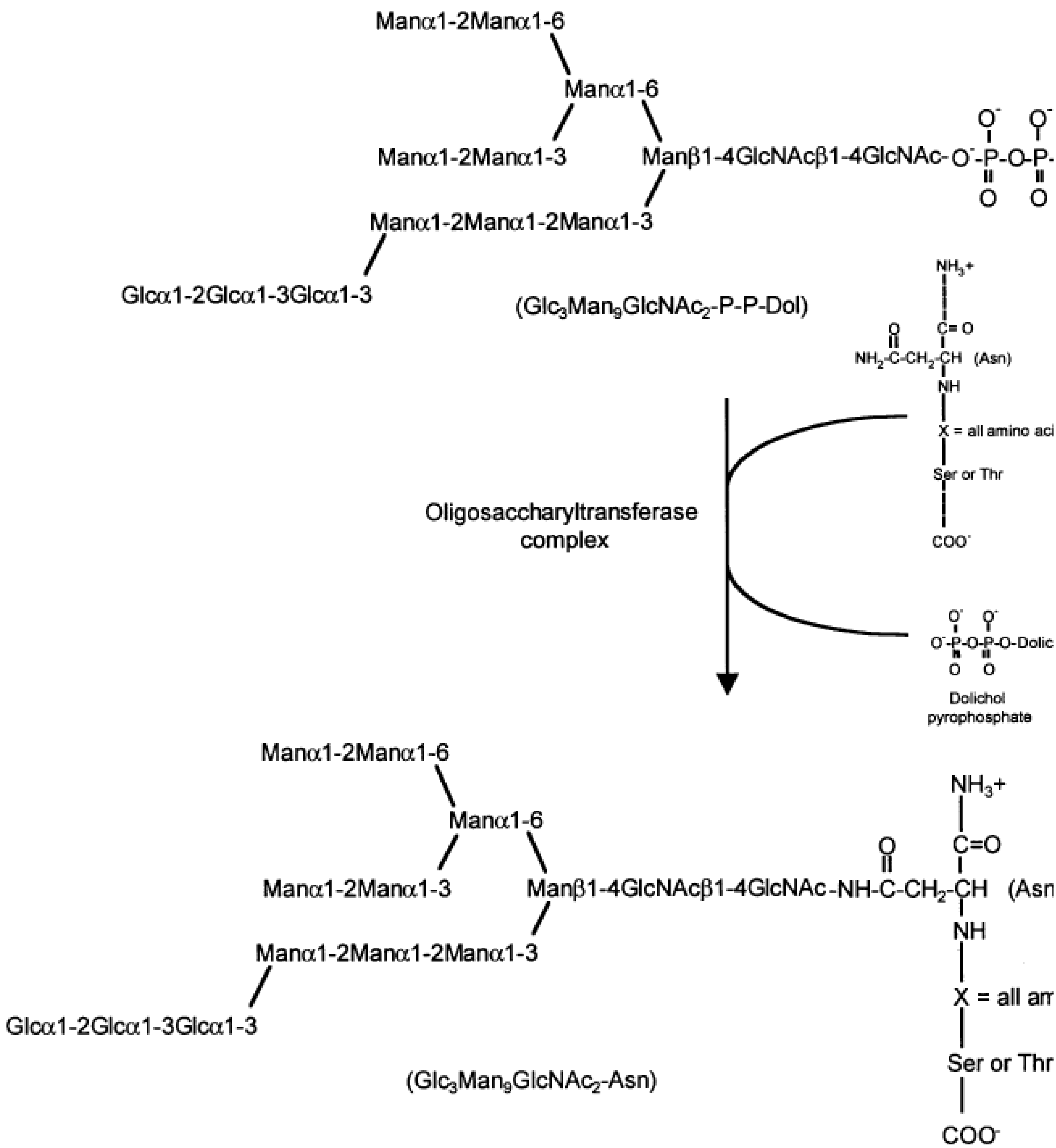

(c)

Figure 1. (*continued*) Structure and biosynthesis of *N*-glycans: (**a**) examples of different types of *N*-glycans; (**b**) steps in assembly of $Glc_3Man_9GlcNAc_2$-P-P-dolichol in RER membrane; (**c**) reaction catalyzed by the oligosaccharyltransferase (OST); (**d**) early-stage trimming reactions of high mannose-type *N*-glycans in the RER and Golgi apparatus; (**e**) late-stage processing of high mannose-type *N*-glycans and their conversion to hybrid- and complex-type chains; (**f**) branching of complex-type *N*-glycans by *N*-acetylglucosaminyltransferases in the Golgi apparatus; (**g**) different types of terminal glycosylation observed in complex-type *N*-glycans; (**h**) biosynthesis of phosphorylated high mannose-type *N*-glycans in lysosomal enzymes.

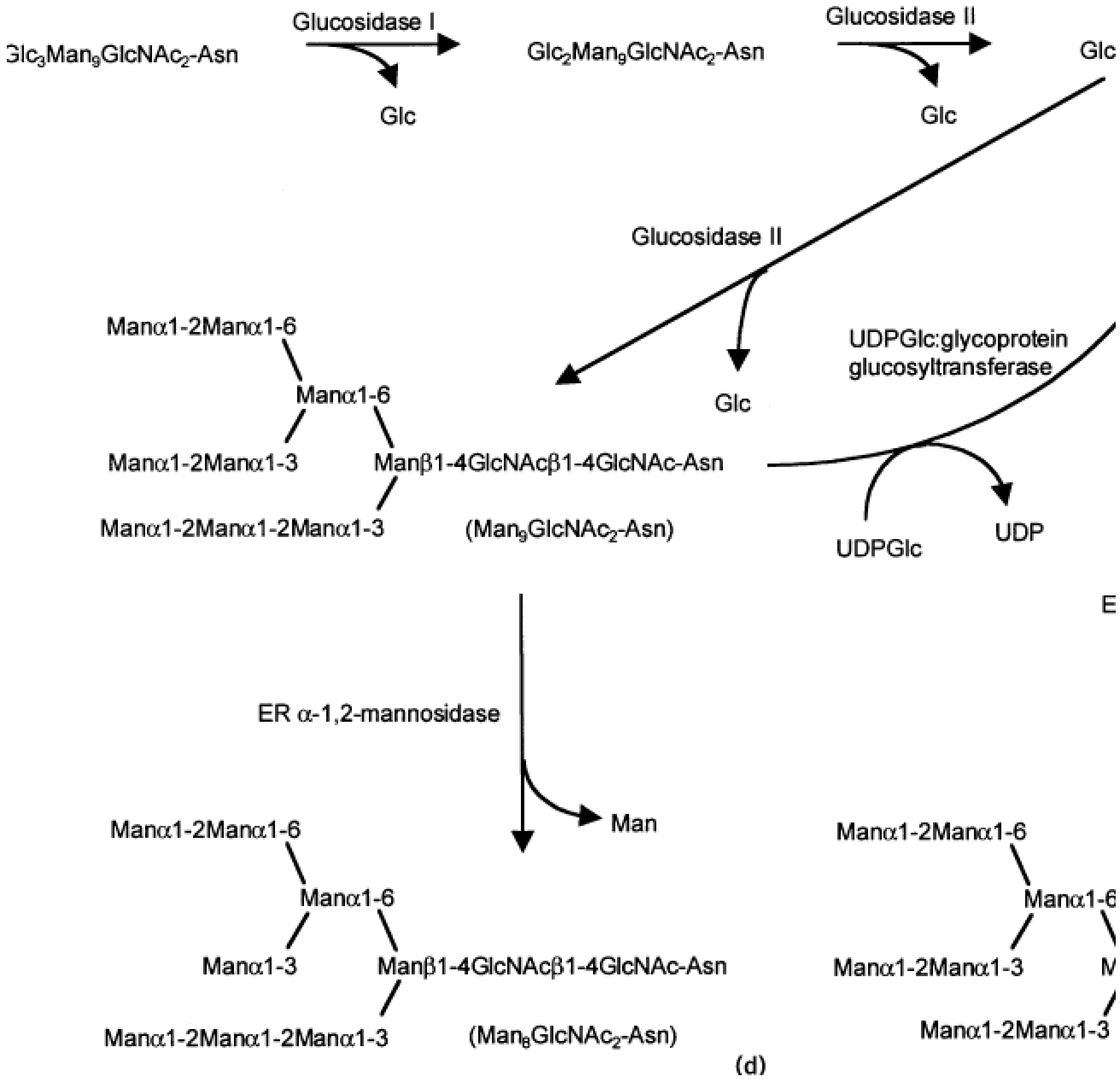

Figure 1. (*continued*) Structure and biosynthesis of *N*-glycans: (**a**) examples of different types of *N*-glycans; (**b**) steps in assembly of $Glc_3Man_9GlcNAc_2$-P-P-dolichol in RER membrane; (**c**) reaction catalyzed by the oligosaccharyltransferase (OST); (**d**) early-stage trimming reactions of high mannose-type *N*-glycans in the RER and Golgi apparatus; (**e**) late-stage processing of high mannose-type *N*-glycans and their conversion to hybrid- and complex-type chains; (**f**) branching of complex-type *N*-glycans by *N*-acetylglucosaminyltransferases in the Golgi apparatus; (**g**) different types of terminal glycosylation observed in complex-type *N*-glycans; (**h**) biosynthesis of phosphorylated high mannose-type *N*-glycans in lysosomal enzymes.

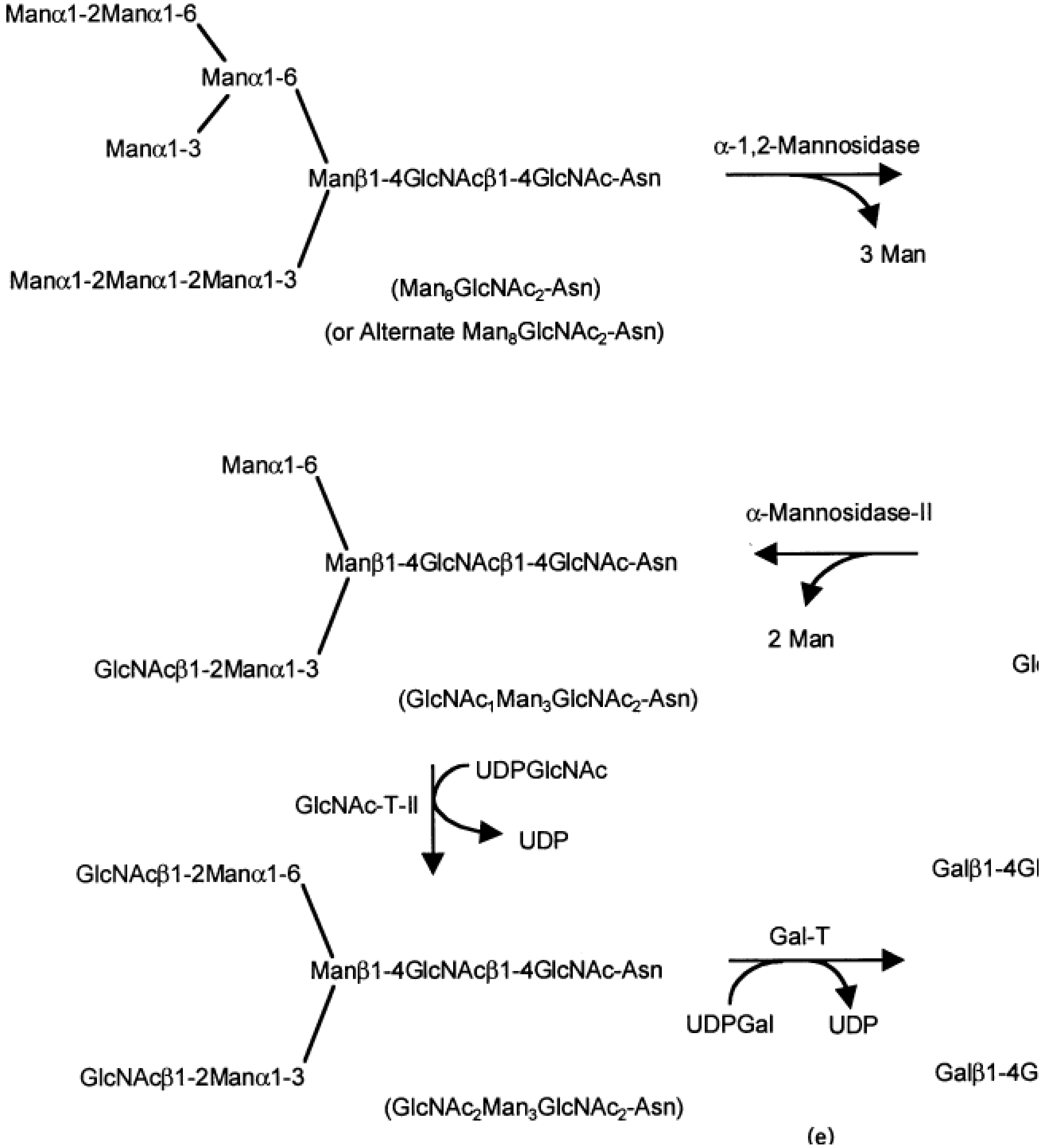

Figure 1. (*continued*) Structure and biosynthesis of *N*-glycans: (**a**) examples of different types of *N*-glycans; (**b**) steps in assembly of $Glc_3Man_9GlcNAc_2$-P-P-dolichol in RER membrane; (**c**) reaction catalyzed by the oligosaccharyltransferase (OST); (**d**) early-stage trimming reactions of high mannose-type *N*-glycans in the RER and Golgi apparatus; (**e**) late-stage processing of high mannose-type *N*-glycans and their conversion to hybrid- and complex-type chains; (**f**) branching of complex-type *N*-glycans by *N*-acetylglucosaminyltransferases in the Golgi apparatus; (**g**) different types of terminal glycosylation observed in complex-type *N*-glycans; (**h**) biosynthesis of phosphorylated high mannose-type *N*-glycans in lysosomal enzymes.

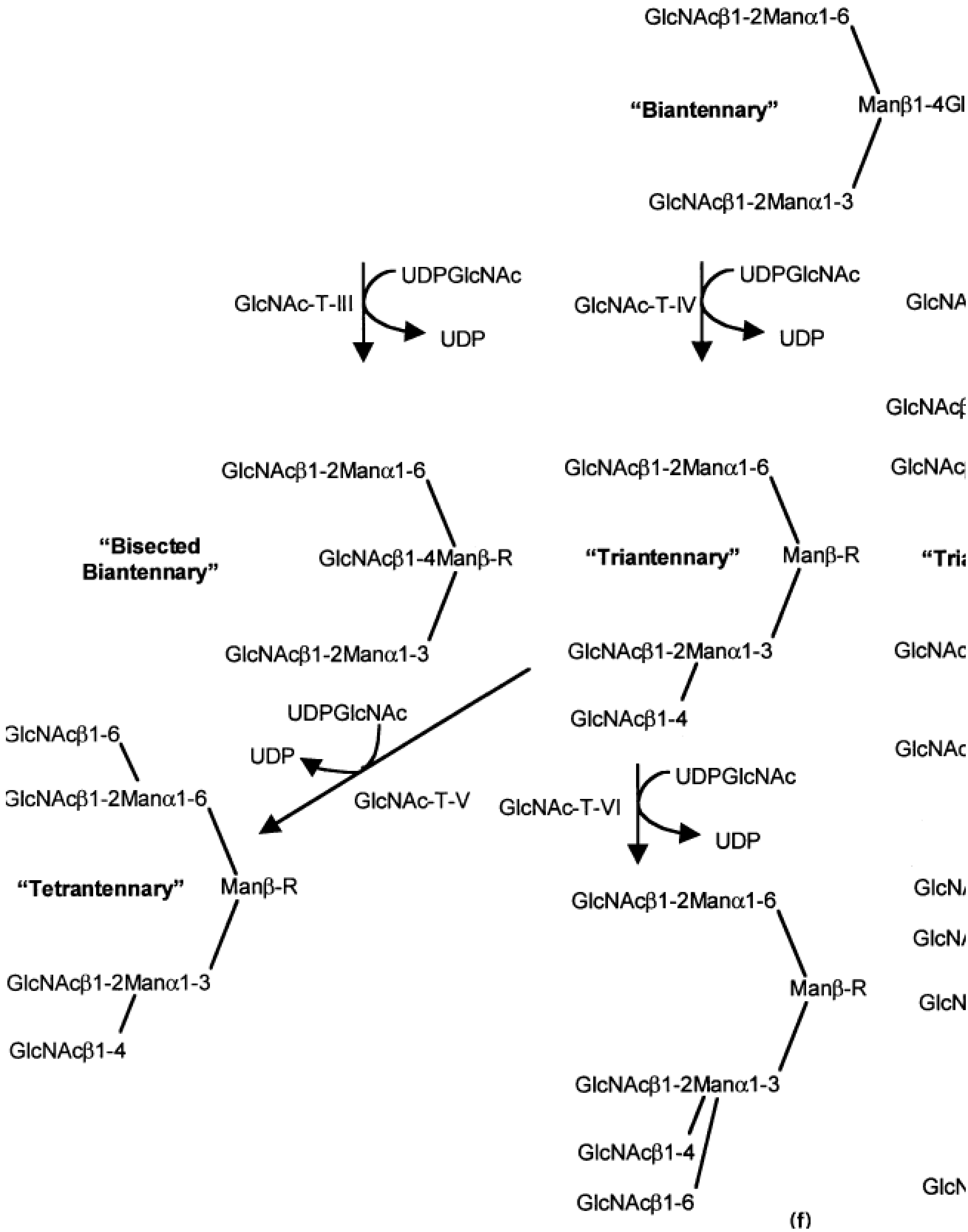

Figure 1. (*continued*) Structure and biosynthesis of *N*-glycans: (**a**) examples of different types of *N*-glycans; (**b**) steps in assembly of $Glc_3Man_9GlcNAc_2$-P-P-dolichol in RER membrane; (**c**) reaction catalyzed by the oligosaccharyltransferase (OST); (**d**) early-stage trimming reactions of high mannose-type *N*-glycans in the RER and Golgi apparatus; (**e**) late-stage processing of high mannose-type *N*-glycans and their conversion to hybrid- and complex-type chains; (**f**) branching of complex-type *N*-glycans by *N*-acetylglucosaminyltransferases in the Golgi apparatus; (**g**) different types of terminal glycosylation observed in complex-type *N*-glycans; (**h**) biosynthesis of phosphorylated high mannose-type *N*-glycans in lysosomal enzymes.

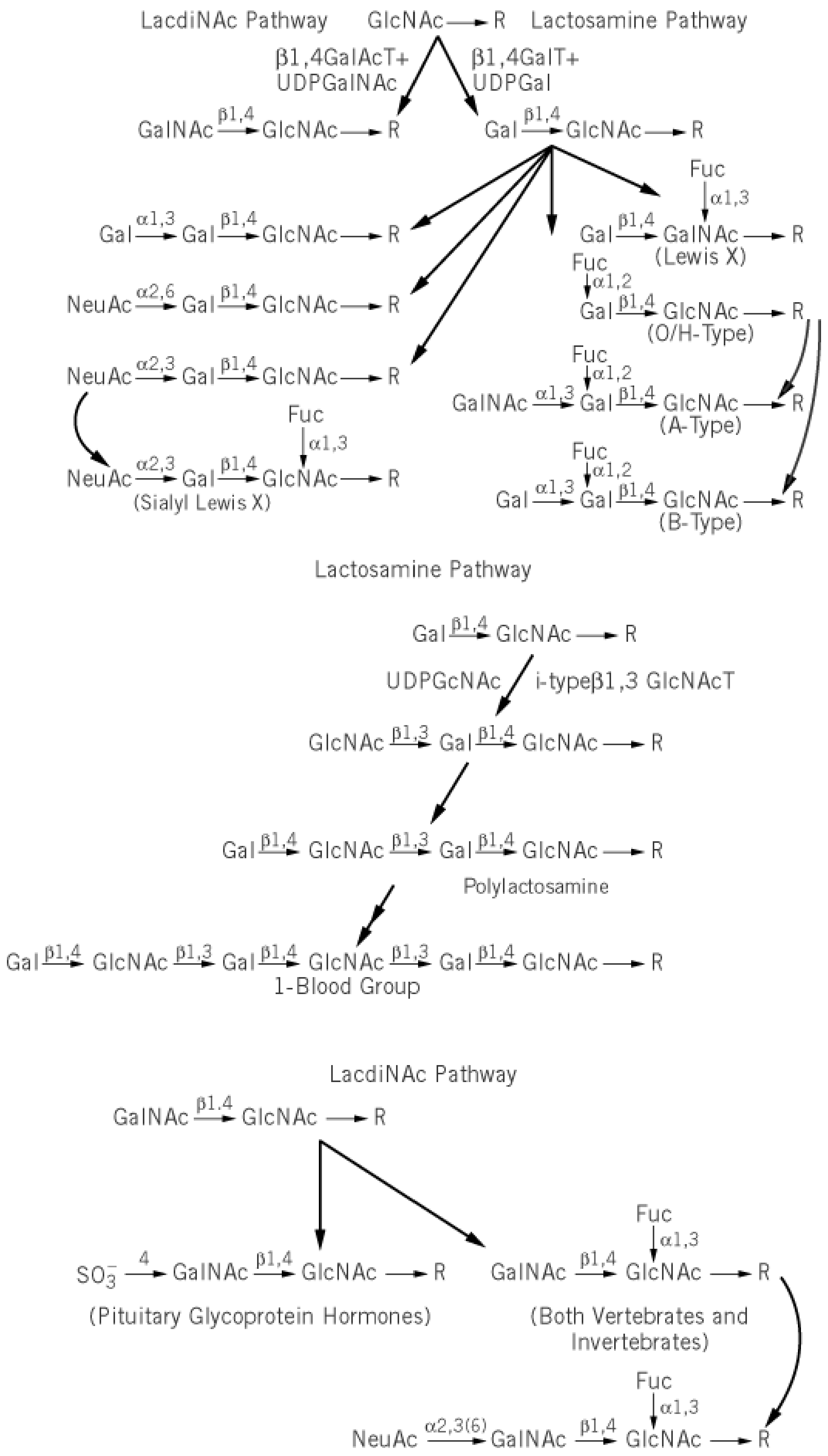
LacdiNAc Pathway
GlcNAc → R
Lactosamine Pathway
β1,4GalAcT+ UDPGalNAc
β1,4GalT+ UDPGal
GalNAc β1,4 GlcNAc → R
Gal β1,4 GlcNAc → R
Gal α1,3 Gal β1,4 GlcNAc → R
Fuc α1,3
Gal β1,4 GalNAc → R
(Lewis X)
NeuAc α2,6 Gal β1,4 GlcNAc → R
Fuc α1,2
Gal β1,4 GlcNAc → R
(O/H-Type)
NeuAc α2,3 Gal β1,4 GlcNAc → R
Fuc α1,2
GalNAc α1,3 Gal β1,4 GlcNAc → R
(A-Type)
Fuc α1,3
NeuAc α2,3 Gal β1,4 GlcNAc → R
(Sialyl Lewis X)
Fuc α1,2
Gal α1,3 Gal β1,4 GlcNAc → R
(B-Type)
Lactosamine Pathway
Gal β1,4 GlcNAc → R
UDPGcNAc
i-typeβ1,3 GlcNAcT
GlcNAc β1,3 Gal β1,4 GlcNAc → R
Gal β1,4 GlcNAc β1,3 Gal β1,4 GlcNAc → R
Polylactosamine
Gal β1,4 GlcNAc β1,3 Gal β1,4 GlcNAc β1,3 Gal β1,4 GlcNAc → R
1-Blood Group
LacdiNAc Pathway
GalNAc β1.4 GlcNAc → R
SO3− 4 GalNAc β1,4 GlcNAc → R
(Pituitary Glycoprotein Hormones)
Fuc α1,3
GalNAc β1,4 GlcNAc → R
(Both Vertebrates and Invertebrates)
Fuc α1,3
NeuAc α2,3(6) GalNAc β1,4 GlcNAc → R

(g)

Figure 1. (*continued*) Structure and biosynthesis of *N*-glycans: (**a**) examples of different types of *N*-glycans; (**b**) steps in assembly of $Glc_3Man_9GlcNAc_2$-P-P-dolichol in RER membrane; (**c**) reaction catalyzed by the oligosaccharyltransferase (OST); (**d**) early-stage trimming reactions of high mannose-type *N*-glycans in the RER and Golgi apparatus; (**e**) late-stage processing of high mannose-type *N*-glycans and their conversion to hybrid- and complex-type chains; (**f**) branching of complex-type *N*-glycans by *N*-acetylglucosaminyltransferases in the Golgi apparatus; (**g**) different types of terminal glycosylation observed in complex-type *N*-glycans; (**h**) biosynthesis of phosphorylated high mannose-type *N*-glycans in lysosomal enzymes.

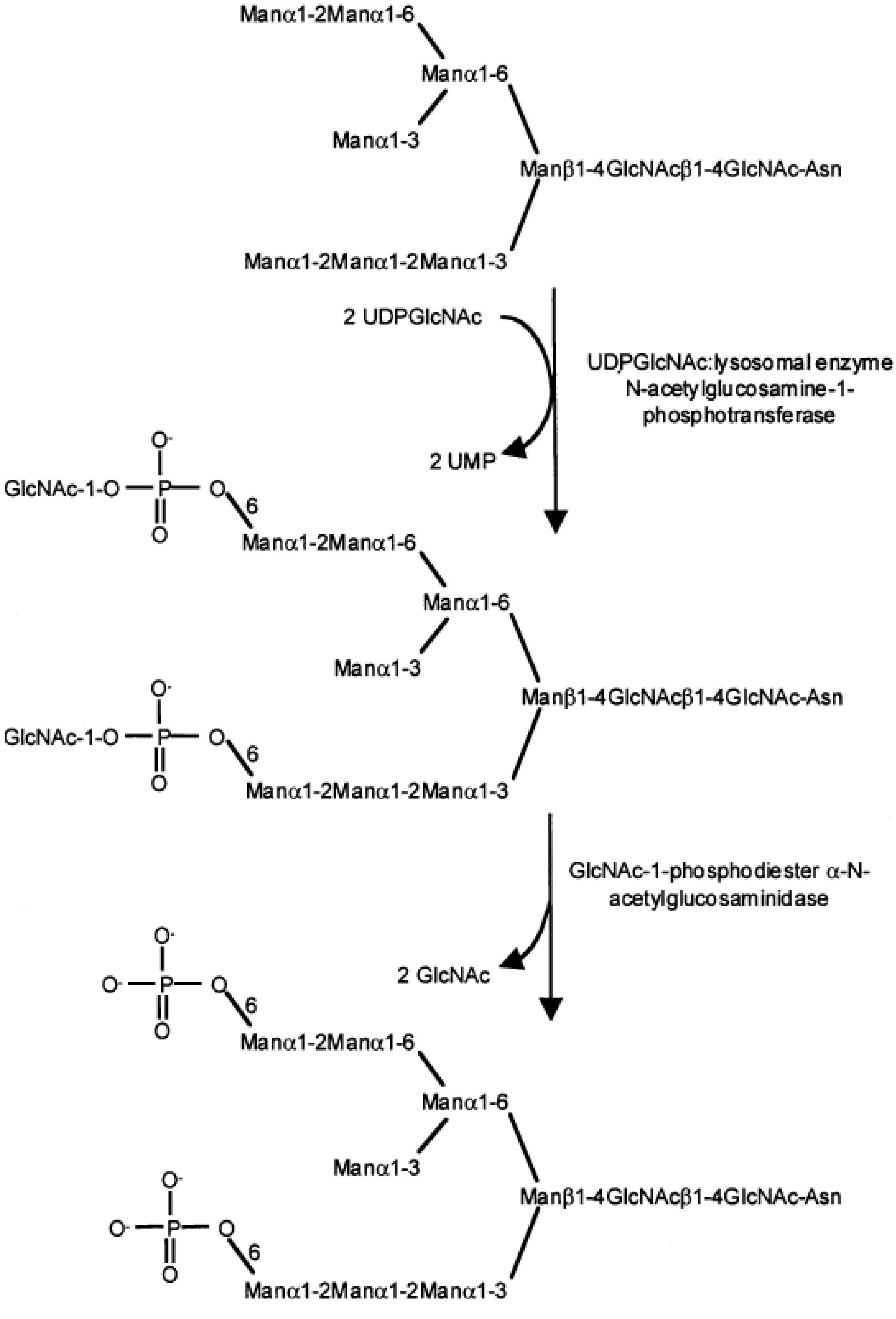

(h)

Figure 1. (*continued*) Structure and biosynthesis of *N*-glycans: (**a**) examples of different types of *N*-glycans; (**b**) steps in assembly of $Glc_3Man_9GlcNAc_2$-P-P-dolichol in RER membrane; (**c**) reaction catalyzed by the oligosaccharyltransferase (OST); (**d**) early-stage trimming reactions of high mannose-type *N*-glycans in the RER and Golgi apparatus; (**e**) late-stage processing of high mannose-type *N*-glycans and their conversion to hybrid- and complex-type chains; (**f**) branching of complex-type *N*-glycans by *N*-acetylglucosaminyltransferases in the Golgi apparatus; (**g**) different types of terminal glycosylation observed in complex-type *N*-glycans; (**h**) biosynthesis of phosphorylated high mannose-type *N*-glycans in lysosomal enzymes.

Inhibitor	Action
Tunicamycin	Inhibits formation of dolichol pyrophosphoryl-GlcNAc from dolichol phosphate and UDPGlcNAc
Australine Castanospermine 1-Deoxynojirimycin N-methyl-deoxynojirimycin DMDP [2R,5R-*bis*(Hydroxymethyl)-3R,4R-dihydroxypyrrolidine]	Inhibits Glucosidase I
Bromoconduritol Castanospermine 1-Deoxynojirimycin (DNJ) N-methyl-deoxynojirimycin	Inhibits Glucosidase II
1-Deoxymannojirimycin (DMJ) N-methyl-deoxynojirimycin DMDP Kifunensine	Inhibits α1,2-Mannosidases
Glcα1-3DMJ (GDMJ)	Inhibits Endomannosidase
Swainsonine Mannostatin	Inhibits α-Mannosidase II
Brefeldin A	Blocks translocation of proteins from ER to Golgi by blocking binding of GDP-ribosylation factor to Golgi and inhibiting GTP-GDP exchange

2. Consensus Sequence for *N*-Glycosylation

The most common structure of *N*-glycans is the presence of GlcNAc-Asn linkages. The presence of these linkages in animal-derived glycoproteins was proven through the pioneering work of R. D. Marshall and A. Neuberger (2). Subsequent studies of many different glycoproteins and the enzymes involved in glycoprotein biosynthesis indicated that the primary **consensus sequence** for *N*-glycosylation of proteins in animals, plants, and yeast is Asn-X-Ser/Thr, where X can be any amino acid except Pro. This consensus sequence is known as the *N*-glycosylation sequon. However, Asn residues within the sequence Asn-X-Cys have also been found to be *N*-glycosylated in some animal glycoproteins (3), suggesting that this may be an alternative sequon in some special cases. For most glycoproteins, most of the Asn-X-Ser/Thr *N*-glycosylation sequons in the extracytoplasmic regions of the protein are *N*-glycosylated. In those cases where the Asn-X-Ser/Thr *N*-glycosylation sequons are not glycosylated, it has been assumed that the site is probably inaccessible to the enzyme machinery that adds the sugar residues to the Asn. In some cases, however, it is clear that amino acid residues flanking the Asn-X-Ser/Thr *N*-glycosylation sequon can modulate the efficiency of *N*-glycosylation (4, 5). The numbers and positions of *N*-glycans in proteins demonstrate tremendous diversity that is glycoprotein-specific. Some glycoproteins, such as hen ovalbumin, contain a single *N*-glycan, whereas other glycoproteins may contain dozens of *N*-glycans. The envelope glycoproteins of **HIV**-1, the AIDS virus, contains approximately two dozen *N*-glycans. The *N*-glycans in some glycoproteins at particular sites may be high mannose-type, whereas at other sites within the same glycoprotein the *N*-glycans may be multiantennary complex type. This phenomenon is referred to as “site-specific *N*-glycosylation.”

Although the *N*-glycosylation sequon is universal among eukaryotes and typically is composed of GlcNAc-Asn linkages, certain types of bacteria also synthesize glycoproteins with other carbohydrates attached to Asn residues within the *N*-glycosylation sequon. For example, Glc-Asn and GalNAc-Asn linkages are found in the halobacterial cell surface glycoproteins and flagellins (6, 7).

3. Synthesis of the Lipid-Linked Oligosaccharide

Many of the early steps in *N*-glycan biosynthesis in yeast, plants, and animals are similar, resulting in the synthesis of a high mannose-type *N*-glycan precursor (8). However, after generation of the high mannose-type *N*-glycan, there is tremendous diversity between phyla in the types of modifications they make to this precursor, as discussed below. *N*-Glycosylation in eukaryotes is initiated in the rough endoplasmic reticulum (RER), and final steps in the pathway are carried out in the Golgi apparatus. Thus, *N*-glycosylation is highly compartmentalized and is associated with the secretory organelles in eukaryotes. *N*-Glycans undergo a series of trimming and processing reactions within these organelles in a highly orchestrated pathway involving the removal and addition of carbohydrate residues. All *N*-glycans arise from a common high mannose-type *N*-glycan precursor on Asn residues. This high mannose-type *N*-glycan precursor arises from the transfer of a preformed precursor oligosaccharide linked to a lipid that has the general formula $Glc_3Man_9GlcNAc_2$-P-P-dolichol. Dolichol is a long-chain polyisoprenoid (Fig. 1b), and it serves as a membrane anchor for assembly of the lipid-linked oligosaccharide. Although glucose (Glc) residues are not commonly found on *N*-glycans in mature glycoproteins, Glc residues are essential components of the lipid-linked oligosaccharide for optimal donor activity.

This lipid-linked oligosaccharide $Glc_3Man_9GlcNAc_2$-P-P-dolichol is partly assembled on the cytoplasmic face of the RER; as the oligosaccharide grows in size by the stepwise addition of sugar residues (8), further elongation occurs in the lumen of the RER (9). The assembly is catalyzed by intrinsic membrane proteins in the RER (10). The first step in the assembly involves the acceptor dolichol monophosphate and the sugar nucleotide donor uridine diphospho-*N*-acetylglucosamine (UDPGlcNAc). The main product of the first reaction is dolichol pyrophosphoryl-GlcNAc and the side-product UMP (Fig. 1b). An important discovery in the elucidation of the *N*-glycosylation pathway was the finding that this first step is inhibited by tunicamycin, a toxic glucosamine derivative antibiotic produced by *Streptomyces lysosuperficus* (11). Because tunicamycin blocks the first step in the assembly process, cells and tissues treated with the drug are unable to synthesize glycoproteins containing *N*-glycans.

The dolichol phosphoryl-GlcNAc serves as a precursor for the assembly of the lipid-linked oligosaccharide and serves as the acceptor for a second reaction in which another GlcNAc residue is added from the donor UDPGlcNAc (Fig. 1b). The resulting main product is dolichol pyrophosphoryl-$GlcNAc_2$, and the side product is UDP. The dolichol pyrophosphoryl-$GlcNAc_2$ is the acceptor for a group of mannosyltransferases in the cytoplasmic face of the RER that add five Man residues in stepwise addition from the donor guanosine diphospho-mannose (GDPMan). The product of this reaction is a lipid-linked oligosaccharide containing 5 Man residues in a structure having the composition $Man_5GlcNAc_2$-P-P-dolichol. This intermediate is translocated into the lumen of the RER, where it is further elongated by Man addition through the donor Dol-P-Man (9). Dol-P-Man is assembled on the cytoplasmic face of the RER from dolichol phosphate and the donor GDPMan. After the addition of four Man residues from Dol-P-Man, the lipid-linked oligosaccharide has the composition $Man_9GlcNAc_2$-P-P-dolichol.

This intermediate $Man_9GlcNAc_2$-P-P-dolichol is further elongated through addition of three Glc residues to $Glc_3Man_9GlcNAc_2$-P-P-dolichol (Fig. 1b). These Glc residues are added from the donor Dol-P-Glc, which itself is assembled on the cytoplasmic face of the RER from the acceptor Dol-P and the donor uridine diphospho-glucose (UDPGlc). The final lipid-linked oligosaccharide has a total of 14 sugar residues and represents the pivotal precursor for the biosynthesis of all *N*-glycans in eukaryotes through the en bloc transfer to Asn residues in glycoproteins by the oligosaccharyltransferase complex in the membrane of the RER. It is interesting to note that 11 of the 14 residues, which are in external positions in the lipid-linked oligosaccharide, are in a-linkage, whereas the 3 core residues are in b-linkage. Since b-linked sugars are usually linear in structure and a-linkages promote turns in the structure, it is likely that the external residues of the lipid-linked oligosaccharide are tightly folded into a compact structure extending from the dolichol pyrophosphoryl core.

4. The Oligosaccharyltransferase

The oligosaccharyltransferase (OST) is a membrane-associated protein assembly that catalyzes the transfer of $Glc_3Man_9GlcNAc_2$-P-P-dolichol to Asn residues within the *N*-glycosylation sequon on nascent polypeptides in the lumen of the RER. Except for trypanosomatid protozoa, which utilize $Man_9GlcNAc_2$-P-P-dolichol, the OST in all other organisms utilizes $Glc_3Man_9GlcNAc_2$-P-P-dolichol as a primary donor. The OST requires Mn^{2+} for activity and catalyzes the formation of a C—N bond between the C-1 position of the reducing GlcNAc residue within $Glc_3Man_9GlcNAc_2$-P-P-dolichol and the amide nitrogen of asparagine with the release of P-P-dolichol (Fig. 1c and Fig. 2). It is likely that the hydroxyl groups of Ser or Thr residues within the *N*-glycosylation sequon participate in the catalysis by activating the amide nitrogen (12, 13). It has been proposed that amino acid residues within the OST force the deprotonation of hydroxyl side chains of Ser or Thr residues, which, in turn, causes them to act as a strong oxyanion for abstraction of proton from the carboxamide nitrogen of asparagine. This possible mechanism explains the conservation of Ser and Thr in the third position of the *N*-glycosylation sequon. The activated asparagine is proposed to attack the $Glc_3Man_9GlcNAc_2$-P-P-dolichol nucleophilically, resulting in displacement of P-P-dolichol from the C-1 of GlcNAc. The fact that Pro residues are not known to occur within functional *N*-glycosylation sequons suggests that close proximity between Ser and Thr residues and the Asn residue is required for optimal OST activity. Pro residues would be expected to introduce a strong bend in the polypeptide backbone, positioning Ser and Thr residues away from Asn.

Figure 2. Schematic of cotranslational *N*-glycosylation of nascent polypeptides in the RER by OST.

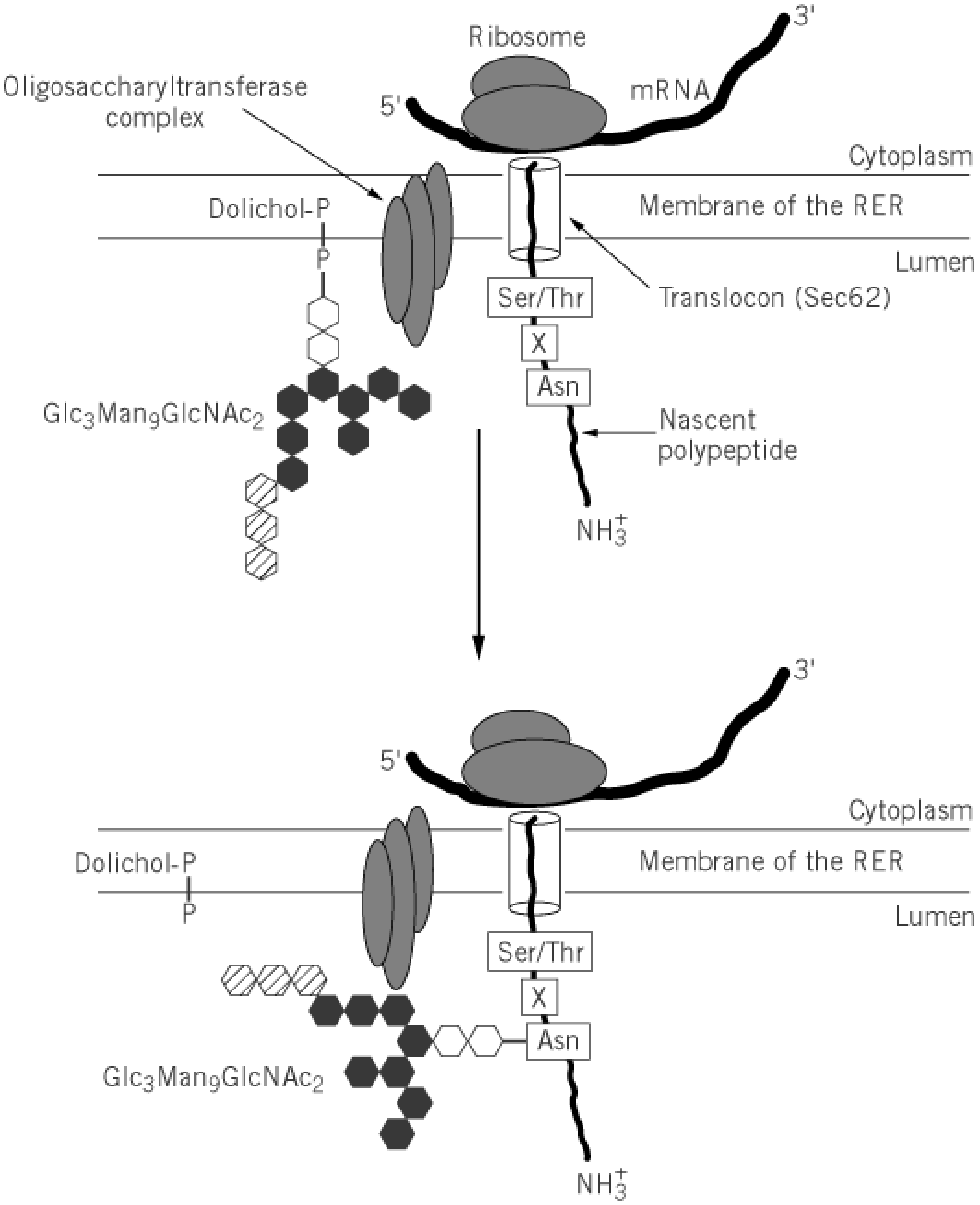

The OST has been purified from many sources (14) and is usually recovered as a protein complex containing from three to six polypeptides. However, other accessory proteins may also be important in efficient activity of the OST. Genetic mutations of genes encoding OST polypeptides have been identified in yeast, and the genes have been **cloned** by complementation (14-16). In yeast the genes identified to date are designated OST1, WBP1, OST3, SWP1, and OST2. Protein homologues of several of these genes have been found in higher animals. All the proteins encoded by these genes in yeast appear to be essential for optimal activity *in vivo*.

The OST is likely to be in close proximity to the translocon or Sec62 pore complex in the RER through which proteins cotranslationally enter the lumen of the RER. The catalytic domain of the OST is functionally located approximately 3–4 nm or 34×10^{-9}m from the lumenal face of the RER and acts on Asn residues within the *N*-glycosylation sequon of nascent polypeptides prior to complete translation of the proteins. Thus, *N*-glycosylation generally occurs as a cotranslational process.

5. Early-Stage Processing Pathway for *N*-Glycans in the RER

Following transfer of the $Glc_3Man_9GlcNAc_2$ to Asn residues, a series of reactions occurs in the lumen of the RER resulting in removal of the 3 Glc residues by glucosidases I and II. These trimming reactions are initiated on the nascent glycopeptide prior to complete translation. The newly synthesized glycoprotein is also subjected to an ER-localized a1,2-mannosidase, which usually removes one of the Man residues (Fig. 1d) (17). As discussed above, the presence of glucosyl residues on the $Glc_3Man_9GlcNAc_2$-P-P-dolichol is essential for optimal donor activity with the OST. But the glucosyl residues on the transferred oligosaccharide $Glc_3Man_9GlcNAc_2Asn$ also serve an important role in **protein folding** and retention in the RER.

6. Role of *N*-Glycosylation in Protein Folding

Following removal of glucosyl residues from $Glc_3Man_9GlcNAc_2Asn$ in newly synthesized glycoproteins, poorly folded glycoproteins are substrates for the enzyme UDPGlc:glycoprotein glucosyltransferase. This enzyme is capable of recognizing the high mannose-type *N*-glycan in poorly folded glycoprotein; it then catalyzes glucosylation of $Man_9GlcNAc_2Asn$ sites, using UDPGlc as a donor to generate the monoglucosylated species $Glc_1Man_9GlcNAc_2Asn$ (18). **Molecular chaperones**, such as calnexin and calreticulin, bind via carbohydrate interactions to monoglucosylated $Glc_1Man_9GlcNAc_2Asn$ (19, 20). The interactions with these chaperones facilitates other molecular interactions, leading to correct protein folding and retarding glycoprotein exit from the endoplasmic reticulum. Interaction with chaperones is an equilibrium binding, however, and the monoglucosylated $Glc_1Man_9GlcNAc_2Asn$ is available as a substrate for glucosidase II, which can remove the Glc residue to regenerate $Man_9GlcNAc_2Asn$. As indicated in Figure 1d, a cycle may develop between UDPGlc:glycoprotein glucosyltransferase and glucosidase II; this cycle continues until the glycoprotein folds in a manner that blocks its interaction with the UDPGlc:glycoprotein glucosyltransferase. The nonglucosylated glycoprotein no longer interacts with calnexin/calreticulin and exits the ER more efficiently. As discussed below, a portion of glycoprotein species with glucosylated high mannose-type *N*-glycans manage to exit the RER, and they are processed by other enzymes within the Golgi apparatus. Many glycoproteins in the RER fail to fold completely and efficiently and are degraded within the RER by proteinases. Thus, the glucosylation and deglucosylation pathway may serve a gate-keeper and quality control function.

7. Processing of *N*-glycans in the Golgi Apparatus

Following early-stage processing in the RER, glycoproteins exit the RER by vesicular transport to the Golgi apparatus. Not all glycoproteins containing glucosylated high mannose-type *N*-glycans are retained in the RER. For those that escape the action of glucosidase II in the RER, the Golgi contains an alternate pathway to facilitate their entry into the processing pathway. The Golgi enzyme, endomannosidase, acts on glucosylated oligosaccharides, such as $Glc_1Man_9GlcNAc_2Asn$ and $Glc_1Man_8GlcNAc_2Asn$ to release the disaccharide Glca1-3Man and to generate $Man_8GlcNAc_2Asn$ and $Man_7GlcNAc_2Asn$, respectively (21). The enzyme can act on a variety of glucosylated high mannose-type chains. The presence of the endomannosidase in the Golgi probably accounts for the inability of chemical inhibitors of glucosidases I and II to block completely the biosynthesis of complex-type *N*-glycans in all cells.

The resulting high mannose-type *N*-glycans, such as $Man_8GlcNAc_2Asn$ and $Man_7GlcNAc_2Asn$, are acted on by a number of a1,2-mannosidases in the cis-Golgi (17), resulting in the release of two to four Man residues and the formation of the processing intermediate $Man_5GlcNAc_2Asn$ (Fig. 1e). Although earlier observations had suggested that the Golgi contained a single a1,2-mannosidase termed mannosidase-I, recent studies have shown that there are a variety of a1,2-mannosidases. The functions of these many different a1,2-mannosidases and their specific roles in the processing pathway are not yet clear.

The resulting $Man_5GlcNAc_2Asn$ is a substrate for a key glycosyltransferase in the biosynthesis of hybrid- and complex-type *N*-glycans. *N*-Acetylglucosaminyltransferase I (GlcNAc-T-1) catalyzes the first committed step in the biosynthetic addition of sugars to the *N*-glycan by generating the GlcNAcb1-2Man linkage on a specific terminal Man residue (Fig. 1d). The action of GlcNAc-T-1 commits *N*-glycans to become either hybrid- or complex-type structures. A critical development in the discovery of a critical step in the biosynthetic process was the identification of mutated Chinese hamster ovary cell lines, termed Lec1 and Clone 15B, that are deficient in GlcNAc-T-1 (22, 23). As a consequence, the biosynthesis of *N*-glycans is halted at the level of $Man_5GlcNAc_2Asn$, and newly synthesized glycoproteins in these cell lines lack any hybrid- or complex-type *N*-glycans. Such mutational studies of Chinese hamster ovary cells have been exploited to generate many derivative cell lines containing mutations in specific aspects of the biosynthetic pathway for *N*- and *O*-glycans (24).

Following the action of GlcNAc-T-1, the product $GlcNAc_1Man_5GlcNAc_2Asn$ is the specific substrate of the medial Golgi enzyme a-mannosidase II, which removes two Man residues resulting in the formation of $GlcNAc_1Man_3GlcNAc_2Asn$ (Fig. 1e). Without the action of a-mannosidase II, *N*-glycans are committed to remain hybrid-type structures. Although early studies had suggested that there was a single a-mannosidase II, a second gene encoding a second a-mannosidase II has been identified (25). Experiments in mice in which the gene for the first a-mannosidase II was deleted have confirmed the presence of this functional alternative a-mannosidase II enzyme (26). The overall relationship between these two a-mannosidases, and whether there may be other related enzymes, is currently unclear. The product of a-mannosidase II action, $GlcNAc_1Man_3GlcNAc_2Asn$, is the substrate for a second *N*-acetylglucosaminyltransferase, GlcNAc-T-II, which adds GlcNAc in b1,2-linkage to the remaining terminal a-mannosyl residue to generate a biantennary complex-type *N*-glycan (Fig. 1e). This biantennary structure is a pivotol precursor for generation of all complex-type *N*-glycans.

8. Terminal Steps of *N*-Glycosylation

The biosynthesis of highly branched complex-type *N* -glycans from the biantennary precursor involves potential reactions with a series of other *N*-acetylglucosaminyltransferases within the medial Golgi apparatus (27). These enzymes, termed GlcNAc-T-III through GlcNAc-T-VII, add GlcNAc residues from donor UDPGlcNAc to the C–2, C–4, and C–6 positions of mannosyl residues. The resulting multiantennary products are indicated in Figure 1f. Not all *N*-glycans are subject to these reactions, since cells differ in their expression of the particular GlcNAc-Ts, and there are site-specific features of branching in glycoproteins.

Following completion of the GlcNAc-T activity within the medial-Golgi apparatus, glycoproteins exit to the trans-Golgi apparatus and trans-Golgi network (TGN), where additional modifications may occur through the actions of terminal glycosyltransferases and sulfotransferases. Some of the potential reactions are indicated in Figure 1g. Again, each cell type differs in the expression and level of these terminal glycosyltransferases, and there are site-specific features of terminal glycosylation in mature glycoproteins. In addition, many of the terminal glycosyltransferases may compete with each other for similar substrates.

In animal cells, it is typical for complex-type *N*-glycans to contain outer galactose (Gal) and sialic acid residues (28). A common sialic acid in humans is *N*-acetylneuraminic acid (NeuAc), but dozens of different sialic acids are known, and many are expressed by other animals. Interestingly, sialic acid is not generally present in plant glycoproteins. Terminal glycosylation of *N*-glycans in plant glycoproteins is different in several ways from those seen in animal glycoproteins (29). Many complex-type *N*-glycans in animal glycoproteins contain a primary terminal motif Galb1-4GlcNAc, known as the lactosamine or LN sequence (Fig. 1e). A second motif, however, known as the lacdiNAc or LDN pathway, has now been identified (30). LDN structures contain the alternative disaccharide GalNAcb1-4GlcNAc-R (Fig. 1e). The outer sugar residues may also be sulfated, as seen, for example, in pituitary hormones, which contain GalNAc-4-sulfate residues (31) (Fig. 1e), and in keratan sulfates, which contain GlcNAc-6-sulfate and Gal-6-sulfate residues. Sulfation of glycoproteins occurs in the trans-Golgi apparatus through the donor phosphoadenosine phosphosulfate (PAPS). PAPS, like the sugar nucleotide donors for glycosyltransferase reactions in the RER and Golgi apparatus, must be transported into those organelles by membrane transporters. These transporters, which are specific for each donor molecule, have been identified by molecular approaches (32).

9. Phosphorylation of *N*-Glycans in Lysosomal Enzymes

In higher eucaryotes, lysosomal hydrolases are directed to the lysosome by a mechanism that depends on specific modification of *N*-linked glycans, which allows sorting of these glycoproteins from others in the secretory pathway. The *N*-linked glycans of lysosomal hydrolases are specifically and uniquely modified in two steps to contain one or more terminal mannose 6-phosphates (M6P) (Fig. 1h). Lysosomal hydrolases bearing the M6P modification then bind to Mannose-6-P-receptors located in the trans-Golgi and are transferred to the endosome by vesicular transport. Once in the endosome, because of the lower pH, the lysosomal hydrolase disassociates from the receptor and is transferred to the lysosome. Once in the lysosome, lysosomal phosphatases remove the phosphate, rendering the process irreversible (33).

The first enzyme in the biosynthesis of the M6P modification is UDP-*N*-acetylglucosamine:lysosomal-enzyme *N*-acetylglucosamine-1-phosphotransferase (abbreviated GlcNAc-phosphotransferase). GlcNAc-phosphotransferase catalyzes the transfer of GlcNAc 1-phosphate from UDP-GlcNAc to specific a1,2-linked mannoses on high mannose oligosaccharides of lysosomal hydrolases. GlcNAc-phosphotransferase is a complex enzyme composed of three polypeptide chains with the subunit structure $a_2b_2g_2$ (34, 35). The specificity of the M6P-dependent lysosomal targeting pathway is a reflection of the substrate specificity of GlcNAc-phosphotransferase, which can only effectively utilize native lysosomal hydrolases as substrates.

The second enzyme in the pathway, *N*-acetylglucosamine-1-phosphodiester a-*N*-acetylglucosaminidase (abbreviated phosphodiester a-GlcNAcase), removes the covering GlcNAc, generating a terminal M6P. Lysosomal enzymes bearing the M6P modification then bind to one of two M6P-receptors in the trans-Golgi network and are transferred to the lysosome. Phosphodiester a-GlcNAcase is a tetramer of identical subunits (36). Unlike GlcNAc-phosphotransferase, phosphodiester a-GlcNAcase does not exhibit any specificity for lysosomal hydrolases as substrates.

Two distinct M6P-receptors have been isolated and characterized (37) (see Mannose 6-P Receptors). A high molecular weight cation-independent M6P-receptor (CI-MPR) was first described. The CI-MPR functions as a monomer, and each monomer binds two mols of M6P. In addition to binding M6P, the CI-MPR is also a high affinity receptor for insulin-like growth factor II (IGF-II) and the urokinase-type plasminogen activator receptor (uPAR). A second receptor has been described that requires divalent cations for binding of M6P (CD-MPR). The CD-MPR functions as a dimer, with each dimer binding two mols of M6P.

Several human diseases of lysosomal hydrolase trafficking result from genetic defects in the enzymes responsible for the biosynthesis of the M6P modification. Mucolipidosis II (MLII) or I-cell disease and mucolipidosis IIIA (classic pseudo-Hurler polydystrophy) result from mutations in the GlcNAc-phosphotransferase a/b-subunit gene. Mucolipidosis IIIC (MLIIIC) or variant pseudo-Hurler polydystrophy results from mutations in the GlcNAc-phosphotransferase g-subunit gene. In the absence of GlcNAc-phosphotransferase, lysosomal enzymes fail to acquire M6P; they enter the secretory pathway, and are secreted from the cell. This mistargeting of lysosomal hydrolases results in a lysosomal deficiency of many lysosomal enzymes and a severe storage phenotype. Patients with partial deficiency of phosphodiester a-GlcNAcase have been described. Like patients with GlcNAc-phosphotransferase deficiency, these patients have greatly elevated serum lysosomal enzyme levels, but do not seem to have a disease as a result of the mistargeting of lysosomal hydrolases.

The presence of the M6P or GlcNAc-1-phosphate modification blocks mannose trimming by Golgi a1,2-mannosidases. This prevents the synthesis of complex-type oligosaccharides and results in the high mannose structures typically found on lysosomal hydrolases.

10. Inhibitors of *N*-Glycosylation

Since the discovery of tunicamycin and its potent inhibition of the *N*-glycosylation pathway, a number of other antibiotics and sugar analogs have been identified that demonstrate specific inhibition of various enzymatic steps in the biosynthetic pathway (38). Most of the inhibitors commonly used today block glycosidase reactions in glycoprotein processing (Table 1). These include the inhibitors of glucosidases I and II, a1,2-mannosidases, the endomannosidase, and a-mannosidase II. Some of these inhibitors demonstrate a high degree of specificity, whereas others are more broadly active toward several enzymes. Another drug that has proven useful in studying *N*-glycosylation pathways is Brefeldin A (BFA). BFA is a fungal metabolite that interferes with protein trafficking between the Golgi apparatus and the trans-Golgi network (TGN), resulting in a blockage in glycoprotein secretion. BFA does not directly inhibit steps in the assembly or processing of *N*-glycans. In general, BFA treatment results in decreased sialylation and fucosylation of glycoproteins in those cells in which these terminal glycosylation steps occur in the TGN.

Table 1. Inhibitors of *N*-Glycosylation and Their Action Sites

Inhibitor	Action
Tunicamycin	Inhibits formation of dolichol pyrophosphoryl-GlcNAcfrom dolichol phosphate and UDPGlcNAc
Australine	
Castanospermine	
1-Deoxynojirimycin	
N-Methyldeoxynojirimycin	
DMDP (2*R*,5*R*-*bis* (Hydroxymethyl)-3*R*,4*R*-dihydroxypyrrolidine)	Inhibits glucosidase I
Bromoconduritol	
Castanospermine	
1-Deoxynojirimycin (DNJ)	
N-Methyldeoxynojirimycin	Inhibits glucosidase II
1-Deoxymannojirimycin (DMJ)	
N-Methyl-deoxynojirimycin	
DMDP	
Kifunensine	Inhibits a1,2-mannosidases
Glca1-3DMJ (GDMJ)	Inhibits endomannosidase

Swainsonine	
Mannostatin	Inhibits a-mannosidase II
Brefeldin A	Blocks translocation of proteins from ER to Golgiby blocking binding of GDP-ribosylation factor to Golgi and inhibiting GTP–GDPexchange

11. Proofreading of N-glycans

N-glycans may have other functions yet to be discovered in early steps of glycoprotein biosynthesis. The presence of specific endoglycosidases in animal cells capable of removing *N*-glycans from glycoproteins (39) suggested that some *N*-glycans may be removed after their addition to protein. These enzymes may be involved in general degradation of glycoproteins. It is also possible, however, that some sites are *N*-glycosylated and the *N*-glycan is subsequently removed in a “quality control” pathway. An enzyme has been identified in animal cells that is capable of catalyzing the de-*N*-glycosylation of proteins, known as a peptide:*N*-glycanase or PNGase; it may be involved in quality control of newly synthesized proteins by removing *N*-glycans from specific sites in a glycoprotein precursor, thereby reducing the number of *N*-glycans in the mature form of the protein. It is presently unclear whether this quality-control pathway operates on all glycoproteins in the ER or whether it specifically recognizes certain *N*-glycans in a restricted set of glycoproteins.

12. Genetic Defects in *N*-glycosylation

In recent years, a number of specific defects in the N-glycosylation pathway have been identified in humans. As mentioned above, the loss of the UDPGlcNAc:lysosomal enzyme *N*-acetylglucosamine-1-phosphotransferase in patients with I-cell disease results in a deficiency of lysosomal hydrolases and a generalized lysosomal storage disease with profound clinical consequences. In recent years, a number of individuals have been identified with decreased *N*-glycosylation of circulating glycoproteins. This deficiency, carbohydrate-deficient glycoprotein syndrome (CDGS), is due to blockage in several steps in the *N*-glycosylation pathway. CDGS is a genetic disease usually associated with major involvement of the central nervous system and mental retardation (40). However, some patients present with gastrointestinal disorder characterized by protein-losing enteropathy. Diagnosis of the disease usually involves identification of decreased glycosylation of serum transferrin, a circulating glycoprotein that normally contains two complex-type *N*-glycans. In CDGS type II patients, there is a deficiency in the Golgi processing enzyme *N*-acetylglucosaminyltransferase II (GlcNAc-T-II). Consequently, these patients synthesize glycoproteins containing the normal number of *N*-glycans, but the glycans have a hybrid-type structure. In contrast, CDGS type I is a more complex disease. Some patients with CDGS type I are unable to synthesize glucosylated dolichol-linked oligosaccharide, leading to accumulation of $_9$GlcNAc$_2$-P-P-dolichol (41). Studies in many systems have shown that the oligosaccharyltransferase is unable to utilize efficiently the Man$_9$GlcNAc$_2$-P-P-dolichol as a donor in comparison with Glc $_3$Man$_9$GlcNAc$_2$-P-P-dolichol (42, 43). Other patients with CDGS type I lack phosphomannomutase, which is required for conversion of mannose-6-phosphate to mannose-1-phosphate in the biosynthesis of GDPMan (44). Still other patients with CDGS type I are deficient in phosphomannose isomerase, the enzyme required for conversion of fructose-6-phosphate to mannose-6-phosphate, eventually leading to GDPMan (45).

Hereditary erythroblastic multinuclearity with positive acidified serum (HEMPAS) lysis test (also known as congenital dyserythropoietic anemia type II) is a disease characterized by decreased *N*-

glycosylation of glycoproteins on erythrocytes, which may be due to a deficiency a-mannosidase II (46). This decreased glycosylation is associated with crenation of the erythrocytes and subsequent hemolysis. Consistent with the possibility that human HEMPAS is associated with deficiency in a-mannosidase II is the finding that mice lacking a functional a-mannosidase II gene also develop a dyserythropoietic anemia associated with decreased *N*-glycosylation of erythrocyte glycoproteins (26).

Targeted genetic mutations in mice involving steps in the *N*-glycosylation pathway have been of great interest in recent years as scientists in the field attempt to unveil the biological functions of *N*-glycans. For example, null mutations in GlcNAc-T-I result in embryonic lethality (47, 48). It is hoped that such studies will begin to uncover many other biological functions of *N*-glycans and other potential enzymes involved in their biosynthesis.

Bibliography

1. R. D. Cummings (1992) in *Glycoconjugates: Composition, Structure and Function* (H. J. Allen and E. C. Kisailus, eds.), Marcel Dekker, New York, pp. 333–360.
2. R. D. Marshall and A. Neuberger (1972) Annu. Rev. Biochem . **41**, 673–702.
3. B. A. Vance, W. Wu, R. K. Ribaudo, D. M. Segal, and K. P. Kearse (1997) J. Biol. Chem. **272**, 23117–23122.
4. E. Bause (1983) Biochem. J. **209**, 331–336.
5. J. L. Mellquist, L. Kasturi, S. L. Spitalnik, and S. H. Shakin-Eshleman (1998) Biochemistry **37**, 6833–6837.
6. P. Messner (1997) Glycoconj. J. **14**, 3–11.
7. J. Lechner and F. Wieland (1989) Annu. Rev. Biochem. **58**, 173–194.
8. R. Kornfeld and S. Kornfeld (1985) Annu. Rev. Biochem. **54**, 631–664.
9. C. B. Hirschberg and M. D. Snider (1987) Annu. Rev. Biochem. **56**, 63–87.
10. J. S. Schutzback (1997) Glycoconj. J. **14**, 175–182.
11. J. S. Tkacz and O. Lampen (1975) Biochem. Biophys. Res. Commun. **65**, 248–257.
12. E. Bause and G. Legler (1981) Biochem. J. **195**, 639–644.
13. B. Imperiali and T. L. Hendrickson (1995) Bioorg. Med. Chem. **3**, 1565–1578.
14. S. Silberstein and R. Gilmore (1996) FASEB J. **10**, 849–858.
15. S. te Heesen, B. Janetzky, L. Lehle, and M. Aebi (1992) EMBO J. **11**, 2071–2075.
16. J. H. Chi, J. Roos, and N. Dean (1996) J. Biol. Chem. **271**, 3132–3140.
17. K. W. Moremen, R. B. Trimble, and A. Herscovics (1994) Glycobiology **4**, 113–125.
18. A. J. Parodi (1998) Braz. J. Med. Biol. Res. **31**, 601–614.
19. D. N. Hebert, B. Foellmer, and A. Helenius (1995) Cell **81**, 425–433.
20. F. E. Ware, A. Vassilakos, P. A. Peterson, M. R. Jackson, M. A. Lehrman, and D. B. Williams (1995) J. Biol. Chem. **270**, 4697–4704.
21. M. J. Spiro, V. D. Bhoyroo, and R. G. Spiro (1997) J. Biol. Chem. **272**, 29356–29363.
22. C. Gottlieb, J. Baenziger, and S. Kornfeld (1975) J. Biol. Chem. **250**, 3303–3309.
23. P. Stanley (1985) Mol. Cell Biol. **5**, 923–929.
24. P. Stanley (1983) Meth. Enzymol. **96**, 157–184.
25. M. Misago, Y. F. Liao, S. Eto, M. G. Mattei, K. W. Moremen, and M. N. Fukuda (1995) Proc. Natl. Acad. Sci. USA **92**, 11766–11770.
26. D. Chui, M. Oh-Eda, Y. F. Liao, K. Panneerselvam, A. Lal, K. W. Marek, H. H. Freeze, K. W. Moremen, M. N. Fukuda, and J. D. Marth (1997) Cell **90**, 157–167.
27. I. Brockhausen and H. Schachter (1997) In *Glycosciences: Status and Perspectives* (H. J. Gabius and S. Gabius, eds.), Chapman and Hall, Weinheim, Germany, pp. 79–113.

28. A. Varki (1998) Trends Cell Biol. **8**, 34–40.
29. P. Lerouge, M. Cabanes-Macheteau, C. Rayon, A. C. Fishette-Laine, V. Gomord, and L. Faye (1998) Plant Mol. Biol. **38**, 31–48.
30. D. H. Van den Eijnden, A. P. Neeleman, H. Bakker, and I. Van Die (1998) Adv. Exp. Med. Biol. **435**, 3–7.
31. L. V. Hooper, S. M. Manzella, and J. U. Baenziger (1996) FASEB J. **10**, 1137–1146.
32. E. Guillen, C. Abeijon, and C. B. Hirschberg (1998) Proc. Natl. Acad. Sci. USA **95**, 7888–7892.
33. S. Kornfeld (1987) FASEB J. **1**, 462–468.
34. M. Bao, J. L. Booth, B. J. Elmendorf, and W. M. Canfield (1996) J. Biol. Chem. **271**, 31437–31445.
35. M. Bao, B. J. Elmendorf, J. L. Booth, R. R. Drake, and W. M. Canfield (1996) J. Biol. Chem. **271**, 31446–31451.
36. R. Kornfeld, M. Bao, K. Brewer, C. Noll, and W. M. Canfield (1998) J. Biol. Chem . **273**, 23203–23210.
37. N. M. Dahms, P. Lobel, and S. Kornfeld (1989) J. Biol. Chem. **264**, 12115–12118.
38. G. P. Kaushal and A. D. Elbein (1994) Meth. Enzymol. **230**, 316–329.
39. T. Suzuki, K. Kitajima, Y. Emori, Y. Inoue, and S. Inoue (1997) Proc. Natl. Acad. Sci. USA **94**, 6244–6249.
40. J. Jaeken (1991) Int. Pediatr. **6**, 56–58.
41. P. Burda, L. Borsig, J. de Rijk-van Andel, R. Wevers, J. Jaeken, H. Carchon, E. G. Berger, and M. Aebi (1998) J. Clin. Invest. **4**, 647–652.
42. L. A. Murphy and R. G. Spiro (1981) J. Biol. Chem. **256**, 7487–7494.
43. J. Stoll, R. Cacan, A. Verbert, and S. S. Krag (1992) Arch. Biochem. Biophys. **299**, 225–231.
44. E. Van Schaftingen and J. Jacken (1995) FEBS Lett. **377**, 318–320.
45. R. Niehues, M. Haslik, G. Alton, C. Korner, M. Schiebe-Sukumar, H. G. Koch, K. P. Zimmer, R. Wu, E. Harms, K. Reiter, K. von Figura, H. H. Freeze, H. K. Harms, and T. Marquardt (1998) J. Clin. Invest. **101**, 1414–1420.
46. M. N. Fukuda, G. F. Gaetani, P. Izzo, P. Scartezzini, and A. Dell (1992) Br. J. Haematol. **82**, 745–752.
47. M. Metzler, A. Gertz, M. Sarkar, H. Schachter, J. W. Schrader, and J. D. Marth (1994) EMBO J. **13**, 2056–2065.
48. E. Ioffe and P. Stanley (1994) Proc. Natl. Acad. Sci. USA **91**, 728–732.

O-Glycosylation

In **eukaryotes**, carbohydrate side-chains are added to certain amino acid residues in some protein sequences to form **glycoproteins** . In N-glycosylation, the sugars are attached in N-linkage to **asparagine residues**, and this type of glycosylation, which is initiated in the endoplasmic reticulum (ER), has been well studied. Glycans may also be added to serine and **threonine residues** in a protein, and because the hydroxyl group of these amino acids forms the link with the sugar, this type of glycosylation has been termed O-glycosylation . The enzymes that initiate glycosylation and add the individual sugars to extend or terminate the chain are glycosyltransferases, which catalyze the basic reaction:

$$\text{nucleotide} - \text{sugar donor} + \text{R-OH receptor} \rightarrow \text{nucleotide} + \text{R-O-sugar}$$

where R is a serine or threonine residue or a sugar already attached to the acceptor protein. In most cases, the nucleotide may be UDP, as for galactose and the hexosamines, or GDP, as for fucose; these donor substances are made in the **cytoplasm**. An exception is sialic acid, which is added from cytadine monophosphate-sialic acid that is made in the nucleus. There are three main types of O-glycosylation in eukaryotes, namely: (*1*) Mucin-type O-glycosylation, in which the proteins normally carry multiple O-linked oligosaccharide chains; (*2*) O-Glycosylation leading to the formation of proteoglycans; and (*3*) O-GlcNAc glycosylation of cytoplasmic and nuclear proteins.This article will focus on O-glycosylation in mammalian cells, especially relating to mucin-type O-glycosylation. Proteins are O-glycosylated, however, even in fungal cells, and these pathways will also be discussed.

1. Mucin-Type O-Glycosylation

This type of glycosylation refers to the covalent attachment of O-glycans to serines and threonines in mucin core proteins, whereby the sugars are added individually and sequentially in the Golgi apparatus. The nucleotide sugar donors are transported into the lumen of the Golgi pathway where the glycosyltransferases are positioned. The genes coding for many of the relevant glycosyltransferases have recently been isolated, **cloned**, and expressed, and it is becoming clear from their specificities that several different enzymes may catalyze the same reaction. Moreover, the existence of enzymes that can add different sugars to the same substrate means that competition can occur for the substrate, providing the locations of the different enzymes overlap in the Golgi pathway. Thus, the locations of the enzymes involved in mucin-type O-glycosylation are as important as their level of activity in determining the final composition of O-glycans added.

1.1. Initiation of Glycosylation

In mammalian cells and as far down the evolutionary scale as *Caenorhabditis elegans*, the first sugar to be added to serine or threonine in alpha linkage is N-acetylgalactosamine (GalNAc). Identifying a specific sequence that defines a glycosylation site has been difficult. Recent developments suggest that this may be largely because not one enzyme but a family of enzymes (UDP-N-acetyl-a-D-galactosamine:polypeptide-N-Acetylgalactosaminyltransferases) are involved in this reaction. These enzymes, referred to here as ppGalNAcTs, catalyze the transfer of GalNAc from UDP-GalNAc to serines and threonine residues (1). The different ppGalNAcTs have distinct but overlapping specificities for the peptide sequence, and the same enzyme can add GalNAc to both serine and threonine residues (2). Thus, the sequences flanking the serine or threonine residue influence whether or not it is glycosylated, but this cannot be inferred merely from a database analysis of in vivo substrates (3).

Knockout strains of the ppGalNAcTs are only just being prepared (4), and some redundancy is to be expected. However, the ppGalNAcTs show well-defined tissue and cell specificity of expression (5), suggesting a differential dependence of each cell type on specific enzymes. The tissue and cell specificity of the ppGalNAcTs also suggests that differences may exist in the sites of glycosylation of the same protein expressed in different cells. Identification of sites that are glycosylated in vivo has been difficult, but some data are now beginning to emerge.

The location in the ER/Golgi pathway where mucin type O-glycosylation is initiated has been controversial. There has been general agreement that GalNAc is not added in the ER, but different methods of analysis have indicated different locations (6, 7). Recent studies using immunoelectron microscopy to localize tagged enzymes in transfected cells suggest that three of the ppGalNAcTs (T1, T2, and T3) are found throughout the Golgi, with the profile of expression being different for each enzyme (8). With mucin proteins, in which hundreds of sugar side chains may be added, it may be that the addition of GalNAc does indeed occur throughout the Golgi. If some chains are initiated later in the pathway, this could contribute to the heterogeneity of composition of the O-glycans that are found in mucin preparations.

In **fungi**, serine and threonine residues are glycosylated via dolichyl phosphate-D mannose (Dol-P-Man) as an intermediate, a reaction that occurs in the ER and has not been observed thus far in higher eukaryotes. The following reactions have been established for *Saccharomyces cerevisiae*:

$$\text{GDP-mannose-Dol-P} \leftrightarrow \text{Dol-P-Man} + \text{GDP}$$

$$\text{Dol-P-Man} + \text{protein(Ser/Thr)} \leftrightarrow \text{protein(Ser/Thr)} - \text{Man} + \text{Dol-P}$$

The protein molecules that are glycosylated may be secreted or are in the cell wall. Although the classification of the yeast O-glycosylation may not fall into any of the categories defined for higher eukaryotes, multiple genes code for enzymes catalyzing the transfer of mannose from Dol-P-Man to serine or threonine residues (Dol-P-Man:protein mannosyl transferases, or PMTs). In this system, the possible redundancy of the enzymes has been investigated by producing multiple mutants, and only a triple disruption is lethal, although some of the double mutants are unable to grow without osmotic stabilization (8).

1.2. Chain Extension in Mucin-Type O-Glycan Synthesis

After the addition of GalNAc to the mucin protein, various core structures are formed by the addition of different sugars (see Fig. 1 of O-Linked Oligosaccharides). Chains are extended from these cores by the addition of N-acetylglucosamine (GlcNAc) and galactose alternately, to give polylactosamine side chains that may be straight or branched (see Figs. 2 and 3 in O-Linked Oligosaccharides). Formation of the different cores varies with the tissue, but a pathway through core 1 and core 2 is commonly used. Two genes that can add GlcNAc in b1,6 linkage to core 1 (to form core 2) have been identified (9). One of the these enzymes can also catalyze the addition of GlcNAc to form the internal branch (shown in Fig. 2 of O-linked oligosaccharides), and the other (the core 2 enzyme) can only catalyze the formation of core 2 from core 1. Where biosynthesis is through core 2, the addition of the GlcNAc is crucial for chain extension.

1.3. Chain Termination

The O-glycans carried on mucins are usually terminated by the addition of sialic acid or fucose, and this may be subject to blood group A or B dependent transferase activity (see Fig. 3A and 3B of O-Linked Oligosaccharides). The number of enzymes that catalyze the addition of sialic acid is steadily increasing and presently is at least ten (10). Not all of these enzymes act on O-glycans, but those acting at the early stages of O-glycosylation are specific for this type of glycosylation. Important enzymes in this category are those adding sialic acid in a2,6 linkage to the first sugar GalNAc, or in a2,3 linkage to galactose in core 1 (see Fig. 2 of O-Linked Oligosaccharides). The sialyltransferase that adds sialic acid in a2,6 linkage to galactose at the end of N-glycans does not add the sugar to O-glycan chains that terminate with sialic acid in a2,3 linkage. Two candidate enzymes exist (ST3 Gal III and ST3 GalIV) that could add sialic acid to galactose at the end of O-glycans, which have been reported to be selective for type I and type 2 chains, respectively. (See Tsuji et al (1996) for further discussion on nomenclature.)

1.4. Localization of Glycosyltransferases Involved in the Biosynthesis of O-Glycans in the Golgi Pathway

Organization of the Golgi apparatus can be separated into three major components: (*1*) the *cis*-Golgi network, (*2*) the Golgi stacks (*cis* medial and *trans*), and (*3*) the *trans* Golgi network, or TGN. The sizes of the various components of the pathway vary with cell type (see Golgi Apparatus). Movement of proteins through the pathway is vectorial, progressing from *cis* to *trans* via nonselective budding transport. Glycosylated proteins leave the *trans* face of the stack to be sorted to their various destinations in the TGN, where further glycosylation may also occur (11).

The glycosyltransferases are themselves type-II membrane glycoproteins, with a short amino-terminal cytoplasmic **domain**, a single transmembrane domain (typically 17 residues), a loosely folded putative stem cell region (50–100 residues), and a tightly folded globular catalytic domain of more than 325 residues, which extends into the lumen of the Golgi apparatus. Early work involving the localization of these enzymes using subcellular fractionation or detection of specific oligosaccharide structures with lectins suggested an orderly compartmentalization of enzymes corresponding to the sequential addition of sugars. More recent studies show that glycosyltransferase organization is more complex, however, and that overlap can occur even between enzymes such as the core 2 enzyme responsible for chain extension and the a2,3 sialyl- transferase ST3Gal I that effects termination (12). These enzymes both use Gal b1,3 -GalNAc-R as a substrate, and changes in their levels of activity affect the final composition of the O-glycans synthesized. Definitive mapping has only been done for a few of the many enzymes involved in O-glycan initiation and biosynthesis. However, with the production of the recombinant enzymes and, in particular, specific monoclonal antibodies directed against them, the relative positions of these enzymes should be established.

The mechanisms involved in sorting the glycosyltransferases, whether these be involved in N- or O-glycosylation, are not fully understood. Two models have been suggested to explain the distribution of these enzymes in the Golgi pathway (13, 14) (see Golgi Apparatus).

1.5. Molecules Carrying Mucin-Type O-Glycans
Although some molecules (eg, erythropoietin) may carry only one O-glycan, most of the molecules carrying carbohydrate side chains attached in this way carry multiple O-glycans and are classified as mucins; the final composition of the molecule is more than 50% carbohydrate. These molecules have a common feature in containing a tandem repeat domain, rich in serine and threonine residues, to which the O-glycans are attached. Of the eight human epithelial mucin genes that have been identified by gene cloning, all but the first (MUC1) are extracellular mucins. MUC1 is a type I transmembrane protein and resembles the membrane-associated selectin ligands (15). It is much larger, however, and the sequence in the repeats is much more conserved. The addition of sugars, even only GalNAc, results in the molecule becoming highly extended, reaching above the glycocalyx, allowing the membrane-associated mucins to influence cell-cell interactions.

The multiplicity of enzymes that can initiate mucin-type O-glycosylation and the sequential nature of the biosynthesis of the O-glycans allow for an almost infinite number of possible glycoforms to be produced from the same core protein, the final structure depending on the profile of expression of the glycosyltransferases. Studies with specific antibodies to the ppGalNAcTs are showing a marked tissue and cell specificity of expression (1, 5), and this also holds true for many of the enzymes involved in biosynthesis of the oligosaccharides, for which studies thus far have depended on looking at messenger RNA expression. Studies on the promoters governing expression of the transferases are only now beginning, but strong indications exist that tissue-specific expression may in some cases depend on the use of alternative **promoters** and alternative splicing, resulting in the production of various mRNAs with different 5′-untranslated regions (16).

1.6. Functions of Mucin-Type Glycoproteins
An obvious function of the extracellular mucins, which form an important component of the mucous layer covering some epithelial cells (eg, lining the gastrointestinal and respiratory tracts), is protection of the underlying epithelium from insult. The O-glycans play a major role in this protective function, not only in the formation of large oligomers, which makes the mucous layer viscous, but also in serving as receptors for invading microorganisms. The membrane-associated MUC1 mucin can also have a protective function but, like the selectin ligands, can also affect cell-cell adhesion.

The O-glycans on the membrane-associated mucins are generally heavily sialylated, and the resulting negative charge results in inhibition of cell-cell interactions unless a specific epitope in the oligosaccharide component can act as a ligand for a **receptor** on another cell, when cell-cell adhesion is enhanced. Study of the interaction of selectins with their glycoprotein ligands has led to detailed definition of the interacting oligosaccharide structure (see O-Linked Oligosaccharides). However, the specific oligosaccharide must be carried on a particular core protein, suggesting an involvement of the protein sequence or structure, either directly or indirectly by allowing clustering of the O-glycans.

1.7. Glycosylation Patterns, Differentiation, and Malignancy

The composition of the side chains added to a mucin core protein can vary not only in different tissues, but also with the differentiation state of a particular cell **phenotype** and with the change to malignancy (see Neoplastic Transformation). Although the changes in malignancy may or may not relate to disease progression, those observed in differentiation are likely to be functional and relate to cell adhesion.

Changes in the expression of the core 2 enzyme have been characterized both in differentiation of T cells and in cancer. Leukosialin is a major glycoprotein expressed on leukocytes, and changes in its composition of added O-glycans occur on activation of human T cells. In resting cells, the dominant O-glycan is a tetrasaccharide (disialylated core 1), whereas in activated T cells the expression of the core 2 enzyme is increased and core 2-based structures are added (17). A similar increase in the activity of the core 2 enzyme is seen in leukocytes from patients with immunodeficiency, as such that seen in Wiscott-Aldrich syndrome (9). Furthermore, the core 2 enzyme is differentially expressed in the thymus, where expression is high in the subcapsular and cortical thymocytes and low in the medullary thymocytes. In this case, the differential expression of core 2 structures correlates with the ability of the cells to interact with a lectin (galectin) synthesized by thymic epithelial cells.

Emphasizing the importance of cell phenotype in defining profiles of glycosylation, the changes in levels of enzymes in malignancy differ in various cancers. In leukemias, the core 2 enzyme can be increased, whereas it may be decreased in breast cancers (18). In breast cancer, there is also an increase in the a2,3 sialyl-transferase that adds sialic acid to core 1, resulting in an increase in the major epitope for sialoadhesin expressed on macrophages. In the colon, where the O-glycans added to the mucins are very large and complex, changes occur in carcinomas that result in increased expression of the sialylated Le^{a} and Le^{x} structures—the ligands for P and E selectins, respectively.

2. O-glycosylation leading to the formation of proteoglycans

Proteoglycans are composed of glycosaminoglycan chains (GAGs) bound to serine residues in a protein core, via a xylose-galactose-galactose bridge. Unlike mucin-type O-glycosylation, threonine residues do not seem to act as acceptors. All GAGs (chondroitin sulfate, dermatan sulfate, heparin and heparan sulfate) except hyaluronic acid are secreted as components of proteoglycans. The post-translational processing of the core protein occurs in the Golgi apparatus (19), where, after chain initiation, monosaccharides are added stepwise from the appropriate UDP-sugars. To attain their final shape, chains are then carried through a series of modifications, including sulfation (see O-Linked Oligosaccharides). There has been more progress in isolating the genes coding for and defining the core proteins of proteoglycans than in isolating the genes coding for the enzymes involved in the biosynthesis of the carbohydrate moieties added to these proteins. The GAGs are large, and where many chains are added there may be only 10% protein in the proteoglycan.

2.1. Initiation of Glycosylation

The initial, rate-limiting step in the synthesis of GAGs is the transfer of xylose from UDP-xylose to a serine residue. This step is catalyzed by UDP-D-xylose: proteoglycan core protein b-D-xylosyl transferase (xyloseT). Attempts to define a sequence in the core protein that will determine whether xylose will be added suggest that, although some limitations can be placed on the sequence flanking the serine (glycine must follow toward the carboxyl end), protein **secondary structure** may play an important role (20). The linking galactose moieties are then added, and the type of GAG to be synthesized is determined by the first hexosamine to be added, which begins the biosynthesis of the main chain.

2.2. Chain Extension

The GAGs consist of hexosamines and either hexuronic acid or L-iduronic acid or galactose units added alternately in unbranched sequence (see O-Linked Oligosaccharides). It seems likely that the enzymes that add the first hexosamine (GalN or GlcN) are different from those acting on the more peripheral regions of the chain. Which hexosamine is added determines which GAG is subsequently synthesized, and sequences in the core protein may direct the choice, as different GAGs can be added to different core proteins in the same cell.

2.3. Functions of Proteoglycans

Proteoglycans may occur intracellularly in **secretory granules**, at the cell surface, and in the extracellular matrix. The functions of proteoglycans are highly diverse, ranging from mechanical functions essential for maintaining the structural integrity of connective tissue, to effects on cell adhesion, motility, proliferation, differentiation, and morphogenesis. Many of these effects depend on binding of proteins to the GAG chains. As with the mucin molecules, these interactions can depend on the charge and are then relatively nonspecific and of low affinity, whereas others, involving a particular oligosaccharide with defined structure, are highly specific. The core protein, in addition to serving as a scaffold for the GAGs, may be involved in anchoring the molecule to the membrane.

3. O-GlcNAc glycosylation of cytoplasmic and nuclear proteins

O-linked N-acetylglucosamine linked to serine or threonine residues was discovered by Torres and Hart (21) and has since been found to be ubiquitous and abundant on nuclear and **cytoskeletal** proteins in virtually all eukaryotes, including fungi (22). This type of glycosylation occurs in the cytoplasm, not in the Golgi apparatus (the site of post-translation modification of the core proteins of mucins and proteoglycans), and it may be extremely important in modifying the activity of intracellular proteins with a wide diversity of functions. Table 1lists some of the classes of proteins that have been shown to be glycosylated in this way.

Table 1. Some Proteins Shown to be Subject to O-GlcNAc Acylation

Proteins involved in transcription (Pol II andtranscription factors)
Cytoskeletal proteins (intermediate filaments,bridging proteins)
Tumor suppressors, oncogenes (p53)
Nuclear pore proteins

3.1. O-GlcNAc and Phosphorylation

O-GlcNAc glycosylation is dynamic; the sugar turns over much more rapidly than does the protein backbone. Most of the proteins undergoing this type of glycosylation are **phosphorylated**, in some instances on the same amino acid residue, so it is suggested that the addition of O-GlcNAc is a regulatory modification analogous to phosphorylation. Many of the sites are similar to those used by some kinases, namely the glycogen synthase kinase and the MAP kinases, and in the *myc* oncogene the site has been mapped to Thr58 in the transactivation domain (23), which is also a major site of phosphorylation and a hot spot for mutagenesis in lymphomas. The glycosylation of **RNA polymerase** II at the mucin-like sequence at the C-terminal domain may indicate a role in transcriptional initiation.

3.2. O-GlcNAc and Protein Interactions

Another function of O-GlcNAc appears to be in mediating cytoskeletal assembly and organization, and a defect in the function has been implicated in Alzheimer's disease (24). Where the GlcNAc is thought to be an alternative to phosphorylation, it is accessible to modification (by a glycosyltransferase that transfers galactose to the hexosamine). When O-GlcNAc is functioning in protein-protein interactions, the sugars appear to be buried in the native molecules and are only accessible after **denaturation** or **proteolysis**.

Whereas about 50% of the sites that are glycosylated are at or near a PVS (Pro-Val-Ser) type of sequence, the other half have no apparent **consensus sequence**. It is not yet clear how many enzymes are involved in this type of glycosylation. However, a gene coding for an O-GlcNAc transferase has now been isolated and characterized. (See Hart et al (1996) for a further discussion).

3.3. Concluding Comments

Addition of sugars in O-linkage to proteins represents a post-translational modification that has far-reaching implications in affecting protein structure and function. The use of recombinant DNA technology to identify and catalog the families of enzymes involved in effecting the modifications shows that the number of genes devoted to this activity in higher eukaryotes is very large indeed. The functions affected by these modifications are also very wide ranging. The relation between structure and function of O-glycosylated proteins is therefore complex, but important tools are being developed, and the challenge is becoming less daunting. One might predict that there will be more entries dealing with the subject in any future issues of this work.

Bibliography

1. T. Sorensen, T. White, H. Wandall, A. K. Kristensen, P. Roepstorff and H. Clausen (1995) J. Biol. Chem. **270**, 24166–24173.
2. H. H. Wandall, H. Hassan, K. Mirgorodskaya, A. K. Kristensen, P. Roepstorff, E. P. Bennett, P. A. Nielsen, M. A. Hollingsworth, J. Burchell, J. Taylor-Papadimitriou, and H. Clausen (1997) J. Biol. Chem. **272**, 23503–23514.
3. A. P. Elhammer, R. A. Poorman, F. Brown, L. L. Maggiora, J. C. Hoogerheide, and F. I. Kezdy (1993) J. Biol. Chem. **268**, 10029–10038.
4. T. Hennet, F. K. Hagen, L. A. Tabak, and J. D. Marth (1995) Proc. Natl. Acad. Sci. USA **92**, 12070–12074.
5. S. Röttger, J. White, H. H. Wandall, J -C. Olivo, A. Stark, E. P. Bennett, C. Whitehouse, E. C. Berger, H. Clausen, and T. Nilsson (1998) J. Cell Sci . **111**, 45–60.
6. S. A. Tooze, J. Tooze, and G. Warren (1988) J. Cell Biol. **106**, 1475–1487.
7. E. G. Berger, T. Mandel, and U. Schilt (1981) J. Histochem. Cytochem . **29**, 364–370.
8. M. Gentzsch and W. Tanner (1996) EMBO J. **15**, 5752–5759.
9. M. F. A. Bierhuizen, K. Maemura, S. Kudo, and M. Fukuda (1995) Glycobiology **5**, 417–425.
10. S. Tsuji (1996) J. Biochem. **120**, 1–13.
11. C. Rabouille, N. Hui, F. Hunte, R. Kieckbusch, E. G. Berger, G. Warren, and T. Nilsson (1995) J. Cell Sci. **108**, 1617–1627.
12. C. Whitehouse, J. Burchell, S. Gschmeissner, I. Brockhausen, K. O. Lloyd, and J. Taylor-Papadimitriou (1997) J. Cell Biol. **137**, 1229–1241.
13. M. S. Bretscher and S. Munro (1993) Science **261**, 1280–1281.
14. T. Nilsson, P. Slusarewicz, M. H. Hoe, and G. Warren (1993) FEBS Lett **330**, 1–4.
15. Y. Shimizu and S. Shaw (1993) Nature **366**, 630–634.
16. M. Sekine, K. Nara, and A. Suzuki (1997) J. Biol. Chem . **272**, 27246–27252.
17. F. Piller, V. Piller, R. I. Fox, and M. Fukuda (1988) J. Biol. Chem. **263**, 15146–15150.
18. I. Brockhausen, J. Yang, J. Burchell, C. Whitehouse, and J. Taylor-Papadimitriou (1995) Eur. J. Biochem. **233**, 607–617.
19. N. Nuwayhid, J. H. Glaser, J. C. Johnson, H. E. Conrad, S. C. Hauser, and C. B. Hirschberg

(1986) J. Biol. Chem. **261**, 12936–12941.
20. T. Brinkmann, C. Weilke, and K. Kleesiek (1997) J. Biol. Chem. **272**, 11171–11175.
21. C. R. Torres and G. W. Hart (1984) J. Biol. Chem. **259**, 3308–3317.
22. M. Machida and Y. Jigami (1994) Biosci. Biotechnol. Biochem. **58**, 344–348.
23. T. Y. Chou, G. W. Hart, and C. V. Dang (1995) J. Biol. Chem. **270**, 18961–18965.
24. L. S. Griffith and B. Schmitz (1995) Biochem. Biophys. Res. Commun. **213**, 424–431.

Suggestions for Further Reading

25. H. Clausen and E. P. Bennett (1996) A family of UDP-GalNAc: polypeptide N-acetylgalactosaminyl-transferases control the initiation of mucin-type O-linked glycosylation. Glycobiology **6**, 635–646.
26. S. J. Gendler. and A. P. Spicer (1995) Epithelial mucin genes. Ann. Rev. Physiol. **75**, 607–634.
27. G. W. Hart, L. K. Kreppel, F. I. Comer, C. S. Arnold, D. M. Snow, Z. Ye, X. Cheng, D. DellaManna, D. S. Caine, B. J. Earles, Y. Akimoto, R. N. Cole, and B. K. Hayes (1996) O-GlcNAcylation of key nuclear and cytoskeletal proteins: reciprocity with O-phosphorylation and putative roles in protein multimerization. Glycobiology **6**, 711–716.
28. R. V. Iozzo and A. D. Murdoch (1996) Proteoglycans of the extracelular environment:clues from the gene and protein side offer novel perspectives in molecular diversity and function. FASEB J. **10**, 598–614.
29. M. Fukuda and O. Hindsgaul (1994) *Molecular Glycobiology*, IRL Press, Oxford.
30. S. Tsuji, A. K. Datta, and J. C. Pauslon (1996) Systematic nomenclature for sialyl transferases. Glycobiology **6**, v–vii.

Golgi Apparatus

The Golgi apparatus receives a varied mixture of newly synthesized proteins and lipids from the endoplasmic reticulum (ER) and sends them to their correct destination in the cell. These molecules share a common pathway through the Golgi apparatus, passing, in sequence, through an ordered array of compartments, each capable of carrying out a specific set of covalent post-translational modifications. In the last compartment, they are separated from each other in preparation for final delivery.

1. Morphology

First described in 1898 by the Italian anatomist Camillo Golgi (1843–1926) using a silver impregnation technique (Fig. 1a) (1), the Golgi apparatus has the same basic structure in all **eukaryotic** cells, comprising a stack of closely apposed and flattened cisternae (Figs. 1d and 1e). Cisternae are often cup-shaped, especially toward the *trans* side (2, 3), and there are typically three to six cisternae in the stack, although up to 40 have been reported (4). Each cisterna is about 1 µm in diameter and comprises a core region, involved in stacking and containing resident enzymes, and a fenestrated rim from which transport vesicles bud and with which they fuse (5). In **plants** and **fungi**, there are multiple copies of the Golgi dispersed throughout the cytoplasm (Fig. 1d) (3). In animal cells these stacks are linked laterally, forming a bifurcating, ribbon-like structure (Figs. 1e and 1f) (6, 7), which forms a compact reticulum most often found in the pericentriolar region of the cell, adjacent to the cell nucleus (Fig. 1a and 1c) (8).

Figure 1. Different views of the Golgi apparatus. (**a**) The original "appareil réticulaire" in a Purkinje cell, described by G
1898 (1) and revealed by his silver impregnation technique. (**b**, **c**) The Golgi reticulum in a living HeLa cell revealed by
Golgi enzyme with the green fluorescent protein (138). (**b**) Phase image. (**c**) Fluorescence image. (**d**) Longitudinal sectio
yeast cell (*Schizosaccharomyces pombe*) fixed with permanganate. Note the dispersed Golgi stacks (arrowheads). (**e**) Ep
the Golgi region of a HeLa cell showing two stacks in the Golgi ribbon. (**f**) Three-dimensional reconstruction of part of t
animal cells. Sections of two Golgi stacks (left and right) are shown linked by tubules and networks connecting equivale
adjacent stacks. (Adapted from Ref. 6, with permission.) Magnification bars: (**b**, **c**) 10 μm, (**d**) 1 μm, (**e**) 0.2 μm.

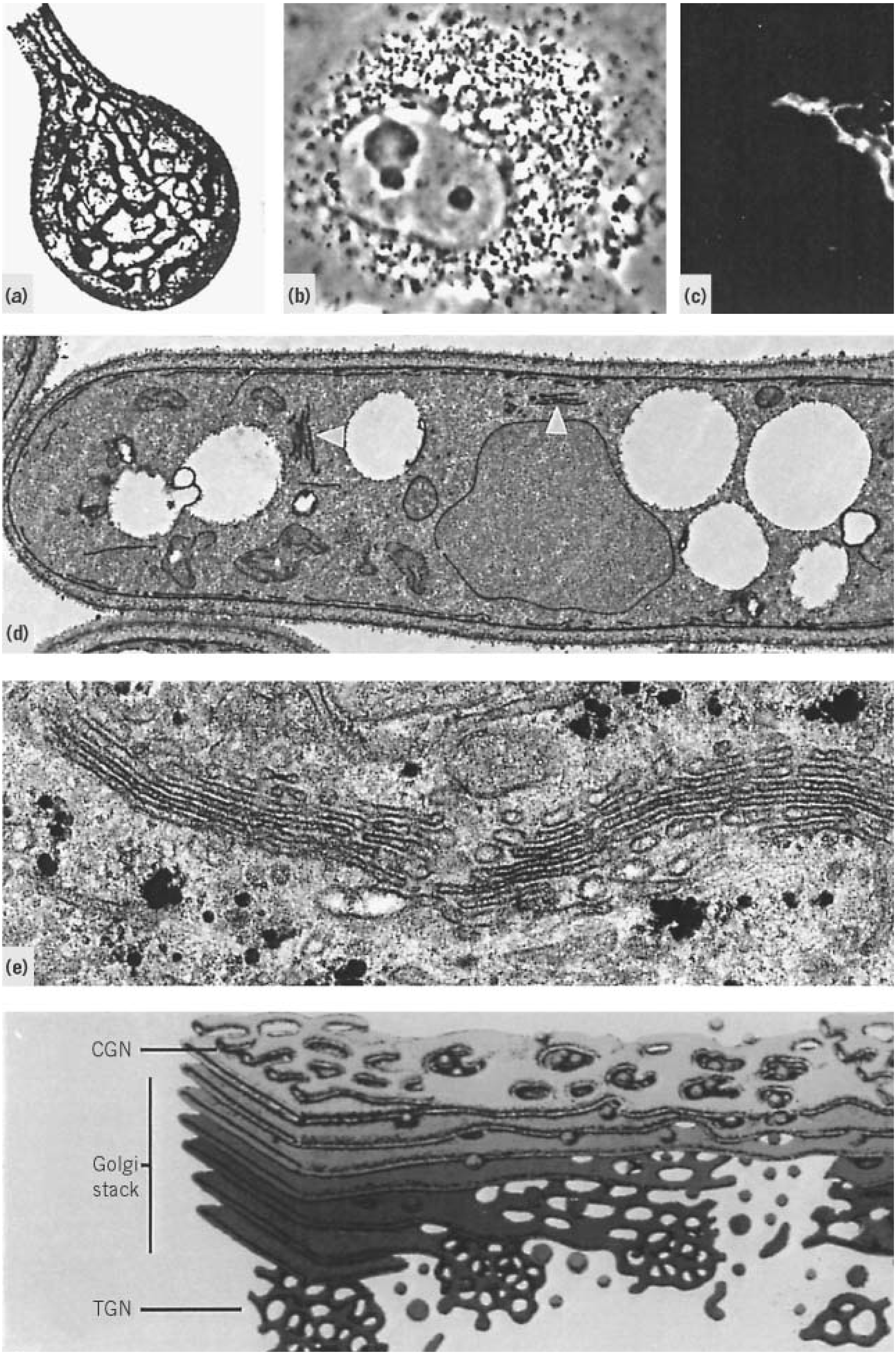
(a)
(b)
(c)
(d)
(e)
CGN
Golgi stack
TGN

Each face of the stack is apposed to a complex and extensive tubular network, best characterized in animal cells (and shown schematically in Fig. 1f). At the *cis* or entry face is the *cis*-Golgi network (CGN) (9), and at the *trans* or exit face is the *trans*-Golgi network (TGN) (10, 11). An intermediate compartment is interposed between the ER and the CGN, which is thought by many to ferry newly synthesized cargo molecules from the exit sites on the ER (the transitional element region) (12) to the CGN (13).

The Golgi apparatus is embedded in a matrix called the "zone of exclusion" because other cytoplasmic structures down to the size of ribosomes are excluded (14). Candidate components of this matrix have been identified, many of which have sequences predicting rod-like, fibrous proteins (15).

2. Biogenesis

The growth and division of the Golgi apparatus has been little studied, with the exception of the partitioning of Golgi membranes during mitosis in animal cells (16). The Golgi ribbon is converted during the early stages of **mitosis** into clusters of small **vesicles** and tubules, as well as free vesicles, a process that is thought to aid the partitioning process (17, 18). Cell-free assays (19, 20) have provided a molecular explanation of at least part of this process (21, 22).

3. Compartmentation

The Golgi apparatus comprises an ordered array of compartments through which newly synthesized proteins pass in sequence. The CGN is the entry point and is thought to be the last quality-control step on the pathway (23, 24). Properly folded cargo proteins proceed on to the stack. Misfolded proteins are returned to the ER for further rounds of folding (25) or degradation (26).

A large number of covalent modifications are carried out by the Golgi apparatus, including glycosylation, acylation, **phosphorylation**, sulfation, and **proteolytic** cleavage (27-30). ***N-Glycosylation*** is the best characterized and comprises a sequence of processing reactions that mark the passage of proteins through the Golgi stack (27, 31). The trimming of the high-mannose oligosaccharides, which are attached co-translationally in the ER, is completed in the early part of the Golgi apparatus. Construction of complex oligosaccharides is initiated in the middle part of the Golgi stack and completed in the late part. The enzymes that carry out these steps are present in two or more adjacent cisternae, generating an overlapping distribution that might help to ensure more complete glycosylation (32). Construction of complex oligosaccharides is completed in the TGN, which also functions to sort proteins and lipids. Those destined for **lysosomes** and **secretory granules** are packaged separately from those destined for the cell surface (see text below).

O-linked oligosaccharides (see O-Glycosylation) and glycolipids (33) are also assembled in a stepwise fashion as they pass, in sequence, through the stacked cisternae. The precise locations at which these steps occur must await cloning and localization of the enzymes involved.

4. Transport Through the Golgi Apparatus

Several models have been proposed to explain the ordered transport of proteins (and some lipids) through the Golgi apparatus. The two extremes are *cisternal maturation* (34) and vesicle-mediated transport (12), illustrated in Figure 2.

Figure 2. Models for transport through the Golgi stack. (**a**) Cisternal maturation envisages a dynamic stack of cisternae i
of cargo molecules, matures into the next one through the retrograde transport of Golgi enzymes. (**b**) Vesicle-mediated tı
cisternae through which a mixture of cargo molecules passes, in sequence, transported from cisterna to cisterna by vesicl

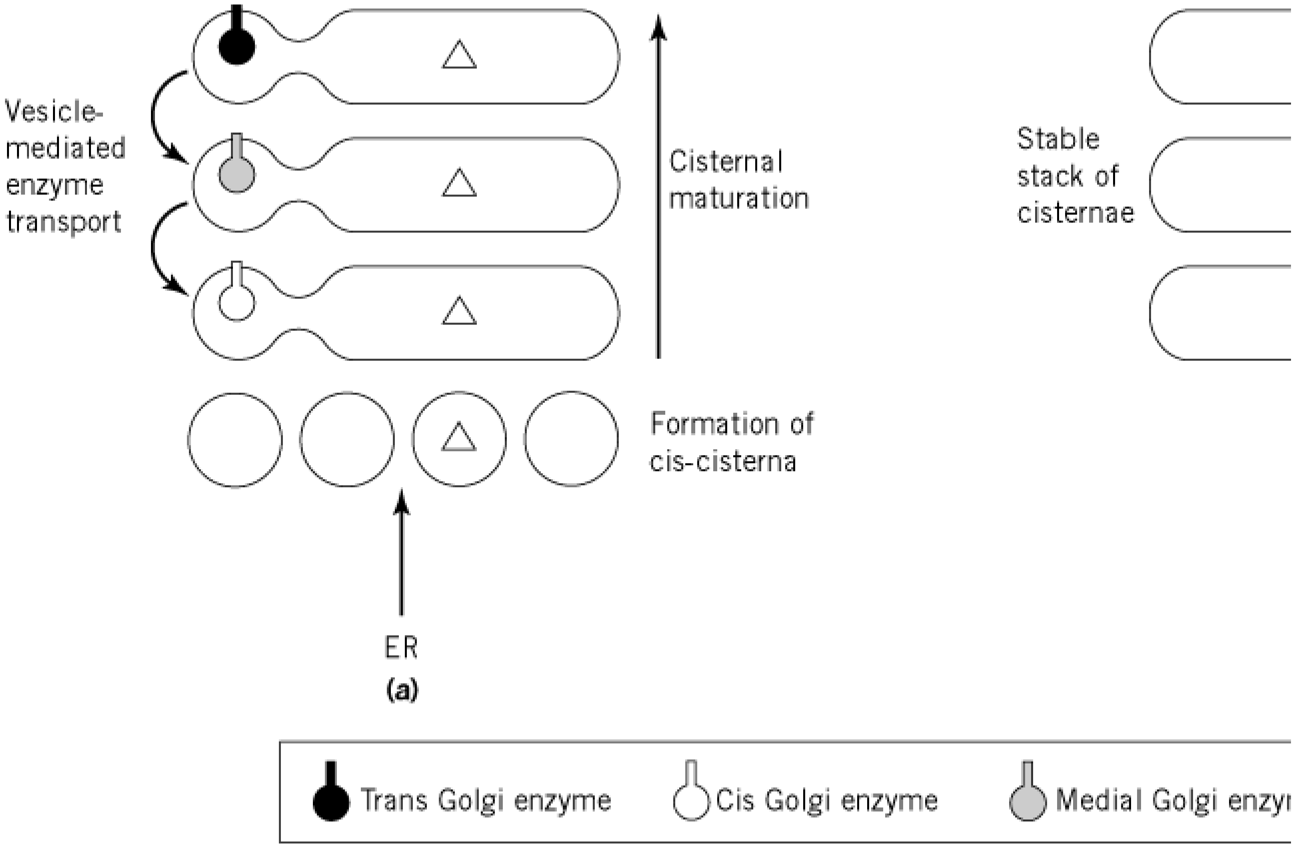

1. Cisternal maturation postulates a dynamic stack of cisternae. The *cis*-most cisterna is assembled by the fusion of transport vesicles from the ER, carrying newly synthesized cargo. Golgi processing enzymes are then delivered back from the next cisterna in the stack, which in turn receives enzymes from the next, and so on throughout the stack. In this way, each cisterna matures into the next one.

2. Vesicle-mediated transport postulates a stable stack of cisternae containing a fixed and ordered array of processing enzymes. The cargo is delivered to each cisterna in turn by **vesicles** that bud from one cisterna and fuse with the next in the stack.

There is still controversy as to whether either model, or a hybrid one, is correct. There is, however, general agreement that the vesicles mediating these pathways are COPI (Coat protomer complex I)-coated vesicles (35).

4.1. COPI-Mediated Budding

Assembly of the coat is thought to be initiated by the GTPase ARF (ADP-ribosylation factor) (36, 37) (Fig. 3). ARF exists in the cytoplasm bound to GDP, which is exchanged for GTP upon binding to Golgi membranes. This is catalyzed by a GEF (guanine nucleotide exchange factor) (38) that is sensitive to brefeldin A (39, 40). Exchange exposes a myristoyl group at the *N*-terminus of ARF, which aids Golgi binding (41). ARF then recruits coatomer , a complex of seven polypeptides (42, 43). This is either direct, through protein–protein interactions (44), or indirect, through the activation of phospholipase D by ARF, which generates phosphatidic acid to which the coatomer can bind (45). Stepwise binding of coatomer complexes is thought to cause incremental deformation of the membrane, generating a coated bud like that thought to occur for **clathrin**-coated vesicles (46). Scission generates a completed COPI vesicle and requires acyl-CoA, but it is otherwise uncharacterized (47). A GAP (GTPase activating protein) catalyzes the hydrolysis of the GTP bound to ARF (48), leading to disassembly of the coat (49) and recycling of the complexes for further rounds of budding.

Figure 3. COPI-mediated budding of transport vesicles. Stepwise assembly of coat subunits (ARF and coatomer) generate a COPI vesicle. GTP hydrolysis releases the coat subunits for further rounds of budding, leaving an uncoated vesicle that can then fuse with the target membrane. Note that proteins such as v-SNAREs, which have to be incorporated into vesicles during budding, have been omitted for clarity.

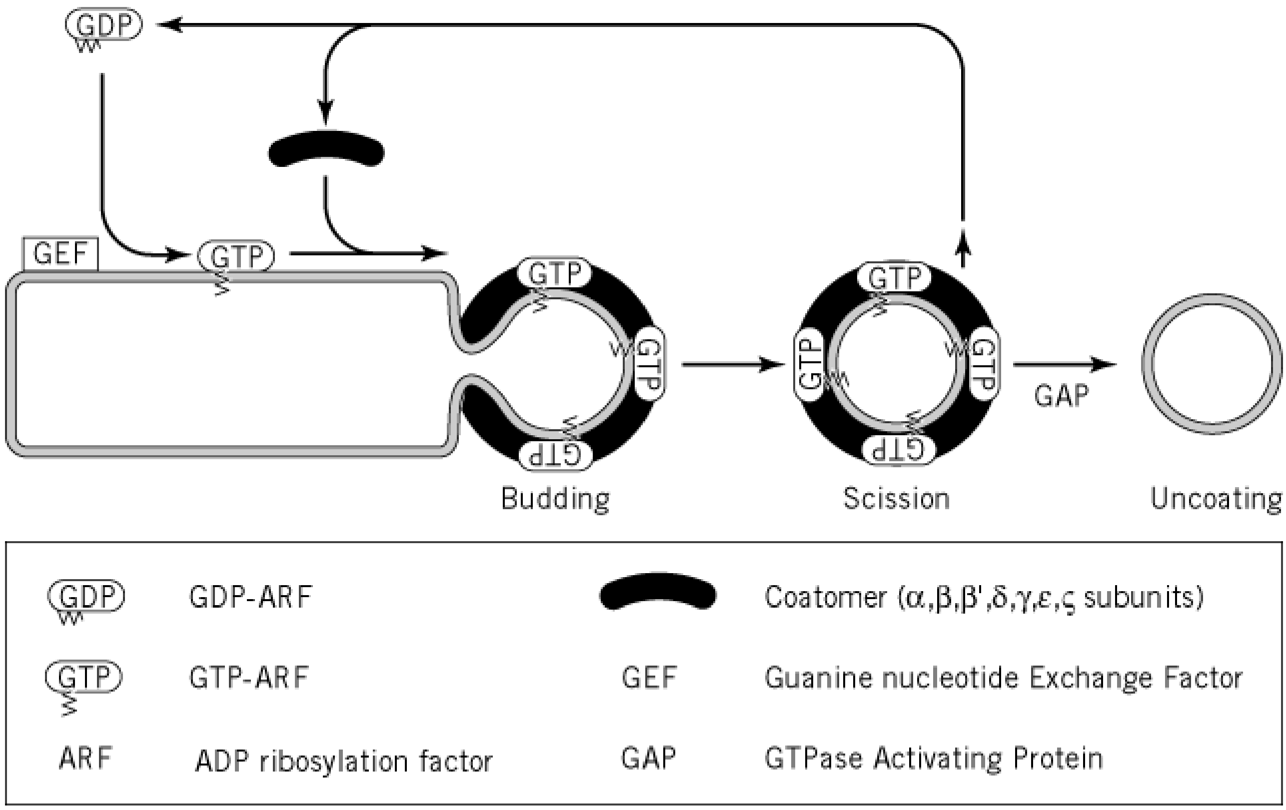

COPI vesicles are also involved in retrograde transport from the Golgi to the ER (see text below) and perhaps also from the ER to the Golgi apparatus (50). COPI coats are found on the TGN but appear not to be involved in transport from this compartment.

There are other types of coated vesicle involved in transport from the ER to the *cis*-Golgi and from the *trans*-Golgi. Two have been characterized at the molecular level. At the *cis*-side of the Golgi apparatus, COPII coats mediate the budding of cargo-carrying vesicles from the ER (50, 51). On the *trans* side, clathrin coats package lysosomal and other proteins during transport to lysosomes or upon recycling from immature granules (see text below). Although the protein constituents of both these coats differ from COPI coats, many of the underlying principles of operation appear to be the same (52). Lipids other than phosphatidic acid, and lipid exchange proteins (53), have also been implicated in budding processes. **Diacylglycerol**, in particular, appears to play a central role (54), although it is unclear whether this role is structural or regulatory.

4.2. Vesicle Docking and Fusion

After budding, Golgi transport vesicles must dock and fuse with the correct compartment. The SNARE hypothesis was put forward to explain the specificity of these transport steps (55) (Fig. 4). This hypothesis postulates a v- (or vesicle) SNARE (SNAP receptor) on each type of transport vesicle that interacts specifically with the t- (or target) SNARE in the recipient membrane compartment. SNAREs were first identified at the presynaptic membrane with which synaptic vesicles fuse during neurotransmission (56-60). Using genetic and biochemical techniques, they have now been identified at many other vesicle-mediated steps in the cell (61).

Figure 4. Targeting and fusion of transport vesicles. Transport vesicles are tethered and then docked specifically using v process. In one model (illustrated), SNAPs mediate the binding of the NSF ATPase to the v–t SNARE pair, and hydroly another model, SNAPs and NSF prime the SNAREs before they can interact with each other (139).

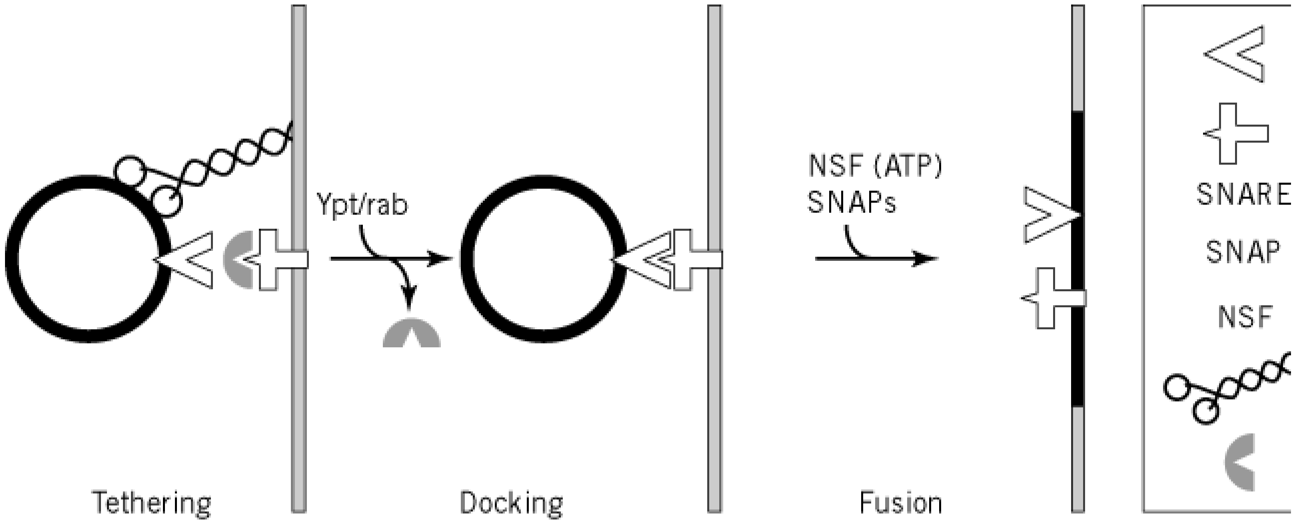

All but one of the SNAREs studied to date are type II membrane proteins, with most of their mass protruding into the cytoplasm (62); the exception has a Cys–Ala–Ala–X box at the *C*-terminus, so it is probably anchored by a long, hydrophobic prenyl group (63) (see Prenylation). Their sequences predict a coiled-coil structure suitable for forming paired complexes (64). Many, perhaps all, t-SNAREs are hetero-oligomers containing, in addition, a member of the SNAP25/sec9 family of proteins (65, 66). Transport vesicles can contain more than one type of v-SNARE, suggesting that multiple SNARE pairs might be used to improve the fidelity of vesicle targeting (63). Assembly of the SNARE pair is a highly regulated process. In some cases, the two membranes are initially brought together by the vesicle docking protein, p115, a process that might facilitate the efficiency with which cognate SNAREs find each other (67).

Some, perhaps all, t-SNAREs exist in an inactive form, complexed to a member of the sec1 family of proteins (68, 69), which is removed during the activation process (70). Activation of SNAREs is triggered by a member of the Ypt/rab family of small GTPases (70, 71), one or more of which is present at each vesicle-mediated transport step (72). They exist in two forms: (a) an inactive, GDP form, complexed with GDI (GDP dissociation inhibitor) in the cytoplasm and (b) an active, GTP form bound to the membrane by a prenyl group (73). Delivery of the GDP form to the correct membrane is mediated by a GDF (GDI displacement factor) (74), followed by exchange of GDP for GTP catalyzed by a GEF (75, 76). Hydrolysis of GTP by a GAP (77, 78) completes the cycle, permitting the ypt/rab to be extracted by GDI and recycled (79-81).

Formation of the cognate SNARE pair is thought to initiate the fusion process catalyzed by the ATPase NSF (*N*-ethylmaleimide-sensitive factor) (82). Binding of NSF to the SNARE pair is mediated by SNAPs (soluble NSF attachment proteins) (83) and leads to ATP hydrolysis, membrane fusion, and break-up of the SNARE pair (84, 85). The precise order of events is still disputed, especially the step at which NSF acts (86, 87). It is also unclear how these events lead to the physical merging of the two lipid bilayers.

More recently, the NSF-like ATPase p97 (88) has been implicated (together with NSF) in the rebuilding of the Golgi apparatus from fragments generated either by mitotic conditions (89) or by drug treatment (90). The fusion role played by p97 is distinct from that played by NSF, but the molecular mechanism is unknown.

5. Protein Sorting

Proteins with very different final locations within the cell are assembled in the ER and sorted in the Golgi apparatus (Fig. 5). Cargo moves to the TGN, where sorting mechanisms separate lysosomal and **secretory granule** proteins from each other and from proteins destined for the cell surface. ER and Golgi proteins have retention mechanisms that inhibit movement beyond the point in the exocytosis pathway at which they usually act. Those molecules that do escape are salvaged by retrieval mechanisms. Retrieval mechanisms also recycle membrane components of the transport machinery. All these mechanisms interpret signals on the proteins undergoing transport. These signals are most often short stretches of sequence that are either read directly by the sorting mechanism or are used to construct the sorting signal.

Figure 5. Protein sorting during transport through the Golgi apparatus. A varied mixture of proteins is assembled in the I
proteins are salvaged, mostly, but not exclusively, from the early part of the Golgi and are returned to the ER. Golgi enzy
Cargo proteins move to the TGN, where they are separately packaged and sent to the plasma membrane, late endosomes

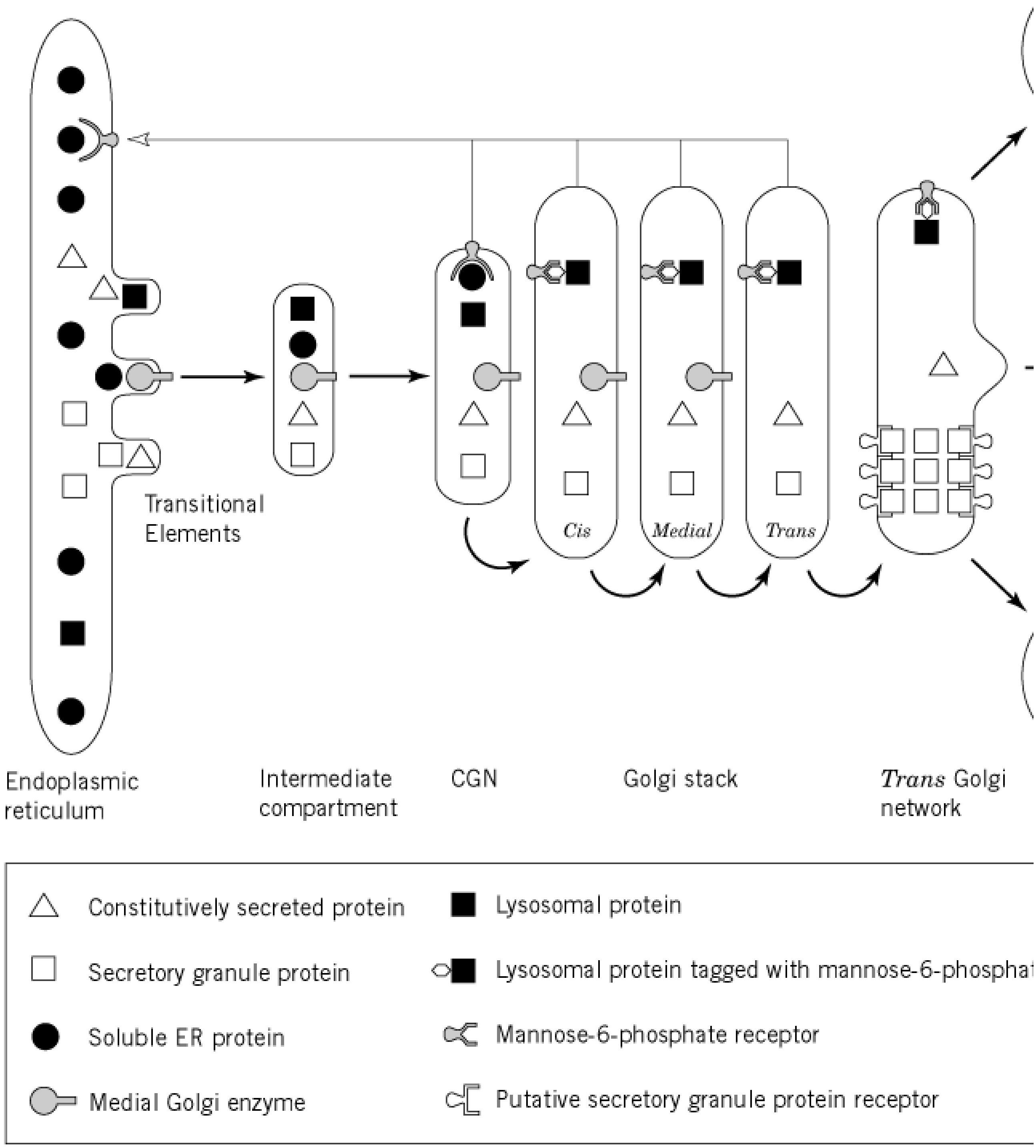

5.1. The Default Pathway
The pathway from the ER to the cell surface was originally designated the default pathway because signals did not appear to be required to transport cargo through the correct sequence of Golgi compartments to the cell surface (91). This is still true for many proteins and many compartmental steps, but there is increasing evidence that some surface cargo can be selectively concentrated, especially during export from the ER (92, 93).

Two types of protein that could be involved in concentrating cargo have been described. The first are **lectin**-like proteins—for example, ERGIC53 (94) and Vip36 (95), which are thought to bind the oligosaccharides attached to many cargo proteins. In the case of ERGIC53, the lectin–cargo complex would be concentrated in transport vesicles because the cytoplasmic tail binds to coat proteins (96). The second are the p24 family of spanning proteins (97, 98), the large lumenal domains of which are thought to bind to cargo molecules by unknown means (97), aided by ancillary proteins (99). This family of proteins is selectively incorporated into transport vesicles, because their cytoplasmic tails contain a dibasic motif that binds coat subunits (100, 101).

5.2. Sorting in the TGN
All cargo molecules share the same pathway up to and including the TGN. It is here that lysosomal (102) and secretory granule proteins (103) are separated from surface cargo. Many soluble lysosomal enzymes are tagged in the early part of the Golgi apparatus with a mannose-6-phosphate signal that is constructed from some of the terminal mannose residues on the high-mannose oligosaccharide by two enzymes that recognize protein features unique to lysosomal enzymes (31, 104). The tagged enzyme moves through the Golgi stack to the TGN, where it binds the large **mannose-6-phosphate receptor** (105). The complex is specifically incorporated into clathrin-coated vesicles, because multiple signals in the cytoplasmic tail of the receptor (106) are recognized by an adaptor (107, 108). The complex is then ferried to a prelysosomal compartment (109) where, eventually, the low pH separates the enzyme from the receptor. The enzyme is delivered to lysosomes, whereas the receptor is recycled for further rounds of transport. Some lysosomal membrane proteins are also ferried in clathrin-coated vesicles. The same adaptor recognizes a signal in the cytoplasmic tail (110).

As well as a direct route to lysosomes from the TGN, there is also an indirect route via the cell surface. For soluble enzymes, this is mediated by the small mannose-6-phosphate receptor (106).

Secretory granule proteins begin to condense in the TGN, probably because of the lower pH of this part of the Golgi apparatus and the presence of calcium ions (111). Condensation is a sorting mechanism, because during this process all other proteins are largely excluded, including, in some cells, the granule proteins destined for other types of secretory granule. The outside of the condensing granule core is thought to bind to sorting **receptors**, thereby enveloping the core with a membrane that buds to form an immature **vacuole**. Maturation proceeds by a process involving vacuole fusion and retrieval of excess membrane, until a mature secretory granule is formed (112).

In polarized cells, there is more than one surface domain, and signals exist to direct surface cargo to one or other of these domains. The signals used include the bound *N*-linked oligosaccharides (113) or sequences within the cytoplasmic tail (114, 115). **GPI-anchored** proteins are thought to form “rafts” that are selectively incorporated into vesicles bound for the apical membrane domain (116).

5.3. Retention in the Golgi Apparatus
Proteins destined to remain in the Golgi apparatus are also synthesized and assembled in the ER. They are transported together with other cargo to the Golgi apparatus, but must then stop in the correct cisterna(e). The retention signal that specifies location within the Golgi apparatus is contained within the membrane-spanning domain and flanking sequences (117) and is thought to inhibit further forward transport in one of two ways. The kin recognition model (118) postulates interaction with other Golgi proteins sharing the same cisterna, generating an oligomer too large to enter the forward-moving transport vesicles. The bilayer thickness model (119) exploits the increasing thickness of Golgi membrane across the stack caused by a gradient of cholesterol. The Golgi protein moves forward until the length of the spanning domain matches that of the bilayer. Different lengths would specify different locations within the stack. There is evidence both for and against each model, but they are not mutually exclusive, and a combination of the two could serve to locate the proteins more precisely in the stack (120).

5.4. Retrieval by Retrograde Transport
Two types of retrieval operate from the Golgi apparatus to the ER. The first is a salvage process, recovering proteins that stray beyond the point in the exocytic pathway at which they operate (121). The need for salvage gave rise to the distillation hypothesis, which could help explain the need for a Golgi stack (122). The second type of retrieval is recycling, mostly of components of the vesicle

fusion machinery.

Salvage of ER proteins is mediated by short signals at the *N*- or *C*-terminus. Soluble proteins in the ER lumen use a *C*-terminal tetrapeptide (123), [KDEL in mammals, HDEL in budding yeast], whereas membrane proteins use either a double-lysine (type I proteins) (124) or a double-arginine (type II proteins) (125) motif (but see Ref. 126). Escaped lumenal proteins bind to the KDEL receptor (127), mostly located in the CGN (128), and this triggers return of the complex (129) in COPI vesicles (130) to the ER, where a change in pH is thought to effect release (131). Escaped membrane proteins with a double-lysine motif are also returned by COPI vesicles, because this motif binds directly to the coatomer component of the COPI coats (132, 133). The mechanism for returning ER proteins with a double-arginine motif is not known.

Salvage of Golgi proteins is less well understood, although there is now good evidence that it occurs (134, 135). Salvage is also an important part of secretory granule biogenesis. During maturation of immature granules, clathrin-coated vesicles recover and return proteins destined for other pathways (136).

Recycling is exemplified by the v-SNAREs. These are present in the target compartment after vesicle fusion and must be recycled to the preceding, donor compartment for further rounds of vesicle budding. The mechanism is not known, but some evidence suggests that they are not passively recycled. Instead, they direct the vesicle to the preceding compartment, in the same way that they directed the earlier vesicles to the target compartment. A t-SNARE would be needed in each of the two compartments linked by the vesicles, but only one v-SNARE. This parsimonious solution to recycling requires a mechanism to switch the specificity of the v-SNARE, depending on which of the two compartments is being targeted (137).

Bibliography

1. C. Golgi (1898) Arch. Ital. Biol. **30**, 60–71.
2. W. G. Whaley (1975) *The Golgi Apparatus*. Cell Biology Monographs, Continuation of Protoplasmatologia, **2**, Springer-Verlag, New York.
3. M. G. Farquhar and G. E. Palade (1981) J. Cell Biol. **91**, 77s–103s.
4. D. W. Fawcett (1981) *The Cell*, 2nd ed., W. B. Saunders, Philadelphia.
5. P. Weidman, R. Roth, and J. Heuser (1993) Cell **75**, 123–133.
6. A. Rambourg and Y. Clermont (1990) Eur. J. Cell. Biol. **51**, 189–200.
7. J. M. Lucocq and G. Warren (1987) EMBO J. **6**, 3239–3246.
8. W. C. Ho, V. J. Allan, M. G. van, E. G. Berger, and T. E. Kreis (1989) Eur. J. Cell. Biol. **48**, 250–263.
9. H. P. Hauri and A. Schweizer (1992) Curr. Opin. Cell. Biol. **4**, 600–608.
10. G. Griffiths and K. Simons (1986) Science **234**, 438–443.
11. M. S. Ladinsky, J. R. Kremer, P. S. Furcinitti, J. R. McIntosh, and K. E. Howell (1994) J. Cell Biol. **127**, 29–38.
12. G. Palade (1975) Science **189**, 347–358.
13. J. Saraste and K. Svensson, (1991) J. Cell. Sci. **100**, 415–430.
14. D. J. Morré and L. Ovtracht (1977) Int. Rev. Cytol. **5**, 61–188.
15. F. A. Barr and G. Warren, (1996) Semin. Cell. Dev. Biol. **7**, 505–510.
16. G. Warren (1993) Annu. Rev. Biochem. **62**, 323–348.
17. G. Warren, T. Levine, and T. Misteli, (1995) Trends Cell Biol. **5**, 413–416.
18. G. Warren and W. Wickner (1996) Cell **84**, 395–400.
19. C. Rabouille, T. Misteli, R. Watson, and G. Warren (1995) J. Cell Biol. **129**, 605–618.
20. T. Misteli and G. Warren (1995) J. Cell Biol. **130**, 1027–1039.

21. T. P. Levine, C. Rabouille, R. H. Kieckbusch, and G. Warren (1996) J. Biol. Chem. **271**, 17304–17311.
22. N. Nakamura, M. Lowe, T. P. Levine, C. Rabouille, and G. Warren (1997) Cell **89**, 445–455.
23. S. M. Hurtley and A. Helenius (1989) Annu. Rev. Cell. Biol. **5**, 277–307.
24. C. Hammond and A. Helenius (1995) Curr. Opin. Cell. Biol. **7**, 523–529.
25. D. N. Hebert, B. Foellmer, and A. Helenius (1995) Cell **81**, 425–433.
26. E. J. Wiertz et al. (1996) Nature **384**, 432–438.
27. J. Roth (1987) Biochim. Biophys. Acta **906**, 405–436.
28. C. Niehrs, R. Beisswanger, and W. B. Huttner (1994) Chem. Biol. Interact. **92**, 257–271.
29. M. F. Schmidt (1989) Biochim. Biophys. Acta. **988**, 411–426.
30. D. F. Steiner, S. P. Smeekens, S. Ohagi, and S. J. Chan (1992) J. Biol. Chem. **267**, 23435–23438.
31. R. Kornfeld and S. Kornfeld (1985) Annu. Rev. Biochem. **54**, 631–664.
32. C. Rabouille et al. (1995) J. Cell. Sci. **108**, 1617–1627.
33. K. Sandhoff and G. van Echten (1994) Prog. Brain. Res. **101**, 17–29.
34. B. Becker, B. Bolinger, and M. Melkonian (1995) Trends Cell Biol. **5**, 305–307.
35. V. Malhotra, T. Serafini, L. Orci, J. C. Shepherd, and J. E. Rothman (1989) Cell **58**, 329–336.
36. T. Serafini, L. Orci, M. Amherdt, M. Brunner, R. A. Kahn, and J. E. Rothman (1991) Cell **67**, 239–253.
37. J. Moss and M. Vaughan (1995) J. Biol. Chem. **270**, 12327–12330.
38. A. Peyroche, S. Paris, and C. L. Jackson (1996) Nature **384**, 479–481.
39. J. B. Helms and J. E. Rothman (1992) Nature **360**, 352–354.
40. J. G. Donaldson, D. Finazzi, and R. D. Klausner (1992) Nature **360**, 350–352.
41. P. A. Randazzo, T. Terui, S. Sturch, H. M. Fales, A. G. Ferrige, and R. A. Kahn (1995) J. Biol. Chem. **270**, 14809–4815.
42. M. G. Waters, T. Serafini, and J. E. Rothman, (1991) Nature **349**, 248–251.
43. T. E. Kreis, M. Lowe, and R. Pepperkok (1995) Annu. Rev. Cell Dev. Biol. **11**, 677–706.
44. L. Y. Zhao et al. (1997) Proc. Natl. Acad. Sci. USA **94**, 4418–4423.
45. N. T. Ktistakis, H. A. Brown, M. G. Waters, P. C. Sternweis, and M. G. Roth (1996) J. Cell. Biol. **134**, 295–306.
46. J. Heuser and L. Evans, (1980) J. Cell. Biol. **84**, 560–583.
47. J. Ostermann et al. (1993) Cell **75**, 1015–1025.
48. E. Cukierman, I. Huber, M. Rotman and D. Cassel (1995) Science **270**, 1999–2002.
49. G. Tanigawa, L. Orci, M. Amherdt, M. Ravazzola, J. B. Helms, and J. E. Rothman (1993) J. Cell. Biol. **123**, 1365–1371.
50. S. Y. Bednarek, L. Orci, and R. Schekman (1996) Trends Cell Biol. **6**, 468–473.
51. C. Barlowe et al. (1994) Cell **77**, 895–907.
52. R. Schekman and L. Orci (1996) Science **271**, 1526–1533.
53. V. A. Bankaitis, J. R. Aitken, A. E. Cleves, and W. Dowhan (1990) Nature **347**, 561–562.
54. B. G. Kearns et al. (1997) Nature **387**, 101–105.
55. T. Sollner et al. (1993) Nature **362**, 318–324.
56. W. S. Trimble, D. M. Cowan, and R. H. Scheller (1988) Proc. Natl. Acad. Sci. USA **85**, 4538–4542.
57. M. Baumert, P. R. Maycox, F. Navone, P. De Camilli, and R. Jahn (1989) EMBO J. **8**, 379–384.
58. M. K. Bennett, N. Calakos, and R. H. Scheller (1992) Science **257**, 255–259.

59. Y. Goda (1997) Proc. Natl. Acad. Sci. USA **94**, 769–772.
60. G. Schiavo, O. Rossetto, and C. Montecucco (1994) Semin. Cell Biol. **5**, 221–229.
61. S. Ferro-Novick and R. Jahn, (1994) Nature **370**, 191–193.
62. J. B. Bock and R. H. Scheller (1997) Nature **387**, 133–135.
63. M. Sogaard et al. (1994) Cell **78**, 937–948.
64. A. Lupas (1997) Trends Biochem. Sci. **21**, 375–382.
65. G. A. Oyler et al. (1989) J. Cell Biol. **109**, 3039–3052.
66. P. Brennwald, B. Kearns, K. Champion, S. Keränen, V. Bankaitis, and P. Novick (1994) Cell **79**, 245–258.
67. S. K. Sapperstein, V. V. Lupashin, H. D. Schmitt, and M. G. Waters (1996) J. Cell Biol. **132**, 755–767.
68. Y. Hata, C. A. Slaughter, and T. C. Sudhof (1993) Nature **366**, 347–351.
69. M. K. Aalto, L. Ruohonen, K. Hosono, and S. Keranen (1991) Yeast **7**, 643–650.
70. V. V. Lupashin and M. G. Waters (1997) Science **276**, 1255–1258.
71. J. P. Lian, S. Stone, Y. Jiang, P. Lyons, and S. Ferro-Novick (1994) Nature **372**, 698–701.
72. K. Simons and M. Zerial (1993) Neuron **11**, 789–799.
73. C. Nuoffer and W. E. Balch (1994) Annu. Rev. Biochem. **63**, 949–990.
74. A. B. Dirac Svejstrup, T. Sumizawa, and S. R. Pfeffer (1997) EMBO J. **16**, 465–472.
75. O. Ullrich, H. Horiuchi, C. Bucci, and M. Zerial (1994) Nature **368**, 157–160.
76. T. Soldati, A. D. Shapiro, A. B. Svejstrup, and S. R. Pfeffer (1994) Nature **369**, 76–78.
77. E. S. Burstein and I. G. Macara (1992) Proc. Natl. Acad. Sci. USA **89**, 1154–1158.
78. T. J. Tan, P. Vollmer, and D. Gallwitz (1991) FEBS Lett. **291**, 322–326.
79. K. Fukui, T. Sasaki, K. Imazumi, Y. Matsuura, H. Nakanishi, and Y. Takai (1997) J. Biol. Chem. **272**, 4655–4658.
80. O. Ullrich, et al. (1993) J. Biol. Chem. **268**, 18143–18150.
81. S. Araki, A. Kikuchi, Y. Hata, M. Isomura, and Y. Takai (1990) J. Biol. Chem. **265**, 13007–13015.
82. M. R. Block and J. E. Rothman (1992) Methods Enzymol. **219**, 300–309.
83. D. O. Clary, I. C. Griff, and J. E. Rothman (1990) Cell **61**, 709–721.
84. D. W. Wilson, S. W. Whiteheart, M. Wiedmann, M. Brunner, and J. E. Rothman (1992) J. Cell Biol. **117**, 531–538.
85. T. Sollner, M. K. Bennett, S. W. Whiteheart, R. H. Scheller, and J. E. Rothman (1993) Cell **75**, 409–418.
86. A. Mayer, W. Wickner, and A. Haas (1996) Cell **85**, 83–94.
87. A. Morgan and R. D. Burgoyne (1995) EMBO J. **14**, 232–239.
88. J. M. Peters, M. J. Walsh, and W. W. Franke (1990) EMBO J. **9**, 1757–1767.
89. C. Rabouille, T. P. Levine, J. M. Peters, and G. Warren (1995) Cell **82**, 905–914.
90. U. Acharya, R. Jacobs, J. M. Peters, N. Watson, M. G. Farquhar, and V. Malhotra (1995) Cell **82**, 895–904.
91. F. T. Wieland, M. L. Gleason, T. A. Serafini, and J. E. Rothman (1987) Cell **50**, 289–300.
92. P. Quinn, G. Griffiths, and G. Warren (1984) J Cell Biol **98**, 2142–2147.
93. W. E. Balch, J. M. McCaffery, H. Plutner, and M. G. Farquhar (1994) Cell **76**, 841–852.
94. C. Arar, V. Carpentier, J. P. Lecaer, M. Monsigny, A. Legrand, and A. C. Roche (1995) J. Biol. Chem. **270**, 3551–3553.
95. K. Fiedler and K. Simons (1996) J. Cell Sci. **109**, 271–276.
96. E. J. Tisdale, H. Plutner, J. Matteson, and W. E. Balch (1997) J. Cell Biol. **137**, 581–593.

97. F. Schimmoller, B. Singer Kruger, S. Schroder, U. Kruger, C. Barlowe, and H. Riezman (1995) EMBO J. **14**, 1329–1339.
98. M. A. Stamnes et al. (1995) Proc. Natl. Acad. Sci. **92**, 8011–8015.
99. M. J. Kuehn, R. Schekman, and P O. Ljungdahl (1996) J. Cell Biol. **135**, 585–595.
100. K. Fiedler, M. Veit, M. A. Stamnes, and J. E. Rothman (1996) Science **273**, 1396–1399.
101. K. Sohn et al. (1996) J. Cell Biol. **135**, 1239–1248.
102. S. Kornfeld and I. Mellman (1989) Annu. Rev. Cell Biol. **5**, 483–525.
103. T. L Burgess and R. B. Kelly (1987) Annu. Rev. Cell Biol. **3**, 243–293.
104. S. R. Pfeffer and J. E. Rothman (1987) Annu. Rev. Biochem. **56**, 829–852.
105. R. Kornfeld (1992) Annu. Rev. Biochem. **61**, 307–330.
106. A. Hille Rehfeld (1995) Biochim. Biophys. Acta **1241**, 177–194.
107. M. S. Robinson (1992) Trends Cell Biol. **2**, 293–297.
108. M. S. Robinson, (1994) Curr. Opin. Cell Biol. **6**, 538–544.
109. G. Griffiths, B. Hoflack, K. Simons, I. Mellman, and S. Kornfeld (1988) Cell **52**, 329–341.
110. S. Honing and W. Hunziker (1995) J. Cell Biol. **128**, 321–332.
111. W. B. Huttner et al. (1995) Cold Spring Harbor Symp. Quantit. Biol. **LX**, 315–327.
112. S. A. Tooze (1991) FEBS Lett **285**, 220–224.
113. P. Scheiffele, J. Peranen, and K. Simons (1995) Nature **378**, 96–98.
114. K. E. Mostov and M. H. Cardone (1995) Bioessays **17**, 129–138.
115. K. Matter and I. Mellman (1994) Curr. Opin. Cell Biol. **6**, 545–554.
116. K. Simons and E. Ikonen (1997) Nature **387**, 569–572.
117. C. E. Machamer (1991) Trends Cell Biol. **1**, 141–144.
118. T. Nilsson et al. (1994) EMBO J. **13**, 562–574.
119. M. S. Bretscher and S. Munro (1993) Science **261**, 1280–1281.
120. H. R. Pelham and S. Munro (1993) Cell **75**, 603–605.
121. G. Warren (1987) Nature **327**, 17–18.
122. J. E. Rothman (1981) Science **213**, 1212–1219.
123. S. Munro and H. R. Pelham (1987) Cell **48**, 899–907.
124. M. R. Jackson, T. Nilsson, and P. A. Peterson (1990) EMBO J. **9**, 3153–3162.
125. M. P. Schutze, P. A. Peterson, and M. R. Jackson (1994) EMBO J. **13**, 1696–1705.
126. D. J. Sweet and H. R. B. Pelham (1992) EMBO J. **11**, 423–432.
127. J. C. Semenza, K. G. Hardwick, N. Dean, and H. R. B. Pelham (1990) Cell **61**, 1349–1357.
128. B. L. Tang, S. H. Wong, X. L. Qi, S. H. Low, and W. Hong (1993) J. Cell Biol. **120**, 325–328.
129. M. J. Lewis and H. R. Pelham (1992) Cell **68**, 353–364.
130. B. Sönnichsen, R. Watson, H. Clausen, T. Misteli, and G. Warren, (1996) J. Cell Biol. **134**, 1411–1425.
131. D. W. Wilson, M. J. Lewis, and H. R. B. Pelham (1993) J. Biol. Chem. **268**, 7465–7468.
132. P. Cosson and F. Letourneur (1994) Science **263**, 1629–1631.
133. F. Letourneur et al. (1994) Cell **79**, 1199–1207.
134. M. H. Hoe, P. Slusarewicz, T. Misteli, R. Watson, and G. Warren (1995) J. Biol. Chem. **270**, 25057–25063.
135. S. L. Harris and M. G. Waters (1996) J. Cell Biol. **132**, 985–998.
136. A. S. Dittie, N. Hajibagheri, and S. A. Tooze (1996) J. Cell Biol. **132**, 532–536.
137. M. J. Lewis and H. R. Pelham (1996) Cell **85**, 205–215.
138. D. T. Shima, H. Haldar, R. Pepperkok, R. Watson, and G. Warren (1997) J. Cell Biol. **137**,

1211–1228.
139. B. J. Nichols, C. Ungermann, H. R. B. Pelham, W. T. Wickner, and A. Haas (1997) Nature **387**, 199–202.

Suggestions for Further Reading

140. H. R. B. Pelham (1989) Control of protein exit from the endoplasmic reticulum. Annu. Rev. Cell Biol. **5**, 1–23.
141. N. K. Pryer, L. J. Wuestehube, and R. Schekman (1992) Vesicle-mediated protein sorting. Annu. Rev. Biochem. **61**, 471–516.
142. J. E. Rothman and G. Warren (1994) Implications of the SNARE hypothesis for intracellular membrane topology and dynamics. Curr. Biol. **4**, 220–233.
143. S. R. Pfeffer (1996) Transport vesicle docking: SNAREs and associates. Annu. Rev. Cell Dev. Biol. **12**, 441–461.
144. J. E. Rothman and F. T. Wieland (1996) Protein sorting by transport vesicles. Science **272**, 227–234.

GPI Anchor

A large number of proteins on the surfaces of eukaryotic cells are covalently linked to a glycosylphosphatidylinositol (GPI) molecule (Table 1). GPI molecules consist of a glycan chain that, contains ethanolamine, glucosamine, and mannose residues linked to the inositol ring of phosphatidylinositol (Fig. 1). The ethanolamine in the GPI molecule is amide-linked to the carboxyl-terminal amino acid residue of the protein after it is translocated across the membrane of the endoplasmic reticulum. The GPI molecule is embedded in the lipid bilayer and is the membrane anchor responsible for retaining the protein at the cell surface. GPI-anchored proteins can be released from the membrane by highly specific phospholipases that cleave the GPI molecule. The complex structure of the GPI molecule (Fig. 1), compared to the other lipids used as membrane anchors, suggests that it has additional functions.

Figure 1. Structure of the GPI anchor. The C-terminal residue of a protein is attached via an amide linkage to the amino group of an ethanolamine phosphate in the GPI molecule (1). A conserved glycan backbone connects the ethanolamine phosphate to the phosphatidylinositol moiety. For simplicity, the sugar residues in the glycan are shown as hexagons. The exact linkages between the sugars and with the phosphatidylinositol and ethanolamine phosphate moieties (i.e., EtNP-6Mana1-2Mana1-6Mana1-4GlcNa1-6*myo*inositol), are highly conserved between protozoa and mammals. In contrast, the side chains (shown as X, Y, and Z) that are attached to the mannose residues in the glycan backbone are highly variable and can contain a variety of other sugars and additional ethanolamine phosphate groups. The hydrophobic part of the phosphatidylinositol (which will be embedded in the lipid bilayer) is shown as a 1-alkyl, 2-acyl structure, although 1,2-diacylglycerol, 1-alkylglycerol, or ceramide are also found. The hydrocarbon chain length and degree of unsaturation are also highly variable among proteins (the example shown here is for human folate-binding protein). The inositol ring can also become acylated (not shown), which makes the GPI anchor insensitive to degradation by PI-phospholipase C (PI-PLC). The sites of action of two different phospholipases that cleave GPI anchors are also shown. PI-PLC is a phospholipase C that can also cleave phosphatidylinositol and is produced by several different pathogenic bacteria [see Phospholipases C]. Although PI-PLC is not involved in physiological release processes, it is widely used in identifying and experimentally manipulating GPI-anchored proteins on cell surfaces. GPI-PLD is a GPI-specific phospholipase D and cannot hydrolyze phosphatidylinositol. GPI-PLD is abundant in mammalian plasma and may be involved in physiologically releasing GPI-anchored proteins from cell surfaces. Ins = *myo*inositol, GlcN = glucosamine, Man = mannose, EtNP = ethanolamine phosphate.

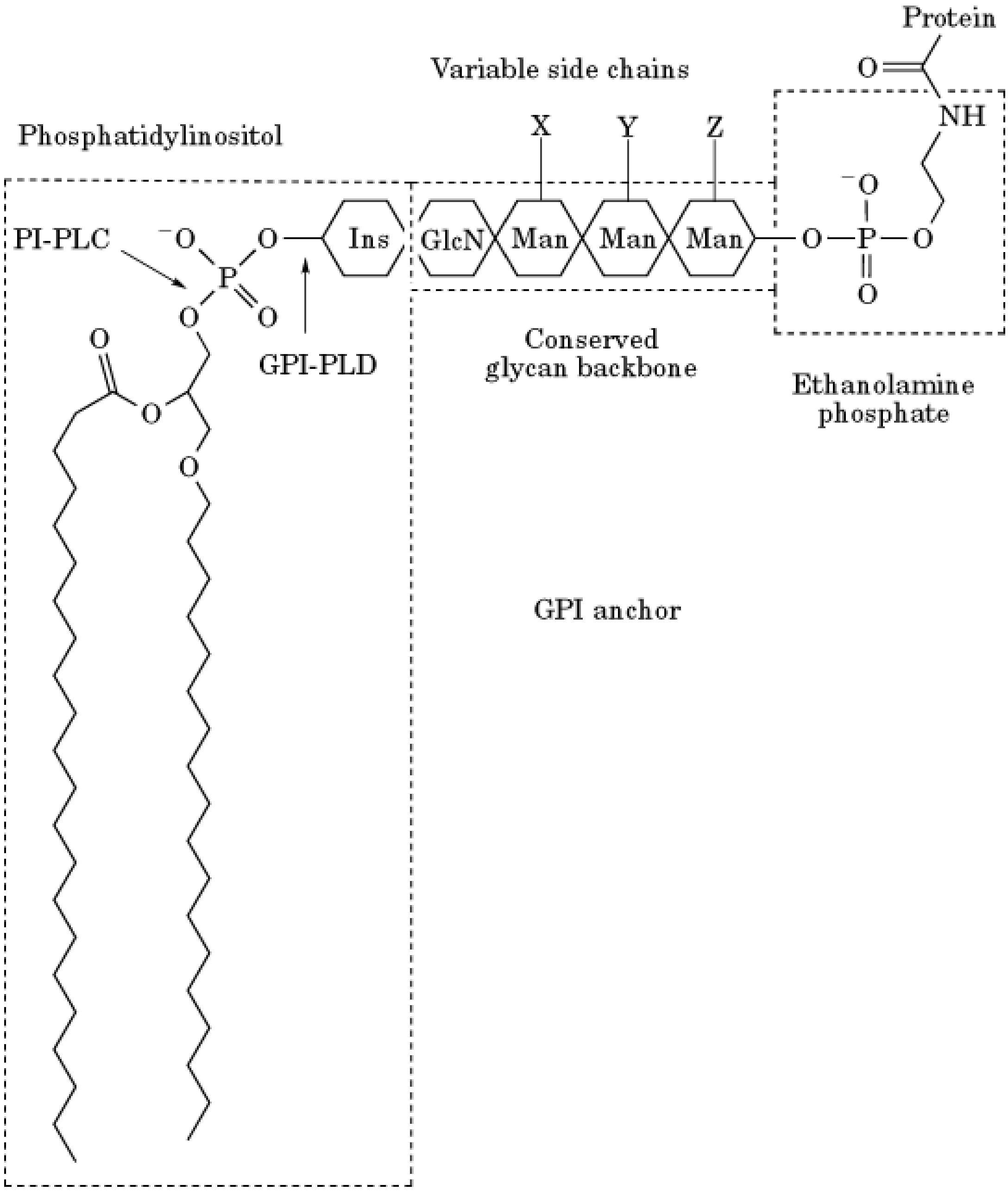

Table 1. Examples of GPI-Anchored Proteins

Alkaline phosphatase and many other ectoenzymes
Variant surface protein of *Trypanosoma brucei*
Heparan sulfate proteoglycan
Scrapie prion protein
Thy-1
TAG-1 and other neural adhesion molecules
Carcinoembryonic antigen
Decay accelerating factor

Folate binding protein
Numerous CD antigens (e.g., CD14, CD16,CD58, CD59, etc.)

Biosynthesis of GPI-anchored proteins takes place in two main stages: (1) The GPI molecule is synthesized by sequential addition of the glycan chain components to a phosphatidylinositol molecule at the cytoplasmic surface of the endoplasmic reticulum. Then, the GPI molecule is translocated across the membrane of the endoplasmic reticulum to the lumenal surface (1-3). (2) The protein is translocated, cotranslationally, into the endoplasmic reticulum. The C-terminal region of the protein contains a special type of "GPI signal peptide" that is recognized and removed by an enzyme (believed to be a transamidase) located on the lumenal surface of the endoplasmic reticulum (4). The same enzyme catalyzes coupling of the terminal ethanolamine of the GPI molecule to the newly exposed carboxyl group in an amide linkage. The attachment process is completed within a few minutes of translation/translocation, and then the GPI-anchored protein is transported through the Golgi apparatus to the cell surface by the conventional **vesicle** transport mechanisms used by other plasma membrane proteins. It should be emphasized that relatively little direct biochemical information is available about the attachment process. Efficient GPI attachment may require precise spatial and temporal coordination of the transamidase with the special GPI signal peptide of the protein and translocation of the GPI precursor. Probably for that reason, reconstitution of GPI-anchoring *in vitro* from purified components presents a formidable technical challenge.

Unlike the other types of lipid anchor, the residue to which the GPI becomes attached (designated site w; see later) is quite variable and relatively difficult to identify from just the amino acid sequence of the protein. Nevertheless, rules for predicting the existence and the location of GPI anchors in a novel protein have been devised on the basis of two sources of information from about twenty naturally occurring, GPI-anchored proteins: (1) comparison of the protein sequence predicted from its gene sequence with the identity of the C-terminal residue in the mature protein, and (2) extensive mutational analysis of the C-terminal region of a limited number of model proteins (4). This region can be divided into three parts:

1. *Hydrophobic C-terminus*. A **hydrophobic** C-terminus is essential for GPI-anchoring, although the minimum number of hydrophobic residues required for GPI-anchoring is quite variable among proteins. In most known GPI-anchored proteins, the hydrophobic region is about 15 to 20 residues long, but it can be as short as eight residues. At first sight this region looks like a hydrophobic polypeptide anchor (see Membrane Anchors), and it may in fact serve this temporary function for the short interval between completion of translation/translocation and attachment of the GPI molecule. Polypeptide anchors are generally a few residues longer, however, and usually terminate in relatively hydrophilic residues. Furthermore, mutations that make this region more like a polypeptide anchor usually result in poor GPI anchoring.
2. *Hydrophilic region*: A hydrophilic region of approximately five to seven residues is located between the hydrophobic region and the attachment site. This region exhibits no strong preference for particular amino acid residues.
3. *Cleavage-GPI attachment site*: There is no strong **consensus sequence**, but there are definite amino acid preferences in the vicinity of the cleavage site: Site w (which becomes the C-terminal residue in the mature protein): Gly, Ala, Ser, Cys, Asp, and Asn preferred. Site w + 1: no preference. Site w + 2: Gly, Ala and Ser preferred. A statistical application of the w/w + 2 preferences predict the attachment site in naturally occurring proteins with approximately 80% accuracy. Apart from its predictive value, this information can be used for engineering novel GPI-anchored proteins. Thus, constructing chimeric polypeptides that contain the extracellular domain of a polypeptide-anchored protein and a GPI signal peptide has permitted expressing many proteins in a GPI-anchored form on the cell surface.

The proteins that use a GPI anchor are quite varied. More than 100 different GPI-anchored proteins have been identified (see Table 1for examples). There is, however, no strong correlation of GPI-anchoring with particular types of protein function. For example, cell surface enzymes and adhesion molecules are found in both GPI-anchored and polypeptide anchored forms. Furthermore, although the potential for reversible membrane binding provided by a lipid anchor is useful for regulating protein distribution inside a cell, it would permit continuous loss of proteins from the cell surface (for a general discussion of factors that can affect membrane affinity of lipid-anchored proteins see Membrane Anchors). It is not known why cell surface proteins use the complex GPI molecule instead of the relatively simple lipid anchors used by cytosolic proteins. Two biophysical properties of the GPI anchor, however, may help to reduce dissociation from the cell surface: (1) The GPI anchor usually contains two relatively long (i.e., >16-carbon) unbranched acyl or alkyl chains, which in combination would have relatively high affinity for the membrane (see Fig. 1). (2) Unlike other types of lipid anchors, there is a long and relatively flexible linking molecule, the glycan backbone (see Fig. 1) between the lipid in the bilayer and the protein. This type of linkage reduces the entropy cost of membrane binding because there are minimal restrictions on translational and rotational motion of the protein (see Membrane Anchors).

Although their functional advantages are uncertain, GPI anchors confer some unusual and well-studied properties on cell-surface proteins: (1) GPI anchors are hydrolyzed by specific phospholipases that remove the hydrophobic lipid group, resulting in a protein that is no longer anchored to the membrane (see Fig. 1). GPI-phospholipase D is a secreted enzyme present in mammalian tissues and plasma and could release proteins from the cell surface. The mechanisms by which this enzyme is regulated are unknown, however (5). (2) Under some conditions, GPI-anchored proteins associate preferentially with particular types of lipid molecule in the membrane lipid bilayer. It has been suggested that GPI-anchored proteins are clustered in particular regions at the cell surface (e.g., microdomains and caveolae), but the size, composition, and functional significance of the clusters are controversial (6). (3) Cross-linking GPI-anchored proteins on the cell surface produces an activating signal in some cell types (7). Because the lipid anchor does not cross the membrane, the mechanism by which the signal is transmitted, and its possible connection to microdomains is currently an area of considerable research interest. (4) In spite of the high membrane affinity of the anchor, GPI-anchored proteins can transfer from one cell to another both *in vitro* and *in vivo* (8, 9). The precise mechanism of this process and its physiological significance are unknown. Intercellular transfer is of considerable therapeutic interest, however, because it offers a relatively efficient method for inserting novel GPI-anchored proteins (natural or engineered) into the surface of a patient's cells *ex vivo* (10).

Bibliography

1. M. J. McConville and M. A. J. Ferguson (1993) Biochem. J. **294**, 305–324.
2. V. L. Stevens (1995) Biochem. J. **310**, 361–370.
3. J. Vidugiriene and A. K. Menon (1994) J. Cell Biol. **127**, 333–341.
4. S. Udenfriend and K. Kodukula (1995) Annu. Rev. Biochem. **64**, 563–591.
5. J.-Y. Li, K. Hollfelder, K.-S. Huang, and M. G. Low (1994) J. Biol. Chem. **269**, 28963–28971.
6. S. Mayor, K. G. Rothberg, and F. R. Maxfield (1994) Science **264**, 1948–1951.
7. D. Brown (1993) Curr. Opinion Immunol. **5**, 349–354.
8. J. L. Miller, M. Giattina, E. J. Blanchette Mackie , and N. K. Dwyer (1998) J. Lab. Clin. Med., **131**, 215–221.
9. S. Ilangumaran, P. J. Robinson, and D. C. Hoessli (1996) Trends Cell Biol. **6**, 163–167.
10. M. E. Medof, S. Nagarajan, and M. L. Tykocinski (1996) FASEB J. **10**, 574–586.

Suggestions for Further Reading

11. M. G. Low (1989) The glycosyl-phosphatidylinositol anchor of membrane proteins, Biochim.

Biophys. Acta **988**, 427–454.
12. M. C. Field and A. K. Menon (1993) In *Lipid Modifications of Proteins* (M. J. Schlesinger, ed.), CRC Press, Boca Raton, pp. 83–134.
13. T. Kinoshita, N. Inoue, and J. Takeda (1995) Defective glycosyl phosphatidylinositol anchor synthesis and paroxysmal nocturnal hemoglobinuria, Adv. Immunol. **60**, 57–103.
14. P. J. Casey and J. E. Buss (eds.) (1995) "Lipid modifications of proteins", In *Methods in Enzymology* **250**, Academic Press, New York.
15. S. Ilangumaran and D. C. Hoessli (1998) *Glycosylphosphatidylinositol-Anchored Biomolecules*, R. G. Landes, Austin, TX.

Gram-Negative Bacteria

Two different groups of bacteria can be distinguished on the basis of the differential Gram-staining. Gram-Positive Bacteria appear bluish-purple, while Gram-negative bacteria are red. The different reactions to Gram-staining are caused by differences in the cell wall structure and composition.

1. The staining procedure and its history

The Danish physician Hans Christian Gram (1853–1938), by profession a pharmacologist and internist, worked temporarily with Friedländer in Berlin and described in 1884 (1) the staining of micrococci in lung tissues with Ehrlich's anilin-water solution of crystal methyl (gentian) violet, a cationic dye. After staining, the preparations were treated with Lugol's solution of iodine in potassium iodide and finally flushed with alcohol briefly. The bluish-purple color was retained by the Gram-positive cocci but discharged from the Gram-negative bacteria. Gram used Bismarckbraun or vesuvin for the counterstain. This method has been modified by many workers, but its essence remains unaltered, and it is still one of the widely used methods of differential staining in bacteriology. At present, the destained Gram-negative bacteria are counterstained with a red dye, e.g. safranin or fuchsin, to make a contrast between the Gram-positive and Gram-negative bacteria (2).

The crystal violet-iodine complex formed during Gram-staining is retained by the cell wall of Gram-positive bacteria, most particularly by the thick layer of peptidoglycan (murein). It is extracted from Gram-negative cells, and from Gram-positive cells of which the peptidoglycan has been removed or loosened by enzymatic (murein hydrolases or peptidases), mechanical, or antibiotic treatment. If the film of Gram-negative cells is too thick, or the bacteria are locally clumped together, the decolorization with alcohol will not be complete. Textbooks mention several exceptions to the rule, and some bacteria are described as being variable in the Gram reaction. Reliable results are dependent on standardization of the preparation of the bacterial films on slides and of performance of the staining procedure. In staining for transmission electron microscopy and energy-dispersive X-ray spectroscopy, the treatment with Gram's iodine solution has been replaced by treatment with trichloro(h^2-ethylene) platinate (3).

2. The Gram-negative cell envelope

The cell envelope of Gram-negative bacteria, eg, the proteobacteria *Escherichia coli* and *Pseudomonas fluorescens*, consists of an outer membrane, which surrounds the periplasm, and the cytoplasmic or inner membrane, which delimits the protoplast. In electron microscopic pictures of thin sections, the two membranes have similar appearances. The space between the outer and the cytoplasmic membranes, the periplasm, contains soluble proteins (enzymes and components of the transport machinery) and the murein sacculus. The latter is a single-layered peptidoglycan network. Peptidoglycan is a characteristic cell-wall component of nearly all eubacteria (bacteria) but not of Archaebacteria (Archaea), and is shown schematically in Fig. 1. Its main function is to preserve the shape and integrity of the cell and to withstand the osmotic pressure of the protoplast. Peptidoglycan consists of long linear glycan chains interlinked with short peptide bridges. The chemical structure and the sequences of aminosugars and of amino acids of the peptide portion are conserved in most Gram-negative bacteria, but can vary in specific taxa, especially in Gram-positive bacteria.

Figure 1. Structure of the peptidoglycan of *Escherichia coli*. N-Acetylglucosamine (GlcNAc) and N-acetylmuramic acid (MurNAc) are interlinked in an alternating sequence by b-1,4 glycosidic bonds forming polysaccharide chains that are crosslinked by peptides consisting of L- and D-alanine, D-**glutamic acid** and *m*-diaminopimelic acid (*m*-A $_2$pm). Murein hydrolases cleave specific bonds: muraminidase; Ý b-N-acetylglucosaminidase;

D,D-carboxypeptidase;

D,D- endopeptidase;

L,D-carboxypeptidase; > N-acetylmuramyl-L-alanine amidase; after J-V Höltje and EI Tuomanen (1991) J. Gen. Microbiol. 137:441–454

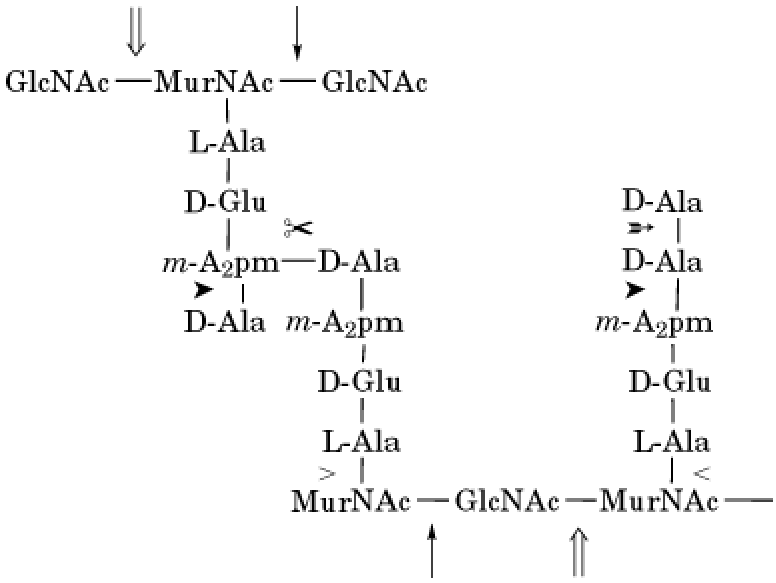

The disaccharide-peptide monomer is synthesized in the cytoplasm as the UDP-activated form and is translocated as N-acetylglucosamine (GlcNAc) b-1,4 N-acetylmuramic acid-(MurNAc)-pentapeptide-pyrophosphoryl-undecaprenol across the cytoplasmic membrane. In a highly controlled process, the precursor is inserted into the murein sacculus by transglycosylation in the glycan chain and subsequent crosslinking by transpeptidation between the penultimate D-alanine residue of one subunit and the *meso*-L-diaminopimelyl residue of another subunit, with release of the terminal alanine (see Fig. 1 and Penicillin-Binding Proteins). Extension of the murein sacculus is the result of a well-regulated balance between lytic and synthetic enzymatic reactions (4). Termination of the glycan strands by formation of a 1,6-anhydro-N-acetylmuramic acid residue is coupled to dephosphorylation of the undecaprenyl-P-P to undecaprenyl-P, which cycles back into the cytoplasm.

The outer membrane is organized asymmetrically. The inner leaflet consists of phospholipids, as in the cytoplasmic membrane. The major component of the outer leaflet is the lipopolysaccharide (LPS), a glycolipid that is anchored in the outer membrane by lipid A. Lipid A is the conservative part of LPS at least in Enterobacteriaceae, eg *Salmonella*, *Shigella*, *Escherichia*, *Enterobacter*, *Klebsiella* etc. and is responsible for the physiological effects of LPS in the infected host cell (endotoxin). The structure of lipid A is shown in Fig. 2(**b**). Lipid A is joined to the core of LPS, which is a spacer to the outermost and variable part of LPS, the O-specific polysaccharide. The latter is the major antigenic determinant of Gram-negative bacteria; it consists of long chains of repeating units of oligosaccharides (Fig. 2**a**). The lipophilic character of the outer membrane is presumably responsible for the exclusion of cell-damaging compounds like the bile salts of the intestine. In several bacteria, the LPS functions as a receptor for bacteriophages, eg **T_4 phage**. The core-lipid A and O-antigen subunits are synthesized as activated precursors in the cytoplasm at the cytoplasmic membrane and exported, attached to bactoprenol pyrophosphate, to the periplasm and the outer membrane (5).

Figure 2. Schematic structure of *E. coli* K-12 lipopolysaccharide (LPS). (**a**) The three parts of LPS and the sugar compositions of the core and O-specific chains. Gal, D-galactose; GlcN, D-glucosamine; Kdo, 3-deoxy-D-*manno*-octulosonic acid; Hep, L-*glycero*-D-*manno* -heptose; GlcNAc, N-acetyl-D-glucosamine; Rha, L-rhamnose; Gal*f*, D-galactofuranose; P, phosphate; P-Etn, phosphoethanolamine; Ac, acetate. (**b**) Structure of lipid A from *E. coli*. The b,1′-6-linked disaccharide of glucosamine is acylated, phosphorylated, and glycosylated with Kdo; the fatty acid residues bound to the disaccharide are laurate and myristate; after C.R.H. Raetz, Figs. 3 and 18A, in F.C. Neidhardt et al., eds., (1996) *Escherichia coli* and *Salmonella*, pp. 1035–1063. ASM Press.

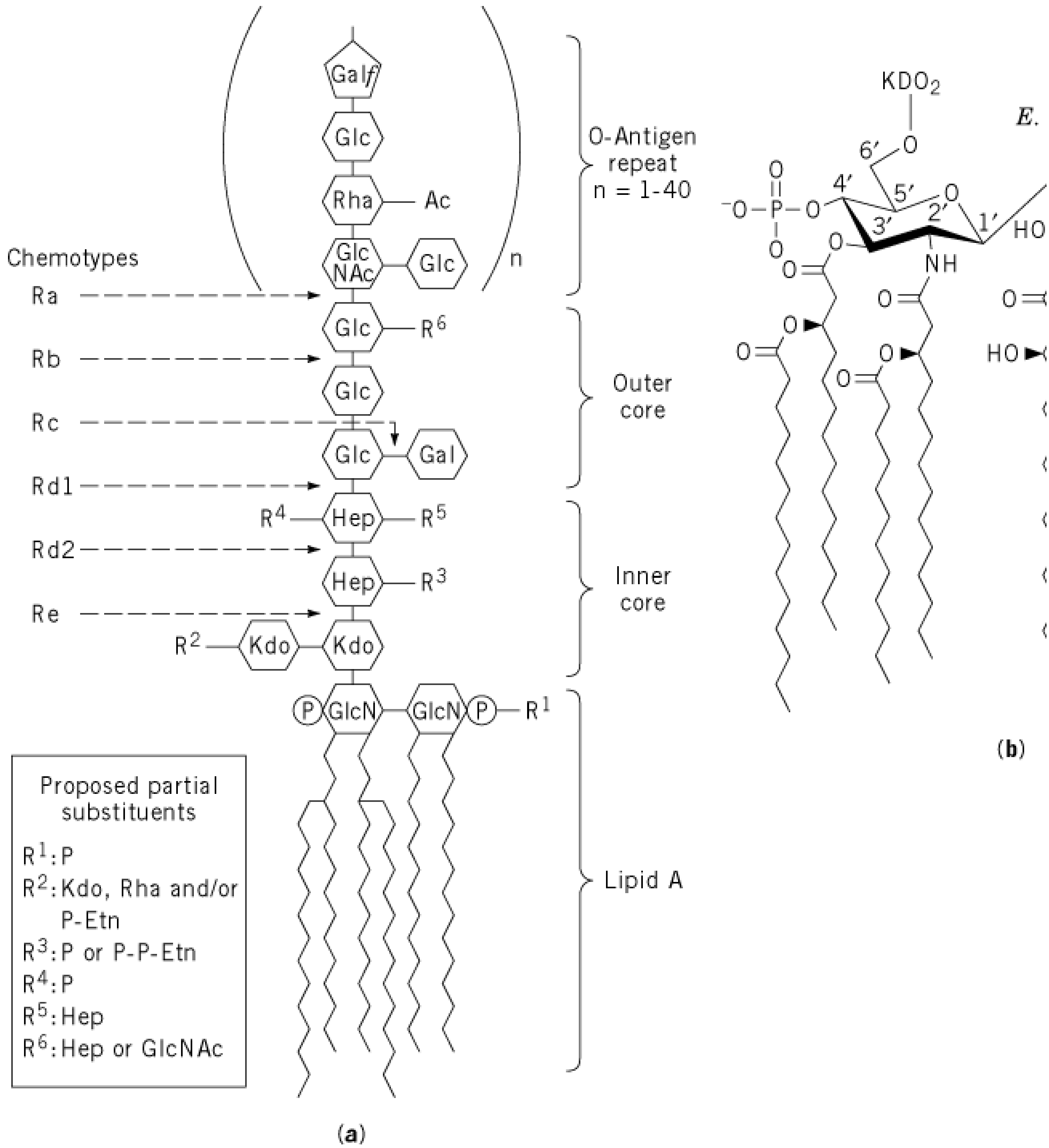

Porins are transmembrane proteins formed of three identical subunits of b-barrels with short alpha-helical domains (see Alpha-helix). They are channels for the entrance and exit of small hydrophilic substances. Some porins are highly substrate-specific. Other outer membrane proteins function as phage receptors or mediate export and import. Covalently bound to peptidoglycan is the lipoprotein. Lipoproteins contain lipids covalently linked to an N-terminal cysteine residue.

The biosynthesis of all the macromolecular components of peptidoglycan and outer membrane starts in the cytoplasm. The pre-proteins and the precursors or building blocks of peptidoglycan or polysaccharides are exported across the cytoplasmic membrane by specific transport systems and are assembled in the periplasm or outer membrane. The energy for assembly cannot be provided in the periplasm by sources of the cytoplasm, so the precursors have to be in an activated state. The precursors of LPS, peptidoglycan, and capsular polysaccharides are transported using undecaprenol phosphate as a cofactor (5).

3. Taxonomy

Although all Gram-negative bacteria have basically the same cell wall structure, they do not form a homogenous taxonomical group. The systematics, and especially the phylogenetic relationships (see Phylogeny) between the bacteria, are based on different principles and features (6, 7). The Gram-reaction, ie the cell-wall type, is only one, but an important, feature of a genus or species, and there are exceptions to the rule. The cyanobacteria, which perform an oxygenic type of photosynthesis, contain a typical outer membrane with LPS. But the murein sacculus is thicker than that of proteobacteria, and in some species a polysaccharide is bound covalently to the murein. This may be one reason why several cyanobacteria stain Gram-positive.

The Gram-negative archaebacteria have cell walls of different composition; these are methanochondroitin ($[4 \rightarrow] - \beta; -\mathrm{D} - \mathrm{GluUA} - [1 \rightarrow 3] - \mathrm{D} - \mathrm{GalNAc} - [1 \rightarrow 3 \text{ or } 4] - D - \mathrm{GalNAc}-$ in *Methanosarcina*), glycoproteins, or heteropolysaccharides composed of uronic acids containing sulfate, glucose, galactose, N-acetygalactosamine, glycine, mannose, and N-acetyl-gulosaminuronic acid groups (3, 7).

Bibliography

1. H. C. Gram (1884) Fortschritte der Medizin **2**, 185–189
2. P. Gerhardt, R. G. E. Murray, W. A. Wood, and N. R. Krieg (1994) *Methods for General and Molecular Bacteriology*, Am. Soc. Microbiol., Washington, D.C., pp. 31–32.
3. T. J. Beveridge and S. Schultze-Lam (1996) Microbiology **142**, 2887–2895.
4. J.-V. Höltje (1998) Microbiol. Mol. Rev. **62**, 181–203.
5. C. R. H. Raetz (1996) *Escherichia coli* and *Salmonella* (F. C. Neidhardt et al., eds.), ASM Press, Washington, D.C., pp. 1035–1063.
6. J. G. Holt, N. R. Krieg, P. H. A. Sneath, J. T. Staley, and S. T. Williams (1994) *Bergey''s Manual of Determinative Bacteriology*, 9th ed., Williams & Wilkins, Baltimore.
7. E. Stackebrandt (1999) *Biology of the Prokaryotes* (J. Lengeler, G. Drews, and H. G. Schlegel, eds.), Thieme Verlag, Stuttgart, pp. 674–720.

Bibliography

1. H. C. Gram (1884) Fortschritte der Medizin **2**, 185–189
2. P. Gerhardt, R. G. E. Murray, W. A. Wood, and N. R. Krieg (1994) *Methods for General and Molecular Bacteriology*, Am. Soc. Microbiol., Washington, D.C., pp. 31–32.
3. T. J. Beveridge and S. Schultze-Lam (1996) Microbiology **142**, 2887–2895.
4. J.-V. Höltje (1998) Microbiol. Mol. Rev. **62**, 181–203.
5. C. R. H. Raetz (1996) *Escherichia coli* and *Salmonella* (F. C. Neidhardt et al., eds.), ASM Press, Washington, D.C., pp. 1035–1063.
6. J. G. Holt, N. R. Krieg, P. H. A. Sneath, J. T. Staley, and S. T. Williams (1994) *Bergey's Manual of Determinative Bacteriology*, 9th ed., Williams & Wilkins, Baltimore.
7. E. Stackebrandt (1999) *Biology of the Prokaryotes* (J. Lengeler, G. Drews, and H. G. Schlegel, eds.), Thieme Verlag, Stuttgart, pp. 674–720.

Gram-Positive Bacteria

Gram-positive bacteria appear bluish-purple in the Gram stain, while Gram-Negative Bacteria are red. The crystal violet-iodine complex formed during Gram-staining is retained by the cell wall of Gram-positive bacteria.

Gram-positive eubacteria (bacteria) are found in several taxonomic groups. Typical representatives are both endospore-forming and nonsporing rods of the genera *Bacillus, Clostridium, Arthrobacter, Lactobacillus, Mycobacterium, Nocardia* and *Streptomyces*. A few archaebacteria (Archaea), such as *Methanobacterium formicicum*, also stain Gram-positive. The Gram reaction depends on both the structural formats and the chemical composition of the cell envelope (see Gram-Negative Bacteria). Gram-positive bacteria have a broader range of cell-wall types than do Gram-negative bacteria (1).

1. Type I Gram-positive cell wall

This type of cell wall consists of a thick peptidoglycan layer mixed with teichoic acids. Peptidoglycan (murein) is a polymer of glycan strands of N-acetyl-D-glucosamine and N-acetylmuramic acid linked in alternating sequence by b-1,4 linkages. The glycan strands are cross-linked by peptide chains of varying complexity, which are bound in amide links to the carboxyl group of the lactic acid residue of muramic acid (Fig. 1**a**). In Gram-positive bacteria, the amino acid composition of the peptides cross-linking the glycan strands (interpeptide bridges; Fig. 1**a**) vary considerably. In these interpeptide bridges, D-amino acids dominate, while aromatic, branched-chain, and sulfur-containing amino acids, plus histidine, arginine, and proline, are absent. In the tetrapeptide of Gram-positive bacteria, diaminopimelic acid can be replaced by lysine.

Figure 1. Schematic structure of polymers in cell walls of Gram-positive bacteria. A. Peptidoglycan with an polyglycine interpeptide bridge, $[Gly]_5$ in *Staphylococcus aureus.* B. Teichoic acid of the ribitol-phosphate type. C. Lipoprotein with fatty acids (R_1 to R_3) linked directly or via glycerol to the terminal cysteinyl residue.

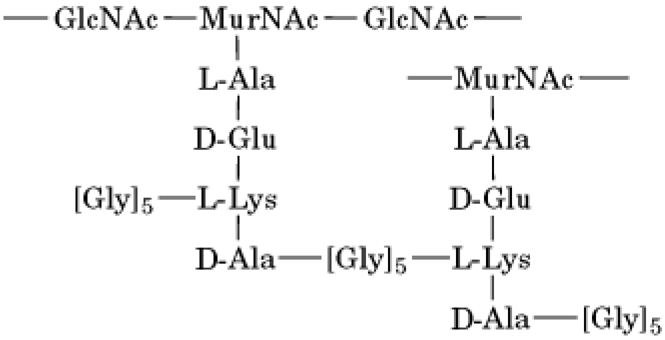

A

B

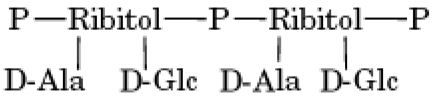

C

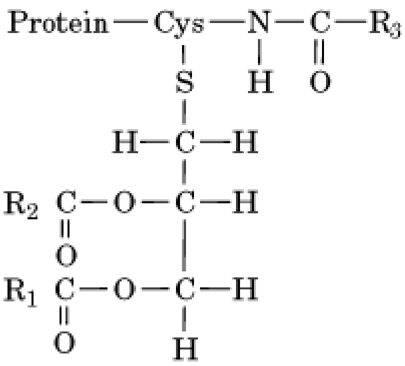

Teichoic acids are polymers consisting of glycerol phosphate or ribitol phosphate that are substituted with sugars and/or amino acids (Fig. 1**b**). They are covalently bound to the peptidoglycan and are exposed on the cell surface. Several Gram-positive bacteria produce, in addition to teichoic acids, *lipoteichoic acids*, which are not covalently bound to peptidoglycan but are associated with the cytoplasmic membrane through **hydrophobic** interactions. They consist of poly C1-3-glycerol phosphate linked to diglucosyl-1-3-diacylglycerol. Lipoteichoic acid penetrates the peptidoglycan and reaches the cell surface. *Teichuronic acids* of Gram-positive bacteria contain hexuronic acids (glucoronic acid or N-acetylmannosamine uronic acid) instead of polyol phosphate. Teichoic, teichuronic, and lipoteichoic acids are highly-charged polymers. Lipoproteins are present in both Gram-negative and Gram-positive cell walls. The terminal cysteine residue of the protein moiety is bound to fatty acids directly or via glycerol residues (Fig. 1**c**). Proteins are also constituents of the Gram-positive cell wall, eg **porins** and surface layer-forming proteins.

Activated precursors of the cell wall polymers are transferred across the cytoplasmic membrane (CM) bound to undecaprenol phosphate (undec-P), which was synthesized from mevalonic acid. The undec-P is recycled via undec-P-P and undec.

2. Type II Gram-positive cell wall

This type of cell wall is represented by the *Corynebacterium-Mycobacterium-Nocardia* group of bacteria. These bacteria have a thick peptidoglycan layer that is, however, penetrated by glycolipids. The muramic acid may be N-glycosylated. Long chains of *lipoarabinomannan* are anchored in the cytoplasmic membrane and penetrate the peptidoglycan layer. The external layer of the cell wall consists of lipooligosaccharides, phenolic glycolipids, glycopeptidolipids, and mycolic acids esterified to arabinogalactan, which is attached to the peptidoglycan. Mycolic acids are long-chain

(40–90 C-atoms) alcohols and fatty acids partially unsaturated and substituted with keto-, methoxy-, epoxy- and OH-groups (2).

The type II of Gram-positive cell wall stains Ziehl-Neelsen positive (acid-alcohol fastness). A mixture of the dye basic fuchsin and phenol is heated on the microscopic slides and penetrates the lipid layer. The slides are subsequently washed in distilled water and decolorized with acid-alcohol. By this procedure the fuchsin is removed from other bacteria and cells but is retained by the acid-fast bacteria. When the cells of these bacteria are treated with alkaline ethanol the lipid content of the cell wall is reduced and the cells became non-acid-alcohol-fast but remained Gram-positive. This result shows that the Gram-positive staining depends on a thick peptidoglycan layer.

3. Type III Gram-Positive Cell Wall

This type of cell wall is present in few Archaea, eg *Methanobacterium formicicum*, containing pseudomurein (1). The glycan strands of pseudomurein are composed of alternating b-N-acetyl-L-talosamine-uronic acid b-1 ← 3 N-acetyl-D-glucosamine and the tetrapeptide contains L-amino acids (Fig. 2).

Figure 2. **Pseudomurein in some methanogenic Archaea**. GlcNAc, N-acetyl-D-glucosamine; NAcTalNUA, b-N-acetyl-L-talosamine uronic acid; Orn, ornithine; Ser, serine; Thr, threonine; Ala, alanine; Lys, lysine; Glu, glutamic acid.

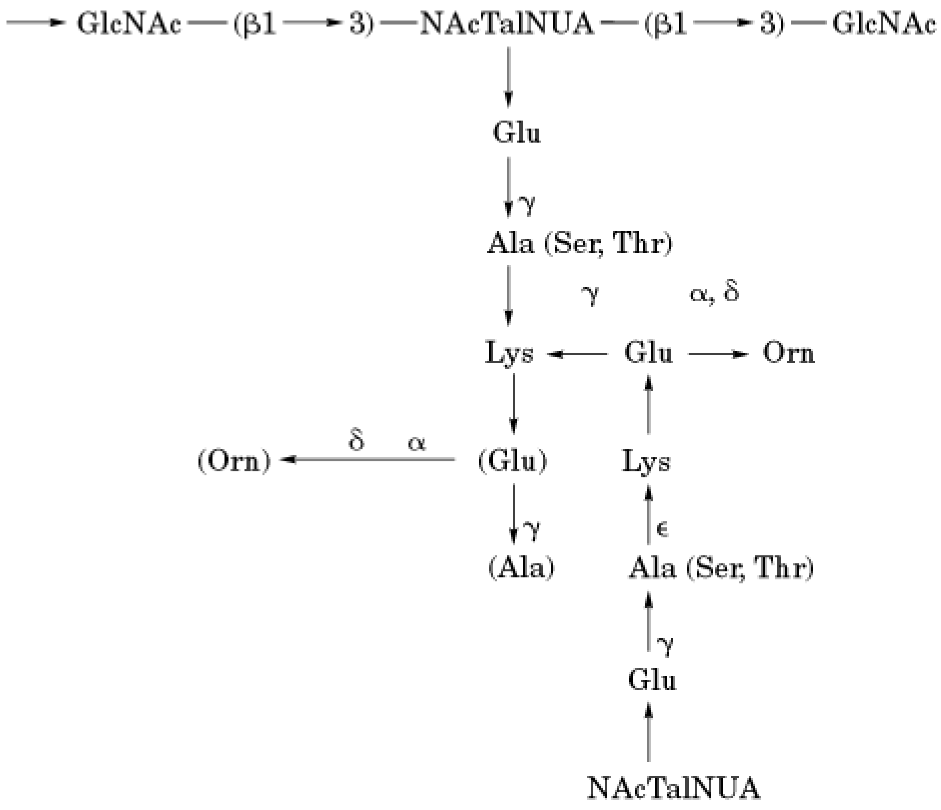

Bibliography

1. E. Stackebrandt (1999) In *Biology of the Prokaryotes* (J. Lengeler, G. Drews, and H. G. Schlegel, eds.), Thieme Verlag, Stuttgart, pp. 674–720.
2. P. J. Brennan and H. Nikaido (1995) Annu. Rev. Biochem. **64**, 29–63.

Greek Key Motif

The Greek key motif describes a particular topology for arranging four **b-strands** into an antiparallel **b-sheet** in protein structures (Fig. 1). The name comes from the similarity between this b-strand topology and a decorative pattern used in ancient Greece (also called the Greek key). A common **domain** structure in proteins is the Greek key b-barrel, a type of **antiparallel b-barrel**, where two Greek key b-sheets fold together to form an eight-stranded antiparallel b-barrel.

Figure 1. Schematic representation of the topology of the Greek key motif in proteins, with individual b-strands of the b-sheet depicted as arrows. The *N*- and *C*-termini of the motif are labeled.

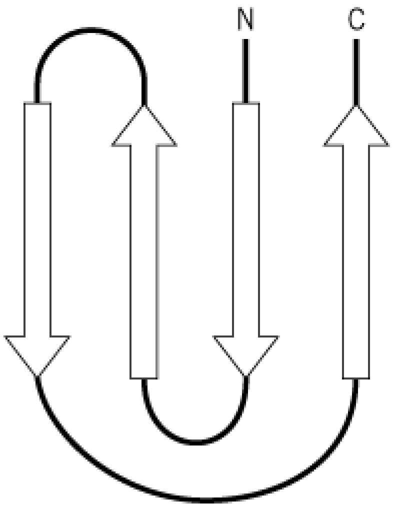

[See also Beta-Sheet and Antiparallel Beta-Barrel Motifs and compare with Beta-meander and Jelly roll motif.]

Suggestion for Further Reading

C. Branden and J. Tooze (1991) *Introduction to Protein Structure*, Garland, New York.

Green Fluorescent Protein (GFP)

GFP is a bioluminescent protein derived from the jellyfish *Aequorea victoria*. The **gene** was **cloned** in 1991, and the protein was found to have the unique property of emitting green light upon illumination with long-wave ultraviolet light without any requirement for additional cofactors or other substrates (1, 2). This has made its gene a most useful reporter gene. The 27-kDa GFP protein has a novel barrel-like protein structure comprised of 11 b-**strands** that surrounds and protects a cyclic tripeptide chromophore at its center (3). When excited by light at 470 nm, this chromophore **fluoresces** with an emission maxima of 509 nm that can be readily observed using conventional fluorescein isothiocyanate fluorescence optics.

The unique and robust properties of GFP have made it valuable for a wide range of applications. Most importantly, detection of light emission from GFP does not require any cell fixation or cell permeabilization, allowing for the first time visualization of a reporter gene in living cells. This feature has made GFP an exceptionally powerful tool in cell and transgenic biology, because expressing cells simply glow green under conventional fluorescence microscopy and confocal microscopy. Furthermore, GFP is observed in living cells, so dynamic events may be followed by making real-time or time-lapse observations. GFP has now been used as a reporter gene in cells from bacteria to human. Importantly, high levels of GFP expression have not been associated with any cellular toxicity; indeed, transgenic mice with ubiquitous expression of GFP thrive without problems. However, prolonged exposure of living cells with long-wave ultraviolet light might cause cell damage, and there may be nuclear damage caused by the generation of free radicals upon GFP excitation.

The b-barrel-like structure of GFP acts to protect its active site and has allowed numerous *N*-terminal and *C*-terminal fusion genes to be made and expressed, without loss of fluorescent activity. Consequently, GFP may be used to study the behavior of tagged proteins within living cells. Proteins have been tagged for a wide range of applications in different organisms. A few of the many examples include tagging ribonucleoprotein particles in *Drosophila* to study their trafficking into the developing egg chamber (4), tagging the histone H2B protein to study the dynamics of chromosome behavior in living human tumor cells (5), and studying **cytoskeletal** dynamics by binding GFP to F-actin in the slime mold Dictyostelium (6).

The second major use of GFP has been for cell-lineage analysis in developmental biology. GFP has not been found to be toxic in any cell type, and the fluorescence does not bleach when excited with 480-nm light. Furthermore, the protein is highly stable; for example, protein **translated** from messenger RNA microinjected into a Xenopus oocyte may still be detected at the feeding tadpole stage of development 5 days later. Thus the fate of the progeny of labeled cells can be followed over significant periods of time during development (7).

Following initial studies with the wild-type protein, several variant GFP isoforms have been generated by mutation analysis (2). Some of these mutations have improved the absorption and emission spectra of the protein, which increase the sensitivity and the versatility of the reporter gene. The mutation Ser65Thr results in an increased brightness of emission, faster fluorophore formation, and reduced photobleaching. Other novel isoforms are particularly valuable, because they emit light at new wavelengths; currently, blue-, red-, and cyan-shifted variants are available (Clontech; `www.clontech.com`), and these can be used in dual or multiple labeling studies with appropriate filters. While certain mutations affect GFP function, other 'silent' mutations have been generated that customize the gene for expression in mammalian cells or in bacteria by optimizing **codon-usage** preferences. Advances in GFP technology can be followed at the "Fluorescent protein Newsgroup" on the Internet (`http://www.bio.net/hypermail/FLUORESCENT-PROTEINS`).

The applications of GFP as a reporter gene are largely determined by its stability and sensitivity. The b-barrel-like structure that protects the chromophore is very stable, resisting temperatures up to 65°C and ionic detergents, and gives high resistance to proteinases (3). The long half-life of GFP makes it ideal for long-term cell-labeling or protein-tagging studies, but it is less suitable for monitoring dynamic changes in gene expression. To circumvent this problem, novel GFP fusion genes have been made with the PEST region of the mouse ornithine decarboxylase gene at the *C*-terminus, which destabilizes the GFP to **protein degradation**; it has a half-life of 1 to 2 hours (8).

Although GFP can be engineered to generate proteins of different half-lives and with different fluorogenic properties, less can be done to improve its sensitivity, because it lacks the ability to amplify its signal through enzymatic turnover of added substrate. In all successful applications thus far, high levels of GFP expression have had to be obtained, achieving of the order of 10^6 molecules per cell or more. The sensitivity of detection is therefore orders of magnitude less than that of other enzyme-based reporter systems, and the detected expression is not tightly coupled to changes in gene transcription.

Bibliography

1. T. Misteli and D. L. Spector (1997) Nature Biotech. **15**, 961–964.
2. A. B. Cubitt et al (1995) Trend Biochem. Sci. **20**, 448–455.
3. G. N. Phillips Jr. (1997) Curr. Opin. Struct. Biol. **7**, 821–827.
4. S. Wang and T. Hazelrigg (1994) Nature **369**, 400–403.
5. T. Kanda, K. F. Sullivan, and G. M. Wahl (1998) Curr. Biol. **8**, 377–385.
6. K. M. Pang, E. Lee, and D. A. Knecht (1998) Curr. Biol. **8**, 405–408.
7. M. Zernicka-Goetz et al. (1996) Development **122**, 3719–3724.
8. Clontechniques (1998) **XIII** (2), 16–17, Clontech Laboratories, Inc., Palo Alto, CA. (HYPERLINK http://www.clontech.com).

Growth Factors

Peptide growth factors provide a critical foundation for intercellular communication in multicellular organisms and are key elements in a complex biological process. But while they promote cell growth, just as often they can have opposite, inhibitory effects on cell proliferation, or instead modulate differentiated cell function. They regulate numerous alternative cell functions that are related to, but sometimes distinct from, cell proliferation. Their activities are often distinct, one from each other, but they can also be significantly redundant; alone, they may exert one activity, but in combination have different, even opposite, effects on cells. To understand their activities, their actions must be defined individually, and then evaluated in the context of complex biological responses.

There are a number of specific characteristics that define the specific properties of a protein growth factor. First and foremost, they are proteins, usually of molecular weights ranging from 5000 to 80,000 daltons. Second, they are ligands that modulate cell function through cell-surface high affinity receptors. On binding the ligand, the receptor activates a **signal-transduction** cascade that, when evaluated on cells in culture, stimulates a proliferative response that includes (but is not limited by) thymidine incorporation into DNA and cell division.

Different peptide growth factors belong to one or another family of structurally related proteins. Hence, numerous proteins that contain sequences homologous to epidermal growth factor (EGF) belong to the EGF family, others with homology to platelet derived growth factor (PDGF) belong to the PDGF family, and still others related to **nerve growth factor** (NGF), **transforming growth factor**-b (TGF b), hepatocyte growth factor (HGF) all belong to the NGF, PDGF, TGF b, or HGF family, respectively. A representative list of these families and some of their members is shown in Table 1.

Table 1. Growth Factor Families

Growth Factor Family	Prototypic Target Cells	Acronyms
Angiopoeitins	Endothelial cells	AP1, AP2
Bone morphogenic proteins	Osteoblasts, osteoclasts, fibroblasts	BMP-1, BMP-2
Brain-derived growth factors	Motor and sensory neurons	BDNF
Ciliary neurotrophic factors	Motor and sensory neurons	CNTF
Colony stimulating factors	Macrophages, granulocytes	M-CSF, GM-CSF
Epidermal growth factors	Epidermal cells, fibroblasts	EGF, TGFA
Erythropoietin	Hematopoeitic stem cells	EPO, TPO
Fibroblast growth factors	Mesenchymal neuroectoderm cells	FGFs and KGFs
Glial-derived neurotrophic factor	Motor and sensory neurons	GDNF
Hepatocyte growth factors	Hepatocytes, endothelial cells	HGF-1, HGF-2
Insulin-like growth factors	Mesenchymal neuroectoderm cells	IGF-1, IGF-2
Interferons	Immunoregulatory cells, fibroblasts	g-IF, a-IF
Interleukins	Immunoregulatory cells, fibroblasts	IL-1, IL-2, IL-3
Neurotrophins	Motor, sensory, autonomic neurons	NGF, NT-2, NT-3
Platelet-derived growth factor	Fibroblasts, mesenchymal cells	PDGF-A. PDGF-B
Tumor necrosis factors	Fibroblasts, inflammatory cells	TNF-A, TNF-B
Vascular endothelial growth factor	Vascular, lymphatic endothelial cells	VEGF-A, B, C, D

When peptide growth factors were first being isolated and identified, they were described either by their biological activity or by the source from which they were purified. Hence, the first fibroblast growth factors (FGFs) were isolated on the basis of their ability to stimulate the proliferation of fibroblasts, NGF by its ability to stimulate nerve cells, TGFs for their ability to transform cells, HGF for its ability to stimulate hepatocytes, and PDGF because it was first purified from platelets. However, the original discovery of a peptide growth factor has seldom reflected the extent of the protein's activities or, in fact, its true physiological function. Few recall that one of the most extensively studied growth factors, EGF, was first named *urogastrone* and was originally characterized for its ability to suppress gastric acid secretion (1). A powerful peptide growth factor in its own right, EGF is a potent growth factor for epithelial cells and yet, in 1962, was isolated and purified on the basis of its ability to cause premature eruption of incisor teeth in mice and not cell proliferation per se (2). Similarly, before the advent of modern cell culture, the detection, isolation, and identification of NGF in 1953 (3), 1960 (4) and 1971 (5), respectively, were based on *in vivo* studies and tissue explants that showed increased neurite outgrowth from nerve ganglia. But is NGF a true nerve growth factor when it stimulates neurite outgrowth, but not nerve cell proliferation? Even more importantly, NGF can stimulate hematopoietic cell colony growth and differentiation (6) and has receptors on the cell surface of fibroblasts, lymphocytes, and numerous mesenchymal cell types that are unrelated to cells of neural lineage (7, 8). The detection of both ligand and receptor in reproductive tissues points to possible functions in reproduction.

In the late 1970s, and throughout the 1980s, the advent of modern methods of cell biology gave investigators the ability to grow numerous cell types in culture, and there was a flurry of activity to define the conditions in which each cell type could grow (9). The first efforts were aimed at replacing serum with tissue extracts so as to identify the active components. Hence, the growth factor literature became saturated with descriptions of "activities" known as fibroblast growth factors, endothelial cell growth factors, cartilage growth factors, milk-derived growth factors, adrenal angiogenic factor, corpus luteum growth factor, brain growth factor, pituitary growth factor, to name only a few. On applying the then developing techniques of molecular cloning, it soon became apparent that all of these seemingly disparate activities were in fact a handful of molecules: FGFs, EGFs, HGFs and PDGFs.

With the realization that, historically, peptide growth factors are a loosely defined collection of molecules that promote cell growth, there have been numerous efforts to rename the field, reorganize its nomenclature, and refine the description of peptide growth factors. While cell biologists have named these molecules "growth factors," immunologists have called them "**interleukins, lymphokines**, and cytokines". Hematologists, in turn, have coined the phrase colony stimulating factors. All descriptions are found throughout the literature and vary from field to field. In the end, the most common usage has remained the historical names given to molecules as they have been identified. When molecules are "rediscovered" because of a new heretofore unknown activity, they are classified according to their original, and ironically sometimes their least important, activity. Hence, when the adrenal angiogenic factor was sequenced and found to be identical to FGF2, it was renamed as such (10). When keratinocyte growth factor (KGF) was sequenced and found to be a member of the FGF family, it was renamed FGF7 (11). As the field has matured, and more structural and biological information has been generated, it has been possible to sort through the pleiotropic activities of growth factors and their sometimes ubiquitous distribution, to rely more heavily on their structural, rather than biological, characteristics for classification (12).

The difficulty in classifying growth factors and the attempts to distinguish them from interleukins, lymphokines, and cytokines is futile and best illustrated by an examination of their range of target cells. It has already been noted that any given growth factor can have numerous activities on any given cell type and that their activities can expand well beyond the context of their original discovery. Even more remarkable, however, is their range of target cells, which can be much greater than originally anticipated. It is here where attempts to delineate functional differences between interleukins, cytokines, and growth factors have failed. Interleukins and cytokines are generally regarded as signaling molecules with activities in the immune system. They were originally thought to be produced by the immune system, for the immune system. Yet many, if not all, interleukins are broad-spectrum proteins that, when studied in detail, regulate numerous processes outside of the immune system. Interleukin 1 (IL1), for example, acts on chondrocytes, astrocytes, fibroblasts, keratinocytes, and some neurons. Best known as a B-cell growth factor, interleukin-6 also regulates mesenchymal cell function. Perhaps even more remarkable is the observation that fibroblasts and other nonimmune cells can be sources of interleukins and not just targets, thus diminishing any differences between interleukins and protein growth factors further. As pleiotropic, ubiquitous biological effectors that control cell proliferation, the terms protein growth factor, cytokine, and interleukin describe near synonymous molecules.

Whatever classification might be conferred to growth factors, cytokines, lymphokines, or interleukins, their activities challenge the foundations of classical sciences like endocrinology, because of their peculiar, and yet necessary, mode of action. Unlike the endocrine system that relies on tissue-to-tissue communication, the growth factor system acts at the cellular level. Thus, while the endocrine pathways rely on blood-borne transportation of signaling molecules to effect change, growth factors mediate alterations in the local biological milieu. This fundamental difference in action has led investigators to rethink how cells communicate and even how they respond to endocrine stimuli. Peptide growth factors, released into the local milieu by one cell, alter the activity of an adjacent cell that is in close proximity (paracrine target) or alternatively the cell from which it derives (autocrine target). The actions of major regulatory peptides are mediated by autocrine and paracrine mechanisms that control growth factors and normal cellular homeostasis. Thus the main difference between the growth factor and cytokine pathways and the endocrine system is in the local action of growth factors. Even lymphokines produced by circulating immune cells act locally, but only after the cell producing it (eg, lymphocytes) has traveled and delivered it to its desired site of action. All growth factors are produced locally to act locally.

With this difference between endocrine and growth factor pathways in mind, it is possible to understand that when growth factors are locally released into biological fluids, they can then act to modify the actions of classic hormones arriving on site from distal sources. Hormone action has long been known to require local cellular factors to permit, mediate, and sometimes modulate responsiveness. For example, insulin-like growth factors and their binding proteins modulate hormone action (13) and TGF-b can modulate adrenal function (14). Furthermore, endocrine hormones can trigger gene expression of growth factors in target cells, which in turn modulate the local milieu and change the cell's responsiveness to further stimulation by the hormone (15).

In view of the fact that peptide growth factors act locally to modulate cell function, it comes as no surprise that there are numerous processes present in the local milieu to control their activities and ensure that their actions do not extend to unwanted targets. Of these processes, four are perhaps the most studied:

- Restricted production and release of the growth factor to limit its action
- Highly regulated receptor gene expression to limit target cell responsiveness
- Circulating inhibitors in blood to sequester and inactivate the ligand
- The binding and sequestration of growth factors at the cell surface and extracellular matrix to keep them in the local milieu

The notion that there is restricted production and release of growth factors and limited receptor expression is best illustrated by the difference between gene expression in embryonic development, fetal growth, and in adult tissues (16). At times as early as before gastrulation, the gene expression of growth factors becomes controlled in both a temporal and spatial fashion, and the role played by growth factors in development is essential in all aspects of patterning, tissue development, and differentiation. As exemplified by studies where the genes for different growth factors have been genetically knocked out, they have been shown to play a critical role during development, but are often suppressed in adult, quiescent tissues. In both cancer and wound healing, however, the genes for these same molecules are activated. In wound healing, they remain regulated until the injury has been resolved. In cancer, activation of these genes leads to uncontrolled cell growth, transformation, abnormal blood vessel growth, and ultimately tumor formation.

One particularly interesting mechanism of controlling growth factor activity appears unique to some of the paracrine factors involved in the injury and inflammatory response. Recent data suggest that molecules like FGF1, FGF2, IL1a, and Il-b can exit the cell independently of the cell's secretory endoplasmic reticulum and Golgi apparatus (17). This protein export process is mechanistically different from protein secretion and is highly specific and regulated. While its physiological significance remains unknown, the selective translocation of certain biological effectors across the plasma membrane presumably restricts their activity and allows the cell to tightly control access to the cell surface and their target cells.

The evidence for natural inhibitors of growth factors is equally compelling. For example, numerous investigators have established that genes encoding high affinity receptors for growth factors encode soluble forms of their high affinity receptors that are generated by alternative splicing of the gene's mRNA or by truncation at the cell surface (18). This form of receptor has no transmembrane domain and no signaling domain. It is secreted by cells and can bind ligand in biological fluids, thus preventing it from interacting with its cell surface (and functional) high affinity receptor. Alternatively, some cells have the ability to produce receptor antagonists that bind, but do not activate high affinity receptors. By virtue of occupying the binding site, molecules like interleukin receptor antagonist (ILRA) and angiopoietin-2 prevent a functional interaction between the ligand and its native receptor.

Perhaps the most remarkable process that appears to control the activity of growth factors stems from the observation that they often appear designed to remain in the local cellular milieu and physically sequestered outside target cells in what is presumed to be a biologically inactive form (19). This observation underlies the need for their action to remain local and predicts the existence of specific signals (eg, enzymes) to render them available to target cells.

The first type of local adhesion is characterized by a noncovalent association of growth factors with the extracellular matrix, the cell surface, or pericellular structures. This binding is often salt- and/or pH-sensitive. Representative examples of growth factors with this type-1 adhesion are shown in Table 2. In contrast, the second type of adhesion is characterized by a covalent association with the extracellular surface, through a transmembrane domain, in the growth factor's precursor. Representative examples of growth factors having this type 2 adhesion are also shown in Table 2.

Table 2. Growth Factors Associated with Cell Surface through Ionic (Type 1) or Transmembrane Domains (Type 2) in Their Precursors

Type 1 Association	Type 2 Association
Fibroblast growth factors	Epidermal growth factors
Transforming growth factor b	Tumor necrosis factors
Colony stimulating factors	G-colony stimulating factors
Insulin-like growth factors	M-colony stimulating factor
Colony stimulating factor	GM-colony stimulating factors
Interleukins 1 and 3	Stem cell growth factor
Hepatocyte growth factors	
g-Interferon	
Vascular endothelial growth factor	
Platelet-derived growth factor	
Bone morphogenic proteins	

Fibroblast growth factors (FGFs) are prototypic examples of type 1 adhesion. They have a high affinity for immobilized heparin, and immunohistochemical techniques localize FGF1 and FGF2 to the extracellular matrix, basement membrane, and cell surface of numerous tissues (20). Indeed, recent studies have identified the binding heparan sulfate proteoglycans that serve to sequester (and possibly deliver) FGFs to its high affinity receptors on target cells. TGFb has also been localized in extracellular and pericellular structures, but it is in what is thought to be a latent, biologically inert form (21). Recent studies have identified three kinds of receptors for this protein, one of which is a high molecular weight proteoglycan anchored onto the plasma membrane through phosphoinositol. Other growth factors with this type 1 adhesion include granulocyte-macrophage colony stimulating factor (GM-CSF), which binds to extracellular matrix and to heparan sulfate-related glycosaminoglycans (GAG), interleukin-3 (IL-3), hepatocyte growth factor (HGF), osteogenin (OTG), and the bone morphogenic proteins (BMP).

Type 2 adhesion is characterized by growth factors that are covalently associated with the plasma membrane because their precursor encodes a transmembrane domain that anchors it to the cell surface. In order to be active, these molecules must either be processed from the precursor to generate an active ligand or must act directly on an adjacent high affinity receptor without being further processed or released. Accordingly, these molecules may have activities that are restricted by availability. The prototypic family (and the most studied) of the growth factors with type 2 adhesion to cells is EGF. It and its structural homologues, TGFa and the heparin-binding EGF, are contained in large precursor proteins that have transmembrane domains that lock them onto the cell surface. Most of the biological studies performed with EGFs have been with the processed unbound forms, so it is less clear if their growth factor activities are maintained when they are unprocessed, at the cell surface. But recent studies using site-directed mutagenesis support the notion that the membrane-bound precursor has growth factor activity and can interact with high affinity receptors on target cells. The ability of growth factors with this type 2 adhesion to elicit a biological response is illustrated by the recent experiment showing that PDGF anchored to the plasma membrane through mutagenesis is still capable of stimulating a mitogenic response (22). Other examples of type 2 adhesion include tumor necrosis factor (TNF) and the hematopoietic factor, CSF-1 and stem cell growth factor, the ligand for the ckit protein. In all instances, each is generated from an integral membrane protein locked onto the cell surface.

It is presumed that a growth factor locked to the cell surface through a transmembrane domain can stimulate a biological response only if it is liberated from its sites of sequestration and delivered to the target cell. The molecular mechanisms that might mediate this regulation are unknown. The extracellular matrix and the various constituents that bind the growth factor are obvious targets for the combined actions of **proteolytic** and glycolytic degradation. These include **plasmins, cathepsins**, collagenases, and a wide array of glycanases, such as heparinases and heparitinases. These enzymes are normally inactive due to the presence of a macroglobulin, plasminogen activator inhibitors, proteinases like nexin, and collagenase inhibitors. In the case of the FGFs, however, it is particularly worthy to note that they are proteinase-resistant when bound to glycosaminoglycans (23). Thus the generation of an FGF-GAG complex by limited proteolysis provides a mechanism to generate a potent biologically active ligand from a pool of sequestered, biounavailable growth factor. Furthermore, glycosaminoglycan binding to some FGFs has been reported to enhance its binding to their high affinity receptor and in some instances is required for delivery (24). The mechanisms that regulate the type 2 adhesion of growth are not known, although there exist proteolytic enzymes capable of releasing the ligand from the cell (25, 26).

In the end, as the peptide growth factors that control cell growth and development have been identified and the mechanisms that regulate their activities better understood, the challenge becomes to characterize how they all act together to control normal cell function. As the use of modern molecular techniques to eliminate combinations of growth factors from the genome genetically becomes more widespread, it should be possible to provide important insight into how these factors act to control normal cell function and, ultimately, their role in whole-body homeostasis.

Bibliography

1. H. Gregory and I. R. Wilshire (1975) Physiol. Chem. **356**, 1765–1774.
2. S. Cohen (1962) J. Biol. Chem. **237**, 1555–1562.
3. R. Levi-Montalcini and V. Hamburger (1952) J. Exp. Zool. **123**, 233–288.
4. S. Cohen (1960) Proc. Natl. Acad. Sci. USA **46**, 302–311.

5. R. H. Angeletti and R. A. Bradshaw (1971) Proc. Natl. Acad. Sci. USA **68**, 2417–2420.
6. H. Matsuda, M. D. Coughlin, J. Bienstock, and J. A. Denburg (1988) Proc. Natl. Acad. Sci. USA **85**, 6508–6512.
7. P. Ernfors, F. Hallbook, T. Ebendal, E. M. Shooter, M. J. Radeke, T. P. Misko, and H. Persson (1988) Neuron **1**, 983–996.
8. M. Bothwell, S. L. Patterson, G. C. Schatteman, S. Thompron et al. (1989) J. Neurosci. **22**, 354–362.
9. A. Baird (1993) Endocrinology **132**, 487–488.
10. D. Gospodarowicz, A. Baird, J. Cheng, G. M. Lui, F. Esch, and P. Böhlen (1986) Endocrinology **118**, 82–90.
11. P. W. Finch, J. S. Rubin, T. Miki, D. Ron, and S. A. Aaronson (1989) Science **245**, 752–755.
12. A. Baird and M. Klagsbrun (1991) Cancer Cells **3**, 239–243.
13. G. Lamson, L. C. Giudice, and R. C. Rosenfeld (1991) Growth Factors **5**, 19–28.
14. J. J. Feige and A. Baird (1992) Prog. Growth Factor Res. **3**, 103–113.
15. J. Massague (1990) Annu. Rev. Cell Biol. **6**, 597–640.
16. M. Goldfarb (1996) Cytokine Growth Factor Rev. **7**, 311–325.
17. A. E. Cleves (1997) Curr. Biol. **7**, 318–320.
18. D. E. Johnson, J. Lu, H. Chen, S. Werner, and L. T. Williams (1991) Mol. Cell Biol. **11**, 4627–4634.
19. J.-J. Feige and A. Baird (1992) Med. Sci. **8**, 805–810.
20. I. Vlodavsky, J. Folkman, R. Sullivan et al. (1987) Proc. Natl. Acad. Sci. USA **84**, 2292–2296.
21. N. L. Thompson, K. C. Flanders, J. M. Smith, L. R. Ellingsworth, A. B. Roberts, and M. B. Sporn (1989) J. Cell Biol. **108**, 661–669.
22. B. A. Lee and D. J. Donoghue (1991) J. Cell Biol. **113**, 361–370.
23. D. Gospodarowicz and J. Cheng (1986) J. Cell Physiol. **128**, 475–484.
24. A. Yayon, M. Klagsbrun, J. D. Esko, P. Leder, and D. M. Ornitz (1991) Cell **64**, 841–848.
25. J. Teixidó, R. Gilmore, D. C. Lee, and J. Massagué (1987) Nature **326**, 883–885.
26. A. Pandiella and J. Massagué (1991) Proc. Natl. Acad. Sci. USA **88**, 1726–1730.

Suggestions for Further Reading

27. A. Baird (1994) Fibroblast growth factors: activities and significance of non-neurotrophin neurotrophic growth factors, Curr. Opin. Neurobiol. **4**, 78–86.
28. M. J. Bissel, H. G. Hall, and G. Parry (1982) How does the extracellular matrix direct gene expression? J. Theor. Biol. **99**, 31–68.
29. M. Y. Gordon (1991) Hemopoietic growth factors and receptors: bound and free. Cancer Cells **3**, 127–133.
30. M. Y. Gordon, G. P. Riley, S. M. Watt, and M. F. Greaves (1987) Comparmentalization of a haematopoietic growth factor (GM-CSF) by glycosaminoglycans in the bone marrow microenvironment, Nature **326**, 403–405.
31. D. C. Lee (1990) TGF-alpha: expression and biological activities of the integral membrane precursor. Mol. Reprod. Dev. **27**, 37–45.
32. J. Massague (1990) Transforming growth factor . A model for membrane anchored growth factors, J. Biol. Chem. **265**, 21393–21396.
33. B. Mroczkowski, M. Reich, K. Chen, G. I. Bell, and S. Cohen (1989) Recombinant human epidermal growth factor precursor is a glycosylated membrane protein with biological activity, Mol. Cell Biol. **9**, 2771–2778.
34. R. Roberts, J. Gallagher, E. Spooncer, T. D. F. Bloomfield, and T. M. Dexter (1988) Heparan sulphate bound growth factors: a mechanism for stromal cell mediated haemopoiesis, Nature

332, 376–378.
35. A. B. Roberts and M. B. Sporn (1990) *The Multifunctional Nature of Growth Factors in Peptide Growth Factors and Their Receptors*, Springer-Verlag, Berlin.
36. K. Tryggvason, M. Höyhtya, and T. Salo (1987) Proteolytic degradation of extracellular matrix in tumor invasion, Biochim. Biophys. Acta **907**, 191–217.
37. S. T. Wong, L. F. Winchell, B. K. McCune et al. (1989) Cell **56**, 495–506.

Growth Hormone

Growth hormone (GH), also called somatotropin or somatotropic hormone, is a protein produced in the anterior pituitary gland and is required for normal growth in vertebrate animals. Its growth promoting action is mediated by insulin-like growth factor-1 (IGF-1) whose synthesis GH stimulates in liver and other target tissues. Growth hormone also has potent metabolic actions in mammals and promotes protein synthesis and lipid degradation while restraining carbohydrate oxidation. GH is comprised of a single chain of ~200 amino acid residues with two internal disulfide bonds and a tertiary structure that includes four alpha helices bundled in an antiparallel fashion. Growth hormone is a member of a family or proteins that are produced in the pituitary glands of all vertebrates and placentae of some mammals. Family members include pituitary prolactin (PRL), placental lactogens (PL), which are also called chorionic somatomammotropins in humans, prolactin-related proteins in ruminants and rodents, proliferins in mice, and somatolactin in fish. Genes that encode most members of the GH family are comprised of five exons and four introns and appear to have arisen by duplication from a single ancestral gene before the appearance of the vertebrates. Splice junctions have been preserved throughout vertebrate evolution. Splicing and processing variants have been described for several members of the family. Growth hormone, PRL, and, presumably, their relatives signal through single-chain membrane receptors that lack intrinsic enzymatic activity, but associate with cytosolic protein tyrosine kinases. Binding of GH to a single-receptor molecule is followed rapidly by the binding of a second receptor molecule to the opposite side of GH to form a trimeric complex that brings the intracellular domains of the two receptor molecules into close apposition and activates associated protein tyrosine kinases of the JAK (Janus kinase) family, particularly JAK2. Similar events occur with PRL signalling and probably the placental lactogens as well. A large number of proteins including the GH receptor and JAK2 become phosphorylated on tyrosine residues to form docking sites for other proteins and initiate signalling cascades. Signalling to the nucleus occurs through the agency of phosphorylated Stat (signal transduction and activation of transcription) proteins and by the MAP kinase and protein kinase C pathways as well.

1. History

GH was discovered in 1921 by Evans and Long (1) as the substance present in extracts of bovine pituitary glands that increased growth in rats when given daily over a period of 3 months. A decade later, Riddle's group prepared by isoelectric precipitation a a pituitary extract that was rich in PRL, a hormone that promotes milk production (2). They subsequently found that the same partially purified extract promoted growth in pigeons and mice and questioned the existence of a separate and unique growth promoting hormone (3). The ensuing controversy foreshadowed later discoveries of the close relationship of GH and PRL in terms of their chemical structures as well as their overlapping biological activities in various assay systems. Available methods of protein purification and hormone assay were quite limited at that time, and, despite continued intense efforts by the Evans group, nearly a quarter of a century elapsed before it was established with virtual certainty that the growth promoting activity of the pituitary gland resided in a single molecular entity. In 1944 Li and Evans

(4) announced the successful isolation of a highly purified preparation of bovine GH that was apparently free of PRL and the activities of other anterior pituitary hormones. Despite its readily demonstrable efficacy in promoting growth in experimental animals, however, no therapeutic benefit to human pituitary dwarfs treated with bovine GH could be demonstrated in the subsequent decade of clinical trials. Knobil and Greep (5) found that GH of bovine or porcine origin was totally ineffective in rhesus monkeys and adopted the then unorthodox view that there might be species differences in the activities of GH. Fortuitously, their work coincided with large scale production of the newly developed Salk polio vaccine that required monkey kidney tissue for growth of the viruses and, hence, the sacrifice of large numbers of rhesus monkeys. They demonstrated that GH isolated from monkey pituitary glands promoted growth and nitrogen retention in hypophysectomized rhesus monkeys. Subsequent findings that GH prepared from monkey or human pituitaries is effective in humans provided the impetus for creation in 1960 of the National Pituitary Agency for large scale collection of human pituitaries at autopsy and centralization of the production of human GH in the United States. Human GH made available through this agency was used for basic research and for the treatment of more than 3,000 patients over the next quarter century (6).

The complete amino acid sequences of GHs derived from human (hGH), monkey (mGH), and bovine (bGH) pituitary glands were known by the early 1970s, and all efforts to modify animal GHs to forms that might be effective in humans or to synthesize human GH by chemical means were unsuccessful. Meanwhile, with the therapeutic need for the scarce hGH and the accumulating wealth of structural information on GH and its related proteins (7), GH was recognized as an attractive model protein for application of the emerging recombinant DNA technology. It was soon shown that GH could be synthesized in bacteria from mammalian DNA fused to a bacterial gene (8). Human GH was the first mammalian protein to be so produced from purely mammalian cDNA (9) and was targeted by the newly formed biotechnology company, Genentech, as the first company to develop and market recombinant protein commercially (10). Approval for clinical use of recombinant human GH was granted by the U.S. Food and Drug Administration in 1985 after several deaths from Creutzfeldt-Jakob disease attributed to pituitary hGH contaminated with the slow virus resulted in a ban on its further administration to human patients. In the decade between 1985 and 1995, ten times as many children were treated with the recombinant hormone as had been treated with the pituitary-derived hormone in the preceding quarter century, and, collectively, they are said to have grown to an additional height of about 4 miles (10). Ready availability of recombinant bovine and porcine GH has also fostered commercial application in agriculture where GH can be used to accelerate growth of domestic livestock, increase feed efficiency, decrease carcass fat, and increase milk yield. Political opposition, however, has limited its use in this regard. Overexpression of GH in transgenic cattle, sheep, and pigs has produced disappointing results, as these animals often become diabetic.

2. Biological Actions

Postnatal growth and the attainment of normal adult size is absolutely dependent upon GH in most species, but guinea pigs and some strains of chickens appear to have evolved alternative mechanisms of growth regulation that appear independent of GH and are not understood. Embryonic growth and growth in the early postnatal period in mammals is also independent of GH. Absence of GH in juvenile animals results in "dwarfism" that varies in severity from less than 25% to 65% of expected adult size. Excessive GH production during the juvenile period leads to a state of giantism in animals and humans, with some afflicted men attaining heights of over 8 feet. Transgenic mice expressing metallothionein-hGH fusion genes attained body weights that were twice more those of littermate controls (11). Cessation of growth in adult animals results from fusion and, hence, is unresponsiveness of the growth plates in the long bones rather than a lack of GH, which continues to be secreted throughout life, albeit it in decreasing amounts with increasing age. Continued overproduction of GH in human adults results in overgrowth of skin and soft tissues and deformities that result from enlargement of those bones that can continue to respond; a condition called acromegly.

The growth-promoting effect of GH is at least partially, and perhaps entirely, attributable to the actions of a growth factor, once known as somatomedin, and now called insulin-like growth factor-1 (IGF-1). GH enhances the synthesis and secretion of IGF-1 in a wide variety of tissues. IGF-1 was so named because of the similarity of both its structure and its biological effects to those of insulin (see **IGF-1**, this volume). Most of the IGF-1 in the blood originates in the liver and circulates tightly bound in a complex that contains two other GH-dependent proteins, the IGF binding protein 3 and an acid-labile protein. IGF-1 is also produced locally by cartilage progenitor cells in the growth plates of the long bones and by other cells that are targets for GH and acts locally in a paracrine or autocrine manner to stimulate cell division and differentiation. This local production and action of IGF-1 appears to be sufficient to account for the stimulation of growth by GH as selective disruption of IGF-1 expression by the liver, which severly reduces the plasma content of IGF-1, does not interfere with normal growth of mice (12). The synthesis of most of the eight different IGF binding proteins that have been described is either positively or negatively regulated by GH. These proteins appear to act as positive or negative modulators of IGF action.

GH is also an important regulator of energy metabolism in most homeothermic animals. It decreases the sensitivity of liver, muscle, and adipose tissue to the actions of insulin (see Insulin, this volume) and promotes the utilization of fat in preference to carboydrates to meet the demands of muscle for energy. Consequently, prolonged administration of GH leads to a reduction of carcass fat while promoting the accumulation of body protein through stimulation of protein synthesis. At the same time that insulin sensitivity is decreased, GH paradoxically increases the responsiveness of the insulin-producing cells of the pancreas to physiological signals for insulin secretion. Excess GH often results in temporary or permanent diabetes mellitus. In many species GH secretion is increased during fasting and, perhaps, facilitates the metabolic adaptations to decreased availability of dietary carbohydrates.

3. Secretion and Metabolism

GH is synthesized and secreted primarily by cells in the anterior pituitary gland called "somatotropes," which appear to arise from the same pool of precursor cells that also give rise to the PRL secreting cells (lactotropes). Some cells appear able to synthesize and secrete both GH and PRL and are called "somatomammotropes" or "lactosomatotropes." Immortalized cells derived from tumors of these cells (eg, GH3 cells) have been widely used as models for studying both synthesis and secretion of peptides. GH is the most abundant hormone produced and stored in the pituitary. Its expression level is about 800 times greater than that of any other pituitary hormone, and it has been estimated to comprise up to 1% of the dry weight of the human pituitary gland. In the living animal, GH is secreted intermittently in pulses spaced about 3 to 4 h apart (13). Positive input for secretion is provided by a 40 to 45 amino acid peptide, the GH releasing hormone (GHRH), which is secreted by neurons in the nearby hypothalamus and reaches the somatotropes through a unique capillary network called the hypophyseal portal system. Negative input for secretion is provided by somatostatin, a 14 amino acid peptide that is synthesized and secreted by other hypothalamic neurons. Pulsatile secretion of GH is throught to result from the periodic coordinated release of GHRH and cessation of somatostain secretion. Various environmental cues (eg, "stress") may evoke additional secretory episodes or abolish one or more secretory pulses depending upon circumstance and the species. Products of GH action, such as IGF-1, in the blood diminish pulse amplitudes by stimulating somatostatin secretion in a typical negative feedback arrangement. In addition, GH may also modulate its own secretion by exerting inhibitory actions on GHRH-secreting neurons. Recently, an additional GH secretagogue, named ghrelin, has been identified. This novel 28 amino-acid peptide is esterified with octanoate at serine 3 and appears to act on both the GHRH-secreting cells of the hypothalamus and the somatotropes.

In mammals, which have been studied more extensively than other vertebrate classes, about half of the GH found in the blood is bound to the GH-binding protein (GHBP) whose structure corresponds to the extracellular portion of the GH receptor (GHR). The GHBP is a product of the GHR gene (see below) and is thought to arise in most species by proteolytic cleavage of the GHR at the extracellular surface. The enzyme responsible appears to be the same metalloprotease that liberates the cytokine, tumor necrosis factor-a, from its transmembrane precursor (14). In rodents, the GHBP is synthesized from an alternatively spliced RNA transcript of the GHR gene. The GHBP increases the apparent biopotency of GH in the intact organism by prolonging its survival time in the blood. When added to isolated tissues or cells, the GHBP reduces bioactivity of GH by competing for hormone with cellular receptors. These effects are not contradictory, as receptor binding leads to complete degradation of the hormone/receptor complex and is likely to serve as the major route of hormone degradation. Some degradation of hormone that reaches the glomerular filtrate also occurs in the kidney. Less than 1% of the GH secreted by the pituitary is excreted intact in the urine.

4. The GH Family of Proteins

GH is a single-chain peptide comprised of 190 to 196 amino acid residues and has a molecular mass of approximately 22,000. Complete amino acid sequence data for hormones from more than 40 different species representing all classes of vertebrates have been determined either by direct analysis of the purified proteins or by deduction from the nucleotide sequences of their cDNAs. Characteristic of all the known GH molecules are the two disulfide bridges that form a long loop by coupling cysteines corresponding to Cys-53 and Cys-165 in the human sequence and a short loop involving Cys-182 and Cys-189. When these cysteine residues are used as reference points and gaps are allowed to maximize alignment of homologous regions, it becomes apparent that more than a third of the amino acid loci in all of the known GH molecules contain identical residues (Fig. 1). Homologies are almost twice as great when conservative substitutions are allowed. Amino acid sequences of GHs from animals as distantly related as humans and sharks have more than 50% identity, although there is considerably more divergence in the GHs within the bony fish. Nevertheless, more than 30 residues in addition to the four cysteines are identical throughout the species, and these appear in clusters with highest conservation in positions between residues 164 and 187 (15). The crystal structure of porcine GH was solved in 1987 (16). In three dimensions, the peptide chain of GH forms into four alpha helices encompassing residues 7 to 34 (helix I), 75 to 87 (helix II), 106 to 127 (helix III), and 152 to 183 (helix IV) (Fig. 2). The alpha helices are tightly packed and arranged in an antiparallel up-up-down-down orientation. The invariant and highly conserved amino acid residues are predominantly found within the alpha helices and presumably contribute to the integrity of the tertiary structure of the molecule. A long loop of 40 amino acids connects helices I and II, and shorter 18 and 24 residue loops connect helices II and III and III and IV, respectively. Short peptide chains are found at the amino and carboxyl termini.

Figure 1. The amino acid sequence of hGH. Shaded boxes indicate conserved amino acids in mammalian GH. The shad lines above or below the peptide chain indicate the amino acid residues present in helices **I, II, III**, and **IV**. (From: H. M Goodman, G. P. Frick, and S. Souza (1996) Species specificity of the primate growth hormone receptor. News Physiol. S 11, 157–160).

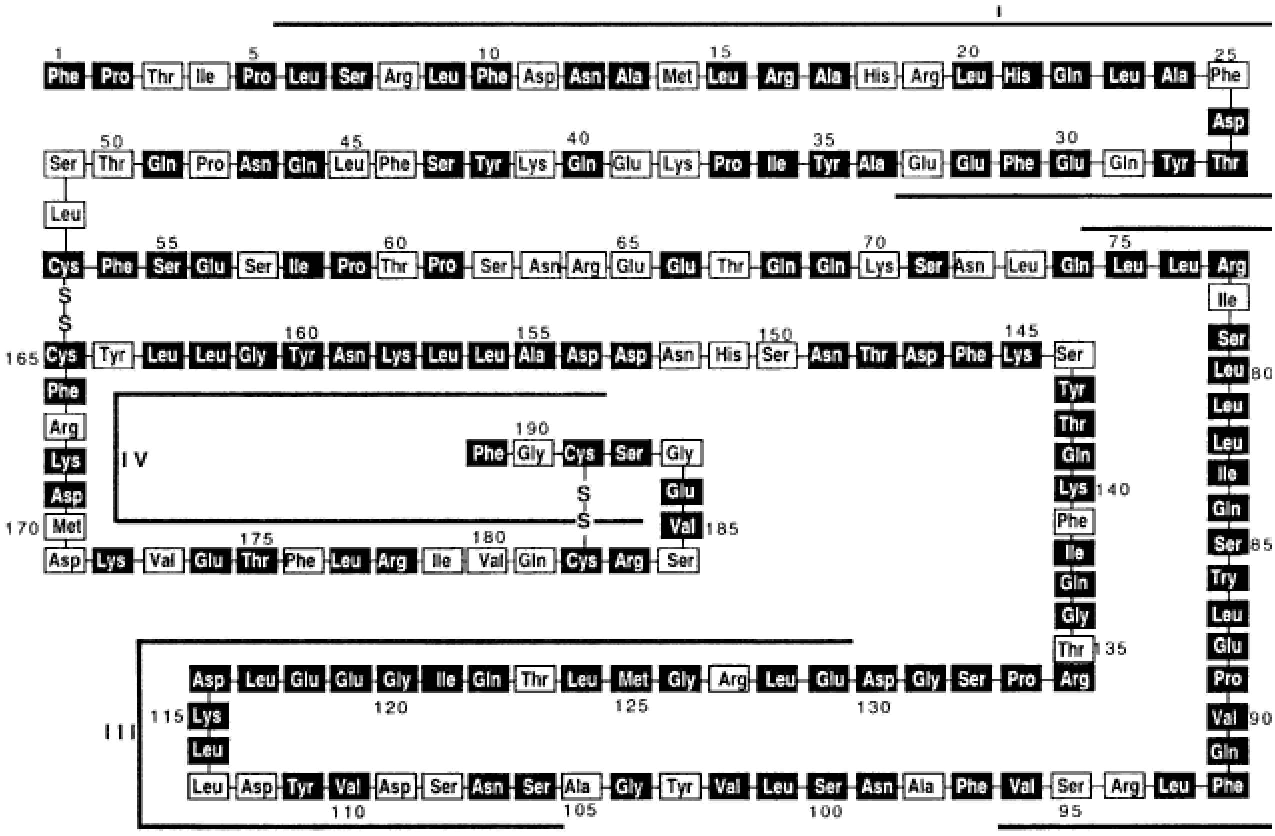

Figure 2. Tertiary structure of GH (modified from ref 14).

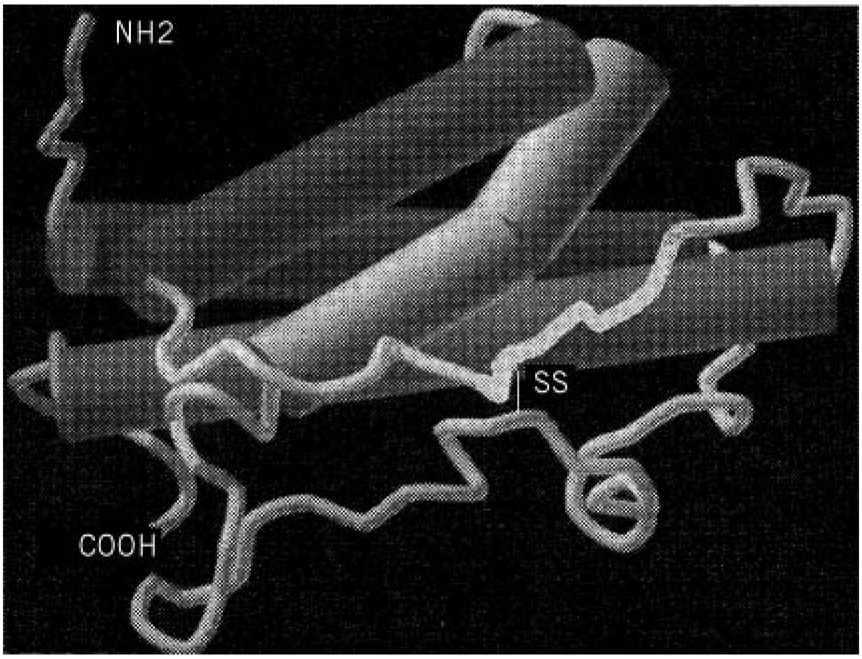

Variant forms of GH have been reported in several species. Of these, the most thoroughly studied is the so-called 20k hGH. This isoform of hGH lacks 15 amino acids (residues 32 to 46) and, consequently, has a molecular mass of 20,000, instead of the 22,000 of the predominant form discussed above (17). The 20k isoform of hGH constitutes only about 10% of the daily GH secretion and may be somewhat less potent than its 22k counterpart in some assay systems. It arises from alternative splicing of the same RNA transcript that codes for the 22k isoform (see below). Another splice variant, a 17.5 kDa form (18), has also been described, but little is known of its physiology. Processing variants include phosphorylated, glycosylated, amidated, and proteolytically cleaved forms (19). Some of these variants are found in the circulation, but their biological importance has not been established. Some modified forms of GH may be artifacts of pituitary storage or purification procedures.

As already indicated, another anterior pituitary hormone, prolactin (PRL), is closely related to GH in both its chemical and biological properties. PRL is found in all vertebrates and has a wide range of biological actions among the various species, including regulation of salt and water balance, growth, and various behaviors and functions associated with reproduction and nurturing of the young (20). PRL is named for its critical role in supporting lactation in mammals. Like GH, PRL consists of nearly 200 amino acid residues and has the same four antiparallel helix bundle tertiary structure as GH. PRL has three intrachain disulfide bridges, two of which correspond to those found in GH, and the third is located near the N terminus. PRL is about 20% identical in amino acid sequence to GH of the same species, a finding that suggested the hypothesis that the two hormones originated from a common ancestral gene (21). *A propos* of this idea, a glycoprotein with a mass of about 26 kDa that appears to be equally related to both hormones has been isolated from pituitary glands of some bony fish (22). It consists of 206 amino acids with about 24% sequence identity with both GH and PRL, and conservation of the two disulfide bridges corresponding to those in GH. Its function has not been established, but it has been named “somatolactin” because of its similarity to both GH and PRL. Somatolactin may be descended from the protein that was ancestral to both GH and PRL and, as of this writing, has not been found in tetrapod or avian pituitary glands.

Additional members of the GH family are expressed in the placenta and, hence, are confined to the mammals. The human placenta secretes a variant form of GH (GH-V), which appears to be the major form of GH present in maternal blood plasma during late pregnancy (23). GH-V differs from pituitary GH (hGH-N, for normal) in 13 of the 191 amino acids in positions that are widely distributed between residues 18 and 149 and, unlike the pituitary hormone, is glycosidated at Asn-140, which is unique to GH-V (24). It has a molecular mass of about 23 kDa. Blood plasma of pregnant women also contains a less abundant 25 kDa GH-like peptide of placental origin, which appears to arise from alternative splicing of the RNA transcript of the hGH-V gene (25) (see below). The human placenta also produces placental lactogen (hPL, more commonly called human chorionic somatomammotropin, hCS), which has both GH-like and PRL-like activities in many assay systems. It is the most abundant peptide produced by the placenta, which, in late pregnancy, may secrete as much as 1g per day. Human CS differs from the pituitary form of hGH in only 28 of the 191 amino acid residues and from hGH-V in only 40 residues, with the carboxyl terminus again showing the greatest degree of identity (24). PLs are also produced by the placentae of other species, notably ruminants and rodents, but apparently are not universally found among the mammals. Four PL and four PRL-related proteins are produced in rodent placentae, and the bovine placenta produces one PL and six PRL-related proteins. The PLs bind to GH or PRL receptors and, at least in cattle, to PL receptors, but, currently, no receptors for PRL-related proteins have been characterized. Bovine and rodent PLs and PRL-related proteins are more similar to PRL than to GH, while the placental lactogen of primates is more closely related to GH.

5. The GH Gene Family

Determination of the structures of the genes that encode the GH family of proteins reveals an even greater similarity and relationship among these proteins than the amino acid sequences. The structure of the GH gene has been determined in mammalian, avian, and piscine genomic libraries. The related PRL, PL, and somatolactin genes have also been sequenced in a variety of species. The mammalian GH genes span about 2 kb and are the smallest in the family, while the somatolactin gene is the largest and extends for about 16 kb. the mammalian PRL genes encompass about 10 kb, and the PL genes resemble those of either GH or PRL, depending upon the species. The genes that encode all of these proteins contain five exons and four introns, and, despite wide variations in the sizes of the introns, the splice junction patterns and the positions of introns with respect to the coding sequences of the protein products have been remarkably conserved. In some suborders of bony fish, eg, the salmonids, however, the fifth exon has been split by insertion of a fifth intron. With the conservation of exon/intron boundaries, the sizes of the first four exons are quite similar, ~0.1, 0.2, 0.1, and 0.2 kb respectively, but exon V ranges from ~3 kb in somatolactin to ~0.3 kb in hGH, giving rise to wide variation in the length of the untranslated 3′ end (15).

The human haploid genome contains five closely-linked GH-related genes at band segment q22–24 on the long arm of chromosome 17 (26, 27) and a single PRL gene on chromosome 6 (28). The hGH-N gene is expressed only in the pituitary and, to a much smaller extent, in some white blood cells (monocytes), while the three hCS genes and hGH-V are expressed only in the placenta. About 67 kb of the hGH gene locus, including intergenic sequences and up- and downstream flanking regions, have been completely sequenced (29). The five gene cluster itself spans about 48 kb (30) and contains the genes for hGH, designated as hGH-N (for normal); two genes for hPL, designated hCS-L (hCS-like) and hCS-A; the gene for hGH-V (for variant); and a third PL gene, hCS-B, arranged in order in the 5′ to 3′ direction. All five genes are transcriptionally oriented in the same direction and are separated by intergenic regions of 6 kb to 13 kb in length. The intergenic regions contain 48 middle repetitive Alu sequences that comprise more than 20% of the nucleotides in the hGH locus (29). A repeated P element consisting of about 1 kb is also found about 2 kb upstream from the promoters of the four placentally expressed genes. The hCS-A and hCS-B genes encode prehormones that differ by one amino acid in the leader sequence have five silent nucleotide differences, but the mature proteins are identical (31). The hCS-B gene also contains a small insertion in the 3′ untranslated region that is not found in hCS-A. The nucleotide sequence of the hCS-L gene shows 93% to 94% homology with the genes for hCS-A and hCS-B, but, because a G to A transition in the splice donor site of the second intron interferes with RNA processing at this site, a complex array of alternatively spliced mRNAs is formed, the majority of which are nonfunctional. One mRNA, however, encodes a 20 kDa protein that may be secreted (32). Expression of the hCS-A and hCS-B genes in the placenta is about 1,000 times higher than that of hGH-V or hCS-L genes (29).

Unlike the primate genome, which contains a single prolactin gene and multiple GH-related genes, the genomes of rodents and ruminants appear to contain a single GH gene and multiple PRL-related genes as judged from their nucleic acid and protein structures. PLs appear to be lacking in other mammalian groups (33). The GH locus and the PRL locus in rodents and ruminants are on separate chromosomes that appear to be homologous with their human counterparts as judged from the colocalization with other known genes. Genes for the numerous PRL-related proteins that are expressed in the placentae of cattle, sheep, rats, and mice map to the same chromosomes as PRL, and, although the entire PRL chromosomal locus has not been sequenced in any of these species, it is likely that they cluster in a fashion analogous to that seen in the human GH locus (34-37).

6. Regulation of GH Gene Expression

There are two aspects to regulation of GH gene expression; both are complex and incompletely understood. One aspect concerns the factors that determine tissue specificity and restricts GH expression to the somatotropes. The other aspect concerns the regulation of the levels of expression by the somatotropes. Expression of hGH-N, but not hGH-V, in the somatotropes is thought to be governed by remote regions of 5′ flanking DNA tens of thousands of bases upstream from the hGH-N gene. These elements, along with somatotrope-specific regulatory proteins, may reorganize the chromatin such that the transactivation factors discussed below have access to the promoter region of the downstream gene (38). Somewhat different control mechanisms may pertain to nonprimates that express only one gene at the GH locus, but, throughout the vertebrates, expression of proteins of the GH/PRL family depends upon the indispensable regulatory protein, Pit-1, which is also sometimes called GHF-1. Pit-1 is a ~290 amino acid protein that is expressed only in certain pituitary cells, the placenta and monocytes that produce GH, and, thus provides cell-specific regulation (39, 40). Pit-1 is also crucial for differentiation and growth of somatotropes during development and for the induction of the GHRH receptor and, hence, sensitivity to hypothalamic control (41). As mentioned earlier, GHRH is the hypothalamic hormone that stimulates the somatotrope to synthesize and secrete GH. In addition, Pit-1 also activates its own transcription and, thereby, maintains the differentiated function of somatotropes, lactotropes, and somatomammotropes (42).

Physiologically, GH synthesis and secretion are driven by GHRH, which acts through receptors on the somatotrope surface to increase the production of cyclic AMP, which binds to and activates protein kinase A. Protein kinase A catalyzes the phosphorylation of a variety of proteins on serine residues and, thereby, increases or decreases their activities. Among the substrates for protein kinase A in the somatotrope are nuclear regulatory factors of the cyclic nucleotide response element binding (CREB) protein family. The hypothalamic peptide somatostatin inhibits GH synthesis and secretion by blocking the actions of GHRH on cyclic AMP production and ion permeability. In addition, peripheral hormones, triiodothyronine from the thyroid gland and glucocorticoids from the adrenal cortex, enhance GH synthesis and secretion. Other paracrine (eg, activin) and circulating factors (insulin, retinoic acid, vitamin D) also act on the somatotrope to modulate GH production either positively or negatively, while yet other regulatory influences, (eg, IGF-I, free fatty acids and glucose) regulate events in the somatotrope through their actions on GHRH and somatostatin secretion.

The proximal promoter includes the TATA box sequence, which for all of the vertebrate GH genes is TATAAAA and for the PRL and somatolactin genes is TATAAAG (15). Regulation is largely conferred by critical nucleotide sequences that lie within a few hundred bases upstream of the cap site in mammalian GH genes and are the elements that bind regulatory proteins. The hGH-N gene has two binding elements for Pit-1, at 80 and 122 base pairs 5′ to the transcription initiation site. These sites are conserved at similar positions in rodent and other GH genes. The ubiquitous zinc finger protein Zn-15 binds to the so-called Z box, a highly conserved sequence located between the Pit-1 elements, and synergizes with Pit-1 (43). Other ubiquitous regulatory factors that bind to the hGH-N promoter include Sp1, AP2 (activator protein 2), NF-1 (nuclear factor-1), USF (upstream stimulatory factor), and the glucocorticoid receptor (42). There is an additional glucocorticoid binding site in the first intron of the hGH-N gene. Glucocorticoid hormones enhance GH expression by augmenting transcription and may also stabilize GH mRNA. The rat GH gene also contains a silencer element whose binding protein is specifically absent in somatotropes (44). Much less is understood concerning control of the the expression of hGH-V. Repression of hGH-V expression in the pituitary may be achieved through the agency of the P element located upstream from each of the placentally expressed genes of the GH family (29).

Despite the high degree of conservation seen in many aspects of the structure and regulation of the GH gene, some different mechanisms appear to apply for regulation of the human and rat genes. The hGH-N gene has two CREB binding sites (45), but these are lacking in the rat GH gene (46). GHRH may, therefore, directly activate the GH gene in humans, but, in rodents, its influence may be exerted indirectly via cyclic AMP response elements (CREs) in the rat Pit-1 promoter and increased synthesis of Pit-1 (47). The human Pit-1 promoter lacks recognizable CREs. The rat GH promoter, but not the hGH-N promoter contains a general hormone response element that binds to thyroid hormone receptors (48) as well as retinoic acid and vitamin D receptors (49). Accordingly, thyroid hormone enhances transcription of the rat GH gene, but not hGH-N.

7. Splice Variants

The preRNA transcripts are processed and spliced to produce mRNA that codes for a prehGH that contains a leader sequence of 26 amino acids that is cotranslationally removed. The first exon/intron boundary is of the class I type, falling between the first and second nucleotides of the glycine codon in hGH-N. The remaining exon/intron boundaries are of the class 0 type and fall between codons.

The translated portion of exon I includes 10 nucleotides: the first three codons and the first nucleotide of codon 4. Exon 2 begins with the second and third nucleotides of codon 4 and contains the codons for the remaining 22 amino acids of the leader sequence and the first 31 residues of the mature protein. Exon 3 codes for residues 32 to 71 of the 22k form of hGH. Exon 4 consists of the codons for residues 72 to 126, and exon 5 codes for the remaining 65 amino acids and the 3′ untranslated region. Codon 46 in exon 3 contains the dinucleotide AG, which can act as an alternate splice acceptor site. In about 10% of the transcripts, the 45 nucleotides at the 5′ end of exon 3 are removed along with the second intron to produce an mRNA that codes for a shorter peptide chain lacking 15 amino acids (residues 32 to 46) and with a mass of 20 kDa (17). A second, and considerably less abundant, splice variant of the hGH-N gene arises from the complete deletion of exon 3 to give rise to a 151 amino acid form with a mass of 17.5 kDa (18). Other mRNA variants lacking exons 3 and 4, and 2, 3, and 4 have been found by reverse transcription-polymerase chain reaction experiments, but it is not known if they are translated or secreted (50).

Although the hGH-V transcript is identical to the hGH-N transcript in the vicinity of the alternate splice site, no alternative splicing of hGH-V occurs at this site. This appears entirely attributable to three nucleotides present only in the hGH-N transcripts and located between the normal and the alternative splice acceptor sites at positions 17, 18, and 24 bases upstream from the alternative site (51). The transcript of hGH-V, however, is subject to alternative splicing in which the 253 nucleotides of intron 4 are retained. Because the reading frame remains open through intron 4 and into exon 5, but with a +1 frame shift, the resulting hGH-V2 transcript codes for a protein in which the 65 carboxyl terminal amino acids are replaced by a different 104 residue carboxyl tail (24). This alternatively spliced transcript represents about one-third of the hGH-V mRNA, but no hGH-V2 protein is secreted, perhaps because a hydrophobic sequence in the new carboxyl tail causes it to be retained within the synctiotrophoblast. Intron 4 may be similarly retained in alternatively spliced transcripts of hCS-A and hCS-B (52) and in bovine GH (53). Alternative splice variants of other species of GH appear not to have been studied extensively.

8. Mechanism of Action

8.1. The GH Receptor

The GH Receptor (GHR) was purified from the richest known source, the rabbit liver, by Waters and Friesen (54). It was cloned from a rabbit cDNA library using an oligonucleotide probe whose construction was based on the amino acid sequence of a fragment of the rabbit GHR (55) and identified using monoclonal antibodies raised against the purified protein in the Waters laboratory (56). Human, rodent, ruminant, porcine, and chicken GHRs were cloned soon thereafter, and the mammalian receptors were found to share 70% or greater sequence identity. The ~4 kb cDNA codes for a 620 amino acid mature protein with an 18 residue leader sequence. Hydropathy analysis indicated a single membrane-spanning region of 24 amino acid residues separating the N-terminal 246 residue extracellular domain from the 350 residue cytosolic domain. The extracellular domain contains seven cysteine residues, of which six are paired in S-S linkage, and five potential N-glycosidation sites. The intracellular domain contains no known catalytic activity but associates with a cytosolic protein tyrosine kinase, Janus kinase-2 (JAK2), which appears to bind to a proline-rich region of the receptor adjacent to the membrane-spanning domain.

The human GHR receptor is a single copy gene on chromosome 5. Its coding and nontranslated 3′ tail are encoded by nine exons, designated 2 to 10, extending over 87 kb. (57). Exon 2 codes for the signal peptide, 3 through 7 for the extracellular domain, exon 8 for the transmembrane domain, exon 9 the beginning of the cytosolic domain, and the long exon 10 (3,400 bp) codes for the bulk of the intracellular domain and the long 3′ untranslated region. At least eight variants of the 5′ untranslated region are found in the human GHR gene (58), and multiple 5′ regions are present in other GHRs indicative of multiple, perhaps tissue specific, promoters. Rodent GHR genes also contain several variants at the 5′ end as well as an additional exon (exon 8A) between exons 7 and 8 (59). Alternative splicing that replaces exons 8, 9, and 10 with exon 8A produces an mRNA that codes for the circulating GH binding protein (GHBP) in rodents (60). The GHBP has a hydrophilic carboxyl tail instead of the transmembrane and cytosolic domains of the GHR.

As with their cognate hormones, the GH and PRL receptors share many similarities in structure (61). The human GH and PRL receptor genes map to the same locus on chromosome 5 (62). The GH and PRL receptors belong to the superfamily of Cytokine/Hematopoietin receptors that includes receptors for erythropoietin, interferon, interleukins 3 and 5, the common subunit of interleukins 2, 4, 7, 9 and 15, the common subunit (gp130) of interleukins 6 and 11, oncostatin, leukemia inhibitory factor, and several others. The relationship is based on both primary and tertiary structural features of the extracellular and cytosolic domains and is also reflected in similarities in the modes of signalling of these receptors. Ligands for these receptors are four helix bundle structures as described for GH.

8.2. GH-Receptor Binding

In a brilliant series of experiments summarized in Wells and colleagues (63) at Genentech mapped the surfaces of the hGH and receptor molecules that come in contact upon binding and determined the stoichiometry of binding to be two receptors per hGH molecule (Fig. 3). High resolution X-ray crystallography of the complex of hGH bound to the extracellular domain of the GHR (64) revealed that virtually identical binding sites on the two receptor molecules bind to nonidentical sites on the surface of the four helix bundle GH molecule and came in contact with each other in their C-terminal regions in a manner that would bring the transmembrane and cytosolic domains in close apposition (Fig. 4). Their data indicated that GH sequentially binds to one receptor molecule at the so called site 1 on GH and then to a second receptor at site 2 on the hormone, the consequences of which produce a receptor dimer and the initial step in signalling. Binding is ordered due to stronger interaction between hGH and the GHR at site 1 than at site 2. Dimerization of the GH receptor upon ligand binding is prototypical of the behavior of the large superfamily of cytokine receptors and provides a basis for understanding how hormone binding can be transduced into a signal by other tyrosine kinase-dependent receptors as well.

Figure 3. Patches on the surface of hGH that bind the hGHR. Key amino acid residues whose mutation to alanine decreases binding are indicated. GH binds to its receptor first at **Site 1** and then at **Site 2**. Note that the orientation of the hGH molecule has been rotated 180° horizontally from that shown in Figure 2 (modified from ref 62).

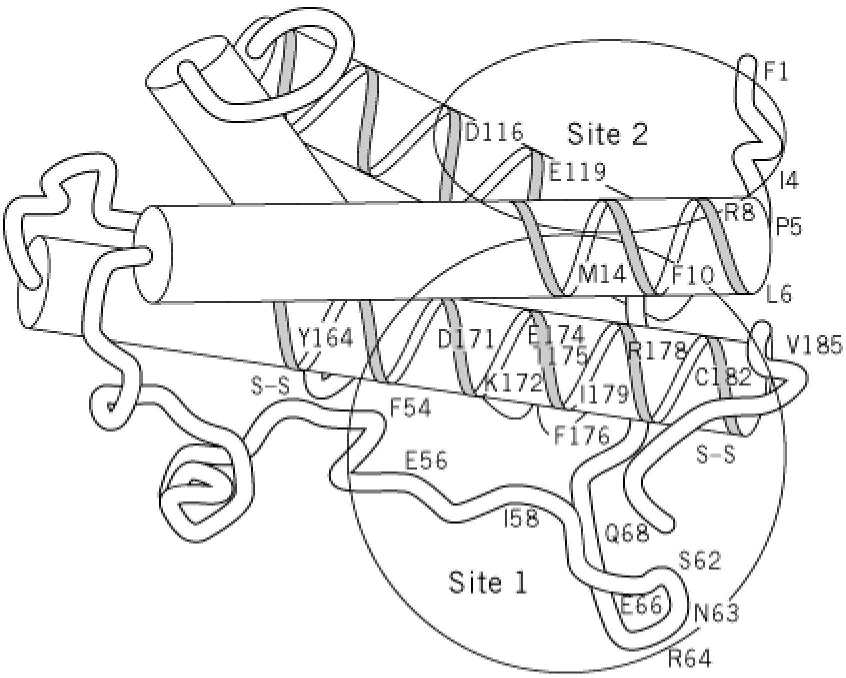

Figure 4. Three-dimensional structure of the GH:GHR complex. Two molecules of the extracellular domain of the GHR, indicated here as **BP1** and **BP2** bind to opposite faces of **hGH** and interact with other in the juxta**membrane** region. (from ref. 62).

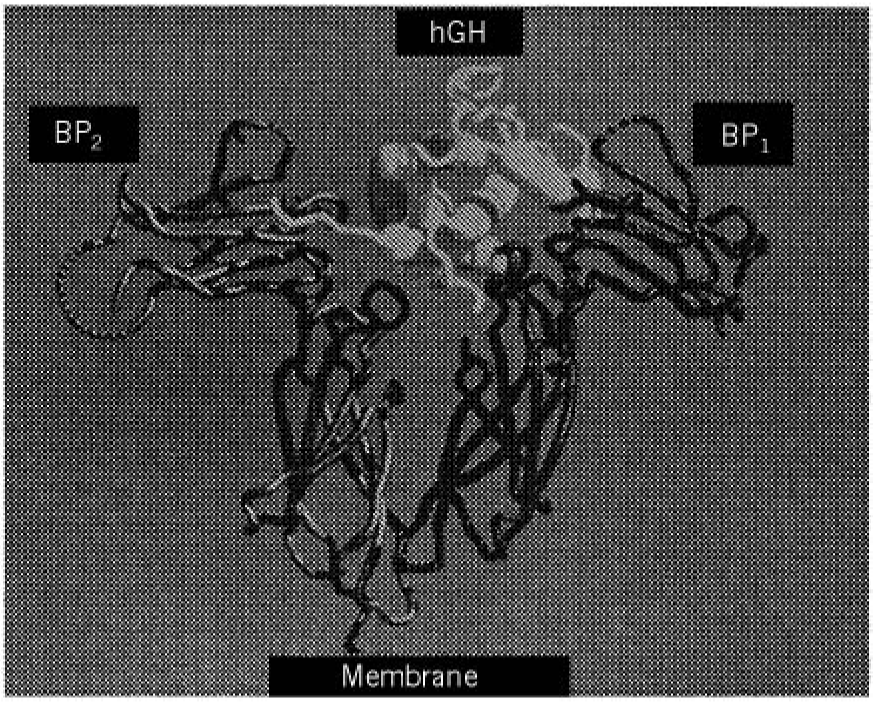

These studies defined the amino acid residues in the GH molecule that contribute to receptor binding either because they come in direct contact with the surface of the receptor or because they contribute to the tertiary structure in a way that presents the interacting amino acids in the proper orientation. "Designer" GH molecules with greater or lesser affinity for lactogenic receptors (65) have been prepared as well as GH molecules with greater affinity for the receptor or an antagonist (G120R) with a mutation in the third helix that interferes with binding at site 2 (66). The region of highest conservation in GH is near the carboxyl terminus, which encompasses amino acids that contribute heavily to site 1. One of the nonconserved amino acids in this region is located at position 171, which in all nonprimate GHs is histidine, but in all primate GHs is aspartic acid. The coordinating residue on the hGHR is arginine in position 43 in place of leucine all other receptors. The incompatibility of His171 in nonprimate hormones with Arg 43 in the human receptor decreases binding affinity 200-fold and is largely responsible for "species specificity" (67).

8.3. Signal Transduction

The primary event in GH signal transduction is the GH-induced dimerization of the GHR, which is thought to bring the cytosolic domains in close apposition resulting in activation and perhaps recruitment of the cytoplasmic tyrosine kinase, Janus kinase-2 (JAK2) and other members of the Janus kinase family (68). Activation of JAK2 results in phosphorylation of tyrosine residues in the GHR and of JAK2 itself. JAK2 appears to associate with the GHR at the N-terminal third of the cytosolic domain, within which is a critical proline-rich region adjacent to the membrane-spanning domain (box 1) that is conserved within the receptor superfamily. Because a relatively large number of cytosolic and nuclear proteins become tyrosine phosphorylated, it is likely that JAK2 has additional substrates or that other tyrosine kinases are recruited and become activated. Phosphorylated tyrosine residues serve as docking sites for other proteins that contain Src Homology 2 (SH2) domains (see **Src Homology 2**, this volume), thereby recruiting other specific proteins that may be substrates for JAK2 or adapter proteins (e.g., SHC or GRB2) that recruit or activate other proteins to the complex and initiate signaling pathways. As with other tyrosine kinase-dependent signalling, multiple pathways appear to be activated (69). One of the most prominent of these pathways involves the Stat proteins (for *s*ignal *t*ransduction and *a*ctivation of *t*ranscription) which, upon activation by tyrosine phosphorylation, form homo- or hetero-dimers with other Stat proteins, migrate to the nucleus, bind DNA, and activate transcription of particular GH-sensitive genes including the early response gene c-fos (70) and the hepatic serine protease inhibitor-1 (Spi-1) gene (71). Activation of JAK2 also directly or indirectly leads to tyrosine phosphorylation of the insulin receptor substrates, IRS-1 and 2, and to activation of phosphatidylinositol-3-kinase and can, thereby, set in motion various metabolic responses to GH (68). Another prominent signaling cascade, the MAP kinase (for *m*itogen *a*ctivated *p*rotein) pathway is also activated. MAP kinases catalyze the phosphorylation on serine residues of diverse proteins including many other protein kinases, Stat proteins, cytoskeletal proteins, and transcription factors such as Elk1, which, when phosphorylated, bind to the c-fos promoter. Stimulation of cells with GH also results in the activation of phospholipase(s), which cleaves membrane phospholipids to release diacylglycerol, which may activate various isoforms of protein kinase C. Protein kinase C catalyzes serine phosphorylation of diverse cellular proteins including DNA regulatory proteins. Finally, GH also causes a rapid increase in intracellular-free calcium (72) by a mechanism that is likely independent of JAK2 as this effect is evident in cells that only express a mutant form of the GHR that cannot bind JAK2 (73). Most of these signalling cascades participate in signal transduction by a variety of hormones, cytokines, and other extracellular signalling molecules, raising the issue of how specific and unique responses to GH are achieved in cells that are also responsive to other agonists. It is likely that the various signalling pathways activated by GH intersect, reinforce, or obtund each other in patterns that are unique to GH and to the particular target cells to produce specific responses to GH.

Bibliography

1. H. M. Evans and J. A. Long (1921) Anat. Rec. **21**, 62–63.
2. O. Riddle, R. W. Bates, and S. W. Dykeshorn (1932) Proc. Soc. Exp. Biol. Med. **29**, 1211–1215.
3. R. W. Bates, T. Laanes, and O. Riddle (1935) Proc. Soc. Exp. Biol. Med. **33**, 446–450.
4. C. H. Li and H. M. Evans (1944) Science **99**, 183–184.
5. E. Knobil and R. O. Greep (1959) Rec. Prog. Horm. Res. **15**, 1–58.
6. S. D. Frasier (1997) J. Pediatr **131**, S1–S4.
7. H. D. Niall, M. L. Hogan, G. W. Tregear, G. V. Segre, P. Hwang, and H. G. Friesen (1973) Rec. Prog. Horm. Res. **29**, 387–416.
8. P. H. Seeburg, J. Shine, J. A. Martial, R. D. Ivarie, J. A. Morris, A. Ullrich, J. D. Baxter, and H. M. Goodman (1978) Nature **276**, 795–798.
9. J. A. Martial, R. A. Hallewell, J. D. Baxter, and H. M. Goodman (1979) Science **205**, 602–607.
10. M. J. Cronin (1997) J. Pediatr. **131**, S5–7.
11. R. D. Palmiter, G. Norstedt, R. E. Gelinas, R. E. Hammer, and R. L. Brinster (1983) Science **222**, 809–814.
12. J. L. Liu, S. Yakar D. LeRoith (2000) Endocrinology **141**, 4436–4441.
13. L. A. Frohman and J. O. Jansson (1986) Endocr. Rev. **7**, 223–253.
14. M. Rand-Weaver, H. Kawauchi, and M. Ono (1992) "Evolution of the structure of the growth hormone prolactin family". In *The Endocrinology of Growth, Development, and Metabolism in Vertebrates*, (M. P. Schreibman, C. G. Scanes, and P. K. T. Pang, eds.,) Academic Press, San Diego, pp. 13–42.
15. Y. Zhang, J. Jiang, R. A. Black, G. Baumann, and S. J. Frank (2000) Endocrinology **141**, 4342–4348.
16. S. S. Abdel-Meguid, H. S. Shieh, W. W. Smith, H. E. Dayringer, B. N. Violand, and L. A. Bentle (1987) Proc. Natl. Acad. Sci. USA **84**, 6434–6437.
17. F. M. DeNoto, D. D. Moore, and H. M. Goodman (1981) Nucleic Acids Res. **9**, 3719–3730.

18. C. M. Lecomte, A. Renard, and J. A. Martial (1987) Nucleic Acid Res. **15**, 6331–6348.
19. U. J. Lewis (1984) Annu. Rev. Physiol. **46**, 33–42.
20. C. S. Nicoll (1974) "Physiological actions of prolactin". In *Handbook of Physiology, Endocrinology*, Vol. **4**, The Pituitary Gland and Its Neuroendocrine Control (E. Knobil and W. H. Sawyer, eds.,) American Physiological Society, Washington, pp. 253–292.
21. H. D. Niall, M. L. Hogan, R. Sayer, I. Y. Rosenblum, and F. C. Greenwood (1971) Proc. Natl. Acad. Sci. U.S.A. **68**, 866–870.
22. M. Rand-Weaver, T. Noso, K. Muramoto, and H. Kawauchi (1991) J. Biochem. **30**, 1509–1515.
23. G. Hennen, F. Frankenne, J. Closset, F, Gomez, G. Pirens, and N. el Khayat (1985) Int. J. Fertil. **30**. 27–33.
24. J. Ray, B. K. Jones, and S. A. Liebhaber (1989) Endocrinology **125**, 566–568.
25. N. E. Cooke, J. Ray. J. G. Emery, and S. A. Liebhaber (1988) Two distinct species of human growth hormone-variant mRNA in the human placenta predict the expression of novel growth hormone proteins. J. Biol. Chem. **263**, 9001–9006.
26. D. L. George, J. A. Phillips III,, U. Francke, and P. H. Seeburg (1981) Hum. Genet. **57**, 138–141.
27. D. Owerbach, W. J. Rutter, J. A. Martial, and J. D. Baxter (1980) Science **209**, 289–291.
28. D. Owerbach, W. J. Rutter, N. E. Cooke, J. A. Martial, and T. B. Shows (1981) Science **212**, 815–816.
29. E. Y. Chen, Y-C. Liao, D. H. Smith, Barrera-Saldaña, R. E. Gelinas, and P. H. Seeburg (1989) Genomics **4**, 479–497.
30. G. S. Barsh P. H. Seeburg, and R. E. Galinas (1983) Nucleic Acids Res. **11**, 3939–3958.
31. H. A. Barrera-Saldaña, P. H. Seeburg, and G. F. Saunders (1983) J. Biol. Chem. **258**, 3787–3793.
32. A. Misra-Press, N. E. Cooke, S. A. Liebhaber (1994) Complex alternative splicing partially inactivate the human chorionic somatomammotropin-like (hCS-L) gene. J. Biol. Chem. **269**, 23220–23229.
33. F. Talamantes, L. Ogren, E. Markoff, S. Woodard, and J. Madrid (1980) Fed. Proc. **39**, 2582–2587.
34. R. Hediger, S. E. Johnson, W. Barendse, R. D. Drinkwater, S. S. Moore, and J. Hetzel (1990) Genomics **8**, 171–174.
35. L. L. Jacson-Grusby, D. Pravtcheva, F. H. Ruddle, D. I. H. Linzer (1988) Endocrinology **122** 2462–2466.
36. A. B. Dietz, M. Georges, D. W. Threadgill, J. E. Womack, and L. A. Schuler (1992) Genomics **14**, 137–143.
37. N. E. Cooke, C. Szpirer, and G. Levan (1986) Endocrinology **119**, 2451–2454.
38. B. K. Jones, B. R. Monks, S. A. Liebhaber, and N. E. Cooke (1995) Mol. Cell Biol. **15**, 7010–7021.
39. C. Lefevre, M. Imagawa, S. Dana, J. Grindlay, M. Bodner, and M. Karin (1987) EMBO J. **6**, 971–981.
40. C. Nelson, V. R. Albert, H. P. Elsholtz, I.-W. Lu, and M. Rosenfeld (1988) Science **239**, 1400–1405.
41. C. Lin, S.-C. Lin, C.-P. Chang, and M. G. Rosenfeld (1992) Nature **390**, 765–768.
42. L. E. Theill and M. Karin (1993) Endocr. Rev. **14**, 670–689.
43. S. N. Lipkin, A. M. Näär, K. A. Kalla, R. A. Sack, and M. G. Rosenfeld (1993) Genes Devel. **7**, 1674–1687.
44. R. J. Roy, P. Gosselin, M. J. Anzivino, D. D. Moore, and S. L. Guerin, (1992) Nucleic Acids Res. **20**, 401–408.

45. A. R. Shepard, W. Zhang, and Eberhard N. L. (1994) J. Biol. Chem. **269**, 18094–1814.
46. F. Argenton, S. Bernardini, S. Puttini, L. Colombo, and M. A. T. Bortousi (1996) Eur. J. Biochem. **238**, 591–598.
47. A. McCormick, H. Rady, J. Fukushima, and M. Karin, (1991) Genes Devel. **4** 1490–1503.
48. A. Sugawara, P. M. Yen, and W. W. Chin, (1994) Endocrinology **135**, 1956–1962.
49. P. Garcia-Villalba, Jimenez-Lara, and A. Aranda (1996) Mol. Cell Biol. **16**, 318–327.
50. A. Palmetshofer, D. Zechner, T. A. Luger, and A. Barta, (1995) Mol. Cell Endocrinol. **22**, 225–234.
51. P. Estes, N. E. Cooke, and S. A. Liebhaber, (1990) J. Biol. Chem. **265**, 19863–1987.
52. J. N. Macleod, A. K. Lee, S. A. Liebhaber, and N. E. Cooke (1992) J. Biol. Chem. **267**, 14219–14226.
53. R. K. Hampson and F. M. Rottman (1987) Proc. Natl. Acad. Sci. U.S.A. **84**, 2673–2677.
54. M. J. Waters and H. G. Friesen (1979) J. Biol. Chem. **254**, 6815–6825.
55. R. Barnard, P. Bundesen, D. Rylatt, and M. J. Waters (1984) Endocrinology **115**, 1805–1813.
56. D. W. Leung, S. A. Spencer, G. Cachianes, R. G. Hammonds, C. Collins, W. J. Henzel, R. Barnard, M. J. Waters, and W. I. Wood (1987) Nature **330**, 537–543.
57. P. J. Godowski, D. W. Leung, L. R. Meacham, J. P. Galgani, R. Hellmiss, R. Keret, P. S. Rotwein, J. S. Parks, Z. Laron, W. I. Wood (1989) Proc. Natl. Acad. Sci. U.S.A. **86**, 8083–8087.
58. R. I. Pekhletsky, B. K. Chernov, and P. M. Rubtsov (1992) Mol. Cell Endocrinol. 90 103–109.
59. A. Edens, J. N. Southard, and F. Talamantes (1994) Endocrinology **135**, 2802–2805.
60. W. C. Smith, J. Kuniyoshi, and F. Talamantes (1989) Mol. Endocrinol. **3**, 984–990.
61. P. A. Kelly, J. Djiane, M. C. Postel-Vinay, and M. Edery (1991) Endocr. Rev. **12**, 235–251.
62. K. C. Arden, J. M. Boutin, P. A. Kelly, J. Dijane, and W. K. Cavenee (1990) Cytogenet. Cell Genet. **53**, 161–165.
63. J. A. Wells, B. C. Cunningham, G. Fuh, H. B. Lowman, S. H. Bass, M. G. Mulkerrin, M. Ultsch, and A. M. de Vos (1993) Rec. Prog. Horm. Res. **48**, 253–275.
64. A. M. de Vos, M. Ultsch, A. A. Kossiakoff (1992) Science **255**, 306–312.
65. B. C. Cunningham and J. A. Wells (1991) Proc Natl Acad Sci U.S.A. **88**, 3407–3411.
66. G. Fuh, B. C. Cunningham, R. Fukunaga, S. Nagata, D. V. Goeddel, and J. A. Wells (1992) Science **256**, 1677–1680.
67. S. C. Souza, G. P. Frick, X. Wang, J. J. Kopchick, R. B. Lobo, and H. M. Goodman (1995) Proc. Natl. Acad. Sci. U.S.A. **92**, 959–963.
68. L. S. Argetsinger, G. S. Campbell, X. Yang, A. Witthuhn, O. Silvennoinen, J. N. Ihle and C. Carter-Su (1993) Cell **74** 237–244.
69. L. S. Argetsinger and C. Carter-Su (1996) Physiol. Rev. **76**, 1089–1107.
70. D. J. Meyer, G. S. Campbell, B. H. Cochran, L. S. Argetsinger, A. C. Larner, D. S. Finbloom, C. Carter-Su, J. Schwartz, (1994) J. Biol. Chem. **269**, 4701–4704.
71. P. L. Bergad, H.-M. Shih, H. C. Towle, S. J. Schwartzenberg, and S. A. Berry (1995) J. Biol. Chem. **270**, 24903–24910.
72. Y. Schwartz, H. M. Goodman, and H. Yamaguchi (1991) Proc. Natl. Acad. Sci. U.S.A. **88**, 6790–6794.
73. N. Billestrup, P. Bouchelouche, G. Allevato, M. Ilondo, and J. H. Nielsen (1995) Proc. Natl. Acad. Sci. U.S.A. **92**, 2725–2729.

Suggestions for Further Reading

74. N. E. Cooke and S. A. Liebhaber (1996) Molecular biology of the growth hormone-prolactin gene system. Vitamins Hormones **50**, 385–459.

75. V. Goffin, K. T. Shiverick, P. A. Kelly, and J. A. Martial (1996) Sequence-function relationships within the expanding family of prolactin, growth hormone, placental lactogen, and related proteins in mammals. Endocrinol. Rev. **17**, 385–410.
76. J. A. Wells and A. M. de Vos (1993) Structure and function of human growth hormone: Implications for the hematopoietins. Annu. Rev. Biophys. Biomol. Struct. **22**, 329–351.
77. R. V. Anthony, R. Liang, E. P. Kayl, and S. L. Pratt (1995) The growth hormone/prolactin gene family in ruminant placentae. J. Reproduct. Fertil. Suppl. **49**, 83–95.
78. J. L. Kostyo ed. (1999). "The endocrine system: Hormonal control of growth", In *Handbook of Physiology*, Oxford University Press, New York.

Gtpases

Regulatory GTPases form a large, evolutionarily related superfamily of enzymes that catalyze the hydrolysis of GTP to GDP and inorganic orthophosphate. The importance of these GTP-binding proteins lies, however, in the diverse regulatory activities that they acquire upon GTP binding and that are terminated by GTP hydrolysis. The GTPases thus act as molecular switches, active in the GTP-bound form and inactive in the GDP-bound form. GTP binding and GTP hydrolysis are both tightly regulated by other proteins (see Guanine Nucleotide Exchange Factors and RGS Proteins). These proteins thus control a GTPase catalytic cycle and determine the fraction of time that the GTPase will spend in the active states. Alternatively, the regulatory proteins can independently turn the switch on or off in response to appropriate signals.

All the GTPases share a conserved structure around the GTP-binding site, with three identifiable regions of conserved amino-acid sequence. More closely related families share further sequence similarities. The individual families of GTPases are defined by the activities that they regulate and by their conserved structures. Each family is discussed under separate entries.

1. Multiple initiation factors and elongation factors required for translation on ribosomes are regulatory GTPases. Their GTP-triggered functions include the recruitment of aminoacyl-tRNAs to the ribosome, participation in peptide bond formation and the associated movement of the nascent protein on the ribosome (see Translation). This structurally and functionally diverse group also includes proteins involved in translocation of nascent proteins across membranes, such as the signal recognition particle. Elongation factor Tu (EF-Tu) from *Escherichia coli* is the historic prototype of the GTPase superfamily. Several proteins involved with co-translational, **signal sequence**-mediated translocation of nascent proteins through membranes are GTP-binding proteins more distantly related to this group.
2. Small, monomeric GTP-binding proteins (SMGs) constitute a large family of structurally related GTPases, most in the 20- to 25-kDa size range. They mediate numerous functions in eukaryotic cells, including activation of protein kinase signaling cascades, regulation of cytoskeleton structure, **nuclear import/export**, budding and docking of membrane **vesicles** involved in subcellular organellar trafficking, and so on.
3. **Heterotrimeric GTP-binding** regulatory proteins, often referred to as G proteins, organize and convey signals from cell surface receptors to cellular effector proteins, such as **adenylyl cyclase**, cyclic GMP phosphodiesterase, **ion channels**, phospholipase C, protein kinases, and so on. Individual G proteins (about 20 in total) display distinct but nonunique selectivity among receptors and effectors. Both the GTP-binding a subunits (~40 kDa), which include a domain similar to the SMGs, and the tightly associated b and g subunits convey signals to distinct effectors.

4. **Dynamins** are GTP-binding cytoskeletal proteins involved in the budding of endocytic vesicles. They are homologous to the other GTP-binding proteins only in the immediate region of the GTP-binding pocket. Dynamins also interact with the bg subunits of the heterotrimeric G proteins.
5. **Tubulins**, the structural proteins of eukaryotic microtubules, are also GTPases but are only distantly related to the regulatory GTPases. Polymerization of microtubules is regulated in part by GTP binding to tubulin.

GTP-Binding Proteins

GTP-binding proteins are members of a superfamily of regulatory proteins whose activity is controlled by binding GTP. They act as conformational molecular switches that regulate numerous and diverse processes throughout the eukaryotes. Many GTP-binding proteins are devoted to signal transduction, mediating information transfer from receptors to intracellular effector proteins. Others regulate such diverse processes as the traffic of membrane proteins and lipids via cytoplasmic transport **vesicles**, the **cytoskeleton**-mediated control of cell morphology, **nuclear import/export**, and such membrane-reforming processes as endocytosis, protein secretion, and budding. In their GTP-bound, active forms, GTP-binding proteins can stimulate or inhibit the activity of cellular effector proteins, recruit effectors to specific intracellular sites, or sequester effectors and thus block their activity. These proteins thus lie at the convergence of multiple regulatory pathways and function as major integrators of cellular information.

GTP-binding proteins are divided into two major classes, each of which is further divided into individual families. Generally, these structurally determined groupings also indicate related functional specialization and biochemical properties. GTP-binding proteins are ubiquitous throughout the eukaryotes, however, and structurally related proteins may perform strikingly different functions in distantly related organisms.

The two major groups of GTP-binding proteins are the heterotrimeric G proteins and the small, monomeric GTP-binding (SMG) proteins. SMGs are also commonly referred to as G proteins, or small G proteins, and the nomenclature is not well established. Heterotrimeric G proteins are composed of a GTP-binding a subunit (~40 to 45 kDa) and a dimer of b and g regulatory subunits (~35 kDa and 7 to 8 kDa). Heterotrimeric G proteins convey signals from receptors at the cell surface to cellular effector proteins (see Heterotrimeric G Proteins). The SMG proteins (20 to 25 kDa) are involved in more diverse functions. In addition to these two major classes, other GTP-binding proteins with related primary structures, tertiary structures, and GTPase cycles include the elongation factors of translation (with bacterial EF-Tu as prototype) and **dynamin** (see Gtpases).

Heterotrimeric G proteins are grouped according to the structures and functions of their a subunits and are named with subscripts originally linked to their functions (1, 2). Members of the G_s family were the first G proteins to be discovered as stimulators (hence “s”) of **adenylyl cyclase**. The G_i's were initially defined as cyclase inhibitors (“i”), but they also perform many other functions. The G_q's stimulate the phosphatidylinositol bisphosphate-specific **phospholipase C-b**'s. Functions of the $G_{12/13}$ family include regulation of the **rho** SMG family and of Na^+/H^+ exchangers. The bg subunits are also diverse: There are 5 Gb subunits and at least 11 Gg subunits in mammals. While not all of the 55 conceivable Gbg dimers occur, their potential diversity is huge.

The SMG proteins cluster in five major subfamilies according to their structure and function. Smaller families also exist, and assignment of some SMGs to families remains uncertain. The ras proteins constitute a family of about five proteins in mammals, although gem/kir proteins are also assigned to this group (3-6). Ras proteins were the first SMGs to be identified, because they are active and frequently observed **oncoproteins** when mutated to constitutively active forms or when overexpressed (7). Ras proteins are the prototypical and best-studied examples of the SMG group (see Oncogenes, Oncoproteins). The rac family (rac, rho, CDC42) are involved in both signal transduction and in the regulation of cytoskeletal control of cell morphology (8, 9). Rab family members (at least 20) are involved in protein secretion and endocytosis (10, 11). ARFs (at least 6) mediate the budding and fusion of intracellular membrane vesicles (12, 13). Ran mediates both inward and outward traffic of macromolecules from the nucleus (14, 15) (see **Nuclear import/export**).

Both heterotrimeric G proteins and SMG proteins act by traversing a tightly controlled cycle of GTP binding and hydrolysis. GTP binding activates G proteins (Fig. 1) (1, 16). Activation is terminated when the bound GTP is hydrolyzed by the G protein's intrinsic GTPase activity. The GDP-bound form is inactive, as is the unliganded form. Each step in this cycle—GTP binding, GTP hydrolysis, and GDP release—is relatively slow, and each can be regulated both positively and negatively. Activation—GDP dissociation and GTP binding—is promoted by guanine nucleotide exchange factors (GEFs). GEFs are also referred to as exchange catalysts. They can be either cell-surface receptors that act in response to extracellular signals or cytosolic proteins that are regulated by **allosteric** ligands or **phosphorylation**. Activation is inhibited by GDP dissociation inhibitors (GDIs), which are regulated independently. Deactivation is also accelerated by GTPase-activating proteins (GAPs), providing a third regulatory input. The net output represents the integration of all three inputs.

Figure 1. The regulatory GTPase cycle for GTP-binding proteins. GTP-binding proteins, G, are converted by GTP to the active state G*-GTP in which they can bind and activate effector proteins. Activation is terminated by hydrolysis of the bound GTP to GDP, which is usually a slow process that is accelerated by GTPase-activating proteins (GAPs). The inactive G–GDP complex is relatively stable, unless nucleotide exchange is catalyzed by a guanine nucleotide exchange factor (GEF). In the case of heterotrimeric G proteins, the GEFs are a family of cell-surface receptors that bind ligands on the extracellular face of the plasma membrane. The inactive, GDP-bound state is stabilized by GDP-dissociation inhibitors (GDI), which in the case of the heterotrimeric G proteins are the Gbg subunits.

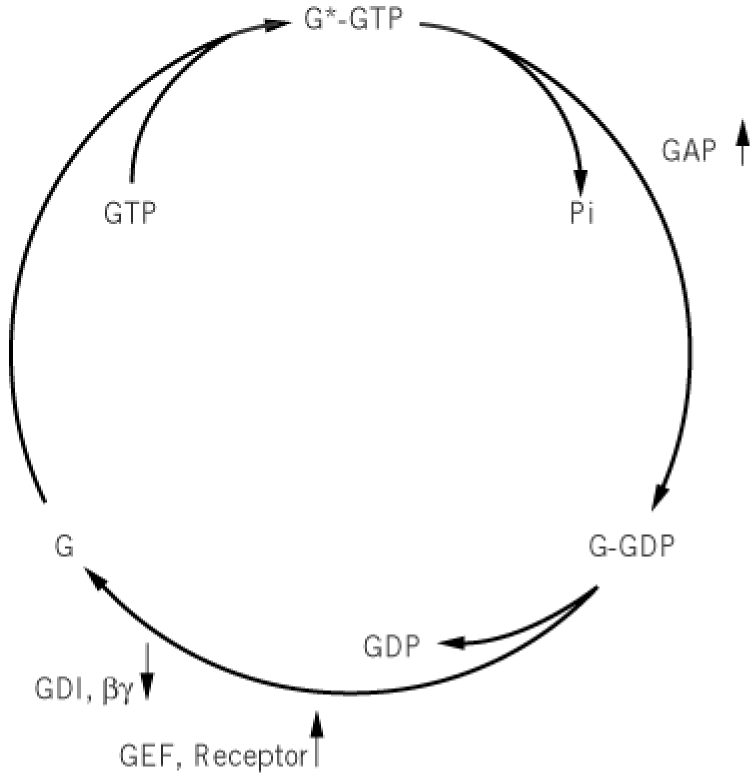

The differing rates of each step in the GTPase cycle, along with their various modes of regulation, allow GTP-binding proteins to operate in one of three conceptually different switching modes: toggles, meters, or timers. (*1*) A GTP-binding protein that traverses the GTPase cycle only once with respect to the process that it regulates behaves as an on/off switch. It is toggled to the active state by GEF-catalyzed activation and maintains its activity until a GAP turns it off. (*2*) A G protein that traverses the GTPase cycle quickly produces a graded signal in which its fractional activation, averaged over time, is a meter of the relative inputs to activation and deactivation. (*3*) A G protein can simply allow a process to occur for a fixed period of time, the lifetime of the bound GTP prior to its hydrolysis. While these basic patterns are formally the same, the distinctive kinetic properties of each determine how a G protein will function in the cell. The ability to work in these three different ways are vital to the functional diversity of G-protein action.

Bibliography

All references are reviews and also serve as suggested reading.

1. E. M. Ross (1989) Signal sorting and amplification through G protein-coupled receptors. Neuron **3**, 141–152.
2. A. G. Gilman (1987) G proteins: transducers of receptor-generated signals, Annu. Rev. Biochem. **56**, 615–649.
3. H. R. Bourne, D. A. Sanders, and F. McCormick (1991) The GTPase superfamily: conserved structure and molecular mechanism. Nature **349**, 117–127.
4. H. R. Bourne, D. A. Sanders, and F. McCormick (1990) The GTPase superfamily I. A conserved switch for diverse cell functions. Nature **348**, 125–132.
5. G. Bollag and F. McCormick (1991) Regulators and effectors of ras proteins. Annu. Rev. Cell Biol. **7**, 601–632.
6. G. M. Bokoch (1996) Interplay between Ras-related and heterotrimeric GTP binding proteins: lifestyles of the big and little. FASEB J. **10**, 1290–1295.
7. M. Barbacid (1987) *ras* Genes. Annu. Rev. Biochem. **56**, 779–827.

8. L. Van Aelst and C. D''Souza-Schorey (1997) Rho GTPases and signaling networks. Genes Dev. **11**, 2295–2322.
9. A. Hall (1998) Rho GTPases and the actin cytoskeleton. Science **279**, 509–514.
10. P. Novick and M. Zerial (1997) The diversity of Rab proteins in vesicle transport. Curr. Opin. Cell Biol. **9**, 496–504.
11. V. M. Olkkonen and H. Stenmark (1997) Role of Rab GTPases in membrane traffic. Intl. Rev. Cytol. **176**, 1–85.
12. M. G. Roth and P. C. Sternweis (1997) The role of lipid signaling in constitutive membrane traffic. Curr. Opin. Cell Biol. **9**, 519–526.
13. A. L. Boman and R. A. Kahn (1995) Arf proteins: the membrane traffic police? Trends Biochem. Sci. **20**, 147–150.
14. J. M. Avis and P. R. Clarke (1996) Ran, a GTPase involved in nuclear processes: its regulators and effectors. J. Cell Sci. **109**, 2423–2427.
15. D. Gorlich and I. W. Mattaj (1996) Nucleocytoplasmic transport. Science **271**, 1513–1518.
16. M. S. Boguski and F. McCormick (1993) Proteins regulating ras and its relatives. Nature **366**, 643–654.

Guanidination

Guanidination is a method for chemical modification of amino groups in proteins. The reaction is relatively slow and proceeds primarily with the e-amino groups of lysine residues, converting them to homoarginine, much less with a-amino groups. The modified amino groups retain their positive charge with increased pK_a. Therefore, structural effects on the modified proteins are usually minimal. The function of the modified protein is usually affected only if the amino group modified intimately participates in the function.

The reaction is followed by amino acid analysis, measuring the appearance of homoarginine and the decrease in lysine. The reaction is quite specific to amino groups, but some side reactions occur with the **thiol** and imidazole groups of cysteine and histidine residues, respectively.

1. Guanidination with *O*-methylisourea

Almost all ε-amino groups of a protein are guanidinated (1) after treatment with 0.5 to 1.0 M *O*-methylisourea [I] at pH 10.1 to 11.0 and 0 to 25°C for 2 to 5 days (Scheme 1):

Scheme 1. x

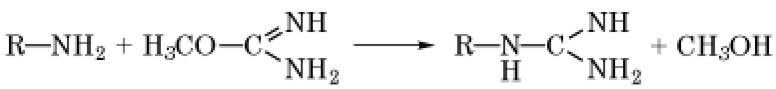

[1] *O*-Methylisourea

2. Guanidination with 1-guanyl-3,4-dimethylpyrazol

1-Guanyl-3,4-dimethylpyrazol [II] guanidinates proteins under milder conditions than *O*-methylisourea (2). Proteins need to be treated with 0.3 to 0.7 M 1-guanyl-3,4-dimethylpyrazol at pH 9.5 and 0°C for 3–7 days (Scheme 2):

Scheme 2. x

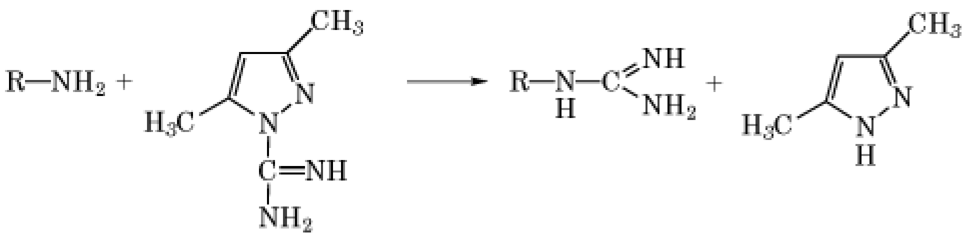

[2] 1-Guanyl-3,5-dimethylpyrazol

Bibliography
1. J.R. Kimmel (1967) Methods Enzymol. **11**, 584–589.
2. A.F.S.A. Habeeb (1972) Methods Enzymol. **25**, 558–566.

Guanidinium Salts

Guanidinium chloride (GdmCl) is one of the most commonly used **denaturants**. Classically, it is employed at 6*M* concentration, at which it unfolds most globular proteins into the form of a random coil. The Gdm^+ ion acts principally by competitively breaking intraprotein hydrogen bonds and forming hydrogen bonds with protein peptide bonds, although the Gdm^+ ion has also a **hydrophobic** character and can interact in this manner with protein nonpolar residues, principally aromatic groups (1).

In using guanidinium ion denaturation, one has to be careful about the selection of the entire salt, since the anion (X^-) exerts its own effect and the net result is the summation of the actions of the Gdm^+ ion and X^-. The effectiveness of Gdm^+ salts in **protein unfolding** follows strictly the Hofmeister series, with the order of denaturing ability being:

$$GdmSCN > GdmCl > GdmCH_3COO > Gdm_2SO_4$$

GdmSCN and GdmCl are strong denaturants, Gdm acetate is much weaker, and Gdm_2SO_4 is a protein stabilizer (1). It is clear that for the SCN^- salt the effect is due to the summation of two denaturing ions; the strong denaturing capacity of Gdm^+ can overcome the weak stabilization by Cl^- and CH_3COO^-. In contrast, the strongly stabilizing SO_4^{2-} ion overcomes the denaturing ability of

Gdm^+. This progression of the Gdm^+ salts along the Hofmeister series is known to reflect their preferential interactions with proteins: GdmCl exhibits preferential binding; Gdm_2SO_4 preferential hydration, ie, is excluded from the accessible surfaces of proteins (2).

Bibliography

1. P. von Hippel and T. Schleich (1969) In *Structure and Stability of Biological Macromolecules* (S. N. Timasheff and G. D. Fasman, eds.), Marcel Dekker, New York, Chap. "6".
2. T. Arakawa and S. N. Timasheff (1984) Biochemistry **23**, 5924–5929.

Guanine Nucleotide Exchange Factors

Guanine nucleotide exchange factors (GEFs) are a structurally diverse group of proteins that are defined by a common function: catalyzing the exchange of bound GDP for GTP on GTP-binding regulatory proteins (see Gtpases and GTP-Binding Proteins). They act on target proteins as diverse as initiation factors and elongation factors of translation, the ras-like monomeric GTP-binding proteins, and the heterotrimeric G proteins. Because the GTP-binding target proteins are activated when GTP binds, the GEFs are stimulatory regulators. The GEFs are also referred to as GDP dissociation stimulators (GDSs), GDP release factors (GRFs), and GDP/GTP exchange catalysts.

The prototypical GEF is the bacterial translational elongation factor EF-Ts, which is the GEF for EF-Tu. GEFs related to EF-Ts are found in all organisms. GEFs for the heterotrimeric G proteins are cell-surface **receptors** that initiate G-protein signaling. They are based on a **hydrophobic** core of seven membrane-spanning **a-helices** that binds ligand on the extracellular face and binds G proteins on the cytoplasmic face. GEFs for the small, monomeric GTP-binding regulatory proteins in eukaryotes also fall into classes specific for their targets. While there is no globally identifiable GEF **consensus sequence** or protein structure, GEFs for a particular class of GTP-binding proteins usually share clear sequence homology, although GEFs are frequently multi-**domain** proteins that combine a GEF domain with domains that fulfill other signaling or protein–protein interaction functions. GEFs may be constitutively active, as are the GEFs for the translation factors. Alternatively, they may be regulated by ligand binding, by **phosphorylation**, by binding of yet other regulatory proteins, or by recruitment to their sites of action when they or their anchors are phosphorylated.

Despite the diversity of their structures and targets, GEFs catalyze GDP/GTP exchange by a common mechanism, shown below (where G is the target GTP-binding protein):

$$\mathrm{GEF} + \mathrm{G{\cdot}GDP} \rightleftharpoons [\mathrm{GEF{\cdot}G{\cdot}GDP}] \overset{\mathrm{GDP}}{\rightleftharpoons} \mathrm{GEF{\cdot}G}$$

$$\overset{\mathrm{GTP}}{\rightleftharpoons} [\mathrm{GEF{\cdot}G{\cdot}GTP}] \rightleftharpoons \mathrm{GEF} + \mathrm{G{\cdot}GTP}$$

Formally, binding of a GEF to its target protein decreases the affinity of the target for guanine nucleotides: It apparently converts the nucleotide binding site to a more “open” configuration. When the GEF binds, dissociation of GDP is accelerated, leaving the GEF bound to the unliganded target. Binding of guanine nucleotide to the target protein must reciprocally decrease its affinity for the GEF, and cytoplasmic GTP is in large excess over GDP, so GTP binds and displaces GEF by the same mechanism. Release of the GEF after it has promoted GDP/GTP exchange allows a single GEF molecule to act sequentially on multiple molecules of target protein. Thus GEFs are true **catalysts** of exchange: They accelerate GDP/GTP exchange but do not alter the equilibrium balance of bound GTP and GDP.

Guanine Quartet

Telomeric DNA plays an important role in stabilizing chromosomes. *Telomeres* refer to the terminal protein-DNA complexes of eukaryotic chromosomes, and the DNA sequences found in telomeres are rich in G and contain a short highly-repetitive sequence, such as $(TTGGGG)_n$. The G-rich strand at the 3′ end exists as a single-stranded overhang and is capable of forming a higher-ordered DNA structure, known as the guanine- or G-quartet, in which four strands associate. There are several ways in which the G-strand can form a very stable four-stranded structure. Indeed, the structures of a number of telomeric sequences have been determined, showing the various forms of the G-quartet structures. The d(GGGGTTTTGGGG) sequence from the protozoa *Oxytricha* forms a hairpin, and two such hairpins joins to make an antiparallel hairpin dimer, thereby resulting in a four-stranded helical structure, with the thymines forming loops at either end. The G-quartet structure was formed by the guanine residues being held together by a cyclic, head-to-tail network of hydrogen bonds and a metal ion (eg, [TEXnical Error]) located at the center. The four guanine residues were found to have a glycosyl conformation that alternates between *anti* and *syn* (see DNA Structure). Another arrangement of the tetra-stranded G-quartet is a fourfold symmetric motif in which the four G-strands are in the parallel orientation (Fig. 1) (1). The polymorphism of the quadruplex structure has been reviewed elsewhere (2). More recently, DNA molecules containing a string of isoguanines have been demonstrated to form very stable parallel tetraplex structures as well.

Figure 1. Side and end views of a parallel G-quartet DNA structure (Nucleic acid data base No. UDD023).

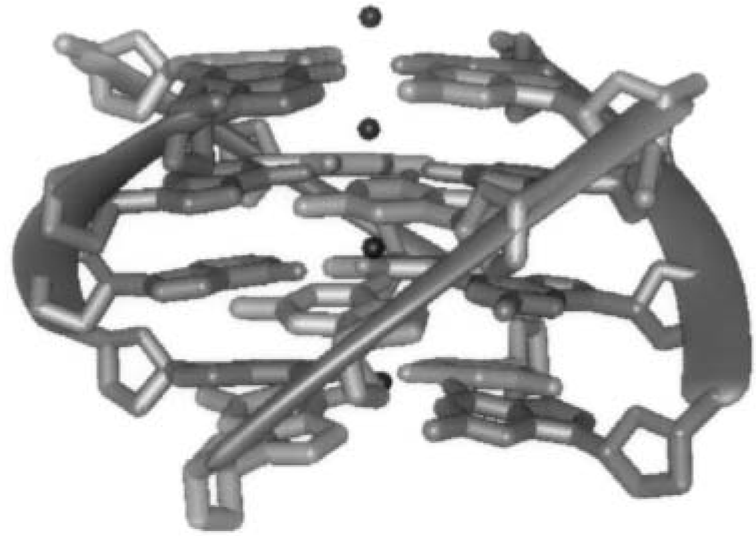

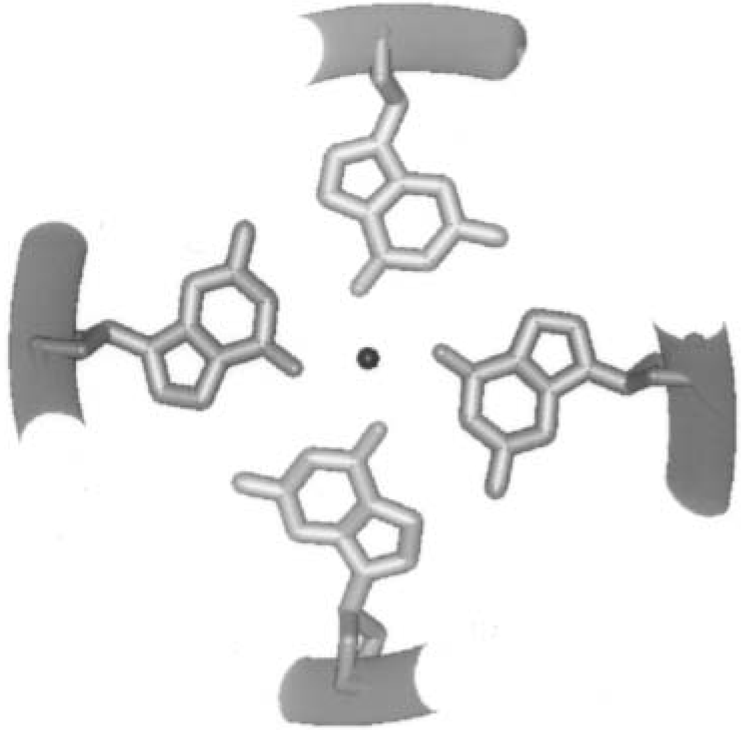

Bibliography

1. K. Phillips, Z. Dauter, A. I. H. Murchie, D. M. J. Lilley, and B. Luisi (1997) J. Mol. Biol. **273**, 171–182.
2. J. R. Williamson (1993) Current Opin. Struct. Biol. **3**, 357–362.

Guanylate Cyclases

Cyclic GMP is synthesized from GTP by the enzyme guanylate cyclase (EC 4.6.1.2) and yields pyrophosphate as a product. Cyclic GMP (cGMP) acts as a second messenger, activating cGMP-dependent protein kinases (see **Phosphorylation protein**) and/or regulating cGMP-sensitive gated **ion channels**. The role of cGMP as an intracellular messenger in vascular smooth muscle relaxation and retinal photo-transduction is well established (see -Monophosphate, cGMP)). Garbers, Goeddel and co-workers (1-3) found that the catalytic centers of guanylyl cyclases are strongly related to eukaryotic class III adenylate cyclases. Thus guanylate cyclases form a single class, in contrast to the four classes of adenylate cyclases, but they are of at least two very different types, linked to the function of the enzyme in the cell and either soluble or membrane-bound in eukaryotic cells. These two forms differ in their structure, regulation, biochemical, and physicochemical properties (4-7).

1. Membrane-bound Guanylate Cyclases

Guanylate cyclases in family I act as sensors and are often **receptors** for hormones, such as atrial natriuretic peptide (ANP), which is involved in controlling of osmotic pressure and sodium excretion in mammals. These guanylate cyclases are complex, membrane-bound enzymes comprising a receptor for specific hormones coupled to a catalytic domain similar in sequence and structure to the catalytic domain of class III adenylate cyclases (1-3). The known guanylate cyclase receptors form several subfamilies (2, 6,8). Those from sea urchins recognize speract and resact , small peptides that stimulate sperm motility and metabolism ((9),(10)). The receptors for natriuretic peptides (ANF) exist in two forms, both of which synthesize cGMP: guanylate cyclase-A (also named ANP-A), which is specific for ANP, and guanylate cyclase-B (or ANP-B) which is stimulated by brain natriuretic peptide rather than by ANP. There are at least three ANP receptors, two with guanylate cyclase activity (ANP-A and ANP-B) and one (ANP-C) that is responsible for clearing ANP from the circulation without a role in signal transduction (11). Intestinal cells contain the receptor for the *Escherichia coli* heat-stable enterotoxin (guanylate cyclase C). The endogenous ligand for this intestinal receptor is a small peptide called guanylin .

Odorant information is encoded by a series of intracellular signal transduction events thought to be mediated primarily by the second messenger cAMP. But a subset of olfactory neurons expresses a cGMP-stimulated phosphodiesterase (PDE2) and a guanylate cyclase of the receptor type (guanylate cyclase D), which demonstrate that cGMP has an important regulatory function in olfactory signaling (see -Monophosphate, cGMP)) (8). Finally, retinal guanylate cyclases (often named retGC) exist in at least two forms, retGC-E and retGC-F. They play a specific functional role in the rods and/or cones of photoreceptors and trigger a protein phosphorylation cascade (see -Monophosphate, cGMP)) (12). They consist of an apparent extracellular domain linked by a single **transmembrane region** to an intracellular domain. They are coupled to guanylate cyclase activating protein-2, which is a Ca^{2+}-binding protein that activates retGC-1 in a Ca^{2+}-sensitive manner (see Calcium Signaling). It is not known whether retGCs act as receptors, but their structures are similar to that of the other plasma membrane-bound guanylate cyclases.

The organization of all these guanylate cyclases is similar: they have an N-terminal extracellular domain that acts as the **ligand-binding** receptor region, then a transmembrane region, followed by a large cytoplasmic C-terminal region that can be subdivided into two domains, a guanylate cyclase catalytic domain and a protein kinase-like domain that is important for controlling the protein phosphorylation cascade linked to the specific signal recognized by the cognate guanylate cyclase (13, 14).

2. Soluble guanylate cyclases

The second family of guanylate cyclases is cytoplasmic and soluble and often designated sGC. They have completely different regulatory functions and always form heterodimers. The two subunits, alpha and beta, are proteins that, although different in length (from 70 to 82 kDa) and sequence, are highly related (15). Two forms of beta subunits are currently known, beta-1, which is expressed in lung and brain, and beta-2, which is more abundant in kidney and liver. The most fascinating feature of these subunits is that they bind a heme **prosthetic group**. Upon binding of nitric oxide (NO) to this heme group, the sGC catalytic activity is stimulated and generates the intracellular signaling molecule cGMP. NO, discovered in 1987, is a signal transduction molecule. Its importance has been emphasized by its role in blood circulation and cardiac muscle functioning (16, 17). Carbon monoxide (CO) also plays a role similar to that of NO (18).

Fifteen conserved cysteine residues of sGC have been mutated to serine by *in vitro* site-directed mutagenesis . All of the resulting recombinant enzymes synthesize cGMP, demonstrating that these residues are not directly involved in catalysis. On the other hand, mutation of two cysteine residues located in the N-terminal, putative heme-binding region of the beta subunit yields proteins that are insensitive to NO and lose their heme prosthetic group. In contrast, mutation of the corresponding cysteine residues of the alpha subunit does not alter their NO responsiveness, indicating that heme binding is probably a specific feature of the N-terminal domain of the beta subunit (19).

3. Similarities Between the Membrane and Soluble Guanylate Cyclases and Class III Adenylate Cyclases

In general, the genetic organizations of both enzyme types have been conserved by the localization of at least one catalytic domain in the carboxy-terminal part of the protein, coupled to a variety (in length and in sequence) of amino-terminal parts. Both forms of guanylate cyclases share a conserved domain that is fundamental for the catalytic activity of the enzyme. A similar domain is also found twice in the different forms of membrane-bound, class III adenylate cyclases from mammals, slime mold, or *Drosophila* (see Adenylate Cyclases). A polypeptide consensus pattern detects both domains of class-III adenylate kinases and guanylate cyclases: Gly-Val-[Leu/Ile/Val/Met]-$X_{0,1}$-Gly-X_5-[Phe/Tyr]-X-[Leu/Ile/Val/Met]-[Phe/Tyr/Trp]-[Gly/Ser]-[Asp/Asn/Thr/His/Lys/Trp]-[Asp/Asn/Thr]-[Ile/Val]-[Asp/Asn/Thr/Ala]-X_5-[Asp/Glu] (1, 3).

The common evolutionary origin of the adenylate cyclases and guanylate cyclases, evidenced by the apparent facility with which it is possible to build up a purine nucleoside triphosphate cyclase of broad specificity, might be relevant to the phylogeny of the catalytic center of class III adenylate cyclases (20). This similarity suggests the existence of a common ancestral purine nucleotide triphosphate cyclase. As a consequence of this interpretation of the sequence data, one might wonder whether evolution has not permitted the existence of some overlap in their specificities because a given cyclase is triggered, under appropriate regulatory conditions, to synthesize either cAMP or cGMP alternatively. This could have been used in cyclic nucleotide-mediated controls existing in eukaryotes, and it might explain the older observations that, in some cases at least, the cAMP and cGMP concentrations vary in opposite directions.

Bibliography

1. M. S. Chang, D. G. Lowe, M. Lewis, R. Hellmiss, E. Chen, and D. V. Goeddel, (1989) Nature **341**, 68–71.
2. D. L. Garbers, (1992) Cell **71**, 1–4.
3. O. Barzu and A. Danchin (1994) Prog. Nucleic Acids Res. Mol. Biol. **49**, 241–283.
4. D. L. Garbers (1990) The New Biologist, **2**, 499–504.
5. D. Koesling, E. Böhme, and G. Schultz, (1991) FASEB J. **5**, 2785–2791.
6. S. Schulz, M. Chinkers, and D. L. Garbers, (1989) FASEB J. **3**, 2026–2035.
7. S. Schulz, P. S. T. Yuen, and D. L. Garbers, (1991) Trends Pharm. Sci. **12**, 116–120.
8. S. Yu, L. Avery, E. Baude, and D. L. Garbers, (1997) Proc. Natl Acad. Sci. USA **94**, 3384–3387.
9. D. L. Garbers, J. K. Bentley, L. J. Dangott, C. S. Ramarao, H. Shimomura, N. Suzuki, and D.

Thorpe, (1986) Adv. Exp. Med. Biol. **207**, 315–357.
10. H. Shimomura, L. J. Dangott, and D. L. Garbers, (1986) J. Biol. Chem., **261**, 15778–15782.
11. M. Chinkers and D. L. Garbers (1991) Adv. Cyclic Nucleic Acid Res. **60**, 553–575.
12. R. B. Yang, D. C. Foster, D. L. Garbers, and H. J. Fulle (1995) Proc. Natl. Acad. Sci. USA **92**, 602–606.
13. J. G. Aparicio and M. L. Applebury (1996) J. Biol. Chem. **271**, 27083–27089.
14. D. Koesling, G. Schultz, and E. Böhme (1991) FEBS Lett. **280**, 301–306.
15. B. Wedel, C. Harteneck, J. Foerster, A. Friebe, G. Schultz, and D. Koesling, (1995) J. Biol. Chem. **270**, 24871–24875.
16. H. Kook, S. E. Lee, Y. H. Baik, S. S. Chung, and J. H. Rhee, (1996) Life Sciences **59**, 41–47.
17. O. W. Griffith and R. G. Kilbourn (1997) Adv. Enzyme Regul. **37**, 171–194.
18. A. Friebe, G. Schultz, and D. Koesling, (1996) EMBO J. **15**, 6863–6868.
19. A. Friebe, B. Wedel, C. Harteneck, J. Foerster, G. Schultz, and D. Koesling, (1997) Biochemistry **36**, 1194–1198.
20. A. Beuve and A. Danchin (1992) J. Mol. Biol. **225**, 933–938.

Guide RNA

Guide RNAs are cofactors for RNA **editing** in kinetoplastid protozoan parasites. They are localized in the mitochondria, where they function to direct insertion and/or deletion of uridylates (U) at specific sites of the pre-messenger RNA to generate the functional mRNA (1-5) (see RNA Editing). The guide RNAs have three domains: (i) the 5′ region sequence is complementary to the substrate pre-mRNA and acts as an "anchor." *In vitro*, this duplex formation is essential for editing to occur (6). (ii) The central domain of the guide RNA contains the information necessary to insert and/or delete uridylates in the pre-mRNA to make the mature edited sequence, which is normally around 30–40 nucleotides in length. (iii) The 3′ end of the guide RNA is characterized by an oligo (U) tail that averages 12 nucleotides in length and is added post-transcriptionally; the function of this tail is unclear. With the development of an *in vitro* system for editing, a critical role in the specificity of editing for the cognate guide RNA has been established (6).

Bibliography

1. R. Benne (1992) Mol. Biol. Rep. **16**, 217–227.
2. G. J. Arts, P. Sloof, and R. Benne (1995) Mol. Biochem. Parasitol. **73**, 211–222.
3. G. J. Arts, H. Vanderspek, D. Speijer, J. Vandenburg, H. Vansteeg, P. Sloof, and R. Benne (1993) EMBO J. **12**, 1523–1532.
4. K. Stuart, T. E. Allen, M. L. Kable, and S. Lawson (1997) Curr. Opin. Chem. Biol. **1**, 340–346.
5. H. Vanderspek, G. J. Arts, R. R. Zwaal, J. Vandenburg, P. Sloof, and R. Benne (1991) EMBO J. **10**, 1217–1224.
6. E. M. Byrne, G. J. Connell, and L. Simpson (1996) EMBO J. **15**, 6758–6765.

Suggestions for Further Reading

7. R. Benne (1996) RNA editing–how a message is changed, Curr. Opin. Genet. Devel. **6**, 221–231.
8. M. L. Kable, S. Heidmann, and K. D. Stuart (1997) RNA editing: getting U into RNA, Trends

Biochem. Sci. **22**, 162–166.
9. P. Sloof and R. Benne (1997) RNA editing in kinetoplastid parasites: what to do with U, Trends Microbiol. **5**, 189–195

Gurken

The *gurken* gene of *Drosophila melanogaster* encodes a protein with homology to the transforming growth factor alpha (TGF-a) class of signaling molecules. During Drosophila oogenesis, the *gurken* gene is **transcribed** in the cells of the germline. The *gurken* messenger RNA accumulates in the oocyte and is **translated** throughout oogenesis. The Gurken protein is transported to the oocyte membrane, and activates the *Drosophila* **epidermal growth factor receptor** (Egfr; also abbreviated DER), which is expressed on the adjacent follicle cells that surround the oocyte. The activation of this major transmembrane receptor regulates the expression of a number of genes in the follicle cells, and thus initiates a series of events that lead to the correct patterning of both the anteroposterior and the dorsoventral axis of the egg and embryo.

The *Drosophila* Egfr is a tyrosine kinase receptor that is used in multiple tissues and at various stages in development to regulate growth, patterning, and differentiation of various cell types. Several ligands have been found to activate the receptor during development (1). Gurken acts as a ligand that is specific to oogenesis. The Gurken protein consists of an extracellular **domain**, which harbors a single epidermal growth factor (EGF)-like domain, a **transmembrane** domain, and a short cytoplasmic domain (2). It is **homologous** to the gene *spitz* of *Drosophila*, which acts as ligand of Egfr in the embryo and in imaginal discs.

During *Drosophila* oogenesis, eggs are produced through the cooperation of the three different cell types that make up individual egg chambers; within each egg chamber, an individual oocyte is connected at its anterior to a group of fifteen nurse cells, and this cluster of 16 cells is surrounded by a follicle cell epithelium (3). Early in oogenesis, *gurken* mRNA is found in the developing oocyte, and the Gurken protein accumulates in the oocyte membrane (4). At this stage, the oocyte occupies only a small part of the volume of the egg chamber, and therefore only a limited number of follicle cells at the posterior of the egg chamber are in contact with the oocyte membrane. In this group of follicle cells, the Egfr is activated by Gurken protein, which results in the specification of these follicle cells as posterior cells. In flies that are mutant for severe loss-of-function **alleles** of *gurken*, Gurken protein is absent, and the follicle cells at the posterior end of the egg chamber are not induced to assume a posterior cell fate. They consequently develop as anterior follicle cells, which results in the production of an egg with two anterior ends. The posterior follicle cells normally send a signal back to the oocyte, which organizes the cytoskeleton of the oocyte and specifies the posterior end of the oocyte. In the mutant egg chambers, no such signal is sent from the follicle cells, and the cytoskeleton of the oocyte is misorganized. RNAs such as bicoid or ***oskar***, which should normally be localized to one end of the egg **RNA localization** are mislocalized in these mutant oocytes, and the embryos that develop inside such eggs have an abnormal antero-posterior pattern (5, 6).

In midoogenesis, the patttern of *gurken* RNA accumulation changes dramatically. At this stage, the oocyte has grown and now occupies about one-third to one-half of the egg chamber. The oocyte nucleus has moved from its initial, symmetric position to one side of the oocyte. The *gurken* RNA accumulates in the region around the oocyte nucleus, and the Gurken protein is now found in a very restricted part of the oocyte membrane, directly overlying the oocyte nucleus (2, 4). At this stage, Gurken activates the Egfr in the lateral follicle cells that contact the oocyte on the side where the nucleus is situated. Activation of the Egfr in these lateral follicle cells induces them to become dorsal follicle cells. In the absence of gurken signaling, the lateral follicle cells develop into ventral follicle cells (7). The ventral follicle cells normally regulate the production of a ventral signal that activates the **Toll** receptor protein on the ventral side of the egg and is responsible for inducing ventral cell fates in the developing embryo. In the strong *gurken* mutants, therefore, the ventralization of the follicle cell epithelium leads to an overproduction of the ventral signal, and consequently to a ventralized embryo (8).

The activation of Egfr in the follicle cells by the Gurken protein therefore has two different functions. In the early egg chamber, activation of the receptor in follicle cells situated at the termini of the egg chamber results in the induction of posterior cell fates. In midoogenesis, activation in the follicle cells on the lateral side of the egg chamber induces dorsal cell fates. The difference in response to receptor activation reflects a prepatterning of the follicle cells along the antero-posterior axis, which, in part, depends on the prior activity of the Notch signaling system (9, 10).

In the establishment of dorsal follicle cell fates, *gurken* signaling presumably leads to the formation of a broad field of dorsal cell fates, but secondary patterning mechanisms appear to operate to lead to the final, complex pattern of cell fates of the mature egg. In addition, *gurken* signaling also interacts with signaling through decapentaplegic (dpp), a molecule with homology to TGF-b. In follicle cells that receive both the *gurken* signal and the *dpp* signal, formation of dorsal appendages is repressed, and formation of operculum cell fate is induced (11, 12). The regulation of the embryonic ventral signal by activation of Egfr seems, however, to be independent of the production of dorsal anterior follicle cell fates. In situations where ectopic activation of Egfr in follicle cells is induced in parts of the follicle cell epithelium, embryos result that show only regional dorsalization, corresponding to the region of the follicle cell epithelium where Egfr was ectopically activated (13).

Bibliography

1. R. Schweitzer and B.-Z. Shilo (1997) Trends Gen. **13**, 191–196.
2. F. S. Neuman-Silberberg and T. Schüpbach (1993) Cell **75**, 165–174.
3. A. C. Spradling (1993) "Developmental genetics of oogenesis", In *The Development of Drosophila melanogaster* (M. Bate and A. Martinez Arias, eds.), Cold Spring Harbor Laboratory Press, Cold Spring Harbor, NY, pp. 1–70.
4. F. S. Neuman-Silberberg and T. Schüpbach (1996) Mech. Dev **59**, 105–113.
5. A. Gonzales-Reyes, H. Elliott, and D. St Johnston (1995) Nature **375**, 654–658.
6. S. Roth, F. S. Neuman-Silberberg, G. Barcelo, and T. Schüpbach (1995) Cell **81**, 967–978.
7. T. Schüpbach (1987) Cell **49**, 699–707.
8. S. Roth and T. Schüpbach (1994) Development **120**, 2245–2257.
9. H. Ruohola, K. A. Bremer, D. Baker, J. R. Sedlow, L. Y. Jan, and Y. N. Jan (1991) Cell **66**, 433–449.
10. A. Gonzales-Reyes and D. St Johnston (1998) Development **125**, 2837–2846.
11. V. Twombly, R. K. Blackman, H. Jin, J. B. Graff, R. W. Padgett, and W. M. Gelbart (1996) Development **122**, 1555–1565.
12. W. M. Deng and M. Bownes (1997) Development **124**, 4639–4647.
13. A. M. Queenan, A. Ghabrial, and T. Schüpbach (1997) Development **124**, 3871–3880.

Suggestions for Further Reading

14. D. Morisato and K. Anderson (1995) Signaling pathways that establish the dorsal-ventral pattern of the Drosophila embryo, Ann. Rev. Gen. **29**, 371–399.
15. R. P. Ray and T. Schüpbach (1996) Intercellular signaling and the polarization of body axes during Drosophila oorgenesis, Genes Dev. **10**, 1711–1723.
16. L. A. Nilson and T. Schüpbach (1998) EGF receptor signaling in Drosophila oogenesis, Curr.

Top. Dev. Biol. **44** (R. Pederson and G. P. Schatten, eds., Academic Press, San Diego) 203–244.

Haldane Relationship

This relationship of enzyme catalysis was first recognized by J. B. S. Haldane in 1930 (1) and is generally known as a Haldane. It relates the kinetic parameters for an enzyme-catalyzed reaction to the equilibrium constant K_{eq} for that reaction. As K_{eq} is a thermodynamic measurement that cannot be altered by an enzyme, the ratio of the rates in the two directions also must not change in the presence of the enzyme; consequently, a Haldane expresses the relationship between the kinetic and thermodynamic properties of an enzymic reaction. Although there are both kinetic and thermodynamic Haldanes (2), the thermodynamic Haldanes do not apply to all kinetic mechanisms and hence this discussion will be restricted to kinetic Haldanes.

For a simple Uni–Uni reaction, A $\rightleftharpoons$P, that is catalyzed by a mutase or isomerase (see **Kinetic mechanisms**), at concentrations of reactants well below the values of their Km (Michaelis constant), the rates of the forward and reverse reactions are given by the expressions $(V_1/K_a)\,A$ and $(V_2/K_p)\,P$, respectively (see Michaelis–Menten Kinetics). Here, A and P represent the concentrations of the reactants, which have K_m values of K_a and K_p, respectively. V_1 and V_2 represent maximum velocities for the forward and reverse reactions, respectively. At equilibrium, the rates of the forward and reverse reactions must be equal, and hence it follows that the relationships given in Equation 1 must hold:

$$\frac{P}{A} = K_{eq} = \frac{V_1 K_p}{V_2 K_a} \qquad (1)$$

In general terms, a Haldane is the ratio of the apparent rate constants for the reactions in the forward and reverse directions when all the substrate concentrations are relatively low. When there is more than one substrate, the apparent rate constant is given by the V/K_m value for the last substrate to add to the enzyme, multiplied by the reciprocals of the dissociation constants for the substrates that added previously. The same definition applies for the products that act as substrates for the reaction in the reverse direction. Thus, for an ordered Bi–Bi mechanism, where substrate A binds to the enzyme before B and product P dissociates before Q:

$$K_{eq} = \frac{V_1}{K_b}\frac{1}{K_{ia}} \Big/ \frac{V_2}{K_p}\frac{1}{K_{iq}} = \frac{V_1 K_p K_{iq}}{V_2 K_{ia} K_b} \qquad (2)$$

For a Bi–Bi ping-pong mechanism, in which substrate A is converted to product P, which dissociates leaving a modified enzyme, before substrate B is bound and converted to product Q, there is a Haldane for each half-reaction (see **Kinetic mechanisms** and **Isotope exchange**). When multiplied together, they give the overall equilibrium constant as shown in Equation 3 (2):

(3)

$$K_{eq} = K_{eq}1 * K_{eq}2 = \frac{V_1/K_a}{V_2/K_p} * \frac{V_1/K_b}{V_2/K_q} = \left(\frac{V_1}{V_2}\right)^2 \frac{K_pK_q}{K_aK_b}$$

Haldane relationships provide a means of checking on the correctness of a proposed kinetic mechanism. The value for K_{eq}, as calculated by using values determined for the kinetic parameters, must be in agreement with the experimentally determined value. They also have implications with respect to the catalytic efficiency of enzymes. It appears that the wide variation in the maximum velocities for enzyme-catalyzed reactions is due to the differences in the K_{eq} values for the reactions, as well as to differences in the physiological concentrations of the substrates, which are usually in the region of their K_m values (3).

Bibliography

1. J. B. S. Haldane (1930) *Enzymes*, Longman, Green & Co. Ltd, London, p. 80. (Reprinted in 1965 by MIT Press, Cambridge, Mass.)
2. W. W. Cleland (1982) Meth. Enzymol. **87**, 366–369.
3. W. W. Cleland (1975) Acc. Chem. Res. **8**, 145–151.

Half-Life, Half-Time

The half-life of a radioisotope or of a chemical reaction can often be described by the time required for the original reactant to decrease to one-half of its original concentration. This parameter is most appropriate for first-order reactions of the type S → P in which the velocity is proportional only to the concentration of [S]:

$$\text{Velocity} = \frac{-d[\text{S}]}{dt} = k_{\text{app}}[\text{S}] \quad (1)$$

The decay of radioisotopes follows this relationship, as do all unimolecular reactions. Even when there is more than one reactant, the reaction occurs with pseudo-first-order kinetics if the other reactants are present in excess and their concentrations do not alter substantially during the course of the reaction (see Kinetics). With first-order reactions, the velocity decreases exponentially with time, as the value of [S] decreases:

$$\ln_e \frac{[\text{S}]}{[\text{S}]_0 - [\text{S}]} = 2.303 \log_{10} \frac{[\text{S}]}{[\text{S}]_0 - [\text{S}]} = k_{\text{app}}t \quad (2)$$

where t is time, k_{app} is the apparent rate constant, and $[S]_0$ is the starting concentration of S. When [S] has reached half the value of $[S]_0$ at the half-life $t_{1/2}$:

$$\ln_e 2 = k_{\text{app}}t_{1/2} \quad (3)$$

$$t_{1/2} = \frac{\ln_e 2}{k_{\text{app}}} = \frac{0.693}{k_{\text{app}}} \tag{4}$$

When known, the half-time can be used to calculate the apparent rate constant for the reaction.

The half-life can also be used to determine the final extent of a reaction. Because the velocity of a first-order reaction decreases exponentially with time (Eq. (2)), it takes a very long time to reach completion or equilibrium. For example, after one to eight half-lives, the extent of a reaction has reached respectively 50, 75, 87.5, 93.75, 96.83, 98.44, 99.23, and 99.61% of completion. After following a reaction for several half-lives, the final extent of reaction can be predicted.

Suggestion for Further Reading

W. P. Jencks (1969) *Catalysis in Chemistry and Enzymology*, McGraw–Hill, New York, pp. 557–564.

Haploid

A *haploid* cell has one complete set of chromosomes characteristic of that species, except for the sex chromosomes (see X-chromosome and Y-Chromosome). It has a ploidy of one. In sexual species, only the **gamete** cells are usually haploid. The normal cell is **diploid** and has complete sets of chromosomes.

Haptens

Haptens are small molecules that can interact with specific **antibodies** but cannot induce an immune response by themselves. They can be rendered **immunogenic** by coupling to a carrier protein that will provide the necessary substrate for **antigen processing and presentation**, whereas the hapten part will contribute the epitopes. The hapten model was put forward and studied extensively by Landsteiner in the 1930s. Many haptens were variations on a cyclic organic compound, especially the phenyl ring that provided a convenient tool to play with a large variety of groups that could be replaced or transposed from one position to another. Among the most popular were 2,4-dinitrophenol and phenylarsonate. Haptens are constructed so to have an active group that can form a covalent interaction with a side chain of the protein carrier, most often a tyrosine residue (for diazotation) or lysine (formation of a covalent bond to the ε**-amino group**). The essence of the elegant work of Landsteiner was to show clearly the exquisite specificity of antibodies, because simply replacing one group by another on the phenyl ring (for instance a NH_2 group by a carbonyl) or changing the position of one group (eg, NH_2 from ortho to meta or para) was sufficient to abolish or at least severely diminish recognition by the antibody. The model also provided a nice structural basis to study cross-reactions, by systematic permutations of groups on the hapten itself or by comparing the antigenicity of the same hapten conjugated to different carriers. This approach was used much later to analyze the so-called “carrier effect” which was a first step toward elucidation of the major histocompatibility complex (MHC) restriction and understanding of the mechanisms of processing and presentation. The hapten model had, however, one major drawback on the impact of the selective theory first proposed by Ehrlich in 1901. The essence of Ehrlich's theory was that introduction of antigen selected antibodies that were supposed to preexist at the lymphocyte surface (which was demonstrated to be true some 60 years later!). As a result of the Landsteiner approach, for about 20 years, in the 1940s and 1950s, it seemed implausible that the immune system might have generated preexisting antibodies to artificial molecules that were created by chemists. This conclusion, however, simply did not take into account the enormous size of the antibody repertoire or the relative degeneracy of antibody recognition, as finally realized later and revisited by the clonal selection theory.

Immunological detection of small molecules of biological interest, such as hormones, neuromediators, or diverse ligands of small size, faces the problem of their immunogenicity and requires that these molecules be first conjugated onto a carrier protein, and there are many examples of this in the recent literature. Once the appropriate antibodies are available, detection of these molecules in a biological sample may be performed by a great variety of inhibition techniques, such as the radioimmunoassay (RIA) or the enzyme-linked immunosorbent assay (ELISA). Conversely, it may happen that small molecules behave spontaneously as immunogens, possibly inducing an undesired hypersensitization. This is the case with some reactive compounds currently used in laboratories, such as **iodoacetamide**, a commonly used alkylating agent that can induce delayed-type hypersensitivity with severe rashes. It is thought to react with cysteine thiol groups of proteins that then behave as carrier and render the small molecule immunogenic. A similar phenomenon is observed with b-lactam antibiotics, of which penicillin is the prototype, occasionally leading to the possible occurrence of anaphylactic reactions.

See also entries Antigen, Epitope, and Immunogen.

Suggestion for Further Reading

O. Mäkelä, I. J. T. Seppälä (1986) "Haptens and carriers". In *Handbook of Experimental Immunology*, Vol. **1**: Immunochemistry (D. M. Weir, L. A. Herzenberg, C. Blackwell, L. A. Herzenberg, eds.), Blackwell, Oxford, U.K., pp. 1–13.

Heat-Shock Response

The heat-shock response represents the orderly cellular response to diverse forms of environmental and physiological stress, which results in the **transcriptional** activation of **genes** encoding **molecular chaperones**, proteinases, and other inducible genes for protection and recovery from stress (Fig. 1). Although the exposure of cells and organisms to heat shock may have its origins with the stress of the primordial environment, the heat-shock response has since adapted to include a diverse array of stresses, including infection with **viruses** and bacteria, exposure to transition heavy metals, amino acid analogues, pharmacologically active small molecules, and oxidants. Common to these stresses are the effects on protein biogenesis defined by events associated with **protein biosynthesis**, **protein folding**, translocation, and assembly into the final native protein or protein complex. Stress challenges protein homeostasis and results in an increased flux of non-native proteins, which, if left unprotected, are prone to misfolding and aggregation. Consequently, through the elevated synthesis of molecular chaperones and proteinases, the heat-shock response responds rapidly and precisely to the intensity and duration of specific environmental and physiological stress signals by repairing protein damage to reestablish protein homeostasis.

Figure 1. Stress activation of heat-shock proteins.

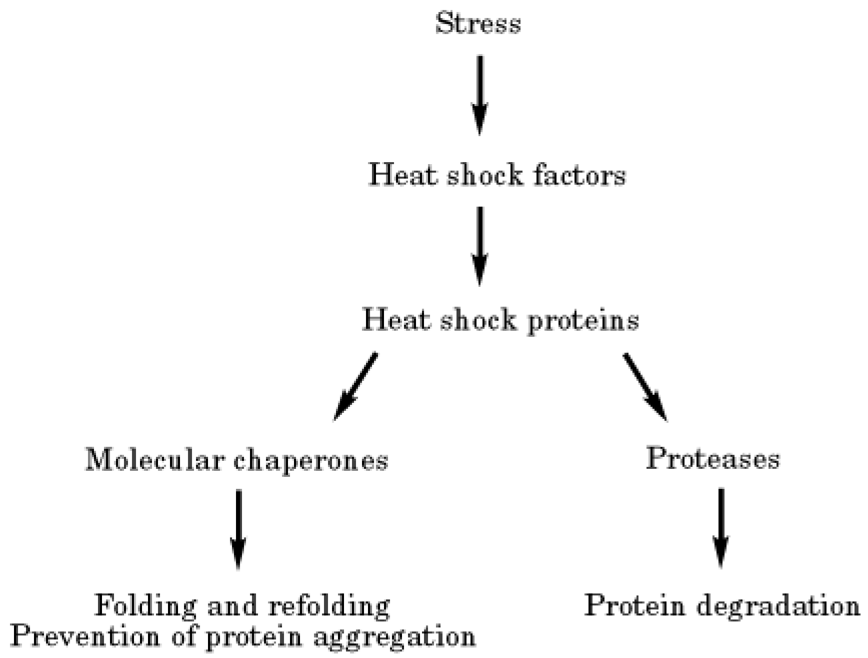

Studies on the heat-shock response have revealed how the cell senses stress and the role of heat-shock proteins in protecting against and repairing protein damage. While prolonged exposures to extreme stress are harmful and can result in cell and tissue death, activation of the heat-shock response by prior exposure to heat shock results in stress tolerance and cytoprotection against stress-induced molecular damage (1). Transient exposure to somewhat elevated temperatures, or reduced levels of chemical stress, cross-protects cells, tissues, and organisms against sustained, normally lethal, exposures to stress. This reveals a valuable survival strategy that “a little stress is good.”

The complexity that underlies the transcriptional regulation of the heat-shock genes is reflected by the diverse array of stress conditions, which can be distinguished into three major categories (Fig. 2): (i) *environmental stresses*, namely, heat shock, amino acid analogues, drugs, oxidative stress, toxic chemicals, heavy metals, and pharmacologically active small molecules; (ii) *nonstress conditions*, namely, the cell cycle, growth factors, serum stimulation, development, differentiation, and activation by certain **oncogenes**; and (iii) *physiologic stress*, *pathophysiologic and disease states*, namely, neuroendocrine hormones, tissue injury and repair, fever, inflammation, infection, ischemia and reperfusion, neural degenerative diseases, and cancer.

Figure 2. Conditions that induce the heat-shock response. Heat-shock gene expression is induced by environmental and physiological stress, nonstressful conditions including cell growth and development, and pathophysiological states.

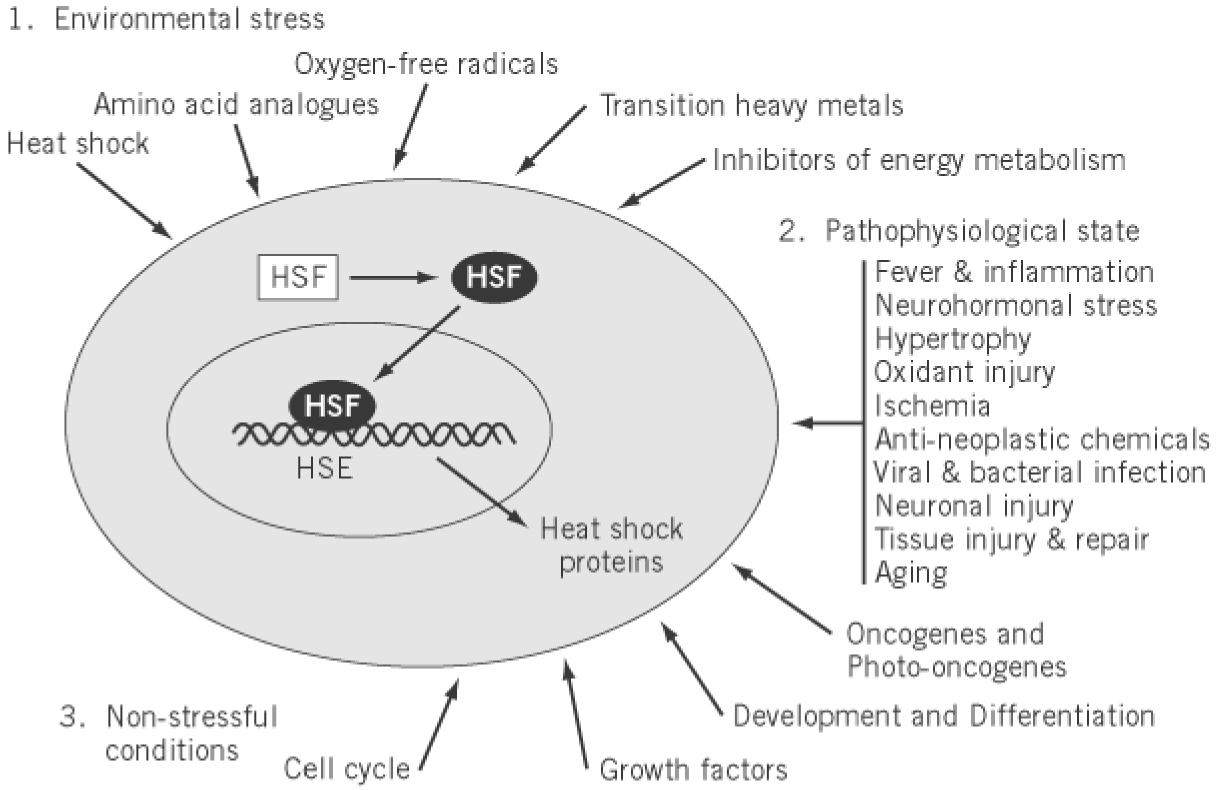

This entry addresses (i) how cells utilize the stress-sensing network of the heat-shock response to regulate the transcription of genes that encode heat-shock proteins and molecular chaperones; (ii) the role of molecular chaperones in protein folding, translocation, and protection against the deleterious consequences of misfolded proteins; and (iii) the role of the heat-shock response and heat-shock proteins in cytoprotection against disease.

1. Stress-Induced Transcriptional Regulation of Heat-Shock Genes in *Escherichia coli*

The heat-shock response in *E. coli* leads to the elevated synthesis of more than 20 proteins (Table 1). Upon temperature elevation, transcriptional activation of the respective heat-shock genes is dependent upon the s factor s32, the product of the rpoH (htpR) gene, which associates with the **RNA polymerase** core enzyme (E) to form the E s32 holoenzyme that binds specifically to **promoters** of most heat-shock genes (2-4). s32 is essential for normal growth; cells lacking s32 are highly restricted in cell growth conditions and are hypersensitive to stress (5). Transcriptional activation of the principal heat-shock genes htpG, **dnaK**, dnaJ, grpE, and groEL/S requires stress-induced changes in the levels of s32. Under normal growth conditions, the concentration of s32 is very low, approximately 10 to 30 copies per cell at 30°C (6) as a result of its short half-life ($t_{1/2}$ = 1min) (7, 8). Following heat shock, s32 levels increase rapidly, due to its increased rate of synthesis of s32 (7, 9-11) and increased stability during heat shock. The consequence of elevated levels of s32 is a burst of heat-shock gene transcription (12-14).

Table 1. A Brief Summary of the Nomenclature, Location, and Function of the Major Chaperone Families

Organism	Chaperone	Compartment	Functions

hsp100	*E. coli*	ClpA,B,C	Cytosol	Roles in stress tolerance; aids in the resolubilization of heat-inactivated proteins from insoluble aggregates; regulates yeast prions
	S. cerevisiae	Hsp 104	Cytosol	
hsp90	*E. coli*	HtpG	Cytosol	Functions in signal transduction (eg, steroid hormone receptor activity); modulates protein kinase activities; refolds and maintains denatured proteins *in vitro*
	S. cerevisiae	Hsp83	Cytosol	
	Mammals	Hsp90	Cytosol	
		Grp94	ER	
hsp70	*E. coli*	DnaK	Cytosol	Functions in lamba phage replication; autoregulates the heat shock response; interacts with nascent chain polypeptides; may facilitate protein degradation by acting as a cofactor in proteolytic systems; dissociates clathrin; functions in interorganellar transport; roles in signal transduction (eg, steroid hormone receptor function); refolds and maintains denatured proteins *in vitro and in vivo* together with the Hdj-1/Hsp40 co-chaperone
	S. cerevisiae	Ssa 1-4	Cytosol	
		Ssb 1,2	Cytosol	
		Kar2	ER	
		Ssc1	Mitochondria	
	Mammals	Hsc70	Cytosol/nucleus	
		Hsp70	Cytosol/nucleus	
		Bip	ER	

		mhsp70	Mitochondria	
hsp60	*E. coli*	groEL	Cytosol	Functions in assembly of bacteriohages and Rubisco; refolds or prevents aggregation of denatured proteins *in vitro*; may facilitate protein degradation by acting as a cofactor in proteolytic systems; functions in folding of organellar proteins
	S. cerevisiae	Hsp60	Mitochondria	
	Plants	Cpn60	Chloroplasts	
	Mammals	Hsp60	Mitochondria	
hsp40	*E.coli*	dnaJ	Cytosol	Chaperone activity, essential co-chaperone activity with Hsp70 proteins to enhance ATPase rate and substrate release
	S. cereviasae	Ydj1	Cytosol/nucleus	
	Mammals	Hdj-1/Hsp40		
		Hdj-2, Hsj-1		
shsp	*E.coli*	IbpA and B	Cytosol	Suppresses aggregation and heat inactivation of proteins *in vitro*; confers thermotolerance through stabilization of microfilaments; possible roles in cell growth and differentiation
	S. cerevisiae	hsp27	Cytosol	
	Mammals	aA and aB-crystallin	Cytosol	
		hsp27	Cytosol	

A complementary stress response to misfolded proteins in the periplasm and outer membrane of *E. coli* is mediated by a second heat-shock factor, sE (s24) (15, 16). Activation of sE leads to the induction of at least 10 additional proteins, four of which have been identified: the periplasmic proteinase degP, s32, the periplasmic peptidyl prolyl cis/trans isomerase fkpA, and sE itself (17-23). Cells lacking sE are sensitive to elevated temperatures, sodium dodecyl sulfate (**SDS**)/ethylenediaminetetraacetic acid (EDTA), and crystal violet (16, 21, 22, 24). The temperature-sensitive phenotype of sE mutants can be restored by activation of a second signal transduction cascade, the Cpx pathway, revealing that *E. coli* has at least two partially overlapping stress signal cascades capable of relieving extracytoplasmic stress (25).

Studies on the regulation of the heat-shock response provide evidence for autoregulation in that the activity and/or levels of heat-shock proteins influences the expression of heat-shock genes. Mutations in the heat-shock proteins dnaK, dnaJ, or GrpE, or reduced expression of groEL/S, enhance heat-shock gene expression at normal growth temperatures and result in an extended heat-shock response after shift to high temperatures (26-28). These cells are defective in the control of s32 synthesis and exhibit increased stability of s32 (8, 27, 29). The degradation of s32 involves dnaK, dnaJ, and GrpE by targeting s32 to the ATP-dependent proteinases FtsH, Lon, **Clp**, and HslVU (30, 31). Negative regulation of s32 is mediated by interaction of a specific region of s32 with dnaK, such that deletion or mutations within this region lead to its sustained synthesis and prolonged half-life (32, 33). The interaction of s32 with dnaK, dnaJ, and GrpE is ATP-dependent, so that dnaJ, in the presence of nucleotide, increases the formation of dnaK–dnaJ–s32 complexes in the ADP state, and GrpE stimulates nucleotide exchange and dissociation of the complex (34, 35). Association of dnaK and dnaJ with s32 prevents s32 from binding to RNA polymerase, resulting in the arrest of heat-shock gene transcription (34, 36-38). In addition to sequestration of s32 from RNA polymerase, the dnaK chaperone machinery autoregulates the *E. coli* heat-shock response by the simultaneous reactivation of heat-aggregated s70 and the preferential assembly of s70 with RNA polymerase (39). The equilibrium between free active s32 and DnaK/DnaJ-bound inactive s32, therefore, constitutes an important feature of the homeostatic control of heat-shock gene regulation in *E. coli*.

2. Stress-Induced Transcriptional Regulation of Heat-Shock genes in Eukaryotes

2.1. Family of Heat-Shock Factors

In higher eukaryotes, stress-induced regulation of the heat-shock response occurs principally by stress-induced activation of heat-shock factors (HSFs) from an inert to a transcription-competent **DNA-binding** state, binding to the heat-shock promoter element, and interaction with components of the basal transcription machinery, thus resulting in inducible transcription (40-43). Among eukaryotes, the complexity of HSF-dependent regulation varies among species, with yeast and *Drosophila* encoding a single HSF gene (44-46), whereas four HSF genes (HSF1 to HSF4) have been isolated and characterized in the mouse, chicken, and human **genomes**, and a distinct but functionally related family of HSFs have been characterized in plants (47-54).

Comparison of the various **cloned** HSF genes reveals an overall sequence identity of 40%, with a high degree of structural conservation (Fig. 3) in the winged helix–turn–helix motif DNA-binding domain (43, 53, 55-57), an extended 80-residue **hydrophobic** repeat (HR-A/B) involved in trimerization (46, 58, 59), and a carboxyl-terminal localized transactivation domain (51, 60-63). With the exception of the HSF in budding yeasts and human HSF4, another hydrophobic repeat (HR-C) is located adjacent to the carboxyl-terminal transactivation domain, which has been suggested to function in suppression of trimer formation by interaction with HR-A/B (50, 64-68). Also positioned between HR-A/B and HR-C are sequences that function as negative regulatory regions that repress either or both DNA binding and transcriptional activation (61, 62, 68). Other features unique to specific HSFs are the presence of an amino-terminal transactivation domain in the *Saccharomyces cerevisiae* HSF and the lack of a functional transactivation domain in human HSF4 (51). A common feature of HSFs other than from *S. cerevisiae* is the negative regulation of DNA binding or transcriptional activity.

Figure 3. General features of heat-shock factors. Schematic representation of HSF1 structural motifs [DNA binding, hydrophobic repeats (HR-A/B and HR-C), and the transcriptional activation domain] and the negative regulatory domains which influence HSF1 activity. The relative positions of these domains are indicated by the amino acid

residues indicated.

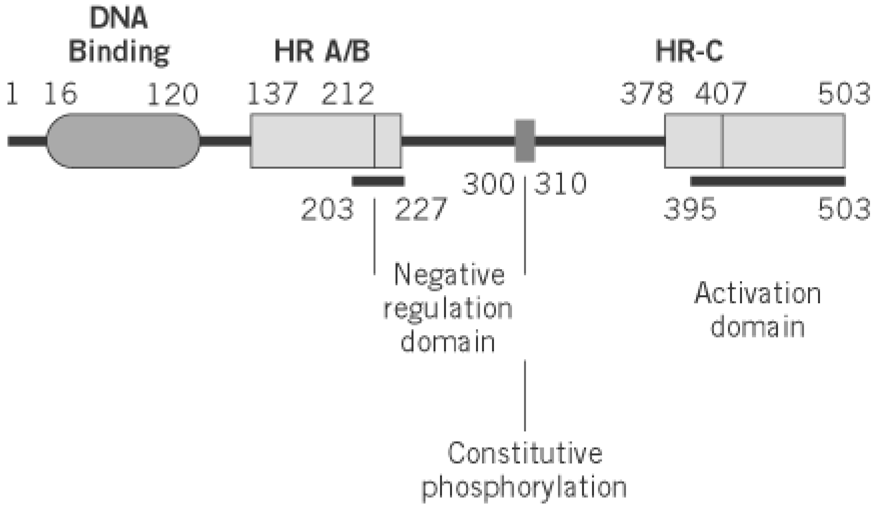

Of the HSFs coexpressed in vertebrates, HSF1 has the properties of the predominant stress-induced transcriptional activator, which acquires both DNA binding and transcriptional activity and is functionally analogous to yeast and *Drosophila* HSF (69, 70). In avian cells, HSF1 and HSF3 are coexpressed and coactivated by chemical and physiological stress, leading to the suggestion of possible redundancy, yet cells deleted for HSF3 and expressing HSF1 are severely compromised for the heat-shock transcriptional response (71-73). HSF3 also interacts with other transcription factors and can be activated, independent of stress, by the Myb oncogene via direct **protein–protein interaction** with the HSF3 DNA-binding domain (74). Myb is a growth-regulated transcription factor; consequently the interaction between Myb and HSF3 reveals a new pathway for genetic crosstalk between cell growth and the stress response. Evidence is also accumulating to indicate that HSF1 may negatively influence the transcriptional activation of other cellular genes, independent of direct binding to heat-shock elements, perhaps via protein–protein interactions with HSF1 (75). Another member of the HSF family, HSF2, in contrast to HSF1, regulates heat-shock gene expression during cell growth and differentiation. HSF2 activity was first described in human erythroleukemia (K562) cells exposed to hemin (76-78), and it was subsequently detected during murine spermatocyte differentiation (79) and embryogenesis (80, 81). The stress-sensing pathway for HSF2 activation is associated with **protein degradation**. HSF2 activity is induced, in a cell-type independent manner, in mammalian tissue culture cells by exposure to specific inhibitors of the **ubiquitin**-dependent proteasome or in cells harboring conditional mutations in components of the proteasome machinery (82). The function of the ubiquitin-dependent proteasome machinery is to degrade short-lived and misfolded proteins; therefore, activation of HSF2 by down-regulation of the protein degradative machinery reveals a requirement for heat-shock proteins, perhaps to prevent misfolding and aggregation of non-native proteins targeted for degradation.

2.2. Regulation and Autoregulation of HSF

Stress-induced activation of HSF1 is a multistep process (Fig. 4). In response to heat shock and other stresses, HSF1 translocates and relocalizes within the nucleus, oligomerizes to a DNA-binding and transcriptionally inert state, becomes inducibly **phosphorylated**, and activates the transcription of heat-shock genes. During prolonged heat shock, HSF1 activity attenuates, as characterized by transcriptional repression of heat-shock genes. Key events during attenuation include the association of HSF1 with the molecular chaperones Hsp70 and Hdj1, interaction with the negative regulator HSBP1, dissociation of HSF1 trimers from DNA, and refolding of the trimer to the monomer. Translocation of HSF1 from the cytoplasm to the nucleus has been described in *Drosophila* and mammalian cells (43, 57, 69, 70, 78, 83-86), yet others have also observed that HSF1 is localized constitutively to the nucleus (86).

Figure 4. Regulation of the heat-shock response. Activation of heat-shock factor (HSF1) is linked to the appearance of n native proteins and the requirement for molecular chaperones (Hsp90, Hsp70, and Hdj1) to prevent the appearance of misfolded proteins. HSF1 exists in the control state as an inert monomer (shown as intramolecularly and negatively regulated for DNA binding and transcriptional activity) and undergoes stepwise activation to (i) a DNA-binding compete state that is transcriptionally inert, (ii) acquisition of inducible phosphorylation, resulting in complete activation and inducible transcription of heat-shock genes, and (iii) attenuation of HSF1 activity. HSF1 activity is negatively regulated heat-shock factor binding protein 1 (HSBP1), which binds to the region of HSF1 corresponding to the heptad repeat, and Hsp70 and Hdj1, which bind to the transcriptional *trans*-activation domain thus repressing HSF1 activity.

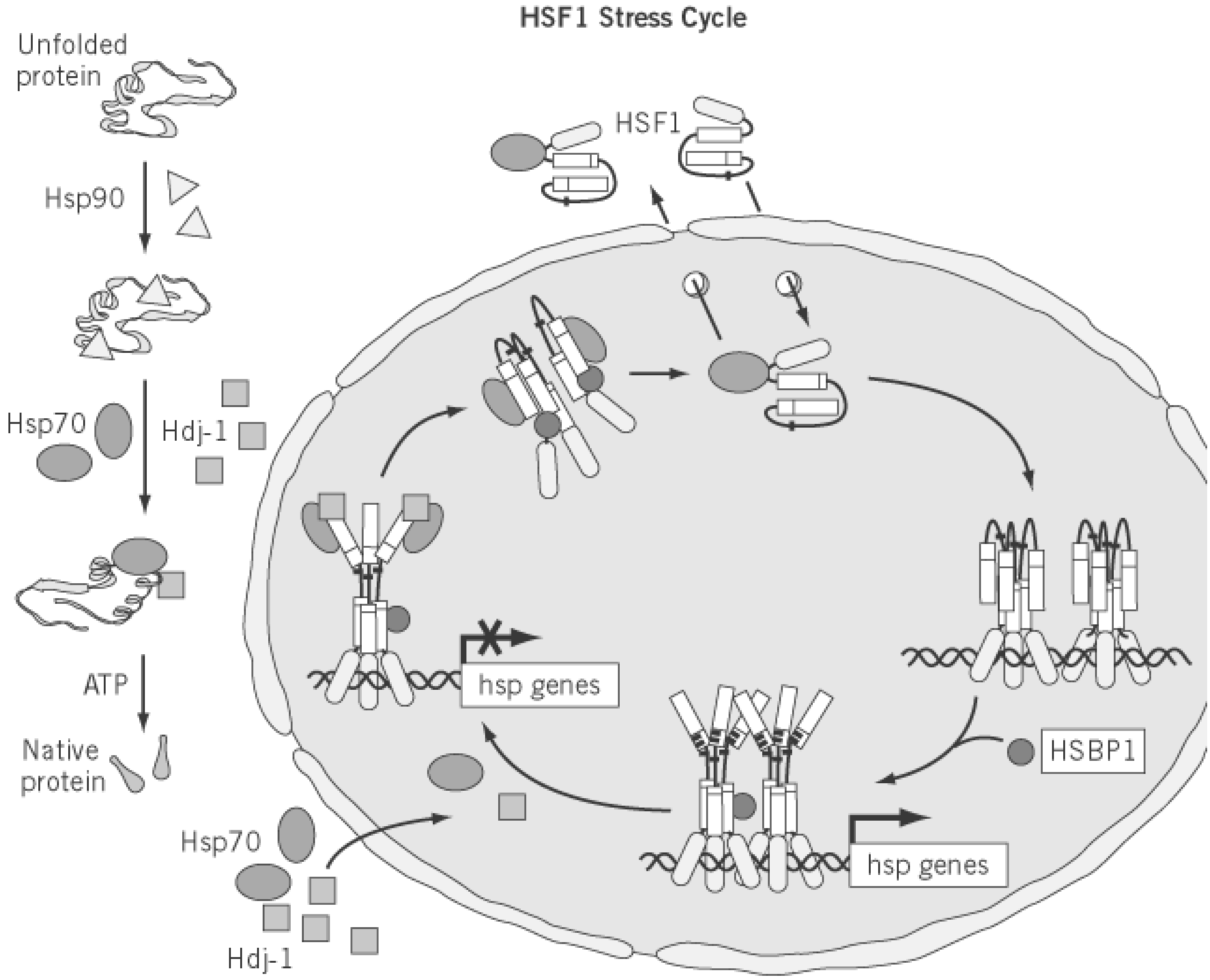

Maintenance of HSF1 in a repressed state is delicately balanced and easily disrupted; for example, overexpression of HSF1 by transient transfection results in constitutively active HSF1; likewise, mutation of a single critical phosphoserine residue has the same derepressing effect (70, 87, 88). Acquisition of HSF1 DNA-binding activity is insufficient to activate transcription, as demonstrated by the effects of the anti-inflammatory drugs sodium salicylate, indomethacin, or ibuprofen, which induce DNA binding-competent trimers that, nevertheless, lack inducible phosphorylation and are transcriptionally active (89-91). Rather than corresponding to a nonfunctional form of HSF1, however, the salicylate-induced HSF1 can be converted *in vivo* to the fully active HSF1 by a subsequent exposure to heat shock (91).

Exposure of human cells to 42°C heat shock results in the rapid and transient inducible transcription of heat-shock genes, with maximal rates of hsp70 and hsp90 transcription occurring within 30 to 60 minutes; thereafter, the rate of heat-shock gene transcription declines rapidly, prior to the loss of HSF1 DNA-binding activity (88, 92, 93). The increased levels of heat-shock messenger RNAs following heat shock result from both transcriptional activation of heat-shock genes and the increased stability of heat-shock messenger RNAs during stress (93, 94). This results in the elevated synthesis and accumulation of heat-shock proteins.

The initial evidence that the eukaryotic heat-shock response is autoregulated was based on the effects of amino acid analogues on *Drosophila* cells. Rather than the expected transient heat-shock response, treatment with azetidine, a proline analogue, resulted in the continuous activation of heat-shock gene expression (95). An explanation for this result was that amino acid analogues induce the heat-shock response as a result of their incorporation into nascent polypeptides that misfold. Such amino acid analogue-containing nascent polypeptides would be expected to associate with Hsp70 (96); the sequestration of Hsp70 by these permanently unfolded polypeptides in turn results in activation of heat-shock gene transcription. However, unlike the heat-shock response, where attenuation is linked to the *de novo* synthesis of heat-shock proteins, Hsp70 synthesized in the presence of amino acid analogues is also misfolded, and therefore nonfunctional as a chaperone, with the consequence that the heat-shock response does not attenuate. These observations led to the proposal that heat-shock proteins are involved in autoregulation of the heat-shock response. Genetic evidence to support the autoregulation of the heat-shock response has shown that overexpression of the yeast Ssa1p (cytosolic Hsp70) dampens the heat-shock response from two different (ssa1 and ssa4) promoters for Hsp70 (97). Likewise, deletion of the ssa1 and ssa2 Hsp70 genes resulted in an unusually high level of expression of another Hsp70 gene (Ssa3p) and other heat-shock proteins in a HSF-dependent manner; these results strongly implicated HSF as a potential target for autoregulation by members of the Hsp70 family (98). The relationship between HSF and Hsp70 was further supported by a search for extragenic suppressors of the temperature-sensitive phenotype of an Hsp70 mutant (ssa1ssa2 strain), which also uncovered HSF as an interactive component of the regulatory response (99). A spontaneous mutant EXA3 that could reverse the growth defect of the Hsp70 mutant (ssa1ssa2) is very closely linked with the gene encoding HSF, and another mutation identified in the genetic screen maps to the HSF gene (100).

Biochemical evidence to support a role for molecular chaperones in the regulation of the heat-shock response have demonstrated that stress-induced HSF1 trimers were associated with Hsp70 (101-105). The Hsp70-HSF complexes are sensitive to ATP, which is typical of chaperone–substrate interactions, and can be reconstituted *in vitro* (101, 105). Through the use of HSF1 deletion mutants and direct *in vitro* binding assays, a site for Hsp70 binding was mapped on the transactivation domain of HSF1 (105). Whereas overexpression of Hsp70 inhibited completely the induction of heat-shock gene transcription, there was little or no effect on the formation of HSF1 trimers or on inducible phosphorylation of HSF1 (103, 105). This demonstrates that Hsp70 can also function as a negative regulator of HSF1 activity and that the repression of heat-shock gene transcription that occurs during attenuation is due to the repression of the HSF1 transactivation domain by direct binding to Hsp70 (101-103, 105). Although Hsp70 has a demonstrated role in the autoregulation of the heat-shock response, other molecular chaperones, such as Hdj1 or Hsp90, have also been implicated in the regulation of HSF1 activity. Hdj1 interacts with HSF1 in higher eukaryotes and negatively regulates HSF1 transcriptional activity (105). A role for members of the DnaJ family in regulation of the heat-shock response is supported by the observation in *S. cerevisiae* that the DnaJ homologue, SIS1, negatively regulates its own expression (106). However, SIS1 autoregulation requires the heat-shock element (HSE) and other sequences, suggesting that additional regulatory molecules might be involved. **HSF** may also associate with Hsp90; such interactions have been detected for yeast, rat, and rabbit Hsp90 (107, 108) but not with human Hsp90 (102, 103, 105).

Identification of the transactivation domain of HSF1 as a chaperone-binding site offers a number of intriguing possibilities for Hsp70 as a competitor for HSF1 interaction with the basal transcriptional machinery (109) or the role of Hsp70 in the conformational change of HSF1. The consequence of Hsp70 binding may render the transactivation domain inaccessible to the transcriptional machinery, thus resulting in the transcriptional repression. A related role for chaperones as regulators of transcriptional activators has also been described for the family of **steroid receptors**, although in this case multiple chaperones are recruited to maintain the activator in a repressed state by formation of a stable chaperone-substrate complex (110). It is tempting to consider that the interactions observed between p53 and Hsp70 (Hsc70) could also reflect a form of chaperone-dependent regulation of the folded state that affects the properties of the transcriptional activator (111).

3. Molecular Chaperones: Roles in Translocation, Protein Folding, and Refolding

3.1. General Features of Molecular Chaperones

Although some proteins refold spontaneously *in vitro* when diluted at low concentrations from **denaturants**, larger, multidomain proteins often have a propensity to misfold and aggregate (see **Protein folding**). Consequently, the challenge within the densely packed environment of the cell is to capture and sequester efficiently non-native proteins that may lead subsequently to either refolding or degradation. Molecular chaperones of the Hsp90, Hsp70, and Hsp60 class accomplish this by capturing non-native intermediates and, together with co-chaperones and ATP, facilitate the appearance of the folded native state (112). The Hsp70 chaperones, for example, recognize stretches in polypeptides that are rich in **hydrophobic** residues and are transiently exposed in early folding intermediates, but typically confined to the hydrophobic core in the native state (113). This contrasts to the Hsp60/GroEL chaperonin, which creates a protected environment with the properties of a "protein-folding test-tube" in which non-native proteins can undergo rounds of binding and release to acquire the native state (114, 115) . The consequence of chaperone interactions with early folding intermediates, therefore, is to shift the equilibrium of protein folding toward on-pathway events and to minimize the appearance of nonproductive intermediates that may have a propensity to aggregate as misfolded species.

The family of molecular chaperones is large; they are diverse in size and apparent structure, yet highly conserved throughout evolution and abundant under nonstress conditions (40, 112, 116). Most chaperones are abundant in growing cells and can attain concentrations of 1% to 5% of total cell protein. They are classified according to molecular size, that is, Hsp100, Hsp90, Hsp70, Hsp60, Hsp40, and small Hsps (Table 1). Biochemical studies on chaperones have shown that a common function of the chaperones Hsp104, Hsp90, Hsp70, the small Hsps, **immunophilins** (FKPB52 and CyP40), the steroid aporeceptor protein p23, and Hip (Hsp70 and Hsp90 interacting protein) is to prevent the *in vitro* aggregation of model protein substrates and to maintain the substrate in an intermediate folded state competent for subsequent refolding to the native state. A distinction among proteins with chaperone activities is that refolding to the native state requires the activity of a specific subset of chaperones, such as Hsp90, Hsp70, or Hsp60/GroEL, which are **nucleotide-binding** proteins, and the regulatory properties of chaperone-specific co-chaperones, such as p23, the immunophilins, which enhance Hsp90, dnaJ, or Hip proteins that associate with Hsp70, and Hsp10/groES, which stimulates Hsp60/groEL. The suggestion that chaperones exist as heteromeric complexes that associate with different folded intermediates allows the substrate to acquire different regulatory states.

3.2. Representative Analysis of the Hsp70 Family

Chaperones are found in nature as functionally related protein families; for example, the eukaryotic Hsp70 proteins are found in the cytoplasm, nucleus, mitochondria, and endoplasmic reticulum, where they maintain proteins in intermediate folded states competent for translocation across the membranes of the mitochondria or endoplasmic reticulum and for subsequent refolding to the native state (116-119). In *E. coli*, the Hsp70 homologue, dnaK, originally identified in a genetic screen for host proteins required for replication of lambda phage, is also required for growth at nonpermissive temperatures (120, 121). Analysis of the structure and functional properties of Hsp70 reveals a multi-domain organization corresponding to a 45-kDa amino-terminal ATPase domain, the 18-kDa carboxyl-terminal peptide-binding domain, and a 7-kDa intra- and interdomain EEVD (Glu–Glu–Val–Asp) regulatory motif (122-124).

Hsp70 interacts with unfolded polypeptides and peptides by binding to arrays of hydrophobic residues in which acidic residues are excluded and the surrounding environment enriched in basic residues (113). Typically, such sites are often buried within the hydrophobic core of folded proteins and are only transiently exposed during protein folding. Affinity of the peptide-binding domain for denatured substrates is dependent on the nucleotide state of the ATPase. Hsp70 exhibits a high affinity for substrate when bound to ADP; upon release of ADP and re-binding of ATP, the affinity for peptides decreases and the substrate is released (125, 126). ATP is hydrolyzed to ADP, and the cycle begins again. The intrinsic ATPase of Hsp70 is exceedingly slow and stimulated by increased temperature, the presence of potassium, calcium, and magnesium ions, the presence of substrates, and the co-chaperones dnaJ and GrpE (126-129). DnaJ stimulates the dnaK ATPase and is required for both the *in vivo* and *in vitro* folding activities of dnaK. dnaJ also functions independently as a chaperone with "holding" activity and has been shown to prevent the aggregation of unfolded rhodanase and **luciferase** in an ATP-independent manner (130). The chaperone activity of DnaJ may not be essential, however, because the human homologue, Hdj-1, neither binds non-native substrates nor prevents protein aggregation. Hdj-1 is necessary for Hsp70-mediated refolding (131). The second dnaK co-chaperone is GrpE, which functions in concert with dnaJ to enhance ADP release, thus allowing the unfolded substrate to dissociate from the dnaK/dnaJ/GrpE complex, also known as the Hsp70 chaperone machine.

3.3. Biochemical Properties in Protein Folding

Among their multitude of biochemical activities, certain chaperones interact with unfolded polypeptides to "hold" non-native proteins in a refolding-competent state, whereas others can also "refold" the polypeptide to its final native state. The relationships between these events in protein folding are indicated in Figure 5. Representatives of the former class include abundant molecular chaperones, such as Hsp90 and the small Hsps. *In vitro*, these heat-shock proteins stably maintain non-native polypeptides in intermediate refoldable states that can then be subsequently refolded by the addition of nucleotide, Hsp70, and Hdj-1 (131, 132). Chaperones of the latter class include Hsp70 and groEL (Hsp60), which can both hold and refold (112, 131). The refolding activity requires accessory proteins or co-chaperones, nucleotide binding, and hydrolysis. In the absence of these co-factors, neither Hsp70 nor groEL are effective in refolding a polypeptide to the native state (124, 131, 133).

Figure 5. Biochemical properties of molecular chaperones in protein folding. The biochemical fate of an unfolded protein is presented schematically. The native protein substrate is denatured (either chemically or thermally) and acquires an unfolded state. Dilution of the denatured protein into buffer containing a nonspecific protein, bovine serum albumin, leads to the aggregated state that is not resolubilized by chaperones (Hsp90, Hsp70, Hdj1) in the presence of ATP. In contrast, dilution of the unfolded protein into the molecular chaperones Hsp70, Hdj1, and ATP results in refolding to the native, enzymatically active state. The holding or intermediate folded state is acquired by dilution into either Hsp90 or Hsp70 alone; subsequent addition of Hsp70, ATP, and the co-chaperone Hdj-1 results in folding to the native state.

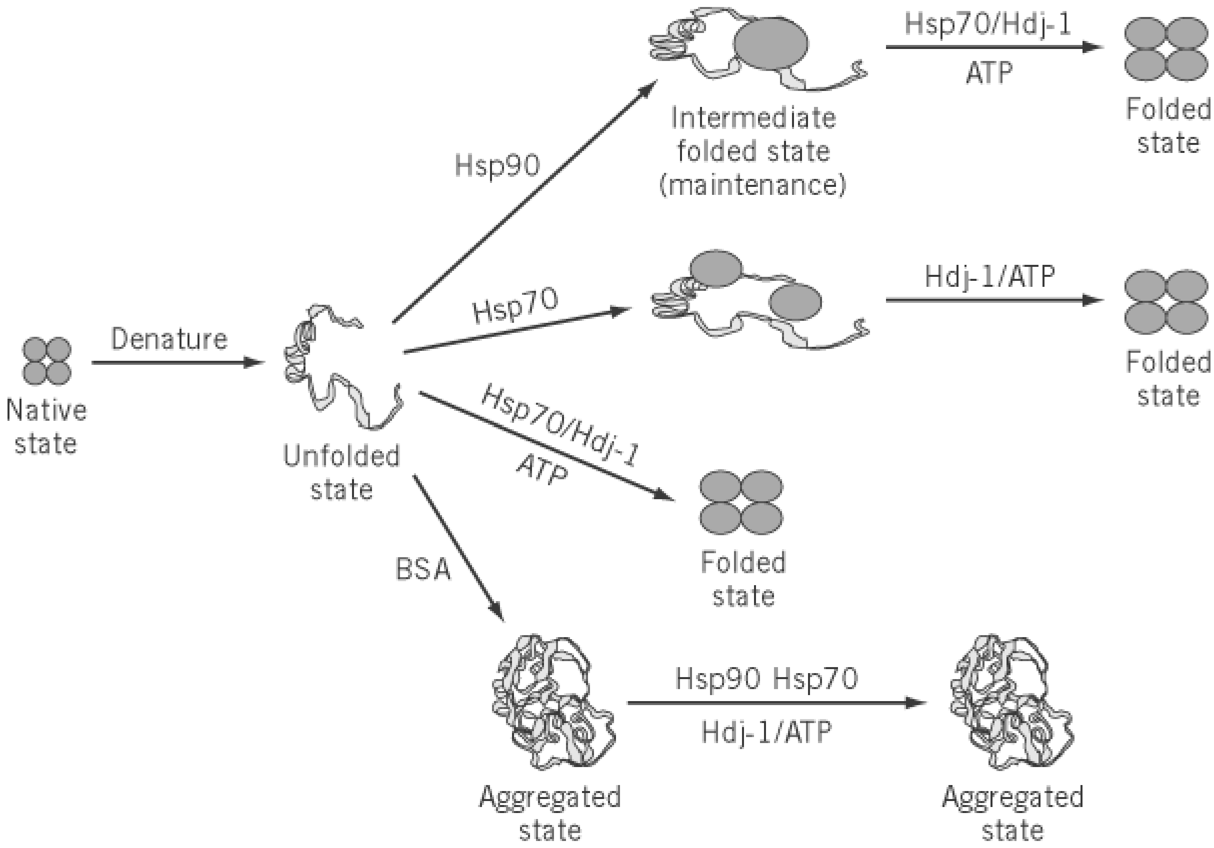

While many of the biochemical properties of molecular chaperones are based on *in vitro* approaches, the situation *in vivo* is more complex due to the coexistence of multiple families of chaperones and diverse substrates within the same subcellular compartments. Most chaperones are expressed constitutively and are relatively abundant in each subcellular compartment, where they function in activities including cell signaling and regulating protein kinase activities. Chaperones including Hsp70, Hsp90, p23, and immunophilins are essential components of steroid aporeceptor complexes and necessary for steroid responsiveness (134, 135). In the unstressed cell, chaperones also modulate the folded state of polypeptides; for example, members of the Hsp70 family have a role in **protein biosynthesis** in translation elongation (117, 136), they maintain mitochondrial-targeted polypeptides as unfolded intermediates in a translocation-competent state, and they facilitate the refolding of translocation-competent proteins in concert with Hsp60 (112, 118). During periods of stress, the expression of many, but not all, chaperones is induced to cope with an increased volume of unfolded proteins. The association of unfolded proteins with chaperones may retard protein aggregation, facilitate refolding of non-native intermediates, and provide an interface with the **protein degradation** machinery.

Molecular chaperones stimulate on-pathway folding, principally by their ability to (a) function as kinetic traps to prevent off-pathway intermediates that may lead to the formation of aggregates and (b) favor folding to the native state (Fig. 5). Chaperones exhibit transient and stable interactions with non-native protein substrates; under normal conditions of cell growth, chaperones are associated with kinases and steroid aporeceptors (137). Mutations that affect protein function often lead to stable complexes with chaperones; for example, mutant forms of p53 are stably associated with Hsp70 (111, 138). In such examples, modulation of the activity or half-life of the chaperone-associated substrate may influence cellular events and pathogenesis. Both the absolute and relative abundance of chaperones influences protein biogenesis in the unstressed cell and during periods of stress, where the expression of many but not all chaperones is induced to cope with an increase in the flux of non-native proteins.

4. Role of Heat-Shock Proteins and Stress-Induced Cytoprotection in Disease

The abnormal expression of heat-shock proteins has been well documented for diseases including ischemia and reperfusion damage, cardiac hypertrophy, fever, inflammation, metabolic diseases, bacterial and viral infection, cell and tissue injury, aging, and cancer (40, 139, 140). Serum **antibodies** to the heat-shock proteins Hsp90, Hsp70, Hsp60, and small heat-shock proteins have been detected in individuals with infectious diseases and autoimmune diseases, including rheumatoid arthritis and insulin-dependent diabetes (141). These observations have led to questions whether stimulation of the immune response is the result of, or causes, cell damage, and whether the appearance of circulating antibodies to heat-shock proteins reflects the organismal response to stress and damage. Although the acute response to stress may be critical for recovery and long-term survival, the chronic expression of heat-shock proteins in diseased tissues may be deleterious to protein biogenesis and have negative effects on cell growth. Because the ability of a cell to survive stress is dependent on both the kinetics of activation and the duration of the response, changes in the environment of the cell will shift the stress-sensing capacity of the heat-shock response, with profound effects on survival, repair, and recovery.

The cytoprotective role of heat-shock proteins offers novel approaches for the treatment of diseases involving metabolic disorders, inflammation, infection, and ischemia (142, 143). Ischemia of the brain, kidney, heart, and liver results from decreased blood flow to tissues; the associated pathology that ensues reflects adaptation to decreased levels of oxygen and nutrients. Expression of heat-shock proteins are rapidly induced, during ischemia and to an even greater degree upon reperfusion associated with the appearance of oxygen-free radicals. Exposure to environmental toxins, such as xenobiotics and aromatic hydrocarbons that promote oxidative damage, could potentiate the damaging effects of ischemia and reperfusion. Cytoprotection and repair against the deleterious effects of stress and trauma can be accomplished by the overexpression of one or more heat-shock protein genes. Yeast cells engineered to overexpress Hsp70, the small heat-shock proteins, or Hsp 104 are also protected against exposure to lethal heat-shock temperatures, H_2O_2, heavy metals, arsenite, anoxia, and ethanol toxicity (1). In vertebrates, modulation of the heat-shock response or the expression of specific heat-shock proteins can limit or prevent the pathologies associated with certain chronic diseases. A class of diseases associated with the appearance of misfolded proteins are the prion diseases, which from yeast to humans are associated with changes in the folded state of the prion that correlates with conversion from a noninfective to an infective state. Among the fascinating features of prion diseases is the epigenetic transmission of an altered protein conformation, thus endowing the infectious prion with unique biological properties. Recent data on the yeast prions Ura3 and Psi, which have features in common with the scrapie prion protein, reveal that the molecular chaperone Hsp 104 has an essential role in solubility of the Psi protein and the regulation of the Psi+ phenotype (144). Whether these observations have direct implications for heat-shock proteins in neurodegenerative diseases remains an exciting dimension for future studies.

In the pathology of myocardial disease, the induction of Hsp70 is associated with both ischemia and reperfusion and therefore could reflect the appearance of damaged proteins during adaptation of the myocardium. The elevated synthesis of heat-shock proteins, therefore, could reflect the response of myocardiocytes to survive the stress by repairing protein damage. For example, the induction of Hsp70 following aortic constriction or work-overload-induced cardiac hypertrophy in animal models could reflect a response to the aberrant synthesis, accumulation, or degradation of proteins or, alternatively, a response to events that occur during the partial reentry of the myocardial cell into the growth cycle (142, 143). Does activation of the heat-shock response reflect protein damage and does this reveal a potential strategy to detect or manipulate the course of events? A correlation between the levels of Hsp70 and the degree of myocardial protection has been demonstrated; moreover, transgenic mice overexpressing Hsp70 exhibited an enhanced resistance to myocardial ischemic stress, thus providing direct evidence for a role of heat-shock proteins in cytoprotection (145-147). These studies reveal that induction of the heat-shock response by the stressed myocardium is proportional to protein damage; therefore a potential strategy would be to enhance the expression of heat-shock proteins such as Hsp70, which in turn may confer a more rapid reestablishment of normal cardiac protein synthesis and myocardial function. The activation of a heat-shock response restores normal cardiac function after injury, possibly by removal of misfolded cardiac proteins and reestablishment of normal cardiac protein synthesis (142).

As an alternative to genetic manipulation to alter heat-shock gene expression, it may be more fruitful to search for small molecules that enhance either the expression or function of heat-shock proteins. Such a pharmacological approach has been suggested, for example, based on experiments using herbimycin-A as an inducer of Hsp70 with protective effects in simulated ischemia on rat neonatal cardiomyocytes (148) and the cytoprotective activity of a hydroxylamine derivative (Bimoclomol) during ischemia and wound healing (149). Other classes of small molecules with heat-shock regulatory properties are nonsteroidal anti-inflammatory drugs (NSAIDs), cyclopentenone prostaglandins, **serine proteinase inhibitors**, and inhibitors of the ATP-dependent **ubiquitin-**dependent proteasome (89, 150, 151). Salicylates and other NSAIDs activate an intermediate form of HSF1, which potentiates the cellular response to stress (89). Pretreatment with NSAIDs such as salicylates or indomethacin (at subthreshold concentrations) both decreases the temperature threshold of the heat-shock response and confers cytoprotection (150). Exposure to aspirin or indomethacin at concentrations comparable to clinical levels results in the priming of human cells for subsequent exposure to heat shock and other stresses, the enhanced transcription of heat-shock genes, and cytoprotection from thermal injury (152). Considering that the expression of heat-shock genes occurs in response to pathological conditions, it would not be surprising if the ability of NSAIDs to activate the DNA-binding activity of HSF and Hsp70 expression contributes to their pharmacological efficacy. Another class of pharmacologically active small molecules in the pathway of arachidonate metabolism are cyclopentenone prostaglandins, which activate the heat-shock response and protect against thermal injury and viral infection (151). It is intriguing to note that this class of molecules has cardioprotective value (153). The development of pharmacologically active small molecules that influence either the regulation or function of heat-shock proteins offers a means to harness the positive cytoprotective value of the heat-shock response.

5. Summary

- Exposure of cells to stresses such as heat shock, oxidant injury, toxic chemicals, and heavy metals causes an imbalance in protein metabolism that challenges the cell to respond rapidly, yet precisely, to minimize the deleterious effects of environmental and physiological stress.
- The heat-shock response, by activation of heat-shock transcription factors, results in the elevated expression of heat-shock genes and the concomitant synthesis of heat-shock proteins and molecular chaperones.
- Molecular chaperones function in a variety of protein biosynthetic events to protect proteins from the deleterious effects of acute or chronic stress by stabilizing and refolding protein folding intermediates or facilitating protein degradation.
- Accumulation of misfolded proteins is of central importance to diseases of protein folding, including **sickle-cell** hemoglobin, cystic fibrosis, and prion diseases, in addition to complex multifactorial diseases, including bacterial and viral infections, myocardial ischemia, neurodegenerative diseases, and cancer.

6. Acknowledgments

The author was supported by a research grant from the NIH and the Fogarty International Fellowship. The assistance of K. Veraldi and S. Fox in preparation of this manuscript is appreciated.

Bibliography

1. D. A. Parsell and S. Lindquist (1994) *The Biology of Heat Shock Proteins and Molecular Chaperones*, Cold Spring Harbor Laboratory Press, Cold Spring Harbor, NY, pp. 457–494.
2. A. D. Grossman, J. W. Erickson, and C. A. Gross (1984) Cell **38**, 383–390.
3. D. W. Cowing et al. (1985) Proc. Natl. Acad. Sci. USA **82**, 2679–2683.
4. M. Bloom et al. (1986) J. Bacteriol. **166**, 380–384.
5. T. Yura, H. Nagai, and H. Mori (1993) Annu. Rev. Microbiol. **45**, 301–325.
6. E. A. Craig and C. A. Gross (1991) Trends Biochem. Sci. **16**, 135–140.
7. A. D. Grossman, D. B. Straus, W. A. Walter, and C. A. Gross (1987) Genes Dev. **1**, 179–184.
8. K. Tilly, J. Spence, and C. Georgopoulos (1989) J. Bacteriol. **171**, 1585–1589.
9. D. B. Straus, W. A. Walter, and C. A. Gross (1987) Nature **329**, 348–351.
10. A. S. Kamath-Loeb and C. A. Gross (1991) J. Bacteriol. **173**, 3904–3906.
11. H. Nagai, H. Yuzawa, and T. Yura (1991) Proc. Natl. Acad. Sci. USA **88**, 10515–10519.
12. S. A. Lesley, N. E. Thompson, and R. R. Burgess (1987) J. Biol. Chem. **262**, 5404–5407.
13. S. Skelly et al. (1987) Proc. Natl. Acad. Sci. USA **84**, 8365–8369.
14. D. B. Straus, W. A. Walter, and C. A. Gross (1987) Nature **329**, 348–351.
15. J. Mecsas et al. (1993) Genes Dev. **7**, 2618–2628.
16. P. E. Rouviere et al. (1995) EMBO J. **14**, 1032–1042.
17. J. W. Erickson et al. (1987) Genes Dev. **3**, 1462–1471.
18. B. Lipinska, S. Sharma, and C. Georgopoulos (1988) Nucleic Acids Res. **16**, 10053–10067.
19. J. W. Erickson and C. A. Gross (1989) Genes Dev. **3**, 1462–1471.
20. Q. P. Wang and J. M. Kaguni (1989) J. Bacteriol. **171**, 4248–4253.
21. S. Raina, D. Missiakas, and C. Georgopoulos (1995) EMBO J. **14**, 1043–1055.
22. D. Missiakas and S. Raina (1997) EMBO J. **16**, 1670–1685.
23. P. N. Danese and T. J. Silhavy (1997) Genes Dev. **11**, 1183–1193.
24. K. Hiratsu et al. (1995) J. Bacteriol. **177**, 2918–2922.
25. L. Connolly A. De Las Penas, B. M. Alba, and C. A. Gross (1997) Genes Dev. **11**, 2012–2021.
26. K. Tilly, N. McKittrick, M. Zylicz, and C. Georgopoulos (1983) Cell **34**, 641–646.
27. D. B. Straus, W. A. Walter, and C. A. Gross (1990) Genes Dev. **4**, 2202–2209.
28. M. Kanemori, H. Mori, and T. Yura (1994) J. Bacteriol. **176**, 4235–4242.
29. A. D. Grossman, D. B. Straus, W. A. Walter, and C. A. Gross (1987) Genes Dev. **1**, 179–184.
30. T. Tomoyasu et al. (1995) EMBO J. **14**, 2551–2560.
31. M. Kanemore, K. Nishihara, H. Yanagi, and T. Yura (1997) J. Bacteriol. **179**, 7219–7225.
32. H. Nagai, H. Yuzawa, M. Kanemori, and T. Yura (1994) Proc. Natl. Acad. Sci. USA **91**, 10280–10284.
33. J. S. McCarty et al. (1996) J. Mol. Biol. **256**, 829–837.
34. K. Liberek and C. Georgopoulos (1993) Proc. Natl. Acad. Sci. USA **90**, 11019–11023.
35. J. Gamer et al. (1996) EMBO J. **15**, 607–617.
36. S. Skelly et al. (1988) Proc. Natl. Acad. Sci. USA **85**, 5497–5501.
37. K. Liberek, T. P. Galitski, M. Zylicz, and C. Georgopoulos (1992) Proc. Natl. Acad. Sci. **89**, 3516–3520.
38. J. Gamer, H. Bujard, and B. Bukau (1992) Cell **69**, 833–842.
39. A. Blaszczak, M. Zylicz, C. Georgopoulos, and K. Liberek (1995) EMBO J. **14**, 5085–5093.
40. R. I. Morimoto, A. Tissieres, and C. Georgopoulos (1990) *Stress Proteins in Biology and Medicine*, Cold Spring Harbor Laboratory Press, Cold Spring Harbor, NY, pp. 1–36.
41. J. T. Lis and C. Wu (1993) Cell **74**, 1–20.

42. R. I. Morimoto (1993) Science **269**, 1409–1410.
43. C. Wu (1995) Annu. Rev. Cell Dev. Biol. **11**, 441–469.
44. G. Wiederrecht, D. Seto, and C. S. Parker (1988) Cell **54**, 841–853.
45. P. K. Sorger and H. R. Pelham (1988) Cell **54**, 855–864.
46. J. Clos et al. (1990) Cell **63**, 1085–1097.
47. S. K. Rabindran, G. Giorgi, J. Clos, and C. Wu (1991) Science **259**, 230–234.
48. K. D. Sarge et al. (1991) Genes Dev. **5**, 1902–1911.
49. T. J. Scheutz et al. (1991) Proc. Natl. Acad. Sci. USA **88**, 6911–6915.
50. A. Nakai and R. I. Morimoto (1993) Mol. Cell. Biol. **13**, 1983–1997.
51. A. Nakai et al. (1997) Mol. Cell Biol. **17**, 469–481.
52. K. D. Scharf et al. (1990) EMBO J. **9**, 4495–4501.
53. L. Nover et al. (1996) Cell Stress Chap. **1**, 215–223.
54. L. Nover and K. D. Scharf (1997) Cell. Mol. Life Sci. **53**, 80–103.
55. C. J. Harrison, A. A. Bohm, and H. C. M. Nelson (1994) Science **263**, 224–227.
56. G. W. Vuister, S. J. Kim, C. Wu, and A. Bax (1994) Biochem. **33**, 10–16.
57. C. Wu, J. Clos et al. (1994) *The Biology of Heat Shock Proteins and Molecular Chaperones*, Cold Spring Harbor Laboratory Press, Cold Spring Harbor, NY, pp. 417–455.
58. P. K. Sorger and H. C. M. Nelson (1989) Cell **59**, 807–813.
59. R. Peteranderl and H. C. M. Nelson (1992) Biochem. **31**, 12272–12276.
60. M. Green, T. J. Scheutz, E. K. Sullivan, and R. E. Kingston (1995) Mol. Cell Biol. **15**, 3354–3362.
61. Y. Shi, P. E. Kroeger, and R. I. Morimoto (1995) Mol. Cell Biol. **15**, 4309–4318.
62. J. Zuo, D. Rungger, and R. Voellmy (1995) Mol. Cell Biol. **15**, 4319–4330.
63. J. Wisniewski, A. Orosz, R. Allada, and C. Wu (1996) Nucleic Acids Res. **24**, 367–374.
64. S. K. Rabindran et al. (1993) Science **259**, 230–234.
65. J. Zuo, R. Baler, G. Dahl, and R. Voellmy (1994) Mol. Cell Biol. **14**, 7557–7568.
66. A. Orosz, J. Wisniewski, and C. Wu (1996) Mol. Cell Biol. **16**, 7018–7030.
67. E. Zandi, T. N. Tran, W. Chamberlain, and C. S. Parker (1997) Genes Dev. **11**, 1299–1314.
68. T. Farkas, Y. A. Kutskova, and V. Zimarino (1998) Mol. Cell Biol. **18**, 906–918.
69. R. Baler, G. Dahl, and R. Voellmy (1993) Mol. Cell Biol. **13**, 2486–2496.
70. K. Sarge, S. P. Murphy, and R. I. Morimoto (1993) Mol. Cell Biol. **13**, 1392–1407.
71. A. Nakai et al. (1995) Mol. Cell Biol. **15**, 5268–5278.
72. M. Tanabe, A. Nakai, Y. Kawazoe, and K. Nagata (1997) J. Biol. Chem. **272**, 15389–15395.
73. M. Tanabe et al. (1998) EMBO J. **17**, 1750–1758.
74. C. Kanei-Ishii et al. (1997) Science **277**, 246–248.
75. C. M. Cahill et al. (1997) Adv. Exp. Med. Biol. **400**, 625–630.
76. N. G. Theodorakis et al. (1989) Mol. Cell Biol. **9**, 3166–3173.
77. L. Sistonen et al. (1992) Mol. Cell Biol. **12**, 4104–4111.
78. L. Sistonen, K. D. Sarge, and R. I. Morimoto (1994) Mol. Cell Biol. **14**, 2087–2099.
79. K. D. Sarge et al. (1994) Biol. Reprod. **50**, 1334–1343.
80. V. Mezger et al. (1994) Dev. Biol. **166**, 819–822.
81. M. Rallu et al. (1997) Proc. Natl. Acad. Sci. USA **94**, 2392–2397.
82. A. Mathew, S. K. Mathur, and R. I. Morimoto (1998) Mol. and Cell Biol. **18**, 5091–5098.
83. J. S. Larson, T. J. Schuetz, and R. E. Kingson (1988) Nature **335**, 372–375.
84. D. D. Mosser, P. T. Kotzbauer, K. D. Sarge, and R. I. Morimoto (1990) Proc. Natl. Acad. Sci.

USA **87**, 3748–3752.
85. V. Zimarino, S. Wilson, and C. Wu (1990) Science **249**, 546–549.
86. J. T. Westwood, J. Clos, and C. Wu (1991) Nature **353**, 822–827.
87. U. Knauf, E. M. Newton, J. Kyriakis, and R. E. Kingson (1996) Genes Dev. **10**, 2782–2793.
88. M. P. Kline and R. I. Morimoto (1997) Mol. Cell Biol. **17**, 2107–2115.
89. D. A. Jurivich, L. Sistonen, R. A. Kroes, and R. I. Morimoto (1992) Science **255**, 1243–1245.
90. C. Giardina and J. T. Lis (1995) J. Biol. Chem. **270**, 10369–10372.
91. J. J. Cotto, M. Kline, and R. I. Morimoto (1996) J. Biol. Chem. **271**, 3355–3358.
92. K. Abravaya, B. Phillips, and R. I. Morimoto (1991) Genes Dev. **5**, 2117–2127.
93. D. D. Mosser, N. G. Theodorakis, and R. I. Morimoto (1988) Mol. Cell Biol. **8**, 4736–4744.
94. N. G. Theodorakis and R. I. Morimoto (1987) Mol. Cell Biol. **7**, 4357–4368.
95. B. J. DiDomenico, G. Bugaisky, and S. Lindquist (1982) Cell **31**, 593–603.
96. R. P. Beckmann, L. A. Mizzen, and W. J. Welch (1990) Science **248**, 850–854.
97. D. E. Stone and E. A. Craig (1990) Mol. Cell Biol. **10**, 1622–1632.
98. W. R. Boorstein and E. A. Craig (1990) Mol. Cell Biol. **10**, 3262–3267.
99. R. J. Nelson, M. F. Heschl, and E. A. Craig (1992) Genetics **131**, 277–285.
100. J. T. Halladay and E. A. Craig (1995) Mol. Cell Biol. **15**, 4890–4897.
101. K. Abravaya, M. P. Myers, S. P. Murphy, and R. I. Morimoto (1992) Genes Dev. **6**, 1153–1164.
102. R. Baler, W. J. Welch, and R. Voellmy (1992) J. Cell Biol. **117**, 1151–1159.
103. S. K. Rabindran et al. (1994) Mol. Cell Biol. **14**, 6552–6560.
104. S. L. Nunes and S. K. Calderwood (1995) Biochem. Biophy. Res. Commu. **213**, 1–6.
105. Y. Shi, D. D. Mosser, and R. I. Morimoto (1998) Genes Dev. **12**, 654–666.
106. T. Zhong, M. M. Luke, and K. T. Arndt (1996) J. Biol. Chem. **271**, 1349–1356.
107. K. Nadeau, A. Das, and C. T. Walsh (1993) J. Biol. Chem **268**, 1479–1487.
108. S. C. Nair et al. (1996) Cell Stress Chap. **1**, 237–250.
109. P. B. Mason Jr.and J. T. Lis (1997) J. Biol. Chem. **272**, 33227–33233.
110. S. P. Bohen and K. R. Yamamoto (1994) *The Biology of Heat Shock Proteins and Molecular Chaperones*, Cold Spring Harbor Laboratory Press, Cold Spring Harbor, NY, pp. 313–334.
111. T. R. Hupp, D. W. Meek, C. A. Midgley, and D. P. Lane (1992) Cell **71**, 875–886.
112. F. U. Hartl (1996) Nature **381**, 571–579.
113. S. Rudiger, L. Germeroth, J. Schneider-Mergener, and B. Bukau (1997) EMBO J. **16**, 1501–1507.
114. A. L. Horwich et al. (1993) Cell **74**, 909–917.
115. M. Mayhew et al. (1996) Nature **379**, 420–426.
116. M. J. Gething (1997) *Molecular Chaperones and Protein-Folding Catalysts*, Oxford University Press, New York, pp. 18–21.
117. E. A. Craig et al. (1994) *The Biology of Heat Shock Proteins and Molecular Chaperones*, Cold Spring Harbor Laboratory Press, Cold Spring Harbor, NY, pp. 31–52.
118. T. Langer and W. Neupert (1994) *The Biology of Heat Shock Proteins and Molecular Chaperones*, Cold Spring Harbor Laboratory Press, Cold Spring Harbor, NY, pp. 53–84.
119. B. Miao, J. Davis, and E. Craig (1997) *Molecular Chaperones and Protein-Folding Catalysts*, Oxford University Press, New York, pp. 3–13.
120. C. Georgopoulos, K. Liberek, M. Zylicz, and D. Ang (1994) *The Biology of Heat Shock Proteins and Molecular Chaperones*, Cold Spring Harbor Laboratory Press, Cold Spring Harbor, NY, pp. 209–249.

121. A. Wawrzynow and M. Zylicz (1997) *Molecular Chaperones and Protein-Folding Catalysts*, Oxford University Press, New York, pp. 481–483.
122. D. B. McKay et al. (1994) *The Biology of Heat Shock Proteins and Molecular Chaperones*, Cold Spring Harbor Laboratory Press, Cold Spring Harbor, NY, pp. 153–177.
123. X. Zhu et al. (1996) Science **272**, 1606–1614.
124. B. C. Freeman, M. P. Myers, R. Schumacher, and R. I. Morimoto (1995) EMBO J. **14**, 2281–2292.
125. K. Liberek, Skowyra, M. Zylicz, and C. Georgopoulos (1991) J. Biol. Chem. **266**, 14491–15596.
126. D. R. Palleros, W. J. Welch, and A. L. Fink (1991) Proc. Natl. Acad. Sci. USA **88**, 5719–5723.
127. K. Liberek et al. (1991) Proc. Natl. Acad. Sci. USA **88**, 2874–2878.
128. S. Sadis and L. E. Hightower (1992) Biochemstry **31**, 9406–9412.
129. M. C. O''Brian and D. B. McKay (1995) J. Biol. Chem. **270**, 2247–2250.
130. H. Schroder, T. Langer, F. U. Hartl, and B. Bukau (1993) EMBO J. **12**, 4137–4144.
131. B. C. Freeman and R. I. Morimoto (1996) EMBO J. **15**, 2969–2979.
132. U. Jakob, M. Gaestel, K. Engel, and J. Buchner (1993) J. Biol. Chem. **268**, 1517–1520.
133. P. Goloubinoff, J. T. Christeller, A. A. Gatenby, and G. H. Lorimer (1989) Nature (London) **342**, 884–889.
134. D. F. Smith (1997) *Molecular Chaperones and Protein-Folding Catalysts*, Oxford University Press, New York, pp. 518–521.
135. W. B. Pratt and M. J. Welsh (1994) Semin. Cell Biol. **5**, 83–93.
136. R. J. Nelson et al. (1992) Cell **71**, 97–105.
137. W. B. Pratt, U. Gehring, and D. O. Toft (1997) *Stress-Inducible Cellular Responses*, Birkhauser Verlag, Basel, pp. 79–95.
138. O. Pinhasi-Kimhi, D. Michalovitz, A. Ben-Zeev, and M. Oren (1986) Nature **320**, 182–184.
139. R. I. Morimoto et al. (1994) *The Biology of Heat Shock Proteins and Molecular Chaperones*, Cold Spring Harbor Laboratory Press, Cold Spring Harbor, NY, pp. 417–455.
140. U. Feige, R. I. Morimoto, I. Yahara, and B. S. Polla (1996) *Stress-Inducible Cellular Reponses*, Birkhauser Verlag, Basel.
141. U. Feige and W. Van Eden (1997) *Stress-Inducible Cellular Responses*, Birkhauser Verlag, Basel, pp. 359–374.
142. I. J. Benjamin and R. S. Williams (1994) *The Biology of Heat Shock Proteins and Molecular Chaperones*, Cold Spring Harbor Laboratory Press, Cold Spring Harbor, NY, pp. 533–552.
143. T. S. Nowak and H. Abe (1994) *The Biology of Heat Shock Proteins and Molecular Chaperones*, Cold Spring Harbor Laboratory Press, Cold Spring Harbor, NY, pp. 553–575.
144. M. M. Patino, J. J. Liu, J. R. Glover, and S. Lindquist (1996) Science **273**, 622–626.
145. R. Mestril et al. (1994) J. Clin. Invest. **93**, 759–767.
146. M. S. Marber et al. (1995) J. Clin Invest. **95**(4), 1446–1456.
147. J. C. L. Plumier et al. (1995) J. Clin. Invest. **95**, 1854–1860.
148. S. D. Morris, D. V. Cumming, D. S. Latchman, and D. M. Yellon (1996) J. Clin. Invest. **97**, 706–712.
149. L. Vigh et al. (1997) Nat. Med. **3**(10), 1150–1154.
150. B. Lee et al. (1995) Proc. Natl. Acad. Sci. USA **92**, 7207–7211.
151. M. G. Santoro (1997) Trends Microbiol. **5**, 276–281.
152. C. Amici, A. Rossi, and M. G. Santoro (1995) Cancer Res. **55**(19), 4452–4457.
153. A. Rossi, G. Elia, and M. G. Santoro (1998) J. Biol. Chem. **273**, 16446–16452.

Hedgehog Signaling

Nusslein-Volhard and Weischaus (1) first identified the *hedgehog* (*hh*) **gene** in their now famous genetic screen that generated many mutations affecting segment number and polarity in Drosophila. Since then, most of the genes discovered in that screen have been **cloned**, and the studies elucidating their functions have provided an in-depth understanding of the molecular mechanisms driving the differentiation of cells with developmentally equivalent properties. The *hh* gene encodes a secreted morphogen that induces an intracellular signaling cascade. This cascade is an integral part of the mechanisms that establish the polarity of the segments during embryogenesis and limb development. *Hh* signaling is well conserved among vertebrates as well, and genes homologous to *hh* have been cloned and studied in various groups, including human, mouse, chicken, Xenopus, and zebrafish (2).

1. Function of *hedgehog* Signaling in Drosophila Development

The *hh* gene plays important roles in both embryogenesis and disc development in *Drosophila melanogaster*. Embryogenesis of Drosophila is a dynamic process involving intricate hierarchical interactions among different gene products whose expression is defined in a temporally and spatially regulated manner. The maternal and zygotic gap gene products lay out the domains from which the insect metameric units evolve. The pair-rule genes, together with the maternal and gap gene activities, establish the repeating embryonic parasegments. The segment polarity genes then specify the anterior and posterior positional information within each evolving segment. Differential expression of the **homeotic** genes expressed within each segment establishes the unique identities of the segments. All of these interactions occurring during embryogenesis define the body plan and serve as a blueprint for pattern formation in latter development.

Hh and ***wingless*** (*wg*, a gene that encodes another signaling morphogen) are two segment polarity genes whose main function is to define the anterior/posterior polarity within each of the embryonic segments. Embryos that lack either *hh* or *wg* function are smaller than wild-type embryos, secrete cuticles that are covered with a lawn of denticles, and do not make naked cuticle (1). This phenotype characterizes many of the segment polarity genes involved in transducing either the *hh* or *wg* signals. The expression of *hh* and *wg* is initiated at the blastoderm by pair-rule gene products in the posterior and anterior compartment of the segments, respectively, and is maintained during gastrulation by interactions among the segment polarity gene products (3, 4). Thus, the loss of *wg* function does not affect initial *hh* expression but causes the gradual loss of *hh* expression at the onset of gastrulation (5-7). Similarly, the loss of *hh* function does not affect the establishment of early *wg* gene expression, but at later stages it results in the loss of *wg* expression along the posterior edge of the anterior/posterior (A/P) segmental boundary (8, 9). Although *hh* is expressed in only two rows of cells that flank the A/P boundary, *hh* mutations affect the development of the entire segment. Genetic studies have demonstrated that these long-range effects of *hh* are mediated through secondary signals such as *wg* and ***decapentaplegic*** (*dpp*) (10-13).

The *hh* signaling pathway is one of the best-studied cascades involved in embryogenesis and limb development, and it is well conserved between insects and vertebrates. In Drosophila, the components identified in this pathway include the putative *hh* receptor *patched* (*ptc*) (14, 15), the coreceptor *smoothened* (*smo*) (16, 17), the transcription factor ***cubitus interruptus*** (*ci*) (18), the **serine/threonine kinases** protein kinase A (PKA) (19) and *fused* (*fu*) (20), *suppressor of fused* (*su (fu)*) (21), *costal*-2 (*cos* -2) (20), and *slimb* (*slmb*) (22), which encodes a protein involved in the **protein degradation** of CI, the protein product of the *ci* gene.

In a developing embryo, *hh* is secreted from the posterior compartment of each segment and binds to its postulated receptor, *ptc*, which is found on the surface of the cells anterior and adjacent to the *hh*-secreting cells. The *hh* precursor protein, HH, is composed of 471 amino acid residues and consists of three functional **domains**: the signal peptide domain (residues 63–83), the N terminus, and the C terminus. The signal peptide is involved in secretion via the endoplasmic reticulum and is cleaved on secretion at the cell surface (5). The 46-kDa full-length HH precursor (F) is not detected in Drosophila embryos or in cell culture, indicating that the signal peptide is cleaved very efficiently on biosynthesis of HH. The resulting 39-kDa HH protein is called Uncleaved (U) and is detected in Drosophila embryos and discs and in cell culture. U undergoes further internal **proteolytic** cleavage, generating a 25-kDa C-terminal protein and the 19-kDa N-terminal fragment that is the active HH molecule responsible for both the short- and long-range *hh* activities. This cleavage is intramolecular and is catalyzed by sequences in the C terminus that are conserved across species and display some similarity to those of serine proteinases (12, 23). Mutation of the invariant histidine residue in this region abolishes HH autocleavage, indicating that the activity of the C terminus is crucial for HH processing (23). The autocleavage occurs between Gly257 and Cys258. In the course of the catalyzed reaction, the nucleophile that attacks the Gly257 carboxyl group is not the usual water molecule, but cholesterol, which consequently remains covalently attached to the N-terminal HH peptide after cleavage. The presence of cholesterol increases the concentration of biologically active HH at the surface of cells secreting HH (24, 25). How the cholesterol-coupled form of HH exerts its short- and long-range effects is not clear. The current hypothesis is that the short-range effect is mediated directly by HH, and that the long-range effect is mediated by the molecules whose expression is induced by HH signaling.

Both genetic and biochemical evidence suggests that the transmembrane protein PTC, the product of the *patched* gene, is the receptor for HH (14, 15, 26). However, *ptc* mutations cause the expression of *hh* target genes—including *wg, dpp*, and *ptc* itself—to be up-regulated and to become independent of an *hh* signal (11, 13, 27-29). This result suggests that *ptc* activity antagonizes the *hh* signal transduction cascade in the absence of an *hh* signal. The gene *smo* also encodes a transmembrane protein and, like *hh*, is a positive regulator of *wg* expression (16, 17). However, SMO does not appear to bind to HH (30). The simplest explanation for these findings is that *ptc* inhibits *smo* activity in the absence of an *hh* signal. When HH binds to PTC, the *ptc* inhibition of *smo* is relieved, and the intracellular cascade can induce *hh* target gene expression. That SMO and PTC **immunoprecipitate** together from cell culture in the presence or absence of HH suggests that PTC-SMO interactions are determined by a conformational change, rather than a dissociation event (31). The activation of *smo* does not require *ptc*, as SMO is constitutively active in a *ptc* mutant background (28, 30).

Genetic epistasis experiments have demonstrated that *Su(fu), fu, cos*-2, and *ci* act downstream from *ptc* and are responsible for transducing the *hh* signal into the nucleus, where *ci* activates the *hh* target genes (8, 20, 32). A perplexing phenomenon associated with *ci* as a transcription factor is that its full-length activated form has never been detected in the nucleus in vivo, not even in the nuclei of cells located at the A/P boundary, where *ci* exerts its transactivation function (18), or in mutants (eg, *ptc, cos*-2, PKA mutants) that exhibit elevated levels of CI protein (29, 33). The accepted explanation for this phenomenon is that cells require undetectable amounts of CI in the nucleus to activate the expression of target genes. CI exists in the cytoplasm as a complex consisting of COS-2, FU, and other unidentified proteins. In the absence of an *hh* signal, this complex is mainly tethered to the cytosolic microtubules (see Microtubule-Associated Proteins (MAPs)) (34-36). CI also exists as two forms: a 155-kDa transcriptionally active form and a 75-kDa N-terminal proteolytic fragment that contains the zinc-finger **DNA-binding** domain. Both forms are detected in the cytosol. In the absence of an *hh* signal, CI is degraded, and the N-terminal fragment of CI is detected in the nucleus, where it functions as a repressor, possibly because it fails to recruit its co-activator Drosophila CBP (cyclic-AMP response element binding protein) (*dCBP*) (34, 37). When the cells receive an *hh* signal, CI dissociates from the microtubule-protein complex, is not degraded, and the full-length form of CI activates *hh* target gene expression (34-36).

A large body of evidence has demonstrated that protein kinase A (PKA) antagonizes *hh* signaling.

PKA mutant clones in the anterior compartment of imaginal discs express *hh* target genes and generate the pattern duplications associated with ectopic *dpp* and *wg* expression (38, 39). As expected, increasing the PKA activity by expressing a constitutively active PKA catalytic subunit antagonizes the *hh*-induced target gene expression along the A/P boundary of the imaginal disc (29, 40). In embryos, PKA has a dual effect on *hh* signaling. Whereas loss of PKA activity leads to increased *hh* target gene expression, the constitutive activity of PKA causes up-regulation of *wg* expression in a *smo*- and *ci*-dependent manner, suggesting that PKA also has a positive function in *hh* signaling during embryogenesis (41). Because an increase in PKA activity does not interfere with *hh* function in either embryogenesis or disc development, it is unlikely that *hh* regulates PKA activity (29, 40, 41). *Ci* is at least one of the direct targets of PKA regulation in the *hh* signaling pathway. In the absence of an *hh* signal, cell culture studies show that CI is **phosphorylated** by the basal PKA activity, and this CI phosphorylation of CI leads to the proteolysis of CI to the N-terminal repressor form (42). When cells receive an *hh* signal, the proteolysis of CI is inhibited, resulting in elevated levels of activated full-length CI. This event leads to the transcriptional activation of target genes in the nucleus, presumably through the interaction with its co-activator *dCBP* (37).

The *hh* gene is also important for the patterning and growth of adult structures. The adult wings and legs are derived from pouches of larval epithelial cells called imaginal discs . Imaginal discs are composed of anterior and posterior compartments derived from groups of cells that originate from the anterior and posterior compartment of certain embryonic segments. Because homozygous *hh* mutants die before hatching, knowledge of *hh* function in patterning the adult appendages was obtained from flies that ectopically express *hh* or from the clonal analysis of *hh* mutant cells. The ectopic expression of *hh* in the anterior compartment of wing and leg discs leads to the duplication of anterior disc patterns or the development of supernumerary wings or legs, depending on the position of the HH-producing clones (10, 43, 44). Loss of endogenous *hh* function in wing and leg discs is associated with loss of patterning in both anterior and posterior compartments and loss of proximal-distal outgrowth that results in smaller appendages (10). The changes in compartment and proximal-distal patterning are mediated by *hh*-induced *dpp* and *wg* (10, 44, 45). In the wing disc, *dpp* is normally expressed along the A/P boundary. Its expression is induced in clones of anterior cells that ectopically express HH, and its expression is abolished in the absence of *hh* function (10, 13, 43). Cells located dorsally in the leg disc express high levels of *dpp*, whereas cells along the ventral A/P boundary express low levels of *dpp* and high levels of *wg*. Dorsal-anterior HH-producing clones induce ectopic *dpp* expression, whereas ventral-anterior HH-producing clones induce ectopic *wg* expression. Similarly, loss of function of *hh* in posterior cells results in a size reduction of the adult leg (10, 45). *Hh* functions similarly in other imaginal discs, such as genital and eye-antennal discs. Loss or gain of function of *hh* is associated with loss or gain of genital and eye-antennal patterns, which is most likely mediated through *dpp* (44, 46, 47).

In the eye disc, pattern formation occurs as a wave of differentiation, the Morphogenetic Furrow (MF), that moves across the disc from posterior to anterior. Undifferentiated cells lie in front of the MF, whereas a patterned array of differentiated photoreceptors and neurons remains behind. HH expression in the cells posterior to the MF drives the progression of the MF, but the mediator of the *hh* signal in the eye-antennal disc is not known. *Dpp* promotes ommatidial differentiation, and its expression is under the control of *hh* before MF formation, after which time, *dpp* autoregulates its own expression and suppresses *wg* expression to promote differentiation behind the MF (5, 23, 48-50).

2. Function of *hedgehog* in Vertebrate Development

Vertebrates carry multiple genes homologous to *hh*, including ***Sonic hedgehog*** (*Shh*), *Indian hedgehog* (*Ihh*), and *Desert hedgehog* (*Dhh*) (51). *Ihh* has been identified in mice, humans, and chicken, and its expression is detected in the developing midgut, lung, and cartilage of the bones. During bone morphogenesis, *Ihh* is expressed in prehypertrophic chondrocytes and controls the balance between ossification and proliferation through a second signal, parathyroid-related protein (PTHrP), which is secreted by perichondrial cells. Ectopic expression of *Ihh* leads to the ectopic induction of PTHrP. Misexpression of *Ihh* or PTHrP results in the disruption of bone development: cartilage elements are broadened, and the bones fail to ossify. On the other hand, premature ossification and insufficient growth of the bones are associated with loss of function of PTHrP or PTH/PTHrP receptor. The genetic analysis of PTHrP-mutant mice indicates that PTHrP is epistatic to *Ihh* and demonstrates that the differentiating prehypertrophic chondrocytes express *Ihh* to induce PTHrP expression in the adjacent perichondrium. The induced PTHrP signal acts as a negative-feedback cue on chondrocytes expressing PTH/PTHrP receptors, to ensure the proliferative status of the cells, and suppresses their early differentiation (52, 53). The mouse *Dhh* gene is involved in spermatogenesis and is proposed to support the survival of sperm cells (54).

2.1. *Sonic hedgehog (Shh)*

Shh is the best-studied *hedgehog* molecule because it is expressed early in embryogenesis and patterns multiple processes during development. These include the establishment of left-right asymmetry in early embryogenesis, specification of ventral neuron fate in the central nervous system, patterning of the dorsal-ventral axis of somites, establishment of the anterior-posterior axis, outgrowth of the limb buds, and eye development. *Shh* expression is first detected in the 8.0 days postcoitum (dpc) mouse embryo, prior to the first somite formation, in the node and the node-derived cells of the head process, which underlies the neural plate. As embryogenesis progresses and the embryo axis extends caudally, *Shh* is detected in the notochord, an extension of the head process, and in the floor plate cells overlying the notochord in the ventral midline of the neural tube. The timing of *Shh* expression in these midline structures matches the inductive activities manifested by the notochord and the floor plate (51, 55). Misexpression and explantation experiments have demonstrated that Shh secreted from the notochord induces the differentiation of floor plate cells and that Shh from both the notochord and the floor plate specifies the ventral neuronal differentiation in the brain and the motor neuron fate in the spinal cord (56-58). Misexpression of *Shh* by the Wnt-1 promoter in mouse embryos results in ectopic floor plate cell differentiation in the dorsal neural tube, as demonstrated by the expression of the floor plate cell marker, *HNF-3b* (hepatocyte nuclear factor 3b) (51). Treatment of neural tube explants with *Shh* conditioned medium also leads to induction of *HNF-3b* (56). Ablation of notochord, loss of *Shh* function, or antibody blockage experimentation provides further evidence that *Shh*, synthesized in the underlying notochord, is required for the induction of floor plate cell differentiation (58-60). The LIM (*l*in-11, *I*sl1, *m*ec-3) homeodomain protein, *Islet-1* (*Isl-1*), is an early ventral neuron marker. Neural tube explants, grown in contact with floor plate tissue or in *Shh*-conditioned medium, acquire ventral neuron fate by expressing *Isl-1*. However, explants from various levels of the neuraxis acquire different identities and express a number of different genes in addition to *Isl-1*, depending on their position along the neural axis. For example, when treated with *Shh*, neural plate cells caudal to the forebrain (rhombencephalon and spinal cord) express both *Isl-1* and *SC1*, which is characteristic of motor neurons, whereas explants from forebrain express *Isl-1* and *Nkx-2.1*, markers that are characteristic of ventral forebrain neurons. The ability of *Shh* to induce different types of ventral neuron fates along the rostrocaudal axis of the neural tube suggests that an early pre-pattern of positional information exists that dictates the differential response to *Shh* (56, 57).

In addition to the patterning of CNS, *Shh* also specifies the dorsal-ventral polarity of somites. Somites originate as spherical balls of epithelial cells derived from paraxial mesoderm flanking the notochord and neural tube. As development proceeds, somites undergo dorsal and ventral differentiation, giving rise to ventral-medial mesochymal sclerotome and dorsal-lateral epithelial dermomyotome. The sclerotome differentiates into axial skeleton including the vertebral column and ribs. The dorsal dermomyotome is subdivided into medial and lateral compartments, which give rise to epaxial (deep back) and hypaxial (limb and body wall) muscles, respectively. The dermis of the back is derived from the superficial epithelial cells that comprise the dermotome. *Shh* is required for both sclerotome differentiation and dermomyotome proliferation. Grafting notochord or floor plate on the dorsal somite enhances sclerotome formation and suppresses dermomyotome formation, suggesting that a substance secreted from the notochord and floor plate specifies ventral sclerotome differentiation (61, 62). Misexpression of *Shh* in the chick dorsal somite results in the dorsal expansion of *Pax-1*, a sclerotomal marker, and down-regulation of the dermomyotomal marker *Pax-*

3 (63) (see Pax Genes). Furthermore, mouse explants co-cultured with *Shh*-expressing cells have increased levels of *Pax-1* and decreased *Pax-3* expression, supporting the hypothesis that *Shh* from axial structures induces ventral sclerotomal cell fate (64). The differentiation and survival of dorsal-medial myotome cells require the inductive functions of both *Shh* from notochord/floor plate and the *wingless* homologue *Wnt* gene products that are derived from the dorsal neural tube (65-68).

The vertebrate limb evolves from both the lateral plate and the lateral edge of the somite. Mesochymal cells from the dorsal-lateral somite adjacent to the presumptive limb bud migrate laterally and give rise to the future limb musculature, and cells from the lateral plate proliferate and develop into the remaining limb tissues, including the bones and tendons. Limb development is a dynamic process orchestrated by multiple inductive signals from the posteriorly located zone of polarization activity (ZPA), the dorsal ectoderm, and the apical ectodermal ridge (AER) that abuts the anterior-posterior axis of the limb, at the distal tip where the dorsal and ventral surfaces meet. *Shh* is expressed in the ZPA and has been shown to establish anterior-posterior polarity in the limb and promote limb outgrowth (69). However, *Shh* alone is not sufficient to induce the expression of its target genes, *Bmp-2* and *Hox* gene cluster, which transduce the *Shh* signal to regulate limb patterning and growth (69, 70). The induction of these genes requires an additional signal, possibly **fibroblast growth factor**-4 (*FGF-4*), that is secreted from the overlying AER (71). *Shh* polarizes and maintains a functional AER. In a similar fashion, AER maintains *Shh* expression in the ZPA, establishing a positive feedback loop and an interdependence between these two inductive signaling centers (71). *Shh* and *FGFs* act together to induce the expression of *Bmp-2*, which relays a signal to induce or maintain *Hox* gene expression (71). Examination of lung and eye development indicates that *Shh* is also an inductive and mitogenic signal governing the growth and differentiation in these organs (72, 73).

3. Comparison of *hedgehog* Signaling in Flies and Vertebrates

The *hh* signaling cascade is well conserved between vertebrates and flies. Homologues of both *ptc* and *smo* have been identified in mammals, and their functions are conserved. Mutations in the mammalian *ptch* and *smo* are associated with familial and sporadic basal cell carcinoma, suggesting that these two homologues function as **tumor suppressor** genes (31, 74-76). Three homologues of *ci* exist in vertebrates: *Gli1, Gli2*, and *Gli3*, which exhibit distinct and overlapping expression patterns during development (77-80). Experiments with *Gli1* antisense and *Gli1* ectopic expression in different systems have shown that Gli1 is the major transcriptional activator that mediates the *Shh* signaling pathway, whereas Gli3 functions as a repressor (81-85). The function of *Gli2* overlaps both *Gli1* and *Gli3* in different developmental processes (85, 86). Mutations in *Gli1* are associated with glioblastoma and skin cancer (87), and those in the *Gli3* gene cause a dominant extra-toe phenotype in mice and are associated with Greg cephalopolysyndactyly syndrome in humans (88-90), suggesting that *Gli1* and*Gli3* function as tumor suppressors. The negative regulation of *Shh* signaling pathways by PKA is also conserved in vertebrates. Ectopic expression of a dominant-negative PKA mutant in the murine dorsal neural tube results in the ectopic expression of *Shh* target genes such as *HNF-3b, path*, and *Gli1*, and the suppression of the dorsal neuronal cell marker *Pax-3* (91). PKA activity has also been shown to antagonize the *Shh* signaling pathway in developing somites (64). Although the *hh* signaling pathways are conserved in most of the systems examined, there are differences between the vertebrate and Drosophila systems. The regulation of CI proteolysis in flies makes CI both an activator and a repressor, whereas in vertebrates it appears that the activation and repression functions are separated into two distinct genes, namely *Gli1* and *Gli3*, respectively. The level of the activated form of CI is regulated post-translationally in flies, whereas the Gli levels are regulated transcriptionally in vertebrates. Continued analysis of these important regulatory cascades will undoubtedly increase our understanding of developmental signaling pathways, their similarities, and their evolutionary divergence.

Bibliography

1. C. Nusslein-Volhard and E. Wieschaus (1980) Nature **287**, 795–801.

2. M. Hammerschmidt, A. Brook, and A. P. McMahon (1997) Trends Genet. **13**, 14–21.
3. S. DiNardo, E. Sher, J. Heemskerk-Jongens, J. A. Kassis, and P. H. O"Farrell (1988) Nature **332**, 604–609.
4. A. M. Arias, N. E. Baker, and P. W. Ingham (1988) Development **103**, 157–170.
5. J. J. Lee, D. P. V. Kessler, S. Parks, and P. A. Beachy (1992) Cell **71**, 33–50.
6. J. Mohler and K. Vani (1992) Development **115**, 957–971.
7. T. Tabata, S. Eaton, and T. B. Kornberg (1992) Genes Dev. **6**, 2635–2645.
8. P. W. Ingham, A. M. Taylor, and Y. Nakano (1991) Nature **353**, 184–187.
9. P. W. Ingham, (1993) Nature **366**, 560–562.
10. K. Basler and G. Struhl, (1994) Nature **368**, 208–214.
11. J. Capdevila and I. Guerrero (1994) EMBO J. **13**, 4459–4468.
12. J. A. Porter, D. P. v. Kessler, S. C. Ekker, K. E. Young, J. J. Lee, K. Moses, and P. A. Beachy (1995) Nature **374**, 363–366.
13. T. Tabata and T. B. Kornberg (1994) Cell **76**, 89–102.
14. J. E. Hooper and M. P. Scott (1989) Cell **59**, 751–765.
15. Y. Nakano, I. Guerrero, A. Hidalgo, A. Taylor, J. R. S. Whittle, and P. W. Ingham (1989) Nature **341**, 508–513.
16. M. v. d. Heuvel and P. W. Ingham (1996) Nature **382**, 547–551.
17. J. Alcedo, M. Ayzenzon, T. V. Ohlen, M. Noll, and J. E. Hooper (1996) Cell **86**, 221–232.
18. T. V. Orenic, D. C. Slusarski, K. L. Kroll, and R. A. Holmgren (1990) Genes Dev. **4**, 1053–1067.
19. D. Kalderon and G. M. Rubbin (1988) Genes Dev. **2**, 1539–1556.
20. A. J. Forbes, Y. Nakano, A. M. Taylor, and P. W. Ingham (1993) Development (Supplement), 115–124.
21. A. Pham, P. Therond, G., Alves, F. B. Tounier, D. Busson, C. Lamour-Isnard, B. L. Bouchon, T. Preat, and H. Tricoire (1995) Genetics **140**, 587–598.
22. J. Jiang and G. Struhl (1998) Nature **391**, 493–496.
23. J. J. Lee, S. C. Ekker, D. P. v. Kessler, J. A. Porter, B. I. Sun, and P. A. Beachy (1994) Science **266**, 1528–1537.
24. J. A. Porter, S. C. Ekker, W.-J. Park, D. P. von-Kessler, K. E. Young, C.-H. Chen, Y. Ma, A. s. Woods, R. J. Cotter, E. V. Koonin, and P. A. Beachy (1996) Cell **86**, 21–34.
25. J. A. Porter, K. E. Young, and P. A. Beachy (1996) Science **274**, 255–259.
26. V. Marigo, R. A. Davey, Y. Zuo, J. M. Cunningham, and C. J. Tabin (1996) Nature **384**, 176–179.
27. A. Martinez-Arias, N. E. Baker, and P. W. Ingham (1988) Development **103**, 157–170.
28. J. Capdevila, M. P. Estrada, E. Sanchez-Herrero, and I. Guerrero (1994) EMBO J. **13**, 71–82.
29. W. Li, J. T. Ohlmeyer, M. E. Lane, and D. Kalderon (1995) Cell **80**, 553–562.
30. Y. Chen and G. Struhl (1996) Cell **87**, 553–563.
31. S. M. Stone, M. Hynes, M. Armanini, T. A. Swanson, Q. Gu, R. L. Johnson, M. P. Scott, D. Pennica, A. Goddard, H. Phillips, M. Noll, J. E. Hooper, F. d. Sauvage, and A. Rosenthal (1996) Nature **384**, 129–134.
32. C. K. Motzny and R. Holmgren (1995) Mech. Dev. **52**, 137–150.
33. J. Hepker, Q.-T. Wang, C. K. Motzny, R. Holmgren, and T. v. Orenic (1997) Development **124**, 549–558.
34. P. Aza-Blanc, F.-A. Ramirez-Webe, and T. B. Kornberg (1997) Cell **89**, 1043–1053.
35. D. J. Robbins, K. E. Nybakken, R. Kobayashi, J. C. Sisson, J. M. Bishop, and P. P. Therond (1997) Cell **90**, 225–234.

36. J. C. Sisson, K. S. Ho, K. Suyama, and M. P. Scott (1997) Cell **90**, 235–245.
37. H. Akimaru, Y. Chen, P. Dai, D.-X. Hou, M. Nonaka, S. M. Smolik, S. Armstrong, R. H. Goodman, and S. Ishii (1997) Nature **386**, 735–738.
38. T. Lepage, S. M. Cohen, F. J. Diaz-Benjumea, and S. M. Parkhurst (1995) Nature **373**, 711–715.
39. D. Pan and G. M. Rubin (1995) Cell **80**, 543–552.
40. J. Jiang and G. Struhl (1995) Cell **80**, 563–572.
41. J. T. Ohlmeyer and D. Kalderon (1997) Genes Dev. **11**, 2250–2258.
42. Y. Chen, N. Gallaher, R. H. Goodman, and S. M. Smolik (1998) Proc. Natl. Acad. Sci. USA **95**, 2349–2354.
43. T. Kojima, T. Michiue, M. Orihara, and K. Saigo (1994) Gene **148**, 211–217.
44. A. L. Felsenfeld and J. A. Kennison (1995) Development **121**, 1–10.
45. F. J. Diaz-Benjumea, B. Cohen, and S. M. Cohen (1994) Nature **372**, 175–179.
46. J. Mohler (1988) Genetics **120**, 1061–1072.
47. E. H. Chen and B. S. Baker (1997) Development **124**, 205–218.
48. J. Royet and R. Finkelstein (1997) Development **124**, 4793–4800.
49. m. Dominguez and E. Hafen (1997) Genes Dev. **11**, 3254–3264.
50. F. Chanut and U. Heberlein (1997) Development **124**, 559–567.
51. Y. Echelard, D. J. Epstein, B. St-Jacques, L. Shen, J. Mohler, J. A. McMahon, and A. P. McMahon (1993) Cell **75**, 1417–1430.
52. A. Vortkamp, K. Lee, B. Lanske, G. V. Segre, H. M. Kronenberg, and C. J. Tabin (1996) Science **273**, 613–621.
53. B. Lanske, A. C. Karaplis, K. Lee, A. Luz, A. Vortkamp, A. Pirro, M. Karperien, L. H. K. Defize, C. Ho, R. C. Mulligan, A.-B. Abou-Samra, H. Juppner, G. V. Segre, and H. M. Kronenberg (1996) Science **273**, 663–666.
54. M. J. Bitgood, L. Shen, and A. P. McMahon (1996) Curr. Biol. **6**, 298–304.
55. E. Marti, R. Takada, D. A. Bumcrot, H. Sasaki, and A. P. McMahon (1995) Development **121**, 2537–2547.
56. H. Roelink, J. A. Porter, C. Chiang, Y. Tanabe, D. T. chang, P. A. Beachy, and T. M. Jessell (1995) Cell **81**, 445–455.
57. J. Ericson, J. Muhr, M. Piaczek, T. Lints, T. M. Jessell, and T. Edlund (1995) Cell **81**, 747–756.
58. J. Ericson, S. Morton, A. Kawakami, H. Roelink, and T. M. Jessell (1996) Cell **87**, 661–673.
59. R. i. Altaba (1992) Development **115**, 67–80.
60. C. Chiang, Y. Litingtung, E. Lee, K. E. Young, J. L. Corden, H. Westphal, and P. A. Beachy (1996) Nature **383**, 407–413.
61. O. Pourquie, M. Coltey, M.-A. Teillet, C. Ordahl, and N. M. Le-Douarin (1993) Proc. Natl. Acad. Sci. USA **90**, 5242–5246.
62. M. Goulding, A. Lumsden, and A. J. Paquette (1994) Development **120**, 957–971.
63. R. L. Johnson, E. Laufer, R. D. Riddle, and C. Tabin (1994) Cell **79**, 1165–1173.
64. C.-M. Fan, J. A. Porter, C. Chiang, D. T. Chang, P. A. Beachy, and M. Tessier-Lavigne (1995) Cell **81**, 457–465.
65. M. E. Pownall, K. E. Strunk, and C. P. Emerson, Jr. (1996) Development **122**, 1475–1488.
66. A. E. Munsterberg, J. Kitajewski, D. A. Bumcrot, A. P. McMahon, and A. B. Lassar (1995) Genes Dev. **9**, 2911–2922.
67. E. Hirsinger, D. Duprez, C. Jouve, P. Malapert, J. Cooke, and O. Pourquie (1997) Development **124**, 4605–4614.
68. M.-A. Teillet, Y. Watanabe, P. Jeffs, D. Duprez, F. Lapointe, and N. M. L. Douarin (1998)

Development **125**, 2019–2030.
69. R. D. Riddle, R. L. Johnson, E. Laufer, and C. Tabin (1993) Cell **75**, 1401–1416.
70. Y. Yang, G. Drossopoulou, P.-T. Chuang, D. Duprez, E. Marti, D. Bumcrot, N. Vargesson, J. Clarke, L. Niswander, A. McMahon, and C. Tickle (1997) Development **124**, 4393–4404.
71. E. Laufer, C. E. Nelson, R. L. Johnson, B. A. Morgan, and C. Tabin (1994) Cell **79**, 993–1003.
72. S. Bellusci, Y. Furuta, M. G. Rush, R. Henderson, G. Winnier, and B. L. M. Hogan (1997) Development **124**, 53–63.
73. A. M. Jensen and V. A. Wallace (1997) Development **124**, 363–371.
74. L. V. Goodrich, R. L. Johnson, L. Milenkovic, J. A. McMahon, and M. P. Scott (1996) Genes Dev. **10**, 301–312.
75. V. Marigo, M. P. Scott, R. L. Johnson, L. V. Goodrich, and C. J. Tabin (1996) Development **122**, 1225–1233.
76. J. Xie, M. Murone, S.-M. Luoh, A. Ryan, Q. Gu, C. Zhang, J. M. Bonifas, C.-W. Lam, M. Hynes, A. Goddard, A. Rosenthal, E. H. Epstein Jr., and F. J. d. Sauvage (1998) Nature **391**, 90–92.
77. K. W. Kinzler, J. M. Ruppert, S. H. Bigner, and B. Vogelstein (1988) Nature **332**, 371–374.
78. D. C. Hughes, J. Allen, G. Morley, K. Sutherland, W. Ahmed, J. Prosser, l. Lettice, G. Allan, M.-G. Mattei, M. Farrall, and R. E. Hill (1997) Genomics **39**, 205–215.
79. J. M. Ruppert, B. Vogelstein, K. Arheden, and K. W. Kinzler (1990) Mol. Cell. Biol. **10**, 5408–5415.
80. C.-c. Hui, D. Slusarski, K. A. Platt, R. Holmgren, and A. L. Joyner (1994) Dev. Biol. **162**, 402–413.
81. J. Lee, K. A. Platt, P. Censullo, and A. R. i. Altaba (1997) Development **124**, 2537–2552.
82. M. Hynes, D. M. Stone, M. Dowd, S. Pitts-Meek, A. Goddard, A. Gurney, and A. Rosenthal (1997) Neuron **19**, 15–26.
83. H. Masuya, T. Sagai, K. Moriwaki, and T. Shiroishi (1997) Dev. Biol . **182**, 42–51.
84. H. Sasaki, C.-c. Hui, M. Nakafuku, and H. Kondoh (1997) Development **124**, 1313–1322.
85. A. R. i. Altaba (1998) Development **125**, 2203–2212.
86. Q. Ding, J. Motoyama, S. Gasca, R. Mo, H. Sasaki, J. Rossant, and C.-c. Hui (1998) Development **125**, 2533–2543.
87. N. Dahmane, J. Lee, P. Robins, P. Heller, and A. R. i. Altaba (1997) Nature **389**, 876–881.
88. T. M. Pohl, M.-G. Mattei, and U. Ruther (1990) Development **110**, 1153–1157.
89. C.-c. Hui and A. L. Joyner (1993) Nature Genetics **3**, 241–246.
90. A. Wild, M. Kalff-Suske, A. Vortkamp, D. Bornholdt, R. Konig, and K.-H. Grzeschik (1997) Hum. Mol. Gen. **6**, 1979–1984.
91. D. J. Epstein, E. Marti, M. P. Scott, and A. P. McMahon (1996) Development **122**, 2885–2894.

Suggestions for Further Reading

92. M. Hammerschmidt, A. Brook, and A. P. McMahon (1997) The world according to *hedgehog*. Trends Genet. **13**, 14–21.
93. P. W. Ingham (1998) Transducing hedgehog: the story so far. EMBO J. **17**, 3505–3511.
94. R. L. Johnson and C. J. Tabin (1997) Molecular models for vertebrate limb development. Cell **90**, 979–990.

HeLa Cells

The HeLa cell line was originated by George Gey and co-workers in 1952 (1) from a cervical adenocarcinoma from a 31-year-old Afro-American female. It has proved to be a very vigorously growing cell line and is one of the most extensively used cell lines in the world. It is lodged at the American Type Culture Collection (ATCC) as CCL-2. It is even more extensively used than many people realize, because it is also guilty of cross-contaminating more cell lines than any other. HeLa was also the first human cell line to be cloned, when HeLa-S3 was isolated by Puck in 1956 (2). HeLa-S3 (Fig. 1) is in the ATCC catalogue as CCL-2.2. HeLa cells were originally propagated in a combination of human and calf serum (see Serum Dependence), but it has been shown that human serum is not necessary, and they are usually maintained in Eagle's Minimal Essential Medium supplemented with 10% fetal bovine serum. HeLa-S3 can be propagated in suspension using low-calcium medium (3).

Figure 1. Sub-confluent culture of Hela-S3 cells. Phase contrast, Olympus CK microscope, 20× objective.

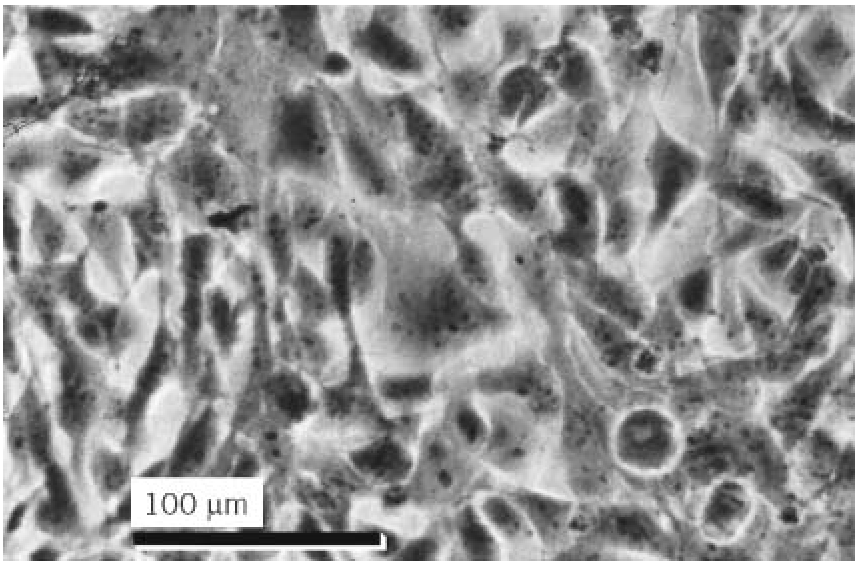

1. Properties

HeLa is a continuous cell line with an **aneuploid** and heteroploid karyotype containing a number of marker chromosomes (4). It expresses the A subtype of glucose-6-phosphate dehydrogenase, which is present in Negroes and absent in Caucasians. The cells are cytokeratin positive, confirming their epithelial origin, contain **papilloma virus** sequences (HPV-18), and have low expression of p53 and normal **retinoblastoma** proteins (5). They have a short population doubling time (18–22 h) and high plating efficiency (60–80% in monolayer).

2. Usage

HeLa cells have been used for propagation and assay of **viruses** and have been shown to be susceptible to **poliovirus**-1,2,3, **adenovirus**-3, encephalomyocarditis, and coxsackievirus B[5]. They have been used in molecular studies (6, 7), in somatic hybridization analysis of senescence (8) and invasion (9), in fermentor culture for biotechnology (10), and for the development of serum-free media (11). As they are deficient in gap-junction communication, they have been used for transfection analysis of gap-junctional proteins (12). They have also been used for studies on molecular signaling (13).

HeLa-S3, a clone of HeLa (2), is one of the more rapidly dividing of the HeLa strains and can be grown in suspension with mechanical agitation. Because it is less well attached than the parental strain, mitotic cells are readily detached by shaking the flask, following partial cell-cycle blockade induced by short-term storage at 4°C, (14, 15). H-HeLa is a subline suitable for the passage and titration of rhinoviruses (16).

3. Cross-Contamination

HeLa was the first human cell line to be propagated widely in a large number of laboratories throughout the world. It is also a vigorously growing cell line with a high plating efficiency and is, therefore, ideally placed to cross-contaminate other cell lines. That this happened was first demonstrated many years ago by **isoenzyme** analysis (17) and subsequently by chromosomal analysis (18). Combined with more recent studies of DNA **fingerprinting**, it is now clear that a large number of continuous cell lines established in the 1960s and 1970s were cross-contaminated with HeLa cells, including lines such as KB (19) and Hep-2 (19, 20), which are still in regular use. The most serious aspect of this is that, although continued use may be quite acceptable in certain circumstances, few authors acknowledge that these lines are HeLa-contaminated, suggesting that a large part of the scientific community is still unaware of this problem, over 30 years after it was first revealed (21). Reports published by the ATCC (22), and the European Collection of Animal Cell Cultures (ECACC) (23), have confirmed that a significant proportion of cell lines in common use may be HeLa cross-contaminants.

Bibliography

1. G. O. Gey, W. D. Coffman, and M. T. Kubicek (1952) Cancer Res. **12**, 364–365.
2. T. T. Puck and P. I. Marcus (1955) Proc. Natl. Acad. Sci. USA **41**, 432–437.
3. R. I. Freshney (1994) *Culture of Animal Cells, a Manual of Basic Technique*, Wiley-Liss, New York, p. 85.
4. T. R. Chen (1988) Cytogenet. Cell Genet. **48**, 19–24.
5. American Type Culture Collection catalogue, ATCC, P.O. Box 1549, Manassas, VA 20108 – 1549 `www.atcc.org`ñ, CCL-2.
6. W. K. Hansen, W. A. Deutsch, A. Yacoub, Y. Xu, D. A. Williams, and M. R. Kelley (1998) J. Biol. Chem. **273**, 756–762.
7. D. A. Jackson and A. Pombo, (1998) J. Cell Biol. **140**, 1285–1295.
8. M. D. Waterfield, M. A. Baker, M. F. Greaves, and E. J. Stanbridge (1986) J. Biol. Chem. **261**, 2418–2424.
9. K. Ess, H. Chen, A. Kier, and R. Brackenbury (1995) J. Cell. Physiol. **162**, 341–347.
10. Y. Chen, T. L. LaPorte, S. S. Wang, and J. Shevitz (1992) Cytotechnology **8**, 85–88.
11. G. J. Blaker, J. R. Birch, and S. J. Pirt (1971) J. Cell. Sci. **9**, 529–537.
12. B. Hertlein, A. Butterweck, S. Haubrich, K. Willecke, and O. Traub (1998) J. Memb. Biol. **162**, 247–257.
13. A. W. Gagnon, L. Kallal, and J. L. Benovic (1998) J. Biol. Chem. **273**, 6976–6981.
14. A. A. Newton and P. Wildy (1959) Exp. Cell Res. **16**, 624–635.
15. B. Lesser and T. P. Brent (1970) Exp. Cell Res. **62**, 470–473.
16. R. R. Rueckert et al. (1971) Virology **44**, 259–270.
17. S. M. Gartler (1967) *Second Decennial Review Conference on Cell, Tissue and Organ Culture*; NCI Monograph, pp. 167–195.
18. W. Nelson-Rees and R. R. Flandermeyer (1977) Science **195**, 1343–1344.

19. S. J. O"Brien, R. Olson, and J. E. Shannon (1977) Science **195**, 1345–1348.
20. T. R. Chen (1988) Cytogenet. Cell Genet. **48**, 19–24.
21. C. S. Stulberg, W. D. Peterson Jr., and W. F. Simpson (1976) Am. J. Hematol. **1**, 237–242.
22. K. S. Lavappa (1978) **14**, 469–475.
23. G. Stacey, B. Bolton A. Doyle, and B. Griffiths (1992) Cytotechnology **9**, 211–216.

Helix–Coil Theory

Unlike many equilibrium folding–unfolding reactions in proteins that can be described adequately by a simple two-state folding mechanism, a-helix formation in polypeptides is not a simple two-state reaction from fully helical molecules to fully unstructured, or random coil, peptides. This multistate behavior results from mixtures of partially helical molecules, primarily with the ends of the peptide "frayed." From the architecture of the a-helix, this is easy to understand. The ends of an a-helix are different from positions in its center because at the *N*-terminus the NH groups, and at the *C*-terminus the C=O groups, are not paired in hydrogen bonds, which are important for stabilizing the helical conformation. Therefore, under optimal helix-forming conditions, the population of helical molecules represent a distribution of partially helical states. Several models, based on simple statistical mechanics, have been developed to describe the macroscopic properties of the system. Collectively, these are known as *helix–coil theories*, although helix to random coil (or nonhelical structure) is a more accurate description of the models.

The two most popular models for the helix–coil transition in peptides were developed independently by Zimm and Bragg (1) and by Lifson and Roig (2) in the late 1950s and early 1960s (see Zimm–Bragg Model and Lifson–Roig Model). The two models share similar features, with a few important differences. For each model, helix formation is a function of three basic parameters: (i) the chain length or number of residues in the polypeptide, (ii) a helix propagation parameter (*s* or *w* value), and (iii) a helix nucleation parameter (s or v^2). In each model, a single unit or residue can exist in only one of two possible conformations [helix or coil (*h* or *c*)] in the Lifson–Roig treatment, and the statistical weights (*v* or *w*) reflect the microscopic equilibrium constant for the transition between *h* and *c*. Helical residues, *h*, flanked on both sides by other *h* residues are assigned a weight *w*, whereas *h* residues at the ends of a stretch of *h* residues are assigned a weight of *v*. The nucleation parameter (v^2 in the Lifson–Roig treatment) reflects the "penalty," considered primarily entropic, to order three consecutive residues into a stabilized helical segment. Figure 1 illustrates this for the simple case of a helical peptide with one hydrogen bond stabilizing the helical conformation. The energetic difficulting in nucleating the a-helix imparts a degree of **cooperativity** to helix formation. Enumeration of all possible combinations of *h* and *c* residues for a polypeptide chain of a given length, along with the assigned statistical weights, provides the partition function for the system. The partition function can then be used to calculate average properties of the population, notably the fraction of helical residues, the average length and number of helical stretches, and other characteristics of the population.

Figure 1. Depiction of a peptide with one helical hydrogen bond formed. The squares represent the backbone peptide bo with the appropriate side chains. The C_a; groups are numbered, and the conformation of each residue is denoted as either peptide, the statistical weights are defined according to the Lifson–Roig model, using the coil state as a reference (weigh weight *v* and internal helical residues *w*.

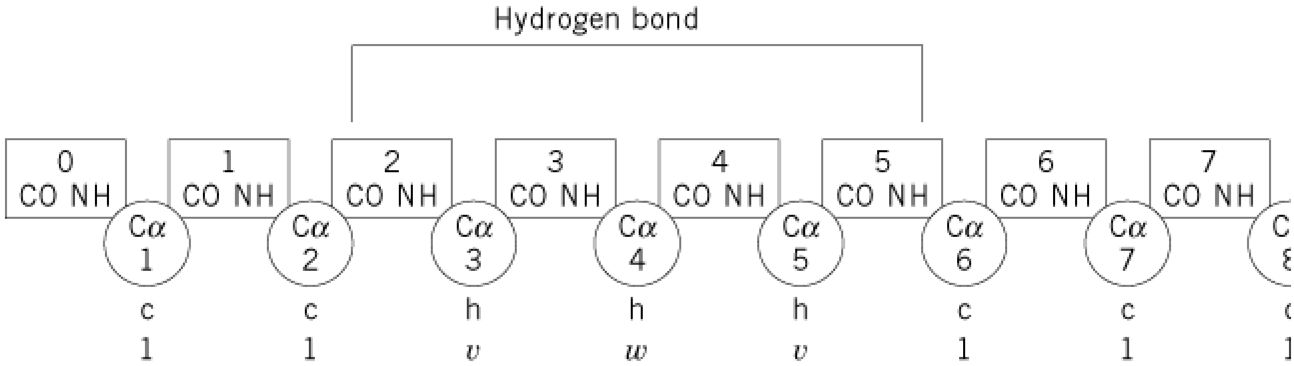

The helix propagation parameter, *w* or *s*, is most closely akin to the helix propensity for a given residue. These helix propensities have recently been measured for all twenty amino acids found in proteins (see Alpha-Helix Formation). The Lifson–Roig model is also amenable to modification (3, 4) to include the energetics of other helix-stabilizing interactions, such as *N*- and *C*-capping and the interactions between side chains. A quantitative determination of these parameters, in conjunction with the Lifson–Roig model for the helix to coil transition, provides a reliable estimate of the amount of helix present in a peptide of any sequence.

Bibliography

1. B. H. Zimm and J. K. Bragg (1959) J. Chem. Phys. **31**, 526–535.
2. S. Lifson and A. Roig (1961) J. Chem. Phys. **34**, 1963–1974.
3. A. J. Doig, A. Charkrabartty, T. M. Klinger, and R. L. Baldwin (1994) Biochemistry **33**, 3396–3403.
4. B. J. Stapley, C. A. Rohl, and A. J. Doig (1995) Protein Sci. **4**, 2383–2391.

Suggestions for Further Reading

5. C. R. Cantor and P. R. Schimmel (1980) *Biophysical Chemistry*, W. H. Freeman, San Francisco. Chapter 20 provides a good introduction to models for helix formation.
6. D. Poland and H. A. Scheraga (1970) *Theory of Helix–Coil Transitions in Biopolymers*, Academic Press, New York. A broad discussion of helix–coil theory. The book also reprints many of the seminal articles on helix–coil theory.

Helix-Turn-Helix Motif

The helix-turn-helix motif was first identified as a conserved sequence element in the repressors encoded by the lambdoid phages of *E. coli* and *Salmonella typhimurium*. Subsequently this element has been found in a large variety of DNA-binding proteins, both in prokaryotes and in eukaryotes, and shows a very high degree of structural conservation. This DNA-binding domain consists of two short a-helices that usually are separated by a glycine residue. This amino acid in concert with its neighbors acts as a flexible hinge allowing the polypeptide chain to bend between the two helices so that they can make hydrophobic contacts with each other. These contacts preserve the relative orientation of the two helices and result in the formation of a compact tertiary structural domain. The distal helix lies in the DNA major groove and the proximal helix contacts the sugar-phosphate backbone. Although the structure of this domain is highly conserved, the orientation of the recognition helix within the major groove is quite variable. This feature suggests that the motif is a structure that possesses a rigidity which is necessary for precise sequence recognition.

Related to the prokaryotic **helix-turn-helix** fold are protein folds of essentially the same fundamental structure, but which contain longer turns or loops. These eukaryotic variants include the homeodomain fold, which contains both a helix-turn-helix element and a short extended minor groove-tracking sequence, the POU-specific domain, and the helix-wing-helix fold. The latter fold contains an extended b sheet immediately following the recognition helix and is typified by hepatocyte nuclear factor 3 (HNF3) and the globular domain of the linker histones, H5 and H1. Whereas the prokaryotic proteins usually bind as homodimers and bind to palindromic DNA targets, the eukaryotic counterparts normally bind as monomers.

Bibliography

"Helix-Turn-Helix Motif" in , Vol. 2, pp. 1105–1106, by Andrew Travers, MRC Laboratory of Molecular Biology, Cambridge; "Helix-Turn-Helix Motif" in (online), posting date: January 15, 2002, by Andrew Travers, MRC Laboratory of Molecular Biology, Cambridge.

Helper Plasmid

In the context of genetic transformation of **plants**, a helper plasmid is a **plasmid** present in Agrobacterium that provides functions required by the **bacteria** for transferring foreign **DNA** to a plant cell. They have been extremely important in plant genetic engineering. Generally, helper plasmids are derivatives of the Ti plasmid that contain an active virulence region, but from which the T-DNA has been removed.

Central to the concept of developing the binary vector system for *Agrobacterium*-mediated plant cell transformation was the finding that the **genes** contained on the T-DNA are not required for its transfer to the plant cell, that this function is provided by gene products of the virulence region of the Ti plasmid, and that they are trans-acting (1). In practice, this means that foreign DNA to be transferred to the plant cell can be **cloned** between the T-DNA border sequences in any plasmid that is stable in *Agrobacterium*. Then, such a plasmid, known as the binary vector, can be transferred to *Agrobacterium* that contains a helper plasmid by **conjugation**, electroporation, or transformation (see Transfection). Helper plasmids are based on deletion derivatives of Ti plasmid that lack the T-DNA. The helper plasmid provides the functions required for transferring the foreign DNA located between the T-DNA borders of the binary vector to the plant cell. The most widely used binary vector/helper plasmid system is the pBin binary vector (2) used in combination with the LBA4404 helper plasmid (1).

Bibliography

1. A. Hoekema, P. R. Hirsch, P. J. Hooykaas, and R. A. Schilperoot (1983) Nature **303**, 179–181.
2. M. W. Bevan (1984) Nucleic Acids Res. **12**, 8711–8721.

Suggestions for Further Reading

3. G. An (1995) In *Agrobacterium Protocols* (K. M. A. Gartland and M. R. Davey, eds.), Humana

Press Totowa, New Jersey. pp. 47–58.
4. F. F. White (1993) "Vectors for gene transfer in higher plants", In Transgenic Plants, Vol. **1** (D. Kung and R. Wu, eds.), Academic Press, San Diego, pp. 15–48.

Helper Virus

Some **viruses** require the gene functions of other viruses to replicate. The viruses that rescue such replication-deficient viruses are known as helper viruses. Adenoviruses, herpes simplex virus 1 and 2 (HSV-1, HSV-2) (see Herpesvirus), cytomegalovirus, and pseudorabies virus are helpers for adeno-associated viruses (AAVs), dependoviruses of *Parvoviridae* family. In addition, hepatitis B virus is a helper virus for hepatitis D virus, and most standard viruses are helpers for their deletion mutants, which are called defective interfering particles. Defective viruses and their helper viruses are usually closely related in many replication processes (see Rous Sarcoma Virus (RSV)). It is now considered, however, that the helper functions are not simple and that they involve the interaction between virus and cells in addition to between defective virus and helper virus.

Genetic analysis of helper functions has been most extensive for adenoviruses. Five regions of the adenovirus genome are required for a permissive AAV infection. They are the E1A, E1B, E2A, E4, and VA regions. The E1A region is required for the *trans*-activation of the AAV p5 and p19 promoters. The E1B-coded 55-kDa transforming protein and the E4 gene product, a 35-kDa protein, are both required for the efficient accumulation of AAV messenger RNAs. Their role in AAV replication is believed to be to stabilize the AAV mRNAs and assist their transport to the cytoplasm. The E2A gene product, an adenovirus DNA-binding protein, and the adenovirus VA RNAs are required primarily for the efficient translation of AAV mRNA to produce the viral capsid protein.

Although a helper virus is necessary for fully permissive AAV infection, helper virus genes appear not to be directly involved in AAV DNA replication. AAV DNA replication may use primarily cellular factors that exist in cells. The role of helper virus gene products may stimulate the synthesis of cellular genes that are required for AAV DNA replication.

Suggestions for Further Reading

K. I. Berns (1996) "*Parvoviridae*: The Viruses and Their Replication". In *Fields Virology*, 3rd ed. (B. N. Fields et al., eds.), Lippincott-Raven, Philadelphia, pp. 2173–2197.

J. M. Taylor (1996) "Hepatitis Delta Virus and Its Replication". In *Fields Virology*, 3rd ed. (B. N. Fields et al., eds.), Lippincott-Raven, Philadelphia, pp. 2809–2818.

Hematopoiesis

Hematopoiesis is a dynamic process in which blood cells of at least eight distinct lineages must be continually replaced from a population of pluripotent hematopoietic stem cells throughout the life span of the animal. The hematopoietic stem cell is a relatively rare cell, estimated to be approximately 0.001% of nucleated bone marrow cells. Stem cells are normally quiescent, in either the G0 or G1 phase of the cell cycle. Hematopoiesis involves the progressive restriction of the developmental potential of hematopoietic progenitors, with a concomitant increase in their proliferative capacity. Conversely, the self-renewal capacity of hematopoietic progenitor cells progressively decreases with the restriction of their developmental potential, with most mature cell types having short life spans and little or no proliferative capacity. In order to produce the correct numbers of mature blood cells, this balance between proliferation and differentiation of hematopoietic progenitors must be tightly controlled. Perturbation of this delicate balance can result in leukemogenesis or in anemias, immunodeficiencies, and other cellular deficiency disorders.

The existence of hematopoietic progenitor and stem cells can be inferred by the progeny they produce. Transplantation of lethally irradiated mice with cells from syngeneic donors has been the classical approach to demonstrate the presence of repopulating hematopoietic stem cells. The first 4 to 6 months after engraftment is characterized by clonal fluctuations in stem cell proliferation and differentiation, followed by the emergence of a stable hematopoietic system, dominated by a small number of totipotent clones. In addition, the extensive self-renewal capacity of these cells can be demonstrated by their ability to reconstitute recipient animals after serial transplantations. Competitive repopulation assays, in which two genetically distinct populations of bone marrow cells are transplanted together into the same recipient, can be used to determine the effects of a specific genetic alteration on the viability of repopulating hematopoietic stem cells.

The earliest restriction in developmental potential of hematopoietic stem cells involves the generation of putative lymphoid- and myeloid-restricted stem cells from the pluripotent myeloid-lymphoid stem cell. Myeloid-restricted stem cells can be detected by the classic spleen colony assay. In this assay, limiting numbers of bone marrow cells are injected into lethally irradiated recipient mice, giving rise to the formation of macroscopic hematopoietic colonies in the spleen within eight days, each derived from a single progenitor cell. These cells, termed CFU-S (colony-forming unit-spleen), are pluripotent and can give rise to all hematopoietic cells of the myeloid lineage. They possess only limited self-renewal capacity, as measured by their ability, on retransplantation, to give rise to secondary spleen colonies. In addition, CFU-S cannot readily confer hematopoietic repopulation and long-term survival of recipient mice. Additionally, progenitor cells that form spleen colonies at day 12 to 14 after transplantation are more potent in terms of repopulating ability than are day 8 CFU-S cells, suggesting that the spleen colony assay detects a range of cells that differ in their proliferative or repopulation potential.

Figure 1. Schematic of adult hematopoiesis.

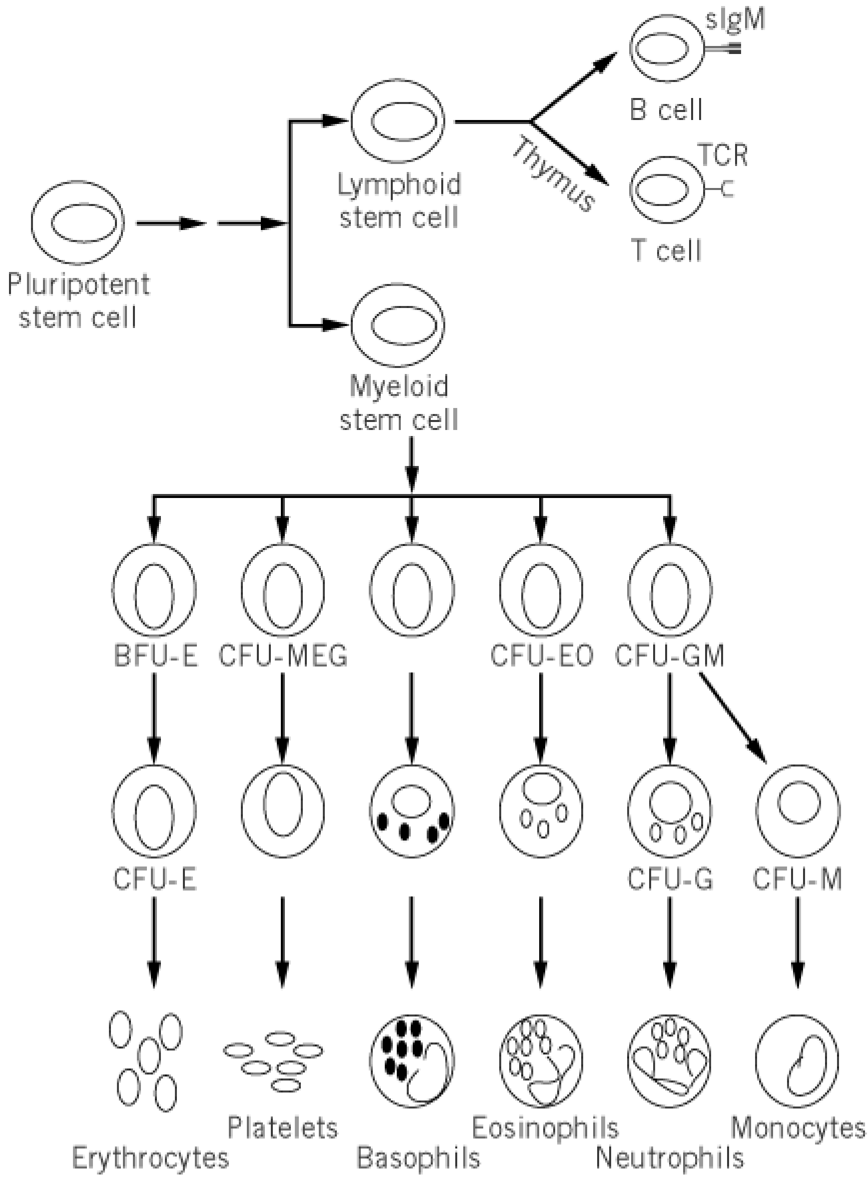

The presence of more restricted hematopoietic progenitor cells can be demonstrated by their ability to form colonies of differentiated blood cells in a semisolid medium in the presence of hematopoeitic growth factors. Multipotential hematopoietic cytokines, including interleukins IL-3 (multipotential CF), IL-4, and granulocyte/macrophage colony stimulating factor (GM-CSF), are capable of supporting the proliferation of multilineage progenitor cells, resulting in the formation of colonies containing multiple hematopoietic lineages. Lineage-specific growth factors, such as erythropoietin, granulocyte CSF (G-CSF), or macrophage CSF (M-CSF or CSF-1), enhance proliferation and differentiation of committed progenitor cells forming colonies of nucleated red blood cells, neutrophils, and macrophages, respectively. A final group of cytokines, including IL-6, IL-11, and Steel (stem cell factor, c-kit ligand), act synergistically with the multilineage and lineage-specific cytokines to enhance colony formation in culture by shortening the G0 period of the hematopoietic progenitors.

During mouse embryogenesis, the first visible sign of hematopoiesis appears in the extraembryonic mesoderm of the day 7.5 yolk sac in the form of blood islands. These blood islands contain primarily primitive erythrocytes, which are large, nucleated cells expressing embryonic hemoglobin, although adult globins are synthesized and accumulate in these cells at later stages of development. Cells of the monocyte-macrophage lineage also appear in the yolk sac. Although the differentiated hematopoietic cells found in the yolk sac are restricted to cells of the erythroid and macrophage lineages, progenitor cells found in the yolk sac at later stages of development can differentiate into various hematopoietic lineages *in vitro* and have been reported to be capable of forming CFU-S *in vivo*, demonstrating the multipotency of these cells. Furthermore, repopulation of recipient animals with yolk sac–derived hematopoietic cells has been reported, suggesting the presence of repopulating hematopoietic stem cells within the yolk sac environment.

Around day 10 of embryonic development, the primary site of hematopoiesis switches from the yolk sac to the fetal liver, the main site of fetal hematopoiesis. The fetal liver produces predominantly cells of the definitive erythroid lineage, expressing adult hemoglobins, as well as some myeloid and lymphoid cells. Various progenitor and stem cells, including CFU-S and pluripotent hematopoietic stem cells capable of long-term repopulation of recipient mice, are all present at a high frequency in the fetal liver. The fetal liver remains the primary erythropoietic organ until shortly before birth, when the major site of hematopoiesis shifts, once again, to the bone marrow. Within the intersinusoidal spaces of the medullary cavity of the bone, hematopoietic cells are found closely associated with the stroma. These cells directly influence hematopoiesis through cell–cell interactions and the production of cytokines, forming a microenvironment that supports blood cell production.

Figure 2. Time course of embryoid body development. Gene expression and presence of hematopoietic precursors are shown.

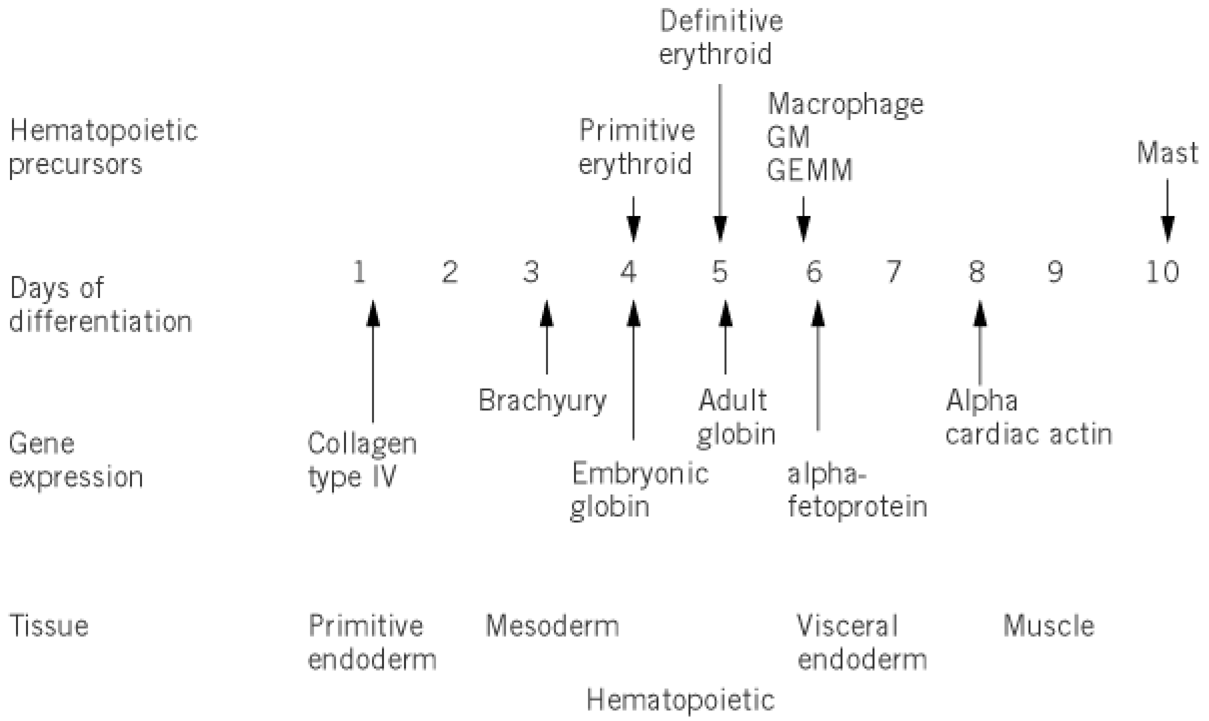

It has long been accepted that, during embryogenesis, the hematopoietic stem cells (HSCS) that originate in the yolk sac migrate to the fetal liver to initiate the second wave of hematopoiesis. However, recent findings of hematopoietic cells in the para-aortic splanchnopleure of mouse embryos prior to colonization of the fetal liver (1-3) suggest the possibility of another source of hematopoiesis in the embryo proper. It is unclear at this time whether the cells involved in primitive hematopoiesis in the yolk sac are precursors to the cells involved in definitive hematopoiesis or whether definitive hematopoiesis develops independently in the embryo proper. Transplantation studies using the adult mouse as a recipient demonstrated HSC activity in the aorta, gonads, and mesonephros (AGM) region of the embryo at day 10, followed by the fetal liver and yolk sac on day 11 (3, 4). These studies suggest that the first definitive HSCs arise in the AGM region and migrate to the fetal liver to establish definitive hematopoiesis. However, transplantation studies utilizing newborn or embryonic mice as recipients demonstrated the presence of HSCs contributing to definitive hematopoiesis in the yolk sac as early as day 9 (5), lending support to previous models. Although the origin of definitive hematopoiesis remains in debate, microenvironment is clearly a crucial element in the regulation of HSC potential.

The study of murine hematopoietic development, and the role of the microenvironment in this process, has been greatly facilitated by the establishment of *in vitro* model systems in which embryonic stem (ES) cells are differentiated to form cells of the hematopoietic system. Coculture of ES cells with primary bone marrow stroma or stromal cell lines results in the formation of a variety of hematopoietic cells including those of the erythroid, myeloid, B, and T cell lineages (6-8). Additionally, if the leukemia inhibitory factor is removed from the medium and the cells are grown in suspension, ES cells will form primitive embryonic structures termed *embryoid bodies* (EBs), which contain a vasculature and closely resemble the visceral yolk sac of the post-implantation embryo. These EBs contain many differentiated cell types, including those of the hematopoietic system, easily detectable by the appearance of visible blood islands containing red blood cells with hemoglobin.

ES-derived EBs express many genes that serve as markers of tissue restriction and lineage commitment during hematopoietic development (9-11), including the full complement of globin genes in the correct temporal order (12). EBs also contain precursors of the primitive erythroid, definitive erythroid, macrophage, neutrophil, and mast cell lineages, as demonstrated by colony-forming assays (10, 11, 13). Later in EB development, differentiated megakaryocytes, neutrophils, eosinophils, and mast cells also appear (14). Additionally, ES cell-derived EBs contain B and T cell precursors (15) and markers indicative of B and T lymphoid cells (16).

The *in vitro* differentiation of ES cells into cells of the hematopoietic system has been utilized to address the question of the origin of primitive versus definitive hematopoiesis. It remains unclear, however, whether primitive and definitive erythrocytes develop from common or distinct precursors in this system (17, 18). Recent evidence from Xenopus suggests the presence of bipotential primitive-definitive hematopoietic progenitors in the vertebrate embryo (19). However, the detectability of primitive erythrocytes in the yolk sac prior to the appearance of hematopoietic progenitor and stem cells in that tissue indicates that the traditional hierarchy of adult hematopoiesis may not apply in the context of primitive hematopoiesis.

The molecular events that regulate the development and maintenance of the hematopoietic system are beginning to come to light. A great deal of the work that forms the basis of this knowledge has been elucidated using the mouse as a model system. The combination of naturally occurring mutations and those generated by homologous recombination in ES cells has produced a battery of mutant ES and mouse lines, which have been instrumental in revealing the molecular biology of hematopoiesis. Furthermore, *in vitro* differentiation of homozygous mutant ES cells has provided additional information regarding the specific role of the targeted genes during hematopoietic development. Some of the genes that have been identified as essential for the development of hematopoietic stem cells during embryogenesis, or the functioning of these cells in the adult, are listed in Table 1.

Table 1. Hematopoietic Mutants

Disrupted Gene	Encoded Protein	Model	Phenotype

CBFa2 (AML1) (42)	Runt homology domain (RHD) TF[a]	KO mice	Block in definitive hematopoiesis
			Stem cell defect
CBFb (43)	Subunit of CBF	KO mice	Same as CBFa2
EKLF (32)	Zinc finger TF	KO mice	Block in definitive erythropoiesis
EpoR (29, 30)	Erythropoietin receptor	KO mice	Block in definitive erythropoiesis
Flk1 (27)	RTK	KO mice/EBs	Stem cell defect
GATA-1 (36, 37)	Zinc Finger TF	KO mice/EBs	Block in primitive erythropoiesis
			Block in definitive erythrocyte maturation
GATA-2 (38, 39)	Zinc Finger TF	KO mice/EBs	Stem cell defect
Kit (20)	RTK	*Dominant White Spotting (W)*	Stem cell defect
			Macrocytic anemia
			Mast cell deficiency
Myb (40)	Myb domain TF	KO mice	Reduced definitive erythroid and myeloid precursors
PU.1 (Spi-1) (41)	Ets domain TF	KO mice	Block in definitive erythroid maturation
			Stem cell defect
Rbtn2 (31)	LIM domain TF	KO mice/EBs	Block in erythroid maturation
Shp-1 (22, 23)	Tyrosine phosphatase	*Motheaten (me)*	Increased myelopoiesis
Steel (20)	Ligand for *c-kit*	*Steel (Sl)*	Same as *W*
Tal-1/SCL (33-35)	Basic HLH TF	KO mice	Lack of erythroid and myeloid precursors

[a] Key: TF, transcription factor; RTK, receptor tyrosine kinase; KO, knockout; EBs, embryoid bodies.

The process of hematopoiesis is controlled by a number of hematopoietic growth factors, which bind to specific cell surface **receptors** and generate a complex series of intracellular signaling events. These signaling events culminate in changes in **gene expression**, which direct the cell toward proliferation or differentiation. The major strategy by which hematopoietic cells interpret extracellular signals is through the activation of receptors that either possess intrinsic **tyrosine kinase** activity or are coupled to cytoplasmic proteins with tyrosine kinase activity. Several of these receptors have been shown to play a role in the regulation of hematopoietic stem cells and to be crucial for the proper development of the hematopoietic system. Naturally occurring mutations in the receptor tyrosine kinase, c-kit (*W*), and its ligand, steel factor (*Sl*), have uncovered an important role for this signaling pathway in the regulation of hematopoietic stem cells (20). In addition to macrocytic anemia and mast cell deficiency, hematopoietic cells from *W* mice show defects in spleen colony formation and in long-term reconstitution of lethally irradiated recipient mice. In contrast, *Sl* mutant mice have a defective microenvironment that is unable to support the growth of normal stem cells. Genetic and biochemical analysis has revealed two other naturally occurring mutations that form part of the Kit-Steel signaling pathway (21). These mouse loci, *motheaten* (*me*) (22, 23) and *micropthalmia* (*mi*) (24, 25), encode a protein tyrosine phosphatase (Shp-1) and a basic helix-loop-helix transcription factor (MITF), respectively.

Gene targeting strategies have also led to the identification of several hematopoietic receptors that are essential for normal hematopoietic development. One of these receptors is Flk1, a receptor tyrosine kinase that binds *vascular endothelial growth factor* (VEGF). Mice homozygous for a mutation in Flk1 lack both mature endothelial and hematopoietic cells (26). In addition, Flk1 -/- ES cells do not contribute to primitive or definitive hematopoiesis *in vitro* or *in vivo* (27), demonstrating a close association between the molecular and cellular regulation of vasculogenesis and hematopoiesis. Gene targeting of STK, a tyrosine kinase receptor of the Met family isolated from a hematopoietic stem cell cDNA library, has demonstrated a role for this receptor in the negative regulation of macrophage activation and nitric oxide production during a cell-mediated immune response (28).

A second class of cell surface receptors that are important for hematopoietic differentiation contains the cytokine receptors, which signal through the Jak/Stat pathway. An example of this class of receptors, which effects the proliferation and survival of erythroid progenitors, is the erythropoietin (epo) receptor. Mice homozygous for mutations in epo or the epo receptor die at embryonic day 13 from a failure of definitive fetal liver erythropoiesis (29, 30). Committed BFU-E (burst-forming unit-erythroid) and CFU-E (colony-forming unit-erythroid) progenitors are present in these mice, suggesting that the epo signaling pathway is necessary for the proliferation and survival of CFU-E progenitors but not for erythroid lineage commitment.

The signaling events generated in response to the engagement of hematopoietic receptors by their respective ligands culminate in changes in gene expression, which direct the cell toward proliferation or differentiation. Genetic analysis in mice has also revealed several transcription factors that are essential for the development of hematopoietic precursors. Collectively, these transcription factors regulate the expression of hematopoietic-specific genes that are important for the differentiation of multiple blood cell lineages from the pluripotential hematopoietic stem cell. Some of these factors are specific for the development of the erythropoietic lineage (GATA-1, EKLF, Rbtn2), suggesting a role in erythroid commitment and/or maturation. Other factors play a more global role in regulating the proliferation versus differentiation of primitive hematopoietic progenitors (PU.1, GATA-2, Myb, SCL/Tal-1). Interestingly, these studies suggest that primitive and definitive hematopoiesis are controlled by somewhat distinct molecular mechanisms. Disruption of genes encoding Rbtn2 (31), SCL/Tal-1 (32-35), GATA-1 (36, 37), or GATA-2 (38, 39) block both primitive and definitive erythropoiesis, whereas mutations in c-myb (40), PU.1 (41), EKLF (32), and CBF a and b (42, 43) affect only definitive erythropoiesis.

The list of mouse mutations effecting the development of the hematopoietic system is growing rapidly. Furthermore, many mutations exist that result in mild alterations in the regulation of adult hematopoiesis rather than in a complete block in hematopoiesis. This finding suggests some redundancy in the pathways that ultimately culminate in proliferation and differentiation of hematopoietic cells. The generation of mice with mutations in multiple genes involved in the regulation of hematopoiesis will be instrumental in the characterization of hematopoietic signaling pathways, as well as in the identification of points at which these pathways intersect.

Bibliography

1. I. E. Godin et al. (1993) Nature **364**, 67–70.
2. A. L. Medvinsky et al. (1993) Nature **364**, 64–67.
3. A. M. Muller et al. (1994) Immunity **1**, 291–301.

4. A. Medivinsky and E. Dzierzak (1996) Cell **86**, 897–906.
5. M. C. Yoder et al. (1997) Immunity **7**, 335–344.
6. T. Nakano, H. Kodama, and T. Honjo (1994) Science **265**, 1098–1011.
7. R. Palacios, E. Golunski, and J. Samaridis (1995) Proc. Natl. Acad. Sci. USA **92**, 7530–7534.
8. J. C. Gutierrez-Ramos and R. Palacios (1992) Proc. Natl. Acad. Sci. USA **89**, 9171–9175.
9. T. McClanahan et al. (1993) Blood **81**, 2903–2915.
10. G. Keller et al. (1993) Mol. Cell. Biol. **13**, 473–486.
11. R. M. Schmitt, E. Bruyns, and H. R. Snodgrass (1991) Genes Dev. **5**, 728–740.
12. M. H. Lindenbaum and F. Grosveld (1990) Genes Dev. **4**, 2075–2085.
13. M. V. Wiles and G. Keller (1991) Development **111**, 259–267.
14. U. Burkert, T. von Ruden, and E. F. Wagner (1991) New Biol. **3**, 698–708.
15. A. J. Potocnik, P. J. Nielsen, and K. Eichmann (1994) EMBO J. **13**, 5274–5283.
16. U. Chen, M. Kosco, and U. Staerz (1992) Proc. Natl. Acad. Sci. USA **89**, 2541–2545.
17. M. Kennedy et al. (1997) Nature **386**, 488–493.
18. T. Nakano, H. Kodama, and T. Honjo (1996) Science **272**, 722–724.
19. J. B. Turpen et al. (1997) Immunity **7**, 325–334.
20. A. Reith, and A. Bernstein (1991) *Genome Analysis 3: Genes and Phenotypes* (K. Davies and S. Tilghman, eds.) 105–133.
21. R. F. Paulson et al. (1996) Nature Genetics **13**, 309–315.
22. L. D. Shultz et al. (1993) Cell **73**, 1445–1454.
23. H. W. Tsui et al. (1993) Nature Genet **4**, 124–129.
24. C. A. Hodgkinson et al. (1993) Cell **74**, 395–404.
25. M. J. Hughes et al. (1993) J Biol Chem **28**, 20687–20690.
26. F. Shalaby et al. (1995) Nature **376**, 62–66.
27. F. Shalaby et al. (1997) Cell **89**, 981–990.
28. P. H. Correll et al. (1997) Genes Function **1**, 69–83.
29. H. Wu et al. (1995) Cell **83**, 59–67.
30. C.-S. Liu et al. (1996) Genes Dev. **10**, 154–164.
31. A. J. Warren et al. (1994) Cell **78**, 45–57.
32. B. Nuez et al. (1995) Nature **375**, 316–322.
33. C. Porcher et al. (1996) Cell **86**, 47–57.
34. L. Robb et al. (1996) EMBO J. **15**, 4123–4129.
35. R. A. Shivdasani, E. L. Mayer, and S. H. Orkin (1995) Nature **373**, 432–434.
36. L. Pevny et al. (1991) Nature **349**, 257–260.
37. M. J. Weiss, G. Keller, and S. H. Orkin (1994) Genes Dev **8**, 1184–1197.
38. F.-Y. Tsai and S. H. Orkin (1997) Blood **89**, 3636–3643.
39. F.-Y. Tsai et al. (1994) nature **371**, 221–226.
40. M. L. Mucenski et al. (1991) Cell **65**, 677–689.
41. E. W. Scott et al. (1994) Science **265**, 1573–1577.
42. T. Okuda et al. (1996) Cell **84**, 321–330.
43. Q. Wang et al. (1996) Cell **87**, 697–708.

Suggestions for Further Reading

44. A. Muller and E. Dzierzak (1993) ES cells as a model of embryonic hematopoiesis? Dev. Biol. **4**, 341–349.

45. S. H. Orkin (1995) Transcription factors and hematopoietic development. J. Biol. Chem. **270**, 4955–4958.
46. R. F. Paulson and A. Bernstein (1995) Receptor tyrosine kinases and the regulation of hematopoiesis. Sem in Immunol **7**, 267–277.
47. L. I. Zon (1995) Developmental biology of hematopoiesis. Blood **86**, 2876–2891.

Hemidesmosomes

Hemidesmosomes are cell junctions that are recognized by their ultrastructural appearance (Fig. 1). Located at the basal cell surface, their most prominent feature in cross section is a dense outer plaque closely applied to the inner surface of the plasma membrane (1). The outer plaque is separated by a less dense region from an inner dense plaque, from which intermediate filaments extend into the cytoplasm. The whole structure forms a circular membrane domain of no more than 0.5 micrometres in diameter and approximately 150 nm deep from the plasma membrane to the inner surface of the inner plaque. The extracellular face of the hemidesmosome is in contact with the lamina lucida of the basement membrane. This region is characterized by the presence of fine anchoring filaments that extend from the plasma membrane across the lamina lucida to the lamina densa. In some sections a linear density called the sub-basal dense plate is seen in the lamina lucida, closely associated with the extracellular face of the hemidesmosomal plasma membrane. Particularly in the epidermis and amnion, the matrix beneath the basement membrane contains numerous banded structures, called anchoring fibrils, which insert into the lamina densa. In favorable sections, filamentous continuity between the anchoring fibrils and the anchoring filaments can be observed. This means that there is continuity of structure in epidermis from the dermis right through to the intermediate filament cytoskeleton of the epidermal cells, in which the hemidesmosome itself provides the transmembrane connection. Such continuity appears to be essential for strong adhesive binding of the epidermis to the dermis, because genetic defects leading to absence or abnormality of anchoring fibrils, anchoring filaments, hemidesmosomes, or basal cell keratin filaments give rise to blistering diseases involving loss of adhesion between the epidermis and the dermis (see below). Although hemidesmosomes appear to resemble half **desmosomes**, they are in fact quite different structures, with a unique and distinct molecular composition (2).

Figure 1. Drawing of an epidermal hemidesmosome seen by electron microscopy. Afib = anchoring fibril; Afil = anchoring filament; Col-dermal collagen fiber; IP = inner plaque; KF = keratin filaments; LD = lamina densa; LL = lamina lucida; SBDP = sub–basal dense plate.

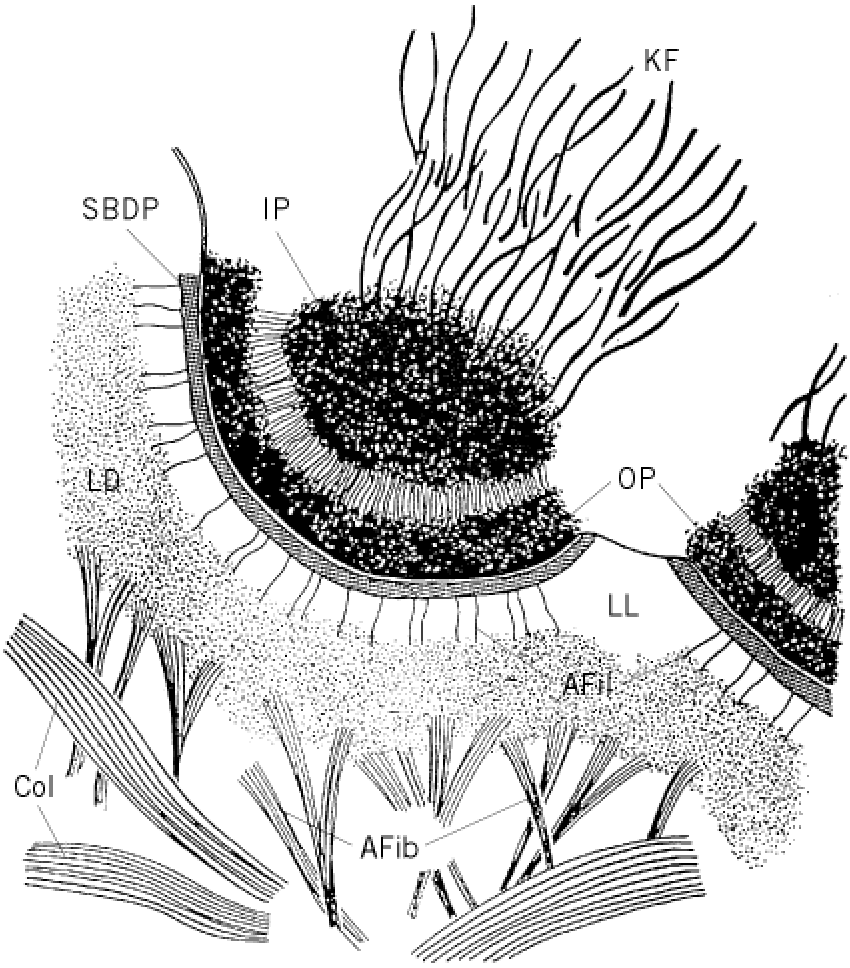

The major molecular components of hemidesmosomes are shown in Figure 2 . The principal adhesion molecule is a6b4 integrin (3), a heterodimer that is extremely abundant on the basal surface of epidermal cells. The b4 subunit is unique among integrin b subunits in having an extremely long cytoplasmic domain of approximately 1000 amino acid residues. The extracellular **domains** of the integrin subunits lie in the lamina lucida of the basement membrane, and their cytoplasmic domains in the hemidesmosomal plaque. The other adhesion molecule is bullous pemphigoid antigen 2 (BPAG2 or BP180), a Type 2 membrane protein whose amino-terminus lies within the desmosomal plaque and the carboxy-terminus in the basement membrane (4). BPAG2 is also referred to as collagen XVII, because it has collagenous repeats in its extracellular domain. a6b4 integrin binds to the truncated **laminin** molecule, laminin 5, which is covalently complexed with laminin 6 or laminin 7 (5). Laminin 5, together with the extracellular domain of BP180, constitutes the anchoring filaments. Laminin 6 and 7 interact with other laminins in the basement membrane and also with nidogen, which links them to other basement membrane components. In addition, they bind to the specific component of anchoring fibrils, collagen VII (6). The anchoring fibrils descend from the lamina densa of the basement membrane into the underlying dermis. The principal plaque components of the hemidesmosome are bullous pemphigoid antigen 1 (BPAG1 or BP230) and plectin (7, 8). Both are members of the plakin family, which also includes desmoplakin, envoplakin, and periplakin of the **desmosome** . BP230 and plectin are believed to be involved in linking between the hemidesmosomal plaque and the intermediate filaments. Although not shown in the diagram, direct interaction between plectin and a6b4 integrin has been demonstrated (9).

Figure 2. Diagrammatic impression of the molecular composition of a hemidesmosome employing information from a

number of sources. a6 = a6 integrin subunit; b4 = b4 subunit; BP180 = 180kDa bullous pemphogoid antigen (BPAG2); BP230 = 230kDa bullous pemphigoid antigen (BPAG1); FN = fibronectin; IF = intermediate filaments; LN 1, 5, 6, 7 = laminins 1, 5, 6, and 7; TAM = tyrosine activation motif.

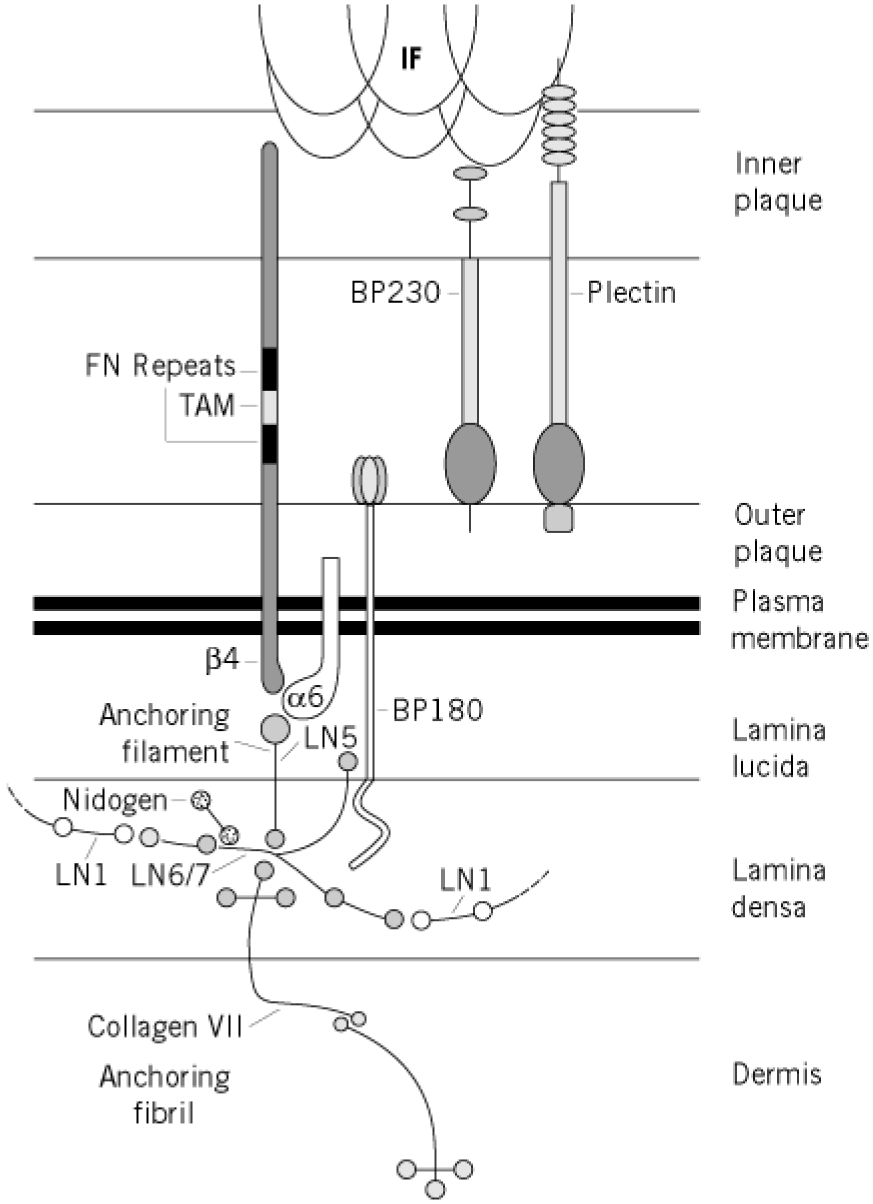

A number of human diseases have been extremely important in elucidating the composition and function of hemidesmosomes. In the **autoimmune** blistering disease bullous pemphigoid, **antibodies** against BPAG1 and 2 are commonly found. Those against an extracellular juxta membrane epitope of BPAG2 have been shown to be pathogenic (10). A number of genetic diseases, collectively known as epidermolysis bullosa (EB), affect basal cells of epidermis and epidermal-basement membrane adhesion. EB simplex involves the basal cell keratins, K5 and K14 (see Keratins). Such mutations disrupt the assembly of the basal cell intermediate filaments and result in cell breakage at a level above the hemidesmosomes (11). The junctional form of EB (EBJ) involves mutations in the a, b, or g chains of laminin 5 or in $a_6 b_4$ integrin (12). This is a lethal disease resulting in epidermal detachment at the level of the basement membrane. EB dystrophica results from mutations of the anchoring fibril component Type VII collagen (13). Anchoring fibrils fail to form, and the epidermis becomes detached below the level of the basement membrane. The importance of plectin in hemidesmosomes has been revealed by the disease EB with muscular dystrophy (14). Here attachment of intermediate filaments from the hemidesmosomal plaque occurs in basal epidermal cells, resulting in epidermal blistering. This is followed later in life by muscular weakening, arising from absence of plectin from the submembrane cytoskeleton of skeletal muscle fibers. Null mutations of a6b4 integrin, plectin, and BP230 produce phenotypes consistent with the defects found in human disease (15-18). This work suggests that BPAG1 forms a similar function to plectin in attaching intermediate filaments to the plaque. The BPAG1 null nutation revealed an additional function for this molecule in the nervous system (17). BPAG1–/– mice develop severe dystonia, resulting in abnormal limb positioning and loss of involvement through muscle and nerve regeneration. This is reminiscent of a hereditary neurodegenerative disease of mice called *dystonia musculorum (dt/dt)*. *dt* is allelic with BP230. It appears that alternative splicing of the amino-terminus of BPAG1 in the nervous system promotes interaction with actin, and its absence results in disorganisation of the neuronal cytoskeleton (19). It is noteworthy that the dermal epidermal junction requires extremely strong adhesion of cells to the extracellular matrix. This may be why hemidesmosomes have two adhesion molecules and two molecules to bridge between the plaque and the intermediate filaments.

Bibliography

1. J. E. Ellison and D. R. Garrod (1984) J. Cell Sci. **72**, 163–172.
2. P. K. Legan et al. (1992) Bioessays **14**, 385–393.
3. A. Sonnenberg et al. (1991) J. Cell Biol. **113**, 907–917.
4. Y. Hirako et al. (1996) J. Biol. Chem. **271**, 13739–13745.
5. M. F. Champliaud (1996) J. Cell Biol. **132**, 1189–1198.
6. H. P. Bächinger et al. (1990) J. Biol. Chem. **265**, 10095–10101.
7. D. H. Klatte et al. (1989) J. Cell Biol. **109**, 3377–3390.
8. G. Wiche et al. (1983) J. Cell Biol. **97**, 887–901.
9. C. M. Neissen (1997) J. Cell Sci. **110**, 1705–1716.
10. Z. Liu et al. (1993) J. Clin. Invest. **92**, 2480–2488.
11. W. H. I. McLean and E. B. Lane (1995) Curr. Opin. Cell Biol. **7**, 118–125.
12. R. A. J. Eady and M. G. Dunhill (1994) Arch. Dermatol. Res. **287**, 2–9.
13. A. M. Christiano et al. (1994) Proc. Natl. Acad. Sci. USA **91**, 3549–3553.
14. W. H. I. McLean et al. (1996) Genes. Dev. **10**, 1724–1735.
15. E. Georges-Labouesse et al. (1996) Nature Genet. **13**, 370–373.
16. R. Van der Neut et al. (1996) Nature Genet. **13**, 366–369.
17. K. Andrä et al. (1997) Genes Dev. **11**, 3143–3156.
18. L. Guo et al. (1995) Cell **81**, 233–243.
19. Y. Yang et al. (1996) Cell **86**, 655–665.

Suggestions for Further Reading

20. D. R. Garrod (1993) Curr. Opin. Cell Biol. **5**, 30–40. (A detailed molecular comparison of desmosomes and hemidesmosomes.
21. K. J. Green and J. C. R. Jones (1996) FASEB. J. **10**, 871–881. (An excellent review.)
22. D. R. Garrod and J. E. Collins (eds.) (1994) *The Molecular Biology of Desmosomes and Hemidesmosomes*, R. G. Landes, Austin, TX. (Articles by some of the leaders in the field.)

Hemizygote

The notion of *hemizygosity* has historical importance in bacterial **genetics**. After the early demonstration by Lederberg of genetic recombination in *Escherichia coli* and the extension of genetic analysis to include a much wider range of unselected markers, a number of complicated anomalies of chromosome segregation began to appear showing that this bacterial system is unconventional. A particular segment of the chromosome of one of the parents, identified by a pair of linked markers, was virtually missing from the **heterozygotes** generated initially and failed to appear in their haploid progeny. These initial **diploids** were incomplete (*hemizygous*). It was first wrongly thought that the missing segment was eliminated from them after their formation. The phenomenon was even given the name of *postzygotic exclusion* . Analysis of this phenomenon led to the discovery of sexuality in bacteria and to the notion of circular chromosome, which resolved the difficulties. To avoid confusion, the term *merozygote* should be used instead of hemizygote for these incomplete and transient heterozygotes.

The term hemizygote should be restricted to a diploid cell or individual in which one of the two copies of a given **gene** has been lost either by deletion or loss of a chromosome. Heterogametic species, in particular human males, are said to be hemizygous for genes located on the X-chromosome and not on the Y-Chromosome (and vice versa).

Suggestions for Further Reading

W. Hayes (1968) *The Genetics of Bacteria and their Viruses*, 2nd ed., Blackwell Scientific Publications, Oxford and Edinburgh, pp. 651–653.

F. Jacob and E. L. Wollman (1961) *Sexuality and the Genetics of Bacteria*, Academic Press, New York, pp. 34–36.

Hemoglobin

Hemoglobin (Hb) is one of the heme-containing oxygen-binding proteins, that generally contain a globin polypeptide chain and a protoheme IX **prosthetic group** that contains a ferrous iron atom. It is found in circulating fluids (blood or hemolymph) of animals, where its fundamental function is transport of molecular oxygen. Its **phylogenetic** distribution is wide, but somewhat capricious. All of the vertebrates, except icefish, have a Hb within their red blood cells that is a tetramer made up of two pairs of two different subunits, each a globin polypeptide chain that contains one heme group. In contrast, invertebrate Hbs are strikingly variable, in their architecture and size, and also in their function. They can be either intracellular or extracellular. Generally, an intracellular Hb is relatively small, whereas extracellular Hbs have a molecular mass ranging from 250 to 3500 kDa. The latter are polymeric and are dissolved directly in the blood plasma, hemolymph, or coelomic fluid. The invertebrate extracellular Hbs have been known traditionally as *erythrocruorins*, but this term lost its significance when it became apparent that there is no particular distinction between the subunits of the extracellular and of the vertebrate Hbs in their prosthetic group, amino acid sequence homology, or three-dimensional protein structure, the globin fold.

1. Vertebrate Hemoglobin

1.1. Structure

The adult form of human Hb, HbA, is composed of two a-subunits and two b-subunits, each of which has one bound heme group (Fig. 1). The a- and b-chains consist of 141 and 146 amino acid residues, respectively. All of the vertebrate Hb chains have similar numbers of residues and homologous amino acid sequences. All adopt very similar globin folds comprised of eight **alpha-helices**, designated A through H, although a-chains lack a-helix D. Early in development, related polypeptide chains replace the a- and b-chains.

Figure 1. The structure of the vertebrate hemoglobins. The molecule is a tetramer composed of two pairs of a- and b-subunits. The a- and b-chains are homologous, have similar globin folds, and each has a bound heme group. How the individual chains are distinguished is described in the text.

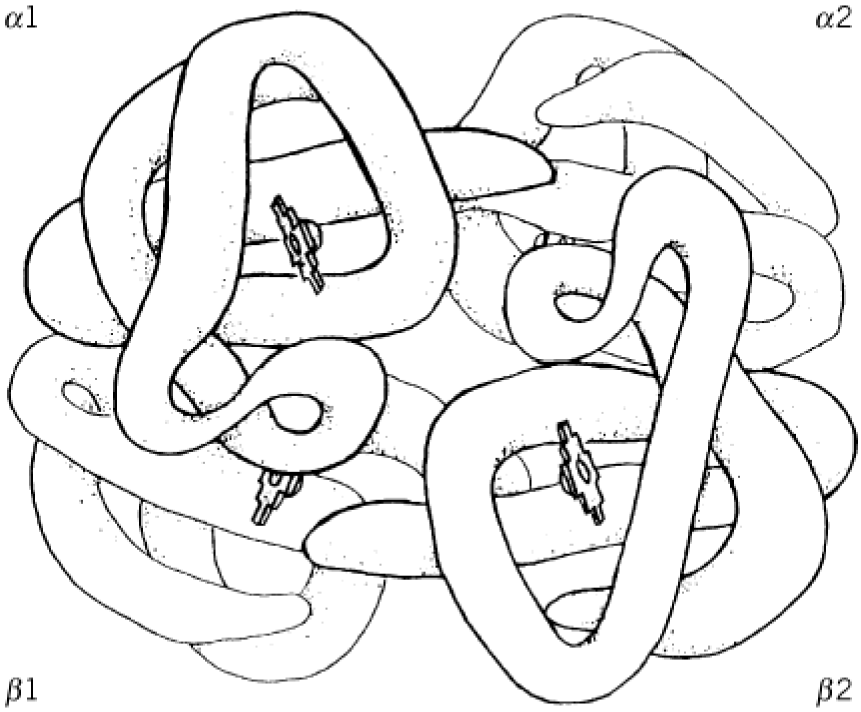

Within the a_2b_2 tetramer, there are relatively few contacts between the pair of a-subunits and the pair of b-subunits, whereas contacts are extensive between the unlike subunits (Fig. 1). If the a-subunits are designated a1 and a2, the b-subunits are numbered so that the distance between the heme iron atoms of the a1/b2 pair is shorter than that in the a1/b1 pair. Because of symmetry, the a1/b1 pair is identical to a2/b2, and a1/b2 is the same as a2/b1 (see Quaternary Structure and Oligomeric Proteins). The tetrameric assembly is stabilized by weak noncovalent bonds, by many van der Waals interactions, a few hydrogen bonds between unlike subunits, and several salt bridges between the two b-subunits.

1.2. Ligand Binding
One molecule of O_2 binds to the sixth coordination site of the iron atom which is on the distal side of the heme group (see Globins and Myoglobin). The heme pocket in the globin fold provides a highly **hydrophobic** environment that maintains the heme iron atom in the ferrous state. Oxidization of the iron atom to ferric to produce methemoglobin destroys its ability to bind oxygen. Upon binding oxygen, the quaternary structure undergoes an extensive change in the relative orientations of the four subunits, especially due to changes in the a1/b2 and a2/b1 interfaces. This switch between two alternative quaternary structures is believed to be involved in the **cooperativity** of oxygen binding. Hb was the primary inspiration of the **concerted model** of allostery, and it remains one of the proteins that best fits that model.

Several other classes of ligand are bound at other specific sites on the deoxy quaternary structure of hemoglobin. These ligands include protons (see Bohr Effect), carbon dioxide, chloride ions, and 2,3-diphosphoglycerate (2,3-DPG). As the ligands bind more avidly to the deoxy form of Hb, they compete in effect with oxygen for binding, and the presence of one of these ligands affects the binding of the others.

1.3. Physiological Function

The physiological functions of vertebrate Hb are (1) transport of oxygen from the lungs to peripheral tissues; (2) transport of carbon dioxide and enhancement of its transport by the blood plasma; and (3) pH regulation (acid–base balance) of the blood.

The transport of oxygen by Hb is well described by its oxygen dissociation curve (or oxygen equilibrium curve), which expresses the dependence of oxygen saturation of Hb (Y) upon the partial pressure of oxygen (P_{O2}) at chemical equilibrium (Fig. 2). The general features of this curve are (1) its sigmoid shape and (2) its shift to the right to higher oxygen partial pressures at higher temperatures or in the presence of the nonheme ligands that bind specifically to deoxy-Hb, protons, CO_2, Cl^-, and 2,3-DPG. The sigmoid shape of the binding curve is ascribed to stepwise enhancement of the oxygen-binding affinity:

$$\mathrm{Hb} + 4\ \mathrm{O_2} \leftrightarrow \mathrm{HbO_2} + 3\ \mathrm{O_2} \leftrightarrow \mathrm{Hb(O_2)_2} + 2\ \mathrm{O_2} \leftrightarrow \mathrm{Hb(O_2)_3} + \mathrm{O_2} \leftrightarrow \mathrm{Hb(O_2)_4} \tag{1}$$

and

$$\begin{aligned} Y &= \frac{[\mathrm{HbO_2}] + 2[\mathrm{Hb(O_2)_2}] + 3[\mathrm{Hb(O_2)_3}] + 4[\mathrm{Hb(O_2)_4}]}{4([\mathrm{Hb}] + [\mathrm{HbO_2}] + [\mathrm{Hb(O_2)_2}] + [\mathrm{Hb(O_2)_3}] + [\mathrm{Hb(O_2)_4}])} \\ &= \frac{K_1 p + 3K_1K_2p^2 + 3K_1K_2K_3p^3 + K_1K_2K_3K_4p^4}{1 + 4K_1p + 6K_1K_2p^2 + 4K_1K_2K_3p^3 + K_1K_2K_3K_4p^4} \end{aligned} \tag{2}$$

Here, $p = P_{O_2}$and K_i (i = 1,2,3,4) are the intrinsic oxygen **association constants** for the *i*th molecule to bind. If the four heme groups of a_2b_2 Hb were equivalent and independent of each other, $K_1 = K_2 = K_3 = K_4$, which would produce a hyperbolic oxygen dissociation curve, like that of myoglobin (Mb) (Fig. 2). Mb is a monomeric globin that contains a single heme group. In contrast, HbA gives a sigmoidal curve in which $K_1 < K_2$, $K_3 \ll K_4$and the ratio of K_4 to K_1 is 500 (2) (Fig. 3). This cooperative binding of oxygen produces the sigmoid curve, in which apparent interactions between the four heme groups of the molecule are mediated by conformational changes in the protein (3). The sigmoidal shape of the oxygen-binding curve contributes to increasing the difference in oxygen saturation between arterial and venous blood and enhances the amount of oxygen released at the tissues (Fig. 2).

Figure 2. Oxygen dissociation curves for hemoglobin (Hb) and myoglobin (Mb). The oxygen concentration is specified by its partial pressure in mm of Hg. The dissociation curve for the monomeric Mb has the expected hyperbolic shape, whereas that for Hb is sigmoid, indicating positive cooperativity in binding the four oxygen molecules by each Hb tetramer. The dissociation curve for Hb is shifted to the left or right upon changing the solution conditions or temperature, as indicated, whereas that for Mb is insensitive to changes in conditions, except for the temperature. The middle of the three curves for Hb is for standard conditions: 37°C, pH 7.4, 40 mm Hg CO_2, and 5 mM 2,3-DPG. The partial pressure of oxygen for arterial blood, 100 mm Hg, and that for mixed venous blood, 40 mm Hg, produce a difference in oxygen saturation of 23%, whereas there would be a much smaller release of oxygen for a hyperbolic curve like that of Mb.

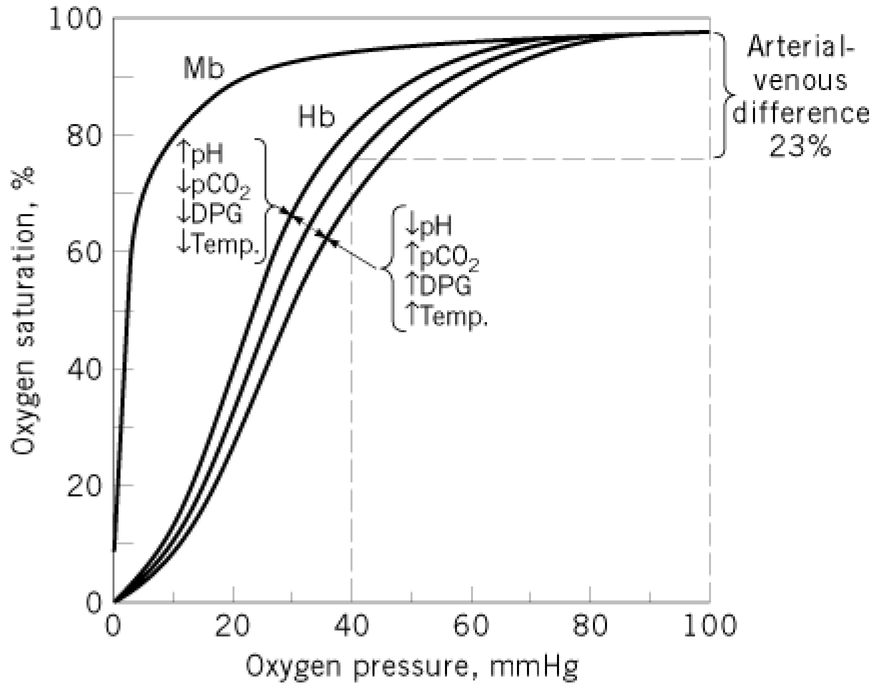

Figure 3. Changes in oxygen affinity of human hemoglobin with oxygen binding at the four heme groups and those upon addition of the cofactors 0.1 M $Cl^{-}$and 2 mM 2,3-DPG. The abscissa indicates the *i*th oxygen molecule to bind, and the ordinate gives the logarithm of the intrinsic association constant for the *i*th step. Open circles correspond to the absence of cofactors, closed circles to their presence. The four-step oxygen binding is illustrated schematically below the graph. Squares and circles represent deoxy and oxy subunits, respectively. Data taken from K. Imai (1982) *Allosteric Effects in Haemoglobin*, Cambridge University Press, London.

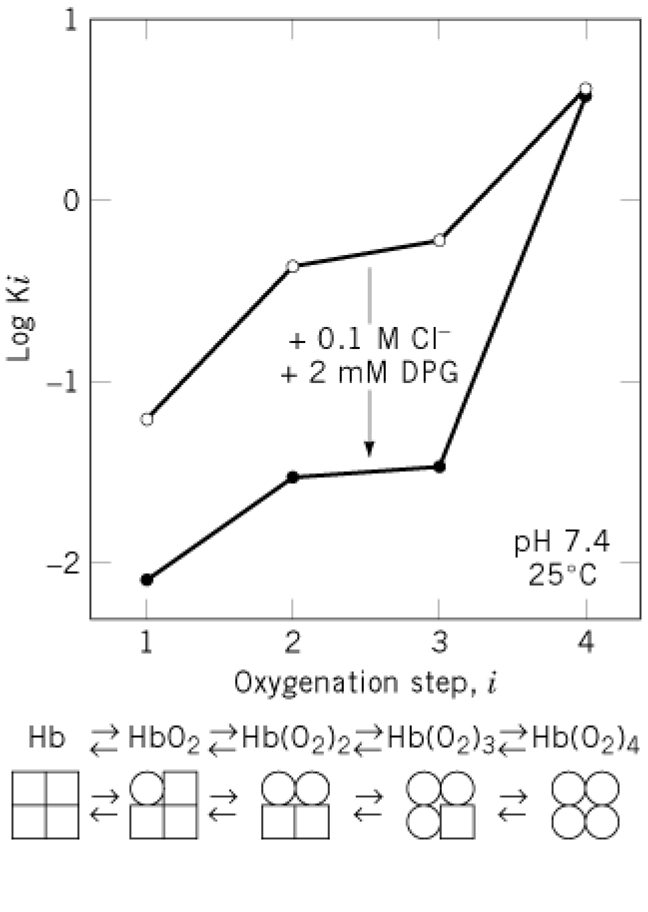

Under physiological conditions, the nonheme ligands lower the oxygen affinity and increase the cooperativity of oxygen binding by HbA. The effect of these ligands on the intrinsic binding constants, K_i, is not uniform with respect to i (Fig. 3). The shift of the oxygen binding curve to higher partial oxygen pressures, that is, the lowering of the overall oxygen affinity upon acidification or upon increasing the CO_2 concentration or temperature has physiological consequences because this enhances the release of oxygen at the peripheral tissues, where such changes result from active metabolism. The effect of pH on the oxygen affinity is known as the Bohr effect. In some cases of chronic hypoxia found in anemia, chronic heart and lung diseases, etc., there is an increase in the intracellular concentration of 2,3-DPG, a decrease in Hb's oxygen affinity, and consequently an enhancement of oxygen release at tissues (4).

Carbon dioxide produced in tissue cells diffuses into the red blood cells and reacts with water, catalyzed by carbonic anhydrase:

$$CO_2 + H_2O \leftrightarrow H_2CO_3 \leftrightarrow H^+HCO_3^- \tag{3}$$

The HCO^-_3bicarbonate ions thus produced move to the blood plasma in exchange for chloride ions and are transported to the lungs. Reaction 3 is greatly shifted to the right when Hb absorbs the protons produced. Moreover, dissolution of the carbon dioxide is greater in the tissue capillaries than in the alveolar because of the uptake of protons upon oxygen release by Hb:

$$HbO_2 + \delta\ H^+ \leftrightarrow Hb(H^+)_\delta + O_2 \tag{4}$$

This oxygen-linked proton binding known as the Haldane effect is the reciprocal expression of the Bohr effect. The release of oxygen in the tissue capillaries enhances the uptake of protons by Hb, thereby causing a further shift of Eq. 3 to the right. Part of the CO_2 is transported linked directly to Hb as a carbamino moiety:

$$Hb(O_2) - NH_2 + CO_2 \leftrightarrow Hb - NHCOOH + O_2 \tag{5}$$

where $–NH_2$is the a-amino groups of the a- and b-chains. This CO_2 binding is also oxygen-linked. Dissociation of oxygen in tissue capillaries enhances the CO_2 binding by Hb, increasing the CO_2 content of the venous blood. The remainder of the CO_2 is dissolved directly in the blood plasma. The major portion (85%) of the total CO_2 is transported as bicarbonate, 10% as the carbamino form, and the remaining 5% as free CO_2. Consequently, as a result of its allosteric properties, Hb plays a key role in CO_2 transport and oxygen transport.

The properties of HbA described here also apply to other vertebrate Hb, except for some slight differences. In some species, 2,3 DPG is replaced by other cellular metabolites, such as ATP, GTP, or **inositol pentaphosphate**, and CO_2 is replaced by bicarbonate ion.

2. Annelid Hemoglobins

Annelida possess giant extracellular HB of molecular mass 3500 kDa. The molecular architecture is a hexagonal bilayer whose diameter is about 30 nm and whose thickness is about 20 nm. The molecule is composed of 12 identical spherical protein units, known as “submultiples,” six of which make one hexagonal layer. These submultiples are assembled to make up an entire molecule using many linker subunits. The submultiple is composed of 16-kDa globin subunits that have the same globin fold as the vertebrate Hb subunits, but the linker subunits are unrelated, heme-free polypeptide chains. The extracellular Hb from the earthworm *Lumbricus terrestris* has been most extensively studied. Its submultiple is a dodecamer composed of three copies of each of four different kinds of globin chains, and 12 such dodecamers are assembled with 36 linker chains and approximately 57 tightly bound calcium ions. Consequently, there are $12 \times 12 (= 144)$heme groups in each molecule. Some of the globin and linker chains have attached carboyhydrates, which are thought to contribute to stabilization of the quaternary structure through their noncovalent, **lectin**-like binding (5, 6).

Annelid Hbs demonstrate a striking diversity of oxygen-binding properties. Most demonstrate a Bohr effect and cooperativity of oxygen binding like those of vertebrate Hb, and sometimes of even greater magnitude, but others have none. The annelid Hb do not respond to cofactors, such as 2,3-DPG or other organic phosphate compounds. Instead, their oxygen affinity is increased by divalent calcium and magnesium ions, which are abundant in the annelid blood. There is some evidence that the functional allosteric unit of annelid Hb is the submultiple.

3. Hemoglobins of Other Species

A great variety of Hbs are found in lower organisms. They can be (1) one-domain monomers, that have a single globin chain of about 16 kDa and one heme group; (2) polymers of such single-domain monomers; (3) two-domain polymers; and (4) multiple-domain polymers. Most of the single-domain monomer Hbs are present in the cytoplasm. Some are in noncirculating cells, whereas others are in coelomic cells of annelida, such as *Glycera*. Although those in noncirculating cells do not apparently participate in oxygen transport, they are still classified as hemoglobins. Leghemoglobin is a monomeric Hb contained in the cytoplasm of root nodules of legumes. It has an extremely high oxygen affinity, which is important for the completely removing of traces of oxygen from the symbiotic bacteria, because nitrogen fixation is a strictly anaerobic process. Consequently, the function of leghemoglobin is to eliminate oxygen, rather than to supply it to tissues.

Finding the single-domain Hb from the gram-negative bacterium *Vitreoscila* was the first indication that the evolutionary origin of globins may date back to the common ancestor with prokaryotes. Hbs isolated from **yeasts** and *Escherichia coli* have two domains, one of which is a globin chain and the other a flavoprotein. The NADH reductase activity of the second domain prevents the heme iron of the first domain from auto-oxidizing to maintain its capability of reversibly binding oxygen. *Chironomus* larvae possess Hbs that are polymorphic in various species, tissues, and developmental stages. Among the 12 Hbs of *C. thummi thummi*, seven exist as homodimers, four as monomers, and one as a monomer or dimer (see Chironomus). The nematode *Ascaris lumbrodoides* Hbs consists of two-domain globin chains, one of which has lost the ability to bind heme. Hbs from nematodes, including *Ascaris*, have extremely high oxygen affinities. The brine shrimp *Artemia salina* Hbs have a molecular mass 250 kDa and are composed of two polypeptide chains, each containing eight heme-binding domains. The blood clam *Scapharca inaequivalvis* has intracellular homodimeric and heterotetrameric Hbs, which bind oxygen cooperatively. The most conspicuous feature of these Hbs is that their globin chains have an additional a-helix at their N-terminus and that the E and F helices are external, exposed to solvent, whereas the G and H helices are internal, involved in subunit interactions. Thus, the clam Hb tetramer is “back to front” relative to the vertebrate Hb tetramer.

The various species of Hb demonstrate oxygen affinities that vary 26,000-fold. The lowest affinity, measured by the value of the partial pressure of oxygen at half saturation, is 26 mm of Hg, that of human Hb at 37°C, whereas that for the highest affinity is only 0.001 mm Hg, for *Ascaris* Hb at 20°C. The species-dependence of the oxygen affinity of Hb is a manifestation of its adaptation to the environments that the organisms inhabit. All of the Hbs have the same protoheme IX heme group, so this tremendous variation in oxygen affinity arises from species differences in the amino acid sequences of the globin moiety. How this is accomplished is not known.

Bibliography

1. G. S. Adair (1925) J. Biol. Chem. **63**, 529–545.
2. K. Imai (1979) J. Mol. Biol. **133**, 233–247.
3. M. F. Perutz (1970) Nature **228**, 726–739.
4. F. A. Oski, A. J. Gottlieb, M. Delivoria-Papadopoulos, and W. W. Miller (1969) N. Engl. J. Med. **280**, 1165–1166.
5. S. Ebina, K. Matsubara, K. Nagayama, M. Yamaki, and T. Gotoh (1995) Proc. Natl. Acad. Sci. USA **92**, 7367–7371.
6. P. D. Martin, A. R. Kuchumov, B. N. Green, R. W. A. Oliver, E. H. Braswell, J. S. Wall, and S. N. Vinogradov (1996) J. Mol. Biol. **255**, 154–169.

Suggestions for Further Reading

7. R. E. Weber (1980) Functions of invertebrate hemoglobins with special reference to adaptations to environmental hypoxia, Am. Zool. **20**, 79–101.
8. K. Imai (1982) *Allosteric Effects in Haemoglobin*, Cambridge University Press, London.
9. S. N. Vinogradov (1985) The structure of invertebrate extracellular hemoglobins (erythrocruorins and chlorocruorins), Comp. Biochem. Physiol. **82B**, 1–15.
10. M. F. Perutz (1989) Mechanisms of cooperativity and allosteric regulation in proteins, Q. Rev. Biophys . **22**, 139–236.
11. T. Gotoh and T. Suzuki (1990) Molecular assembly and evolution of multi-subunit extracellular annelid hemoglobins, Zool. Sci. **7**, 1–16.
12. M. Bolognesi, D. Bordo, M. Rizzi, C. Tarricone, and P. Ascenzi (1997) Nonvertebrate hemoglobins: Structural basis for reactivity, Prog. Biophys. Mol. Biol. **68**, 29–68.
13. M. F. Perutz, A. J. Wilkinson, M. Paoli, and G. G. Dodson (1998) The stereochemical mechanism of the cooperative effects in hemoglobin revisited, Annu. Rev. Biophys. Biomol. Struct . **27**, 1–34.

Hemoglobin Mutations

The study of human hemoglobin mutations opened the era of molecular genetics. In 1949, Linus Pauling and colleagues first described the alteration of the electrophoretic mobility of hemoglobin (Hb) by the **sickle cell** anemia mutation. The basis for the more positive electrical charge of sickle cell hemoglobin (Hb S) was not known, but the fact that it was a property of individual Hb molecules led Pauling to designate sickle cell anemia a molecular disease. In 1956 Vernon Ingram demonstrated that the charge difference is due to substitution of valine for glutamic acid in position six of the b-globin peptide chain. This observation was the first to prove that mutations can alter the amino acid sequence of a polypeptide chain and, by extension, it was proposed that the normal function of **genes** is to specify the primary structures of proteins, a hypothesis that is well established now.

It is no accident that the initial connection between mutations and protein structure emerged from studies of Hb. In higher animals, Hb is the protein that is most readily available in relatively pure form. In the case of mammals, a lysate of washed red cells can be used for Hb classification without further purification. Hb levels are measured as part of routine clinical examinations, and persons with diminished synthetic ability or with functionally aberrant Hb are likely to be identified and studied further. Hb is probably the protein that has been most extensively studied worldwide for genetic variations, and the array of mutations known is remarkable in number and in effect.

1. The Globin Loci

A hemoglobin molecule in vertebrates is tetrameric and consists of two each of two globin subunits. The folded tertiary structure of each globin chain binds one molecule of heme. The two kinds of globin subunits in Hb A, the major human adult Hb (actually present from birth onward), are labeled a-globin and b-globin. The a-globin polypeptide chain consists of 141 amino acid residues, and the b-globin chain has 146 residues. The molecular structure can be written a_2b_2. An additional adult Hb, designated Hb A_2, comprises 2.5% of the total. Its molecular structure is a_2d_2, so Hb's A and A_2 differ only in having different “b-like” globins. Other Hb's present at various stages of human development are fetal Hb's, $a_2{}^Gg_2$ and $a_2{}^Ag_2$, and embryonic Hb's, $a_2\varepsilon_2$, $z_2\varepsilon_2$, and z_2g_2. All of the globin chains resemble each other in amino acid sequence and folding pattern and are similar to myoglobin of muscle, which occurs as a monomer. Genetically, the a and z genes form a cluster on human chromosome 16, and the b, d, ^Gg, ^Ag, and e genes form a cluster on chromosome 11 (Fig. 1). All of the functional genes have three **exons** and two **introns**. In addition to the functional genes, there are several pseudogenes.

Figure 1. Diagrams of the organization of the a-globin complex on chromosome 16 and the b-globin complex on chromosome 11. Functional genes are in black. Gene sizes and relative positions are not drawn to scale.

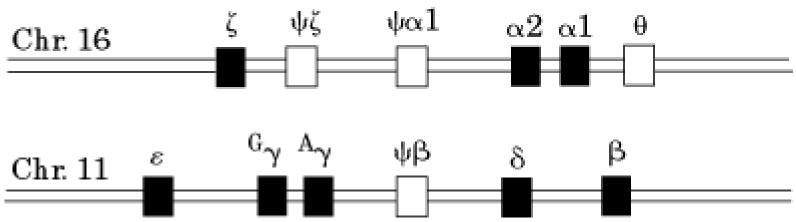

The globin genes constitute a gene family that, along with myoglobin, evolved from a single ancestral gene through gene duplication and evolutionary **divergence**. Recent duplication has occurred in the case of the two a genes, which are identical, and the two g genes, whose products differ by a single codon. The b and d genes are also similar.

An interesting feature of the globin genes is the similarity in order of expression during development with order on the chromosomes. During the embryonic period, the z, ε, g, and a genes are actively transcribed, forming $z_2\varepsilon_2$, z_2g_2, and $a_2\varepsilon_2$ Hb's. The primary Hb during the fetal period is a_2g_2. At about birth, but not as a result of birth, production changes to a_2b_2 and a_2d_2 . The molecular basis for these switches has not been established.

2. Mutations of Hb Genes

Over 500 different mutations have been observed in the Hb loci, exemplifying almost every known mutational mechanism. Those involving the b locus are especially apparent, because this locus becomes active at birth. If a mutation is limited to the b locus, embryonic and fetal development should be normal. In contrast, the a locus is active from the embryonic period. A major defect in its function is likely to interfere with fetal development and lead to abortion. The same is true of the g loci. Defects in function that are limited to the d locus are likely to go unnoticed because of the small amount of Hb A_2 normally made.

The phenotypic consequences of Hb mutations can be classified roughly into four categories: (1) complete absence of a gene product, (2) normal function but diminished amount, (3) abnormal function with or without diminished amount; and (4) normal function and amount. The first group includes genetic deletions, which can extend over two or more loci. Single base-pair substitutions can produce any of the four effects, depending on the site of the substitution. The inability to produce adequate amounts of Hb is known as thalassemia.

3. Absence of a Gene Product

The classical examples are the a- and b-thalassemias that involve deletions of all or part of the a and b genes, respectively. (See Thalassemia.) Other causes are frameshift mutations that involve insertion or deletion of one or two nucleotides, which switch the reading frame. Unless these changes occur very near the C-terminal end of the polypeptide, no recognizable product is produced. Several such mutations, known in the b globin gene, result in b thalassemia.

Single nucleotide substitutions also lead to complete absence of a gene product. In a number of thalassemia mutants, a nucleotide substitution in the coding region of a gene introduces a stop codon, producing a truncated, nonfunctional, and unrecognizable gene product. If a nucleotide substitution occurs at a critical site in a regulatory region, transcription of the gene may not occur. This has been shown in several cases of thalassemia, in which substitutions in the TATA box and other 5′ sites interfere with transcription. Substitutions in the 3′ **poly-A** site leads to absence of product, presumably by interference with translation .

One unusual cause for the absence of b-globin is nonfunction of the switch mechanism that causes transcription to change from the g genes to the d and b genes. In such cases, the g genes continue to function, and transcription of the d and b genes is not initiated. The major Hb is a_2g_2 (fetal Hb or Hb F), and the condition is known as hereditary persistence of fetal hemoglobin. The Hb F is synthesized in amounts adequate for normal function, and homozygotes for this mutation are normal. The responsible mutations occur in two regions. One is a site between the g genes and the d gene. The other sites are in the **promoter** regions of the g genes.

4. Diminished Amount of a Normally Functional Hb

Mutations outside the coding regions of genes substantially suppress transcription without obliterating it completely. Several nucleotide substitutions in the promoter region of the b-globin gene do that, resulting in very low amounts of normal Hb A (so-called b^+–thalassemia). A number of substitutions in the coding region also reduce the amount of globin. In some instances, the globin is quite functional. Hb C results from the substitution of lysine for glutamic acid in residue six of the b-chain. This does not interfere with function but the amount of Hb C produced is less than that of Hb A. Hb C is widespread in West Africa and offers some protection against falciparum malaria. Another polymorphic mutant, Hb E, occurs widely in East Asia and appears to protect against malaria also. Hb E results from a change in codon 26 of the b gene, near the boundary between exon 1 and intron 1. There are several cryptic splice sites in this region. In the case of the Hb E mutation, a cryptic splice site in codon 25 is substantially activated, and only a portion of the primary transcript is spliced correctly. Presumably this mechanism occurs in a number of other mutations that have not been studied so extensively.

5. Functionally Abnormal Globins

The prime example of a functionally abnormal Hb is **sickle cell** Hb (Hb S). Hb S transports oxygen normally. However, in the deoxygenated state, the Hb S molecules aggregate to form long crystal-like structures that disrupt the red cell. The cause is substitution of a **hydrophobic** valine residue in place of glutamic acid in residue six of the b-globin polypeptide chain. This causes the N-terminal part of the b chain to fold differently, leading to aggregation.

Other examples are the mutations that cause **methemoglobinemia** . These involve amino acid substitutions in the heme-binding region. In normal hemoglobins, the Fe of the heme is stabilized in the Fe^{2+} state, which is required for O_2 binding. In Hb M mutations, the Fe is predominantly in the more stable Fe^{3+} form (methemoglobin, metHb). The amount of Hb M made is normal. Therefore a heterozygote has approximately half normal Hb A and half Hb M. Such a person is essentially normal, comparable to a person who is heterozygous for b-thalassemia. The high level of metHb gives them a gray-blue color, however. Hb M mutations are rather rare, and homozygotes have not been observed. Presumably, they would be lethal.

6. Mutations Normal in Function and Amount

The list of these mutations is not extensive because they normally escape detection unless populations are screened. An interesting example is Hb Lisbon, which results from the substitution of aspartic acid for glutamic acid at residue 23 of the a_1-globin. This rare human variant is the standard “wild-type” form in gorillas. All other amino acids are identical in the a_1 globins of the two species.

Another interesting normal variation is the tandem duplication of one of the a-globin genes in populations in the southwest Pacific. Having five copies of the a-globin genes rather than four is a harmless variation.

Suggestion for Further Reading

Web site: *On-Line Mendelian Inheritance in Man*, http://www3.ncbi.nlm.nih.gov/Omim/.

Hemophilia

Hemophilia is the term used to describe uncontrolled bleeding, which may range from mild (bleeding after surgery or significant trauma) to severe (spontaneous bleeding into joints, muscle, and internal organs). Most examples are attributable to one of the two classic inherited hemophilias: the sex-linked disorders hemophilia A and hemophilia B. The most common of these is hemophilia A, which is caused by mutations in the **gene** on the human X-chromosome coding for the blood coagulation cofactor molecule, factor VIII (see Blood Clotting). Hemophilia B is caused by mutations to another X-chromosome-encoded gene, that for the zymogen of the blood coagulation serine proteinase factor IX. Less common congenital bleeding disorders are caused by mutations in the genes coding for other proteinase components of the blood coagulation system (factors VII, X, XI, and prothrombin), the cofactor molecule factor V, fibrinogen, and the serpin a_2-antiplasmin. Other causes of bleeding are due to defects in platelet aggregation caused by mutations in the genes coding for the integrin a_{IIb} b_3 (glycoprotein IIb-IIIa, the platelet-fibrinogen binding site), the cell adhesion molecule von Willebrand factor, or its platelet binding-site glycoprotein Ib-IX.

The molecular basis of both hemophilia A and B has been studied extensively. Historically, bleeding defects have provided the basis for defining the reactions of the blood coagulation pathways and, more recently, elucidating of structure–function relationships in the coagulation factors. Hemophilias A and B have also been valuable models in the study of mutational mechanisms. All possible types of gene disruption have been detected, including point mutations, deletions, insertions, duplications, and inversions, and they can lead to either absence of the protein, reduced levels of protein, protein with reduced functional activity, or nonfunctional protein.

In various populations, the frequency of hemophilia A is 1 in 510×10^3 male births. Over 80 point mutations in the factor VIII gene have been detected. Of these, 27 cause severe hemophilia and are mainly nonsense mutations, while 29 cause moderate to severe hemophilia and all are missense mutations. The most functionally interesting of the latter are those that lead to normal levels of protein but with severely reduced activity, that is, with reduced specific activity, which account for 5% of the total point mutations. These are all mutations of the Arg residue at the P1 position, immediately preceding the peptide bond to be cleaved, of the thrombin cleavage sites of factor VIII, and involve the hypermutable CpG dinucleotide (which is susceptible to 5-methylcytosine deamination) (see CpG Islands).

The frequency of hemophilia B is one-sixth that of hemophilia A. More than 300 point mutations have been detected, 40% of which lead to factor IX with reduced specific activity; these mutations affect all the **domains** of factor IX. The mutations that can be most readily rationalized in structure–function terms include those leading to abnormal post-translational modification of the Gla domain (ie, generation of **g-carboxyglutamic acid** and b-hydroxyaspartic acid residues), mutation of the arginine residues at the proteolytic activation sites, and mutations affecting the active-site serine residue. Over half of these mutations are in CpG dinucleotides, with C → T or G → A transition mutations.

Suggestion for Further Reading

E. G. D. Tuddenham and D. N. Cooper (1994) *The Molecular Genetics of Haemostasis and Its Inherited Disorders*, Oxford Monographs on Medical Genetics No. 25, Oxford University Press.

Hepatitis B Virus

Hepatitis B virus (HBV) is one of the hepadnaviruses and causes acute, self-limited or persistent infection that can potentially be passed vertically from carrier mother to infant, or horizontally by the percutaneous and transmucosal exchange of infected blood and body fluids. Persistent infection by HBV is often associated with chronic liver disease that can lead to the development of hepatocellular carcinoma (HCC). The neonatal transmission route is thought to be an important mechanism for HBV persistence because of the immunological immaturity of the infected host. The concomitant infection is usually self-limited, with clearance of virus particles from the liver and blood and the development of lasting immunity to reinfection.

HBV is a spherical particle, 42 nm in diameter (Fig. 1). The genome of HBV is a circular DNA duplex of 3.2 kbp that replicates by **reverse transcription** (see HIV (Human Immunodeficiency Virus) and Rous Sarcoma Virus (RSV)) of a pre-genome RNA and contains a single-stranded gap region of variable length in one strand. DNA replication and transcription of viral genes and the mechanism of virion assembly within infected hepatocytes have been unraveled so some extent, but less is known about the virus–cell interactions that control virus attachment, uncoating, and entry into susceptible cells, as well as the integration of HBV DNA into the host cell genome. Although viral sequences implicated in the interaction of the virion with the cellular membrane are located in a variable region of the amino-terminal part of the pre-S1 domain, the cellular receptor for HBV has not yet been fully characterized.

Figure 1. Schematic diagram of a hepatitis B virus particle.

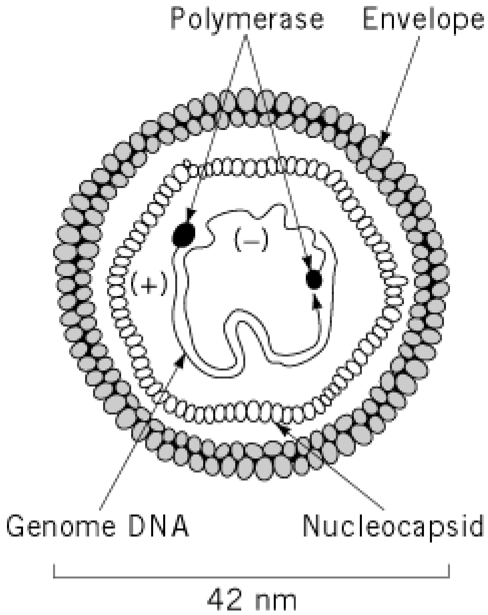

Nucleotide sequences and those amino acid sequences deduced from HBV DNA from different virus subtypes (adw, adr, ayw, ayr) have revealed a compact, overlapping coding organization of the genome, where the entire genome is coding (Fig. 2). Four open reading frames (ORFs) are localized on one viral strand in the same transcriptional polarity. Two of them, the C and S regions, specify structural proteins: the 183-residue nucleocapsid protein HBcAg and the 226-residue envelope major protein HBsAg, respectively. The smallest ORF, X, codes for a trans-acting 154-residues regulatory protein that interacts with various cellular proteins and may play a major role in hepatic cell transformation. Overlapping these coding regions, the largest ORF, P, encodes a viral polymerase of 843 residues, which is necessary for viral replication and has activities of **DNA polymerase**, **reverse transcriptase**, plus ribonuclease H. This overlapping of the P region is a characteristic feature and, with its unusual overlapping of coding and regulatory sequences (such as **promoters**, two specific enhancers, and a poly A termination signal), makes this virus unique. In addition to the central homologous region, two strong homology blocks in the amino- and carboxy-terminal parts of the X protein might correspond to a conservative selective pressure for functional activity of the X as a *trans*-regulator, and of the viral ribonuclease H encoded by *C*-terminal sequences of P, which overlap with the 5′ end of the X protein.

Figure 2. Genetic organization and transcription map of the hepatitis B virus genome. The HBV DNA was derived from virus of the adr subtype, with a nucleotide sequence of 3215 bp. The positions of promoters and two enhancers are indicated by and *f*, respectively. The four different transcripts are indicated with a poly(A) tail (~). The terminal protein domain of polymerase (•) is attached to the 5′ end of the minus strand (—). DR1 and DR2 represent 11-bp direct repeats.

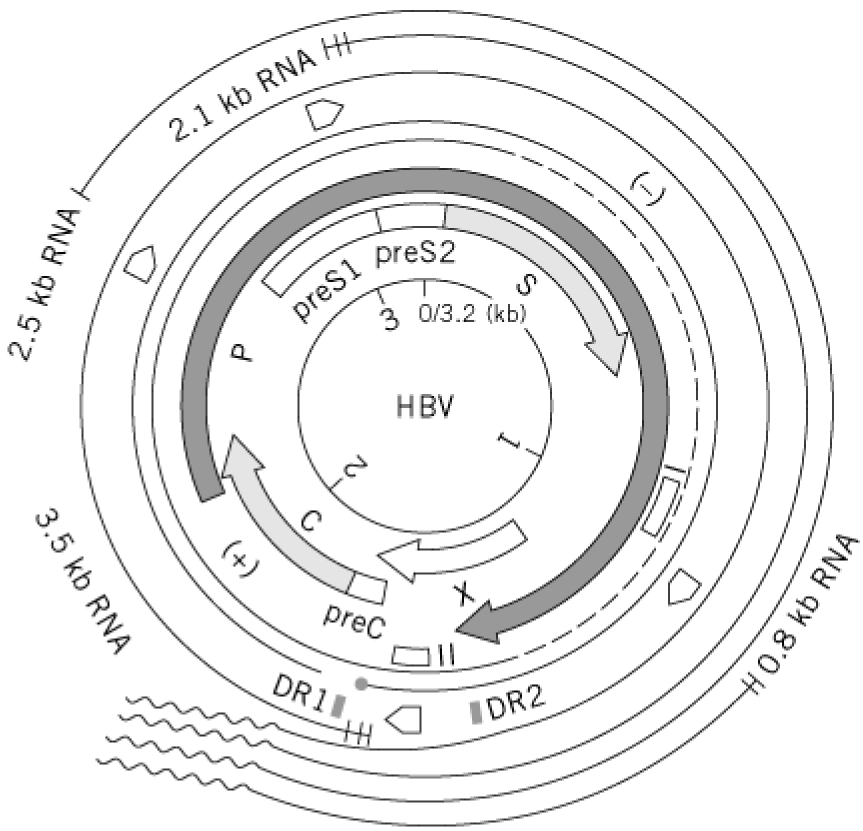

Another important characteristic of HBV is a high mutation rate due to the lack of a proofreading function of the reverse transcriptase that replicates its genome. This may increase the production of mutated variants during persistent infection, which enables the virus to escape from the host immune response or enables a growth advantage of mutant viral genomes. Substantial nucleotide and amino acid sequence heterogeneity in different isolates of HBV, plus specific mutations in the HBV genome in individual patients, have been observed, and partially deleted HBV genomes have also been observed in human hepatocellular carcinoma. However, there is no experimental evidence that these defective HBV genomes might harbor oncogenic potential, nor that any particular HBV subtype might be more oncogenic than others. Comparison of the HBV genome with those of animal hepadnaviruses reveals extensive homologies among mammalian hepadnaviruses (WHV, GSHV), which share a basically identical genomic organization.

The antibody response to HBV envelope antigen (HBsAg) is well characterized to be **T-cell-dependent** and plays an important role in clearance of the circulating virus and preventing their attachment and uptake by susceptible hosts. The role of the antibody response to the nucleocapsid (HBcAg and its derivative in serum, HBeAg) and nonstructural proteins (X and P) in HBV pathogenesis is less clear yet. Persistent infection of HBV is mainly caused by a weak antiviral immune response that cannot kill or cure all of the infected cells. Alternatively, chronic hepatitis may be caused by an inappropriate T-cell response that can kill but cannot cure the infected hepatocytes without enough production of cytokines to clear the infection.

Suggestion for Further Reading

D. Ganem (1996) "*Hepadnaviridae* and Their Replication". In *Fields Virology*, 3rd ed. (B. N.Fields et al., eds.), Lippincott-Raven, Philadelphia, pp. 2703–2737.

Heptad Repeat

Fibrous proteins of the a-type, as well as many globular proteins, contain a heptad repeat of the form $(a–b–c–d–e–f–g)_n$ in which nonpolar amino acid residues are found with high probability in positions *a* and *d*. Regions displaying a heptad repeat invariably have the a**-helix** conformation and give rise to a **coiled-coil** molecule in which the apolar residues in *a* and *d* in several chains pack in a regular manner along the axis (1) (Fig. 1) (see also Cytokeratins). Electrostatic interactions between charged residues in positions *e* and *g* of adjacent polypeptide chains help to specify the relative orientation and axial stagger of the chains. Various positions within the heptad repeat are not occupied equally by different amino acids (1-3), and this has provided the basis for distinguishing between two- and three-stranded coiled-coils in fibrous proteins (4). Consider the *a*, *d*, *e*, and *g* positions in turn. Leucine, lysine, asparagine, and arginine residues occur more commonly in position *a* in two-stranded coiled-coils than in three-stranded ones, whereas the reverse is true for alanine, glutamine, serine, and threonine. In the *d* positions, leucine is favored in two-stranded coiled-coils, but isoleucine, serine, threonine, and valine are found more commonly in the three-stranded conformations. In *e* positions, glutamic acid, isoleucine, and glutamine are more commonly observed in two-stranded ropes than three-stranded ones, but the reverse is true for phenylalanine, leucine, serine, tryptophan, and tyrosine. Finally, in position *g*, glutamic acid, glutamine, and arginine are favored in two-stranded ropes, whereas isoleucine, leucine, asparagine, tryptophan, and tyrosine occur significantly more frequently in three-stranded coiled-coils.

Figure 1. Heptad repeat seen in axial projection for two- and three-stranded a-helical coiled-coils. Residues in positions *a* and *d* are generally apolar and are shielded from water as a result of systematic close packing along the axis of the rope-like structure so formed (dotted lines). Interchain ionic interactions are also possible, the most common type being those that occur between oppositely charged residues in positions *e* and *g* (dashed lines).(From Ref. 66, with permission.)

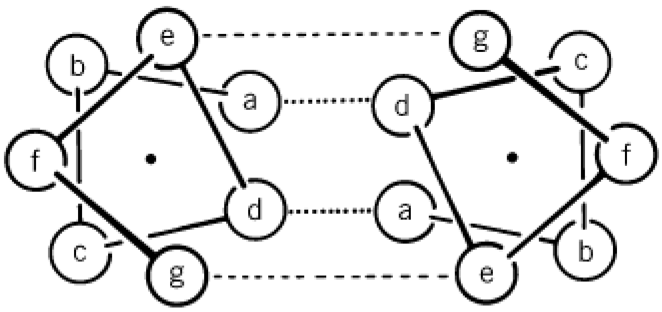

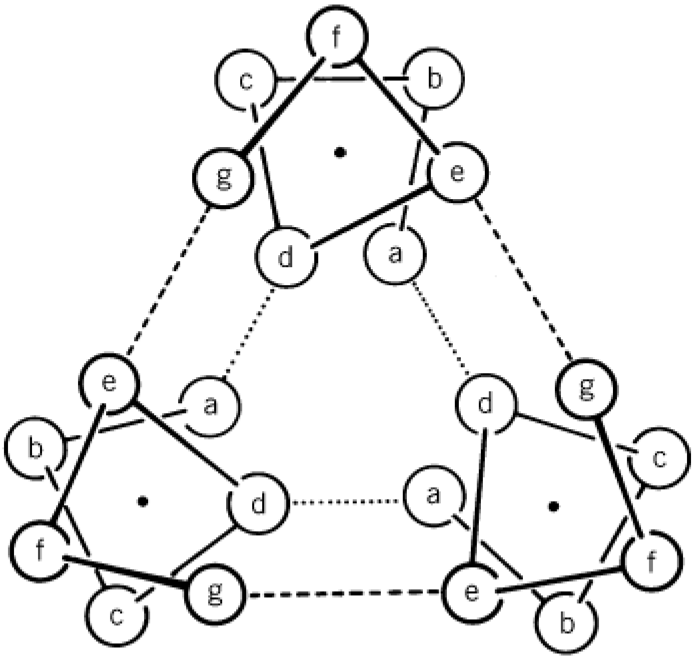

Groupings of amino acids also clearly provide a means for distinguishing one multichain coiled-coil from another (Table 1). These figures indicate, for instance, that in two-stranded structures the acidic residues occur very infrequently in position *a* but quite commonly in position *d*. In contrast, basic residues are found commonly in *a* but much less so in *d*. In three-stranded coiled-coils, the preferences for the charged residues are almost reversed in these positions. In all cases the *a* and *d* positions are occupied by apolar residues at a frequency of about 75%. In three-stranded structures the occupancy of charged residues in positions *e* and *g* is reduced, and the occupancy of apolar residues is increased. This trend continues as the number of strands in the coiled-coil rope increases.

Table 1. Percentage of Apolar (ap), Acidic (ac), and Basic (ba) Residues in Positions *a*, *d*, *e*, and *g*

Position	Group	Two-Stranded Structure	Three-Stranded Structure
a	ap	72.6	77.5
a	ac	1.4	3.1
a	ba	13.8	2.2

d	ap	76.1	79.3
d	ac	6.3	1.0
d	ba	3.8	3.9
e	ap	16.9	20.9
e	ac	27.9	22.9
e	ba	23.7	22.5
g	ap	20.0	25.8
g	ac	32.3	22.7
g	ba	19.0	17.3[a]

[a] Acidic residues (ac) are aspartic acid and glutamic acid; basic residues (ba) are arginine and lysine; apolar residues (ap) are leucine, isoleucine, valine, methionine, phenylalanine, tyrosine, and alanine.

A run of consecutive heptad repeats is frequently interrupted, sometimes by a region of sequence with different structural characteristics and sometimes by the insertion/deletion of a few residues in an otherwise perfect and continuous heptad substructure. Analysis shows, however, that the vast majority of such discontinuities fall into one of three categories (5): (i) the deletion of three residues (a " *stutter*"), (ii) the insertion of one residue (a "*skip*") which is structurally equivalent to two stutters, and (iii) the deletion of four residues (a " *stammer*"). Stutters lead to a local unwinding of the coiled-coil structure, whereas the stammer results in a local overwinding. A skip thus leads to a longer distance axially over which the coiled-coil is partially unwound.

Bibliography

1. C. Cohen and D. A. D. Parry (1986) -Helical coiled-coils—a widespread motif in proteins. Trends Biochem. Sci. **11**, 245–248.
2. J. F. Conway and D. A. D. Parry (1990) Structural features in the heptad substructure and longer range repeats of two-stranded -fibrous proteins. Int. J. Biol. Macromol. **12**, 328–334.
3. J. F. Conway and D. A. D. Parry (1991) Three-stranded -fibrous proteins: the heptad repeat and its implications for structure. Int. J. Biol. Macromol. **13**, 14–16.
4. D. N. Woolfson and T. Alber (1995) Predicting oligomerization states of coiled coils. Protein Sci. **4**, 1596–1607.
5. J. H. Brown, C. Cohen and D. A. D. Parry (1996) Heptad breaks in -helical coiled coils: stutters and stammers. Proteins Struct. Funct. Genet. **26**, 134–145.
6. C. Cohen and D. A. D. Parry (1990) -Helical coiled-coils and bundles: how to design an -helical protein. Proteins Struct. Funct. Genet. **7**, 1–15.

Suggestions for Further Reading

7. C. Cohen and D. A. D. Parry (1990) -Helical coiled-coils and bundles: how to design an -helical protein. Proteins Struct. Funct. Genet. **7**, 1–15.
8. A. Lupas (1996) Coiled-coils: new structures and new functions. Trends Biochem. Sci. **21**, 375–382.

Hermaphrodite

In the animal kingdom, natural selection has promoted the development of two opposite sexes, the male and female genders. In most species, individuals belong to either sex, developing either a female **phenotype** with female external genitalia: a uterus, tubes, and two ovaries, or, depending on the presence of a testis-determining factor, a male phenotype with male external genitalia: epididymis and a testis (see Sex). In a hermaphrodite, either in a true hermaphrodite or pseudohermaphrodite , elements of both genders are present in one individual. Some nematodes are physiologically true hermaphrodites (eg, *Caenorhabditis elegans*). Here, the molecular switch to determine whether a male or hermaphrodite is formed depends on an X-chromosome counting system (1), which involves primarily the xol-1 (2, 3) and tra-1 (4) genes. In mammals, however, male and female organs are not normally present in one individual.

Due to the severity of the aberration, different types of hermaphrodites can be found. The clinical appearance of a hermaphrodite is characterized by intermediate sex forms of the external genitalia and **germ line** cells. Gonads that diagnose a true hermaphrodite are ovary and testis, or a combination of the two, the ovotestis. The combination of an ovary and ovotestis is most commonly found in hermaphrodites, followed by the combination of two ovotestes. When close to an ovary, the tubes and rudiments of an uterus are most commonly detected; when close to a testis, a vas deferens and an epididymis are present. In some cases, however, with a lower frequency of appearance, the opposite gender organs, or none, are developed: Tubes and uteri and/or vas deferens and epididymis are found, together with an ovotestis. This can occur because sex differentiation is highly dependent on hormones. As sexual organs are formed from primordial **germ cells**, as well as from soma cells, the gonadal sex does not fit to the genetical and/or cytological sex under certain circumstances.

Besides true hermaphrodites, there are also pseudohermaphrodites, in which all other organs are female but a testis has developed. Due to the higher temperature in the body than in the scrotum, these cells are prone to the development of cancer and will be removed.

Regarding the karyotype of hermaphrodites, those with a Y-Chromosome are more likely to develop a testis than those without. The ovotestis contains both ovarian and testicular cells. The ovarian cells are in many cases normal, and primary follicles are also found. In contrast, the testicular cells show histological aberrations in true hermaphrodites, regardless of whether these cells are found in a testis or an ovotestis.

Regarding the hormone production of hermaphrodites, they are characterized by normal levels of estrogens and gestagens. However, the levels are also dependent on the amount of normal ovarial stroma present in the hermaphrodite. Spermatogenesis does not occur, but testosterone is produced, although it does not reach the levels of normal males. The reduced amounts are responsible for the virilization. There is only one case reported in which a hermaphrodite became a father. However, there are hermaphrodites that are fertile after removal of the testicular tissue and can give birth to children. This certainly does not depend solely on the presence of an ovary, but also on a physiological development of at least one of the tubes and of the uterus. Interestingly, all children born from female hermaphrodites were male. Roughly half the hermaphrodites were identified before the third year of life, but many hermaphrodites were identified only during or after puberty.

During embryogenesis, germ cells become either spermatogonia or oogonia, depending on their genetic constitution. The **genotype** sex normally determines which type of gonads are developed. Further differentiation depends on the hormonal secretion of the gonads themselves, which consequently determines the **phenotypic** sex. The primordial gonad develops to an ovary, and the inner and external genitalia also tend to feminize, so long as the production of male hormones is not stimulated. In the case of secretion of male hormones, especially testosterone and mullerian inhibiting hormone, mullerian ducts do not develop; instead, wolfian ducts are formed that change the fate of the organs, and epididymis, vas deferens, and seminal vesicles evolve.

In cattle and goats, a special situation is found in a male and female twin. Due to the transfer of anastomosae, the development of mullerian ducts is inhibited in the female twin, which results in an infertile female. The external genitalia are female, but the uterus is rudimentary or missing. The male twin is fertile under normal circumstances. Apart from these special cases in twin births in cattle and goats, the biological reason for pathological hermaphroditism in mammals is still unclear.

Other genetically determined disorders related to gender are the Turner (X0) syndrome (5, 6) and surplus X-chromosomes, such as the XXY constitution (Klinefelter syndrome), which can now be detected using **PCR** techniques (7). Due to the absence of the Y-chromosome, the Turner syndrome is mostly linked with a female phenotype, although a mild masculinization has been reported (8). An additional X-chromosome leads to infertility and a reduced IQ. Additional Y-chromosomes, as found in XYY karyotypes, lead to extreme tallness, but not necessarily to crime, as was assumed in former times. In every case, the presence of a Y-chromosome leads automatically to a male phenotype, regardless of how many X-chromosomes were inherited. However, it must be kept in mind that it is not the Y-chromosome itself that triggers the development of male fate, but the SRY gene (see Sex). Mutations within this gene can disrupt its function and consequently lead to female development, even though a Y-chromosome is present.

Bibliography

1. M. Nicoll, C. C. Akerib, and B. J. Meyer (1997) Nature **388**, 200–204.
2. L. M. Miller, J. D. Plenefisch, L. P. Casson, and B. J. Meyer (1988) Cell **55**, 167–183.
3. N. R. Rhind, L. M. Miller, J. B. Kopczynski, and B. J. Meyer (1995) Cell **80**, 71–82.
4. C. P. Hunter and W. B. Wood (1990) Cell **63**, 1193–1204.
5. T. Ogata and N. Matsuo (1995) Hum. Genet. **95**, 607–629.
6. C. Geerkens, W. Just, K. R. Held, and W. Vogel (1996) Hum. Genet. **97**, 39–44.
7. A. Kleinheinz and W. Schulze (1994) Andrologia **26**, 127–129.
8. R. Medlej, J. M. Lobaccaro, P. Berta, C. Belon, B. Leheup, J. E. Toublanc, J. Weill, C. Chevalier, R. Dumas, and C. Sultan (1992) J. Clin. Endocrinol. Metab. **75**, 1289–1292.

Herpesvirus

Herpesviruses are large DNA **viruses** whose genomes consist of a large linear double-stranded DNA molecule, 125 kbp to 229 kbp in length. Their hosts range from lower vertebrates to humans. At present, approximately 100 herpesviruses have been isolated and at least partially characterized. In humans, five viruses [herpes simplex virus 1 (HSV-1) and 2 (HSV-2), varicella zoster virus (VZV), human cytomegalovirus (HCMV) and Epstein–Barr virus (EBV)] have been identified as members of the herpesvirus family, *Herpesviridae*. In the past decade, however, three new herpesviruses, namely, human herpesvirus 6, 7, and 8 (HHV-6, HHV-7, and HHV-8), were isolated from healthy people and AIDS patients. These human herpesviruses are responsible for a wide variety of diseases.

Although herpesviruses share common features in their structure, gene organization, replication style, and so forth, the family *Herpesviridae* is further divided into three subfamilies, *Alphaherpesvirinae*, *Betaherpesvirinae*, and *Gammaherpesvirinae*. *Alphaherpesvirinae* includes HSV-1, HSV-2, VZV, pseudorabies virus, equine herpesvirus 1 (EHV-1), and so on. They have a relatively short replication cycle, induce cytocidal damage in infected cells, and establish latency primarily in sensory ganglia. *Betaherpesvirinae* includes HCMV, HHV-6, HHV-7, and so on, and is characterized by its restricted host range, long replication cycle, and slow spread of infection from cell to cell in culture. They can establish latency in lymphoreticular cells, secretory glands, kidneys, and other tissues. *Gammaherpesvirinae* contains EBV, HHV-8 (Kaposi's sarcoma-associated herpesvirus), herpesvirus saimiri (HVS), and so on. They replicate in lymphoid cells, and latency is frequently demonstrated in lymphoid tissue. A most important feature of this subfamily is that some are associated with naturally occurring malignant tumors.

The virions of herpesviruses consist of four morphological elements: an inner core, an icosahedral capsid with 162 capsomers, a surrounding amorphous layer, known as the tegument, and an envelope containing a number of **glycoproteins**. The tegument of the HSV virion is known to contain about 20 distinct structural proteins, some of which have important regulatory functions for the initiation of viral replication. The genomes of eight human herpesviruses have been entirely sequenced, and the complete DNA sequences are also available for several animal herpesviruses, including EHV-1, EHV-2, HVS, and mouse CMV. Although the number of viral genes encoded in the genomes varies, a set of approximately 40 genes is conserved in all herpesviruses. These encode capsid proteins, envelope glycoproteins, proteins involved in DNA cleavage/packaging, and enzymes such as **DNA polymerase**, DNA helicase, DNA primase, uracil-DNA glycosylase, dUTPase, ribonucleotide reductase, and protein kinase. The herpesvirus genomes contain a number of accessory genes that are dispensable for viral replication in cell culture. For example, 45 of 84 HSV genes have been shown to be nonessential. These accessory gene products are supposed, however, to be important for viral growth and spread in their natural hosts.

The principal strategy of herpesvirus replication is similar in all of them and can be summarized as follows: (i) Fusion of the virion envelope with the plasma membrane occurs at the cell surface in a pH-independent manner; (ii) viral capsids with a portion of the tegument are transported to a **nuclear pore**, where viral DNA is released into the nucleus, circularized, and then **transcribed** by cellular **RNA polymerase** II; (iii) viral gene expression is coordinately regulated and sequentially ordered in a cascade fashion; (iv) viral DNA replicates by a **rolling circle** mechanism, and unit-length viral DNA is cleaved from newly synthesized concatemers and packaged into preformed empty capsids; (v) full capsids pass through the inner and outer membranes of the nuclear envelope by budding and reenvelopment and associate with tegument proteins in the perinuclear region; (vi) enveloped virions accumulate in the endoplasmic reticulum and then mature in the Golgi apparatus; and finally, (vii) mature virions are released into the extracellular space by exocytosis.

All herpesviruses have the ability to persist in their natural hosts throughout life. During latency, the viral genomes are present in the form of an **episome** in the nucleus, and only a small subset of viral genes is transcribed. The synthesis of specific viral proteins appears to be essential for some herpesviruses to maintain latency, but not for others. Various stimuli, such as stress and immunosuppression, induce reactivation, which triggers viral replication and shedding of infectious virus. The molecular mechanism of herpesvirus reactivation remains to be elucidated.

Suggestions for Further Reading

B. Roizman (1996) "Herpesviridae" . In *Fields Virology*, 3rd ed. (B. N. Fields et al., eds.), Lippincott-Raven, Philadelphia, pp. 2221–2230.

B. Roizman and A. E. Sears (1996) "Herpes Simplex Viruses and Their Replication". In *Fields Virology*, 3rd ed. (B. N. Fields et al., eds.), Lippincott-Raven, Philadelphia, pp. 2231–2295.

Y. Becker and G. Darai (1994) *Pathogenicity of Human Herpesviruses due to Specific Pathogenicity Genes*, Springer-Verlag, Berlin.

Heterochromatin

The term *heterochromatin* was originally used to describe chromatin that stained intensely with particular dyes. This is in contrast to the rest of chromatin, which stained less well and is called euchromatin. Heterochromatin comes in two varieties, constitutive, which is permanently heterochromatic, and facultative, which can change its state. The chromatin regions of centromeres and telomeres are examples of constitutive heterochromatin. In contrast, the inactive X-chromosome (see Barr Body, X-Chromosome Inactivation) and the vast bulk of inactive chromatin in any chromosome are composed of facultative heterochromatin.

The most common observed consequence of heterochromatin formation is the repression of transcription, either in the heterochromatin itself or in regions of chromatin adjacent to the heterochromatin domain. The variability in gene expression at the border of the heterochromatin is described as "position effect variegation." Three explanations have been offered for this phenomenon. The first is that special proteins, such as heterochromatin protein 1 (HP1, see following text), cause heterochromatin to adopt its distinct structure and that these proteins can "spill over" into regions of normal chromatin and exert repressive effects on gene expression. The second is that heterochromatin represents the sequestration of chromosomal domains in specialized nuclear compartments from which the transcriptional machinery is excluded, for example, the chromocenter. The third applies only to *Drosophila* and other insects with polytene chromosomes in that, following placement adjacent to heterochromatin, a gene undergoes fewer rounds of replication than normal. Fewer copies of the gene would cause a concomitant reduction in transcription. Most investigators accept that heterochromatin-specific proteins diffuse onto normal chromatin and thereby influence the gene expression of juxtaposed genes. Although initially defined from work on insects, there is an increasing body of evidence that heterochromatin domains exist in all eukaryotic chromosomes, including those of yeast. Moreover, it is clear that metazoans have used this type of chromosomal organization for the developmental regulation of gene expression.

An approach to the molecular basis of heterochromatin formation has been to look for mutations in *Drosophila* or more recently in *Saccharomyces cerevisiae* that enhance or suppress position effects on gene expression (modifiers of position effect variegation). Modifiers of position effect variegation include mutations in the genes encoding the chromosomal proteins involved in forming heterochromatin. Using this approach, the gene encoding a nonhistone protein, HP1, was identified (see Chromocenter). Mutations of the HP1 gene reduce position effects on gene expression (1). HP1 is preferentially associated with the heterochromatin regions of polytene chromosomes. Other proteins homologous to HP1 include Polycomb, which is also chromatin-associated and from genetic experiments it is known that it influences the expression of many genes in normal chromatin (2). Neither HP1 nor Polycomb interacts with DNA directly, but they presumably recognize some aspect of nucleosome or chromatin fiber structure. Recent experiments reveal that certain proteins that affect position effect variegation, for example, SUV38H1, are histone methyltransferases that selectively modify lysine #9 in histone H3 (3), and that the resulting modified histone is a preferential target for binding by HP1 (4). Combined with earlier data that overexpression of this enzyme leads to HP1 redistribution from heterochromatin (5), as does the histone hyperacetylation via inhibition of histone deacetylases (6), these data strongly support a model that idiosyncratically modified nucleosomes form a landing pad for HP1. Polycomb and HP1 share a common amino acid sequence known as the chromodomain (chromatin modification) (see Chromocenter). This domain is highly conserved through evolution and can be found even in yeast. For example, the *S. pombe* SW16 gene encodes a chromodomain protein. The SW16 protein is involved in the assembling the chromosomal domain containing the transcriptionally silent mating type cassettes.

Position effect variegation also depends on the presence of normal levels of the histone proteins and posttranslational modifications of the N-terminal tails of the core histones, such as acetylation. The histones are needed for forming nucleosomes and for subsequently forming higher order structures. Acetylating the N-terminal tails alters the interaction of the histones with DNA and, potentially, the folding of nucleosomal arrays. Position effect variegation also depends on proteins that recognize nucleosomal arrays, but not naked DNA, such as HP1 and Polycomb (see Position Effect). HP1 is associated only with inactive chromosomal regions, but Polycomb interacts with at least 50 different sites within *Drosophila* chromosomes, including developmentally important loci encoding homeodomain proteins. However, mutations in a second gene family that interacts with the histone proteins allow genes associated with Polycomb to remain active. Thus, Polycomb is likely to exert its effects on gene expression via chromatin structures dependent on the histone proteins (7, 8).

Position effect variegation is recognized now as a universal phenomenon in eukaryotic chromosomes. Genes integrated into yeast chromosomes near the silent mating loci or close to the telomeres are repressed in a way that reflects their proximity to these sites in the chromosome. This silencing effect spreads over at least 5 to 10 kbp of contiguous DNA, but not as much as 20 to 30 kbp in yeast. As in *Drosophila*, the genes influencing the position effect in yeast encode structural components of chromatin or enzymes associated with the modification of chromatin (see Position Effect).

Examples of mammalian chromosomal regions that contain heterochromatin are also the centromere and the telomere (9). The telomeres of mammalian chromosomes have an unusual chromatin structure in which nucleosomes are closely packed (see Telomere). Mammalian telomeres consist of the sequence $(TTAGGG)_n$ repeated for 10 to 100 kbp. Heterochromatin at the centromere contains tandemly repeated simple sequence “satellite” DNA, for example the a-satellite DNA at the human centromere (see Centromeres). This a-satellite heterochromatin plays a structural role by mediating attachment of the kinetochore. In these instances, specialized heterochromatin structures have an important architectural role and protective function in the chromosome.

Occasionally, an entire nucleus becomes heterochromatinized. One example is the inactivation of the erythrocyte nucleus in chicken. Here the special linker histone variant H5, which represses transcription and compacts nucleosomal arrays very effectively, accumulates. Histone H5 is more arginine-rich than the normal linker histone H1 found in somatic cells. This increase in arginine content probably strengthens the interaction of H5 with DNA and stabilizes chromatin structure. In this instance, the assembly of a specialized heterochromatin structure reflects the terminal differentiation of this particular specialized cell type.

Bibliography

1. P.B. Singh, J. Cell Sci. **107**, 2653–2668 (1994).
2. S.C.R. Elgin, Curr. Opinion Cell Biol. **2**, 437–445 (1990).
3. S. Rea et al., Nature **406**, 596–599 (2000).
4. M. Lachner et al., Nature **410**, 116–120 (2001).
5. M. Melcher et al., Mol. Cell. Biol. **20**, 3728–3741 (2000).
6. A. Taddei, C. Maison, D. Roche, and G. Almouzni, Nat. Cell Biol. **3**, 114–120 (2001).
7. H.W. Brock and M. van Lohuizen, Curr. Opin. Genet. Dev. **11**, 175–181 (2001).
8. B. Zink and R. Paro, Nature **337**, 468–471 (1989).
9. D. Shore, Curr. Opin. Genet. Dev. **11**, 189–198 (2001).

Additional Reading

10. Wolffe A., *Chromatin: Structure and Function*, 3rd ed., Academic Press, London, U.K., 1998.

Heteroduplex

Two single-stranded nucleic acid polymers with at least partial complementarity can form duplexes with stretches of double helix, corresponding to the regions of nucleotide sequence homology, interleaved with unpaired stretches, corresponding to noncomplementary regions. Two types of single-stranded loops are introduced by noncomplementarity in the heteroduplex (Fig. 1). A loop in only one of the strands indicates a deletion. A loop composed of single-strand regions in both strands indicates a region of sequence incompatibility. A heteroduplex can be composed of two DNA strands, one DNA strand and one RNA strand, or two RNA strands. *In vivo*, heteroduplexes (DNA–DNA) can arise in the process of recombination or as a consequence of errors (mismatches) in DNA replication (DNA–DNA) or transcription (DNA–RNA). Hybridization of nucleic acids of different origins leads to heteroduplexes *in vitro*.

Figure 1. Loops in a heteroduplex indicate either a deletion or a region of noncomplementarity in the two strands.

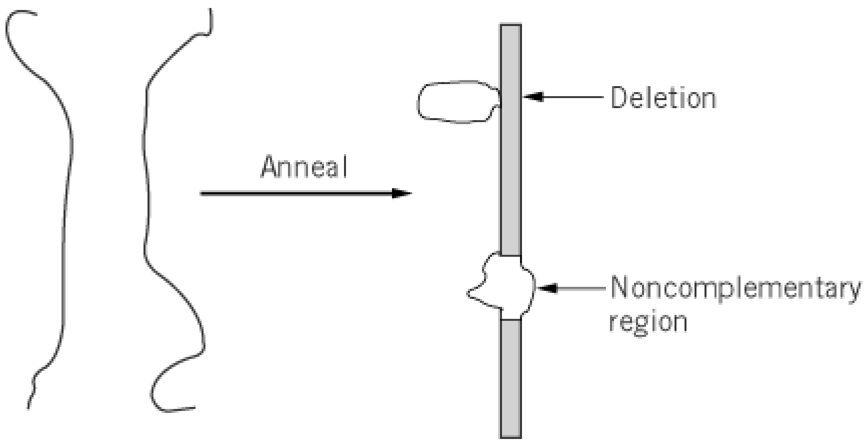

The level of sequence homology in the heteroduplex can be evaluated by monitoring the change in ultraviolet **absorbance** on heteroduplex formation or by selective enzymatic digestion of single-stranded regions, followed by hydroxyapatite chromatography. These techniques are analogous to those used for studies of reassociation kinetics (1).

Electron microscopy can used to visualize the regions of sequence homology in the heteroduplex, even though nucleic acids are not sufficiently dense to be easily observable directly in the electron microscope. The heteroduplex is spread on the surface of the electron microscope grid. Heavy metals and proteins are applied to the nucleic acid by one of several techniques, thereby making the polymers visible in the electron microscope.

Bibliography

1. R. J. Britten, D. E. Graham, and B. R. Neufeld (1974) Meth. Enzymol. **29**, 363.

Suggestion for Further Reading

2. R. W. Davis, M. Simon, and N. G. Davidson (1971) Electron microscope heteroduplex methods for mapping base sequence homology in nucleic acids, Meth. Enzymol. **21**, 413–428.

Heterokaryon

A *heterokaryon* is a combined cell with two separate **nuclei**. Pontecorvo (1) who worked with the **fungus** *Aspergillus nidulans*, which lacks a sexual cycle, observed that genetic recombination occurs during cell division in **mitosis** and employed it in the genetic analysis of fungi. If asexual **spores** from two genetically dissimilar strains of a filamentous fungus are planted very close together on the surface of a solid medium, the emerging hyphae fuse at points of contact. This fusion is followed by the transfer of nuclei from one hypha to the other, so that *heterokaryons* are formed whose hyphae contain nuclei from both strains. As the heterokaryotic hyphae grow, the nuclei multiply independently.

When asexual spores are formed, however, each initial sporogenous cell receives only one nucleus of one type or the other. Subsequent multiplication of these cells thus produces chains of spores. Each chain consists of genetically identical spores, homokaryons, although the spores of adjacent chains may differ in phenotype. Very occasionally, however, two of the nuclei in the heterokaryotic hyphae fuse to form a single **diploid** nucleus. This nucleus multiplies as such and is incorporated into spores in the same way as the haploid nuclei, so rare chains of diploid spores arise which, on subsequent germination, yield diploid individuals. If the haploid parental strains differ in complementary nutritional requirements, eg, one of genotype Ab (requiring B in the growth medium) and the other aB (requiring A), the diploid nucleus (Ab/aB) will possess genetic determinants to synthesize both and B substances needed for growth of the parents. Therefore the existence of diploid spores can be recognized and cultures obtained from them by plating on media lacking the growth factors A and B (2).

Cell fusion is usually carried out by treating a suspension of cells with some inactivated **viruses** or with polyethylene glycol, to alter the plasma membrane of cells so that they are induced to fuse with each other.

Heterokaryons provide a way of mixing the components of two separate cells to study their interactions (see Hybrid Cell).

Bibliography

1. G. Pontecorvo (1954) Caryologia, suppl. 6, 192–200.
2. J. A. Roper (1992) Experientia **8**, 14–15.

Heterosis

Heterosis is the phenomenon in which **heterozygotes** exhibit superiority of fitness over homozygotes . This superiority often occurs in the areas of viability, longevity, fecundity, and resistance to disease. Therefore, heterosis is sometimes referred to as “hybrid vigor”. Heterosis occurs when two different, often **inbred** strains are crossed. The effect of homozygous deleterious alleles is reduced in the heterozygotes produced through the cross. The increase in vigor may be due to overdominance or superiority of the heterozygote for particular gene differences, or to the introduction of favorable dominant alleles to loci previously homozygous for deleterious recessive **alleles**. Therefore, the terms “heterosis” and “overdominance” are used interchangeably; both confer heterozygotes with an evolutionary advantage over homozygotes.

When survival or reproduction is lowered with recessive alleles, such alleles are eliminated faster from inbred homozygous populations than from outbred, heterozygous populations. Homozygous deleterious alleles will first increase, and then natural selection will tend to remove the deleterious alleles, resulting in less genetic variation and greater average fitness as the heterozygous alleles increase. However, deleterious recessive genes will not be totally eliminated by selection, because they will not be exposed to selection in the heterozygotes.

The major histocompatibility complex (MHC) genes in humans and mouse are known to have extremely high numbers of alleles (Figure 1) (1). Since the number of alleles is much greater than expected if the alleles were all equivalent functionally, it has been long speculated that positive selection is operating on these complex genes. By making combinatorial sets of different alleles, an organism can become resistant to viral infection, which confers superiority of fitness over the homozygote. Thus, the MHC genes are counted as one example of overdominance.

Figure 1. The protein structure of the MHC human protein, HLA Class IA. The residues involved in binding antigen are shown by the closed circles (1).

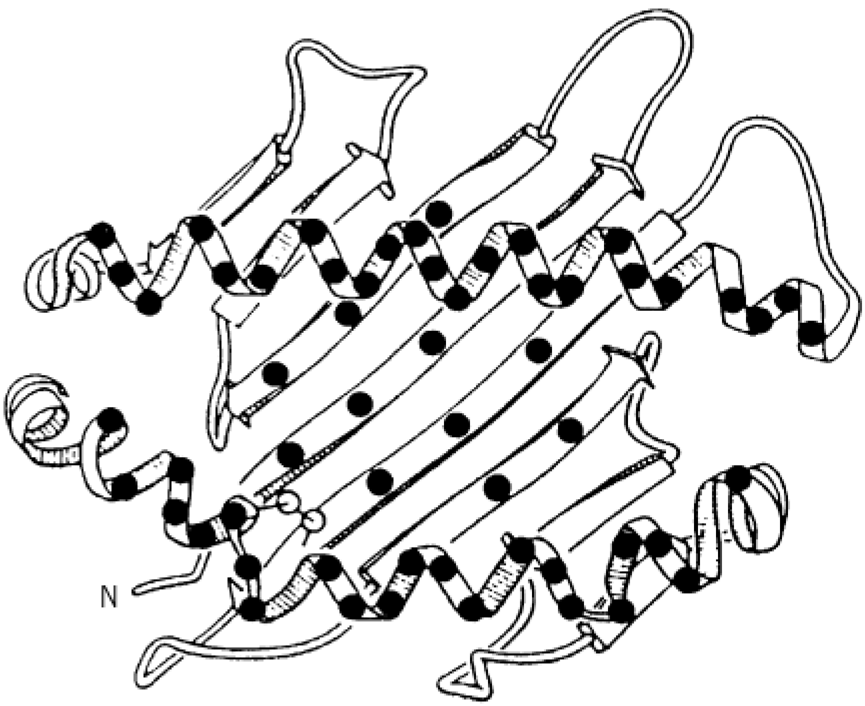

Hughes and Nei (2) examined the numbers of synonymous and nonsynonymous substitutions in the MHC genes. They found that the number of nonsynonymous substitutions, which change the amino acid, was significantly greater than that of synonymous substitutions in the **antigen**-recognition sites, even though the opposite occurred elsewhere. They concluded that positive selection, most probably by overdominance or heterosis, is operating only on the antigen recognition sites.

Bibliography

1. T. Gojobori and T. Imanishi (1991) Transplantation Now **4**, 26.
2. A. L. Hughes and M. Nei (1988) Nature **335**, 167–170.

Heterotrimeric G Proteins

Heterotrimeric G proteins are **GTP-binding** regulatory proteins that amplify, integrate, and transmit information from cell-surface receptors to cellular signaling proteins, known as effectors. G-protein signaling pathways are found in all eukaryotes; but they have been best studied in animals, where their number is greatest. Animals express over a thousand G-protein-coupled receptors that bind a variety of ligands: biogenic amines and lipids, **peptides**, **protein hormones**, odorants, and other compounds. Fungi use G proteins to convey signals from receptors for pheromones and nutrients, and higher plants may use G proteins in response to pathogens or light.

G proteins convey information by traversing a tightly controlled cycle of GTP binding and hydrolysis. G proteins are activated when GTP binds to the Ga subunit; but GTP binding is extremely slow, unless it is promoted by an agonist-bound receptor. GTP-activated G protein can then bind and activate the effector. Activation is terminated when the G protein hydrolyzes bound GTP to GDP, which does not activate (see Gtpases). Signal amplitude is thus a balance between receptor-stimulated GTP binding and GTP hydrolysis.

G proteins are defined by their GTP-binding a subunits, which are primarily responsible for selective recognition of receptors and effectors (Table 1). Vertebrate genomes encode about 20 Ga subunits, while ***Caenorhabditis*** *elegans* has closer to 30. Plants and fungi have only one or two. Diversity is further enhanced in some cases by alternative splicing of RNA transcripts. Ga subunits form heterotrimers by reversible binding to Gbg dimers. Vertebrates express at least 5 Gb's and 12 Gg's. Although possible combinations of Gb with Gg and of Ga with Gbg dimer are limited by both their cellular expression and intrinsic affinity, the potential number of heterotrimers still numbers over 100. Gabg trimers are bound firmly to the inner face of the plasma membrane, with the exception of transducin in photoreceptor membranes. Membrane attachment depends on Gbg, although Ga subunits are somewhat **hydrophobic** and are further modified by two lipid groups (see Membrane Anchors).

Table 1. Heterotrimeric G Proteins in Animals[a]

Family	Ga Genes	Splicing Products
s	s	2 “long,” 2 “short”
	olf	
i	i1	
	i2	
	i3	
	z	
	o	A,B
	t1 (transducin)	
	t2 (transducin)	
	g (gustducin)	
q	q	(3 in *Drosophila*)
	11	

	14
	15 / 16 (orthologous)
12	12
	13
	con (concertina, *Drosophila*)

[a] This list is most representative of vertebrates, although flies and roundworms also have members of each family. In the roundworm *C. elegans*, for example, there are also 13 "worm-specific" Ga subunits that are expressed primarily in sensory neurons (57). Ga subunits have been identified in the coelenterates, but not yet in sponges or protozoa. Ga subunits in fungi and plants do not fall neatly into any of the animal classes.

The Gabg trimer is quite stable, with **dissociation constants** (K_d) for release of Gbg estimated at 10^{-9}M or less. GTP binding decreases this affinity and drives dissociation, to form free Ga-GTP plus free Gbg. Thus, activation of a Ga by receptor-promoted GTP binding also releases an active Gbg subunit, which regulates a distinct spectrum of effectors. Activation of Ga allows Gbg to generate a second signaling output that can be subsequently quenched by Ga-GDP.

1. Ga Subunits

Ga subunits are globular proteins with molecular weights in the range 39 to 44 kDa (1). They are based on two discrete structural **domains**. The GTP-binding domain, formed by the *N*-terminal and *C*-terminal thirds of Ga, has a tertiary structure and amino acid sequence similar to the small monomeric G proteins (see GTP-Binding Proteins), and it is therefore referred to as the ras-like domain, in analogy to $p21^{ras}$. The middle third of the Ga sequence folds into a discrete **a-helix**-rich domain that acts in part as a cover to the GTP-binding site. Ras-like domains and helical domains can be expressed separately in bacteria and will associate with each other in solution (2). The linkage between the two domains is crucial. The more *C*-terminal linker peptide is also one of three "switch" regions that undergo profound conformational change upon activation; it is referred to as switch I. It resides near switch II, which is totally in the ras-like domain. The switch regions are involved in the binding of Gbg, a family of related proteins known as regulators of G-protein signaling, or RGS proteins, and effectors (1). The second major interaction site involves the *N*- and *C*-termini of Ga proteins, which are close together in the folded structure. This region is involved in recognition of receptors and effectors, Gbg, and RGS proteins. In the inactive heterotrimer, the *N* -terminus of Ga lies as an a-helix along the side of the Gb subunit. The *N*-terminus is apparently quite flexible, however, because its conformation or orientation is apparently different in the abg trimer, free Ga-GDP, or activated free Ga or when bound to an RGS protein.

The *N*-terminal helix of Ga contains two important covalent lipid modifications. The terminal amino group of Ga subunits is blocked by lipid: in the Ga_i family by a **myristoyl** amide group that is added shortly after translation; in Ga_s by an unidentified but hydrophobic modification; and in the Ga_q family by an unidentified modification. In addition, a cysteine residue close to the *N*-terminus is linked to a **palmitoyl group** in all Ga's except Ga_t. In contrast to myristoylation, palmitoylation occurs through a thioester linkage and is therefore reversible. Palmitoyl groups turn over in cells and, in several cases, palmitate turnover is promoted by G-protein activation, so that depalmitoylation follows G-protein activation and repalmitoylation ensues thereafter. Myristoylation and the unknown modification of Ga_s are important for establishing high-affinity interactions with effectors, Gbg, and RGS proteins. The regulatory roles of palmitoylation are less clear. Palmitoylation contributes to the overall hydrophobicity of Ga's, and the absence of palmitate may explain in part the solubility of Ga_t (3). Palmitoylation contributes to membrane attachment, but it is unclear whether this contribution reflects interaction with a specific anchoring protein (Gbg perhaps) or merely an increase in hydrophobicity. It also enhances the affinity for Gbg and decreases the affinity for RGS proteins (4).

Ga-GTP regulates effectors that include enzymes that synthesize or degrade second messengers, **ion channels**, protein **kinases**, regulators of small G proteins, and transport proteins (Table 2). The list is growing constantly. Thus far, it appears that individual Ga subunits have relatively restricted ranges of effector targets. Thus, Ga_s stimulates **adenylyl cyclase** (5), but other targets have not been identified. G_t stimulates cyclic GMP phosphodiesterase (6). G_q family members all stimulate **phospholipase C**-b's (7), and there is one report of G_q stimulation of Bruton's **tyrosine kinase** (8). Ga_i is relatively unique in that it can inhibit two different effectors: several of the adenylyl cyclase **isoforms** (5) and, at least in some cases, some of the same K^+ channels that are stimulated by Gbg (9).

Table 2. G-Protein-Regulated Effectors[a]

Effector	a	bg	GAP
Adenylyl cyclase	s, i↓	↓	–
Cyclic GMP phosphodiesterase (PDE)	t		"co-GAP"
Phospholipase C	q		+
GIRK K^+ channel	i↓		
PI-3-kinase			
Ca^{2+} channel		↓	
Rho GEF	13(12)		+
Protein kinases	q?	↓	
Transporters	?	?	

[a] The arrows indicate whether the activity is increased or decreased by the G protein. Question marks indicate uncertainty of direct interactions. GAP activity of effectors has not been assayed in all cases. Cyclic GMP PDE is shown as a co-GAP because it potentiates the GAP activity of RGS9. The list of known G-protein-regulated effectors is constantly growing.

2. Gbg Subunits

Gbg is a stable heterodimer of a ~35kDa Gb subunit and a ~8kDa Gg subunit, which fold and associate shortly after translation. Nascent Gb will denature if g is not present, and, once formed, Gbg can only be dissociated under denaturing conditions. In the native dimer, Gb is a torus of seven pie-wedge domains known as a b-propeller, because each wedge is composed almost exclusively of **b-strands** . The sequence of Gb is a sevenfold repeat of the "WD40" motif. However, each blade of the propeller is not one individual WD repeat, but is composed of roughly half of each of two adjacent repeats. The ~8kDa Gg subunit is extended across the face of the b-propeller, and the Gg *N*-terminus binds the *N*-terminus of Gb in an extended coiled coil. Gbg binds to Ga along the face of the b-propeller opposite to Gg, with the central hole in the propeller aligned with the switch II region of Ga. The other substantial Ga–Gbg contact is between the *N*-terminal a-helix of Ga and the edge of Gb (10-12). Specificity in Gbg dimer formation is still poorly understood, and most Gbg dimers form readily. In mammals, Gb_{1-4} are strikingly **homologous** to each other, and Gb_5, the most divergent, is still identical in over 50% of its residues. Gg's are much more diverse.

Although Gbg subunits were initially considered to be nonspecific inhibitors of G-protein activation, it is now clear that they regulate as many or more effectors as do the Ga's (Table 2) and fulfill many other signaling functions as well (12). Gbg can either stimulate or inhibit different isoforms of adenylyl cyclase, activate PIP $_2$-specific phospholipase C-b, open K^+ channels and close Ca^{2+} channels, and either activate or inhibit both **tyrosine kinases** and **serine/threonine protein kinases** . New Gbg-mediated functions are being discovered regularly. Gbg regulates effectors when it is released from the Gabg trimer upon activation, reflecting the preferential binding of Gbg to the inactive, GDP-bound Ga. Full dissociation of Ga-GTP from Gb may actually be an extreme outcome of a conformational change that alters the Ga–Gbg interface to allow Gbg to regulate effectors while remaining in physical contact with Ga.

In addition to controlling effector proteins, Gbg exerts multiple regulatory effects directly on Ga's. First, Gbg is required for stable membrane attachment of Ga. Gbg binds tightly to bilayers, in part because of *C*-terminal prenylation of the g subunit (see text below). Sprang proposed a plausible orientation of Gabg with respect to the bilayer, so that both the prenylated *C*-terminus of Gg and the lipid-modified *N*-terminus of Ga can interact directly with lipids (10). Next, Gbg is essentially required for regulation of Ga by receptors, in part by anchoring and orienting Ga with respect to the membrane surface. Anchoring Ga at the membrane surface increases its local concentration at the receptor several thousandfold, increasing its apparent affinity for the receptor proportionately. Direct effects of Gbg on receptor–Ga interactions are also likely. Last, Gbg binds preferentially to Ga in its inactive, GDP-bound conformation, thereby slowing dissociation of GDP from Ga. Gbg is thus a GDI (GDP-dissociation inhibitor) for its Ga partner, suppressing the basal signal output when there is no stimulatory input from the receptor (see text below). Gbg generally decreases the rate of dissociation of GDP from Ga about 10-fold, and even greater effects may occur in cells. Through a combination of these mechanisms, Gbg can facilitate the appropriate activation of a Ga by receptor and suppress its basal activation, thereby decreasing the background signal while permitting a rapid and efficient response to agonist.

Gbg contributes to agonist-dependent desensitization of receptor signaling by recruiting members of a family of protein kinases that phosphorylate G-protein-coupled receptors to initiate their desensitization and down-regulation. G-protein-coupled receptor kinases (GRKs) selectively **phosphorylate** agonist-liganded receptors at one or more serine or threonine residues in the *C*-terminal region or in the third cytoplasmic loop. Phosphorylation recruits scaffolding proteins, known as *arrestins*, which both inhibit interactions with Ga and link receptors to nascent clathrin-coated pits to initiate their endocytosis (13, 14).

The selectivity of Gbg among receptors, Ga subunits, and effectors—and the structural basis thereof—remains unclear. It has not been possible to isolate abg trimers with a unique subunit composition except from specialized cells. One exception, Gb_1g_1, is found exclusively in photoreceptors and interacts well only with Ga_t, but such selectivity is unusual. *In vitro* studies have usually failed to observe marked selectivity of Gbg dimers in any context. The results of cellular studies have been mixed. Most notably, Kleuss et al. (15, 16) found that suppression of individual Gb or Gg molecules by microinjection of **antisense** messenger RNA leads to receptor-selective inhibition of Gbg signaling functions.

In addition to its controlled release from Ga, the availability and activity of Gbg is also controlled independently. Phosducin, a ubiquitously expressed protein that is unrelated to Ga, binds Gbg with high affinity and blocks its interactions with other proteins. Phosducin is thought to act as a Gbg chelator, and its ability to bind Gbg is regulated by protein kinase A-catalyzed phosphorylation (17). Phosphorylation of phosducin decreases its affinity for Gbg, thereby regulating Gbg in response to cellular cyclic AMP. Gbg is also known to bind both actin and **calmodulin**-Ca^{2+}, but it is unclear whether these interactions actually convey regulatory information to or from Gbg.

3. Regulatory GTPase Cycle

The regulatory GTPase cycle, proposed by Cassel and Selinger in 1977 (18, 19), provides the biochemical mechanism of G-protein signaling. Its kinetic parameters determine the rates of signal initiation and termination and the signal amplitude, both basal and agonist-stimulated (Fig. 1). Each step is tightly controlled. A G protein traverses the GTPase cycle relatively quickly with respect to the duration of the signal that it mediates, undergoing repeated activation, deactivation, and nucleotide exchange. The signal amplitude is therefore proportional to the fraction of time that the G protein spends in the GTP-bound, active state. The amplitude can be increased by accelerating GDP release and GTP binding or by inhibiting GTP hydrolysis. Similarly, the amplitude is decreased by inhibiting nucleotide exchange or by stimulating GTP hydrolysis. The rate of steady-state GTP hydrolysis and the fractional activation of the G protein at steady state are therefore independent: A G protein can cycle quickly or slowly, while maintaining either a high or low fractional regulatory activity.

Figure 1. The regulatory GTPase cycle. GTP-binding proteins are converted by binding GTP to the active state G*–GTP such that they can in turn bind and activate effector proteins. Activation is terminated by hydrolysis of bound GTP to GDP, usually a slow process that is accelerated by GTPase-activating proteins, GAPs. The inactive G–GDP complex is relatively stable unless nucleotide exchange is catalyzed by a receptor. The inactive, GDP-bound state is stabilized by Gbg subunits.

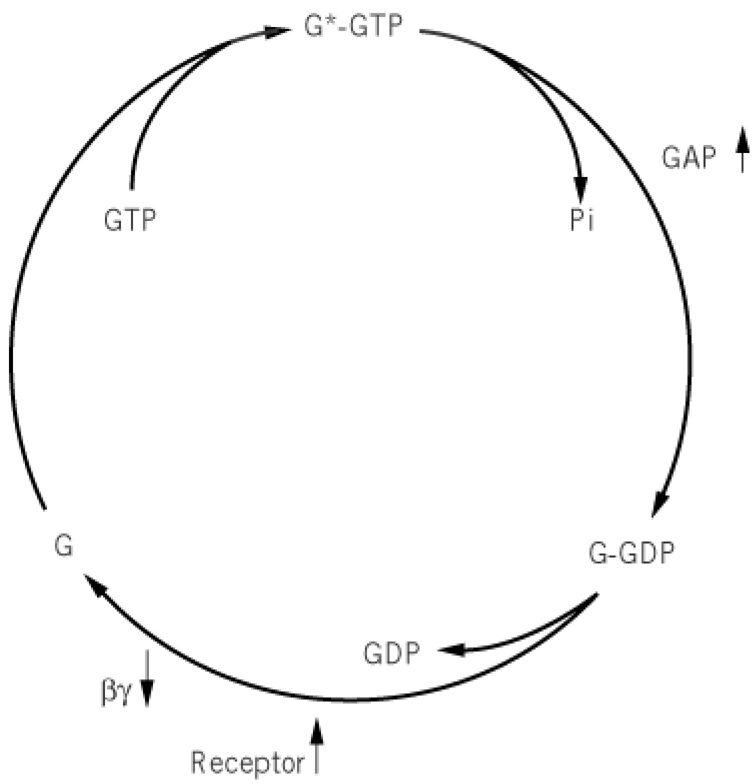

3.1. GDP–GTP Exchange

The release of bound GDP and the binding of GTP is a slow process in which the initial release of GDP is rate-limiting under physiological conditions. *In vitro*, dissociation of GDP can take minutes to hours, and a G protein retains a molecule of bound GDP after purification. Once the GDP has dissociated, GTP binding is fast under most experimental conditions. Association rate constants are estimated at 10^6 to $10^8 M^{-1} \cdot min^{-1}$, so the binding of GTP at a 50 μ *M* cytosolic concentration takes place in a second or less. Activation of the G protein subsequent to binding of GTP is also fast, although a GTP-bound but nonactivated Ga subunit can be prepared at low temperatures or in the absence of divalent cations. Unliganded G proteins can be prepared *in vitro*, although harsh conditions may be required to strip the GDP (20).

G-protein-coupled receptors initiate signaling by accelerating GDP/GTP exchange. Agonist-liganded receptor initially binds to G-GDP to form a transient low-affinity complex of receptor, G protein, and GDP, from which the GDP dissociates [(a) in equation 1]. In the absence of added guanine nucleotide, the resulting receptor–G-protein complex [(b) in equation 1] is itself relatively stable; this maintains the nucleotide binding site in an “open” conformation. In the presence of GTP, a second transient complex, receptor–G–GTP [(c) in equation 1] forms and activates the G protein. At this point, the receptor can dissociate (to leave free, activated G protein) and is itself free to catalyze further G-rotein activation. In cases where receptor-catalyzed GDP/GTP exchange occurs much more rapidly than G-protein deactivation, a single agonist-bound receptor can maintain the activation of multiple G-protein molecules and consequently generate considerable signal amplification. In specialized cells, such as photoreceptors, several thousandfold amplification can be achieved in this way (21).

$$\mathrm{R + G{\cdot}GDP} \rightleftharpoons \underset{(a)}{\mathrm{[R{\cdot}G{\cdot}GDP]}} \overset{\mathrm{GDP}}{\rightleftharpoons} \underset{(b)}{\mathrm{R{\cdot}G}} \overset{\mathrm{GTP}}{\rightleftharpoons} \underset{(c)}{\mathrm{[R{\cdot}G^{*}{\cdot}GTP]}} \rightleftharpoons \mathrm{R + G^{*}{\cdot}GTP}$$

Formally, receptor-catalyzed GDP/GTP exchange reflects the **negative cooperativity** of binding of receptors and guanine nucleotides to G proteins: Each decreases the G protein's affinity for the other, and the decreased affinity appears as an increased rate of dissociation (22). According to this mechanism, a receptor can accelerate the exchange of any guanine nucleotides, and it is the high cellular ratio of GTP to GDP that drives exchange in the physiological direction.

GDP/GTP exchange is also modulated by Gbg, which exerts two separate effects in the GTPase cycle. First, Gbg is a GDP-dissociation inhibitor (GDI) for Ga subunits. By stabilizing the binding of GDP to Ga, Gbg decreases the frequency of spontaneous GDP/GTP exchange and thus suppresses background noise in G-protein signaling pathways. Gbg can also inhibit receptor-stimulated GDP/GTP exchange and thereby inhibit G-protein signaling. Release of Gbg when one G protein is activated can inhibit the activation of another, with the extent of inhibition determined by the relative affinities of the two Ga's for Gbg. Second, and in seeming contrast to its inhibitory effects, Gbg is essentially required for the activation of G proteins by receptors. As discussed above, this effect reflects the membrane anchoring role of Gbg, but it may also have a direct regulatory component.

3.2. GTP Hydrolysis

Ga subunits catalyze hydrolysis of bound GTP by facilitating direct attack by water on the g phosphoryl group, and GTP hydrolysis is followed quickly by dissociation of inorganic orthophosphate (1). The intrinsic rates of hydrolysis of bound GTP vary markedly, however. For G_s, G_i, and G_o, GTP hydrolysis proceeds with a rate constant of 3 to $4 min^{-1}$, such that the active state has a half-life of 10 to 15 s. G_q is somewhat slower, with a half-life of 1 min. G_z is slowest, with a half-life of about 7 min. These rates are still much faster than those of the small, monomeric G proteins, evidently because the helical domain of heterotrimeric G proteins provides a catalytically important arginine residue that the small GTP binding proteins lacks.

If GTP hydrolysis is the primary deactivating event in G protein signaling, the rate of hydrolysis of bound GTP observed *in vitro* should be commensurate with the rate of signal termination upon removal of receptor agonist. This is true in some systems, such as adenylyl cyclase. In others, however, physiological termination of a signal is much faster than the rate at which G-protein-bound GTP is hydrolyzed by the appropriate G protein *in vitro* (23). This discrepancy was resolved by the discovery of GTPase-activating proteins, GAPs, which accelerate the hydrolysis of Ga-bound GTP up to several hundredfold (24).

The first GAP for a heterotrimeric G protein to be identified was also a G-protein-regulated effector, and two such effectors are now known to have GAP activity. Phospholipase C-b's both are regulated by G_q and act as a G_q GAP. PLC-b1 binds Ga_q-GTP with a K_d of ~2nM and increases its rate of hydrolysis more than 50-fold (24, 25). A G_{13}-regulated effector, a GEF for the monomeric G protein rho, is also a G_{13} GAP (26). The second group of G-protein GAPs comprises the RGS proteins. About 30 mammalian RGS proteins have been identified, and RGS proteins are found throughout the eukaryotes. They are GAPs for members of the G_i and G_q families, but with a specificity that is otherwise still poorly understood. RGS proteins have not been demonstrated to have effector activity, although definable functional domains of many RGS proteins outside the conserved GAP domain suggests that they may have other functions. The binding interface between RGS proteins and the switch II region of Ga subunits is similar in overall structure to that between GAPs for the small, monomeric GTP-binding proteins and their targets. However, GAPs for the small G proteins contribute the necessary arginine residue that is provided by the helical domain in Ga subunits (1).

The physiological functions of G-protein GAPs are still largely speculative. GAPs can obviously inhibit G proteins by decreasing the lifetime of the active state, and one role of inducible RGS proteins is attenuation of G-protein signals. The yeast RGS protein Sst2p, which is induced by the **mating** factor signaling pathway, is clearly a feedback inhibitor that is induced by mating factor and serves to turn off the mating response after its induction. GAPs are also clearly required for fast responses to the removal of agonists, and they contribute indirectly to the speed of the stimulatory phase of the GTPase cycle also (24, 27, 28). Such kinetic effects are more likely functions for the GAP activities of effector proteins.

4. Mechanism-Based Tools for G-Protein Research

Knowledge of the regulatory GTPase cycle has led to the development and use of highly specific tools for modulation of G-protein function in cells and *in vitro*. These tools include guanine-nucleotide analogs, bacterial toxins, and a wide array of mutations that can interrupt or alter specific reactions in the GTPase cycle.

4.1. Guanine Nucleotides

Nonmetabolizable analogs of GTP and GDP are used both as manipulators and as probes of G-protein signaling. Prototypes are GTPgS and Gpp(NH)p, GTP analogs that bind and activate G proteins but do not undergo chemical hydrolysis. Because they bind with relatively high affinity (particularly GTPgS), they lock G proteins in the active state. In cells and in membranes, they activate slowly in the absence of agonists, but more quickly in response to receptor-mediated nucleotide exchange. [^{35}S]GTPgS is also the standard radioligand used for quantifying G proteins. The Ga-[^{35}S]GTPgS complex is efficiently trapped on nitrocellulose filters, providing a convenient assay method. GDPgS, which mimics GDP and also binds tightly to Ga subunits, blocks activation and acts as a signaling antagonist. All three compounds are quite useful for intervention in G-protein pathways, but they have little, if any, selectivity among different G proteins, from the small monomeric G proteins through to the heterotrimeric G proteins. Greater specificity can be achieved by using a specific receptor agonist to accelerate nucleotide exchange, so that in a short time interval only the G-protein target of that receptor will bind the nucleotide. An alternative to nonhydrolyzable GTP analogs, a combination of Al^{3+} and F^-, activates heterotrimeric G proteins directly by binding as the AlF^-_4 ion to the Ga-GDP complex in place of the g-phosphoryl group of GTP. Al/F thus converts G-GDP to the active form. While activation by Gpp(NH)p or GTPgS requires nucleotide exchange, Al/F activates almost immediately. Moreover, Al/F is selective for heterotrimeric G proteins and does not bind to monomeric G proteins under normal conditions. **X-ray crystallographic** studies showed that GDP/Al/F $_4$ is not a true analog of GTP, but instead is an analog of the octagonal bipyramidal transition state that occurs during GTP hydrolysis (1). The reason that small monomeric G proteins do not bind Al/F is that they are such poor GTPases that they have low affinity for the transition state structure, although they can bind Al/F if a GAP is present to stabilize the transition state (29).

4.2. Toxins

Cholera toxin and pertussis toxin are widely used in G protein research because they are highly specific probes for G_s and for G_i or G_o, respectively. They **ADP-ribosylate** the a subunits of these G proteins with distinct chemistry, specificity, and effect, and they can be used both *in vitro* and in cells. Cholera toxin, after entering the cell through the endocytic pathway, catalyzes the ADP-ribosylation of an arginine residue at the GTP-binding site of Ga_s, thereby blocking the hydrolysis of bound GTP. G_s that has been ADP-ribosylated by cholera toxin is thus constitutively activated by cellular GTP. Cholera toxin is a specific activator of G_s signaling pathways because the cognate arginine residue in other Ga subunits is ADP-ribosylated much less efficiently. Pertussis toxin specifically ADP-ribosylates a conserved cysteine residue near the *C*-terminus of Ga_i, Ga_o, and Ga_t, thereby rendering the modified Ga insensitive to receptor. Thus, while the Ga retains its intrinsic regulatory and GTPase activities, it cannot be activated, and its function in cells is consequently blocked. Pertussis toxin is most useful for defining G_i-mediated pathways in cells, because the cysteine target residue is absent in the G_s, G_q, and G_{12} families. Pertussis-toxin treatment of cultured cells can also be used to create a functionally G_i-free background in which to study mutant G_i family members whose target cysteine residue has been replaced.

4.3. Mechanism-Based Mutants in G Proteins

Knowledge of the structure and genetics of the Ga family has yielded a group of reasonably reliable mutations that can be used to block GTP hydrolysis, to compromise GTP binding, or to block interaction with effectors or GEFs (1). Constitutively activating mutations that interfere with GTP hydrolysis are the oldest member of this class; the first is based on a naturally occurring, activating mutation of Gly12 in $p21^{ras}$ that makes it oncogenic. The corresponding mutation in Ga subunits also activates, but usually to a lesser extent. In Ga subunits, mutation of a conserved glutamine residue to leucine or of a conserved arginine (the cholera toxin modification site) to cysteine will produce constitutively active proteins that are expressed at normal levels and are otherwise unaltered. The leucine mutant is also insensitive to the GAP activity of RGS proteins (30). Apparent constitutive activation in cells can also be achieved by mutations that increase the rate of GDP/GTP exchange by destabilizing GDP binding (31). Strong dominant negative mutations in Ga subunits have been based on the mutation of Val17 in $p21^{ras}$. This mutation, which presumably acts by creating a nonactivating Ga that chelates receptors, has been less widely used.

Mutations can alter the specificity with which a Ga recognizes specific receptors or effectors. Experience with chimeric mutations that replace either the *N*- or *C*-terminal few amino acids of a Ga with those of another have permitted the construction of G proteins that can respond to receptors of interest and regulate effectors of interest in transfected cell lines. While the construction of these chimeras is not yet standard, the regions of interest for a specific interactions are reasonably well-defined, and enough mutants have been created to guide investigators in new cases.

5. G-Protein-Regulated Effectors

Heterotrimeric G proteins stimulate or inhibit a wide variety of effector proteins: enzymes that synthesize or degrade second messengers, protein kinases, ion channels, exchange factors for monomeric G proteins and, probably, a fairly large number of transporters (Table 2). As suggested by this list, the structures of effector proteins vary widely: They are either integral or peripheral membrane proteins that can be monomeric, homo-oligomeric, or hetero-oligomeric.

The mechanisms of effector regulation by G proteins also vary widely. Regulation can be stimulatory or inhibitory, additive, or synergistic, and both a and bg subunits independently regulate different spectra of effectors. Moreover, multiple isoforms of individual effectors often display differential sensitivity to regulation by Ga and/or Gbg subunits or by other signaling inputs. Individual isoforms are differentially expressed according to cell type, developmental stage, or acute regulatory signals. Such diversity allows a cell to respond to a single G-protein input with unique second messenger outputs, depending on the array of effector isoforms that it expresses. Last, an effector may also act as a GAP to regulate the GTPase activity of the Ga subunit by which it itself is regulated. A receptor can thus modulate the amplitude and speed of the inputs it receives.

5.1. Adenylyl Cyclase

Adenylate cyclase catalyzes the formation of cyclic AMP, the prototypical and ubiquitous second messenger. Eukaryotic adenylyl cyclase is itself the prototypical G-protein-regulated effector. Its stimulation by the concerted action of hormones and guanine nucleotides led to the discovery of G proteins (32, 33). At least 10 isoforms of adenylyl cyclase are found in vertebrates, all of which are stimulated by the activated form of Ga $_s$. Individual isoforms may be inhibited by the activated form of Ga$_i$, and they may be either stimulated or inhibited by (or insensitive to) Gbg. Cell-specific expression of these cyclase isoforms allows the construction of flexible signaling networks in which receptor-initiated signals to different G proteins can combine additively, synergistically, or negatively, to produce an integrated cyclic AMP signal. In addition to direct G-protein regulation, adenylyl cyclase isoforms can be further regulated by calmodulin, by Ca^{2+} itself, or by phosphorylation by several protein kinases (34). In yeast, adenylyl cyclase is regulated by a monomeric, ras-related G protein in response to nutritional signals (35).

Adenylyl cyclase in animals is a monomeric, integral membrane protein whose architecture is based on a pseudodimeric structure (36, 37). Each half of the adenylyl cyclase molecule is a cluster of six membrane-spanning a-helices, followed by a cytoplasmic domain. The active site and the site of all known regulatory interactions are contained within the pseudodimer of the two cytoplasmic domains, C1 and C2. Both Ga$_i$, Ga $_s$, and Gbg bind to C1:C2 dimers, expressed either separately or when fused. Determinants of sensitivity to G_s, G_i, and Gbg are found in distinct and nonoverlapping binding sites in the C1:C2 pseudodimer. The function of the membrane-spanning domain is unknown. Its apparent similarity to membrane transport proteins suggests that it may have an evolutionary history as a transporter. The possibility that an adenylyl cyclase from paramecium is an ion channel (38) is at least consistent with this idea. It is of evolutionary interest that adenylyl cyclase in yeast, which is stimulated by a ras-like monomeric G protein, is a large (~200kDa) soluble protein that is only vaguely related to animal cyclases in the catalytic domains (39).

5.2. Cyclic GMP Phosphodiesterase

A distinct cyclic GMP phosphodiesterase (PDE) is found in vertebrate photoreceptor cells (rods and clones), where it degrades cyclic GMP in response to light signals to cause the closure of cyclic GMP-gated cation channels (6). Retinal PDE is stimulated by the active form of G_t (transducin), which in turn is activated by the photobleached (meta II) form of rhodopsin, a receptor whose ligand is the covalently bound, light-sensing chromophore retinal. G $_t$-sensitive PDE is a heterotetramer of an ab catalytic dimer and two inhibitory g subunits, to which activated G $_t$ binds. In contrast to adenylyl cyclase, which is activated by the binding of Ga_s, the PDE is stimulated by the dissociation of the g subunits when they are sequestered by Ga_t-GTP. The rhodopsin-G $_t$-phosphodiesterase pathway is also unusual in that its components are expressed at extraordinarily high levels in photoreceptor membranes, where rhodopsin represents about 70% the total membrane protein and G $_t$ is about half of the remainder (40).

5.3. Phospholipase C-<b>b<b>

PIP_2-specific **phospholipase C**-b (PLC-b) isozymes are peripheral membrane proteins that are stimulated either by Ga_q family members, by Gbg, or by both, depending on the PLC-b isoform (7). They hydrolyze PIP_2 to the second messengers **diacylglycerol**, an activator of protein kinase C, and inositol-1,4,5-trisphosphate, which releases stored Ca^{2+} into the cytoplasm (see **Inositol triphosphates**). PLC-bs, approximately 150 kDa in size, are based on a core catalytic domain that is common to all PIP_2-selective PLCs. In addition, the PLC-bs also contain a long, *C*-terminal extension that binds Ga_q and mediates its stimulatory interaction (41). Gbg subunits bind at sites in the *N*-terminal half of the molecule. Differential stimulation of PLC-b activity by Ga or Gbg depends on the isoform. Both *in vitro* and *in vivo*, PLC-b-1 is primarily Ga_q-sensitive; PLC-b-2 and b-3 are also markedly stimulated by Gbg; regulation of PLC-b4 has not been described in detail, but it does respond to Ga_q. In cells, stimulation of Ga_i also can lead to PLC-b stimulation, but the response is mediated by Gbg. Sensitivity of PLC activation to pertussis toxin is therefore indicative of Gbg signaling. PLC-bs were the first G-protein-coupled effectors to be shown to have intrinsic GAP activity, which is specific for G_q, its activator (25). Such intrinsic GAP activity in an effector is presumably involved in rapid temporal control of signaling and in determination of receptor specificity, rather than in autoinhibition (24). The G $_q$ PLC-b pathway, while ubiquitous in animals, is particularly important for vision in mollusks and arthropods, where, in photoreceptor cells, rhodopsin regulates a G_q that in turn stimulates a PLC-b.

5.4. Inward Rectifier K^+ Channels

G-protein-gated, inward rectifier K^+ channels (GIRKs), which are found in heart, neurons, and other cells, cause a cellular hyperpolarization that is particularly important in the control of neurons, cardiac muscle, and smooth muscle. GIRKs are stimulated by Gbg subunits that in most cases are released by stimulation of Ga_i, so that GIRK activation is usually sensitive to pertussis toxin (12). A Ga_i-regulated K^+ channel is either a homotetramer or heterotetramer of members of the GIRK protomer family. Free Gbg binds directly to the GIRK channel, and addition of GDP-bound (inactive) Ga can inhibit GIRK stimulation by binding Gbg and blocking its action. It has been reported that activated Ga_i can inhibit GIRK-mediated currents, although it is not clear how this inhibition relates to the ability of nonactivated Ga_i to chelate bg and thus terminate its activating effect (9).

5.5. Other Ion Channels

Voltage-gated Ca^{2+} channels of the N and P/Q (dihydropyridine-insensitive) type are inhibited by Gbg. These are hetero-oligomeric channels that have a complex quaternary structure of integral and peripheral protein components. The location of the binding sites for Gbg are not known, but are presumed to lie in the b subunit, whose different isoforms determine the sensitivity to Gbg (42, 43). Some voltage-gated Na^+ channels are also stimulated by Gbg, perhaps by a direct binding mechanism (44).

5.6. Protein Kinases

Direct regulation of protein kinases by G proteins was first demonstrated in the yeast *Saccharomyces* *cerevisiae*, where Gbg (Ste4p, Ste18p) released from the Ga subunit (Gpa1p) in response to a pheromone receptor activates an ERK signaling cascade to control the mating response (45). An increasing number of protein kinases are now known to be regulated by G proteins in all eukaryotes, and these signaling pathways are under intense study.

At least three groups of protein kinases are regulated by G proteins, and their activation can lead to control of cell growth, cell differentiation, or acute physiological responses. First, Gbg both stimulates and inhibits different serine/threonine kinases in several MAP/ERK kinase cascades in animals and fungi, and probably in plants too. In the case of Raf1, Gbg probably stimulates the kinase activity directly, but other protein kinases may simply be recruited to their sites of action by Gbg. Second, the G-protein-coupled receptor kinases that initiate desensitization and endocytosis of G-protein-coupled receptors also bind directly to Gbg. Binding to Gbg localizes these kinases to the plasma membrane and facilitates the phosphorylation of receptors, although it is not known whether Gbg actively increases protein kinase catalytic activity (14). In animal cells, activation of G-protein pathways also leads to increased phosphorylation of protein tyrosine residues by a combination of indirect mechanisms and, probably, direct stimulation of the kinases. Both Ga_q and Gbg have been reported to stimulate the activity of Bruton tyrosine kinase (8, 46).

5.7. Phosphatidylinositide-3-kinase

Phosphatidylinositide-3-kinases (PI-3-Ks) catalyze the phosphorylation of PI-4,5-P_2 to PI-3,4,5-P_3, which activates at least one protein kinase and may trigger other cellular responses. PI-3-Ks are heterodimers of a catalytic subunit, which is a member of a conserved family of PI-3-K isozymes and one of a diverse group of regulatory subunits (47). The G-protein-regulated PI-3-K has unique regulatory and inhibitory subunits not closely related to other members of the family. It is stimulated directly by Gbg, and both subunits are required for regulation by Gbg.

5.8. Rho GEF

A guanine nucleotide exchange factor (GEF) for the Rho class of small monomeric G proteins is both stimulated by G_{13} and acts as a GAP for G_{12} and G_{13} (26, 48).

5.9. Transporters

Transporters of Na^+/H^+, glucose, Mg^{2+}, and Ca^{2+} have all been reported to be regulated, positively or negatively, by G-protein signaling pathways (49-52). In some cases, their behaviors are consistent with direct regulation by either Ga or Gbg subunits.

6. G-Protein-Coupled Receptors

G-protein-coupled receptors (GPCRs) bind G proteins at the inner face of the plasma membrane and, in response to extracellular agonists, catalyze the exchange of GDP for GTP. GPCRs make up a huge multigene family of proteins whose members are found throughout the eukaryotes. Genes for GPCRs in humans number about 1000, exclusive of the multiple odorant receptors expressed in olfactory epithelium, and account for over 1% of the total genome. Appropriately, GPCRs respond to a diverse range of agonists: biogenic amines, lipids, peptides, chemically diverse pheromones, nucleotides and nucleosides, protein hormones, Ca^{2+}, odorants and tastants, photons (with the help of an attached 11-*cis*-retinal chromophore), and proteinases (by exposure of endogenous agonist peptides) (53, 54).

The GPCRs share a common overall structure and mechanism of action. They are based on a common core structure, a bundle of seven hydrophobic, bilayer-spanning helices in the plasma membrane. The *N*-terminus, usually glycosylated, is extracellular, and the *C*-terminus is cytoplasmic. Both are of variable length. Interhelix loops are short, with the exception of the third cytoplasmic loop, which links a-helices 5 and 6: It can contain up to about 200 amino acid residues. Thus, while the membrane-spanning domain of GPCRs has a minimal size of less than 30 kDa, receptors range in total size to more than 100 kDa. The high-resolution protein structure of a GPCR is not yet known, but a low-resolution structure is available for visual rhodopsin (55). This structure orients the a-helices with respect to each other; and it distinguishes their packing from that of bacteriorhodopsin, an unrelated seven-helix **proton pump**. The rhodopsin structure has been combined with biochemical data, comparison of similar receptors, and the results of numerous mutagenesis experiments, to produce a useful model of a receptor's hydrophobic core (56).

The amino acid sequences of GPCRs in animals are most highly conserved in the membrane-spanning helices and short loops. Several signature sequences are identifiable in these regions, and receptors closely related by sequence usually bind similar extracellular ligands (54). Animal GPCRs include three subfamilies. The major subfamily accounts for receptors for most ligands, including those for most small molecules, proteins, and many peptides. The other two families are the receptors for glutamate and for a group of peptide hormones. Enough GPCR sequences are now available that it is frequently possible to predict the ligand specificity of a receptor from just its sequence. GPCRs in fungi and slime molds are also based on a bundle of seven membrane-spanning a-helices, but any homology of these receptors to animal receptors or to each other is not obvious. Their evolutionary origins are uncertain. Higher plants probably also use seven-span receptors to regulate heterotrimeric G proteins, but identification of candidate proteins as legitimate GPCRs is not yet certain.

The GPCR family is extraordinarily important to drug design: About 30% of prescription drugs act on GPCRs. Both because of this impetus and because of basic interest in their function and biology, extraordinary efforts have gone toward detailed analysis of these receptors and their ligand-binding sites. Ligand-binding sites have been mapped chemically, by mutagenesis and by the study of responses to structurally defined ligands. Experimental approaches have been complemented by intense molecular modeling. Two general structures have emerged. In receptors for small ligands such as biogenic amines, the ligand-binding site is a relatively deep cleft on the extracellular face of the bundle of membrane-spanning helices. Ligands make contact with residues from multiple helices, and it is thought that these contacts initiate the levering of the helices that constitutes receptor activation. Receptors for other ligands, notably the ab dimeric glycoprotein hormones, have extensive *N*-terminal domains that themselves have ligand-binding activity. These *N*-terminal ligand-binding domains may position the ligand near the external face of the helices to promote helix–helix levering.

In contrast to the external ligand-binding site, the cytoplasmic site on GPCRs that binds and regulates G proteins has been harder to identify. Mutagenesis experiments—mostly the creation of chimeric receptors that use segments of one receptor to alter the G protein specificity of another—suggest that the second and third intracellular loops are the primary components of the G-protein-binding site. Other mutations in the third loop can create constitutively active receptors. In those cases where the third intracellular loop is large, regions near spans 5 and 6 are more important for G-protein regulation, and the central segment fulfills other functions. It has not been possible to identify sequence motifs that determine specificity among G proteins, even when the general regions important for selectivity have been established. This divergence of sequence in receptors that bind the same G protein suggests that receptor subfamilies acquired specificity for extracellular ligands prior to the evolution of the multiple G-protein families.

The process of GPCR activation by ligand is best understood as a conformational equilibrium: An unliganded receptor is usually in an inactive conformation, but the binding of agonist favors the activated state. Partial agonists promote activation incompletely. In any case, the active receptor can catalyze nucleotide exchange on the correct Ga subunit. In constitutively active mutant receptors, an unliganded receptor can catalyze nucleotide exchange. As predicted, these mutants generally bind agonist ligands more tightly than do the wild-type receptor, indicating that they are constitutively in the agonist-favored conformation. The coupling of receptors and G proteins leads to a stereotyped effect of guanine nucleotides on the affinity of agonist binding. As discussed above, binding of an active (agonist-liganded) receptor to G protein drives dissociation of guanine nucleotide to form an agonist–receptor–G-protein complex that can be dissociated by the addition of GTP (or GDP) (equation 1). The receptor–G-protein complex displays higher affinity for agonist than does free receptor. Because addition of guanine nucleotide to membranes drives dissociation of this complex, to leave free receptor and nucleotide-bound G protein, nucleotides are often observed to decrease the affinity of receptors to agonist—but not antagonis—ligands. The nucleotide-driven decrease in agonist affinity has become a useful test for whether a receptor of unknown mechanism interacts with a G protein (22).

Cells regulate their level of response to G-protein stimulation in large part by modulating the expression and activity of the appropriate GPCRs. GPCRs undergo acute desensitization upon stimulation as a result of phosphorylation of serine and threonine residues on their cytoplasmic faces, usually in the third cytoplasmic loop or in the *C*-terminal region. Phosphorylation is catalyzed both by second messenger-activated protein kinases and by a group of GPCR kinases (GRKs). GRKs preferentially phosphorylate receptors in their agonist-bound forms. Phosphorylation limits receptor interaction with G proteins to varying extents. More importantly, phosphorylation helps recruit inhibitory proteins, known as arrestins, which both further inhibit receptor activity and promote receptor-endocytosis and consequent degradation by linking receptors to clathrin, the major coat protein of coated pits (13, 14).

Bibliography

1. S. R. Sprang (1997) Annu. Rev. Biochem. **66**, 639–678.
2. D. W. Markby, R. Onrust, and H. R. Bourne (1993) Science **262**, 1895–1901.
3. E. M. Ross (1995) Curr. Biol. **5**, 107–109.
4. Y. Tu, J. Wang, and E. M. Ross (1997) Science **278**, 1132–1135.
5. R. K. Sunahara, C. W. Dessauer, and A. G. Gilman (1996) Annu. Rev. Pharmacol. Toxicol. **36**, 461–480.
6. L. Stryer (1986) Annu. Rev. Neurosci. **9**, 87–119.
7. W. D. Singer, H. A. Brown, and P. C. Sternweis (1997) Annu. Rev. Biochem. **66**, 475–509.
8. K. Bence, W. Ma, T. Kozasa, and X.-Y. Huang (1997) Nature **389**, 296–299.
9. W. Schreibmayer, C. W. Dessauer, D. Vorobiov, A. G. Gilman, H. A. Lester, N. Davidson, and N. Dascal (1996) Nature **380**, 624–627.
10. M. A. Wall, D. E. Coleman, E. Lee, J. A. Iñiguez-Lluhi, B. A. Posner, A. G. Gilman, and S. R. Sprang (1995) Cell **83**, 1047–1058.
11. D. G. Lambright, J. Sondek, A. Bohm, N. P. Skiba, H. E. Hamm, and P. B. Sigler (1996) Nature **379**, 311–319.
12. D. E. Clapham and E. J. Neer (1997) Annu. Rev. Pharmacol. Toxicol. **37**, 167–203.
13. O. B. Goodman Jr., J. G. Krupnick, F. Santini, V. V. Gurevich, R. B. Penn, A. W. Gagnon, J. H. Keen, and J. L. Benovic (1996) Nature **383**, 447–450.
14. J. G. Krupnick and J. L. Benovic (1998) Annu. Rev. Pharmacol. Toxicol. **38**, 289–319.
15. C. Kleuss, J. Hescheler, C. Ewel, W. Rosenthal, G. Schultz, and B. Wittig (1991) Nature **353**, 43–48.
16. C. Kleuss, H. Scherübl, J. Hescheler, G. Schultz, and B. Wittig (1993) Science **259**, 832–834.
17. P. H. Bauer, S. Müller, M. Puzicha, S. Pippig, B. Obermaier, E. J. M. Helmreich, and M. J. Lohse (1992) Nature **358**, 73–76.
18. D. Cassel and Z. Selinger (1976) Biochim. Biophys. Acta **452**, 538–551.
19. D. Cassel, H. Levkovitz, and Z. Selinger (1977) J. Cyclic Nucleotide Res. **3**, 393–406.
20. K. M. Ferguson and T. Higashijima (1991) Methods Enzymol. **195**, 188–192.
21. P. A. Liebman, K. R. Parker, and E. A. Dratz (1987) Annu. Rev. Physiol. **49**, 765–791.
22. E. M. Ross (1992) In *An Introduction to Molecular Neurobiology* (Z. W. Hall, ed.), Sinauer Associates, Sunderland, Mass., pp. 181–206.
23. G. E. Breitwieser and G. Szabo (1988) J. Gen. Physiol. **91**, 469–493.

24. E. M. Ross (1995) Rec. Prog. Hormone Res. **50**, 207–221 [Abstract].
25. G. Berstein, J. L. Blank, D.-Y. Jhon, J. H. Exton, S. G. Rhee, and E. M. Ross (1992) Cell **70**, 411–418.
26. T. Kozasa, X. Jiang, M. J. Hart, P. M. Sternweis, W. D. Singer, A. G. Gilman, G. Bollag, and P. C. Sternweis (1998) Science **280**, 2109–2111.
27. G. H. Biddlecome, G. Berstein, and E. M. Ross (1996) J. Biol. Chem. **271**, 7999–8007.
28. N. Zerangue and L. Y. Jan (1998) Curr. Biol. **8**, 313–316.
29. R. Mittal, M. R. Ahmadian, R. S. Goody, and A. Wittinghofer (1996) Science **273**, 115–117.
30. D. M. Berman, T. M. Wilkie, and A. G. Gilman (1996) Cell **86**, 445–452.
31. T. Iiri, P. Herzmark, J. M. Nakamoto, C. Van Dop, and H. R. Bourne (1994) Nature **371**, 164–168.
32. E. M. Ross and A. G. Gilman (1977) J. Biol. Chem. **252**, 6966–6969.
33. E. M. Ross and A. G. Gilman (1980) Annu. Rev. Biochem. **49**, 533–564.
34. R. Taussig, W.-J. Tang, J. R. Hepler, and A. G. Gilman (1994) J. Biol. Chem. **269**, 6093–6100.
35. T. Toda, I. Uno, T. Ishikawa, S. Powers, T. Kataoka, D. Brock, S. Cameron, J. Broach, K. Matsumoto, and M. Wigler (1985) Cell **40**, 27–36.
36. J. J. G. Tesmer, R. K. Sunahara, A. G. Gilman, and S. R. Sprang (1997) Science **278**, 1907–1916.
37. J. Krupinski, F. Coussen, H. A. Bakalyar, W.-J. Tang, P. G. Feinstein, K. Orth, C. Slaughter, R. R. Reed, and A. G. Gilman (1989) Science **244**, 1558–1564.
38. J. E. Schultz, S. Klumpp, R. Benz, W. J. Schurhoff-Goeters, and A. Schmid (1992) Science **255**, 600–603.
39. S. Marcus, M. Wigler, H. P. Xu, R. Ballester, M. Kawamukai, and A. Polverino (1993) Ciba Found. Symp. **176**, 53–61.
40. H. E. Hamm and M. D. Bownds (1986) Biochemistry **25**, 4512–4523.
41. S. G. Rhee and K. D. Choi (1992) In *Advances in Second Messenger and Phosphoprotein Research* (J. W. Putney, Jr. ed.), Raven Press, New York, pp. 35–61.
42. S. Herlitze, D. E. Garcia, K. Mackie, B. Hille, T. Scheuer, and W. A. Catterall (1996) Nature **380**, 258–262.
43. S. R. Ikeda (1996) Nature **380**, 255–258.
44. J. Y. Ma, W. A. Catterall, and T. Scheuer (1997) Neuron **19**, 443–452.
45. J. Kurjan (1992) Annu. Rev. Biochem. **61**, 1097–1129.
46. S. Tsukada, M. I. Simon, O. N. Witte, and A. Katz (1994) Proc. Natl. Acad. Sci. USA **91**, 11256–11260.
47. L. R. Stephens, A. Eguinoa, H. Erdjument-Bromage, M. Lui, F. Cooke, J. Coadwell, A. S. Smrcka, M. Thelen, K. Cadwallader, P. Tempst, and P. T. Hawkins (1997) Cell **89**, 105–114.
48. M. J. Hart, X. Jiang, T. Kozasa, W. Roscoe, W. D. Singer, A. G. Gilman, P. C. Sternweis, and G. Bollag (1998) Science **280**, 2112–2114.
49. M. E. Maguire and J. J. Erdos (1980) J. Biol. Chem. **255**, 1030–1035.
50. R. Hooley, C.-Y. Yu, M. Symons, and D. L. Barber (1996) J. Biol. Chem. **271**, 6152–6158.
51. R. A. Hall, R. T. Premont, C.-W. Chow, J. T. Blitzer, J. A. Pitcher, A. Claing, R. H. Stoffel, L. S. Barak, S. Shenolikar, E. J. Weinman, S. Grinstein, and R. J. Lefkowitz (1998) Nature **392**, 626–630.
52. M. Kuroda, R. C. Honnor, S. W. Cushman, C. Londos, and I. A. Simpson (1987) J. Biol. Chem. **262**, 245–253.
53. S. Watson and S. Arkinstall (1994) *The G-Protein Linked Receptor Facts Book*, Academic Press, San Diego.
54. C. D. Strader, T. M. Fong, M. R. Tota, D. Underwood, and R. A. F. Dixon (1994) Annu. Rev.

Biochem. **63**, 101–132.
55. V. M. Unger and G. F. X. Schertler (1995) Biophys. J. **68**, 1776–1786.
56. J. M. Baldwin, G. F. X. Schertler, and V. M. Unger (1997) J. Mol. Biol. **272**, 144–164.
57. C. I. Bargmann and J. M. Kaplan (1998) Annu. Rev. Neurosci. **21**, 279–308.

Suggestions for Further Reading

58. D. E. Clapham and E. J. Neer (1997) G protein subunits. Annu. Rev. Pharmacol. Toxicol. **37**, 167–203.
59. H. G. Dohlman, J. Thorner, M. G. Caron, and R. J. Lefkowitz (1991) Model systems for the study of seven-transmembrane-segment receptors. Annu. Rev. Biochem. **60**, 653–688.
60. A. G. Gilman (1987) G proteins: Transducers of receptor-generated signals. Annu. Rev. Biochem. **56**, 615–649.
61. T. Gudermann, F. Kalkbrenner, and G. Schultz (1996) Diversity and selectivity of receptor–G protein interaction. Annu. Rev. Pharmacol. Toxicol. **36**, 429–459.
62. Y. Kaziro, H. Itoh, T. Kozasa, M. Nakafuku, and T. Satoh (1991) Structure and function of signal-transducing GTP-binding proteins. Annu. Rev. Biochem. **60**, 349–400.
63. J. G. Krupnick and J. L. Benovic (1998) The role of receptor kinases and arrestins in G protein-coupled receptor regulation. Annu. Rev. Pharmacol. Toxicol. **38**, 289–319.
64. E. M. Ross (1989) Signal sorting and amplification through G protein-coupled receptors. Neuron **3**, 141–152.
65. S. R. Sprang (1997) G protein mechanisms: insights from structural analysis. Annu. Rev. Biochem. **66**, 639–678.

Hfr'S And F-Primes

1. Bacterial Sex

Immediately after its discovery by Lederberg and Tatum in 1946 (1), bacterial mating was found to be unorthodox. Conventional sex mixes the entire **genomes** of both parents. But fertile strains of *Escherichia coli* K-12 donated only parts of their chromosomes during mating, transferring them into the other partner, the recipient, to recombine with its genome. The genetic determinant of this donor ability was also unusual: It was able to transfer itself rapidly from cell to cell as an autonomous unit without any associated chromosomal genes. This determinant was named the F (or sex) factor, later shown to be a **plasmid**, and the recombination process it enabled proved to be the key to our understanding of the genetic and physical organization of the bacterial chromosome (see F Plasmid).

2. Hfr's

Cultures of F^+ strains were able to transfer the F factor itself at high frequency to F^- recipients, thereby converting them to F^+ donors, but chromosomal markers were transferred much less efficiently, generating recombinant progeny at frequencies of about one per million parental cells. By chance, certain isolates from an F^+ culture were found with the opposite character: They had virtually lost the ability to transfer donor ability but now generated recombinants at greatly elevated frequencies. They were consequently called Hfr (high-frequency recombination) strains (Fig. 1**a**).

Figure 1. Bacterial genetics by Hfr's and F-primes. (**a**) Genetic donor types. Left to right: An F^+ cell containing the autonomous F plasmid; an Hfr, in which F has integrated into the chromosome; a primary F′ strain, in which F has excised with a portion of chromosome; a secondary F′ strain, diploid for the chromosomal portion carried by the F′ as a result of transfer to a wild-type recipient (ie, merodiploid). The arrow indicates the origin (*oriT*) and orientation of F transfer. (**b**) Mapping by interrupted mating. Following donor-recipient contact, the Hfr chromosome breaks at *oriT* (open arrow) to initiate transfer of a single donor strand into the recipient; concomitant replication in the donor restores its chromosome (not shown). The entering strand recombines with the resident chromosome, replacing the mutant alleles (*leu*, *his*, *arg*) with wild-type counterparts, and recombinants are selected by plating on medium with streptomycin (to stop growth of donors) and without one of the amino acids (to stop growth of nonrecombinant recipients). The recombination frequency declines as distance from *oriT* increases, owing to random breakage, and recombinant formation after sampling is prevented by forced breakage, allowing measurement of distances between *oriT* and the gene. For a given Hfr, the map can be read directly from the time-of-entry data. The combined results from several matings (F^-×Hfr1, Hfr2, Hfr3) showed that the *E. coli* chromosome is genetically circular.

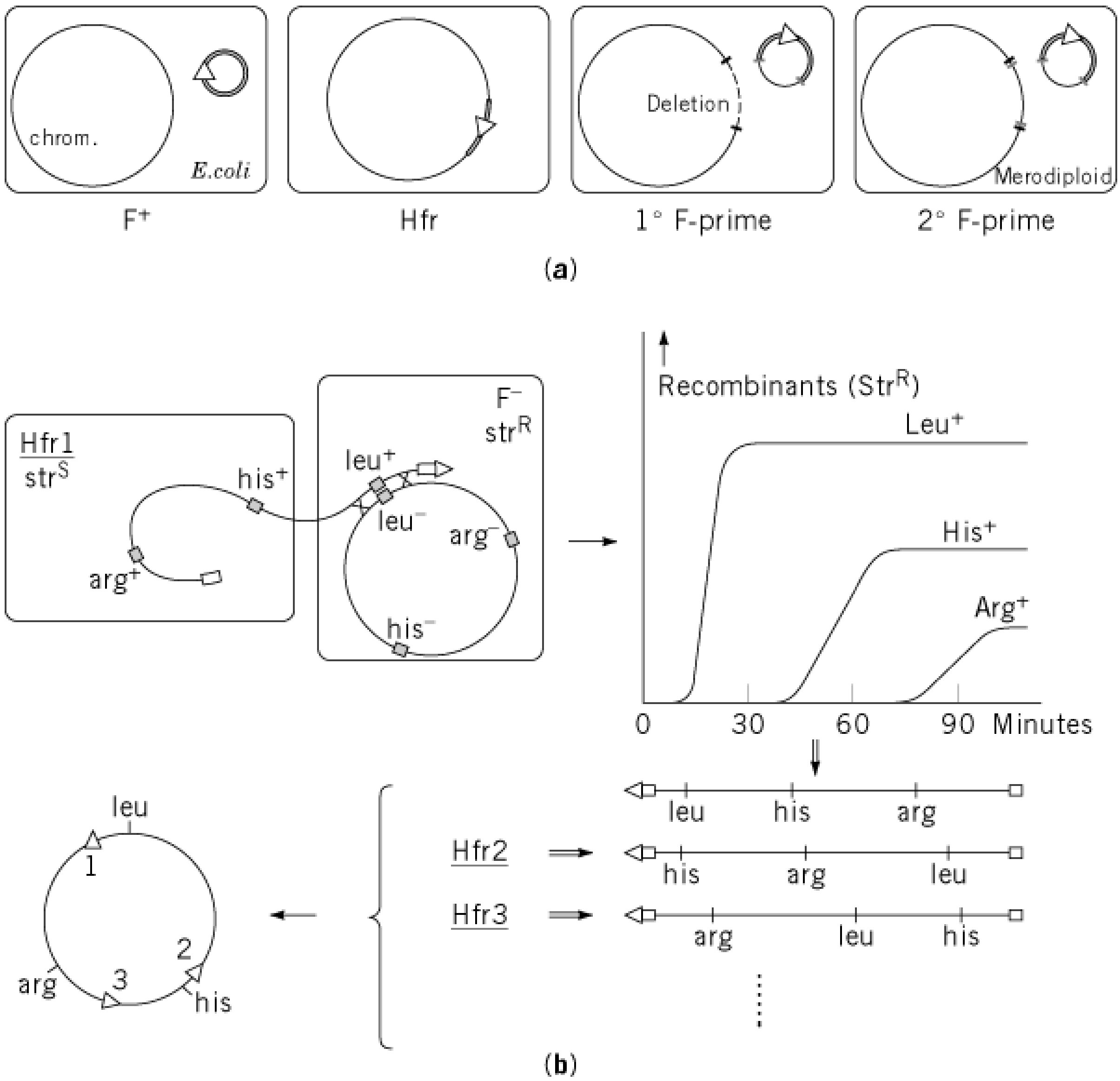

3. F-Primes

Although Hfr strains were generally stable, F^+ “revertant” derivatives identical to the original strain were readily isolated. Some of these derivatives showed an intermediate **phenotype**: They transferred not only the F^+ character at high frequency, but a small set of chromosomal markers as well, so that the normally haploid recipient became merodiploid, that is, **diploid** for only a part of its genome. Such derivatives were termed F-primes (F′; Fig 1**a**).

The physical basis of these early observations is now understood, even if some aspects of the transfer mechanism itself continue to present challenges (see **Conjugation**). The molecular basis of Hfr and plasmid-prime formation was worked out almost entirely using the F plasmid in *E. coli* K12, and we therefore focus our discussion mostly on F. Host gene mobilization involving other plasmids in other bacterial genera conform, in general, to the F pattern. Nevertheless, Hfr's and primes derived from other plasmids justify inclusion in this chapter on the grounds of their utility, and we briefly describe methods for isolating them.

4. The Nature of Hfr Transfer

Wollman and Jacob (2) exploited the one-way transfer of DNA by developing the interrupted mating experiment to map genes (Fig. 1 **b**); in doing so, they revealed the nature of Hfr transfer. Mating is started by mixing cultures of Hfr and F^- strains. Samples of the mixture are taken at intervals and mating pairs ruptured by violent shaking; portions are then plated on agar to select for growth of recombinants. Each Hfr strain introduced its markers into the F^- recipient in a precise order and at a fixed time. Recombination frequencies were greatest for markers transferred early ($\sim10^{-1}$) and declined progressively for later entering markers (to $\sim10^{-5}$); this presumably reflects the sensitivity of conjugal pairs to spontaneous breakage. The results established the linkage relationships of various markers as a simple function of time of entry into the recipient. Moreover, collation of the results from matings with several Hfr strains indicated that the *E. coli* genome consists of a single, circular linkage group (Fig. 1**b**) (3). This striking genetic result has been corroborated by various biophysical means and confirmed by DNA sequencing of the entire genome (4).

Hfr donors transferred donor ability at only very low frequencies and in association with late-entering markers. This observation, together with the time of entry results, suggested that Hfr strains arose by a single recombinational crossover between a circular F plasmid and a circular chromosome, such that the F was integrated into the chromosome (Fig. 1**a**) (5, 6). During mating, the F is broken to provide the leading end, or origin of transfer (*oriT*), which passes into the recipient, while the genes that encode the mating functions are left at the other end, which is therefore the last, and least likely, to enter (Fig. 1**b**). The order of entry for a given Hfr is determined simply by the site and orientation of F integration into the chromosome. The donor ability of F^+ cultures is then explained by the formation of many different Hfr's, each with F integrated at a distinct site, so that the F^+ population as a whole transfers all markers at about the same rate.

The recombination process is completed in the recipient, where a portion of the linear DNA transferred can be substituted for the equivalent segment of the recipient's circular chromosome by homologous recombination; if different alleles are present in the recombining region, the result is formation of a genetic recombinant.

5. Genesis of Hfr Strains

As more Hfr's were isolated and their points of origin determined, it became clear that certain sectors of the chromosome were favored for insertion of F (7). Moreover, the ability of F^+ strains to generate recombinants was severely reduced in *recA* mutants (8), implying a need for homologous recombination in Hfr formation. The reasons became evident later, when **electron microscopic** analysis of heteroduplexes formed between F and other extrachromosomal DNAs showed that F carries four known transposable elements: Tn*1000*, IS*2*, and two IS*3*s (9). About 13 IS*2*s and 6 IS*3*s are scattered throughout the *E. coli* chromosome, and their locations correspond with the origins of transfer of most Hfr's (10). Thus, homologous recombination via a single crossover between F and the chromosome is the dominant mode of Hfr formation by F (Fig. 2). Nevertheless, other mechanisms exist, as suggested by the isolation of Hfr's in which the F is flanked by copies of Tn*1000*, implying integration by replicative transposition (11).

Figure 2. Hfr and F′ formation. Homologous recombination between a transposable element on F and one on the chromosome, situated between two genes, **a** and **b**, integrates F, while the same process involving a different pair of elements excises it to form an F-prime. Transposition into targets on either the chromosome or the same plasmid creates other varieties of F-prime (not shown; see Ref. 9). Notice how these simple recombination events have changed the relationship of **a** and **b**; the Type I event has placed them on different molecules, while the Type II has reversed their order. This genome has evolved.

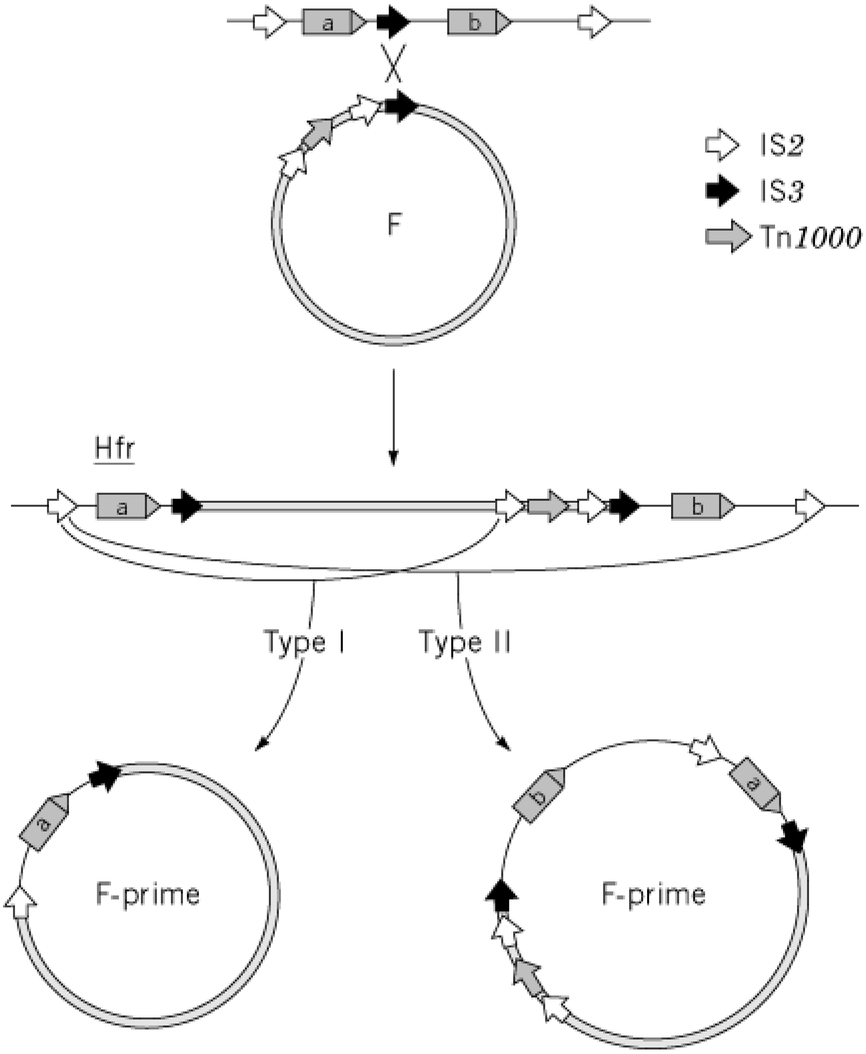

It is not only in their role as portable regions of homology that the transposable elements of F promote recombination in *E. coli*. At some point in the evolution of F, one of the IS*3*s transposed into the *finO* regulator gene (12), resulting in constitutive overexpression of the transfer system and the high transfer frequencies that enabled Lederberg and Tatum to find recombinants. F and *E. coli* K-12 thus owe their preeminence in the development of molecular genetics to these transposition events.

6. Genesis of F-Primes

Adelberg and Burns (13) observed that one Hfr “revertant”, which now transferred maleness at high efficiency, had undergone alterations in both its F plasmid and its chromosome, such that each now recombined with the other at very high frequency, as if they retained "memories" of each other. The molecular basis of the memory was in fact an exchange of segments upon excision of F (14, 15).

The various forms that these exchanges take are shown in Figure 2. Once again, the patches of sequence homology provided by the transposable elements play a major role (9). Recombination between two transposable elements, one in F and one in the chromosome, excises a plasmid that now carries one chromosomal flank but has left a dispensable part of itself in the chromosome (16). Plasmids formed in this way are termed Type I F-primes. Alternatively, recombination between chromosomal sequences on both sides of the F integration site creates an undeleted F-prime, termed Type II. Any chromosomal repeated sequence is sufficient: Type II F-primes that arose by recombination between IS5 elements (17) or between **ribosomal** RNA genes (18) have been found. Type I F-primes may also arise by transposition of Tn*1000* into a chromosomal target, with associated deletion of F sequences on the other side of the transposon. Type II RP4-primes might also be formed this way: An RP4::mini-Mu plasmid integrated by transposition can be excised by replicative transposition of one of the bordering mini-Mu elements into chromosomal DNA (19). An unusual event, in which F *oriT* had apparently undergone recombination with certain chromosomal loci, generated Type I F-primes lacking the *tra* operon (20).

F-prime formation has been likened to *in vivo* cloning. There is in principle no limit to the amount of chromosomal DNA that an F-prime can carry, and F-primes carrying up to 30% of the chromosome have been found. In practice however, large F-primes tend to be unstable or growth inhibitory.

Spontaneous rearrangements may be capable of generating a great variety of F-primes from a given Hfr. After excision of the initial F-prime, intramolecular transposition may delete or invert parts of the chromosomal sequence, or the F-prime may reintegrate elsewhere in the chromosome, effectively transposing its chromosomal DNA, only to re-excise as a different F-prime with a new juxtaposition of chromosomal sequences (21, 22). The potential consequences for evolution of the host genome alone are obvious (23), even without considering the possibilities raised by transfer to other species (24-26).

7. Utility of Hfr's and F-Primes

The major use of Hfr's has been the long-range mapping of genetic markers, and circular maps of several **gram-negative** bacteria have been established. How long their utility in this regard will continue is not certain, given the increasing rate at which entire microbial genomes are being sequenced. Hfr mating is still, however, an efficient way to assign new mutations to approximate locations on the chromosome, and it may often be the most convenient way of constructing genetically marked strains.

Whereas Hfr's find their main use in mapping, F-primes have been most important in analysis of function. Transfer of the appropriate F-prime to mutant strains allows tests of complementation and **dominance** at roughly equivalent copy numbers, as illustrated by the central role played by *F′lac* plasmids in deducing the basis of regulated expression of the ***lac*** operon (27). F-primes have also been particularly useful in studies of the biology of plasmids themselves, as surrogates for parent plasmids that confer no readily observable phenotype. Plasmid-primes mobilized by the promiscuous conjugation system of RP4 are used for mutagenesis of many species, as vehicles for delivering transposons or mutant genes for allele replacement (28).

8. Isolating Hfr's

The relatively frequent formation of *E. coli* Hfr strains by F integration is not usually mimicked by other plasmid-host pairs. Therefore various selective methods for isolating strains with integrated plasmids have been developed.

8.1. Treatment with Mutagens

Nitrosoguanidine treatment enabled isolation of Hfr-ColV strains of *E. coli* (29) and Hfr-FP2 strains of *Pseudomonas aeruginosa* (30). Ultraviolet irradiation stimulates Hfr formation by F in *E. coli*. Why these treatments promote Hfr formation is unknown; stimulation of recombination by **DNA damage** might play a part.

8.2. Selection for a Plasmid-Borne Marker Under Conditions in Which the Plasmid Cannot Replicate
Treatment of an *Erwinia* strain carrying F′*lac* with **acridine** orange, which specifically inhibits F replication, led to isolation of an Hfr strain (31). Growth at high temperatures of cells carrying temperature-sensitive (*ts*) IncP plasmids allowed isolation of Hfr's in *P. aeruginosa* (32) and *Rhodobacter capsulatus* (33). Exploiting restricted host range has served the same purpose; Hfr's have been selected after transfer of a hybrid plasmid, containing the ColE1 replicon linked to the RP4 *tra* region, into species of *Rhodobacter* (34) and *Methylobacillus* (35), in which ColE1 cannot replicate. Tn*10*-mediated transposition of the *E. coli* chromosome into a *ts* vector carrying the *tra* region generated Hfr's of any predetermined origin and orientation (36).

8.3. Rescue of Replication-Defective Chromosomes by Plasmid Replicons
Strains of *E. coli* and *Salmonella typhimurium* with *dnaA*ts mutations are unable to grow at 42°C because initiation of chromosome replication is blocked. Temperature resistance results from the integration of plasmids able to assume control of chromosome replication, and this can be used to select Hfr strains. Several R and Col plasmids, as well as F, have given rise to Hfr's in this way (see Ref. 37 for review).

8.4. Incorporation of a Transposon into the Conjugative Plasmid
This approach, which recalls the formation of Hfr's by Tn *1000* transposition, is more generally applicable. Two plasmids in particular have been used to transfer chromosomal DNA in a wide variety of gram-negative bacteria. RP4 carrying either the prophage Mu transposon or its mini-Mu derivative is integrated into the chromosome by replicative transposition, such that the inserted RP4 is flanked on each side by a copy of the Mu element (19). R68.45 carries a tandem duplication of IS21: Cutting between the IS21 elements and pasting into a chromosomal target site integrates the conjugative plasmid, once again flanked by copies of the transposon (38).

8.5. Conjugational Transposons
Conjugation determinants are inserted into a transposon, and strains are selected that carry the transposon at various sites in the chromosome. Each derivative is an Hfr. Yakobsen and Guiney (39) created bipartite Hfr derivatives of *R. meliloti*: Tn5 carrying *oriT* of RP4 was transposed into the chromosome, and RP4 transfer functions were provided by a plasmid, permitting oriented transfer of chromosomal DNA. This approach essentially recapitulates the mobilization of nonconjugative plasmids, such as ColE1, by self-transmissible ones, such as F. Alternative systems in which all the transfer functions are inserted into the transposon have also been constructed (40).

8.6. Transposons as Regions of Portable Homology
Again mimicking natural F integration, this time by homologous recombination, a plasmid carrying a transposable element can be transferred to a recipient that already has the transposable element inserted into its chromosome; growth of exconjugants in conditions restrictive for plasmid replication (temperature-sensitivity, narrow host range, etc.) allows the direct selection of Hfr strains. This approach has been used to obtain Hfr's by integration of F′ *ts*::Tn10 in *S. typhimurium* (41) and R91-5::Tn5 in *Pseudomonas putida* (42). It lends itself both to the generation of banks of Hfr derivatives and to the isolation of individual Hfr's with predetermined origins of transfer.

8.7. Potential Problems
Three potential problems beset the isolation of useful Hfr strains: (i) paucity of insertion sites, (ii) instability, and (iii) deleterious integration. Homology-based integration depends on the chance that the transmissible plasmid and the chromosome have sequences in common, and it also leaves the integrated DNA susceptible to **RecA**- or **resolvase**-mediated excision (43). Fortunately, the transposon-based strategies for Hfr isolation largely overcome these problems: Because transposon

target specificity is usually very low, the range of Hfr's obtainable is, for practical purposes, unlimited; and spontaneous transposon excision is sufficiently rare to permit formation of stable Hfr's. Most conjugative plasmids are of somewhat higher copy number than F, and their integration is often poorly tolerated (32, 43, 44). Here again, a transposon-based strategy solves the problem, because incorporation of transfer functions in a transposon uncouples them from the replicon, as described above.

9. Isolating F-Primes

As in the case of Hfr's, several techniques for isolating particular plasmid-primes have been developed to overcome the limitations of natural mechanisms. One of the earliest used was the selection for early transfer of a marker normally transferred late in an Hfr cross (15). F-primes carrying proximal markers can also be selected by using a *recA* mutant recipient to impair integration of the selected marker (45). This approach has been used to select an R-prime in *P. aeruginosa* (46), and a variation of it in which recombination is prevented by transfer to a recipient of a different species has led to the isolation of many R-primes (eg, Ref. 47). Some recombinants, formed by mating one Hfr strain with another that had been converted to the F^- phenocopy state by prolonged incubation in stationary phase, proved to be “double males,” containing two integrated Fs: recombination between them created F^- primes carrying the intervening DNA (48). A similar event appears to be responsible for the formation of certain R-primes.

The above methods all rely on genetic maneuvers to select spontaneously formed plasmid-primes. A quite distinct method has been used to produce finer gradations in the range of F-primes created. It is based on the essentially random cleavage of host DNA that occurs during **phage P1** infection and consists of simply **transducing** F (or R) DNA into F^- cells (49). It has been used thus far to create shorter versions of existing F-primes, for genetic analysis (50), and to isolate an R′lac plasmid directly by infection of an Hfr strain (51).

10. Prospects

With the radical, and no doubt permanent, shift to physical mapping and sequencing as the preferred means of analyzing genomes, Hfr's and plasmid-primes will now serve mainly as adjuncts to other methods. Even the role of F-primes in genetic complementation has been largely taken over by convenient low copy-number cloning vectors. Nevertheless, these traditional methods should continue to be useful during the initial stages of genetic characterization of new organisms able to host promiscuous conjugative plasmids, such as RP4. Moreover, recent insights into the roles of gene mobilization in the pathogenicity of bacteria underline the importance of understanding the mechanisms of plasmid–chromosome interactions (52). It is not unreasonable to anticipate novel ones. It is also interesting to speculate on giant plasmid-primes as the origin of multichromosome bacteria (53, 54).

Bibliography

1. J. Lederberg and E. Tatum (1946) Nature **158**, 558.
2. E. L. Wollman and F. Jacob (1955) C. R. Acad. Sci. **240**, 2449–2451.
3. F. Jacob and E. L. Wollman (1958) Symp. Soc. Exp. Biol. **12**, 75–92.
4. F. R. Blattner et. al. (1997) Science **277**, 1453–1474.
5. A. L. Taylor and E. A. Adelberg (1961) Biochem. Biophys. Res. Commun. **5**, 400–404.
6. A. M. Campbell (1962) Adv. Genet. **11**, 101–145.
7. R. Curtiss,III and D. R. Stallions (1969) Genetics **63**, 27–38.
8. R. C. Clowes and E. E. M. Moody (1966) Genetics **53**, 717–726.
9. N. Davidson, R. C. Deonier, S. Hu, and E. Ohtsubo (1975) In *Microbiology—1974* (D. Schlessinger, ed.), ASM, Washington, D.C., pp. 56–65.

10. M. Umeda and E. Ohtsubo (1989) J. Mol. Biol. **208**, 601–614.
11. M. S. Guyer, R. R. Reed, J. A. Steitz, and K. B. Low (1981) Cold Spring Harbor Symp. Quant. Biol. **45**, 135–140.
12. K.-C. Cheah and R. A. Skurray (1986) J. Gen. Microbiol. **132**, 3269–3275.
13. E. A. Adelberg and S. N. Burns (1960) J. Bacteriol. **79**, 321–330.
14. A. Richter (1957) Genetics **42**, 391.
15. F. Jacob and E. A. Adelberg (1959) C. R. Acad. Sci. **249**, 189–191.
16. P. A. Sharp, M.-T. Hsu, E. Ohtsubo, and N. Davidson (1972) J. Mol. Biol. **71**, 471–497.
17. M. S Timmons, A. M. Bogardus, and R. C. Deonier (1983) J. Bacteriol. **153**, 395–407.
18. D. L. Blazey and R. O. Burns (1983) J. Bacteriol. **156**, 1344–1348.
19. F. van Gijsegem and A. Toussaint (1982) Plasmid **7**, 30–44.
20. R. G. Hadley and R. C. Deonier (1980) J. Bacteriol. **143**, 680–692.
21. J. M. Buysse and S. Palchaudhuri (1984) Mol. Gen. Genet. **193**, 543–553.
22. E. Ohtsubo and M.-T. Hsu (1978) J. Bacteriol. **134**, 795–800.
23. M. Riley and A. Anilionis (1978) Annu. Rev. Microbiol **32**, 519–560.
24. K. E. Sanderson and C. A. Hall (1970) Genetics **64**, 215–228.
25. M. Mergeay and J. Gerits (1978) J. Bacteriol. **135**, 18–28.
26. L. A. Wiater, A. Marra, and H. A. Shuman (1994) Plasmid **32**, 280–294.
27. F. Jacob, D. Perrin, C. Sanchez, and J. Monod (1960) C. R. Acad. Sci. **250**, 1727–1729.
28. R. Simon, U. Priefer, and A. Pühler (1983) Biotechnology **1**, 784–791.
29. P. L. Kahn (1968) J. Bacteriol. **96**, 205–214.
30. H. Herrmann and E. Günter (1984) Mol. Gen. Genet. **197**, 286–291.
31. A. K. Chatterjee and M. P. Starr (1973) J. Bacteriol. **116**, 1100–1106.
32. C. Riemann, M. Rella, and D. Haas (1988) J. Gen. Microbiol. **134**, 1515–1523.
33. A. Colbeau, J.-P. Magnin, B. Cauvin, B. T. Champion, and P. M. Vignais (1990) Mol. Gen. Genet. **220**, 393–399.
34. S. V. Kameneva, T. P. Politseva, N. V. Belavina, and S. V. Shestakov (1986) Genetika **22**, 2664–2672.
35. I. G. Serebrijski, S. M. Kazakova, and Y. D. Tsygankov (1989) FEMS Microbiol. Lett. **59**, 203–206.
36. V. Fran, A. Conter, and J.-M. Louarn (1990) J. Bacteriol. **172**, 1436–1440.
37. C. Reimann and D. Haas (1993) In *Bacterial Conjugation* (D. B. Clewell, ed.), Plenum Press, New York, pp. 137–188.
38. N. S. Willets, C. Crowther, and B. W. Holloway (1981) Plasmid **6**, 30–52.
39. E. A. Yakobson and D. G. Guiney (1984) J. Bacteriol. **160**, 451–453.
40. D. A. Johnson (1988) Plasmid **20**, 249–258.
41. F. G. Crumley, R. Menzel, and J. R. Roth (1979) Genetics **91**, 639–655.
42. A. D. Strom, R. Hirst, J. Petering, and A. Morgan (1990) Genetics **126**, 497–503.
43. C. Riemann and D. Haas (1986) Mol. Gen. Genet. **203**, 511–519.
44. D. Haas and B. W. Holloway (1976) Mol. Gen. Genet. **144**, 243–251.
45. B. Low (1968) Proc. Natl. Acad. Sci. USA **60**, 160–167.
46. B. W. Holloway (1978) J. Bacteriol. **133**, 1078–1082.
47. R. W. Hedges, A. E. Jacob, and I. P. Crawford (1977) Nature **267**, 283–284.
48. A. J. Clark (1963) Genetics **48**, 105–120.
49. J. Pittard and E. A. Adelberg (1963) J. Bacteriol. **85**, 1402–1408.

50. N. J. Marsh and D. E. Duggan (1972) J. Bacteriol. **109**, 730–740.
51. A. Nishimura, Y. Nishimura, and L. Caro (1973) J. Bacteriol. **116**, 1107–1112.
52. S. Falkow (1996) In *Escherichia coli and Salmonella. Cellular and Molecular Biology*, 2nd ed. (F. C. Neidhardt et al., eds.), ASM Press, Washington, D.C., pp. 2723–2729.
53. W. Hayes (1968) *The Genetics of Bacteria and Their Viruses*, 2nd ed., Blackwell Scientific Publications, Oxford, p. 674.
54. C. Rosenberg, P. Boistard, J. Denarié, and F. Casse-Delbart (1981) Mol. Gen. Genet. **184**, 326–333.

Suggestions for Further Reading

55. F. C. Neidhardt et al., eds. (1996) *Escherichia coli and Salmonella. Cellular and Molecular Biology*, 2nd ed., ASM Press, Washington, D.C. Chapters 126–129 in Vol. **2**, Section C provide a comprehensive treatment of the subject, centered on *E. coli*, as well as an exhaustive bibliography.
56. C. Reimann and D. Haas (1993) "Mobilization of chromosomes and non-conjugative plasmids by cointegrative mechanisms."In *Bacterial Conjugation*, (D. B. Clewell, ed.), Plenum Press, New York. An excellent starting point for accessing the available information on conjugal transfer in a wide range of bacteria.
57. W. Hayes (1968) *The Genetics of Bacteria and Their Viruses*, 2nd ed. Blackwell Scientific Publications, Oxford Chapters 22 ("Conjugation") and 24 ("Sex Factors and Other Plasmids") of this textbook is a lucid account of the historical development of the subject, written by one of its pioneers.
58. T. D. Brock (1990) *The Emergence of Bacterial Genetics*. Cold Spring Harbor Laboratory Press, Cold Spring Harbor, New York. Chapter 5 ("Mating") is another historical perspective. The science, enlivened by anecdote, is treated more lightly than in Hayes, but without sacrifice of rigor or clarity.

High Mobility Group (HMG) Proteins

The major proteins of chromosomes and chromatin are the histones, but other, nonhistone chromosomal components are also present, in much lower amounts. The most abundant and best characterized of these is the class of high mobility group (HMG) proteins. (The name is an operational definition coined when the proteins were first isolated in the 1970s as proteins that were soluble in 2% trichloroacetic acid or 5% perchloric acid and migrated with a high mobility in polyacrylamide gel electrophoresis .) HMG proteins in metazoans fall into three structurally and functionally distinct classes: the HMG 1, 2 family, HMG 14 and 17, and the HMG I(Y) family. (The numbering is also a legacy from the past!) They appear to be present in all cells of higher eukaryotes. They are relatively abundant, being present in the nucleus on average at about 1 molecule per 10 to 15 nucleosomes [considerably less for HMG I(Y)]. All have intriguing properties, and their cellular roles are not fully understood, but they are likely to play important roles in **gene** expression. None of the three classes shows specificity for particular DNA sequences; instead, they bind to particular structures in DNA or to chromatin. Both HMG 1,2 and HMG I(Y) have "architectural" roles, and both bind primarily to DNA in the minor groove, although they are wholly unrelated in amino acid sequence and structure. The early work on these proteins is described in a definitive book (1). A recent review (2) gives a comprehensive account of more recent work and is an excellent source of references up to 1996, which in general will not be duplicated here. For more general background, the reader should consult two volumes on chromatin (3, 4).

1. The HMG 1 and 2 Family

In vertebrates this class consists of HMG1 (molecular mass ~25,000Da) and two closely related forms of HMG2, which are a few residues shorter. They are the products of **homologous** genes and show a high degree of evolutionary conservation. They have a tripartite structure consisting of two tandem homologous regions of about 80 amino acid residues (the two DNA-binding "HMG boxes") and a long acidic tail of about 30 (HMG 1) or 20 (HMG 2) consecutive **aspartic** and glutamic acid residues linked to the second box by a short basic region. HMG 1 and 2 bind to DNA with a "structure-preference" rather than a sequence preference. They bind to bent or bulged DNA and to DNA kinked by the antitumor drug *cis*-platin, in preference to linear DNA; they also prefer four-way junctions, **supercoiled** DNA and DNA minicircles, and they stabilize DNA loops (the juxtaposed ends probably resemble crossovers in supercoiled DNA). They bend linear DNA, as shown by the ability to cause circularization (in the presence of DNA Ligaseto join the ends) of short DNA fragments (~80bp) that will not circularize unaided, and they constrain negative supercoils in relaxed circular DNA. The ability to distort DNA, as well as to recognize DNA distortions reflected in these properties, is likely to reflect the *in vivo* role(s) of HMG 1 and 2.

Relatively abundant HMG-box proteins that bind to DNA without sequence specificity also occur in yeast (NHP6A and B), insects (eg, HMG-D and HMG-Z in *Drosophila*; HMG1a and b in *Chironomus*), and plants (HMGa, etc.). In all these cases, the proteins contain only one HMG box and the acidic tail is often shorter than in vertebrate HMG1,2 (eg, 10 residues in HMG-D). All these proteins bind preferentially to distorted DNA substrates (although the *Chironomus* HMG 1a and 1b bind A-T-rich linear and four-way junction DNA with equal affinity). The HMG-box motif also occurs in a large and growing number of sequence-specific transcription factors, as a single copy, with no acidic tail, and embedded in unrelated sequence (5, 6). The first examples were the product of the male sex-determining gene on the mouse Y chromosome (SRY) and the lymphocyte enhancer binding protein (LEF-1). The specificity of these proteins for their DNA targets resides in the HMG box. They also bind to four-way DNA junctions, and they bend linear DNA containing their DNA binding sites (7). The estimated bend angles are ~130° for LEF-1 and ~90° for mouse and human SRY. Proteins with two or more HMG boxes bind DNA with relatively low sequence specificity. These include the **RNA polymerase** I transcription factor UBF (upstream binding factor; 4–6 HMG boxes, depending on source, and a very long acidic tail) and the mitochondrial factors mtTF1 and ABF2.

This diverse group of sequence-specific and non-sequence-specific HMG-box DNA-binding proteins is united by the ability to distort and bend DNA, which is probably central to their biological roles. They are regarded as "architectural elements in the assembly of nucleoprotein structures" (7). Their properties are analogous to those of the bacterial IHF (integration host factor) and **HU proteins**. Indeed HMG-D, NHP6A and HM can all functionally replace HU in *Escherichia coli*, and HMG 1 and 2 can functionally replace HU in facilitating assembly of the invertasome during Hin-mediated recombination .

Protein structures have been determined by NMR for the A and B HMG boxes of HMG 1, the HMG boxes of *Drosophila* HMG-D and the transcription factor Sox4, and for the HMG boxes of SRY and LEF-1 complexed with oligonucleotides. Although there are slight differences that might be significant, the protein folds are all generally very similar, showing that there is no gross change in the HMG-box structure on binding to DNA. The HMG box is L-shaped, the relative positions of the two arms being fixed by a tightly packed **hydrophobic** cluster; Figure 1 shows the A-box of HMG1 (8). The "long" arm contains an *N*-terminal extended **b-strand** packed against **a-helix** III in the *C*-terminal half of the molecule; the "short" arm consists of a-helices I and II. DNA binding occurs on the concave face of the protein, which interacts in the minor groove of the DNA. The SRY/DNA and LEF-1/DNA structures (9, 10) show that the protein partially intercalates into the minor groove and causes the DNA to bend toward the major groove, away from the protein (Fig. 2). The minor groove is also opened up (becomes wider and shallower), forming a larger surface for interaction with the protein, and the DNA is locally untwisted. The protein thus sits on the *outside* of the bend and is very reminiscent of the way in which the **TATA box**-binding protein TBP interacts with DNA. In both structures a bulky hydrophobic residue (Ile in SRY, Met in LEF-1) intercalates between base pairs near the center of the DNA to cause bending. Binding is stabilized by interaction of a basic region *C*-terminal to the box with the major groove opposite the widened minor groove. All HMG boxes are likely to bind to DNA in essentially the same way, except that the role of intercalation in the non-sequence-specific proteins is less clear. Sequence-specific and non-sequence-specific HMG boxes also show characteristic differences in residues at key positions in the *N*-terminal b-strand.

Figure 1. Structure of the HMG box in the A-domain of HMG1 (residues 11-83 of the protein) determined by NMR spectroscopy (8).

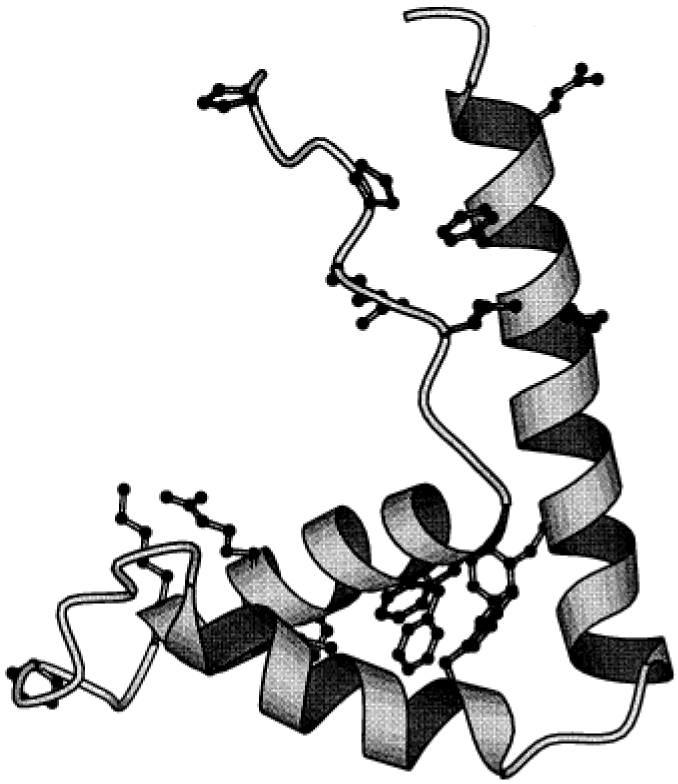

Figure 2. Structure of the LEF-1 HMG box complexed with DNA complex, determined by NMR spectroscopy (10).

The isolated A and B boxes of HMG 1 bend and distort DNA like the entire protein; there are slight differences between them that might be related to the small differences in structure between the two boxes (8). Tandem boxes have a higher affinity for DNA than single boxes and are more effective than single boxes in DNA binding and bending; the basic linker between the boxes and the acidic tail further enhances the affinity (eg, Ref. 11). The acidic tail works in the opposite direction on most DNA substrates *in vitro*, by lowering the affinity of the HMG boxes for DNA, possibly by general charge repulsion, and possibly by interacting electrostatically with the DNA-binding face of the box (es). The acidic tail of HMG-D, however, increases the affinity and selectivity of the protein for mini-circles (<100bp), which are highly constrained and effectively present a "pre-bent" substrate (12); the same is true for HMG 1. Perhaps the tail stabilizes a conformation of the protein that is suited to recognition of a highly predistorted substrate.

Surprisingly little is known for certain about the binding of HMG 1 and 2 to chromatin. Early observations on micrococcal nuclease (**Staphylococcal nuclease**) digestion products of chromatin (3, 4) suggested that HMG 1 and 2 were associated with linker DNA, and that that there was a population of HMG1-containing nucleosomes lacking histone H1. This led to the suggestion that HMG 1 binds to sites normally occupied by H1, but the evidence for this is still circumstantial. However, binding of H1 and HMG 1 to nucleosomes reconstituted on to the *Xenopus* 5 S rRNA gene resulted in similar protection of chromatosome length DNA against micrococcal nuclease digestion (see Chromatin and Nucleosome), which was interpreted in terms of a shared structural role (13). The finding that, like HMG 1, H1 and its globular domain would also bind to synthetic four-way junctions (14) has been taken to reinforce this (the four-way junction is assumed to mimic the crossover of the entering and exiting duplexes around the dyad of the nucleosome). However, it is not clear that the two proteins are recognizing the same features of the four-way junction. Moreover, given the nature of H1 binding to the nucleosome (see Nucleosome or Chromatin), even if H1 and HMG 1 bind in the same general vicinity, the details of their interactions in chromatin would be expected to be very different. *In vivo* evidence for a shared *functional* role in at least some circumstances is more compelling. In *Drosophila* early embryos, where cell division is rapid, H1 is absent and the condensed chromosomes contain HMG-D (which has only one HMG box). At later stages, the chromosomes contain H1 rather than HMG-D, and gene transcription, which was previously absent, starts (15). This apparently reciprocal relationship suggests that H1 and HMG-D may have a common function at different stages of embryogenesis in *Drosophila*, although not necessarily an identical binding site on the nucleosome. Rigorous reconstitution studies are needed to settle the question of how HMG 1 and 2 bind to chromatin. It is, of course, possible that they function only at **promoters** or enhancers, where a nucleosome is absent. For example, by bending DNA they might facilitate the interaction of two proteins, bound on either side of the kink, that is required for some functional purpose; or they could facilitate the binding of a protein that binds best to a DNA bend, by pre-bending the DNA in an essentially catalytic role; or they might also stabilize a DNA loop, such as might be formed to bring enhancer and promoter elements into proximity.

HMG 1 and 2 have been variously implicated in DNA replication, transcription, DNA repair and recombination, and, given their versatility in DNA distortion and recognition of distorted DNA, this is not altogether surprising. In recent *in vitro* studies of V(D)J recombination of immunoglobulin biosynthesis (see Gene Rearrangement), HMG 1 and 2 were found to stimulate V(D)J cleavage (16) and to be components of a stable post-cleavage complex between synapsed recombination signals (17). An obvious question is whether HMG 1 and 2 have roles in transcriptional activation; distinct roles for the HMG boxes and the acidic tails might be envisaged. *In vitro* studies (for references see Ref. 2) have given conflicting answers. It has been suggested that activation might result from stabilization of an activated conformation of the TFIID-TFIIA initiation complex on the promoters of activated genes; or, based on *in vitro* binding assays, that HMG 1 and 2 might act indirectly to promote transcription by promoting the binding of various transcription factors to their cognate DNA binding sites, probably by bending the DNA. *In vivo* results (transfection experiments) show enhancement of transcription by HMG 1 and suggest that the acidic tail acts as a transactivation domain, although this is not the case for the heterologous mammalian HMG 1 expressed in yeast (2). However, HMG 1 and 2 have also been reported to repress transcription by RNA polymerase II *in vitro*—either by interacting with TBP in the presence of a TATA-box-containing oligonucleotide and thus preventing binding of TFIIB and formation of a preinitiation complex, or by acting later, after the assembly of the TBP-TFII promoter complex. There are now several examples of facilitation of transcription factor binding to DNA by HMG 1 and 2, and this seems likely to be important. For example, binding of the progesterone receptor to an oligonucleotide containing the progesterone response element is enhanced ~10–fold by HMG 1 and 2, and HMG 2 stimulates the sequence-specific binding of the octamer transcription factors Oct 1 and Oct 2, by interacting with the POU domains (2). HMG 1 stimulates DNA binding of human HOXD9, by interaction with the **homeobox** domain (18), and of the tumor suppressor p53 (19). Ternary complexes between the transcription factor, HMG protein, and DNA are likely, but in at least some cases the HMG must be only weakly bound, because such complexes cannot be detected by gel electrophoresis.

2. The HMG I(Y) Family

HMG I and Y are isoforms generated by alternative splicing, differing only in HMG Y (96 amino acid residues) having an 11-residue deletion compared with HMG I (107 residues). HMG C (105 residues) is the third member of this family and is related (~50% sequence identity) to HMG I(Y). Like HMG 1 and 2, they appear to function as "architectural" transcription factors, but the two classes are structurally unrelated. The proteins are subject to post-translational modifications, notably **cell cycle**-dependent reversible **phosphorylation**, probably by p34cdc2/cyclin ("cdc2 kinase"). They are expressed at higher levels (~15 to 50 times) in transformed and undifferentiated cells than in differentiated somatic cells, relatively independent of cellular growth rate; there is also a correlation with increased metastatic tumor potential. Further background and references may be found in Ref. 2.

The HMG I(Y) proteins have a distinctive primary structure containing three regions designated "A-T hooks," separated by flexible chain. HMG C is similar in the A-T hook regions, but much less so elsewhere. The A-T hook binds to the minor grooves of A-T-rich sequences, occupying 5 or 6 bp; three tandem AT hooks would therefore occupy 15 to 18 bp of continuous A-T DNA. The **consensus sequence** of the A-T hook motif is -Pro-Arg-Gly-Arg-Pro- flanked by basic residues; the motif also occurs in a number of unrelated DNA-binding proteins in a range of species. The polypeptide backbone structure is predicted to be similar in shape to the drugs distamycin A, netropsin, and Hoechst 33258, which bind to the minor groove of B DNA and can displace HMG I(Y) from A-T-rich DNA. The structural similarity is borne out by NMR spectroscopy (see text below). In addition to minor groove binding—although in completely different ways—HMG I(Y) also shares with HMG 1 and 2 the property of binding to A-rich non-**B-form** DNA, such as four-way junctions, in preference to the corresponding duplexes (20). HMG I(Y) also bends DNA (but in this case bending is attributed simply to asymmetric charge neutralization on one face of the DNA duplex by the basic amino acid side chains in the A-T hook DNA-binding domains) and supercoils relaxed circular DNA in the presence of **topoisomerase** I, probably through strand unwinding, the mechanism of which is unclear. Removal of the negatively charged *C*-terminal domain increases supercoiling by 8- to 10-fold, apparently without affecting the affinity of HMG I(Y) for A-T-rich DNA (2).

Earlier studies suggested a variety of roles for HMG I(Y) proteins (2). More recently, more direct experiments point to a role in transcriptional regulation (negative or positive) of a number of mammalian genes with A-T-rich promoter or enhancer sequences. In positive regulation, HMG I(Y) has been proposed to act as an "architectural" transcription factor that bends DNA and contacts components of a multiprotein complex, as well as promoting contacts between other members. A well-documented example (21) is the involvement of HMG I(Y) in the virus-induced expression of the human b-interferon gene (IFN-b). HMG I(Y) appears, through a combination of DNA bending and protein-protein interactions, to mediate the assembly of a complex containing HMG I(Y) and the transcription factors NF-kB and ATF-2/c-Jun, all bound simultaneously to two separate "positive regulatory domains" (PRDII and IV) of DNA in the 5′ promoter/enhancer region of the b-interferon gene. NF-kB binds to the major groove and HMG I(Y) to the minor groove. The structure of a 39-residue peptide containing the second and third DNA-binding domains complexed with a 12-bp oligonucleotide containing a 5-bp A-T tract from the PRDII element of the b-interferon enhancer has recently been determined by NMR spectroscopy (22) and reveals extensive hydrophobic and polar contacts in the minor groove centered around an Arg-Gly-Arg motif. In contrast to the HMG box–DNA complexes (see text above), the minor groove is not widened and the DNA is not bent. However, this is a short piece of DNA and, although the protein does not directly cause bending at its binding site, as the HMG box does, bending might well be induced outside the binding site and would be apparent only with a longer DNA segment. Principles similar to those involved at the b-interferon promoter are likely to prove a common feature of the role of HMG I(Y) in many systems—for example, in the function of HIV-1 pre-integration complexes (23).

The situation with respect to the binding of HMG I(Y) to chromatin is not clear. The proteins will bind to nucleosome core particles *in vitro*, at up to four molecules per nucleosome, in a noncooperative manner. However, they bind to A-T-rich DNA in preference to mixed-sequence nucleosomes and, as pointed out (2), if A-T sequences were present in the linker DNA—or in a nucleosome-free region—that would probably be the preferred binding site for HMG I(Y) in chromatin. There is an intriguing possible connection between HMG I(Y) and chromatin structure through histone H1 (see Histones). *In vitro* H1 will bind preferentially to A-T-rich fragments of naked DNA, possibly through "-SPKK-" (Ser-Pro-Lys-Lys) motifs in the *C*-terminal tail, and can be displaced by HMG I(Y). In the nucleus, scaffold attachment regions of chromatin are A-T-rich and have been suggested to be focal points for displacement of H1 by HMG I(Y), perhaps leading to "open chromatin" domains (24); in neoplastic cells, greatly increased levels of HMGI(Y) might contribute to altered patterns of gene expression. This is still speculation, but it is highly suggestive that HMG I(Y) co-localize (as shown by immunofluorescence) with A-T-rich scaffold regions in metaphase chromosomes, which contain the interphase scaffold attachment regions brought together (25).

3. HMG 14 and 17

These evolutionarily related proteins are present in all tissues of most higher organisms. Their precise cellular roles are not understood, although various lines of evidence suggest that they facilitate transcription of chromatin, and it now appears that this is at the level of higher-order structure. Early work reported a correlation between DNAse I-sensitivity of chromatin, which itself correlates with transcriptional competence (see Chromatin), and the presence of HMG 14 and 17 (see Refs. 2 and 3 for background). HMG 14 and 17 contain, respectively, 98 and 89 amino acid residues and have a high content of lysine, alanine and proline and a negatively charged *C*-terminal region (although there is no continuous run of acidic residues, as in HMG 1 and 2). They bind to nucleosomes in preference to free DNA through a 30-residue, basic sequence that is conserved within the HMG 14 and HMG 17 classes, but differs in detail between the two (2). HMG 14 and 17, despite their common ancestry, are only 60% identical in sequence and are likely to perform different roles in the cell.

Two copies of HMG 14 and 17 bind cooperatively to 146-bp nucleosome core particles (see Nucleosome) at roughly physiological ionic strength, presumably by recognizing particular structural features. In native chromatin, nucleosomes containing only HMG 14 or HMG 17 are clustered in runs of, on average, six nucleosomes, potentially giving functionally distinct domains along the chromatin fiber, the significance of which is not yet clear (26). The free proteins appear to be unstructured in solution but could well become structured upon interaction with the nucleosome core. Binding of HMG 14 is weakened by **phosphorylation** of Ser 6, which is an early event in the induction of immediate-early genes on mitogenic stimulation (27). Footprinting and cross-linking data have led to a model for the location of the two HMG 14 or 17 molecules on the core particle, in which the HMG proteins are bound by their basic *N*-terminal regions to sites 20 or 30 base pairs from the end of the core particle DNA and then loop under one of the DNA ends to contact, in each case, a major groove adjacent to the dyad on the central turn of DNA (2). This could explain why HMG 14 and 17 stabilize nucleosome core particles, by preventing charge repulsion that would lead to unraveling of the ends. In contrast, HMG 14 and 17 appear to destabilize chromatin higher-order structure in some way, although they do not prevent its formation (2), consistent with the facilitating effect of HMG 14 and 17 on transcription. When tested for activator function as fusions to DNA-binding proteins in yeast, HMG 14 and 17 did not act as classical transcription factors, despite an acidic *C*-terminal region. However, transcription from minichromosomes assembled in *Xenopus* or *Drosophila* embryo extracts was stimulated by HMG 14 and 17, in contrast with transcription from naked DNA, consistent with a role for HMG 14 and 17 in destabilizing chromatin structure (2). Enhancement of transcription from assembled SV40 minichromosomes by HMG14 was interpreted as relief of H1-mediated repression, resulting in unfolding, for which the acidic *C*-terminal region of HMG 14 is needed (28). Specific interactions with the *N*-terminal tail of H3 may be involved (29)—yet another role for the *N*-terminal tails (see Chromatin).

Bibliography

1. E. W. Johns (1982) *The HMG Chromosomal Proteins*, Academic Press, London.
2. M. Bustin and R. Reeves (1996) Prog. Nucleic Acid Res. and Mol. Biol. **54**, 35–100.
3. K. van Holde (1988) *Chromatin*, Springer-Verlag, New York.
4. A. P. Wolffe (1995) *Chromatin: Structure and Function*, 2nd ed., Academic Press, New York.
5. V. Laudet, D. Stehelin, and H. Clevers (1993) Nucleic Acids Res. **21**, 2493–2501.
6. A. D. Baxevanis and D. Landsman (1995) Nucleic Acids Res. **23**, 1604–1613.
7. R. Grosschedl, K. Giese, and I. Pagel (1994) Trends Genet. **10**, 94–100.
8. C. H. Hardman et al. (1995) Biochemistry **34**, 16596–16607.
9. M. H. Werner, J. R. Huth, A. M. Gronenborn, and G. M. Clore (1995) Cell **81**, 705–714.
10. J. J. Love et al. (1995) Nature **376**, 791–795.
11. K. D. Grasser et al. (1998) Eur. J. Biochem. **253**, 787–795.
12. D. Payet and A. A. Travers (1997) J. Mol. Biol. **266**, 66–75.
13. K. Nightingale, K. Dimitrov, R. Reeves, and A. P. Wolffe (1996) EMBO J. **15**, 548–561.
14. P. Varga-Weisz, K. van Holde, and J. Zlatanova (1993) J. Biol. Chem. **268**,20699.
15. S. S. Ner and A. A. Travers (1994) EMBO J. **13**, 1817–1822.

16. D. C. van Gent, K. Hiom, T. T. Paull, and M. Gellert (1997) EMBO J. **16**, 2665–2670.
17. A. Agrawal and D. G. Schatz (1997) Cell **89**, 43–53.
18. V. Zappavigna et al. (1996) EMBO J. **15**, 4981–4991.
19. L. Jayaraman et al. (1998) Genes Dev. **12**, 462–472.
20. D. A. Hill and R. Reeves (1997) Nucleic Acids Res. **25**, 3523–3531.
21. W. Du, D. Thanos, and T. Maniatis (1993) Cell **74**, 887–898.
22. J. R. Huth et al. (1997) Nat. Struct. Biol. **4**, 657–665.
23. C. M. Farnet and F. D. Bushman (1997) Cell **88**, 483–492.
24. K. Zhao, E. Kas, E. Gonzalez, and U. K. Laemmli (1993) EMBO J. **12**, 3237–3247.
25. Y. Saitoh and U. K. Laemmli (1994) Cell **76**, 609–622.
26. Y. V. Postnikov et al. (1997) J. Mol. Biol. **274**, 454–465.
27. J. M. Barratt, C. A. Hazzalin, E. Cano, and L. C. Mahadevan (1994) Proc. Natl. Acad. Sci. USA **91**, 4781–4785.
28. H. F. Ding, M. Bustin, and U. Hansen (1997) Mol. Cell. Biol. **17**, 5843–5855.
29. L. Trieschmann, B. Martin, and M. Bustin (1998) Proc. Natl. Acad. Sci USA **95**, 5468–5473.

Suggestions for Further Reading

30. D. M. Crothers (1993) Architectural elements in nucleoprotein structures. Curr. Biol. **3**, 675–676.
31. K. D. Grasser (1998) HMG1 and HU proteins: architectural elements in plant chromatin. Trends Plant Sci. **3**, 260–265.
32. R. Grosschedl (1995) Higher-order nucleoprotein complexes in transcription: analogies with site-specific recombination. Curr. Opin. Cell Biol. **7**, 362–370.
33. S. S. Ner, A. A. Travers, and M. E. Churchill (1994) Harnessing the writhe: a role for DNA chaperones in nucleoprotein complex formation. Trends Biochem. Sci. **19**, 185–187.

High-Performance Liquid Chromatography (HPLC)

HPLC is a modern high-resolution liquid **chromatographic** technique best described as high-performance liquid chromatography because the essence of the technique is the high resolution of the separations achieved by using uniform microparticulate, chromatographic supports and well-designed equipment. HPLC has also been called high-pressure or high-speed liquid chromatography but these acronyms do not reflect the essential features of the technique.

The development of HPLC has been in several areas including theory, special columns, and equipment. Though the theoretical principles of HPLC were firmly established by Martin and Synge (1) in the early 1950s, HPLC in practice did not appear until the late 1960s because of instrumental problems. Horváth et al. (2) constructed one of the first practical HPLC apparatuses for use in their research on **nucleotides** . Subsequently, dramatic developments in packing materials, particle sizes (as small as 3 µm), narrow-bore columns (as small as 0.5 mm inner diameter for microbore columns) and high column inlet pressures (up to 12,000 psi) have been achieved for high resolution and efficiency.

HPLC is carried out in all classical modes of column chromatography involving a liquid mobile phase. The most important are liquid-solid adsorption, liquid-liquid and organo-bonded partition, **ion-exchange**, **size-exclusion**, and affinity chromatography . HPLC has the advantages over classical liquid chromatography that the columns are reusable, the sample introduction can be automated, flow rates can be controlled precisely, and detection and quantification can be achieved by using continuous flow detectors. These features have led to improved analytical accuracy and precision.

The widespread application of HPLC in biochemical studies is evidenced by countless publications in the field. For example, HPLC is widely used by molecular biologists to isolate **nucleic acids** from synthetic oligonucleotides to natural **plasmids** (see reviews 3, 4 and Chapter 11.1 in 5), and by protein biochemists to purify **peptides** and proteins (see reviews 6–10 and Chapter 11.2 in 5). Those requiring more detailed practical information are directed to the reviews cited previously and also to a number of excellent monographs (5), (11-13).

Bibliography

1. A. J. P. Martin and R. L. M. Synge (1941) Biochem. J. **35**, 1358–1368.
2. C. Horváth, B. A. Preiss, and S. R. Lipsky (1967) Anal. Chem. **39**, 1422–1428.
3. M. Colpan and D. Riesner (1988) in *Modern Physical Methods in Biochemistry, Part B* (A. Neuberger and L. L. M. Van Deenen, eds.), Elsevier, Amsterdam, pp. 85–105.
4. P. R. Brown (ed.) (1984) *HPLC in Nucleic Acid Research* (Chromatographic Science, Vol.**28**), Marcel Dekker, New York.
5. A. Fallon, R. F. G. Booth, and L. D. Bell (1987) *Applications of HPLC in Biochemistry*, Elsevier, Amsterdam.
6. W. S. Hancock (1984) Handbook of HPLC for the Separation of Amino Acids, Peptides, and Proteins, Vols.**I** and **II**, CRC Press, Boca Raton.
7. M. T. W. Hearn and M. I. Aguilar (1988) in *Modern Physical Methods in Biochemistry, Part B* (A. Neuberger and L. L. M. Van Deenen, eds.), Elsevier, Amsterdam, pp. 107–142.
8. A. R. Kerlavage (ed.) (1989) *The Use of HPLC in Receptor Biochemistry*, Alan R. Liss, New York.
9. C. T. Mant and R. S. Hodges (eds.) (1991) *High-Performance Liquid Chromatography of Peptides and Proteins: Separation, Analysis, and Conformation*, CRC Press, Boca Raton.
10. R. M. Chicz and F. E. Regnier (1990) in *Guide to Protein Purification* (M. P. Deutscher, ed.), *Methods in Enzymology* 182, Academic Press, New York, pp. 392–421.
11. H. Engelhardt (ed.) (1986) *Practice of High Performance Liquid Chromatography: Applications, Equipment and Quantitative Analysis*, Springer-Verlag, Berlin.
12. U. D. Neue (1997) *HPLC Columns: Theory, Technology, and Practice*, Wiley-VCH, New York.
13. A. Weston and P. R. Brown (1997) *HPLC and CE: Principles and Practice*, Academic Press, San Diego.

Hill Coefficient, Plot

The Hill coefficient is used to provide a quantitative measure of cooperativity of ligand binding. It is usually estimated graphically from a Hill plot. A hypothetical example of a Hill plot is shown in Figure 1. To construct a Hill plot, y, the fractional saturation of the binding sites by a ligand X, is determined experimentally. The data are plotted as log (y/ 1–y) versus log $[X]_f$. The Hill coefficient,

n_H, is given by the slope of this plot at log $(y/1–y) = 0$—that is, at $y = 0.5$ or 50% saturation of the X binding sites.

Figure 1. Hill plot. A hypothetical Hill plot for positively cooperative binding of ligand X to a macromolecule with two binding sites for X is shown. The data are presented as points, and the limiting asymptotes with slope 1 at high and low extents of ligand binding are shown as lines. The intrinsic stepwise binding constants, K_1 and K_2, given by the intercepts at <rf>log</rf>[X] = 0, are 0.1 and 10, respectively. The Hill coefficient is 1.8.

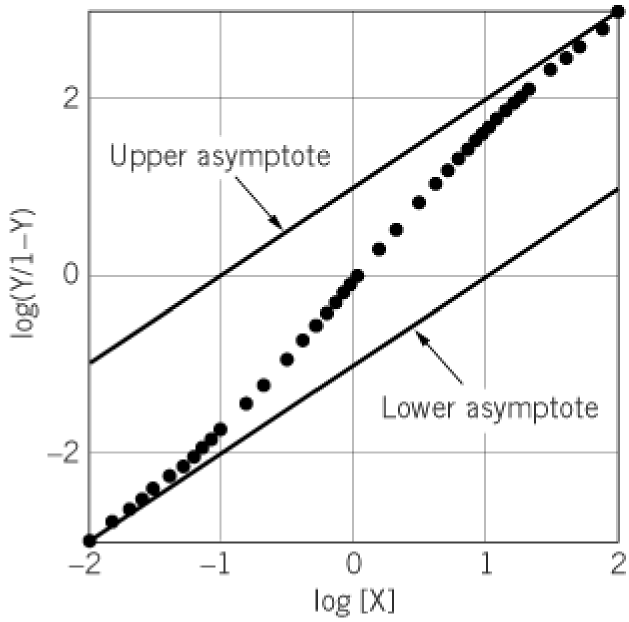

The value of the Hill coefficient provides two important items of information. First, its value relative to 1 indicates the type of cooperativity. For noncooperative ligand binding, $n_H = 1$. For positively cooperative ligand binding, $n_H > 1$; and for negatively cooperative ligand binding, $n_H < 1$. Second, for positively cooperative ligand binding, the value of n_H puts an upper limit on the numbers of interacting binding sites for X. For example, for a tetrameric protein with four binding sites for X, $n_H \leq 4$.

The Hill plot was initially developed by A. V. Hill in the context of proposing a mechanism for the positive cooperativity of oxygen binding to hemoglobin (1). The central concept of his proposal was recognition that cooperativity in ligand binding requires interactions between multiple binding sites. In the limit that the cooperativity between n binding sites is very strong, then only unliganded and fully n-liganded species of the protein exist. This can be expressed by the binding reaction

$$P_n + nX \rightleftharpoons (P \cdot X)_n \tag{1}$$

An apparent association constant may be written as

$$K = \frac{[(P \cdot X)_n]}{[P_n][X]^n} \tag{2}$$

The fractional saturation, y, is then given by

$$\bar{y} = \frac{[X]^n}{(1/K) + [X]^n} \tag{3}$$

Equation 3 can be converted into a form useful for graphical analysis by taking the ratio of bound sites to free sites, $y/(1–y)$, and taking the logarithm

$$\log(\bar{y}/[1-y]) = n\log[X]_f + \log K \tag{4}$$

Equation 4 is the basis for the Hill plot.

Analysis of the properties of Equation 4 as a function of [X] shows that the slope approaches +1 at both small and large values of y (2-4). These are shown as the lines in Figure 1 that are labeled lower asymptote and upper asymptote, respectively. As described below, in principle these asymptotes provide information about ligand binding. However, accurate determinations of the asymptotes in practice are difficult because they require measurements at very low and very high extents of ligand binding. For this reason, most uses of the Hill plot focus on the slope at 50% saturation with ligand X, the Hill coefficient.

The Hill coefficient can usually be determined with good precision for cooperative binding systems, and it provides an accurate phenomenological description of the cooperativity. For systems with two interacting binding sites for X (eg, dimeric proteins), it may be possible to determine apparent dissociation constants for each site from the Hill plot (see text below). For larger numbers of interacting binding sites, it may be possible to determine the dissociation constants for the first and last ligands bound and the interaction energy between these sites. However, determinations of dissociation constants for other ligand bindings steps are not in general possible. (See Ref. 3 for discussion relative to oxygen binding to hemoglobin.)

To understand the relations between cooperative ligand binding and the Hill coefficient, it is instructive to consider the case of a symmetrical dimer with one binding site for ligand X on each subunit. The stepwise occupancy of the binding sites can be written

$$P_2 + X \overset{K_1}{\rightleftharpoons} P_2X + X \overset{K_2}{\rightleftharpoons} P_2X_2 \tag{5}$$

where K_1 and K_2 are intrinsic stepwise association constants defined by the equations

$$K_1 = \frac{[P_2X]}{[P_2][X]}, \qquad K_2 = \frac{2[P_2X_2]}{[P_2X][X]} \tag{6}$$

The Hill coefficient at $y = 0.5$ is given by

$$n_H = \frac{2}{1 + (K_1/K_2)^{1/2}} \tag{7}$$

For $(K_1/K_2) > 1$, $n_H < 1$, indicating negative cooperativity. For $(K_1/K_2) < 1$, $n_H > 1$, indicating positive cooperativity. The value of n_H cannot exceed 2. The intercepts of the asymptotes in Figure 1, when $\log[X] = 0$ are $\log K_1$ (lower) and $\log K_2$ (upper). Thus they provide values for the intrinsic stepwise binding constants for the initial and final ligand binding steps. Although this is a general result, experimental determination of the asymptotes is in practice difficult. An analogous treatment of cooperativity in the kinetic behavior of a symmetric dimeric enzyme using Weber's approach of coupling free energies (4) has been presented and shows the relations between the magnitude of the coupling free energies and the value of the Hill coefficient (5). A treatment of the Hill coefficient in the context of the concerted allosteric model is presented on page 135 of Ref. 3 .

Bibliography

1. A. V. Hill (1910) J. Physiol. (London) **40**, iv–vii.
2. J. T. Edsall and H. Gutfreund (1983), *Biothermodynamics: The Study of Biochemical Processes at Equilibrium*, Monographs in Molecular Biophysics and Biochemistry, (H. Gutfreund, ed.), Wiley, New York, p. 248.
3. J. Wyman and S. J. Gill (1990), *Binding and Linkage: Functional Chemistry of Biological Macromolecules*, University Science Books, Mill Valley, CA.
4. G. Weber (1992), *Protein Interactions*, Chapman and Hall, New York, p. 293.
5. G. D. Reinhart (1988) Biophys. Chem. **30**, 159–172.

Hirudin

Hirudin is a protein inhibitor of thrombin in the saliva of the medicinal leech *Hirudo medicinalis* [see Proteinase inhibitors, protein and Serine proteinase inhibitors]. The target enzyme here seems obvious. It is a single polypeptide chain of 65 amino acid residues crosslinked by three disulfide bridges. It combines extremely tightly ($K_I 10^{-14}$M) with thrombin. The crystal structure of a thrombin-hirudin complex reveals that hirudin is not a standard-mechanism canonical inhibitor. The active site of thrombin is embedded in a canyon restricting the entry of many substrates and of most trypsin inhibitors that do not inhibit thrombin. Hirudin blocks the active site, but none of its residues embeds into the S_1 cavity, a hallmark of standard-mechanism canonical inhibition. The highly flexible COOH terminus of hirudin (residues 50–65) binds to the fibrinogen-binding exosite of thrombin. Many hirudin-based drugs block this fibrinogen-binding exosite rather than the active site of thrombin.

Suggestion for Further Reading

M. G. Grütter et al. (1990) Crystal structure of the thrombin-hirudin complex: A novel mode of serine protease inhibition. EMBO J. **9**, 2361–2365.

His Operon

Energy equivalent to about 41 ATP molecules is required to synthesize one molecule of the amino acid histidine (1). The considerable metabolic cost of histidine biosynthesis presumably accounts for the evolution of multiple strategies to regulate the rate of synthesis of the amino acid in response to environmental changes. Checkpoints regulate both the flow of intermediates through the biosynthetic pathway and the amounts of histidine-biosynthetic enzymes present. Expression of the genes for these enzymes is regulated in bacterial cells by mechanisms that are both general (metabolic regulation, elongation control) and specific (attenuation control, segmental stabilization of the distal part of the messenger RNA).

1. Structural organization of the operon

In *Escherichia coli* and *Salmonella typhimurium* the enzymes responsible for the biosynthesis of histidine are encoded by eight genes tightly clustered in a single, large operon (*his* operon). In both species, transcription produces a single polycistronic mRNA about 7300 nucleotides long, extending from a primary **promoter** (*hisp1*) to a Rho-independent terminator. Two weak internal promoters, *hisp2* and *hisp3*, are located within the *hisC* and *hisF* genes, respectively. The structural organization of the operon is essentially the same in the two species, and in both the translational stop codon of each **cistron** overlaps the translational initiation codon of the downstream cistron (2). This organization allows ribosomes to initiate the translation of a new cistron without moving away from the mRNA after terminating translation of the preceding one. Such a translational coupling mechanism probably guarantees equimolar synthesis of the corresponding gene products (3).

2. Control of transcription initiation and elongation

Transcription of the *his* operon is about four-fold more efficient in bacteria growing in minimal-glucose medium than when growing in rich medium. This form of control, called *metabolic regulation*, adjusts the expression of the operon to the amino acid supply in the cell. It is mediated by the “alarmone” guanosine 5′-diphosphate 3′-diphosphate (ppGpp), which is the effector of the stringent response (see Stringency). The alarmone regulates the *his* operon positively by stimulating the primary promoter *hisp1* under conditions of moderate amino acid starvation (4).

In addition to this general metabolic control, *his* operon transcription is specifically regulated by attenuation of transcription, a mechanism in which a regulatory element, located upstream of the first structural gene of the cluster, modulates the level of expression of the histidine biosynthetic enzymes in response to the intracellular levels of charged histidyl-transfer RNA, His-tRNA ^{His} (see Transfer RNA) (5). The *his*-specific regulatory element is transcribed in a 180-nucleotide RNA leader, which exhibits two prominent features: (i) a 16-residue coding sequence including seven consecutive codons specifying histidine, and (ii) overlapping regions of dyad symmetry capable of folding into mutually exclusive, alternative **secondary structures** that signal either transcription termination or antitermination (6, 7). Six RNA segments are involved in base pairing (Fig. 1 A to F) and the stem-loop structure formed by the E and F RNA regions, plus the adjacent run of uridylate residues, constitutes the attenuator, a strong Rho-independent transcription terminator (Fig 1). Translational control of *his* operon transcription is determined by ribosome occupancy of the leader RNA, which in turn depends, given the peculiar composition of the *his* leader peptide, on the availability of His-tRNA ^{His}. High levels of His-tRNA^{His} allow rapid movement of ribosomes up to the B segment; in this case, formation of the C:D and E:F stem-loop structures will result in premature transcription termination (Fig. 1, Attenuation). In the presence of low levels of charged tRNA^{His}, ribosomes stall at the consecutive histidine codons of the leader peptide and prevent the A:B pairing by masking the A segment. Base pairing between the B and C and between the D and E RNA regions prevents formation of the attenuator and determines the antitermination conformation (Fig. 1, Transcription). In the case of severe limitation of the intracellular pool of all charged tRNAs, translation of the leader peptide fails to initiate: under these conditions, the A:B, C:D and E:F stem-loop structures form sequentially, producing a strong transcription termination (Fig. 1, Superattenuation). **RNA polymerase** pauses after synthesis of the first RNA hairpin (A:B). This pausing is believed to synchronize transcription and translation of the leader region by halting the elongating RNA polymerase until a ribosome starts translation of the leader peptide (8). The pause hairpin (Fig. 1) is the only portion of the structure thought to form when RNA polymerase resides at the pause site.

Figure 1. Regulation of translation of the *his* operon messenger RNA. Top: the nucleotide sequence of the leader region *typhimurium* from the transcription initiation site (+1) to the first structural gene, *hisG*. Brackets above the nucleotide se segments (A to F) capable of forming alternative, mutually exclusive secondary structures. The convergent arrows indic structure required for transcriptional pausing at the downstream site indicated by a vertical arrow (see text). The amino a peptide and of the amino-terminal region of *hisG* are shown. Bottom: Schematic representation of the different conform (see text). The run of U's at the 3′ end indicates the formation of the terminator hairpin E:F. The position of the terminati (UAG) in each RNA configuration is also indicated.

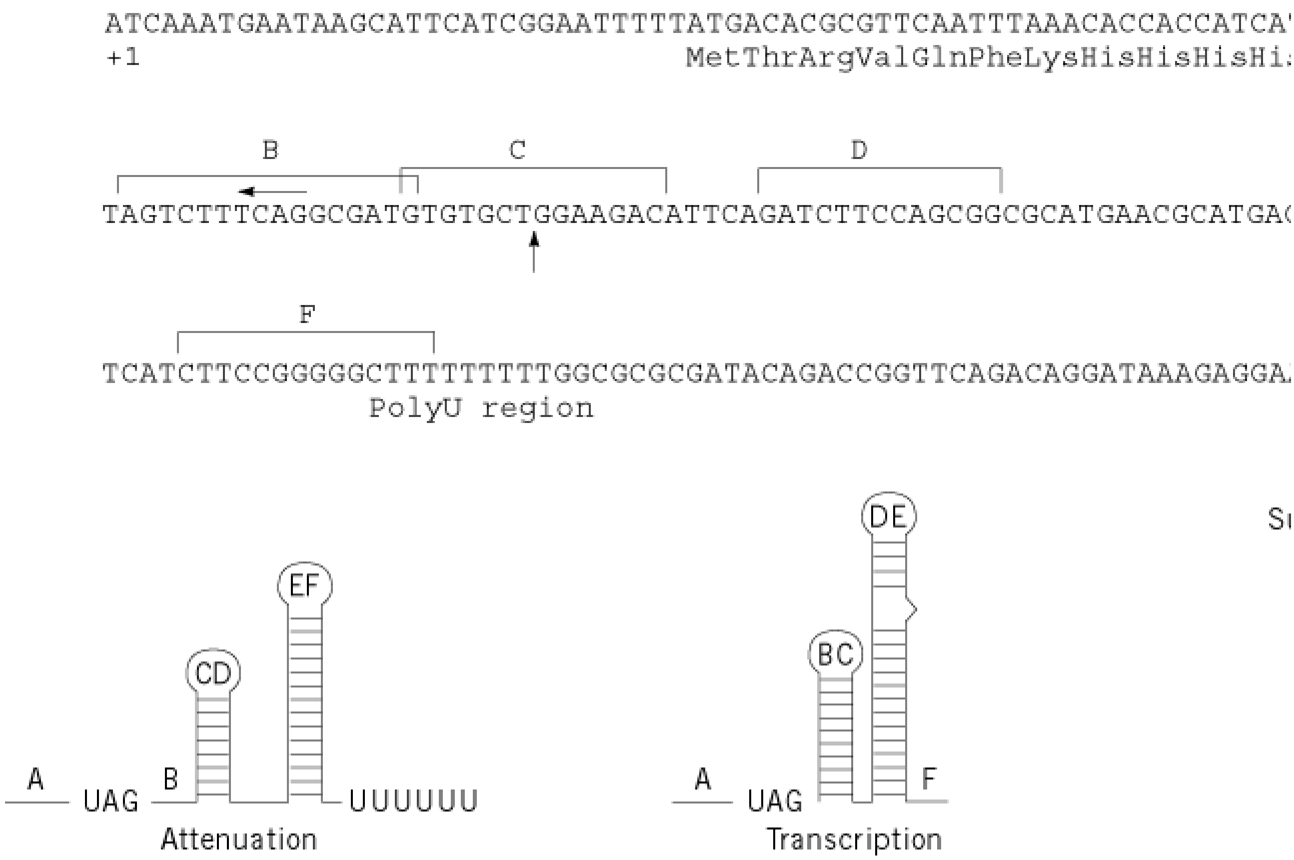

Because the absolute amount of charged tRNA^{His} controls the level of *his* attenuation (5), mutants exhibiting high *his* operon expression contain defects in tRNA ^{His} biosynthesis, aminoacylation with histidine, or tRNA ^{His} modification and processing. The *hisR* gene encodes the single cellular tRNA^{His}; and mutations in the *hisR* promoter reduce the total cellular content of tRNA^{His} molecules by about 50% and thereby cause increased readthrough transcription of the *his* attenuator (9). The *hisS* gene encodes histidyl-aminoacyl tRNA synthetase, which aminoacylates tRNA ^{His} molecules with histidine. Mutations that lower the activity of the histidyl-tRNA synthetase or decrease the enzyme's affinity for histidine, tRNA^{His}, or ATP, affect the level of *his* attenuation by reducing the percentage of tRNA^{His} molecules charged with histidine (10). The *hisT* gene encodes pseudouridine synthase I, which catalyzes the formation of pseudouridine residues in the anticodon region of several tRNA species, including tRNA^{His}. Although the undermodified tRNA ^{His} molecules are charged with histidine to the same extent as in wild-type strains, transcription termination at the *his* attenuator is greatly decreased, because the slow rate of translation of the consecutive histidine codons causes stalling of ribosomes (11).

The overall contribution of the internal promoter *hisp2* to the expression of the distal genes of the operon is negligible when transcription proceeds from *hisp1*, because *hisp2* is inhibited by transcription readthrough, a phenomenon known as *promoter occlusion* (12). *hisp2* is also subjected to metabolic regulation, although to a lesser extent than *hisp1*.

Elongation of the *his*-mRNA is modulated by a non-specific mechanism operating at the level of intracistronic *transcription termination elements* (TTEs) (13). These elements consist of cytosine-rich and guanosine-poor RNA regions and are the binding-activation sites of the transcription-termination Rho factor, which is responsible for polar effects in polycistronic operons (14). A premature arrest of translation, produced by nonsense mutations, favors the binding of Rho to the TTE on the nascent transcript. The subsequent interaction of Rho with the elongating RNA polymerase causes a premature release of transcripts. Polarity results, with reduced expression of the genes located downstream from the TTE.

3. Decay and Segmental Stabilization of the *his*-mRNA

The primary 7300-nucleotide *his*-mRNA has a half-life of about 3 minutes in cells growing in minimal-glucose medium and is degraded in a net 5′ → 3′ direction. Three major processed species, 6300, 5000, and 3900 nucleotides long, encompassing the last seven, six, and five cistrons, respectively, are generated in the decay process (12). The 6300- and the 5000-nucleotide RNAs, which have half-lives of 5 and 6 minutes, respectively, have heterogeneous 5′ ends generated by ribonuclease E cleavage (see RNA Degradation In Vitro). The 3900-nucleotide processed RNA species has a unique 5′ end and an uncommon stability, having a half-life of about 15 minutes. This RNA species is generated by specific processing events requiring sequential cleavages by two different endonucleases. RNase E triggers the process by cleaving at a major target site located in the *hisC* cistron, 620 nucleotides upstream of the 5′ end of the processed species. Subsequently, ribonuclease P cleaves the processed RNA species generated by RNase E at a site located 76 nucleotides upstream of the start codon of the *hisB* cistron, producing the mature 5′ end. The observation that the RNase P-catalyzed reaction requires the presence of ribosomes suggests that translation of the *hisB* cistron might favor formation of the structure recognized by RNase P (15).

Bibliography

1. M. Brenner and B. N. Ames (1971) In *Metabolic Pathways* (H. J. Vogel, ed.), Academic Press, Inc., N.Y., vol. **5**, pp. 349–387.
2. M. S. Carlomagno, L. Chiariotti, P. Alifano, A. G. Nappo, and C. B. Bruni (1988) J. Mol. Biol. **203**, 585–606.
3. C. Yanofsky, T. Platt, I. P. Crawford, B. P. Nichols, G. E. Christie, H. Horowitz, M. Van Cleemput, and A. M. Wu (1981) Nucleic Acids Res. **9**, 6647–6668.
4. J. C. Stephens, S. W. Artz, and B. N. Ames (1975) Proc. Natl. Acad. Sci. USA **72**, 4389–4393.
5. F. Blasi and C. B. Bruni (1981) Curr. Top. Cell. Regul. **19**, 1–45.
6. W. M. Barnes (1978) Proc. Natl. Acad. Sci. USA **75**, 4281–4285.
7. P. P. Di Nocera, F. Blasi, R. Di Lauro, R. Frunzio, and C. B. Bruni (1978) Proc. Natl. Acad. Sci. USA **75**, 4276–4280.
8. C. L. Chan and R. Landick (1989) J. Biol. Chem. **264**, 20796–20804.
9. H. M. Johnston, W. M. Barnes, F. G. Chumley, L. Bossi, and J. R. Roth (1980) Proc. Natl. Acad. Sci. USA **77**, 508–512.
10. J. A. Lewis and B. N. Ames (1972) J. Mol. Biol. **66**, 131–142.
11. C. F. Singer, G. R. Smith, R. Cortese, and B. N. Ames (1972) Nature New Biol. **238**, 72–74.

12. P. Alifano, C. Piscitelli, V. Blasi, F. Rivellini, A. G. Nappo, C. B. Bruni, and M. S. Carlomagno (1992) Mol. Microbiol. **6**, 787–798.
13. P. Alifano, F. Rivellini, D. Limauro, C. B. Bruni, and M. S. Carlomagno (1991) Cell **64**, 553–563.
14. P. Alifano, M. S. Ciampi, A. G. Nappo, C. B. Bruni, and M. S. Carlomagno (1988) Cell **55**, 351–360.
15. P. Alifano, F. Rivellini, C. Piscitelli, C. M. Arraiano, C. B. Bruni, and M. S. Carlomagno (1994) Genes Dev. **8**, 3021–3031.

Suggestions for Further Reading

16. M. Winkler (1996) "Biosynthesis of histidine. In" *Escherichia coli and Salmonella typhimurium*, 2nd Ed. (F. C. Neidhart, ed.), American Society for Microbiology, Washington DC, pp 485–505.
17. P. Alifano, R. Fani, P. Liò, A. Lazcano, M. Bazzicalupo, M. S. Carlomagno, and C. B. Bruni (1996) Histidine biosynthetic pathway and genes: Structure, regulation and evolution. Microb. Rev. **60**, 44–69.

Histidine (His, H)

The amino acid histidine is incorporated into the nascent polypeptide chain during **protein biosynthesis** in response to two **codons**—CAU and CAC—and represents approximately 2.2% of the residues of the proteins that have been characterized. The histidyl residue incorporated has a mass of 137.14 Da, a **van der Waals volume** of 118 Å ^{3}, and an accessible surface area of 194 Å^2. His residues are changed during divergent evolution with average frequency; they are interchanged in **homologous** proteins most frequently with asparagine and glutamine residues.

The side chain of His residues consists of a b-methylene carbon and an imidazole group:

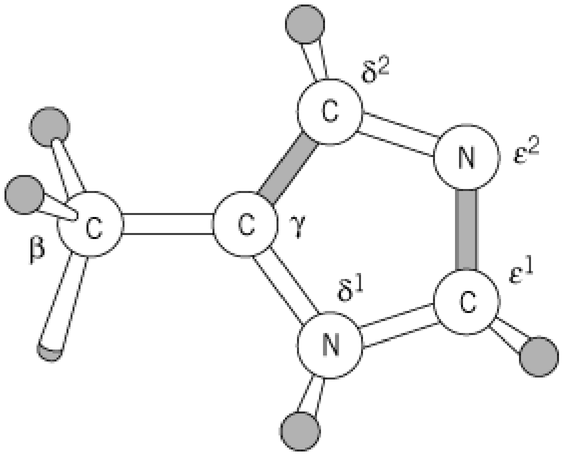

The imidazole groups possesses several special properties that make it extremely effective as a nucleophilic catalyst. It is an amine, which is much more reactive than hydroxide ion in terms of basicity. Furthermore, it is a tertiary amine, which is intrinsically more nucleophilic than primary or secondary amines. The enhanced reactivity of tertiary amines is usually canceled by their greater steric hindrance, but in imidazole the atoms bonded to the two nitrogen atoms are held back in a five-membered ring and cause relatively little steric hindrance. Imidazole has a pK_a value near 7, so it is one of the strongest bases that can exist at neutral pH. A weaker base would have a lower nucleophilic reactivity, whereas a stronger base would be protonated to a greater extent at neutral pH and would be correspondingly less reactive.

In the nonionized form of the imidazole ring, the nitrogen atom with the hydrogen atom is an electrophile and a donor for **hydrogen bonding**, while the other nitrogen atom is a nucleophile and a hydrogen bond acceptor. Consequently, this one side chain is extremely versatile, almost the chemical equivalent of being ambidextrous. Not surprisingly, His residues are often found at the active sites of enzymes and involved directly in catalysis.

The two nitrogen atoms of the His side chain are designated here as d1 and ε2, but they are also known, respectively, as p and q or as N-1 and N-3. The latter designation is often ambiguous, because biochemists usually assign the number 1 to the nitrogen atom adjacent to the C_g, whereas organic chemists tend to reverse the numbers. The nonionized imidazole ring can exist as two tautomers, with the hydrogen atom on either the d1 and ε2 nitrogen atom. In model peptides, the hydrogen atom is usually predominantly on the ε2 nitrogen atom, which has a pK_a value about 0.6 pH unit higher than that of the d1 atom. The relative affinities of the two nitrogen atoms for protons can vary with their local environment, however, and both forms are found in folded proteins.

The nonionized His side chain is readily protonated, with a p K_a value near 7 at the second N atom, which destroys its nucleophilicity. The positive charge is shared by the two N atoms by resonance:

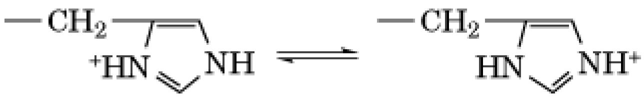

The $C_{\varepsilon}{}^{1}$ atom, between the two N atoms, is observed to exchange its hydrogen atom slowly with aqueous solvents, indicating that it has a very small probability of being deprotonated:

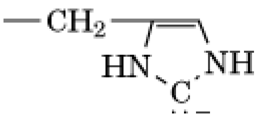

This hydrogen exchange reaction provides a useful probe of the environments of His residues in proteins. His residues are especially useful in ^{1}H-**NMR** studies of proteins because the hydrogen atom on the $C_{\varepsilon}{}^{1}$ atom is usually well resolved from the multitude of resonances of the other hydrogen atoms in proteins. Its resonance is usually shifted by about 1 ppm to a lower field strength on protonation of the side chain, often making it relatively easy to determine the pK_a values of individual His residues, even in large proteins.

His is one of the residues least favoring the *alpha*-**helical** conformation in model peptides, but it occurs in a-helices in native protein structures slightly more frequently than in *beta* **-sheets** or reverse turns .

The imidazole group is, in principle, capable of undergoing numerous chemical modification reactions, but most of these occur much more readily with **amino** and thiol groups, so very few are suitable for modifying His residues specifically. The imidazole nitrogen atoms have an intrinsic affinity for metal ions, especially zinc, iron, and copper. His residues are frequently involved in binding such ligands to proteins, as in metal-requiring enzymes, **zinc fingers**, myoglobin, and hemoglobin.

Suggestions for Further Reading

E. A. Barnard and W. D. Stein (1959) The roles of imidazole in biological systems, Adv. Enzymol. **20**, 51–110.

M. Tanokura (1983) ^{1}H-NMR study on the tautomerism of the imidazole ring of histidine residues. I. Microscopic p K values and molar ratios of tautomers in histidine-containing peptides, Biochim. Biophys. Acta **742**, 576–585.

Histocompatibility

The transplantation of tissue from one individual to another most often results in an adverse immune reaction between the host and the transplanted tissue, leading to graft rejection. The inclusion of lymphoid effector cells in a tissue graft can lead to graft-versus-host disease as well. These phenomena stem primarily from discordant expression of MHC cell surface molecules encoded by **polymorphic** class I and class II loci of the major histocompatibility complex (MHC). Graft acceptance or rejection is most strongly associated with identity or difference at class I loci, followed by class II and so-called minor histocompatibility antigens, as described below. The clinical evaluation of donor–host compatibility involves "tissue typing" individuals to determine the alleles present at the HLA-A, -B, and -DR loci. In practice, perfect matches at these loci are rare (requiring identity at as many as six independent loci, because **gene** products from maternal and paternal chromosomes are co-dominantly expressed); the majority of transplants rely mainly on the use of immunosuppressive agents postoperatively to increase graft survival. Host individuals are additionally screened for the presence of serum **antibodies** to MHC molecules, arising from prior exposure to non-self MHC through a blood transfusion or pregnancy.

Allograft rejection involves a variety of phenomena; the discussion here is confined to mismatched donor–host class I alleles (whose gene products have often been referred to as "classical transplantation antigens") as the basis for tissue incompatibility. MHC class I molecules present peptide **antigens** to the clonally expressed T-cell receptors (TCRs) of cytotoxic T lymphocytes (CTLs). The composition of the peptides presented by a given class I molecule is influenced by allomorph-specific peptide binding preferences, which in turn are a function of polymorphic amino acid residues found in the peptide-binding region of the class I molecule. Under typical circumstances, CTLs are rendered tolerant to the self class I/self peptide complexes expressed in an individual. The presence of an allograft introduces a new cohort of class I/peptide complexes into the host system, and the array of peptides displayed on the cells of the graft will reflect the binding preferences of the donor's class I allomorphs. Among these allo-MHC/peptide complexes are potentially numerous **epitopes** to which the host individual is not tolerant, thereby marking cells of the transplanted tissue for destruction by circulating CTL.

The cellular immune response to non-self class I/peptide complexes is termed "alloreactivity." The molecular basis for TCR recognition of allo-MHC molecules has long been an area of intensive study and debate in immunology. The preceding paragraph implies a scheme in which allorecognition is a peptide-specific phenomenon and fundamentally similar to the recognition of self class I+foreign peptide. In this view, conserved regions of the majority of class I molecules are themselves likely to provide similar molecular surfaces for contact with the TCR, regardless of the class I allomorph being considered. Specific interactions thus occur between variable regions of the TCR and the class I-bound peptide. There is now considerable evidence to support this model of allorecognition (1). However, allotypic residues on the surface of a class I molecule may also provide critical determinants for allorecognition by some TCR (2), and it is possible that both modes of recognition are utilized in the polyclonal T-cell response to an allograft.

The peptide-based nature of allorecognition also accounts for the involvement of "minor histocompatibility antigens" in graft rejection. Even when genetically nonidentical donor and host are HLA matched, they also manifest differences stemming from the expression of variants of several other polymorphic proteins. A well-known example is the H-Y antigen, encoded on the Y-Chromosome of males, which presents a barrier to successful male-to-female transplantation. This protein is expressed in nearly all tissues and differs in amino acid sequence from its X-chromosome homologue (present in both males and females) (3). Consequently, some H-Y antigen-derived peptides that are presented by MHC class I molecules (3, 4) will constitute novel epitopes in a female host receiving tissue from a male donor, provoking a cellular immune response. The total number of human minor histocompatibility loci and the identity of the proteins they encode remain as yet undetermined.

Bibliography

1. L. A. Sherman and S. Chattopadhyay (1993) Annu. Rev. Immunol. **11**, 385–402.
2. R. Brock, K. H. Wiesmuller, G. Jung, and P. Walden (1996) Proc. Natl. Acad. Sci. USA **93**, 13108–13113.
3. W. Wang et al. (1995) Science **269**, 1588–1590.
4. O. Rotzschke, K. Falk, H. J. Wallny, S. Faath, and H. G. Rammensee (1990) Science **249**, 283–287.

Histone Acetylation

Acetylation of chromatin by histone acetyltransferases (HATs), using acetyl coenzyme A as the acetyl donor, occurs at the e-amino groups of particular lysine side chains in the *N*-terminal basic tails of the core histones, with varying consequences. Histone deacetylases (HDACs) remove the acetylation. Histone acetylation has roles in chromatin assembly linked to DNA replication, in gene transcription, where the histones are hyperacetylated, and, apparently paradoxically, in heterochromatin (1). In the centric heterochromatin of the polytene chromosomes of the fruit fly *Drosophila* (2) and at the silent mating type loci in the yeast *Saccharomyces cerevisiae* (3), the histones are hypoacetylated, as might be expected, but an acetyl group on Lys12 in the exposed *N*-terminal tail of H4 (see Nucleosome) is essential for heterochromatin formation and may act as a recognition site for the assembly of other heterochromatin proteins. The importance of the pattern of site-specific acetylation, rather than the overall number of acetyl groups, is becoming increasingly clear, but is still poorly understood. Elevated levels of Lys16 acetylation on H4 in the male X-chromosome in *Drosophila* appears to be important, in some way, in **dosage compensation**, which results in a doubling of transcription from X-linked genes in the male (4).

Histone H4 deposited with H3 at the **replication fork** by the core histone **molecular chaperone** CAF-1 (chromatin assembly factor 1) during chromatin assembly is acetylated at Lys5 and Lys12 primarily, by a so-called B-type (deposition-linked) acetyltransferase. Deacetylation occurs soon after deposition. Transcription-related hyperacetylation occurs in chromatin at lysines 5, 8, 12, and 26 in H4, and lysines 9 and 14 in H3. Its role appears to be to "open" chromatin, primarily by destabilizing higher-order structure, thus permitting access by the transcription machinery. Suggestions of the interactions that might be disrupted have come recently from the high-resolution structure of the nucleosome core particle. Because the *N*-terminal tails are not bound within the nucleosome core, acetylation is unlikely to act at this level. The facilitation of **transcription factor** binding due to acetylation observed in *in vitro* assays with mononucleosomes (eg, Ref. 5) may be due to disruption of nonspecific interactions of the histone tails with the DNA gyres, in the absence of any possibilities for higher-order structure formation. Direct evidence that acetylation *per se* does result in increased transcription has come from studies of the *hsp*26 gene reconstituted using a *Drosophila* embryo extract into chromatin with either unacetylated or acetylated histones (6). In nuclei, large domains of chromatin-encompassing active genes appear to be acetylated; this state precedes transcription, and the chromatin is said to be in a transcriptionally competent state. In at least one well-documented case (7), the chicken b-globin gene cluster, the genes are embedded in a domain of greater than 30 kbp, where the histones are hyperacetylated and which shows increased sensitivity to the **nuclease** DNase I (see Chromatin), suggesting a less compact structure.

1. Histone Acetylases

The finding that the *Tetrahymena* HAT, HAT-A, is **homologous** to a yeast transcriptional co-activator, GCN5 (8), solved the mystery of how acetylation might be targeted to particular regions of chromatin. It has since been shown that the acetyltransferase activity of GCN5 (which functions as the GCN5-Ada2-Ada3 complex) is essential for its activator activity (9, 10) and that acetylation occurs in the **promoter** region. GCN5 also functions with Ada proteins in the yeast SAGA complex, which also contains Spt proteins (transcriptional regulators) (SAGA = *S*pt3–*A*da–*G*CN5–*A*cetyltransferase) and is involved in the regulation of many yeast genes. It is now clear (1) that a growing number of proteins known to be transcriptional co-activators and co-activator-associated proteins have HAT activity [eg, p300/CBP, P/CAF (a human homologue of GCN5), the TFIID component $TAF_{II}250$, which is likely to be associated with all promoters during transcriptional initiation, and many others]. (CBP = cAMP response element binding protein; CAF = CBP–associated factor.) Most, including GCN5, function within large complexes, where one subunit recognizes a DNA-bound transcription factor and another has acetyltransferase activity. p300/CBP interacts with transcription factors in many different signaling pathways (eg, nuclear hormone receptors, c-Fos, c-Jun/v-Jun), and acetylation is therefore the end point of many signal transduction pathways. Acetylation of different histones, and different sites within a particular histone, may turn out to require different HATs; GCN5 *in vivo* acetylates preferentially Lys8 and Lys16 of H4 and Lys14 of H3 (11). Histones may not be the only targets of all of the enzymes designated as histone acetyltransferases, for example, HMG 1 and HMG I(Y) are known to be acetylated *in vivo*. The transcription factor/tumor suppressor p53 is acetylated both *in vitro* and *in vivo* by p300, its coactivator. Two general transcription initiation factors, TFIIEb and TFIIF, can also be acetylated by P/CAF and p300 (12). Because the HAT activities that have recently been studied are tethered to sequence-specific DNA binding proteins at promoters (and enhancers), their effect will necessarily be local. It is not clear how this relates to whole domain acetylation over tens of kilobases. One possibility is that the loosening/disruption of the chromatin structure close to the promoter might be transmitted down the 30-nm filament (see Chromatin) through disruption of cooperative interactions, and that the temporarily loosened tails become targets for a pool of untargeted acetylases. There are other possibilities, and this area needs further study. Various models for how histone acetylases and deacetylases selectively affect gene expression have recently been discussed (13).

The first structure of a HAT catalytic subunit (Hat1 from the yeast *Saccharomyces cerevisiae*, which was the first HAT to be isolated) has recently been determined, complexed with acetyl CoA (14); *in vivo* Hat1 exists as a heterodimer with the regulatory subunit HAT2. Hat1's sequence preference for acetylation is Lys12>Lys5, and it acetylates free rather than nucleosomal histones, so it seems likely to be a deposition-related HAT. Nonetheless, Hat1 in both yeast and human cells appears to be primarily nuclear, rather than cytoplasmic as is generally assumed (see Refs. 14 and 15). Hat1 has sequence motifs in common with the GCN5-related superfamily of *N*-acetyltransferases (the GNAT superfamily) and should therefore be an excellent model for the other HATs. Indeed the Hat1 structure explains mutagenesis data on other HATs, such as Gcn5 and CBP; some of the mutations map to the acetyl CoA binding site. The structure of a HAT with a histone or histone tail bound is now needed to reveal the basis of the site specificity of acetylation, which is in the meantime suggested by modeling (14); the structure of a Hat1/Hat2 complex would also be of considerable interest. Hat2 is similar to the p48 subunit of CAF-1 (see Chromatin) and to similar subunits in histone deacetylase HD1 in humans and a related deacetylase in *Drosophila*. These related proteins may be histone-binding subunits.

2. Histone Deacetylases

Histone deacetylases (HDACs) are enzymes that remove acetyl groups, which generally results in repression of transcription. They also appear to be targeted to particular sites by gene regulatory proteins, in this case repressors, in organisms from yeast to mammals. (Intriguingly, the yeast deacetylase RPD3, which is also a repressor of **silencing** at telomeres and mating type loci, specifically deacetylates Lys5 and Lys12 in H4 *in vitro*, consistent with the requirement for Lys12 in an acetylated form for heterochromatin.) Like the HATs, HDACs function in the context of large complexes in which interaction of the HDAC and repressor appears to be mediated by corepressors. In yeast the deacetylase RPD3 is complexed with the corepressor sin3. The mammalian homologue, mSin3, has four paired amphipathic helix (PAH) domains that can interact with several repressors and corepressors. One is the Mad/Max repressor (Mad antagonizes the transcriptional activation and transformation functions of the **Myc oncoprotein**); another is N-CoR, a repressor for the thyroid hormone receptor, which exists in a complex with mSin3A and the mammalian homologue of RPD3. Progress in this rapidly evolving field has been succinctly summarized (1, 16). The finding that the 5-methylcytosine binding protein, MeCP2, recruits Sin3 (17, 18) and a deacetylase suggests a way of ensuring that chromatin in methylated (inactive) regions of the genome remains unacetylated and in a stable higher-order structure.

Bibliography

1. M. Grunstein (1997) Nature **389**, 349–352.
2. B. M. Turner, A. J. Birley, and J. Lavender (1992) Cell **69**, 375–384.
3. M. Braunstein et al. (1996) Mol. Cell. Biol. **16**, 4349–4356.
4. J. R. Bone et al. (1994) Genes Dev. **8**, 96–104.
5. M. Vettese-Dadey et al. (1996). EMBO J. **15**, 2508–2518.
6. K. P. Nightingale, R. E. Wellinger, J. M. Sogo, and P. B. Becker (1998) EMBO J. **17**, 2865–2876.
7. T. R. Hebbes, A. W. Thorne, and C. Crane-Robinson (1988) EMBO J. **7**, 1395–1402.
8. J. E. Brownell et al. (1996) Cell **84**, 843–851.
9. M.-H. Kuo et al. (1998) Genes Dev. **12**, 627–639.
10. L. Wang, L. Liu, and S. Berger (1998) Genes Dev. **12**, 640–653.
11. M.-H. Kuo et al. (1996) Nature **383**, 269–272.
12. A. Imhof et al. (1997) Curr. Biol. **7**, 689–692.
13. K. Struhl (1998) Genes Dev. **12**, 599–606.
14. R. N. Dutnall, S. T. Tafrov, R. Sternglanz, and V. Ramakrishnan (1998) Cell **94**, 427–438.
15. A. Verreault, P. D. Kaufman, R. Kobayashi, and B. Stillman (1997) Curr. Biol. **8**, 96–108.
16. M. J. Pazin and J. T. Kadonaga (1997) Cell **89**, 325–328.
17. X. Nan et al. (1998) Nature **393**, 386–389.
18. P. L. Jones et al. (1998) Nat. Genet. **19**, 187–191.

Suggestions for Further Reading

19. J. E. Brownell and C. D. Allis (1996) Special HATs for special occasions. Linking histone acetylation to chromatin assembly and gene activation. Curr. Opin. Genet. Dev. **6**, 176–184.
20. P. A. Grant et al. (1998) The SAGA unfolds: convergence of transcription regulators inchromatin-modifying complexes. Trends Cell Biol. **8**, 193–197.
21. G. A. Hartzog and F. Winston (1997) Nucleosomes and transcription: recent lessons from

genetics. Curr. Opin. Genet. Dev. **7**, 192–198.
22. P. Kaufman (1996) Nucleosome assembly: the CAF and the HAT. Curr. Opin. Cell Biol. **8**, 369–373.
23. S. Y. Roth and C. D. Allis (1996) Histone acetylation and chromatin assembly: a single escort, multiple dances? Cell **87**, 5–8.
24. B. M. Turner (1998) Histone acetylation as an epigenetic determinant of long-term transcriptional competence. Cell. Mol. Life Sci. **54**, 21–31.
25. P. A. Wade, D. Pruss, and A. P. Wolffe (1997) Histone acetylation: chromatin in action. Trends Biochem. Sci. **22**, 128–132.

Histone Fold

The histone-fold motif is a protein structure feature common to all four histones that was first revealed in the structure of the core histone octamer (1). The mode of interaction of this motif with DNA, suggested by the octamer structure, is shown in detail in the structure of the nucleosome core particle (2). The histone fold has since been recognized in the structures of several other proteins, spanning the evolutionary range from archaebacteria to mammals, that are involved, like the histones, in **DNA:protein recognition** and protein–protein interactions . Some of the histone-fold proteins thus far identified show little or no sequence homology with the histones (3).

The histone fold consists of a long central a-helix connected by loops to two shorter a-helices. It may have arisen by gene duplication of a **helix–strand–helix motif**, with helix fusion resulting in the long central a-helix (4). The histones in the nucleosome core particle occur as heterodimers through extensive interactions between the two histone folds in a "handshake motif," with extensive **hydrophobic** interactions between the nonpolar faces of the two long amphipathic a-helices. The same basic fold occurs in the homodimeric archaeal histone HMfB (from the hyperthermophile *Methanothermus fervidus*) (5), which shows some sequence similarity to the histones, and in the presence of DNA forms tetramers similar to the H3 $_2$H4$_2$ tetramer (see Histones). In HMfB, however, there are no regions similar to the extensions to the basic fold in H3 that contribute to the organization of the DNA in the nucleosome core particle.

Strikingly, the histone fold has also been found to occur in other proteins. The first reports were for **TATA box**-binding protein-associated factors (TAFs), components of the transcription initiation factor TFIID. The 2 Å X-ray crystallography structure of the complex of TAF(II)42 and TAF(II)62 from *Drosophila* showed that it was a tetramer (a dimer of heterodimers), with the interacting regions (which constitute a relatively small part of the total protein) organized in histone folds similar to those of H3 and H4 (6) (Fig. 1). The finding that human TAF(II)20 (homologous to *Drosophila* TAF(II)30a) probably also contains a histone-fold motif similar to that in H2B (7) (no H2A homologues have been found) led to the suggestion that there is a histone octamer-like TAF complex within human TFIID, composed of a tetramer of TAF(II)80 and TAF(II)31 and two homodimers of TAF(II)20 (in *Drosophila* a tetramer of TAF(II)62 and TAFII42) and two homodimers of TAF(II)30a) (6, 7). Surprisingly, three histone-like TAFs also occur amongst the 20 subunits of the P/CAF acetyltransferase complex (see Histone Acetylation), namely, TAF(II)31, TAF(II)20 / 15 and PAF65a (similar to human TAF(II)80), which resemble H3, H2B, and H4, respectively, and an octamer-like structure has again been suggested (8). The yeast 1.8-MDa SAGA (*S*pt-*A*da- *G*CN5-*a*cetyltransferase) acetyltransferase complex, which is similar to the human P/CAF complex, also contains three histone-fold TAFs with homology to H2B, H3, and H4 as integral components (9), and the Spt3 protein appears to have histone folds in its *N*- and *C*-terminal regions, which have been suggested to interact intramolecularly (10). X-ray crystallography has recently shown that yet another pair of TAFs, human TAF(II)18 and TAF(II)28, which show only weak homology to histones, also form a heterodimer through a histone fold (9). The histone-fold motif thus appears to be widespread, and it may simply be a robust structural motif particularly well-suited to protein dimerization in large complexes. It remains to be seen, however, whether histone octamer-like TAF structures have a particular role to play in processes involving histones. Despite the presence of the histone fold, any interaction of TAFs with DNA is likely, *a priori*, to be different from that in the nucleosome core because the arginine side chains of the core histones that insert into the minor groove of the surrounding DNA are absent; in the case of *Drosophila* TAF(II)42 and TAF (II)62, they are replaced by serine and glutamate. The **four-helix-bundle** interface and the orientation of the two heterodimers within the TAFII tetramer are also different from those in the $H3_2H4_2$ tetramer, although this in itself might not necessarily preclude DNA binding.

Figure 1. Drawings of the histone folds in H3 and H4, and *Drosophila* TAF(II)42 and TAF(II)62. (**a**) The TAF(II)42/TA heterodimer from which the $H3_2H4_2$ tetramer in chromatin is formed; (**b**) the tetramer TAF(II)42 $_2$.TAF(II)62$_2$ (residues TAF62).(Adapted from Ref. 6 and reproduced with permission.)

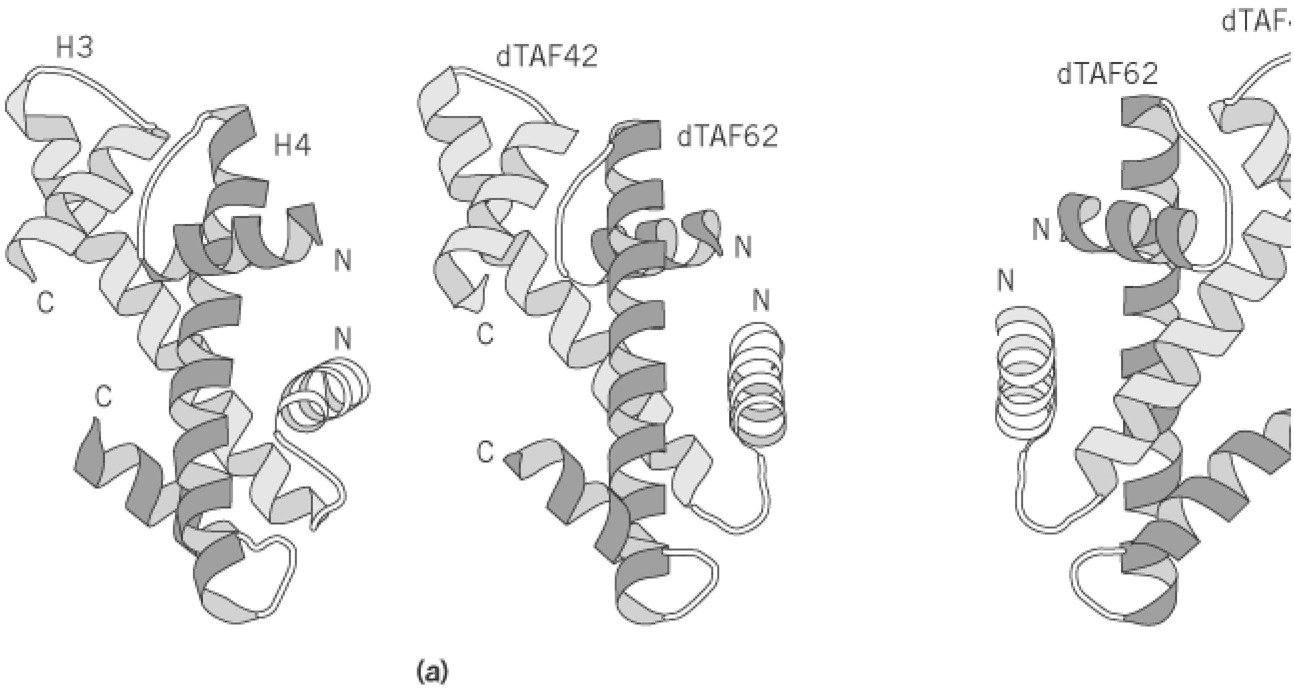

Although no high-resolution structural data are yet available, it seems likely, on the basis of sequence homology with H2A and H2B, that the histone-fold motif also occurs in two subunits of the trimeric mammalian transcription factor CBF [CCAAT-binding factor (11)] and its yeast homologue HAP (CCAAT boxes are widespread promoter elements; see CAAT Box) and in the human protein NC2 [negative cofactor 2 (12); also known as DRAP1] and its yeast homologue, which repress transcription of class II genes by binding to TBP and to DNA and inhibiting preinitiation complex formation by preventing TFIIB binding. It is striking that the histone fold already present in the *Archaea* has been adapted not only for DNA packaging in eukaryotes but also apparently as a dimerization motif in gene regulatory proteins, which sometimes show little, if any, sequence similarity. This is reminiscent of the “winged helix” DNA-binding motif in the globular domain of histone H5 (see Histones), which is also found in bacterial **cyclic AMP receptor protein** and the liver transcription factor HNF3g, a member of a large family of transcription factors (the

HNF/forkhead family) from several organisms.

Bibliography

1. G. Arents et al. (1991) Proc. Natl. Acad. Sci. USA **88**, 10148–10152.
2. K. Luger et al. (1997) Nature **389**, 251–260.
3. A. D. Baxevanis and D. Landsman (1998) Nucleic Acids Res. **26**, 372–375.
4. G. Arents and E. N. Moudrianakis (1995) Proc. Natl. Acad. Sci. USA **92**, 11170–11174.
5. M. R. Starich, K. Sandman, J. N. Reeve, and M. F. Summers (1996) J. Mol. Biol., **255**, 187–203.
6. X. Xie et al. (1996) Nature **380**, 316–322.
7. A. Hoffmann et al. (1996) Nature **380**, 356–359.
8. V. V. Ogryzko et al. (1998) Cell **94**, 35–44.
9. P. A. Grant et al. (1998) Cell **94**, 45–53.
10. C. Birck et al. (1998) Cell **94**, 239–249.
11. S. N. Maity and B. deCrombrugghe (1998) Trends Biochem. Sci. **23**, 174–178.
12. A. Goppelt, G. Stelzer, F. Lottspeich, and M. Meisterernst (1996) EMBO J. **15**, 3105–3116.

Suggestions for Further Reading

13. S. K. Burley, X. Xie, K. L. Clark, and F. Shu (1997) Histone-like transcription factors in eukaryotes. Curr. Opin. Struct. Biol. **7**, 94–102.
14. A. Hoffmann, T. Oelgeschlager, and R. G. Roeder (1997) Considerations of transcriptional control mechanisms: Do TFIID-core promoter complexes recapitulate nucleosome-like function? Proc. Natl. Acad. Sci. USA, **94**, 8928–8935.
15. K. Struhl and Z. Moqtaderi (1988) The TAFs in the HAT, Cell **94**, 1–4.

Histones

Histones are small basic (positively charged) proteins that are complexed with DNA in the nucleus of almost all eukaryotic cells (not dinoflagellates or mammalian spermatozoa) and serve to package the DNA into nucleosomes in chromatin. It has recently become clear that they also play an important regulatory role in gene transcription and repression. Together, the histones occur in a mass roughly equal to that of DNA. There are five histone types, falling into two functional classes: the core histones (H3, H4, H2A, and H2B) and the larger linker histones (H1 and its variants). Two copies of each of the core histones form the histone octamer that constitutes the protein core of the nucleosome, around which are wound two complete left-handed superhelical turns of DNA. The nucleosome is stabilized by the binding of one molecule of the histone H1 class, which also plays a role in stabilization of the higher-order structure of chromatin. It is becoming clear that H1 may also play a specific role in the regulation of some genes. Both the core histones and H1 undergo dynamic reversible modification. Acetylation of the core histones plays an important role in processes as diverse as transcription, nucleosome assembly, and heterochromatin formation (see Histone Acetylation). Histone H1 is **phosphorylated** during S-phase and mitosis in the cell cycle, and its extreme cell-type specific variants in avian erythrocytes and sea urchin sperm are phosphorylated up until the final stages of chromatin compaction. Two volumes contain a wealth of information about the histones (1, 2).

1. Core Histones: The Histone Octamer

The core histones [molecular masses ~11,300Da (H4) to 15,300 (H3)] show a high degree of evolutionary sequence conservation, consistent with their role as organizing structural components in a common mode of DNA packaging in eukaryotes. Histones H3 and H4 are the most conserved proteins known, with only two (conservative) amino acid differences out of 102 residues between pea and calf H4. All the core histones have high contents of the basic amino acids lysine and arginine (whose side chains are protonated, and hence positively charged, at neutral pH). H2A and H2B are relatively lysine-rich, and H3 and H4 are relatively arginine-rich. The basic residues are unevenly distributed along the amino acid sequence and are concentrated toward the *N*-terminal regions of about 25 to 40 residues. These regions (the *N*-terminal "tails") are implicated in stabilization of chromatin higher-order structure and are essential for a number of vital functions. They are also the sites of several post-translational modifications, including acetylation, which has been well-studied (see Histone Acetylation).

The four core histones exist in chromatin as an octamer that is structurally organized as a tetramer of H3 and H4 ($H3_2H4_2$) and two dimers of H2A and H2B (H2A.H2B). The octamer may be isolated as an entity from chromatin at high ionic strength (eg, 2 M NaCl), which disrupts the electrostatic interactions between the histones and DNA and, in addition, preserves the association of tetramers and dimers (3). At physiological ionic strength, in the absence of DNA, the isolated octamer falls apart into tetramers and dimers. The structure of the octamer, determined to 3.1 Å resolution by X-ray crystallography (4), reveals two distinctive features of the histone associations (Fig. 1). First, the four histones (which have no obvious sequence homology) share a common fold, now designated the "histone fold." This comprises a long central a-helix and two shorter flanking a-helices connected by loops. Second, the histone pairs H3, H4 and H2A, H2B share a common mode of association as heterodimers in a "handshake motif," creating a crescent-shaped structure. Two H3.H4 heterodimers interact through a-helical regions on H3 to form the rather flat tetramer, which resembles a twisted horseshoe; H2A.H2B dimers flank this on each face, through interactions between a-helical regions on H2B and H4. The octamer crystal structure confirmed the presence of a left-handed helical ramp (for DNA binding) on the octamer surface, which had been inferred from earlier work (5), and suggested how the histone fold might form DNA contacts. The details of the interaction of the octamer with DNA have since been observed directly in the high-resolution structure of the nucleosome core particle (see Nucleosome), which also reveals the positions of the histone tails that were not visible in the structure of the octamer alone, because they are disordered. Intriguingly, the histone fold has since been found embedded in much larger proteins, notably several TAFs (TATA-box binding protein-associated factors) and transcription factors (see Histone Fold).

Figure 1. The structure of the histone octamer at 3.1 Å resolution, showing the histone folds (4).

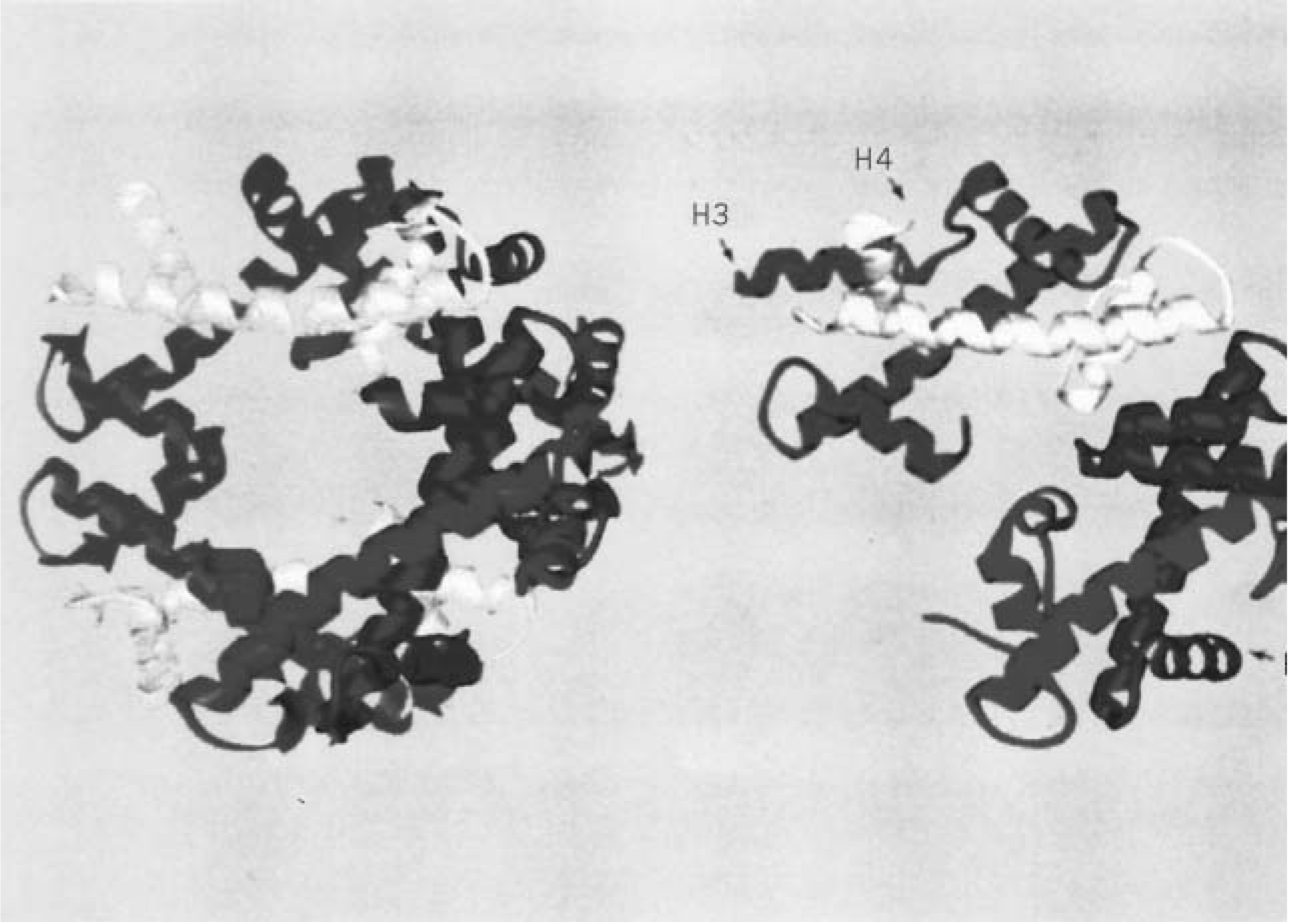

The *N*-terminal histone tails of the core histones are well-conserved, despite being external to the structured core of the octamer, suggesting some structural or functional role. The tails do not appear to be required for nucleosome core integrity and may be removed by **proteolysis** without causing structural disruption. There is good evidence that they play a role, together with the basic tails of H1, in stabilization of chromatin higher-order structure. In the structure of the nucleosome core particle (6) (see Nucleosome) they form few, if any, contacts within the nucleosome core, but are extended from it and are well-placed to interact with neighboring nucleosomes or other chromosomal components. The role of the tails has been extensively studied genetically in yeast (7) (see Nucleosome). It is increasingly recognized that the tails may function as recognition sites for protein factors important for chromatin function. For example, particular sequences in the *N*-terminal tails of H4 (residues 16 to 29) and H3 (residues 4 to 20) are required, together with other proteins (Rap1, Sir2, Sir3, and Sir4) for transcriptional **silencing** (through formation of a more repressed chromatin structure) at yeast telomeres and silent mating type loci (see Chromatin). The amino-termini of H3 and H4 are also required for a1–a2 repression in yeast (a regulatory mechanism involved in distinguishing **diploid** from haploid yeast cells) (8) and for the action *in vitro* of at least one chromatin remodeling machine, *Drosophila* NURF (9).

The *N*-terminal tails are the sites of several types of post-translational modification, the best studied of which is acetylation (see Histone Acetylation). It is involved in transcription and chromatin assembly, the acetylation patterns being different in the two cases, and could also provide additional markers for specific recognition by various partner proteins. The specific acetylation of Lys12 only in heterochromatin in *Drosophila* and yeast could perform such a role. Transcription-linked hyperacetylation, primarily on H4 and H3, is believed to result in relaxation of the repressive higher-order structure by disruption of internucleosome contacts. Crystal contacts in the nucleosome core particle suggest contacts that might be involved (6) (see Nucleosome). Other post-translational modifications have been less well studied and are less well understood (1, 2). Phosphorylation occurs constitutively at the *N*-terminal serine of H2A and, in a small proportion of histones, at Ser 10 and Ser 28 of H3 in response to mitogen stimulation in mammalian cells (10). Phosphorylation and acetylation appear to coexist in the same nucleosomes after mitogen stimulation and might act synergistically to disrupt internuclesomal contacts involving H3 tails and to facilitate transcription. The role of other modifications of the core histones (methylation of lysine side chains, and—in the case of H2B—**ADP-ribosylation**) is unclear; ADP-ribosylation may have a role in DNA repair, probably by disruption of chromatin structure. Also unclear is the role of ubiquitination of lysine side chains near the *C*-terminus of H2A and H2B (ie, covalent attachment of the small protein ubiquitin through an isopeptide linkage), but it appears not to be related to the well-recognized role of ubiquitination as a signal for **protein degradation**.

Core histone variants, the products of distinct genes, are found in all organisms. Their precise role is not clear, but they presumably allow fine-tuning of nucleosome structure and stability for particular purposes. A well-documented example is the developmental pattern of expression of five H2A variants and four H2A variants, which changes through the cleavage, blastula, and gastrula stages of sea urchin embryogenesis (11). Significantly, there is no variation in H3 and H4, which form the structural core of the nucleosome. During spermatogenesis in the same organism, there is a global replacement of somatic H2B with the larger and more basic sperm-specific variant spH2B, which has a long *N*-terminal extension with several "-SPKK-" (-Ser/Thr-Pro-X/Lys-Lys/Arg-) motifs (see text below) and helps in the tight compaction of chromatin in the sperm head. On fertilization, this is phosphorylated and then replaced during subsequent cell divisions with somatic variants. *Drosophila* has two evolutionarily conserved H2A variants: H2A.X, which has a *C*-terminal extension (like wheat H2A1, which has 19 extra residues and binds to linker DNA), and H2A.vD, which is essential for *Drosophila* development and has counterparts in mammals (H2A.Z), chickens (H2A.F/Z), and the ciliated protozoan *Tetrahymena* (hv1), where it is found in actively transcribed chromatin. H2A.Z is interesting because it has an *N*-terminal tail resembling that of H4 and indeed is acetylated more than the canonical H2A, thus providing obvious additional possibilities for regulation of function. For further details, see Ref. 2.

A class of more extreme so-called core histone variants are really hybrid proteins, with a region of histone sequence fused to a wholly unrelated region of unknown function. Two such proteins are the mammalian centromere-specific protein CENP-A (the yeast homologue is CSE4) and macroH2A. CENP-A (molecular mass ~17,000Da) is similar to H3 in its *C*-terminal domain, but has a highly divergent *N*-terminal region and appears to be associated, although not solely, with a- satellite DNA (12). Assuming that it replaces the normal H3, it presumably imparts special properties to centromeric chromatin. MacroH2A is a highly conserved protein in which the *N*-terminal third resembles H2A and the *C*-terminal two-thirds contains a coiled-coil protein dimerization motif. There are two macroH2A subtypes, which are (a) highly conserved and (b) identical in the histone region. It came as a surprise to find that one subtype is localized to the inactive X-chromosome (in mouse) and is distributed throughout the chromatin (13); it is tempting to speculate that the coiled-coil might have a role in protein oligomerization and condensation of chromatin. MacroH2A is thus one more distinctive component of the inactive X-chromosome, the others being heavily **methylated** DNA, hypoacetylated H4, and association with a large ***cis*-acting** nuclear RNA (termed Xist).

2. Linker Histones/Histone H1

Linker histones (H1 and its variants and subtypes) in higher eukaryotes are larger than the core histones (molecular mass ~20,000 to 25,000 Da) and are particularly lysine-rich. They have a tripartite domain structure, in which a central globular domain of about 80 amino acid residues, which is highly conserved between species, is flanked by basic *N*- and *C*-terminal domains ("tails") that are much more divergent. In the absence of DNA, the tails are disordered and may be selectively removed by proteolysis, leaving the globular domain intact. In a typical mammalian H1, the *N*- and *C*-terminal tails are about 40 and 100 residues long, respectively; the lengths differ in some species-specific and cell-type-specific variants. Nucleosomes released from chromatin by digestion with micrococcal nuclease (**Staphylococcal nuclease**) are rapidly trimmed by further digestion so that the ~200 bp of DNA is reduced to ~166 bp, giving a chromatosome. If H1 is removed before digestion, however, only 146 bp remain protected, as digestion proceeds to the limit nucleosome core particle. The globular domain of H1 alone is sufficient to protect 166 bp, so this is the region of H1 that binds close to the nucleosome core, stabilizing the nucleosome and protecting an extra 20 bp from digestion. The basic *C*-terminal tail (and possibly also the *N*-terminal tail) binds to the linker DNA between adjacent nucleosomes (hence the name *linker histones*), partially neutralizing its negative charge and promoting folding of the nucleosome filament into a higher-order structure, the 30-nm filament; H1 is located on the inside of the 30-nm filament (see Chromatin). The role of H1 is thus to stabilize both the nucleosome and an ordered higher-order chromatin structure. H1 may be phosphorylated (see text below) and poly-ADP-ribosylated; the role of the latter modification is not clear, but it is probably involved in DNA repair .

There are many subtypes and more extreme sequence variants of H1, which all share the same domain organization. These may coexist in the same cell type (eg, there are six H1 subtypes in chicken erythrocytes), and the assumption is that they might stabilize different chromatin higher-order structures. This would be likely to occur only if they were clustered along a chromatin filament, and this indeed appears to be the case for one of the seven H1 variants in the interphase polytene chromosomes in the Dipteran insect ***Chironomus*** *thummi* (14). Information is lacking for other systems or for other H1s in *Chironomus*. There are several instances of changes in linker histone variants during developmentally regulated processes (11, 15). During sea urchin embryogenesis, six distinct H1 subtypes are produced at particular stages; and *Xenopus* has an embryonic form of H1, namely B4, that is very different from the normal somatic H1. The *C*-terminal tail is less basic, and this might result in a less condensed chromatin structure in *Xenopus* embryos, compatible with rapid nuclear division and DNA replication. Extreme variants may also be produced to shut down transcription in particular cell types, and they appear to be associated with more stable chromatin higher-order structures (see Chromatin). For example, in transcriptionally inert mature avian erythrocytes, H5 (which binds more tightly than H1, probably due to its higher arginine content, although it has shorter *N*- and *C*-terminal tails) has largely replaced H1; and in sea urchin sperm, somatic H1 is replaced by a larger and more basic sperm-specific H1, namely spH1, which, together with sperm-specific core histones, is very effective in condensation of the DNA. (In mammalian sperm, histones are replaced by protamines, small arginine-rich proteins, rather than by specialized histone variants.) $H1^{0}$, an H1 variant whose appearance in mammalian cells appears to correlate with terminal differentiation (eg, in neurons), is much more similar to H5 than to H1 in its globular domain.

The globular domains of histones H1 and H5 (GH1 and GH5) can bind to the body of the nucleosome (see text above) and protect an additional 20 bp beyond the core particle length from digestion. The structure of GH5, determined by X-ray crystallography, shows a "winged helix" motif (a variant on the **helix–turn–helix** DNA-binding motif) which is also found in two proteins that bind to specific DNA sequences, namely the liver transcription factor HNF_3g (hepatocyte nuclear factor 3g,) and the prokaryotic protein **cyclic AMP receptor protein** (CRP) (16). It consists of a three-helix bundle with a b-hairpin (or "wing") at its *C*-terminus. Based on the X-ray crystal structures of these proteins bound to DNA, the likely mode of binding of GH5 to DNA, in the major groove, has been deduced. Biochemical evidence points to a second DNA binding site on GH5, and this has been identified on the opposite face of the globular domain (17) (Fig. 2). It is likely that the two sites are occupied in the nucleosome by two of the three duplexes (the central turn and the entering and exiting DNA) that are present in the vicinity of the dyad axis of the nucleosome. Current evidence for bulk nucleosomes (18) suggests that GH5 bridges the central turn, close to the dyad, and one of the entering/exiting duplexes. The orientation proposed would place the *C*-terminal tail of H1 directed toward linker DNA, as expected from various lines of evidence. A different mode of binding of the globular domain to the reconstituted *Xenopus* 5 S nucleosome has been proposed, but it is not yet clear whether this is a special property of the 5 S nucleosome (see Nucleosome). The existence of two binding sites on the globular domain is probably the basis of its preference (over linear DNA) for four-way DNA junctions (19), which mimic a pair of duplexes at the DNA crossover point near the nucleosome dyad.

Figure 2. The structure of the globular domain of histone H5 (GH5) showing the two clusters of basic residues at the two proposed DNA-binding sites on opposite faces of the domain (17). Binding to DNA at one site is by analogy with the structures of HNF3g and CRP (see text).

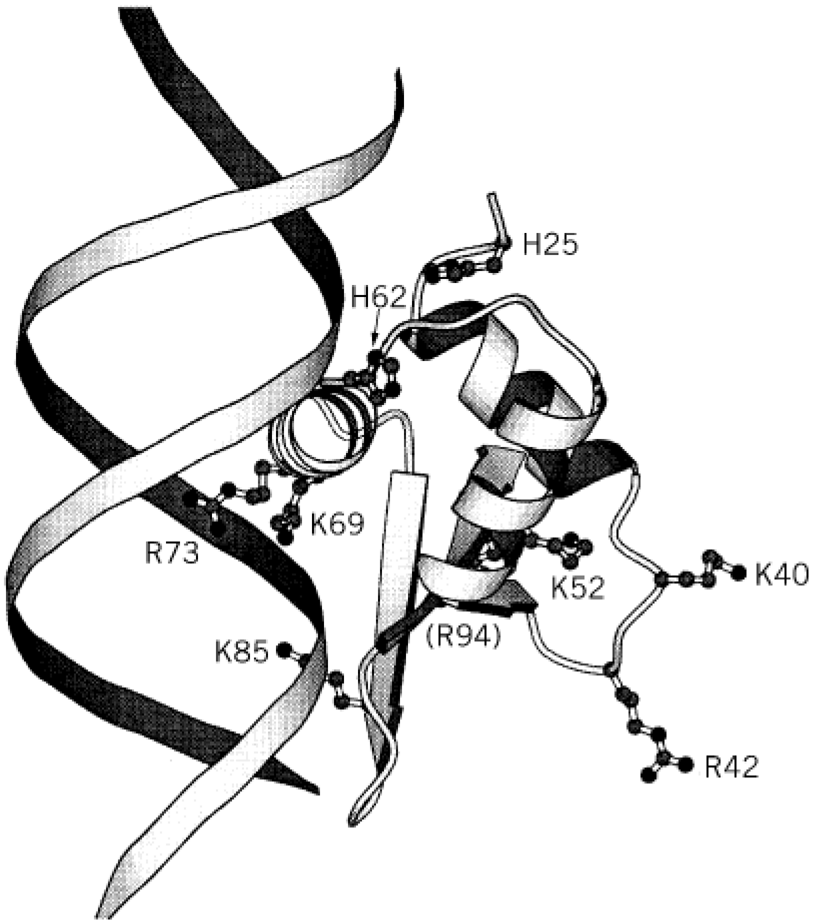

There is no high-resolution structural information for the *N*- and *C*-terminal tails of H1 or any of its variants. The role of the *N*-terminal tail (~40 amino acid residues in the canonical H1) is unclear, but there is some evidence that it may anchor the globular domain correctly in the presence of the *C*-terminal tail. The basic *C*-terminal tails (~90 to 130 amino acid residues, depending on the variant) have unusually high contents (~50%) of the basic residues lysine and arginine, as well as relatively high contents of alanine and proline. They are essential for chromatin condensation and are believed to bind to linker DNA. They are disordered in the free protein, but they are likely in the presence of DNA to exist as a-helical segments rich in lysine and alanine, the segments being separated by proline residues (20). The proline residues are often embedded in so-called “-SPKK-” sequence motifs (-Ser/Thr-Pro-X/Lys-Lys/Arg-), where the serine is a potential phosphorylation site. There is some phosphorylation at S-phase of the cell cycle and considerably more at mitosis, probably due to the action of the cyclin-dependent kinase, $p34^{cdc2}$ (21). The role of phosphorylation is likely to be to loosen the interactions between the H1 tails and linker DNA, and at mitosis to permit other factors and interactions to drive chromosome condensation. Some members of the repertoire of H1s produced during different stages of sea urchin embryogenesis lack -SPKK- motifs, suggesting that the binding of different H1s may be differentially regulated. Phosphorylation also plays a role in the control of chromatin transitions unrelated to the cell cycle, namely, in the late stages of avian erythropoiesis, or sea urchin sperm spermatogenesis, where there is no cell division and where special histone variants that bind more tightly than somatic H1 (ie, H5 and spH1, respectively) suppress transcription by promoting chromatin condensation. H5 and spH1 are phosphorylated at the -SPKK- motifs (of which there are six copies in the *N*-terminal tail of spH1 and further copies in the C-tail) until the final stage of maturation, when a final dephosphorylation step in the spermatozoon or mature erythrocyte results in the final stage of chromatin condensation and even closer chromatin packing in the sperm head or erythrocyte nucleus; removal of the phosphate increases the net positive charge on the histone and promotes histone–DNA interactions, leading to condensation. An analogous situation exists in the amitotic nucleus of *Tetrahymena* (22).

There are two very atypical H1s, or—in one case—candidate H1, in lower eukaryotes, which lack the characteristic domain organization of the canonical H1. The ciliated protozoan *Tetrahymena thermophila*, which has a transcriptionally active but amitotic **macronucleus** and a transcriptionally inert mitotic **micronucleus**, contains a small, basic, macronuclear protein of 163 residues, designated H1, that appears to share some of the functions of linker histones. (A set of distinctive polypeptides appears to substitute for H1 in the micronucleus.) The macronuclear H1 condenses chromatin in the nucleus, and phosphorylation at 'TPVK' sites results in an increase in nuclear volume, suggesting that phosphorylation loosens interactions with chromatin, as expected (22, 23). It lacks the distinctive globular domain of the canonical H1, however, although its *C*-terminal region has similarities to the *C*-terminal tail of H1. Exactly how the *Tetrahymena* H1 is bound to chromatin is unclear. An unusual, but quite different, domain organization also occurs in a candidate H1 identified from the recently determined complete sequence of the yeast (*Saccharomyces cerevisiae*) genome. Previous attempts to isolate H1 from yeast had been unsuccessful, and one view was that because the linker length of yeast chromatin was virtually zero (chromatin repeat length ~166 base pairs) there was no requirement for neutralization of linker DNA charge or, therefore, for a canonical linker histone. Analysis of the yeast genome revealed an open reading frame (the *HHO1* gene) encoding a protein (Hho1p) with regions of sequence homology to the globular domain of H1, which is regarded as a candidate H1 (24). It has *two* globular domains of about 80 residues, with a basic *N*-terminal extension and a basic connecting linker with some resemblance to the *C*-terminal tail of the canonical H1. Recombinant Hho1p appears to have some of the distinctive properties of H1 in a standard chromatin reconstitution, namely protection of an additional ~20bp of DNA beyond the core particle length against exonuclease digestion (25). Its unique structure, however, means that there are likely to be differences in its detailed mode of binding to chromatin compared with canonical H1, and it is by no means clear at present whether Hho1p functions as a true H1 or is instead a transcription factor with domains homologous to the globular domain of H1 [cf. some TAFs, which have sequence homology to core histones (see Histone Fold); or even $HNF3_g$ which contains the same structural fold as in the globular domains of H5 and H1 (see text above), although in that case there is no sequence homology between the two proteins].

Gene disruptions and deletions have been used to ask whether H1 is essential. Disruption ("knockout") of the $H1^0$ gene in mouse appeared to be without consequence; it is likely, however, that one or some of the six other subtypes compensate (26); in other words, there is functional redundancy. Deletion of the entire complement of somatic H1 genes has not been achieved. Early *Xenopus* embryos contain the unusual H1 variant B4 (see text above) which is later replaced by somatic H1; elimination of B4 had little effect on nuclear assembly or on the development of the organism (27). Deletion of the single gene for the atypical macronuclear H1 of *Tetrahymena* was not lethal, but was not without effect either (23). Vegetative growth, general transcription, and general nucleosome repeat length were unaffected, but there were changes in the nuclear volume (presumably consistent with the role of the protein in chromatin condensation and packing in the nucleus), in the efficiency of meiotic division, and, significantly, in the transcriptional regulation of specific genes. However, although some genes were activated, consistent with the expected repressive role for H1, others were repressed (eg, the CyP gene, which encodes a thiol proteinase). One explanation would be that the binding of the *Tetrahymena* H1 is needed in some nucleosomes to position them in such a way that certain sequences necessary for the binding of activators are exposed. In yeast, deletion of the yeast *HHO1* gene had no detectable effect on cell growth, viability, or mating, or on telomeric silencing, basal transcriptional repression, or efficient **sporulation** (25, 28). It also did not affect transcription of the SW1/SNF-dependent *SUC2* gene or the repression of the silent a1/a2 genes, or activation at a distance of a GAL1 promoter (28). It remains to be seen whether the Hho1p protein is really a *bona fide* H1 or a transcription factor evolutionarily related to the globular domain of histone H1, despite assuming some of the functional properties of H1 in an *in vitro* assay (25). These and other studies suggest strongly that H1 and its variants probably have roles beyond that of simple repression and stabilization of higher-order structure in chromatin. Gene-specific effects of H1 are clear in one well-documented case, namely, the 5 S rRNA genes of *Xenopus laevis*. Replacement of the unusual embryonic variant B4 with the somatic H1 during embryogenesis has been shown to be causal for the selective repression of the oocyte 5 S, leaving the somatic genes active (29). Gene-specific effects of H1, in addition to a general, default, repressive role, may turn out to be more common than might have been imagined.

Bibliography

1. K. van Holde (1988) *Chromatin*, Springer-Verlag, New York.
2. A. P. Wolffe (1995) *Chromatin: Structure and function*, 2nd ed., Academic Press, London.
3. J. O. Thomas and R. D. Kornberg (1975) Proc. Natl. Acad. Sci. USA **72**, 2626–2630.
4. G. Arents et al. (1991) Proc. Natl. Acad. Sci. USA **88**, 10148–10152.
5. A. Klug et al. (1980). Nature **287**, 509–516.
6. K. Luger et al. (1997) Nature **389**, 251–260.
7. M. Grunstein (1997) Nature **389**, 349–352.
8. L. Huang, W. Z. Zhang, and S. Y. Roth (1997) Mol. Cell. Biol. **17**, 6555–6562.
9. P. T. Georgel, T. Tsukiyama, and C. Wu (1997) EMBO J. **16**, 4717–4726.
10. M. J. Barratt, C. A. Hazzalin, E. Cano, and L. C. Mahadevan (1994) Proc. Natl. Acad. Sci. USA, **91**, 4781–4785.
11. D. Poccia (1986) Int. Rev. Cytol. **105**, 1–65.
12. K. F. Sullivan, M. Hechenberger, and K. Masri (1994) J. Cell Biol. **127**, 581–592.
13. C. Costanzi and J. R. Pehrson (1998) Nature **393**, 599–601.
14. E. Mohr, L. Trieschmann, and U. Grossbach (1989) Proc. Natl. Acad Sci USA **86**, 9308–9312.
15. S. Khochbin and A. P. Wolffe (1994) Eur. J. Biochem. **225**, 501–510.
16. V. Ramakrishnan (1994) Curr. Opin. Struct. Biol. **4**, 44–50.
17. F. A. Goytisolo et al. (1996) EMBO J. **15**, 3421–3429.
18. Y.-B. Zhou et al. (1998) Nature **395**, 402–405.
19. P. Varga-Weisz et al. (1994) Proc. Natl. Acad. Sci. USA **91**, 3525–3529.
20. D. J. Clark, C. S. Hill, S. R. Martin, and J. O. Thomas (1988) EMBO J. **7**, 69–75.
21. R. W. Lennox and L. H. Cohen (1988) In *Chromosomes and Chromatin*, Vol. **1** (K. W. Adolph, ed.) CRC Press, Boca Raton, FL. pp. 33–56.
22. S. Y. Roth and C. D. Allis (1992) Trends Biochem. Sci. **17**, 93–98.
23. X. T. Shen and M. A. Gorovsky (1996) Cell **86**, 475–483.
24. S. C. Ushinsky et al. (1997) Yeast **13**, 151–161.
25. H. G. Patterton et al. (1998) J. Biol. Chem. **273**, 7268–7276.
26. A. M. Sirotkin et al. (1995) Proc. Natl. Acad. Sci. USA **92**, 6434–6438.
27. M. Dasso, S. Dimitrov, and A. P. Wolffe (1994) Proc. Natl. Acad Sci. USA **91**, 12477–12481.
28. D. Escher and W. Schaffner (1997) Mol. Gen. Genet. **256**, 456–461.
29. P. Bouvet, S. Dimitrov, and A. P. Wolffe (1994) Genes Dev. **8**, 1147–1159.

Suggestions for Further Reading

30. V. Ramakrishnan (1997) Histone structure and the organization of the nucleosome. Ann. Rev. Biophys. Biomol. Struct. **26**, 83–112.
31. V. Ramakrishnan (1997) Histone H1 and chromatin higher-order structure. Crit. Rev. Eukaryot. Gene Expr. **7**, 215–230.
32. K. van Holde and J. Zlatanova (1996) The linker histones and chromatin structure: new twists. Prog. Nucleic Acid Res. Mol. Biol. **52**, 217–259.
33. A. A. Travers (1999) Towards a higher order structure for chromatin—the location of the linker histone in the nucleosome. Trends Biochem. Sci. (in press).
34. R. D. Cole (1987) Microheterogeneity in H1 histones and its consequences. Int. J. Protein Res. **39**, 433–449.

HIV (Human Immunodeficiency Virus)

Human immunodeficiency virus (HIV), a causative virus of acquired immune deficiency syndrome (AIDS), is a member of the *Lentivirus* genus of the family *Retroviridae* (see Rous Sarcoma Virus (RSV)). The first isolate was reported in 1983 and was named lymphadenopathy-associated virus (LAV). Other isolates, such as human T-lymphotropic virus type III (HTLV-III) and AIDS-associated retrovirus (ARV), were reported in 1984. These HIV isolates were later categorized as HIV-1, because a serologically unique HIV isolate was discovered in 1986 and designated as HIV-2. Great sequence variation, especially in the env gene, is characteristic of HIV, and at least nine subtypes of HIV-1 (A to I) and/or five of HIV-2 (A to E) have been classified.

HIV virions are spherical and about 110 nm in diameter. The HIV virion has a lipid-bilayer envelope, and approximately 72 knobs (spikes) protrude from the envelope. Each knob is composed of oligomeric surface protein (SU:gp120 in HIV-1 and gp130 in HIV-2) and transmembrane protein (TM:gp41 in both HIV-1 and HIV-2). Inside the envelope, the capsid proteins (CA:p24) form the bullet-shaped capsid shell. The matrix protein (MA:p17) is present between the envelope and CA. The nucleocapsid protein (NC:p9) binds to the viral genome. SU, TM, MA, CA, and NC are the major structural proteins. Two identical copies of single-stranded RNA of positive polarity are contained in a HIV virion as the genome. The enzymes proteinase (PR), **reverse transcriptase** (RT) (see Rous Sarcoma Virus (RSV) and Hepatitis B Virus), and integrase (IN) are also contained in the capsid shell.

The genome RNA of about 9.2 kb is, like cellular messenger RNAs, capped at the 5′ end (see Cap) and tailed by poly(A) at the 3′ end. The genome has short direct repeats (R) and unique sequences at both ends (U5 at the 5′ end and U3 at the 3′ end). These sequences are important to form long terminal repeats (LTRs) during replication. The coding sequences of HIV have three major genes of retroviruses: gag, pol, and env. The gag gene codes for MA, CA, and NC; the pol gene codes for PR, RT, and IN; the env gene codes for SU and TM. It is characteristic of HIV to have accessory genes. Two of them, tat and rev, are essential for replication in both HIV-1 and HIV-2. HIV-1 has vif, vpr, nef, and vpu, while HIV-2 has vif, vpr, nef, and vpx instead of vpu as nonessential accessory genes.

The replicative cycle starts with an interaction between the virion and the cell surface receptor. The principal receptor for HIV is the CD4 molecule, which is expressed on CD4-positive T lymphocytes, macrophages, and so on. The CD4-binding sites on the virion are on SU (gp120). The next crucial step after binding is fusion of the virion envelope and the plasma membrane. It has been postulated that an *N*-terminal hydrophobic **domain** in TM is the actual fusion protein, which needs to be exposed by a conformational change in the envelope glycoproteins caused by SU binding to CD4.

Interestingly, an additional cell-surface molecule, actually a chemokine receptor like CCR5 or CXCR4, is needed to initiate the fusion process. These chemokine receptors are referred to as “co-receptors” for HIV infection. Once the nucleoproteins get into the cytoplasm, synthesis of the minus-strand DNA starts using RT and host transfer RNA^{Lys} attached near the 5′ end of the viral genome as a primer. Synthesis of viral DNA is similar to that of other mammalian and avian retroviruses, but lentiviruses, including HIV, start the plus-strand DNA synthesis at two sites; one is a polypurine tract near U3 like many other retroviruses, and the other is a central polypurine tract at the end of pol gene. Double-stranded viral DNA with the LTR (see Rous Sarcoma Virus (RSV)) on both ends is carried to the nucleus as preintegration complex. Presumably, nuclear localization signals in MA and/or Vpr play an important role in nuclear translocation of the preintegration complex. While mammalian and avian retroviruses require cell division for efficient virus production, HIV can infect nondividing, terminally differentiated cells. Linear double-stranded viral DNA is the substrate for IN and the direct precursor of integrated provirus.

Integrated proviral DNA has an LTR on both ends. Full-length viral RNA is transcribed from the U3/R boundary in the 5′LTR to the R/U5 boundary in the 3′LTR, and 5′-capped and 3′-poly(A)-tailed viral RNA serves as both genome RNA and mRNA for translation. The mRNA undergoes complex RNA splicing. The env and accessory gene products are translated from spliced mRNAs. The env gene products (Env) are translated as a precursor protein, gp160, in the rough endoplasmic reticulum, processed to gp120 (SU) and gp41 (TM), and expressed on the cell surface. The gag and pol gene products (Gag and Pol) are translated from unspliced mRNA. The pol gene is not in the same reading frame as gag gene, however, and pol gene products are translated as a Gag–Pol fusion protein by ribosomal frameshifting at the gag–pol boundary. Viral assembly occurs just below the plasma membrane. Virions bud out from the cells, covered by the plasma membrane (viral envelope) with SU and TM. Viral proteinase (PR) digests Gag and Gag–Pol fusion proteins to MA, CA, NC, PR, RT, and IN, and the virions are matured.

Suggestion for Further Reading

P. A. Luciw (1996) "Human Immunodeficiency Viruses and Their Replication. In" *Fields Virology*, 3rd ed. (B. N. Fields et al., eds.), Lippincott-Raven, Philadelphia, pp. 1881–1952.

Hofmeister Series

The Hofmeister (or *lyotropic*) series, first described by Hofmeister in 1888, is the ordering of ions in their effectiveness in salting out proteins (see Precipitation). Since then, it has been established that the same order is maintained in the effects of these ions on **nucleic acid** and protein stability (see **Stabilization and destabilization by co**), association–dissociation equilibria between macromolecules, enzyme activity, and various other biological and biochemical functions (1). The ordering is as follows:

← Stabilization   Unfolding →
← Salting in   Salting out →

Anions:

$$SO_4^{2-} < CO_3^{2-} < F^- < CH_3COO^- < Cl^- < Br^- < NO_3^- < ClO_4^- < I^- < SCN^-$$

Cations:

$$NH_4^+ < Rb^+, K^+ < Na^+, Cs^+ < Li^+ < Mg^{2+} < Ca^{2+} < Ba^{2+}$$

Anions and cations are essentially independent of each other in these actions, and their effects are additive. For example, it has been found that LiBr is a good salting in agent, whereas NaCl is a salting out agent (2). Reshuffling the ions gives the result that both NaBr and LiCl have no effect on the solubility, in other words, the salting in capacity of one ion (Li^+ or Br^-) is compensated by the salting out characteristic of the co-ion (Cl^- or Na^+).

Bibliography

1. P. von Hippel and T. Schleich (1969) In *Structure and Stability of Biological Macromolecules* (S. N. Timasheff and G. D. Fasman, eds.), Marcel Dekker, New York, "Chap. 6".
2. D. R. Robinson and W. P. Jencks (1965) J. Am. Chem. Soc. **87**, 2470–2479.

Holocentric Chromosome

Holocentric or polycentric chromosomes have centromeric heterochromatin (see Centromeres) distributed at multiple sites along the length of the chromosome (1). Organisms with holocentric chromosomes include nematodes, such as *Ascaris*, insects, such as *Lepidoptera*, and **plants** in the genus *Lazula*. Spindle fibers attach along the whole length of holocentric chromosomes (Fig. 1). Sites of attachment of the spindle to centromeric chromatin are interspersed with noncentromeric segments, as in *Ascaris*, or all the chromatin in the chromosome is competent for attachment, as in the coccid bugs (2). In this latter case, centromeric functions are appropriately described as diffuse. In some organisms, like *Lazula*, localized centromeric function might be retained in mitotic chromosomes but shift to different positions in meiotic chromosomes. Mammalian tissue culture chromosomes also persist and segregate when they have multiple centromeres, but in this case only one centromere remains functional (4).

Figure 1. Monocentric and holocentric chromosomes. (a) Monocentric chromosomes have a single site of chromosomal attachment to the spindle. (b) Holocentric chromosomes have multiple sites of attachment to the spindle.

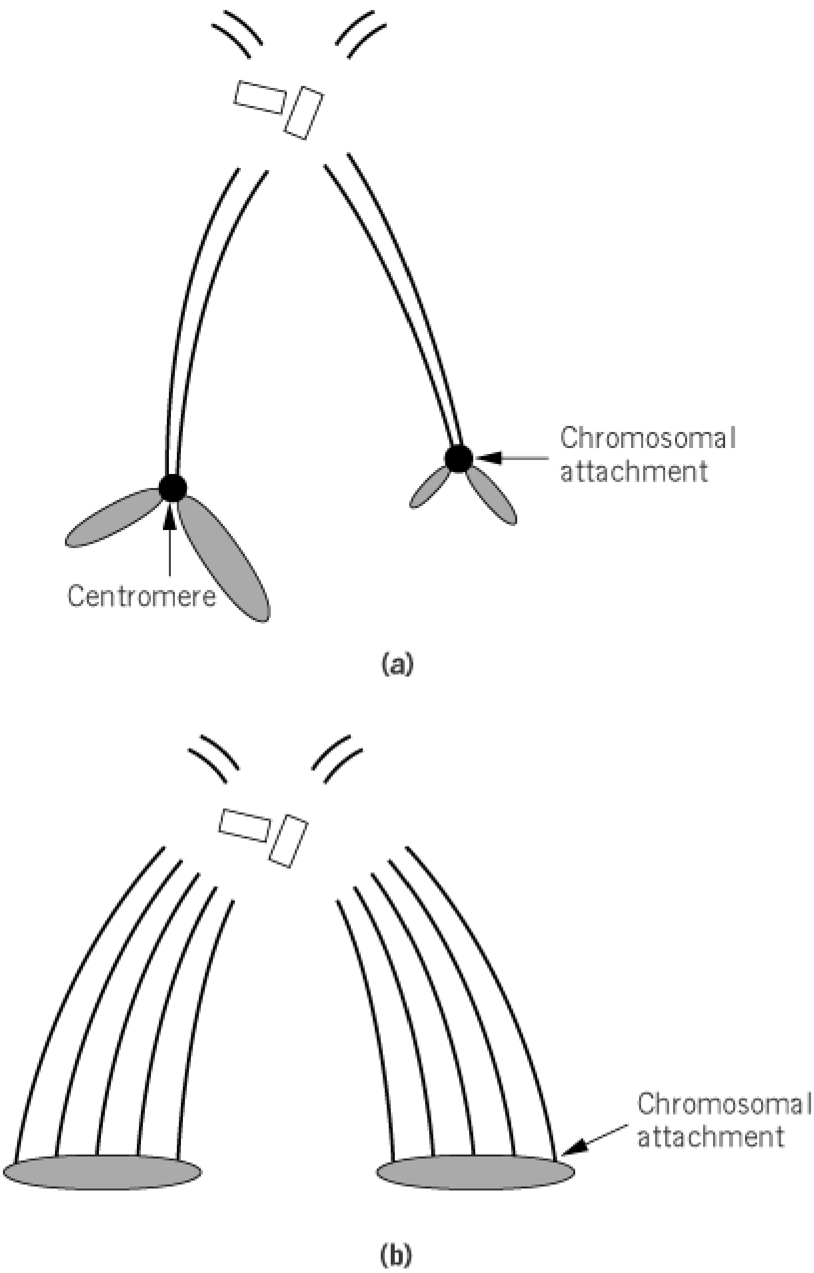

Bibliography

1. S. Dimpinelli and C. Coday (1989) Trends Genet. **5**, 310–314.
2. S. Hughes-Schrader (1948) Adv. Genet. **2**, 127–203.
3. J. P. Braselton (1981) Chromosoma **82**, 143–153.
4. B. K. Vig (1984) Chromosoma **90**, 39–45.

Suggestion for Further Reading

5. R. P. Wagner, M. P. Maguire, and R. L. Stallings (1993) *Chromosomes. A synthesis*, Wiley-Liss, New York.

Holoenzyme, Apoenzyme

A number of enzymes rely on the presence of a **prosthetic group** at their active site in order for them to be catalytically active (see Coenzyme, Cofactor). For example, aminotransferases require pyridoxal phosphate. Prosthetic groups are small molecules that are covalently or tightly bound at the active site. They provide groups that the protein component of the enzyme does not possess, but that are essential for catalysis. The enzyme with a prosthetic group bound is referred to as a holoenzyme, whereas after removal of the prosthetic group, the protein component alone is termed an apoenzyme. Thus,

$$\text{Holoenzyme} = \text{apoenzyme} + \text{prosthetic group} \quad (1)$$

The term apoenzyme is also applied to **allosteric** enzymes such as aspartate transcarbamoylase from which the regulatory subunits have been removed.

Homeobox Genes

Homeobox genes play fundamental roles in development and evolution. They are perhaps the best examples of key regulators of gene transcription that are at the heart of the genetic circuitry, regulating different pathways. Homeobox genes have been highly conserved throughout evolution and are involved in the genetic control of the body plan, the determination of cell fate, and several other basic developmental processes. Common among the hundreds of different homeobox genes known today is a highly homologous, 180-bp structural motif, the homeobox . The homeobox encodes a 60-amino acid residue polypeptide chain, the ***homeodomain***, that represents the **DNA-binding** domain of the respective proteins.

1. History of Homeobox Genes

Homeotic mutations lead to segmental transformations, suggesting that they are involved in the genetic control of a body plan. The first homeotic mutant, bithorax, was discovered in 1915 (1). This *Drosophila* **gene** was later shown to be part of a gene cluster termed the bithorax complex (BX-C) (2). Single mutations in the bithorax complex induced major modifications in the body plan, for example, generating four-winged flies. In 1983, the first homeobox gene locus, *Antennapedia*, was isolated (3), which is part of the ***Antennapedia* complex** (Antp). Comparative sequence analysis of the first three cloned homeobox genes, *Antennapedia*, *fushi tarazu*, and **Ultrabithorax**, established a common DNA motif, coined the homeobox (4, 5). This motif was not confined to *Drosophila*, but was also found in vertebrates, including mice and humans. In 1984, the first homeobox gene in the mouse was **cloned** by cross-hybridization using a *Drosophila* homeobox probe (6).

2. Structure and Function of the Homeodomain

The highly conserved **homeodomain** is typically composed of 60 amino acid residues. Figure 1 shows the amino acid **consensus sequence** based on 346 different homeodomain sequences (7). Comparison of the X-ray crystallography structures of the homeodomains of **engrailed** and other homeobox genes of the yeast **mating-type** proteins revealed a **helix-turn-helix** binding motif (8), suggesting that all homeodomains bind to DNA in the same manner. The three **alpha-helical** regions are composed of residues 10–22, 28–38 and 42–58 of the homeodomain (see Fig. 1). Helix 3, the recognition a-helix, binds to the major groove of DNA, whereas helices 1 and 2 lie close to each other in an antiparallel orientation outside the double helix. Thus, only a small number of residues in helix 3 (in particular, that at position 50) and in the *N*-terminal arm are responsible for the specificity of contacts with the DNA. Furthermore, *in vitro* binding studies with protein extracts of the locus *Antennapedia* showed that the homeodomain binds as a monomer to its DNA-binding site, dissociated only slowly, with an estimated half-life of 90 min (9). Other examples suggest that homeobox proteins may dimerize. Transcriptional regulation of homeodomain proteins *in vivo* was first demonstrated for bicoid, interacting with its target gene hunchback (10-12).

Figure 1. The primary and secondary structures of the homeodomain. The homeodomain contains three well-defined a-helices and a more flexible fourth helix. The schematic illustration of the structure represents a composite derived from the structures of the Antennapedia, engrailed, and MATa2 homeodomains. The amino acid consensus sequence is based on 346 homeodomain sequences. For each position, the amino acid encountered most frequently is listed at the top, while other amino acids are listed beneath in decreasing order of frequency of occurrence. Amino acids occurring fewer than 5 times (1.5%) are not shown. The symbols on top indicate highly conserved positions: ▽ are the most highly conserved positions, with only one or two amino acids found at that position. *ƒ* indicates highly conserved positions with three to five different amino acids found at a particular position, and * indicates conserved positions, with not more than nine different amino acids.

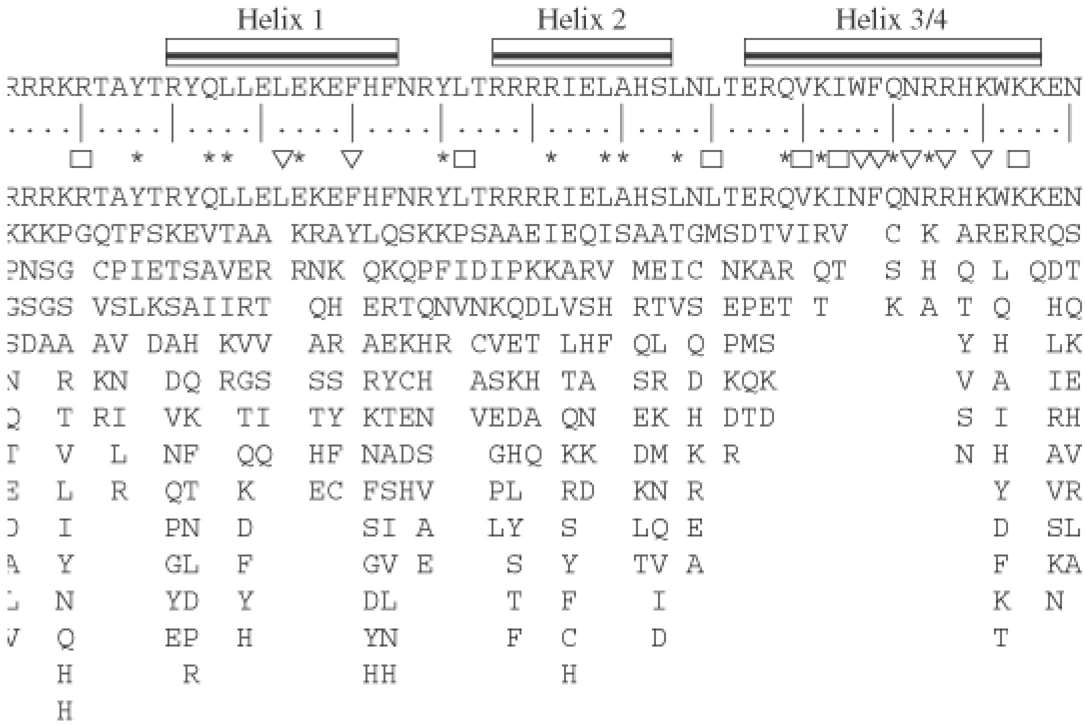

3. HOX Gene Clusters

Homeobox genes are clustered in *Drosophila* and organized in two separate clusters, the bithorax (BC-C, 2) and *Antennapedia* (Antp) complexes (13, 14), and are referred to as *HOM-C complexes* . The genes of these two gene clusters have been termed *HOX genes*. HOX genes play a critical role in pattern formation. The order of HOX genes within each cluster correlates with the temporal order of expression of these genes, which are expressed along the anteroposterior axis of the embryo. Interestingly, homeobox genes with sequence similarity to *Drosophila* **HOX genes** are also clustered in vertebrates. Both humans and mice have four HOX gene clusters, which reside on different chromosomes. They are termed *Hoxa* to *Hoxd* in mice and *HOXA* to *HOXD* in humans (15). Altogether, 38 genes reside in these four gene clusters, and all are orientated in the same 5′–3′ direction of transcription (16, 17). Furthermore, in mammals the order of HOX genes within a cluster dictates the time of expression.

4. Homeotic Mutations

The term *homeotic mutations* actually refers to HOX gene mutations within the homeotic clusters. For example, a homeotic mutation in the *Antennapedia* gene complex transforms an antenna into a leg. A mutation in the *bithorax* gene results in a fly with four wings. A mutation in human HOXD13 results in synpolydactyly. Some of the mouse HOX mutations have been shown to lead to only relatively mild phenotypes. This may be due to functional compensation or to different parallel regulatory pathways.

In a broader sense, homeotic mutations may encompass mutations of all homeobox genes. Homeotic mutations may represent the classic examples of loss-of-function mutations or gain-of-function mutations. It is interesting that missense mutations causing loss-of-function mutations are often concentrated in the homeodomain or in other functionally important parts of the protein. In contrast, nonsense mutations leading to gene truncations are distributed more widely across the genes. Also, a 50% reduction in the gene product (haploinsufficiency) or overexpression may lead to different clinical phenotypes, suggesting that correct dosage is crucial at certain times in development. This was shown for the first time for PAX6, which leads to aniridie when underexpressed and to other severe eye abnormalities when overexpressed (18, 19) (see Pax Genes).

5. Homeodomain Gene Families

Using degenerate oligonucleotide probes or amplification by **PCR**, a wide variety of novel homeobox genes that represent non-HOX homeobox genes have been identified. Some of these “isolated” (“orphan”) homeodomain gene families contain additional highly conserved domains. Examples of these conserved motifs are the **paired-**, **POU-**, LIM-, engrailed-, and **zinc-finger** motifs, which specify the individual classes of homeobox genes. Each of the two independent DNA-binding domains contacts a specific short sequence on the major groove of the DNA double helix. Examples of the homeobox genes with a paired domain include several members of the PAX gene family (PAX 2, 3, 6); POU domain genes are **P**it1, **O**ct1, and **u**nc 86; genes with a LIM motif include the nematode lin-11 and putative human **oncogene** rhombotin1; the engrailed class of homeobox genes includes EH1-5, and a gene with a zinc-finger motif is the human ATBF1 gene.

A homeobox page on the different homeobox genes is maintained by Thomas R. Bürglin and can be accessed via the Internet (site currently unavailable).

6. Homeobox Genes in Disease

In the last few years, gene disruption experiments in transgenic mice, as well as positional cloning in humans, have defined a number of homeobox genes associated with genetic diseases and congenital syndromes. The first human HOX gene mutation, HOXD13, was described in families with synpolydactyly (webbing and duplication of fingers) (20). Here the homeodomain was still intact, and the affected members of these families had an expansion of 7–10 additional alanine residues. RIEG, a bicoid -related homeobox gene, was shown to be involved in Rieger syndrome, a complex human disorder with dental, ocular, and further abnormalities (21). Just recently, the chick and *Xenopus* homologues of RIEG (Pitx2) were shown to determine the left–right asymmetry of internal organs in vertebrates (22). SHOX, a **paired**-related gene, was shown to play a major role in human growth (23), affecting the height in Turner and Léri-Weill syndrome patients, Langer dwarfism, and idiopathic short stature patients. The MSX1/MSX2 family of genes has been found to be mutated in some forms of craniosynostosis (24). PAX2 and PAX6 genes play a role in eye development, and PAX3 in the Waardenburg syndrome, the most common form of inherited deafness (25). Two gene families in particular, Emx and Otx, have been reported to play a role in brain development, and EMX2 mutations, for example, have been associated with schizencephaly (26).

7. Evolutionary Conservation

Because of their fundamental importance in embryonic development, homeobox genes have been highly conserved throughout evolution. Homeobox genes have been found in plants, fungi, insects, and vertebrates. Both the **secondary structures** and tertiary structures of homeodomains of different species have been highly conserved. The two HOM-C clusters in *Drosophila*, and the four HOX clusters in mice and humans, arose by gene duplication and **divergence** from a common ancestral cluster (27). Such a single gene cluster was found in *Amphioxus*, the closest invertebrate relative of the vertebrates.

Functional homology between *Drosophila* and mouse HOX genes has been shown by gene knockout and transgenic mice (28, 29). Most striking are the gene transfer experiments carried out between mouse and *Drosophila*. They demonstrated, for example, that the mouse HOXb-6 gene can induce antennal legs when ectopically expressed in *Drosophila* (30). The ability to compare and extrapolate among species as diverse as *Drosophila*, mice, and humans is also highlighted in experiments with the mutants of eyeless (ey) in *Drosophila*, small eye (Pax6) in mice, and Aniridia (PAX6) in humans, which share a 90% sequence identity in their homeodomains. The murine Pax6 is not only strongly homologous to the *Drosophila* PAX6, but both can induce ectopic eye structures on the wings, legs, and antennae by targeted expression (31).

Bibliography

1. C. Bridges and T. H. Morgan (1923) Carnegie Inst. Wash. Publ. **327**, 1–251.
2. E. B. Lewis (1978) Nature **276**, 565–570.
3. R. L. Garber, A. Kuroiwa, and W. J. Gehring (1983) EMBO J. **2**, 2027–2036.
4. M. P. Scott and A. J. Weiner (1984) Proc. Natl. Acad. Sci. USA **81**, 4115–4119.
5. W. McGinnis, M. S. Levine, E. Hafen, A. Kuroiwa, and W. J. Gehring (1984) Nature **308**, 428–433.
6. W. McGinnis, C. P. Hart, W. J. Gehring, and F. H. Ruddle (1984) Cell **38**, 675–680.
7. T. R. Bürglin (site currently unavailable).
8. A. Laughon and M. P. Scott (1984) Nature **310**, 25–31.
9. M. Affolter, A. Percival-Smith, M. Müller, W. Leupin, and W. J. Gehring (1990) Proc. Natl. Acad. Sci. USA **87**, 4093–4097.
10. W. Driever and C. Nüsslein-Volhard (1989) Nature **337**, 138–143.
11. W. Driever, G. Thoma, and C. Nüsslein-Volhard (1989) Nature **340**, 363–367.
12. G. Struhl, K. Struhl, and P. M. Macdonald (1989) Cell **57**, 1259–1273.
13. T. C. Kaufman, R. Lewis, and B. Wakimoto (1980) Genetics **27**, 309–362.
14. T. C. Kaufman, M. Seeger, and G. Olsen (1990) Adv. Gen. **27**, 309–362.
15. D. Duboule, ed. (1994) *Guidebook to the Homeobox Genes*, IRL Press, Oxford.
16. M. Kessel and P. Gruss (1990) Science **249**, 374–379.
17. R. Krumlauf (1992) BioEssays **14**, 245–252.
18. T. Jordan, I. Hanson, D. Zaletayev, S. Hodgson, J. Prosser, A. Seawright, N. Hastie, and V. van Heyningen (1992) Nat. Gen. **1**, 328–332.
19. A. Schedl, A. Ross, M. Lee, D. Engelkamp, P. Rashbass, V. van Heyningen, and N. D. Hastie (1996) Cell **86**, 71–82.
20. Y. Muragaki, S. Mundlos, J. Upton and B. R. Olsen (1996) Science **272**, 548–551.
21. E. V. Semina, R. Reiter, N. J. Leysens, W. L. M. Alward, K. W. Small, N. A. Datson, J. Siegel-Bartelt, D. Bierke-Nelson, P. Bitoun, B. U. Zabel, J. C. Carey, and J. C. Murray (1996) Nat. Gen. **14**, 392–399.
22. A. K. Ryan, B. Blumberg, C. Rodriguez-Esteban, S. Yonei-Tamura, K. Tamura, T. Tsukui, J. de la Peña, W. Sabbagh, J. Greenwald, S. Choe, D. P. Norris, E. J. Robertson, R. M. Evans, M. G.

Rosenfeld, and J. C. I. Belmonte (1998) Nature **394**, 545–551.

23. E. Rao, B. Weiss, M. Fukami, A. Rump, B. Niesler, A. Mertz, K. Muroya, G. Binder, S. Kirsch, M. Winkelmann, G. Nordsiek, U. Heinrich, M. H. Breuning, M. B. Ranke, A. Rosenthal, T. Ogata, and G. A. Rappold (1997) Nat. Gen. **16**, 54–63.
24. D. Davidson (1995) Trends Gen. **11**, 405–411.
25. D. Engelkamp and V. van Heyningen (1996) Curr. Opin. Gen. Dev. **6**, 334–342.
26. E. Boncinelli (1997) Curr. Opin. Gen. Dev. **7**, 331–337.
27. C. Kenyon (1994) Cell **78**, 175–180.
28. M. Kessel and P. Gruss (1991) Cell **67**, 89–104.
29. H. LeMouellic, Y. Lallemand, and P. Brûlet (1992) Cell **69**, 251–264.
30. J. Malicki, K. Schughart, and W. McGinnis (1990) Cell **63**, 961–967.
31. G. Halder, P. Callaerts, and W. J. Gehring (1995) Science **267**, 1788–1792.

Suggestions for Further Reading

32. D. Duboule, ed. (1994) *Guidebook to the Homeobox Genes*, IRL Press, Oxford.
33. E. Boncinelli (1997) Homeobox genes and disease, Curr. Opin. Gen. Dev. **7**, 331–337.

Homeostasis

Homeostasis is the tendency of an organism to maintain an equilibrium among its internal physiological functions and between the organism and its environment. Metabolism within the cell is regulated to maintain a constant inner environment. Organ systems for respiration, digestion, metabolism, and excretion all work to maintain homeostasis within the organism. Some vertebrates (birds and mammals) also have homeostatic mechanisms to maintain their internal temperatures.

Suggestions for Further Reading

G. G. Simpson and W. S. Beck (1965) *Life, an Introduction to Biology*, 2nd ed., Harcourt, Brace, and World, New York, p. 106.

H. W. Smith (1953) *From Fish to Philosopher*, Little, Brown, Boston. (A wonderful little book on the function and evolution of excretory systems in vertebrates.)

A. S. Romer (1962) *The Vertebrate Body*, 2nd ed., W. B. Saunders, Philadelphia.

Homeotic Genes

Homeotic genes are required during the development of plants and animals to control the differentiation of repeated homologous structures, such as vertebrae or flower organs. Mutations in homeotic genes result in the transformation of one of these homologous structures into the likeness of another structure normally present in a different position. Although most homeotic genes encode transcription factors (see below), a homeotic gene should be considered as such using anatomical, and not molecular, criteria.

The term “homeosis” was first coined to describe certain spontaneous aberrations seen in the wild in which one part of a homologous series is transformed into the likeness of another (1). In plants, it is frequent to observe these transformations between the different organs of the flower (petals transformed into stamens). In animals, these transformations can happen between appendixes (antenna into leg transformations in insects), parts of a segment (a lumbar vertebra into a thoracic one in vertebrates), or result in the formation of supernumerary organs in more anterior or posterior positions (extra mammary glands). Bateson also included under the term homeosis certain bilateral transformations in which both primordia develop in an animal in which normally only the left or the right primordia gives rise to the adult structure (tusk of the Narwhal; ovary and oviduct of fowl). The first homeotic mutant in animals, *bithorax*, was described in the fruit fly *Drosophila melanogaster* by Bridges and Morgan in 1923. In bithorax mutant flies, part of the metathorax transforms into mesothorax (haltere into wing). Mutations in many genes resulting in homeotic transformations of organs or segments have been isolated in plants, insects, and vertebrates. All these mutant transformations fit within Bateson's anatomical definition of homeosis, and, therefore, the genes that mutate to give such phenotypes are termed “homeotic genes.”

In animals, the concept of a homeotic gene is associated historically with that of homeobox and Hox gene from which it should be distinguished. The association originates from the early studies in *Drosophila* of the molecular nature of the homeotic genes. Genetic analysis had showed that some homeotic genes are in different locations in the genome, but many cluster in two complexes: the Antennapedia complex contains homeotic genes required for the development of the head and the anterior thorax, and the Bithorax complex contains genes required for the development of more posterior segments. Molecular analysis of the homeotic genes of the Bithorax and Antennapedia complexes showed that they encode transcription factors with a common protein domain (2, 3). Because this new protein domain was first found in homeotic genes and was common to all of them, it was called the homeodomain, and the DNA sequence encoding it was called homeobox. Despite this historical link, not all homeotic genes encode homeodomain proteins and vice versa. In animals there are homeobox genes required for segmentation or dorsal-ventral specification that, when mutated, do not result in homeotic transformations. In plants, this lack of correlation is more evident as most homeotic genes are encoded by transcription factors of the **MADS** domain class, and the mutation of homeoproteins like “knotted” does not result in homeotic transformations (4).

According to their similarity, homeodomain sequences can be classified into at least 30 classes (5). The homeodomains encoded by the genes of the Antennapedia and Bithorax complexes are most related by sequence, and homologues of these genes have been found not only in vertebrates and arthropods but also in unsegmented worms like *Caenorhabditis elegans* (6, 7). These evolutionarily related genes are required for the specification of structures along the anterior–posterior axis and have in common the property of being organized in clusters. To reflect this common function and evolutionary origin, the term “Hox genes” was coined. Hox genes are expressed in the anterior-posterior axis of the organism in a collinear order with their location in the cluster. Genes located 3′ in the cluster are expressed in more anterior positions than those located more 5′. Hox genes are homeotic genes; however, certain mutations in Hox genes affect cell properties like migration or cell differentiation, without resulting in clear homeotic transformations.

In plants, the ABC model explains satisfactorily how the homeotic genes form the different organs of the flower (8). According to this model, there are three classes of homeotic genes (termed A, B, and C) acting in combination to form the four flower organs: petals, sepals, stamens, and carpels. These organs are arranged in concentric rings known as whorls. The first (outer) whorl is formed by sepals that express class A genes during development; the second whorl is formed by petals that express A and B genes; the third is formed by stamens that express B and C genes; and the fourth (innermost) is formed by carpels that express C genes. This restricted spatial expression can be represented by the following formula: 1A, 2AB, 3BC, 4C, where numbers represent whorls and letters represent the gene class expressed in those whorls. The ABC model also proposes that the A and C genes repress each other; so, in a class A mutant, C genes are expressed in the region where A genes are normally expressed, and vice versa. In contrast, the mutation of B genes does not affect the spatial expression of A or C genes. With this premise, most of the available expression and mutant data can be explained. In an A mutation C genes will be expressed in all four whorls (1C, 2BC, 3BC, 4C), resulting in a flower expressing C in the outer whorl, which consequently develops as carpels; expressing BC in the second and third whorls, which develop as stamens; and expressing only C in the fourth whorl, which then develop as carpels. With the same logic, a mutation in C leads to a flower composed of sepals, petals, petals, sepals (1A, 2AB, 3AB, 4A). Class B mutants lead to flowers composed of sepals, sepals, carpels, carpels (1A, 2A, 3C, 4C). A triple mutant lacking one gene of each class lacks all the floral organs, and the whorls develop as leaves.

A common characteristic of all homeotic genes is their capability to organize the development of entire segments or structures. To reflect this property, the homeotic genes have been named "selector genes" (9) (and also "identity genes") as they are high in a genetic hierarchy and can "select" what kind of organ is formed in a certain position. Homeotic genes have this property because they control groups of downstream genes, which are ultimately responsible for the shape of the organs by controlling cell behaviors like cell division, adhesion, etc. In *Drosophila*, where more are known, the downstream genes encode diverse proteins, such as signaling molecules, adhesion molecules, transcription factors, etc. (10).

One property that is essential for a homeotic gene is that it is active only in a subset of the homologous series of organs. Where a certain homeotic gene is active is controlled in both plants and animals at the transcriptional level. Only the organ primordia in which a particular homeotic gene is expressed will have the set of characteristics that this gene confers. In a loss of function mutant for this homeotic gene, the characteristics of the organ are replaced with those of another homologous organ. On the other hand, if the function of a homeotic gene is activated in the primordia of a homologous organ that normally does not express it, this organ will have a homeotic transformation.

There is a complex system involved in activating, modulating, and maintaining homeotic gene expression. The best known example is the regulation of Hox gene expression. In *Drosophila* it is the segmentation genes that activate spatially restricted patterns of Hox gene expression (11). Vertebrate Hox gene expression is thought to be initiated by the retinoic acid morphogen (12). Recent studies show that besides the Retinoic acid receptors, the vertebrate caudal homologs are activators of Hox expression in frogs and mice (13, 14). There is a group of genes have been well characterized in both vertebrates and invertebrates that are responsible for the maintenance of Hox gene expression. These are mainly positive regulators, the *Trithorax* genes, and negative regulators, the *Polycomb* genes. Mutations in the Trithorax and Polycomb genes result in homeotic transformations; therefore, they must also be considered homeotic genes. In plants, some genes required for the formation of the floral meristem act as early activators of flower homeotic genes (15, 16). Interestingly, a negative homeotic gene regulator has been isolated in plants that is homologous to a *Polycomb* gene (17).

Most homeotic genes studied to date encode transcription factors, but, as homeosis is an anatomical concept, it is possible that other classes of genes result in homeotic transformations. In fact, the transformations of wing toward notum observed in mutants for the signalling gene *wingless* have been considered a homeotic transformation (18).

Bibliography

1. W. Bateson (1894) MacMillan & Co, London.
2. M. P. Scott and A. Weiner (1984) Proc. Natl. Acad. Sci. U.S.A. **81**, 4115–4119.
3. W. McGinnis, *et al.* (1984) Nature **308**, 428–433.
4. J. A. Long, *et al.* (1996) Nature **379**, 66–69.

5. C. Kappen, K. Schughart, and F. H. Ruddle (1993) Genomics **18**, 54–70.
6. C. Kenyon (1994) Cell **78**, 175–180.
7. R. Krumlauf (1994) Cell **78**, 191–201.
8. D. Weigel and E. M. Meyerowitz (1994) Cell **78**, 203–209.
9. A. García-Bellido (1975) CIBA Foundation Symposium ed. Cell Patterning, Vol. **29**, Elsevier, Amsterdam. 161–182.
10. Y. Graba, D. Aragnol, and J. Pradel (1997) BioEssays **19**, 379–388.
11. M. Bienz and J. Müller (1995) BioEssays **17**, 775–784.
12. H. Marshall, *et al.* (1996) FASEB J. **10**, 969–978.
13. H. V. Isaacs, M. E. Pownall, and J. M. Slack (1998) Embo J. **17**, 3413–27.
14. M. Houle, *et al.* (2000) Mol. Cell Biol. **20**, 6579–86.
15. D. Wagner, R. W. Sablowski, and E. M. Meyerowitz (1999) Science **285**, 582–4.
16. M. A. Busch, K. Bomblies, and D. Weigel (1999) Science **285**, 585–7.
17. J. Goodrich, *et al.* (1997) Nature **386**, 44–51.
18. G. Morata and P. A. Lawrence (1977) Dev. Biol. **56**, 227–240.

Suggestions for Further Reading

19. S. B. Carroll (1995) Homeotic genes and the evolution of arthropods and chordates. Nature, **376**, 479–485.
20. Y. Graba, D. Aragnol, and J. Pradel (1997). *Drosophila* Hox complex downstream targets and the function of homeotic genes. BioEssays **19**, 379–388.
21. R. Krumlauf (1994) *Hox* genes in vertebrate development. Cell **78**, 191–201.
22. D. Weigel and E. M. Meyerowitz (1994) The ABCs of floral homeotic genes. Cell **78**, 203–209.

Homokaryon

A *homokaryon* is a hyphal cell, mycelium, organism or **spore** of **fungi** in which all the **nuclei** are genetically identical. The alternative situation is a heterokaryon.

Homological Modeling

Proteins that have similar amino acid sequences, or primary structures, adopt the same fold, or conformation of the **polypeptide** backbone, similar tertiary structures. In other words, the relationship of the three-dimensional protein structure to the amino acid sequence (see Protein Structure Prediction) does not have a one-to-one correspondence, but one-to-many. Therefore, when the 3-D structure of one of the proteins encoded by a **gene family** is known, it can be assumed that all of the other **homologous** protein members of the family adopt essentially the same fold. This is a strictly empirical observation that has held valid for natural proteins, and it provides the basis for homological modeling. It is not easy to give a precise numerical threshold, but two proteins with sequences that are identical at 30% or more of the amino acid residues over a span of more than 100 residues, are almost certainly homologous to each other and belong to the same family (1). Again, this is an empirical rule deduced from natural proteins, which have evolved from a common **evolutionary** ancestor by the accumulation of individual mutations, and it need not be applicable to *de novo* designed proteins. In fact, if the sequence is deliberately designed in one step, the fold of a protein can be converted from totally **alpha-helical** to beta-sheet while keeping the sequences 50% identical (2). There is, however, no guarantee that *de novo*-designed proteins will fold to a unique 3-D structure.

Homological modeling begins with alignment of a query sequence against the sequence of a protein homologue of known structure (see Aligning Sequences). The sequence alignment is best performed by a mathematical technique called dynamic programming. The two sequences aligned may contain insertions or deletions (indels) here and there, shown as gaps in one of the sequences. As the sequence similarity decreases, the number of gaps increases, and the entire alignment becomes less certain. If the structure is modeled according to an incorrect alignment, the resulting model will also be incorrect. Thus, a sequence identity of 40 to 50% or more is usually required for accurate homological modeling. Given the sequence alignment, the query amino acid sequence is mounted onto the known structure, which supplies a template backbone, and the necessary amino-acid side chains are replaced according to the sequence alignment.

Once a proper protein of known structure has been found for a query sequence, the main problems of homological modeling are twofold. The first is to fill in any missing polypeptide backbone by generating an appropriate loop structure. The other is to put all of the new side chains into the correct orientation. If the query structure has residues inserted, there is no template for that part of the sequence. The procedure for generating loops should generate additional polypeptide backbone that joins its two termini smoothly to the template structure and also has an energetically favorable conformation. Indels generally occur at the protein surface, so there are few interactions or steric hindrance to guide the structural design. The orientations of the new side chains of interior residues are determined by the packing of all of the atoms within the protein interior. A simple way to incorporate the new side chains is to adjust their conformation against the fixed conformations of nonsubstituted side chains and the polypeptide backbone. The conformations can also be selected from those observed most frequently in known protein structures, collected in “rotamer libraries,” and from those calculated to have the most favorable energies. A “dead-end elimination” algorithm is more advanced (3). More automatically, the simulated annealing method (4) can be applied to the entire model structure, allowing even the backbone conformation to vary, while seeking the energetically most stable and optimum conformation as a whole. Several computer packages for homological modeling are commercially available.

Bibliography

1. C. Sander and R. Schneider (1991) Proteins: Struct Function Genet. **9**, 56–68.
2. S. Dalal, S. Balasubramanian, and L. Regan (1997) Nat. Struct. Biol. **4**, 548–552.
3. A. Desmet, M. D. Maeyer, B. Hazes, and I. Lasters (1992) Nature **356**, 539–542.
4. A. Sali and T. L. Blundell (1990) J. Mol. Biol. **212**, 403–428.

Homologous Chromosomes

Each **diploid** somatic nucleus contains two copies of each chromosome, known as homologues. The existence of pairs of homologous chromosomes is important for providing at least two copies of any particular gene. This provides the cell with two opportunities to generate a functional gene product. However, it also creates the problem of segregating the homologous chromosomes into the **gametes**. Homologous chromosomes always pair during the first meiotic cell division, when they have to be separated to help create haploid gametes (Fig. 1). In certain instances, homologous chromosomes also pair in the somatic **interphase**. This pairing is common in *Dipteran* insects and in some **plants** (1). The techniques of fluorescent ***in situ*** **hybridization** (FISH) and confocal microscopy (see Denaturation Mapping) allow for the definition of chromosomal territories within the nucleus. Homologous chromosomes frequently occupy adjacent territories in insects and plants (2). Nevertheless, homologues do not often pair in the interphase of mammalian cells. Homologous chromosomes are occasionally found in contact with the same nuclear structures, such as the nucleolus or the nuclear membrane, but the distances between homologues are quite variable (3).

Figure 1. Homologous chromosomes during meiosis. (a) Homologous chromosomes align during the pachytene of the first meiotic division. (b) Homologous chromosomes are separated during the anaphase of the first meiotic division.

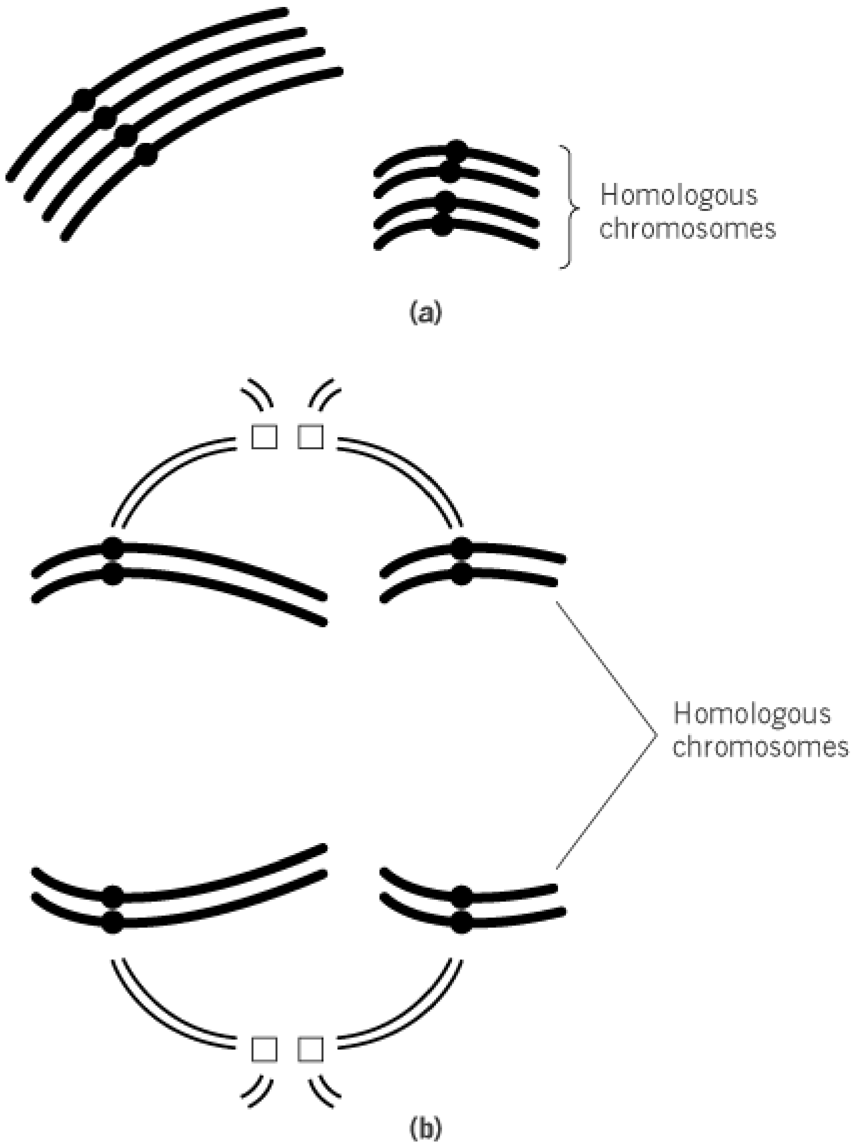

Pairing of homologous chromosomes in **meiosis** occurs simultaneously with the beginning of chromosome condensation early in the **prophase** of the first meiotic division. In *Coprinus*, a **fungus**, the interaction between homologues, known as **synapsis** begins on the longitudinally aligned chromosomes at points towards the ends of the chromosomes and moves towards the centromere. It is probable that there are specific sites within the chromosome that have evolved to mediate chromosomal pairing (4). How homologous sequences are positioned next to each other during this chromosomal alignment process is also unknown, but recognition of similar nucleoprotein structures is likely to be involved (see Chromocenter). However heterochromatin association does not have a major role in this process, nor do the specialized chromosomal structures found at centromeres and telomeres. The end result of chromosomal adjustment is stable physical linkage of the homologues by the synaptonemal complex (SC) (5). This is a ribbonlike structure consisting of two electron-dense lateral elements (25 nm wide) that are separated by a less dense central region (105 nm wide). The major components of the SC are synthesized during the meiotic prophase. Most of the chromatin is located outside of the SC in loops attached to the lateral elements. The SC has important functions in providing a structural framework for efficient recombination, thereby stabilizing the crossover sites where chromatin bridges form at **chiasmata** (sites of **crossing-over** between homologous DNA sequences). SCs might also introduce constraints on the formation of chiasmata so that they cannot occur too close together. Visualization of SCs under the **electron microscope** after special staining procedures is a useful for revealing any misalignments of chromosomes due to deletions and duplications. This is a useful adjunct to conventional analysis of chromosomal bands.

Bibliography

1. B. John (1976) Chromosoma **46**, 279–286.
2. L. Avivi and M. Feldman (1989) Hum. Genet. **55**, 281–285.
3. L. Manmelides (1984) Proc. Natl. Acad. Sci. USA **181**, 3123–3128.
4. R. S. Hawley (1980) Genetics **94**, 625–637.
5. C. B. Gillies (1984) CRC Crit. Rev. Plant Sci. **2**, 81–116.

Suggestion for Further Reading

6. R. P. Wagner, M. P. Maguire, and R. L. Stallings (1993) *Chromosomes. A Synthesis* Wiley-Liss, New York.

Homologous Recombination

Homologous, or generalized, recombination requires extensive nucleotide sequence homology between the interacting chromosomes or chromosomal segments. Recombination occurs anywhere within the homologous region, although the frequency varies throughout the region. Near hot spots of recombination, such as the **Chi sites** of *Escherichia coli*, recombination occurs at higher than average frequency. Cold spots, near which recombination occurs at lower than average frequency, are also known.

Homologous recombination plays multiple biological roles. It was first recognized by its production of new combinations of **alleles** from genetically marked parental chromosomes. Later, it was recognized that it plays an important role in the segregation of replicated homologues in the first meiotic division (without further replication sister chromatids subsequently segregate in the second meiotic division). Finally, homologous recombination is the principal method by which double-strand DNA breaks are repaired with fidelity, at least in microorganisms (see DNA Repair).

Homologous recombination can be classified in numerous ways. One way distinguishes reciprocal recombination (crossing over) from nonreciprocal recombination (gene conversion). Reciprocal recombinant types are produced in a single event in the former, but not in the latter. A strict classification requires assessing all of the parental chromosomes entering the event and all of the progeny chromosomes emerging from it. These are most readily assessed in meiosis of certain **fungi** (ascomycetes) that enclose the four products of meiosis, spores, in a sac called an ascus.

Consider a cross between marked parental chromosomes *a b c* and +++. After DNA replication, recombination may occur between a nonsister pair before the first meiotic division. After the two meiotic divisions, four meiotic products emerge.

In gene conversion, an *a*+*c* recombinant chromosome is produced but the reciprocal type, + *b* +, is not. In a crossover, both an *a*++ recombinant chromosome and its reciprocal type +*bc* are produced. Both a gene conversion and a crossover may occur in the same event. In a population of meioses, statistical association of the two events is commonly observed; that is, among the meioses that have a gene conversion at *b*, a higher frequency of crossing over occurs in the *ab* or *bc* interval than in the population as a whole.

Many models have been proposed for homologous recombination. Most models attempt to account for gene conversion and crossing over as alternative outcomes of a common initial event. Common themes in most models of homologous recombination are (1) an initiating break, either single-stranded or double-stranded, in one parental chromosome; (2) the formation of a single-strand end on that chromosome; (3) invasion of the single-stranded tail into the homologous chromosome and the displacement of the identical (or nearly identical) single strand, to form a displacement or D-loop; (4) formation of a more complex joint molecule, such as a Holliday junction; and (5) resolution of this intermediate into one or two progeny chromosomes.

The joint molecule intermediates contain hybrid DNA; that is, DNA with one strand from each parent. If the parental DNA molecules differ genetically in this region, the hybrid DNA is heteroduplex; that is, it contains a noncomplementary nucleotide sequence. If the parental chromosomes differ at a single base pair, the heteroduplex contains a simple mismatch. Mismatch repair converts the heteroduplex to a homoduplex of one or the other parental type and produces a gene convertant. More complex differences between the parental DNA molecules, such as deletions, insertions, or multiple base-pair changes, also produce heteroduplex DNA acted upon by repair enzymes to produce gene convertants. In the absence of such mismatch repair, the heteroduplex DNA is replicated and produces a postmeiotic segregant, that is, a meiotic product that produces two genetic types at the first mitotic division.

D-loops may arise by a single-strand invading tail with a 3′-end, which primes DNA synthesis. Such synthesis is necessary to repair a double-strand break that has been enlarged into a double-strand gap by loss of nucleotides. If the double-strand gap occurs at a site of genetic difference between the parental chromosomes, DNA synthesis templated by the intact chromosome repairs the double-strand gap and produces a gene convertant without mismatch repair.

In many models of homologous recombination, resolution of a Holliday junction in alternate ways gives crossing over (or not) with respect to markers flanking the site of hybrid DNA formation. This feature accounts for the statistical association of crossing over and gene conversion, yet allows for gene conversion without crossing over. These two types of events may, however, sometimes occur by distinct mechanisms. For example, a single-strand invasion without formation of a Holliday junction could readily give a gene convertant, but not a crossover.

Models of homologous recombination can be classified as follows: (1) In breakage-and-reunion there is no loss or resynthesis of nucleotides except for that associated with mismatch repair. This mechanism is exemplified by the Holliday model and, with the addition of limited DNA synthesis, the double-strand gap repair model. (2) In break-copy mechanisms, one parental DNA is broken, and one of its ends primes DNA synthesis (copying) using the other parental DNA as template. This mechanism occurs in recombination of bacteriophages, bacteria, and some types of mitotic double-strand break repair. (3) In copy-choice recombination the initial stage of DNA replication is templated by one parental chromosome, but then replication switches to the other parental DNA at a homologous point. This type of recombination may occur in RNA viruses.

Another type of homologous recombination, single-strand annealing, occurs in the special cases of deletion between direct repeats in a chromosome or in other instances when DNA can be lost, for example, in phage recombination. In this case, a double-strand break may occur between the direct repeats. Resection of one strand at each end exposes complementary single strands that anneal and produce hybrid DNA with one strand from each copy of the repeat. Appropriate trimming of single-strand ends, filling of gaps, and ligations produce a recombinant. This occurs between homologous regions on separate chromosomes if two initiating breaks occur at appropriate places.

Single-strand annealing is an example of a nonconservative recombination event, that is, when two homologous segments or chromosomes interact to produce only one segment or chromosome. In conservative recombination, exemplified by breakage-and-reunion mechanisms, two parental chromosomes produce two progeny chromosomes, one or both of which is recombinant.

Homologous recombination is a complex process promoted, in the cases studied, by multiple enzymes. A central activity, exemplified by the RecA protein of *E. coli*, promotes the association of homologous nucleotide sequences. RecA protein promotes the formation of D-loops from single-strand tails and a homologous duplex. Proteins of related amino acid sequence and function are widespread in many organisms, ranging from bacteria to humans. Other enzymes prepare substrates for RecA protein. For example, the RecBCD enzyme of *E. coli* generates a single-strand intermediate from linear duplex DNA. Other enzymes resolve recombination intermediates into products. For example, the RuvC protein of *E. coli* cleaves a Holliday junction near the exchange point into two separate duplexes. Their nicks are ligated by DNA ligase to produce intact, possibly recombinant DNA molecules.

Suggestions for Further Reading

1. R. Kucherlapati and G. R. Smith (eds.) (1988) *Genetic Recombination*, American Society for Microbiology, Washington, D.C.
2. D. F. R. Leach (1996) *Genetic Recombination*, Blackwell Science, Oxford, England.

Homology

Homology is a similarity due to a shared common ancestor in . Therefore, homology is the result of ; in contrast, is a consequence of . Originally, homology was used for morphological characters, such as organs. For example, homologous organs were defined as organs that are related to each other through a common descent, even though now they perhaps exhibit different functions. At the present time, however, the term is used in relation to molecular traits, in particular, **nucleotide sequences** and amino acid sequences.

Any two sequences can be compared by alignment, where maximum similarity is used as the basis of measurement (see). Once the alignment is made, the proportion of identical nucleotides, site by site, can be computed. This proportion is the simplest measure for the “degree of sequence similarity.” When the proportion is statistically significant, it is reasonable to say that the two sequences being compared are homologous, because the probability that the similarity was derived by mere chance is, in most cases, extremely small. In general, if the proportion of identical sites is at least 25–30% in an amino acid sequence, or over 40% in a nucleotide sequence, the two sequences may be said to be homologous. This is because there is an extremely high possibility that this similarity is due to a common ancestor and a very low probability that it occurred randomly. The degree of sequence similarity can then be called the "degree of homology."

By using sequence similarity, one can search for homologous sequences in the nucleotide and amino acid . A given sequence is used as a query sequence and is compared with a sequence in an entry of the database by sliding one site in each comparison, until all possible comparisons have been made. This procedure is repeated for all entries of the database. Only the entries where the sequence homology is statistically significant to the query sequence are noted. This search is called a "homology search." In practice, algorithms called "dynamic programming" are used to make the homology search more efficient.

The homology search is particularly useful for predicting the function of a newly identified gene or protein. This is based on the following logic: In general, conservation of a sequence is known to be stronger for functionally important regions of a protein. If we search a sequence and find a region where conservation is strong, it is reasonable to conclude that the region is functionally important and that the function is possibly shared by the homologous sequences. Doolittle constructed his own public database of amino acid sequences, which were deduced from nucleotide sequences (1). He conducted a primitive homology search by using a viral **oncogene** (*sis*) as a query sequence and then found homology with human (Figure 1). He found that the homology was very high, and for this reason he proposed that the *sis* gene may have a function as a . Following Doolittle's prediction, experiments confirmed the hypothesis (2). In fact, it was found that the *sis* gene was the host gene that was inserted into the viral genome. This was the first report in which a homology search was successful for predicting biological function of an unknown sequence. Since then, the homology search has become a very popular tool in molecular biology.

Figure 1. Sequence homology between mouse PDGF gene and viral *sis* oncogene. Identical amino acids are indicated by similar amino acids by a period.

```
PDGF(mouse): MNRCWALFLPLCCYLRLVSAEGDPIPEELYEMLSDHSIRSFDDLQRLLHRD
                                  .:::::::::.::: :::::::::::::. :
V-sis       :                MTLTWQGDPIPEELYKMLSGHSIRSFDDLQRLLQGD

PDGF(mouse): DLNMTRAHSGVELESSSRGRRSLGSLAAAEPAVIAECKTRTEVFQISRNLI
             ::::::.::: :::: .::.::::::..::::.:::::::::::::.::
V-sis:       DLNMTRSHSGGELESLARGKRSLGSLSVAEPAMIAECKTRTEVFEIS----
```


Bibliography

"Homology" in , Vol. 2, pp. 1165–1166, by T. Gojobori; "Homology" in (online), posting date: January 15, 2002, by T. Gojobori, National Institute of Genetics, Shizuoka, Japan.

1. R. F. Doolittle (1981) Science **214**, 149–159.
2. T. F. Deuel, J. S. Huang, S. S. Huang, P. Stroobant, and M. D. Waterfield (1983) Science **221**, 1348–1350.

Homozygote

The **phenotype** of a **diploid** cell may depend upon the interaction of two **alleles** of a gene because a **recessive** gene can express itself only in the absence of its **dominant** allele (note, however, that some genes are neither dominant or recessive). This brings us to two very important words in the language of genetics, *homozygote* and **heterozygote** that describe the general genetic constitution of diploid cells.

A homozygote is a zygote, or other diploid cell, derived from the union of two **gametes** of identical **genotype**. In practice, however, homozygosity requires evidence from genetic crosses that a particular pair of genes is identical, and it is obviously impossible to prove that *all* the thousands of pairs of genes in what appears to be a homozygous individual are in fact identical. So the words homozygote and heterozygote have a narrower connotation and denote the relationship between specific homologous chromosome regions or genes.

We say that a diploid cell is homozygous for gene *A*, which means that it has the genetic constitution either *AA* or *aa*, or, as it is usually written, *A*/*A* and *a*/*a*, where *A* and *a* are two distinguishable alleles. A cell may be homozygous for gene *A* but heterozygous for gene *B* (*AB*/*Ab*).

Hoogsteen Base Pairing

Nucleic acid bases can form a variety of base pairs. In all canonical duplex structures including B-DNA, A-DNA, and Z-DNA, the so-called Watson–Crick base pairs are found. The Watson–Crick base-pairings of guanine with cytosine and adenine with thymine are shown in Figure 1. The G to C and A to T complementarities are provided by specific hydrogen bond donors and acceptors between the bases. In a G:C base pair three hydrogen bonds are found between G-O6 and C-N4, G-N1 and C-N3, and G-N2 and C-O2 positions, and in an A:T base pair two hydrogen bonds are found between A-N6 and T-O4, and A-N1 and T-N3 positions. The two C1′ atoms within a G:C base pair and an A:T base pair are equidistant (~10.5 Å). Thus the G:C and A:T base pairs in the Watson–Crick conformation are nearly iso-structural, from the point of the view of the sugar-phosphate backbone.

Figure 1. Schematic illustration of the A:T and G:C Watson–Crick and Hoogsteen base pairs. Hydrogen bonds are shown as dashed lines, and the distance between two C1′ atoms (shown as open squares) is drawn with a thin line. The numbering system of the purine and pyrimidine rings is shown.

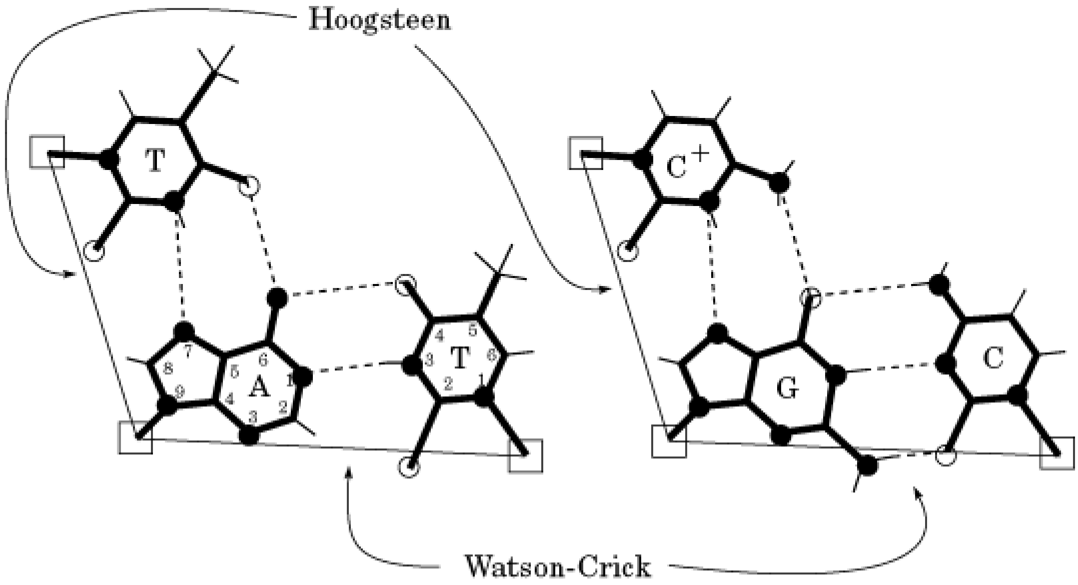

In earlier crystallographic analyses of nucleic acid base pairs, it was found that an A:T base pair can also adopt a different conformation. Instead of using the N1 position of adenine to base pair with N3 of thymine, the N7 position of adenine was used. This type of A:T base pair was named Hoogsteen base pair (1). A striking difference between those two types of base pairs is that the C1′–C1′ distance in the Hoogsteen base pair of 8.65 Å is significantly shorter than that of the Watson–Crick base pair of 10.5 Å. Therefore the Hoogsteen base pair is not compatible structurally with the Watson–Crick base pair in B-DNA. The incorporation of a Hoogsteen base pair in B-DNA destabilizes the duplex structure. A similar G:C Hoogsteen base pair is not stable unless the C is protonated at the N3 position.

However, certain chemical modifications may enhance the stability of the Hoogsteen base pair. It was shown that the modified nucleoside 3-isodeoxyadenosine (iA) forms a stable base pair with thymine (T) using the Hoogsteen conformation, and the iA:T base pair is fully compatible with the normal Watson–Crick base pair as evident from the stable duplex of $d(CG[iA]TCG)_2$ shown by NMR analysis (2). Another modification which stabilizes the Hoogsteen base pair involves the use of 8-amino-adenine in which the amino group at the C8 position can form an additional hydrogen bond with the O2 of thymine (3). Those modified bases may find applications when the Hoogsteen base pairing is needed in nucleic acid structures.

The binding of protein or drug to DNA may induce alternative base pairs, including Hoogsteen base pair, to form. It has been shown that the quinoxaline bis-intercalator antibiotics triostine A and echinomycin bind to -XCGY- sequences with the drug bracketing the CG dinucleotide base pairs. In the structure of the triostine-CGTACG and triostine-GCGTACGCT complexes, the A:T and G:C$^+$ base pairs adjacent to the quinoxaline rings adopt Hoogsteen base pairs (4). The molecular basis for the Hoogsteen base pair in the structure is to improve the stacking interactions between the quinoxaline ring and the adjacent base pairs. It is likely that such a conformational rearrangement from the Watson–Crick to Hoogsteen base pairs may occur in other biological systems.

An important role for the A:T and G:C$^+$ Hoogsteen base pairs is found in the structure of a nucleic acid triple helix. The formation of a poly(A).poly(U).poly(U) triplex requires that the third strand of poly(U) is bound to the poly(A) strand of the poly(A).poly(U) duplex using Hoogsteen base pairing. The T.A.T. and the C.G.C$^+$ triple base pairs are shown in Figure 1. (Note that the triple C.G.C. base pair is not stable unless the second C is protonated.)

It should be pointed out that Hoogsteen base pairing is not restricted in DNA. In transfer RNA, the nucleic acid bases are often modified and involved in tertiary interactions. For example, in yeast $tRNA^{Phe}$ the nucleotide at position 58 is 1-methyl-adenosine, which is base paired with T54 (5). Because the N1 position of this adenine is methylated, it cannot participate in the normal Watson–Crick base pair. Instead m^1 A58 and T54 form a reverse Hoogsteen base pair. It is likely that those noncanonical base pairs, including Hoogsteen and reverse Hoogsteen base pairs, will be found in higher-ordered RNA structures.

Bibliography

1. K. Hoogsteen (1963) Acta Crystallogr. **16**, 907–916.
2. B. Bhat, Neelma, N. J. Leonard, H. Robinson, andA. H.-J. Wang (1996) J. Am. Chem. Soc. **118**, 3065–3066.
3. K. Kawai, I. Saito, and H. Sugiyama (1998) Tetrahedron Lett. **39**, 5221–5224.
4. A. H.-J. Wang et al. (1984) Science **225**, 1115–1121.
5. S. H. Kim et al. (1974) Science **185**, 435–440.

Horizontal Gene Transfer

In general, **genes** are transferred from one generation to the next in a vertical fashion, from parent to progeny through the gametes donated from each parent to form the zygote from which the offspring develops (see Vertical Gene Transfer). In horizontal gene transfer, a gene is transferred from one species to another, often with a **virus** or bacterium acting as the vehicle (Fig. 1). In vertical gene transfer, the genes must originate in germline cells in order to be transferred. In horizontal gene transfer, the gene may originate in a somatic cell, but the receiving cell must be a germline cell in order for the transferred gene to be passed on to the next generation. Strictly speaking, transfers of genes between somatic cells of two species are not called horizontal gene transfer.

Figure 1. Illustration of horizontal gene transfer and how it affects the (**a**) species and (**b**) gene phylogenetic trees.

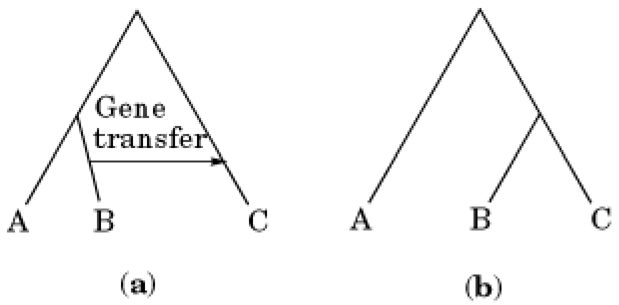

Horizontal gene transfer is often difficult to detect. It is often suspected, however, when there is marked discontinuity in the phylogenetic tree for a gene, such as the appearance of a gene in one species, but not in any of its most closely related species. Discrepancies between the phylogenetic trees for species and for genes can also indicate that horizontal gene transfer may have occurred.

The **nucleotide sequences** of entire genomes show that horizontal gene transfers must have occurred often. When the complete genome sequences of three representative species from the three major organismic worlds, namely, *Escherichia coli* (Eubacterium), *Methanococcus jannaschi* (Archaebacterium), and *Saccharomyces cerevisiae* (Eukaryote) were compared with each other, approximately 60% of all the genes of the archaebacterial genome are closer to those of the eubacterium than to those of eukaryotes, whereas about 30% of the archaebacterial genes were closer to eukaryotes. The remaining 10% of the genes are archaebacteria-specific (1). Therefore, the archaebacterial genome looks like a mosaic structure, a mixture of genetic material from various genomes. At present, only horizontal gene transfer can explain the mosaic features of the genomes. It implies that a tremendous amount of horizontal gene transfer should have taken place during long-term evolution. Genomes appear to have a robustness that allows major changes in gene order and arrangement without loss of function. This provides an environment in which horizontal gene transfer can occur and provides a source for the emergence of new gene systems and new gene interactions. Thus, the unit of function appears to be the gene, and the positions of genes in the genome have little effect on function. There appear to be only rare examples in which a set of genes must work as a unit. This elasticity of the genome allows it to absorb any disturbances caused by horizontal gene transfer, and it demonstrates the evolutionary significance of the genome itself.

Bibliography

1. H. Watanabe, T. Gojobori, and M. Kin-Ichiro, (1997) Gene **205**, 7–18.

Hormone Receptors

Hormones regulate a wide variety of physiological functions, encompassing intermediary metabolism, growth, and cell differentiation. In contrast to the diversity of their phenotypic effects, they have only two fundamental mechanisms of action, depending on their physical chemical characteristics. The lipophilic steroid hormones and thyroid hormones (vitamin D_2 and retinoic acid have similar modes of action) are **hydrophobic** and primarily act intracellularly, modulating gene transcription, whereas the peptide hormones, adrenaline, and melatonin are hydrophilic and act primarily at the cell membrane, triggering a cascade of signal transduction events leading to intracellular regulatory effects. The first step, and a prerequisite for the elicitation of the hormonal effect of both lipophilic or hydrophilic hormones, is binding of the hormone to its appropriate **receptor** protein. The hormone receptors have the following characteristics: (a) high specificity, so that the receptors can recognize their specific ligand and discriminate between the incoming signals; (b) high affinity for their ligand (K_D values in the range of 10^{-7} to 10^{-10}M); and (c) limited capacity (no more than a few thousand receptor molecules per cell).

1. Lipophilic Hormones

The hydrophobic hormones appear to diffuse across the membrane into the cell (although there are claims of a specific transport mechanism) and bind with high affinity and specificity to their respective receptor protein (see Estrogen Receptors). These receptors, also known as nuclear receptors, belong to a large family of proteins with similar structures, characterized by various functional **domains**, through which the biological activity of the molecule is expressed (Fig. 1). The central DNA-binding domain is responsible for recognition and specific interaction with specific **palindromic** DNA sequences, the hormone response elements. Characteristic of DNA-binding domains are those comprised of two **zinc finger** structures: One is on the amino-terminal side making specific contact with the DNA major groove, and the other is responsible for the specific homodimerization of the activated receptor. Other important domains are (a) the ligand-binding domain, which is at the carboxy terminus of the receptor, (b) nuclear import, export motifs, (c) **heat-shock** protein binding sites, and (d) **transactivation** domains, which can be at either the *N*- or *C*-terminal regions of the receptor. In the absence of hormone, the receptor is complexed to other proteins, such as the heat shock protein hsp90, immunophilins, and smaller peptides. Upon hormone binding, the complex dissociates and the receptor protein is released and forms homodimers, which then bind to the hormone response elements (HREs) (see Hormone Response Elements, Glucocorticoid Response Element). The HREs are enhancer elements that are activated by the ligand–receptor complex. The result of this binding is stimulation (or, in some cases, inhibition) of transcription of the appropriate gene. The mechanism is not yet elucidated, but it also involves interaction of the hormone–receptor complex with other nuclear proteins, such as transcription factors, “adaptor proteins,” “coactivators,” and transacetylases (1-4). The primary transcript is subsequently processed (see RNA Splicing), and the resulting messenger RNA is **translated** into the respective protein. The nature of the protein determines the phenotypic expression of the hormone action: For example, if the protein is an enzyme involved in gluconeogenesis, the blood glucose level will change; if it is a growth factor, cell replication will be affected.

Figure 1. Mechanism of action of lipophilic hormones. (**a**) Mechanism of action of lipophilic hormones. (**b**) Receptors of lipophilic hormones. [From Ref. 10, with permission (slightly modified).]

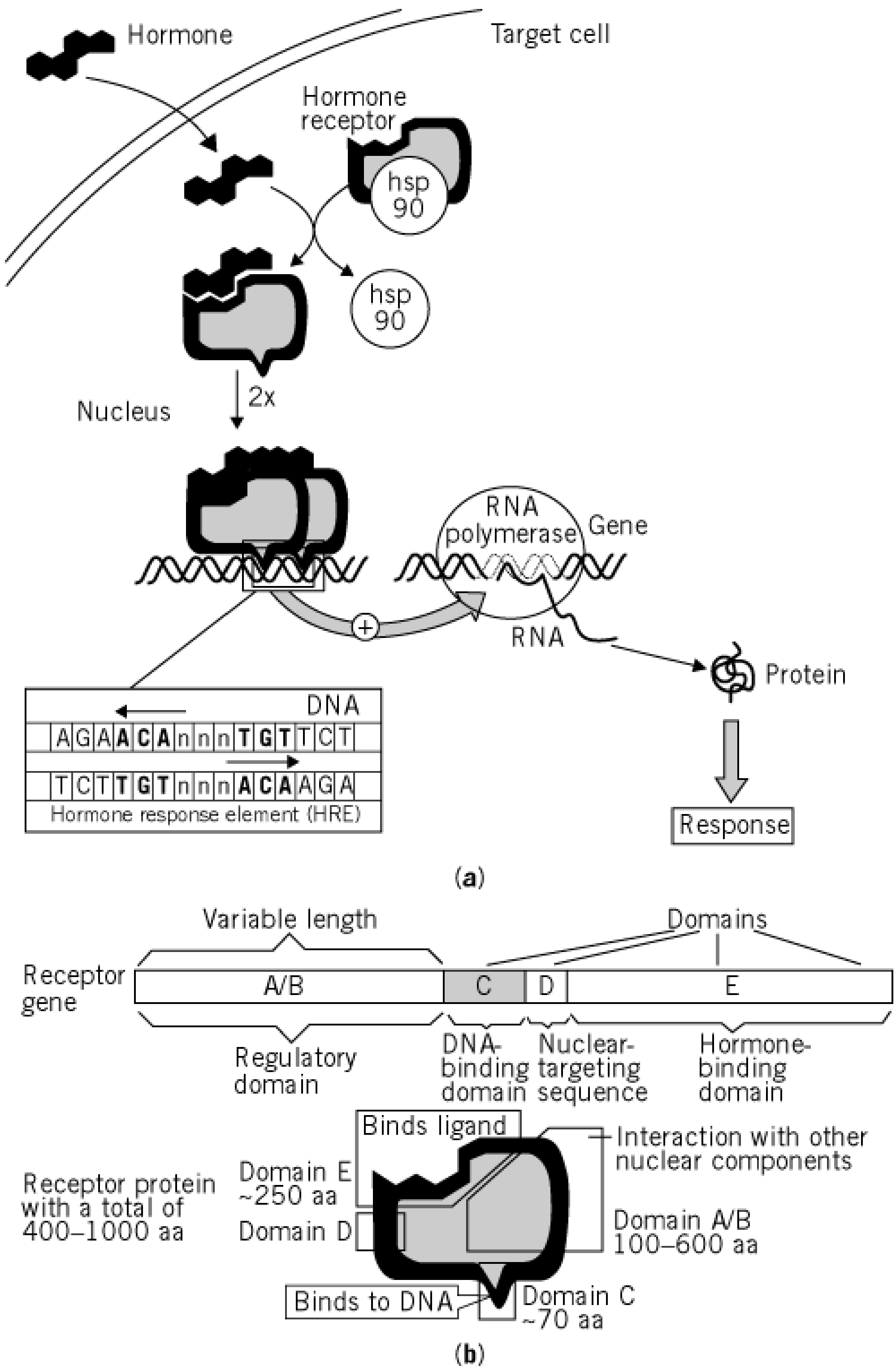

The effects of steroid hormones are usually long-term, needing hours to be exerted. It is becoming increasingly evident, however, that some steroid hormones act very rapidly, by binding to membranes and altering the intracellular concentrations of Ca^{2+}, Na^{+}, and other ions (5). The nature of the membrane-binding sites (eg, whether they are parts of a pore complex) is not known.

2. Hydrophilic Hormones

The hydrophilic hormones are not able to penetrate the cell and instead interact with membrane receptors (see Hormone Receptors) (Fig. 2). Two types of membrane receptors for hydrophilic hormones have been characterized, Type I and Type III. The third type, Type II, represents ion channels, which are mainly regulated by neurotransmitters.

Figure 2. Mechanism of action of hydrophilic hormones. [From Ref. 10, with permission (slightly modified).]

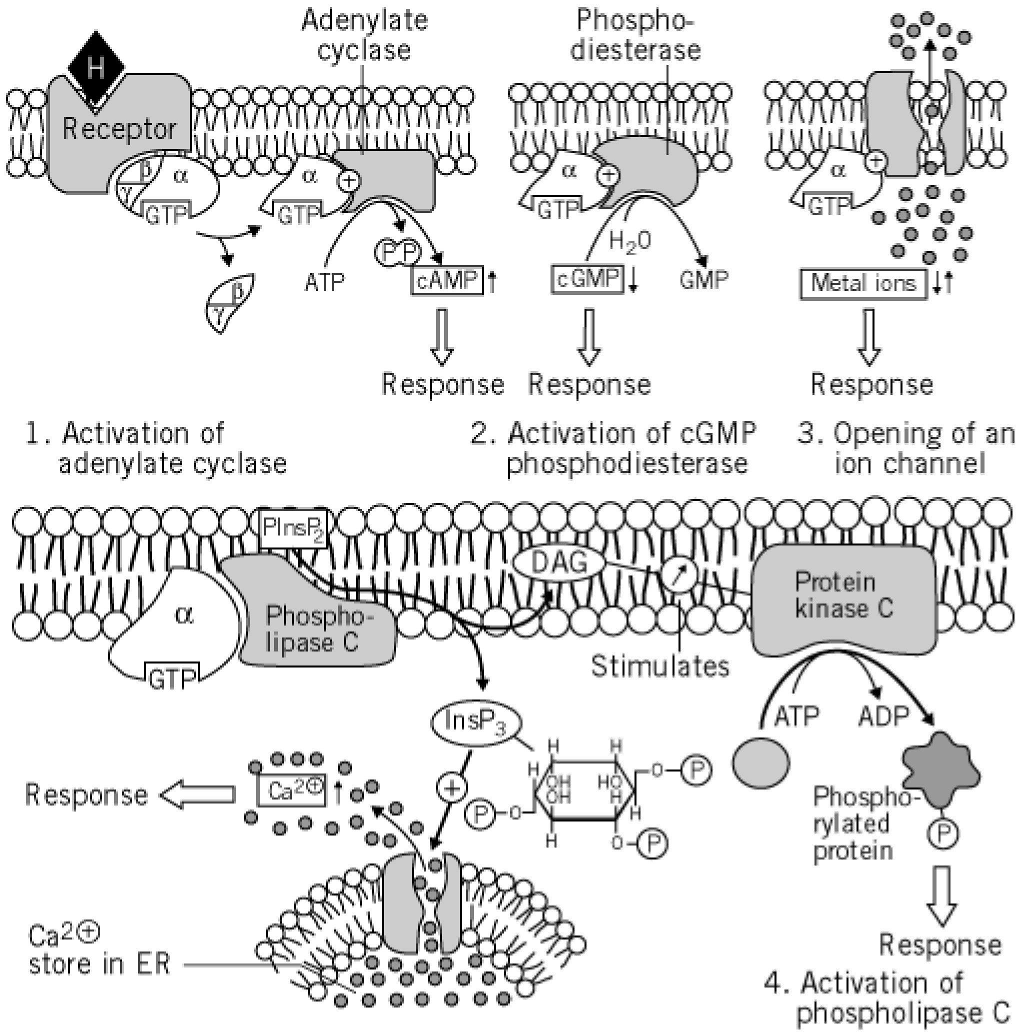

2.1. Type III Receptors

These receptors are integral membrane proteins, with seven **a-helical** domains spanning the membrane, an extracellular domain that is important for ligand recognition, and an intracellular one important for signal transduction. Binding of the cognate ligand induces a conformational change in the receptor that is further transmitted through a family of guanine nucleotide-binding proteins (**G proteins**) associated with the receptor (Fig. 2). The G proteins are trimers of a, b, and g subunits. In the resting state, the a subunit has GDP bound. Interaction of the hormone with the receptor leads to exchange of GDP for GTP on the a subunit and dissociation of the G complex into a separate a-subunit and a b/g dimer. The free a subunit is the effector molecule that activates enzymes involved in the production of second messengers, such as the adenylate cyclases, which catalyze 3′,5′-**cyclic AMP** synthesis from ATP, and **phospholipase C**, which catalyzes the production of inositol 1,4,5-triphosphate (IP_3) and **diacylglycerol** (DAG) from phosphatidyl inositol bisphosphate. Cyclic AMP and DAG are **allosteric** modulators of protein kinases A and C, respectively, whereas the hydrophilic IP_3 reaches the endoplasmic reticulum and acts there by releasing Ca^+_2 from storage sites (6-8). Activation of the protein kinases leads to **phosphorylation** at serine/threonine residues of a large variety of proteins (see Serine/Threonine Kinases and Phosphatases), which are activated in their various functions, such as enzymes, structural proteins, and transcription factors.

The free a subunit of the G protein, due to its intrinsic GTPase activity, hydrolyzes its bound GTP to GDP. When the hormonal stimulus ceases, the GDP is not replaced by GTP, and the G-protein trimer is reconstituted. Consequently, the system thus returns to its initial inactive condition.

2.2. Type I Receptors

These receptors are best exemplified by the insulin receptor. It is composed of two identical a subunits that are extracellular and two identical b subunits, with extracellular, transmembrane, and intracellular domains. The intracellular domains possess intrinsic protein kinase activity. Binding of the cognate ligand induces a conformational change and dimerization of the receptor molecule. This leads to activation of the kinase activity of the receptor and phosphorylation of tyrosine residues within the kinase domain and at other sites of the receptor (see Tyrosine Kinases and Phosphatases). These last sites create docking sites for downstream signal transduction molecules containing **SH2 domains**, which are activated by a variety of mechanisms (eg, tyrosine phosphorylation, conformational changes). Subsequently, by way of intermediate second messenger molecules, they trigger metabolic processes, gene transcription, and DNA replication . The importance of second messenger formation is that the original hormonal signal is amplified by two to three orders of magnitude and that multiple signal effects are integrated by using the same second messenger.

3. Medical Disorders

A series of endocrine diseases result from genetic defects of the receptors for both the lipophilic and the hydrophilic hormones. They are manifested as resistance syndromes, with elevated blood levels of the specific hormone, because the regulatory feedback inhibitory cycle is not functioning. Mutations have been found in various domains of the receptors, leading to partial or total loss of response to hormonal stimuli. In more rare cases, the receptors have lost their function, but in addition they inhibit the action of the wild-type receptor (dominant negative mutants). Table 1 shows an overview of diseases caused by mutations in genes coding for members of the nuclear hormone receptor family.

Table 1. Some Diseases Caused by Mutations in Genes Coding for Members of the Nuclear Hormone Receptor Superfamily[a]

Mutant Receptors	Disease	Remarks
Androgen	Androgen insensitivity syndrome (AIS)	Complete AIS leads to a complete female phenotype.
Glucocorticoid	Glucocorticoid resistance syndrome	Symptoms of fatigue, hirsutism, and hypertension.
Mineralocorticoid	Mineralocorticoid resistance syndrome	Rare autosomal disease, with symptoms of hyponatraemiaand dehydration.
Estrogen	Estrogen resistance syndrome	Only one case with complete resistance has beenreported. Symptoms of incomplete epiphysal closure, prolonged linear growth.
Thyroid hormone	Thyroid hormone	Caused by mutations in the b-

	resistance syndrome	receptor gene.Goiter, learning disabilities, hearing defects, delayed bone maturation, mentalretardation.
Vitamin D_3 (calcitriol)	Vitamin D_3 resistancesyndrome	Severe rickets, secondary hypocalcemia, hyperparathyroidism.

[a] Ref. 9, with permission (slightly modified).

Bibliography

1. U. Clever and P. Karlson (1960) Exp. Cell Res. **20**, 623–626.
2. M. Beato, P. Herrlich, and G. Schutz (1995) *Cell* 83, 851–857.
3. D. M. Heery et al. (1997) Nature **387**, 733–736.
4. J. Iorchia et al. (1997) Nature **387**, 677–683.
5. M. Wehling (1994) Annu. Rev. Physiol. **59**, 365–393.
6. A. Hall (1990) Science **249**, 635–640.
7. W. J. Tang and A. G. Gilman (1992) Cell **70**, 869–872.
8. N. DiVecha and R. F. Irvine (1995) Cell **80**, 269–278.
9. A. Baniahmad, M. Eggert, and R. Renkawitz (1997) In *Transcription Factors in Eukaryotes* (A. G. Papavissiliou, ed.), Springer, Heidelberg.
10. J. Koolman and K.-H. Rohm (1996) *Color Atlas of Biochemistry*, Thieme, Stuttgart.

Suggestions for Further Reading

11. R. E. J. Ribeiro, P. J. Kushner, and J. D. Baxter (1995) The nuclear hormone receptor gene superfamily. Annu. Rev. Med. **46**, 443–453.
12. M. G. Parker (1993). *Steroid Hormone Action*, IRL Press, Oxford, U.K.
13. R. White and M. G. Parker (1998) Molecular mechanisms of steroid hormone action. Endocrine-Related Cancer, **5**, 1–4.

Hormone Response Elements

Lipophilic hormones are able to enter cells and exert their actions by binding to specific **receptors** . Binding of hormones of this type, such as the **steroids**, retinoic acid, thyroid hormone and vitamin D_3, results in the activation of their receptors, which then bind to specific response elements and activate gene transcription . The detailed discussion of this process for one specific hormone and its response elements is provided in Glucocorticoid response element. This article describes the relationships between the different response elements for these various hormones (1).

In each case, the particular response element confers a specific response to a particular hormone because the response element binds only the receptor for that hormone, and not other receptors (2, 3). Thus, the glucocorticoid response element (GRE) binds the glucocorticoid receptor–glucocorticoid hormone complex and hence mediates response to glucocorticoid hormone (Table 1, part a). However, alteration of an A residue at the third position of the palindromic GRE sequence to a T residue converts the GRE into an ERE (estrogen response element), which binds the estrogen receptor–hormone complex and therefore activates gene expression in response to estrogen (Table 1, part a). Similarly, while the glucocorticoid and estrogen response elements have a 3-bp space between the two halves of the response element, the removal of this space to make the two halves of the response element contiguous with one another results in a thyroid hormone response element (TRE) that binds the thyroid hormone receptor. Hence, relatively small changes in sequence can affect the receptor that is bound by the response element and therefore result in it mediating a different pattern of gene expression.

Table 1. Relationships Among Various Hormone Response Elements

(a) Palindromic repeats	
Glucocorticoid	RGRACANNNTGTYCY[a]
Oestrogen	RGGTCANNNTGACCY
Thyroid	RGGTCA——TGACCY
(b) Direct Repeats	
9-*cis*-Retinoic acid	$AGGTCAN_1AGGTCA$
All-*trans* retinoic acid	$AGGTCAN_2AGGTCA$
	$AGGTCAN_5AGGTCA$
Vitamin D_3	$AGGTCAN_3AGGTCA$
Thyroid hormone	$AGGTCAN_4AGGTCA$

[a] N indicates that any base can be present at that position, R indicates a purine ie A or G, Y indicates a pyrimidine ie. C or T. A dash indicates that no base is present, the gap having been introduced to align the sequence with the other sequences.

Although a response to thyroid hormone can be obtained by having the palindromic element illustrated in Table 1, part a, most thyroid hormone response elements are of a different form, in which the GGTCA sequence is directly repeated, with a 4-bp gap between the two direct repeats (Table 1, part b). As with the palindromic elements, the spacing between these direct repeats can affect the nature of the receptor that is bound: Direct repeats with a spacing of 1, 2, or 5 bp produce a response to different forms of retinoic acid, a 3-bp spacing produces a response to vitamin D_3, and a 4-bp space results in a response to thyroid hormone. Detailed structural studies of the different receptors involved have recently revealed the manner in which their different structures allow them to recognize these different response elements specifically (4).

Hence, a family of related response elements that bind a family of related receptor proteins allow different genes to respond to different, but related, lipophilic hormones.

Bibliography

1. M. Beato (1989) Cell **56**, 335–344.
2. D. J. Mangelsdorf, C. Thummel, M. Beato, P. Herrlich, G. Schutz, K. Umesono, B. Blumberg, P. Castner, M. Mark, P. Shambon, and R. M. Evans (1995) Cell **83**, 835–839.

3. M. G. Parker (1993) Curr. Opin. Cell Biol. **1**, 512–518.
4. F. Rastinejad, T. Pearlmann, R. M. Evans, and P. B. Sigler, (1995) Nature **375**, 203–211.

Suggestions for Further Reading

5. H. Gronemeyer and V. Laudet, (1995) Nuclear receptors. Protein Profile **2**, 1173–1308.
6. H. Gronemeyer, and D. Moras (1995) How to finger DNA. Nature **375**, 190–191.
7. D. J. Mangelsdorf, and R. M. Evans (1995) The RXR heterodimers and orphan receptors (1995). Cell **83**, 841–850.

Hormones

Hormones are chemical signaling molecules that regulate metabolism, growth, and differentiation in multicellular organisms (1). Hormones are produced in specialized cells of the endocrine glands and reach their target cells by way of the blood circulation. The term "hormone" is sometimes applied loosely to encompass various other regulatory compounds, including those of lower animals and plants, that show comparable effects. Several hormones (primarily steroid hormones and thyroid hormones) are transported in the circulation while bound to specific binding proteins. These proteins serve as hormone depots, releasing the hormone when needed and also protecting it from rapid inactivation. Most hormones are either steroids (see Steroid Hormones) or peptides and proteins (see Peptide Hormones) (Table 1). Adrenaline, the thyroid hormones, and melatonin are hormones derived from amino acids. In insects and crustaceans, peptide hormones, steroid hormones (ecdysteroids), and sesquiterpenoid derivatives (juvenile hormones) have been isolated.

Table 1. List of Hormones and Sites of Production

Hormones	Site of Production
Steroids	
Glucocorticoids (cortisol, corticosterone)	Adrenal cortex
Mineralocorticoids (aldosterone)	Adrenal cortex
Androgens (testosterone)	Testis
Estrogens (17b-estradiol)	Ovary (follicles)
Progestins (progesterone)	Ovary (corpus luteum)
Calcitriol[a]	Kidneys
Peptide and Proteo Hormones (Partial List)	
Parathormone	Parathyroids
Insulin	Pancreas
Glucagon	Pancreas
Ocytocin	Neurohypophysis
Vasopressin	Neurohypophysis
Melanotropin	Pars intermedia of hypophysis

Somatotropin	Adenohypophysis
Corticotropin	Adenohypophysis
Thyrotropin	Adenohypophysis
FSH (folitropin)	Adenohypophysis
LH (lutropin)	Adenohypophysis
Amino Acid Derivatives	
Thyroxin, triiodothyronine	Throid gland
Adrenaline	Adrenal cortex
Melatonin	Epiphysis

[a] Steroid derivative, not a steroid, but with molecular action like steroid hormones.

The steroid hormones are derived from cholesterol by a series of enzymatic reactions that take place in the cytosol and in mitochondria of primarily cells of the adrenal cortex, ovary, and testis. In some cases, the steroid hormone must be subjected to modification in the target tissue, either to be activated or to produce a more active derivative. The steroid hormones are inactivated mainly in the liver in various ways—for example, by reduction of keto groups or unsaturated double bonds, ring hydroxylation, oxidation of hydroxyl groups, and cleavage of the side chain. They are excreted after being conjugated to sulfuric or glucuronic acids. Most of the peptide and proteohormones are synthesized in the form of precursor proteins (prohormones) and are stored in the endocrine cell. Before being released into the circulation, the prohormones are cleaved to the active hormone. Their inactivation involves **proteolytic** cleavage by intracellular proteinases. The production and release of many hormones is controlled by "tropic" hormones produced by the hypophysis, an endocrine "master" gland; this phenomenon is known as *hormone hierarchy*. The hypophysis responds to chemical signals (metabolites, hormones) from the periphery or to neuroendocrine stimuli from the hypothalamus (liberins, which act positively on hypophysial hormone release, and statins, which inhibit their release). From an evolutionary standpoint, the endocrine system developed earlier than the other two major regulatory systems of higher organisms, the nervous and the immune systems.

The molecular mechanism of hormone action depends on the physical chemical characteristics of the hormones. Steroid and thyroid hormones, which are **hydrophobic**, can enter the cell and bind intracellularly to their respective hormone receptors (2-4). These proteins belong to the superfamily of nuclear receptors and are present in the quiescent cell as complexes with other proteins, among them **heat-shock** proteins. This complex dissociates upon binding of the hormone ligand, the receptor homodimerizes, and it then binds to specific nucleotide sequences, the hormone response elements (HRE). These represent receptor-activated enhancer elements situated at varying distances from the **promoter** of the hormonally regulated genes. Interaction of the hormone–receptor homodimer complex with the HRE results, in a still undefined way, in either stimulation or inhibition of gene transcription, and consequently of expression of the gene. The nature of the protein synthesized determines the **phenotypic** effect. The hydrophilic hormones (peptide and proteohormones, adrenaline and melatonin) cannot enter the cell, but bind to membrane hormone receptors. This results, by way of a **G-protein** effector system, in activation of enzyme systems (eg, adenylate cyclase, **phospholipase C**) generating second messengers, which are **allosteric** effectors of protein kinases primarily (5-7) (see Phosphorylation, Protein). The hormonal effect depends upon the nature of the phosphorylated protein. One class of membrane receptors eg, the insulin receptor, first dimerizes upon binding the hormone and is then autophosphorylated; in this state, it can phosphorylate and activate other intracellular proteins (see Hormone Receptors).

Analogues of hormones can be either more or less potent than the natural hormones, or they can be inhibitors of hormone action; many have been synthesized and used in research or as therapeutics.

The more potent analogues of steroid hormones exhibit higher affinity for the cognate receptor than the natural hormone or greater stability, due to lower rates of inactivation and excretion. Important examples of such analogs are diethylstilbestrol, an estrogen, and dexamethasone and triamcinolone, glucocorticoids. Competitive inhibitors also bind with high affinity to the receptor but cannot elicit the hormonal effect; they can inhibit receptor homodimerization, binding of the receptor to hormone response elements, or interaction of the receptor with the transcriptional machinery. Some such inhibitors (Fig. 1) that have found clinical application include the antiestrogen ICI 182780 used in treatment of breast cancer, the antiandrogen cyproteron in prostate cancer and hirsutismus, and RU486, an antiprogesterone compound used in pregnancy termination.

Figure 1. Synthetic hormone antagonists.

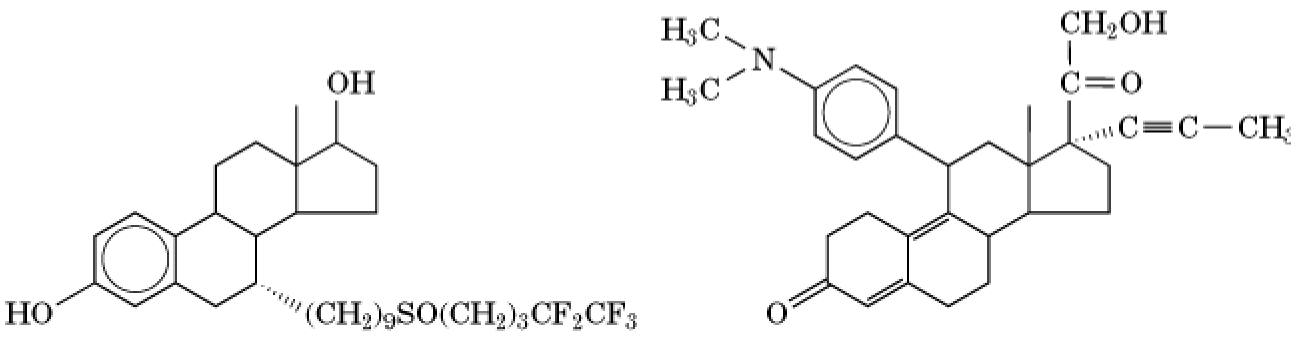

Bibliography

1. E. T. Baulieu and P. A. Kelly (eds.) (1990) *Hormones: From Molecules to Disease*, Hermann, Paris.
2. E. M. Evans (1988) Science **240**, 889–895.
3. D. J. Mangelsdorf et al. (1995) Cell **83**, 835–839.
4. M. Beato, P. Herrlich, and G. Schutz (1995) Cell **83**, 851–857.
5. A. Hall (1990) Science **249**, 635–640.
6. W. J. Tang and A. G. Gelman (1992) Cell **70**, 869–872.
7. N. Divecha and R. F. Irvine (1995) Cell **80**, 269–278.

Suggestions for Further Reading

8. J. D. Wilson and D. W. Foster, eds. (1992) *Williams Textbook of Endocrinology*, 8th ed., Saunders, London.
9. M. G. Parker (1993) *Steroid Hormone Action*, IRL Press, Oxford, U.K.
10. R. L. J. Ribeiro, P. J. Kushner, and J. D. Baxter (1995) The nuclear hormone receptor superfamily. Annu. Rev. Med. **46**, 443–453.

Hotspot

DNA sequence analysis can be used to reveal the distribution of mutations within a gene due to spontaneous mutagenesis or following treatment by specific chemicals. Such mutation spectra reveal that neither spontaneous nor induced mutagenesis is random, but mutations cluster in specific regions within a gene. Those DNA sites at which a large number of mutants occur are referred to as "hot spots." For example, Halliday and Glickman (1) found that 71% of the 729 spontaneous mutants in the *lac I* gene of *E. coli* carried mutations in a small region (positions 620–632) with base sequence $[5'TGGC3']_3$. In contrast, 98% of ICR-191-induced mutations in the *lac I* gene were +1 and –1 frameshift mutations in runs of repetitive G.C base pairs (2).

There are several possible explanations for genetic hot spots. A trivial one is that there could be a selection bias that favors the detection of mutations at some sites in preference to those at others, but this is probably not true of most observations in the literature. The most likely explanations of most hot spots are unequal distribution of premutational lesions in the gene, differences in processing of lesions in different regions, or some sort of differential DNA repair process. The frameshift mutations produced by N_2-(acetylamino)fluorene (AAF, Fig. 1) provide an example in which the reasons for hot spots have been explored in some detail, especially by Fuchs and co-workers (3). This model carcinogen forms adducts on the C8 position of guanine bases. However, the distribution of AAF-induced mutations fails to correspond to the distribution of AAF adducts in DNA. Only 19% of the DNA adducts appear at the sites of mutational hot spots, even though these sites produce 89% of the mutations (4). Subsequent studies have suggested that these hot spots result from differences in processing of DNA damage at particular sites, with premutational events being more readily converted into a mutation at hot spots than at other sites in DNA.

Figure 1. Structure of AAF (2-acetylaminofluorene).

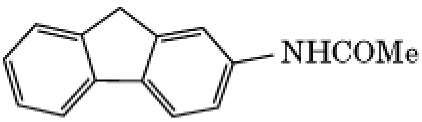

Bibliography

1. J. A. Halliday and B. W. Glickman (1991) Mutat. Res. **250**, 55–71.
2. M. P. Calos and J. H. Miller (1984) J. Mol. Biol. **153**, 39–66.
3. G. R. Hoffmann and R. P. P. Fuchs (1997) Chem. Res. Toxicol. **10**, 347–359.
4. R. P. P. Fuchs (1984) J. Mol. Biol. **177**, 173–180.

HU And Related Proteins

The bacterial type-II DNA-binding proteins include the abundant HU and integration host factor (IHF) proteins and the phage-encoded TF1. They are believed to condense their cognate **genomes** by binding at multiple sites and inducing coherent bends. HU and TF1 possess little, if any, binding sequence specificity, but IHF, which is also required for site-specific **recombination, DNA replication**, and transcription, binds at specific sites characterized by a limited **consensus sequence**.

All proteins of this type bind to DNA as dimers and bend the DNA to a substantial extent. In particular, IHF induces a bend angle of at least 160°, and possibly in excess of 180°, within the 2 1 / 2 turns of double helix that comprise its binding site. IHF is normally a heterodimer, while HU can exist either as a homo- or as a heterodimer. In both IHF and HU, the two ~10 kDa subunits intertwine to form a compact core, from which two long beta-sheet ribbon arms extend. These arms track along the minor groove from the inside to the outside of the wrapped DNA, where they terminate at the two substantial kinks. In addition to these interactions via the b arms, IHF also clamps the hairpin by minor-groove contacts with **alpha-helices** from both subunits in the core of the dimer. All the contacts to the DNA are either in the minor groove or are part of an extensive network of electrostatic interactions with the backbone phosphate groups.

The two kinks are induced by the partial intercalation between adjacent base pairs of an absolutely conserved proline sidechain located at the tips of the b arms. In the IHF–DNA complex, the DNA bend is maintained by two distinct mechanisms. On the outside of the bend, the hydrophobic intercalation stabilizes the opening of the minor groove. On the inside, charge neutralization counteracts the enhanced repulsion between the phosphates on opposite sides of the narrowed grooves.

The sequence dependency of IHF binding is determined by the conformation of DNA rather than by base-specific contacts. The “consensus” sequence consists of two short elements separated by approximately half a turn in only one of the two half-sites. The conserved sequence CAA at the kink site can accommodate the severe distortion induced by the protein better than other short sequences, and so is favored.

Suggestion for Further Reading

P. A. Rice, S. Yang, K. Mizuuchi, and H. A. Nash (1996) Crystal structure of an IHF–DNA complex: a protein-induced U-turn. Cell **87**, 1295–1306.

Hybrid Cell

A heterokaryon, with two separate **nuclei**, eventually proceeds to **mitosis**. This produces a *hybrid cell* in which the two nuclear envelopes have been disassembled, allowing all the chromosomes to be brought together in a single large nucleus. Although such hybrid cells can be cloned to produce hybrid cell lines, the initial hybrid cells are unstable and lose chromosomes. For unknown reasons, mouse-human hybrid cells predominantly lose human chromosomes (see Hybridomas). The loss is random and gives rise to a variety of hybrid cell lines, each of which contains only one or a few human chromosomes. This phenomenon has been used in mapping the locations of genes in the human genome.

Hybrid Dysgenesis

Hybrid dysgenesis is a syndrome observed in *Drosophila* that results from the high-frequency germline transposition of a particular *Drosophila* transposable element called the P element (1). The phenotypes associated with hybrid dysgenesis include a high frequency of mutation and sterility. Hybrid dysgenesis results when males from a strain that contains P elements in its genome are crossed with females from a non-P strain. The lack of high-frequency transposition when P^+ (or P^-) strains are crossed among themselves results from the fact that the P element encodes, in addition to a transposase, an inhibitor of transposition. Thus, hybrid dysgenesis occurs only when the egg is from a P^- strain, lacking the P element and its inhibitor, and when the P-element-containing DNA arrives via sperm without the inhibitor.

Regulation at several levels can account for hybrid dysgenesis. Transposition of the P element is restricted to the germ line because an intact transposase protein is produced only in the germ line. Transposase is encoded by four separate exons whose messenger RNA needs to be assembled by RNA splicing. This splicing event can occur only in the germ line because a somatic protein that binds to Exon 2 RNA near the 5′ splice site inhibits splicing in somatic tissue (2, 3). Another level of control of P element transposition is the transposition inhibitor encoded by the P element itself (1). This inhibitor derives from the P element mRNA, so the transposition inhibitor is related to, but is not identical to, transposase. The mechanism of inhibition appears to involve repression of transcription, which decreases the amount of available transposase.

The high-frequency P-element transposition in the germline that leads to hybrid dysgenesis thus results from the germline-specific synthesis of transposase from the DNA of the sperm of a P^+ male in the absence of a transposition inhibitor; the inhibitor is lacking in the maternal cytoplasm because this fly lacks a P element to generate the inhibitor.

Bibliography

1. W. R. Engels (1996) Curr. Top. Microbiol. Immunol. **204**, 103–124.
2. F. A. Laski, D. C. Rio, and G. M. Rubin (1986) Cell **44**, 7–19.
3. C. W. Siebel and D. C. Rio (1990) Science **248**, 1200–1208.

Hybrid Individual

A hybrid is the offspring of genetically different individuals. The term is used often to refer to the offspring of distantly related members of the same species or of closely related species. The potential production of fertile hybrids is a fundamental criterion to assign different individuals, strains, or races to a single biological species.

A *heterozygote* is an individual whose nuclei carry at least two different versions of at least part of the genetic information. The difference may consist in the nucleic acid sequence, the number of chromosomes, or the order of the genes in the chromosomes.

1. Mendelian Hybrid

In a restricted sense, a Mendelian hybrid is the result of crossing two true-breeding strains (homozygotes) (see Homozygote, True Breeding).

A hybrid may involve two **alleles** *A* and *a* of a single gene (a monohybrid *Aa*), or two pairs of alleles at two different genes (the dihybrid *AaBb*), and so on. Hybrids produce characteristic Mendelian segregations in crosses with each other or with their parents (see Mendelian Inheritance, **Crosses**).

Genes that appear in heterozygosis in a polyhybrid may be carried in the same or different chromosomes. The dihybrid *AaBb* is said to be in the *cis-configuration*, or the *coupling* phase, when it contains two dominant alleles on the same chromosome and two recessive alleles on the homologous chromosome of the diploid; to make a graphic distinction, the genotypes of the homologous chromosomes are separated by a slash: *AB/ab*. The dihybrid *AaBb* is said to be in the *trans-configuration*, or the *repulsion* phase, when each chromosome carries a dominant and a recessive allele: *Ab/aB*. When two genes are sufficiently close in the same chromosome, their alleles do not form the random combinations expected from Mendelian inheritance; alleles in the same chromosome tend to remain together.

Hybrids may be larger, more vigorous, or more resistant to adverse conditions than their parents. This phenomenon, called heterosis or *hybrid vigor*, occurs frequently in plants and animals and has led to the commercial production of hybrid seed for agriculture. Depending on the actual techniques that are used, hybrid seed may be too expensive and replaced in practical application by "*double hybrid* seed," the offspring of two hybrids, each with different parents.

Hybridization, Nucleic Acids

Shortly after the discovery of the double helix, it was found that the two strands of DNA could be separated and that duplex DNA could be reformed. Further it was found that DNA from different sources could be combined to form hybrid duplexes (1). Hybridization techniques have become one of the workhorses of molecular biology (2). The properties that promote formation of duplexes from partially or exactly complementary single-stranded nucleic acids are the foundation of hybridization techniques. A requirement for most hybridization experiments is labeled nucleic acid, which provides a detectable signal reporting the quantity of hybrid duplex formed with high sensitivity. Many techniques in nucleic acid chemistry rely on formation of a hybrid duplex composed of single-stranded nucleic acids from different origins.

Hybridization techniques vary markedly in their details, but there are features common to all. Under appropriate solution conditions, two nucleic acid strands with at least partial sequence complementarity can form a hybrid duplex. Each strand may be either DNA or RNA. Most hybridization experiments consist of a minimum of three steps: (*1*) preparation of the target, (*2*) formation of the hybrid duplex, and (*3*) detection of the hybrid duplex. Each step can be technically challenging, and proper procedure requires multiple accompanying control experiments.

The nucleic acids to be hybridized should be free of interfering contaminants. If any of them are part of a duplex, a denaturation step, either by heat or alkali, is included. Frequently, a partial degradation step prior to denaturation is included in the procedure. The degradation is accomplished either by shear or by endonuclease digestion. Selection of the temperature and solution conditions for the hybridization reaction is critical in determining the outcome (see Stringency). Under high stringency conditions, only regions that are highly complementary will form hybrid duplexes. As the stringency is lowered, the fraction of bases participating in hybrid duplexes will increase because of the greater tolerance for defect in sequence alignment under such conditions.

The power of hybridization techniques comes from the dependence of the stability of the hybrid duplex on the extent of complementarity of the constituent strands. The stability of the hybrid duplex depends strongly on solution conditions and temperature, which must be designed carefully to achieve the desired level of sequence discrimination. Most hybridization solutions contain EDTA to bind divalent cations, a polymer utilized to enhance hybrid formation (presumably via an excluded volume effect), and a **denaturant**, usually formamide, in a pH buffered salt solution. The combination of solution conditions (especially the formamide and NaCl concentrations) and temperature defines the stringency of the hybridization reaction. Optimizing the stringency of the reaction is of paramount importance in the success of any hybridization experiment. Defining the optimum depends on the objectives of the experiment. High stringency conditions reduce the stability of the hybrid duplex and select for high sequence homology. Such conditions are used when high target specificity is desired. Low stringency conditions tolerant greater sequence variability. Lower stringency conditions are useful when it is desirable to relax sequence selectivity, such as when probing for a family of related sequences.

When hybridization is performed in solution, the selective detection of hybrid duplexes is difficult. Some progress has been made on this issue by application of fluorescence **energy transfer** techniques; however, selective detection of hybrids remains problematic. This has limited the application of solution hybridization. Its primary application is for formation of heteroduplexes that are subsequently analyzed to determine the extent of sequence complementarity. Another difficulty encountered in solution hybridization is the competition between formation of the hybrid duplex and reformation of the original duplex. There are several approaches to address this problem. For example, when RNA–DNA hybrids are formed, high formamide concentrations (80%) can be used; DNA–DNA duplexes are more destabilized under such conditions. The most common way to circumvent the competitive equilibrium problem is by immobilization of the denatured nucleic acid on a surface. Immobilization prevents reassociation of the denatured duplex. Immobilization of a target nucleic acid forms the basis for a wide variety of probe hybridization techniques. It is in these techniques that the true utility of hybridization for studying nucleic acids is realized.

Traditionally, hybridization reactions have been confined to formation of RNA–DNA and DNA–DNA duplexes. The recent and rapid developments in synthesis of unnatural nucleic acid analogues with base and backbone modifications is expanding the number of possible combinations of duplexes that can be formed. These developments are likely to be exploited in new hybridization reactions. Also, the recent development of triplex-forming nucleic acids for use as probes has expanded the range of reactions that can be usefully included under the heading hybridization.

Bibliography

1. B. J. McCarthy and R. B. Church (1970) Annu. Rev. Biochem. **39**, 131–150.
2. J. Sambrook, E. F. Fritsch, and T. Maniatis (1989) *Molecular Cloning: A Laboratory Manual*, 2nd ed., Cold Spring Harbor Press, New York.

Suggestion for Further Reading

3. P. Tijssen (1993) *Hybridization with Nucleic Acid Probes: Part 1*, *Theory and Nucleic Acid Preparation; Part 2, Probe Labeling and Hybridization Techniques*, Elsevier, Amsterdam.

Hybridomas

Classical seminal studies by Köhler and Milstein in 1975 (1) led to the generation of monoclonal antibodies with defined specificity. Hybridoma methodology was based primarily on fusing murine immune lymphocytes with a malignant myeloma lymphocyte cell line that possessed certain important genetic and biochemical properties. This important methodology was necessitated by the fact that immune antibody-producing B lymphocytes were difficult to maintain as stable cell lines under tissue culture conditions. However, fusion of antibody-producing cells with a malignant myeloma cell line resulted in proliferative cells that can be maintained indefinitely.

Spontaneous fusions between lymphocytes are rare events, so the frequency of fusion was increased to generate large numbers of fused cells by using surface-active agents such as inactivated Sendai virus or the chemical polyethylene glycol (PEG). Upon mixing immune lymphocytes with myeloma cells and the fusing reagent, a selection system was mandatory to eliminate unfused parental cells and to assay for appropriately fused cells that synthesized antibodies with the desired specificity. The tissue culture selection process was dependent on the procurement of myeloma cell lines that no longer synthesized an immunoglobulin and lacked genes for **thymidine kinase** (TK) and/or **hypoxanthine-guanine-phosphoribosyl transferase** (HGPRT). These enzymes catalyze important steps in the salvage pathway used in DNA synthesis by dividing cells. Unfused myeloma cells are unable to proliferate in the HAT selection medium (containing hypoxanthine, aminopterin, and thymidine) because aminopterin inhibited the *de novo* DNA biosynthetic pathway, forcing the cells to use the nonfunctional salvage pathway. Fused myeloma cells proliferate in HAT medium because the immune lymphocytes (fusion partner) furnish the essential TK and HGPRT enzymes for the salvage pathway. Thus, cells that survived incubation with HAT medium represented a successful immune B-cell–myeloma cell fusion, usually on a 1:1 cellular basis. The second phase in hybridoma production was the selection of those fused cells that synthesized and secreted antibody of the desired specificity. This was generally achieved by diluting fused cell populations to a single cell and then generating clones by proliferation of the single cell. The extracellular fluid or media from the single cell and resulting progeny were assayed for the appropriate antigen binding. The methods and techniques used to detect monoclonal antibody activity are usually based upon some variation of the solid-phase immunoassay (eg, ELISA or radioimmunoassay formats).

Hybridoma methodology and consistent generation of relatively large amounts of monoclonal antibodies with defined specificities has proven to be a source of important immunological reagents.

1. The provision of adequate quantities of monoclonal antibody has facilitated the routine determination of primary structures of both the H and L chains at the protein level.
2. Various monoclonal antibodies can be crystallized on a regular basis, providing atomic, 2- to 3-Å resolution structures by **X-ray crystallographic** procedures. In general, **Fab** fragments (four-domain substructures of antibodies, including the variable domains of both chains) with bound ligand crystallize most efficiently. Approximately 100 resolved structures of monoclonal antibodies (Fab fragments) have now been reported.
3. This methodology provides large homogeneous hybridoma cell populations from which messenger RNA responsible for the synthesis of H and L chains can be obtained. Through development of polynucleotide primers, polymerase chain reaction (**PCR**) technology can be used to generate complementary DNA copies for sequencing at the gene level.
4. Gene cloning experimentation with antibody genes has been important in successful site-directed mutagenesis studies. Such studies have been critical in deciphering structure–function relationships governing antibody activity.
5. Hybridoma methodology has led to the development of antibody derivatives, such as single-chain antibodies (2). The latter represent ~25,000–Da structures containing only the variable domains of the H and L chains of a specific antibody molecule. Variable domains constituting single-chain antibodies are usually attached covalently through the use of flexible polylinkers (10 to 15 amino acid residues) that are encoded in the single-chain synthetic gene. Single-chain genes are subsequently incorporated into the appropriate plasmids and expressed in either **prokaryote** or **eukaryote** cell lines.
6. Antigen–antibody interactions can now be studied on a homogeneous basis, yielding important information regarding the thermodynamics of binding.
7. The provision of monoclonal antibodies by hybridoma technology has led to the development of standard diagnostic procedures as well as therapeutically useful immunochemical reagents.

Monoclonal antibodies of defined specificity generated through hybridoma methodology have been used to solve many issues related to structure–function relationships within the antibody molecule. Based on studies with monoclonal antibodies, the property of Fab (active site) segmental flexibility within the IgG class of antibodies was solved. Homogeneous binding at both active sites within a bivalent molecule ruled out **allosteric** effects within antibody molecules. Thus, binding at one active site does not influence antigen binding at the adjacent site. Conformational changes transmitted throughout the molecule subsequent to binding of antigen were dismissed as an explanation for such important phenomena as **complement** binding and fixation. In all cases, the availability of monoclonal antibodies proved important to examine definitively these important questions.

Although hybridoma technology has been the method of choice to produce monoclonal antibodies of defined specificity, new techniques have now emerged. Similar to the construction of single-chain antibodies, gene segments encoding the H- and L-chain variable domains are genetically fused to genes encoding a **bacteriophage** coat protein (3). The engineered bacteriophage infect bacteria, and the resulting phage particles express active antibody products on their surface. The resulting phage display library expresses many different antigen-binding domains. Phage that specifically bind antigen are selected and used to infect bacteria in a second cycle. Each selected phage produces a monoclonal antigen-reactive particle. Primary structures of the variable domains can be determined, and those genes can be fused to the antibody constant region genes to reconstruct a monoclonal antibody. Such genes transfected into myeloma cell lines are expressed, and the antibody products are secreted. Phage display methodology has important implications for the future.

Bibliography

1. G. Köhler and C. Milstein (1975). Nature **256**, 495–497.
2. R. E. Bird, K. D. Hardman, J. W. Jacobson, S. Johnson, B. M. Kaufman, S.-M. Lee, T. Lee, S. H. Pope, G. S. Riordan, and M. Whitlow (1988) Science **242**, 423–426.
3. I. Roitt, J. Brostoff, and D. Male (1996) *Immunology*, 4th ed. Mosby, London, p. 28.9.

Hydration

The total hydration of a protein (or nucleic acid) is the effective amount of water immobilized by (bound to) a protein molecule or other macromolecule. This consists of a summation of interactions of water molecules with individual sites on the accessible surface of a protein molecule. Such interactions vary from (1) very strong ones, such as water molecules trapped within cavities on a protein molecule and involved in the actual folded structure of the protein, (2) weak interactions, such as water molecules that hydrate charged and other **polar groups** on the surface of a protein molecule; and (3) very weak interactions that comprise water molecules whose rotation or translation is momentarily perturbed by the proximity of a protein molecule (by weak attraction or repulsion). This last type of interaction is primarily **entropic** in nature and reflected by a very small value of the **free energy**. The summation of all these interactions manifests itself as effective binding (ie, immobilization of the water by the protein) that may have a small fractional value at each protein surface site, but which sums up to some whole numbers over the entire molecule.

Total hydration is very difficult to measure, and its values may be a function of the techniques used. X-ray crystallography detects the more strongly interacting water molecules. The NMR technique that detects water molecules whose freezing is perturbed by the presence of the protein (1) and vapor pressure osmometry (2) give similar values of total hydration. These values are of similar magnitude to those obtained from equilibrium dialysis in those cases in which there is total exclusion of ligand from the protein surface. Furthermore, a measurement of site occupancy by the ligand by a contact detecting technique (total binding), when combined with equilibrium dialysis, yields the total hydration (see Eq. 1 of Binding). See also Preferential Hydration.

Bibliography
1. I. D. Kuntz and W. Kauzmann (1974) Adv. Protein Chem. **28**, 339–345.
2. H. B. Bull and K. Breese (1974) Arch. Biochem. Biophys. **161**, 665–670.

Hydrodynamic Volume

Measurement of the hydrodynamic properties of a biological macromolecule can provide low resolution information about its size and shape. This information can be useful in modeling any interactions in which the macromolecule is involved. Among the techniques used for hydrodynamic measurements are **light scattering, sedimentation velocity** and sedimentation equilibrium centrifugation, and size exclusion chromatography. The hydrodynamic properties of a macromolecule are often expressed in terms of a macromolecular volume (see Stokes Radius). In considering the volume of a macromolecule, however, one must include not only the macromolecule itself but also the role of solvent. Solvent that is “trapped” is an inherent part of a macromolecule and will, therefore, be reflected in measurements of its transport properties. A simple model of hydration of a biological macromolecule is shown in Figure 1. As indicated, water may be bound either at the surface of the macromolecule or in interior spaces. Some solvent molecules may be bound specifically, and others may be simply trapped. In the thermodynamic treatment of this bound water, no distinction is made between the various classes of bound-water molecules. Instead, they are treated as a smooth surface or as internal pools. In any hydrodynamic measurement, these water molecules remain tightly associated with the macromolecule, so the total volume of the macromolecule derived from such studies will necessarily include the bound solvent. A mathematical treatment of hydrodynamic volume in which the bound water molecules are explicitly included is provided here, based on References 1-3.

Figure 1. A cartoon diagram of a macromolecule with bound water. The water can be associated with the surface of the macromolecule or may be accumulated in “pools” in the interior of the molecule. The thermodynamic treatment of this water presented here does not distinguish between these different types of bound-water molecules.

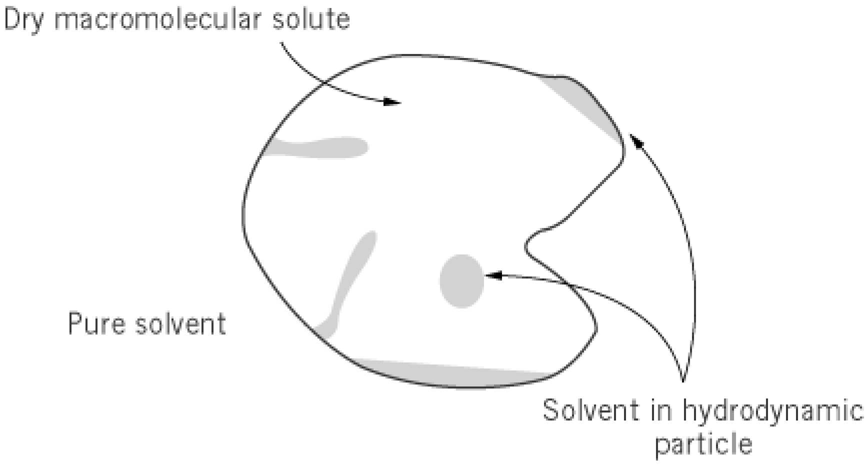

Assume that a given macromolecule has d_1 grams of water bound per gram of macromolecule. If V^*_1 is the average specific volume of this water in cm^3/gm, and if a solution consists of g_1 grams of water and g_2 grams of anhydrous macromolecule, the total volume of the solution can be calculated using the following equation:

$$V_{tot} = (g_1 - g_2\delta_1)\overline{V}_1^{\Delta} + g_2V_2 + \delta_1 V_1^* g_2 \tag{1}$$

where V_{D1} is the specific volume of pure water in cm^3/gm. The first term in the equation is the volume of unbound water; it is assumed to have the same specific volume as pure water. The second term is the volume occupied by the macromolecule; the specific volume of the macromolecule in solution, V_2, is not necessarily equivalent to the specific volume of the pure solid macromolecule. The third term is the volume of bound water. The sum of the second and third terms is the volume of the hydrated macromolecule. This volume can be calculated using the following equation:

$$V_h = \frac{M}{N_0}(V_2 + \delta_1 V_1^*) \tag{2}$$

where M is the **molecular weight** of the macromolecular solute and N_0 is Avogadro's number. Unfortunately, this equation is not very useful, since the terms V_2, d_1, and V^*_1 are not known. These variables can, however, as indicated below, be replaced by those that are experimentally accessible.

The **partial specific volume** of a solute is the change in solution volume when a small increment of the solute is added, at the limit of infinite dilution. This quantity is determined experimentally by measuring the density of a solution as a function of the weight concentration of the solute. The expected result of this measurement can be derived from Equation (1)

$$\overline{V}_2 = \left[\frac{\partial V_{tot}}{\partial g_2}\right]_{g_1,T} = -\delta_1\overline{V}_1^{\Delta} + V_2 + \delta_1 V_1^* \tag{3}$$

This derivation assumes that the macromolecule is sufficiently dilute that the degree of its hydration is independent of its concentration. Using this equation, we can replace V_2 and V^*_1 in Equation (2) to yield

$$V_h = \frac{M}{N_0}(\overline{V}_2 + \delta_1 \overline{V}_1^{\Delta}) \tag{4}$$

The term V_{D1} represents the specific volume of water, which is a pure substance, and can be replaced by its partial specific volume, V_1, which is simply the inverse of the density of pure water. It follows that the hydrated volume of the macromolecule is

$$V_h = \frac{M}{N_0}(\overline{V}_2 + \delta_1 \overline{V}_1) \tag{5}$$

The partial specific volume of the macromolecular solute, V_2, can be measured directly by determining the change in solution volume as a function of added macromolecular solute. The final term is the hydration, and d_1 is an unknown, but it can be reasonably estimated.

Direct determination of the partial specific volumes (V_2 in Eq. (5)) of macromolecules is accomplished by determining the change in solution volume as a function of added macromolecular solute. This can be a difficult measurement and may require a large amount of material. The availability of accurate microbalances can minimize the latter difficulty. Partial specific volumes can also be determined by ultracentrifugation in various mixtures of H_2O/D_2O with varying densities (3). The advantages of this technique are that it as both rapid and requires very little material. The partial specific volumes of proteins can also be reasonably estimated from their amino acid compositions, using estimates of specific volumes of individual amino acid residues (4).

Hydration of biological macromolecules (d_1 in Eq. (5)) has been measured using a variety of techniques, including NMR spectroscopy of frozen samples and **calorimetric** studies. Results from these studies on proteins indicate that the variation in bound water is related to the amino acid composition of the protein. Based on these results, methods for calculating the amount of water bound to a protein from its amino acid composition have been developed. Results of the calculations are in good agreement with the results of experimental measurement (5).

Bibliography

1. C. Tanford (1961) *Physical Chemistry of Macromolecules*, Wiley, New York, pp. 339–341.
2. C. R. Cantor and P. R. Schimmel (1980) *Biophysical Chemistry*, Part II, Freeman, San Francisco, pp. 550–555.
3. S. J. Edelstein and H. Schachman (1973) Meth. Enzymol. **27**, 82–98.
4. E. J. Cohn and J. T. Edsall (1943) *Proteins, Amino Acids and Peptides as Ions and Dipolar Ions*, Reinhold, New York, p. 157.
5. I. D. Kuntz Jr.and W. Kauzmann (1974) Adv. Protein Chem., **28**, 239–345.

Hydrogen Bond

A hydrogen bond is an attractive interaction between the donor pair X—H and the acceptor atom Y, where H is a hydrogen atom that is covalently bound to an electronegative atom X but attracted to another electronegative atom, Y. The hydrogen bond is commonly represented by a dotted line, as in X—H¼Y. The electron density in the X—H bond is attracted more to X, so X has a partial negative charge and H a partial positive charge, which has been demonstrated by neutron and X-ray diffraction studies of hydrogen bonded crystals. Since the hydrogen bond involves at least three and sometimes four atoms, physically it is characterized by the bond length (—H¼Y—), the angle formed by X—H¼Y, and the enthalpy of formation, D *H*. Typical donors are F—H, >NH, —NH_2, —OH, —COOH, and less frequently, —S—H, → C—H groups. Hydrogen bonds involving C—H are among the weakest. The acceptors are commonly —N, > C=O, —C—F, > NH, > O, and p-electron systems of unsaturated or aromatic hydrocarbons. Examples of hydrogen bonded pairs commonly found in biological structures are [P—OH¼O=P], [O—H¼O=C], [N—H¼O=C], and [O—H¼O—H] (1).

Historically, the presence of associative interactions among certain types of organic and inorganic molecules was recognized in the early 1900s. The remarkable unusual properties of liquid water were attributed to the network of hydrogen-bonded H_2O molecules (for a summary of the early history and references, see Ref. 2). The idea of a hydrogen bond provided an extra valence for the hydrogen atom, which already has a closed electron shell structure. The early observations were summarized in a unified view and presented as the "hydrogen bond" by L. C. Pauling (3).

1. Methods of Detection

For their ease and sensitivity, the vibrational spectroscopy techniques of infrared (IR) and, less frequently, Raman spectroscopy, plus NMR, are the preferred methods for detecting the presence of hydrogen bonds. Neutron diffraction from single crystals gives the most precise elucidation of the hydrogen bond geometry, as it detects the hydrogen atom directly, in contrast to X-ray crystallography, where the presence of a hydrogen bond can be inferred only by the shorter than normal distance between the heavier atoms X and Y (1, 2, 4, 5).

1.1. X-H Stretching Mode in Infrared Spectroscopy

A low frequency shift in IR spectra in the frequency range of 1500–4000 cm^{-1} that is highly temperature-dependent and accompanied by a dramatic increase in absorbance is usually taken as evidence of hydrogen bonds involving O—H or N—H groups as donors. Bending of X—H¼Y bonds in and out of the plane causes absorbance in the region of 1700–1800 cm^{-1} and 400–900 cm^{-1}, respectively. The stretching and bending vibrations of H¼Y hydrogen bonds have much lower resonance frequencies of 50–600 cm^{-1} and less than 50 cm^{-1}, respectively (1). Such spectral changes allow the determination of an equilibrium constant for formation of the hydrogen bond, and its temperature dependence can give the enthalpy of formation. The low frequency vibrational modes make important contributions to the thermodynamic properties of hydrogen-bonded systems.

1.2. Deshielded Proton Signals in NMR

NMR spectroscopy can detect hydrogen bonds because the hydrogen atoms involved are less shielded and consequently resonate at a lower magnetic field. In the case of nucleic acids, these hydrogen atoms are known to have typical chemical shifts of 9–15 ppm downfield of the internal standard (6). If the acceptor group is of aromatic p electrons, the resonance is shifted upfield relative to non-hydrogen-bonded atoms.

1.3. Position of the H Atom by Neutron and X-Ray Diffraction

Neutron diffraction gives the most accurate positions of hydrogen atoms, as they scatter about half as much as C, N, and O atoms. In contrast, hydrogen atoms are barely detectable by X-ray diffraction, and hydrogen bonds are evident primarily from the closeness of the X and Y atoms. On the other hand, there are much more X-ray crystallography data available than neutron diffraction data. The controversy over the existence of weak C—H¼O (or N, S, Cl) hydrogen bonds has been discussed (7).

2. Energetics

2.1. Enthalpy of Formation

The enthalpy of formation of typical hydrogen bonds is commonly determined as the temperature dependence of the association constant for hydrogen-bonded dimers in isolation. The values measured range from a few to 100 kJ/mol, and the majority are in the range 20–30 kJ/mol (Table 1). The bond energy of a hydrogen bond is therefore less than 0.1 that of typical C━C or C━N covalent bonds.

Table 1. Thermodynamics of Hydrogen Bond Formation

Species	–D*H*, kJ/mol	–D*S*, e.u./mol-H bond
Formic acid dimer (gas)	28	18
Acetic acid dimer (gas)	31	18
Propionic acid dimer (gas)	32	18
Stearic acid dimer (liquid)	28	14
Water (gas)	18–21	
Water (liquid)	14	
Methanol (gas)	13–25	
Methanol (liquid)	20	
Ethanol (gas)	17	
Ethanol (liquid)	~17	
Ammonia (gas)	~17	
HF (gas)	28–29	
HCN (gas)	14	

2.2. Hydrogen Bond Potential

Typical potential-energy curves for hydrogen bonds are presented in Figure 1. The first curve (**a**) demonstrates that most common unsymmetric potential, where the H atom is more strongly associated with atom X than with Y. The second curve (**b**) illustrates a symmetric case, where H is bonded equally to X and to Y. As the potential barrier becomes lower, the position of the hydrogen atom becomes sensitive to environmental factors. The third curve (**c**) illustrates the rare case where the potential-energy curve has a single minimum, and the hydrogen bond is truly centric; a good example of this may be found in intramolecular, symmetric hydrogen bonds illustrated in Figure 2.

Figure 1. Potential-energy curves of hydrogen-bonded systems: (**a**) a typical case of an unsymmetric potential, where the H atom is more strongly bonded to X; (**b**) a symmetric case such as Fig. 1**c**; and (**c**) a rare case of a centric potential.

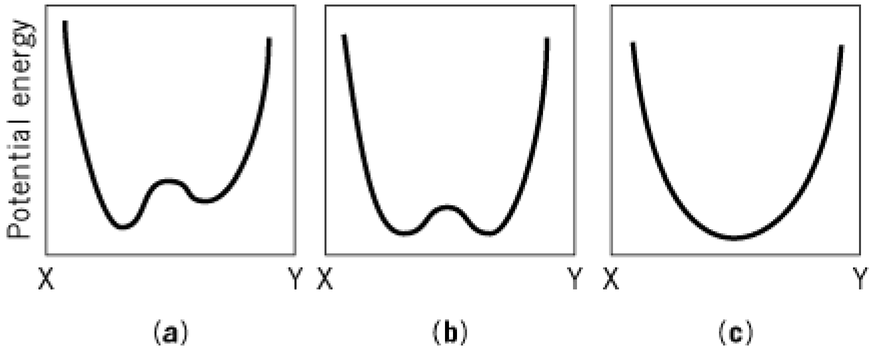

Figure 2. Schematic illustration of various geometries of hydrogen-bonded complexes: (**a**) a strong hydrogen bond between hydrogen fluoride and fluoride anion; (**b**) a cyclic dimer of aliphatic acids; (**c**) a symmetric example of intramolecular hydrogen bonding; (**d**) a hydrogen bond network of water molecules; (**e**) an example of a multi-centered hydrogen bond system. Taken from 9 with permission.

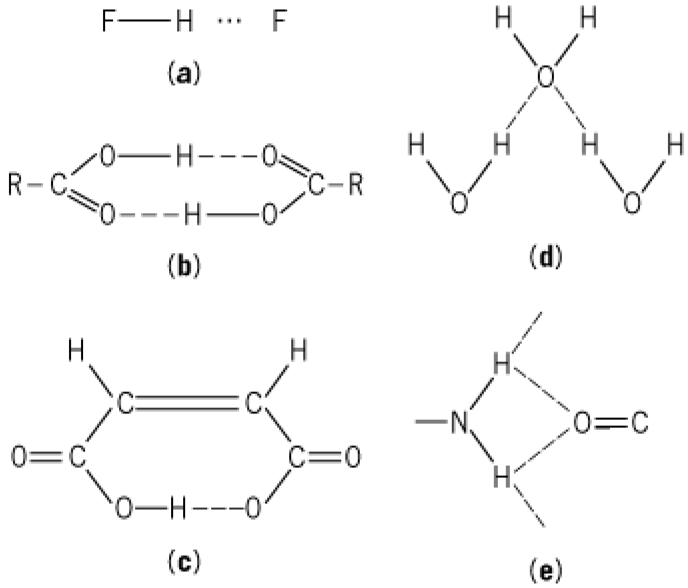

The Morokuma potential decomposes the total hydrogen bond energy into the following terms and evaluates the relative contribution of each term from the distance between the atoms, r: (*1*) electrostatic (r^{-1}), (*2*) polarization (r^{-4}), (*3*) exchange repulsion (r^{-12}), (*4*) charge transfer <rf>exp</rf>($-r$), and (*5*) dispersion interactions ($r^{-6} + r^{-8} + r^{-10}$) (1, 8) (see Electrostatic Interactions and van der Waals Interactions). The dependence of the total hydrogen bond energy calculated for a water dimer in the gas phase is given in Figure 3 in terms of the individual interactions above.

Figure 3. Decomposition of the total hydrogen bond energy of the water dimer, demonstrating an important contribution of the electrostatic term. (Taken from Ref. 1 with permission.)

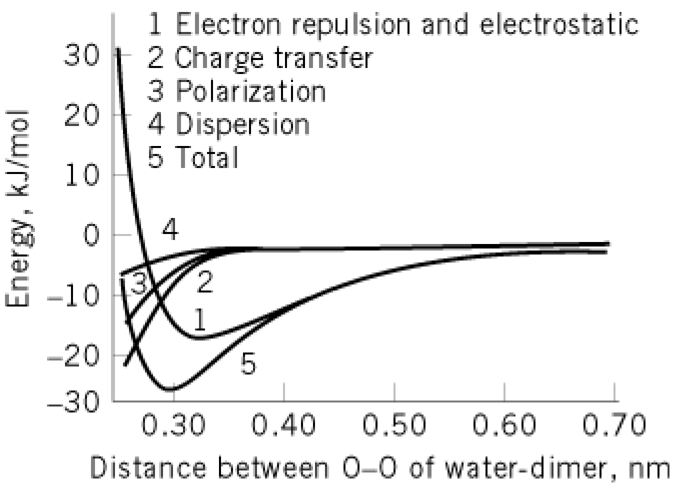

3. Hydrogen Bond Geometry

The acceptor Y atom of a hydrogen bond often has electrons in lone pairs that are directional, and consequently the hydrogen bond is also highly directional. Because of this property, the hydrogen bond is often a determining factor for the geometry of hydrogen-bonded crystals and in the conformation of polymers. In Figure 2, the geometries of a variety of hydrogen-bonded molecular complexes are presented in simplified forms. The distinction between inter- and intramolecular hydrogen bonds is important for small molecules, because the geometric constraints are more severe for the latter. For small molecules in solution, hydrogen-bonded pairs are constantly changing their counterparts, due to the low potential and activation energies of hydrogen bonds.

3.1. Bond Length

The distance parameters of X—H¼Y hydrogen bonds may be defined in several ways. When the position of the H atom is known, the distance between H and Y is defined as the hydrogen bond length. When it is not known, the distance between X and Y is a less sensitive, but in many cases still a good, guide for the presence of a hydrogen bond. For example, high resolution neutron diffraction studies indicate that nonbonded distances between two O atoms of <0.30 , 0.34, and >0.37 nm correspond to respective hydrogen bond probabilities of nearly 100%, about 50%, and almost 0% (1, 9). The strength of a hydrogen bond is no more than 0.1 that of a common covalent bond, so the geometries of weak to moderate hydrogen bonds are sensitive to their environment. The hydrogen bond distance H¼Y can vary by as much as ±20% from the averages given in Table 2. For example, a compilation of more than 120 bond lengths determined by neutron diffraction studies gave a distribution of O—H distances of 0.095–0.120 nm, of H¼O from 0.120 to 0.200 nm (1).

Table 2. Bond Lengths in Typical Hydrogen Systems

Hydrogen-Bonded Systems	X—H	X—Y	H¼Y	Examples
O—H¼O	~0.100nm	0.275 nm	~0.17	Ice
N—H¼O	~0.090nm	0.299 nm	~0.21	Urea
O—H¼N	~0.110nm	0.278 nm	~0.17	Acetoxime
N—H¼N	~0.090nm	0.308 nm	~0.22	Guanine·HCl·$\frac{1}{2}H_2O$

In the nucleosides and nucleotides, some of the H¼Y distances are as follows (1):

P—OH¼OP	0.155–0.169 nm	
P—OH¼OH	0.165–0.189 nm	
O_W—H¼OP		0.166–0.188 nm
P—O—H¼O_W	0.159–0.168 nm	
Other O—H¼O	0.174–0.218 nm	
N—H¼O=P	0.158–0.189 nm	
N—H¼O=C	0.169–0.232 nm	
N—H¼N	0.173–0.223 nm	
NH—H¼O=P	0.167–	

	0.207 nm
NH—H¼O=C	0.168–0.273 nm
NH—H¼N	0.185–0.276 nm

3.2. Bond Angle

Although the three atoms involved in an X—H¼Y hydrogen bond tend to lie on a straight line, and unless there are two or more acceptors, the final geometry is a compromise of all the environmental factors. A hydrogen bond is therefore sometimes said to be "soft." As a result, the angle formed by the three atoms X—H¼Y is close to 180° for a strong hydrogen bond, and the flexibility about this angle increases as the bond becomes weaker. Bifurcated hydrogen bonds cannot be linear. Figure 4 (10) illustrates the distribution of X—H¼Y angles.

Figure 4. The distribution of hydrogen bond angles. The three atoms involved in the formation of a hydrogen bond have preferred configuration for the hydrogen bond to be most effective. The distribution on the left is normalized with respect to the statistical factor of 2 p sin f. (Taken from Ref. 9 with permission.)

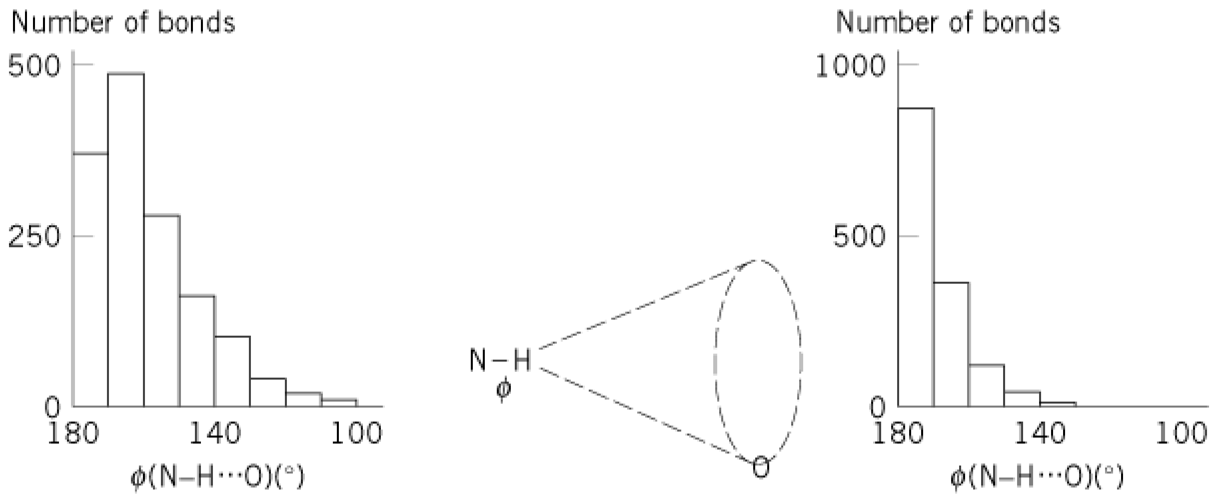

A very good example of the geometry of a hydrogen-bonded dimer is found in acetic acid in the gas phase, which is similar to scheme **b** of Figure 2. The O—H¼O angle is 180°, and the O—H and H¼O bond lengths are 0.104 and 0.164 nm, respectively.

4. Hydrogen Bonds in Molecular Biology

4.1. Hydrogen Bonds in Water

Water is well known to differ from the liquids formed by comparable molecules, such as H_2S, in its higher melting and boiling temperatures, its greater heat of fusion and of evaporation, and in its greater viscosity, properties that are important for life on earth. The hydrophobic effect that is one aspect of the interactions between nonpolar molecules and groups in water is a result of the physical properties of hydrogen-bonded networks in liquid water. When nonpolar molecules dissolve in water, they create a cavity within the hydrogen-bonded network of water molecules, which disrupts the network and forces a rearrangement of the water molecules; this reduces the entropy of the system. It is thermodynamically preferable for the nonpolar molecules to associate, thereby reducing the total area of the water–solute interface and minimizing the disruption of the hydrogen-bonded network of water.

4.2. Hydrogen Bonds in Protein Structure

Hydrogen bonds in folded protein structures are formed primarily (about 90%) between the N—H and C=O groups of the polypeptide backbone, and about 85% of these are in either alpha-helix or beta-sheet . In the a-helix, hydrogen bonds are formed between peptide groups every four residues apart; in the case of b-sheets, every two residues. The average hydrogen bond length (H¼O) is shorter for b-sheets (0.197 nm) than for the a-helix (0.206 nm). Three-centered, bifurcated hydrogen bonds are observed in helices, but are not as common as in small molecules. Polar side chains with hydrogen atoms, such as those of tyrosine, serine, threonine, lysine, arginine, glutamic acid, aspartic acid, glutamine, and asparagine, can act as hydrogen bond donors. Turn structures, such as **beta**- and gamma-turns, are also stabilized by main-chain hydrogen bonds (11, 12). The concept of low-barrier hydrogen bonds has been introduced to explain the fast and efficient proton transfer within and between proteins (13), but their presence, although persuasive in the gas phase, is still controversial and not supported by an NMR study (14).

4.3. Hydrogen Bond Network in the Active Site of Serine Proteinases

A hydrogen bond network was proposed in the active sites of serine proteinases on the basis of the X-ray crystallographic structure of chymotrypsin, so as to explain the unusual chemical reactivity of the serine residue at its active site (15, 16). At neutral pH, the hydroxyl group of an ordinary serine residue is not able to carry out an electrophilic attack on the carbonyl carbon of peptide bonds. That the active site Ser195 residue is in an activated state because of its participation in a hydrogen bond network with Asp102 and His57 has been well accepted. In the process of hydrolyzing a substrate peptide bond, the carbonyl group of the susceptible bond forms a covalent bond with the hydroxyl group of Ser195, to form an acyl intermediate, cleaving the peptide bond, and permitting the amino-terminus of the carboxyl-terminal portion of the peptide to form a hydrogen bond with His57. The amino group is then replaced by a water molecule, which will cleave the covalent bond to Ser195 and the amino-terminal portion of the substrate will dissociate, to complete the proteolysis reaction.

Hydrogen bond networks are also present in the active sites of carboxyl proteinases and in the functions of DNA-binding proteins, such as **zinc fingers**. The importance of hydrogen bonds in the subunit interactions of oligomeric proteins has been discussed thoroughly by Perutz (17).

4.4. Hydrogen Bonds in Nucleic Acids

The importance of hydrogen bonds in **nucleic acids** is twofold. Hydrogen bonds between the bases stabilize the **double-helix** structures of DNA and RNA, but a more important aspect is that hydrogen bonds are formed only between specified pairs of adenine:thymine, A:T (uracil for RNA) and guanine:cytosine, G:C. Formation of hydrogen bonds only between such specified pairs permits the basic mechanism of transmission of genetic information in the nucleic acids. The biological significance of the Watson–Crick model of DNA was in the specific hydrogen-bonding patterns between A:T and G:C complementary nucleotide pairs, which have been amply verified. There are other possibilities of hydrogen bond patterns among the four bases, but, under physiological conditions, the **Watson–Crick base pairs** are the most stable. An important aspect is that the G:C base pair is more stable than the A:T pair, in part because of the greater number of hydrogen bonds.

4.5. Hydrogen Bonds in Carbohydrates and Lipids

Carbohydrate molecules have a large number of —OH groups, all of which are candidates for forming hydrogen bonds. There is no doubt that the conformations of carbohydrates, and especially those of polymeric carbohydrates, are strongly influenced by hydrogen bond formation. Formation of hydrogen-bonded (often three-centered) structures in their fibrous and crystalline states is discussed by Jeffrey (1). The functional groups in lipid molecules that can form hydrogen bonds are limited to the hydrophilic head groups. Consequently, the conformational variation of lipid molecules through hydrogen bond formation is rather limited, compared to the preceding examples.

5. Prospectives

The importance of hydrogen bonds in chemistry and especially in biology is increasingly appreciated because of the advance of our knowledge of the natural and synthetic multimolecular systems known as supra-molecular systems. These complex structures are stabilized by multitudes of weak secondary interactions such as **van der Waals**, **electrostatic**, chelating, and hydrogen bonding interactions. The importance of supramolecular structures resides in the fact, as well as in our expectation, that a structure held together weakly and therefore dynamically will exert more subtle functions than will other developed molecules and molecular systems. The hydrogen bond is based on neutral groups and strongly controls the geometry of the resulting molecular associations, which will be important in controlling the structure and activity of synthetic and hybrid structures once the nature of hydrogen bond is understood more precisely. New methods are emerging for the study of hydrogen bonded systems with completely different perspectives. For example, the strength and specificity of hydrogen bonding can now be measured using scanning probe techniques applied to a group of molecules (18) and at the single-molecule level (19).

Bibliography

1. G. A. Jeffrey (1997) *An Introduction to Hydrogen Bonding*, Oxford Univ. Press, New York.
2. G. C. Pimentel and A. L. McClellan (1960) *The Hydrogen Bond*, Freeman, San Francisco.
3. L. C. Pauling (1960) *The Nature of Chemical Bond and the Structure of Molecules and Crystals: An Introduction to Modern Structural Chemistry*, Cornell Univ. Press, Ithaca.
4. P. Schuster, G. Zundel, and C. Sandorfy (1976) *The Hydrogen Bond: Recent Developments in Theory and Experiments*: Vol. **1** I, *Theory*; Vol. **2**, *Structure and Spectroscopy*; Vol. **3**, *Dynamics*, *Thermodynamics and Special Systems*, North-Holland, Amsterdam.
5. G. A. Jeffrey and W. Saenger (1991) *Hydrogen Bonding in Biological Structures*, Springer-Verlag, Berlin.
6. C. W. Hilbers (1979) "Hydrogen-bonded proton exchange and its effect on NMR spectra of nucleic acids", in *Biological Applications of Magnetic Resonance*, R. G. Shulman, ed., Academic Press, New York, Chapter "1", pp. 1–44.
7. R. Taylor and O. Kennard (1982) J. Am. Chem. Soc. **104**, 5063–5070.
8. U. C. Singh and P. A. Kollman (1985) J. Chem. Phys. **83**, 4033–4040.
9. C. Ceccarelli, G. A. Jeffrey, and A. Taylor (1981) J. Mol. Struct. **70**, 255–271.
10. R. Taylor, O. Kennard, and W. Versichel (1984) J. Am. Chem. Soc. **106**, 244–248.
11. S. N. Vinogradov (1980) "Structural aspects of hydrogen bonding in amino acids, peptides, proteins, and model systems", in *Molecular Interactions*, H. Ratajczak and W. J. Orville-Thomas, eds., Wiley, New York, Vol. **2**, pp. 179–229.
12. G. E. Schulz and R. H. Shirmer (1979) *Principles of Protein Structure*, Springer-Verlag, New York.
13. R. A. Copeland and S. I. Chan (1989) Proton translocation in proteins, Annu. Rev. Phys. Chem. **40**, 671–698.
14. E. L. Ash, J. L. Sudmeier, E. C. De Fabo, and W. W. Bachovchin (1997) A low-barrier hydrogen bond in the catalytic triad of serine proteases? Theory versus experiment, Science **278**, 1128–1132.
15. D. M. Blow, J. J. Birktoft, and B. S. Hartley (1969) Role of a buried acid group in the mechanism of action of chymotrypsin, Nature **221**, 337–340.
16. C. Branden and J. Tooze (1991) *Introduction to Protein Structure*, Garland Publishing, New York, p. 237.
17. M. Perutz (1992) *Protein Structure: New Approaches to Disease and Therapy*, Freeman, New York.
18. A. Noy, D. V. Vezenov, and C. M. Lieber (1997) Chemical force microscopy, Annu. Rev. Mat. Sci. **27**, 381–421.
19. A. Ikai (1996) STM and AFM of bio/organic molecules and structures, Surf. Sci. Rep. **26**, 261–332.

Hydrogen Exchange

Hydrogen exchange is the interchange of hydrogen atoms between a molecule of interest, usually a peptide, **protein**, or **nucleic acid**, and water. Usually the exchange is detected because the hydrogens are different isotopes, the normal protium (^{1}H), or deuterium (^{2}H = D), or tritium (^{3}H = T). Designating the two isotopes as H and H′, the remainder of the macromolecule as M, and O as the oxygen atom of water, the reaction can be represented as

$$\mathrm{MH} + -\mathrm{OH'} \rightarrow \mathrm{MH'} + -\mathrm{OH} \quad (1)$$

Hydrogen exchange experiments provide information about the flexibilities of biological macromolecules. These are not static structures but exhibit a flexibility that is often important in their function. They undergo spontaneous thermal fluctuations and folding and unfolding processes, and they may display variations of their conformations. These motions vary with the binding of other molecules, with **allosteric** interactions, and with other environmental influences. All of these affect the rates of hydrogen exchange, whose measurement then helps to elucidate the dynamic structure of the molecule. For example, it is possible to measure the rate of base-pair opening in the DNA **double helix**, which is prerequisite for **replication** and transcription .

Rates of exchange of different types of hydrogen atoms are quite variable. Those attached to oxygen atoms of sugars in carbohydrates or of serine, threonine, and tyrosine residues in proteins exchange so rapidly that they are difficult to measure. Exchange of hydrogens attached to carbon is too slow. Those of most experimental interest are attached to nitrogen, as in the CONH peptide backbone or the asparagine and glutamine $CONH_2$ side chains of peptides and proteins and in the amino (NH_2) and imino (NH) groups of the nucleic acid bases **adenine**, **thymidine**, **uracil**, **guanine**, and **cytosine**. These exchange in milliseconds, or even faster with appropriate catalysts, when free and accessible to the solvent, but much slower, by as much as 10^{12}-fold, when buried in the interior of a macromolecule and inaccessible to solvent. These retardations reveal information about the stability of the folded macromolecular structure. The rate at which exchange actually occurs provides information about molecular dynamics.

1. Rates and Mechanisms of Chemical Exchange in Model Small Molecules

The rate of exchange R_{ex} or the rate of disappearance of MH and the formation of MH′ [Eq. (1)] is given by Eq. (2), where $[\mathrm{MH}]_{eq}$ and $[\mathrm{MH'}]_{eq}$ are the equilibrium concentrations of MH and MH′ and k_{ex} is the rate constant for the reaction (see Molecular Dynamics). For the amide groups of peptides and proteins, it is observed that k_{ex} has the form in Eq. (3), corresponding to acid catalysis by H^+ and base catalysis by OH^-. The catalytic constants are k_H and k_{OH}, respectively, and a term that is usually too small to detect, except in solvents less polar than water, corresponds to water catalysis. For the NH group of a typical amide, $k_H \sim 10^{-1} M^{-1} s^{-1}$ and $k_{OH} \sim 10^7 M^{-1} s^{-1}$. A graph of log k_{ex} versus pH is shown in Fig. 1. This shows a minimum given by Eq. (4), where $K_w = [\mathrm{H^+}][\mathrm{OH^-}] = 10^{-14}\ \mathrm{M}^2$.

$$R_{ex} = -\frac{d([\mathrm{MH}] - [\mathrm{MH}]_{eq})}{dt} = \frac{d([\mathrm{MH'}] - [\mathrm{MH'}]_{eq})}{dt} = k_{ex}([\mathrm{MH}] - [\mathrm{MH}]_{eq}) \tag{2}$$

$$k_{ex} = k_{\mathrm{H}}[\mathrm{H}^+] + k_{\mathrm{OH}}[\mathrm{OH}^-] + k_w \tag{3}$$

$$pH_{min} = \frac{1}{2}\log\left(\frac{k_{\mathrm{H}}}{K_w k_{\mathrm{OH}}}\right) \tag{4}$$

The mechanism of the base-catalyzed reaction involves removing the amide NH hydrogen atom [Eq. (5)], to create the imidate anion (the conjugate base of the amide), which then abstracts an H^+ from water to regenerate the amide [Eq. (6)]. The mechanism of the acid-catalyzed reaction depends on the amide. For the $CONH_2$ side chains of asparagine and glutamine residues, the exchange occurs simply by transient protonation of the nitrogen, which produces an unstable conjugate acid of the amide, followed by removal of a different hydrogen as H^+ [Eq. (7)]. For backbone CONH groups, exchange occurs by attachment of H^+ to the oxygen atom, which is much more basic than the nitrogen (see Kinetics), and produces another conjugate acid [Eq. (8)], followed by removal of H^+ from nitrogen, to produce the imidic acid, the unstable **tautomer** of an amide [Eq. (9)]. Attachment of a solvent H^+ to the nitrogen, followed by removal of H^+ from oxygen, regenerates the amide, but with its H exchanged [Eq. (10)].

$$\mathrm{RC(=O)NHR' + OH^- \rightarrow RC(-O^-) = NR'(imidate) + H_2O} \tag{5}$$

$$\mathrm{RC(-O^-) = NR' + H_2O \rightarrow RC(=O)NHR' + OH^-} \tag{6}$$

$$\mathrm{RC(=O)NH_2 + H^+ \rightarrow RC(=O)NH_3^+ \rightarrow RC(=O)NH_2 + H^+} \tag{7}$$

$$\mathrm{RC(=O)NHR' + H^+ \rightarrow RC(-OH) = NHR'^+} \tag{8}$$

$$\mathrm{RC(-OH) = NHR'^+ \rightarrow RC(-OH) = NR'(imidic\ acid) + H^+} \tag{9}$$

$$\mathrm{RC(-OH) = NR' + H^+ \rightarrow RC(-OH) = NHR'^+ \rightarrow RC(=O)NHR' + H^+} \tag{10}$$

The rates vary with the substitution pattern in the amide (1). Table 1lists logarithms of relative rate constants k_{H} and k_{OH} for various amino acid residues (2). Electron-withdrawing groups increase k_{OH} because they stabilize the negative charge that is created in the imidate anion. They also decrease k_{H} because they destabilize the positive charge created in either mechanism. As a result, pH_{min} [Eq. (4)] is decreased and the minimum in Fig. 1 moves to the left. Rates also increase with increasing temperature. In acid, the activation energy is 14 kcal/mol. In base, at constant pH, the apparent activation energy is 17.5 kcal/mol, but this greater value largely results from the temperature-dependence of K_w.

Figure 1. pH dependence of the value of the intrinsic exchange rate constant k_{ex} for the backbone amide of a typical peptide.

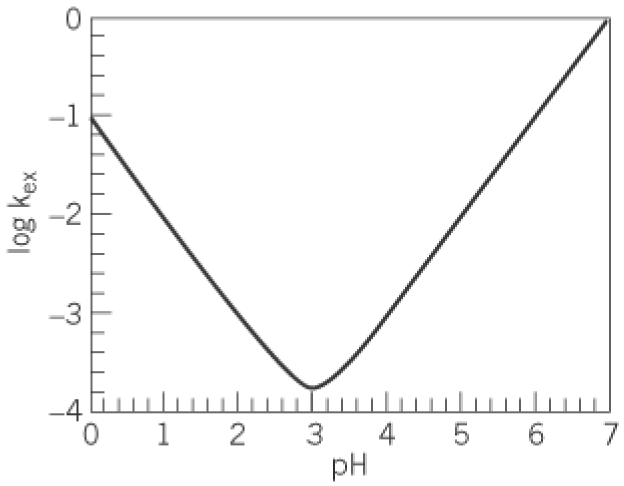

Table 1. Rate Constants for Acid- and Base-Catalyzed Hydrogen Exchange in $CH_3C(=O)NH_aCHRC(=O)NH_bCH_3$, relative to R=$CH_3$[a]

R	$\log_{10}k_{H,a}$	$\log_{10}k_{H,b}$	$\log_{10}k_{OH,a}$	$\log_{10}k_{OH,b}$
CH_3	≡0	≡0	≡0	≡0
($(CH_2)_3NHC(NH_2)_2^+$	–0.59	–0.32	0.08	0.22
CH_2CONH_2	–0.58	–0.13	0.49	0.32
$CH_2CO_2^-$	0.9	0.58	–0.30	–0.18
CH_2COOH	–0.9	–0.12	0.69	0.6
CH_2SH	–0.54	–0.46	0.62	0.55
$CH_2S\text{-})_2$ (Cys_2)	–0.74	–0.58	0.55	0.46
H	–0.22	0.22	0.27	0.17
$(CH_2)_2CONH_2$	–0.47	–0.27	0.06	0.20
$(CH_2)_2CO^-{}_2$	–0.9	0.31	–0.51	–0.15
$(CH_2)_2COOH$	–0.6	–0.27	0.24	0.39
CH_2Im (His)	–	–	–0.10	0.14
$CH_2ImH^+(His \cdot H^+)$	–0.8	–0.51	0.8	0.83
$CH(CH_3)CH_2CH_3$	–0.91	–0.59	–0.73	–0.23
$CH_2CH(CH_3)_2$	–0.57	–0.13	–0.58	–0.21

$(CH_2)_4NH_3^+$	–0.56	–0.29	–0.04	0.12
$(CH_2)_2SCH_3$	–0.64	–0.28	–0.01	0.11
CH_2Ph	–0.52	–0.43	–0.24	0.06
Cis-$(CH_2)_3N_a$ (Pro)	(H_a absent)	–0.19	(H_a absent)	–0.24
Trans-$(CH_2)_3N_a$ (Pro)	(H_a absent)	–0.85	(H_a absent)	0.60
CH_2OH	–0.44	–0.39	0.37	0.30
$CH(OH)CH_3$	–0.79	–0.47	–0.07	0.20
CH_2Indol (Trp)	–0.40	–0.44	–0.41	–0.11
$CH_2C_6H_4OH$ (Tyr)	–0.41	–0.37	–0.27	0.05
$CH(CH_3)_2$	–0.74	–0.30	–0.70	–0.14
N-term[b]	–	–1.32	–	1.62
C-term[c]	0.96	–	–1.8	–
C-term[d]	~0.05	–	–	–

[a] Ref. 2.

[b] For $^+H_3NCH_2CONHCH_3$.

[c] For $CH_3C(=O)NHCH_2CO^-{}_2$.

[d] For $CH_3C(=O)NHCH_2COOH$.

The mechanisms of exchange in nucleic acids are analogous, except that the equivalent of Eq. (7) never contributes. The imino NH groups of uracil, thymidine, and guanine are sufficiently acidic that they can be removed by OH^- at every encounter, in a diffusion-controlled reaction that has a rate constant k_{OH}~$10^{10}M^{-1}s^{-1}$. Weaker bases, such as components of the buffer, also remove these hydrogen atoms. Acid-catalyzed exchange proceeds by protonation of oxygen, followed by deprotonation of the NH, to produce the iminol tautomer (**1**, R = H or CH_3, or **2**; Fig. 2) as a transient intermediate. Acid catalysis for guanine is masked by conversion to the conjugate acid. Exchange of an amino NH_2 group of adenine, guanine, or cytosine is catalyzed by acid and base, and there is also a pH-independent rate near neutrality. The base-catalyzed reaction involves slow removal of an NH by OH^-. The acid-catalyzed reaction involves attachment of H^+ to a ring nitrogen, followed by removal of one of the amino hydrogen atoms by water, to produce an abnormal tautomer (**3**, **4**, **5**; Fig. 2) as a transient intermediate. In the pH-independent region, that NH is removed by OH^- instead of water, to form the same intermediate. In each of these substrates, the acid catalysis is masked at low pH by complete conversion of substrate to its conjugate acid.

Figure 2. Abnormal tautomers of nucleic acid bases that are transient intermediates in hydrogen exchange.

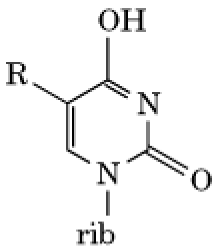

1

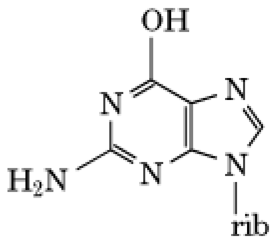

2

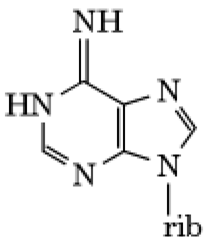

3

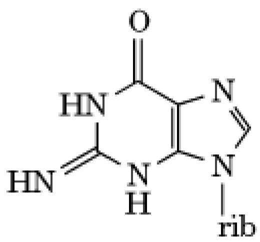

4

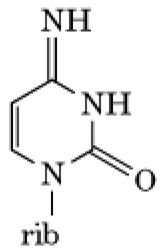

5

Because charged species, either cationic or anionic, must be formed as intermediates, the local environment affects the rate of hydrogen exchange. For example, nearby charges stabilize or destabilize the charged intermediate by electrostatic interactions. These charges include the phosphate backbone of nucleic acids and the side chains of acidic or basic residues in proteins. However, their effect is moderated by ions of salts that screen the interaction. As a result, the intrinsic rates are affected by the ionic strength of the solution. Moreover, the charges on nearby sites titrate with pH, leading to a variability of k_{ex} that is more complicated than in Fig. 1. Another effect on rates arises in less polar solvents, where those charged intermediates are less stable and lead to a reduction in rate. This may also contribute to a retardation of exchange in the nonpolar, **hydrophobic** interior of a protein. It is widely believed that the major retardation of exchange in biological macromolecules occurs when the hydrogen atom is involved in a hydrogen bond to some adjacent group. Generally, that hydrogen bond must be broken to expose the NH to solvent and render it susceptible to exchange. But simple interpretation is confounded by the fact that hydrogen bonding and inaccessibility usually occur simultaneously in folded macromolecules (see Nonpolar).

2. Mechanisms of Chemical Exchange in Macromolecules

An NH group at the surface of a macromolecule and hydrogen-bonded only to water has an intrinsic exchange rate characteristic of a model small molecule. Hydrogen atoms that are protected in the interior of a macromolecule and by internal hydrogen bonding exchange more slowly. The degree of this retardation provides information about the stability of the macromolecular structure and the flexibility that permits exchange.

The process by which inaccessible hydrogen atoms gain access to water so that they can undergo exchange is still a matter of debate, but there are two limiting and extreme models. According to the solvent-penetration model, water and catalytic H^+ or OH^- gain access to the interior of the macromolecule through channels, perhaps generated transiently by conformational fluctuations. Then the rate of exchange is governed by the extent to which those buried hydrogen atoms come into contact with the solvent atoms. According to the other model, called the local-unfolding model, cooperative motion of a segment of the molecule breaks a set of hydrogen bonds and other interactions that hold the macromolecule in its stable conformation. Thereby, the NH groups of that segment are exposed to solvent, where they can undergo exchange. This model agrees nicely with the dynamic nature of macromolecular structure, although it does not explain why exchange is not decreased substantially by incorporating the macromolecule into a crystal lattice, and it is an oversimplification to assume a single unfolded state from which exchange occurs. Macromolecules probably achieve a variety of unfolded states, from those involving only minor local fluctuations to those involving global unfolding.

The local-unfolding model can be analyzed kinetically, as in Eq. (11). Here k_{unfold} is the rate constant for the motion that converts the closed to the open form, k_{fold} is the rate constant for reversion back to the closed form, and k_{ex} is the rate constant for hydrogen exchange, as in Eqs. (2), (3). The general expression for the observed rate constant is given by Eq. (12). Two limiting behaviors can be distinguished:

$$\text{closed} \underset{k_{fold}}{\overset{k_{unfold}}{\rightleftarrows}} \text{open} \xrightarrow{k_{ex}} \text{exchanged product} \quad (11)$$

$$k_{obs} = \frac{k_{unfold}k_{ex}}{k_{fold} + k_{ex}} \quad (12)$$

If $k_{ex} \gg k_{fold}$, then k_{obs} [Eq. (12)] simplifies to k_{unfold}. The rate-limiting step is the opening to produce the locally unfolded state, from which exchange is rapid. Under these conditions, called "EX1," the rate is independent (except insofar as k_{unfold} is pH-dependent) of the concentrations of acid or base catalyst, which enter into Eq. (3). In principle, these conditions can be induced at high pH, where k_{ex} becomes sufficiently large. In practice, it is rare to achieve these conditions for a protein without **denaturation**, and exchange generally occurs from the totally unfolded conformation. In contrast, this is possible for DNA, and extrapolation to high pH or catalyst concentration provides k_{unfold}, the rate at which the double helix breaks the hydrogen bonds and allows an NH group to exchange.

If $k_{fold} \gg k_{ex}$, then k_{obs} [Eq. (12)] simplifies to $K_{op}k_{ex}$, where $K_{op} = k_{unfold}/k_{fold}$ is the equilibrium constant, [open]/[closed], for forming the locally unfolded state. These conditions are called "EX2", and they correspond to exchange that occurs only during that fraction of the time when the macromolecule is unfolded. Because k_{ex} can be approximated by the value (including acid or base catalysis, according to pH) for an appropriate model small molecule (1, 2), then the experimentally determined value of k_{obs} provides an estimate of K_{op}. Moreover, conversion to the corresponding **free energy**, D$G°$ = $-RT \ln K_{op}$, provides a measure of the energy that stabilizes the closed native state of the macromolecule or of the energy required to allow the local unfolding. Alternatively, k_{ex}/k_{obs} (= $1/K_{op}$) can be called a protection factor P, which represents the extent to which exchange is retarded in the native state.

3. Applications

Study of hydrogen exchange has the advantage that the measurement need not perturb the macromolecule and involves only the normal solvent, water. Separate samples can be exposed to a labeling pulse for varying time periods. Then the exchange is quenched by adjusting the pH to trap the label, and the subsequent time course of the loss of label from each site is monitored. The pulse conditions can be chosen to label selectively the sites of interest for the particular application.

Hydrogen exchange has long been used to provide information about the tertiary structures of proteins and about protein dynamics. Characteristic patterns of protection factors are associated with hydrogen atoms in **a-helices** or **b-sheets** . To the extent that hydrogen exchange also involves cooperative unfolding of an entire structural **domain**, all of the hydrogens in that domain should show the same protection factor.

Other aspects that have been investigated include the quaternary structure of proteins and their interactions with small molecules and other macromolecules. For example, selective labeling allows recognizing the segments involved in allosteric transitions in such proteins as hemoglobin. Because exchange of some NH atoms requires local unfolding, the observed rates also provide information about the stability of the native structure and the way it responds to changes in the environment. Intermolecular interactions that have been probed include protein–peptide interactions, enzyme–substrate and enzyme–inhibitor binding, protein–protein interactions, such as those between cytochrome ***c*** and cytochrome *c* peroxidase or between a protein and an antibody or a chaperonin, and protein–nucleic acid interactions.

One of the most recent applications is characterization of transient intermediates in **protein folding**. Exposed hydrogen atoms in a deuterated protein that is undergoing refolding are labeled during a rapid pulse with normal water. Then the pattern of a normal hydrogen isotope trapped in the refolded native protein can be analyzed to infer the structure of the intermediate. This method has been applied to several proteins, including **ribonuclease A**, cytochrome *c*, **barnase**, and hen egg white lysozyme.

For duplex DNA, it is possible to measure k_{unfold}, the rate of base-pair opening. Most rate constants measured are between 2×10^{1} and $2\times10^{3}s^{-1}$, but lower values are evidence of unusual structural features. It is also possible to study the influence of **intercalators** and of **triple helices**.

4. Methods of Measurement

The simplest method for detecting hydrogen exchange is measuring the overall extent of exchange by measuring the isotopic content of the macromolecule. This is achieved by counting the radioactivity of tritium or by UV-visible or vibrational spectroscopy that is sensitive to isotopic content. These methods measure only the total content of isotope, however, and cannot distinguish among the various hydrogen atoms in the macromolecule.

Methods involving various aspects of nuclear magnetic resonance (NMR) distinguish the individual hydrogen atoms in a molecule, and methods for assigning each signal have been developed. Two-dimensional Fourier-transform NMR is especially powerful at spreading out the spectrum so that each site is resolved. Pulse methods have been developed to select only particular nuclei, such as those attached to ^{15}N. Then the simplest method for measuring rates of exchange is transferring the sample to D_2O and watching the disappearance of each NH signal.

Three other techniques utilize the unique capability of NMR to detect exchange and measure rates under equilibrium conditions, when no net reaction is proceeding. The derivatives in Eq. (2) are zero, but an NH remains in an MH site for an average time of $1/k_{ex}$. (1) The signal of an NH that is exchanging with solvent H_2O displays an NMR broadening that increases with the exchange rate, until the signal becomes so broad that it disappears into the base line. (2) The signal of a CH adjacent to an NH is split into a doublet. As the NH exchange rate increases, the doublet components broaden, overlap, and coalesce into a broad single peak that then sharpens. This method provides rate constants for small molecules but is much less suitable for macromolecules, where the CH signals are not resolvable. (3) Various pulse sequences also label H_2O or individual NH signals with a characteristic magnetization (saturation or inversion). As hydrogen atoms exchange among these sites, the magnetization is transferred from one site to another. Analysis of the magnitude and time course of these transfers provides the rate constants for exchange. All of these techniques have the further advantage of not being limited by rapid exchange during mixing.

Mass Spectrometry is used to measure the overall exchange process because the different isotopes slightly alter the molecular weight of the macromolecule. It has only recently been applied to measuring hydrogen exchange rates at individual sites because it is necessary to cleave the macromolecule into small pieces that can be analyzed individually. This must be done under conditions that preserve the label, using enzymes that function at 0°C and at pH_{min} (Fig. 1), and then the fragments are separated and analyzed for isotopic content.

Bibliography

1. R. S. Molday, S. W. Englander, and R. G. Kallen (1972) Biochemistry **11**, 150–158.
2. Y. Bai, J. S. Milne, L. Mayne, and S. W. Englander (1993) Proteins **17**, 75–86.

Suggestions for Further Reading

3. S. W. Englander and N. R. Kallenbach (1984) Hydrogen exchange and structural dynamics of proteins and nucleic acids. Q. Rev. Biophys. **16**, 521–655 (an extensive, broad review).
4. C. L. Perrin (1989) Proton exchange in amides: Surprises from simple systems, Acc. Chem. Res. **22**, 268–275 (review of mechanisms of exchange in models, with NMR methods).
5. C. K. Woodward (1994) Hydrogen exchange rates and protein folding, Curr. Opinion Struct. Biol. **4**, 112–116.
6. M. Guéron and J.-L. Leroy (1995) Studies of base pair kinetics by NMR measurement of proton exchange, Methods Enzymol. **261**, 383–413. (applications to nucleic acids).
7. S. W. Englander, T. R. Sosnick, J. J. Englander, and L. Mayne (1996) Mechanisms and uses of hydrogen exchange. Curr. Opinion Struct. Biol. **6**, 18–23 (brief recent review including methods and applications).

Hydrogen Isotopes

Hydrogen is element number 1 in the periodic table and the most abundant element in the universe. Hydrogen has a valence state of 1 (1); it occurs mainly in nature in combination with oxygen as water in all living organisms and is present in all organic matter.

Three isotopes of hydrogen exist in nature: ^1H (protium, with an abundance of 99.985%), ^2H (deuterium, with an abundance of 0.015%), and ^3H (*tritium* , which exists naturally only in trace amounts) (see Radioactivity and Radioisotopes). Stable deuterium, which was first prepared by Urey (1), is used as heavy water (^2H_2O or D_2O) for contrast variation in **neutron scattering**, altering the density of aqueous solvents, and in studying hydrogen exchange reactions in macromolecules, as well as in moderating (slowing down) neutrons in some nuclear reactors. It is also used as a proton source in nuclear magnetic resonance spectroscopy and imaging.

Among the hydrogen isotopes, only tritium is **radioactive**, with a half-life of 12.35 years (2). It decays by beta-minus emission to ^3H, which is stable. Tritium yields one beta particle per decay, with an energy of 0.0186 MeV maximum, 0.00568 MeV on average. Tritium is produced in a nuclear reactor by irradiation of enriched lithium targets according to the reaction $^6Li(n,a)^3H$, or by irradiation of ^3H gas targets according to the reaction $^3He(n,p)$ ^3H. Tritium is used as an ingredient in thermonuclear weapons, in luminous lighting (airport runway lights, exit signs and luminous paints), and as a tracer in biomedical studies.

Tritium was first made available for biological research by the U.S. Atomic Energy Commission in

1948. The first tritium uptake studies in humans were conducted in 1951. Streptomycin and tetracycline were first labeled with tritium (2), and tritiated water was first used to measure total-body water in 1956 (3). Hundreds of different tritiated compounds are now commercially available in generous amounts and with high specific activity from commercial suppliers. Methods for tritium labeling typically involve exchange, substitution, or addition reactions, such as exchange by heterogeneous catalysis, exchange by homogeneous catalysis, exchange catalyzed by radiation, substitution by chemical reduction, or hydrogenation.

The short range of tritium's weak beta particle, its low toxicity, relatively low cost, and usefulness for high resolution autoradiography make it a convenient choice for tracer studies. A frequently encountered problem is pH-dependent loss of tritium by exchange with solvent water.

In molecular biology, tritium is widely used as a tracer and label for **nucleic acid** precursors. One of the most common tritiated compounds used is ^{3}H-**thymidine**, which may be introduced into the laboratory animal by direct injection or added to excised tissues. The metabolism and uptake of ^{3}H-thymidine is used to monitor DNA replication. Tritiated thymidine has also been used to study the effectiveness of therapeutic drugs that either stimulate or block DNA synthesis, such as chemotherapeutic agents. Tritium-labeled amino acids are incorporated into proteins and are used to follow protein biosynthesis.

The presence of tritium may be determined by liquid scintillation counting or chromatography. In autoradiography, specimens containing tritiated compounds may be coated with photographic emulsion and incubated under refrigeration to expose the emulsion to tritium beta particles. The emulsion is then developed and fixed, and the tissues are stained for microscopy to identify the labeled organelles (4) (see Autoradiography).

Bibliography

1. D. R. Lide and H. Pr. Frederikse, eds. (1995) *CRC Handbook of Chemistry and Physics*, CRC Press, Boca Raton, Fla.
2. Knolls Atomic Power Laboratory (1966) *Chart of the Nuclides*, 15th editor, available from General Electric Company, San Jose, Calif.
3. F. A. Odekwa, D. D. Kozoll, and K. A. Meyer (1963) J. Nucl. Med. **4**, 60.
4. L. G. Caro and R. P. Van Tubergen (1962) J. Cell. Biol. **15**, 173–188.

Suggestions for Further Reading

5. *The Radiochemical Manual*, 2nd ed. (1966) Amersham, Bucks, England.
6. National Council on Radiation Protection and Measurement (1979) *Tritium and Other Radionuclide Labeled Organic Compounds Incorporated in Genetic Material*, NCRP Report No. 63, Washington D.C.,

Hydrogenase

Hydrogenases are enzymes that catalyze the reversible oxidation of molecular hydrogen and play an important role in the anaerobic metabolism of microorganisms. Hydrogen uptake and production occur in sulfate-reducing **bacteria** and fermentative **anaerobes**, as well as in aerobic **nitrogen-fixing** bacteria, photosynthetic bacteria, and **cyanobacteria** (1). Three distinct categories of hydrogenases have been described:

- *Iron hydrogenases.* With two [4Fe-4 S] centers in addition to a special type of [4Fe-4 S] center.
- *Nickel–iron hydrogenases.* With a nickel center coordinated to a sulfur atom, two [4Fe-4 S] centers, and a [3Fe-xS] center.
- *Nickel–iron-selenium hydrogenases.* With a nickel center coordinated to a selenium atom as well as two [4Fe-4 S] centers.

Bibliography

1. D. S. Patil (1994) Methods. Enzymol. **243**, 68–94.

Hydrolase

Hydrolases are enzymes that catalyze the hydrolysis of a range of bonds. They frequently show broad specificity, and this characteristic has posed problems in naming them. The systematic name for an enzyme that performs a hydrolytic reaction includes the term hydrolase, whereas the trivial name is formed by the addition of the suffix *ase* to the name of the substrate or the class of substrate on which the enzyme acts. Those hydrolases that act on carboxylic esters, thiolesters, phosphomonoesters, phosphodiesters, phosphotriesters, diphosphomonoesters, **DNA** and **RNA** have been classified as a group that acts on ester bonds. The glycosidases hydrolyze *O*-glycosyl, *N*-glycosyl, and *S*-glycosyl compounds; etherases act on ether and thioether bonds; peptidases hydrolyze aminoacylpeptide, dipeptide, and dipeptidylpeptide bonds. Other categories of hydrolase are the serine carboxypeptidases and serine proteinases, which contain a DIFP (diisopropyl fluorophosphate)-sensitive a serine residue at their active sites, the thiol proteinases, the carboxyl proteinases, and the metalloproteinases There are also hydrolases that act on C—N , rather than peptide, bonds, and the substrates for these enzymes include amides, cyclic amides, linear amidines, cyclic amidines, and nitriles. Other hydrolases act on acid anhydrides and C—C , halide, P—N , S—N , and C—P bonds.

Hydropathy

a -helices can be identified in the primary structure of a membrane protein with a relatively high confidence using hydropathy analysis, in which each residue is assigned a characteristic hydrophobicity value. Hydropathy is a term that refers to the spectrum of amino acid side chains in the hydrophilicity–hydrophobicity scale. It was originally coined by Kyte and Doolittle(1) in an article describing an algorithm that identifies helical transmembrane spans and that came to be widely used. Their scale is based on the transfer free energies from water to vapor of model compounds for the amino acid side chains, as well as on the exterior–interior distribution of amino acids in protein structures. The hydropathy values of some residues were adjusted subjectively by the authors. Another frequently used hydrophobicity scale has been devised by Engelman, Steitz, and Goldman(2). This is a physicochemical scale based on the free energies of transfer from water to oil of amino acid residues that are parts of a helix. These free energy changes have been corrected for unfavorable hydrophilic contributions due to polar atoms and protonation/deprotonation events of charged residues upon transfer to the nonpolar phase. A number of other scales exist. A useful review on hydrophobicity scales has been written by Eisenberg(3), and references to recent literature are provided by Wimley and White(4), who have measured the free energies of transfer of all 20 amino acid residues from the interface of a lipid bilayer to water.

To calculate a hydropathy profile, the hydrophobicity of a chosen number of residues within a window is summed and divided by the number of residues in the window. The resulting score is assigned to the residue in the middle of the window, after which the window is moved on by one residue and the procedure is repeated. An example of a hydropathy prediction is shown in Figure 1. In the cases of bacteriorhodopsin, cytochrome oxidase, and bacterial photosynthetic reaction center, this simple analysis correctly identified the approximate positions of all the transmembrane helices, with no false positives.

Figure 1. A Kyte–Doolittle hydropathy analysis of subunits I **(a)** and II **(b)** of the bovine cytochrome *c* oxidase, with the true locations of the transmembrane helices marked beneath the plot. A window length of 11 residues was used. The *C*-terminal peripheral domain of subunit II is indicated. Helix VII of subunit I is least well predicted. It contains only 17 residues, whereas hydropathy analysis suggested a length of about 26 that partially overlaps the residues seen in the actual helix in the X-ray structure.

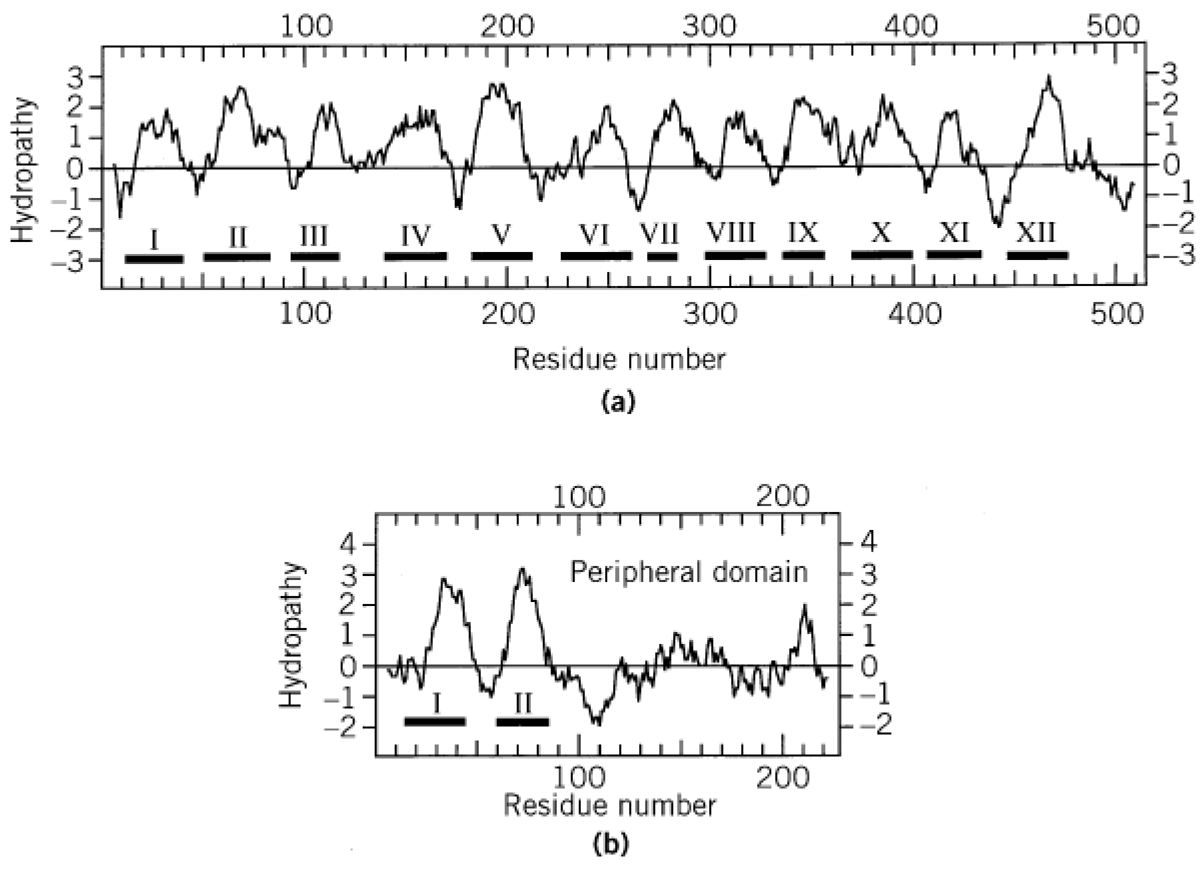

Several more advanced methods for prediction of transmembrane helices have been developed. In addition to the hydropathy analysis, these make use of, for example, the observation that deletions and insertions occur in **homologous** sequences only outside the transmembrane sequences. Thus, use of a multiple sequence alignment, instead of a single sequence, as the input for the algorithm improves the prediction. Likewise, the modern algorithms make use of statistical analyses of amino acid preferences within transmembrane helices and in their flanking loops.

The “positive inside” rule has been incorporated into the prediction protocols to determine the orientation of the polypeptide in the membrane. This rule is based on the fact that **arginine** and lysine residues occur more frequently in the loops between transmembrane helices that reside in the inner side of the membrane (and are shorter than 60 residues) than in the loops on the outer surface of the membrane.

Bibliography

1. J. Kyte and R. F. Doolittle (1982) A simple method for displaying the hydropathic character of a protein. J. Mol. Biol. **157**, 105–132.
2. D. M. Engelman, T. A. Steitz, and A. Goldman (1986) Identifying nonpolar transbilayer helices in amino acid sequences of membrane proteins. Annu. Rev. Biophys. Biophys. Chem. **15**, 321–353.
3. D. Eisenberg (1984) Three-dimensional structure of membrane and surface proteins. Annu. Rev. Biochem. **53**, 595–623.
4. W. C. Wimley and S. H. White (1996) Experimentally determined hydrophobicity scale for proteins at membrane interphases. Nature Struct. Biol. **3**, 842–848.

Hydrophilic

Most biological molecules contain electronegative atoms such as O, N, or S. These molecules or groups are polar and can act as hydrogen bond acceptors or donors, allowing them to interact more or less strongly with other such polar groups, with groups possessing charges of opposite sign, or with solvent water, which is equipped with partial positive and negative charges. Molecules or groups that bear full electrostatic charges, such as the NH^{+}_{3} and COO^{-} groups of amino acids in neutral solution, are extremely polar and especially difficult to remove from water. Hydrophilicity, or hydrophilic character, provides a quantitative index of a molecule's polarity, by indicating the difficulty of removing it from solvent water.

Hydrophilicity

When biological molecules combine or react with each other, or change shape, their interactions with the solvent change. The noncovalent binding of **ligands** by enzymes, antibodies, and other **receptors**, eg, involve removal of the interacting partners from the solvent to which they were previously exposed; also, the ease of breaking and making chemical bonds depends on the strength of interaction of the reactants and products with solvent. Most biological molecules contain electronegative atoms such as O, N, or S, which can act as hydrogen bond acceptors or donors and allow them to interact more or less strongly with solvent water; they are said to be hydrophilic . The rates and equilibria of most biological processes, including binding interactions and metabolic transformations, are therefore strongly influenced by changing interactions with the surrounding solvent, which typically is ~80% water in intracellular fluid. Many biological compounds are so polar that their removal from solvent water, an operation essential to measuring the strength of their solvation by water, or *hydrophilicity*, is difficult. The very difficulty of measuring hydrophilicity suggests the magnitude of the solvation forces and the potential magnitude of their influence on rates and equilibria.

Hydrophilicity can be defined as the dimensionless equilibrium constant for the transfer of a molecule between the dilute vapor phase, in which intermolecular contacts are negligible, to dilute aqueous solution, in which each solute molecule is completely surrounded by solvent water. The concentration is measured in the same units, such as moles/liter, in each phase. Hydrophilic character is simply $\log_{10}$ of the equilibrium constant for transfer from vapor to water (1). Hydrophilicity and hydrophilic character values provide the simplest measure of a molecule's affinity for watery surroundings, since they do not depend on any reference phase in which the molecule interacts with other partners. In that sense, they differ from hydrophobicity, which involves a second solvent that is immiscible with water, and with which the solute molecule interacts more or less strongly (see Partition Coefficient). Hydrophilic character also differs from solubility, in which the reference phase is the pure solute in liquid or crystalline form: Such an arbitrary reference is of questionable value if different solute molecules are to be compared against each other.

Hydrophilic character can be determined in some cases by measuring the water solubility of a gas under an atmosphere of known partial pressure, or conversely, by measuring the concentration of a solute in the gas space over an aqueous solution of known concentration (Fig. 1). In more typical cases, of the kind often encountered in biological molecules, the concentration of gas in the vapor phase may be too low to detect directly. In such cases, a large volume of carrier gas (usually argon or nitrogen) is bubbled through an aqueous solution of known concentration, then through an efficient trap, which may be water itself. From the amount of solute collecting in the trap, plotted as a function of the measured volume of carrier gas that has passed through the system, it is a simple matter to calculate the concentration of solute in the vapor phase. Using radioisotope labels, UV spectroscopy, or high-field NMR measurements, it is possible in this way to examine molecules as hydrophilic as **peptides** (2) or guanidino compounds (3), and to determine water-to-vapor distribution coefficients as low as 10^{-10}. A scale of such equilibrium constants for simple organic compounds *in uncharged form* is shown in Figure 2. More extreme values are beyond direct measurement. However, there is much evidence to suggest that the free energy of solvation by water tends to be an additive function of a molecule's constituent groups (1), allowing values for complex molecules to be estimated by considering their substituents. From the behavior of methylamine and acetic acid, eg, it can be inferred that the concentration of glycine in the vapor phase, over a 1- *M* aqueous solution, is approximately $10^{-14}M$, even though that value is too low to measure directly.

Figure 1. The equilibrium for transfer of a molecule from dilute aqueous solution to the vapor phase. Hydrophilicity is the reciprocal of this equilibrium constant, and it measures the affinity of a molecule for watery surroundings.

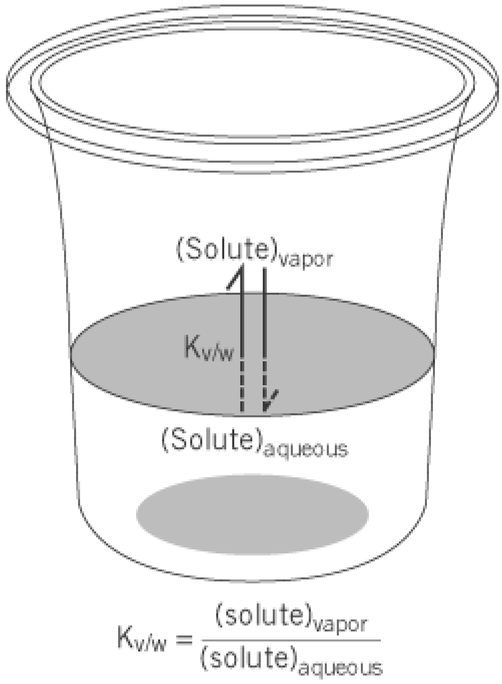

Figure 2. Scale of hydrophilicities for simple organic compounds in uncharged form.

$$Keq = \frac{\text{Moles/liter (vapor)}}{\text{Moles/liter (aqueous)}}$$

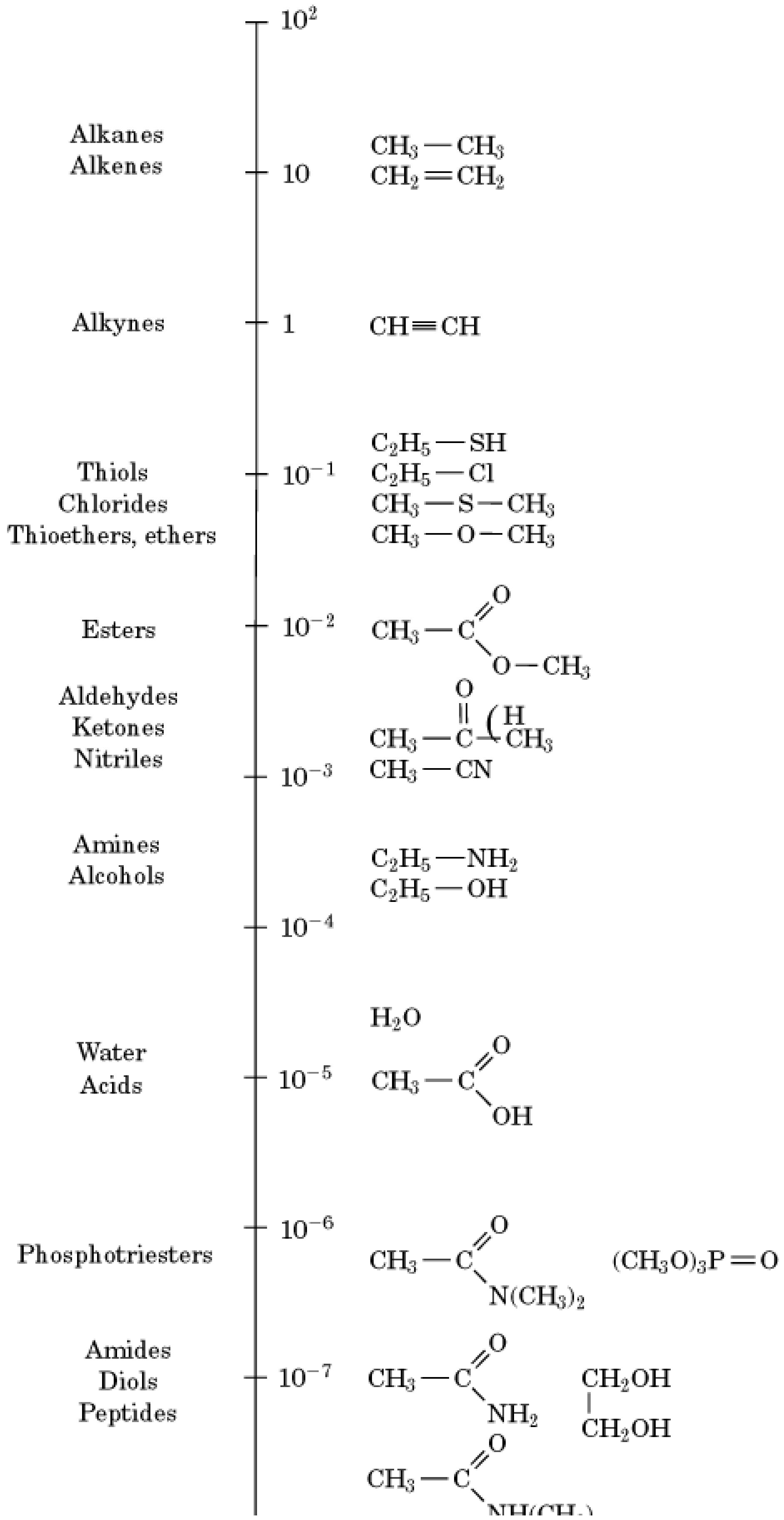

These methods have revealed that the hydrophilicities of the protein amino acid side-chains, expressed in terms of their equilibria of transfer from the vapor phase to neutral aqueous solution at 25°C, span a range of approximately 10^{16}-fold(3, 5). These values are as follows:

	$\log_{10} K_{v \to w,pH7}$
Glycine	–1.75
Leucine	–1.68
Isoleucine	–1.58
Valine	–1.46
Alanine	–1.43
Proline	–1.10
Methionine	–1.09
Phenylalanine	–0.56
Cysteine	0.91
Threonine	3.59
Serine	3.72
Tryptophan	4.32
Tyrosine	4.49
Glutamine	6.90
Lysine	7.00
Asparagine	7.12
Histidine	7.55
Glutamate	7.50
Aspartate	8.05
Arginine	14.65

These values were found to be closely related to the tendencies of the corresponding amino acids found at the surfaces of proteins, as revealed by their structures determined by X-ray crystallography. Figure 3 shows the relationship between hydrophilicity and the nominal transfer free energy of each side-chain from the interior to the surface of a protein, as indicated by the relative populations of surface and buried residues for each amino acid. In addition, a remarkable bias in the genetic code was noted, such that purines (usually A) serve as the second code letter for all the more hydrophilic amino acids (3, 4). Figure 4 shows the amino acid side-chains in order of increasing hydrophilicity, alongside the code letters at the second position for each of the amino acids, but the significance of this correlation is not understood.

Figure 3. Tendencies of the 20 amino-acid residues to appear at the surfaces of globular proteins, compared with their free energies of transfer from the vapor phase to neutral aqueous solution (3, 4).

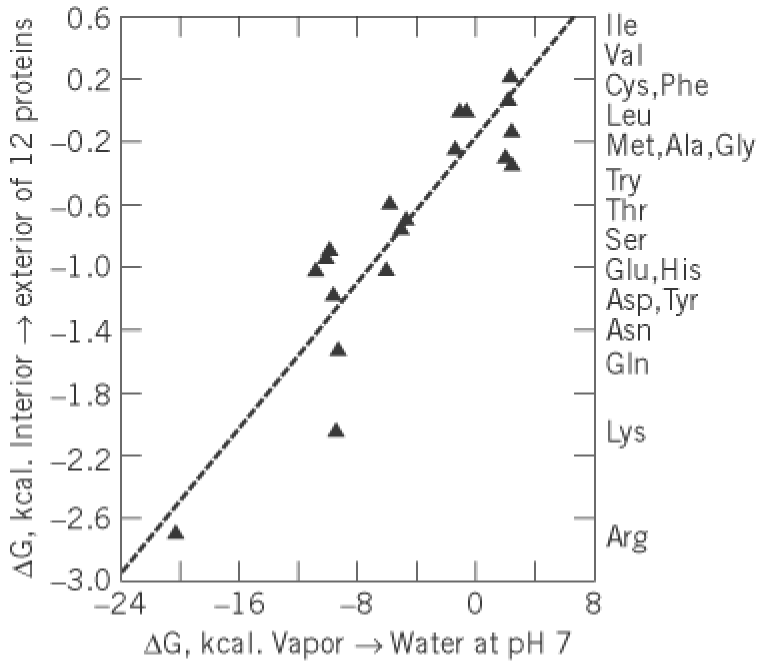

Figure 4. Code letters and anticode letters at the second position for each of the amino acids.

		2nd codeletter (mRNA)	2nd anticodeletter (DNA)
	Gly	G	C
	Leu	U	A
	Ile	U	A
	Val	U	A
	Ala	C	G
	Phe	U	A
	Cys	G	C
	Met	U	A
	Thr	C	G
	Ser	C(G)	G(C)
	Trp	G	C
	Tyr	A	T
	Gln	A	T
	Lys	A	T
	Asn	A	T
	Glu	A	T
	His	A	T
	Asp	A	T
Most hydrophilic	Arg	G	C

The close relationship observed between hydrophilicity and protein structure (Fig. 3) suggested that this scale might have some value in predicting **protein folding**. It was also used to propose a scale of hydropathy values for predicting the relative tendencies of different parts of a protein sequence to be found in membranes (6). More recently, this scale of hydrophilicities has been compared and contrasted with scales of hydrophobicity, obtained by reference to condensed phases including 1- *n*-octanol and to cyclohexane (7). Completion of a three-sided cycle allows estimation of equilibria of transfer between the vapor phase and cyclohexane, a pure measure of **van der Waals** forces. As expected, these are found to be roughly proportional to the accessible surface area. Since the interiors of protein molecules represent condensed phases, scales of hydrophobicity can be considered more directly related to folding equilibria than are scales of hydrophilicity using the vapor phase as a reference. Hydrophilicity, on the other hand, is more amenable to theoretical study because it does not entail the involvement of a second condensed phase in addition to water.

Bibliography

1. J. Hine and P. K. Mookerjee (1975) J. Org. Chem. **40**, 292–298.
2. R. Wolfenden (1978) Biochemistry **17**, 201–204.
3. R. Wolfenden, L. Andersson, P. M. Cullis, and C. C. B. Southgate (1981) Biochemistry **20**, 849–855.
4. R. Wolfenden, P. M. Cullis, and C. C. B. Southgate (1979) Science **206**, 575–577.
5. P. R. Gibbs, A. Radzicka, and R. Wolfenden (1991) J. Amer. Chem. Soc. **113**, 4714–4715.
6. J. Kyte and R. F. Doolittle (1982) J. Mol. Biol. **157**, 105–132.
7. A. Radzicka and R. Wolfenden (1988) Biochemistry **27**, 1664–1670.

Suggestion for Further Reading

8. R. Wolfenden (1983) Waterlogged molecules. Science **222**, 1087–1093.

Hydrophobic Chromatography

1. The Basic Principle

Hydrophobic chromatography (HC) is a chromatographic method for the characterization, separation, and isolation of proteins and cells (1). It is based on **hydrophobic** (water-repelling) interactions between (a) hydrocarbon chains of different lengths and shapes that are anchored on inert beads and (b) the hydrophobic "pockets" or "patches" that are found on the accessible surface of proteins. Such hydrocarbon chains interact with the protein molecules submerged in water and bind them to minimize the surface of the hydrophobic area that is exposed to the water. This binding brings about the release of "ordered" water molecules, which forms the basis for the hydrophobic interactions. It turns out that proteins can be distinguished and resolved from one another by HC, because they differ in the size, number, and water repellence of their hydrophobic "patches" or "pockets." This basic principle in chromatography (2, 3) is also known as hydrophobic interaction chromatography and **reversed-phase** high-performance liquid chromatography (HPLC). It has now become a very powerful method of separation and has been used for research in biochemistry, molecular biology, and biotechnology—for example, in the preparation and characterization of drugs such as enzymes, hormones, antibodies, and receptors.

2. The Development of HC

HC was developed as a result of an unexpected observation made while attempting to make use of affinity chromatography (AC) (4). The basic concept in AC is based on the use of the specific affinity between the biorecognition site of a protein (an enzyme, an antibody, a receptor, etc.) and one of its biospecific ligands (a substrate, an inhibitor, a hormone, or a regulatory metabolite) that is covalently linked to an inert matrix backbone and can be regarded as an immobilized “bait” for the protein. The column with the immobilized bait is then used to “fish out” the desired protein from a mixture. While developing the basic principles of AC, it was observed that the purification of a desired protein is often improved by interposing a hydrocarbon chain (an “arm”) between the ligand and the matrix backbone (4, 5). It was presumed that such an arm relieves the steric restrictions imposed by the backbone on the ligand, thereby increasing its flexibility as well as its availability to the protein (5, 6). It was also implied that the hydrocarbon arms do not alter the inert nature of the matrix, a condition that obviously has to be ensured to preserve a strictly biospecific (active-site mediated) adsorption of the extracted protein. This assumption seemed reasonable at the time (at least with water-soluble proteins), because it had been shown in the case of lysozyme that “most of the markedly nonpolar and hydrophobic side chains ¼ are shielded from the surrounding liquid by more polar parts of the molecule” and that, as predicted by Sir Eric Rideal and Irving Langmuir, “lysozyme is quite well described as an oil drop with a polar coat” (7).

For the purification of enzymes involved in glycogen metabolism, glycogen (the “bait”) was anchored onto beaded agarose . Unexpectedly, two glycogen-coated agarose preparations that differed only in the length of the hydrocarbon chains bridging the ligand and the agarose bead (Seph-C_8-glycogen and Seph-C_4-glycogen) exhibited different behaviors: Whereas the column material with eight-carbon-atom bridges adsorbed glycogen phosphorylase *b*, that with four-carbon-atom bridges did not even retard it (2). Control experiments revealed that both the adsorption of the enzyme by Seph-C_8-glycogen and its exclusion by Seph-C_4-glycogen could be reproduced with columns that contained no glycogen whatsoever (Seph-C_8-NH_2 and Seph-C_4-NH_2), indicating that free w-aminooctyl chains (which had not reacted with glycogen) were mainly responsible for the retention of phosphorylase on Seph-C_8-glycogen and also raising the possibility that the very length of the hydrocarbon chain determines the retention power of these columns.

3. Homologous Series of Alkylagarose Columns

To challenge this working hypothesis, a homologous series of alkylagarose columns was synthesized, and their retention power was tested with two enzymes, glycogen phosphorylase *b* and glyceraldehyde-3-phosphate dehydrogenase (Fig. 1). This “homologous series of alkylagarose columns” (Seph-C_n) refers to a set of columns that are identical in their ligand density, net charge, and ultrastructure. Such a set of columns can be considered as a series of consecutive controls in which each column differs from the preceding one in the series only in having hydrocarbon chains one carbon atom longer. In general, under the same experimental conditions, different proteins display different adsorption profiles on the Seph-C_n columns (1-3). For example, under the conditions used to retain phosphorylase *b* ($n \geq 4$), D-glyceraldehyde-3-phosphate dehydrogenase was not even retarded on any of the columns tested ($n = 14$). Thus, while Seph-C_1 and Seph-C_2 would not distinguish between the two enzymes and would exclude both of them, Seph-C_3 would begin to resolve them, and Seph-C_4 would separate them efficiently, indicating that the ability to bind and to discriminate between two proteins (ie, to resolve and separate them) is a function of the number of carbon atoms in the hydrocarbon chains of the columns (Fig. 1). In addition, the above results showed that it is possible to adjust the tightness of adsorption of a given protein and avoid an overly strong retention, which would then require drastic conditions for elution that might **denature** the eluted protein. Finally, these studies illustrated the use of “deforming agents” (local, fully reversible **denaturants** that loosen the structure of the proteins) as efficient and delicate eluents in detaching adsorbed proteins from HC columns.

Figure 1. Preferential adsorption of glycogen phosphorylase *b* on alkylagarose columns varying in the length of their alk

chains. Samples containing D-glyceradehyde-3-phosphate dehydrogenase (GAPD) and glycogen phosphorylase *b* were a onto the columns. Nonadsorbed proteins were washed off, then (*arrow*) a deforming buffer (Def.) was applied, which el phosphorylase from Seph-C_4 but not from Seph-C_6. Acetic acid (0.2 M) was needed to detach glycogen phosphorylase *b* Seph-C_6, which in this case came out in an inactive (denatured) form.

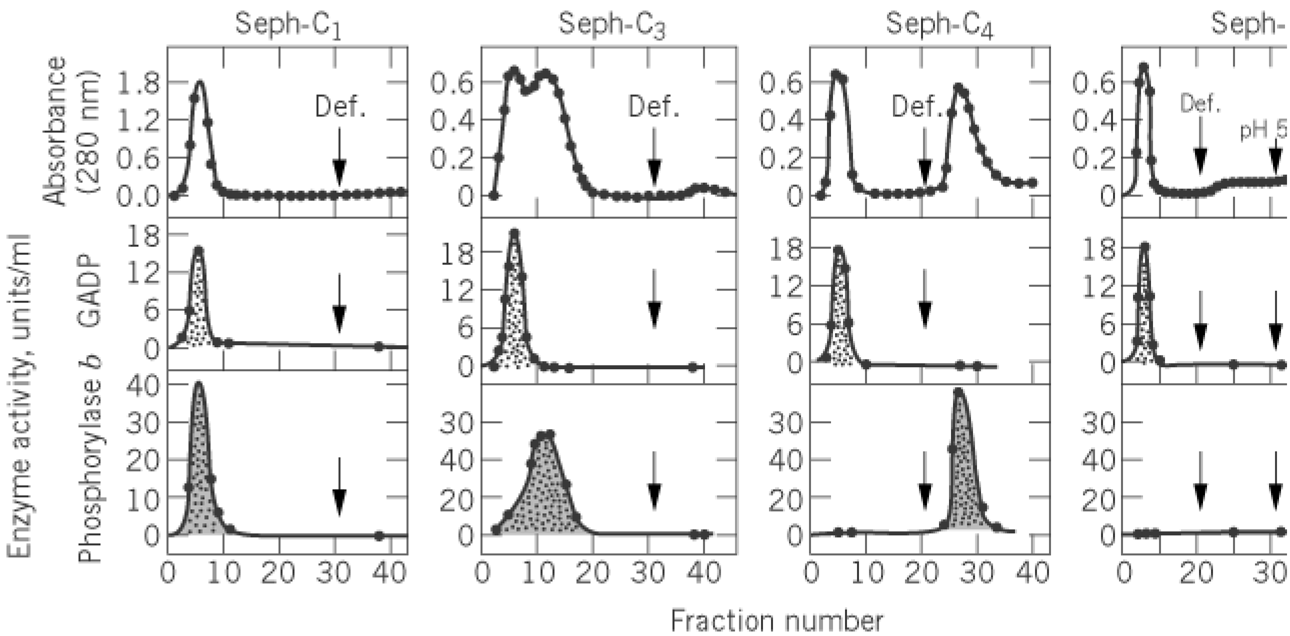

HC provides now a general, systematic approach to the purification of water-soluble, as well as lipophilic, proteins. This approach makes use of homologous series of alkylagaroses and their derivatives (Seph-C_n-X where X = H, NH_2, COOH, OH, C_6H_5, etc.; Fig. 2) to achieve resolution and purification of proteins and cells. Each member in these series offers flexible hydrophobic arms or “yardsticks” that interact with accessible hydrophobic “patches” or “pockets” in the various proteins, retaining only some proteins out of a mixture. Further resolution is then achieved by gradually changing the nature of the eluent. The wide applicability of this type of chromatography in protein purification and in separating cells is now well accepted. Procedures for the synthesis and the characterization of Seph-C_n (n = 112) are described in Ref. 1.

Figure 2. Examples of homologous series of alkylagarose derivatives (Seph-C_n-X) that can be used for HC (1).

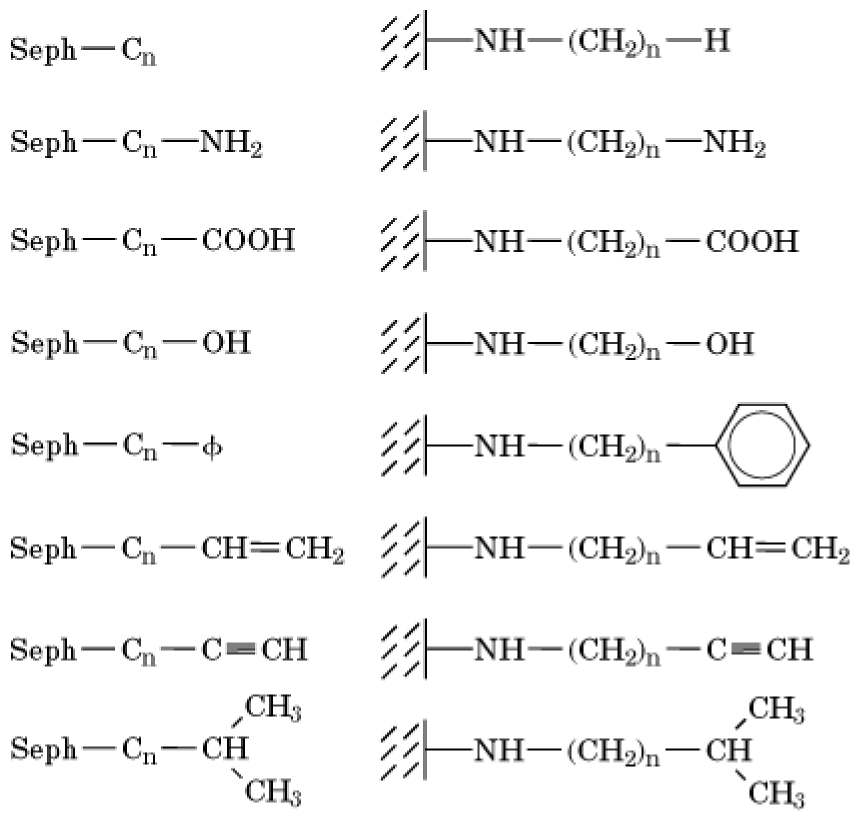

4. Selecting a Column for a Given Purification—the Exploratory Kit

The selection of a suitable substituted agarose within a given homologous series (eg, Seph-C_n) is achieved by means of an exploratory group of column materials designed for this purpose (1). Each column in the kit contains one member of the series. If, under certain conditions, a specific protein is adsorbed onto hydrocarbon chains X carbon atoms long, and if a change in the eluent promotes exclusion from Seph-C_x, then this is the column of choice. An example of an adsorption-elution profile of glycogen phosphorylase, *b*, on the Seph-C_n series, is given in Figure 3a. As seen in this figure, as the length of the hydrocarbon chains increases, less protein is excluded from the column. While Seph-C_0 and Seph-C_1 exclude all the protein, Seph-C_2 and Seph-C_3 retard it, whereas Seph-C_4 and higher members of the series retain the protein. By passage of a 0.4 M imidazolium-citrate buffer, a “deformer” for glycogen phosphorylase *b* (8, 9), it is possible to elute the enzyme quantitatively from the Seph-C_4 column, but not from higher members in the series. In fact, recovery of the enzyme from Seph-C_6 was achieved only with a drastic eluent, 0.2 M CH_3COOH, which displaces the enzyme but also denatures it. On the basis of such results, Seph-C_4 should be chosen for the preparative purification of this enzyme; and indeed this column allowed a 60- to 100-fold purification in one step, with >95% recovery of enzyme activity (Fig. 3b).

Figure 3. Hydrophobic chromatography (**a**) Adsorption profile of glycogen phosphorylase *b* on a Seph-C_n kit. The filled circles indicate the amount of protein passing straight through the column. Empty circles indicate the amount of protein eluted by a “deforming buffer.” (**b**) Preparative purification of the enzyme from a muscle extract. Absorbance (empty circles) and specific activity (filled circles) were monitored. Nonadsorbed protein was removed by washing, and elution with the “deforming buffer” was initiated at the fraction indicated by the arrow (1, 2).

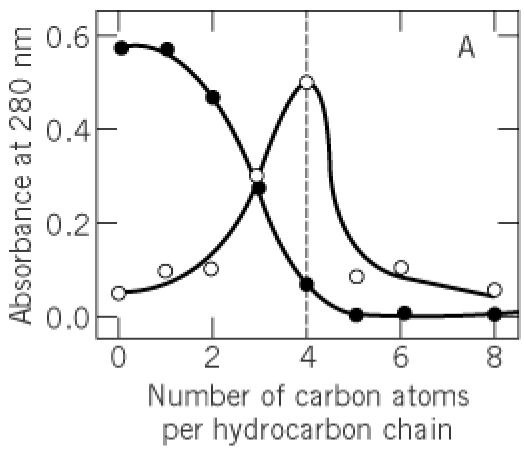

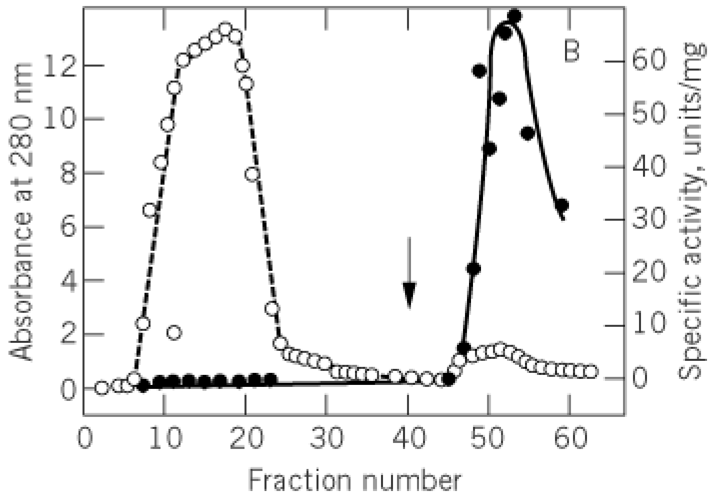

5. Means of Elution

Studies aimed at the optimization of elution from alkylagaroses have shown that proteins can be desorbed from such columns by a variety of means: polarity-reducing agents, specific deformers, mild detergents, low concentration of denaturants, alteration in pH or temperature, and changes in ionic strength and ionic composition. Because the availability of hydrophobic crevices or patches on the surface of a protein appears to depend on its conformation, and because the retention of proteins by alkylagaroses depends largely on the lipophilicity, size, shape, and number of these crevices and patches, the above-mentioned means of elution may function either by directly disrupting the hydrophobic interactions between the column material and the protein or by changing the conformation of the protein. In fact, both mechanisms may often operate simultaneously. High selectivity in elution may also be achieved by using biospecific ligands, such as coenzymes, substrates, specific metal ions, and allosteric effectors, which often bring about ligand-induced conformational changes in proteins.

6. Useful Features of Hydrophobic Chromatography

The important features of hydrophobic chromatography are as follows: (i) It provides an independent criterion for the resolution of macromolecules. (ii) It provides means for gradually adjusting the adsorption forces and thereby avoiding an overly strong retention. (iii) It can be used for the detection of conformational changes in proteins when these are reflected in the size or distribution of hydrophobic crevices or patches. A potential use of these column materials may be in the purification and study of lipophilic membrane-bound proteins that have accessible hydrophobic regions used for their localization within the membrane. (iv) It provides a basis for the development of automatic consecutive fractionators (1) for the purification of proteins.

7. On the Mechanism of Action of Alkylagaroses

In their functional conformation, water-soluble proteins are folded so as to "bury" as many as possible of their hydrophobic side chains in the interior of the molecule and to expose as many as possible of their polar, charged side chains to interaction with water. It is now clear, however, that complete burying of all hydrophobic groups is generally not achieved, leaving some hydrophobic groups exposed at the surface of the protein. Together with hydrophobic components of charged amino acids, such as the ($-CH_2-$), stretches of lysine and glutamic acid residues, or the phenyl ring of tyrosine residues, these form hydrophobic "patches" or "pockets" at the surface of the molecule (Fig. 4). A sufficiently large hydrophobic patch may constitute a binding site for the hydrocarbon chains implanted on the hydrophilic agarose matrix and form "hydrophobic bonds," freeing "ordered" water molecules and allowing them to interact with each other (10-12). The available hydrophobic patches and pockets of different proteins vary in number, size, shape, and lipophilicity, and these variations are reflected in the relative affinities of different proteins for a specific alkylagarose. It is the properties of such patches, and perhaps their distribution on the surface of different proteins, that play a major role in the resolution of proteins on alkylagaroses.

Figure 4. Schematic representation of the surface of a protein molecule with an exposed hydrophobic amino acid residue (tryptophan) and hydrophobic "pockets" or "patches" (*hatched*). The scheme also illustrates how hydrophobic constituents of several nonhydrophobic amino acids bearing hydrophobic functional groups can together form a site capable of accommodating a hydrophobic hydrocarbon chain (1).

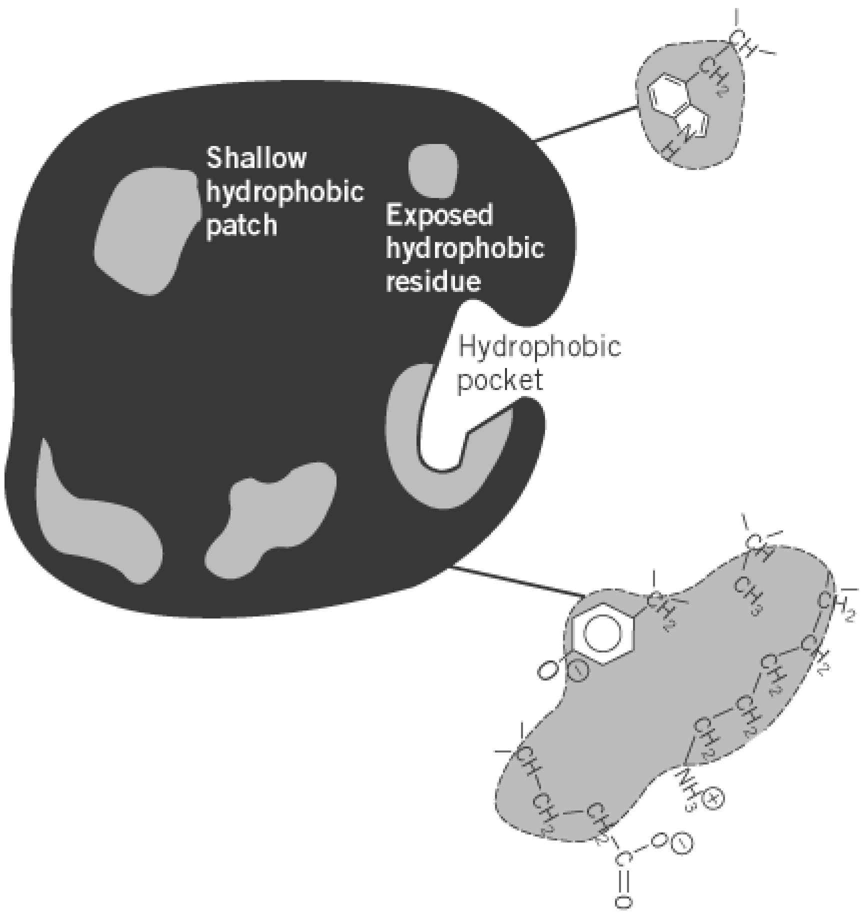

Bibliography
1. S. Shaltiel (1984) Methods Enzymol. **104**, 69.
2. Z. Er-el, Y. Zaidenzaig, and S. Shaltiel (1972) Biochem. Biophys. Res. Commun. **49**, 383.
3. S. Shaltiel and Z. Er-el (1973) Proc. Natl. Acad. Sci. USA **70**, 778.
4. P. Cuatrecasas, M. Wilchek, and C. B. Anfinsen (1968) Proc. Natl. Acad. Sci. USA **61**, 636.
5. P. Cuatrecasas (1970) J. Biol. Chem. **245**, 3059.
6. P. Cuatrecasas and C. B. Anfinsen (1971) Annu. Rev. Biochem. **40**, 259.
7. D. C. Phillips (1966) Sci. Am. **November**, 78.
8. S. Shaltiel, J. L. Hedrick, and E. H. Fischer (1966) Biochemistry **5**, 2108.
9. J. L. Hedrick, S. Shaltiel, and E. H. Fischer (1969) Biochemistry **8**, 2422.
10. G. S. Hartley (1936) *Aqueous Solutions of Paraffin-Chain Salts* Hermann, Paris.
11. H. S. Frank and M. W. Evans (1945) J. Chem. Phys. **13**, 507.
12. W. Kauzmann (1959) Adv. Protein Chem. **14**, 1.

Hydrophobic Effect

Cooks and physicists are aware of the tendency of oil to separate from water, a solvent that is very self-cohesive. In biology, this effect is expressed in the tendency of uncharged (or nonpolar) molecules to escape from water by entering less polar surroundings, or by adhering to each other (Fig. 1). This phenomenon, termed the *hydrophobic effect* (1, 2), is believed to play a decisive role in maintaining the stability of biological membranes, in the proper folding of protein molecules (see Protein Stability), and in determining the relative affinities of hormones, antibodies, and substrates for proteins that bind them. The tendency of any particular nonpolar molecule or chemical group at equilibrium to favor transfer from water to a nonpolar phase, such as a hydrocarbon solvent, is termed its hydrophobicity.

Figure 1. A partial view of the origins of the hydrophobic effect.

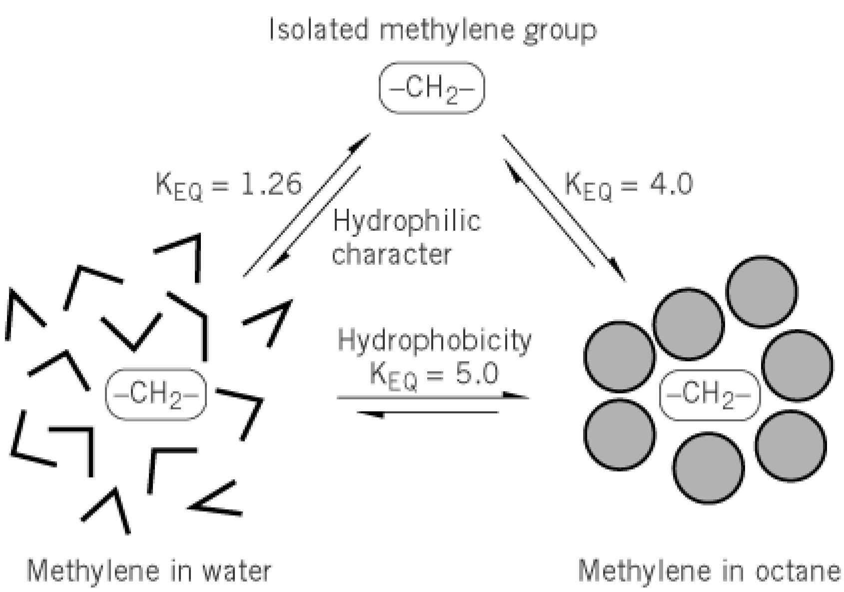

The physical origins of the hydrophobic effect remain controversial, because the properties of water as a solvent are not yet fully understood. It is of interest to ask whether nonpolar molecules, such as methane or ethane with no polar groups, tend to leave water and enter less polar solvents (octane is a familiar example) mainly because they are repelled by water; or whether they do so because they are attracted to the less polar solvent (or to each other). That question can be addressed by referring to an absolute standard, the vapor phase, that neither attracts nor repels solutes, and in which "solute" molecules exist in isolation most of the time. Using the vapor phase as a reference, single molecules of methane are found to exhibit an appreciable tendency to leave water, as indicated by their equilibria of transfer from water to the vapor phase. For methane, this equilibrium constant is 27 in favor of the vapor phase at 25°C. This tendency increases gradually with the size of a normal alkane, as can be seen in the series $CH_4$27, $C_2H_6$20, $C_3H_8$29, C_4H_{10}38, C_5H_{12}51, C_6H_{14}74, C_7H_{16}83. For each CH_2 increment, transfer to the vapor phase is enhanced by an average factor of 1.26. In contrast, each CH_2 increment enhances the equilibrium of transfer from the vapor phase to a nonpolar solvent by a factor of 4.0. As a result, each CH_2 increment increases the distribution coefficient for transfer from water to a nonpolar solvent by a factor of 5.0 (Fig. 2). Similar behavior has been observed in the normal series of hydrocarbons, esters of acetic acid, amines, and alcohols (3). In summary, single molecules of hydrocarbons have an appreciable tendency to leave water and enter the vapor phase, where they exist in isolation. These molecules are thus truly "hydrophobic" in the sense that they have an absolute tendency to escape from water. That is hardly surprising, since water is among the most self-cohesive molecules known, with an extremely high surface tension. However, this tendency to leave water is only slightly enhanced by increasing the size of the hydrocarbon (addition of a $-CH_2$ increment), whereas increasing size greatly enhances the tendency of a nonpolar solute to leave water and enter a nonpolar solvent. One is led to conclude that attraction to the nonpolar solvent also plays a major role in the hydrophobic effect, and this is believed to be due to van der Waals interactions, or London dispersion forces.

Figure 2. Analysis of the hydrophobic effect in terms of the equilibrium affinity of a solute for water and for a nonpolar liquid. (**a**) Electrons are more strongly attracted by the oxygen atom of the water molecule, leaving partial negative charges near the corners of a tetrahedron, and partial positive charges at the other two corners. (**b**) Water molecules are strongly attracted to each other by their partial charges, forming H-bonds between H and O atoms. As a result, liquid water is very self-cohesive. (**c**) Nonpolar molecules, like oil drops, break up the structure of water in which they are dissolved. The self-cohesiveness of water encourages these molecules or groups to coalesce, so that the part of the solvent can return to its preferred structure. This is called the hydrophilic effect.

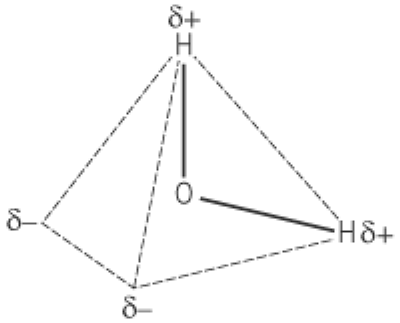

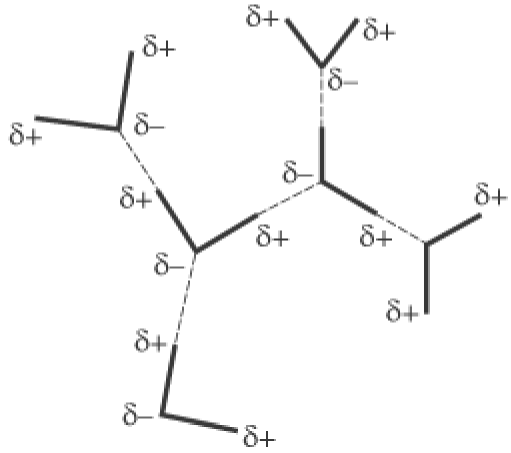

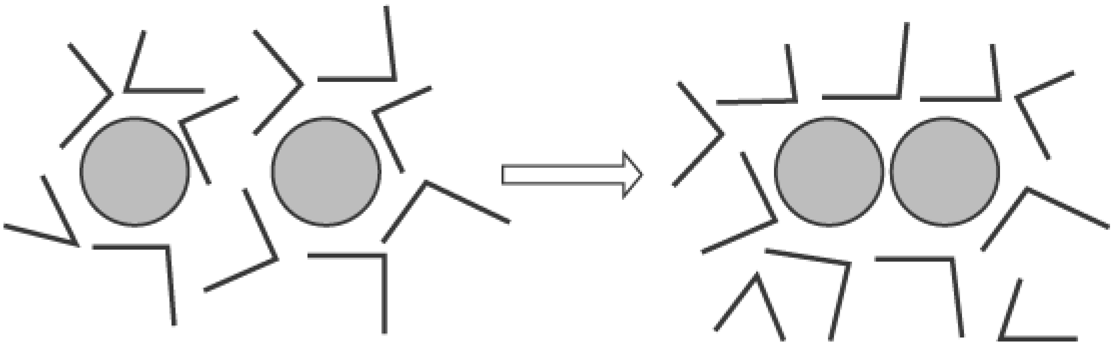

The hydrophobic effect is unique, among the noncovalent forces involved in maintaining biological structures, in that it grows stronger with increasing temperature (1, 4), ie, **enthalpy** is released (D *H* is positive) when the force takes effect. If there is a net free energy of attraction (ie, D*G* is negative), then **entropy** must be released (*T*D*S* must be positive and greater in magnitude than D*H*), since D*G* = D*H*–*T*D*S*. If a protein's stability were dependent entirely on the hydrophobic effect, then the protein would be expected to lose its structure at low temperatures, and some proteins do in fact undergo "cold denaturation" (see **Protein denaturation**). There has been continuing interest in the probable structural origins of the entropy (and enthalpy) increases that accompany the formation of hydrophobic interactions. Changes in the properties of water in the immediate neighborhood of the solute almost certainly account, at least in part, for the loss of entropy that accompanies the introduction of a nonpolar molecule or methylene increment into water from the vapor phase or a nonpolar solvent. Frank and Evans (5) suggested that this might imply formation around solutes of a kind of *clathrate* or *iceberg* structure, in which water molecules were more ordered than in the bulk solute. These authors did not suggest that water surrounding a solute resembled Ice I in any literal sense, nor does current experimental evidence seem to support such a possibility. Entropy losses associated with introducing nonpolar solutes into water might also arise, at least in part, from restrictions on the mobility of solutes when they are introduced into a structured aqueous environment. In normal aliphatic compounds of increasing size, solubility might (according to this view) be reduced by progressive restrictions on internal rotation, and compounds with internal rotations already restricted would not be affected to the same extent. In apparent accord with this view, steroids and cycloalkanes display lower activity coefficients in water than nonrigid compounds of similar size, with reference to both nonpolar solvents and to the vapor phase (6), and the alicyclic amino acid proline is more hydrophilic than would be expected for an amino acid with an aliphatic side-chain of the same size (7). These effects could alternatively be due, at least in part, to the reduced surface area of cyclic as compared with open-chain compounds, resulting in the imposition of less severe restrictions on the solvent. These uncertainties illustrate the general difficulty of deconvoluting thermodynamic functions, which describe equations of state, without making assumptions that are themselves open to question. A clearer view of the origins of the structural origins of the hydrophobic effect awaits a more complete understanding of the properties of water and aqueous solutions.

All molecules, even those that are truly nonpolar, are attracted to each other by London dispersion forces. These forces are responsible for the fact that octane, and the lipid molecules present in biological membranes, are liquids at room temperature. They also make a major contribution to the hydrophobic effect discussed above, and to the resulting tendencies of protein molecules to adopt the specific structures needed for their activities. Anyone who has observed the wheels of a locomotive, or two cyclists riding a tandem bicycle, has a rough mental image of the London dispersion force. If we picture two atoms of argon near each other, it is easy to imagine that temporary fluctuations in the distribution of electrons around one of these atoms may, at any given instant, place a partial negative charge toward the other atom. In response to this fluctuation, electrons in the orbitals of the neighboring atom tend to adjust slightly, placing a partial positive charge in the vicinity of the first atom and creating a small electrostatic attraction between them. A moment later, the roles may be reversed, but a net attraction remains. Because of the small charges involved, and their fluctuating character, London dispersion forces are individually weak and intensely dependent on the distances separating the atoms. These forces reach a maximum at an optimal distance equivalent to the sum of the **van der Waals** radii of the two atoms (typical van der Waals radii are 0.10 nm for H, 0.16 nm for C, 0.135 nm for O, 0.145 nm for N, and 0.17 nm for S). Beyond that distance, their mutual attraction falls off with the 6th power of the distance separating the two atoms. At distances closer than optimal, repulsion between the electron clouds of the two atoms builds up rapidly (unless they are able to share their electrons in a covalent bond), with the 12th power of the distance separating the atoms. The number and aggregate strength of the attractions between nonpolar molecules can be considerable, even though they are individually weak. They account for a substantial part of the hydrophobic effect discussed above and are thus largely responsible for maintaining the integrity of biological membranes and the proper folding of protein molecules.

Bibliography

1. W. Kauzmann (1959) Adv. Prot. Chem. **14**, 1–45.
2. C. Tanford (1974) *The Hydrophobic Effect*, Wiley, New York, pp. 1–11.
3. R. Wolfenden and C. A. Lewis (1976) J. Theor. Biol. **59**, 231–235.
4. G. Némethy and H. A. Scheraga (1962) J. Chem. Phys. **36**, 3382–3400.
5. H. S. Frank and M. W. Evans (1945) J. Chem. Phys. **13**, 507–532.
6. M. Osinga (1979) J. Amer. Chem. Soc. **101**, 1621–1622.
7. P. R. Gibbs, A. Radzicka, and R. Wolfenden (1991) J. Amer. Chem. Soc. **113**, 4714–4715.

Suggestions for Further Reading

8. J. T. Edsall and H. A. McKenzie (1978) Water and proteins. I. The significance and structure of water, its interaction with electrolytes and non-electrolytes. II. The location and dynamics of water in protein systems and its relation to their stability and properties. Adv. Biophys. **10**, 137–207.
9. W. P. Jencks (1969) *Catalysis in Chemistry and Enzymology*, McGraw-Hill, New York, pp. 393–436.
10. W. Kauzmann (1959) Some factors in the interpretation of protein denaturation. Adv. Prot. Chem. **14**, 1–45.
11. C. Tanford (1974) *The Hydrophobic Effect*, Wiley, New York, pp. 1–11.

Hydrophobic Electrophoresis

Although aqueous buffers are the appropriate solvents for gel electrophoresis of native hydrophilic macromolecules, separations of **hydrophobic** species require the presence of detergents or miscible organic solvents. Uncharged or amphoteric detergents are compatible with the formation of a gel and electrophoresis. Alternatively, charged detergents can be added to the buffer and have a negligible effect on electrophoresis, so long as conductance is not greatly elevated. The most widely used detergent for that purpose is the strongly dissociating and denaturing detergent, **SDS**. However, the **molecular sieving** of charged detergent micelles in electrophoresis as a function of gel concentration needs to be considered, as well as the generation of moving boundaries in discontinuous buffer systems, with the detergent as a leading or trailing ion (see Disc Electrophoresis). Miscible organic solvents are particularly suitable for relatively hydrophobic gels, such as some of the "Hydrolink" gels (1) or the new spongelike copolymer gel media(2).

When it is desirable to preserve native or relatively undissociated structures and their biological activities, gel electrophoresis must be conducted in "nondenaturing detergents," ie, under conditions that render the particular detergent relatively innocuous with regard to the disruption and inactivation of active structures and complexes. For that purpose, seven groups of amphoteric or uncharged detergents are particularly useful(3). Their effectiveness in solubilization depends sharply on their concentration, critical micelle concentration (cmc) and micellar weights, and the protein/detergent ratio.

Bibliography

1. R. J. Molinari, M. Connors, and R. G. L. Shorr (1993) Adv. Electrophoresis **6**, 44–64.
2. M. G. Harrington, K. H. Lee, E. Bailey, and L. E. Hood (1994) Electrophoresis **15**, 187–199.
3. L. M. Hjelmeland and A. Chrambach (1984) Methods Enzymol. **104**, 305–318.

Suggestion for Further Reading

4. L. M. Hjelmeland and A. Chrambach (1981) Electrophoresis and electrofocusing in detergent containing media: A discussion of basic concepts. Electrophoresis **2**, 1–11.

Hydrophobic-Interaction Chromatography

Hydrophobic (literally meaning "water hating") describes nonpolar compounds that have little affinity for polar molecules, such as water, and self-associate in a polar environment because of the hydrophobic effect . Hydrophobic interactions are energetically favorable because of an increase in **entropy** ($\Delta S > 0$) that originates when the solvent water molecules leave the more ordered structure around the nonassociated nonpolar compounds for the more unstructured, bulk polar environment. If matrices in a chromatography column provide hydrophobic surfaces to interact with analytes and one can separate mixtures of molecules with hydrophobic moieties, we are dealing with hydrophobic-interaction chromatography.

The principle of hydrophobic-interaction chromatography was originally known (1) by the name "**salting-out** chromatography," but it acquired its current name only after the synthesis of specific stationary phases in the early 1970s (2-4). In hydrophobic-interaction chromatography, retention is promoted by high concentrations of an appropriate salt, and elution is achieved with low salt concentrations. The matrices in the column are very hydrophilic and have only a very mild hydrophobicity. The increase in concentration of a salting-out salt drives the analytes out of the mobile phase and onto the stationary phase, much like the precipitation of highly water-soluble proteins or hydrophilic polymers that occurs under conditions of high ionic strength (see Salting In, Salting Out and Preferential Hydration).

Although many view hydrophobic-interaction chromatography as an extension of reversed-phase chromatography to an aqueous mobile phase without organic modifiers, there are a number of basic differences between these two separation techniques. In hydrophobic-interaction chromatography, the matrix is hydrophilic and is substituted with short-chain groups, such as phenyl, butyl, or octyl (see Ref. 5 for a list of different matrices), and the mobile phase is usually an aqueous salt solution. In reversed-phase chromatography, the matrix is an octyl (C8) or octadecyl (C18)-derived silica, and the mobile phase is usually a mixture of water and a less polar organic modifier (eg, methanol or acetonitrile). These two techniques exploit the different sources of the hydrophobicity of proteins. Hydrophobic-interaction chromatography depends on surface hydrophobic groups, which arise from the protein's **tertiary** and quaternary structures, and is carried out under conditions that maintain the integrity of the protein conformation. Reversed-phase chromatography is carried out on the unfolded protein, in which nearly all the hydrophobic groups are exposed to the matrix, and depends on the protein's primary structure. Proteins frequently **denature** under conditions of reversed-phase chromatography because organic solvents are needed for elution and/or because of the strength of the interaction with the stationary phase, whereas the mild elution conditions and mild hydrophobic interaction of hydrophobic-interaction chromatography matrices allow the elution and recovery of native proteins.

The most interesting aspect of hydrophobic-interaction chromatography is the frequent increase of retention with increasing temperature because this chromatographic method is an entropy-driven process. This is the opposite of any other type of retention chromatography. It should also be pointed out that the proteins are loaded onto the hydrophobic-interaction chromatography column using a buffer with a high salt concentration as the starting mobile phase and are then eluted by a gradient with decreasing ionic strength. This is the opposite of the procedure employed in ion-exchange chromatography .

Hydrophobic-interaction chromatography is extremely useful for purifying proteins and peptides. The principle of this chromatographic method is orthogonal to those of ion-exchange and size-exclusion chromatography methods. Therefore it is used effectively in schemes that combine all three chromatographic methods to separate proteins from complex mixtures. However, the solubilities of proteins in high-salt buffers are limited by the salting-out effect. This constrains the applications of hydrophobic-interaction chromatography for preparative purposes. A detailed operational protocol is beyond the scope of this article, so interested readers are directed to excellent reviews [5, 6, and chapter 13 (pp. 250–259) of Ref. 7].

Bibliography

1. A. Tiselius (1948) Ark. Kemi. Mineral. Geol. **B26**, 1.
2. S. Shaltiel and Z. Er-el (1973) Proc. Natl. Acad. Sci. USA **70**, 778–781.
3. B. H. J. Hofstee (1973) Anal. Biochem. **52**, 430-448.
4. S. Hjertén, J. Rosengren, and S. Pahlman (1974) J. Chromatogr. **101**, 281–288.
5. K.-O. Eriksson (1989) in *Protein Purification: Principles, High Resolution Methods, and Applications* (J.-C. Janson, and L. Rydén, eds.), VCH, New York, pp. 207–226.
6. R. M. Kennedy (1990) in *Guide to Protein Purification* (M. P. Deutscher, ed), *Methods in Enzymology* **182**, Academic Press, New York, pp. 339–343.
7. U. D. Neue (1997) *HPLC Columns: Theory, Technology, and Practice*, Wiley-VCH, New York.

Hydrophobicity

A molecule is said to be *hydrophobic* if it has a tendency to move from the polar solvent water to a nonpolar, oily surrounding. The tendency of a molecule or chemical group to undergo transfer at equilibrium from water to a nonpolar phase, such as a hydrocarbon solvent, is termed its *hydrophobicity*. The inverse properties are hydrophilic and hydrophilicity. Hydrophobicity is important in allowing drugs to cross membranes, and its analysis has therefore been important in the development of the pharmaceutical industry (1, 2). The relative hydrophobicities of the amino acids are of particular interest to biochemists and molecular biologists, because of their role in **protein folding**. Thus, the least hydrophobic amino acids are found almost exclusively at the accessible surfaces of proteins in which they occur, exposed to solvent water, whereas the interiors of proteins are almost uniformly composed of hydrophobic amino acids (3). For reasons that are not yet fully understood, but may be related to protein folding, the hydrophobicities of amino acids are also associated with a pronounced bias in the composition of the genetic code (4) (see also Hydrophilicity).

Hydrophobicity is usually expressed quantitatively as either the equilibrium constant or as the negative Gibbs **free energy** (-RT ln K_{eq}) for transfer of a solute from dilute aqueous solution to the nonpolar phase. This dimensionless equilibrium constant, the partition coefficient, is determined experimentally by measuring the concentration of the solute that is dissolved in each phase after thorough mixing, at equilibrium. After mixing equilibrium is achieved, a separatory funnel or similar device is used to separate the phases before measuring their solute content. A simple device for performing these experiments rapidly, with small volumes of material, is illustrated in Figure 1. Some solutes show a pronounced tendency to self-associate, either in water or in the nonpolar solvent. Self-association is indicated by an increasing tendency to favor one phase, that in which aggregation occurs more readily, as the solute concentration is increased. When such behavior is encountered, partition coefficients must be extended to sufficient dilution to avoid self-association in both phases. The results can then be used as a basis for calculating the concentration-independent distribution coefficient between phases, the hydrophobicity.

Figure 1. A simple apparatus for measuring hydrophobicity, consisting of a submersible magnetic stirrer, 20-mL scintillation vial, and lead cap to hold the vial in place. Measurements are made using aqueous solutions buffered in a pH range in which the solute is uncharged, using the solute at high dilution to avoid self-association, and a sensitive method of detection (typically NMR or radioisotopic assay). To estimate effective K_{dist} at pH 7, the observed K_{dist} is corrected for the fraction of solute that is ionized.

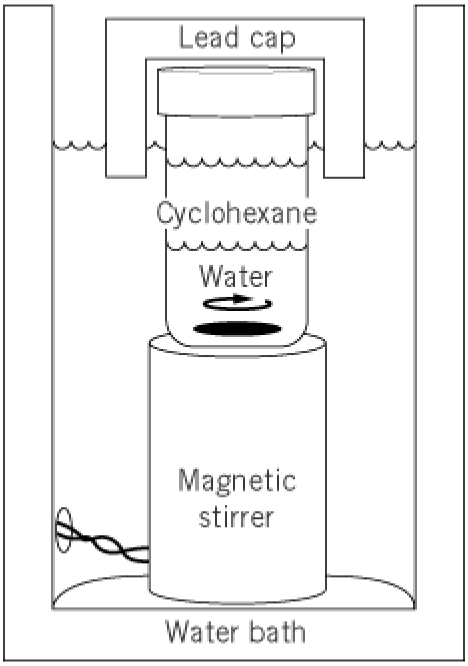

Certain immiscible solvents, such as 1-*n*-butanol and 1-*n*-octanol, are much more polar than others and are miscible with water to a considerable extent. Figure 2 shows that when a distribution measurement has been performed using octanol, the nonpolar phase contains 2.3 *M* water; in contrast, water-saturated cyclohexane contains only $1.6 \times 10^{-3} M$ water. Solutes experience relatively little change in surroundings in passing between wet octanol and water, so there is a “leveling” effect that tends to result in distribution coefficients that approach unity. To provide a more sensitive measure of differences in solute polarity, the nonpolar solvent that is used as a reference in these experiments should be as nonpolar as possible, ideally a liquid hydrocarbon such as cyclohexane. Adopting a scale of this kind, the side-chains of the amino acids that occur in proteins vary in their distribution coefficients between cyclohexane and neutral aqueous solution over a range of 4×10^{14}, from arginine (the most polar) to leucine and isoleucine (the least polar). For octanol-to-water distribution, the range is only 3×10^{2}. There is also evidence of specific interactions between solutes and octanol, as might be expected from the **hydrogen-bonding** potential of octanol's hydroxyl groups (2).

Figure 2. Solvents compared with respect to their water content at saturation, at 25°C.

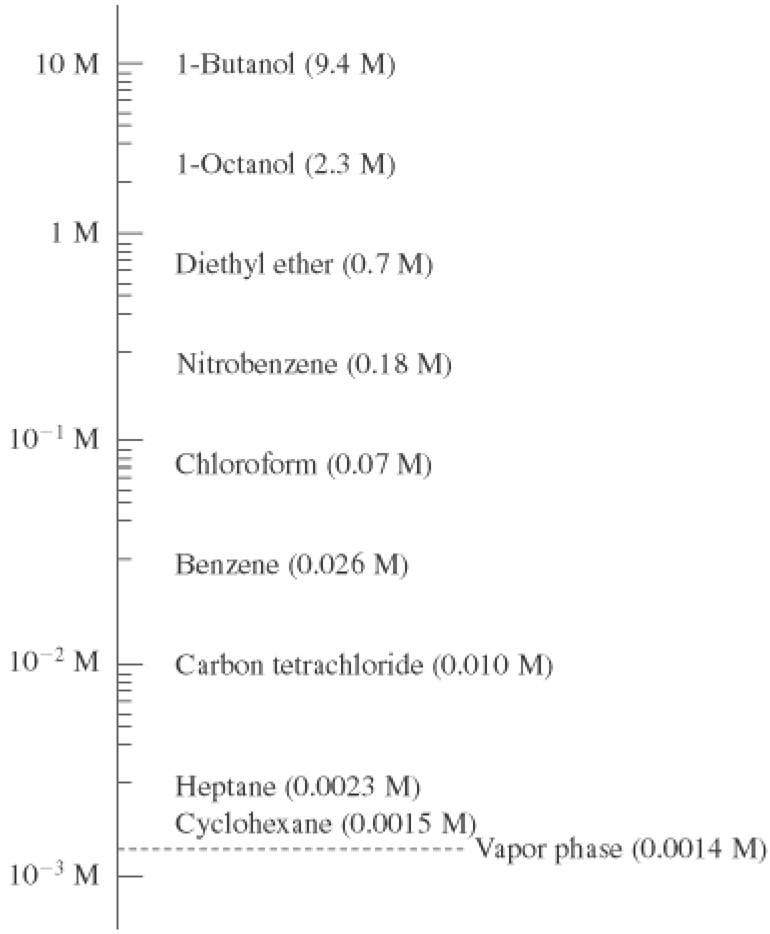

For a highly polar compound, such as a carboxylic acid or an amine, the solute may partition so strongly in favor of water that the concentration in cyclohexane is difficult to detect. Sensitivity can be improved by using a very large volume (eg, 1000 mL) of the nonpolar phase to extract the solute from a small amount (1 mL) of water, separating the phases, then "back-extracting" the solute into a small volume (1 mL) of water. After appropriate correction, distribution coefficients as large as 10^7 can be measured in this way using NMR, UV spectroscopy or radioisotope methods as a means of detection. Ionization tends to render a solute extremely polar, and its hydrophobicity is then more easily determined at pH values where the compound is uncharged. Its hydrophobicity at pH 7 can then be calculated by multiplying the value for the uncharged compound by the fraction that is actually uncharged at pH 7.

Many molecules are found to exhibit behavior consistent with the view that a molecule's hydrophobicity, expressed as free energy, is a roughly additive function of the hydrophobicities of its constituent chemical groups. A comprehensive collection of early data from the literature, with correlations and exceptions noted, has been published by Hansch and Leo (2). More recently, data have been collected for the amino acid side-chains (3), **nucleic acid** bases (5), phosphoric acid esters and amides (6), *cis*- and *trans*- peptide bonds (7) and carbohydrates (8). The hydrophobicities of the reactants and products of hydrolysis of ATP have been shown to differ to such an extent that ATP hydrolysis, which is highly exergonic in water (see Adenylate Charge), becomes endergonic in its absence, ie, changing the solvation can be considered to provide the entire driving force for ATP hydrolysis (8).

Hydrophobicities of the amino acid side chains occurring in proteins, expressed as $\log_{10}$ of the equilibrium constant at 25°C, for transfer from neutral aqueous solution to cyclohexane (3), are

Leucine	3.62
Isoleucine	3.62
Valine	2.97
Proline	2.51
Phenylalanine	2.19
Methionine	1.73
Tryptophan	1.71
Alanine	1.33
Cysteine	0.93
Glycine	0.69
Tyrosine	–0.10
Threonine	–1.89
Serine	–2.49
Histidine	–3.42
Glutamine	–4.07
Lysine	–4.08
Aparagine	–4.88
Glutamate	–5.00
Aspartate	–6.41
Arginine	–10.97

Proline differs from the other amino acids in that its nitrogen atom is involved in a secondary amide linkage. From a family of related compounds, it can be inferred that proline is 2.9-fold less hydrophobic than valine (9), placing its value at 2.51 on the above scale.

It is of interest to compare the hydrophobicities of the amino acids that occur in proteins with their tendencies to appear in buried positions or at the surfaces of proteins. Such a comparison, shown in Figure 3, suggests that there is a close correlation. It should be noted that the slope of the line is very shallow, consistent with the view that the environment of buried amino acid residues is much less nonpolar than cyclohexane, especially in the case of the more polar amino acids.

Figure 3. Distributions of amino-acid side-chains, from surface to buried positions in proteins (10), treated as an equilibrium constant ($K_{exposed>buried}$), compared with distribution coefficients for the corresponding side-chains from neutral aqueous solution to cyclohexane (3).

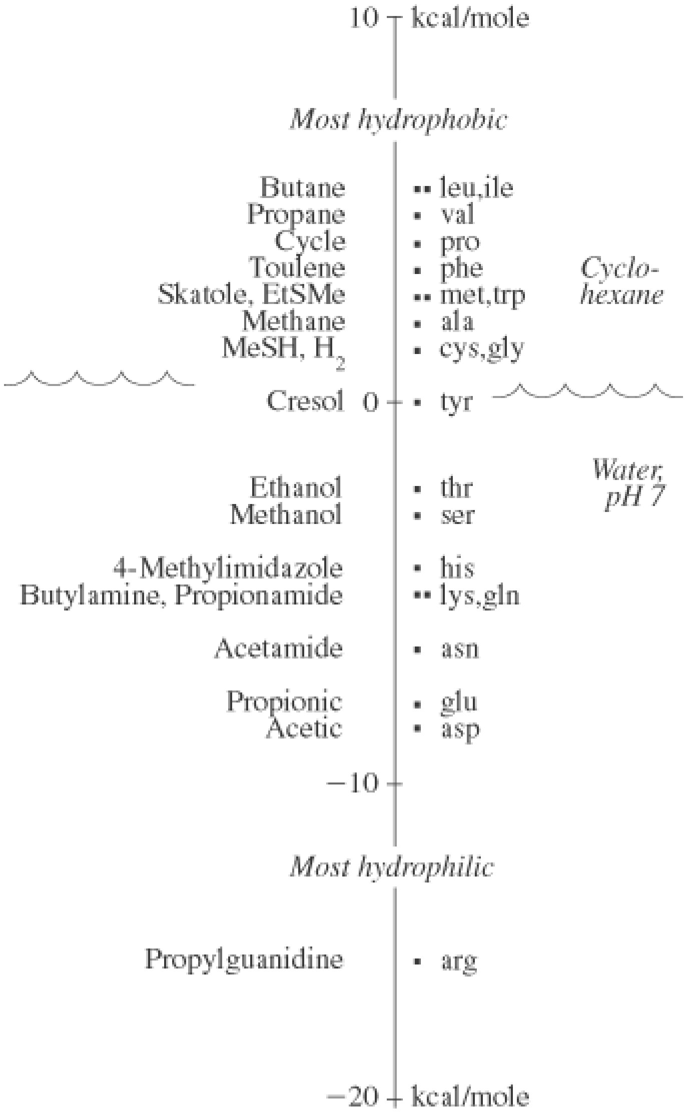

Bibliography

1. A. J. Leo, C. Hansch, and D. Elkins (1971) Chem. Rev. **71**, 525–680.
2. C. Hansch and A. J. Leo (1979) *Substituent Constants for Correlation Analysis in Chemistry and Biology*, Wiley, New York.
3. A. Radzicka and R. Wolfenden (1988) Biochemistry **27**, 1664–1670.
4. R. Wolfenden, L. Andersson, P. M. Cullis, and R. Wolfenden (1979) Science **206**, 575–577.
5. P. M. Cullis and R. Wolfenden, Biochemistry **20**, 3024–3028.
6. R. Wolfenden and R. Williams (1983) J. Amer. Chem. Soc. **105**, 1028–1031.
7. A. Radzicka, L. Pedersen, and R. Wolfenden (1987) Biochemistry **27**, 4358–4362.
8. R. Williams and R. Wolfenden (1985) J. Amer. Chem. Soc. **104**, 4345–4351.
9. P. R. Gibbs, A. Radzicka, and R. Wolfenden (1991) J. Amer. Chem. Soc. **113**, 4714–4715.
10. C. Chothia (1976) J. Mol. Biol. **105**, 1–18.

Suggestion for Further Reading

11. R. Wolfenden (1983) Waterlogged molecules. Science **222**, 1087–1093.

Hydroxyapatite Chromatography

Hydroxyapatite, also known as hydroxylapatite and abbreviated as HA, is a modified form of crystalline calcium phosphate, $Ca_{10}(PO_4)_6(OH)_2$, that has proven to be a very useful inorganic matrix for purifying and fractionating diverse macromolecules. Hydroxyapatite chromatography was introduced by Tiselius et al. in 1956 (1). Bernardi (2, 3) undertook extensive studies of **protein** behavior on hydroxyapatite, worked out standard procedures for the operation of HA columns, and discussed the mechanisms of adsorption and elution. Gorbunoff (4-6) extended Bernardi's work and deduced a mechanism of protein–HA interaction based on three fundamental conclusions:

1. Adsorption and elution cannot be regarded as simple reversals of a single process.
2. **Amino** and carboxyl groups act differently in the adsorption of proteins to HA.
3. Elution of basic and acidic proteins by different salts occurs by different mechanisms.

Briefly, in the adsorption of proteins to HA columns equilibrated with phosphate buffer, amino groups act through nonspecific electrostatic interactions between their positive charges and the general negative charges on the HA column, whereas carboxyl groups are repelled electrostatically from the negative charge of the column and by binding specifically to calcium sites on the column. Basic proteins are eluted as a result of normal Debye–Hückel charge screening by F^-,Cl^-,ClO_4^-,SCN^- and phosphate anions, or by specific displacement by Ca^{2+} and Mg^{2+} ions. Acidic proteins are eluted by displacement of their carboxyl groups from HA calcium sites by ions, such as fluoride or phosphate, that form stronger complexes with calcium than carboxyl groups.

Hydroxyapatite chromatography provides a unique fractionation method that has properties distinct from other separation techniques, such as preparative electrophoresis, ion-exchange chromatography and **size-exclusion chromatography** . Therefore HA chromatography has been used to advantage in purification schemes, frequently as a final purification step, and is used widely in biochemical research (see Ref. 7, a booklet provided by Calbiochem). The reader requiring more detailed and practical information is directed to the excellent review by Gorbunoff (8).

Bibliography

1. A. Tiselius, S. Hjertén, and Ö. Levin (1956) Arch. Biochem. Biophys. **65**, 132–155.
2. G. Bernardi (1971) Methods Enzymol. **22**, 325–339.
3. G. Bernardi (1973) Methods Enzymol. **27**, 471–429.
4. M. J. Gorbunoff (1984) Anal. Biochem. **136**, 425–432.
5. M. J. Gorbunoff (1984) Anal. Biochem. **136**, 433–439.
6. M. J. Gorbunoff and S. N. Timasheff (1984) Anal. Biochem. **136**, 440–445.
7. T. L. Brooks (1985) *Hydroxylapatite: Fast Flow and High Resolution*, Calbiochem Biochemicals, San Diego.
8. M. J. Gorbunoff (1990) in *Guide to Protein Purification* (M. P. Deutscher, ed.), *Methods in Enzymology* **182**, Academic Press, New York, pp. 329–339.

Hydroxylation (Lysine, Proline)

The principal posttranslational modifications of the polypeptides of collagen are the hydroxylation of proline and lysine residues to yield 4-hydroxyproline, 3-hydroxyproline (Hyp) and hydroxylysine (Hyl), plus glycosylation of the hydroxylysyl residues (Fig. 1). These modifications are catalyzed by three hydroxylases and two glycosyl transferases. The reactions occur until the polypeptides form the triple-helical collagen structure, which prevents any further modification reactions.

Figure 1. Structures of 4-hydroxyproline, 3-hydroxyproline, and hydroxylysine, as the free amino acids.

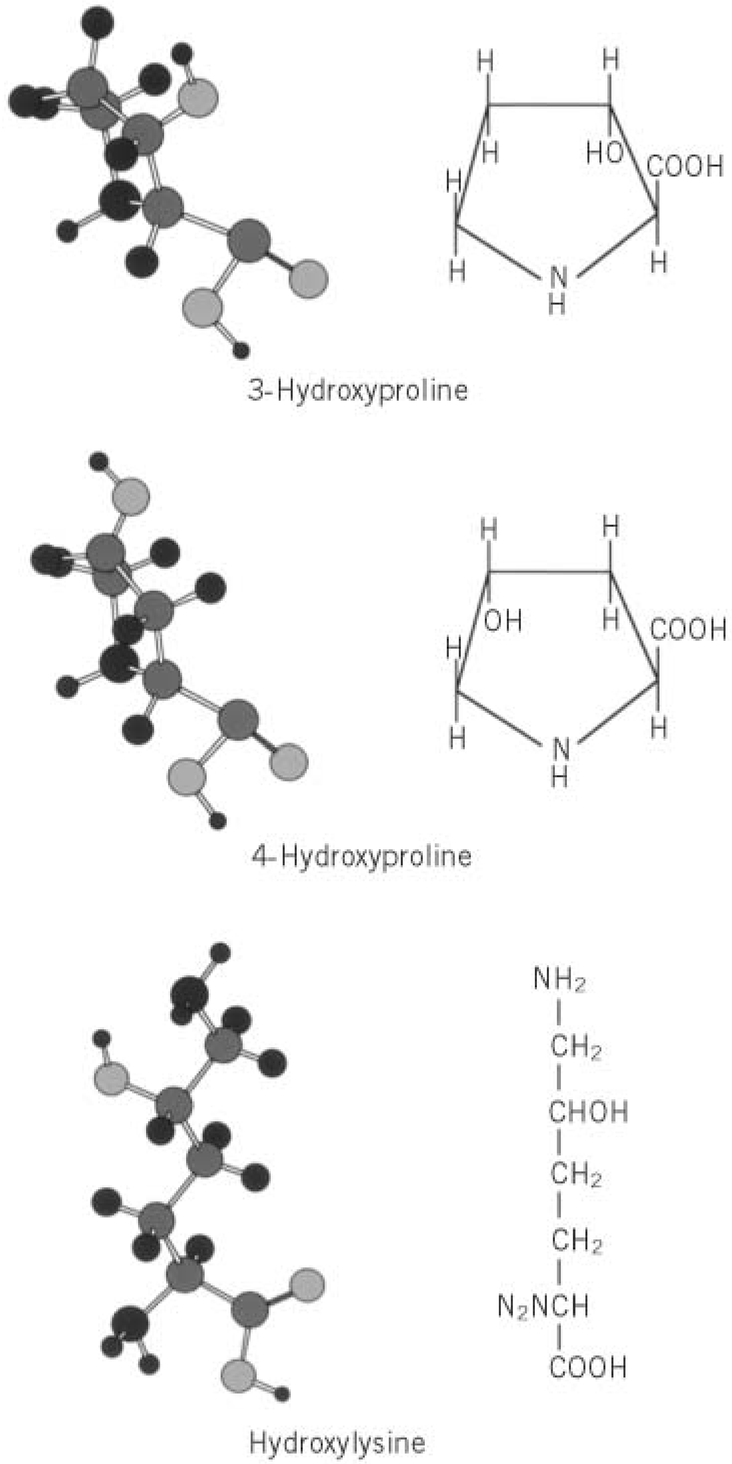

The hydroxylation of prolyl and lysyl residues in polypeptides is catalyzed by three separate glycoprotein members of the 2-oxoglutarate dioxygenase family of enzymes: prolyl 4-hydroxylase, prolyl 3-hydroxylase, and lysyl hydroxylase (Fig. 2). All three enzymes require a nonhelical polypeptide substrate. The minimum substrate structures for these enzymes are the triplets –X–Pro–Gly–,–Pro–Hyp–Gly–, and –X–Lys–Gly–, respectively. The activities of both prolyl 4-hydroxylase and lysyl hydroxylase are influenced by the adjacent amino acids and by peptide chain length.

Figure 2. Hydroxylation reactions on proline and lysine residues of collagen.

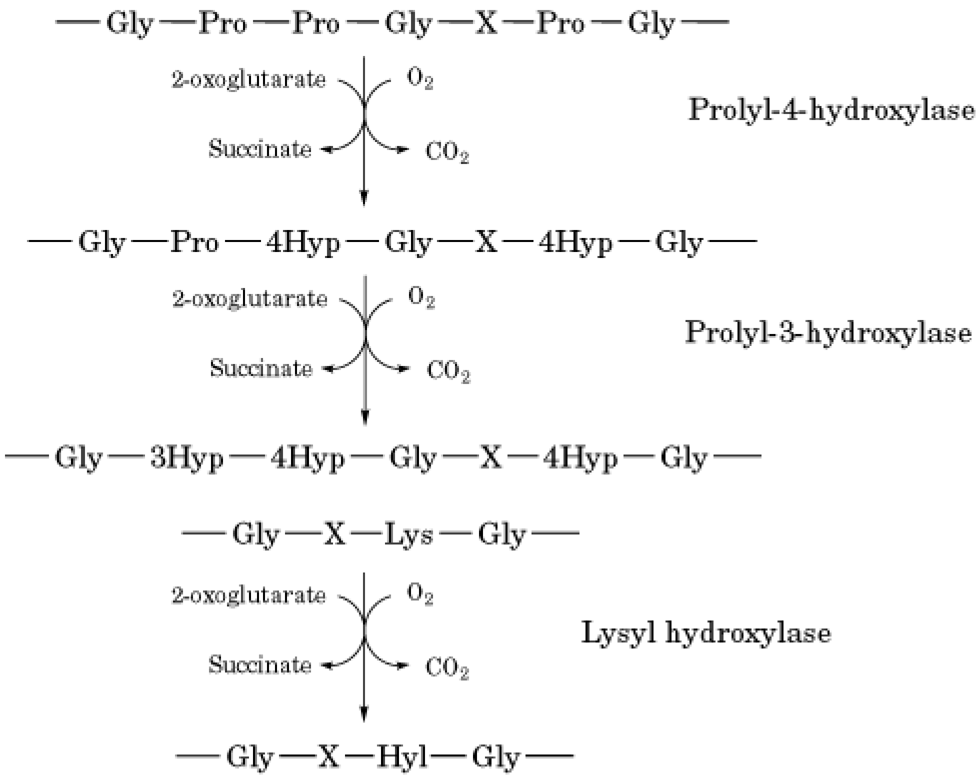

The reaction mechanisms of all three hydroxylase enzymes are similar, and each requires as cosubstrates Fe^{2+} , 2-oxoglutarate, and molecular O_2. The 2-oxoglutarate is stoichiometrically decarboxylated during hydroxylation; one atom of the O_2 molecule is incorporated into succinate and the other, into the hydroxyl group formed on the proline or lysine residue. The main function of ascorbate in the collagen hydroxylase reaction may well be to act as an antioxidant for the oxidation of Fe^{2+} to Fe^{3+} . Ascorbate is not consumed, and the hydroxylation reaction may proceed in its absence. The iron chelator, a,a′-dipyridyl, is a potent inhibitor of these hydroxylase reactions. In its presence, nonhydroxylated collagen is synthesized (in the case of type I collagen) or nonhelical chains may be secreted (in the case of type IV collagen).

1. Prolyl 4-Hydroxylase

The active prolyl 4-hydroxylase in vertebrates is a tetramer of molecular weight 240,000, and consists of two copies of each of two different types of subunits (a subunits, 64 kDa; b subunits, 60 kDa). It has two catalytic sites, one per pair of dissimilar subunits. The peptide- and 2-oxoglutarate-binding sites are located on the a subunit, while the ascorbate-binding sites may be composed of both a and b subunits. The principal contribution to the catalytic sites is from the a subunits, but some parts of the large catalytic sites may come from both the a and b subunits. The avian and mammalian a subunit sequences are highly conserved. The b subunit has proved to be a highly unusual multifunctional polypeptide that in isolation is protein disulfide isomerase (PDI).

2. Prolyl 3-Hydroxylase

Prolyl 3-hydroxylase (procollagen proline, 2-oxoglutarate 3-dioxygenase) requires a specific substrate sequence, catalyzing hydroxylation of prolyl residues only in the sequence –Pro–Hyp–Gly–. Prolyl 3-hydroxylase requires the same specific cofactors as does prolyl 4-hydroxylase. The reason for this modification is unknown, and the relative abundance of 3-hydroxyproline varies markedly in the different collagens. The individual chains of type I collagen each contain a single 3-hydroxyproline residue, while type IV collagen can contain up to 20 residues per 1000 amino acids.

3. Lysyl Hydroxylase

The enzyme lysyl hydroxylase (procollagen-lysine, 2-oxoglutarate 5-dioxygenase) catalyzes the hydroxylation of lysyl residues at the d carbon atom (Fig. 1) in –X–Lys–Gly–triplet sequences by a mechanism similar to that described for prolyl 4-hydroxylase. The hydroxyl groups of the hydroxylysyl residues have two important functions—they act as attachment sites for carbohydrate residues (either galactose or glucosyl-galactose), and they play a role in the formation of intra- and intermolecular collagen crosslinks (see Collagen). The hydroxylysine content of the a chains of the different collagen types varies from 5 to 70 residues per 1000 amino acids.

The enzyme lysyl hydroxylase in vertebrates is a **glycoprotein** containing asparagine-linked carbohydrate moieties. The enzyme is a dimer of 190,000 Da, composed of two monomers with different carbohydrate contents. The polypeptide chain of chick lysyl hydroxylase consists of 710 amino acids, with a 20-residue signal sequence. It is not very similar in sequence to the homologous, catalytically important a subunit of prolyl 4-hydroxylase, even though the enzymes share the same cofactor and substrate specificities.

N-Hydroxysuccinimide

N-Hydroxysuccinimide [I] is employed as an **acetylating** or acylating agent in its acetylated [II] or ester [III] forms. The activated ester is prepared by reacting *N*-hydroxysuccinimide with **carbodiimide**-activated carboxyl groups. Acetylation of amino groups in proteins is conducted under milder conditions with *N*-acetylsuccinimide [II] or *N*-hydroxysuccinimide acetate than with acetic anhydride.

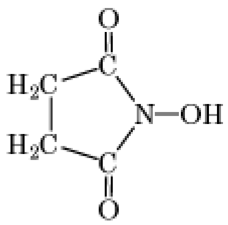

[I] *N*-Hydroxy-succinimide

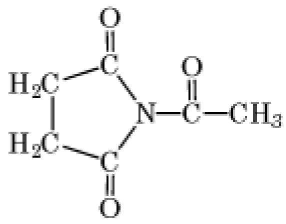

[II] *N*-Acetyl-succinimide

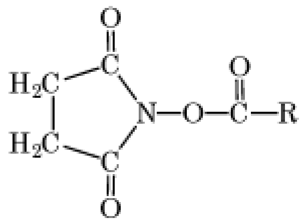

[III] *N*-Hydroxysuccinimide ester

Various *N*-hydroxysuccinimide esters are prepared and employed to acylate proteins. These reactions are used for chemical modification and labeling of proteins (1). *N*-Hydroxysuccinimide esters are often employed as one part of the reactive groups in **bifunctional reagents** for cross-linking proteins (2). *N*-Hydroxysuccinimide esters are also employed to prepare activated column resins for affinity chromatography. *N*-Hydroxysuccinimide esters of amino acids are obtained by condensing of N-protected amino acids and *N*-hydroxysuccinimide with carbodiimide, and they are widely employed for peptide synthesis.

Bibliography

1. Y.W. Shing and A. Ruoho (1981) Anal. Biochem. **133**, 171–175.
2. T.H. Ji (1983) Methods Enzymol. **91**, 580–609.

Hypersensitive Site

DNase 1 hypersensitive sites are the first place this **nuclease** introduces a double-strand break in chromatin (see DNase 1 Sensitivity). These sites usually involve small segments of DNA sequences (100 to 200 bp) and are two or more orders of magnitude more accessible to DNase 1 cleavage than inactive chromatin (1, 2). DNase 1 hypersensitive sites result from the assembly of specific nucleoprotein complexes that generally contain transcription factors flanked by positioned nucleosomes. DNase I hypersensitive sites also reflect the stable association of a transcription factor on the surface of a nucleosome (3). DNase I hypersensitive sites and nucleosome arrays are usually detected by DNase 1 or **micrococcal nuclease** digestion, followed by indirect end-labeling methodologies to map the hypersensitive site relative to a site of restriction enzyme cleavage (Fig. 1). As the most accessible regions of chromatin to non-histone DNA-binding proteins, DNase I hypersensitive sites generally denote DNA sequences with important functions in the nucleus.

Figure 1. A scheme for mapping the position of DNase I hypersensitive sites in chromatin relative to restriction endonuclease cleavage sites.

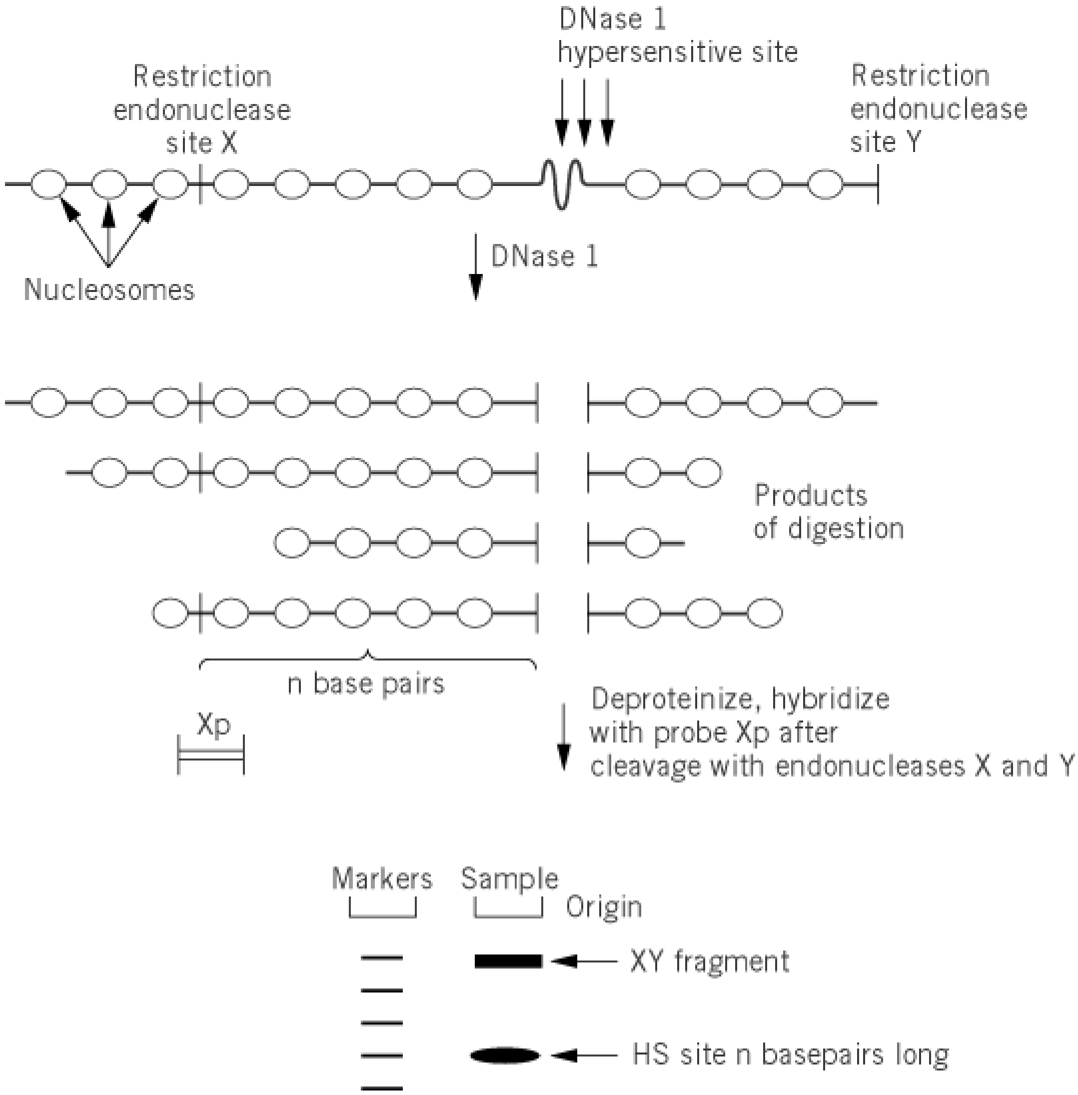

DNase 1 hypersensitive sites were first detected in the SV40 minichromosome, at the region that functions as an **origin of replication**, and in *Drosophila* chromatin (4). In general, these sites are accessible to all enzymes or reagents that cut duplex DNA. These sites have been mapped to a large number of functional segments of DNA, including **promoters**, enhancers, **locus control regions**, transcriptional **silencers**, origins of replication, recombination elements, and structural sites within or around telomeres (5).

These sites often fall into a hierarchy of patterns around regulated genes. Twelve DNase I hypersensitive sites are found in the chicken b-**globin** locus that contains four globin genes (5′-s-b^H-b^A-e-3′) and covers more than 65 kbp of DNA (Fig. 2). One site is present in all cells, independent of whether the genes are transcriptionally active or not. Three sites, upstream of the s-globin gene, were present only in erythroid cells destined to express the globin genes. These sites were initially without clear functional significance. However, a similar site was found between the b^A and e genes that corresponds to an enhancer element. Four sites were found over the promoters of each gene, depending on whether the gene was transcriptionally active, and three sites were found downstream of the genes, corresponding to transcription termination elements (the b ^{A} gene excluded). It is important to note that the formation of DNase I hypersensitive sites at the promoters of the globin genes is a relatively late step in the commitment of these genes to become transcriptionally active. However, it is clear that the formation of such sites precedes the actual initiation of transcription by

RNA polymerase. Indeed, the generation of these sites may account for a component of the general nuclease sensitivity of a gene (see DNase 1 Sensitivity) (6).

Figure 2. DNase I hypersensitive sites of the chicken b-globin locus. Contiguous genes are indicated as open arrows, the three distinct types of DNase I hypersensitive sites present in all cells specific to erythroid cells, and those that are developmentally regulated within the erythroid lineage are indicated.

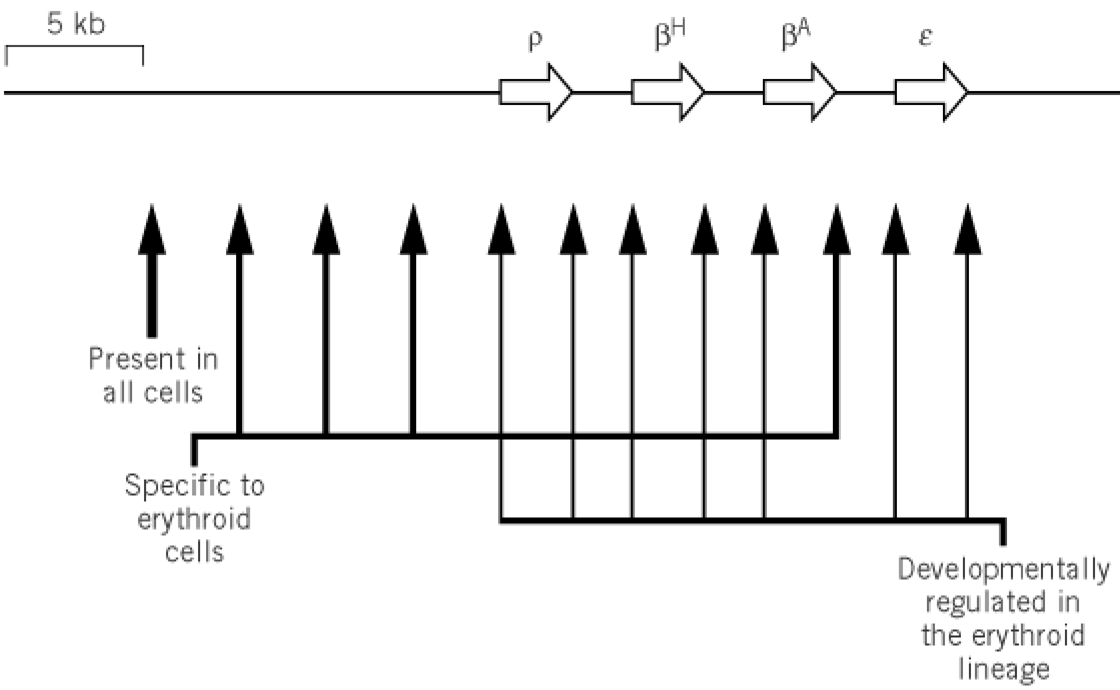

One of the most thorough dissections of a DNase I hypersensitive site was carried out by Elgin and colleagues (4). The *Drosophila* **heat-shock** protein *hsp26* gene is very rapidly activated transcriptionally by raising the temperature of a fly to a stressful level (a heat shock of 34°C). Two DNase I hypersensitive sites exist at the promoter of the *hsp26* gene, including recognition sequences for the promoter-specific, heat-shock transcription factor (HSTF, a leucine zipper protein) (Fig. 3). Following heat shock, HSTF binds to these sites. In contrast, transcription factor TFIID is bound to the TATA box before and after heat shock. TFIID alone is insufficient to cause the *hsp26* gene to be transcribed, and the specific association of the HSTF protein is also required. High-resolution analysis revealed that a nucleosome is positioned between the proximal and distal binding sites for HSTF, i.e. between the two DNase I hypersensitive sites. In this case, the exact position of histone-DNA contacts within this nucleosome depends on the DNA sequence to which the histones bind (from –300 to –140 relative to the start site of transcription at +1), and also on adjacent DNA sequences. These are repeats of the type $(CT)_n.(GA)_n$, which bind a specific *transacting* factor, the GAGA protein (7). The $(CT)_n.(GA)_n$ repeat regions are located to either side of the positioned nucleosome at –347 to –341 and at –135 to –85. The GAGA factor bound to these repeats may function as a "bookend" to determine exactly where the nucleosome will be positioned. Recent evidence suggests that the GAGA factor might function through ATP-dependent mechanisms to direct the assembly of a particular chromatin architecture actively. Transcription of the gene is regulated through the association of the HSTF with recognition elements at –51,–170,–269, and –340. The sites at –170 and –269 will be wrapped around the core histones in rotational frames that prevent HSTF association. However, the wrapping of DNA around the nucleosome will also bring the HSTF molecules bound to the sites at –340 and –51 into juxtaposition, and the histones may potentially facilitate transcription by causing a clustering of HSTF activation domains. Direct evidence for transcriptional activation mediated by this nucleosome is yet to be established. It is clear, however, that the positioning of a nucleosome in this particular way allows key transcription factors to obtain access to essential regulatory elements in spite of the assembly of the gene into chromatin.

Figure 3. The specific chromatin organization of the *Drosophila* hsp26 promoter. Key cis-acting elements are indicated relative to the start site of transcription (hooked arrow). The organization of these sites on a specific nucleosomal scaffold is indicated together with the interactions necessary to prevent or activate transcription. A tethered RNA polymerase II molecule is released through events initiated by the binding of HSTF.

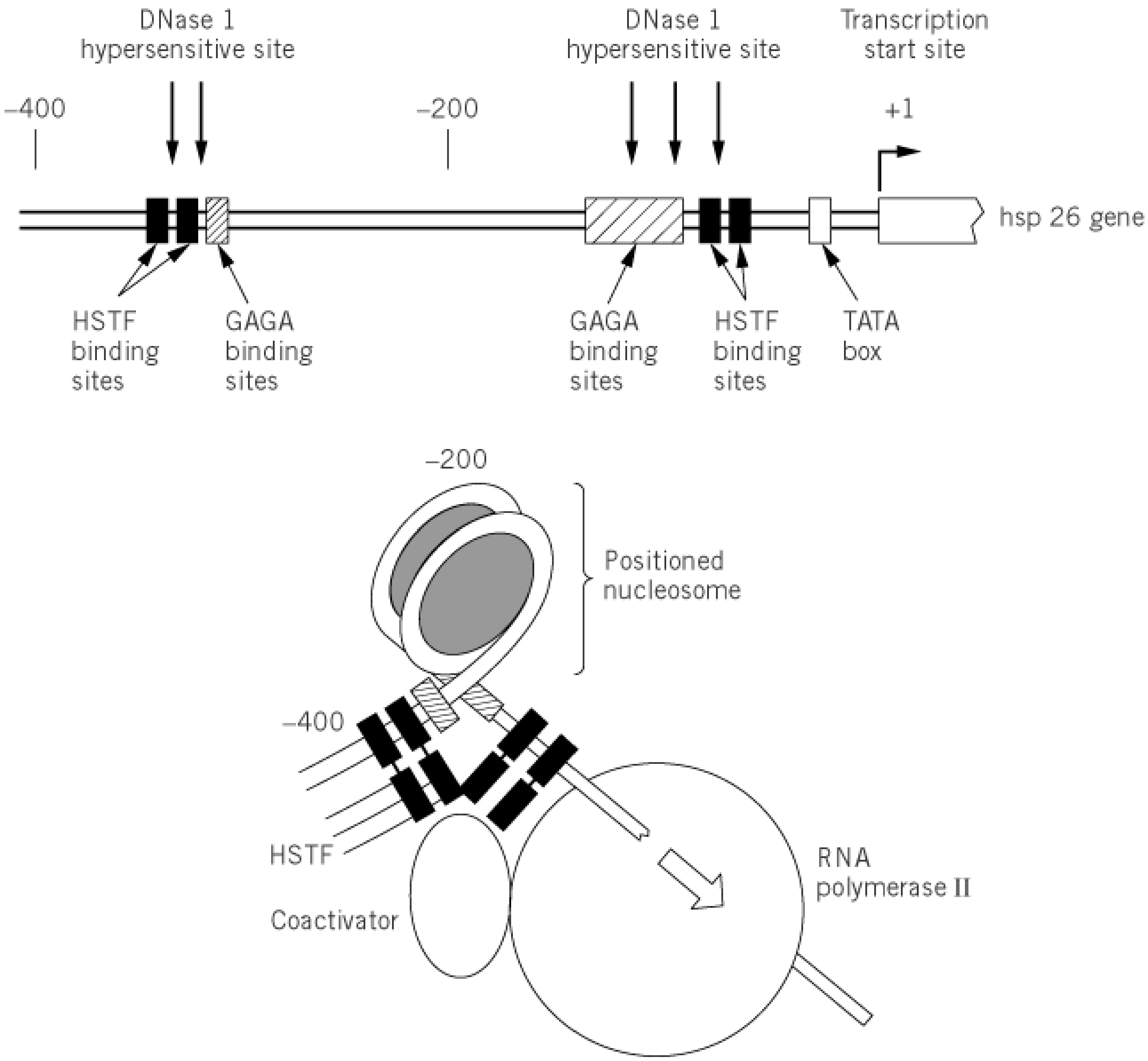

For a DNase I hypersensitive site on the vitellogenin genes, nucleosome positioning directed by the DNA sequence occurs between –300 and –140 relative to the start site of transcription at +1. The binding sites for the stimulatory transcription factors, the estrogen receptor and nuclear factor *1*, lie outside the region of DNA that is wrapped around the histones, at –300 to –330 and at –120 to –110, respectively (8). When these sites are brought together either by positioning a nucleosome in between them (or artificially by deleting the intervening DNA), transcription is enhanced about 5- to 10-fold. This moderate stimulatory effect is much more significant than it might appear because assembling a nonspecific chromatin structure would normally lead to a >20–fold repression of transcription as the binding sites for transcription factors are occluded by the histones. Thus in the vitellogenin gene example, nucleosome positioning has two roles: (1) to provide a scaffold that allows transcription factors to communicate more effectively; and (2) to prevent the formation of repressive histone-DNA interactions that may prevent any transcription factor from gaining access to a chromatin template.

DNase I hypersensitive sites have proven very useful in defining important DNA sequences. Among these are the four strongly nuclease-sensitive sites located 10 to 20 kbp upstream of the cluster of human b-globin genes. These sites, known as locus control regions (LCRs), represent ***cis*-acting** elements that allow genes integrated into a chromosome to be expressed independently of chromosomal position, i.e. position effects are abolished. A consequence of this is that LCRs allow each copy of a gene integrated in multiple copies to be expressed equivalently, so that gene expression is **copy-number** dependent. Therefore the LCR functions to control gene activity over an entire chromatin **domain**.

Bibliography
1. C. Wu et al. (1979) Cell **16**, 797–806.
2. J. D. McGhee et al. (1981) Cell **27**, 45–55.
3. J. Wong et al. (1997) EMBO J. **16**, 7130–7145.
4. S. C. R. Elgin (1988) J. Biol. Chem. **263**, 19259–19262.
5. D. S. Gross and W. T. Garrard (1988) Ann. Rev. Biochem. **57**, 159–197.
6. M. Reitman and G. Felsenfeld (1990) Mol. Cell. Biol. **10**, 2774–2786.
7. Q. Lu, L. L. Wallrath, H. Granok, and S. C. R. Elgin (1993) Mol. Cell. Biol. **13**, 2802–2814.
8. C. Schild, F.-X. Claret, W. Wahli, and A. P. Wolffe (1993) EMBO J. **12**, 423–433.

Hypervariable Locus

In general terms, a "hypervariable locus " is a genetic locus that shows a great degree of variability, or **polymorphism**, in the genomes of a population. High degrees of polymorphism occur at hot spots of mutation or recombination, or they can be the consequence of a continuously varying strong natural selection pressure on a locus, such as that exerted on the **major histocompatibility locus**. The term "hypervariability" is normally used, however, to indicate the instability of minisatellites, which is related to their sequence of 15 to 60 bp being tandemly repeated. The mutation frequency for changes in the number of tandem repeats has been estimated to vary between 10^2 and 10^4 per kbp per generation, which is one to three orders of magnitude higher than the rate of point mutation (1). **Unequal crossing over** within such a tandem repeat is likely to be an important generator of asymmetrical new alleles (2). Jeffreys noted that the core of his first hypervariable minisatellite shared some sequence characteristics with the **Chi sequence** of lambda phage, a signal for homologous recombination, which is probably achieved by binding a **Rec** protein that locally unwinds and nicks DNA (3). The hypothesis that minisatellites are recombination hotspots has been partially confirmed by the observation that most highly variable human minisatellites tend to be located in the subtelomeric regions of chromosomes (see Telomere), precisely those that exhibit high recombination rates (4).

Changes in the lengths of minisatellite repeats occur both in the **germline** and in **somatic cells**, possibly by sister chromatid exchanges. Somatic length mutations may represent markers of tumor cell progression and variation (5). With some hypervariable minisatellites, no difference has been found between the frequency of germline mutations in **oocytes** or **spermatocytes**. Given the large difference in the number of **mitosis** events that follow **meiosis** in the female and male germlines, it would seem that the cause of mutation is not always mitosis-dependent (6). Also, for some minisatellites, closely related **alleles** show the same flanking DNA sequences, whereas for other minisatellites flanking **haplotype** switching is observed. It should be concluded that recombinational events within minisatellites are not always the cause of length mutation.

Another mechanism possibly responsible for length mutation is slippage of the **DNA polymerase** during replication of the minisatellite, with the consequence of variation in one or very few units (7). A computer simulation to estimate the expected number and size range of alleles under a stepwise, replication slippage mutation model explained the available data better with the shorter microsatellites than with minisatellites (8).

Recently, methods have been devised for analyzing mutant alleles of single minisatellites by the polymerase chain reaction (**PCR**). Several features of the variability observed, such as its polarity, the addition of elements without evidence of **crossing over**, and rearrangement of elements with respect to their sequence in the homologous chromosome, suggest the involvement of complex **gene-conversion**-like events in the generation of mutant alleles (9).

Bibliography

1. A. J. Jeffreys, V. Wilson, and S. L. Thein (1985) Nature **314**, 67–73.
2. A. J. Jeffreys, N. J. Royle, V. Wilson, and Z. Wong (1988) Nature **332**, 278–281.
3. G. R. Smith (1983) Cell **34**, 709–710.
4. A. P. Jarman and R. A. Wells (1989) Trends Genet. **5**, 367–371.
5. M. Perucho et al. (1995) Cold Spring Harbor Symp. Quant. Biol. **59**, 339–348.
6. A. J. Jeffreys et al. (1995) Electrophoresis **16**, 1577–1585.
7. G. Levinson and G. A. Gutman (1987) Mol. Biol. Evol. **4**, 203–221.
8. M. D. Shriver, L. Jin, R. Chakraborty, and E. Boerwinkle (1993) Genetics **134**, 983–993.
9. A. J. Jeffreys et al. (1994) Nature Genet. **6**, 136–145.

I-Motif

The complementary DNA strand of the telomere TTGGGG sequence, CCCCAA, adopts an unusual DNA structure at low pH. The structure was first proposed by a NMR analysis (1) and later confirmed by X-ray crystallography (2) of cytosine-rich sequences under low pH conditions. It contains a highly unusual, mutually intercalated, four-stranded structure. This structure has been dubbed the i-motif, where two parallel duplexes intercalate with one another in an antiparallel orientation (Fig. 1). Each parallel duplex consists of hemiprotonated $C:C^+$ base pairs. It is unclear whether such a structural motif is associated with any biological function at present.

Figure 1. Side and end views of the structure of the i-motif (Nucleic Acids Database UDF062).

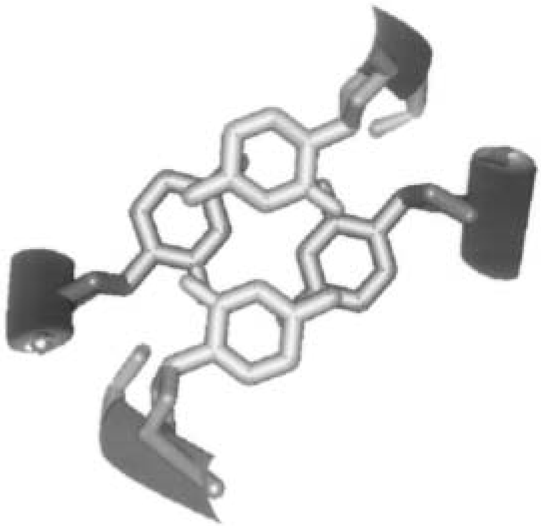

Bibliography

1. K. Gehring, J. L. Leroy, and M. Gueron (1993) Nature **363**, 561–565.
2. L. Chen, L. Cai, X. Zhang, and A. Rich (1994) Biochemistry **33**, 13540–13546.

Ideogram

An ideogram is a diagrammatic representation of the karyotype that shows all of the pairs of homologous chromosomes in the nucleus. The pairs of chromosomes are lined up in order of size, so that the centromeres are aligned and the short arm is uppermost. An ideogram is a useful point of reference for analyzing mutations.

Idiotypes

The concept of the idiotype of **immunoglobulins** emerged in the early 1960s from two different approaches, one by Oudin with rabbit **antibodies**, the other by Kunkel and analysis of the immunochemical characteristics of human myeloma proteins. At the time, Oudin had described the allotypic specificities as defining **antigenic** characteristics of a group of individuals within a given animal species. This was observed for rabbit immunoglobulins and was the consequence of **allelic** variants of both the heavy and light chains. It was then found that when rabbit antibodies prepared against *Salmonella typhi* were injected into another rabbit expressing the same (known) allotypes, they induced the synthesis of antibodies that specifically recognized the anti-*Salmonella* antibodies raised in the first rabbit. It was also shown that they did not react with normal rabbit serum taken before the *Salmonella* injection, thereby excluding that they identified a new allotypic specificity. Idiotypic specificities were thus defined as antigenic specificities characteristic of one antibody (the idiotype) produced by one animal and specific for one given antigen. Antibodies produced by the second animal were termed **anti-idiotypic antibodies**. Idiotypes are also referred to as Ab1 while anti-idiotypes are referred to as Ab2, in a simplified nomenclature.

At the same time, Kunkel was comparing the immunochemical characteristics of human myeloma proteins with those of normal immunoglobulins. He found that antibodies raised against one given myeloma protein, which cross-reacted against normal immunoglobulins, became specific for the immunizing protein once extensively adsorbed on normal immunoglobulins. This was taken as indicative of determinants specific for any given monoclonal product, although it was not entirely clear whether it was also linked to the pathological “abnormal” nature of the myeloma protein.

Structural analysis confirmed, as anticipated, that idiotypic determinants, or idiotopes, were present on the Fab fragments and, more precisely, on the variable regions of H and/or L chains (see Immunoglobulin Structure), depending on the idiotype. Extensive analysis of idiotype structure performed by a combination of immunochemical and structural analysis of anti-**hapten** antibodies revealed several types of idiotopes. Some Ab1–Ab2 interactions could be inhibited by a hapten of Ab1, indicating that the corresponding idiotopes were part of the antibody combining site, whereas other were not. Genetic analysis also revealed that some idiotypic specificities were common to several idiotypes, whereas others were strictly specific for one given Ab1, leading to the distinction of public and private idiotypes, a notion that was directly related to the dual origin of antibody diversity, germline encoded and somatically generated. Idiotypy was studied extensively when it was discovered that the cascade Ag(X) → Ab1 → Ab2 could be continued and amplified in a large idiotypic network of interactions, providing a basis for autoregulation of the immune system. An especially interesting observation was that Ab2 could induce certain Ab3 molecules that resembled Ab1 in that they could bind the original Ag(X) antigen. This led to the definition of the “internal image” of the antigen, proposed by Jerne, containing the idea that the collection of normal immunoglobulins of an individual could represent a huge population of internal images of the outside antigen world. It also stimulated approaches of idiotypic vaccines that could have been used in place of classical antigens, an interesting idea whenever antigens were either difficult to identify or poorly immunogenic.

See also entries Autoimmunity, and Autoimmune Diseases.

Suggestions for Further Reading

A. Coutinho (1995) The network theory: 21 years later. Scand. J. Immunol. **42**, 3–8.
C. A. Bona (1996) Internal image concept revisited. Proc. Soc. Exp. Biol. Med. **213**, 32–42.

IgA

Immunoglobulin A (IgA), accounts for about 10% to 15% of the circulating **immunoglobulins**. The main feature of IgA is its presence in high concentrations in all mucosal secretions (intestine, lung, colostrum, tears, etc.), and for this reason it is generally considered of prime importance in fighting pathogens, against which it constitutes a first line of defense. The presence of elevated amounts of IgA in secretions correlates with their special structural features, namely their ability to dimerize and to have an extra Ig secretory component added upon passage through epithelial cells.

The basic Ig structure of IgA is a classical H_2 L_2 monomer in which the heavy chains are a chains, composed of the usual V_H region and three C_H domains. In humans there are two **isotypes**, IgA1 and IgA2, encoded by distinct C_H genes. As a result, the two isotypes differ from each other by small amino acid sequence differences and by the length of their hinge regions. In addition, the IgA2 isotype has two **allelic** variants, recognized by specific antisera as two distinct allotypes, IgA2 m(1) and IgA2 m(2). The IgA2 m(1) has a special structural feature, because its heavy chain lacks the cysteine residue that is covalently **disulfide-bonded** to the light chains in other isotypes; consequently, the H–L interactions are exclusively noncovalent, whereas the light chains are covalently dimerized. Carbohydrate moieties account for about 10% of the molecule and are mostly attached in the vicinity of the hinge region. In the serum, the IgA are essentially monomeric, whereas they polymerize in the vicinity of epithelial cells, with the formation of dimers (major), but also trimers and tetramers. When polymerized, the IgA gains an extra chain, termed the J chain [which as not the same as the **J (joining) region**], which is disulfide-bonded to part of the IgA heavy chains. Once dimerized, the IgA molecule is covalently bound to the poly-Ig receptor, expressed at the basal pole of the epizthelial cell. This complex is internalized, and the polymerized IgA is released at the apical pole of the cell in the lumen of the corresponding organ upon **proteolytic** cleavage between two **domains** of the poly-Ig receptor, so that one subunit remains covalently linked to the IgA polymer, forming the so-called secretory component. Besides allowing the IgA to migrate through the epithelial cell, the secretory component is thought to protect the immunoglobulin from cleavage by proteinases. The local concentration of IgA may be very high and, due to its polymerized state, this Ig has an increased avidity for antigen. Because of its abundance in colostrum, it is of crucial importance for passive antibody transfer to the newborn and thus ensures a temporary protection against pathogens, because the immune system will remain immature for some time. It should be recalled, however, that the protective effect of colostrum and/or milk greatly varies from one species to the other. Whenever the placental barrier is easily passed by an active transfer of IgG, the importance of colostral IgA is minimized. In humans, protection is ensured by transplacental transfer. An example of the reverse situation is seen in cattle.

Mucosal immunity, as immunologists like to refer to it whenever IgA is involved, is presently a rapidly expanding field. It has not been studied sufficiently, considering that it appears to be of prime importance in fighting against pathogenic microorganisms.

See also entries Class Switching, Isotype, and J Chain.

Suggestions for Further Reading

M. E. Lamm (1997) Interaction of antigens and antibodies at mucosal surfaces. Annu. Rev. Microbiol. **51**, 311–340.

J. Mestecky and J. R. McGhee (1987) Immunoglobulin A: molecular and cellular interactions involved in IgA biosynthesis and immune response. Adv. Immunol. **40**, 153–245.

B. A. Hendrickson et al. (1996) Lack of association of secretory component with IgA in J chain-deficient mice. J. Immunol. **157**, 750–754.

IgD

IgD is an immunoglobulin that is present on the surface of mature B cells. Its circulating concentration is in the range of 40–400 µg/mL, which does not contribute significantly to the overall amount of secreted Ig (compare with the 10 mg/mL range for IgG). IgD exists as only one isotype and is exclusively a d_2k_2 or d_2l_2 monomer. The d chain in humans has three **constant domains**, whereas there are only two in murine species, in which Cd_2 is replaced by an unusually long hinge region. The main characteristic of IgD is to be essentially coexpressed at the surface of the same B cell with IgM. This does not contradict the clonal selection theory, because the two B-cell receptors express the same variable regions and hence have the same antibody specificity. This is because the switch region that is located at the 5′ position of all C gene isotypes is absent from the Cd locus. Coexpression of m and d chains results from alternative splicing, thus leading to both IgM and IgD that are associated to same k or l chains within a given B cell. Occasionally, clones expressing solely IgD without IgM can be encountered. This is most apparent in rare myeloma cells that are IgD producers. In that case, the absence of IgM probably results from a deletion of the Cm genes at the genomic level. This seems also to be the case of a recent observation of B cells detected in human tonsils that express exclusively IgD and have surprisingly accumulated an unusually large number of somatic mutations. Despite their very peculiar specialization as surface Ig, the role of IgD is still very poorly understood, although some arguments point to their possible role in B-cell induction of **tolerance**.

See also entries Isotype.

Suggestions for Further Reading

F. R. Blattner and P. H. Tucker (1984) The molecular biology of IgD. Nature **307**, 417–422.

J. Wienands, J. Hornbach, A. Radbruch, C. Riesterer, and M. Reth (1990) Molecular components of the B cell antigen receptor complex of class IgD differ partly from those of IgM. EMBO J. **9**, 449–455.

C. C. Goodnow et al. (1988) Altered immunoglobulin expression and functional silencing of self-reactive B lymphocytes in transgenic mice. Nature **334**, 482–484.

Y.-J. Liu et al. (1996) Normal human IgD$^+$IgM$^-$ germinal center Bcells can express up to 80 mutations in the variable region of their IgD transcripts. Immunity **4**, 603–613.

IgE

IgE is the immunoglobulin most commonly known as the main cause of anaphylaxis or, more generally speaking, of the immediate hypersensitivity states, such as asthma, hay fever, atopic dermatitis, and other well-known manifestations of atopic patients. IgE is present in normal individuals at very low concentrations, normally somewhat less than 1 µg/mL. This concentration may be considerably elevated in patients suffering from one or another form of immediate hypersensitivity, and also in patients with internal parasite infections. This points to a major role as support of anaphylactoid states and suggests a possible role in the defense against parasites, a view that has been seriously reinforced of late.

IgE is a monomer of molecular formula $\epsilon_2 k_2$ or $\epsilon_2 l_2$. It may, as all the other Ig subclasses, be expressed as cell-surface or circulating Ig, and it has an elevated carbohydrate content (>10% by weight). The ε chains have four constant Cd **domains**, and the molecular weight of IgE averages 180 kDa. IgE does not fix **complement** and is heat-labile. Its role in driving the immediate hypersensitivity reactions is due to the fixation of circulating IgE antibodies on **Fc receptors** of very high affinity; FcRεI is located on several cell types, mostly basophils and mast cells. These large cells contain granules that contain a high concentration of pharmacologically active substances, like histamine, neutral proteinases, proteoglycans, and **tumor necrosis factor a**; (TNFa). Contact of an antigen (here denominated an allergen) with specific IgE fixed to such cells of an atopic patient who has already been sensitized will activate the target cell and release the pharmacologically active substances, thus initiating a large cascade of secondary reactions. Histamine will bind selectively to H1-type receptors and exert various deleterious effects, such as vasodilatation, local exudation, and spasmogenic activity of intestinal, uterine, or bronchial muscles, depending on the localization of the target. TNFa liberated upon mast-cell activation may have a beneficial effect in antimicrobial defense. Other mediators are synthesized as a response to IgE triggering. Those include prostaglandins, PGD2, leukotrienes, and so on, and a large number of **cytokines** that considerably amplify the response and especially initiate a strong inflammatory reaction. Fixation of IgE on other cell types, like eosinophils, **macrophages**, or platelets, can also occur through the FcεRII, which is of lower affinity than FcεRI, and trigger liberation of many mediators, including free radicals that may be beneficial by helping to fight against pathogens, although most of the effects are quite aggressive for the host tissues.

Discovery of the two main populations of helper T cells, Th1 and Th2, which drive a fine regulation of the immune response through a complex network of cytokines, has opened the way to a reinvestigation of the possibility of modulation of the expression of IgE, which is of prime importance for atopic patients, but also to fight more effectively against parasites, which remain quite elusive pathogens to date. IgE production is essentially driven by cytokines of the Th2 group, particularly interleukin 4, which was shown to favor the **class switch** to this Ig class.

See also entries Antibody, Class Switching, Immunoglobulin, and Isotype.

Suggestions for Further Reading

B. J. Sutton and H. J. Gould (1993) The human IgE network. Nature **366**, 421–428.

T. Mossmann and R. L. Coffman (1989) Th1 and Th2 cells. Different patterns of lymphokine secretion lead to different functional properties. Annu. Rev. Immunol. **7**, 145–174.

IgG

IgG is the major class of immunoglobulin (Ig) and has long been taken as the basic Ig model. IgG are found either as free circulating molecules in the bloodstream, where they account for about 70% of total Ig, or anchored at the B-cell surface, constituting the B-cell receptor in association with the IgaIgb heterodimer signaling module. They contain two g and two light chains, either k or l, and about 2% by weight of carbohydrate, located on the CH $_2$ **domains**. IgG is expressed as four distinct subclasses, termed IgG1, IgG2, IgG3, and IgG4 in humans, resulting from the presence of the corresponding g1 to g4 heavy chains encoded by separate germline Cg genes. The four **isotypes** have minor structural differences, both in the length of their hinge region and in primary structure, which remain 95% identical; this suggests that the amplification of g isotypes is a rather recent event. IgG subclasses also exist in other species. In the mouse there are also four discrete isotypes called IgG1, IgG2a, IgG2b, and IgG3. That there is no correspondence between the various human and mouse isotypes confirms that the subclass expansion is characteristic of each animal species and occurred after they diverged. The different isotypes are endowed with somewhat different biological properties. All except for IgG4 bind **complement**. The first component of the complement cascade, C1q, has a binding site on the C $_H$2 domain. This site becomes accessible once the antibody molecule has interacted with antigen, presumably as the result of an opening of the Fab–Fc angle, which is made possible because of the flexibility of the hinge region (see Immunoglobulin Structure). The IgG subclasses bind to different **Fc receptors**. The major subclass is IgG1, followed by IgG2. Expression of the various subclasses during development follows different kinetics, with IgG2 and IgG4 being synthesized only slowly after birth. Allotypic markers termed Gm factors have long been identified on IgG and have provided an interesting basis for studying human population genetics.

IgG can be cleaved, in the native state, by a variety of **proteolytic** enzymes, due to the flexibility of the hinge region and to the somewhat accessible short regions that separate the various domains. Porter (1) reported the isolation of Fab and Fc fragments upon cleavage with papain; IgG may also be cleaved with **pepsin**, which largely destroys the C_H2 domain, leaving a $(Fab')_2$ fragment, which has two pieces slightly larger than an Fab **disulfide-bonded** through the inter-heavy-chain bridges that have remained untouched, and the Fd′ fragment, which covers roughly the C_H3 COOH-terminal domain. Cleavage with **plasmin** cleaves off the last C_H3 domain, leaving a major Facb fragment (for antibody and complement binding). Finally, it is possible in a limited number of cases to release the variable V_H-V_L domains noncovalently bound as the Fv fragment, which contains one intact antibody combining site. The three-dimensional protein structures of the isolated domains are quite independent of their interactions with other parts of the IgG molecule. Extensive protein engineering has been made on this structure, by introducing the corresponding complementary DNAs into vectors that are expressed in bacteria or other systems, such as the baculovirus. Extensive phage display libraries have been constructed that provide a huge combination of V_H–V_L pairs having an almost infinite set of discrete recognition Ig-like molecules.

During the early phases of the primary immunization, IgM is rapidly replaced by IgG upon class switching, a molecular mechanism that operates at the genomic level, leading to the replacement of one isotype by the other, without changing the variable regions and thus conserving the antibody specificity. Somatic hypermutations occur primarily in IgG molecules, so they become increasingly adapted to the exquisite recognition of **epitopes** of the immunizing antigen. This implies both an enzymatic mechanism for mutations and a strong selection exerted by the antigen itself on IgG-producing B cells. Some of the selected clones with high affinity will ultimately differentiate into plasma cells and produce circulating IgG, whereas others will become memory cells, expressing membrane IgG of high affinity that will rapidly react in a subsequent reexposure to the antigen, initiating a secondary response.

See also entries Antibody, B Cell, Class Switching, Immune Response, and Immunoglobulin.

Bibliography

1. R. R. Porter (1959) The hydrolysis of rabbit -globulin and antibodies with crystalline papain. Biochem. J. **73**, 119–126.

Suggestion for Further Reading

2. D. Burton (1990) Antibody: the flexible adaptor molecule. Trends Biochem. Sci. **15**, 64–69.

IgM

Immunoglobulin M (IgM) is the first immunoglobulin to appear after immunization, the first to occur in ontogeny and in phylogeny, and the first to be expressed at the surface of B cells during their differentiation. Most of these properties are a result of the fact that the genes encoding their C_H regions are the closest to the V_H locus. IgM is built on the classical H_2L_2 model as either m_2k_2 or m_2l_2 monomers (see Immunoglobulin Structure). As such, these monomers are expressed at the B-cell surface, where they represent, associated with the Iga–Igb heterodimer signaling module, the B-cell receptor that interacts with the immunogen upon primary immunization. In the serum, most of the circulating IgM is a pentamer, $(m_2k_2)_5$ or $(m_2l_2)_5$, in which monomers are covalently **disulfide-bonded**, a linkage that involves the addition of theJ chain, similar to that present in the IgA dimer. The constant region of the m chain does not contain a hinge region, but instead has an additional C domain, as compared with IgG. IgM has a high content of carbohydrate (10% to 12% by weight) which is bound at ***N*-glycosylation** sites of the first three Cm domains.

The basic monomer has a molecular weight of 180 kDa, and the pentamer has a molecular weight of about 970 kDa. Because of their size, circulating IgM subclasses were originally designated as macroglobulins. They are found in a lymphoproliferative disease, the Waldenstrom macroglobulinemia, where they are overexpressed as the result of the malignant amplification of an IgM-producing B-cell clone. In normal serum, IgM accounts for 10% to 15% of the total circulating immunoglobulins. IgM behaves as expected as decavalent antibodies for binding to **epitopes**, provided that they are located on a small antigen, such as a hapten. On larger antigens, as a result of steric hindrance, IgM pentamers will interact with at most five molecules of antigen. Individual antibody-combining sites are most often of low affinity but the pentamerization potentiates the binding efficiency, demonstrated by the “avidity” of the antibody, a typical immunologist parameter not really defined in mathematical terms. IgM is very efficient in **complement** binding and thus is highly lytic for cellular targets, which may be bacteria or eukaryotic cells like red blood cells; in this case one uses the term *hemolysins*, rather than *hemagglutinins*, when the complement component is not participating in the final reaction.

The so-called natural antibodies are most often of the IgM type. This is the case of natural anti-A and anti-B hemagglutinins, described as the classical **alloantibodies** responsible for major transfusion incompatibilities. More generally speaking, natural antibodies are frequently endowed with **autoimmune** recognition properties and thus may bind a large variety of molecules, such as tubulin, actin, double-stranded DNA, and so on. These natural antibodies are harmless and most likely represent the basic repertoire of germline-encoded immunoglobulins, which therefore have nearly no somatic mutations. As a result, their specificity is very low, which makes them bind many antigens, although usually only weakly. Why these antibodies are not aggressive to the organism is still subject to debate, although the combination of two parameters, low affinity and low concentration, is possibly the answer.

As already mentioned, IgM is the first group of isotypes to be produced upon primary immunization. Whenever the antigen is T-dependent, which is the most frequent situation, IgM is rapidly replaced by IgG, which will warrant a better affinity because of the acquisition and selection of somatic hypermutations. Immunization with polysaccharides, which are essentially T-independent antigens, will thus be limited to the production of IgM antibodies. In phylogeny, IgM is also the first group of immunoglobulin classes that have been identified in primitive fishes. It should be mentioned that the classical immune response, with the existence of circulating antibodies, seems to have occurred with the lower vertebrates. Invertebrates have, however, other types of responses to fight very efficiently against pathogens.

See also entries Antibody, Immune Response, Immunoglobulin, and J Chain.

Suggestion for Further Reading

A. C. Davis and M. J. Shulman (1989) IgM-molecular requirements for its assembly and function. Immunol. Today **10**, 118–128.

Illegitimate Recombination

Illegitimate recombination includes those events that do not fall into any of the more clearly defined categories of recombination (homologous recombination, **site-specific recombination**, and transposition). Illegitimate recombination may itself include an assortment of types of events. Parental DNA molecules or DNA segments in illegitimate recombination often share a few homologous base pairs. Some of these events result from DNA replication errors and others from joining broken DNA ends. Illegitimate recombination generates deletions and translocations and therefore can have profound genetic consequences.

One type of illegitimate recombination widely studied in bacteria results from slippage between the template and newly replicated DNA strands. The prototype for this mechanism is that suggested by Streisenger et al. (1) for generating frameshift mutations at points of repeated nucleotides. For example, DNA containing on one strand A_5 can generate A_4 or A_6 by loss or gain of a base pair by the following proposed mechanism. Replication pauses within the repeat. The newly synthesized strand unwinds and anneals with the template, but out of register, leaving one or more nucleotides as a single-stranded loop on either the template or the newly synthesized strand. Replication resumes, and this newly synthesized strand has fewer or more nucleotides than the parent. In the absence of repair synthesis, another round of faithful replication fixes the mutation.

A similar event can occur between direct repeats of any sequence that may or may not be separated by intervening base pairs. If the repeats do not themselves have internal repeats, interaction between them produces a deletion or duplication of one copy of the repeat plus the intervening sequence. One could imagine that these events occur by homologous recombination where the repeats are out of register (unequal crossing over), but in *Escherichia coli* these events are independent of known homologous recombination functions. The events are not reciprocal, that is, a deletion is not formed concurrently with a duplication. Deletions can occur between repeats separated by thousands of base pairs, although the frequency decreases as this separation becomes larger (2).

Linear DNA introduced into mammalian cells by transfection often undergoes illegitimate recombination by integration into the genome or by end-joining. End-joining has been extensively studied and occurs by ligation of the ends without any apparent requirement for homology. If excision of nucleotides from one or both ends occurs before or after transfection, a few homologous base pairs may be exposed, and annealing may occur between them. Filling of gaps and ligation can generate a novel joint. These events may be paradigms for integration of exogenous linear DNA and for chromosomal translocations. These events typically occur between DNA molecules sharing little or no homology and may occur between broken chromosome ends that swap partners and rejoin.

The DNA ends that provoke illegitimate recombination may be generated by a variety of mechanisms. Linear DNA may be introduced into cells, as in transfection. Restriction Enzymes may be induced to cut DNA at special sites in cells. DNA **topoisomerases** make transient double-strand breaks that may be illegitimately rejoined. This process is stimulated by topoisomerase inhibitors. Pausing or termination of DNA replication generates single-strand gaps whose ends may provoke illegitimate recombination, perhaps after conversion of the gap into a double-strand break. The variety of mechanisms that generate breaks may account for the variety of types of illegitimate recombination observed in cells.

Illegitimate recombination is not entirely a haphazard process. Regulated forms of this process occur in generating functional immunoglobulin genes by gene rearrangements and in eliminating micronuclear DNA in *Tetrahymena* **macronucleus** development. Other types of recombination previously considered illegitimate are recognized now as site-specific recombination and transposition. Further studies of illegitimate recombination may reveal unappreciated mechanisms and the biological roles of these events.

Bibliography

1. G. S. Sreisinger et al. (1967) Cold Spring Harbor Symp. Quant. Biol. **31**, 77–84.
2. S. T. Lovett et al. (1994) Mol. Gen. Genet. **245**, 294–300.

Suggestions for Further Reading

3. N. D. Allgood and T. J. Silhavy (1988) "Illegitimate recombination in bacteria", In *Genetic Recombination* (R. Kucherlapati and G. R. Smith, eds.), American Society for Microbiology, Washington, D.C., pp. 309–330.
4. D. Erhlich (1989) "Illegitimate recombination in bacteria", In *Mobile DNA* (D. E. Berg and M. M. Howe, eds.), American Society for Microbiology, Washington, D.C., pp. 799–832
5. S. D. Ehrlich et al. (1993) Mechanisms of illegitimate recombination, Gene **135**, 161–166.
6. M. Meuth (1989) "Illegitimate recombination in mammalian cells", In *Mobile DNA* (D. E. Berg and M. M. Howe, eds.), American Society for Microbiology, Washington, D.C., pp. 833–860.
7. D. Roth and J. Wilson (1988) "Illegitimate recombination in mammalian cells", In *Genetic Recombination* (R. Kucherlapati and G. R. Smith, eds.), American Society for Microbiology, Washington, D.C., pp. 621–653.

Imaginal Disc

The past decade has witnessed enormous progress in understanding the molecular mechanisms that control the development of imaginal discs in insects. Lessons obtained from the studies of imaginal discs are being used to unravel mechanisms underlying vertebrate development, because many **genes** and developmental pathways are conserved throughout evolution.

The development of imaginal discs is a feature unique to the holometabolous insects (beetles, moths, flies, and butterflies). The life cycles of holometabolous insects include four stages: embryo, larva, pupa, and adult (also known as *imago*). Development through these stages does not occur simply by increasing the sizes of exiting structures; instead, it involves a dramatic transformation from larva to adult. The transformation is achieved by the replacement of larval tissues with a special population of cells, known as *imaginal discs*, which form sac-like structures residing inside the larva. Imaginal discs have been studied most extensively in the fruit fly *Drosophila melanogaster* (1-4). There are 10 major pairs of imaginal discs, which give rise to adult cuticular structures of the head and the thorax, and a single genital disc, which forms the adult genitalia. The location of the imaginal discs in the mature larva (third instar stage) is illustrated in Figure 1. Studies in *Drosophila* have shown that imaginal discs are initially set aside during embryogenesis, apart from most embryonic cells that will contribute to the larva. In the embryo, the imaginal disc precursor cells can be visualized by the expression of molecular markers or by their particular sizes, shapes, and movement. The imaginal discs appear in the newly hatched larva as local thickenings of the epidermis and, in the case of the wing disc, contain around 40 cells (5). Subsequently, the imaginal disc cells proliferate rapidly during larval stages. By the end of the larval stage, the largest imaginal disc, that of the wing, contains approximately 50,000 cells (6). During pupation, the imaginal disc cells go through morphogenetic movements, in response to a pulse of the molting hormone ecdysone, to give rise to specific adult structures, accompanied by the breaking-down of the larval tissues.

Figure 1. Locations of imaginal discs in a third instar larva, and the morphology of several major imaginal discs. There are 10 major pairs of imaginal discs, which give rise to adult cuticular structures of the head and the thorax, and a single genital disc, which forms the adult genitalia. (After Ref. 86)

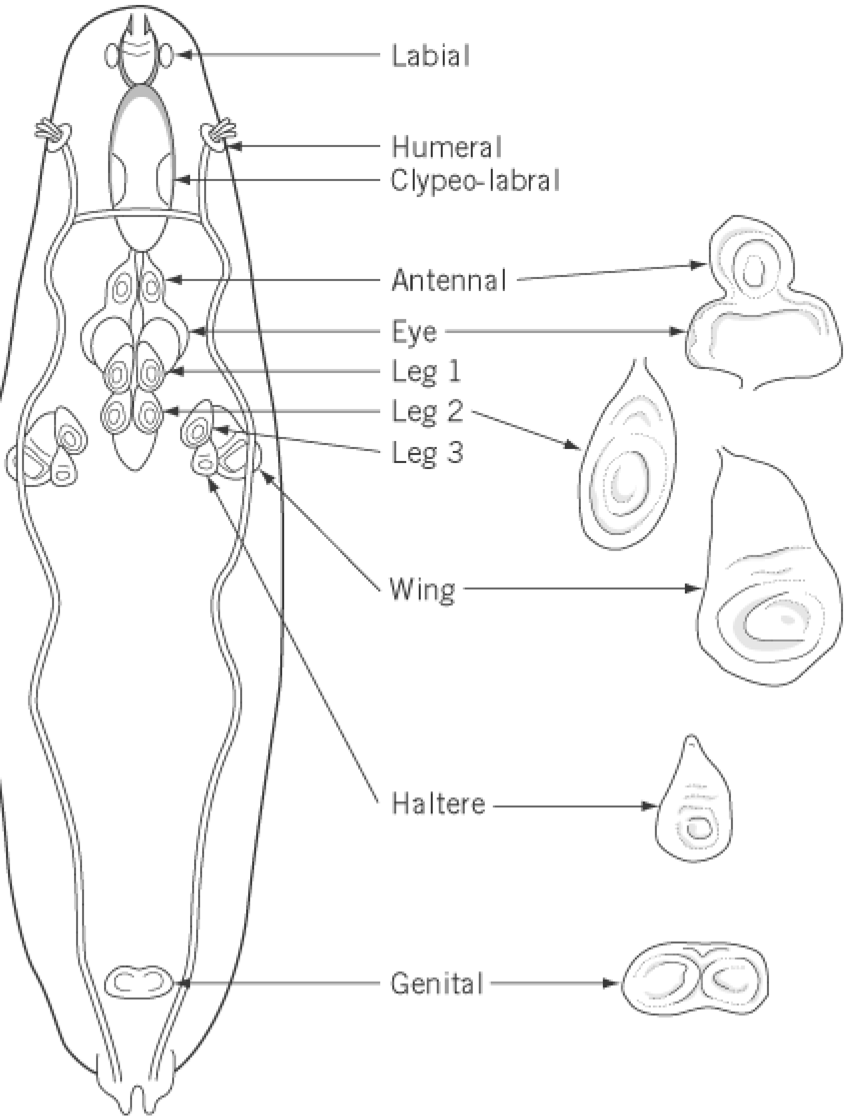

The molecular studies of imaginal discs in *Drosophila* have been addressing the following major questions. First, how are the imaginal disc precursor cells set aside (or established) during embryogenesis? Second, how is the growth of imaginal discs in the larva regulated? Third, how do developmental patterns form in the mature imaginal disc along its anterior–posterior, dorsal–ventral, and proximal–distal axes? And fourth, how is the identity of a given imaginal disc specified? The following is a brief summary of our current understanding on these topics.

1. Establishment of the Imaginal Disc Precursor Cells in the Embryo

The fate of imaginal disc precursor cells is determined by intersecting anterior–posterior and dorsal–ventral signals in the embryo. These signals are provided by two sets of patterning genes along the embryonic anterior–posterior and dorsal–ventral axes. Along the anterior–posterior axis, a regulatory hierarchy involving gap genes, pair-rule genes, and segment polarity genes determines the different cell fates. In particular, the activities of several segment polarity genes, including ***wingless*** (*wg*), ***engrailed*** (*en*), *patched* (*ptc*), and ***hedgehog*** (*hh*), are required for the consolidation of the parasegment boundaries, which appear during early development of the embryo (7, 8). Among these genes, *wg*, encoding a secreted molecule of the Wnt family of proteins (9), is required for the establishment of the thoracic wing and leg discs, which originate from primordia spanning the parasegment boundaries (10, 11). Like the anterior–posterior axis, the embryonic dorsal–ventral axis is also patterned by a hierarchy of maternal and zygotic genes. In particular, the decapentaplegic (dpp) protein, a member of the **transforming growth** factor b (TGF-b) gene family of signaling molecules (12), and other molecules in the dpp signaling pathway function to specify dorsal cell fates (13, 14). In contrast, the DER protein, the *Drosophila* **EGF receptor** homologue, and other genes in the DER signaling pathway are required to specify ventral cell fates (15, 16). The positions of the thoracic disc precursor cells along the dorsal–ventral axis are determined by the combined repressing activities of the dpp and the DER proteins, which limit the thoracic disc precursor cells to lateral positions of the embryo (17). Therefore, the thoracic disc precursor cells are established by the intersecting signals of Wg along the anterior–posterior axis, and dpp and DER along the dorsal–ventral axis.

2. Regulation of the Imaginal Disc Growth in the Larva

As mentioned above, imaginal discs increase their number of cells by thousands of fold during larval development. Misregulation of disc growth can result in imaginal discs with abnormal sizes and morphology. Genetic studies have identified a large number of mutants that are either defective or excessive in disc growth. The disc overgrowth mutants are of particular interest, because they may provide genetic models for tumor suppressor genes in humans. Recessive mutations in several dozens of genes have been identified that cause two types of disc overgrowth phenotypes: hyperplasia and neoplasia (18-20). Hyperplastic discs retain the normal epithelial organization and the capacity to differentiate, whereas the neoplastic discs do not. These several dozens of genes are known as tumor suppressor genes in *Drosophila*, and over 10 of them have been characterized molecularly. For example, one of these genes, *lethal(1)discs large* (*dlg*), is the first identified member of a evolutionary conserved family of proteins, called membrane-associated guanylate kinase homologues (MAGUKs) (21). In *Drosophila*, *dlg* is localized at and required for the formation of septate junctions in epithelial cells, and loss of *dlg* function causes epithelia to lose their organization and overgrow (22). Further studies of these *Drosophila* tumor suppressor genes are likely to shed light on general mechanisms in the regulation of cell proliferation.

3. Pattern Formation in the Imaginal Discs

3.1. Anterior–Posterior Patterning

Previous studies have shown that imaginal discs are subdivided into distinct cell populations, called compartments (23, 24). The compartmental boundary serves as a line of lineage restriction, and cells in one compartment do not intermingle with cells in the other. The anterior and posterior compartments of the thoracic discs can be traced back to the embryonic stage when the disc precursor cells are specified initially along the anterior–posterior axis of the embryos (25). In these discs, the posterior compartment is defined by the expression of the transcription factor *engrailed* (*en*) (26), which activates the expression of *hedgehog* (*hh*) in the same compartment (27, 28). In the wing disc, the hedgehog protein synthesized in the posterior compartment diffuses a short distance into the anterior compartment to induce the expression of *dpp* in a stripe of cells just anterior to the anterior–posterior boundary (27, 29). The decapentaplegic protein in turn acts as a long-range morphogen to organize the growth and patterning of the whole wing (30, 31) (Figure 2). The leg disc is very similar to the wing disc, except that in the leg disc the induction of *dpp* by the hedgehog protein is limited to the adjacent dorsal anterior cells, whereas the adjacent ventral anterior cells are induced by the hedgehog protein to express *wg* (32, 53). In addition, *dpp* and *wg* mutually repress the transcription of each other (Figure 3) (34, 35). The unpaired genital disc consists of three primordia, the female genital, the male genital, and the anal primordia. Each primordium of the genital disc is divided into anterior and posterior compartments. Here, *hh*, *dpp*, and *wg* are used to pattern each primordium in a manner similar to how they function in the leg disc (36, 37). In contrast to the wing, leg, and genital discs, the eye disc is not divided into any lineage-restricted compartments. Pattern formation in the eye disc is accompanied by movement of the morphogenetic furrow (MF), a morphological distinguishable indentation, which sweeps across the eye disc from posterior to anterior. Cells anterior to the MF are undifferentiated, whereas cells posterior to the MF undergo cellular differentiation (37). The initiation of eye disc differentiation is regulated by interactions between the positive regulator *dpp* and the negative regulator *wg*. Subsequently, the progression of differentiation requires *hh*. Despite the lack of the anterior and posterior compartments, the regulatory relationships between *hh*, *dpp*, and *wg* are retained in the eye disc. It has been shown that *dpp* and *wg* suppress the expression of each other, and the hedgehog protein produced by cells posterior to the MF induces *dpp* expression within the MF (39, 40).

Figure 2. Axis formation and gene expression in the developing wing. In the first instar larva, the wing disc has already posterior compartment is identified by the expression of *engrailed* (26). In the second instar larva, the dorsal–ventral axi identified by the expression of *apterous* (33). The dorsal-specific expression of *apterous* is maintained during third larva begins to be expressed in a region slightly anterior to the anterior–posterior boundary (87). The dorsal and ventral surfac of the late third instar disc: the perspective ventral surface folds under the dorsal one, while the wing blade unfolds and l wing blade region (X) is placed at the tip of the wing.(After Ref. 54.)

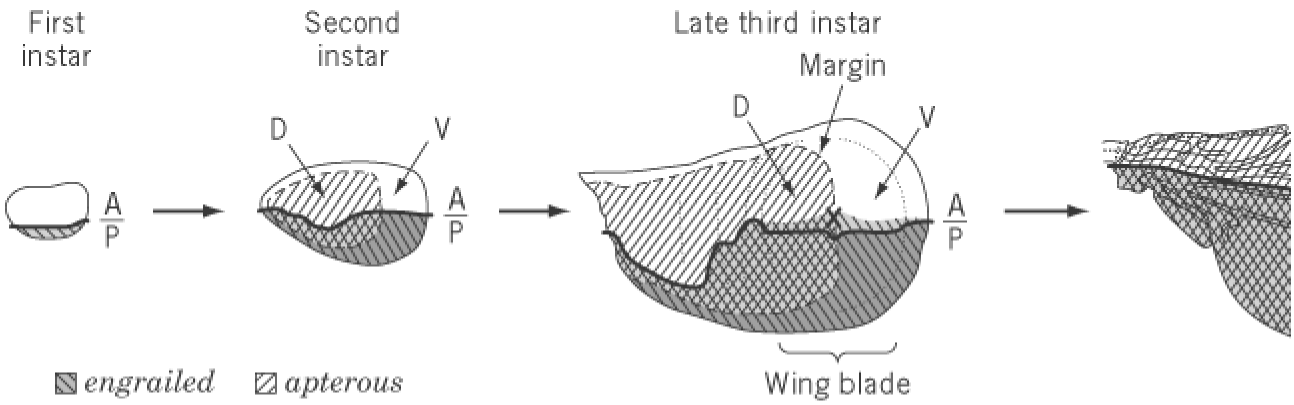

Figure 3. Spatial expression and regulatory interaction between *hedgehog* and other genes in the leg imaginal disc. The l cells diffuses across the anterior–posterior compartment boundary; it induces the adjacent dorsal anterior cells to express anterior cells to express *wingless* (32, 55). The central region of the disc, where *decapentaplegic* and *wingless* are coexpr and *aristaless* and defines the distal tip of the leg (68-70).(After Ref. 32.)

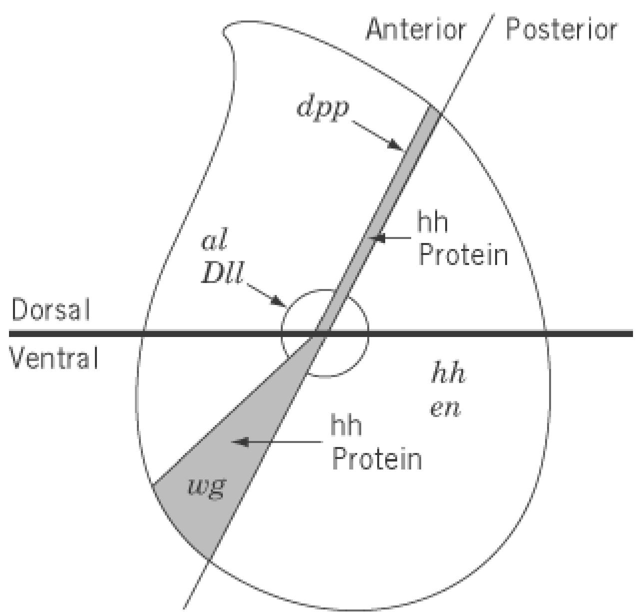

Several other components of the hedgehog signal transduction pathway have been identified. Positively-acting components of the pathway include the seven transmembrane protein smoothened

(41), the kinase fused (42), and the transcription factor **cubitus interruptus** (43); negatively-acting components of the pathway include the transmembrane protein patched (44, 45), protein kinase A (46-49), and the **kinesin**-related protein costal2 (50). The current model suggests that the patched and smoothened proteins constitute the receptor for the hedgehog signal (51). The cubitus interruptus protein, which is expressed only in the anterior cells due to the repression by the engrailed protein in the posterior compartment, forms a protein complex with the fused and costal2 proteins (50, 52). In some anterior cells, the cubitus interruptus protein is cleaved to generate a truncated form that translocates to the nucleus and represses *dpp* transcription. The hedgehog protein inhibits the proteolysis of the cubitus interruptus protein, leading to the expression of *dpp* in a stripe of anterior cells adjacent to the anterior–posterior boundary (53).

3.2. Dorsal–Ventral Patterning

During the second instar larval stage, the wing disc is also divided into dorsal and ventral compartments (23). The dorsal–ventral compartmental boundary lies at the future wing margin, which separates the upper surface of the wing from the lower one. Wing formation depends on the interactions between the dorsal and ventral cells (54). The dorsal selector gene *apterous* (*ap*), which encodes a LIM **homeodomain** protein, is expressed and required in the dorsal cells (33, 55-57), and it activates the expression of *fringe* (*fng*) in these cells (58). The fringe protein acts through two ligands of the **Notch** receptor, *Serrate* and *Delta* (59-63), to restrict the expression of downstream genes *wg* and *vestigal* (*vg*) along the dorsal–ventral boundary, which in turn coordinate wing growth and patterning (64-66).

3.3. Proximal–Distal Patterning

Besides the anterior–posterior and dorsal–ventral axes, appendages (wing and leg) also possess a proximal–distal axis. It appears that interactions between the anterior–posterior and dorsal–ventral axes of the disc are critical for patterning along the proximal–distal axis (67). In the leg, the hedgehog protein secreted from the posterior compartment induces the adjacent dorsal anterior cells to express *dpp* and ventral anterior cells to express *wg*. The region where *wg* and *dpp* are coexpressed expresses *Distal-less* and *aristaless*, which defines the most distal part of the leg (68-71). Accordingly, a secondary proximal–distal axis can be induced when a new intersection point of *wg* and *dpp* expression is generated in the leg disc. Similarly in the wing disc, the intersection of *dpp* expression along the anterior–posterior boundary and *wg*–*vg* expression along the dorsal–ventral boundary corresponds to the distal tip of the wing.

4. Specification of the Imaginal Disc Identity

Although patterning of all imaginal discs share some common features, the identity of an individual imaginal disc is specified by the **homeotic** and other selector genes. Homeotic genes in the **Bithorax** and **Antennapedia** complexes are involved in the specification of head and thoracic discs (72). For example, ***Ultrabithorax*** (*Ubx*) is expressed in the haltere, but not in the wing disc, and specifies the haltere fate (73-75). Loss of *Ubx* function in the haltere results in a haltere-to-wing transformation, generating the famous four-winged fly (76). The homeotic gene *Antennapedia* (*Antp*) specifies the leg disc, and ectopic expression of *Antp* in the eye–antenna disc results in antenna-to-leg transformation (77, 78). However, homeotic genes are not the only genes that are used to specify disc identity. The *Drosophila* ***Pax*** family gene *eyeless* (*ey*), which encodes a protein containing a paired domain and a homeodomain, is required for the determination of the eye disc fate (79). Ectopic expression of *ey* can induce ectopic eye development in other imaginal discs (80). Several genes have been shown to act downstream of *ey* in this process, including *eyes absent*, *sine oculis*, and *dachshund* (81, 82).

Studies of imaginal disc development in *Drosophila* have shed new light on various aspects of vertebrate development. For example, gene expression and functional studies suggest a striking similarity between fly appendages and vertebrate limbs (32, 67, 83, 84). The dorsal–ventral boundary of the wing disc is analogous to the apical ectoderm ridge (AER), which is a major signaling center for the developing vertebrate limb. The posterior compartment of the wing disc is analogous to the zone of polarizing activity (ZPA), the source of the morphogen, sonic hedgehog, that patterns the anterior–posterior axis of the vertebrate limb bud. In addition, several key regulatory genes in patterning imaginal discs have been implicated in human diseases. For example, mutations in the human *patched* gene are responsible for basal cell carcinoma, a common form of human cancer (85).

Bibliography

1. S. M. Cohen (1993) In *The Development of Drosophila melanogaster* (M. Bate and A. Martinez Arias, eds.), Cold Spring Harbor Laboratory Press, Cold Spring Harbor NY, pp. 747–841.
2. P. J. Bryant (1978) In *The Genetics and Biology of Drosophila* (M. Ashburner and T. R. F. Wright, eds.), Academic Press, London, pp. 229–335.
3. H. Oberlander (1985) In *Comprehensive Insect Physiology, Biochemistry and Pharmacology*, Vol. **2** (G. A. Kerkut and L. I. Gilbert, eds.), Pergamon Press, Oxford, pp. 151–182.
4. J. R. S. Whittle (1990) In *Seminars in Cell Biology*, Vol. **1**, (P. W. Ingham, ed.), Saunders, Philadelphia, pp. 241–252.
5. M. M. Madhavan and H. A. Schneiderman (1977) Wilhem Roux"s Arch. **183**, 269–305.
6. J. W. Fristrom (1972) In *The Biology of Imaginal Discs* (H. Ursprung and R. Nothiger, eds.), Springer-Verlag, Berlin, pp. 109–154.
7. J. Hooper and M. P. Scott (1992) In *Early Embryonic Development of Animals*, Vol. **18**, (W. Hennig, ed.), Springer-Verlag, Berlin, pp. 1–48.
8. A. Martinez Arias (1993) In *The Development of Drosophila melanogaster* (M. Bate and A. Martinez Arias, eds.), Cold Spring Harbor Laboratory Press, Cold Spring Harbor, NY, pp. 517–608.
9. R. Nusse and H. E. Varmus (1992) Cell **69**, 1073–1087.
10. S. M. Cohen (1990) Nature **343**, 173–177.
11. B. Cohen, A. A. Simcox, and S. M. Cohen (1993) Development **117**, 597–608.
12. D. M. Kingsley (1994) Genes Dev. **8**, 133–146.
13. E. L. Ferguson and K. V. Anderson (1992) Cell **71**, 451–461.
14. D. Morisato and K. V. Anderson (1995) Annu. Rev. Genet. **29**, 371–399.
15. E. Raz and B. Z. Shilo (1993) Genes Dev. **7**, 1937–1948.
16. N. Perrimon and L. A. Perkins (1997) Cell **89**, 13–16.
17. S. Goto and S. Hayashi (1997) Development **124**, 125–132.
18. E. Gateff (1994) Int. J. Dev. Biol. **38**, 565–590.
19. E. Gateff et al. (1996) Int. J. Dev. Biol. **40**, 149–156.
20. K. L. Watson, R. W. Justice, and P. J. Bryant (1994) J. Cell Sci. Suppl. **18**, 19–33.
21. D. F. Woods and P. J. Bryant (1991) Cell **66**, 451–464.
22. D. F. Woods and P. J. Bryant (1989) Dev. Biol. **134**, 222–235.
23. A. Garcia-Bellido, P. Ripoll, and G. Morata (1973) Nature New Biol. **245**, 251–253.
24. P. A. Lawrence and G. Morata (1976) Dev. Biol. **50**, 321–337.
25. A. Martinez-Arias and P. A. Lawrence (1985) Nature **313**, 639–642.
26. T. Kornberg, I. Siden, P. O"Farrell, and M. Simon (1985) Cell **40**, 45–53.
27. J. J. Lee, D. P. von Kessler, S. Parks, and P. A. Beachy (1992) Cell **71**, 33–50.
28. T. Tabata, S. Eaton, and T. B. Kornberg (1992) Genes Dev. **6**, 2635–2645.
29. T. Tabata and T. B. Kornberg (1994) Cell **76**, 89–102.
30. J. Capdevila and I. Guerrero (1994) EMBO J **13**, 4459–4468.
31. D. Nellen, R. Burke, G. Struhl, and K. Basler (1996) Cell **85**, 357–368.
32. N. Perrimon (1995) Cell **80**, 517–520.

33. B. Cohen, M. E. McGuffin, C. Pfeifle, D. Segal, and S. M. Cohen (1992) Genes Dev. **6**, 715–729.
34. W. J. Brook and S. M. Cohen (1996) Science **273**, 1373–1377.
35. J. Jiang and G. Struhl (1996) Cell **86**, 401–409.
36. E. H. Chen and B. S. Baker (1997) Development **124**, 205–218.
37. F. Casares, L. Sánchez, I. Guerrero, and E. Sánchez-Herrero (1997) *Dev. Genes Evol.* 216–228.
38. T. Wolff and D. F. Ready (1993) In *The Development of Drosophila melanogaster* (M. Bate and A. Martinez Arias, eds.), Cold Spring Harbor Laboratory Press, Cold Spring Harbor, NY, pp. 1277–1326.
39. U. Heberlein and K. Moses (1995) Cell **81**, 987–990.
40. J. E. Treisman and U. Heberlein (1998) Curr. Top. Dev. Biol. **39**, 119–158.
41. J. Alcedo, M. Ayzenzon, T. Von Ohlen, M. Noll, and J. E. Hooper (1996) Cell **86**, 221–232.
42. T. Préat et al. (1990) Nature **347**, 87–89.
43. S. Eaton and T. B. Kornberg (1990) Genes Dev. **4**, 1068–1077.
44. J. E. Hooper and M. P. Scott, Cell **59**, 751–765 (1989).
45. R. G. Phillips, I. J. Roberts, P. W. Ingham, and J. R. Whittle (1990) Development **110**, 105–114.
46. D. Pan and G. M. Rubin (1995) Cell **80**, 543–552.
47. J. Jiang and G. Struhl (1995) Cell **80**, 563–572.
48. W. Li, J. T. Ohlmeyer, M. E. Lane, and D. Kalderon (1995) Cell **80**, 553–562.
49. T. Lepage, S. M. Cohen, F. J. Diaz-Benjumea, and S. M. Parkhurst (1995) Nature **373**, 711–715.
50. J. C. Sisson, K. S. Ho, K. Suyama, and M. P. Scott (1997) Cell **90**, 235–245.
51. D. M. Stone et al. (1996) Nature **384**, 129–134.
52. D. J. Robbins et al. (1997) Cell **90**, 225–234.
53. P. Aza-Blanc, F. A. Ramirez-Weber, M. P. Laget, C. Schwartz, and T. B. Kornberg (1997) Cell **89**, 1043–1053.
54. S. S. Blair (1995) Bioessays **17**, 299–309.
55. J. A. Williams, S. W. Paddock, and S. B. Carroll (1993) Development **117**, 571–584.
56. F. J. Diaz-Benjumea and S. M. Cohen (1993) Cell **75**, 741–752.
57. S. S. Blair, D. L. Brower, J. B. Thomas, and M. Zavortink (1994) Development **120**, 1805–1815.
58. K. D. Irvine and E. Wieschaus (1994) Cell **79**, 595–606.
59. S. Artavanis-Tsakonas, K. Matsuno, and M. E. Fortini (1995) Science **268**, 225–232.
60. J. F. de Celis, A. Garcia-Bellido, and S. J. Bray (1996) Development **122**, 359–369.
61. F. J. Diaz-Benjumea and S. M. Cohen (1995) Development **121**, 4215–4225.
62. D. Doherty, G. Feger, S. Younger-Shepherd, L. Y. Jan, and Y. N. Jan (1996) Genes Dev. **10**, 421–434.
63. R. J. Fleming, Y. Gu, and N. A. Hukriede (1997) Development **124**, 2973–2981.
64. J. Kim, K. D. Irvine, and S. B. Carroll (1995) Cell **82**, 795–802.
65. V. M. Panin, V. Papayannopoulos, R. Wilson, and K. D. Irvine (1997) Nature **387**, 908–912.
66. J. Kim et al. (1996) Nature **382**, 133–138.
67. W. J. Brook, F. J. Diaz-Benjumea, and S. M. Cohen (1996) Annu. Rev. Cell Dev. Biol. **12**, 161–180.
68. G. Campbell, T. Weaver, and A. Tomlinson (1993) Cell **74**, 1113–1123.
69. K. Basler and G. Struhl (1994) Nature **368**, 208–214.
70. F. J. Diaz-Benjumea, B. Cohen, and S. M. Cohen (1994) Nature **372**, 175–179.

71. T. Lecuit and S. M. Cohen (1997) Nature **388**, 139–145.
72. A. Garcia-Bellido (1977) Am. Zool. **17**, 613–629.
73. P. A. Beachy, S. L. Helfand, and D. S. Hogness (1985) Nature **313**, 545–551.
74. G. Struhl (1982) Proc. Natl. Acad. Sci. USA **79**, 7380–7384.
75. S. D. Weatherbee, G. Halder, J. Kim, A. Hudson, and S. Carroll (1998) Genes Dev. **12**, 1474–1482.
76. E. B. Lewis (1978) Nature **276**, 565–570.
77. S. Schneuwly, R. Klemenz, and W. J. Gehring (1987) Nature **325**, 816–818.
78. G. Gibson and W. J. Gehring (1988) Development **102**, 657–675.
79. R. Quiring, U. Walldorf, U. Kloter, and W. J. Gehring (1994) Science **265**, 785–789.
80. G. Halder, P. Callaerts, and W. J. Gehring (1995) Science **267**, 1788–1792.
81. F. Pignoni et al. (1997) Cell **91**, 881–891.
82. R. Chen, M. Amoui, Z. Zhang, and G. Mardon (1997) Cell **91**, 893–903.
83. S. S. Blair (1997) Curr. Biol. **7**, R686–R390.
84. K. D. Irvine and T. F. Vogt (1997) Curr. Opin. Cell Biol. **9**, 867–876.
85. R. L. Johnson et al. (1996) Science **272**, 1668–71.
86. D. Fristrom and J. W. Fristrom (1993) In *The Development of Drosophila melanogaster* (M. Bate and A. Martinez Arias, eds.), Cold Spring Harbor Laboratory Press, Cold Spring Harbor, NY, pp. 843–897.
87. S. S. Blair (1992) Development **115**, 21–33.

Suggestions for Further Reading

88. S. M. Cohen (1993) "Imaginal disc development." In *The Development of Drosophila melanogaster* (M. Bate and A. Martinez Arias, eds.), Cold Spring Harbor Laboratory Press, Cold Spring Harbor, NY, pp. 747–841.
89. P. A. Lawrence and G. Struhl (1996) Morphogens, compartments, and pattern: lessons from *Drosophila*? Cell **85**, 951–961.
90. W. J. Brook, F. J. Diaz-Benjumea, and S. M. Cohen (1996) Organizing spatial pattern in limb development. Annu. Rev. Cell Dev. Biol. **12**, 161–180.
91. K. D. Irvine and T. F. Vogt (1997) Dorsal–ventral signaling in limb development. Curr. Opin. Cell Biol. **9**, 867–876.
92. J. E. Treisman and U. Heberlein (1998) Eye development in Drosophila: formation of the eye field and control of differentiation. Curr. Top. Dev. Biol. **39**, 119–158.

Immortalization

Cell lines isolated from normal tissue continue to proliferate for a fixed number of cell population doublings, after which the culture undergoes senescence; that is, it will undergo a culture age-dependent cessation of growth (1). Such cell lines are called *finite cell lines*, in contrast to *continuous cell lines* (see Cell Line). Several potential explanations have been proposed for their limited lifespan *in vitro*: nutritional deficiency, cumulative genetic damage, delayed interaction with an infectious agent, or genetically programmed aging. Although there are, undoubtedly, cell lines that die out soon after isolation, due to nutritional deficiency or infectious agents such as mycoplasma, there is now overwhelming evidence that the replicative lifespan is programmed into cells (2-4). This has been established by **somatic cell** hybridization and microcell fusion experiments, which have shown that there are at least ten dominant **genes** that will re-establish a finite lifespan in continuous cell lines after fusion with cells from a finite cell line (5, 6). The identity of these genes is not clear, but their interaction with cell cycle regulators has been suggested (7). As finite cells show progressive shortening of their telomeres with successive generations in culture, until replication is no longer possible, regulation of telomerase (8-10) or an alternative mechanism for maintenance of telomere length (11), is now the most likely regulator of replicative lifespan. The vast majority of continuous cell lines from tumors (11, 12) re-express telomerase, which is capable of regenerating the truncated telomere at each cycle, thereby preventing cessation of cell division. Reintroduction of the telomerase gene extends the lifespan (13, 14) and may, ultimately, prove to be the most satisfactory means of immortalizing cells, particularly if under the control of a regulatable promoter.

Agents used to immortalize cell lines, such as irradiation, mutagens, **oncogenes**, or viral genes such as **SV40 virus** large T Antigen, adenovirus E1a, or HPV E7, interact with cell-cycle regulatory proteins, such as p53 and **retinoblastoma** proteins and the cyclin/Cdk complexes, either directly or via mutation (15). Mutations may be induced directly by irradiation; alternatively, interactions with p53 and other genome guardian proteins may allow spontaneous mutations to be propagated and not repaired or eliminated from the cell population. While these mutational events may lead directly to inactivation of senescence genes, it is also possible that reduced cell cycle control and DNA surveillance allows cells to proceed beyond their normal lifespan, allowing time for small minority populations of cells expressing telomerase to appear, particularly if one of the mutations was in a telomerase repressor (16).

Senescence was first described with human diploid fibroblasts but has been shown to occur for other cell types (10) and other species (17). There is a general relationship between the proliferative lifespan *in vitro*, the age of the donor individual, and the average lifespan of the species. Cell lines derived from embryos and young individuals will generally survive longer than cell lines from older donors; moreover, cell lines from long-lived species generally survive longer than those from short-lived species, although this correlation is less well established than that with donor age. Not all cell lines will senesce; notable exceptions are cell lines derived from mice or from tumors of many species. In these cases, evidence of senescence can still be seen, but transformed cells appear within the population and eventually overgrow, producing continuous cell lines. Such immortalized cell lines have been generated spontaneously from many species, such as Syrian (18) and Chinese hamsters (19), cows (20), and monkeys (21, 22), but rarely from normal human or chick cells. Because spontaneous immortalization is such a rare event in normal human cell lines, when it does occur, it begs the question as to whether the cell lines from which immortal lines do arise are really normal, or whether they were already genetically predisposed by one or more initiating mutations in a positively acting **oncogene** by or deletion or inactivation of a negatively acting tumor suppressor gene.

Transformation is a term with many different meanings, depending on the context in which it is used (see Neoplastic Transformation). Transformation of cultured cells implies a heritable **phenotypic** change resulting from a spontaneous or experimentally induced genomic alteration. It is usually associated with an increased life-span and alterations in growth control, and it may, but does not always, give rise to a tumorigenic cell line. There are at least three discernible processes: immortalization, development of aberrant growth control, and neoplastic transformation. A cell line may become immortal without becoming neoplastic or losing many aspects of normal growth control, such as contact inhibition, density limitation of cell proliferation, or anchorage dependence. Examples of this are NIH-3T3 primitive mouse embryo mesodermal cells and BHK21 baby hamster kidney fibroblasts. However, both of these may progress to fully transformed lines: 3T3 cells spontaneously (23) (by maintenance at high cell density) and BHK21 by infection with a transforming virus, such as **polyoma** (10). It is not clear whether immortalization is a prerequisite for neoplastic transformation or aberrant growth control, although life-threatening progressive neoplasia almost certainly requires immortalization of one or more stem lines of the tumor.

Immortalization can be defined as the acquisition of an infinite lifespan, usually taken as in excess of 100 population doublings, while, in this context, transformation implies loss of growth control mechanisms, such as growth factor or serum dependence, G1 cell cycle arrest, contact inhibition of cell motility, density limitation of cell proliferation, dependence of cell proliferation on anchorage to, and spreading on, a substrate, and increased production of secreted proteinases such as plasminogen activator. Neoplastic transformation implies that the cells will grow as an invasive tumor *in vivo* and usually incorporates all, or most of, the growth control aberrations listed above. It is possible, therefore, that there are only two stages, immortalization and transformation, which need not have a fixed temporal relationship to one another.

Immortalization can also be induced by agents that interfere with growth regulatory genes, or senescence genes (5, 6). These may be physicochemical agents, such as high energy irradiation (24), oncogenes (25) or viral genes, such as SV40 large T antigen (26), E1a from adenovirus, E6 and E7 from papilloma viruses (27), and Epstein–Barr virus genes (28). Viral immortalization can be achieved by transfection of the appropriate viral genes or infection with whole virus. The second has biohazard safety implications and requires, for safe handling, demonstration that the immortalized cells do not produce infectious virus. For this reason, transfection of cloned genes, most commonly SV40 large T antigen, is generally preferred. Typically, transfected cultures arrest at the M1 stage of the cell cycle, but a few morphologically altered clones will continue to proliferate. These can be picked or selected as resistant if cotransfected with a selectable marker, such as resistance to G418 or hygromycin B (29). These clones are usually pooled and subsequently undergo crisis (M2), a cessation of growth, from which a small fraction of cells may grow through to form a continuous cell line. The frequency of occurrence of immortalization within a cell population may be as low as 1×10^9, or as high as 1×10^5.

Continuous cell lines have many advantages for routine culture (Table 1), mostly due to their higher growth rate and saturation density, their ability to proliferate in suspension, and their high plating efficiencies. These properties are associated with transformation, however, and continuous cell lines, which are immortalized but not transformed, will not give such high yields or plating efficiencies. As some interference with normal growth control mechanisms is implied in both immortalized and transformed cells, no continuous cell line can be said to be normal. However, cell lines that are immortalized, but not neoplastically transformed, may be said to be closer to the normal phenotype. In both cases, regrettably, there is a tendency to lose lineage markers and the capacity to differentiate (30, 31). However, there are a number of cases where differentiation and lineage markers are retained (24, 32) and there are good prospects for normal **gene expression**, post-transcriptional and post-translational modification, and phenotypic expression. Such cell lines may be useful for the production of proteins by protein engineering, such as factor VIII (33), or as vectors for further transfection studies. The advent of telomerase-induced immortalization, particularly if the gene is introduced with a promoter that is temperature- or hormone-sensitive, may prove to be the best way forward for generating immortalized cell lines capable of both indefinite replication and expression of differentiation under appropriate conditions.

Table 1. Properties of Transformed Cells[a]

Growth Characteristics	Genetic Properties	Structural Alterations	Neoplastic Properties
Immortal	High spontaneous mutation rate	Modified actin cytoskeleton	Tumorigenic

Anchorage independent: clone in agar, may grow in stirred suspension	Aneuploid	Loss of cell-surface-associated fibronectin	Angiogenic
Loss of contact inhibition	Heteroploid	Increased lectin agglutination.	Enhanced proteinase secretion, eg, plasminogen activator
Growth on confluent monolayers of homologous cells "focus" formation	Overexpressed or mutated oncogenes	Modified extracellular matrix	Invasive
Reduced density limitation of growth: high saturation density, high growth fraction at saturation density	Deleted or mutated suppressor genes	Altered expression of cell adhesion molecules (cadherins, integrins)	
Low serum requirement	Stable or elongated telomeres	Disruption in cell polarity	
Growth-factor-independent	Overexpressed telomerase or ALT genes		
High plating efficiency			
Shorter population doubling time			

[a] Modified from Freshney: *Culture of Animal Cells. A Multimedia Guide,* 1999 Wiley-Liss, New York.

Bibliography

1. L. Hayflick and P. S. Moorhead (1961) Exp. Cell Res. **25**, 585–621.
2. S. Goldstein, S. Murano, H. Benes, E. J. Moerman, R. A. Jones, and R. Thweatt (1989) Exp. Geront. **24**, (5–6) 461–468.
3. S. E. Holt, J. W. Shay, and W. E. Wright (1996) Nature Biotechnol. **14**, (July) 836–839.
4. M. Sasaki, T. Honda, H. Yamada, N. Wake, and J. C. Barrett (1994) Cancer Res. **54**, 6090–6093.
5. O. Pereira-Smith and J. Smith (1988) Proc. Natl. Acad. Sci. USA **85**, 6042–6046.
6. T. Ogata, D. Ayusawa, M. Namba, E. Takahashi, M. Oshimura, and M. Oishi (1993) Mol. Cell. Biol. **13**, 6063–6043.
7. G. H. Stein, L. F. Drullinger, R. S. Robetorye, O. M. Pereira-Smith, and J. R. Smith (1991) Proc. Natl. Acad. Sci. USA **88**, 11012–11016.
8. J. W. Shay, H. Werbin, and W. E. Wright (1994) Mol. Cell. Diff. **2**, 1–21.
9. C. W. Greider and E. H. Blackburn (1996) Sci. Am. (Feb.) **274**, 92–97.
10. P. Konig and D. Rhodes (1997) Trends Biochem. Sci. (Feb.) **22**, 43–47.

11. T. M. Bryan and R. R. Reddel (1997) Eur. J. Cancer **33**, 767–773.
12. S. Bachetti and C. M. Counter (1995) Intl. J. Oncol. **7**, 423–432.
13. A. G. Bodnar, M. Ouellette, M. Frolkis, S. E. Holt, C.-P. Chiu, G. B. Morin, C. B. Harley, J. W. Shay, S. Lichsteiner, and W. E. Wright (1998) Science **279**, 349–352.
14. H. Vaziri and S. Benchimol (1998) Curr. Biol. **8**, 279–282.
15. E. K. Parkinson (1996) in *Culture of Immortalized Cells*, R. I. Freshney, and M. G. Freshney eds., Wiley-Liss, New York, pp. 1–23.
16. M. Oshimura and J. C. Barrett (1997) Eur. J. Cancer **33**, 710–715.
17. R. J. Hay and B. L. Strehler (1967) Exp. Gerontol. **2**, 123.
18. I. Macpherson, and M. Stoker (1962) Virology **16**, 147.
19. T. T. Puck, S. J. Cieciura, and A. Robinson (1958) J. Exp. Med. **108**, 945–956.
20. P. Del Vecchio and J. R. Smith (1981) J. Cell. Physiol. **108**, 337–345.
21. H. Hopps, B. C. Bernheim, A. Nisalak, J. H. Tjio, J. E. Smadel (1963) J. Immunol. **91**, 416–424.
22. Y. Gluzman (1981) Cell **23**, 175–182.
23. D. Brouty-Boyé, R. W. Tucker, J. Folkman (1980) Intl. J. Cancer, **26** 501–507.
24. N. A. Punchard, D. Watson, R. Thompson, and M. Shaw (1996) in *Culture of Immortalized Cells*, R. I. Freshney, M. G. Freshney eds., Wiley-Liss, New York, pp. 203–237.
25. T. L. Morgan, D. Yang, D. G. Fry, P. J. Hurlin, S. K. Kohler, V. M. Maher, and J. J. McCormick (1991) Exp. Cell Res. **197**, 125–136.
26. L. V. Mayne, T. N. C. Price, K. Moorwood, J. F. Burke (1996) in *Culture of Immortalized Cells*, R. I. Freshney, M. G. Freshney eds., Wiley-Liss, New York, pp. 77–93.
27. G. A. Seigel (1996) In Vitro Cell Dev. Biol.—Animal **32**, 66–68.
28. B. J. Bolton and N. K. Spurr (1996) in *Culture of Immortalized Cells*, R. I. Freshney and M. G. Freshney eds., Wiley-Liss, New York, pp. 283–298.
29. J. Sambrook, E. F. Fritsch, and T. Maniatis (1989) *Molecular Cloning, a Laboratory Manual*, 2nd ed., **3** vols. Cold Spring Harbor Laboratory Press, Cold Spring Harbor, NY.
30. H. C. Isom and I. Georgoff (1984) Proc. Natl. Acad. Sci. USA **85**, 9783–9787.
31. D. Wynford-Thomas (1996) in *Culture of Immortalized Cells*, R. I. Freshney, M. G. Freshney eds., Wiley-Liss, New York, pp. 183–201.
32. J. F. Burke, T. N. C. Price, and L. V. Mayne (1996) in *Culture of Immortalized Cells*, R. I. Freshney, M. G. Freshney, eds. Wiley-Liss, New York, pp. 299–313.
33. F. Moldovan, H. Benanni, J. Fiet, O. Cussenot, J. Dumas, C. Darbord, and H. R. Soliman (1996) In Vitro Cell Dev. Biol.—Animal **32**, 16–23.

Immune Response

The immune response is a complex sequence of events initiated by the introduction of an immunogen in an organism. In vertebrates, it is the consequence of the stimulation of B and/or T lymphocytes, leading either to the production of specific **antibodies** from B cells or to the occurrence of effector **T cells**—for example, cytotoxic T lymphocytes. Immunologists classically make a clear distinction between immune responses that are characterized by antibody production and those that result primarily in the emergence of cytotoxic T cells or delayed-type hypersensitivity, which are depicted as humoral and cellular immunity, respectively. In fact, penetration of complex

antigens, such as most bacteria and **viruses**, trigger both types of immune responses. Furthermore, antibody responses directed against T-dependent antigens, the most common case, require cellular cooperation between B and T cells, and the humoral and cellular responses are quite intricate.

It must be realized that both the nature and the intensity of the immune response is largely dependent on the nature, dose, and mode of penetration of the antigen. For example, when given subcutaneously or intravenously, proteins stimulate a good circulating antibody response, provided that they are given in an immunogenic range of doses. If given orally, mucosal antibody production will occur preferentially. By contrast, intradermal injection will induce delayed hypersensitivity, mediated by T lymphocytes. The level of response may be substantially increased by admixing antigen with adjuvants that ensure a long-lasting liberation of antigen, in addition to providing nonspecific stimulation of the immune system.

Whatever the nature of the response, it always follows basic principles that are most simply quantified in a classical humoral response. Following antigen administration, two parameters may be followed: One is the disappearance of antigen from the body fluid, and the other is the occurrence of circulating antibodies. After a first immunization, the blood concentration of antigen decreases rapidly within a few hours, remains somewhat steady for a few days, and then rapidly decreases again, until it is no longer detectable. This occurs after 5 to 7 days, when antibodies start to be produced. As they circulate in the bloodstream, they bind to the remaining antigens, and the immune complexes are eliminated (which may be a major problem for individuals suffering renal failure). The antibodies that first appear are IgM. Their yield increases for a few days, until they are replaced by IgG antibodies that result from class switching of the isotype. The antibody titer slowly diminishes and becomes barely detectable. This is a typical primary response. As B cells start making IgG antibodies in germinal centers of peripheral lymph nodes, they rapidly accumulate somatic hypermutations so that antibodies with higher affinity will occur and be positively selected by antigen. A fraction of these B cells will constitute the long-lived memory cells that will react immediately upon a second administration of antigen. The secondary response then takes place, characterized by a rapid elevation of the IgG antibody titer, which will remain high for a much longer period of time. If a different antigen were used instead of the first one, a typical primary response would have been observed, and this is illustrative of the high specificity of the immune response. Antigen may be given several times, ensuring a successive boost of responses, leading to a hyperimmunized state.

The general kinetics described above are typical of T-dependent soluble antigens. With polysaccharides, there is no secondary response, and the antibodies remain essentially of the IgM type (with some IgG2a and IgA2 in humans). The immune response to particulate antigens, such as bacteria, is generally more complex, due to antigenic diversity. The respective contribution of humoral and cellular responses is largely dependent on the microorganism.

See also entries Antibody, Antigen, Immunogen, and Immunization.

Suggestions for Further Reading

P. F. Searle and L. S. Young (1996) Immunotherapy II: antigens, receptors and costimulation. Cancer Metastasis Rev. **15**, 329–349.

J. Mestecky, S. M. Michalek, Z. Moldoveanu, and M. W. Russell (1997) Routes of immunization and antigen delivery systems for optimal mucosal immune responses in humans. Behring Inst. Mitt. **98**, 33–43.

Immunity

Immunity may be defined as a resistant state conferred on a living organism by a wide variety of cells and molecules that tend to eliminate pathogens or aggressive agents, thus ensuring the individual's integrity. Immunologists often make a distinction between natural, or innate, and adaptive immunity, although the latter is also quite “natural” when understood as a basic physiological phenomenon. It might be advisable to use instead the concept of nonspecific versus specific, but even this is not entirely satisfactory, because the limits are not so clear. This is well illustrated by the opposed views that were expressed at the end of the nineteenth century by those, like Metchnikoff, who supported the cellular basis for immunity, centered on the phagocytic properties of the macrophage and those, like Ehrlich, who gave a major role to circulating **antibodies**, thus supporting humoral immunity. In fact, both mechanisms are part of the organism defenses; and the macrophage, which was initially considered to have nonspecific phagocytic potentialities, turned out to be able to acquire some specificity by opsonisation—that is, the binding of antibodies of the various isotypes to its **Fc receptors**. Much more recently, the ability of macrophages to process and present protein antigens proved definitively that all these partners could be linked and that a clear-cut distinction was primarily a scholastic dispute. Defense mechanisms are quite diversified in the living world, although vertebrates have developed a highly complex immune system endowed with an adaptive response that can face a huge potential antigenic repertoire because of a sophisticated genetic organization that may express at any given time millions of different and specific **immunoglobulins** or **T cell receptors** (TCRs) produced by B cells and T cells, respectively. Invertebrates have also developed immune defenses against pathogens that involve, in addition to phagocytic cells or soluble enzymes, mechanisms like those described in insects, which have a limited repertoire of genetically encoded peptides endowed with diverse bacteriolytic, antiviral, or antiparasite activities.

One may consider that the defense mechanisms that operate in vertebrates are organized on successive levels. The first one involves cutaneous and mucosal barriers that ensure a physical protection, as well as a chemical one, including enzymes such as lysozyme that can have a bactericidal effect. The second level is used whenever pathogens have entered the bloodstream. Examples of efficient but nonspecific mechanisms that can be mobilized quickly are (a) phagocytosis by monocytes and macrophages, (b) inflammatory reaction that produces many cytolytic factors, (c) lytic activity initiated by components of the **complement** cascade, (d) natural killer (NK) cells, and (e) various **cytokines**, with special reference to interferons that block viral replication, and so on. Simultaneously, the adaptive immune response is initiated, leading to the occurrence of the first wave of IgM antibodies, which are soon replaced by more efficient IgG, and/or to the emergence of cytotoxic T lymphocytes, which are of prime importance in destroying virus-infected cells. Vaccination will reinforce immunity by stimulating a specific immune response to major dangerous pathogens, allowing the organism to react quickly with the appropriate B- and T-cell responses when a natural infection takes place.

See also entries Antigen, Antibody, Autoimmunity, Immunogen, Immune Response.

Suggestions for Further Reading

M. C. Carroll and A. P. Prodeus (1998) Linkages of innate and adaptive immunity. Curr. Opin. Immunol. **10**, 36–40.

H. Kohler and S. Paul (1998) Superantibody activities: new players in innate and adaptive immune responses. Immunol. Today **19**, 221–227.

Immunity, Transposon

For some transposable elements, the frequency at which they insert into a target DNA that already contains a copy of the element is much reduced from their frequency of insertion into that same DNA lacking a copy of the transposable element (Fig. 1). This inhibition does not represent a global inhibition of transposition within the cell: The inhibition is specifically cis-acting on the DNA that contains the transposable element. This inhibition is called *transposition immunity* or *target immunity*. Although target immunity is usually evaluated in intermolecular transposition reactions, it is likely that a principal function of this phenomenon is to discourage intramolecular transposition—that is, to prevent the insertion of a mobile element into itself or into adjacent donor backbone. Target immunity has the effect of discouraging insertions locally and promoting insertion at a distance from the donor site of the mobile element .

Figure 1. Target immunity. For some elements such as Mu and Tn7, the frequency with which they insert into a target DNA already containing a copy of the element is much reduced. A target DNA already containing a copy of the transposon is a poor target because the target binding protein (small circle) is not effectively bound to the immune target. Binding of the target protein is discouraged by transposition proteins that bind specifically to the transposon ends in the immune target DNA.

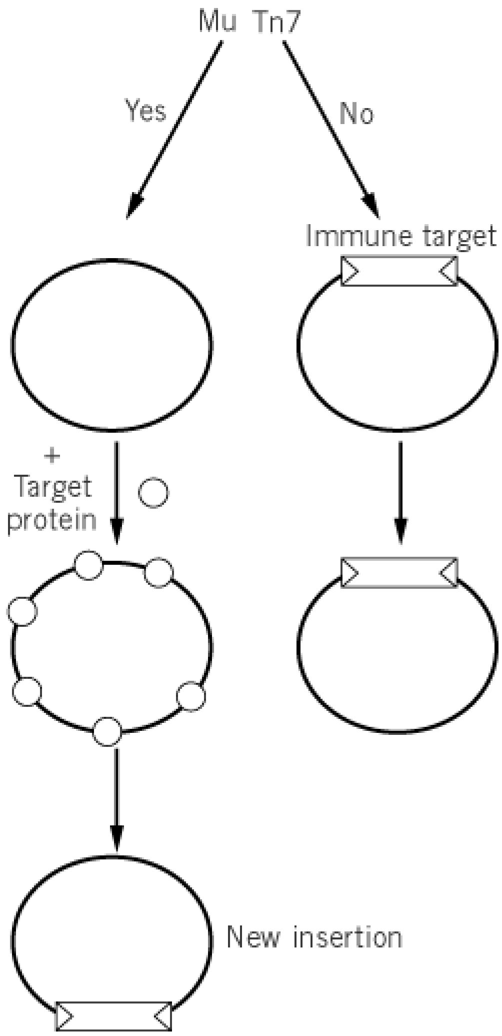

Target immunity has been observed for a number of bacterial elements. The phenomenon was first observed with Tn3-like transposons and subsequently with bacteriophage **Mu** (1), and Tn7 (2, 3), a **drug-resistance** element. Phage Mu uses multiple rounds of transposition to set up replication forks that promote phage replication during lytic growth. Through transposition immunity, Mu ensures that new insertions made during the replication process will not be into extant copies of Mu, destroying these copies; thus transposition immunity facilitates Mu replication.

The mechanism of immunity has been dissected *in vitro* with Mu (4, 5), and Tn7 (6, 7). Common features of these elements are that the activity of the transposase is controlled by an ATP-dependent regulatory protein that interacts with the transposase and the target DNA via an ATP-dependent **DNA-binding** activity. Transposition occurs when the transposase interacts with this regulatory protein in an ATP-bound state on the target DNA. The ATP state of the regulatory protein is key to its activity, promoting transposition when it exists in an ATP-bound state on the target DNA and being inactive in a non-ATP state removed from the target DNA. As described below, the state of the ATP regulatory protein appears to be the key to immunity. A reasonable model is that the establishment of immunity involves discouraging the interaction of the ATP-dependent regulatory protein with the target DNA (Fig. 1).

In all systems examined, target immunity is imposed on a potential target DNA by the DNA sequence ends of the transposon—that is, the *cis*-acting recombination sequences at the ends of the transposon that are the transposase recognition sites. An attractive model for immunity is that when the transposase interacts with transposon end sequences on the potential target DNA, it exists on the target DNA in high local concentration and actively discourages the interaction of the ATP-dependent regulatory protein with the target DNA, thus effectively clearing the target DNA of targeting protein and discouraging transposition into that DNA. The ends of the transposon with bound transposase appear to interact with the target protein by simple protein–protein interactions facilitated by DNA looping (5, 7).

It seems likely that different forms of the transposase will interact with the target protein to execute transposition and transposition immunity. In Tn7, for example, immunity can be imposed by one of the protein components of the transposase, while actual transposition requires collaboration between both protein subunits of the transposase (7). In other cases, such as Mu, different forms of transposase, for example in different oligomeric states, may signal these different reactions.

Retroviruses also show a form of immunity in that intramolecular insertion is discouraged, although they show no inhibition for insertion into DNAs containing retroviral ends (8). The ability to block intramolecular insertion has been correlated with a requirement for a particular human protein (9), but the role of this protein and the mechanism of retroviral immunity remain to be established.

Bibliography

1. A. Darzins, N. E. Kent, M. S. Buckwalter, and M. J. Casadaban (1988) Proc. Natl. Acad. Sci. USA **85**, 6826–6830.
2. L. K. Arciszewska, D. Drake, and N. L. Craig (1989) J. Mol. Biol. **207**, 35–52.
3. B. Hauer and J. A. Shapiro (1984) Mol Gen Genet. **194**, 149–158.
4. K. Adzuma and K. Mizuuchi (1988) Cell **53**, 257–266.
5. K. Adzuma and K. Mizuuchi (1989) Cell **57**, 41–47.
6. R. J. Bainton, K. M. Kubo, J.-N. Feng, and N. L. Craig (1993) Cell **72**, 931–943.
7. A. Stellwagen and N. L. Craig (1997) EMBO J. **16**, 6823–6834.
8. M. S. Lee and R. Craigie (1994) Proc. Natl. Acad. Sci. USA **91**, 9823–9827.
9. M. S. Lee and R. Craigie (1998) Proc. Natl. Acad. Sci. USA **95**, 1528–1533.

Immunization

Immunization occurs as the result of the penetration of an immunogen in an organism, leading to the stimulation of the immune system and the production of **antibodies** and/or T-cell effectors that specifically recognize the initiating antigen. Immunization may occur naturally, upon penetration of a pathogen, bacteria, virus, or parasite, and requires several days before becoming fully effective fighting the invader. This may be too slow to ensure efficient protection, and this led to the development of systematic vaccinations against major pathogens. The word *vaccination* originates from the first vaccine that was directed against smallpox, using the cross-reactive vaccinia virus. Used on a worldwide basis, it led to the complete eradication of this severe disease, and thus is no longer in use. Major vaccines used in humans include tetanus, **diphtheria**, measles, **polio**, mumps, rubella, **influenza**, rabies, **hepatitis B**, and a few others. Vaccines are most frequently administered by injection, but sometimes orally, as in the case of the live attenuated poliovirus vaccine. A vaccine may be used as the full pathogen after it has been inactivated, or as an attenuated genetic variant. One also can use a purified molecule that has been isolated from the pathogen or genetically engineered.

For laboratory purposes, immunization generally aims at producing antibodies for immunochemical analysis. Conventional polyspecific antibodies are generally prepared in mice, guinea pigs, rabbits, or goats. There is no standard immunization procedure, but only some general guide lines that define basic conditions for good immunogenicity. Besides using an appropriate dose, the antigen might have to be conjugated to a carrier protein. Use of adjuvant, most frequently the complete Freund's adjuvant, is admixed with the immunogen. Finally, repeated injections will increase both the affinity and the titer of the antibodies generated.

See also entries Antigen, Antigen Processing, Presentation, Antibody, Immune Response, and Immunogen.

Suggestions for Further Reading

W. M. McDonnell and F. K. Askari (1997) Immunization. JAMA **278**, 2000–2007.

E. Manickan, K. L. Karem, and B. T. Rouse (1997) DNA vaccines. A modern gimick or a boon to vaccinology? Crit. Rev. Immunol. **17**, 139–154.

Immunoaffinity Chromatography

Immunoaffinity chromatography (IAC) is a widely used method for the selective extraction of **antibodies** or other biomolecules on the basis of the biospecific affinity between an antibody (Ab) and its antigen (Ag) (1). The antigen may be a small molecule (a hapten) or a macromolecule (M) such as an enzyme, a hormone, a growth factor, and so on. IAC has been used for many years for the purification of antibodies by immobilized antigens and also for the purification of antigens (enzymes, receptors, hormones, growth factors, etc.) by antibodies anchored to inert carriers. The antibodies used can be polyclonal, provided that a pure antigen is injected to obtain the antibodies and that strict specificity is ascertained. It is often advisable to use anti-peptide (sequence-oriented) polyclonal antibodies to reduce the danger of heterogeneity in the specificity of the antibody population. Monoclonal antibodies are usually a very good choice because they are homogeneous and directed against a distinct epitope. Under ideal conditions, antibody columns allow separation of specific peptides or proteins from crude mixtures in one step. The procedure for an IAC purification involves the same steps described for affinity chromatography.

A major difficulty in the use of immobilized antibodies is the high affinity of some antibodies for their antigens. This sometimes makes the recovery of active enzymes difficult, because the harsh conditions that are required in the elution step bring about either an inactivation of the enzyme or the loss of an important regulatory function. Among the eluents that have (and are) being used in IAC are buffers with a low pH (2.2) or a high pH (11.5), **chaotropes** (5 M KSCN), or mild **denaturants** such as urea (3.5 to 8 M) or **guanidinium** salts (2–6 M). Therefore, attempts are sometimes made to purify by exclusion (also known as "reverse immunoadsorption"). In this procedure, the contaminating proteins are the ones to be adsorbed and removed, while the desired protein is excluded (2).

With the introduction of monoclonal antibodies in IAC, it became possible to use homogeneous immunoglobulins not only directed against a distinct antigenic determinant (3, 4) and to tailor their affinity. A lowered affinity permits milder conditions for elution and reduces the possibility of irreversible denaturation during the elution step. As expected, the use of monoclonal antibodies has had a significant impact in biochemistry, in molecular biology, and in medicine.

Bibliography

1. M. A. J. Godfrey (1997) In *Affinity Separations* (P. Matejtschuk, ed.), IRL Press, Oxford University Press, New York, p. 141.
2. J. A. Weare, J. T. Gafford, N. S. Ur, and E. G, Erdos (1982) Anal. Biochem. **123**, 310.
3. G. Kohler and C. Milstein (1975) Nature (London) **256**, 495.
4. J. W. Goding (1980) J. Immunol. Methods **39**, 285.

Immunoassays

Immunoassays are a collection of techniques for measuring biological or synthetic materials, using **antibodies** specific for those materials. Immunoassays are also applied in reverse, in which a purified antigen or hapten is used to quantify an uncharacterized antibody preparation. The common element in all immunoassays is the interaction of an antibody with a ligand. The assay methods differ in the accessory chemical reactions that take place prior to, or as a consequence of, ligand binding, and in the instrumentation used to detect the binding event or subsidiary reaction. Radioimmunoassays and enzyme-linked immunosorbent assays (ELISA) are especially widely used types of immunoassay. Others are complement fixation, agglutination, Farr Assay, and Ouchterlony Double Diffusion. They are listed as separate entries and not discussed here. Below, we sketch the principles underlying the most common immunoassay methods relevant to molecular biology.

1. Fluorescence Quench

The emission of a photon as a molecule returns to its electronic ground state from an excited state produces **fluorescence**. "Quenching of fluorescence" refers to chemical interactions that allow an excited state to dissipate its energy through a nonradiative mechanism (see Fluorescence Quenching). Common mechanisms that can cause quenching include collisions with solvent, protonation or deprotonation reactions, resonance energy transfer, and collisions or static contact with quenchers. Quenchers encompass a huge variety of substances, from molecular oxygen to heme proteins, and the binding of a quencher to an antibody can easily be measured. Quenchers most relevant to immunoassays are aromatic organic molecules, which are frequently used as haptens. These molecules are thought to cause nonradiative deexcitation by transiently accepting electrons from the excited state of a fluorophore.

Tryptophan is the only strongly fluorescent naturally occurring amino acid, and antibody sequences usually show an abundance of exposed Trp residues in the antigen-combining site (1). Consequently, binding of a quenching antigen or hapten to an antibody nearly always causes decrease of Trp fluorescence from the antibody. Furthermore, the fluorescence decrease is generally linear with the number of combining sites filled; hence it is a direct measure of the degree of saturation of the antibody (2). Bound and free Ab as a function of added ligand can be calculated and displayed as a Scatchard Plot or used for direct fitting to a binding equation to determine the antibody valency and the association equilibrium constant for binding the ligand. Fluorescence quench on antigen binding is a very desirable technique for immunoassay, because it allows direct measurement of antibodies and antigens interacting in solution and can be performed without chemical labeling of the molecules under study with reporter groups.

2. Fluorescence Anisotropy or Fluorescence Polarization

This method relies on the change in molecular tumbling rate that occurs when an antibody–antigen complex forms. Fluorescence anisotropy is most appropriate for antibody-antigen pairs that are of different molecular size (3), and may be applicable even if no overt change in fluorescence signal results from complex formation.

Plane-polarized light absorbed by a fluorophore will (to a first approximation) be emitted with the same plane of polarization, unless the fluorophore molecule reorients during the lifetime of its excited state. Since the tumbling rate is a function of molecular size, polarization of emitted light is very sensitive to complex formation. A small molecule will tumble rapidly, hence the orientation of an excited state fluorophore will randomize, and fluorescence emission will be isotropic. In contrast, a large molecule will tumble slowly; hence emission from a fluorophore will remain polarized. A small molecule that binds to a large molecule will take on the tumbling characteristics of the large molecule. For example, anisotropic emission from a fluorescent tag on a small antigen will sharply increase on complexation with a large antibody. To use this principle for a quantitative immunoassay, fluorescence anisotropy is measured separately for the free antigen and fully complexed antigen. Between these two limiting values, anisotropy will be linear with the extent of antigen complexation; hence the degree of complex formation in a test sample may be inferred from the observed anisotropy.

Fluorescence anisotropy is measured by exciting a fluorophore with polarized light and observing fluorescence intensity through a polarizing filter oriented parallel ($I_{\parallel}$;) or perpendicular ($I_{\perp}$;) to the excitation plane. The relative intensities from the parallel and perpendicular emissions are used to calculate anisotropy or polarization from the equations:

$$\text{Anisotropy} = \frac{I_{\parallel} - I_{\perp}}{I_{\parallel} + 2I_{\perp}} \quad (1)$$

$$\text{Polarization} = \frac{I_{\parallel} - I_{\perp}}{I_{\parallel} + I_{\perp}} \quad (2)$$

Although polarization and anisotropy are very closely related, equations relating observed intensities to ligand binding and other phenomena are generally simpler when expressed in terms of anisotropy; hence this is the preferred parameter. Fluorophores used for anisotropy measurements of proteins, such as fluorescein and **dansyl**, typically have excited-state lifetimes of 5 ns. This lifetime is on the same order as the tumbling times of protein antigens. The small, globular protein lysozyme, for example, also has a rotational correlation time of 5 ns (4); hence a fluorescein label on lysozyme would show considerable depolarization of fluorescence. Intact IgG has a rotational correlation time of 220 ns; hence its complex with the labeled lysozyme would show strong fluorescence anisotropy.

One complication to the fluorescence anisotropy technique is the occurrence of local motions affecting the fluorophore, often referred to as "segmental flexibility." The timescale for these local motions can be sufficiently fast to reorient the fluorophore and depolarize emission, even if the fluorophore is attached to a large, slowly tumbling macromolecule (5).

3. Phosphorescence or Time-Resolved Fluorescence

Phosphorescence is a fluorescence phenomenon in which, for quantum-mechanical reasons, the excited state of a fluorophore cannot easily return to the ground state by emission of a photon. Emission does occur, but on a much longer timescale than is normal for fluorescence. Because of this long lifetime, the presence of even small amounts of quenching agents such as O_2 is sufficient to suppress observation of any signal from naturally phosphorescent biological compounds. Phosphorescence is measured by exciting a sample with a pulsed light source, waiting an interval for short-lived fluorescence states to decay, then integrating photon counts during the remaining dark period before the next pulse. This ability to resolve short-lived from long-lived fluorescence is the chief advantage of a phosphorescent probe, as background phosphorescence of biological samples is almost nil. By contrast, the steady-state fluorescence background is often quite high, and the signal-to-background ratio in short-lived fluorescence-based assays is a more common limitation of sensitivity of an assay than the absolute magnitude of the signal.

Europium is the most common phosphorescent probe in time-resolved fluorescence immunoassays (6). This metal ion is attached to antibodies or antigens through bifunctional linker molecules containing a chelate moiety at one end and a group reactive with protein residues at the other. In a typical assay, a trapping antibody is immobilized on a solid support, antigen in a test sample is allowed to bind, and then the Eu^{3+}-labelled antibody is allowed to bind the trapped antigen. After washing away unbound reagents, Eu^{3+} is extracted from the antibody in low pH buffer containing phosphorescence enhancing agents (7). These agents act both by sequestering the Eu^{3+} ion from quenchers and transferring absorbed light to the Eu^{3+} ion. The fluorescence emission is integrated repetitively over several hundred microseconds, using a stroboscopic fluorimeter. Comparison of the response from the test sample to a standard curve constructed with known concentrations of analyte allows determination of the concentration of analyte in the test sample.

4. Chemiluminescence

Chemiluminescence is a phenomenon related to fluorescence, in which an electronic excited state of a molecule is reached through a chemical reaction. Emission of a photon, which is optically detected, returns the molecule to the ground state. A chemiluminescent immunoassay involves an antibody or antigen that has been covalently tagged with a molecule capable of participating in a chemiluminescent reaction. The tag remains inert through immunologic steps such as antigen or secondary antibody binding. Subsequent mixing with a trigger solution initiates the luminescent reaction.

A chemiluminescent immunoassay to detect an antigen typically begins with immobilization of a capture antibody on a solid support. The test sample is added, followed by the tagged detection antibody. Luminol was the first luminogenic tag to be used for an immunoassay (8), but derivatized acridinium esters are now more common (9, 10). Unbound reagents are washed away, and luminescence is determined in a luminometer. This device combines two automated functions (11). First, trigger solutions (alkaline H_2O_2 in the case of acridinium labels) are added to the sample to initiate the luminescence reaction. Mixing is usually complete in less than 1 s. Next, a detector, usually with photon-counting electronics, measures light emission from the sample over a defined time interval, typically 10 s. As with other immunoassays, the response of a test sample is compared to the responses from a set of standards to determine the analyte concentration in the test sample.

Because photon emission from luminescent tags can be induced to occur quantitatively over the span of a minute, as compared to radioactive decay of isotopic isotopes, which continues over months in the case of ^{125}I, chemiluminescent assays are inherently very sensitive. ELISA assays that use a luminogenic substrate, which are sometimes referred to as “chemiluminescent immunoassays,” are perhaps the most sensitive of all assays. Combination of an enzyme tag on the antibody and a luminogenic enzymatic reaction yields a degree of amplification that can detect as little as 1000 molecules of analyte (12).

Bibliography

1. E. A. Padlan (1990) Proteins **7**, 112–124.
2. H. N. Eisen (1964) Meth. Med. Res. **10**, 115–121.
3. E. Haber and J. C. Bennett (1962) Proc. Natl. Acad. Sci. USA **48**, 1935–1942.
4. B. P. Maliwal and J. R. Lakowicz (1984) Biophys. Chem. **19**, 337–344.
5. W. B. Dandliker and G. A. Feiger (1961) Biochem. Biophys. Res. Commun. **5**, 299–304.
6. K. Pettersson, H. Siitari, I. Hemmilä, E. Soini, T. Lövgren, V. Hänninen, P. Tanner, and U.-H. Stenman (1983) Clin. Chem. **29**, 60–64.
7. I. Hemmilä, S. Dakubu, V.-M. Mukkala, H. Siitari, and T. Lövgren (1984) Anal. Biochem. **137**, 335–343.
8. J. S. A. Simpson, A. K. Campbell, M. E. T. Ryall, and J. S. Woodhead (1979) Nature **279**, 646–647.
9. I. Weeks, I. Behesgti, F. McCapra, A. K. Campbell, and J. S. Woodhead (1983) Clin. Chem. **29**, 1474–1479.
10. I. Weeks, M. Sturgess, R. C. Brown, and J. S. Woodhead (1986) Meth. Enzymol. **133**, 366–387.
11. P. E. Stanley (1986) Meth. Enzymol. **133**, 587–603.
12. L. J. Kricka (1993) Clin. Biochem. **26**, 325–331.

Suggestions for Further Reading

13. J. R. Lakowicz (1983) *Principles of Fluorescence Spectroscopy*, Plenum Press, New York. (Rigorous but very readable description of fluorescence and other optical techniques and their use in biological applications.)
14. C. P. Price and D. J. Newman, eds. (1997) *Principles and Practice of Immunoassay*, 2nd ed., Macmillan, London. (Comprehensive treatment covering many types of immunoassay.)
15. E. P. Diamandis and T. K. Christopoulos, eds. (1996) *Immunoassay*, Academic Press: New York.
16. R. F. Masseyeff, ed. (1993) *Methods of Immunological Analysis*, VCH, New York. (An ambitious 12-volume series that is truly a comprehensive treatment of immunoassay methods. Volume **1**, W. H. Albert and N. A. Staines, eds., *Fundamentals*, contains many treatments that are of general utility regardless of instrumental method.)

Immunoelectron Microscopy

In molecular biology, the location of specific molecules in organelles and cells at the microscopic level has gained prominence in recent years through the development of a wide range of cytochemical techniques. These techniques are based upon the property that specific markers can be chemically coupled to a wide variety of molecules. Examples are fluorescent markers for light microscopy and electron-dense markers, such as ferritin or colloidal gold, for electron microscopy. The use of poly- and monoclonal antibodies has widened the possibility of localization to essentially every particle that can invoke an immunogenic response. The antibodies produced can be bound to markers used in microscopy and the distribution of the molecules of interest visualized directly by 1-, 2-, or 3-step labeling procedures (1).

Immunocytochemistry is the application of antibodies in labeling protocols and must be performed in an aqueous environment to ensure that the antigen detectability is accurate and reproducible. Hence, cryotechniques are much preferred over the classical technique of chemical fixation, dehydration, and plastic embedment, which usually results in a loss of antigenicity. Along with cryofixation and cryosectioning, the use of colloidal gold is now commonplace. Colloidal gold has numerous advantages, among which are (i) it is electron dense and easily visualized in electron microscope images; (ii) various sizes of gold particles can be obtained, allowing double-labeling experiments; (iii) it can be easily complexed with a wide variety of ligands; and (iv) the maintenance of bioactivity of complexed molecules is excellent. Typically, the primary antibody binds to the antigen of interest and is visualized by labeling with a secondary antibody to which colloidal gold is conjugated in analogy to the use of fluorescent antibodies in immunofluorescence. With immunogold labeling, certain considerations should be addressed before starting (2). (i) Where is the antigen located? Additional preparative steps may be necessary to make the antigen accessible to the gold antibody. (ii) What is the nature of the antibody? A monoclonal antibody may not bind the antigenic site if the site is modified during electron microscope preparation; this problem is generally much less severe with cryotechniques. Polyclonal antiserum, which contains a number of different antibodies directed against more than one epitope on the antigen, is less susceptible to conformational changes or modification of the antigen. (iii) From which species were the antibodies derived? Care should be exercised to ensure that antibodies are raised to pure undenatured antigens in a species compatible with the labeling system.

A recent advance in photooxidation has allowed for precise correlative immunolocalization on the same specimen using fluorescent light and immunoelectron microscopies (3). With use of this technique, proteins can first be localized to individual cells or tissue types at the light microscope level with an antibody containing a suitable fluorescent label such as eosin. Subsequently, the protein can be further localized at the electron microscope level by illuminating the fluorophore in the presence of oxygen and diaminobenzidine. Fluorophores with a relatively poor quantum yield, such as eosin, produce reactive oxygen intermediates that oxidize the diaminobenzidine, producing a brown osmophilic polymer. Preparation of these specimens for electron microscopy by osmium fixation yields a highly localized osmium stain at the antigen. Fluorescence photooxidation can also be used with nucleic acid sequences by using biotinylated probes and an eosin–streptavidin conjugate (see Streptomycin).

Bibliography

1. M. J. Dykstra (1993) *A Manual of Applied Techniques for Biological Electron Microscopy*, Plenum Press, New York.
2. J. R. Harris (1991) *Electron Microscopy in Biology*, IRL Press, Oxford.
3. T. J. Deerinck et al. (1994) J. Cell Biol. **126**, 901–910.

Immunoelectrophoresis

If an antibody specific for the protein of interest is available, immunological detection and immunoelectrophoresis are the preferred methods for identification of that protein. Specifically, since the immuno-reactive site on a protein need not be affected by any post-translational modifications of a protein, immunological identification is the principal method for the recognition of a particular gene product in an electrophoretic pattern. Blotting of protein gel electrophoresis patterns to a membrane, with subsequent exposure of the blot to antibody, is the primary tool of immunological identification. More than any other factor, it is responsible for the possibility to construct protein databases from the hundreds to thousands of spots separable by two-dimensional gel electrophoresis .

Immunoelectrophoresis is the electrophoresis of one or more macromolecule in gels containing specific antibodies against them. Depending on the relative concentrations of the antibody and macromolecule, plus their affinity for each other, they interact to form complexes, which can then **immunoprecipitate** within the gel. The precipitates are visible within the gel. In this way, it is possible to quantify the amount of macromolecule present, by measurement of the size of the “rocket” produced and comparison with a known standard concentration (1). The antigenic relationships between proteins can be inferred from the precipitation patterns generated when the two are subjected to immunoelectrophoresis in adjacent wells of the gel, so that their precipitation patterns overlap (Fig. 1). If the overlapping rockets behave independently, the two molecules responsible are not immunologically related. If, however, they generate “fused rockets,” at least some of the same antibody molecules recognize both macromolecules. Crossed immunoelectrophoresis (Fig. 1) consists of an initial gel electrophoresis separation of the macromolecules of interest, followed by their electrophoresis at a right angle to the initial separation into a gel containing the antibody; this technique can yield particularly high resolution (3).

Figure 1. Crossed immunoelectropherogram of human serum. First dimension: Electrophoresis occurred in 1% (w/v) agarose, sodium barbital buffer, pH 8.6, 0.02 *M* ionic strength, at 10 V/cm and 15°C, for 70 min, with the anode to the left. The circular well where the sample of human serum was applied is visible at the right. Second dimension: Electrophoresis occurred in the same gel and gel buffer, but containing 12.5 μl rabbit antibody against human serum/cm^2 of gel, at 2 V/cm, for 20 h, with the anode at the top. The antibody is isoelectric at pH 8.6 and therefore stationary during electrophoresis. (Fig. 3 of (1)).

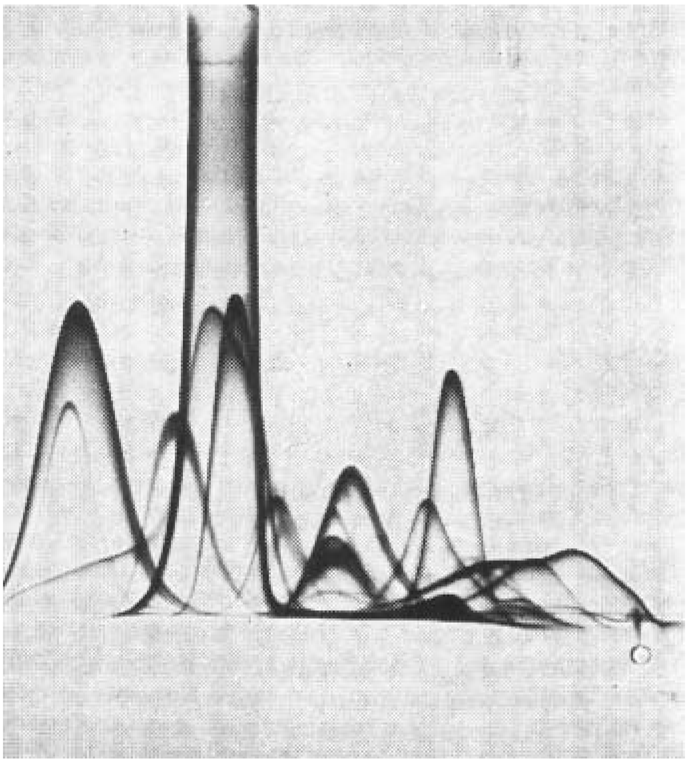

Bibliography

1. N. H. Axelsen, J. Kroll, and B. Weeke (1973) Scand. J. Immunology, Supplement 1, **2**, 1–169.
2. J. Clausen (1969) In *Immunochemical Techniques for the Identification and Estimation of Macromolecules* (T. S. Work and E. Work, eds.), North Holland, Amsterdam, pp. 400–572.
3. C.-B. Laurell (1972) Scand. J. Clin. Lab. Invest., Supplement 124, **29**, 21–37.

Suggestion for Further Reading

4. C.-B. Laurell (1965) Antigen-antibody crossed electrophoresis. Anal. Biochem. **10**, 358–361.

Immunogen

Immunologists make the distinction between antigen and immunogen. This came from the observation that small molecules termed haptens could interact with **antibodies**, even though they were unable by themselves to stimulate an immune response. Raising anti-hapten antibodies therefore necessitates preparing a conjugate of the hapten with a carrier protein. On this basis, it was proposed to distinguish antigenicity from immunogenicity and, consequently, an antigen from an immunogen. Antigenicity describes the chemical structures that contribute to interaction with an antibody, whereas immunogenicity defines the properties of a molecule for inducing an immune response. Natural immunogens, as opposed to chemically derived hapten conjugates, possess the dual properties of inducing the immune response and interacting with the resulting antibodies. Thus one must consider that a protein molecule, which is recognized by the antibodies through its epitopes, also behaves as its own carrier. This simply results from the antigen processing/presentation mechanisms that take place in the antigen-presenting cells.

Because immunogenicity is linked to the presentation phenomenon, which is genetically regulated because it involves the active participation of molecules of the Major histocompatibility complex (MHC), it is largely dependent upon the genetic constitution of the animal that receives the antigen. It has long been noticed that one strain of mice will not respond to a given antigen, whereas another one would develop an excellent response. This was strictly correlated with the presence of certain **alleles** of the MHC genes and provided a clear demonstration that the immune response was under strict (dominant) genetic control. This is why two outbred individuals, chosen at random, will respond differently to the same antigen. See Antigen Processing, Presentation for a more comprehensive explanation of immunogenicity.

Finally it should be remembered that, depending on the conditions used for immunization, the same antigen may reveal itself as immunogenic or not. One important parameter is the dose of antigen given. Either too low or too high a dose may prevent immunization and even induce a **tolerant** state, so the correct dose must be carefully defined before deciding whether a molecule is immunogenic or not. Another parameter is the route of injection, which conditions the secondary lymphoid organs that will be encountered by the antigen. Also, immunogenicity may be greatly enhanced by the addition of adjuvants to the antigen solution. Immunogenicity therefore results from a large variety of causes and is far from depending solely on the nature of the immunogen.

See also entries Antibody, Antigen, Antigen Processing, Presentation, Epitope, Haptens, Immune Response, and Immunity.

Suggestions for Further Reading

M. Sela (1969) Antigenicity: some molecular aspects. Science, **166**, 1365–1374.

H. O. McDevitt et al. (1972) Genetic control of the immune response. Mapping of the Ir-1 locus. J. Exp. Med. **135**, 1259–1278.

Immunoglobulin

Immunoglobulins (Igs) are **glycoproteins** synthesized by B lymphocytes that are the agents for B-cell recognition in the immune system. They are expressed either at the surface of B lymphocytes, where they represent the B-cell receptor (BCR), or in a soluble form in the body fluids, especially in the bloodstream, where they are also designated as **antibodies**. Immunoglobulins exert a dual function: (a) They recognize native **epitopes** on the antigen surface and (b) they are endowed with biological or effector functions such as **complement** fixation, **active transport** through the placental barrier in mammals, fixation to a variety of cells that express specific receptors for the various Ig isotypes [**Fc receptors** (FcRs)], and so on. The number of potential epitopes that immunoglobulins may recognize is enormous. This is the repertoire problem. By contrast, the number of effector functions is very limited, which immediately raises a major problem for the organization of the Ig molecules, which must accommodate a high diversity of antibody combining sites at one end and rather conserved structures at the other end. This difficulty has been solved by a very special structural organization of Ig, which is the consequence of a very sophisticated organization of the **genes** that encode the Ig polypeptide chains.

1. The Basic IgG Topological Model

Immunoglobulins have a multichain structure characterized by the basic pattern of IgG, the major Ig class or isotype, which contains two identical heavy (H) **polypeptide chains** and two identical light (L) chains (Fig. 1). This basic pattern was defined in the 1960s as the result of many independent workers, but predominantly by Porter and Edelman, who received the Nobel Prize in 1972, and by Hilschmann, who reported the first amino acid sequences of human light chains. The H chains have a molecular weight of about 52 kDa, and the L chains have a molecular weight of 23 kDa. The IgG molecule is symmetrical and contains two identical antibody-combining (or antigen-binding) sites. It contains about 2% by weight carbohydrates, which are located on the COOH-terminal half of the heavy chains. B cells are clonally organized, so that each one makes an Ig of one particular specificity; the entire population of Ig of one individual is extremely heterogeneous. Hence, structural studies had to be performed primarily on monoclonal materials, either derived from the product of malignant cells (myeloma proteins) or from monoclonal antibodies. Until the beginning of the 1980s, most structural data were derived from amino acid sequencing, thereafter by DNA sequencing of complementary DNA or **genomic** DNA.

Figure 1. Topological model of the IgG molecule. The symmetrical molecule contains two identical H and two identical L chains, each having a variable (VH and VL) and a constant (CL, CH) region. The constant region of the heavy chain contains three homology regions (CH1, CH2, CH3) and a flexible hinge between CH1 and CH2, which makes the molecule accessible to proteolytic enzymes that will release the Fab (antigen binding) and Fc (crystallizable) fragments. Homology regions provide the structural basis to the domain organization of Ig molecules.

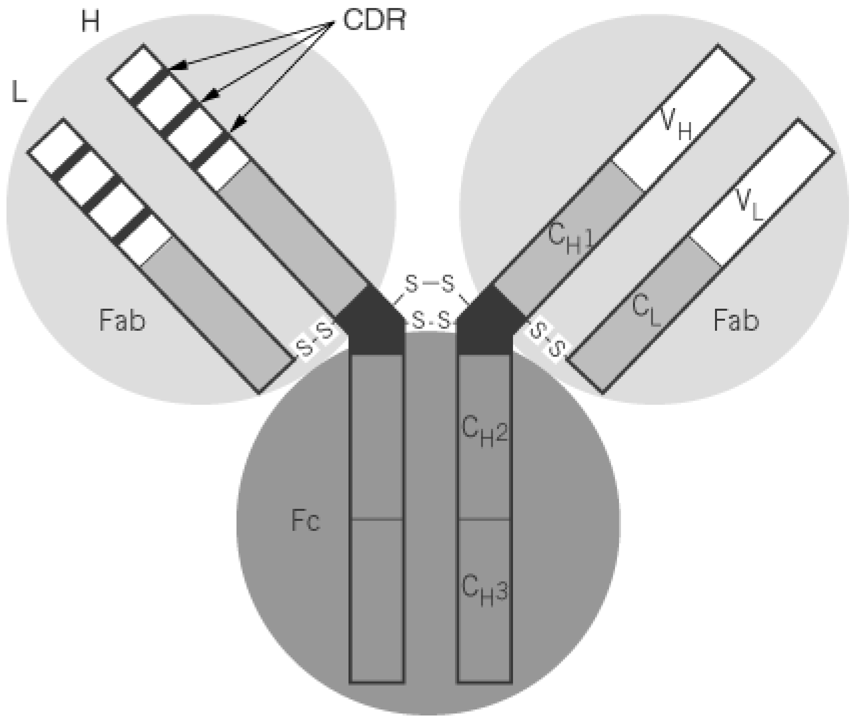

Structural analysis revealed that Igs were built in a very peculiar way, with a general organization centered on a pseudo-unit or homology region of about 110 amino acid residues containing an intrachain disulfide bond. The light chain contains two such regions: one NH_2-terminal, which is highly variable from one L chain to another, the so-called **variable region** or V_L, and one COOH-terminal, which is highly conserved between the various chains, termed C_L. There are two types of light chains, **kappa** (k) **and lambda** (l), built on the same model, but encoded by genes at different loci, K and L, respectively. The relative proportion of either type varies extensively from one animal species to another. In the mouse, k chain Ig account for 95% of the total, whereas the proportion is inverted in cattle or horses. In humans, the k/l ratio is approximately 60/40. Heavy chains are built on the same principle: They contain a V_H region of somewhat similar size and contain a C_H region that contains three homology regions, termed C_H1, C_H2, and C_H3. The NH_2-terminal half of the heavy chain, composed of V_H-C_H1 and designated the Fd fragment, is covalently bound by a disulfide bond to the light chain. The ensemble Fd-L is the Fab (for antigen binding fragment), whereas the COOH-terminal halves of the two heavy chains form the Fc (for crystallizable fragment) because they were initially obtained by Porter upon cleavage with papain. The complete IgG therefore contains two Fab fragments, each having one identical antigen binding site, because the molecule is a symmetrical one, and one Fc; each of these fragments has roughly the same molecular weight of 150 kDa. The short section of the heavy chains located between the Fab and the Fc fragments is flexible and, for that reason, accessible to **proteolytic** cleavage, and it is called the *hinge region*. Within both the V_H and V_L, cumulative sequence data have revealed the presence of **hypervariable** regions that have been shown to interact directly with epitopes and that were for this reason called *complementarity determining regions*, or CDR (see Immunoglobulin Structure).

2. Domain Organization and the Basic Ig Fold

The special general architecture of Ig, characterized by the existence of the homology regions, is of particular interest for several reasons. First, it strongly suggests that this is the result of a long series of gene duplications from an ancestral gene that might have encoded a basic 110-residue polypeptide chain from which constant and variable regions would have evolved, making possible the dual functions of Ig. Second, the gene duplication phenomenon has allowed effector functions to be amplified by the emergence of other immunoglobulin **isotypes**, which fall into five classes in higher vertebrates, termed IgG, IgM, IgA, IgD, and IgE. These molecules differ from each other structurally by the nature of the constant region of their heavy chains, which are g, m, a, d, and ε, respectively, whereas their light chains are the same. In the course of immunization, antibodies are the first of the IgM class, and there is a **class switch** later on to the production of another isotype, usually IgG, which represents 70% of circulating Ig. Because the V_H region is conserved during this switch and because the light chain remains unchanged, the antibody specificity is maintained, whereas new specialized biological functions have occurred, as described separately under specific headings.

The existence of homology regions has not only provided a basis for understanding the molecular evolution of immunoglobulins, but has also raised the point that, if these regions had diverged and been selected for the emergence of new biological functions, they had to be endowed with thermodynamic autonomy, so that each may acquire a three-dimensional (3-D) structure independently of the others; this is a prerequisite to achieve separate and specialized functions. This was the essence of the **domain** hypothesis, proposed in 1970 by Edelman, which was later fully verified when X-ray crystallography studies of antibodies and antibody–antigen complexes were reported. In fact, because of the presence of a floppy hinge region in the IgG molecule, it was not possible to get crystals of a complete molecule but, instead, of the separated Fab and Fc fragments, which turned out to have the same general multiglobular structure, precisely centered on each homology region or domain. This led to the definition of the domain "immunoglobulin fold", depicted in Fig. 2 and well-defined from the 3-D structure of a light chain. Both the V and the C domains are similarly organized as a b-barrel, characterized by two planes containing antiparallel **b-sheets** stabilized by the intrachain disulfide bond. The various **b-strands** are connected by loops of variable length, and the V domain has extra loops that contribute the antigen binding site. There are other some minor differences between the V and the C domains, because nine b-strands are present in the V_H and V_L domains, whereas only seven are in C_L and C_H1 and eight are in C_H2 and C_H3. All CDRs are located in loops, and the 3-D analysis of an antibody–antigen complex confirms that all participate in antigen binding. The immunoglobulin fold was subsequently identified in many other proteins, including many molecules of immunological interest, providing a basis for the definition of the immunoglobulin superfamily.

Figure 2. Schematic organization of light-chain V and C domains, indicating the basic immunoglobulin fold. Arrows indicate the antiparallel b-strands as arranged in each domain as two distinct b-pleated sheets tightly anchored by an intrachain disulfide bond.(From Ref. 1959, with permission.)

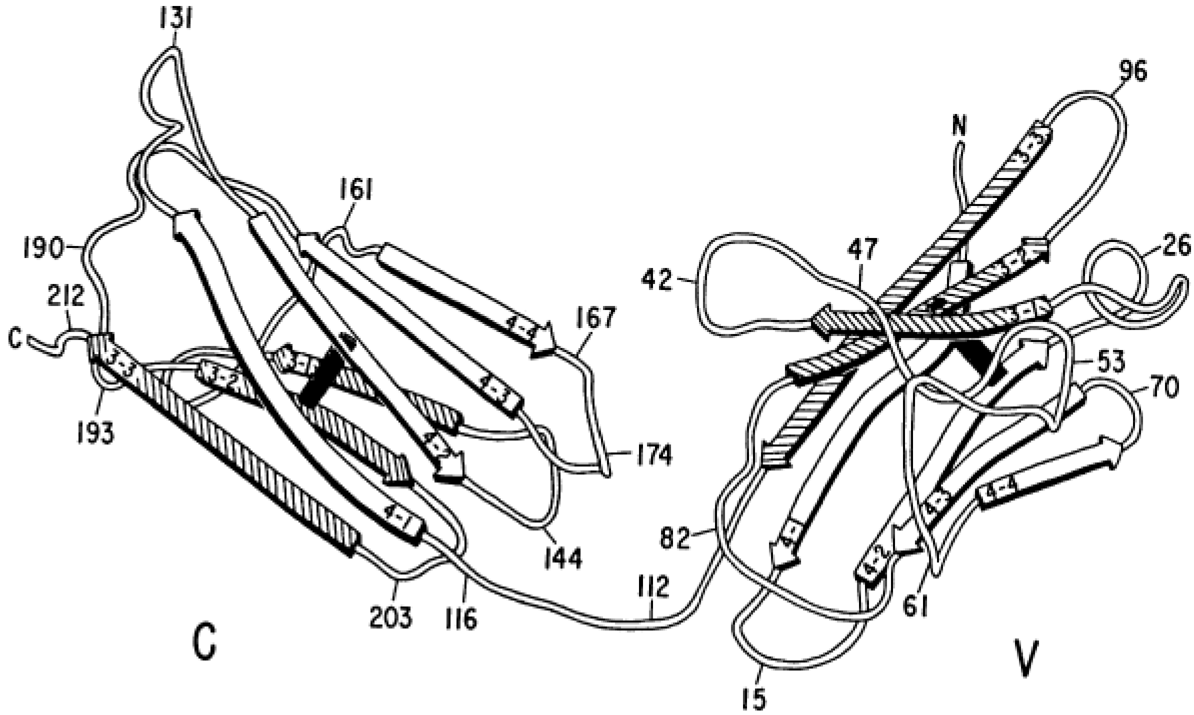

Suggestions for Further Reading

R. R. Porter (1959) The hydrolysis of rabbit gammaglobulin and antibodies by crystalline papain. Biochem. J. **73**, 119–126.

G. M. Edelman and M. D. Poulik (1961) Studies on structural units of the -globulins. J. Exp. Med. **113**, 861–884.

J. B. Fleischman, J. B. Pain, and R. R. Porter (1962) Reduction of gammaglobulins. Arch. Biochem. Biophys. Suppl **1**, 174–180.

G. M. Edelman, B. A. Cunningham, W. E. Gall, P. D. Gottlieb, U. Rutishauser, and M. J. Waxdal (1969) The covalent structure of an entire gamma G immunoglobulin molecule. Proc. Natl. Acad. Sci. USA. **63**, 78–85.

N. Hilschmann and L. Craig (1965) Amino acid sequence studies with Bence-Jones proteins. Proc. Natl. Acad. Sci. USA **53**, 1403–1409.

W. J. Dreyer and J. C. Bennett (1965) The molecular basis of antibody formation: a paradox. Proc. Natl. Acad. Sci. USA. **54**, 864–869.

T. T. Wu and E. A. Kabat (1970) An analysis of the sequences of the variable regions of the Bence-Jones proteins and myeloma light chains and their implications for antibody complementarity. J. Exp. Med. **132**, 211–250.

L. M. Amzel and R. J. Poljak (1979) Three-dimensional structure of immunoglobulins. Annu. Rev. Biochem. **48**, 961.

Immunoglobulin Biosynthesis

The biosynthesis of immunoglobulins (Igs) is a particularly complex process, because it necessitates a long sequence of events: (a) Ig gene rearrangements that take place during early B-cell differentiation in bone marrow; (b) assembly of heavy (H) and light (L) **polypeptide chains** to form the basic H_2L_2 monomer; (c) transport to the cell surface, through the various intracellular compartments that permit the protein core to be sequentially glycosylated; (d) pentamerization for the IgM isotype, dimerization for IgA, with binding of the J chain; and (e) shedding of the final Ig as a circulating antibody. In addition to these steps, one must also include **classing**, **switching** of isotype, and the alternative splicing that allows the heavy chain to be synthesized in either membrane or secreted forms (see Membrane Proteins and Protein Secretion).

The phenomenon of Ig gene rearrangement is described in other entries (see Gene Rearrangement, Allelic Exclusion, B Cell, V Genes, and Recombinase). In brief, before transcription, any Ig gene must first rearrange the various elements that will encode the **variable regions** of both the H and L chains. This takes place in bone marrow, where the **antigen-independent** early steps of B-cell differentiation, which are mostly devoted to Ig gene rearrangement, a highly controlled sequential succession of events ($D \rightarrow J_H$, $V_H \rightarrow D - J_H$and $V_L \rightarrow D - J_L$), occur. As a result of these rearrangements, a membrane-bound IgM is expressed at the surface of the immature B cell. Finally, as the cell leaves the marrow to enter the periphery, coexpression of IgD and IgM occurs in mature B cells. Further differentiation to plasma cells is **antigen**-driven. At this terminal stage, Igs are secreted as circulating antibodies. Expression of other isotypes implies that the switch mechanism has been operative, leading the way to all remaining steps of Ig biosynthesis mentioned above.

Each heavy and light chain is translated separately on discrete **polysomes** of the endoplasmic reticulum. This is a rapid process, as for most polypeptides (about 1 min for H, and 30 s for L). The heavy chain is retained by BiP, a **heat-shock** protein, Hsp70, until it binds a light chain. Two pathways have long been known, depending on the isotype and the animal species. In the first, most frequent one, half-molecules (HL) are formed that rapidly dimerize. In the other, heavy chains dimerize, and then H_2L and finally H_2L_2 are formed. All these events take place in the ergastoplasm cisternae where the first carbohydrate, an *N*-acetylglucosamine, is added. Monomers are transported to the Golgi apparatus after formation of an ergastoplasmic vesicle. Subsequent carbohydrates are added, and the glycosylated monomer is included in Golgi vesicles that will fuse at the plasma membrane of the cell. After addition of a fucose residue, the molecule is either shed or anchored at the cell surface, depending upon whether this heavy chain is of the membrane or secreted type.

All surface isotypes are expressed as H_2L_2 monomers. Pentamerization of secreted IgM takes place just before leaving the cell, in the immediate vicinity of the plasma membrane, simultaneously with formation of a disulfide bond to the J chain. Dimerization of the IgA isotype occurs in mucosal plasma cells, where disulfide bonding to the J chain takes place. This causes covalent binding to the poly-Ig receptor, expressed at the basal pole of the epithelial cell. After internalization, the complex is transported through the epithelial cell, and the polymerized IgA is released at the apical pole of the cell in the lumen of the corresponding organ, along with **proteolytic** cleavage between two **domains** of the poly-Ig receptor, so that one subunit remains covalently linked to the IgA polymer, forming the so-called secretory component. Besides allowing the IgA to migrate through the epithelial cell, the secretory component is thought to protect the immunoglobulin from cleavage by proteolytic enzymes.

See also entries Antibody, B Cell, Gene Rearrangement, and Immunoglobulin.

Suggestions for Further Reading

T. K. Blackwell and F. W. Alt (1989) Mechanism and developmental program of immunoglobulin gene rearrangement in mammals. Annu. Rev. Genet. **23**, 605–636.

E. S. Vitetta and J. W. Uhr (1973) Synthesis, transport, dynamics and fate of cell surface Ig and alloantigens in murine lymphocytes. Transpl. Rev. **14**, 50–75.

R. Wall and M. Kuehl (1983) Biosynthesis and regulation of immunoglobulins. Annu. Rev. Immunol . **1**, 393–422.

Immunoglobulin Structure

The **immune** system has evolved to recognize the entire organic world by producing complementary **immunoglobulins**, or **antibodies**, to identify and defend the vertebrate body against foreign substances (for a general reference, see (1)); an entry point to the many web sites containing information about antibodies is `http://www.antibodyresource.com`). Antibody molecules, like enzymes and many other proteins, have specific binding sites that interact with **ligands**, often in a true lock-and-key manner (see Antibody–Antigen Interactions). They also interact with other molecules involved in intercellular signaling, for example, the **Fc receptor**. Antibodies are part of a superfamily of proteins, some but not all of which participate in the immune response. Molecules related to antibodies that appear on cell surfaces mediate cell–cell recognition and signaling processes to trigger proliferation of particular cells in response to antigenic challenge.

The mechanism by which antibody diversity is created is now understood in considerable detail at the genetic (or sequence) level and at the protein structural level (see Immunoglobulin Biosynthesis). Common features of immunoglobulins were first recognized physicochemically and serologically, then described in terms of their amino acid sequences, and only much later revealed in atomic detail by X-ray crystallography . Limited **proteolytic** digestion and cleavage of disulfide bonds shows that antibodies contain multiple **polypeptide chains** (Fig. 1). The chains are classified by size into light (L) chains (about 23 kDa) and heavy (H) chains (about 60 kDa). Systematic internal **homologies** in the amino acid sequences suggest that immunoglobulins are composed of multiple copies of related units, each forming an individual, quasi-independent, three-dimensional structure, or **domain**, that has a common folding pattern. Light chains contain two domains, and heavy chains contain four or five. Heavy chains were distinguished originally on the basis of their amino acid sequences into k and l classes or **isotypes**. In humans, k and l light chains are present in comparable proportions. In the mouse, k light chains predominate.

Figure 1. Domain structures of the most common immunoglobulins. Most immunoglobulins contain both light and heavy chains, each of which comprises one variable domain and varying numbers of constant domains. The combination of two light plus two heavy chains is a higher order building block, of which immunoglobulins of different classes (IgG, IgA, IgM, IgD and IgE) show different states of oligomerization. Additional chains are linkers where necessary.

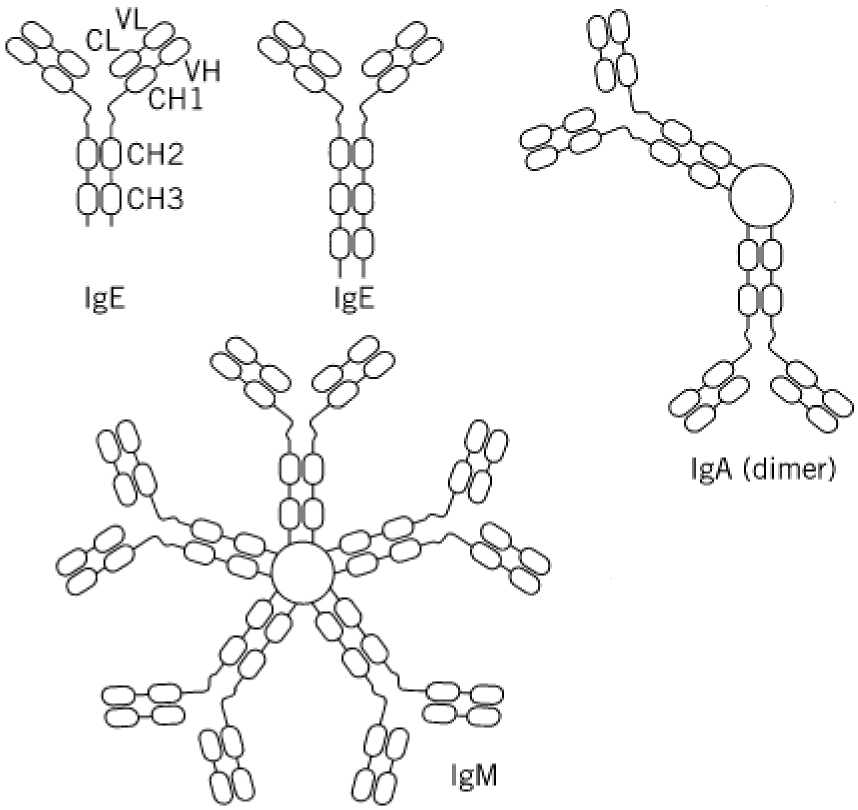

Different types of antibody molecules show variations on a general structural theme. They are multichain proteins built from domains about 100 amino acid residues long known as the immunoglobulin fold. Before the first crystal structure determinations of immunoglobulins, Kabat and co-workers identified the regions involved in antigen binding by analyzing the distribution of variability in aligned immunoglobulin sequences (2). Two types of domains were recognized on the basis of the variability of their sequences: variable (V) and constant (C) domains. Within the variable domains, they noticed regions of still greater variability called the hypervariable regions or complementarity determining regions (CDR), which they correctly and presciently predicted would be responsible for antibody specificity for different antigens. The regions of the variable domain outside the CDRs are called the **framework regions**. The framework provides a scaffolding of nearly constant structure to which the antigen-binding loops are affixed.

Indeed, when the first structures of immunoglobulin domains were determined by X-ray crystallography, it appeared that both constant and variable domains had a similar, double beta-sheet structure in the framework region, that the hypervariable regions corresponded to surface loops in the variable domains, and that these loops did indeed interact with bound antigens. In almost all immunoglobulin domains, a conserved disulfide bond links the two sheets, and a **tryptophan residue** packs against it. Chothia and Lesk subsequently carried out the three-dimensional analog of the sequence comparisons of Kabat and coworkers by using the crystal structures (3). This led to some revision of the boundaries between the framework and CDR regions.

Different classes of immunoglobulins–IgG, IgA, IgM, IgD, and IgE–differ in their assembly from chains and domains. Figure 1 shows the domain structures of the different classes of immunoglobulins. Molecules in the class best known structurally, the IgGs, usually have two heavy chains that contains four domains and two light chains that contain two domains. The antigen-combining site in most IgGs is formed from three loops from the light chain and three from the heavy chain. Each IgG has two copies of the binding site, one from each light chain–heavy chain pair, which permits multiple interactions with antigens to form aggregates.

The IgG molecule contains four polypeptide chains, two identical light chains, each containing one variable and one constant domain, denoted V_L and C_L, and two identical heavy chains, containing one variable and three constant domains, denoted V_H, C_{H1}, C_{H2}, and C_{H3} (see Fig. 2). The C_{H1} and C_2 domains are linked by a segment of polypeptide chain called the hinge region. The angle between the V_L–V_H domain pair and the C_L–C_{H1} domain pair is called the elbow angle. These joints are usually flexible in solution. Immunoglobulins also contain carbohydrate moieties introduced by ***N*-glycosylation** that are not shown.

Figure 2. A schematic diagram of the structure of an IgG molecule (**a**), showing the distribution of domains in the heavy and light chains and (**b**) the interchain disulfide bridges, and the definitions of the fragments - Fab, Fab′ and Fc - produced by limited proteolytic cleavage.

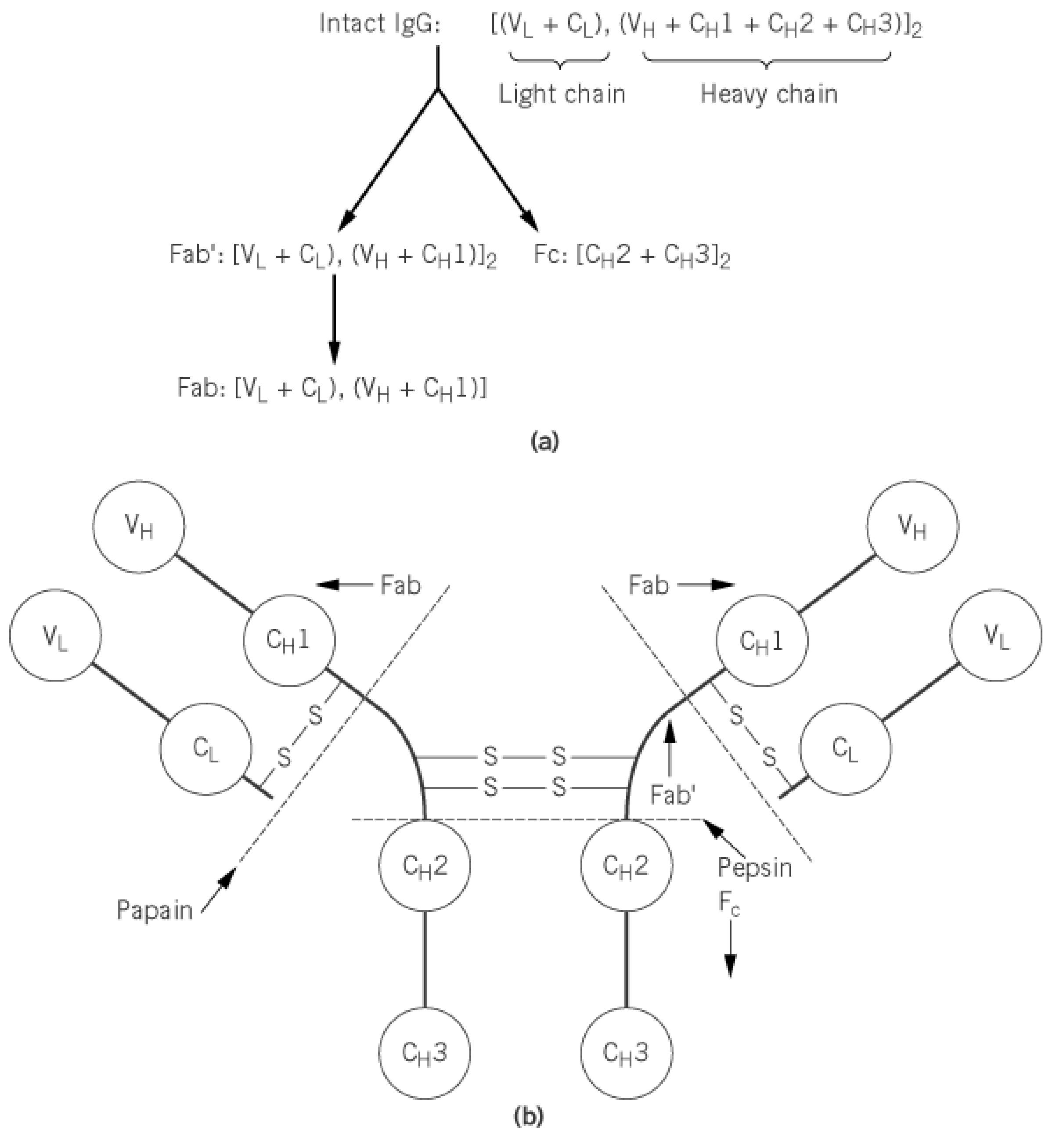

Figure 2 defines the fragments produced by limited proteolytic cleavage. Most of the structural analysis has been carried out on Fab fragments (4). Single-chain Fv fragments, in which the C-terminus of the V_H domain is linked by a flexible peptide to the N-terminus of the V_L domain, or vice versa, are important in protein engineering (5).

The interactions between the different polypeptide chains in an IgG include the disulfide bonds (see Fig. 2) and the interfaces between corresponding domains–V_L–V_H, C_L–C_{H1}, and C_{H3}–C_{H3}, but not C_{H2}–C_{H2}–that pack together to form extensive **van der Waals** contacts. It is characteristic of proteins that interior interfaces are formed by the packing of complementary surfaces. This complementarity of fit fixes the relative spatial disposition of the pieces that interact. A tendency to conserve the residues involved in these interfaces explains why different light and heavy chains pair fairly freely to form complete immunoglobulins. In the V_L –V_H interaction, conservation of the relative geometry has the additional important consequence that, to a reasonable first approximation, the double b-sheet frameworks of V_L and V_H domains form a scaffolding of nearly constant structure on which the antigen-binding site is erected.

Figures 3 and 4 show the **secondary structures** and tertiary structures, respectively, of the V and C domains. Each has the form of a double b-sheet “sandwich.” In immunoglobulin domains, the two sheets are oriented so that their strands approximately parallel. Figure 5 shows the interface between V_L and V_H domains (6).

Figure 3. The folding patterns of (**a**) variable domains and (**b**) constant domains. The domains shown are the V_L and C_H Strands of b-sheet are shown as polygonal ribbons, and the loops joining them as lines that join the C_{alpha} atoms of succ domain contains two b-sheets. One domain is shown in solid lines and the other in broken lines.

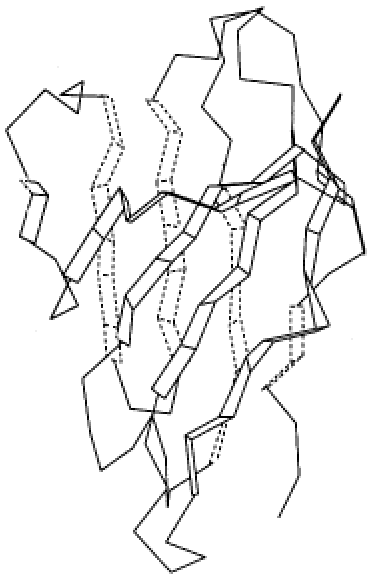

(a)

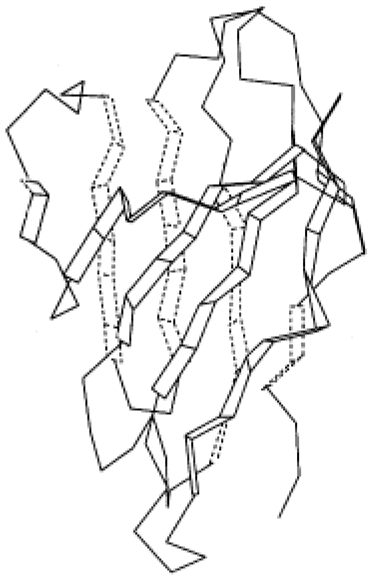

(a)

Figure 4. Schematic representations of typical hydrogen-bonding patterns of (**a**) V_L, (**b**) V_H and (**c**) C domains. The two opened like a book. Strands in the upper sheets in this figure were indicated by ribbons with broken lines in Figure 3. Str in this figure correspond to the strands drawn with solid lines in Figure 3.

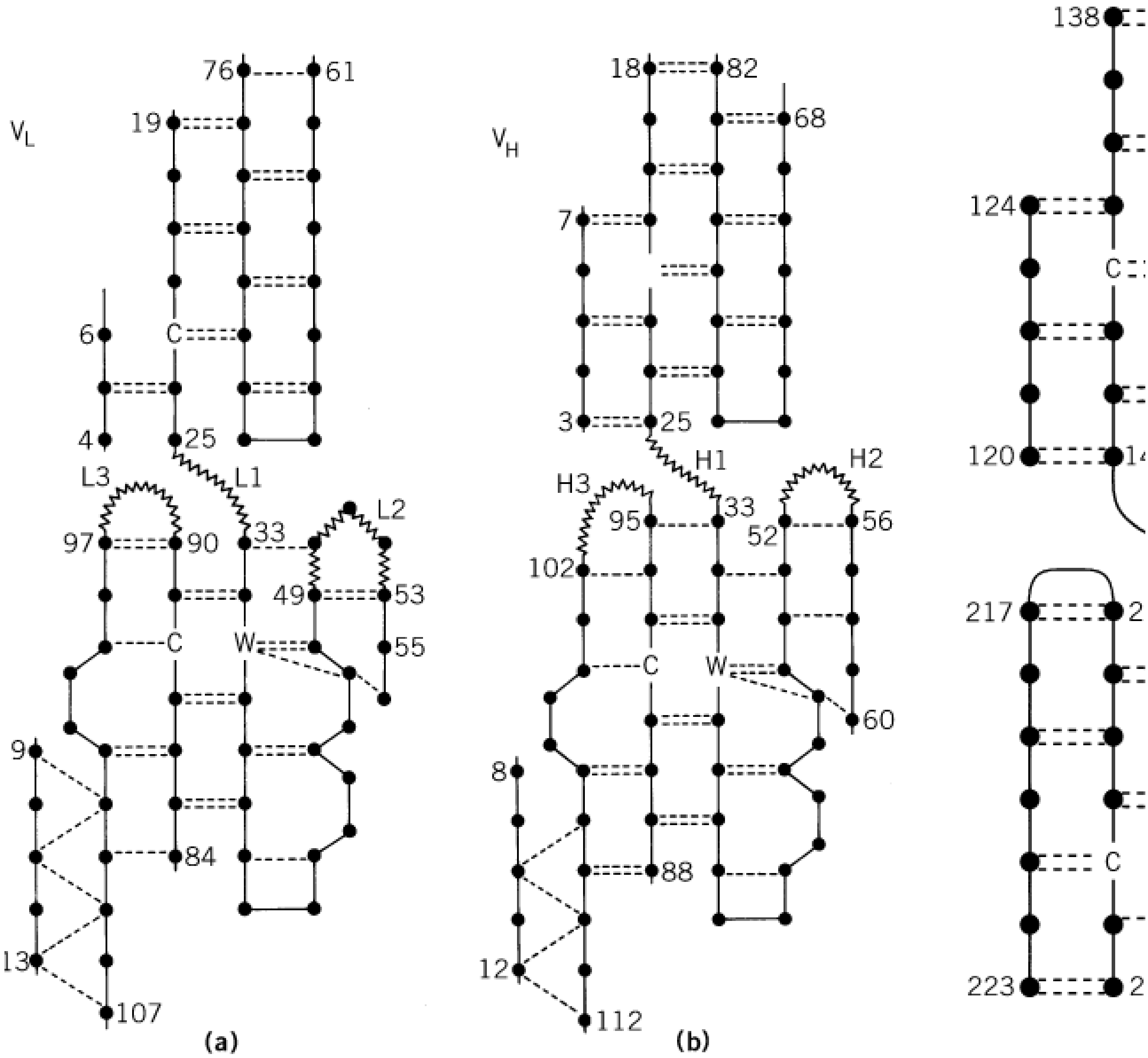

Figure 5. The interface between the V_L and V_H domains in the antilysozyme antibody D1.3 (8). The V_L domain is trace
V_H domain by a broken line. In this perspective, the antigen-binding site is on the upper surface of the molecule. Side cl
the V_L chain that contact bound antigen are shown with filled circles, and those from the V_H chain with open circles. Th
strongly twisted.

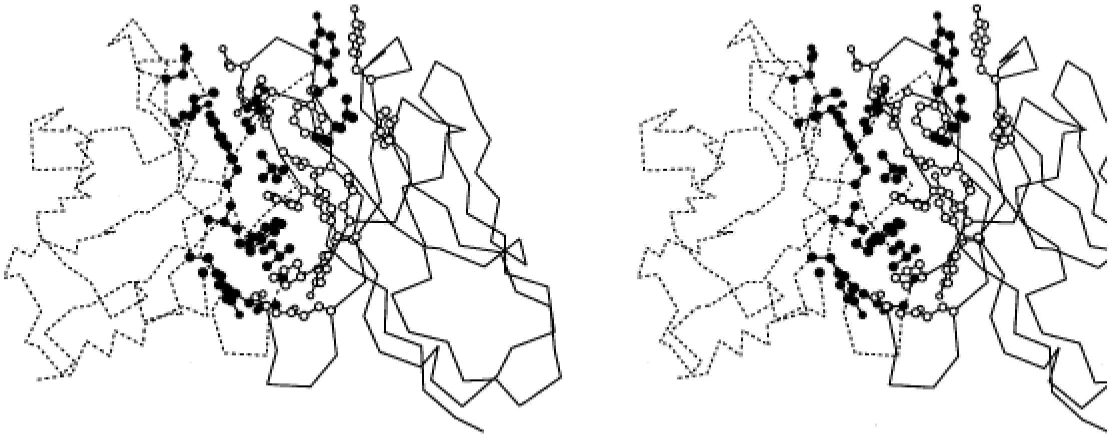

0.1. The Antigen-Binding Site
The study of antibody antigen-binding sites lies at the intersection of two topics of interest. One is th immune response: What is the relationship among the sequences of immunoglobulins generated by t genetic combination and somatic mutation and the three-dimensional conformations of the resulting sites? The second is the question of how the recognition and binding of an antigen by antibodies rela understanding of protein–ligand interactions, and the extent to which we can quantitatively explain a specificity at the level of interatomic interactions.

Most antibody antigen-binding sites are formed primarily from six loops–three from the V_L domain V_H domain. The three loops from the V_L domain are called L1, L2, and L3, in order of their appeara acid sequence. Alternatively, they are called CDR1, CDR2, and CDR3. V_H domains contain three cc loops H1, H2, and H3. In contrast, the antibodies of the camel and related animals contain only heav V_H CDRs suffice to create the antigen-binding site. This observation has obvious applications to sele artificial antibodies for therapy. Four of the loops, L2, H2, L3, and H3, are "**hairpins**," in that they li antiparallel strands of a single b-sheet, connecting strands of sheet that are hydrogen-bonded to each L1 and H1 bridge a strand from one of the two b-sheets to a strand in the other (Fig. 6).

Figure 6. The V_L domain of REI, indicating the antigen-binding loops L1, L2, and L3.

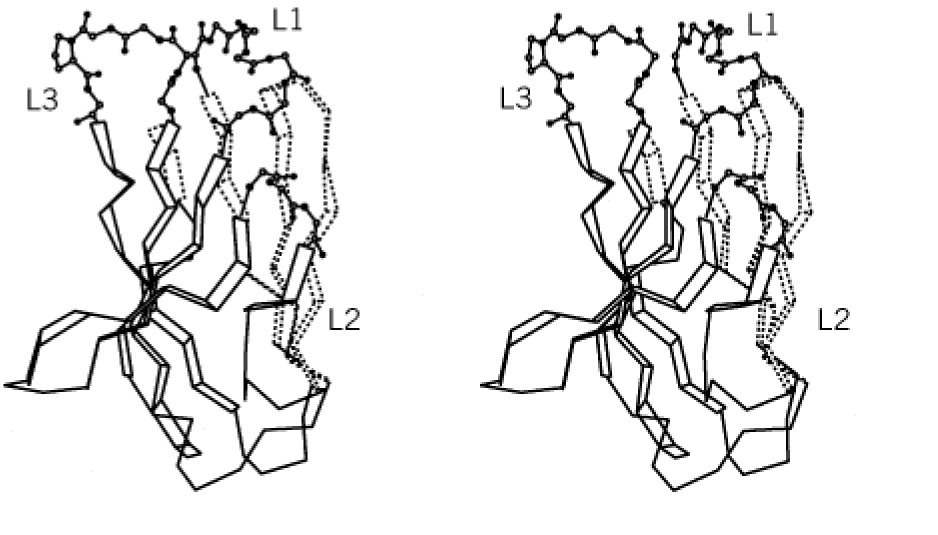

PC603 (Fig. 7) and the other the complex between Fab HyHEL-5 and hen egg white lysozyme (Fig orientations were chosen looking down onto the antigen-binding site, that is, an "antigen's-eye view chain loops are on the left and the heavy-chain loops are on the right. Reading clockwise starting at

loops appear in the order L1, L2, H3, H1, H2, and L3. The arrangement of the loops is roughly sym
opposite H1, L2 is opposite H2, and L3 opposite H3. The central position of H3 is noteworthy.

Figure 7. The spatial distribution of antigen-binding loops, or CDRs, in the antigen-binding site of McPC603. PC = t
phosphorylcholine. The orientation is chosen to give a view down onto the antigen-binding site, an “antigen's-eye viev

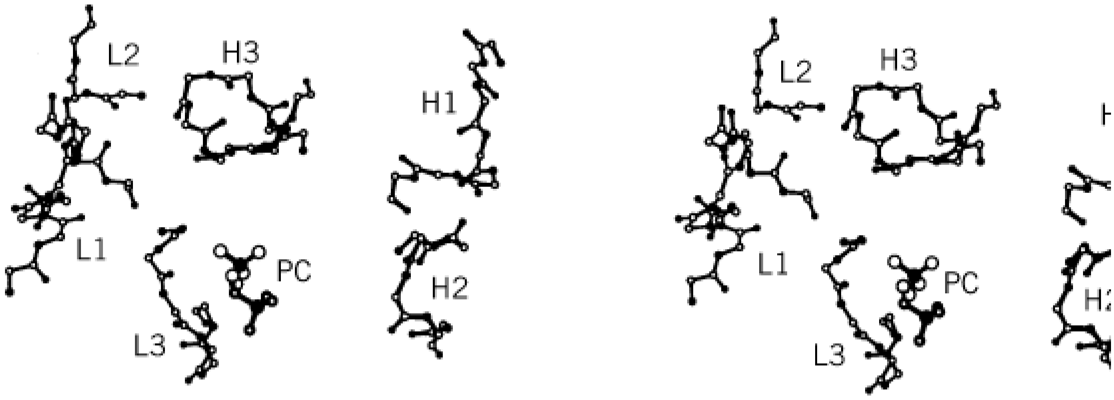

Figure 8. Interactions between HyHEL-5 and hen egg white lysozyme. Residues in lysozyme that make contact with t
in bold ball-and-stick representation. Residues in the antibody that make contact with the lysozyme are shown in skele
Broken lines indicate hydrogen bonds between antigen and antibody.

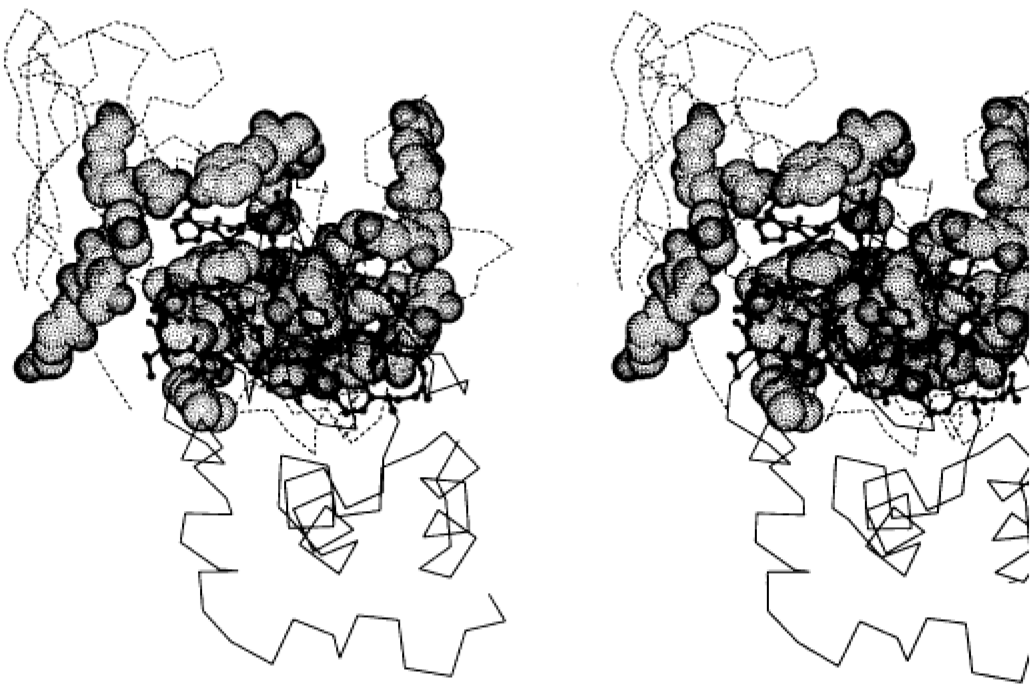

In many cases, antigen-antibody interactions involve the rigid association of the two structures. In
mechanism analogous to “induced fit” takes place, in which the structures of the free and ligated ai
significant structural changes. The structures of complexes between antibodies and protein antigen
antibodies specific for different **epitopes** of lysozyme and one specific for **neuraminidase**, demon
general features of the interactions are similar to those seen when other proteins associate without
conformational changes (7) (see Protein–Protein Interactions). The number of residues in contact g

from 27 to 39, distributed approximately equally between antibody and antigen. The accessible sur the antibody–antigen interface varies between 1250 and 1940 Å^2, and the interfaces are densely pa many cases several buried water molecules occupy sites within the interface. There are typically 1(bonds across the interface.

In the complex between Fab D1.3 and hen egg white lysozyme, for example, the interface is a relat dimensions $20\ \text{Å} \times 30$, although one glutamine side chain from the lysozyme inserts into a pocke (8). A total of 17 residues from the antibody make contact with a total of 17 residues from the lyso pairs of residues are in contact. Of the 17 residues from the antibody, three are framework residues adjacent to CDRs.

In the lysozyme–antibody complexes of known structure, there is rather little change in structure o relative to their unliganded states. Therefore, these complexes fit the picture of recognition by fairl have preformed complementarity. This is not observed, however, in complexes of antibodies and o clipped out of protein structures, because the latter are flexible in solution. In the complex between nine-residue region from influenza virus hemagglutinin (9), the peptide in the complex has the con type I b-turn, somewhat different from its conformation in the native hemagglutinin structure. Con structure of the Fab fragment of the antibody in free and liganded forms shows that there has also b rearrangement of the structure of loop H3. The relative orientations of V_L and V_H domains change antigen by a rotation, typically of about 3°, but up to 11° in known structures.

Another peptide–Fab complex, B13I2 (10), contains the seven-residue epitope of a 19-residue anti; to the C-helix of myohemerythrin. The residues of the peptide in the complex have the conformatio turn, not helical as in the native protein. What is most significant is that the antibody cross-reacts v protein, which it could not do while retaining its native structure. It is interesting that apomyoheme more strongly to the antibody. Apomyohemerythrin lacks the iron atoms, one of which binds to res C-helix in the native state. This implies that myohemerythrin changes conformation to bind the ant removal of a stabilizing interaction–a barrier to conformational change–enhances binding. (The str B13I2–myohemerythrin complex has not been determined.)

0.3. The Sequence Repertoire of the Immune System

Analysis of sequences of the loci on human chromosomes that carry the genes for antibodies and c these results with the amino acid sequences of expressed antibodies reveal what genetic resources t system possesses and how it uses them. The following discussion is restricted to human sequences

The gene for the variable region of the light chain is formed during B-cell development by combin segment. The k locus contains more than 40 functional V_k; segments and 5 J_k segments. The l locu functional V_l segments and 4 J_l segments. The gene for the variable region of the heavy chain is fo combinatorial joining of three segments: V_H (variable), D (diversity) and J (joining). Each individu approximately 51 functional V_H segments (11), 25 D segments, and six functional J segments. Des number of possibilities implied by these various combination, they apparently are not used with eq Comparing a database of expressed antibodies with the set of V_k germ-line sequences, of a total of germ-line V_k segments, only about 11 are used frequently, and others appear in only a minority of $_l$ sequences, 10% of the functional V_l gene segments produce 50% of the expressed V_l repertoire (

The nonuniform appearance of sequences is also reflected in a bias in the structures of the hyperva the associated primary antibodies. As discussed later, antigen-binding loops of antibodies usually h conformations chosen from a small repertoire of discrete canonical structures. The antibodies studi show strong preferences for particular main-chain conformations in their light-chain hypervariable

corresponding analysis of the V_H segments–which code for a region containing the first two hyper
the V_H domain–revealed similar nonuniform structural preferences (14). For example, sequences c
segments, which code for the part of the V_H domain that includes loops H1 and H2, suggest that th
different canonical structures of H1 and six of H2, potentially producing 18 different structures. H
sequences contain only seven different combinations of canonical structures of H1 and H2 (14).

0.4. Somatic Mutation and the Maturation of the Antibody Response

The distribution of residues that differ from their germ-line identities in expressed antibodies has b
Tomlinson and co-workers (15) by comparing sequence diversity on a residue-by-residue basis bet
antibodies and mature ones. Whereas the diversity in the germ-line antibodies is greatest in H3 anc
center of the antigen-binding site (because of junctional diversity in gene assembly; see Immunogl
Biosynthesis), somatic mutations spread the diversity to its periphery. In almost all cases, somatic
isolated single-residue substitutions, not insertions or deletions. The total change is less than the ty
between germ-line segments, that is, if one thinks of the germ-line segments as "islands in a seque
somatic mutations extend the domains of the individual germ-line segments, rather than filling in t
them. Thus, there was no ambiguity in identifying the germ-line segment from which each mature
Somatic mutation is a perturbation of a germ-line segment rather than a major reconfiguration of th
site.

Wedemeyer et al. (16) studied the maturation of an anti-nitrophenyl phosphonate catalytic antibod
crystallography. They solved the structures of the germ-line and somatically mutated Fab fragment
without ligand. Their results reveal both the sites of mutation and the structural effects. There are n
sequence changes between germ-line and mature antibody, three in the light chain and six in the he
the light chain mutants is in the L1 loop. The other two are at positions near in the sequence to L1
heavy-chain mutants appears in H2, three are in regions adjacent to or in contact with the antigen-b
two are surface residues at the opposite ends of the domains, which presumably have little effect o
binding site. No mutation is at a position directly in contact with the antigen. No mutation appears
although there are extensive contacts between H3 and the hapten. The conformations of two of the
loops (H1 and H2) differ between germ-line and mature antibody.

The antigen-binding site of the mature antibody has a similar conformation with and without boun
conformation that is complementary to the hapten. This structure is shared by the ligated state of th
antibody, but the unligated state of the germ-line antibody differs in conformation, that is, the gern
adopt the hapten-binding conformation, but this is induced by the ligand. In contrast, the mature an
conformation even in the absence of ligand.

Wedemeyer et al. (16) suggest that conformational flexibility in the primary antibody response rep
mechanism for generating antibody diversity. Indeed, it is possible that still other conformations o
antibody might be induced by alternative, related ligands. In this way the same primary antibody c
starting point for alternative maturation pathways to produce secondary antibodies to different liga
there is no direct structural evidence that this happens, nor how different the induced conformation

0.5. Structures of Loops in Proteins

The many known protein structures demonstrate that generally loops connecting strands of a b-she
characteristic sets of conformations, which depend on their lengths, sequences, and interactions wi
surroundings. For short hairpins in proteins, the conformation is usually determined primarily by t
sequence of the loop itself (17). For a polypeptide chain to reverse direction in a "tight" turn, it usu
advantage of a special residue, such as Gly or Pro, that allows a nonstandard main-chain conforma
Conformations of many short hairpins depend on the length and position of such a special residue.
also applies to many of the shorter CDR hairpins, L2, L3, and H3. H2 is exceptional, however, in t
residue strongly influences its conformation (18).

Medium-sized loops fall into two classes (19). The conformations of those that have ends close tog usually determined by hydrogen-bonding interactions of polar atoms that point into the interior of t typical V_k L3 loop, illustrated in Figure 9, exemplifies this case.) The conformations of more exte as H1, depend on the packing of bulky side chains against or into the core of the protein. In H1, for 29 of the heavy chain is usually a Phe, which is packed into the framework (see Fig. 10).

Figure 9. The most common canonical structure of V_k; L3, that from REI. This shows the characteristic *cis*-proline p C-terminus and the polar side-chain at the residue just before the loop that forms hydrogen bonds to stabilize the conf region.

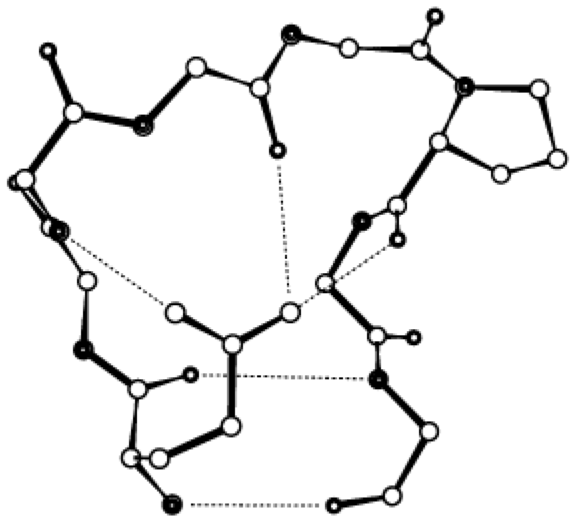

Figure 10. The H1 loop of Fab J539. An important contribution to stabilizing the conformation of this loop is the pac Phe29 into the region between the two sheets.

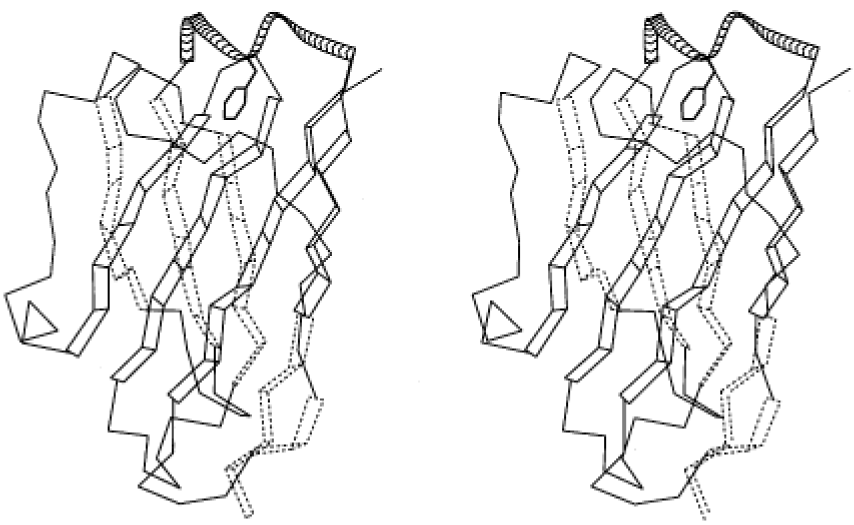

The Canonical Structure of Antigen-Binding Loops of Antibodies

Studies of immunoglobulin structures have shown that their antigen-binding loops have only a sm discrete main-chain conformations. These conformations are determined by a few particular resid outside the loop but interacting with it. Among corresponding loops of the same length, only these be conserved that maintain the conformation of the loop (20). The conserved residues may be thos special main-chain conformations or that form special hydrogen-bonding or packing interactions. residues in the sequences of the loops are left free to vary to modulate the surface topography and distribution of the antigen-binding site.

The biological significance of this robustness of the main-chain conformation of the antigen-bindi play a role in tuning antibodies by somatic mutation. In the system as it has evolved, a change in a antigen-combining site in most cases produces only a conservative structural change. This is what in a system that already shows affinity and requires only "fine-tuning." Consider the alternative. I completely altered the main-chain conformation of the loops, the effect would produce a successi primary responses, rather than a secondary response whose structures are perturbed in only minor important) ways from a set of already selected primary antibodies. One should not underestimate tiny structural changes to produce very large effects on binding affinity.

The ability to isolate the determinants of loop conformation in a few particular residues in the seq it possible to analyze the distribution of loop conformations in the many known immunoglobulin out of the six hypervariable regions of antibodies–L1, L2, L3, H1, and H2–have only a few main- conformations or "canonical structures" H3 is discussed separately later. Most sequence variation surface by altering the side chains on the same canonical main-chain structure. Sequence changes sets of positions switch the main chain to a different canonical conformation.

As an example, Figure 9 shows the L3 loop from V $_k$ REI. There is a proline residue at position 9 peptide bond. Hydrogen bonds between the side chain of the residue at position 90, just N-termina main-chain atoms of residues in the loop stabilize the conformation. The side chain is a Gln in RE other V_k chains. The combination of this loop length, one of these polar side chains at position 90 constitute the "signature" of this conformation in this loop, from which it can be recognized in a s immunoglobulin for which the structure has not been experimentally determined. The conformati 10) illustrates a nonhairpin loop, which joins strands in separate sheets. Its conformation is stabili inward-pointing side chains against the framework. General support for the canonical structural d antigen-binding loops has come from analysis of known sequences and structures of immunoglob conformations observed in the relatively few known immunoglobulin structures account for the lo proportion of all immunoglobulins.

When the canonical structural model was proposed, analysis of the large compilation of immunog sequences of Kabat and co-workers (21) showed that over 90% of the hypervariable regions in V the same length and contain the "signature" residues of a known canonical structure and therefore have conformations close to those found in the currently known immunoglobulin structures. Indee was conservative in that it includes only those hypervariable regions that matched the sequence re exactly. Of course one was dealing then with a limited number of known structures, and the mode overturned if subsequent structural determinations produced an unbounded proliferation of main-c conformations. However, the conclusion that the repertoire is limited and discrete is justified, alth canonical structures have appeared. Recently, 244 hypervariable regions in 49 immunoglobulin Fa structures determined at resolutions of between 1.7 and 3.1 Å were analyzed according to their str (22). Some 85%, and even more in subsequent work, were clustered into groups identified as kno structures and had very similar conformations. The structures on which the canonical structure an primarily human and mouse antibody fragments. However, analysis of the sequences of shark and suggest that the basic pattern of canonical structures goes back to the very early stages in the evol immune system (23). These observations suggest that the main-chain conformations of five of the regions–L1, L2, L3, H1, and H2–are described by a small repertoire of canonical structures. Most present among the immunoglobulin structures already known, and the main-chain conformations o an immunoglobulin of unknown structure can very often be predicted from the sequence by the pr specific residues (24).

A roster of current canonical structures is available (20). Its accuracy and completeness depend o
determination of the sets of residues responsible for the observed conformations and (2) the assun
changes in the identities of residues at other sites do not significantly affect the conformation of tl
results have been tested and refined by using them to predict the atomic structures of binding sites
immunoglobulin structures before determining them by X-ray crystallography (24).

0.6.1. Precision of the Canonical Structural Model

Qualitatively, the canonical structure model states that the main-chain conformations of five of th
binding loops fall into small, discrete clusters. It is important to know quantitatively how similar a
exemplars of the same canonical structure in different antibodies, for a proper understanding of th
mechanism of immune recognition and for the designing or modeling antibody structures. The tw
addressed are, what is the spread in the main-chain conformations of the canonical structures and
spread in their positions and orientations with respect to the framework? When the canonical struc
initially proposed, this question was difficult to answer, partly because the differences in observec
were comparable with the experimental error. Some of the structures had been determined only at
resolution and, even more seriously, some contained qualitative errors.

Now, the precision of canonical structures has been examined by analyzing and comparing of the
the antigen-binding loops in 17 immunoglobulins for which accurate structures have been determi
resolution (20). The structures used were determined to a resolution of 1.6 to 2.3 Å and refined to
greater than 21%. These contain 7 V_l, 10 V_k, and 15 V_H chains. Although the hypervariable regio
particular immunoglobulins do not cover all of the known canonical structures, they do include al
ones. The results indicate that the main-chain conformations of different examples of the same ca
in different antibodies are usually conserved to within about 0.3 to 0.4 Å rms deviation, which is a
degree of similarity.

0.6.2. The H3 Loop is Even More Variable

H3, the third hypervariable region of the heavy chain, is far more variable in length, sequence, an
the other antigen-binding loops (21). Therefore, it cannot be included in the canonical structural d
conformational repertoire that applies to the three hypervariable regions of V_L chains and the first
chains. Because the H3 loop falls in the region of the V-D-J join in the assembly of the immunogl
chain gene (Fig. 11), several mechanisms contribute to generating its diversity, including combina
V_H, D, and J gene segments and alternative splicing patterns at the junctions.

Figure 11. The roles of the V, D, and J gene segments in determining the immunoglobulin fold. Loop H3 arises fro
the V-D-J join in the assembly of the heavy chain gene. In the V_H domain of McPC603 shown here, the region enco
segment coincides almost exactly with the H3 loop region.

Figure 12. Two H3 loops with alternative torso conformations: (**a**) McPC603 - the bulged torso conformation, (**b**) 4 nonbulged torso conformation.

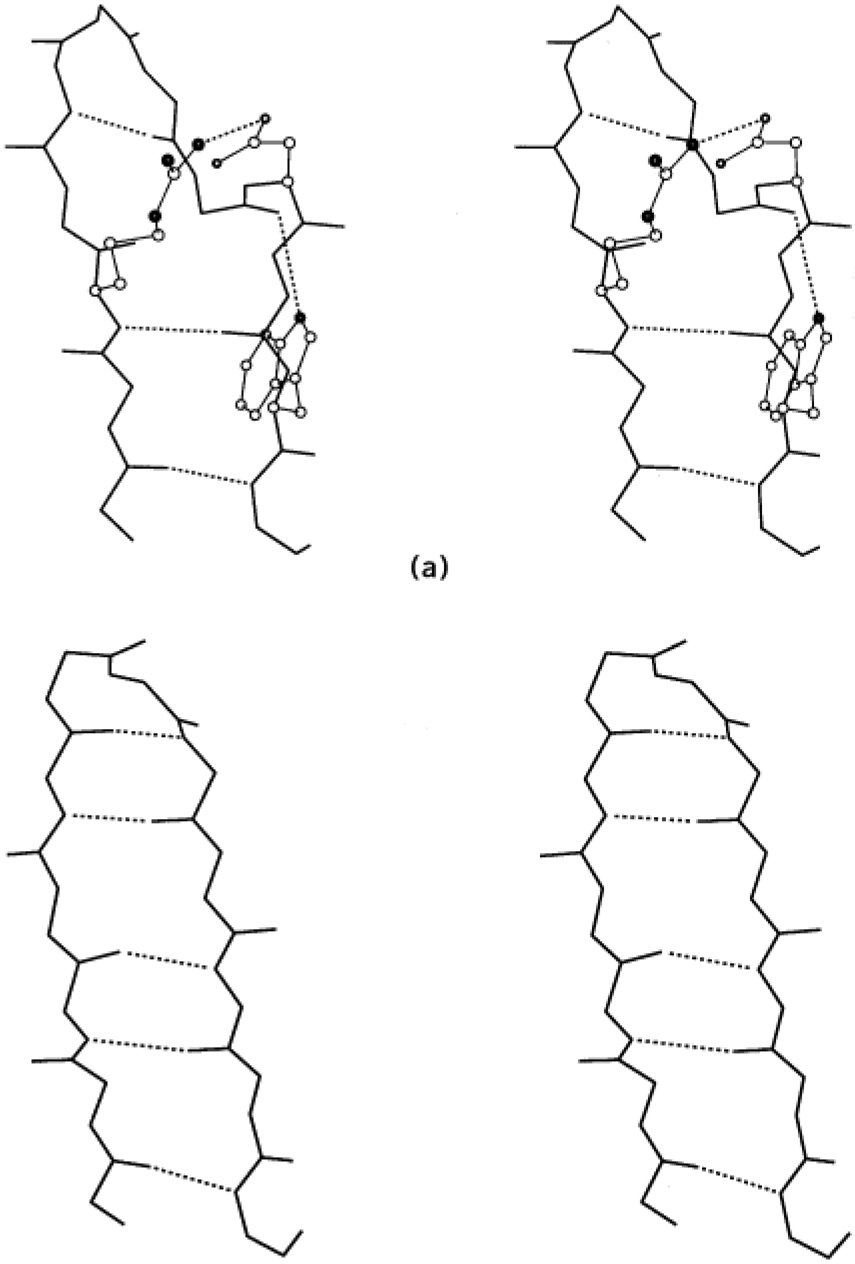

(a)

(b)

In expressed antibodies, H3 is prominently at the center of the antigen-binding site (see figs. 7,8) central position, H3 makes significant interactions with other loops with the framework, with the partner, and with ligands, which influence its conformation. Thus H3, in contrast to the other five binding loops, has a conformation that depends strongly on its molecular environment. Indeed, a containing the V_H domain of antibody B1-8 combined with two different V_L domains has two ve conformations of H3 (25). This important observation implies that general rules governing the cc H3 (unlike the other five antigen-binding loops) must involve interactions outside the local regio

To include all residues that contribute to determinants of the conformation of the H3 region and l conserved residues Cys92 and Gly104 provide useful landmarks to identify the H3 region in a ne H3 region is defined as the residues from Cys92 to Gly104. Analysis of the conformations of H3 divided the H3 region into a torso section comprising a head, the apex of the loop, and residues p framework–four residues starting from the conserved Cys92 and from the N-terminus and six res

C-terminus. For H3 structures that contain more than 10 residues, there are two main classes of t conformations (see Fig. 11). In the major class, the conformation of the torso has a **b_{12}-bulge** at a few H3 regions, the torso does not contain a bulge, but continues the regular hydrogen-bonding b-sheet.

The choice of bulged or nonbulged torso conformation is dictated primarily by the sequence. A b formed whenever residues are present that permit formation of a salt bridge between the side cha Lys residue at position 94 and Asp101, unless a residue at position 93 forms the salt bridge. Inde the torso region were chosen as the largest set of residues proximal to the framework that have a repertoire of conformations, as in the canonical structure model of other antigen-binding loops. I heads or apices of the H3 loops have a very wide variety of conformations. In shorter H3 regions containing the nonbulged torso conformation, the heads follow the rules relating sequence to stru hairpins. For longer H3 regions containing the bulged torso conformation, there are many very d conformations of the head, which can be catalogued but are difficult to classify.

Accurately predicting the conformation of the torso of the H3 region from amino acid sequence i most cases. Predicting the conformation of the head is possible in some cases. However, our und sequence–structure relationships has reduced the uncertainty to no more than a few residues at th region, but these residues appear in a crucial position within the antigen-binding site!

0.7. Prediction of Antigen-Binding Sites

The possibility of accurately predicting the three-dimensional structures of immunoglobulins at t is centrally important for engineering antibodies with prescribed specificity. Several methods for structures of antigen-binding sites have been proposed. Some apply information from known stru are based on *a priori* methods.

The canonical structural analysis of the conformations of the hypervariable loops suggests a mod all but the apex of the H3 loop: Construct the frameworks by standard **homology modeling** techn Then identify, if possible, canonical structures of the loops and graft them onto the modeled fram

Another procedure for predicting the structures of antigen-binding loops relies on conformationa calculations. The main-chain conformation of an antigen-binding loop attached to a given frame constraint that the chain must connect two fixed end points with a specified number of residues. fewer than about six residues, it is possible to enumerate a fairly complete set of feasible main-ch chain conformations, which bridge the given end points and do not make steric collisions within between the loop and the rest of the molecule. The search procedure can be fine enough to incluc the correct one in the many possibilities enumerated. To choose one of them as the predicted con possible to estimate conformational energies and to evaluate the accessible surface areas of each context of the remainder of the protein and set criteria for selecting the most favorable one. Typi conformational energy calculations include terms representing hydrogen bond, van der Waals, ar interactions. Accessible surface area calculations estimate the interaction between the protein anc Note that these procedures are completely general, independent of the current state of the structu

Procedures for conformation generation and evaluation have been implemented in a number of c programs. An application to predict all six antigen-binding loops of McPC603 and HyHEL-5 has (29). The resulting models of the antigen-binding loops of McPC603 and HyHEL-5 have rms de range 0.3 to 2.6 Å (backbone) and 1.4 to 4.1 Å (all atoms).

Jones and Thirup (30) developed an alternative approach to modeling loops, based on selecting l proteins in the database of known structures that span the given end points and overlap with pept termini. For this procedure to be useful, it is required (1) that the loops in immunoglobulin antige appear in other proteins in the database; (2) that the geometrical relationship between the loop an that flank it are the same in immunoglobulin antigen-binding sites and proteins in the database co of the same conformation; and (3) if several loops are found in the database that properly join the flanking an antigen-binding loop, it must be possible to select the correct one. This problem is th faced in methods in which loop conformations are generated *a priori*. If the selection from candi identified from homologous regions of other immunoglobulins by database searching is based on patterns in the sequences, the procedure reduces in effect to the canonical structural method.

The main-chain conformations of most antigen-binding loops recur in other antibody structures (course, one of the elements of the canonical structural model) and also in unrelated proteins (18, exceptions are unusually long loops, such as L1 of McPC603 or H3 of KOL. In other words, the loops whose structures commonly appear in antibodies are not unique to antibody structures. Ho geometrical relationship between the loop and its flanking peptides usually differs when compari binding loop with a loop of similar conformation in an unrelated protein (except for short hairpin conformation). In these cases it would not be possible to build a correct model of an unknown im A protocol that combines these approaches, by using a CONGEN procedure alone for short loops supplements it with database search techniques for longer loops, has been described (32).

1. Conclusions: How Does the Immune System Generate and Then Refine Molecules of Genera

Based on the studies of sequences and structures, we can provide some fairly detailed answers to about what the immune system is doing at the structural level. Here we are concerned with the ge diversity in structure and thereby in affinity and specificity but do not treat the cellular mechanis which challenge by antigens elicits the proliferation of those cells that produce antibodies that bi Immunoglobulin Biosynthesis).

The antigen-combining site has a main-chain conformation determined by the canonical structure L2, L3, H1, and H2, plus the more variable H3. The number of potential main-chain structures in binding site is equal to the product of the number of possible canonical structures for loops L1, L H2, and of the number of possible structures of H3. Although putting numbers into these stateme large numbers of potential antibody sequences, there are preferences for structure at the level of canonical structures. Because only a relatively few residues are required to fix the canonical stru chain, most of the antigen-binding loop residues can be freely decorated with side chains to vary topography and charge distribution of the binding site.

The immune system is one of many biological examples of molecular recognition. Individual ant complexes fit the classical ideas of lock-and-key complementarity and induced fit, but the system more complex than, for example, enzymes, in which the lock and key are in most cases fixed and within the lifetime of the organism. In the primary immune response, the immune system achieve many keys by providing many locks, but to achieve the spectacular affinity of the secondary resp mechanism to perturb the locks for better fit. The integration of the immune response over the sy involving both sequence and structural dimensions together with the clinical and biotechnologica makes it a fascinating topic to study.

2. Acknowledgment

We thank Drs. I. Tomlinson and E. Gherardi for a critical reading of this manuscript.

Bibliography

1. A. K. Abbas, A. H. Lichtman, and J. S. Pober *Cellular and Molecular Immunology*, 3rd ed., Philadelphia, 1997.

2. T. T. Wu and E. A. Kabat (1970) J. Exp. Med. **132**, 211–249.
3. C. Chothia and A. M. Lesk (1987) J. Mol. Biol. **196**, 901–917.
4. E. Padlan (1996) Adv. Protein Chem. **49**, 57–133.
5. R. Glockshuber, M. Malia, I. Pfitzinger, and A. Plückthun (1990) Biochemistry **29**, 1362–13
6. C. Chothia, J. Novotny, R. E. Bruccoleri, and M. Karplus (1985) J. Mol. Biol. **186**, 651–663
7. J. Janin and C. Chothia (1990) J. Biol. Chem. **265**, 16027–16030.
8. T. N. Bhat, G. A. Bentley, G. Boulot, M. I. Green, D. Tello, W. Dall'acqua, H. Souchon, F. A. Mariuzza, and R. J. Poljak (1994) Proc. Natl. Acad. Sci. USA **91**, 1089–1093.
9. J. M. Rini, U. Schulze-Gahmen, and I. A. Wilson (1992) Science **255**, 959–965.
10. R. L. Stanfield, T. M. Fieser, R. A. Lerner, and I. A. Wilson (1990) Science **248**, 712–719.
11. I. M. Tomlinson, G. P. Cook, N. P. Carter, R. Elaswarapu, S. Smith, G. Walter, L. Buluwela and G. Winter (1994) Hum. Mol. Genet. **6**, 853–860.
12. J. P. L. Cox, I. M. Tomlinson, and G. A. Winter (1994) Eur. J. Immunol . **24**, 827–836.
13. O. Ignatovich, I. M. Tomlinson, P. T. Jones, and G. Winter (1997) J. Mol. Biol. **268**, 69–77.
14. C. Chothia, A. M. Lesk, E. Gherardi, I. Tomlinson, G. Walter, J. D. Marks, M. B. Llewelyn, (1992) J. Mol. Biol. **227**, 799–817.
15. I. M. Tomlinson, G. Walter, P. T. Jones, P. H. Dear, E. L. L. Sonnhammer, and G. Winter (1 Biol. **256**, 813–817.
16. G. J. Wedemayer, P. A. Patten, L. H. Wang, P. G. Schultz, and R. C. Stevens (1997) Science 1669.
17. B. L. Sibanda, T. L. Blundell, and J. M. Thornton (1989) J. Mol. Biol . **206**, 759–777.
18. A. Tramontano, C. Chothia, and A. M. Lesk (1989) Proteins: Struct. Function Genet. **6**, 382-
19. A. Tramontano, C. Chothia, and A. M. Lesk (1990) J. Mol. Biol. **215**, 175–182.
20. B. Al-Lazikani, A. M. Lesk, and C. Chothia (1997) J. Mol. Biol. **273**, 927–948.
21. E. A. Kabat, T. T. Wu, H. M. Perry, K. S. Gottesman, and C. Foeller (1991) *Sequences of Pr Immunological Interest*, 5th ed., Public Health Service, N.I.H, Washington, D.C..
22. A. C. R. Martin and J. M. Thornton (1996) J. Mol. Biol. **263**, 800–815.
23. S. Barré, A. S. Greenberg, M. F. Flajnik, and C. Chothia (1994) Nat. Struct. Biol. **1**, 915–92
24. C. Chothia, A. M. Lesk, A. Tramontano, M. Levitt, S. J. Smith-Gill, G. Air, S. Sheriff, E. A. Davies, W. R. Tulip, P. M. Colman, S. Spinelli. P. M. Alzari, and R. L. Poljak (1989) Nature
25. X. Y. Pei, P. Holliger, A. G. Murzin, and R. L. Williams (1997) Proc. Natl. Acad. Sci. USA
26. H. Shirai, A. Kidera, and H. Nakamura (1996) FEBS Lett . **399**, 1–8.
27. V. Morea, A. Tramontano, M. Rustici, C. Chothia, and A. M. Lesk (1998) J. Mol. Biol. **275**,
28. A. Sali (1995) Mol. Med. Today **1**, 270–277.
29. R. E. Bruccoleri, E. Haber, and J. Novotny (1988) Nature **335**, 564–568.
30. T. A. Jones and S. Thirup (1986) EMBO J. **5**, 819–822.
31. A. Tramontano and A. M. Lesk (1992) Proteins: Struct. Function Genet. **13**, 231–245.
32. A. C. R. Martin, J. C. Cheetham, and A. R. Rees Proc. Natl. Acad. Sci. USA **86**, 9268–9272.
33. G. Winter, A. D. Griffiths, R. E. Hawkins, and H. R. Hoogenboom (1994) Ann. Rev. Immun 455.
34. P. G. Schultz and R. A. Lerner (1995) Science **269**, 1835–1842.

Immunophilin

Cytosolic receptor proteins for immunosuppressant drugs in mammals of the cyclosporin and peptidomacrolide type have been named immunophilins because of their putative involvement in the signaling mechanism of the cellular immune response (1). It was further pointed out that the immunophilin/immunosuppressant complex is active, not the individual free drug or receptor. A composite surface formed by the bound drug and by the surrounding immunophilin residues functions by binding other cellular proteins involved in signal transduction. Initially, because of the limited knowledge about the diversity of these enzymes, the groups of immunophilic receptor proteins coincided with the enzyme classes of peptidyl prolyl cis/trans isomerases (PPIase), cyclophilins, and FK506-binding proteins (FKBP). Now, cyclophilins and FKBP have been isolated that display only modest affinity for these drugs or cannot form active enzyme/drug complexes. Furthermore, the new PPIase families of trigger factors and parvulins do not bind the immunosuppressive drugs at all. On the other hand, there are now also many other proteins that have considerable affinity for the immunosuppressants and are not PPIase (2). To avoid confusion with nomenclature, the term immunophilin should be limited to PPIases with proven involvement in immunosuppression.

Bibliography

1. R. F. Standaert, A. Galat, G. L. Verdine, and S. L. Schreiber (1990) Nature **346**, 671–674.
2. G. Fischer (1994) Angew. Chem., Int. Ed. Engl. **33**, 1415–1436.

Suggestions for Further Reading

3. G. Wiederrecht and F. Etzkorn (1994) The immunophilins, Perspect. Drug Discovery Design **2**, 57–84.
4. S. L. Schreiber and G. R. Crabtree (1992) The mechanism of action of cyclosporin-A and FK506, Immunol. Today **13**, 136–142.
5. S. H. Snyder and D. M. Sabatini (1995) Immunophilins and the nervous system, Nature Med. **1**, 32–37; summarizes immunophilins of the nervous system.

Imprinting

1. Mammalian Imprinting: From Genomes to Genes

Sexual reproduction, which involves the fusion of two gametes produced by two distinct individuals, is the most common form of reproduction encountered among higher eukaryotes. Although sexual reproduction has obvious long-term benefits, such as being a powerful source of genetic variability and in triggering evolution, many short-term disadvantages, including what is called the “cost of meiosis” (1), could have acted against its maintenance during evolution. In this regard, one can view imprinting as a way to “maintain” sexual reproduction, by providing an absolute short-term advantage. Parental imprinting, also known as genomic or gametic imprinting, is a genetic effect in which the expression (behavior) of **genomes, chromosomes**, or chromosomal regions differs according to their parental origin. As a result, individuals from species in which imprinting occurs require a contribution of both parental genomes to develop properly. This phenomenon is observed in many biological systems, from bugs, where sexual determination involves the inactivation and sometimes even the loss of the whole paternal genome (2), to mammals, which will be the main subject of this review.

In mammals, evidence that maternal and paternal genomes are imprinted to function differentially during development initially came from the study of parthenogenetic and androgenetic mouse embryos generated by pronuclear transplantations (3-5). In general, parthenogenetic embryos (two maternal genomes) fail to develop normal extraembryonic components, whereas androgenetic embryos (two paternal genomes) have a very poorly developed embryo proper. Mouse genetic studies involving the analysis of maternal and paternal disomies and/or duplications of defined chromosome regions have subsequently demonstrated that this phenomenon does not affect the whole genome *per se*, but rather only specific regions (6). Ten regions on six mouse autosomes have been shown to be subject to imprinting [chr 2, 6, 7, 11, 12, and 17, (6)]. The maternal and paternal duplications for five of the imprinted regions have distinct consequences, indicating that there are in total 15 known imprinting effects. One cannot exclude the possibility, however, that there are additional imprinted regions with phenotypic effects too subtle to be detected.

Further investigations have revealed that the genetic basis for these imprinting effects is likely to be the genes themselves, because some of the genes lying within these regions are subject to imprinting, which means that they are monoallelically expressed, either from the paternal or the maternal chromosome, depending on the gene. In the same way, monoallelic expression can occur in most tissues of the individual or can be restricted to a very specific developmental stage and/or cell lineage. Now, more than 25 imprinted genes have been identified in mouse, and most of these are conserved in human (Table 1). Despite the growing list of imprinted genes and their more detailed characterization, the function of imprinting remains a mystery. The abnormalities displayed by parthogenetic and androgenetic mouse embryos underscore, however, that imprinting plays a pivotal role in development.

Table 1. List of Imprinted Genes in Human and Mouse and Some of Their Characteristics[a]

				Human		
Gene	**Function**	**Chr**	**Exp**	**Specificity**	**Methylation**	**Ch**
Human Chromosome11/Mouse Chromosome 7						
IGF2/Igf2	Growth factor		pat	Mostly monoallelic except in choroid plexus,leptomeninges and adult liver		
INS2/Ins2	Insulin		pat + mat			
H19	Noncoding RNA		mat	Mostly monoallelic except in early placentae	Hypermethylation of the paternal allele	
HASH2/Mash2	Transcription		mat	Mostly monoallelic		

	factor					
KVLQT1/Kvlqt1	Potassium channel		mat	Mostly monoallelic except heart		
$p57^{KIP2}$	Cyclin-cdk inhibitor		mat	Mostly monoallelic with weak expression of thepaternal allele in most tissues; biallelic in fetal brain		
IPL/Ipl	Role in apoptosis?		mat	Mostly monoallelic with some mosaicism		
IMPT1/Impt1	Metabolite transporter?		mat	Allelic bias		
Human Chromosome15/Mouse Chromosome 7						
ZNF127/Zfp127	Zinc-finger protein		pat	Mostly monoallelic	Hypermethylation of the maternal allele	
ZNF127A S/Zfp127as						pat
NECDIN/Necdin			pat	Mostly monoallelic		Hypermet of the mat allele
SNRPN/Snrpn	Splicing		pat	Mostly monoallelic	5′ Region methylated on the maternal allele 3′ region methylated on the paternal allele	
PAR-SN	No ORF		pat	Monoallelic (lymphoblast)		
PAR-5			pat	Monoallelic (fibroblast)		
IPW	No ORF		pat	Mostly monoallelic		
PAR-1			pat	Monoallelic (fibroblast)		
UBE3A/Ube3A	Ubiquitin protein ligase		mat	Moallelic only in brain	No allelic methylation identified	
DST			mat	Moallelic only in brain		
UBE3A/DST-antisense	Regulation of UBE3A imprinting?		pat	Expressed and monoallelic only in brain		
Miscellaneous Genes						
p73	Tumor	1p36	mat	Mostly monoallelic	NT	

	suppressor					
IGF2R/Igf2r	IGF2 receptor	6q25-26	mat + pat	Mostly biallelic.	Region 2 hypermethylated on the maternal allele	17
				Some cases of monoallelic expression		
Igf2r−antisense	Regulation of Igf2r imprinting?					17
MAS/Mas	Cell surface receptor	6q25-26		Monoallelic only in adult breast	17	
PEG1-MET/Peg1-Mest	a/b Hydrolase fold family	7q32	pat	Monoallelic in fetus, biallelic in blood	Maternal methylation	6
HTR2	Serotonin receptor	13q14	mat	Monoallelic (fibroblast)	Maternal methylation	14
U2af1-rs1	Splicing	NC				11
Peg3/Pw1	?					7
Grf1	Regulates synthesis and release of growth hormone					9
Peg5/neuronatin						2
Impact						18
XIST/Xist	X-inactiva-tion	X				X

[a] The first part of the table corresponds to the human chromosome 11/mouse chromosome 7 cluster; the second part of the table corresponds to the human chromosome 15/mouse chromosome 7 cluster; and the third part of the table corresponds to miscellaneous genes. Chr, chromosomal localization; Exp, allele expressing the gene; pat, paternal; mat, maternal. Specificity: specificity of the monoallelic expression. Methylation: allelic methylation. Noted as G when inherited from the gametes, S (somatic) when not. NC (in the case of U2af1-rs1 in man) indicates not conserved at the location homologous to that in mouse. Blank cells indicate not tested or not published results.

This is also true in humans, because the presence of two paternal genomes without a maternal one results in the formation of hydatidiform moles (7), which is essentially equivalent to that found with the androgenetic embryos in the mouse. In addition, the deregulation of imprinting causes disease, and the expression of several inherited diseases is strongly influenced by the sex of the transmitted parent. The best-known examples are the Beckwith–Wiedemann syndrome (BWS) and the Prader–Willi and Angelman syndromes (PWS and AS) (8). BWS is often associated with lack of a biparental inheritance of chromosome 11p15 and is characterized by pre- and postnatal overgrowth, including hemihypertrophy, visceromegaly, and macroglossia (enlarged tongue), and an increased probability of developing childhood cancers, the most frequent ones being Wilm's tumor and adenocortical carcinoma. The involvement of imprinting in this syndrome was suggested by the preferential maternal transmission of mutations in BWS (9, 10) as well as the occurrence of paternal uniparental disomies (UPDs) of chromosome 11p in several sporadic cases of BWS (11).

PWS and AS are two clinically distinct syndromes that share a chromosomal location (15q11-q13) but display opposite parental origins of transmission. PWS is characterized by hypotonia, hypogonadism, variable mental retardation and obesity (12), while the AS clinical features include hyperactivity, ataxic gait, "puppet-like" arm movements, bouts of inappropriate laughter, seizures, EEG abnormalities and severe mental retardation with absence of speech (13, 14). Most (60% to 70%) PWS and AS cases are associated with *de novo* cytogenetic deletions of the 15q11-q13 region. In PWS, the deletion occurs exclusively on paternal chromosome 15 (15), whereas AS chromosome 15q11-q13 deletions are of maternal origin (16). Maternal and paternal uniparental disomy (UPD) also occur in some PWS (17) and AS (18) cases, respectively. Roughly 25% of PWS patients display UPD with both chromosomes 15 being inherited from the mother and no chromosome 15 being derived from the father. Only about 5% of AS cases result from paternal UPD and maternal nullisomy for chromosome 15. These observations indicate that the gene(s) responsible for PWS are expressed only from the paternal chromosome, whereas the AS gene(s) are transcribed from the maternal chromosome.

The list of human diseases resulting from abnormal imprinting will no doubt expand as the catalogue of imprinted genes (see Table 1) becomes more complete. The identification of other loci subject to genomic imprinting requires some knowledge of the properties specific to such regions.

2. Characteristics of Imprinted Regions and Genes

The occurrence of imprinting and its consequent monoallelic expression implies that both alleles of the same gene can be recognized and differentially regulated within the same nucleus. The fact that imprinting occurs in laboratory inbred mouse strains, which are genetically identical at all loci, indicates that the basis of imprinting must be epigenetic. Imprinting is a two-step process that must fulfill two conditions. The first step is the apposition of the mark, the imprint, which will allow one allele of a gene (or a chromosomal region) to be distinguished from its homologue. This "labeling" must occur during gametogenesis, which is the only stage where both alleles are physically separated. The question remains as to which allele, the repressed or the expressed one, carries the imprint, although recent evidence suggests that it is the silent allele that is modified in the gamete (see text below). The second step of the process is the reading of the imprint in the appropriate developmental stage and/or tissue, which implies that the imprint has not been erased during development and is stably maintained. Stability is one of the required characteristics of imprinting. Once established, the imprint must indeed be clonaly inherited and maintained through cell divisions. Reversibility is the other necessary property of impritinting, because the imprint must be erased and properly reestablished at each generation. Both stability and reversibility are features of, and can be explained by, epigenetic modification of the chromatin.

Differential **methylation** of the cytosine residue in **CpG** dinucleotides is an attractive candidate as the "label" of imprinted genes and regions, because it is an epigenetic modification that is reversible and heritable, and it can play a role in the regulation of gene (19, 20). The association of DNA methylation with transcriptional activity and chromatin conformation is most evident in the case of the mammalian X chromosome, where the **promoters** of several **housekeeping genes** on the inactive X chromosome are enriched for 5-methylcytosine. These results suggest that repression of gene activity can be mediated through methylation of 5′ regulatory elements. This association is less clear for tissue-specific autosomal genes where, despite a significant body of suggestive evidence, there is no direct proof that DNA methylation modulates transcriptional activity.

A significant difference in the degree of methylation between the paternal and maternal genomes has been elegantly demonstrated by Rougier et al. (21). These authors used **antibodies** to 5-methylcytosine to label metaphase chromosomes in mouse preimplantation embryos, and they observed distinct differences in the labeling patterns at the one-cell stage. The **euchromatic** arms of the maternal chromosomes were intensely stained and demonstrated an R-like banding pattern. In contrast, the antibody staining of the paternal set of chromosomes was quite faint (21). While these data demonstrate the marked difference in global DNA methylation between the two parental chromosome complements in preimplantation development, more direct evidence of a role for DNA methylation in the process of epigenetic marking has been derived by the analysis of sites of allelic methylation within imprinted genes. Most imprinted genes indeed display parent-specific methylation (Table 1). For some of them, including *H19* and *SNRPN* (22-25), methylation is associated with the repressed allele, whereas for others, like *Igf2*, it is the expressed allele that is methylated (26). Strong evidence for the pivotal role of DNA methylation in the regulation of imprinted gene expression comes from studies in mice bearing a disruption of the DNA methyltransferase gene (Dnmt), the enzyme responsible for the maintenance of cytosine methylation (27). Such mice display embryonic lethality and a content of 5-methylcytosine that is reduced to about 30% of wild-type levels (27). Moreover, the expression of several imprinted genes in Dnmt -/- mice is abnormal with, for example, activation of the normally repressed paternal *H19* allele and silencing of the normally active paternal *Igf2* allele (28). While these results clearly indicate the functional role of allelic DNA methylation in imprinted gene expression, the imprinting of some genes, such as *Mash2*, appears normal in Dnmt-/- mice, suggesting the possibility of different mechanisms of imprinting in terms of its association with methylation (29).

Another property of imprinted regions is asynchronous DNA replication. Chromosome replication banding studies generally indicate that homologous regions on both autosomes of a pair replicate at the same time in the S phase of the cell cycle (30). Using this approach, Izumikawa et al. first observed that this was not the case for the imprinted chromosomal region 15q11-q13 (31). That imprinted chromosomal regions replicate asynchronously has been confirmed in other replication banding studies (32, 33) and by using a different assay of DNA replication involving the technique of fluorescence in situ hybridization (FISH) (34). The use of the FISH assay has revealed that DNA replication asynchrony is a feature of other imprinted regions (34-36). The parental origin of the earlier replicating allele was investigated for several probes from different imprinted regions, and it was generally found that DNA replication occurs earlier on the paternal homologue (34, 37-39). The patterns of allele-specific replication have also been investigated in the cells of PWS and AS patients (34, 37-40), with one important finding being that the DNA replication of various probes from the PWS/AS region is synchronous in the cells of PWS and AS UPD individuals (37-40), suggesting the requirement of a biparental contribution for the regulation of replication asynchrony (38). These findings led to the suggestion that allelic cross-talk might be involved in the normal pattern of imprinting. As several such cross-talk models of transcriptional regulation involve pairing of homologous chromosomes, the possibility that the maternal and paternal chromosome 15 homologues physically associate during somatic cell division was investigated.

Three-dimensional analysis of FISH in spatially intact nuclei was performed by laser scanning confocal microscopy to determine the distance between homologous chromosomes in cell cycle-fractionated human lymphocytes (41). The results demonstrated that in normal cells the chromosome 15 homologues pair during the late S phase. The most tightly paired region was observed to be 15q11-q13, consistent with the hypothesis that allelic cross-talk could be involved in the normal pattern of imprinting in chromosome 15q11-q13 (41). Homologous association was also observed at the imprinted IGF2 locus on chromosome 11p15 (41), suggesting that the physical association of chromosome homologues is another manifestation of imprinting in normal human somatic cells and that regulation in *trans* could play an important role in the establishment and/or maintenance of imprinting.

The hypothesis that *trans*-sensing effects may play some role in the regulation of imprinting has been confirmed to some extent at the molecular level using mouse models, where imprinted genes have been modified or deleted by **gene-targeting** mutagenesis (42, 43). Crosses between mouse strains bearing different *H19* deletions revealed that transmission through the maternal germline affects the DNA methylation pattern of the paternal *Igf2* allele. In these crosses, where the maternal (active) *H19* allele is deleted, the paternal copy of *Igf2* is hypomethylated relative to that in wild-type animals (42). It has also been shown that imprinted expression of another gene, *Ins2*, which is tightly linked to *Igf2*, can be affected by the *trans* allele (43). In the latter experiments, the level of transcription of the maternal copy of a reporter gene (Lac Z) construct inserted at the *Ins2* locus depended on what was present on the paternal copy. Expression of the maternal copy of LacZ was repressed in the case where the paternal copy was an insertion of a different reporter (Neo), but not in mice where the paternal homologue is wild type. These results suggest that interaction between two alleles in *trans* can modulate both allele-specific transcription and DNA methylation and thus play a fundamental role in the establishment and/or maintenance of imprinting.

The properties of imprinted regions summarized above underscore the fundamental role of epigenetic modification of chromatin in the establishment and the maintenance of the imprint. There is, in addition, some molecular evidence for allele-specific changes in chromatin structure at imprinted loci. For the imprinted gene *U2af1-rs1* (see Table 1), there is a correlation between imprinted expression and an “open” or “active” chromatin expression, because the gene shows both expression and the presence of nuclease-hypersensitivity at sites in the promoter region of the paternal, but not the maternal, allele (44). No such allele-specific differences in nuclease sensitivity has been identified for the imprinted *Igf2* gene (45), however, suggesting that differential chromatin structure, at least as assayed by these approaches, is not a general feature of imprinted genes. Alternatively, these discrepant findings may reflect different mechanisms of imprinting for *U2af1-rs1* and *Igf2*. Further evidence for an association between imprinting and chromatin structure at the global level comes from the observation of sex-specific meiotic recombination frequencies in imprinted regions (46, 47).

3. A Catalog of Imprinted Genes and Their Characteristics

Although the occurrence of imprinting in mammals was demonstrated in 1984 (3, 4), one had to wait several years for the first imprinted genes to be described. As it is often the case in biological research, several papers, published at approximately the same time, reported imprinting of three genes, *Igf2r, Igf2*, and *H19* (48-50). These are the most studied of the imprinted genes in terms of understanding imprinting mechanisms (see text below). Since these initial reports, the number of genes identified as imprinted has continuously increased. There were eight reported by 1994 (51), and four years later more than 25 genes are identified as being monoallelically expressed in a parental-dependent way, at least at some point during development (Table 1). Due to limited space, these cannot be described in detail here, and only a few have been chosen as examples.

Igf2r was mapped to mouse chromosome 17, in a region known to contain the Tme locus, a **maternal-effect** mutation that results in the death of embryos at day 15 of gestation (52). **Northern blot** hybridizations of RNA from embryos having inherited a deletion of Tme from their mother or their father showed that only the maternal allele of *Igf2r* is expressed (48). Methylation analysis of a 130-kbp region spanning the *Igf2r* locus has identified two CpG island regions that display allelic methylation (26). Region 1, which corresponds to the 5′ end of the transcription unit, is hypermethylated on the transcriptionally silenced, paternal allele. Region 2, localized in the second **intron** of the gene, shows the opposite pattern, with hypermethylation of the expressed, maternal allele. Only the region 2 hypermethylation profile is inherited from the gametes and remains constant in all developmental stages and must therefore represent the imprint for the *Igf2r* gene. The functional role of this region in the imprinted expression of *Igf2r* was demonstrated by generating transgenic mice carrying a yeast artificial chromosome (YAC) from that region, which successfully reproduced methylation and expression of the endogenous *Igf2r* (53). Deletion of region 2 from these transgenes results in loss of imprinting and biallelic expression of *Igf2r*. Moreover, the region 2 CpG island was shown to be responsible for the expression of an **antisense** RNA (AS) whose expression profile is opposite to that of *Igf2r*. Only the paternal allele is normally transcribed and, in the case where *Igf2r* biallelic expression is associated with deletion of region 2, both alleles are repressed. It has been suggested that the antisense is the “imprintor” gene that regulates in *cis* the imprinted expression of *Igf2r* (54) (see text below).

Evidence for the imprinting of *Igf2* came initially from genetic studies of knockout mice generated to investigate the potential role of this gene during development. Heterozygotes having inherited the deletion from the father are smaller in size than normal animals and are indistinguishable in appearance from homozygotes (55). In contrast, when the mutation is transmitted through the mother, the heterozygotes are phenotypically normal. Molecular analysis of *Igf2* expression in genotyped embryos using ribonuclease protection assay subsequently confirmed that the paternal *Igf2* gene is transcriptionally active, whereas the maternal transcript is not detectable, except in choroid plexus and leptomeninges (49).

H19 is an abundant RNA in the developing mouse embryo. Despite the absence of coding potential of *H19*, it is conserved significantly between human and mouse (56). Overexpression of *H19* in transgenic mice results in late prenatal lethality, suggesting that its dosage must be strictly controlled during development (57). In addition, *H19*, like *Igf2*, was mapped to mouse chromosome 7, in a region known to display an imprinting effect. Imprinted expression of *H19* was assessed using a ribonuclease protection assay that could distinguish between **polymorphic** alleles from different mouse subspecies. Only the maternal allele was shown to be expressed in liver and skeletal muscle of neonates and adults (50). Fine mapping subsequently localized *H19* less than 90 kbp from *Igf2*, with both genes having the same transcriptional orientation (58). Thus, both genes are physically clustered and imprinted, although in the opposite direction. In addition, *Igf2* and *H19* display a very similar, if not identical, pattern of expression during development (59). These findings led to the hypothesis that *H19* and *Igf2* operate from a common set of regulatory elements (60). Indeed, two endoderm-specific **enhancers**, located distal to *H19*, were shown to be responsible for the maternal expression of *H19* and the paternal expression of *Igf2* (61). The choice of the gene (*H19* or *Igf2*) to be activated by these enhancers is dictated by their methylation status. Both *H19* and *Igf2* have a region of hypermethylation on the paternal chromosome (23, 62). Only in the case of *H19*, however, is the methylation inherited from the gamete, suggesting a role as the imprint to distinguish the two alleles of *H19* (63). This paternal-specific *H19* methylation is thought to result in the strong preference for *Igf2* expression on the paternal chromosome. Methylation of *H19* on the paternal allele thus indirectly triggers the expression of *Igf2*. On the maternal chromosome, the preference for *H19* expression could well result from its closer proximity to the enhancers, a possibility that has been demonstrated by creating transgenic mice with duplicated and mislocated enhancers (64). *H19* can therefore be classified as a gene that is directly imprinted, whereas *Igf2* is imprinted indirectly, leading to the suggestion that the role of *H19* is to regulate the expression of *Igf2* and other flanking genes. This role for *H19* is analogous to that of an imprintor as mentioned above (54).

As shown above, initial reports of imprinted genes were based on genetic evidence: either the observation of a parental effect associated with a mutation (*Igf2*), or the mapping of a gene to a region known to display an imprinting effect (*Igf2r* and *H19*). This latter “strategy” has led to the identification of other clusters of imprinted genes, including that of mouse chr. 7/human chr. 11 *H19/Igf2* cluster and the mouse chr. 7/human chr. 15 cluster (Table 1).

The human 11p15 region, which contains *H19* and *IGF2*, is associated with the Beckwith–Wiedemann syndrome (BWS). *IGF2* has long been a strong candidate for this syndrome, since it is highly expressed in the tissues that are the most affected in BWS. Moreover, *IGF2* imprinting is lost in 80% of BWS cases, resulting in biallelic expression of the gene (65), a finding that could explain the overgrowth characteristic associated with this syndrome. However, no chromosome rearrangment or mutation affecting the expression of *IGF2* alone has been identified in BWS patients, and the search for additional candidate gene(s) has led to a detailed transcription and imprinting map of the region. *p57* ^{KIP2}, an imprinted gene (66) that encodes a cyclin-dependant kinase (CDK) inhibitor, is the first gene shown to be mutated in BWS patients (67). *KVLQT1* was identified by positional cloning and mapped between *p57* ^{KIP2} and *IGF2*. *KVLQT1* is disrupted by chromosomal rearrangements in BWS patients (68) and is imprinted, with predominant maternal expression in most tissues. One exception is heart, where biallelic expression is observed. In several specimens, including different fetal tissues, however, monoallelic expression is not complete and, although the maternal allele is predominately expressed, residual expression from the paternal gene is detected. This "weak" or "leaky" imprinting is even more pronounced in the case of the mouse homologue *Kvlqt1*. While early expression of the gene is maternal in origin, this strong maternal bias is gradually lost in a tissue-specific manner as embryogenesis proceeds. Adult animals show complete biallelism (69). *IMPT1*, an other imprinted gene lying in the human 11p15.5/mouse distal 7 regions, also shows an allelic bias ("unequal allelic expression") toward the maternal allele (70).

Incomplete imprinting has also been reported for *UBE3A*, the gene involved in Angelman syndrome. This gene displays highly tissue-specific imprinting, with predominant maternal expression in brain, but the paternal allele still expresses [TEXnical Error] of the total (71). In that case, this is likely to be due to the presence of different cell populations in the brain samples studied, one displaying complete monoallelic expression and a second, less abundant one, showing normal, biallelic expression; in mouse, *Ube3A* imprinting was shown to be restricted not only to brain but, more specifically, to certain types of neurons (72). Whether similar explanations are valid for most cases of incomplete imprinting remains to be determined. Most techniques used so far to study the imprinting status of genes, such as Northern blot, reverse transcriptase–polymerase chain reaction (**RT-PCR**), or ribonuclease protection, are performed on tissue samples or even whole individuals (embryos), which implies a mixture of several cell types. Analysis at the cellular level will require the use of more sophisticated technologies, like single-cell PCR or RNA-FISH. As suggested by the recent description of "weakly" imprinted genes, more detailed analyses of the expression pattern of genes may prompt us to reconsider our definition of imprinting. Will any gene showing monoallelic expression in a reasonable number of cells at any developmental stage or in any tissue be considered as imprinted? One important point to keep in mind, however, is that if imprinting implies monoallelic expression at some point during development or in some cell types, monoallelic expression doesn't necessarily indicate imprinting. This is evident from the observation that genes such as those encoding the olfactory receptors (73) and the lymphokine IL-2 (74) are monoallelically expressed but cannot, however, be considered as imprinted, because their expression can be from either the maternal or the paternal allele (random allelic expression).

It may also be very difficult to exclude that any gene is imprinted, because of the difficulty in analyzing the status of allelic expression in all cell populations within any tissue at any developmental stage. In other words, if the demonstration of nonrandom allelic expression is the molecular proof of imprinting, the "failure" to detect such an expression pattern is not proof of the absence of imprinting. One example that illustrates this problem is the Angelman syndrome gene, *UBE3A*. This gene was shown to be responsible for Angelman syndrome based on its chromosomal localization and the presence of point mutations in several patients. However, *UBE3A* displayed biallelic expression in fibroblasts and lymphocytes since the only cell types that had initially been tested, this gene was considered as not imprinted. It was shown only later that *UBE3A* is indeed imprinted, but that this is restricted to brain (71, 75) or, even more specifically, to certain types of neurons (72).

4. Mechanisms of Imprinting

Imprinted genes appear to be preferentially organized into clusters, rather than dispersed throughout the genome, although this may be biased by the fact that the search for imprinted genes has been mostly based on their localization within a region displaying an imprinting effect. This organization into clusters, along with additional molecular evidence, suggests that each imprinted gene is not regulated independently from the other member of the cluster and that cis-acting elements are crucial for their concerted regulation. Two main types of *cis*-elements will be described here, imprinting centers and imprintors, and their relation to each other will be discussed.

4.1. Imprinting Center

As mentioned above, PWS and AS are two distinct syndromes that map to the chromosome 15q11-q13 region. Analysis of several patients carrying distinct rearrangements has allowed definition of two nonoverlapping regions responsible for these syndromes, with the AS region being smaller and lying distal to the PWS region (76). However, small deletions of less than 50 kbp within the PWS interval, in the 5′ region of the paternally expressed *SNRPN* gene (Table 1), were shown to be associated not only with PWS upon paternal transmission, but also with AS when transmitted maternally (77). These deletions affect the methylation profile and the gene expression pattern of the entire PWS region and, probably, although this has not yet been proven, the AS region. In such PWS patients, both chromosomes carry a maternal-specific methylation profile, and the paternally expressed genes of the region, such as *SNRPN, PAR-1*, and *PAR-5*, are transcriptionally silent (78). In AS patients, these genes are expressed biallelically (79) and the paternal methylation pattern is found on both chromosomes. The expression profile of the maternally expressed, AS gene *UBE3A* has not been tested, but it is expected to be silenced on both alleles. Because of these long-range effects, the deletions are thought to affect an imprinting control region, the imprinting center (IC), and are called “imprinting mutations.” Fine mapping of the IC has led to the identification of alternative *SNRPN* 5′ exons, the BD exons, which are spliced to exon 2 of *SNRPN*, skipping the first exon and giving rise to another transcript, different from the *SNRPN* transcript but also paternally expressed (80).

In general, AS imprinting mutations result from the deletion of the BD exons, while PWS imprinting mutations are associated with deletion of at least *SNRPN* exon 1 (80), indicating that the IC has a bipartite structure. One model presented to explain how the IC regulates the imprinting process in PWS and AS invokes a mechanism of imprint switching (77, 80). In this model, the *SNRPN* exon 1 acts as an initiation site, functioning in the paternal germline to switch the chromosome epigenetic state from maternal to paternal. Mutation or deletion of this region causes a failure in the imprint switch during paternal gametogenesis, leading to PWS, because the paternally inherited chromosome has a maternal imprint. The other *cis* element of the bipartite IC would function via an interaction in *trans* with a female-specific factor in the maternal-to-paternal switch of epigenetic states. Mutation or deletion of this structure results in a failure of switching in the maternal germline and a chromosome 15 abnormality where the maternally transmitted chromosome carries a paternal imprint. An individual inheriting this chromosome would have AS due to the lack of a normal maternal contribution of the 15q11-q13 region. While the elements that control the imprint switching process remain to be identified, it has been proposed that the BD exons regulate imprint switching in the maternal germline (80).

It would appear that imprinting mutations may also be involved in the molecular pathogenesis of BWS (36). The evidence for this comes from a translocation family where *IGF2* is expressed biallelically, rather than paternally, although monoallelic DNA methylation of sites in the 3′-end of the gene is observed in most individuals and tissues. Such an uncoupling of allelic DNA methylation from transcription suggests that the disease results from an imprint mutation.

4.2. Imprintors

The findings that only a subset of imprinted genes display a site(s) of allelic methylation that are inherited from the gametes has led to the concept of imprintor genes (54). Such genes inherit the allelic methylation signal from the gametes and thereby act in *cis* to control the expression of the other imprinted “target” genes in the domain by a mechanism of promoter/enhancer competition, as discussed above for the coordinate regulation of *H19* and *Igf2* (60), with *H19* acting as the imprintor in this domain. This concept has also been invoked to explain the regulation of *Igf2r* and its antisense (53). In the latter case, the maternal allele-specific methylation of a CpG island within region 2 (see above) is inherited from the mother and persists in embryonic and adult tissues (26). This region 2 corresponds to a promoter for an antisense that is specifically transcribed from the paternal allele, but repressed on the maternal, strongly suggesting involvement of the antisense in the regulation of *Igf2r* imprinting (53). In the context of the model of Barlow (54), the antisense acts as the imprintor in the *IGF2r* domain.

There is also evidence to indicate that antisense may also play a role in imprinting at the AS locus due to the recent observation of a *UBE3A* antisense transcript (81). This antisense, which also encompasses another sense transcript that is downstream of *UBE3A*, displays the opposite pattern of allelic expression (paternal), and this only in brain. In other tissues where *UBE3A* is biallelically expressed, such as lymphocyte and fibroblast, the antisense is silenced, suggesting that expression of the two transcripts is mutually exclusive (81). These findings once again implicate a role for antisense in regulation of imprinted gene expression and suggest, in two cases, that the putative imprintor is an antisense, although this does not hold true for *H19*. One property shared by the *Igf2r* and *UBE3A* antisense transcripts and *H19* is that these do not have protein coding potential, which does not contradict their acting as imprintors, given that the sole function of an imprintor is to regulate the imprinted expression of other genes.

4.3. Relation Between Imprinting Centers and Imprintors

There are two difficulties with the imprint switch model as it relates to the mechanism of action of the IC in the AS/PWS region. The first is that the BD exons display paternal allele-specific expression, making it difficult to understand how these might function to initiate switching in the maternal germline. Because of this puzzling observation and because these alternative *SNRPN* exons are not conserved in mouse, an alternative model involving competition for a common set of regulatory elements has been proposed to explain the mechanism of the IC (82).

The latter model was proposed initially to explain the opposite imprinting of *H19* and *Igf2* (60) (see above). In the case of the bipartite IC in the AS/PWS region, the element that overlaps the region spanning the BD exons elements is a *cis*-acting maternal epigenetic mark. This *cis*-acting site is extensively methylated in the female germline and represses the paternal genes via spreading of DNA methylation (82). Deletion of this *cis*-acting element would cause AS by transmission of an unmethylated maternal chromosome which thus carries a paternal epigenotype. The *SNRPN* promoter would somehow maintain the PWS region in an unmethylated state in the soma, and its deletion would result in a failure of the maintenance of this state and cause PWS. A neuronal enhancer would also be located in the PWS/AS region to explain the repression of maternally expressed genes, including *UBE3A*, on the maternal chromosome. *SNRPN* and *UBE3A* would compete for this enhancer, with access of *UBE3A* to this enhancer being regulated by the methylation status of the *SNRPN* promoter, which is normally paternally methylated (82). There is, however, evidence to suggest that the region spanning the BD exons is biallelically methylated (83) and that some sites in the PWS region are more methylated on the paternal chromosome (24, 77). Both these findings contradict the enhancer-competition model to explain imprinting in chromosome 15q11-q13 (83).

A different concept of the imprintor, which includes aspects of both models, has been presented to explain the action of the PWS/AS IC (54). On the one hand, the paternally expressed *SNRPN* transcripts encoded that contain the alternative BD exons could function as the imprintor expression competition with *UBE3A*. Alternatively, an imprintor gene encoded from within the AS critical region, but not from the IC, would compete for expression with *UBE3A* (54). The finding of a *UBE3A* antisense provides some support for this latter version of the imprintor model.

The arguments summarized above indicate that, despite much progress, the function and mechanism of action of imprinting centers is not yet understood. Neither the imprint switch, the imprintor, nor the original enhancer-competition model explain an important property of the IC—that is, how these centers act over extensive (1–2 Mb) genomic regions. A mouse model, in which the region syntenic to the PWS-IC has been deleted, not only has some features of PWS, but also displays lack of expression of several paternally expressed genes, including *Ndn*, a gene that is about 1 Mb proximal of the IC (84). Further characterization of these mutant mice should be quite useful in further studies of the function of the IC during development. Finally, the observation that a fragment spanning the *SNRPN* exon 1 can function as a **silencer** element in transgenic *Drosophila* suggests that elements within the IC may regulate imprinting via a silencing mechanism that is evolutionarily conserved (85). It remains to be determined, however, if the silencing element identified by this approach can act over genomic distances in the Mbp size range, as would be predicted for the functional element of an IC.

5. Evolution and Function

Although evidence is accumulating that clearly implicates parental imprinting in developmental and pathological processes, its function in normal development raises more questions than provides answers. Several theories have been developed to explain the acquisition and, more importantly, the maintenance (fixation) of imprinting in mammals. One of these is the subtle and precise control on gene expression that imprinting allows during development. Imprinting has also been described as having evolved from a host defense mechanism (86) and, alternatively, as a surveillance mechanism for chromosome loss (87). However, these hypotheses are often dismissed, because there is no explanation for the fact that imprinting, as described here, is restricted to mammals. In contrast, the parental conflict theory is based on the hallmark manifestation of mammalian evolution—that is, the acquisition of a placenta, which mediates the interaction between the embryo and the mother during intrauterine growth (88). Following the latter theory, the evolutionary interest of the father is to promote growth of its own progeny by maximizing the amount of resource extracted from the mother. On the other hand, it is in the interest of the mother to maximize her total number of surviving offspring without showing favoritism toward the offspring of particular males. This is particularly true for offspring within litters from several fathers. This theory predicts that paternally controlled genes would favor fetal growth, whereas maternally controlled genes would tend to reduce offspring size. This is in agreement with the global observation that androgenetic embryos display abnormal extraembryonic tissues and that parthenogenetic embryos have a poorly developed embryonic portion. At the molecular level, the case of *Igf2/Igf2r* also favors this theory; *Igf2*, a paternally expressed gene, is involved in fetal growth, whereas *Igf2r*, which is maternally transcribed, is supposed to facilitate the degradation of *IL2*. A systematic analysis of the effects of UPDs on fetal growth has, however, shown several contradictions to the predictions of the conflict model (89).

As the number of imprinted genes identified will increase, theories proposed for the evolution of imprinting will probably multiply. The general picture emerging presently is that more genes than initially suspected are imprinted. Whether the imprinted status is “necessary” for their function remains, however, to be determined. Some can be imprinted as “bystanders” because of their location in an imprinted region. It also becomes more and more evident that imprinting is not an “all or nothing” phenomenon. It can affect genes with a high cellular specificity and/or only partially, with the “silent” allele still expressed, albeit at a low level. As a result, we might then consider imprinted expression to be the rule rather than an exception.

Bibliography

1. P.-H. Gouyon, S. Maurice, X. Reboud, and I. Till-Bottraud (1993) La Recherche **24**, 70–76.
2. J. J. Bull (1983) *Evolution of Sex Determining Mechanisms*, Benjamin Cummings, Menlo Park, CA.
3. J. McGrath and D. Solter (1984) Cell **37**, 179–183.
4. M. A. H. Surani, S. C. Carton, and M. L. Norris (1984) Nature **308**, 548–550.
5. D. Solter (1988) Annu. Rev. Genet. **22**, 127–146.

6. B. M. Cattanach and J. Jones (1994) J. Inherit. Metab. Dis. **17**, 403–420.
7. S. D. Lawler, S. Povey, R. A. Fisher, and V. J. Pickthal (1982) Ann. Hum. Genet. **46**, 209–222.
8. M. Lalande (1997) Annu. Rev. Genet. **30**, 173–195.
9. C. Moutou, C. Junien, I. Henry, and C. Bonaiti-Pellie (1992) J. Med. Genet. **29**, 217–220.
10. D. Viljoen and R. Ramesar (1992) J. Med. Genet. **29**, 221–225.
11. I. Henry, C. Bonaiti-Pellie, V. Chehensse, C. Beldjord, C. Schwartz, G. Utermann, and C. Junien (1991) Nature **351**, 665–667.
12. M. G. Butler (1990) Am. J. Med. Genet. **35**, 319–332.
13. J. Clayton-Smith and M. E. Pembrey (1992) J. Med. Genet. **29**, 412–415.
14. C. Rougeulle and M. Lalande (1998) Neurogenetics **1**, 229–237.
15. M. G. Butler and C. G. Palmer (1983) Lancet **1**, 1285–1286.
16. J. H. Knoll, R. D. Nicholls, R. E. Magenis, J. M. Graham, M. Lalande, and S. A. Latt (1989) Am. J. Med. Genet. **32**, 285–290.
17. R. D. Nicholls, J. H. Knoll, M. G. Butler, S. Karam, and M. Lalande (1989) Nature **342**, 281–285.
18. S. Malcolm, J. Clayton-Smith, M. Nichols, S. Robb, T. Webb, A. L. Armour, A. J. Jeffreys, and M. E. Pembrey (1991) Lancet **337**, 694–697.
19. A. Razin and H. Cedar (1994) Cell **77**, 473–476.
20. R. Jaenisch (1997) Trends Genet. **13**, 323–329.
21. N. Rougier, D. Bourc'his, D. Molina Gomes, A. Niveleau, M. Plachot, A. Pàldi, and E. Viegas-Péquignot (1998) Genes Dev. **12**, 2108–2113.
22. M. Brandeis, T. Kafri, M. Ariel, J. R. Chaillet, J. McCarrey, A. Razin, and H. Cedar (1993) EMBO J. **12**, 3669–3677.
23. A. C. Ferguson-Smith, H. Sasaki, B. M. Cattanach, and M. A. Surani (1993) Nature **362**, 751–755.
24. C. C. Glenn, S. Saitoh, M. T. Jong, M. M. Filbrandt, U. Surti, D. J. Driscoll, and R. D. Nicholls (1996) Am. J. Hum. Genet. **58**, 335–346.
25. R. Shemer, Y. Birger, A. D. Riggs, and A. Razin (1997) Proc. Natl. Sci. USA **94**, 10267–10272.
26. R. Stoger, P. Kubicka, C. G. Liu, T. Kafri, A. Razin, H. Cedar, and D. P. Barlow (1993) Cell **73**, 61–71.
27. E. Li, T. H. Bestor, and R. Jaenisch (1992) Cell **69**, 915–926.
28. E. Li, C. Beard, and R. Jaenisch (1993) Nature **366**, 362–365.
29. T. Caspary, M. A. Cleary, C. C. Baker, X.-J. Guan, and S. M. Tilghman (1998) Mol. Cell. Biol. **18**, 3466–3474.
30. R. Drouin, G. P. Holmquist, and C.-L. Richer (1994) Adv. Hum. Genet. **22**, 47–115.
31. Y. Izumikawa, K. Naritomi, and K. Hirayama (1991) Hum. Genet. **87**, 1–5.
32. M. S. Lin, A. Zhang, and A. Fujimoto (1995) Hum. Genet. **96**, 572–576.
33. R. Drouin, M. Boutouil, R. Fetni, G. P. Holmquist, P. Scott, C.-L. Richer, and N. Lemieux (1997) Chromosoma **106**, 405–411.
34. D. Kitsberg, S. Selig, M. Brandeis, I. Simon, I. Keshet, D. J. Driscoll, R. D. Nicholls, and H. Cedar (1994) Nature **364**, 459–463.
35. O. W. Smrzka, I. Fae, R. Stoger, R. Kurzbauer, G. F. Fischer, T. Henn, A. Weith, and D. P. Barlow (1995) Hum. Mol. Genet. **4**, 1945–1952.
36. K. W. Brown, A. J. Villar, W. Bickmore, J. Clayton-Smith, D. Catchpoole, E. R. Maher, and W. Reik (1996) Hum. Mol. Genet. **5**, 2027–2032.
37. J. H. Knoll, S. D. Cheng, and M. Lalande (1994) Nat. Genet. **6**, 41–46.
38. J. M. LaSalle and M. Lalande (1995) Nat. Genet. **9**, 386–394.

39. P. H. Gunaratne, M. Nakao, D. H. Ledbetter, J. S. Sutcliffe, and A. C. Chinault (1995) Genes Dev. **9**, 808–820.
40. L. M. White, P. K. Rogan, R. D. Nicholls, B.-L. Wu, B. Korf, and J. H. M. Knoll (1996) Am. J. Hum. Genet. **59**, 423–430.
41. J. M. LaSalle, and M. Lalande (1996) Science **272**, 725–728.
42. T. Forné, J. Oswald, W. Dean, J. R. Saam, B. Bailleul, L. Dandolo, S. M. Tilghman, J. Walter, and W. Reik (1997) Proc. Natl. Acad. Sci. USA **94**, 10243–10248.
43. B. Duvillié, D. Bucchini, T. Tang, J. Jami, and A. Pàldi (1998) Genomics **47**, 52–57.
44. R. Feil, M. D. Boyano, N. D. Allen, and G. Kelsey (1997) J. Biol. Chem. **272**, 20893–20900.
45. R. Feil, M. A. Handel, N. D. Allen, and W. Reik (1995) Dev. Genet. **17**, 240–252.
46. W. P. Robinson, and M. Lalande (1995) Hum. Mol. Genet. **4**, 801–806.
47. A. Pàldi, G. Gyapay, and J. Jami (1995) Curr. Biol. **5**, 1030–1035.
48. D. P. Barlow, R. Stoger, B. G. Herrmann, K. Saito, and N. Schweifer (1991) Nature **349**, 84–87.
49. T. M. DeChiara, E. J. Roberston, and A. Efstratiadis (1991) Cell **64**, 849–859.
50. M. S. Bartolomei, S. Zemel, and S. M. Tilghman (1991) Nature **351**, 153–155.
51. M. S. Bartolomei (1994) Nature Genet. **6**, 220–221.
52. K. Artzt, D. P. Barlow, W. Dove, K. Fisher-Lindahl, M. Lyon, J. Klein, and L. M. Silver (1991) Mamm. Genome **1**, S281–S301.
53. A. Wutz, O. W. Smrzka, N. Schweifer, K. Schellander, E. F. Wagner, and D. P. Barlow (1997) Nature **389**, 745–749.
54. D. P. Barlow (1997) EMBO J. **16**, 6899–6905.
55. T. M. DeChiara, A. Estratiadis, and E. J. Robertson (1990) Nature **345**, 78–80.
56. C. I. Brannan, E. Claire Dees, R. S. Ingram, and S. M. Tilghman (1990) Mol. Cell. Biol. **10**, 28–36.
57. M. E. Brunknow and S. M. Tilghman (1991) Genes Dev. **5**, 1092–1101.
58. S. Zemel, M. S. Bartolomei, and S. M. Tilghman (1992) Nat. Genet. **2**, 61–65.
59. R. Ohlsson, F. Hedborg, L. Holmgren, C. Walsh, and T. J. Ekstrom (1994) Development **120**, 361–368.
60. M. S. Bartolomei, A. L. Webber, M. E. Brunkow, and S. M. Tilghman (1993) Genes Devel. **7**, 1663–1673.
61. P. A. Leighton, J. R. Saam, R. S. Ingram, C. L. Stewart, and S. M. Tilghman (1995) Genes Dev **9**, 2079–2089.
62. T. Sasaki, R. Scott Hansen, and S. M. Gartler (1992) Mol. Cell. Biol. **12**, 3819–3826.
63. K. D. Tremblay, J. Saam, R. S. Ingram, S. M. Tilghman, and M. S. Bartolomei (1995) Nature Genet. **9**, 403–413.
64. A. L. Webber, R. S. Ingram, J. M. Levorse, and S. M. Tilghman (1998) Nature **391**, 711–715.
65. R. Weksberg, S. D. R., F. Y. L., S. Q. L., and S. J. (1993) Nat. Genet. **5**, 143–150
66. I. Hatada, J. Inazawa, T. Abe, M. Nakayama, Y. Kaneko, Y. Jinno, N. Niikawa, H. Ohashi, Y. Fukushima, K. Iida, C. Yutani, S.-i. Takahashi, Y. Chiba, S. Ohishi, and T. Mukai (1996) Hum. Mol. Genet. **5**, 783–788.
67. I. Hatada, H. Ohashi, Y. Fukushima, Y. Kaneko, M. Inoue, Y. Komoto, A. Okada, S. Ohishi, A. Nabetani, H. Morisaki, M. Nakayama, N. Niikawa, and T. Mukai (1996) Nature Genet. **14**, 171–173.
68. M. P. Lee, R.-J. Hu, L. A. Johnson, and A. P. Feinberg (1997) Nature Genet. **15**, 181–185.
69. T. D. Gould and K. Pfeifer (1998) Hum. Mol. Genet. **7**, 483–487.
70. D. Dao, D. Frank, N. Qian, D. O"Keefe, R. J. Vosatka, C. P. Walsh, and B. Tycko (1998) Hum. Mol. Genet. **7**, 597–608.

71. C. Rougeulle, H. Glatt, and M. Lalande (1997) Nature Genet. **17**, 14–15.
72. U. Albrecht, J. S. Sutcliffe, B. M. Cattanach, C. V. Beechey, D. Amstrong, G. Eichele, and A. L. Beaudet (1997) Nature Genet. **17**, 75–78.
73. A. Chess, I. Simon, H. Cedar, and R. Axel (1994) Cell **78**, 823–834.
74. G. A. Holländer, S. Zuklys, C. Morel, E. Mizoguchi, K. Mobisson, S. Simpson, C. Terhorst, W. Wishart, D. E. Golan, A. K. Bhan, and S. J. Burakoff (1998) Science **279**, 2118–2121.
75. T. H. Vu and A. R. Hoffman (1997) Nature Genet. **17**, 12–13.
76. J. S. Sutcliffe, Y.-h. Jiang, R.-J. Galjaard, T. Matsuura, P. Fang, T. Kubota, S. L. Christian, J. Bressler, B. Cattanach, D. H. Ledbetter, and A. L. Beaudet (1997) Genome Res **7**, 368–377.
77. K. Buiting, S. Saitoh, S. Gross, B. Dittrich, S. Schwartz, R. D. Nicholls, and B. Horsthemke (1995) Nat. Genet. **9**, 395–400.
78. J. S. Sutcliffe, M. Nakao, S. Christian, K. H. Orstavik, N. Tommerup, D. H. Ledbetter, and A. L. Beaudet (1994) Nat. Genet. **8**, 52–58.
79. S. Saitoh, K. Buiting, P. K. Rogan, J. L. Buxton, D. J. Driscoll, J. Arnemann, R. König, S. Malcolm, B. Horsthemke, and R. D. Nicholls (1996) Proc. Natl. Acad. Sci. USA **93**, 7811–7815.
80. B. Dittrich, K. Buiting, B. Korn, S. Rickard, J. Buxton, S. Saitoh, R. D. Nicholls, A. Poustka, A. Winterpacht, B. Zabel, and B. Horsthemke (1996) Nature Genet. **14**, 163–170.
81. C. Rougeulle, C. Cardoso, M. Fontes, L. Colleaux, and M. Lalande (1998) Nature Genet. **19**, 15–16.
82. S. M. Tilghman, T. Caspary, and R. S. Ingram (1998) Nature Genet. **18**, 206–208.
83. A. Schumacher, K. Buiting, M. Zeschnigk, W. Doerfler, and B. Horsthemke (1998) Nature Genet. **19**, 324–325.
84. T. Yang, T. E. Adamsom, J. L. Resnick, S. Leff, R. Wevrick, U. Francke, N. A. Jenkins, N. G. Copeland, and C. I. Brannan (1998) Nature Genet. **19**, 25–31.
85. F. Lyko, K. Buiting, B. Horsthemke, and R. Paro (1998) Proc. Natl. Acad. Sci. USA **95**, 1698–1702.
86. D. P. Barlow (1993) Science **260**, 309–310.
87. J. H. Thomas (1995) Proc. Natl. Acad. Sci. USA **92**, 480–482.
88. T. Moore and D. Haig (1991) Trends Genet. **7**, 45–49.
89. L. D. Hurst and G. T. McVean (1997) Trends Genet. **13**, 436–443.

In Situ Hybridization

The spatial distribution of a target nucleic acid in a tissue, cell, or chromosome can be visualized by in situ hybridization techniques. As with other hybridization techniques, there are many variations. Each procedure shares a set of common steps: (*1*) fixing the sample to preserve its structure, (*2*) limited proteinase digestion that provides access to the hybridization probe, (*3*) addition of the hybridizing probe, (*4*) washing to remove unhybridized probe, and (*5*) detection of hybrids.

Small probes are usually preferred over larger probes for *in situ* hybridization. The probe must **diffuse** efficiently into the sample so that the hybridization reaction can occur. The advantage imparted by faster diffusion of small probes is partially countered by their tendency to be lost in the washing step. Because the stability of the hybridized duplex depends on concentration for short oligonucleotides, the dilution that accompanies the washing step can result in release of some of the probe from the hybrid duplexes.

Visualization is difficult when a small number of target molecules are present. This limited most of the applications of the method to hybridization of messenger RNA. Low copy-number DNA and RNA are, however, physiologically important. Viral DNA also may be present in cells in low copy number. The need to increase the sensitivity of the technique to permit visualization of low copy-number targets has led to incorporation of amplification techniques into *in situ* hybridization techniques. Several amplification techniques have been employed, with polymerase chain reaction (**PCR**) being the most widely applied.

Radioisotope or **fluorescence** detection of the hybrid duplex can be employed, but the current method of choice is bioluminescence or chemiluminescence . A biotin label is detected by streptavidin coupled to alkaline phosphatase or horseradish peroxidase. These enzymes catalyse several reactions that can begin a cascade of reactions leading to production of light. Because biotin is a natural metabolite, high background signals may be observed in some tissues. One of the many alternatives is a digoxigenin label that is recognized and bound by a specific antibody linked to alkaline phosphatase or horseradish peroxidase. Counter staining permits identification of cellular structures and, in turn, observation of the distribution of hybrid duplexes within the cell or tissue.

Suggestions for Further Reading

D. G. Wilkinson, ed. (1993) *In situ Hybridization: A Practical Approach*, IRL Press, New York.

J. Gu, ed. (1995) *In situ Polymerase Chain Reaction and Related Technology*, Eaton Press, Natick, MA.

L. Kricka, ed. (1992) *Nonisotopic DNA Probe Techniques*, Academic Press, San Diego.

Inborn Errors of Metabolism

Inborn errors of metabolism is the term applied to genetic disorders caused by loss of function of an enzyme. Enzyme activity may be low or lacking for a variety of reasons, such as lack of transcription and translation of the corresponding gene, improper folding of the polypeptide, unstable tertiary structure, a defective active site, failure to bind the corresponding coenzyme under physiological conditions, or failure to enter into complexes with other proteins. A single good copy of the gene is often sufficient, and many inborn errors are therefore recessive traits. The severity of the phenotype is highly variable among inborn errors, depending on the role of the biochemical pathway in metabolism. A few inborn errors can be treated by diet. Most cannot. Inborn errors were the first genetic disorders to be considered for gene therapy.

1. Early Recognition of Inborn Errors

The phrase *inborn errors of metabolism* appears to have been first used by A.E. Garrod in the Croonian Lectures of 1908, published as a monograph with that title in 1909. In 1902, Garrod published an account of a patient with alkaptonuria and speculated that it was due to an inherited derangement of metabolism. Subsequently, he encountered other rare patients who suffered from apparent metabolic defects. The fact that the parents of such patients were often related to each other suggested that the metabolic defects might be inherited as recessive traits. In his 1909 publication, he suggested four candidate disorders as examples of inborn errors: alkaptonuria, albinism, pentosuria, and cystinuria. Although the sciences of genetics and biochemistry were in their infancies at the time, Garrod was remarkably perceptive in recognizing the possibility of inherited variations in metabolism.

Garrod's prescient observations were largely ignored except as a footnote in the biochemical literature. The geneticists were not ready for biochemistry, nor were biochemists quite ready to deal with genetics. Enzymes were just being identified as the important agents in metabolism, and little was known about the enzymes themselves or other protein functions. Nothing was known about the chemical nature of genes or how they act. It was not until the late 1930s that geneticists began to employ biochemical approaches to study what genes do. Soon thereafter, G.W. Beadle, E.L. Tatum, and others, based primarily on studies of *Neurospora*, observed that each mutant form studied appeared to be defective in a specific enzymatic conversion. Their work led to the *one gene-one enzyme* hypothesis, which equates the action of each genetic locus with the activity of a single enzyme.

We know now that many proteins are not enzymes. Also, many enzymes are complexes of different proteins. (Some RNA molecules have enzyme activity—the ribozymes—but these will not be considered here and are not active in metabolic pathways as that term is usually defined.) We also know now that genes are composed of DNA and their function is to code for the primary structure of proteins. The inborn errors of metabolism envisioned by Garrod are readily explained by the role of genes in coding for specific enzymes or enzyme subunits. Errors in metabolism reflect loss of activity of a particular enzyme due to an error in a gene that codes for that enzyme. The terms *metabolic block* and *metabolic error* are used as synonyms for inborn errors of metabolism.

2. Some Properties of Enzymes

It is helpful to consider how enzymes function if one is to understand the many variations that lead to malfunction. First, the polypeptide chain that is coded by a gene must be folded into the correct three-dimensional structure. Protein folding is a consequence of the amino acid sequence and the interaction of the side chains with each other and with water. Many detrimental mutations act by substituting one amino acid for another, interfering with the electrostatic and hydrophobic interactions of the functional enzyme. In the case of glucose 6-phosphate dehydrogenase deficiency, hundreds of mutant forms have been identified. A common feature of many is decreased stability of the folded enzyme.

To function, enzymes must have an active site that determines substrate access and binding. They often require coenzymes, small organic molecules that bind and help carry out the chemical transformations at the active site of the enzyme. Some coenzymes are made by the host organism. Others, of which the B vitamins are examples, must be supplied in the diet in higher animals. The coenzymes must bind at specific sites on the apoenzymes to form active holoenzyme. Mutation at those sites can reduce or abolish the affinity of the enzyme for the coenzyme. In some instances when the affinity is reduced, increase in the coenzyme level can compensate. For example, homocystinuria results from a defect in cystathionine synthase, which catalyzes the conversion of homocysteine to cystathionine. The homocysteine substrate accumulates and is excreted in urine as homocysteine. Some cases are treatable with large doses of vitamin B_6, which is converted to the coenzyme pyridoxal phosphate and increases the level of active enzyme. In other patients, the molecular defect is in another part of the enzyme, or the enzyme may be missing. Vitamin B_6 is of no value in those cases. The two types of cases are not distinguishable clinically apart from the response to therapy.

Coenzymes that are synthesized in the body may also be absent due to defects in their synthesis. This causes loss of activity of the enzymes of which they are a normal part. An example is found in phenylketonuria (PKU). PKU is a classic inborn error of metabolism usually caused by mutation of the phenylalanine hydroxylase gene. This enzyme uses tetrahydrobiopterin as a coenzyme. In a small proportion of cases, the genetic defect is in synthesis of tetrahydrobiopterin. The end result is the same. Phenylalanine cannot be broken down by the normal pathway and accumulates, causing the classic features of PKU.

Many enzymes and other proteins function as dimers, higher multimers, or part of a multisubunit complex. This imposes a requirement that the monomeric form have a configuration that permits complex formation. Changes in the amino acid sequence can alter the ability of a monomeric enzyme to enter into complexes, either with itself to form an active dimer or with other subunits to form a complex. The mutant subunit might still have activity under some circumstances, but the conditions under which the substrate is encountered inside a cell may be very different.

This list of protein functions is not exhaustive. Many properties of an enzyme can be affected by structural changes. Any change that substantially or completely blocks the activity so that a metabolic conversion does not occur can be the cause of an inborn error of metabolism.

3. Metabolic Errors and Phenotypes

Although some inborn errors are relatively benign, many are quite detrimental, often fatal. The impact of a metabolic error depends greatly on the metabolic pathway and on the ability of other metabolic and physiological systems to compensate for the error. Alkaptonuria is relatively benign. The pathway that is blocked is in the catabolic breakdown of homogentisic acid, and no essential products are missing because of this block. Homogentisic acid is not reabsorbed by the kidneys and is excreted in the urine, preventing accumulation of high levels in the body. Over time, oxidation products of homogentisate are deposited in joints, causing a form of arthritis. In contrast, the block in phenylketonuria is in the conversion of phenylalanine to tyrosine. Phenylalanine is efficiently reabsorbed by the kidneys and accumulates to high levels in the blood, generating by-products that interfere with development of the central nervous system.

Several blocks in the breakdown of gangliosides are responsible for degenerative diseases of the central nervous system (e.g., Tay-Sachs disease). In these instances, breakdown occurs in the lysosomes. The large gangliosides accumulate in the lysosomes, which become very large, eventually interfering with cell function and ultimately causing death. Such disorders are examples of lysosomal storage diseases. A characteristic of these disorders is an initially normal phenotype, followed by degeneration as the lysosomes store increasing amounts of material.

Another group of metabolic blocks depends on environmental agents for expression. Galactosemia is one of the earliest known examples. Affected persons cannot metabolize galactose, which comes from lactose in milk. The galactose 1-phosphate that accumulates interferes with other metabolic processes and can lead to death unless milk is avoided. Other rare individuals are homozygous for absence of functional plasma cholinesterase. If succinyldicholine is administered as a muscle relaxant during electroshock or other treatment, they have very prolonged recovery of muscle function.

4. Inborn Errors and Genetics

In most cases, if a locus that codes for an enzyme has one normal allele, a normal phenotype results; it is haplosufficient. Two nonfunctional alleles are required for the metabolic error to occur. This means that the condition is inherited as a recessive trait. If q is the frequency of the mutant allele, the frequency of homozygotes would be q^2, and the frequency of heterozygous "carriers" would be $2pq$. For $q = 0.01$, the frequency of homozygotes therefore is $q^2 = 0.0001$ and $2pq = 0.0198$. The bulk of the recessive alleles in the population are in heterozygous combination and not subject to elimination by selection. Some genes that code for enzymes are haploinsufficient. The mutant allele is associated with a modified phenotype and is transmitted therefore in pedigrees as a dominant trait. The phenotype of the heterozygote need not be identical to the homozygous mutant phenotype, which might be more severe.

With the advent of prenatal diagnosis for nearly all metabolic errors, once the gene is identified, the frequency of affected children born can be substantially reduced if a mating is known to be at risk. Identification of such matings usually occurs because of a prior pregnancy that involved an affected offspring. Without massive population screening of normal persons, however, the frequency of matings at risk will not change.

5. Treatment of Inborn Errors

Reference has been made to treatment of phenylketonuria and galactosemia by elimination of components of diet. Some forms of homocystinuria respond to high levels of dietary vitamin B_6. The number of inborn errors that are managed by diet is small. Because inborn errors are usually associated with loss of activity of a single enzyme, the idea of enzyme replacement has been an enticing goal for many years. How to do this technically is a major challenge. The principle has been demonstrated in a sense in a boy with phenylketonuria who received a liver transplant for reasons unrelated to the PKU. The condition was cured. Because PKU is effectively treated by diet, liver transplants are not considered an appropriate therapy.

There are a number of inborn errors of great severity that are candidates for gene therapy. The first attempts at gene therapy involved a patient with adenosine deaminase deficiency, which causes severe immunodeficiency. The gene is well characterized and can be incorporated into viral vectors. The results were very promising, but a satisfactory protocol has yet to be achieved. Another candidate disorder is Lesch-Nyhan syndrome, which is due to loss of activity of hypoxanthine phosphoribosyl transferase (hprt). Patients are mentally retarded and engage in self-mutilation. A very low level of hprt activity is sufficient to prevent the disorder. Gene therapy need not be very efficient in order to be effective. Success has been elusive, however.

Despite the disappointments in early attempts at gene therapy, it remains the most promising approach for metabolic errors as well as for certain other genetic disorders.

Additional Reading

HarrisH., *Garrod"s Inborn Errors of Metabolism*, Oxford University Press, London, U.K., 1963, xi+207 pp. Included are reprints of the original 1902 and 1909 publications of Garrod.

Scriver C.R., Beaudet A.L., Sly W.S., Valle D., eds., *The Metabolic and Molecular Bases of Inherited Disease*, 7th ed., McGraw-Hill, New York, 1995.

Strachan T. and Read A.P., *Human Molecular Genetics*, 2nd ed., Wiley-Liss, New York, 1999.

On-Line Mendelian Inheritance in Man: http://www3.ncbi.nlm.nih.gov/Omim/. This database can be searched for any inborn error of metabolism. It provides an up-to-date description of research and links to related sites.

Inclusion Bodies

Inclusion bodies are insoluble, biologically inactive aggregates of partially folded **protein**, which are often produced when a heterologous or recombinant protein is overexpressed, especially in the popular and frequently used *Escherichia coli* bacteria (see Expression Systems). Inclusion body formation is frequently seen in both **Gram-negative** and Gram-positive bacteria, but less often in yeast, insect, or mammalian cells. Inclusion bodies are also called *refractile bodies* because they refract light and are visible in the phase-contrast **microscope**. Usually, there is only one inclusion body per cell, which can span the whole diameter of the cell, depending on the expression level of the protein. Inclusion bodies can occur in both the cytosolic and **periplasmic** location in bacteria. If the initial expression level is sufficiently high, the inclusion bodies tend to be a rather homogeneous aggregate of the overexpressed protein. However, several other proteins are also found as coprecipitants, such as elongation factor EF-Tu, outer membrane proteins, and small **heat-shock** proteins.

Systematic analysis of inclusion body formation shows no correlation with the size, relative hydrophobicity, or number of proline residues (see Cis/Trans Isomerization) in the protein. However, the relative charge and the number of amino acid residues that prefer the turn conformation correlate reasonably well with the tendency for inclusion body formation. Also, there is an excellent correlation between inclusion body formation and high expression level of the protein. Even native, cytosolic proteins can form inclusion bodies at a sufficiently high expression level. A kinetic model has been suggested that takes these observations into account. It states that inclusion body formation is dependent on the relative rates of **protein biosynthesis**, **protein folding**, and aggregation.

Overexpression of a particular protein can be deleterious to cell viability (1). The protein may have a biochemical activity that is directly toxic, or the overexpression state itself is toxic. This is marked by an inability of the cell to recover after a period of overexpression. One major contributing factor is the observed destruction of ribosomes (2). Finally, a word of caution. The most abundant *E. coli* protein is elongation factor EF-Tu, reaching 5% to 10% of the total cellular protein. Any protein that is expressed at higher levels challenges the biosynthetic capacity of the cell, especially if it is made from a gene with a high portion of rare **codons**. The most negative consequences are less growth capacity and high error levels in translation.

1. How Can the Formation of Inclusion Bodies Be Avoided?

In most cases, the native, soluble form of a protein is desired in high quantity and purity. It is therefore important to avoid inclusion body formation, which requires that the protein be solubilized, generally in a **denatured** state, and then folded. Furthermore, the quality of protein folded from inclusion bodies can be inferior (3).

There are several ways to avoid inclusion body formation. First, fermentation parameters can be varied, such as the richness of the medium, its pH, and the level of aeration or micronutrients. A major improvement is often seen when the growth temperature is lowered. Second, the expression level of the protein can be varied. This can be done by selecting an appropriate expression **vector** with sufficiently weak **promoter** and/or translation initiation elements. Also, an expression vector that allows regulated but variable steady-state levels of gene expression can be used (4). However, most overexpression systems are inducible, so that varying the level of **inducer** may suffice. Third, coexpression of protein folding modulators, such as the **molecular chaperones** GroES/EL can help. Coexpression of the **DnaK/DnaJ** chaperones may help when GroES/EL is ineffective. Also, coexpression of *E. coli* thioredoxin can counteract inclusion body formation (3). Other folding modulators of potential use are peptidyl-prolyl ***cis/trans*** **isomerases** and thiol/disulfide oxidoreductases. Fourth, genetic engineering can improve soluble expression. The simplest solution is to fuse the protein of interest to other proteins that are known to improve the yield of soluble protein, such as the bacterial thioredoxin and IgG binding domains of *S. aureus* protein A (see Fusion Gene, Fusion Protein). A more sophisticated approach involves the rational design of higher solubility by the introduction of specific point mutations by site-directed mutagenesis, and elimination of amino acid sequences involved in aggregation. Finally, a **signal sequence** can cause the transport of the protein of interest to the **periplasm** or to the extracellular medium, where the environment favors the folding of some proteins.

2. How Can Inclusion Bodies Be Used?

Even inclusion body formation can be turned into an advantage so long as the protein can be refolded. The primary advantage is the ease of purification of inclusion bodies; those with a recombinant protein fraction of more than 60% can be isolated by centrifugation of crude cell lysate at moderate rotor speeds (5000 to 12,000 g). The purity of an inclusion body protein can be improved further by resuspension and centrifugation in a buffer containing 2% sodium deoxycholate (5). Inclusion bodies are often the only way to obtain a protein that is highly toxic in its native form. Any protein can usually be isolated via inclusion bodies if it is fused to an amphiphilic extension (6) or if it is expressed at a sufficiently high level (eg, using T7 promoter vectors). Also, host strains with a defective **heat-shock** response or with a mutation in an important molecular chaperone system may be useful. Inclusion bodies are often an advantage when the yield of the native protein is low because of extensive **proteolysis**.

The key to efficient use of inclusion bodies is to know how to solubilize and refold the protein in high yield. The strong denaturants 4 to 6 M **guanidinium chloride** or 6 to 10 M urea are the most common solubilizing reagents. Another method uses detergents, such as cetylmethylammonium chloride or sarkosyl, or alkaline solution (7). Often, it is necessary to use **thiol** reagents along with the **chaotropes** to facilitate reduction of nonnative disulfide bonds.

All methods for folding the solubilized and denatured protein are based on the removal or dilution of the denaturant and reducing agent. This can be done by one-step dilution, by dialysis or, as when sarkosyl is used, by the addition of a micelle-forming detergent (eg, **Triton X-100**) that sequesters the protein-bound sarkosyl (8).

A major drawback to most *in vitro* folding approaches is the presence of aggregation side reactions, which compete with the proper folding reaction. It is therefore often necessary to refold at low protein concentration or to use pulse renaturation techniques (9). Furthermore, low temperatures or the composition of the refolding buffer may affect the yield of native protein. A major improvement can be observed when the denatured protein is refolded on a solid support, which effectively prevents aggregation by protein-protein contacts (10, 11).

Molecular chaperones, such as GroES/EL, have also been used for *in vitro* refolding of denatured proteins. A promising new development is the advent of refolding chromatography, where immobilized chaperones or fragments thereof are used for refolding of protein. Elaborate "artificial" chaperone systems have also been constructed, applying nonprotein refolding agents or changes in the physical environment (6). A combination of detergents and cyclodextrins has been used to mimic the two-step action of GroES/EL in protein folding. Systems have also been made that are based on temperature-jump techniques or refolding on a solid support.

Bibliography

1. B. Miroux and J. E. Walker (1996) J. Mol. Biol. **260**, 289–298.
2. H. Dong, L. Nilsson, and C. G. Kurland (1995) J. Bacteriol. **177**, 1497–1504.
3. T. Yasukawa et al. (1995) J. Biol. Chem. **270**, 25328–25331.
4. L. M. Guzman, D. Belin, M. J. Carson, and J. Beckwith (1995) J Bacteriol **177**, 4121–4130.
5. L. Rao et al. (1996) Anal. Biochem. **241**, 173–179.
6. J. G. Thomas, A. Ayling, and F. Baneyx (1997) Appl. Biochem. Biotech. **66**, 197–238.
7. J. Suttnar et al. (1994) J. Chromatog. B **656**, 123–126.
8. J. V. Frangioni and B. G. Neel (1993) Anal. Biochem. **210**, 179–187.
9. R. Rudolph (1996) In *Protein Engineering: Principles and Practice* (J. L. Cleland and C. S. Craik, eds.), Wiley-Liss, Inc., New York, pp. 283–298.
10. T. E. Creighton (1986) In *Protein, Structure, Folding and Design*, (D. Oxender, ed.), Alan R Liss, New York, pp. 249–257.
11. A. Holzinger, K. S. Phillips, and T. E. Weaver (1996) Biotechniques **20**, 804–808.

Suggestions for Further Reading

12. R. S. Donovan, C. W. Robinson, and B. R. Glick (1996) Optimizing inducer and culture conditions for expression of foreign proteins under the control of the *lac* promoter. J. Industrial Microbiol. **16**, 145–154.
13. G. Georgiou (1996) "Expression of proteins in biotechnology." In *Protein Engineering: Principles and Practice* (J. L. Cleland and C. S. Craik, eds.), Wiley-Liss, Inc., New York, pp. 101–127.
14. C. Kurland and J. Gallant (1996) Errors of heterologous protein expression. Curr. Op. Biotech. **7**, 489–493.
15. R. Rudolph (1996) "Successful protein folding on an industrial scale". In *Protein Engineering: Principles and Practice* (J. L. Cleland and C. S. Craik, eds.), Wiley-Liss, Inc., New York, pp. 283–298.
16. R. Rudolph and H. Lilie (1996) *In vitro* folding of inclusion body proteins. FASEB J. **10**, 49–56.
17. J. G. Wall and A. Plückthun (1995) Effects of overexpressing folding modulators on the *in vivo* folding of heterologous proteins in Escherichia coli. Curr. Op. Biotech. **6**, 507–516.

Indel

An "indel" is a site of insertion or deletion in aligned, homologous protein or nucleotide sequences (1). Mutational events in nucleic acid sequences include insertions and deletions, as well as base substitutions. Often, it is not possible to distinguish between insertional or deletional events, because this would require either access to the (presumably dead) common ancestor of the aligned sequences or else a sufficient number of related sequences to reveal the nature of a particular event in a recently derived lineage. In globular proteins, indels are largely restricted to sites (usually loops) at the protein surface (2). A gapped region of a sequence alignment may actually have a history of multiple insertions and deletions, and it is then a fruitless exercise to try to retrace the actual events. Indel is therefore a useful term as it avoids the need to make an error-prone assignment of the actual mutational event(s). The most sensitive algorithms for aligning sequences allow for the possibility of indels being placed at any position in any sequence, using gap penalties to apply a cost to indel insertion, to limit their frequency (3, 4).

Bibliography

1. D. Sankoff and J. B. Kruskal (1984) *Time Warps, String Edits and Macromolecules: The Theory and Practice of Sequence Comparison*, Addison-Wesley, Reading, MA, p. 11.
2. S. Pascarella and P. Argos (1992) J. Mol. Biol. **224**, 461–471.
3. S. B. Needleman and C. D. Wunsch (1970) J. Mol. Biol. **48**, 443–453.
4. T. F. Smith and M. S. Waterman (1981) Adv. Appl. Math. **2**, 482–489.

Suggestion for Further Reading

5. D. Sankoff and J. B. Kruskal (1984) *Time Warps, String Edits and Macromolecules: The Theory and Practice of Sequence Comparison*, Addison-Wesley, Reading, MA.

Induced Fit

The specificity of enzymes is of importance for their function and involves the fit of a substrate into the active site of the enzyme. The concept of enzyme specificity, which implies that there is a close steric relationship between an enzyme and its substrate, was proposed in 1894 by Emil Fischer, who developed the lock and key hypothesis of enzyme action. He explored the idea that the active site of an enzyme was simply a rigid template for the substrate and this would account for the ability of an enzyme to act on only one or a limited number of substrates.

The lock and key hypothesis was accepted for several decades. But it was questioned in 1958 by Koshland (1), who recognized that it did not account for the low activity of many enzymes with water, which is always present at a concentration of 55 *M*, as a substrate or for the failure of enzymes to act on compounds whose structure was similar to that of the normal substrate. He proposed that:

- The active site of an enzyme is not necessarily a template for the substrate.
- The binding of the substrate at the active site produces a structural, or conformational, change.
- Conformational change brings about the correct alignment of the catalytic groups of the enzyme with those of the substrate so that a reaction occurs.

The induced fit concept can explain why molecules of a structure similar to that of the normal substrate can combine at the active site, but not undergo reaction, because they lack the structural features required for catalysis.

An early, and now classical, demonstration of substrate-induced conformational change is the binding of glucose to hexokinase (2). This enzyme has two lobes, and between them is a cleft in which the active site is located. The binding of glucose induces the rotation of the two lobes and closure of the cleft; these movements have the effect of excluding water and facilitating transfer of the phosphoryl group from ATP to glucose, rather than to water. Kinetic evidence for conformational changes with hexokinase comes from studies on the ATPase activity of the enzyme that occurs in the absence of glucose. This activity is low relative to the rate of phosphorylation of glucose, but is stimulated by lyxose. This sugar does not undergo phosphorylation, but interacts at the binding site for glucose to increase the maximum velocity of the reaction and lower the Km for $MgATP^{2-}$(3). The ability of substrates to cause conformational changes at the active site of enzymes has now been demonstrated by a variety of techniques, including X-ray crystallography. These changes are also a characteristic feature of the catalytic function of **allosteric** enzymes.

Bibliography

1. D. E. Koshland (1960) Adv. Enzymol. **22**, 45–97.
2. C. M. Anderson, F. H. Zucker, and T. A. Steitz (1979) Science **204**, 375–380.
3. G. DelaFuente, R. Lagunas, and A. Sols (1970) Eur. J. Biochem. **16**, 226–233.

Influenza Virus

Influenza viruses, which belong to the family of *Orthomyxoviridae*, are enveloped **viruses** with single-stranded, negative-sense RNA as the genome. The lipid envelope of influenza viruses is derived from the plasma membrane of the host cell in which the virus was grown. Influenza A and B viruses each contain eight species of RNA segments (Fig. 1), whereas influenza C virus contains seven segments. Influenza A, B, and C viruses are divided on the basis of antigenic differences between their nucleoprotein (NP) and matrix (M) proteins. Influenza A viruses are further subdivided into subtypes based on the antigenic differences of the hemagglutinin (HA) and neuraminidase (NA) glycoproteins (currently into 15 HA and 9 NA subtypes). Influenza A and B viruses grown in eggs or tissue-culture cells have a spherical structure, are 80 to 120 nm in diameter with some pleomorphism, and exhibit variation throughout the life cycle. Viruses freshly isolated from humans or animals exhibit greater heterogeneity and pleomorphism, including the presence of greatly elongated forms.

Figure 1. Schematic diagram of influenza A virus particle.

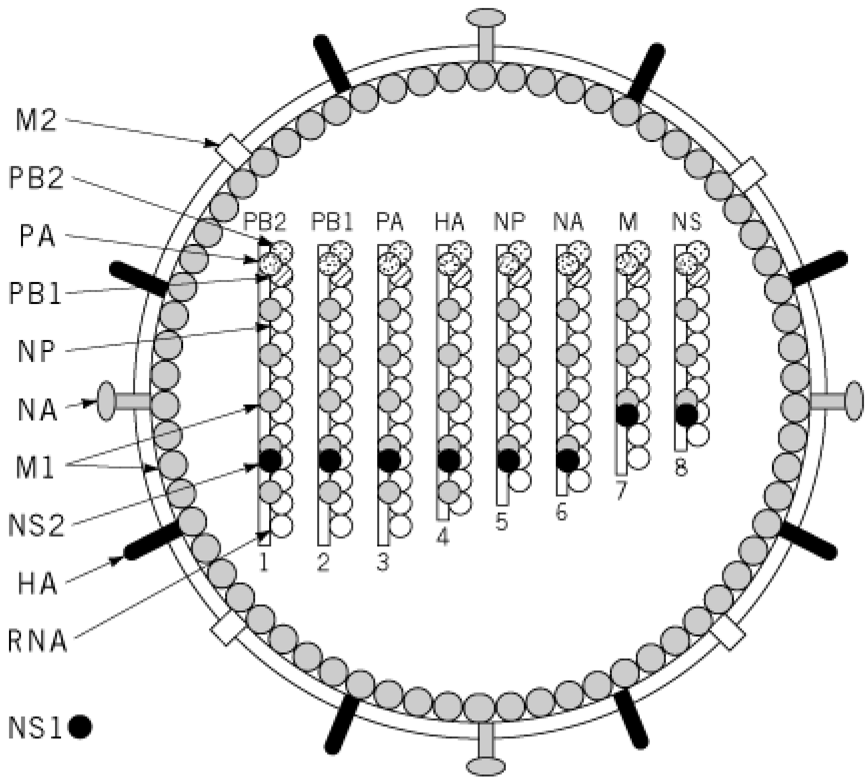

Influenza A and B virus envelopes each contain two kinds of 10- to 14-nm spikes radiating outward (the HA and the NA) (Fig. 1). The HA has a trimeric rod-shaped structure, while the NA has a tetrameric mushroom-shaped structure. The HA has the receptor (sialic acid)-binding and fusion activities. The NA has a neuraminidase activity that cleaves the virus receptor. Influenza A virus envelope also contains a tetrameric M2 **ion channel**, while influenza B virus contains a NB ion channel. The influenza C virus envelope contains only single spikes (HE), organized into orderly hexagonal arrays, that have both hemagglutinin and esterase activities.

The first isolation of the Influenza A virus from swine was reported in 1931, and that from humans was reported in 1933. The complete **nucleotide sequence** of the influenza virus was first reported for the A/PR/8/34 (PR8) strain in 1982, and it contains 13,588 nucleotides. The PR8 virus RNA segment 1 (2341 nucleotides) codes for PB2 (759 residues, 30 to 60 molecules/virion), 2 (2341 nucleotides) for PB1 (757 residues, 30 to 60 molecules/virion), 3 (2233 nucleotides) for PA (716 residues, 30 to

60 molecules/virion), 4 (1778 nucleotides) for HA (566 residues, 500 molecules/virion), 5 (1565 nucleotides) for NP (498 residues, 1000 molecules/virion), 6 (1413 nucleotides) for NA (454 residues, 100 molecules/virion), 7 (1027 nucleotides) for M1 (252 residues, 3000 molecules/virion), and M2 (97 residues, 20 to 60 molecules/virion) via splicing, 8 (890 nucleotides) for NS1 (230 residues, nonstructural) and NS2 (121 residues, 130 to 200 molecules/virion) via splicing (Fig. 1).

The viral transcription and replication takes place in the nucleus of the infected cell. The PB1, PB2, and PA proteins form a tetramer that has RNA-dependent **RNA polymerase** (replicase and transcriptase) activity. The PB2 protein has **endonuclease** activity and cuts the host mRNA to generate 10- to 13-nucleotide-long capped-RNA primer for the viral transcription (known as “cap snatching”). The viral RNA genomes and the NP protein form helical ribonucleoprotein (RNP) complexes. Twelve nucleotides at the 3′ end and 13 at the 5′ end of the RNA genomes are well-conserved among all influenza viruses, and they comprise the **promoter** where the virus polymerase binds and starts transcription and replication. The genomes also form a “panhandle structure,” in which the ends of an otherwise single-stranded RNA are held together by base pairing. The M1 is thought to underlie and probably integrate into the inner layer of the lipid bilayer. The M1 also interacts with the RNP, as well as with the HA and the NA. The NS1 protein is not incorporated into the virion. It interferes with the splicing and nuclear export of the cellular mRNAs. It also regulates the viral translation. The NS2 (it is currently known as NEP) has a nuclear export signal (NES, see Nuclear Import, Export).

Influenza virus is a major causative agent of the acute respiratory influenza illness, which is sometimes lethal for the elderly. In the pandemic of 1918 to 1919, called Spanish influenza, 20 to 40 million people were killed by infection with influenza A virus (H1N1). Influenza A viruses naturally infect humans, swine, horses, seals, a wide variety of birds, and some other mammalian species. Wild aquatic birds are probably the primordial reservoir of all influenza A viruses. On the other hand, influenza B viruses infect only humans. Influenza C virus infects humans and swine.

Immunity to influenza is long-lived and is subtype-specific. The HA contains the major neutralizing antigenic **epitopes**. The accumulation of point mutations (antigenic drift) alters the antigenicity of the HA. The appearance of new subtypes occurs by the reassortment of the HA or the NA gene among influenza A viruses (antigenic shift). Inactivated influenza vaccines are currently used widely worldwide, but live attenuated vaccines are being developed. Amantadine hydrochloride is a licensed antiviral agent for prophylactic and therapeutic use against all influenza A virus subtypes in humans.

Genetic manipulation of influenza A and B viruses has been successful, and some influenza A virus vector systems also have been developed.

Suggestions for Further Reading

R. A. Lamb and R. M. Krug (1996) "*Orthomyxoviridae*: The Viruses and Their Replication". In *Fields Virology*, 3rd ed. (B. N. Fields et al., eds.), Lippincott-Raven, Philadelphia, pp. 1353–1395.

B. R. Murphy and R. G. Webster (1996) "Orthomyxoviruses". In *Fields Virology*, 3rd ed. (B. N. Fields et al., eds.), Lippincott-Raven, Philadelphia, pp. 1397–1445.

Initiation Codon

Protein biosynthesis starts using the specific genetic code, named the initiation codon or start codon. In general, the AUG codon is used universally in both prokaryotes and eukaryotes. Occasionally, GUG is used as an alternate initiation codon in about 10% of bacterial genes, and very rarely is UUG also used. In eukaryotes, UUG is never used, but CUG, ACG, and GUG are occasionally or rarely used as an alternate initiation codon. There is only one known case in bacteria in which AUU functions as an initiation codon. The initiation codon is recognized by the specific transfer RNA referred to as initiator tRNA, $tRNA^{iMet}$ (eukaryotes) or $tRNA^{fMet}$ (prokaryotes) and is decoded as *N*-formyl methionine (fMet) (see fMET (N-Formyl Methionine)).

In prokaryotes, polycistronic genes are often regulated cooperatively at the translational level. This phenomenon, referred to as translational coupling, is observed when the downstream initiation codon overlaps the upstream stop codon in the sequence AUGA, or the downstream initiation codon is sequestered by the RNA stem structure. Ribosomes can enhance translation initiation of these downstream genes by slippage of the 30S ribosomal subunit or by unwinding the inhibitory RNA stem structure.

Initiation Complex

Initiation of protein synthesis is believed to be a rate-limiting step, because it requires multiple initiation factors and specific signals on messenger RNA that coordinately interact and function to form initiation complexes. The obvious difference between prokaryotic and eukaryotic mechanisms is based on the difference of where the ribosome enters the mRNA. Prokaryotic mRNAs are often polycistronic, and ribosomes can gain entry to the mRNA directly at the translation start site within the mRNA sequence to form initiation complexes, while eukaryotic mRNAs are monocistronic and ribosomes must gain entry to mRNA at its Cap and move downstream to the translation start site to form initiation complexes (see Scanning Hypothesis). Correct recognition of the site for initiation complex formation by prokaryotic ribosomes is mediated by complementary base-pairing between the **Shine–Dalgarno** sequence on mRNA and the anti-Shine–Dalgarno sequence on the 3′ terminus of 16S rRNA. The eukaryotic initiation process is in sharp contrast to the prokaryotic process, because it involves numerous initiation factors. This reflects the fact that specific protein factors are required for 5′ Cap recognition by the ribosome and for scanning of the ribosome to the downstream initiation site (1).

An initiation complex is first formed as a preinitiation complex composed of the small ribosomal particle (30S for prokaryotes, 40S for eukaryotes), **fMet-**transfer RNA, initiation factors, and GTP at the start site of mRNA. Upon formation of proper preinitiation complexes, the large ribosomal particle (50S for prokaryotes or 60S for eukaryotes) joins the preinitiation complex, to form the initiation complex (2). During this step, GTP is hydrolyzed to GDP while the fMet-tRNA-carrier factors, IF-2 (prokaryotes) and eIF-2 (eukaryotes), dissociate from the ribosome, leaving fMet-tRNA at the P site of the ribosome.

Although the translation of virtually all eukaryotic cellular mRNAs and the majority of viral RNAs is initiated via the scanning ribosome mechanism, there is a small, yet not insignificant, number of RNAs (particularly viral RNAs) that are translated by an internal initiation mechanism [see Internal Ribosome Entry Site (IRES)(3)].

Initiation of protein synthesis is a good target for regulating gene expression. Most of the bacterial ribosomal proteins are negatively autoregulated at the initiation step of their synthesis. When present in excess over rRNA, a set of ribosomal proteins (**translational repressors**) bind to their own mRNA and stop its translation. The ribosomal protein-binding site on its mRNA (or **operator**) overlaps the ribosome binding site, thereby blocking the formation of initiation complexes. The operator consists of a specific RNA structure that mimics the rRNA structure where the ribosomal protein (repressor) binds. Like the ribosomal protein repressor, *E. coli* threonyl-tRNA synthetase (ThrRS) is negatively autoregulated at the translation level when in excess of its substrate $tRNA^{thr}$. ThrRS binds to the leader region of its own mRNA at the translational initiation site and represses its translation by preventing ribosome binding. The ThrRS operator mimics the structure $tRNA^{thr}$.

Initiation of protein synthesis in eukaryotes can be regulated by **phosphorylation** of eIF-2a by mammalian protein kinase PKR (4). The PKR activity was originally detected as the enzyme responsible for double-stranded (ds) RNA-dependent protein synthesis inhibition in **poliovirus**-infected HeLa Cells, and in cell-free translation systems made from rabbit reticulocytes. The target of dsRNA's mysterious ability to inhibit protein synthesis initiation was eventually shown to be the protein kinase PKR, which blocks protein synthesis by phosphorylating initiation factor eIF-2a. Higher eukaryotic cells possess an intrinsic defense system that is mediated by interferon. Interferon release by virus-infected cells sensitizes neighboring cells by inducing the transcription of genes that encode anti-viral products. Some of these, notably the protein kinase PKR and 2,5A synthase, act at the level of protein synthesis. (2,5A synthase makes an oligonucleotide that activates a latent ribonuclease.) Viruses, in turn, have elaborated products (e.g., the VA RNA produced by adenovirus) that neutralize these cellular defenses, thereby enabling the production of viral proteins and progeny virions.

Recruitment of the 40S small ribosomal subunit to eukaryotic mRNA is mediated by interactions between a limited set of translation initiation factors (2). One of these factors, eIF-3, is a 40S subunit-associated factor comprised of at least eight subunits in mammalian cells that interacts with the mRNA-associated initiation factor eIF-4F (Fig. 1). eIF-4F consists of two core subunits. These are the mRNA **5′-Cap**-binding protein eIF-4E and the large subunit eIF-4G. Recent studies on eIF-4G have revealed that it binds to eIF-4E and eIF-3, as well as to the **poly(A)**-binding protein (Pab1p in yeast) (5). The multipurpose adapter nature of eIF-4G allows it to recruit the 40S ribosome to mRNA via the simultaneous association of eIF-4G with both eIF-4E and eIF-3 (Fig. 1). Knowledge of eIF-4E's interaction with the 5′-Cap permits an understanding of cellular and viral strategies to control Cap-stimulated translation. For example, cells express a small family of inhibitory proteins that regulate eIF-4E assembly. These are called the 4E-binding proteins [4E-BPs (6)]. The 4E-BPs share an amino acid motif with the *N*-terminal domain of eIF-4G that is known to be required for eIF-4G's interaction with eIF-4E. In their nonphosphorylated form, the 4E-BPs act as competitive inhibitors of the eIF-4G-eIF-5E interaction (Fig. 1).

Figure 1. Control of initiation complex formation via Cap binding in eukaryotes (7). (**a**) eIF-4E recruits the 40S subunit of mRNA by protein interaction with eIF-4G and eIF-3. (**b**) Regulation of initiation complex formation by phosphorylati eIF-4E binding proteins, 4E-BPs.

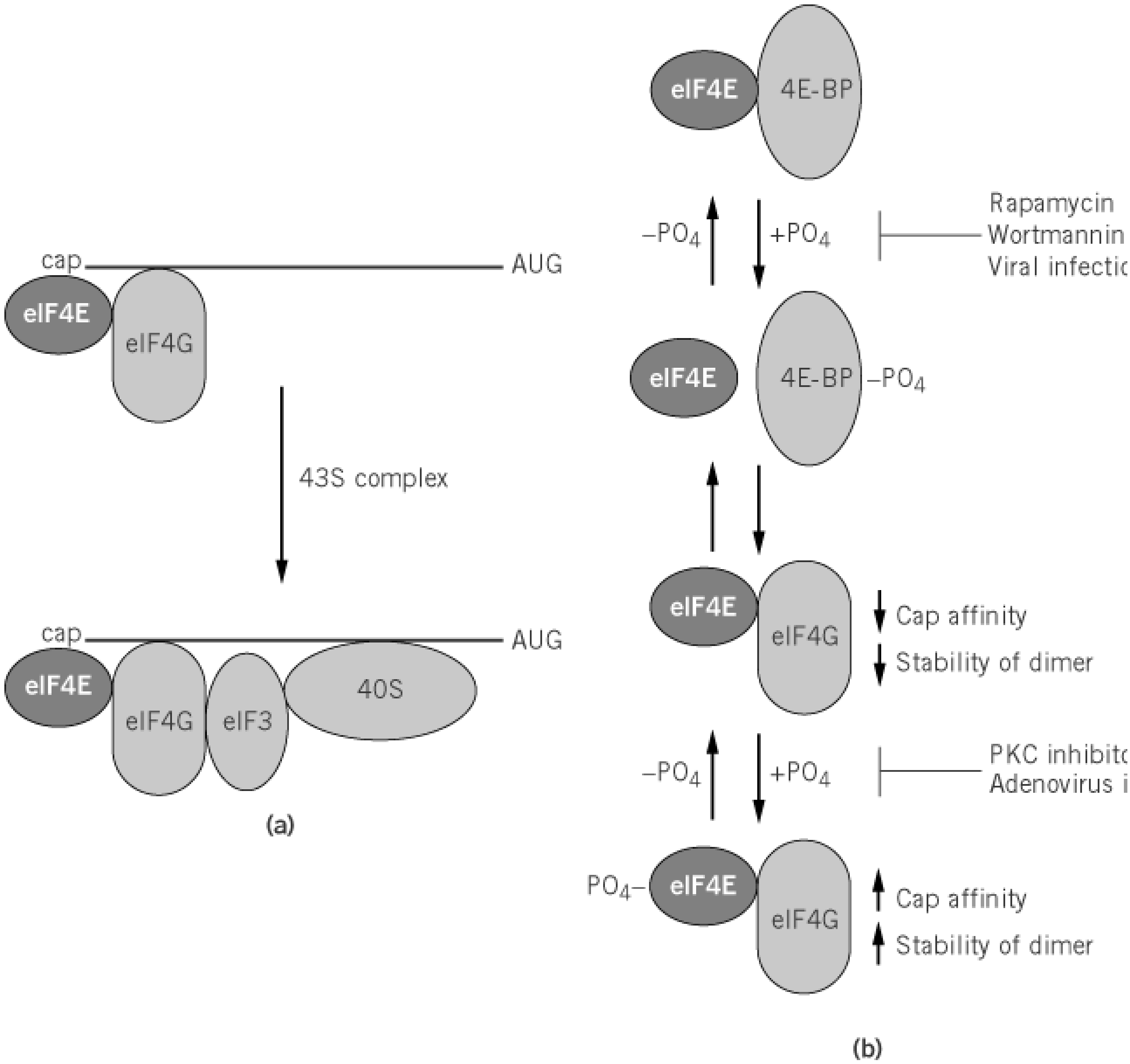

Bibliography

1. W. C. Merrick and J. W. B. Hershey (1996) In *Translational Control* (J. W. B. Hershey, M. B. Mathews and N. Sonenberg, eds.), Cold Spring Harbor Press, Cold Spring Harbor, NY, pp. 31–69.
2. R. J. Jackson (1996) In *Translational Control* (J. W. B. Hershey, M. B. Mathews, and N. Sonenberg, eds.), Cold Spring Harbor Press, Cold Spring Harbor, NY, pp. 71–112.
3. E. Ehrenfeld (1996) In *Translational Control* (J. W. B. Hershey, M. B. Mathews, and N. Sonenberg, eds.), Cold Spring Harbor Press, Cold Spring Harbor, NY, pp. 549–573.
4. H. D. Robertson and M. B. Mathews (1996) Biochimie **78**, 909–914.
5. M. W. Hentze (1997) Science **275**, 500–501.
6. A. Pause et al. (1994) Nature **371**, 762–767.
7. A. B. Sachs, P. Sarnow, and M. W. Hentze (1997) Cell **89**, 831–838.

Suggestions for Further Reading

8. M. Springer, C. Portier, and M. Grunberg-Manago (1997) In *RNA Structure and Function* (R. W.

Simons and M. Grunberg-Manago, eds.), Cold Spring Harbor, Laboratory, Cold Spring Harbor, NY, pp. 377–413.
9. A. B. Sachs, P. Sarnow, and M. W. Hentze (1997) Cell **89**, 831–838.

Initiation Factor (IF)

Formation of an initiation complex for translation of protein biosynthesis on 70 S ribosomes in bacteria involves, in addition to initiator fMet-$tRNA^{fMet}$, messenger RNA, and GTP, the cooperative interaction of three proteins, initiation factors IF-1, IF-2 and IF-3 (Table 1). Until now, no convincing data have indicated the existence of additional factors. Numerous *in vitro* experiments demonstrate that IF-1 and IF-3 shift the ribosome-dissociation equilibrium from 70 S ribosomes toward dissociation into 30 S and 50 S subunits. Under physiological conditions, the ribosomal subunit equilibrium is toward 70 S formation, and IF-1 serves to increase the rate constant for both the dissociation and association of 70 S ribosome, whereas IF-3 shifts the equilibrium strongly toward dissociation by binding to the 30 S particle. IF-3 also selects the initiator tRNA in the presence of the initiation codon triplet, as well as on a natural mRNA template. IF-3 action distinguishes the initiator transfer RNA from elongator tRNAs by specific domains in the tRNA and not by its formyl methionine (fMet). Part of the information is located in the anticodon stem and loop region. IF-3 has been shown to destabilize selectively polynucleotide-primed 30 S complexes formed with elongator tRNAs. The third initiation factor, IF-2, directs fMet-$tRNA^{fMet}$ binding to the 30 S subunit. This initiation factor might also exclude noninitiator tRNAs from the P site, while allowing formylated charged initiator tRNA to enter. This reaction is stimulated by IF-1 and GTP. In addition, IF-2 helps the association of the two subunits and has a GTPase activity in the presence of ribosomes. The process of initiation complex formation in prokaryotes is summarized in Fig. 1 (1).

Figure 1. The initiation pathway of protein synthesis in prokaryotes.

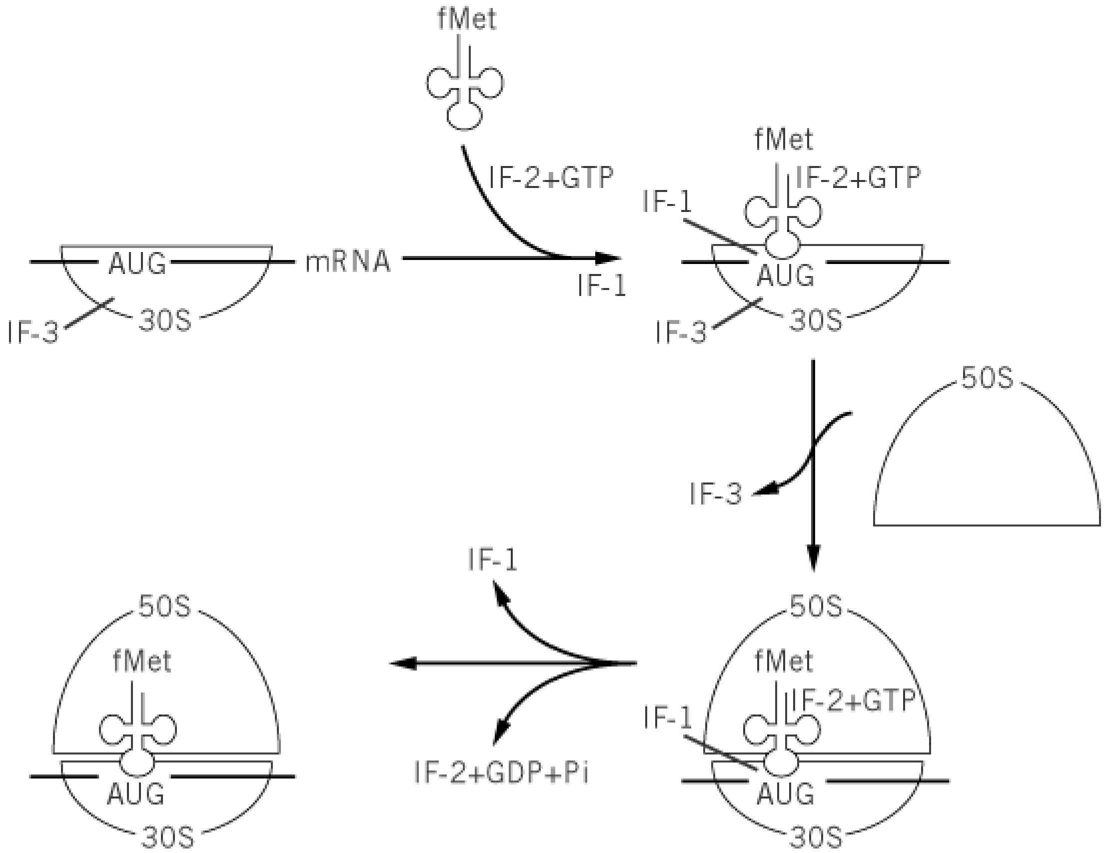

Table 1. ***Escherichia coli*** **Initiation Factors**

Factor	Molecular Mass	Number of Amino Acids	Gene	Function
IF-1	8,119	71	*infA*	Promotes IF-2 and IF-3 functions
IF-2a	97,300	889	*infB*	Binds fMet-tRNA and GTPase
IF-2b	79,700	732	*infB*	
IF-3	20,668	181	*infC*	Ribosome dissociation and mRNA binding; increasesthe specificity of the initiation complex for fMet-tRNA

In the absence of tRNA or initiation factors, the 30 S particle by itself binds to the proper initiation region on mRNAs. The sequence of events directed by initiation factors shows that IF-1 and IF-3 are released before or during the joining of the subunits, whereas IF-2 is released after their joining and requires GTP hydrolysis. The three factors are present in cells at sufficiently high concentration to saturate the free 30 S particle. The steady-state levels of initiation factors are coordinately regulated in exponentially growing bacteria relative to one another and relative to ribosome levels. All levels rise as a function of increasing growth rate, suggesting that the cellular levels of initiation factors are under metabolic control. Neither IF-2 and IF-3 synthesis is under stringent control *in vivo*.

All of the initiation factor genes have been cloned and mapped: *infA* for IF-1, *infB* for IF-2, and *infC* for IF-3. They are dispersed on the bacterial chromosome and, with the exception of *infA*, are associated with other components of the protein biosynthesis apparatus (threonyl and phenylalanyl-tRNA synthetase, and ribosomal protein L20 and L35 for IF-3; $tRNA^{fMet}$, NusA, and ribosomal protein S15 for IF-2). The *infB* gene produces two forms of IF-2, IF-2a (97.3 kDa), and IF-2b (79.7 kDa), using two in-frame initiator codons. Both forms are implicated in fMet-tRNA binding to 30 S ribosomes and possess a ribosome-dependent GTPase activity. The meaning of the existence of two forms of IF-2 in bacteria, as well as their functional difference, is not known.

The eukaryotic initiation steps are promoted by at least 10 different initiation factors, some of which are themselves complexes of numerous protein subunits. Figure 2 summarizes where the more important of the initiation factors function in the pathway (2). eIF-1A and eIF-3 are involved in the dissociation of ribosomes; eIF-2 and eIF-2B are primarily concerned with $tRNA^{iMet}$ binding to 40 S subunits; eIF-4A, eIF-4B, and eIF-4F promote mRNA binding and scanning; and eIF-5A is involved in the junction step. Essentially all the initiation factor polypeptide cDNAs have been **cloned** and sequenced (Table 2).

Figure 2. The initiation pathway of protein synthesis in eukaryotes.

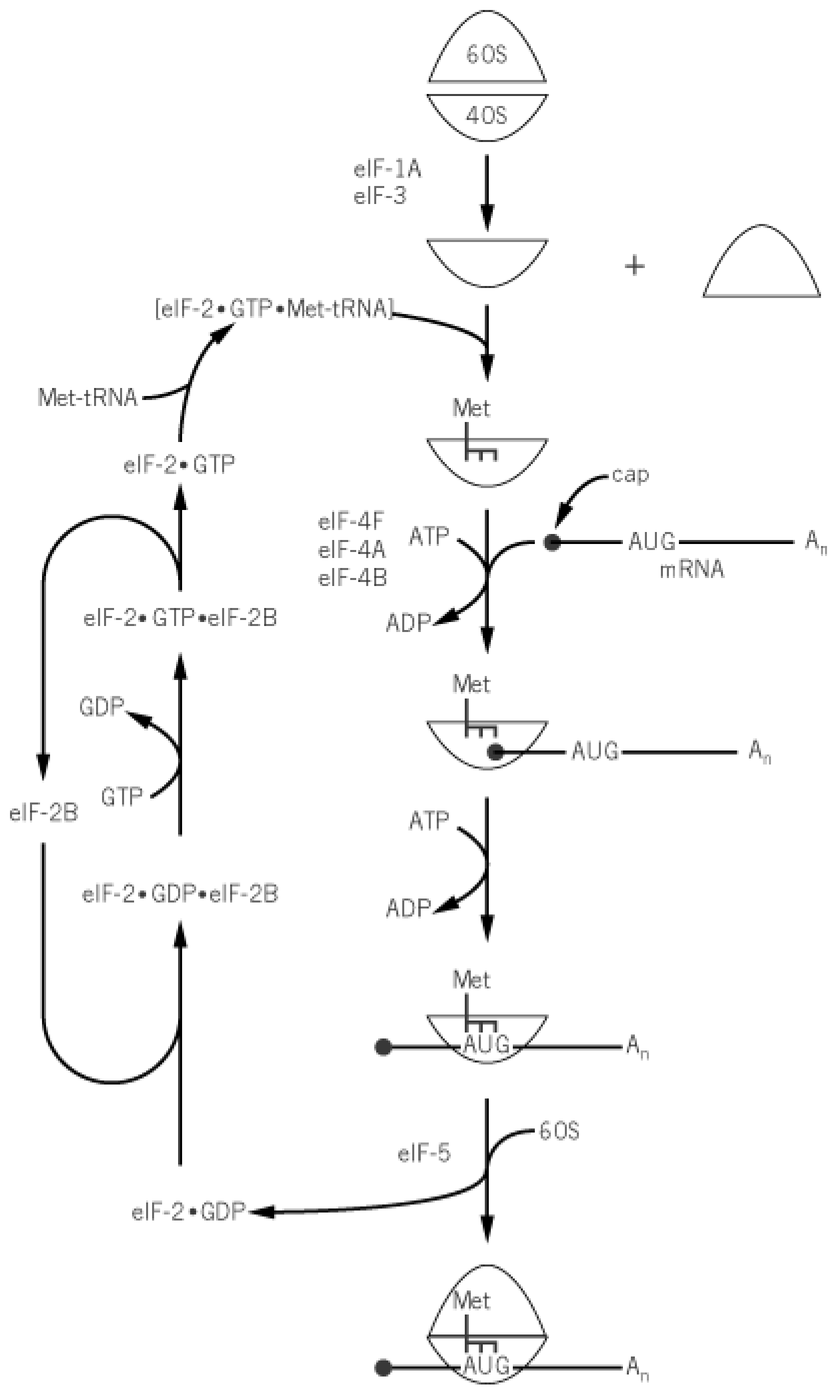

n pathway of protein synthesis in eukaryotes. [Full View]

Table 2. Eukaryotic Initiation Factors (2)

Factor	Subunit	Molecular Mass (kDa)	Function
eIF-1		12.6	Enhances initiation complex formation
eIF-1A		16.5	Ribosomal dissociation; promotes Met-$tRNA^{iMet}$ binding

eIF-2		125	Binds Met-tRNA^{iMet}and GTP
	a	36.1	Phosphorylated subunit
	b	38.4	Binds Met-tRNA^{iMet}
	g	51.8	Binds GTP; Met-tRNA^{iMet}
eIF-2B		270	Guanine nucleotide exchange factor for eIF-2
	a	33.7	
	b	39.0	Binds GTP
	g	58	Binds ATP
	d	57.1	Binds ATP
	e	80.2	Phosphorylated subunit
eIF-2C		94	Stabilizes ternary complex in presence of RNA
eIF-3		650	Dissociates ribosomes; promotes Met-tRNA^{iMet} and mRNA binding
	p35	35	Highly phosphorylated
	p36	36.5	
	p40	39.9	
	p44	35.4	RNA binding motif
	p47	47	
	p48	52.5	Identical to Int-6 (oncogene) homologue
	p66	64.0	Binds RNA
	p110	105.3	
	p116	98.9	Major phosphorylated subunit
	p170	166.5	
eIF-4A		44.4	ATPase, helicase, binds RNA
eIF-4B		69.8	Binds RNA, promotes helicase activity
eIF-4F		250	Binds 5′ Cap, helicase
	eIF-4E	25.1	Cap-binding subunit
	eIF-4A	44.4	ATPase, helicase
	eIF-4G	153.4	Binds eIF-4A, eIF-4E, eIF-3, and Pab1p
eIF-5		48.9	Promotes GTPase with eIF-2 and ejection of eIFs
eIF-6		25	

eIF-2 forms a ternary complex with Met-tRNA^{iMet} and GTP that binds to the 40 S ribosome, where it is established by eIF-1A and eIF-3. The resulting 43 S preinitiation complex then interacts with mRNA prepared by eIF-4F, eIF-4A, and eIF-4B. eIF-4F is a heterodimeric complex that binds to the -Cap structure of mRNA. It is composed of one molecule each of eIF-4E, eIF-4A, and eIF-4G. eIF-4E is of lower abundance in the cell than the other subunits and initiation factors, thereby making the eIF-4F complex rate-limiting under most circumstances. eIF-4A is an RNA-dependent ATPaseand binds RNA only weakly. Its sequences contain ATP-binding elements found in the **DEAD box** family of RNA Helicases. eIF-4B is an RNA-binding protein that contains two **RNA-binding** motifs: the RNP consensus octamer and hexamer elements and an arginine-rich domain. eIF-4F (bound to the 5′ Cap) together with eIF-4B possess RNA helicase activity dependent on ATP hydrolysis. When mRNA secondary structure is melted, the 40 S ribosome is able to bind to the 5′ Cap region and begin scanning. Proper interaction of the Met-tRNA ^{iMet} anticodon with the AUG initiator codon is monitored by eIF-5, which promotes GTP hydrolysis, followed by the ejection of initiation factors and junction of the 40 S initiation complex with 60 S subunits. eIF-2 leaves as a complex with GDP and requires eIF-2B-catalyzed exchange of the GDP for GTP in order to promote another round of initiation.

Bibliography

1. D. E. Draper (1996) In *Escherichia coli and Salmonella*, 2nd ed. (R. Curtiss III et al., eds.), American Society for Microbiology Press, Washington, D.C., pp. 902–908.
2. W. C. Merrick and J. W. B. Hershey (1996) In *Translational Control* (J. W. B. Hershey, M. B. Mathews, and N. Sonenberg, eds.), Cold Spring Harbor Laboratory Press, Cold Spring Harbor, NY, pp. 31–69.

Suggestion for Further Reading

3. M. Springer, C. Portier, and M. Grunberg-Manago (1997) In *RNA Structure and Function* (R. W. Simons and M. Grunberg-Manago, eds.), Cold Spring Harbor Laboratory Press, Cold Spring Harbor, NY, pp. 377–413.

Initiation Of DNA Replication

How replication of a chromosome is initiated has been a major subject of molecular genetics, because the regulation of chromosomal replication occurs primarily at the stage of initiation (see DNA Replication). Molecules that might be involved in the initiation of replication of the bacterial circular chromosome were proposed by Jacob et al. in 1963 (1). They assumed that each replicon consists of two elements participating in positive regulation of the initiation: (1) a *cis*-acting DNA signal (the replicator, which is now called the replication origin), and (2) a *trans*-acting protein factor (the initiator), which would interact directly with the replicator. The positive regulation for the initiation of chromosomal replication arose from the observation that **protein biosynthesis** is required for the initiation of each round of replication in *Escherichia coli*. Later, it was found that initiation occurs when each individual cell reaches a fixed amount of cell mass relative to the number of the replication origins, regardless of the growth rate (2). To explain these phenomena, the initiator accumulation theory was proposed (3). In this model, an initiator is synthesized and accumulates in the cell at the same rate as the cell mass increases, and initiation takes place every time a certain number of initiators accumulate for each replication origin. The model also proposed that the initiator should act as a repressor of its own **gene expression** to maintain the cellular content of the protein (autogenous regulation) as constant and so it is accumulated in concert with an increase in cell mass. Although Jacob and his colleagues merely stated that the model was a simplified one, their far-sighted hypothesis has now proven to be correct concerning the prokaryotic replicons, those of bacteria, **bacteriophage**, and **plasmids** (see DNA Replication).

1. Initiation of Bacterial Plasmid Replication

The replication of bacterial plasmids and phage has been shown to start from a unique site on the replicon (the origin, see Replication Origin), and most plasmids and phage encode a gene, often designated *rep*, for a replicon-specific protein required for the initiation of DNA replication. The replicon-specific Rep proteins have been shown to recognize specific sequences at the origin and to act positively to recruit host-encoded replication enzymes (4). The initiation frequency of the replication of plasmids is regulated so as to maintain a steady-state **copy number** characteristic of the particular plasmid in a given host bacterium (5). The majority of plasmids in **Gram-negative** bacteria contain direct repeats of the Rep binding sequence (iterons) within the origin. Many of these plasmids also contain indirect repeats of sequences related to the iterons within the **promoter** region of the *rep* gene, and the expression of the Rep protein is autoregulated, as proposed in the initiator accumulation theory. Direct repeats within the functional origin of an iteron-containing plasmid, when inserted into a plasmid normally compatible with the iteron-containing plasmid, show strong incompatibility with the plasmid. In addition, insertion of additional homologous iterons into an iteron-containing plasmid results in a reduction of the copy number of the plasmid. Based on these observations, it was proposed initially that replication begins when a sufficient amount of Rep protein is accumulated to cover the iterons at the origin, and additional Rep binding sequences reduce the effective amount of the initiator (6). However, extensive studies conducted on the regulation of initiation of the iteron-containing plasmids have revealed properties that argue against the simple titration model (5). For example, increasing the concentration of the Rep protein of several plasmids *in vivo* did not result in a proportional increase in the copy number. Several Rep proteins have been shown to exist as two forms; dimers that bind to the iterons in the origin and monomers that regulate its own expression. Although new models that modify the simple titration model to explain the regulation of the initiation of plasmid replication have been proposed, much remains to be learned to understand it completely (5).

2. Initiation of Replication of Bacterial Chromosome

A number of genes have been identified as being involved in the initiation of chromosomal replication in bacteria. The functions of these genes during the initiation process have now been well defined through genetic and biochemical studies in *E. coli* (4, 7). DnaA protein was found to function at the first step in the initiation process by binding to specific DNA repeats (the DnaA box) in the replication origin of the chromosome (*oriC*), and then opening the double strand for formation of the primosome, the machinery for the first primer synthesis (see DNA Replication). The combination of a DnaA box and DnaA protein functioning as *cis* and *trans* regulatory elements, respectively, in the initiation of chromosomal replication was subsequently found to be common in **eubacteria** (7, 8).

Expression of the *E. coli dnaA* gene is negatively regulated by the DnaA protein itself, by the protein binding to DnaA boxes located in the promoter region of the gene, and the concentration of the DnaA protein is kept proportional to the origin concentration. Overproduction of the DnaA protein stimulated the initiation of chromosomal replication up to two-fold, and that stimulation was proportional to the increase in the DnaA protein concentration within this limited range. DnaA overproduction also resulted in a two-fold increase in minichromosome (*oriC* plasmid) copy number. Thus, *E. coli* DnaA protein is considered to fulfill the qualifications required for an initiator that controls the timing of initiation of replication during the cell cycle, and the time of initiation is assumed to be set by the DnaA protein accumulating to a threshold level (9). However, it should be noted that other factors affecting initiation control have been identified. The characteristic of *oriC* of enterobacteria is the presence of many GATC sequences, which are sites for the Dam **restriction-modification** methylase. It was found that newly replicated *oriC* DNA strands are not methylated during up to one-third of the cell cycle after the replication. Such hemi-methylated DNA tends to bind to the cell membrane and does not act as a template for activation by DnaA protein. Furthermore, initiation of replication occurs more or less at random in relation to the cell cycle in a mutant lacking Dam methylase (7). The DnaA protein can be modified in different ways by binding ATP or ADP. Phospholipids were found to reactivate the inactive form (ADP–DnaA) *in vitro* by exchanging ADP for ATP. Initiation from *oriC* seemed to be inhibited *in vivo* in a mutant in which the synthesis of phospholipids was limited (10).

The *dnaA* gene is also autoregulated in *Bacillus subtilis*. However, expression of the *B. subtilis dnaA* gene is coupled to initiation of replication of the chromosome. It is assumed that the autorepression by interaction of DnaA protein with many DnaA boxes near the promoter is so strong in *B. subtilis* that the gene is expressed only when the chromosome undergoes vigorous conformational changes during the replication of the gene itself (11). In *B. subtilis*, fewer than one *oriC* plasmid/cell is allowed to coexist with the chromosome. Introduction of extra copies of DnaA boxes would be incompatible with chromosomal replication. This stringent control of the initiation observed may be ascribed to the strong negative control of *dnaA* expression. Accumulation of the DnaA protein to a threshold level was shown to be prerequisite for the initiation of replication in *B. subtilis*. However, control of the timing of the initiation may require other factors, because the DnaA protein seems to be synthesized only in the early stage of the replication cycle in this cell. Although the role of DnaA as a key factor for regulation of initiation is clear in both *E. coli* and *B. subtilis*, the overall view of the regulation of the timing of initiation is not still clear. And, different devices to control the timing seem to have been evolved in two bacteria.

3. Initiation in Eukaryotes

A unique initiator protein (T Antigen) has been identified to regulate the initiation of replication of the eukaryotic **SV40 virus**. However, no single initiator protein like bacterial DnaA has been found for eukaryotic chromosomes. Instead, multiprotein complexes have been identified to initiate replication of the multiple replicons of eukaryotes. Furthermore, a complex network of protein–protein interactions (complex formation) and protein modifications (**phosphorylation**) regulates the initiation (see DNA Replication).

Bibliography

1. F. Jacob, S. Brenner, and F. Cuzin (1963) Cold Spring Harbor Symp. Quant. Biol. **28**, 329–348.
2. W. D. Donachie (1968) Nature **219**, 1077–1079.
3. L. Sompayrac and O. Maaloe (1973) Nature New Biol. **241**, 133–135.
4. A. Kornberg and T. A. Baker (1992) *DNA Replication*, 2nd ed., W. H. Freeman and Company, New York.
5. D. R. Helinski, A. E. Toukdarian, and R. Novick (1996) in *Escherichia coli and Salmonella* (F. C. Neidhard, ed.), American Society for Microbiology, Washington, DC, pp. 2295–2324.
6. H. Tsutsui and K. Matsubara (1981) J. Bacteriol. **147**, 509–516.
7. W. Messer and C. Weigel (1996) In *Escherichia coli and Salmonella* (F. C. Neidhard, ed.), American Society for Microbiology, Washington DC, pp. 1579–1601.
8. H. Yoshikawa and N. Ogasawara (1991) Mol. Microbiol. **5**, 2589–2597.
9. J. Herrick, M. Kohiyama, T. Atlung, and F. G. Hansen (1996) Mol. Microbiol . **19**, 659–666.
10. W. Xia and W. Dowhan (1995) Proc. Natl. Acad. Sci. USA **92**, 783–787.
11. H. Yoshikawa and R. G. Wake (1993) In *Bacillus subtilis and Other Gram-positive Bacteria* (L. Sonenshein, J. A. Hoch, and R. Losick, eds.), American Society for Microbiology, Washington, DC, pp. 507–528.

Inositol Lipids and Phosphates

*Myo*inositol, a carbohydrate first found in the mid-1800s in muscle, was defined in the 1930s as a growth factor for yeasts and mammals and then as a component of membrane phospholipids (phosphoinositides) (1, 2). In the 1950s, Hokin and Hokin found that secretory stimuli often accelerate phosphoinositide turnover in their target cells (2, 3). This initial observation led ultimately to recognition of inositol lipids and phosphates as crucially important regulatory molecules in eukaryote cells.

1. *Myo*inositol

*Myo*inositol is one of nine stereoisomeric hexahydroxycyclo-hexanes (the inositols). Several inositols occur in nature, but only *myo*inositol is used widely in the headgroups of membrane phospholipids and in water-soluble inositol polyphosphates. When in the preferred “chair” configuration, *myo*inositol has five equatorial hydroxyl groups (1-6): only the 2-OH is axial (Fig. 1) (1, 2, 4). IUPAC recommendations decree that D- *myo*inositol 1-phosphate (abbreviated as Ins1*P*; the same molecule as L-*myo*inositol 3-phosphate) is the reference molecule for the numbering of biological *myo*inositol derivatives (4). Inositol is made biosynthetically by cyclization of the central metabolite glucose 6-phosphate (by way of 5-ketoglucose 6-phosphate) to Ins3*P*, which is then dephosphorylated (1).

Figure 1. The configuration of, and carbon atom numbering (D-configuration) in, *myo*inositol. The mirror plane () identifies the plane of symmetry through the 2- and 5-carbons of the inositol ring.

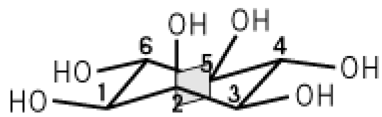

It is not clear how evolution “selected” *myo*inositol (from here on simply termed *inositol*) to take on multiple biological roles. Maybe inositol's stereochemistry gives its derivatives some biologically desirable property. Alternatively, evolution may have “needed” a conveniently synthesized and stable polyol, and selected a molecule that comes, by a very short route, from a ubiquitous cell constituent.

The stereochemical versatility of inositol has allowed biology to put it to many uses. Because it has an axis of symmetry through its 2- and 5-carbons (Fig. 1), addition of one substituent to C-1, C-3, C-4, or C-5 immediately renders every carbon in the ring stereochemically unique. For example, Ins1*P* and Ins3 *P* are enantiomers, as are the inositol tetrakisphosphates Ins(1,3,4,5)P_4 and Ins(3,4,5,6)P_4 (L-Ins(1,3,4,5)P_4) (1, 4). Thus, the possible variety of stereochemically (and biologically) unique inositol derivatives can be almost endless.

2. Inositol lipids and phosphates: variety and evolution

Inositol seems to be essential to all eukaryotic cells, and some members of both bacterial kingdoms (Eubacteria and Archaebacteria) also contain inositol lipids and phosphates. Many of the functions of the inositol lipids are becoming understood in remarkable detail, but only a few functions have been definitively ascribed to particular inositol polyphosphates.

Before about 1950, cells were thought to contain a single inositol glycerophospholipid, namely phosphatidylinositol (PtdIns; *sn*-1,2-diacyl-glycero-3-phospho-D-1-*myo*inositol) (Fig. 2). This is generally the most abundant inositol glycerophospholipid, and it and its phosphorylated derivative often have a 1-arachidonyl, 2-stearoyl acyl fatty acyl pairing in mammalian cells. Seven other glycerophosphoinositides, all of which are phosphorylated derivatives of PtdIns, have been identified since 1949 (Fig. 2). Figure 3 summarizes the likely metabolic and functional interrelationships between these glycerolipids.

Figure 2. The “simple” inositol glycerolipids of eukaryotic cells.

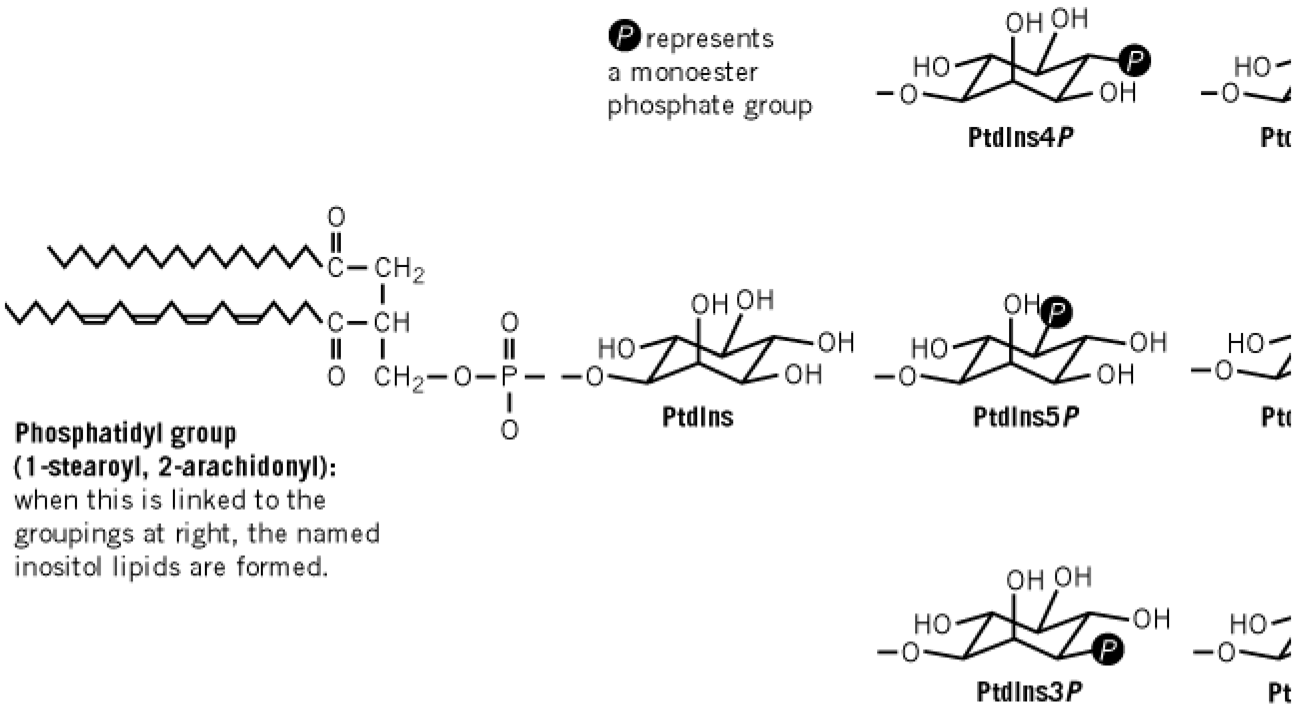

Figure 3. Likely pathways involved in eukaryotic glycerophosphoinositide-based signaling. Substrates of signaling path in shaded ovals, and proven or probable second messengers are in shaded boxes. Note that PtdIns serves as the common and that PtdIns(4,5)P_2 3-kinase signaling pathways and PtdIns(4,5)P_2-directed (Type I) and PtdIns-directed (Type III) in functions.

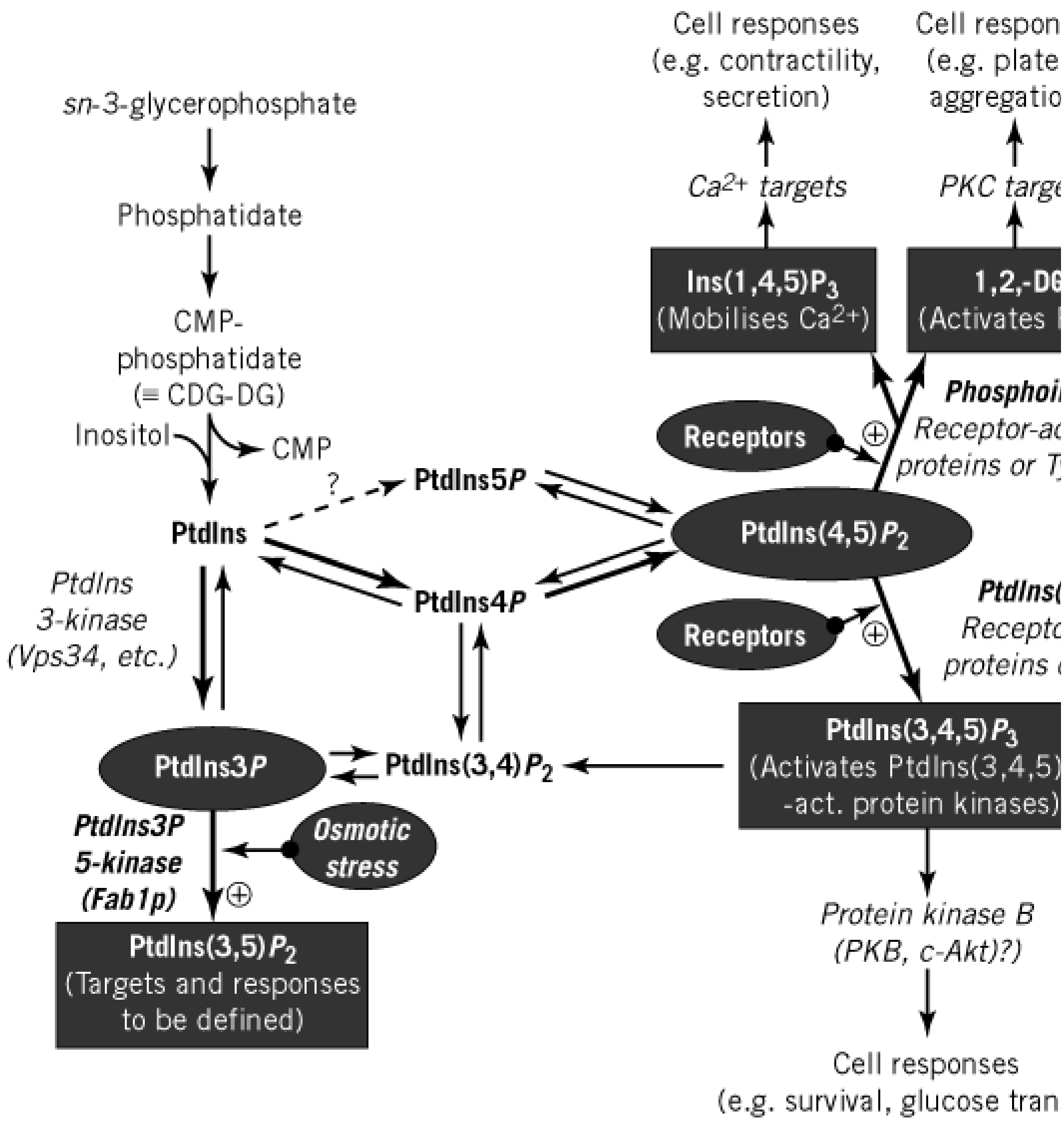

In addition to these relatively simple membrane lipids, the membrane-penetrating lipid anchors of many cell-surface (glyco)proteins and their precursors are PtdIns glycans of varying complexity (see GPI Anchor). Some eukaryotic cells, notably plants and yeasts, also contain complex sphingolipids with inositol-containing headgroups. Although these do not yet have proven functions, their metabolism in yeast is somehow linked to vesicle trafficking (5).

Cells also contain many water-soluble inositol (poly)phosphates. For example, Dictyostelium and mammalian cell lines, such as WRK1 (mammary tumor) and HL60 (myeloid), contain 25 or more different inositol phosphate species (eg, ref. 6). Figure 4 summarizes the metabolic links between many of these inositol phosphates, primarily as in mammalian cells. A variety of inositol phosphate interconversion pathways have been reported from plants and yeasts, including a remarkably direct conversion of Ins(1,4,5)P_3 to InsP_6, apparently by a single enzyme (7). Plant seeds store much of the phosphate essential to their successful germination and development as phytate (an insoluble bivalent cation complex of InsP_6), alleged to be the most abundant phosphate ester in nature.

Figure 4. Pathways of inositol polyphosphate interconversion in eukaryote cells. For simplicity, individual inositol monophosphates and bisphosphates on the dephosphorylation pathways have been omitted.

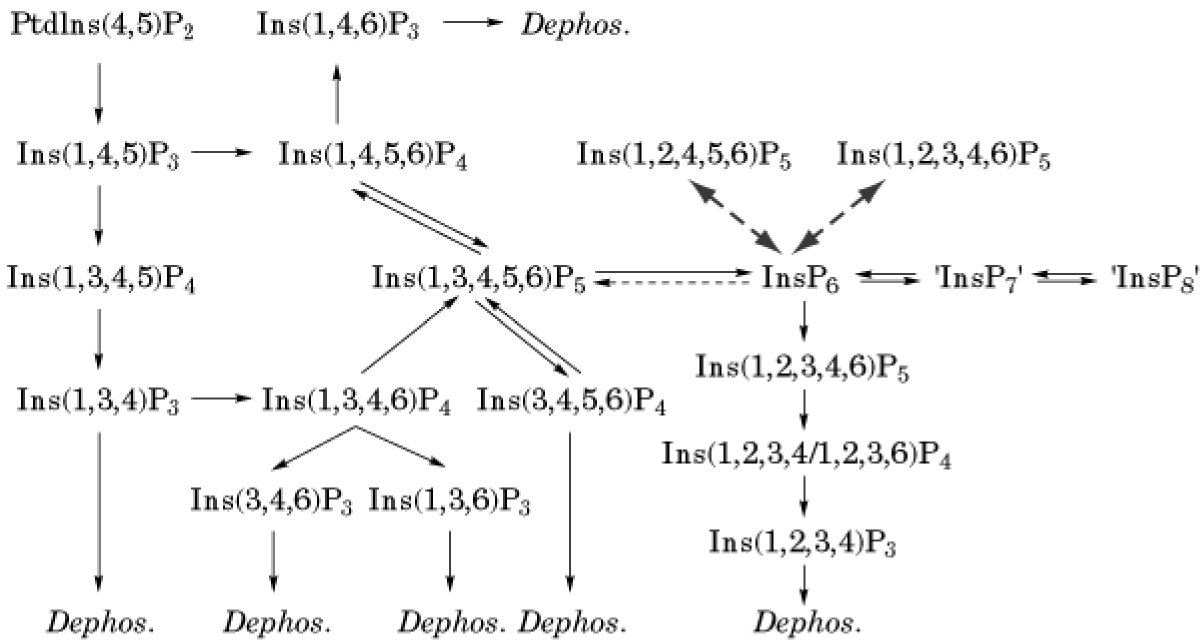

Some families of Eubacteria have additional inositol-containing phospholipids, the best characterized being the PtdIns mannosides of mycobacteria. Archaebacteria, which inhabit some of the most hostile environments on the planet, have glycerophospholipids that are very distinctive, both because the steric configuration of the diradylglycerol backbone of these lipids is opposite to that of the eukaryotic and eubacterial lipids and because they use very different, and chemically very stable, hydrocarbon side chains. Again, however, some of these have inositol headgroups (8). Moreover, hyperthermophilic archaebacteria use inositol in another remarkable way. When they are exposed to temperatures that are even more extreme than usual, they synthesize very high cytosolic concentrations (~0.5M) of the K^+ salts of water-soluble inositol phosphate derivatives, such as dimyoinositol 1,1′-(3,3′)-phosphate, as cytoprotective solutes (9).

When the primeval cells from which all later organisms evolved were emerging, a fairly early step was almost certainly enclosure of the newly evolving cellular metabolic machinery within a selectively permeable membrane envelope made of amphiphilic lipids. The fact that *myo*inositol, an unusually stable cyclic polyol, is a component both of the diether lipids of Archaebacteria and of the (mainly) diacyl-glycerolipids of Eubacteria (some) and eukaryotes suggests that it was recruited into membrane lipids very early. This probably happened before the two-billion-year-old evolutionary radiation that gave rise to the major biological kingdoms, making inositol a very ancient cell component.

Only since the early 1980s, however, has it been recognized how inositol's stereochemical versatility has let cells employ its derivatives for many different jobs. Throughout this recent period, frequent discoveries of “new” inositol-containing cell constituents have regularly been followed by the definition of “new” functions for inositol derivatives.

3. Inositol lipids and phosphates in signaling

One of the most essential characteristics of cells is their ability to respond with changes in their behavior to chemical changes in their environment. Many of these extracellular chemical signals cannot penetrate the plasma membrane, and so the cell surface receptors that respond to them couple to transmembrane signal transduction mechanisms that pass information to the cell interior. Inositol lipids play essential roles as the metabolic substrates and/or the output signals of at least two, and maybe three or more, widespread cell signaling systems.

3.1. Signaling through Phospholipase C Activation

The best characterized of these signaling pathways uses receptor activation of PtdIns(4,5) P_2 hydrolysis by phosphoinositidase C (phospholipase C, PLC) to make the second messengers inositol 1,4,5-trisphosphate (Ins(1,4,5) P_3) and 1,2-diacylglycerol, as outlined in Fig 3 (top right). Despite extensive early work by the Hokins (3), only in the 1970s was it realized that inositol lipid hydrolysis has the properties of a coupling reaction that links cell-surface receptors to the intracellular mobilization of Ca^{2+} (2) (see Calcium Signaling). PtdIns(4,5)P_2 hydrolysis was then identified as the primary stimulated reaction (10). Meanwhile, Nishizuka defined the polyunsaturated 1,2-diacylglyerol (1,2-DG) liberated from PtdIns(4,5)P_2 as a second messenger that activates many members of the protein kinase C family (11). Finally, Streb et al. showed that Ins(1,4,5) P_3 released Ca^{2+} from an intracellular store (12). We now know that Ins(1,4,5)P_3 triggers intracellular Ca^{2+} release through the intrinsic cation **channels** of at least four subtypes of Ins(1,4,5)P_3 “receptor” that are expressed primarily in various elements of the endoplasmic reticulum (13).

These revelations established two new principles. First, chemical species very different from nucleotide cyclic phosphates (see -cyclic AMP, cAMP); -Monophosphate, cGMP)) and the Ca^{2+} ion, the prototypic intracellular messenger molecules that were recognized between the mid-1950s and the mid-1970s, can function as “second messengers.” Second, receptor-generated intracellular messenger molecules need not be water-soluble and thus mobile within the cell. Instead, protein kinase C homes to the 1,2-DAG that is formed at the plasma membrane as a consequence of PtdIns (4,5)P_2 hydrolysis. There it is activated by simultaneous interactions with 1,2-DAG, anionic aminophospholipids, notably phosphatidylserine, in the inner leaflet of the plasma membrane, and the ambient concentration of cytoplasmic Ca^{2+}.

There are numerous excellent reviews of the PLC signaling pathway and the extraordinary variety of receptors that harness it (eg, refs. 11-15; and see Phospholipases C): some of the important receptors that harness this signaling pathway are listed in Table 1(see also Acetylcholine Receptor, Rhodopsin). There is a substantial family of PLCs that can hydrolyze PtdIns(4,5)P_2, and these are activated by two or more fundamentally different mechanisms (16). PLCs of the b-family are activated by some subfamilies of receptors in the 7-span or “serpentine” superfamily. Different serpentine receptors activate PLC-bs, either through the GTP-ligated a-subunits of heterotrimeric G proteins of the G_Q subfamily (**pertussis toxin**-insensitive) or bg-subunit dimers that are liberated following activation of G proteins in the G_i/G_o subfamily (**pertussis toxin**-sensitive). PLCs of the g-subfamily are attracted to the cytoplasmic face of the plasma membrane by certain phosphotyrosine-containing peptide motifs that are made by activated **tyrosine kinases**, and there they are tyrosine-phosphorylated: these two events cooperate to activate PtdIns(4,5)P_2 hydrolysis by the PLCgs (16). PLCds exist alongside PLCbs and PLCgs in animal cells, but only PLCds seem to be present in yeasts and plants. To some degree, the PLCds remain a puzzle, particularly because we still do not fully understand how they are activated. They can be activated by increases in cytosolic (Ca^{2+}) that are fairly large but physiologically plausible, but there may be other activating factors yet to be discovered.

Table 1. Stimuli that Transmit Signals into Target Cells at Least in Part Through Phosphoinositide-Based Signaling Pathways

PLC-Catalyzed PtdIns(4,5)P_2 Hydrolysis

Platelet-derived growth factor (PDGF)	Angiotensin I (AT$_1$receptor)
	Endothelins (3 receptors)
Adrenergic (a$_1$receptor)	Rhodopsin (invertebrates only)
Histamine (H$_1$ receptor)	
Acetylcholine (muscarinic, 2 subtypes)	Thromboxane A$_2$
	Interleukin 8
Vasopressin (V$_1$receptor)	Glutamate (metabotropic receptors)
Oxytocin	
Substance P and other tachykinins	Some taste receptors?
PtdIns(3,4,5)P_3 Synthesis Catalyzed by Type I Phosphoinositide3-Kinases	
Platelet-derived growth factor (PDGF)	The ab/CD3 antigen receptor complex of T lymphocytes
Insulin	
IGF-1	*f*MetLeuPhe
Colony-stimulating factor-1 (CSF-1)	
PtdIns3P 5-Kinase-Catalyzed PtdIns(3,5)P_2 Synthesis	
Hyperosmotic stress (yeast)	

A particularly clear illustration of the essential nature of the phospholipase C signaling pathway has emerged from genetic studies of the visual systems of insects (eg, *Drosophila*), which use rhodopsin-linked phospholipase C activation as their primary signaling pathway in response to the light activation of rhodopsin (17). Fly retinas show a striking set of genetic defects in this signaling pathway. They do not function properly if they lack: (1) a receptor-coupled phosphoinositidase C; (2) a diacylglycerol kinase and CDP-diacylglycerol synthase necessary for the resynthesis of PtdIns from the hydrolyzed PtdIns(4,5)P_2; or (3) a PtdIns transfer protein that is assumed somehow to maintain the PtdIns supply to the photoreceptor membranes (see Table 2and ref. 5).

Table 2. Biological Effects for Eye Function in *Drosophila* of Mutations in, or Changes in, the Expression Level of Proteins Involved in Phosphoinositide-Based Signaling (See Ref. 3 for References to Original Observations)

Gene or Protein	Target Protein	Phenotype
NorpA	PLC-b, coupled to light-activated rhodopsin	Eye elements fail to generate a light-triggered receptor potential
RdgA	Diacylglycerol kinase	Photoreceptors degenerate
RdgB	PtdIns transfer protein	Light-induced degeneration of photoreceptors
Cds	CDP-diacylglycerol	Reduced signal gain

	synthase (a step in PtdIns biosynthesis)	during photoreception; light-dependent degeneration of photoreceptors
Type-I PtdIns(4,5)P_2 3-kinase	Organ-targeted Type I PI3K	Eye size correlates positively with the concentration of expressed PI3K

3.2. Signaling through 3-Phosphorylation of PtdIns(4,5)P_2 to Phosphatidyl-inositol 3,4,5-Trisphosphate (PtdIns(3,4,5)P_3)

In the late 1980s, eukaryote cells yielded up both PtdIns3 *P* and phosphoinositide 3-kinases that can make PtdIns3 *P* from PtdIns (generically abbreviated below as PI3Ks). Soon, however, it was found that some PI3Ks can use PtdIns, PtdIns4*P*, and PtdIns(4,5)P_2 as substrates and so can also make two other novel lipids: PtdIns(3,4)P_2 and PtdIns(3,4,5)P_3. Moreover, neutrophils stimulated by the chemotactic attractant *f*MetLeuPhe (see Chemotaxis) were seen to make a lipid with the charge of a phosphatidylinositol trisphosphate (PtdIns P_3): this proved to be PtdIns(3,4,5)P_3.

Soon came recognition that many activated receptor tyrosine kinases (see Growth Factors; Platelet-Derived Growth Factor; Insulin) and a few G-protein-coupled serpentine receptors (especially those in hematopoietic cells) can very rapidly (within seconds) stimulate a subset of PI3Ks that phosphorylate PtdIns(4,5)P_2 to PtdIns(3,4,5)P_3 (see Table 1). These are now known as the Type I subfamily (18).

The PtdIns(3,4,5)P_3 generated in response to receptor stimulation, which is the most highly charged membrane phosphoinositide present in cells, is presumed to be located in the inner leaflet of the plasma membrane. This identified it as another potential receptor-generated signaling molecule. Several key observations soon combined to confirm this view (18-20). First, the PtdIns (4,5)P_2 3-kinase responsible for PtdIns(3,4,5) P_3 synthesis in response to activated tyrosine kinases is a heterodimer of a catalytic subunit (p110) and a **SH2 domain**-containing regulatory subunit (p85). Immediately after the activation of some growth factor receptors, this p110/p85 PI3K becomes physically complexed with the activated receptor tyrosine kinase. This binding is mediated by the SH2 domain of p85, which recognizes a particular phosphotyrosine-containing motif (typically *P*Tyr-Met-Asp/Pro-Met) in the cytoplasmic “tail” of the activated receptor tyrosine kinase. Interaction with this motif localizes the kinase to the inner surface of the plasma membrane, where it becomes tyrosine-phosphorylated and is activated. Second, mutations of the “kinase insert” sequence of the platelet-derived growth factor (PDGF) receptor abolish this *P*Tyr-containing motif and reduce the growth-stimulating and survival-promoting activity of PDGF. Third, the tyrosine kinase activities of the activated insulin and insulin-like growth factor I receptors phosphorylate insulin receptor protein 1 (IRS-1), generating multiple PI3K-activating motifs. This activation of PI3K activity is essential both for the survival-promoting activities of these hormones and for a number of their classical actions on carbohydrate metabolism (19, 20). Fourth, overexpressed or constitutively active PI3Ks are growth-promoting and can be oncogenic (18). Finally, neutrophils contain a different Type I PtdIns(4,5)P_2-directed PI3K, which is activated by the G protein bg–subunit complexes that are released following activation of some G protein–coupled receptors (eg, the *f*MetLeuPhe receptor) (21).

The fungal metabolite wortmannin A was a key reagent in many of these studies. Interest in this compound was aroused when it was found to inhibit multiple, and apparently unrelated, cell responses to external stimulation. These included:

1. The rapid oxidative burst characteristic of stimulated neutrophils;
2. Insulin-stimulated glucose uptake into target tissues, notably adipose and skeletal muscle, which is achieved primarily by fusion of vesicles enriched in glucose-permeable channels with the plasma membrane;
3. Maintenance of cell survival in response to “growth/survival factors” such as IGF1; and
4. Activation of the formation of lamellipodia at the leading edge of migrating cells (see Cytoskeleton).

Once it was realized that wortmannin is a very potent inhibitor of the Type-I PI3Ks that make PtdIns(3,4,5)P_3, this became an obvious candidate as the immediate activator of some or all of these responses. Although subsequent studies showed that wortmannin can be a less than scrupulously precise pharmacological reagent, other evidence has subsequently confirmed that many of the biological responses that are most sensitive to wortmannin inhibition are indeed consequences of PI3K activation. Used carefully, therefore, this compound has remained valuable for the initial identification of responses that might be consequences of receptor-stimulated PtdIns (3,4,5)P_3 synthesis.

Some details of how cells sense and respond to a PI3K-driven rise in PtdIns(3,4,5)P_3 concentration as a regulatory signal have been elucidated. Most notably, accumulation of PtdIns(3,4,5)P_3 very quickly leads to activation of protein kinase B (PKB, also known as c-Akt), a **serine-threonine protein kinase** and the product of a proto-oncogene (22). To become fully activated, cytosolic PKB must become firmly localized to the inner face of the plasma membrane and must be phosphorylated on two widely separated residues (Thr473 and Ser308). PKB physically associates with the plasma membrane, primarily through a direct interaction between its pleckstrin homology (PH) domain and the normal PtdIns(4,5)P_2 complement of that membrane, but this association may be strengthened by newly formed PtdIns(3,4,5)P_3.

Receptor-stimulated formation of PtdIns(3,4,5)P_3 triggers phosphorylation of the membrane-bound PKB. In this process, one PtdIns(3,4,5)P_3-activated protein kinase (phosphoinositide-dependent kinase 1; PDK1) phosphorylates PKB on Thr308, and another may phosphorylate it on Thr473 (Fig. 2; refs. 23, 24). The interaction that activates PDK1 seems to be between the newly formed PtdIns(3,4,5)P_3 and a PtdIns(3,4,5)P_3-selective PH domain in PDK1.

A substantial number of other candidate target proteins avidly and selectively bind PtdIns(3,4,5)P_3: these include the so-called centaurins (25, 26) and Bruton's tyrosine kinase, an enzyme essential for normal B lymphocyte development (27). Which, if any, of these serve as directly-controlled regulatory targets of this receptor-responsive polyphosphoinositide remains to be determined (20).

4. Phosphoinositides and membrane trafficking

The earliest work on receptor-stimulated phosphoinositide turnover, in the 1950s and 1960s, focused primarily on its possible relationship to the triggering of secretory processes (3). The emphasis then moved to unraveling the central roles of phosphoinositides in signaling. Recently, however, there has been a remarkable resurgence of interest in how phosphoinositides contribute to intracellular membrane and protein trafficking (28).

4.1. PtdIns(4,5)P_2 Synthesis and Exocytosis

It has long been known that **secretory vesicles** (eg, adrenal medullary chromaffin "granules") support rapid PtdIns4*P* biosynthesis, and recently it was recognized that **exocytotic** secretory processes in yeast and in mammalian cells fail in the absence of a functional cytosolic "PtdIns transfer protein" (PITP). In yeast, *Sec14*, one of many ***Sec*** genes implicated in secretory protein transit early in the pathway between the Golgi apparatus and the plasma membrane, encodes a PITP and, in permeabilized PC12 cells (which mimic catecholamine secretion by adrenal medulla), a PITP is among the proteins that are needed to reconstitute ATP-driven exocytotic secretion.

PtdIns is made at the endoplasmic reticulum but is involved in signaling at the plasma membrane. Soon after the discovery of PITPs in the 1970s, it was recognized that these molecules might serve as "ferries" that move PtdIns around cells (2), an idea that was recently validated (29, 30). PITPs bind PtdIns and/or phosphatidylcholine, one molecule at a time, and shuttle these lipids across the cytosol from membrane to membrane. Mammals have two very similar PITPs (a and b), either of which can support PtdIns(4,5)P_2-dependent signaling and exocytosis. Although the yeast protein encoded by *Sec14* is functionally quite similar, it has an unrelated amino acid sequence.

A second cytosolic protein that is essential for catecholamine secretion by PC12 cells is a PtdIns4*P* 5-kinase. Successful exocytosis, therefore, requires PtdIns to be delivered to the secretory vesicle membrane and phosphorylated to PtdIns(4,5)P_2 (31). Accumulation of a substantial amount of PtdIns(4,5)P_2 in the secretory vesicle membrane may somehow "prime" the vesicles, switching them to a state in which they can fuse with the plasma membrane in a subsequent Ca^{2+}-activated exocytosis step.

4.2. PtdIns3P and Membrane Trafficking

PtdIns3*P*, by contrast, is somehow implicated in vesicular protein sorting to the vacuole of yeast and the lysosomes of mammalian cells (which are functionally homologous organelles), and also in membrane fusion between elements of a membrane vesicle compartment (the "early" endosomes) that plays a central role in the import into eukaryotic cells of macromolecules such as the iron-carrier protein transferrin. This first became apparent when the protein encoded by *vps34*, one of many genes whose disruption interferes with vesicular protein sorting in cells, was identified as a PtdIns-specific PI3K: Vps34p and other Vps34p-like PI3Ks make up the Type III PI3K subfamily. It is not clear how PtdIns3*P* contributes to the membrane fusion and fission events in these membrane trafficking processes. However, detailed studies of EEA1, a protein characteristic of early endosomes, have shown that a **zinc finger**like protein domain known as a "FYVE finger" serves as a highly selective PtdIns3*P*-binding domain; similar FYVE finger domains are present in several other mammalian and yeast proteins involved in membrane trafficking processes (32, 33).

The importance of the 3-phosphorylation of PtdIns by Type III PI3Ks was further emphasized when it was discovered that the PtdIns3 *P* that Vps34p makes is the substrate for the synthesis of phosphatidylinositol 3,5-bisphosphate (PtdIns(3,5)P_2), the most recently discovered of the polyphosphoinositides (34, 35). Whereas PtdIns3*P* synthesis is a constitutive activity of unstressed cells—as it should be if it is involved in the continuous vesicle-mediated protein flows into cells from the exterior and from Golgi to lysosomes—PtdIns(3,5)P_2 synthesis is acutely regulated. In both fission and budding yeasts, hyperosmotic stress provokes a striking acceleration of PtdIns(3,5)P_2 synthesis (35). The exact function of this striking response is yet to be defined.

5. Inositol lipid-binding domains in proteins

One common theme that has emerged particularly strongly from many recent studies of the functions of inositol lipids and phosphates is the involvement of stereospecific, high-affinity interactions between particular polyphosphorylated inositol lipid or phosphate species and **protein**

domains whose primary function appears to be the selective recognition of these molecules. Many of these domains are members of a large family of so-called pleckstrin homology (or PH) domains (15, 36), but see also the mention above of 'FYVE fingers.'

PH domains have a characteristic cluster of basic amino acid residues that, in each protein, ligates a particular subset of polyphosphorylated inositol derivatives [eg, (37)]. For example, the PH domains of PKB/Akt and of Bruton's tyrosine kinase preferentially bind PtdIns(4,5)P_2 and PtdIns(3,4,5)P_3, respectively (23, 27). As the name suggests, the prototypic PH domain was found in pleckstrin: this is an abundant platelet cytosol protein that becomes heavily phosphorylated by protein kinase C downstream of receptors (eg, for thrombin) that activate phospholipase C but whose function is still not entirely clear. A major function of PH domains is to mediate noncovalent binding of proteins to the cytoplasmic surfaces of polyphosphoinositide-containing membranes—notably the plasma membrane, but also other structures such as exocytotic secretory vesicles—so as to localize them at their functional sites. Some such effects are likely to be constitutive, as when a PH domain-containing protein homes to the steady-state complement of plasma membrane PtdIns(4,5) P_2. In other circumstances, PH domains probably play a major regulatory role. For example, PtdIns(3,4,5) P_3-binding PH domains will relocate proteins to the plasma membrane, often for activation, only after cells have been exposed to a PtdIns(3,4,5)P_3-generating stimulus.

6. The Functions of inositol phosphates

Although the biological function of Ins(1,4,5)P_3 is clear, why cells contain so many other inositol polyphosphates remains uncertain. That eukaryotic cells commit substantial genetic resources and metabolic energy to complex inositol polyphosphate interconversion pathways (see Fig. 4) surely indicates that at least some of these molecules have important cellular functions, but few of these are established with any certainty. Some of these are summarized in Table 3, and discussion of others can be found in recent reviews (5, 6, 15, 36, 42, 43).

Table 3. Defined and Probable Functions of Some Inositol Polyphosphates and Glycerophosphoinositol Polyphosphates (See the Text for Further References)

Compound	Function	References
Ins(1,4,5)P$_3$: formed by hydrolysis of PtdIns(4,5) P_2	Signaling, through Ins(1,4,5)P_3-stimulated Ca^{2+} mobilization	(13, 14)
Ins(1,4,5,6)P$_4$: formed from Ins(1,4,5)P_3 by Ins(1,4,5)P_3 3-kinases	Modulation of Ca^{2+} entry following depletion of intracellular Ca^{2+} stores? Modulation of GTPase-activating protein	(15)
Ins(3,4,5,6)P$_4$	Slowly accumulates during stimulation of PLC-coupled receptors. Inhibits a Ca^{2+}/**calmodulin**-dependent and kinase-regulated epithelial Cl^- channel	(38)
Ins(1,3,4,5,6)P$_5$ (often	Modulation of O_2 binding to avian	(39)

mimicked experimentally with InsP_6)	and reptilian **hemoglobins**	
GroPIns4 *P* (and/or **GroPIns(4,5) P_2**)	Accumulate in Ras-transformed cells, inhibit adenylate cyclase	(40)
Several pyrophosphate derivatives of InsP_6 (shown as InsP_7 and InsP_8 in Fig. 4)	Widespread, rapid metabolic turnover of pyrophosphate groups, high free energy of hydrolysis, exact structures vary between cell types	(41)

Bibliography

1. R. Parasarathy and F. Eisenberg (1986) Biochem. J. **235**, 313–322.
2. R. H. Michell (1975) Biochim. Biophys. Acta **415**, 81–147.
3. L. E. Hokin and M. R. Hokin-Neaverson (1989) Biochim. Biophys. Acta **1000**, 465–469.
4. IUPAC (1989) Biochem. J. **258**, 1–2.
5. R. H. Michell (1997) Essays Biochem. **32**, 31–47.
6. P. J. Hughes and R. H. Michell (1993) Curr. Opin. Neurobiol . **3**, 383–400.
7. P. P. Ongusaha, P. J. Hughes, J. Davey, and R. H. Michell (1998) Biochem. J. **335**, 671–680.
8. Y. Koga, M. Nishihara, H. Morii, and M. Akagawa-Matsushita (1993) Microbiol. Rev. **57**, 164–182.
9. L. O. Martins, R. Huber, H. Huber, K. O. Stetter, M. S. DaCosta, and H. Santos (1997) Appl. Environ. Microbiol. **63**, 896–902.
10. J. A. Creba, C. P. Downes, P. T. Hawkins, G. Brewster, R. H. Michell, and C. J. Kirk (1983) Biochem. J. **212**, 733.
11. Y. Nishizuka (1990) Nature **334**, 661–665.
12. M. J. Berridge (1987) Ann. Rev. Biochem. **56**, 159–194.
13. K. Mikoshiba (1997) Curr. Opin. Neurobiol. **7**, 339–345.
14. M. J. Berridge (1993) Nature, **361**, 315–325.
15. N. Divecha and R.F. Irvine (1995) Cell **80**, 269–278
16. S. B. Lee and S. G. Rhee (1995) Curr. Opin. Cell Biol . **7**, 183–189.
17. R. Ranganathan, D. M. Malicki, and C. S. Zuker (1995) Ann. Rev. Neurosci. **18**, 283–317.
18. B. Vanhaesebrock, S. J. Leevers, G. Panayatou, and Waterfield (1997) Trends Biochem. Sci. **22**, 267–272.
19. L. Stephens, T. R. Jackson, and Hawkins, P. T. (1993) Biochim. Biophys. Acta **1179**, 27–75.
20. A. Toker and L. C. Cantley (1997) Nature **387**, 673–676.
21. L. R. Stephens, A. Eguinoa, H. Erdjument-Bromage, M. Lui, F. Cooke, J. Coadwell, A. S. Smrcka, M. Thelen, K. Cadwallader, P. Tempst, and P. T. Hawkins (1997) Cell **89**, 105–114.
22. B. Marte and J. Downward (1997) Trends Biochem. Sci. **22**, 355–358.
23. D. Stokoe, L. R. Stephens, T. Copeland, P. R. Gaffney, C. B. Reese, G. F. Painter, A. B. Holmes, F. McCormick, and P. T. Hawkins (1997) Science **277**, 567–570.
24. D. R. Alessi and P. Cohen (1998) Curr. Opin. Genet. Devel. **8**, 55–62.
25. L. P. Hammonds-Odie, T. R. Jackson, A. A. Profit, I. J. Blader, C. W. Turck, G. D. Prestwich, and A. B. Theibert (1996) J. Biol. Chem. **271**, 18859–18868.

26. K. Tanaka, S. Imajoh-Ohmi, T. Sawada, R. Shirai, Y. Hashimoto, S. Iwasaki, K. Kaibuchi, Y. Kanaho, T. Shirai, Y. Terada, K. Kimura, S. Nagata, and Y. Fukui (1997) Eur. J. Biochem. **245**, 512–519.
27. M. Fukuda, T. Kojima, H Kabayama, and K. Mikoshiba, (1996) J. Biol. Chem. **48**, 30303–30306.
28. P. De Camilli, S. D. Emr, P. S. McPherson, and P. Novick (1996) Science **271**, 1533–1539.
29. S. Cockcroft (1997) FEBS Lett. **410**, 44–48.
30. K. W. A Wirtz (1997) Biochem. J. **324**, 353–360.
31. J. C. Hay, P. L. Fisette, G. H. Jenkins, K. Fukami, T. Takenawa, R. A. Anderson, and T. F. J. Martin (1995) Nature **374**, 173–177.
32. J.-M. Gaullier, A. Simonsen, A. D''Arrigo, B. Bremnes, H. Stenmark, and R. Aasland (1998) Nature **394**, 432–433.
33. V. Patki, D. C. Lawe, S. Corvera, J. V. Virbasius, and A. Chawla (1998) Nature **394**, 433–434.
34. C. A. Whiteford, C. A. Brearley, and E. T. Ulug (1997) Biochem. J. **323**, 597–601.
35. S. K. Dove, F. Cooke, M. R. Douglas, L. G. Sayers, P. Parker, and R. H. Michell (1997) Nature, **390**, 187–192.
36. M. Fukuda and K. Mikoshiba (1997) BioEssays **19**, 593–603.
37. M. Hyvonen and M. Saraste (1997) EMBO J. **16**, 3396–3404.
38. I. I. Ismailov, C. M. Fuller, B. K. Berdiev, V. G. Shlyonsky, D. J. Benos, and E. Barrett (1996) Proc. Natl. Acad. Sci. USA **93**, 10505–10509.
39. H. Yanase, S. Cahill, J. J. M. Dellano, L. R. Manning, K. Schneider, B. T. Chait, K. D. Vandegriff, R. M. Winslow, and J. M. Manning (1994) Protein Sci. **8**, 1213–1223.
40. M. Falasca, A. Carvelli, C. Iurisci, R-G. Qiu, M. H. Symons, and D. Corda (1997) Mol. Biol. Cell. **8**, 443–453.
41. C. Albert, S. T. Safrany, M. E. Bembenek, K. M. Raddy, K. K. Reddy, J. R. Falck, M. Brocker, S. B. Shears, and G. W. Mayr (1997) Biochem. J. **327**, 553–560.
42. F. S. Menniti, K. G. Oliver, J. W. Putney, and S. B. Shears (1993) Trends Biochem. Sci. **18**, 53–56.
43. N. Sasakawa, M. Sharif, and M. R. Hanley (1995) Biochem. Pharmacol. **50**, 137–146.

Insertion Sequence Elements

Insertion sequence (IS) elements are small (0.75 to 1.5 kbp) transposable elements found in bacteria (1). They usually encode only a transposase gene and special sequences at the tips of the element on which the recombinase acts to move the element from place to place. IS elements thus structurally resemble, for example, P elements from *Drosophila*, the widespread Tc1/mariner elements, and Ac elements from maize, although IS elements are generally much smaller. Like P, Tc1/mariner, and Ac elements, IS elements alter DNA in the host genome upon insertion and can cause gene inactivation.

IS elements were among the first nonmaize transposable elements discovered, being identified in bacteria in the late 1960s as the cause of highly polar mutations in bacterial operons and also as components of translocatable antibiotic-resistance segments. It was possible to manipulate bacterial

DNA molecules at this time because of their relatively small size, something that was not possible for other organisms such as maize, and the direct characterization of the DNA of these polar mutations revealed that they resulted from an insertion of a discrete piece of DNA.

Some IS elements also associate to form what are called *composite elements* in which two ISs flank a region of DNA that encodes a selectable trait, for example an antibiotic-resistance determinant (Fig. 1). The action of transposase at the two external edges of the IS elements can move the entire IS–drug resistance gene–IS element from place to place (Fig. 1). Each IS element can also move independently, although this does not result in movement of the antibiotic resistance determinant. IS elements are found as individuals at various positions in bacterial chromosome.

Figure 1. IS elements can associate to form composite transposons. IS elements encode information to promote their translocation, a transposase (arrow) and special sequences at their ends (triangles). Composite transposons are formed by two IS elements flanking a drug resistance determinant, here tetracycline. When the inside (I) and outside (O) ends of an individual IS element are the substrates for recombination, the IS element alone translocates. When the outside (O) ends of the two ISs flanking the antibiotic resistance determinant are the substrates for recombination, the entire IS–drug resistance–IS segment translocates.

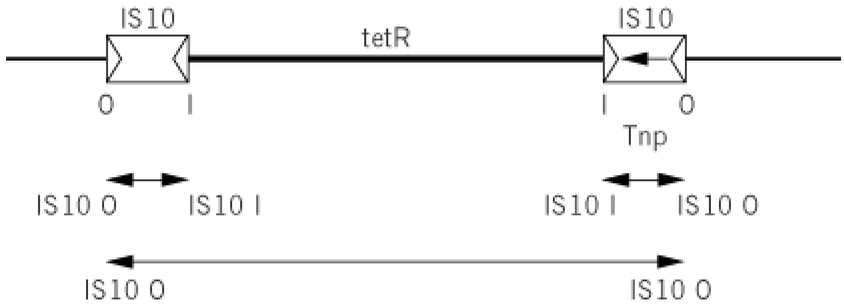

Particularly well-studied IS sequences are IS10 (2) and IS50 (3). The composite transposon Tn10 consists of two IS10 elements flanking a DNA segment that encodes a tetracycline-resistance determinant. The composite transposon Tn5 is composed of two IS50 elements flanking a **kanamycin**-resistance encoding segment. Both of these elements translocate by a cut-and-paste mechanism, in which the element is excised from the donor DNA and then inserts into the target DNA. They and their derivatives have also been invaluable reagents in the genetic analysis of bacteria (4). The strategy of using transposon mutagenesis to tag genes physically to allow **gene** isolation has been a very valuable technique.

Another class of IS elements—members of the IS3 family that includes IS3 and IS911—have an interesting strategy for expressing transposase. The element contains two open reading frames, OrfA and OrfB. OrfA encodes the DNA-binding determinant that directs this protein to the ends of the transposon, but OrfA has no transposase activity. The actual transposase OrfAB results from a frameshifting event near the end of OrfA that joins OrfA and OrfB (5). The amount of transposase, and thus the frequency of transposition, is determined by the amount of frameshifting. These elements also appear to transpose by an unusual mechanism (6, 7). Transposition begins by cleavage at one end of the transposon, exposing a 3′OH end of the element, followed by an intramolecular attack of that 3′OH end to just outside the 5′ end of that same strand; note that this is the same chemistry as is involved in other transposition reactions, the only difference being that the joining reaction is intramolecular, rather than intermolecular. By either another such single-strand cleavage and intramolecular joining, or by replication, a double-stranded DNA circle results in which the IS ends are closely juxtaposed, with just a few nucleotides separating them. This “circle junction” version of the IS element then interacts with the target site and is inserted by breakage at 3′ ends of the transposon and joining the exposed ends to the target DNA.

It should be appreciated that although some of the well-studied elements and widely used bacterial elements such as Tn10 and Tn5 contain IS elements, certainly not all bacterial transposable elements contains IS sequences. Tn3, Mu phage, and Tn7 are all examples of bacterial elements that lack IS sequences, and these elements do not associate to form composite transposons.

Bibliography

1. E. Ohtsubo and Y. Sekine (1996) Curr. Top. Microbiol. Immunol. **204**, 1–26.
2. N. Kleckner, R. Chalmers, D. Kwon, J. Sakai, and S. Bolland (1996) Curr. Top. Microbiol. Immunol. **204**, 49–82.
3. W. S. Reznikoff (1993) Annu. Rev. Microbiol. **47**, 945–963.
4. C. M. Berg and E. Berg (1995) In *Mobile Genetic Elements* (D. J. Sherratt, ed.), IRL Press, Oxford, England, pp. 38–68.
5. M. Chandler and O. Fayet (1993) Mol. Microbiol. **7**, 497–503.
6. P. Polard and M. Chandler (1995) Genes Dev. **9**, 2846–2858.
7. B. Ton-Hoang, P. Polard, and M. Chandler (1998) EMBO J. **17**, 1169–1181.

Insulin

Insulin is a peptide hormone that is secreted by the b-cells of the islets of Langerhans in the pancreas. The principal role of this hormone is the regulation of glucose metabolism and homeostasis by regulating the concentrations and activities of numerous enzymes involved with catabolism and anabolism. The molecule (MW 5808) consists of two polypeptide chains, A and B, linked by two disulfide bonds (Fig. 1). Reduction of these disulfide bonds results in the loss of biological activity.

Figure 1. The processing of pro-insulin (top) to the two polypeptide chains of insulin linked by disulfide bonds (bottom). The sequence of the pro-insulin polypeptide chain is shown, by one-letter abbreviations, only near the sites of cleavage by the convertases PC1 / 3 and PC2 and the carboxypeptidase; the remainder of the connecting C peptide that is removed proteolytically is shown as the solid line only.

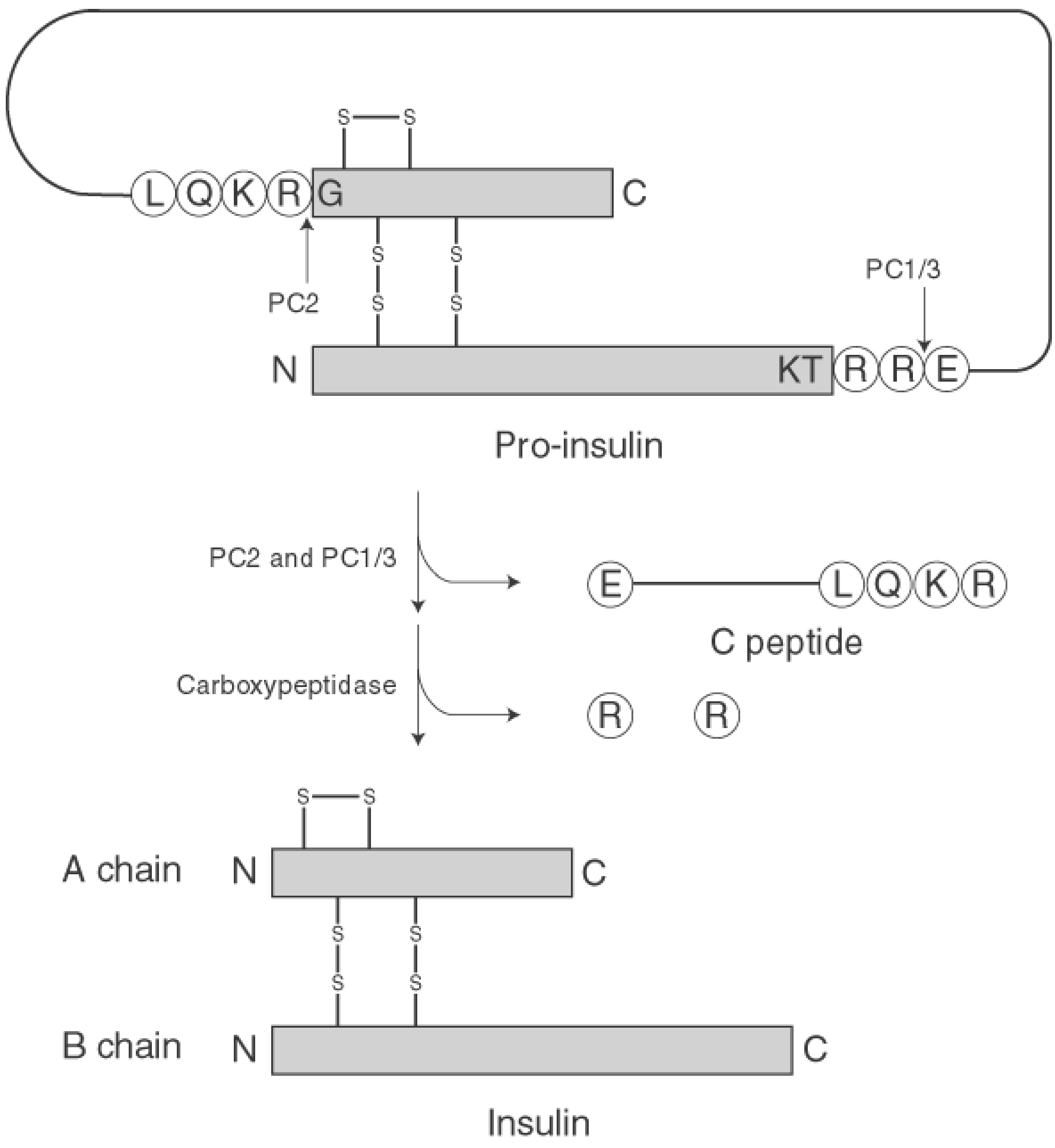

In humans, the insulin **gene** is located on chromosome 11. Several **alleles** coding both normal and pathological forms of insulin have been identified. An individual's genes are co-dominantly expressed. Insulin is synthesized initially on **polyribosomes** of the rough endoplasmic reticulum (ER) as pre-pro-insulin (see Polyproteins), a single-chain precursor protein of molecular weight 11,500. The *N*-terminal signal peptide of 23 or 24 primarily **hydrophobic** residues is cleaved immediately by signal peptidase after penetration of the peptide into the ER lumen. The resulting pro-insulin (MW 9000) undergoes **protein folding** and disulfide bond formation. It is then transported to the Golgi apparatus and is sorted into **clathrin**-coated **secretory granules**. **Posttranslational modification** by **membrane**-bound endoproteinases, pro-hormone convertases PC-2 and PC-1 / 3, and a carboxypeptidase converts proinsulin into equimolar amounts of insulin and free C peptide (Fig. 1). Other than to facilitate proper folding, the C peptide has no known function. The insulin stored in the mature secretory granules assumes a hexameric quaternary structure with two bound zinc ions (1). In response to plasma glucose levels, the mature granule translocates to the cell membrane, fuses with the membrane, and discharges its contents. Other than glucose, several other substances (eg, mannose, ribose, arginine, and leucine) also stimulate release.

Upon secretion by the pancreas, insulin is directly infused into the portal vein and the liver, where it exerts its primary metabolic effects. Monomeric insulin generates intracellular effects by binding to its plasma-membrane receptor (see Peptide Hormones). The precise signal transduction mechanisms (see Signal Transduction) are still not completely known (2).

The principal target tissues of insulin are liver, muscle, and fat. In most tissues, insulin increases the number of plasma membrane glucose **transporters**, such as GLUT 4 (3, 4), but glucose uptake in the liver is also increased because of the increased activity of regulatory enzymes that play a role in glycolysis. Glycogenolysis is inhibited. Glucokinase, **phosphfructokinase** -1, pyruvate kinase, and insulin-dependent **phosphodiesterase** are all involved. In addition, specific **phosphatases** increase the activity of glycogen synthase and thus lead to increased glycolysis. Glucose-6-phosphatase is inhibited. Overall, hepatocyte glucose and its phosphorylated forms are increased, resulting in lower blood levels of glucose. The actions are complex, because all the metabolic pathways must be coordinated and maintained to effect homeostasis.

The insulin-receptor gene is located on chromosome 19. The insulin receptor (see Hormone Receptors Peptide Hormones) is a **tyrosine kinase** and comprised of two identical extracellular a-subunits (MW 135 kDa) and two identical transmembrane b-subunits (MW 95 kDa). The a-subunit contains the insulin-binding domain, and the membrane-spanning b-subunit transduces the signal. After the hormone-receptor complex is formed, it is internalized by endocytosis mechanisms. The receptor is recycled back to the membrane, while the insulin molecule is degraded (5).

Mutations occur in some forms of diabetes mellitus in both the genes for insulin and its receptor (6), as well as defects in ER and Golgi processing (7). The mutations may result in impaired binding, impaired transmembrane signaling, altered endocytosis and recycling, or impaired transport of the receptor to the cell membrane. Diabetes is thus a catabolic disease caused by an apparent insulin deficiency. There are genetic components to both type I (insulin dependent) and type II (insulin independent) diabetes. Moreover, type I diabetes can result from an **autoimmune** response that destroys the pancreatic b-cells and insulin production (8).

Therapy consists of the subcutaneous administration of insulin. Protein engineering of human insulin production in *Escherichia coli* now provides the therapeutic drug. Use of insulin-secreting cell lines as **gene therapy** is presently only in the early stages of development (9).

Bibliography

1. H. R. Petty (1993) *Molecular Biology of Membrane: Structure and Function*, Plenum, New York, pp. 255–262.
2. P. Stralfors (1997) BioEssays **19**, 327–335.
3. O. Ezaki (1997) Biochem. Biophys. Res. Commun. **241**, 1–6.
4. J. E. Rice, C. Livingstone, and G. W. Gould (1996) Biochem. Soc. Trans. **24**, 540–546.
5. G. D. Holman and M. Kasuga (1997) Diabetologica **40**, 991–1003.
6. D. A. Brooks (1997) FEBS Lett. **409**, 115–120.
7. D. Accili (1995) Diabetes-Metabolism Rev. **11**, 47–62.
8. A. A. Alzaid (1996) Acta Diabetologica **33**, 87–99.
9. M. Tiedge and S. Lenzen (1995) Experimental and Clinical Endocrinology and Diabetes **103S**, 46–55.

Insulin-Like Growth Factors

The insulin-like growth factors (IGFs) are among the most ubiquitous class of peptide growth factors in the body and are found in most tissues and in blood. Two types, IGF-I and -II, have been purified from serum, each with molecular masses of approximately 7.6 kDa. Liver is a major site of their expression, both in fetal and postnatal life, although almost all tissues have been shown to express these peptides in the human and animal fetus (1, 2); this suggests a predominantly autocrine or paracrine role, in which the IGF affects primarily the same cell or only nearby cells. In the fetus, the most abundant isomer is IGF-II, but in some species, such as rat, but not humans, IGF-II is absent from adult serum and is replaced by IGF-I. In humans, IGF-II persists throughout life, although the relative abundance of IGF-I increases postnatally. A high-affinity type 1 IGF receptor is ubiquitous in developing tissues and recognizes IGF-I with an order of magnitude greater binding affinity than it does IGF-II. Consequently, IGF-I is a more potent **mitogen** with a half-maximal response on most cell types at approximately 1 to 3 nM. The IGFs also have proven roles in the control of cell differentiation and are preventive of apoptosis in many cell types. In postnatal life, synergy between endogenous IGF-I and trophic endocrine hormones facilitates endocrine glandular function. For example, thyroid-stimulating hormone synergizes with IGF-I to support thyroxine synthesis, while a synergy of IGFs with follicle stimulating hormone allows sex steroid production in the ovary (3). The type 1 IGF receptor has an intracellular tyrosine kinase domain that is capable of **phosphorylating** the insulin receptor substrate proteins (IRS-1 and -2). IGFs are able to activate the proto- **oncogene** *ras* in many cell types, which subsequently signals gene transcription changes in cell nuclei, often by a mitogen-activated protein (MAP) kinase pathway, but also by the activation of phosphoinositol-3 kinase (see Inositol Lipids and Phosphates), culminating in the activation of the transcription factors *fos*, *jun*, and *myc*. An additional high-affinity receptor that specifically binds IGF-II, the type II or cation-independent **mannose-6-phosphate receptor**, is ubiquitous but has no consistent intracellular signaling pathway or biological endpoint.

The IGFs are seldom found in free form but are complexed to one of six distinct classes of specific binding protein, termed IGFBP-1 to -6. These are found both in serum and in extracellular fluids, and they serve not only as carrier proteins to extend the biological half-life of the ligands but also modulate their biological actions by either interacting or competing with the type 1 IGF receptors. While all six IGFBPs have a conserved core structure, differences in their *N*- and *C*-termini confer individual relative binding affinities for IGF-I and -II and an ability to interact with both the extracellular matrix and the cell surface (4). Two of these IGFBPs, IGFBP-1 and -2, contain an **integrin**-binding motif that allows binding to the cell surface a_5b_1 integrin, which is the fibronectin receptor. The ability of these IGFBPs to potentiate IGF action is related to their integrin-binding activity, which may facilitate an advantageous presentation of the ligand to its high-affinity receptor. All IGFs except IGFBP-1 also contain heparin-binding **domains**, allowing binding to sulfated glycosaminoglycans in the extracellular matrix and on the cell membrane. The majority of IGF-I and -II in blood is carried on IGFBP-3. From the second half of fetal development, IGFBP-3, together with an IGF molecule, is associated with an acid-labile subunit in the circulation to generate a tertiary complex of 150 kDa. In this form, IGFs cannot leave the circulation; the fraction accessible to extracellular fluids is carried by IGFBP-1, -2, -4, and -5.

A large proportion of the IGF:IGFBP complexes in extracellular fluids and stored within the extracellular matrix are probably inaccessible to the cell-surface receptors. Their availability depends on modification of the IGFBPs by specific proteinases, resulting in a reduced binding affinity for IGFs. Such proteinases have been identified for IGFBPs-2 to -5. An IGFBP-3-degrading proteinase appears in maternal serum from the second trimester of human pregnancy until term, which reduces the amount of IGF carried by IGFBP-3 and increases its transcapillary passage in association with other IGFBPs (5). A naturally occurring tissue proteinase can also remove the three *N*-terminal amino acid residues from IGF-I, resulting in a much reduced binding affinity for IGFs. Thus, while IGF-I and -II are present in the circulation, this serves predominantly as an extracellular store.

Controlled **proteolysis** of IGFBPs and extracellular matrix molecules is likely to be the key regulatory step in the bioavailability and subsequent actions of IGF-I and -II.

1. IGF gene structure

1.1. IGF-I

The human IGF-I **gene** is located on the long arm of chromosome 12 (6). It comprises at least five exons (see Introns, Exons) spread over more than 90 kbp (7). The gene encodes two precursor forms of IGF-I, represented by transcripts with distinct 3′ regions that arise by alternative splicing of the premessenger RNA (Fig. 1). Each transcript includes sequences of the three 5′ exons (exons 1, 2, and 3) but only one of the two 3′ exons (exons 4 and 5) of the gene. The resulting precursors, IGF-Ia and IGF-Ib, have identical amino-terminal segments of 48 residues that are encoded by exons 1 and 2. The identities of IGF-Ia and -Ib are maintained in their mature IGF-I regions, which comprise 70 amino acid residues encoded by exons 2 and 3, and in the first 16 residues at their *C*-terminus, encoded by exon 3. They are different in the remainder of their C-terminus, where IGF-Ia has an additional 19 amino acid residues encoded by exon 5 and IGF-Ib has an additional 61 residues encoded by exon 4.

Figure 1. **Schematic representation of human IGF-I and -II precursor proteins**. The hatched areas in IGF-Ia and IGF-Ib highlight the alternative sequences arising from alternative splicing (exon 3 to exon 4 in IGF-Ia, and exon 3 to exon 5 in IGF-Ib). The hatched area in the predicted IGF-II variant highlights the area at the juncture of the B and C domains close to an RNA splice site, where differences in the variant human IGF-II molecule tend to occur.

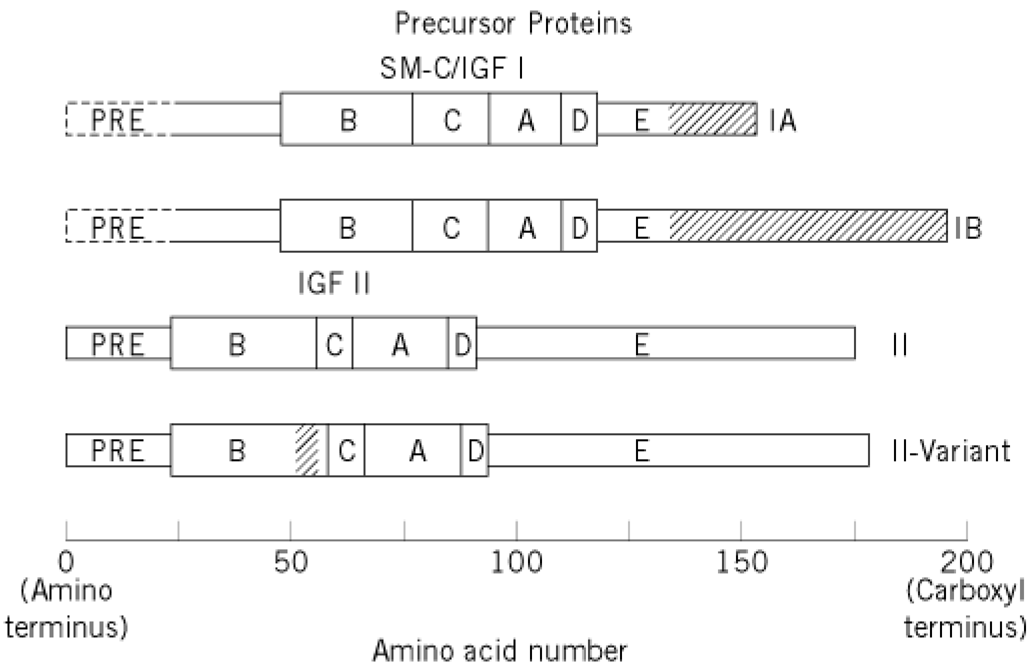

The rat IGF-I gene has six exons, of which five are **homologous** to those of the human gene, with extensive identity of nucleotide sequences (8). The two alternative **signal sequences** (I and IA) encode variant amino-termini for the pre-pro-IGF-I signal peptide, depending on which translation initiation codon is used *in vivo*. IGF-I cDNA clones with alternative 5′-untranslated regions have also been identified in the mouse (9) and other species. Like the human gene, the rat IGF-I gene encodes two precursors, represented by distinct mRNA transcripts. The rat IGF-Ia precursor is analogous to the human product, having a *C*-terminus encoded by exons 3 and 5. However, the *C*-terminal region of rat IGF-Ib is dissimilar to that of human IGF-Ib (which is encoded by exons 3 and

4), comprising sequences encoded by exons 3, 4, and 5 (Fig. 2).

Figure 2. **Representation of alternative splicing resulting in the formation of alternative IGF-I precursor peptides in the rodent**. Exons are represented by the open boxes. Introns are represented by a thin line. The rodent (and human) IGF-I gene contains five exons. It is assumed that translation is initiated at the indicated ATG codon. Exon 2 contains the signal peptide and residues 1 to 25 of the B domain. Exon 3 contains the remainder of the B domain; the complete C, A, and D domains; and residues 70 to 86 of the E domain (hatched). Exons 4 and 5 contain alternate sequences for the remainder of the E domain and the 3′-untranslated region. Splicing of exon 3 to exon 5 gives rise to the IGF-Ia precursor (protein-coding region of exon 5 is stippled). The IGF-Ib precursor arises by splicing exon 3 to exon 4 (protein-coding region of exon 4 is solid), which is spliced to exon 5. Pro-IGF-Ib terminates earlier in exon 5 than pro-IGF-Ia (indicated by the vertical line in the stippled area of exon 5).

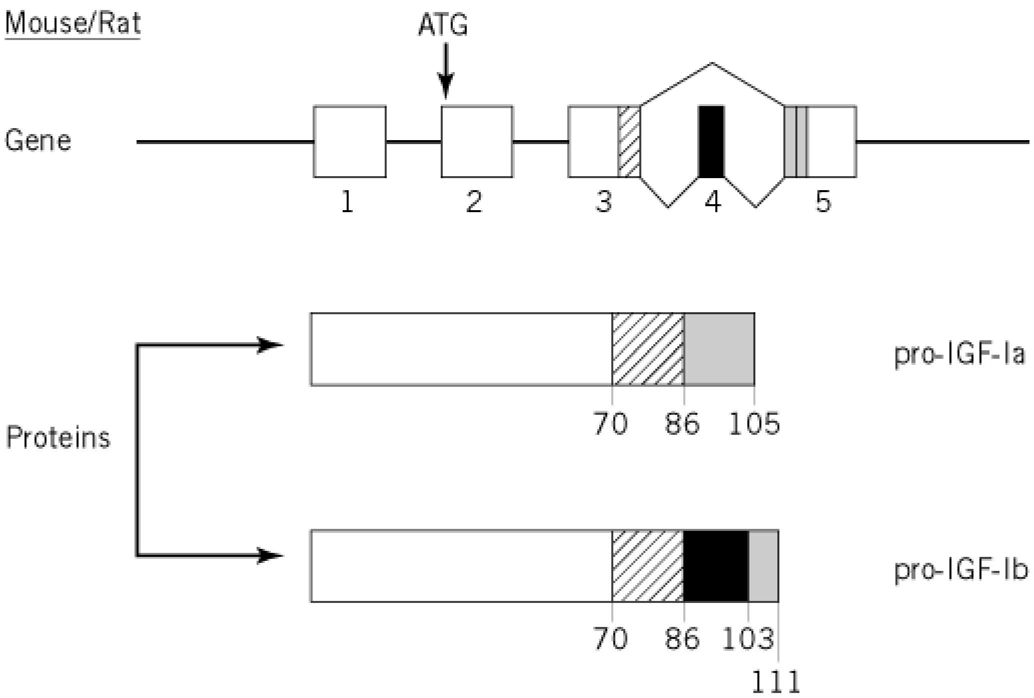

Messenger (mRNA) species encoding IGF-I of at least three size classes are detected by **Northern blot** analysis, ranging from approximately 0.8 kb to 7.8 kb. At least three factors contribute to this size heterogeneity. Alternative splicing pathways can account for two classes of transcripts encoding the precursors IGF-Ia and IGF-Ib. Additionally, transcripts have been identified with distinct 5′-untranslated sequences in mouse and rat and with variable lengths of 3′-untranslated sequences. Using probes that distinguish IGF-Ia and -Ib mRNAs in tissues of humans, it was shown that transcripts encoding both precursors are represented within each of the three size classes of IGF-I transcripts. In all rodent tissues, transcripts encoding IGF-Ia are more abundant than those encoding IGF-Ib, although the relative abundance of these mRNA species differs between hepatic and nonhepatic tissues; transcripts encoding IGF-Ib represent approximately 13% of IGF-I mRNAs in the liver of adult rats but only 2 to 5% of the total elsewhere. When growth hormone was given to hypophysectomized rats, the levels of both mRNA types were elevated coordinately in nonhepatic tissues, but in liver IGF-Ib mRNA was raised threefold more than that of IGF-Ia mRNA. The functional significance of the two pre-pro-IGF-I precursors remains unknown. Most of the heterogeneity in IGF-I transcript size is due to differing lengths of 3′-untranslated sequences. These arise from multiple polyadenylation signal sequences previously within exon 5 of the rat gene, and they may affect the stability of IGF-I mRNAs, providing a mechanism for posttranscriptional regulation of expression. Evidence for multiple polyadenylation sites in IGF-I gene also exists for the mouse, human, and sheep proteins.

1.2. IGF-II

The IGF-II genes in human, rat, and mouse each encodes a 180-residue precursor (pre-pro-IGF-II), consisting of a 24-residue *N*-terminal signal peptide, a 67-residue mature IGF-II, and an 89-residue *C*-terminal pro-peptide. As with pre-pro-IGF-I, the pre- and pro-peptide fragments are removed during protein biosynthesis. Sequences for the cDNA diverge within the 5′ and 3′ noncoding regions, indicating the existence of IGF-II transcripts differing in their untranslated sequences. The human IGF-II gene is found on the short arm of chromosome 11, where it is closely linked to the insulin locus (10). The rodent IGF-II gene is similarly adjacent to the insulin gene on chromosome 1 in the rat, or chromosome 7 in the mouse (11). The genes for both human and rat IGF-II cover at least 30 kbp and 12 kbp, respectively, and contain multiple exons and **promoters**. Exons E4, E5, and E6 encode pre-pro-IGF-II protein, while exons EI, E2, and E3 are noncoding and used differentially, forming alternative, 5′-untranslated regions of different RNA molecules (Fig. 3). The human IGF-II gene uses three additional noncoding exons. Consensus eukaryote promoter sequences, such as a TATA box and GC boxes (SPI recognition sequences), are present in the regions upstream of human and rat exons E2 (promoter P2) and E3 (promoter P3). The promoter region (Pl) upstream of rat, human, and mouse exon EI lacks TATA and GC boxes, and the transcription start sites are heterogeneous. The region upstream of human exon I (Pl) lies within 1.4 kbp of the insulin gene. A polyadenylation signal, conforming to the **consensus sequence** AATAAA, is located 20 nucleotides from the 3′ end of exon 6, and further potential polyadenylation sites are also present in exon 6 of both the human and rat IGF-II genes.

Figure 3. **Schematic representation of the rat IGF-II gene**. Transcripts arising at each of three promoters and terminat
Proptein-coding regions are solid, untranslated regions are open.

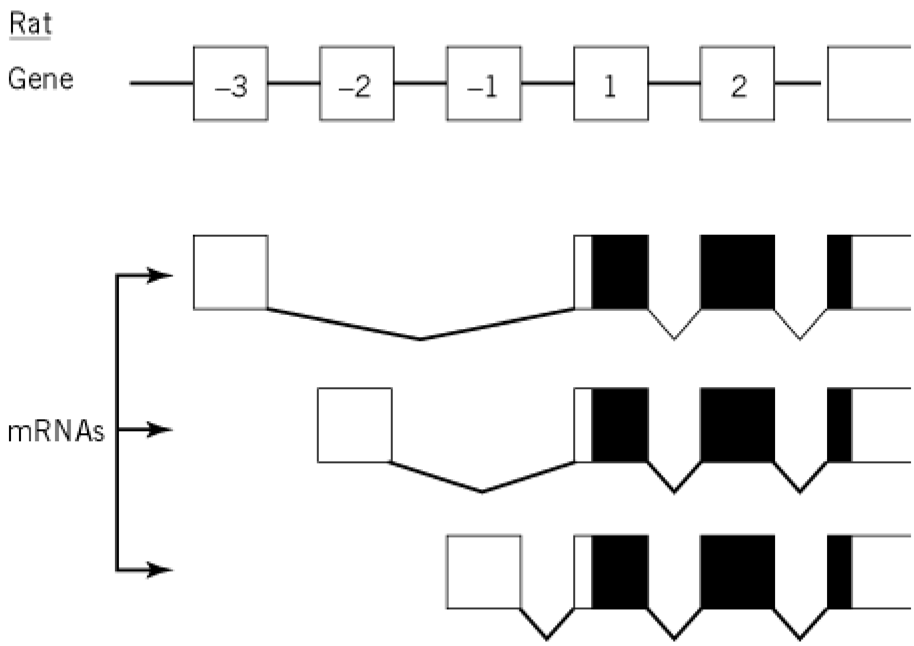

IGF-II mRNAs differ predominately in their 5¢-untranslated sequences, with the major transcripts in and 4.8 kbp, and in rodents approximately 3.8, 4.6, and 8.6 kbp. These arise from the promoters P1, of the noncoding exon EI, E2, or E3 spliced to the three coding exons, E4, E5, and E6, with transcrip polyadenylation site. Transcripts derived from P2 are most abundant in human tissues, whereas those tissues. Transcripts arising from P1 are least abundant in both species. Termination of transcription a (consensus AATAAA) in exon 6 gives rise to short transcripts of 1 to 3 kb found in rat and human ti

IGF-II cDNAs encoding variant proteins have been found in humans (12). These transcripts arise by weak splice-acceptor site upstream of the major splice-acceptor site of exon 5. The additional nine n sequences predict the replacement of Ser-29 with the tetrapeptide Arg–Leu–Pro–Gly, and this IGF-I

(13). The expression of IGF-II is regulated by p53 through interaction with the IGF-II P3 promoter, tumorigenesis when variant p53 forms are present (14).

2. Structure of IGF-I and -II peptides

The IGFs are single-chain polypeptides that show amino acid sequence homology with pro-insulin. allows the recognition of equivalents of the insulin B, C, and A domains within the IGFs, together w domain, which is not found in pro-insulin (Fig. 4). All amino acid residues common between species IGFs with the exception of residue A21, which is Asn in insulin but Ala in the IGFs. Conservation o in a tertiary structure similar to that of insulin, and the **hydrophobic** core of insulin, consisting of A B24 Phe, is also conserved. The most obvious differences from pro-insulin are in the C domain. The insulin are identical. IGF-I consists of 70 amino acid residues, with a predicted molecule weight of 7 detected by mass spectrometry (15). Its isoelectric point is 8.8. Human IGF-II consists of 67 amino a molecular weight of 7469, which was reported as 7440 by mass spectrometry. IGF-II has an isoelect between predicted and detected sizes may be due to covalent changes caused by the extraction proce

Figure 4. **Structural homology of insulin, pro-insulin, and IGF**. Schematic representation of the three-dimensional s insulin (with additional C chain) and the insulin-like growth factors (with C chain and D chain) demonstrating their clo

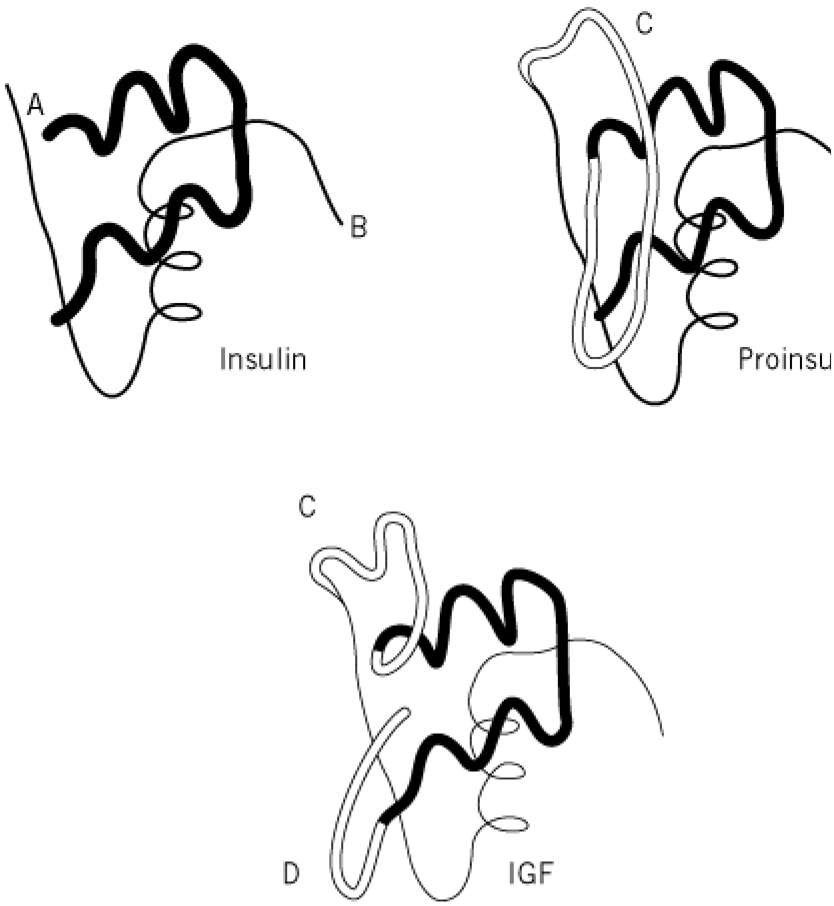

There are two different IGF-I precursors, one derived from exons 1, 2, 3, and 5 (IGF-Ia) and the othe (16). They differ in their *C*-terminal precursor sequence (E domain) and result in identical mature pe IGF-I lacking the first three *N*-terminal residues [des(1–3)IGF-I] was reported by Sara et al. (17) in Des(1–3)-IGF-I has a 100-fold reduction in affinity for IGFBPs-1 and -2 as compared to IGF-I. The is only two to three times lower than is intact IGF-I. Studies on receptor interaction and biological a and recombinant des(1–3)IGF-I. The truncated molecule has a much increased biological activity an intact IGF-I. The *in vivo* half-life of the peptide is shorter than that of intact IGF-I in the rat, due to tl in growth-deficient animals it stimulates growth in length more than does recombinant IGF-I (18).

Variation also exists in IGF-II molecules. Jansen et al. (19) isolated and characterized a cDNA deriv liver encoding an IGF-II variant in which B29 Ser is replaced by the sequence Arg–Leu–Pro–Gly as This cDNA was obtained from the same library that contained the cDNA encoding classical IGF-II a splicing of the pre-mRNA. The peptide has been isolated from human serum and found to constitute (13). Its functional characteristics have shown a two- to threefold reduction in affinity for purified IC placenta and reduced mitogenicity. Another IGF-II variant described by Zumstein et al. (20) is a 10-l Ser is substituted by Cys–Gly–Asp, and it contains the first 21 residues of the *C*-terminal precursor e substitution does not occur at an intron-exon junction, allelic variation must be responsible for its oc been found in human spinal fluid, serum, and brain (21-23). Presumably these molecules represent u precursor forms.

3. IGF binding proteins

The amino acid sequences at the NH_2- and COOH-termini of the six IGFBPs are highly conserved, v terminus of exon I, including 12 cysteines, identical in human and rat IGFBP-1–5 (4) (Fig. 5). Huma in a Gly–Cys–Gly–Cys–Cys segment that is conserved in other IGFBPs. Species differences also oc terminal segment. In the COOH-terminal region, 18 residues, including four cysteines, out of 28 are human and rat. Related molecules designated by some as IGFBPs-7 to -10 have been identified, but biologically meaningful homology. The middle region of the IGFBP proteins, corresponding to the C most of exon 2, is not conserved in different IGFBPs. It includes N-glycosylation sites that are used additional cysteine residues in IGFBP-4. IGFBP-1, -2, and -3 proteins are encoded by four exons; IC comprised exclusively of 3′-untranslated sequences. There is no evidence that alternative splicing co variation. The IGFBPs do not appear to be synthesized as larger precursor proteins.

Figure 5. **Alignment of the amino acid sequences of the six rat IGFBPs**. Amino acid residues are shown in one-lette maximal homology alignment. Identical residues at corresponding positions in more than three of the IGFBPs are show residues are marked by asterisks, except for the additional two cysteines (underlined) present only in IGFBP-4. The RG indicated by an arrow. The internal amino acid sequences that could not be aligned were grouped by parentheses.

```
                                     *   *          *          *           * **   *         *
Rat IGFBP-1              APQPWHCAPCTAERLELCPPVP-AS-CPEISRPAGCGCCPTCALPLGAACGVA
Rat IGFBP-2               EVLFRCPPCTPERLAACGPPPDAP-CAELVREPGCGCCSVCARQEGEACGVY
Rat IGFBP-3      GAGAVGAGPVVRCEPCDARALAQCAPPPTAPACTELVREPGCGCCLTCALREGDACGVY
Rat IGFBP-4               DEAIHCPPCSEEKLARCRPPVG---CEELVREPGCGCCATCALGLGMPCGVY
Rat IGFBP-5              LGSFVHCEPCDEKALSMC-PPSP-LGC-ELVKEPGCGCCMTCALAEGQSCGVY
Rat IGFBP-6                ALAGCPGC----(GPGVQEEDAGSPAD)----GCAETGGCFRREGQPCGVY

(VLEPPPPATSSLSGSQHEEAKAAVASEDELAESPEMTEEQLLDSFHLMAPSREDQPILWNAISTYSSMRAREITDL
(EKRRVGATPQQVADSEDDHSEGGLVENHVDGTMNMLGGSSAGRKPPKSGMKELAVFREKVNEQHRQMGKGAKHLSL
(ANASAASNLSAYLPSQPSPGNTTESEEDHNAGSVESQVVPSTHRVTDSKFHPLHSKMEVIIKGQARDSQRYKVDYE
(TELSEIEAIQESLQTSDKDESEHPNNSFNPCSAHDHRCLQKHMAKVRDRSKMKVVGTPREEPRPVPQG)
(LNEKSYGEQTKIERDSREHEEPTTSEMAEETYSPKVFRPKHTRISELKAEAVKKERRKKLTQSKFVGGAENTAHPR
(QRARGPSEETTKESKPHGGASRPRDRDRQKNPRTSAAPIRPSPVQDGEMG)

 *                                *          *          * *                  ↓
PCQRELYKVLERLAAAQQKA--GD-E-IYKFYLPNCNKNGFYHSKQCETSLDGEAGLCWCVYPWSGKKIPGSLETRG
PCQQELDQVLERISTMRLPDDRGPLEHLYSLHIPNCDKHGLYNLKQCKMSLNGQRGECWCVNPNTGKPIQGAPTIRG
PCRREMEDTLNHLKFLNVLSPRGV-------HIPNCDKKGFYKKKQCRPSKGRKRGFCWCVDKYGQPLPGYDTKGKD
SCQSELHRALERLAASQ--S-RTH-EDLFIIPIPNCDRNGMFHPKQCHPALDGQRGKCWCVDRKTGVKLPGGLEPKG
PCRRHMEASLQEFKASPRMVPRAV-------YLPNCDRKGFYKRKQCKPSRGRKRGICWCVDKY-GNKLPGMEYVDG
PCRRHLDSVLQQLQTE-VF--RGGANGL---YVPNCDLRGFYRKQQCRSSQGNRRGPCWCVDPM-GQPLPVSPDGQG
```

The major carrier protein for IGFs in blood is IGFBP-3 (24). It is also able to bind an acid-labile non predominant 150-kDa IGFBP complex in adult serum. Concentrations of ALS in human plasma are a longer half-life in the circulation when it is associated with the 150-kDa complex. The human IGF of four protein-coding exons homologous to those of the IGFBP-1 and IGFBP-2 genes, and a fifth ex gene is located on chromosome 7, 20 kbp from the IGFBP-1 gene, in tail-to-tail orientation. The tran 132 bp upstream from the adenine–thymine–guanidine (ATG) translation initiation codon. IGFBP-3 abundantly in liver but was also present at high levels in kidney, stomach, heart, adrenal, ovary, and contains a TATA box 30 bp upstream from the transcription initiation site, a GC element (97 bp ups overlap the GC element.

The human IGFBP-1 gene is 5.2 kbp in length and contains four protein-coding exons. It has been lo mRNA is abundant in decidua in late pregnancy but was not detected in placenta. The other major si where a 1.5-kb mRNA transcript is found. IGFBP-1 mRNA was increased 100-fold in rat liver two d streptozotocin and was reversed after three days of insulin treatment. The increase in hepatic IGFBP kidney results primarily from increased transcription of the IGFBP-1 gene. Insulin treatment decreas and IGFBP-1 mRNA levels within one hour, most likely by direct effects on gene transcription. IGF potentiating effects *in vitro*. The presence of an Arg–Gly–Asp (RGD) sequence at the COOH-termin with cell-surface receptors for proteins in the extracellular matrix. Serine **phosphorylation**–dephosp biological action of IGFBP-1. Dephosphorylation decreases the affinity of IGFBP-1 for IGF-I, prom inactive complex.

The IGFBP-2 gene has been localized to human chromosome 2 and to the homologous mouse chrom genes are organized into four exons, each of which contains coding sequences. The human gene is 3 large size of intron 1 (27 kbp). In Northern blots of RNA from fetal rats, a 1.5-kb IGFBP-2 mRNA w kidney, and lung and was less abundant in intestine, muscle, heart, and skin. In midgestation rat brai the epithelium of the choroid plexus, suggesting that IGFBP-2 might participate in the transport of I IGFBP-2 mRNA in rat liver increased 10-fold after 48 hours of fasting, which was reversed after one mRNA was increased 10- to 20-fold in streptozotocin-treated rats, and this was reversed by insulin t sequence at its COOH-terminus. Human IGFBP-2 binds IGF-II with 10-fold greater affinity than IG similar for rat IGFBP-2. IGFBP-2 inhibits the mitogenic effects of IGFs *in vitro*.

The IGFBP-4 gene is located on chromosome 17, and IGFBP-4 mRNA has been estimated as 2.5 kb
hybridization is seen in liver, and a weaker hybridization signal exists with RNA from adrenal, testes
hypothalamus, and brain cortex. In addition to the 18 cysteine residues found in other IGFBPs, IGFE
the nonconserved middle region of the molecule. Glycosylated and nonglycosylated forms of IGFBI
serum.

The IGFBP-5 gene is located on human chromosome 5. In adult rat tissues, a 6-kb IGFBP-5 mRNA
present at high levels in lung, heart, and stomach. A 1.7-kb transcript, presumably differing in the le
also been reported. IGFBP-5 binds IGF-II with 10-fold higher affinity than IGF-I.

IGFBP-6 was purified from human cerebrospinal fluid and human and rat serum. It lacks two (huma
cysteine residues found in other IGFBPs. Human, but not rat, IGFBP-6 contains a potential *N*-glycos
IGF-II with high affinity and IGF-I with greater than 70-fold lower affinity. The human IGFBP-6 ge
IGFBP-6 mRNA is widely expressed in tissues of adult male rats, with a 1.3-kb transcript that is abu
intestine, adrenal, kidney, stomach, spleen, heart, brain, and liver.

4. Selective deletions of IGF genes

Gene deletion by homologous recombination is a powerful way of examining the morphological and
factor deficiency. Some of the most dramatic findings from gene targeting have been obtained with t
Homologous recombination has been used to disrupt either the IGF-I, the IGF-II, or the type 1 IGF r
interbreeding, combination gene "knockouts" have then been obtained. Deletion of the IGF-I gene yi
birthweight about 60% of normal, of which some died within six hours of birth (25). Some of the mu
the females were infertile due to a failure of ovarian follicular development. Using a similar strategy
IGF-II gene is parentally **imprinted** and is only transmitted from the male allele in the majority of ti
plexus and meninges, where both alleles of the gene are active (26). IGF-II-deficient homozygotes h
to animals lacking IGF-I, demonstrating that both isomers have a role in prenatal growth. However,
humans, there is a single published record of a natural deletion of the IGF-I gene, which was associa
retardation and short stature in the child (27).

Deletion of the type 1 IGF receptor, which is primarily responsible for both the mitogenic signaling
IGF-II, yielded homozygous animals that were only 45% of normal weight at delivery and died with
to a failure to breathe and probably resulted from a widespread muscle hypoplasia, including that of
increase in neuronal cell density in the spinal cord and brainstem of the mutant animals, while the sk
the stratum spinosum, and bone ossification was delayed by about two fetal days. Double gene knoc
type 1 receptor genes resulted in a similar phenotype to that found after deletion of the receptor alon
type 1 receptor yielded a subgroup of animals with only 30% of normal birth weight at term and gro
This suggests that an additional receptor to the type 1 form may also contribute to IGF-II signaling.
receptor is deleted in a naturally occurring gene deletion identified by the lack of the imprinted locus
embryonic stage (29). Whether this receptor can contribute to IGF-II signaling *in vivo* is not clear.

The aforementioned series of studies demonstrates that neither IGF-I nor IGF-II is crucial for key m
development, but that they act as "true" growth factors, contributing to the expansion of stem cell po
differentiation.

Bibliography

1. V. K. M. Han, P. K. Lund, D. C. Lee, and A. J. D''Ercole (1988) J. Clin. Endocrinol. Metab. **66**,
2. A. L. Brown, D. E. Graham, S. P. Nissley, D. J. Hill, A. J. Strain, and M. M. Rechler (1986) J .E
3. D. J. Hill and J. Hogg (1989) In *Clinical Endocrinology and Metabolism, Perinatal Endocrinolc*
Bailliere Tindall, London U.K., pp. 579–625.
4. R. H. McCusker and D. R. Clemmons (1992) In *The Insulin-Like Growth Factors, Structure anc*

Schofield, ed.), Oxford University Press, Oxford, U.K., pp. 110–150.
5. L. C. Giudice, E. M. Farrell, H. Pham, G. Lamson, and R. G. Rosenfeld (1990) J. Clin. Endocrin
6. J. E. Brisenden, A. Ullrich, and U. Francke (1984) Nature **310**, 781–784.
7. P. Rotwein, K. M. Pollock, D. K. Didier, and G. G. Krivi (1986) J. Biol. Chem. **261**, 4828–4832
8. A. Shimatsu and P. Rotwein (1987) Nucleic Acids Res. **15**, 7196–7197.
9. G. I. Bell, M. M. Stempien, N. M. Fong, and L. B. Rall (1986) Nucleic Acids Res. **14**, 7873–788
10. K. L. O''Malley and P. Rotwein (1988) Nucleic Acids Res. **16**, 4437–4446.
11. P. Rotwein and L. J. Hall (1990) DNA and Cell Biol. **9**, 725–735.
12. P. N. Schofield and V. E. Tate (1987) Development **101**, 793–803.
13. B. Hampton, W. H. Burgess, D. R. Marshak, K. J. Cullen, and J. F. Perdue (1989) J. Biol. Chem
14. L. Zhang, F. Kashanchi, Q. Zhan, S. Zhan, J. N. Brady, A. J. Fornace, P. Seth, and L. J. Helman
15. J. L. Van den Brande, C. M. Hoogerbrugge, K. Beyreuther, P. Roepstorff, J. Jansen, and S. C. va Endocrinol. **122**, 683–695.
16. P. Rotwein (1986) Proc. Nat. Acad. Sci. U.S.A. **83**, 77–81.
17. V. R. Sara et al. (1986) Proc. Nat. Acad. Sci. U.S.A. **83**, 4904–4907.
18. C. Gillespie, L. C. Read, C. J. Bagley, and F. J. Ballard (1990) J. Endocrinol . **127**, 401–405.
19. M. Jansen, F. M. A. van Schaik, H. van Tol, J. L. Van den Brande, and J. S. Sussenbach (1985)
20. P. P. Zumstein, C. Luthi, and R. E. Humbel (1985) Proc. Nat. Acad. Sci. U.S.A. **82**, 3169–3172.
21. G. K. Haselbacher and R. Humbel (1982) Endocrinology **110**, 1822–1824.
22. G. K. Haselbacher, M. E. Schwab, A. Pasi, and R. E. Humbel (1985) Proc. Nat. Acad. Sci. U.S.
23. L. K. Gowan, B. Hampton, D. J. Hill, R. J. Schlueter, and J. F. Perdue (1987) Endocrinology **12**
24. S. Rajaram, D. J. Baylink, and S. Mohan (1997) Endocrine Rev. **18**, 801–831.
25. J-P. Liu, J. Baker, A. S. Perkins, E. J. Robertson, and A. Efstratiadis (1993) Cell **75**, 59–72.
26. T. M. De Chiara, A. Efstratiadis, and E. J. Robertson (1990) Nature **345**, 78–80.
27. K. A. Woods, C. Camacho-Hubner, D. Barter, A. J. Clark, and M. O. Savage (1997) Acta Paedia
28. J. Baker, J-P. Liu, E. J. Robertson, and A. Efstratiadis (1993) Cell **75**, 73–82.
29. D. P. Barlow, R. Stoger, B. G. Herrmann, K. Saito, and N. Schweifer (1991) Nature **349**, 84–87.

Suggestions for Further Reading

30. W. H. Daughaday and P. Rotwein (1989) Endocrine Rev. **10**, 68–91.
31. J. S. Sussenbach (1989) Prog. Growth Factor Res. **1**, 33–48.
32. P. N. Schofield (ed.) (1992) *The Insulin-Like Growth Factors: Structure and Biological Functio* U.K.

Integrases

Integrases represent a subset of DNA (poly)nucleotidyltransferase enzymes each of which catalyzes the insertion of a specific extra**chromosomal** segment of **DNA** into the genome of its host. They form central elements in the replicative cycles of several prokaryotic and eukaryotic **viruses** and in the intracellular translocation of retrotransposons. The best studied of these are the integrases encoded by the pol gene of various retroelements, such as the retroviridae, and those of temperate bacteriophages, most notably lambda phage. The different strategies employed to break and reunite the host DNA with the incoming polynucleotide distinguish two distinct families of integrases. A key difference is whether or not the reaction takes place by forming a covalent integrase-DNA intermediate. In the lambda Int family of site-specific recombinases, the integrase forms a transient covalent linkage with the 3′-ends of the bacteriophage and host DNA at the points of recombination. In contrast, retroviral integrase (IN) catalyzes DNA insertion via a noncovalent intermediate, using a process that is chemically similar to the “cut and paste” mechanism of classical transpositional recombination. Unraveling DNA integration in molecular terms will necessitate understanding just how the underlying chemical steps are harnessed by each distinct integrase nucleoprotein complex to meet the different DNA site specificities and topologies demanded by their diverse genetic rearrangements.

1. Retroviral Integrases

1.1. DNA Integration Mechanism

DNA integration is a critical step in the replicative cycle of all single-stranded (ss) RNA retroviruses, including notably **HIV**-1, the causative agent of AIDS. Following **reverse transcription**, the resultant complementary DNA copy of the retroviral ssRNA genome must be inserted into a chromosome of the infected host cell to elicit a productive infection. The retroviral integrase (IN) catalyzes two consecutive nucleophilic substitution reactions in this process (Fig 1a; Steps 1 and 2) at the phosphodiester bonds that ultimately form the sites of attachment between the viral and host DNA. The first reaction, known as 3′-OH end processing, results in the nucleolytic expulsion of the two external nucleotides from both 3′-ends of the linear viral cDNA. Here, the 5′-phosphoryl group of the leaving dinucleotide is transferred directly to the electronegative group of the attacking nucleophile, generally donated by a water molecule. In the second step (polynucleotidyl transfer), the recessed 3′-OH groups are in turn coordinated as nucleophiles to attack specific positions on the phosphodiester backbone of the host DNA. In line with the displacement of a host 5′-phosphoryl group, a direct transesterification with the attacking viral 3′-OH end results in the insertion of the viral DNA at this site.

Figure 1. Comparison of retroviral cDNA and bacteriophage l DNA integration. Both mechanisms involve two consecutive nucleophilic substitution reactions (Steps 1 and 2), shown side-by-side at bottom of figure. (a) Retroviral IN. Step 1: Endonucleolytic 3′-OH end processing. The two outermost bases of the cDNA adjacent to a subterminal CA dinucleotide are removed from both 3′-termini, yielding a staggered intermediate with 5′-protrusions. Step 2: Polynucleotidyl transfer. Each processed 3′-OH end is reattached in a staggered fashion to opposite strands of the host DNA (for HIV-1 at phosphodiester bonds positioned 5 bp apart). Gap repair, probably by host proteins, results in duplication of the host DNA (shown in gray) at the proviral junction. (b) Bacteriophage l Int. Step 1: Breakage of partner strands. A pair of Int protomers (ovals) attack the scissile phosphodiester bonds (black dots) at parallel positions on the juxtapositioned recombination strands, resulting in the formation of covalent 3′-phosphotyrosine linkages and free 5′-OH ends. Step 2: Polynucleotidyl transfer (resolution). Each 5′-OH end rejoins with the 3′-phosphoryl of its facing partner strand by branch migration and resolution of the covalent protein–DNA intermediate. Recombination intermediates with the target DNA (shown in gray) are drawn to emphasize the crossover sites [after (20)] rather than its topological structure, which more accurately corresponds to a **Holliday junction** intermediate.

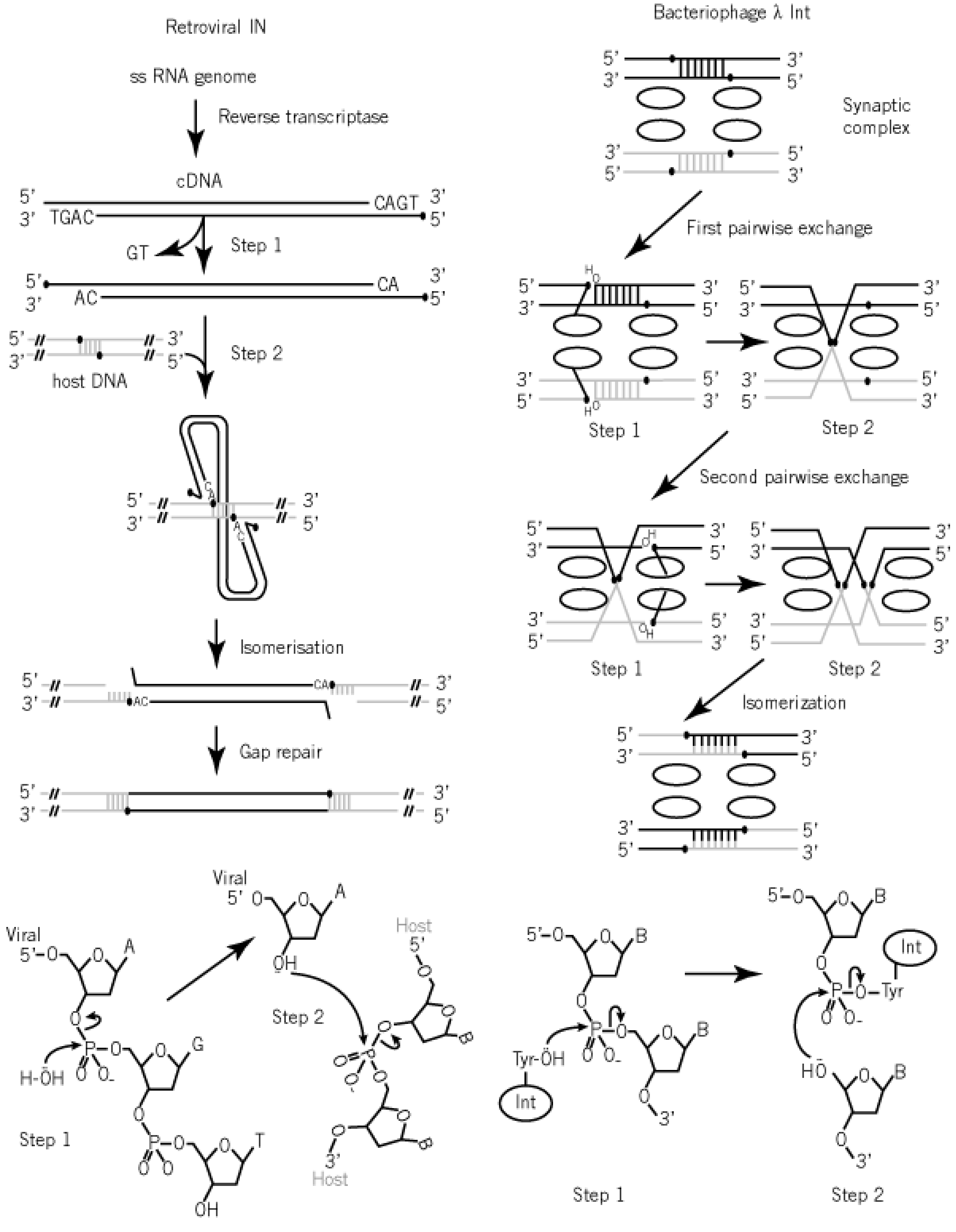

(a) (b)

Two notable hallmarks of this type of DNA integration mechanism persist at the borders of the resultant proviral–host DNA junction. First, the provirus is two bases shorter than the preintegrated cDNA, where its 3′-boundaries with the host DNA are delineated at each end by a highly conserved CA-3′ dinucleotide. Secondly, a region of 4 to 6 bp of host DNA is duplicated at the junction of proviral attachment that arises from the staggered integration of each viral end on opposite stands of the host DNA. The length of this duplication is specific to each retrovirus rather than its host.

Although retroviral DNA integration is clearly nonrandom, it may occur at any one of a large number of potential sites within the genome, which are dictated principally by the accessibility and structure of the chromatin (1). Yeast retrotransposons (Ty elements) integrate much more precisely, despite an essentially identical DNA integration mechanism, at or near nonessential genes or transcriptionally "silent" regions of the genome. Ty3 cDNA is drawn into the required locus by protein–protein interactions between a component of the Ty3 integration complex, possibly the Ty3 IN itself, and a polIII promoter-bound protein complex composed minimally of the transcription factors TFIIIB and TFIIIC, thus securing the DNA integration functions at that site (2). A similar, but as yet unsubstantiated, proposition has been put forward for HIV-1 IN, which interacts functionally with integrase interactor 1 (INI 1), a homologue of the yeast transcription factor SNF5, which could potentially direct integration into regions of open chromatin (3).

Unlike bacteriophage integrases, the IN proteins of retroelements cannot excise the integrated viral template from the host genome. Instead, viral propagation occurs via new generations of transcribed ssRNA progeny, which are packaged into virions with retroviral proteins and released to infect a new host cell. Nevertheless, IN can resolve the partial integration intermediates formed in this process and catalyzes the excision of the viral DNA from "one-ended" intermediates of a Y-type structure by a process named "disintegration" (4). During excision of the viral part, the broken target DNA strand is resealed by a similar phosphoryl transfer mechanism to that of the forward integration reaction, although the "reverse" process differs in the sense that it displays a relaxed specificity for viral sequences.

1.2. The IN Protein

Retroviral cDNA (>8 kb) exists in the cytoplasm of infected cells as a high molecular weight preintegration complex (PIC) and copurifies with several retroviral, and at least some host proteins. One of these is the high mobility group (**HMG**) protein HMG1(Y) (5), which among other global activities bends DNA and stimulates the concerted integration activity of purified IN (6). Increasing evidence suggests that such accessory proteins contribute important architectural features necessary to guide the integration functions of the PIC (7). Nonetheless, purified IN alone encompasses all of the minimal requirements for catalyzing both nucleophilic substitution (end processing and transfer) reactions with synthetic viral termini *in vitro* (reviewed in Ref. 8).

Although the IN-catalyzed functions exhibit some degree of specificity for the nucleotide sequence (s) of the viral termini and for the CA dinucleotide in particular, purified IN does not bind preferentially to its cognate sequence. The factors within the virion that direct IN to the two distal termini of the nascent cDNA and coordinate their concerted integration at a discrete host target site remain to be established. Neither function is reproduced efficiently *in vitro* with the purified protein.

Structure-function studies on deleted derivatives of the integrase indicate that the protein is organized into three major **domains** (Fig. 2a). Although crystallizing the full length protein has proven difficult because of its inherent aggregative properties, now the structures of each of the isolated domains of the human immunodeficiency virus type-1 (HIV-1) integrase have been determined independently.

1. The N-terminal region (residues 1 to 50) bears a highly conserved HHCC motif (His-X_{3-7}-His-X_{23-32}-Cys-X_2-Cys) that binds Zn^{2+} stoichiometrically (9). Contrary to the organization of a classical **zinc finger**, its structure more closely resembles that of helical DNA-binding proteins that possess a helix-turn-helix (HTH) motif and is most akin to that of the trp repressor (10) (see TRP Operon). The helical bundle arrangement is ordered by Zn^{2+}, which is tetrahedrally coordinated by the conserved His and Cys residues. The binding of Zn^{2+} stimulates multimerization and the catalytic functions of the integrase (9, 11). The N-terminus is essential for 3-OH processing and integration but is dispensable for the disintegration reaction, which minimally requires the core region.

2. The central **protease**-resistant core domain (residues 50 to 212) comprises a minimal active site for the polynucleotidyl transfer reaction. This domain carries a triad (D,D,E or Asp,Asp,Glu) of essential catalytic residues (organized Asp-$X_{39\text{-}58}$-Asp-X_{35}-Glu) that coordinate a divalent cation (Mg^{2+}, and also Mn^{2+}) necessary for phosphoryl transfer. The core domain binds and catalyzes the resolution of Y-structure disintegration intermediates but cannot alone catalyze the forward reactions of the integration mechanism with linear DNA substrates. Several residues of the core are highly conserved in retroviral and retrotransposon integrases and in analogous prokaryotic transposases (12). Most remarkable is its structural homology to the ribonuclease H and RuvC enzymes, comprising a central 5-stranded beta-sheet flanked by **alpha-helical** regions (13). Despite the fact that these proteins do not catalyze DNA integration or transposition, nonetheless, they are involved in similar transesterification reactions using aspartic acid and glutamic acid catalytic residues. The catalytic residues superimpose well on the corresponding structures, indicating a general structural fold for a topologically related superfamily of DNA nucleotidyltransferases, all of which catalyze nucleophilic substitutions at the phosphodiester bonds of polynucleotides.
3. The C-terminal region is less well conserved both in sequence and in size and exhibits an independent nonspecific DNA-binding activity. Several integrases also possess C-terminal nuclear localization signals that, it is proposed, direct the active uptake of the large PIC structure through the undisrupted nuclear membrane [eg (14)] (see Nuclear Import, Export). The organization of its 5 beta-strands into a b-barrel consisting of two antiparallel b-sheets is very similar in structure to Src-homology 3 (SH3) domains, which are often associated with protein–protein interactions (15) (see SH2, SH3 Domains). It is likely that the basic character of this domain that has solvent-exposed lysine and arginine residues is involved in long-range electrostatic interactions with the negatively charged DNA phosphate groups. A saddle-shaped groove formed between two of the b-strands may provide a channel for this interaction (16).

Figure 2. Structure and functional organization of the domains of (a) retroviral (HIV-1) IN and (b) bacteriophage l Int proteins. Numbering is of the amino acid residues.

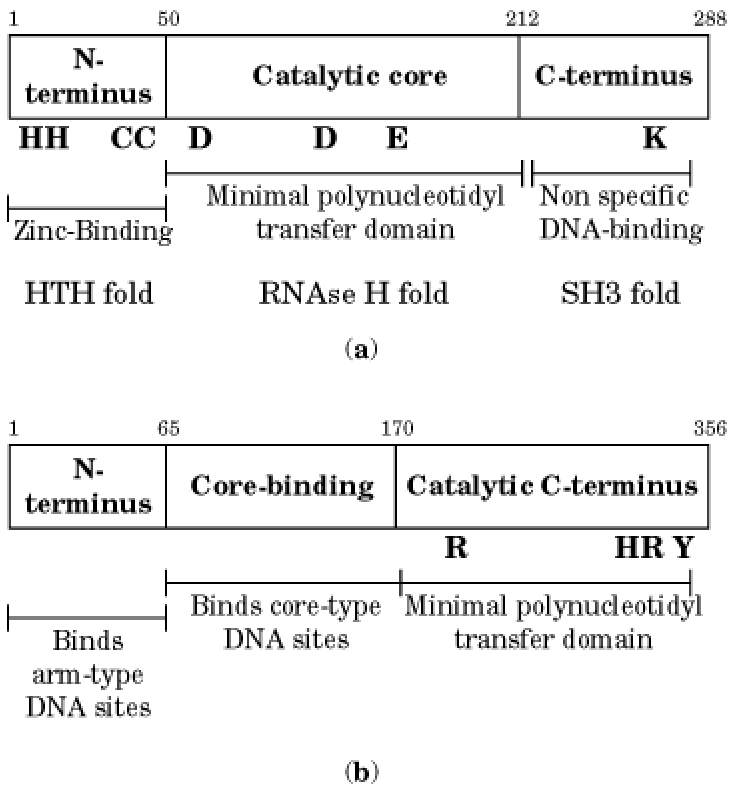

All three domains form dimers when analyzed as isolated polypeptide chains. Most likely, interactions between the domains of IN play a central role in forming the requisite multimeric configuration (17). The precise oligomeric form adopted by the protein *in vivo* is still not known, although high-order assemblies have been implicated in forming stable, catalytically active nucleoprotein complexes *in vitro* [eg (18)]. Despite progress made in this respect via protein–DNA cross-linking studies (19), the overall three dimensional view of these nucleoprotein intermediates remains sketchy.

2. Bacteriophage Lambda Integrase

2.1. DNA Integration Mechanism

The chromosomal integration of the viral genomes of temperate bacteriophages, exemplified by the reaction catalyzed by lambda integrase (Int), is a conservative site-specific recombination mechanism in which the recombination partner (*att*) sites are reciprocally exchanged by a set of isoenergetic cleavage and rejoining reactions (20). Like retroviral integration (see previous discussion), each strand-exchange reaction takes place via two consecutive nucleophilic substitutions, except, in this case, (1) a covalent Int–DNA intermediate is formed with each of the four recombination strands, and (2) the strand exchange is precise, neither adding nor deleting nucleotides at the site of insertion (Fig. 1b). Integrative recombination takes place through two sequential sets of such strand exchanges. Each is begun by the nucleophilic attack of Int at equivalent positions on the donor (*att*P) and target (*att*B) recombination strands. The energy of the primary substitution reaction is conserved via a 3′-phosphotyrosine (Fig. 1b, Step 1), which, after strand migration, is subsequently resolved by the exposed 5′-OH end of the corresponding recombination partner (Fig. 1b, Step 2). This second substitution results in covalently rejoining the two strands, and, in doing so, liberates the unmodified Int protein. Excision of the integrated viral genome (between *att*L and *att*R sites generated by the original recombination) is also catalyzed by Int. Although this occurs by the same reaction chemistry, the stimulation of excision versus integration is accomplished with the assistance of other viral and host factors. Xis and Fis promote excision, whereas IHF is required for both.

2.2. The Int Protein

The bacteriophage l integrase (Int) is a 40-kDa (356 amino acid residue) site-specific DNA-binding protein that has type I topoisomerase activity. It recognizes *att* regions that contain two distinct types of Int binding sites distributed over ~270 bp: (1) a central, imperfectly symmetrical region equating to the crossover site (~30 bp) that consists of two inverted “core” DNA-binding sites, separated by the 7 bp that delineate the overlap between the boundaries of the points of recombination, and (2) more distant flanking motifs, termed “arm” DNA-binding sites. In conjunction with other accessory protein-binding sites, arm sites are control points through which the higher order synaptic complex may adopt the appropriate **tertiary conformation** for the correct positioning and hence, efficient recognition of the core-binding sites.

Several structure-function studies have pinpointed the primary DNA-binding properties of l Int to within discrete domains of the protein (Fig. 2b). The N-terminus (residues 1 to 169) is required for site-specific binding to the core site but is devoid of catalytic activity, whereas the first 64 residues are sufficient to bind tightly to arm-type DNA substrates. The central domain (residues 65 to 170) recognizes core-type sites, albeit with a low binding affinity. The C-terminal domain (residues 170 to 356) contains the minimal catalytic site required for polynucleotidyl transfer. Sequence alignments show that several residues are highly conserved with other site-specific recombinases (21), particularly in the position of the catalytic tyrosine residue, Tyr342, and three essential active-site residues (Arg212, His308, and Arg311, or R-H-R). Its overall topology is that of a mixed a-b structure comprising a bundle of seven a-helices cradled by seven b-strands (organized into one b-sheet at the foot of the structure and two flanking beta-turns) (22). The catalytic R-H-R triad clusters at the base of a shallow groove, proposed as the DNA-binding surface, that runs along one face of the protein. These residues are separated by ~20 Å from the catalytic tyrosine residue, which is located on an exposed and highly flexible 17-residue loop. The speculative function of the loop may be to bend backward bringing the Tyr342 nucleophile into the vicinity of the clustered R-H-R residues (cis-acting) or alternatively to extend outward and reach into the catalytic pocket of a paired Int protomer (trans -acting).

Bibliography

1. R. Craigie (1992) Trends Genet. **8**, 187–190.
2. J. Kirchner, C. M. Connolly, and S. B. Sandmeyer (1995) Science **267**, 1488–1491.
3. G. V. Kalpana, S. Marmon, W. Wang, G. R. Crabtree, and S. P. Goff (1994) Science **266**, 2002–2006.
4. S. A. Chow, K. A. Vincent, V. Ellison, and P. O. Brown (1992) Science **255**, 723–726.
5. C. M. Farnet and F. D. Bushman (1997) Cell **88**, 483–492.
6. A. Aiyar, P. Hindmarsh, A. M. Skalka, and J. Leis (1996) J. Virol. **70**, 3571–3580.
7. S-Q. Wei, K. Mizuuchi, and R. Craigie (1997) EMBO J. **16**, 7511–7520.
8. C. Vink and R. H. A. Plasterk (1993) Trends Genet. **9**, 433–437.
9. R. Zheng, T. M. Jenkins, and R. Craigie (1996). Proc. Natl. Acad. Sci. USA **93**, 13659–13664.
10. M. Cai, R. Zheng, M. Caffrey, R. Craigie, G. M. Clore, and A. M. Gronenborn (1997) Nat. Struct. Biol. **4**, 567–577.
11. S. P. Lee and M. K. Han (1996) Biochemistry, **35**, 3837–3844.
12. O. Fayet, P. Ramond, P. Polard, M. F. Prère, and M. Chandler (1990) Mol. Microbiol. **4**, 1771–1777.
13. F. Dyda, A. B. Hickman, T. M. Jenkins, A. Engleman, R. Craigie, and D. R. Davies (1994) Science **266**, 1981–1986.
14. S. P. Moore, L. A. Rinckel, and D. J. Garfinkel (1998) Mol. Cell. Biol. **18**, 1105–1114.
15. A. P. Eijkelenboom, R. A. Lutzke, R. Boelens, R. H. Plasterk, R. Kaptein, and K. Hard (1995) Nat. Struct. Biol. **2**, 807–810.
16. P. J. Lodi et al. (1995) Biochemistry **34**, 9826–9833.
17. M. D. Andrake and A. M. Skalka (1996) J. Biol. Chem. **271**, 19633–19636.
18. I. K. Pemberton, M. Buckle, and H. Buc (1996) J. Biol. Chem. **271**, 1498–1506.
19. T. S. Heuer and P. O. Brown (1998) Biochemistry **37**, 6667–6678.
20. W. M. Stark, M. R. Boocock, and D. J. Sherratt (1992) Trends Genet. **8**, 432–439.
21. S. E. Nunes-Düby, H. Y. Kwon, R. S. Tirumalai, T. Ellenberger, and A. Landy (1998) Nucleic. Acid. Res. **26**, 391–406.
22. H. J. Kwon, R. Tirumalai, A. Landy, and T. Ellenberger (1997) Science **276**, 126–131.

Suggestions for Further Reading

23. A. Landy (1989) Dynamic, structural, and regulatory aspects of l site-specific recombination. Annu. Rev. Biochem. **58**, 913–949.
24. K. Mizuuchi (1997) Polynucleotidyl transfer reactions in site-specific DNA recombination, Genes to Cells **2**, 1–12.
25. P. Rice, R. Craigie, and D. R. Davis (1996) Retroviral integrases and their cousins, Curr. Opinion Struct. Biol. **6**, 76–83.

Integrative Suppression

Initiation Of DNA Replication of a replicon depends on an interaction between an initiator **protein** and a replication origin sequence specific for each replicon. In *Escherichia coli*, the DnaA protein binds to the origin and melts the duplex DNA strands to recruit the machinery for DNA synthesis, and it is the sole essential protein required specifically for the initiation of the chromosomal replication. **Conditional lethal** *dnaA* mutants defective in the initiation of replication under nonpermissive conditions can be rescued if the initiator gene and the replication origin of another replicon are integrated somewhere in the host chromosome. Such cells can survive by initiating chromosome replication from the origin of the integrated replicon, instead of the native origin. This phenomenon is called integrative suppression. In contrast, integration of the other replicon cannot relieve mutations in genes that are required for the replication of the integrated replicon.

The integrative suppression of *E. coli dnaA* mutations was observed using **plasmid** replicons, such as **F factor** and R1, and phage replicons, such as P2 (1). Furthermore, deletion mutants of the *dnaA* gene or the *oriC* sequence could be obtained. Similar integrative suppression was reported recently for *Bacillus subtilis* (2). The initiation site and frequency of chromosome replication could be changed artificially using integrative suppression mutations, and the regulation of cell cycle progression in bacteria has been studied based on the **phenotypic** changes in the mutants (2, 3).

Bibliography

1. W. Messer and C. Weigel (1996) in *Escherichia coli and Salmonella* (F. C. Neidhard, ed.), American Society for Microbiology, Washington, DC, pp. 1579–1601.
2. A. K. M. Hassan et al. (1997) J. Bacteriol. **179**, 2494–2502.
3. K. Nordstrom, R. Bernander, and S. Dasgupta (1991) Mol. Microbiol. **5**, 769–774.

Integrins

Integrins are a large family of related, transmembrane, cell surface **receptor** proteins that bind extracellular matrix (ECM) and cell adhesion molecules (CAMs). Almost all cell types express some type of integrin, as these receptors are often responsible for positioning cells within their specific environment by associating them with ECMs or CAMs on adjacent cells. Integrins play crucial roles in cell–matrix and cell–cell interactions important in the development and function of organisms ranging from plants to Drosophila to humans. Many cells require an attachment to the extracellular matrix to survive and grow. Cells also make use of integrins during migratory events that are important in neural development, inflammation, and metastasis.

1. Integrin structure

Integrins are noncovalently associated heterodimers consisting of an alpha and a beta subunit, both of which span the membrane lipid bilayer. The ligand binding site outside the cell requires contributions from both subunits. Both subunits have a single membrane-spanning domain and short cytoplasmic domains. The latter interact with the actin cytoskeleton and transmit signals to the interior of the cell. When ligand is bound, integrins signal across the membrane by altering actin polymerization and activating a tyrosine kinase. The name *integrin* derives from the way that these receptors “integrate” fibrils of ECM on the outside of the cell in direct register with actin filaments underneath the plasma membrane.

Alpha subunits range in size from approximately 200 to 120 kDa and are 25% to 45% identical in amino acid sequence. The alpha subunits are characterized by a series of 3 to 4 repeated EF-hand motifs in the extracellular domain that are important for binding divalent cations. Mn^{2+} and Mg^{2+} ions are required for integrin binding, and disruption of integrin activity with EDTA is often used to dislodge tissue culture cells from the substratum. These divalent cations participate in the binding of ligand. Some integrin alpha subunits contain an extra inserted **domain** in the N-terminus, called an *I domain*, which is thought to expand the **ligand binding** ability of integrins. Some alpha subunits are proteolytically cleaved in the extracellular domain near the membrane, and the resulting heavy and light chains are linked by disulfide bonds. Just cytoplasmic to the transmembrane domain, all alpha subunits have a highly conserved GFFKR motif (-Gly-Phe-Phe-Lys-Arg-) whose function is unknown. Other than this sequence, the cytoplasmic domains of the alpha subunits are generally not highly conserved. Differential RNA splicing is known to occur for some alpha subunit messenger RNA (eg, alpha-6, alpha-7), and the alternative splicing variants have specific patterns of expression and may have altered binding properties as well.

The beta subunits are about 95 to 120 kDa in size, with the notable exception of the 200-kDa beta-4 subunit. The amino acid sequences, again about 40% to 50% identical between subunits, include four conserved cysteine-rich domains in the extracellular region. The short cytoplasmic domain (40 to 50 amino acid residues) is generally more conserved in the beta subunits, except for beta-4, which has an intracellular domain of 1000 residues containing fibronectin type III domains. Interestingly, the beta-4 integrin interacts with intermediate filaments rather than with the actin cytoskeleton as other integrins do. Splice variants of the beta subunit mRNA have been identified which, in the case of the beta-1 subunit, is thought to result in different signaling properties, with one such variant displaying a dominant negative activity. The beta-1 subunit cytoplasmic domain also contains NPXY motifs (-Asn-Pro-X-Tyr-), thought to be important in mediating endocytosis by clathrin-coated vesicles.

2. Integrin Signal Transduction

A conformational change is propagated across the lipid bilayer to alter proteins associated with the cytoplasmic domains. The beta-1 subunit, and probably also other beta subunits, interacts with the actin cytoskeleton via associations with the proteins talin and alpha-**actinin**. These proteins colocalize at structures called *focal adhesions* (adhesion plaque, focal contact), which are areas closely opposed to the substratum in cultured cells. Protein tyrosine kinases also associate with focal adhesions, and *focal adhesion kinase* associates with the cytoplasmic domain of the beta-1 subunit and is activated on integrin ligation. This kinase activity is thought to alter the dynamics of actin and to signal to the nucleus to regulate **gene expression**. Integrins also bring about cellular alkalization and can lead to increases in the cytoplasmic calcium ion concentration and activation of protein kinase C (see Calcium Signaling). A variety of enzymes are known to increase their activity after integrin stimulation, including phospholipase A2, the GTPase **Rho**, and phosphatidyl inositol phosphate kinase (PIP 5-kinase), and enzymes associated with the Ras/MAP kinase pathway.

Growth Factors, such as platelet-derived growth factor, are known to synergize with ECM integrin ligands to stimulate cellular replication, and this results from a convergence of signaling pathways. Other cell surface receptors may interact with integrins and activate integrin signaling.

Integrin activity is regulated post-translationally in a cell-specific manner. For example, transfection of the same alpha-2 complementary DNA into different cell types that express the beta-1 subunit can result in either an inactive **receptor**, a collagen receptor, or a dual-function collagen and laminin receptor. The activity appears to be regulated by altering the integrin conformation, but the factors controlling this process are not understood. Activating antibodies have been generated that bind to the extracellular domain of integrins and activate increased ligand binding. Intracellular changes can also activate integrins through an inside-out signaling mechanism. For example, in T lymphocytes, the alpha-l/beta-2 integrin is activated to bind I-CAM only after the T cell receptor binds antigen. In this way, the T cell becomes more adhesive to endothelial cells lining the blood vessels in the area surrounding the antigen. This type of affinity modulation is also seen in platelets, where ADP or thrombin can induce high-affinity fibrinogen binding in the alpha-IIb/beta-3 integrin, which is important for blood clotting. Tyrosine phosphorylation of the beta-1 subunit by pp60src inhibits ligand binding.

Regulation of integrin function is crucial to many processes in development. For example, decreasing integrin expression in skin epithelial cells leads to their movement away from the basal lamina and their terminal differentiation. Inactivation of integrins in retinal neurons is correlated with the timing of axon pathfinding, and this may lead to a turn by the growth cone away from ECM ligands and towards CAM ligand.

3. The Integrin Family

At least 16 alpha subunits and 8 beta subunits, constituting at least 21 heterodimers, have been discovered to date. Different alpha-beta combinations give rise to receptors with different ligand-binding specificity, although not all possible alpha-beta pairings have been detected (Table 1). Receptors are often multifunctional, with abilities to bind more than one ligand. In addition, there is an apparent redundancy in function among the heterodimers. For example, at least seven integrin laminin receptors have been identified. It has become clear that some integrins bind to different sites on the same ligand and bind different ligand isoforms with varying avidity. For example, integrin alpha-5/beta-1 binds to the RGD site in fibronectin, but the alpha-4/beta-1 receptor binds to an LDV motif in an alternately spliced fibronectin. Some beta subunits are able to pair with multiple alpha subunits and, likewise, some alpha subunits are capable of forming heterodimers with more than one beta subunit.

Table 1. Integrin Heterodimers and Some of Their Ligands

	b1	**b2**	**b3**	**b4**	**b5**	**b6**	**b7**	**b8**
a**1**	**C**,[a] L_1							
a**2**	**C, L_1**, a**3, Ch**							
a**3**	**L_5,C,F,E,** a**2,3,T**							
a**4**	**VCAM, F_{LDV}**,a**4,T**, O, W						**VCAM,F_{LDV}**, MadCAM	
a**5**	**F_{RGD},T**							
a**6**	**L_1,L_5**			**L_1,L_5**				
a**7**	**L_1**							
a**8**	**F_{RGD}, Tn**, O							
a**9**	**C, L_1**							
a**10**	**C**							
aV	**V,F_{RGD}**		**Fb,F,V,OB,**		**V**	**F_{RGD}**		**V**

		W, T	
a**L**	**ICAM 1,2,3**		
aM	**C3bi,FX,Fb**		
a**X**	**FB, C3bi**		
a**D**	ICAM3		
a**IIB**		**Fb,F,V W, ICAM**	
a**E**			a**E**

[a] Key: C, collagens; F, fibronectin (RGD site or LDV site indicated); L, laminin (isoform number indicated); V, vitronectin; VCAM, vascular cell adhesion molecule 1; T, thrombospondin; Tn, tenascin/cytotactin; ICAM, intercellular adhesion molecule 1,2,3; MadCAM, mucosa addressin cell adhesion molecule. Fb, fibrinogen; W, von Willebrand factor; FX, factor X; C3bi, inactivated component of complement 3B; O, osteopontin; B, bone sialoprotein; Ch, chondroadherin.

The beta-1 family of integrins includes receptors for fibronectin, laminins, collagens, vitronectin, thrombospondin, and a variety of other matrix ligands. These integrins mediate many types of interactions between cells and the ECM. Beta-1 integrins are involved in important basic developmental cellular movements, such as **gastrulation**. Beta-1 laminin receptors are important in the development of neurons and muscle cells, from migration of neuroblasts and myoblasts to axon and dendrite outgrowth to synapse formation. The alpha-2/beta-1 collagen/laminin receptor mediates the contraction of collagen gels by resident cells during the remodeling of the interstitial ECM, and the alpha-5/beta-1 receptor has been implicated in organizing fibronectin networks. The alpha-4/beta-1 receptor, which binds both fibronectin and the vascular **cell adhesion molecule**-1 (VCAM-1), allows white blood cells to bind to inflamed endothelial cells (which express VCAM-1) and to exit out of the blood vessel to mediate an immune response. Some beta-1 integrins are also thought to interact with each other or to associate with other integrins on adjacent cells.

The beta-2 integrins are expressed by white blood cells and mediate cell–cell interactions important to the immune response by interacting with immunoglobulin super family molecules (ICAMs) and other ligands. Once neutrophils are activated, the alpha-L/beta-2 on their surface adheres to ICAMs on the endothelial cell surface, working in concert with the alpha-4/beta-1 receptor to allow the cell to exit the circulation. Beta-3 integrins include vitronectin receptors on bone and blood vessel endothelial cells (alpha-v/beta-3), and the alpha-IIA/beta-3 fibrinogen receptor important in platelet aggregation. Angiogenesis can be blocked by inhibitors of the alpha-v/beta-3 receptor on endothelial cells, which causes them to undergo apoptosis, and this same receptor is also involved in phagocytotic processes.

Other beta-subunit families, although smaller and less well characterized, may prove to be equally important. For example the alpha-6/beta-4 integrin is part of the hemidesmosomes in epithelial cells that attach cells to anchoring filaments made of laminin-5, and the beta-8 integrins are abundantly expressed on neurons.

The importance of integrins is underscored by genetic studies in a variety of species. In the fruit fly *Drosophila melanogaster*, integrin homologues were first identified as “position-specific antigens” with interesting patterns of expression during development. Loss of function of one beta subunit results in the myospheroid **phenotype**, where muscle cells cannot adhere to the matrix and assume a nonfunctional rounded shape. Loss of the alpha-PS3 gene results in numerous defects in tissue morphogenesis and cellular movements. Another alpha subunit is required for short-term memory in flies, suggesting a new role for integrins at the synapse. Nematode mutants show defects in cellular migrations, and mouse **knockout strains** in individual subunits have thus far proved lethal. For example, knockout of the alpha-4 subunit results in lethality at embryonic day 10, in part because of defective heart formation. Cellular interactions during heart development may require interactions between alpha-4/beta-1 and VCAM-1. Beta-1 subunit mutants fail to implant in the uterus. In humans, nonfunctional beta-2 subunit results in leukocyte adhesion deficiency disease, which renders patients prone to bacterial infections. Loss of the beta-3 subunit results in a clotting disorder called Glanzmann's thrombasthenia, and mutations in the alpha-6/beta-4 heterodimer lead to a blistering skin disease known as epidermolysis bullosa.

Suggestions for Further Reading

R. O. Hynes and A. D. Lander (1992) Contact and adhesive specificities in the associations, migrations and targeting of cells and axons. Cell **68**, 303–322.

M. A. Schwartz, M. D. Schaller, and M. H. Ginsberg (1995) Integrins: emerging paradigms of signal transduction. Ann. Rev. Cell Dev. Biol. **11**, 549–599.

E. Ruoslahti (1996) RGD and other recognition sequences for integrins. Ann. Rev. Cell Dev. Biol. **12**, 697–715.

Interallelic Complementation

1. What counts as allelic?

The use of complementation tests for defining the gene as a unit of function is explained under the headings Complementation and Complementation tests. It was assumed as a general rule in those articles that complementation between two mutants occurs only when their mutations are in different **genes** (**cistrons**). Complementation tests carried out, for example, on auxotrophic (nutritionally exacting) mutants of the budding **yeast** *Saccharomyces cerevisiae* or the filamentous **fungus** *Neurospora crassa*, indeed split the mutants cleanly into different complementation groups. Little or no complementation occurs within groups, and universal complementation occurs between them (see Fig. 3 of Complementation Tests). However, the patterns that emerge from complementation tests are not always clear-cut, and many examples can be cited of complementation between mutants that one would want to call allelic on other grounds.

An **allele** is a particular form of a gene, and so what counts as allelic complementation depends on how the gene is defined. As a working rule, most would agree to define the gene as a segment of DNA that is transcribed into a single molecule of RNA, although that definition needs qualification to accommodate various special systems of gene organization. It may also be considered reasonable to include within the definition those adjoining *cis*-acting, nontranscribed DNA sequences that regulate gene transcription, though this extension of the definition may lead to difficulties in deciding how far the gene's territory extends and whether it is allowed to overlap with other genes.

In the great majority of the eukaryotic organisms studied, genes that have protein-encoding functions are virtually always units of translation and of transcription. Each gene specifies just one polypeptide chain. In bacteria, however, and in the nematode *Caenorhabditis*, many genes are organized in operons, which are units of transcription that contain two or several nonoverlapping sequences each of which is translated into a different polypeptide chain. Thus, the *Escherichia coli lac* operon messenger RNA encodes b-**galactosidase** (*LacZ*), b-galactoside permease (*LacY*), and galactoside **transacetylase** (*LacA*). Here the term gene refers to the single-protein units rather than the whole unit of transcription. Even though *LacZ* and *LacY* are within the same unit of transcription, they have sufficient independence of function to rank as separate genes, and the normal phenotype of a $Z-Y+/Z+Y-$ partial diploid (see Complementation Tests) poses no problem and is not counted as allelic complementation.

Attention was first focused on allelic complementation as a result of intensive studies of auxotrophic (nutritionally exacting) mutants of microorganisms, first in the fungus *Neurospora crassa* and then in budding yeast and bacteria. The *Neurospora* mutants gave the main early encouragement to the view that each gene is responsible for the specificity (at first rather vaguely defined, but later taken to mean amino acid sequence) of a single enzyme. Each enzyme was expected to catalyze a single reaction, and indeed, nearly all auxotrophic mutants were defective in carrying out just one biosynthetic step. The finding, in *Escherichia coli*, that **tryptophan synthetase** deficiency results from mutation of either of two clearly distinct genes was clarified by the demonstration that this enzyme consists of two different polypeptide chains, one for each gene. Subsequently it was recognized that "one gene—one polypeptide" was a better working hypothesis than "one gene—one enzyme."

2. Complementation Maps

Because genes were expected to encode single polypeptide chains, there was no obvious possibility of allelic complementation. That would require recombination between polypeptide chains, which did not occur. However, as more mutants were screened, it was commonly found that, although most mutants defective in some single biosynthetic step were indeed noncomplementing in all pairwise combinations, testing of larger numbers revealed a few that showed complementation with some of the other members of the series, though still noncomplementing with most of them.

The complementation relationships within a series of mutants of the same enzyme were summarized in the form of complementation maps, in which mutants were represented as linear segments, nonoverlapping or overlapping depending on whether or not they complemented one another. Figure 1 shows a relatively simple example. Each group of mutants had some unity and justified their being called allelic because many or most of them were noncomplementing with all of the others. The overlaps in the complementation maps were crucial because they made it difficult to consider that the series of mutants falls in more than one gene, perhaps encoding different polypeptide components of the same enzyme. In principle, the overlaps could represent deletions of DNA that extended between genes, but deletions as a general explanation could be ruled out on two grounds. First, the mutational sites of "overlapping" mutations often recombined in **meiosis**. Secondly, they could, in many cases, undergo reverse mutation to wild type.

Figure 1. Complementation matrix and complementation map for a set of 42 *Neurospora crassa arg-1* mutants that are deficient in the enzyme argininosuccinate synthetase. The number of mutants in each of the complementation classes A–F is shown in parenthesis (1).

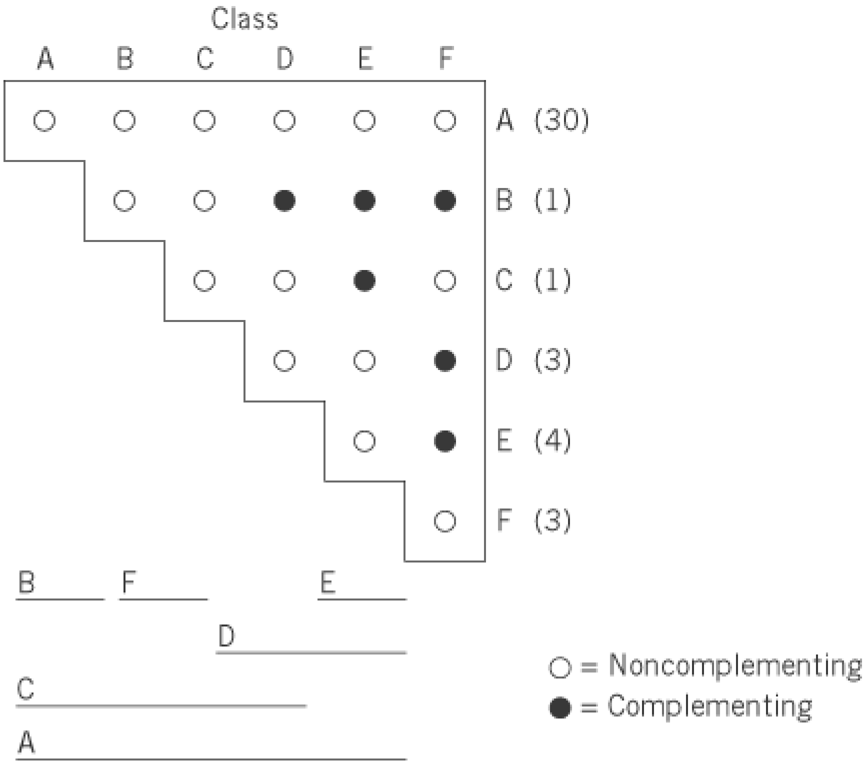

Up to a point, it was possible to place all of the segments of most complementation maps in a simple line (eg, Fig. 1), encouraging the view that perhaps the map had some relationship to the linear structure of the gene. But with the inclusion of more mutants, it usually became impossible to accommodate all of them without making the map two-dimensional with closed loops and tails. And where a complementation map and a fine-structure gene map were both available, usually a simple and consistent relationship did not exist between the two (3).

No general theory explains the many and various forms of complementation maps, but at least some special explanations have emerged from studies of particular cases. Much depends on the whether the enzyme (or other protein) gene product has one function or several.

3. Dimeric/Oligomeric Enzymes with Single Functions—Conformational Correction

In the first *Neurospora* examples, it was clear that the mutations affect single enzymes that catalyze single reactions. Thus the *ad-4* mutants, unable to make adenine, are defective in adenylosuccinase (4), and the *am* mutants that require a-amino nitrogen lack NADP-specific glutamate dehydrogenase (GDH) (5). Within each of these mutant series, some pairs show complementation, and in both cases it was shown that, under certain conditions, some degree of enzymatic activity could be obtained from mixed protein preparations of complementing mutants. The mutually complementing *am* mutants produce inactive, but physically nearly normal, forms of GDH protein, and active GDH is readily obtained by freezing and thawing mixtures of purified complementing mutant proteins in the presence of 0.1 M sodium chloride. This is a procedure that brings about dissociation and reassociation of protein subunits in other systems (6). NADP-specific GDH is a hexamer (six identical polypeptide subunits), and the enzymically active complementation products are mixed hexamers, though the complex mixture of hybrid proteins (all combinations from 5:1 to 1:5) was resolved only partly into its components (7).

The hybrid protein hypothesis for allelic complementation had already gained support from experiments by Schlesinger and Levinthal (8) on mutants of *Escherichia coli* deficient in alkaline phosphatase, a dimeric enzyme. Here a mixture of two individually almost inactive mutant forms of the enzyme dissociated to monomers by acidification and then allowed to reassociate was to form highly active mixed dimers (8).

Crick and Orgel (9) proposed that individually inactive monomers of dimeric enzymes might remedy each other's defects through mutual correction of their folded conformation. This is especially likely when the enzyme involved is allosteric and switches between active and inactive forms by ligand binding. One likely reason for mutational inactivation of an allosteric enzyme is excessive stabilization in the inactive form. Allosteric proteins are generally dimeric or oligomeric and, according to the simplest version of allosteric theory, their constituent monomers shift their conformation in a concerted, all-or-none, fashion. If so, one would expect that the conformational preference of the majority or more strongly stabilized component would prevail in a mixed oligomer. The idea is explained diagrammatically in Fig. 2a. It receives some support from studies of the *Neurospora am* mutants. Neurospora NADP-GDH is indeed an allosteric enzyme and, in most of the complenting pairs of mutants, one partner produces a GDH variety that is potentially active, but switches to the active conformation only under unphysiologically extreme conditions. In the best investigated examples, the other partner is a form of the protein that is unconditionally inactive because it has lost an essential side-chain in a substrate-binding site (see Enzymes), but is conformationally nearly normal. The potential activity of the first component was realized upon **hybridization** with the second (6). Another *am* mutant (10) that complements either of the first two kinds is best interpreted as producing a GDH variety that cannot form stable hexamers by itself.

Figure 2. Two modes of complementary interaction between mutant derivatives of the same protein. (a) Formation of mixed oligomers (shown here as trimers) that have one mutant monomer potentially active (+) but stabilized in an inactive conformation and the other always inactive but conformationally normal. In the mixed trimer (hetero-oligomer), the activity of the (+) component is realized by conformational correction. (b) Formation of active enzyme by association of two independently folded fragments. The shapes depicted in this figure are imaginary.

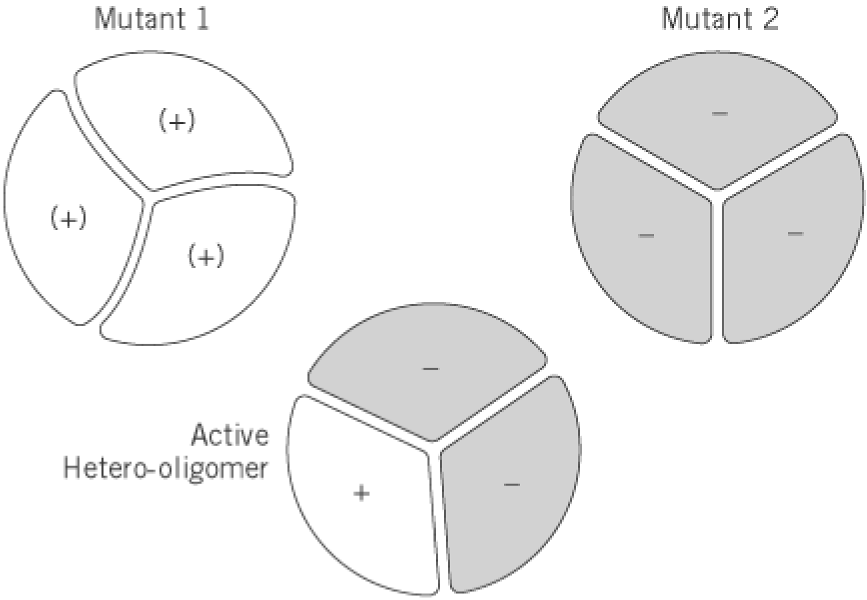

(a)

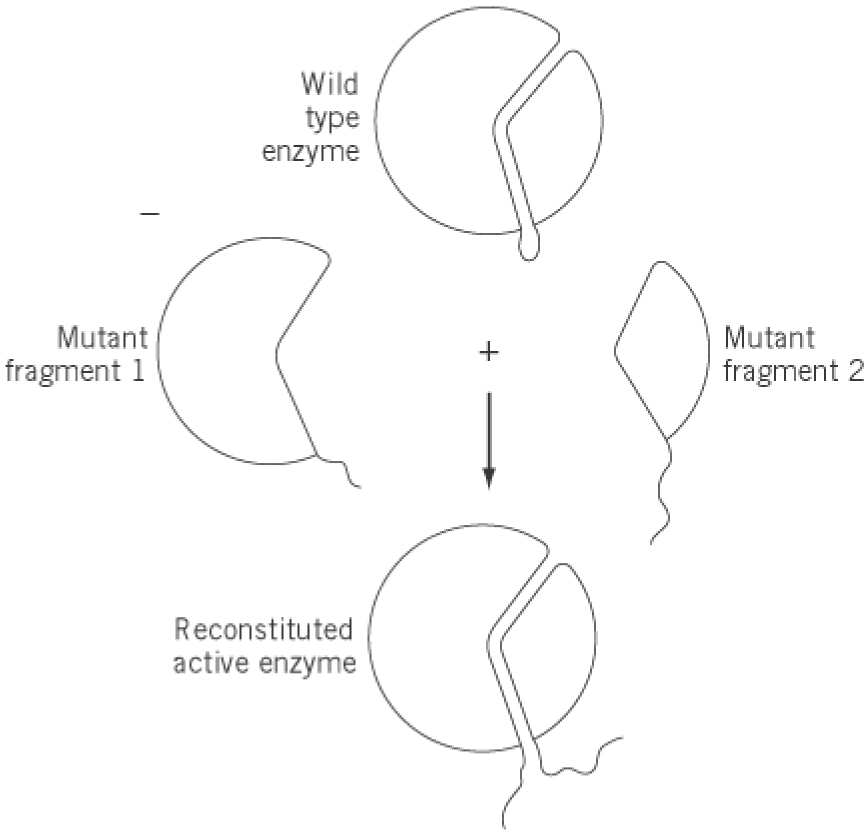

(b)

These examples of allelic complementation still leave some possibility of rescuing complementation as a criterion for allelism. Instead of insisting that alleles should never complement each other, one can adopt a softer criterion, namely that they should never complement to form a truly wild-type protein product. Then, the *cis*/*trans* criterion for allelism survives in modified form, and the crucial *cis-trans* difference is no longer between function and no function but between full function and (perhaps marginally) subnormal function. In the case of the *Neurospora am* mutants, it was fairly easy to demonstrate that their complementation products are subwild and have relatively low activity per unit protein and reduced **thermostability**. But this amended criterion for allelism is not always easy to apply. The best indication that a series of mutants belongs to a single gene is that, notwithstanding complementation between some pairs, a substantial proportion fails to complement any of the others.

On the conformational correction hypothesis, complementation maps that relate to single enzymatic functions must be presumed to represent interactions within the three-dimensional structures of proteins. Though most are too complex to interpret, a limited number of nonoverlapping segments can be explained in terms of global properties of mutant proteins, as in the case of the *Neurospora am* mutants mentioned previously. In any case, conformational correction applies only when the protein is a dimer or oligomer.

4. Fragment Complementation with a Monomeric Enzyme

At one time allelic complementation was seen as diagnostic of a dimeric or oligomeric gene product. What was overlooked, however, was the possibility of piecing together a functional monomeric protein from fragments. There is good evidence from several sources that this happens.

The best known example (11) involves *Escherichia coli* b-**galactosidase**, the *LacZ* product. This enzyme consists of a single, long (1025-residue) polypeptide chain. Mutants that have deletions of the N-terminal ("upstream") end of the chain complement virtually any mutant that has a defect in a substantial section at the C-terminal or downstream end (the w-region) provided that the deletion does not extend into that region. The uptream deletions were called w-donors and the downstream deletions complementing mutants w-acceptors. The latter class includes chain-terminating mutants in which the w region is hardly present at all. Thus an interaction between complementary fragments of a single polypeptide chain, called in this case w-complementation, result in reconstituting active enzyme.

The general explanation for complementary interaction of polypeptide fragments is that each of the two polypeptide sequences, whether continuous as in the wild type or separated as in w-complementation, fold up independently to form three-dimensional "**domains**"—protein globules that fit closely and stably together like two pieces of a three-dimensional jigsaw puzzle. Their mutual affinity enables the initially separated domains to find one another when synthesized in the same cell or, indeed, when mixed *in vitro*. w-Complementation creates a fully active and stable b-galactosidase, and the lack of a covalent connection between the two fragments does not matter. The overlap between them increases the molecular weight of the enzyme somewhat but does not impede its function.

Now, complementation between *LacZ* sequences is used routinely in **plasmid** technology (12). An *E. coli lacZ* deletion mutant, M15, lacks just 30 amino acid residues at the N-terminus of the b-galactosidase chain, and this nearly complete polypeptide is complemented by many different short N-terminal fragments that evidently can repair the N-terminal (a) domain. A number of different cloning plasmids have been constructed so as to encode one of these a fragments, and, if introduced into M15, signal their presence by producing active a-complemented b-galactosidase and the appearance of blue colonies on a growth medium containing a substance that is cleaved by the enzyme to give the color, **X-gal**.

It is still not clear how important interactions between polypeptide fragments, as opposed to formation of mixed oligomers, will prove to be an explanation of allelic complementation. For oligomeric proteins, the two possibilities are not mutually exclusive. Their occurrence together within the same allelic series could be responsible for the complexity of some complementation maps.

5. Enzymes with Multiple Functions

Another explanation for allelic complementation, which applies more commonly than at one time thought, is that the protein product of the gene has several enzymatic functions, usually involved with different steps in the same biosynthetic pathway. An amino acid replacement that eliminates one enzymatic activity does not necessarily have any critical effect on the others. In terms of protein structure, this means presumably that the polypeptide chain is folded into a number of domains that function largely independently. In this kind of situation, different mutant alleles can in principle complement one another without mutual conformational correction or even the formation of mixed oligomers, though these interactions may also occur.

The genetic control of multifunctional enzymes has been most thoroughly investigated in filamentous fungi and budding yeast because extensive collections of relevant mutants have been available in these organisms. Here we briefly review three examples, two from the yeast *Saccharomyces cerevisiae* and one from *Neurospora crassa*.

Schweizer and his colleagues (13, 14) collected a large number of yeast mutants that had lost the ability to synthesize fatty acids. The pathway of synthesis, starting with acetic and malonic acids and leading to long-chain fatty acids, could be divided biochemically into six steps, corresponding to separately assayable enzymatic activities. The whole pathway was catalyzed by a protein complex composed of just two long polypeptide chains. The mutants were assigned by genetic mapping and complementation tests to two genes, *fas1* and *fas2*, unlinked to each other Every *fas1* mutant complemented every *fas2* mutant. Extensive complementation also occurred within *fas1* and within *fas2*. The complementation maps are shown in Fig. 3. Three complementation groups in each map are complementary in all combinations, and these correspond to losses of different single enzymatic activities. In both *fas1* and *fas2*, there are also mutants that failed to complement any of the others and some that have more restricted overlaps in the map. The comprehensively noncomplementing mutants are mostly chain terminators or, less often, frameshifts, which failed to synthesize a complete polypeptide chain (see Frameshift Mutation) and, as a result have lost all the enzyme activities normally associated with it. Although the different domains of the polypeptide chains could function independently so long as complete chains were produced, a shortened chain failed to form any of the active domains.

Figure 3. Complementation relationships of *Saccharomyces cerevisiae fas* mutants deficient in one or more activities of the fatty acid synthesizing enzyme complex. By complementation testing, they split into two distinct groups, *fas1* and *fas2*, that correspond to two unlinked genes and two different polypeptide chains. Within each group are three mutually complementing classes that correspond to losses of three different enzymatic activities of a single polypeptide chain and numerous mutants (mostly chain-terminating) that fail to complement all of the others (13, 14).

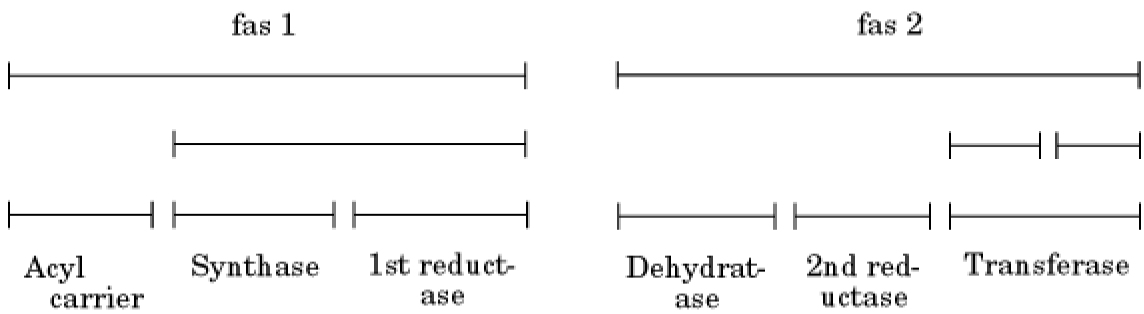

The *Neurospora* example, probably the most complex and extensively analyzed of any, involves the pathway for synthesizing aromatic compounds. Mutants blocked in this pathway have to be supplied with a complete mixture of essential aromatic metabolites (phenylalaline, tyrosine, tryptophan, and *p*-aminobenzoic acid) because they cannot make the common precursor of the benzene ring, chorismic acid. The pathway segment relevant here comprises the five steps leading to enol-pyruvylshikimic acid phosphate, the immediate precursor of chorismate. The five distinct enzymatic activities were at first thought to be due to separate proteins encoded by a close cluster of genes because a number of closely linked and mutually complementing mutants were found that lack single enzymatic activities. However, doubt was thrown on the separate gene interpretation by the numerous mutants that failed to complement two or more of the single-activity groups.

The complementation map is shown in Fig. 4. The map shows a polarized pattern, and all the overlaps start at the left (DHS reductase) end of the map and extend for different distances to the right. The situation became much clearer following the biochemical demonstration that the entire complex of reactions is catalyzed by a dimeric multifunctional enzyme that has just one kind of polypeptide chain. As with yeast *fas1*/*fas2*, the mutants represented as overlaps on the complementation map are largely chain terminators. But the aro protein differs from the *fas1*/*fas2* complex in the polarized pattern of its complementation map. The obvious explanation for this is that the gene, as represented in Fig. 4), is transcribed and translated from right to left, and prematurely terminated forms of the polypeptide chain retain the enzymatic activities of the domains upstream of the termination point. A remaining anomaly is that, to give coherence to the complementation map, the EPSP synthetase segment has to be placed at the N-terminus of the chain, upstream of DHQ synthetase, whereas in the actual polypeptide chain the two segments are the other way round. The fact that the enzymatic complex is a dimer opens the door to further complications. There is the possibility of conformational interactions between monomers, and the unanswered question of how prematurely terminated monomers are accommodated in the dimeric structure.

Figure 4. Relationships among *Neurospora crassa* mutants that are deficient in one or more of five steps in the synthesis aromatic ring, depicted in the upper line (EPSP, the precursor of chorismic acid, is enolpyruvyl shikimic acid phosphate) different enzymatic activities (second line) are properties of different domains of a single polypeptide chain. The complementation map below shows five classes of *aro* mutants, each of which is deficient in a single enzyme activity, complementing each other in all combinations, and "polar" mutants each of which lacks two or more activities. The num mutants found in each class in the first screen are shown in parentheses. Initially no singly deficient mutants were found DHQase class because this function is duplicated by a catabolic DHQase. The missing class was found after the latter en had been eliminated by mutation (15).

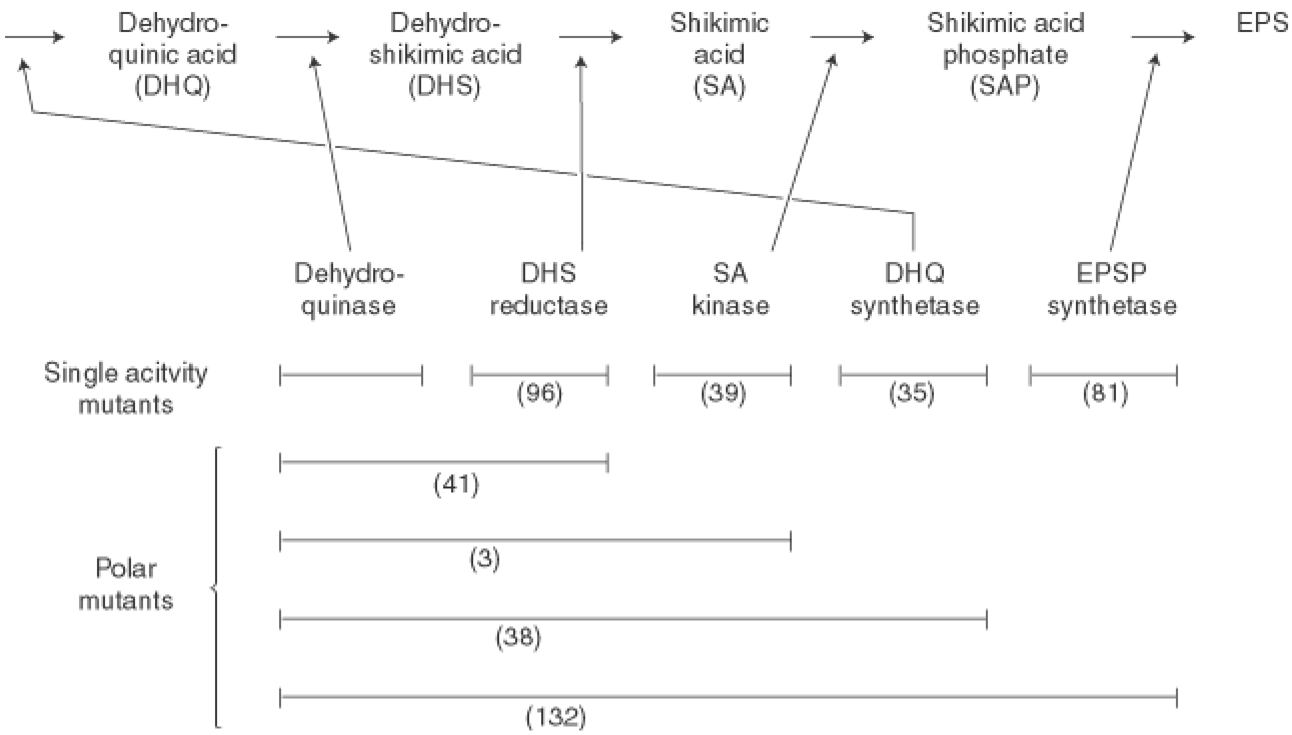

The second example of polarized complementation, this time from yeast, provides a link to similar situations in insects and mammals. Among several classes of **uridine** or **cytidine**-requiring (URA) mutants, the *URA2* group, a tightly linked group, that maps to a first approximation to the same chromosome locus (*URA2*), includes two mutually complementing subgroups, A and C, and other mutants (B) that complement neither (16). When the mutational sites were placed in order in a recombinational gene map, the A and C subgroups mapped in two close but nonoverlapping segments, whereas nearly all of the B mutations, which eliminate both A and C functions, mapped within the C segment. It was shown that the B overlapping class consists mostly of chain-terminating mutations, with some frameshifting insertions or deletions, which are expected to eliminate or make nonsense of "downstream" polypeptide sequences. Essentially the same situation has been found in two other fungi, *Neurospora* and the ink-cap mushroom *Coprinus*.

The enzymological explanation of all three fungal examples is the same. The protein gene product is multifunctional, and has two enzymatic activities, carbamoyl phosphate synthase (CPSase) and **aspartate** *trans* **carbamoylase** (ATCase), that catalyze the first two steps of the pyrimidine biosynthetic pathway. The yeast *URA2*-A mutants lacked ATCase, the C mutants lacked CPSase, the B mutants lacked both, and the same applied to the analogous mutant classes in the other two fungi. The polypeptide also has a third enzymatic activity, glutamine amidotransferase (GATase), an initially unrecognized component of CPSase activity. The single polypeptide chain is synthesized from the GATase/CPSase end, so that downstream chain-terminating mutations could eliminate ATCase and not CPSase, and upstream terminators could only eliminate both.

A similar situation applies in the pyrimidine biosynthetic pathway of *Drosophila*. The difference here is that the analogous gene product has an additional enzyme function, dihydro-orotase, that catalyzes a further step in the pathway, as well as GATase, CPSase and ATCase (17). The gene is called *rudimentary* (*r*) referring to the effect on the wings and bristles of the fly, which are sensitive indicators of pyrimidine limitation. The *r* series of mutants provided the first demonstration in *Drosophila* of allelic complementation comparable to the fungal examples (18). Later work showed that generally the mutually complementing *r* mutants are deficient in different enzymatic activities of the single-gene product.

Multifunctional enzymes encoded by single genes (sometimes called "cluster genes" to point out their superficial resemblance to gene clusters) are not uncommon in higher organisms. For example, the first steps of pyrimidine biosynthesis in the mouse are catalyzed by a single protein very like the *Drosophila r* gene product, and in *Drosophila* a single protein (encoded by the *Gart* gene) is responsible for catalyzing several steps of purine synthesis, not all of them sequential. If complementation between mutant alleles has not been a feature of these other systems, it is because the necessary collections of viable mutants have not been obtained.

Although a degree of complementation between different mutant derivatives of multifunctional enzymes is to be expected, it is not clear whether it always, or even ever, results in maximally efficient enzymatic function. The catalysis of several sequential reactions by a single protein suggests that the organism's metabolism derives some benefit from the proximity of the different catalytic protein domains. In the fungal examples just reviewed, the separated enzymatic activities function together well enough to support normal growth under laboratory conditions, but this is perhaps not a very stringent test.

6. Single Genes that Encode More Than One Protein

Investigation of the exon-intron structures of genes has brought the realization that a single gene, that is, with a single primary RNA transcript, can encode two or more different proteins that have different and complementary functions as a result of different modes of splicing of the pre-mRNA (see Alternative Splicing). The different protein products always, at least in the known examples, have much of their amino acid sequence in common, but two alternative products may each have sequences that the other lacks. Mutations in these differentiating segments affect different functions and should show complementation. Thus the *Drosophila Passover* gene (19) encodes two alternative proteins respectively required for normal synaptic connections in the neural system and for some other function necessary for viability. Certain mutations, although allelic in the sense that they affect the same primary transcript, show complementation because they damage different proteins (Fig. 5).

Figure 5. Complementation between alleles at the *Passover* gene of *Drosophila melanogaster* due to alternative modes o splicing introns from the pre-mRNA. The *pas*^{V} (recessive lethal) and *pas*^{N} (recessive neural dysfunction) mutations complement each other to produce a wild-type phenotype. They fall within exons that are mutually exclusive in the diffe spliced mRNAs. Mutations (*pas*^{VN}) that fall within the common upstream exons complement neither *pas*^{V} nor *pas*^{N}. Fill open boxes represent translated and untranslated exon sequences, respectively, and the lines between them are introns (1

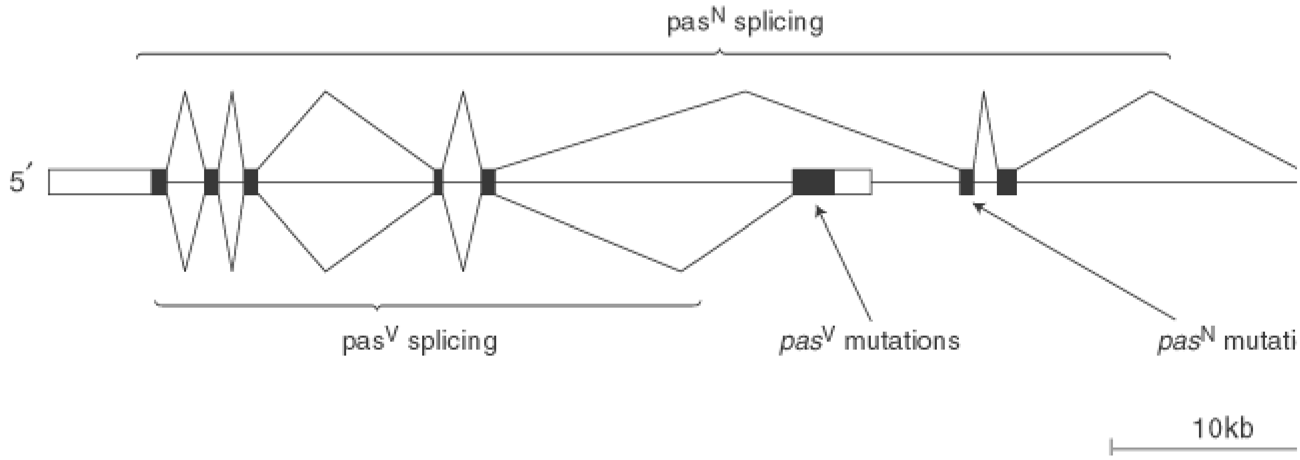

7. Morphologically Pleiotropic Genes

Pleiotropic means having two or more distinct effects. If a pleiotropic gene mutates so as to lose one its functions and not the other(s), then there are obvious possibilities for allelic complementation. This point has already been made in connection with genes that encode multifunctional enzymes, and it also applies to pleiotropic genes that have effects at the morphological level.

A good example is provided by the *dumpy* (*dp*) gene of *Drosophila melanogaster* (20). Different recessive mutant alleles of this gene, when homozygous, have three different effects: (l) a skewing of the thoracic bristles (called “vortex”, *v*); (2) a shortening and oblique orientation of the wings (*o*); and (3) recessive lethality (*l*). In some alleles, two or three of these functional defects occur together. *o*, *v*, and *ov* alleles complement *l* in diploids, whereas *ol*, *vl* and *ovl* do not. In combination, the effects of the alleles are additive. Each partner supplies that part of normal gene function that it possesses and the other lacks. No new function is created but each allele merely contributes what it can do by itself. A somewhat similar mutational effect but with less variety was discovered many years earlier by N. P. Dubinin in his investigation of the *Drosophila* **achaete-scute** locus (21). Here different mutations eliminated different bristles, and heterozygotes with two scute mutant alleles lacked only those bristles that were missing in both parental homozygotes.

The whole array of *dp* mutants can be attributed to a single gene on two grounds. The mutants that have lost two or three functions cannot be due to deletions overlapping more than one gene because they all form wild-type recombinants in crosses with the single-function mutants; and the sites of the different mutations, mapped by recombinational analysis, do not fall into functionally different segments but are rather intermingled.

To the extent that their multiple functions can be separately affected by mutation, pleitropic morphology-determining genes, such as *dp* in *Drosophila*, bear some formal similarity to the “cluster genes” of fungi. But *dp*, at least, is not resolvable into single-function segments, and the reason for its pleiotropy is likely to be different. Another, better understood *Drosophila* gene, ***Ultrabithorax*** (*Ubx*), that encodes a regulatory protein and is differentially expressed in different tissues, may provide a better model.

The *Ultrabithorax* (*Ubx*) gene in *Drosophila* plays a vital role in establishing segment identity in the developing fly embryo (22). It is expressed in a zone extending from the end of the abdomen to the middle of the second thoracic segment. Loss of *Ubx* function by mutation causes lethal transformation of the third thoracic and first abdominal segments to likenesses of the second thoracic segment. Mutations of less drastic effect in the *Ubx* gene cause losses of *Ubx*+ function in specific **parasegments**, which comprise the posterior half of one segment and the anterior half of the next segment to the rear. These mutations, it is thought, affect parasegment-specific enhancer sequences that are necessary in some way for the local transcription of *Ubx*. Fly embryos homozygous for a recessive mutation called **bithorax** (*bx*), located within the *Ubx* large intron (Fig. 6), fail to transcribe *Ubx* in parasegment 5 that covers the anterior half of the third thoracic segment (T3). T3 normally carries vestigial wings (“balancers” or halteres). The true wings are on the second thoracic segment (T2). In *bx*/*bx* flies, the front half of T3 becomes T2-like, and the front half of the haltere is expanded, tending toward the wing. Another recessive mutant, postbithorax (*pbx*), that maps just upstream of the *Ubx* transcriptional start point, has an analogous effect on *Ubx* expression in parasegment 6 that covers the posterior half of T3. When homozygous, *pbx* causes wing-like enlargement of the posterior half of the haltere. The homozygous double mutant *bx pbx*/*bx pbx*, develops (when it develops at all) into a four-winged fly. Both the *cis* and the *trans* double heterozygotes, *pbx bx*/++ and *bx* +/+ *pbx* are phenotypically normal.

Figure 6. Complementation by transvection in *Drosophila melanogaster*. (a) The normal expression of the *Ubx*+ gene in the posterior thoracic segment depends on an enhancer (○) located in a *Ubx* intron. (b) In the *bithorax* (*bx*) allele (recessive, causing partial segmental transformation with enlarged halteres), this enhancer has been disrupted (Ä). The $Ubx^{M \times 6}$ allele (recessive lethal) has a deletion that takes out the *Ubx* promoter (P). The complementation of the two alleles to give a very nearly wild-type fly (24) is due to the enhancer, still present in *Ubx*M × 6, that acts in *trans* on the promoter P. (c) The effect is due to close somatic pairing of chromosomes. When this is disrupted by a structural rearrangement, the *bx* mutant phenotype reappears. The position of the upstream enhancer disrupted in *pbx* mutants is also shown. *bx* and *pbx* complement each other fully in *trans* (see text).

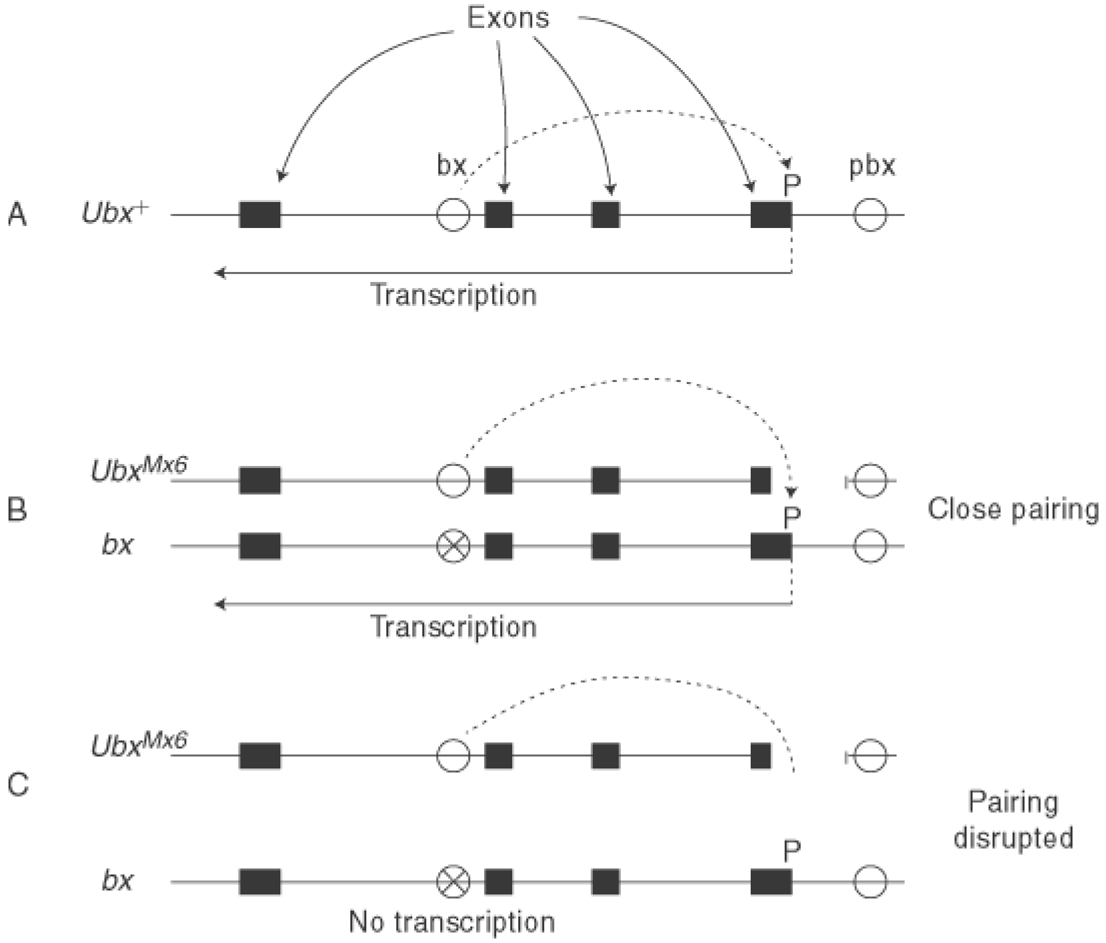

Based on their complementation in *trans*, one might, in the absence of further information, regard *bx* and *pbx* as mutations in different genes, This, indeed, is how they were originally interpreted. However, neither allele is complemented to more than a very limited extent by a *Ubx* null mutant allele, and so by this criterion they are functionally part of *Ubx*—complementary regulators of the same transcription unit. So *bx* and *pbx* can be regarded as alleles of *Ubx*, and the wild-type *bx*/*pbx* phenotype provides an example of another kind of allelic complementation, based on its tissue-specific controls of expression, not on the structure of the gene product or on the multiplicity of its effects (though it does have multiple effects).

The *Ubx* gene bears on the topic of allelic complementation in another and more surprising way. E. B. Lewis (23) discovered that *Ubx*/*bx* heterozygotes have a more extreme mutant phenotype when the somatic pairing of homologous chromosomes (which is characteristic of flies) is disrupted by a structural rearrangement with a breakpoint close to the *Ubx* locus. He called this phenomenon ***transvection***. The idea is that the two mutant alleles somehow help each other toward normal function when they are physically close. It has been found in a few other *Drosophila* genes as well as *Ubx*.

More recently, the *Ubx*/*bx* phenomenon has been reinvestigated and given a new interpretation (24). One of the *Ubx* alleles used in the recent work, $\mathrm{Ubx}^{\mathrm{M\times6}}$, is null (and recessive lethal) by virtue of a deletion that removes the promoter region of the gene. Compared with other null *Ubx* alleles, it shows unusually strong complementation with the standard *bx* allele, which has a *gypsy* transposable element (see Transposon) inserted into the largest *Ubx* intron, disrupting an enhancer of *Ubx* transcription in parasegment 5. The $Ubx^{\mathrm{M\times6}}$/*bx* heterozygote is very nearly wild type morphologically except when the somatic pairing of the homologous chromosomes is impeded by a structural rearrangement, when the front half of the haltere becomes enlarged. The proposed explanation of the strong complementation is that the bx^{+} enhancer, still present in the *Ubx* allele, acts in *trans* on the enhancer-deficient *bx* allele. The idea is shown in Fig. 6. Enhancers are usually supposed to act only in *cis* and bind proteins that help to form the transcriptional initiation complex at the gene promoter on the same chromosome, but this interpretation of transvection suggests that, with close pairing of homologues (as occurs in *Drosophila* polytene chromosomes), an enhancer on one homologue can reach across and help to activate the allele on the other chromosome of the pair. In the case of this particular *Ubx*/*bx* interaction, the *trans* effect may have been particularly strong because, as a result of the deletion in the *Ubx* allele, there was no competition for the services of the enhancer from a promoter in *cis*.

If we grant that the enhancer is a part of the gene (difficult to deny when it is within one of the gene's introns), then transvection is yet another mechanism for allelic complementation.

Bibliography

1. D. G. Catcheside and A. Overton (1959) Cold Spring Harbor Symp. Quant. Biol. **23**, 137–140.
2. U. Leupold and H. Gutz (1965) In Genetics Today (Proc. 11th Int. Congr. Genetics) **2**, 31–33.
3. M. E. Case and N. H. Giles (1960) Proc. Natl. Acad. Sci. USA **46**, 657–676.
4. D. O. Woodward, C. W. H. Partridge, and N. H. Giles (1958) Proc. Natl. Acad. Sci. USA **44**, 1237–1244.
5. J. R. S. Fincham (1962) J. Mol. Biol. **4**, 257–274.
6. A. Coddington, T. K. Sundaram, and J. R. S. Fincham (1966) J. Mol. Biol. **17**, 503–512.
7. D. H. Watson and J. C. Wootton (1978) Biochem. J. **175**, 1125–1133.
8. M. J. Schlesinger and C. Levinthal (1963) J. Mol. Biol. **7**, 1–12.
9. F. H. C. Crick and L. E. Orgel (1964) J. Mol. Biol. **8**, 161–165.
10. J. R. S. Fincham and A. J. Baron (1977) J. Mol. Biol. **110**, 627–642.
11. A. Ullman and D. Perrin (1970) In *The Lactose Operon* (edited by J. R. Beckwith and D. Zipser, eds.), Cold Spring Harbor Laboratory Press, Cold Spring Harbor, New York, pp. 143–172.
12. J. Sambrook, E. F. Fritsch, and T. Maniatis (1989) *Molecular Cloning*, 2nd ed. Cold Spring Harbor Laboratory Press, Cold Spring Harbor, New York pp. 4.7–4.9.
13. P. Tauro et al. (1974) Mol. Gen. Genet. **12**, 131–148.
14. A. Knobling, D. Schiffman, H. D. Sickinger, and E. Schweitzer (1975) Eur. J. Biochem. **56**, 359–367.
15. H. W. Rines, M. E. Case, and N. H. Giles (1969) Genetics **61**, 789–800.
16. M. Denis-Duphil and J. G. Kaplan (1976) Mol. Gen. Genet. **145**, 259–271.
17. J. N. Freund and B. P. Jarry (1987) J. Mol. Biol. **193**, 1–13.
18. O. G. Fahmy and M. J. Fahmy (1959) Nature **184**, 1927–1929.
19. S. H. Krishnan, E. Frei, A. P. Schalet, and R. J. Wyman (1995) Proc. Natl. Acad. Sci. USA **92**, 2021–2025.
20. E. A. Carlson (1959) Genetics **44**, 347–373.
21. N. P. Dubinin (1933) J. Genet. **26**, 37–58.
22. P. A. Lawrence (1992) *The Making of a Fly*, Blackwell Scientific, Oxford.
23. E. B. Lewis (1955) Amer. Nat. **89**, 73–89.
24. A. Martinez-Laborda, A. Gonzales-Reyes, and G. Morata (1992) EMBO J. **11**, 3543–3562.

Interband

The dense bands of polytene chromosomes stain more intensely with **DNA**-sensitive dyes, indicating that the DNA concentration and hence the compaction of chromatin are greater in these regions. These bands broadly correlate with the number and positions of known genetic loci (1). Nevertheless, each band contains much more DNA than found in a typical gene. In certain well-defined cases, a band contains small clusters of genes, such as those encoding the chorion proteins. In contrast, the interband regions contain less condensed DNA and chromatin, as has been shown directly for the *Notch* gene. In situ hybridization reveals that the 5′ regulatory regions of the *Notch* gene lie in the interband, and the gene itself occupies a single cytologically defined band (2). Transcriptionally active bands become differentiated structures known as **puffs**, in which the chromosomal structure is disrupted as a consequence active transcription.

Bibliography

1. B. H. Judd and M. W. Young (1973) Cold Spring Harbor Symp. Quant. Biol. **38**, 573–579.
2. M. C. Rykowski, S. J. Parmalee, D. A. Agard, and J. W. Sedat (1988) Cell **54**, 46–72.

Suggestion for Further Reading

3. D. DePomerai (1990) *From Gene to Animal* 2nd ed., Cambridge University Press, Cambridge, UK.

Intercalation

Virtually any molecule with sufficiently large aromatic chromophore will bind to the double-helical DNA structure by insertion of the flat chromophore between the base pairs . The primary driving force for intercalative binding is stacking (charge-transfer and dipole-induced dipole) interactions between the intercalator and the adjacent base pairs, and many compounds have larger and more electron-deficient chromophores than a DNA base pair. The residence time of the intercalator at a particular site varies widely according to its structure, ranging from a few milliseconds to many hours. Intercalation disrupts the DNA structure, forcing the base pairs apart by about 3.5 Å and unwinding the helix by 10–25° (depending on the structure of the intercalator) (1). **Acridines** are classic examples of DNA intercalators, and this DNA interaction is considered integral to their activity as frameshift mutagens.

A wide range of other planar polyaromatic molecules apart from acridines have been shown to intercalate and also to cause frameshift mutations (2, 3). The most common types of frameshift mutations involve the gain or loss of one or two base pairs, typically in repetitive sequences of DNA. In these cases, every codon after the mutation site is altered within a coding region, typically resulting in the formation of truncated proteins because of the generation of nonsense mutations. Nonfunctional gene products are thus a common result of frameshift mutations, and these may have major phenotypic effects, depending upon the role of that specific gene function in cell viability and metabolism.

In 1966, Streisinger et al. (4) developed a model in which he suggested that frameshift mutations are generated because of a localized pairing out of register, or slippage, during DNA replication. This slippage occurs at repetitive runs of one or more bases, leaving an unpaired base or a few bases out of register, ultimately resulting in the incorporation of an inappropriate number of bases during DNA replication. Intercalating agents may bind to the DNA bulges associated with the mispairing, thereby stabilizing these structures and enhancing the spontaneous rates of frameshift mutagenesis at this site. This model, albeit with modifications, still provides a useful explanation of most of the data available to the present day (5, 6).

Bibliography

1. L. P. G. Wakelin (1986) Med. Res. Rev. **6**, 275–340.
2. W. A. Denny, P. M. Turner, G. J. Atwell, G. W. Rewcastle, and L. R. Ferguson (1990) Mutat. Res. **232**, 233–241.
3. L. R. Ferguson, P. M. Turner, and W. A. Denny (1990) Mutat. Res. **232**, 337–343.
4. G. Streisinger, Y. Okada, J. Emrich, J. Newton, et al. (1966) Cold Spring Harbor Symp. Quant. Biol. **31**, 77–84.
5. L. R. Ferguson and W. A. Denny (1990) Mutagenesis **5**, 529–540.
6. G. R. Hoffmann and R. P. P. Fuchs (1997) Chem. Res. Toxicol. **10**, 347–359.

Interferons

1. General Introduction to the Interferon System

Interferons (IFNs) are members of the group of secretory proteins called cytokines and are defined by their ability to interfere with viral infection. However, IFNs are multifunctional proteins that also inhibit cell proliferation, regulate cell differentiation, regulate apoptosis (programmed cell death), and modulate activities of the immune system. A wide range of cell types produce IFNs in response to infection by viruses, bacteria, and mycoplasma. Noninfectious agents such as growth factors, other cytokines, and double-stranded RNA (dsRNA) molecules also induce IFN expression. In fact, dsRNA may be a physiologically relevant mediator of IFN synthesis since it is an important intermediate in viral replication. IFNs are extremely potent biological response modifiers with specific activities of at least 10^6 units per milligram of protein, with 1 unit defined as the amount of IFN necessary to inhibit virus replication by 50%.

IFNs were originally classified according to the cell types that generally produce them. The type I IFNs (IFNa and IFNb) are usually produced by leukocytes and fibroblasts, respectively, while type II IFN (IFNg) is produced by lymphocytes. However, cloning of individual human type I IFN genes has shown that the family is rather large and includes 15 different IFNa subtypes (with four pseudogenes), one IFNb, and two IFNw (with five pseudogenes). Type I IFNs are acid-stable, have similar protein structure and biological activities, bind and transduce signals through a common multiprotein cell surface receptor, are induced in response to viral and other inducers, and share a common gene locus on human chromosome 9. All the genes for type I IFNs are devoid of introns. In contrast, the single type II IFN, IFNg, is acid-labile, and its expression is limited mainly to T cells and NK cells. The structural gene for IFNg is located on human chromosome 12 and contains three introns.

Although IFNs share similar biological actions, there are distinctive differences in the biological actions of type I and type II IFNs. For example, only IFNg induces class II histocompatibility antigens (all IFNs induce class I expression) and inhibits the Th2 subset of helper T cells, thereby altering the balance between the humoral and cellular immune responses. Therefore, while IFNg is more active in immunomodulation than type I IFNs, type I IFNs in general are more efficient antiviral agents. Thus, although all IFNs are antiviral, the biological roles of the different IFNs in vivo are distinct, as shown in mouse models for infectious disease. Mice lacking a functional type I IFN system (by knockout of one of the type I IFN receptor genes) were highly sensitive to a wide variety of viral infections (1, 2). In contrast, mice lacking a functional type II IFN system (by knockout of the IFNg gene or a IFNg receptor gene) were more sensitive to bacterial and parasitic infections, but generally remained resistant to viral infections (1).

IFNs are not directly antiviral, but elicit their biological effects by first binding to specific receptors on the surface of target cells. The interaction of the ligand with its cognate receptor transduces signals to the nucleus that results in new gene expression: the transcription of new mRNAs and their translation into new proteins. While many of the proteins induced by type I and type II IFNs are distinct, there is a certain degree of overlap. Nonetheless, the IFN-induced proteins are ultimately responsible for biological actions of IFNs. The transcription of some IFN-induced genes does not require de novo protein synthesis, such as the family of immediate early genes called IFN-stimulated genes (ISGs). Other IFN-induced genes require protein synthesis and are involved in the delayed response to IFNs, such as class II histocompatibility antigens and IFN-response factors (IRFs).

2. IFN Receptors

All type I IFNs (IFN a, b and w) bind to a ubiquitously expressed cell surface receptor, varying in number from 500 to 20,000 high-affinity ($K_d \approx 20–100$ pM) receptors/cell (3, 4). The cDNAs coding for two subunits of the type I IFN greceptor, IFNAR1 and IFNAR2, have been cloned; both of these are located on human chromosome 21 (5-8). The human IFNAR1 chain (~110–135 kDa glycoprotein) is a 557–amino acid protein, with a 100–amino acid intracellular domain and a 21–amino acid transmembrane segment. The IFNAR1 chain is a signal transducing subunit, but does not directly bind IFN (9). The major ligand binding chain of the type I IFN receptor is IFNAR2, which exists as three different polypeptides due to alternative splicing and differential use of polyadenylation sites (7). The longest form, IFNAR2c (~100 kDa glycoprotein), is a 515–amino acid protein that acts as a functional receptor in type I IFN signaling.

Two subunits of the type II IFNg receptor, IFNGR1 and IFNGR2, have also been cloned (10-12). The human IFNGR1 chain (90-kDa glycoprotein) is the ligand-binding subunit of the receptor and is a 472–amino acid protein with a cytoplasmic domain of 221 amino acids and a 23–amino acid transmembrane segment. The gene for IFNGR1 is located on human chromosome 6. Although transfection of the human IFNGR1 gene into murine cells confers high-affinity ligand binding, a species-specific component (IFNGR2) encoded by human chromosome 21 is necessary for a fully functional receptor. The human IFNGR2 chain (~65-kDa glycoprotein) is a 316–amino acid polypeptide with a 66–amino acid cytoplasmic domain and a 24–amino acid transmembrane segment.

Cytokine receptors have been classified into two groups on the basis of structural similarity in their extracellular domains. The class I cytokine receptor family includes receptors for growth hormone, prolactin, erythropoietin, interleukins-2, -3, -4, -6, and -7, granulocyte-CSF, and granulocyte macrophage-CSF and are typified by conserved tryptophan, NH2-terminal and COOH-terminal cysteine pairs, and a membrane proximal WSxWS box. The IFNAR1, IFNAR2, IFNGR1, IFNGR2 and the interleukin (IL)-10 receptor constitute the type II cytokine receptor family, based on a characteristic 200–amino acid extracellular domain (13). These receptors have no inherent enzyme activity, but on ligand binding generate cytoplasmic signals in combination with JAK tyrosine kinases and STAT proteins. Members of this family in general have a ligand binding chain with either low or high affinity, and at least one chain involved in signal transduction, which has either relatively low binding affinity for the cytokine or no detectable binding activity at all. Receptor activation by this family of cytokines requires the ligand-dependent interaction between receptor subunits to form oligomers.

3. Signal Transduction by IFNs Through the JAK-STAT Pathway

IFNs elicit their biological effects by transducing a signal to the nucleus, which results in selective gene expression (14, 15). ISGs are a family of genes that are transcriptionally activated within minutes by IFNs. ISG transcriptional activation is regulated through the tyrosine phosphorylation of STAT proteins (for *S*ignal *T*ransducers and *A*ctivators of *T*ranscription), which is mediated by members of the Janus family of nonreceptor protein tyrosine kinases (JAKs) (16-19). JAKs are so named because they have a functional kinase domain as well as a second kinase-like domain, and hence are two-faced like the Roman god Janus. JAKs constitutively associate with membrane proximal regions of the intracellular domains of IFN receptor subunits to provide catalytic activity and transduce intracellular signals by phosphorylating a variety of substrates on tyrosine residues (20). In the case of the type I IFN receptor, the TYK2 and JAK1 Janus kinases are constitutively bound to the IFNAR1 and IFNAR2 subunits, respectively (8, 21). On ligand binding the JAKs cross-phosphorylate each other, with Tyk2 becoming phosphorylated first on type I IFN addition. In the case of the IFNg receptor, the JAK1 and JAK2 kinases are constitutively bound to the IFNGR2 and IFNGR1 subunits, respectively, and on ligand binding JAK1 appears to be activated first (22, 23). The activated JAKs phosphorylate specific tyrosine residues within the cytoplasmic tails of the IFN receptor chains to provide docking sites for STAT proteins (24, 25). STAT proteins are transcription factors and hence contain DNA-binding domains (with the exception of STAT2, which apparently can only function in a complex with STAT1). STAT proteins also contain src homology-2 (SH2) regions (19), which are modular noncatalytic domains of about 100 amino acids that are found in various cytoplasmic signaling proteins. SH2 domains recognize phosphotyrosine motifs, with specificity dictated by the primary sequence immediately COOH-terminal from the phospho-Tyr (26). The separate docking sites for the binding domains of SH2 domains from different signaling molecules have been mapped on many receptors and cytoplasmic signaling proteins.

Type I IFNs activate STAT1 and STAT2 by inducing their phosphorylation on discrete tyrosine residues. These STATs dimerize, complex with a 48-kDa DNA-binding protein, and then move into the nucleus, recognizing a highly conserved IFN-stimulus response element (ISRE) in the promoter of ISGs to directly activate these genes (27, 28). This conserved 15-base pair element (consensus: AGTTTCNNTTTCNC/T) is present in the promoters of nearly 20 type I IFN-inducible genes examined so far and is both necessary and sufficient for gene induction.

As an added complexity, some type I IFN-inducible genes like IRF-1 do not contain an ISRE and are activated by STAT1 dimers (29). Type I IFNs also activate STAT3, the transcription factor for acute phase response genes. STAT3 recognizes a conserved promoter element found within these genes and is activated by a wide variety of cytokines, suggesting that it may integrate diverse signals into common transcriptional responses (25, 30-32). STAT3 binds directly to the tyrosine-phosphorylated IFNAR1 chain and also undergoes IFN-dependent tyrosine phosphorylation (25). In addition, other members of the STAT family (STAT4, STAT5, and STAT6) have been reported to be activated by type I IFNs in a cell type–restricted manner (33, 34). Although much is known about the role of STAT1-STAT2 dimers in ISG transcriptional activation, the physiological role of other STAT protein complexes in IFN-induced gene expression is not known.

For type II IFNs, a variety of response elements have been described for genes regulated by IFNg. Most notable is the IFNg-activated sequence (GAS, consensus: TTNCNNNAA), which is found in IFNg-induced genes such as the genes for guanylate binding protein, interferon response factor (IRF)-1, and the Fcg receptor I. IFNg induces the oligomerization of the IFNGR1 and IFNGR2 chains of its cognate receptor and the activation of JAK1 and JAK2 kinases (35). The cytoplasmic tail of the IFNGR1 chain undergoes tyrosine phosphorylation and hence provides a docking site for STAT1. Subsequently, STAT1 also undergoes phosphorylation, forms homodimers, translocates to the nucleus, and binds to the GAS element, resulting in the transcriptional activation of IFNg-induced genes. As is the case for type I IFNs, IFNg also activates several members of the STAT family, but the physiological relevance of this remains to be established.

Besides STATs, a number of other *trans*-acting factors (such as IFN-regulatory factors 1 and 2, IFN consensus sequence-binding protein, etc.) also appear to regulate IFN-inducible gene expression. For example, type I IFNs activate nuclear factor kB (NF-kB) (36). Active DNA-binding forms of NF-kB are dimers of various members of the Rel/NF-kB family of polypeptides (p50, p52, c-Rel, v-Rel, RelA, and RelB). NF-kB normally exists as a dormant complex in the cytoplasm through the binding of inhibitor of kB (IkB) proteins. Viruses, cytokines, and lipopolysaccharides induce inactive NF-kB/IkB complexes to dissociate, allowing NF-kB to enter the nucleus and bind DNA. NF-kB binds to sites in the promoters and enhancers of key cellular genes regulating apoptotic, immune, and inflammatory responses. NF-kB suppresses apoptosis (37-40), and hence activation of NF-kB by IFN protects cells from apoptotic death (36). Blockage of NF-kB nuclear translocation and activation by the introduction of super-repressor forms of IkB enhances apoptotic killing by IFN.

The signal transduction pathway activated by many other cytokines is similar to that of IFNs but involves different combinations of JAKs (there are four: JAK1, JAK2, JAK3, and TYK2) and STAT proteins (there are seven STATs). Thus, the IFN-activated JAK/STAT pathway serves as a paradigm for understanding cytokine signal transduction in general. The critical roles that JAK1, TYK2, STAT1, STAT2, and STAT3 play in type I IFN signaling on the one hand, and that JAK1, JAK2, and STAT1 play in type II IFN signaling on the other hand, have been demonstrated through the use of cell lines with defined individual defects in these signaling components (20, 35, 41). Although the tyrosine phosphorylation of STATs is responsible for transcriptional activation of IFN-stimulated genes, serine phosphorylation events are also critical for optimal IFN-induced transcription and for the biological response to IFN (42-45). A variety of serine kinases have been implicated in IFN signaling, including protein kinase C isoforms, the mitogen-activated protein kinase cascade, phosphatidylinositol 3-kinase, RNA-dependent protein kinase (PKR), and protein kinase B (PKB)/Akt (43, 45-50).

4. IFN-Stimulated Genes and Their Functions

Since there is overlap in the signal transduction pathways activated by all IFNs, there is significant overlap in the genes induced by type I and type II IFNs. However, distinctive expression, as well as significant overlap, of gene transcripts regulated by either type I (a, b) or type II (g) IFNs has been demonstrated by the use of oligonucleotide arrays corresponding to more than 6,800 human genes (51). A short discussion of some of the well-characterized gene products induced by IFNs (there are over 30 different products identified so far) follows (52).

a. Protein Kinase R (PKR) This type I IFN-induced protein kinase requires dsRNA for activity. Activated PKR phosphorylates several key cellular proteins, most notably the eukaryotic initiation factor-2a, resulting in the cessation of polypeptide chain initiation. The major cellular function of PKR appears to be growth control by regulating the rates of cellular and viral protein synthesis.
b. 2′,5′ Oligoadenylate Synthetase (OAS) OAS is a family of type I IFN-induced enzymes that require dsRNA as a cofactor. OAS catalyzes the formation 2′-5′ oligoadenylates and thereby activates RNase L, which cleaves viral and cellular RNAs.
c. Mx Proteins Mx proteins are type I IFN-inducible proteins that are involved in the inhibition of myxovirus (such as influenza virus) replication in mice by a poorly defined pathway. Mx genes and proteins have been identified in other species, including humans, but their antiviral activity is broader than that of murine Mx.
d. Indoleamine 2,3-Dioxygenase (IDO) IDO is a type I and type II IFN-inducible intracellular enzyme that degrades tryptophan to kynurenine and plays a role in the inhibition of the growth of intracellular parasites such as *Toxoplasma gondii*.
e. IFN-Regulatory Factor-1 (IRF-1) IRF-1 is a type I and type II IFN-inducible transcription factor that binds to a DNA element found in the IFNb promoter. IRF-1 appears to play a key regulatory role in growth control and tumorigenesis.

f. Class I Histocompatibility Antigens Class I antigens are induced by both type I and type II IFNs and are broadly expressed on almost all cell types. Class I antigens play critical roles in antigen recognition by cytotoxic T cells (CD8+).

g. Class II Histocompatibility Antigens Class II antigens are induced by IFNg and have a restricted tissue distribution (present on B cells, macrophages, and activated T cells). These antigens participate in antigen recognition by helper T cells (CD4+).

5. Conclusion

This article has focused on the present understanding of the highly complex IFN system. IFNs were the first cytokines to be discovered (over 40 years ago) and characterized. Rapid advances have been made in the last decade on the structure and regulation of IFN genes, the characterization and cloning of the components of the multisubunit IFN receptors, and the signal transduction pathways by which IFNs exert their effects. However, many gaps remain in our knowledge. Future work will undoubtedly refine our understanding of this complex cytokine system.

6. Literature Cited

An apology is made to colleagues whose work was not cited due to space restrictions.

Bibliography

1. U. Muller et al., Science **264**, 1918–1921 (1994).
2. C.M. Owczarek et al., J. Biol. Chem. **272**, 23865–23870 (1997).
3. C. Vanden Broecke and L.M. Pfeffer, J. Interferon Res. **8**, 803–811 (1988).
4. L.C. Platanias, L.M. Pfeffer, R. Cruciani, and O.R. Colamonici, J. Immunol. **150**, 3382–3388 (1993).
5. G. Uze, G. Lutfalla, and I. Gresser, Cell **60**, 225–234 (1990).
6. P. Domanski et al., J. Biol. Chem. **270**, 21606–21611 (1995).
7. G. Lutfalla et al., EMBO J. **14**, 5100–5108 (1995).
8. D. Novick, B. Cohen, and M. Rubinstein, Cell **77**, 391–400 (1994).
9. O.R. Colamonici et al., J. Biol. Chem. **269**, 9598–9602 (1994).
10. S. Hemmi et al., Cell **76**, 803–810 (1994).
11. M. Aguet, Z. Dembic, and G. Merlin, Cell **55**, 273–280 (1988).
12. J. Soh et al., Cell **76**, 793–802 (1994).
13. J.F. Bazan, Proc. Natl. Acad. Sci. U.S.A. **87**, 6934–6938 (1990).
14. A.C. Larner, A. Chaudhuri, and J.E. Darnell Jr., J. Biol. Chem. **261**, 453–459 (1986).
15. A.C. Larner et al., Proc. Natl. Acad. Sci. U.S.A. **81**, 6733–6737 (1984).
16. M. Muller et al., Nature **366**, 129–135 (1993).
17. L. Velazquez, M. Fellous, G.R. Stark, and S. Pelligrini, Cell **70**, 313–322 (1992).
18. C. Schindler, K. Shuai, V.R. Prezioso, and J.E. Darnell Jr., Science **257**, 809–813 (1992).
19. X.Y. Fu, Cell **70**, 323–335 (1992).
20. J.N. Ihle et al., TIBS **19**, 222–229 (1994).
21. O.R. Colamonici et al., J. Biol. Chem. **269**, 3518–3522 (1994).
22. D. Kaplan et al., J. Biol. Chem. **271**, 9–12 (1996).
23. M. Sakatsume et al., J. Biol. Chem. **270**, 17528–17534 (1995).
24. A.C. Greenlund, M.A. Farrar, B.L. Viviano, and R.D. Schreiber, EMBO J. **13**, 1591–1600 (1994).

25. C.H. Yang et al., J. Biol. Chem. **271**, 8057–8061 (1996).
26. T. Pawson and J. Schlessinger, Curr. Biol. **3**, 434–442 (1993).
27. R.L. Friedman and G.R. Stark, Nature **314**, 637–639 (1985).
28. N.C. Reich et al., Proc. Natl. Acad. Sci. U.S.A. **84**, 6394–6398 (1987).
29. R. Pine, A. Canova, and C. Schindler, EMBO J. **13**, 158–167 (1994).
30. G.S. Campbell et al., J. Biol. Chem. **270**, 3974–3979 (1995).
31. T. Boulton et al., Proc. Natl. Acad. Sci. U.S.A. **92**, 6915–6919 (1995).
32. Z. Zhong, Z. Wen, and J.E. Darnell Jr., Science **264**, 95–98 (1994).
33. E. Fasler-Kan et al., Eur. J. Biochem. **254**, 514–519 (1998).
34. J.D. Farrar et al., J. Biol. Chem. **275**, 2693–2697 (2000).
35. J.E. Darnell Jr., I.M. Kerr, and G.R. Stark, Science **264**, 1415–1421 (1994).
36. C.H. Yang et al., Proc. Natl. Acad. Sci. U.S.A. **97**, 13631–13636 (2000).
37. A.A. Beg et al., Nature **376**, 167–170 (1995).
38. A.A. Beg and D. Baltimore, Science **274**, 782–784 (1996).
39. D.J. Van Antwerp et al., Science **274**, 787–789 (1996).
40. C.Y. Wang, M.W. Mayo, and A.S. Baldwin Jr., Science **274**, 784–787 (1996).
41. C.H. Yang, A. Murti, and L.M. Pfeffer, Proc. Natl. Acad. Sci. U.S.A. **95**, 5568–5572 (1998).
42. L.M. Pfeffer et al., Proc. Natl. Acad. Sci. U.S.A. **88**, 7988–7992 (1991).
43. N.C. Reich and L.M. Pfeffer, Proc. Natl. Acad. Sci. U.S.A. **87**, 8761–8765 (1990).
44. H. Akai and A.C. Larner, J. Biol. Chem. **264**, 3252–3255 (1989).
45. C.R. Faltynek et al., J. Biol. Chem. **264**, 14305–14311 (1989).
46. L.M. Pfeffer, B. Strulovici, and A.R. Saltiel, Proc. Natl. Acad. Sci. U.S.A. **87**, 6537–6541 (1990).
47. M. David et al., Science **269**, 1721–1723 (1995).
48. S. Uddin et al., J. Immunol. **158**, 2390–2397 (1997).
49. L.M. Pfeffer et al., Science **276**, 1418–1420 (1997).
50. C.H. Yang et al., J. Biol. Chem. **276**, 13756–13761 (2001).
51. S.D. Der, A. Zhou, B.R. Williams, and R.H. Silverman, Proc. Natl. Acad. Sci. U.S.A. **95**, 15623–15628 (1998).
52. D.H. Kalvakolanu and E.C. Borden, Cancer Invest. **14**, 25–53 (1996).

Additional Reading

53. Pfeffer L.M., *Mechanisms of Interferon Action*, CRC Press, Boca Raton, Fla., 1987.
54. Pestka S., Langer J.A., Zoon K.C., and Samuel C.E., Rev. Biochem. **56**, 727–777 (1987).
55. Darnell J.E. Jr., Kerr I.M., and Stark G.R., Science **264**, 1415–1421 (1994).
56. Ihle J.N. et al., TIBS **19**, 222–229 (1994).
57. Kalvakolanu D.H. and Borden E.C., Cancer Invest. **14**, 25–53 (1996).
58. Leaman D.W., Prog. Mol. Subcell. Biol. **20**, 101–42 (1998).
59. Sen G.C., Semin. Cancer Biol. **10**, 93–101 (2000).

Interleukin-1 Motif

The interleukin-1 motif is a common protein motif found in protein structures. It is present in those of interleukin-1, fibroblast growth factors, and Kunitz-type trypsin inhibitors. The motif is characterized by an unusual pseudo-threefold symmetry. The secondary structure of the interleukin-1 motif has 12 b-strands that form six **hairpins**. Three of the hairpins form a six-stranded **antiparallel b-barrel** with a **hydrophobic** core; the other three form a hairpin triplet structure that caps the barrel (Fig. 1). There is little sequence identity between proteins adopting this three-dimensional structure, apart from a preference for large hydrophobic residues in those regions of the sequence that form the core.

Figure 1. Schematic representation of the backbone structure of human interleukin-1b (1) showing the characteristic fold. Strands are shown as arrows, and connecting loops are in yellow. The three roughly equivalent repeating b-structural uni shown in different colors (red, green, and blue) to highlight their similarity. Two orthogonal orientations are shown. (**Le** The six-stranded b-barrel forms the lower half of the structure and is capped by the triangular array of b-hairpins. (**Right** view is shown looking down the axis of the triangular array and b-barrel showing the pseudo-threefold symmetry of the structure. This figure was generated using Molscript (2) and Raster3D (3, 4). See color insert.

The interleukin-1 motif is sometimes called a b-trefoil, because it can be dissected into three equivalent Y-shaped (or trefoil) b-structural units. However, the b-trefoil terminology should not be confused with the "trefoil peptide domain" that represents a very different structural motif of gastrointestinal protective peptides. Furthermore, it should be noted that the known structures of all other interleukins (apart from interleukin-1) are **four-helix bundles**.

[See also Beta-Sheet and Antiparallel Beta-Barrel Motifs.]

Bibliography

1. J. P. Priestle, H.-P. Schar, and M. G. Grutter (1989) Proc. Natl. Acad. Sci. USA **86**, 9667–9671.
2. P. J. Kraulis (1991) J. Appl. Crystall. **24**, 946–950.
3. E. A. Merritt and M. E. P. Murphy (1994) Acta Crystallogr. **D50**, 869–873.
4. D. J. Bacon and W. F. Anderson (1988) J. Mol. Graphics **6**, 219–222.

Suggestions for Further Reading

5. M. B. Swindells and J. M. Thornton (1993) A study of structural determinants in the interleukin-1 fold. Protein Eng. **6**, 711–715.
6. A. G. Murzin, A. M. Lesk, and C. Chothia (1992) -Trefoil fold: patterns of structure and sequence in the Kunitz inhibitors, interleukins-1 and -1 , and fibroblast growth factors. J. Mol. Biol. **223**, 531–543.

Interleukins

Multicellular organisms are composed of a few hundred cell types whose survival, growth, differentiation, and effector function in specific tissues or organs need to be exquisitely controlled. This is accomplished mostly by a myriad of secreted regulatory proteins, broadly classified as cytokines (1), that are secreted locally and modulate the cell physiology of each tissue. Cytokines embrace a wide variety of regulatory proteins that include growth factors, colony-stimulating factors, interleukins, lymphokines, monokines, and interferons . Typically, the molecular masses of cytokines range from a few thousand to a few tens of thousands. Cytokines, in contrast to hormones, are synthesized locally in a transient manner, often by a variety of nonspecialized cells, and function locally at their sites of production. In general, their half-life is short. Classical hormones (eg, insulin), on the other hand, are produced by specialized cells within particular organs, are disseminated throughout the body via the circulatory system, and act at a distance from their sites of production.

The interleukins constitute a subset of cytokines that are produced by and regulate cells involved in immune defense mechanisms. The generic term interleukin (IL) and a corresponding numbering system of nomenclature were introduced in 1979 (2) to reflect that these regulatory proteins are communicating signals for leukocytes, and not just lymphocytes. However, this system has not been completely successful, because now it has been shown that some interleukins may be produced by nonleukocytes and act on other cell types. At present, new leukocyte regulatory proteins are always assigned IL numbers upon establishing a gene sequence. IL-18 is the most recent.

1. General Properties of Interleukins

Table 1 lists the major biological actions of the interleukins. These proteins, which have been characterized most thoroughly in the human and mouse systems, are noted for their pleiotropy and redundant biological activity. The receptors for many of the interleukins, such as IL- 1, -2, -3, -5, and -6, have been well characterized. Typically, they consist of multiple protein subunits. Shared signalling receptor subunits are seen for a number of cytokines, for example, IL-3/IL-5/granulocyte-macrophage colony stimulating factor and also IL-2/IL-4/IL-7/IL-9/IL-15 (see Fig. 1.). To illustrate this further, Fig. 1 shows the structure of the IL-6 receptor complex as a paradigm for the interleukins. The biological activity of IL-6 is exerted upon binding with low affinity to its cognate receptor (IL-6 receptor or alpha-subunit) located on the surface of its target cells. Then, the low-affinity IL-6/IL-6 receptor complex binds with high affinity to the beta-subunit of the receptor complex, the **signal-transducing** molecule gp130, to exert the biological activities of this interleukin. The subunit gp130 is also shared by IL-11 and even other cytokines (eg, ciliary neurotrophic factor, leukemia inhibitory factor, oncostatin M, and cardiotropin-1) which, in part, explains the overlapping activities of these cytokines at the molecular level.

Table 1. Biological Actions of the Interleukins

Interleukin	Action	References
IL-1a/b	Stimulates thymocyte proliferation; acute phaseresponse	5, 6
IL-2	Supports proliferation and activation of T lymphocytes	7
IL-3	Stimulates hematopoiesis; production of cells in all myeloid lineages	8
IL-4	Stimulates proliferation of B lymphocytes	9
IL-5	Activation and differentiation of eosinophils; accessory factor neutrophils	10, 11
IL-6	Stimulates hemopoietic progenitor cells, B-lymphoid, and myeloma cells; induction of acute phase protein synthesis in the liver	12, 13
IL-7	Stimulates proliferation of thymocytes, T lymphocytes including cytotoxic T cells, and early B-lymphocyte precursors	14
IL-8	Stimulates chemotaxis by neutrophils and other cell types	15
IL-9	Stimulates growth of T-lymphoid cell lines; activation of mast cells; potentiates prolferative effect of IL-2 on fetal lymphocytes	16
IL-10	Suppresses cytokine production by T lymphocytes	17, 18
IL-11	Hematopoietic growth factor; induces acute phase protein synthesis	19
IL-12	Stimulates cytokine production by natural killer cells and T cells	20
IL-13	Regulates the function of monocytes and B cells; anti-inflammatory action	21
IL-14	Stimulates proliferation of B cells	22
IL-15	Stimulates proliferation of T cells	23
IL-16	Lymphocyte chemoattractant factor; modulates T-cell activation	(24)
IL-17	Stimulates production of proinflammatory and hemopoietic cytokines in epithelial, endothelial, fibroblastic, or stromal cells	25
IL-18	Stimulates proliferation of T cells; induces IFN-g production	26

Figure 1. Structure of the Inteleukin-6 receptor complex as a paradigm for interleukins. IL-, interleukin; R, receptor; CN
leukemia inhibitory factor; OM, oncostatin-M, GM-CSF, granulocyte macrophage-colony stimulating factor; gc, commo

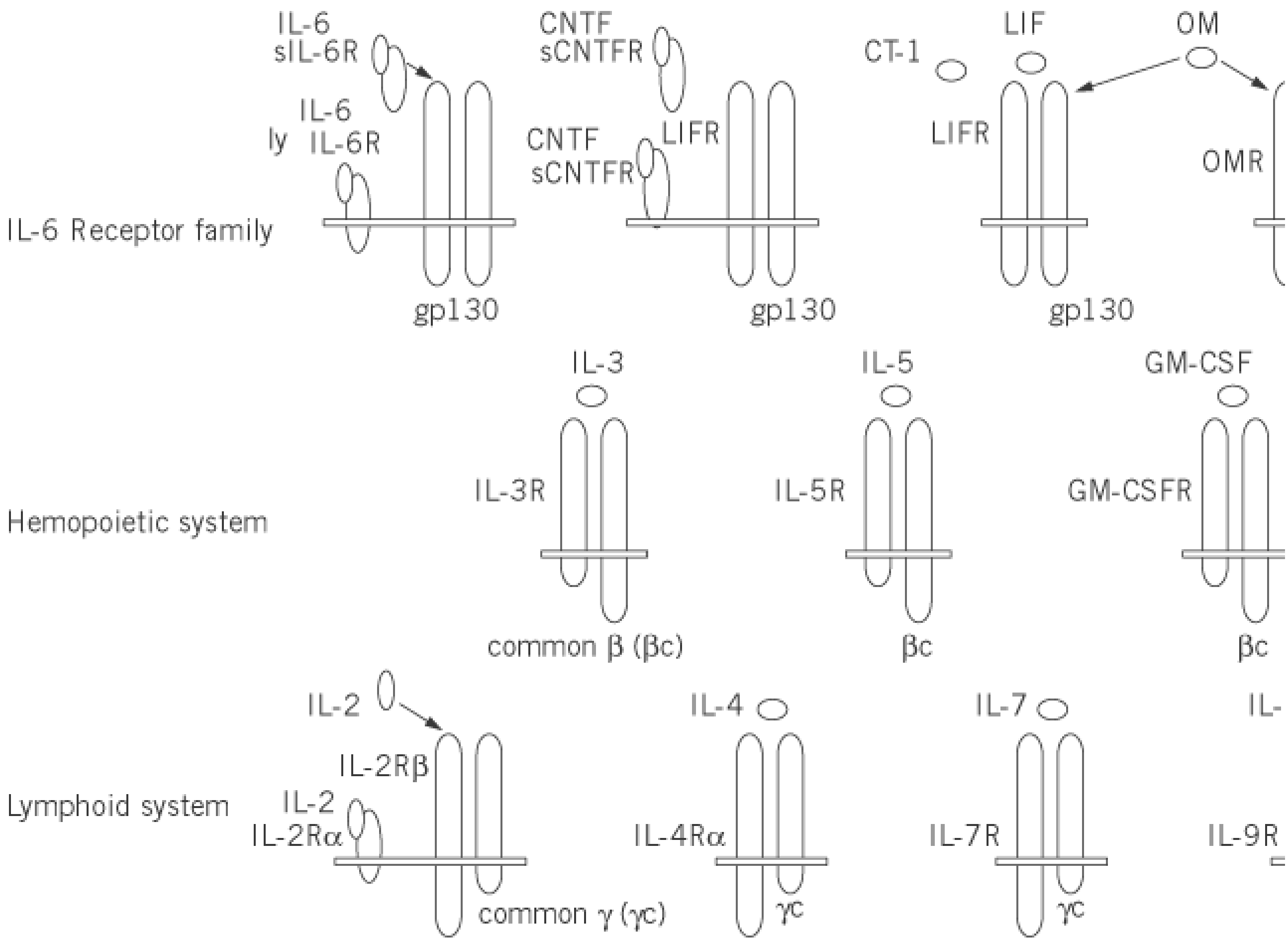

The signal-transduction mechanisms used by the interleukins is presently being unraveled. Although binding of interleukin to its cognate receptor complex stimulates protein **tyrosine kinase** activity, the receptors themselves do not possess any intrinsic tyrosine kinase activity. Rather, nonreceptor tyrosine kinases, such as members of the **src** and **JAK** families, may become associated with the interleukin receptor signaling subunits (typically, binding a ligand to its receptor induces the dimerization of signaling subunits) leading to phosphorylation of tyrosine residues of the signalling subunit. These events lead to the activation of multiple signal-transduction pathways, such as the **STAT**, Ras-**MAP kinase** and phosphatidyl inositol kinase pathways (3, 4).

Recent reviews for all of the interleukins that outline their role in pathogenesis and disease therapy are listed in Table 1. Other features of the interleukins are listed in Table 2. For access to current information regarding the interleukins (as well as other cytokines), the reader is referred to the following internet web sites:

GroCyte home page: (site currently unavailable)

COPE (Cytokines Online Pathfinder Encyclopedia) home page: http://bioinfo.weizmann.ac.il/cgi-bin/cope/cope.pl

Table 2. Properties of Interleukins

	Molecular	Amino	Glycosylation[c]	Cysteines and	Three-

Interleukin[a]	Weight ($\times 10^{-3}$)[b]	Acid Residues	pI	N-	O-	Disulfide Connectivities[d]	Structure[e]	Dimensic Structur
IL-1a (IL1A Human)	18	159	5.3	1N-		1	IL-1R type I	X ray (2I
							IL-1R type II	
IL-1b (IL1B Human)	17.4	153	6.0	1N-		2	IL-1R type I	X ray (1I NMR (6I
							IL-1R type II	
IL-2 (IL2 Human)	15.4	133	7.2		O-	3	IL-2Ra (low affinity)	X ray (1ITB), NMR (1I
						(Cys58–Cys105)	IL-2Rb and gc (high affinity)	
IL-3 (IL3 Human)	15	133	7.3	2N-		2	IL-3Ra	NMR (1J
						(Cys16–Cys84)	IL-3Rb	
IL-4 (IL4 Human)	15	129	9.1	2N-		6	IL-4R	X ray (1HIK), NMR (1RCB)
						(Cys2–Cys126), (Cys23–Cys64), (Cys45–Cys98)		
IL-5 (IL5 Human)	13.1 (26.2 homodimer)	115 (130 homodimer)	7.3	2N-		2 per chain (4 involved in interchain disulphide homodimer)	IL-5Ra IL-3Rb	X ray (1HUL)
						(Cys44–Cys86)		
IL-6 (IL6 Human)	20.8	183	6.4	2N-		4	IL-6Ra (low affinity)	X ray, (1ALU)
						(Cys43–Cys49)	gp130 (high affinity)	NMR (1I
						(Cys72–Cys82)		
IL-7 (IL7 Human)	17.4	152	8.4	3N-		6	IL-7R	Theoretic model
							IL-2Rgc	(1IL7)
							Possibly	

						another	
IL-8 (IL8 Human)	8–8.9	69–77	8.5–9.0		4	IL-8RA	NMR (1I
						IL-8RB	
					(Cys12–Cys39)		
					(Cys14–Cys55)		
IL-9 (IL9 Human)	14.1	126	8.6	4N-	10	IL-9R	
						IL-2Rgc	
IL-10 (IL10 Human)	18.6	160	7.8	1N-	4	IL10R	X ray (1I
						Possibly others	
IL-11 (IL11 Human)	19.1	178	11.3		0	IL-11Ra	
						gp130	
						Possibly one other	
IL-12-p35 subunit (I12AHuman)	22.5	197	6.4	3N-	7	IL12Rb$_2$	
IL-12-p40 subunit (I12BHuman)	34.7	306	5.4	4N-	10	IL12Rb$_1$	
IL-13 (IL13 Human)	12.3	112	8.5	4N-	4	IL13Ra$_1$,a$_2$	Theoretic model
					(Cys28–Cys56)	IL4Ra	(3ITR, 3I
					(Cys44–Cys70)		
IL-14 (IL14 Human)	53	483	8.8	3N-	34		
IL-15 (IL15 Human)	12.8	114	4.4	2N-	4	IL15Ra	
					(Cys54–Cys104)	IL-2Rb & gc	
					(Cys61–Cys107)		
IL-16 (IL16 Human)	13.3	130	4.7		1	CD4	NMR (1I
IL-17 (IL17 Human)	15.1	132	8.3	1N-	6	IL17R	

IL-18 (IL18 Human)	18.3	158	4.8			4	IL18R

[a] SwissProt database accession filename is shown in parenthesis: http://www.expasy.ch/srs5/.

[b] Molecular weight calculated from the amino acid weight of the expressed functional protein.

[c] Includes potential N-glycosylation sites (ie, Asn-X-Ser/Thr motif).

[d] Cysteine comnnectivities determined experimentaly and, in some cases by homology.

[e] Pdb database filename is shown in parenthesis: http://www.pdb.bnl.gov/.

[f] Genbank database accession filename is shown in parenthesis: http://www.expasy.ch/srs5/.

Bibliography

1. S. Cohen, P. E. Bigazzi, and T. Yoshida (1974) Cell. Immunol. **12**, 150–159.
2. L. A. Aarden et al. (1979) J. Immunol. **123**, 2928–2929.
3. P. C. Heinrich et al. (1998) Biochem. J. **334**, 297–314.
4. K. D. Liu, S. L. Gaffen, and M. A. Goldsmith (1998) Curr. Opinion Immunol . **10**, 271–278.
5. F. S. di Giovine and G. W. Duff (1990) Immunol. Today **11**, 13–20.
6. C. A. Dinarello (1997) Cytol. Growth Factor Rev. **8**, 253–265.
7. K. A. Smith (1988) Science **240**, 1169–1176.
8. J. W. Schrader (1998) In *The Cytokine Handbook*, 3 rd ed. (A. Thomson, ed.), Academic Press, San Diego, pp. 105–132.
9. J.-L. Boulay and W. E. Paul (1992) Curr. Opinion Immunol. **4**, 294–298.
10. K. Takatsu (1992) Curr. Opinion Immunol. **4**, 299–306.
11. C. J. Sanderson, H. D. Campbell, and I. G. Young (1988) Immunol. Rev. **102**, 29–50.
12. R. J. Simpson et al. (1997) Protein Sci. **6**, 929–955.
13. T. Kishimoto, S. Akira, M. Narazaki, and T. Taga (1995) Blood **86**, 1243–1254.
14. R. Murray (1996) Curr. Opinion Hematol. **3**, 230–234.
15. M. Baggiolini, B. Dewald, and B. Moser (1994) Adv. Immunol. **55**, 97–179.
16. J.-C. Renauld et al. (1993) Adv. Immunol. **54**, 79–97.
17. R. de Waal Malefyt et al. (1992) Curr. Opinion Immunol. **4**, 314–320.
18. M. Howard and A. O"Garra (1992) Immunol. Today **13**, 198–200.
19. X. Du and D. A Williams (1997) Blood **89**, 3897–3908.
20. G. Trinchieri (1993) Immunol. Today **14**, 335–338.
21. G. Zurawaski (1994) Immunol. Today **15**, 19–26.
22. J. L. Ambrus et al. (1993) Proc. Nat. Acad. Sci. USA **90**, 6330–6334.
23. S. Bulfone-Paus et al. (1997) Nat. Med. **3**, 1124–1128.
24. T. Kishimoto (1996) J. Immunol. Methods **196**, 103–104.
25. F. Fossiez et al. (1996) J. Exp. Med. **183**, 2593–2603.
26. M. T. Gillespie and N.J. Horwood (1998) Cytol. Growth Factor Rev. **9**, 109–116.

Suggestions for Further Reading

27. A. W. Thomson (ed.) (1998) *The Cytokine Handbook* 3rd ed., Academic Press, San Diego.
28. N. A. Nicola (ed.) (1994) *Guidebook to Cytokines and Their Receptors*, Oxford University Press, Oxford.

Intermediate Filaments

Intermediate filaments (IFs), which are about 10 nm in diameter, are so named because they were thought to be intermediate in size between the well-known microtubules and the **actin**-containing microfilaments. They are ubiquitous components of virtually all eukaryotic cells (Fig. 1), being found not only in the **cytoplasm** but also within the cell nucleus. The IF are dynamic structures capable of assembling and disassembling during cell division and of making and breaking interactions with microtubules, microfilaments, and other cellular components.

Figure 1. Electron micrograph of vimentin IF showing long sinuous filaments about 10 nm in diameter. Bar = 100nm. (From Ref. 4, with permission.)

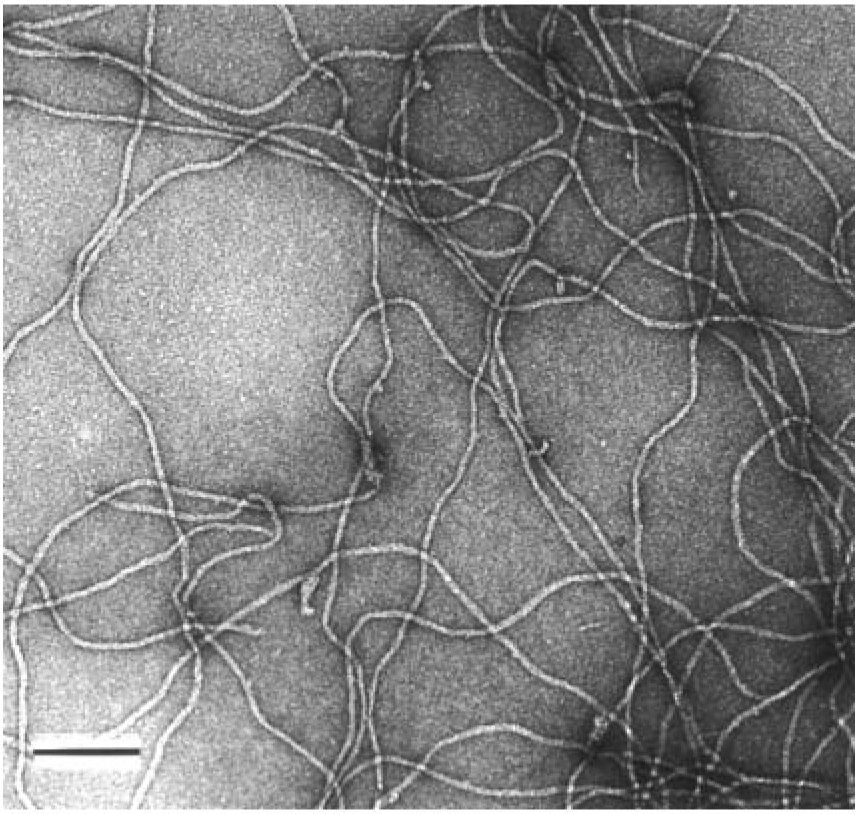

Sequence analysis of IF protein chains has shown common and variable **domains**. In essence, each protein has a largely conserved central, **heptad repeat**-containing domain that separates regions at either end of the chain that are chemically and structurally diverse (Fig. 2). These similarities and differences, together with subsequent data on their **gene** structures, have allowed a simple classification system to be formulated. Type Ia and IIa IF chains occur in hard a- keratin, type Ib and IIb chains occur in epidermal keratin, type III chains occur in **desmin, vimentin**, glial fibrillary acidic protein and peripherin, type IV chains occur in a-internexin and light-, medium- and heavy-neurofilament chains, type V chains occur in the nuclear **lamins**, and type VI chains occur in nestin. The lamin group is unique in their nuclear localization and in the insertion of six additional heptads within the central domain. (Note, however, that invertebrate IF also contain a six-heptad insert in the same place.) One IF family, the cytokeratins, is discussed in detail in that entry. The keratins form obligate heterodimeric structures (type I/type II) in contrast to the homodimeric conformations of type III IF (and type IV and type V IF too). Nonetheless, heterodimers of the form III/IV and III/VI are also found *in vivo* . The heptad-containing regions thus form a coiled-coil rope of predicted length 45.7 nm in hard a-keratin, 46.2 nm in epidermal keratins, and 45.3 nm in vimentin, other type III molecules and in type IV molecules too. Type V IF molecules are about 52 nm in length. The values for epidermal keratin and vimentin are determined from an analysis of the disposition of the residues that are cross-linked (1-3). Electron micrographs of rotary shadowed IFs have been obtained that are in agreement with these values. Scanning transmission electron microscopy (STEM) data indicate that native IFs *in vivo* contain about 32 chains in cross section, although some aggregates with about 16, 24, and 40 chains have also been observed *in vitro*. This has been taken to indicate that the IF may contain an eight-chain protofibrillar substructure. *In vitro* two, three, four, or five such protofibrils may aggregate, but *in vivo* it seems more probable that only the 32-chain (four-protofibril) possibility occurs. The data thus show that the rod domains form the core of the IF and that the *N*- and *C*-terminal domains lie on the surface, where they may interact with other elements of the cell. As noted before, some types of IF in either the cytoplasm or the nucleus are able to assemble and reassemble during certain stages of the cell cycle, most particularly **mitosis**. It now seems clear that **phosphorylation** generally plays a significant role in this process. Almost all IF chains contain phosphorylation sites in their *N*- and *C*-terminal domains. Phosphorylation resulting from the action of a range of possible **kinases** results in the disassembly of preformed IF or prevents formation of IF *in vitro*. Conversely, dephosphorylation allows reassembly to proceed. The complete story is somewhat more complicated than indicated here, but without doubt phosphorylation/dephosphorylation plays a central role in regulating the formation of IF.

Figure 2. Domain structures of intermediate filaments of type III (vimentin and peripherin) and type IV (a-internexin an While the rod domains of all IF proteins, segments 1 (or 1A and 1B) and 2, are **homologous** (though distinct), the *C*-tern proteins display considerable variation. KSP, for example, refers to the multiple Lys–Ser–Pro motifs that are important a glutamic acid-rich regions.(From Ref. 4, with permission.)

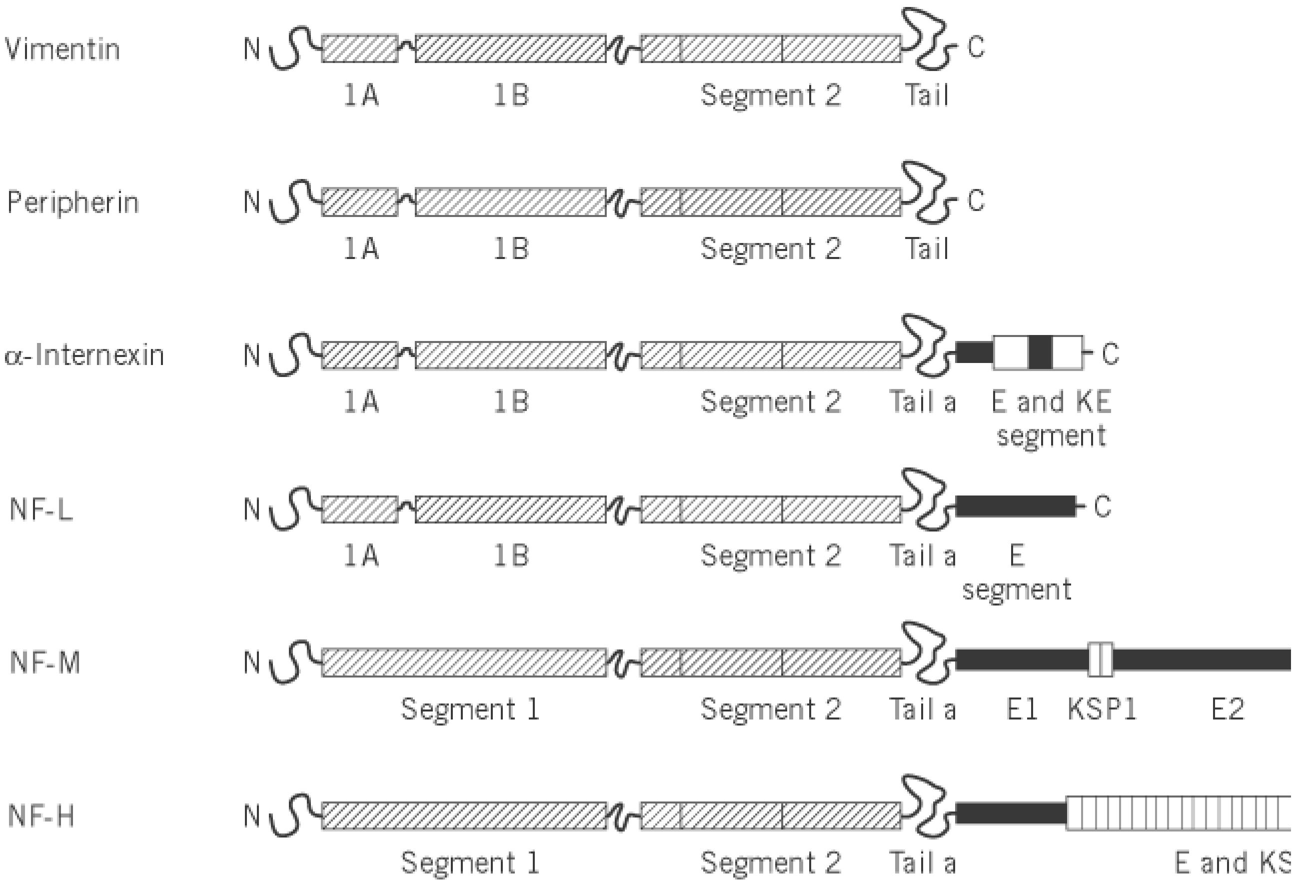

IF function has long been a controversial topic, but real progress has been made in recent years. Consider, for example, just one of the IFs, namely, neurofilaments. The long, highly phosphorylated *C*-terminal domains in the medium and heavy neurofilament chains (NF-M and NF-H) are critically involved in determining the caliber of the axon, as well as its organization and function. The *C*-terminal sequences, when phosphorylated, are believed to control slow axonal transport down the microtubule and to have enhanced flexibility that allow them to modulate the density of the neurofilaments, as well as their separations. Overexpression of NF-L and NF-H produce experimental phenotypes that resemble motor neuron disease. Furthermore, mutations in the 52 –Lys–Ser–Pro–phosphorylation sites in the *C*-terminal domain of NF-H are the proximal cause of some cases of sporadic amyotrophic lateral sclerosis. The *C*-terminal domains of the NF-M and NF-H chains are known to interact with the *C*-terminal ends of the a- and b-tubulin subunits in microtubules, although microtubule-associated proteins such as q (**tau protein**) and MAP2 are also believed to be intimately involved in this phosphorylation-regulated interaction. Terminal domains in other IF proteins are also important in specifying their functions.

Bibliography

1. P. M. Steinert, L. N. Marekov, R. D. B. Fraser, and D. A. D. Parry (1993) Keratin intermediate filament structure: crosslinking studies yield quantitative information on molecular dimensions and mechanism of assembly. J. Mol. Biol. **230**, 436–452.
2. P. M. Steinert, L. N. Marekov, and D. A. D. Parry (1993) Conservation of the structure of keratin intermediate filaments: molecular mechanism by which different keratin molecules integrate into pre-existing keratin intermediate filaments during differentiation. Biochemistry **32**, 10046–10056.
3. P. M. Steinert, L. N. Marekov, and D. A. D. Parry (1993) Diversity of intermediate filament structure: evidence that the alignment of coiled-coil molecules in vimentin is different from that in keratin intermediate filaments. J. Biol. Chem. **268**, 24916–24925.
4. D. A. D. Parry and P. M. Steinert (1990) *Intermediate Filament Structure*, Springer-Verlag, Heidelberg.

Suggestions for Further Reading

5. D. A. D. Parry and P. M. Steinert, 1995 *Intermediate Filament Structure*, Springer-Verlag, Heidelberg.
6. R. D. Goldman and P. M. Steinert (eds.) (1990) *Cellular and Molecular Biology of Intermediate Filaments*, Plenum Press, New York.
7. E. Fuchs and K. Weber (1994) Intermediate filaments: structure, dynamics, function and diseases. Annu. Rev. Biochem. **63**, 345–382.

Intermediate Junction

The intermediate or adherens junction (see Cell Junctions) is a cell–cell adhesive that occurs in a number of different forms. The category includes the zonula adherens of simple epithelial cells (1), forming a subapical ring beneath the tight junctions, spot-like punctae adherentes (2) of small intestinal mucosa, and the ribbon-like fasciae adherentes of the intercalated discs of cardiac muscle

(3). Ultrastructurally, these junctions are characterized by membrane separation of 20 nm and a cytoplasmic plaque or membrane undercoat that is associated with the actin or microfilament cytoskeleton. The principal functions of adherens junctions are (i) cell adhesion, (ii) organization of the basolateral domain/terminal web of epithelia, (iii) signal transduction, and (iv) contractility.

The principal adhesion molecules of adherens junctions are classical cadherins such as E-cadherin and *N* -cadherin (Figs. 1 and 2) (4). These mediate homophilic binding between the apposed plasma membranes of adjacent cells. The cytoplasmic domains of cadherins are linked to the actin cytoskeleton via molecules known as **catenins** (5). b-Catenin is a member of the armadillo family of junctional/signaling molecules (6); a-catenin is an actin-binding protein that binds to E-cadherin via b-catenin (7). a-catinin is related to vinculin, another actin-associated protein located in intermediate junctions (8). Alternatively, g-catenin or plakoglobin may participate in this linkage in place of b-catenin. A large number of other proteins that participate in actin cytoskeletal assembly and function have also been found in association with junctions of the adherens type (see Table 1). The actin filaments extend toward the membrane with the barbed ends outwards after heavy myosin decoration. Several candidates for actin-capping and -binding proteins are present. These include vinculin, ezrin, radixin and moesin, and a-actinin (9). E-cadherin may be found in epithelial cells as a complex with fodrin, adducin, and ankyrin, members of the submembrane cytoskeleton. The latter group of molecules also form complexes with the basolaterally located sodium potassium Na^+/K^+ ATPase. These associations between adhesive components of the adherens junction and components of the membrane cytoskeleton of the basolateral epithelial cell membrane are believed to be important in establishing epithelial cell polarity (10). It is significant that the **tyrosine kinases** c-src and c-yes associate with the junction, since tyrosine **phosphorylation** appears to be an important regulator of the adhesive function of E-cadherin and adherens junctions. In particular, tyrosine phosphorylation of b-catenin had been shown to down-regulate the adhesive function of the junction, resulting in loss of cell adhesion, and to promote invasive behaviour on epithelial cells (11). Tyrosine phosphorylation of another armadillo protein, p120, also appears to regulate junctional adhesion (12). Association of the epidermal growth factor receptor (EGF-R) tyrosine kinase with b-catenin has been reported (13). This emphasizes the role of tyrosine phosphorylation in regulating the function of the junction.

Figure 1. Zonulae adherentes of mouse small intestine stained with a monoclonal antibody to E-cadherin. The zonula form of the junction is evident in transverse sections of cells (arrowheads). In vertical sections, the concentration of stain in the junctions is clearly seen (large arrows), as well as the presence of weaker staining along with the entire lateral borders of the cells (small arrows).(Reproduced from Ref. 23, with permission of Chapman and Hall.)

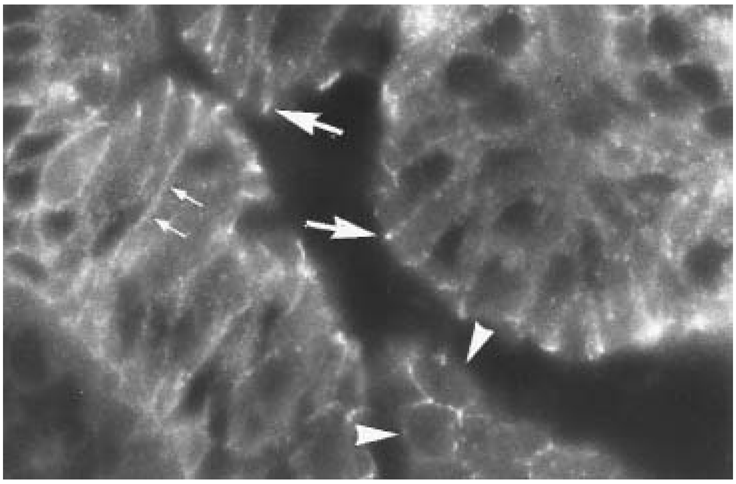

Figure 2. Diagram showing the various cellular roles of the adherens junction protein b-catenin. (1) b-Catenin associates with the cytoplasmic domain of the adhesion molecule, E-cadherin where its function is to provide a regulatory link, via a-catenin, to the actin cytoskeleton. This link is essential for the adhesive function of E-cadherin in the intermediate junction. (2) Cytoplasmic b-catenin, when phosphorylated by GSK3b, associates with APC protein and is degraded. (3) Wnt or wingless signaling inhibits GSK3b, allowing unphosphorylated b-catenin to associate with LEF-1 transcription factor to enter the nucleus and regulate gene activity.

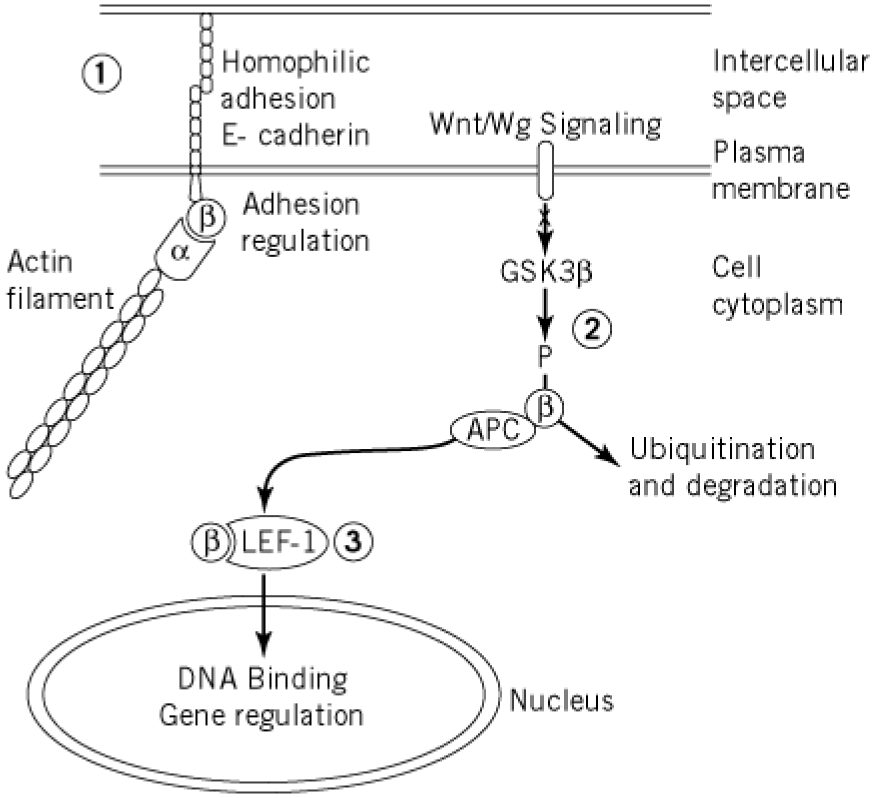

Table 1. Components of the Zonula Adherens Junction in Simple Epithelial Cells[a]

	MW (M_r) ($\times 10^3$)	Function
E-cadherin	120	Calcium-dependent cell adhesion molecule.
b-Catenin	88	Mediates E-cad, binding to cytoskeleton. Signaltransduction.
Plakoglobin (gamma-catenin)	83	Mediates E-cad, binding to cytoskeleton. Signaltransduction.
Armadillo (*Drosophila*)	116	Mediates cad binding to cytoskeleton. Signaltransduction.
p120	120	Signal transduction.
Vinculin	130	Actin-associated protein.
a-Catenin	102	Links E-cad, to cytoskeleton via b-cat.
a-Actinin	100	Actin binding protein.

Ezrin	85	
Radixin	82	Membrane-actin cytoskeleton interaction
Moesin	75	
Fodrin (spectrin)	240 / 220	Membrane skeletal protein: binds ankyrin, actin,band 4.1, adducin.
Ankyrin	200–220	Links membrane to cytoskeleton
Protein 4.1	78	Links spectrin to actin and membrane.
Adducin	103+93	Mediates actin-spectin binding.
Zyxin	82	Actin binding (via a actin).
Tropomyosin	35	Actin binding.
Myosin II	260	Actin binding contractile.
c-src	60	Tyrosine kinase
c-yes	60	Oncogene products

[a] The proteins in this table may be found to be associated with cell–cell adhesive junctions of the zonula adherens type but are not restricted to the zonula adherens.

b-Catenin, like other members of the armadillo family, including plakoglobin or g-catenin and the *Drosophila* armadillo protein itself, have a dual function as adherens junction components and in signal transduction and the regulation of gene activity. These proteins participate in the wingless signaling pathway in *Drosophila* and the Wnt pathway in vertebrates. Thus, both b-catenin and g-catenin have been shown to cause axis duplication when overexpressed in Xenopus embryos (14). Furthermore, each may form a complex with the LEF-1 transcription factor and enter the cell nucleus to regulate gene expression (15). The adenomatous polyposis coli (APC) **tumor suppressor** protein, another member of the armadillo family, is important in regulating the cytoplasmic level of b-catenin. Thus, b-catenin may associate either with E-cadherin at the cell surface or with APC (16). In the latter complex, it is targeted for attachment to ubiquitin and **protein degradation**. This complex forms when b-catenin is phosphorylated by the **serine-threonine kinase** glycogen kinase synthase kinase-3 b (GSK3b). However, dephosphorylation causes dissociation of the b-catenin-APC complex and increases the cytoplasmic level of b-catenin. This promotes complex formation with T-cell-factor/lymphoid enhancer-binding factor 1 (TCF/LEF-1) and entry into the nucleus. Activation of this signaling pathway may occur either by Wnt signaling or through mutation of APC (17). Mutations of the latter are associated with familial adenomatous polyposis coli, where patients form numerous colonic polyps, an important risk factor in colorectal cancer. The equivalent pathway in *Drosophila*, the wingless signaling pathway, is important in development of segment polarity (18). Mutations of E-cadherin and b-catenin are also important in tumor promotion. Inherited mutations in E-cadherin have been shown to predispose affected individuals to carcinomas (19).

The contractile function of the actin microfilament ring associated with adherens junctions is important in aspects of morphogenesis during embryonic development. In neural tube rolling in the amphibian embryo, for example, contraction of apicolateral microfilament rings in the cuboidal epithelial cells of the neural plate results in curvature of the epithelium by narrowing of the apical surface (20, 21). The adhesive components of the adherens junctions to which the microfilament rings attach bind the cells together. It has also been shown that reagents, such as cytochalasin, that affect actin microfilament assembly modulate the permeability of tight junctions (See Tight Junction) in simple epithelia. This may indicate that the zonula adherens plays a role in regulating the function of tight junction (22).

Bibliography

1. M. G. Farquhar and G. E. Palade (1963) J. Cell Biol. **17**, 375–412.
2. D. Drenckhan and H. Franz (1986) J. Cell Biol. **102**, 1843–1852.
3. T. Volk and B. Geiger (1984) EMBO J. **3**, 2249–2260.
4. K. Boller et al. (1985) J. Cell Biol. **100**, 327–332.
5. M. Ozawa et al. (1989) EMBO J. **8**, 1711–1717.
6. P. D. McCrea et al. (1991) Science **254**, 1359–1361.
7. A. Nagafuchi et al. (1991) Cell **65**, 845–857.
8. B. Geiger et al. (1981) J. Cell Biol. **91**, 614–628.
9. S. Tsukita et al. (1993) J. Cell Biol. **123**, 1049–1053.
10. E. Rodriguez-Boulan and W. J. Nelson (1989) Science **245**, 718–725.
11. J. Behrens et al. (1993) J. Cell Biol. **120**, 757–766.
12. M. J. Ratcliffe et al. (1997) J. Biol. Chem. **272**, 31894–31901.
13. H. Hotschuctzky et al. (1996) J. Cell Biol. **127**, 1375–1380.
14. N. Funayama et al. (1995) J. Cell Biol. **128**, 959–968.
15. J. Behrens et al. (1996) Nature **382**, 638–642.
16. B. Rubinfeld et al. (1997) Science **275**, 1790–1792.
17. V. Korinek et al. (1997) Science **275**, 1784–1787.
18. M. Van de Wetering et al. (1997) Cell **88**, 789–799.
19. P. Guilford et al. (1998) Nature **392**, 402–405.
20. P. C. Baker and T. E. Schroeder (1967) Dev. Biol. **15**, 432.
21. P. Karfunkel (1971) Dev. Biol. **25**, 30.
22. J. L. Madara et al. (1986) J. Cell Biol. **102**, 2125–2136.
23. D. R. Garrod and J. E. Collins (1992) "Intercellular Junctions and Cell Adhesion in Epithelial Cells. In" *Epithelial Organization and Development* (T. P. Fleming, ed.), Chapman and Hall, London, pp. 1–52.

Suggestions for Further Reading

24. D. R. Garrod and J. E. Collins (1992) "Intercellular Junctions and Cell Adhesion in Epithelial Cells. In" *Epithelial Organisation and Development* (T. P. Fleming, ed.), Chapman and Hall, London, pp. 1–52.
25. A. Ben-Ze ‘ev (1999) "Focal Adhesion and Adherens Junctions: Their Role in Tumourgenesis". In *Adhesive Interactions of Cells* (D. R. Garrod, M. A. J. Chidgey, and A. J. North, eds.), JAI Press. Greenwich, CT, pp. 135–163.
26. A. I. M. Barth et al. (1997) Cadherins, catenins and APC protein: interplay between cytoskeletal complexes and signalling pathways. Curr. Opin. Cell Biol. **9**, 683–690.

Internal Guide Sequence

In the group I self-splicing introns, the 5′ splice site is determined by the formation of intramolecular base pairing (1). The site is located in the 5′ half of the stem in a stem-loop structure known as P1. A short, **intron**-encoded sequence in the 3′ half of the P1 stem is called the internal guide sequence (or

IGS) and pairs with the end of the 5′ exon (see "Splice Sites"). The name suggests that it binds to both splicing junctions to bring the two exon ends together, but this original idea has been proven to be unnecessary. The functionally similar element in group II introns is the exon-binding site (or EBS). Intron-encoded guide sequences have also been observed at the RNA Editing sites of glutamate receptors by the double-stranded RNA adenosine deaminase.

In connection with the RNA world hypothesis, a resemblance between the **codon-anticodon** interaction and the IGS-exon pairing has been pointed out (2). It has been reported that an **fMet-**oligo RNA in which the RNA sequence is complementary to an artificial IGS created in a group I intron-derived **ribozyme** can be hydrolyzed at the acylation bond, mimicking a prototype of **peptidyl transfer**.

Bibliography

1. T. R. Cech (1993) In *The RNA World* (R. F. Gesteland and J. F. Atkins, eds.), Cold Spring Harbor Laboratory Press, Cold Spring Harbor, NY, pp. 239–269.
2. H. F. Noller (1991) Nature **353**, 302–303.

Internal Ribosome Entry Site (IRES)

Most eukaryotic messenger RNAs have the Cap structure at 5′ termini (see Cap), where 40 S **ribosomal** subunits enter the mRNA with association with the eIF-4F complex (cap-binding protein complex; see Initiation Factor (IF)). The 40S initiation complex then scans the 5′ untranslated region (or 5′UTR) to find the initiation codon (see Scanning Hypothesis). The mRNAs of picornaviruses, represented by poliovirus, however, have no 5′-Cap structure, but contain an internal ribosome entry site (IRES) on the 5′-untranslated region (UTR), which functions as an alternative entry site for the ribosome (1). Upon infection, poliovirus produces a proteinase that cleaves eIF-4G, the largest subunit of eIF-4F, thereby shutting down the Cap-dependent initiation of cellular mRNAs, while activating the viral translation by IRES-dependent initiation. Picornavirus mRNA has a long 5′UTR (600 to 1200 nucleotides), and the IRES corresponds to the 3′ proximal 450-nucleotide region that involves multiple stem-loop structures (Fig. 1). One motif that may act as the actual ribosome binding site is a pyrimidine-rich region of about 20 nucleotides preceding an AUG triplet with a spacer of 20 to 25 nucleotides. In some types of picornavirus, including poliovirus, ribosomes do not initiate translation at this AUG triplet but at the next available AUG. On the other hand, the other picornaviruses, such as encephalomyocarditis virus, initiate translation at the first AUG. The IRES-dependent initiation requires a subset of ordinal initiation factors, as well as specific cellular factors such as La protein and polypyrimidine-tract binding protein. Viruses other than picornavirus, such as hepatitis C virus (HCV) and plant RNA viruses, also contain IRES. In addition, at least two cellular mRNAs, **antennapedia** mRNA of *Drosophila* and BiP mRNA of mammals, show IRES activities. No sequence resemblance has been noted among the IRES of picornavirus, HCV, and the cellular mRNAs.

Figure 1. Schematic representation of the predicted stem-loop structure of the poliovirus IRES (1).

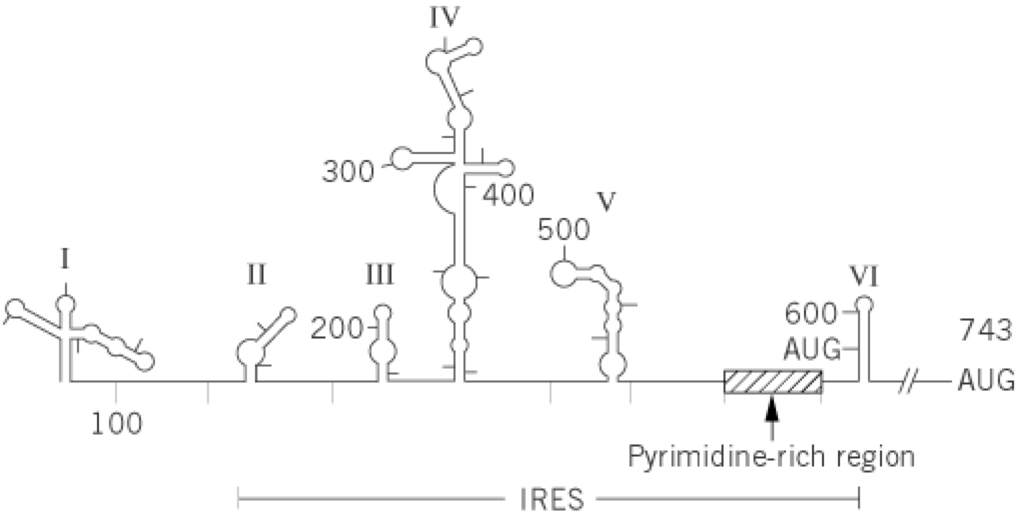

Bibliography

1. E. Ehrenfeld (1996) In *Translational Control* (J. W. B. Hershey, M. B. Mathews, and N. Sonenberg, eds.), Cold Spring Harbor Laboratory Press, Cold Spring Harbor, NY, pp. 549–573.

Suggestion for Further Reading

2. R. J. Jackson (1996) In *Translational Control* (J. W. B. Hershey, M. B. Mathews and N. Sonenberg, eds.), Cold Spring Harbor Laboratory Press, Cold Spring Harbor, NY, pp. 71–112.

Interspersed DNA Elements

To understand the architecture of the human genome, we need a complete definition of all *interspersed DNA elements*, the families of sequences repeated throughout the genome, as these make up the majority of human DNA. These repeat sequences are arbitrarily classified into CpG Islands, Sines (short interspersed DNA sequence elements comprising Alu sequences in primates), Lines (long interspersed DNA sequence elements), **minisatellites** and **microsatellites**. All these entities are repeated many times in the genome, and are arbitrarily defined as about 10^4 copies or more per **diploid** genome.

Introns, Exons

Introns are sections of primary RNA **transcripts** that are removed as part of the maturation of functional **messenger** RNA or, rarely, of ribosomal RNA. They are also known as *intervening sequences*. The sections between the introns that are retained in the mature RNA product are called *exons*. Introns occur very widely in the nuclear genes of **eukaryotes**, and nuclear introns command the most attention. But there are two other, rather different kinds of intron, called **Group I** and Group II, that have been found in eukaryotic **organellar** genomes and occasionally in **bacteria** and **bacteriophage**. Introns of another kind have been found in a few species of **Archaebacteria** (1), but these are not covered in this article.

1. Eukaryotic Nuclear Introns

1.1. Occurrence and Detection

Introns are found in some **genes** of all eukaryotes thus far studied, but their frequency and average size increase enormously as genomes become larger and organisms more complex. In the budding **yeast** *Saccharomyces cerevisiae*, most genes do not have introns, and, where they occur, the introns are seldom more than 100 bp long. In filamentous **fungi**, such as *Neurospora* and *Aspergillus*, most genes that have been sequenced so far have introns but seldom more than two or three and usually in the size range 50 to 100 bp. The nematode worm *Caenorhabditis elegans* has some much longer introns, but the transcribed sequences still consist mostly of exons. In the fruit fly *Drosophila* many genes are interrupted by long introns, sometimes kilobases long. In mammals most genes are often expanded 100-fold or more by numerous introns that far exceed the exons in average length, though their coding sequences may not amount to more than a few kilobases. Some examples of exon/intron proportions and arrangements from a number of representative eukaryotes are presented in the article on Gene Structure.

Introns are defined by comparisons between the sequences, or restriction maps of chromosomal (genomic) DNA and complementary DNA (cDNA) obtained by **reverse transcription** of processed mRNA. cDNA is also used as a probe to search for homology with ordered genomic restriction fragments. Some of the first discovered introns were made visible by electron microscopy of artificially constructed genomic DNA/cDNA or genomic DNA/mRNA heteroduplexes. The introns appeared as unpaired single-stranded loops (Fig. 1). Shorter introns are identified, at least tentatively, as segments interrupting **open reading frames** with intron consensus sequences at their ends (Table 1).

Figure 1. Two ways of detecting introns (**a**) Comparison of restriction-site maps of the rabbit b-globin gene and cDNA, reverse transcribed from the b-globin messenger RNA (2). A second, smaller intron was not revealed by this analysis and is not shown in the diagram. (**b**) The appearance of a heteroduplex formed between chicken ovalbumin gene DNA and its mRNA, drawn from the electron micrograph of Dugaiczyk *et al.* (3).

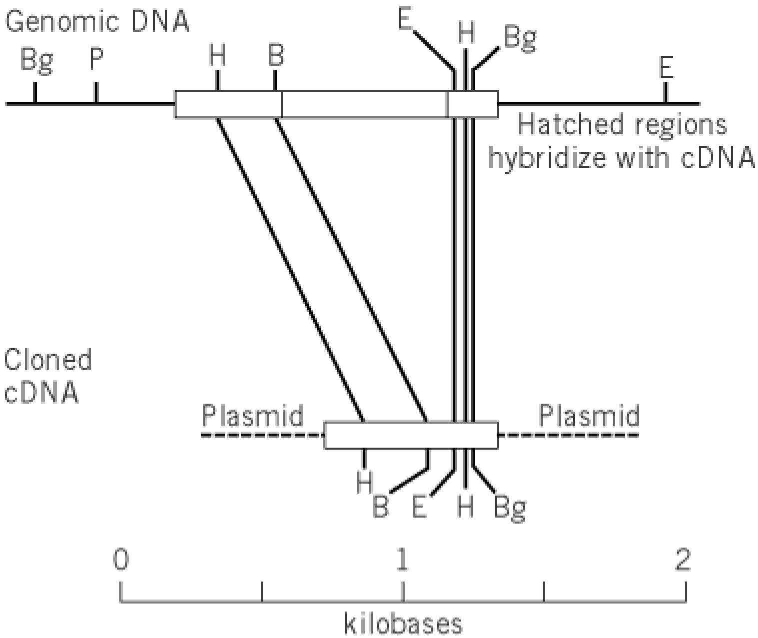

(a)

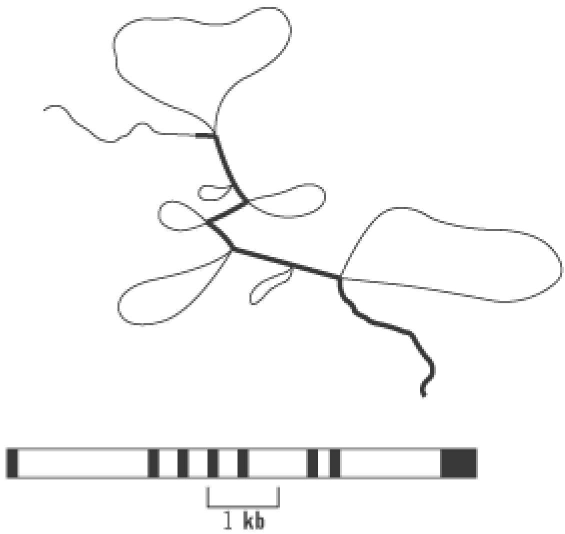

(b)

Table 1. Intron Consensus Sequences in Various Organisms [a], [b]

Organism	5′ Splice	Branch Point	3′ Splice
Vertebrates	AG/*GU*AAGU	UNCUR*A*C	(Y-rich)NC*AG*/G
Saccharomyces	AG/*GU*AUGU	*UACUAAC*	(Y-rich)*YAG*/
Plants	AG/*GU*AAGU	UA-rich	(U-rich)UGC*AG*/GU

[a] From Ref. 4.

[b] Key: Y = pyrimidine; R = purine; N = any nucleotide. underlined residues are invariant, or nearly so. The slash (/) divides exon from intron.

Although the internal sequences of nuclear introns bear no relationship to each other (or, indeed, to anything else), they show some consensus at or near to their 5′ and 3′ (i.e., upstream and downstream) termini, sometimes called the donor and receptor sites (Table 1). At the upstream end, the consensus is 5′-GUAUGU for *Saccharomyces* and 5′-GUPuAGU in mammalian introns. The GU is nearly universal, and the following bases are somewhat variable (U in the messenger RNA corresponds to T in the DNA coding strand). Introns are terminated virtually universally at their downstream (3′) ends by YAG (Y for pyrimidine), usually immediately preceded by a pyrimidine-rich sequence. Some 15 to 40 bp upstream of the 3′ AG is a sequence called (for reasons that will emerge) the *branch point*, which in yeast has the invariant sequence 5′-UACUAACA, reduced in other fungi to CURAC, and represented in mammals by the barely recognizable YXYYRAY (X standing for any base and R for either purine). The conserved A is most important. The somewhat different consensus sequences in different groups of organisms are shown in Table 1).

Intron excision occurs in two steps. First, the upstream guanosine 5′-phosphate is cleaved from the upstream exon and condensed with the 2′-hydroxyl group of the branch-point adenosine to form a loop, often called a **"lariat" structure**, still joined to the downstream exon (see Fig. 4 later). Then the freed 3′-hydroxyl of the upstream exon attacks the phosphate diester link between the lariat and the downstream exon to free the lariat and join the two exons. This sequence of interactions is catalyzed by an array of five **small nuclear ribonucleoprotein** complexes (snRNPs), U1, U2, U4, U5, and U6, each of which contains a short unique RNA molecule and a number of proteins, some of which, the Sm proteins, are RNA-binding. Collectively the U complexes form a supercomplex, called the spliceosome.

To a considerable extent, the process of splicing can be explained in terms of **Watson–Crick base pairing** between RNA sequences, shown by suppression of the effects of **mutation** in splicing sequences by compensating changes in U-RNAs or by chemical cross-linking of the paired sequences. Just as with **codon**–anticodon pairings in messenger RNA translation, most of the RNA–RNA pairings must be too weak to hold by themselves, and presumably they act by guiding much stronger protein–RNA and protein–protein interactions, about which much remains to be learned. The course of events has been most thoroughly worked out for *Saccharomyces*. With only minor variations, it is the same in mammals and presumably in eukaryotes generally. (see **Splicing RNA**).

1.2. Splicing Options

Some intron excision is regulated in all eukaryotes that have introns in tissue or cell-specific ways. Thus, in *Saccharomyces* yeast, which has relatively few introns, the splicing-out of the intron in the *MER1* gene, which functions in meiotic recombination, depends on the protein product of the **meiosis**-specific *MER2* (5). In *Drosophila*, one of the three introns in the transposase gene of the mobile **P-element** is spliced out only in the **germ line**, which explains why the element does not transpose in somatic tissues (6). Sexual development in the fly depends on a splicing cascade. The *Sexless* (*Sxl*) gene product, produced only in females, promotes both the splicing of its own pre-mRNA and that of the *transformer* (*tra*) gene, so that the latter encodes a protein which, acting together with the product of another gene *tra2*, splices the sexless (*sxl*) pre-mRNA to produce mRNA for female development (Fig. 2). The alternative ("default") splicing option is female-determining (8). In mammals that have their abundant introns, the splicing of pre-mRNAs in different ways in different tissues is almost more the rule than the exception. Two other examples of alternative patterns of pre-mRNA splicing are illustrated under Gene Structure and Interallelic Complementation.

Figure 2. Two examples of splicing option control from *Drosophila*. (**a**) The female-specific *Sxl* (*sex-lethal*) protein binds at the 3′ end of intron 1, blocking the otherwise favored male splicing option and diverting splicing action of U2AF to a splice site in exon 2, bypassing a stop codon and allowing formation of functional female-specific mRNA. See text for further explanation. (**b**) *tra-2* and female-specific *tra* proteins bind to a splicing-enhancer region (shown horizontally hatched) in exon 4 of the *dsx* (doublesex) gene to activate splicing at the 3′ end of intron 3, thus preempting the otherwise favored alternative of splicing exon 3 directly to exon 5. The two modes of splicing result in two functional mRNAs, one for males and one for females. There is a polyadenylation signal at the 3′ end of exon 4, thus effectively terminating the female mRNA at this point. Information from Ref. 7.

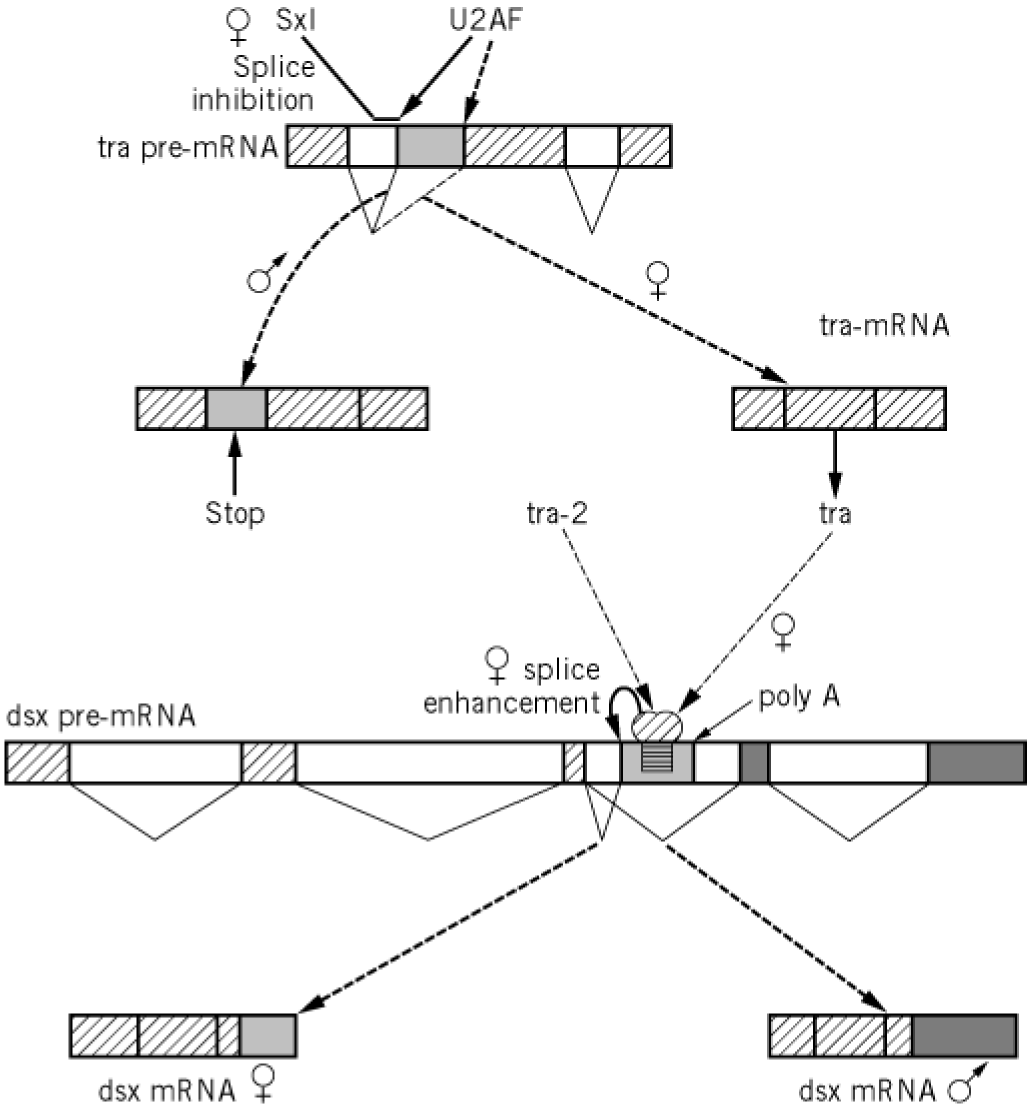

So far as it is understood, selective splicing of introns depends mostly on splicing enhancers, RNA motifs to which proteins bind to facilitate splicing at nearby sites. A family of RNA-binding proteins, the so-called SR proteins, have been especially implicated in enhancer function (7, 9). Characteristically, they have two kinds of domains, one RNA-binding and the other rich in arginine-serine dipeptide sequences (hence the designation SR). The latter, it is thought, are involved in protein–protein binding and recruiting of components of the splicing apparatus.

One of the most thoroughly investigated systems of splicing control by an enhancer is the final step of the *Drosophila* sex-determining splicing cascade, alluded to previously (10) (Fig. 2). The enhancer sequence that determines male-type splicing of Drosophila *dsx* mRNA and interacts with the protein products of *tra* and *tra2* is located in the fourth exon between 300 and 570 base pairs downstream of the splice junction that it controls. It includes six tandemly arranged approximate tandem repeats, each 13 bp, with an 18-bp purine-rich sequence between the fifth and sixth repeats. Both of the repeats and the purine-rich element are necessary for efficient splicing of the preceding intron. *In vitro* protein–RNA binding studies have shown that the *tra2* protein binds to the repeats and the *tra* protein to the purine-rich segment (10). Both are proteins that have SR domains, and their binding to the RNA is reinforced by cooperative interaction with one or more other SR proteins, which would not bind specifically to the enhancer by themselves. It is thought that the whole SR complex so formed binds to splicing factors, perhaps U2 components, and relays them to the 3′ splice site located 300 to 320 bp upstream (Fig. 2). A problem to which evolution has presumably found an answer is that of reconciling the two quite different functions of the *dsx* splice enhancer. On the one hand, it has to provide binding sites for the splice-promoting proteins, and on the other hand, it encodes a part of the amino acid sequence of the female-specific *dsx* protein that has its own special functions.

Purine-rich splice-enhancer sequences are found in other genes, including some from mammals (11). Binding to SR proteins, either site-specific or more general in function, is likely to be a general property of splice enhancers.

A different method of splice-site regulation is exemplified by the first step of the Drosophila sex cascade (12). The *Sxl* protein, which acts in the female on *tra* pre-mRNA to produce the female-specific messenger, is a kind of degenerate SR protein that retains its RNA-binding domain but has lost its SR domains. It binds with high affinity and specificity to the polypyrimidine tract adjacent to the 3′ splice site of the third *tra* intron to the exclusion of a complete SR protein, called U2AF, which is necessary for recruiting the U2 complex, a function that SR-less *Sxl* protein is unable to perform. As a result, the third exon becomes spliced to the fifth instead of the fourth exon ((12); Fig. 2).

In both of the Drosophila examples just reviewed, the splicing control is exercised at the 3′ end of the intron. Other splicing options involve choices among different 5′ splice sites. It is presumed that, here too, the options are controlled by specific RNA-binding proteins, particularly of the SR class, that have either enhancing or inhibitory effects on specific splice sites. A very great deal remains to be discovered in this field.

2. Group I and Group II Introns

These introns are most commonly found within the genes of mitochondria and chloroplasts and more rarely in **bacteria** and **bacteriophages** (Table 2). **Group I introns** are particularly prevalent in mitochondrial DNA of fungi, also accompanied at least in *Saccharomyces* by group II (Fig. 3). Both groups are common in **plastid** DNA of many kinds of photosynthetic eukaryotes. Group I introns are found particularly in transfer RNA genes. With the exceptions shown in the Table 2, they are not found in nuclear genes.

Figure 3. Group I and group II introns in mitochondrial genes of *Saccharomyces cerevisiae*. *COB* and *COX1* encode cytochrome b and subunit 1 of cytochrome oxidase. The L-rDNA transcript is processed to form large ribosomal RNA. Open, stippled, and hatched boxes represent, respectively exons, group I introns, and group II introns. Straight arrows indicate intron open reading frames. Note that several of them start in upstream exons. Curved arrows indicate that the protein products facilitate the splicing of their own introns or, in one case, an intron in another gene. The asterisks indicate high-frequency transfer to intronless alleles. This diagram is a composite. These introns are not all present together in any one yeast strain. Information from Ref. 1.

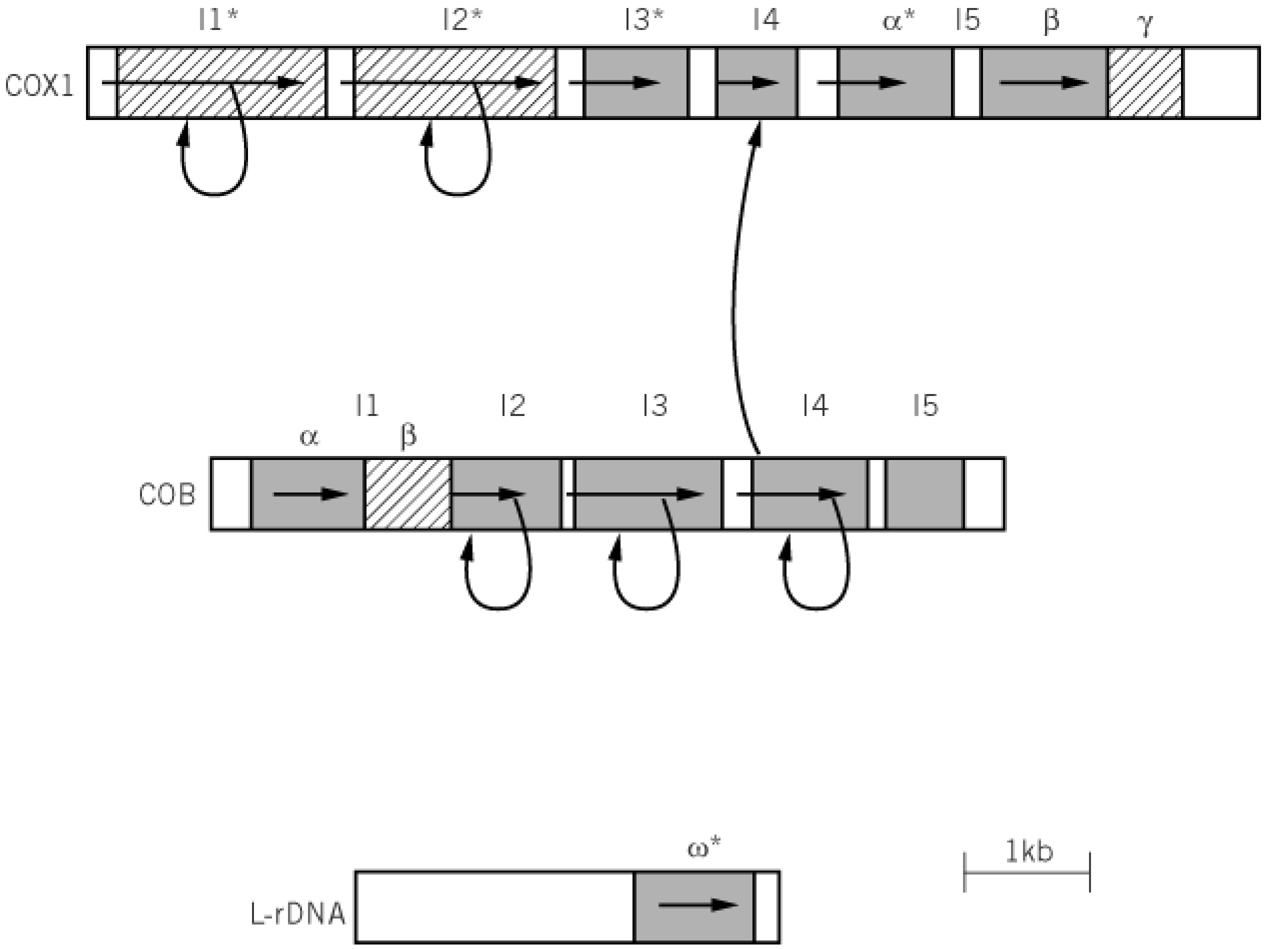

Table 2. Distribution of Group I and Group II Introns[a]

	Group I	Group II
Mitochondrial		
Yeasts	*Saccharomyces*	*Saccharomyces*
	Schizosaccharomyces	
	Klyveromyces	
Sea anemone	*Metridium*	
Filamentous fungi	*Neurospora*	
	Podospora	
	Aspergillus	
Bacteria	*Agrobacterium*	*Calothrix Escherichia*
Blue-green algae	*Anabaena*	
	Cyanophora	
Bacteriophage	T4 (*E. coli*)	
	SPO1 (*Bacillus subtilis*)	

Chloroplast		
Flowering plants	*Nicotiana*	*Nicotiana* (tobacco)
	Zea (corn)	
	Vicia (bean)	
Liverwort	*Marchantia*	*Marchantia*
Algae	*Dictyota* (brown seaweed)	
	Vaucheria	
		Bryopsis (green,filamentous)
	Ochromonas (yellow-greenunicell)	
	Chlamydomonas	*Chlamydomonas* (greenunicells)
	Chlorella	
		Euglena
Nuclear		
Slime mold	*Physarum*	
Ciliate	*Tetrahymena*	

[a] 1, 13, and references therein.

Group I and group II introns differ fundamentally from the common introns of nuclear pre-mRNAs in their requirements for splicing. They have characteristic internal secondary structures that differ between the two groups, in the form of double-stranded stems, stabilized by base-pairings, and single-stranded loops. This internal structure, it is thought, serves the same purpose in aligning the intron ends for splicing as does base pairing with the RNAs of the snRNPs in splicing nuclear introns.

At least some group I and (to a lesser extent) group II introns act as **ribozymes** to catalyze their own splicing *in vitro* without the aid of protein, though mostly under unphysiological conditions, such as high temperature and high magnesium ion and general salt concentration. *In vivo*, their splicing is facilited by proteins, generally called *maturases*, some of which are encoded in open reading frames within the introns themselves (1, 13, 14). This has been shown genetically for some of the *Saccharomyces* introns (Fig. 3), where mutations in the open reading frames result in failure to splice, a deficiency that can be remedied by the same kind of nonmutant introns acting in *trans*. For example, in the *Saccharomyces cerevisiae cob* and *cox1* genes, that respectively encode cytochrome b and subunit 1 of cytochrome oxidase, numerous introns, some group I and some group II, depend mostly for their splicing on intron-encoded proteins, and some require nuclear-encoded proteins, either instead or in addition.

Groups I and II are distinguished from one another in their secondary structures, in the nature of the proteins encoded by their open reading frames (see later), and in the chemistry of their splicing reactions (Fig. 4). In Group I, the phosphodiester linkage at the 3′ end of the upstream exon is attacked by the 3′-hydroxyl of a free guanosine molecule. A trans-esterification reaction leaves the junction cleaved with a free 3′-hydroxyl on the exon side and the guanosine attached to the free 5′ end of the intron. Then, in a second transesterification step, the 3′-hydroxyl of the upstream exon reacts with the phosphodiester bond at the 3′ end of the intron (always a guanylate residue), releasing the intron, sometimes but not always as a circle, and ligating the exons together (Fig. 4). In one case, a group I intron in the fungus *Podospora anserina*, the excised circles reverse-transcribed into DNA, has embarked on a damaging career of its own, replicating freely in the mitochondria and causing senescence (1).

Figure 4. The modes of excision of group I, group II, and nuclear introns compared. Based on Ref. 1 by permission.

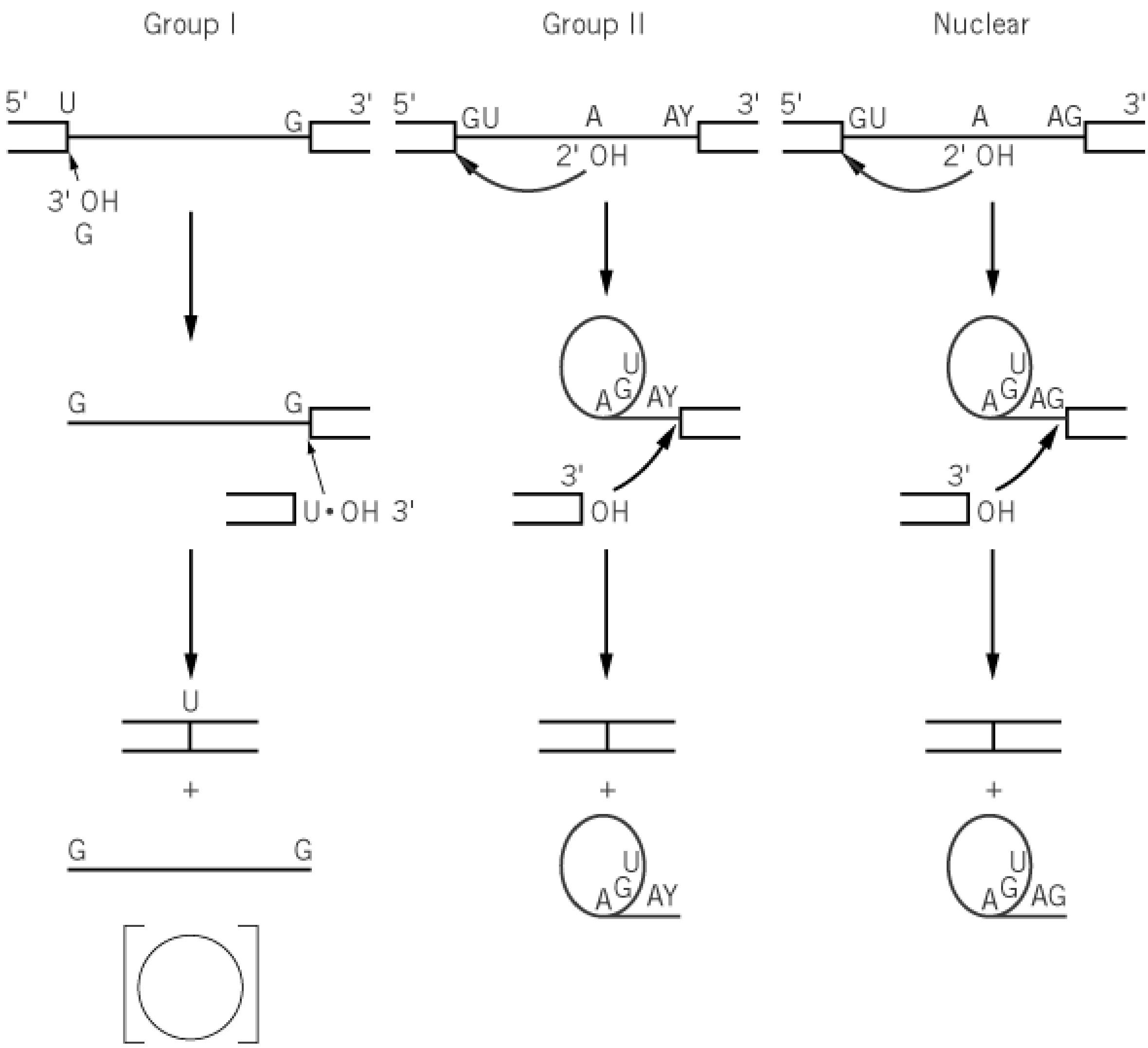

The splicing of group II introns is similar to that of nuclear pre-mRNA introns (Fig. 4), and a lariat intermediate is formed. G is always at the 5′ end of the intron (consensus GUGYG), and generally AY (not AG) is at the 3′ end. A crucial A also serves as a branch-point residue, although the sequence surrounding it, usually composed of U and/or C residues, has little similarity to the corresponding sequences of nuclear introns. The 5′ G interacts with the branch-point A to form the lariat and then, again as in nuclear introns, the free 3′-hydroxyl of the upstream exon attacks the phosphodiester linkage at the 3′ end of the intron to fuse the exons and release the intron as a lariat.

An extraordinary feature of group I introns, found also but less frequently in group II, is their ability to transpose as DNA from one allele to another. The transposition is conservative in the sense that the recipient acquires the intron without the donor losing it. One of the most thoroughly investigated examples involves the group I w-intron in the mitochondrial large rRNA gene of some strains of *Saccharomyces cerevisiae* (14). When a strain possessing the intron (w+) is crossed with one that lacks it (w–) (the mitochondria of the two strains are distinguished by drug resistance or other markers), the progeny emerging from the cross have recombined as well as predominantly parental-type mitochondrial genomes, virtually all now carrying w. And although most of the mitochondrial genetic markers are inherited from either parent with equal probability, two drug-resistance markers, chloramphenicol and **erythromycin** resistance, located within the rRNA gene and hence close to w, are inherited predominantly from the w+ parent. Apparently w is unilaterally transferred from one mitochondrial genome to the other and carries flanking DNA of variable length along with it. The explanation for this conversion (and coconversion) is that w includes an open reading frame that encodes a double-strand **endonuclease** that is specific for a site within the rRNA gene. This enzyme makes a double-strand break in the mitochondrial DNA of the w– parent, which is then enlarged to a gap that is repaired by copying from the w+ parent (1, 14). This explanation bears a strong resemblance to the double-strand break model currently proposed for recombination in meiosis.

The high-frequency transposition of w is strictly homologous, that is to say, it is targeted to a sequence similar to the that from which it came, a process sometimes called “homing.” The same property has been identified in a number of other group I introns (Fig. 3), and the same explanation applies to these, namely, the intron encodes an endonuclease that makes a double-stranded cut at or close to the intron's home site. As indicated before, at least some of the group I-encoded endonucleases also act as maturases to facilitate splicing.

The open reading frames in the approximately 20% of group II introns that possess them encode proteins of quite a different family. Virtually all have a consensus domain, called X, a possible but unproved function of which is maturase activity (15). Many of them also have two other recognizable domains, one characteristic of **reverse transcriptase** and the other **zinc-finger**-like with double-strand endonuclease activity specific for the homing site (16). The transposition of the yeast *COX1* intron, which has been analyzed *in vitro*, occurs by reverse transcription, primed by the 3′ OH-terminated transcribed DNA strand on one side of the double-strand break, followed by ligation of the 3′ end of the single-strand, reverse transcript into the recipient DNA and the repair synthesis of its complementary strand (Fig. 5).

Figure 5. Proposed mechanisms of “homing” transposition of group I (a) and group II (b) introns. Dotted lines are RNA, broken lines new synthesis, and thick segments intron sequence. After Refs. 1 and 14 by permission.

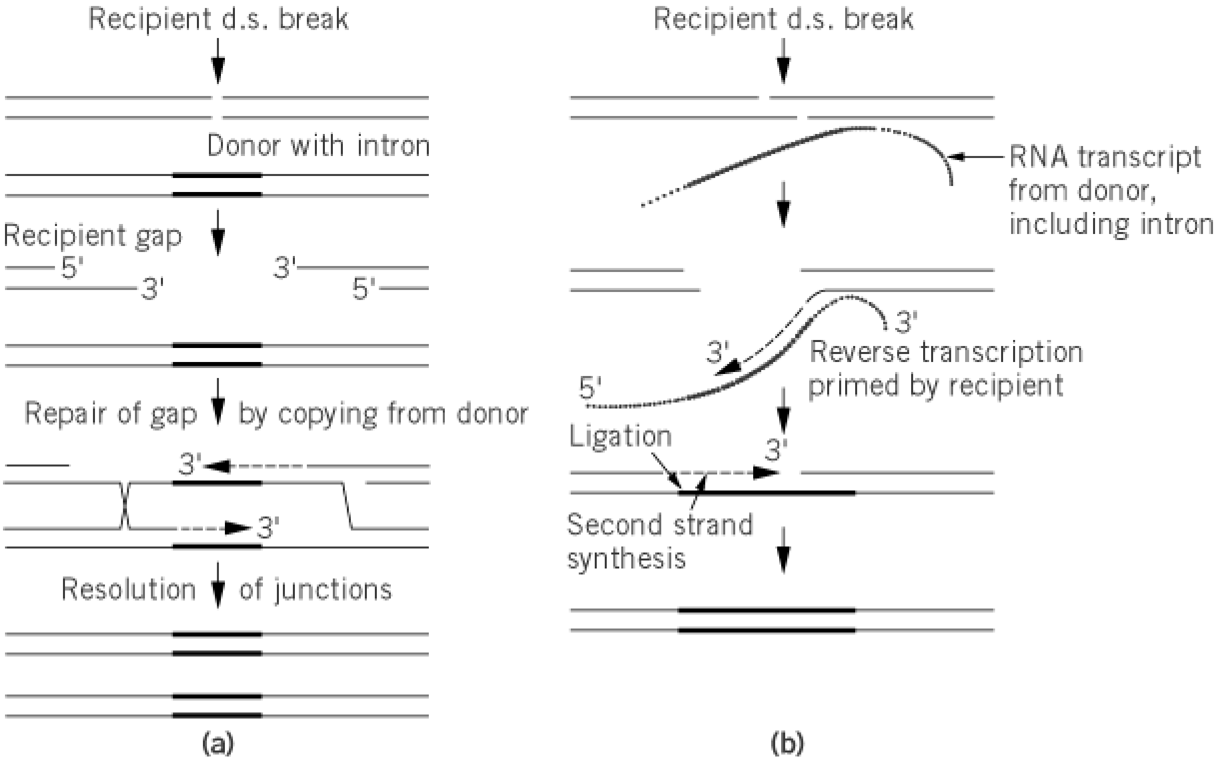

An interesting feature of many of the open reading frames in both class I and class II introns is that, although they are mainly within the intron, they start in the upstream exon (Fig. 3). This mutual adaptation of exon and intron must mean that their association is very ancient and that the intron cannot be a recent invader. This conclusion is borne out by observations of positional conservation of some group I introns over great lengths of evolutionary time. However, their patterns of distribution that have similar kinds of introns present in diverse genes and homologous genes with different sets of introns are hard to explain except on the assumption that both group I and group II introns can move, even if rarely, to new sites. In some instances, such movement has been directly demonstrated. To further complicate the picture, there is evidence that open reading frames within introns can sometimes transpose from one intron to another (17). Again, the most plausible, though unsubstantiated, explanation for such events is that transcripts can be reverse-transcribed and the cDNAs reintegrated into the genome, usually into sequences homologous to those from which they came from but occasionally at nonhomologous, that is, ectopic, sites.

3. Uses for Introns

From the elaborate mechanisms that organisms have evolved to cope with introns, one would suppose that they must confer some benefit. There are several ways in which they can contribute to the function of the organism.

First, introns in nuclear genes give additional flexibility to gene function. Splicing options allow a gene to encode two or more different proteins to serve different functions at different times. Some sequences are in common and others are unique. Some examples were given before and others can be found in the articles on Gene Structure and **Allelic Complementation**. Investigating the control of pre-mRNA splicing is still at an early stage, but it promises to reveal a degree of complexity to rival that existing in control of gene transcription.

Secondly, introns can be involved in controlling transcription. There are fairly numerous examples of downstream enhancers located in introns of genes. One, the *bithorax* enhancer within the *Drosophila Ubx* gene, is mentioned under Gene Structure.

Thirdly, there are several examples, which may become much more numerous as more of the very long introns in mammalian genes are sequenced, of open reading frames that encode significant looking protein sequences, "nested" within the introns of other genes. An example is cited in the article on Gene Structure. The *Drosophila Gart* gene, identified because of its function in **purine biosynthesis**, has an open reading frame in its largest intron that encodes cuticle protein, used at the pupation stage. Here the mRNAs of *Gart* and the nested gene are transcribed from opposite strands of the DNA, and therefore, presumably, cannot, both be produced at the same time. There are also a few examples of genes nested within mitochondrial introns. The sea anemone *Metridium senile* harbors a group I intron within its mitochondrial gene for subunit 5 of NADH dehydrogenase, and this intron includes the genes for subunits 1 and 3 of the same enzyme (18). In this case all three genes use the same DNA strand for transcription, and so the excised intron becomes a bicistronic mRNA for the nested genes.

A less well-substantiated, but very real possibility is that introns are sometimes used as timing devices for gene expression. Transcription is not instantaneous. In *Drosophila* it has been estimated that it proceeds at the rate of about 1.4 kb per minute. This implies that, for a gene expanded to 60 kb because of its intron content, as is sometimes the case in *Drosophila* and often in mammals, there is an interval of nearly an hour between the start and completion of transcription. There is one example in *Drosophila* where intron length is crucial (19). Two genes, *knirps* (*knr*) and *knirps-like* (*knr-1*) encode very similar proteins but differ greatly in intron length, about 1 kb in *kni* and 19 kb in *knr-1*. The gene *kni* is essential at the blastoderm stage of embryonic development, when nuclear division proceeds very rapidly. Mutants that have no functional *kni* can be partially rescued by transcription of *knr-1* cDNA, which lacks introns, but not by genomic *knr-1*, presumably because the latter does not have time to be transcribed between one nuclear division and the next. Although it has not been demonstrated, it may be that for some developmental genes a long lead-time between transcription-induction and expression of the protein product is appropriate. In all events, organisms have become adjusted to the various transcriptional times of their genes, and hence to some extent depend on maintaining their accustomed intron lengths.

4. The Origin of Introns

Discussion about the origin of introns has been dominated by the idea, first put forward by Walter Gilbert (20), that exons were once separate genes and that introns are the present-day relics of the gaps between them when they were first brought together early in evolution. This is sometimes called the "introns early" hypothesis. The strongest evidence in favor of this view is the observation that where proteins consist of different **domains**, somewhat separate in the three-dimensional structure, and distinct even if mutually dependent functions, they are encoded by different exons (20). The heavy and light chains of immunoglobulins are good examples. And where pre-mRNA are spliced in different ways to yield functionally different protein products, it is clear that at least some of the introns mark the boundaries between rearrangeable protein domains that are functionally distinct modules. It is also true (see Gene Structure) that numerous multifunctional genes in eukaryotes are clearly homologous to separate single-function genes in bacteria, which are generally seen as more akin to the earliest organisms (though, in fact, they have been evolving for just as long as anything else).

There are difficulties, however, in imagining how introns that have an elaborate splicing-out mechanism could have evolved independently in such a similar form in all of the spaces between originally separate domains when they were first brought together. The alternative, the "introns late" hypothesis, is that genes, however complex their functions and however they were formed, came into existence without the benefit of introns and that the introns came in later, perhaps in a form akin to present-day group II introns, which are both mobile and similar to nuclear introns in their splicing mechanism. Natural selection could explain the correlation between intron positions and interdomain regions, since that these are likely to be the positions where any disruption due to insertion would do the least damage.

Comparisons between homologous genes in different organisms give contradictory messages. Some introns have retained their positions, although not their internal sequences, over vast tracts of evolutionary time, but others come and go even between quite closely related organisms, often into and out of positions that cannot be considered boundaries between functionally distinct domains. The strict introns-early hypothesis, if anyone held strictly to it, would suppose that every intron position that we see now was there from the origin of the gene and that the reason that all the positions are not occupied now is that introns can be lost, most plausibly by gene conversion, when patches of cDNA replace the intron-containing genomic sequences. But as has been pointed out (22), if introns were present in the primeval gene in all their present-day positions, the exons must have been so short as to be incapable of encoding any functionally distinct part of a protein.

An unanswered, perhaps unanswerable, question is whether the longest introns were always so long and, if not, how they grew.

Bibliography

1. A. M. Lambowitz and M. Belfort (1993) Annu. Rev. Biochem. **62**, 587–622.
2. A. J. Jeffries and R. A. Flavell (1977) Cell **12**, 1097–1108.
3. A. Dugaiczyk et al. (1979) Proc. Natl. Acad. Sci. USA **76**, 2253–2257.
4. W. Filipowicz, in Ref. 22.
5. J. A. Engelbrecht, K. Voelker-Meiman, and G. S. Roeder (1993) Cell **66**, 1257–1268.
6. C. W. Siebel, L. D. Fresco, and D. C. Rio (1992) Genes Dev. **6**, 1386–1401.
7. J. Valcarcel, R. Singh, and M. R. Green, in Ref (22).
8. B. S. Baker (1989) Nature **340**, 521–524.
9. J. L. Manley and R. F. Tacke (1996) Genes Dev. **10**, 1569–1579.
10. K. W. Lynch and T. Maniatis (1995) Genes Dev. **9**, 284–293.
11. Q. Sun et al. (1993) Genes Dev. **7**, 2598–2608.
12. J. Valcarcel, R. Singh, and P. D. Zamore et al. (1993) Nature **362**, 171–176.
13. T. R. Cech (1990) Annu. Rev. Biochem. **59**, 543–568.
14. B. Dujon (1989) Gene **82**, 91–114.
15. F. Michel and J. L. Ferat (1995) Annu Rev. Biochem. **64**, 435–461.
16. S. Zimmerly, H. Guo, P. S. Perlman, and A. M. Lambowitz (1995) Cell **82**, 545–554.
17. C. H. Sellem, Y. d"Aubenton-Carafa, J. L. Rossingnol, and L. Belcour (1996) Genetics **143**, 777–788.
18. C. T. Beagley, N. A. Okada, and D. R. Wolstenholme (1996) Proc. Natl. Acad. Sci. USA **93**, 5619–5923.
19. M. Rothe M. Pehl H., Taubert, and H. Jackle (1992) Nature **359**, 156–159.
20. W. Gilbert (1978) Nature **271**, 501.
21. C. C. F. Blake, (1979) Nature **277**, 598 and Inter.Rev. Cytol. **95**, 149–185.
22. A. Stoltzfus, J. M. Logsdon Jr., J. D. Palmer, and W. F. Doolittle (1979) Proc.Nat. Acad. Sci. USA **94**, 10739–19744.

Inverse Folding Problem

This problem arose from attempts to design proteins *de novo*. Here one begins by selecting a certain known target protein structure, for example, the globin fold, and freely designs amino acid sequences (primary structures) that should adopt this conformation spontaneously. There will be a number of sequences compatible for a particular target because **homologous** proteins are known to adopt the same fold (see Homological Modeling). A solution becomes unique, however, if one searches for the sequence that would fold and would give the most stable structure. Such a sequence is likely to differ even from the native sequence of the target structure. In this procedure, one starts from a 3-D structure and works toward a sequence (Fig. 1), opposite to the direction of **protein folding** and protein structure prediction, where one starts with the sequence and tries to find the 3-D structure.

Figure 1. Inverse folding problem. Given a particular 3-D structure, search for any amino acid sequence that would preferably adopt the fold. Note that the thinking is reversed in direction compared with that of protein folding.

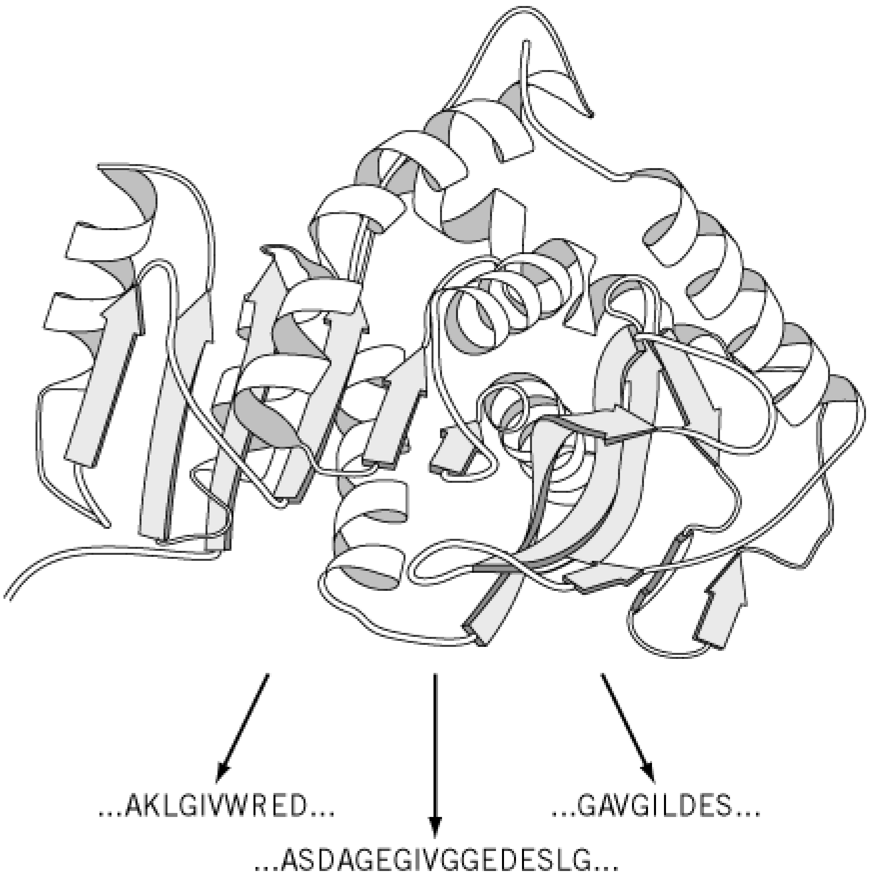

One of the obstacles in solving the inverse folding problem is dealing with the amino acid residue side chains. The protein backbone can be fixed just the same as in the target structure, but the side chains vary with the sequence. At each stage, the optimal packing of the atoms of the side chains within the protein interior needs to be determined. To avoid this annoying task, a simplified treatment of side chains has been introduced (1); each of the 20 side chains of the normal amino acids is represented by one point (the C_b atom for all residues except glycine), and its bulkiness and other physicochemical properties are effectively included in the interaction potential used, which is called the “mean-force energy potential” or the “Sippl potential.” The position of the C_b atom is fully determined by the dihedral angles of the backbone alone (see Ramachandran Plot), so it is not necessary to worry about the side-chain conformation. The Sippl potential is a function of the distance between the C_b atoms of two side chains and of the amino acid type. The quality of the side-chain packing is given quantitatively by the sum of the interaction energies estimated by the Sippl potential between the side chains. The applicability of the Sippl potential has been established by the "Sippl test (2)." The native amino acid sequence *a* of one structure (A) is selected from a structural library of various known structures and mounted onto another structure (B) that is larger in size than A. Mounting sequence *a* onto structure B is possible with various alignments, shifting residues one-by-one without introducing any gaps. Each time, the total energy of the structure is estimated by using the Sippl potential. Upon completion, structure B is replaced by the next structure of the structural library, including structure A itself. If the native combination of sequence and structure gives the lowest energy among all the alternatives, it is concluded that the potential function is effective and useful. The Sippl test has been performed successfully with various Sippl-type potentials (3, 4), but this is not sufficient for the inverse folding problem. The Sippl test is a recognition test for sequence recognizing structure, just opposite to the inverse folding problem of structure recognizing sequence.

Another difficulty with the inverse folding problem is whether the energy values of different systems (proteins with different sequences) can be compared to each other (5, 6). Of course, it is almost meaningless to compare the energy of two different substances, such as ethane and ethanol. Apart from the absolute energy, however, the energy of protein stability is defined as the energy difference between the folded and **unfolded** protein states, which can be compared among different proteins. Ota et al. (7) introduced a simple approximation to estimate the energy of protein stabilization in combination with the Sippl-type potential energy and applied the method to analyzing the thermal stability of mutant proteins. Similar treatments could conceivably deal with the inverse folding problem and achieve the *de novo* design of proteins.

Bibliography

1. M. J. Sippl (1990) J. Mol. Biol. **213**, 859–883.
2. M. Hendlich, P. Lackner, S. Weitckus, H. Floeckner, R. Froschauer, K. Gottsbacher, G. Casari, and M. J. Sippl (1990) J. Mol. Biol. **216**, 167–180.
3. C. Ouzounis, C. Sander, M. Scharf, and R. Schneider (1993) J. Mol. Biol. **232**, 805–825.
4. Y. Matsuo, H. Nakamura, and K. Nishikawa (1995) J. Biochem. **118**, 137–148.
5. M. J. Rooman and S. J. Wodak (1995) Protein Eng. **8**, 849–858.
6. G. M. Crippen (1996) Struct. Function Genet. **26**, 167–171.
7. M. Ota, S. Kanaya, and K. Nishikawa (1995) J. Mol. Biol. **248**, 733–738.

Inversion, Chromosomal

The major sources of variation in the eukaryotic genome are chromosomal breakages and reunions, leading to inversions and translocations. If two breaks occur in a chromosome and the excised fragment is rotated 180° before being reunited, then an inversion occurs. Three breaks in a chromosome can lead to an intrachromosomal translocation. In humans, both pericentric (the position of the centromere is changed) and paracentric (the position of the centromere is not changed) inversions occur in 1 to 2% of the population. Surprisingly often these gross chromosomal inversions do not have any **phenotypic** consequence (1). Most of these inversions are pericentric and involve nonrandom chromosomal breakpoints (Fig. 1).

Figure 1. Chromosomal inversions. Those that change the position of the centromere are called pericentric inversions (**a**), and those that maintain the position of the centromere are called paracentric (**b**).

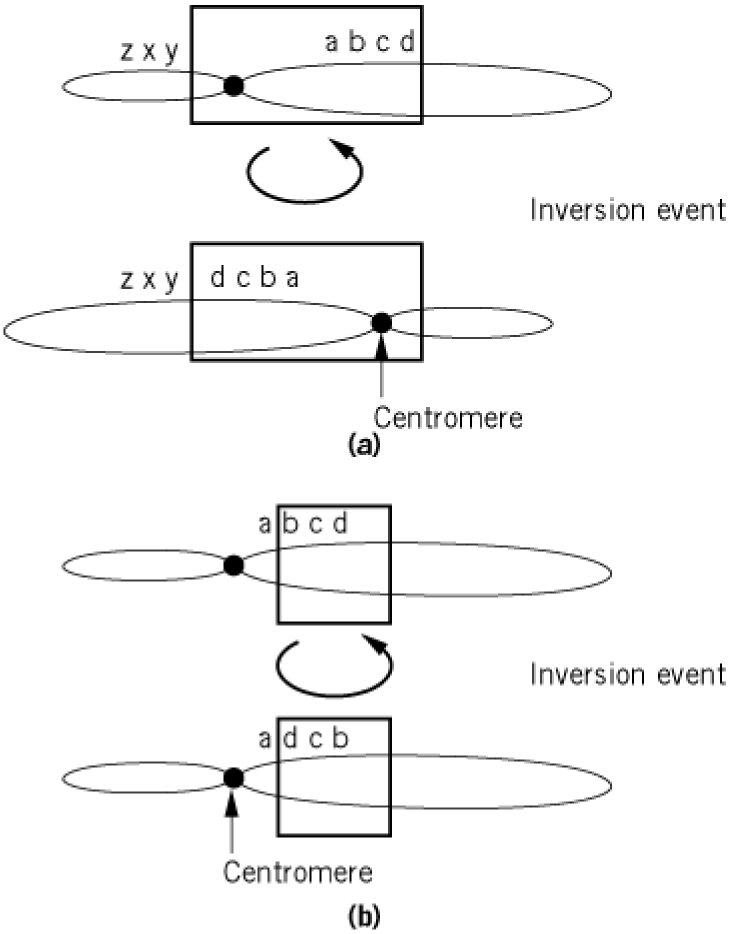

The polytene chromosomes of *Drosophila* are especially suited for studying gross chromosomal rearrangements. It has been shown that the evolution of distinct species of *Drosophila* was associated with the accumulation of many paracentric and pericentric inversions, so that on average two new inversions can be identified in each species (2). Comparison of the chromosomal banding patterns of humans with that of various apes also reveals that several chromosomes have undergone inversions leading to detectable differences (3). Inversions have also been well documented in **plants** and **fungi**. Nevertheless, inversions are an unwelcome occurrence for sexually reproducing organisms because of the consequence for **meiosis**. Chromosomal inversions cause homologous chromosomes to become locally heterozygous, which can create problems during the chromosomal alignment process that happens in meiotic **prophase**. This heterozygosity is normally overcome by the formation of an inversion loop, so that chromosomal alignment is maintained where possible. Inversions also create problems for the appropriate segregation of chromosomal material if **crossovers** occur within the inversion loop.

In humans, fertility is reduced because paracentric inversion prevents appropriate chromosomal segregation when a crossover occurs within an inversion loop. The products of a paracentric inversion are an acentric fragment and a dicentric chromosome, which breaks during **anaphase**. Only the two chromatids that are not involved in the crossover remain normal. The embryos generated from **gametes** without the full complement of chromosomes are generally inviable. With pericentric inversions, the risk of producing an abnormal embryo is increased, depending on the origin of the gamete. The products of a pericentric inversion have gene duplications and deficiencies.

These duplications potentially lead to defective gametes. With male gametes, there is a 4% risk of abnormality, and with female gametes there is an 8% risk. This presumably reflects the greater contribution of the female gamete and the maternal chromosomes to early embryonic development. Comparable decreases in fertility are found in flowering plants. This leads to a strong evolutionary selection against chromosomal inversion (4).

Bibliography

1. D. S. Moorehead (1976) Am. J. Human. Genet. **28**, 294–301.
2. H. Carson (1983) Genetics **103**, 465–489.
3. J. J. Yunis and O. Drakash (1982) Science **215**, 1525–1529.
4. S. Wright (1977) *Evolution and Genetics of Populations*, Vol. **4**: Variability within and among natural populations, University of Chicago Press, Chicago.

Suggestion for Further Reading

5. M. S. Clark and W. J. Wall (1996) "Chromosomes". *The Complex Code*, Chapman and Hall, London.

Inverted Repeats

A repeat, or repeating, **nucleotide sequence** is any of two or more identical segments of a longer sequence or identical segments in a double-stranded **DNA**. If two such DNA fragments are inserted into a long DNA duplex with opposite polarity (one “head on,” the other “tail on”), the corresponding pair are known as inverted repeats . The various types of repeats are schematically outlined in the Figure for Tandem Repeats. The sequences of the pair of inverted repeats, if read from the same strand, are complementary to one another. Inverted repeats placed immediately after one another make a palindrome. If the separation between the inverted repeats is comparatively short (up to a few tens of bases), the repeats may correspond to a hairpin in a RNA transcript generated from such a structure, or to a cruciform structure in DNA under torsional constraint (1).

Inverted repeats are an important element of several types of mobile DNA elements, or transposons (2). They are located at the ends of the transposons when integrated into a genome. For example, bacterial **insertion sequences** (IS) are flanked by 10- to 40-bp inverted repeats. The insertion sequences themselves can make a pair of inverted repeats, as in the case of the bacterial transposon Tn10, which is flanked by 1400-bp IS10 sequences of opposite polarity. The inverted repeats are involved in the recombination events that occur during integration or excision of the transposons.

Bibliography

1. Y. Timsit and D. Moras (1996) Q. Rev. Biophys. **29**, 279–307.
2. *Mobile DNA* (1989) (D. E. Berg and M. M. Howe, eds.) ASM, Washington, D.C.

Suggestion for Further Reading

3. B. Alberts, D. Bray, J. Lewis, M. Raff, K. Roberts and J. D. Watson (1994) *Molecular Biology of the Cell*, 3rd ed., Garland Publishing Inc., New York.

Inverted Terminal Repeat

The movement of transposable elements from place to place in genomes results from the actions of a special element-encoded recombinase on special DNA sequences at the tips of the element. In virtually all such elements, these special recombination sequences at the ends of the transposon include transposase binding sites arranged as inverted repeats. It is these sites that define where the breakage and joining events must occur. Because identical (or nearly identical) terminal sequences are arranged as inverted repeats, the disposition of the transposase at both ends relative to the transposon ends is identical, so that the breakage and joining will occur in the same relative positions at both ends.

The terminal inverted repeats are usually composed of special sequences at the extreme tips of the transposon that signal exactly where that breakage and joining should occur, plus more internal binding sites for the transposase (1, 2) (Fig. 1). In some elements, there are multiple binding sites for the transposase, including the one that is part of the terminal inverted repeat and others internal (3). These interior sites probably play a role in loading the transposase appropriately onto the termini and may be dispensable after the initial stages of transposition have occurred, for example, after synapsis of the transposon ends. For some elements, a binding site for a host factor important for recombination may also be part of the terminal repeat.

Figure 1. The ends of IS10. Special sequences at the ends of the element specify the position of transposase binding and also provide signals to prompt DNA breakage and joining. Transposase binding is specified by sequences from position 6 to position 23, and the positions from 6 to 13 are most critical. Although particular sequences at positions 1, 2, and 3 are not required for transposase binding, they are necessary to prompt the chemical steps of DNA breakage and joining. The identity of positions 4 and 5 is not critical. The outside and inside ends of IS10 have the same transposase binding motifs, but the outside end has in additional a binding site for integration host factor (positions 30–42), a bacterial protein, that is a cofactor in reactions involving the outside ends.

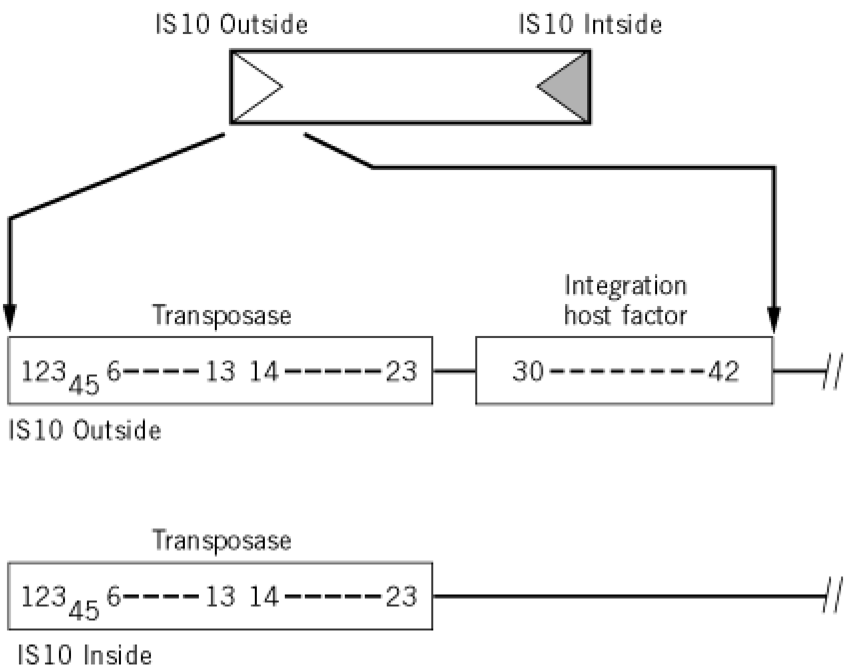

Although multiple transposase binding sites may be present, breakage and joining is restricted to the terminal inverted repeats because of the presence of a transposase binding site adjacent to the special sequences at the extreme tips of the element that provoke cleavage (1, 2). Alteration of these "cleavage signal" nucleotides generally blocks cleavage, but transposase binding still occurs. Often there is a spacer region of a few nucleotides between the transposon binding site and the cleavage nucleotides at the tip.

Bibliography
1. D. Haniford and N. Kleckner (1994) EMBO J. **13**, 3401–3411.
2. J. Sakai, R. M. Chalmers, and N. Kleckner (1995) EMBO J. **14**, 4374–4383.
3. B. D. Lavoie and G. Chaconas (1996) Curr. Top. Microbiol. Immunol. **204**, 83–102.

Iodine Isotopes

Iodine is element number 53 in the periodic table and has valence states of 1, 3, 5, or 7 (1). Iodine is an essential element in humans in small amounts, and lack of iodine causes thyroid goiter. The thyroid concentrates iodine, synthesizes and stores the thyroid hormone **thyroxine**, and releases it to maintain physiological balance. Excessive exposure to chemical iodine can cause skin, eye, and mucous membrane irritations. Iodine compounds are used as chemical reagents, as antimicrobial agents, as radiopharmaceuticals in medicine, and in photographic chemicals.

Thirty-five isotopes of iodine have been identified (2), ranging in atomic mass from ^{108}I (half-life = 36 ms) to ^{142}I (half-life = 0.25 s) (see Radioactivity and Radioisotopes). Only one isotope of iodine is stable (^{127}I). The longest lived isotope (^{129}I) has a half-life of 15.7 million years.

The four most important radioactive isotopes of iodine (or *radioiodine*) for biomedical use are: ^{123}I, ^{124}I, ^{125}I, and ^{131}I (Table 1). Each radioiodine is prepared uniquely and has a variety of different applications, advantages, and disadvantages (3). Iodine is a useful **radiolabel** for many studies, as it can be chemically incorporated into proteins relatively easily. All radioiodine compounds must be handled with care, as radioiodine is volatile and readily concentrated in the human thyroid gland.

Table 1. Principal Radioisotopes of Iodine in Medicine and Research: Their Radioactive Emissions, Yields, and Energies (2)

Element	Mass (amu)[a]	Physical Half-life	Beta-Particle Yield	Average Beta Energy (MeV)[b]	Gamma-Ray Yield	Gamma Energy (MeV)
Iodine	123	13.22 hours	—	—	0.833	0.159
	124	4.18 days	0.229	0.824	0.453	0.511
					0.611	0.603
					0.101	0.723

				0.105	1.691
125	59.6 days	—	—	0.0667	0.0355
131	8.021 days	1.0	0.182	0.0606	0.284
				0.812	0.364
				0.0727	0.637

[a] Atomic mass units.

[b] Million electronvolts.

High purity iodine-123 is usually produced in an accelerator by the reaction ^{127}I(*p*,5*n*) ^{123}Xe→^{123}I + b^{-}, or by the reaction ^{124}Xe(*p*,g) ^{123}I. Iodine-124 is an undesirable impurity in ^{123}I preparations. Iodine-123 is used as a diagnostic imaging agent in nuclear medicine for thyroid imaging and uptake studies. Its relatively short half-life of 13 h. is a disadvantage for transportation from site of production to hospitals for clinical use.

Iodine-124 can be prepared in an accelerator by deuteron bombardment of tellurium according to the reaction ^{124}Te(*d*,2*n*) ^{124}I. Iodine-124 is a positron (beta-plus) emitter having useful applications in positron-emission tomography in diagnostic nuclear medicine. Iodine-124 has also been used as a label for 5-iodo-2′-deoxyuridine, an analog of thymidine, for DNA uptake studies, and tumor imaging. It has potential application as a therapeutic radionuclide.

Carrier-free ^{125}I is prepared in a reactor using an ^{124}Xe target according to the reaction ^{124}Xe(*n*,g) ^{125}Xe → ^{125}I + b^{-}. It may also be prepared in an accelerator by deuteron bombardment of tellurium according to the reaction ^{124}Te(*d*,*n*) ^{125}I. Iodine-125 emits low energy (0.035 MeV) gamma rays and thus is *not* useful for external imaging. However, ^{125}I is used extensively to **radiolabel** small specimens and proteins for a variety of applications in molecular biology, including radioimmunoassay, autoradiography, and fluorography. Iodine-125 is a common label for 5-iodo-2′-deoxyuridine in DNA uptake and **hybridization** studies. It has possible applications as a therapeutic radionuclide because of the high linear energy transfer of Auger electrons emitted by ^{125}I-labeled DNA in cell nuclei. Iodine-125 is also used in permanent seed implants (brachytherapy) for treatment of slowly growing tumors, such as carcinoma of the prostate.

Iodine-131 may be prepared in an accelerator according to the reaction ^{130}Te(*d*,*n*) ^{131}I. It is more commonly prepared in a reactor by tellurium capture according to the reaction ^{130}Te(*n*,g) ^{131}Te → ^{131}I + b^{-}, or as a ^{235}U fission product. Iodine-131 was discovered and used for thyroid function studies in 1938 (4). It was the first radioisotope to be approved (in 1951) by the U.S. Food and Drug Administration for human use as a new drug.

Today, ^{131}I is used extensively in clinical nuclear medicine for many purposes (3). These include thyroid uptake studies (555 kBq, or kilobecquerels, administered), scans with metastatic thyroid cancer in athyroid patients, and treatment of benign thyroid disease (185 MBq), for thyroid carcinoma ablation (5.55 GBq), and as a labeled monoclonal antibody in targeted-cell therapy of lymphoma and leukemia (up to 30 GBq). Other applications are radioiodine labels for dyes, macromolecules, proteins, and hormones, including ^{131}I-norcholesterol for diagnosis of aldosterone-producing tumors in the adrenals and ^{131}I-metaiodobenzylguanidine for imaging pheochromocytoma and other neuroendocrine tumors. Iodine-131 has the advantage of a relatively long half-life (8.021

days) for production, transportation, and labeling, but the disadvantage of abundant gamma rays, which can be a radiation hazard.

Bibliography

1. D. R. Lide and H. Pr. Frederikse, eds. (1995) *CRC Handbook of Chemistry and Physics*, CRC Press, Boca Raton, Fla.
2. Knolls Atomic Power Laboratory (1966) *Chart of the Nuclides*, 15th ed., available from General Electric Company, San Jose, Calif.
3. J. C. Harbert (1996) in *Nuclear Medicine: Diagnosis and Therapy*, J. C. Harbert, W. C. Eckelman, and R. D. Neuman, eds., Chapter "20", pp. 407–427.
4. M. Brucer (1990) *A Chronology of Nuclear Medicine*, Heritage Publications, Inc., St. Louis, Mo.

Suggestions for further reading

5. L. K. Bustad, ed. (1964) *Biology of Radioiodine*, Pergamon Press, Oxford.
6. J. C. Harbert, W. C. Eckelman, and R. D. Neumann (1996) *Nuclear Medicine: Diagnosis and Therapy*, Thieme Medical Publishers, New York.

Iodoacetamide, Iodoacetate

Iodoacetamide and iodoacetate are two of the most common reagents used for chemically modifying thiol groups irreversibly. They have a long history, dating back to 1874 when it was reported that bromoacetate injected subcutaneously into frogs killed them, as a result of progressive respiratory and cardiac depression; iodoacetate was subsequently found to be more reactive. These studies were important in elucidating the mechanism of glycolysis, which led to the realization that iodoacetate and other such compounds acted by reacting with the thiol groups of proteins, in this case at the active site of the enzyme glyceraldehyde-3-phosphate dehydrogenase. Iodoacetamide became popular because it can cross cell membranes much more readily than can iodoacetate and therefore is more potent with cells and organs.

Both iodoacetamide and iodoacetate react rapidly and specifically with the ionized form of thiol groups, to generate very stable adducts:

$$-S^- + I - CH_2CONH_2 \rightarrow -S - CH_2CONH_2 + I^- \tag{1}$$

$$-S^- + I - CH_2CO_2^- \rightarrow -S - CH_2CO_2^- + I^- \tag{2}$$

These adducts are commonly known as the carboxamidomethyl and carboxymethyl, respectively. They are stable to conditions routinely used to hydrolyze proteins to their substituent amino acids, except that the carboxamidomethyl group gets hydrolyzed to the carboxymethyl (see Amino Acid Analysis).

The reaction with iodoacetamide or iodoacetate occurs by the thiolate anion attacking and displacing the iodine atom in a nucleophilic reaction. Consequently, the rate of the reaction increases with increasing pH, up to just beyond the pK_a of the thiol group, which typically is about 9 for most biological substances. The pH dependence of the rate of the reaction can be used to measure the apparent pK_a value of the thiol group, although there are exceptional cases in catalytic proteins where the results are misleading, presumably because the protein modifies the energy of the transition state for the reaction (1). The reaction occurs rapidly with thiol groups. The second-order rate constant for reaction at 25°C of iodoacetamide with a fully ionized cysteine thiol group, with a pK_a of about 8.7, is approximately 25 $s^{-1}M^{-1}$. Consequently, the half-time for modification of such a thiol group upon adding 0.1 M iodoacetamide is only 0.3 sec. Iodoacetate reacts about three times less rapidly than does iodoacetamide.

It is important to realize that protons are released by the reaction. Frequently, high concentrations of a thiol reagent are used to reduce all cysteine residues, and then a large excess of iodoacetate or iodoacetamide is added to react with both the protein and the reagent. In this case, the pH will drop and the rate of the reaction will slow, and even stop before completion, unless very high concentrations of a buffer are present.

The two reagents differ only in one being an amide, and neutral, and the other an acid, and negatively charged. This charge difference is useful for counting residues of thiol groups in a protein. Mixtures of the two reagents are reacted with a protein containing *N* thiol groups, to produce a spectrum of molecules with net charge differences of 0 to *N*. If this spectrum is resolved by electrophoresis, isoelectric focusing, ion-exchange chromatography, or other techniques dependent only upon the charge of the protein, the number of species with different charges present can be counted, giving the integer value of *N*.

Both iodoacetamide and iodoacetate also react with amino groups, but at a lower rate, and primarily at very alkaline pH values, where the reactive nonionized amino groups are present. Both lysine and histidine residues can be modified in this way. The reaction of **ribonuclease A**, which has no free thiol groups, with the two histidine residues at its active site, each reacting with different N atoms, was important in demonstrating the specificity of the interactions that could take place in enzyme-active sites (2). They can also react with the sulfur atom of **methionine residues** to generate the positively charged sulfonium salt, but at a much lower rate (3). This rate is essentially independent of pH, however, so it can become the predominant modification reaction of a protein at very low pH values. The reactions of iodoacetamide and iodoacetic acid can be used in diagonal methods to isolate specifically cysteine- and methionine-containing peptides.

Many variants of iodoacetate and iodoacetamide have been devised by adding further groups with absorbance and fluorescence properties that serve as reporters of structure in proteins.

Bibliography

1. J. W. Nelson and T. E. Creighton (1994) Biochemistry **33**, 5974–5983.
2. R. G. Fruchter and A. M. Crestfield (1967) J. Biol. Chem. **242**, 5807–5812.
3. H. G. Gundlach, S. Moore, and W. H. Stein (1959) J. Biol. Chem. **234**, 1761–1764.

Suggestions for Further Reading

4. J. L. Webb (1966) *Enzyme and Metabolic Inhibitors*, Vol. **III**, "Chapter 1", Academic Press, New York.
5. F. R. N. Gurd (1967) Carboxymethylation. Methods Enzymol. **11**, 532–541.

Ion Channel Receptors

A diverse group of neurotransmitter receptors are ligand-gated **ion channels**. These can be subgrouped into receptors that are either excitatory (acetylcholine, glutamate, serotonin) or inhibitory [g-aminobutyric acid (GABA), glycine]; they have similar structural features, but different regulatory properties. These receptors are characterized by fast- and short-acting responses to ligand. Additionally, these receptors are subject to targeting by docking proteins that induce aggregation. The increased permeability to ions results in the influx of second messengers, resulting in activation of downstream targets.

1. Receptor Structure

Because it was one of the first receptors studied in detail, more is known about the nicotinic acetylcholine receptor than any other (1). This receptor consists of four different **polypeptide chains**, with the composition $a_2$bgd. Each subunit has a single **transmembrane** domain. Although the structure of the channel is not known, the five subunits are thought to assemble together to form a pore, with the neurotransmitter binding site located in the extracellular domain of the asubunits. Numerous mutational analyses have led to an understanding of the molecular dynamics of the regulation of the channel by ligands. Thus, acetylcholine binding induces a conformational change, opening the gate to allow influx of Na^+ and K^+ ions (1).

The structures of the inhibitory ligand-gated anion channels are similar to the nicotinic cholinergic receptor. Both GABA and glycine activate Cl^- channels, in a manner analogous to the regulation of K^+ and Na^+ channels by acetylcholine.

2. Regulation of Ligand-Activated Channels

Ligand-activated channels are generally found to be clustered on the postsynaptic side of a synapse. Recent studies have suggested that the clustering is mediated by interactions with a group of targeting proteins, such as PSD-95 and GRIP, that contain PDZ domains. These regions are **domains** involved in protein-protein interactions and are known to interact with specific sequences in the *C*-terminal regions of transmembrane proteins (2).

Ligand-gated ion channels are also known to be regulated by **phosphorylation**. The primary structures of these receptors contain numerous **consensus sequences** for various protein kinases. Both *in vivo* and *in vitro* experiments have demonstrated phosphorylation of both excitatory and inhibitory receptors, by both **tyrosine kinases** and **serine/threonine kinases**. These phosphorylations are likely to play a role in modulating the activation of the receptor by ligands, and they may have consequences for understanding long-term modulation of receptor function (3).

See also Calcium Signaling.

Bibliography

1. A. Karlin (1993) Curr. Opin. Neurobiol. **3**, 289–309.
2. H.-C. Kornau, P. H. Seeburg, and M. B. Kennedy (1997) Curr. Opin. Neurobiol. **7**, 368–373.
3. T. C. Smart (1997) *Curr. Opin. Neurobiol.* **7**, 358–367.

Ion Pair

An ion pair is two molecules or groups of opposite electric charge in close proximity due to favorable electrostatic interactions between them. The term ion pair is generally used in all fields of liquid chemistry, in contrast to a salt bridge, but in biochemistry the term frequently refers to a salt bridge.

Ion-Exchange Chromatography

Ion exchange is the reversible interchange of ions of the same charge between a solution and a solid, insoluble material in contact with it. It proceeds by equivalents. One chemical equivalent of one kind of ion enters the solid, and one chemical equivalent of another kind of ion must leave. Therefore, electrical neutrality is always maintained. An ion exchanger consists of an insoluble matrix to which charged groups have been covalently bound. The charged groups associate with mobile counterions. These counterions are reversibly exchanged with other ions of like charge (ie, ion exchange) without altering the matrix. Two main forms of ion exchangers are commonly used: anion exchangers and cation exchangers. Positively charged exchangers have negatively charged counterions (anions) available for exchange and so are termed anion exchangers. Negatively charged exchangers have positively charged counterions (cations) and are termed cation exchangers.

Ion-exchange chromatography is an inclusive term for all **chromatographic** separations of ionic substances carried out by using an insoluble ion exchanger as the stationary phase. As an ionic solution passes over and through the exchanger, ions from the solution exchange for those already on the solid matrix. This technique came into prominence during World War II as a separation procedure for the rare earth and transuranium elements. The technique was first used by Taylor and Urey (2) to separate lithium and potassium isotopes using zeolite resins, and Samuelson (3) demonstrated the potential of synthetic resins. In the mid 1950s, Sober and Peterson (4-6) synthesized the diethylaminoethyl (DEAE) and carboxymethyl (CM) derivatives of cellulose, still in use today for ion-exchange chromatography of proteins.

Although all ion exchanges are reversible, the equilibrium distributions vary widely, and this variation makes ion-exchange chromatography possible. In other words, the basic principle of ion-exchange chromatography involves competition between different ions of the same charge for binding to an oppositely charged chromatographic matrix, the ion exchanger. The interaction between the analytes and the ion exchanger depends on several factors: the charge properties of the analytes; the ionic strength and the nature of the particular ions in solution; the pH; and the presence of other additives in the mobile phase, such as organic solvents. Because retention in ion-exchange chromatography involves an electrostatic interaction between the fixed charges of the ion-exchange matrix and those of the analytes, it is clear that the more highly charged an analyte, the more strongly it binds to a given, oppositely charged ion exchanger. Similarly, more highly charged ion exchangers, those with a greater degree of substitution with charged groups, bind analytes more effectively than weakly charged ones. It should be mentioned that the terms strong and weak ion exchangers derive from the pK_a values of their charged groups and do not say anything about the strength with which they bind analytes. At pH values far from the pK_a, binding equally strong either to a weak or a strong ion exchanger. In addition to the ion exchange effect, other types of binding also occur in the ion-exchange process. These effects are generally small and are mainly due to **van der Waals** forces and polar interactions.

Because of its versatility, its high resolving power, its high capacity, and its straightforward basic principle, ion-exchange chromatography is one of the chromatographic techniques used most often in biochemical studies [see section IV of Ref. 1 (pp. 170–270), Ref. 7]. Detailed operational protocols and the lists of its applications are beyond the scope of this volume, and the interested reader is directed to several excellent reviews (7-10).

Bibliography

1. C. T. Mant and R. S. Hodges (eds.) (1991) *High-Performance Liquid Chromatography of Peptides and Proteins: Separation, Analysis, and Conformation*, CRC Press, Boca Raton.
2. T. I. Taylor and H. C. Urey (1938) J. Chem. Phys. **6**, 429–438.
3. O. Samuelson (1939) Z. Anal. Chem. **116**, 328.
4. H. A. Sober and E. A. Peterson (1954) J. Am. Chem. Soc. **76**, 1711–1712.
5. E. A. Peterson and H. A. Sober (1956) J. Am. Chem. Soc. **78**, 751–755.
6. H. A. Sober, F. J. Gutter, M. M. Wycoff, and E. A. Peterson (1956) J. Am. Chem. Soc. **78**, 756–763.
7. E. Karlsson, L. Rydén, and J. Brewer (1989) in *Protein Purification: Principles, High Resolution Methods, and Applications* (J.-C. Janson, and L. Rydén, eds.), VCH, New York, pp. 107–148.
8. E. F. Rossomando (1990) in *Guide to Protein Purification* (M. P. Deutscher, ed.), *Methods in Enzymology* **182**, Academic Press, New York, pp. 309–317.
9. H. F. Walton (1992) in *Chromatography* (E. Heftmann, ed.) (*Journal of Chromatography Library*, Vol. **51A**), Elsevier, Amsterdam, pp. A227–A265.
10. J. Swadesh (1997) in *HPLC: Practical and Industrial Applications* (J. Swadesh, ed.), CRC Press, Boca Raton, pp. 171–243.

Ionization

Ionizable groups in biological macromolecules are either protonated or deprotonated to have positive or negative ionic charges, depending on the pH condition of the solvent. At a neutral pH, the phosphate groups in nucleic acids are all ionized, and the bases are almost neutral. In contrast, in proteins at a neutral pH, the charge states of the ionizable groups are exquisitely dependent on the individual pK_a values of the ionizable residues. They directly affect the electronic structures around active sites, and the stabilities of protein structures (see Electrostatic Interactions).

The degree of ionization of an acid, i, is $10^{-pK_{ai}}/(10^{-pK_{ai}}+10^{-pH})$, and the degree of ionization of a base, j, is $10^{-pH}/(10^{-pK_{aj}}+10^{-pH})$. Therefore, the total net change of an amphoteric molecule, such as a protein, is given by

$$-\sum_i 10^{-pK_{ai}}/(10^{-pK_{ai}}+10^{-pH})+\sum_j 10^{-pH}/(10^{-pK_{aj}}+10^{-pH})$$

The charge state of an ionizable group is governed by its intrinsic acidity and also by the electrostatic environment, which depends on the ionic strength of the solvent. When an ionizable group is surrounded by other anions, the pK_a value increases. In contrast, when it is surrounded by cations, the pK_a value decreases. Therefore, when a salt bridge is formed between an acid and a base, the pK_a of the acid decreases, and the pK_a of the base increases. Thus, each ionizable group in a protein has a unique pK_a value, and this changes with changes in the ionization of nearby groups. The apparent pK_a value is determined by titration experiments or estimated by theoretical calculations based on the tertiary molecular structure. Even when the only structural information about a protein is its amino acid composition, the total net charge of the protein can be approximated, and the isoionic point estimated, by using only the intrinsic pK_a^{int} values, listed in Table 1 of Electrostatic interactions.

Iron-Binding Proteins

Iron is the most abundant transition metal in the earth's crust, but it is poorly available as a nutrient because it forms insoluble ferric hydroxides in the presence of O_2 at neutral pH. Organisms have coped with this challenge by evolving various uptake strategies based on chelation. Once internalized, free iron is quite toxic to cells: Fe^{2+} and Fe^{3+} ions react with H_2O_2 and O^-_2 to generate hydroxyl radicals, which indiscriminately oxidize cellular constituents. Hence, there is a clear need for some form of iron homeostasis (1).

Microbial iron metalloregulation (2) is best understood in *Escherichia coli*. In this bacterium, the ferric uptake regulation (*fur*) gene regulates many genes, including more than a dozen associated with siderophoric biosynthesis and transport. The monomeric Fur protein is approximately 18 kDa in mass and binds a single Fe^{2+} ion. With Fe^{2+} bound, Fur targets a GATAATGATAATCATTATC **consensus sequence** near the **promoter** of iron-regulated genes and acts as a dimeric repressor.

Corynebacterium diphtheriae (and other bacterial and fungal pathogens) experiences a state of iron starvation upon entering a mammalian host, and it responds by producing diphtheria toxin at maximal rates. The diphtheria *tox* repressor (DtxR) plays the primary role in regulating toxin biosynthesis. Fe^{2+}-activated DtxR is a functional dimer, which binds at the *tox* **operator** locus. **X-Ray crystallographic** structures of DtxR suggest that ferrous ions cause a caliper-like conformational change in the relative orientation of the monomers in the dimeric protein structure, leading to a decrease in the distance between the two DNA-recognition alpha-helices to match that in the target DNA (3) (see DNA-Binding Proteins and Repressors).

Bacteria sequester iron during times of plenty and produce bacterioferritins. Mammalian analogs of these iron storage proteins, ferritins, are much better understood.

Bibliography

1. G. Winkelmann, D. van der Helm, and J.B. Neilands (eds.) (1987) *Iron Transport in Microbes, Plants and Animals*, VCH, Weinheim, Germany.
2. J. H. Crosa (1997) Microbiol. Mol. Biol. Rev. **61**, 319–336.
3. N. Schiering, X. Tao, H. Zeng, J. R. Murphy, G.A. Petsko, and D. Ringe (1995) Proc. Natl. Acad. Sci. USA **92**, 9843–9850.

Suggestions for Further Reading

4. H. Sigel and A. Sigel (series eds.) (1974–1998) *Metal Ions in Biological Systems*, Dekker, New

York, Vols. **1–35**.
5. R. J. Cousins (1994) Metal elements and gene expression, Annu. Rev. Nutr. **14**, 449–469.

Iron-Response Elements

The messenger RNAs for iron-binding proteins, such as the transferrin receptor and both subunits of ferritin, contain so-called iron-response elements (IREs). These are RNA structures that contain a stem and a loop that has the **consensus sequence** CAGUGX (1). The transducer proteins, termed iron-responsive proteins (IRPs), bind to the IRE loop when the free iron concentration is low, whereas they are inactivated by high cellular iron levels. Formation of the IRE–IRP complex has a variety of physiological effects, as indicated in Table 1. IRP-binding stabilizes the transferrin mRNA against **RNA degradation**. Regulation of the transferrin receptor expression occurs at the **transcriptional** level. On the other hand, ferritin IRE–IRP complexes block association of the small **ribosomal** subunit with the mRNA of both ferritin subunits and prevent their translation. Consequently, regulation of ferritin expression occurs at the translational level.

Table 1. Physiological Effects of Key Mammalian IREs

mRNA-Containing IRE	Low [Fe]	High [Fe]
Transferrin receptor	Fe uptake Ý	Fe uptake ↓
Ferritin H- and L-chains	Fe storage ↓	Fe storage Ý
5-Aminolevulinate synthase	[porphyrin] ↓	[porphyrin] normal

5-Aminolevulinate synthase, the first enzyme in the heme biosynthetic pathway, is also regulated by IRPs. One of its two IRPs is strikingly homologous to aconitase, an iron-sulfur enzyme in the Krebs cycle. Interestingly, nitric oxide inhibits iron uptake by both IRPs (they remain active and capable of IRE recognition) and hence functions as a vertebrate hormone.

Bibliography
1. M. W. Hentze and L. C. Kühn (1996) Proc. Natl. Acad. Sci. USA **93**, 8175–8182.

Suggestions for Further Reading
2. H. Sigel and A. Sigel (series eds.) (1974–1998) *Metal Ions in Biological Systems*, Dekker, New York, Vols. **1–35**.
3. R. J. Cousins (1994) Metal elements and gene expression, Annu. Rev. Nutr. **14**, 449–469.

Iron–Sulfur Proteins

This class of proteins comprises several types of proteins and enzymes that contain iron atoms coordinated by sulfur atoms in clusters of different types (Fig. 1). The simplest FeS proteins are the rubredoxins (1Fe, no inorganic sulfur) and the ferredoxins (2Fe, 3Fe and 4Fe). In more complex FeS proteins, other **prosthetic groups** (FAD, FMN, heme, Mo, Ni, etc.) are present, in addition to the iron-sulfur cluster(s). Thus, FeS proteins fulfill several roles: **electron transfer** and storage, catalysis, structural, and regulatory functions (1, 2).

Figure 1. Schematic structures of iron-sulfur clusters found in FeS proteins as determined by X-ray crystallography studies: (**a**) the $Fe(S\text{-}Cys)_4$ unit in rubredoxin; (**b**) the 2Fe–2S cluster in eukaryotic ferredoxins and in Rieske proteins; (**c**) the cubane-like 4Fe–4S structure of bacterial ferredoxins, HiPIPS, IRPs, and active aconitase; (**d**) the cuboidal 3Fe–4S structure found in some bacterial ferredoxins, in inactive aconitase, and in some complex redox enzymes; (**e**) the P cluster of dinitrogenase; (**f**) the FeMoCo cofactor of dinitrogenase.

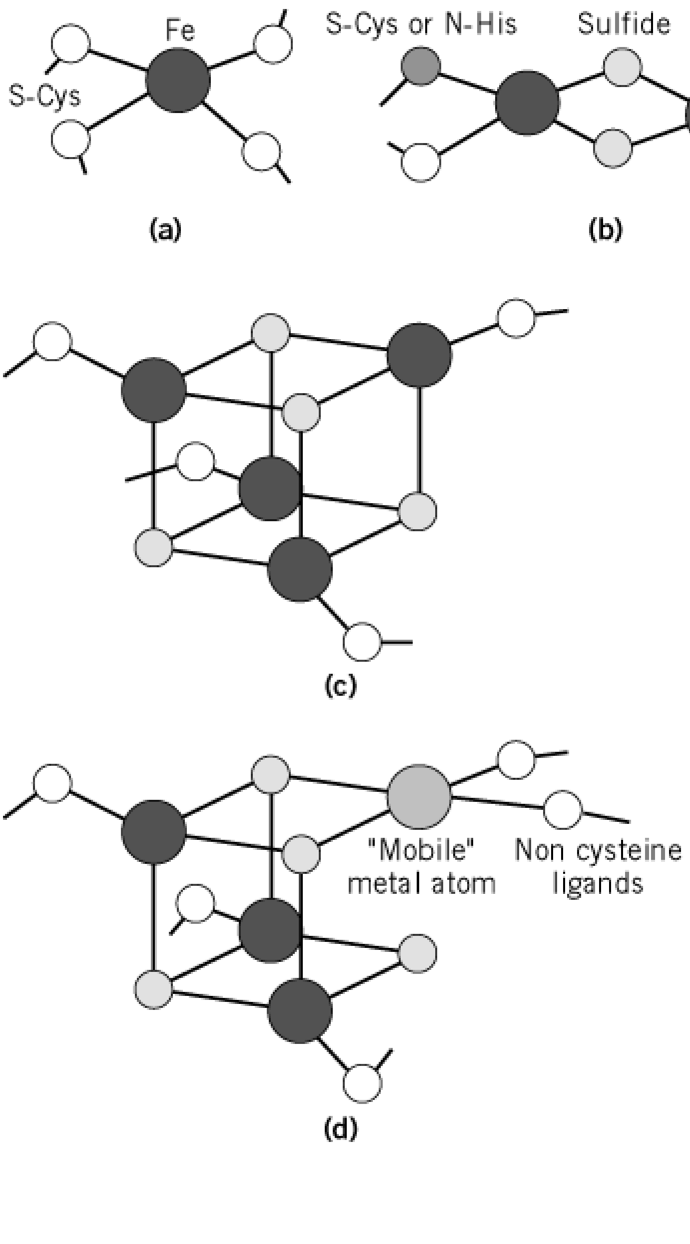

1. High Potential Electron Carriers: Rubredoxins, HiPIPs, and Rieske Proteins

The simplest of all FeS proteins is rubredoxin, containing a single Fe atom ligated by a four-cysteine-residue unit (Fig. 1a), and no inorganic sulfide, in a polypeptide of 50 to 60 amino acid residues. Rubredoxins are found in strictly anaerobic bacteria and archea (*Clostridia*, *Desulfovibriacee*, *Pyrococcales*) and have oxidation/reduction potentials (+30 to 60 mV, relative to the hydrogen electrode) that appear to be too high to be relevant for bacterial metabolism. Although assumed to function as electron carriers, the redox partners of rubredoxins in anaerobes have not been identified. Recently, a rubredoxin–oxygen oxidoreductase was found to function *in vitro* at the end of a soluble electron transfer chain that couples NADH oxidation to oxygen consumption in *Desulfovibrio gigas*. There is another protein in *D. gigas* containing a single $Fe(Cys)_4$ unit in each of its two small subunits, named desulforedoxin. Rubredoxin-like proteins that contain two $Fe(Cys)_4$ clusters are also found in *Pseudomonacee*. These aerobic rubredoxins transfer electrons to enzymes that catalyze the oxidation of alkanes.

Photosynthetic microorganisms such as *Chromatium spp* and *Rhodospira spp* contain the so-called HiPIPs (high-potential iron–sulfur proteins). These proteins contain a single, cysteine-coordinated 4Fe–4S cubane-like structure (Fig. 1c), but these protein structures favor the high-potential 3+/2+ transition of the metal cluster (reduction potentials +90 to +450mV), rather than the 2+/1+ transition typical of [4Fe–4S] clusters in bacterial ferredoxins.

Among the high-potential FeS proteins of the **mitochondrial** and photosynthetic electron transfer chains, a singularity is represented by the so-called “Rieske” protein in the cytochromes b-c_1 and b_6-f complexes. These “Rieske” proteins contain a 2Fe–2S cluster with two histidine and two cysteine ligands in a unique binding motif (Fig. 1b). The same type of coordination is found in other FeS proteins, most notably in ferrochelatase (found in the intermembrane space of mitochondria and required for inserting iron in tetrapyrroles) and in some bacterial dioxygenases.

2. Complex FeS Proteins

The redox properties of FeS clusters are utilized in multielectron transfer systems, which can be made more efficient by combining donors and acceptors into a single, often multimeric structure. This evolutionary advantage led to the appearance of complex FeS proteins, in which 4Fe–4S or 2Fe–2S clusters are combined with other inorganic or organic cofactors.

Desulfovibriacee and some *Clostridia* also contain what apparently amounts to a natural chimeric protein, in which a rubredoxin-like **domain** is linked to a domain that contains a binuclear, oxo-bridged iron center, such as those found in ribonucleotide reductase or in hemerythrin—hence the trivial names of these proteins: rubrerythrin and nigerythrin. Rubrerythrin was found to have ferroxidase activity, and an oxygen-scavenging function was hypothesized for these proteins. Yet another combination of metallic clusters has been found in *D. gigas* desulfoferrodoxin, a protein in which a desulforedoxin site is associated with an iron site having nitrogen ligands. No biological function is known for desulforedoxin or desulfoferrodoxin.

Nitrogenase components 1 and 2 represent the best-known examples of combinations of different and unusual metal–sulfur centers. In the dimeric component 2 (dinitrogenase reductase), a 4Fe–4S cluster (Fig. 1c) is bound at the dimer interface. Each of the subunits provides two of the coordinating cysteine residues, and the cluster structure and properties are modified upon adenylylation of the dimer. The a_2b_2 nitrogenase component 1 (the true dinitrogenase) contains a number of the so-called P-clusters (derived from 4Fe–4S cubanes) (Fig. 1e), again harbored jointly by adjacent subunits. In the same intersubunit fashion, dinitrogenase also binds FeMoCo, the metal cluster at which the multielectronic reduction of dinitrogen to ammonia occurs. FeMoCo is a modified double cubane structure, in which one of the corners is occupied by a Mo rather than a Fe atom, and is coordinated also by histidine and by an isocitrate molecule (Fig. 1f). Another elementary process in bacterial physiology is hydrogen evolution, which uses an enzyme containing an Ni–FeS cluster, along with 4Fe–4S clusters.

FeS proteins containing multiple iron centers and organic cofactors (most typically flavins and pterins) abound in the electron transport chains of both prokaryotes and eukaryotes. These membrane-bound enzymes are typically made up of several subunits, with a variety of arrangements, and types of clusters and cofactors spanning a broad range of reduction potential values, often modulated through the binding of suitable effectors. Also, an active role for FeS clusters in energy transduction has been proposed. Soluble complex iron–sulfur enzymes play key roles in bacterial metabolism (glutamate synthase or anaerobic ribonucleotide reductase) and in the assimilation pathways of inorganic nutrients in plants (as in sulfite, nitrate, and nitrite reductases), often in conjunction with unique cofactors. A mammalian soluble protein of great complexity is xanthine oxidase, containing flavin, iron–sulfur, and a molybdopterin cofactor. Formylmethanofuran dehydrogenases are FeS proteins found in methylotrophs, which contain Mo or W and a pterin dinucleotide.

3. FeS Proteins Having No Electron-Transfer Function

There is a remarkable structural similarity between the $Fe(Cys)_4$ unit found in rubredoxin-like proteins and the $Zn(Cys)_4$ unit found in DNA-binding **zinc fingers**, and transcription factors containing a $Fe(Cys)_4$ unit have been reported for a number of organisms. No DNA-binding activity has been reported for rubredoxins themselves. Examples of FeS proteins displaying the ability of binding polynucleotides are not limited to rubredoxin-like proteins. *Escherichia coli* endonuclease III contains a single 4Fe–4S cluster, which apparently only plays a structural role.

To alleviate the toxicity of the byproducts of aerobic respiration, *E. coli* induces the synthesis of protective enzymes, and this induction is controlled by the regulatory FeS proteins SoxRS, OxyR, and ArcAB. ArcAB, Fnr, SoxRS, and OxyR function in concert, so that *E. coli* can optimize its energy production and growth rate. Fnr and SoxRS are DNA-binding proteins, and they utilize 4Fe–4S and 2Fe–2S clusters as direct sensors of the redox environment (3).

Perhaps the best-known example of the regulatory function of FeS proteins is represented by the RNA-binding proteins involved in iron homeostasis in mammalian cells. When cells are depleted of iron, iron regulatory proteins IRP1 and IRP2 bind with high affinity to specific RNA stem-loop structures (**iron responsive elements**, IREs) in messenger RNA transcripts. Binding of IRPs to IRE stabilizes the mRNA coding for the transferrin receptor against degradation, while blocking the translation of the mRNA coding for the iron-storage protein, ferritin. In the presence of iron, IRP1 assembles a 4Fe–4S cluster and loses its IRE-binding properties, whereas IRP2 is rapidly subject to **protein degradation**. Thus, the presence of iron allows synthesis of ferritin (as well as of d-aminolevulinate synthase, mitochondrial succinate dehydrogenase, and aconitase), while repressing the synthesis of the transferrin receptor and therefore diminishing iron import into the cell (4).

The role of iron in citrate isomerization catalyzed by aconitase was recognized many years ago, and aconitase was found to contain a 4Fe–4S cluster, which can be converted reversibly to an inactive 3Fe–4S form (Fig. 1d). This conversion is made easier by the absence of a coordinating cysteine residue to the “labile” iron atom. Also complex FeS proteins are not limited to redox reactions. A FAD and 4Fe–4S enzyme from *Clostridium aminobutyricum* catalyzes the reversible dehydration of 4-hydroxybutyryl-CoA to crotonyl-CoA, a reaction involving the cleavage of an unactivated C–H bond; similar activities have been reported for other bacteria.

4. Processing of FeS Proteins and Cluster Assembly

From a chemical standpoint, iron–sulfur clusters are among the easiest cofactors to assemble. Synthetic FeS complexes containing 1, 2, 4, or more iron atoms and an appropriate complement of sulfide readily self-assemble in mixtures of iron, thiol groups, and a suitable source of sulfide (1). This observation, plus the positive charge of the pyrite-like fundamental unit of FeS clusters, and evolutionary considerations, prompted some hypotheses on a role of FeS clusters in the emergence of life in the reducing and acidic environment near submarine hot springs in primordial oceans (5).

A different situation is encountered in the cell, where the toxicity of iron and sulfide must be accounted for, and where **protein folding** or assembly of multimeric proteins must occur, along with **protein targeting** of nuclear-encoded proteins to the appropriate compartments. In cells and organelles, sulfide may be derived from cysteine or from thiosulfate through appropriate enzymes, while the actual carriers of iron remain unknown. FeS proteins are imported into organelles as metal-free precursors, and cluster insertion and acquisition of a native structure are very often assisted by more or less complex scaffolding systems. These scaffolding systems are most relevant when assembly of interprotein multimetallic clusters (as in dinitrogenase) or of multiple-component, multiple-cofactor enzymes is required.

Bibliography

1. H. Beinert, R. H. Holm, and E. Münck (1997) Science **277**, 653–659.
2. M. K. Johnson (1998) Curr. Opin. Chem. Biol. **2**, 173–181.
3. E. Hidalgo, H. Ding, and B. Demple (1997) Trends Biochem. Sci. **22**, 207–210.
4. T. A. Rouault and R. D. Klausner (1996) Trends Biochem. Sci. **21**, 174–177.
5. G. Wächtershäuser (1992) Prog. Biophys. Mol. Biol. **58**, 85–201.

Suggestions for Further Reading

6. R. H. Holm, P. Kennepohl, and E. I. Solomon (1996) Structural and functional aspects of metal sites in biology. Chem. Rev. **96**, 2239–2314.
7. D. M. Kurtz (1997) Structural similarity and functional diversity in diiron-oxo proteins. J. Biol. Inorg. Chem. **2**, 159–167.
8. H. Beinert, M. C. Kennedy, and C. D. Stout (1996) Aconitase as iron–sulfur protein, enzyme and iron-regulatory protein. Chem. Rev. **96**, 2335–2373.
9. R. Cammack (1992) Iron–sulfur clusters in enzymes: themes and variations. Adv. Inorg. Chem. **38**, 281–322.
10. D. H. Flint and R. M. Allen (1996) Iron–sulfur proteins with nonredox functions. Chem. Rev. **96**, 2315–2334.

Isochores

The vertebrate genome is compartmentalized into compositionally homogeneous regions, the *isochores* , originally identified (1) as segments of DNA longer than 300 kb that are homogeneous in base composition over segments at least 3 kb long. Isochores can be arranged into several families distinguished by different base compositions, as shown initially by density gradient centrifugation of DNA molecules derived from isochores through the breaks occurring during DNA preparation. Typical of the genomes of most mammals, the human genome has two GC-poor isochore families, L1 and L2 (which have few G and C bases, primarily A and T), which together represent 62% of the genome. Two GC-rich families H1 and H2 represent, respectively, 22 and 9% of the genome, and a very GC-rich H3 family represents only 3–4%. The remaining 4% of the genome consists of satellite and **ribosomal** DNA (2).

The localization of specific genes to defined isochores indicates that genes are not distributed randomly in the human genome. The density of genes is low in GC-poor isochores, increases with increasing GC content in the H1 and H2 families, and reaches a maximum in the very GC-rich family H3, where the gene concentration is at least 20-fold higher than in the GC-poor isochores. The H3 family corresponds to **telomeric** bands of **metaphase** chromosomes, and the L1 + L2 families correspond to **Giemsa bands**, whereas reverse bands comprise both GC-poor and GC-rich isochores.

1. Isochores and Evolution

The compositional distributions of large genome fragments (greater than 100 kb, such as those comprising standard DNA preparations) of **exons** and their codon positions and of **introns** are correlated with each other. They represent compositional patterns and are very different between the genomes of cold- and warm-blooded vertebrates, mainly because the former are much less heterogeneous in base composition and never reach the high GC levels attained by the latter. Only small compositional differences are found among the genomes of either cold- or warm-blooded vertebrates. Compositional patterns allow defining two modes of genome evolution: a conservative mode with no compositional change and a transitional (or shifting) mode with compositional changes. The conservative mode is observed among both cold- and warm-blooded animals. The transitional mode comprises both major and minor compositional changes. In vertebrate genomes, the major changes are associated with GC-rich and very GC-rich isochores in mammalian and avian genomes. Thus, the compositional changes reflect genome **phenotypes** differing not only between warm and cold-blooded vertebrates (eg, *Xenopus* versus mammals and birds), but also between mammals and birds (human and mouse versus chicken), and even among mammals. For a comprehensive review, see refs. 3 and 4.

Bibliography

1. G. Macaya, J-P Thiéry, and G. Bernardi (1976) J. Mol. Biol. **108**, 237–254.
2. D. Mouchiroud et al. (1991) Gene **100**, 181–87.
3. G. Bernardi (1993) Mol. Biol. Evol. **10**, 186–204.
4. G. Bernardi (1995) Ann. Rev. Genetics **29**, 445–476.

Isochromosome

Isochromosomes are chromosomes that contain multiple identical chromosomal arms. They may arise during the cell cycle when the two sister chromatids of an **acrocentric** or telocentric chromosome remain fused at their centromeres, leading to the creation of a **metacentric** isochromosome. Alternatively, if homologous chromosomes fail to pair during the first division of **meiosis**, the centromere of the univalent chromosome might split transversely, i.e., between the two arms, which results in two telocentric chromosomes that could be segregated during cell division. These telocentric chromosomes are unstable, and they may fuse to form an isochromosome in which one whole chromosome arm is deleted and the other duplicated. Isochromosomes in humans have been used to demonstrate that the centromere has variable activity, dependent on chromosomal context. For example, an isochromosome X containing two centromeres can be stably inherited through **cell division** if one is inactivated.

Suggestion for Further Reading

M. S. Clark and W. J. Wall (1996) *Chromosomes. The Complex Code*, Chapman and Hall, London, pp. 43–44.

Isocratic Elution Chromatography

Continuous elution of analytes in a **chromatographic** separation with only one mobile phase (a single solvent or a constant-composition solvent mixture) throughout the separation is known as isocratic-elution chromatography. This method is frequently very time-consuming, and the analytes are eluted as broad bands if they are strongly adsorbed on the column. Therefore, it is common to follow an initial period of isocratic separation with an elution gradient, in which the polarity of the initial mobile phase is progressively changed by the continuous programmed addition of increasing quantities of a second mobile phase to speed up the rate of elution and to sharpen eluent zones that are trailing or fronting. A description of the theory of isocratic-elution chromatography is beyond the scope of this article, and interested readers are directed to the excellent chapter written by Jandera and Churácek (1).

Bibliography

1. P. Jandera and J. Churácek (1985) *Gradient Elution in Column Liquid Chromatography: Theory and Practice* (*Journal of Chromatography Library*, Vol. **31**), Elsevier, Amsterdam, pp. 1–55.

Isoelectric Focusing

Conventional isoelectric focusing (IEF) in soluble, amphoteric buffers known as carrier ampholytes (CAs) was reported by Svensson-Rilbe in 1961 (1-3). In this technique, the macromolecules of interest are subjected to electrophoresis in a continuous pH gradient. They migrate electrophoretically toward the pH of their isoelectric point (pI), where they have zero mobility. Therefore, the system comes to equilibrium, with each species of macromolecule tightly focused at its pI; any diffusion away is reversed by the electrophoretic migration. At about the same time, Meselson et al. (4) described **isopycnic centrifugation**, a related high-resolution technique that is another member of a family called isoperichoric focusing by Kolin (5). Unlike conventional **chromatographic** and **electrophoretic** techniques, where peaks of material are constantly dissipated by diffusion, IEF and isopycnic centrifugation have built-in mechanisms opposing this. As the analyte reaches an environment (the *perichoron* in Greek) in which its physicochemical parameters are equal (*iso*) to those of its surroundings, it focuses, or condenses, in an ultrathin zone, kept stable and sharp in time by two opposing force fields: diffusion (tending to dissipate the zone) and external fields (voltage gradients in IEF or centrifugal fields in isopycnic centrifugation) forcing the “escaping” analyte back into its “focusing” zone.

Both conventional IEF using carrier ampholytes and the new version using immobilized pH gradients (IPG) (6) rely on the equation for resolving power (expressed as DpI, i.e., the difference in isoelectric points between a protein and a just resolved, nearest contaminant) (7):

$$\Delta \mathrm{pI} = 3.17\sqrt{(D_t[\partial(\mathrm{pH})/\partial x]/E[\partial u/\partial(\mathrm{pH})])}$$

where D_t is the protein translational diffusion coefficient, E is the voltage gradient (V/cm) applied, $\partial(\mathrm{pH})/\partial x$ is the slope of the pH gradient along the separation axis, and $\partial u/\partial(\mathrm{pH})$ is the titration curve of the protein in terms of its mobility as a function of pH. Experimental conditions minimizing DpI offer the greatest resolution, which are shallow pH gradients and high voltage gradients. The best DpI attainable is of the order of 0.01 pH unit in CA-IEF but 0.001 in IPG, where more shallow pH gradients and higher voltages are possible. Consequently, complex mixtures of macromolecules can be resolved into very many species, and what appears to be a single species by many separation techniques is frequently resolved into several by IPG (Fig. 1). A brief description of both methods will be given.

Figure 1. An example of the separations possible with isoelectric focusing. This soluble form of the **receptor** for epidermal growth factor (EGF) gave a single band on SDS-PAGE, but it was resolved by IPG into three major isoforms and several minor bands. The pH gradient was from pH 5 to pH 8, in a 10-cm-long 5% T, 4% C **polyacrylamide gel** equilibrated with 30% ethylene glycol. A total of 50 µg of protein was loaded at the anode, and focusing was carried out with the cathode uppermost. The resulting gels were stained with Coomassie Brilliant Blue R-250 (in ethanol, acetic acid, and copper sulfate) on the left and by Western blotting on the right. The pI values of the major components are indicated.(From Ref. 18, with permission.)

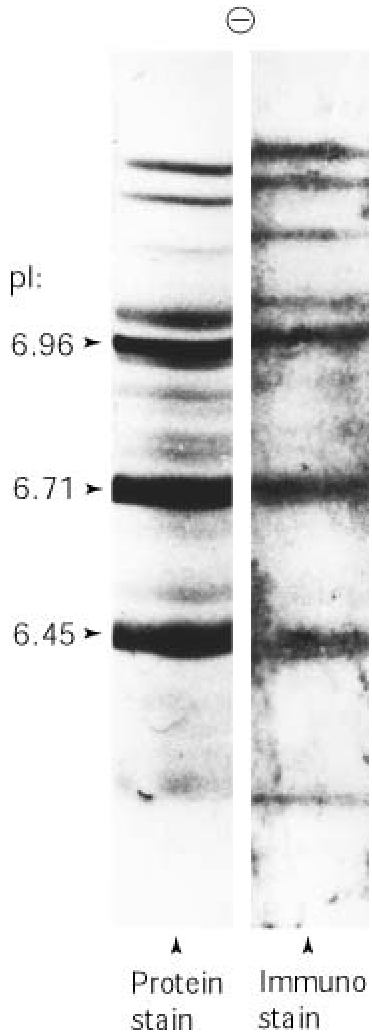

1. Conventional Isoelectric Focusing in Soluble, Amphoteric Buffers

Carrier ampholytes set up the pH gradient for IEF by distributing themselves electrophoretically at their isoelectric points. For a range of pH values, an appropriate mixture of ampholytes is necessary. They must not only be amphoteric, but must also have suitable buffering power and conductivity at their pI (7). The hallmark of a carrier ampholyte is the absolute value of the difference between its pI and the p K_a of its buffering groups; the smaller this value, the greater its conductivity and buffering capacity at its pI (8). Very few natural compounds have this property.

A breakthrough came in 1964 with Versterberg's synthesis of Ampholines (trade name of the commercial product from LKB). They are “oligoprotic amino carboxylic acids, each containing at least four weak protolytic groups, at least one being a carboxyl group and at least one a basic nitrogen atom, but no peptide bonds” (9). Figure 2 reports a hypothetical general structural formula of these ampholytes. Very narrow pH ranges of ampholytes are produced, except for the very extreme pH 2.5 to 4 and pH 9 to 11 ranges, by subfractionating the “wide pH-range” mixture in multicompartment electrolyzers. The synthesis of Ampholines is a genuine “chaotic” process, in that very heterogeneous mixtures of different oligoamines (typically pentaethylene hexamine, tetraethylene pentamine, and triethylene tetramine, including their branched isomers) were reacted with an a-b unsaturated acid (typically acrylic acid) at an appropriate ratio (usually 2 N atoms/1 carboxyl group); b-propionic acid residues result. By this synthetic approach, >600 ampholyte species could be generated in the pH 3 to 10 interval. Subsequently, Pharmalyte species containing >5000 chemically distinct amphoteres in the pH 2.5 to 11 interval were produced. Almgren (10) had predicted theoretically (assuming equimolar distribution of the CA species, even distribution of their DpI along the pH scale, and the same DpK_a) that only 30 amphoteres/pH unit had to be present to generate a stepless pH course. Because the oligoamines prepared had pK_a values well distributed along the pH scale, they could provide the buffering power and conductivity required for IEF. Additionally, the extra p K_a value of the “titrant” acrylic acid grafted onto the oligoamino backbone endowed acidic carrier ampholytes with extra buffering power. This is one of the reasons why focusing with CA buffers is usually more successful in acidic pH ranges than alkaline. The other reasons are that this synthesis generates fewer alkaline ampholytes and that open-face IEF gel slabs at pH >8 absorb atmospheric CO_2, unless submerged under a thin layer of light paraffin oil.

Figure 2. Composition of ampholines. (**a**) Representative chemical formula (aliphatic oligo-amino, oligo-carboxylic aci(**b**) Portions of hypothetical titration curves of Ampholines. (**c**) Different pH cuts for wide- and narrow-range carrier ampholytes.(Courtesy of LKB Producter AB.)

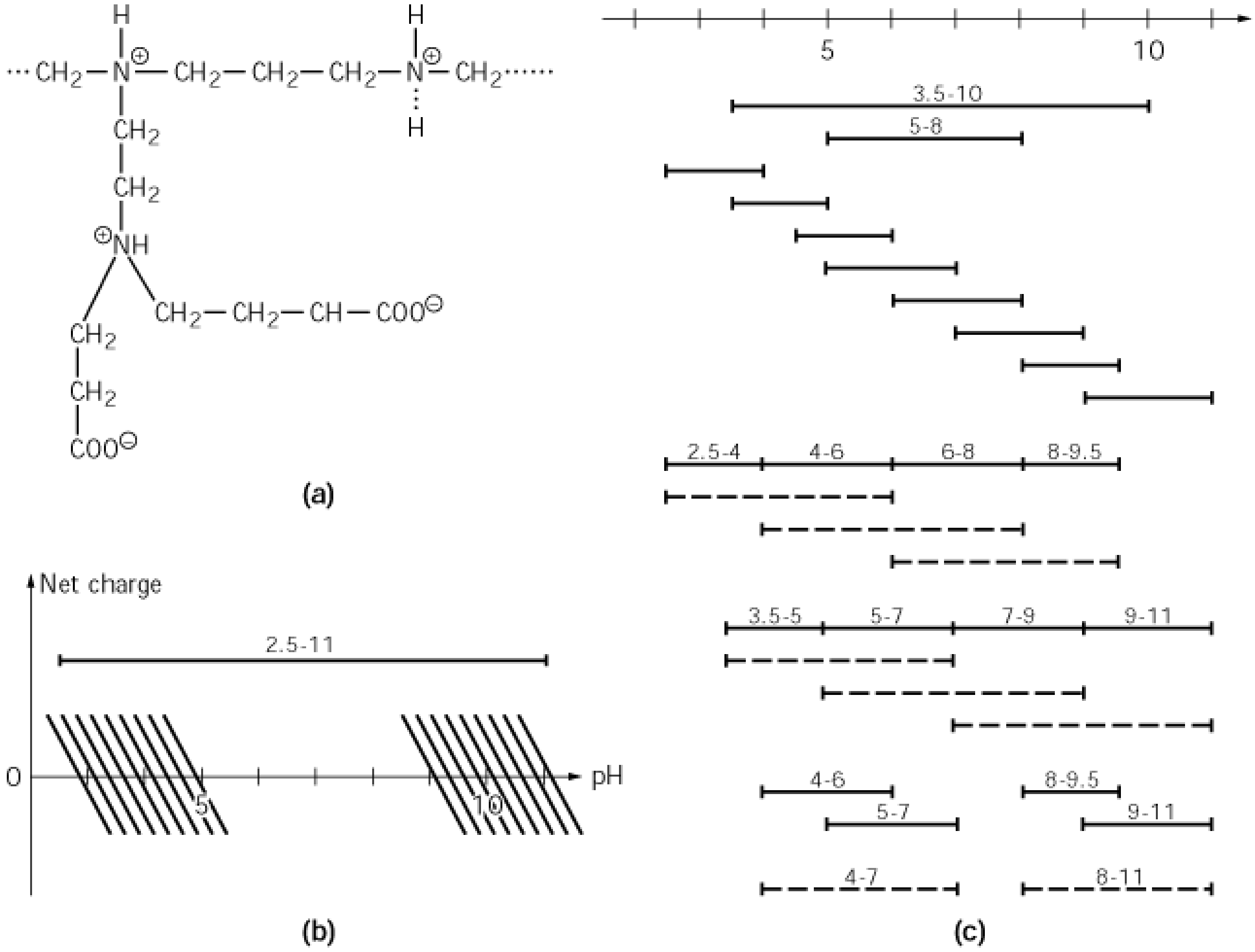

CA–IEF offers unrivaled resolving power in a vast number of separations and is now a standard technique in molecular biology. In addition to its current uses, at least two particular applications are worth mentioning: (a) its use in **two-dimensional** (2-D) electrophoresis to generate 2-D maps (11, 12) and (b) for generating titration curves of macromolecules. In the latter case, the CA–IEF slab gel is focused to generate the desired pH gradient. The slab is then turned 90° and the sample is loaded in a long, thin trench spanning from anode to cathode. The sample is then subjected to electrophoresis perpendicular to the stationary pH gradient. As a result, each protein exhibits its own pH/mobility curve in the gel slab (13).

There are, however, a number of problems with the CA–IEF gels: They have uncertain chemical environments of low ionic strength and uneven buffering capacity and conductivity; cathodic drift results in extensive loss of proteins at the gel cathodic extremity upon prolonged runs; and the pH gradients possible are limited by the nature of the carrier ampholytes available. The low ionic strength within the gel often induces near-isoelectric precipitation and smears of proteins, even in analytical runs with small amounts of protein. For all these reasons, the technique of IPG was launched in 1982 (6).

2. Immobilized pH Gradients

Immobilized pH gradients (IPGs) are unique in that they are based on the insolubilization of the entire set of buffers and titrants responsible for generating and maintaining the pH gradient along the separation axis. Contrary to CA–IEF, where a multitude of soluble, amphoteric buffers is expected to create and sustain the pH gradient during the electrophoretic run, IPGs are based on only a few well-defined, nonamphoteric buffers and titrants, able to perform in a highly reproducible manner.

Advantages of the IPG technique are: (a) increased resolution (by at least one order of magnitude); (b) unlimited stability of the pH gradient; (c) flexibility in the choice of pH interval; (d) increased loading ability; (e) high reproducibility; (f) minimal distortion by salts in the sample; (g) full control of pH, buffering capacity and ionic strength; and (h) easy separation of sample from buffering ions in preparative runs.

In IPGs, the pH gradient exists prior to the IEF run and is copolymerized, and thus immobilized, within the polyacrylamide matrix. This is achieved by using, as buffers, a set of six nonamphoteric weak acids and bases, having the general chemical composition $CH_2CH—CO—NH—R$, where R denotes either two different weak carboxyl groups, with pK_a values of 3.6 and 4.6, or four tertiary amino groups, with pK_a values of 6.2, 7.0, 8.5, and 9.3 (available under the trade name Immobiline from Pharmacia-LKB). A more extensive set, comprising 10 chemicals (with the addition of a pK_a 3.1 acidic buffer, a pK_a 10.3 alkaline species, and two strong titrants, a pK_a 1 acid and a pK_a >12 quaternary base), is available as “pI select” from Fluka AG, Buchs, Switzerland. During gel polymerization, these buffering species are efficiently incorporated into the gel (84% to 86% conversion efficiency at 50°C for 1 h). Immobiline-based pH gradients can be cast in the same way as conventional gradient polyacrylamide gels, by using a density gradient to stabilize the Immobiline concentration gradient, with the aid of a standard two-vessel gradient mixer (see Transverse Gradient Gel Electrophoresis (Tgge)). The buffers are not amphoteric, but are bifunctional: At one end of the molecule is located the buffering (or titrating) group, and at the other is the acrylic double bond, which will participate in the polymerization process. Acidic and alkaline Immobilines have different temperature coefficients ($\partial pK_a/\partial T$), so temperature affects Immobiline pH gradients, as do the ionic strength and additives that change the water structure (chaotropic agents, such as urea) or lower its dielectric constant. The largest changes are due to the presence of urea: Acidic Immobilines increase their pK_a values in 8 M urea by as much as 0.9 pH units, and basic Immobilines increase their pK_a values by only 0.45 pH unit. Detergents in the gel (up to 2% *w/v*) do not alter the Immobiline pK_a, suggesting that acidic and basic groups attached to the gel are not incorporated into surfactant micelles. For generating extended pH gradients, one should use two additional strong titrants having pK_a values well outside the desired pH range: QAE (quaternary amino ethyl)-acrylamide (pK_a >12) and AMPS (2-acrylamido-2-methyl propane sulfonic acid, pK_a ≈1).

With the IPG technology, ultranarrow (0.1), narrow (1.0), and extended (up to 8.0) pH gradients can be engineered with high precision and reproducibility. Recipes have been tabulated listing 58 1-pH-unit-wide gradients, separated by 0.1 pH unit increments, starting with the 3.8 to 4.8 pH interval and ending with the pH 9.5 to 10.5 range (14). If a narrower pH gradient is needed, it can be derived from any of the 58 pH intervals tabulated by a simple linear interpolation of intermediate Immobiline molarities. Recipes for gradients with pH spans from 2 pH units up to 6 pH unit spans are available (15). All the formulations are normalized to give the same average value of buffering power of 3mequiv.$L^{-1}pH^{-1}$, adequate for producing highly stable pH gradients. For pH intervals covering >4pH units, the best solution is to mix a total of 10 Immobiline species, 8 of them buffering ions and two the strong acidic and basic titrants. Nonlinear (eg, concave and convex exponential, as well as sigmoidal) IPG gradients can be generated and optimized (16).

After casting, IPG gels should be washed extensively, so as to remove nonpolymerized material, salts, and polymerization catalysts. This also produces clean matrices, devoid of toxic materials (eg, unreacted acrylic double bonds) that could modify proteins by reacting with thiol groups and terminal amino groups. As IPG gels are cast onto plastic supports and are rather thin (0.5 mm) and porous, they can be stored dry and then reswollen with any desired additives just prior to use. IPG are very reproducible and effective at very alkaline pH values, up to pH 12, where CA–IEF would simply fail; histones could thus be focused to steady state (17).

Bibliography

1. H. Svensson (1961) Acta Chem. Scand. **15**, 325–341.
2. H. Svensson (1962) Acta Chem. Scand. **16**, 456–466.
3. H. Svensson (1962) Arch. Biochem. Biophys. Suppl. 1, 132–140.
4. M. Meselson, F. W. Stahl, and J. Vinogradov (1957) Proc. Natl. Acad. Sci. USA **43**, 581–585.
5. A. Kolin (1977) In *Electrofocusing and Isotachophoresis* (B. J. Radola and D. Graesslin, eds.), de Gruyter, Berlin, pp. 3–33.
6. B. Bjellqvist, K. Ek, P. G. Righetti, E. Gianazza, A. Görg, W. Postel, and R. Westermeier (1982) J. Biochem. Biophys. Methods **6**, 317–339.
7. H. Rilbe (1973) Ann. N.Y. Acad. Sci. **209**, 11–22.
8. P. G. Righetti, M. Fazio, and C. Tonani (1988) J. Chromatogr . **440**, 367–377.
9. O. Vesterberg (1973) Ann. N.Y. Acad. Sci. **209**, 23–33.
10. M. Almgren (1971) Chem. Scripta **1**, 69–75.
11. D. S. Young and N. G. Anderson (Guest Eds.) (1982) (Special Issue on 2-D Gel Electrophoresis) Clin. Chem. **28**, 737–1092.
12. L. Anderson and N. Anderson (Guest Eds.) (1984) (Special Issue on 2-D Gel Electrophoresis) Clin. Chem. **30**, 1897–2108.
13. P. G. Righetti (1996) In *Current Protocols in Protein Science* (J. E. Coligan, B. M. Dunn, H. L. Ploegh, D. W. Speicher, and P. T. Wingfield, eds.) Vol. **1**, suppl. 3, Wiley, New York, pp. 7.3.13–7.3.26.
14. P. G. Righetti, A. Bossi, and C. Gelfi (1998) In *Gel Electrophoresis of Proteins. A Practical Approach* (B. D. Hames ed.), IRL Press, Oxford, U.K., pp. 127–187.
15. P. G. Righetti (1989) In *Protein Structure, A Practical Approach* (T. E. Creighton, ed.), IRL Press, Oxford, U.K., pp. 23–63.
16. E. Giaffreda, C. Tonani, and P. G. Righetti (1993) J. Chromatogr. **630**, 313–323.
17. A. Bossi, C. Gelfi, A. Orsi, and P. G. Righetti (1994) J. Chromatogr. A **686**, 121–128.
18. E. Wenisch, P. G. Righetti, and W. Weber (1992) Electrophoresis **13**, 668–673.

Suggestions for Further Reading

19. P. G. Righetti (1983) *Isoelectric Focusing: Theory, Methodology and Applications*, Elsevier, Amsterdam, pp. 1–386.
20. P. G. Righetti (1990) *Immobilized pH Gradients: Theory and Methodology*, Elsevier, Amsterdam, pp. 1–400.
21. H. Rilbe (1996) *pH and Buffer Theory. A New Approach*, Wiley, Chichester, pp. 1–192.

Isoelectric Point (PI)

The isoelectric point is the pH at which the total net charge of an amphoteric molecule becomes zero. The isoelectric point depends on the ionic strength of the solvent, the counterion species, and the solute concentration, whereas the isoionic point is the isoelectric point in the absence of counterions and at low solute concentrations. The isoelectric point is readily measured as the pH at which the molecule is immobile in an electrophoresis experiment (see Isoelectric Focusing). The isoelectric point approaches the isoionic point at low ionic strength, when all bound ions are removed. At the isoelectric point, amphoteric molecules aggregate and become insoluble because there are no electrostatic repulsions between molecules with the same net charge.

Isofunctional Proteins

In some instances, it is necessary for an organism to produce two or more forms of the same protein, *isofunctional proteins* that have the same function, so as to optimize their metabolic regulation. Cells generally have two primary mechanisms for regulating their metabolic reaction rates in response to changes in the levels of various metabolites: (i) **allosteric** inhibition or activation of the activities of certain enzymes and (ii) regulation of the biosynthesis of the enzymes.

1. Regulation of Biosynthetic Pathways

Consider a linear sequence of reactions

$$A \longrightarrow B \longrightarrow C \longrightarrow D \longrightarrow E \longrightarrow M$$

leading to the synthesis of the essential metabolite M. In the presence of excess M in the intracellular pool, the enzyme carrying out the conversion A → B will often be subject to **feedback inhibition** by M if, as is generally the case, this enzyme is an allosteric protein. M may also **repress** the synthesis of the enzymes of the entire pathway. These control phenomena are economical and efficient ways of keeping the pool size of M relatively constant and do not cause any detrimental side effects.

Now consider a branched reaction biosynthetic sequence, such as that of the aspartate family of amino acids:

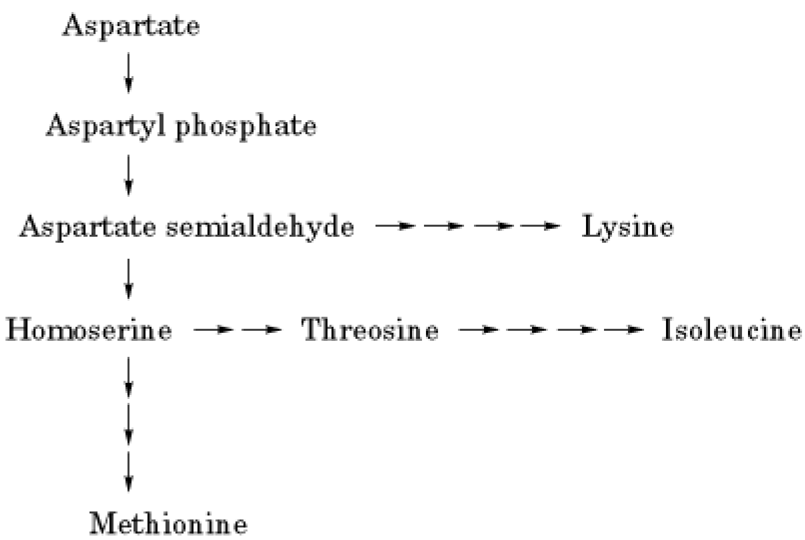

Regulation of this pathway by feedback inhibition of the first enzyme, aspartokinase, or by repressing expression of the enzymes of the entire pathway by the various end products (lysine, threonine, isoleucine, and methionine) could not ensure balanced production of all end products when one or just a few are present in excess. The solution to this potential dilemma differs according to the organism studied, but that of *Escherichia coli* illustrates the use of isofunctional proteins.

2. Three Aspartokinases in *Escherichia Coli*

Of all the natural amino acids occurring naturally as protein constituents, only two, L-lysine and L-threonine, influence the aspartokinase activity of crude extracts of *E. coli*. Neither totally inhibit the activity, and the total inhibition, when they are present simultaneously, is the sum of that observed for each independently because one aspartokinase is sensitive to inhibition by lysine and another is sensitive to threonine (1). The synthesis of the enzyme aspartokinase is repressed by lysine, and that of the latter is subject to a multivalent repression by threonine and isoleucine ((1),(2)). A third aspartate kinase is inhibited by none of the end-products of the pathway, but its synthesis is repressed by methionine (see Methionine Regulon). The three aspartokinases are highly homologous and share a common ancestor (3-5).

The rational solution in *E. coli* to the dilemma posed by the regulation of branched biosynthetic pathways was the synthesis of multiple, *isofunctional* enzymes that catalyze the synthesis of the common precursor, aspartyl phosphate. Each of these enzymes is independently subject to feedback inhibition and to repression by different end-product metabolites. Another example is encountered in the *E. coli* biosynthetic pathway of aromatic amino acids. Three distinct isofunctional 3-deoxy-d-arabino-heptulosonate-7-phosphate synthetases are, respectively regulated by allosteric inhibition and/or repression by the three end products, phenylalanine, tyrosine, and tryptophan (6) (see TRP Operon).

Bibliography

1. E. R. Stadtman et al. (1961) J. Biol. Chem. **236**, 2033–2038.
2. G. N. Cohen and J-C. Patte (1963) Cold Spring Harbor Symp. Quant. Biol. **28**, 513–515.
3. M. Cassan et al. (1986) J. Biol. Chem. **261**, 1052–1057.
4. M. Katinka et al. (1980) Proc. Natl. Acad. Sci. USA **77**, 5730–5733.
5. M. M. Zakin et al. (1983) J. Biol. Chem. **258**, 3028–3031.
6. A. J. Pittard (1996) In *Escherichia coli and Salmonella; Cellular and Molecular Biology* (F. C. Neidhardt, ed.), ASM Press, Washington, DC, Vol. **I**, p. 460.

Suggestion for Further Reading

7. G. N. Cohen (1994) *Biosyntheses*, Chapman and Hall, New York and London, pp. 147–200.

Isoionic Point (Isoionic pH)

The isoionic point is the pH at which the total net charge of an amphoteric molecule becomes zero in pure water. The ideal isoelectric point is that in the complete absence of salt and at very low solute concentrations. No counterions should be present except for the protons and the hydroxyl ions of the solvent. Any metal ions bound to the macromolecules should be removed. The isoionic point can be estimated from the pK_a values of the individual ionizable groups.

Isoleucine (Ile, I)

The amino acid isoleucine is incorporated into the nascent polypeptide chain during **protein biosynthesis** in response to three **codons**—AUU, AUC, and AUA—and represents approximately 5.2% of the residues of the proteins that have been characterized. The isoleucyl residue incorporated has a mass of 113.16 Da, a **van der Waals volume** of 124 $Å^3$, and an accessible surface area of 182 $Å^2$. Ile residues are frequently changed during divergent evolution; they are interchanged in **homologous** proteins most frequently with valine, leucine, and threonine residues.

The Ile side chain is nonpolar with no functional or reactive groups:

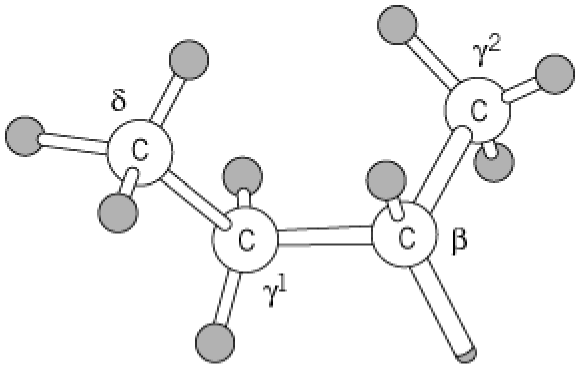

Consequently, Ile is one of the most **hydrophobic** amino acid residues, and 60% of Ile residues are completely buried in native protein structures. Ile residues do not favor the **alpha-helical** conformation in model peptides, and they occur most frequently in the beta-sheet type of **secondary structure** in native proteins. Note that the Ile side chain has a center of asymmetry, at C^b, and that only the one isomer occurs naturally and is incorporated into proteins.

Suggestions for Further Reading

T. E. Creighton (1993) *Proteins: Structures and Molecular Properties*, 2nd ed., W. H. Freeman, New York.

Isomer

The word isomer indicates that two molecules share the same elemental formula, being derived from the Greek isos, for "equal" and meros for "part." The importance of isomers in chemistry and biochemistry derives from the historical importance of elemental analysis in determining structural identity. A simple example of isomers is ethanol and dimethyl ether, both compounds having the elemental formula C_2H_6O (Fig. 1).

Figure 1. The structural differences between the isomers ethanol and dimethyl ether. These demonstrate how two molecules having the same elemental formulas can have different covalent structures.

Structural isomers

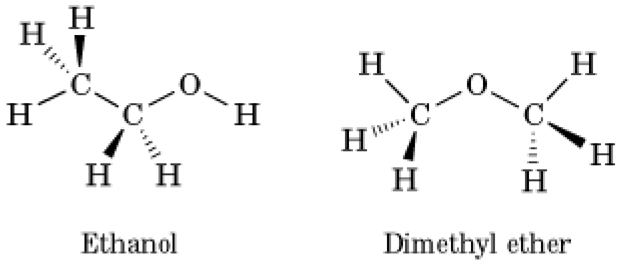

Since two molecules of common elemental formula can differ in many ways, many times the mode of differentiation is indicated. Ethanol and dimethyl ether are structural isomers, as are glucose and fructose, because the number and type of bonds are different. Geometric isomers differ in geometrical arrangement of bonds, eg, fumarate and maleate. Stereoisomers, diastereomers, and enantiomers are specialized cases of isomerism, where the differences in the molecules are determined solely by the spatial orientation of the bonds. Tautomers are another specialized class of isomers that are differentiated by their ability to equilibrate rapidly.

A common mistake is to regard conformers as isomers. Conformers are generated by rotation about a single bond and not a difference in the structure or configuration of the bonds present, which is required for isomerism (1).

Bibliography

1. E. L. Eliel et al. (1967) *Conformational Analysis*, Wiley-Interscience, New York, p. 1.

Suggestions for Further Reading

2. K. Mislow (1962) In *Comprehensive Biochemistry, I: Atomic and Molecular Structure* (M. Florkin and E. H. Stotz, eds.), Elsevier, Amsterdam, pp. 192–241.
3. B. Testa (1982) In *Stereochemistry* (C. Tamm, ed.), New Comprehensive Biochemistry 3, Elsevier, Amsterdam, pp. 1–48.

Isomerases

Isomerases form a broad group of enzymes that catalyze intramolecular rearrangements. The subdivisions within this class are:

- *Racemases*. Act on amino acids and hydroxy acids with **chiral** centers.
- *Epimerases*. Act on carbohydrates and their derivatives, as well as other compounds with chiral centers.
- *Isomerases*. Catalyze cis trans isomerization reactions, keto-enol transformation, the interconversion of aldoses and ketoses, shifts of double bonds, and the rearrangement of disulfide bonds.
- *Mutases*. Transfer acyl, phosphoryl, amino, and other groups from one intramolecular position to another

Isomorphous Replacement

To determine the structure of a macromolecule using X-ray crystallography, an electron density map of the structure is computed as a Fourier summation:

$$\rho(xyz) = \frac{1}{V}\sum_h \sum_k \sum_\ell |F(hk\ell)| \times \exp[-2\pi i(hx + ky + \ell z) + i\alpha(hk\ell)] \quad (1)$$

where r(*x y z*) is the electron density at position *x*, *y*, *z* in the unit cell and *F*(*h k* ℓ) is the amplitude of the structure factor for reflection *h k* h. Apart from correction factors, *vbm*0;*F*(*hk*h) *vbm*0; = <*rad*><*rcd*>*I*(*hk*h)</*rcd*></*rad*>, where *I*(*h k* h), is the intensity measured for the reflection *h k* h. The phase angle for this reflection is a(*h k* h). The value of a(*h k* h) cannot be derived directly from the experimental data for macromolecular structures (see Phase Problem). Several methods do exist, however, to find the values for the phase angles. For macromolecular structures, such as proteins, isomorphous replacement is the oldest and the most general method. It was applied for the first time by Perutz to solve the structure of hemoglobin (1).

It requires the X-ray diffraction pattern of native protein crystals and also of one or more derivatives that contain heavy atoms attached to the native protein. The attachment must be isomorphous, which means that the structure of the protein itself should not be affected by the binding of the heavy atom reagents. A first check for isomorphism is comparing the unit cell dimensions of the native and derivative crystals. An easy way to introduce heavy atoms is to soak a native crystal in an appropriate solvent that contains the heavy atom. It uses the large voids and channels filled with the solvent that are present between protein molecules in a crystal. Small reagents easily diffuse into the crystal and reach reactive sites on all of the molecular surfaces.

After processing the diffraction data, the position of the heavy atoms in the unit cell must be found. This can be done with a difference Patterson summation which has as coefficients (D*F*)^2 = (*vbm*0;F_{PH}*vbm*0;–*vbm*0;F_P*vbm*0;)^2 and all phase angles equal to zero:

$$P(uvw) = \frac{1}{V}\sum_h \sum_k \sum_\ell \{\Delta F(hk\ell)\}^2 \cos[2\pi(hu + kv + \ell w)]$$

where *u*, *v*, and *w* are coordinates in the Patterson cell [see Patterson Map]. F_{PH} and F_P are the amplitudes of the structure factor for one reflection of the derivative and the native structure, respectively.

After determining and refining the heavy atom position and parameters, the heavy atom contribution of the vector $\mathbf{F_H}$ to the structure factor can be calculated. The knowledge of F_{PH}, F_P and $\mathbf{F_H}$is sufficient to determine the phase angle of the reflection from the crystal that contains only the protein. In principle, this is done by a circle construction method due to Harker. In this method, the structure factors are regarded as vectors in a plane (Argand diagram). The length of such a vector is equal to the amplitude of the structure factor and its direction is given by the phase angle of the reflected beam. For each reflection, a circle is drawn whose radius is F_P (Fig. 1). Next, the vector $\mathbf{F_H}$

is pointed to the center of this F_P circle. A second circle is drawn with radius F_{PH} whose center is at the origin of vector $\mathbf{F_H}$. The points of intersection of the two circles are possible end points of the structure factor of the protein, because only at those positions is the principle of isomorphous replacement obeyed: $\mathbf{F_P} + \mathbf{F_H} = \mathbf{F_{PH}}$.

Figure 1. The Harker construction for determining the protein phase angle in the isomorphous replacement method.

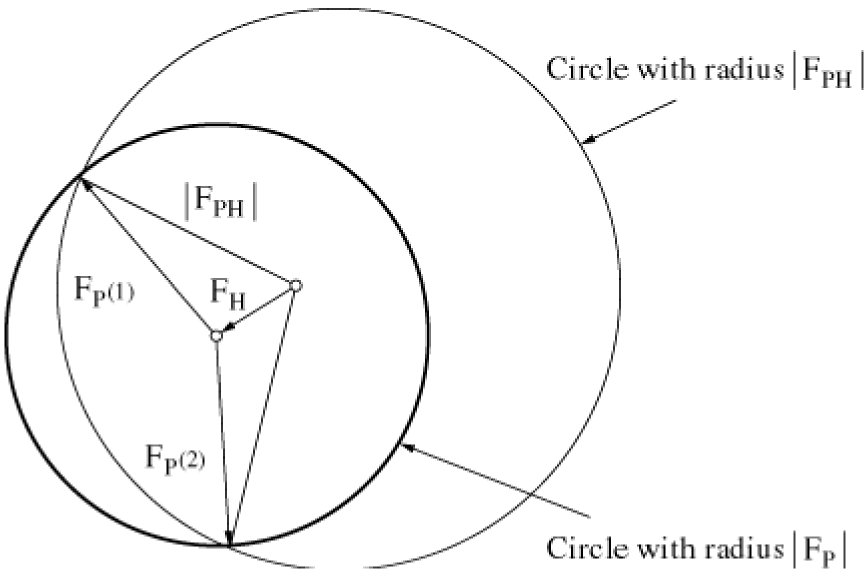

The choice between the two possible vectors, $\mathbf{F_P}$ (1) and $\mathbf{F_P}$ (2), can be made by repeating the procedure with a second, or even further, heavy atom derivatives. This is called multiple isomorphous replacement (MIR). Because of experimental errors and nonideal isomorphism, the correct phase angle may differ somewhat from the exact point of intersection. Therefore, weighting probabilities are introduced in most procedures for calculating the phase angle, depending on the degree of closure of the vector triangle $\mathbf{F_P} + \mathbf{F_H} = \mathbf{F_{PH}}$ (2). With only one derivative, the method is called single isomorphous replacement (SIR). With SIR, the protein electron density map is calculated from $\mathbf{F_P}$ (1) + $\mathbf{F_P}$ (2). It is expected that the correct values for the many $\mathbf{F_P}$'s contribute to a correct electron density map and the incorrect values contribute to noise.

Bibliography

1. D. W. Green, V. M. Ingram, and M. F. Perutz (1954) Proc. Roy. Soc. A **225**, 287–307.
2. D. M. Blow and F. H. C. Crick (1959) Acta Crystallogr. **12**, 794–802.

Suggestion for Further Reading

3. J. Drenth (1999) *Principles of Protein X-ray Crystallography*, Springer, New York, Chap. "7".

Isopropyl-1-Thio-b-D-Galactopyranoside

Escherichia coli grown in lactose (1-4-b-galactosyl-glucose) produces about a thousand times more **b-galactosidase** than when grown in glucose. What happens? The kinetics of the process could be revealing, but lactose is a substrate of b-galactosidase. Lactose is hydrolyzed into glucose and galactose by this enzyme, and it is also isomerized. In fact, one of the isomerization products, *allolactose* (1-6-b-galactosyl-glucose) is the actual **inducer**. Lactose itself does not induce! Therefore, lactose is badly suited for the kinetic study of this induction process.

What would possibly be an ideal inducer that is not hydrolyzed by b-galactosidase? The German biochemist Otto Meyerhof had left a collection of glycosides in Paris when fleeing the German army in 1940. One of them was phenyl-1-thio-b-D-glucopyranoside, synthesized in 1912 by Konrad Delbrück in Emil Fischer's laboratory in Berlin. In contrast to ordinary glycosides, it is stable under extreme conditions. Jacques Monod found the collection after the war. He picked up the idea and interested two German chemists, Dietmar Türk and Burckhardt Helferich in Bonn, in synthesizing a whole set of 1-thio-b-D-galactopyranosides. The best inducer was isopropyl-1-thio-b-D-galactopyranoside (IPTG). Because IPTG is not measurably hydrolyzed by b-galactosidase, it was called a gratuitous inducer. Using IPTG, it could be shown that induced b-galactosidase synthesis starts three minutes after addition of the inducer and continues from then on at with a constant rate (1) (see Lac Operon). Later, **radiolabeled** IPTG was used to isolate Lac repressor (see Lac Repressor) (2). See Lac Operon for further details and reference 3 for its general history.

Bibliography

1. J. Monod (1956) In *Enzymes: Units of Biological Structure and Function*, Academic Press, New York, pp. 7–28.
2. W. Gilbert and B. Müller-Hill (1966) Proc. Natl. Acad. Sci. USA **56**, 1891–1898.
3. B. Müller-Hill (1996) *The lac Operon. A Short History of a Genetic Paradigm*, de Gruyter, Berlin.

Isoschizomer

Isoschizomers are distinct, different restriction endonucleases (see Restriction Enzymes and Restriction–Modification Systems) that recognize the same DNA sequence and cleave at the same position in the DNA. Isoschizomers are derived from different organisms and sometimes have different amino acid sequences. For example, R•*Eco*RI (from *Escherichia coli*) and R•*Rsr*I (from *Rhodobacter sphaeroides*) are isoschizomers that both recognize the duplex DNA sequence G ^ AATTC and cleave (designated by the caret symbol " ^ ") the phosphodiester bond after the G on each strand (G ^ AATTC). Another isoschizomeric pair are the type IIs enzymes *Ksp*632I and *Ear* I, which recognize CTCTTC and cleave (1/4) to the right side (3′) of the sequence (1). The (1/4) designation indicates that the (5′–3′) strand is cleaved one nucleotide residue to the right of the canonical sequence and that the complementary strand is cleaved on the same side 4 nucleotide residues beyond the site.

Except in a few cases, like the R•*Eco*RI/R•*Rsr*I pair, isoschizomers show little amino acid sequence similarity to one other. DNA methyltransferases (MTases; see Methyltransferase, DNA), the companion enzymes of endonucleases, isolated from different organisms and having the same DNA sequence and methylation specificity, are referred to as *isoprostomers* or *isomethylators* (2). For example, M•*Eco*RI and M•*Rsr*I both recognize GAATTC and methylate the second adenine base to give GAmATTC, where mA represents the methylated adenine product.

A related type of isomeric restriction endonucleases is termed *neoschizomer* or *heteroschizomer* (2). These endonucleases are also derived from different organisms and have the same sequence specificity, but cleave at different positions within the sequence. For instance, R•*Asp*718I and R•*Kpn*I are neoschizomers that produce G ^ GTACC and GGTAC ^ C cleaved sequences, respectively. Another neoschizomeric pair are R•*FoK*I and R•*Sts*I, which recognize the sequence dGGATG and cleave (9/13) and (10/14) nucleotides beyond the recognition sequence, respectively (3). MTases that have the same sequence specificity but methylate at different positions are termed *heteroprostomers* (2). For example, M•*Hpa*II and M•*Msp*I both recognize CCGG, but M•*Hpa*II methylates the first C to give mCCGG and M•*Msp*I, the second C to give CmCGG.

Depending on the particular endonuclease or MTase, one **isoenzyme** may provide a more economical or suitable alternative to another. Some isomers are less costly to produce, have less star activity, can be more easily freed of nuclease contamination, or have greater stability or different sensitivities to methylation. Isomeric endonucleases and MTases are useful in several applications. For example, some isoschizomers can be used to analyze the methylation state of DNA. For instance, to determine the level of 5-methylcytosine in CG dinucleotides in mammalian genomes, isoschizomers with different sensitivities to methylation may be used. R•*Msp*I, R•*Hpa*II, and R•*Hap*II all recognize and cut after the first C of C ^ CGG. R•*Msp*I cuts at methylated sequences CmCGG, whereas the isoschizomers R•*Hpa*II and R•*Hap* II do not. In a related example, MTase isomers can be used to modulate endonuclease activity. M•*Hpa*II (CmCGG) and M•*Msp*I (mCCGG) are a heteroprostomeric pair. M•*Msp*I methylation inhibits R•*Msp*I and R•*Hpa*II but not R•*Hap*II, whereas M•*Hpa*II methylation inhibits R•*Hpa*II and R•*Hap*II but not M•*Msp*I.

Neoschizomers are also useful in molecular cloning. For instance, R•*Sac*I generates a 5′ overhang, staggered cut on cleavage of the canonical sequence GAGCT ^ C. Its neoschizomer, R•*Eco*ICRI, generates a blunt cut: GAG ^ CTC. *Blunt-end* DNA generated by R•*Eco*ICRI can be ligated (see DNA Ligase) to other blunt-end DNA fragments, thereby eliminating the need for compatibility of cohesive termini for ligation of DNA fragments produced by R•*Sac*I cuts. The existence of restriction–modification isoenzymes expands our capacity to manipulate DNA.

Bibliography

1. A. Pingould, J. Alves, and R. Geiger (1993) in *Methods in Molecular Biology*, Vol. **16**, *Enzymes of Molecular Biology*, M. M. Burrell, ed., Humana Press, Inc., Totowa, N.J., p. 167.
2. C. Kessler and V. Manta (1990) Gene **92**, 1–248.
3. R. J. Roberts and S. E. Halford (1993) in *Nucleases*, 2nd ed., (S. M. Lynn, R. S. Lloyd, and R. J. Roberts, eds.,) Cold Spring Harbor Laboratory Press, New York, pp. 35–88.

Isotachophoresis

Isotachophoresis (also known as “stacking”) is an application of discontinuous buffer systems for electrophoresis in which sequential moving boundaries of all the components present (the stack) are set up and displaced in the electric field at a single velocity. In principle, such a system does not differ from the stacking phase of disc electrophoresis . The sequential leading and trailing ion moving boundaries may be separated from each other by proteins or other ionic species with intermediate net mobilities (“spacers”). Both amino acids and carrier ampholyte mixtures (see Isoelectric Focusing) have been used as spacers between stacked protein zones. At equilibrium, contiguous zones of stacked proteins or spacers migrate at the same velocity; hence the name *isotachophoresis* . The width of each zone is proportional to the amount of protein or spacer in the zone. Thus, when the sample load is increased, the distance between the leading and trailing edges of a moving boundary (the zone within the stack) increases, making it possible to isolate a homogeneous protein from the center of each zone of the "extended stack." The concentration of protein is "regulated" at very high values by the mobilities and concentrations of the ions constituting the discontinuous buffer system that generates the stack, and so isotachophoresis is an ideal preparative technique. Theoretically, isotachophoresis is not only synonymous with steady-state stacking and disc electrophoresis but becomes also mechanistically the same as isoelectric focusing when the concentration of the common counterion approaches zero.

The spaced zones can be detected by differences in their temperature or conductance, because each moving boundary at the steady-state is characterized by a specific field strength that provides an equal ("iso") mobility in spite of the differences in net mobility between components of the stack. Such detectors affixed to capillaries are the preferred instrumentation of analytical isotachophoresis, and they preceded by many years the use of absorbance and fluorescence detectors in capillary zone electrophoresis.

Suggestions for Further Reading

F. M. Everaerts, J. L. Beckers, and P. E. M. Verheggen (eds.) (1976) *Isotachophoresis*. Elsevier, Amsterdam.

G. Baumann and A. Chrambach (1976) Gram-preparative protein fractionation by isotachophoresis: Isolation of human growth hormone isohormones. Proc. Natl. Acad. Sci. USA **73**, 732–736.

A. Chrambach and L. M. Hjelmeland (1984) "Some recent conceptual advances in moving boundary electrophoresis and their practical implications. In" *Electrophoresis '83* (H. Hirai, ed.),W. de Gruyter, Berlin, pp. 81–97.

A. Adam and C. Schots (eds.) (1980) *Biochemical and Biological Applications of Isotachophoresis* . Elsevier, Amsterdam.

Isotope Exchange at Equilibrium

Measuring the rate of exchange of isotopes between substrates and products in the presence of an enzyme has been very useful for determining the **kinetic mechanisms** of enzyme-catalyzed reactions. It relies on the incorporation of **radioactive** atoms from a substrate (or product) into the product (or substrate) under conditions where there is no net reaction. Thus, it differs from other kinetic techniques that rely on the measurement of the rates of product formation. The procedure that is utilized depends on the mechanism under study

A single-site ping-pong mechanism consists of two partial reactions, so the overall reaction is a double displacement (see **Kinetic mechanisms**); First, substrate A is converted to P, leaving a modified form of the enzyme that then converts substrate B to product Q. For the first partial reaction

$$\mathrm{E} + \mathrm{A} \rightleftharpoons (\mathrm{EA} - \mathrm{FP}) \rightleftharpoons \mathrm{F} + \mathrm{P}$$

the addition of only substrate A to the enzyme will result in the release of P and the production of a modified form of the enzyme F. The maximum amount of P that can be released is equivalent to the enzyme concentration and that will occur only when the equilibrium of the partial reaction lies far to the right or the concentration of A is high. Usually, the concentration of enzyme that is used to detect a partial exchange reaction is low and in the micromolar region, so the release of P is small. In the absence of substrate B, the system is at thermodynamic equilibrium, and the A and P reactants are shuttling back and forth. Thus, on the addition of isotopically labeled P (or A), it will be converted to A (or P) and the isotope is incorporated into A (or P). Given sufficient time, the label will be distributed in the same proportions in A and P, and the specific radioactivities of A and P will be identical. The rate at which A is converted to P must be the same as that for the conversion of P to A. It is this partial exchange reaction in the absence of the other substrate that characterizes a ping-pong mechanism. But it is important to demonstrate that the exchange reaction occurs with both halves of the reaction, ie, with both A/P and with B/Q. If only one exchange reaction occurs, it could be due to the presence of an impurity in the enzyme preparation.

The equation for the initial rate of the exchange reaction observed between A and P, starting with labeled A, v_{A-P}, is given by the expression

$$v_{A-P} = \frac{(V_1 K_{ia}/K_a)AP}{K_{ia}P + K_{ip}A + AP} \tag{1}$$

Here, V_1 is the maximum rate of the enzyme-catalyzed reaction, A and P are the concentrations of the two reactants, and K_a is the $\boldsymbol{K_m}$ of A. The equation has the same form as that for the initial velocity of a ping-pong mechanism (see **Kinetic mechanisms**), except that the denominator contains **dissociation constants** for the EA (K_{ia}) and FP (K_{ip}) complexes (1). In the absence of the formation of a dead-end FA complex (see Substrate Inhibition), a plot of $1/v$ against $1/A$ at different concentrations of P yields a family of parallel straight lines (see Lineweaver–Burk Plot). Analysis of the kinetic data can give values for K_{ia} and K_{ip} as well as for the apparent maximum velocity of the isotope exchange reaction, which is equal to either V_1K_{ia}/K_a or V_2K_{ip}/K_p, where V_2 is the maximum rate of the reverse reaction. An equation of the same form applies for measurement of the initial rate of the B–Q exchange:

$$v_{B-Q} = \frac{(V_1 K_{ib}/K_b)BQ}{K_{iq}B + K_{ib}Q + BQ} \tag{2}$$

The maximum velocity of the exchange reaction, relative to the maximum velocities of the overall chemical reactions, depends on the values of the dissociation and Michaelis constants. But there is a relationship between the maximum rates of the chemical (V_1 and V_2) and exchange (V_{A-P} and V_{BQ}) reactions (Eq. 3):

$$\frac{1}{V_{A-P}} + \frac{1}{V_{B-Q}} = \frac{1}{V_1} + \frac{1}{V_2} \tag{3}$$

A further relationship that holds for a single-site ping-pong mechanism is given in Equation 4:

$$\frac{1}{V_{A-Q}} = \frac{1}{V_{A-P}} + \frac{1}{V_{B-Q}} \tag{4}$$

The addition of both substrates or both products to measure the rate of the overall exchange reaction would reduce the rate of exchange of the partial exchange reactions because of the formation of the FB and/or EQ complexes, which would reduce the concentration of the forms of enzyme that participate in the partial exchange reactions.

The procedure that is utilized for the study of exchange reactions with sequential reactions differs from that for a ping-pong mechanism, because sequential mechanisms do not exhibit partial exchange reactions. The technique is applied by allowing the sequential reaction to come to equilibrium and then disturbing that equilibrium by the addition of a small chemical concentration of a highly **radiolabeled** reactant. The initial rate of the exchange of the label from substrate to product is measured as a function of the concentration of a substrate–product pair that is increased in its equilibrium ratio. For the Bi–Bi reaction

$$A + B \rightleftharpoons P + Q$$

K_{eq} is equal to $(P)\,(Q)/(A)/(B)$ and it is possible to raise the concentration of any one of four pairs of reactants, P/A, P/B, $Q/\,A$, or Q/B, without disturbing the equilibrium. The exchange rate can be measured for any one of three possible pairs, but for the most part, exchanges are measured between like substrate–product pairs with the absolute concentration of the same pairs being raised in constant ratio. For the creatine kinase reaction

$$\text{Creatine} + \text{MgATP}^{2-} \rightleftharpoons \text{phosphocreatine} + \text{MgADP}^{-}$$

the three possible exchanges would be creatine-phosphocreatine, ATP-phosphocreatine, and ATP-ADP. No atoms are exchanged between creatine and ADP.

The exchange patterns for ordered and rapid equilibrium, random mechanisms are given in Table 1. A straightforward ordered mechanism is characterized by the fact that the A–Q exchange is inhibited as the concentration of the B/P pair is increased (1). This result contrasts with that for a rapid equilibrium, random mechanism where there is no inhibition of the A–Q exchange rate with increasing concentrations of the B/P pair. The latter mechanism is further characterized by the equality of all three exchange reactions, as demonstrated for the creatine kinase reaction (2). This will not be the case unless catalysis is the sole rate-limiting step of the reaction sequence (3). An enzyme that catalyzes a Bi–Bi reaction which conforms to a rapid equilibrium, random mechanism has distinct binding sites for each of the two substrates involved in the reaction. Thus, it becomes possible for one substrate and the product of the other substrate to be present on the enzyme at the same time. Two such dead-end complexes could form. The one involving the smaller substrate and smaller product (EBQ) will always form, whereas the other dead-end complex may, or may not, do so. Increasing the concentration of the reactant pair that is involved in dead-end complex formation will lead to inhibition of all three exchanges.

Table 1. Isotope Exchange Patterns

Mechanism	Varied Substrate–ProductPair	Exchange Measured	Type of Double-reciprocal Plot
Ordered	A/Q	A – Q	Linear
		B – P	Linear
	B/P	A – Q	Substrate inhibition[a]
		B – P	Linear
Rapid equilibrium, random	A/Q	A – Q	Linear
		B – P	Linear
	B/P	A – Q	Linear
		B – P	Linear

B/Q	A – Q	Substrate inhibition
	B – P	Substrate inhibition
	A – P	Substrate inhibition

[a] This term is used to describe the fall-off in the initial rate of isotope exchange as the concentration of a substrate–product pair is raised in constant ratio.

The equations that describe the initial rates of isotope exchange for sequential reaction mechanisms are considerably more complex than those for the partial exchange reactions with a ping-pong mechanism. The equations for ordered (2), and rapid equilibrium, random (3) and partly random (4) mechanisms have been presented, and these references also contain a more complete discussion of isotope exchange at equilibrium for sequential reaction mechanisms.

Bibliography

1. W. W. Cleland (1986) Invest. Rates Mech. Reactions **6**, 791–870.
2. J. F. Morrison and W. W. Cleland (1966) J. Biol. Chem. **241**, 673–683.
3. P. F. Cook, G. L. Kenyon, and W. W. Cleland (1981) Biochemistry **20**, 1204–1210.
4. G. R. Ainslie and W. W. Cleland (1972) J. Biol. Chem. **247**, 946–951.

Isotope Filtering, Editing

Selective detection of the nuclear magnetic resonance (NMR) signals of hydrogen atom (proton) spins that are **scalar coupled** to another type of nucleus produces an isotope-filtered, or isotope-edited, proton NMR spectrum. NMR experiments are now well established as a means of determining the tertiary structures of biological macromolecules and examining the complexes formed between these molecules and various ligands. Most such experiments involve observation of proton (^1H) NMR signals, often with the goal of determining nuclear Overhauser effects (NOEs) between specific atoms of the system. As the size of the molecule increases, the number of hydrogen atoms in the structure increases. The proton NMR spectrum then becomes so crowded that resolution of a particular signal from nearby signals is difficult. Achieving the necessary resolution is further hindered because the widths of the NMR spectral lines generally also increase with increasing molecular size. One way to overcome these difficulties is to introduce ^{13}C and ^{15}N atoms into the molecule at nearly 100% abundance, rather than the much lower natural abundance. The ^1H NMR signals for protons directly attached to these isotopes can be detected selectively, producing a proton spectrum of the system that is simplified and, thus, easier to analyze for the desired information.

A wide variety of experimental methods are available to achieve isotope editing or filtering of one-, two- or three-dimensional NMR spectra (1-5). All experimental methods depend on the existence of a substantial spin coupling (J-coupled) interaction between ^{13}C or ^{15}N atoms and the hydrogen atoms that are attached to them. The one-bond coupling constant $^1J_{CH}$ is typically 120–160 Hz, whereas $^1J_{NH}$ for the peptide proton–peptide amide nitrogen interaction is about 90 Hz; thus, the necessary conditions for a successful isotope filtering experiment are well met in systems that have been enriched in these isotopes. The filtering experiments can potentially also be extended to other isotopes. For example, Cd^{2+} in metalloproteins couples strongly to nearby hydrogen atoms, and the proton NMR signals for these can be deduced by an isotope filtering experiment that relies on Cd-H coupling.

A particularly powerful application of isotope filtering is the study of complexes formed between a receptor and a **ligand**. If the receptor molecule is used in a form in which carbon and nitrogen positions are enriched to high levels with ^{13}C and ^{15}N, isotope editing would permit selective detection of the proton signals from the receptor when a complex forms between the receptor and a ligand. Alternatively, positions of the ligand could be enriched with these isotopes, in which case an isotope editing experiment with the receptor-ligand complex would display proton signals from the only ligand (6, 7). (See also Triple Resonance, Nuclear Overhauser Effect (NOE).)

Bibliography

1. R. H. Griffey and A. G. Redfield (1987) Quart. Rev. Biophys. **19**, 51–82.
2. L. P. McIntoch and F. W. Dahlquist (1990) Quart. Rev. Biophys. **23**, 1–38.
3. G. Otting and K. Wuthrich (1990) Quart. Rev. Biophys. **23**, 39–96.
4. S. W. Fesik and E. R. P. Zuiderweg (1990) Quart. Rev. Biophys. **23**, 97–131.
5. H. Oschkinat, T. Muller, and T. Dieckmann (1994) Angew. Chem. Int. Ed. Engl. **33**, 277–293.
6. S. W. Fesik (1988) Nature **332**, 865–866.
7. G. Wider, C. Weber, and K. Wuthrich (1991) J. Am. Chem. Soc. **113**, 4676–4678.

Suggestions for Further Reading

8. J. Cavanagh, W. J. Fairbrother, A. G. Palmer III, and N. J. Skelton (1995) *Protein NMR Spectroscopy*, Academic, San Diego.
9. *NMR of Proteins* (1993) (G. M. Clore and A. M. Gronenborn, eds.), CRC Press, Boca Raton.
10. K. Wuthrich (1976) *NMR in Biological Research: peptides and proteins*, American Elsevier, New York.

Isotope

Isotype specificities were first described by Oudin for **immunoglobulins** as a characteristic of one molecule of one given animal species. Immunoglobulin isotypes designate the different classes or subclasses that differ from each other by the structures of their heavy chains, leading to the classical IgG, IgM, IgD, IgA, and IgE, corresponding to the g, m, d, a, and ε heavy chains, respectively. IgG are furthermore divided into four subclasses that are also discrete isotypes, numbered from IgG1 to IgG4, whereas IgA has two subclasses, IgA1 and IgA2. The word also applies to light chains, with the **kappa (k) and lambda (l) light chain** isotypes. Each isotype is encoded by a separate constant-region gene that is split in as many **domains** (including the hinge regions) as are present in the corresponding chain. Kappa and lambda chains are present in all Ig classes and subclasses, whereas heavy chains are isotype-specific. The discrete isotypes have distinct effector functions, such as **complement** fixation, active transplacental transfer, and binding to discrete **Fc receptors**, thereby ensuring a selective fixation to different cell types.

During immunization, IgM antibodies appear first, a few days after immunogen administration. They are rapidly replaced by IgG that will acquire somatic hypermutations, thus becoming of higher affinity. Replacement of IgM by IgG involves rearrangement at the DNA level, known as isotype class switching . The switch may involve any switch region present at the 5′ position of each CH region gene (with the exception of IgD), leading to the expression of either isotype. Targeting of the isotype that will be involved in switching is under the control of **cytokines** produced by T cells and therefore only occurs in T-dependent **immune responses**.

See also entries **Antibody, Class switching, IgA, IgD, IgE, IgG**, and IgM.

Suggestion for Further Reading

J. B. Natvig and H. G. Kunkel (1973) Human immunoglobulin: classes, subclasses, genetic variants and idiotypes. Adv. Immunol. **16**, 1–59.

52. A. L. Osterman, H. B. Brooks, J. Rizo, and M. A. Phillips (1997) Biochemistry 36, 4558–4567.
53. S. Matsufuji, T. Matsufuji, N. M. Wills, R. F. Gesteland, and J. F. Atkins (1996) EMBO J. 15, 1360–1370.
54. S. Elias, B. Bercovich, C. Kahana, P. Coffino, M. Fischer, W. Hilt, D. H. Wolf, and A. Ciechanover (1995) Eur. J. Biochem. 229, 276–283.
55. Y. Murakami, N. Tanahashi, K. Tanaka, S. Omura, and S. Hayashi (1996) Biochem. J. 317, 77–80.
56. Y. Murakami, T. Ichiba, S. Matsufuji, and S. Hayashi (1996) J. Biol. Chem. 271, 3340–3342.
57. T. Ichiba, S. Matsufuji, Y. Miyazaki, and S. Hayashi (1995) Biochim. Biophys. Acta 1262, 83–86.
58. U. Rosander, I. Holm, B. Grahn, H. Loup-Rein, M.-O. Mattsson, and O. Heby (1995) Biochm. Biophys. Acta 1264, 121–128.
59. E. S. Canellakis, A. A. Paterakis, S. C. Hu, C. A. Panagiotidis, and D. A. Kyriakidis (1993) Proc. Natl. Acad. Sci. USA 90, 7129–7133.
60. S. Hua, X. Li, P. Coffino, and C.C. Wang (1995) J. Biol. Chem. 270, 10264–10271.
61. S. G. Reddy, S. M. McIlheran, B. J. Cochran, L. L. Woreth, L. A. Bishop, P. J. Brown, V. P. Knutson, and M. K. Haddox (1996) J. Biol. Chem. 271, 24945–24953.
62. X. Li, B. Stebbins, L. Hoffman, G. Pratt, M. Rechsteiner, and P. Coffino (1996) J. Biol. Chem. 271, 4441–4446.
63. X. Li and P. Coffino (1996) J. Biol. Chem. 271, 4447–4451.
64. E. Mamroud-Kidron and C. Kahana (1994) FEBS Lett. 356, 162–164.
65. J. J. Palvimo, M. Partanen, and O. A. Janne (1996) Biochem. J. 316, 993–998.
66. A. P. Kumar, P. K. Mar, B. Zhao, R. L. Montgomery, D. C. Kang, and A. P. Butler (1995) J. Biol. Chem. 270, 4341–4348.
67. M. S. Abrahamsen, R. S. Li, W. Dietrich-Goetz, and D. R. Morris (1992) J. Biol. Chem. 267, 18866–18873.
68. C. Wrighton and M. Busslinger (1993) Mol. Cell. Biol. 13, 4657–4669.
69. C. Bello-Fernandez, G. Packham, and J. L. Cleveland (1993) Proc. Natl. Acad. Sci. USA 90, 7804–7808.
70. K. E. Tobias, J. Shor, and C. Kahana (1995) Oncogene 11, 1721–1727.
71. M. Selvakumaran, D. Liebermann, and B. Hoffman (1996) Blood 88, 1248–1255.
72. K. E. Tobias and C. Kahana (1995) Cell Growth and Differentiation 6, 1279–1285.
73. G. Packman and J. L. Cleveland (1994) Mol. Cell. Biol. 14, 5741–5747.
74. S. Gaubatz, A. Imhof, R. Dosch, O. Werner, P. Mitchell, R. Buettner, and M. Eilers (1995) EMBO J. 14, 1508–1519.
75. J. A. Mosheir, M. Skunca, W. Wu, S. Moppana, F. J. Rauscher, and J. Dosescu (1996) Nucleic Acids Res. 24, 1149–1157.
76. U. M. Wallon, L. Person, and O. Heby (1995) Mol. Cell. Biochem. 146, 39–44.
77. S. Pyronnet, S. Vagner M. Bouisson, A.C. Prats, N. Vaysse, and L. Pradayrol (1996) Cancer Res. 56, 1742–1745.
78. M. Fogelpetrovic, S. Vujcic, J. Miller, and C. W. Porter (1996) FEBS Lett. 391, 89–94.
79. L. M. Shantz, R.-H. Hu, and A. E. Pegg (1996) Cancer Res. 56, 3265–3269.
80. D. Rousseau, R. Kaspar, I. Rosenwald, L. Gehrke, and N. Sonenberg (1996) Proc. Natl. Acad. Sci. USA 93, 1065–1070.

Orphons

Orphons are a class of dispersed, solitary genetic elements of the genome derived from tandem multigene families. These displaced elements arise from genes that do or do not code for proteins, including those of histones in the sea urchin *Lytechinus pictus*; ribosomal genes in *Saccharomyces cerevisiae*; ribosomal genes and H3 histone genes in *Drosophila melanogaster* (1); the amylase multigene family of mice (2); the spliced-leader small RNA gene family of *Trypanosoma brucei* (3) and of the nematode *Angiostrongylus cantonensis* (4); and the human 28S ribosomal DNA (5).

An interesting case is that of the human immunoglobulin V kappa gene regions. They have been transposed during evolution from the site of the kappa locus on chromosome 2 to chromosomes 1, 22, and other chromosomes. These orphons are very similar and may have derived from a single ancestral gene. The DNA sequences at the junction of chromosome 22 and other orphon regions are direct and inverted repeats and in one case an Alu sequence repeat. These unusual features may have predisposed the orphon regions to transposing by serving as target sites for enzymes involved in recombination (6).

Bibliography

1. G. Childs et al. (1981) Cell 23, 651–663.
2. S. Bodary et al. (1985) J. Mol. Biol. 182, 1–10.
3. M. Parsons, R. G. Nelson, and N. Agabian (1986) Nucleic Acids Res. 14, 1703–1718.
4. G. W. Joshua, F. B. Perler, and C. C. Wang (1995) Nucleic Acids Res. 23, 1030–1035.
5. J. Munro, R. H. Burdon, and D. P. Leader (1986) Gene 48, 65–70.
6. P. Borden, R. Jaenichen, and H. G. Zachau (1990) Nucleic Acids Res. 18, 2101–2107.

Orthologous Genes

Orthologous genes are two or more genes whose follows the speciation process, and they have usually the same function in each resulting species; that is, a particular gene in the ancestral will be duplicated in the two different species following speciation and will usually be maintained in each, because both species will require the function of that gene (Fig. 1) (1). These genes differ from , which diverged before or after speciation as a result of and usually have different functions. For example, the genes for the a and b polypeptide chains of hemoglobin and that for myoglobin are homologous but paralogous, whereas the hemoglobin a chains from different species are orthologous; similarly, the b chains and myoglobins from different species are orthologous. Only comparisons of orthologous genes can be used to reconstruct species phylogenies.

Figure 1. Generation of orthologous and paralogous genes (1).

It is often difficult to distinguish orthologous genes from paralogous genes. However, analysis has shown that some genes have a single version in a genome. Therefore, if this is the case in two or more species, there is a strong probability that these genes are orthologous. If the gene is a member of a known , there is a distinct probability that it is a paralogous gene, depending on the number of genes in the family, because the gene could be a product of gene duplication before or after speciation.

Orthologous gene pairs are useful for estimating the rate of nucleotide substitution and species phylogenies. When the time since two species diverged (T_s) is known from the fossil record, it follows that the orthologous pairs should also have diverged at the time of species divergence. Therefore, the rate of nucleotide substitution for the gene (v) can be estimated by dividing the number of nucleotide substitutions (K_n) between orthologous gene pairs by two times of the divergence time between the two species $v = K_n/(2T_s)$.

Two homologous genes sampled from the gene family between two species are often paralogous, rather than orthologous. If the two genes are paralogous, the divergence time of these genes (T_g) must have been earlier than the speciation time ($T_g > T_s$). If the divergence time of those genes is mistakenly assumed to be the divergence time between the species, the divergence time of the genes will be underestimated and will lead to overestimation of the rate of nucleotide substitution ($K_n/(2T_g) > v$). Thus, it is important to use only orthologous genes in estimating the rate of nucleotide substitution and the times of speciation.

There have been many recent advances in genome analysis, and as a result complete genomes are known. Those of two species can be compared to determine whether the physical order of genes in the genomes is conserved between different species. To accomplish this, it is vital to distinguish orthologous genes from paralogous genes. By focusing on orthologous genes, it is possible to trace changes in gene location during evolution because of the one-to-one correspondence in gene location between genomes, unless gene duplication takes place after speciation.

Bibliography

“Orthologous Genes” in , Vol. 3, p. 1731, by T. Gojobori; “Orthologous Genes” in (online), posting date: January 15, 2002, by T. Gojobori, National Institute of Genetics, Shizuoka, Japan.

1. H. Watanabe, H. Mori, T. Itoh, and T. Gojobori, (1997) J. Mol. Evol. 44, 57–64.

Oskar Gene

The oskar is a maternal effect gene in Drosophila melanogaster whose primary function is to organize a specialized cytoplasm, termed the germ plasm or pole plasm, at the posterior pole of the maturing egg (1). This germ plasm contains factors required for abdomen formation and germ-cell formation. The oskar messenger RNA is synthesized during oogenesis. It is deposited into the egg, where it becomes localized to the posterior pole through sequences in its 3′ untranslated region (UTR). Only posteriorly localized RNA is translated into Oskar protein. The site of Oskar protein synthesis determines where germ plasm is assembled, and the quantity of Oskar protein determines how many germ cells form. oskar is a member of the posterior group of genes (named for their effect on development of the abdomen in the posterior half of the embryo). Most of the posterior group genes facilitate localization and translation of oskar mRNA, while a small number of posterior genes act together with Oskar in the assembly of the germ plasm or are specifically required for either germ cell or abdomen formation.

1. oskar Protein and RNA Structure

oskar encodes a 2.9-kb mRNA that is expressed in the germ line of the adult female and is present at the posterior pole of early embryos. oskar mRNA has a 14-nucleotide 5′ UTR and a 1045-nucleotide 3′ UTR. Two different in-frame start codons are used to produce Oskar protein isoforms of 606 amino acids residues (69 kDa) and 468 residues (54 kDa). The short isoform has full oskar activity, although the long isoform is necessary to maintain localization of the oskar mRNA at the posterior of the oocyte (2, 3). The 3′ UTR contains regulatory elements for RNA localization and translation, while the region between the two start codons contains sequences necessary for translational regulation (4). The Oskar protein is novel, in that no known sequence or structural motifs are present. The only known homologue is from Drosophila virilis (5).

2. oskar RNA Localization and Translation

Oskar protein synthesis is regulated at the level of mRNA localization and translation and occurs during oogenesis. Each Drosophila ovary consists of approximately 16 ovarioles, each of which contains a series of developing egg chambers. At the tip of each ovariole, a germ-line stem cell produces a new stem cell and a cystoblast by asymmetric cell division. Each cystoblast undergoes four rounds of division with incomplete cytokinesis, giving rise to 15 nurse cells and the oocyte. The nurse cell–oocyte cluster is interconnected by cytoplasmic bridges called ring canals and surrounded by somatic follicle cells. oskar RNA is produced in the nurse cells and deposited into the developing oocyte, where it accumulates from the earliest stages of oogenesis. By stage 8 of oogenesis, the RNA is concentrated at both the anterior margin and the posterior pole of the oocyte. By stage 10, oskar RNA is localized exclusively to the posterior pole, where it remains until it is degraded in the early embryo after germ-cell formation [see Fig. 1 (6, 7)]. Oskar protein is translated once the mRNA becomes localized to the posterior pole, while unlocalized RNA is translationally repressed. This ensures that protein is made only at the posterior pole of the oocyte and embryo (2, 3).

Figure 1. A Drosophila melanogaster ovariole. oskar mRNA is detected by in situ hybridization. In the earlier stages of oogenesis (top of figure), oskar mRNA accumulates in the oocyte. As each egg chamber matures, the oskar mRNA is localized within the oocyte to the posterior pole (center and bottom of figure). Anterior is to the top, posterior is to the bottom.

The site where oskar RNA is localized and Oskar protein is synthesized determines where germ cells form and the posterior body region, the abdomen, develops. Therefore processes that lead to the localization of oskar RNA are directly linked to the establishment of anterior–posterior polarity within the oocyte. All aspects of oskar RNA localization are mediated by sequences within the oskar 3′ UTR (8). Early aspects of oskar RNA transport into the oocyte and localization to the posterior pole of the oocyte require the correct organization of the microtubule network. Genes involved in the polarization of the early microtubule network that extends from the nurse cells to the oocyte also affect the transport of oskar into the oocyte. These genes include egalitarian, Bicaudal-D, (coiled-coil domain protein), orb (an RNA-recognition motif protein with similarity to mammalian CEBP), and cytoplasmic dynein (9). Subsequently, the establishment of anterior–posterior polarity within the oocyte is controlled by cell–cell signaling between the oocyte-bound Gurken protein, a member of the transforming growth factor-a (TGF-A) family, and its receptor, the Drosophila EGF receptor (DER or torpedo). Mutations in either gene disrupt localization of oskar RNA to the posterior pole, presumably by altering the polarity of the microtubule network within the oocyte. Indeed, inhibitors of the microtubule, but not of the microfilament, cytoskeleton disrupt the localization of oskar RNA during oogenesis (10). Other maternal effect genes that affect oskar localization and affect the microtubule organization in the oocyte include cappuccino (for min homologue), spire, and mago nashi (a novel protein that is highly conserved from plants to humans). A role of microfilaments in oskar mRNA localization is suggested by the effect that mutations in the tropomyosin II gene (an actin-binding protein) have on oskar RNA localization (11). It has been proposed that the actin cytoskeleton is required for high levels of oskar mRNA localization or the firm anchoring of the RNA at the posterior pole (11).

Staufen, a double-stranded RNA-binding protein, has been proposed as the best candidate to mediate directly the localization of oskar RNA. staufen mutants do not affect the organization of the cytoskeleton, and Staufen protein and oskar RNA colocalize during oogenesis (12). A direct physical interaction between Staufen and oskar RNA has not been demonstrated. Staufen is also required for localization of bicoid mRNA to the anterior of the oocyte and prospero RNA to the apical side of dividing neuroblasts (12).

oskar mRNA that is not localized to the posterior pole is translationally repressed. If the RNA is translated prematurely, posterior body patterning will be specified throughout the embryo. Translational repression is mediated through specific RNA-binding sites in the 3′ UTR of oskar mRNA. The RNA-binding protein Bruno (which corresponds to arrest gene independently identified on the basis of its early arrest maternal effect phenotype) binds specifically to Bruno response elements (BREs) in the oskar RNA (13). The bicaudal-C protein (a KH-domain protein) has also been implicated in repressing translation of unlocalized oskar RNA. Only at the posterior pole, where oskar RNA is localized, is the RNA translationally active. Activation of translation depends on derepression mediated through sequences between the two alternative start codons of the oskar mRNA (4). Translation of oskar RNA or the stability of Oskar protein is further dependent upon the gene aubergine as well as upon the Vasa protein, an RNA helicase that interacts physically with Bruno protein (14, 15).

3. Role of oskar in Germ Plasm Assembly

Homozygous mutant oskar females are viable, but produce embryos that lack germ plasm. These embryos fail to form germ cells and do not develop an abdomen. Mislocalization of the oskar coding region (via the RNA localization element in the 3′ UTR of bicoid mRNA) to the anterior of the oocyte results in the assembly of ectopic germ plasm, a mirror image duplication of the abdomen, and formation of ectopic germ cells (16). Thus oskar is both necessary and sufficient for assembly of germ plasm and for formation of both the abdomen and germ cells.

Assembly of the germ plasm is also dependent upon other factors that act downstream of oskar. Vasa is a DEAD-box helicase that physically interacts with Oskar. The products of the tudor and valois genes are also required for germ plasm assembly. Vasa, Tudor, and Oskar are components of electron-dense particles, known as polar granules, that are found only in the germ plasm (17).

The effect of *oskar* on abdomen formation is mediated through the *nanos* gene. Oskar is responsible for localizing *nanos* mRNA to the posterior pole of the embryo, where Nanos protein is translated and acts to facilitate abdomen formation through repression of the *hunchback* mRNA. While the mechanism of *nanos* localization to the posterior pole is not clear, *oskar* is both necessary and sufficient for *nanos* localization. Overexpression of *oskar* or mislocalization of the *oskar* mRNA results in an excess of *nanos* activity at the site of *oskar* localization.

oskar also recruits several factors to the posterior pole that play a role in germ-cell formation. These include: *germ cell-less* mRNA, which encodes a protein that associates with the nuclear envelope; mitochondrial large ribosomal RNA (*mtlrRNA*) that is found outside of the mitochondria, where it associates with polar granules during the early stages of embryogenesis; and *polar granule component 1* (*pgc1*), which codes for an untranslated RNA. A number of different experiments suggest that *germ cell-less* and *mtlrRNA* are required for germ-cell formation (18, 19), while antisense experiments with *pgc1* suggest a role for this gene in germ-cell migration or development (20). Other maternal factors localized to the posterior pole in an *oskar*-dependent manner include maternal *hsp83* mRNA, whose RNA is stabilized in the posterior depending on the germ plasm; the cell cycle regulator *cyclin B*; *outspread*; and the Fat-facets protein that is a sequence-specific de-ubiquitinating proteinase. The roles of these genes in germ-cell formation, migration, or development are unclear.

Bibliography

1. R. Lehmann and C. Nüsslein-Volhard (1986) *Cell* **47**, 141–52.
2. C. Rongo, E. R. Gavis, and R. Lehmann (1995) *Development* **121**, 2737–2746.
3. F. H. Markussen, A. M. Michon, W. Breitwieser, and A. Ephrussi (1995) *Development* **121**, 3723–3732.
4. N. Gunkel, T. Yano, F. H. Markussen, L. C. Olsen, and A. Ephrussi (1998) *Genes Dev.* **12**, 1652–1664.
5. P. J. Webster, J. Suen, and P. M. Macdonald (1994) *Development* **120**, 2027–2037.
6. J. Kim-Ha, J. L. Smith, and P. M. Macdonald (1991) *Cell* **66**, 23–35.
7. A. Ephrussi, L. K. Dickinson, and R. Lehmann (1991) *Cell* **66**, 37–50.
8. J. Kim-Ha, P. J. Webster, J. L. Smith, and P. M. Macdonald (1993) *Development* **119**, 169–178.
9. M. McGrail and T. S. Hays (1997) *Development* **124**, 2409–2419.
10. N. J. Pokrywka and E. C. Stephenson (1995) *Dev. Biol.* **167**, 363–370.
11. M. Erdelyi, A. M. Michon, A. Guichet, J. B. Glotzer, and A. Ephrussi (1995) *Nature* **377**, 524–527.
12. D. St. Johnston, D. Beuchle, and C. Nüsslein-Volhard (1991) *Cell* **66**, 51–63.
13. J. Kim-Ha, K. Kerr, and P. M. Macdonald (1995) *Cell* **81**, 403–412.
14. P. J. Webster, L. Liang, C. A. Berg, P. Lasko, and P. M. Macdonald (1997) *Genes Dev* **11**, 2510–2511.
15. J. E. Wilson, J. E. Connell, and P. M. Macdonald (1996) *Development* **122**, 1631–1639.
16. A. Ephrussi and R. Lehmann (1992) *Nature* **358**, 387–392.
17. W. Breitwieser, F. H. Markussen, H. Horstmann, and A. Ephrussi (1996) *Genes Dev.* **10**, 2179–2188.
18. T. A. Jongens, B. Hay, L. Y. Jan, and Y. N. Jan (1992) *Cell* **70**, 569–584.
19. S. Kobayashi, R. Amikura, and M. Okada (1993) *Science* **260**, 1521–1524.
20. A. Nakamura, R. Amikura, M. Mukai, S. Kobayashi, and P. F. Lasko (1996) *Science* **274**, 2075–2079.

Suggestions for Further Reading

21. A. Ephrussi, and R. Lehmann (1992) Induction of germ cell formation by oskar [see comments]. Nature 358, 387–392.

22. N. Gunkel, T. Yano, F. H. Markussen, L. C. Olsen, and A. Ephrussi (1998) Localization-dependent translation requires a functional interaction between the 5¢ and 3¢ ends of oskar mRNA. Genes Dev. 12, 1652–1664.

23. J. Kim-Ha, P. J. Webster, J. L. Smith, and P. M. Macdonald (1993) Multiple RNA regulatory elements mediate distinct steps in localization of oskar mRNA. Development 119, 169–178.

24. C. Rongo and R. Lehmann (1996) Regulated synthesis, transport and assembly of the Drosophila germ plasm. Trends Genet. 12, 102–109.

25. P. J. Webster, L. Liang, C. A., Berg, P. Lasko, and P. M. Macdonald (1997) Translational repressor bruno plays multiple roles in development and is widely conserved. Genes Dev. 11, 2510–2521.

Ouchterlony Double Diffusion

A direct extension of the precipitin reaction to immunoassays is the Ouchterlony double diffusion technique (1). Here, two or more wells are cut in an agar slab and filled with either antigen or antibody. The two materials slowly diffuse throughout the slab. As the antibody and antigen molecules encounter each other and react, a precipitate forms in the gel. Because of the highly cooperative nature of immunecomplex lattice formation, the precipitate forms an extremely sharp line between the two wells. The position of the precipitin line, compared to lines generated from other dilutions of antigen or antibody, gives a semiquantitative measure of the relative concentration of the reactant. However, the true value of the Ouchterlony technique is the remarkable number of details that can be inferred from the precipitin patterns formed. From the presence of multiple lines, or complex precipitin patterns formed at the intersection with multiple antigen or antibody wells in the agar slab, conclusions can be drawn about such properties as antigen heterogeneity, antigen molecular weight, shared antigenic determinants, and cross-reactivity of different antisera (2). The Ouchterlony technique is now obsolete, but it is commonly described in older literature.

Bibliography

1. Ö. Ouchterlony (1948) Acta Pathol. Microbiol. Scand. 25, 186–191.

2. Ö. Ouchterlony and L.-Å. Nilsson (1986) "Immunodiffusion and immunoelectrophoresis", in Handbook of Experimental Immunology, 4th ed., Vol. 1: Immunochemistry, D. M. Weir, ed., Blackwell, Oxford, pp. 32.1–32.50.

Ovalbumin

The major protein in egg-white is ovalbumin. It has the typical highly ordered structure of a serpin (see Fig. 1 in that entry), but has lost the ability to refold the loop that would correspond to its reactive center; consequently it has no proteinase inhibitor activity. Its smallness relative to other serpins, and its conformational stability, make it suitable as a marker for gel electrophoresis. The stability is only relative, however; its reactive-center loop can be cleaved proteolytically to produce a form known as plakalbumin. It is likely that the induced insertion of this loop, like that that occurs in other serpins, explains a conformation, with increased stability, that forms on long-term storage: S-ovalbumin.

Suggestions for Further Reading

P. E. Stein, A. G. W. Leslie, J. T. Finch, and R. W. Carrell (1991) Crystal structure of uncleaved ovalbumin at 1.95 Å, J. Mol. Biol. 221, 941–959.

P. G. W. Gettins, P. A. Patston, and S. T. Olson (1996) Serpins: Structure, Function and Biology, R. G. Landes, Georgetown, TX, pp. 135–137.

Overlay Assay: Enzyme Zymography of Plasminogen Activators and Inhibitors

Zymography is a gel-based enzymatic assay useful for detection and semi-quantitative analysis of proteases and is performed using overlay or co-polymerization techniques (1, 2). In overlay assays, samples are fractionated by SDS-PAGE and, after removal of SDS, the polyacrylamide gel is overlaid on an agarose indicator gel containing protein substrate. Enzyme diffusion into the indicator gel occurs during incubation of the gel sandwich and results in degradation of protein substrate. The indicator gel is then stained to reveal zones of proteolysis, which appear as cleared bands on a dark background. In co-polymerization techniques, protein substrate is incorporated directly into the polyacrylamide gel matrix and, after electrophoresis and SDS removal, gels are incubated floating in buffer (2). In either method, specificity or sensitivity is tailored by modification of acrylamide gel pore size, substrate choice, incubation time, buffer conditions, and by inclusion of activators or inhibitors in gels or buffers.

Overlay assays are advantageous when substrate preference involves proteins that either bind poorly to acrylamide (albumin, casein) or are irreversibly denatured by SDS (collagen type I) and, thus, are not amenable to co-polymerization methods; gelatin, in contrast, is readily incorporated into the polyacrylamide gel matrix, and co-polymerization has been used extensively for assay of gelatinases (2). Overlay methods are also more appropriate for initial quantitative evaluations because enzyme activity is confined within the gel sandwich and, thus, not susceptible to diffusional loss to surrounding buffer, as may occur with co-polymerization assays (1). Furthermore, overlay assays are the method of choice for analysis of complex proteolytic systems in which zymogens, co-substrates, or endogenous inhibitors are relevant, as multiple components can be incorporated into indicator gels.

Representative of a complex proteolytic system is application of the overlay assay to analysis of the plasminogen activator (PA), inhibitor (PAI) system (3, 4). Briefly, samples containing PAs (urokinase [uPA], tissue plasminogen activator [tPA]) and their endogenous inhibitor (PAI) are resolved by SDS-PAGE on 10% gels. Gels are washed with Triton X-100, to remove SDS and allow protein renaturation, and then overlaid on an indicator gel containing plasminogen (zymogen) and fibrin (protein substrate). During incubation, PAs diffuse into the indicator gel, cleave plasminogen to form plasmin, a serine protease that degrades fibrin. After staining of the indicator gel, lytic zones (PA) appear as cleared bands on a dark background (zymography). In contrast, if exogenous PA is also incorporated into the indicator gel, then lysis occurs everywhere except where inhibitor is present; thus, lytic-resistant zones (PAI) appear as dark bands on a clear background (reverse zymography).

1. Materials and Methods

1.1. Materials

Fibrinogen (plasminogen-rich) from Organon Teknika, Holland; SeaKem garose and Gelbond support backing from FMC BioProducts, Rockland, ME; human uPA and tPA from American Diagnostica, Greenwich, CT. All reagents prepared using ultra-pure water.

1.2. Sample Preparation and SDS-PAGE

Samples were prepared, as appropriate, in 2X Laemmli sample buffer without reducing agent or heating (4). Proteins were resolved by 10% SDS-PAGE (0.75 mm thick slab gels; 20 mA constant current) as previously described (5). After electrophoresis, gels were washed twice (2.5% Triton X-100, 200 mL/gel, 30 min each) to remove SDS and carefully overlaid on indicator gels.

1.3. Preparation of Fibrin Indicator Gel

Plasminogen-rich fibrinogen (5 mg/mL) was solubilized in 0.85% saline (prewarmed to 37°C) with gentle mixing (inversion several times over 1–2 h). Agarose (1%) was separately prepared in PBS (pH 7.4) by heating in a boiling water bath. Dissolved agarose was removed from heat and cooled to 60°C; 15mL of thrombin stock (260 U/mL) and 5 mL fibrinogen solution were then added to the hot agarose (25 mL) in rapid succession and with constant swirling. The agarose-fibrin solution was quickly poured onto the hydrophilic side of a Gelbond support film (~13 × 17cm) using a 25 mL glass pipet and a continuous, vertical motion from left to right; the Galbond support film had been previously stabilized on a glass plate (see below). The agarose indicator gel was allowed to solidify for at least 30 min at room temperature before overlay with the acrylamide gel. Final gel composition was ~0.8% agarose, 0.08% plasminogen-rich fibrinogen, and 0.1 U/mL thrombin (4).

1.4. Fibrin Zymography

Washed polyacrylamide gels were carefully overlain on fibrin indicator gels and incubated (37°C, 18–20 h) in closed containers containing water-moistened paper towels to provide a humidified atmosphere. After incubation, the acrylamide gels were carefully removed, and the indicator gel was stained (<5min; 0.1% amido black, 70% methanol, 10% acetic acid), destained (70% methanol, 10% acetic acid), and allowed to air dry.

1.5. Reverse Zymography

For detection of PAIs, the indicator gel also contained uPA (0.8 U/mL).

1.6. Notes and Tips

1) Excessive or too vigorous mixing during fibrinogen solubilization results in protein flocculation; 2) volume loss during agarose heating should be reconstituted using ultra-pure water; 3) Galbond has hydrophilic (spreads water) and hydrophobic (beads water) surfaces; water placed in the center of a glass plate adheres the hydrophobic surface of the Gelbond providing a flat stable surface for gel pouring and subsequent handling of gel sandwiches; 4) Work quickly, fibrin polymerization and agarose solidification occur rapidly; delay in pouring produces inhomogeneities within the indicator gel; 5) when disassembling glass plates after electrophoresis, cut the bottom of the acrylamide gel for later orientation; 6) acrylamide gels enlarge and become fragile during washing; handle with care; 7) to position acrylamide gels carefully grasp the upper corners; overlay from bottom to top in a continuous motion to avoid air trapping; 8) avoid repositioning of the polyacrylamide gel when constructing the gel sandwich as artifactual lysis and streaking may result; 9) volumes given are for one full-sized indicator gel; 10) up to two indicator gels can be simultaneously prepared; extra gels can be stored at 4°C for 3–4 days in sealed plastic bags humidified with a damp paper towel.

2. Results and Discussion

Samples containing PAs can be readily analyzed by fibrin zymography using a gel overlay assay (Fig. 1). In such assays PAs and PAIs are resolved by electrophoresis on 10% polyacrylamide gels in the absence of reducing agent or heating. Omission of reducing agent is necessary because SDS may cause artifactual activation of thiol-dependent proteases (i.e., lysosomal thiol cathepsins) as well as inactivation of disulfide-stabilized proteases (i.e., plasminogen activators). Similarly, heating is avoided to preclude artifactual aggregation, activation, or inactivation of susceptible proteases.

Figure 1. Schematic of fibrin overlay assay. (a) Preparation of the fibrin indicator gel. (b) Overlay of the indicator gel (fibrin zymography). For details see MATERIALS AND METHODS section.

During electrophoresis the partially denatured protease migrates with respect to molecular weight. SDS removal after electrophoresis by the nonionic detergent Triton X-100 allows proteins to renature and regain activity. Wash times should be kept to a minimum and accurately monitored to avoid excessive leaching of protease and to assure reproducibility between experiments, respectively.

The gel sandwich should be constructed without repositioning of the acrylamide gel and should be incubated in a humidified atmosphere to avoid gel drying. Incubation times and conditions (temperature, pH) vary depending on the intrinsic properties of the protease being examined as well as its concentration in biological samples. For quantitative purposes, standard curves should be constructed to determine dose-time relationships with respect to size of the lytic zone. Overlay assay of PAs requires incubation for 6–18 h and is temperature-dependent (37°C).

Indicator gels require only brief staining (<5 min) and, after drying, are readily photographed by back lighting. Overlay zymography of PAs demonstrates fibrinolytic zones at molecular weights corresponding to uPA (45 kDa) and tPA (70 kDa) as well as some high (110 kDa) molecular weight bands (Fig. 2A), presumably representing complexes of PA-PAI (3,4). In contrast, reverse zymography demonstrates fibrinolytic-resistant zones at a molecular weight (50 kDa) corresponding to PAI (Fig. 2B). Protease/inhibitor identification can be verified by parallel zymograms in which indicator gels contain PA-specific antibodies or inhibitors i.e., amiloride to inhibit uPA and erythina to inhibit tPA, as has been described elsewhere (4).

Figure 2. Amido black-stained indicator gels. (a) Fibrin zymogram demonstrating uPA (45 kDa), tPA (70 kDa), and higher molecular weight PA complexes (open and closed triangles). (b) Reverse zymogram demonstrating PAI (50 kDa) as well as uPA shadow (45 kDa). Samples 1–4) were from conditioned media of bovine corneal endothelial cells at different growth stages (4).

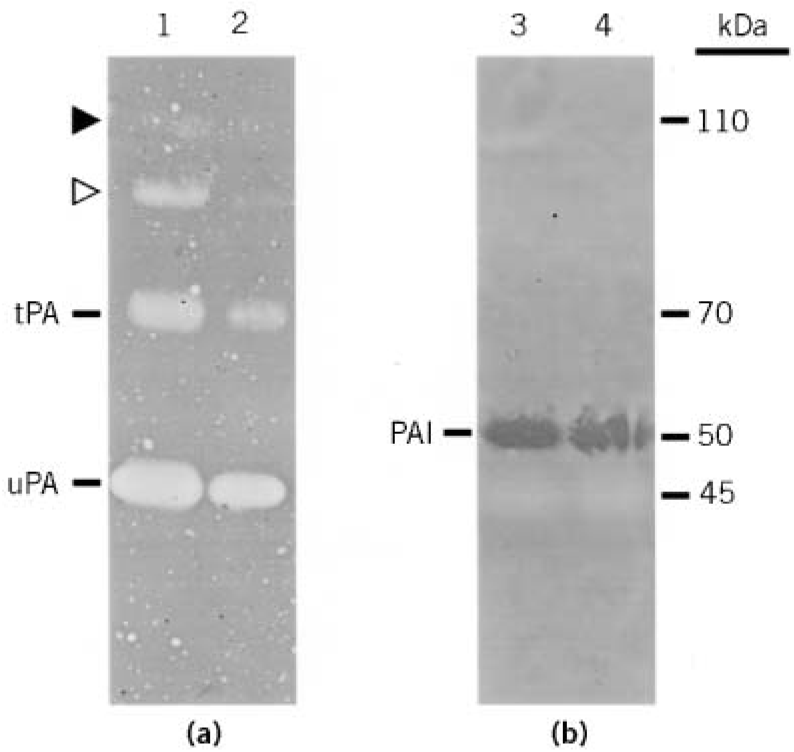

In summary, overlay zymography is a versatile assay for the detection and semi-quantitative investigation of proteases, which is readily applicable to complex systems. Unique to the overlay method is the opportunity to incorporate into the indicator gel multiple components including activators, inhibitors, antibodies, zymogens, co-factors, and allosteric modifiers. This enables highly sensitive and specific assays to be developed and, thus, affords extensive biochemical investigation of diverse proteolytic systems.

Bibliography

1. M. S. Lantz and P. Cibrowski (1994) Meth. Enzymol. 235, 563–594.
2. G. S. Makowski and M. L. Ramsby (1996) Anal. Biochem. 236, 353–356.
3. D. J. Loskutoff, J. A. van Mourik, L. A. Erickson, and D. Lawrence (1983) Proc. Natl. Acad. Sci. U.S.A. 80, 2956–2960.
4. M. L. Ramsby and D. L. Kreutzer (1993) Invest. Ophthalmol. Vis. Sci. 34, 3207–3219.
5. 5. G. S. Makowski and M. L. Ramsby (1997) in Protein Stucture: A Practical Approach (T.E. Creighton, ed.), IRL Press, Oxford, UK, pp. 1–27.

Suggestions for Further Reading

6. P. A. Andreasen, B. Georg, L. R. Lund, A. Riccio, and S. Stacey (1990) Mol. Cell. Endocrinol. 68, 1–19.
7. K. Dano, P. A. Anderson, J. Grondahl-Hansen, P. Kristensen, L. S. Nielsen, and L. Skriver (1985) Adv. Cancer Res. 44, 139–266.
8. L. A. Erickson, D. A. Lawrence, and D. J. Loskutoff (1984) Anal. Biochem. 137, 454–463.
9. J. D. Vassalli, A. P. Sappino, and D. Belin (1991) J. Clin. Invest. 88, 1067–1072.
10. M. L. Ramsby, P. C. Donshik, and G. S. Makowski (2000) Inflammation 24, 45–71.

Oxidation/Reduction Potential

Many of the fundamental physiologic reactions in a cell, both in the metabolic pathways of degradation and in the storage of energy via production of ATP, involve the transfer of electrons from one molecule, the donor (or reducing agent), to another, the acceptor (or oxidant). They are thus called redox reactions and are catalyzed by redox enzymes.

1. Redox Reactions and Redox Couples

The molecule donating an electron is the reductant (red) and becomes oxidized in the reaction, whereas the molecule accepting the electron is the oxidant (ox) and becomes reduced. In fact, each redox exchange:

is composed of two reactions:

The reductant and its corresponding oxidized form constitute a redox couple, in which both partners participate in the redox reaction. Each redox couple is characterized by a standard oxidation-reduction potential ( ) that quantitatively defines its tendency to lose an electron. In a redox reaction, the redox couple that has the higher affinity for the electron will be the oxidant, whereas the couple having a greater tendency to donate electrons will be the reductant. The same redox couple may therefore be either a reductant or an oxidant, depending on the redox potential of the second redox couple in the reaction. Examples of such a mechanism occur in the mitochondrial and the anaerobic bacterial electron transfer chains and in the photosynthesis pathway in chloroplasts, where the reductant of the (i)th step is the oxidant of the (i-1)th step.

2. Electrode Potential

The redox potential can be measured electrochemically as the electromotive force generated by connecting a half-cell of the redox sample with a reference half-cell. The reference half-cell consists of a platinum electrode immersed in a 1 M H^+ solution and saturated with H_2 gas at 1 atmosphere; the sample half-cell consists of an electrode immersed in a solution of the redox couple under standard conditions (1 M of the electron donor and acceptor, 25°C, and pH 7). The electrodes are connected to a voltmeter. A salt bridge (KCl solution) enables electrical continuity between the half-cells. The electrons flow in the direction determined by the redox potential of the sample relative to the reference. This is the voltage observed at the beginning of the experiment (standard concentration of 1 M), as the redox potential of the hydrogen electrode is arbitrarily taken as 0 V. The redox potentials ( ) of redox couples are thus expressed relative to the $\frac{1}{2}H_2/H^+$ couple.

For a redox reaction ($ox + e^- \rightleftharpoons red$), the Nernst equation relates the concentration of the redox species with the redox potential:

where E is the redox potential, $E°$ is the redox potential for components in their standard state at pH 0, R is the gas constant (8.3144 J K^{-1} mol), F is the Faraday constant (9.65×10^4 J V^{-1} mol), n is the number of electrons transferred, and T is the absolute temperature. In biology, the equation is generally written as

where E_h is the redox potential referred to the standard hydrogen electrode, $E_{m,x}$ is the mid-point redox potential (when [ox] = [red] ≠ standard state) at a defined pH (x) of and 2.303 RT/F = 0.06 for 29.4°C. The value of E_m for a defined redox couple depends on the relative stability of the oxidized and reduced states: the more negative the value of E_m, the more stable is the oxidized form and the stronger is the electron donor. Conversely, any factor stabilizing the reduced form makes the couple a better electron acceptor, having a more positive redox potential.

3. Redox Potential, Free Energy, and Equilibrium Constant

The change in free energy associated with a redox reaction ($red_1 + ox_2 \rightleftharpoons ox_1 + red_2$) is related to the difference in redox potentials of the reactants by the formula:

in which n is the number of electrons transferred, F is the energy change as 1 M of electrons falls through a potential of 1 V (23.06 kcal V^{-1} mol^{-1}), and $\Delta E°'$ is the difference in redox potentials of the reactants in volts. $\Delta G°'$ is the free energy change per mole and is expressed in kilocalories.

We know that at constant temperature and pressure a reversible reaction proceeds until an equilibrium is attained, defined by

in which $[ox_1]$, $[red_1]$, $[red_2]$, and $[ox_2]$ are the reactant concentrations, and K_{eq} is the equilibrium constant of the reaction at a certain constant temperature. K_{eq} is related to the $\Delta G°'$ free energy change by;

where R is the gas constant (1.987 cal mol^{-1} K^{-1}) and T is the absolute temperature (K).

We can also say that:

Knowing the redox potentials of a redox couple, the last relationships make it possible to calculate the equilibrium concentrations. Conversely, the redox potential of a solution can be calculated from the relative concentrations of the redox couples at equilibrium.

4. How to measure the redox potential

The oxidation of a reductant (red$_1$) by an oxidant (ox$_2$), at fixed temperature and pH, can be followed potentiometrically by measuring the variation of the electromotive force of a solution of the reductant as it is titrated with the oxidant. In practice, with a Pt electrode connected with a reference electrode (ie, a calomel electrode), the redox potential of the red$_1$ solution is recorded after each addition of ox$_2$. The redox potential increases as the value of [ox$_1$]/[red$_1$] increases and is equal to E_m when the initial reductant is half oxidized, [ox$_1$] = [red$_1$] = 50%. When [ox$_1$] is close to 100%, the redox potential varies rapidly, and the titration comes to an end; the point of equivalence has then been reached, i.e. an equivalent of ox$_2$ has been added to red$_1$. In biological systems, the redox proteins generally carry colored groups that have substantial absorbance in the visible range of wavelengths. This allows precise determination by absorption spectroscopy of the relative concentrations of the oxidized and reduced species.

Many molecules can act as oxidizing and reducing agents in nonbiological redox reactions, whereas in the metabolic pathways of living organisms, few molecules have been conserved during the evolution as redox agents for many different substrates.

The oxidation/reduction potentials of some biologically relevant compounds and free redox groups are presented in Table 1.

Table 1. Oxidation/Reduction Potentials of Some Biologically Relevant Compounds and Free Redox Groups

Redox Couple	$E_{m,\,7}$ (mV)
	–320
	–230
	–200
	–219
	–190
	–115
	0.0[a]
	+60
	+100
	+110
	+150

+360
+480
+480
+770
+820

[a] Taken as reference.

Suggestions for Further Reading

J. G. Morris (1968) A Biologist"s Physical Chemistry, Edward Arnold Ltd., London, "Chapter 12".

D. G. Nicholls and S. J. Ferguson (1992) Bioenergetics 2, Academic Press, "Chapter 3".

Oxidoreductases

Oxidoreductases form a large class of enzymes that catalyze the oxidation of one substrate, with the concomitant reduction of another. For these donor-acceptor reactions, the electron acceptor may be a pyridine nucleotide (eg, NAD), cytochrome, oxygen, quinone or others. The term dehydrogenase is used to describe oxidation-reduction reactions whenever possible, whereas the term oxidase is restricted to enzymes for which oxygen is an acceptor. Dehydrogenases act on primary and secondary alcohols, as well as hemiacetals. They also convert aldehydes to the corresponding acids, and these reactions may involve phosphorylation of the acid or acylation of coenzyme A (CoA). Oxo groups may be oxidized by the addition of water, followed by the cleavage of a bond or dehydrogenation. Dehydrogenases can introduce double bonds by direct dehydrogenation at a single bond. They function as oxidases by utilizing oxygen for the deamination of amino acids that can also undergo direct dehydrogenation reactions. In addition, they can dehydrogenate secondary amines to form double bonds and oxidize NADH or NADPH as well as nitrogenous substrates and donors with sulfur or heme groups.

Oxygen-Binding Proteins

Oxygen-binding proteins are defined as proteins that reversibly bind O_2. They are exclusively metalloproteins.

1. Classification

The classification of oxygen-binding proteins and some of their properties and distribution are presented in Table 1. Protoheme IX is the common oxygen-binding site for myoglobins (Mb), IDO-like Mb, hemoglobins (Hb), compact Hb, and FixL. Dioxygen is bound at the ferrous ion at the center of the heme group (see Myoglobin). The vinyl group normally at position 2 of protoheme IX is replaced by a formyl group in the chlorocruoroheme carried by chlorocruorin (Chl). Hemerythrin (Hr), myohemerythrin (myoHr), and hemocyanin (Hc) are nonheme proteins. The oxygen-binding site for Hr and myoHr is a binuclear iron center, and that for Hc is a binuclear copper center.

Table 1. Classification of Oxygen-Binding Proteins

Name	O_2 Binding Site	Protein Folding	Molecular Mass, kDa	Aggregation State	Color		Distrib
					Deoxy	Oxy	
Myoglobin	Protoheme IX	Globin	17 or 34	Monomer or dimer	Purple	Red	Vertebr muscle gastrop radular
IDO-like myoglobin	Protoheme IX	Unknown	40 or 80	Monomer or dimer	Purple	Red	Gastro buccal
Hemoglobin	Protoheme IX	Globin	17, 34, or 44	Monomer or dimer	Purple	Red	Bacteri unicellu eukaryo and pla
	Protoheme IX	Globin	65	Tetramer	Purple	Red	Vertebr cell
	Protoheme IX	Globin	3500	144mer	Purple	Red	Anneli plasma
Compact hemoglobin	Protoheme IX	Unknown	13–15	Monomer	Purple	Red	Cyanob protozo green a
FixL	Protoheme IX	Unknown	110	Dimer	Similar to Hb or Mb		Rhizobi Bradyrh
Chlorocruorin	Chlorocruoroheme	Globin	3500	144mer	Greenish red	Greenish red	Blood p four po families
Myohemerythrin	Binuclear Fe center	4-a-Helix bundle	14	Monomer	Colorless	Violet	Sipunc muscle
Hemerythrin	Binuclear Fe center	4-a-Helix bundle	40–110	3, 4 or 8mer	Colorless	Violet	Red cel phyla o inverte
Hemocyanin	Binuclear Cu center	a-Helices and b-barrel	450–3300	6, 12, 24, 36, or 48mer	Colorless	Blue	Arthrop plasma
	Binuclear Cu center	Unknown	3500–8700	10 or 20mer	Colorless	Blue	Mollus plasma

The hemoglobins in protozoa (*Paramecium* and *Tetrahymena*), green algae (*Chlamydomonas*), and cyanobacteria are not authentic hemoglobins because their polypeptide chains are about 20% shorter and without substantial amino acid sequence similarities. Several pieces of evidence suggest that the structures of these “compact hemoglobins” differ from the “globin fold” (see Globins), and it is generally considered that they arose from a different evolutionary ancestor (see Convergent Evolution). Likewise, IDO-like Mb evolved from a common ancestor of indoleamine dioxygenase, a heme-containing enzyme that degrades tryptophan. Based on the gene structures and amino acid sequences, myoglobins and hemoglobins are divided into three distinct evolutionary groups: (1) “universal globins”, 17-kDa polypeptide chains, that have about 150 amino acid residues; (2) “truncated globins” or “compact globins”, 13 kDa, that have about 120 residues per chain; and (3) “IDO-like Mb” (1). The second group has been known as “truncated globin”, but “compact globin” is more appropriate because these proteins have no detectable amino acid homology with the universal globins.

2. Distribution, Structure, and Function

Figure 1 illustrates the distribution of oxygen-binding proteins in a simplified phylogenetic tree. Hr and Hc are distributed within certain animal phyla, such as Sipuncula, Brachiopoda, Annelida, Arthropoda, and Mollusca. Hb, the most widely distributed, occurs in bacteria to vertebrates, and even in plants, but only intermittently. The principal physiological function of the circulating proteins (vertebrate Hb, annelid Hb, Chl, Hr, and Hc) is to transport O_2 from the lungs or gills to peripheral tissues. The function of the noncirculating proteins (Mb and myoHr), and probably also of IDO-like Mb, is oxygen storage and intracellular transport.

Figure 1. Phylogenetic distribution of oxygen-binding proteins. Abbreviations undefined in the text are Er, erythrocruor same as Chl (chlorocruorin). Erythrocruorin was the name used for what is now called annelid extracellular hemoglobin. hemoproteins of yeast, paramecium, and legume root nodules are designated as Mb in this figure, they are sometimes de Hb, because they are not contained in muscle and Hb is a more comprehensive name of oxygen carrier. From Van H Miller (1995) (see Reading List).

See Myoglobin for details of Mb and IDO-like Mb and Hemoglobin for details of Hb. The other oxygen-binding proteins are described here.

2.1. Compact Hemoglobin

Only a limited number of structure and functional studies of compact Hb have been carried out. The physiological role of these proteins is uncertain. It is proposed that Hb from the cyanobacterium *Nostoc cummune* is an oxygen scavenger in nitrogen fixation.

2.2. FixL

The FixL that occurs in *Rhizobium meliloti* and *Bradyrhizobium japonicum* is a chimeric protein consisting of a heme-containing domain and a protein kinase domain. Its proposed function is to sense oxygen through its heme domain and to transduce this signal by controlling the phosphorylation of transcriptional activator FixJ, which in turn induces the expression of the genes for nitrogen fixation, thereby providing oxygen-dependent control of nitrogen fixation (2). The heme domain has no significant sequence similarities to globins, suggesting that it arose independently.

2.3. Chlorocruorin

Chl has only a limited phylogenetic distribution. It is found in the blood plasma of four families of polychaeate annelids, the *Sabellidae*, *Serpulidae*, *Chlorhaemidae*, and *Ampharetidae*. The protein structure of Chl is essentially the same as that of extracellular annelid Hb, except for the change in the heme group (3). The vinyl to formyl replacement at position 2 of protoheme produces the characteristic greenish color and low oxygen affinity of Chl due to the enhanced electron-withdrawing properties of the formyl group. Chl shows highly cooperative oxygen binding. As with annelid Hb, its oxygen affinity is pH-dependent (see Bohr Effect) and is increased by divalent cations like Mg^{2+} and Ca^{2+} (4).

2.4. Hemerythrin (Hr) and Myohemerythrin

Hr has been found only in four phyla of marine invertebrates: Priapulia, Sipuncula, Brachiopoda, and one family of annelida, Magelonidae. It is contained in red cells called “hemerythrocytes” that float in the coelomic fluid. A noncirculating Hr is found in muscle fibers of sipunclids and is called “myoHr”, in analogy to myoglobin. Coelomic Hr is found predominantly as the octamer, but also as tetramers, trimers, and dimers. The octamer is composed of two different subunits that have different amino acid sequences (5). The octamer has a mass of 108 kDa, the shape of a square doughnut, and consists of two rings of four subunits each, whose rings are associated in a face-to-face, isologous manner (see Quaternary Structure). Each 13.5-kDa subunit consists of four parallel alpha-helices twisted in a left-handed bundle (6) (see Four-Helix Bundle Motif). The tertiary structure of myoHr (13.9 kDa) is similar to that of one Hr subunit. MyoHr and each subunit of Hr contains a site that has two iron atoms, which bind one O_2 molecule. The iron atoms are bound directly to seven amino-acid side chains of the protein. One of the O_2 atoms binds to one of the iron atoms, and the other oxygen atom forms a hydrogen bond with the oxo bridge that connects the two iron atoms.

The oxygen affinity of myoHr is higher than that of coelomic Hr of the same species. Octameric Hr from two brachiopods (*Lingula unguis* and *Lingula reevii*) show notable cooperativity in oxygen binding and have Hill coefficients of 1.8 to 2.2 (see Hemoglobin), whereas other Hrs are essentially noncooperative, irrespective of their state of aggregation. It has been suggested that the allosteric unit of *L. unguis* octameric Hr is the entire molecule (7). Effects of intracellular cofactors, such as H^+, CO_2, Mg^{2+}, Ca^{2+}, and Cl^-, on the oxygen affinity have been observed with some Hrs, but their physiological significance is not clear.

2.5. Hemocyanin

Hc is found in the blood plasma of two phyla, arthropod and mollusk. The oxygen-binding site of Hc is composed of a pair of copper ions, each of which is liganded by three histidine residues of the protein. It was long thought that O_2 binds as a peroxo ion, serially bridging the two Cu(II) ions, but now there is direct evidence that the mode of O_2 binding is a m-h^2:h^2 coordination, in which both oxygen atoms are bound to both of the copper ions and the O–O axis perpendicular to the Cu–Cu axis.

Arthropod and mollusk Hc exhibit similar optical and ligand-binding properties, but their molecular architectures are quite different. All arthropod Hcs are composed of hexamers. Each 75-kDa polypeptide chain carries one oxygen-binding site. These aggregate into 1, 2, 4, 6, or 8 hexamers, depending on the species, and no intermediate aggregation states are observed in each case. With this mode of assembly, one Hc molecule has from 6 to 48 oxygen-binding sites and a molecular mass ranging from 450 to 3300 kDa. Each hexamer is a “trimer of dimers,” and the shape is a trigonal antiprism. Each polypeptide chain consists of three domains. The first and second are a-helical, whereas the third has an irregular structure that contains a 7-strand b-barrel (see Beta-Sheet). The O_2-binding site is in the second domain.

In contrast to the arthropod Hc, those from mollusks are organized entirely differently. The molecule is composed of one or more cylindrical units, each containing 10 subunits. Each subunit is a long polypeptide chain of 350 to 440 kDa composed of seven or eight globular folded regions, each of which binds one O_2 molecule. It is not known whether each such region is composed of more than one domain, so it is called instead a “functional unit.” Its three-dimensional structure is not yet known.

The quaternary structures of both arthropod and mollusk Hc are stabilized by many calcium ions. The Hc oxygen affinity varies, depending on the species, especially in the Arthropoda, and reflects adaptations to the great variety of life styles and environments of the animals. Most Hcs demonstrate a distinct Bohr effect and varying degrees of cooperativity in oxygen binding. The Hill coefficient ranges between 1 and 12. A higher degree of aggregation is not necessarily accompanied by greater cooperativity. The oxygen dissociation curves of the Hcs that have large multimeric structures are not compatible with the classic allosteric concerted model of Monod, Wyman, and Changeux but are described best by a "nesting" model (8). This assumes that the allosteric units capable of transitions between two states, r and t, are in turn nested within larger structural units that are in equilibrium between two global states, R and T. In addition to the structural calcium ions, other calcium ions, plus magnesium ions, regulate the oxygen affinity.

There is very little sequence similarity between arthropod subunits and molluscan functional units. This and their very different molecular architectures indicate that they probably evolved independently.

Bibliography

1. K. Fukami-Kobayashi, M. Mizutani, and M. Go (1995) In Tracing Biological Evolution in Protein and Gene Structures (M. Go and P. Schimmel, eds.), Elsevier, Amsterdam, pp. 271–282.
2. M. A. Gilles-Gonzalez, G. S. Ditta, and D. R. Helinski (1991) Nature 350, 170–172.
3. A. N. Qabar, M. S. Stern, D. A. Walz, J.-T. Chiu, R. Timkovich, J. S. Wall, O. H. Kapp, and S. N. Vinogradov (1991) J. Mol. Biol. 222, 1109–1129.
4. K. Imai and S. Yoshikawa (1985) Eur. J. Biochem. 147, 453–463.
5. H. Yano, K. Satake, Y. Ueno, K. Kondo, and A. Tsugita (1991) J. Biochem. (Tokyo) 110, 376–380.
6. K. B. Ward, W. A. Hendrickson, and G. L. Klippenstein (1975) Nature 257, 818–821.
7. K. Imai, H. Takizawa, T. Handa, and H. Kihara (1995) In Structure and Function of Invertebrate Oxygen Carriers (S. N. Vinogradov and O. H. Kapp, eds.), Springer-Verlag, New York, pp. 179–189.
8. C. A. Robert, H. Decker, B. Richey, S. J. Gill, and J. Wyman (1987) Proc. Natl. Acad. Sci. USA 84, 1891–1895.

Suggestions for Further Reading

9. M. C. M. Chung and H. D. Ellerton (1979) The physicochemical and functional properties of extracellular respiratory hemoglobins and chlorocruorins, Prog. Biophys. Mol. Biol. 35, 53–102.
10. K. E. Van Holde and K. I. Miller (1995) Hemocyanins, Adv. Protein Chem. 47, 1–81.
11. T. Suzuki and K. Imai (1998) Evolution of myoglobin, Cell. Mol. Life Sci. 54, 979–1004.
12. D. M. Kurtz (1992) Molecular structure/function relationships of hemerythrins, Adv. Comp. Environ. Physiol. 13, 151–171.
13. K. E. van Holde and K. I. Miller (1995) Hemocyanins, Adv. Protein Chem. 47, 1–81.

Oxytocin

Oxytocin (MW 1007) is a peptide hormone released by the posterior pituitary gland that displays a wide spectrum of biological activities, including a role in reproduction and social behavior (1). It stimulates uterine contraction and lactation, activates myometrial GTPase and phospholipase C, and increases sodium excretion. It consists of only nine amino acid residues, with Cys1 and Cys6 linked by a disulfide bond and with an amidated C-terminus:

The complementary DNA (cDNA) encoding the precursor for human oxytocin has been cloned and DNA sequenced (2). This indicated that the genes for oxytocin and vasopressin are linked on the same human chromosome, 20, and arose through gene duplication (3). The gene for the oxytocin precursor, pro-oxyphysin, is composed of two introns and three exons. The initial gene product contains oxytocin, plus a carrier protein, neurophysin.

The majority of oxytocin is produced in the neurohypophysis and magnocellular neurons of the paraventricular and supraoptic nuclei of the hypothalamus. It is processed proteolytically from its precursor form during transport along the axonal projections to the posterior pituitary. The enzymes and the mechanisms of the specific posttranslational modifications involved in the production of active peptides from the precursor protein are still not completely known. The process by which the prohormones are packaged into the membrane-bound secretory granules and transported down the axon supraopticohypophyseal tract is the subject of ongoing investigation. The hormone and its associated neurophysin are secreted from nerve terminals of the neurohypophysis into the portal system of the neurohypophysis by calcium-dependent exocytosis, although the molecules responsible are not yet known. Oxytocin secretion is initiated by depolarizing electric impulses on the cell membranes. That is followed by calcium influx into the cell, fusion of the secretory granules with the cell membrane, and exocytotic extrusion of the hormone.

The relationship of oxytocin to its four types of receptors (4) and subsequent signaling is not completely understood (5). The human receptor has been sequenced (6); however, its structure analyzed, and its binding sites identified (7).

Oxytocin is primarily associated with lactation and parturition in females. It is used clinically to induce labor or augment labor, when appropriate, because it stimulates the contractions of uterine smooth muscle. Oxytocin release is stimulated by a baby's cry or suckling, and this subsequently releases prolactin, which causes milk to be released, by stimulating the contraction of myoepithelial cells in milk ducts of mammary glands and thereby forcing milk from alveoli in the breast. Oxytocin has been implicated in other functions. These include mating and maternal behavior, natriuresis, modulation of the cholesterol/phospholipid ratio in membranes, and even memory. However, the elimination of oxytocin in transgenic mice did not change their reproductive and maternal behavior (8, 9). Both male and female homozygous knockouts are fertile, and the females are capable of parturition; cross reactivity of vasopressin with the oxytocin receptors explains this apparent contradiction. Milk release was absent, but it was correctable by oxytocin injection. In males, the importance of oxytocin is even less well understood. It has been suggested that oxytocin is involved in prolactin release, penile erection, and various aggressive sexual behaviors.

Bibliography

1. R. Ivell and J. A. Russell, editors (1995) Oxytocin: Cellular and Molecular Approaches in Medicine and Research (Advances in Experimental Medicine and Biology, vol. 235), Plenum, New York.
2. E. Mohr (1995) Vitamins and Hormones 51, 235–266.
3. Y. Hara et al. (1990) Mol. Brain Res. 8, 319–324.
4. R. Ivell et al. (1997) Biochem. Soc. Trans. 25, 1058–1066.
5. C. Barberis et al. (1998) J. Neuroendocrinology 156, 223–229.
6. T. Kimura et al. (1992) Nature 356, 526–529.
7. B. Mouillac et al. (1995) in ref. 1, pp. 301–307.
8. K. Nishimori et al. (1996) Proc. Natl. Acad. Sci. USA 93, 11699–11704.

9. W. S. Young III et al. (1996) J. Neuroendocrinology 8, 847–853.

P Element

The P element is a transposable element in *Drosophila* that can insert into many different positions in the genome (1). In addition to being an element whose transposition mechanism has been interesting to dissect, its transposition is controlled in interesting ways at several levels. Manipulation of P-element transposition has also been an immensely powerful tool for *Drosophila* genetics (2). One widespread use of P elements is to make physically tagged mutations that have allowed the ready isolation of the affected genes through the physical marker provided by the P element. Also, P-element transposition has provided a widely used method for introducing sequences into the *Drosophila* genome.

P elements were discovered by studying the phenomenon hybrid dysgenesis that results when males from certain strains of *Drosophila* are crossed with females of certain different strains. In the germline of the progeny of such crosses, there is a high frequency of mutations and also sterility. Characterization of mutations resulting from such crosses revealed that they resulted from the insertion of a novel 2.9-kbp piece of DNA, the P element (see Fig. 1 in Transposable Elements). Transposition of this element is usually restricted to the germline, because the transposase is assembled from four exons by RNA splicing in the P-element messenger RNA, and factors in somatic cells can both inhibit transcription and block splicing. Hybrid dysgenesis results from a cross of a P-element male with a non-P-element-containing female. The use of the maternal non-P-element strain is important because, in addition to making transposase, the P element also produces a transposition inhibitor from the unspliced P-element RNA, so transposition is inhibited in eggs of P^+ strains.

P-element transposition is promoted by the P-element transposase (3) and a collaboration with at least one host protein that also interacts with the ends of the P element (4). Interestingly, this host protein is related to other proteins involved with DNA repair. The nature of the collaboration between these proteins that promotes transposition is not yet known. P-element transposition occurs via a “cut and paste” mechanism, in which the element is excised from the donor site and then inserted into the target site. The donor gap resulting from transposon excision can be repaired by double-strand break repair using a sister homologue as a template (5).

The P element has been an immensely powerful tool in studying *Drosophila*. Not long after the discovery and molecular characterization of the P element, it was used in a landmark experiment to introduce novel DNA sequences into the *Drosophila* genome (6). A special P-element derivative was constructed that had, in addition to transposase, a further gene whose activity could be scored visually by inspection of flies. It was found that injection of this modified P element into embryos could result in its integration into the germline and expression in adult flies. Such P-element-mediated transformation is now a commonly used method in *Drosophila* analysis (2). P-element derivatives are also widely used as mutagens, so that the mutations generated are physically tagged with the element; this makes isolation of the target DNA containing the mutated gene very straightforward.

Bibliography

1. W. R. Engels (1996) Curr. Top. Microbiol. Immunol. 204, 103–124.

2. K. Kaiser, J. W. Sentry, and D. J. Finnegan (1995) *Mobile Genetic Elements* (D. J. Sherratt, ed.) IRL Press, Oxford, pp. 69–100.
3. E. L. Beall and D. C. Rio (1998) *EMBO J.* **17**, 2122–2136.
4. E. L. Beall and D. C. Rio (1996) *Genes Dev.* **10**, 921–933.
5. W. R. Engels, D. M. Johnson-Schlitz, W. B. Eggleston, and J. Sved (1990) *Cell* **62**, 515–525.
6. G. M. Rubin and A. C. Spradling (1982) *Science* **218**, 348–353.

P22 Bacteriophage

The *Salmonella typhimurium* phage P22 is a double-stranded DNA phage of the Podoviridae family that has played a key role in the development of molecular biology. Studies with P22 have contributed to our understanding of genetic exchange, control of gene expression, and biological self-assembly. It has proven itself to be a valuable laboratory tool for genetic manipulation of its host, *Salmonella*. P22 is classified as a lambdoid phage because it shares life cycle similarities with the *Escherichia coli* lambda phage. Comparison of the similarities and differences between P22 and the other lambdoid phage has served to illuminate both the common themes and the range of diversity that nature employs in problem solving (1).

P22 was originally isolated as a lysogen of *Salmonella*, and it has played a key role in the development of bacterial genetics. In 1952, Zinder and Lederberg discovered the phenomenon of generalized transduction of *Salmonella* genes by P22 (2). This observation led to studies on the mechanism of the establishment of lysogeny, which contributed to our current understanding of repressors and anti-repressors. Studies of the assembly of P22 have been instrumental in framing the concepts that guide our thinking about common mechanisms in biological assembly (3). In addition, the well-defined and readily manipulable genetics of P22 have allowed it to lead the way in the development of genetic analysis of protein folding and assembly (3-6).

Bacteriophage P22 is a temperate virus, meaning that following infection two distinct life cycles are available to it: the lytic or the lysogenic life cycles. In the lytic life cycle, a series of viral genes are expressed that ultimately result in the production of several hundred progeny virions per cell. The progeny virions are released approximately one hour after infection, through lysis of the host cell (Fig. 1). In the alternative pathway, termed the lysogenic pathway, the phage chromosome integrates into the host chromosome, and expression of the phage structural genes is suppressed (see Lysogeny). The integrated phage is called a prophage, which is replicated and passed to the daughter cells during cell division. In response to an appropriate environmental signal, such as irradiation with ultraviolet light, the prophage can excise itself, enter the lytic cycle, and generate progeny phage. The decision between whether an infecting phage enters the lytic or lysogenic pathway depends on a number of factors, the most important of which seems to be the number of infecting virions, or multiplicity of infection.

Figure 1. Electron micrograph of a section through a bacteriophage P22-infected *Salmonella typhimurium* cell approximately 30 min after infection. The electron-dense progeny phage within the cell contains double-stranded DNA, whereas the infecting phage that remain attached to the cell at 1 and 8 o'clock do not.

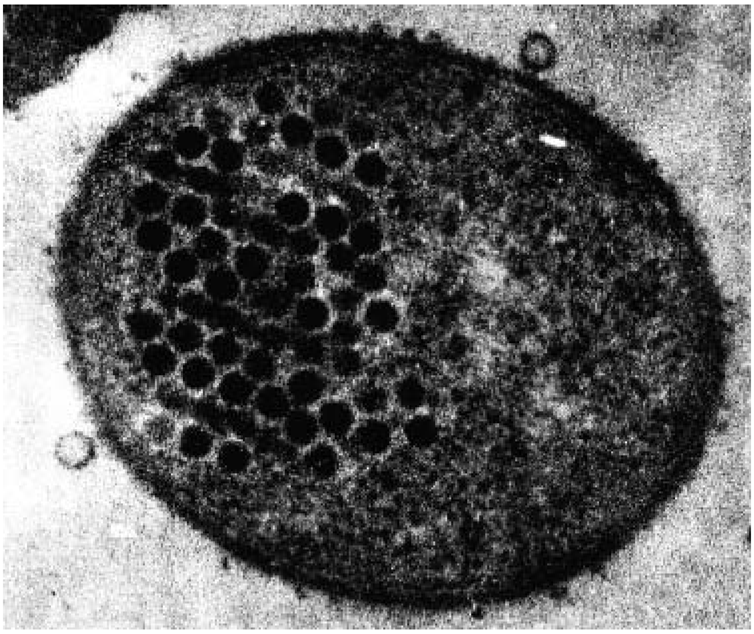

1. Structure

The P22 virion consists of two distinct structural elements: the capsid and the tail. The dsDNA phage genome is contained within the capsid and is thereby protected from environmental insult. The capsid of the P22 virion is a T = 7 icosahedral symmetry lattice approximately 600 Å in diameter, composed of ~420 identical copies of the 47-kDa gene product 5 (gp5) coat protein (7). The capsid itself is a very stable structure, resistant to elevated temperature and drying, as well as nucleases and proteinases. Interestingly, this stability does not arise directly from the coat protein subunits, but rather from their intersubunit contacts (8). The coat protein subunits themselves, prior to polymerization into the capsid, are only modestly stable. The tail is composed of up to six trimers of the 72-kDa gp9 tailspike protein. The tailspike protein serves as the organelle for attachment of the virus to the host cell during infection and is itself also a very stable structure (9).

The 27×10^6–kDa linear dsDNA genome is contained within the capsid of the phage in a highly condensed liquid-crystalline state. The close packing of the phosphate groups in the condensed form requires charge neutralization, which is accomplished through the binding of Mg^{2+} ions. Although the precise packing of the DNA within the capsid is not known, the B form of DNA structure appears to be retained (10).

The structure of the tailed vertex of the phage is surprisingly complex. The tailspike trimers are attached to the capsid through a connector region. The connector is composed of a macromolecular complex composed of 12 subunits of the gp1 portal protein, as well as the connector proteins, gp4, gp10, and gp26. The 83-kDa gp1 portal protein is arranged as a dodecameric complex, approximately 180 Å in diameter with a central channel approximately 30 Å in diameter (11). It is thought that the DNA enters and exits the head through the central channel of the portal complex. Portal complexes have been identified in nearly all the dsDNA-containing bacteriophage. Although there has been debate as to whether portal complexes are composed of 12 or 13 subunits, the existence of the portal complex at an icosahedral vertex poses an interesting structural dilemma: The portal complex exhibits 12- or 13-fold symmetry, but is located at a fivefold symmetrical vertex, resulting in a symmetry mismatch. This means that there cannot be a simple 1:1 interaction between portal and capsid subunits during assembly and function. Although the exact manner in which the portal protein interacts with the capsid is unknown, it has been suggested that such an arrangement would make it possible for the portal complex to rotate within the capsid during DNA translocation

(12).

The tailspike protein folds and assembles independently of the capsid, and then adds subsequently to the capsid to render the phage infectious. The unique biochemical properties of the tailspike protein, coupled with the well-defined genetics of the bacteriophage system, have made it an ideal subject for *in vivo* studies of protein folding. The tailspike folds in a multistep pathway, in which partially folded intermediates associate to form an SDS-sensitive protrimer (13). The protrimer then matures into a very stable SDS-insensitive trimer. The reason for this stability is that the central region of each subunit of the trimer is folded into a right-handed b-helix structure, and the C-terminal regions interdigitate to form b-sheet structures (14, 15). The ability to identify readily and quantify the ratio of partially folded and fully folded proteins by the simple technique of SDS-PAGE analysis has allowed the isolation and characterization of a series of mutations that destabilize the partially folded intermediates. Because these mutations have no effect on the stability of the final fully folded trimer, these mutants have been termed temperature-sensitive for folding (*tsf*) mutants. Analysis of these mutants has lent support to the idea that protein folding and assembly takes advantage of transient interactions between amino acid residues that do not play a critical role in the stability of the final structure. At restrictive temperatures, the *tsf* mutant proteins form aggregates, indicating that aggregation occurs through the interaction of partially folded protein molecules and that alterations in the lifetime of the protein folding intermediates can result in aggregation (6, 16-18).

2. The Infection Process

P22 initially infects the host *Salmonella* cell through the binding of the tailspike to the O-antigenic repeating units of the bacterial lipopolysaccharide. The interaction of the tailspike protein with this receptor defines the host range. Once bound, the tailspike slowly destroys the receptor by cleaving the au (1, 3)-O-glycosidic bond between rhamnose and galactose units. The virion carries up to six tailspikes, but only three are used for binding during infection (9, 19, 20). Once bound, the phage moves laterally across the cell surface through repeated cycles of binding and release, presumably until it locates a second receptor, at which point binding becomes irreversible (21).

The dsDNA is then injected into the host cell in a linear fashion (22). The phage-encoded pilot proteins gp7, gp16, and gp20 are required to ensure that the DNA crosses the plasma membrane in an infectious form. Although the mechanism of their action remains unknown, they translocate from the phage into the host cell during infection (23). Following infection, the dsDNA circularizes by homologous recombination between the terminal redundancy regions, yielding a circular dsDNA that represents a single copy of the phage genome (24).

3. The Lysogenic Pathway

In the lysogenic state, the bacterial chromosome carries an integrated copy of the bacteriophage chromosome, termed a prophage. In the prophage, the genes responsible for growth of the phage and subsequent death of the host are repressed through the action of a specific repressor system. This repression results in a phenomenon known as *immunity*. If a host cell carrying a lysogen is subsequently superinfected by a phage carrying the same repressor system as the prophage, it too will be unable to grow. P22 maintains the prophage in a quiescent state through the action of two repressor proteins (Fig. 2). In this regard, P22 differs from phage, which has only a single repressor, cI. The two P22 repressor proteins are called *c2* and *mnt*, and they give rise to two immunity systems. The *immC* region is similar to the immunity region of l. The P22 c2 repressor acts at O_L and O_R to prevent transcription of the early genes. The unique *immI* region includes an antirepressor, *ant*, and its regulators *mnt* and *arc*. Mnt acts to repress the transcription of the ant antirepressor. If *mnt* is turned off, ant is synthesized. Ant binds to and inactivates the c2 repressor protein, with the result that the prophage enters the lytic pathway. The production of ant itself is regulated through the action of the *arc* gene. In *arc* mutants, high levels of ant are produced, and these levels block phage development. The arc and mnt proteins are two members of a small family of proteins that use antiparallel b-sheet motifs rather than helix–turn–helix motifs to bind their operator DNA (25, 26) (see DNA-Binding Proteins).

Figure 2. Genetic map of bacteriophage P22. The genes are positioned above the line (not to scale), with their function indicated above. Promoter regions and the loci of repressor action are indicated below the line. The c2 repressor protein inhibits synthesis of the early genes, P_l and P_r. The anti-terminators 24 and 23 result in expression of the early and late genes, respectively. Note that genes with related functions are clustered.

The *ant* gene lies downstream of P_{late} and is transcribed during the lytic cycle as part of the late operon, but Ant protein is not synthesized. An additional promoter P_{sar} lies within the *ant* gene and directs the synthesis of a 69-nucleotide long antisense RNA that binds to the *ant* messenger RNA and inhibits its translation (27, 28).

In order to form a stable lysogen, the phage genome has to integrate into the host; otherwise it would be diluted out during cell division. Integration occurs preferentially at a particular site, attB, in the host chromosome and requires the action of the phage-encoded integrase (Int) protein and the host-encoded integration host factor (IHF). The circular phage chromosome carries a similar site, termed attP (29). A single crossover event catalyzed by the Int protein results in integration. For entry into the lytic cycle, excision proceeds by the reverse mechanism but, to ensure that excision does not take place prematurely, requires the additional function of the *xis* gene product, which overlaps *int* in the genetic map (30).

Entry into the lysogenic pathway is controlled by the genes *c1* and *c3*. These gene products stimulate the production of the c2 repressor protein immediately after infection. C1 binds to the P_{RE} (promoter repressor establishment) promoter as a tetramer and stimulates *c2* synthesis (31). High-level expression of c2 appears to be required for entry into the lysogenic pathway, and this is the probable reason that a high multiplicity of infection favors lysogeny.

In addition to the immunity conferred by the immI and immC repressor systems, the phage employs three other mechanisms to prevent superinfection. The first is a modification of the host O antigen, which inhibits the adsorption of P22. This function is encoded by the a1 gene (32). The genes sieA and sieB (superinfection exclusion) block superinfection. Expression of SieB appears to lead to abortive infection; while the superinfecting phage enters the cell, and early functions are normally expressed, late function expression is inhibited. The sieA protein is an 18-kDa protein that partitions into the membrane and acts to block DNA from crossing the periplasmic space and entering the host cell (33). It therefore excludes virion DNA from entering the cells, regardless of the identity of the DNA.

4. The Lytic Pathway

In the lytic pathway, P22 enters the *Salmonella* host cell and begins the process of reproduction. In P22, as in l, the proteins involved in the lytic cycle are expressed sequentially. Control of the timing of the production of mRNA transcripts is achieved through the use of anti-termination proteins that allow the RNA polymerase to ignore encoded termination signals. To take advantage of this, the P22 genome is organized so that these regulatory proteins can exert their influence on a large number of genes (34). The genes themselves are clustered into functional units; for example, all the genes involved in assembly are clustered into the late operon and are under the control of a single regulatory protein. Like lambda, the early genes of P22 are arranged into two operons, P_L and P_R, which flank the P22 c2 repressor gene. The genes in these operons encode proteins involved in DNA replication, recombination, integration, and the regulation of gene expression. Gene 24, which is transcribed off P_L, is similar in function to the lambda N gene. It functions to prevent the termination of transcription at genetically defined sites in the chromosome and allows for complete transcription of the early genes (35, 36). Gene 23, which is transcribed off P_R, is analogous to gene Q in lambda and allows transcription of the late genes (37). The late genes that are driven off the P_{late} promoter code for the proteins necessary for head and tail assembly.

5. Generalized Transduction

Transduction is a process by which bacterial DNA is carried from one cell to another by a phage particle. Generalized transducing particles contain DNA derived entirely from the host-cell chromosome. Bacteriophage P22 transducing particles originate when the host chromosome, rather than the phage chromosome, serves as the substrate for packaging. During a lytic infection, the phage chromosome is replicated as a concatamer, and the concatamers are resolved as the double-stranded DNA is packaged by a headful mechanism. The products of phage genes 2 and 3 are required for packaging and act as a complex. Genetic evidence suggests that gp3 is responsible for recognizing a unique site or region termed a pac site. Packaging proceeds in an ATP-dependent reaction until the head is full, at which point the gp2/gp3 complex cuts the DNA; packaging then continues into another empty phage head. This model is the "sequential packaging model." The P22 head can package 105% of a phage genome, accounting for the observed terminal redundancy and circular permutation of the genetic map (38-41).

Within the *Salmonella* chromosome, there are a minimum of five to six sites, called pseudo-pac sites, which are recognized by the gp2/gp3 complex as pac sites. The nonrandom distribution of pseudo-pac sites therefore leads to a nonrandom distribution of transduced markers (42). Mutants that map in gp3, termed HT mutants, have been isolated in which up to 50% of the phage heads carry host DNA. These mutants have proven extremely valuable for studying the genetics of *Salmonella*. The 44-kbp length of the packaged DNA corresponds to about 50 genes and has made possible linkage analysis and genetic mapping of the *Salmonella* chromosome.

6. Specialized Transduction

Specialized transducing particles carry both host and phage DNA linked in a continuous stretch in a single particle. There are two mechanisms by which specialized transducing particles can arise: from aberrant prophage excision or by insertion into the phage genome of host translocatable elements. P22 has more latitude in its ability to mediate specialized transduction than does bacteriophage l. Because P22 packaging does not use unique ends, it can package extremely long stretches of DNA by segmenting them into multiple heads. If a host cell is multiply infected, an intact oversized genome can be generated by recombination.

7. Capsid Morphogenesis

During P22 morphogenesis, properly folded associated tailspike trimers add to the dsDNA-containing head, to generate an infectious virion. However, the filled capsid is not the first structure that is assembled (Fig. 3). The gp5 coat protein subunits are first assembled into a structure termed a procapsid (37). Like the mature virion, the procapsid has T = 7 icosahedral symmetry, and the portal protein is present at a single vertex in the form of a dodecameric complex (43, 44). However, the procapsid does not contain DNA. The interior volume is filled with approximately 300 copies of the gp8 scaffolding protein. Studies with conditional lethal mutants have demonstrated that the presence of the scaffolding protein facilitates coat protein polymerization and ensures a proper structure. In the absence of scaffolding protein, a variety of morphologically aberrant polymers are formed, while assembly proceeds with high fidelity (45). The procapsid is approximately 10% smaller in diameter and is less stable than the mature head. During DNA packaging, the scaffolding protein exits, and the lattice expands. Three-dimensional single-particle reconstructions from cryoelectron microscopy of the procapsid and mature form revealed that there are ~25 Å diameter holes situated at the center of the hexavalent capsomeres in the procapsid and that these holes are closed during expansion. No proteins are added to the procapsid to close the holes; instead, they are closed by domain movements within the coat protein subunits (46). These holes are likely candidates for the exit ports for the scaffolding protein during DNA packaging (43). The freed scaffolding protein is recycled to participate in further rounds of assembly (47). Thus, the scaffolding protein functions as an “assembly molecular chaperone” whose presence is transiently required to provide positional information. The use of scaffolding proteins is a common theme in the assembly of the lambdoid phages and is also required for the assembly of the herpesviruses.

Figure 3. The morphogenetic pathway of the bacteriophage P22 capsid. The first structure formed is a procapsid, which
coat, scaffolding, and portal proteins. The “pilot” proteins are also incorporated at this stage. The concatameric DNA is
with the exit of the scaffolding protein. The addition of gp4, gp10, and gp26 stabilizes the head, and tailspike binding re

The scaffolding protein of P22, as well as all well-characterized scaffolding proteins, is a highly α-helical molecule that forms oligomers in solution (48). In the case of P22, dimerization of the scaffolding protein plays a key role in assembly. In both P22 and the herpes virus, the region of interaction between the coat and scaffolding protein has been mapped to the C-terminal end of the molecule. In addition to its role in assembly, it has been suggested that the scaffolding protein may function to exclude the chance incorporation of cellular proteins during head assembly, because the presence of cellular proteins within the capsid would result in a decreased internal volume and preclude the encapsidation of a complete P22 genome. P22 scaffolding protein regulates its own levels of biosynthesis, which is decreased if there is a large free pool, but up-regulated if all the scaffolding protein is incorporated into procapsids (49-51). This post-transcriptional control might be a mechanism to insure that all procapsids contain a full complement of scaffolding protein, despite the fact that a full complement is not strictly required for assembly (52).

During morphogenesis, the dsDNA is packed into the procapsid, the scaffolding protein exits, and the capsid lattice expands. The exact sequence of these events is not known, but the expansion is an exothermic process, suggesting that the capsid is “spring loaded” (53). Interestingly, the portal protein is part of the gauge that determines when the head is full; mutants in the gp1 portal protein have been identified that result in packaging a piece of P22 DNA up to 5% larger than normal (54). Following DNA packaging, the portal vertex is closed by the addition of the protein products of genes 4, 10, and 26. These proteins, which add sequentially, serve to stabilize the DNA within the capsid and also to provide the site for tail attachment (55).

There are two genes that are essential for lysis, genes 13 and 19. Gene 13 encodes an 11-kDa protein whose function is to disrupt the cell membrane by forming pores and to allow the hydrolytic enzymes access to the cell wall. Mutations in gene 13 have been isolated that delay lysis for up to several hours, despite the fact that the phage-encoded lysozyme is being produced. Gene 19 encodes the P22 lysozyme, a 16-kDa monomeric protein that attacks and degrades the peptidoglycan layer of the cell wall, leading to cell lysis. The bacteriophage P22 lysozyme is very similar to the well-studied T4 lysozyme with respect to structure and function.

Procapsid-like particles of P22 can be assembled in vitro from purified proteins (52). This has made it possible to perform sophisticated physical chemical studies of virus assembly. These studies have revealed that capsid assembly is a nucleation-limited reaction (56), proceeds along a well-directed pathway (56), and can be inhibited by the binding of small molecules to the coat protein subunits (57).

Over the past 30 years, the bacteriophage P22 system has contributed to our understanding of gene expression, protein folding and assembly, and basic virology. It appears that the lessons that we can learn from these systems is limited only by the creativity of the investigator.

Bibliography

1. A. Campbell (1994) Annu. Rev. Microbiol. 48, 193–222.
2. N. D. Zinder and J. Lederberg (1952) J. Bacteriol. 64, 679–699.
3. J. King, R. Griffin-Shea, and M. T. Fuller (1980) Q. Rev. Biol. 55, 369–393.
4. J. Jarvik and D. Botstein (1975) Proc. Natl. Acad. Sci. USA 72, 2738–2742.
5. J. King and M. H. Yu (1986) Methods Enzymol. 131, 250–266.
6. J. King, C. Haase-Pettingell, A. S. Robinson, M. Speed, and A. Mitraki (1996) Faseb J. 10, 57–66.
7. S. Casjens (1979) J. Mol. Biol. 131, 1–14.
8. P. E. Prevelige, Jr., J. King, and J. L. Silva (1994) Biophys. J. 66, 1631–1641.
9. V. Israel (1976) J. Virol. 18, 361–364.

10. K. L. Aubrey, S. Casjens, and G. J. Thomas, Jr. (1992) Biochemistry 31, 11835–11842.
11. C. Bazinet, J. Benbasat, J. King, J. M. Carazo, and J. L. Carrascosa (1988) Biochemistry 27, 1849–1856.
12. R. W. Hendrix (1978) Proc. Natl. Acad. Sci. USA 75, 4779–4783.
13. D. P. Goldenberg, D. H. Smith, and J. King (1983) Proc. Natl. Acad. Sci. USA 80, 7060–7064.
14. D. P. Goldenberg and T. E. Creighton (1994) Curr. Biol. 4, 1026–1029.
15. S. Steinbacher, R. Seckler, S. Miller, B. Steipe, R. Huber, and P. Reinemer (1994) Science 265, 383–386.
16. C. A. Haase-Pettingell and J. King (1988) J. Biol. Chem. 263, 4977–4983.
17. A. Mitraki, B. Fane, C. H. Haase-Pettingell, J. Sturtevant, and J. King (1991) Science 253, 54–58.
18. M. A. Speed, T. Morshead, D. Wang, and J. King (1997) Protein Sci. 6, 99–108.
19. V. Israel (1978) J. Gen. Virol. 40, 669–673.
20. S. Iwashita and S. Kanegasaki (1976) Eur. J. Biochem. 65, 87–94.
21. U. Baxa, S. Steinbacher, S. Miller, A. Weintraub, R. Huber, and R. Seckler (1996) Biophys. J. 71, 2040–2048.
22. M. Rhoades, L. A. MacHattie, and C. A. Thomas, Jr. (1968) J. Mol. Biol. 37, 21–40.
23. V. Israel (1977) J. Virol. 23, 91–97.
24. D. Botstein and M. J. Matz (1970) J. Mol. Biol. 54, 417–440.
25. M. J. Burgering, R. Boelens, D. E. Gilbert, J. N. Breg, K. L. Knight, R. T. Sauer, and R. Kaptein (1994) Biochemistry 33, 15036–15045.
26. B. E. Raumann, M. A. Rould, C. O. Pabo, and R. T. Sauer (1994) Nature 367, 754–757.
27. T. H. Wu, S. M. Liao, W. R. McClure, and M. M. Susskind (1987) Genes Dev. 1, 204–212.
28. S. M. Liao, T. H. Wu, C. H. Chiang, M. M. Susskind, and W. R. McClure (1987) Genes Dev. 1, 197–203.
29. L. Smith-Mungo, I. T. Chan, and A. Landy (1994) J. Biol. Chem. 269, 20798–20805.
30. J. M. Leong, S. E. Nunes-Duby, A. B. Oser, C. F. Lesser, P. Youderian, M. M. Susskind, and A. Landy (1986) J. Mol. Biol. 189, 603–616.
31. Y. S. Ho, D. Pfarr, J. Strickler, and M. Rosenberg (1992) J. Biol. Chem. 267, 14388–14397.
32. M. Gough and J. V. Scott (1972) Virology 50, 603–605.
33. B. Hofer, M. Ruge, and B. Dreiseikelmann (1995) J. Bacteriol. 177, 3080–3086.
34. M. M. Susskind and D. Botstein (1978) Microbiol. Rev. 42, 385–413.
35. S. Hilliker and D. Botstein (1975) Virology 68, 510–524.
36. J. W. Roberts, C. W. Roberts, S. Hilliker, and D. Botstein (1976) in R. Losick and M. Chamberlin, eds., RNA Polymerase, Cold Spring Harbor Laboratory, Cold Spring Harbor, NY.
37. D. Botstein, C. H. Waddell, and J. King (1973) J. Mol. Biol. 80, 669–695.
38. B. K. Tye, J. A. Huberman, and D. Botstein (1974) J. Mol. Biol. 85, 501–528.
39. B. K. Tye and D. Botstein (1974) J. Supramol. Struct. 2, 225–238.
40. S. Casjens and M. Hayden (1988) J. Mol. Biol. 199, 467–474.
41. S. Casjens, W. M. Huang, M. Hayden, and R. Parr (1987) J. Mol. Biol. 194, 411–422.
42. H. Schmieger (1982) Mol. Gen. Genet. 187, 516–518.
43. B. V. Prasad, P. E. Prevelige, E. Marietta, R. Chen, D. Thomas, J. King, and W. Chiu (1993) J. Mol. Biol. 231, 65–74.
44. P. A. Thuman-Commike, B. Greene, J. Jakana, B. V. V. Prasad, J. King, P. E. Prevelige, Jr., and W. Chiu (1996) J. Mol. Biol. 260, 85–98.
45. W. Earnshaw and J. King (1978) J. Mol. Biol. 126, 721–747.

46. P. E. Prevelige, Jr., D. Thomas, K. L. Aubrey, S. A. Towse, and G. J. Thomas, Jr. (1993) Biochemistry 32, 537–543.

47. J. King and S. Casjens (1974) Nature 251, 112–119.

48. M. H. Parker, W. F. Stafford III, and P. E. Prevelige, Jr. (1997) J. Mol. Biol. 268, 655–665.

49. J. King, C. Hall, and S. Casjens (1978) Cell 15, 551–560.

50. S. Casjens and M. B. Adams (1985) J. Virol. 53, 185–191.

51. S. Casjens, M. B. Adams, C. Hall, and J. King (1985) J. Virol. 53, 174–179.

52. P. E. Prevelige, Jr., D. Thomas, and J. King (1988) J. Mol. Biol. 202, 743–757.

53. M. L. Galisteo and J. King (1993) Biophys. J. 65, 227–235.

54. S. Casjens, E. Wyckoff, M. Hayden, L. Sampson, K. Eppler, S. Randall, E. T. Moreno, and P. Serwer (1992) J. Mol. Biol. 224, 1055–1074.

55. H. Strauss and J. King (1984) J. Mol. Biol. 172, 523–543.

56. P. E. Prevelige, Jr., D. Thomas, and J. King (1993) Biophys. J. 64, 824–835.

57. C. M. Teschke, J. King, and P. E. Prevelige, Jr. (1993) Biochemistry 32, 10658–10665.

Suggestions for Further Reading

58. M. M. Susskind and D. Botstein (1978) Molecular genetics of bacteriophage P22. Microbiol. Rev. 42, 385–413. (An outstanding review of the genetics of bacteriophage P22).

59. P. E. Prevelige Jr. and J. King (1993) Assembly of bacteriophage P22: a model for dsDNA virus assembly. Prog. Med. Virol. 40, 206–221.

P53

p53 is a well-characterized tumor suppressor gene. It is located on human chromosome 17p13.1 and encodes a polypeptide chain of 375 amino-acid residues. Like the retinoblastoma gene, loss of p53 function results in the onset of oncogenesis (see Oncogenes and Neoplastic Transformation). p53 is a transcription factor that regulates the expression of cell-cycle regulatory proteins. The p53 protein contains an N-terminal transactivation domain, a central DNA-binding domain, and a C-terminal regulatory domain. The C-terminal domain of p53 mediates oligomerization of the protein, which is essential for its DNA-binding activity. This domain also mediates its interaction with other cellular factors that enhance the DNA-binding activity of the protein.

P53 plays a pivotal role during the execution of apoptosis (programmed cell death) pathways induced by DNA damage caused by agents, such as ultraviolet or ionizing radiation (Fig. 1). Current models suggest that DNA damage results in up-regulating p53 gene transcription and accumulation of this protein in the cell (1). Accumulation of p53 appears to result in the enhanced transcription of a group of genes, such as the cell cycle-dependent kinase inhibitor p21/WAF-1/cip-1, that are responsible for stalling the cell cycle in either the G_1 or G_2/M-phase. This mechanism provide the cell with valuable time to make critical repairs in its genetic material. In the event that the necessary repairs cannot be made, the p53 protein initiates a "suicidal" apoptotic program, resulting in cell death, to prevent clonal expansion of a cell with a mutated genome.

Figure 1. Proposed function of p53. (a) P53 is not required for normal cell division. (b) In response to DNA damage,

p53 levels increase and arrest the cell at the first of two “checkpoints” in the G_1 phase of the cell cycle. If all of the repairs have been made to the DNA, the cell divides normally and completes the cell cycle. However, if the cell still contains mutated or duplicated DNA sequences, it dies by a suicidal apoptotic mechanism to prevent its expansion). (
In those cells that have mutated or lost p53 genes, the arrest at G_1 does not occur, and the cells that have mutated genomes proliferate and become cancerous.

Malignant cells have evolved novel strategies to destroy p53 function, and approximately 50% of human tumors contain mutations or deletions in this gene. Normal p53 protein binds to DNA and transactivates the transcription of a distinct set of target genes. Mutated forms of p53 cannot bind DNA in this fashion, however, and therefore behave abnormally. A second mechanism by which normal p53 function is subverted in a cancerous cell is through the MDM2 protein. The MDM2 protein binds to p53, and it is amplified in many tumor cells. When these two proteins are bound, p53 cannot mediate growth arrest at the cell cycle checkpoints (as described previously), which leads to rapid clonal expansion of cells that have unstable, mutated genomes.

Bibliography

1. L. J. Ko and C. Prives (1996) Genes Dev. 10, 1054–1072.

P-Glycoproteins

The best characterized form of drug resistance in human cells is due to the overexpression of P-glycoprotein (P-gp). This 170-kDa plasma membrane protein is a member of the ATP Binding Cassette (ABC) superfamily of transport proteins; it can extrude a range of hydrophobic anticancer drugs from the cell against a concentration gradient, and thus protect the cell. Consequently, cells that overexpress P-gp show reduced intracellular concentrations of drugs and greater resistance to them (1). Molecular probes developed to identify P-gp in cancer tissues also strongly suggest that, at least in hematological malignancies, P-gp plays a significant role in multiple drug resistance (MDR) in the clinic.

The mammalian *mdr* gene family consists of two members in humans and three in rodents (2). Of the two human genes, *MDR1* and *MDR2*, only *MDR1* confers drug resistance. The sequences of the mouse *mdr1* and *mdr3* are 80% identical to the *MDR1* human gene product, and they are also capable of conferring resistance to drugs, as are their hamster homologues, *pgp1* and *pgp2*. The human *MDR1* gene encodes a 1280-amino acid membrane protein, P-gp. Hydropathy plots of this protein have led to a secondary structure model for P-gp (see Fig. 1) in which it consists of 12 putative transmembrane regions, with two ATP-binding domains on the cytoplasmic face of the membrane. Each half of the protein consists of six hydrophobic transmembrane putative alpha-helices and one ATP-binding domain; the two halves are 43% identical (3).

Figure 1. A hypothetical two-dimensional model of human P-glycoprotein and its functional domains. This model, with ATP sites (nucleotide binding domains), is based on hydropathy analysis of the amino acid sequence. The ATP sites are indicated. The N-linked glycosylation sites are indicated by wavy lines, and the known phosphorylation sites are shown show the regions labeled with photoaffinity analogues. Filled circles represent amino acid residues in which mutations h transport specificity. This figure is adapted from Ref. 1.

Drug resistance conferred by the human and rodent P-gp's has been extensively studied. However, there continue to be controversies and alternate models vis-à-vis the mechanism by which an extremely broad range of substrates are expelled from the cells. The most widely accepted model is that the P-gp uses ATP to power a molecular pump to remove chemotherapeutic agents from the cell (1). According to this hypothesis, chemotherapeutic agents diffuse down a concentration gradient into the cell, and the pump either acts as a “flipase” to expel them as they enter the bilayer, or the drugs are first transported from the cytosol to the membrane and subsequently pumped out from the membrane. An alternate mechanism has also been suggested in which changes in the intracellular pH and membrane potential alter the transmembrane partitioning or intracellular sequestering of the drugs (4). As these are the two principal models on which most current work is based, the evidence on which each is based will be considered briefly.

The alternative partitioning model is essentially a passive diffusion model (4). The central notion is that the drugs are sufficiently hydrophobic to cross the membrane spontaneously. The subsequent asymmetric distribution of these drugs is then a consequence of the asymmetry of the chemical potential (pH and membrane potential). It is argued that because the cytosol of tumor cells is acidic, the drugs (most of which are weak bases, with pK_a values 7.4 to 8.2) get protonated and are trapped in the cytosol. Conversely, an increased cytosolic pH would decrease the intracellular accumulation of drugs. Experimental evidence in support of this scenario comes from a number of observations. In model systems such as phospholipid vesicles, it is possible to modulate the transmembrane distribution of some of the drugs implicated in MDR by altering the pH. The cytosolic pH is higher in tumor cells exhibiting MDR and those transfected with P-gp. Verapamil, which reverses MDR, causes a partial acidic shift in the pH of cells. The model suffers, however, from a number of shortcomings. It cannot explain how drugs that are not weak bases are effluxed. A number of cells exhibiting MDR do indeed show pH shifts in agreement with the model, but a significant number of cells do not show these changes. More importantly, even where these changes in pH do occur, they are in most instances not of a magnitude sufficient to explain the several hundred-fold increase in resistance that these cells display.

The active transport model for MDR is more attractive and based on a large body of currently available evidence ([5], [6]). Drug binding and photoaffinity studies show a direct interaction between P-gp and many of the substrates. The drugs stimulate the ATPase activity of P-gp in proportion to its ability to transport those drugs. Specific amino acid substitutions alter the substrate specificity of P-gp. Additionally, purified P-gp reconstituted into phospholipid vesicles is capable of drug transport, even in the absence of electrochemical gradients. MDR is a complex phenomenon, and it is conceivable that the changes in electrochemical gradients may be the result of epiphenomena during the prolonged selection of cells in cytotoxic drugs. Perhaps the best prospect of resolving this issue lies in the use of transient expression systems. A vaccinia virus-based expression system has been developed recently that allows high-level expression of P-gp in many mammalian cells ([7]). The use of this system clearly excludes the pleiotropic effects associated with the use of drugs in selecting cultured cells.

Studies with both cultured cells and transient expression systems provide compelling evidence that the substrates interact directly with P-gp. Table 1 lists some of the agents that interact with P-gp. This has also been demonstrated by the use of diverse substrate analogs that photoaffinity label the P-gp and yielded valuable information on the direct interaction of P-gp with its substrates: ^{125}I-labeled iodoazylazidoprazoin (IAAP), an analog of prazosin ([8]); ^{125}I-labeled iodomycin, an analog of daunorubicin ([9]); ^{3}H-labeled azidopine ([10]); and 6-O-[2-[3-(4-azido-3-[^{125}I]iodophenyl) propionamido]ethylcarbamyl] forskolin (AIPPF), an analog of forskolin ([11]). While the nature of these interactions is still unknown, photoaffinity experiments with these analogs and site-directed mutagenesis analysis indicate that the interaction is probably in the regions of transmembrane segments 5, 6, 11, and 12.

Table 1. List of Selected Substrates and Modulators of P-Glycoprotein

Substrates of P-glycoprotein	Agents that Reverse Multidrug Resistance
Vinca alkaloids	Calcium channel blockers
Vinblastine	Verapamil
Vincristine	Dihydropyridines
Anthracyclines	Azidopine
Daunorubicin	Antiarrhythmics
Doxorubicin	Quinine
Epipodophyllotoxins	Quinidine
Etoposide	Antihypertensives
Teniposide	Reserpine
Antibiotics	Yohimbine

Dactinomycin	Antibiotics
Actinomycin D	Hydrophobic cephalosporins
Other cytotoxic agents	Immunosuppressants
Mytomycin	Cyclosporine A
Taxol	FK506
Topotecan	Steroid hormones
Colchicine	Progesterone
Emetine	Megestrol acetate
Gramicidin D	HIV protease inhibitors
Puromycin	Sequinavir
Valinomycin	Indinavir
	Ritonavir

The notion that the energy of ATP hydrolysis is utilized by P-gp to pump drugs actively is central to the active pump model. Consequently, the substrate-stimulated ATPase activity of P-gp has been studied in considerable detail. P-gp consists of two transmembrane segments and two ATP-binding sites. Each ATP site is comprised of three conserved regions: Walker A and Walker B motifs and a hydrophobic dodecapeptide-a signature of ABC superfamily members, also called the "C" region. ATP hydrolysis is abolished by chemical modification with N-ethylmaleimide or mutations in the conserved residues of the Walker A or Walker B region. Orthovanadate, which behaves as an analogue of inorganic phosphate, inhibits the ATPase by trapping Mg-ADP at the catalytic site. Mutational analysis and chemical modification have established that both sites can bind and hydrolyze ATP. Moreover, the interaction of the two sites is essential for ATP hydrolysis and drug transport. Purified P-gp catalyzes substrate-stimulated ATP hydrolysis. The protein, however, also has a basal ATPase activity in the absence of substrate, which may be due to activation by endogenous lipids or peptides. Based on current evidence, an alternating catalytic model of ATP hydrolysis proposes that, while both sites bind ATP, only one site at any given time acts as a catalytic site. The conformation of this site is presumed to prevent the other from hydrolyzing ATP (12).

1. P-glycoproteins in normal cells

The wide distribution of P-gp in normal human tissues, such as the blood–brain barrier, liver, kidney, intestine, adrenal glands, and testes, has long prompted speculation on the role of P-gp in normal cells (1, 5). There is also a more urgent need to understand the normal physiological role of P-gp. Effective inhibitors of P-gp-mediated drug transport are being developed and entering clinical trials. The safe use of these inhibitors requires that the functions of P-gp in normal physiology be understood so as to anticipate, and eventually limit, the potential side effects arising from their use. In recent years, the use of knockout mice (Mouse) with disrupted P-gp genes provided a direct method of studying these functions.

Mice with disruptions of each of the three P-gp-encoding genes (mdr1a, 1b, and mdr2) have been obtained (13). Under laboratory conditions, all the knockout mice are healthy, fertile, normal anatomically and histologically, and have a normal life span. The most striking result obtained with the mice homozygous for a disrupted mdr1a gene was the role of P-gp as an active extruder of molecules that pass the blood–brain barrier. For example, ivermectin, an excellent P-gp substrate, accumulates to levels over 100-fold higher in the brains of mdr1a(–/–) mice than in mdr1a(+/+) mice. The tolerance of mdr1a(–/–) mice to ivermectin was also reduced 100-fold. The results from the double knockout mice (mdr1a + mdr1b) are particularly important because, unlike humans, mice have two functional drug-transporting genes, and only a double knockout can tell us about the untoward effects that may be expected by use of powerful MDR reversal agents. The double knockouts have not yet been analyzed in detail, but there are no gross physiological, anatomical, or pathological abnormalities. Particularly important is the fact that gross disturbances in corticosteroid metabolism, pregnancy, and bile formation, which would reasonably be expected to occur based on earlier speculations of the function of P-gp, are absent in these mice. These studies suggest a protective role against chemical toxicity for P-gp in humans.

Bibliography

1. M. M. Gottesman and I. Pastan (1993) Ann. Rev. Biochem. 62, 385–427.
2. W. F. Ng, F. Sarangi, R. L. Zastawy, L. Veinot-Drebot, and V. Ling (1989) Mol. Cell. Biol. 9, 1224–1232.
3. C-J. Chen, J. E. Chin, K. Ueda, D. P. Clark, I. Pastan, and M. M. Gottesman (1986) Cell 47, 381–389.
4. P. D. Roepe (1995) Biochim. Biophys. Acta 1241, 385–405.
5. M. M. Gottesman, C. A. Hrycyna, P. V. Schoenlein, U. A. Germann, and I. Pastan (1995) Annu. Rev. Genet. 29, 607–649.
6. F. J. Sharom (1997) J. Membrane Biol. 160, 161–175.
7. M. Ramachandra, S. V. Ambudkar, I. Pastan, M. M. Gottesman, and C. A. Hrycyna (1996) Mol. Biol. Cell. 7, 1485–1498.
8. L. M. Greenberger (1993) J. Biol. Chem. 268, 11417–11425.
9. A. Demmer, H. Thole, P. Kubesch, T. Brandt, M. Raida, R. Fislage, and B. Tummler (1997) J. Biol. Chem. 272, 20913–20919.
10. E. P. Bruggemann, U. A. Germann, M. M. Gottesman, and I. Pastan (1989) J. Biol. Chem. 264, 15483–15488.
11. D. I. Morris, L. M. Greenberger, E. P. Bruggeman, C. Carderelli, M. M. Gottesman, and I. Pastan (1994) Mol. Pharmacol. 46, 329–337.
12. A. E. Senior, M. K. Al-Shawi, and I. L. Urbatsch (1995) FEBS Lett. 377, 285–289.
13. P. Borst and A. H. Schinkle (1996) Eur. J. Cancer 32, 985–990.

Suggestions for Further Reading

14. M. M. Gottesman, I. Pastan, and S. V. Ambudkar (1996) Curr. Opin. Genet. Dev. 6, 610–617. A recent review of the molecular biology, biochemistry, and energetics of P-glycoprotein, with a very helpful annotated list of references.
15. W. Stein (1997) Physiol. Rev. 77, 545–590. An excellent review on the kinetics of P-glycoprotein drug transport function, which includes very detailed and often quantitative discussions.

P-Loop

The P-loop is a fingerprint sequence that characterizes ATP- or GTP-binding proteins and is part of the nucleotide–binding motif (1). The characteristic P-loop sequence is Gly–X–X–Gly–X–Gly–Lys–Thr/Ser, where X is any residue. In the three-dimensional protein structures that have a P-loop sequence, such as adenylate kinase, the loop is located between a β-strand and an α-helix and forms a binding site for the phosphate group of the nucleotide—hence the name P-loop. The loop wraps around the phosphate, with the glycine residues adopting conformations that are forbidden for other residues. The backbone amides and the conserved lysine residue interact with the phosphate of the nucleotide.

The P-loop fingerprint sequence is used to identify ATP- or GTP- binding proteins from their primary structure (1). It has also been used to classify a broad group of protein structures, the nucleoside triphosphate hydrolase fold (2), which has a P-loop structure within an a/b domain comprising a central b-sheet surrounded by a-helices. Different families within this classification have varying numbers of b-strands and different connectivities.

[See also Nucleotide Binding Motif.]

Bibliography

1. M. Saraste, P. R. Sibbald, and A. Wittinghofer (1990) TIBS 15, 430–434.
2. A. G. Murzin, S. E. Brenner, T. Hubbard, and C. Chothia (1995) J. Mol. Biol. 256, 126–143.

Paired Helical Filaments

Alzheimer's disease is characterized by amyloid plaques and intraneuronal inclusions or tangles in the cell body and the proximal axon and dendrites (1). The tangles are comprised of paired helical filaments (PHFs) (Fig. 1), but these bear no relationship to the neurofilament type of intermediate filaments (IFs). Indeed, PHF are composed of tau (protein), a microtubule-associated protein that is hydrophilic, rich in proline, glycine, serine and threonine residues, and normally highly soluble. In the PHFs, however, the t protein is in an abnormal state of phosphorylation. In adult humans, t is not a single protein but a family of six variants encoded by the same gene generated by alternative splicing. All of the t chains have a related domain structure, a fundamental part of which is three or four tandem repeats, each of which is normally involved in microtubule-binding. These repeats are about 31 or 32 residues in extent and are only imperfectly preserved (2), but they have homology with other microtubule-associated proteins. The human isoforms of t vary also in their N-terminal regions, in that some contain an insert of 29 or 58 residues. Trojanowski and Lee (2) thus note that the largest t isoform contains 441 residues and has a 58-residue N-terminal insert and four tandem microtubule-binding repeats; the smallest isoform is 352 residues long and has no N-terminal insert and only three microtubule-binding repeats. The normal role of t *in vivo* is to stabilize the microtubules in the axon, thus facilitating microtubule-based axonal transport. t can readily be phosphorylated by the action of a variety of kinases; however, specific kinases acting on a serine residue in the first repeat domain cause the dissociation of t from microtubules. Although there is no evidence that any part of t adopts a regular secondary structure, its assembly into PHF is thought to be mediated through the repeat domains. The paired helical filaments thus formed consist of two filaments, each about 10 nm in diameter. They coil around one another with a pitch length of about 150 nm (Fig. 1). Individual t molecules have been observed in the electron microscope, where they appear as rodlike structures with lengths of about 35 nm. Proteolytic removal of the N-terminal region and part of the C-terminal region of t results in PHF with their fuzzy coats removed. Each strand in section appears to have a three-domain C-shaped structure. This also implies that the repeat domains form the core of the PHF and that the terminal ends of the t chains lie on the outer surface.

Figure 1. Electron micrographs of paired helical filaments (PHFs) from Alzheimer brains. (a) PHF from neurofibrillary
et al. (5), stained with 1% phosphotungstic acid. This preparation contains homogeneous long filaments that still retain t
coat." The cross-over repeat is 75 to 80 nm, and the width varies between a minimum of about 10 nm and a maximum
Greenberg and Davies (6). This preparation results in soluble filaments of shorter length than in (a) and is more heterog
nm repeat and a width varying between 8 and 18 nm; (2) is a straight filament with width 8 nm; (3) is a twisted filament
diameter (up to 25 nm); (4) is a straight filament with a wide diameter (18 nm); (5) is a twisted rodlike particle about 80
crossover period. In many cases the particles appear to be broken apart across the filament—for example, the two rod
of (3) and the short stub to the right of it, or the two straight rods above particle (3). Bar = 100 nm. (From Wille et al. (3)
Mandelkow.)

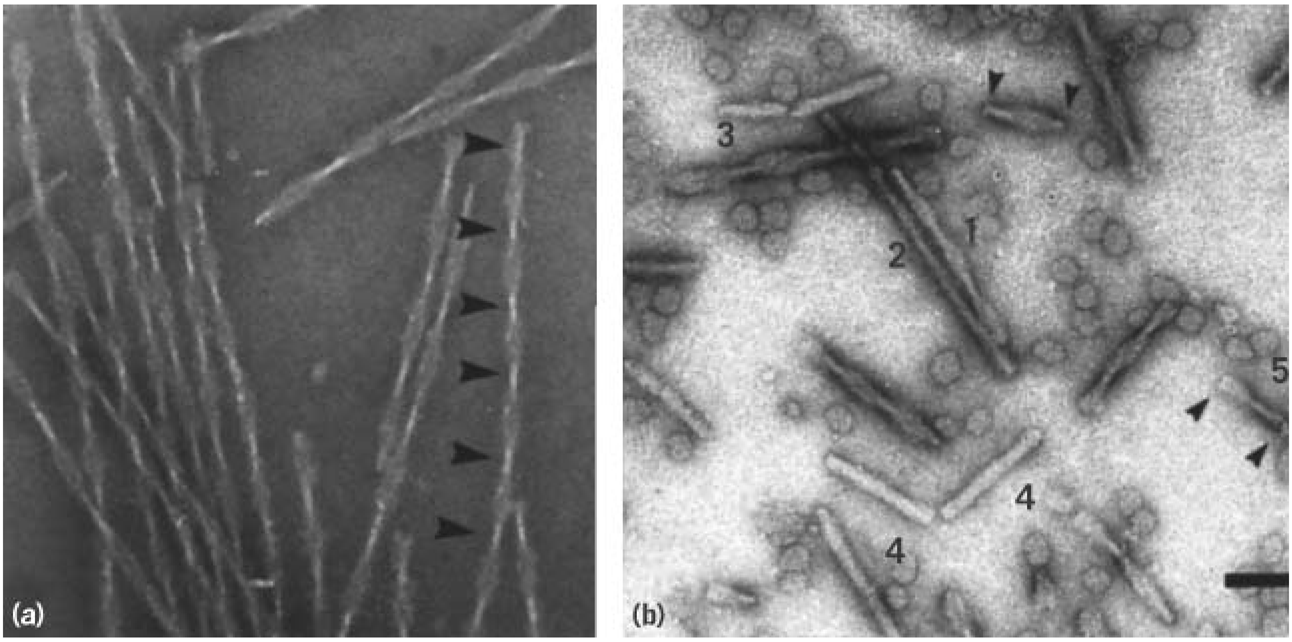

A major problem in this field had been the difficulty in reassembling the entire t molecule in vitro into a structure that closely resembles native PHF, although this has now been achieved. Wille et al. (3) and Schweers et al. (4) have described the reproducible formation of PHF from recombinant t protein and from constructs containing three of the repeating domains. Their results showed that the state of phosphorylation of t was not a determinant of PHF formation, that the repeat domain in t can form antiparallel dimers cross-linked by disulfide bonds to their cysteine residues, and that PHF can be formed from these dimers. Inhibition of dimer formation resulted in no PHF formation, indicating that it might be the key initial step. Schweers et al. (4) have concluded that two residues of particular importance in t are the serine in the first repeat (residue 262 in the htau40 isoform) and the cysteine in the third repeat (residue 322 in htau40): phosphorylation of the serine residue leads to dissociation of t from the microtubules and allows other modes of aggregation to occur, whereas oxidation of the cysteine leads to dimer formation followed by PHF assembly.

Bibliography

1. M. L. Shelanski and C. M. Troy (1990) "The Cytoskeleton in Neurological Disease". In Cellular and Molecular Biology of Intermediate Filaments (R. D. Goldman and P. M. Steinert, eds.), Plenum Press, New York, pp. 451–465.
2. J. Q. Trojanowski and V. M.-Y. Lee (1995) Phosphorylation of paired helical filament tau in Alzheimer''s disease neurofibrillary lesions: focusing on phosphatases. FASEB J. 9, 1570–1576.
3. H. Wille, G. Drewes, J. Biernat, E.-M. Mandelkow and E. Mandelkow (1992) Alzheimer-like paired helical filaments and antiparallel dimers formed from microtubule-associated protein tau in vitro. J. Cell Biol. 118, 573–584.
4. O. Schweers, E.-M. Mandelkow, J. Biernat, and E. Mandelkow (1995) Oxidation of cysteine-322 in the repeat domain of microtubule-associated protein t controls the in vitro assembly of paired

helical filaments. Proc. Natl. Acad. Sci. USA 92, 8463–8467.

5. C. Wischik, R. Crowther, M. Stewart, and M. Roth (1985) Subunit structure of paired Relical filaments in Alzheimer's disease. J. Cell Biol. 100, 1905–1912.

6. S. E. Greenberg and P. Davies (1990) A preparation of Alzheimer paired helical filaments that displays distinct tau-proteins by polyacrylamide-gel electrophoresis. Proc. Natl. Acad. Sci. USA 87, 5827–5831.

Suggestions for Further Reading

7. M. Goedert, R. Jakes, M. G. Spillantini, and R. A. Crowther (1994) "Tau protein and Alzheimer's disease". In Microtubules (J. S. Hyams and C. W. Lloyd, eds.), Wiley-Liss, New York, 183–200.

Pair-rule Genes

Pair-rule genes play critical roles in the formation of the Drosophila melanogaster body plan, which consists of fourteen contiguous segments arranged along the anterior-posterior axis. This basic plan is established by a cascade of segmentation gene activities that generate spatially repeated patterns of gene expression before the completion of cellularization. Most pair-rule genes are initially expressed in patterns of seven evenly spaced stripes about four nuclei wide that represents the first evidence of a segmental body plan. These stripe patterns are established by integrating crude positional cues provided by asymmetrically localized maternal factors and proteins encoded by the gap genes. These cues are in the form of gradients of transcription factors that interact directly with pair-rule regulatory regions, resulting in position-specific activation or repression. In several cases, pair-rule genes have been shown to contain discrete enhancers that direct the expression of single stripes of pairs of stripes. Each enhancer responds in a unique way to the asymmetric cues, and the seven stripe entire pattern represents the sum of effects of all enhancers. Once initial stripes are established, they are refined by interactions among the pair-rule genes themselves, creating a system of overlapping patterns. This system then directs the expression of segment polarity genes in patterns of fourteen stripes about one cell wide. The fourteen stripe patterns mark cells that will form borders between segmental compartments, and, thus, establish the body plan of the mature animal.

Pair-rule genes were first identified as members of a class of zygotic recessive mutations that affect the organization of the Drosophila body plan (1). Loss of function mutants in pair-rule genes contain only seven segments, and close examination of specific defects in the body plan indicates that every other segment is missing. For example, embryos with reduced even-skipped (eve) gene function contain only odd-numbered segments ("even" numbered segments are "skipped"). Other pair-rule genes lack odd-numbered segments or contiguous portions of adjacent segments that overlap every other border between two segments. These mutant phenotypes suggest that the fourteen segment body plan is established by a mechanism involving genes that specify patterns of cell fate decisions with a pair-rule periodicity.

Most pair-rule genes encode proteins with well-characterized DNA-binding motifs, and, thus, function as transcription factors in Drosophila development (Table 1). Many of these genes are expressed in patterns that appear as seven or eight transverse stripes that encircle the cellularizing blastoderm (2-4). The stripes are evenly spaced along the anterior-posterior axis in positions coincident with regions of the body plan that are disrupted in loss of function mutants. This suggests that the pair-rule genes function for the most part within their domains of expression. Interstripe regions where the genes are not expressed are also important for normal development because near reciprocal phenotypes can be generated by ubiquitous expression of pair-rule gene products (5).

Table 1.

Pair-rule Gene:	Protein Motif:	Reference:
hairy (h)	helix-loop-helix	(68)
even-skipped (eve)	homeodomain	(4, 69)
fushi tarazu (ftz)	homeodomain	(70)
runt (run)	runt-domain	(71)
paired (prd)	homeodomain, paired domain	(72, 73)
odd-skipped (odd)	zinc finger	(74)
odd-paired (opa)	zinc finger	(75)
sloppy-paired (slp)	forkhead domain	(76)
outstretched (os)	secreted protein	(77)
odd Oz (odz)	EFG-repeats, TM tyrosine kinase	(78)
tenascin^{M} (ten^{M})	EGF-repeats, ECM protein	(79)

Since the striped patterns of the pair-rule genes represent the first evidence of a metameric body plan, at least some of them must be generated de novo. It has been suggested that reiterated patterns such as stripes might be generated by reaction diffusion mechanisms (6-9). This model is supported by experiments in purely chemical systems that create striped patterns as the result of self-organizing processes (10). However, genetic experiments suggest that pair-rule genes are not self-organizing but are part of a hierarchy of genes that establishes polarity and segmental patterning along the anterior-posterior axis. This hierarchy is initiated by maternal effect genes that establish polarity by depositing mRNAs into the poles of the oocyte during late stages of oogenesis (11). Immediately after fertilization, the mRNAs are translated and their protein products diffuse toward the middle of the embryo creating gradients of proteins with high concentrations at the poles. These gradients direct the zygotic transcription of the gap genes, which are expressed in one or two broad domains along the anterior-posterior axis (Fig. 1). The maternal gradients and gap gene expression domains overlap, creating different combinations and concentrations of these factors according to position along the anterior-posterior axis.

Figure 1. (A) Spatial relationship between stripes of expression of the pair-rule genes even-skipped (eve) and fushi tarazu (ftz) and the positions of gap protein expression domains along the anterior posterior axis of Drosophila. Anterior is to the left. The gap genes hunchback (hb), giant (gt), Kruppel (Kr) and knirps (kni) are expressed in one or two broad domains in response to maternal gradients such as bicoid (bcd) that emanate from the poles of the embryo. (B). A double in situ hybridization experiment detects eve (red) and ftz (black) mRNAs. These genes are expressed in reciprocal patterns that establish the segmental body plan.

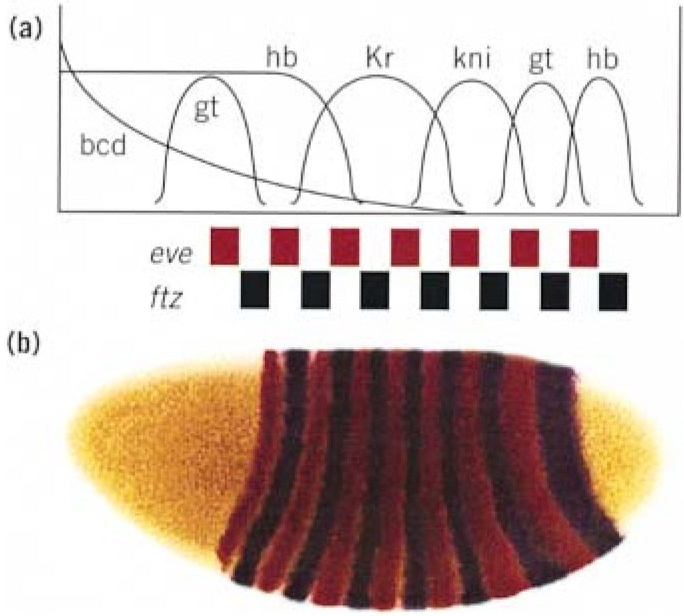

Striped patterns of the pair-rule genes are differentially disrupted in embryos lacking the functions of individual maternal effect, gap, and other pair-rule genes (12-16). These experiments are difficult to interpret, however, because removing the function of a single gene causes pattern shifts and disruptions in many other genes. Several experimental approaches have been used to unravel the mechanisms involved in pair-rule patterning. Regulatory interactions can be inferred from transgenic experiments that ubiquitously misexpress segmentation genes under the control of a heat shock inducible promoter (5, 17-20). When short heat pulses are used and the timing of pattern disruptions carefully monitored, it is possible to determine if a gene directly affects the expression of a given target or if intermediary genes must be expressed to induce the response (21, 22). Ectopic expression is also possible using enhancers that activate position-specific expression during early development (23-25). Finally, promoter truncation and P-element transformation assays (26) have identified two classes of cis-regulatory regions (enhancers) that are important for pair-rule patterning in the blastoderm. Enhancers of the first class specify the placement of individual stripes by responding primarily to gradients of maternal effect and gap proteins. Enhancers of the second class specify complete patterns of seven stripes but are active after the first striped patterns are established. These enhancers respond to transcriptional cues provided by the pair-rule genes themselves and are thus important for mechanisms that maintain and refine initial patterns.

1. Regulatory Mechanisms That Control the Initiation of Individual Pair-Rule Stripes

An important breakthrough in understanding how pair-rule patterns are established arose from the analysis of *hairy (h)* mutations caused by translocation breakpoints in the 5' regulatory region of the gene (27). Breakpoints located near the transcription start site cause the deletion of seven segmental units (like *h* null alleles), but those further away delete only a subset of segments. Thus, the regulatory elements controlling *h* function at different positions along the anterior posterior axis are physically separable, suggesting that individual stripes are independently controlled by discrete enhancers. This hypothesis was confirmed by a series of P-element transformation experiment with *h* lacZ reporter genes, which identified discrete enhancer elements that independently control the expression of single stripes or pairs of stripes (28, 29). Similar studies led to the identification of modular enhancers in the *eve* regulatory region (30-32). Interestingly, enhancers that control stripes 2, 3, and 7 are located upstream of the *eve* coding region; those that control the other four stripes are located downstream (Fig. 2).

Figure 2. Stripe-specific enhancers in the eve locus. A map shows the positions of enhancers (rectangles) identified by promoter truncation and P-element mediated transformation experiments. Simple patterns of one or two stripes of reporter gene expression are driven five discrete enhancers. The initial patterns of seven eve stripes represents the sum of the activities of these enhances. A separate enhancer directs a seven stripe pattern that appears after the initial pattern is established. This enhancer is important for maintaining and refining the pattern.

These enhancers control the positioning of individual stripes or pairs of stripes by responding to positional cues set up by the maternal effect and gap genes. The best characterized stripe enhancer controls the expression of eve stripe 2. Truncation analysis has narrowed this enhancer to a 480 base pair (bp) sequence that is sufficient to drive a stripe of lacZ reporter gene expression at the position of stripe 2 (33) (Fig. 3A). Trans-acting factors involved in regulating this enhancer were identified by crossing flies containing the stripe 2 lacZ transgenes into embryos lacking maternal and gap-gene functions. These experiments suggest that the maternal effect gene bicoid (bcd) and the gap gene hunchback (hb) are required for activation, while the gap genes giant (gt) and Kruppel (kr) are required for setting the anterior and posterior borders of the stripe (13, 34). The expression patterns of the proteins encoded by these genes are consistent with their genetically identified functions (Fig. 1A). bcd and hb completely overlap the position of stripe 2, and gt and Kr about the anterior and posterior borders, respectively. Repressive interactions between gt and Kr are important for maintaining the spacing where stripe 2 is expressed (20, 25). All four proteins contain DNA-binding domains and have been shown to bind in vitro multiple sites in the stripe 2 enhancer (34, 35) (Fig. 3B). Most binding sites for activator proteins are located within 50 bp of repressor sites. Mutating binding sites for bcd or hb causes a reduction in expression levels, and deleting gt sites causes a dramatic expansion of the stripe response into anterior regions of the embryo (33, 36, 37). These experiments suggest that the stripe 2 enhancer functions as a binary switch that controls region-specific activation by directly responding to combinations of asymmetrically localized regulatory factors.

Figure 3. (A) lac Z reporter gene expression directed by the 480 bp eve stripe 2 enhancer. Genetic experiments suggest that this enhancer is activated by bicoid (bcd) and hunchback (hb). The anterior and posterior borders of this stripe are

set by repression involving the gap proteins giant (gt) and Kruppel (Kr), respectively (see Fig. 1). (B) Positions of binding sites for proteins that regulate this enhancer. Activator sites are shown below the line, with repressor sites above. These sites enable the enhancer to make on/off decisions based on the combinations and concentrations of these proteins in a given nucleus.

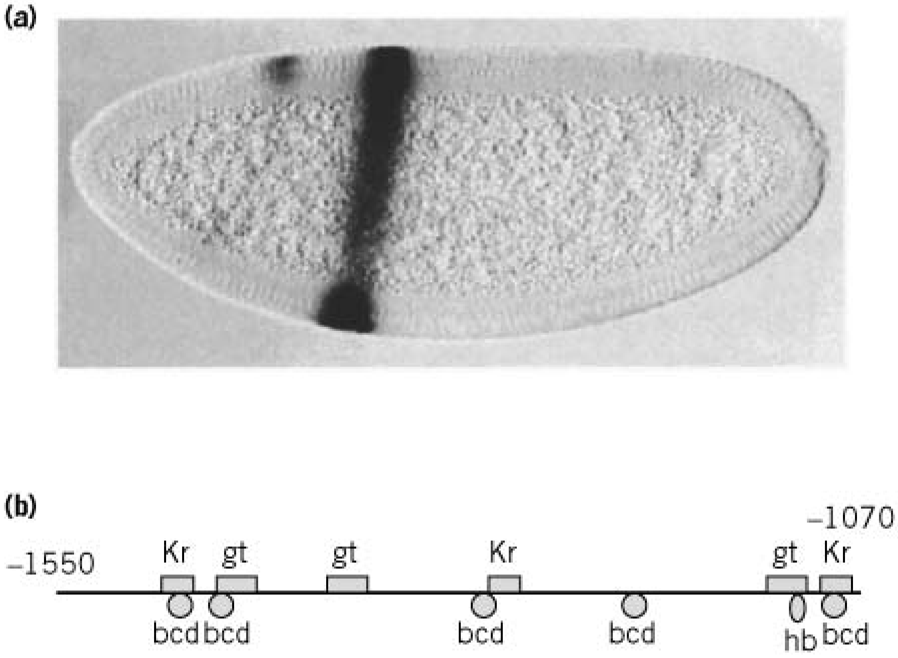

Several other stripe-specific enhancers have been characterized in detail (38-40). These analyses suggest a general model for the initial establishment of individual stripes (41). In this model, factors involved in activating individual stripes are broadly distributed, and stripe borders are set by repressive interactions mediated by gradients of gap proteins. Activations and repression events involve direct binding to closely linked sites within each enhancer. The close linkage of repressor to activator sites suggests that the repressors function over short distances to interfere with the binding or activity of activator proteins. Consistent with this hypothesis, increasing the spacing between activator and repressor sites to an interval greater than ~100 bp can prevent gap protein-mediated repression from occuring (42, 43).

Short-range repression is also important for ensuring that individual enhancers function independently in the context of complex promoters. This has been tested by transgenic experiments using reporter genes that contain the eve stripe 2 enhancer and another 500 bp enhancer that regulates stripes 3 and 7 (40). In the wild-type gene, these two enhancers are separated by a ~1,700 bp sequence. When this sequence is deleted so that the enhancers are juxtaposed, there is a severe disruption of the pattern driven by the reporter gene (44). Inserting shorter spacer sequences (160 bp and 300 bp) between the enhancers restores the correct expression pattern. These results suggest that transacting factors bound to one enhancer interfere with the activity of other enhancers and that spacing between enhancers prevents such interface in the wild-type gene.

2. Regulatory Mechanisms That Maintain and Refine Striped Patterns

Because different mechanisms control the establishment of individual eve and h stripes, they are expressed in a specific temporal order while the embryo is going through the process of cellularization. Each enhancer contributes to a final pattern of seven stripes that are each approximately four to five nucleus diameters wide (Figure 4A). By the end of cellularization, these initial patterns are refined until individual stripes are two or three cells wide. During this process, some seven stripe patterns are replaced by fourteen stripes, either by splitting the initial stripes or by activating new stripes in interstripe regions. Precise overlaps between specific genes are established so that each row of nuclei within a segmental unit contains a unique combination of pair-rule proteins. Genetic experiments suggest that positive interactions among the pair-rule genes maintain the stripes during this process, while negative interactions control spatial refinement. For example, there is a premature loss of *eve* stripes in *eve* and *paired* (*prd*) mutants, suggesting roles for these genes in maintaining the striped pattern (45, 46). In contrast, there is a significant posterior expansion of *eve* stripes in *run* mutants, suggesting that repression by *run* is important for refining the stripes (13, 31). Ubiquitous expression of *run* via heat shock causes a rapid repression of *eve*, consistent with this hypothesis (32). In contrast, *ftz* stripes are prematurely lost in *ftz* and *run* mutants, and expanded in *h* mutants, suggesting that these genes maintain and refine the *ftz* pattern (12, 47, 48).

Figure 4. (A) Interactions among pair-rule genes that maintain and refine initial striped patterns. Four parasegmental units are shown. Arrows represent positive interactions, blunted lines negative. The process of maintenance and refinement narrows stripes from four to five nuclei wide to two to three wide. (B) Spatial relationship between refined pair-rule patterns and the expression pattern of the segment polarity gene *en*. *en* is expressed in cells that contain specific combinations of pair-rule proteins. B is colinear with A.

The molecular mechanisms involved in these interactions are only beginning to be understood. Promoter truncation and P-element transformation experiments have identified enhancers in eve and ftz that direct reporter gene expression in patterns of seven stripes (31, 32, 49). These stripes appear late in the process of cellularization, persisting through the stages of gastrulation and germ band elongation. This timing is consistent with a role for these enhancers in maintaining and refining initial striped patterns. An example is a 300 bp eve enhancer that directs a late pattern of seven stripes coincident with the endogenous pattern (46, 50). This enhancer is inactive in embryos that lack eve or prd function, suggesting that a combination of autoregulation and cross regulation by prd activates transcription of this enhancer. The enhancer contains binding sites for both proteins; mutating these sites causes a loss of expression, suggesting that direct DNA-binding is required for activation (46, 50).

Another autoregulatory element involved in pair-rule refinement is 430 bp ftz enhancer (AE) that contains multiple ftz binding sites; when these sites are mutated, the enhancer is inactivated (51). Further experiments strongly indicate that the in vivo activation of this enhancer involves direct binding by ftz. These experiments take advantage of the fact that the ftz protein, which contains a glutamine residue at position 50 of the homeodomain, binds in vitro with high affinity to a specific class of binding sites (CCATTA) (52, 53). Other homeodomain proteins, such as bed, contain lysine at this position and prefer a different sequence (GGATTA). Changing a single CCATTA binding site in the ftz AE to GGATTA causes a significant loss of AE activity (51). However, activity is restored in trans by a ftz rescue construct in which the glutamine at position 50 is replaced with a lysine residue. This experiment confirms the importance of this residue in specific DNA recognition by homeodomain proteins and demonstrates conclusively that direct DNA-binding by ftz is required for the activity of this enhancer.

It is worth noting, however, that the 430 bp AE represents only a small part of a complex 2,600 bp upstream element (UE) that is important for ftz stripe maintenance (54-57). A separate enhancer, the zebra element (ZE), also direct reporter gene expression in late cellularizing embryos (49). Together, these enhancers integrate positive inputs provided by ftz, the ftz-cofactor Ftz-F1, and run, as well as negative inputs mediated by h that refine the stripes from the posterior (48, 58, 59). Binding sites for gap proteins and other ubiquitously distributed factors such as tramtrack (ttk), have also been identified in these regions, but their exact roles in ftz patterning are still unclear (56, 60).

3. Functions of the Striped Patterns of the Pair-Rules Genes

Precise overlapping patterns of the pair-rule genes are established by the end of cellularization. These patterns comprise a coordinated system that controls the expression of the segment polarity class of segmentation genes. An example is the segment polarity gene engrailed (en), which is expressed in fourteen stripes one cell wide (61, 62). Cells that express en will remain segregated from neighboring cells lacking en throughout development. This segregation establishes a border between the anterior and posterior compartments within each parasegmental unit. Genetic and misexpression experiments suggest that odd and even-numbered stripes within the en pattern are regulated by different mechanisms involving pair-rule genes (21-23, 63-66) (Fig 4). Oddnumbered stripes are activated in cells that contain eve and prd protein, and the anterior and posterior borders of these stripes are set by sloppy-paired (slp) and run respectively. Even numbered stripes are activated in cells than contain ftz and prd protein, and the anterior and posterior borders of these stripes are probably set by slp and odd-skipped (odd), respectively. Very little is known, however, about the cis components that control the expression of either set of stripes or any other segment polarity gene.

In summary, the pair-rule genes make up an integrated system that transduces asymmetrically localized positional information into fourteen stripe patters that establish the segmental body plan of Drosphila. Significant progress has been made in unraveling certain aspects of the mechanisms involved, but the complexity of the system suggests that a full understanding will not possible using only a reductionist approach. Recent attempts have been made to use computer modeling to integrate individual components of the pair-rule system into a gene circuit method (67). This method has successfully generated a complete pattern of seven stripes at the position using quantitative data representing the expression patterns of the maternal and gap proteins. In the future, this type of analysis will be important for synthesizing molecular data and predicting mechanisms that can then be tested experimentally.

Bibliography

1. C. Nusslein-Volhard and W. Wieschaus (1980) Nature 287, 795–801.
2. S. B. Carroll and M. P. Scott (1985) Cell 43, 47–57.
3. E. Hafen, A. Kuroiwa, and W. Gehring (1984) Cell 37, 833–841.
4. P. M. Macdonald, P. Ingham, and G. Struhl (1986) Cell 47, 721–34.
5. G. Struhl (1985) Nature 318, 677–80.
6. A. M. Turing, (1990) Bull. Math. Biol. 52, 153–97.
7. S. A. Newman (1993) Bioessays 15, 277–83.
8. T. C. Lacalli (1990) J. Theor. Biol. 144, 171–94.
9. A. Hunding, S. A. Kauffman, and B. C. Goodwin (1990) J. Theor. Biol. 145, 369–84.
10. Q. Ouyang and H. L. Swinney (1991) Nature 352, 610–612.
11. D. St Johnston and C. Nusslein-Volhard (1992) Cell 68, 201–19.
12. S. B. Carroll and M. P. Scott (1986) Cell 45, 113–26.
13. M. Frasch and M. Levine (1987) Genes. Dev. 1, 981–95.
14. M. Klingler and J. P. Gergen (1993) Mech. Dev. 43, 3–19.
15. K. L. Hooper, S. M. Parkhurst, and D. Ish-Horowicz (1989) Development 107, 489–504.
16. T. Gutjahr, E. Frei, and M. Noll (1993) Development 117, 609–23.
17. G. Struhl (1989) Ciba. Found. Symp. 144, 65–86.
18. E. Eldon and V. Pirrotta (1991) Development 111, 367–378.
19. H. M. Krause, R. Klemenz, and W. J. Gehring (1988) Genes. Dev. 2, 1021–36.
20. R. Kraut and M. Levine (1991) Development 111, 611–21.
21. A. S. Manoukian and H. M. Krause (1992) Genes. Dev. 6, 1740–51.
22. A. S. Manoukian and H. M. Krause (1993) Development 118, 785–96.
23. M. Fujioka, J. B. Jaynes and T. Goto (1995) Development 121, 4371–82.
24. D. Kosman and S. Small (1997) Development 124, 1343–54.
25. X. Wu, R. Vakani and S. Small (1998) Development 125, 3765–74.
26. G. M. Rubin and A. C. Spradling (1982) Science 218, 348–53.
27. K. Howard, P. Ingham and C. Rushlow (1988) Genes. Dev. 2, 1037–46.
28. G. Riddihough and D. Ish-Horowicz (1991) Genes. Dev. 5, 840–54.
29. K. R. Howard and G. Struhl (1990) Development 110, 1223–31.
30. M. Fujioka, Y. Emi-Sarker, G. Yusibova, T. Goto, and J. Jaynes (1999) Development 126, 2527–38.
31. T. Goto, P. Macdonald, and T. Maniatis (1989) Cell 57, 413–22.
32. K. Harding, T. Hoey, R. Warrior, and M. Levine (1989) Embo. J. 8, 1205–12.
33. S. Small, A. Blair, and M. Levine (1992) Embo. J. 11, 4047–57.
34. S. Small, R. Kraut, T. Hoey, R. Warrior and M. Levine (1991) Genes. Dev. 5, 827–39.
35. D. Stanojevic, T. Hoey and M. Levine (1989) Nature 341, 331–5.
36. D. Stanojevic, S. Small, and M. Levine (1991) Science 254, 1385–7.
37. D. N. Arnosti, S. Barolo, M. Levine, and S. Small (1996) Development 122, 205–14.
38. M. J. Pankratz, E. Seifert, N. Gerwin, B. Billi, U. Nauber, and H. Jackle (1990) Cell 61, 309–17.

39. J. A. Langeland and S. B. Carroll (1993) Development 117, 585–96.
40. S. Small, A. Blair, and M. Levine (1996) Dev. Biol. 175, 314–24.
41. S. Small, and M. Levine (1991) Curr Opin Genet Dev 1, 255–60.
42. A. D. Johnson (1995) Cell 81, 655–8.
43. S. Gray, and M. Levine (1996) Curr Opin Cell Biol 8, 358–72.
44. S. Small, D. N. Arnosti, and M. Levine (1993) Development 119, 762–72.
45. M. Frash, R. Warrior, J. Tugwood, and M. Levine (1988) Genes Dev 2, 1824–38.
46. M. Fujioka, P. Miskiewicz, L. Raj, A. A. Gulledge, M. Weir, and T. Goto (1996) Development 122, 2697–707.
47. K. Howard, and P. Ingham (1986) Cell 44, 949–57.
48. C. Tsai, and P. Gergen (1995) Development 121, 453–62.
49. Y. Hiromi, A. Kuroiwa, and W. J. Gehring (1985) Cell 43, 603–13.
50. J. Jiang, T. Hoey, and M. Levine (1991) Genes. Dev. 5, 265–77.
51. A. F. Schier, and W. J. Gehring (1992) Nature 356, 804–7.
52. A. Percival-Smith, M. Muller, M. Affolter, and W. J. Gehring (1990) Embo J. 9, 3967–74.
53. J. Treisman, P. Gonczy, M. Vashishtha, E. Harris, and C. Desplan (1989) Cell 59, 553–62.
54. Y. Hiromi, and W. J. Gehring (1987) Cell 50, 963–74.
55. L. Pick, A. Schier, M. Affolter, T. Schmidt-Glenewinkel, and W. J. Gehring (1990) Genes. Dev. 4, 1224–39.
56. W. Han, Y. Yu, N. Atlan, and L. Pick (1993) Mol Cell Biol 13, 5549–59.
57. A. F. Schier, and Gehring W. J. (1993) Embo J 12, 1111–9.
58. A. Guichet, J. W. Copeland, and M. Erdelyi et al. (1997) Nature 385, 548–52.
59. Y. Yu, W. Li, and K. Su et al. (1997) Nature 385, 552–5.
60. C. R. Dearolf, J. Topol, and C. S. Parker (1989) Genes. Dev. 3, 384–98.
61. T. Kornberg, I. Siden, P. O'Farrell, and M. Simon (1985) Cell 40, 45–53.
62. P. H. O'Farrell, C. Desplan, and S. DiNardo et al. (1985) Cold Spring Harb. Symp. Quant. Biol. 50, 235–42.
63. D. E. Coulter, and E. Wieschaus (1988) Genes. Dev. 2, 1812–23.
64. S. DiNardo, and P. H. O'Farrell (1987) Genes. Dev. 1, 1212–25.
65. M. P. Weir, B. A. Edgar, T. Kornberg, and G. Schubiger (1988) Genes Dev. 2, 1194–203.
66. K. M. Cadigan, U. Grossniklaus, and W. J. Gehring (1994) Genes. Dev. 8, 899–913.
67. J. Reinitz, and D. H. Sharp (1995) Mech. Dev. 49, 133–58.
68. C. A. Rushlow, A. Hogan, S. M. Pinchin, K. Howe, M. Lardelli, and D. Ish-Horowicz (1989) Embo. J. 8, 3095–103.
69. M. Frasch, T. Hoey, C. Rushlow, H. Doyle, and M. Levine (1987) Embo. J. 6, 749–59.
70. A. Laughon, S. B. Carroll, F. A. Storfer, P. D. Riley, and M. P. Scott (1985) Cold Spring Harb. Symp. Quant. Biol. 50, 253–62.
71. M. A. Kania, A. S. Bonner, J. B. Duffy, and J. P. Gergen (1990) Genes. Dev. 4, 1701–13.
72. G. Frigerio, M. Burri, D. Bopp, S. Baumgartner, and M. Noll (1986) Cell 47, 735–46.
73. J. Treisman, E. Harris, and C. Desplan (1991) Genes. Dev. 5, 594–604.
74. D. E. Coulter, E. A. Swaykus, M. A. Beran-Koehn, D. Goldberg, E. Wieschaus, and P. Schedl (1990) Embo. J. 9, 3795–804.
75. M. J. Benedyk, J. R. Mullen, and S. DiNardo (1994) Genes. Dev. 8, 105–17.
76. U. Grossniklaus, R. K. Pearson, and W. J. Gehring (1992). Genes. Dev. 6, 1030–51.
77. A. Levine, A. Bashan-Ahrend, O. Budai-Hadrian, D. Gartenberg, S. Menasherow, and R. Wides (1994) Cell 77, 587–98.

78. S. Baumgartner, D. Martin, C. Hagios and R. Chiquet-Ehrismann (1994) Embo J. 13, 3728–40.
79. D. Harrison, P. McCoon, R. Binari, M. Gilman, and N. Perrimon (1998) Genes. Dev. 12, 3252–63.

Suggestions for Further Reading

80. P. Lawrence (1992) The making of a fly, Blackwell Scientific Publications, Cambridge, MA.
81. M. Pankratz and H. Jackle (1993) "Blastoderm Segmentation. The Development of Drosophila melanogaster" (M. Bate and A. Martinez-Arias, eds.), Cold Spring Harbor Press.
82. S. Small (1997) "Mechanisms of segmental pattern formation in Drosophila melanogaster. Progress in Development Biology". (J. Collier, ed.) Oxford and IBH Publishing, pp. 137–178.
83. D. St Johnston and C. Nusslein-Volhard (1992) The origin of pattern and polarity in the Drosophila embryo. Cell: 201–19.

Palindrome

A palindromic word or text reads the same in both directions. Strictly speaking, this definition applies only to the same line of the text. The term "palindrome" is traditionally applied to double-stranded DNA (which is "two lines") when the nucleotide sequence is read forward from one strand and backward from the other, complementary strand. The reading proceeds in the same direction in terms of chemical polarity, 5′ to 3′, because DNA is an antiparallel duplex. A more appropriate name for such double-stranded palindromes that is also frequently used is a "sequence or element with complementary symmetry."

The palindromes in the double-stranded sense as discussed above are not only built of two identical sequences, but they also have complementary symmetry (twofold rotational symmetry). One example, the recognition site for the BamHI restriction enzyme, is shown in Fig. 1. Such a peculiar structure is typical of restriction sites. It guarantees that both strands—not just one—will be cut by the enzyme, either simultaneously or after a second approach by the enzyme. Nucleotide sequences of various lengths with complementary symmetry are rather common. For example, they comprise the consensus sequences of many repressor-binding sites, or operators (1).

Figure 1. A nucleotide sequence with complementary symmetry (a) and a double-stranded palindrome (b)—the element with twofold rotational symmetry. Hydrogen bonds between the strands in (b) are not shown.

The condition of identity and complementarity of the two strands of the palindrome also makes the halves of each strand complementary to one another, with the potential for each strand to fold back on itself, forming a hairpin structure. In a palindromic DNA duplex, such hairpins could be made in both strands, so that a cruciform structure is formed (2) (see Fig. 2). The loops of the cruciforms generally could be any size and not necessarily complementary symmetric, as the sequences in the stems of the cruciform. Another obvious property of palindromes is the identity of their double-stranded halves, except for their being placed in opposite polarity, like inverted repeats, but without interruption between the repeats. (Various types of repeats are compared in the scheme presented in Tandem Repeats.) Generally speaking, any head-to-head (or tail-to-tail) fusion of identical fragments of a double-stranded DNA would generate a palindrome. For example, very long palindromes are formed in the process of gene amplification (3), in the size range of many kilobases. Complementary symmetries generally separated by rather long interruptions are characteristic of many transposable elements (4). A whole family of transposable elements also exists: the foldback element transposons, which are about 1 kb in size. These transposons are essentially made of inverted repeats with a very small middle loop region—almost a palindrome.

Figure 2. Schematic presentation of a hairpin structure in a single-stranded DNA or RNA (a) and of a cruciform structure (b). The double lines correspond to antiparallel complementary strands in the duplex parts of the structures.

Palindromes that read the same in both directions of the same strand, ie, proper (or true), palindromes also are known. These sequences possess a mirror symmetry, for example, ATGAGTA. Such elements are frequently encountered in intervening sequences, or introns (5), and may be interpreted as a device to avoid complementary folding of the sequence. Indeed, the absence of complementary sequence elements in the mirror-symmetric sequences of the true palindromes like AT¼TA and TG¼GT causes the sequences to be located in the single-stranded regions of the RNA secondary structure.

Another class of mirror-symmetry palindromes are the polypurine and polypyrimidine stretches in the H-form structure (6, 7). This partially triplex structure is formed in a normal DNA duplex at lowered pH or under torsional stress. The locally separated polypyrimidine strand folds back and binds to the duplex by Hoogsteen hydrogen bonds. The sequence of this third strand can be incorporated into the structure only if it is mirror-symmetric to the sequence of the polypyrimidine strand of the Watson-Crick duplex.

Bibliography

1. P. P. Papp, D. K. Chattoraj, and T. D. Schneider (1993) J. Mol. Biol. 233, 219–230.
2. Y. Timsit and D. Moras (1996) Q. Rev. Biophys. 29, 279–307.
3. J. L. Hamlin et al. (1991) Prog. Nucl. Acid Res. Mol. Biol. 41, 203–239.
4. Mobile DNA (1989) (D. E. Berg and M. M. Howe, eds.) ASM, Washington, D.C.
5. J. S. Beckmann, V. Brendel, and E. N. Trifonov (1986) J. Biomol. Struct. Dynam. 4, 391–400.
6. S. M. Mirkin et al. (1987) Nature 330, 495–497.
7. M. D. Frank-Kamenetskii and S. M. Mirkin (1995) Annu. Rev. Biochem. 64, 65–95.

Suggestion for Further Reading

8. B. Alberts, D. Bray, J. Lewis, M. Raff, K. Roberts, and J. D. Watson (1994) Molecular Biology of the Cell, 3rd ed., Garland Publishing Inc., New York.

Palmitoylation

Palmitoylation is a post-translational modification process in which eukaryotic and viral proteins become ester- or thioester-linked to the 16-carbon saturated fatty acid, palmitic acid. Palmitoylation occurs on the thiol group of cysteine residues (S-palmitoylation) or on the hydroxyl groups of serine and threonine residues (O-palmitoylation). S-palmitoylation (see Fig. 1) of cysteine residues close to the N- or C-terminus provides a membrane anchor for some cytosolic proteins, and is important for their correct localization within the cell. However, S-palmitoylation also occurs on polypeptide-anchored and integral membrane proteins, and its role in these proteins is uncertain.

Figure 1. Modification of a cysteine or serine residue by a palmitoyl group. An internal cysteine residue in the protein is thioester-linked to the 16-carbon saturated fatty acid, palmitic acid to give an S-palmitoyl group. Palmitic acid can also be ester-linked to serine (or threonine) residues to give an O-palmitoyl group. The cysteine and serine residue in each figure is indicated by a dotted line.

In contrast to the other lipid modifications of proteins (see Membrane Anchors), palmitoylation has proven relatively difficult to study. Even though palmitoylation was discovered more than 20 years ago and occurs on at least 50 different types of proteins, this process is still poorly understood at the biochemical level [for a comprehensive description of the early work in this area, see the review articles by Schmidt (1989) and Towler et al (1988)]. Apart from detailed studies of S-palmitoylation of cysteine residues in signal transduction components (eg, Src family tyrosine kinases, G-protein ÿ subunits, Ras proteins, etc; see below), many of the initial reports of protein palmitoylation have not been substantiated in the last decade, and their functional significance is difficult to assess. There is essentially no recent information on O-palmitoylation of proteins. The lack of recent progress in these areas is due to several reasons.

1. For most of the "palmitoylated" proteins, the evidence for palmitoylation is based solely on the incorporation of ^{3}H-labeled palmitate into cellular proteins followed by immunoprecipitation, SDS-PAGE, and autoradiography. It is usually possible to distinguish ester, or O-palmitoylation of serine and threonine from thioester or S-palmitoylation of cysteine in the ^{3}H-labeled proteins by selective chemical deacylation procedures. However, more detailed analysis of ^{3}H-labeled palmitoylated peptides is generally not practicable, because their unpredictable chromatographic behavior makes them very difficult to purify. This technical problem has thwarted attempts to identify the precise location of the incorporated ^{3}H-label in most of the palmitoylated proteins. Indeed, for several "palmitoylated" proteins, it was subsequently shown that the incorporated palmitate is part of a completely different structure, the GPI anchor.
2. The ^{3}H-labeled palmitate can be converted to other fatty acids before incorporation into some of the proteins. This suggests that the acyltransferase responsible for acylating the protein may be non selective and/or that different cells contain variable amounts of distinct acyltransferases with different specificities.
3. Protein S-palmitoyltransferase activities that can catalyze the transfer of a palmitoyl group from palmitoyl CoA to cysteine residues in protein or model peptide substrates have been identified in mammalian membrane fractions (1–5). Removal of the palmitoyl group by thioesterase activities has also been described. However, none of these activities has been thoroughly characterized at the molecular level, and it is difficult to tell if they are responsible for palmitoylation/depalmitoylation *in vivo*. Non enzymatic palmitoylation (autoacylation) of cysteine residues by palmitoyl CoA was also reported for several proteins, and this may account for some of the difficulties encountered in isolating and characterizing the protein S-palmitoyltransferase(s).
4. The criteria that determine which particular cysteine residue(s) in a protein will become palmitoylated are also uncertain. The presence of other lipid anchors (eg, prenyl or myristoyl groups; see below) on neighboring residues will facilitate cysteine palmitoylation presumably as

a result of transient anchoring to membranes. These observations suggest that localization of “exposed” cysteine residues close to the bilayer surface, rather than a well-defined sequence motif, is the determinant for palmitoylation (4). S-palmitoylation of cysteine residues in polypeptide-anchored and integral membrane proteins could simply be the accidental result of proximity to the bilayer surface, where palmitoyl CoA and other molecular species of acylCoA are likely to be abundant.

As a consequence of the experimental problems identified above, there is relatively little information on the functional significance of palmitoylation for most proteins. However, site-directed mutagenesis studies, on a small number of proteins that are involved in signal transduction, demonstrated that a palmitoyl group can act as membrane anchor and may play a role in regulating distribution of proteins between membranes and the cytoplasm as well as their association with lipid rafts (6) (for a general discussion of factors that can affect membrane affinity of lipid-anchored proteins, see Membrane Anchors). In some G protein ÿ subunits and src-related tyrosine kinases, it has been shown that palmitoylation of cysteines near the N-terminus is dependent on prior myristoylation of the N-terminal glycine (7-9). Palmitoylation of ÿ subunits can also be increased by receptor activation (10, 11). Similarly, palmitoylation of cysteine residues near the C-terminus of some Ras proteins is dependent on prior farnesylation (see Prenylation). Because farnesyl and myristoyl groups are both relatively weak anchors, the increase in membrane affinity resulting from palmitoylation has a major effect on the amount of these proteins bound to the membrane (12, 13). Furthermore, biophysical studies indicate that addition of palmitate not only increases binding affinity, but also increases the stability of membrane anchoring by reducing the rate of dissociation from the membrane (14, 15). Palmitoylation also occurs on cysteine residues in polypeptide-anchored proteins (eg, the transferrin receptor and CD4; see Table 1) and integral proteins with multiple transmembrane regions (eg, rhodopsin and some types of adrenergic receptor). As expected, preventing palmitoylation of these proteins by mutagenesis of the appropriate cysteine residues has no discernible effect on membrane anchoring. However, cysteine mutagenesis often has no, or relatively subtle, effects on the functional properties of the protein either, and the biological significance of palmitoylation remains uncertain in these cases.

Table 1. Examples of Palmitoylated Proteins

G protein ÿ subunits
Src family tyrosine kinases (e.g. $p59^{fyn}$, $p56^{lck}$ etc.)
GAP-43 (neuromodulin)
H- or N-Ras proteins
G protein-coupled receptors (e.g. rhodopsin, $ÿ_{2A}$, $ÿ_2$–adrenergic receptors etc.)[a]
Transferrin receptor[a]
CD4[a]
Viral envelope proteins[a]
Myelin proteolipid protein[a, b]
Mucus glycoproteins[b]

[a] Integral or polypeptide-anchored proteins.

[b] O-palmitoylation; all other examples are S-palmitoylation.

Bibliography

1. L. Berthiaume and M. D. Resh (1995) J. Biol. Chem. 270, 22399–22405.
2. L. Liu, T. Dudler and M. H. Gelb (1996) J. Biol. Chem. 271, 23269–2376.
3. J. T. Dunphy, W. K. Greentree, C. L. Manahan, and M. E. Linder (1996) J. Biol. Chem. 271, 7154–7159.
4. J. T. Dunphy, H. Schroeder, R. Leventis, W. Greentree, J. K. Knudsen, J. R. Silvius, and M. E. Linder (2000) Biochim. Biophys. Acta 1485, 185–198.
5. J. A. Duncan and A. G. Gilman (1996) J. Biol. Chem. 271, 23594–23600.
6. S. Moffett, D. A. Brown, and M. E. Linder (2000) J. Biol. Chem. 275, 2191–2198.
7. M. Y. Degtyarev, A. M. Spiegel, and T. L. Z. Jones (1994) J. Biol. Chem. 269, 30898–30903.
8. A. M. Shenoy-Scaria, L. K. Timson Gauen, J. Kwong, A. S. Shaw, and D. M. Lublin (1993) Mol. Cell. Biol. 13, 6385–6392.
9. L. Alland, S. M. Peseckis, R. E. Atherton, L. Berthiaume, and M. D. Resh (1994) J. Biol. Chem. 269, 16701–16705.
10. S. M. Mumby, C. Kleus, and A. G. Gilman (1994) Proc. Natl. Acad. Sci. U.S.A. 91, 2800–2804.
11. M. Y. Degtyarev, A. M. Spiegel, and T. L. Z. Jones (1993) J. Biol. Chem. 268, 23769–23772.
12. K. Cadwallader, H. Paterson, S. G. MacDonald, and J. F. Hancock (1994) Mol. Cell. Biol. 14, 4722–4730.
13. M. H. Gelb (1997) Science 275, 1750–1751.
14. S. Shahinian and J. R. Silvius (1995) Biochemistry 34, 3813–3822.
15. G. Milligan, M. Parenti, and A. I. Magee (1995) TIBS 20, 181–186.

Suggestions for Further Reading

16. D. A. Towler, J. I. Gordon, S. P. Adams, and L. Glaser (1988) The biology and enzymology of eukaryotic protein acylation. Annu. Rev. Biochem. 57, 69–99.
17. M. F. G. Schmidt (1989) Fatty acylation of proteins. Biochim. Biophys. Acta 988, 411–426.
18. P. J. Casey and J. E. Buss (1995) Lipid Modifications of Proteins, Meth. Enzymol. 250.
19. R. S. Bhatnagar and J. I. Gordon (1997) Understanding covalent modification of proteins by lipid; Where cell biology and biophysics mingle. Trends Cell Biol. 7, 14–20.
20. J. T. Dunphy and M. E. Linder (1998) Signalling function of proteins palmitoylation. Biochim. Biophys. Acta 1436, 245–261.

Papain

Papain is a thiol proteinase that is obtained from the latex of the papaya tree (1) (Fig. 1). It has an essential cysteine residue at its active site that must be in the reduced form in order to be active. For this reason, it is often used in the presence of a reducing agent, such as b-mercaptoethanol or dithiothreitol . Papain has broad specificity and will hydrolyze peptide bonds adjacent to almost any amino acid residue, although it shows a trypsin -like preference for arginine and lysine residues. Its activity is optimal around pH 6. It is inactivated by reagents that react with thiol groups, such as iodoacetate or iodoacetamide, as well as silver and mercuric ions and p-chloromercuribenzoate.

Other inhibitors include leupeptin, a peptide aldehyde that is a general thiol proteinase inhibitor, and E-64, an epoxide compound isolated from *Aspergillus japonicus* (Fig. 2). Leupeptin also inhibits some serine proteinases, whereas E-64 is more specific and has a strong affinity only for thiol proteinases. The epoxide group of the latter forms a thioether with the active site thiol group of the enzyme. It has little reactivity for thiol groups not in active sites.

Figure 1. The three-dimensional structure of the thiol proteinase papain. Only the polypeptide backbone is indicated schematically as a ribbon, with arrows for b-strands and coils for a-helices.

Figure 2. Chemical structure of E-64, an inhibitor of some thiol proteinases. Its chemical name is L-trans-epoxysuccinyl-leucylamide-(4-guanidino)-butane. The epoxy group forms a thioether linkage with the active-site thiol group of papain or cathepsin B.

Papain is used to degrade proteins in the presence of a reducing agent (2). Because it has broad specificity, it can generate many small peptides from a large protein. For this reason, it is usually employed to digest the intermediate-sized peptides that are generated by treating a protein with a proteinase of narrow specificity such as trypsin (see Peptide Mapping). Papain is used commercially in a popular brand of meat tenderizer.

Bibliography

1. A. J. Barrett (1986) Biomed. Biochim. Acta 45, 1363–1374.
2. D. W. Cleveland, S. G. Fischer, M. W. Kirschner, and U. K. Laemmli (1977) J. Biol. Chem. 252, 1102–1106.

Papovavirus

The virion of the Papovaviridae family of viruses contains a double-stranded circular DNA as the genome, has an icosahedral capsid, and can induce tumors in animals. The name papovavirus is derived from papillomavirus, polyomavirus, and vacuolating virus (the old name of SV40). The particle and genome sizes of papillomaviruses are slightly greater than those of polyomaviruses, measuring 55 nm in diameter instead of 45 nm, and about 8000 base pairs in length instead of about 5000. On this basis, the papovaviruses are divided into two genera, Polyomavirus and Papillomavirus. BKV, JCV, SV40, LPV, murine polyomavirus, hamster polyomavirus, and many others are classified in the former genus.

Papillomaviruses were isolated as agents that induce warts in many animals, including rabbits, goats, cattle, dogs, deer, and so on. Papillomaviruses were also isolated from human warts in late 1970s. Presently, more than 70 viruses are classified as human papillomavirus (HPV). A subgroup of about 20 HPVs has been associated with lesions of the anogenital tract. These HPVs can be further divided into two groups: the low-risk HPV group, including HPV 6 and HPV 11, which are associated with benign lesions, such as condyloma acuminata, and the high-risk group, including HPV16, HPV18, HPV33, and others, which are associated with malignant lesions that can progress to cancer. The high-risk HPV can efficiently immortalize human squamous epithelial cells in vitro and transform established rodent cells. The genes of the high-risk group HPVs that are responsible for the transforming activity are E6 and E7, which are ubiquitously conserved among all papilloma viruses, including those of animal origins. The E7 gene products of the high-risk HPVs bind and inactivate retinoblastoma family proteins more efficiently than those of the low-risk HPVs and HPVs associated with benign skin lesions. This binding is mediated through the amino acid sequence of the E7 gene product, which is commonly detected in the T antigens of SV40 and polyomaviruses. The only E6 gene products of the high-risk groups bind to p53 protein through an interaction with cellular E6-AP protein, and they subsequently cause ubiquitin-mediated protein degradation of the p53 protein. The consequent deregulation of cellular growth control by E6 and E7 genes is considered to be the molecular basis of carcinogenesis by the high-risk HPVs.

Suggestions for Further Reading

H. zur Hausen (1996) Papillomavirus infections-a major cause of human cancers. Biochim. Biophys. Acta 1288, F55–F78.

P. M. Howley (1996) "Papillomavirinae: The Viruses and Their Replication". In Fields Virology, 3rd ed. (B. N. Fields et al., eds.), Lippincott-Raven, Philadelphia, pp. 2045–2076.

Paralogous Genes

Paralogous genes are two or more genes that emerged during evolution from a common ancestral gene by gene duplication within a species. Usually, they acquire different functions; well-known examples are the a and b-hemoglobin polypeptide chains and that of myoglobin. They contrast with orthologous genes, which have not been duplicated within species, but retain the same function and have descended during evolution by the process of speciation only. Both orthologous and paralogous genes are homologous, but a comparison of paralogous genes from different species will not reflect the process of species divergence. Paralogous genes are usually present as members of a gene family within a genome. For more details, see Orthologous Genes.

Parasexual Cycle

The parasexual cycle allows new allele combinations to be formed independently of whether the organism can undergo a sexual cycle and meiosis. The parasexual cycle involves the fusion of haploid nuclei, mitotic recombination, and random chromosome losses. Parasexuality was discovered by Giorgio Pontecorvo (1) and has been demonstrated with several fungi and, in a modified form, with cultured cells of multicellular animals.

The parasexual cycle is sketched in Fig. 1, taking a filamentous Ascomycete as a model. Fusion of haploid cells to form a heterokaryon occurs spontaneously in many fungi in a process called hyphal anastomosis. In many fungi this process occurs with certain pairs of strains said to be vegetatively compatible and fails with others. Compatibility requires the strains to carry certain combinations of alleles at certain genes. Heterokaryons can be prepared in the laboratory by fusion of protoplasts and other techniques in fungi without anastomosis and in many other organisms.

Figure 1. Parasexual cycle in filamentous Ascomycetes. Nuclei are followed from the haploid parents above to the haploid segregants below, through cell fusion, nuclear fusion, and haploidization. Recombinant nuclei are indicated by different shading patterns.

Two haploid nuclei in a heterokaryon may fuse to form a diploid nucleus. This process occurs seldom or not at all in vegetative heterokaryons, although it may be very quick after the fusion of gametes in the sexual cycle. Diploid cells are usually very hard to distinguish from heterokaryotic cells carrying the same genetic markers, but they may be very easily distinguished from haploid cells. In fungi in which all spores are uninucleate, colonies grown from diploid and haploid spores are distinguished easily with the help of appropriate genetic markers.

The diploid nuclei of many fungi are unstable because the loss of one chromosome of each pair is not deleterious. A slow process of haploidization takes place during mitotic growth as random chromosome losses convert the diploid into haploids through intermediates called aneuploids. The resulting haploid nuclei contain random combinations of the chromosomes of the two original haploid nuclei. The frequency of chromosome loss is increased by treatments with benomyl and other agents.

In addition, mitotic recombination occurs sporadically between the duplicated chromosomes of the diploid and the aneuploids and produces new combinations of their genetic markers (see Mitotic Recombination). The chromosomes in the final haploid nuclei are composed of random combinations of chromosome segments from the two original haploid nuclei (Fig. 2).

Figure 2. Chromosome events during the parasexual cycle. The chromosomes are followed from the haploid parents above to the haploid segregants below, through diploidization, mitotic recombination, and chromosome loss.

As a result of the parasexual cycle, genes in different chromosomes exhibit recombination frequencies of 50 % while those that are close to each other in the same chromosome appear more or less tightly linked.

Fusion of cultured cells from different mammals gives rise first to heterokaryons and then to anfiploid nuclei, which contain all the chromosomes of the original cells. Chromosome losses reduce the number of chromosomes in these anfiploids, but not necessarily at random: chromosomes of *Homo sapiens* are lost more frequently than those of *Mus musculus* from their anfiploids. The correlation between the presence or absence of certain genetic markers and certain chromosomes in the segregants is a powerful technique for the quick assignment of genes to chromosomes (see Cell fusion, Hybridomas).

Bibliography

1. G. Pontecorvo (1956) Annu. Rev. Microbiol. **20**, 151–168.

Suggestions for Further Reading

2. G. Sermonti (1969) *Genetics of Antibiotic-Producing Microorganisms*, Wiley-Interscience, London (see Parasexuality, pp. 175–228).
3. A. J. Clutterbuck (1992) Sexual and parasexual genetics of *Aspergillus* species. Biotechnology **23**, 3–18.
4. C. J. Bos (1996) "Somatic recombination" In *Fungal Genetics* (C. J. Bos, ed.), Marcel Dekker, New York, pp. 73–95.

Parsimony

Parsimony is one of the principles of phylogenetic tree reconstruction in which the phylogeny of a group of species or genes is inferred to be the branching pattern that requires the smallest number of evolutionary changes (1). Of course, no one knows whether evolution actually occurred in this way, but the parsimony principle appears to work reasonably well, particularly for comparisons of closely related species or genes, but it tends to lose its effectiveness in comparison to more remotely related species or genes. For the latter comparisons, double mutational changes (due to reverse mutations) have accumulated to such an extent that the parsimony principle cannot detect all changes.

The merit of using the parsimony principle is that we can infer the amino acid or nucleotide sequences of all the intermediate stages in the continuous lineage between the ancestor and the present species. The intermediate stages may be trustworthy, however, only when closely-related genes are compared.

Bibliography

1. M. Ridley, (1997) *Evolution*, 2nd ed., Blackwell Science, USA.

Parthenogenesis

Parthenogenesis is the development of a zygote without fertilization. Parthenogenesis can be induced experimentally by a number of procedures (1), but it occurs naturally in some species. A special case of parthenogenesis is called arrhenotoky. This is the mechanism of sex determination in many insects. Fertilized eggs develop into diploid females, while unfertilized eggs develop parthenogenetically as haploid males. Arrhenotoky occurs in the four insect orders: Hymenoptera, Homoptera, Thysanoptera, and Coleoptera (2). In the Hymenoptera, arrhenotoky is the only mechanism of sex determination.

In addition to arrhenotoky, or male haploidy, another form of parthenogenesis, called thelytoky, in which the unfertilized eggs develop as females. It can be either (a) cyclic, in which parthenogenetic and bisexual generations alternate, or (b) complete (3). Cyclic parthenogenesis is found among some insects, such as aphids (4), and in a few vertebrates (5). Complete parthenogenesis has appeared many times during evolution in a variety of phyla. The phylum Rotifera appears to be entirely parthenogenetic. There are even parthenogenetic species of vertebrates (6).

In arrhenotoky, the unfertilized eggs develop as haploid males, but in thelytoky the unfertilized eggs develop as diploid females (or polyploid females in some cases). In order for the unfertilized haploid eggs to develop as diploids, the genetic content of the cells must be doubled. Because parthenogenesis has arisen independently many times during evolution, this problem has been solved in a variety of ways (7). The failure of the second meiotic division during gametogenesis results in the production of diploid eggs. Meiosis can also proceed normally, with the fusion of two of the meiotic products producing a diploid egg. In other species, haploid eggs are produced, but fusion of haploid nuclei occurs during the early cleavage stages to restore diploidy.

Bibliography

1. Y. Fuyama (1986) Genetics 112, 237–248.
2. M. J. D. White (1948) Animal Cytology & Evolution, Cambridge University Press, Cambridge, U.K. p. 267.
3. Reference 2, p. 280.
4. A. F. Shull (1925) Am. Nat. 59, 138–154.
5. S. B. Hedges, J. P. Bogart, and L. R. Maxson (1992) Nature 356, 708–710.
6. L. D. Densmore, C. C. Moritz, J. W. Wright, and W. M. Brown (1989) Evolution 43, 969–983.
7. Reference 2, p. 281.

Suggestions for Further Reading

8. M. J. D. White (1948) Animal Cytology & Evolution, Cambridge University Press, Cambridge, U.K. pp. 280–302.
9. C. D. Darlington (1937) Recent Advances in Cytology, The Blakiston Company, Philadelphia, pp. 434–478.

Partial Specific (Or Molar) Volume

The volumes of macromolecules can be determined from their structures in several different ways (see Molecular Surface, Volume; Isoleucine (Ile, I); Accessible Surface). In solution, the volumes relevant to thermodynamics are the partial specific and partial molar volumes. They involve not only the volume of the macromolecule itself, but also the contribution of solute–solvent interactions (hydration). In general, macromolecule solutions are systems with two or more components, containing the macromolecule, water, salts, etc. However, it is more convenient to reduce any such system to a binary one; one component is the solvent, ie water plus salts, etc., the other is the solute, ie a protein. At constant temperature T and pressure P, the total volume V of such a binary solution comprising g_1 grams of solvent and g_2 grams of solute is expressed as follows:

(1)

where v_1 and v_2 are partial specific volumes of solvent and solute, respectively, as defined by

(2)

(3)

These parameters measure the change in volume upon adding further solvent or solute to the aqueous system.

The partial specific volume can be determined experimentally by measuring the densities of the solution containing the macromolecule (in units of g cm^{-3}) as a function of its concentration. A variety of techniques have been used for density measurements: The majority of specific volume data have been obtained by pycnometry and digital densimetry (mechanical oscillator technique). Except for some rare cases, the plot of V vs g_2, which should be a straight line according to Equation (1), is not straight, due to solute–solute interactions. This means that the specific volumes of the solvent and solute are not the same as those of the pure phases of these components in most cases, and it is necessary to measure directly the values of v_1 and v_2. In practice, the apparent specific volume f_2 is defined instead of the partial specific volume, by assuming the specific volume of solvent in the solution to be the same as that of solvent in the pure phase v_1^0

(4)

The relation between apparent and partial specific volumes is as follows:

(5)

From this equation, it is apparent that the apparent and partial specific volumes become equal at infinite dilution (g_2 = 0). Usually, values of v_2 and f_2 at infinite dilution (denoted as v_2^0 and f_2^0) are used as the appropriate quantity for a protein molecule in solution not involved in intermolecular interactions with other protein molecules. When the molecular weight M_2 of a solute is known, the partial and apparent molar volumes V_2 and F_2, respectively, can be calculated using the equations $V_2 = v_2M_2$ and $f_2 = f_2M_2$, respectively.

In two-component solutions, the partial specific volume of folded proteins falls in the range of 0.69 to 0.76 cm^3 g^{-1}, depending on their structure and amino acid composition (see Table 1 of Compressibility). The majority exhibit values in the range of 0.72 to 0.75 cm^3 g^{-1}, which are within the range of the partial specific volumes of amino acids, which range from 0.559 cm^3 g^{-1} for aspartic acid to 0.819 cm^3 g^{-1} for leucine and isoleucine (Table 1). If we assume the additivity principle of volume, the apparent specific volume of a protein may be estimated from its amino acid composition by using the equation $f_2 = \Sigma f_i w_i / \Sigma w_i$, where f_i is the apparent specific volume of the ith amino acid residue (Table 1) and w_i its weight percent (Ref. 1). In spite of a number of simplifications and assumptions, this method yields relatively rather accurate results. It should be noted, however, that the partial specific and apparent volumes are thermodynamic quantities, and changes in the environment (solvent composition, temperature, pressure, etc.) may cause significant changes in this volume.

Table 1. Apparent specific volumes of amino acid residues at 25°C (Ref. 1)

Residue	Apparent specific volume ($cm^3 g^{-1}$)
Ala	0.732
Arg	0.756
Asn	0.610
Asp	0.573
Cys	0.630
Gln	0.667
Glu	0.605
Gly	0.610
His	0.659
Ile	0.876
Leu	0.876
Lys	0.775
Met	0.739
Phe	0.766
Pro	0.748
Ser	0.596
Thr	0.676
Trp	0.728
Tyr	0.703
Val	0.831

The partial specific volume of a protein in water is expressed as the sum of three contributions (Ref. 2): (1) the constitutive volume estimated as the sum of van der Waals volumes of the constitutive atoms (v_c); (2) the volume of the cavities in the molecule due to imperfect atomic packing (v_{cav}); (3) the volume change due to solvation or hydration (Dv_{sol}).

(6)

The value of Dv_{sol} is usually negative, because hydration processes involve the contraction of solvent water. The volume change on transferring a protein from one solvent to another is calculated as the difference in v_2^0 between the two solvents. The volume change due to any conformational change of protein is also defined as the difference in v_2^0. In such a case, v_c does not change, so the observed volume change is ascribed primarily to differences in v_{cav} and Dv_{sol}. In general, processes increasing the solvent accessible surface area, eg, unfolding and dissociation into subunits, are expected to produce negative volume changes due to increased hydration. Most experimental data meet this expectation, but some data show no change or even slightly positive volume changes. It is noteworthy that the volume change observed at a given protein concentration, which is based on $\bar{v}_2$, may differ, even in its sign, from the result obtained at infinite dilution.

The partial specific volume measured at constant molality of the added cosolvent (eg, salts or organic compounds) is a useful quantity, as it is a truly thermodynamic volume. In practice, however, the measurement of this volume often accompanies difficulties in sample preparation, and most experiments (especially ultracentrifugation or small-angle X-ray scattering) are usually done with solutions that have been subjected to dialysis to equilibrium against the solvent. At equilibrium, the chemical potentials of diffusible components are equal on the two sides of a membrane, but the molalities of the components are not necessarily identical mainly due to Donnan effects and preferential binding of solvent components to protein. The apparent isopotential specific volume $\phi_2'^0$, which is measured at constant chemical potential of the solvent components (equilibrium dialysis systems), can be obtained from the density differences between the protein solutions and the dialyzate by the same procedures as used for ϕ_2^0. However, $\phi_2'^0$ is not a partial quantity in the thermodynamic sense, since the molalities of the diffusible components are not held constant, but this specific volume is operationally very useful because it reflects preferential protein–solvent interactions. In a two-component system or a dilute buffer system where Donnan effects and/or preferential solvent interactions are absent, ϕ_2^0 and $\phi_2'^0$ should be identical. In the presence of high concentration of a third component, however, large differences between these two specific volumes occur, as is shown in Table 2. The difference between ϕ_2^0 and $\phi_2'^0$ was derived theoretically by Casassa and Eisenberg (3):

(7)

where $\bar{v}_1$ and $\bar{v}_3$ are partial specific volumes of components 1 (water) and 3 (cosolvent), respectively; ξ_1 and ξ_3 represent preferential interaction parameters in terms of the number of grams of component 1 (or 3) that must be added per gram of component 2 to maintain components 1 and 3 at constant chemical potential. Then, the values ξ_1 and ξ_3 can be calculated with two specific volumes ϕ_2^0 and $\phi_2'^0$, which are usually measured by digital densimetry within an accuracy of ±0.002 $cm^3\,g^{-1}$ at isomolal and isopotential conditions of solvent components (Ref. 4). Positive values of ξ_3 or negative ξ_1 indicate the preferential binding of component 3 to protein; the opposite, negative ξ_3 or positive ξ_1, indicates that water interacts more favorably with the protein, ie, there is preferential hydration (Fig. 1). Whether preferential binding or preferential hydration occurs depends on the affinity of the cosolvent for the protein. As seen in Table 2, preferential hydration is observed for cosolvents having a potential ability to stabilize and crystallize proteins, whereas preferential binding occurs with denaturants. Thermodynamic properties such as solubility (phase separation), stability, and chemical equilibrium are subject to preferential solvent interaction, because it is directly linked to the chemical potential of the protein.

Figure 1. Schematic illustration of solvent component distributions in mixed solvents. (a) Preferential binding: Cosolvent (additive) is present in the solvation shell of protein at a greater local concentration than in the bulk solvent. (b) Preferential hydration: Exclusion of cosolvent from the protein surface results in enrichment of water in the solvation shell. [Taken from G. C. Na and S. N. Timasheff (5).]

Table 2. Apparent specific volumes of proteins and DNA at constant molality and constant chemical potential of various cosolvents (Ref. 6)

Solvent	Temperature (°C)	f_2^0 (cm^3 g^{-1})	f_2^0 c(cm^3 g^{-1})	x_3 (g^{-1})
Chymotrypsinogen A				
30% glycerol, 10 mM HCl	20	0.727	0.745	–0.123
1 M sucrose, 1 mM HCl	20	0.736	0.773	–0.138
10% PEG1000, pH 3	20	0.732	0.743	–0.07
6 M GdmCl	20	0.729	0.712	0.15
8 M urea	20	0.730	0.720	0.08
Bovine serum albumin				
1 M Na_2SO_4, pH 5.6	20	0.735	0.788	–0.074
2 M glucose, pH 6	20	0.727	0.750	
30% glycerol	25	0.729	0.744	–0.101
30% sorbitol	25	0.738	0.761	–0.092

20% propylene glycol, pH 2	25	0.740	0.726	0.211
1 M GdmCl	20	0.735	0.729	0.025
6 M GdmCl	20	0.717	0.724	0.06
DNA (calf thymus)				
0.20 M NaCl (NaDNA)	25	0.503	0.540	
0.20 M CsCl (CsDNA)	25	0.446	0.503	

The specific volumes f_2^0 and f_2^0 of nucleic acids are very small (around 0.5 $cm^3 g^{-1}$) and remarkably influenced by solvent composition (especially salt concentration) because they are polyelectrolytes with high charge densities (Table 2).

Bibliography

1. A. A. Zamyatnin (1984) Ann. Rev. Biophys. Bioeng. 13, 145–165.
2. W. Kauzmann (1959) Adv. Protein Chem. 14, 1–63.
3. E. F. Casassa and H. Eisenberg (1964) Adv. Protein Chem. 19, 287–395.
4. J. C. Lee, K. Gekko, and S. N. Timasheff (1979) Methods Enzymol. 61, 26–49.
5. G. C. Na and S. N. Timasheff (1981) J. Mol. Biol. 151, 165–178.
6. H. Durchschlag (1986) In Thermodynamic Data for Biochemistry and Biotechnology (H. J. Hinz, ed.), Springer-Verlag, Berlin, pp. 45–128. Contains details of specific volumes and their tabulation.

Particle Electrophoresis

As a result of the rising interest of molecular biologists in cells and organelles, the analytical separation and the preparative fractionation of those species by electrophoresis becomes increasingly important. Their large size makes gel electrophoresis difficult, as gels with very large pores are required. Specialized electronic devices for their separation on an analytical scale have been developed (1). Common capillary zone electrophoresis instrumentation has also been applied to particles up to 10 µm in diameter (2). Effective resolution of particles on the basis of differences in their size and shape, using solutions of polymers of various types and molecular weights for molecular sieving is possible (3), but the selection of the appropriate polymer is arbitrary at present. The resolving power is best when the particle diameter is less than the effective pore size (or “screening length”) of the polymer network in solution, and the separation of different particles is due to a differential occupation of available spaces in the network. By contrast, resolution is poor when the particle diameter exceeds that pore size, and separation is then due to a differential displacement of the network by the particle.

On preparative scales, separations in free solution are compatible with available instrumentation, such as free-flow electrophoresis apparatus (4) or automated gel electrophoresis apparatus in its preparative mode in conjunction with polymer solutions is feasible (5). In both analytical and preparative electrophoresis, sedimentation of the particles becomes an impediment to electrophoretic resolution only when the particle size surpasses about 8 μm in diameter (2). In those applications, electrophoretic separations in a microgravity environment are feasible (6).

Bibliography

1. A. W. Preece and K. A. Brown (1989) Adv. Electrophoresis 3, 351–404.
2. S. P. Radko, M. M. Garner, G. Caiafa, and A. Chrambach (1994) Anal. Biochem. 223, 82–87.
3. D. Tietz, A. Aldroubi, H. Pulyaeva, T. Guszczynski, M. M. Garner, and A. Chrambach (1992) Electrophoresis 13, 614–615.
4. J. Bauer and G. Weber (1996) Electrophoresis 17, 526–528.
5. E. Gombocz and E. Cortez (1995) Appl. Theor. Electrophoresis 4, 197–209.
6. R. S. Snyder and P. H. Rhodes (1990) Proc. 4th Eur. Symp. Life Sci. Res. Space, Trieste, Italy, pp. 411–415.

Suggestion for Further Reading

7. A. Budde, E. Knippel, G. Gruemmer, J. Treichel, H. Brockmann, E. Donath, and H. Baeumler (1996) Electrophoretic fingerprinting and multiparameter analysis of cells and particles. Electrophoresis 17, 507–511.

Partition Coefficient

A molecule's partition coefficient is the equilibrium constant for its transfer between two phases that are immiscible (eg, water and cyclohexane). This equilibrium constant is measured by analyzing both phases after equilibrium has been achieved by stirring or shaking, and then dividing the molar concentration in the first phase by the molar concentration in the second. To avoid (or detect) the occurrence of aggregation (eg, formation of dimers) in either phase, the experiment must be carried out at a series of concentrations and the results extrapolated to infinite dilution. Aggregation in either phase is signaled by a tendency of the apparent equilibrium constant to increase in favor of one phase, that in which aggregation is greatest, as the total concentration of solute increases. Such partition coefficients depend on the particular temperature at which they were measured and are used in determining hydrophobicity. See also Transfer Free Energy.

Parvalbumin

Parvalbumin binds calcium with high affinity and appears to be involved in buffering of intracellular Ca^{2+} signals. It is a small protein (10–12 kDa) that is present in muscle, brain, kidney, testis, and adipose tissue. The various parvalbumin proteins can be classified into two evolutionarily distinct groups: the a-lineage and the b-lineage. Both types of proteins have, however, similar structures and functions. Parvalbumins are members of the EF-Hand Motif family of calcium-binding proteins.

1. Biological Function

Parvalbumin was first identified in skeletal muscle cells, and its function is best understood in these cells. For muscle cells to relax after a stimulus, the Ca^{2+} signal must be quenched by active transport of the Ca^{2+} ions into the sarcoplasmic reticulum. Parvalbumin has been implicated in skeletal muscle relaxation after a single twitch, as well as after a tetanic (continuous) contraction, and it may facilitate Ca^{2+} translocation in the sarcoplasm. There is still some controversy, however, over whether parvalbumin can exchange Ca^{2+} and Mg^{2+} ions fast enough to be involved in relaxation after a single twitch.

The function of parvalbumin in other cell types is less clear. It may act as a Ca^{2+} buffer to protect cells from damage due to calcium overload, particularly in the nervous system. It may also play an indirect role in Ca^{2+} signal transduction by affecting the nature of the incoming signal. For instance, it could modulate how quickly the signal builds, or how long the signal lasts. Parvalbumin may also be involved in cell growth and the cell cycle.

Oncomodulin is a b-lineage parvalbumin of particular interest, because it is found in abundance in certain cancer cells. It is normally found only in the preimplantation embryo and in the placenta. The function of this protein is completely unknown. However, its expression is cell cycle-dependent, and oncomodulin antisense oligonucleotides inhibit cell growth when injected into chemically transformed fibroblasts.

2. Ion-Binding Properties

Parvalbumin's two functional EF-hands will bind either Ca^{2+} or Mg^{2+} ions. Two main types of metal-binding loops are found in parvalbumins. The most common is the Ca^{2+}/Mg^{2+} “mixed” binding loop. These sites bind Ca^{2+} with high affinity ($K_{Ca} = 10^7$ to $10^9 M^{-1}$), and Mg^{2+} with moderate affinity ($K_{Mg} = 10^3$–$10^5 M^{-1}$) (1). Binding is competitive, and at basal physiological ion concentrations ($[Ca^{2+}] = 1 - 10 \times 10^{-8}$M; $[Mg^{2+}] = 1 \times 10^{-3}$M), mixed sites are occupied by Mg^{2+}. Exchange between bound Ca^{2+} and Mg^{2+} is slow (2, 3). The second type of binding loop is the Ca^{2+}-specific loop. The Ca^{2+} affinity of these sites is lower than in mixed sites ($K_{Ca} = 10^5 - 10^7 M^{-1}$), and the Mg^{2+} affinity is significantly reduced ($K_{Mg} = 10^1 - 10^2 M^{-1}$) (4). These sites are metal-free under basal physiological conditions, and can therefore bind Ca^{2+} quickly. Oncomodulin is the only member of the parvalbumin subfamily that has a Ca^{2+}-specific site paired with a mixed site.

3. Structure

Parvalbumins are the only known members of the EF-hand family with three such motifs (a prototypical functional domain is composed of only two). However, the N-terminal EF-hand of parvalbumin does not bind Ca^{2+} and is therefore considered to be a nonfunctional ancestral site. The protein is largely helical, with six alpha-helices, labeled A through F. The functional calcium-binding loops occur between helices C and D and between helices E and F. The loop between helices A and B is shorter than the functional loops (10 residues rather than 12), and as mentioned above, does not bind metal ions.

Parvalbumin was the first EF-hand protein whose high resolution three-dimensional structure was determined (5). To date, all the known parvalbumin structures have metal bound. Structures of parvalbumin bound to both Ca^{2+} and Mg^{2+} are available (6-13). The overall structure of the protein is very similar irrespective of which ion is bound. The two a-helices flanking each functional binding loop (the C/D pair and the E/F pair) are nearly perpendicular to each other, while the A and B helices, which flank the non-functional binding site, are nearly antiparallel (Fig. 1). However, there are some differences between the binding loops with bound Ca^{2+} and those occupied by Mg^{2+}, particularly in the position of the highly conserved glutamic acid residue that is the final residue of the binding loop. In parvalbumin and all other EF-hand calcium-binding proteins studied to date, this glutamic acid is a bidentate calcium ligand. In the Mg^{2+}-bound parvalbumin structures, this glutamic acid is a monodentate ligand (14). This difference reflects the preference of the Mg^{2+} ion for six ligands, whereas the Ca^{2+} ion can accommodate seven or even eight ligands. The apo structure is of questionable physiological importance, since almost all parvalbumin binding loops are occupied by Mg^{2+} under basal physiological conditions. NMR studies indicate, however, that apo-parvalbumin has a structure very similar to that seen for the ion-bound states (15). This is consistent with its proposed role as a calcium buffer, which requires high Ca^{2+} affinity but not the conformational change associated with the transduction of a calcium signal into a mechanical or metabolic response (see Calmodulin).

Figure 1. Ribbon representation of $(Ca^{2+})_2$-parvalbumin using the coordinates of 1PVA (7).

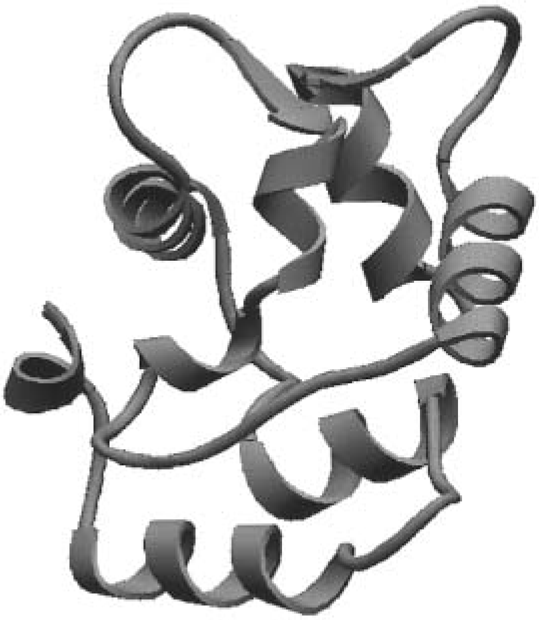

Bibliography

1. J. Haiech, J. Derancourt, J.-F. Pechere, and J. G. Demaille (1979) Biochemistry 18, 2752–2758.
2. Y. Ogawa and M. Tanokura (1986) J. Biochem. 99, 73–80.
3. Y. Ogawa and M. Tanokura (1986) J. Biochem. 99, 81–89.
4. M. Milos, J.-J. Schaer, M. Comte, and J. A. Cox (1986) Biochemistry 25, 6279–6287.
5. R. H. Kretsinger and C. E. Nockolds (1973) J. Biol. Chem. 248, 3313–3326.
6. J.-P. Declercq, B. Tinant, J. Parello, and G. Etienne (1988) J. Mol. Biol. 202, 349–353.
7. J.-P. Declercq, B. Tinant, J. Parello, and J. Rambaud (1991) J. Mol. Biol. 220, 1017–1039.
8. F. R. Ahmed, D. R. Rose, S. V. Evans, M. E. Pippy, and R. To (1993) J. Mol. Biol. 230, 1216–1224.

9. V. D. Kumar, L. Lee, and B. F. P. Edwards (1990) Biochemistry 29, 1404–1412.

10. P. C. Moews and R. H. Kretsinger (1975) J. Mol. Biol. 91, 201–228.

11. F. Roquet, B. Tinant, J.-P. Declercq, R. Rambaud, and J. Parello (1992) J. Mol. Biol. 223, 705–720.

12. A. L. Swain, R. H. Kretsinger, and E. L. Amma (1989) J. Biol. Chem. 264, 16620–16628.

13. C. A. McPhalen, A. R. Sielecki, and J. Santarsiero (1994) J. Mol. Biol. 235, 718–732.

14. T. C. Williams, D. C. Corson, K. Oikawa, W. D. McCubbin, C. M. Kay, and B. D. Sykes (1986) Biochem. 25, 1835–1846.

Suggestion for Further Reading

15. T. L. Pauls, J. A. Cox, and M. W. Berchtold (1996). The Ca^{2+}-binding proteins parvalbumin and oncomodulin and their genes: new structural and functional findings. Biochim. Biophys. Acta 1306, 39–54.

Pathogenesis In Fungi

1. Pathogenesis and Virulence

To understand how a given organism is able to infect its host, it is important to determine which aspect(s) of the biology of the fungus differs from nonpathogenic fungi. According to Bulmer and Fromtling, "Pathogenicity is the capacity of an organism to damage, ie, to produce disease in another animal or plant" (1). This property is the result of a direct interaction between the pathogen and the host. In many ways, pathogenicity and virulence are very broadly defined terms. If one considers all the possible gene products required for growth on or within a host, those that contribute to disease symptoms and host-range specificity, and those that govern their regulation, then we may be considering hundreds (or thousands) of potential components. Furthermore, the ability of an organism to adapt quickly to new environmental challenges is itself likely to be an effective virulence mechanism, in that it enables the pathogen to take advantage of new opportunities.

One of the most cited examples of virulence in the fungal world is the ability to switch morphological forms. While some fungi are pathogenic as yeast or conidial forms [eg, Histoplasma capsulatum, Coccidioides immitis, and Blastomyces dermatitidis and Coccidioides immitis (2–4)], numerous correlations between hyphal growth and pathogenicity have been cited for many of the fungal pathogens. In fact, mutants incapable of switching to hyphal growth are often revealed as nonpathogenic: cpg-1 deletions in C. parasitica (5), deletions of fuz7 in U. maydis (6), or cph1/efg1 homozygous deletions in C. albicans (7). The ability to switch morphological forms is referred to as dimorphism and is governed by a number of external factors including nitrogen, pH, temperature, and intracellular biochemical pathways (eg, level of cAMP) (8). Similarly, correlations between a strain's ability to myceliate and its virulence (defined by the LD50, lethal dose to obtain 50% killing of the host) have also been cited as strong virulence factors.

Pathogen-produced products which contribute in some way to either the establishment or continuation of the disease process have also been cited as virulence factors. Historically, secretion of degradative enzymes such as elastase and certain proteinases (9, 10) have been cited as potential virulence factors using a variety of methods to correlate disease progression with levels of expression. Paracoccidioides brasiliensis has been shown to alter its level of virulence with the production of a-1,3 glucan, suggesting that this polymer may act as a protective layer (11). Genes that contribute to adherence of the fungus to its host have also been regarded as virulence factors (12). Numerous genetic mutants or strain isolates have been analyzed in in vivo experiments to identify underlying gene products causing changes in pathogenicity. In fungus–plant interactions, the pathogen may produce a substance that specifically detoxifies plant-secreted antifungal compounds. For example, G. graminis deletion mutants have been generated that are relatively resistant to the production of avenacin by oat roots but retain full pathogenicity to wheat, which does not synthesize saponins (13); isolates of Nectria haematococca are similarly able to detoxify the pea phytoalexin, pisatin, using a cytochrome P450 mechanism (14). Furthermore, the biosynthetic pathway leading to melanin production in M. grisea correlates with altered virulence in this fungus; strains with reduced melanin content are less virulent (15). In some instances, these factors are reported to increase the pathogen's ability to penetrate host tissue (as in the case of melanin or proteinase production), while in others they may simply contribute to the overall fitness of the organism in vivo. For example, some auxotrophies are known to decrease virulence in vivo but play little or no role in vitro. Mutations in the URA3 and ADE2 genes of C. albicans and C. neoformans attenuate virulence in vivo (16, 17).

Alternatively, pathogen-induced factors that result in direct attacks upon the host are also known. The best-characterized system of host-selective toxin production by a plant fungus is in Cochliobolus. Different species of this genus are known to produce plant-specific toxins: T-toxin, HC-toxin, and victorin, of which only HC-toxin production has been deleted and shown to be nonpathogenic on maize (reviewed in Ref. 18).

One area in which there is sparse molecular information, but a great deal of inferential information, is in the interactions between the host immune system and pathogen. Research directed toward understanding the role of the unique polysaccharide capsule of Cryptococcus neoformans pathogenicity has uncovered a large difference in ability to phagocytose capsulized versus acapsular C. neoformans mutants in vitro, although it is not yet clear whether the ability to engulf a cell correlates with killing (4). Additionally, macrophages appear to recognize and engulf wild-type, single, and double mutants of the MAPK pathway in C. albicans equally well; however, only wild-type strains were able to switch morphologies, adding further support that dimorphism plays a significant role in virulence in this organism (7). It is tempting to speculate that in the chs3 C. albicans cell wall mutant, prolonged survival in vivo (19) had more to do with a change in its interaction with the host immune system than with any other factor. If, in fact, the host defense system plays a more significant role in disease progression than has been realized, it will be interesting to determine whether factors such as increased lipid content cited as a virulence factors in strains of Coccidioides immitis, Histoplasma capsulatum, and Blastomyces dermatidtidis (1, 20) is a result of an alteration in the interaction rather than a simple defense on the part of the fungus.

2. Signal Transduction and Pathogenesis

Signal transduction pathways play an important role in the cellular biology of all eukaryotic organisms, including fungi. The ability of a pathogen to receive signals from its environment and transmit those signals intracellularly to alter development or enable biochemical pathways so as best to take advantage of those changes has been recognized as a significant partner in pathogenesis of the organism. Some of the pathways have been carefully worked out in S. cerevisiae and S. pombe with regard to cell cycle, filamentation, stress, and the pheromone response. It appears that the molecules required to relay a signal from the external environment to the appropriate transcription factors within the nuclei of many of the filamentous fungi are highly homologous to those described in other organisms. Some of the molecules have been identified and isolated on the basis of sequence homology, and some by complementation or the use of similar screens. While the precise targets of many of these molecules have yet to be discovered, it is becoming clearer that many of the pathways in yeast are similarly conserved in more distantly related organisms.

Virulence and signal transduction pathways are inescapably intertwined in the biology of fungi and their pathogens. In the filamentous fungi, signal transduction pathways have been identified that regulate conidiation in *A. nidulans*, virulence in *C. albicans*, *C. parasitica*, *U. maydis*, and *M. grisea*, and mating. While only a few of the components have been identified in the filamentous fungi to date, there is much anticipation that most, if not all, of the players will eventually be isolated and characterized. Although their exact developmental pathways may be very different in the different fungi, it is important to keep in mind the similarities in order to appreciate the conservation of function across the biological world.

2.1. MAP Kinase Pathway

Signal transduction involves the activation of a receptor molecule at the surface of a cell, which transmits the signal inward toward associated proteins at the cytoplasmic interface of the plasma membrane. Changes in these proteins are relayed via a small number of known pathways (either by a cascade of kinases or by the release of a second messenger), which in turn activate a number of protein targets, some of which are themselves transcriptional activators. Subsequent alterations in transcription of whole sets of genes then reprogram the cell's "transcriptome," resulting in a particular cellular response to the initial signal. That signal may be any of a number of ligands that tells the cell something about its external environment: for example, nutritional availability, osmolarity, presence of compatible mating partners, or light. In one common pathway observed in all eukaryotes, a heterotrimeric G protein activates a mitogen-activated protein (MAP) kinase module that results in the further activation of target proteins, among which is a transcription factor. In some cells, multiple MAPK signaling pathways can be operating simultaneously, altering the organisms' transcriptome moment-by-moment. A MAP kinase pathway influence on pathogenicity has been shown for the corn smut, *U. maydis*, in which tumor production and completion of the sexual cycle is dependent upon successful compatible mating (21). Appressorium formation and pathogenic growth of *M. grisea in planta* also require a functional MAP kinase pathway (22). Because the components of these pathways are so highly conserved, one of the central questions that remains unanswered is how specificity is achieved and how that affects the pathogenicity of the organism.

2.2. Cyclic AMP Pathway

A second common pathway that impinges upon pathogenicity is the cyclic AMP-mediated pathway, which begins with a plasma membrane-bound sensor molecule (none of which has been isolated for the filamentous fungi to date). Upon a functional receptor–ligand interaction, a signal is transmitted to a heterotrimeric GTP-binding protein, possibly through a conformational change in the membrane protein. Second messenger cyclic AMP (cAMP) is produced via adenylate cyclase, which then alters the activity of cAMP-dependent protein kinase A (PKA) by binding to the regulatory subunit of PKA. This releases the catalytic subunits, which continue to activate downstream targets (including transcriptional regulatory proteins). A few components of this pathway have been identified in filamentous fungi. Mutants in *uac1* (adenylyl cyclase of *U. maydis*) have been shown to be defective in their ability to switch from budding to filamentous growth and, in addition, were unable to cause disease on corn (reviewed in (Ref. 23)); disruption of *adr1* (catalytic subunit of PKA) results in nonpathogenesis, whereas inactivation of *uka1* (catalytic subunit of PKA) has apparently little or no effect on growth, morphology, or pathogenesis. Disruption of *fil1* (G a subunit of *U. hordei*) also prevented normal hyphal to bud switching. Interestingly, of the four G a proteins isolated from *U. maydis*, only one, *gpa3*, was shown to be required for pathogenic development, disruption of the other three displayed no obvious phenotypes. Furthermore, *gpa3* mutants were unable to respond to pheromone signals strongly suggesting that a single G a subunit may play a role in multiple signaling pathways as has been observed in *S. cerevisiae* and *C. albicans*. Mutants disrupted in the catalytic subunit of *M. grisea* (CPKA) were shown to be unable to form appressoria on artificial surfaces, and they were also unable to infect rice unless exogenous cAMP was administered (23).

3. Strategies to Identify Virulence Factors

3.1. Gene Knockouts

There are a number of molecular genetic strategies that can be used to identify genes responsible for virulence in fungi (24). In a standard experiment, genetic manipulations are made such that the chromosomal copy of a gene in question is replaced by a marker gene. The growth rate of these strains is then compared to the normal wild-type strain and subsequently tested *in vivo* to determine the potential of the “knocked out” gene to cause disease. Proper controls wherein additional strains containing the chromosomal knockout, but also harboring a transformant carrying a reintroduced wild-type copy of the gene, or a heterozygote, is also compared in order to ensure that the effects observed are due to the presence or absence of a specific gene product and not some other underlying mechanism. It should be noted that due to the frequency of ectopic integration in filamentous fungi, these experiments may be difficult to interpret. They have been successfully accomplished for a wide variety of gene products in the dimorphic fungus, *C. albicans*. Using a modification of the original “ura-blaster” strategy (25), it is possible to knockout both copies of a given gene in this perpetually diploid organism. Genes in cell wall biosynthesis, signal transduction, and so on, have been identified as involved in virulence in such tests (7, 19, 26). This directed approach to virulence determination has also been successful in *A. nidulans* (27), *Gaeumannomyces graminis* (28), and *C. neoformans* (29), for example. Using this approach, there is the potential to knockout each gene in a given organism systematically and test its pathogenicity *in vivo*.

3.2. Gene Transfer

Virulence factors have also be identified by their ability to confer pathogenicity upon a related species or strain that was previously nonpathogenic. In this approach, a library is constructed and transformed into a nonpathogenic organism. Entire library pools are then tested for changes in related events that are suspected of having influences upon pathogenicity (adherence properties, toxin production, proteinase activity, etc.), and gene products are identified and then retested for altered virulence relative to the existing host strain. This approach has been successful in identifying a gene conferring adhesion properties from *C. albicans* to *S. cerevisiae* (30).

3.3. Gene Expression

This may be accomplished in a number of different ways. First is to identify all the genes expressed during an infection, by complementary DNA cloning, differential display analysis, or promoter fusions (all of which are technically feasible in the filamentous fungi). The idea is that crucial genes will be expressed sometime during or immediately prior to the establishment of an infection. These genes can then be further screened for their role in virulence, using a variety of knockout or deletion strategies. The *MPG1* protein of *M. grisea* was identified using this approach and confirmed to be important in the development of fungal infection structures (31). Using a differential display approach, two genes from *U. maydis* (32) and six genes from *C. albicans* have been identified that are differentially induced during infection (33). As additional sequence information becomes available for other fungal genomes, the use of promoter fusions as an approach will probably become somewhat more popular. Following the initial identification of clones that express a viable fusion, sequence analysis of the upstream sequences encoding the fusion will reveal the target gene. Conceivably, libraries in which the reporter proteins are cell surface-directed will aid in the initial identification of positive clones in this type of model.

One of the most fascinating stories concerning pathogenicity in fungal biology involves the interaction between *Cryphonectria parasitica* (chestnut blight fungus) and a hypovirus. These fungi, which have wreaked havoc upon the chestnut forests of the northeastern United States, are themselves infection-susceptible to a hypovirus that causes reduced virulence of the fungus for the plant. In addition to causing reduced virulence, the virus causes altered colony morphology, reduced pigmentation, and attenuated asexual sporulation. Differential display analysis of infected and noninfected isolates identified a candidate gene, *cpg1* whose reduced expression in infected isolates appears to correlate with pathogenicity (5, 34).

3.4. Mutagenesis

Historically, a traditional genetic approach in which mutations are isolated and further characterized has proven beneficial in the understanding of pathogenesis of fungi. One of the more recent strategies to understanding and defining virulence factors has come from alterations in transposon-mediated mutagenesis screens. Transposons are relatively small fragments of DNA that are capable of recombining nearly randomly into different sites within a single genome. They have proven useful in creating large number of "insertional" mutant libraries that are easily screened for loss-of-function phenotypes. Unfortunately, filamentous fungi appear to lack such elements. However, restriction enzyme-mediated integration (REMI) has been be used to create insertional mutants in filamentous fungi. Pathogenicity genes were identified for Cochliobolus heterostrophus (35) and Ustilago maydis (36) using REMI.

A modification of this method, called signature-tagged mutagenesis, has been used successfully in bacterial pathogenesis to identify insertional mutants that fail to grow in vivo (37). In this method, every insertional mutant carries with a unique oligomer tag that identifies it from all other mutants. After inoculating a mouse and recovering all survivors, DNA is prepared and hybridized to colony blots of the original input pool. Mutants not surviving are not recovered and are easily identified as not hybridizing. Identification of the gene into which the insertional tag is present is performed by sequencing. One of the only drawbacks to this approach is that only nonessential genes may be recovered, because insertions into essential genes are by definition lethal in culture.

3.5. Use of In Vivo Models

The use of in vivo models to confirm the role of individual genes in virulence is an important aspect of this field. However, it is important to recognize the difference between the establishment of infection and the maintenance of infection. Both are clearly critical factors in host–pathogen interactions, yet targets should be different, though somewhat overlapping. Second, the size of the inoculum is a well-established variable in disease models. It is not inconceivable that certain genes play a more significant role at low inocula in certain situations while other virulence genes are turned on under conditions of high inocula. Third, it is important to remember that virulence is multifactorial and results from a balance between the pathogen and the host immune system. Comparisons across different fungal backgrounds or different host models should proceed with caution.

4. Fungal Virulence Genes as Targets for Antifungal Therapy

It is not enough that we understand how an organism grows and develops or produces disease; it is our ability to use this information to circumvent those processes that will enable humanity to control and manage diseases produced by microorganisms. Compounds aimed toward inhibiting functions of known or suspected virulence factors have been suggested as likely to be effective in reducing disease even though many of the virulence genes identified to date have been shown to be nonessential for growth and reproduction of the organism in vitro. A compound directed toward such a nonessential target would likely prevent fungal growth until the compound were either removed or inactivated. In clinical situations where prophylaxis is appropriate, a reduction in anticipated fungal pathogen virulence could significantly influence patient outcome, because the disease will not likely gain entry initially. Unfortunately, the human patient population that often contracts fungal diseases is often immune-debilitated. From an agricultural view, inhibition of fungal growth will probably lead to increased production over a short season, making these attractive targets. Another consideration in choosing virulence factors as targets is the likelihood that parallel and/or redundant pathways may exist. With all of this, virulence genes are important to consider as potential drug targets.

Strategies for identifying fungal virulence genes as potential targets for drug development and/or vaccine development include many of the cloning strategies identified earlier. Furthermore, the use of bioinformatics and genome sequencing has made it possible to identify potential candidates based on previously known motifs, which may then be tested in vivo for specific disease.

Bibliography

1. G. S. Bulmer and R. A. Fromtling (1983) "Pathogenic Mechanisms of Mycotic Agents". In Fungi Pathogenic for Humans and Animals, Part B, (D. H. Howard, eds.), Marcel Dekker, New

York.
2. J. E. Loyd, R. M. DesPrez, and R. A. Goodwin, Jr. (1990) *Histoplasma capsulatum*. In *Principles and Practice of Infectious Diseases* (G. L. Mandell, R. G. B. Douglas, and J. E. , eds.), Churchill Livingstone, New York, pp. 1989–1999.
3. S. W. Chapman (1990) *Blastomces dermatitidis*. In *Principles and Practice of Infectious Diseases* (G. L. Mandell, R. G. Douglas, and J. E. Bennett, eds.), Churchill Livingstone, New York.
4. D. A. Stevens (1990) *Coccidioides immitis*. In *Principles and Practice of Infectious Diseases* (G. L. Mandell, R. G. B. Douglas, and J. E. Bennett, eds.), Churchill Livingstone, New York, pp. 2008–2017.
5. S. Gao and D. L. Nuss (1996) Proc. Natl. Acad. Sci. USA **93**, 14122–14127.
6. F. Banuett and I. Herskowitz (1994) Genes Dev. **8**, 1367–1378.
7. H.-J. Lo et al. (1997) Cell **90**, 939–949.
8. S. Gold, G. Duncan, K. Barrett, and J. W. Kronstad (1994), Genes Dev. **8**, 2805–2816.
9. K. J. Kwon-Chung, D. G. Lehman, and C. P. T. Magee (1985) Infect. Immun. **49**, 571–575.
10. J. W. Rippon and G. L. Peck (1967) J. Invest. Dermatol. **50**, 54–58.
11. G. San-Blas and D. Vernet (1977) Infect. Immun. **15**, 897–902.
12. H. J. Watts, F. S. H. Cheah, V. Hube, D. Sanglard, and N. A. R. Gow (1998) FEMS Micro. Lett. **159**, 129–135.
13. P. Bowyer, B. R. Clarke, P. Lunness, M. J. Daviels, and A. E. Osbourn (1995) Science **267**, 371–374.
14. K.-M. Weltring, B. G. Turgeon, O. C. Yoder, and H. D. VanEtten (1988) Gene **68**, 335–344.
15. R. J. Howard and B. Valent (1996) Annu. Rev. Microbiol. **50**, 491–512.
16. W. A. Fonzi and M. Y. Irwin (1993) Genetics **134**, 717–728.
17. J. R. Perfect, D. L. Toffaletti, and T. H. Rude (1993) Infect. Immun. **61**, 4446–4451.
18. D. G. Panaccione (1993) Trends Microbiol. **1**, 14–20.
19. C. E. Bulawa, D. W. Miller, L. K. Henry, and J. M. Becker (1995) Proc. Natl. Acad. Sci. USA **92**, 10570–10574.
20. R. A. Cox, L. R. Mills, G. K. Best, and J. F. Denton (1972) Infect. Immun. **5**, 449–453.
21. T. Spellig, B. M. , F. Lottspeich, R. W. Frank, and R. Kahmann (1994) EMBO J. **13**, 1620–1627.
22. J.-R. Xu and J. E. Hamer (1996) Genes Dev. **10**, 2696–2706.
23. J. W. Kronstad (1997) Trends Plant Sci. **2**, 193–199.
24. L. H. Hogan, B. S. Klein, and S. M. Levitz (1996) Clin. Microbiol. Rev. **9**, 469–488.
25. E. Alani, L. Cao, and N. Kleckner (1987) Genetics **116**, 541–545.
26. L. Yaar, M. Mevarech, and Y. Koltin (1997) Microbiology **143**, 3033–3044.
27. M. A. Stringer, R. A. Dean, T. C. Sewall, and W. E. Timberlake (1991) Genes Dev. **5**, 1161–1171.
28. P. Bowyer, B. R. Clarke, P. Lunness, M. J. Daniels, and A. E. Osbourn (1995) Science **267**, 371–374.
29. Y. C. Chang and K. J. Kwon-Chumng (1994) Mol. Cell. Biol. **14**, 4912–4919.
30. M. Barki, Y. Koltin, M. Yanko, A. Tamarkin, and M. Rosenberg (1993) J. Bacteriol. **175**, 5683–5689.
31. N. J. Talbot, D. J. Ebbole, and J. E. Hamer (1993) Plant Cell **5**, 1575–1590.
32. R. Bohlmann, F. Schauwecker, C. Basse, and R. Kahmann (1994) Plant Microbe Interact. **3**, 239–245.
33. B. Cormack and F. S. (1995) J. Cell. Biochem. (Suppl. **19B**) abstract B4-202, 156.

34. L. Zhang, A. C. L. Churchill, P. Kazmierczak, D. H. Kim, and N. K. Van Alfen (1993) Mol. Cell. Biol. 13, 7782–7792.

35. S. W. Lu et al. (1994) Proc. Natl. Acad. Sci. USA 91, 12649–12653.

36. M. Bolker, H. U. Bohnert, K. H. Braun, J. Gorl, and R. Kahmann (1995) Mol. Gen. Genet. 248, 547–552.

Patterson Map

Patterson maps give structural information in X-ray crystallography, even if the phases of the reflections are not known (see Phase Problem). With the Patterson function $P(uvw)$, a vector map is calculated. Vectors between atoms in the real structure show up as vectors from the origin to maxima in the Patterson map (Fig. 1). The size and shape of the unit cell in this map is identical to the crystal unit cell.

(1)

where u, v, and w are relative coordinates in the Patterson cell; h, k, and ℓ are the indices of the reflections; V is the volume of the unit cell; and is the amplitude of the structure factor of reflection $h\,k\,\ell$. Calculation of the Patterson function from Eq. 1 does not require knowledge of the phase angles of the reflections and can always be calculated from the experimental diffraction data because, apart from correction factors, , where $I(h\,k\,\ell)$ is the intensity of reflection $hk\ell$.

Figure 1. Example of a simple Patterson map. (a) A two-dimensional unit cell with three atoms. (b) The corresponding

For very simple chemical compounds, it is possible to derive the real structure from the Patterson map. A protein Patterson map, however, has too many overlapping vectors to extract any structural information. However, protein Patterson maps are extremely useful for understanding the molecular replacement technique. They are also employed in isomorphous replacement to locate the attached heavy atoms. The difference between the amplitudes of the reflections for the native and heavy atom crystals is used in the calculation, to produce a difference Patterson map. Such a map should result only from the heavy atoms, and it should be interpretable because the number of heavy atoms attached is usually small and therefore they form a simple structure.

Suggestion for Further Reading

J. Drenth (1999) Principles of Protein X-ray Crystallography, Springer, New York.

Pax Genes

Nine Pax genes have been isolated from vertebrates through sequence homology to a region in the

Drosophila gene *paired*, which codes for a DNA-binding domain. This domain of 126–amino acid residues is highly conserved and is known as the paired box. Binding sites for Pax proteins have been found in the promoter regions of genes coding for proteins as functionally varied as other transcription factors, crystallins, receptors, peptide hormones and cell adhesion proteins. Pax proteins are expressed in restricted regions during embryonic development. Pax genes are subdivided on the basis of the presence or absence of two further conserved sequences: a paired-type homeobox and an octapeptide coding region. These elements are keys to the functions of Pax proteins in morphogenetic processes such as (1) establishing the competence of tissues to particular developmental fates, (2) commitment of cells to particular developmental fates, and (3) the regionalization of the central nervous system.

1. Structure and Biological Activity of Pax Proteins

1.1. Classes of Pax Proteins

Pax proteins are transcription factors that regulate gene transcription. All nine Pax proteins contain the paired box, a 136–amino acid residue domain with DNA-binding activity that has sequence similarity to a domain found in the Drosophila protein paired (1) (reviewed in (2)). As well as the paired domain, Pax proteins also carry one or both of two other conserved domains: the paired-type homeodomain and the octapeptide sequence (Fig. 1). The presence or absence of these other conserved domains is used to classify the Pax proteins into four groups (Fig. 1). The amino acid sequences of the conserved domains of a Pax protein are more similar to those within the same class than those of Pax proteins from different classes (2). Additionally, when Pax proteins have similar functions in a particular tissue, for example, Pax-2 and Pax-5 in the midbrain/hindbrain boundary, they come from the same class.

Figure 1. Structure of Pax proteins.

1.2. Pax Proteins Directly Regulate the Expression of Many Types of Genes

Pax proteins regulate gene transcription by binding to specific sequences in the enhancer and promoter regions upstream of the coding regions of the gene. This results in the initiation of transcription, which subsequently results in synthesis of the protein. The paired domain binds to DNA; thus it is crucial to the regulation of gene transcription. Changes to the amino acid sequence in this domain have been demonstrated to strongly inhibit the binding of Pax proteins to DNA (3, 4). The specific DNA sequences that Pax proteins bind to have been found in the enhancer and promoter regions of genes coding for many classes of proteins (Table 1). This is consistent with the fact that Pax genes are important regulators of organogenesis in the developing embryo.

Table 1. Types of Genes Whose Expression is Regulated by Pax Proteins

Gene	Protein Product Type	Promoter Bound By	Reference
En1	Transcription Factor	Pax-2, -5, -8	(105)
En2	Transcription Factor	Pax-2, -5, -8	(105)
Crystallin (various)	Structural Protein	Pax-6	(106)
NCAM	Cell Adhesion Protein	Pax-6	(107)
Insulin	Peptide Hormone	Pax-6	(69)
Glucagon	Peptide Hormone	Pax-6	(69)
Thyroperoxidase	Enzyme	Pax-8	(84)
IgH	Immunoglobulin Subunit	Pax-5	(79)
CD19	Receptor	Pax-5	(76)
c-met	Receptor	Pax-3	(60)
p53	Cell Cycle/Apoptosis Regulator	Pax-5	(101)

2. Developing Processes Regulated by Pax Proteins

Pax proteins have important roles in regulating organogenesis, commitment of cells to particular developmental pathways, and the regionalization of the central nervous system (summarized in Table 2). Pax proteins help mediate these processes by (1) enabling an embryonic tissue to be competent to interact with other tissues, (2) conferring regional identity to a portion of tissue that later forms a new embryonic structure, (3) commitment of cells to a lineage with a particular differentiation pathway, (4) maintenance of boundaries between regions that have separate developmental fates, and (5) conferring multipotency to precursor cells (15, 85).

Table 2. Summary of Pax Gene Null Mutation Phenotypes in Mouse Mutants

Gene	Null Mutation	Heterozygous Phenotype	Homozygous Phenotype	Reference
Pax-1	Undulated, targeted	Normal	Hypoplasia of vertebral bodies and discs	(52, 53, 108)
Pax-2	KrD, targeted	Small kidneys, optic coloboma	No kidneys or genital tracts, optic oloboma	(25, 26, 28, 30, 31, 73)
Pax-3	Splotch	Lack of pigmentation	No limb muscle, neural crest derivatives absent or hypoplasic, persistent truncus arteriosus	(45, 58-64, 22-60, 62, 109, 110)
Pax-4	Targeted	Normal		(66)
Pax-5	Targeted	Normal	No B cells, cerebellar and inferior colliculous defects	(26-28, 77, 78)
Pax-6	Sey, Sey[Neu], rSey, targeted	Microphthalmia, corneal and iris defects	No eyes or olfactory bulbs, forebrain and motorneuron/interneuron specification defects	(7-9, 14, 15, 30, 31, 35-38, 47, 67)
Pax-7	Targeted	Normal	No muscle satellite cells, maxillary process, nasal capsule	(22, 46, 85)
Pax-8	Targeted	Normal	Absence of thyroid	(83)
Pax-9	Targeted	Normal	Absence of teeth	(55, 81)
Pax-2/Pax-5	Double homozygous	—	Absence of isthmic organizer, cerebellum and inferior colliculus	(26, 28)
Pax-3/Pax-7	Double homozygous	—	Neuronal specification defects (somitic derivatives not reported)	(22)
Pax-1/Pax-9	Compound heterozygous, double homozygous	—	Absence of vertebral bodies and discs, teeth	(51)

The roles of Pax proteins in these processes have been studied in mice having natural or targeted mutation of the Pax genes (Table 2). One property of Pax genes is that, for some developmental processes, two fully functional copies of the genes are required for normal differentiation of the tissue. Thus, developmental abnormalities in kidney, optic nerve, eye and pigmentation are found in mice heterozygous for mutations in particular Pax genes. These defects are broadly consistent with human syndromes in which one copy of the corresponding PAX genes are mutated. This characteristic, known as haploinsufficiency, results in autosomal-dominant phenotypes that are not the result of novel gene function but, rather, the consequence of depleted levels of functional protein. Increased levels of Pax protein can also alter developmental fate; extra Pax-6 genes results in developmental defects of the eye (5).

2.1. Pax-6 is Necessary for Early Eye Development

The embryonic eye is formed from an extension of the developing forebrain known as the optic vesicle, which is the precursor tissue for the retina, and a portion of the ectoderm, the lens ectoderm, that overlies this optic vesicle (reviewed in (6)). A crucial early process of eye development is the induction of the lens ectoderm by the optic vesicle to form firstly the lens placode, then a vesicle and finally the mature lens. In animals homozygous for the natural Pax-6 null mutations Sey (7-9), Sey^{Neu} (9) and rat rSey (10), lens development fails to occur. Pax-6 is expressed in the presumptive lens ectoderm and in the induced lens placode (11, 12). This pattern of expression strongly suggested that Pax-6 proteins is part of the mechanism that allows the ectoderm to respond to a lens induction signal from the optic vesicle. This notion was supported by explant recombination experiments between homozygous rSey and wild-type tissue which showed that the homozygous ectoderm failed to respond to optic vesicle interactions but that homozygous mutant optic vesicle could still induce lens ectoderm (13). A conclusive study of this interaction employed conditional knockout in mice to specifically ablate functional Pax-6 genes in the lens while leaving fully functional Pax-6 in the optic vesicle and other tissues (14). Lens ectoderm with no functional Pax-6 underwent an initial response resulting in increased expression of the transcription factor Sox-2, then its development arrested. Although optic vesicle development is arrested in the natural Pax-6 mutants, optic vesicles in the conditional knockout mice underwent development to form not one but several retinas. Thus, the optic vesicle is also required for correct placement of the retina, but not further development of the retina.

Development of the optic vesicle into the retina is characterized by the sequential generation of mature retinal cell types from stem cells in the original neuroectodermal layer (reviewed in (6)). An important feature of this process is the prevention of differentiation of all the stem cells into differentiated cells, so that a stem cell population is retained for the generation of later appearing cell types. However, specific ablation of Pax-6 in the retina by conditional knockout, results in all the stem cells of the retina differentiating into the first cell type to appear, the amacrine cells, and the consequent arrest of further retinal development (15). Thus, Pax-6 is necessary for maintenance of this stem cell population.

2.2. Pax Proteins and Patterning the Central Nervous System

Pax proteins are one of many classes of regulator proteins that control the generation of neural tissue. They are part of the mechanism that specify certain neuronal populations. Moreover, some structures in the CNS require Pax proteins for their survival. Pax proteins also modulate the extracellular environment of certain structures resulting in well-demarcated boundaries with neighboring tissues.

The neural tube and hindbrain exhibit particularly striking patterns of Pax gene expression. Pax-6 is expressed in most of the neural tube but is missing in the most dorsal and ventral margins (11, 16). Pax-3 and Pax-7 are expressed in the dorsal neural tube (17, 18). Combinations of transcriptional regulators including the Pax proteins are specified in individual cells on the basis of positional information provided by opposing concentration gradients of secreted peptide factors (reviewed in (19)). Sonic hedgehog, is secreted from the ventral margin of the neural tube, known as the floorplate, and from the notochord while BMP proteins diffuse from the dorsal margin of the neural tube (the roofplate) and the overlying ectoderm is the second group of signals. Additionally, transcriptional regulator expression can be modulated by other transcriptional regulators. Gain or loss of function for individual transcriptional regulators can change the specification of restricted neuronal types. Deletion of functional Pax-6, which is normally expressed in the middle of the neural tube, results in the respecification of the motor neurons supplying the hypoglossal nerve and some ventral interneurons (16, 20). Inappropriate expression of Pax-6 in the ventral neural tube respecifies a population of Nkx-2.2-expressing neurons by repressing expression of the transcriptional regulator (21). Loss of functional Pax-3 and Pax-7 genes results in one population of neurons inappropriately expressing the transcriptional regulator En-1 and the respecification of some ventral commisure neurons to other fates (22). Ectopic expression of Pax-3 in the ventral neural tube prevents the formation of the floorplate (23).

Pax-2 and Pax-5 are required for the maintenance of the isthmic organizer, which forms the boundary between the midbrain and hindbrain. This structure is required for the development of the inferior colliculus and the cerebellum (reviewed in (24)). Development of regions of the optic tectum and cerebellum were hypoplasic in both Pax-2 (25, 26) and Pax-5 null (27) mutant homozygous mouse embryos. These results suggested that Pax-2 and Pax-5 had similar, but not redundant, functions in the maintenance of the isthmic organizer. Generation of Pax-2/Pax-5 double null mutant homozygotes led to the complete absence of isthmic organizer, colliculus and cerebellum (26, 28, 29) and the extension of tissues adjoining these missing structures into the consequent space.

Pax proteins have an instructive role in the establishment of the boundary between the developing optic nerve tract and the retina. Both these structures form from the optic vesicle. The more medial portion, the optic stalk, is the optic nerve tract anlage and the more lateral, the optic cup, forms the retina. The developing optic nerve tract is characterized by expression of Pax-2 (25, 30). Absence of functional Pax-2, results in the extension of Pax-6 expression into the more medial portion of the optic vesicle and ultimately the generation of retinal epithelial cells (25, 30, 31). When functional Pax-6 is missing, the Pax-2 expression domain is shifted into the lateral optic vesicle (30). Furthermore, binding of Pax-6 protein to the Pax-2 promoter represses transactivation and binding of Pax-2 protein to Pax-6 promoter also represses transactivation (30).

In the forebrain, Pax-6 has been shown to establish the correct boundaries between the structures in the forebrain and between the forebrain and midbrain. In Pax-6 null mutant homozygotes, the caudal forebrain develops markers characteristic of the midbrain (32-34). The dorso-anterior aspect of the forebrain, the telencephalon, develops into the cerebral cortex and the striatum. Lack of functional Pax-6 leads to alterations in its boundary with the thalamus (35), defects in the developing cortical-striatal boundary (36, 37) and altered radial glia differentiation (38). The telencephalon phenotype is, in part, a function of modulation of the levels of the extracellular matrix proteins R-cadherin and tenascin (36) resulting in the loss of a well demarcated boundary with neighboring tissues.

2.3. Pax Genes Regulate Migration of Neural Crest Cells

The neural crest lays a crucial role in vertebrate development. Structures derived from neural crest cells include many peripheral neurons, including those in the spinal ganglia (dorsal root, sensory and autonomic), some of the bones of the skull, elements of the inner ear, cardiovascular structures and melanocytes (the pigmented cells) (reviewed in (39)). Neural crest cells migrate from the dorsal region of the neural tube and brain vesicles just after the fusion of their neural folds. This migratory process is influenced by three Pax proteins: Pax-3, Pax-6 and Pax-7. The migration of neural crest cells is blocked at thoracic and lumbar levels in homozygous splotch Pax-3 null mutant embryos and is severely impaired in cervical regions (40-42). This results in small or absent spinal ganglia, deficient ensheathing of peripheral nerves and the absence of melanocytes (43). Lack of neural crest migration into cardiac tissue results in the failure of the separation of the aorta and the pulmonary artery into two separate blood vessels (44, 45). Pax-7 and Pax-6 play similar roles to Pax-3 in the generation of more anterior neural crest-derived craniofacial structures. The maxillary process and nasal capsule are missing in Pax-7 null homozygotes (46) and Pax-6 null allele homozygotes lack lateral nasal processes (47).

2.4. Pax-1 and Pax-9 and Vertebral Body Formation

The vertebral column is derived from the sclerotome compartment of somites (48). Pax-1 and Pax-9 are expressed in the sclerotomes of the differentiated somites (1, 49), as a result of sonic hedgehog protein signaling from the notochord and the neural tube (50). Some Pax-1 expressing cells then migrate ventromedially to surround the notochord and differentiate to form the vertebral bodies and intervertebral discs (1, 49). The cells fated to form the vertebral bodies condense to form cartilage in a process known as chondrogenesis as evidenced by Sox-9 and collagen II expression (51). It is the fate of this cell population that Pax-1 and Pax-9 regulate. Mouse embryos homozygous for the natural null Pax-1 mutation undulated (52, 53) and the targeted Pax-1 null allele (54) exhibit vertebral body hypoplasia and fusions due to inhibited chondrogenesis and agenesis of the intervertebral discs. Hypoplasia is particularly pronounced in the posterior portion of each vertebra, and heterozygotes for Pax-1 null alleles have hypoplasic cervical and lumbar vertebrae (54). When embryos are homozygous for targeted null alleles of both Pax-1 and Pax-9, chondrogenesis does not occur because decreased proliferation and increased apoptosis leads to the disappearance of the vertebral body fated cell population (51). However, homozygotes for the Pax-9 targeted null allele have a normal vertebral column (55). These studies show that Pax-1 and Pax-9 have partially redundant roles in the vertebral bodies, but that Pax-1 acts uniquely in intervertebral disc formation and in normal chondrogenesis of the posterior of each vertebra.

2.5. Pax-3 Requirement for the Migration of Limb Muscle Precursor Cells

The skeletal muscles of the trunk and limbs are derived from the dermomyotome of the somatic mesoderm (reviewed in (48)). The myotome, which develops from the dermomyotome, forms the muscles of the back and ribcage. Precursors of limb muscle migrate from the leading lateral edge of the dermomyotome into the developing limb bud and coalesce into dorsal and ventral premuscle masses. These premuscle masses then form mature musculature. Both Pax-3 (56, 57) and Pax-7 (18, 46) are expressed in the dermomyotome with Pax-3 expressed more strongly in the lateral portion and Pax-7 in the medial portion. Loss of functional Pax-3 results in the failure of limb muscle precursors to make the transition from epithelium to mesenchyme and migrate into the limb (58, 59). This failure in migration is due in part because Pax-3 transactivation is required for the expression of the SF/HGF receptor c-met (60-62). SF/HGF protein is expressed in the limb buds and limb muscle precursor cells do not migrate in embryos homozygous for the null allele for c-met (63). Additionally, apoptotic cells are seen in the somites of mice homozygous for the Pax-3 null allele splotch at the developmental stages that limb muscle precursors emigrate from the somite (64).

2.6. Pax-4 and Pax-6 Mediate Endocrine Cell Specification in the Pancreas

The endocrine cell populations of the pancreas are found in the Islets of Langerhans (reviewed in (65)). The a, b, d and PP cell lineages synthesize glucagon, insulin, somatostatin and pancreatic polypetide, respectively. Pax-4 is expressed in the b (insulin-producing) and d (somatostatin-producing) cells (66), and Pax-6 is expressed in all four lineages (67). Inactivation of both copies of the Pax-4 gene resulted in the failure of insulin- and somatostatin-producing cell populations to differentiate and resulted in increased numbers of glucagons-producing cells (66). The latter finding is consistent with the discovery that Pax-4 protein binding to the enhancer of the glucagon gene represses transcription (68). Pax-6 homozygous null mutants lack glucagon-expressing cells and fail to form islets of Langerhans (67, 69). Moreover, Pax-6 protein transactivates the glucagon and insulin promoters and also binds to the somatostatin promoter (69). In embryos lacking both functional Pax-4 and Pax-6 genes, endocrine pancreatic cells fail to develop altogether (67). Hence the actions of Pax-4 and Pax-6 are required to generate the full complement of endocrine pancreas cell types from a single endocrine pancreatic progenitor population.

2.7. Pax-2 is Required for Mesenchymal-to-Epithelial Transitions in the Urogenital System

The development of the definitive kidney commences when a mesenchymal structure, known as the metanephric mesenchyme, induces the ureter to bud out from the caudal Wolffian duct (reviewed in (70)). Contact by the ureter induces the metanephric mesenchyme to differentiate into the glomerulae which are the proximal and distal tubular epithelial structures seen in the nephrons of the kidney. The metanephric mesenchyme expresses Pax-2 (71, 72). Pax-2 is necessary to allow the metanephric mesenchyme to undergo mesenchymal-to-epithelial transitions since mice that are homozygous for either the targeted Pax-2 null mutation (73) or the natural KrD mutation (31). Moreover, genital structures of epithelial morphology such as the vas deferens and seminal vesicles in the male and the uterus and vagina in the female are also missing in mice homozygous for these mutations. Pax-2's role in kidney formation is dosage dependent, kidneys in heterozygous mice are hypoplasic.

2.8. Pax-5 and the B-Cell Lineage

The B-cell lineage is one of the two cell types that mediate the immune response. Pax-5 is expressed in B cells until terminal differentiation (74) (reviewed in (75)). In Pax-5 null allele homozygotes, differentiation is arrested at a very early stage prior to the initiation of expression of the early marker, CD19 (27). In fact, the CD19 gene's promoter contains Pax-5 binding sites (76). However, the Pax-5 (-/-) pre B cells can populate the thymus when injected into Rag-2 (-/-) mutants (77), and can be diverted to other fates in vitro (78). Pax-5 is thus required for the generation and maintenance of an immature B-cell population. The finding that Pax-5 represses expression from the Immunoglobulin Heavy Chain gene (IgH) enhancer (79) suggests that downregulation of Pax-5 expression may be an important part of terminal differentiation.

2.9. Roles of Pax Proteins in Other Tissues

Pax genes have been found, from developmental defects observed in null-mutant homozygote embryos, to participate in the regulation of other developmental processes that are less studied. Nevertheless, the roles Pax genes play here are similar to the others described above.

Pax-1 and Pax-9 are required for full development of tissues derived from the third and fourth pair of pharyngeal pouches such as the thymus, parathyroid gland and the ultimobranchial bodies. These structures are completely missing from Pax-9 null allele homozygotes (55) and mice with no functional Pax-1 have a reduced thymus with 50 to 80% fewer T-cells (80).

Pax-9 plays a crucial role in the generation of teeth at the tooth germ stage. It is expressed at discrete sites in the mesenchyme along the developing mandible due to inductive signaling by FGF-8 and antagonistic signaling by BMP-2 and -4 (81). Only Pax-9 expressing portions of the mesenchyme can initiate tooth formation (81) in an in vitro assay; its absence in Pax-9 null mutant homozygotes prevents further development of tooth primordia (55).

The thyroid gland is formed from two cell populations: endodermal cells that express Pax-8 and pharyngeal-derived mesenchymal cells that form the parathyroid (82). Ablation of functional Pax-8 prevents the endodermal cells participating in thyroid development resulting in thyroid agenesis (83). Moreover, Pax-8 protein can transactivate the promoters of thyroglobulin and thyroperoxidase (84).

The olfactory bulbs differentiate from the nasal placode, which is induced in a Pax-6 dependent process. These structures are missing in Pax-6 null allele homozygotes (79, 47).

Finally, satellite cells are missing in the muscle tissue of Pax-7 null mutant homozygotes (85). However, the muscle stem cell population is unaffected.

3. Pax Genes and Human Disease

3.1. Human Syndromes Resulting from Mutation of Pax Genes

PAX gene mutations have been implicated in a number of syndromes over the last decade. The symptoms of these conditions are broadly consistent with the observations in heterozygous null mutant mice.

Two syndromes are known to result from mutations at the Pax-6 locus: Aniridia and Peter's anomaly. Aniridia is a syndrome in which the iris fails to develop fully (86-88). This is consistent with the iris malformations in heterozygous Sey mice (7, 8). Significantly, the posterior layer of the iris is derived from the optic cup, which expresses Pax-6. Peter's anomaly is a defect in the formation of the cornea that renders it opaque (89). The cornea develops from ectodermal tissue that expresses Pax-6 and forms over the lens after its formation.

The symptoms of Waardenburg's Syndrome 1 are pigmentation defects and hearing loss, which occurs as a result of PAX-3 mutation (90, 91). These defects occur as a result of the impaired migration or differentiation of neural crest cells, which give rise to structures of the inner ear and to the melanocytes. Sufferers of this syndrome are deaf, however mice heterozygous for the Splotch null mutation of Pax-3 are not (91).

In humans, disruption of PAX-2 function leads to optic nerve colobomass, renal hypoplasia and vesicouretal reflux (92, 93). This syndrome is consistent with the optic nerve and kidney phenotypes in mice heterozygous for the targeted Pax-2 null mutation (73).

3.2. Pax Genes and Cancer

Transcription factors that are inappropriately expressed or mutated play a significant role in tumorigenesis. Some studies have identified PAX genes as tumor promoters in certain cancers. The potential for PAX genes to promote neoplasia was shown in a study where Pax-1, -2, -3 and -6 transformed 3T3 cells could form tumors when injected subcutaneously into nude mice (94). Moreover, the cells transformed in focus assays.

Chromosome translocations leading to fused genes that contain some PAX sequences is one way by which PAX genes may promote tumorigenesis. Rhabdomyosarcomas are soft-tissue tumors with a muscle morphology found in the young. Characteristic of this sarcoma is a translocation from chromosome 13 to the PAX-3 locus in chromosome 2 GALILI (95). This results in a fusion of sequences of a forkhead-class gene to the homeobox of PAX-3, which expresses a chimeric protein that can transactivate gene expression at PAX-3 binding sites in their enhancers (96) (97)s. More recently a PAX-7 to forkhead translocation was isolated from a rhabdomyosarcoma (98). The effect of a translocation like this may put expression of the chimeric gene under a different, looser regulation. Alternatively, the resultant fusion proteins may simply have better transactivator potential than their parent proteins. A recent study found that the PAX-3/forkhead fusion protein was unresponsive to the PAX-3 repressor protein, hDaxx (99).

In other cases, the genetic lesion does not change the coding sequences of the PAX gene but only the promoter-enhancer region. An example of this is the translocation of the Em enhancer of the IgH gene to the PAX-5 locus in diffuse large-cell lymphomas (100). PAX-5 has been shown to directly repress the transcription of p53 (101) whose protein is crucial for initiation of apoptosis and cell cycle control. Another is the elevated PAX-2 and PAX-8 expression in Wilm's tumor (102-104).

4. Conclusion

Over the last twelve years, the Pax genes have been identified, their patterns of expression characterized, and many of their functions analyzed. Functional analyses have been helped by the fortuitous discovery of natural Pax rodent and zebrafish mutants, which complemented the targeted mutational studies. All Pax genes display restricted patterns of expression in both neural and nonneural structures. Some Pax genes have similar functional roles in the development of certain tissues. The best example of this is Pax-2 and Pax-5 in the morphogenesis of the midbrain-hindbrain boundary. Pax protein functions in some morphogenetic processes are sensitive to gene dosage, and the malformations seen in heterozygous mouse mutants and in the corresponding human syndromes resulting from mutation of the cognate PAX gene are strikingly similar. Thus haploinsufficiency is a conserved feature of Pax function in different species.

Pax proteins play important roles in certain morphogenetic processes. One of these is in conferring competence to respond to inductive influences. Examples include the competence of ectodermal tissue to be induced to form lens or nasal placode tissue, metanephric mesenchyme to form kidney epithelial structures, and the competence of dermomyotome cells to form a migratory myogenic cell type. Pax proteins also function in cell specification, examples being the B cells, pancreatic endocrine cells, the neural e developing crest, and certain neuronal cell types. In these cases, Pax proteins also help to mediate the survival of these cell types, since null mutations of Pax genes also lead to the disappearance of the cell types.

Studies in coming years will identify more structures whose genesis requires the actions of Pax genes particularly in the developing brain. Studies will also focus on Pax protein interactions with other nuclear proteins in forming transcriptional complexes, which is poorly characterized at present. Yet other studies will investigate the control of the expression of Pax genes.

Bibliography

1. U. Deutsch, G.R Dressler, and P. Gruss, Cell 53, 617–625 (1988).
2. C. Walther et al., Genomics 11, 424–434 (1991).
3. G. Chalepakis et al., Cell 66, 873–884 (1991).
4. K.J Vogan, D.J Epstein, D.G. Trasler, and P. Gros, Genomics 17, 364–369 (1993).
5. A. Schedl et al., Cell 86, 71–82 (1996).
6. D. Jean, K. Ewan, and P. Gruss, Mech. Dev. 76, 3–18 (1998).
7. B.L Hogan et al., J. Embryol Exp. Morphol. 97, 95–110 (1986).
8. B.L Hogan, E.M Hirst, G. Horsburgh, and C.M. Hetherington, Development 103, 115–119 (1988).
9. R.E Hill et al., Nature 354, 522–525 (1991).
10. T. Matsuo et al., Nat. Genet. 3, 299–304 (1993).
11. C. Walther and P Gruss, Development 113, 1435–1449 (1991).
12. H.S Li et al., Dev. Biol. 162, 181–194 (1994).
13. M. Fujiwara, T. Uchida, N. Osumi-Yamashita, and K Eto, Differentiation 57, 31–38 (1994).
14. R. Ashery-Padan, T. Marquardt, X. Zhou, and P. Gruss, Genes Dev. 14, 2701–2711 (2000).
15. T. Marquardt et al., Cell 105, 43–55 (2001).
16. J. Ericson et al., Cell 90, 169–180 (1997).
17. M.D Goulding et al., Embo J. 10, 1135–1147 (1991).
18. B. Jostes, C. Walther, and P. Gruss, Mech. Dev. 33, 27–37 (1990).
19. T.M. Jessell, Nat. Rev. Genet. 1, 20–29 (2000).
20. N. Osumi et al., Development 124, 2961–2972 (1997).
21. J. Briscoe, A. Pierani, T.M Jessell, and J. Ericson, Cell 101, 435–445 (2000).
22. A. Mansouri and P. Gruss, Mech. Dev. 78, 171–178 (1998).
23. P. Tremblay, F. Pituello, and P. Gruss, Development 122, 2555–2567 (1996).
24. H Nakamura, Trends Neurosci. 24, 32–39 (2001).
25. M. Torres, E. Gomez-Pardo, and P. Gruss, Development 122, 3381–3391 (1996).
26. M. Schwarz et al., Proc. Natl. Acad. Sci. U.S.A. 94, 14518–14523 (1997).
27. P. Urbanek et al., Cell 79, 901–912 (1994).
28. P. Urbanek, I. Fetka, M.H Meisler, and M. Busslinger, Proc. Natl. Acad. Sci. U.S.A. 94, 5703–5708 (1997).
29. M. Schwarz et al., Mech. Dev. 82, 29–39 (1999).
30. M. Schwarz et al., Development 127, 4325–4334 (2000).
31. S.A. Keller et al., Genomics 23, 309–320 (1994).
32. J.C. Grindley et al., Mech. Dev. 64, 111–126 (1997).
33. G.S. Mastick, N.M. Davis, G.L. Andrew, and S.S. Easter, Development 124, 1985–1997 (1997).
34. N. Warren and D.J. Price, Development 124, 1573–1582 (1997).
35. A. Stoykova, R. Fritsch, C. Walther, and P. Gruss, Development 122, 3453–3465 (1996).
36. A. Stoykova, M. Gotz, P. Gruss, and J. Price, Development 124, 3765–3777 (1997).
37. A. Stoykova, D. Treichel, M. Hallonet, and P Gruss, J. Neurosci. 20, 8042–8050 (2000).
38. M. Gotz, A. Stoykova, and P Gruss, Neuron 21, 1031–1044 (1998).
39. C. LaBonne and M. Bronner-Fraser, Annu. Rev. Cell Dev. Biol. 15, 81–112 (1999).
40. T. Franz and R. Kothary, Brain Res. Dev. Brain Res. 72, 99–105 (1993).
41. T. Franz, Anat. Embryol. (Berlin) 187, 371–377 (1993).
42. G.N. Serbedzija and A.P. McMahon, Dev. Biol. 185, 139–147 (1997).

43. T. Franz, Acta Anat. (Basel) 138, 246–253 (1990).
44. T. Franz, Anat. Embryol. (Berlin) 180, 457–464 (1989).
45. S.J. Conway, D.J. Henderson, and A.J. Copp, Development 124, 505–514 (1997).
46. A. Mansouri, A. Stoykova, M. Torres, and P. Gruss, Development 122, 831–838 (1996).
47. J.C. Grindley, D.R Davidson, and R.E. Hill, Development 121, 1433–1442 (1995).
48. B. Brand-Saberi and B. Christ, Curr. Top. Dev. Biol. 48, 1–42 (2000).
49. C. Ebensperger et al., Anat. Embryol. (Berl) 191, 297–310 (1995).
50. A.G Borycki, L. Mendham, and C.P. Emerson, Development 125, 777–790 (1998).
51. H. Peters et al., Development 126, 5399–5408 (1999).
52. R. Balling, U. Deutsch, and P. Gruss, Cell 55, 531–535 (1988).
53. J. Wallin et al., Development 120, 1109–1121 (1994).
54. B. Wilm et al., Proc. Natl. Acad. Sci. U.S.A. 95, 8692–8697 (1998).
55. H. Peters, A. Neubuser, K. Kratochwil, and R. Balling, Genes Dev. 12, 2735–2747 (1998).
56. B.A. Williams and C.P. Ordahl, Development 120, 785–796 (1994).
57. M.D. Goulding, A. Lumsden, and P. Gruss, Development 117, 1001–1016 (1993).
58. E. Bober et al., Development 120, 603–612 (1994).
59. M. Goulding, A. Lumsden, and A.J. Paquette, Development 120, 957–971 (1994).
60. J.A Epstein et al., Proc. Natl. Acad. Sci. U.S.A. 93, 4213–4218 (1996).
61. G. Daston, E. Lamar, M. Olivier, and M. Goulding, Development 122, 1017–1027 (1996).
62. X.M Yang, K. Vogan, P. Gros, and M. Park, Development 122, 2163–2171 (1996).
63. F. Bladt et al., Nature 376, 768–771 (1995).
64. A.G. Borycki et al., Development 126, 1665–1674 (1999).
65. H. Edlund, Diabetes 50, S5–9 2001).
66. B. Sosa-Pineda et al., Nature 386, 399–402 (1997).
67. L. St-Onge et al., Nature 387, 406–409 (1997).
68. S.B. Smith, H.C. Ee, J.R. Conners, and M.S. German, Mol. Cell Biol. 19, 8272–8280 (1999).
69. M. Sander et al., Genes Dev. 11, 1662–1673 (1997).
70. M. Horster et al., Pflugers Arch. 434, 647–660 (1997).
71. G.R Dressler et al., Development 109, 787–795 (1990).
72. H.O. Nornes et al., Development 109, 797–809 (1990).
73. M. Torres, E. Gomez-Pardo, G.R. Dressler, and P. Gruss, Development 121, 4057–4065 (1995).
74. B. Adams et al., Genes Dev. 6, 1589–1607 (1992).
75. S.L. Nutt, A.G. Rolink, and M. Busslinger, Cold Spring Harb. Symp. Quant. Biol. 64, 51–59 (1999).
76. Z. Kozmik et al., Mol. Cell Biol. 12, 2662–2672 (1992).
77. A.G. Rolink, S.L. Nutt, F. Melchers, and M. Busslinger, Nature 401, 603–606 (1999).
78. S.L Nutt, B. Heavey, A.G. Rolink, and M. Busslinger, Nature 401, 556–562 (1999).
79. M. Singh and B.K Birshtein, Mol. Cell Biol. 13, 3611–3622 (1993).
80. J. Wallin et al., Development 122, 23–30 (1996).
81. A. Neubuser, H. Peters, R. Balling, and G.R Martin, Cell 90, 247–255 (1997).
82. D. Plachov et al., Development 110, 643–651 (1990).
83. A. Mansouri, K. Chowdhury, and P. Gruss, Nat. Genet. 19, 87–90 (1998).
84. M. Zannini, H. Francis-Lang, D. Plachov, and R. Di Lauro, Mol. Cell Biol. 12, 4230–4241 (1992).

85. P. Seale et al., Cell 102, 777–786 (2000).
86. C.C Ton et al., Cell 67, 1059–1074 (1991).
87. T. Glaser, D.S Walton, and R.L Maas, Nat. Genet. 2, 232–239 (1992).
88. T. Jordan et al., Nat. Genet. 1, 328–332 (1992).
89. I.M Hanson et al., Nat. Genet. 6, 168–173 (1994).
90. M. Tassabehji et al., Nature 355, 635–636 (1992).
91. K.P. Steel and R.J. Smith, Nat. Genet. 2, 75–79 (1992).
92. P. Sanyanusin et al., Nat. Genet. 9, 358–364 (1995).
93. L.A. Schimmenti et al., Am. J. Med. Genet. 59, 204–208 (1995).
94. C.C. Maulbecker and P Gruss, EMBO J. 12, 2361–2367 (1993).
95. D.N. Shapiro et al., Cancer Res. 53, 5108–5112 (1993).
96. W.J. Fredericks et al., Mol. Cell Biol. 15, 1522–1535 (1995).
97. J.E. Sublett, I.S. Jeon, and D.N. Shapiro, Oncogene 11, 545–552 (1995).
98. R.J. Davis and F.G. Barr, Proc. Natl. Acad. Sci. U.S.A. 94, 8047–8051 (1997).
99. A.D. Hollenbach, J.E. Sublett, C.J. McPherson, and G. Grosveld, EMBO J. 18, 3702–3711 (1999).
100. M. Busslinger et al., Proc. Natl. Acad. Sci. U.S.A. 93, 6129–6134 (1996).
101. E.T. Stuart, R. Haffner, M. Oren, and P. Gruss, EMBO J. 14, 5638–5645 (1995).
102. G.R. Dressler and E.C. Douglass, Proc. Natl. Acad. Sci. U.S.A. 89, 1179–1183 (1992).
103. M.R. Eccles et al., Cell Growth Differ. 3, 279–289 (1992).
104. A. Poleev et al., Development 116, 611–623 (1992).
105. D.L. Song, G. Chalepakis, P. Gruss, and A.L Joyner, Development 122, 627–635 (1996).
106. A. Cvekl and J. Piatigorsky, Bioessays 18, 621–630 (1996).
107. B.D. Holst, Y. Wang, F.S. Jones, and M.G. Edelman, Proc. Natl. Acad. Sci. U.S.A. 94, 1465–1470 (1997).
108. H. Koseki et al., Development 119, 649–660 (1993).
109. T. Franz et al., Anat. Embryol. (Berl) 187, 153–160 (1993).
110. M. Goulding et al., Genomics 17, 355–363 (1993).

Pedigree

A pedigree is a family tree, a graphical presentation of biological descent (Fig. 1). Each generation is represented in a separate row. Males are presented by squares and females are represented by circles; alternative respective symbols are ♂, representing the shield and spear of Mars, and ♀, the mirror of Venus. Horizontal lines join parents and sets of sibs; vertical lines indicate descent. Sibs are ordered according to birth from left to right. Double horizontal lines call attention to parents that are closely related (inbreeding); sometimes they are used to join monozygotic twins as well. Filled, colored, or shaded symbols indicate affected individuals in pedigrees that represent the inheritance of certain traits; partly modified symbols indicate unaffected heterozygous carriers. Several sibs can be pooled together by indicating their number within a single symbol. A pedigree may be described in words, but this is usually impractical.

Figure 1. Conventional symbols used in the representation of pedigrees.

In the analysis of pedigrees, attention must be given to inconstant phenotypes due to effects of the environment or the rest of the genotype of the affected individuals on the expression of the allele. Some alleles are unstable and change from one generation to the next (see Trinucleotide Repeats). Because of the small size of human families, linkage has to be deduced from the pooled results of many groups of sibs (see Lod scores).

PEG (Polyethylene Glycol)

PEG is a polyether polymer commonly used to induce the precipitation or crystallization of macromolecules and viruses. In spite of its name, polyethylene glycol, it has hydroxyl groups only at each end of the polymeric chain:

Except for these ends, the polymer is essentially nonpolar. The ether oxygen atom is only slightly polar and hydrogen bonds with water just sufficiently to make PEG water-soluble. PEG is produced by the simple polymerization of ethylene oxide,

and is available in different lengths, whose molecular weights vary from 200 to 20,000, depending on the polymerization process. The average number of monomers in each molecule may be estimated by dividing the molecular weight of the polymer by 44, the molecular weight of the monomer.

PEG precipitates proteins because it is a large, water-soluble polymer that is excluded from the surfaces of macromolecules simply because of its large physical size, a phenomenon known as steric exclusion (see Excluded Volume). A large polymer cannot penetrate the interior of a folded protein or other macromolecule, so it is effectively excluded from a shell around the macromolecule. The thickness of the shell is defined by the center of the polymer at its point of closest approach to the macromolecule. The presence of the polymer in effect increases the concentration of the macromolecule because the macromolecule is excluded from the volume of the solution occupied by the polymer. When the solubility limit of the macromolecule is reached, it precipitates or crystallizes.

Water molecules are smaller and penetrate within this shell of solvent around the macromolecule from which PEG is excluded. As a result, a zone enriched in water is formed around the protein molecule. The end result is preferential hydration of the macromolecule and preferential exclusion of the polymer (1). Solely on this basis, PEG would be expected to stabilize the folded conformation of the macromolecule (see Stabilization And Destabilization By Co-Solvents). However, PEG is a relatively nonpolar molecule that interacts favorably with the nonpolar surfaces exposed when a macromolecule unfolds, and the net effect is that PEG destabilizes folded proteins (1, 2).

Bibliography

1. T. Arakawa and S. N. Timasheff (1985) Biochemistry 24, 6756–6762.
2. G. G. Hammes and P. R. Schimmel (1967) J. Am. Chem. Soc. 89, 442–446.

Penicillin

The penicillins are antibacterial agents belonging to the group known as the b-lactam antibiotics. Penicillin was first discovered about 70 years ago by Alexander Fleming as a metabolic by-product of the fungus Penicillium notatum (1). Since then, other fungi have been shown to produce several different structural types of penicillins. All penicillins share a common bicyclic nucleus that is composed of fused b-lactam and thiazolidine rings (Fig. 1). This compound, known as 6-aminopenicillanic acid, is a cyclic peptide formed by the condensation of L-cysteine and D-valine. An important structural feature of the penicillins is the acyl side-chain attached to 6-aminopenicillanic acid (represented by R in Fig. 1). The different members of the penicillin family are distinguished by their acyl side chains, some examples of which are shown in Figure 1b. The derivatives known as penicillin G and penicillin V are natural penicillins, namely, fungal metabolites. The medical application of penicillin in the 1940s highlighted the birth of the antibiotic era, and subsequent misuse of this and other antibiotics has led to the current drug resistance crisis (2) (see Antibiotic Resistance).

Figure 1. (a) The structure of the penicillin nucleus; R represents a hydrogen atom in the case of 6-aminopenicillanic acid. (b) Examples of acyl side chains of natural and semisynthetic pencillins.

Comparative studies indicated that the structure of the acyl side chain significantly influenced the antibacterial spectra and physical properties of penicillin. The development of semisynthetic penicillins was an important event in penicillin development. Nayler (3) has presented a historical account of the discovery of semisynthetic penicillins. Semisynthetic antimicrobial agents are derivatives of a natural product that have been deliberately modified chemically. In the case of the semisynthetic penicillins, the natural product is the penicillin nucleus, 6-aminopenicillanic acid. The discovery of methods to produce large amounts of 6-aminopenicillanic acid in the late 1950s was the pivotal event that led to the development of semisynthetic penicillins. The subsequent synthetic chemical acylation of 6-aminopenicillanic acid gave rise to numerous new penicillins with novel properties, and this approach was essential to keep up with the growing demands to solve problems faced by medical applications. For example (see Fig. 1), this technology gave rise to agents that exhibited broad-spectrum antibacterial activity (eg, ampicillin and carbenicillin), agents that could be administered orally (eg, ampicillin), and agents that were resistant to the action of b-lactamase (eg, methicillin).

Penicillin inhibits the synthesis of the bacterial cell wall polymer known as peptidoglycan or murein. This topic has been reviewed recently by Höltje (4, 5). Peptidoglycan is a single large macromolecule that completely envelopes bacterial cells. It represents an exoskeleton that supports the underlying cytoplasmic membrane. In this regard, it serves an absolutely essential function in preventing osmotic lysis of the bacterial cells. The actual targets of penicillin are membrane-bound enzymes, known as penicillin-binding proteins (PBPs), that catalyze the transpeptidation reaction in the final stage of peptidoglycan polymerization. Transpeptidation creates crosslinkages between adjacent peptide chains in the peptidoglycan polymer. The amide group in the b-lactam ring of penicillin represents a structural analogue of the D-alanyl-D-alanine peptide bond involved in the transpeptidation reaction. Penicillin is a suicide substrate for PBPs, and the interaction of penicillin with its PBP target results in the formation of a stable penicilloylated enzyme derivative. For details of the mechanism of action of penicillin, see Penicillin-Binding Proteins (see Fig. 1 of that article).

Penicillin is bactericidal. The lethal effect of penicillin treatment is normally associated with bacterial cell lysis (4, 5). This lysis is catalyzed by one or more bacterial enzymes known as peptidoglycan hydrolases. These enzymes cleave chemical bonds in peptidoglycan. Their normal physiological functions are poorly understood. It is believed that the activities of at least some of these hydrolases create openings in the completely closed peptidoglycan molecule, to permit the insertion of new subunits during the growth of bacterial cells. The terminal stage of peptidoglycan synthesis is consequently proposed to be a coordinated process catalyzed by two classes of enzymes: the PBPs and the peptidoglycan hydrolases. These enzymes are further proposed to form a multienzyme complex. Therefore, bacteria are killed by penicillin in a two-step process. In the first step, penicillin inhibits activities of the PBPs involved in peptidoglycan polymerization. In the second step, the peptidoglycan hydrolases become uncoupled from the peptidoglycan biosynthetic process and cause lysis of the bacteria.

It has long been recognized that penicillin kills only actively growing bacteria (6). More recent studies have confirmed that the bactericidal effect of penicillin is directly dependent on the bacterial growth rate (7). The first application of penicillin in genetics was based on this concept. Lederberg and Zinder (8) and Davis (9) independently developed a technique, known as penicillin selection, for the isolation of auxotrophic mutants of *Escherichia coli*. The procedure involves inoculating a sample of *E. coli* containing rare auxotrophic mutants into a minimal medium lacking the nutritional factor(s) required by the mutants. Only the wild-type cells in the population are capable of growing in this medium, and the majority of these are subsequently killed by the addition of a lethal dose of penicillin. The auxotrophic mutants are tolerant to penicillin and are readily recovered by screening the survivors of the penicillin treatment.

The basis for the pencillin tolerance of amino acid–deprived cells has been investigated. Amino acid deprivation of *E. coli* results in the coordinate inhibition of a variety of metabolic activities in a phenomenon that has been called the "stringent response" (10) (see Stringent Control). The stringent response is probably a strategy to restrict energy consumption in an effort to promote the survival of bacteria during periods of starvation. Amino acid–deprived *E. coli* accumulate a novel nucleotide, guanosine 3′,5′-bispyrophosphate (ppGpp), which is believed to mediate the stringent response. Membrane phospholipid synthesis, cell wall peptidoglycan synthesis, and penicillin-induced lysis are among the many metabolic activities that are inhibited during the stringent response (11, 12). Moreover, the activities of the membrane peptidoglycan polymerases and peptidoglycan hydrolases have been shown to be dependent on ongoing phospholipid synthesis. Therefore, the inhibition of phospholipid synthesis by ppGpp results in the inhibition of the membrane-associated reactions in peptidoglycan metabolism and is the direct cause of the penicillin tolerance of starved *E. coli*.

The concept of penicillin selection can be applied more broadly. It can be used in any situation where it is possible to design culture conditions that do not permit the growth of the cells to be selected. For example, penicillin selection can be used to select cells that have been spontaneously cured of transposon insertions. Therefore, cured cells can be selected from a population of cells that carry the transposon Tn5 (which encodes kanamycin resistance) by growing the culture in a medium containing both kanamycin and ampicillin. The ampicillin will kill only those cells that carry Tn5, and cured cells can be isolated by screening the surviving population.

Genetic elements encoding b-lactamases (see Penicillin-Binding Proteins) are currently widely employed as selective markers in molecular biological applications. Consequently, penicillin derivatives, especially ampicillin, are among the most common chemicals encountered in a molecular biology laboratory. Penicillin selection is attractive because these antibiotics are relatively inexpensive and are highly effective because of their bactericidal action. In medical applications, penicillin derivatives are considered to be of low toxicity. They are allergenic, however, and the development of either immediate or delayed hypersensitivities are the most frequent and serious problems associated with penicillin therapy. It is notable that anaphylaxis to penicillin has been reported after nontherapeutic exposure (13). It is therefore conceivable that exposure to penicillin in the laboratory could result in hypersensitive reactions in sensitized individuals, and those who are known to be allergic to penicillin should be alerted to this possibility.

Bibliography

1. A. Fleming (1929) Br. J. Exp. Pathol. 10, 226–236.
2. S. B. Levy (1992) The Antibiotic Paradox. How Miracle Drugs are Destroying the Miracle, Plenum Press, New York.
3. J. H. C. Nayler (1991) in 50 Years of Penicillin Application. History and Trends, H. Kleinkauf and H. von Döhren, eds., Public Ltd., Czech Republic, pp. 64–74.
4. J.-V. Höltje (1995) Arch. Microbiol. 164, 243–254.
5. J.-V. Höltje (1996) Microbiology 142, 1911–1918.
6. G. L. Hobby, K. Meyer, and E. Chaffee (1942) Proc. Soc. Exp. Biol. Med. 50, 281.
7. E. Tuomanen, R. Cozens, W. Tosch, O. Zak, and A. Tomasz (1986) J. Gen. Microbiol. 132, 1297–1304.
8. J. Lederberg and N. Zinder (1948) J. Am. Chem Soc. 70, 467–468.
9. B. D. Davis (1949) Proc. Natl. Acad. Sci. USA 35, 1–10.
10. M. Cashel, D. R. Gentry, V. J. Hernandez, and K. E. Rudd (1996) in Escherichia coli and Salmonella typhimurium. Cellular and Molecular Biology, F. C. Neidhardt, R. Curtiss III, J. L. Ingraham, E. C. C. Lin, K. B. Low, B. Magasanik, W. S. Reznikoff, M. Riley, M. Schaechter, and H. E. Umbarger, eds., ASM Press, Washington, DC, pp. 1458–1496.
11. D. G. Rodionov, A. G. Pisabarro, M. A. De Pedro, W. Kusser, and E. E. Ishiguro (1995) J. Bacteriol. 177, 992–997.
12. D. G. Rodionov and E. E. Ishiguro (1995) J. Bacteriol. 177, 4224–4229.
13. M. Blanca, J, Garcia, J. M. Vega, A. Miranda, M. J. Carmona, C. Mayorga, F. Moreno, and C. Juarez (1996) Clin. Exp. Allergy 26, 335–340.

Suggestions for Further Reading

14. J.-V. Höltje. (1998) Growth of the stress-bearing and shape-maintaining murein sacculus of Escherichia coli, Microbiol. Mol. Biol. Rev. 62, 181–203.
15. J. M. Ghuysen (1991) Serine-lactamases and penicillin-binding proteins, Annu. Rev. Microbiol. 45, 37–67.

Penicillin-Binding Proteins

The concept of antibiosis originated with Ehrlich and the sulfa drugs. It was firmly established by Fleming, Florey, and Chain, who discovered the use of penicillin. The chemical structure of penicillin has some remarkable features: its β-lactam amide bond is equivalent to a peptide bond extending between two carbon atoms that have the D configuration (see Stereochemistry), in the a position to a free carboxyl group . Penicillin kills bacteria because it inactivates specialized acyl serine transferases that are involved in the assembly and metabolism of the cell-wall peptidoglycan. It immobilizes the catalytic center in the form of a stable serine ester-linked penicilloyl enzyme derivative (Fig. 1). Variants of penicillin, such as ampicillin, also exist.

Figure 1. The structure of penicillin and its reaction with the active-site serine residue of acyl-serine transferases. The re
of the reaction is shown at left, and the resulting penicilloyl enzyme is shown at right. If the penicilloyl enzyme is stable,
enzyme is a penicillin-binding protein. Alternatively, if the penicilloyl enzyme is hydrolyzed rapidly, the enzyme is a b-

The bacterial cell-wall peptidoglycan is a covalently closed, net-like polymer (1). Linear glycan strands are made up of alternating b-1,4-linked units of N-acetylglucosamine and N-acetylmuramic acid. The carboxyl groups of the N-acetylmuramic acid residues are amide linked to the amino terminal L-alanine residues of peptide units L-alanyl-g-D-glutamyl-L-diaminoacyl-D-alanine. Neighboring peptide-substituted glycan strands are crosslinked by peptide bridges that extend from the D-alanine at the carboxyl end of one peptide to the side-chain amino group of the diamino acid residue of another peptide. The nature of the diamino acid residue and the composition of the peptide bridge vary according to the bacterial species.

In Escherichia coli, the diamino acid residue is meso-diaminopimelic acid, and the peptide bridges are direct D-alanyl-(D)-meso-diaminopimelic acid bonds. The immediate biosynthetic precursor of the cell-wall peptidoglycan is lipid II (2), in which a disaccharide peptide unit is linked to a $C_{55}H_{89}$ undecaprenyl lipid carrier via a pyrophosphate bridge involving C_1 of N-acetylmuramic acid, and the peptide borne by N-acetylmuramic acid is a pentapeptide that terminates with a D-alanyl-D-alanine sequence. From this precursor, glycosyltransferases catalyze glycan chain elongation by displacement of the pyrophosphate linked to C1 of N-acetylmuramic acid by the 4-hydroxyl group of N-acetylglucosamine. Then acyl serine transferases catalyze peptidoglycan crosslinking at the expense of the D-alanyl-D-alanine bond of the pentapeptide units. This reaction proceeds via formation of a peptidyl (L-alanyl-g-D-glutamyl-L-diaminoacyl-D-alanyl) enzyme intermediate linked as an ester to a serine residue at the active site, with the concomitant release of the carboxy terminal D-alanine residue of the pentapeptide. It is achieved by the transfer of the peptidyl moiety to the side-chain amino group of the diamino acid residue of another peptide. Because the reaction involves breaking a D-alanyl-D-alanine bond, the acyl serine transferases are classified as DD-transpeptidases.

Acyl serine transferases are also involved in the control of the extent of peptidoglycan crosslinking. DD-carboxypeptidases hydrolyze the D-alanyl-D-alanine peptide bonds of pentapeptide units by transferring the peptidyl moiety of the acyl-enzyme intermediate to water. DD-endopeptidases hydrolyze the interpeptide bonds, which in some bacteria extend between two D centers in a position to a free carboxylate, as, for example, the D-alanyl-(D)meso-diaminopimelic acid bonds in the E. coli peptidoglycan.

Penicillin has similarities to the above substrates and is a suicide substrate of the DD-(trans, carboxy, endo)peptidases. These DD-peptidases attack and rupture the b-lactam amide bond of penicillin but produce a serine ester-linked penicilloyl enzyme that is almost completely inert and inactive. The catalytic center turns over very slowly—one time or less per hour—and the inactivated enzymes are detectable as penicillin-binding proteins (PBPs).

In some cases, proteins acquired the ability to catalyze the hydrolysis of the serine ester-linked penicilloyl enzyme, which resulted in a remarkable defensive mechanism by producing enzymes, (the b-lactamases), with the ability to hydrolyze penicillin and other b-lactam antibiotics. On good b-lactam substrates, the catalytic center of these b-lactamases can turn over 1000 times or more per second.

The DD-peptidases and serine b-lactamases form a superfamily of penicilloyl serine transferases (3). They are an exemplary model of molecular evolution. Numerous changes in their amino acid sequences, and gene fusion with the genes for several polypeptides of different origins, resulted in a prolific expansion of groups, classes, and subclasses of these enzymes, with multiple personalities. They share structural motifs. Some have similar enzymatic activity but varying substrate specificities. Others catalyze distinct reactions and fulfill different functions.

1. Protein Structure

The DD-peptidases and b-lactamases presumably diverged from a common ancestor while retaining the same basic protein structure (4). Similarities in their overall amino acid sequences are almost nonexistent, but folding invariably brings three common motifs of the polypeptide chains close to each other in the tertiary structure, forming the catalytic center at the boundary between an all-a domain and an a/b domain, which consists of a five-stranded beta-sheet covered by alpha-helices on both faces. With “x” denoting a variable amino acid residue, motif 1 has the sequence -Ser-x-x-Lys- (where Ser is the active-site serine), is at the amino end of an a-helix, and occupies a central position in the cavity. Motif 2 has the consensus sequence [Ser/Tyr]-x-[Asn/Asp/Cys] and is on a loop between two a-helices on one side of the cavity. Motif 3 has the sequence [Lys/His]-[Thr/Ser]-Gly and is on the innermost strand of the b-sheet on the other side of the cavity. The relative positions of these three motifs are well conserved in the various proteins.

2. Penicillin targets in *Escherichia coli*

E. coli possesses nine PBPs. PBPs 4, 5, 6, and 7 are monofunctional DD-carboxypeptidases that are not essential for viability. PBPs 1a, 1b, 1c, 2, and 3 are multidomain proteins (3) in which a transmembrane spanner is linked to the amino end of a non-penicillin-binding (n-PB) module that is linked to the amino end of an acyl serine transferase, penicillin-binding (PB) module. The two modules comprise a single polypeptide chain that folds on the exterior of the plasma membrane (Fig. 2). There are two classes: A and B (see text below).

Figure 2. Design and membrane topology of multimodular penicillin-binding proteins (PBPs) of class A and class B. Indicated are the five motifs of the n-PB modules of class A PBPs ƒ, the three motifs of the n-PB modules of class B PBPs ○ , and the intermodule junction sites D. For more details on the class-specific motifs, see text. The PB modules bear the characteristic motifs of the penicilloyl serine transferase superfamily. Some PBPs have inserts and N- and C-terminal extensions, which are not shown.

PBP1a and PBP1b of class A (850 and 844 amino acid residues, respectively) combine the transglycosylase (n-PB module) and the DD-transpeptidase (PB module) activities that are required for peptidoglycan assembly. Each catalyzes the conversion of lipid II into polymeric peptidoglycan in in vitro assays (5). Loss of either PBP1a or PBP1b is tolerated, but loss of both is fatal (6). Under these extreme conditions, PBP1c (770 amino acid residues) does not rescue *E. coli* from death.

PBP2 and PBP3 of class B (633 and 588 amino acid residues, respectively) are inert on lipid II (7). They combine in a single polypeptide chain a cell cycle (n-PB) module and an acyl serine transferase (PB) module. Both modules are essential, and loss of neither PBP2 nor PBP3 is tolerated. The genes for PBP2, the DD-carboxypeptidase PBP5, and the integral membrane protein RodA cluster at the 14-min region of the chromosome; these proteins prescribe traits as complex as cell-wall expansion and cell-shape maintenance (8). PBP3, MraW, FtsL, FtsQ, FtsA, the cytoskeletal FtsZ, and FtsW (an analog of RodA)—the encoding genes of which cluster at the 2-min region of the chromosome—prescribe traits as complex as septum formation (9).

3. The Multimodular PBP Family

Sixty-three multimodular PBPs of various bacterial species (10) comprise two classes, A and B, with distinct amino acid sequence signatures in their n-PB modules but conserved motifs in their acyl serine transferase-PB modules. The junction sites between the n-PB and PB modules usually have the carboxy terminal sequence Asp-x-x-x-Gln (Fig. 2). There is a clustering into several subclasses of A and B, corresponding to Gram-negative and Gram-positive bacteria.

Based on these observations, the cores of the n-PB modules (n-PB cores) of the multimodular PBPs start at the amino end of the first motif and terminate at the intermodule junction site. The cores of the associated PB modules (PB cores) start about 70 residues N-terminal of the Ser-x-x-Lys motif—at the carboxy end of the intermodule junction site (where insertions occasionally occur), and they terminate about 70 residues C-terminal of the Lys-[Thr/Ser]-Gly motif; PBPs also have C-terminal extensions. In *E. coli* PBP1b, motif 3 of the PB core has the sequence Lys-Thr-Gly at residues 698–700, residues 762–780 are essential, but residues 781–844 are dispensable (11). (In *Streptococcus pneumoniae* PBP2x (the structure of which is known at low resolution [(12)]), motif 3 of the PB core has the sequence Lys-Ser-Gly at residues 547–549, and residues Ser617–Asp750 form a carboxy terminal module with its own fold.

The multimodular PBPs are fully integrated hybrids. In contrast to the monofunctional PBPs, which are autonomous folding entities, the PB modules of multimodular PBPs have lost the ability to fold by themselves (13-15). They require the assistance of the associated n-PB modules, which implies precise and specific module-module interactions. Correct folding (in terms of penicillin binding) of the associated n-PB and PB modules of *E. coli* PBP3 is independent of the transmembrane spanner (13). In contrast, the cell septation activity of *E. coli* PBP3 is dependent on the membrane-anchor module, indicating that the membrane anchor and its cytosolic tail have more sophisticated functions than that of a simple anchoring device (16).

4. Evolution of Multimodular Class A PBPs

The n-PB cores of the class A PBPs form a continuum of homologous sequences, and they have an extended amino acid sequence signature in the form of five motifs, indicative of conserved transglycosylase activity. In *E. coli* PBP1a, motif 1 starts at residue 86 with the sequence Glu-Asp-Ser-Arg-Phe-x-Glu-His-x-Gly, motif 2 starts at residue 117 with the sequence Gly-Ala-Ser-Thr-Ile-Thr-Gln-Gln, motif 3 starts at residue 139 with the sequence Arg-Lys-x-x-Glu, motif 4 starts at residue 156 with the sequence Lys-x-Glu-Ile-Leu-x-Gly-Tyr-x-Asn, motif 5 starts are residue 221 with the sequence Arg-Arg-x-x-x-Val-Leu-, and Gly284 is at the amino end of the intermodule junction site. Residues Glu86 of motif 1 and Glu143 of motif 3 are almost certainly important components of the transglycosylase catalytic center.

The associated PB cores of the class A PBPs of Gram-negative bacteria cluster into two subclasses: A1 (prototype: *E. coli* PBP1a) and A2 (prototype: *E. coli* PBP1b), which form a supercluster. Those of Gram-positive bacteria cluster into three subclasses: A3 (prototype: *S. pneumoniae* PBP1a), A4 (prototype: *S. pneumoniae* PBP2a), and A5 (prototype: *S. pneumoniae* PBP1b).

Although performing the same transglycosylase-transpeptidase activities, PBPs of subclasses A1 and A2 in Gram-negative bacteria and PBPs of subclasses A3, A4, and A5 in Gram-positive bacteria are almost certainly paralogous. They prescribe distinct, subtle traits in peptidoglycan assembly in these two groups of bacteria that sometimes are difficult to detect.

5. Evolution of Multimodular Class B PBP

The class B PBPs evolved differently than did class A PBPs (10). The n-PB and PB cores underwent adaptive evolution in such a concerted manner that, in Gram-negative bacteria, an n-PB core of subclass B2 (prototype *E. coli* PBP2) or B3 (prototype *E. coli* PBP3) is linked to a PB core of subclass B2 or B3, respectively. In Gram-positive bacteria, an n-PB core of subclass B1 (prototype: *Enterococcus faecium* PBP3), B4 (prototype *S. pneumoniae* PBP2x), or B5 (prototype *S. pneumoniae* PBP2b) is linked to a PB core of subclass B1, B4, and B5, respectively.

This unique combination of the n-PB and PB cores indicates that they have different functions in cell morphogenesis (n-PB module) and peptidoglycan crosslinking (PB-module). The Gram-negative PBPs of subclasses B2 and B3 are paralogous, and the Gram-positive PBPs of subclasses B1, B4, and B5 are also paralogous. In contrast, the Gram-negative PBPs of subclasses B2 or B3 may be orthologous to the Gram-positive PBPs of subclass B5 or B4, respectively.

The Gram-positive PBPs of subclass B1 have no equivalent in the Gram-negative bacteria. They are endowed with unique properties, and they represent an important mechanism of resistance to penicillin. These PBPs have a very low affinity for the drug. They allow the strains that (over) produce them to grow in the presence of penicillin at concentrations sufficient to inactivate the PB modules of all the other PBPs of class A and class B. To all appearances, they are able to perform the basic functions required for cell-wall peptidoglycan assembly in a cell cycle-dependent fashion in conjunction (presumably) with the transglycosylase-n-PB module of class A PBPs (or with monofunctional transglycosylases).

The question of how the class B PBPs function in cell morphogenesis is still open. Yet the unique amino acid sequences of their n-PB modules (10) and the three-dimensional structure of *S. pneumoniae* PBP2x (12) are worthy of reflection. The n-PB cores of all class B PBPs have three conserved motifs. In *S. pneumoniae* PBP2x, motif 1 starts at residue 76 and has the sequence Arg-Gly-x-x-x-Asp-Arg-Asn-Gly, motif 2 starts at residue 186 and has the sequence Arg-x-Tyr-Pro-x-Gly, motif 3 starts at residue 215 and has the sequence Gly-x-x-Gly-x-Glu-x-x-x-Asn, and Gly258 is the amino end of the intermodule junction site. The n-PB module of PBP2x is shaped like a pair of sugar tongs; motifs 1, 2, 3 and the amino half of the intermodule junction site are located in the head of the sugar tongs (which fits into a noncatalytic groove of the PB module), and the long polypeptide stretch that extends between motifs 1 and 2 is well exposed at the surface of the protein.

Other class B PBPs probably adopt the same basic folded structure but with subclass- and species-specific variations. The acyl serine transferase-PB module of class B PBPs probably prescribes traits related to peptidoglycan crosslinking, and this activity might be regulated by the associated n-PB module itself, in conjunction with other components of the morphogenetic networks.

6. Penicillin-Oriented Evolution

Evolution is occurring before our eyes. The massive use of b-lactam antibiotics functions to fuel the emergence of b-lactamases of widely varying specificities by the alteration of a limited number of amino acid residues in the wild-type enzymes (17). Oriented evolution also results in the spread of low-affinity PBPs of subclass B1 among enterococcal and staphylococcal pathogens (18, 19). Strains close to the squirrel *Staphylococcus sciuri* might be the source of the PBP2a-encoding gene in human MRSA (methicillin-resistant *S. aureus*) strains (20). Multimodular PBPs also evolve into variants having a decreased affinity for the drug. Penicillin-resistant *S. pneumoniae* strains possess PBPs that are reduced-affinity variants of PBP1a of subclass A3, PBP2x of subclass B4, and PBP2b of subclass B5 (21). These altered PBPs are the products of mosaic genes in which sensitive sequence blocks are replaced by homologous, resistant blocks from related, naturally penicillin-resistant species by transformation and recombination events (22). The origin of the foreign DNA sequences is unknown, but several sources are probably involved.

7. Penicillin Sensory Transducers

BlaR is a bipartite protein involved in the inducibility of b-lactamase synthesis in *Bacillus licheniformis* (23). An amino terminal module is embedded in the plasma membrane via a four-helix bundle. Loops connecting the transmembrane segments are exposed to the outer and inner faces of the membrane, respectively; the carboxy end of the fourth transmembrane segment is fused to an extracellular penicilloyl serine transferase module. This module possesses the three typical motifs described earlier (Ser402-x-x-Lys, Tyr476-x-Asn, and Lys539-Thr-Gly), and it shares 32% identity with the Oxa-2 class D b-lactamase.

As an independent entity, the penicilloyl serine transferase module of BlaR is a high-affinity PBP. As a component of the full-size BlaR, it adopts a different conformation, and reception of the penicillin-induced signal does not involve penicilloylation of the active-site Ser402. These properties suggest that a class D b-lactamase acquired a new property—penicillin binding—via local structural changes. Fusion of this PBP to another polypeptide then resulted in a hybrid that performs another function: gene regulation.

Signal emission in the cytosol is probably mediated by the intracellular loop that connects transmembrane segments 3 and 4. This loop has no recognizable site of methylation/demethylation and no recognizable site that could be associated with a histidine kinase, but it possesses the His-Glu-Leu-Tyr-His consensus sequence of a neutral zinc peptidase (see Metalloproteinases). This putative peptidase might adopt an active conformation in response to the signal transmitted via the four a-helix bundle. Following this hypothesis, BlaR would be another example of control of gene activity via proteolytic degradation of key regulatory proteins.

Penicillin receptors similar to the *B. licheniformis* BlaR are involved in the inducibility of the synthesis of b-lactamase and low-affinity PBP2a of subclass B1 in *S. aureus* (24). Gram-negative bacteria have developed a different mechanism: b-lactamase synthesis is the result of the b-lactam-induced, peptidoglycan hydrolase-mediated derailment of the peptidoglycan recycling process (25).

Bibliography

1. J. M. Ghuysen (1968) Bact. Rev. 32, 425–464.
2. J. van Heijenoort (1996) In *Escherichia coli* and *Salmonella*, 2nd ed., ASM Press, Washington, D C, pp. 1025–1034.
3. J. M. Ghuysen (1991) Annu. Rev. Microbiol. 45, 37–67.
4. J. A. Kelly, A. P. Kuzin, P. Charlier, and E. Fonzé (1998) Cell. Mol. Life Sci. 54, 353–358.
5. M. Matsuhashi (1994) New Comprehensive Biochem. 27, 55–72.
6. J. I. Kato, S. Hideho, and Y. Hirota (1985) Mol. Gen. Genet. 200, 272–277.
7. M. Adam, C. Fraipont, N. Rhazi, M. Nguyen-Distèche, B. Lakaye, J. M. Frère, B. Devreese, J. Van Beeumen, Y. van Heijenoort, J. van Heijenoort, and J. M. Ghuysen (1997) J. Bacteriol. 179, 6005–6009.
8. D. Joseleau-Petit, D. Thévenet, and R. D''Ari (1994) Mol. Microbiol. 13, 911–917.
9. M. Vicente, M. J. Gomez, and J. A. Ayala (1998) Cell. Mol. Life Sci. 54, 317–324.
10. C. Goffin and J. M. Ghuysen (1998) Microbiol. Mol. Biol. Rev. 62, 1079–1093.
11. F. Lefèvre, M. H. Rémy, and J. M. Masson (1997) J. Bacteriol. 179, 4761–4767.
12. S. Pares, N. Mouz, Y. Pétillot, R. Hakenbeck, and O. Dideberg (1996) Nature Struct. Biol. 3, 284–289.
13. C. Goffin, C. Fraipont, J. Ayala, M. Terrak, M. Nguyen-Distèche, and J. M. Ghuysen (1996) J. Bacteriol. 178, 5402–5409.
14. E. C. Y. Wu, W. E. Alborn Jr., J. E. Flokowitsch, J. Hoskins, S. Unal, L. C. Blaszczak, D. A. Preston, and P. L. Skatrud (1994) J. Bacteriol. 176, 443–449.
15. M. Mollerach, P. Partoune, J. Coyette, and J. M. Ghuysen (1996) J. Bacteriol. 178, 1774–1775.
16. L. M. Guzman, D. S. Weiss, and J. Beckwith (1997) J. Bacteriol. 179, 5094–5103.
17. K. Bush and G. Jacoby (1997) J. Antimicrob. Chemother. 39, 1–3.

18. B. Bergi-Bächi (1994) Trends Microbiol. 2, 389–393.
19. D. Raze, O. Dardenne, S. Hallut, M. Martinez-Bueno, J. Coyette, and J. M. Ghuysen (1998) Antimicrob. Ag. Chemother. 42, 534–539.
20. S. Wu, C. Piscitelli, H. de Lencastre, and A. Tomasz (1996) Microb. Drug Resist. 2, 435–441.
21. R. Hakenbeck and J. Coyette (1998) Cell. Mol. Life Sci. 54, 332–340.
22. C. G. Dowson, J. T. Coffey, and B. G. Spratt (1994) Trends Microbiol. 2, 361–366.
23. K. Hardt, B. Joris, S. Lepage, R. Brasseur, J. O. Lampen, J. M. Frère, A. L. Fink, and J. M. Ghuysen (1997) Mol. Microbiol. 23, 935–944.
24. B. Joris, K. Hardt, and J. M. Ghuysen (1994) New Comprehensive Biochem. 27, 505–516.
25. C. Jacobs, J. M. Frère, and S. Normark (1997) Cell 88, 823–832.

Suggestions for Further Reading

26. J. V. Höltje (1998) Growth of the stress-bearing and shape-maintaining murein sacculus of Escherichia coli. Microbiol. Mol. Biol. Rev. 62, 181–203.
27. J. Lutkenhaus and S. G. Addinall (1997) Bacterial cell division and the Z ring. Annu. Rev. Biochem. 66, 93–116.
28. N. Nanninga (1998) Morphogenesis of Escherichia coli. Microbiol. Mol. Biol. Rev. 62, 110–129.

Pepsin, Pepsinogen

Pepsin is a carboxyl proteinase that is secreted from the chief (or peptic) cells that are part of the oxyntic glands, located on the lining of the stomach (1). It is synthesized as a 42.5-kDa zymogen precursor, pepsinogen, which is stored in the chief cells and released in response to neural and hormonal signals activated by eating. Once pepsinogen enters the acidic environment of the stomach, it undergoes a change in conformation that exposes its active site. This allows pepsinogen to catalyze the hydrolysis of the peptide bond between residues 16 and 17 of its own polypeptide chain. Subsequently, residues 17 to 44 are also removed proteolytically, and the resultant 35-kDa protein is pepsin. It is active at acidic pH and has broad specificity, with preference for hydrolysis of peptide bonds involving tryptophan, phenylalanine, leucine, and methionine residues, especially when they are adjacent to other hydrophobic amino acids. It is often used to digest proteins under acidic conditions in order to obtain peptides linked by disulfide bonds. Disulfide rearrangement, which can sometimes occur at neutral or alkaline pH, is minimized at acidic pH. Pepsinogen is stable at neutral pH and becomes activated at acidic pH, whereas pepsin is stable at acid pH but becomes inactivated at neutral pH.

Pepsin is inhibited by pepstatin, p-bromophenacyl bromide, diazoketones, and various epoxides. It has been reported that pepsin can catalyze transpeptidation reactions, which could, in principle, cause confusion when trying to sequence proteins. This has not been a major problem in practice, however.

Bibliography

1. M. Plebani (1993) Crit. Rev. Clin. Lab. Sci. 30, 273–328.

Pepstatin

This naturally occurring peptide analogue was discovered by screening culture filtrates of the mold actinomyces for inhibitors of the proteolytic enzyme pepsin (1). It also inhibits other carboxyl proteinases, but not serine, thiol, or metalloproteinases. Its chemical structure is: isovaleryl-valyl-valyl-statine-alanyl-statine [where statine is the unusual residue (3S,4S)-4-amino-3-hydroxy-6-methylheptanoic acid] (Fig. 1, see top of next page). Analogues of pepstatin (also called pepstatin A) have been obtained from *Streptomyces* strains with variable inhibitory properties toward different carboxyl proteinases, and a range of synthetic pepstatins have been prepared that have quite remarkable affinities for specific carboxyl proteinases (2). Pepstatin is often used to prevent unwanted proteolysis when isolating proteins under acidic conditions. It is effective at a concentration of about 1 mg/mL.

Bibliography

1. H. Umezawa et al. (1970) J. Antibiot. 23, 259–262.
2. T. Aoyagi and H. Umezawa (1975) In Proteases and Biological Control (E. Reich, D. B. Rifkin, and E. Shaw, eds.), Cold Spring Harbor Laboratory Press, Cold Spring Harbor, NY, pp. 429–454.

Peptidases

Peptidases are enzymes that catalyze the hydrolysis of peptide bonds—that is, the -CONH- bonds that link amino acids in peptides, polypeptides, and proteins. According to the Enzyme Commission of the International Union of Biochemistry and Molecular Biology, they are Class 3, subgroup 4 (peptide hydrolase) enzymes (E.C. 3.4). Some peptidases only act on small substrates—di-, tri-, or oligopeptides—while others act preferentially on protein substrates. The latter are more properly referred to as proteinases (also known as proteases, proteolytic enzymes). Some peptidases cleave peptide bonds involving the amino acids at either the beginning or end, i.e., the amino terminal (N-terminal) or carboxy terminal (C-terminal)—of a peptide chain. They are therefore called exopeptidases and, depending on their particular specificity, are either aminopeptidases or carboxypeptidases. Other peptidases cleave internal bonds in a polypeptide chain and are called endopeptidases. Most peptidases are relatively specific and will only act at peptide bonds in which a particular amino acid or type of amino acid (acidic, basic, neutral, hydrophobic, etc.) contributes either the -CO or -NH group. Some have broad specificity, especially when acting on unfolded, denatured proteins, but they can be highly specific or not active at all with folded, native proteins.

Figure 1. Chemical structure of pepstatin [isovaleryl-valyl-valyl-(3S,4S)-4-amino-3-hydroxy-6-methylheptanoyl-alanyl-amino-3-hydroxy-6-methylheptanoic acid], a transition-state analogue inhibitor of certain carboxyl proteinases, such as cathepsin D, and many microbial carboxyl proteinases. Because its structure resembles the tetrahedral intermediate that of substrate hydrolysis, it forms a tightly bound complex with the active site of each of these enzymes. See Pepstatin, previ

Peptidases have myriad functions. They activate or inactivate peptide hormones; they degrade dietary proteins and peptides; they participate in structural growth and remodeling by degrading collagen and other structural proteins; they protect against infectious agents; and they induce blood clotting. They regulate blood pressure, play an important role in fertilization, and control the cell cycle. They are ubiquitous and enormously diverse. As might be expected, inappropriate peptidase activity could have devastating consequences, so there are numerous peptidase inhibitors and other biological means of curtailing peptidase activity (see Proteinase Inhibitors).

While all peptidases catalyze peptide bond hydrolysis, they do not all do this the same way. In order to act under various conditions, four different mechanisms have evolved, and peptidases are classified as carboxyl proteinase, thiol proteinase, serine proteinase, and metalloproteinase, depending on the particular mechanism they employ. Even within these classes, there are many thematic variations such that it seems that there are almost as many peptidases as there are peptides.

Peptidases have a host of commercially significant uses ranging from “clot busters” (both in blood vessels and in drain pipes) to meat tenderizers. Peptidase inhibitors represent a multibillion dollar pharmaceutical market where they are important in controlling high blood pressure, as well as preventing the progress of acquired immune deficiency syndrome (AIDS).

Peptide

Peptides, sometimes referred to as oligopeptides, are oligomers in which the repeating units are amino acids. Peptides have a defined sequence of amino acids that are linked together by formation of peptide bonds. In contrast to polypeptides and proteins, peptides consist of a small number of amino acids. The distinction between a peptide and a polypeptide is somewhat arbitrary, but generally a peptide has between 2 and 50 amino acid residues. A peptide of two amino acids may be more specifically referred to as a dipeptide, three repeating units as a tripeptide, four repeating units as a tetrapeptide, and so on.

Most peptides are unstructured, described as having a random coil conformation, but others have highly ordered secondary and tertiary structure similar to that observed in larger proteins. The more structured peptides often incorporate disulfide bonds. Many peptides have important biological functions. For example, the pentapeptide leucine-enkephalin (Fig. 1) is a neurotransmitter with opiate-like activity; the hormone insulin is formed from two disulfide cross-linked peptide chains;

and the major toxins from venomous spiders and cone shells are disulfide-rich peptides (Fig. 2). Naturally occurring peptides are usually produced by hydrolysis or cleavage of precursor proteins, through the action of peptidases or proteinases.

Figure 1. Chemical structure of the pentapeptide Leu-enkephalin, which has the sequence Tyr–Gly–Gly–Phe–Leu.

Figure 2. Schematic representation of the structure of the 16-residue a-conotoxin PnIA (1), showing the backbone and disulfides. The two turns of a-helix are depicted as a coil. The two disulfide bonds are shown in ball-and-stick representation. This figure was generated using Molscript (2) and Raster3d (3, 4).

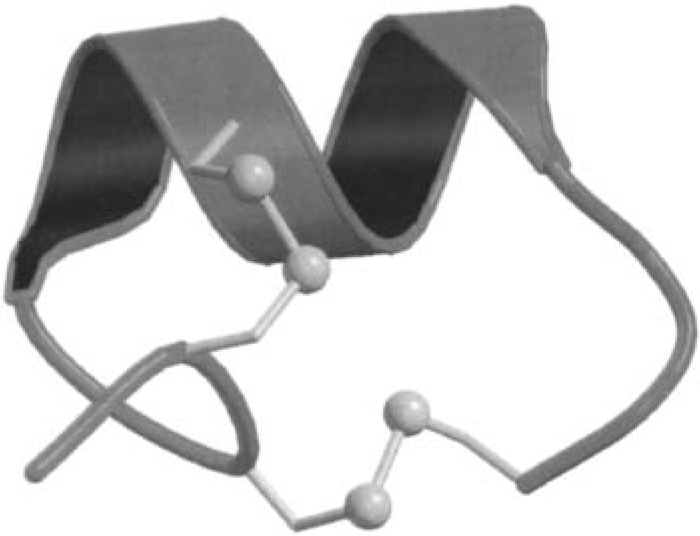

[See also Polypeptide chain]

Bibliography

1. Hu et al. (1996) Structure 4, 417–423.
2. P. J. Kraulis (1991) J. Appl. Crystallogr. 24, 946–950.
3. E. A. Merritt and M. E. P. Murphy (1994) Acta Crystallogr. D50, 869–873.
4. D. J. Bacon and W. F. Anderson (1988) J. Mol. Graphics 6, 219–222.

Suggestions for Further Reading

5. M. Bodanszky (1988) Peptide Chemistry, Springer-Verlag, New York.
6. P. D. Bailey (1990) An Introduction to Peptide Chemistry, Wiley, Chichester.

Peptide Antibiotic Biosynthesis

Peptide antibiotics include a variety of peptide structures with diverse biological properties (1). Historically, the first antibacterial compounds identified were peptides (penicillin, gramicidin, tyrocidine). New such peptides have been characterized steadily, including actinomycin (antitumor); cyclosporin (immunosuppressant); destruxin (insecticide); ferrichrome (siderophore); pepstatin, antipain, and bestatin (proteinase inhibitors); microcystin (phosphatase inhibitor); and defensin and magainin (anti-infectives).

Their biosynthesis may occur either (i) on ribosomes by direct transcription, translation, and post-translational processing of peptide antibiotic genes (see Protein biosynthesis)—for example, nisin—or (ii) without ribosomes but on a multienzyme system, using the thiotemplate mechanism. The structural complexity of peptide antibiotics ranges from modified amino acids to polypeptide chains of up to 50 amino acid residues (2). Ribosomal systems can incorporate only the L isomer of the 20 normal amino acids, plus selenocysteine, while there are no such limitations to the nonribosomal systems, which can use hydroxy acids, fatty acids, and amines. Nevertheless, peptides of ribosomal origin are known to include D amino acid residues, cyclic side chains, and disulfide bonds. All nonribosomal peptides also originate from linear precursors, but a variety of types of cyclization are known. Identification of the biosynthetic origin is crucial for subsequent genetic analysis, and the structural properties of compounds arising from the two types of pathway are compared in Table 1.

Table 1. Structural Features of Peptide Antibiotics of Ribosomal and Nonribosomal Origin

Feature	Ribosomal Path	Nonribosomal Path
Size (amino acids)	No size limitation	2 to about 50, 4 to 10 dominating
amino acid constituents	21 protein amino acids and modified amino acids	Various types of amino acids modified amino acids including 2-, 3-, and 4-amino compounds (more than 300 known)
D-Amino acids	Not more than one, epimerized post-translationally	Often several, either incorporated directly, or epimerized during synthesis
Non-amino acid constituents	Acyl residues, amines originating from decarboxylation	Various acyl residues, including aromatic acids, hydroxy acids
Cyclic structures	Rare; frequent disulfide cycles, thioether cycles	More frequent than linear structures, various peptide bond cyclizations, but also lactones
Modifications	Hydroxylation,	N-Methylation,

	dehydration (Ser, Thr), side-chain cyclization (Cys to thiazoles, Thr to oxazoles, Glu to pyroGlu)	hydroxylation, side-chain cyclization (Cys to thiazole), glycosylation, side-chain crosslinking (aromatic rings)
Unusual constituents	Not known	Urea type of peptide bond, phospho-amino acids, amino-modified fatty-acid-derived components (lipopeptides), mixed polyketide structures
Biosynthesis	Gene can be identified; consider splicing, processing, and posttranslational modification; often prepropeptides detected	Nonribosomal enzyme systems present; peptide families are frequent in the same or related organisms, biosynthesis of rare precursors needed
Sources	Various animals and plants, sometimes bacteria	Mainly bacteria and lower fungi, occasionally plants and insects

1. Ribosomal Biosynthesis

Peptide antibiotics that are synthesized initially on ribosomes comprise a rapidly expanding field of research (3, 4). The compounds synthesized in this way range from linear polypeptide chains to compact multicyclic peptides with several disulfide bonds or thioether linkages (lantibiotics). Their genes are usually isolated by reverse genetics, and they usually reside within gene clusters, together with genetic information for their post-translational modification and export, and for resistance of the host to their actions. Genes for typical animal peptides, like defensins, are present in multiple copies with minor differences in sequence (5). The signals for their targeting and processing are critical for their functions in innate immunity. A peptide from the venom from the spider Agelenopsis aperta is activated by epimerization of a specific residue (6).

Internal cyclizations other than disulfide bond formation have been restricted to bacterial sources, and the enzymes involved in formation of thiazolines (microcin B) and lantibiotic ethers (dehydration of serine and threonine residues to dehydroalanine and dihydrobutryine, respectively, followed by addition of the thiol group of cysteine) are being characterized (7). The post-translational modification of these antibiotics takes place on a membrane-attached multienzyme complex, which also facilitates their export and their role in intercellular communication.

2. Synthesis by Peptide Synthetases

The biosynthesis of peptide antibiotics by nonribosomal systems, on peptide synthetases, requires a considerable amount of information, and these multienzyme complexes are among the largest protein structures known, with masses up to 1700 kDa, corresponding to a 45.5 kbp open reading frame, to synthesize cyclosporin (see Gene Structure). Synthesis of each amino acid residue of such a peptide antibiotic requires a minimum of three catalytic domains: (i) the activating adenylate domain, (ii) the carrier protein, and (iii) the condensing domain, which collectively are referred to as a module (see Thiotemplate Mechanism Of Peptide Antibiotic Synthesis). The nonribosomal code for the amino acid sequence of the peptide is determined by the substrate specificity of the activating domain. Selection and activation of the appropriate amino acid is followed by its attachment as a thioester to the 4′-phosphopantetheine prosthetic group attached to the adjacent carrier domain (8), it is then linked covalently to the next amino acid, on the adjacent module. The thioester intermediates may be subjected to various modifications, such as epimerization, N-methylation, and hydroxylation, catalyzed by additional domains introduced into the module structure. The intermediates in the reaction are covalently attached to the peptide synthetase, and only the final product is released. Examples of known peptide synthetases are compiled in Table 2.

Table 2. Nonribosomal Peptide Synthetase Systems

Peptide	Organism	Structural Type[a]	Gene Cloned	Enzymology
		Linear		
Bacilysin	Bacillus subtilis	P-2-M	(+)	(+)
ACV	Streptomyces clavuligerus Aspergillus nidulans Penicillium chrysogenum Acremonium chrysogenum	P-3	+	+
Bialaphos	Streptomyces hygroscopicus	P-3	+	+
Anguibactin	Vibrio anguillarum	R-P-2-M	+	–
Phaseolotoxin	Pseudomonas syringae pv. ph.	P-4-M	(+)	–
Ardacin	Kibdelosporangium aridum	P-7-M	(+)	–
Pyoverdin	Pseudomonas aeruginosa	R-P-8-M	+	–
		Cyclopeptides		
Enterobactin	Escherichia coli	P-C-E-3	+	+
HC-toxin	Cochliobolus carbonum	C-4	+	+
Tentoxin	Alternaria alternata	C-4	–	+
Echinocandin	Aspergillus nidulans	R-C-6	–	(+)
Microcystin	Microcystis aeruginosa	C-7	(+)	–
Iturin	Bacillus subtilis	C-8	(+)	–
Gramicidin S	Bacillus brevis	$C\text{-}(P\text{-}5)_2$	+	+
Tyrocidin	Bacillus brevis	C-10	+	+
Cyclosporin	Tolypocladium niveum	C-11-M	+	+
Mycobacillin	Bacillus subtilis	C-13	–	+
		Lactones		
Actinomycin	Streptomyces chrysomallus	$R\text{-}(L\text{-}5)_2\text{-}M$	+	+
Destruxin	Metarhizium anisopliae	L-6	+	(+)
Etamycin	Streptomyces griseus	R-L-7	–	(+)
Surfactin	Bacillus subtilis	L-8	+	+
Quinomycin	Streptomyces echinatus	$(R\text{-}P\text{-}4)_2$	–	+

R106	Aureobasidium pullulans	L-9	–	(+)
Syringomycin Syringostatin	Pseudomonas syringae	R-L-9	(+)	–
SDZ90-215	Septoria sp	L-10	–	+
		Depsipeptides		
Enniatin	Fusarium sp	C-$(P_2)_3$-M	+	+
Beauvericin	Beauveria bassiana	C-$(P_2)_3$-M	–	+
		Branched polypeptides		
Bacitracin	Bacillus licheniformis	P-12-C-7	+	+
Nosiheptide	Streptomyces actuosus	R-P-13-C-10-M	–	+
Thiostrepton	Streptomyces laurentii	R-P-17-C-10-M	–	+
		Branched peptidolactones		
Lysobactin	Lysobacter sp.	P-11-L-9	(+)	+
A21798A	Streptomyces roseosporus	R-P-13-L-10	(+)	+
A54145	Streptomyces fradiae	R-P-13-L-10	–	+
Tolaasin	Pseudomonas tolaasii	R-P-18-L-5	(+)	–

[a] The abbreviations used are: P, peptide; C, cyclopeptide; L, lactone; E, ester; R, acyl; M, modified. The structural types are defined by the number of amino-, imino-, or hydroxy acids in the precursor chain. The ring sizes of cyclic structures are indicated in the number following C, L, or E, defining the type of ring closure. The abbreviations used for unusual amino acids and other compounds are listed in the abbreviations footnote on the first page.

Current applications of such enzyme systems are the enzymatic synthesis of peptide analogues, taking advantage of the relatively low stringency of the nonribosomal code—this is, the specificities of the peptide synthetases (9). Efforts are being made to alter the modular construction of peptide synthetases so as to generate new enzyme systems capable of synthesizing novel peptides.

Bibliography

1. H. Kleinkauf and H. von Döhren (eds.) (1990) Peptide Antibiotics, de Gruyter, Berlin.
2. H. Kleinkauf and H. von Döhren (1997) "Peptide Antibiotics". In H. Kleinkauf and H. von Döhren, (eds.), Products of Secondary Metabolism, Vol. 7 of H. Rehm, L. G. Reed, A. Pühler, P. Stadler (eds.), Biotechnology, 2nd ed., Verlag Chemie, Weinheim, pp. 277–322.
3. R. E. W. Hancock and R. Lehrer (1998) Trends Biotechnol. 16, 82–88.
4. W. F. Broekaert et al. (1997) Crit. Rev. Plant Sci. 16, 297–323.
5. C. L. Bevins et al. (1996) Genomics 31, 95–106.
6. S. D. Heck et al. (1996) Proc. Natl. Acad. Sci. USA 93, 4036–4039.
7. R. W. Jack, F. Götz, and G. Jung (1997) "Lantibiotics". In H. Kleinkauf and H. von Döhren (eds.), Products of Secondary Metabolism, Vol. 7 of H. Rehm, L. G. Reed, A. Pühler, P. Stadler (eds.), Biotechnology, 2nd ed., Verlag Chemie, Weinheim, pp. 323–368.
8. M. A. Marahiel, T. Stachelhaus, and H. D. Mootz (1997) Chem. Rev. 97, 2651–2674.

9. H. von Döhren, U. Keller, J. Vater, and R. Zocher (1997) Chem. Rev. 97, 2675–2705.

Peptide Bond

The peptide bond is the chemical link that connects amino acids to form the polypeptide chains of peptides and proteins. The repeating units of these linear polymers, the 20 amino acids, are naturally occurring chemical entities comprising an amino group, a carboxyl group, a hydrogen, and a side chain of variable chemistry. These four groups are connected to a central carbon atom, denoted C_a (or C_{alpha}) (Fig. 1). Peptide bonds are formed by condensation of the carboxyl group of one amino acid with the amino group of another amino acid, giving rise to a dipeptide. Repeated condensation of amino acids produces tripeptides, tetrapeptides, and so on. Proteins can incorporate many thousands of peptide-linked amino acids.

Figure 1. General scheme for formation of a dipeptide XY from two amino acids, X and Y, by reaction of the carboxyl group of amino acid X with the amino group of amino acid Y. The R group attached to C_a is variable, depending on the type of amino acid (R_x and R_y). The peptide bond of the dipeptide product is boxed, and its partial double bond character is depicted.

In vivo, peptide bond condensation occurs at the C-terminus of the growing polypeptide chain to produce proteins having specific sequences defined in the genetic code. This reaction is catalyzed in a process called translation, by enzymes of the cell's protein biosynthesis machinery. Synthetic peptides and proteins can also be produced by chemical peptide synthesis. In contrast to *in vivo* protein biosynthesis, solid-phase synthesis usually occurs by condensation of amino acids to the N-terminus of the growing polypeptide chain. Peptide bonds can be broken down, or hydrolyzed, by enzymes such as peptidases and proteinases.

Each peptide unit in a polypeptide chain has three chemical bonds. The central peptide bond is not freely rotatable, because it has partial double bond character (Fig. 1). This imposes planarity on the peptide bond, so that only two discrete conformations are available. These two conformations, defined by the angle w (Fig. 2), are called the cis and trans configurations. Of these two, the trans configuration is energetically preferred, and is much more commonly observed, unless the following residue is proline (see Cis/Trans Isomerization).

Figure 2. Section of a polypeptide structure showing two peptide bonds (–CONH–) and one amino acid residue (–NH–C_a(R)(H)–CO–). The dihedral angles w, f, and y of the peptide backbone are labeled.

The single bonds on either side of the peptide bond are rotatable. The angle around the N–C_a bond of a peptide is called phi (f), and the angle of the C_a–**C** bond is called psi (y). Certain combinations of f and y, defined as the "allowed" regions of a f/y or Ramachandran Plot, are preferred and energetically favored over others. The allowed f/y angles define the conformations of regular secondary structure such as a-helix or b-strand that are stabilized by backbone hydrogen bonds between peptide bond units.

[See also Polypeptide Chain and Protein Structure.]

Suggestions for Further Reading

A. G. Walton and J. Blackwell (1973) Biopolymers, Academic Press, New York.

C. Branden and J. Tooze (1991) Introduction to Protein Structure, Garland, New York.

Peptide Hormones

The first identified peptide hormone, secretin, was found in 1902 by Baylis and Starling. They discovered that the bioactive compound stimulated the secretion of saliva, and thus they named the factor secretin. Because the compound was produced by one tissue and transported by the blood to a distant organ, where it stimulated the saliva secretion, it was called a hormone based on the Greek word hormao, which means "to stimulate". Since then it has been found that many physiological functions in the body are controlled by such communication with the endocrine and neural systems (1). That is, the regulation, integration, or coordination of various metabolic activities and bodily functions of tissues and organs involve the synthesis of low concentrations (micromolar to picomolar) of biochemical signals or messengers that can be disseminated and transported throughout the organism, to effect the required changes through receptors at distant target cells. Such regulation of function also requires that the production of the hormone be self-limiting; consequently, it requires both negative and positive feedback loops and interactive modulation of G-coupled systems (see GTP-Binding Proteins) of neurotransmitter (see Neuropeptides) systems to affect functional balance, or homeostasis. Through modulation, downregulation, desensitization, upregulation, and receptor cross-talk, hormones in some cases interact with the central nervous system (CNS) to influence neuronal function, to alter behavior, and to control other hormones. In other cases, one function can be influenced by several different hormones. All operate primarily under the hierarchical control of the central nervous, endocrine, and immune systems. Although hormones were originally defined as material that is secreted by endocrine glands, the term is now often applied to hormones that are expressed in other tissues or are formed from precursors located in other tissues. For example, angiotensin, which maintains the water and electrolyte balance and controls blood pressure, is produced by converting angiotensinogen in the blood with renin secreted by the juxtaglomerular cells in the kidney.

1. Biosynthesis, Secretion, and Interaction with Receptors

A peptide hormone is first synthesized on the ribosome as a pre-pro-hormone following transcription and translation of the genetic information (2) of the messenger RNA. This precursor of high molecular weight contains an N-terminal signal peptide, which guides the protein to the rough endoplasmic reticulum (ER), where the signal peptide is removed proteolytically by a signal peptidase, in a form of co-translational processing. The pro-hormone, or hormone precursor (see Polyproteins), that is produced usually does not possess much biological activity. Most pro-hormones and pro-neuropeptides contain within their polypeptide chains several smaller peptides with various biological activities. These pro-hormones normally undergo posttranslational processing, protein folding, disulfide bond formation, or chemical modification, such as N-glycosylation, O-glycosylation, acetylation, or amidination, when they are processed through the Golgi apparatus. The pro-hormones undergo specific proteolytic cleavage by endoproteinases or processing enzymes and then are sorted (3) into secretory granules. The polypeptide hormone is stored in the secretory vesicles and, in some cases, may undergo further processing by enzymes.

Almost all of the cleavage sites in the precursor protein contain a dibasic sequence, Lys–Arg or Arg–Arg, that is recognized by the processing enzymes. The Kex-2 proteinase of yeast, kexin, was the first enzyme found to cleave at Lys–Arg and Arg–Arg sequences. Subsequent use of the kex-2 gene as a probe (see Probe Hybridization) led to the cloning of similar gene products from mammalian cells (4). Investigations demonstrated that these convertases, which cleave at the C-terminal side of Lys–Arg and Arg–Arg sequences, play an important physiological role. Differential processing of a single precursor protein in two different tissues can now be explained by the presence or relative concentrations of different posttranslational enzymes in tissues. For example, pro-opiomelanocortin (POMC) is differentially processed in the anterior and intermediary pituitaries (5). In the anterior and intermediary pituitary, ACTH and b-LPH are the predominant products because PC-1/3 (pro-protein convertase) is most prevalent. In the intermediary pituitary, however, alpha-melanocyte-stimulating hormone (a-MSH), corticotropin-like intermediary peptide (CLIP), and b-endorphin are secreted because PC-2 is more prevalent there (see Fig. 1).

Figure 1. Processing of the pro-opiomelanocortin (POMC) to produce ACTH (adrenocorticotropic hormone), B-LPH (b-lipotropin), A-MSH (a-melanocyte stimulating hormone), CLIP (corticotropin-like intermediary peptide), g-LPH, and b-endorphin. The pro-protein convertase PC-1 / 3 carries out the initial cleavages in the anterior and intermediary pituitary, whereas convertase PC-2 is present primarily in the intermediary pituitary.

The hormone within the secretory vesicles is released from the vesicles by exocytosis upon stimulation by extracellular signals provided by neurotransmitters or other hormones, wherupon the hormone is transported by the blood or extracellular fluid to the target cells. Once a hormone is secreted, it usually binds to a specific plasma protein carrier, which prolongs its half-life because the complex reduces the rate of hormone destruction by plasma proteinases.

The release of the peptide is normally controlled by a feedback mechanism. In the case of ACTH, for example, the secretion of corticoid is stimulated by ACTH, but on the other hand, corticoid suppresses CRF and ACTH secretion from hypothalamus. In turn, ACTH suppresses CRF secretion.

The type of endocrine hormone secretion is classified by the distance between the cells that secrete the peptide and its target cells. Classically, endocrine hormones act at a distant target, while paracrines act upon nearby cells, and an autocrine acts upon the cell that secreted it. Many hormones often function in all three ways, however, making such distinctions difficult. Hormones secreted by neural cells and neurons are called neuroendocrines.

When the hormone reaches its target cell, it binds to its specific receptor in the cell membrane. Each receptor is a membrane protein complex and consists of three domains, (1) extracellular, (2) transmembrane, and (3) intracellular domains. The tertiary structure of the receptor is essential for specific binding of the ligand. This interaction induces structural changes in the receptor that result in activation of an intracellular enzyme that generates a transient increase in concentration of a signaling compound (see Signal Transduction), such as cyclic AMP (cAMP), cyclic GMP (cGMP), diacylglycerol (DAG), or inositol triphosphate, IP_3. The elevated concentration of these second messengers and of the phosphorylated forms of proteins triggers the appropriate metabolic response. Proteins are phosphorylated on serine, threonine, or tyrosine residues by cAMP-dependent protein kinase (PKA), DAG-activated protein kinase C (PKC), or tyrosine kinases.

Many hormone receptors have a common structure in which the single polypeptide chain passes back and forth through the membrane seven times, forming seven transmembrane alpha-helices. For these receptors, the hormone-binding signal is transmitted or transduced to the interior of the cell by binding the receptor-ligand complex to a series of G-proteins (see Heterotrimeric G Proteins). G-proteins bind GDP or GTP. When G-proteins bind to their receptors, GTP exchanges with GDP bound to the a-subunit of the G-protein. The Ga–GTP complex binds adenylate cyclase, activating the enzyme. The activation of adenylate cyclase produces cAMP in the cytosol and leads to the activation of PKA and the phosphorylation of enzymes. Many classes of G-proteins exist, such as G_s and G_i, stimulatory and inhibitory G-proteins, respectively. A second class of G-protein coupled-receptor synthesizes DAG and IP3 as second messengers. The hormone-receptor complex interacts with G-proteins, and this is followed by the G-protein activation of phospholipase C-g (PLCg). PLCg hydrolyzes phosphatidylinositol bisphosphate to IP3 and DAG. IP3 binds to the endoplasmic reticulum and opens the calcium channels so that stored calcium flows into the cytosol and activates enzymes. On the other hand, the DAG binds and activates PKC and also opens calcium channels. PKC phosphorylates serine and threonine residues, thereby modulating the catalytic effect of the corresponding enzymes.

One receptor, that of ANF (atrial natriuretic factor), is coupled to the production of cGMP by guanylate cyclase. Another ANF receptor lacks guanylate cyclase activity and is thought to play a role in the clearance of ANF. Yet another type of receptor is the heterotetrameric insulin receptor. It is composed of two a- and two b-subunits. The a-subunits protrude outside the membrane and contain the binding sites, while the b-subunits penetrate through the membrane in a single transmembrane a-helix and contain tyrosine-kinase activity. When insulin binds to the receptor, intramolecular phosphorylations are triggered, and this autophosphorylation enhances its ability to phosphorylate enzymes that induce the physiological response (Fig. 2). (see also Heterotrimeric G Proteins).

Figure 2. General mechanism of action of peptide hormones that bind to receptors and thereby alter the activity of adenylate cyclase through heterotrimeric G-proteins. The peptide hormone binds to the extracellular part of the receptor embedded in the plasma membrane. This is transmitted to the abg heterotrimeric G-protein, which dissociates in the Gbg-dimer and the Ga subunit, which binds to adenylate cyclase and alters its activity accordingly.

2. Methods of Isolation and Structure Determination

The structure of a peptide hormone was first demonstrated by de Vigneaud in 1953, when he determined the structure of oxytocin and confirmed it by total chemical synthesis. In 1954, the structure of insulin was determined by Sanger. The chemical structure of secretin was not determined until 1966, 60 years after its initial discovery. Because peptide hormones exist in such small concentrations, it was difficult then to isolate, purify, and analyze them. Subsequent development of better detection methods with higher sensitivities, such as radioimmunoassay (RIA), made possible the rapid isolation and structure determination of a large number of peptide hormones and neuropeptides. Later gene cloning provided the sequence of the complementary DNA of hormone precursors by using a DNA probe (see Probe Hybridization) based on the known peptide sequence. This also provides the structure of previously undetected protein isoforms. For example, in the case of endothelin-1 (ET-1), which had been isolated from cultured endothelium cells of blood vessels, screening of the human chromosomal DNA library revealed the existence of genes for three isoforms: ET-1, ET-2, and ET-3. Each isoform consists of 21 amino acid residues, and they have high sequence homology. Another method of detecting new peptide hormones is by screening the DNA sequence of the precursor protein. In this case, another new peptide hormone that is linked in the precursor molecule can be detected. In the precursor of glucagon, two amino acid sequences that resemble glucagon were found, GLP-1 and GLP-2. Another example is the case of calcitonin gene-related peptide (CGRP), which stimulates the formation of cAMP. Analysis of the gene of the precursor protein of calcitonin (CT), which modulates serum calcium concentrations, revealed that the CT gene consists of five introns and six exons. As a consequence of alternative splicing of the RNA transcripts (see Transcription), the mRNA for the CT precursor is found in the thyroid but the mRNA for CGRP is formed in the nervous system.

As a result of the progress in gene technology, the chemical structures of a large number of hormone receptors have now been determined. Most of their intrinsic ligands also have been identified. However, there are still receptors for which no ligands are known. New techniques are being developed to search for new bioactive peptides that serve as ligands for such orphan receptors. In 1998 (6), a prolactin-releasing factor or peptide was found in the search for the ligand for one such orphan receptor that is expressed in the human pituitary. The 31-residue peptide stimulates the pituitary to release prolactin.

3. Synthesis and Conformational Analysis

After the isolation and structure determination of a peptide hormone has been achieved, the peptide is often chemically synthesized to confirm the structure. With the synthesized material, structure-activity relationships can be explored to design drugs for treating individuals with peptide-hormone deficiencies or with malfunctioning peptides. The technique of combinatorial chemistry has recently made it possible to synthesize millions of compounds and to screen them for activity rapidly and efficiently (7). In addition, gene technology has provided a means of producing human peptide sequences, such as insulin, in *Escherichia coli*, yeast, or other expression systems. This has afforded the opportunity to produce peptide hormones and receptors that are uniformly labeled with ^{13}C and ^{15}N isotopes for nuclear magnetic resonance (NMR) analysis. These labeled compounds can then be used to investigate the interaction between ligand and receptor, as well as to study the conformational changes that occur upon binding. Consequently, the ongoing study of the tertiary structures by NMR and X-ray crystallography is now providing more details regarding the mechanisms of hormonal action.

Bibliography

1. A. W. Norman and G. Litwack, editors (1987, 1997) *Hormones*, 1st and 2nd eds., Academic Press, New York.
2. W. W. Chin (1995) In *Principles and Practice of Endocrinology and Metabolism*, 2nd ed., J. B. Lippincott, Philadelphia, pp. 8–41.
3. M. J. Perone, S. Windeatt, and M. G. Castro (1997) *Histology and Histopathology* **12**, 1179–1188.
4. S. P. Smeekens (1993) *Bio/Technology* **11**, 182–186.
5. M. G. Castro and E. Morrison (1997) *Critical Rev. Neurobiol.* **11**, 35–57.
6. S. Hinuma (1998) *Nature* **393**, 272–276.
7. C. Pinilla et al. (1995) *Biopolymers* **37**, 221–240.

Peptide Libraries

Peptide libraries were first introduced during the mid-1980s as a means to elucidate the details of antibody–antigen recognition (1, 2). Prior to that time, epitope mapping required fragmentation analysis, either at the protein or DNA level, which was a laborious and time-consuming process. Geysen et al. (1) demonstrated that synthetic peptide libraries could be prepared and screened by enzyme-linked immunosorbent assay (ELISA) to elucidate antibody–epitope recognition to the resolution of a single amino acid residue. This was the first case in which a problem in molecular recognition was elucidated using a synthetic library and is often cited as a critical development in the emergence of combinatorial libraries.

The first generation of synthetic peptide libraries was limited in size to a few hundred peptides, due to the need for each library member to be prepared as a discrete compound. However, the combination of mixture-synthesis techniques (1-4), reliable strategies for identifying active species from complex mixtures (3, 4), and advances in peptide sequencing methods quickly led to the routine preparation and screening of libraries containing millions of distinct peptide sequences. Several reports of ten-residue peptide libraries containing more than 10^{12} peptides have even appeared (5, 6). When coupled with an increasing availability of unnatural amino acid building blocks, peptide libraries of this scale and complexity became valuable tools for identifying novel peptide agents for a wide range of applications (eg, see Refs 7 and 8). Soluble and solid-phase peptide libraries continue to find applications in the identification of antigenic determinants. In addition, they have been used to identify receptor ligands (5, 9-14), inhibitors of enzymatic activity (15), and novel antibacterial agents (3, 7, 14). Many of these applications have employed standard assay formats (eg, soluble activity or binding assays), requiring complex deconvolution or iterative synthesis and screening cycles to identify the active species from complex synthetic pools (see Combinatorial Synthesis).

Split synthesis methods for preparing one-bead, one-compound (OBOC) peptide libraries have overcome many of the limitations of standard assay formats and pooling strategies. Because each bead carries a single compound in amounts approaching several nanomoles, assays can be performed directly on the resin beads that detect interactions of bead-linked compound with a soluble target. A typical assay utilizes ELISA methodologies to indicate beads bearing compounds that interact with the target (16). Positive beads may be selected manually, or more sophisticated instrumentation may be employed to detect and isolate active beads (17). Alternatively, the OBOC format is amenable to off-bead assays through the use of cleavable linkers inserted between the peptide and the solid-phase support (18, 19). In an off-bead assay, the peptide is released from the resin bead, but proximity to the bead is maintained through use of a diffusion-limiting matrix or a positional array. For example, distribution of the library and a test cell line within a soft agar matrix, followed by partial peptide release, leads to the formation of locally high concentrations of peptide in the agar surrounding each bead. Zones of reduced cell growth (or another reporting mechanism such as color change) surrounding single beads are used to identify peptides having the desired activity. Beads producing a zone of activity are removed and analyzed by standard Edman Degradation or mass spectrometric analysis to determine the sequences of the active peptides. This approach has been used for identifying peptide ligands for G-protein-coupled receptors (20), as well as cytotoxic peptides that may have application as anticancer agents (19). This represents but a few examples of the unique screening methods that have been developed using peptide chemistry coupled with the OBOC library format. Other notable examples include the use of a fluorescence-activated cell sorter (FACS) (17) (see Flow Cytometry) to identify active beads, as well as direct visualization of cancer cells binding to peptides on beads (21).

The initial excitement surrounding synthetic peptide libraries has been tempered in recent years. Peptides are linear, highly flexible polymers with fixed side-chain spacing. In contrast, most proteins adopt complex three-dimensional structure that place active chemical groups in positions that cannot be approximated by linear peptides. As a result, many targets fail to yield hits from short peptide libraries. The introduction of constraints into the peptide chain, including cyclization or use of domain scaffolds with defined structural propensities (Fig. 1a), may increase the success rate for some targets. In addition, altering the polymer backbone can change the spacing of the side chains (22-25). Although unnatural amino acids can be used to shift the side-chain spacing (eg, b-amino acids), the problems enumerated above associated with a linear and flexible polymer remain. A wide range of peptidomimetics that employ novel backbones have emerged to address this issue (Fig. 1b) (26-28). Such compounds also address a second major criticism of peptides: They are ill-suited for in vivo applications due to poor pharmacokinetic properties. By utilizing building blocks with physicochemical properties compatible with uptake and absorption, peptidomimetics have moved a step closer to lead compounds for drug discovery. The true utility of peptidomimetics for drug discovery remains unknown, but their potential for use as research tools is high.

Figure 1. Structural aspects of peptide libraries. a) Illustration of one structural bias, a b-turn (top), that can be introduced in a peptide library, and two approaches for creating libraries based on this structural scaffold. They are cyclization (bottom left) and the use of constrained dipeptide surrogates (bottom right). b) Examples of various peptidomimetics.

See also Combinatorial Libraries, Libraries, Combinatorial Synthesis, Affinity Selection, DNA Libraries, Genomic Libraries, cDNA Libraries, Expression Libraries, and Phage Display Libraries.

Bibliography

1. H. M. Geysen, R. H. Meleon, and S. J. Barteling (1984) Proc. Natl. Acad. Sci. USA 81, 3998–4002.
2. R. A. Houghten (1985) Proc. Natl. Acad. Sci. USA 82, 5131–5135.
3. R. A. Houghten, C. Pinilla, S. E. Blondelle, J. R. Appel, C. T. Dooley, and J. H. Cuervo (1991) Nature 354, 84–86.
4. C. Pinilla, J. R. Appel, P. Blanc, and R. A. Houghten (1992) Biotechniques 13, 901–905.
5. R. A. Houghten and C. T. Dooley (1993) NIDA Res. Monogr. 134, 66–74.
6. C. Pinilla, J. R. Appel, and R. A. Houghten (1994) Biochem. J. 301, 847–853.
7. S. E. Blondelle, E. Takahashi, P. A. Weber, and R. A. Houghten (1994) Antimicrob. Agents Chemother. 38, 2280–2286.
8. K. S. Lam, M. Lebl, V. Krchnak, S. Wade, F. Abdul-Latif, R. Ferguson, C. Cuzzocrea, and K. Wertman (1993) Gene 137, 13–16.
9. C. T. Dooley, N. N. Chung, B. C. Wilkes, P. W. Schiller, J. M. Bidlack, G. W. Pasternak, and R. A. Houghten (1994) Science 266, 2019–2022.
10. R. A. Houghten (1993) Gene 137, 7–11.
11. C. T. Dooley, R. A. Kaplan, N. N. Chung, P. W. Schiller, J. M. Bidlack, and R. A. Houghten (1995) Pept. Res. 8, 124–137.
12. C. T. Dooley, N. N. Chung, P. W. Schiller, and R. A. Houghten (1993) Proc. Natl. Acad. Sci. USA 90, 10811–10815.
13. C. T. Dooley and R. A. Houghten (1993) Life Sci. 52, 1509–1517.
14. R. A. Houghten, J. R. Appel, S. E. Blondelle, J. H. Cuervo, C. T. Dooley, and C. Pinilla (1992) Biotechniques 13, 412–421.
15. J. Vagner, G. Barany, K. S. Lam, V. Krchnak, N. F. Sepetov, J. A. Ostrem, P. Strop, and M. Lebl (1996) Proc. Natl. Acad. Sci. USA 93, 8194–8199.
16. K. S. Lam, M. Lebl, and V. Krchnak (1997) Chem. Rev. 97, 411–448.
17. M. C. Needels, D. G. Jones, E. H. Tate, G. Heinkel, L. M. Kochersperger, W. J. Dower, R. W. Barrett, and M. A. Gallop (1993) Proc. Natl. Acad. Sci. USA 90, 10700–10704.
18. M. Lebl, M. Patek, P. Kocis, V. Krchnak, V. J. Hruby, S. E. Salmon, and K. S. Lam (1993) Int. J. Pept. Protein Res. 41, 201–203.
19. S. E. Salmon, R. H. Liu-Stevens, Y. Zhao, M. Lebl, V. Krchnak, K. Wertman, N. Sepetov, and K. S. Lam (1996) Mol. Diversity 2, 57–63.
20. C. K. Jayawickreme, G. F. Graminski, J. M. Quillan, and M. R. Lerner (1994) Proc. Natl. Acad. Sci. USA 91, 1614–1618.
21. M. E. Pennington, K. S. Lam, and A. E. Cress (1996) Mol. Diversity 2, 19–28.
22. R. J. Simon, R. S. Kania, R. N. Zuckermann, V. D. Huebner, D. A. Jewell, S. Banville, S. Ng, L. Wang, S. Rosenberg, C. K. Marlowe, et al. (1992) Proc. Natl. Acad. Sci. USA 89, 9367–9371.
23. A. B. Smith III, T. P. Keenan, R. C. Holcomb, P. A. Sprengeler, M. C. Guzman, J. L. Wood, P. J. Carroll, and R. Hirschmann (1992) J. Am. Chem. Soc. 114, 10672–10674.
24. C. Y. Cho, E. J. Moran, S. R. Cherry, J. C. Stephans, S. P. A. Fodor, C. L. Adams, A. Sundaram, J. W. Jacobs, and P. G. Schultz (1993) Science 261, 1303–1305.

25. M. Hagihara, N. J. Anthony, T. J. Stout, J. Clardy, and S. L. Schreiber (1992) J. Am. Chem. Soc. 114, 6568–6570.

26. M. A. Gallop, R. W. Barrett, W. J. Dower, S. P. A. Fodor, and E. M. Gordon (1994) J. Med. Chem. 37, 1233–1251.

27. E. M. Gordon, R. W. Barrett, W. J. Dower, S. P. A. Fodor, and M. A. Gallop (1994) J. Med. Chem. 37, 1385–1404.

28. L. A. Thompson and J. A. Ellman (1996) Chem. Rev. 96, 555–600.

Peptide Mapping

Peptide mapping allows rapid overall evaluation of a protein's primary structure from limited analysis of the peptides produced by proteolysis. Only a single amino acid difference between two peptides caused by mutation or posttranslational modification alters the physical properties of the peptide in which that difference occurs. So peptide mapping is a very sensitive way of detecting differences between closely related proteins. The peptides produced by a specific proteinase are separated into a pattern ("peptide map"), and the maps of related proteins are compared. Single differences, such as the Glu/Val difference between normal/sickle cell hemoglobins that was early recognized by peptide mapping (1) or the relationships between isozymes are found rapidly (2). Subsequent refinements in the methods and resolution of mapping produced excellent one- and two-dimensional (2-D) techniques that have been reviewed (3) and much used. The classical peptide mapping methods of two-dimensional fingerprinting and Cleveland maps are described in those articles. These classical approaches are still practical when the amounts of protein are sufficient, but molecular biology now centers on different approaches.

One extension increases the sensitivity, as required by present-day and future needs, to evaluate proteins available only in very small amounts. This has become possible by modern separation techniques, such as capillary HPLC (4), capillary electrophoresis (5), and high-resolution two-dimensional gel electrophoresis (6, 7). A further extension is to rely on mass spectrometry, using laser desorption instruments, triple quadrupoles, ion-trap devices, or other techniques, and perform the mapping, detection, and analysis in one step. In this manner, using entire peptide mixtures or preselected fragments, direct determination of the total masses of peptide fragments from a protein gives a unique "fingerprint" and is expected soon to be the mapping method of general choice. Combined with databases of peptides from all known proteins, it allows direct identification of any protein that has been characterized from the same or a closely related source (8-10). Then, mass spectrometric peptide mapping and simultaneous data bank screening will constitute a powerful technique as a descendant of the classical peptide mapping idea. In the near future, when crucial genomes are completely sequenced, the work remaining will center on identifying of each gene product and on proteome analysis to correlate gene expression with predicted protein structures stored in data banks.

1. Liquid chromatography

When reverse-phase HPLC was introduced in the mid-1970s, column chromatographic methods largely replaced paper and thin-layer plate separations. Further miniaturization and additional separation techniques have since continuously altered the separation methods (4), but the principle of peptide mapping by comparing efficient separations of peptides remains. In many cases, the resolution now is so high that complex peptide mixtures are separated completely by single-column chromatographic steps, thereby reintroducing one-step mapping methods. Instruments are also so reproducible that repeated runs, even at different times, are virtually identical, thereby introducing mapping comparisons on the same instrument on different occasions. The principle of peptide mapping has gained further momentum, which is expected to continue in present and future stages of proteome research with all of its gene product characterizations.

The principle is still to compare two or more expressed proteins by suitable proteolytic digests, followed by identical instrument runs, and subsequently evaluating all peak positions and heights of the resulting patterns. The era of peptide mapping has moved from spots or bands on solid supports and multiple but simultaneous separations to peak positions on microcolumns after successive separations. In addition to detecting structural differences, many other applications of this technique are now in use, for example, epitope mapping, determination of glycosylation, phosphorylation, or oxidation sites, and assignment of disulfide bonds. Peptide mapping is used extensively for quality control and characterization of recombinant DNA -derived products.

The major advantages in using microcolumn methods for peptide mapping are speed (often minutes), sensitivity (femtomole amounts, even with detection by UV absorbance), and ease of recovery for further characterization by amino acid analysis, Edman Degradation, and mass spectrometry. Several high-performance separation media have been developed that allow rapid HPLC resolution of peptides and proteins. The classical silica-based stationary phase HPLC column has been used extensively for nearly twenty years in numerous applications, and alternative materials, such as divinylbenzene cross-linked polystyrene (11), have since emerged. Frequently, the stationary phase is packed in microbore columns with a narrow inner diameter (on the order of 1 to 2 mm), with low flow rates (down to 40 µL/min), small elution volumes (40 to 60 µL), better detector response (5- to 20-fold higher) than conventional HPLC columns, and requiring only picomole quantities of protein. However, the current trend is toward further miniaturization and smaller inner diameters, leading to still lower detection limits, but also toward implementation of powerful detection techniques, such as Z-shaped flow cells for efficient UV absorbance, laser-induced fluorescence, electrochemical detection, and mass spectrometry.

Capillary reverse-phase HPLC is conducted with column inner diameters of between 350 and 75 µm and at flow rates of 4 to 0.2 µL/min. The low flow rates necessitate special technical solutions for recovering separated peptides. Such a system has recently been developed [MicroBlotter (12, 13)] for subpicomole peptide mapping after digestion of proteins in gels (14, 15) or on membranes after blotting (16) and for isolating peptides for microsequence analysis. The capillary outlet intermittently touches a strip of poly(vinylidene difluoride) (PVDF) membrane while moving along the strip. After sample collection, the PVDF strip is aligned with the chromatogram to excise spots that correspond to peptide candidates for structural analysis.

The protein to be analyzed is still digested with trypsin, Lys-C proteinase, or another suitable proteolytic enzyme. Protocols for microdigestion in small volumes (1 to 10 µL) and for recovering peptides from small samples (a few picomoles or less) have been developed (17). After digestion, the proteolytic peptides are derivatized with fluorescent tags (18) for detection. Generally, however, separation problems may arise from precolumn derivatization, and the digest is often injected directly onto the column after adjusting the pH to that of the mobile phase at the start of chromatographing. The most widely used solvent systems still consist of gradients of acetonitrile (often 0 to 60%, v/v) in aqueous trifluoroacetic acid (TFA) (often 0.1% v/v), but several other chromatographic solvents have also been suggested, for example, heptafluorobutyric acid instead of TFA, hydrochloric acid, sodium phosphate buffer at acidic or neutral pH, and ammonium bicarbonate, ammonium acetate, triethylammonium phosphate, or 1.0% sodium chloride at neutral pH. The most common detection technique is still UV absorbance, normally at both 214 and 280 nm, the latter for identification of peptides that contain tryptophan and tyrosine residues. Alkylation of cysteine with [^{14}C]- iodoacetic acid or 4-vinylpyridine is common to prevent disulfide formation and peptide aggregation and to promote convenient detection of cysteine-containing peptides in the resulting map. A practical example of capillary HPLC peptide mapping (Fig. 1) illustrates how in *vivo* oxidation of a recombinant protein hormone after intravenous administration is detected (17)

Figure 1. Capillary HPLC tryptic peptide maps of recombinant human growth hormone (lower profile) and of the same protein recovered from rat serum taken 15 (middle profile) and 45 (upper profile) min after an intravenous dose of the preparation. Arrows link methionine-containing peptides (right in each pair) with their corresponding oxidized forms (left in each pair), showing the increase in oxidized form with time *in vivo*. The peptides were separated with a 320 μm×15cm reverse-phase (C_{18}) column. From Ref. 17 with permission.

2. Capillary electrophoresis

Capillary electrophoresis in different separation modes, often capillary zone electrophoresis (CZE), provides a further powerful approach to peptide mapping (19), that has high sensitivity (low femtomole level) and short separation time (minutes). More than 10^6 theoretical plates are achieved and used to generate reproducible peptide patterns suitable for mapping experiments (Fig. 2). Capillary electrophoresis is also a suitable complement to reverse-phase HPLC for identifying peptides because the separation mechanism is different, based on mass-to-charge ratio and hydrophobic interaction, respectively. Consequently, peptide fragments not resolved by reverse-phase HPLC are often completely resolved by CZE. Similarly, reverse-phase HPLC may resolve peptides not separable by CZE (21).

Figure 2. Peptide mapping of a fraction from a brain extract by capillary electrophoresis, to illustrate reproducibility with time and use of mapping for peptide identification. The separation in (*a*) reveals that the fraction contains a mixture of short peptides, the one at the arrow is suspected to be a neuroactive peptide, Gly-Pro-Glu. After adding of the corresponding synthetic peptide, reanalysis in (*b*) reveals that the synthetic peptide (arrow) comigrates with the

biological peptide component. Considering that the time between separations (a and b) is >2 weeks, the repetitive pattern confirms the reproducibility of the system on a sensitive scale (0.1 to 2 pmol analyzed). From Ref. 20 with permission.

Fused silica capillaries that have charged surfaces in which electroendosmosis takes place are commonly employed, typically with inner diameters of 20 to 200 µm and lengths of 20 to 100 cm. Small inner diameters are best suited for peptide mapping because the more narrow the capillary, the better the resolution. For peptide separations, sodium phosphate buffer, pH 2.5, is a good electrolyte that allows sensitive detection at short wavelengths (190–200 nm) because of its high UV transparency. Including short-chain, ion-pairing reagents (hexanesulfonic or heptanesulfonic acid) in the buffer improves resolution, in particular of hydrophobic peptides, and has been tested in peptide mapping (Fig. 3). The voltages applied range from 5 to 30 kV, and electric field strengths range from 200 to 500 V/cm. Separations are influenced by a combination of electrophoretic mobility and electroendosmosis. CZE can be used preparatively, and the components separated in the peptide map can be further characterized by amino acid analysis, Edman degradation, or mass spectrometry (5, 23). In particular, electrospray mass spectrometry has gained recent popularity as an on-line detection technique with simultaneous tandem mass spectrometric capability for peptide structure information at the low femtomole level (24–26).

Figure 3. Tryptic peptide mapping of recombinant human erythropoietin in phosphate buffer, pH 2.5, with 100 mM heptanesulfonic acid by capillary electrophoresis. The maps from two different expression systems are shown, the upper without glycosylation (*E. coli*), the lower with (Chinese Hamster Ovary cells) but subsequently treated with N-glycanase. Although 16 peaks have identical migrations, indicating identical primary gene products, peaks a–f differ and can be attributed to differences at specific sites in the eukaryotic form. From Ref. 22 with permission.

3. Mass spectrometry

Protein fingerprinting by determining the masses of all the peptides generated by proteolysis of polypeptide chains separated by gel electrophoresis has recently emerged as an extremely powerful tool for protein identification. It combines sensitivity and high throughput (8). Complex protein mixtures of crude cell lysates can be separated with 2-D gel electrophoresis systems (27). For identification, the amount of protein in many 2-D gel spots is well below 1 picomole and thus too small for the commonly used sequencer technology, but it is accessible to recently developed sequencer instruments (down to 100 femtomole by cartridge miniaturization and capillary HPLC for phenylthiohydantoin detection; see Edman Degradation) using matrix-assisted laser desorption/ionization (MALDI) (28) or electrospray (29) mass spectrometry, recently extended by nanoelectrospray ionization (30, 31). As a consequence, a novel type of “peptide mapping” of proteins has emerged, using their fragment masses and efficient algorithms to search peptide-mass databases, which permits structural assignment, protein identification, and determination of minor differences (32-34).

As in traditional peptide mapping, the first step in this procedure is proteolytic cleavage of the protein (commonly, still with trypsin), either in solution, in a gel (14, 15), or on a membrane after blotting on nitrocellulose or PVDF membranes (16). The MALDI mass analysis and the database search are highly automated (35), which increases the throughput and makes multiple protein identifications efficient (Fig. 4). If the protein is still unknown after the database search, the peptides are further analyzed by tandem mass spectrometry (36, 37). Using the nanoelectrospray ion source, sequence stretches up to 16 residues obtained from as little as 5 ng of protein digested with trypsin in a gel have been reported (10).

Figure 4. Peptide mapping by automated MALDI mass spectrometry and database searching after in-gel digestion with trypsin of a yeast protein recovered from a 2-D gel system. Ion signals whose measured masses match the

calculated masses of protonated tryptic peptides are indicated with circles. Sequence coverage is greater than 70%. Terminal Arg (R) and Lys (K) sequence tags are marked by arrows. Also shown is a magnification of one of the tryptic peptide peaks that reveals the resolution of molecules containing different natural isotopes. From Ref. 35 with permission.)

4. Conclusion

Peptide mapping, complemented with Edman degradation and mass spectrometry, involves principles from the 1950s and earlier. But they have survived in the newest phases of modern molecular biology and now position themselves at the front of developments by providing rapid and sensitive identification of minor differences among related, alternatively synthesized, and posttranslationally modified gene products at femtomole and soon attomole levels.

Bibliography

1. V. M. Ingram (1956) Nature *178*, 792–794.
2. H. Jörnvall (1970) Eur. J. Biochem. *16*, 41–49.
3. W. J. Gullick (1986) In *Practical Protein Chemistry: A Handbook* (A. Darbre, ed.), Wiley, Chichester, U.K., pp. 207–225.
4. R. L. Moritz et al. (1994) Methods *6*, 213–226.
5. T. Bergman, B. Agerberth, and H. Jörnvall (1991) FEBS Lett. *283*, 100–103.
6. A. Görg, W. Postel, and S. Günther (1988) Electrophoresis *9*, 531–546.
7. J. E. Celis et al. (1996) FEBS Lett. *398*, 129–134.
8. S. D. Patterson and R. Aebersold (1995) Electrophoresis *16*, 1791–1814.
9. D. F. Hunt et al. (1992) Science *255*, 1261–1263.
10. M. Wilm et al. (1996) Nature *379*, 466–469.
11. N. B. Afeyan et al. (1990) J. Chromatogr. *519*, 1–29.
12. M. L. Kochersperger, K.-L. Hsi, and P.-M. Yuan (1994) Protein Sci. *3*, Suppl. 1, 98, 265-M.
13. K.-L. Hsi et al. (1995) Protein Sci. *4*, Suppl. 2, 150, 540-M.
14. J. Rosenfeld et al. (1992) Anal. Biochem. *203*, 173–179.
15. U. Hellman et al. (1995) Anal. Biochem. *224*, 451–455.
16. J. Fernandez et al. (1992) Anal. Biochem. *201*, 255–264.
17. J. E. Battersby et al. (1995) Anal. Chem. *67*, 447–455.
18. J.-Y. Chang et al. (1982) Eur. J. Biochem. *127*, 625–629-M.

19. J. P. Landers (1993) Trends Biochem. Sci. 18, 409–414.
20. T. Bergman (1993) In Methods in Protein Sequence Analysis (K. Imahori and F. Sakiyama, eds.), Plenum, New York, pp. 21–28.
21. J. Bullock (1993) J. Chromatogr. 633, 235–244.
22. R. S. Rush et al. (1993) Anal. Chem. 65, 1834–1842.
23. A.-C. Bergman and T. Bergman (1996) FEBS Lett. 397, 45–49.
24. J. F. Banks, Jr.and T. Dresch (1996) Anal. Chem. 68, 1480–1485.
25. J. F. Kelly, L. Ramaley, and P. Thibault (1997) Anal. Chem. 69, 51–60.
26. H. R. Morris et al. (1996) Rapid Commun. Mass Spectrom. 10, 889–896.
27. W. F. Patton et al. (1990) Biotechniques 8, 518–527.
28. M. Karas and F. Hillenkamp (1988) Anal. Chem. 60, 2299–2301.
29. J. B. Fenn et al. (1989) Science 246, 64–71.
30. M. S. Wilm and M. Mann (1994) Int. J. Mass Spectrom. Ion Processes 136, 167–180.
31. M. Wilm and M. Mann (1996) Anal. Chem. 68, 1–8.
32. W. J. Henzel et al. (1993) Proc. Natl. Acad. Sci. USA 90, 5011–5015.
33. D. J. C. Pappin, P. Hojrup, and A. J. Bleasby (1993) Curr. Biol. 3, 327–332.
34. M. Mann, P. Hojrup, and P. Roepstorff (1993) Biological Mass Spectrom. 22, 338–345.
35. A. Shevchenko et al. (1996) Proc. Natl. Acad. Sci. USA 93, 14440–14445.
36. D. F. Hunt et al. (1986) Proc. Natl. Acad. Sci. USA 83, 6233–6237.
37. K. Biemann and H. A. Scoble (1987) Science 237, 992–998.

Suggestions for Further Reading

38. Methods in Protein Structure Analysis. Proceedings from the conference series with the same name, usually published biannually. Latest issue now in press (J. Prot. Chem.), from the XIth conference at Annecy, 1996.
39. Techniques in Protein Chemistry. Proceedings from the annual meetings of the Protein Society, usually published yearly by Academic Press.
40. ABRF News. Proceedings from the workshops of the Association of Biomolecular Resource Facilities.

Peptide Nucleic Acids

Peptide nucleic acids (PNA) are DNA mimics in which the phosphoribose backbone of DNA has been substituted by a pseudopeptide backbone to which the normal nucleobases are tethered. An 8-mer thymine oligoamide was first described in 1991. The name PNA was coined when it was demonstrated that this molecule forms a triple helix with a polyadenine DNA strand and that a PNA of mixed sequence that contains all four DNA bases forms duplexes with DNA and RNA that obey the Watson–Crick basepair rules. In 1994, it was reported that two PNAs that have complementary base sequences hybridize into a double-helical structure. PNA has attracted great attention within medicinal chemistry and molecular biology, and also in fields, such as organic and physical chemistry because of its interesting chemical and physical properties. Because it binds efficiently and sequence-specifically to single-stranded RNA and DNA and, under certain conditions, also to double-stranded DNA, PNA has great potential for diagnostic and pharmaceutical applications.

1. Chemistry and Synthesis

The backbone of PNA is based on 2-aminoethylglycine linkages that mimic the normal phosphodiester backbone of DNA (1). A methylene carbonyl linker connects the standard nucleotide bases to this backbone at the amino nitrogens (Fig. 1). This chemistry has some interesting consequences. In contrast to DNA or phosphorothioate oligonucleotides, PNA is a nonionic molecule. In addition, it is achiral, which avoids diastereomeric structures and the need to develop stereoselective synthesis reactions. Schemes for protecting reactive groups on the PNA monomers are based on either Boc or Fmoc chemistry (see Peptide Synthesis). In both cases, oligomers can be assembled using established, solid-phase peptide synthesis procedures and a (methylbenzhydryl) amine polystyrene resin as solid support (2). PNA oligomers are cleaved from the support by treatment with either anhydrous hydrogen fluoride or trifluoromethanesulfonic acid, as in traditional peptide chemistry, followed by purification using HPLC. Modifications of PNA are obtained by coupling amino acids during solid-phase synthesis or by attaching other compounds that contain a carboxylic acid group to the exposed N-terminal amino group. The ease with which PNAs are modified should facilitate optimization of specific functional requirements.

Figure 1. Comparison of the chemical structures of (a) DNA and (b) PNA. B = nucleobase.

2. Physical-Chemical Properties

PNA has proven very potent as a DNA mimic capable of participating in both duplex and triplex formation. Moreover, it displays various interesting properties beyond those of natural DNA.

2.1. PNA-DNA/RNA Duplexes

The properties of PNA-DNA duplexes have been extensively investigated using the mixed-sequence pentadecamer H-TGTACGTCACAACTA-NH_2 (3). This PNA oligomer forms a duplex with complementary DNA that is antiparallel, has the amino-terminus of PNA facing the 3' end of DNA, and has a T_m (melting temperature) of 70°C. The corresponding DNA-DNA complex has a T_m of only 53°C. PNA also binds to the parallel, complementary, DNA target, although it has lower affinity (T_m = 56°C). The preference for antiparallel orientation is a general feature of mixed-sequence PNA-DNA duplexes. Kinetic binding studies have shown that antiparallel PNA-DNA duplex formation is very fast, faster than formation of a corresponding DNA-DNA duplex, whereas considerably slower kinetics were observed for formation of parallel PNA-DNA complexes (4). The thermal stability of PNA-RNA duplexes is generally higher than that of PNA-DNA duplexes, and the rate of association between PNA and RNA is somewhat faster than that between PNA and DNA.

The greater thermal stability of PNA-DNA/RNA duplexes compared to the corresponding DNA-DNA duplexes is predominantly ascribed to the lack of electrostatic repulsions between the two strands. This hypothesis is based on the observation that PNA-DNA and DNA-DNA duplexes have equal thermal stability (melting temperatures) at ionic strengths above 1 M Na^+. As expected, the stability of PNA-DNA hybrids is little affected by changes in ionic strength, except in the limit of low ionic strength, where the stability increases. The higher stability of PNA-DNA compared with DNA-DNA duplexes at low ionic strength is due to a more favorable entropy change linked to duplex formation, which is attributed to a release of counterions from the DNA polyanion as PNA binds (5).

The sequence-specificity of PNA binding to nucleic acids is manifested in the considerably lower stabilities of heteroduplexes that contain mismatches. The effect of base-pair mismatches in the middle of a pentadecamer PNA-DNA duplex revealed decreases in T_m of 8 to 20°C for single mismatches (3). Similar decreases in T_m were observed in PNA-RNA for the corresponding mismatches. Thus, the sequence discrimination of a PNA oligomer is equal to, or even better than, that of a DNA oligomer.

2.2. $(PNA)_2$-DNA Triplexes

Homopyrimidine PNA or PNA oligomers that have a high pyrimidine content bind complementary purine DNA by forming $(PNA)_2$-DNA triplexes (6), virtually without forming of any duplex. Monophasic, well-defined melting curves are obtained for these very stable complexes (T_m > 70°C for decamer PNAs), where the binding is most probably governed by standard Watson–Crick and Hoogsteen base pairing. Triplex formation involving cytosine in the homopyrimidine PNA is pH-dependent (lower pH increases hybrid stability), as expected if C^+GC triplets with one cytosine protonated are being formed. It is interesting to note that experiments still indicate a $(PNA)_2$-DNA stoichiometry even at pH 9, where cytosine is not expected to be protonated. This suggests that only a single hydrogen bond of cytosine is sufficient or that its pK_a is drastically changed.

2.3. Binding to Double-Stranded DNA: Strand Invasion

The high stability of $(PNA)_2$-DNA triplexes enables the PNA to dissociate double-stranded DNA (dsDNA). For example, homopyrimidine PNA oligomers displace the pyrimidine strand of dsDNA at the target site and form a $(PNA)_2$-DNA triplex with the DNA homopurine target. The expelled DNA pyrimidine strand forms a single-stranded loop (Fig. 2). PNA-DNA complexes formed by strand invasion are characterized by high thermodynamic stability and high specificity, which seems contradictory. The strand invasion reaction, however, is kinetically controlled, which allows screening by the PNA for the target sequence, without becoming trapped in thermodynamically stable but incorrectly matched complexes. Although restricted to low ionic strength, this is an interesting binding property of PNA that is being pursued extensively, and several applications have been demonstrated.

Figure 2. Schematic general model of the possible mechanisms of PNA_2-DNA triplex formation by strand invasion of a DNA duplex.

The mechanism of formation of strand-displacement complex involving a PNA(pyrimidine)$_2$-DNA (purine) triplex has been investigated by gel retardation assay using DNA restriction fragments that contain single PNA targets (7). The reaction obeys pseudo-first-order kinetics, and a single mismatch in a 10mer PNA reduces the binding rate constants by more than a factor of 100. For the polynucleotide system poly(dA):poly(dT) and PNA-thymine oligomers, the PNA binding reaction was studied in real time by circular dichroic (CD) spectroscopy (8). This revealed somewhat complex reaction kinetics and also demonstrated the presence of at least one intermediate species. The rate-limiting step is a transient opening of a few base pairs in the DNA duplex (as reflected by the size of the activation barrier). Quite remarkably, the reaction is second-order in PNA concentration, indicating that both PNA strands are involved in the precursor complex. Possibly, the two PNAs are associated loosely with the DNA duplex before the base-pair opening step. Interestingly, intercalators bound to the starting duplex DNA increase the PNA binding rate, even at higher salt concentration, presumably by facilitating initiation of PNA invasion at the intercalation site. Even if the formation of strand-displacement complexes is highly dependent on the ionic strength, complexes formed at low ionic strength are generally stable kinetically at salt concentrations up to 0.5 M NaCl.

PNA targeted to dsDNA sequences other than purine-rich stretches was recently investigated, but such complexes have reduced stability (9). With purine-rich PNA sequences, duplexes formed by the invasion into dsDNA at a complementary pyrimidine target (making a PNA-DNA duplex) have been detected by CD spectroscopy, and by a gel electrophoretic mobility-shift assay. Somewhat surprisingly, cytosine-rich and alternating thymine-cytosine PNA oligomers bind to their corresponding duplex DNA sequence of intact dsDNA by forming PNA-$(DNA)_2$ triplexes. The pH-dependence indicates that this probably involves Hoogsteen base pairing. These recent findings suggest that there are vast possibilities for using PNA to target a variety of base sequences of dsDNA, although more studies are necessary to assess the details of the various binding mechanisms.

2.4. PNA-PNA Duplexes and PNA-PNA-PNA Triplexes

Complementary PNA decamers that contain all four nucleobases form stable antiparallel duplexes very high in thermal stability (PNA–PNA T_m = 67°C; PNA–DNA T_m = 51°C, DNA–DNA T_m = 33.5°C for identical decamer sequences) that have a high sequence specificity that demonstrates Watson–Crick base pairing (10). As observed for PNA-DNA duplexes, the antiparallel PNA-PNA orientation is preferred, although the parallel PNA-PNA complex is still considerably stable (T_m = 47°C. Moreover, a PNA$_3$ triplex that has two pyrimidine decamers and one purine decamer was detected by optical spectroscopy and mass spectrometry, and the CD spectrum indicates a helical structure similar to (DNA)$_3$ and (PNA)$_2$-DNA triplexes (11).

The base pairing in PNA-PNA duplex formation occurs rapidly on a subsecond timescale. Once formed, some PNA-PNA duplexes undergo a conformational transition (10). Although PNA in complexes with DNA or RNA adopts right-handed helical structures as a result of the hybridization, PNA-PNA duplexes, which are devoid of intrinsic chiral constituents, are believed to exist as a racemic mixture of right- and left-handed helices. However, the attachment of a chiral amino acid to the C-terminus of one strand can induce inversion into one predominating helical sense among the PNA-PNA duplexes, which was detectable as a slowly growing CD signal upon mixing. Such a chiral bias depends on the PNA sequence at the C-terminus (a G-C base pair is preferred) and on the nature of the terminal chiral amino acid. The D and L forms of amino acids give rise to mirror image CD spectra of PNA (Fig. 3a), indicating that helices of opposite handedness are formed, The nature of the side chain (hydrophobic or hydrophilic) also decides the preferred helical sense. Helix reorganization occurs on a timescale of minutes at room temperature and exhibits first-order kinetics. The reaction shows a high entropic activation barrier, as would be expected for a transition from one helical sense to another. PNA-PNA duplex helicity that originates from a chiral amino acid at the PNA terminus can propagate about 10 base pairs (chiral persistence length,) or approximately one helical turn.

Figure 3. CD-spectra of GTAGATCACT·AGTGATCTAC duplexes. (a) PNA-PNA duplex with terminal D-lysine (light gray) and L-lysine (dark gray). (b) PNA-DNA antiparallel (light gray), PNA-RNA antiparallel (dark gray), and PNA-DNA parallel ( ). (c) PNA-PNA (light gray) and DNA-DNA (dark gray).

3. Structure of PNA Complexes

The unique chemical and physical properties of PNA have inspired investigations of structural details of PNA-nucleic acid hybrids by various techniques, including NMR, X-ray crystallography, CD, and linear dichroic (LD) spectroscopy.

3.1. Dichroic Spectroscopy of PNA-DNA Hybrids

The CD of PNA-DNA and PNA-RNA duplexes provided the first indications of the overall base-pair geometry in these complexes (3). The CD spectra of DNA-DNA, antiparallel PNA-DNA, and antiparallel PNA-RNA duplexes are all similar, suggesting that PNA participates in forming right-handed helices that have base-pair geometry not much different from that found in B-DNA or A-DNA helices (Fig. 3b). In contrast, the spectra of parallel PNA-DNA and PNA-RNA complexes deviate more from the DNA-DNA spectrum, suggesting different base stacking (Fig. 3b).

Earlier, LD and CD showed that PNA-T_8 with poly(dA) forms a right-handed PNA_2-DNA triplex, in which the base triplets are arranged with their planes approximately perpendicular to the helix axis, similar to the standard poly$(dT)_2$-poly(dA) triplex (6). Further, the PNA_2-DNA triplex has a remarkably rigid structure, indicating efficient stacking interactions. The high thermal stability of $(PNA)_2$-DNA triplexes is expected because of the absence of interstrand repulsions, and it is assisted by hydrophobic and dipolar interactions, and possibly also by intrabackbone hydrogen bonds (see later). Titration experiments with PNA-T_8 added to poly(dA) show by LD and CD that no duplex stretches are present at subsaturation ratios but that segments of $(PNA)_2$-DNA triplexes are distributed evenly on the poly(dA) strand separated by flexible single-stranded regions. Only close to the saturation point, 2:1 PNA to DNA bases, does the complex become rigid due to complete formation of triplex and stacking between each PNA triplex segment.

A helical structure of PNA-PNA complexes has also been suggested. The CD spectrum of PNA-PNA resembles that of the corresponding DNA-DNA duplex (Fig. 3c) in shape and amplitude, so it is inferred that the structures similar in their base-stacking interactions and degree of organization (10).

3.2. NMR and X-Ray Crystal Structures of PNA-Containing Complexes

Three-dimensional molecular structures have recently been reported for several PNA complexes (Fig. 4). The structures of PNA-RNA hexamer (12) and PNA-DNA octamer (13) duplexes have been determined by NMR. The structures of a nonamer $(PNA)_2$-DNA (14) triplex and a hexamer PNA-PNA (15) duplex were determined by X-ray crystallography. Some general conclusions can be drawn from these structures. It is clear from the heteroduplexes, that binding of PNA still allows the backbone of the nucleic acid partner to retain a nearly "normal" conformation. The RNA strand in the RNA-PNA duplex, has approximately an A-conformation with C3′-endosugar puckering, whereas the DNA in the PNA-DNA duplex is closer to B-form with C2′-endosugar puckering (see DNA Structure). It is striking, however, that the base-pair positions in both duplexes are more A-like in their helical displacement, but, in contrast to a canonical A-form helix, are more perpendicular to the helical axis. The two duplexes also show a larger pitch—about 13 base-pairs for the PNA-DNA duplex—than the usual 10 to 11 base pairs observed in nucleic acid duplexes.

Figure 4. Structures of PNA duplexes and triplexes. (A) and (B). Solution structures of PNA-DNA octamer duplex (A) and PNA-RNA hexamer duplex (B). (C) and (D). X-ray crystallographic structures of a PNA-PNA duplex (C) and of PNA_2-DNA nonamer triplex (D). Figure kindly provided by Dr. Scott Carter.

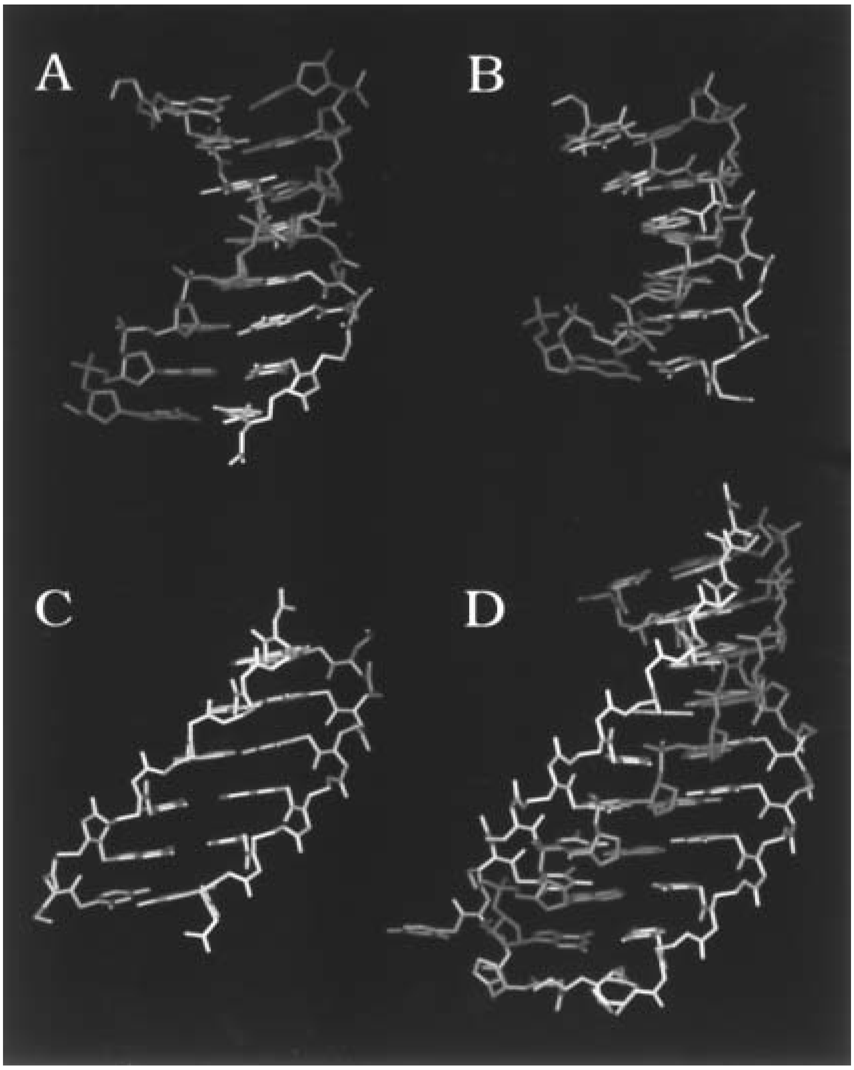

The crystal structure of the $(PNA)_2$-DNA triplex reveals hydrogen bonds between phosphate groups of the DNA backbone and amide protons in the PNA backbone of the Hoogsteen strand. These contacts could be important for the ability of homopyrimidine PNA oligomers to form very stable triplexes with complementary oligonucleotides. Moreover, the two PNA strands in the triplex structure are nearly identical and resemble the PNA strand in the PNA-DNA duplex. Both the $(PNA)_2$-DNA triplex and especially the PNA-PNA duplex show very wide (26 Å and 28 Å, respectively) helices with a large pitch (16 and 18 bases per turn in the triplex and duplex, respectively), strongly suggesting that this latter type of helix is the natural conformation of helices that have PNA backbones. It is further notable that the base pairs in the PNA-PNA duplex exhibits interbase-pair stacking overlaps close to A-form. Thus, it is clear that PNA helices have a structure of their own that resembles, but is also distinctly different from, known nucleic acid helices.

4. Structure–Activity Studies

Because PNA has demonstrated unique hybridization properties toward complementary oligonucleotides, it has been of the utmost interest to understand what structural elements are responsible for its behavior. Furthermore, it is important to know what kind of chemical modifications can be accomplished and accommodated while retaining binding to DNA and RNA.

A large number of studies on backbone-modified PNAs show that any minor deviations from the original aminoethylglycine backbone can be tolerated. Extensions in any of the three possible linking directions impair stability of its complexes, and the restricted flexibility imposed by the secondary amido group in the nucleobase linker is also necessary because reducting this to a tertiary amine is deleterious to the hybridization potency (16). Isomerization to the retroinverse structure, which essentially moves a methylene group from the ethylene to the glycine moiety, also results in PNAs of low hybridization efficiency. However, there is much freedom in the way substituents may be placed in the a-position of the glycine moiety of the PNA backbone. Backbones based on natural amino acids other than glycine result in fair to good DNA mimicking properties. Even cyclic substituents, such as cyclohexyl substitution at the aminoethyl linker, are acceptable, provided the right stereoisomer is chosen. By using PNA monomers that have incorporated natural amino acids, chemical functionality can be introduced into the backbone and the physical properties of the PNAs, such as hydrophilicity, hydrophobicity, ionic character, etc. might be finely tuned and controlled. It is believed that this greatly facilitates the optimization of pharmacokinetic behavior, for example (see later).

PNA-DNA chimeras are potentially interesting because they may allow DNA-recognizing enzymes (such as ribonuclease H and DNA polymerase) to interact with the DNA part, while the PNA part would provide high binding affinity and specificity. For this purpose, a linker is necessary that connects the two oligomers to allow stacking between the neighboring bases in the PNA and DNA parts of the chimera. Successful reports describe the synthesis of PNA-DNA chimeras of both DNA-3′-N-PNA and DNA-5′-C-PNA type junctions (17). Such chimeras hybridize to complementary oligonucleotides less efficiently than pure PNAs, but they are able to activate ribonuclease H.

5. A Possible Genetic Drug?

The potential use of PNA as an antisense or antigene drug for sequence-specific modulation of gene expression has bright prospects. Oligonucleotide analogs can be designed to recognize and hybridize to complementary sequences in a particular messenger RNA and thereby inhibit its translation (see also Antisense Oligonucleotides). Alternatively, oligonucleotides can be targeted to dsDNA and interfere there with transcription of a particular gene (the antigene strategy). These two approaches are depicted in Figure 5. In vitro assays examining the effect of PNA on DNA replication, transcription, and translation all look quite promising. The sequence specificity is high, and the biological stability of PNA is sufficient (18). Drawbacks include the poor cellular uptake of PNA and the sensitivity of strand invasion complexes to salt concentrations, which must be addressed before general applications can be developed. Moreover, the pharmacological properties of PNAs have not yet been thoroughly investigated.

Figure 5. Principles of the antisense and antigene gene-targeting strategies. In normal cells (a), DNA is transcribed into which then is translated into protein. When the cells are treated with an antisense oligomer (b), hybridization to a sequence specific mRNA inhibits expression of the protein at the level of translation. Treatment of the cells with an antigene oligo complementary to a sequence in the DNA leads to inhibition of transcription of the gene into mRNA.

5.1. Transcription Arrest by PNA

When targeting genomic DNA by the antigene strategy, inhibition should in theory be obtained by the formation of just one PNA-DNA complex in each haploid genome. Because pyrimidine PNAs form extremely stable, strand-invasion complexes upon binding to dsDNA, they should be excellent antigene agents (18). It has been shown that such complexes indeed arrest transcription by both prokaryotic and eukaryotic RNA polymerases in vitro. PNA bound to the promoter clearly blocks the access of the polymerase protein to the DNA, whereas PNA bound within the coding region of a gene sterically blocks polymerase progression (Fig. 6a). In therapeutic applications, several issues are, however, still unclear. First, to bind dsDNA, a polypurine target must be present in the gene of interest. This, of course, limits the number of possible targets. Second, and this could be more serious, the formation of strand-displacement complexes occurs very slowly at physiological salt concentration. Modifications of PNA by intercalators or positively charged lysine residues may, however, improve the binding rates. Furthermore, chemically linking the end of the Watson–Crick and Hoogsteen PNA strands to each other or incorporating pH-independent pseudoisocytosines into the Hoogsteen strand can increase the association rates with dsDNA. It was found that binding of PNA to supercoiled plasmid DNA is much faster than to linear DNA, indicating that the DNA topology is an important parameter for the rate of binding. Because transcriptionally active chromosomal DNA is usually negatively supercoiled, this could be of relevance for PNA binding in vivo. It has also been shown that binding of PNA to dsDNA is enhanced when the DNA is being transcribed, probably because of partly ssDNA in the transcription bubble.

Figure 6. Translational arrest and transcriptional inhibition. (a) Translation initiation is blocked by either a duplex- or a triplex-forming PNA, whereas a triplex-forming PNA is required for translation elongation arrest of the ribosome. (b) Transcriptional inhibition is accomplished by homopyrimidine PNAs that form invasion triplexes either at the promoter or the coding region of the gene.

5.2. PNA as an Artificial Promoter

Even though not considered an antigene effect, the ability of PNA to activate transcription is worth mentioning in this context. The resemblance between PNA strand invasion hybrids and transcriptional initiation complexes allows transcription to start on the looped-out strand of the PNA-DNA complex. Experiments with *Escherichia coli* RNA polymerase show that the looped-out DNA strand acts as a template, and the length of the resulting transcripts corresponds exactly to run-off transcripts initiated at the bound PNA. Such a “PNAmoter” is very strong and might have the potential to activate genes *in vivo*, provided that strand invasion is accessible inside cells. As mentioned, PNA also arrests transcription, but the two processes differ as to the size of the displacement loop. Although arrest works for decamer targets, transcriptional initiation requires a larger loop.

5.3. Translational Arrest by PNA

Because PNA-RNA complexes are not recognized by ribonuclease H, PNA-mediated antisense effects depend on mechanisms involving steric blocking of RNA processing, transport into the cytoplasm, or translation. Studies performed in vitro show that translational initiation is blocked by a PNA that forms either a duplex (mixed sequence) or a triplex (pyrimidine-rich), whereas arrest of translational elongation by the ribosome requires a triplex-forming homopyrimidine PNA (Fig. 6). Antisense properties in a cellular context have been possible to assess by microinjection of PNA directly into cultured cells (circumventing the cellular uptake problem), and sequence-specific effects have been confirmed (18).

Bacteria have attracted relatively little attention as targets for antisense agents. However, the demonstration of gene- and sequence-specific antisense inhibition by PNA in *E. coli* opens possibilities for antisense antibacterial drugs and gene-function analysis in bacteria (19). In view of the resistance to current antibiotics displayed by an increasing number of strains of pathogenic bacteria, the possibility of novel antibiotics seems especially important.

5.4. Delivery and Biological Stability of PNA

The prospect of using PNA as a genetic drug makes sense only if PNA is delivered efficiently to cells and distributed so that it interacts with the target mRNA or DNA. Studies conducted with cells in culture indicate that PNA uptake is slow and that PNA ends up in endosomal compartments (18). Using a liposome system as an in vitro cell model, the PNA penetration properties based on passive diffusion have been investigated in detail and are slow (requiring days) (20). Therefore, PNA molecules need to be modified somehow, either by conjugation to ligands so that active receptor-mediated cellular uptake channels might be exploited or by attachment to moieties that make them attracted to the membrane, so that the local concentration of PNA near or within the cell membranes increases. It has been found that a PNA conjugated to an antibody for transferrin transports across the blood-brain barrier, possibly via the transferrin receptor (21). Most other DNA analogs also show poor uptake properties, similar to those observed with PNA. It is always important, however, to extend uptake studies to *in vivo* situations. Surprisingly, phosphorothioate oligonucleotides, which are taken up only inefficiently in cell culture, have favorable pharmacokinetic behavior in animal models (18).

Agreeing with its chemical remoteness to natural nucleic acids or peptides, PNA exhibits resistance to degradation by cellular nucleases and proteinases and remains intact when incubated in serum or cellular extracts. Thus, PNA has ample biological stability for drug development. Furthermore, no signs of general toxicity by PNA have been observed thus far.

6. PNA as a Diagnostic Tool

An increasing number of applications have been described that confirm the potential for PNAs to facilitate the development of novel methodologies in molecular biology, diagnostics, and related fields. A few of these applications are described here.

6.1. PNA-Directed PCR Clamping

The high stability and sequence selectivity of PNA-DNA complexes have been exploited in analyzing single base-pair mutations in DNA by employing PCR amplification (22). PNA directed toward the primer binding site, the region adjacent to the primer site, or toward the middle of the PCR region, decreases amplification because PNA cannot function as a primer for DNA polymerase. The most efficient and discriminative clamping was observed, as might have been expected, with homopyrimidine PNA decamers. Formation of such PNA_2-DNA triplexes inhibit the polymerase at any PNA binding site. With this technique, a single mismatch in the primer site is detectable.

6.2. PNA and S1 Nuclease as Artificial Restriction Enzymes

PNAS in combination with S1 nuclease have been used as “artificial restriction enzymes” (23). Hybridization of a homopyrimidine PNA oligomer to the complementary target on dsDNA leads to strand displacement of the noncomplementary DNA strand. Upon treatment with nuclease S1, the single-stranded DNA is cut into well-defined fragments. The binding of two PNA molecules to two adjacent targets on the same or opposite DNA strands led to an opening of the entire region, including the intervening base pairs, and thereby provided an accessible substrate for the nuclease and considerably increased the sensitivity to cleavage.

6.3. PNA-Mediated Nucleic Acid Purification

PNA oligomers that carry six histidine residues can be used to purify target nucleic acids by nickel affinity chromatography (24). Moreover, PNAs linked to biotin in combination and streptavidin-coated magnetic beads can be used to purify genomic DNA of *Chlamydia trachomatis* directly from urine samples. This “purification by hybridization” approach offers a number of advantages over traditional purification methods. One drawback, however, is that it requires knowledge of a target sequence and a dedicated capture oligomer must be synthesized for each different target nucleic acid. Short pyrimidine PNAs form unprecedently stable triplexes with complementary nucleic acids. Because being short means that their target sequence is prevalent in large nucleic acids, such short PNAs can be used as generic capture probes to purify large nucleic acids. It has been shown that a biotin-tagged PNA-thymine heptamer purifies human genomic DNA efficiently from whole blood by a simple and rapid procedure.

7. Mimic of DNA

Studies of PNA and its complexes with nucleic acids add new perspectives to our understanding of

DNA and also RNA. The base-pair stacking in the PNA-DNA and PNA-RNA duplexes is similar to that of the pure nucleic acid duplexes, showing that neither the absence of backbone charge nor absence of chirality in one of the strands markedly affects the helical stacking. Thus, the helicity can be considered a result of the stacking interaction (mainly dipolar interactions between the nucleobases) in combination with strains from the backbone, rather than arising from phosphate–phosphate repulsion that strives to increase the separation of negative charges along the backbone. An important manifestation of the preferred helical structure is also the helical stacking in PNA-PNA duplexes (10, 11). It is speculated that the helical shape of nucleic acids was selected in evolution because it allows better exposure of signature features of the bases on the helical surface without loss in secondary structure stability and thereby facilitates protein recognition.

The structural similarity between PNA-DNA and DNA-DNA duplexes offers the opportunity to investigate the forces responsible for binding different ligands to dsDNA (25). Assuming that the main binding forces can be divided into electrostatic interactions and hydrophobic contributions, the effect of replacing the negatively charged DNA backbone with a neutral peptide backbone could help assess the role of the phosphate groups in binding a given ligand. Typical molecules that intercalate or bind to grooves exhibit strongly reduced affinities for PNA-DNA complexes. None of the intercalators studied exhibited any significant binding, whereas classical minor groove binders bind weakly to PNA-DNA complexes. No simple ligand has been found that binds to PNA-PNA duplexes. These findings illustrate the importance of electrostatic attractions for ligand binding to DNA.

8. PNA and Prebiotic Chemistry

Identifying the first genetic molecule could provide the key to understanding the origin of life. The difficulties in spontaneously forming nucleotides under prebiotic conditions might be used to argue that nucleic acids (DNA or RNA) were not the first genetic materials on the primitive earth. Therefore, it has been proposed that one or more genetic systems composed of simpler monomers may have preceded the RNA world, an era in which RNA molecules would have acted as both the genetic material and the catalyst. Then, genetic takeover would have allowed the development of RNA-controlled life. PNA is an example of an oligomer that could have preceded RNA because it is simpler than RNA but exhibits all of the important properties of nucleic acids with respect to information storage. PNA oligomers can act as templates for polymerizing of the complementary activated RNA mononucleotides, and an RNA oligonucleotide template facilitates the synthesis of complementary PNA strands. These experiments suggest that transitions between different genetic systems may occur without loss of information. A continuous transition from one genetic system to another is possible only if it is possible to form chimeras, that is, mixed molecules that contain building blocks of both systems. In fact, template-directed formation of PNA-DNA chimeras has been demonstrated (26).

PNA is attractive as a primordial macromolecule because it is simple and stable, but, not least, also because PNA is achiral. Introducing and maintaining homochirality on the primitive earth is often considered a crucial issue. How would the first RNA and DNA molecules (which are chiral) have formed from a random racemic mixture of chemically related subunits, including all the possible optical isomers? One possibility is that some physical selection mechanism resulted in forming a chiral environment before the origin of life, or, which may be more likely, that a general chiral bias was active during evolution and led to a final complete selection of handedness (27). Because homochirality is required for the function of enzymes and nucleic acids, an adaptive process might have selected for homochirality at some stage in prebiotic chemical evolution. The discovery of PNA-PNA helices with the handedness determined by a terminal chiral seed suggests that a molecular precursor of RNA could have provided a mechanism for chiral amplification (28).

9. Concluding Remarks

The development of PNA has had implications for many areas of DNA chemistry, biology, and technology, ranging from basic molecular recognition, self-assembly, chiral induction, and genetic therapeutic drugs, to our understanding of the structure and function of Nature's genetic material, DNA, and speculation on its prebiotic predecessors and origin. Even some novel materials have their origin in PNA (29). Therefore, PNA should be viewed as a DNA mimic and also as a structural and self-recognizing system in its own right.

Bibliography

1. P. E. Nielsen (1991) Science 254, 1497–1500.
2. K. L. Christensen et al. (1995) J. Peptide Science 3, 175–183.
3. M. Egholm et al. (1993) Nature 365, 566–568.
4. K. Jensen, H. Orum, P. E. Nielsen, and B. Norden (1996) Biochemistry 36, 5072–5077.
5. S. Tomac et al. (1996) J. Am. Chem. Soc. 118, 5544–5552.
6. S. K. Kim et al. (1993) J. Am. Chem. Soc. 115, 6477–6481.
7. V. V. Demidov et al. (1995) Proc. Natl. Acad. Sci. 92, 2637–2641.
8. P. Wittung, P. E. Nielsen, and B. Norden (1996) J. Am. Chem. Soc. 118, 7049–7054.
9. P. Wittung, P. E. Nielsen, and B. Norden (1997) Biochemistry 36, 7973–7979.
10. P. Wittung et al. (1994) Nature 368, 561–563.
11. P. Wittung, P. E. Nielsen, and B. Norden (1997) J. Am. Chem. Soc. 119, 3189–3190.
12. S. C. Brown, S. A. Thomson, J. M. Veal, and D. G. Davis (1994) Science 265, 777–780.
13. M. Leijon et al. (1994) Biochemistry 33, 9820–9825.
14. L. Betts, J. A. Josey, J. M. Veal, and S. R. Jordan (1995) Science 270, 1838–1841.
15. H. Rasmussen et al. (1997) Nat. Struct. Biol. 4, 98–101.
16. B. Hyrup et al. (1994) J. Am. Chem. Soc. 116, 7964–7970.
17. K. H. Petersen et al. (1995) Bioorg. Med. Chem. Lett. 5, 1119–1124.
18. H. Knudsen and P. E. Nielsen (1997) Anticancer Drugs 8, 113–118.
19. L. Good and P. E. Nielsen (1998) Nat. Biotechnol. 16, 355–358.
20. P. Wittung et al. (1995) FEBS Lett. 365, 27–29.
21. W. M. Partridge, R. J. Boado, and Y.-S. Kang (1995) PNAS 92, 5592–5596.
22. H. Orum et al. (1993) Nucleic Acid Res. 21, 5532–5336.
23. V. Demidov et al. (1993) Nucleic Acid Res. 21, 2103–2107.
24. H. Orum et al. (1995) BioTechniques 19, 472–480.
25. P. Wittung et al. (1994) Nucleic Acid Res. 22, 5371–5377.
26. S. L. Miller (1997) Nat. Struct. Biol. 4, 167–169.
27. B. Norden (1978) J. Mol. Evol. 11, 313–332.
28. A. W. Schwartz (1994) Curr. Biol. 4, 758–760.
29. R. H. Berg, S. Hvilsted, and P. S. Ramanujam (1996) Nature 383, 505–507.

Suggestion for Further Reading

30. M. Eriksson and P. E. Nielsen (1996) PNA-nucleic acid complexes. Structure, stability and dynamics, Q. Rev. Biophys. 29, 369–394.

Peptide Synthesis

The chemical synthesis of small proteins has only recently become feasible with reliability. Progress in this field has depended on the development of the solid phase procedure and the automated synthesizer by Merrifield to reduce the labor and errors associated with repetitive manual procedures. Difficulties in generating pure peptides arose from accumulated byproducts resulting from synthetic difficulties in chain assembly and deprotection of side-chain functionality. Advances in analytical and purification technologies have provided tools for addressing these problems. A variety of strategies have been developed to overcome the synthetic difficulties, and several laboratories have invested sufficiently in the optimization of the technology to produce synthetic small proteins of sufficient purity as to remove any doubts regarding their biological effects (1).

One of the first examples where a small synthetic protein had a major impact on a biological problem of clinical significance was the development of human immunodeficiency virus (HIV) proteinase inhibitors. Although the gene sequence for the 99-residue protein which dimerized to give the active proteinase, was identified when the DNA sequence of the gene for HIV was determined, cloning and expressing of HIV proteinase proved to be exceptionally difficult for pharmaceutical groups, even for those with records of considerable previous success in biotechnology. Synthetic HIV proteinase, a 99-residue homodimer prepared in the laboratory of Stephen Kent (2), was used in the initial determination of HIV proteinase specificity and inhibitor screening. The availability of this synthetic protein certainly expedited the development of HIV proteinase inhibitors used for the treatment of acquired immune deficiency syndrome (AIDS). This example and others would argue that chemical synthesis of small proteins may be more rapid than cloning and expression for some proteins, and it can provide ready access to sufficient quantities (hundreds of milligrams) of protein for screening or biophysical studies. In fact, the first X-ray crystallography structure (3) of HIV proteinase complexed with an inhibitor, MVT-101, used synthetic HIV proteinase and set the record for the largest synthetic molecule whose structure was confirmed by crystallography.

1. Solution Versus Solid Phase

Traditional approaches to peptide synthesis were based on solution methods using convergent synthetic schemes, with isolation and characterization of each intermediate. This provided well-defined products with confidence in their final structures, but at the price of increased labor and losses at each synthetic step in separating product from reagents and byproducts. Until recently, the synthesis of small proteins (60 to 100 residues) has been dominated by fragment condensation in solution with maximal protection of side chains. The desired protein sequence is divided into peptide segments of about 10 residues, which is about the maximum length of peptide readily prepared by stepwise addition in solution. After each reaction, the product is isolated and fully characterized before proceeding with the next reaction. Once the set of fragments has been prepared, they are combined pairwise to generate segments of approximately 20 residues. These are then combined pairwise to generate fragments of approximately 40 residues, and this fragment condensation continues until the desired sequence is obtained. The protecting groups on side chains are then removed to give the fully unprotected peptide chain, which is allowed to fold, resulting in the desired protein. First, the 80-residue protein is divided into eight 10-residue segments that are prepared by stepwise elongation requiring nine coupling and nine deprotection steps, with isolation of each intermediate to give a completely protected fragment with both amino and carboxyl termini protected. Depending on the role of the segment, either its N- or C-terminus is deprotected and reacted with its adjacent fragment. This process is continued until the entire protein is assembled, deprotected, purified, and allowed to fold.

The solid-phase approach utilizes a polymeric protecting group that allows the use of excess reagents to force reactions to near completion by the mass action law and trivial isolation of polymeric product by filtration and washing. Intermediates are not isolated, and purity of the final product depends on complete reaction at each synthetic step and minimization of side reactions during the buildup of the oligomeric peptide and subsequent removal from the polymer with deprotection, to give the desired product. The advent of high-performance liquid chromatography (HPLC) with more sophisticated techniques such as nuclear magnetic resonance (NMR), capillary electrophoresis, and mass spectrometry for purification and characterization of the intermediates and final products allows routine synthesis of peptides in the 50- to 100-residue range. Because of the difficulties in purification of larger peptides and small proteins with only minor differences in structure from byproducts, the unambiguous synthesis of larger peptides and small proteins is best accomplished by assembly of fragments that have been purified and fully characterized. This prevents accumulation of side products with only minor structural differences that can be difficult to remove in the final mixture. Initially, chain assembly was relatively easy to optimize, and the majority of undesirable side products in the final cleavage were due to incomplete deprotection of side chains. Considerable effort over two decades was devoted to understanding the sequence-dependent problems leading to truncated sequences or those missing a residue, but these efforts were hampered by the polymeric support itself, which limited application of the normal methods for characterizing intermediates. This effort has led to the current state of the technology, in which average reaction yields are estimated to be greater than 99.5%. Such yields are essential if multiple sequential chemical reactions are performed without isolation and purification of intermediate products.

Automation of the solid-phase reaction was initiated almost immediately once a viable synthetic scheme for peptides was evolved, and the first automated synthesizer was announced by Merrifield and Stewart in 1965 (4). Continuous development of synthesizers and the associated chemistry allows the automated addition of 75 residues per day to a growing peptide chain (5). In many cases, the repetitive yields are sufficiently high that useful products can be isolated from the synthetic mixture by HPLC when small proteins are prepared. If one desires to be more confident that the observed properties are uniquely determined by the targeted sequence, then a more conservative approach utilizing fragment condensation is still required.

Illustrative are the solid-phase protocols for the two strategies (Boc and Fmoc) commonly used for the synthesis of peptides. The Boc strategy (Fig. 1) is often combined with a 1% to 2% cross-linked polystyrene support and a benzyl ester linkage to the polymer, requiring strong acid such as hydrogen fluoride for deprotection. The procedure favored by most synthetic laboratories uses an acid-labile linkage similar to the p-methoxybenzyl ester linkage of the Wang resin and a base-labile amino protecting group, the fluorenylmethyloxycarbonyl (Fmoc), on the added amino acids (Fig. 2). One can use side-chain protection with similar acid lability to the Wang linkage to give free peptide upon cleavage, or use more stable side-chain protection to give the protected peptide for fragment condensation after purification and characterization. In the latter case, a final deprotection with strong acid such as HF is required.

Figure 1. A common implementation of the BOC strategy for peptide synthesis.

Figure 2. The alternative FMOC/Wang support strategy which allows ready synthesis of protected peptide fragments as

2. Orthogonal and Selective Protection

Because many of the 20 common amino acids have side chains containing chemically reactive groups (carboxyl, hydroxyl, imidazole, indole, phenol, amine, guanidinium) which could compete for selective peptide bond formation, they must be protected temporarily during assembly to make sure that only the desired a-amino and a-carboxyl groups react to join the protected amino acid to the growing peptide chain with the desired linkage. It is essential that these side-chain protecting groups are stable (orthogonal) to the conditions used for removal of the amino protecting group (Fig. 3) in chain elongation and yet be readily removable at the end of the synthesis. Much effort has been expended developing compatible sets of protecting groups for the 20 naturally occurring amino acids. The peptide chain is routinely assembled stepwise from the C- to N-terminus because one can best preserve the chiral integrity of the component amino acids by activating the carboxyl group of a urethane-protected amino acid [ROCO-, where R = t-butyl (Boc), R = benzyl (Z), and R = fluorenylmethyl (Fmoc)] for coupling with the N-terminal amine of the growing peptide chain. After the addition of a protected amino acid, the a-amino protecting group must be removed in order to provide the amine nucleophile for the next reaction. This must be accomplished while retaining the side-chain protecting groups of the growing peptide chain. This leads to the concept of orthogonal protection, in which the a-amino group is protected with a group that can be removed selectively by a mechanism that does not affect the side-chain protecting groups. A common example in solid-phase synthesis would be the use of the Fmoc group, which can be removed repetitively from the a-amino groups under basic conditions, and the use of acid-labile protecting groups, such as Boc or OtBu, on the side chains that must remain throughout chain elongation. If one attempts to couple a peptide to another peptide by activation of the carboxyl group of one of the two, the chiral integrity of the amino acid whose carboxyl group is activated (which is analogous to coupling an acetyl amino acid, which can form a cyclic intermediate, leading to rapid exchange and inversion of the alpha carbon) is often compromised by racemization, consequently, a mixture of peptides with R and S configurations at the activated amino acid results. This leads to the use of special procedures for coupling peptides, as well as a strong priority to favor glycine or proline as the C-terminal residues in fragment coupling, due to their resistance to racemization. Chemical or enzymatic ligation of peptide fragments offers an alternative approach to simple chemical activation of the C-terminal carboxyl group of one fragment and nucleophilic attack by the N-terminal amino group of the other fragment.

Figure 3. Urethane protecting groups for amino groups in common usage. Boc, t-butyloxycarbony; Z, carbobenzoxy (or benzyloxycarbonyl); Fmoc, fluorenylmethyloxycarbonyl.

3. Coupling Reagents

The choice of one of the numerous reagents to activate the carboxyl group for nucleophilic attack by the amine function, to produce the peptide bond, depends on numerous factors. When coupling peptide fragments, reagents that minimize racemization are preferred; a traditional favorite in solution chemistry for coupling fragments has been the azide group. A common procedure is activation by a combination of a diimide, such as 1,3-diisopropylcarbodiimide (DIC) or 1,3-dicyclohexylcarbodiimide (DCCI), with hydroxybenzotriazole (HOBt), or through the use of an activated derivative of HOBt, such as TBTU, to generate the activated HOBt ester in situ. Incorporation of multiple sequential sterically hindered amino acids (valine, isoleucine, aminoisobutyric acid, etc.) often require the use of special coupling reagents, such as acid fluorides, HATU, etc.) to provide reasonable reaction rates and efficient coupling yields.

4. Minimal Versus Maximal Protection

In order to get selectivity in the reaction, all reactive groups except the two that are desired to react can be protected transiently with chemically labile protecting groups. This is referred to as maximal protection and would be preferred, except for incomplete removal and side reactions associated with deprotection of the fully protected peptide product containing a heterogeneous set of protecting groups. In solid-phase synthesis, assembly of the correct sequence is often quite facile, but incomplete removal of the protecting groups can lead to an intractable mixture. By careful control of reaction conditions (aqueous, pH, etc.), one can eliminate some of the side-chain protection to minimize problems associated with protecting group removal. This is referred to as minimal protection and is preferred if selective acylation of the amino terminus by the carboxyl of the N-terminal peptide can be achieved.

5. Chemical Ligation

Certain groups of chemical functionality have exceptional affinities for selective reaction, particularly in the formation of small rings. Recent developments have led to the synthesis of large peptide fragments by solid-phase synthesis, removal from the polymeric support and of most, if not all, side-chain protecting groups, and then selective coupling of the unprotected fragments based on chemical ligation. The most developed strategy for this approach is the use of an N-terminal cysteine residue with a special reactive C-terminal group on the other peptide. This approach was initially conceived by Kemp in his thiol capture strategy (7) and was reduced to a practically successful general approach by the groups of Kent (8-10) and Tam (11-13). For illustrative purposes, the native chemical ligation procedure of Dawson et al. (9) is described (Fig. 4), because it seems to have had the most practical impact. In this case, solid-phase synthesis is used to prepare two unprotected peptide segments that are combined in aqueous solution. The C-terminal fragment contains an N-terminal cysteine residue, and the C-terminal peptide fragment is prepared as the thioester. The thioester is displaced by the thiolate anion of a Cys residue. If the Cys is N-terminal, an acyl migration through formation of a five-membered ring occurs to generate the desired stable amide bond. If the sulfur atom of a Cys residue within the peptide chain is involved, then the thioether formed is capable of being displaced by other thiols, until the fragment migrates to the N-terminal Cys, when the stable rearrangement can occur. An alternative strategy, using an N-terminal b-bromoalanine of fragment two and the C-terminal thioester of fragment one to give the same covalent thioester intermediate by thioesterification, has been explored by Tam et al. (12)

Figure 4. Native chemical ligation of two unprotected peptide fragment using thiol–thioester exchange with ligation at the N-terminal cysteine residue (9).

While many proteins contain cysteine residues, and some have them optimally spaced for fragment assembly, many do not, and one of the research goals in this area is the extension of these concepts to allow coupling at residues other than the N-terminus of cysteine residues. Some success has been achieved with ligation at X–Gly and Gly–X sites (14), as well as at X–His sites (15). Another development that bodes well for the chemical synthesis of larger proteins is the adaptation of chemical ligation to solid-phase using agarose as the polymeric support. This should allow repetitive ligation of smaller fragments to generate the larger protein stepwise on the polymer.

6. Applications

One might question why one would want to prepare small proteins when one can easily express the genetic message in a variety of biological systems, including eukaryotic systems that include post-translational modification. Limitations of normal expression systems to the 20 common amino acids restricts chemical modification of the parent protein for a variety of biophysical and pharmaceutical applications. Incorporation via molecular biology of novel amino acids as spectroscopic probes, or to introduce conformational constraints, is feasible using the suppressor mutation approach pioneered by the Schultz group (16-18). In this case, however, steric limitations of the protein biosynthetic machinery preclude the use of certain unusual amino acids or constrained dipeptides (19), which are readily accessible via organic synthesis. The quantities of protein obtained by this approach are generally small, requiring assay methods (enzymatic or spectroscopic) that are sensitive as well as specific.

6.1. Peptide Libraries

The explosion of combinatorial chemistry in the pharmaceutical industry as a paradigm for drug discovery was foreshadowed in the use of peptide libraries by Geysen (20) to map peptide epitopes or antigenic sites on proteins. Numerous strategies (21-23) to synthesize mixtures of thousands to millions of peptides and allow selection of those with the desired activities (24) have developed over the past 20 years. Combinatorial synthesis of individual compounds for assay has developed rapidly, because it eliminates the problem of deconvolution of the mixture to identify the individual compound responsible for the observed activity. It also simplifies the pharmacological evaluation of compounds, due to concerns over synergy or the inhibition of activity that is potentially possible in the bioassay of mixtures. Nevertheless, the most effective strategy for lead generation and optimization will be determined by the cost and efficiency of the biological screen versus that of synthesis.

Bibliography

1. T. W. Muir and S. B. Kent (1993) Curr. Opin. Biotech. 4, 420–427.
2. J. Schneider and S. B. Kent (1988) Cell 54, 363–368.
3. M. Miller, B. K. Sathyanarayana, A. Wlodawer, M. V. Toth, G. R. Marshall, L. Clawson, L. Selk, J. Schneider, and S. B. H. Kent (1989) Science 246, 1149–1152.
4. R. B. Merrifield and J. M. Stewart (1965) Nature 207, 522–523.
5. M. Schnolzer, P. Alewood, A. Jones, D. Alewood, and S. B. Kent (1992) Int. J Peptide Protein Res. 40, 180–193.
6. L. A. Carpino, D. Sadat-Aalaee, H. G. Chao, and R. H. DeSelms (1990) J. Am. Chem. Soc. 112, 9651–9652.
7. D. S. Kemp and R. I. Carey (1993) J. Org. Chem. 58, 2216–2222.
8. M. Schnolzer and S. B. Kent (1992) Science 256, 221–225.
9. P. E. Dawson, T. W. Muir, I. Clark-Lewis, and S. B. Kent (1994) Science 266, 776–779.
10. T. W. Muir, P. E. Dawson, and S. B. Kent (1997) Methods Enzymol. 289, 266–298.
11. C.-F. Liu and J. P. Tam (1994) J. Am. Chem. Soc. 116, 4149–4153.
12. J. P. Tam, Y. A. Lu, C. F. Liu, and J. Shao (1995) Proc. Natl. Acad. Sci. USA 92, 12485–12489.
13. C. F. Liu, C. Rao, and J. P. Tam (1996) J. Am. Chem. Soc. 118, 307–312.
14. L. E. Canne, S. J. Bark, and S. B. H. Kent (1996) J. Am. Chem. Soc. 118, 5891–5896.
15. L. S. Zhang and J. P. Tam (1997) Tetrahedron Lett. 38, 3–6.
16. C. J. Noren, S. J. Anthony-Cahill, M. C. Griffith, and P. G. Schultz (1989) Science 244, 182–188.
17. D. Mendel, J. Ellman, and P. G. Schultz (1993) J. Am. Chem. Soc. 115, 4359–4360.
18. J. A. Ellman, D. Mendel, and P. G. Schultz (1992) Science 255, 197–200.
19. S. Hanessian, G. McNaughton-Smith, H.-G. Lombart, and W. D. Lubell (1997) Tetrahedron 53, 12789–12854.
20. H. M. Geysen (1985) Immunol. Today 6, 364–369.
21. R. A. Houghten, C. Pinilla, S. E. Blondelle, J. R. Appel, C. T. Dooley, and J. H. Cuervo (1991) Nature 354, 84–86.
22. K. S. Lam, S. E. Salmon, E. M. Hersh, V. J. Hruby, W. M. Kazmierski, and R. J. Knapp (1991) Nature 354, 82–84.
23. A. Furka (1995) Drug Dev. Res. 36, 1–12.
24. G. Koppel, C. Dodds, B. Houchins, D. Hunden, D. Johnson, R. Owens, M. Chaney, T. Usdin, B. Hoffman, and M. Brownstein (1995) Chem. Biol. 2, 483–487.

Suggestions for Further Reading

25. B. Merrifield (1993) Life During a Golden Age of Peptide Chemistry, American Chemical Society, Washington, D.C.
26. B. Gutte, ed., (1995) Peptides: Synthesis, Structures and Applications, Academic Press: New York.

27. M. Bodansky (1984) Principle of Peptide Synthesis, Springer-Verlag, New York.
28. M. Bodansky and A. Bodansky (1984) The Practice of Peptide Synthesis, Springer-Verlag, New York.

Peptidyl Prolyl Cis/Trans Isomerases

Only a few cis/trans isomerizations are catalyzed by enzymes. Most of these enzymes catalyze isomerization of C=C double bonds. However, the highly abundant and ubiquitously distributed peptidyl prolyl cis/trans isomerases (PPIases) have evolved to accelerate the rotation about a formal single bond. They catalyze the cis/trans isomerization of imide peptidyl-proline bonds and are inactive toward the -CONH- peptide moiety. In enzyme nomenclature, PPIases are classified under EC number 5.2.1.8.

Initially, PPIases were identified in the cytosol of kidney cells from their ability to accelerate the cis to trans isomerization of chromogenic tetrapeptides of the type succinyl-Ala-Xaa-Pro-Phe-4-nitroanilides (where Xaa is any natural amino acid) by an assay that utilizes the conformational specificity of chymotrypsin (1). Briefly, in this cis/trans assay, the trans prolyl bond isomer of the substrate succinyl-Ala-Ala-Pro-Phe-4-nitroanilide (about 92% of the total) is cleaved completely at the anilide bond in a few seconds when high concentrations (≫ mM) of the proteinase are used. The remaining cis isomer of the peptide (8%) is resistant to chymotrypsin until it undergoes cis to trans isomerization. When monitored by the absorbance of the released product (4-nitroaniline), the isomerization is the rate-limiting step for proteolyzing the cis isomers indirectly. It can be quantified as a first-order reaction with a half-time of about 90 s at 10°C. This kinetic phase, which is equivalent to a quasi-irreversible cis to trans isomerization, has an accelerated rate in the presence of catalytic amounts of a PPIase. The calculated rate constants depend linearly on the PPIase concentration. This assay could not demonstrate catalysis in both directions, but this was possible with NMR (2, 3). The standard assay was greatly improved by dissolving the assay peptides in LiCl/trifluoroethanol to increase the fraction of cis isomer (4).

PPIases were initially anticipated to be fold/rearrangement catalysts for proteins bearing cis prolyl bonds in the native state because the slow trans to cis interconversion following protein synthesis on the ribosome will seriously limit the rate of in vivo protein folding. Indeed, PPIases increase the rate of the slow kinetic phases in vitro refolding of many denatured proteins known to be limited in rate by prolyl isomerization. In support of a physiological role in protein folding, the involvement of a PPIase in triple-helix formation in type I procollagen was shown in chick embryo fibroblasts in cellulo (5). However, the biological functions of PPIases are not yet well understood, and they may have more general roles than affecting only de novo protein folding.

According to our current knowledge, the enzyme class of PPIases comprises three families with unrelated amino acid sequences: cyclophilins (abbreviated Cyp), FK506-binding proteins (abbreviated FKBP), and parvulins. An additional subfamily, the prokaryotic trigger factors, exhibits weak sequence similarity to FKBP proteins but lacks FK506-binding ability (6). The amino acid sequences of several dozen different PPIases are known, encompassing molecular masses from 10.1 kDa (92 amino acids in length) for E. coli parvulin (7) to 158 kDa for the NK-TR1 cyclophilin of human, large granular lymphocytes (8). Typically, Escherichia coli cells harbor two cyclophilins, four FKBP-like PPIases, the archetype of parvulins, along with the SurA protein containing two parvulin domains, and the ribosome-bound trigger factor. Among the 470 predicted coding regions in the free-living bacterium Mycoplasma genitalium, which has the smallest known genome of any free living organism, a trigger factor homologue is the sole PPIase present (9).

Members of the PPIase families resemble perfectly evolved enzymes for catalytic efficiency (10). For oligopeptide substrates, both the Michaelis constant, K_m, and the turnover number, k_{cat}, are large and yield values of k_{cat}/K_m of up to $>10^7\ M^{-1}\ s^{-1}$. These bimolecular rate constants approach the diffusion-controlled limits for enzyme reactions (see Enzymes). With $k_{cat}/K_m = 1.1 \times 10^6\ M^{-1}\ s^{-1}$, the *E. coli* trigger factor catalyzing refolding of a denatured ribonuclease T1 variant exemplifies a particularly efficient catalysis in protein folding (11). This efficacy results from having extended secondary binding sites to bind the unfolded protein substrate favorably. These subsites encompass the two protein domains flanking the central PPIase domain of the enzyme. Many of the PPIase enzymes are specific only for certain amino acid residues flanking the proline in the primary structure, but this is less important with the cyclophilins. Conversely, a hydrophobic side chain of the amino acid preceding the proline enhances catalysis by FKBPs.

PPIases applied in catalytic amounts cannot alter the *cis/trans* equilibrium of the substrates, as expected. When protein refolding is hindered by misfolding and protein aggregation, an increase of the yield of native protein is not obtained by supplementing the refolding buffer with a PPIase. Thus, an important aspect of chaperones is missing in PPIases (12).

Immunosuppressive compounds, like cyclosporin A, FK506 and rapamycin, bind tightly to the respective active site of cyclophilins and FKBPs and inhibit their enzymatic activities reversibly and competitively and have inhibition constants in the picomolar to micromolar range. Cross-inhibition of the different classes does not occur. At the present time, no specific reversible inhibitors for parvulins and trigger factors have been reported.

Definitive identification of the natural substrates of PPI-ases has not been reported yet. Nevertheless, a number of binding proteins, which may include the putative cellular substrates, were identified by chemical cross-linking, affinity chromatography, the yeast two-hybrid screen, and by co-purification. For example, the nuclear parvulin-like PPIase Pin1 has affinity for NIMA protein kinase in the two-hybrid system. The catalytic activity of this isomerase is involved in cell-cycle control in eukaryotes (13). For the trigger factor family, association with nascent chains derived from secreted and cytosolic proteins and specific affinity for the 50S subunit of the *E. coli* ribosome are indicated by cross-linking and fractionation of enzyme activity (6, 14, 15). On the other hand, the same PPIase has been detected as an indispensable component of the heterooligomeric complex of the chaperone GroEL with the degradable fusion protein CRAG. This system has been used to determine the requirements for rapid degradation of abnormal, misfolded proteins by the proteinase ClpP in *E. coli* cells (16). When a trace of copurifying protein of the ryanodine receptor was analyzed, it became obvious that intracellular calcium release channels on the endoplasmic or sarcoplasmic reticulum (ryanodine receptor, RyR) and the inositol 1,4,5-triphosphate receptor constitute heterooligomeric complexes of the type $((RyR)_4(FKBP12)_4)$ with either cytosolic FKBP12 or FKBP12.6 (17, 18). A dysfunctional state, associated with the impairment of the receptor-mediated Ca^{2+} retardation of the channel, arises from inhibiting PPIase activity with both FK506 and rapamycin (19). Furthermore, FKBPs and cyclophilins in the range of 40 to 60 kDa were found as components of the unactivated steroid receptor complex, associated with the hsp90 component of the receptor (20). Interestingly, two members of different families of proteins that assist protein folding, an enzyme and a chaperone, coexist as binding partners in this receptor complex.

Bibliography

1. G. Fischer, H. Bang, and C. Mech C. (1984) Biomed. Biochim. Acta 43, 1101–1111.
2. D. Kern et al. (1995) Biochemistry 34, 13594–13602.
3. R.M. Justice, Jr. et al. (1990) Biochem. Biophys. Res. Commun. 171, 445–450.

4. J.L. Kofron et al. (1991) Biochemistry 30, 6127–6134.
5. B. Steinmann, P. Bruckner, and A. Superti-Furga (1991) J. Biol. Chem. 266, 1299–1303.
6. G. Stoller et al. (1995) EMBO J. 14, 4939–4948.
7. J.U. Rahfeld et al. (1994) FEBS Lett. 352, 180–184.
8. S.K. Anderson et al. (1993) Proc. Natl Acad. Sci. USA 90, 542–546.
9. C.M. Fraser et al. (1995) Science 270, 397–403.
10. J.J. Burbaum, R.T. Raines, W.J. Albery, and J.R. Knowles (1989) Biochemistry 28, 9293–9305.
11. C. Scholz et al. (1997) EMBO J. 16.
12. G. Kern, D. Kern, F.X. Schmid, and G. Fischer (1994) FEBS Lett. 348, 145–148.
13. K.P. Lu, S.D. Hanes, and T. Hunter (1996) Nature 380, 544–547.
14. Q.A. Valent et al. (1995) EMBO J. 14, 5494–5505.
15. T. Hesterkamp, S. Hauser, H. Lutcke, and B. Bukau (1996) Proc. Natl Acad. Sci. USA 93, 4437–4441.
16. O. Kandror, O.M. Sherman, M. Rhode, and A.L. Goldberg (1995) EMBO J. 14, 6021–6027.
17. H.B. Xin et al. (1995) Biochem. Biophys. Res. Commun. 214, 263–270.
18. A.P. Timerman et al. (1996) J. Biol. Chem. 271, 20385–20391.
19. A.R. Marks (1996) Trends Cardiovasc. Med. 6, 130–135.
20. T. Ratajczak and A. Carrello (1996) J. Biol. Chem. 271, 2961–2965.

Suggestions for Further Reading

21. J.E. Kay (1996) Structure-function relationships in the FK506-binding protein (FKBP) family of peptidyl-prolyl cis/trans isomerases, Biochem. J. 314, 361–385; an important reference source about FKBPs.
22. G. Fischer (1994) Peptidyl-prolyl cis/trans isomerases and their effectors, Angew. Chem., Int. Ed. Engl. 33, 1415–1436.
23. F.X. Schmid (1993) Prolyl isomerase: Enzymatic catalysis of slow protein-folding reactions, Ann. Rev. Biophys. Biomol. Struct. 22, 123–143; summarizes PPIase catalysis in protein folding.
24. A. Galat and S. M. Metcalfe (1995) Peptidylproline cis/trans isomerases, Prog. Biophys. Mol. Biol. 63, 67–118; contains an exhaustive bibliography of many aspects of PPIases.

Peptidyl Transferase

Peptidyl transferase is an integral part of the large subunit of ribosomes and catalyzes peptide-bond formation in the elongation step of translation during protein biosynthesis. Peptide-bond formation involves an acyl group O-to-N migration and converts an ester to an amide. Peptidyl-transfer RNA in the P site is the ester bond of high energy content that donates its peptidyl group to the amino group of aminoacyl-tRNA bound in the A site of the ribosome. The peptidyl transferase reaction is often measured by the puromycin reaction, in which puromycin acts as the acceptor substrate to form peptidyl-puromycin. In bacteria, peptidyl transferase activity can be detected in the 50 S ribosomal subunit, and several ribosomal proteins are thought to play a role in the activity. The primary activity of peptidyl transfer, however, is a ribozyme activity encoded in the 23 S rRNA. The peptidyl transferase activity of *Escherichia coli* and *Thermus aquaticus* ribosomes are resistant to conventional protein extraction procedures (1), and the formation of a G-C pair between G2252 in the conserved hairpin loop of *E. coli* 23 S rRNA and C74 in the 3 terminal region of tRNA is a prerequisite for the peptidyl transfer reaction. These findings suggest that not all the large subunit proteins are necessarily required for peptidyl transferase activity. It has been shown recently that *E. coli* 23 S rRNA synthesized by *in vitro* transcription with T7 RNA polymerase exhibits the primary peptidyl transfer activity in the absence of any ribosomal proteins *in vitro*, and that the truncated domain V transcript alone has this activity (2).

Peptidyl transferase is also involved in the termination reaction of protein synthesis and hydrolyzes the ester bond between the peptide chain and tRNA at the P site of the ribosome (see Release Factor). Peptidyl transferase is inhibited by various antibiotics, such as chloramphenicol, lincomycin, carbomycin (prokaryotes), and cycloheximide (eukaryotes).

Bibliography

1. H. F. Noller, V. Hoffarth, and L. Zemniak (1992) Science 256, 1416–1419.
2. I. Nitta, Y. Kamada, H. Noda, T. Ueda, and K. Watanabe (1998) Science 281, 666–669.

Suggestion for Further Reading

3. K. S. Wilson and H. F. Noller (1998) Cell 92, 337–349.

Perinuclear Space

The perinuclear space is the lumenal space between the inner and outer nuclear envelope bilayers that separate the nucleus from the cytoplasm. The width of the space is between 100 Å and 500 Å. Because the outer nuclear membrane is continuous with the endoplasmic reticulum, the perinuclear space is continuous with the lumen of the endoplasmic reticulum.

Permissive Condition

The condition under which a conditional lethal mutant grows is called the permissive condition, in contrast to the nonpermissive condition or restrictive condition, which restricts growth (see Conditional Lethal Mutations).

Peroxidase

Peroxidases occur throughout the biosphere and catalyze the oxidation of various substrates at the expense of peroxide. Peroxidases are involved in plant growth hormone metabolism, the production of thyroxine, neutrophil-mediated detoxification reactions, prostaglandin biosynthesis, and lignin degradation, to name a few. Although peroxidases are found in plants, animals, and microorganisms, the most thoroughly understood are the nonmammalian heme-containing peroxidases. They all are single polypeptide chains in the range of 30 to 40 kDa and contain a single ferric protoporphyrin IX as the prosthetic group. Based on sequence analysis and now X-ray crystallographic structures, the nonmammalian peroxidases have been divided into three classes (1): intercellular (Class I), extracellular fungal (Class II), and extracellular plant peroxidases (Class III). The extracellular enzymes are glycosylated, and in the case of Class III enzymes there often are many isozymes with varying degrees of glycosylation. The extracellular peroxidases contain two calcium-binding sites and at least four disulfide bonds, presumably for the additional stability required of secreted enzymes.

Now a wealth of structural information is available about peroxidases because of recent crystal structure determinations. Coupled with the cloning and expression of several peroxidases in recombinant systems, this has opened the way for using protein engineering methods to study structure–function relationships.

1. Catalytic Cycle

The overall peroxidase cycle occurs in three distinct steps:

(1)

(2)

(3)

where P is the enzyme porphyrin whose heme iron is indicated, and S is the substrate. In Step 1, the peroxide removes two electrons from the enzyme to give what is called Compound I. In doing so, the peroxide O–O bond is broken, produces water, and the second peroxide-derived oxygen atom remains coordinated to the iron. One electron is removed from the iron to give the oxy-ferryl intermediate (Fe^{4+} = O), and a second electron is removed from the porphyrin to give a porphyrin p cation radical. In some peroxidases, an amino acid side chain is oxidized to a radical rather than the porphyrin. Normally, the formation of Compound I is quite easy to follow because the resting enzyme is red/brown in color, whereas Compound I is green. In Step 2, the porphyrin radical is reduced, producing a substrate radical, S·. Because of porphyrin reduction, Compound II is no longer green, but red. Finally in Step 3, Compound II is reduced by a second substrate molecule. In plant peroxidases, the substrates are normally small aromatic molecules. Once substrate radicals form, they dimerize or disproportionate in nonezymatic reactions.

2. Three-Dimensional Structures

From 1980 to 1993, only one nonmammalian heme peroxidase crystal structure was known, cytochrome c peroxidase. Since then an additional six structures have been determined (2), and there may well be more on the way. Representative examples of Class I, II, and III peroxidases are shown in Fig. 1. The sequence identity can be as low as 15% between peroxidases, yet the crystal structures have a similar fold independent of sequence homology or phylogenetic origin. This underscores the important "rule" in structural biology that tertiary structure is far more conserved than primary structure. All of the various peroxidases consist of a core of 10 alpha helices, two of which, the B and F helices, sandwich the heme plane. The various peroxidases differ in structure primarily on the surface. For example, Class III peroxidases have two additional a-helices on the surface (F′ and F″), whereas cytochrome c peroxidase has a beta-sheet structure. It is thought that these additional helices in the Class III enzymes may play a role in substrate binding.

Figure 1. Representative crystal structures from each of the three primary classes of nonmammalian heme peroxidases: (CCP, cytochrome c peroxidase); Class II (LIP, lignin peroxidase); Class III (PNP, peanut peroxidase). The a-helices are as labeled cylinders, and the beta structure as shaded ribbons.

3. Active-Site Structures

Not surprisingly, the active sites of heme peroxidases are highly conserved (Fig. 2). The proximal pocket contains the His residue coordinated to the heme iron. This His ligand donates a hydrogen bond to the conserved Asp residue. It is thought that this interaction imparts a greater imidazolate character to the His ligand, resulting in extra negative charge on the His residue that stabilizes the Fe^{3+} state of the heme. This is one reason that peroxidases exhibit a lower redox potential in the Fe^{3+}/Fe^{2+} couple than the globins, even though the globins and peroxidases both use a His ligand. Directly adjacent to the His ligand, Most peroxidases have an aromatic residue stacked parallel to and in contact with the His ligand. This residue is Phe in most peroxidases, but Trp in the two known Class I peroxidase structures. For the class I peroxidases, the Trp indole ring N atom donates a hydrogen bond to the conserved proximal Asp residue (Fig. 2).

Figure 2. The active site structure of ascorbate peroxidase, a representative example of a nonmammalian heme peroxidase.

The B helix provides key catalytic residues on the opposite, distal side of the heme. It is thought that the distal His and Arg residue operate in concert to help cleave the peroxide O–O bond. Stacked parallel to the distal heme surface is a conserved aromatic residue, which is Phe in the known crystal structures, except for the Class I peroxidases, which use Trp.

4. Catalytic Mechanism

Most of the effort in understanding the peroxidase mechanism has centered on the formation of Compound I. It is thought that the distal His and Arg residues operate in concert to ensure that the peroxide O–O bond is cleaved heterolytically (3; Fig. 3). The distal His operates as an acid/base catalyst by removing a proton from the incoming peroxide and delivering it to the peroxide O2 atom. As shown in Fig. 3, the distal His donates a hydrogen bond to an invariant Asn residue, which ensures that the Nd2 of the distal His is free to accept a proton from the incoming peroxide. The Arg residue may help to stabilize a developing negative charge on the leaving O2 atom. The net result is heterolytic fission of the peroxide O–O bond. This leaves behind an “oxene” O atom that contains only six valent electrons, a potent oxidant. The oxene center removes one electron from the iron atom, to give Fe^{4+} and one from a neighboring organic group, normally the porphyrin. The crystal structure of Compound I (4) shows that the distal Arg residue swings in to hydrogen-bond with the iron-linked oxygen atom. This may account in part for the stability of the $Fe^{4+} = O$ center in Compound I.

Figure 3. The catalytic mechanism of Compound I formation.

The formation of Compound I is stoichiometric and has a second-order rate constant of between 10^7 and 10^8 M^{-1} s^{-1} for most heme peroxidases. Site-directed mutagenesis has been used to probe this mechanism by amino acid substitution of key catalytic groups in the active site. Changing the distal His to Leu (6) lowers the rate of Compound I formation by 10^5, demonstrating that the distal His is indeed a critical residue. Somewhat surprisingly, the nature of the proximal ligand is not important for Compound I formation because a Gln that replaces the proximal His residue affects only the stability of Compound I and not the rate of formation (6).

5. Enzyme Substrate Complexes

All of the known heme peroxidase structures show that one heme edge is accessible to small aromatic molecules that are typical peroxidase substrates. It is generally thought that small substrates interact at this site and deliver electrons directly to the heme, resulting in reduction of the Compound I porphyrin radical or Compound II $Fe^{4+}=O$ center. Nevertheless, there is no direct structural evidence for this view. To date, only the structures of two heme peroxidase-substrate complexes are known. Manganese peroxidase oxidizes Mn^{2+} to Mn^{3+}, and the Mn^{3+} operates in a complex with dicarboxylic acids as a diffusible oxidant of lignin. The crystal structure of manganese peroxidase (7) shows that Mn^{2+} coordinates with protein carboxylates and one heme propionate. Cytochrome c peroxidase is unusual among the known heme peroxidase structures because its substrate is another protein, cytochrome c. The crystal structure of the cytochrome c peroxidase–cytochrome c complex (8) has provided important insights into the nature of interprotein electron transfer reactions.

6. Heme Halo Peroxidases

The crystal structure of one heme halide peroxidase is known (9). Chloroperoxidase (CPO) is secreted by the mold *Caldariomyces fumago* where it functions to chlorinate 1,3-cyclopentanedione to the natural product 2,2-dichloro-1,3-cyclopentanediol (caldariomycin). The catalytic cycle of CPO is similar to other heme peroxidases. However, in CPO the oxidizing power of Compound I is used to oxidize Cl^- ions to HOCl, and then the HOCl operates as an organic chlorinating agent. Traditional heme peroxidases cannot catalyze this reaction probably because the redox potential of Cl^- is too high. However, CPO operates at very low pH (3) where the redox potential and hence the reactivity of Compound I may be significantly increased over other peroxidases that operate closer to physiological pH.

CPO consists of a single 30-kDa polypeptide chain, one heme group, and one disulfide bond. The crystal structure shows at least 14 different sites of glycosylation. The fold is unlike that of other heme peroxidases, and the proximal ligand is a Cys residue not His. This is very similar to cytochromes P450, which also use a Cys ligand. As a result, CPO shares spectral features characteristic of P450s. The most significant is the 450-nm band in the visible absorption spectrum when the enzyme is reduced in the presence of carbon monoxide to give the Fe^{2+}–CO complex.

6.1. Reactions Catalyzed by Chloroperoxidase

CPO is one of the most diverse of the known heme enzymes. In addition to operating as a chloroperoxidase, CPO exhibits activities characteristic of traditional heme peroxidases, catalase, and cytochrome P450s:

Halogenation (normal function)	$RH + H_2O_2 + Cl^- + H^+ \rightarrow R\text{-}Cl + 2H_2O$
Dehydrogenation (heme peroxidases)	$2RH + H_2O_2 \rightarrow R\text{-}R + 2H_2O$
H_2O_2 decomposition (catalase)	$2H_2O_2 \rightarrow O_2 + 2H_2O$
Oxygen insertion (P450)	$R + H_2O_2 \rightarrow R\text{-}O + H_2O$

Sulfoxidation and epoxidation reactions catalyzed by CPO proceed with a high degree of enantioselectivity (10, 11). Even the typical peroxidase dehydrogenation reactions proceed with enantioselectivity, something other peroxidases cannot do. The CPO crystal structure provides some insights into these unusual functional properties. Although CPO is a helical protein, the overall fold is unique not the typical peroxidase fold. In addition, the heme is accessible from the top distal surface, not the heme edge. Bracketing the distal heme pocket near the $Fe^{4+}=O$ center are two key

Phe residues and other hydrophobic groups that form a shallow pocket that is the most probable site for substrate binding (Fig. 4). The asymmetrical nature of this pocket can account for the observed enantioselectivity.

Figure 4. The active site structure of chloroperoxidase. Glu183 most likely serves the same acid/base catalytic role as the distal His in traditional heme peroxidases. The two Phe residues shown help form the substrate binding site that enables this enzyme to catalyze enantioselective sulfoxidation, epoxidation, and electron transfer reactions.

Like other peroxidases, CPO forms Compound I with an Fe^{4+}=O center and porphyrin radical. The catalytic groups, however, are quite different in CPO. Directly adjacent to the peroxide binding site, CPO has a Glu residue rather than His, and there is no active-site Arg in CPO.

7. Other Heme Peroxidases

Although the nonmammalian heme peroxidases have received most of the attention, the heme-containing peroxidases are very diverse. Mammals produce well-known peroxidases like myeloperoxidase, lactoperoxidase, and thyroid peroxidase. Although these peroxidases contain heme and have active sites similar to the nonmammalian heme peroxidases, these enzymes are larger and have different three-dimensional structures (12). The best understood is myeloperoxidase. The function of myeloperoxidase in white blood cells and the related eosinophil peroxidase is to oxidize halides and thiocyanate ions to produce HOCl, HOBr, and HOSCN, which are potent antipathogen oxidizing agents. The marine worm *Amphitrite ornata* produces a dehalogenating heme-containing peroxidase (13). *Mycobacterium tuberculosis*, the causative agent in tuberculosis, produces a heme catalase/peroxidase that metabolizes the most widely used antituberculosis drug, isoniazid. Strains resistant to isoniazid have a point mutation in the catalase/peroxidase, which implicates the peroxidase as a drug activator (14). Other bacteria, such as *Pseudomonas aeruginosa*, produce a cytochrome c peroxidase that contains two heme groups (15).

8. NonHeme Peroxidases

A number of peroxidases do not have heme as the prosthetic group. The fungus Curvularia inaequalis produces a chloroperoxidase that utilizes vanadium (VO_3) as a cofactor (16). Vanadium bromoperoxidases are also well known in algae (17). NADH peroxidase uses a flavin (18), and glutathione peroxidase is unique in utilizing an essential selenocysteine residue at the active site to oxidize glutathione and reduce hydroperoxides (19). There also are peroxidases that contain no metal center or other cofactors, such as the haloperoxidase of Pseudomonas pyrrocinia (20). In many of these, a detailed understanding is just developing based on recent advances in cloning and expression of these unusual and interesting peroxidases.

Bibliography

1. K. G. Welinder (1992) Curr. Biol. 2, 388–393.
2. M. Gajhede, D. J. Schuller, A. Henriksen, A. T. Smith, and T. L. Poulos (1997) Nat. Struct. Biol. 4, 1032–1038.
3. T. L. Poulos (1987) Adv. Inorg. Biochem. 7, 1–36.
4. S. L. Edwards, H. X. Nguyen, R. C. Hamlin, and J. Kraut (1987) Biochemistry 26, 1503–1511.
5. J. E. Erman, L. B. Vitello, M. A. Miller, A. Shaw, K. A. Brown, and J. Kraut (1993) Biochemistry 32, 9798–9806.
6. K. Choudhury, M. Sundaramoorthy, A. Hickman, T. Yonetani, E. Woehl, M. F. Dunn, and T. L. Poulos (1994) J. Biol. Chem. 269, 20239–20249.
7. M. Sundaramoorthy, K. Kishi, M. H. Gold, and T. L. Poulos (1994) J. Biol. Chem. 269, 32759–32767.
8. H. Pelletier and J. Kraut (1992) Science 258, 1748–1755.
9. M. Sundaramoorthy, J. Terner, and T. L. Poulos (1995) Structure 3, 1367–1377.
10. S. Colonna, N. Gaggero, L. Casella, G. Carrea, and P. Pasta (1992). Tet. Asymm. 3, 95–106.
11. E. J. Allain, L. P. Hager, L. Deng, and E. Jacobsen (1993). J. Am. Chem. Soc. 115, 4415–4416.
12. R. Fenna, J. Zeng, and C. Davey (1995) Arch. Biochem. Biophys. 316, 653–656.
13. Y. P. Chen, S. A. Woodin, D. E. Lincol, and C. R. Lovell (1996) J. Biol. Chem. 271, 4609–4612.
14. Y. Zhang, B. Heym, B. Allen, D. Young, and S. Cole (1992) Nature 358, 591–593.
15. V. Fulop, C. J. Ridout, C. Greenwood, and J. Hajdu (1995) Structure 3, 1225–1233.
16. A. Messerschmidt and R. Wever (1996) Proc. Natl. Acad. Sci. USA 93, 392–396.
17. B. E. Krenn, M. G. Tromp, and R. Wever (1989) J. Biol. Chem. 264, 19287–19292.
18. T. Stehle and G. E. Schulz (1992) J. Mol. Biol. 224, 1127–1141.
19. O. Epp, R. Ladenstein, and A. Wendel (1983) Eur. J. Biochem. 133, 51–69.
20. C. Wolfframm, F. Lingens, R. Mutzel, and K. H. van Pee (1993) Gene 130, 131–135.

Suggestion for Further Reading

21. T. L. Poulos and R. Fenna (1994) Met. Biol. 30, 25–75. Review that leads back to primary literature.

Pertussis Toxin

Among the several virulence factors implicated in the pathogenesis of whooping cough, a major role is played by pertussis toxin (PT), which is also a major determinant in the development of antipertussis protective antibodies (1). PT is active on a variety of cells and causes a wide range of effects, due to the ADP-ribosylation of different trimeric cytosolic G proteins involved in cell signal transduction (2).

PT is composed of five different subunits: S1 (21 kDa) is the catalytic part, and S2, S3, two copies of S4, and S5 form the cell-binding pentamer B. Despite the heterogeneity of the components of B and lack of an appreciable primary structure similarity, the overall structural organization of PT is closely similar to those of other oligomeric toxins having B units (3-7). The B pentamer is disk-shaped, and its subunits fold in six antiparallel strands with a-helices lining the central pore (6). S2 and S3 possess additional domains with a lectin-like fold, which were suggested to determine the different sugar-binding properties of PT being different from those of cholera toxin and enterotoxins (6). In fact, PT binds to glycoproteins, such as fetuin , having an Asn-linked branched mannose core with terminal N-acetylglucosamine (8).

At variance from cholera toxin, the carboxyl terminus of S1 enters the B oligomer central pore only halfway, and there are fewer protein–protein contacts (4, 6). The similarity with cholera toxin is very high in the active site, with overlapping glutamate and tyrosine residues essential for activity. His35 occupies a central position in the NAD-binding cavity of PT, as is also the case with the active sites of diphtheria toxin and exotoxin A from *Pseudomonas*. Little information is available on the internalization of PT or the mechanism of membrane translocation of S1 (8). That the structural and functional organization of PT is similar to that of cholera toxin, entertotoxins, and shiga toxins suggests there are further similarities in their mode of cell penetration.

Reduction of the S1 subunit in the presence of detergents frees an ADP-ribosyltransferase activity specifically directed toward the a subunit of several trimeric G proteins. At variance from cholera toxin and entertotoxin, PT catalyzes the ADP-ribosylation of a cysteine residue present in a Xaa-Cys-Gly-Leu-Xaa motif contained in the carboxyl-terminal part of the a subunit of several trimeric G proteins, including G_i, G_o, and G_{gust} G_s has a tyrosine residue in the position of the cysteine and is not modified by PT. Another difference from cholera toxin is that the S1 enzymic activity is greatly enhanced by ATP and other adenine nucleotides (9). The result of the S1-catalyzed ADP-ribosylation of G_i and G_t is different from the cholera toxin or entertotoxin modification of G_s because the carboxyl-terminal cysteine residue of G_i and G_t is centered in the area of interaction between the G protein and plasma membrane receptor. As a consequence, the inhibitory physiological effects normally mediated by these G proteins are not transmitted. The PT oligomer B has biological functions independent of the ADP-ribosyltransferase activity, such as that of inducing the proliferation of T lymphocytes (10).

Bibliography

1. R. Sekura, J. Moss, and M. Vaugham (1985) *Pertussis Toxin*, Academic Press, New York.
2. M. Domenighini, M. Pizza, and R. Rappuoli (1995) *Bacterial Toxins and Virulence Factors in Disease* (J. Moss et al., eds.), Marcel Dekker, New York, pp. 59–80.
3. T. Sixma et al. (1993) J. Mol. Biol. 230, 890–918.
4. R. G. Zhang et al. (1995) J. Mol. Biol. 251, 563–573.
5. M. E. Fraser, M. M. Chernaia, Y. V. Kozlov, and M. N. G. James (1994) Nature Struct. Biol. 1, 59–64.
6. P. E. Stein et al. (1994) Structure 2, 45–57.
7. A. G. Murzin (1993) EMBO J. 12, 861–867.

8. H. R. Kaslow and D. Burns (1992) FASEB J. 6, 2684–2690.
9. J. Moss et al. (1986) Biochemistry 25, 2720–2725.
10. M. Tamura et al. (1983) J. Biol. Chem. 258, 6756–6761.

Pest Regions

One of several features of proteins that have been proposed lead to their rapid protein degradation is the presence of so-called PEST regions, protein domains that are enriched in proline, glutamic acid, serine, and threonine residues. These regions were first described by Rechsteiner and co-workers in the mid-1980s after searching for structural features of proteins that correlate with short half-lives. They developed a computer-based algorithm rating the presence of at least one P, E, S, or T residue in a hydrophilic stretch of at least 12 amino-acid residues and flanked by a positively charged residue. Consequently, PEST regions do not represent a specific sequence per se, but they are instead a general feature of the relevant protein domains. Less than 10% of mammalian proteins of known amino acid sequence have such PEST regions, but a high percentage of short-lived proteins do. In some cases, proteins become more stable after removal of their PEST regions, and a few examples have been shown where transplantation of PEST regions into long-lived proteins causes their rate of degradation to be increased.

The mechanism by which PEST sequences may influence degradative rates has remained elusive. Some PEST-containing proteins are degraded by proteasomes in a ubiquitin-dependent manner, and they require different E2 and E3 enzymes (see Ubiquitin). On the other hand, PEST regions may simply correlate with rapid hydrolysis because they often contain consensus sequences for known protein kinases, and phosphorylation often signals ubiquitin conjugation and degradation. Also, proline-rich hydrophilic domains are likely to exist as unfolded loops on the surface of protein structures and to be more susceptible to interactions with molecular chaperones, kinases, and other proteinases. Theories involving degradation by calpains and proline endopeptidase have, however, proved false.

Suggestions for Further Reading

S. Rogers, R. Wells, and M. Rechsteiner (1986) Amino acid sequences common to rapidly degraded proteins: the PEST hypothesis, Science 234, 364–368.

M. Rechsteiner and S. W. Rogers (1996) PEST sequences and regulation by proteolysis, Trends Biochem. Sci. 21, 267–271.

Phage Display Libraries

Phage display libraries are a variant of expression libraries in which cloned DNA inserts are expressed as polypeptide fusion proteins with bacteriophage capsid proteins, so that the foreign proteins are "displayed" on the exterior of the modified virus particle (Fig. 1) (1-3). Because the virus also contains a DNA genome, a physical linkage is maintained between the displayed peptide and its encoding DNA sequence. This linkage is the core of the power of phage display. Although the displayed proteins behave in many respects as soluble factors, they remain associated with their DNA code as part of an infectious particle. Thus, even trace amounts of display phages with desired activity can be amplified by infection, and the active peptide sequences can be decoded by DNA sequencing.

Figure 1. Schematic illustration of phage display. A double-stranded copy of the phage genome is cleaved enzymatically, and foreign DNA is inserted in-frame into a capsid gene. After introduction of recombinant phage DNA into bacterial cells, novel fusion phage are generated with foreign peptides displayed as capsid fusion proteins on the phage surface.

Several different bacterial viruses have been modified to serve as phage display vectors. By far the most common type of vector is derived from the filamentous Ff bacteriophage (4). The popularity of this virus is due first to the fact that it packages a relatively small single-stranded DNA genome, providing some advantages in mutagenesis and DNA sequencing, and second to the robust technologies that have been developed for display of both short peptides and larger proteins. Other viruses that have been adapted for phage display include lambda phage and T4 phage. Future directions in this field will likely include vector construction using human enteric bacteriophages for the purpose of mucosal vaccine development. In addition, certain human viruses could conceivably be modified as viral display vectors for human gene therapy applications.

Filamentous phage display vectors fall into two categories. First are the phage vectors, which accommodate foreign DNA fused to one of several capsid genes within the phage genome. Phage vectors are adequate for peptide display, but larger polypeptide–capsid fusion proteins tend to interfere with phage assembly or infectivity. This interference can be tolerated if the phage can incorporate a preponderance of normal capsid proteins, with only a small proportion of fusion capsid proteins present. Such a situation occurs in the second category of vectors, called “phagemids,” in which the foreign DNA and the capsid gene are both cloned into a special type of plasmid containing the phage DNA-packaging signal. Foreign DNA is thus cloned as a gene fusion with the phagemid capsid protein. A phagemid is not infectious by itself, but in the presence of a “helper” phage the phagemid DNA can be packaged into an infectious virus particle that displays a mixture of normal and fusion capsid proteins. Using phage and phagemid vectors, a great number of foreign sequences have been expressed as viral capsid fusion proteins, including peptides, antibodies, enzymes, DNA-binding proteins, RNA-binding proteins, and regulatory proteins (reviewed in Ref. 4). Furthermore, any of these proteins can be diversified to form combinatorial phage display libraries, which can then be screened to identify novel proteins with desirable properties.

Phage display screening is a robust technology that typically operates through affinity selection of phage-encoded molecules that interact with target proteins (1). A phage display library typically expresses billions of different peptides or polypeptides. The active minority of the library can be fractionated from the noninteracting majority by affinity partitioning over a solid-phase target. Phages that bind are then readily eluted and amplified by infection of a suitable bacterial host, and further rounds of selection can be performed. This iterative selection process provides a powerful means to obtain specific peptide aptamers, as well as sequence–activity relationship (SAR) data for any target of interest.

Phage display has proven to be a powerful means of obtaining functional probes to study any target of interest. Thus, peptide aptamers can be used to characterize target function in much the same way that antibodies have been used historically to detect, trap, and inhibit their targets. However, unlike animal-based antibody technologies, phage display can yield peptide or antibody functional probes without requiring immunogenicity or immunization by the target. Furthermore, the complexity of modern phage display libraries exceeds the genetically encoded complexity of the immune system. Thus, phage display technologies are likely to continue to find increasing applications throughout the biological and medical sciences.

See also Combinatorial Libraries, Libraries, Combinatorial Synthesis, Affinity Selection, DNA Libraries, Genomic Libraries, cDNA Libraries, Expression Libraries, and Peptide Libraries.

Bibliography

1. G. P. Smith (1985) Science 228, 1315–1317.
2. S. F. Parmley and G. P. Smith (1988) Gene 73, 305–318.
3. W. Markland, B. L. Roberts, M. J. Saxena, S. K. Guterman, and R. C. Ladner (1991) Gene 109, 13–19.
4. B. K. Kay, J. Winter, and J. McCafferty (1996) Phage Display of Peptides and Proteins, Academic Press, San Diego.

Suggestions for Further Reading

5. J. D. Watson (1987) Molecular Biology of the Gene, 4th ed., Benjamin-Cummings, Menlo Park, CA.
6. J. Sambrook, E. F. Fritsch, and T. Maniatis (1989) Molecular Cloning: A Laboratory Manual, 2nd ed., Cold Spring Harbor Laboratory Press, Cold Spring Harbor, NY.
7. D. J. Kenan, D. E. Tsai, and J. D. Keene (1994) Trends Biochem. Sci. 19, 57–64.
8. (1996) Combinatorial Chemistry, Methods in Enzymology, vol. 267, Academic Press, San Diego.
9. L. A. Thompson and J. A. Ellman (1996) Chem. Rev. 96, 555–600.
10. B. K. Kay, J. Winter, and J. McCafferty (1996) Phage Display of Peptides and Proteins, Academic Press, San Diego.

Phagocytosis

Phagocytosis is the ability of a cell to internalize large particles, as exemplified by the feeding of phagocytic amoebae, which is one type of endocytosis. Phagocytosis is initiated by the binding of large extracellular particles (eg, bacteria) to specific cell-surface receptors, either directly or indirectly. Indirect recognition involves host-derived opsins, such as antibody or complement fragments, that coat the particles and serve as ligands for some phagocytic receptors. The best-characterized opsins are antibodies that bind to surface antigens on infectious microorganisms and form an antibody coat in which the tail region of each antibody molecule (the Fc region) is exposed. Binding of the antibody-coated particles to specific Fc receptors on phagocytic cells initiates phagocytosis. Ligands for other receptors, including complement receptors (see Complement System), integrins, cell-surface lectins, and certain glycosylphosphatidylinositol (GPI)-anchored proteins [eg, CD14 (1)], also activate phagocytosis.

A common feature of the phagocytic events mediated by these various receptors is that particle internalization depends on the polymerization of actin. Activated cell-surface receptors transmit signals to the cytoplasm that induce actin polymerization (2, 3). During Fc receptor-mediated phagocytosis at least, these activation signals involve the small GTP-binding proteins Rac/Rho/CDC42 and tyrosine kinases. The localized polymerization of actin at the site of particle attachment to the cell pushes plasma membrane around the particle, allowing further opsin-receptor interactions (zippering) and the progressive development of the particle within a membrane invagination tightly apposed to the particle surface. When engulfment is completed, the forming phagocytic vesicle, or phagosome, is sealed and detaches from the cell surface.

In most cases the phagosome fuses with resident compartments of the endocytic pathway (endosomes and lysosomes) to acquire the spectrum of hydrolases that digest the phagosome content. The resulting digestion products are transferred to the cytosol and used to synthesize cellular constituents or are secreted from the cell. In multicellular organisms, phagocytosis is primarily associated with defense against infection by ingesting invading microorganisms and the scavenging of senescent, damaged, or apoptotic cells (1) and cellular debris. These functions are generally performed by specialized white blood cells, such as macrophages and neutrophils, that act as “professional” phagocytes. These cells are extremely active. In humans, for example, macrophages remove around 10^{11} senescent red blood cells every day. However, most cells are capable of phagocytosis when challenged with appropriate ligands.

Many invasive bacterial, fungal and protozoan pathogens use phagocytosis to enter cells. Some, such as *Listeria* and *Yersinia*, use cadherins or integrins, respectively, as receptors to initiate endocytic events similar to those described previously. Others, such as *Shigella*, secrete proteins that activate phagocytosis directly. Then the fate of the phagocytic vesicle varies according to the nature of the pathogen internalized. *Listeria*, *Shigella*, and *Trypanosoma cruzi* induce lysis of the phagosome membrane to gain access to the cytoplasm. Other agents (*Legionella*, *Salmonella*, *Mycobacterium avium*) reside and replicate within phagocytic vesicles and produce components that prevent fusion with lysosomes, thus avoiding the hydrolytic consequences of endocytosis, or modify the environment within the phagosome to minimize the effects of the hydrolytic environment (4, 5).

(See also Endocytosis, Pinocytosis, Macropinosomes.)

Bibliography

1. A. Devitt, O. D. Moffatt, C. Raykundalia, J. D. Capra, D. L. Simmons, and C. D. Gregory (1998) *Nature* 392, 505–509.

2. S. Greenberg (1995) Trends Cell Biol. 5, 93–99.
3. K. Ireton and P. Cossart (1998) Curr. Opinion Cell Biol. 10, 276–283.
4. Y. K. Oh, C. Alpuche Aranda, E. Berthiaume, T. Jinks, S. I. Miller, and J. A. Swanson (1996) Infect. Immun. 64, 3877–3883.
5. S. Sturgill-Koszycki et al. (1994) Science 263, 678–681.

Phalloidin

Phalloidin is a cyclic heptapeptide found in the highly poisonous mushroom *Amanita phalloides*. Phalloidin binds with very high affinity to F-actin and stabilizes these filaments by preventing depolymerization. It contains several uncommon amino acids and is resistant to all proteolytic enzymes tried thus far. While phalloidin has the ability to be highly toxic to a cell due to the changes that it will induce in actin polymerization, it is now known that the toxicity of *Amanita phalloides* is due mainly to the a-and b-amanitins (potent inhibitors of RNA polymerase II), since phalloidin is not absorbed from the gastrointestinal tract (1). Nevertheless, phalloidin has been an extremely important drug in answering structural, biochemical, and cell biological questions about actin.

Phalloidin does not bind to monomeric actin (G-actin), but binds with a 1:1 stoichiometry to protomers within the F-actin filament. This is the opposite mode of binding of DNase I (see DNase 1 Sensitivity), which binds with high affinity to G-actin but not to F-actin. As a result of this selective binding, both may be used to assay the concentrations of G- vs F-actin within a fixed cell. The phalloidin-stabilized filament resists depolymerization that would otherwise be induced by a reduction of the actin concentration, by chaotropic agents, *cytochalasins*, heat denaturation, and proteolysis (2). The critical concentration is the concentration of the monomeric species of actin at which it is in equilibrium with *polymers*, and this is about 10^{-6} M for muscle actin. Phalloidin reduces this critical concentration by a factor of about 25. These properties of phalloidin have made it a very useful tool for labeling actin filaments within a cell (using fluorescent derivatives of phalloidin) and for stabilizing actin filaments used in structural and biophysical studies.

Bibliography

1. A. Jaeger, F. Jehl, F. Flesch, P. Sauder, and J. Kopferschmitt (1993) J. Toxicol. Clin. Toxicol. 31, 63–80.
2. T. Wieland and H. Faulstich (1978) CRC Crit. Rev. Biochem. 5, 185–260.

Phase Problem

To determine the structure of a molecule by X-ray crystallography, after collecting and processing the data, the electron density $\rho(x\ y\ z)$ in the crystal unit cell can be calculated at every position $x\ y\ z$

(1)

To use this equation requires that the values of both $F(hk\ell)$ and $a(hk\ell)$ for each reflection $hk\ell$ are known. The $F(hk\ell)$'s are easily found because (apart from corrections) they are proportional to the square root of the measured scattered intensities $I(hk\ell)$. The phase problem is that the phase angles $a(hk\ell)$ are not provided directly by the experimental data. This fundamental problem greatly delayed the use of X-ray crystallography initially, but it is hardly a problem anymore. For small molecules, it has long been solved by direct methods. In the crystallography of macromolecules, several methods exist to determine the phase angles of the reflections:

1. isomorphous replacement
2. molecular replacement
3. MAD (multiple-wavelength anomalous dispersion)

Classical direct methods are applicable to macromolecular crystals only if the protein is small and the X-ray data can be collected to high resolution (1).

Bibliography

1. G. M. Sheldrick et al. (1993) Acta Crystallogr. D49, 18–23.

Suggestion for Further Reading

2. J. Drenth (1999) Principles of Protein X-ray Crystallography, Springer, New York.

Phase Variation, Pili

Certain enterotoxigenic strains of *Escherichia coli* produce pilus-like appendages called colonization factor antigens (CFAs) that are longer than common type I pili. Production of type I pili or CFA is mutually exclusive in these bacteria and thus represents a specialized example of bacterial phase variation. That displayed by type IV pili of *Neisseria gonorrhoeae* is the best-characterized system. The N-terminal domain of *N. gonorrhoeae* pilin is hydrophobic and highly conserved among different variants. Other regions of the pilin molecule, however, known as minicassettes, vary widely in amino acid sequence. There is also wide variation at the DNA level between the various copies of the genes that encode a particular pilin protein. In *N. gonorrhoeae* the expression of the *pilE* gene is controlled at transcription by a two-component regulatory system; this comprises the transcriptional activator PilA and the sensor component PilB, which phosphorylates PilA. If Pil$^+$ and Pil$^-$ respectively represent the phenotypes when functional pili are assembled or not on the bacterial cell surface, then phase variation represents the fluctuation that occurs between Pil$^+$ and Pil$^-$. There are several types of phase variation (1).

1. The first arises because the expressed protein has two possible sites (P^+ and P^S) at which subsequent processing can take place. When cleaved proteolytically at P^+, the pilin protein assembles into normal pili (Pil$^+$). In contrast, when it is cut at P^S it no longer contains the hydrophobic region required for assembly. The protein is secreted and lost from the cell, so there is no pili formation (Pil$^-$).

2. The second type of phase variation is similar to the first in that it again gives rise to a pilin protein that is aberrant and not capable of forming pili *in vivo*. Although the pilin gene is present in multiple copies in the chromosome, generally only one of these has a promoter and is expressed. This gene is designated *pilE*, where *E* represents expression. Those gene copies that are not expressed are termed *pilS*, where *S* represents silent. Both the *pilE* and *pilS* genes contain a number of internal repeated DNA sequences. Homologous recombination, which involves exchanges of the interior regions of the genes, can lead to unequal exchange of DNA because of the repetitive nature of the sequences. As a result, the PilE protein produced may be larger in size than normal. As before, this cannot be processed in such a way that pili formation is possible, hence the phenotype is Pil$^-$.

3. The third mechanism of phase variation concerns the *pilC* gene. The expressed protein PilC, which has been detected by immunoelectron microscopy at the tip of the pili, is an important protein in the assembly and functioning of intact mature pili. Towards the 5′ end of the *pilC* coding sequence there is a long run of G bases. Slipped-strand mispairing during synthesis alters the number of G bases and generates a frameshift mutation. This again gives rise to Pil$^-$ phenotype. Note, however, that pili of normal appearance are produced in this case and that another phase-variable pilus-associated protein replaces PilC in its assembly function, but it lacks the ability to bind to epithelial cells (2). Phase variation probably evolved to allow the bacterium to escape the immune response of its host and to allow it to adapt to new cell types (1).

Bibliography

1. A. A. Salyers and D. D. Whitt (1994) Bacterial Pathogenesis: A Molecular Approach, ASM Press, Washington, D.C.
2. T. Rudel, D. Facius, R. Barten, I. Scheuerpflug, E. Nonnenmacher, and T. F. Meyer (1995) Role of pili and the phase-variable PilC protein in natural competence for transformation of Neisseria gonorrhoeae. Proc. Natl. Acad. Sci. USA 92, 7986–7990.

Phenotypic Lag

After a cell sustains a mutation, there may be a delay of one or more generations before the mutant phenotype is expressed. This delay has two causes. First, a recessive mutation may be complemented by the wild-type allele on another chromosome. In mitotically dividing diploid cells, at least a one-generation delay occurs before the phenotype is expressed. Under most laboratory conditions, haploid organisms also have more than one chromosome per cell and show a lag of one or two generations. Secondly, when a mutation that gives rise to a mutant protein first appears, the cell may have many copies of the wild-type protein. Expression of the mutant phenotype may be delayed until these preexisting proteins are diluted or degraded. A classical example from *Escherichia coli* genetics is resistance to bacteriophage T1. Resistance is conferred by mutations that alter the phage receptor on the cell surface, but several generations are needed before the preexisting sensitive receptors are diluted. Even dominant phenotypes may fail to be expressed until the cellular concentration of the wild-type protein falls. Phenotypic lag complicates the determination of mutation rates from fluctuation tests (1-4).

Bibliography

1. S. E. Luria and M. Delbrück (1943) Genetics 28, 491–511.
2. P. Armitage (1952) J. R. Stat. Soc. B 14, 1–40.
3. A. L. Koch (1982) Mutat. Res. 95, 129–143.

4. F. M. Stewart, D. M. Gordon, and B. R. Levin (1990) Genetics 124, 175–185.

Phenylalanine (Phe, F)

The amino acid phenylalanine is incorporated into the nascent polypeptide chain during protein biosynthesis in response to two codons—UUU and UUC—and represents approximately 3.9% of the residues of the proteins that have been characterized. The phenylalanyl residue incorporated has a mass of 147.18 Da, a van der Waals volume of 135 Å^3, and an accessible surface area of 218 Å^2. Phe residues are changed infrequently during divergent evolution; they are interchanged in homologous proteins most frequently with tyrosine and leucine residues.

Phe is one of the three amino acids with an aromatic ring in its side chain:

which has absorbance and fluorescence spectral properties that are very useful in quantifying proteins and analyzing their structural properties. The other two—tyrosine and tryptophan—predominate, however, so Phe residues are useful only in their absence. The aromatic ring of Phe residues is comparable chemically to that of benzene or toluene; consequently, it is largely nonpolar (except for the tendency of the electrons of the peripheral H atoms to be drawn into the aromatic ring) and is chemically reactive only under extreme conditions that are not applicable to proteins.

Tyr residues occur primarily within the interiors of folded protein structures, and approximately 50% are totally buried; normally, they are still rotating rapidly by 180° rotations about the C_b–C_g single bond. They tend to occur primarily in alpha-helices, although also in beta-sheets, and they favor the a-helical conformation in model peptides.

Suggestion for Further Reading

T. E. Creighton (1993) Proteins: Structures and Molecular Properties, 2nd ed., W. H. Freeman, New York.

Phenylketonuria

The metabolic disorder phenylketonuria (PKU) was first described in 1934 by A. Følling, who was investigating the excretion of ketone bodies in the urine of two mentally retarded children. The reagent in use, acidified $FeCl_3$, typically turns a purple-red color with ketones. The urine of these children turned bright blue-green instead. Examination of additional mentally retarded children uncovered eight more who were similar, both clinically and in their urine reactions. Følling subsequently demonstrated that the responsible urinary constituent was phenylpyruvic acid, thus the name phenylketonuria. In addition to mental retardation, affected children share a number of clinical features, including irritability, seizures, eczema, and a “mousy odor.” They tend to be more lightly pigmented than others in the same family.

The rarity of this disorder in the general population and the occurrence of more than one affected person in a sibship suggested recessive inheritance. The equal occurrence of males and females and the fact that the parents and other relatives were unaffected was consistent with autosomal recessive inheritance.

1. The Biochemistry of PKU

F{ø}lling suggested that patients who have PKU have a block in metabolism of phenylalanine, and in 1947 G.A. Jervis proposed that the metabolic error is in the conversion of phenylalanine to tyrosine. He subsequently proved this hypothesis by showing that liver from a PKU patient cannot make the conversion. Thus, PKU was among the earliest examples of a metabolic error, a term proposed by A.E. Garrod in 1909, and it has served as a model for other metabolic defects.

Phenylalanine is efficiently reabsorbed in the kidneys, leading to maintenance of very high blood levels. In normal persons, the blood phenylalanine is ca. 60 µM. The level in PKU patients can be 40 times higher. This leads to formation and excretion of otherwise rare metabolites of phenylalanine, such as phenylpyruvic acid, phenylacetic acid, and o-hydroxyphenylacetic acid. These metabolites very likely contribute to the clinical features of PKU by interfering with various metabolic and developmental processes.

Phenylalanine hydroxylase (PAH; L-phenylalanine-4-monooxygenase; EC 1.14.16.1) is the enzyme that is ordinarily nonfunctional in PKU. The predicted polypeptide molecular weight is 51,862 daltons, but the enzyme is usually a homotetramer. It catalyzes the oxidation of L-phenylalanine, using tetrahydrobiopterin as a cofactor (Fig. 1). Production of PAH occurs almost entirely in the liver. A large number of PAH alleles are known. Some produce completely inactive PAH; others produce PAH that has reduced or normal activity. Persons whose allelic combinations produce PAH activity <1% of normal have classical PKU. If there is some activity, a mild form of the disorder may result. Heterozygotes, with one normal and one inactive allele, are phenotypically normal even though the total enzymic activity is reduced.

Figure 1. Three enzymes that are important in the conversion of phenylalanine to tyrosine. Additional enzymes and cofactors are required to form BH_4. Reduced activity of phenylalanine hydroxylase (PAH) can result from structural modifications of PAH or from deficiency of BH_4.

2. Treatment of PKU

Humans cannot make phenylalanine or tyrosine and must depend on diet for these two essential amino acids. The phenylalanine content of foods is in excess of body requirements for protein synthesis, and the surplus is metabolized via tyrosine. This suggested the possibility of reducing the accumulation of phenylalanine by reducing the dietary intake. Such efforts, initiated in 1953 by H. Bickel, ultimately proved successful. The low-phenylalanine diet must be introduced soon after birth of an affected infant in order to avoid permanent damage to the developing central nervous system.

With the development of an effective method of treatment, the urgency of neonatal diagnosis became apparent. In the early 1960s, R. Guthrie developed a microbial test using whole blood from a heel stick. This rapid and inexpensive test made large-scale screening possible, and required screening of newborns for elevated blood phenylalanine has become widespread in western countries. Once the central nervous system has matured fully, persons with PKU are somewhat less sensitive to increased blood levels of phenylalanine. This includes not only regulation of protein intake but also avoidance of the artificial sweetener aspartame, which is a dipeptide derivative of aspartic acid and phenylalanine. However, long-term studies have shown benefits of continued treatment of adults.

Although dietary regulation has been highly successful, it is not a perfect treatment. Treated patients show mildly depressed IQ compared to non-PKU controls. One suggested cause is increased dysmyelination with age in the presence of elevated blood phenylalanine. Also, tyrosine is lower in PKU patients, treated or untreated, and this may lead to deficiency of neurotransmitters.

In view of the single gene and its single protein product that are defective in PKU, this disorder would seem a good candidate for gene therapy. It has not been considered a high priority, however, because of the effectiveness of dietary restriction of phenylalanine. When procedures for gene therapy have been sufficiently developed and tested, it is likely that they will be applied to PKU. Introduction of functional PAH genes during the neonatal period should cure the metabolic defect. This, in effect, was the case with one young boy who received a liver transplant for reasons unrelated to his PKU status.

The successful treatment of PKU by diet has led to the problem of maternal PKU, which occurs in successfully treated women who are homozygous for PKU and whose offspring therefore are heterozygous. The developing fetus, although genetically normal (but heterozygous), depends on the mother to regulate blood phenylalanine. The fetus is also highly susceptible to moderate increases in blood phenylalanine. Prior to conception and during pregnancy, a PKU mother must regulate her blood phenylalanine levels rigorously to avoid damage to the fetus. The recommended maximal level is 360 μM.

One consequence of introducing screening was the recognition that some children have levels of phenylalanine that are above normal but that do not reach the levels that lead to pathology and that do not require dietary management. These cases of "hyperphenylalaninemia," defined as plasma levels >120 μM, are often due to homozygosity for PAH alleles that have low but nonzero enzyme activity. In other instances, the hyperphenylalaninemia is transient in neonates and disappears with time.

3. Other Defects That Interfere with Metabolism of Phenylalanine

In rare instances, high levels of blood phenylalanine are due to deficiencies of PAH activity caused by other loci. The cofactor 5,6,7,8-tetrahydrobiopterin (BH_4) is produced from 7,8-dihydrobiopterin (BH_2) by the enzyme dihydropteridine reductase (DHPR). The gene that codes for DHPR is on chromosome 4 at 4p15.31. In one form of PKU, loss of activity of this gene leads to absence of BH_4 and therefore to inactivity of PAH (Fig. 1). Because BH_4 is a cofactor in several other reactions that are important to brain function, dietary management of blood phenylalanine levels does not restore a normal phenotype. Such cases occur in 1 to 2 births per million.

A second rare variant of PKU is due to deficiency of 6-pyruvoyl tetrahydropterin synthase (Fig. 1), one of several enzymes necessary for BH_2 synthesis. This enzyme is coded by a gene on chromosome 11 at 11q22.3-q23.3. As in the case of DHPR deficiency, the neurological effects are not prevented by management of diet.

4. Molecular Genetics of PAH

The gene that codes for PAH is on chromosome 12 at 12q24.1. It is some 90 kb long with 13 exons. The messenger RNA is 2,677 nt long, consisting of 472 nt in the 5′ untranslated region, 1,356 nt (452 codons) in the coding sequence, and 849 nt in the 3′ untranslated region. Exons 1 to 12 are relatively small, varying in size from 57 nt to 197 nt. Exon 13 has 890 nt, of which 41 are coding. Introns vary in size from 1.0 kb to 23.5 kb.

Some 200 distinct mutations associated with PKU have been identified in the PAH gene. There are presumed to be many more that are associated with unrecognized hyperphenylalaninemia or that are normal variants. Some normal variants are known, and in a few instances they are polymorphic. Of the mutations that cause PKU, approximately three-fourths are nucleotide substitutions that lead to amino acid substitutions or premature chain termination. Another 25 or more are nucleotide substitutions that interfere with normal splicing of the RNA transcript. A number of small gene deletions have also been identified. A high frequency of mutations is found in exon 7, thought to be due to ascertainment bias rather than mutational hotspots. Almost any change in amino sequence in this region of the PAH molecule is likely to interfere with function.

A relatively small number of these mutations account for the majority of the cases of PKU, and particular mutations may be prevalent only in a limited population. Because several different mutations may occur with relatively high frequencies in a population, most so-called homozygotes are in fact compound heterozygotes, that is, the two alleles involve different mutations. Both, however, are nonfunctional. Comparison of mutations in European and Asian populations shows quite different spectra, indicating that most of the extant mutations arose after separation of the major races.

5. Population Genetics of PKU

The frequency of patients with PKU varies considerably among populations. In Norway, where PKU was first discovered, the frequency is ca. 1 in 14,000 births. Among Northern Europeans in general, the frequency is ca. 1 in 10,000 births, with a higher incidence of 1/4,500 in Ireland. Among U.S.

whites, the frequency is 1/8,000. The frequency among African-Americans is ca. 1/50,000. The frequency is very low in Ashkenazi Jews and Asians. A frequency of homozygotes of 1/10,000 corresponds to a gene frequency of 0.01 and a frequency of heterozygotes of 2%.

Investigation of PKU has been aided by the discovery of eight polymorphic DNA variants within the PKU gene. These were originally recognized as restriction fragment length polymorphisms, although now PCR is used for some sites. One of the sites involves different numbers of short tandem repeats, providing several alleles. Altogether, there are about 800 possible combinations (haplotypes) of "alleles" at these sites, of which only about 75 have been observed. Within a population, many fewer are observed, and usually only a few reach substantial frequencies.

The study of mutant-allele–haplotype associations in a variety of populations has provided insight into the origin and spread of the genes in historic and prehistoric periods. For example, the mutation R261Q is widespread in Europe but is always associated with haplotype **1**. In general, haplotype 1 has a normal PAH allele. The interpretation is that this particular mutation arose on a haplotype 1 chromosome, and all R261Q mutations are descended from that single mutational event. In contrast, the R408W mutation occurs in northwest Europe on a haplotype 1 background and in eastern Europe on a haplotype 2 background. This suggests that two independent mutations occurred, one in a Celtic population and the other in a Slavic population.

Additional Reading

Scriver C.R., Kaufman S., Eisensmith R.C., and Woo S.L.C., The hyperphenylalaninemias, in C.R. Scriver, A.L. Beaudet, W.S. Sly, and D. Valle, eds., The Metabolic and Molecular Bases of Inherited Disease, 7th ed., vol. I, McGraw-Hill, New York, 1995, pp. 1015–1075.

On-Line Mendelian Inheritance in Man: http://www3.ncbi.nlm.nih. gov/htbin-post/Omim/dispmim?261600

PAH locus database: http://www.mcgill.ca/pahdb/

Phosphate Buffers

Phosphate buffers are commonly used in biological work. Phosphoric acid, , has pK_a values of about 2, 7, and 12. All three hydroxyl groups are identical and, indeed, all four oxygen atoms are identical on the NMR time scale as a result of rapid hydronations and dehydronations. Thus, 2 is the pK_a for the first H^+ to dissociate, even though it is coming equally from each of three groups. The next pK_a is raised to 7 because it is much harder for H^+ to dissociate from the charged ion than from the neutral H_3PO_4 molecule and, similarly, for the third pK_a. Hence, the Henderson–Hasselbalch equation for orthophosphate is

(1)

The large separation of the pK_a values means that, for a buffer of $H_2PO_4^-$ and HPO_4^{2-}, the concentrations of H_3PO_4 and PO_4^{3-} are negligible, and the pK_a values of 2 and 12 become irrelevant.

An advantage of phosphate as a buffer is that salts such as NaH_2PO_4 and Na_2HPO_4 are solid and both can be weighed out in the appropriate quantities; hence, the reproducible preparation of phosphate buffers need not involve adjustments of pH. Care must be taken, however, that the salt used, hydrate or anhydrous, does not lose or gain water on storage. Another advantage is that phosphate is transparent in the UV, down to wavelengths at which proteins may be estimated by their peptide bond absorbance, where carboxylate ions also absorb.

The main disadvantage is that with a doubly charged buffering species, the pK_a of 7.2 is three times more sensitive to changes in ionic strength than a buffer with only singly and zero charged components. Another disadvantage is that phosphate can support algal or fungal growth as a nutrient. Phosphate will also sequester and precipitate many cations, especially Ca^{2+} (see Calcium Signaling).

1. Diphosphate (pyrophosphate)

A variant of phosphate buffer is diphosphate (pyrophosphate). The acid, , has two strongly acidic groups, with pK_a values near 2, as with orthophosphate. The groups generated are electron-withdrawing, and so the next group has its pK_a lowered from the 7.2 of orthophosphate to 6.2 (at an ionic strength of 0.1 M; with its more strongly charged ions, the dissociation constants of diphosphate are even more sensitive than orthophosphate to changes in ionic strength). The group, however, is slightly electron-donating, so that the final pK_a is raised to 8.4. Hence, the Henderson–Hasselbalch equation for pyrophosphate in the neutral pH region is

(2)

Diphosphate can be hydrolyzed to orthophosphate, and the equilibrium strongly favors orthophosphate, but diphosphate is stable for long periods of time in neutral and alkaline conditions, even on heating.

Phosphatidylinositol

Phosphatidylinositol, generally abbreviated as PI or PtdIns, is a glycerophospholipid that has myo-inositol (one of nine stereoisomers of hexahydroxycyclohexane) as the polar head group. It is found in the membranes of eukaryotes and some eubacteria. Because of the anionic phosphodiester group, it contributes to the negative charge of the phospholipid bilayer. The free hydroxyl groups of PI can be phosphorylated or glycosylated to produce a wide variety of inositol phospholipids with specific functions. Two distinct types of inositol phospholipid have particularly important functions in eukaryotes that are described in separate entries:

1. Phosphatidylinositol phosphates are key components of several intracellular signaling pathways, either as the intact molecule or after they are cleaved by phospholipase C to 1,2-diacylglycerol and an inositol phosphate

2. Glycosylphosphatidylinositols (GPIs) can be covalently attached to the C-terminus of many proteins and are responsible for anchoring them to the membrane (see Membrane Anchors and GPI Anchor). GPIs may also occur in a “free form” without attached protein. Although the role of these free GPIs in mammalian cells is uncertain, they are an essential part of te protective coat used by many protozoal parasites.

Phosphatidylinositol Kinases

Phosphoinositides serve important functions in controlling the regulation of growth and differentiation in cells, as well as serving as substrates for the generation of inositol trisphosphate, IP_3 (see Inositol Lipids and Phosphates). In response to a variety of growth factors and cytokines, phosphatidylinositol (PI) is phosphorylated sequentially, to form the polyphosphoinositide PI-3,4,5-P_3 (PIP_3). These phosphorylations are catalyzed by the enzyme PI 3-kinase. The lipid products of this enzyme are not substrates for phospholipases, but instead have direct regulatory properties themselves.

PI 3-kinase has a number of domains for protein–protein interactions that contribute to its regulation and localization. The enzyme consists of a catalytic (p110) and regulatory (p85) subunit. p85 has two SH2 domains and one SH3 domain, which play a crucial role in regulation of the activity and targeting of the enzyme. Upon growth factor-receptor activation, p85 is recruited to receptors phosphorylated on tyrosine residues, or their substrates. The occupancy of these SH2 domains in p85 causes activation of the enzyme, while also serving to target it to the plasma membrane, or in some cases to intracellular membranes, where its lipid products can bind to proteins (1).

The generation of 3-phosphoinositides appears to play an important role in signal transduction. Activation of PI 3-kinase is necessary for the full expression of a number of tyrosine kinase receptors, including those for insulin, nerve growth factor, and others (1). Activation of the enzyme has been shown to prevent apoptosis in a number of cell types. Moreover, a retrovirus encoding PI 3-kinase was found to induce hemangiosarcomas in chickens, and mutations in the enzyme were associated with increased life span in *Caenorhabditis elegans*. Many advances in identifying the role of PI 3-kinase have come from the use of pharmacological inhibitors, such as wortmannin (1).

The targets of the lipid products of PI 3-kinase have received a great deal of attention. PI 3-kinase appears to play a universal role in membrane trafficking, perhaps explaining its wide importance in signal transduction. Cell adhesion molecules can also cause its activation, linking these events to changes in the actin cytoskeleton. Although there have been numerous reports on the essential role that PI 3-kinase plays in most aspects of signal transduction, most attention has focused on downstream changes in phosphorylation. There have now been a number of protein kinases that are activated after PI 3-kinase activation. One group belongs to the calcium-independent protein kinase C family members, especially z and q. Additionally, PIP_3 can induce a phosphorylation cascade. This involves the activation of the serine/threonine kinases PDK and Akt, which is also known as protein kinase B (PKB). It is now thought that PIP_3 can bind to the pleckstrin homology (PH) domain of these kinases, effectively recruiting them to the plasma membrane or intracellular membranes for activation. While PDK appears to be controlled mainly by targeting, it can phosphorylate and activate Akt, which in turn can phosphorylate a variety of intracellular substrates, including transcription factors, other kinases, proteins controlling apoptosis, and others (1).

Bibliography

1. A. Toker and L. C. Cantley (1997) Nature 387, 673–676.

Phosphofructokinase

Phosphofructokinase, or PFK (EC 2.7.1.11), is one of the best characterized allosteric enzymes. It catalyzes the step of glycolysis in which fructose-6-phosphate (FRU-6P) is phosphorylated to fructose-1,6-bisphosphate (FRU-1,6P_2) using either ATP or pyrophosphate (PP_i) as a phosphate donor. This enzyme is present in most types of eukaryotes and eubacteria but occurs rarely in archaebacteria. PFKs from animals, yeast, and most bacteria use ATP as a phosphate donor. Those that use PP_i are found in plants, protozoa, and some bacteria, often in addition to ATP-dependent enzymes. The amino acid sequences of most of the ATP-dependent PFKs are homologous, indicating that they form an evolutionary gene family. This family includes both “small” bacterial enzymes and “large” enzymes from mammals and yeast. It is a good model of enzyme evolution and of the appearance of “new” regulatory functions. PFK in most organisms is a highly regulated enzyme that has several allosteric effectors, and it controls (at least in part) the rate of glycolysis. The PFK from *Escherichia coli* has become a paradigm for the concerted allosteric model (1). X-ray crystallography, site-directed mutagenesis, and enzyme kinetic studies on bacterial ATP-dependent PFKs have also explained their catalytic and regulatory properties in some detail.

1. Isoenzymes

In humans (and probably in other mammals), there are three homologous types of PFK polypeptide chains, the muscle M, liver L, and platelet P isozymes. They are encoded by different genes, located on chromosomes 21, 1, and 10, respectively. All have several introns. The few cases of alternative splicing reported always lead to deletion of one exon and formation of a nonfunctional enzyme. Even though the M, L, and P type proteins are different, they share enough similarities assemble into active, multiple, heterologous oligomers, usually tetramers. The many different PFK isoforms generated in this way have somewhat different catalytic and regulatory properties, such as saturation by ATP and Fru-6P or sensitivity to allosteric effectors (2). Some species, such as *E. coli*, also have other minor proteins with PFK activity, but have unrelated amino acid sequences indicating that they do not belong to the main family of PFKs.

2. Metabolic Role

The reaction catalyzed by PFK, using either ATP or PP_i, is irreversible under physiological conditions. Its complex regulation by adenine nucleotides and by various metabolites indicates that PFK controls the production of cellular energy and the carbon flux between glucose and pyruvate. In several instances, the activity of PFK is coupled to that of pyruvate kinase because Fru-6P, the substrate of PFK, is an allosteric activator of one form of pyruvate kinase. This coupling is stronger in bacteria, where phosphoenolpyruvate (PEP), the substrate of pyruvate kinase, is the allosteric inhibitor of PFK. In some microorganisms (Gram-positive bacteria and mycoplasms, but not *E. coli*), the genetic expression of these two enzymes is coordinated. They catalyze reactions seven steps apart in glycolysis. In these cases, the genes that code for PFK and pyruvate kinase are adjacent on the chromosome and constitute an operon under transcriptional control by the same promoter (3).

The enzymatic (and sometimes genetic) coupling between two enzymes that each catalyze irreversible phosphoryl transfer steps is probably crucial for controlling the glycolytic flux, especially in anaerobes that use glycolytic fermentation as their main energy-producing pathway.

3. Primary Structures and Evolution

Most of the ATP-dependent PFKs, whether from animals, yeasts, or bacteria, have homologous sequences and belong to an evolutionary gene family. The simplest members of this family are bacterial PFKs whose polypeptide chains are about 35 kDa. Mammalian PFKs are approximately twice as large, about 80 kDa, and have an internal sequence repeat. Their N- and C-terminal halves are homologous and both resemble bacterial PFKs. This suggests that they have been produced by tandem gene duplication and fusion (4). All of the important active site residues are conserved in the N-terminal half, indicating a catalytic function, whereas replacement of several crucial residues, notably that of Asp127 by Ser, suggests that the C-terminal half is inactive. Yeast PFK is composed of two types of related chains, a of 108 kDa and b of 105 kDa. Each has a segment homologous to mammalian PFKs and unrelated N- and C-terminal extensions. These chains have formed by duplication of a mammalian-like gene followed by independent acquisition of terminal extensions (Fig. 1). The distribution of residues crucial for catalysis, plus various kinetic studies, suggest that the active site is carried by the N-terminal half of the b-chain and that the a-chain has only a regulatory role. Homologous residues are referred to here by their numbers in the *E. coli* enzyme.

Figure 1. Evolution of PFKs suggested by the comparison of their primary sequences. The unrelated segments are represented by thin lines. Among the homologous segments, those that have retained a catalytic function are open, and those that have lost their catalytic abilities and evolved to acquire a regulatory function are crossed. The special weak crossing on the N-terminal segment of the yeast a chain reflects that the evidence in favor of a pure regulatory role is weaker than for the other eukaryotic PFKs.

PP_i-dependent PFKs are made of two homologous chains, each of which has a segment distantly related to bacterial PFKs. This suggests that all PFKs might derive from the same ancestral protein (Fig. 1). The conservation of critical residues indicates that the catalytic site is on the b-chain and that the a-chain is regulatory.

4. Quaternary Structure

Bacterial and mammalian PFKs are active as tetramers and are inactivated upon dissociation into dimers (see Quaternary Structure). The allosteric inhibition of the PFK from *Thermus thermoaquaticus* by PEP involves such a dissociation. The crystal structures of bacterial PFKs explain why an oligomeric state is required for activity. The Fru-6-P binding site is at the interface between two subunits. The fructose moiety interacts with one subunit and the 6-phosphate group with the other (5). Under some conditions, tetrameric mammalian PFKs associate further into octamers and even more complex structures. They are active, but the role of this aggregation is not clear. PP_i-dependent PFKs also have a tetrameric structure that contains two a- and two b-chains. Yeast PFK is active only as an octamer that has four a- and four b-chains.

5. Catalytic Mechanism of Phosphoryl Transfer

Experiments with chiral (^{16}O, ^{17}O, and ^{18}O)-ATP have shown that transfer of the g-phosphate from ATP to Fru-6P occurs directly within a ternary complex (6) without a phosphoryl–enzyme intermediate. Steady-state kinetics are compatible with a random order of substrate binding, and the pH-dependence of the maximum velocity suggests that $Mg^{2+}\cdot ATP^{4-}$ is the most active ionic form (7).

X-ray crystallography of bacterial PFKs and site-directed mutagenesis suggest that several PFK active site groups are involved in catalyzing phosphoryl transfer (Fig. 2). The deprotonated side chain of Asp127 acts as a base and abstracts a proton from the 1-OH group of Fru-6P so as to increase its nucleophilicity. Mutation of Asp127 to Ser decreases the catalytic rate constant 10^4-fold (8). The transferred phosphoryl group is stabilized by interactions with the magnesium ion, by the positive charge of Arg72, and by a hydrogen bond to Thr125. The deprotonated side chains of Asp103 and Asp129 hold the magnesium ion that contributes electrostatic catalysis. The amide NH of Gly104 makes a hydrogen bond with the bg-oxygen bridge to facilitate cleavage of the O–P bond (5). X-ray crystallography also shows that the active site of *E. coli* PFK takes two conformations, one “open” that binds substrates and releases products and one “closed” in which catalysis occurs (5). Rapid kinetics have shown that conformational changes indeed occur in *E. coli* PFK upon substrate binding (and/or product release) and that these changes are slow enough to be rate-limiting in some conditions for the catalytic cycle (9).

Figure 2. The transition state of the reaction catalyzed by PFK with the main interactions with the active site as suggested by X-ray crystallography (5) and site-directed mutagenesis. The residues shown are conserved in all of the active PFKs except for Thr125, replaced by a serine in eukaryotic PFKs, which conserves an OH group. The partial covalent bonds are indicated by broken lines, and the hydrogen and electrostatic bonds by dotted lines.

6. Purification and assay of activity

Most PFKs are purified by affinity chromatography using a nucleotide analog covalently coupled to a resin. The usual assay measures the formation of Fru-1,6P$_2$ by coupling it to the disappearance of

NADH using aldolase, triosephosphate isomerase, and glycerol-phosphate dehydrogenase (10, 11).

7. Regulation of activity

The catalytic activities of all PFKs are sensitive to pH, ionic strength, divalent metal ions and/or their chelators (the real substrate is the ATP – Mg^{2+} complex), and phosphate, , and K^+ ions (10, 11). In addition, PFKs often have complex regulatory properties, such as sensitivity to allosteric effectors and/or a cooperative saturation by the substrate Fru-6P. Only a few (eg, that from Dictyostelium discoideum) follow Michaelis–Menten kinetics under all conditions studied.

7.1. Allosteric Effectors

The activities of PFKs are modulated by several allosteric effectors that differ among various organisms (Table 1). Most of these effectors do not modify the maximum velocity, but affect only the saturation by Fru-6P, influencing the cooperativity and/or half-saturating concentration. All PFKs are activated by an increase in levels of ADP and/or AMP, which would express a shortage of cell energy (see Adenylate Charge). In addition, most eukaryotic PFKs are strongly inhibited allosterically by ATP, and show nonhyperbolic ATP saturation. Because of this inhibition by ATP, PFK in the liver is almost inactive with the *in vivo* concentrations of Fru-6P and ATP, and the total PFK activity is much too low to account for the glycolytic flux measured *in vivo*. This discrepancy between the expected and measured glycolytic flux led to the discovery of the most potent allosteric activator of eukaryotic PFKs, Fru-2,6P_2, which relieves allosteric inhibition by ATP (12). The concentration of Fru-2,6P_2 in mammalian cells is controlled by hormones that act on cell metabolism through cAMP and protein kinase A. Fru-2,6P_2 decreases when cAMP increases. This hormonal control of PFK activity via Fru-2,6P_2 regulates the balance between the degradation of glycogen and the synthesis of glucose and/or lipids. Fru-1,6P_2 also activates PFKs, but with a much lower affinity than Fru-2,6P_2 (12).

Table 1. The Main Effects of PFK in Different Organisms

PFKs from	Activation	Inhibition
Bacteria	ADP or GDP[a]	PEP
Mammals[b]	AMP.ADP	Citrate
	Fru-2.6P_2	ATP
Yeast	AMP.ADP	Citrate
	Fru-2.6P_2	ATP

[a] ADP is probably the physiological effector, but GDP has been used to activate bacterial PFKs in many kinetic studies because ADP is also a competitive inhibitor of the substrate ATP.

[b] The three different isotypes of PFK in mammalian cells are sensitive to the same effectors but to varying extents.

Most eukaryotic PFKs are also allosterically inhibited by citrate, the first metabolite in the Krebs cycle. Citrate inhibition is responsible for the “Pasteur effect” in yeast, a decrease of glucose consumption upon shift from anaerobic to aerobic growth. Indeed, the reoxidation of NADH by oxygen via the respiratory chain raises the level of the Krebs cycle intermediates, and the citrate inhibition of PFK decreases the rate of glycolysis.

Bacterial PFKs are insensitive to citrate, but are sensitive to feedback inhibition by PEP, the penultimate end product of glycolysis.

7.2. Appearance of “New” Regulatory Functions upon Evolution of Sites

The variety of allosteric effectors of PFKs can be explained by their evolution. Bacterial PFKs originally possessed an active site that binds both ATP and Fru-6P, plus an effector site that binds ADP or PEP. After the gene duplication and fusion that doubled the polypeptide chain, the active site on the N-terminal half retained its function, whereas that on the C-terminal active site evolved into a regulatory site (Fig. 1). The Fru-6P subsite became the activation site for Fru-2,6P_2 and the ATP subsite became an inhibitory site. Similarly, evolution could have modified an inhibitory site for PEP in bacterial PFKs into one for citrate in eukaryotic PFKs. The evolution from bacterial to eukaryotic PFKs has also created the structural elements needed for communication between the active site and the “new” regulatory sites.

7.3. The Cooperativity of *E. coli* PFK toward Fru-6P and the Concerted Model of Monod, Wyman, and Changeux

The steady-state kinetics of *E. coli* PFK were the first to be analyzed according to the concerted allosteric model. Quantitative agreement between experimental data and predictions from the model was remarkable (1). According to the model, the protein is in equilibrium between two conformational states, R and T. The active R state has a much higher affinity for Fru-6P and for the activator ADP (or GDP), whereas the inactive T state has a much higher affinity for the inhibitor PEP. In the absence of ligand, the equilibrium between the R and T states of free PFK largely favors T, and the a ratio $T_0/R_0 = 4\times10^6$ (1). The simplicity of the concerted model is that a unique transition between the two states R and T is involved in both the cooperativity toward Fru-6P and the influence of allosteric effectors. Some bacterial PFKs show sigmoïdal saturations by Fru-6P only in the presence of the inhibitor PEP, confirming that the transition into an inactive state induced by PEP and the cooperativity toward Fru-6P are related.

The crystal structure of the complex between a bacterial PFK and an analog of the inhibitor PEP shows that the latter is bound to a regulatory site remote from the active site and that the protein has changed its quaternary conformation. The change induced by PEP closes the Fru-6P binding site (13). This is consistent with the observation that PEP inhibits by decreasing PFK's apparent affinity for Fru-6P. Some residues that bind PEP are also involved in binding the allosteric activator ADP when PFK is in its active conformation. The opposite effects of binding activators and inhibitors to a single effector site result because it has two mutually exclusive conformations, that agree with the concerted allosteric model. The quaternary structure of the inactive conformation is less stable, which explains the PEP-induced dissociation of the PFK from *T. thermoaquaticus*

However, the transition between the two states R and T seen by X-ray crystallography cannot explain entirely the cooperativity of *E. coli* PFK toward Fru-6P. In the absence of ligand, free PFK is not in the inactive T_0 state because (1) its crystal structure is that of the R state (14), and (2) it binds Fru-6P with high affinity and without any cooperativity (15). Presteady-state kinetics show that binding substrates and/or effectors to *E. coli* PFK is accompanied by conformational changes within the R state, which are slow enough to be rate-limiting for the catalytic cycle. Thus, the cooperativity of *E. coli* PFK is in part independent of the transition between the crystallographic R and T states and is due to a change in the rate-limiting step from a conformational change at low Fru-6P concentrations to phosphoryl transfer at high Fru-6P (9). Such a kinetic origin of cooperativity explains observations with some mutants that are difficult to fit with the concerted model, such as values of the Hill coefficient larger than the number of Fru-6P binding sites (16) and reversal of the influence of effectors, when PEP becomes an activator (17) and GDP an inhibitor.

7.4. Phosphorylation of Mammalian PFKs by Protein Kinase A

Mammalian PFKs are phosphorylated on specific sites by protein kinase A. This produces changes in kinetic properties and in the tendency to aggregate into octamers, but the physiological role of this phosphorylation is unknown.

Bibliography

1. D. Blangy, H. Buc, and J. Monod (1968) J. Mol. Biol. 31, 13–35.
2. G. A. Dunaway, T. P. Kasten, T. Sebo, and R. Trapp (1988) Biochem. J. 251, 677–683.
3. P. Branny, F. De la Torre, and J.-R. Garel (1993) J. Bacteriol. 175, 5344–5349.
4. R. A. Poorman, A. Randolph, R. G. Kemp, and R. L. Heinrikson (1984) Nature 309, 467–469.
5. Y. Shirakihara and P. R. Evans (1988) J. Mol. Biol. 204, 973–994.
6. R. L. Jarvest, G. Lowe, and B. V. L. Potter (1981) Biochem. J. 199, 427–432.
7. I. Auzat, G. Le Bras, and J.-R. Garel (1994) Protein Peptide Lett. 1, 179–182.
8. H. Hellinga and P. R. Evans (1987) Nature 327, 437–439.
9. I. Auzat, E. Gawlita, and J.-R. Garel (1995) J. Mol. Biol. 249, 478–492.
10. D. Kotlarz and H. Buc (1982) Methods Enzymol. 90, 60–70.
11. K. Uyeda (1979) Adv. Enzymol. 48, 193–244.
12. E. Van Schaftigen (1987) Adv. Enzymol. 59, 315–395.
13. T. Schirmer and P. R. Evans (1990) Nature 343, 140–145.
14. W. R. Rypniewski and P. R. Evans (1989) J. Mol. Biol. 207, 805–821.
15. D. Deville-Bonne and J.-R. Garel (1992) Biochemistry 31, 1695–1700.
16. I. Auzat, G. Le Bras, and J.-R. Garel (1995) J. Mol. Biol. 246, 248–253.
17. F. T. K. Lau and A. R. Fersht (1987) Nature 326, 811–812.

Suggestions for Further Reading

18. P. R. Evans (1992) "Activity and allosteric regulation in bacterial phosphofructokinase", Proceedings from The Robert A. Welch Foundation Conference on Chemical Research XXXVI, pp 39–54. A reference that may be difficult to find but has an outstanding short and clear synthesis of the structure, catalytic mechanism, regulation, and evolution of phosphofructokinases.
19. L. A. Fothergill-Gilmore and P. A. M. Michels (1993) Evolution of glycolysis, Prog. Biophys. Mol. Biol. 59, 105–235. An exhaustive comparison of glycolytic enzymes from various species with fine sections on the structure, evolution, and expression of the genes that code for phosphofructokinases and a very complete list of references.

Phospholipases

Phospholipases hydrolyze membrane phospholipids (see Lipases). The lipid substrates for these enzymes are usually quite specific. Hormone-regulated phospholipase C (PLC) can hydrolyze a number of membrane phospholipids, including phosphatidylcholine and phosphatidylethanolamine. Phosphatidylinositol (PI) and its phosphorylated derivatives (polyphosphoinositides) are the most common substrates involved in second messenger generation, producing soluble inositol phosphates, such as inositol trisphosphate (IP_3), that are involved in calcium signaling.

Phospholipase D enzymes usually prefer phosphatidylcholine as substrate, generating phosphatidic acid and choline. Phosphatidic acid has been proposed to mediate a variety of biological responses involved in mitogenesis and protein trafficking (1).

The turnover of polyphosphoinositides occurs in a cycle of hydrolysis and resynthesis, called the “PI cycle.” PI is phosphorylated sequentially on the 4 and 5 hydroxyl groups of the inositol ring, to produce PI-4,5-P_2. Upon hormonal activation, PLC subsequently catalyzes the phosphodiesteratic cleavage of this lipid, resulting in the generation of diacylglycerol and IP_3 in the cell. After its degradation, PI can be resynthesized by the phosphorylation of diacylglycerol to PA, via the activity of a diacylglycerol kinase and the subsequent synthesis of PI via PI synthase. Thus, this cycle results in the generation of two potential second messengers, the membrane-associated diacylglycerol, which can activate protein kinase C, as well as IP_3, which can lead to the mobilization of intracellular calcium levels.

Several forms of PI-PLC have been identified (1). These proteins all exhibit an absolute requirement for calcium and are equally capable of hydrolyzing PI and the polyphosphoinositides PIP and PI-4,5-P_2. These proteins exist in three subfamilies, b, g, and d, each with multiple members. They have a number of conserved and divergent domains, reflecting their differential regulation. All three subclasses have a pleckstrin homology (PH) domain, which probably mediates some type of interaction with lipids in the membrane, and an EF-hand motif, presumably involved in calcium binding. Moreover, there are two additional conserved domains, designated X and Y, that contain the catalytic core of the enzyme; there is also a conserved C2 domain, also likely to be required for calcium interaction. PLCg, which is regulated by tyrosine kinase receptors, contains two SH2 domains and one SH3 domain and has been shown to undergo phosphorylation of tyrosine residues. PLCb is responsible for regulation through G-protein-coupled receptors and is generally regulated by a subunits of the Gq family of heterotrimeric G proteins, linked to a subset of such receptors. Additionally, their bg subunits have also been shown to regulate PLCb, although the efficacy of this activation is not comparable to that seen with Gqa. PLCb can also act as an activator of the GTPase activity of Gq, effectively behaving as a GTPase activating protein (GAP).

Bibliography

1. W. D. Singer, H. A. Brown, and P. C. Sternweis (1997) Annu. Rev. Biochem. 66, 475–509.

Phospholipases C

1. Historical Perspective

The phosphatidylinositol (PI)-specific phospholipases C have emerged as key and determining components of the PI cycle of signal transduction. In this pathway, the action of any of several extracellular agents (including hormones, cytokines, neurotransmitters, and xenobiotics) results in activation of PI-specific phospholipases C that cleave phosphatidylinositol bisphosphate (PIP_2) (1-3). This results in the formation of inositol trisphosphate (IP_3) and diacylglycerol (DAG), which act as important second messengers involved in the regulation of calcium signaling and protein kinase C, respectively (Fig. 1).

Figure 1. Regulation and function of the phosphatidylinositol (PI) cycle. The scheme illustrates two mechanisms for

activation of the PI cycle through (1) direct phosphorylation of phospholipase C g by tyrosine kinase receptors, and (2) G proteins in the case of G-protein-coupled receptors. The two products of PIP_2 hydrolysis, IP_3 and diacylglycerol (DAG) function as second messengers in activating calcium release and protein kinase C, respectively. Resynthesis of PIP_2 from DAG completes the PI cycle.

Early insight into the PI cycle came from studies by Hokin and Hokin, who identified turnover of inositol phospholipids in cells stimulated with acetylcholine. Work over the ensuing decades resulted in the delineation of the biochemical components of the PI cycle and the realization of its intimate connection to changes in calcium levels in the cells. Thus, it became appreciated that specific phospholipases of the C type were activated in response to acetylcholine and other hormones. It was also appreciated that PIP_2 was the preferred substrate in this pathway and that this was coupled to changes in calcium homeostasis (3). It was then determined that the IP_3 product of this reaction acted directly on specific receptors internal to the cell to cause changes in the levels of free calcium. Contemporaneously, a direct connection was made between DAG and protein kinase C, demonstrating a second messenger function for DAG (4, 5).

2. Regulation of Phospholipase C

PI-specific phospholipases C have been purified and cloned. They exist as a family of related phospholipases with close similarity in catalytic activity and preference for PIP_2 as a substrate, but with distinct mechanisms of regulation (1). Notably, the two best-studied members of the family, phospholipase Cb and phospholipase Cg, are coupled through distinct mechanisms to two different classes of membrane receptors. G protein–coupled receptors regulate phospholipase Cb through direct activation by hetero-trimeric G proteins. On the other hand, phospholipase Cg is tyrosine phosphorylated (see Phosphorylation, Protein) by transmembrane tyrosine kinase receptors (and also by nonreceptor tyrosine kinases) through interactions with specific SH2 modules in phospholipase Cg that are recognized by specific SH2-binding domains in the tyrosine kinases (Fig. 1).

2.1. Role of Phospholipases C in Signal Transduction and Cell Biology

Given their intimate coupling to two major classes of transmembrane receptors, phospholipases C serve a critical role in allowing the ligands of these receptors to regulate the intracellular levels of calcium and the activity of protein kinase C. This is accomplished by the activity of the two products of the phospholipase C reaction. IP_3 is a hydrophilic and diffusable small molecule that interacts specifically and with high affinity with the IP_3 receptor in the endoplasmic reticulum. This results in release of calcium from stores in the endoplasmic reticulum into the cytosol. In turn, free calcium appears to coordinate a variety of cellular responses through the activation of various enzymes, including protein kinases and phosphodiesterases (see Calcium Signaling). Simultaneously, DAG, which is formed in the membrane, activates several members of the protein kinase C family. Protein kinase C is capable of phosphorylating a variety of substrates that result in the regulation of diverse biological responses. Protein kinase C is also activated potently by phorbol esters, which are plant toxins that cause a myriad of cellular responses, including effects on blood cell activation, cell growth regulation, tumor promotion, memory formation, immune responses, inflammatory reactions, hormone release, and neurotransmission, most likely through activation of protein kinase C (4). Therefore, the two products of the phospholipase C reaction serve as critical second messengers, often acting in synergy to regulate a variety of cellular responses.

Bibliography

1. S. G. Rhee, P. G. Suh, S. H. Ryu, and S. Y. Lee, (1989) Science 244, 546–550.
2. P. W. Majerus, T. M. Connolly, H. Deckmyn, T. S. Ross, T. E. Bross, H. Ishii, V. Bansal, and D. Wilson (1986) Science 234, 1519–1526.
3. M. J. Berridge, P. H. Cobbold, and K. S. R. Cuthbertson, (1988) Phil. Trans. Roy. Soc. Lond. 320, 325–343.
4. Y. Nishizuka (1992) Science 258, 607–614.
5. R. M. Bell (1986) Cell 45, 631–632.

Suggestions for Further Reading

6. M. Berridge (1993) Inositol trisphosphate and calcium signalling. Nature 361, 315–324.
7. N. Divecha and R. Irvine (1995) Phospholipid signaling. Cell 80, 269–278.

Phosphorous Isotopes

Phosphorus is element number 15 in the periodic table and has valence states of 3 or 5 (1). Seventeen isotopes have been identified (2), ranging in atomic mass number from ^{26}P to ^{42}P, most of which have physical half-lives of seconds or milliseconds and do not have important applications. Only one stable isotope of phosphorus is found in nature (^{31}P).

The most important radioactive isotope of phosphorus is ^{32}P (half-life = 14.29 days) (see Radioisotopes). It undergoes beta-minus decay to ^{32}S, which is stable. Phosphorus-32 yields one beta particle per decay, with an energy of 1.71 MeV maximum, 0.695 MeV on average. Another useful radioisotope of phosphorus is ^{33}P (half-life = 25.4days). It yields one beta particle per decay, with an energy of 0.1667 MeV maximum, 0.0486 MeV on average.

Phosphorus-32 is usually prepared in an accelerator by bombarding a stable sulfur target with deuterons according to the reaction $^{34}S(d,a)^{32}P$. It may also be prepared by accelerator deuteron bombardment of ^{31}P according to the reaction $^{31}P(d,p)^{32}P$ or by reactor neutron-activation according to $^{31}P(n,g)^{32}P$. Carrier-free radioisotope is prepared by reactor production according to the reaction $^{32}S(n,p)^{32}P$.

Phosphorus-32 was first made by Fermi in 1934 using neutrons from a radium–beryllium source (3). In 1935, Hevesey made ^{32}P by the same method and studied the metabolism of phosphorus compounds in rats (3). Hevesey also studied blood volume using ^{32}P-labeled red blood cells. When it was found that ^{32}P killed blood cells, Lawrence produced it in a cyclotron and in 1938 was the first to use it as a therapeutic radioisotope for treatment of leukemia in humans (3). Phosphorus-32 is presently used as an effective treatment for polycythemia vera (4, 5), for treatment of painful bone metastases from prostate and other cancers (6), for restenosis stents in treating heart disease, and in colloidal form for direct intratumoral injection, or infusional brachytherapy (7). The systemic use of ^{32}P has been limited by concerns over potential leukemogenic effects.

As a diagnostic agent, ^{32}P has been used to study skeletal growth and bone tumor kinetics. In molecular biology, ^{32}P is used primarily to label nucleic acids, which have one phosphorous atom per nucleotide, and for phosphorylation of proteins. Phosphorus-32 is readily detected by beta-particle liquid scintillation counting, Cerenkov radiation detectors, autoradiography, and fluorography.

Bibliography

1. D. R. Lide and H. Pr. Frederikse, eds. (1995) CRC Handbook of Chemistry and Physics, CRC Press, Boca Raton, Fla.
2. Knolls Atomic Power Laboratory (1996) Chart of the Nuclides, 15th ed., available from General Electric Company San Jose, Calif.
3. M. Brucer (1990) A Chronology of Nuclear Medicine, Heritage Publications, Inc., St. Louis, Mo.
4. J. Lazlo (1974) Postgrad. Med. 55, 168–173.
5. C. Parmentier and P. Gardet (1994) Nouv. Rev. Fr. Hematol. 36, 189–192.
6. E. B. Silberstein (1993) Semin. Oncol. 20 (suppl. 2), 10–21.
7. S. E. Order et al. (1996) Ann. Acad. Med. Singapore 25, 347–351.

Suggestion for Further Reading

8. H. N. Wagner, Jr. (1968) Principles of Nuclear Medicine, W. B. Saunders Co., Philadelphia.

Phosphorylase Kinase

Phosphorylase kinase (E.C. 2.7.1.38) catalyzes the phosphorylation of residue Ser14 in relatively inactive glycogen phosphorylase b, converting it to the much more active phosphorylase a. Its discovery in 1955 by Fischer and Krebs, and their later demonstration that the enzyme converting phosphorylase a to b is a protein phosphatase that removed the phosphate, provided a firm basis for further investigation of the first metabolically interconvertible enzyme system to be discovered. These investigators and their colleagues characterized phosphorylase kinase and demonstrated that it was itself activated by phosphorylation by cyclic AMP (cAMP)-dependent protein kinase (cAPK), thus suggesting the famous cascade system for the regulation of glycogen metabolism by hormones. In addition, it was discovered in this same laboratory that Ca^{2+} is required for activity, and later by Drummond et al. that the activation of glycogenolysis is coordinated to muscular contraction by the release of calcium from the endoplasmic reticulum in response to nervous stimulation (see Calcium Signaling). It was not until 1978 that the small calcium-binding protein calmodulin was found to be an integral part of phosphorylase kinase responsible for the allosteric activation by Ca^{2+}. Calmodulin was designated subunit d because three other subunits, the regulatory a and b and the catalytic g, were already known. Each is present in four copies, so the holoenzyme may be represented as $a_4b_4g_4d_4$ with an overall molecular weight of 1.3 million. This enormous protein presents a formidable challenge to investigators, but the subunits have been isolated and their primary sequences determined, while progress is being made on their functions and on the complex regulation of this enzyme. The gene for the catalytic domain of subunit g has been cloned, and the structure of the subunit determined by X-ray crystallography, so the molecular basis of the catalytic activity has been elucidated. The comprehensive review by Picket-Gies and Walsh (1) covers the literature until 1986 and can be used as the essential reference for this article. It is suggested for further reading.

1. Structure and Function

The molecular weights of the subunits have been determined by sequence analyses (2) and are a = 138,422, b = 125,205, g = 44,673, and d = 16,680. Various analyses by electron microscopy of $a_4b_4g_4d_4$ show a bilobed butterfly-like structure that may be cleaved by trypsin into two halves, suggesting that the subunits are arranged as a bridged dimer of octamers ($a_2b_2g_2d_2$), while another study found a “chalice” form. These observations have been reconciled by a three-dimensional model that can account for all views (3). Essentially there are three twofold axes of symmetry relating the four abgd_protomers, resulting in a tetrahedral arrangement. Proteolytic digestion suggests that the b subunits play an essential role in holding the holoenzyme together, but there are additional interactions of other subunits. Lithium bromide causes dissociation into two complexes, agd_and gd;_both of these have activity toward phosphorylase b equal to that of the holoenzyme.

The determination of the amino acid sequences of all four subunits provided valuable insights into their various functions. The g subunit proved to have substantial homology with the catalytic subunit of cAPK. There is an additional C-terminal region (approximately residues 286 to 386) that can be removed by chymotrypsin, to yield a catalytic domain (residues 1 to 285) with full activity and no calmodulin/Ca^{2+} sensitivity. The C-terminal or regulatory domain contains two calmodulin-binding domains, suggesting a double binding mode that accounts for the unusual phenomenon that calmodulin binds to the isolated g subunit in the absence of calcium, becoming subunit d, and suppresses its activity. Troponin C, which is homologous to calmodulin, also binds to the g subunit and may provide a more direct link between the neural activation of skeletal muscle contraction and glycogenolysis. The a and b subunits are highly homologous, suggesting a common ancestral protein. Both have calmodulin-binding domains, but apparently only one extrinsic calmodulin binds per pair of a/b units, known as d subunits, in the intact holoenzyme in the presence of excess calcium, resulting in four d subunits in all. The b subunit contains two sites for phosphorylation by cAPK, on Ser26 and Ser700. The two sites appear to be phosphorylated equally rapidly, and either one results in an increase in activity of the holoenzyme, but a total of only one phosphate per subunit is found. The rate of phosphate incorporation into the b subunit is 5- to 10-fold faster than that into the a subunit and is a prerequisite for the latter, suggesting a conformational change. The a subunit is phosphorylated at Ser1018 by cAPK, with resultant increases in activity. Both the a and b subunits have several sites for autophosphorylation, but the evidence that this phenomenon has significance for *in vivo* regulation is ambiguous.

Kinetics of the phosphorylase kinase reaction were studied using a tetradecapeptide from phosphorylase b (residues 5 to 18) that contained the phosphorylatable Ser14 in order to avoid substrate-directed effects. The kinetic mechanism was found to be rapid equilibrium random Bi–Bi, indicating that either ATP or the protein can bind first and that the phosphoryl transfer step in the ternary complex is rate-limiting. Several studies on the effects of deleting or substituting various amino acid residues of the peptide permit one to conclude that the kinase shows a marked preference for peptides having the natural sequence around Ser14, while the latter is also important because a Thr14 peptide has a very low rate of phosphorylation. Because the first 18 residues of phosphorylase b are disordered, it is not surprising that the corresponding peptide, presumably in a random conformation, should be a good substrate for the kinase. The kinase must, however, recognize more than just the N-terminal peptide, because the intact protein substrate has a K_m at least fivefold lower and a maximum velocity (V_{max}) fivefold greater. Phosphorylase kinase will also phosphorylate Ser7 of glycogen synthase, but this is also the target for other kinases, including cAPK (which does not act on phosphorylase), so the physiological significance of its action on this and several other proteins is not known.

The high-resolution structure of the crystallized catalytic domain of the g subunit has been determined by Johnson et al. (4) and compared to other protein kinases (5). The structure is very similar to that of cAPK and contains the same catalytic residues in equivalent positions. These include Lys57 to interact with the phosphates of ATP and Asp167 to interact with the Mg^{2+} of ATP/Mg^{2+}. An N-terminal lobe, mostly b-sheet, is connected to the a-helical C-terminal lobe by polypeptide chain, allowing opening and closing of the active site cleft between the two lobes. The suggested catalytic mechanism is that Asp149 abstracts a proton from the substrate serine residue and the resultant alcoholate ion attacks the terminal phosphate of ATP. In cAPK, an activation segment has Thr197 phosphate, which interacts with Arg165, next to the catalytic Asp166, and other basic residues, but in phosphorylase kinase this is replaced by Glu182, which forms an ionic link with Arg148 of the catalytic loop and serves the same function of maintaining Asp149 and other catalytic residues in the correct orientation.

2. Regulation

Because so many results from *in vitro* studies may have no physiological significance, only those most likely to apply *in vivo* will be considered here. Because nearly all the phosphorylase and 20% to 40% of the kinase are associated with the glycogen particle in muscle, the kinase action on phosphorylase must occur with the latter bound to glycogen by its catalytic face, leaving the control face with Ser14 exposed to the cytosol (see Glycogen Phosphorylase). It is relevant, then, that glycogen decreases the K_m for phosphorylase b 10-fold; and this is likely to be via conformational changes in the substrate, because glycogen has no effect on phosphorylation of the tetradacapeptide containing residues 5 to 18. The allosteric inhibitor of phosphorylase b, glucose-6-phosphate, also inhibits kinase activity on the protein, but not on the peptide, suggesting augmentation of the metabolite feedback. There is a good correlation between the increase of Ca^{2+} levels due to nervous or electrical stimulation, muscle contraction, and the activation of both phosphorylase kinase and its substrate, and this occurs without changes in either the level of cAMP or the phosphorylation state of the kinase. The molecular basis is the allosteric activation due to binding of Ca^{2+} to the d subunit and, at higher Ca^{2+} levels, of the binding of Ca^{2+}-calmodulin to the a/b_subunits (the d subunits). In contrast, the administration of adrenaline can cause coordinated changes in cAMP levels, activation of cADK and phosphorylase kinase, and formation of phosphorylase a. A point still in contention is whether or not Ca^{2+} is still an obligate requirement for kinase catalysis, as in vitro experiments suggest, but the increased affinity for the metal ion after phosphate incorporation into the b and_a_subunits may allow low endogenous levels to suffice. Heilmeyer (2) summarizes current knowledge of regulation, including a possible role for an allosteric ATP/Mg^{2+} site on the a subunit that may stimulate binding of the same substrate to the g subunit by displacing inhibitory ADP. He suggests that an ancestral gd phosphorylase kinase, responsive only to Ca^{2+}, could not handle all the signals needed to regulate the conversion of phosphorylase b to a. The addition of the two regulatory subunits b and_a permitted regulation by cAMP-dependent phosphorylation, extrinsic calmodulin, and substrate binding (ATP/Mg^{2+}).

Bibliography

1. C. A. Pickett-Gies and D. Walsh (1986) *The Enzymes*, Vol. 17, 3rd. ed. pp. 395–459.
2. L. M. G. Heilmeyer, (1991) Biochim. Biophys. Acta *1094*, 168–174.
3. M. T. Norcum, et al. (1994) J. Mol. Biol. *241*, 94–102.
4. D. J. Owen, et al. (1995) Structure *3*, 467–482.
5. L. N. Johnson, M. E. M. Noble, and D. J. Owen (1996) Cell *85*, 149–158.

Phosphorylation, Protein

Phosphorylation is a common, and usually reversible, post-translational modification of proteins. The amino acid residues that can be phosphorylated are listed in Table 1. Protein phosphorylation is either an intermediate step in the course of an enzymatic reaction or a more durable modification that regulates protein properties. This entry focuses on regulatory protein phosphorylation. In this context, the phosphorylation reaction is catalyzed by protein kinases, which form a specific class of phosphoryl-transferases, generally transferring the phosphoryl group from the g position of ATP (Fig. 1a, see exceptions below) to the side chain of an amino acid residue. The dephosphorylation reaction corresponds to the transfer of the phosphoryl group to a water molecule (ie, the hydrolysis of the phosphoester bond). Both reactions are energetically favorable and occur readily in the presence of the appropriate catalyst, a protein kinase or phosphatase. In a living cell, the level of phosphorylation of a protein is the result of a dynamic equilibrium between its rates of phosphorylation and dephosphorylation. As mentioned above, the phosphoryl donor is usually ATP, in complex with Mg^{2+}. In vitro, for some protein kinases, ATP or Mg^{2+} can be replaced by GTP or Mn^{2+}, respectively. In somewhat artificial conditions (eg, very low levels of ATP and high levels of ADP), protein kinases can catalyze the transfer of phosphoryl group from the phospho-amino acid of a protein to ADP, generating ATP. Although secreted proteins or peptides are known to be phosphorylated, the regulatory phosphorylation reactions that have been well-characterized to date take place within cells.

Figure 1. Major pathways of regulatory protein phosphorylation/dephosphorylation. (a) The most general case, observed in all types of living organisms, corresponds to phosphorylation of serine, threonine, or tyrosine residues by protein kinases using ATP/Mg^{2+} as phosphoryl donor. The dephosphorylation is catalyzed by a protein phosphatase,

usually distinct from the protein kinase. The activity of both the protein kinase and phosphatase can be regulated by intracellular or extracellular stimuli. The phosphorylated or the dephosphorylated forms of the protein substrate, or both, may be responsible for the biological response observed. (b) Although not as common as the previous phosphorylation system, the two-component system is widespread in eubacteria and has also been found in archaebacteria and eukaryotes. A "sensor protein kinase" autophosphorylates histidine residues in response to an environmental stimulus, using ATP/Mg^{2+} as phosphoryl donor. The phosphate is then transferred to an aspartate residue of a "response regulator," which may be located on the same polypeptide chain as the sensor kinase, or on a distinct one. The phosphorylated response regulator triggers the biological response. (c) The third phosphotransferase system has been described in bacteria only. In this system coupled to sugar transport, the phosphoryl group is transferred successively from phosphoenolpyruvate (PEP) to histidine and cysteine residues of several proteins (indicated with roman numerals) and to an incoming sugar. In addition to its function in sugar metabolism, this system has been shown to be coupled to several biological responses. HPr, histidine-containing phosphocarrier protein (see the text for references); Pi, inorganic phosphate; P, phosphate.

Table 1. Amino Acid Residues That Can Be Phosphorylated in Proteins

Acceptor group	Amino acid	Product
Alcohol	Serine, threonine	Phosphoester
Phenol	Tyrosine	Phosphoester
Basic amino acid	Histidine, arginine, lysine	Phosphoramidate
Thiol	Cysteine	Phosphate thioester
Acyl	Aspartate, glutamate	Mixed phosphate-carboxylate acid anhydride

1. Historical Perspective

Regulation by protein phosphorylation was discovered by Edmund Fischer and Edwin Krebs in the course of their studies of glycogen metabolism between 1955 and 1958 (1, 2). It was known from the work of Carl and Gerty Cori that glycogen phosphorylase, the enzyme that degrades glycogen, exists in two forms, an active form (phosphorylase a) and an inactive form (phosphorylase b). Fischer and Krebs showed that the only difference is that phosphorylase a is phosphorylated and they identified phosphorylase kinase, the protein kinase that phosphorylates phosphorylase b on Ser14, transforming it into the active phosphorylase a (Fig. 2). The same authors later showed that cyclic AMP, the intracellular second messenger formed under the action of epinephrine or glucagon, exerts its effects on glycogen catabolism by activating a protein kinase. This protein kinase, cyclic AMP-dependent protein kinase (or protein kinase A, PKA), phosphorylates and activates phosphorylase kinase. In skeletal muscle, they demonstrated that phosphorylase kinase is also activated by Ca^{2+}-calmodulin, allowing the coupling of metabolic events with contraction. Although it was originally thought that these reactions might be specific for the regulation of glycogen, the subsequent work of Paul Greengard and others showed that phosphorylation of proteins accounts for the action of many extracellular signals, and several protein kinases activated by cyclic GMP, Ca^{2+}-calmodulin and Ca^{2+}-lipids were discovered (3-5). During the same period, the protein phosphatases involved in the regulation of glycogen metabolism started to be studied methodically (6). This opened a new field, because it is now apparent that regulation of protein phosphatases is as important as regulation of protein kinases in the control of cell function. Another major step in the study of protein phosphorylation was the discovery of phosphorylated tyrosine residues by Tony Hunter in 1979 (7). Phosphotyrosine raised considerable interest when it was discovered that it is increased in cells transformed by viruses, and that v-src, and v-abl, two major viral oncogenes, are tyrosine kinases. Shortly thereafter, it was shown that growth factor receptors, which are transmembrane proteins, have an intrinsic tyrosine kinase activity associated with their intracellular domain (8) (see Tyrosine Kinase Receptors). This tyrosine kinase activity is stimulated upon binding of the growth factor to the extracellular domain of the receptor. Thus, it became evident that, in spite of its low abundance in normal cells, phosphotyrosine residues are a key step in the control of cell growth and differentiation. More recently, molecular cloning of genes has identified a very large number of protein kinases and phosphatases in all living organisms that have been studied. It is now apparent that protein phosphorylation is a fundamental mechanism of signal transduction used by all cells to regulate the properties of their proteins in response to external or internal clues. The list of fundamental biological processes regulated by protein phosphorylation would be nearly endless, but would include gene expression, energy production and storage, cell division and differentiation, as well as synaptic plasticity in the nervous system, which is thought to underlie learning and memory.

Figure 2. Regulation of glycogen degradation. The main pathways regulating glycogen degradation, the study of which led to the discovery of protein phosphorylation, are illustrated. Glycogen is degraded stepwise by glycogen phosphorylase. Schematically, glycogen phosphorylase exists in either a dephosphorylated inactive form (b) or a phosphorylated active form (a). The transformation of b-form to a-form is catalyzed by phosphorylase kinase. Phosphorylase kinase itself is activated by two independent pathways. In skeletal muscle, Ca^{2+} entering the cell during the action potential binds to calmodulin and activates phosphorylase kinase directly. In addition, phosphorylase kinase is activated by phosphorylation by cAMP-dependent protein kinase (PKA). PKA is directly stimulated by cyclic AMP (cAMP), which is generated in response to the stimulation of adenylyl cyclase by various seven transmembrane-segment G-protein-coupled receptors (e.g. receptors for epinephrine or glucagon). Dephosphorylation and inactivation of glycogen phosphorylase is catalyzed by several enzymes, the study of which led to the description and classification of protein phosphatases. See the text for references. Pi, inorganic phosphate; , phosphatase; ↑, activation.

2. Phosphorylation in Prokaryotes

Studies of protein phosphorylation in prokaryotes initially lagged behind those in eukaryotic cells. However, the paramount role of regulation by protein phosphorylation is now recognized in both Archea and Bacteria (9, 10). Bacteria possess ATP-dependent phosphorylation systems, using protein kinases that have sequence homologies with those of eukaryotes. These protein kinases phosphorylate serine or threonine residues and are, in many cases, regulated by cellular metabolites, rather than by second messengers. An original enzyme of bacteria is isocitrate dehydrogenase kinase/phosphatase of enteric bacteria, which has combined phosphatase and kinase activities located on the same polypeptide chain (11). A second system of protein phosphorylation in eubacteria corresponds to the sensor kinase/response regulator, often termed the two-component system (12). In such systems, a sensor kinase, generally membrane-associated, phosphorylates itself on a histidine residue in response to external stimuli [eg, chemoattractant, nutrient, osmotic pressure, etc. (Fig. 1b)]. The phosphoryl group is then transferred to an aspartic acid residue located on a distinct protein or on the same polypeptide chain, the response regulator, triggering the appropriate biochemical response. This type of signal transduction seems to be evolutionarily very ancient, because it has now been also identified in Eucarya and Archea (10). In the third phosphorylation system, described thus far only in bacteria, the phosphoryl group donated by phosphoenolpyruvate (PEP) is passed down a chain of phosphorylatable proteins (9). Phosphorylation of these proteins occur on histidine and cysteine residues (Fig. 1c). Such PEP-dependent systems are implicated in a wide variety of regulations, including carbohydrate metabolism, transcription, and adenylate cyclase. Protein phosphatases are less well-characterized in prokaryotes. Relatives of the PPP phospho-serine/threonine protein phosphatase gene family have been identified in Archea and in eubacterial bacteriophages (10). Finally, it should be noted that bona fide tyrosine phosphorylation has been demonstrated in bacteria, as well as the presence of potential tyrosine phosphatases that bear a similar sequence signature to that of eukaryotic tyrosine phosphatases in their active site (10).

3. Phosphorylation in Eukaryotes

Regulatory protein phosphorylation in eukaryotes occurs primarily on serine, threonine, and tyrosine residues (Fig. 1a). The great majority of the protein kinases responsible for the phosphorylation of these residues have a conserved catalytic domain that belongs to a single gene family. It has been estimated that more than a thousand different protein kinases can be coded in the genome of higher eukaryotes (13, 14). The genome of *Saccharomyces cerevisiae* contains genes for 113 such conventional protein kinases (15). Interestingly, a number of lipid kinases have a catalytic domain related to that of conventional protein kinases. Some of these enzymes are capable of autophosphorylation; and at least one of them, DNA-PK, is a genuine protein kinase, stimulated by the ends of double-stranded DNA (16). In addition, histidine kinases related to the bacterial two-component system have been identified in several eukaryotes (Fig. 1b). They are, for example, involved in the responses of yeast to osmotic shock (17) and of plants to ethylene (18). An original group of serine kinases related to histidine kinases corresponds to the mitochondrial protein kinase that phosphorylates a-ketoacid dehydrogenases (11).

The catalytic domains of regulatory protein phosphatases in eukaryotes belong to several gene families: Serine/threonine phosphatases belong to two gene families of metal-requiring enzymes, PPP and PPM (19), whereas tyrosine and dual-specificity phosphatases form a superfamily of genes that have a common signature sequence in their active site (Cys–X_5–Arg) and a common catalytic mechanism. These enzymes are grouped in four families: classical phosphotyrosine phosphatases (PTPs), low-molecular-weight PTPs, VH1-like dual-specificity phosphatases, and cdc25-like dual-specificity phosphatases (20).

4. Specificity of Protein Phosphorylation

Protein kinases display a high degree of substrate specificity. First, the vast majority phosphorylate either serine/threonine or tyrosine side chains, whereas only a few kinases have a dual specificity, for both threonine and tyrosine. In addition, protein kinases are highly sensitive to the immediate environment of the phosphorylated residue (21). Thus, specific consensus sequences have been identified for many of them (Table 2). In some cases, the specificity also depends on higher-order determinants, such as interactions between the protein substrate and the protein kinase at sites located at distance from the phosphorylated residue. In living cells, the proximity between the protein kinase and its substrate plays an important role. This is achieved by specific targeting mechanisms, which enrich the kinase concentration at particular sites of the cell (22, 23). There are also a number of scaffolding proteins that associate several enzymes, including kinases and/or phosphatases and their substrates (24). In the case of protein phosphatases, the nature of the sequence surrounding the phospho-amino acid to be dephosphorylated seems generally less critical than in the case of protein kinase, and the role of higher-order determinants, as well as that of targeting processes, appears fundamental (25, 26). It should be pointed out that, with the exception of some monosubstrate systems, there is no perfect match between the substrate specificity of most protein kinases and phosphatases, implying a complex intertwining of the regulation by these enzymes.

Table 2. Examples of Consensus Phosphorylation Sites for Protein Kinase

cAMP-dependent protein kinase	Arg/Lys-Arg-Xxx-Ser*
Ca^{2+}-calmodulin-dependent kinase II	ArgXxxXxxSer*/Thr*
Protein kinase C	Arg/Lys (Xxx)1-2 Ser*/Thr* Xxx-Arg/Lys
Casein kinase 1	Acid-Xxx-Xxx-Ser*
Casein kinase 2	Ser*/Thr* Xxx-Xxx Asp/Glu
MAP-kinases, cyclin-dependent kinases	Ser*/Thr* Pro
EGF-receptor tyrosine kinase	Glu/Asp-Tyr*-Hyd

5. Methods to Study Protein Phosphorylation

5.1. General Methods to Study the State of Phosphorylation of Proteins

(detailed descriptions of methods can be found in Ref. 27-30). The most commonly used approach is metabolic radiolabeling of cells of interest with ^{32}P-orthophosphoric acid (sometimes called "front-phosphorylation"). ^{32}Pi is taken up by cells, incorporated into endogenous ATP (as well as in many other phosphorylated molecules), and used to phosphorylate proteins, lipids, and nucleic acids. Labeled phosphoproteins can be studied by electrophoresis (usually two-dimensional gel electrophoresis) or following immunoprecipitation with specific antibodies. However, proteins are often phosphorylated on several sites, which can have different physiological meanings, and other approaches are required to analyze independently the phosphorylation of each of them (see below). Moreover, the amount of ^{32}P incorporated in a given site does not reflect directly the stoichiometry of phosphorylation of this site, but rather the turnover rate of the phosphoryl group. That is, a site phosphorylated at a high stoichiometry but with a low turnover rate (eg, "constitutive phosphorylation") will appear poorly labeled, whereas a residue phosphorylated at a low stoichiometry, but with a high turnover rate, will appear intensely labeled. The levels of labeling are also dependent on the specific activity of the intracellular ATP pools, which may vary, depending on the cell population or physiological status. Therefore, other methods have been developed to avoid these pitfalls. In "back-phosphorylation" assays, proteins of interest are isolated in conditions in which their phosphorylation state is preserved. They are then phosphorylated stoichiometrically *in vitro* with g^{32}P-ATP and a purified kinase, active on the phosphorylation site of interest. Thus, the higher the level of phosphorylation of the site *in vivo*, the lesser radioactive phosphate is incorporated *in vitro*. The use of this method is limited, however, by the requirement for a highly active purified protein kinase and by its low sensitivity. An alternative approach that is enjoying considerable success is the use of phosphorylation-state-specific antibodies. Some of these antibodies react with a phosphorylated amino acid, almost independently of its sequence environment. For example, antibodies specific for phospho-tyrosine are extremely useful tools in the study of protein tyrosine phosphorylation. Moreover, specific antibodies can be raised against synthetic phosphopeptides encompassing the phosphorylation site of a protein of interest. Such antibodies are specific for a given protein phosphorylated at a particular site, and they provide powerful tools that can be used for immunoblotting, immunocytochemistry, and other approaches.

Phosphoproteins are often studied by one- or two-dimensional electrophoresis. In nondenaturing conditions (eg, isoelectrofocusing), the presence of a phosphorylated residue shifts the electrophoretic mobility of the protein toward a more acidic form. In the presence of SDS, phosphorylation of a protein may have no effect on its electrophoretic mobility, or it may increase its mobility and its apparent size. The slowing of the protein mobility by phosphorylation during SDS-PAGE is often attributed to a decrease in the charge density due to decreased binding of SDS to the phosphorylated protein. In contrast, it is noteworthy that phosphorylation at specific sites may increase the mobility of some rare proteins in SDS-PAGE.

5.2. Methods for Identifying the Phosphorylated Amino Acid(s)

Following prelabeling with ^{32}P or in vitro phosphorylation with g^{32}P-ATP, the nature of the phosphorylated residues can be determined by acid hydrolysis of the peptide bonds and separation of phospho-serine, phospho-threonine, and phospho-tyrosine by thin-layer electrophoresis. Phospho-histidine and phospho-aspartate are extremely acid-labile and cannot be identified by this approach. On the other hand, the resistance of phospho-tyrosine to alkaline pH is used to study this phospho-amino acid preferentially. The phosphopeptides generated by partial proteolysis of a ^{32}P-labeled phosphoprotein with specific endoproteinases can be studied by two-dimensional phosphopeptide maps (usually a combination of thin-layer electrophoresis and chromatography). Such two-dimensional phosphopeptide maps are very useful for comparing the sites phosphorylated on the same protein under various circumstances, in vivo or in vitro. Phosphopeptides can also be separated by high-performance liquid chromatography (HPLC) and, if sufficient amounts of material are recovered, submitted to automatic protein sequencing, allowing the identification of the phosphorylated residue and its surrounding protein sequence. The use of powerful technologies of matrix-assisted laser desorption/ionization (MALDI) mass spectrometry now provides an interesting alternative approach to identify phosphorylation and other post-translational modifications. Site-directed mutagenesis of individual residues (replacement of a "phosphorylatable" residue by a "nonphosphorylatable" one—for example, replacement of a serine or a threonine by alanine, or of a tyrosine by a phenylalanine) is often used to test the phosphorylation of a precise residue. Although this approach is extremely useful, it should be kept in mind that the information obtained is indirect and that such mutations may have consequences on other properties of the protein other than preventing phosphorylation of the mutated residue.

6. Effects of Phosphorylation on the Properties of Proteins

The effects of phosphorylation on the properties of many proteins are known to be functionally important. They include the activation or inhibition of enzymes, the opening or closing of ion channels, the increase or decrease in the activity of transcription factors, the aggregation or disassembly of cytoskeletal components, and many other effects. There are only a few cases, however, in which the precise molecular mechanism by which phosphorylation of a specific residue brings about the functional changes observed is known in detail. The consequences of the phosphorylation of an amino acid residue can be local, or they can be amplified in the three-dimensional protein structure. Phosphorylation can also alter the interactions of a protein with others. A phosphate group being bulky and highly charged (two negative charges at physiological pH), its presence alters dramatically the properties of the amino acid side chain to which it is bound. It is often attempted to mimic the consequence of phosphorylation of a residue by its mutation to a negatively charged amino acid (aspartate or glutamate). In some cases, such mutations reproduce some of the effects of phosphorylation, while they prevent the normal phosphorylation of the corresponding residues. However, the size and the charge of the carboxyl group are less than those of a phosphoryl group, accounting for the many failures of this approach.

6.1. Local Effects of Phosphorylation on the Properties of Proteins

One example of a protein in which phosphorylation modifies dramatically the activity of an enzyme by a local action on the active site is isocitrate dehydrogenase (IDH), an enzyme regulated by phosphorylation in plants and bacteria. In the unphosphorylated state, IDH is active and catalyses the oxidative decarboxylation of isocitrate to a-ketoglutarate, a critical step in the Krebs citric acid cycle. In the presence of high levels of ATP, IDH is switched off by phosphorylation, and citrate is funneled to the glyoxylate cycle, a biosynthetic pathway that allows plants and bacteria to grow on acetate. *Escherichia coli* IDH is phosphorylated on Ser113 by an enzyme that is also able to dephosphorylate the same residue (a tandem kinase/phosphatase; see above). Ser113 is located in the substrate binding site, near the active site of the enzyme (31). Phosphorylation of this serine prevents isocitrate binding by steric hindrance and electrostatic repulsion (Fig. 3a).

Figure 3. Effects of phosphorylation on proteins. (a) Local effects of phosphorylation on isocitrate dehydrogenase (IDH). IDH transforms isocitrate into a-ketoglutarate, with concomitant production of CO_2 and reduction of NAD^+ in NADH. In *E. coli* IDH, phosphorylation of serine-113 in the active site prevents the binding of the substrate and inactivates the enzyme. (b) Allosteric activation of glycogen phosphorylase by phosphorylation. Phosphorylase is a homodimer; phosphorylation of Ser14 in both subunits leads to rearrangement of the amino-terminal region, modification of the subunit interaction, and changes in the tertiary and quaternary structure of the enzyme, making the active site more accessible to the substrate. (c) Regulation of SH2-domain binding by tyrosine phosphorylation. When particular protein sequences are phosphorylated on tyrosine residues, they bind with high affinity to specific SH2 domains. The presence of phosphotyrosine is necessary for the binding, but the specificity of the interaction is achieved by the recognition by the SH2 domain of the residues on the carboxy-terminal side of the phosphorylated tyrosine (Xxx +1, +2, +3). See the text for references. P, phosphate.

Another example of a well-studied local effect of phosphorylation is provided by the structural studies of protein kinases themselves (32). For the protein kinases to be active peptide loop in the vicinity of the active site, termed the activation loop or T loop, must be correctly positioned. In many protein kinases, the correct positioning of the activation loop requires its phosphorylation on one or two residues. Interestingly, in some cases the phosphorylation appears constitutive (eg, protein kinase A), whereas in others (eg, mitogen-activated protein kinases, MAP kinases) the phosphorylation of the activation loop is a fundamental regulatory step, catalyzed by a specific activating protein kinase.

6.2. Effects of Phosphorylation on the Overall Structure of Proteins

Phosphorylation of a single residue can have dramatic consequences on the tertiary structure and quaternary structure of a protein, as demonstrated by the study of the X-ray crystallography structure of glycogen phosphorylase in the phosphorylated and nonphosphorylated states (33). Phosphorylase is a homodimer, and phosphorylation occurs on a serine in the amino-terminal region of each peptide chain (Ser14), located strategically at the subunit interface. Phosphorylation of this serine leads to the reorganization of the amino terminus of each subunit and the modification of its interaction with the other subunit. As a consequence, the enzyme is stabilized in a form in which the active site, located at a distance from the phosphorylated serine, becomes more accessible to the substrate (Fig. 3b). In this case, the effects of phosphorylation on the structure of the enzyme are comparable to those occurring during classical allosteric activation, except that the effects of phosphorylation are due to a covalent modification of the enzyme, and not to ligand binding.

6.3. Effects of Phosphorylation on Protein–Protein Interactions

Protein phosphorylation can have dramatic regulatory effects on protein–protein interactions, as disclosed by the study of protein tyrosine phosphorylation. Indeed, a 100-residue domain first identified in Src, after which it was termed Src-homology 2 (SH2), and then found in many other proteins, was shown to bind specific peptides phosphorylated on tyrosine (34, 35). Phosphorylation of the tyrosine residue is necessary for binding, but the specificity of the interaction is achieved by the recognition of additional residues, located on the carboxy-terminal side of the phosphorylated tyrosine, by the SH2 domain (Fig. 3c). Binding of SH2 domains to specific peptide sequences phosphorylated on tyrosine residues allows the clustering of enzymes directly or via adapter proteins, around activated growth-factors receptors. Such enzymes, including phosphatidylinositol-3-kinase, phospholipase Cγ, or guanine-nucleotide exchange factors, are thus brought into the vicinity of their membrane-associated substrates. SH_2-mediated clustering triggers the cascades of reactions responsible for the effects of growth factors. SH2 domains can also have very different functions, such as maintaining a protein in an inactive state, as in the case of Src-family tyrosine kinases (36, 37). A carboxy-terminal phosphorylated tyrosine is involved in an intramolecular interaction with the SH2 domain, placing the enzyme in a closed conformation unable to reach its substrates. Activation results from dephosphorylation of the carboxy-terminal tyrosine, or by displacement of the SH2 domain by a competing phosphopeptide. Additional domains that interact specifically with phosphorylated proteins have been identified, including PTB domains (phosphotyrosine-binding) (38) and 14–3–3 proteins, whose interaction with their partner proteins appears to require phosphorylation of the latter on a serine residue (39).

7. The Place of Protein Phosphorylation in the Signal Transduction Networks

Many signal transduction systems in cells use several modules whose hierarchical organization allows powerful amplification and precise modulation. Protein phosphorylation is involved in most of these transduction systems, either as an output mechanism, altering the properties of target proteins, or as a module of information processing. Indeed, phosphorylation reactions in cells often occur in cascades in which activation of a first protein kinase phosphorylates and activates a second protein kinase, which, in turn, phosphorylates and activates a third kinase, and so on. This situation may account in part for the very large number of protein kinases, and it apparently has a number of interesting properties (40, 41). First, phosphorylation cascades allow amplification of the signal: One molecule of the first activated kinase can phosphorylate several secondary kinases, which can each phosphorylate several tertiary kinases, and so on. Another property of these cascades is to acquire kinetic properties, such as positive or negative cooperativity, similar to those of allosteric enzymes, even if the kinases composing the cascade themselves follow classical Michaelis–Menten kinetics. Thus, protein kinase cascades can convert graded inputs into switch-like outputs (42). Finally, the kinase cascades provide many levels of regulation and possible cross-talks between different regulatory pathways. Thus, it is likely that the organization of protein kinases in cascades confers strong evolutionary advantages, as attested by the very high degree of conservation of many of these cascades.

8. Examples of Phosphorylation Dysfunction in Human Diseases

As mentioned above, virtually all intracellular biological processes are regulated to some extent by protein phosphorylation. Thus, it is not surprising that dysfunction of these reactions may be responsible for some pathological states, including in humans. Protein kinases and phosphatases regulate cell growth, and a number of mutations leading to the uncontrolled activation of phosphorylation pathways are oncogenic (43, 44). Several oncogenes are tyrosine kinases (eg, v-Src, v-Fyn, v-ErbB, Met) or serine/threonine kinases (eg, Raf1, Mos) that are activated by mutation, whereas it is the loss of function of protein tyrosine and phospholipid phosphatase PTEN that is oncogenic (45). Loss of function of protein kinases is also responsible for various genetic diseases, including immune deficiency by the absence of γ-globulins [mutation of a nonreceptor tyrosine kinase in Bruton's disease (46)], intestinal palsy [mutation of a receptor tyrosine kinase Ret in Hirschprung's disease (47)], or myotonic dystrophy [mutation of a serine/threonine kinase (48)]. Conversely, protein phosphatases are used as weapons by some pathogenic organisms. For example, one of the virulence genes of *Yersinia* bacteria, including the agent of bubonic plague, is a phosphotyrosine phosphatase (49). Some environmental toxins exert their effects by stimulating protein kinases irreversibly (eg, stimulation of protein kinase C by oncogenic phorbol esters) or inhibiting protein phosphatases (inhibition of serine/threonine phosphatases by okadaic acid or microcystins, which are responsible for food poisoning) (50). On the other hand, the immunosuppressant drugs that have allowed the recent progress in organ grafting, cyclosporin A and FK506, act by inhibiting calcineurin, a Ca^{2+}/calmodulin-dependent protein phosphatase (51). Thus, the large number of protein kinases and phosphatases, and their involvement in numerous biological functions, has prompted many investigators to try to develop specific inhibitors or activators of these enzymes as potential therapeutic tools.

Bibliography

1. E. G. Krebs (1993) Angew. Chem. (Engl.) 32, 1122–1129.
2. E. H. Fischer (1993) Angew. Chem. (Engl.) 32, 1130–1137.
3. J. F. Kuo and P. Greengard (1970) J. Biol. Chem. 245, 2493–2498.
4. M. B. Kennedy and P. Greengard (1981) Proc. Natl. Acad. Sci. USA 78, 1293–1297.
5. Y. Takai, A. Kishimoto, Y. Iwasa, Y. Kawahara, T. Mori, and Y. Nishizuka (1979) J. Biol. Chem. 254, 3692–3695.
6. P. Cohen (1994) Bioessays 16, 583–588.
7. T. Hunter (1996) Biochem. Soc. Trans. 24, 307–327.
8. H. Ushiro and S. Cohen (1980) J. Biol. Chem. 255, 8363–8365.
9. M. H. Saier, Jr., L. F. Wu, and J. Reizer (1990) Trends Biochem. Sci. 15, 391–396.
10. P. J. Kennelly and M. Potts (1996) J. Bacteriol. 178, 4759–4764.
11. K. M. Popov, J. W. Hawes, and R. A. Harris (1997) Adv. Second Messenger Phosphoprotein Res. 31, 105–111.
12. L. A. Alex and M. I. Simon (1994) Trends Genet. 10, 133–138.
13. T. Hunter (1987) Cell 50, 823–829.
14. S. K. Hanks and T. Hunter (1995) FASEB J. 9, 576–596.
15. T. Hunter and G. D. Plowman (1997) Trends Biochem. Sci. 22, 18–22.
16. K. O. Hartley, D. Gell, G. C. M. Smith, et al. (1995) Cell 82, 849–856.

17. T. Maeda, S. M. Wurgler-Murphy, and H. Saito (1994) Nature 369, 242–245.
18. C. Chang, S. F. Kwok, A. B. Bleecker, and E. M. Meyerowitz (1993) Science 262, 539–544.
19. D. Barford (1996) Trends Biochem. Sci. 21, 407–412.
20. E. B. Fauman and M. A. Saper (1996) Trends Biochem. Sci. 21, 413–417.
21. B. E. Kemp and R. B. Pearson. (1990) Trends Biochem. Sci. 15, 342–346.
22. D. Mochly-Rosen (1995) Science 268, 247–251.
23. M. C. Faux and J. D. Scott (1996) Trends Biochem. Sci. 21, 312–315.
24. T. Pawson and J. D. Scott (1997) Science 278, 2075–2080.
25. P. J. Kennelly and E. G. Krebs (1991) J. Biol. Chem. 266, 15555–15558.
26. M. J. Hubbard and P. Cohen (1993) Trends Biochem. Sci. 18, 172–177.
27. T. Hunter, ed. (1991) Methods Enzymol. 200.
28. T. Hunter, ed. (1991) Methods Enzymol. 201.
29. A. C. Nairn and S. Shenolikar (1995) Neuroprotocols 6, 2–111.
30. A. A. Boulton, G. B. Baker, and H. C. Hemmings, Jr., eds, (1996) Neuromethods: Post-translational Modifications. Humana Press, Totowa, NJ.
31. J. H. Hurley, A. M. Dean, J. L. Sohl, D. E. Koshland, Jr., and R. M. Stroud (1990) Science 249, 1012–1016.
32. L. N. Johnson, M. E. M. Noble, and D. J. Owen (1996) Cell 85, 149–158.
33. L. N. Johnson (1992) FASEB J. 6, 2274–2282.
34. L. E. M. Marengere and T. Pawson (1994) J. Cell Sci. 107, 97–104.
35. T. Pawson (1995) Nature 373, 573–580.
36. W. Q. Xu, S. C. Harrison, and M. J. Eck (1997) Nature 385, 595–602.
37. F. Sicheri, I. Moarefi, and J. Kuriyan (1997) Nature 385, 602–609.
38. M. M. Zhou, K. S. Ravichandran, E. T. Olejniczak, et al. (1995) Nature 378, 584–592.
39. A. J. Muslin, J. W. Tanner, P. M. Allen, and A. S. Shaw (1996) Cell 84, 889–897.
40. E. Shacter, E. R. Stadtman, S. R. Jurgensen, and P. B. Chock (1988) Methods Enzymol. 159, 3–19.
41. S. Swillens, J. M. Boeynaems, and J. E. Dumont (1988) Methods Enzymol. 159, 19–27.
42. J. E. Ferrell, Jr. (1996) Trends Biochem. Sci. 21, 460–466.
43. G. A. Rodrigues and M. Park (1994) Curr. Opin. Genet. Dev. 4, 15–24.
44. T. Hunter (1997) Cell 88, 333–346.
45. J. Li, C. Yen, D. Liaw, et al. (1997) Science 275, 1943–1947.
46. S. Tsukada, D. J. Rawlings, and O. N. Witte (1994) Curr. Opin. Immunol. 6, 623–630.
47. G. Romeo, P. Ronchetto, Y. Luo, et al. (1994) Nature 367, 377–378.
48. Y.-H. Fu, D. L. Friedman, S. Richards, et al. (1993) Science 260, 235–238.
49. K. Guan and J. E. Dixon (1990) Science 249, 553–556.
50. C. MacKintosh and R. W. MacKintosh (1994) Trends Biochem. Sci. 19, 444–448.
51. J. Liu, J. D. Farmer, W. S. Lane, J. Friedman, I. Weissman, and S. L. Schreiber (1991) Cell 66, 807–815.
52. R. B. Pearson and B. E. Kemp (1991) Methods Enzymol. 200, 62–81.
53. Z. Songyang, K. P. Lu, Y. T. Kwon, et al. (1996) Mol. Cell. Biol. 16, 6486–6493.

Phosphotransferase

Phosphotransferases form a large group of enzymes that are involved with the transfer of a g-phosphoryl group from ATP, or another nucleoside triphosphate, to an acceptor molecule (see Kinase). They are divided into groups according to the identity of the phosphoryl group acceptor. These acceptors can be alcohols and carboxylic acids, as well as nitrogenous and phosphorylated compounds . All phosphotransferases have an essential requirement for a bivalent metal ion (see Metal-Requiring Enzymes).

Photolyase/Photoreactivation

Photoreactivation is the reversal of the effects of ultraviolet (UV) light (200 to 300 nm) by simultaneous or subsequent exposure of the organism to near UV-visible (300 to 500 nm) light (1, 2). Photoreactivation prevents the induction by UV light of growth delay, mutation, and cell death. Although several factors contribute to the phenomenon of photoreactivation, the main mechanism involved is the reversal of UV-induced pyrimidine dimers in DNA by the enzyme called photoreactivating enzyme, or DNA photolyase (3). DNA photolyase is the only known enzyme to employ light energy to catalyze a chemical reaction (3).

The two major lesions induced in DNA by UV light are cyclobutane pyrimidine dimers (Pyr<>Pyr) and [6–4] photoproducts (Pyr[6–4]Pyr) (Fig. 1). There are separate photolyases that are specific for Pyr<>Pyr and for [6–4] photoproducts (4, 5), but no known enzyme can act on both lesions. The structures and reaction mechanisms of the two types of photolyases are similar and may be summarized as follows. Each consists of a single polypeptide chain of 55 to 65 kDa containing a chromophore that acts as a photoantenna (folate or deazaflavin) and a catalytic cofactor ($FADH_2$) (6-9). It binds to the photodamage in DNA in a light-independent manner, producing a relatively stable enzyme-substrate complex. Upon exposure to light, the enzyme breaks the bonds that link the two pyrimidines to one another, generates standard canonical bases as products, and then dissociates from the repaired DNA. In contrast to many other enzymatic reactions that involve electron transfer, catalysis by photolyase involves a cyclic electron transfer and is not a redox reaction, in that upon completion of the enzymatic reaction the redox states of the enzyme and the substrate remain the same (6).

Figure 1. The two major photoproducts produced in DNA by ultraviolet light from (a) thymine dinucleotide: (b) the cyclobutane thymine dimer, and (c) the [6–4] photoproduct. Similar photoproducts arise from other adjacent dipyrimidines in DNA.

1. Evolution

Photolyases are flavoproteins, yet the primary sequences of the apoenzymes do not reveal any obvious homology to the signature sequences found in other flavoproteins (4). Instead, photolyases have remarkable sequence homology to blue-light photoreceptors (10), which regulate circadian rhythms in organisms ranging from mustard to humans (11-13). It appears that the necessity for the flavin cofactor to function from the light-excited state has imposed unique constraints on the flavin binding site of photolyase/blue-light photoreceptor family of proteins, such that the active-site geometry of these proteins is different from all other flavoproteins that carry out catalysis with ground-state flavin.

The distribution of the members of the photolyase/blue-light photoreceptor family in the biological world does not fit a readily defined pattern of evolutionary selection. The coliform bacterium *Escherichia coli* contains photolyase, but the soil bacterium *Bacillus subtilis* does not. The budding yeast *Saccharomyces cerevisiae* has the enzyme, but the fission yeast *S. pombe* does not. *Drosophila melanogaster* possesses cyclobutane pyrimidine dimer photolyase, [6–4] photolyase, and blue-light photoreceptor (14), while humans lack photolyase but express two blue-light photoreceptor proteins. Table 1 shows the expression pattern of this class of proteins in select members of the “three kingdoms of life”: bacteria, archaea, and eukarya. No general rules emerge from this table. The only rules that appear to have arisen from investigations of these groups of proteins are the following. (i) Cyclobutane photolyase has been detected in bacteria, plants, and animals through marsupial animals (15), but it has not been found in placental mammals such as human (16) and mouse. (ii) The [6–4] photolyase has been found in plants, insects (*Drosophila*), and some vertebrates (*Xenopus*, rattlesnake), but not in mammals such as human or mouse, nor in bacteria. (iii) Blue-light photoreceptors have been found in plants (*Arabidopsis*, mustard) and animals (*Drosophila*, human, and mouse), but not in bacteria. (iv) Of all bacterial and eukaryotic viruses investigated, photolyase has, so far, been found only in a grasshopper virus.

Table 1. Distribution of the Photolyase/Blue-Light Photoreceptor Family of Proteins in the Biological World

	Bacteria		Archaea			Eucarya	
	E. coli	B. subtilis	M. thermoauto	M. janaschii	S. cerevisiae	D. melanogaster	H. sapiens

Photolyase	Yes	No	Yes	No	Yes	Yes	No
[6–4] Photolyase	No	No	No	No	No	Yes	No
Cryptochrome	No	No	No	No	No	Yes	Yes

The tissue distribution of photolyase in animals that possess the gene is rather surprising. It is highly expressed in *Drosophila* ovaries, where it is expected to protect germ cells from UV damage. However, it is also expressed in all internal organs of opossum, including high levels of expression in the brain. Considering the nocturnal nature of the opossum, and the low probability even in bright daylight of UV and photoreactivating light penetrating the skull of the opossum, this expression pattern remains enigmatic.

2. Structure

Photolyases consist of a single polypeptide of 500 to 700 amino acid residues and two noncovalently bound cofactors/chromophores. One of the chromophores is always flavin adenine dinucleotide (FAD), and the other is either pterin (methenyltetrahydrofolate in the case of *E. coli* and *S. cerevisiae* photolyases) or deazariboflavin. Deazariboflavin is considered an ancient molecule, and photolyases with this cofactor have been found only in a few organisms that are capable of synthesizing this uncommon cofactor: *Aspergillus nidulans, Streptomyces griseus*, and *M. thermoautotrophicum*. Most other photolyases characterized to date, including those from *E. coli, S. cerevisiae, D. melanogaster*, and marsupials, contain a pterin as the second chromophore. Only two [6–4] photolyases have been characterized in detail, those of *D. melanogaster* and *X. laevis*, and both contain a pterin as the second chromophore (17). Blue-light photoreceptors from mustard, *A. thaliana*, and humans contain FAD and a pterin (11, 12).

The structures of *E. coli* and *A. nidulans* photolyases have been determined (18, 19). Even though the two enzymes are only 39% identical in sequence, they have remarkably similar structures, such that the traces of C^{a} atoms are superimposable. The enzymes consist of two well-defined domains: an *N*-terminal a/b domain, which is connected to the *C*-terminal alpha-helical domain through a long inter-domain loop. The folate or the deazaflavin chromophores are located in a crevice separating the two domains. In the *E. coli* enzyme, the folate is close to the surface of the protein and hence is not tightly bound to the enzyme; furthermore, its orientation is not optimal for energy transfer to the FAD cofactor. In contrast, the deazariboflavin chromophore in *A. nidulans* photolyase is deeply buried between the two domains, and it has a more favorable orientation relative to FAD for efficient energy transfer between the chromophores. Thus even though center-to-center distances between the two chromophores in the two photolyases are about 17 Å, the energy transfer from the second chromophore to FAD is more efficient (97% to 70%) in *A. nidulans* photolyase than in that of *E. coli* (20). The helical domain is made up exclusively of a-helices that are packed in two rather compact clusters. The FAD is buried between these clusters, and the flavin and adenine rings of the cofactor are in the unusual *cis* conformation in both photolyases.

The crystal structures of both enzymes also reveal how they bind to DNA. A plot of the surface potential of the enzyme reveals a longitudinal groove traversing both the a/b and the a-helical domains that is paved with positive charges. At its center is a hole that has the shape and size appropriate for cyclobutane pyrimidine dimer. The bottom of the hole is made up by the flavin ring. These structural features suggest that the DNA is in the positively charged groove through ionic interactions between the DNA backbone and the positive charge of the side chains and that the dimer “flips out” of the duplex into the hole within the enzyme. Following repair, the flipped-out dinucleotide would undergo a conformational change upon transformation of the dimer into two monomers, which would force the bases out of the hole and assist the repaired DNA to dissociate from the enzyme. Biochemical data indicate that [6–4] photolyase also employs a "flip-out" mode of complex formation during catalysis.

3. Reaction Mechanism

Photolyase works by the classical Michaelis–Menten kinetic mechanism; that is, the enzyme and substrate form a noncovalent complex that is converted to an enzyme–product complex after catalysis and eventually dissociates to yield product and free enzyme. The light-dependence of this catalysis step is unique to photolyase.

3.1. Binding

Photolyase, unlike some other high-specificity DNA-binding proteins, does not rely on diffusion along the linear DNA molecule to recognize its substrate. Similarly, the enzyme, in contrast to most proteins that bind to DNA in a sequence-specific manner and hence require double-stranded DNA, binds to its cognate lesions in single- and double-stranded DNA with almost equal affinities (2, 1). This property of the enzyme, combined with the fact that the enzyme can bind the photoproduct even in a dinucleotide form and repair it with high affinity, are consistent with a model in which the enzyme binds mostly to the backbone of the damaged strand and flips-out the photolesion into the catalytic hole for repair.

3.2. Catalysis

A most extraordinary aspect of catalysis by photolyase is its absolute dependence on light. According to the Woodward–Hoffman rule on symmetry in molecular orbitals, the symmetry of molecular orbitals in a chemical reaction is conserved between reactants and products. A corollary of this rule is that photochemically allowed reactions that proceed from the lowest unoccupied molecular orbitals (LUMO) are thermally forbidden; and conversely, thermally allowed reactions that proceed from the highest-occupied molecular orbitals (HOMO) are photochemically forbidden. In line with these rules, the cyclobutane ring of Pyr<>Pyr is stable at pH 1 and 160 °C for 6 h, but it is reversed to pyrimidine monomers with 240 nm light with a quantum yield of about 1.0. Surprisingly, however, even though photolyase utilizes light energy to catalyze the repair, the reaction is not a photochemical reaction in the strict sense, because it does not involve photoexcitation of the pyrimidine dimer, either directly or indirectly. Consequently, splitting of Pyr<>Pyr by photolyase does not break the rule of conversation of orbital symmetry. The enzyme accomplishes this feat by converting the Pyr<>Pyr into a radical, which then readily proceeds, thermally, to monomers. Light (300 to 500 nm) is used simply to excite the cofactor of the enzyme into a strong reductant capable of donating an electron to the relatively inert Pyr<>Pyr.

Having thus stated the general features of catalysis, the specifics for Pyr<>Pyr photolyase can be summarized as shown in Figure 2. The enzyme binds to its substrate independent of light, and the reaction proceeds upon exposure to light as follows (6). First, a photon is absorbed by the photoantenna (pterin or deazaflavin) to excite the chromophore to the excited singlet state. Second, the photoantenna transfers the energy by dipole–dipole interactions to $FADH^-$ with either 70% (pterin) or 97% (deazaflavin) efficiency. Third, the excited singlet state of $FADH^-$ transfers an electron to Pyr<>Pyr with about 100% efficiency, generating flavin neutral radical and Pyr<>Pyr radical anion. Fourth, the Pyr<>Pyr radical anion splits to pyrimidine monomers, concomitant with electron transfer back to restore the flavin to its catalytically active state. The reaction is a photoinitiated cyclic electron transfer, which results in bond rearrangement without changing the redox status of the reactants.

Figure 2. Photoreactivation photocycle for photolyase. The active site of the enzyme complexed to substrate is shown. (
pterin) absorbs a near-UV photon. (2) The excited singlet-state pterin transfers energy to $FADH^-$ by dipole–dipole inter

FADH⁻ transfers an electron to the thymine dimer (4). The thymine dimer anion radical collapses to two thymines, conc the flavin neutral radical.

The [6–4] photolyase functions in a similar manner (17, 22), with one important exception. Formation of [6–4] photoproduct encompasses joining of C6 of the 5′ base to the C4 of the 3′ base via a sigma bond, accompanied by transfer of the group at the C4 position (–NH or –OH) of the 3′ base to the C5 position of the 5′ base. Thus, simple cleavage of these new bonds would not restore the bases to normal. Hence, before the photoinduced cleavage of these bonds, the enzyme converts the “open form” of [6–4] photoproduct to an oxetane intermediate in which the NH or OH that was transferred to the C5 position of the 5′ base is shared by the C5 of the 5′ base and the C4 of the 3′ base (22). When the oxetane intermediate receives an electron from the active-site flavin, the resulting radical intermediate collapses to the two original bases, with back electron transfer to restore the flavin radical to its catalytically active form (Figure 3).

Figure 3. [6–4] Photolyase photocycle. Upon binding to the enzyme, the open form of the [6–4] photoproduct is conver photocycle proceeds as follows: (1) The photoantenna absorbs a photon and (2) transfers energy to the catalytic cofactor 4] photoproduct; (4) the photoproduct radical splits into two normal bases, concomitant with electron transfer back to th

The blue-light photoreceptors that exhibit 40% to 60% sequence identity to photolyases (10) have absolutely no repair activity (11). They are photoreceptors for regulating plant growth or for photoentrainment of the circadian clock in animals (13). However, the reaction mechanism of these molecules is not known at present.

Bibliography

1. A. Kelner (1949) Proc. Natl. Acad. Sci. USA 35, 73–79.
2. R. Dulbecco (1949) Nature 163, 949–950.
3. C. S. Rupert, S. Goodgal, and R. M. Herriott (1958) J. Gen. Physiol. 41, 457–471.
4. G. B. Sancar, F. W. Smith, M. C. Lorence, C. S. Rupert, and A. Sancar (1984) J. Biol. Chem. 259, 6033–6038.
5. T. Todo, H. Takemori, H. Ryo, M. Ihara, T. Matsunaga, O. Nikaido, K. Sato, and T. Nomura (1993) Nature 361, 371–374.
6. G. Payne and A. Sancar (1990) Biochemistry 29, 7715–7727.
7. M. S. Jorns, G. B. Sancar, and A. Sancar (1984) Biochemistry 23, 2673–2679.
8. J. L. Johnson, S. Hamm-Alvarez, G. Payne, G. B. Sancar, K. V. Rajagopalan, and A. Sancar

(1988) Proc. Natl. Acad. Sci. USA 85, 2046–2050.
9. A. P. M. Eker, J. K. C. Hessels, and J. O. van de Velde (1988) Biochemistry 27, 1758–1765.
10. M. Ahmad and A. R. Cashmore (1993) Nature 366, 162–166.
11. K. Malhotra, S. T. Kim, A. Batschauer, L. Dawut, and A. Sancar (1995) Biochemistry 34, 6892–6899.
12. D. S. Hsu, X. Zhao, S. Zhao, A. Kazantsev, R. P. Wang, T. Todo, Y. F. Wei, and A. Sancar (1996) Biochemistry 35, 13871–13877.
13. Y. Miyamoto and A. Sancar (1998) Proc. Natl. Acad. Sci. USA 95, 6097–6102.
14. T. Todo, H. Ryo, K. Yamamoto, H. Toh, T. Inui, H. Ayaki, T. Nomura, and M. Ikenaga (1996) Science 272, 109–112.
15. S. Yasuhira and A. Yasui (1992) J. Biol. Chem. 267, 25644–25647.
16. Y. F. Li, S. T. Kim, and A. Sancar (1993) Proc. Natl. Acad. Sci. USA 90, 4389–4393.
17. X. Zhao, J. Liu, D. S. Hsu, S. Zhao, J.-S. Taylor, and A. Sancar (1997) J. Biol. Chem. 272, 32580–32590.
18. H. W. Park, S. T. Kim, A. Sancar, and J. Deisenhofer (1995) Science 268, 1866–1872.
19. T. Tamada, K. Kitadokoro, Y. Higuchi, K. Inaka, A. Yasui, P. E. de Ruiter, A. P. M. Eker, and K. Miki (1997) Nature Struct. Biol. 4, 887–891.
20. S. T. Kim, P. F. Heelis, T. Okamura, Y. Hirata, N. Mataga, and A. Sancar (1991) Biochemisty 30, 11262–11270.
21. I. Husain, G. B. Sancar, S. R. Holbrook, and A. Sancar (1987) J. Biol. Chem. 262, 13188–13197.
22. S. T. Kim, K. Malhotra, C. A. Smith, J.-S. Taylor, and A. Sancar (1994) J. Biol. Chem. 269, 8535–8540.

Suggestions for Further Reading

23. G. B. Sancar (1990) DNA photolyases: physical properties, action mechanism, and roles in dark repair. Mutation Res. 236, 147–160.
24. A. Sancar (1994) Structure and function of DNA photolyase. Biochemistry 33, 2–9.
25. P. F. Heelis, R. F. Hartman, and S. D. Rose (1995) Photoenzymatic repair of UV- damaged DNA: a chemist"s perspective. Chem. Soc. Rev. 24, 289–297.
26. M. Ahmad and A. R. Cashmore (1996) Seeing the light: the discovery of cryptochrome. Plant Mol. Biol. 30, 851–861.
27. A. Sancar (1996) "No “End of History” for photolyases" Science 272, 48–49.

Photon Correlation Spectroscopy

Dynamic light scattering is a method for measuring the diffusion of macromolecules within a solution due to Brownian motion. It differs from “classical” or “static” light scattering, which permits the measurement of the molecular weight and radius of gyration of macromolecules from the light they scatter at varying scattering angles. Dynamic light scattering measures instead the intensity fluctuations of the scattered light on the timescale of 10^{-3} to 10^{-9} s. The frequencies of these fluctuations depend on how rapidly the molecules are moving by diffusion. These measurements require lasers, which provide light of high intensity, collimation, monochromaticity, and, most importantly, spatial and time coherence; the last attributes mean that the light is emitted from the laser as a continuous wave rather than as short bursts.

The physics underlying dynamic light scattering is complicated (1). In simple terms, the moving macromolecules will Doppler-broaden the otherwise monochromatic incident radiation. The scattered intensity will fluctuate because of beating interference of scattered waves of different, but similar, wavelengths; the situation is analogous to the fluctuations in intensity of a radio channel caused by interference from another radio channel of a very close wavelength. This broadening of the originally monochromatic light is why the technique is often referred to as quasi-elastic light scattering (QLS). The detector sends the intensity signal to a special computer, called an autocorrelator, which compares or correlates the intensity at different times; for this reason, the technique has another term, photon correlation spectroscopy (PCS). How rapidly the intensity fluctuates over short periods of time, or delay times, t, is represented by how a parameter known as the normalized intensity autocorrelation function, $g^{(2)}$ (t), decays as a function of t. The superscript “(2)” is used to indicate that it is an intensity, as opposed to an electric field “(1)” autocorrelation function. Many data sets of $g^{(2)}$(t) as a function of t are accumulated and averaged. The degree of averaging necessary depends on the incident laser intensity and the size and concentration of the scattering macromolecule (at a given concentration; larger molecules scatter more). For globular proteins, sufficient data can usually be acquired within one to several minutes.

Analysis of how the normalized intensity autocorrelation function $g^{(2)}$(t) decays as a function of t can be used to evaluate the translational diffusion coefficient, D_t. For dilute solutions of spherical or near-spherical (ie, globular) macromolecules, the variation of $g^{(2)}$(t) with t can be represented by the simple logarithmic equation

(1)

where the parameter k is known as the Bragg wave vector, whose magnitude is defined by

(2)

where n is the refractive index of the medium, q is the scattering angle, and l is the wavelength of the incident light. Consequently, the value of D_t can be found from a plot of ln[$g^{(2)}$(t) – 1] versus t. Figure 1 illustrates an example for the motility protein dynein.

Figure 1. Dynamic light scattering of a solution of dynein. The channel number is a measure of the delay time, q (see Eq. (1) of the text).

Two important practical conditions need to be noted: (1) the value of D_t is sensitive to the temperature, which needs to be accurately controlled or, at the very least, monitored during the measurement; and (2) the scattering signal is very sensitive to the presence of trace amounts of dust or aggregation products; solutions and the scattering cell or cuvette need to be scrupulously clean and free of particulates. The samples must be filtered and centrifuged and the vessels washed. Special filling devices have been constructed to minimize this dust problem (2).

The value of D_t can be converted to the standard conditions of water at 20.0°C and extrapolated to zero sample concentration (see Diffusion). An additional extrapolation is necessary if the macromolecule is not globular. There is an extra term on the right-hand side of equation 1 that arises from rotational diffusion at finite angles q. This term approaches zero as q does. Therefore, it is necessary to make the measurements of D_t at a number of angles q and to extrapolate to zero angle (or Bragg vector k). The extrapolations to zero sample concentration and to zero angle q (or k) can be performed simultaneously on a biaxial extrapolation plot known as a dynamic Zimm plot (3). If an angular extrapolation is not necessary, a scattering angle of 90° is usually chosen, and fixed-angle instruments are usually set at this angle. At low angles, the problems due to contamination with large particles (see (2) above) are accentuated.

If a sample is heterogeneous, it is possible, at least in principle, to obtain a distribution of diffusion coefficients after various assumptions and mathematical manipulation of the autocorrelation data; these methods have been reviewed (4), and several commercially available computer programs are available. A more simple way of representing heterogeneity is with the polydispersity factor (PF), which is obtained by comparing linear with quadratic or more complex fits of the normalized autocorrelation function decay data (5).

Measurements can be made very rapidly with dynamic light scattering, and it is possible to follow biomolecular assembly–disassembly processes that occur on a timescale of minutes. An example of the swelling of southern bean mosaic virus in response to the removal of bound Ca^{2+} ions is given in Fig. 2 (6).

Figure 2. Following the dynamics of a process using dynamic light scattering: effect of removal of calcium ions (by adding EGTA at 10 min) on the hydrodynamic radius (R_H) of southern bean mosaic virus (adapted from Ref. 6).

Bibliography

1. W. Brown, ed. (1993) *Dynamic Light Scattering. Theory and Applications*, Oxford Univ. Press, U.K.
2. A. H. Sanders and D. S. Cannell (1980) *Light Scattering in Liquids and Macromolecular Solutions*, V. Degiorgio, M. Corti, and M. Giglio, eds., Plenum Press, New York, pp. 173–182.
3. W. Burchard (1992) in *Laser Light Scattering in Biochemistry*, S. E. Harding, D. B. Sattelle, and V. A. Bloomfield, eds., Royal Society of Chemistry, Cambridge, U.K., pp. 3–22.
4. R. M. Johnsen and W. Brown (1992) in *Laser Light Scattering in Biochemistry*, S. E. Harding, D. B. Sattelle, and V. A. Bloomfield, eds., Royal Society of Chemistry, Cambridge, U.K., pp. 77–91.
5. P. N. Pusey (1974) in *Photon Correlation and Light Beating Spectroscopy* (H. Z. Cummings and E. R. Pike, eds.) Plenum Press, New York, pp. 387–428.
6. M. Brisco, C. Haniff, R. Hull, T. M. A. Wilson, and D. B. Sattelle (1986) *Virology* **148**, 218–220.

Suggestions for Further Reading

7. S. E. Harding, D. B. Sattelle, and V. A. Bloomfield, eds. (1992) *Laser Light Scattering in Biochemistry*, Royal Society of Chemistry, Cambridge, U.K.
8. K. S. Schmitz (1990) *An Introduction to Dynamic Light Scattering by Macromolecules*, Academic Press, New York (a comprehensive introductory treatise, although demanding some familiarity with mathematics).
9. K. E. Van Holde (1985) *Physical Biochemistry*, 2nd ed., Prentice-Hall, Englewood Cliffs, N.J.

Photosynthesis

Photosynthesis is the energy transduction process whereby solar light energy is converted into a chemical form and used for the synthesis of organic molecules. Photosynthesis takes place in higher plants, algae, and certain bacteria. It involves light-induced redox processes in which carbon dioxide becomes reduced. The ability to use water as an electron source distinguishes the oxygenic photosynthetic organisms—eukaryotic plants and algae, plus prokaryotic cyanobacteria and prochlorophytes, from the nonoxygenic photosynthetic bacteria. Photosynthetic organisms evolved more than 3.5 billion years ago, and they are the origin of current biomass, as well as of fossil fuels.

In all types of photosynthetic organisms, the photosynthesis reaction can be divided into two major phases: (1) the light reactions and (2) the carbon fixation reactions (the Calvin cycle). The light reactions lead to the production of ATP and NADH or NADPH. These molecules are required for the subsequent CO_2 fixation and the formation of trioses, glucose, and more complex carbohydrates. The primary energy conversion is driven by redox-active pigment-protein complexes known as photosynthetic reaction centers. Together with light-harvesting complexes and electron transport components, such as cytochromes, iron-sulfur proteins, and quinones, the reaction centers catalyze electron and proton transport across a biological membrane to create a proton motive force. In analogy with the respiratory process in mitochondria and bacteria, this proton motive force drives the synthesis of ATP (adenosine triphosphate) by the enzyme ATP synthase.

In oxygenic photosynthesis, $NADP^+$ is reduced by electron transfer from two reaction centers, photosystem II and photosystem I, which are coupled in series (Fig. 1). The electrons are supplied by photosystem II through its unique ability to oxidize water, leading to release of molecular oxygen. The nonoxygenic photosynthetic bacteria contain only one reaction center and typically use organic or inorganic compounds as reductant to reduce NAD(P). They perform cyclic electron transport to produce ATP. Two groups of reaction centers (type I and type II) are present among the various photosynthetic bacteria and have been shown to be highly analogous to photosystem I and photosystem II of oxygenic photosynthesis, respectively (1).

Figure 1. Light-driven, noncyclic electron transport in oxygenic photosynthesis. Two types of photosynthetic reaction c
linked in series, connected by a cytochrome b_6f complex, to extract electrons and protons from water and to make them
reduction of $NADP^+$ and ultimately CO_2. The quinone reduction is driven by a type II reaction center called photosyste
the reaction center responsible for creating sufficient reduction potential to reduce $NADP^+$ via FeS centers is a type I rea
called photosystem I. Photosystem II and photosystem I are evolutionary related to the type II reaction center of purple b
type I reaction center of green sulfur bacteria, respectively (see Fig. 2). Both types of reaction center are depicted as hav
cofactors arranged around two fold symmetry axis as revealed by X-ray crystallography (3, 6). Chl is chlorophyll a; Ph
(in the case of photosynthetic bacteria these cofactors are either bacteriochlorophyll or bacteriopheophytin). A "special"
interacting chlorophylls, which acts as the primary electron donor (P_D), is called P680 for photosystem II and P700 for p
is plastoquinone in photosystem II and phylloquinone in photosystem I. Fe is a nonheme iron; F_X, F_A, F_B are low potent
centers, and F_D is ferredoxin. $(Mn)_4$ is the cluster of manganese atoms involved in the oxidation of water; Y_Z and Y_D are
tyrosine residues—the former are on the main route of electron transfer. Arrows show electron transfer paths. The two p
are functionally connected by the cytochrome b_6f complex, which oxidizes the reduced quinone (QH_2, plastoquinol) an
copper-containing extrinsic protein, plastocyanin (PC). Because quinones are normally 2 electron/2 proton acceptors, th
cytochrome complex accepts two electrons, one reducing an iron–sulfur center (FeS) and the other reducing a low pote
cytochrome (cyt b). The reduced FeS center donates an electron to cytochrome f (cyt f). The other electron participates in q
dependent cyclic electron transport, involving high and low potential b-type cytochromes, which functions as a proton p
developed from reference 1.

In eukaryotic organisms, photosynthesis occurs in specialized cell organelles (chloroplasts) enclosed by a double outer membrane (envelope) and an internal membrane system (thylakoid membrane). This organelle contains, like mitochondria, its own DNA. The thylakoid membrane harbors the two photosystems, the light-harvesting antenna, electron transport components, and the ATP synthase (CF_0–CF_1). Despite their prokaryotic nature, cyanobacteria have a photosynthetic thylakoid membrane that is differentiated from the plasma membrane. In nonoxygenic photosynthetic bacteria, various forms of invaginations of the cell membrane give rise to so-called chromatophores, to which the photosynthetic light reactions are confined. The reduction of CO_2 and the subsequent enzymatic reactions of the Calvin cycle take place in the cytoplasm of prokaryotic cells or in the soluble stromal compartment of chloroplasts. The photosynthetic apparatus is remarkably adaptable to various stress conditions, in particular to short- and long-term changes in light intensity. Under severe light stress, however, photosystem II can suffer from oxidative damage leading to (photo)inhibition of photosynthesis.

1. Photosynthetic Reaction Centers

Photosynthetic bacteria are rudimentary in a general biological perspective, but they have been extremely useful as simple experimental model organisms to elucidate the structure and function of the photosynthetic light reactions and to understand the evolution of photosynthesis (2). These bacteria can be classified into two major groups based on their types of reaction centers: (1) green-sulfur bacteria (eg, *Chlorobium limicola*) and heliobacteria (eg, *Heliobacterium chlorum*, *Heliobacillus mobilis*) use low potential iron–sulfur clusters as electron acceptors, and their reaction centers are designated FeS type or type I; and (2) purple bacteria (eg, *Rhodobacter sphaeroides*, *Rhodopseudomonas viridis*, *Rhodospirillum rubrum*, *Chromatium vinosum*) and green gliding bacteria (*Chloroflexus aurantiacus*) have type II reaction centers with pheophytin and two quinone molecules as electron acceptors.

X-ray crystallographic, functional, and genetic analyses have revealed that photosystem I and photosystem II of oxygenic photosynthesis are closely related to the bacterial type I and type II reaction centers, respectively (Fig. 1).

The reaction center is the most vital part of the photosynthetic apparatus in which the primary light-induced redox processes take place (1). The type I and II reaction centers have a similar basic architecture, and they function using essentially the same mechanistic principle. Both use a “special pair” of chlorophyll or bacteriochlorophyll molecules as the primary electron donor (P_D) and a (bacterio-) chlorophyll (type I) or a (bacterio-)pheophytin (type II) as primary electron acceptor (P_A). When excited by light, P_D donates an electron to P_A within a few picoseconds, and the radical pair $P^+_D P^-_A$ is formed:

The primary donor and acceptor are arranged in the reaction center in such a way that the primary charge separation occurs across the lipid bilayer of the photosynthetic membrane.

The stability of this primary charge separation is ensured by rapid transfer of the electron from P_A to the secondary electron acceptors, A_1, A_2, and so on and by passing an electron to P^+_D from secondary electron donors, D_1, D_2, and so forth:

In type I reaction centers, A_1 is a quinone, while A_2 is a low potential 4Fe–4 S cluster (F_X). The donors are typically c-type cytochromes or the copper protein plastocyanin (in oxygenic electron transport only) (see Electron Transfer Proteins). In the type II reaction center, quinones constitute both the A_1 (Q_A) and A_2 (Q_B) acceptors. These are normally plastoquinone or, in purple bacteria, ubiquinone. In the bacterial type II centers, **cyt**ochromes are often the electron donors, while in oxygenic photosynthesis the electrons are provided by the unique system of water oxidation. The primary donor of photosystem II (P680) is a powerful oxidant in its P680$^+$ form. In fact, P680$^+$ is the most oxidizing species found in living organisms (E_m = +1.1V), enabling extraction of electrons from water (see Electron Transfer Proteins and Redox Enzymes). Oxidation of water requires the accumulation of four oxidizing equivalents, which are necessary to abstract four reducing equivalents from two water molecules to produce one molecule of dioxygen (O_2). The water-oxidation system involves a cluster of four manganese atoms that are converted to higher valence in a stepwise manner by four separate photochemical events (the S-state cycle) involving P680 and a redox-active tyrosine residue in the reaction center.

1.1. Type II Centers

Determination of the high-resolution three-dimensional structure of the purple bacterial reaction center was a landmark in photosynthesis research (3). The structure revealed an approximately twofold symmetrical relationship of the prosthetic groups (Fig. 1) and the two protein subunits (L and M) that bind them. These two subunits each possess five transmembrane helices and have very similar structures, forming a heterodimeric structure. The two bacteriochlorophylls of the primary electron donor, P_D, form a special pair at the periplasmic side of the chromatophore membrane. Following the structure across the membrane, the next cofactors are two additional bacteriochlorophylls, then two bacteriopheophytins, followed by two quinones in the Q_A and Q_B sites near the cytoplasmic surface. All the duplicated cofactors (Fig. 1) are related by a twofold axis passing through the special pair P_D and a nonheme iron located midway between the two quinones. Notably, despite this approximate twofold symmetry, the electron transfer to Q_B via Q_A occurs exclusively along one branch, while the other branch is inoperational (Fig. 1). It is still not clear whether the bacterial chlorophyll located between the primary donor and the bacteriopheophytin is directly involved in the charge separation process as a redox-active species. The symmetry of the reaction center is broken by the H subunit, which has a single membrane-spanning alpha-helix and a globular domain at the cytoplasmic side of the membrane. Furthermore, there is a four-heme cytochrome present on the periplasmic side in most purple bacteria.

Functional and compositional analyses of oxygenic photosynthesis have revealed that photosystem II carries out electron transfer reactions similar to those occurring in the reaction centers of purple bacteria (3). On the acceptor side, photosystem II has pheophytin and Q_A, Q_B plastoquinone molecules, as well as the nonheme iron (Fig. 1), and electron transfer occurs with similar rate constants. Furthermore, the two protein subunits of the photosystem II reaction center (D_1 and D_2) show homology with the L and M proteins and form a heterodimeric structure similar to the bacterial reaction center. This has been confirmed by the structure of photosystem II obtained at 0.8 nm resolution by electron microscopy. In contrast to the bacterial reaction center, two photosystem II complexes are tightly associated to form a dimeric structure (4).

P680 is probably a dimer of chlorophyll molecules, but the relative orientation of the chromophores and their degree of exciton interaction seem to differ somewhat from the bacterial primary donor. Most significantly, photosystem II differs in its donor properties, allowing the extraction of electrons from water (Fig. 1). Most experimental observations suggest a close association between the active manganese cluster and the reaction center heterodimer.

Despite all the redox components required for the light-induced electron transfer from water to plastoquinone being associated with the D_1/D_2 reaction center heterodimer, photosystem II contains as many as 25 different subunits (1). These are encoded either by chloroplast or nuclear genes designated psbA-X. Closely associated with the reaction center is cytochrome b559, which is not a part of the main electron transfer chain but instead protects against photodamage. Most subunits are integral membrane proteins and span the membrane, but three extrinsic proteins are located at the inner thylakoid surface to stabilize the manganese cluster and to sequester the Ca^{2+} and Cl^- ions that are also required for water oxidation. A peculiar feature of the complex is the relatively large number (up to 10) of small proteins with only one membrane-spanning segment. Two chlorophyll-a-binding proteins, CP47 and CP43, serve as inner light-harvesting antenna closely associated with the reaction center. Each contains 40 chlorophyll-a molecules and possesses 6 transmembrane domains; they are complemented by an outer antenna constructed of various pigment-protein complexes, depending on the taxonomic group (see text below).

1.2. Type I Centers

Of the type I reaction centers, photosystem I is the best characterized, partly due to the 0.4 nm-resolution structure of the complex obtained from a thermophilic cyanobacterium (6). Notably, the basic three-dimensional structural arrangement of photosystem I is the same as for the type II center, despite its different content of redox-active groups. Photosystem I has the twofold symmetry with the axis passing through the chlorophyll-a dimer of the primary donor (P700) and a 4Fe–4 S center (Fig. 1). Two additional pairs of acceptor chlorophyll molecules occur along this axis. A fourth pair of chlorophyll molecules appears to connect those of the reaction center and of the light-harvesting antenna. The photosystem I reaction center is a heterodimer composed of two large reaction center subunits (PsaA and PsaB), each possessing 11 membrane-spanning segments. In contrast to the type II center, the two reaction center subunits also harbor the inner light-harvesting antenna of about 100 chlorophyll-a molecules. The 22 a-helices of the PsaA and PsaB proteins are arranged in such a way that 5 helices from each subunit form a central reaction center portion, in analogy with the D_1/D_2 and L/M heterodimers. The additional 12 a-helices are located on either side of this central portion and harbor the antenna chlorophylls. This arrangement should be compared to the inner chlorophyll-a antenna of photosystem II composed of two distinct proteins, CP47 and CP43, together comprising

12 membrane spanning helices (4).

Photosystem I is also a multisubunit complex of both nuclear and chloroplast genetic origin, with up to 15 different subunits (PsaA- PsaM) (5). PsaC, an extrinsic subunit at the outer stromal surface (Fig. 1), provides ligation for two acceptor FeS clusters (F_A and F_B). There are also subunits providing docking sites for ferredoxin and plastocyanin (see Azurin) at the acceptor and donor sides of the reaction center, respectively. The eukaryotic photosystem is complemented by an outer antenna of chlorophyll a/b -binding proteins (LHCI). In cyanobacteria, but probably not in plants, the photosystem I complex is trimeric.

No structural information is yet available for the nonoxygenic type I reaction centers of green sulfur bacteria or heliobacteria. There is compelling evidence that these photosynthetic bacteria have homodimeric reaction centers despite the same overall arrangement of the redox active groups as in photosystem I. It is therefore assumed that these bacterial reactions centers are evolutionarily more primitive and ancestral to the heterodimeric reaction centers (7, 8).

1.3. Evolutionary Aspects of Photosynthesis

The occurrence of two different but analogous reaction centers, composed of two related, yet distinct protein subunits, provides insight into the evolution of photosynthesis (1, 7, 8). In the beginning, there was probably a primordial reaction center composed of one single subunit (Fig. 2), which may have evolved to a homodimeric structure with both electron transfer branches operational. Then a gene duplication took place in early evolution, the heterodimeric reaction centers were generated by divergent evolution, and one of the electron transfer branches was closed. It is assumed that the ancestral reaction center contained both quinone and iron–sulfur acceptors, but that the latter were lost in the type II centers. Later the two types of reaction centers were linked to pave the way for current oxygenic photosynthesis (Fig. 2). It is not clear when the ability to oxidize water was acquired, but no single type II reaction center able to split water has been identified. The chloroplast of eukaryotic photosynthetic organisms is generally assumed to have its evolutionary origin in symbiotic ancestors of cyanobacteria.

Figure 2. Evolution of photosynthetic reaction centers. A primordial reaction center containing both quinones and Fe-S centers as electron acceptors, evolved into type I and type II centers, where the latter lost their FeS component. Gene duplications and divergence gave rise to homodimeric, finally heterodimeric, reaction centers where only one electron transfer route is operational. In cyanobacteria, the two types of reaction centers merged to pave the way for oxygenic photosynthesis (see Fig. 1). The scheme is developed from References 6 and 7.

2. Light-Harvesting Protein Complexes

The evolution of type I and type II reaction centers has been matched by the development of a multitude of different light-harvesting pigment-protein systems. This enables photosynthetic organisms to use the entire solar spectrum and provides versatility with respect to the surrounding light environment. In bacteria there are typically 40 chlorophyll-containing molecules per reaction center, while in plants this number could be several hundred (2). The correct organization of the various pigments within the antenna systems is crucial in order to ensure efficient energy transfer. Following absorption of a photon by one of the antenna pigments, the excitation moves from pigment to pigment via so-called resonance energy transfer, until being trapped in the reaction center. These ultrafast processes can now be followed by femtosecond (10^{-15} s) flash spectroscopy.

Purple bacteria have two types of light-harvesting protein complexes, designated LHI and LHII (9). They are composed of two small proteins (a and b) that each span the membrane once and bind bacteriochlorophyll a and carotenoids. LH1 is closely associated with the reaction center (L, M, and H subunits). LH2 is located more peripherally and functions as an outer and variable antenna. The structure of LH2 has been determined to high resolution by X-ray crystallography (9). The complex has a donut shape with 9 a-subunits forming a hollow cylinder with 1.8 nm inner and 3.4 nm outer radii. All the pigments are located between these cylinder walls. The bacteriochlorophylls are ligated to histidine residues. Eighteen molecules form an overlapping ring located toward the outer membrane surface, while nine are located more toward the inner portion of the membrane. The latter are perpendicular to the other bacteriochlorophylls and with the bacteriochlorophyll ring parallel to the membrane surface. The carotenoids are arranged in close association with the bacterial chlorophylls. This ring of chlorophylls allows the excitation to become delocalized over a large area, thereby facilitating the energy transfer to LHI, which is likely to have a structure similar to LHII. Purple bacteria can also contain bacteriochlorophyll-*b*, in addition to bacteriochlorophyll-*a*. Typically, purple bacteria can harvest light in a very broad interval of the spectrum, even above 1000 nm.

Green sulfur bacteria have a peculiar antenna system, chlorosomes, which appear as bag-like structures on the inside of the cytoplasmic membrane (2). They contain a complex mixture of bacteriochlorophylls *c*, *d*, and *e* assembled into rod elements approximately 5–10 nm in diameter. Notably, chlorosomes contain very few proteins, and the polymeric structures are maintained primarily by pigment–pigment interactions. A water-soluble baseplate bacteriochlorophyll-*a*-protein complex sandwiched between the chlorosomes and the cytoplasmic membrane provides the link between the chlorosome antenna and the reaction center chlorophylls. Green sulfur bacteria can absorb light up to 850 nm. Heliobacteria do not contain an outer antenna but manage with the inner bacteriochlorophyll *a* antenna of its type I reaction center.

Cyanobacteria use water-soluble protein structures known as phycobilisomes as outer light-harvesting antenna (10). A phycobilisome contains several hundreds of phycobilin pigments (phycocyanin, phycoerythrin, and allophycocyanin) covalently bound to the phycobiliproteins. The organization of a phycobilisome involves rod-like structures composed of 5 to 6 elements that are connected to a tricylindrical core of phycobiliproteins carrying allophycocyanin. The excitation energy migrates, via the core, from the peripheral rod sections to the CP47/CP43 inner chlorophyll-*a* antenna, and finally to the D_1/D_2 reaction center. The phycobilosomes are located at the outer thylakoid membrane surface facing the cytoplasm and connected to photosystem II via nonpigmented linker proteins.

The plant photosystems have chlorophyll *a/b*-binding (CAB) proteins as their outer light-harvesting antenna (10). Altogether there are ten different but related nucleus-encoded CAB proteins: 6 associated with photosystem II and 4 with photosystem I. These are all integral membrane proteins, each with a molecular weight of about 25 kDa and with three transmembrane-spanning regions. The CAB proteins noncovalently bind approximately half of the chlorophyll *a* and all of the chlorophyll-*b*, as well as a majority of the carotenoids. Most attention has been paid to the major CAB protein complex of photosystem II, designated LHCII. It is the most abundant thylakoid protein complex and, apart from a crucial function in light harvesting, is essential for maintaining the thylakoid membrane organization and to adjust the antenna of photosystem II in response to short- and long-term fluctuations in the light environment. LHCII normally exists as a trimer. Each monomer has been estimated to bind up to 14 chlorophyll molecules, one chlorophyll molecule for every 15 amino acids, indicating a very tight packing. The structure of LHCII has been determined to 0.34 nm resolution by electron crystallography (11).

Green algae have basically the same outer light-harvesting antenna as plants. In brown algae, the CAB proteins are homologous to the plant CAB proteins. Interestingly, the CAB proteins are not unique to eukaryotic organisms, since the prokaryotic prochlorophytes have a similar kind of light-harvesting proteins. On the other hand, eukaryotic red algae have no CAB proteins, but phycobilisomes similar to those of cyanobacteria.

The carotenoids of the various light-harvesting complexes and reaction centers not only play a role in light-harvesting but are also essential as protectants against oxidative damages.

3. Electron Transport

3.1. Oxygenic Photosynthesis

Photosystem I and photosystem II are linked in series via plastoquinone, the cytochrome b_6f complex, and plastocyanin (Fig. 1). When the secondary plastoquinone acceptor of photosystem II

(Q_B) has received two electrons, it is protonated and leaves its binding site on the D_1 protein. This Q_B site is the major target for several commercial herbicides, such as atrazine and diuron. The reduced plastoquinone interacts with the Q_0 site of cytochrome b_6f. This cytochrome complex is analogous to the mitochondrial cytochrome bc_1, whose structure has been solved to high resolution. The photosynthetic cytochrome complex contains four redox centers: one heme c (f), two hemes b, and a high potential Rieske 2Fe–2 S cluster. The redox components are ligated to three protein subunits: cytochrome f and cytochrome b_6, which are both plastid-encoded, and the nucleus-encoded Rieske FeS protein. Altogether, the complex contains at least five subunits. It performs quinol oxidation via cytochrome b_6f, involving a so-called Q cycle, which translocates twice the number of protons that could be translocated by the plastoquinone/plastoquinol oxidoreduction alone. The electrons are eventually linked via cytochrome f, the FeS center and plastocyanin to photosystem I, reducing $P700^+$. The final step in noncyclic electron transfer is the reduction of $NADP^+$, which is mediated by ferredoxin and the ferredoxin-$NADP^+$ reductase, a flavoprotein.

Noncyclic electron transport gives rise to proton transport into the inner (lumen) thylakoid compartment, via cytochrome b_6f and the plastoquinone/plastoquinol oxidoreduction (Fig. 1). In addition, protons are translocated into the lumen as a consequence of the oxidation of water. Cyclic electron transfer leading to transmembrane proton transport can occur around photosystem I and cytochrome b_6f, although the precise mechanism is still under debate. The proton motive force created by non-cyclic or cyclic electron transport substantiate the chemiosmotic coupling theory of ATP formation.

3.2. Nonoxygenic Photosynthesis

The simplest form of electron transport occurs in purple bacteria (2). The electrons from the quinol formed at the reaction center are transported back to the primary donor via a cytochrome bc_1 complex and at least one other cytochrome. This light-driven cyclic electron transfer is coupled to ATP production via a proton motive force. Purple bacteria do not possess noncyclic electron transport in the classical sense. A reductant can donate electrons into the quinone pool or to a cytochrome, but these reductants are not sufficiently strong to reduce NAD^+ directly. Instead, this is performed via "reversed" electron transport involving a NADH dehydrogenase enzyme. Some of the energy from the light-mediated cyclic electron transfer is used to drive these reactions.

Photosynthetic bacteria containing type I reaction centers are able to perform non-cyclic electron transport using other compounds as reductants, for example, simple sulfur components (2). The iron-sulfur centers on the acceptor side have redox potentials that are sufficiently low to allow reduction of NAD^+. In addition, sulfur bacteria and heliobacteria can perform cyclic electron transport coupled to ATP formation.

4. Carbon Dioxide Fixation and Photorespiration

The conversion of carbon dioxide to carbohydrates occurs in a cyclic process, called the Calvin cycle or the photosynthetic carbon reduction cycle. These reactions take place in the cytoplasm of prokaryotic cells or in the stroma of chloroplasts, mediated by at least a dozen enzymes. In the first step, ribulose-1,5-bisphosphate (RuBP) reacts with a molecule of carbon dioxide, thereby forming two identical C3 molecules of 3-phosphoglycerate, 3-PGA. This reaction is catalyzed by ribulosebisphosphate carboxylase (Rubisco), which is the most abundant protein on earth, and in eukaryotes consists of eight copies each of a small and a large subunit. In subsequent reactions, 3-PGA is converted into hexose and pentose phosphates, which requires 3 mol of ATP and 2 mol of NADPH per mole of CO_2 fixed. Hexose phosphates are converted to starch or are exported from the chloroplast via the phosphate translocator as triose phosphates. RuBP is regenerated from 3-PGA in reactions requiring further input of NADPH and ATP. The activities of some of the Calvin cycle enzymes are regulated and coupled to the redox state of the electron transport chain via thioredoxin (12).

A proportion of RuBP is oxygenated by Rubisco, which also can function as an oxygenase, in a potentially wasteful reaction (in terms of quantum efficiency of CO_2 fixation), to form phosphoglycolate and 3-phosphoglycerate. This reaction is called photorespiration. The major part of the carbon flow to glycolate is returned, via the photosynthetic carbon oxidation cycle, back into the Calvin cycle. Production of 1 mol of CO_2 results in the net consumption of 7 mol of ATP and 4 mol of NADPH. Although photorespiration lowers the quantum efficiency of CO_2 fixation, it is an important side reaction because it can dissipate excess energy under unfavorable conditions, thereby preventing oxidative damage to the photosynthetic apparatus. In addition, photorespiration provides a link between the carbon and nitrogen cycles and can provide additional ATP to the mitochondria and the cytosol. Under conditions of a short supply of carbon dioxide, such as under conditions of water stress when the leaves close their stomata to reduce water loss or at elevated temperatures, photorespiration is enhanced.

In the so-called C4 plants, photorespiration is strongly reduced (12), and the primary carboxylation reaction is of phosphoenolpyruvate (PEP), involving an enzyme that has a much higher affinity for CO_2 than Rubisco. In this carboxylation reaction, 4-carbon carboxylic acids are formed (hence the name C4 plants) in specialized mesophyll cells and are then transported to the bundle sheath cells. There they are decarboxylated, and the concentrated CO_2 is assimilated into the Calvin cycle via Rubisco. The photorespiration is kept low because of both the elevated CO_2 levels and the very low proportion of oxygen-evolving photosystem II centers in the bundle sheath cells.

5. Thylakoid Membrane Organization

5.1. Thylakoid Membrane Heterogeneity

The thylakoid membrane is a lipid bilayer that is composed mainly of galactolipids with an unusually high level of unsaturation and encloses an aqueous compartment, the lumen. The thylakoid membrane shows a strong lateral heterogeneity (5), in terms of both protein and lipid compositions (Fig. 3). A substantial amount of the membrane is folded into stacks ("grana stacks"), where the outer membrane surfaces are in close contact. The extent of stacking varies greatly with plant species and light conditions. The stacked regions contain mainly photosystem II, whereas the unstacked, stroma-exposed membranes contain photosystem I and the ATP synthase (Fig. 3). The intermediate electron carrier cytochrome b_6f is distributed over both membrane regions. Destacking of the membrane and randomization of the protein complexes occurs when divalent cations (mainly Mg^{2+}) are depleted. In cyanobacteria, there is no thylakoid stacking or lateral segregation between the photosystems.

Figure 3. Schematic model of thylakoid membrane organization and its lateral heterogeneity. The thylakoid membrane is a lipid bilayer that encloses an aqueous compartment, the lumen. The protein and protein complexes within the thylakoid membrane are unequally distributed over the stacked and stroma-exposed membrane regions.

5.2. Biogenesis and Maintenance of the Thylakoid Membrane

Chloroplasts develop from structurally very simple proplastids, which consist of an envelope, a nucleoid with DNA fibrils, a small number of ribosomes, and some flattened thylakoid membrane sacs that appear to be continuous with the inner membrane of the envelope. Development of the proplastid requires light, several chromophores, and multiple nuclear genes, all acting together through several signal transduction chains in a tightly regulated process. When leaves develop in total darkness, so called etioplasts are formed, which contain no chlorophyll and no thylakoid membrane system. These etioplasts consist of lipid-rich cube-like structures called prolamellar bodies, containing mainly the light-regulated enzyme protochlorophyllide reductase and its pigment substrate protochorophyllide. Within a day of illumination of the etioplast, chlorophyll is synthesized and an active thylakoid membrane system is formed.

Biogenesis of the thylakoid membrane system involves the synthesis of at least 70 to 85 proteins of the four main photosynthetic protein complexes (5). Many of these proteins are encoded in the nucleus; after synthesis in the cytosol, they are imported into the chloroplast and targeted and inserted into the thylakoid membrane. To increase targeting efficiency to the chloroplast and to prevent missorting to other organelles, these nucleus-encoded proteins are synthesized with a signal sequence that is recognized by a receptor on the outer envelope surface (13). After nucleotide triphosphate-driven import into the chloroplast, this signal sequence is cleaved off by a stromal peptidase . Targeting to the thylakoid is facilitated by a second signal sequence, or via information within the mature protein. Different pathways for targeting and insertion into the membrane have been found, and a number of structurally important components, such as the Sec machinery and a signal recognition particle (SRP) have been identified (14). It should be noted that most chloroplast-encoded proteins do not contain a signal sequence. The chloroplast-encoded thylakoid proteins are inserted into the membrane either co-translationally or post-translationally, possibly by mechanisms similar to those in *Escherichia coli*. Most proteins that form the central functional core of each photosynthetic complex are chloroplast-encoded, whereas the more peripheral proteins are nuclear-encoded. To achieve the proper stoichiometry of the different proteins, regulation of synthesis takes place at transcriptional, translational, and post-translational levels, via various signal transduction chains and through feedback mechanisms.

The two photosystems and the cytochrome b_6f complex contain in total at least 15 different cofactors and many different pigments. The biosynthesis of these cofactors and pigments is tightly linked to the synthesis and accumulation of the proteins. Very little is understood, however, about the mechanisms of this coordination.

It has become clear that, in addition to the proteins of the photosynthetic complexes, there must be a fairly large number of proteins involved in the biogenesis and maintenance of the complexes.

Several functions must be performed during these processes: synthesis and ligation of cofactors, membrane insertion, folding, and degradation of proteins. Notably, these auxiliary proteins are mostly located in the stroma-exposed thylakoid regions (Fig. 3).

Recently, members of several classes of these enzymes have been discovered, and most of these auxiliary proteins are encoded in the nuclear genome. Some of these genes have an eukaryotic origin, whereas many originate from prokaryotic chloroplast predecessors. Sequencing of various bacterial genomes, such as those of *Synechocystis* 6803 and *E. coli* and the ongoing sequencing of the higher plant genome of *Arabidopsis thaliana* and other plant species, will prove helpful in identification of the components involved in biogenesis of the photosynthetic apparatus.

5.3. Short- and Long-Term Adaptation to the Environment

The photosynthetic apparatus is constantly regulating its activity, in response to both the quantity and the quality of light, as well as the varying demands for metabolic end products of the light and dark reactions (NADPH, ATP, glucose, etc). The two photosystems operate in series but do not have the same action spectrum. Photosystem II can use light at wavelengths below 680 nm, whereas photosystem I can use wavelengths up to 700 nm. Maximal absorption of the outer antenna of photosystem I (LHCI) is 5 nm red-shifted (thus lower energy level) compared to that of photosystem II (LHCII). Thus, changes in color of the light will affect the relative activities of the two photosystems. For optimal quantum use, it is important to balance the activities of the two photosystems, and several short- and long-term adaptive and regulatory processes must occur. The demand for ATP and reducing equivalents by the dark reaction shows several-fold variations on changing environmental conditions, such as cold, heat, or water stress, and also during different stages of plant development (e.g., vegetative growth, senescence).

On a short-term timescale (milliseconds to minutes), light energy can be redistributed via disconnection of the major CAB protein (LHCII) from photosystem II (5). This process is driven by redox-controlled phosphorylation of LHCII. The disconnected LHCII can migrate along the thylakoid membrane to photosystem I and thereby redistribute absorbed light energy. This reversible process is called the *state transition*. Some of the light absorbed by CAB proteins can also be dissipated in the form of heat. This heat dissipation is probably occurring through formation of exciton traps through the reversible conversion of xanthophyll pigments. Furthermore, cyclic electron flow from photosystem I back into the plastoquinone pool could help to balance the activities of the two photosystems and to alter the ATP/NAPDH ratio.

If the short-term adaptations are not sufficient, the quantities of the structural components of the photosynthetic apparatus are changed through the regulated biosynthesis and proteolysis. Various signal transduction chains that respond to different environmental conditions exist to make these dynamic changes possible.

5.4. Light-Induced Stress, Photoinhibition and Repair

If the adaptation and regulatory processes described above are not sufficient, damaging oxidative reactions can occur. Several scavenging mechanisms, such as superoxide dismutases and exciton transfer to carotenoids, are present in the thylakoid to quench toxic oxygen species. The main target for photoinhibitory damage of the photosynthetic apparatus is photosystem II, especially its D_1 reaction center protein. Consequently, the D_1 protein has a much shorter lifetime than any other photosynthetic protein. Photoinactivation of photosystem II function can occur either on its donor side, when electron donation to P680 is limiting, or on its acceptor side, when the quinones become overreduced. Since photosystem II is not functional without the D_1 protein, plants have evolved a very efficient repair mechanism. Two important features of this repair mechanism are (1) a controlled disassembly of photosystem II, to ensure that the other, undamaged, protein subunits of photosystem II are not proteolyzed and can be recycled; and (2) tightly coupled proteolysis and synthesis of the D_1 protein through an as-yet unidentified mechanism.

Bibliography

1. J. Barber and B. Andersson (1994) Nature 370, 31–34.
2. R. E. Blankenship, M. T. Madigan, and C. E. Bauer (1995) Anoxygenic Photosynthetic Bacteria, Kluwer Academic Publishers, Dordrecht.
3. J. Deisenhofer, O. Epp, K. Miki, R. Huber, and H. Michel (1985) J. Mol. Biol. 180, 385–398.
4. K.-H. Rhee, E. P. Morris, J. Barber, and W. Kühlbrandt (1998) Nature 396, 283–286.
5. B. Andersson and J. Barber (1994) in Advances in Molecular and Cell Biology, E. E. Bittar, ed., JAI Press, Greenwich, CT, Vol. 10, pp. 1–53.
6. W.-D. Schubert, O. Klukas, N. Krauss, W. Saenger, P. Fromme, and H. T. Witt (1997) J. Mol. Biol. 272, 741–769.
7. R. E. Blankenship (1992) Photosynth. Res. 33, 91–111.
8. W. F. J. Vermaas (1994) Photosynth. Res. 41, 285–294.
9. G. McDermott, S. M. Prince, A. A. Freer, A. M. Hawthornthwaite-Lawless, M. Z. Papiz, R. J. Cogdell, and N. W. Isaacs (1995) Nature 374, 517–521.
10. D. J. Simpson and J. Knoetzel (1996) in Advances in Photosynthesis, D. R. Ort and C. F. Yocum, eds., Kluwer Academic Publishers, Dordrecht, Vol. 4, pp. 493–506.
11. W. Kühlbrandt, D. N. Wang, and Y. Fujiyoshi (1994) Nature 367, 614–621.
12. G. Edwards and D. Walker (1983) C_3, C_4: Mechanisms, and Cellular and Environmental Regulation of Photosynthesis, Blackwell Scientific Publications, Oxford.
13. B. D. Bruce and K. Keegstra (1994) in Advances in Molecular and Cell Biology, E. E. Bittar, ed., JAI Press, Greenwich, CT, Vol. 10, pp. 389–430.
14. D. J. Schell (1998) Annu. Rev. Plant. Physiol. Plant Mol. Biol. 49, 97–126.

Suggestions for Further Reading

15. B. Andersson and J. Barber (1992) Too much of a good thing; light can be bad for photosynthesis, Trends Biochem. Sci. 17, 61–66.
16. W. Nitschke and A. W Rutherford (1991) Photosynthetic reaction centres: variations on a common structural theme? Trends Biochem. Sci. 16, 241–245.
17. R. Bassi, D. Sandonà, and R. Croce (1997) Novel aspects of chlorophyll a/b-binding proteins, Physiol. Plant. 100, 769–779.
18. Y. Cohen, S. Yalovsky, and R. Nechushtai (1995) Integration and assembly of photosynthetic protein complexes in chloroplast thylakoid membranes, Biochim. Biophys. Acta 1241, 1–30.
19. K. J. van Wijk, B. Andersson, and E.-M. Aro (1996) Kinetic resolution of the incorporation of the D_1 protein into PSII and localisation of assembly intermediates in the thylakoid membranes of spinach chloroplasts, J. Biol. Chem. 217, 9627–9636.

Photosynthetic Reaction Center

The photosynthetic reaction center is a redox-active complex of pigments and proteins that is the most vital part of the photosynthetic apparatus. All reaction centers have similar basic architectures, and their functions follow essentially the same mechanistic principles. They use a “special pair” of chlorophyll molecules as a primary electron donor (P_D) and a chlorophyll or pheophytin as the primary electron acceptor (P_A). On excitation by light, P_D donates an electron to P_A, and a radical pair is formed. This primary charge separation is stabilized by transfer of the electron to secondary acceptors and by passing an electron from secondary donors. The donors and acceptors are arranged in the reaction center in such a way that the primary charge separation occurs across the lipid bilayer of a photosynthetic membrane. The redox components are ligated to two distinct, but related, membrane-spanning proteins. In oxygenic photosynthesis in plants, algae and cyanobacteria, two reaction centers, photosystem I and photosystem II, are coupled in series. Photosystem I belongs to the type I reaction centers, which contain FeS clusters as electron acceptors and are also found in nonoxygenic green sulfur photosynthetic bacteria. Photosystem II belongs to the type II reaction centers, which contain quinone acceptors and are also present in purple bacteria. The two types of reaction centers are thought to be related evolutionarily. The structures of photosynthetic reaction centers are known primarily through X-ray crystallography, in particular from the elucidation of the reaction center of purple bacteria. See Photosynthesis for further details.

Phylogenetic Tree

A phylogenetic tree is a tree-like presentation of the phylogenetic relationships among species or genes. In particular, a phylogenetic tree can be constructed by using evolutionary distances between amino acid or nucleotide sequences (see Sequence Analysis). The tree obtained by this construction is called a “molecular phylogenetic tree” or simply a “phylogenetic tree.”

The methods for constructing a phylogenetic tree can be separated into two major categories, depending on the target traits. These are character-based methods and distance-based methods (1, 2). For example, the maximum-likelihood (ML) method (3) for constructing a phylogenetic tree is a character-based method, whereas the neighbor-joining (NJ) method (4) is a distance-based method. In most instances, the following procedures are used to construct a phylogenetic tree: First, the nucleotide (or amino acid) sequences to be compared are aligned simultaneously with each other. When the number of sequences to be compared is more than two, the alignment is called a “multiple alignment.” A character-based method, such as the ML method, can then be used immediately. For the distance-based methods, on the other hand, the number of nucleotide or amino acid substitutions is estimated for all possible combinations of sequence pairs. Using the substitution numbers as evolutionary distances, one is able to use distance-based methods, such as the NJ method.

Phylogenetic trees are either rooted and unrooted trees (see Fig. 1). The rooted tree has an ancestral node, but the unrooted tree is just a network without any ancestral node. The ML methods give a rooted tree, whereas the NJ methods produce a network or unrooted tree. It is, however, possible to identify the ancestral node in a phylogenetic tree that has been constructed by the NJ method. If a particular gene sequence is known to be apparently the most remotely related one to other sequences, it is included as an outgroup into a set of sequences to be compared when a phylogenetic tree is constructed. Then, the branching point between the outgroup and all other sequences can be identified as an ancestral point. Note that if the outgroup is related very remotely to other genes, the substitution numbers may not be estimated correctly because of the so-called saturation effect.

Figure 1. Schematic representation of (a) rooted and (b) unrooted phylogenetic trees.

When a phylogenetic tree is constructed by using gene sequences, the tree obtained (the “gene tree”) may be different from the tree of species (the “species tree”) that has been constructed utilizing information other than sequences, such as the fossil record. In particular, if paralogous genes are included in the analysis, the phylogenetic tree will not be the same as the species tree. This is because paralogous genes, by definition, do not follow the speciation process. Thus, special attention to paralogous genes is required when the species tree is inferred from the gene tree. A species tree can be constructed only by comparing orthologous genes.

Bibliography

1. M. Nei, (1987) Molecular Evolutionary Genetics, Columbia Univ. Press, New York.
2. R. F. Doolittle, (1996) Methods Enzymology 183, 659–669.
3. J. Felenstein, (1981) J. Mol. Evol. 17, 368–376.
4. N. Saitou, and M. Nei, (1987) Mol. Biol. Evol. 4, 406–425.

Phylogeny

Phylogeny is the evolutionary relationship among organisms or genes that takes into account the time and the divergence process from a common ancestor. When evolutionary relationships among organisms are studied by the techniques of molecular biology, the subject and the phylogeny obtained are called “molecular phylogeny” (1). Molecular phylogeny can be studied by immunological methods, protein electrophoresis, DNA-DNA hybridization, and amino acid and nucleotide sequences. For example, the immunological method utilizes the fact that cross-reactions in antibody–antigen interactions are stronger for closely related organisms than for distantly related ones. With this method, however, quantitative analysis has been difficult. Now the numbers of nucleotide or amino acid substitutions are used, as evolutionary distances, primarily to reconstruct the phylogeny of genes or proteins (see Phylogenetic Tree).

Previously in the study of phylogeny, controversy existed between cladistics and phenetics. Cladistics is the study of the pathway of evolution, in which the ancestor–descendant relationship is always discussed with the topology of a rooted phylogenetic tree, called a “cladogram” (see Phylogenetic Tree). On the other hand, phenetics is the study of the relationship among a group of organisms on the basis of the degree of similarity between their molecular, phenotypic, and anatomic traits. A tree-like network presenting phenotypic relationships is called “phenogram.” When a molecular clock exists, it is generally considered that a phenogram and a cladogram at the molecular level become identical to each other.

When the phylogeny of closely related organisms or genes is studied, for example, for individuals or alleles within a given population, it may be better to call it genealogy rather than phylogeny. Molecular genealogy is important for the study of genetic relationships among individuals or their alleles. The coalescence time is the shortest time for individuals or alleles to share the common ancestor in a given genealogy, and this can give us useful information about the time and degree of genetic diversity in the ancestral population (2).

Bibliography

1. W. H. Li and D. Graur, (1991). *Fundamentals of Molecular Evolution*, Sinauer Associates, Sunderland, MA.
2. M. Nei, (1987) *Molecular Evolutionary Genetics*, Columbia Univ. Press, New York.

Physarum

The acellular slime mold *Physarum polycephalum* has been studied in the laboratory extensively as a model eukaryotic organism. This soil amoeba has provided insights into many basic cellular functions. It is most famous for its complex developmental and sexual cycle. In the laboratory, it can be maintained in several forms, including a plasmodium that is basically an enormous singe cell containing several thousands of synchronously dividing nuclei. A simplified schematic of its developmental cycle is shown in Figure 1.

Figure 1. Schematic diagram of the *Physarum* developmental cycle.

In conditions that are not limiting in terms of food or moisture, Physarum is usually found in the plasmodium form. When the food supply begins to dwindle, the cell can either migrate to find more or begin the process of sporulation. In early stages of sporulation, cytoplasmic projections are formed that are filled with haploid nuclei. As the process continues, structures called fruiting bodies are constructed, and the nuclei packed in a protective shell and become spores. A mature fruiting body can rupture and spread the spores over the immediate area, where they remain dormant until conditions become right for germination or they get carried to a more favorable place by wind or insects.

When conditions are optimal, the spore germinates, releasing a haploid cell. This amoeba can search for food and can transform into a flagellate swimming form if it encounters water. Interestingly, this transition between the amoeba and myxoflagellate form occurs quickly and does not require additional protein biosynthesis, only rearrangement of existing components. If the amoeba encounters unfavorable conditions, it can change into a dormant and resistant form called a cyst. Amoebae can also mate or fuse with others, and the resulting cell grows into the plasmodium.

The Physarum genome is complex. The nuclei in the plasmodium form are a mixture of haploid and diploid. There has also been reported extrachromosomal linear DNA that can be maintained even upon transformation into yeast cells (1). There appear to be substantial differences between strains and under different growth conditions. One strain was reported to have about 70 chromosomes, containing a total of 1 to 5 × 10^9 base pairs of DNA (2).

A wide variety of genetic tools have been developed for manipulation of Physarum. Mutations can be created, and the resulting phenotypes analyzed in many ways. Extrachromosomal plasmids have been constructed into a family of vectors useful in stable or transient expression of heterologous genes. Multiple selectable markers systems are available, allowing the construction of strains in which complementation can be used to analyze the functions and interactions of proteins. Homologous recombination has been shown to occur, allowing gene knock outs and gene replacements to be made.

Of particular interest in Physarum is a complex system of photoreceptors and signaling that controls the onset of sporulation (3). The naturally synchronous cell cycle of Physarum plasmodium has been especially interesting, because fluctuations of inositol phosphate levels appear to be involved in its control (4).

Studies using the acellular slime mold Physarum polycephalum as a model eukaryotic organism have made contributions to our understanding of basic cell functions. Interesting insights will continue to be made using this social amoeba in the laboratory.

Bibliography

1. P. Kunzler (1985) Nucleic Acids Res. 13, 1855–1869.
2. J. Mohberg (1977) J. Cell Sci. 24, 95–108.
3. C. Starostzik and W. Marwan (1994) J. Bacteriol. 176, 5541–5543.
4. M. Belyavskyi and H. W. Sauer (1992) Eur. J. Cell Biol. 58, 371–376.

Suggestions for Further Reading

5. H. C. Aldrich and J. W. Daniel, eds. (1982) Cell Biology of Physarum and Didymium, two volumes, Academic Press, New York.
6. W. F. Dove, J. Dee, S. Hatano, F. B. Haugli, and K. E. Wohlfarth-Bottermann, eds. (1986) The Molecular Biology of Physarum polycephalum, Plenum Press, New York.
7. W. Sauer (1982) Developmental Biology of Physarum, Cambridge University Press, Cambridge, U.K.

Pili

Adhesion pili are fairly stiff, filamentous structures, typically about 6.8 nm in diameter and about 1 µm in length, that protrude from a bacterium and provide specific attachment sites between the bacterium and some target cell (Fig. 1). The pili (or fimbriae as they are also known) terminate in a flexible fibrillum about 2.5 nm in diameter. The link between the bacterium and the cell is maintained during mechanically challenging situations *in vivo*, but the pili undergo significant structural rearrangement as a consequence. Single-particle reconstruction work has shown that the pilus may unwind without depolymerizing to produce a fibrillum-like structure, thus generating a filament as much as five times its original length whilst maintaining a high degree of structural coherence (1). A wide variety of pili exist *in vivo*, and these include the mannose-binding type I pili of the *Enterobacteriaceae* family and the gonococcal type IV pili. The data suggest that pili from all sources have a conserved structure and a similar morphology.

Figure 1. Electron micrographs of (left) negatively stained and (right) metal-shadowed P pili from *E. coli* that cause pyelonephritis. The 2.5-nm-diameter fibrillum extending from the end of the pilus is clearly shown at right. Bar = 50 nm. (Courtesy of E. Bullitt and L. Makowski.)

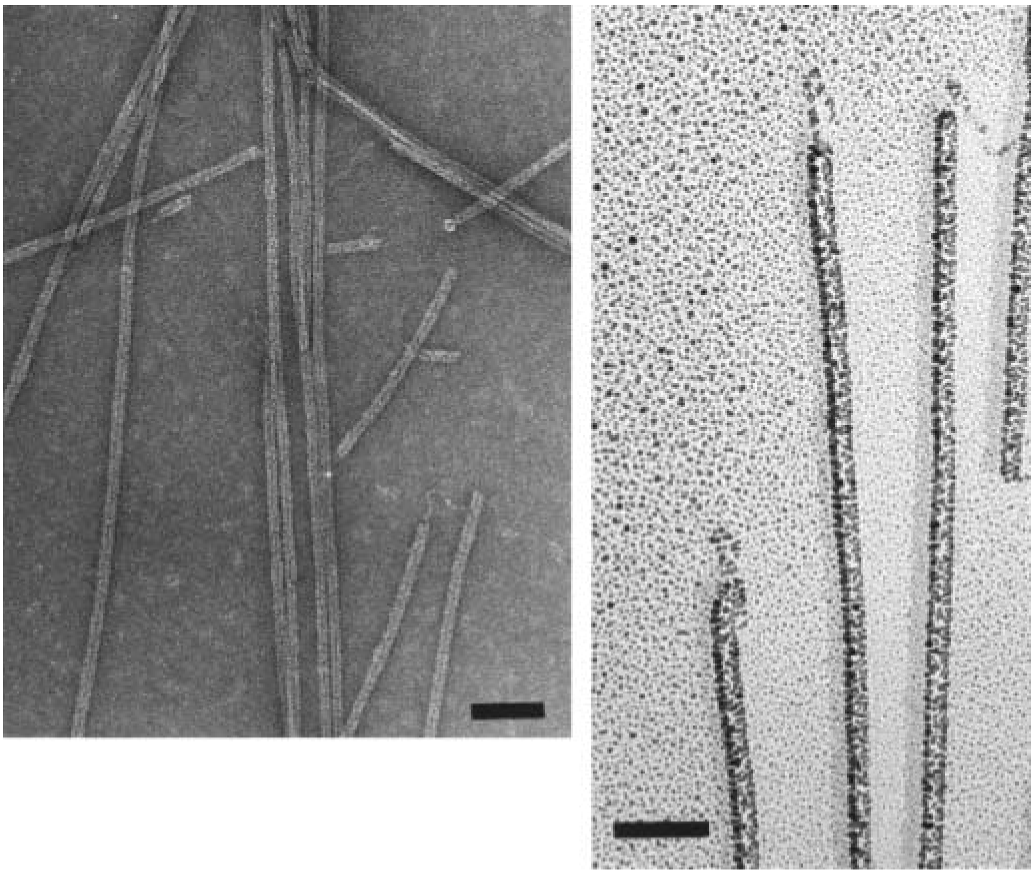

P pili, the surface appendages of *Escherichia coli*, have been particularly well characterized by X-ray fiber diffraction, scanning transmission electron microscopy (STEM), and three-dimensional reconstruction methods (1, 2), and for that reason they are described here in more detail. The pilus of diameter 6.8 nm contains approximately 1000 copies of a single protein (PapA) of molecular weight 16.5 kDa (Fig 2). Pili-terminating fibrillae are composed of proteins known as PapE, PapF, and PapK. The former two proteins position PapG at the tip of the fibrillus: PapG is a digalactose-binding molecule and is responsible for binding to the host (1). PapA, PapE, and PapF are similar in sequence, especially at their C-termini where they bind to PapD, the periplasmic molecular chaperone. The crystal structure of PapD (3) reveals a pair of domains, each comprising an antiparallel b-barrel, linked by a hinge region. PapH appears to stabilize the attachment of the pilus to the outer membrane of the bacterium. The assembly of P pili also requires PapC, an outer membrane protein.

Figure 2. Schematic of the position of proteins in P pili. (From Ref. 4, with permission.)

Fiber X-ray diffraction patterns from orientated pili are consistent with a helical structure having about 33 subunits in 10 turns (2). This helix is characterized by an axial repeat of 24.45 nm, a pitch length of 2.445 nm, a rise per subunit of 0.742 nm, and 3.30 subunits per turn. Measurements of the mass-per-unit length determined using STEM were consistent with each subunit comprising a single PapA molecule. Three-dimensional reconstruction methods yielded similar helical parameters based on a structure with 23 subunits in seven turns (axial repeat of 17.43 nm, a pitch length of 2.49 nm, a rise per subunit of 0.758 nm, and 3.28 subunits per turn: Fig. 3). These values are also very similar to those reported for type I pili from E. coli (pitch length 2.32 nm and 3.125 subunits per turn), in which a single pilin (FimA) predominates. This protein has about 25% sequence identity with PapA and would be expected to have a similar three-dimensional conformation. Using rotary shadowing, the handedness of the P pili helix has been determined. The three-start helix with a pitch length of about 9 nm has been visualized directly and is left-handed. Hence, the fundamental one-start helix is right-handed. The pili have an off-centered helical cavity (the radial coordinate of the center of the cavity is about 0.5 nm) with approximate dimensions 2.5 by 1.5 nm (1). Channels emanating out from the cavity link it to the outside of the pilus. The shape of the PapA molecule is not yet known, but it has been suggested that its long axis may lie along the same direction as the one-start helix, thus facilitating a possible structural transition to the more extended helical form arising from the response of the pili to mechanical stress. Bullitt and Makowski (1) have proposed that the relatively stiff pilus can be transformed to a flexible fibrillum if the interactions between the PapA molecules on adjacent turns of the one-start helix are broken and if there is a rotation of the domains along the direction of the one-start helix. PapA, as well as some of the other Pap proteins, would thus be expected to be elongated under these conditions. Because the mass-per-unit-length of a fibrillum is about one-fifth of that of the pilus, it is possible that the pilus could be extended fivefold. As a result, many pili with different lengths would be able to bind the cell simultaneously, thus providing stronger adhesion than if the pili were of fixed length. In that case they would have a greater chance of being broken individually when under shear.

Figure 3. Three-dimensional reconstruction of P pili from electron microscopy and image analysis. P pili are 6.8 nm in diameter and have a helical symmetry with 23 subunits in seven turns. The pitch length of the helix is 2.49 nm, and the axial rise per residue is 0.758 nm. *E. coli* may utilize plastic deformation of P pili to withstand shear forces in the host cell environment, extending the pilus to a thin fibrillum-like structure to maintain attachment to the target cell. Bar = 2.5 nm. (Courtesy of E. Bullitt and L. Makowski.)

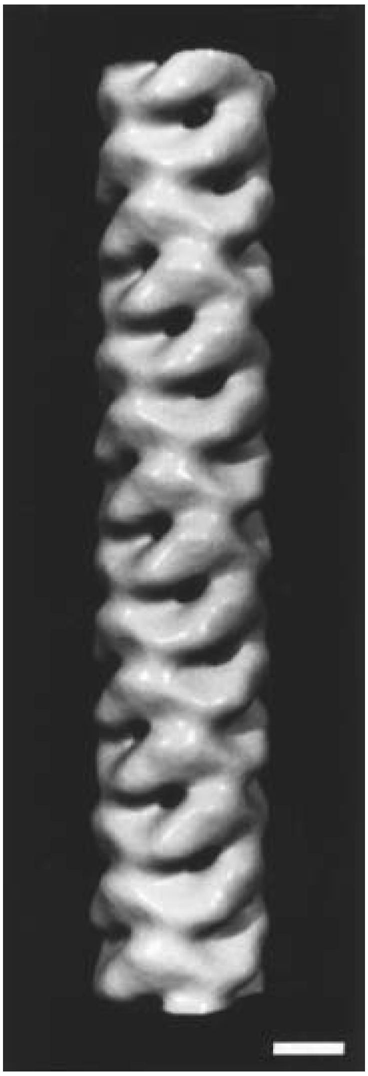

Bibliography

1. E. Bullitt and L. Makowski (1995) Structural polymorphism of bacterial adhesion pili. Nature (London) 373, 164–167.
2. M. Gong and L. Makowski (1992) Helical structure of P pili from Escherichia coli: evidence from X-ray fiber diffraction and scanning transmission electron microscopy. J. Mol. Biol. 228, 735–742.
3. A. Holmgren and C. I. Branden, (1989) Crystal structure of chaperone protein PapD reveals an immunoglobulin fold. Nature (London) 342, 248–251.
4. M. J. Kuehn, F. Jacob-Dubuisson, K. Dodson, L. Slonim, R. Striker, and S. J. Hultgren (1994) Genetic, biochemical, and structural studies of biogenesis of adhesive pili in bacteria. Methods Enzymol. 236, 282–306.

Suggestion for Further Reading

5. M. J. Kuehn, F. Jacob-Dubuisson, K. Dodson, L. Slonim, R. Striker, and S. J. Hultgren (1994) Genetic, biochemical, and structural studies of biogenesis of adhesive pili in bacteria. Methods Enzymol. 236, 282–306.

Pinocytosis

Pinocytosis is a form of endocytosis that is mediated by several different vesicular mechanisms and is responsible for both receptor-mediated and fluid-phase endocytosis. Clathrin -mediated endocytosis is the best-characterized pinocytic pathway and, in some cell types at least, is the major pathway for pinocytosis.

0.1. Clathrin-Dependent Endocytosis

The uptake of most receptor-bound ligands and extracellular fluid is mediated by endocytic clathrin-coated vesicles, typically 100 to 150 nm in diameter (1). These form constitutively from plasma membrane clathrin-coated pits during most of the cell cycle, but their formation, in common with other membrane trafficking events, does not occur during mitosis. Clathrin-coated vesicle assembly is initiated by the multifunctional AP-2 adaptor protein complex. The recruitment of AP-2 from the cytosol is poorly understood, but it may involve binding to inositol phospholipids and possibly to a polypeptide receptor [two related adaptor complexes, AP-1 and AP-3, are involved in vesicular transport from intracellular compartments (2)]. Membrane-bound AP-2 provides sites for attachment of cytosolic clathrin triskelions, which assemble either as flat lattices or invaginating lattice structures (see Clathrin). Clathrin assembly is required to drive membrane invagination at the cell surface, although local concentrations of specific lipids also contribute to membrane deformation.

AP-2 also provides binding sites for a spectrum of other proteins that are required structurally or catalytically for the formation of coated vesicles. These include amphyphysin, dynamin, EPS-15, synaptojanin, AP180/CALM, and the endophilins (SH3p4, SH3p8, SH3p13) (3). The precise roles of these proteins are still being established. Dynamin is currently the best characterized. This 100-kDa GTPase is recruited to coated pits via the SH3 domain of amphyphysin and is required for pinching off (scission of) invaginated coated vesicles (1). GTP hydrolysis is required for a conformational change in dynamin that leads to fusion of the membrane at the neck of an invaginated vesicle. Cells that express dominant-negative mutant forms of dynamin do not internalize transferrin and other ligands taken up by receptor-mediated endocytosis. Moreover, the Shibire mutant of Drosophila melanogaster has a temperature-sensitive defect in dynamin. At the nonpermissive temperature, Shibire mutants are paralyzed because they cannot recycle clathrin-coated vesicles, which is required to regenerate synaptic vesicles. Dynamin has also been implicated in forming of caveolae and non-clathrin vesicles (4, 5), but these processes are not well understood, and the full extent of dynamin function is still to be clearly established. Rab5 and RabGDI are also required for coated vesicle budding (6), and this may reflect some quality-control mechanism to ensure that endocytic-coated vesicles also include the correct SNARE proteins and allow the subsequent targeting and fusion of the vesicles with early endosomes.

Clathrin-dependent endocytosis is inhibited by treatments that interfere with the functions of the regulatory proteins, such as cytosol acidification, hypertonic medium, or K^+-depletion, or by overexpressing modified forms of key protein components (clathrin hub domains, GTP-bound dynamin, amphyphysin-SH3 domains, Eps15 AP-2-binding domains), all of which act as dominant negatives (7). Under these conditions clathrin-dependent, receptor-mediated endocytosis (e.g., transferrin uptake) is blocked. Although the overexpression, for example, of dominant-negative dynamin blocks clathrin-dependent endocytosis, fluid-phase endocytosis is unaffected or only partially affected, suggesting that there is also a clathrin-independent pathway for constitutive endocytosis. Although this clathrin-independent pathway may be active to some extent under normal conditions (its contribution to total endocytosis may vary in different cell types ranging from <10% in baby hamster kidney cells to 50% in hepatocytes), its activity may be up-regulated when clathrin-dependent endocytosis is effectively blocked (8). The molecular basis of this clathrin-independent pathway is not known, but there are several other pathways that could mediate fluid-phase uptake (see later).

Following endocytosis, clathrin-coated vesicles must be uncoated to allow fusion with early endosomes. Uncoating, which is ATP-dependent and requires the proteins auxilin and hsc70, releases clathrin, AP-2, and the other vesicle components, allowing them to be reused (9).

0.2. Clathrin-Independent Endocytosis

Caveolae, or plasmalemmal vesicles, are flask-shaped (60 to 80 nm in diameter) invaginations seen on the cytoplasmic aspect of the plasma membrane in many cell types. It is believed that they form by the oligomerization of a coat protein, caveolin (VIP-21). The function of caveolae is unclear. In endothelial cells, they mediate transcytosis, but in other cells they may provide an alternative endocytic route, although their net contribution to total endocytosis is likely to be small. Caveolae function in the concentration of a subset of cell-surface proteins, including GPI-anchored molecules, such as the folate receptor, and may internalize these components. Caveolae have also been implicated in the entry of SV40 virus. The caveolar membrane has a characteristic lipid composition distinct from the bulk of the plasma membrane and includes a relatively high cholesterol content. Thus drugs that preferentially bind cholesterol, such as filipin or nystatin, disrupt caveolae structurally and functionally. This distinctive membrane lipid composition also includes a concentration of the ganglioside GM1. GM1 functions as the receptor for cholera toxin and, in keeping with this, the endocytic uptake of cholera toxin is caveolae-mediated. Dynamin (see previous) has also been implicated in the pinching off required to release caveolae into the cytosol, presumably using the same mechanism as in clathrin-mediated endocytosis (4, 5). Caveolae also function in calcium signalling and signal transduction, and purified caveolae contain heterotrimeric G proteins, Src family protein kinases, and protein kinase C. Certain cell types, for example lymphocytes, lack VIP-21/caveolin and identifiable caveolae, suggesting that caveolar function is not essential for cell viability. The fate of internalized caveolae is unclear, and it has been suggested that they may fuse with early endosomes.

Bibliography

1. S. L. Schmid (1997) Annu. Rev. Biochem. 66, 511–548.
2. G. Odorizzi, C. R. Cowles, and S. D. Emr (1998) Trends Cell Biol. 8, 282–288.
3. O. Cremona and P. De Camilli (1997) Curr. Opinion Neurobiol. 7, 323–330.

4. J. R. Henley, E. W. Krueger, B. J. Oswald, and M. A. McNiven (1998) J. Cell Biol. 141, 85–99.
5. P. Oh, D. P. McIntosh, and J. E. Schnitzer (1998) J. Cell Biol. 141, 101–114.
6. H. McLauchlan, J. Newell, N. Morrice, A. Osborne, M. West, and E. Smythe (1998) Curr. Biol. 8, 34–45.
7. H. Riezman, P. G. Woodman, G. van Meer, and M. Marsh (1997) Cell 91, 731–738.
8. H. Damke, T. Baba, D. E. Warnock, and S. L. Schmid (1994) J. Cell Biol. 127, 915–934.
9. S. E. Holstein, H. Ungewickell, and E. Ungewickell (1996) J. Cell Biol. 135, 925–937.
10. R. G. Parton (1996) Curr. Opinion Cell Biol. 8, 542–548.
11. E. Stang, J. Kartenbeck, R. G. Parton (1997) Mol. Cell. Biol. 8, 47–57.

Plant Genetic Engineering

Plant genetic engineering is defined as the creation of a complete plant containing a fragment of foreign DNA stably inserted into its nuclear genome. During the last 15 years, the majority of the world's most significant crop plants have been transformed. Apart from a significant impact on plant research in general, the products of transgenic plants are currently entering the marketplace and, indeed in some cases, are achieving market dominance.

Plant transformation relies on inserting foreign DNA into a single plant cell, followed by regenerating that cell into a complete plant. Often this process relies on totipotency, the unique ability of isolated plant cells, when cultured in the presence of plant hormones, to divide to form an undifferentiated callus that, in turn, is induced to form shoots and roots and thus a complete plant. Two general means are available for transferring foreign DNA to plant cells, *Agrobacterium*-mediated transformation and naked DNA uptake.

Agrobacterium is a soil bacterium that contains a tumor-inducing Ti plasmid. During *Agrobacterium*-mediated transformation, a defined fragment of the Ti plasmid, the so-called transferred or T-DNA (see T-Complex, T-DNA, T-Region, T-Strand), is transferred from the bacterium to the infected plant cell and integrated stably into the plant nuclear genome. The T-DNA is delimited by 25-bp imperfect border repeats. Transformation vectors based on the T-DNA have been developed and can be grouped into two types, cointegrative and binary. Cointegrative vectors are based on a Ti plasmid in which the body of the T-DNA within the border sequences has been replaced by a defined sequence of DNA. Foreign DNA contained on an appropriate plasmid is introduced into *Agrobacterium* and integrated into the cointegrative vector by recombination. Binary vectors are based on plasmids stable in both *Escherichia coli* and *Agrobacterium*. They contain T-DNA border sequences between which foreign DNA can be cloned to be transferred to the plant genome. Then, the binary vector is transferred to a host *Agrobacterium* that contains a Ti helper plasmid which contains functions necessary for gene transfer to plant cells, but lacks a T-DNA. Because cointegrative vectors are based on Ti plasmid, they are very stable in *Agrobacterium*, but they can be difficult to work with in practice. On the other hand, binary vectors can be handled with relative ease, although they are unstable in *Agrobacterium* and continued antibiotic resistance selection is required to maintain them (1).

Transformation using *Agrobacterium* requires direct contact between the plant cell and the infecting bacteria. In practice, this is achieved by cocultivation of *Agrobacterium* with isolated plant cells or explants, such as leaves, roots, or tubers. In this case, bacteria are incubated with plant material, and transformation occurs over a period of about two days. Then, the plant material is washed to remove excess bacteria and cultured further to allow plant regeneration (1). Recently, a novel nontissue culture approach of transformation has been described using the model plant Arabidopsis. Here the developing floral buds of intact plants are vacuum infiltrated with the Agrobacterium. The plants are washed, allowed to recover, and selfed. From progeny seeds, transgenic plants can be selected by growth on antibiotics to which resistance is encoded by the foreign DNA contained on the transformation vector (2). It has been generally assumed that Agrobacterium-mediated transformation is limited to the obvious natural hosts of Agrobacterium, the dicotyledonous plants. Recently, however, it has been established that Agrobacterium can be used effectively to create transgenic monocotyledonous plants, such as rice (3).

Naked DNA uptake was developed for two reasons: (1) as a means of transforming plants whose cells, or tissues, are not amenable to culture and to high-frequency Agrobacterium transformation; (2) because of the possibility of using nonspecialized plant transformation vectors in transformation. Naked DNA transformation uses standard bacterial plasmids as vectors. The only requirement is that the plasmid contains a gene linked to a plant-specific promoter that is functional in transgenic plants. Several methods are available to transfer foreign DNA into plants. The two techniques used most frequently with isolated cells, treatment with polyethylene glycol and electric discharge or electroporation (see Transfection), achieve relatively high frequencies of transformation, which generally result in measurable activity of the transferred gene constructs after approximately one day. This allows transient expression assays, for example, to test the expression of specific promoter/gene constructs. Cells transformed in this manner can also be regenerated to intact plants as described previously. Naked DNA can also be introduced into plant cells by particle bombardment. This involves coating gold or tungsten particles with DNA and using a gas or electric discharge to project the particles into target cells. This can be used to study transient expression in intact tissue, but its greatest practical application has been to insert foreign DNA into explants from which shoot or root organogenesis can occur (4).

In both Agrobacterium-mediated transformation and naked DNA uptake, the foreign DNA stably integrates into the nuclear genome of the plant. Agrobacterium-mediated transformation can result in inserting a single unrearranged fragment of DNA that represents the T-DNA. In transgenic cells resulting from naked DNA uptake, however, the DNA might be rearranged and can occur as multimers.

Upon insertion into the genome, a gene linked to a plant-specific promoter is expressed in a pattern determined by that promoter. A variety of reporter genes have been developed to allow direct selection for the growth of transgenic material (for example, resistance to kanamycin, hygromycin, or herbicides) or for screening for expression (for example, histochemical staining with b-glucuronidase or fluorescence resulting from expression of the jellyfish green fluorescent protein). An increasing variety of promoters are available to produce expression in most plant tissues (for example, the 35 S-RNA promoter derived from cauliflower mosaic virus) or expression in a tissue-specific manner (for example, tapetum-specific expression). Recently promoter constructs have been developed so that the expression of specific genes can be induced in defined tissues following the external application of an inducing substance, such as glucocorticoids (5).

Gene expression can also be inactivated in transgenic plants, by the expression of either antisense oligonucleotides (6) or sense constructs of the target gene, a phenomenon known as cosuppression. The exact mechanism by which cosuppression occurs is not known nor is the reason for the instability of transgenic expression that often occurs in some plant lines (7).

In addition to transferring foreign genes to the genomes of plants, transformation in plants can be considered a form of insertional mutagenesis. This is the basis of gene tagging, where a defined sequence of DNA inserts into the genome and knowledge of this sequence allows recovering the flanking plant sequence from mutant genomes by hybridization, PCR, or plasmid rescue. Either transposable elements transferred to a novel plant host or T-DNA can be used in gene tagging. The latter has the advantage of producing single insertions, simplifying genetic analysis, but requires screening large numbers of mutant individuals following a transformation experiment. The transposable element approach has the advantage of using populations of mutant individuals produced by genetic crossing. Each individual contains multiple transposon insertions, thus reducing the number of mutants that need to be screened for a mutant phenotype. The construction of gene tags can vary. For example, at their borders they can contain a reporter gene lacking a promoter, so that expression of the reporter gene occurs only if it is inserted into the genome near a promoter (8, 9). Another example is the use of a tag that contains transcriptional enhancers, so that expression of flanking genes becomes activated following insertion of the tag into the plant genome (10).

Plant genetic engineering has had a profound effect on basic plant biology. Transgenic plants have been used to study the mechanism of gene expression and the developmental and biochemical consequences of the expression or inhibition of the expression of various genes (11).

The creation of transgenic plants has begun to have a profound effect on agriculture because of the steady appearance of genetically engineered crop plants. These include plants tolerant of herbicides or resistant to insect predation and viral infection. Interestingly, plants altered in developmental events or biochemical processes have also gained a place in the agronomic marketplace. Possibly the most widely known example of this is the tomato engineered, using antisense technology, so that the polygalacturonidase gene, which is normally involved in the softening of fruit, is not expressed during fruit development. These tomatoes have delayed ripening (12). Another interesting example is the potatoes engineered so that they contain changed starch content and quality for industrial processes (13). The acreage of transgenic crops plants is steadily increasing worldwide (14). This technology is, however, not without its opponents. Concerns have been raised as to transfer of the transgenes from transgenic plants to local plant relatives, increasing the weediness of certain plant species, and the creation of products that may induce unexpected allergies in consumers.

Bibliography

1. J. Draper, R. Scott, P. Armitage, and R. Walden (1989) Plant Genetic Transformation and Gene Expression. A Laboratory Manual, Blackwell Scientific, Oxford.
2. F. F. White (1993) Transgenic Plants, Vol. 1 (D. Kung and R. Wu, eds.), Academic Press, San Diego, pp. 15–48.
3. Y. Hiei, S. Ohte, T. Komari and T. Kumashiro (1994) Plant J. 6, 271–282.
4. N. Bechtold, J. Ellis, and G. Pelletier (1993) C. R. Acad. Sci. Paris, Life Sciences 316, 1194–1199.
5. T. Aoyama, C. H. Dong, Y. Wu, M. Carabelli, G. Sessa, I. Ruberti, G. Morelli, and N-H Chua (1995) Plant Cell 7, 1775–1785.
6. A. R. van der Krol, J. N. Mol, and A. R. Stuitje (1988) Gene 72, 45–50.
7. S. P. Kumpatla, M. B. Chandrasekharan, L. Iyer, G. Li, and T. C. Hall (1998) Trends Plant Sci. 3, 97–104.
8. M. A. Haring, C. M. Rommers, H. J. J. Nijkamp, and J. Hille (1991) Plant Mol. Biol. 16, 449–461.
9. J. F. Topping, W. Wei, M. C. Clark, P. Muskett, and K. Lindsey (1995) Methods Mol. Biol. 49, 63–79.
10. H. Hayashi, I. Czaja, H. Lubepow, J. Schell, and R. Walden (1992) Science 258, 1350–1353.
11. T. ap Rees (1995) Trends Biotech. 13, 375–378.
12. M. G. Kramer and K. Redenbaugh (1994) Euphytica 79, 293–297.
13. R. G. F. Visser et al. (1991) Mol. Gen. Genet. 225, 289–296.
14. USDA Animal and Plant Health Inspection Service. Internet http://www.aphis.usda.gov/bbep/bp.

Suggestions for Further Reading

15. R. Walden (1989) Genetic Transformation in Plants, Prentice-Hall, Englewood Cliffs, NJ.

16. M. J. Chrispeels and D. E. Sadava (1994) *Plants, Genes and Agriculture*, Johns and Barlett.
17. S. D. Kung and R. Wu (1992) *Transgenic Plants*, Vols. 1 and 2, Academic Press, San Diego.
18. C. Tudge (1988) *Food Crops of the Future*, Blackwell Scientific Press.

Plant Hormones

Development of higher organisms—plants as well as animals—is largely based on a coordinate division, expansion, and differentiation of cells. This coordination is primarily based on cell-to-cell communication over short and long distances and is orchestrated by messengers of various chemical nature. One class of signaling molecules contains the hormones, characterized by their ability to exert, most often, specific effects over a distance and by their capacity to act at very low concentrations. This entry presents a brief overview of the current state of the art in the field of plant hormones, or phytohormones.

Since the first discovery of phytohormones, approximately 70 years ago, dedicated efforts of plant physiologists and biochemists have produced a wealth of data on their chemical nature, pathways of biosynthesis and metabolism, possible conjugates, transport mechanisms throughout the plant, and physiological functions (1). Studies have been based traditionally on the correlation of the effects observed upon exogenous application of hormones with changes in their endogenous concentration. A major disadvantage of this approach is that it remains uncertain whether the effect reflects the normal physiological role of the hormone. Another problem arises from the fact that the distribution of the growth regulator over the entire plant body is largely unpredictable. Moreover, problems of uptake and rapid metabolism were not uncommon. The use of inhibitors had the additional drawback of potential lack of specificity. In the past decade, our knowledge of the molecular basis of plant hormone biology has made a giant leap forward, mainly owing to molecular genetic studies of mutants in thale cress (*Arabidopsis thaliana* (L.) Heynh.). Molecular techniques have allowed the unraveling of mechanisms by which phytohormones control tissue-specific and developmentally regulated responses. Genetic engineering enables changes in internal concentration or perception of a hormone in a temporally and spatially controlled manner. Moreover, several applications in agriculture and horticulture are being explored (2–4). Introduction of bacterial hormone biosynthesis genes (mainly from *Agrobacterium tumefaciens*) into plants has confirmed much of the classical view of hormone action (5).

Our current understanding of the biosynthesis, perception, signal transduction, control of gene expression, and effects of each class of phytohormones are presented in the separate entries. Six classes of compounds are recognized as true phytohormones: auxins, cytokinins, gibberellins, abscisic acid, ethylene, and brassinosteroids. Other growth regulators, such as polyamines, oligosaccharides, and salicylic and jasmonic acids, also influence plant growth and development. For a description of their effects, see recent reviews (6–8).

It is important to stress that plant hormones do not play exclusive roles in development, but that they instead act coordinately at different stages. The most direct indication for this characteristic is their overlapping physiological roles (1). This cross-talk is most certainly based on molecular interactions between factors regulating signal transduction and feedforward or feedback loops of different hormone pathways. Moreover, environmental cues exert an additional level of control on plant hormone abundance and activity. Thus, hormone signaling pathways are probably integrated with those participating in phototransduction, control of the biological clock, nutrient sensing, and stress (9). Given the redundancy of involvement of signaling intermediates, such as G proteins, phosphorylation cascades, and calcium signaling mechanisms should exist to maintain accuracy of individual signaling chains (10). Much of the specificity might derive from a restricted spatial distribution of signaling components together with their assembly in complexes, called transducons. The latter would consist of a module of receptors, receptor targets, and downstream signaling factors, presumably coupled by 14–3–3 proteins (11). Such scaffolding proteins have been demonstrated in signaling pathways in bacteria and in yeast (12, 13). Interactions between different transduction cascades could be exerted by components that navigate between them—for example, second messengers or mobile protein kinases (14).

With the current progress in sequencing of the genome of Arabidopsis, plus the technical advances that allow rapid map-based cloning, creation of large tagged-mutant collections (15), and production of knockout mutants by homologous recombination (16), it can be predicted that the molecular controls of hormonal pathways and their target genes will be unraveled at a dazzling pace in the next few years. The puzzle of inter- and intracellular hormonal networking will soon come of age.

Bibliography

1. P. J. Davies (1995) Plant Hormones: Physiology, Biochemistry and Molecular Biology, Kluwer, Dordrecht, The Netherlands.
2. C. Mariani, V. Gossele, M. De Beuckeleer, M. De Block, R. B. Goldberg, W. De Greef, and J. Leemans (1992) Nature 357, 384–387.
3. R. Ayub, M. Guis, M. Ben Amor, L. Gillot, J.-P. Roustan, A. Latché, M. Bouzayen, and J.-C. Pech (1996) Nature Biotechnol. 14, 862–866.
4. G. L. Rotino, E. Perri, M. Zottini, H. Sommer, and A. Spena (1997) Nature Biotechnol. 15, 1398–1401.
5. H. J. Klee and C. P. Romano (1994) Crit. Rev. Plant Sci. 13, 311–324.
6. J. A. Ryals, U. H. Neuenschwander, M. G. Willits, A. Molina, H.-Y. Steiner, and M. D. Hunt (1996) Plant Cell 8, 1809–1819.
7. R. A. Creelman and J. E. Mullet (1997) Plant Cell 9, 1211–1223.
8. R. Walden, A. Cordeiro, and A. F. Tiburcio (1997) Plant Physiol. 113, 1009–1013.
9. T. H. Thomas, P. D. Hare, and J. van Staden (1997) Plant Growth Regul. 23, 105–122.
10. A. J. Trewavas and R. Malhó (1997) Plant Cell 9, 1181–1195.
11. P. C. Sehnke and R. J. Ferl (1996) Curr. Biol. 6, 1403–1405.
12. T. W. Grebe and J. Stock (1998) Curr. Biol. 8, R154–R157.
13. I. Herskowitz (1995) Cell 80, 187–197.
14. D. M. Braun and J. C. Walker (1996) Trends Biochem. Sci. 21, 70–73.
15. N. Bechtold, J. Ellis and G. Pelletier (1993) C. R. Acad. Sci. Paris (Life Sci.) 316, 1194–1199.
16. K. Yoon, A. Cole-Strauss, and E. B. Kmiec (1996) Proc. Natl Acad. Sci. USA 93, 2071–2076.

Suggestions for Further Reading

17. C. H. Bornman, ed. (1997) Special volume: Hormones, regulating and signalling substances in plant growth and development. Physiol. Plant. 100, 407–738.
18. J.-P. Kader, ed. (1998) Special issue: Arabidopsis thaliana. Plant Physiol. Biochem. 36, 1–197.
19. K. Palme, ed. (1994) Signals and Signal Transduction Pathways in Plants, Kluwer, Dordrecht, The Netherlands.
20. F. B. Salisbury and C. W. Ross (1992) Plant Physiology, 4th ed. Wadsworth Publishing Company, Belmont (CA).
21. J. van Staden, ed. (1997). Special issue: Opinion on current research in cytokinin physiology. Plant Growth Regul. 23, 1–134.

Plasmalemma

Plasmalemma (plasma+Gr. lemma = pellicle) is a membrane structure that is synonomous with the plasma membrane of cells. There are other usages of the term. In sea urchin eggs, it is the vitelline membrane covering the hyaline plasma layer; upon fertilization the vitelline membrane thickens and becomes the fertilization membrane, which separates from the plasma membrane lying just beneath. In amoeba, it is the outermost membrane, which also contains many filamentous structures. In plants, it is the external membrane of the cytoplasm; under osmotic stress in hypertonic salt solutions, plant cells undergo plasmolysis, where the plasmalemma separates from the cellulose wall of the cell. (See also Membranes.)

Suggestion for Further Reading

H. Davson (1964) A Textbook of General Physiology, 3rd ed. Little Brown, Boston. (Contains a concise description of the various cell membranes and their physiological characteristics.)

Plasminogen

Plasminogen is one of the most abundant zymogens of serine proteinases in mammalian species; it is expressed constitutively in the liver and is present in blood at 200 µg/mL. The activated proteinase, plasmin, is one of the most active, because of its broad substrate specificity. The activation system for plasminogen is therefore a powerful and potentially promiscuous proteolytic system, which consequently has mechanisms for its strict regulation. The most fundamental of these is the ability of plasminogen to bind to various insoluble matrices (ie, fibrin and certain cell-surface components), a process regulating both the activation of plasminogen (see Plasminogen Activators) and the inhibition of plasmin.

The binding properties of plasminogen are mediated by its various kringle domains. Plasminogen is a mosaic protein composed of a 77-residue N-terminal domain, five kringle modules, and the serine proteinase domain. The kringle modules each contain a binding site for lysine or other w-amino carboxylic acids. Kringle 1 binds these ligands with the highest affinity (dissociation constant K_d = 10 µM for 6-aminohexanoic acid) and represents the archetype for this binding site. It contains both anionic and cationic centers, with an intervening hydrophobic depression (1, 2). The cationic center is not present in all kringles, such as kringle 5, and these have a preference for ligands lacking a carboxylate function. Therefore, plasminogen can interact with the side chains of internal lysine residues, as well as those at the C-termini of proteins degraded by proteinases with a specificity for basic residues, including trypsin, or plasmin itself. The latter mechanism may act to amplify the plasminogen activation system.

The gross conformation of plasminogen is dramatically affected by kringle-binding ligands (3). In the absence of such ligands, it adopts a compact conformation, due to poorly understood interactions between the N-terminal domain and the kringle modules. Exogenous kringle-binding ligands disrupt these interactions and cause an extension of the molecule to approximately double its length. This conformational change can also be accomplished by proteolytic removal of the N-terminal peptide, generating Lys78-plasminogen (to discriminate between them, the native molecule is often referred to as Glu1-plasminogen). The conformation of plasminogen has a very marked effect on its activation, with the extended or "open" form being activated at least 10-fold more efficiently. The absolute difference in activation rates may be much larger, as the "closed" form is in equilibrium with the "open" form in the absence of exogenous ligands. Thus the physiologically relevant substrate form of plasminogen is thought to be that bound to various surfaces in the "open" conformation.

Plasmin free in solution is very rapidly inhibited by the serpin α_2-antiplasmin, which is dependent largely on an initial interaction between the C-terminal region of the inhibitor with the lysine-binding site of plasmin kringle 1 (4). Hence, plasmin inhibition is decreased when these sites are occupied by binding to fibrin or cell surfaces (5). Plasmin and plasminogen have moderate affinities for these surfaces (K_d ~1 µM),. with dissociation half-lives of the order of minutes. Thus binding of plasminogen and subsequent dissociation of plasmin, respectively, regulate the activation and inhibition of this proteolytic system.

One final notable feature of plasminogen is its potential to attain proteolytic activity in the absence of the activation cleavage at Arg561–Val562. The non-enzymatic bacterial protein streptokinase binds to the serine proteinase domain of plasminogen and induces a conformational change, with the formation of a functional active site. This has full activity against peptide substrates, but the specificity of the complex against macromolecular substrates is changed from that of plasmin to that of a plasminogen activator. Therefore, "catalytic" amounts of streptokinase can rapidly lead to full activation of plasminogen. Although this property is used clinically to generate plasmin activity *in vivo*, an equivalent endogenous mechanism has not been detected.

Bibliography

1. I. I. Mathews, P. Vanderhoff-Hanaver, F. J. Castellino, and A. Tulinsky (1996) Biochemistry 35, 2567–2576.
2. M. R. Rejante and M. Llinás, (1994) Eur. J. Biochem. 221, 939–949.
3. W. F. Mangel, B. H. Lin, and V. Ramakrishnan (1990) Science 248, 69–73.
4. W. E. Holmes, L. Nelles, H. R. Lijnen, and D. Collen (1987) J. Biol. Chem. 262, 1659–1664.
5. V. Ellis, N. Behrendt, and K. Danø, (1991) J. Biol. Chem. 266, 12752–12758.

Plasminogen Activators

Mammalian species have two plasminogen activators, urokinase- or urinary-type plasminogen activator (uPA) and tissue-type plasminogen activator (tPA), that are the products of separate genes and members of the chymotrypsin family of serine proteinases. Both are mosaic proteins with a modular structure similar to that of the blood coagulation proteinases to which they are closely related [Blood Clotting]. The two plasminogen activators provide an excellent example of the regulatory potential made available by the modular construction of these proteinases. Although catalyzing the same reaction, i.e., specific hydrolysis of Arg560–Val561 of plasminogen, gross differences in the organization of the N-terminal modules of the plasminogen activators, together with subtle differences in the serine proteinase domain, lead to remarkably different functional properties. These are reflected in their biological roles with tPA being predominantly responsible for plasmin-catalyzed fibrin dissolution, whereas uPA is thought to be responsible for generating plasmin activity in the context of extracellular matrix degradation and thus to be involved in tissue remodeling and invasive cell migration (e.g. tumor invasion and metastasis; vascular remodeling) (see Urokinase).

1. tPA

tPA is composed of five independent domains; an N-terminal fibronectin type-I (finger) module, an EGF-like module, two kringle modules and the serine proteinase domain. It is secreted primarily by vascular endothelial cells as a single-chain glycoprotein of 527 residues (M_r 65,000). This single-chain form also undergoes a plasmin-catalyzed “activation” cleavage (Arg275-Ile276) to give a disulfide-bridged two-chain molecule. However, uniquely among the serine proteinases, the catalytic activities of these two forms are very similar. They vary by approximately 10–20–fold in the absence of cofactors, but in the presence of fibrin [see “Fibrinogen”] as a cofactor their activities are essentially indistinguishable. Molecular modeling and mutagenesis studies suggest that the “active zymogen” nature of tPA is largely due to Lys429 (Lys156 in chymotrypsin numbering); in the absence of a proteolytically exposed N-terminal a-amino group at Ile276, it can form a salt-bridge with Asp477, substituting for the interaction between the a-amino group of Ile16 with Asp194 in chymotrypsin (1). The crystal structure of two-chain tPA is compatible with this hypothesis (2).

Fibrin has a dramatic effect on the activities of both forms of tPA. The catalytic efficiency increases up to 1000-fold, as a result of a large reduction in the K_m (Michaelis constant) for plasminogen and a more modest increase in the value of the catalytic rate constant k_{cat} (3). More than one mechanism appears to be responsible for these kinetic effects. Fibrin principally enhances plasminogen activation by provides a template for the coincident binding of enzyme and substrate in a ternary complex. In contrast to the binding of uPA to uPAR, the interactions between tPA and fibrin responsible for this binding are complex and not fully elucidated. The fibronectin type-I and the lysine-binding properties of the second kringle module are involved, with sites in the serine proteinase domain also implicated. Secondary to this template effect, fibrin also appears to induce conformational changes in the serine proteinase domain of single-chain tPA, bringing it to catalytic equivalence with two-chain tPA, and increasing its activity against small peptide substrates. Whether these are direct effects or result from the significant interdomain interactions that exist in tPA is presently undetermined.

In addition to its fibrinolytic role, analysis of tPA$^{-/-}$ knock-out mice has revealed a role for tPA in the brain, in both normal and neurodegenerative situations. The proteolytic activity of tPA is implicated in the plasticity and reorganization of synapses involved in various learning processes, although it is not known whether plasminogen activation is required in these processes or whether tPA acts on other substrates. tPA is also involved in neuronal cell death following excitotoxin stimulation of the hippocampus and in ischemic stroke. The former process is known to require plasminogen activation, with plasmin acting to degrade laminin, an important extracellular matrix component in the central nervous system (4).

Bibliography

“Plasminogen Activators” in , Vol. 3, pp. 1865–1866, by Vincent Ellis, Ph.D., University of East Anglia, School of Biological Sciences, Norwich, United Kingdom, NR4 7TJ; “Plasminogen Activators” in (online), posting date: January 15, 2002, by Vincent Ellis, Ph.D., University of East Anglia, School of Biological Sciences, Norwich, United Kingdom, NR4 7TJ.

1. K. Tachias and E.L. Madison (1997) J. Biol. Chem. 272, 28–31.
2. D. Lamba, M. Bauer, R. Huber, S. Fischer, R. Rudolph, U. Kohnert and W. Bode (1996) J. Mol. Biol. 258, 117–135.
3. M. Hoylaerts, D.C. Rijken, H.R. Lijnen and D. Collen (1982) J. Biol. Chem. 257, 2912–2919.
4. Z.L. Chen and S. Strickland (1997) Cell 91, 917–925.

Suggestions for Further Reading

5. K. Danø, P.A. Andreasen, J. Grøndahl-Hansen, P. Kristensen, L.S. Nielsen and L. Skriver. (1985) Plasminogen activators, tissue degradation and cancer. Adv. Cancer Res. 44, 139–266.
6. H.R. Lijnen and D. Collen (1998) "t-Plasminogen activator", in Handbook of Proteolytic Enzymes, A.J. Barrett, F. Woessner and N. Rawlings, eds., Academic Press, London, pp 184–190.

Plasmogamy

Plasmogamy occurs when two different cells fuse with each other and the cytoplasm of both is joined. During fertilization , plasmogamy occurs when the sperm has entered the cell membrane of the egg and a male and a female pronucleus develop. However, plasmogamy in animal reproduction is unusual in that the amount of cytoplasm of the two gametes is disparate. The oocyte is one of the biggest cells in the body and contains most of the cytoplasm, whereas the spermatozoon is a very specialized cell that contains only very small amounts.

The length of time it takes the sperm head to fuse with the oocyte cytoplasm depends on the species. In general, fusion takes place during meiosis of the oocyte. These divisions are necessary, as the primordial germ cells remain diploid until ovulation commences at the beginning of puberty under the influence of follicle-stimulating hormone (FSH) and luteinizing hormone (LH). During growth and oogenesis, the oocyte becomes temporarily tetraploid and undergoes two meiotic divisions, resulting in the extrusion of polar bodies. Formation of the first polar body involves a cytoplasmic protrusion at the animal pole. The cytoplasm is not divided equally among the two cells, however, and the polar bodies contain less material than the remaining oocyte. The first polar body in a number of different species appears to be a maturized cell. The second polar body appears after the second meiotic division and contains a variable amount of cytoplasmic contents. In most cases, however, the fate of the polar bodies is a degenerative process. During this stage of fertilization, the formation of crenations along the vegetal pole occurs, along with redistribution of cytoplasmic compounds.

Upon sperm entry, which is the first step that can be considered a unification in which the cytoplasms are joined, a number of events are triggered. Sperm entry itself is mediated by an adhesion protein named fertilin (previously known as PH-30). The a subunit of fertilin is involved in mediating the binding of sperm and egg plasma membranes (1); there is also evidence for adhesive activity of an egg b1 integrin-mediated interaction (2). These gene products are expressed by the ADAM gene family and are processed during sperm maturation (3, 4).

The first measurable event during plasmogamy is a rapid depolarization of the plasma membrane on sperm entry. This process is used in some species to prevent more than one spermatozoon from entering the egg. In sea urchins, eggs with a fertilization potential greater than 0 mV are not polyspermic. Maintaining a potential of +5 mV causes a block of fertilization. If the applied voltage is lowered below 0 mV, fertilization will occur and, if the potential is maintained below –30 mV, the eggs will become polyspermic. These observations indicate that a rapid change in the potential of the plasma membrane is a first reaction of the egg to sperm entry. The change in polarity occurs concomitantly with the influx of calcium (see Calcium Signaling). The release of calcium and of the cortical granules occurs in a sort of wave, starting from the point of sperm entry. Within the cell, the pH is raised, which is assumed to be another factor of egg activation, along with enhancing or initiating protein biosynthesis, DNA replication, messenger RNA polyadenylation, glucose-6-phosphate dehydrogenase activity, potassium conductance, glycogenolysis, and thymidine uptake. These events go together with the pronucleus development and chromatin condensation. The cortical granule reaction does not seem to be affected by the raised pH.

Exocytosis of the cortical granules is another event that occurs during plasmogamy. The contents of the granules trigger the conversion of the ZP2 and ZP3 glycoprotein receptors for sperm to ZP2f and ZP3f, respectively, which are the inactivated forms. In the mouse, rabphilin-3A is involved in the process of calcium-dependent exocytosis on fertilization (5).

There are several explanations for the calcium release mechanism: It can be mediated by inositol triphosphate (IP_3) or be IP_3-independent, or it can be mediated by G-protein or tyrosine kinase-linked enzymes. It has been shown that IP_3 and diacylglycerol are involved in a number of signal transduction processes and that IP_3 is involved in the autocatalytic cycle of calcium release at fertilization (6). These observations have led to the assumption that the sperm induces an initial production of IP_3, but the mechanism of IP_3 generation has not been elucidated. In addition to this theory, the production of IP_3 and diacylglycerol is assumed to be linked to proteins, as their involvement was shown in several species in which G-proteins triggered the formation of IP_3. Up until now, however, no corresponding molecules were found that could support this kind of sperm-induced egg activation. It was also shown, in sea urchins, that ryanodine is able to induce calcium release through ryanodine receptors, which are distantly related to the IP_3 receptors. In experiments with agonists and antagonists of the IP_3 receptor, the involvement of both systems in calcium release was observed. When the IP_3-induced calcium release was blocked, however, other systems were not able to compensate. At this time, it must be assumed that a number of mechanisms act together to induce calcium release, but the main triggering mechanism is still not clear.

Bibliography

1. J. P. Evans, R. M. Schultz, and G. S. Kopf (1997) Dev. Biol. 187, 94–106.
2. J. P. Evans, G. S. Kopf, and R. M. Schultz (1997) Dev. Biol. 187, 79–93.
3. R. Yuan, P. Primakoff, and D. G. Myles (1997) J. Cell. Biol. 137, 105–112.
4. D. G. Myles, and P. Primakoff (1997) Biol. Reprod. 56, 320–327.
5. N. Masumoto, T. Sasaki, M. Tahara, A. Mammoto, Y. Ikebuchi, K. Tasaka, M. Tokunaga, Y. Takai, and A. Miyake (1996) J. Cell. Biol. 135, 1741–1747.
6. M. J. Whittaker, and R. F. Irvine (1984) Nature 312, 636–639.

Suggestion for Further Reading

7. F. J. Longo, ed. (1997) *Fertilization*, 2nd ed., Chapman & Hall, London, Weinheim, New York, Melbourne, Madras, pp. 49–65; provides further information concerning early events during plasmogamy.

Plastocyanin

Plastocyanins belong to the family of cupredoxins [ie, relatively small (~10 kDa, 97–104 amino acid) blue single copper proteins, including azurins] involved in electron transfer (1). They are

DNA to protein, it also plays a vital structural role in many ribonucleoprotein particles and, as is now recognized, can itself have catalytic activity. Whereas in the hypothetical RNA world, RNA would have acted unaided by other macromolecules, RNA almost invariably functions in modern organisms associated with RNA-binding proteins, a wide variety of which have now been identified. Although many RNA-binding proteins are uncharacterized structurally and do not fall into known categories, primary sequence analysis has led to the identification of a number of recurring RNA-binding motifs in functionally diverse RNA-binding proteins (1, 2). Interestingly in most cases, these are structurally and therefore probably evolutionarily distinct from DNA-binding motifs. RNA molecules are classified into various types based on their function or localization, such as transfer RNA (tRNA), messenger RNA (mRNA), ribosomal RNA (rRNA), viral RNA (vRNA), small nuclear RNA (snRNA), and small cytoplasmic RNA (scRNA). Table 1 gives some examples of RNA-binding proteins associated with each form, and Table 2 summarizes with examples the known RNA-binding motifs. Understanding how RNA-binding proteins specifically interact with their target RNA to form functional complexes is a key problem in structural biology, that has ramifications throughout molecular biology from transcription to protein biosynthesis and from replication of viruses to development of embryos and genetic disease.

Table 1. Selected RNA-Binding Proteins, their RNA Targets, and their Functions

RNA	RNA binding proteins	Function
tRNA	tRNA (m^5U54)methyl-transferase	General tRNA modification
	tRNA-guanine transglycosylase	Specific tRNA modification
	aminoacyl-tRNA synthetase	tRNA aminoacylation
	met-tRNAf^{met} formyltransferase	Prokaryote translation initiation
	IF3	Prokaryote translation initiation
	EF-Tu	tRNA transport to ribosome
M1 RNA	C5 protein	Subunit of E. coli Rnase-P endoribonuclease
mRNA/hnRNA	RNA polymerase II	Transcription
	GreA	Transcription termination
	hnRNP proteins	Pre-mRNA binding
	Sex-lethal	Pre-mRNA splicing
	mRNA capping enzyme	5′ capping enzyme
	E. coli RNase III	RNA processing
	ds RNA adenosine deaminase	mRNA editing
	CBP20, CPB80	Nuclear cap-binding protein subunits
	eIF-4F	Cytoplasmic cap binding protein
	Poly-A-polymerase, CStF	3′ poly-adenylation
	Poly-A-binding protein (PABP)	mRNA stability
	aCP-1, aCP-2	a-Globin mRNA stability
	Staufen	mRNA localization

	Endo-, exoribonucleases	mRNA degradation
	IRE-binding protein, E. coli	Translational regulation
	Threonyl-tRNA synthetase, T4 regA	Translational regulation
	Thymidylate synthase	Translational regulation
rRNA	RNA polymerase III	rRNA transcription
	Nucleolin	rRNA processing
	Nucleolar 2′-O-methyltransferase	rRNA modification
	TFIIIa	5s rRNA storage
	Sx, Lx	Small and large subunit ribosomal proteinss
snRNA	B, B′, D1, etc.	Core snRNP proteins (Sm-proteins)s
	U1A, U2B″, etc.	Specific SnRNP proteinss
	Human RNA helicase A	RNA helicases
vRNA	RNA-dependent RNA polymerase	Replications
	Viral nucleocapsid proteins	Assembly, protections
	MS2 coat protein	Viral capsid, translational repressors
	dsRNA-dependent protein kinase	Translation regulations
	Reverse transcriptase	Copying RNA to DNAs
RNA ligase	DNA ligase	Ligating RNAs
	HIV-Tat	Transcriptional activators
scRNA		
SRP RNA	Signal recognition particle proteins	Targeting of secretory proteinss
gRNA	TUTase	mRNA editings

Table 2. Various RNA-Binding Domains and Sequence Motifs[a, b]

Sequence Motif	Representative Proteins and Reference Describing Structure (in parentheses)	Target RNA
RNP domain	U1A spliceosomal protein (7)	U1 snRNA
	(9,10)	U1A protein mRNA
(RNA recognition motif)	U1 70k spliceosomal protein (1,6)	U1 snRNA
	hnRNP protein C (1)	mRNA precursor
		mRNA

	hnRNP protein A1[a]	precursor
	Poly(A)-binding protein (1)	mRNA poly(A) tail
dsRNA-binding motif	*E. coli* RNase III (12)	RNA transcript
	Drosophila Staufen (11)	Maternal bicoid mRNA
KH domain	hnRNP protein K (1)	mRNA precursor
	Fragile X protein (13)	Unknown
	Vigilin (14)	tRNA?
Zn-finger	TFIIIA (18)	5 S rRNA
S1 domain	Polynucelotide phosphorylase (15)	
	Ribosomal protein S1	mRNA
	Initiation factor 1	
Sm domain	Spliceosomal core proteins (2)	snRNAs
OB domain	Class IIb aminoacyl tRNA synthetase (19–21)	tRNA
RGG box	hnRNP proteins (1)	mRNA precursor
Alu binding module	SRP 14 / 9 heterodimer	Alu domain of SRP RNA

[a] Y. Shamoo, U. Krueger, L. M. Rice, K. R. Williams, and T. A. Steitz (1997) *Nature Struct. Biol.* **4**, 215–222; R.-M. Xu, L. Jokhan, X. Cheng, A. Mayeda, and A. R. Krainer (1997) *Structure* **5**, 559-570.

[b] M. Görlach, M. Friedrichs, G. Dreyfuss, and L. Mueller (1992) *Biochemistry* **31**, 9254.

Some of the important questions concerning the nature of protein-RNA recognition can be illustrated by considering tRNAs (see Transfer RNA). They function as adaptor molecules that specify amino acid residues corresponding to particular triplet codons. There are 20 aminoacyl-tRNA synthetases, one for each amino acid, and each of these enzymes must specifically recognize and aminoacylate only its cognate tRNA with its cognate amino acid (3, 4). In contrast, the prokaryotic elongation factor Tu (EF-Tu), which introduces aminoacylated tRNA (aa-tRNA) into the A-site of the ribosome, binds to all aa-tRNA (except initiator-Met tRNA and selenocysteinyl-tRNA) and hence must recognize features common to all elongator aa-tRNAs (5). These are two extreme examples of tRNA recognition mechanisms that are essential in maintaining the fidelity and efficiency of protein biosynthesis. The various tRNAs are transcribed as precursor RNA molecules and must be processed correctly by specific nucleases and a surprisingly large number of different base-modifying enzymes to form mature molecules. These modifying enzymes also have diverse specificities. Some recognize almost all tRNA [eg, tRNA (m^5U54)methyltransferase]. Others recognize a subset of tRNA (eg, tRNA-guanine transglycosylase), even a unique tRNA species.

A wide variety of RNA-binding proteins are involved in producing, processing, transporting, translating, and degrading mRNA, the most abundant single-stranded RNA in cells. mRNA in eukaryotes is capped at the 5′ end and polyadenylated at the 3′ end, and introns must be correctly excised by the splicing machinery. Mature mRNAs are transported from the nucleus to the cytoplasm for translation. Gene expression is regulated at the transcriptional level and also at the translational level by a variety of mechanisms mediated by mRNA-binding proteins. The controlled degradation of mRNA is also an important process, involving a complex set of endo- and exonucleases. All of these processes must interact precisely with a large number of specific or nonspecific RNA-binding proteins and enzymes.

RNA is an essential structural and functional component of many ribonucleoproteins (RNP). Assembly of these RNP requires specific recognition of RNA structure and/or base identity by RNP protein subunits. The ribosome itself contains RNA molecules, which are matured by splicing and modifying enzymes in the nucleolus in association with small nuclear RNP (snoRNP). The rRNA may actually play the key catalytic role in peptidyl transfer. Pre-mRNA splicing is a complicated regulated process, involving a number of small nuclear RNPs containing snRNA that form a dynamic complex known as the spliceosome. The substrate of the spliceosome is not naked RNA, but pre-mRNA (also known as heterogeneous nuclear RNA, hnRNA) complexed with various proteins that form particles known as hnRNP. The mammalian signal recognition particle (SRP) is an scRNP consisting of a 300-nucleotide 7 S RNA associated with six protein subunits. It binds to signal peptides at the N-terminal end of secreted proteins as they emerge from the ribosome and directs the nascent-chain/ribosome complex to receptors on the endoplasmic reticulum membrane in eukaryotic cells. Systems homologous to SRPs are found in all living cells. Ribonuclease P, a tRNA-processing endonuclease, is an RNP in which the RNA component plays the catalytic role. Telomerase is a complex enzyme consisting of template RNA and protein subunits that adds multiple repeats of a particular sequence onto the ends of chromosomal DNA. Many viruses contain RNA as their genetic element, and virally-coded RNA-binding proteins play essential roles in the very diverse modes of replication and assembly of viruses.

How do RNA-binding proteins recognize their RNA-binding sites? RNA is distinguished from DNA most readily by the presence of the ribose 2′-OH and because the extended RNA double helix is predominantly in the A-form and has helical parameters significantly different from DNA, which is normally in the B-form. These general features permit nonspecific double-stranded RNA-binding proteins to recognize their correct nucleic acid substrate (eg, dsRNA-dependent protein kinase). On the other hand, specific RNA-binding proteins have more difficulty recognizing undistorted A-form RNA, which is characterized by a deep, narrow major groove and a shallower minor groove. The bases in the major groove are not readily accessible to protein side chains for specific recognition by hydrogen bonding except near the beginning or ends of helices. By contrast, the readily accessible minor groove contains less information for base discrimination. This problem is in reality bypassed by the fact that most cellular RNA is single-stranded, which forms irregular structures comprising short helices resulting from Watson-Crick pairing of short complementary stretches interspersed with hairpins, internal loops, bulges, or pseudoknots. Many RNA-binding proteins specifically recognize irregular RNA structures whose bases are more exposed for hydrogen bonding or stacking interactions with protein side chains. Indeed, the irregularities may be specifically induced or enhanced by the protein/RNA interaction. Some RNA molecules fold further into complex tertiary structures (eg, tRNA) whose unique three-dimensional shape may be sufficient to define specific backbone interactions with an RNA-binding protein (eg, seryl-tRNA synthetase recognizing $tRNA^{Ser}$).

1. Domains and Motifs Found in RNA-Binding Proteins

The majority of the known RNA-binding proteins have modular structures that contain an RNA-binding domain combined with other auxiliary domains (1, 2). Four RNA-binding sequence motifs have been found in RNA-binding proteins from diverse species; therefore, it is considered that they arose early in evolution. These correspond to (1) the RNP domain, (2) the KH domain , (3) the dsRNA-binding domain, and (4) the S1 domain. X-ray crystallography has shown or NMR that they contain an a/b fold similar to those found in some ribosomal protein subunits, and it has been suggested that these RNA-binding motifs may have evolved from ribosomal proteins. This might help to explain why RNA-binding domains are generally distinct from DNA-binding domains. Notable exceptions are the zinc finger, OB fold, and homeodomain. It is an interesting observation that many known RNA-binding proteins are all b or a/b proteins that contain an exposed b-sheet. The crystalline structure of the complex between U1A protein and an RNA hairpin discussed later suggests why a b-sheet is a good RNA-binding surface.

1.1. RNP Domain

The RNP domain, also known as RNA recognition motif (RRM) or RNP-consensus sequence (RNP-CS) type RNA-binding domain, is found in more than 200 distinct RNA-binding proteins from diverse species (1, 2, 6). It is also the second most common protein sequence motif in the entire genome of the nematode Caenorhabditis elegans. These facts suggest that this module appeared early in evolution. The RNP domain is about 80 amino acid residues long and contains two highly conserved short sequence motifs called RNP octamer (RNP1) and RNP hexamer (RNP2). Some proteins contain only a single RNP domain, but others contain multiple copies. For example, the protein that binds to the polyadenylate (poly A) tail of mRNA in eukaryotes contains four tandem copies of the RNP domain.

The three-dimensional structure of the RNP domain first determined for U1A spliceosomal protein, indicated that it consists of a four-stranded antiparallel b-sheet flanked on one side by two a-helices. The RNP1 and RNP2 motifs are located in the two middle b-strands of the sheet, and the side chains of the three highly conserved aromatic residues within RNP1 and RNP2 are projected onto the surface of the b-sheet (in U1A one of these residues is replaced by a glutamine) (7). U1A protein is a protein component of U1 snRNP, a large RNA-protein complex involved in pre-mRNA splicing, and binds to an RNA hairpin that contains 10 nucleotides in the loop. The crystal structure of a complex between U1A protein and an RNA hairpin representing its binding site has been determined at 1.9 Å resolution (8). The RNA hairpin loop binds to the surface of the b-sheet as an open structure, and the first seven nucleotides of the loop are fitted into a groove formed on the surface of the b-sheet (Fig. 1). The polypeptide loop between the b2 and b3 strands protrudes through the RNA loop. The bases of the seven nucleotides are splayed, and the protein-RNA contacts are made almost exclusively by RNA bases. These seven bases stack on an adjacent base, a protein side chain, or both and also form an intricate hydrogen-bond network with protein side chains and the amide and carbonyl groups of the protein main chain. U1A protein also binds to the 3′ untranslated region of its own pre-mRNA and prevents its polyadenylation by directly interacting with poly-A polymerase. The binding site contains two internal loops, each with the AUUG(CU)AC heptamer found in U1 snRNA hairpin II (6, 9, 10).

Figure 1. Crystal structure of a complex between U1A spliceosomal protein and its hairpin RNA binding site in U1 snRNA (8). The contact surface of the protein molecule is shown, whereas the RNA is a skeletal model. The AUUGCAC sequence in the ten-nucleotide loop fits into the groove on the surface of the b-sheet and binds tightly through stacking and hydrogen bond interactions with the protein.

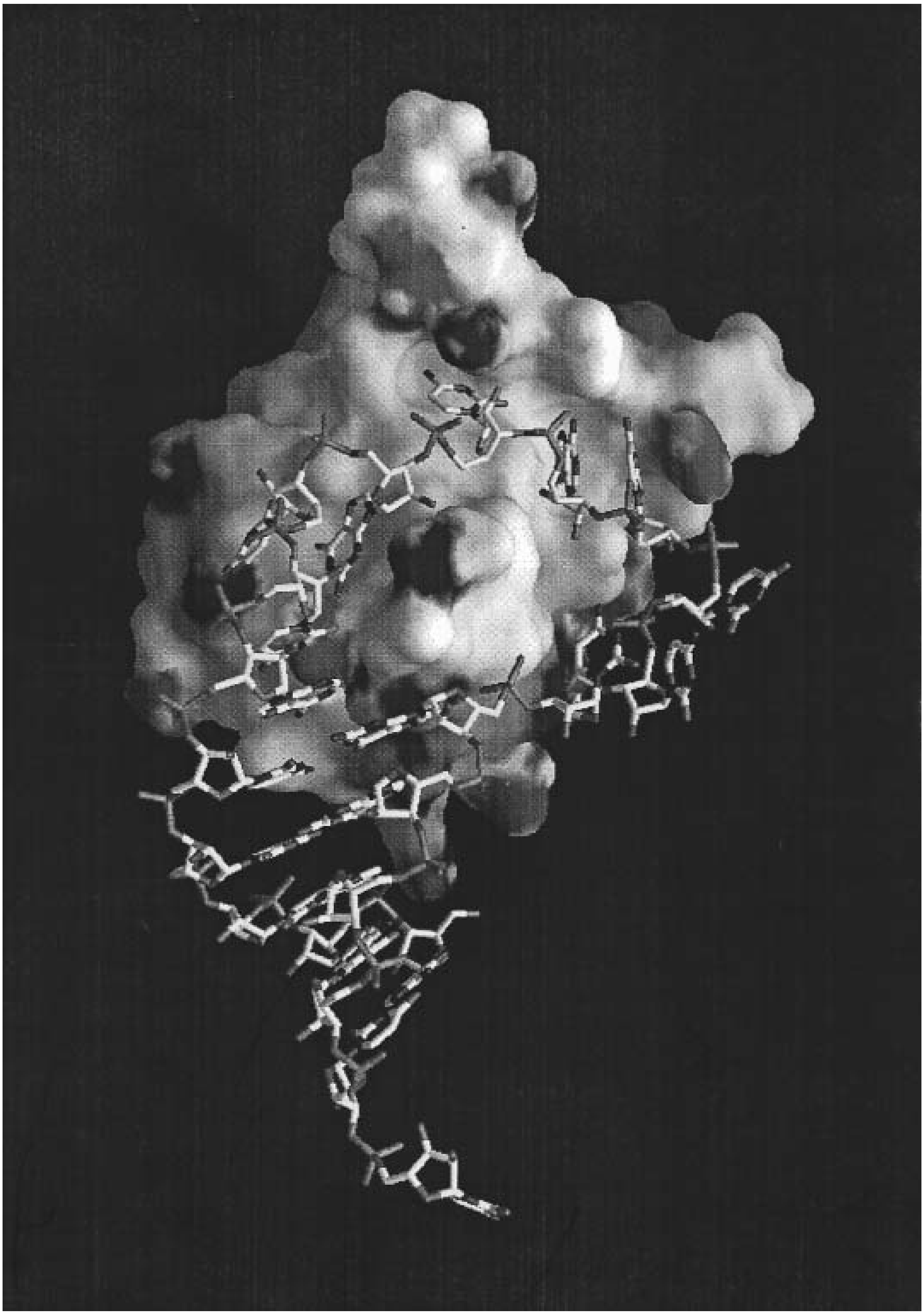

1.2. Double-Stranded RNA-Binding Domain (dsRBD)

The dsRBD is a short sequence motif found in multiple copies in RNA-binding proteins from diverse origins including *Escherichia coli*, *Drosophila*, *Xenopus*, and mammals. In the *Drosophila* embryo, Staufen protein binds to maternal bicoid mRNA and plays an important role in establishing the anterior-posterior polarity through mRNA localization (11). *E. coli* ribonuclease III is an important enzyme involved in processing ribosomal and transfer RNA. The dsRBD is also found in adenosine deaminase, which is a key enzyme in RNA Editing, and in the double-stranded RNA-dependent protein kinase, which plays an important role in viral gene expression. The NMR structures of dsRBD from RNase III and Staufen protein show that the module contains a three-stranded antiparallel b-sheet that has two a-helices packed on one side (11, 12). The dsRDB shows strong similarities to the N-terminal domain of *Bacillus stearothermophilus* ribosomal protein S5 at the levels of both amino acid sequence and three-dimensional structure (11). This strongly suggests that dsRBD may have evolved from a ribosomal protein. It is not yet known how this domain binds RNA, but site-directed mutagenesis experiments suggest that loops between b1 and b2 and between b3 and a2 may be involved in RNA-binding. The major groove of dsRNA is narrow and deep, and the bases are not accessible by protein side chains for sequence-specific interactions. It is likely that each dsRBD binds to the minor groove or to the phosphate backbone in the major groove. Biochemical experiments suggest that a set of dsRDB, together with some auxiliary domains, may recognize a structural feature of folded RNA.

1.3. KH Domain

Heterogeneous nuclear ribonucleoprotein (hnRNP) K is one of the nuclear proteins that bind to precursors of mRNA (1). There are three copies of a sequence motif within hnRNP K, and homologous sequences have been found in many proteins from diverse species, from bacteria to man, that interact with RNA. Human Fragile X (FMR1) gene contains two copies of the KH domain. A mutation in one of these is responsible for severe hereditary mental retardation (1, 13). The natural RNA target of the FMR1 gene product has not been identified, but the mutation that causes severe hereditary mental retardation abolishes the binding of poly(U) to the FMR1 protein. This suggests that the ability of FMR1 to bind to RNA is essential for its *in vivo* function. Two proteins that contain three copies of the KH domain are associated with the 3′ untranslated region of a-globin mRNA. These proteins affect the *in vivo* half-life of the a-globin mRNA. Ribosomal protein S3 from *E. coli* and other bacteria contains the KH domain, suggesting that the KH domains found in higher organisms have evolved from a ribosomal protein (1). The NMR structure of the KH domain from human vigilin has an a/b structure that contains a three-stranded b-sheet with three a-helices (14).

1.4. S1 Domain

Ribosomal protein S1 from *Escherichia coli* contains six copies of a short sequence motif of approximately 80 amino acid residues. S1 protein is directly involved in RNA binding because it can be cross-linked to mRNA in the translational initiation complex. The S1 domain has been found in proteins from bacteria and eukaryotes, including polynucleotide phosphorylase, initiation factor 1 (IF1), NusA, ribonucleases II and E from *E. coli*, yeast RNA helicase PRP22, eukaryotic initiation factor eIF2a, and eIF2a kinase inhibitor. An NMR study of the S1 domain of polynucleotide phosphorylase shows that this domain consists of a five-stranded antiparallel b-barrel (15).

1.5. MS2 Bacteriophage Coat Protein

One of the best studied examples of an RNA-binding protein is the MS2 bacteriophage coat protein. The MS2 phage contains a genomic RNA 3569 nucleotides long, packaged into an icosahedral protein shell that consists of 180 copies of the coat protein. A capsid protein dimer binds to an RNA hairpin formed near the ribosome-binding site of the virally encoded replicase gene, thereby inhibiting translation of the replicase mRNA. The interaction also triggers assembly of the coat protein and packaging of the genomic RNA. A synthetic RNA hairpin that represents the binding site was soaked into a crystal of the empty phage particle, and its structure was determined to 2.8 Å resolution (16). The RNA, which contains a tetraloop and a bulged adenosine, binds to the surface of the continuous b-sheet across the dyad axis. The side chain of a tyrosine residue stacks onto a cytidine in the tetraloop, and the bulged adenosine and an adenosine in the tetraloop bind to equivalent sets of residues from each subunit.

1.6. Zinc-Containing RNA-Binding Proteins

Transcription factor IIIA is a transcriptional activator of the 5 S rRNA gene, but it also binds to its gene product 5 S to rRNA, and functions as a storage or transport protein (17). It contains nine zinc fingers, each of which folds into a domain that contains two b-strands and one a-helix stabilized by the coordination of two histidine and two cysteine residues to a zinc ion. Crystallographic analyses of zinc finger proteins in complex with dsDNA show that the a-helix fits into the major groove of the

DNA and forms many sequence-specific contacts with the DNA bases (18). It is believed that 5 S rRNA folds into a branched double helix that contains many bulges which may widen the major groove of RNA to permit entry of the recognition helices. The HIV nucleocapsid protein is another example of a zinc-containing, RNA-binding protein. Others are *E. coli* alanyl-tRNA synthetase and tRNA guanine transglycosylase (28).

1.7. Other RNA-Binding Modules

The bases of the anticodon loops of $tRNA^{Asp}$ and $tRNA^{Lys}$ are splayed over the surface of a b-barrel domain of their cognate tRNA synthetases and are recognized in a sequence specific manner (see later) (19, 20). Many structural homologues of this b-barrel domain, which is known as the OB-fold, have been found in proteins that bind oligonucleotides (both ssRNA and ssDNA) or oligosaccharides (21).

The Sm proteins that form the core of spliceosomal small nuclear ribonucleoprotein particles (snRNP) contain a conserved sequence motif. It is predicted that this domain has an a/b fold, but its structure is yet to be determined (2). Some hnRNP proteins contain multiple repeats of an Arg-Gly-Gly (RGG) sequence that are believed involved in RNA binding (1).

The crystal structure of the SRP 9/14 heterodimer, which binds to the Alu domain of the mammalian signal recognition particle RNA, has been determined. SRP9 and SRP14 are structurally homologous and contain the same a-b-b-b-a fold, related to but distinct from the dsRNA-binding module. The heterodimer has pseudo two-fold symmetry and is saddle-like, comprising a strongly curved six-stranded amphipathic b-sheet. The four helices are packed on the convex side, and the exposed concave surface is lined with positively charged residues.

Both HIV tat and rev proteins bind the TAR and RRE elements, respectively, to their target RNA sequences, by arginine-rich peptides. The solution structure of a 14-residue arginine-rich peptide from BIV tat complexed with BIV TAR has been determined by NMR (26). The peptide forms a b-hairpin that interacts in the RNA major groove.

2. tRNA-Binding Proteins

2.1. Aminoacyl-tRNA Synthetases

The fidelity of protein synthesis depends to a large extent on the extreme specificity with which aminoacyl-tRNA synthetases charge their cognate tRNA with their cognate amino acid. In *E. coli*, there are at least 46 different tRNA molecules that have anticodons which correspond to the various amino acids. The seryl-tRNA synthetase, for example, has to charge the six serine isoacceptors (including one for selenocysteine) selectively and ignore the others. Because tRNA superficially have similar secondary and tertiary structures, what is the molecular basis for the specific recognition between aminoacyl-tRNA synthetases and tRNA? In many cases, extensive biochemical studies have revealed the so-called tRNA identity elements (see Aminoacyl tRNA Synthetases).

A more detailed picture of specific tRNA recognition and catalysis by aminoacyl-tRNA synthetases is emerging from crystallographic studies of aminoacyl tRNA synthetases complexed with various combinations of their three substrates: ATP, cognate amino acid, and cognate tRNA, plus the activated amino acid intermediate, the aminoacyl-adenylate. Now crystal structures are known of 14 of the 20 aminoacyl tRNA synthetases, five of which are in complexes with cognate tRNA (3, 4). The three systems, for which the most extensive structural data exists on protein-tRNA recognition, are the class I glutaminyl system and the class II aspartyl and seryl systems. These show strikingly different modes of specific synthetase-tRNA interaction but share certain general features, including a fairly large synthetase-tRNA interactive interface characterized by (1) nonspecific backbone contacts, often involving basic residues, both of which increase binding affinity and aid correct positioning and orienting the tRNA; (2) discriminatory base-specific interactions restricted to a few regions, principally the anticodon and the acceptor stem. The second general feature is mutual induced fit by which protein-RNA contacts are made as a result of conformational changes in either or both macromolecules. This includes ordering of protein loops and reorienting and stabilizing domains (eg, SerRS), base-pair breaking in the acceptor stem, and 3′-end distortion (eg, tRNA^{Gln}) and destacking of bases in the anticodon loop (eg, tRNA^{Gln}, tRNA^{Asp}).

2.2. Glutaminyl-tRNA Synthetase (GlnRS)

GlnRS is a monomeric class I synthetase whose specificity for tRNA^{Gln} is largely determined by interactions with identity elements in the tRNA acceptor stem and anticodon stem-loop, both of which have severe distortions from the structure found in uncomplexed tRNA. In the E. coli complex, the tRNA anticodon stem is extended from five to seven base pairs by two extra non-Watson–Crick base pairs (23). The three anticodon bases (CUG) are splayed to fit into three separate recognition pockets formed at the interface between distal two b-barrel domains of the protein. In the active site of the synthetase, the tRNA is oriented so that specific interactions can be made within the acceptor stem's minor groove to identity determinants in base pairs 2 and 3. On the other hand, the tRNA 3′-end reaches the catalytic center only by forming an unusual hairpin turn. This conformation requires breaking the first U1-A72 base pair and is stabilized, in part, by a hydrogen bond between the discriminator base G73 and the phosphate of A72.

2.3. Aspartyl-tRNA Synthetase (AspRS)

AspRS is a dimeric class IIb synthetase that binds two tRNAs symmetrically, although each tRNA interacts predominantly with only one subunit. In contrast to class I, class II synthetases interact with the acceptor stem of their cognate tRNA from the major groove side (27) by the so-called motif 2 loop, which in yeast AspRS makes base-specific interactions with the discriminator base G73 and base pair U1-A72 (19). The major groove side recognition also means that the single-stranded 3′-end of the tRNA enters the synthetase active site without significant distortion from its normal helical path, again in strong contrast to class I. Anticodon recognition by AspRS is performed by an N-terminal, five-stranded, b-barrel domain (OB fold) (21). The normal compact structure of the free tRNA anticodon loop undergoes a large conformational change, and the five anticodon loop bases are exposed to the exterior. The three anticodon bases (GUC) lie across the b-sheet surface and are recognized by specific hydrogen bonding interactions (19). Recent crystallographic results on another closely related class IIb synthetase complexed with its cognate tRNA, T. thermophilus lysyl-tRNA synthetase, show a very similar interaction between the anticodon of tRNA^{Lys} (CUU) and the N-terminal, b-barrel domain of LysRS (20). Whereas the central U35 interacts identically in the two systems (by stacking with a conserved phenylalanine residue and hydrogen bonding with conserved glutamine and arginine residues), the specificity for base 36 and to a lesser extent for base 34 is idiosyncratic for each synthetase.

2.4. Seryl-tRNA Synthetase (SerRS)

SerRS is also a dimeric class II synthetase, but its mode of tRNA recognition differs significantly from that of AspRS (Fig. 2). SerRS is characterized by a unique 100-residue, N-terminal domain that is folded into a 60 Å long, solvent exposed and flexible, antiparallel coiled coil, known as the helical arm (24, 25). The variety of serine anticodons from two distinct groups means that the serine isoacceptors share no common anticodon base. Thus, the anticodon is not an identity element of tRNA^{Ser}, whereas the long variable arm is, a feature shared only by tRNA^{Leu} and tRNA^{Tyr}. The main features of the recognition of tRNA^{Ser} by T. thermophilus SerRS are (1) the tRNA binds across the two subunits of the dimer; (2) upon tRNA binding the helical arm of the synthetase is stabilized in a new orientation and binds between the TΨC loop and the long, variable arm of the tRNA; (3) contacts with the tRNA long, variable-arm backbone extend until the sixth base pair, explaining the need for a minimum length of the tRNA variable arm; (4) the synthetase makes many backbone contacts, but few base-specific interactions, and is principally recognizing the unique shape of tRNA^{Ser}. The unique shape of tRNA^{Ser} is largely determined by bases 20A and 20B inserted into the D-loop, both of which play novel roles in tertiary interactions in the tRNA core. In particular, the base of G20B is stacked against the first base pair of the long variable arm and thus defines the spatial orientation of the latter; (5) the anticodon stem loop is not in contact with the synthetase; (6)

the motif 2 loop of SerRS (longer than that of AspRS) makes base contacts down to the fourth base pair within the acceptor stem's major groove, but they are, however, only weakly discriminatory (25).

Figure 2. Overall view of the ternary complex of seryl-tRNA synthetase, tRNA^{Ser}(GGA), and a nonhydrolyzable analog monomer 1 is in yellow, and monomer 2 is in blue. Only the backbone and its secondary structure are shown (arrows ar tRNA backbone is in red, and the bases are in green. The tRNA is viewed looking down the anticodon stem, which is no in the figure. The long variable arm of the tRNA crosses the helical arm of monomer 2 perpendicularly and emerges at t the Ser-AMS molecule is represented by spheres. See color insert.

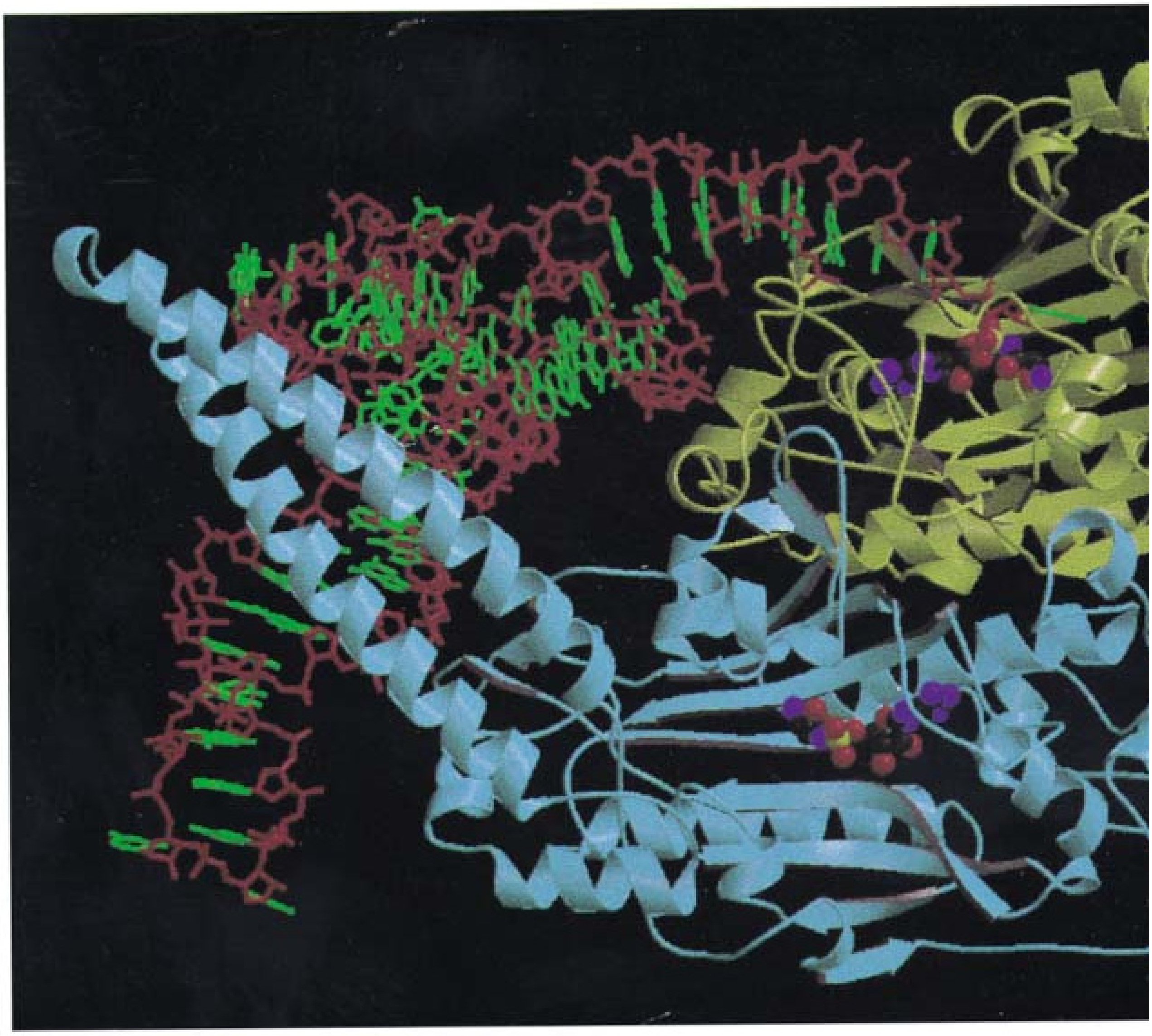

2.5. Elongation Factor EF-Tu

EF-Tu is a G-protein that, in the activated GTP-bound state, binds all aminoacylated elongator tRNA with higher affinity than uncharged tRNA and delivers them to the ribosome. The crystalline structure of the ternary complex of yeast tRNA^{Phe}, T. aquaticus EF-Tu and GDPNP has recently been determined and reveals how activated EF-Tu contacts relatively limited and conserved regions of aa-tRNA (6). The only parts of the aa-tRNA in contact with EF-Tu are the aminoacylated CCA end, the 5′ phosphate, and the T-stem helix. The long stem of the L-shaped tRNA projects away from the protein, so that the entire complex is extremely elongated. The CCA-3' end binds in a cleft between domains 1 and 2 of EF-Tu, and conserved residues from domain 2 interact with the base and phosphate of A76. Main-chain hydrogen bonds from EF-Tu are made to the ester group linking the carboxyl group of the amino acid to the 3'OH of the ribose and to the free amino group of the amino acid. The amino acid itself projects into a pocket formed between domains 1 and 2. The tRNA 5' phosphate is bound by conserved basic residues in helix B of domain 1 and from domain 2. One side of the T-stem helix is packed against a depression between domains 1 and 3. The contacts are made by nonconserved residues from domain 3.

It has been pointed out that the EF-Tu.GTP.tRNA^{Phe} ternary complex extraordinarily similar in shape to that of the elongation factor EF-G.GDP binary complex. This mimicry suggests that the two complexes might bind to the same ribosomal state.

Bibliography

1. C. G. Burd and G. Dreyfuss (1996) Science 265, 615–621.
2. K. Nagai (1994) Curr. Opinion Struct. Biol. 6, 53–61.
3. J. G. Arnez and D. Moras (1994) RNA-protein interactions (ed, K. Nagai and I. W. Mattaj, eds.), IRL Press, Oxford, pp. 52–81.
4. S. Cusack (1995) Nature Struct. Biol. 2, 824–831.
5. P. Nissen, M. Kjeldgaard, S. Thirup, G. Polekhina, L. Reshetnikova, B. Clark, and J. Nyborg. (1995) Science 270, 1464–1472.
6. K. Nagai, C. Oubridge, N. Ito, J. Avis, and P. Evans (1995) Trends Biochem. Sci. 20, 235–240.
7. K. Nagai, C. Oubridge, T.-H. Jessen, J. Li, and P. R. Evans. (1990) Nature 348, 515–520.
8. C. Oubridge, N. Ito, P. R. Evans, C. H. Teo, and K. Nagai (1994) Nature 372, 432–438.
9. F.-H. T. Allain, C. C. Gubser, P. W. A. Howe, K. Nagai, D. Neuhaus, and G. Varani (1996) Nature, 380, 646–650.
10. C. W. G. van Gelder, S. I. Gunderson, E. J. R. Jansen, W. C. Boelens, M. Polycarpou-Schwartz, I. W. Mattaj, and W. J. van Venrooij (1993) EMBO J. 12, 5191–5200.
11. M. Bycroft, S. Grünert, A. G. Murzin, M. Proctor, and D. St. Johnston (1995) EMBO J. 14, 3563–3571.
12. A. Kharrat, M. J. Macias, T. J. Gibson, M. Nilgens, and A. Pastore (1995) EMBO J. 14, 3572–3584.
13. H. Siomi, M. Choi, M. C. Siomi, R. L. Nussbaum, and G. Dreyfuss. (1994) Cell 77, 33–39.
14. G. Musco, G. Stier, C. Joseph, M. A. C. Morelli, M. Nilges, T. J. Gibson, and A. Pastore (1996) Cell 85, 237–245.
15. M. Bycroft, T. J. P. Hubbard, M. Proctor, S. M. V. Freund, and A. G. Murzin (1997) Cell 88, 1–20.
16. K. Valegård, J. B. Murray, P. G. Stockley, N. J. Stonehouse, and L. Liljas (1994) Nature 371, 623–626.
17. J. Miller, A. D. McLachlan, and A. Klug (1985) EMBO J. 4, 1609–1614.
18. N. P. Pavletich and C. O. Pabo (1991) Science 252, 809–817.
19. J. Cavarelli, B. Rees, M. Ruff, J. C. Thierry, and D. Moras (1993) Nature 362, 181–184.
20. S. Cusack, A. Yaremchuk, and M. Tukalo (1996) EMBO J. 15, 6321–6334.
21. A. G. Murzin (1993) EMBO J. 12, 861–867.
22. M. A. Rould, J. J. Perona and T. A. Steitz (1991) Nature 352, 213–218.
23. V. Biou, A. Yaremchuck, M. Tukalo, and S. Cusack (1994) Science 263, 1404–1410.
24. S. Cusack, A. Yaremchuk, and M. Tukalo (1996) EMBO J. 15, 2834–2842.
25. J. D. Puglisi, L. Chen, S. Blanchard, and A. D. Frankel (1995). Science 270, 1200–1203.

26. M. Ruff et al., (1991) Science 252, 1682–1689.
27. C. Romier, K. Reuter, D. Suck, and R. Ficner (1996) EMBO J. 15, 2850–2857.

Suggestions for Further Reading

28. K. Nagai and I. W. Mattaj (1994) RNA-Protein Interactions, IRL Press, Oxford.
29. R. Gestland and J. Atkins (1993) The RNA world, Cold Spring Harbor Press, Cold Spring Harbor, New York.
30. D. E. Draper (1995). Protein-RNA recognition, Annu. Rev. Biochem. 64, 593–620.
31. D. Söll and U. L. RajBhandary (1995) tRNA, Structure, Biosynthesis and Function, ASM Press, Washington, D.C.

ROESY Spectrum

A conventional nuclear Overhauser effect (NOE) experiment in nuclear magnetic resonance (NMR) spectroscopy involves detection of changes in the intensities of NMR signals associated with a particular spin of the molecule being examined, when other spins are perturbed in some way. The changes in signal intensity are the result of altered populations of nuclear spin energy levels associated with both sets of spins and reflect their physical proximity. There may be magnetic interactions between spins while they are in coherent states and these may lead to changes of signal intensity. This second kind of Overhauser effect is detected in a "rotating frame" NOE (or ROE) experiment. The ROE may be determined in a one-dimensional format or be incorporated into multidimensional experiments. A two-dimensional (2D) ROE experiment is often referred to as ROESY (rotating frame Overhauser effect spectroscopy). In such a 2D experiment, the appearance of a cross peak at the chemical shift coordinate (A, B) requires that there be a ROE between the spins characterized by these chemical shifts (δ_A, δ_B). The power of experiments that produce ROEs or NOEs is that changes in signal strength are strongly dependent on the distance between interacting spins. Thus, the observation of a ROE or NOE provides a constraint that can be used to define the tertiary structure of the macromolecule being studied.

For the standard NOE experiment wherein the detected signal intensity changes arise from alterations of spin energy level populations, the effect is given by

(1)

where $f_I\{S\}$ indicates the NOE on the signal from spin I when there is a perturbation of level populations associated with spin S; I_0 is the normal intensity of the signal for spin I observed from a sample at thermal equilibrium before the analyzing RF pulse, and I_p is the intensity of the same signal when there has been a perturbation of spins S before the analyzing pulse. The value of $f_I\{S\}$ depends on the gyromagnetic ratios of spins I and S, how these spins move in the sample, the strength of the magnetic field used for the NMR experiment, and the details of how the energy level populations associated with spin S are perturbed during the course of an experiment. Values of $f_I\{S\}$ ranging from 0.5 to -1.0 are possible when both I and S are protons. It should be noted that, given the definition of $f_I\{S\}$, some set of experimental conditions may exist for which $f_I\{S\}$ becomes zero. Under these conditions, there is little or no change in signal intensity, even though spins I and S might be very close to each other. These conditions are typically experienced when the mass of the molecule under study is in the range of 500–2000 D.

In contrast, the ROE on signal intensities is always positive for near-neighbor nucleus-nucleus interactions and thus remains detectable under all experimental conditions (1-3). This very significant advantage is countered, however, by the need to correct the experimental data for various artifacts and by the possibility that coherence transfers may produce effects that are unrelated to the ROE. Analysis of ROE data in conjunction with conventional NOE data may provide important insights into existing chemical exchange processes (4). Although most ROESY experiments with biological macromolecules involve interactions between hydrogen ^{1}H atoms, useful heteronuclear ROESY experiments also are feasible (5). The elements of the ROESY experiment can be built into experiments that produce three-dimensional or higher NMR spectra. (See also Nuclear Overhauser Effect (NOE), NOESY Spectrum.)

Bibliography

1. A. A. Bothner-By, R. L. Stephens, J. M. Lee, C. D. Warrren, and R. W. Jeanloz (1984) J. Am. Chem. Soc. 106, 811–813.
2. A. Bax and D. G. Davis (1985) J. Magn. Reson. 63, 207–213.
3. D. Neuhaus and M. P. Williamson (1989) The Nuclear Overhauser Effect in Stuctural and Conformational Analysis, V.C.H., New York, Chapter "9", pp. 307–350.
4. J. Fejzo, W. M. Westler, S. Macura and J. L. Markley (1991) J. Magn. Reson. 92, 20–29.
5. G. W. Kellogg and B. I. Schweitzer (1993) J. Biomol. NMR 3, 577–595.

Suggestions for Further Reading

6. C. J. Bauer, T. A. Frenkiel, and A. N. Lane (1990) J. Magn. Reson. 87, 144–152.
7. T. E. Bull (1992) Prog. NMR Spectroscopy 24, 377–410.
8. D. Canet (1996) NMR Concepts and Methods, Wiley, New York, Chapter "4", pp. 139–196.
9. J. Cavanagh, W. J. Fairbrother, A. G. Palmer III, and N. J. Skelton (1995) Protein NMR Spectroscopy, Academic Press, San Diego.

Rolling Circle DNA Replication

In DNA replication, the DNA polymerase cannot initiate the synthesis of a new DNA strand and must rely on a priming device. In general, an RNA primer is synthesized at or near a replication origin to start synthesis of the leading strand. However, a DNA primer terminus can be generated by a nuclease-generated nick at a specific place in some circular duplex DNA, and replication will then proceed unidirectionally, as shown in Figure 1. This mode of replication is called rolling circle replication and is found for replication of the replicative form (RF) form of bacteriophage single-stranded genomes of Gram-negative bacteria and of the multicopy plasmids of Gram-positive bacteria (see Single-Stranded DNA Replication). Rolling circle replication is also observed in the late stage of the replication of the lambda phage genome and in the process of the conjugative transfer of bacterial plasmids.

Figure 1. Scheme for rolling circle replication (see text for details).

DNA synthesis initiates using the free 3'-OH end at the nick as a primer, and a replication fork proceeds around the template. In the process, the newly synthesized strand displaces the old strand from the template. In the case of replication of the RF form of single-stranded phage genomes and of plasmids of Gram-positive bacteria, the displaced old strand is cleaved off after one round of replication and is converted into the circular, double-stranded form. In contrast, in phage lambda replication, the replication fork proceeds a number of revolutions around the template without cleavage of the displaced strand, and the displaced strand becomes double-stranded as it is peeled off. The linear concatemer thus created is cleaved into one unit length and packaged into the phage particles. In the conjugation process of plasmids, this displaced strand is transferred into the new cell.

The initial nick of rolling circle replication is introduced by an endonuclease specific for each system. The similarity of the amino acid sequences of the initiator endonucleases and of the proteins (known as relaxases) involved in the initiation and termination of conjugative DNA strand transfer clearly indicate that they are evolved from a common ancestor (1, 2).

Bibliography

1. T. V. Ilyina and E. V. Koonin (1992) Nucl. Acids Res. 20, 3279–3285.
2. D. R. Byrd and S. W. Matson (1997) Mol. Microbiol. 25, 1011–1022.

Rossmann Fold

In the 1970s, Rossman and colleagues (1, 2) identified, analyzed, and characterized the similarity between the protein structures of lactate dehydrogenase and malate dehydrogenase, two enzymes that bind the dinucleotide NAD. Both protein structures incorporate two b–a–b–a–b protein motifs, and each half of the bound dinucleotide binds to one of these units. The b–a–b–a–b structural motif, which forms a parallel b-sheet surrounded by a-helices, is referred to as either a Rossmann fold or a mononucleotide-binding motif.

[See also Nucleotide Binding Motif.]

Bibliography

1. S. T. Rao and M. G. Rossmann (1973) J. Mol. Biol. 76, 241–256.
2. M. G. Rossmann, D. Moras, and K. W. Olsen (1974) Nature 250, 194–199.

R_0T Curve

1. DNA–RNA Hybridization

During purification of messenger RNA, its quantity and the extent of purification can be determined by hybridization techniques. This also permits determining the size of the mRNA independently by gel electrophoresis.

Hybridization involves annealing a large excess of RNA with double-stranded DNA previously radiolabeled by nick translation or during its synthesis. Such labeling techniques result in a high specific radioactivity, so the necessary excess of RNA can be obtained easily. Heating double-stranded DNA denatures it to its single-stranded components and slow cooling of these single strands permit renaturation. This technique is used in C_0t curves to characterize DNA samples. Hall and Spiegelman (1) demonstrated that the same experiment can be performed with heat-denatured DNA and the corresponding mRNA, and slow cooling produces DNA–mRNA hybrids that were observed in cesium chloride density gradient centrifugation. When mRNA was heated with genetically unrelated DNA, no hybrid molecules were formed.

1.1. Kinetics of Association

DNA–RNA hybridization is a second-order reaction (see Kinetics). If t is the time, D the concentration of single-stranded DNA in moles of nucleotides/liter, R the concentration of excess mRNA in the same units, and k the rate constant for the reaction, then the equation describing the reaction is the following:

The value of k is expressed in units of .

DNA self-reassociation is avoided by using a low concentration with RNA in excess. Then the RNA hybridizes much faster than the DNA, and its concentration remains practically constant throughout the reaction. The reaction follows pseudo-first order kinetics, and the equation above simplifies to the following:

R_0 is the mRNA concentration at .

By substituting at , the integrated equation becomes

When 50% of the DNA (cDNA) strands have been converted into DNA-RNA hybrids, at D becomes $D_0/2$, and R_0t becomes $R_0t_{1/2}$. This yields

from which the value of k can be derived by

Therefore the velocity of the association reaction is inversely proportional to the value $R_0t_{1/2}$, which itself is directly related to the size of a pure RNA or DNA molecule.

1.2. Determining mRNA size and evaluating a given mRNA in an RNA mixture

Knowing the size a of a given mRNA, the unknown size x of another mRNA is determined by the following equation:

For ovalbumin mRNA, which is 2000 nucleotides long, the $R_0t_{1/2}$ value is $4 \times 10^{-3} M^{-1} s^{-1}$. For prolactin mRNA (900 nucleotides long) the $R_0t_{1/2}$ value is accordingly smaller: $1.8 \times 10^{-3} m^{-1} s^{-1}$ (2).

The values of $R_0t_{1/2}$ allow determining the fraction of a certain mRNA in a mixture by comparing hybridization of the corresponding cDNA with the corresponding “pure” mRNA and with the same mRNA in a mRNA mixture. Because the size of the studied mRNA is constant, its reassociation rate depends only on its concentration in the mixture, according to the equation

The course of hybridization is monitored by determining the number of DNA–RNA hybrids at various reaction times. This is done in two ways (2):

1. by applying the reaction mixture to a chromatography column of hydroxyapatite in 0.05 M phosphate buffer at pH 6.8 and at a temperature of 60°C. The single-stranded DNA elutes with 0.14 M phosphate buffer, whereas the double-stranded DNA–RNA molecules elutes with 0.45 M phosphate buffer.
2. by digestion with S1 nuclease, which digests single-stranded DNA, whereas RNA–DNA hybrids remain unaffected and are precipitated with trichloroacetic acid.

2. Determining the Number of Different Sequences in mRNA Transcribed from a cDNA Library

To judge whether a cDNA library is representative, ie, whether the number of different clones carrying a particular cDNA insert reflects the relative fraction of the corresponding mRNA molecules in the cell from which the library has been prepared, the number of different mRNA sequences in the mRNA population is determined. This is done by hybridizing highly labeled cDNA with an excess of mRNA. The amount of hybridized DNA at any time t is plotted as a function of R_0t. The kinetic curve yields the number of kinetic classes of mRNA molecules and their $R_0t_{1/2}$ values. The values are corrected to obtain the values that would have been obtained if each of the classes had been considered on its own. The values are also corrected for the nonspecific poly-dA sequences in the cDNA from the mRNA poly A tails, which do not contribute to hybridization. Then the corrected $R_0t_{1/2}$ values are used to determine the number of different sequences in each kinetic class by comparing them with the values of mRNA of known complexity ((3),(4)).

References

1. B. D. Hall and S. Spiegelman (1961) Proc. Natl. Acad. Sci. USA 47, 134–146.
2. R. A. Maurer (1980) J. Biol. Chem. 255, 854–859.
3. J. O. Bishop et al. (1974), Nature 250, 199–204.
4. S. J. Flint (1980) In J. H. Setlow and A. Hollaender, eds., Genetic Engineering, Plenum Press, New York, Vol. 2, pp. 47–82.

Rous Sarcoma Virus (RSV)

Rous sarcoma virus (RSV) was discovered in the extract of chicken sarcoma by Dr. P. Rous in 1911 as the first infectious reagent that causes tumors, and it is now known to be the prototype oncogenic retrovirus (Oncovirinae). It is widely accepted that ALV (avian leukosis virus), a replication-competent retrovirus carrying the genes gag (internal structural proteins), pol (reverse transcriptase and DNA endonuclease) (see HIV (Human Immunodeficiency Virus) and Hepatitis B Virus), and env (envelope glycoproteins), had once picked up a gene present in the chicken chromosome, now designated as cellular src (c-src), during its replication cycle as a rare event. RSV therefore carries an extra gene designated viral src (v-src) (because it is derived from c-src) at the extreme 3′ region of the genome, and it can be expressed from a subgenomic messenger RNA produced by RNA splicing (Fig. 1). By changing from c-src upon its integration into the virus genome and by accumulation of mutations during the subsequent propagation of virus, this virus gene had acquired the ability to cause neoplastic transformation in chickens. High-level expression of c-src, however, does not cause such transformation. The products of both these v-src and c-src genes are now known to be tyrosine-kinases, with molecular weights of 60 kDa, and $p60^{v\text{-}src}$ has much higher kinase activity than does $p60^{c\text{-}src}$.

Figure 1. Proviral DNA structure of Rous sarcoma virus. The line at the top indicates the chromosomal DNA containing proviral DNA. SD, splicing donor site; and SA, splicing acceptor site. Three transcripts are produced from the LTR promoter, as shown below.

This prototype virus, however, is exceptional among RNA tumor viruses in that it is replication-competent. All the other oncogenic retroviruses acquired proto-oncogenes at the expense of a part of their genomes that is essential for virus replication, and they therefore require the association of other replication-competent virus such as ALV (often called helper virus) for their propagation. Because of the advantage of this exceptional genome structure, RSV has been historically used in laboratory for the analysis of neoplastic transformation in cell culture; virus titers, which were originally assayed by sarcoma formation in the injected chicken, are now determined much more easily by formation of a focus (a group of transformed cells) in infected chicken embryo fibroblasts (CEFs). RSV-infected CEF assume refractile morphology and acquire the ability to grow in soft agar (anchorage-independent growth). These phenotypes unique to cellular transformation are maintained even after cell divisions, because the virus genome is also replicated as a proviral DNA that is integrated into the host chromosome.

One of the breakthroughs in oncogene research was the isolation of unique temperature-sensitive mutants of RSV. These mutant RSVs were replication-competent independent of the temperature, but the transformation phenotypes of the infected cells were temperature-dependent. At 37°C, infected cells assume fully transformed morphology, while cells become flatter and assume very similar morphology to that of uninfected CEF at 40°C to 41°C. These observations led to the discovery of oncogenes and revealed the following basic ideas about them:

1. RSV encodes a gene responsible for the initiation of cellular transformation (the oncogene now known to be v-src, described above).
2. The oncogene is not necessary for the viral replication.
3. Continuous function of the oncogene is necessary for the maintenance of cellular transformation. (This observation excluded another hypothesis, the "hit and run theory," in which the virus infection process is supposed to cause irreversible phenotypic changes to the host cells.)

It is also noteworthy that RSV-based avian retrovirus vectors are now widely used as a powerful tool for basic research. By transfecting plasmid DNA carrying a proviral DNA in which the v-src sequence was substituted with an exogenous gene, replication-competent virus vectors expressing the exogenous gene can be recovered from the culture fluid of the transfectants and used to introduce foreign genes into several avian primary cells, embryos, or adults quite efficiently.

Suggestion for Further Reading

J. M. Coffin, S. H. Hughes, and H. E. Varmus (1997) *Retroviruses*, Cold Spring Harbor Laboratory Press, Cold Spring Harbor, NY.

S-Adenosyl-L-Methionine

S-Adenosyl-L-methionine (AdoMet), one of nature's most intriguing biological objects, is a sulfonium compound, first described by Cantoni (1), that is synthesized in every cell from L-methionine and adenosine triphosphate (ATP) by methionine adenosyl transferase (MAT).

(1)

MAT catalyzes a most unusual reaction where ATP serves as the donor of its adenosine moiety, while its triphosphate chain is cleaved nonrandomly by the intrinsic triphosphatase activity of MAT itself, with the a and the b phosphates yielding inorganic pyrophosphate (PP_i) and the g phosphate yielding orthophosphate, P_i (2). It is noteworthy that the triphosphatase activity of MAT is stimulated by AdoMet (3). MAT is found in every cell, and the amino acid sequences of enzymes isolated from species that are separated by more than a billion years in evolutionary divergence (see Divergent Evolution), such as *Escherichia coli* (4) and humans (5, 6), exhibit an extraordinary degree of homology.

Elucidation of the structure of AdoMet as a sulfonium compound and clarification of the mechanism of its biosynthesis revealed that, in the reaction catalyzed by MAT, the chemical energy of the pyrophosphate bonds in ATP is utilized for the synthesis of a new class of energy-rich compounds. At physiological pH, the free energy of hydrolysis of a sulfonium compound is equivalent to that of the pyrophosphate bond in ATP (see Adenylate Charge, Free Energy Relationships), and the reaction is essentially irreversible, because it is accompanied by the release of a proton (7).

AdoMet was first identified as the source of methyl groups for biological transmethylation reactions (8), but it was anticipated that the energetic equivalence of the bonds linking the three ligands to the sulfur atom would enable AdoMet to function biologically as a source of either alkyl or adenosyl groups, thereby endowing AdoMet with unique biochemical versatility (9). Experimentally, Tabor et al. (10, 11) made the important discovery that *S*-adenosylpropylamine, a sulfonium compound resulting from the enzymatic decarboxylation of AdoMet (12), can serve as a donor of propylamine in the synthesis of spermidine from putrescine, and of spermine from spermidine (11). AdoMet decarboxylase is particularly interesting from the mechanistic point of view, since it has a covalently bound pyruvate that is required for activity (13). AdoMet decarboxylase and the propylaminetransferases are widely distributed in nature having been found in bacteria, yeast (14), and vertebrates. The synthesis of polyamines is of great biological importance although, quantitatively, it is less significant than biological transmethylation.

The biochemical availability of the groups linked to the sulfonium center of AdoMet was demonstrated by Nishimura et al. (15), who showed that AdoMet can serve as a donor of the aminobutyryl group to S-RNA, and more recently by Knappe (16) and by Reichardt and collaborators, who demonstrated that AdoMet can serve as an adenosine donor (17, 18). Finally Adams and Yang (19, 20) discovered in fruit ripening that AdoMet is cleaved to thiomethyl-adenosine and 1-aminocyclopropane-1-carboxylic acid. This reaction is of great biological significance, in that 1-aminocyclopropane-carboxylic acid is further metabolized to ethylene, a plant hormone that initiates fruit ripening and regulates many aspects of plant growth and development. Thiomethyl-adenosine is cleaved phosphorolytically to adenine and thiomethyl ribose 1-phosphate, in the first step of a salvage pathway that results in the regeneration of methionine (21).

In these reactions, AdoMet functions as a donor of one of the three ligands attached to the sulfonium atom. In addition, it has been shown that its 6 amino group is utilized in the synthesis of 7,8-diaminopelargonic acid, an intermediate in the synthesis of biotin (22). The mechanism of this reaction is entirely unknown, but it demonstrates the biochemical versatility of AdoMet.

In addition, AdoMet plays a role as a positive or as a negative allosteric effector (see Allostery) in the regulation of the key reactions that affect the metabolism of homocysteine. This amino acid can either be remethylated to methionine by 5-methyl-tetrahydrofolate (see Aminopterin, Methotrexate, Trimethoprim, and Folic Acid) or conjugated with serine to yield cystathionine. As an inhibitor of methylene-tetrahydrofolate reductase (23, 24), AdoMet regulates the availability of methyl-tetrahydrofolate, the key intermediate needed for the methylation of homocysteine in the de novo synthesis of methionine, whereas as an allosteric effector of cystathionine synthase (25) AdoMet favors commitment of homocysteine to the transulfuration pathway.

Quantitatively, AdoMet's role of serving as a methyl donor predominates. With the exception of the de novo synthesis of methionine, AdoMet is the sole source of the methyl groups utilized by a myriad of substrate-specific methyltransferases for the synthesis of a great variety of compounds, such as creatine, phospatidylcholine, yeast sterols, plant alkaloids, fungal and bacterial antibiotics, ubiquinone, triterpenes, lignins, and methyl chloride. AdoMet is also the source of the methyl groups required for the post-translational modification of proteins and nucleic acids.

Inversion of configuration at the stereospecific sulfonium center is a constant feature of the enzymatic methyl group transfer reactions (26-29). This indicates that methyltranferases, and by extrapolation alkyltransferases in general, operate by a mechanism involving direct transfer of the methyl, or alkyl, group from the sulfonium atom to the acceptor substrate, thus precluding a methylated intermediate or a ping-pong mechanism (see Enzymes).

S-Adenosyl-L-homocysteine (AdoHcy) is a product (30) and consequently a competitive inhibitor (31, 32), of all the reactions in which AdoMet participates as a methyl donor. AdoHcy also regulates fruit ripening by inhibiting the formation of ethylene (33) from AdoMet. In eukaryotes and most prokaryotes, the only pathway for the further metabolism of AdoHcy is catalyzed by adenosylhomocysteine hydrolase (AdoHcyase), an enzyme that, first shown by de la Haba and Cantoni (34), catalyzes the reversible hydrolysis of AdoHcy to homocysteine and adenosine. The equilibrium of this reaction lies far in the direction of synthesis; physiologically, however, the reaction proceeds in the hydrolytic direction because homocysteine and adenosine are efficiently removed by methionine synthase and by adenosine deaminase, respectively. It was shown by Eloranta (35) that in most tissues the activity of AdoHcyase is 100 to 1000 times greater than the activity of MAT and that consequently the intracellular concentration of AdoHcy is 20 to 100 times smaller than that of AdoMet.

The mechanisms regulating the utilization of AdoMet by many different competing reactions are not well understood. Many methyltransferases have been purified and studied in detail. The kinetics of most are relatively simple, and the physiological activity of these enzymes appears to be related directly to the availability of methyl acceptor substrates, to their affinity (K_m) for AdoMet, and to their inhibition constant (K_i) for AdoHcy. Comparison of these parameters in a number of enzymes revealed that the kinetic features of different methyltransferases can be very different, and they appear to vary independently. This led to the suggestion that the intracellular ratio of AdoMet/AdoHcy, also known as the "methylation ratio," might play a key role in the regulation of AdoMet utilization (36).

The validity of this hypothesis can be explored by modulating experimentally the intracellular AdoMet/AdoHcy ratio. This ratio will decrease whenever inhibition of the enzymes responsible for the removal of adenosine and/or homocysteine shifts the equilibrium of AdoHcyase towards AdoHcy synthesis, or when removal of AdoHcy generated by methyltransfer reactions is prevented by inhibition of AdoHcyase. It is also possible to take advantage of the broad specificity of AdoHcyase for adenosine by supplying adenosine analogs, like 3-deazaadenosine (DZA), that, being adenosine deaminase-resistant, can be converted to 3DZAHcy (37). Modulation of the AdoMet/AdoHcy ratio or the generation of analogues containing groups other than adenosine in response to the administration of various AdoHcyase inhibitors and/or substrates, indicates that in different tissues the physiological responses may be ascribed to the inhibition of specific methyltransferases (38). These results therefore appear to support the hypothesis that the utilization of AdoMet by various competing reactions is regulated by the intracellular AdoMet/AdoHcy ratio. It should be noted, however, that interpretation of these experiments is complex because the accumulation of AdoHcy and/or of other analogues may also result in an increase in the intracellular level of AdoMet, due to feedback inhibition of AdoMet-dependent methyl or alkyl transferases.

Unexpectedly and most importantly, AdoMet has been found to be a safe and effective agent in the treatment of certain forms of clinical depression (39, 40). While it has been clearly established that administration of AdoMet results in a significant increase in the concentration of AdoMet in the cerebrospinal fluid (CSF) (41), it has not been determined whether the therapeutic effects of AdoMet are related to its ability to function as a methyl donor. In the absence of an animal model for depressive disorders, it has unfortunately been possible only to formulate hypotheses to account for the mode of action of AdoMet in such illnesses.

Bibliography

1. G. L. Cantoni (1953) J. Biol. Chem. 204, 403–416.
2. G. L. Cantoni and J. Durell (1957) J. Biol. Chem. 225, 1033–1048. (Abstract)
3. S. H. Mudd (1962) J. Biol. Chem. 237, PC1372–PC1375.
4. G. D. Markham, J. Deparasis, and J. Gatmaitan (1984) J. Biol. Chem. 259, 14505–14507.
5. S. Horikawa and K. Tsukada (1991) Biochem. Int. 25, 81–90.
6. L. Alvarez, F. Corrales, A. Martin-Duce, and J. M. Mato (1993) Biochem. J. 293, 481–486.
7. G. L. Cantoni (1960) in Onium compounds. Handbook of Comparative Biochemistry (M. Florkin and H. Mason, eds.), Academic Press, New York, p. 181.
8. G. L. Cantoni and P. J. Vignos, Jr. (1954) J. Biol. Chem. 209, 647–659.
9. G. L. Cantoni (1952) in A Symposium on Phosphorus Metabolism (W. D. McElroy and B. Glass, eds.), Vol. 2, p. 129, Johns Hopkins Univ. Press, Baltimore MD.
10. H. Tabor, C. M. Rosenthal, and C. W. Tabor (1958) J. Biol. Chem. 233, 907–914.
11. C. W. Tabor and H. Tabor (1984) Ann. Rev. Biochem. 53, 251–282.
12. C. Kutzbach and E. L. R. Stokstad (1971) Biochim. Biophys. Acta 250, 459–477.
13. G. D. Markham, C. W. Tabor, and H. Tabor (1982) J. Biol. Chem. 257, 12063–12068.
14. K. K. Kashiwagi, S. K. Taneja, T. Y. Liu, C. W. Tabor, and H. Tabor (1990) J. Biol. Chem. 265,

22321–22328.
15. S. Nishimura, Y. Taya, Y. Kuchino, and Z. Ohashi (1974) Biochem. Biophys. Res. Commun. 57, 702–708.
16. J. Knappe, F. A. Neugebauer, H. P. Blaschkowski, and M. Ganzler (1984) Proc. Natl. Acad. Sci. USA 81, 1332–1335.
17. R. Eliasson, M. Fontecave, H. Jornvall, M. Krook, E. Pontis, and P. Reichard (1990): Proc. Natl. Acad. Sci. USA 87, 3314–3318.
18. J. Harder, R. Eliasson, E. Pontis, M. D. Ballinger, and P. Reichard (1992) J. Biol. Chem. 267, 25548–25552.
19. D. O. Adams and S. F. Yang (1979) Proc. Natl. Acad. Sci. USA 76, 170–174.
20. Y. Yu, D. O. Adams, and S. F. Yang (1979) Arch. Biochem. Biophys. 198, 280–286.
21. P. S. Backlund, Jr., C. P. Chang, and R. A. Smith (1982) J. Biol. Chem. 257, 4196–4202.
22. G. L. Stoner and M. A. Eisenberg (1975) J. Biol. Chem. 250, 4037–4043.
23. D. A. Jencks and R. G. Matthews (1987) J. Biol. Chem. 262, 2485–2493.
24. K. Hashinaka and M. Yamada (1992) Arch. Biochem. Biophys. 293, 40–45.
25. J. D. Finkelstein, W. E. Kyle, J. J. Martin, and A.-M. Pick (1975) Biochem. Biophys. Res. Commun. 66, 81–87.
26. J. Luthy, J. Retey, and D. Arigoni (1969) Nature 221, 1213–1215.
27. H. G. Floss, L. Mascaro, M. Tsai, and R. W. Woodard (1979) in Transmethylation Elsevier/North Holland, New York, p. 135.
28. J. W. Cornforth, S. A. Reichard, P. Talalay, H. L. Carrell, and J. P. Glusker (1987) Lancet 99, 7292–7300.
29. G. de la Haba et al. (1959) J. Am. Chem. Soc. 81, 3975–3980.
30. G. L. Cantoni and E. Scarano (1954) J. Am. Chem. Soc. 76, 4744–4745.
31. K. D. Gibson, J. D. Wilson, and S. Udenfriend (1961) J. Biol. Chem. 236, 673–679.
32. R. T. Borchardt (1977) in The Biochemistry of Adenosylmethionine (F. Salvatore, E. Borek, V. Zappai, H. G. Williams-Ashman, and F. Schlenk, eds.), Columbia Univ. Press, New York, p. 151.
33. G. Miura and P. K. Chiang (1985) Anal. Biochem. 147, 217–221.
34. G. de la Haba and G. L. Cantoni (1959) J. Biol. Chem. 234, 603–608.
35. T. O. Eloranta (1977) Biochem. J. 166, 521–529.
36. G. L. Cantoni and P. K. Chiang (1980) in Natural Sulfur Compounds (D. Cavallini, G. E. Gaull, and V. Zappia, eds.), Plenum Press, New York, p. 67.
37. H. H. Richards, P. K. Chiang, and G. L. Cantoni (1978) J. Biol. Chem. 253, 14476–14480.
38. P. K. Chiang and G. L. Cantoni (1979) Biochem. Pharmacol. 28, 1897–1902.
39. G. M. Bressa (1994) Acta Neurol. Scand. Supplement 154, 7–14.
40. G. L. Cantoni, S. H. Mudd, and V. Andreoli (1989) Trends Neurosci. 12, 319–324.
41. T. Bottiglieri and K. Hyland (1994) Acta Neurol. Scand. Supplement 154, 19–26.

S1 Nuclease

S1 nuclease is a 32-kDa nuclease that is specific for hydrolyzing of single-stranded RNA or DNA molecules into 5′-mononucleotides. It is a zinc-requiring metalloprotein that is inactivated by chelating agents, such as EDTA and citrate, and by phosphate concentrations as low as 10 mM. Its enzyme activity is optimal at pH 4.0 to 4.3, half at pH 4.9, and negligible above pH 6.0. The protein is thermostable (1) and resistant to several denaturing agents, such as urea, SDS, and formamide (2, 3). Digestion of single-stranded DNA is five times more efficient than that of single-stranded RNA, and 75,000 times more efficient than digestion of double-stranded DNA. The low level of cleavage of double-stranded DNA is minimized by increasing the ionic strength to about 0.2 M salt (2, 4-6), whereas it is increased by negative supercoiling of the double-helical DNA, UV irradiation, and depurination (3, 6-9).

Because S1 nuclease does not degrade double-stranded DNA or DNA–RNA hybrids, it is used widely to remove single-stranded regions from such duplexes. It is extremely useful for (1) measuring the extent of specific hybridization between single strands of DNA and/or RNA; (2) probing the existence of duplex DNA regions; (3) removing cohesive, sticky ends generated by restriction enzymes from single-stranded protruding DNA; (4) increasing the specificity of nucleic acid hybridization (10); (5) localizing intron, exon boundaries; (6) isolating of duplex regions in single-stranded viral genomes (11, 12); (7) probing strand breaks in duplex DNA molecules (2, 9, 13); (8) cleaving double-stranded regions that have lower duplex stability (14, 15); (9) localizing inverted repeat sequences (14, 15); (10) introducing deletion mutations at D loops in duplex DNA; and (11) mapping the genomic regions involved in interactions with DNA-binding proteins (16). Its most frequent use in mapping DNA sequences that encode RNA is described further here, because it exemplifies the potential and limits of the technique.

1. Mapping DNA sequences that encode RNA

A method for mapping RNA molecules onto the DNA templates from which they were transcribed was first described by Berk and Sharp (17, 18). The rationale is illustrated in Figure 1. An RNA transcript R is complementary to nucleotides of the coding strand of a DNA, D. Hybridization of the denatured DNA and RNA leads to a hybrid duplex molecule that has single-stranded overhangs. These are removed by digestion with S1 nuclease. The size of the resulting DNA fragment, that is, the value of n, can be determined by subjecting it to electrophoresis on a polyacrylamide gel like those used in DNA sequencing. S1 nuclease does not remove the poly A track or the cap of eukaryotic messenger RNA when they are base-paired, but the 5′-cap structure, it has been thought, sterically hinders S1 digestion of single-stranded mRNA at the phosphodiester bond adjacent to the first nucleotide (19). When mapping is done with an end-labeled probe, one can determine the polarity and the map position of the RNA on the corresponding DNA sequences (19). This strategy is very useful for mapping the 5′-end of mRNA transcripts, thereby identifying promoter sequences (Fig. 2), and mapping the exons in spliced eukaryotic mRNA (Fig. 3).

Figure 1. Rationale for S1-nuclease mapping

Figure 2. Mapping of 5′-proximal promoter sequences. Promoter sequences localized upstream of the 5′ terminus of eukaryotic spliced RNAs can be mapped after hybridization of RNA preparations with a labeled DNA template (corresponding to the coding strand) that contains the putative promoter sequences (as suggested by DNase hypersensitivity, sequence analysis, etc.). In this example, DNA fragment XYZ encodes an RNA complementary to sequence YZ. The promoter sequences are localized in X. The 5′-end of the RNA delineates the X-Y junction. The first step consists of preparing a single-stranded, 5′-labeled DNA probe (XY) that contains the 5′-proximal promoter sequences and does not cover the 3-end of the RNA molecule. This conserves the 5′-labeled end (the dark sphere) after S1 digestion. Then, this DNA strand (top) is hybridized to the mRNA (bottom). The DNA and RNA overhangs are digested by S1 nuclease, and hybridized regions are protected. The S1- digested hybrid is denatured before to analysis by denaturing gel electrophoresis. Only the labeled DNA fragments are visualized by autoradiography. Left lane: control undigested labeled probe (XY); right lane: S1-digested sample in which only the protected Y region of labeled probe is protected. The length of the protected DNA fragment (Y) is smaller than that of the initial probe (XY). The difference in size (X) identifies the starting point (5′-end) of the RNA molecule.

Figure 3. Mapping exon-intron junctions. In this example, a spliced mRNA composed of two exons is hybridized with the complementary, labeled DNA template (coding strand). Following hybridization of complementary sequences, a loop of single-stranded DNA (corresponding to the intron) is generated. Upon incubation of the partial DNA–RNA duplex with S1 nuclease, the free 3′ and 5′ exon-proximal DNA overhangs and the loop are digested. The size of the resulting DNA–RNA hybrid, which contains only exon sequences, is determined by gel electrophoresis in a nondenaturing buffer. Establishing the individual sizes of the two exons requires gel electrophoresis under denaturing conditions to dissociate the hybrid strands. Only the labeled DNA fragments are observed by autoradiography.

Labeling the DNA fragmant

Determining the size of the S1-resistant DNA fragment relies on measuring a difference in size between the initial DNA probe and the protected segment. The DNA is usually detected specifically by autoradiography, which requires that it be radiolabeled and that the label be within the protected segment and survive the S1 nuclease digestion. Cloned DNA fragments are labeled uniformly or specifically at either the 5' or 3' termini. Labeling at the 5' terminus is usually done with polynucleotide kinase in the presence of γ-^{32}P-ATP, whereas 3' labeling is achieved with α^{32}P-nucleoside triphosphates and either the Klenow fragment of Escherichia coli DNA polymerase I, T4 polynucleotide kinase, or nucleotidyl terminal transferase.

2. Preparing single-strand templates

The previous labeling methods label both strands, so it is necessary to purify the labeled coding strand or to use conditions that favor hybridization between the RNA and DNA strands (see later). Generally, the best results are obtained with separated strands. After denaturation, the two strands of a DNA fragment may be separated by electrophoresis in polyacrylamide or agarose gels if they have different base compositions. It is not possible to predict how each strand will migrate, however, so the S1 mapping must be done with each strand. Hybridization of polyUG to the denatured strands may accentuate differences in their electrophoretic mobilities (20, 21). The double-stranded DNA fragment is digested asymmetrically from its two ends, so that the two single strands have different mobilities after denaturation (see Fig. 3). Alternatively, single-stranded DNA may be isolated by cloning in filamentous bacteriophage or plasmid vectors based upon such phage (see DNA Sequencing).

2.1. Use of Double-Stranded DNA Fragments

The rate of hybridization of RNA molecules to single strands of DNA is similar to that of DNA single-strand renaturation (22, 23). Therefore, the rate of hybridization is maximal in the presence of a high salt concentration (1 M NaCl) and a temperature corresponding to the melting temperature (T_m) of 25 to 30°C. In practice, hybridization is often done in the presence of formamide to decrease the T_m and to hybridize at a lower temperature (24, 25). The melting temperature of duplex DNA molecules can be calculated (26) from the base composition, the ionic strength, and the formamide concentration by using the equation

(1)

At high concentrations of formamide (70 to 80%), the T_m of a DNA-DNA duplex is 5 to 10°C lower than the T_m of the corresponding RNA–DNA hybrid (26). Under such conditions, a hybridization temperature between these two T_m values considerably favors association of the RNA with its coding DNA strand. Most RNA–DNA hybridizations are done at temperatures between 40 and 60°C with a buffer that provides constant pH and ionic strength, such as 0.04 M NaCl and 1 mM EDTA. To establish the optimal conditions for hybridization, the T_m of the DNA duplex used should be determined experimentally. Then, hybridization with the RNA is done at a temperature 2 to 4°C higher. The best results are usually obtained when excess DNA is used. Under such conditions, RNA–DNA hybridization is nearly complete in 3 hours with adenovirus 2 DNA (35 kbp) at a concentration of 10 µg/mL (27). Extrapolating, it can be predicted that nearly complete hybridization of a DNA that has n kilobases will be obtained under similar conditions in 3 hours at a DNA concentration of (n/3.5) mg/mL.

In practice, the labeled, double-stranded DNA and the RNA molecule are mixed and reextracted together once. After resuspending the pellet in "double-strand hybridization buffer" of 50 mM PIPES (pH 6.4), 1 mM EDTA, 0.4 M NaCl, 80% formamide, the mixture is incubated at 65°C to denature the nucleic acids. Then, it is transferred to the appropriate temperature for hybridization.

2.2. Use of Single-Stranded DNA Fragments

The probe and the target single-stranded DNA are resuspended in a "single-strand hybridization buffer" of 0.3 M PIPES (pH 6.4), 30 mM EDTA, 2.5 M NaCl, and incubated as before.

Bibliography

1. T. Ando (1966)) Biochim. Biophys. Acta 114, 158–168.
2. V. M. Vogt (1973) Eur. J. Biochem. 33, 192–200.
3. H. Hofstetter, A. Schambock, Van den Berg, and C. Weissmann (1976) Biochim. Biophys. Acta 454, 587–591.
4. T. E. Shenk, R. P. W. Rhodes, and P. Berg (1975) Proc. Natl. Acad. Sci. USA 72, 989–993.
5. V. M. Vogt (1980) in Methods in Enzymology, 65, (L. Grossman and K. Moldave, eds.),

Academic Press, New York, pp. 248–255.
6. P. Beard, J. F. Morrow, and P. Berg (1973) J. Virol. 12, 1303–1313.
7. G. N. Godson (1973) Biochim. Biophys. Acta 308, 59–67.
8. M. Mechali, A. M. Recondo, and M. Girard (1973) Biochem. Biophys. Res. Commun. 15, 1306–1320.
9. K. Shishido and T. Ando (1975) Biochim. Biophys. Acta 390, 125–132.
10. B. J. Bratina, M. Viebahn, and T. M. Schmidt (1996). Methods Mol. Cell. Biol. 6.
11. K. Shishido and Y. Ikeda (1970) J. Biochem. 67, 759–765.
12. K. Shishido and Y. Ikeda (1971) Biochem. Biophys. Res. Commun. 44, 482–489.
13. J. E. Germond, V. M. Vogt, and B. Hirt (1974) Eur. J. Biochem. 16, 591–600.
14. D. M. Lilley (1980) Proc. Natl. Acad. Sci. USA 77, 6468–6472.
15. N. Panayotatos and R. Wells (1981) Nature 289, 466–470.
16. R. Meyer, J. Grassberg, J. Scott, and A. Kornberg (1980) J. Biol. Chem. 255, 2897–2901.
17. A. J. Berk and P. A. Sharp (1977) Cell 12, 721–732.
18. A. J. Berk and P. A. Sharp (1978) Proc. Natl. Acad. Sci. USA 75, 1274–1278.
19. R. F. Weaver and C. Weissman (1979) Nucleic Acids Res. 7, 1175–1193.
20. G. S. Hayward (1972) Virology 49, 342–344.
21. R. W. Goldbach, R. F. Evans, and P. Borst (1978) Nucleic Acids Res. 5, 2743–2754.
22. J. G. Wetmur and N. Davidson (1968) J. Mol. Biol. 31, 349–370.
23. R. J. Britten and D. E. Kohne (1968) Science 161, 529–540.
24. Bonner, K. Kugn, and Bekw (1967) Biochemistry 6, 3650–3653.
25. B. L. McConaughy, C. D. Laird, and B. I. McCarthy (1969) Biochemistry 8, 3289–3295.
26. J. Casey and N. Davidson (1978) Nucleic Acids Res. 5, 1539–1552.
27. P. A. Sharp, A. J. Berk, and S. M. Berget (1980) Methods in Enzymology 65, (L. Grossman and K. Moldave, eds.), Academic Press, New York, pp. 750–768.

Salt Bridge (Salt Linkage, Ionic Bond)

A salt bridge is a pair of ionized groups with opposite charge that are in very close proximity in a macromolecule and contact each other at their van der Waals radii. The ion pair is stabilized by attractive electrostatic interaction and may even have some hydrogen bond character. Intra- and intermolecular salt bridges are frequently observed in proteins (1) and at protein–protein and protein–nucleic acid interfaces (2).

Bibliography

1. D. J. Barlow and J. M. Thornton (1983) J. Mol. Biol. 168, 867–885.
2. C. O. Pabo and R. T. Sauer (1992) Ann. Rev. Biochem. 61, 1053–1095.

Saltatory DNA Replication

Particles of SV40 virus are produced in permissive simian cells. Infection of nonpermissive rodent cells by SV40 results in integration of the viral genome into the host chromosome. The transformed rodent cells have no free SV40 genomes, but SV40 genomes are produced when these nonpermissive cells are fused with permissive simian cells. The chromosomes from the monkey cells provide replicative functions not present in the rodent cells, making SV40 DNA replication possible in the heterokaryons. Repeated rounds of initiation of DNA replication from the integrated SV40 replication origins result in polytenization of that region (see Polytene Chromosome), which may liberate a linear DNA duplex containing the integrated SV40 genome. The liberated DNA will then recombine with itself to form a circular viral genome. In cell lines with tandem duplications of the integrated SV40 DNA, the efficiency of infectious virus formation is increased because of the terminal duplication of the liberated linear DNA. In the absence of tandem duplication, cyclization by nonhomologous recombination may form mutants with deletion of viral DNA or insertion of host DNA (1).

Bibliography

1. A. Kornberg and T. A. Baker (1992) In DNA Replication, 2nd ed., W. H. Freeman, New York, pp. 690–699.

Salting In, Salting Out

The effect of salts on protein solubility is described by the salting in, salting out effect (1): The dependence of the solubility of a protein on salt concentration is one in which, for any salt, at low salt concentration the solubility of a protein increases; then, after the protein passes a point of maximal solubility, the further addition of salt reduces its solubility (see Precipitation). Typical patterns are shown in Figure 1 (2).

Figure 1. The solubility of carboxyhemoglobin in various electrolytes at 25°C. (Reprinted from (2) with permission of The American Society of Biological Chemists.)

This complex dependence has been decomposed into two contributions (3). At low salt concentration, proteins are salted in; in other words, their solubility increases. For any protein, this is independent of the nature of the salt and is simply the consequence of the fact that proteins carry positively and negatively charged groups on their accessible surface. These are surrounded by an atmosphere of the ions of the salt, which increases the solubility according to the simple Debye–Hückel equation. Thus, if s_s and s_w are the solubilities of the protein in salt solution and pure water, respectively, the salting in is described by the following equation:

(1)

where Z is the net charge of the protein, I its ionic strength, and [illegible] a combination of constants.

At high salt concentration (approximately > 0.5 M), salting in becomes saturated, and the effect of salting out takes over, ie, the protein solubility decreases, following the law that the logarithm of the solubility (S, usually given in units of grams of protein per 1000 cm^3 of solvent) is linear in salt concentration expressed as ionic strength:

(2)

where b and K_s are empirical constants. The parameter K_s, called the salting out constant, is characteristic of the particular salt. The order of salting out effectiveness is close to invariant for most proteins and follows the Hofmeister series (2). The magnitude of K_s is defined by the preferential interaction of the particular salt with the protein, as

(3)

where m_s is the molal concentration of the salt (3). (Salts that induce preferential hydration (negative binding in equilibrium dialysis; see Binding) reduce the solubility of proteins. Conversely, a solvent system that shows preferential binding increases the solubility of proteins.

Bibliography

1. E. J. Cohn and J. D. Ferry (1943) In Proteins, Amino Acids and Peptides (E. J. Cohn and J. T. Edsall, eds.), Van Nostrand Reinhold, New York, pp. 586–622.
2. A. A. Green (1932) J. Biol. Chem. 95, 47–66.
3. T. Arakawa and S. N. Timasheff (1985) Meth. Enzymol. 114, 49–77.

Salvage Pathways To Nucleotide Biosynthesis

Most nucleotide biosynthesis in most cells occurs via the nearly ubiquitous de novo synthetic pathways, starting from amino acids and their derivatives (see Purine Ribonucleotide Metabolism and Pyrimidine Ribonucleotide Metabolism). However, most cells possess capabilities for taking up nucleosides and nucleobases and converting them to nucleotides. Because these processes involve reutilization of previously synthesized purine and pyrimidine rings, they are called salvage pathways. These pathways are much shorter and simpler than the de novo pathways. On the other hand, there is much more variability from organism to organism, and from tissue to tissue in the same organism, in salvage synthetic capabilities. The metabolic importance of salvage pathways has come to light, first, along with the realization of the serious consequences of hereditary deficiencies in certain salvage enzymes and, second, with the many ways in which salvage pathways are being exploited to create or enhance the effectiveness of chemotherapy against a variety of diseases.

1. Transport of Nucleosides and Nucleobases

Substrates for salvage pathways can come from intracellular nucleic acid degradation (see DNA Degradation In Vivo). For most cells, however, salvage precursors are derived from the extracellular environment. An extreme example is protozoan parasites, which derive all their nucleic acid precursors from salvage substrates in the blood of infected organisms. In fact, these parasites have evolved to the extent that they completely lack de novo pathways and are totally dependent on salvage (1, 2); development of specific salvage inhibitors now constitutes one of the most active research areas of biochemical parasitology.

Nucleosides are hydrophilic molecules and do not readily diffuse through membranes; to an extent, the same is true for nucleobases. Thus, most cells contain specific transporter systems, which take up these molecules by facilitated diffusion (3, 4). In recent years, however, concentrative transport systems have been described, especially for nucleosides. These systems depend on sodium and involve cotransport of the nucleoside with Na^+. Most animal cells contain a broad-specificity nucleoside transporter that functions by facilitated diffusion, the active transport systems being limited primarily to specialized cells, for example, those that take up and use adenosine as a physiological regulator. The nucleobase transport systems are less well characterized, and the question of whether cells contain multiple base transporters or a single broad-specificity transporter has not yet been resolved.

2. Salvage Pathways

Nucleobases are anabolized by phosphoribosyltransferases , which use 5-phosphoribosyl-1-pyrophosphate (PRPP),

while nucleosides are anabolized primarily by kinases

Nucleosides can also be salvaged by a nucleoside phosphorylase followed by a phosphoribosyltransferase.

In principle, this route could be used for nucleotide synthesis, starting with a base, given that nucleoside phosphorylases are readily reversible. However, these enzymes generally act within cells in the direction of nucleoside degradation.

Salvage enzymes vary considerably in tissue distribution and specificity. Mammalian cells salvage purines primarily at the free base level through the action of two phosphoribosyltransferases: hypoxanthine guanine phosphoribosyltransferase (HGPRT), which converts hypoxanthine and guanine to inosinic acid (IMP) and GMP, respectively; and adenine phosphoribosyltransferase (APRT), which specifically converts adenine to AMP. HGPRT is the enzyme missing in cells of males suffering from Lesch–Nyhan syndrome (see Purine Ribonucleotide Metabolism). Pyrimidines, by contrast, are more likely to be salvaged at the nucleoside level. In the de novo pathway, orotic acid is converted to orotidylate by a phosphoribosyltransferase, but comparable pyrimidine salvage enzymes are of extremely limited distribution.

Protozoa that rely on nucleotide salvage pathways, particularly for purines, bear a distinctive set of enzymes— nucleoside hydrolases. These organisms take up purine nucleosides from the blood of infected animals, for example, and then hydrolyze the nucleoside to ribose plus the base; the base is then salvaged by a phosphoribosyltransferase (5). Because the nucleoside hydrolases are quite distinct from known proteins, they are being explored as targets for drugs that would specifically inhibit the growth of an infecting parasite by blocking this salvage route, which is essential for the parasite but not the host.

As discussed more thoroughly below, nucleoside and base analogues are widely used as antiviral, antimicrobial, and anticancer drugs. Because of the interest in developing or improving the effectiveness of drugs that act as DNA synthesis inhibitors, there has been particular emphasis on the deoxyribonucleoside kinases (6). Four such enzymes, with overlapping specificities, are found in human cells. Properties and subcellular distributions of these enzymes are summarized in Table 1. It is of particular interest that deoxycytidine kinase (dCK) is also the principal enzyme for utilization of purine deoxyribonucleosides (the K_m values are much higher for the purines than for deoxycytidine; hence the name of the enzyme).

Table 1. Properties of the Human Deoxyribonucleoside Kinases

Enzyme Cycle Regulation	Natural Substrates	Intracellular Distribution	Cell Cycle Regulation
Deoxycytidine kinase (dCK)	dCyd, dAdo, dGuo	Cytosol	Constitutive
Thymidine kinase 1 (TK1)	dThd, dUrd	Cytosol	S-phase-specific
Thymidine kinase 2 (TK2)	dThd, dUrd, dCyd	Mitochondria	Constitutive
Deoxyguanosine kinase (dGK)	dGuo, dAdo, dIno	Mitochondria[0]	Constitutive

Source: Arnér and Eriksson (6)

A key to understanding some clinical disorders is knowledge of the tissue distribution of salvage enzymes. For example, the immunodeficiency state that results from adenosine deaminase deficiency can be related to this factor (see Purine Ribonucleotide Metabolism). Most or all tissues in an affected individual accumulate adenosine and deoxyadenosine as a result of the genetic block to purine catabolism. Nucleoside salvage enzymes are particularly active in the reticuloendothelial system, where apoptosis leads to degradation and reutilization of cell components, including nucleic acids. Thus, blood cells accumulate excessive amounts of ATP, and in particular, dATP, which interferes with white cell proliferation as part of the immune response, through its inhibition of ribonucleotide reductase.

A salvage enzyme of considerable interest is the family of thymidine kinases specified by herpes viruses. As exemplified by the herpes simplex thymidine kinase, these enzymes have two distinctive properties. First, they are bifunctional enzymes, with thymidylate kinase activity as well. Thus, the enzyme is evidently designed to catalyze two sequential reactions. Second, the nucleoside kinase activity has much broader substrate specificity than most cellular nucleoside kinases. As discussed below, antiviral chemotherapeutic strategies exploit this distinctive property.

3. Salvage Enzymes as Selectable Markers

Because nearly all cells possess de novo nucleotide synthetic capabilities, the salvage enzymes are usually not required for cell viability. In addition, a large number of nucleobase and nucleoside antimetabolites are available, most of them inhibitors of specific enzymes (see Nucleotides, Nucleosides, And Nucleobases). These factors create favorable conditions for the use of salvage enzymes as selectable genetic markers, ie, genetic characteristics that promote the selective survival or growth of desired cell types. For example, the mammalian enzyme encoding HGPRT is widely used as a selectable marker in genetic analysis. 6-Thioguanine is metabolized by HGPRT to give the thiol analogue of inosinic acid, which is toxic. Cells lacking HGPRT can be selected for because they grow in 6-thioguanine-containing medium, while other cells are killed. Hence, one can estimate mutation rates by culturing wild-type cells in the presence of thioguanine and enumerating the cells that grow. Another advantage of this gene for genetic analysis is that it is carried on the X-chromosome. Thus, in male-derived cell lines, only one mutation, rather than two independent events is required to give the resistant phenotype.

A comparable selectable marker is the gene encoding thymidine kinase. 5-Bromodeoxyuridine is anabolized similarly to thymidine;

(1)

However, incorporation of bromodeoxyuridine into DNA is a lethal event. Thus, thymidine kinase deficiency leads to a BrdUrd-resistant phenotype. Because many large DNA viruses encode a thymidine kinase, this is a useful system for manipulating viral genes, for example, the use of vaccinia virus as a vector in the generation of multivalent vaccines (7).

On the other hand, one can select for the presence of active salvage enzymes. The best example is the use of “HAT medium” in somatic cell genetic analysis and in preparing monoclonal antibodies. These techniques involve fusing cells of differing origins and culturing in HAT medium to select for those cells that have undergone fusion. HAT is an acronym for the medium's constituents,— hypoxanthine, aminopterin, and thymidine. Aminopterin inhibits dihydrofolate reductase, blocking the synthesis of tetrahydrofolate needed for de novo synthesis of purine nucleotides and thymidine nucleotides. Thus, cells can grow in HAT medium only if they express active thymidine kinase and HGPRT, for salvage synthesis of thymidine and purine nucleotides, respectively. In monoclonal antibody production, one of the cell lines to be fused lacks thymidine kinase, and the other lacks HGPRT. Thus, only cells resulting from a fusion event have functional copies of both enzymes and can grow.

A final example relates to the use of a selectable marker to force expression of a nonselected marker. For cloning into expression systems in mammalian cells, one often incorporates into the cloning vector the *Escherichia coli xpt* gene, which encodes a distinctive phosphoribosyltransferase that acts on xanthine and guanine. During and after transfection of cells with the recombinant DNA, the cells are cultured in the presence of mycophenolic acid, which blocks de novo guanine nucleotide synthesis by inhibiting IMP dehydrogenase, the enzyme that converts IMP to XMP (which would then be converted to GMP). Thus, the only cells that can grow are those that have taken up and expressed the *xpt* gene, which bypasses this metabolic block. Being carried on the same vector, the gene of interest is also cloned and/or expressed, even though its expression was not directly selected for.

4. Salvage Enzymes and Molecular Pharmacology

A large number of antiviral, antibacterial, antiparasitic, and anticancer drugs act by inhibiting or otherwise manipulating pathways in nucleotide metabolism and thereby interfering with nucleic acid synthesis. Several examples are cited in Nucleotides, nucleosides, and nucleobases. In most cases, the active species is a nucleotide. Because nucleotide molecules are charged, and because specific transport systems for nucleotides don't exist, these molecules penetrate membranes poorly, if at all.

Therefore, in order to generate a therapeutically effective nucleotide intracellularly, its precursor must be administered extracellularly as a nucleobase or nucleoside analogue. Effective use of such drugs demands extensive understanding of salvage pathways in the target cell, subcellular distribution of the enzymes involved, degradative enzymes that might compete with the pathway leading to the desired nucleotide analogue, levels of the target enzyme, and cell-cycle regulation of all the enzymes involved (8).

As an example of the factors involved, consider the fluorinated pyrimidines, 5-fluorouracil (FUra) and 5-fluorodeoxyuridine (FdUrd), analogues used for decades in treating various cancers. It was established in 1958 (9) that these drugs are converted *in vivo* to 5-fluorodeoxyuridine monophosphate (FdUMP), an analogue of deoxyuridine monophosphate, the substrate for thymidylate synthase (Fig. 1; see Deoxyribonucleotide Biosynthesis And Degradation), and that FdUMP is a potent inhibitor of thymidylate synthase and, hence, of DNA replication. Figure 1 shows also the metabolic pathways that both activate these analogues and divert them from their desired endpoint (10). From the figure, one can see that coadministration with FdUrd of a thymidine phosphorylase inhibitor should increase the effectiveness of the analogue by blocking its catabolism. Note that there are multiple routes for activation of FUra; note also that FUra can enter pools of RNA precursors which, in principle, could limit its selectivity by diminishing the specificity of its effect against DNA synthesis. There is evidence, however, that, in some tumors, the effectiveness of FUra actually depends in part on its incorporation into RNA, where it stimulates translational miscoding.

Figure 1. Metabolism of fluorinated pyrimidines by salvage and other enzymes. dR-P is deoxyribose-5-phosphate, dR-1-P deoxyribose-1-phosphate, and R-1-P ribose-1-phosphate. Enzymes are 1, thymidylate synthase; 2, dihydrofolate reductase; 3, serine transhydroxymethylase; 4, thymidine kinase; 5, thymidine phosphorylase; 6, uridine phosphorylase; 7, uridine kinase; 8, uridylate kinase; 9, nucleoside diphosphate kinase; 10, ribonucleoside diphosphate reductase; 11, RNA polymerase.

Bibliography

1. R. L. Berens, E. C. Krug, and J. J. Marr (1995) in Biochemistry of Parasitic Organisms and its Molecular Foundation (J. J. Marr and M. Muller, ed.), Academic Press, London, pp. 89–117.
2. D. J. Hammond and W. E. Gutteridge (1996) Mol. Biochem. Parasitol. 13, 243–261.
3. P. G. W. Plagemann, R. M. Wohlhueter, and C. Woffendin (1988) Biochim. Biophys. Acta 947, 405–443.
4. D. A. Griffith and S. M. Jarvis (1996) Biochim. Biophys. Acta 1286, 153–181.
5. D. W. Parkin (1996) J. Biol. Chem. 271, 21713–21719.
6. E. S. J. Arnér and S. Eriksson (1995) Pharmacol. Ther. 67, 155–186.

7. D. W. Grosenbach and D. E. Hruby (1995) in Methods in Molecular Genetics: Molecular Virology Techniques, Part B (K. W. Adolph, ed.), 7B, 45–64.

8. R. I. Christopherson and S. D. Lyons (1990) Medicinal Res. Rev. 10, 505–549.

9. S. S. Cohen, J. G. Flaks, H. D. Barner, M. Loeb, and J. Lichtenstein (1958) Proc. Natl. Acad. Sci. USA 44, 1004–1012.

10. B. Ardalan and R. Glazer (1981) Cancer Treatment Reviews 8, 157–167.

Suggestions for Further Reading

11. Reference 8 above is a thorough review of purine and pyrimidine analogues as chemotherapeutic agents.

12. G. B. Elion (1989) Science 244, 41–47; describes the history of the development of 6-thioguanine as an antileukemic drug, allopurinol as a gout treatment, and acyclovir as an antiviral agent.

13. H. Mitsuya, ed. (1997) Anti-HIV Nucleosides: Past, Present, and Future, R. G. Landes Co., Georgetown, TX. An informative reference, with five review articles discussing strategies for developing more effective nucleoside analogues for treating HIV infections.

Sarkosyl

Sodium N-lauroylsarcosine, or Sarkosyl, is a detergent that is structurally related to SDS, except that Sarkosyl has an additional polar and rigid peptide bond linkage within the hydrophobic backbone (Fig. 1). Such rigidity added to the N-terminus of the hydrophobic chain could lead to a decrease in its ability to be inserted freely into hydrophobic membrane bilayers and proteins. This could explain why Sarkosyl is milder than SDS in its ability to denature and disrupt membrane and protein structures. Because of a similar difference in side-chain structure, the bile acid detergent CHAPS is rendered milder than the strongly denaturing sodium cholate, which inactivates integral membrane proteins, such as the serotonin 1A receptor (1). The relatively mild nature of Sarkosyl has been exploited at least in a few cases. Important examples include the purification of Escherichia coli RNA polymerase sigma factors by solubilizing inclusion bodies (2) and the solubilization and purification of the scrapie protein, the prion PrP^{Sc} (3, 4). Although comparison of the structural features of Sarkosyl with those of other detergents suggests that it might be effective in solubilizing functionally active membrane proteins, the major use of Sarkosyl has been to isolate DNA and RNA. The principal reason for this is that Sarkosyl is highly efficient in dissociating nucleosomes and ribosomes (5). The detergent also denatures nucleic acids and inhibits certain enzymes, such as deoxyribonucleases and ribonucleases, which could degrade these molecules.

Figure 1. The structure of Sarkosyl.

Bibliography

1. P. Banerjee, J. B. Joo, J. T. Buse, and G. Dawson (1995) Chem. Phys. Lipids *77*, 65–78.
2. R. R. Burgess (1996) Methods Enzymol. *273*, 145–149.
3. K. U. Grathwohl, M. Horiuchi, N. Ishiguro, and M. Shinagowa (1996) Archiv. Virol. *141*, 1863–1874.
4. T. Muramoto, M. Scott, F. E. Cohen, and S. B. Prusiner (1996) Proc. Natl. Acad. Sci. USA *93*, 15457–15462.
5. C. H. Chang and D. S. Luse (1997) J. Biol. Chem. *272*, 23427–23434.

Satellite DNA

The regions adjacent to the centromeres in chromosomes of higher eukaryotes are composed of very long blocks of highly repetitive DNA, in which simple sequences are repeated a thousand times or more. Often, these repeated sequences have a base composition very different from that of the remainder of the DNA, so they can be separated from the bulk DNA by cesium chloride density gradient centrifugation of slightly fragmented DNA. For this reason, such DNA is referred to as satellite DNA. The localization of satellite DNA near the centromeres allows localization of the centromeres by *in situ* hybridization and autoradiography in squashed metaphase cells, using radiolabeled RNA copies of the satellite sequence (2).

Different satellites can occur in the same species. For example, *Drosophila virilis* possesses three centromeric satellites (1) whose sequences are highly related. None of these satellite sequences is a pure repeat of the basic consensus sequence. The reason behind the evolution of several sequences is not clear.

Usually, satellite DNA is not transcribed into messenger RNA, as it lacks promoter sites where RNA chains can be initiated. DNA polymerase must recognize the satellite sequences, however, because the DNA from centromeres is replicated at the same rate as the rest of the chromosomal DNA. It is assumed that the satellite sequences bind particular proteins essential for the centromere's function of holding the daughter chromatids together during metaphase, such as playing a role in the assembly of the kinetochores responsible for their attachment to the mitotic spindle or guiding the topoisomerase that eventually separates the sister chromatids (see DNA Topology). Thus satellite sequences are examples of structural rather than genetic regions of DNA.

Bibliography

1. J. G. Gall and D. D. Atherton (1974) J. Mol. Biol. *85*, 633–634.
2. M. L. Pardue and J. G. Gall (1970) Science *168*, 1356–1358.

Satellites

Satellites are subviral agents that depend for their replication on co-infection of a host cell with a helper virus (HV). The nucleotide sequences of the nucleic acids of satellites are substantially different from those of their HV or their hosts, although some satellites may share with their HV short sequences, often at the termini. Thus, satellites are different from defective interfering particles or RNAs, which are wholly derived from the genome of the HV. One chimeric replicon with sequences derived from both a satellite and a HV has been described (1). The relationship between helper virus and satellite is usually specific in that only one HV species, or a group of related species, can sustain the replication of a particular satellite species; on the other hand, a particular HV may sustain the replication of different, unrelated satellites. There is no correlation between the taxonomic relationships of satellites and those of their HVs. Thus, satellitism may have evolved independently several times. The presence of a satellite may modulate the level of accumulation and the pathogenicity of the HV. Because of these properties, satellites can be considered as molecular parasites of their HVs. Satellites are not needed for the normal multiplication of HVs, but there are satellite-like RNA molecules that may be necessary for completion of the HV's life cycle under natural conditions. Examples are the satellite-like single-stranded RNAs associated with groundnut rosette umbravirus or with beet necrotic yellow vein benyvirus, which are needed for transmission of the HV by their respective aphid or fungal vector.

Satellites are a heterogeneous group, rather than a single taxonomic unit. There are satellites that encode proteins that are expressed *in vivo*, and others that are noncoding. When the encoded protein is a structural protein that encapsidates the satellite nucleic acid, the satellite is called a **satellite virus**. Satellite viruses are found as distinct nucleoprotein components in preparations of the HV. The first satellite virus was described in 1962 associated with tobacco necrosis virus (TNV) (2). Satellites that do not encode their structural proteins are called **satellite nucleic acids**. The first satellite nucleic acid was described associated with tobacco ringspot nepovirus in 1969 (3). The different groups of satellite viruses and nucleic acids, and their abbreviations, are listed in Table 1.

Table 1. Satellites and Their Types, with Indication of Size of Nucleic Acid and Accession Number of Typical Sequence Variants[a]

Satellite	Size (nt)	Accession
Viruses		
Subgroup I		
Tobacco necrosis satellite virus (STNV)	1239	J02399
Panicum mosaic satellite virus (SPMV)	826	M17182
St. Augustine decline satellite virus (SSADV)	824	L10083
Tobacco mosaic satellite virus (STMV)	1058	M24782
Maize white line mosaic satellite virus (SMWLMV)	1168	M55012
Subgroup II		
Chronic bee-paralysis associated satellite virus (CPVA)	~ 1100	NR
Nucleic acids		
ssRNA satellites		
Large satRNAs with messenger properties		

Arabis mosaic nepovirus (ArMV) large sat-RNA	1104	D00664
Chicory yellow mottle nepovirus (CYMV) large sat-RNA	1165	D00686
Grapevine bulgarian latent nepovirus (GBLV) sat-RNA	~ 1500	NR
Grapevine fanleaf nepovirus (GFLV) sat-RNA	1114	D00442
Myrobalan latent ringspot nepovirus (MLRV) sat-RNA	~ 1400	NR
Strawberry latent ringspot nepovirus (SLRV) sat-RNA	1118	X69826
Tomato black ring nepovirus (TBRV) sat-RNA	1374	X05689
Bamboo mosaic potexvirus (BaMV) sat-RNA	836	L22762
Small linear satellite RNAs		
Turnip crinkle carmovirus (TCV) sat-RNA	230	X12749
	355[b]	X12750
Cucumber mosaic cucumovirus (CMV) sat-RNA	335	M18872
Peanut stunt cucumovirus (PSV) PSV sat-RNA	393	Z98198
Pea enation mosaic enamovirus (PEMV) sat-RNA	717	U03564
Tobacco necrosis necrovirus (TNV) small sat-RNA	620	NR
Chicory yellow mottle nepovirus (CYMV) small sat-RNA	457	D00721
Artichoke mottled crinkle tombusvirus (AMCV)sat-RNA	~700	NR
Cymbidium ringspot tombusvirus (CyRSV) sat-RNA	619	D0072
Tomato bushy stunt tombusvirus (TBSV) sat-RNA	822	Af022788
Small circular satellite RNAs		
Barley yellow dwarf luteovirus (BYDV) sat-RNA	322	M63666
Arabis mosaic nepovirus (ArMV) small sat-RNA	300	M21212
Tobacco ringspot nepovirus (TRSV) sat-RNA	359	M14879
Lucerne transient streak sobemovirus (LTSV) sat-RNA	324	X01984
Rice yellow mottle sobemovirus (RYMV) sat-RNA	212	AF039909
Solanum nodiflorum mottle sobemovirus (SNMV) sat-RNA	377	J02386
Subterranean clover mottle sobemovirus (SCMV) sat-RNA	332	M33000
Velvet tobacco mottle sobemovirus (VTMoV) sat-RNA	366	J02439
dsRNA satellites		
M satellite of *Saccharomyces cerevisiae* virus L-A	1801	U78817
Satellite of *Trichomonas vaginalis* virus T1	497	U15991
ssDNA satellites		
Tomato leaf curl geminivirus (TLCV) sat-DNA	682	U74627

[a] nt, nucleotides; ss, single-stranded; ds, double-stranded; NR, not reported.

[b] A chimeric replicon with sequences derived from both satellite and helper virus.

1. Satellite viruses

All known satellite viruses have a single-stranded RNA of 800 to 1200 nucleotides. In addition to the open reading frame (ORF) encoding their coat protein, some satellite viruses contain further ORFs; it remains unclear if the encoded products have any role *in vivo* (4). The structure of their isometric, 17-nm diameter particles, built of 60 protein subunits, differs from that of their HV. The particle structures of STNV, STMV and SPMV (see Table 1) have been determined at high resolution by X-ray crystallography (5). In spite of the different structures of the TNV virus particle and of the coat protein of its satellite STNV, both are able to bind specifically to zoospores of the vector fungus *Olpidium brassicae*.

Best-characterized are the satellites of the tobacco necrosis satellite virus (STNV) subgroup. The 1000- to 1200-nucleotide RNA of STNV has no methylated cap structure or genome-linked protein (Vpg protein) at its 5' end. Unlike most plant virus RNAs, it has a phosphorylated 5' terminus. Interference with the accumulation of the TNV has been described for STNV. The particles of STNV may also contain a noncoding satellite RNA of about 620 nucleotides, which depends on TNV for its replication and on STNV for its encapsidation. This is a good example of the complexity of the dependence relationships in satellitism.

Satellite viruses are also found associated with chronic bee-paralysis virus (CPV) (6). Its RNA consists of three species, about 1.1 kb, which can be encapsidated in 17-nm isometric particles built of coat proteins encoded by the satellite or by CPV. The satellite interferes with CPV replication.

2. Satellite nucleic acids

Satellite nucleic acids are single-stranded RNA, single-stranded DNA, or double-stranded RNA satellites associated to viruses of the same type of nucleic acid. Most of the characterized satellites are associated with plant viruses, and most are single-stranded RNA.

2.1. Single-Stranded RNA Satellites

These are classified into three subgroups.

(i) Subgroup I includes satellites with messenger properties. The RNA molecules are between 0.8 and 1.5 kb in size. These satellites encode nonstructural proteins that are expressed *in vivo*. The most studied satellites of this subgroup are those associated with nepoviruses. Large single-strand RNA satellites of nepoviruses have a 3' terminal Poly A sequence and a 5' terminal Vpg protein that, in the analyzed instances, is indistinguishable from that on the HV genome and, therefore, is encoded by it. The encoded nonstructural proteins of different satellite RNAs share some conserved domains, and in some cases have been shown to be needed for replication of the satellite RNA. It may be speculated that these proteins are needed to adapt the virus replication complex to the satellite RNA. For most large satellite RNAs of nepoviruses, effect on the accumulation or pathogenicity of the HV has not been shown. This may depend on the experimental system: the large satellite RNA of ArMV was shown to modulate the symptoms of the HV, depending on the species of host plant. Another satellite RNA in this subgroup has been found associated with bamboo mosaic potexvirus. The encoded nonstructural protein is not essential for satellite replication (7). Interestingly, this protein shares significant sequence similarity with the structural protein of the satellite virus of PMV, suggesting an evolutionary relationship between the satellite virus and the satellite RNA.

(ii) The second subgroup of single-stranded RNA satellites are small, linear RNAs, of less than 800 nucleotides and with no circular forms. Although they may contain potential ORFs, and *in vitro* translation products have been described for some variants of the satellite RNA of CMV, evidence is strong that these molecules are noncoding RNAs. Thus, their biological functions must depend on the RNA structure, which would mediate the direct interaction of the satellite RNA with components of the HV and/or the host plant. Experimental analyses of secondary structure have been done for the satellite RNAs of CMV and TCV, and there is evidence that several have highly-paired secondary structures. This may account for the high survivability of satellite RNAs *in vivo* and *in vitro*, as well as for their high infectivity. Most satellite RNAs in this subgroup modify the symptoms induced by the HV. The most frequent modification is symptom attenuation, but modulation to more severe symptoms (eg intense chlorosis or necrosis) also occurs. Symptom modulation depends on the triple interaction between the strain of satellite RNA, strain of HV, and species or genotype of the host plant. For the satellite RNA of CMV, there has been an extensive analysis of symptom determinants in the satellite RNA. For the satellite RNAs of CMV and TCV, the HV and host determinants have been identified as well. The presence of the satellite RNA often results in depression of the accumulation of the HV, but the relationship between this and the attenuation of symptoms is unclear: depression of HV accumulation also occurs when the interaction between satellite RNA and HV results in symptom exacerbation. Also, for some combinations of satellite RNA and HV, symptom attenuation is not accompanied by a reduction in the accumulation of the HV. The satellite RNA may also interfere with movement of the HV within the infected plant, as shown for the satellite RNA of TCV (8).

(iii) The third subgroup of single-stranded RNA satellites are small circular RNAs. These satellite RNAs actually occur as both circular and linear molecules. The HV may encapsidate circular forms (for sobemoviruses) or linear forms (for nepoviruses and luteoviruses). In both cases, replication is through a rolling circle mechanism (see Rolling Circle DNA Replication). Small circular single-stranded RNA satellites interfere with the accumulation and symptoms induced by the HV. These satellites have been described under the heading Virusoids.

The single-stranded RNA satellites may replicate by different mechanisms than their HV. Thus, the replication machinery of the HV must be adapted to the replication of the satellite RNA. Satellite-encoded factors (for the large, encoding satellites) or unidentified host factors may play a role in modifying the virus replication complex. It is to be noted that for those systems that have been analyzed in detail, the efficiency of satellite RNA replication depends on the HV, as well as on the host plant.

Because of the attenuation of the symptoms of HV, single-stranded RNA satellites have been proposed as efficient agents for the biocontrol of HV-induced plant diseases, both in classical cross-protection programs and by engineering transgenic plants. The high genetic variability of satellite RNAs under experimental and natural conditions, and the possibility of their evolution from attenuating to highly pathogenic types, should be considered when evaluating the potential risks of such control programs.

2.2. Double-Stranded RNA Satellites

Other nucleic acid satellites are the double-stranded RNA satellites associated with viruses in the family *Totiviridae*. Of these, the best studied are the M satellites, which are responsible for the killer phenotype and for immunity to the killer toxin associated with the L-A virus of *Saccharomyces cerevisiae*. The multiplication of the M satellite depends on both the helper virus L-A and on host chromosomal genes.

2.3. Single-Stranded DNA Satellites

A 682-nucleotide, circular, single-stranded DNA satellite has been found associated with tomato leaf curl geminivirus (TLCV). The satellite DNA contains no ORF, is encapsidated in TLCV particles, and is totally dependent for its replication on the replication-associated protein of TLCV. It shows no sequence similarity with the HV DNA, except for a motif that is universally conserved in geminiviruses and involved in single-stranded DNA replication, and for the binding site for the replication-associated protein. At odds with most RNA satellites, this satellite DNA can be supported by distantly related geminiviruses (9).

Satellites have been considered interesting models to approach the analysis of fundamental aspects of virology, such as virus replication, encapsidation, pathogenesis, recombination, and variability. Also, the often complex dependence relationships between satellites and HV pose interesting questions about evolution. Because of this, much research has focused on satellites. Still, major questions remain largely unanswered: (i) how satellites are replicated by the replication machinery of the HV, (ii) how they affect the accumulation (ie, replication and/or movement) of the HV, (iii) how they modify symptoms of the HV, and (iv) what is their origin, evolution, and fate in populations of their HV.

Bibliography

1. A. E. Simon and S. H. Howell (1986) EMBO J. 5, 3423–3428.
2. B. Kassanis (1962) J. Gen. Microbiol. 27, 477–488.
3. I. R. Schneider (1969) Science 166, 1627–1629.
4. G. Routh, J. A. Dodds, L. Fitzmaurice, and T. E. Mirkov (1995) Virology 212, 121–127.
5. N. Ban, S. B. Larson, and A. McPherson (1995) Virology 214, 571–583.
6. H. A. Overton, K. W. Buck, L. Bailey, and B. V. Ball (1982) J. Gen. Virol. 63, 171–179.
7. N. S. Lin, Y. S. Lee, B. Y. Lin, C. W. Lee, and Y. H. Hsu (1996) Proc. Natl. Acad. Sci. USA 93, 3138–3142.
8. Q. Z. Kong, J. L. Wang, and A. E. Simon (1997) Plant Cell 9, 2051–2063.
9. I. B. Dry, L. R. Krake, J. E. Rigden, and M. A. Rezaian (1997) Proc. Natl. Acad. Sci. USA 94, 7088–7093.

Suggestions for Further Reading

10. C. W. Collmer and S. H. Howell (1992) Role of satellite RNA in the expression of symptoms caused by plant viruses. Annu. Rev. Phytopathol. 30, 419–442.
11. R. I. B. Francki (1985) Plant virus satellites. Ann. Rev. Microbiol. 39, 151–174.
12. C. Fritsch, M. A. Mayo, and O. Hemmer (1993) Properties of satellite RNA of nepoviruses. Biochimie 75, 561–567.
13. F. Garcia-Arenal and P. Palukaitis (1999) Structure and functional relationships of satellite RNAs of cucumber mosaic virus. In P. K. Vogt (Ed.), Satellites and defective viral RNAs. Curr. Topics Microbiol. Immunol. 239, 37–63.
14. M. J. Roossinck, D. Sleat, and P. Palukaitis (1992) Satellite RNAs of plant viruses: structures and biological effects. Microbiol. Rev. 56, 265–279.
15. R. B. Wickner (1996) Double-stranded RNA viruses of Saccharomyces cerevisiae. Microbiol. Rev. 60, 250–265.

Scalar Coupling

Nuclear magnetic resonance (NMR) spectra of liquid or gaseous samples of a molecule are usually more complex than would be expected based on the number of chemically distinct nuclei in the molecule. The additional complexity (fine structure) in the spectra arises from spin-spin coupling, also called J-coupling, spin-spin splitting, or scalar coupling. The exact resonance frequencies of NMR transitions associated with a particular nucleus depend on the magnetic field at that nucleus, which is the sum of many components. The largest part is provided by the magnetic field of the NMR instrument, as modified by the chemical shift effects of the electrons of the subject molecule and the electrons of surrounding molecules. (See Chemical Shift.) Smaller contributions to the total magnetic field are made by other nuclei in the vicinity of the subject nucleus. Surrounding nuclei are usually “spin 1/2” nuclei and, according to quantum mechanics, these nuclei can have only a “spin-up” or “spin-down” state. Either of these states will potentially contribute to the magnetic field experienced at a neighboring nucleus, with the result that the NMR signals associated with that nucleus may be a collection of signals (a multiplet). Each line of the multiplet represents a particular combination of neighboring nuclear spin orientations. Analysis of multiplet structure can provide important details of a molecule, because scalar coupling effects are dependent on the number and relative orientations of the coupled nuclei. Scalar coupling is a necessary condition for coherence transfer experiments such as correlation spectroscopy (COSY) and total correlation spectorscopy (TOCSY), and it is fundamental to isotope-filtering NMR experiments.

Consider the one-dimensional proton NMR spectrum of N-acetyltryptophan shown in Figure 1. The proton (hydrogen atom) attached to C-4 of the indole ring of this molecule has a shielding parameter that corresponds to 7.53 ppm. The NMR spectrum of proton H-4 is more complicated than would be expected because H-4 feels the orientation of adjacent proton H-5. Two possible orientations exist for H-5, so H-4 experiences two different magnetic fields, and these are represented in the proton NMR spectrum as two signals at slightly different frequencies.

Figure 1. A portion of the proton NMR spectrum of N-acetyltryptophan corresponding to the protons attached to the indole ring, obtained at 500 MHz. (The full spectrum is given in Figure 3 of NMR.) The acetylated amino acid was dissolved in d$_6$-DMSO.

The size of the scalar coupling effect is measured in terms of a parameter called the scalar coupling constant, or spin-spin coupling constant, usually symbolized J and always measured in Hz. Subscripts may follow the J that denote the identities of the spins whose interaction is represented by the coupling constant. A superscript may precede the J that indicates the number of chemical bonds that separate the interacting nuclei. Experiments show that J can be either positive or negative. Not all NMR experiments are sensitive to the sign of J, however, and often only the magnitude of J is discussed. In the case of proton H-4 of N-acetyltryptophan, the spin-spin coupling interaction between H-4 and H-5, represented by the symbol has a value for the coupling constant of about +7Hz.

The value of a spin-coupling constant depends on several factors, including the gyromagnetic ratios of the interacting nuclei and the nature of the chemical bonding between them. The larger the product of the gyromagnetic ratios of the coupling partners, the larger the J_{AB}. A tendency exists for coupling constants to decrease with the number of intervening bonds, that is, $^1J_{AB} > {}^2J_{AB} > {}^3J_{AB}$. $^3J_{AB}$ has an important dependence on the dihedral angle between the first and third covalent bonds, which can be the source of useful stereochemical information. Table 1 indicates the ranges observed for various spin coupling constants between spin 1/2 nuclei that make up biological macromolecules.

Table 1. Typical Values for Coupling Constants, $^{n}J_{AB}$)

Chemical System	J, Hz
	$^{2}J_{HH}$, –15 to –10
(1)	
	$^{3}J_{HH}$, 2 to 12 (depends on dihedral angle)
(2)	
	$^{3}J_{HH}$, 7 to 9 (ortho) $^{4}J_{HH}$, 1.5 to 2.5 (meta) $^{5}J_{HH}$, 0 to 1 (para)
(3)	
^{13}C-H	$^{1}J_{CH}$, 125 to 250 (depends on carbon hybridization)
^{13}C-C-H	$^{2}J_{CH}$, –5 to 5
	$^{1}J_{CC}$, ~55
(4)	
	$^{1}J_{CC}$, 30 to 40
(5)	
^{15}N-H	$^{1}J_{NH}$, 80 to 100
	$^{1}J_{CN}$, ~11

(6)

$^1J_{CN}$, ~15

(7)

A detailed understanding of the spin-spin coupling phenomenon requires a quantum-mechanical treatment. An important result of such an analysis is that J-coupling between nuclei that have the same chemical shift is not observable experimentally in most of the commonly performed NMR experiments with liquids. Thus, the spin coupling constant between two protons of a methyl group, which is a two-bond proton-proton interaction ($^2J_{HH}$), is not observable in a standard one-dimensional proton NMR spectrum.

An observed spin-spin coupling constant of $^nJ_{AB}$ is potentially made up of two types of contributions. Interactions between the A and B nuclei and the electrons that bind A and B to each other and to the remainder of the molecule provide the means whereby the orientation of one nuclear spin is sensed by the other. There are several possible mechanisms by which nuclei-electron interactions can take place; in all cases, the fine structure introduced by them, as reflected by J values, is independent of the laboratory magnetic field used for the NMR experiment (B_o) and, for all practical purposes, independent of the orientation of the molecule being studied in this magnetic field. A direct through-space interaction between spin 1/2 nuclei is also possible. This nuclear dipole–nuclear dipole interaction is strongly dependent on internuclear distance and on orientation of the molecule relative to B_o. Importantly, in samples where sufficient molecular motion exists so that all possible orientations relative to the magnetic field are rapidly sampled, this contribution to spin-spin coupling averages to zero, leaving only the electron-mediated contributions. These are the conditions that normally obtain in nonviscous solutions at magnetic fields less than ~12 T and normal laboratory temperatures. In organized systems (such as liquid crystals) or in very high magnetic fields, sufficient ordering may exist that the dipole-dipole contribution to J is not completely averaged away, and an appreciable structure-dependent contribution to the observed coupling constant through this mechanism will be present.

Often, the multiplet structure produced in an NMR spectrum by J-coupling is undesirable because it provides no useful information. A variety of experimental techniques, generally known as decoupling, can be used to remove the effects of spin-spin coupling from an NMR spectrum. Under decoupling conditions, the spectrum is simplified, perhaps reduced to single peaks at the positions corresponding to the chemical shifts (shielding parameters) of the nuclei being examined. Bear in mind, however, that decoupling methods do not remove spin-spin couplings. These are fundamental aspects of the electronic and geometrical properties of the sample that cannot be removed by external intervention. Only the effects of spin coupling—multiplicity in NMR spectra—are removed by a decoupling procedure. The ^{13}C spectrum shown in Figure 4 of NMR was obtained with proton decoupling. Because proton-^{13}C spin coupling effects are absent from the spectrum, the spectral line positions depend only on the ^{13}C chemical shifts.

Suggestions for Further Reading

R. J. Abraham, J. Fisher and P. Loftus (1988) Introduction to NMR Spectroscopy, Wiley, New York.

F. A. Bovey (1988) Nuclear Magnetic Resonance Spectroscopy, Academic, San Diego.

R. K. Harris (1983) Nuclear Magnetic Resonance Spectroscopy: a physicochemical view, Pitman, Marshfield, Mass.

S. W. Homans (1992) A Dictionary of Concepts in NMR, Clarendon, Oxford.

R. Kitamaru (1990) Nuclear Magnetic Resonance: principles and theory, Elsevier, New York.

R. S. Macomber (1998) A Complete Introduction to Modern NMR Spectroscopy, Wiley, New York.

C. H. Yoder and C. D. Schaeffer, Jr. (1987) Introduction to Multinuclear NMR, Benjamin/Cummings, Menlo Park.

Scanning Electron Microscopy

The scanning electron microscope (SEM) has been used for three decades to produce direct, 3-D topographic images of biological samples. Until recently, the resolution in SEM has been too low to directly observe most macromolecules. Advances in specimen preparation, which are sufficient to preserve fine structural details at the molecular level, and instrumentation have extended the possible spatial resolution from 5–10 nm to 2–4 nm. In the SEM, the image is constructed by using a fine electron beam that is raster-scanned over the surface of a specimen. Secondary electrons from the specimen are emitted through excitation caused by primary electrons in the beam striking the specimen. The intensity of the secondary electrons is detected and used to modulate the brightness of another electron beam synchronously scanned over the surface of a cathode ray tube (1). Even though its resolution does not approach that routinely attained in the TEM, the high-resolution SEM (HRSEM) has the advantage of high contrast and high signal-to-noise. However, it must be noted that the SEM provides information only about the surface, whereas the TEM will provide information about the internal structure as well. To increase HRSEM signal yield, enhance contrast, and reduce charging artifacts, coating the specimen with a thin metal layer is performed. However, it is possible to view the fracture surface of a frozen hydrated specimen directly in the SEM without coating the surface with metal (2). For high-resolution work, the metal coat must be thin, with a grain size small enough to reduce decoration artifacts while still producing a high-resolution secondary electron signal.

The preparation of biological specimens can be broadly divided into two methods, chemical and cryo. Though easier to perform, chemical fixation is slower than cryofixation and consideration of pH and osmotic strength must be made. Furthermore, the more widespread adoption of high-pressure freezing to inhibit ice crystal formation has made cryofixation more attractive. One advance that has permitted cryo-HRSEM to characterize biological specimens at near molecular resolution is the employment of an in-lens field emission gun as the source of the electron beam (3). The beam diameter from such a gun is less than 1 nm. However, practical resolution has not achieved this dimension because of the nature of the metal coat and beam damage during observation in the HRSEM. Furthermore, the resolution is limited by the penetration of the electron beam into the specimen, since secondary electrons are emitted from a volume around the site at which the probe meets the specimen. HRSEM can be performed at either low voltage with bulk specimens, or high voltage with thin specimens. The low-voltage electron beam penetrates less deeply into bulk specimens, resulting in the high-contrast signal being generated at only a few nanometers radius from the point of beam impact. Hence, high topographic spatial resolution can be achieved (1). On the other hand, the beam diameter can be made smaller at high voltage, therefore representing a greater potential for high-resolution scanning of thin specimens (4).

HRSEM is being used more often to probe fine details of biological specimens than in the past. Cryo-HRSEM has been used to visualize surface features of reovirus particles (5). It was found that because SEM imaged only the surface of each particle, obscuring of structural detail by the internal structure or by the opposite surface was avoided, an important consideration with large structures such as viruses. Further results with cryo-HRSEM provided evidence that topographical views of actin filaments, microtubules, and clathrin cages could show individual subunits, thus permitting identification by molecular morphology (6). The success in visualizing the 3-D surface architecture of these cytoskeletal elements was attributed to controlled freeze-drying, thin metal coating, cryo-transfer and cryo-observation. In order for SEM visualization to be accomplished, the ice surrounding frozen samples must be removed, either by freeze-drying (ice sublimation in a vacuum) or freeze-substitution (ice dissolved by a chemical solvent), followed by critical point drying. It was found for cytoskeletal structures that freeze-drying provided a superior topography. HRSEM of mitochondria showed a greater variation of cristae morphology than previously recognized and also elucidated how serial-section TEM produced unreliable results because of limited resolution (7).

Bibliography

1. D. C. Joy and J. B. Pawley (1992) Ultramicroscopy 47, 80–100.
2. J. B. Pawley, P. Walther, and S.-J. Shih (1990) J. Microscopy 161, 327–335.
3. T. Nagatani et al. (1987) Scanning Microscopy 1, 901–909.
4. R. Herman and M. Muller (1991) Scanning Microscopy 5, 653–664.
5. V. E. Centronze et al. (1995) J. Struct. Biol. 115, 215–225.
6. Y. Chen et al. (1995) J. Microscopy 179, 67–78.
7. P. J. Lea et al. (1994) Microsc. Res. Tech. 27, 269–277.

Scanning Hypothesis

Most cellular messenger RNAs initiate translation via a scanning mechanism in eukaryotes. According to the scanning hypothesis (1), eukaryotic ribosomes bind to the 5′ end of the mRNA and subsequently migrate along the mRNA until they encounter an AUG codon embedded in an appropriate context, whereupon translation initiation occurs. One of the first steps in initiation of translation of most mRNAs in mammalian cells is recognition of the Cap structure and the interaction with it of eIF-4F. At some point in this process, the small ribosomal subunit with associated factors binds to the mRNA and scans to the initiation codon. The scanning model postulates that the 40S ribosomal subunit stops at the first AUG if that codon occurs in a favorable context. But if the first AUG codon occurs in a suboptimal context—for example, in the absence of the critical purine at position –3 or a G at position +4—some 40S subunits will bypass the first AUG and initiate instead at a downstream site. Two independently initiated proteins may thus be produced from one mRNA by context-dependent leaky scanning. Sometimes ribosomal leaky scanning is used for protein expression. For example, translation of the hepatitis B virus pol gene from the viral pre-genome RNA involves such a mechanism (2).

In addition, internal start codons in eukaryotes can be reached by a reinitiation mechanism, originally thought to be the exclusive trait of eubacterial ribosomes. Reinitiation at a downstream codon may be possible when the 5-proximal AUG triplet is followed shortly by a terminator codon and fails to form the proper initiation complex (3).